THE SENSES

A COMPREHENSIVE REFERENCE

VOLUME EDITORS

DAVID SMITH, STUART FIRESTEIN, GARY BEAUCHAMP

ADVISORY BOARD

ALLAN I. BASBAUM, RON HOY, AKIMICHI KANEKO,
GORDON M. SHEPHERD, GERALD WESTHEIMER

VOLUME 1

OLFACTION AND TASTE

EDITORIAL ADVISORY BOARD

Dr Allan I. Basbaum
University of California, San Francisco, CA, USA

Dr Akimichi Kaneko
Keio University, Tokyo, Japan

Dr Gordon M. Shepherd
Yale University, New Haven, CT, USA

Dr Gerald Westheimer
University of California, Berkeley, CA, USA

Volume Editors

Volume 1: Vision I

Dr Richard H. Masland
Harvard University, Boston, MA, USA

Dr Thomas D. Albright
Salk Institute, San Diego, CA, USA

Volume 2: Vision II

Dr Thomas D. Albright
Salk Institute, San Diego, CA, USA

Dr Richard H. Masland
Harvard University, Boston, MA, USA

Volume 3: Audition

Dr Peter Dallos
Northwestern University, Evanston, IL, USA

Dr Donata Oertel
University of Wisconsin, Madison, WI, USA

Volume 4: Olfaction and Taste

Dr Stuart Firestein
Columbia University, New York, NY, USA

Dr Gary K. Beauchamp
Monell Chemical Senses Center, Philadelphia, PA, USA

Volume 5: Pain

Dr M. Catherine Bushnell
McGill University, Montreal, Quebec, Canada

Dr Allan I. Basbaum
University of California, San Francisco, CA, USA

Volume 6: Somatosensation

Dr Jon H. Kaas
Vanderbilt University, Nashville, TN, USA

Dr Esther P. Gardner
New York University, New York, NY, USA

Introduction to Volumes 1 and 2

We have tried in these two volumes to cover most of the major topics in visual neuroscience, starting from molecular fundamentals and progressing to perception and cognition. We are fortunate to begin with an essay by Gerald Westheimer, one of the founders of the modern field and a scholar of great depth. The first volume continues with chapters on visual ecology and the mechanics of vision in animals other than mammals – comparative subjects that should inform thinking about all aspects of vision in any species. Our colleagues in those areas have outdone themselves and we are grateful for their thorough and entertaining contributions.

The chapters on the mammalian retina are, in general, shorter and more focused. In selecting the authors we have sought the leaders and innovators in each specialized area and we are fortunate that so many of them are represented here. We have urged them to provide continuity in their chapters and believe that they succeed in creating a deep and coherent portrait of the circuitry and fundamental functions of the retina. The final chapters of this volume leave the retina and enter the brain. They ask: where does the output of the retina go next, and what happens to it in the early stages of central vision? Here, we begin to encounter some of the limitations of current methods, notably that studies of visual coding have lagged behind the gains made using molecular and imaging techniques. A striking example is our inability to specify the different visual coding patterns transmitted to the brain by the approximately 12 structural types of retinal ganglion cells. Current approaches to the coding problem are illustrated in several chapters; but the problem is far from solved and represents a major task for the next generation.

The second volume moves beyond brain structures and mechanisms involved in light detection, retinal processing, and low-level analysis of visual image features, to address central representations associated with the perceptual interpretation of visual images. In recent years, visual neuroscience has made great strides in understanding how salient visual attributes are represented in the cerebral cortex. Recent advances are reflected here in an extended series of chapters written by leaders in their respective subfields, which collectively explore the cortical representations of luminance, color, motion, and shape. Consistent with one of the major recent trends in the field, these chapters do a fine job of integrating data and comparing perspectives gained via visual psychophysics, neurophysiology, and functional brain imaging.

In addition to representing and abstracting key properties of visual attributes, such as color and motion, vital processing stages in the visual cortex include (i) extracting the spatial layout of surfaces in the visual scene and (ii) recognizing objects. The former falls under what has come to be called 'mid-level visual processing' and recent progress is reflected here in a chapter on the topic of surface depth ordering by cues for transparency and occlusion. Object recognition, by contrast, has long been regarded a facet of 'high-level visual processing'. We have included an extended chapter that canvasses this captivating subfield with timely discussions of visual memory and perceptual constancies. One particularly intriguing and well-studied aspect of high-level vision is face recognition, and we have included a chapter that delves into this topic in some detail.

Among the most important discoveries in central visual processing over the past couple of decades is the degree to which neuronal representations of visual attributes are modifiable by shifts of attention and by experience. The field of visual attention has been particularly prolific and we have accordingly included a series of detailed chapters that address varieties of attention and their neurophysiological manifestations in the visual cortex. Perceptual learning – an experience-dependent change in the way visual features are represented –

is an emerging area of study, and we have included a chapter that nicely interweaves evidence regarding perceptual effects, neuronal response properties, and underlying mechanisms.

Finally, one of the main functions of visual processing is to influence movements of the body. Sensorimotor integration and plasticity are broad areas of study, which deserve their own volume, but we have included herein an article on a topic that is both representative of the field and one of its most deeply plowed zones – the vestibulo-ocular reflex (VOR).

The breadth and depth of topics addressed by the chapters in these two new volumes on the visual system attest to the fact that this field has developed greatly since the time Donald Hebb observed that "we know virtually nothing about what goes on between the arrival of an excitation at a sensory projection area and its later departure from the motor area of the cortex." In recent years, much of this development has been driven by technology – for example, the use of ever-better techniques for cell labeling and tracing of neuronal connections, and the refinement of procedures for recording neuronal activity in behaving animals. A long-awaited bridge has also been extended between the fields of experimental psychology and physiology, which has lead in part to a powerful union of visual psychophysics and cellular neurophysiology.All indications are that the next edition of these volumes will contain chapters that build on still newer technical and conceptual developments, such as the large-scale application of molecular genetic tools to probe visual functions at the systems level, and the use of imaging techniques that enable monitoring of activity simultaneously from large populations of neurons. Indeed, we have much to look forward to.

Richard H. Masland and Thomas D. Albright

Introduction to Volume 3

Producing a handbook, indeed any compendium that purports to represent the state of the art, is a perilous undertaking. Never mind prospective authors who are reluctant to write yet another review, or contributors who enthusiastically accept an invitation but fail to deliver, or the perennially late. Such perils of editorship are expected. The real culprit is the task itself. If a field or subject is mature enough to afford definitive summary, the likelihood is high that it is already stale. If, however, the subject is vibrant and still evolving, trying to summarize it is akin to chasing a mirage. While one writes the gospel according to Peter, Paul is sure to publish a bit that makes Peter's tome somewhat dated. Auditory neuroscience is vibrant and not all the questions are answered. So, as with most books of this sort, this volume provides a glimpse of a field in transition. The reader will find that many chapters hint at some tentativeness. We hope that a lack of final conclusions on some topics will inspire further work.

When we entered the field 35–45 years ago, it was not difficult to master most of what was known about the subject in relatively short order. Then, hearing science was largely the domain of engineers, physicists, and psychologists, and practitioners were few. The subject has meanwhile flourished and expanded to become an integral part of mainstream biology. Relying on all the powerful techniques developed for cell biology and neuroscience with the full incorporation of molecular and genetic approaches, and often introducing some that have been borrowed from the physical sciences, hearing research has emerged as one of the most interesting and complex subjects in all of biology. It is hoped that this volume conveys some of this interest as well as the palpable excitement that permeates the field.

The ear is a remarkable organ. It is a multistage transducer and nonlinear feedback system that conducts mechanical vibrations, slow and fast, first from air to fluid and then from fluid to cells that can convert minute movements to electrical signals that are recognized by the nervous system. The ear could not be more sensitive; if it were, sound would be drowned by thermal noise. It produces a frequency resolution akin to placing 29 new keys between each two adjacent keys of the piano. This book describes some of the special features that allow the ear to perform these feats.

The brain does not receive complete information from the ear directly but uses input from the cochlea to compute what it really cares about, namely where sounds emanate and what they mean. These computational tasks are complicated and are only just beginning to be understood. It is no accident that our external ears sit far apart on our heads; we use the difference in time of arrival to compute the sound's angle of incidence. Those tiny time differences can be used only if the firing of neurons can encode them. Neither is it an accident that our ears are asymmetrical top–bottom and front–back; differences in the way the ears reflect sounds into and away from the ear canal distinguish sounds coming from front or back, up or down. As the head and ears grow, the brain has to keep recalibrating its computations. Perhaps most remarkable, and least well understood, is how a human being uses an onslaught of rapidly changing sounds to learn what another is thinking.

Like the field, the volume evolved too during its planning and production stages. Some subjects were split into smaller chunks, some cameos were added, and several were removed. We allowed, even encouraged, a degree of multiple coverage of certain subjects, particularly those very lively ones where different viewpoints and orientations could be instructive. It is our hope that we have produced an accurate compendium of the field in the first decade of the third millennium that will inspire others to take up the job of discovering how animals hear and understand what is going on in their acoustic environment.

Peter Dallos and Donata Oertel

Introduction to Volume 4

This volume of the *The Senses: A Comprehensive Reference* provides a current review of the chemical senses of taste and smell. Historically, these were considered the minor senses. Descriptions of them were often combined in textbooks both because the natural stimuli are chemicals and because not much was known about them compared with vision and audition. Presumably, they were less studied since it did not seem so bad if humans lost their ability to smell or taste; blindness and deafness were much more serious concerns. However, one might justifiably argue that if all animal life were considered, these are the most important senses. Taste is devoted to a single overwhelmingly important function: it insures that an organism takes in appropriate nutrients and avoids poison. The sense of smell has more varied functions. It too is involved with recognizing food and motivating its intake but it also plays a critical role in monitoring the environment for danger and, perhaps most importantly, in regulating social and sexual activities. Thus, without these two senses most animals would neither eat nor mate! For humans, we have been learning more about the crucial roles taste and smell play in regulating food choice and intake, modulating social interactions, surveying the chemical environment, and providing pleasure. Loss or alteration of smell and taste are not trivial afflictions.

Fortunately, research in the chemical senses is no longer neglected. Indeed, the remarkable rate of progress may, at first blush, even make the idea of a handbook seem absurd. By the time you read these chapters there will be tens of new publications not covered in this book. But in fact it is all those papers that make a compendium like this useful, even if necessarily incomplete. Not long ago one could start out in the fields of olfaction or taste and come up to speed in the literature quite easily. Indeed, for some of us that was one of the attractions of the field. The advent of new techniques, their successful application to questions in chemical sensing, the attraction of investigators from other fields, suddenly transformed the chemical senses from the most mysterious to the most investigated of the sensory systems. Now it is critical to be able to read papers in molecular biology, anatomy, physiology, imaging, psychophysics, genetics, bioinformatics, genomics. . .

So the value of a handbook is as a quick but inclusive reference that will bring even senior investigators rapidly up to speed in an unfamiliar area. In this respect, the contributors to this volume have done an admirable job. Chapters cover all of the above topics in the context of specific systems in olfaction and taste, they cover historical literature (now anything published before 1995 it seems), and provide the kind of background that will facilitate appreciation of the up-to-date advances that appear monthly, if not weekly, in our dynamic field.

This handbook will also, we hope, serve new entrants in the field, especially students and postdoctoral fellows. Each chapter has extensive citations that are an excellent guide to the current literature, and will remain so for many years. The authors have endeavored not only to review the current state of the field, but also to identify important questions and remaining mysteries. Although there have been amazing advances in the past decade and a half, there are even more questions, and more interesting questions, than there were when the last edition of this Handbook appeared.

So, how about the next edition? What will it contain? Will it appear in print or only electromagnetically? What are the advances that will be chronicled in that edition? Who will the chapter authors be? This is a remarkable era in the chemical senses. Our bet is that it is only beginning. We thank the authors for their work to chronicle its current progress and to set the stage for future discoveries.

Gary K. Beauchamp

Introduction to Volume 5

"*There is no coming to consciousness without pain.*" Carl Gustav Jung

It has been argued that pain, unlike audition, vision, somatosensation, and olfaction, is not a primary sense, but instead is more of an emotional experience. Most researchers of pain, however, consider pain to be a complex perception evoked by noxious stimuli. Pain is probably far more complicated than the other perceptual modalities described in this series. For example, in the setting of tissue or nerve injury, where pain is persistent, the stimulus that evokes pain can change. In fact, under these conditions innocuous stimuli can readily evoke the perception of pain.

But even these unusual characteristics do not capture the features that make pain among the most complex of perceptions. The International Association for the Study of Pain defines pain as "An unpleasant sensory and emotional experience associated with actual or potential tissue damage, or described in terms of such damage." In other words, although there is a very discrete anatomical and physiological basis for the detection and transmission of messages that are interpreted as painful, what makes the experience of pain so special is that there is always a profound emotional quality to the experience. For all of these reasons, pain is unquestionably one of the most interesting subjects to address in the *The Senses: A Comprehensive Reference*.

Pain in general, and pain research in particular, is especially exciting as it brings together elements of so many disciplines. This volume is comprehensive. It includes a wealth of information on the molecular biology, anatomy, physiology, and biochemical bases of 'pain', both in the normal and injury setting. But this volume also addresses the critical cognitive component of the pain experience, including some of the most provocative cerebral imaging studies that for the first time are providing insights into the gestalt of brain activity that occurs when pain is experienced. There are chapters on the pharmacological basis of the placebo, on the utility of hypnosis for the treatment of pain, and even an essay on consciousness and pain.

This is not a 'how to treat' clinical textbook. Nevertheless, the editors are advocates of the new mantra in the field, namely that *chronic* pain is not a symptom of disease, but rather is a disease entity itself, a disease of nervous system function. Therefore, in addition to covering the fundamentals of acute 'pain' processing, from the nociceptor to cortical activation, we also cover, in depth, the changes that occur in the setting of injury, including molecular, structural, and biochemical alterations in the properties of nociceptors and central nervous system pathways. Some of the particularly intractable clinical pain conditions are discussed. These chapters not only provide insights into pathophysiology but also clues to pain management.

Of course, a variety of compendia have recently appeared, and many also provide comprehensive reviews of the field. With this in mind, the editors have made a concerted effort to produce a final product that is different. Too often the excitement that epitomizes the field of pain research is buried within, or indeed omitted from, the typical edited book. Some textbooks include the proverbial 'box' that highlights an interesting topic, but these are generally very limited. We wanted to bring these topics to the forefront. Our approach is to include, in association with each major chapter, at least one or two cameos that illustrate fascinating and provocative areas of basic and clinical neuroscience that intersect the study of pain.

A few years ago we knew almost nothing about the cortical mechanisms that underlie the pain experience. Today in 2007, some scientists, albeit the minority, believe that cortical imaging can provide an objective measure of the pain experience. A few years ago, the tetrodotoxin-resistant subtype of voltage-gated sodium

channel, NaV1.8, was considered the Holy Grail for the next breakthrough in pain management. How fast things change. The discovery that a loss of function mutation of NaV1.7 underlies a condition of congenital insensitivity to pain and that a gain of function mutation underlies the excruciatingly painful condition of erythromelalgia has dramatically altered the focus, not only of the science community but also of the pharmaceutical industry. The pace of discovery in pain research is indeed remarkable. We hope that this volume conveys the excitement inherent in this discovery process and, most importantly, that it stimulates the next generation of basic and clinical scientists to unravel the mystery of the pain experience.

Allan I. Basbaum and M. Catherine Bushnell

Introduction to Volume 6

When we read the word 'touch' we think of hands: an empty hand extended in friendship, a lover's caress, a mother cuddling her infant child, the 'high fives' of teammates slapping each others' hand celebrating victory in sporting events. Touch means contact between our body and another person, object, plant, or animal. Contact deforms the skin in ways that convey information to the brain about the identity of external entities; their size, shape, compliance, texture, and temperature. Because the hand is the most densely innervated part of the human body, it is not surprising that we use the hand more than any other body part to glean information beyond ourselves that allows us to interact with our surroundings in meaningful ways.

The sense of touch is unique in that it is not merely receptive, but it is crucial for guiding motor behavior. We interact with the environment to acquire tactile information, and use that knowledge to modify the world. Touch is essential for guiding the behavior of our hands. This dual sensory and motor role of touch has been beautifully depicted by the seventeenth century Spanish artist Jusepe de Ribera (1591–1652) in a canvas entitled '*The Sense of Touch*' (Figure 1). Here we see a blind man holding a sculpted head in his left hand as he palpates the face with his right hand. The surface contours and features of the head that are sensed by receptors in the hand are transformed by the brain into a mental image of the object. However, this object is not found in this form in nature, but was actually created by the hand of the sculptor, guided by touch. The painting itself is,

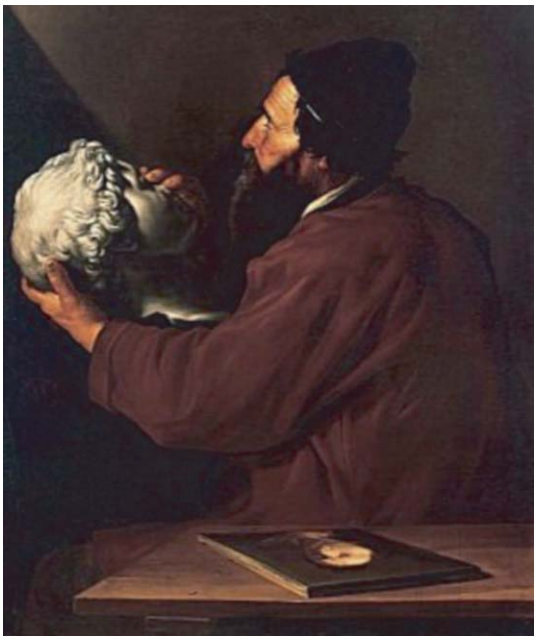

Figure 1 The Sense of Touch, c. 1615–16 by Jusepe de Ribera. Reproduced with permission from The Norton Simon Foundation © 2002.

of course, another work of the hand in which direct vision of the world, or the world of the artist's imagination, is transformed by the actions of the hand into an image on canvas delineated by skilled hand movements.

In this volume we have attempted to summarize current knowledge about the sense of touch. The various chapters have been selected to provide insight into the neurobiological mechanisms that underlie tactile sensations. We begin with an examination of the psychophysics of touch, the ability of humans to perceive the world through deformation of the skin by external stimuli. We then describe the various sensory receptors in the skin that transduce mechanical and thermal events into a pattern of nerve impulses that convey discrete bits of tactile information to the central nervous system. We explore how the information is integrated and transformed in the brain to give rise to conscious sensations of touch. In higher centers of the cerebral cortex, the sensory signals are further transformed by cognitive mechanisms such as attention, experience, and prediction, as well as by motor behaviors as we interact with the world in meaningful and useful manners. These subjective actions allow us to feel what we are particularly interested in, and to shape the information in ways that are useful for accomplishing the desired goals.

Most of the chapters in this volume deal with the sensory capabilities of the hand of humans and monkeys. However, we have also included chapters on touch in other parts of the body, and in other species, to highlight those properties of touch unique to primate hands, and those generalizable to touch as a sensory modality. We hope that this volume will provide a valuable resource to students encountering this subject for the first time, as well as to the expert audience who have contributed so much to our understanding of the sense of touch.

Esther P. Gardner and Jon H. Kaas

Dedication to Volume 4

David V. Smith (1943–2006)

David Smith was prominent among a cohort of taste physiologists born in the 1940s on three continents, who have collectively defined – or trained those who defined – gustatory activity in the central nervous system. They learned from the founders of our discipline: Yngve Zotterman, Carl Pfaffmann, Lloyd Beidler, and Masayasu Sato. Equipped with self-styled microelectrodes, they extended recordings from peripheral axons to the small, medial neurons of this ancient sense and taught us how taste selects from a perilous chemical environment to compose a healthy body.

Even as David made his way from his boyhood home in Memphis to study psychology in Knoxville forces were aligning in a competition that was to become the central motif of his career: labeled-line versus patterning. It was a binary that always concerned David, but never consumed him, as it did others of his era. It was our primary topic of professional conversation when David and I explored the South Pacific for a month in the early 1970s, and still the focus of a chapter we wrote three decades later. However voluminous the data, however sophisticated the analyses, they have never been sufficient to seal a victory, and now the issue, still unresolved if indeed a resolution exists, lies exhausted at the periphery of the field (see Chapter 4.17 A Perspective on Chemosensory Quality Coding by M. Frank)

David was always respectful of the coding arguments from both sides, as he was of those who made them. However, he could never divorce his thinking from the central discovery of gustatory electrophysiology – that taste cells are broadly tuned – and permit himself to favor a labeled-line strategy that would seem poorly suited to that finding. Thus, David remained an advocate of patterning even as he vowed unsuccessfully, three times in my presence, never to entertain the topic again.

David trained with Don McBurney in psychophysics, then with Pfaffmann in the electrophysiological techniques that became central to his life's work. He experimented on blowflies, frogs, mice, rats, rabbits, cats, and humans, but David's primary focus was on the hamster hindbrain. Over 30 years, David generated a body of data from the hamster that complemented each component that others had revealed in rats: anatomical connections, membrane qualities, coding principles, neurotransmitters, and centrifugal influences (see Chapter 4.12

Neurotransmitters in the Taste Pathway by R. Bradley). David's thinking was creative and original; his techniques precise; his analyses sophisticated and unbiased. He did not work in large groups – across all his publications David has a mean of fewer than 1.5 co-authors – but over time he worked with scores of colleagues, learning their techniques, sharing his, and always pressing for deeper understanding (see Chapter 4.15 Central Neural Processing of Taste Information by D. Smith and S. Travers).

His objective pursuit of information absent personal agendas made David a trusted colleague and leader. The Association for Chemoreception Sciences (AChemS; Minneapolis) elected him Executive Chairperson (now 'President') in 1985. David directed the neuroscience program at the University of Wyoming in the 1970s and 1980s, the Taste and Smell Center at Cincinnati in the 1980s and 1990s, served as Vice-Chair of Anatomy and Neurobiology at the University of Maryland School of Medicine in the 1990s and 2000s, then completed his life cycle, returning to Memphis as endowed Department Chair of Anatomy and Neurobiology at the Tennessee Health Science Center. In each role, David was fair, collegial, yet demanding, as he was as Executive Editor of *Chemical Senses*.

David was in the fullness of his personal and professional life, living in the city that had called him home, surrounded by appreciative colleagues and by his wife Michiko, whose devotion David requited. In my last chat with the healthy David in 2005, he expressed as much satisfaction with his life as his modesty would permit. It was all too brief.

Thomas R. Scott

Dedication to Volume 6

During the course of one year, the somatosensory community lost three major colleagues: Kenneth Johnson, Stanley Bolanowski, and Tim Pons. All three had been invited to contribute to this Volume, but sadly they passed away before this was possible. References to their work abound in various chapters, but do not substitute for their unique achievements and voices. We all miss them dearly, and would like to dedicate this Volume to their memory.

Esther P. Gardner and Jon H. Kaas

Permission Acknowledgments

The following figures is produced with kind permissions of Nature Publishing Group http://www.nature.com/nature.

Fig 1, 2 from Evolutionary transition from stretch to hearing organs in ancient grasshoppers.
Fig 3 from Eocene evolution of whale hearing.
Fig from Molecular Basis of Mechanosensory Transduction.
Fig 1 from Force generation by mammalian hair bundles supports a role in cochlear amplification.
Fig 7 from Reduced climbing and increased slipping adaptation in cochlear hair cells of mice with Myo7a mutations.
Fig 1 from TRPA1 Is a candidate for the mechanosensitive transduction channel of vertebrate hair cells.
Fig 2 from Hearing: Tightrope act.
Fig 1 from Origin of receptor potential in inner hair cells of the mammalian cochlea – evidence for Davis' theory.
Fig 2 from Transmitter release at the hair cell ribbon synapse.
Fig 2 from He et al. (2002). Motility-associated hair-bundle motion in mammalian outer hair cells.
Fig 1 from Mode of action of the efferent olivocochlear bundle on the inner ear.
Fig 1 from Time-intensity trading' in locust auditory interneurons.
Fig 1, 4 from Precise inhibition is essential for microsecond interaural time difference coding.
Fig 1 from Incremental training increases the plasticity of the auditory space map in adult barn owls.
Fig 1 from Olfactory receptor antagonism between odorants.
Fig 1 from Deficient pheromone responses in mice lacking a cluster of vomeronasal receptor genes.
Fig 1 from Ultrasensitive pheromone detection by mammalian vomeronasal neurons.
Fig 2 from Ultrasensitive pheromone detection by mammalian vomeronasal neurons.
Fig 1 from Spinothalamic lamina I neurons selectively sensitive to histamine: a central neural pathway for itch.
Fig 2 from A thalamic nucleus specific for pain and temperature sensation.
Fig 1 from Mechanisms of Disease: neuropathic pain—a clinical perspective l.
Fig 1 from Mechanisms of disease: neuropathic pain–a clinical perspective.
Fig 1a, 1b and 4c from Multiplicative computation in a visual neuron sensitive to looming.
Fig 1 from Dendritic territories of cat retinal ganglion cells.
Fig 1, 3 from Neuronal correlate of pictorial short-term memory in the primate temporal cortex.
Fig 1, 2 from Neuronal correlate of visual associative long-term memory in the primate temporal cortex.
Fig 1 from Complex objects are represented in macaque inferotemporal cortex by the combination of feature columns.
Fig 1 adapted from Neural organization for the long-term memory of paired associates.
Fig 1b and g from Spatially organized representation of hue in macaque V2.
Fig 1a and b from Multiple processing streams in occipito-temporal visual cortex.
Fig 1 from Changed perceptions in Braille readers.
Image courtesy of Goodenough, Beyond the gap: functions of unpaired connexin channels.

The following material is produced with kind permissions of American Association for the Advancement of Science http://www.sciencemarg.org.

Fig 1 from The evolutionary convergence of hearing in a parasitoid fly and its cricket host.).
Fig 2 from Cochlear microphonic audiograms in the "pure tone" bat Chilonycteris parnellii parnellii.

Fig 1 from Initiation of behavior by a single neurons: the role of behavioural context.
From 2 from Statistical learning by 8-month-old infants.
Fig 4c from Insect Sex-Pheromone Signals Mediated by Specific Combinations of Olfactory.
Fig 1a and b from MHC class I peptides as chemosensory signals in the vomeronasal organ.
Fig 2 from Encoding pheromonal signals in the accessory olfactory bulb of behaving mice.
Fig 1 from Smell Identification Ability: Changes with Age. 21.
Fig 7 from Neurodegeneration in Normal Brain Aging and Disease. Science of Aging Knowledge Environment.
Fig 1 from "Myelinated nociceptive afferents account for the hyperglyesia".
Fig 1 from A cortical region consisting entirely of face-selective cells.
Fig 1 from Nelissen K. et al. (2006) (A, B) and Vanduffel W. et al. (2002) (C). AAAS.
Fig 1 adapted from Ocular responses to linear motion are inversely proportional to viewing distance.
Fig 2d, c from Central projections of identified, unmyelinated (C) afferent fibers innervating mammalian skin.
Fig 4 is adapted from MAL Layer specific somatosensory cortical activation during active tactile discrimination.

The following material is produced with kind permissions of Taylor and Francis Ltd http://www.tandf.co.uk/journals.
Tab 1 from A survey of public health policy on bilateral fittings and comparison with market trends: The evidence-base required to frame policy.
Fig 1 from the Physiology of Fishes.
Fig 8 is adapted from "Ligand screening of olfactory receptors" - In G protein coupled receptors: structure, function, and ligand screening.
Fig 1 from Ultrastructure of the organ of Jacobson and comparative study with olfactory mucosa. Acta Otolaryngol.
Fig 1 from Marine and Freshwater Behaviour and Physiology.

1.01 The Visual System and Its Stimuli

G Westheimer, University of California, Berkeley, CA, USA

© 2008 Elsevier Inc. All rights reserved.

1.01.1	Conceptual Foundations	1
1.01.2	The Visual Stimulus	2
1.01.3	The Compression of Information	2
1.01.4	Seeing Objects in Space	3
1.01.5	The Experimental Problem: Efficient Specification of Stimulus Variables	5
1.01.6	Information Theory and Prior Probability	6

Once it became accepted, a millennium ago, that vision takes place not by the emanation of probing rays from the eyes but by the transmission into the eye and acceptance at the retina of light from the outside, the general program of vision research was laid out: learning how to relate our perception of things to the objects generating them.

The outer bounds of this program pose very profound questions indeed, and have commanded the attention of the deepest thinkers. Just what is a valid description of the outside world? How to get a grip on what constitutes a percept? Notions range the gamut from Immanuel Kant's demand that our knowledge of the *Ding an sich* is entirely indirect, predicated on the structure of our mind, to, at the other extreme, the willful ignoring of any subjective content of percepts by behaviorists.

However, if the problem is defined a little more narrowly, it becomes tractable. We accept that there is a world outside of us and that there are commonly agreed-on ways of characterizing it, a job vision researchers leave essentially to physicists. We also accept that all of us have personal experiences that can be grouped under the rubric of percepts, talked about, compared, and – by observing the report and behavior of others, including animals – used as data for scientific investigation.

1.01.1 Conceptual Foundations

A central issue stems from Johannes Mücler's law of specific nerve energy: not how discharges in the optic nerve fibers are initiated, but their central connections characterize a sensory input as visual. From this follows the posing of the question as to the adequate stimulus, a concept widely discussed in the early days of sensory research and defined as the environmental variable for which the energy needed to initiate a response is minimal. For human vision it is the electromagnetic radiation in a one-octave wide band centered on a wavelength around 550 nm. It was called light well before electromagnetic radiation had been invented and had its own stand-alone standard, the candle, whose physical properties were defined only after physicists had come to involve themselves with such devices as radiometers. No better illustration can be found of how natural science begins and then expands around the human experience. Nor of how the visual system has evolved to match what matters in the organism's environment and best enables to deal with it. The wavelength range and maximum sensitivity within it parallels that of the ambient radiation, that is, sunlight for terrestrial animals and shifted toward shorter wavelengths in the case of deep aquatic ones.

By 1860, Fechner, a seminal figure in this area, had enunciated that the task of sensory science is to find a functional relationship between the physical, and the mental worlds and he called it psychophysics. In a nice nineteenth-century touch that has served twentieth-century vision science so well, he allowed the subject to go forward on two separate tracks: the functional relationship between the outside world and some intermediate corporal stages, and then between the latter and the mind. Because not too much was known in Fechner's time about the central neural stages of vision, he left us free to select structures to identify as the intermediate stage. It could be the retina, the primary visual cortex, or other cortical areas. The second part of Fechner's program, the relationship between physiological states of the brain and our conscious experiences, involves questions that vision scientists by and large have laid aside, although a resurgence of interest in consciousness is beginning to change that. One way of

circumventing it has been the short-circuit of substituting overt behavior for the psycho in Fechner's psychophysics – the program of vision research then becomes uncontestable, both to those favoring a severely physicalist approach and to those demanding that subjective experiences be included in the portfolio. It is just that the latter group insist that there is also place for personal, not physically substantiable, observations, say, the unique yellow in the spectrum, or Gestalt grouping. Or, in Hering's memorable phrase, if one wants to figure out what a watch does, it helps, in addition to studying its cogs, wheels, and springs, to look at its face.

1.01.2 The Visual Stimulus

Regardless of the end point, the practice of vision research starts with the world of stimuli. Even the most subject-oriented of vision researchers, Goethe in his *Farbenlehre*, devoted to cataloging light and color experiences, could not entirely dispense with the manipulation of stimuli. Of the three involved class of parameters, time had been standardized since antiquity, for defining the parameters of space we turn to geometry, and for the specifications of light and color to classical physics.

But it is salutary to remember that human vision played a role in the evolution of knowledge in the fields of geometry and classical physics. It is not coincidental that the all-time greats in the physics of light – Isaac Newton, Thomas Young, James Clerk Maxwell, and Lord Rayleigh – all manifested an interest in vision and made notable contributions to it. Neither can the more formal side of defining the outside world, geometry, be seen as proceeding independently of the rules and structure of our visual system. A straight line is not defined by logical inference from previously defined premises – the usual operation within closed logico-deductive system in mathematics – but is an axiom based entirely on intuition. Used in fundamental discussions by thinkers from Kant to Hilbert, the German word *Anschauung* is indispensable here: sometimes translated as apperception, it means an intuitive, unmediated perceptual grasp of something, not further analyzable. There is a component of *Anschauung* in the axioms of geometry and indeed in the representation of space in our mind. The manifold of colors is also three dimensional but it unfolds in an entirely different manner in our mind than the visual space of objects.

At the outset, the most direct physical standards are employed to characterize what impinges on our eyes when we open them, and hence the stimuli used in vision research to probe the visual system. If the specific visual functions to be investigated are not known beforehand, we would in theory want to have available the full panoply of information about the outside world confronting the eyes, namely the temporal sequence and wavelength distribution in the energy directed to the eye from all the points in the three-dimensional object space. This is a five-dimensional manifold (energy in ergs, along with time, wavelength, and the three space dimensions). For most vertebrates, the additional dimension of polarization can be ignored. The coherence property of the radiation, to which in principle some light-detecting mechanisms are not indifferent, seems not to be utilized.

1.01.3 The Compression of Information

Such a complete catalog is outside the capability of any organism to process. Thus compromises have to be introduced to winnow it down. As species evolve, the uptake is narrowed by making choices at many junctions:

- Three hundred sixty degree panoramic vista, or only forwardly directed vision with binocular overlap for purposes of depth perception?
- Equal but limited resolution over the whole field or specialized high-resolution locus with an eye movement scanning ability?
- Fine differentiation in the wavelength dimension or economy in the number of photopigments?
- High sensitivity to weak stimuli and to small differences, or robustness to overload?

In all these cases, a particular balance has been struck between cost of processing and the information available to the animal. In the wavelength dimension, many mammalian eyes manifest a particularly ingenious solution: two separate systems with different portfolios. The energy emitted by a star and directed to the eye might, for spectroscopic purposes, be broken down into erg s^{-1} for as fine a set of wavelength bins as the resolution of the spectroscope permits and should also be detected in as small a quantity as feasible. So we have two parallel systems: scotopic and photopc.

The scotopic system has high sensitivity and, because all the light is funneled through a single photopigment, it has no ability to dissect in the wavelength dimension. It involves a simple light specification: find the product of the incident energy and the scotopic luminosity at each wavelength and arrive at a single number that denotes the stimulus strength for that star (Figure 1). We have an illustration of information compression with its twin consequences: (1) economy of signal transmission (there is only one value – scotopic lumens) and (2) inability to reconstitute the original input (as regards chromaticity, scotopic signals are monovariant).

For photopic vision, the same principle holds, except now the photopic luminosity is used to arrive at the luminance, in lumens, by the same process of multiplication and summing over the spectrum. In addition, trichromacy enters. For purposes of color discrimination, it suffices to calculate two chromaticity coefficients, because light is filtered through just three classes of photopigments and it is the ratio of their output that counts. This is again a process of information reduction, though this time not as severe as for scotopic vision. However, once it is done, the full spectral emission curve has been discarded and cannot be reconstituted. The associated loss of information is best exemplified by the phenomenon of metamerism, in which a whole host of wavelength distributions that yield the same chromaticity coefficients are no longer distinguishable. However, because there is variability in the cone pigments between species, and even among the normal of the same species, not to mention genetic deficiencies, characterizing a stimulus in terms of the standardized color coordinates is inappropriate in some circumstances of thorough color vision analysis.

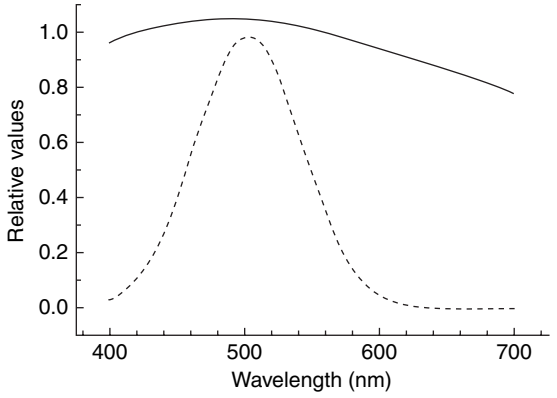

Figure 1 A star like our sun has an emission spectrum (in units of watts, W) given by the solid line. To derive its luminous energy for scotopic vision, the ordinates of each point on this curve are multiplied by the height of the scotopic luminosity curve, shown by the dashed line, at that wavelength and the product summed over the whole spectrum. Units of the luminosity curve are lumens/watt and the product therefore is a single number in luminosity units embodying the stimulus strength of this star for rod vision. The detailed shape of the star's emission spectrum has been discarded in the process and is no longer available. This is an example of compression within a stimulus domain, with the dual consequence of efficiency of operation and loss of information.

Thus the process of compressing information about the world of stimuli is intimately intertwined with the current knowledge of the structure and function of the visual system – when this is still evolving, the process is incomplete and in danger of being circular. This applies also to the physical description of the domain of stimuli. Just imagine if it turned out that some eyes are sensitive to a hitherto unsuspected or perhaps even unknown variable of electromagnetic radiation, say circular polarization or photon entanglement. All previous relevant experiments would then have an element of uncertainty because that particular dimension of a stimulus had been left unspecified. Fortunately, vision science these days is unlikely to be susceptible to such concerns, but other sensory modalities certainly are not.

1.01.4 Seeing Objects in Space

One subset of the visual world that has received more attention than the rest is that of space. As pointed out earlier, there is something special about our appreciation of the layout of stimuli in three dimensions. Regardless of whether we think it has been arrived at through learning or we began with an innate sense of it (i.e., whether we lean toward an empiricist or a nativist standpoint), we all see objects arrayed in different locations simultaneously, there is an extensive quality here that can be counterpoised to those of brightness and color, to which the word intensive is traditionally applied. That this arraying is in three dimensions – no less than three quantities are needed for a full specification – is a given fact, no further analyzable. But the mode of specifying locations within space certainly is, and the subject has been analyzed by some of the finest scholarly and scientific minds.

Since Euclid it has been the convention to posit points as the beginning elements of space, and since Descartes to construct a rectangular coordinate

system to house them. Once an origin has been chosen, three numbers uniquely define the location of a point. For monocular vision it is convenient to set the origin at the center of the eye's entrance pupil and to have the vertical axis accord with gravity, aligning the eye and head with it. But other coordinate systems may at times be more expedient (Figure 2). Where binocular vision is involved, one can place the origin at the bisection point of the line joining the centers of the entrance pupils (or perhaps the centers of rotation) of the two eyes, and draw the radius vector from that point to the object point. The three coordinates could now be r, the distance along the radius vector, and θ and ϕ, the angles of rotation around the vertical and horizontal axes, respectively. Such a construction makes overt that the distance from the observer and the angle made with the head's mid-sagittal plane have more perceptual import than the Cartesian coordinates. One can go even further and define the distance from the observer not by the linear measure along the radius vector but by the angle of parallax between the lines of sight of the two eyes to the object point. Here is a coordinate system based on three angles: laterality, elevation, and binocular parallax. In many instances it may be a better map than any other for the neural representation of space in the primary visual cortex.

It should be noted that the spatial transformations described so far differ only in the specification of coordinates; simple equations relate them. Nor has any compression been introduced, like the one which leads from the full spectral distribution to just one luminosity and two color values. But, of course, the specification of the light-emitting property of the three-dimensional world surrounding an observer, point by point, is an astronomical undertaking and almost never warranted. If the visual mechanism being studied is adequately accessed through one eye, and if the observation distance is kept constant, only two dimensions of visual angle are needed. Further reduction is possible if a repertoire of configurations is utilized, each of which requires only a smaller set of parameters. Paradigmatic is the line, which needs only the coordinates of each end point or, equivalently, coordinates of one end plus length and orientation. A huge range of visual mechanisms, neural and psychophysical, have been investigated with stimuli whose geometrical and luminance properties are simply described as lines, bars, circles, and rectangles at given positions, having identified luminance, chromaticity, or contrast values on a given background.

To underline how helpful it can be to pick the most appropriate coordinate system, consider the task of specifying the location of a point on the circumference of a regular spiral. The x, y, and z values in rectangular Cartesian coordinates will, of course, provide the desired information but they may

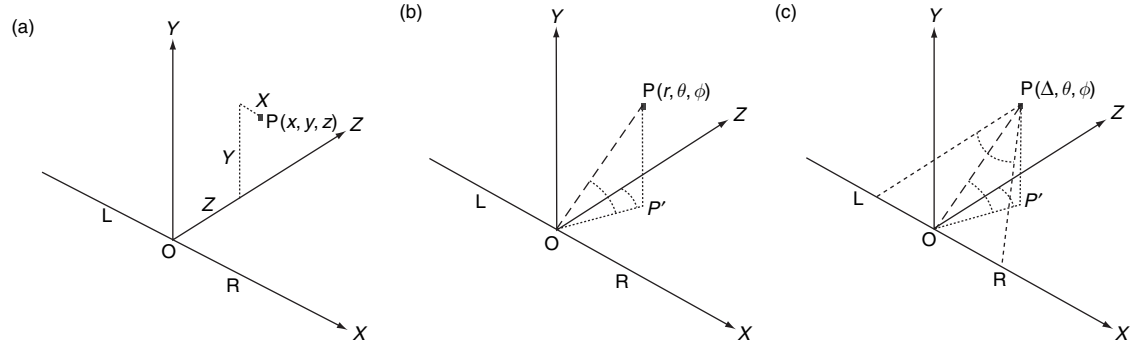

Figure 2 An example of transformation of stimulus specification in spatial vision. Information is fully conserved but rearranged to conform better to the anatomical or functional layout of the visual system. A point P is located in the upper right quadrant of the visual field. O is the location of the bisection of the interocular distance, and the head's mid-sagittal plane is aligned with the vertical. (a) Three-dimensional Cartesian coordinates: displacement of point from mid-sagittal plane of head (x), from the horizontal plane of regard (y), and along the z axis (z). (b) Here P is defined by the length of OP, that is, the radial distance r, and the orientation of line OP is defined by the two angles, θ between OP′ and OZ, describing laterality or azimuth, and ϕ between OP and OP′, describing elevation. (c) Coordinate r in the middle panel is replaced by the angle Δ between the lines from the right and left eyes to point P. In a given individual, because the distance RL is fixed, this angle is uniquely related to r. If the eyes are directed to a point at infinity on the z axis, the triangular coordinates of the point P in the binocular visual field yield an anatomically meaningful representation, binocular disparity Δ, azimuth θ, and elevation ϕ.

be quite opaque. Instead, if the orientation of the axis, the pitch, and the radius of is circumscribing cylinder have been previously fixed, how much more directly related to the situation is it to state the number of steps up the spiral and the angle within the turn! The advantage of coordinates intrinsic to the actual structure rather than more generic ones like the Cartesian becomes even more evident in the case of regular changes in radius as in a wood screw.

1.01.5 The Experimental Problem: Efficient Specification of Stimulus Variables

Reduction to a manageable set of variables can take many forms, usually predicated by prior knowledge of the sorting that the visual system does on the incoming signals. For example, when light or chromaticity are studied, pattern and shape variables are subsidiary, and vice versa. But it is surprising to recognize just how big the task is to specify the stimulus in even a narrowly defined experiment. Take the case in which a single gray Gabor patch is employed to probe a visual function. Its center location in the visual field has a distance from the eye and two angular coordinates. The underlying grating has orientation, mean light level ($cd\,m^{-2}$), amplitude, spatial frequency, and phase. Its modulating Gaussian envelope has standard deviation in two dimensions. It is a huge parameter space even though just a single basic pattern is employed to map the sensitivity profile of the human observer or perhaps a neuronal element (Figure 3).

Occasionally, more radical transformations in the spatial domain are encountered, which at their best involve no loss of information, that is, are fully reversible, yet produce an entirely different depiction of the world of visual stimuli than the pattern of light (and color) distributed before us in three-dimensional space as ordinarily regarded. A popular example is the Fourier transformation, which was borrowed from optics and holography. It is just one example of what are called kernel functions, in which the point-by-point energy distribution is sifted through, or convoluted with, a complete set of basis functions, covering space in an altogether different manner, in this particular case sinusoidal gratings in the full range of spatial frequencies. It results in a distribution providing the amplitudes and phases of all the gratings which, were super-imposed, would reconstruct the original world. It might be mentioned parenthetically that the widely utilized power spectrum is an incomplete description of the visual world because it contains no information on spatial phase.

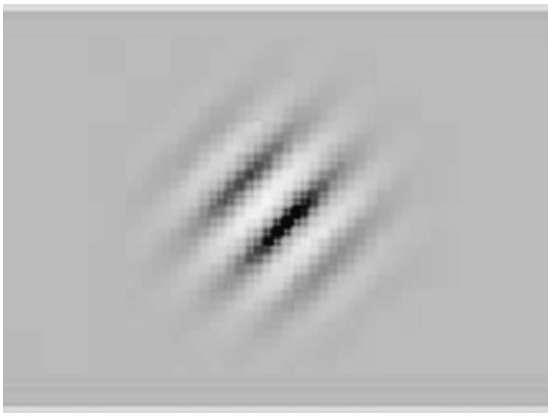

Figure 3 The Gabor patch is a popular stimulus used in vision research, yet needs a surprisingly large number of parameters for its specification. Even in the simple situation when it is black and white and shown in a plane perpendicular to the line of sight (1) the location of its center has three coordinates; (2) the underlying grating has orientation, amplitude, spatial frequency, and phase; (3) the Gaussian envelope has standard deviation in two directions unless it is circular; and (4) the background has luminance measured in $cd\,m^{-2}$. To these may have to be added the orientation of the display plane if it is not normal to the line of sight and, should color be of concern, chromaticity values of the pattern and background. As with all stimulus patterns, using Gabor patches in place of other alternatives implies the premise that this particular template has a singular value as a probe.

In principle, the manner of representation should not matter as long as certain safeguards are obeyed, particularly that it is complete and that it allows the full reconstruction of the original. However, once nonlinearities enter, the basis functions with which the object scene is analyzed need to be matched to the operations that are being performed. For example, if the retina subjects the incoming light to a center/surround filtering, and that operation is nonlinear, analysis by other means, say a set of elongated Gabor functions, will yield results that no longer allow predictions of the response to other kinds of stimuli.

This is not a trivial issue, because the essence of research into sensory processing is not just to report on a single experiment, no matter how rigorous the methodology and clean-cut the result. For exploring details of connectivity and cellular mechanisms, such as mapping of receptive fields of individual neural units, a limited test set, of course, can still be of value. But, in

principle, the aim is to predict how the visual apparatus and the whole organism will behave in more general situations, extrapolating from the ones tested in the laboratory. In the beginning, most of the research proceeded using stimuli that have firm footing in physics – white or monochromatic light and patterns based on classical geometry. However, as our understanding increased, stimuli were employed whose properties accommodate more sophisticated rules such as a logarithmic rather than linear progression in the light levels, or patterns that hug the well-documented spatial profiles of the neural stage being investigated, for example, circular difference of Gaussians in the retina, and bars and edges in the primary visual cortex.

However, there are widely expressed concerns that such stimuli, which include also random dot kinematograms and stereograms, are still too artificial and may not fully reveal the systems' performance under natural conditions. Exposing the visual system to natural scenes, for the purposes of analyzing it, may indeed reveal responses that were not predictable from those to simpler, more generic stimuli. But, while extending the range this does not solve the question of generalization from a particular class of stimuli to other, less predicable, ones.

1.01.6 Information Theory and Prior Probability

If the mission of vision science is to study the way the system gathers information about the environment – preparatory to its utilization for the organism's responses or storage for comparison with later input – it should not surprise that the movement launched under the banner of information theory was eagerly embraced. As famously formulated by Shannon, the unit of information, the bit, is the yes or no, or 0 or 1, binary answer to a single question. To make calculations for multiple events easier, they are performed in the realm of logarithms in which association rules are additive rather than multiplicative, so that the answer to two questions gives twice the information. Shannon went on to calculate the reduction of uncertainty, that is, the information gained, for the specification of a single letter of the English alphabet, which is $\log_2(26) = 4.7$ bits. Many areas of communication engineering gained clarity and precision by having apparently intractable situations laid out in such a lucid fashion. In particular, cost-effectiveness of various ways of communication could be compared and optimization achieved by minimizing duplication, technically called redundancy. Information is passed along channels usually after having been subjected to reexpression in a different form, that is, recoded. Concepts such as channel capacity and coding efficiency were developed. The analogy with what takes place in the passage from light reaching the retina to nerve impulses sent into the brain is so obvious that it would have been a dereliction of duty to neglect this new branch of scholarship. Information theory in its mathematical form can be used wherever data are adequately characterized and numerically presented, and this holds in many situations in vision science. Pixels, coding algorithms, and redundancy rules can be defined on the basis of the laws of optical physics as well as the structure of the eye's optics and the functional modules of the retina.

Looked at more closely, however, information theory contains some complexities, tackled right at the outset by Shannon. Though there are 26 letters in the alphabet, they do not occur equally often, so that more information is gained (or uncertainty diminished) when a q comes up than an e. This is taken into account by weighting each letter according to its frequency; as formally defined in Shannon's theory, the information content of an event depends on the set of prior probabilities of the elements of the ensemble. Thus the information gained when a letter of the alphabet is revealed depends on the frequency of its occurrence and this obviously will depend on the kind of text; similarly, the information content of being shown a particular word will depend on prior familiarity with the subject being treated.

Numerical specification of information transfer requires knowledge of the set of prior probabilities associated with the particular circumstances. It follows that the application of this approach will be successful (i.e., helpful in illuminating the operation of the visual system) to the degree that the situation allows quantitative expression about the elements of the ensemble and of their prior probabilities. Channel capacity, coding efficiency, and other such concepts are more meaningful when they involve readily quantifiable stimulus sets and output measurements, for example, impulses in a nerve fiber or an observer's yes and no responses in a psychophysical trial, than when a decision concerns, say, the identification of a face.

Prior probabilities also enter in the deployment of Bayesian inference, a brand of statistics that is being resurrected following years of neglect. In orthodox

statistics one estimates the probability that an encountered event might have arisen from one particular model. For example, how often would one get one's result under a null hypothesis, that is, that the operation in the test situation is indistinguishable from that in control situations? In Bayesian statistics this process is inverted: one tries to estimate the most likely of a range of models to give rise to the particular event, and for this purpose it is necessary to weight each model with its prior probability. Where this knowledge is available, Bayesian statistics is a powerful tool and to be preferred over the classical approach. But, where not, its point is missed.

This formulaic layout of both information theory and Bayesian statistics exposes the fundamental difficulty of studying perception via the inverse method, that is, inferring the stimulus from the givens of the percept. The state of the organism at any one time is compatible with (i.e., could have arisen from) a range of possible stimulus conditions, and to narrow these down one needs an idea of how likely each of them might be. An observer sees a set of black and white stripes; did they originate from:

1. the belly of a Bengal tiger?
2. the flank of a zebra?
3. the tail of a skunk? or
4. a Gabor patch shown on a monitor in an experimental setup?

The answer and the kind of response (fright, wonder, turning away, pressing the left button on a computer mouse) will depend on the context or, to use the technical phrase, the prior probability. At most times the direct (defined stimulus → observed response) research approach is preferred over the inferential (measured response → likely stimulus), but in some scientific enterprises, epidemiology for example, such a choice is not available.

Any benefits to our understanding of visual science from these modern approaches still lie in the future. But even if they turn out to be slim, they will have had the salutary effect of making us realize how much the traditional way of studying a sensory system, the one employing stimuli conceived in physics or derived from previous knowledge of the system's operation, needs to be supplemented. It has served well but its limitations are becoming more apparent as it is being recognized how far from invariant the apparatus is: properties change depending on its previous history and concurrent inputs. There are extensive interconnections within each neural stage of the visual stream, as well as between the stages in the form of feedback and top-down pathways. As a consequence, in the alert, behaving organism the state of the circuit in which it is imbedded is as much a factor in the response of a neural element in the central visual system as the immediate incoming signal from the eye. In the road ahead, approaches will be needed that transcend the time-honored simple input → output ones that have enabled the construction of the rich knowledge base of the visual sense so eloquently related in the chapters of the present volume.

1.02 Evolution of Vertebrate Eyes

R D Fernald, Stanford University, Stanford, CA, USA

© 2008 Elsevier Inc. All rights reserved.

1.02.1	**Introduction**	9
1.02.2	**Structural and Functional Adaptations in Eyes**	10
1.02.2.1	General Constraints	10
1.02.2.2	Optical Constraints	11
1.02.2.3	Lenses: Multiple Protein Types and Gene Sharing	12
1.02.2.4	Capturing Photons: The Opsin/Retinal Solution	13
1.02.3	**Evolutionary Origins**	15
1.02.3.1	Developmental Evidence about Eye Evolution	15
1.02.3.2	Developmental Evidence about Eye Evolution	16
1.02.3.3	Functional Evidence about Eye Evolution	18
1.02.3.4	Other Solutions to Capturing Photons	19
1.02.4	**How Did Eyes Evolve?**	20
References		21

Glossary

monophyletic A group of organisms or traits arising from a single, inferred common ancestor or ancestral trait.

polyphyletic A trait which evolved independently in different organisms.

phylogeny The evolutionary relatedness amongst organisms.

photoreceptor Specialized type of neuron found in the eye capable of converting light into a neural signal.

phototransduction The process of converting light energy into neural energy.

1.02.1 Introduction

Sunlight provides energy essential for all life on earth and is a profoundly important selective force, which has driven the evolution of processes that harvest the sun's energy. However, equally important, light is the premier source of information for many species driving evolution of light-sensing organs, including eyes that harvest information. So since the beginning of biological evolution on our planet over 5 billion years ago, sunlight has both fueled and informed life. Light, and the light/dark cycle from the rotating earth may be second only to sex as the most important selective force that has acted on biological organisms. One of the most remarkable evolutionary consequences of sunlight has been the evolution of mechanisms that convert photons into signals useful to organisms. Understanding the evolutionary history of eyes, however, has been vexed, because their fossil remains give limited information about their function and origins. So in understanding the genetic, biochemical, and structural remnants of eye evolution, Ernst Mayr's dictum: "evolution is an affair of phenotypes" provides a guide. This is particularly true when trying to uncover commonalities amongst the varieties of eyes and mechanisms to convert photons into energy useful to their owners.

How did eyes evolve? Darwin knew that eyes offered a special challenge to evolutionary thinking stating "... that the eye ... could have been formed by natural selection seems, I freely confess, absurd in the highest possible degree" (Darwin, C., 1859). This is the most frequently cited quote of Darwin about eyes but he also wrote: "Reason tells me, that if

numerous gradations from a simple and imperfect eye to one complex and perfect can be shown to exist, each grade being useful to its possessor, as is certainly the case; if further, the eye ever varies and the variations be inherited, as is likewise certainly the case; and if such variations should be useful to any animal under changing conditions of life, then the difficulty of believing that a perfect and complex eye could be formed by natural selection, though insuperable by our imagination, should not be considered as subversive of the theory" (Darwin, C., 1859). Though understanding eye evolution challenges the imagination, several new findings have changed our fundamental understanding about the origins of eyes.

New insights about eye evolution at the molecular level are the discovery of clusters of genes implicated in eye development that are conserved in eyes across large phylogenetic divides. Moreover, it is now clear now that vertebrate genomes contain nearly twice as many genes encoding light-transducing opsin proteins as previously known. But most importantly, physiologists have identified two fundamentally different kinds of photodetection systems in single organisms. In fact, within the eye of vertebrates, there are now known to be two fundamentally different kinds of phototransduction cascades, apparently collaborating to interpret information from light signals. Taken together, these new insights provide a much clearer story about how and how often eyes arose during evolution.

1.02.2 Structural and Functional Adaptations in Eyes

1.02.2.1 General Constraints

Walls G. L. (1942), in his monumental book provided remarkable insights about the many features of the vertebrate eye with detailed drawings showing the range and variety of vertebrate eye phenotypic characteristics. The variety of adaptations in eyes produced by selective pressures for vision in different habitats is truly astonishing. But eye structures depend critically on the physical properties of light which sets limits on how light can be collected and focused. For example, eyes have evolved to be sensitive to only a narrow range of wavelengths, relative to the broad spectrum of energy produced by sunlight (see Figure 1). This is probably because early evolution occurred in water that reduces light dramatically as a function of wavelength (Fernald, R. D., 1988). Selection favored biochemical mechanisms sensitive in this limited range of wavelengths and set the sensitivity for subsequent evolution of light detection. Many species have long lived on land where they are exposed to the broader spectrum of electromagnetic radiation from the sun, yet most animal eyes transduce light only within the original narrow band dictated by water. Some insects and species of fish and birds later evolved additional receptor types for ultraviolet light (e.g., Viltala, J. *et al.*, 1995) in response to the terrestrial

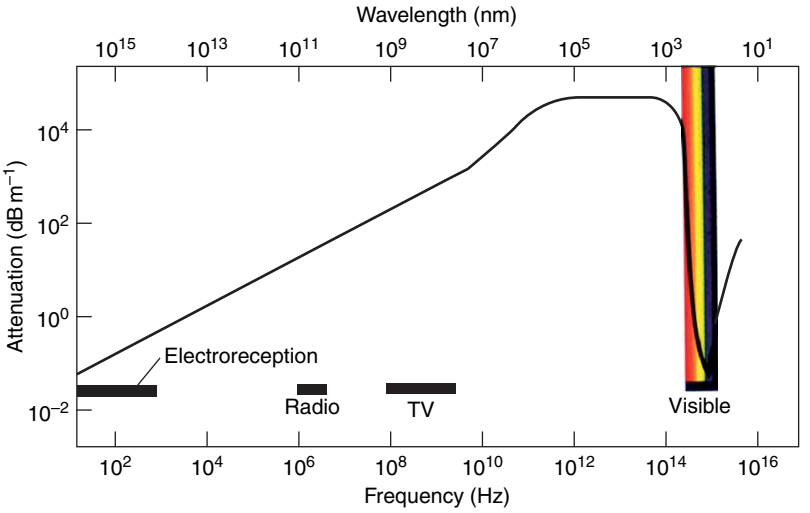

Figure 1 The attenuation (decibels per meter) of electromagnetic (EM) radiation by water as a function of wavelength (nm; top) and frequency (Hz; bottom). Significant amounts of EM radiation cannot pass through water except in two ranges: under 10^3 Hz and from 10^{14} to 10^{15} Hz. Animals have exploited these two ranges for communication: weakly electric fish communicate using the low range and visible light used by all eyes is in the upper range. Adapted from Fernald, R. D. 1988. Aquatic Adaptations in Fish Eyes. In: Sensory Biology of Aquatic Animals (*eds.* J. Atema, R. R. Fay, A. N. Popper, and W. N. Tavolga), pp. 185–208. Springer.

environment. Thus the narrow range of wavelength sensitivity is a residual reflection of our aquatic origins and illustrates how early evolutionary solutions persist in the evolved organs.

Among animals, of the ~33 animal phyla, about one-third have no specialized light-detecting organ, one-third have light sensitive organs, and the remaining third have eyes (Land, M. F. and Nilsson, D. E., 2002). Image-forming eyes have appeared in six of the 33 extant metazoan phyla (Cnidaria, Mollusca, Annelida, Onychophora, Arthropoda, and Chordata), and these six contribute about 96% of the known species alive today (Land, M. F. and Fernald, R. D., 1992), suggesting that eyes contribute to evolutionary success. Existing eyes range in size from a fraction of a millimeter to tens of centimeters in diameter and the range of types and locations suggests that they can evolve relatively easily (see below).

1.02.2.2 Optical Constraints

Only three types of image forming optical systems have evolved in eyes (Figure 2): images formed by shadows, by refraction (e.g., lens and/or cornea), or by reflection as first systematically studied by Land M. F. (1981). Since physical laws governing light fundamentally limit how an eye can function, similar structures have evolved in distinctly unrelated animals such as fishes and cephalopods. The chambered or camera eyes in these two lineages are very similar in a large number of details, despite the fact that their owners are phylogenetically quite distant (Packard, A., 1972; Fernald, R. D., 2006). Both evolved spherical lenses to achieve sufficient refractive power for focusing light underwater, but the inverted retinal layers of fishes and all vertebrates are distinctly different from the noninverted, somewhat simpler retinae of cephalopods. Moreover, each group uses a different family of opsin molecules and different transduction cascades to process photons. Macroscopically, these eye types and the animals bearing them are not homologous, even though there are striking similarities and even some homologies at the molecular and developmental levels. This seeming contradiction lies at the heart of understanding eye evolution.

The greatest variety of eyes has been found in invertebrates, which have both camera eyes (e.g., cephalopods) and compound eyes (e.g., *Drosophila*). Moreover, invertebrates also have the greatest variety in eye number and location in particular species. Whereas vertebrates have paired, chambered, lensed eyes on the head, invertebrates species may have multiple, nonpaired eyes and eyes in remarkable locations. For example, certain butterflies have light-detecting organs located such that darkness signals successful copulation (Arikawa, K. *et al.*, 1996a; 1996b). In addition, Nordström K. *et al.* (2003) described a visual system in the planula of a box

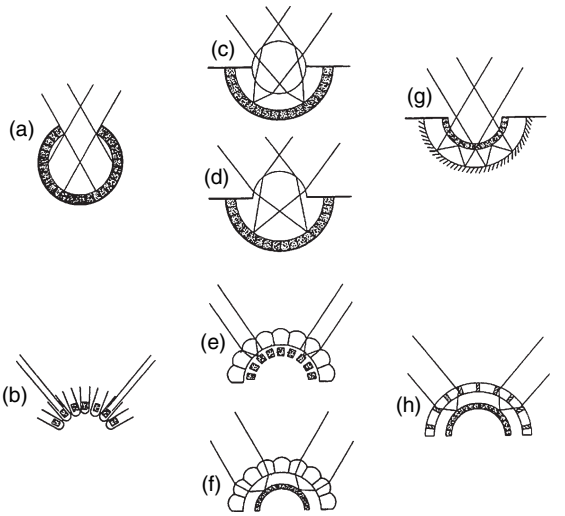

Figure 2 Major eye optical types found in animals. Chambered eyes (top: (a), (c), (d), and (g)) and compound eyes (bottom: (b), (e), (f), and (h)). Eyes form images using shadows (a, b), refraction (c–f), and reflection (g, h). The simple pit eye (a) led to the lensed eyes in fish and cephalopods (c) and terrestrial animals (d). Scallop eyes (g) are chambered but use concave mirror optics to produce an image. The simplest compound eye (b) found in bivalve molluscs led to the apposition compound eye (e) found in bees and crabs, the refracting superposition compound eye (f) of moths and krill and the reflecting superposition eye (h) found in decapod shrimps and lobsters. Adapted from Land, M. F. and Nilsson, D. E. 2002. Animal Eyes. Oxford University Press.

jellyfish *Tripedalia cystophora*, with eyecups directly connected to motor cilium meaning no nervous system processes visual information, making the eyes a complete sensory–motor system.

There is great variation in the capacities of eyes depending ultimately on their structure. For example, resolution of an image, as measured in degrees subtended differs by about 13-fold among vertebrates and even more between vertebrates and invertebrates. Eagles have the greatest acuity that is around 10 000-fold greater than that found in planaria (Land, M. F. and Nilsson, D. E., 2002). Similarly, a comparison of relative sensitivities among vertebrates reveals a range of 4×10^5 between highly sensitive deep sea animal vision and human foveal vision (Land, M. F. and Nilsson, D. E., 2002).

Another remarkable adaptation is differential wavelength sensitivity of photoreceptor types producing what we call hue or color discrimination. The selective pressures for evolution of wavelength discrimination appear to have been quite pervasive. Probably, the added value of better contrast detection, which increases the likelihood of recognizing food, mates, and predators, would have been enhanced with chromatic information (e.g., Nagel, M. G. and Osorio, D., 1993; Osorio, D. and Vorobyev, M., 1996). Indeed, recent work comparing eight primate taxa suggests that trichromatic vision evolved where leaf consumption was critical (Lucas, P. W. *et al.*, 2003). In support of this idea, many species of diurnal reptiles and birds have colored retinal filters, made of oil droplets, which appear to have evolved to increase the number of colors that can be discriminated, suggesting selective pressure for improved color vision (Vorobyev, M., 2003).

1.02.2.3 Lenses: Multiple Protein Types and Gene Sharing

Eyes collect light through an aperture, and focus it with a lens onto photoreceptor cells specialized to convert photons into neural signals. Some eyes exist without pupils and even without lenses (e.g., *Nautilus*), but eyes that evolved to give their owners a clear view of the environment over a short timescale do have lenses. Since lenses are constructed of tightly packed proteins, their evolutionary relationships might provide some insight into eye evolution.

In vertebrates, lenses are formed from modified epithelial cells which have high concentrations of soluble proteins, known as 'crystallins' because they are packed into arrays. In contrast, in most invertebrates, lens proteins are secreted by specialized cells in the eye. Interestingly, lenses of mitochondrial origin have been found in the two pairs of eyes of the parasite *Neoheterocotyle rhinobatidis* (Rohde, K. *et al.*, 1999). Despite very different cellular origins, to function optically lens proteins must be distributed to produce a radial gradient of refractive index that is low at the edge of the lens and high in the center (see Kroeger, R. H. H. *et al.*, 1999). An exact gradient of refractive index is essential for vision in animals living in water but such gradients are also found in lenses of terrestrial vertebrates and invertebrates. Perhaps most remarkably, cephalopods assemble their spherical lens from two distinct embryological sources, yet manage to produce the obligatory gradient of refractive index (Jagger, W. S. and Sands, P. J., 1999).

Until quite recently, the 10 or so crystallin proteins found in lenses were thought to be unique to lens tissue, presumed to have evolved for this function and formed a closely related phylogenetic family. Of the large number of crystallins, alpha and beta–gamma crystallins are indeed specialized lens proteins in vertebrates, related to heat shock protein and schistosome egg antigen, respectively. However, the many remaining vertebrate lens proteins are a not conserved but rather are a diverse group, many of which are used as enzymes elsewhere in the body. Surprisingly, most of these taxon-specific lens proteins are actually products of the same genes as the enzymes, a double use that has been termed 'gene sharing' by Wistow G. (1993a; 1993b). For example, a crystallin protein in the duck lens was shown to be similar to a metabolic enzyme, argininosuccinate lyase. Both the lens protein and the metabolic enzyme are encoded by the same gene, not from duplicated genes and such sharing might be a prelude to gene duplication. Such molecular opportunism is so effective that it has also occurred both in cephalopods (Tomarev, S. I. and Zinovieva, R. D., 1988) and in *Drosophila* (Janssens, H. and Gehring, W. J., 1999). One possibility is that since lenses need the production of a relatively large amount of protein, genes that have been successfully upregulated in other tissues might be preferentially selected.

Remarkably, the brittlestar (*Ophiocoma wendtii*), form crystal lenses as a part of their skeletal armor from calcite crystals. The crystals, oriented to bring light onto the photoreceptive surfaces in the body, focus the light much as corrective lenses might and effectively concentrate the light by ~50 times (Aizenberg, J. *et al.*, 2001).

The common cellular strategy of assembling lenses from diverse, phylogenetically unrelated proteins seems to be a convergent evolutionary solution that has occurred in many vertebrates independently. The exquisite gradient of the refractive index, which evolved in vertebrates and invertebrates alike resulted because it is the only way known to make an optically useful lens. What remains unknown is how such diverse protein species are assembled and folded to preserve key properties of transparency and refractive index gradient along the axis of the lens. The challenge for understanding lens development is to identify mechanisms responsible for organizing diverse proteins into a functioning lens. However, since lenses appear to have evolved along independent lines, their phylogenetic relationships do not provide a useful window into eye evolution.

1.02.2.4 Capturing Photons: The Opsin/Retinal Solution

Transducing light is the essential function of visual systems and an ancient molecule, opsin, in association with other key players has a long evolutionary history. Vertebrate opsins, also called visual pigments, appeared before eyes (Land, M. F. and Fernald, R. D., 1992) and evolved along at least seven lines, diverging from an ancestral type, before teleost fish diverged from other vertebrates (e.g., Hisatomi, O. *et al*, 1994) and indeed before deuterostomes split from the protostomes (Terakita, A., 2005). This suggests that a common ancestor had multiple opsin genes, which has been recently confirmed (see below). The exact sequence along which opsins evolved is still open to interpretation (e.g., Okano, H. *et al*., 1992), but it is clear that they evolved in parallel.

Opsins are seven transmembrane proteins (30–50 kDa) that associate with a nonprotein moiety, the chromophore, retinal. Among the ~1000 opsin forms that have been described to date, the phylogenetic differences among the seven major groups correspond to specific functional classifications (Figure 3). These classes differ in several ways but perhaps most importantly in their transduction via different G proteins. For example, although both vertebrate and invertebrate photosensitive opsin receptors are G-coupled (e.g., heterotrimeric guanine nucleotide-binding protein-coupled), and both use 11-*cis*-retinal or a close variant as their chromophore, vertebrate rod-and-cone opsins signal through photoreceptor-specific, G proteins called transducins. In contrast, invertebrate opsins signal through the G_q family of G proteins. In addition, photic responses are terminated differently. In vertebrates, excitation is followed by a combination of phosphorylation of the excited opsin, the binding of arrestin proteins which is then followed by regeneration of the active chromophore form needed for photosensitivity (Figure 4). The process in invertebrates is quite different where the G protein is inactivated by its target, phospholipase C.

Opsin function is very well understood (e.g., Menon, S. T. *et al*., 2001) and the adaptive radiation of pigment types due to natural selection for particular wavelength responses has been described for some special cases (e.g., east African cichlids, Sugawara, T. *et al*., 2002; squirrelfish, Yokoyama, S. and Takenaka, N., 2004). Moreover, the evolutionary relationships among rhodopsin molecules is well-known and some

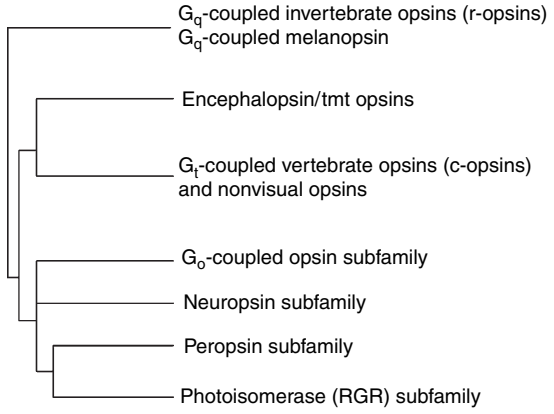

Figure 3 A simplified schematic molecular phylogenetic tree inferred by the neighbor-joining method showing the seven known opsin subfamilies. RGR, retinal G-protein-coupled receptor; TMT, teleost multiple tissue. Adapted from Terakita, A. 2005. The opsins. Genome Biol. 6, 213.

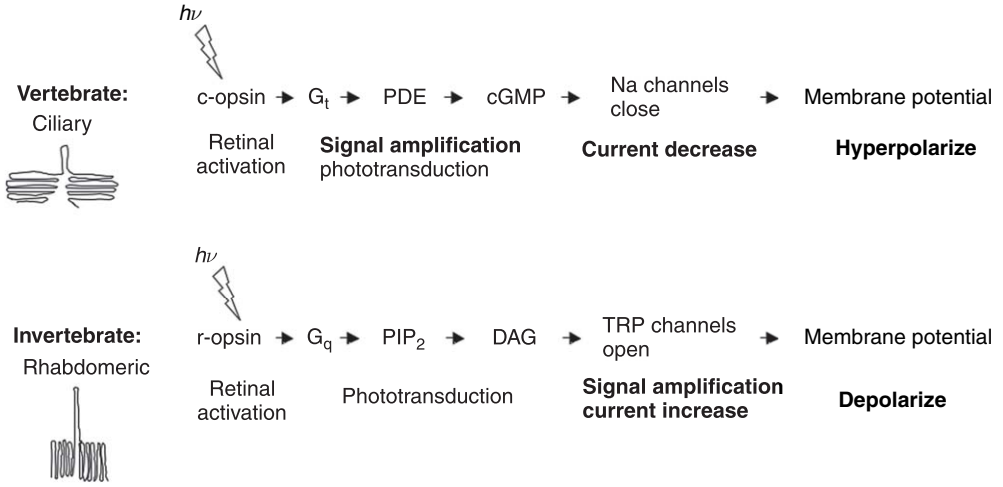

Figure 4 Schematic illustration showing the key differences between a simplified representation of (top) canonical vertebrate ciliary phototransduction and (bottom) invertebrate rhabdomeric phototransduction where $h\nu$ represents incident photon energy. The two different opsin types (c-opsin and r-opsin) are contained in distinctly different membrane types, ciliary, and rhabdomeric. The opsins are coupled to different families of G proteins that act via different types of transduction cascades. Amplification occurs during phototransduction in ciliary receptors and during channel opening in rhabdomeric receptors. These cascades produce signals of different sign. cGMP, cyclic guanosylmophosphate; DAG, diacylglycerol; G_q, guanine nucleotide-binding protein α15; G_t, transducin; PDE, phosphodiesterase; PIP_2, phosphatidylinositol-4,5-biphosphate.

of this is based on understanding the interaction between retinal and opsin (Marsh, L. and Griffiths, C. S., 2005). However, there has been considerable variance in spectral sensitivities that likely resulted from specific selective advantages for one solution over another. Detailed comparisons between terrestrial vertebrates and insects, for example, reveal that there are not unique solutions to encoding both spatial and spectral information. Mammals and bees use long-wavelength receptors for luminance and color vision while flies and birds have evolved separate sets of photoreceptors for the two purposes (Osorio, D. and Vorobyev, M., 2005).

Primate photopigments also offer examples of relatively recent evolutionary change in these important molecules. For example, Old World monkeys, apes, and humans have trichromatic vision, while New World monkeys are polymorphic, having dichromatic or trichromatic color vision (Jacobs, G. H., 1996). In this context, *Homo sapiens* may be unique in the polymorphism found in our color vision system (e.g., Neitz, M. *et al*, 1996). The variance in number and kinds of photopigments in the human retina might reflect the reduced selective pressure on color vision. The subtlety of selective pressures on chromatic detection is clear in many species. For example, in the bluefin killifish, the relative abundance of cone types depends on whether the animals live in springs or swamps (Fuller, R. C. *et al*., 2003). The novel differential spectral sensitivity in these populations is produced epigenetically through differential expression of cone classes in the retina, rather than via modification of the spectral tuning of opsin molecules, showing that there are different ways to achieve different kinds of chromatic sensitivity.

Another kind of mechanism modifying wavelength sensitivity in cone photoreceptors that depends on life history changes has been described in Pacific salmon (*Oncorhynchus gorbuscha*) and in winter flounder (*Pseudopleuronectes americanus*). As salmon grow and move from being planctivores living in surface waters where ultraviolet (UV) light is abundant to fish-eating predators in deeper waters where blue-green light prevails, they remodel their UV-sensitive cones with insertion of an opsin that is tuned to blue wavelengths (Cheng, C. L. and Flamarique, I. N., 2004). A similar mechanism has been previously reported in winter flounder (*Pseudopleuronectes americanus*) in which a single opsin type in juveniles, located in hexagonally arranged single cones is replaced by three different opsin types in photoreceptors arranged in a square array after the animal has metamorphosed into an adult (Evans, B. I. and Fernald, R. D., 1993; Evans, B. I. *et al*., 1993).

These examples and abundant others show that animals have evolved eyes with resolution, sensitivity

and wavelength detection to match their needs. Specifically, wavelength sensitivity can change with such life history changes and be quite different in closely related species. The best understood visual transduction mechanisms are those used for the main visual input in both vertebrates and invertebrates. The role of the five other opsin families and their mechanisms of visual transduction are beginning to be understood although a great deal remains mysterious.

1.02.3 Evolutionary Origins

1.02.3.1 Developmental Evidence about Eye Evolution

Logically, eyes might be monophyletic, having evolved from a single progenitor, or polyphyletic, having arisen more than once during evolution. Once it was understood that opsin played a role in phototransduction in all eyes that had been investigated, eyes were thought to have a single, monophyletic origin. The notion was that a phylogenetic tree of one important functional protein, opsin would link all eye types together. However, Salvini-Plawen L. V. and Mayr E. (1977) took a completely different perspective and compared overall structure, photoreceptor types, developmental origins of eye tissue, position of receptor axons, and other anatomical markers among eyes using existing fauna. Based on this analysis, they came to the conclusion that eyes evolved not once but at least 40 different times, and possibly many more (reviewed in Land, M. F. and Fernald, R. D., 1992). This 'multiple-origins' hypothesis, based on morphological evidence was unchallenged for 20 years until results comparing developmental pathways at the molecular level revealed a major surprise. Specifically, Gehrig and co-workers showed that *pax6* could induce ectopic eyes in fruit flies, leading them to dub this a 'master regulatory gene' (Halder, G. *et al*, 1995). Based on these results, Gehring W. J. and Ikeo K. (1999) proposed that because a single, well-conserved gene, *pax6*, could initiate eye construction in mice and flies, eyes must have arisen from a single ancestor. Did eyes appear many times in the course of evolution making them polyphyletic, as claimed by Salvini-Plawen and Mayr based on phenotype or have all eyes 'descended' directly from a common, primitive form, making them monophyletic, as claimed by Gehring *et al.* based on genes controlling development? Since this original debate erupted, there have been several important discoveries showing that eyes must have arisen more than once and, that we carry the evidence in our own eyes!

By the Cambrian period (570–500 million years ago), eyes were present in the form of very simple eyecups, useful for detecting light but not for processing directional information. Although the causes are unknown, explosive speciation, or the 'Big Bang' of animal evolution happened during the Cambrian (Conway-Morris, S., 1998). Existing eye types improved radically, coincident with the appearance of carnivory and predation. The evolution of ocular structures has proceeded in two stages (see Figure 2; Land, M. F. and Fernald, R. D., 1992). First was the production of simple eye spots which are found in nearly all the major animal groups and contain a small number of receptors in an open cup of screening pigment (Land, M. F. and Fernald, R. D., 1992). This kind of detector cannot play a role in recognizing patterns but rather for distinguishing light from dark. The second stage in eye evolution is the addition of an optical system that can produce an image. As noted above, image-forming eyes occur in 96% of known species distributed among the six phyla. Although there are basically only three methods of forming an image, among the known eye types are at least 11 distinct optical systems producing images, the most recently described is a telephoto lens, identified in the chameleon in 1995. Indeed, six of the optical systems have only been discovered in the past 25 years.

Since camera-type eyes are demonstrably superior in several respects (Nilsson, D. E., 1989), why do not all animals have them? Camera-type eyes require big heads and bodies to hold them, which likely restricted the number of animals that have followed this evolutionary path. Also, it is probable that, having evolved one eye type, conversion to another type requires intermediate stages that are much worse or useless when compared with the existing design. This would make a switch essentially lethal to animals that depend on seeing. Although this argument makes sense intuitively, some existing cases of novel optical combinations suggest this is probably not the whole story.

For teaching purposes, textbooks tend to group animal eyes into two groups, the camera-type or 'simple' eyes and the compound eyes, which does reflect a real and fundamental difference in visual systems. However, such a dichotomy conceals a remarkable diversity of optical systems subsumed under each heading.

For example, Nilsson D. E. and Modlin R. (1994) described a mysid shrimp (*Dioptromysis paucispinous*) that has a combined simple and compound eye: partly compound with multiple facets exactly like the eye of an insect, and partly simple with a single lens focusing an image on a sheet of receptors like that of a human. These shrimp are about 5 mm long with nearly spherical eyes at the ends of stalks. In addition to the facets (~800–900) there is a single giant facet facing the shrimp's tail, which the shrimp frequently rotates forward probably to get a better look at something since that facet has ~5 times the acuity (but much lower sensitivity) than the rest of the eye. It is as if the shrimp were carrying a pair of binoculars for the occasional detailed look at something ahead of it. The discovery that simple and compound eye types can be found in a single animal raises the question of how a developmental program could produce this outcome.

1.02.3.2 Developmental Evidence about Eye Evolution

Classical experimentation directed at understanding ocular development focused on vertebrate eyes, a specialized extension of the brain. Experimental models were primarily limited to mice and chicks due to their extensive prior exploitation as model organisms. The beautiful images available today make the often subtle but distinctive morphological changes during eye development seem much more obvious than they were when first observed since it is now possible, with scanning electron microscopy and sophisticated methods of controlling the state of tissue development, to watch unfolding of the production of an eye.

Eyes develop from the prospective forebrain, beginning in the eyefields, which are made up of cells of the anterior neural plate. As the prosencephalon grows, this region moves forward until the optic groove forms, and the neuroectoderm of the groove locally contacts the surface ectoderm, inducing the lens placode. As the placode invaginates to form the lens vesicle, the optic vesicle forms the bilayered optic cup, which ultimately becomes the eye. The interaction between the optic vesicle and the lens placode was identified as the 'organizer of the lens' by Spemann H. (1924). The presumptive lens arises from the lens placode, a thickening of the ectoderm in contact with the optic vesicle. Coincident with this change is the onset of expression of proteins that will form the lens. Other structures of the eye are formed by large- and small-scale tissue movements, caused and accompanied by the expression of tissue-specific genes at that site. The cornea arises from the surface ectoderm over the lens and from migrating mesenchyme derived from the neural crest. Many of the original observations about the role of specific tissue bits in these processes resulted from exquisite embryonic manipulations related to transplantation experiments. For example, Nieuwkoop P. D. (1963) identified, among other things, the source tissue essential for the induction of eye production.

With macroscopic changes described, the next challenge has been to synthesize the phenomenological, macroscopic morphological observations with molecular explanations of eye development and understand what this tells us about evolution. The morphological process of eye development has been viewed as a set of steps toward a final tissue arrangement but underlying this apparently straightforward sequence of large-scale events are distributions of gene expression with substantial overlap in both time and space. Gene expression is closely regulated, and we know that specific genes and gene products are used repeatedly, making the causal relationships among the players difficult to conceptualize. Nonetheless, progress in characterizing the genes responsible for particular steps in eye development has been reasonably rapid, as shown in several recent reviews (Harland, R., 2000; Chow, R. L. and Lang, R. A., 2001; Graw, J., 2003). Functions for at least 15 transcription factors and several signaling molecules have been described in human and mice eyes, based on developmental disorders and/or molecular manipulations (e.g., Graw, J., 2003). As with other molecular actors, the transcription factors and signaling molecules are expressed during ocular development are also essential for normal development in a wide range of other tissues. This suggests that a particular combination of expression patterns and their timing is important for the proper functioning of these genes in eye development.

It is known that the paired box gene 6 (*pax6*), a member of the family of genes that encode transcription factors with a homeodomain and a paired domain, appears to be important in eye formation across many species. The remarkable demonstration that *pax6* can induce eyes where they should not be ('ectopic') in *Drosophila* (Halder, G. *et al.*, 1995), and similar subsequent demonstration in vertebrates (Chow, R. L. *et al.*, 1999), led to the suggestion that there might be 'master control genes' responsible for

development and differentiation of ocular tissue in many species. Subsequent work has shown, however, that 'master control gene' is a misnomer since a suite of genes are required, collectively, to initiate eye development, all of which are essential. Moreover, as noted above, the genes in question actually have dynamic spatial and temporal expression during many stages of eye development, in addition to expression for essential purposes in other tissues and organs in the brain and elsewhere. Nonetheless, it is remarkable that some of the same genes appear in the context of eye development, despite great evolutionary distance among the owners of the eyes. How this might have occurred is discussed below.

For *Drosophila* eyes, the story has become considerably more complex. It seems that not one but a collection of seven genes, encoding transcription factors and two signaling molecules collaborate to make eyes (reviewed in Kumar, J. P., 2001). These nuclear factors (*eyeless* (*ey*), *twin of eyeless* (*toy*) – both of which are *pax6* homologs, *sine oculus* (*so*), *eyes absent* (*eya*), *dachshund* (*dac*), *eye gone* (*eyg*), and *optix*) and signaling systems, including the Notch and receptor tyrosine kinase pathways, act via a complex regulatory network that is reasonably well understood (see Kumar, J. P., 2001; Figure 1). The master gene hypothesis is not supported, because deletion of any of these genes causes loss or radical reduction in the *Drosophila* compound eye and, surprisingly, any gene except *sine oculus,* in collaboration with certain signaling molecules, can cause ectopic expression of an eye in a limited set of imaginal disks. This means that the whole troupe is needed to produce a reasonable eye. Why this might be so is suggested by recent work showing that the *eya* gene products are phosphatases, the first case in which a transcription factor can itself dephosphorylate other proteins to fine tune gene expression (Li, X. *et al*., 2003). This elegant work demonstrated the details of interactions among *Six1*, *Dach*, and *Eya* in the formation of the kidney, muscle, and inner ear, as well as eyes, suggesting that this suite of genetically interacting proteins has been recruited repeatedly during evolution for organogenesis of different structures.

It is difficult to abandon the heuristic of hierarchical regulatory processes in development originally proposed by Lewis to characterize homeotic properties of bithorax and antennapedia genes but molecular analysis of eye development shows that this concept may not be useful. Instead, eye development appears to need new ways of thinking about how complex tissues are made and how such organs arose in evolution. The widespread and redundant activities of specific genes during ocular development (e.g., Chauhan, B. K. *et al*., 2002; Baumer, N. *et al*., 2003) suggest that hierarchies, if they exist, are unknown and the more likely scenario is the orchestrated activity of a suite of molecular actors.

As described above, the diversity of eyes confirms their dynamic evolutionary past. Explosive speciation, or the 'Big Bang' of animal evolution happened during the Cambrian (Conway-Morris, S., 1998), when existing eye types appear to have improved radically, coincident with the onset of carnivory and predation. Many selective forces were likely at work (Fernald, R. D., 2000), including perhaps the first instances where light enabled behavioral signals (Parker, A. R., 1998) so no predominant selective force can be claimed. The rapidity of eye evolution has always been a question, but, using a simulation, Nilsson D. E. and Pelger S. (1994) suggested that about 2000 sequential changes could produce a typical image-forming eye from a light sensitive patch. With reasonable estimates, this suggests that an eye could evolve in less than half a million years making the virtual explosion of eyes during the Cambrian seem quite reasonable (Land, M. F. and Nilsson, D. E., 2002). After the Cambrian, three phyla emerged: arthropods, mollusks, and chordates. Although these groups all use the opsin molecule to capture light, details of the structure and function of their eyes differ considerably.

One of the most interesting developmental differences among extant eyes is the embryonic origin of the different structures comparing the camera eyes in vertebrate and cephalopod eyes (summarized in Nilsson, D. E., 1996). Cephalopod eyes form from an epidermal placode through successive infoldings, whereas vertebrate eyes emerge from the neural plate and induce the overlying epidermis to form the lens as described above. It is also noteworthy that the cephalopod eyes lack a cornea, which is present in all vertebrates whether aquatic or not. In addition to the differences in embryonic origin, photoreceptor cells divide into either ciliary or microvillar structures to provide the membrane surface for the opsin molecule (Salvini-Plawen, L. V. and Mayr, E., 1977). Microvilli predominate in invertebrates, whereas vertebrate photoreceptors are ciliary. Physiological responses are also quite different, with the microvillous receptors of arthropods and mollusks depolarizing to light, and the ciliary receptors of vertebrates hyperpolarizing to light. In phototransduction, vertebrate photoreceptors exploit

cyclic guanosine 5′-monophosphate (GMP) as a second messenger system, while invertebrates use inositol trisphosphate (Fernald, R. D., 2000). And, even though opsin is the key molecule for detecting light, mechanisms for regeneration (e.g., reisomerization) of the chromophore/opsin system are dramatically different among phyla (Gonzalez-Fernandez, F., 2003).

1.02.3.3 Functional Evidence about Eye Evolution

Until recently, the photo detection systems we understood well were localized primarily to eyes and pineal glands and a few other sites in the body such as the skin. For each of these, a canonical opsin and related transduction cascade were known. Specifically, ciliary structures associated with specific G proteins are known from vertebrate eyes and microvilli associated with inositol phosphate signaling cascades are known from invertebrate eyes (see above). Then, in several laboratories, each of these phototransduction cascades was found in unexpected organisms. Arendt D. *et al.* (2004) found that the polychete ragworm (*Platynereis dumerilii*) in addition to the rhadomeric photoreceptors in its eyes, had ciliary photoreceptors in the brain. This group also showed that the typical types of opsins associated with each photoreceptor type were both expressed in the ragworm and localized only with that type (e.g., vertebrate c-opsin in the brain and invertebrate r-opsin in the eye). This means that the two main types of 'eyes' exist in a worm.

The idea that two kinds of photoreceptors might exist in an invertebrate was first suggested by the pioneering work of Gorman who, with co-workers showed physiological and morphological data suggesting both types of photoreceptors exist in a scallop, *Pecten irradians* (Gorman, A. L. F. and McReynolds, J. S., 1969; Gorman, A. L. F. and McReynolds, J. S., 1971). These investigators found depolarizing and hyperpolarizing responses to light stimuli from cells located in different layers of the scallop retina, with depolarizing potentials arising from the proximal layer and hyperpolarizing potentials form the distal layer. The investigators interpreted their data solely with respect to the various kinds of selective advantages each response type might have but did not consider the evolutionary implications though their data support the existence of the two canonical receptor types in one organism.

Somewhat earlier, in vertebrates, a parallel set of results appeared. A small population of intrinsically photosensitive retinal ganglion cells were been discovered that play key roles in the regulation of nonvisual photic responses. Surprisingly, these rely on melanopsin (see Figure 3), an opsin first identified in vertebrate melanophores, brain and eyes by Provencio I. *et al.* (1998). The melanopsin in the retina was found to underlie photosensitive ganglion cells discovered by Berson D. M. *et al.* (2002), shown to be required for normal light-induced circadian phase shifting (Panda, S. *et al.*, 2002) and yet could not function without the presence of normal rods and cones (Ruby, N. F. *et al.*, 2002). Taken together, this meant that signals from the photosensitive ganglion cells were being combined with those from rods and cones somewhere in the visual system.

Photosensitive ganglion cells were then thought to comprise a nonimage-forming system that can detect the presence or absence of light but not much more. Subsequent functional analyses showed that retinal melanopsin functions via a phototransduction cascade that resembles invertebrate opsins and, in another similarity to invertebrates has intrinsic photoisomerase activity (Panda, S. *et al.*, 2005; Qiu, X. *et al.*, 2005). Adding to the remarkable set of discoveries, melanopsin-expressing ganglion cells in the primate retina have been shown to signal color and radiance levels to the lateral geniculate nucleus (Dacey, D. M. *et al.*, 2005). So, not only do vertebrates carry a version of the invertebrate visual transduction system with them, but it is used in a variety of ways, including to provide information to the 'image-forming' visual system.

There are several remarkable conclusions to be drawn from this work. First, these findings show that at least two kinds of photoreception existed in the Urbilateria, before the split into three Bilateria branches at the Cambrian (Figure 5), and, importantly, each of these branches still carry versions of these two systems. It is noteworthy that cryptochromes, also discovered very recently (Cashmore, A. R. *et al.*, 1999) are another photoreceptive system that is not based on opsin, has no molecular amplification and is found in both plants and animals. To date, cryptochromes have been shown to play a role in circadian rhythms (Green, B. C., 2004) and control of the iris muscle in birds (Tu, D. D. *et al.*, 2004) as well as many functions in plants.

Second, the two independently evolved light transduction pathways that coexist in both vertebrates and invertebrates now collaborate in collecting and processing information from photons. Although the evolutionary statement, 'survival of the

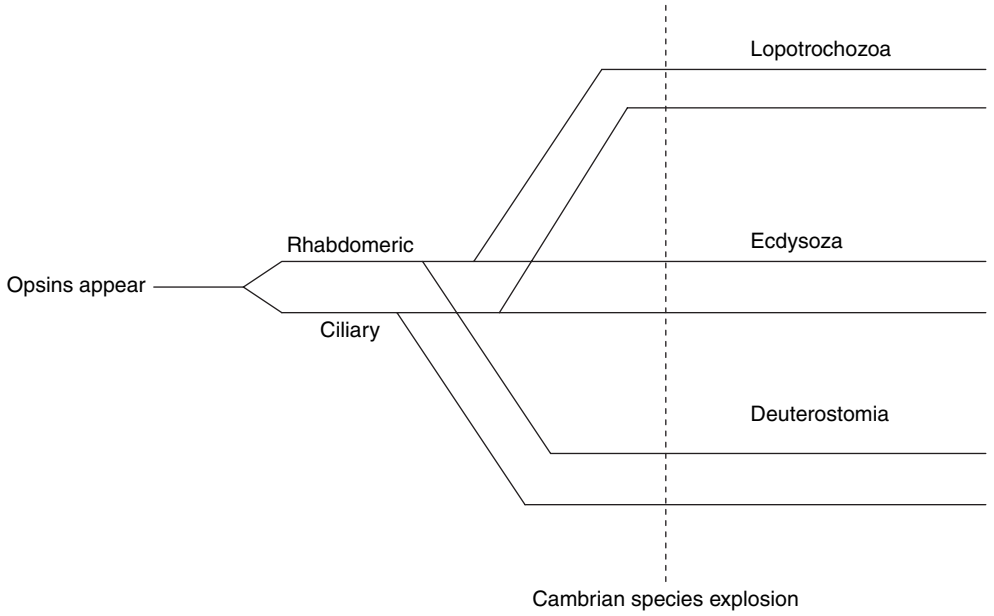

Figure 5 Schematic phylogeny of the Bilateria showing that the distinct rhabdomeric and ciliary organizaton of opsins preceded the split of the urbilateria. Adapted from Nilsson, D.-E. 2005. Photoreceptor evolution: ancient siblings serve different tasks. Curr. Biol. 15, R94–R96.

fittest' suggests a single survivor in an evolutionary race, here we see two contenders coexisting and even working together to inform adult organisms about information contained in light.

Third, since seven families of opsin have been described in vertebrates, including humans (see Figure 3 above), we can expect more surprises in how animals detect and use light. The additional opsins discovered recently have not yet been functionally characterized but the evidence suggests that there are no more opsins to be discovered (Kumbalasiri, T. and Provencio, I., 2005). Even so, figuring out how existing opsins might work together is an important challenge.

1.02.3.4 Other Solutions to Capturing Photons

As described, a persistent issues in the evolution of eyes is whether eyes evolved once or many times. Though it seems quite clear now that there were at least two kinds of phototransduction (e.g., ciliary and rhabdomeric) before the urbilateria split into three families (see Figure 4), energy and information are harvested in archaea and eukaryotic microbes using a system that clearly arose independently, via convergent evolution. Microbial, or type 1 rhodopsins, named to distinguish them from the visual pigments or type 2 rhodopsins, function to harvest light for energy, to guide phototaxis and probably many yet undiscovered functions (Spudich, J. L. *et al.*, 2000). While the number of known type 2 ('visual') rhodopsins has increased as described over the past several years (see above), the number of known type 1 rhodopsins has rapidly increased with the harvesting and genetic sequencing of ocean samples from a handful to over 800 (Spudich, J. L. and Jung, K. H., 2005). These type 1 rhodopsins are widely dispersed on the planet, found in organisms living in both fresh and sea water, salt flats, and glacial seas among others.

There are several fundamental differences between types 1 and 2 rhodopsins. First, there is no evident phylogenetic relationship between the genetic sequences of type 1 and type 2 rhodopsins. As more type 1 opsins are discovered, a connection may become apparent, but given the current state of knowledge, this seems unlikely. Second, the type 1 rhodopsins reveal convergent solutions to the mechanisms for converting photon energy. Both rhodopsin types consist of seven transmembrane domain proteins and, in each, retinal is attached in a Schiff base linkage via a lysine residue in the seventh helix (Spudich, J. L. *et al.*, 2000). However, type 1 rhodopsin (25–30 kDa) has a different organization of its intramembrane domains from type 2 rhodopsin (35 kDa), which reflects the fundamental difference in their signaling cascades.

Whereas type 1 rhodopsins function within the membrane to pump ions or signal to other integral membrane proteins, type 2 rhodopsins signal via G proteins, receptor kinases via the cytoplasmic loops (see above and Spudich, J. L. *et al.*, 2000). Retinal is used in association with both apoproteins but these are photoisomerized quite differently. In the familiar, type 2 rhodopsins, 11-*cis*-retinal is transformed to all trans upon absorbing light while in type 1 rhodopsins, all-*trans*-retinal is transformed to 13-*cis* when absorbing light.

Taken together, the remarkable convergence of type 1 and 2 rhodopsins suggests that in the course of evolution, an opsin apoprotein, associated with retinal has been discovered and exploited twice. Clearly, when the seven transmembrane protein is appropriately solvated with retinal, it is useful for transforming the energy of photons into more useful forms. This also suggests that progenitors of the type 1 opsins may have existed in earliest evolution before the divergence of archaea, eubacteria, and eukaryotes. This means that the light-driven ion transport mechanism for deriving energy used in association with retinal 1 preceded the evolution of photosynthesis as a means for using the sun's energy (Spudich, J. L. and Jung, K. H., 2005). We can now wonder whether a proto eye-like structure using rhodopsin 1 remains to be found that would allow a comparison of an additional independent solution to extracting information from light.

1.02.4 How Did Eyes Evolve?

Eyes exist in a variety of shapes, sizes, optical designs, and locations on the body, but they all provide similar information about wavelength and intensity of light to their owners. Different tissues have been recruited to build lenses and retinas across the phyla (Fernald, R. D., 2006). In contrast, all eyes share the same mechanism of absorbing photons since the opsin–chromophore combination has been conserved across phylogeny. Despite new findings yielded by powerful molecular techniques, all evidence still suggests that eyes have a polyphyletic origin, particularly since the discovery that two photodetection systems had evolved prior to the split of the urbilateria into three families. Clearly, eye as we know them contain homologous molecules responsible for many structural, functional and even developmental features. Given a growing list of homologous gene sequences among molecules in the eye across vast phylogenetic distances, the challenge is now to discover what makes the eyes of *Drosophila*, squid, and mouse so different. Understanding what makes eyes different may be a bigger challenge than finding what they have in common.

It seems increasingly evident that as eyes evolved, different functional mechanisms have been generated by recruiting existing gene programs. From genome sequencing, we know that there are far fewer genes in organisms than previously thought, so the use and reuse of genes and their products in combinatorial assemblies as reported for known genomes make sense. In the development of eyes, this seems to be the rule not the exception. Specifically, in the evolution of eyes, it seems likely that light sensitivity evolved early in the Cambrian in the form of a proto-opsin molecule in association with the chromophore, retinal. This molecular combination, sensitive to light, became associated with the genes *pax6* (Sheng, G. *et al.*, 1997), and possibly, *eya* (based on its phosphatase activity (Li, X. *et al.*, 2003)). One can imagine that this combination was recruited and worked well in early evolved eyespots and other light-sensing organs. It would not be surprising, for example, to find these genetic players in the recently described eye without a nervous system (Nordström, K. *et al.*, 2003).

Important insights about how regulatory gene networks might have evolved comes from what is called the 'hox paradox' (Wray, G. A., 2002). During development, orthologous genes are expressed in superficially similar domains during embryonic development of very different organisms (e.g., *Drosophila*; mouse) yet these embryos produce adults that are anatomically quite distinct having very few structures with common ancestors. Though not completely resolved, one resolution of this paradox is that there has been evolutionary convergence in the use of some genes and hence apparent homology (Wray, G. A., 2003). It seems that this is the likely scenario for the evolution of eyes. Some genes have been recruited into regulatory gene networks repeatedly, possibly committed early in evolutionary history and kept because they simply work well.

As different eye types evolved over time, there was probably repeated recruitment of particular gene groups, not unlike improvisational groups of actors, interacting to produce candidates for selection. The evolutionary fiddling through which various combinations or routines were tried could have led to numerous parallel evolutionary paths for eyes as we now envisage.

From this, two different mechanisms for transmitting the photic information to surrounding cells were

selected for, one in ciliary and one in rhadomeric photoreceptors. These two systems are likely present in all organisms as described above for worms and mice. The big surprise is that both of these transduction systems persisted with each selected as the primary visual system for a major branch of animals. So, the answer to the question of whether eyes evolved from a single prototypical eye (monophyletic), or whether they evolved repeatedly (polyphyletic), appears to be that quite evidently eyes arose at least twice and probably many times. And, as described above, given the vast number of organisms using rhodopsin 1, we should not be surprised if additional eyes appear in the biological world in the future.

References

Aizenberg, J., Tkachenko, A., Weiner, S., Addadi, L., and Hendler, G. 2001. Calcitic microlenses as part of the photoreceptor system in brittlestars. Nature 412, 819–822.

Arendt, D., Tessmar-Raible, K., Snyman, H., Dorresteijn, A. W., and Wittbrodt, J. 2004. Ciliary photoreceptors with a vertebrate-type opsin in an invertebrate brain. Science 306, 869–871.

Arikawa, K., Scholten, D. G. W., and Stavenga, D. G. 1996a. Spectral origin of the red receptors in the retina of the butterfly *Papilio xuthus*. Zool. Sci. (Tokyo) 13, 118.

Arikawa, K., Suyama, D., and Fujii, D. 1996b. Light on butterfly mating. Nature 382, 119.

Baumer, N., Marquardt, T., Stoykova, A., Speiler, D., Treichel, D., Ashery-Padan, R., and Gruss, P. 2003. Retinal pigmented epithelium determination requires the redundant activities of Pax2 and Pax6. Development 130, 2903–2925.

Berson, D. M., Dunn, F. A., and Takao, M. 2002. Phototransduction by retinal ganglion cells that set the circadian clock. Science 295, 1070–1073.

Cashmore, A. R., Jarillo, J. A., Wu, Y. J., and Liu, D. 1999. Cryptochromes: blue light receptors for plants and animals. Science 284, 760–765.

Chauhan, B. K., Reed, N. A., Yang, Y., Cermak, L., Reneker, L., Duncan, M. K., and Cvekl, A. 2002. A comparative cDNA microarray analysis reveals a spectrum of genes regulated by Pax6 in mouse lens. Genes Cells 7, 1267–1283.

Cheng, C. L. and Flamarique, I. N. 2004. Opsin expression: new mechanism for modulating colour vision – single cones start making a different opsin as young salmon move to deeper waters. Nature 428, 279.

Chow, R. L. and Lang, R. A. 2001. Early eye development in vertebrates. Annu. Rev. Cell Dev. Biol. 17, 255–296.

Chow, R. L., Altmann, C. R., Lang, R. A., and Hemmati-Brivanlou, A. 1999. Pax-6 induces ectopic eyes in a vertebrate. Development 126, 4213–4222.

Conway-Morris, S. 1998. The Crucible of Creation: The Burgess Shale and the Rise of Animals. Oxford University Press.

Dacey, D. M., Liao, H. W., Peterson, B. B., Robinson, F. R., Smith, V. C., Pokorny, J., Yau, K. W., and Gamlin, P. D. 2005. Melanopsin-expressing ganglion cells in primate retina signal colour and irradiance and project to the LGN. Nature 433, 698–699.

Darwin, C. 1859. The Origin of Species by Means of Natural Selection. John Murray.

Evans, B. I. and Fernald, R. D. 1993. Retinal transformation at metamorphosis in the winter flounder (*Pseudopleuronectes americanus*). Vis. Neurosci. 10, 1055–1064.

Evans, B. I., Harosi, F. I., and Fernald, R. D. 1993. Photoreceptor spectral absorbance in larval and adult winter flounder (*Pseudopleuronectes americanus*). Vis. Neurosci. 10, 1065–1071.

Fernald, R. D. 1988. Aquatic Adaptations in Fish Eyes. In: Sensory Biology of Aquatic Animals (*eds*. J. Atema, R. R. Fay, A. N. Popper, and W. N. Tavolga), pp. 185–208. Springer.

Fernald, R. D. 2000. Evolution of eyes. Curr. Opin. Neurobiol. 10, 444–450.

Fernald, R. D. 2006. Casting a genetic light on the evolution of eyes. Science 313, 1914–1918.

Fuller, R. C., Fleishman, L. J., Leal, M., Travis, J., and Loew, E. 2003. Intra specific variation in retinal cone distribution in the bluefin killifish, *Lucania goodei*. J. Comp. Physiol. A 189, 609–616.

Gehring, W. J. and Ikeo, K. 1999. Pax 6: mastering eye morphogenesis and eye evolution. Trends Genet. 15, 371–377.

Gonzalez-Fernandez, F. 2003. Interphotoreceptor retinoid-binding protein – an old gene for new eyes. Vision Res. 43, 3021–3036.

Gorman, A. L. F. and McReynolds, J. S. 1969. Hyperpolarizing and depolarizing receptor potentials in the scallop eye. Science 165, 309–310.

Gorman, A. L. F. and McReynolds, J. S. 1971. Photoreceptors in primitive chordates: fine structure, hyperpolarizing receptor potentials, and evolution. Science 172, 1052–1054.

Graw, J. 2003. The genetic and molecular basis of congenital eye defects. Nat. Rev. Genet. 4, 876–888.

Green, B. C. 2004. Cryptochromes: tailored for distinct functions. Curr. Biol. 14, R847–R849.

Halder, G., Callaerts, P., and Gehring, W. J. 1995. New perspectives on eye evolution. Curr. Opin. Genet. Dev. 5, 602–629.

Harland, R. 2000. Neural induction. Curr. Opin. Genet. Dev. 10, 357–362.

Hisatomi, O., Kayada, S., Aoki, Y., Iwasa, T., and Tokunaga, F. 1994. Phylogenetic relationships among vertebrate visual pigments. Vision Res. 34, 3097–3102.

Jacobs, G. H. 1996. Primate photopigments and primate color vision. Proc. Natl. Acad. Sci. U. S. A. 93, 577–581.

Jagger, W. S. and Sands, P. J. 1999. A wide-angle gradient index optical model of the crystalline lens and eye of the octopus. Vision Res. 39, 2841–2852.

Janssens, H. and Gehring, W. J. 1999. Isolation and characterization of drosocrystallin; a lens crystallin gene of *Drosophila melanogaster*. Dev. Biol. 207, 204–214.

Kroeger, R. H. H., Campbell, M. C. W., Fernald, R. D., and Wagner, H. J. 1999. Multifocal lenses compensate for chromatic defocus in vertebrate eyes. J. Comp. Physiol. A 184, 361–369.

Kumar, J. P. 2001. Signalling pathways in *Drosophila* and vertebrate retinal development. Nat. Rev. Genet. 2, 846–857.

Kumbalasiri, T. and Provencio, I. 2005. Melanopsin and other novel mammalian opsins. Exp. Eye Res. 81, 368–375.

Land, M. F. 1981. Optics and Vision in Invertebrates. In: Handbook of Sensory Physiology (*ed*. H. Autrum), pp. 471–592. Springer.

Land, M. F. and Fernald, R. D. 1992. The evolution of eyes. Annu. Rev. Neurosci. 15, 1–29.

Land, M. F. and Nilsson, D. E. 2002. Animal Eyes. Oxford University Press.

Li, X., Oghi, K. A., Zhang, J., Krones, A., Bush, K. T., Glass, C. K., Nigam, S. K., Aggarwal, A. K., Maas, R., Rose, D. W., and Rosenfeld, M. G. 2003. Eya protein phosphatase activity regulate Six1–Dach–Eya transcriptional effects in mammalian organogenesis. Nature 426, 247–253.

Lucas, P. W., Dominy, N. J., Riba-Hernandez, P., Stoner, K. E., Yamashita, N., Loria-Calderon, E., Petersen-Pereira, W., Rojas-Duran, Y., Salas-Pena, R., Solis-Madrigal, S., Osorio, D., and Darvell, B. W. 2003. Evolution and function of routine trichromatic visionin primates. Int. J. Org. Evol. 57, 2636–2643.

Marsh, L. and Griffiths, C. S. 2005. Protein structural influences in rhodopsin evolution. Mol. Biol. Evol. 22, 894–904.

Menon, S. T., Han, M., and Sakmar, T. P. 2001. Rhodopsin: structural basis of molecular physiology. Physiol. Rev. 81, 1659–1688.

Nagel, M. G. and Osorio, D. 1993. The tuning of human photopigments may minimize red-green chromatic signals in natural conditions. Proc. R. Soc. Lond. B Biol. Sci. 252, 209–213.

Neitz, M., Hagstrom, S. A., Kainz, P. M., and Neitz, J. 1996. L and M cone opsin gene expression in the human retina: relationship with gene order and retinal eccentricity. Invest. Ophthalmol. Vis. Sci. 37, S448.

Nieuwkoop, P. D. 1963. Pattern formation in artifically activated ectoderm (*Rana pipens* & *Ambystoma punctatum*). Dev. Biol. 7, 255–279.

Nilsson, D. E. 1989. Optics and Evolution of the Compound Eye. In: Facets of Vision (*eds*. D. G. Stavenga and R. C. Hardie), pp. 30–73. Springer.

Nilsson, D. E. 1996. Eye ancestry: old genes for new eyes. Curr. Biol. 6, 39–42.

Nilsson, D.-E. 2005. Photoreceptor evolution: ancient siblings serve different tasks. Curr. Biol. 15, R94–R96.

Nilsson, D. E. and Modlin, R. 1994. A mysid shrimp carrying a pair of binoculars. J. Exp. Biol. 189, 213–236.

Nilsson, D. E. and Pelger, S. 1994. A pessimistic estimate of the time required for an eye to evolve. Proc. R. Soc. Lond. B Biol. Sci. 256, 53–58.

Nordström, K., Wallen, R., Seymour, J., and Nilsson, D. E. 2003. A simple visual system without neurons in jellyfish larvae. Proc. R. Soc. Lond. B Biol. Sci. 270, 2349–2354.

Okano, H., Hayashi, S., Tanimura, T., Sawamoto, K., Yoshikawa, S., Watanabe, J., Iwasaki, M., Hirose, S., Mikoshiba, K., and Montell, C. 1992. Regulation of *Drosophila* neural development by a putative secreted protein. Differentiation 52, 1–11.

Osorio, D. and Vorobyev, M. 1996. Colour vision as an adaptation to frugivory in primates. Proc. R. Soc. Lond. B Biol. Sci. 263, 593–599.

Osorio, D. and Vorobyev, M. 2005. Photoreceptor spectral sensitivities in terrestrial animals: adaptations for luminance and colour vision. Proc. Biol. Sci. 272, 1745–1752.

Packard, A. 1972. Cephalopods and fish: the limits of convergence. Bio. Rev. 47, 241–307.

Panda, S., Nayak, S. K., Campo, B., Walker, J. R., Hogenesch, J. B., and Jegla, T. 2005. Illumination of the melanopsin signaling pathway. Science 307, 600–604.

Panda, S., Sato, T. K., Castrucci, A. M., Rollag, M. D., DeGrip, W. J., Hogenesch, J. B., Provencio, I., and Kay, S. A. 2002. Melanopsin (Opn4) requirement for normal light-induced circadian phase shifting. Science 298, 2213–2216.

Parker, A. R. 1998. Colour in Burgess Shale animals and the effect of light on evolution in the Cambrian. Proc. R. Soc. Lond. B Biol. Sci. 265, 967–972.

Provencio, I., Jiang, G., De Grip, W. J., Hayes, W. P., and Rollag, M. D. 1998. Melanopsin: an opsin in melanophores, brain, and eye. Proc. Natl. Acad. Sci. U. S. A. 95, 340–345.

Qiu, X., Kumbalasiri, T., Carlson, S. M., Wong, K. Y., Krishna, V., Provencio, I., and Berson, D. M. 2005. Induction of photosensitivity by heterologous expression of melanopsin. Nature 433, 745–749.

Rohde, K., Watson, N. A., and Chisholm, L. A. 1999. Ultrastructure of the eyes of the larva of *Neoheterocotyle rhinobatidis* (Platyhelminthes, Monopisthocotylea), and phylogenetic implications. Int. J. Parasitol. 29, 511–519.

Ruby, N. F., Brennan, T. J., Xie, X., Cao, V., Franken, P., Heller, H. C., and O'Hara, B. F. 2002. Role of melanopsin in circadian responses to light. Science 298, 2211–2213.

Salvini-Plawen, L. V. and Mayr, E. 1977. On the evolution of photoreceptors and eyes. Evol. Biol. 10, 207–263.

Sheng, G., Thouvenot, E., Schmucker, D., Wilson, D. S., and Desplan, C. 1997. Direct regulation of rhodopsin 1 by Pax-6/eyeless in *Drosophila*: evidence for a conserved function in photoreceptors. Genes Dev. 11, 1122–1131.

Spemann, H. 1924. Über Organisatoren in der tierischen Entwicklung. Naturwissenschaften 48, 1092–1094.

Spudich, J. L. and Jung, K. H. 2005. Microbial Phodopsins: Phylogenetic and Functional Diversity. In: Handbook of Photosensory Receptors (*eds*. W. R. Briggs and J. L. Spudich), pp. 1–21. Wiley-VCH.

Spudich, J. L., Yang, C. S., Jung, K. H., and Spudich, E. N. 2000. Retinylidene proteins: structures and functions from archaea to humans. Annu. Rev. Cell Dev. Biol. 16, 365–392.

Sugawara, T., Terai, Y., and Okada, N. 2002. Natural selection of the rhodopsin gene during the adaptive radiation of East African Great Lakes cichlid fishes. Mol. Biol. Evol. 19, 1807–1811.

Terakita, A. 2005. The opsins. Genome Biol. 6, 213.

Tomarev, S. I. and Zinovieva, R. D. 1988. Squid major lens polypeptides are homologous to glutathione S-transferases subunits. Nature 336, 86–88.

Tu, D. D., Batten, M. L., Palczewski, K., and Van Gelder, R. N. 2004. Nonvisual photoreception in the chick retina. Science 306, 129–131.

Viltala, J., Korpimaki, E., Palokangas, P., and Koivula, M. 1995. Attraction of kestrels to vole scent marks visible in ultraviolet detection. Nature 373, 425–427.

Vorobyev, M. 2003. Coloured oil droplets enhance colour discrimination. Proc. R. Soc. Lond. B Biol. Sci. 270, 1255–1261.

Walls, G. L. 1942. The Vertebrate Eye and its Adaptive Radiation. The Cranbrook Institute of Science.

Wistow, G. 1993a. Lens crystallins: gene recruitment and evolutionary dynamism. Trends Biochem. Sci. 18, 301–306.

Wistow, G. 1993b. Identification of lens crystallins: a model system for gene recruitment. Methods Enzymol. 224, 563–75.

Wray, G. A. 2002. Do convergent developmental mechanisms underlie convergent phenotypes? Brain Behav. Evol. 59, 327–336.

Wray, G. A. 2003. Transcriptional regulation and the evolution of development. Int. J. Dev. Biol. 47, 675–684.

Yokoyama, S. and Takenaka, N. 2004. The molecular basis of adaptive evolution of squirrelfish rhodopsins. Mol. Biol. Evol. 21, 2071–2078.

Further Reading

Fernald, R. D. 2004. Eyes: variety, development and evolution. Brain Behav. Evol. 64, 141–147.

Jacobs, G. H. 1998. A perspective on color vision in platyrrhine monkeys. Vision Res. 38, 3307–3313.

Land, M. F. 2000. On the functions of double eyes in midwater animals. Philos. Trans. R. Soc. Lond. B Biol. Sci. 355, 1147–1150.

Land, M. F. and McLeod, P. 2000. From eye movements to actions: how batsmen hit the ball. Nat. Neurosci. 3, 1340–1345.

Nordström, K., Larsson, T. A., and Larhammar, D. 2004. Extensive duplications of phototransduction genes in early vertebrate evolution correlate with block (chromosome) duplications. Genomics 83, 852–872.

Wistow, G. J., Shaughnessy, M. P., Lee, D. C., Hodin, J., and Zelenka, P. S. 1993. A macrophage migration inhibitory factor is expressed in the differentiating cells of the eye lens. Proc. Natl. Acad. Sci. U. S. A. 90, 1272–1275.

1.03 Vision in Birds

G R Martin, University of Birmingham, Birmingham, UK

D Osorio, University of Sussex, Brighton, UK

© 2008 Elsevier Inc. All rights reserved.

1.03.1	**Introduction**	25
1.03.2	**Fundamental Constraints on Bird Eyes**	26
1.03.2.1	Size and Information Capacity	26
1.03.2.1.1	Costs of increasing eye size	27
1.03.2.1.2	Eye-size allometry and ecology	27
1.03.2.2	The Ambient Light Environment and Light Adaptation	27
1.03.3	**Describing and Comparing Optical Structure of Avian Eyes**	28
1.03.3.1	Optical Design	29
1.03.3.1.1	Eye size	29
1.03.3.1.2	Contributions of lens and cornea	30
1.03.3.1.3	Amphibious habits and optical design	30
1.03.3.2	Accommodation	31
1.03.4	**The Kiwi: Regressive Evolution of a Bird Eye**	31
1.03.5	**Visual Fields**	32
1.03.5.1	Describing Visual Fields	32
1.03.5.1.1	Difficulties in estimating visual fields and binocular overlap	34
1.03.5.2	Types of Avian Visual Field	35
1.03.5.2.1	Type 1 fields	35
1.03.5.2.2	Type 2 fields	36
1.03.5.2.3	Type 3 fields: owl eyes	36
1.03.5.3	Visual Fields and Eye Movements	36
1.03.5.4	The Function of Binocularity	36
1.03.5.4.1	Binocularity and optic flow fields	40
1.03.5.4.2	Binocular vision and nocturnality	41
1.03.5.4.3	The blind area above the head and eye size – sunshades in birds	42
1.03.6	**Photoreceptors and the Retina**	42
1.03.6.1	Photopigments and Photoreceptors	42
1.03.6.2	Oil Droplets	43
1.03.6.2.1	Spectral properties of oil droplets and the benefits of narrowing spectral tuning curves	44
1.03.6.2.2	Variation in oil droplet pigmentation	44
1.03.6.3	Photoreceptor Densities and Distributions	45
1.03.6.4	Variation of Receptor Spectral Sensitivities and Densities	45
1.03.7	**Functions of the Different Types of Avian Cone**	46
1.03.7.1	Double Cones and Avian Luminance	46
1.03.7.2	Single Cones and Tetrachromacy	47
1.03.7.3	Specialization of Single Cones and UV Sensitivity	48
1.03.8	**Concluding Remarks: A Wing Guided by an Eye?**	48
References		48

1.03.1 Introduction

Rochon-Duvigneaud A. (1943, p. 453) captured the essence of a bird as "a wing guided by an eye." Both in popular imagination and in science, the phrase unites the defining characteristics of birds, flight with vision as the primary sense. Wings are the essential attribute of all birds or, for flightless birds, their ancestors.

Wings and vision diversified together, to give the range of ecology and behavior of living birds (Gill, F. B., 2007). Bats have remarkable powers of echolocation (Nachtigall, P. E. and Moore, P. W. B., 1988), but compared with birds their ecology and behavior is restricted. Vision provides spatial information at the speed, resolution, and range necessary to guide flight and the other behaviors that make birds so interesting (Perrins, C. M., 1990; Davies, M. N. O. and Green, P. R., 1994; Gill, F. B., 2007).

But how does an eye guide a wing so successfully? All eyes, irrespective of optical structure and evolutionary origins, perform the same essential tasks. They capture light and determine three primary attributes: the direction of the source, its intensity, and its spectrum. Although visual perception requires complex central neural processes, the eye exerts fundamental constraints on the information made available to the brain. Basic performance criteria of eyes that are essential for understanding visual physiology, and how vision is matched to behavioral needs, include (1) the absolute threshold in dim light, (2) the intensity or chromatic contrast thresholds for discriminating between two sources, (3) the spatial resolution, (4) the rate at which information is acquired, and (5) the cyclopean and binocular visual fields. These limits to vision set by the eye are essential for understanding visual physiology, and how vision is matched to behavior and ecology.

Rochon-Duvigneaud alluded to visual abilities in the second part of his description of a bird, ". . . ce qui exige la précision et la vitesse des fonctions rétiniennes" [the requirement for precision and speed in retinal processing]. Here he recognized the two main functional divisions of an eye: (1) an optical imaging system and (2) a photoreceptor array (retina) that starts image analysis. Rochon-Duvigneaud chose to emphasize the primary importance of the retina in determining visual capability (see Sections 1.03.6 and 1.03.7, and these have been reviewed by Meyer D. B. (1977) and Granda A. M. and Maxwell J. H. (1979)). However, as we show here, the relationship between behavioral ecology and visual mechanisms is reflected in both optics and retinal structure.

Sections 1.03.2, 1.03.3, 1.03.4 and 1.03.5 describe the optics of bird eyes and how the ways in which they vary affect the key properties of the image. Subsequent discussions suggest how these variations may be interpreted as adaptations to particular behaviors and ecological conditions. Among these image properties is the visual field, that is, the volume of space imaged on the retina, which limits visual information that is available at any one instant. The two monocular visual fields are combined to provide the total visual field (the cyclopean field), but they also overlap to provide a region of binocular vision. Section 1.03.5 concludes by summarizing the behavioral and ecological factors that are associated with different types of visual field.

1.03.2 Fundamental Constraints on Bird Eyes

1.03.2.1 Size and Information Capacity

In retrieving optical information from the environment, all eyes are constrained by the same fundamental problems that limit sensitivity and spatial resolution. In essence, there is always a trade-off between these two fundamental visual capacities; if there are few quanta in the image, then resolution cannot be high, and if the eye is designed to achieve high spatial resolution, it cannot do so at low light levels (Land, M. F. and Nilsson, D.-E., 2002). However, while this fundamental problem cannot be overcome, it can be mitigated by optical design, by topographical variation in the way that the retina samples the image, and by flexibility in the way that photoreceptors are pooled to sample the image at different light levels (Snyder, A. W. *et al.*, 1977). Optically, a bigger eye is better; a large pupil admits more light and has a higher diffraction limit to spatial resolution (Land, M. F. and Nilsson, D.-E., 2002; chapter 3). This raises fundamental questions about the selective forces that influence eye size and how information gain can be optimized for a particular set of environmental conditions within an eye of a particular size. Phototransduction and photoreceptors are metabolically costly (Laughlin, S. B., 2001a; 2001b), and it is clear that eyes should optimize the use of each photoreceptor cell. Shannon information encoded by each receptor is a good measure for predicting the trade-off between photon catch and receptor size (and hence spatial resolution) for natural images (Snyder, A. W. *et al.*, 1977; 1986; Hateren, J. H. van, 1992). Maximization of information capacity may account for features such as topographical variation in the receptor array, flexible neural pooling with light adaptation (Snyder, A. W. *et al.*, 1977; Srinivasan, M. V. *et al.*, 1982; Hateren, J. H. van, 1992), and the operation of pupils (Laughlin, S. B., 1992).

A clear example of how the retina can have specialized regions that sample the image in different ways is seen in the foveae and linear retinal areas in many bird species (reviewed by Meyer, D. B., 1977). Particularly striking examples of such regional specialization are the deep foveae of raptors, which act as telephoto lenses. These foveae are thought to achieve high resolution and low sensitivity in the fovea, while higher sensitivity and lower resolution are achieved outside the fovea (Snyder, A. W. and Miller, W. H., 1978). Overall birds have many types of retinal regional specializations, which have been interpreted with respect to both ecology and behavior (reviewed by Meyer, D. B., 1977). These include multiple foveae and linear areas in which a high density of photoreceptors and ganglion cells are arranged in an approximately horizontal band across the field of view serving lateral vision. But there may also be an area of the retina in which large and low-density ganglion cells serve forward vision. Both arrangements have been described in the retinae of shearwaters (Procellariidae) (Hayes, B. *et al.*, 1991; Hart, N. S., 2004). Photoreceptors and the Retina discusses regional specialization of receptors and color vision.

1.03.2.1.1 Costs of increasing eye size

Given that vision is important to birds, a simple prediction based on the above sections is that their eyes should be absolutely large. However, increased eye size is not without costs: as eye size increases, there will be a corresponding increase in receptor numbers, which has a metabolic cost (Laughlin, S. B., 2001a; 2001b), and eye mass will also increase. One of the fundamental constraints upon the evolution of birds has been selection for both reduced body mass and the distribution of mass toward the body core. This is a manifestation of the high power to low body mass ratio, which is considered to be one of the most important constraints that has shaped the evolution of birds (King, A. S. and King, D. Z., 1980). Single-chambered eyes are essentially heavy fluid-filled chambers. In flying birds, their increased size is probably countered by selection against (1) having a disproportionately heavy head, which is likely to destabilize flight, and (2) an absolute increase in body mass (King, A. S. and King, D. Z., 1980).

1.03.2.1.2 Eye-size allometry and ecology

The metabolic and weight costs of increasing eye size need to be compensated by advantages. Given that both absolute sensitivity (quantum catch) and spatial resolution can theoretically benefit from increasing size, it is of interest which criterion is in practice most significant. This clearly requires careful comparative analysis of the behavior and ecology of individual species or taxa at the level of the family or order, but some general trends have been discerned by comparing gross differences across a range of taxa.

Consideration of selection for eye size needs to take account of the overall relationship between eye size and body size. For 104 species of flying birds (each from a different family, with body masses between 6 g and 4.9 kg), eye mass scales as $(\text{body mass})^{0.68}$ (Brooke, M. D. L. *et al.*, 1999). This scaling is close to that for brain size, so that the ratio of eye mass to brain mass is fixed. An interesting observation was that there is no clear relationship between flight speed and eye size (Brooke, M. D. L. *et al.*, 1999), as might be expected if visual ability (e.g., integration time or spatial resolution) were related to speed of movement.

If body size is taken into account, avian eye size among certain taxa appears to be best predicted by the time at which the birds are active and to a lesser extent by the foraging strategy (Garamszegi, L. A. *et al.*, 2002). This general conclusion is supported by findings that passerines with comparatively large eyes start singing earlier in the day (Thomas, R. J. *et al.*, 2002) and shorebirds with large eyes tend to forage at night (Thomas, R. J. *et al.*, 2006). However, both diurnal raptors (Accipitridae) and nocturnal owls (Strigidae) have larger eyes than other families (Brooke, M. D. L. *et al.*, 1999; Garamszegi, L. A., *et al.*, 2002), indicating that more-detailed analyses within these and other taxa are necessary to determine how eye size is related to behavior and ecology at a more specific level.

1.03.2.2 The Ambient Light Environment and Light Adaptation

No bird is active at a fixed illumination intensity. When an eagle forages with full sunlight illumination, light levels could be 10^9-fold higher than those experienced by an owl in the same area under starlight (Martin, G. R., 1990). The eagle may experience a 1000-fold range of light levels between sunrise and noon, while the owl may experience a 10^6-fold range between sunset and a moonless night. To operate across these light ranges, eyes use both optical and retinal mechanisms to adjust sensitivity and resolution.

It is clear, however, that optical mechanisms to cope with light level changes are restricted. The pupil, controlled by the iris, is the only mechanism able to adjust retinal illuminance. This has a restricted dynamic range, and its effect may be

attenuated by the oil droplets (see Section 1.03.6.2). Although it can probably equilibrate rapid changes in retinal illumination between sun and shade, the pupil cannot compensate for the full-range light levels. For example, in rock pigeon (*Columba livia*; henceforth pigeon), the pupil can change retinal illumination by about 16-fold, which is similar to the range of the iris effect in humans (Marshall, J. *et al.*, 1973). Species that constrict the pupil to a pinhole or slit achieve a wider range of control. Such pupils are common among mammals, but among birds they occur only in skimmers (Rynchopidae) (Walls, G. L., 1942; Zusi, R. L. and Bridge, D., 1981). A small pupil increases diffraction and so is optically undesirable in a good eye (Laughlin, S. B., 1992). This view seems to be supported by the king penguin (*Aptenodytes patagonicus*), whose pupil does have a large dynamic range but is probably mainly adapted for seeing well in dim light at depth (see Section 1.03.3.1.3). The king penguin's fully constricted pupil forms a pinhole (diameter ≈0.65 mm) and when dilated ≈12.7 mm, which achieves a 300-fold range of retinal illumination (Martin, G. R., 1999). The penguin's pupil may allow the retina to remain dark adapted when the bird is at the surface. This will ensure that when at depth on a foraging dive and the pupil is fully dilated, the eye will be appropriately adapted to the ambient illumination. King penguins regularly dive to 200–300 m where light levels, even at midday, are equivalent to lower night-time levels (Martin, G. R., 1999).

1.03.3 Describing and Comparing Optical Structure of Avian Eyes

Vertebrate eyes have two principal refractive components, lens and cornea, separated by a variable aperture (Figure 1). This simple design embodies a number of degrees of freedom, which are capable of producing a range of optical performance. Variations in optical design can involve (1) the shape and relative positions of the principal refractive surfaces, (2) the effective refractive index of the lens, (3) the relative and absolute sizes of optical components, and (4) the size of the pupil aperture. The outcome is that when viewing the same scene, retinal images in different eyes can have quite different characteristics. In particular, images may differ in absolute size and brightness, and the angular extent of the proportion of space imaged upon the retina. That is the monocular retinal visual field.

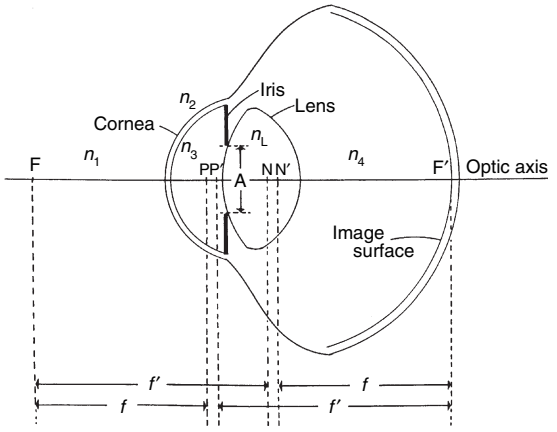

Figure 1 The general optical design of birds' eyes showing the main optical parameters defined in a schematic eye model. N, N′ are the nodal points; P, P′ are the principal points; F, F′ are the focal points of the optical system. They describe the points in a perfect optical system, through which a bundle of light rays would appear to pass and focus. They are shown positioned along the optic axis, which is assumed to be the axis of symmetry for the optical system. The distance *f* and *f′* between the nodal points and the focal points are the anterior and posterior focal lengths. The reason why there are two focal lengths for an eye is that the object and image points occur in media of different refractive index: n_1 (air) and n_4 (vitreous humor); n_2 and n_3 are the refractive indices of the cornea and aqueous humor; and n_L is the calculated equivalent bulk refractive index of the lens. An amphibious eye in water will have a single focal length and the cornea will not have any power since the refractive index of water and of the aqueous humor are equal. *A* is the diameter of the pupil defined by the margins of the iris. A schematic eye model such as this will only apply to paraxial rays that are close to the optic axis; it will not accurately describe optical parameters for peripheral rays. From these schematic eye parameters the refractive power of the cornea F_C, the lens F_L, and the whole eye F_E are calculated, and these are the important tools for making comparisons of the kind shown in Tables 1 and 2 and discussed in the text.

A useful basis for describing the general optical structure of an eye is the schematic eye model (Hughes, A., 1977; Martin, G. R., 1983; Hughes, A., 1986; Land, M. F. and Nilsson, D.-E., 2002). A diagram usually accompanies this mathematical description of the optics (Figure 1). The model normally represents a hypothetical average for a given species. Figure 2 illustrates schematic eyes of five species, namely, tawny owl (*Strix aluco*), common starling (*Sturnus vulgaris*), ostrich (*Struthio camelus*), Manx shearwater (*Puffinus puffinus*), and pigeon. Schematic eye models are also available for barn owl (*Tyto alba*) and chicken (*Gallus domesticus*;

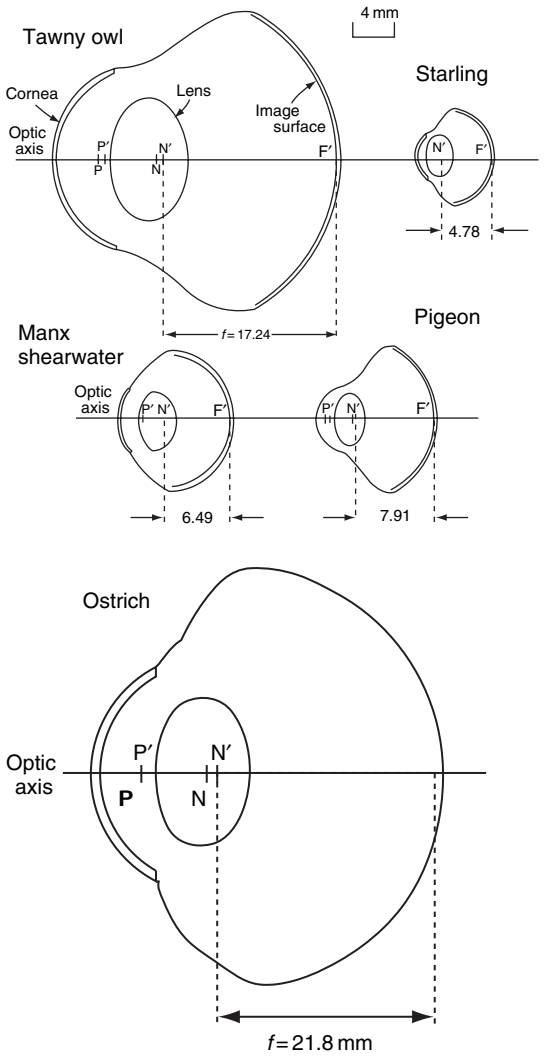

Figure 2 Scaled diagrams of the schematic eye models of five bird species. Also shown is the overall shape of the eye in an approximately horizontal plane. Symbols as in Figure 1. All numerical values are in millimeters. Tawny owl (*Strix aluco*; Martin, G. R., 1982), common starling (*Sturnus vulgaris*; Martin, G. R., 1986a), rock pigeon (*Columba livia*; Marshall, J. *et al.*, 1973; Martin, G. R. and Brooke, M. D. L., 1991), manx shearwater (*Puffinus puffinus*; Martin, G. R. and Brooke, M. D. L., 1991), and ostrich (*Struthio camelus*; Martin, G. R. *et al.*, 2001).

Schaeffel, F. and Howland, H. C., 1988; Schaeffel, F. and Wagner, H., 1996). Description of an eye by a small number of key variables allows interspecific comparisons of optical structure and performance. These in turn allow correlations with key environmental variables, and hence an exploration of how vision may be related to behavioral and ecological variables.

1.03.3.1 Optical Design

1.03.3.1.1 Eye size

Ostriches have eyes that are amongst the largest of any land vertebrate, with an axial length ≈39 mm, but overall there is wide variation of eye size among birds (Brooke, M. D. L. *et al.*, 1999). Figure 2 presents scaled schematic eye diagrams of eyes whose size differs over a fivefold range. The most important optical parameter associated with eye size is the anterior focal length (or posterior nodal distance, PND) as this determines the retinal area over which the image is spread. Miller W. H. (1979) showed that a large PND is essential for an eye to achieve the maximum theoretical limit of visual resolution. This is because there is a lower limit (about 1.5 μm) to diameter of a photoreceptor, which (in the absence of a diffraction limit) sets a maximum packing density of the retinal sampling (see Section 1.03.2.1).

Thus, it is a simple prediction that high-resolution eyes should be absolutely large, as does indeed seem to be the case. The highest psychophysical resolution known in any animal is for the Australian wedge-tailed eagle (*Aquila audax*), whose eye has an axial length of about 33 mm (PND 22 mm; Reymond, L., 1985). By comparison, the larger eyes of ostriches have an estimated maximum resolution (based on retinal ganglion cell density and image size) about seven times lower than that of the eagle. This suggests that large eye size in ostriches is associated with high sensitivity (nocturnal or crepuscular) vision, rather than high-resolution diurnal vision as in the eagle (Boire, D. *et al.*, 2001).

The ostrich eye supports the argument that a relatively large eye size is often associated with nocturnality (see Section 1.03.2.1.2), allowing high absolute sensitivity rather than high spatial resolution. Among birds tawny owls provide the best test of this. Their eyes are ≈29 mm long and their absolute visual threshold has been behaviorally determined (Martin, G. R., 1977; 1986b). The tawny owl has an absolute visual threshold which is similar to that of a nocturnal mammal, the domestic cat (*Felis domesticus*), and is about 2.5 times lower than that of humans and about 100 times lower than that of pigeons. Owl eyes are not, however, the most sensitive in the animal kingdom; that accolade goes to some deep-sea invertebrates whose relative sensitivity is nearly 100 times greater (Land, M. F. and Nilsson, D.-E., 2002). The advantage that a large eye brings the owl is that although its retina is dominated by rod photoreceptors, at high (daytime) light levels its resolving power

is similar to that of the smaller, and cone-dominated, eye of pigeons. The resolution of an owl eye markedly exceeds the resolution of a pigeon as light levels fall (Martin, G. R., 1986b). Thus, the tawny owl appears to have a good eye as defined by Land M. F. and Nilsson D.-E. (2002) in that it combines both relatively high resolution and high sensitivity. So far, few bird eyes have been studied by the behavioral measures, plus analysis of optics, that are necessary to compare the trade-off between resolution and sensitivity in other species.

1.03.3.1.2 Contributions of lens and cornea

Table 1 compares key parameters of the eyes of the five species illustrated in Figure 2. That these eyes differ in their total refractive power is a manifestation of eye size, since a smaller eye must have a higher refractive power to bring the image of a distant object to focus on the retina. Of more interest is the ratio of the power of the lens to that of the cornea ($F_L : F_C$). This parameter reflects how the two optical components (lens and cornea) contribute to the total power, and it does vary substantially between species.

Starling, owl, and ostrich eyes have an $F_L : F_C$ ratio that is close to unity, that is, the lens and cornea contribute approximately equal refractive power. These eyes share a similar optical design, despite the nearly fivefold difference in length, differences in their shapes, and of course behavioral differences between the three species. In short, these eyes are approximate scaled versions of a single optical design. An $F_L : F_C$ ratio of unity is not, however, universal. In pigeon the cornea contributes about 2.5 times the refractive power of the lens, while in the Manx shearwater the situation is almost reversed, with the lens contributing considerably more than the cornea. These differences in optical structure are functionally significant in that the total refractive power of the pigeon and shearwater eyes differ markedly. Although their eyes are of equal size, the effective focal length of shearwaters is less than that of pigeons, and therefore, the retinal image is smaller. Pigeons, by virtue of a larger image, have the potential for higher spatial resolution, whereas shearwaters have a smaller and hence brighter image, with the potential for greater sensitivity. A similar effect is achieved within a single eye by telephoto optics in the deep foveae of raptors, which increase the effective focal length of the eye and hence image size at the expense of brightness (Snyder, A. W. and Miller, W. H., 1978).

1.03.3.1.3 Amphibious habits and optical design

Species that need to see both in air and underwater are faced with a specific optical problem. Immersion abolishes the refractive power of the cornea, because it now separates media (water and aqueous humor) of near-identical refractive index. If an amphibious eye is to focus both in air and in water, the lens must be able to compensate for the loss of corneal refraction. Should an aerial eye, like that of a starling, be immersed in water, its lens would need 124 diopters of additional refractive power.

This consideration led Sivak J. G. (1976) to propose that eyes designed for well-focused vision in air and water should have a relatively flat cornea, and hence low power. The lens may then more easily compensate for the effects of immersion. Such an optical design is indeed found in penguins (Sivak, J. G., 1976; Martin, G. R. and Young, S. R., 1984; Martin, G. R., 1999), and in the albatrosses (*Diomedea* spp.). However, the scaling of eyes, as discussed above (see Section 1.03.3.1.1), also predicts that the absolute power of the cornea should decrease as eye size increases.

Table 2 shows that ostriches, king penguins, and two albatross species have similar-sized eyes.

Table 1 Comparison of eye size (axial length) and certain schematic eye parameters in five species of birds

	F_{EYE} (D)	F_L (D)	F_C (D)	$F_L : F_C$	Axial length (mm)	Focal length (mm)
Starling	209	112.5	124.6	0.90	7.92	4.78
Shearwater	154	108.6	68.1	1.60	11.82	6.49
Pigeon	126	38.7	95.9	0.40	11.62	7.91
Tawny owl	58	29.9	35.7	0.84	28.50	17.24
Ostrich	45.9	27.5	25.4	1.08	39.01	21.8

Schematic eyes for these species are show diagrammatically in Figure 2, where sources are also given. Focal length is the anterior focal length (posterior nodal distance, PND); Refractive powers are in diopters (D).

Table 2 Eye axial length, corneal refractive power (F_C in diopters, D), and radius of corneal curvature (R, mm) in 11 species of bird

	Axial length (mm)	F_C *(D)*	*R (mm)*
Ostrich	38	25.4	13.23
King penguin	25	10.2	32.9
Grey-headed albatross	37	22.8	14.7
Black-browed albatross	39	23.3	14.4
Tawny owl	28.5	35.7	9.4
Humboldt penguin	18.7	29.8	11.3
Rock hopper penguin		17.7	19.1
Gentoo penguin		15.1	22.4
Manx shearwater	11.82	68.1	4.9
Rock pigeon	11.62	95.9	3.5
Common starling	7.92	124.6	2.70

Sources are given in Figure 2 and Table 3 with the exception of rockhopper and gentoo penguins (Sivak, J. G., 1976).

Albatrosses make shallow dives but appear to detect food from the surface, whereas king penguins often forage at great depth. Ostriches and albatrosses, whose vision is likely to be adapted primarily to aerial conditions, share a similar eye design and have corneas of relatively low refractive power compared with smaller-eyed birds (Table 1). In these large birds the relatively low corneal power can be attributed to scaling of the basic aerial avian eye. However, king penguins have a cornea of even lower refractive power that can be interpreted as an adaptation to the demands of vision in both air and water. Unfortunately, no psychophysical data are available for any penguin to determine whether similar resolution is achieved in both air and water.

It is also noteworthy that when any eye enters water the brightness of the retinal image decreases. This is because the magnifying effect of the cornea on the pupil is lost, and so the effective entrance pupil decreases. In addition, diving to any depth results in a marked decrease in illumination. King penguins dive to light levels equivalent to night at the surface and are in effect nocturnal foragers (Martin, G. R., 1999). Thus, the large size of king penguin eyes may be primarily an adaptation to low light levels, while the relatively low-power cornea could be described as an adaptation to reduce the accommodative demand upon the lens when moving between air and water. There is, however, another possibility. The pinhole pupil of a king penguin eye in air (see Section 1.03.2.2) will give a large depth of focus, and it may be that its eye is in fact primarily for aquatic conditions (emmetropic in water), with the optics effectively bypassed at the surface.

1.03.3.2 Accommodation

The larger the eye, the higher the requirement for an accommodative mechanism, since smaller eyes have a greater depth of field than larger ones (Land, M. F., 1981; Martin, G. R., 1994a). Accommodation in mammals relies on deformation of the lens, whereas birds can control accommodation using both the lens and the cornea (Glasser, A. and Howland, H. C., 1996; Ott, M., 2006). It is not clear under which circumstances a particular mechanism is used. For example, it may be that for certain distances only the cornea is used, and for others the lens and cornea work in tandem. The iris is an important component of this system. It causes the deformation of the lens by squeezing the annular pad (Figure 1), which in turn causes the anterior lens surface to bulge, and hence to increase in refractive power. It is also not clear how independent the two functional effects of the iris are: accommodation and control of image brightness. There are marked interspecific differences in the density of the muscle fibers involved in the mechanisms of accommodation in birds, for example, they are described as bulky and strong in chicken but scarcely developed in pigeon (Glasser, A., 2003); the functional significance of these differences is not known. It is argued that in all birds accommodation serves to increase the power of the cornea and/or the lens (Glasser, A. *et al.*, 1994; 1995). However, in the relaxed eye all parts of the retina are not necessarily focused at infinity. In common starlings the frontal visual field appears to be emmetropic for near objects when the lateral field focuses at infinity (Martin, G. R., 1986a). Similarly, in the frontal parts of the pigeon, visual field resolution is best for a viewing distance of 100 mm and cannot focus more distant objects (Rounsley, K. J. and McFadden, S., 2005).

1.03.4 The Kiwi: Regressive Evolution of a Bird Eye

Writing in the *Origin of Species*, Darwin C. R. (1859, p. 186) described eyes as "Organs of extreme perfection and complication" and argued that they set a particularly difficult challenge to his theory of evolution. That challenge has been addressed (Land, M. F. and Fernald, R. D., 1992; Nilsson, D. E. and Pelger, R. F., 1994), but Darwin's concern about perfection permeates twentieth-century surveys of vertebrate eyes (e.g., Walls, G.

L., 1942; Rochon-Duvigneaud, A., 1943; Duke-Elder, S., 1958). It is therefore interesting that under certain conditions eyes regress in evolution, leading to blindness in species such as the cave fish (*Astyanax mexicanus*) (Jeffery, W. R., 2005; Leys, R. *et al.*, 2005).

Although blind cave dwellers are familiar, there are few well-documented instances of partial regression of eye structure and vision, and here kiwis (*Apteryx* spp.) are a good example (Martin, G. R. *et al.*, 2007). Nocturnality along with freedom from some of the constraints on eye size that are faced by flying birds (see Section 1.03.2.1.1) might predict that kiwis should have large eyes. Flightless Struthioniformes (ostriches and allies) and Sphenisciformes (penguins) have among the largest of any vertebrates (see Section 1.03.3.1.1).

The five living kiwi species have evolved in New Zealand over a period of 80 million years without terrestrial mammals (Tennyson, A. J. D. *et al.*, 2003; Wilson, K.-J., 2004). Kiwis are nocturnal, flightless, cursorial birds of the forest floor, where they forage for soil and surface-dwelling invertebrates (Marchant, S. and Higgins, P. J., 1990). Little is known about their senses, although they use smell to find food (Wenzel, B., 1968).

Kiwi eyes are able to accommodate, showing that the optical system is functional (Howland, H. C. *et al.*, 1992), but their axial length and equatorial diameter (both ≈7.0 mm) are exceptionally small with respect to body mass (see Section 1.03.2.1.1; Brooke, M. D. L. *et al.*, 1999). The eye shape is similar to that of diurnal birds such as starlings and pigeons, not like the tubular eyes of owls (Martin, G. R., 1986b; Hall, M. I. and Ross, C. F., 2007). These small eyes are probably limited to the detection of gross detail within a nocturnal scene (Land, M. F. and Nilsson, D.-E., 2002). Furthermore, the visual fields are very small, and visual centers in the brain are almost absent. There is no discernable visual wulst, which is the main visual center in the forebrain (Reiner, A. *et al.*, 2004), whereas the relatively large olfactory and tactile centers (Martin, G. R. *et al.*, 2007) reflect a high concentration of tactile receptors around the bill tip, where the nostrils are (uniquely in birds) situated (Cunningham, S. J., 2006; Martin, G. R. *et al.*, 2007).

Kiwi is then the exception that proves the rule that vision is important to birds. Other ratites, such as the moa, cassowary, rhea, and ostrich, have large eyes (Worthy, T. H. and Holdaway, R. N., 2002). It seems safe to conclude that reduced vision is a derived characteristic in kiwi and a good example of adaptive regressive evolution (Jeffery, W. R., 2005). There is, however, a comparison to be made with nocturnal mammals such as rodents that, like kiwi, rely mainly on touch and smell. Perhaps vision cannot meet the perceptual challenges of nocturnal life on the forest floor.

1.03.5 Visual Fields

Among vertebrates, the eyes occupy many different locations in the skull (Walls, G. L., 1942). Frontal eyes, as in humans, have approximately parallel optical axes; colloquially the eyes look in the same direction. The two eyes receive very similar views. No birds, including owls (see Section 1.03.5.2.3), have eyes with parallel optical axes. Instead each eye views a different part of visual space, with various degrees of overlap. Visual fields of birds are diverse: the total visual fields and the areas of binocular overlap differ markedly in their size and location. These differences may have important consequences for behavior.

This section reviews the topography of visual fields in birds and discusses their functions. It is based on data obtained by an ophthalmoscopic reflex technique (Martin, G. R. and Katzir, G., 1994a), which has been applied to a wide range of species (Table 3). The technique allows visual field topography to be determined in alert birds and so represents visual field topography as it is in nature.

1.03.5.1 Describing Visual Fields

A visual field is the three-dimensional (3D) space within which the eyes can receive visual information at any one instant. Visual fields are described by an angular coordinate system based on conventional latitude and longitude and centered on the head. The center of the coordinate system is the intersection of the bird's median sagittal plane with the midpoint of a line joining the optical center of each eye (the nodal points). The equator is aligned in the median sagittal plane. The field is visualized by its projection onto the surface of a sphere that is centered on the head. As in cartography, mapping 3D visual fields on a flat surface causes distortions (Leys, R. *et al.*, 2005). To understand spatial relationships between features in the visual field, the spherical projection can be viewed from different directions, much as a globe can be viewed from various directions (Figure 3). Sections through the visual fields in different planes that pass through the center of the projection (approximately the center of the head) allow straightforward quantitative comparisons of field dimensions: for example, (1) the angular width

Table 3 Bird species (13 orders; 19 families; 31 species) and their visual field types

Struthioniformes
- Struthionidae
  - Ostrich *Struthio camelus* (type 1) (Martin, G. R. and Katzir, G., 1995)
- Apterygidae
  - Brown kiwi *Apteryx mantelli* (Martin, G. R. *et al.*, 2007)
  - Great spotted kiwi *Apteryx haastii* (Martin, G. R. *et al.*, 2007)

Spheniscidae
- Spheniscidae
  - Humboldt penguin *Spheniscus humboldti* (type 1) (Martin, G. R. and Young, S. R., 1984)
  - King penguin *Aptenodytes patagonicus* (type 1) (Martin, G. R., 1999)

Procellariiformes
- Diomedeidae
  - Black-browed albatross *Diomedea melanophris* (type 1) (Martin, G. R., 1998)
  - Gray-headed albatross *Diomedea chrysostoma* (type 1) (Martin, G. R., 1998)
- Procellariidae
  - Manx shearwater *Puffinus puffinus* (type 1) (Martin, G. R. and Brooke, M. D. L., 1991)
  - White-chinned petrel *Procellaria aequinoctialis* (type 1) (Martin, G. R. and Prince, P. A., 2001)
  - Antarctic prion *Pchyptila desolata* (Martin, G. R. and Prince, P. A., 2001)

Ciconiiformes
- Ardeidae
  - Cattle egret *Bubulcus ibis* (Martin, G. R. and Katzir, G., 1994a)
  - Reef heron *Egretta gularis* (Martin, G. R. and Katzir, G., 1994a)
  - Squacco heron *Ardeola ralloides* (Martin, G. R. and Katzir, G., 1994a)
  - Black-crowned night heron *Nycticorax nycticorax* (Katzir, G. and Martin, G. R., 1998)

Phoenicopteriformes
- Phoenicopteridae
  - Lesser flamingo *Phoeniconaias minor* (Martin, G. R. *et al.*, 2005)

Anseriformes
- Anatidae
  - Mallard *Anas platyrhynchos* (type 2) (Martin, G. R., 1986c)
  - Northern shoveler *Anas clypeata* (type 2) (Guillemaine, M. *et al.*, 2002)
  - Wigeon *Anas penelope* (type 1) (Guillemaine, M. *et al.*, 2002)
  - Blue duck *Hymenolaimus malacorhynchos* (type 1) (Martin, G. R. *et al.*, 2007)
  - Pink-eared duck *Malacorhynchus membranaceus* (type 2) (Martin, G. R. *et al.*, 2007)

Falconiformes
- Accipitridae
- Short-toed snake eagle *Circaetus gallicus* (type 1) (Martin, G. R. and Katzir, G., 1999)

Charadriiformes
- Burhinidae
  - Stone-curlew *Burhinus oedicnemus* (type 1) (Martin, G. R. and Katzir, G., 1994b)
- Scolopacidae
  - Woodcock *Scolopax rusticola* (type 2) (Martin, G. R., 1994b)
- Laridae
  - Black skimmer *Rynchops niger* (type 1) (under review)

Columbiformes
- Columbidae
  - Rock pigeon *Columba livia* (type 1) (Martin, G. R. and Young, S. R., 1983)

Strigiformes
- Strigidae
  - Tawny owl *Strix aluco* (type 3) (Martin, G. R., 1984)

Caprimulgiformes
- Steatornithidae
  - Oilbird *Steatornis caripensis* (type 1) (Martin, G. R. *et al.*, 2004b)
- Caprimulgidae
  - Paraque *Nyctidromus albicollis* (type 1) (Martin, G. R. *et al.*, 2004a)

(*Continued*)

Table 3 (Continued)

Coraciiformes
Bucerotidae
Southern ground hornbill *Bucorvus leadbeateri* (type 1) (Martin, G. R. and Coetzee, H. C., 2004)
Southern yellow-billed hornbill *Tockus leucomelas* (type 1) (Martin, G. R. and Coetzee, H. C., 2004)
Passeriformes
Sturnidae
European starling *Sturnus vulgaris* (type 1) (Martin, G. R., 1986a)

In all species visual fields have been determined using the same ophthalmoscopic reflex method. Taxonomy follows Sibley C. G. and Monroe B. L. (1990).

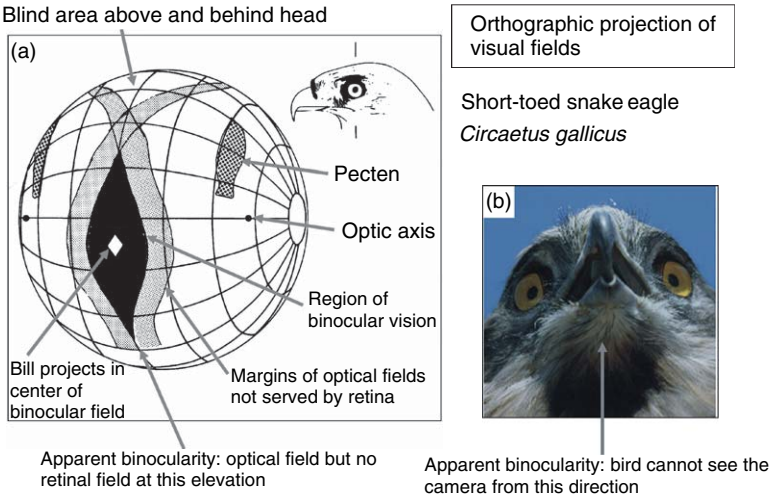

Figure 3 Depiction of visual fields. Example based on data for short-toed snake eagle (*Circaetus gallicus*). (a) Perspective view of an orthographic project of the visual field showing the binocular sector to the front of the head and the blind area above and the margins of the optical fields that are not served by retina. The projection of the optic axes, pectens, and of the bill are also shown. It should be imagined that the bird is placed at the center of a transparent sphere that surrounds the head and the projections of the various features are drawn onto the surface, the orientation of the head is depicted in the inset drawing, but the median sagittal plane of the bird lies is in the same plane as the equator of the projection that is vertical and contains the projection of the bill. (b) Photograph of a bird taken at a position in the sagittal plane below the bird that lies outside of the retinal visual field. This gives the impression that the bird has binocular vision at this point since it is possible to see into the eye. However, there is no retina serving vision at this elevation and so the bird could not see the camera.

of the binocular field in the plane of the bill or at the horizontal; (2) the angular width of the blind area above or behind the head; and (3) the total angular width of the visual field in a particular plane (the cyclopean field; see example in Figure 4).

1.03.5.1.1 Difficulties in estimating visual fields and binocular overlap

Casual examination of the eyes to estimate visual field parameters can be misleading, especially in exaggerating binocular overlap in the frontal field. Figures 3 and 4 exemplify this problem. The photograph in Figure 3(b) suggests that the bird is looking binocularly at the camera. However, the functional visual field (Figure 3(a)) determined by the ophthalmoscopic reflex (see Section 1.03.5) shows that although it is indeed possible to see into the eye (and hence the pupil is visible), the image falls outside the retina. In fact the eagle's optics produce a binocular field that is 40° wide in the horizontal plane, but functionally the field is only 20° (Figure 4). Similarly Figure 3 shows that there are elevations where it is possible to see into both eyes, but the eagle is blind because there is no retina. In summary, the frontal binocular field width is not maximized within the optics. A similar situation

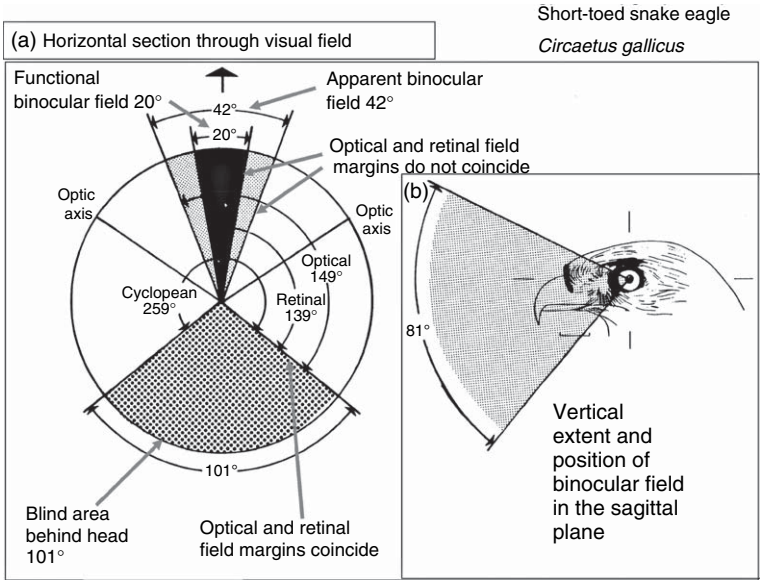

Figure 4 Depiction of visual fields. Example based on data for short-toed snake eagle (*Circaetus gallicus*). (a) Horizontal section through the visual field showing the key features in a single plane. The median sagittal plane of the bird is vertical and perpendicular to the plane of the drawing, and the bill points in the direction of the arrow at the top. Key features of the visual field are indicated. (b) The vertical extent of the visual field in the median sagittal plane (which is in the same plane as the drawing) relative to the bird's head as depicted in the drawing. In this plane the visual field is always binocular.

applies to other species, including ostriches, herons, and owls. The Function of Binocularity discusses the reasons to forego maximizing binocularity.

While there is a deficiency in frontal binocularity, to the rear of the head, in all birds examined, the margins of the optical and retinal fields coincide (e.g., Figure 4), to make maximum use of the optical image.

1.03.5.2 Types of Avian Visual Field

For the frontal field, and particularly the binocular field, there are three main types of visual field topography. It is hypothesized that the topography is determined primarily by feeding ecology or the requirements of provisioning young, rather than phylogeny or ecology (Martin, G. R. *et al.*, 2005). Of prime importance is the need for precise visual control of bill position, when attacking prey or feeding chicks, which is associated with a type 1 field (Figure 3). This applies whether the bird forages in air or water or is primarily diurnal or nocturnal. Birds species that exemplify different types of visual fields and their foraging ecology are depicted in Figures 5(b)–5(d).

1.03.5.2.1 Type 1 fields

Type 1 fields occur in diverse species (Table 3). The projection of the bill falls either centrally or just below the center of the frontal binocular region. This region is narrow and vertically extended, with a maximum width of 20–30°. Although the direction of the bill is approximately central within the binocular field, this does not necessarily mean that the bird can see its bill. Species that lunge or peck at food with the bill (e.g., pigeon, herons, albatrosses, and penguins) or take prey in the feet (eagles) probably cannot see their bill. Only for those that forage with open mandibles (e.g., starling) or manipulate and inspect items held in the bill (e.g., hornbills (Bucerotidae) and skimmers (Rynchopidae)) is the bill visible (Figure 5(b)).

The vertical extent of the binocular region in type 1 fields varies considerably. It is 80° in an eagle (Figure 3) but in herons extends 180° from directly above to directly below the head when the bill is horizontal (Figure 6). This arrangement allows a heron that is standing with the head horizontal to observe prey at its feet. The bird can remain motionless until prey is within striking distance. The extended binocular field gives rises to the often-illustrated ability of bitterns (*Botaurus*, *Ixobrychus* spp.) to look forward while the bill points skyward in a cryptic posture. Type 1 fields have a blind area to the rear of the head, which varies in width from about 40° in herons to 100° in eagles.

Apart from herons and raptors a number of species that need to locate their bill precisely have type 1

fields. Flamingos are filter feeders (see Section 1.03.5.2.2), but parents feed chicks by dripping liquid directly into the mouth, which requires precise bill position (Figure 5(b)). Similarly, Antarctic prions (*Pachyptila desolata*) filter feed on the wing and have to place their bill precisely at the water surface (Martin, G. R. and Prince, P. A., 2001). The prion has a type 1 field with the bill positioned in the lower half of the binocular region, and a 50° bind area behind the head. Skimmers (*Rynchops*) have an extraordinary method of foraging where the beak is held open in flight. The skimmer's lower mandible ploughs through the water and snaps shut when it touches an object (Zusi, R. L., 1996). The skimmer has a type 1 visual field and is one of the few species described that can see its bill tip. This arrangement could allow accurate bill placement and identification of what has been seized (Figure 5(b)).

1.03.5.2.2 Type 2 fields

Type 2 fields are characterized by a frontal binocular field $\leq 10°$ wide. The bill falls at the periphery or outside the visual field. Unlike many type 1 fields, full use is made of the available optical image, with no blind margin. The binocular field extends through approximately 180° in the sagittal plane, approximately from the horizontal in front of the head to the horizontal behind. This gives panoramic vision with complete coverage of the celestial hemisphere. There is no blind area above or to the rear.

Type 2 fields are typically found in species whose foraging is guided by nonvisual cues and also have precocial self-feeding chicks. Examples are filter-feeding ducks (e.g., mallard (*Anas platyrynchos*), shoveler (*Anas clypeata*), and pink-eared duck (*Malacorhynchus membranaceus*)) (Figure 5(d)) and long-billed probing shorebirds (Charadridae), which locate prey by touch with the bill tip (Gottschaldt, K. M., 1985; Piersma, T. *et al.*, 1998; Nebel, S. *et al.*, 2005).

1.03.5.2.3 Type 3 fields: owl eyes

Owls (Strigidae, Tytonidae) have a broad frontal binocular field $\approx 50°$ wide, with the bill tip just below the lower periphery (Figure 5(c)). An extensive blind area to the rear of the head reaches a maximum width of approximately 160° directly behind. The eye position appears to be frontal, as in humans, but in fact the eyes diverge by 55°. Moreover, as for type 1 fields, the binocular region is considerably narrower than it might appear, and not maximized within the optical image. Owls seize prey with their feet, which swing into the binocular area just before the strike. While the visual fields of owls are distinct from those of other species, it is not clear which aspects of their behavior and ecology underlie this specialization. It has been argued that extensive binocular overlap is associated with the nocturnality (Walls, G. L., 1942; Tansley, K., 1965). However, as we have mentioned, the binocular overlap is smaller than might be expected. Other nocturnal birds including oilbirds and nightjars (Caprimulgidae) and night herons (*Nycticorax* spp.) have type 1 visual fields (Figure 5(c)). Owl eyes are discussed further in Section 1.03.5.4.2.

1.03.5.3 Visual Fields and Eye Movements

In many species, eye movements are virtually absent (e.g., owls (Martin, G. R., 1984) and albatrosses (Martin, G. R. and Prince, P. A., 2001)), and where they do occur, they are nonconjugate (Wallman, J. and Pettigrew, J. D., 1985), which allows a wide range of visual field configurations (see examples in hornbills; Martin, G. R. and Coetzee, H. C., 2004). A notable change in visual field topography is the abolition of frontal binocularity and a corresponding reduction in the width of the blind area to the rear. This is exemplified in herons where the maximum eye movement amplitude is about 18° in the horizontal plane (Figure 7). The functional significance of visual field changes produced by eye movements is not clear. Increased visual coverage to the rear of the head may be significant. Although head movements are often important, as for humans, eye movements probably allow high-acuity regions to track or inspect a target.

1.03.5.4 The Function of Binocularity

The extent and position of binocular overlap and its relationship to visual foraging have received particular attention. The frontal binocular field of 20–30° is common to all type 1 fields (Section 1.03.5.3) and seems to be a general solution to a common problem. Nonetheless, the arrangement is not universal, which suggests that it is not concerned primarily with the flight control. Narrower binocular fields, linked to panoramic vision of the celestial hemisphere, are found in species that are both fast flying and maneuver within both open and woodland habitats (European woodcock, *Scolopax rusticola*, and mallard).

General accounts are influenced by the assumption that binocular vision (two eyes viewing the same location) results in stereopsis (Hughes, A., 1977).

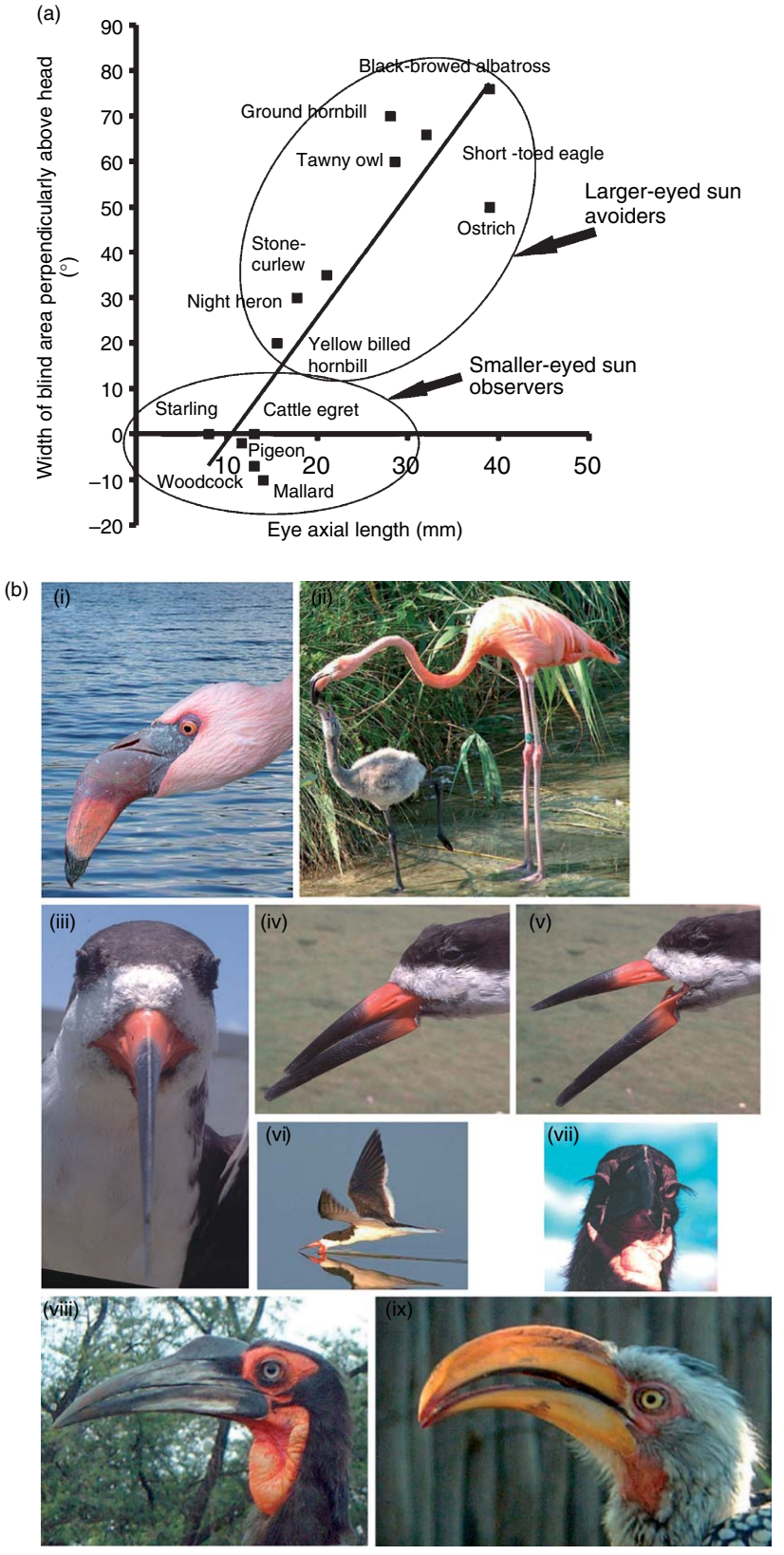

Figure 5 (*Continued*)

(c)

(d)

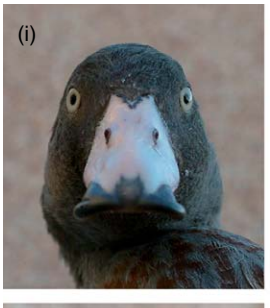

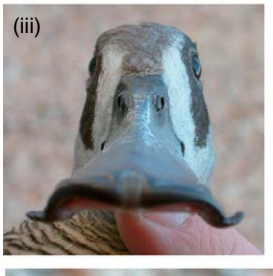

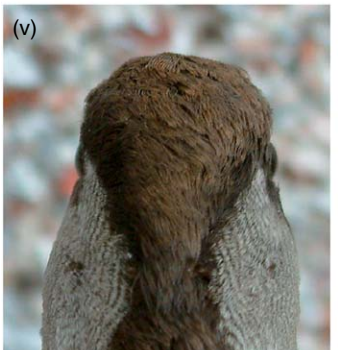

However, for birds the assumption that binocularity inevitably results in stereopsis is questionable (McFadden, S. A., 1993; 1994; Davies, M. N. O. and Green, P. R., 1994). The pigeon has depth perception and is sensitive to disparities of about 1 arc minute (compared to 4 s in humans), but it is doubtful that this ability is used in foraging (McFadden, S. A., 1993). Motion-parallax is probably an important source of depth information for birds (Kral, K., 2003) and cannot easily be ruled out. Although owls do have stereopsis (Nieder, A. and Wagner, H., 2000; Willigen, R. F. *et al.*, 2003), it is unlikely to provide a general

Figure 5 (a) Eye size and sunshades. The width of the blind area perpendicularly above the head as a function of eye axial length in 13 species of terrestrial birds. Positive values indicate the width of a blind area and negative values the width of a binocular field. All measurements employed the same ophthalmoscopic reflex technique and show values when the head is eld in its typical posture for the species. The line is the linear regression. The Spearman correlation between the two variables is significant ($r = 0.85$, $P < 0.005$, $n = 13$). Species are grouped as larger-eyed sun avoiders that have a blind area above the head and posses optic adnexa (eye lashes, eye brows) capable of shading the eye, and smaller-eyed sun observers that have vision above the head and do not have optic adnexa. (b) Examples of bird species whose visual fields are described in the text and in Table 3. Filter feeding. Flamingos (i) feed with their head upside down and filter microscopic particles from the water surface. This technique would not seem to require accurate bill placement guided by visual cues. However, flamingo visual fields show the characteristics of birds that feed by accurate visually guided pecking in which the bill is placed centrally within the binocular field. It is argued that this visual field configuration is necessary when feeding the chick. This entails accurately dripping crop-milk into the juvenile's open bill (ii) and this presumably can only be achieved by guidance from visual cues. Tactile feeding. Skimmers (iii–v) are unique in their feeding technique. They forage apparently blindly with the lengthened lower mandible trailing in the water as the bird flies a level straight course (iv). Birds may feed by both night and day. The bill is snapped shut on a prey item when triggered by tactile or vestibular cues produced when the mandible strikes prey. Skimmers' visual fields also show the characteristics of birds that feed by accurately visual guided pecking, but it is argued that this configuration is necessary not for accurate bill placement but for visual inspection of prey items caught during blind trawling. Precision-pecking and visually guided manipulation of items. Hornbills (viii, ix) have massive down-curved bills that are used to locate and excavate for, and manipulate, a wide range of prey and other food items. The birds have type 1 visual fields with binocular vision about the bill and eye movements of relatively large amplitude that can bring about marked changes in visual field configuration. All hornbills have relatively large eyes and have some of the most elaborate sun shade optical adnexa found in birds, including extensive brows and eye lashes (vii). (c) Examples of bird species whose visual fields are described in the text and in Table 3. Nocturnally active birds. Although apparently facing similar visual challenges in the nocturnal and crepuscular environment, these birds exhibit a wide range of visual field configurations that are probably related to particular foraging techniques. Oilbirds (i, ii) are arguably the most nocturnal of all birds and rarely, if ever, see daylight since they roost in caves during the day and only emerge to forage at night to feed on fruit in the tropical rain forest canopy. Although their eyes are relatively large and protrude noticeably from the skull, their visual fields show the characteristics of type 1 fields (Table 3), suggesting that accurate bill placement toward items may be guided by visual cues. However, these birds are also thought to employ olfactory cues in determining the general location of ripe fruits. A similar visual field configuration is found in nightjars (iii, iv), which take insect prey on the wing from the open airspace in twilight and at night. Despite being totally nocturnal kiwi (v) have relatively very small eyes and the smallest binocular and total visual fields yet recorded in a bird. It is possible that vision in these flightless birds has been subject to regressive evolution and that locomotion and food finding are guided primarily by olfactory and tactile cues gained from the bill tip. In contrast owls (vi) have the most frontally placed eyes and the broadest binocular field yet described in birds (type 3 field), and these are thought to be correlated with prey capture using the feet and with the use of auditory cues to locate prey. Owls are unique among birds in having elaborate external ear structures (placed at the edge of the feathers of the facial disk and just behind the eyes), which function to locate sounds accurately, mainly in the region in front of the head. Although owls appear to have forward-facing eyes, the optic axes diverge by nearly 50°, also because the retina does not serve the whole of the available optical field, the degree of binocular overlap appears to be much broader than it functionally is (see Figures 3 and 4). (d) Duck species feed using a range of different foraging techniques. In blue ducks (i, ii) although the eyes are set relatively high in the skull, the visual field shows the typical characteristics of a visually guided forager (type 1 field), but these birds also gain near-comprehensive vision around the head. Blue ducks feed on mobile and sessile prey in fast-flowing mountain rivers and are thought to be visually guided toward individual items. On the other hand, pink-eared ducks (iii, iv) filter feed on small items taken from the surface of often highly turbid waters. In these birds the eyes are set very high on side of the skull and this results in a very narrow area of binocularity that extends from directly in front of the head to directly behind (v), giving the birds comprehensive visual coverage of the hemisphere about the head. However, the birds cannot see their own bill tip, suggesting that bill position does not rely on accurate visual guidance. It is argued that such comprehensive vision is only possible since these birds cannot only feed themselves without relying on visual cues to guide the bill, but also that juvenile birds are precocial and self-feeding and do not need provisioning by the parent, unlike the example of the filter-feeding flamingos that need to provision their young.

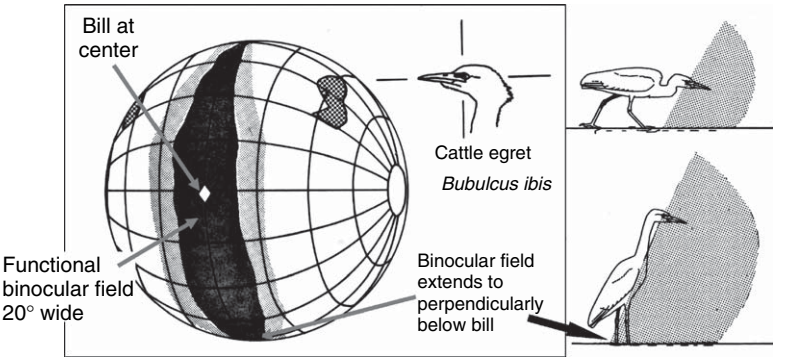

Figure 6 Depiction of visual fields. Example based on data for cattle egret (*Bubulcus ibis*). The diagram shows a perspective view of an orthographic project of the visual field showing the binocular sector that extends from perpendicularly above to perpendicularly below the horizontal plane. The drawings to the right depict postures typical of birds when foraging, and the shading indicates the extent of the binocular field in the in the median sagittal plane. This indicates that the birds can gain extensive visual coverage below the bill, allowing binocular viewing of objects at or close to its feet when the bill is held horizontal.

account for binocularity in birds. Instead it is likely that binocularity is related to the need to analyze optic flow fields (Martin, G. R. and Katzir, G., 1999).

1.03.5.4.1 Binocularity and optic flow fields

The functional importance of binocular overlap may lie not in the fact that each eye can image the same portion of the frontal field simultaneously, but as a result of each monocular field projecting contralaterally. This allows the monocular field to encompass a pole in the linear optic flow field during forward motion (Gibson, J. J., 1986).

Symmetrical flow fields are thought to be important for the control of locomotion in birds, mammals, and insects. The optic flow about a pole gives robust information about the point where the animal is heading, and the time to contact that point (Lee, D. N., 1980; Gibson, J. J., 1986; Davies, M. N. O. and Green, P. R., 1994; Lee, D. N., 1994). Birds need to determine both heading and time to contact rapidly and accurately since they often move at speed toward objects: their heads when pecking, their bodies when approaching objects in flight, and when striking prey with the feet. Flow field variables are known to control landing responses in some, but not all, bird species (Davies, M. N. O. and Green, P. R., 1994). Neurons that respond selectively to various types of flow field, including symmetrically expanding images, are found in the nucleus rotundus (homologue of mammalian pulvinar) of the pigeon forebrain (Frost, B. J. *et al.*, 1994, Sun, H. and Frost, B. J., 1998). These neurons may be functionally equivalent to similar neurons that control self-motion in insects (Krapp, H. G. and Hengstenberg, R., 1996; Srinivasan, M. V., 1996).

In normal forward motion the visual field of an eye must extend contralaterally in order to contain a flow field pole. For forward movement toward a relatively distant target, the disparity of viewpoint of two eyes with overlapping contralateral fields is negligible. The two eyes then should theoretically receive virtually identical optical flow fields, but as the motion signals are likely to be affected by differences in contrast and other image parameters, integration will increase their reliability. Furthermore, for close objects, movement with respect to a target (as in pecking or bill striking) may be precisely specified by the fact that the optic image of the target can be symmetrically positioned with respect to the centers of expansion of each flow field (Lee, D. N. *et al.*, 1991).

Why then is the maximum width of the binocular field in type 1 fields only 20–30°? It can been suggested that this width gives sufficient flow field information for rapid approaches toward objects during foraging, while maximizing the width of the peripheral, and hence cyclopean, visual field (Martin, G. R. and Katzir, G., 1999). In birds such as skimmers, mallard, and woodcocks the binocular overlap at the elevation of the horizontal in flight is only about 10°, which seems sufficient for the control of flight and landing. As mentioned above (see Section 1.03.5.2.1; Figures 3 and 6) in many species the binocular field width could be doubled if full use was made of the optical image. It is interesting that many insects, including flies (Land, M. F. and Eckert, H., 1985), have a binocular overlap of about 10°.

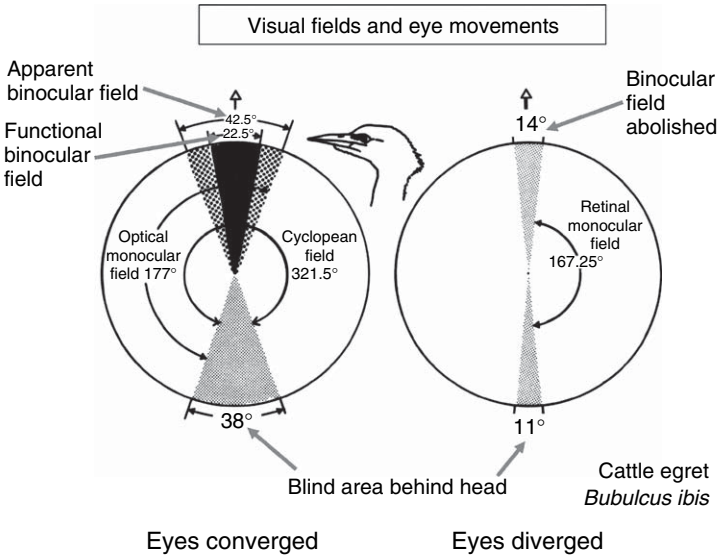

Figure 7 Visual fields and eye movements. Example based on data for cattle egret (*Bubulcus ibis*). Each diagram depicts a section through the visual fields in the horizontal plane. In this plane the margins of the field of each eye can move by up to 18° as a result of eye rotation. When the two eyes are fully rotated to the front of the bird's head (i.e., to the top of the diagram), there is a binocular overlap of 22° (left), but when the eyes are rotated backward, the binocular field is abolished and there is a blind sector 14° wide (right). The eyes can move independently of each other, and therefore, a wide variety of visual field configurations are possible. For example, if one eye is fully forward and the other rotated fully back, then 4° of binocular overlap remains, but this is not symmetrically displaced about the median sagittal plane.

Insects mostly lack stereopsis, and given the importance of optic flow to their flight control (Krapp, H. G. and Hengstenberg, R., 1996; Srinivasan, M. V., 1996), similar reasons may underlie binocularity in insects and birds. As mentioned above (see Section 1.03.5.2.1; Figures 3 and 6) in many species the binocular field width could be doubled if full use was made of the optical image. It is therefore pertinent to consider why the image is not fully used.

In lateral-eyed animals, frontal vision is in fact peripheral vision with respect to the optics of each eye. In all optical systems image quality declines toward the periphery, owing to increases in spherical and other aberrations. There is no information on optical quality in the periphery of any bird eye, but it is a reasonable hypothesis that frontal vision requires the bird to use part of the visual field away from the periphery. No advantage is gained by having contralateral vision to the image periphery since the region that is viewed contralaterally with poor quality optics is covered by more central portions of the ipsilateral eye.

1.03.5.4.2 Binocular vision and nocturnality

The visual fields of owls pose an interesting problem. The wide binocular field described as type 3 (see Section 1.03.5.2.3) has been found only in owls (Figure 5(c)). Broad binocular fields of about 50° have long been associated with the nocturnal and/or the predatory habit of these birds (Walls, G. L., 1942; Tansley, K., 1965). However, similar frontal visual fields are absent in diurnal raptors, such as short-toed snake eagle, which take prey in the feet, or in both flying and flightless nocturnal species such as oilbird (*Steatornis caripensis*), nightjars, night herons, and kiwis. Two factors may account for the particular visual field characteristics of owls: eye size and the use of hearing in the location and capture of prey.

Low light levels favor eyes with a large aperture compared to focal length ratio (i.e., low *f*-number), which produce a bright image but requires a large absolute pupil size to maximize photon catch (Martin, G. R., 1985; Land, M. F. and Nilsson, D.-E., 2002). The consequence of these two requirements is that the eye must be absolutely large, with the attendant costs in mass (see Section 1.03.2). Owl eyes are remarkably long (≈29 mm axial length in tawny owl compared to ≈24.0 mm in human), but their tubular in shape will save weight (Martin, G. R., 1982). If eyes of this length were placed so as to point more laterally, the total skull width would increase greatly; in fact owl eyes protrude more from the skull

than all other birds examined. Eye position therefore may, at least in part, be a matter of the geometry of squeezing a large eye into a small skull.

An additional factor may be associated with the elaborate external ear structures of owls, which function in the accurate sound localization (Payne, R. S., 1971; Konishi, M., 1973; Norberg, R. A., 1978). Owls are unique in the possession of these structures, and they alone may displace the eyes forward in the skull. Furthermore, these large external structures prohibit vision to the rear of the head.

1.03.5.4.3 The blind area above the head and eye size – sunshades in birds

The preceding sections show how the demands of feeding behavior and flight control give a restricted range of frontal binocularity. There is, however, considerable variation in the topography of the total visual field, especially in the extent of the cyclopean field in the horizontal plane and in the width of the blind area above the head (Martin, G. R. and Katzir, G., 2000).

The width of the blind area above the head is a function of eye size (Figures 5(a) and 5(b)). Smaller-eyed birds because of their panoramic vision are unable to avoid imaging the sun, but larger-eyed birds, such as the eagle shown in Figure 3, seem frequently to adopt strategies that avoid imaging the sun. The relationship between eye-size and the width of the blind area may be explained if viewing the sun becomes an increasing problem as eye size increases. The image of the sun can act as a light source within the eye. Scattered light from this image inside the chamber produces the phenomenon that is known in humans as disability glare (Ho, A. and Bilton, S. M., 1986; Dickinson, C. M., 1991) that can prevent target detection, particularly when the original object is of low contrast (Le Claire, J. *et al.*, 1982). In support of this hypothesis is the observation that only in larger-eyed birds are found external structures (eye lashes and enlarged brows, Figure 3(b)) that can shade the eye. The reason why glare is especially problematic for large eyes is not obvious, but it may be that the effects are felt disproportionately in retinae adapted for high resolution. In smaller eyes that have not evolved to achieve the highest resolution, light scattered from an image of the sun upon the retina may not degrade image contrast sufficiently that the benefits of gaining comprehensive visual coverage are outweighed by a reduction in the ability to gain spatial information across the whole of that visual field.

1.03.6 Photoreceptors and the Retina

1.03.6.1 Photopigments and Photoreceptors

Birds have one rod and four types of cone photopigment, which belong to the five ancient genetic families of vertebrate opsins (see Vision in Fish). All have a retinal (A1) chromophore. Spectrophotometric measurements show that the sensitivity maxima (λ_{max}) of four of the five photopigments are conserved across a wide range of avian species, namely, RH1 (λ_{max} 500 nm) that is found in rods, RH2 (λ_{max} 505 nm), SWS2 (λ_{max} 470 nm), and LWS (λ_{max} 565 nm) (fig. 9b; Yokoyama, S. and Yokoyama, R., 1996; Hart, N. S., 2001; Hart, N. S. and Hunt, D. M., 2007). SWS1 pigments fall into two classes according to whether a key site (amino acid 90) has a cysteine or a serine residue, which respectively give λ_{max} values of 365 and 410 nm (Wilkie, S. E. *et al.*, 2000). Spectral sensitivity of SWS1 can therefore be inferred from the opsin DNA, which facilitates the study of the phylogeny (Ödeen, A. and Håstad, O., 2003; Hart, N. S. and Hunt, D. M., 2007). This shows that in birds the 410 nm (VS) variant is the primitive form and that UV sensitivity has evolved independently on at least four occasions (see Section 1.03.6.4).

A penguin (*Spheniscus humboldti*) provides a likely exception to the general uniformity of avian photopigment, with 403, 450, and 543 nm pigments reported (Bowmaker, J. K. and Martin, G. R., 1984). It seems probable that the penguin's LWS pigment is blue shifted and the MWS pigment is absent (see Section 1.03.6.4).

Birds have three morphologically distinct types of photoreceptor: rods, single cones, and double cones (Walls, G. L., 1942; Cserhati, P. *et al.*, 1989). Double cones are widespread in vertebrates (see Vision in Fish; Walls, G. L., 1942), but absent from mammals. Four types of single cone (Figures 8 and 9) are distinguished on the basis of their spectral sensitivity LWS, MWS (containing RH2 pigment), SWS (containing SWS2 pigment), and UV/VS (containing SWS1 pigment and according to whether λ_{max} is near 365 or 410 nm). This nomenclature is potentially confusing because names of cones are similar but do not always match the photopigment. Double cones contain the LWS pigment. Each cone has a specific type of oil droplet in the proximal part of the outer segment (Figures 8 and 9; Bowmaker, J. K., 1977; Cserhati, P. *et al.*, 1989; Hart, N. S., 2001).

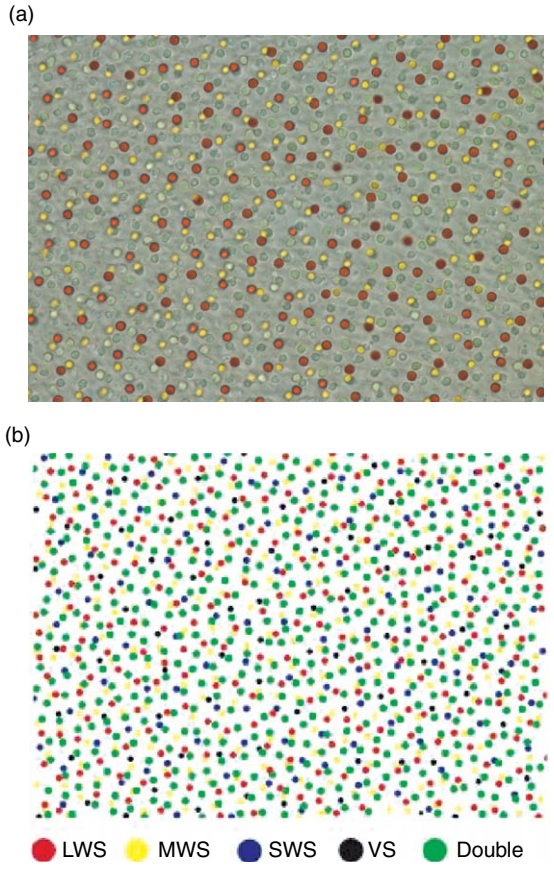

Figure 8 Images of a chicken retina showing the distributions of different cone types as revealed by their oil droplets. (a) Unstained retinal whole mount. Red oil droplets in LWS cones and yellow droplets in the MWS cones are clearly visible. Other types are less readily distinguished in this image but can be identified under UV illumination and by fluorescence. (b) Locations of all five types of cone taken from a different chicken retina. Courtesy of Dr. N. S. Hart.

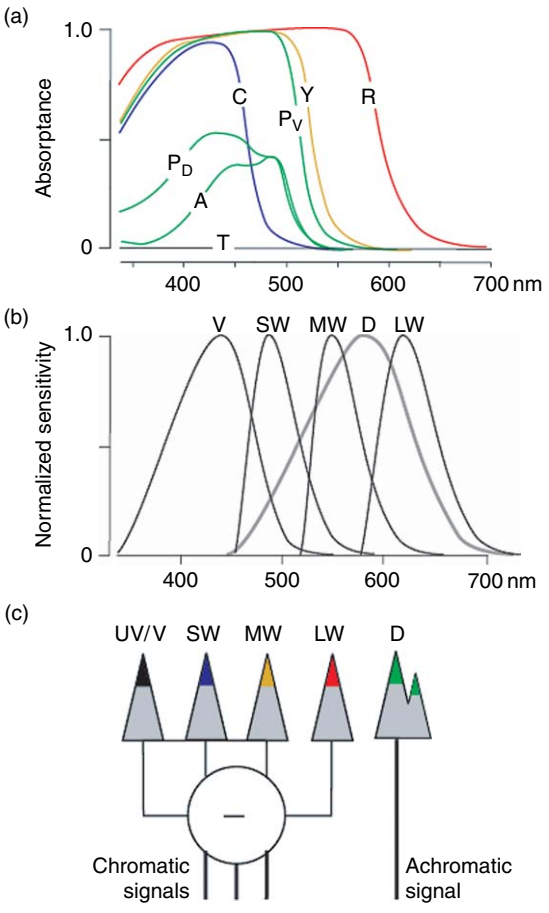

Figure 9 (a) Spectral absorptances of cone oil droplets measured in the peafowl (*Pavo cristatus*) by Hart N. S. (2002). Compare to Figure 8. The droplets are identified as follows: T-type (transparent) in UV/VS cones; C-type (colorless) in SWS cones; Y-type (yellow) in MWS cones, R-type (red) in LWS cones, and P-type (pale) and A-type (accessory) in the principal and accessory members of the double cone pair, respectively. P_V droplets occur in the ventral retina and therefore view the celestial hemisphere. P_D-type droplets occur in the dorsal retina less dense and resemble the A-type droplets. Cutoff wavelengths of the droplets are approximately given as follows: T: none; C: 450 nm; Y: 500 nm; R: 570 nm; P_V: 500 nm in the ventral retina (Hart, N. S., 2002). All these droplets have very high maximum absorbances. The P-type droplets in the dorsal retina and A-type droplets are less dense and cut off at about 480 nm. (b) Photoreceptor spectral sensitivities for a peafowl (Hart, N. S., 2002). The double cone spectral sensitivity curve resembles that of human L cones but will be affected by the specific type of oil droplet present (panel a). These sensitivities represent the primitive state in having a VS (410 nm) pigment. Oscine passerines (other than corvids), parrots, rhea, and gulls have a UVS (360 nm) pigment. (c) Diagram of how two main types of visual signal may be derived from the five types of cone. The four types of single cones serve at least three chromatic mechanisms, while the double cones (D) serve an avian luminance mechanism. Whilst supported by current evidence (see Section 1.03.7), this model may well be elaborated in future.

Spectral filtering by pigmented oil droplets sharpens the tuning of avian LWS, MWS, and SWS cones (Figure 9; Hart, N. S. and Vorobyev, M., 2005). The double cone oil droplet blocks UV, so that the double cone spectral sensitivity resembles that of human L cones. The UV/VS cone oil droplet is transparent. The next section looks further at oil droplets and their pigments.

1.03.6.2 Oil Droplets

Lungfish and many terrestrial vertebrates including marsupials, but not eutherian mammals, have oil droplets in their cone outer segment, which lie immediately proximal to the disks that contain photopigment (Walls,

G. L., 1942; Goldsmith, T. H. *et al.*, 1984; Cserhati, P. *et al.*, 1989). In some vertebrate groups oil droplets are all transparent, and in others, including birds they may be colored (Figures 8 and 9(a)). Where they are colored, oil droplets probably have at least two functions: (1) for focusing (or guiding) light and (2) for spectral filtering. This filtering may be beneficial in excluding damaging UV light and/or for color vision. Direct evidence (e.g., by depleting pigments from oil droplets, Wallman, J. 1979; Bowmaker, J. K. *et al.*, 1993) for the proposed benefits from oil droplets is limited, but there is relevant theoretical work.

The high refractive index of oil droplets compared to cytoplasm suggests a role in focusing or guiding light within the outer segment. The small size (<3 μm diameter) of oil droplets means that waveguide effects are important, so they cannot be understood as a conventional lens (Enoch, J. M., 1980). A physical model using microwaves guided by optics made of plastic (Govardovskii, V. I. *et al.*, 1981) shows that oil droplets can enhance propagation of near-axial rays within the outer segment and reduce the effective intensity off-axis rays. The overall effect is to enhance type I Stiles–Crawford effects (Enoch, J. M., 1980), and hence to reduce the effect of changes in pupil size (see Section 1.03.2.2). Consistent with this finding, a theoretical model suggests that oil droplets may concentrate light within the outer segment (Ives, J. T. *et al.*, 1983).

1.03.6.2.1 Spectral properties of oil droplets and the benefits of narrowing spectral tuning curves

Avian oil droplets contain carotenoids (except for UV/VS cones), which absorb light between the near UV and a longer wavelength (Goldsmith, T. H. *et al.*, 1984). When UV absorption by other optical media is taken into account, the oil droplets act as filters that block short-wavelength light (Hart, N. S. and Vorobyev, M., 2005). One benefit of blocking short wavelengths is to prevent UV photodamage (Young, R. W., 1994). As each cone type has its own specific oil droplet filter, this means that the eye can admit near UV light without damaging longer-wavelength-sensitive receptors. By comparison, mammals are often blind to UV light, because the lens blocks wavelengths below 400 nm. This interpretation is consistent with the relatively low density of pigmentation in double cone oil droplets in the dorsal as compared with the ventral retina of the peafowl (Figure 9(a); Hart, N. S., 2002).

Birds have six types of oil droplets (Figures 8 and 9): T-type (transparent) in UV/VS cones, C-type (colorless) in SWS cones; Y-type (yellow) in MWS cones, R-type (red) in LWS cones, and P-type (pale) and A-type (accessory) in the principal and accessory members of the double cone pair, respectively.

Whereas blocking UV may be the main role of clear double cone oil droplets, in the single cones it seems likely that narrowing and red-shifting spectral sensitivities is important (Figure 9). Thus, LWS cones have a 565 nm visual pigment, but the oil droplet shifts the receptor peak sensitivity (λ_{max}) to around 600 nm; MWS cones have a 500 nm pigment but λ_{max} ~530 nm; and SWS cones a 470 nm pigment and λ_{max} 490 nm. This spectral narrowing has a substantial cost to photon catch (>75% for the LWS cones), and it seems likely that the corresponding benefit is for color vision.

The likely benefits of oil droplets for color vision are, however, not clear. Spectral filtering by oil droplets substantially increases the number of colors (i.e., visual spectra) that theoretically can be discriminated (Vorobyev, M., 2003). Naturally occurring spectra do not, however, occupy the full range of discriminable colors. The advantages are greatest where there is fine detail in the spectra. Some avian plumage colors for example are notably brilliant, and calculations suggest that oil droplets can improve their discriminability compared to unfiltered cone pigments (Vorobyev, M. *et al.*, 1998). However, given the lack of taxonomic variation in oil droplets (see below), and the fact that many groups of birds lack bright plumage, this is not a likely explanation of their primary evolutionary function. Most natural spectra vary smoothly (Maloney, L. T., 1986) in which case the loss of light may more than offset the benefits for color discriminability (Hateren, J. H. van, 1993). An alternative explanation is that narrowing the spectral sensitivity of photoreceptors may be beneficial for color constancy (Worthey, J. A. and Brill, M. H., 1986; Osorio, D. *et al.*, 1997; Vorobyev, M. *et al.*, 1998).

Behavioral tests might resolve questions about the function of oil droplet pigmentation. These are possible because dietary carotenoid deprivation removes oil droplet pigmentation. One study of Japanese quail in optomotor tests shows that effects are consistent, with deprived birds having inferior color vision when compared to normal birds (Wallman, J., 1979).

1.03.6.2.2 Variation in oil droplet pigmentation

In most avian species studied a single type of cone has a single type of oil droplet (Bowmaker, J. K. *et al.*, 1997; Hart, N. S., 2001). However, data are limited,

mainly to passerines and gallinaceous birds. The high refractive index of oil droplets means that it is difficult to measure their absolute optical density, but there is some variation within and between species. As one might expect, pigmentation is relatively weak in nocturnal birds (Hart, N. S., 2001). The wedge-tailed shearwater (*Puffinus pacificus*) has weakly or unpigmented droplets in the high-acuity visual streak dorsal to the equator (and hence in the ventral visual field; Hart, N. S., 2004). Another arrangement that is not unexpected is to have more densely pigmented P-type oil droplets on the double cones in the ventral retina, which views the sky, than the dorsal retina, as is found in the peacock (*Pavo cristatus*; Hart, N. S., 2002). It is likely that such density gradients are at least partly caused by incident light intensity. An experimental study showed that chickens raised in bright illumination have higher pigment density in their oil droplets than do birds raised in dim light (Hart, N. S. *et al.*, 2006).

The most complex retina known is in the pigeon where there are two clearly defined regions: the red sector, which views the ventral–frontal visual field, and presumably is concerned with locating food, and the yellow sector that occupies the remainder of the retina. In the red sector, double cone oil droplets cut off at either about 550 or 525 nm, whereas in the yellow sector, double cone oil droplets cut off between 470 and 500 nm (Bowmaker, J. K., 1977; see also next section).

1.03.6.3 Photoreceptor Densities and Distributions

Receptor densities have been recorded in species including passerines, budgerigar, and chickens, either from oil droplet counts in a retinal whole mount or by spectrophotometry (Figure 8; Hart, N. S. *et al.*, 2000a; Hart, N. S., 2001). Usually 40–50% of the receptors are double cones but range from 30% for pigeon red sector retina to 75% for an owl (*Strix varia*; Bowmaker, J. K., 1977; Braekevelt, C. R. *et al.*, 1996). Of the single cones, LWS and MWS are present in approximately equal numbers and UV/VS least frequent, with SWS densities ranging between these two values (Bowmaker, J. K., 1977; Bowmaker, J. K. *et al.*, 1997; Hart, N. S., 2001). Pigeon yellow sector retina falls within the typical range, with 50% double cones and 12% each of LWS and MWS cones, but the red sector is atypical with 30% double cones and ~25% for each of the LWS and MWS cones (Bowmaker, J. K., 1977). It should be noted that visual thresholds are likely to be proportional to the square root of receptor density (Kelber, A. *et al.*, 2003), so that effects of variations on color vision are relatively small.

Aside from the overall density of the different types of photoreceptor, the layout of the receptor mosaic is of interest, both from a developmental point of view and with regard to retinal sampling. Having six types of receptor poses a problem for spatial sampling because any one type of cone is likely to undersample the image (Snyder, A. W. and Miller, W. H., 1977; Snyder, A. W. *et al.*, 1986). Theory suggests that an orderly cone mosaic, as found in many fish, optimizes coding of spatial information (Lythgoe, J. N., 1979; Bossomaier, T. R. *et al.*, 1985). By comparison, the array of human L and M cones appears to be random (Williams, D. R. and Hofer, H., 2003). It seems possible from published images of retinas that birds are intermediate, they are less orderly than fish, but there is evidence for nonrandom distributions of MWS and LWS cones in starling (Hart, N. S. *et al.*, 2000b). UVS cones in budgerigar are said to be nonrandomly distributed (Wilkie, S. E. *et al.*, 1998).

1.03.6.4 Variation of Receptor Spectral Sensitivities and Densities

It is readily apparent that avian visual optics vary between species and that often this variation reflects visual ecology (see Sections 1.03.2, 1.03.3, and 1.03.5). By comparison, it seems that spectral sensitivities of avian photoreceptors are conservative with little evidence for adaptive variation (Hart, N. S., 2001; Hart, N. S. and Hunt, D. M., 2007). Thus, a strictly marine bird the wedge-tailed shearwater has very similar spectral receptors to a peacock (Hart, N. S., 2002; 2004). There are, however, some exceptions.

First, humboldt penguin (*S. humboldti*) probably has only three types of visual photopigment, with 80% double cones and probably three types of single cone. Pigment sensitivity maxima are at 403, 450, and 543 nm, and the longest wavelength oil droplet cuts off below 525 nm (Bowmaker, J. K. and Martin, G. R., 1984; Suburo, A. M. and Scolaro, J. A., 1999). It seems likely that this eye reflects the lack of long wavelengths in water.

A more widespread mode of variation is in the spectral sensitivity of the SWS1 pigment. As mentioned above (see Section 1.03.6.1), there are two main forms of this pigment with sensitivity maxima

at about 365 nm (UV) and 410 nm (VS). The UV form occurs in most oscine passerines (but not corvids), in a gull (*Larus* sp.), ostrich (but not rhea (*Rhea Americana*)), and parrots (Psittaciformes). The VS form is found in the suboscine and corvid groups of passerines, and most other avian lineages (Ödeen, A. and Håstad, O., 2003). That there may be adaptive variation in the spectral tuning of the UV/VS cones is perhaps not surprising as theoretical considerations suggest that small shifts in the spectral composition and intensity of illumination will affect the relative merits of these two types of pigment (Vorobyev, M. *et al*., 1998). There is, however, no obvious explanation for the observed pattern of variation.

1.03.7 Functions of the Different Types of Avian Cone

Given that birds have five types of cone photoreceptor, it may be that receptors are specialized for particular behaviors, or aspects of visual perception. Identification of visual pathways is a key aspect of work on primate vision. Here a familiar distinction is between the magnocellular pathway, originating from the parasol-type retinal ganglion cells, and the parvocellular pathway originating from the midget retinal ganglion cells (Kaplan, E., 2003). Regarding the evolutionary basis for the presence of separate visual pathways, an obvious question is whether the functional divisions are specific to particular groups, such as primates, or have emerged separately in separate lineages: that is, by convergent evolution. As predominantly diurnal and arboreal animals, primates are in many ways the most bird-like of mammals, so that comparisons are of particular interest.

The primate magnocellular system combines M (green) and L (red) cone outputs to give a luminance signal, which is used for motion and many aspects of form recognition (Livingstone, M. and Hubel, D., 1988; Kaiser, P. K. *et al*., 1990; Logothetis, N. K., *et al*., 1990). The magnocellular system signal has relatively high contrast sensitivity, but spatial resolution is limited by spatial pooling of cone outputs in the parasol ganglion cells (Kaplan, E., 2003). By comparison, the parvocellular system has relatively low contrast sensitivity, but midget ganglion cells do not pool cone outputs (at least in the central visual field). This system can encode high spatial frequencies and the red–green chromatic signal, which is based on spectral opponency between L and M cone signals. Further types of primate retinal ganglion cell encode S (blue) cone signals including blue–yellow opponent signals (Dacey, D., 2000).

There is little work on physiology of avian retinal ganglion cells, but there are studies of specialization of the cone photoreceptors themselves. Starting from receptor spectral sensitivities (Hart, N. S., 2001), one can use stimuli that give well-specified receptor excitations and so isolate subsets of receptors (Osorio, D. *et al*., 1999a; 1999b; Goldsmith, T. H. and Butler, B. K., 2003; 2005). The emerging picture suggests that the double cones have a role comparable to that of the primate M-cell pathway. They provide an avian luminance signal, which is used for motion detection and certain aspects of form vision (Campenhausen, M. von and Kirschfeld, K. 1998; Osorio, D. *et al*., 1999b; Jones, C. D. and Osorio, D., 2004; Goldsmith, T. H. and Butler, B. K., 2005). Avian single cones are used for color vision, and birds may have a tetrachromatic color vision based on the four single cones. The following sections review the evidence for functional specialization of the avian cones.

1.03.7.1 Double Cones and Avian Luminance

In human psychophysics techniques such as the minimally distinct border are used to determine the spectral sensitivity of visual mechanisms. The relative brightness of two colors regions is adjusted until a sensitivity minimum or null is reached (Kaiser, P. K., 1971; Livingstone, M. and Hubel, D., 1988; Kaiser, P. K. *et al*., 1990). This establishes that certain visual tasks are predominately color-blind (i.e., they do not use chromatic signals) and shows that the achromatic signal that is used has the spectral sensitivity characteristic of the luminance mechanism or M-cell system (see Section 1.03.7).

In birds nulling techniques have been used with optokinetic responses (i.e., motion perception), in quail and pigeons (Wallman, J., 1979; Campenhausen, M. von and Kirschfeld, K., 1998), and with texture perception in poultry chicks (Jones, C. D. and Osorio, D., 2004). There are also comparable studies of spectral inputs to motion-sensitive neurons in pigeons (Sun, H. and Frost, B. J., 1997). These studies generally suggest that the tasks in question is color blind, but Wallman J. (1979) gives evidence for a chromatic input to optokinetic responses in quail (*Coturnix coturnix*). Also, the spectral sensitivity resembles that of the double cones and is unlikely

to be attributable to any one type of single cone (Osorio, D. *et al*., 1999b; Jones, C. D. and Osorio, D., 2004). A single measurement of spectral sensitivity does not, however, readily distinguish a mechanism that combines an appropriately weighted sum of single cone outputs from a double cone signal. A distinction could be made by tests of the effects of selective adaptation, but to our knowledge this has not been done.

The notion that the double cones give an avian luminance signal is reinforced by evidence that they do not contribute to color vision, which we outline in the following section.

1.03.7.2 Single Cones and Tetrachromacy

The narrow spectral tuning of the single cones (Figure 9), and their comparatively even spacing across the spectrum, indicates that they are adapted for coding spectral information, and hence for color vision. Color vision requires comparison of the outputs for two or more spectral types of receptor. For a range of species there is evidence that color vision is served by chromatic mechanisms, with low sensitivity to brightness (Vorobyev, M. and Osorio, D., 1998; Kelber, A. *et al*., 2003). Also we know that humans are trichromatic, in that signals from each of the three cone types are used independently so that spectra are coded with three degrees of freedom. However, within the 3D human color space the two dimensions that represent chromaticity (i.e., hue and saturation) appear to be more relevant to color perception than the achromatic axis (brightness). This is why 2D chromaticity diagrams, such as the CIE *xy* color triangle, that represent a gamut of colors of approximately equal brightness proves useful.

By analogy with human trichromatic color vision, it is a plausible hypothesis that birds are tetrachromatic. Within the 4D avian color space one can plot a 3D chromatic tetrahedron, which is analogous to a human color triangle (Goldsmith, T. H., 1990; Kelber, A. *et al*., 2003). Tests of tetrachromacy are, however, elusive. The key prediction is that two lights of differing spectral composition will have the same color (i.e., they are metamers) only if each of the receptor mechanisms (i.e., cone types) gives the same response to each of the two lights. A mismatch in one mechanism could not be offset by a complementary adjustment to another. It should be noted that the receptor mechanisms used may be contingent on a number of factors, such as the illumination level, the visual task, and the visual field used. There is no *a priori* reason for having a single type of color vision.

Behavioral investigation of color vision benefits from the knowledge of receptor spectral sensitivities, and these are now available for many bird species (see Section 1.03.6; Hart, N. S., 2001; Hart, N. S. and Hunt, D. M., 2007). Two principal methods are used to investigate receptor inputs to avian color vision, both of which support the view (Goldsmith, T. H., 1990) that birds use four single cones to give tetrachromatic color vision. Direct but inconclusive evidence comes from studies that isolate specific subsets of receptors by combinations of illumination and reflectance spectra (Osorio, D. *et al*., 1999b). This method can show whether birds have specific chromatic mechanisms. Thus, week-old poultry chicks probably have at least three opponent mechanisms: L versus M, L+M versus S, and S versus VS (Osorio, D. *et al*., 1999b). Separate evidence from studies with spectra that differ only in the UV suggests that VS/UV receptors contribute to color vision of starling and quail (Smith, E. L. *et al*., 2002). These studies give evidence for tetrachromacy but are not conclusive and do not rule out a role for the double cones.

Clear, if less direct, evidence for tetrachromacy comes from spectral sensitivity data for pigeon, budgerigar (*Melopsittacus undulatus*), and a passerine (Pekin robin, *Leiothrix lutea*; Vorobyev, M. and Osorio, D., 1998; Goldsmith, T. H. and Butler, B. K., 2003; 2005). In tests of spectral sensitivity subjects discriminate between two stimuli: a uniform adapting field, which is approximately achromatic, and a field where monochromatic light is added to a central region (and so appears nonuniform). The procedure gives the minimum intensity of a given wavelength that is detectable against the background, and when tests are repeated across the spectrum they generate a spectral sensitivity curve. Under light-adapted conditions, spectral sensitivities for a wide range of animals, including birds, are consistent with a model where discrimination thresholds are set by chromatic (i.e., opponent) signals derived from single cone mechanisms, achromatic mechanisms are much less sensitive, and there is no evidence for a role for double cones (Vorobyev, M. and Osorio, D., 1998; Goldsmith, T. H. and Butler, B. K., 2003; Kelber, A. *et al*., 2003; Goldsmith, T. H. and Butler, B. K., 2005). This model does not predict visual thresholds for Pekin robin in low light conditions, or for the pigeon red field, where achromatic signals appear to be more important in setting spectral sensitivity thresholds.

1.03.7.3 Specialization of Single Cones and UV Sensitivity

Aside from their role in color vision, one can ask whether a given sensory receptor contributes to specific behavior. In birds particular attention is given to UV/VS cones. In part this work is stimulated by the interest in the idea that birds perceive the world in a way different from ourselves. More specifically, there is evidence that plumage that is used in visual displays reflects more strongly in the UV than do other types of plumage (Hausmann, F. *et al*., 2003). By filtering illumination, and by the using UV blocking filters (i.e., sunblock) painted on plumage, it can be shown that UV wavelengths are used in courtship behavior and foraging behaviors (Cuthill, I. C., 2006). For example, the attractiveness of male starlings and zebra finches to females is altered according to whether or not the UV is in the illumination (Bennett, A. T. D., *et al*., 1996; 1997), and the attractiveness of male bluethroats (*Luscinia svecica*) is reduced by blocking UV reflectance from their blue throat patches (Andersson, S. and Amundsen, T., 1997). These findings are of interest, in part because there is great variation in the proportion of UV in natural illumination, and so have implications for how male birds select display sites. There is, however, no clear evidence that the UV signal is of special significance compared to those from the other single cones. It would be interesting to know whether the UV signal is perceived as an aspect of chromaticity or brightness.

1.03.8 Concluding Remarks: A Wing Guided by an Eye?

This chapter opened with the phrase, "A bird is a wing guided by an eye," coined by Rochon-Duvigneaud A. (1943) to capture the essence of a bird. The discussion that followed shows clearly that birds use their eyes for far more than the guidance of flight and that some birds do not use their eyes to guide flight. The discussion also showed that although some general principles regarding the optical structure of eyes can be discerned, and rules regarding the form and function of visual fields have been proposed. The study of bird eyes presents many challenges, which are met by a number of techniques and approaches, but key among them are comparative studies that relate eye design to ecology and behavior. It is sobering to note that aspects of eye structure and/or visual fields are discussed for <1% of all bird species currently recognized. Each species represents an independently evolving lineage, in which vision is likely to have become finely tuned by natural selection to the challenges presented by the ecology and behavior of the species. We have some idea of the general principles that have governed the design of eyes and their placement in the skull, but we are far from knowing the subtle variations that natural selection has built around these general designs.

References

Andersson, S. and Amundsen, T. 1997. Ultraviolet colour vision and ornamentation in bluethroats. Proc. R. Soc. Lond. B 264, 1587–1591.

Bennett, A. T. D., Cuthill, I. C., Partridge, J. C., and Lunau, K. 1997. Ultraviolet plumage colors predict mate preferences in starlings. Proc. Natl. Acad. Sci. U. S. A. 94, 8618–8621.

Bennett, A. T. D., Cuthill, I. C., Partridge, J. C., and Maier, E. J. 1996. Ultraviolet vision and mate choice in zebra finches. Nature 380, 433–435.

Boire, D., Dufour, J.-S., Théoret, H., and Ptito, M. 2001. Quantitative analysis of the retinal ganglion cell layer in the ostrich, *Struthio camelus*. Brain Behav. Evol. 58, 343–355.

Bossomaier, T. R., Snyder, A. W., and Hughes, A. 1985. Irregularity and aliasing: solution? Vision Res. 25, 145–147.

Bowmaker, J. K. 1977. The visual pigments, oil droplets and spectral sensitivity of the pigeon. Vision Res. 17, 1129–1138.

Bowmaker, J. K. and Martin, G. R. 1984. Visual pigments and oil droplets in the penguin, *Spheniscus humboldti*. J. Comp. Physiol. A 156, 71–77.

Bowmaker, J. K., Heath, L. A., Wilkie, S. E., and Hunt, D. M. 1997. Visual pigments and oil droplets from six classes of photoreceptor in the retinas of birds. Vision Res. 37, 2183–2194.

Bowmaker, J. K., Kovach, J. K., Whitmore, A. V., and Loew, E. R. 1993. Visual pigments and oil droplets in genetically manipulated and carotenoid deprived quail: a microspectrophotometric study. Vision Res. 33, 571–578.

Braekevelt, C. R., Smith, S. A., and Smith, B. J. 1996. Fine structure of the retinal photoreceptors of the barred owl (*Strix varia*). Histol. Histopathol. 11, 79–88.

Brooke, M. D. L., Hanley, S., and Laughlin, S. B. 1999. The scaling of eye size with body mass in birds. Proc. R. Soc. Lond. B 266, 405–412.

Campenhausen, M. von and Kirschfeld, K. 1998. Spectral sensitivity of the accessory optic system of the pigeon. J. Comp. Physiol. A 183, 1–6.

Cserhati, P., Szel, A., and Rohlich, P. 1989. Four cone types characterized by anti-visual pigment antibodies in the pigeon retina. Invest. Ophthalmol. Vis. Sci. 30, 74–81.

Cunningham, S. J. 2006. Foraging Sign, Bill Morphology and Prey Detection in the North Island Brown Kiwi (Apteryx Mantelli). BSc (Hons) Research Report. Palmerston North, New Zealand Massey University.

Cuthill, I. C. 2006. Color Perception. In: Bird Coloration. Vol. 1. Mechanisms and Measurement (*eds*. G. E. Hill and K. J. McGraw) pp. 3–40. Harvard University Press.

Dacey, D. 2000. Parallel pathways for spectral coding in primate retina. Annu. Rev. Neurosci. 23, 743–775.

Darwin, C. R. 1859. On the Origin of Species by Means of Natural Selection, or the Preservation of Favoured Races in the Struggle for Life, 1st edn. John Murray.

Davies, M. N. O. and Green, P. R. 1994. Multiple Sources of Depth Information: An Ecological Approach. In: Perception and Motor Control in Birds: An Ecological Approach (*eds*. M. N. O. Davies and P. R. Green), pp. 339–356. Springer-Verlag.

Dickinson, C. M. 1991. Optical Aids for Low Vision. In: Vision and Visual Dysfunction (*ed*. W. N. Charman), pp. 183–228. Macmillan.

Duke-Elder, S. 1958. System of Ophthalmology: Vol. 1. The Eye in Evolution. Henry Kimpton.

Enoch, J. M. 1980. Vertebrate receptor optics and orientation. Doc. Ophthalmol. 48, 373–388.

Frost, B. J., Wylie, D. R., and Wang, Y. C. 1994. The Analysis of Motion in the Visual Systems of Birds. In: Perception and Motor Control in Birds: An Ecological Approach (*eds*. M. N. O. Davies and P. R. Green), pp. 248–269. Springer.

Garamszegi, L. A., Moller, A. P., and Erritzoe, J. 2002. Coevolving avian eye size and brain size in relation to prey capture and nocturnality. Proc. R. Soc. Lond. B 269, 961–967.

Gibson, J. J. 1986. The Ecological Approach to Visual Perception. Erlbaum.

Gill, F. B. 2007. Ornithology. Freeman.

Glasser, A. 2003. How Other Species Accommodate. In: Current Aspects of Human Accommodation (*eds*. R. Guthoff and K. Ludwig), pp. 13–38. Kladen Verlag.

Glasser, A. and. Howland, H. C. 1996. A history of studies of visual accommodation in birds. Q. Rev. Biol. 71, 475–509.

Glasser, A., Murphy, C. J., Troilo, D., and Howland, H. C. 1995. The mechanism of lenticular accommodation in chicks. Vision Res. 35, 1525–1540.

Glasser, A., Troilo, D., and Howland, H. C. 1994. The mechanism of corneal accommodation in chicks. Vision Res. 34, 1549–1566.

Goldsmith, T. H. 1990. Optimization, constraint, and history in the evolution of eyes. Q. Rev. Biol. 65, 281–322.

Goldsmith, T. H. and Butler, B. K. 2003. The roles of receptor noise and cone oil droplets in the photopic spectral sensitivity of the budgerigar, *Melopsittacus undulatus*. J. Comp. Physiol. A 189, 135–142.

Goldsmith, T. H. and Butler, B. K. 2005. Color vision of the budgerigar (*Melopsittacus undulatus*): hue matches, tetrachromacy, and intensity discrimination. J. Comp. Physiol. A 191, 933–951.

Goldsmith, T. H., Collins, J. S., and Licht, S. 1984. The cone oil droplets of avian retinas. Vision Res. 24, 1661–1671.

Gottschaldt, K. M. 1985. Structure and Function of Avian Somatosensory Receptors. In: Form and Function in Birds Vol. 3 (*eds*. A. S. King and J. Mclelland), pp. 375–461. Academic Press.

Govardovskii, V. I., Golovanevskii, E. I., Zueva, L. V., and Vasil'eva, I. L. 1981. Role of cellular organoids in photoreceptor optics (studies on microwave models). Zh. Evol. Biokhim. Fiziol. 17, 492–497 (in Russian).

Granda, A. M. and Maxwell, J. H. 1979. Neural Mechanisms of Behaviour in the Pigeon. Plenum.

Guillemaine, M., Martin, G. R., and Fritz, H. 2002. Feeding methods, visual fields and vigilance in dabbling ducks (Anatidae). Funct. Ecol. 16, 522–529.

Hall, M. I. and Ross, C. F. 2007. Eye shape and activity pattern in birds. J. Zool. (Lond.) 271, 437–444.

Hart, N. S. 2001. Variations in cone photoreceptor abundance and the visual ecology of birds. J. Comp. Physiol. A 187, 685–697.

Hart, N. S. 2002. Vision in the peafowl (Aves: *Pavo cristatus*). J. Exp. Biol. 205, 685–697.

Hart, N. S. 2004. Microspectrophotometry of visual pigments and oil droplets in a marine bird, the wedge-tailed shearwater *Puffinus pacificus*: topographic variations in photoreceptor spectral characteristics. J. Exp. Biol. 207, 1229–1240.

Hart, N. S. and Hunt, D. M. 2007. Avian visual pigments: characteristics, spectral tuning, and evolution. Am. Nat. 169, S7–S26.

Hart, N. S. and Vorobyev, M. 2005. Modelling oil droplet absorption spectra and spectral sensitivities of bird cone photoreceptors. J. Comp. Physiol. A 191, 381–392.

Hart, N. S., Lisney, T. J., and Collin, S. P. 2006. Cone photoreceptor oil droplet pigmentation is affected by ambient light intensity. J. Exp. Biol. 209, 4776–4787.

Hart, N. S., Partridge, J. C., Cuthill, I. C., and Bennett, A. T. D. 2000a. Visual pigments, oil droplets, ocular media and cone photoreceptor distribution in two species of passerine bird: the blue tit (*Parus caeruleus* L.) and the blackbird (*Turdus merula* L.). J. Comp. Physiol. A 186, 375–387.

Hart, N. S., Partridge, J. C., and Cuthill, I. C. 2000b. Retinal asymmetry in birds. Curr. Biol. 10, 115–117.

Hateren, J. H.van 1992. A theory of maximizing sensory information. Biol. Cybern. 68, 23–29.

Hateren, J. H.van 1993. Spatial, temporal and spectral pre-processing for colour vision. Proc. R. Soc. Lond. B 251, 61–68.

Hausmann, F., Arnold, K. E., Marshall, N. J., and Owens, I. P. 2003. Ultraviolet signals in birds are special. Proc. R. Soc. Lond. B 270, 61–67.

Hayes, B., Martin, G. R., and Brooke, M. D. L. 1991. Novel area serving binocular vision in the retinae of procellariiform seabirds. Brain Behav. Evol. 37, 79–84.

Ho, A. and Bilton, S. M. 1986. Low contrast charts effectively differentiate between types of blur. Am. J. Optom. Physiol. Opt. 63, 202–208.

Howland, H. C., Howland, M., and Schmid, K. L. 1992. Focusing and accommodation in the brown kiwi (*Apteryx australis*). J. Comp. Physiol. A 170, 687–689.

Hughes, A. 1977. The Topography of Vision in Mammals of Contrasting Life Style: Comparative Optics and Retinal Organization. In: Handbook of Sensory Physiology. Vol. VII/5 (*ed*. F. Crescitelli), pp. 613–756. Springer-Verlag.

Hughes, A. 1986. The Schematic Eye Comes of Age. In: Visual Neuroscience (*eds*. J. Pettigrew, K. J. Sanderson, and W. R. Levick), pp. 60–89. Cambridge University Press.

Ives, J. T., Normann, R. A., and Barber, P. W. 1983. Light intensification by cone oil droplets: electromagnetic considerations. J. Opt. Soc. Am. 73, 1725–1731.

Jeffery, W. R. 2005. Adaptive evolution of eye degeneration in the Mexican blind cavefish. J. Hered. 96, 185–196.

Jones, C. D. and Osorio, D. 2004. Discrimination of oriented visual textures by poultry chicks. Vision Res. 44, 83–89.

Kaiser, P. K. 1971. Minimally distinct border as a preferred psychophysical criterion in visual heterochromatic photometry. J. Opt. Soc. Am. 61, 966–971.

Kaiser, P. K., Lee, B. B., Martin, P. R., and Valberg, A. 1990. The physiological basis of the minimally distinct border demonstrated in the ganglion cells of the macaque retina. J. Physiol. 422, 153–183.

Kaplan, E. 2003. The M, P, and K Pathways of the Primate Visual System. Chapter 30. In: The Visual Neurosciences (*eds*. L. M. Chalupa and J. S. Werner), pp. 481–493. MIT Press.

Katzir, G. and Martin, G. R. 1998. Visual fields in the black-crowned night heron *Nycticorax nycticorax*: nocturnality does not result in owl-like features. Ibis 140, 157–162.

Kelber, A., Vorobyev, M., and Osorio, D. 2003. Animal colour vision: behavioural tests and physiological concepts. Biol. Rev. 78, 81–118.

King, A. S. and King, D. Z. 1980. Avian Morphology: General Principles. In: Form and Function in Birds (*eds*. A. S. King and J. McLelland), pp. 10–89. Academic Press.

Konishi, M. 1973. Locatable and non-locatable acoustic signals for barn owls. Am. Nat. 107, 775–785.

Kral, K. 2003. Behavioural-analytical studies of the role of head movements in depth perception in insects, birds and mammals. Behav. Processes 64, 1–12.

Krapp, H. G. and Hengstenberg, R. 1996. Estimation of self-motion by optic flow processing in single visual interneurons. Nature 384, 463–466.

Land, M. F. 1981. Optics and Vision in Invertebrates. In: Handbook of Sensory Physiology Vol. VII/6B (*ed*. H. -J. Autrum), pp. 471–592. Springer.

Land, M. F. and Eckert, H. 1985. Maps of the acute zones of fly eyes. J. Comp. Physiol. A 156, 525–538.

Land, M. F. and Fernald, R. D. 1992. The evolution of eyes. Annu. Rev. Neurosci. 15, 1–29.

Land, M. F. and Nilsson, D.-E. 2002. Animal Eyes. Oxford University Press.

Laughlin, S. B. 1992. Retinal information capacity and the function of the pupil. Ophthalmic Physiol. Opt. 12, 161–164.

Laughlin, S. B. 2001a. Energy as a constraint on the coding and processing of sensory information. Curr. Opin. Neurobiol. 11, 475–480.

Laughlin, S. B. 2001b. The Metabolic Cost of Information – A Fundamental Factor in Visual Ecology. In: Ecology of sensing (*eds*. F. G. Barth and A. Schmid), pp. 170–185. Springer.

Le Claire, J., Nadler, M. P., Weiss, S., and Miller, D. 1982. A new glare tester for clinical testing: results comparing normal subjects and variously corrected aphakic patients. Arch. Ophthalmol. 100, 153–158.

Lee, D. N. 1980. The optic flow field: the foundation of vision. Phil. Trans. R. Soc. Lond. B Biol. Sci. 290, 169–179.

Lee, D. N. 1994. An Eye or Ear for Flying. In: Perception and Motor Control in Birds: An Ecological Approach (*eds*. M. N. O. Davies and P. R. Green), pp. 270–291. Springer.

Lee, D. N., Reddish, P. E., and Rand, D. T. 1991. Aerial docking by hummingbirds. Naturwissenschaften 78, 526–527.

Leys, R., Cooper, S. J., Strecker, U., and Wilkens, H. 2005. Regressive evolution of eye pigment gene in independently evolved eyeless subterranean diving beetles. Biol. Lett. 1, 496–499.

Livingstone, M. and Hubel, D. 1988. Segregation of form, color, movement, and depth: anatomy, physiology, and perception. Science 240, 740–749.

Logothetis, N. K., Schiller, P. H., Charles, E. R., and Hurlbert, A. C. 1990. Perceptual deficits and the activity of the color-opponent and broad-band pathways at isoluminance. Science 247, 214–217.

Lythgoe, J. N. 1979. The Ecology of Vision. Clarendon Press.

Maloney, L. T. 1986. Evaluation of linear models of surface spectral reflectance with small numbers of parameters. J. Opt. Soc. Am. A 3, 1673–1683.

Marchant, S. and Higgins, P. J. 1990. Handbook of Australian, New Zealand and Antarctic Birds. Vol. 1 Part B. Oxford University Press.

Marshall, J., Mellerio, J., and Palmer, D. A. 1973. A schematic eye for the pigeon. Vision Res. 13, 2449–2453.

Martin, G. R. 1977. Absolute visual threshold and scotopic spectral sensitivity in the tawny owl *Strix aluco*. Nature 268, 636–638.

Martin, G. R. 1982. An owl's eye: schematic optics and visual performance in *Strix aluco* L. J. Comp. Physiol. A 145, 341–349.

Martin, G. R. 1983. Schematic Eye Models in Vertebrates. In: Progress in Sensory Physiology Vol. 4 (*ed*. D. Ottoson), pp. 43–81. Springer.

Martin, G. R. 1984. The visual fields of the tawny owl, *Strix aluco* L. Vision Res. 24, 1739–1751.

Martin, G. R. 1985. Eye. In: Form and Function in Birds. Vol. 3 (*eds*. A. S. King and J. McLelland), pp. 311–373. Academic Press.

Martin, G. R. 1986a. The eye of a passeriform bird, the European starling (*Sturnus vulgaris*): eye movement amplitude, visual fields and schematic optics. J. Comp. Physiol. A 159, 545–557.

Martin, G. R. 1986b. Sensory capacities and the nocturnal habit of owls (Strigiformes). Ibis 128, 266–277.

Martin, G. R. 1986c. Total panoramic vision in the mallard duck, *Anas platyrhynchos*. Vision Res. 26, 1303–1306.

Martin, G. R. 1990. Birds by Night. T & A D Poyser.

Martin, G. R. 1994a. Form and Function in the Optical Structure of Bird Eyes. In: Perception and Motor Control in Birds: An Ecological Approach (*eds*. M. N. O. Davies and P. R. Green), pp. 5–34. Springer.

Martin, G. R. 1994b. Visual fields in woodcocks *Scolopax rusticola* (Scolopacidae; Charadriiformes). J. Comp. Physiol. A 174, 787–793.

Martin, G. R. 1998. Eye structure and amphibious foraging in albatrosses. Proc. R. Soc. Lond. B 265, 1–7.

Martin, G. R. 1999. Eye structure and foraging in king penguins *Aptenodytes patagonicus*. Ibis 141, 444–450.

Martin, G. R. and Brooke, M.de L. 1991. The eye of a procellariiform seabird, the Manx shearwater, *Puffinus puffinus*: visual fields and optical structure. Brain Behav. Evol. 37, 65–78.

Martin, G. R. and Coetzee, H. C. 2004. Visual fields in hornbills: precision-grasping and sunshades. Ibis 146, 18–26.

Martin, G. R. and Katzir, G. 1994a. Visual fields and eye movements in herons (Ardeidae). Brain Behav. Evol. 44, 74–85.

Martin, G. R. and Katzir, G. 1994b. Visual fields in the stone curlew *Burhinus oedicnemus*. Ibis 136, 448–453.

Martin, G. R. and Katzir, G. 1995. Visual fields in ostriches. Nature 374, 19–20.

Martin, G. R. and Katzir, G. 1999. Visual field in short-toed eagles *Circaetus gallicus* and the function of binocularity in birds. Brain Behav. Evol. 53, 55–66.

Martin, G. R. and Katzir, G. 2000. Sun shades and eye size in birds. Brain Behav. Evol. 56, 340–344.

Martin, G. R. and Prince, P. A. 2001. Visual fields and foraging in procellariiform seabirds: Sensory aspects of dietary segregation. Brain Behav. Evol. 57, 33–38.

Martin, G. R. and Young, S. R. 1983. The retinal binocular field of the pigeon (*Columba livia*): English racing homer. Vision Res. 23, 911–915.

Martin, G. R. and Young, S. R. 1984. The eye of the humboldt penguin, *Spheniscus humboldti*: visual fields and schematic optics. Proc. R. Soc. Lond. B 223, 197–222.

Martin, G. R., Ashash, U., and Katzir, G. 2001. Ostrich ocular optics. Brain Behav. Evol. 58, 115–120.

Martin, G. R., Jarrett, N., Tovey, P., and White, C. R. 2005. Visual fields in flamingos: chick-feeding versus filter-feeding. Naturwissenschaften 92, 351–354.

Martin, G. R., Jarrett, N., and Williams, M. 2007. Visual fields in blue ducks and pink-eared ducks: visual and tactile foraging. Ibis 149, 112–120.

Martin, G. R., Rojas, L. M., Ramirez Figueroa, Y. M., and McNeil, R. 2004a. Binocular vision and nocturnal activity in oilbirds (*Steatornis caripensis*) and pauraques (*Nyctidromus albicollis*): Caprimulgiformes. Ornitol. Neotrop. 15(Suppl.), 233–242.

Martin, G. R., Rojas, L. M., Ramirez, Y., and McNeil, R. 2004b. The eyes of oilbirds (*Steatornis caripensis*):

pushing at the limits of sensitivity. Naturwissenschaften 91, 26–29.
Martin, G. R, Wilson, K.-J., Wild, M. J., Parsons, S., Kubke, M. F., and Corfield, J. 2007. Kiwi forego vision in the guidance of their nocturnal activities. PLoSOne 2(2): e198. doi:10.1371/journal.pone.0000198.
McFadden, S. A. 1993. Constructing the Three-Dimensional Image. In: Vision, Brain and Behavior in Birds (*eds*. H. P. Zeigler and H.-J. Bischof), pp. 47–61. MIT Press.
McFadden, S. A. 1994. Binocular Depth Perception. In: Perception and Motor Control in Birds: An Ecological Approach (*eds*. M. N. O. Davies and P. R. Green), pp. 54–73. Springer.
Meyer, D. B. 1977. The Avian Eye and Its Adaptations. In: Handbook of Sensory Physiology. Vol. VII/5 (*ed*. F. Crescitelli), pp. 549–611. Springer.
Miller, W. H. 1979. Ocular Optical Filtering. In: Handbook of Sensory Physiology.? Vol. VII/6A (*ed*. H. J. Autrum), pp. 69–143. Springer.
Nachtigall, P. E. and Moore, P. W. B. 1988. Animal Sonar: Processes and Performance. Plenum.
Nebel, S., Jackson, D. L., and Elner, R. W. 2005. Functional association of bill morphology and foraging behaviour in calidrid sandpipers. Anim. Biol. 55, 235–243.
Nieder, A. and Wagner, H. 2000. Horizontal-disparity tuning of neurons in the visual forebrain of the behaving barn owl. J. Neurophysiol. 83, 2967–2979.
Nilsson, D. E. and Pelger, R. F. 1994. A pessimistic estimate of the time required for an eye to evolve. Proc. R. Soc. Lond. B 256, 53–58.
Norberg, R. A. 1978. Skull asymmetry, ear structure and function and auditory localization in Tengmalm's Owl, *Aegolius funereus*. Phil. Trans. R. Soc. Lond. B 282, 325–410.
Ödeen, A. and Håstad, O. 2003. Complex distribution of avian color vision systems revealed by sequencing the SWS1 opsin from total DNA. Mol. Biol. Evol. 20, 855–861.
Osorio, D., Marshall, N. J., and Cronin, T. W. 1997. Stomatopod photoreceptor spectral tuning as an adaptation for colour constancy in water. Vision Res. 37, 3299–3309.
Osorio, D., Miklósi, A., and Gonda, Zs. 1999a. Visual ecology and perception of coloration patterns by domestic chicks. Evol. Ecol. 13, 673–689.
Osorio, D., Vorobyev, M., and Jones, C. D. 1999b. Colour vision of domestic chicks. J. Exp. Biol. 202, 2951–2959.
Ott, M. 2006. Visual accommodation in vertebrates: mechanisms, physiological response and stimuli. J. Comp. Physiol. A 192, 97–111.
Payne, R. S. 1971. Acoustic location of prey by barn owls. J. Exp. Biol. 54, 535–573.
Perrins, C. M. 1990. The illustrated encyclopaedia of birds. Headline.
Piersma, T., Aelst, R., Kurk, K., Berkhoudt, H., and Maas, L. R. M. 1998. A new pressure sensory mechanism for prey detection in birds: the use of principles of seabed dynamics? Proc. R. Soc. Lond. 265, 1377–1383.
Reiner, A., *et al.* 2004. Revised nomenclature for avian telencephalon and some related brainstem nuclei. J. Comp. Neurol. 473, 377–414.
Reymond, L. 1985. Spatial visual acuity of the eagle *Aquila audax*: a behavioural, optical and anatomical investigation. Vision Res. 25, 1477–1491.
Rochon-Duvigneaud, A. 1943. Les yeux et le vision des vertébrés. Masson.
Rounsley, K. J. and McFadden, S. 2005. Limits of visual acuity in the frontal field of the rock pigeon (*Columba livia*). Perception 34, 983–993.
Schaeffel, F. and Howland, H. C. 1988. Visual optics in normal and ametropic chickens. Clin. Vision Sci. 3, 83–86.
Schaeffel, F. and Wagner, H. 1996. Emmetropization and optical development of the eye of the barn owl (*Tyto alba*). J. Comp. Physiol. A 178, 491–498.
Sibley, C. G. and Monroe, B. L. 1990. Distribution and Taxonomy of Birds of the World. Yale University Press.
Sivak, J. G. 1976. The role of the flat cornea in the amphibious behaviour of the blackfoot penguin. Can. J. Zool. 54, 1341–1345.
Smith, E. L., Greenwood, V. J., and Bennett, A. T. 2002. Ultraviolet colour perception in European starlings and Japanese quail. J. Exp. Biol. 205, 3299–3306.
Snyder, A. W. and Miller, W. H. 1977. Photoreceptor diameter and spacing for highest resolving power. J. Opt. Soc. Am. 67, 696–698.
Snyder, A. W. and Miller, W. H. 1978. Telephoto lens system of falconiform eyes. Nature 275, 127–129.
Snyder, A. W., Bossomaier, T. R., and Hughes, A. 1986. Optical image quality and the cone mosaic. Science 231, 499–501.
Snyder, A. W., Laughlin, S. B., and Stavenga, D. G. 1977. Information capacity of eyes. Vision Res. 17, 1163–1175.
Srinivasan, M. V. 1996. Flies go with the flow. Nature 384, 411.
Srinivasan, M. V., Laughlin, S. B., and Dubs, A. 1982. Predictive coding: a fresh view of inhibition in the retina. Proc. R. Soc. Lond. B 216, 427–459.
Suburo, A. M. and Scolaro, J. A. 1999. Environmental adaptations in the retina of the Magellanic Penguin: photoreceptors and outer plexiform layer. Waterbirds 22, 111–119.
Sun, H. and Frost, B. J. 1997. Motion processing in pigeon tectum: equiluminant chromatic mechanisms. Exp. Brain Res. 116, 434–444.
Sun, H. and Frost, B. J. 1998. Computation of different optical variables of looming objects in pigeon nucleus rotundus neurons. Nat. Neurosci. 1, 296–303.
Tansley, K. 1965. Vision in Vertebrates. Chapman Hall.
Tennyson, A. J. D., Palma, R. L., Robertson, H. A., Worthy, T. H., and Gill, B. J. 2003. A New Species of Kiwi (Aves, Aptertygiformes) from Okarito, New Zealand. Rec. Auckland Mus. 40, 55–64.
Thomas, R. J., Székely, T., Cuthill, I. C., Harper, D. G. C., Newson, S. E., Frayling, T. D., and Wallis, P. D. 2002. Eye size in birds and the timing of song at dawn. Proc. R. Soc. Lond. B 269, 831–883.
Thomas, R. J., Székely, T., Powell, R. F., and Cuthill, I. C. 2006. Eye size, foraging methods and the timing of foraging in shorebirds. Funct. Ecol. 20, 157–165.
Vorobyev, M. 2003. Coloured oil droplets enhance colour discrimination. Proc. R. Soc. Lond. B 270, 1255–1261.
Vorobyev, M. and Osorio, D. 1998. Receptor noise as a determinant of colour thresholds. Proc. R. Soc. Lond. B 265, 351–358.
Vorobyev, M., Osorio, D., Bennett, A. T., Marshall, N. J., and Cuthill, I. C. 1998. Tetrachromacy, oil droplets and bird plumage colours. J. Comp. Physiol A 183, 621–633.
Wallman, J. 1979. Role of the Retinal Oil Droplets in the Color Vision of Japanese quail. In: Neural Mechanisms of Behavior in Pigeon (*eds*. A. M. Granada and J. H. Maxwell), pp. 327–351. Plenum.
Wallman, J. and Pettigrew, J. D. 1985. Conjugate and disjunctive saccades in two avian species with contrasting oculomotor strategies. J. Neurosci. 5, 1418–1428.
Walls, G. L. 1942. The Vertebrate Eye and Its Adaptive Radiation. Cranbrook Institute of Science.
Wenzel, B. 1968. Olfactory prowess of kiwi. Nature 220, 1133–1134.
Wilkie, S. E., Robinson, P. R., Cronin, T. W., Poopalasundaram, S., Bowmaker, J. K., and Hunt, D. M. 2000. Spectral tuning of anan violet- and ultraviolet-sensitive visual pigments. Biochemistry 39, 7895–7901.

Wilkie, S. E., Vissers, P. M., Das, D., Degrip, W. J., Bowmaker, J. K., and Hunt, D. M. 1998. The molecular basis for UV vision in birds: spectral characteristics, cDNA sequence and retinal localization of the UV-sensitive visual pigment of the budgerigar (*Melopsittacus undulatus*). Biochem. J. 330, 541–547.

Williams, D. R. and Hofer, H. 2003. Formation and Acquisition of the Retinal Image. In: The Visual Neurosciences (*eds*. L. M. Chalupa and J. S. Werner), pp. 795–810. MIT Press.

Willigen, R. F.van der, Frost, B. J., and Wagner, H. 2003. How owls structure visual information. Anim. Cogn. 6, 39–55.

Wilson, K.-J. 2004. Flight of the Huia: Ecology and Conservation of New Zealand's Frogs, Reptiles, Birds and Mammals. Canterbury University Press.

Worthey, J. A. and Brill, M. H. 1986. Heuristic analysis of von Kries color constancy. J. Opt. Soc. Am. A 3, 1708–1712.

Worthy, T. H. and Holdaway, R. N. 2002. The Lost World of the Moa: Prehistoric Life in New Zealand. Canterbury University Press.

Yokoyama, S. and Yokoyama, R. 1996. Adaptive evolution of photoreceptors and visual pigments in vertebrates. Ann. Rev. Ecol. Syst. 27, 543–567.

Young, R. W. 1994. The family of sunlight-related eye diseases. Optom. Vision Sci. 71, 125–144.

Zusi, R. L. 1996. Family Rynchopidae (Skimmers). In: Handbook of the Birds of the World. Vol. 3. Hoatzin to Auks (*eds*. J. del Hoyo, A. Elliott, and J. Sargatal), pp. 668–677. Lynx Edicions.

Zusi, R. L. and Bridge, D. 1981. On the slit pupil of the black skimmer. J. Field Ornithol. 52, 338–340.

Further Reading

Norberg, R. A. 1968. Physical factors in directional hearing in *Aegolius funereus* (Strigiformes), with special reference to the significance of the asymmetry of the external ears. Arkive Zool. 20, 181–204.

1.04 Vision in Fish

J K Bowmaker, University College London, London, UK

E R Loew, Cornell University, Ithaca, NY, USA

© 2008 Elsevier Inc. All rights reserved.

1.04.1	**Introduction**	54
1.04.2	**Evolutionary Origin of Visual Pigments**	54
1.04.3	**Lamprey**	55
1.04.4	**Rays and Sharks**	56
1.04.5	**Chondrosteans/Acipenseriformes**	56
1.04.6	**Holosteans**	56
1.04.7	**Lungfish and Coelacanth**	57
1.04.8	**Teleosts**	58
1.04.8.1	Multiple Opsins	58
1.04.8.2	Rh2 (Middle-Wave Green-Sensitive) Opsin Duplication	59
1.04.8.3	SWS2 (Short-Wave Blue/Violet-Sensitive) Opsin Duplication	63
1.04.8.4	SWS1 (Short-Wave Violet/Ultraviolet-Sensitive) Opsin Duplication	64
1.04.8.5	LWS (Long- to Middle-Wave Red/Green-Sensitive) Opsin Duplication	66
1.04.8.6	Ontogenetic Changes in Visual Pigment Complement	67
1.04.8.7	Simple Opsin Expression/Cellular Trajectories	67
1.04.8.8	Complex Opsin Expression/Cellular Trajectories	67
1.04.8.9	Short-Wavelength Shifts: Salmonids and the Lingcod	68
1.04.8.10	Long-Wavelength Shifts: Yellowfin Tuna	69
1.04.9	**Adaptive Significance**	70
References		73

Glossary

Actinopterygii A vertebrate class including all the rayed-finned fish.

agnathostomes Primitive jawless fish represented today by lamprey and hagfish.

apoptosis Programmed cell death where a series of biochemical processes lead to characteristic changes in cell morphology and cell death.

chondrostei Primitive rayed-finned cartilaginous fish showing some ossification, including sturgeons and paddlefish.

elasmobranchs Cartilaginous fish including sharks, skates, and rays.

flexion in larval fish A developmental stage when there is a bending upward of the notochord tip as part of the process of caudal-fin formation.

gnathostomes Jawed vertebrates.

holostei Primitive bony fish including bowfins and garfish.

microspectrophotometry A technique in which a narrow beam of light is passed through an isolated rod or cone in order to measure the absorption of the visual pigment.

notochord A flexible, rod-shaped body found in embryos against which the body muscles act and replaced in adults by the vertebral column.

ontogeny The study of the origin and the development of an organism from the fertilized egg to its adult form.

phylogeny The study of evolutionary relatedness among various groups of organisms.

porphyropsins All visual pigments based on Vitamin A_2.

pseudogene A region of DNA that can be recognised as a gene or part of a gene, but has lost protein-coding ability or is otherwise no longer expressed in the cell.
rhodopsins All visual pigments based on Vitamin A_1.
Sarcopterygii A vertebrate class including the lobed-finned fish (coelacanths and lungfish) and all terrestrial vertebrates.
teleosts All 'modern' bony fish, but excluding the primitive chondrosteans and holosteans.

1.04.1 Introduction

About half of all living vertebrates are fish and the vast majority of these are teleosts. Perhaps surprisingly, freshwater fish make up about 40% of total fish species, yet rivers and lakes make up less than 1% of the earth's water. The remaining 60% of fish species occupy marine environments, though the oceans comprise about 97% of all the water on earth (Horn, M. H., 1972). This implies that freshwaters offer much greater opportunities for speciation with a wide variety of habitats and the possibility of population isolation in contrast to the rather more uniform open ocean. This is not to deny the great variation in coastal waters and coral reefs, and the major changes that occur with depth in the ocean, not generally available to freshwater fish.

These great variations in spacelight in the aquatic environment offer a singular prospect for studying the evolution of color vision in vertebrates. Water color in the seas can vary from clear blue oceanic water to green coastal waters, and freshwaters show an even wider range of colors due to dissolved organic material (DOM), ranging from clear blue lake waters through to heavily peat-stained brown river waters. This broad range of aquatic habitats has led to many variations in the visual system of fish, notably in the arrangement and variety of rod and cone photoreceptors in the retina. The cone complement of fish retinas is highly variable, with species possessing cones from a single spectral class to others possessing four or more spectrally distinct classes. In addition, different morphological types of cone are present, with at least two types of single cone, and double cones in which the two halves may be spectrally identical or spectrally different.

There have been many recent reviews of vision in fish, focused primarily on teleosts (see Douglas, R. H. and Djamgoz, M. B. A., 1990; Bowmaker, J. K., 1995; Partridge, J. C. and Cummings, M. E., 1999; Douglas, R. H., 2001; Marshall, N. J. *et al.*, 2003; Bowmaker, J. K. and Hunt, D. M., 2006; Hunt, D. M. and Bowmaker, J. K., 2006; Partridge, J. C. *et al.*, 2006). The aim of this chapter is to highlight some of the recent advances in our understanding of fish vision and visual pigments, concentrating on the evolutionary consequences of opsin gene duplication and the presence of multiple cone pigments and how this is reflected in the changes in visual sensitivity observed in many teleosts during development. Recently there has also been an increased interest in the visual pigments and visual capabilities of the more primitive fish groups such as lamprey and sturgeon, as well as in the living fossils, coelacanths, and lungfish.

1.04.2 Evolutionary Origin of Visual Pigments

Comparative studies across all of the major vertebrate groups have established that, in addition to a rod class of pigment, there are four spectrally distinct classes of cone pigment encoded by distinct opsin genes: a long- to middle-wave class (LWS) maximally sensitive in the red–green spectral region from about 490 to 570 nm, a middle-wave class (Rh2) sensitive in the green from about 480 to 535 nm, a short-wave class (SWS2) sensitive in the blue–violet from about 410 to 490 nm, and a second short-wave class (SWS1) sensitive in the violet–ultraviolet from about 355 to 440 nm (Yokoyama, S., 2000). These cone classes have arisen through a series of gene duplications from an ancestral single opsin gene. By applying estimates of the rate of gene divergence, it is suggested that the appearance of the four classes occurred very early in vertebrate evolution, about 450–500 million years ago (MYA). This is close to the time of one of the major steps in vertebrate evolution, the appearance of jaws.

1.04.3 Lamprey

Primitive jawless fish, agnaths, are represented today by lampreys and hagfish. Studies of the northern hemisphere lampreys (*Petromyzon* and *Lampetra* spp.) have established that these species contain only two classes of photoreceptor classified as rods with a single class of cone maximally sensitive at longer wavelengths (Govardovskii, V. I. and Lychakov, D. V., 1984; Ishikawa, M. *et al.*, 1987; Negishi, K. *et al.*, 1987; Hárosi, F. I. and Kleinschmidt, J., 1993). Electrophysiological data suggest that the rods may function at both scotopic and photopic levels (Govardovskii, V. I. and Lychakov, D. V., 1984). In the southern hemisphere species, *Mordacia mordax*, only a single class of rod photoreceptor has been identified (Collin, S. P. *et al.*, 2004).

In contrast to these species with limited photoreceptor classes, the southern hemisphere species, *Geotria australis*, in addition to rods, has multiple spectral classes of cone (Collin, S. P. *et al.*, 2003a). Microspectrophotometry (MSP) has identified two spectrally distinct classes of cones containing porphyropsins with a wavelength of maximum absorbance, λ_{max}, at about 610 and 515 nm, along with rods with λ_{max} at about 505 nm. Further study of the genetic complement of visual pigment opsins in *Geotria* (Collin, S. P. *et al.*, 2003b) has identified five opsin genes. Three of these are orthologous to the LWS, SWS2, and SWS1 opsin genes of jawed vertebrates, but the remaining two, RhA and RhB, appear to be equally distantly related to the gnathostome Rh1 and Rh2 gene families. Collin S. P. *et al.* (2003b) proposed that the gene duplication that gave rise to the true rod Rh1 gene and the middle-wave-sensitive cone Rh2 gene of jawed vertebrates occurred after the separation of the gnathostomes from the agnaths. However, this assertion has been questioned (Collin, S. P. and Trezise, A. E. O., 2006; Pisani, D. *et al.*, 2006), with further phylogenetic analyses suggesting that the RhA lamprey gene is orthologous to the Rh1 gene (Figure 1).

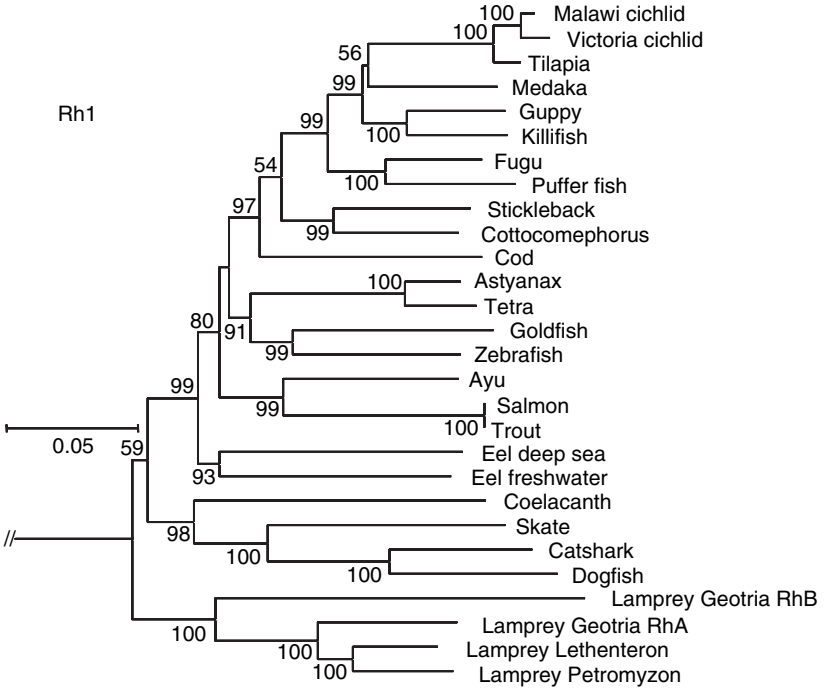

Figure 1 Phylogeny of teleost's Rh1 (rod) opsin genes. Nucleotide sequences were aligned by ClustalW, and the tree was generated by the neighbor-joining method (Saitou, N. and Nei, M., 1987). The bootstrap confidence values (1000 replicates) are shown for each branch. The *Drosophila* Rh4 sequence (M17719) was used as an outgroup (not shown). The scale bar is equal to 0.05 substitutions per site. Sequences were obtained from GenBank accession numbers AY775114, AY673768, AY775108, AB180742, Y11147, AY296738, AF201471, CR704557, BT028623, U97266, AF385832, U12328, AB245433, L11863, AF109368, AB086404, AF201470, AF201470, L78008, L78007, AF131253, U81514, Y17585, Y17586, AY366494, AY366493, AB116382, U67123.

The status of the lamprey RhB gene is less clear. The debate about the evolution of rod opsins and scotopic vision will continue, and it raises the intriguing question as to what defines a rod and a cone and also how to classify the photoreceptors in lampreys that contain the RhA and RhB opsins. Are these cell types defined by their opsin content, the isoforms of the proteins involved in visual transduction, or the physiological parameters of excitation and adaptation?

1.04.4 Rays and Sharks

Although traditionally elasmobranchs were thought to be primarily adapted for scotopic vision in having an all-rod retina (Walls, G. L., 1942), their phylogenetic position, radiating early (about 400 MYA) from the main gnathostome lineage, would imply that they have the potential of retaining all of the four vertebrate cone opsin classes. Indeed, it is clear that most, if not all, sharks and rays possess at least a single class of cone (Cohen, J. L., 1990), as is the case for the guitarfish, *Rhinobatos lentiginosus,* where MSP found a single spectral class of cone with a λ_{max} identical to that of the rod (Gruber, S. H. *et al.*, 1990). However, some skates may have pure rod retinas (Ripps, H. and Dowling, J. E., 1990; Govardovskii, V. I. and Lychakov, L. V., 1977) and in two species of *Raja*, the rods function at both scotopic and photopic levels (Dowling, J. E. and Ripps, H., 1990; Ripps, H., and Dowling, J. E., 1990), superficially similar to the rods of northern hemisphere lamprey (Govardovskii, V. I. and Lychakov, L. V., 1984).

In contrast, electroretinography from the retina of the common sting ray, *Dasyatis pastinaca* (Govardovskii, V. I. and Lychakov, L. V., 1977), revealed a spectral sensitivity with three peaks, suggesting cone visual pigments with λ_{max} at 476, 502, and 540 nm. Further, studies of horizontal cells from a related species, the red stingray *Dasyatis akajei* (Toyoda, J. I. *et al.*, 1978), identified three layers of horizontal cells in which the innermost layer consisted of chromatically coded C-type cells. More recently, MSP studies have demonstrated that two species of shovelnose rays (*Rhinobatos typus* and *Aptychotrema rostrata*) (Hart, N. S. *et al.*, 2004) and the blue-spotted maskray, *Dasyatis kuhlii* (Theiss, S. M. *et al.*, 2007), possess three spectral classes of single cone with λ_{max} at about 460–480, 490–500, and 550–560 nm. All three species have rods with λ_{max} close to 500 nm. These data clearly suggest that these species of ray have at least a trichromatic color vision system.

1.04.5 Chondrosteans/ Acipenseriformes

This ancient order of ray-finned fish consists of 25 species in two families, the sturgeons (Acipenseridae) and the paddlefish (Polyodontidae). The retinas of all but a single species of sturgeon and paddlefish contain rods and single cones with no evidence of paired elements (the stellate sturgeon is all cone; Govardovskii, V. I. and Zueva, L. V., 1987). Within a species there is little morphological difference between cones shown by MSP to contain different visual pigments (see below). Interestingly, all of the cones have a colorless oil droplet although there is a report of a small cone without a droplet in the Siberian sturgeon (Govardovskii, V. I. *et al.*, 1991).

All knowledge of the cone visual pigments in these groups comes from MSP (for a recent review, see Sillman, A. J. and Dahlin, D. A., 2004). From the position of the λ_{max}, it appears that the adults express at least one LWS, Rh2, and SWS2 gene in individual cones, in addition to an Rh1 gene in the rods. In the absence of genomic data it is uncertain how many Rh2 or SWS2 genes there are, but the lack of appreciable variability within each spectral group suggests that if there were multiple genes being expressed, they are isochromatic or at least differ little in the visual pigment they yield.

In freshwater, most adult sturgeon and paddlefish are bottom feeders quite at home in dim, muddy, highly turbid environments. For this reason, and their relatively small eyes and documented highly developed sense of smell, it is surprising to find that these species have retained such an apparently complex potential color vision capability.

1.04.6 Holosteans

These primitive fish, diverging from the chondrosteans about 250–300 MYA, were dominant in both marine and freshwater environments in the Triassic some 200 MYA. However, only two surviving genera, both inhabiting freshwaters in North America, have survived. The Amiidae have a single surviving representative, the bowfin *Amia calva.* The Lepisosteidae are the gars with seven surviving species.

No opsin data are available for either of these groups; however, some inferences can be drawn

from MSP data. In *Amia*, Burkhardt D. A. *et al.* (1983) identified double cones containing pigments with λ_{max} at 624 nm and 556 nm and single cones with λ_{max} at 457 nm, the pigments best fit by Vitamin A_2 visual pigment templates. This suggests the expression of LWS, Rh2, and SWS2 opsins. Only adult individuals were examined and no data on the presence or absence of an SWS1 gene are available.

The longnose gar, *Lepisosteus osseus*, has the full complement of opsin group expression even in the adult. Previously only two classes of cone pigment had been reported with λ_{max} at about 623 and 535 nm (Levine, J. S. and MacNichol, E. F., 1979; Burkhardt D. A. *et al.*, 1983), presumably representing LWS and Rh2 cone classes, but a recent MSP study of adult longnose gar (Loew, E. R., unpublished observations) identified five cone pigments with λ_{max} at 631, 541, 441, 427, and 365 nm. These most likely represent expression of LWS, Rh2, SWS2, and SWS1 opsin groups. Of particular interest is the presence of what could be the expression of two SWS2 genes (the 427 and 441 nm pigments) suggesting an early gene duplication (see below).

1.04.7 Lungfish and Coelacanth

The exact phylogenetic relationship between lungfish (Dipnoi), coelacanths (Crossopterygei, Coelacanthimorpha), and tetrapods remains unclear (e.g., Thomson, K. S., 1993; Meyer, A., 1995), but lungfish and coelacanths occupy a unique evolutionary link between terrestrial vertebrates such as reptiles and birds, and aquatic vertebrates such as teleosts and elasmobranchs. These groups diverged in the early Devonian about 350–400 MYA.

There are only three extant species of lungfish, geographically separated in Australia, South America, and Africa. The retinal organization of the Australian species, *Neoceratodus forsteri*, has recently been studied in some detail. The retina contains, in addition to rods, multiple classes of cones distinguished by brightly colored oil droplets (Robinson, S. R., 1994; Bailes, H. J. *et al.*, 2006), a feature common to reptiles and birds. At least three morphologically distinct cone classes can be identified: about 75% with a large red droplet, about 15% with a yellow pigmented ellipsoid region, and about 5% with a small clear droplet (Figure 2). This strongly suggests that *N.*

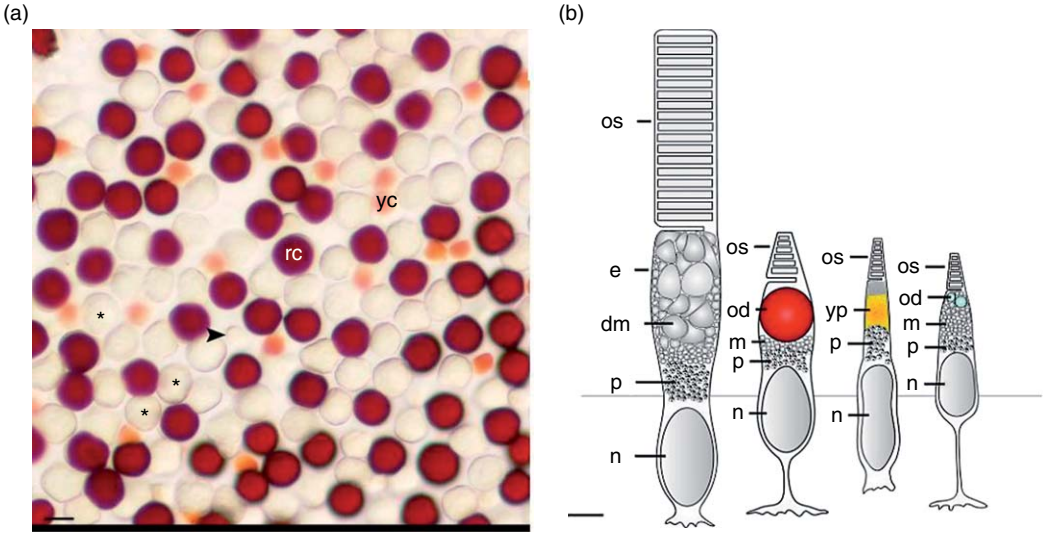

Figure 2 Photoreceptors of the Australian lungfish, *Neoceratodus forsteri*. (a) Retinal wholemount of a fresh retina showing all four morphological photoreceptor types at the level of the ellipsoid. The large, clear photoreceptors (asterisks) are rods; the red (rc) and yellow (yc) cones are easily distinguishable by the color of their intracellular inclusions. One clear cone (arrowhead) can be identified because it is noticeably smaller than the rod photoreceptors. (b) Schematic summary of photoreceptor types drawn to scale. dm, distended mitochondria; e, ellipsosome; m, mitochondria; n, nucleus; od, oil droplet; os, outer segment; p, paraboloid; yp, yellow pigment. Scale bars = 10 μm. Reproduced from Bailes, H. J., Robinson, S. R., Trezise, A. E. O., and Collin, S. P. 2006. Morphology, characterization, and distribution of retinal photoreceptors in the Australian lungfish *Neoceratodus forsteri* (Krefft, 1870). J. Comp. Neurol. 494, 381–397, with permission from John Wiley & Sons Ltd.

forsteri has the potential for at least trichromatic color vision and recent analysis of visual pigments by MSP (Marshall, J. *et al.*, 2006a) has identified four spectrally distinct cone pigments in addition to a rod pigment. In adults, three porphyropsin cone pigments are present with λ_{max} at 479, 557, and 620 nm, whereas young fish have an additional UV-sensitive cone pigment with λ_{max} at 374 nm. The Australian lungfish has therefore retained the four vertebrate ancestral cone pigments with the potential for tetrachromatic color vision, at least at a juvenile stage. The presence of the colored oil droplets also implies that this feature is ancient and may represent the ancestral composition of cones (Walls, G. L., 1942; Robinson, S. R., 1994). Morphologically different cone classes may also be present in the African and South American lungfish (Walls, G. L., 1942; Ali, M. A. and Anctil, M., 1973), but their spectral properties have not been examined.

In contrast to lungfish that live in shallow freshwater rivers, the two extant species of coelacanth are found in relatively deep waters between 100 and 400 m in the Indian Ocean. Their retinae are more typical of deep-sea fish and are rod-dominated with cones comprising only about 1–2% of the photoreceptors (Millot, J. and Carasso, N., 1955; Locket, N. A., 1973). However, these may possibly be divided into three morphological classes. The rarest cone class (type 1 of Locket), with only about 22 mm^{-2}, contains an oil droplet that is probably colorless (Millot, J. and Carasso, N., 1955). The extracted rod pigment with λ_{max} at 473 nm (Dartnall, H. J. A., 1972) is typical of deep-sea fish and its sensitivity may be correlated with the maximum transmission of oceanic water, around 470–480 nm. Recently two opsin genes have been isolated from both species of *Latimeria* (Yokoyama, S. *et al.*, 1999; Yokoyama, S. and Tada, T., 2000.), which are orthologous to the Rh1 and Rh2 vertebrate opsins. These genes have been expressed and have λ_{max} at 485 and 478 nm, respectively. Yokoyama S. *et al.* (1999) also isolated a pseudogene derived from the SWS1 class, but no evidence was found for either an LWS or a SWS2 gene. Yokoyama S. *et al.* (1999) suggested that because of their spectral closeness, the 473 nm pigment extracted by Dartnall H. J. A. (1972) was in fact the Rh2 pigment, but this cannot be the case. Extraction techniques typically yield only rod pigments and given the very low numbers of cones in the retina of *Latimeria*, the extracted 473 nm pigment must be the Rh1 pigment, which has λ_{max} at 485 nm when expressed. The 12 nm discrepancy between the two values is surprising, given that extracts of rod pigments from deep-sea fish typically agree with direct measurements of visual pigment absorbance by MSP. It has also been suggested (Yokoyama, S. *et al.*, 1999) that the presence of the Rh1 and Rh2 pigments could give the coelacanth rod-/cone-based color vision within the narrow spectral window available at depth in the ocean. Given the very low density of cones, this seems an unlikely scenario and it is more probable that the cones will give a very limited luminance response at photopic levels.

The two extant species of coelacanth are nocturnal piscivorous predators living at depth in the ocean (Fricke, H. and Hissmann, K., 2000), but their Devonian ancestors likely lived in a coastal wetland environment (Thomson, K. S., 1993) and presumably possessed a typical vertebrate polychromatic photopic visual system. Comparisons of the Rh1 and Rh2 opsin genes from both coelacanth species suggest that the migration to the deep sea occurred about 200 MYA (Yokoyama, S. and Tada, T., 2000). The change in habitat to the relatively dim monochromatic deep sea presumably resulted in the loss of color vision along with the loss of function of the other three cone opsin genes.

1.04.8 Teleosts

The numbers of teleost species far exceed those of any other fish group and comprise about 96% of all living fish species. The teleost radiation began in the Cretaceous about 150 MYA and by the end of the Cretaceous, it had become the dominant fish in both oceanic and freshwater habitats. Teleost vision ranges from tetrachromatic color vision in many shallow water freshwater fish to pure rod vision in the majority of deep-sea fish. Adult epipelagic teleosts tend to be trichromatic or dichromatic, having lost or no longer expressing either the LWS or the SWS1 opsins or both. In contrast, fish living in highly turbid or deeply stained waters tend to lose or not express the shorter-wave opsins, but retain the LWS and Rh2 opsin genes. In more extreme conditions, fish may become cone monochromats expressing only the Rh2 or LWS genes.

1.04.8.1 Multiple Opsins

Unlike most other vertebrate groups, many teleost families have duplicated their cone opsin genes to produce a range of functional opsins within each

opsin gene class. There is evidence that the Actinopterygii (ray-finned fish) have more genes than other vertebrate groups and it has been suggested that a whole-genome duplication occurred early in the evolution of ray-finned fish, in the Devonian around 350 MYA, after their divergence from the sarcopterygian lineage (Meye, A. R. and Schartl, M., 1999; Christoffels, A. *et al.*, 2004; Furutani-Seiki, M. and Wittbrodt, A. V., 2004). Thus the sarcopterygian fish, which includes coelacanth and lungfish, and all land vertebrates (amphibians, reptiles, birds, and mammals), tend to have only half the number of genes compared with actinopterygian fish. However, the evolution of gene families is an active process in which gene duplication (whether by whole-genome duplication or simple duplication of a limited number of genes) will be accompanied by the subsequent mutation of genes, leading either to the decay of some genes into pseudogenes and eventually junk DNA or to a divergent gene with a new function (neofunctionalization) (Ohno, S., 1970). In groups such as cichlids and cyprinids, mutations in the duplicated genes have led to functional spectral shifts in the pigments, but at least in puffer fish (tetraodontids) there is evidence that one of their duplicated Rh2 genes is a pseudogene that has suffered a loss of function relatively recently (Neafsey, D. E. and Hartl, D. L., 2005). Gene duplication in teleost opsin genes is most notable within the Rh2 gene family, but also occurs in both the LWS and SWS2 classes. Evidence for duplication of the SWS1 gene is limited and has been reported only in the ayu (*Plecoglossus altivelis*, an osmerid salmonid) (Minamoto, T. and Shimizu, I., 2005).

1.04.8.2 Rh2 (Middle-Wave Green-Sensitive) Opsin Duplication

One of the most striking examples of opsin gene duplication is found in the cichlid populations of the African Great Lakes. These species are notable for their diversity, particularly in their color patterns. Lake Malawi has more than 700 species of cichlids that have evolved from a common ancestor within the last million years (Meyer, A., 1993; Turner, G. F. *et al.*, 2001). Their rapid evolution is thought to be the result of sexual selection and the evolution of mate choice. Most species are sexually dimorphic and visual communication is crucial for mate choice (for reviews see Seehausen, O., 2000; Kocher, T. D., 2004).

Typically, adult African cichlids possess three cone visual pigments, with nonidentical double cones maximally sensitive at longer wavelengths and shorter-wavelength-sensitive single cones (Fernald, R. D. and Liebman, P. A., 1980; Van der Meer, H. J. and Bowmaker, J. K., 1995; Carleton, K. L. *et al.*, 2000; Carleton, K. L. and Kocher, T. D., 2001; Parry, J. W. L. *et al.*, 2005; Jordan, R. *et al.*, 2006). Measurements of cone spectral sensitivities by MSP from a relatively small sample of species from Lake Malawi suggest that cichlids inhabiting rock and sand habitats have significantly different cone visual sensitivities (Carleton, K. L. and Kocher, T. D., 2001). The Mbuna (rock-dwelling) species tend to have double cones with maximum sensitivities at about 535 and 488 nm and ultraviolet- or violet-sensitive single cones with λ_{max} at about 370 or 420 nm. In contrast, non-Mbuna species that are more sand-dwelling may be less sensitive to short wavelengths, possessing double cones with maximum sensitivities at about 570 and 535 nm and blue-sensitive single cones with λ_{max} at about 450 nm (Levine, J. S. and MacNichol, E. F., 1979; Carleton, K. L. *et al.*, 2000; Parry, J. W. L. *et al.*, 2005; Jordan, R. *et al.*, 2006). However, in some species, notably *Pseudotropheus acei* (an Mbuna species), rare additional cones have been identified suggesting that at least seven spectrally distinct cone pigments may be expressed in the retina (Figure 3 and Table 1) (Parry, J. W. L. *et al.*, 2005).

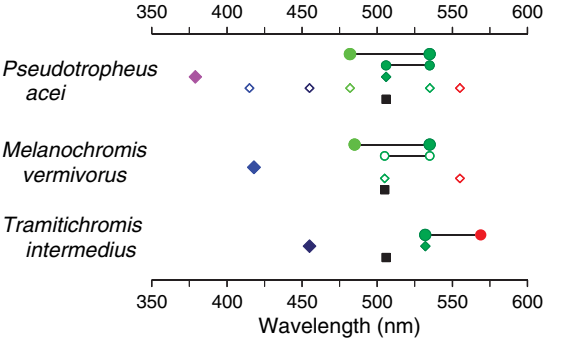

Figure 3 Distribution of the different cone types in three species of cichlids from Lake Malawi. Filled circles: double cones; size reflects relative frequency. Open circles: rare or individual double cones. Filled diamonds: single cones; size reflects relative frequency. Open diamonds: rare or individual single cones. Filled squares: rods. The color code reflects the four cone opsin gene classes: red, LWS; green, Rh2; blue, SWS2, and violet, SWS1. Data from Parry J. W. L., Carleton, K. L., Spady, T., Carboo, A., Hunt, D. M., Bowmaker, J. K. 2005. Mix and match color vision: tuning spectral sensitivity by differential opsin gene expression in Lake Malawi cichlids. Curr. Biol. 15, 1734–1739.

Table 1 Peak absorbances of the cone visual pigments identified in African cichlids and in medaka and killifish

	LWS	*Rh2Aα*	*Rh2Aβ*	*Rh2B*	*SWS2A*	*SWS2B*	*SWS1*
Expressed							
Metriaclima zebra[a]		528	519	484		423	368
Oreochromis niloticus[b]	560	528	517	472	456	425	360
MSP							
Metriaclima zebra[c]		533		488			368
Pseudotropheus acei[a]	566	534	505	482	452	415	378
Melanochromis vermivorus[a]	556	534	504	485		418	
Tramitichromis intermedius[a]	569	532			455		
		Rh2-B	Rh2-C	Rh2-A			
Oryzias latipes medaka[d]	561	516	492	452	439	405	356
Lucania goodie bluefin killifish[e]	573	540			455	405	360

[a]Parry J. W. L. *et al.* (2005).
[b]Spady T. C. *et al.* (2006).
[c]Carleton K. L. and Kocher T. D. (2001).
[d]Matsumoto Y. *et al.* (2006).
[e]Fuller R. C. *et al.* (2004; 2003).
The expressed cone pigment data are from gene sequences amplified from retinal cDNA, expressed in mammalian cells, and regenerated with 11-*cis*-retinal *in vitro* (Parry, J. W. L. *et al.*, 2005; Spady, T. C. *et al.*, 2006).

Analysis of the opsin gene complement from two species, *Metriaclima zebra* (Mbuna) and the Nile tilapia (*Oreochromis niloticus*) (Parry, J. W. L. *et al.*, 2005), has demonstrated that of the seven genes, three are from the Rh2 gene class, two from the SWS2 class, with single representatives of the LWS and SWS1 gene classes. The Nile tilapia is considered to be the riverine equivalent of the ancestors of the lake cichlids. In order to correlate opsin gene sequences with the different pigments identified by MSP, all seven gene sequences have been amplified from retinal cDNA, expressed in mammalian cells, and regenerated with 11-*cis*-retinal *in vitro* (Parry, J. W. L. *et al.*, 2005; Spady, T. C., *et al.*, 2006).

The data demonstrate that gene duplication in the green-sensitive Rh2 gene of cichlids has occurred on at least two occasions (Figure 4). There was a relatively ancient duplication, leading to Rh2A and Rh2B genes, which occurred after the divergence of the Acanthopterygii from other teleosts, sometime between 260 MYA (Kumazawa, Y. *et al.*, 1999) and 115–200 MYA (Furutani-Seiki, M. and Wittbrodt, J., 2004). The two genes have diverged such that their expressed cone pigments may be separated by as much as 50 nm. The Rh2A pigments have λ_{max} as long as about 535 nm, whereas the Rh2B pigments absorb maximally at shorter wavelengths around 480 nm. The second, much more recent duplication of the Rh2A gene probably occurred within the past 10 MYA only in the intralacustrine cichlid radiation (Kocher, T. D. *et al.*, 1995). The duplication has led to two spectrally distinct classes, Rh2Aα and Rh2Aβ, with λ_{max} around 525–535 nm and 505–520 nm, respectively (Parry, J. W. L. *et al.*, 2005; Spady, T. C., *et al.*, 2006).

Since adult cichlids express predominantly only three of the seven available opsins, the question arises as to what function maintains the presence of the other genes. Genes that are not expressed would be expected to evolve free of any constraints of selective pressure and would build up random mutations leading to nonfunctionality. The functional opsins may be differentially expressed spatially and/or temporally. Regional variations of cone pigments across the retina and ontogenetic changes in cone opsin expression are not uncommon both in teleosts and mammals. Variations in expression across the retina have not been described in these cichlids, but ontogenetic changes have been established, at least in tilapia. Using quantitative methods to determine levels of gene expression, Spady T. C. *et al.* (2006) have shown that larval tilapia primarily express four of the seven opsins – SWS1, Rh2B, Rh2Aα, and LWS – at approximately equal levels (Figure 5). However during development there is a major switch in expression with a marked downregulation of the SWS1 and Rh2B genes and a significant upregulation of the SWS2A and LWS gene. Adult tilapia primarily express only three opsins: SWS2A, Rh2Aα, and LWS, with the LWS noticeably dominant.

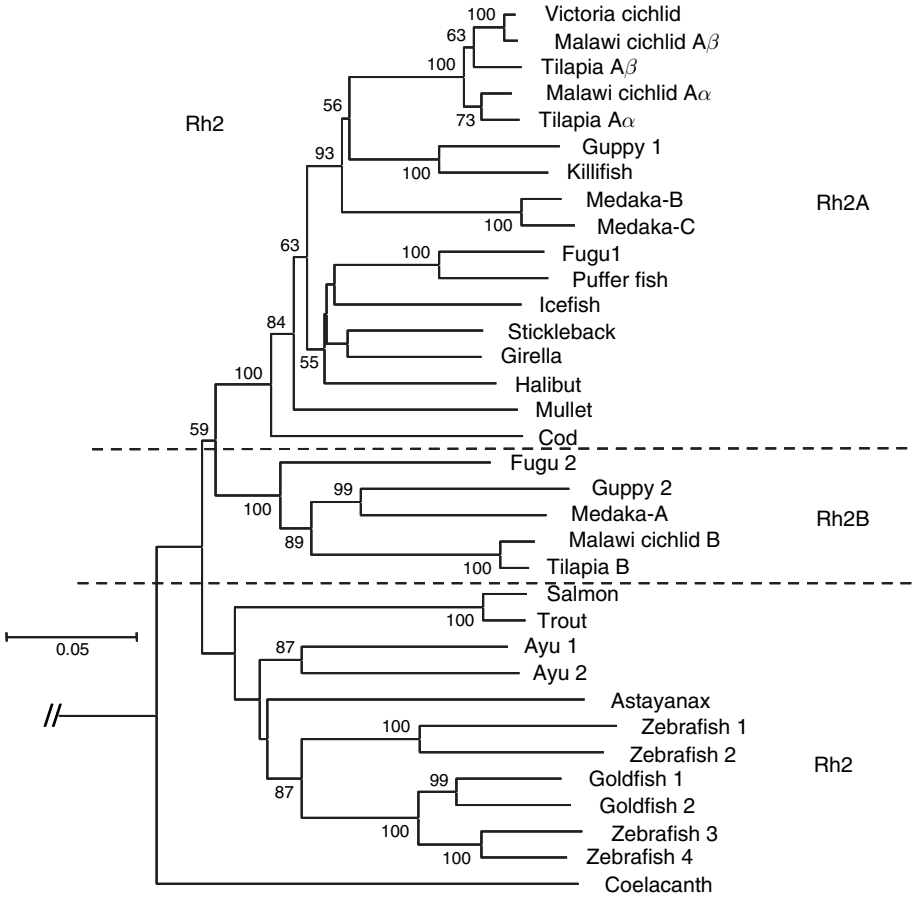

Figure 4 Phylogeny of teleost's Rh2 cone opsin genes. Nucleotide sequences were aligned by ClustalW, and the tree was generated by the neighbor-joining method (Saitou, N. and Nei, M., 1987). The bootstrap confidence values (1000 replicates) are shown for each branch. The *Drosophila* Rh4 sequence (M17719) was used as an outgroup (not shown). The scale bar is equal to 0.05 substitutions per site. The dashed lines indicate the divergences of the three classes of Rh2 gene. Sequences were obtained from Genbank accession numbers AY673755, DQ088650, DQ235682, DQ088651, DQ235683, DQ234859, AY269739, AB223054, AB223055, AF226989, AY598944, AY771354, BT027598, AB158259, AF156263, Y18680, AF385824, AY599603, DQ234858, AB223053, DQ088652, DQ235681, AY214132, AF425076, AB098703, AB098704, AH004622, AB087805, AB087806, L11865, L11866, AB087807, AB087808, AF131258.

From this it can be inferred that larval tilapia are potentially tetrachromatic with sensitivity extending into the near ultraviolet, but that adults are limited to trichromacy and are primarily long-wave-sensitive. This supposition is supported by MSP data (Loew, personnel communication) where larval fish have been shown to possess at least four spectral cone classes, including UV-sensitive small single cones, whereas adults possess only three spectral cone classes, double cones that are either red/red or red/green and blue-sensitive single cones. The presence of red/red and red/green double cones reflects the predominant expression of the LWS gene in the adult fish. (Ontological variation in cone pigments is discussed more fully below.)

Phylogenetic analysis indicates that the duplication into Rh2A and Rh2B occurred early in the radiation of teleosts, at least before the divergence of the Paracanthopterygii (including gadids) and the Acanthopterygii (including cichlids) (Figure 4), which is thought to have occurred somewhere between 260 MYA (Kumazawa, Y. *et al.*, 1999) and 115–200 MYA (Furutani-Seiki, M. and Wittbrodt, J., 2004). Thus all of the orders within the percomorph teleosts should show evidence of the Rh2A and Rh2B genes, and these have been identified in the guppy (*Poecilia reticulata*, Atherinomorpha,

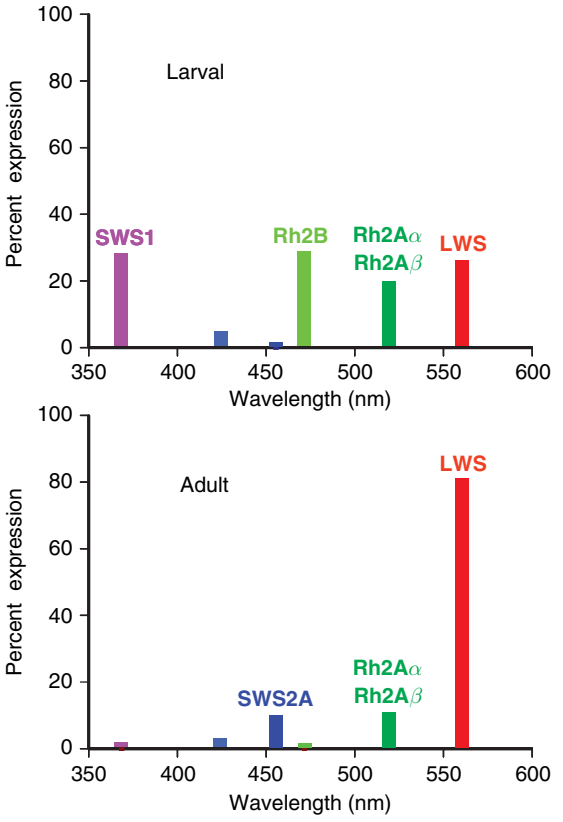

Figure 5 Relative cone opsin expression profiles for larval and adult tilapia, *Oreochromis niloticus*. At larval stages, four of the seven cone opsin genes are predominately expressed giving the potential for tetrachromatic color vision. In the adult there is a marked downregulation of the SWS1 gene with a greatly enhanced expression of the LWS gene. Adult tilapia are potentially trichromatic. Data from Spady T. C., Parry, J. W. L., Robinson, P. R., Hunt, D. M., Bowmaker, J. K., and Carleton, K. L. 2006. Evolution of the cichlid visual palette through ontogenetic subfunctionalization of the opsin gene arrays. Mol. Biol. Evol. 23, 1–10.

Cyprinodonti-formes) (Hoffmann, M. *et al.*, 2006) and medaka (*Oryzias latipes*, Atherinomorpha, Beloniformes) (Matsumoto, Y. *et al.*, 2006), which has a pattern of cone opsin genes very similar to the African cichlids. In medaka, the orthologous gene to the cichlid Rh2B gene has been confusingly designated Rh2A with λ_{max} at 452 nm, and, as in the cichlids, the orthologous gene to the Rh2A is duplicated, the two genes termed Rh2B and Rh2C with λ_{max} at 516 and 492 nm, respectively (Table 1). It is notable that the three Rh2 pigments in medaka are substantially displaced to shorter wavelengths than the cichlids (as are the two SWS2 pigments). The phylogeny of these Rh2 genes implies that the second duplication in medaka and the cichlids is independent (Figure 4). However, it is possible that the duplications have a common origin and subsequent gene conversion has removed any trace of long divergence (Matsumoto, Y. *et al.*, 2006).

In the guppy, although there are data for both the cone visual pigments from MSP (Archer, S. N. *et al.*, 1987; Archer, S. N. and Lythgoe, J. N., 1990) and the opsin genes (Hoffmann, M. *et al.*, 2006), it is not straightforward to match the two sets of data. MSP identified shorter-wave-sensitive pigments with λ_{max} around 360, 408, and 464 nm and an apparent polymorphism of cone pigments in the red/green spectral region with cones having λ_{max} at about 533, 548, and 572 nm. Differences were found between individual fish in the occurrence of these three longer-wave pigments. Hoffmann M. *et al.* (2006) suggest that the variations in the longer-wave pigments is a result of gene duplication and polymorphism of the guppy's LWS gene (see below) and that the Rh2A and Rh2B cone pigments have similar absorbance or are differentially expressed during development. However, given the data from cichlids and medaka, it is as likely that the 464 and 533 nm pigments are expression of the Rh2B and Rh2A genes, respectively.

The orthologous gene to the Rh2A cichlid gene has been identified in a number of other percomorphs, but in many instances the Rh2B orthologue has not been identified or has been reduced to a pseudogene. It is not clear whether this is because the gene has been lost or simply missed in the analysis of opsin genes. Within the Tetraodontiformes, the fugu (*Takifugu rubripes*) and the puffer fish (*Tetraodon nigroviridis*) possess a functional orthologue of the cichlid Rh2A gene (Figure 4), but the orthologue of the Rh2B has apparently been truncated to a pseudogene relatively recently (Neafsey, D. E. and Hartl, D. L., 2005). In five species of Antarctic notothenioid ice fish (Pointer, M. A. *et al.*, 2005), MSP has identified only a single spectral class of green-sensitive cone with λ_{max} close to 490 nm. Only a single Rh2 gene was isolated from one of the species (*Dissostichus mawsoni*) and *in vitro* expression and regeneration of the gene gave a similar peak absorbance to that obtained by MSP. These data together suggest that at least in this suborder of percomorphs, the duplicate Rh2B gene may have been lost.

A further group of percomorphs in which both MSP and molecular genetics of cone opsins are available are the killifish (Atherinomorpha, Cyprinodontiformes). In the bluefin killifish (*Lucania goodei*) five cone pigments have been identified by MSP and five cone opsins isolated (Table 1) (Fuller, R. C. *et al.*, 2003; 2004). This species apparently has only a single Rh2 gene that is orthologous to the cichlid Rh2A and is expressed as a green-sensitive 537 nm pigment. Again, as in the ice fish, has this species lost the Rh2B variety or has it simply been missed? In the closely related killifish, *Fundulus heteroclitus*, only four spectral classes of cone have been identified by MSP (Novales Flamarique, I. and Hárosi, F. I., 2000). The two short-wave pigments with λ_{max} at 363 and 400 nm are presumably expressed from SWS1 and SWS2B genes and the long-wave 563 nm pigment from an LWS gene. However, the middle-wave pigment with λ_{max} at 463 nm could be the expression of either an SWS2A or an Rh2B gene. If it is the SWS2A gene, then these data would suggest that there is no expression of any of the Rh2 genes in this species.

Gene duplication of the Rh2 gene has also occurred independently within the cyprinids (Figure 4). Goldfish express two Rh2 genes that yield cone pigments spectrally separated by only about 6 nm when reconstituted with 11-*cis* retinal (505 and 511 nm) (Johnson, R. L. *et al.*, 1993). Zebrafish have a double duplication leading to four spectrally distinct Rh2 genes arranged in a tandem array, with expressed pigments, again based on 11-*cis* retinal, with λ_{max} ranging from 467 to 505 nm (Chinen, A. *et al.*, 2003; 2005a). In zebrafish there are clear changes in the temporal and spatial pattern of expression of the four pigments in the embryo during the first few days post fertilization (Takechi, M. and Kawamura, S., 2005), but the functional significance of this is difficult to determine. It is most likely that the opsins are coexpressed at various stages during development. In adult goldfish, we have been unable to show that the two Rh2 opsins are expressed in separate classes of cone with the λ_{max} of the green half of double cones and the long single green cones being identical (unpublished observations). This is in contrast to the ayu (an osmerid salmonid) where its two Rh2 genes are expressed separately in one half of the double cones and in long single cones (Minamoto, T. and Shimizu, I., 2005), though their λ_{max} have not been determined.

1.04.8.3 SWS2 (Short-Wave Blue/Violet-Sensitive) Opsin Duplication

Phylogenetic analysis shows that the SWS2 gene duplicated in the early ancestry of the Acanthopterygii in a similar fashion as the Rh2 gene (Figure 6). Mutations have led to two spectrally distinct subfamilies, the SWS2A having λ_{max} around 440–455 nm and SWS2B with λ_{max} at shorter wavelengths between about 405 and 425 nm. These opsin genes and their expressed pigments have been identified in cichlids (Carleton, K. L. and Kocher, T. D., 2001; Parry, J. W. L. *et al.*, 2005; Spady, T. C. *et al.*, 2006), medaka (Matsumoto, Y. *et al.*, 2006), and the killifish (Fuller, R. C. *et al.*, 2003; 2004). In medaka and killifish, the SWS2B pigments have λ_{max} at 405 nm and in cichlids around 415–425 nm. A duplication of the SWS2 gene has not been reported in teleosts outside of the Acanthopterygii, though the two blue-sensitive pigments of the longnose gar (441 and 427 nm) may be another example. If both these two pigments prove to be an expression of SWS2 genes, then it is likely that this duplication in the Holostei occurred independently of the duplication in the Acanthopterygii.

In teleosts other than Acanthopterygii, although SWS2 gene duplication is not apparent, a similar dichotomy in the spectral location of SWS2 pigments appears to have occurred in cyprinids. In goldfish the SWS2 pigment reconstituted with 11-*cis* retinal has λ_{max} at 441–443 nm (Johnson, R. L. *et al.*, 1993; Chinen, A. *et al.*, 2005b) (453 nm as a porphyropsin (Hárosi, F. I. and MacNichol, Y., 1974; Bowmaker, J. K. *et al.*, 1991) similar to the λ_{max} of the blue-sensitive cone pigments of carp (Hárosi, F. I., 1985), roach, *Rutilus rutilus* (Avery, J. A. *et al.*, 1983; Downing, J. E. G. *et al.*, 1986), and tench, *Tinca tinca* (Loew, E. R. and Lythgoe, J. N., 1978). In contrast, zebrafish SWS2 pigment has λ_{max} at 407–416 nm (Nawrocki, L. *et al.*, 1985; Robinson, J. *et al.*, 1995; Palacios, A. G. *et al.*, 1996; Cameron, D. A., 2002; Chinen, A. *et al.*, 2003) and the Japanese dace, *Tribolodon hakonensis* (Hárosi, F. I. and Hashimoto, Y.,1983), and rudd, *Scardinius erythrophthalmus* (Whitmore, A. V. and Bowmaker, J. K., 1989), similarly have a blue-sensitive cone pigment with λ_{max} around 405–415 nm. (Rudd have also been reported to have a blue-sensitive cone with λ_{max} at 450–460 nm (Loew, E. R. and Dartnall, H. J. A., 1976).) Chinen A. *et al.* (2005) have reconstructed the likely ancestral SWS pigment of the goldfish and zebrafish, which, when expressed with 11-*cis* retinal, has a maximum absorbance at 430 nm, indicating that mutations

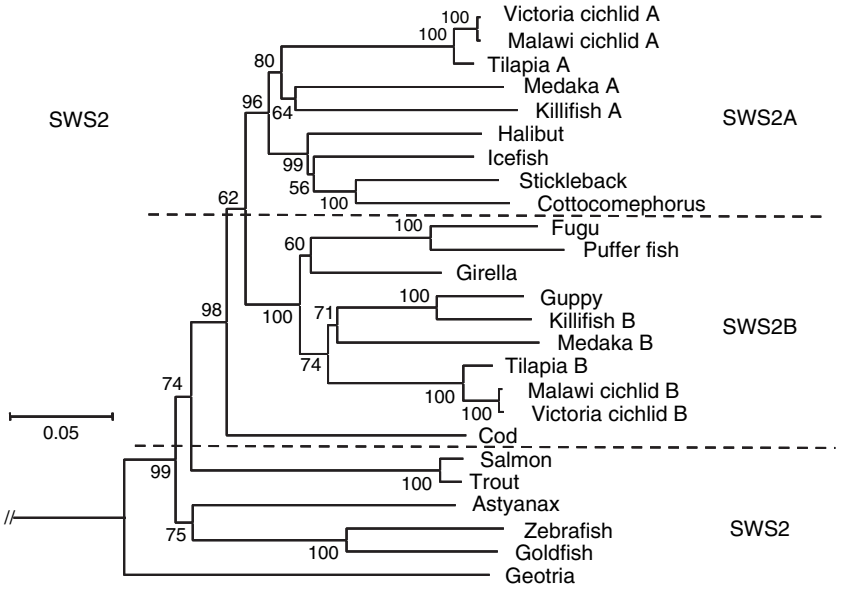

Figure 6 Phylogeny of teleost's SWS2 cone opsin genes. Nucleotide sequences were aligned by ClustalW, and the tree was generated by the neighbor-joining method (Saitou, N. and Nei, M., 1987). The bootstrap confidence values (1000 replicates) are shown for each branch. The *Drosophila* Rh4 sequence (M17719) was used as an outgroup (not shown). The scale bar is equal to 0.05 substitutions per site. The dashed lines indicate the divergences of the three classes of SWS2 gene. Sequences were obtained from Genbank accession numbers AY673763, AF247114, AF247116, AB223056, AY296737, AF316497, AY771356, BT027452, AJ430479, AY598947, AY598948, AB158256, DQ234860, AY296736, AB223057, AF247120, AF317674, AY673708, AF385822, AY214134, AF425075, AF134762, AF109372, L11864, AY366492.

have occurred in both species to displace the pigment to longer and shorter wavelengths, respectively.

Although data are somewhat limited, it is noticeable that both in some groups of the Acanthopterygii and in the cyprinids, teleost groups that diverged over 100 MYA, the blue-sensitive cone pigments, appear to fall into two spectral groups centered around 410–420 and 440–450 nm. Is this a limitation of the data or are these locations driven by ecological factors or determined by structural constraints on opsins? Outside of teleosts, the short-wave-sensitive cone pigments of birds also fall into these two spectral locations. All avian species studied to date have a blue-sensitive pigment (SWS2) with λ_{max} close to 450 nm, and birds that lack a true UV-sensitive cone possess a violet-sensitive pigment with λ_{max} at about 405–420 nm (Okano, T. *et al.*, 1992; Bowmaker, J. K. *et al.*, 1997; Hart, N. S., 2001). In the avian retina, the violet-sensitive pigments are the expression of an SWS1 opsin and are not the product of the SWS2 opsin. Indeed, this would appear to be the case in all vertebrate groups with the exception of teleosts. In mammals, including humans, where the S-cone pigment has λ_{max} at about 420 nm (Dartnall, H. J. A. *et al.*, 1983; Oprian, D. D. *et al.*, 1991; Merbs, S. L. and Nathans, J., 1992; Fasick, J. I. *et al.*, 1999), all the short-wave-sensitive pigments are SWS1 pigments and the SWS2 gene has been completely lost.

1.04.8.4 SWS1 (Short-Wave Violet/Ultraviolet-Sensitive) Opsin Duplication

Duplication of SWS1 genes appears to be rare within teleosts and all the reported SWS1 pigments are expressed as true UV-sensitive pigments with λ_{max} between 350 and 380 nm (Parry, J. W. L. and Bowmaker, J. K., 2000; Cowing, J. A. *et al.*, 2002; Chinen, A. *et al.*, 2003; Parry, J. W. L. *et al.*, 2005; Matsumoto, Y. *et al.*, 2006; Spady, T. C. *et al.*, 2006). The exception to this is the smelt, ayu (*P. altivelis*), where two SWS1 genes have been identified (Minamoto, T. and Shimizu, I., 2005), but one of the pair (SWS1-1) is expressed at a very low level and could not be identified by *in situ* hybridization (Figure 7). The spectral sensitivity of the two opsins is not known and it may be that they are spectrally identical. It would appear that the tuning mechanisms that have evolved in other vertebrate groups to

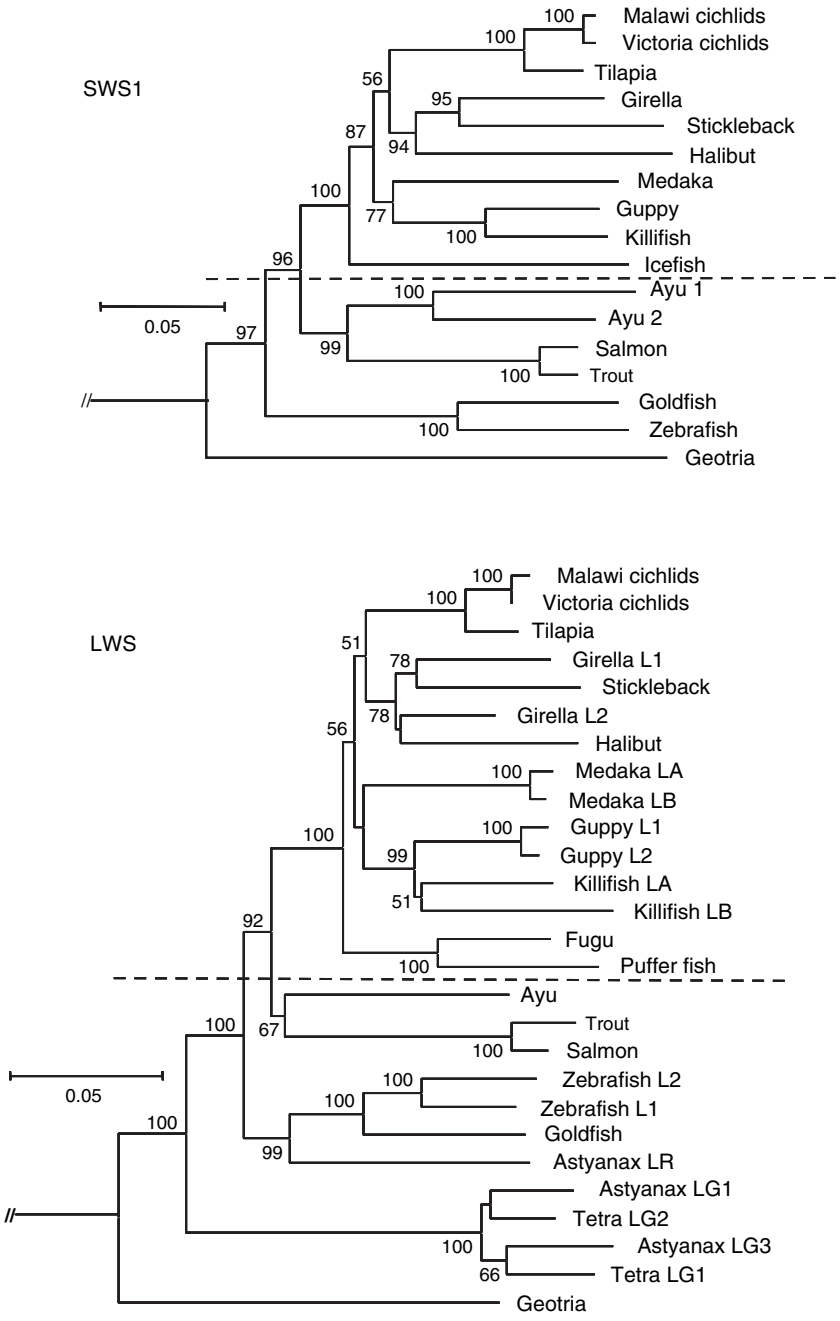

Figure 7 Phylogeny of teleost's SWS1 cone opsin genes. Nucleotide sequences were aligned by ClustalW, and the tree was generated by the neighbor-joining method (Saitou, N. and Nei, M., 1987). The bootstrap confidence values (1000 replicates) are shown for each branch. The *Drosophila* Rh4 sequence (M17719) was used as an outgroup (not shown). The scale bar is equal to 0.05 substitutions per site. Sequences were obtained from Genbank accession numbers AF191219, AY673728, AF191221, AB158257, BT028514, AF156264, AB223058, DQ234861, AY296735, AY927654, AB098705, AB098706, AY214133, AF425074, D85863, AF109373, AY366495. Phylogeny of teleost's LWS cone opsin genes. Nucleotide sequences were aligned by ClustalW, and the tree was generated by the neighbor-joining method (Saitou, N. and Nei, M., 1987). The bootstrap confidence values (1000 replicates) are shown for each branch. The *Drosophila* Rh4 sequence (M17719) was used as an outgroup (not shown). The scale bar is equal to 0.05 substitutions per site. Sequences were obtained from Genbank accession numbers AF247126, AY673749, AF247128, AB158261, BT027981, AB158260, AF316498, AB223051, AB223052, DQ168660, DQ168659, AY296740, AY296741, AY598942, AY598943, AB098702, AF425073, AY214131, AB087804, AB087803, L11867, M90075, U12024, AB239250, U12025, AB239249, AY366491.

tune SWS1 opsins to longer wavelengths above 400 nm (Yokoyama, S. *et al.*, 2000; Shi, Y. S. *et al.*, 2001; Cowing, J. A. *et al.*, 2002; Shi, Y. S. and Yokoyama, S., 2003; Hunt, D. M. *et al.*, 2004; Parry, J. W. L. *et al.*, 2004; Wilkie, 2000 #5625) have not been achieved in teleosts, where violet sensitivity is achieved through SWS2B opsins.

1.04.8.5 LWS (Long- to Middle-Wave Red/Green-Sensitive) Opsin Duplication

Duplication of the LWS gene appears to have occurred independently in a number of groups (Figure 7). Within the Acanthopterygii, duplication has been identified in girella (Perciformes) (Miyazaki, T. *et al.*, 2005) and the Atherinomorphs, medaka (Beloniformes) (Matsumoto, Y. *et al.*, 2006), killifish (Cyprinodontiformes) (Blow and Yokoyama, Genbank accession numbers AY296735–AY296741), and guppy (Cyprinodontiformes) (Hoffmann, M. *et al.*, 2006). These duplications appear to have occurred independently, but it is possible that they have a common origin, at least within the Atherinomorphs, and subsequent gene conversion has removed any trace of long divergence. Outside of the Acanthopterygii, LWS gene duplication also occurs in zebrafish (Cypriniformes) (Chinen, A. *et al.*, 2003) and the cave fish *Astyanax* (Characiformes) (Yokoyama, R. and Yokoyama, S., 1990).

In *Astyanax* three LWS genes have been identified, and based on the known tuning sites between primate L- and M-cones, it is clear that one of the genes (r007, LR in Figure 7) corresponds to a red-sensitive pigment with λ_{max} at about 565 nm and that the other two similar genes (g101 and g103, LG1 and LG3 in Figure 7) correspond to a green-sensitive pigment with λ_{max} at about 535 nm (Yokoyama, R. and Yokoyama, S., 1990; Kleinschmidt, J. and Hárosi, F. I., 1992; Yokoyama, S. and Radlwimmer, F. B., 2001; Parry, J. W. L. *et al.*, 2003). This is a striking illustration of convergent evolution, where exactly the same amino acid substitutions are found tuning between the 535 and 565 nm cone pigments in both primates and *Astyanax*. Another characid, a tetra, *Paracheirodon innesi* is reported similarly to have the two g-variations of the LWS gene (Kasai and Oshima, Genbank accession numbers AB239249 and AB239250). Somewhat surprisingly, phylogenetic analysis implies that the divergence of the red and green versions of the LWS gene occurred at the base of the teleosts, before the separation of the characids and cyprinids from the Acanthopterygii, but homologous genes to the green genes of the characids have not been identified in any other teleost groups.

In zebrafish the two LWS genes have been expressed with λ_{max} at 558 and 548 nm (Chinen, A. *et al.*, 2003), but there is no evidence from MSP for two spectrally distinct populations of LWS cones, though different groups report slightly different λ_{max} ranging from 556 to 570 nm (Nawrocki, L. *et al.*, 1985; Robinson, R. *et al.*, 1993; Cameron, D. A., 2002). Also, two LWS genes have been identified in killifish, but their spectral sensitivities have not been published and again there is no evidence of two populations of LWS cones in the retina (Fuller, R. C. *et al.*, 2004). In both zebrafish and killifish, the lack of evidence for two populations of LWS cones may simply be that the rather limited MSP data are insufficient to distinguish two pigments separated perhaps by only a few nanometers or that the two pigments are coexpressed. In medaka the duplicated genes have similar spectral sensitivities (Matsumoto, Y. *et al.*, 2006). In the guppy, at least two LWS genes are present (Hoffmann, M. *et al.*, 2006) and MSP of cones gives three potential λ_{max} at about 533, 548, and 572 nm (Archer, S. N. and Lythgoe, J. N., 1990). As suggested above, the 533 nm pigment may represent an Rh2A gene, leaving the two longer cone pigments as candidates for LWS genes. However, Archer S. N. and Lythgoe J. N. (1990) suggested that the 548 nm cones might be coexpressing the 533 and 572 nm pigments. The precise arrangement of pigments will only be resolved with further work on the expression of the isolated opsin genes.

Duplication of the LWS gene would seem to be the most likely explanation for the observation from MSP that at least in three species of pike, *Esox niger*, *Esox lucius*, and *Esox masquinongy* (Esocidae), the two halves of the long-wave-sensitive double cones (nonidentical twins) contain LWS pigments spectrally separated by about 15 nm, with λ_{max} at about 616 and 630 nm (Loew, E. R. *et al.*, 2006). These pigments are porphyropsins and there is no evidence that the spectral difference is a result of a small inclusion of a rhodopsin in the shorter half of the twin cone. The Esocidae are highly divergent both from the cyrinids and from the Acanthopterygii and the presumed LWS gene duplication in pike must be independent of the duplications within the other groups.

1.04.8.6 Ontogenetic Changes in Visual Pigment Complement

To the extent that visual pigments set the boundary for visual perception of both intensity and color, it should not be surprising that as the visual tasks and environment of a fish change during their development, so should their visual capabilities. This idea was initially supported by extraction studies on rods, showing chromophore shifts between rhodopsins and porphyropsins, and therefore peak absorbance shifts that are associated with changing environmental parameters such as the spectrum of the background spacelight, day length, temperature (e.g., see reviews of Bridges, C. D. B., 1972 and Bowmaker, J. K., 1995). That cones could also exchange chromophores was confirmed later using MSP (for a review, see Bowmaker, J. K., 1995). Almost all of the early work was carried out on mature fish or salmonids at the parr-to-smolt transition. However, a rich literature has developed directed specifically at larval-to-juvenile-to-adult transitions, from the points of view of chromophore shifting, opsin expression, and cellular changes. This is facilitated by the ability to determine opsin genotype and phenotype at the molecular level while also being able to determine expression patterns in time and space. To the visual ecologist interested in adaptive significance, these capabilities, when applied to temporal metamorphoses, are of particular use, since the visual world and tasks of most larvae are simple compared to those of adults, making modeling far easier (see below).

1.04.8.7 Simple Opsin Expression/Cellular Trajectories

The term simple is used here to describe trajectories not involving opsin switching in differentiated cones, as described for cichlids and others in this chapter. A good example of how available techniques can be applied to this kind of system can be found in the winter flounder, *Pleuronectes americanus* (Percomorpha). Early studies used histology and MSP to follow the retinal and visual pigment changes taking place during premetamorphic and postmetamorphic periods (Evans, B. I. and Fernald, R. D., 1993; Evans, B. I. *et al.*, 1993; see also Evans, B. I., 2004). Opsin expression studies using reverse transcriptase polymerase chain reaction (RT-PCR) on pre- and postmetamorphic stages have been added to this (Mader, M. M. and Cameron, D. A., 2004). The first cells to appear during ontogeny in premetamorphic fish are single cones with λ_{max} at about 520 nm expressing a single Rh2 opsin gene. With development are added rods at 509 nm expressing an Rh1, single cones at 461 nm expressing an SWS2, and double cones with 529 and 547 nm pigments expressing Rh2 and LWS opsin, respectively. No evidence of a UV pigment was found at any stage, although the presence of an SWS1 gene cannot be excluded. Interestingly, the authors suggest that a single Rh2 opsin produces both the 520 nm pigment in the premetamorphic fish and the 529 nm pigment in one member of the postmetamorphic double cone. They base this on their inability to identify more than one Rh2 product using RT-PCR and cross-reactivity of *in situ* probes. However, since flounders are percomorphs (and closely related to halibut, see Figure 4), they have the potential of possessing both an Rh2A and an Rh2B opsin gene and it may be that a second Rh2 gene is present, but has yet to be isolated.

The finding that cones precede rods during ontogeny appears to be the rule, although the first pigment(s) to be expressed may vary. An Rh2 opsin appears first in winter flounder as well as in the sturgeon and catfish (based on λ_{max} position determined by MSP (Sillman, A. J. *et al.*, 1993; Sillman, A. J. and Dahlin, D. A., 2004)). This is followed by rods and other single-cone classes that can express any of the other opsin gene classes. Last to develop are paired cones, either twin or double. For other species, such as goldfish (Stenkamp, D. L. *et al.*, 1996; 1997) and zebrafish (Raymond, P. A. *et al.*, 1993; 1995), the order appears to be LWS, Rh2, SWS2, and SWS1, although more recent evidence suggests that the blue opsin is expressed first in zebrafish (Takechi, M. and Kawamura, S., 2005).

1.04.8.8 Complex Opsin Expression/Cellular Trajectories

Not all species show the successive addition of photoreceptor classes, each expressing a single opsin type, as described for the winter flounder. Rather, there can be expression shifts within already present photoreceptors, as well as cone additions and apoptotic losses. For many years the only examples of an opsin change in a preexisting photoreceptor producing an ontogenetic λ_{max} shift were the eels, *Anguilla rostrata* and *Anguilla anguilla* (Beatty, D. D., 1975; Wood, P. and Partridge, J. C., 1993), and the cardinal fish, *Apogon brachyrammus* (Munz, F. W. and McFarland, W. N., 1975). From the above discussion,

it is obvious that changes in opsin expression, with or without the loss or gain of new cone types, are quite common in both marine and freshwater fishes. The most frequently observed alterations are in the expression of short-wavelength opsins and the presence of UV cones. The only published reports of changes involving long-wavelength opsin expression are for the goatfish, *Upeneus tragula* (Percomorpha) (Shand, J., 1993) and yellowfin tuna, *Thunnus albacares* (Percomorpha) (Loew, E. R. *et al.*, 2002). Examples of the kinds of shifts in both opsin expression and retinal structure are given below.

1.04.8.9 Short-Wavelength Shifts: Salmonids and the Lingcod

More is known about the developmental and life history changes in retinal architecture and visual pigment complement in salmonids than for any other group. Early literature concentrated on rhodopsin/porphyropsin shifts in rods (see Bridges, C. D. B., 1972) and later the cones (see, e.g., Bowmaker, J. K. and Kunz, Y. W., 1987; Hawryshyn, C. W. and Hárosi, F. I., 1994; Cheng, C. L. *et al.*, 2006). Most of the changes involve the loss and gain of UV photoreceptors and their correlation with life history events. Whereas there remains some controversy about the timing and pattern of loss, it appears that UV cones can follow two paths during development. In the Pacific salmonids studied by Cheng C. L. *et al.* (2006) only single cones are present at hatching and all express an SWS1 opsin. Downregulation of UV opsin expression later in development is associated either with the loss of the UV cell through apoptosis (this is associated with the well-documented loss of small corner cones as seen at the parr-to-smolt transition) or with the increased expression of a blue opsin gene leading to a shift in spectral sensitivity. The latter process was confirmed both by MSP and by *in situ* labeling (Cheng, C. L. and Novales Flamarique, I., 2004). The pattern is somewhat different for the Atlantic salmon, but changes in overall spectral sensitivity at the short-wavelength end of the spectrum seem to be a common feature among salmonids.

The lingcod, *Ophiodon elongatus* (Percomorpha), also shows changes in SWS1 and SWS2 opsin expression (see Table 2 containing unpublished data used with the permission of Lyle Britt). The larvae are near-surface diurnal planktivores, whereas adults can be found from the surface to depths in excess of 400 m (Allen, M. J. and Smith, G. B., 1988). At the time of hatching, only the UV cones are present, although they are few and disappear very quickly. At preflexion there is definite expression of UV-, violet-, green-, and red-sensitive cones (all single cones), presumably expressing SWS1, SWS2(B), Rh2, and LWS opsin genes, respectively. Between preflexion and flexion, there is a rapid loss of UV cones, presumably due to downregulation of the SWS1 gene and most likely apoptosis of the UV cells.

At the time of prejuvenile-to-juvenile transformation, all of the violet-sensitive cones show a spectral shift toward the blue, which can be interpreted as

Table 2 Visual pigments (λ_{max} in nm ± SD) versus developmental stage for the lingcod

Photoreceptor	*Preflexion*	*Flexion*	*Postflexion*	*Prejuvenile*	*Transformation*	*Juvenile*	*Adult*
Rod		500 ± 1	500 ± 1	499 ± 2	501 ± 3	500 ± 2	499 ± 2
Single cones							
UV	364 ± 9						
Violet	405 ± 4	402 ± 2	402 ± 1	407 ± 6			
Violet/blue					421 ± 19		
Blue						460 ± 5	461 ± 1
Green	514 ± 1	512 ± 1	512 ± 2	513 ± 2	517 ± 2	521 ± 1	523 ± 1
Yellow	564 ± 6	564 ± 2	565 ± 1	568 ± 3	565 ± 5		
Double cones							
Green member					519 ± 2	522 ± 1	522 ± 4
Yellow member					567 ± 4	565 ± 4	563 ± 7
Twin cones					519 ± 3	520 ± 2	521 ± 3

Note that the rods do not appear until the flexion stage, which is similar to that reported for a number of other species (e.g., tuna (see below) and salmonids (see above)). The same is true for a number of other Pacific Northwest marine species. However, in several species rods were present at the preflexion stage along with single cones (Britt, L. L. *et al.*, 2001).
From Britt, L. L., 2006.

a change in opsin gene expression and coexpression from the SWS2 opsin gene to either a second SWS2(A) opsin gene or an Rh2 opsin. By the end of this transformation, which takes only about 48 h, all of the violet-sensitive cones have become blue-sensitive. There is also an apparent small long-wave shift in the green-sensitive single cones from about 512 to 522 nm. This may well reflect a switch between two Rh2 opsin genes. The final adult complement consists of the expression of the LWS, an Rh2, and probably the SWS2A opsin genes. These MSP data suggest the ontological expression of at least six cone opsin genes, somewhat similar to that described earlier for cichlids. Lingcod, more closely related to the cottoids, is, like the cichlids, a percomorph, where gene duplication of both Rh2 and SWS2 opsin genes has occurred (see Figures 4 and 6). In salmonids, there is no evidence of transformation or coexpression in the green Rh2 or red LWS cones. The adaptive significance of the two sequential changes in short-wavelength sensitivity remains obscure.

1.04.8.10 Long-Wavelength Shifts: Yellowfin Tuna

The retinas of postflexion through adult tuna are highly developed, containing rods and single and twin cones (Margulies, D., 1997). The adult eye is large and together with a high cone density endows tuna and billfish with the highest visual acuity reported in fishes (Tamura, T. and Wisby, W. J., 1963; Nakamura, E. L., 1968; 1969). The single cones contain a visual pigment with λ_{max} at 426 nm and the identical twin cones and rods contain pigments with λ_{max} around 485 nm (Loew, E. R. *et al.*, 2002). Preliminary analysis of the opsin genes has identified single LWS and SWS2 genes and at least two Rh2 genes (Carleton, K. R., personnel communication). The SWS2 gene and an Rh2 gene presumably correlate with the 426 and 485 nm adult cone pigments, respectively. However, no LWS cones have been seen in adult yellowfin tuna in spite of extensive searching (note that LWS cones have been reported in marlin (Fritsches, K. A. *et al.*, 2003)), but an LWS visual pigment has been identified by MSP in larval yellow perch (Loew, E. R. *et al.*, 2002).

In yellowfin tuna, the retinal anatomy of first feeding through flexion larvae is quite different from the adult (see Margulies, D., 1997). Only single cones are found in first feeders, with rods not becoming evident until late flexion/early postflexion. Small twin cones appear during postflexion and greatly increase in size through the juvenile stages. Associated with these retinal and developmental changes are changes in prey type. A summary of visual pigment findings for yellowfin tuna cones at different developmental stages is presented in Figure 8 (Loew, E. R. *et al.*, 2002). The visual pigment complement for subadults is complex. At flexion (6–9 mm standard length, SL), when there are no observable rods and only single cones present, there is a broad range of λ_{max} essentially spanning the wavelength range from 418 to 575 nm. With increasing SL there is a decrease in overall range of single cone λ_{max} with some suggestion of clustering around the 426 nm single-cone adult value, and an absence of values in the 430 to 480 nm range. A second convergence leads to a single-cone cluster around 485 nm at 43 mm SL. Twin cones are first evident at the early juvenile 1 stage (21 mm SL). Here too, there is λ_{max} heterogeneity that converges to the 485 nm adult value by the end of the juvenile 1 stage.

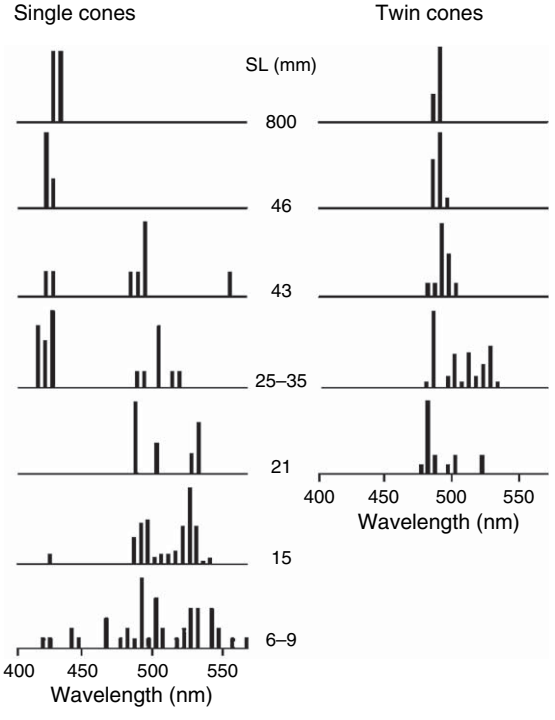

Figure 8 Cone visual pigments versus standard length (SL) for yellowfin tuna. Reproduced from Loew, E. R., McFarland, W. N., and Margulies, D. 2002. Developmental changes in the visual pigments of the yellowfin tuna, *Thunnus albacares*. Mar. Freshw. Behav. Physiol. 35, 235–246, with permission from Taylor & Francis.

Combining the MSP and molecular data, one can conclude that the SWS2 gene produces the 426 nm pigment, the Rh2 gene produces the 485 nm pigment, and the LWS gene produces a pigment with λ_{max} greater than 560 nm. The presence of measured pigments with λ_{max} substantially below 426 nm suggests the presence of an additional SWS1 gene that has yet to be identified. As with lingcod, tuna are percomorphs and so may have the possibility of at least six cone opsin genes.

1.04.9 Adaptive Significance

Knowledge of the overall spectral sensitivity of a fish at a particular life-history stage still needs to be rationalized in terms of its adaptive significance. This requires information on the visual tasks performed at that stage in a particular photic environment. As described above for cichlids (see also Carleton, K. L. *et al.*, 2006), this can be a very complex process, having to take into account differences in the turbidity and spectral characteristics of the water and the great variation in the size, shape, and spectral characteristics of relevant targets (e.g., conspecifics). Whereas some models have been developed, which try to take all these factors into account when deciding which complement of visual pigments is most efficient under a given set of conditions and tasks (see Loew, E. R. and Zhang, H., 2006; Marshall, J. *et al.*, 2006b), the degree of complexity in a group like the cichlids can be quite confounding. However, examination of relatively simple systems can lead to broad generalizations. The main visual task of larval fish is prey detection. For obligate diurnal planktivores this occurs in the top few meters of the water column in both marine and freshwater environments. Feeding usually takes place within a horizontal band over a few body lengths. Unless the fish is very close to an object, the background is basically featureless and described by the average horizontal radiance. For freshwater species the presence of a UV pigment in the larval/juvenile has been seen as an adaptation for planktivory (Bowmaker, J. K. and Kunz, Y. W., 1987; Browman, H. I. *et al.*, 1994; see reviews by Bowmaker, J. K., 1991; Beaudet, L. and Hawryshyn, C. W., 1999; Partridge, J. C. and Cummings, M. E., 1999). This is supported by the loss of UV cells with the transition to demersal piscivory (e.g., the perch, Loew, E. R. and Wahl, C. M., 1991), or a switch from UV to violet or blue opsin expression (e.g., salmonids, Cheng, C. L. *et al.*, 2006) and lingcod (Britt, L. L., personal communication). The cessation of LWS expression in yellowfin tuna and goatfish at the planktivory–piscivory transmission has already been mentioned, but this is not so easily explained since the optical characteristics of plankton contributing to contrast are not as spectacular at longer wavelengths (McFall-Ngai, M. J., 1990; Johnsen, S., 2001).

Recently, a unifying adaptive imperative, based on the above examples, as well as an extensive study of Northern Pacific larval species (Britt, L. L. *et al.*, 2001; Britt, L. L., personal communication) has been proposed involving contrast enhancement for chlorophyll-containing targets (McFarland, W. N. and Loew, E. R., personal communication). Whereas transparency seems to be an adaptive feature of zooplankton, most prey on chlorophyll-containing phytoplankton that can easily be seen through the otherwise transparent body (Figure 9). The increase in contrast, at least to our eyes, has led to the following generalizations:

1. In addition to an SWS1 and/or SWS2 opsin gene useful for both chlorophyll and UV contrast enhancement, diurnal larval planktivores in clear blue oceanic waters will express at least one longer-wave opsin gene that may or may not be turned off with age.
2. In addition to one or more longer-wave opsins, diurnal larval planktivores in green coastal or freshwater will express at least one SWS1 or SWS2 opsin gene useful for both chlorophyll and UV contrast enhancement that may or may not be turned off with age. These ideas were tested using the model of Loew E. R. and Zhang H. (2006).

Assume a single spherical target having a chlorophyll reflectance spectrum (Figures 9(b) and 9(c)) subtending 2° of visual angle and being viewed horizontally against the background spacelight at 2 m depth. The calculated background spectra are seen in Figure 10 for both clear oceanic (Figure 10(a), no dissolved chlorophyll or DOM) and a typical freshwater (Figure 10(b), 1 mg m^{-3} chlorophyll and 0.2 mg l^{-1} DOM). Using an iterative process, the program answers the question: which set of visual pigments maximizes the visibility of the target viewed against the spectrally defined background as the target is moved away from the eye? These solutions are seen in Figures 11 and 12 for clear blue oceanic water and a typical freshwater, respectively. For a straight luminosity task, a single visual pigment matching

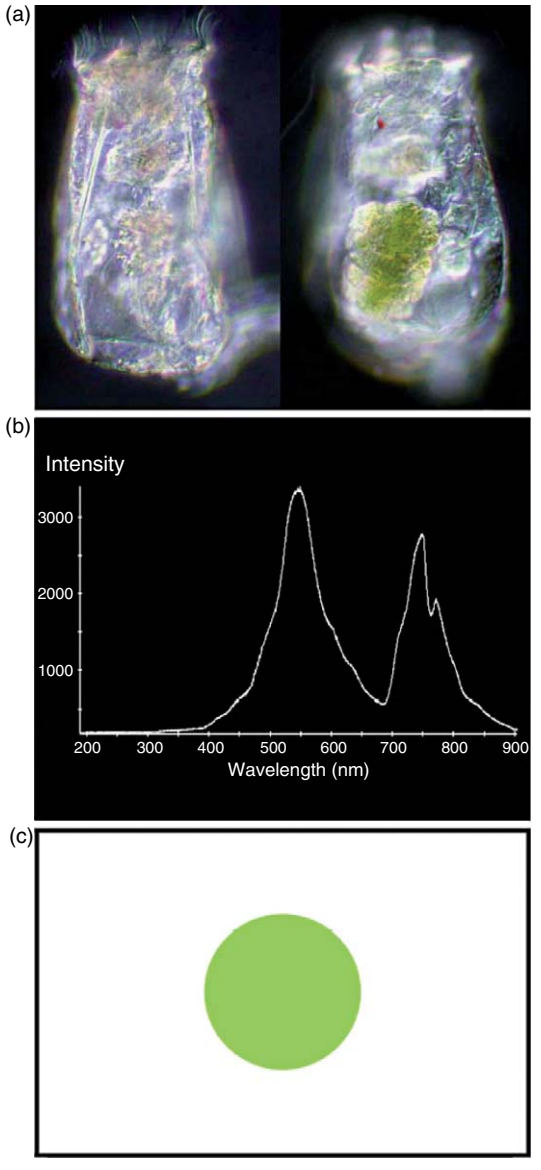

Figure 9 (a) A starved (left) and fed (right) rotifer showing the visibility of the chlorophyll-containing prey in the gut. (b) The reflectance spectrum of chlorophyll in the gut measured using an Ocean Optics USB 2000 spectroradiometer fitted to an Olympus microscope. (c) A colored target generated using the reflectance spectrum (see Loew, E. R. and Zhang, H., 2006, for methodology).

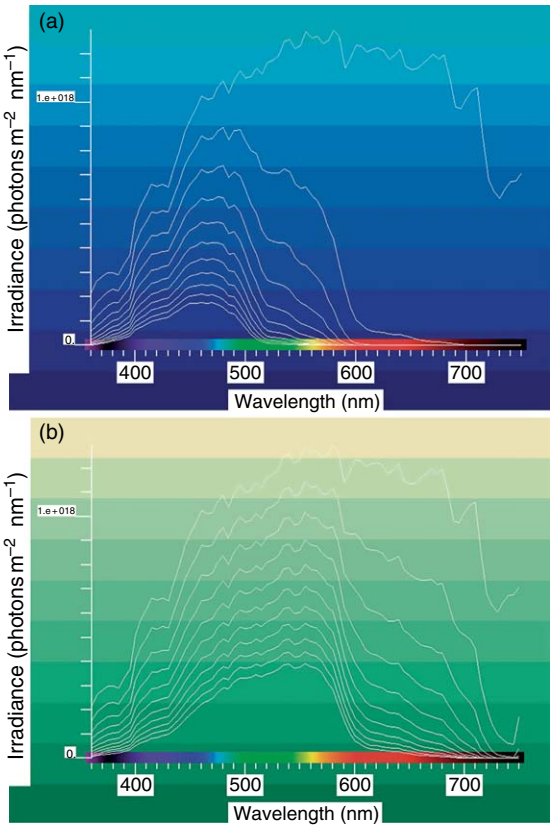

Figure 10 Calculated downwelling irradiance at 0.2 m intervals from the surface for (a) clear blue oceanic and (b) a typical freshwater. See text for explanation.

the background spacelight gives the best contrast as expected (Figures 11, 12(a), and 12(b)). For a chromaticity detection task, two pigments, one at long and the other at short wavelengths, provide the best contrast solution for this chlorophyll target (Figures 11, 12(c), and 12(d)). Note that in both water types the predicted LWS pigments should have λ_{max} greater than 600 nm to be optimal. The fact that pelagic species like tuna do not achieve this range may indicate an inability to utilize Vitamin A_2 as a chromophore. The predicted short wavelength pigments have somewhat longer λ_{max} than those measured in both freshwater and pelagic larvae. This may be due to a compromise between the need to use both chlorophyll and UV cues in prey detection.

The solutions given by this and most other models are best used for generating testable hypotheses as given above and should not be treated as reality. In addition to spectral data for the macro- and micro-environment and relevant targets in those environments, and the usual phenotypic data derived from MSP, electrophysiological or gene expression techniques, future studies should also include opsin genotype data, if a complete picture of the potential for color vision is to be derived.

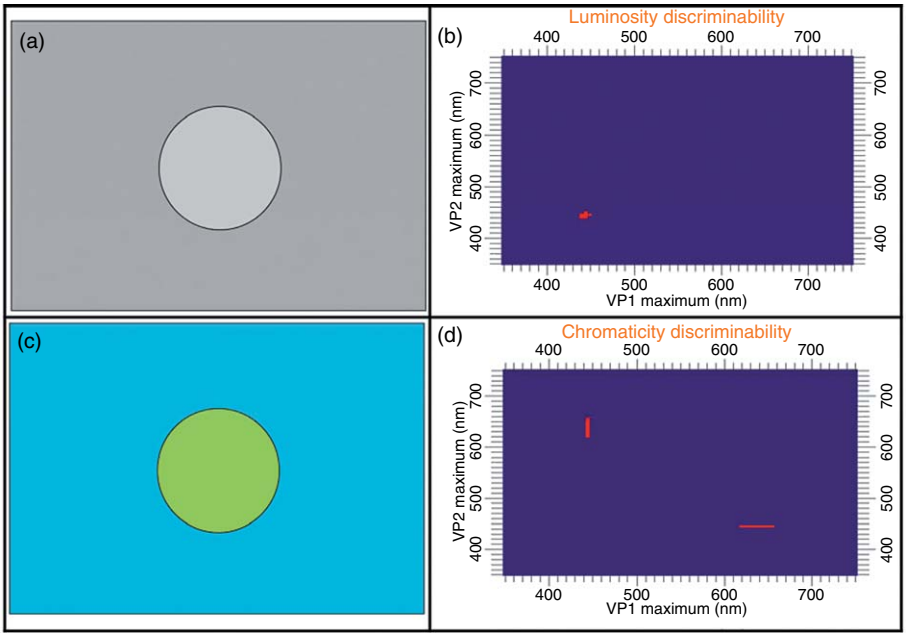

Figure 11 (a) Luminosity contrast of the chlorophyll target seen in Figure 10 viewed horizontally at a distance of 1.0 m at 2.0 m depth in clear blue oceanic water. (b) The solution to the question, which visual pigment will maximize the distance from the eye that the target can be detected against the background spacelight using brightness alone? (c) The calculated color appearance of the target to a human observer under the viewing conditions given for (a). (d) The solution to the question, which set of visual pigments will maximize the distance from the eye that the target can be detected against the background spacelight using color contrast alone?

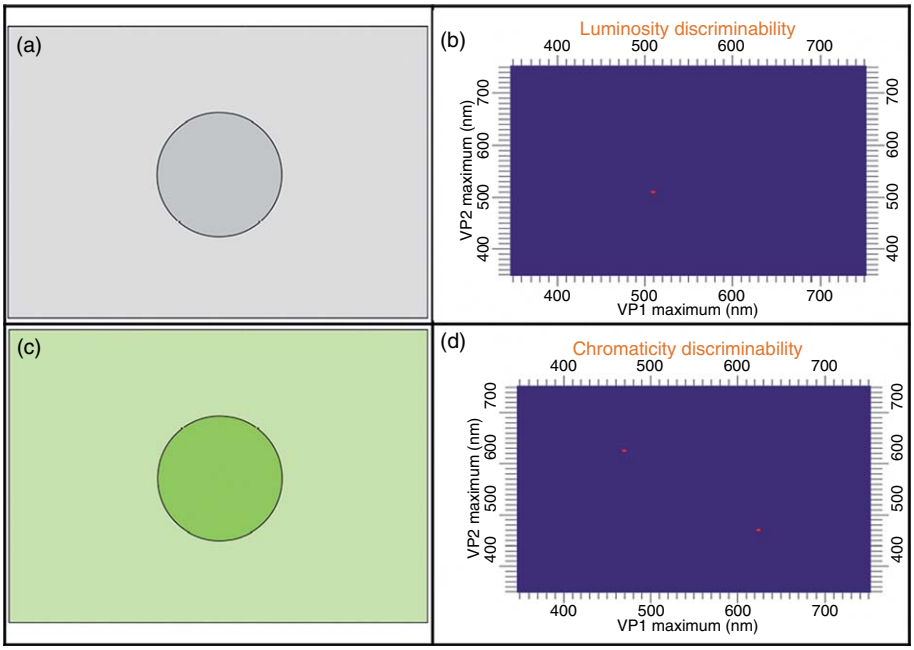

Figure 12 (a) Luminosity contrast of the chlorophyll target seen in Figure 10 viewed horizontally at a distance of 1.0 m at 2.0 m depth in a typical freshwater. (b) The solution to the question, which visual pigment will maximize the distance from the eye that the target can be detected against the background spacelight using brightness alone? (c) The calculated color appearance of the target to a human observer under the viewing conditions given for (a). (d) The solution to the question, which set of visual pigments will maximize the distance from the eye that the target can be detected against the background spacelight using color contrast alone?

References

Ali, M. A. and Anctil, M. 1973. Retina of South American lungfish, *Lepidosiren paradoxa* Fitzinger. Can. J. Zool. 51, 969–972.

Allen, M. J. and Smith, G. B. 1988. Atlas and zoogeography of common fishes in the Bering Sea and northeastern Pacific. NOAA Tech. Rept. NMFS 66, 151.

Archer, S. N. and Lythgoe, J. N. 1990. The visual pigment basis for cone polymorphism in the guppy, *Poecilia reticulata*. Vision Res. 30, 225–233.

Archer, S. N., Endler, J. A., Lythgoe, J. N., and Partridge, J. C. 1987. Visual pigment polymorphism in the guppy *Poecilia reticulata*. Vision Res. 27, 1243–1252.

Avery, J. A., Bowmaker, J. K., Djamgoz, M. B. A., and Downing, J. E. G. 1983. Ultraviolet sensitive receptors in a freshwater fish. J. Physiol. 334, 23P.

Bailes, H. J., Robinson, S. R., Trezise, A. E. O., and Collin, S. P. 2006. Morphology, characterization, and distribution of retinal photoreceptors in the Australian lungfish *Neoceratodus forsteri* (Krefft, 1870). J. Comp. Neurol. 494, 381–397.

Beatty, D. D. 1975. Visual pigments of the American eel, *Anguilla rostrata*. Vision Res. 15, 771–776.

Beaudet, L. and Hawryshyn, C. W. 1999. Ecological Aspects of Vertebrate Visual Ontogeny. In: Adaptive Mechanisms in the Ecology of Vision (*eds*. S. N. Archer, M. B. A. Djamdoz, E. R. Loew, J. C. Partridge, and S. Vellerga), pp. 413–437. Kluwer.

Bowmaker, J. K. 1991. The Evolution of Visual Pigments and Photoreceptors. In: Evolution of the Eye and Visual System, Vol. 2 (*eds*. R. L. Gregory and J. R. Cronly-Dillon), pp. 63–81. Vision and Visual Dysfunction. Macmillan.

Bowmaker, J. K. 1995. The visual pigments of fish. Prog. Ret. Eye. Res. 15, 1–31.

Bowmaker, J. K. and Hunt, D. M. 2006. Evolution of vertebrate visual pigments. Curr. Biol. 16, R484–R489.

Bowmaker, J. K. and Kunz, Y. W. 1987. Ultraviolet receptors, tetrachromatic colour vision and retinal mosaics in the brown trout (*Salmo trutta*): age-dependent changes. Vision Res. 27, 2101–2108.

Bowmaker, J. K., Heath, L. A., Wilkie, S. E., and Hunt, D. M. 1997. Visual pigments and oil droplets from six classes of photoreceptor in the retinas of birds. Vision Res. 37, 2183–2194.

Bowmaker, J. K., Thorpe, A., and Douglas, R. H. 1991. Ultraviolet-sensitive cones in the goldfish. Vision Res. 31, 349–352.

Bridges, C. D. B. 1972. The Rhodopsin–Porphyropsin Visual System. In: Photochemistry of Vision, Vol. VII/1 (*ed*. H. J. A. Dartnall), pp. 417–480. Handbook of Sensory Physiology, Springer.

Britt, L. L., Loew, E. R., and McFarland, W. N. 2001. Visual pigments in the early life stages of Pacific Northwest marine fishes. J. Exp. Biol. 204, 2581–2587.

Browman, H. I., Novales Flamarique, I., and Hawryshyn, C. W. 1994. Ultraviolet photoreception contributes to prey search behavior in two species of zooplanktivorous fishes. J. Exp. Biol. 186, 187–198.

Burkhardt, D. A., Gottesman, J., Levine, J. S., and Macnichol, E. F. 1983. Cellular mechanisms for color coding in holostean retinas and the evolution of color vision. Vision Res. 23, 1031–1041.

Cameron, D. A. 2002. Mapping absorbance spectra, cone fractions, and neuronal mechanisms to photopic spectral sensitivity in the zebrafish. Vis. Neurosci. 19, 365–372.

Carleton, K. L. and Kocher, T. D. 2001. Cone opsin genes of African cichlid fishes: tuning spectral sensitivity by differential gene expression. Mol. Biol. Evol. 18, 1540–1550.

Carleton, K. L., Hárosi, F. I., and Kocher, T. D. 2000. Visual pigments of African cichlid fishes: evidence for ultraviolet vision from microspectrophotometry and DNA sequences. Vision Res. 40, 879–890.

Carleton, K. L., Spady, T., and Kocher, T. D. 2006. Visual Communication in East African Cichlid Fishes: Diversity in a Phylogenetic Context. In: Communication in Fishes (*eds*. F. Ladich, S. P. Collin, P. Moller, and B. G. Kapoor), Vol. 2, pp. 485–516. Science Publishers.

Cheng, C. L. and Novales Flamarique, I. 2004. Opsin expression: new mechanism for modulating colour vision. Nature 428, 279.

Cheng, C. L., Novales Flamarique, I., Hárosi, F. I., Rickers-Haunerland, J., and Haunerland, N. H. 2006. Photoreceptor layer of salmonid fishes: transformation and loss of single cones in juvenile fish. J. Comp. Neurol. 495, 213–235.

Chinen, A., Hamaoka, T., Yamada, Y., and Kawamura, S. 2003. Gene duplication and spectral diversification of cone visual pigments of zebrafish. Genetics 163, 663–675.

Chinen, A., Matsumoto, Y., and Kawamura, S. 2005a. Reconstitution of ancestral green visual pigments of zebrafish and molecular mechanism of their spectral differentiation. Mol. Biol. Evol. 22, 1001–1010.

Chinen, A., Matsumoto, Y., and Kawamura, S. 2005b. Spectral differentiation of blue opsins between phylogenetically close but ecologically distant goldfish and zebrafish. J. Biol. Chem. 280, 9460–9466.

Christoffels, A., Koh, E. G. L., Chia, J. M., Brenner, S., Aparicio, S., and Venkatesh, B. 2004. Fugu genome analysis provides evidence for a whole-genome duplication early during the evolution of ray-finned fishes. Mol. Biol. Evol. 21, 1146–1151.

Cohen, J. L. 1990. Vision in Elasmobranchs. In: The Visual System of Fish (*eds*. R. H. Douglas and M. B. A. Djamgoz), pp. 465–490. Chapman and Hall.

Collin, S. P. and Trezise, A. E. O. 2006. Molecular evidence for dim-light vision in the last common ancestor of the vertebrates – response. Curr. Biol. 16, R320–R320.

Collin, S. P., Hart, N. S., Shand, J., and Potter, I. C. 2003a. Morphology and spectral absorption characteristics of retinal photoreceptors in the southern hemisphere lamprey (*Geotria australis*). Vis. Neurosci. 20, 119–130.

Collin, S. P., Hart, N. S., Wallace, K. M., Shand, J., and Potter, I. C. 2004. Vision in the southern hemisphere lamprey *Mordacia mordax*: spatial distribution, spectral absorption characteristics and optical sensitivity of a single class of retinal photoreceptor. Vis. Neurosci. 21, 765–773.

Collin, S. P., Knight, M. A., Davies, W. L., Potter, I. C., Hunt, D. M., and Trezise, A. E. O. 2003b. Ancient colour vision: multiple opsin genes in the ancestral vertebrates. Curr. Biol. 13, R864–R865.

Cowing, J. A., Poopalasundaram, S., Wilkie, S. E., Robinson, P. R., Bowmaker, J. K., and Hunt, D. M. 2002. The molecular mechanism for the spectral shifts between vertebrate ultraviolet- and violet-sensitive cone visual pigments. Biochem. J. 367, 129–135.

Dartnall, H. J. A. 1972. Visual pigment of the coelacanth. Nature 239, 341–342.

Dartnall, H. J. A., Bowmaker, J. K., and Mollon, J. D. 1983. Human visual pigments: microspectrophotometric results from the eyes of seven persons. Proc. R. Soc. Lond. B 220, 115–130.

Douglas, R. H. 2001. The Ecology of Teleost Fish Visual Pigments: A Good Example of Sensory Adaptation to the Environment? In: Ecology of Sensing (*eds*. F. G. Barth and A. Schmid), pp. 215–235. Springer.

Douglas, R. H. and Djamgoz, M. B. A. 1990. The Visual System of Fish, p. 526. Chapman and Hall.

Dowling, J. E. and Ripps, H. 1990. On the duplex nature of the skate retina. J. Exp. Zool. Suppl. 5, 55–65.

Downing, J. E. G., Djamgoz, M. B. A., and Bowmaker, J. K. 1986. Photoreceptors of cyprinid fish: morphological and spectral characteristics. J. Comp. Physiol. A 159, 859–868.

Evans, B. I. 2004. A Fish's Eye View of Habitat Change. In: The Senses of Fishes (*eds*. G. Von der Emde, J. Mogdans and B. G. Kapoor), pp. 1–30. Kluwer.

Evans, B. I. and Fernald, R. D. 1993. Retinal transformation at metamorphosis in the winter flounder (*Pseudopleuronectes americanus*). Vis. Neurosci. 10, 1055–1064.

Evans, B. I., Hárosi, F. I., and Fernald, R. D. 1993. Photoreceptor spectral absorbance in larval and adult winter flounder (*Pseudopleuronectes americanus*). Vis. Neurosci. 10, 1065–1071.

Fasick, J. I., Lee, N., and Oprian, D. D. 1999. Spectral tuning in the human blue cone pigment. Biochemistry 38, 11593–11596.

Fernald, R. D. and Liebman, P. A. 1980. Visual receptor pigments in the African cichlid fish, *Haplochromis burtoni*. Vision Res. 20, 857–864.

Fricke, H. and Hissmann, K. 2000. Feeding ecology and evolutionary survival of the living coelacanth *Latimeria chalumnae*. Mar. Biol. 136, 379–386.

Fritsches, K. A., Litherland, L., Thomas, N., and Shand, J. 2003. Cone visual pigments and retinal mosaics in the striped marlin. J. Fish Biol. 63, 1347–1351.

Fuller, R. C., Carleton, K. L., Fadool, J. M., Spady, T. C., and Travis, J. 2004. Population variation in opsin expression in the bluefin killifish, *Lucania goodei*: a real-time PCR study. J. Comp. Physiol. A 190, 147–154.

Fuller, R. C., Fleishman, L. J., Leal, M., Travis, J., and Loew, E. 2003. Intraspecific variation in retinal cone distribution in the bluefin killifish, *Lucania goodei*. J. Comp. Physiol. A 189, 609–616.

Furutani-Seiki, M. and Wittbrodt, J. 2004. Medaka and zebrafish, an evolutionary twin study. Mech. Devel. 121, 629–637.

Govardovskii, V. I. and Lychakov, L. V. 1977. Photoreceptors and visual pigments of Black Sea elasmobranchs. Zh. Evol. Biokhim. Fiziol. 13, 162–166.

Govardovskii, V. I. and Lychakov, D. V. 1984. Visual cells and visual pigments of the lamprey, *Lampetra fluviatilis*. J. Comp. Physiol. A 154, 279–286.

Govardovskii, V. I. and Zueva, L. V. 1987. The photoreceptors and visual pigments of some sturgeons. Zh. Evol. Biokhim. Fiziol. 23, 865–686.

Govardovskii, V. I., Byzov, A. L., Zueva, L. V., Polisczuk, N. A., and Baburina, E. A. 1991. Spectral characteristics of photoreceptors and horizontal cells in the retina of the Siberian sturgeon *Acipenser baeri* Brandt. Vision Res. 31, 2047–2056.

Gruber, S. H., Loew, E. R., and McFarland, W. N. 1990. Rod and cone pigments of the Atlantic guitarfish, *Rhinobatos lentiginosus garman*. J. Exp. Zool. S5, 85–87.

Hárosi, F. I. 1985. Ultraviolet- And Violet-Absorbing Vertebrate Visual Pigments: Dichroic and Bleaching Properties. In: The Visual System (*eds*. J. S. Levine and A. Fein), pp. 41–55. Alan Liss.

Hárosi, F. I. and Hashimoto, Y. 1983. Ultraviolet visual pigment in a vertebrate: a tetrachromatic cone system in the dace. Science 222, 1021–1023.

Hárosi, F. I. and Kleinschmidt, J. 1993. Visual pigments in the sea lamprey, *Petromyzon marinus*. Vis. Neurosci. 10, 711–715.

Hárosi, F. I. and MacNichol, E. F. 1974. Visual pigments of goldfish cones. Spectral properties and dichroism. J. Gen. Physiol. 63, 279–304.

Hart, N. S. 2001. The visual ecology of avian photoreceptors. Prog. Ret. Eye Res. 20, 675–703.

Hart, N. S., Lisney, T. J., Marshall, N. J., and Collin, S. P. 2004. Multiple cone visual pigments and the potential for trichromatic colour vision in two species of elasmobranch. J. Exp. Biol. 207, 4587–4594.

Hawryshyn, C. W. and Hárosi, F. I. 1994. Spectral characteristics of visual pigments in rainbow trout (*Oncorhynchus mykiss*). Vision Res. 34, 1385–1392.

Hoffmann, M., Tripathi, N., Henz, S. R., Lindholm, A. K., Weigel, D., Breden, F., and Dreyer, C. 2006. Opsin gene duplication and diversification in the guppy, a model for sexual selection. Proc. R. Soc. Lond. B Published online, Sept 2006.

Horn, M. H. 1972. The amount of space available for marine and freshwater fishes. Fish. Bull. 70, 1295–1297.

Hunt, D. M. and Bowmaker, J. K. 2006. Visual Pigments and Visual Communication in Deepwater Environments. In: Communication in Fishes (*eds*. F. Ladich, S. P. Collin, P. Moller, and B. G. Kapoor), Vol. 2, pp. 457–483. Science Publishers.

Hunt, D. M., Cowing, J. A., Wilkie, S. E., Parry, J. W. L., Poopalasundaram, S., and Bowmaker, J. K. 2004. Divergent mechanisms for the tuning of shortwave sensitive visual pigments in vertebrates. Photochem. Photobiol. Sci. 3, 713–720.

Ishikawa, M., Takao, M., Washioka, H., Tokunaga, F., Watanabe, H., and Tonosaki, A. 1987. Demonstration of rod and cone photoreceptors in the lamprey retina by freeze replication and immunoflourescence. Cell Tis. Res. 249, 241–246.

Johnsen, S. 2001. Hidden in plain sight: the ecology and physiology of organismal transparency. Biol. Bull. 201, 301–318.

Johnson, R. L., Grant, K. B., Zankel, T. C., Boehm, M. F., Merbs, S. L., Nathans, J., and Nakanishi, K. 1993. Cloning and expression of goldfish opsin sequences. Biochemistry 32, 208–214.

Jordan, R., Kellogg, K., Howe, D., Juanes, F., Stauffer, J., and Loew, E. 2006. Photopigment spectral absorbance of Lake Malawi cichlids. J. Fish. Biol. 68, 1291–1299.

Kleinschmidt, J. and Hárosi, F. I. 1992. Anion sensitivity and spectral tuning of cone visual pigments *in situ*. Proc. Natl. Acad. Sci. 89, 9181–9185.

Kocher, T. D. 2004. Adaptive evolution and explosive speciation: the cichlid fish model. Nat. Rev. Genet. 5, 288–298.

Kocher, T. D., Conroy, J. A., McKaye, K. R., Stauffer, J. R., and Lockwood, S. F. 1995. Evolution of NADH dehydrogenase subunit 2 in East African cichlid fish. Mol. Phylo. Evol. 4, 420–432.

Kumazawa, Y., Yamaguchi, M., and Nishida, M. 1999. Mitochondrial Molecular Clocks and the Origin of Euteleostean Biodiversity: Familial Radiation of Perciforms May Have Predated the Cretaceous/Tertiary Boundary. In: The Biology of Diversity (*ed*. M. Kato), pp. 35–52. Springer.

Levine, J. S. and MacNichol, E. F. 1979. Visual pigments in teleost fishes: effects of habitat, microhabitat and behaviour on visual system evolution. Sens. Processes 3, 95–130.

Locket, N. A. 1973. Retinal structure in *Latimeria chalumnae*. Phil. Trans R. Soc. Lond. B 266, 493–521.

Loew, E. R. and Dartnall, H. J. A. 1976. Vitamin A1/A2-based visual pigment mixtures in cones of the rudd. Vision Res. 16, 891–896.

Loew, E. R. and Lythgoe, J. N. 1978. The ecology of cone pigments in teleost fish. Vision Res. 18, 715–722.

Loew, E. R. and Wahl, C. M. 1991. A short-wavelength sensitive cone mechanism in juvenile yellow perch, *Perca flavescens*. Vision Res. 31, 353–360.

Loew, E. R. and Zhang, H. 2006. Propagation of Visual Signals in the Aquatic Environment: An Interactive Windows©-Based Model. In: Communication in Fishes (*eds*. F. Ladich, S. P. Collin, P. Moller, and B. G. Kapoor), Vol. 2, pp. 281–302. Science Publishers.

Loew, E. R., Davies, W. L., Hunt, D. M., and Bowmaker, J. K. 2006. Different LWS opsins expressed in individual members of twin cones in teleosts. Invest. Ophthalmol. Vis. Sci. 47, e-abstract.

Loew, E. R., McFarland, W. N., and Margulies, D. 2002. Developmental changes in the visual pigments of the yellowfin tuna, *Thunnus albacares*. Mar. Freshw. Behav. Physiol. 35, 235–246.

Mader, M. M. and Cameron, D. A. 2004. Photoreceptor differentiation during retinal development, growth, and regeneration in a metamorphic vertebrate. J. Neurosci. 24, 11463–11472.

Margulies, D. 1997. Development of the visual system and inferred performance capabilities of larval and early juvenile scombrids. Mar. Freshw. Behav. Physiol. 30, 75–98.

Marshall, N. J., Jennings, K., McFarland, W. N., Loew, E. R., and Losey, G. S. 2003. Visual biology of Hawaiian coral reef fishes. III. Environmental light and an integrated approach to the ecology of reef fish vision. Copeia 3, 467–480.

Marshall, J., Vorobyev, M., Collin, S. P., Bailes, H. J., and Hart, N. S. 2006a. Tetrachromatic colour vision in the Australian lungfish *Neoceratodus forsteri*. Perception, Suppl. 35, 168.

Marshall, J., Vorobyev, M., and Siebeck, U. E. 2006b. What Does a Reef Fish See When It Sees a Reef Fish? Eating ''Nemo''©. In: Communication in Fishes (*eds*. F. Ladich, S. P. Collin, P. Moller, and B. G. Kapoor), Vol. 2, pp. 393–422. Science Publishers.

Matsumoto, Y., Fukamach, S., Mitam, H., and Kawamura, S. 2006. Functional characterization of visual opsin repertoire in medaka (*Oryzias latipes*). Gene 371, 268–278.

McFall-Ngai, M. J. 1990. Crypsis in the pelagic environment. Am. Zool. 30, 175–188.

Merbs, S. L. and Nathans, J. 1992. Absorption spectra of human cone pigments. Nature 356, 433–435.

Meyer, A. 1993. Phylogenetic relationships and evolutionary processes in East African cichlid fishes. Trends Ecol. Evol. 8, 279–284.

Meyer, A. 1995. Molecular evidence on the origin of tetrapods and the relationships of the coelacanth. Trends Ecol. Evol. 10, 111–116.

Meyer, A. and Schartl, M. 1999. Gene and genome duplications in vertebrates: the one-to-four (-to-eight in fish) rule and the evolution of novel gene functions. Curr. Opin. Cell Biol. 11, 699–704.

Millot, J. and Carasso, N. 1955. Note préliminaire sur l'oeil de *Latimeria chalumnae* (Crossoptérygien-Coelacanthide). Comp. Rend. Acad. Sci. 241, 576–577.

Minamoto, T. and Shimizu, I. 2005. Molecular cloning of cone opsin genes and their expression in the retina of a smelt, Ayu (*Plecoglossus altivelis*, Teleostei). Comp. Biochem. Physiol. B 140, 197–205.

Miyazaki, T., Yamauchi, M., Takami, M., and Kohbara, J. 2005. Putative ultraviolet-photosensitivity in the retina of 1-year-old nibbler *Girella punctata*: based on molecular and histological evidences. Fish. Sci. 71, 159–167.

Munz, F. W. and McFarland, W. N. 1975. Part I: Presumptive cone pigments extracted from tropical marine fishes. Vision Res. 15, 1045–1062.

Nakamura, E. L. 1968. Visual acuity of two tunas, *Katsuwonus pelamis* and *Euthynnus affinis*. Copeia 1, 41–49.

Nakamura, E. L. 1969. Visual acuity in yellowfin tuna, *Thunnus albacares*. Proceedings of the FAO conference on fish behaviour in relation to fishing techniques and tactics pp. 19–27. Norway.

Nawrocki, L., BreMiller, R., Streisinger, G., and Kaplan, M. 1985. Larval and adult visual pigments of the zebrafish, *Brachydanio rerio*. Vision Res. 25, 1569–1576.

Neafsey, D. E. and Hartl, D. L. 2005. Convergent loss of an anciently duplicated, functionally divergent Rh2 opsin gene in the fugu and *Tetraodon* pufferfish lineages. Gene 350, 161–171.

Negishi, K., Teranishi, T., Kuo, C. H., and Miki, N. 1987. Two types of lamprey retina photoreceptors immunoreactive to rod- or cone-specific antibodies. Vision Res. 27, 1237–1241.

Novales Flamarique, I. and Hárosi, F. I. 2000. Photoreceptors, visual pigments, and ellipsosomes in the killifish, *Fundulus heteroclitus*: A microspectrophotometric and histological study. Vis. Neurosci. 17, 403–420.

Ohno, S. 1970. Evolution of Gene Duplication. Springer.

Okano, T., Kojima, D., Fukada, Y., Shichida, Y., and Yoshizawa, T. 1992. Primary structures of chicken cone visual pigments: vertebrate rhodopsins have evolved out of cone visual pigments. Proc. Natl. Acad. Sci. 89, 5932–5936.

Oprian, D. D., Asenjo, A. B., Lee, N., and Pelletier, S. L. 1991. Design, chemical synthesis, and expression of genes for the three human color vision pigments. Biochem. 30, 11367–11372.

Palacios, A. G., Goldsmith, T. H., and Bernard, G. D. 1996. Sensitivity of cones from a cyprinid fish (*Danio aequipinnatus*) to ultraviolet and visible light. Vis. Neurosci. 13, 411–421.

Parry, J. W. L. and Bowmaker, J. K. 2000. Visual pigment reconstitution in intact goldfish retina using synthetic retinaldehyde isomers. Vision Res. 40, 2241–2247.

Parry, J. W. L., Carleton, K. L., Spady, T., Carboo, A., Hunt, D. M., and Bowmaker, J. K. 2005. Mix and match color vision: tuning spectral sensitivity by differential opsin gene expression in Lake Malawi cichlids. Curr. Biol. 15, 1734–1739.

Parry, J. W. L., Peirson, S. N., Wilkens, H., and Bowmaker, J. K. 2003. Multiple photopigments from the Mexican blind cavefish, *Astyanax fasciatus*: a microspectrophotometric study. Vision Res. 43, 31–41.

Parry, J. W. L., Poopalasundaram, S., Bowmaker, J. K., and Hunt, D. M. 2004. A novel amino acid substitution is responsible for spectral tuning in a rodent violet-sensitive visual pigment. Biochemistry 43, 8014–8020.

Partridge, J. C. and Cummings, M. E. 1999. Adaptations of Visual Pigments to the Aquatic Environment. In: Adaptive Mechanisms in the Ecology of Vision (*eds*. S. N. Archer, M. B. A. Djamgoz, E. R. Loew, J. C. Partridge, and S. Valerga), pp. 251–283. Kluwer.

Partridge, J. C., White, E. M., and Douglas, R. H. 2006. The effect of elevated hydrostatic pressure on the spectral absorption of deep-sea fish visual pigments. J. Exp. Biol. 209, 314–319.

Pisani, D., Mohun, S. M., Harris, S. R., McInerney, J. O., and Wilkinson, M. 2006. Molecular evidence for dim-light vision in the last common ancestor of the vertebrates. Curr. Biol. 16, R318–R319.

Pointer, M. A., Cheng, C. H. C., Bowmaker, J. K., Parry, J. W. L., Soto, N., Jeffery, G., Cowing, J. A., and Hunt, D. M. 2005. Adaptations to an extreme environment: retinal organisation and spectral properties of photoreceptors in Antarctic notothenioid fish. J. Exp. Biol. 208, 2363–2376.

Raymond, P. A., Barthel, L. K., and Curran, G. A. 1995. Developmental patterning of rod and cone photoreceptors in embryonic zebrafish. J. Comp. Neurol. 359, 537–550.

Raymond, P. A., Barthel, L. K., Rounsifer, M. E., Sullivan, S. A., and Knight, J. K. 1993. Expression of rod and cone visual pigments in goldfish and zebrafish: a rhodopsin-like gene is expressed in cones. Neuron 10, 1161–1174.

Ripps, H. and Dowling, J. E. 1990. Structural features and adaptive properties of photoreceptors in the skate retina. J. Exp. Zool. Suppl. 5, 46–54.

Robinson, S. R. 1994. Early vertebrate colour vision. Nature, 367, 121.

Robinson, J., Schmitt, E. A., and Dowling, J. E. 1995. Temporal and spatial patterns of opsin gene expression in zebrafish (*Danio rerio*). Vis. Neurosci. 12, 895–906.

Robinson, J., Schmitt, E. A., Hárosi, F. I., Reece, R. J., and Dowling, J. E. 1993. Zebrafish ultraviolet visual pigment: absorption spectrum, sequence, and localization. Proc. Natl. Acad. Sci. 90, 6009–6012.

Saitou, N. and Nei, M. 1987. The neighbor-joining method: a new method for reconstructing phylogenetic trees. Mol. Biol. Evol. 4, 406–425.

Seehausen, O. 2000. Explosive Speciation Rates and Unusual Species Richness in Haplochromine Cichlid Fishes: Effects Of Sexual Selection. In: Advances in Ecological Research (*eds*. A. Rossiter and H. Kawanabe), Vol. 31, pp. 237–274. .

Shand, J. 1993. Changes in the spectral absorption of cone visual pigments during the settlement of the goatfish *Upeneus tragula*: the loss of red sensitivity as a benthic existence begins. J. Comp. Physiol. A 173, 115–121.

Shi, Y. S. and Yokoyama, S. 2003. Molecular analysis of the evolutionary significance of ultraviolet vision in vertebrates. Proc. Natl. Acad. Sci. 100, 8308–8313.

Shi, Y. S., Radlwimmer, F. B., and Yokoyama, S. 2001. Molecular genetics and the evolution of ultraviolet vision in vertebrates. Proc. Natl. Acad. Sci. 98, 11731–11736.

Sillman, A. J. and Dahlin, D. A. 2004. The Photoreceptors and Visual Pigments of Sharks and Sturgeons. In: The Senses of Fishes (*eds*. G. Von Der Emde, J. Mogdans, and B. G. Kapoor), pp. 31–54. Kluwer.

Sillman, A. J., Ronan, S. J., and Loew, E. R. 1993. Scanning electron-microscopy and microspectrophotometry of the photoreceptors of ictalurid catfishes. J. Comp. Physiol. A 173, 801–807.

Spady, T. C., Parry, J. W. L., Robinson, P. R., Hunt, D. M., Bowmaker, J. K., and Carleton, K. L. 2006. Evolution of the cichlid visual palette through ontogenetic subfunctionalization of the opsin gene arrays. Mol. Biol. Evol. 23, 1–10.

Stenkamp, D. L., Barthel, L. K., and Raymond, P. A. 1997. Spatiotemporal coordination of rod and cone photoreceptor differentiation in goldfish retina. J. Comp. Neurol. 382, 272–284.

Stenkamp, D. L., Hisatomi, O., Barthel, L. K., Tokunaga, F., and Raymond, P. A. 1996. Temporal expression of rod and cone opsins in embryonic goldfish retina predicts the spatial-organization of the cone mosaic. Invest. Ophthalmol. Vis. Sci. 37, 363–376.

Takechi, M. and Kawamura, S. 2005. Temporal and spatial changes in the expression pattern of multiple red and green subtype opsin genes during zebrafish development. J. Exp. Biol. 208, 1337–1345.

Tamura, T. and Wisby, W. J. 1963. The visual sense of pelagic fishes, especially on visual axis and accommodation. Bull. Mar. Sci. Gulf Caribb. 13, 433–448.

Theiss, S. M., Lisney, T. J., Collin, S. P., and Hart, N. S. 2007. Colour vision and visual ecology of the blue-spotted maskray, *Dasyatis kuhlii* Müller & Henle, 1814. J. Comp. Physiol. A 193, 67–79.

Thomson, K. S. 1993. The origin of the tetrapods. Am. J. Sci. 293A, 33–62.

Toyoda, J. I., Saito, T., and Kondo, H. 1978. Three types of horizontal cells in stingray retina: their morphology and physiology. J. Comp. Neurol. 179, 569–579.

Turner, G. F., Seehausen, O., Knight, M. E., Allender, C. J., and Robinson, R. L. 2001. How many species of cichlid fishes are there in African lakes? Mol. Ecol. 10, 793–806.

Van der Meer, H. J. and Bowmaker, J. K. 1995. Interspecific variation of photoreceptors in four coexisting haplochromine cichlid fishes. Brain Behav. Evol. 45, 232–240.

Walls, G. L. 1942. The Vertebrate Eye and Its Adaptive Radiation. Cranbrook Institute of Science.

Wilkie, S. E., Robinson, P. R., Cronin, T. W., Poopalasundaram, S., Bowmaker, J. K. and Hunt, D. M. 2000. Spectral tuning of avian violet- and ultraviolet-sensitve visual pigments. Biochem. 39, 7895–7901.

Whitmore, A. V. and Bowmaker, J. K. 1989. Seasonal variation in cone sensitivity and short-wave absorbing visual pigments in the rudd, *Scardinius erythrophthalmus*. J. Comp. Physiol. A 166, 103–115.

Wood, P. and Partridge, J. C. 1993. Opsin substitution induced in retinal rods of the eel (*Anguilla anguilla* (L.)): a model for G-protein-linked receptors. Proc. R. Soc. Lond. B 254, 227–232.

Yokoyama, S. 2000. Molecular evolution of vertebrate visual pigments. Prog. Ret. Eye. Res. 19, 385–419.

Yokoyama, S. and Radlwimmer, F. B. 2001. The molecular genetics and evolution of red and green color vision in vertebrates. Genetics 158, 1697–1710.

Yokoyama, S. and Tada, T. 2000. Adaptive evolution of the African and Indonesian coelacanths to deep-sea environments. Gene 261, 35–42.

Yokoyama, R. and Yokoyama, S. 1990. Convergent evolution of the red- and green-like visual pigment genes in fish, *Astyanax fasciatus*, and human. Proc. Natl. Acad. Sci. 87, 9315–9318.

Yokoyama, S., Radlwimmer, F. B., and Blow, N. S. 2000. Ultraviolet pigments in birds evolved from violet pigments by a single amino acid change. Proc. Natl. Acad. Sci. 97, 7366–7371.

Yokoyama, S., Zhang, H., Radlwimmer, F. B., and Blow, N. S. 1999. Adaptive evolution of color vision of the Comoran coelacanth (*Latimeria chalumnae*). Proc. Natl. Acad. Sci. 96, 6279–6284.

1.05 Phototransduction in Microvillar Photoreceptors of *Drosophila* and Other Invertebrates

R C Hardie and M Postma, University of Cambridge, Cambridge, UK

© 2008 Elsevier Inc. All rights reserved.

1.05.1	**Introduction**	80
1.05.2	**Photoreceptor and Retinal Morphology**	80
1.05.3	**Electrophysiology**	82
1.05.3.1	Invertebrate Photoreceptors Depolarize	82
1.05.3.2	Voltage-Clamped Light-Induced Current	82
1.05.3.3	Potassium Channels	85
1.05.3.4	Other Channels and Transporters	86
1.05.3.5	Intracellular Recordings of Voltage Responses	86
1.05.3.6	Electroretinogram	86
1.05.4	**Molecular Components of the Phototransduction Cascade**	87
1.05.4.1	Strategies for Gene Discovery	87
1.05.4.2	Rhodopsin	88
1.05.4.2.1	Chromophore	90
1.05.4.2.2	Invertebrate rhodopsins are bistable	91
1.05.4.3	Visual Pigment Cycle	92
1.05.4.3.1	Arrestins terminate active metarhodopsin	92
1.05.4.3.2	Arrestin translocation	93
1.05.4.3.3	Rhodopsin kinase and phosphatase	93
1.05.4.3.4	Arrestin phosphorylation	94
1.05.4.4	Heterotrimeric G Protein	95
1.05.4.4.1	G protein β and γ subunits	96
1.05.4.4.2	G_q translocation	97
1.05.4.5	Phospholipase C (NORPA)	97
1.05.4.5.1	Phospholipase C is also a GTPase-activating protein	98
1.05.4.5.2	Measuring phospholipase C activity	98
1.05.4.6	Light-Sensitive Channels *trp* and *trpl*	99
1.05.4.6.1	Structure of TRP and TRPL	100
1.05.4.6.2	Channel properties	101
1.05.4.6.3	*trp* and *trpl* phenotypes	102
1.05.4.6.4	TRPL translocation	103
1.05.4.7	INAF, a Novel Protein Required for TRP Function	103
1.05.4.8	Scaffolding Protein INAD	103
1.05.4.9	Myosin Kinase NINAC	104
1.05.5	**Messengers of Excitation**	104
1.05.5.1	Evidence for Activation by Lipid Messengers	104
1.05.5.2	PIP_2 Depletion	106
1.05.6	**Ca^{2+}-Dependent Feedback and Mechanisms of Adaptation**	108
1.05.6.1	Ca^{2+} Signals	109
1.05.6.1.1	Ca^{2+} signals are dominated by Ca^{2+} influx	109
1.05.6.1.2	Ca^{2+} transients in the rhabdomeres	110
1.05.6.1.3	Ca^{2+} buffers and homeostasis	110
1.05.6.2	Ca^{2+}-Dependent Negative Feedback	111
1.05.6.2.1	Calmodulin	113
1.05.6.2.2	Protein kinase C INAC	114

1.05.7	**Phosphoinositide Metabolism**	114
1.05.7.1	rdgA, Cytidine-5′-Diphosphate – Diacylglcerol Synthase, and Phosphatidylinositol Synthase	115
1.05.7.2	rdgB and Phosphatidylinositol Kinases	115
1.05.8	**Molecular Strategies of Quantum Bump Generation and Adaptation**	116
1.05.8.1	Compartmentalization and Local Signaling	116
1.05.8.2	Fast Nonlinear Response Kinetics	117
1.05.8.3	Quantum Bump Latency	118
1.05.8.4	Refractory Period	118
1.05.8.5	Adaptation	119
1.05.9	**Phototransduction Mechanisms in Other Invertebrates**	120
1.05.9.1	Other Arthropods	120
1.05.9.1.1	Limulus	120
1.05.9.1.2	Bee and crayfish	121
1.05.9.2	Mollusks	121
1.05.9.3	Annelids	122
1.05.10	**Conclusion**	122
References		123

Glossary

ankyrin repeats Protein-binding motifs.
Arr1 Arrestin 1.
Arr2 Arrestin 2.
ATP Adenosine 5′-triphosphate.
BAPTA 1,2-bis(*o*-aminophenoxy)ethane-*N*,*N*,*N*′,*N*′-tetraacetic acid, fast Ca^{2+}-specific chelator.
Ca orange Calcium indicator.
Ca ATPase ATP-dependent Ca^{2+} pump.
CaCaM Ca^{2+} calmodulin.
***caged Ca*$^{2+}$** Photolabile compound with tightly bound Ca^{2+} which can be released by photolysis.
Calliphora Blowfly.
calnexin Gene encoding a Ca^{2+}-binding, chaperone protein.
calphotin Gene encoding a Ca^{2+}-binding protein.
CalX *Drosophila* sodium/calcium exchanger, belonging to NCX family.
CaM Calmodulin.
CaMKII Calmodulin kinase II.
CBS Calmodulin-binding site.
CC Coiled-coil region.
CDP–DAG Cytidine 5′-diphosphate–diacylglycerol.
CDP–DAG synthase Enzyme that converts PA into CDP–DAG.
cds Gene encoding CDP–DAG synthase.
cGMP Cyclic guanosine 3,5-monophosphate.
clathrin A major constituent of the protein coat of vesicles formed during endocytosis.
CMP Cytidine 5′-monophosphate.
CNG Cyclic nucleotide gated.
CTP Cytidine 5′-triphosphate.
DA Dark adapted.
DAG Diacylglycerol.
DAG lipase Enzyme that converts DAG into PUFAs.
DGK Diacylglycerol kinase.
diptera Flies which only have a single pair of wings on the mesothorax.
Drosophila Fruitfly.
***EC*$_{50}$** The half-maximal concentration for excitation.
eGFP Enhanced green fluorescent protein.
EGTA Ethylene glycol tetraacetic acid, a slow Ca^{2+} chelator.
ER Endoplasmatic reticulum.
ERG Electroretinogram.
Fluo-3 Calcium indicator.
FRET Fluorescence resonance energy transfer.
G Heterotrimeric G protein.
GAP GTPase-activating protein.
GDP Guanosine 5′-diphosphate.
GPRK1 G protein-coupled receptor kinase.
***G*$_q$** PLC-activating G protein.
GTP Guanosine 5′-triphosphate.
GTPase GTP-hydrolyzing protein.
***G*α** Heterotrimeric G protein alpha subunit.
***G*β** Heterotrimeric G protein beta subunit.
***G*γ** Heterotrimeric G protein gamma subunit.

IC_{50} The half-maximal concentration for inhibition.
immunogold labeling Antibody labeling using colloidal gold, visible in electron microscope.
ina *i*nactivation *n*o *a*fterpotential gene.
INAC Eye-specific PKC encoded by *inaC* gene.
INAD Scaffolding protein encoded by *inaD* gene.
INDO-1 Calcium indicator.
$InsP_3$ Inositol 1,4,5 trisphosphate.
$InsP_3R$ $InsP_3$ receptor.
ipRGC Intrinsically photosensitive retinal ganglion cells.
Kir2.1 PIP_2-sensitive inward rectifier ion channel.
LA Light adapted.
laza Lazaro, gene encoding LPP.
LIC Light-induced current.
Limulus Horseshoe crab.
LMC Large monopolar cells (first-order visual interneurons).
LPP Lipid phosphate phosphohydrolase.
M Metarhodopsin.
Na/K ATPase Sodium–potassium pump.
NCKX Potassium-dependent sodium/calcium exchanger.
NCX Na/Ca exchanger with 3Na:1Ca stoichiometry.
nina no inactivation no afterpotential gene.
NINAC Class III myosin.
norp no receptor potential gene.
NORPA Eye-specific PLC encoded by *norpA* gene.
ocelli Small, dorsally located simple eyes.
ommatidium Cluster of photoreceptor cells and accessory cells underlying each facet lens of the compound eye.
opsin Light-sensitive transmembrane G protein-coupled receptor.
P Ionic permeability.
PA Phospatidic acid.
PC Phosphatidylcholine.
PDA Prolonged depolarizing afterpotential.
PDZ domain (PSD95, disks large, zonula adherens) protein binding domain, five of which are found in the scaffolding protein INAD.
phosrestin Alternative name for arrestin.
PI Phosphatidylinositol.
Pi Phosphate.
PI kinase Enzyme that phosphorylates PI-producing PIP.
PI synthase Enzyme that converts CDP–DAG into PI.
PIP Phosphatidylinositol 4-phosphate.
PIP kinase Enzyme that phosphorylates PIP-producing PIP_2.
PIP_2 Phosphatidylinositol 4,5-bisphosphate.
PITP PI transfer protein.
PKA Protein kinase A.
PKC Protein kinase C.
PLC Phospholipase C.
PLCβ Phospholipase Cβ.
PLD Phospholipase D.
PUFA Polyunsaturated fatty acid.
quantum bump Single-photon response.
R Rhodopsin.
R1–6 Major class of fly photoreceptor cells.
R7 and 8 Minor classes of fly photoreceptor cells.
rdg retinal degeneration gene.
3-hydroxy retinal Chromophore of dipteran opsins.
3-hydroxy retinol Sensitizing pigment.
RGS Regulator of G protein signaling.
rhabdomere Light-absorbing structure of the photoreceptor cell.
RK Rhodopsin kinase.
RyR Ryanodine receptor.
scaffolding protein A protein that binds multiple other proteins of different types.
serotonin A monoamine neurotransmitter.
Shab Potassium channel gene.
Shaker Potassium channel gene.
Shal Potassium channel gene.
signalplex The INAD complex (also referred to as transducisome).
SMC Submicrovillar cisternae.
thapsigargin Endoplasmic reticulum Ca^{2+}-ATPase inhibitor.
TRP Light-activated nonspecific cation channel encoded by *trp* gene.
trp *t*ransient *r*eceptor *p*otential gene.
TRPL Light-activated nonspecific cation channel encoded by *trpl* gene.
trpl *t*ransient *r*eceptor *p*otential-*l*ike gene.
TRPγ TRP homologue.
UV Ultraviolet light.
WT Wild type.

1.05.1 Introduction

The task of encoding visual information poses photoreceptors with a number of formidable and often conflicting challenges. They must maximize their sensitivity, by being able to absorb a high fraction of the incident light; at the same time they may need to optimize visual acuity, by keeping the cross-sectional area of the light-capturing organelle close to the wavelength of light. Maximum sensitivity also requires the ability to detect single photons, reliably and as rapidly as possible. In addition, they must be able to light adapt in order to operate over the vast environmental range of intensities, which span more than 10 orders of magnitude from starlight to direct sunlight. In the course of evolution, two major classes of ocular photoreceptors have become specialized to perform these functions: ciliary photoreceptors, typified by vertebrate rods and cones (see Phototransduction in Rods and Cones), and the microvillar, or rhabdomeric photoreceptors of many invertebrate groups, including arthropods and most mollusks.

Ciliary and microvillar photoreceptors diverged very early in metazoan evolution (Arendt, D., 2003), and their separate evolutionary histories have resulted in rather different biological solutions to the challenges photoreceptors face. Although all known ocular photoreceptors use rhodopsin to absorb the incident light energy, and a G-protein-coupled signaling cascade to transduce this into changes in conductances in the plasma membrane, the detailed biochemical pathways are quite distinct. Where studied, the transduction cascade of ciliary photoreceptors leads to metabolism of cyclic GMP (cGMP) and modulation of cyclic nucleotide-gated ion channels (CNG channels), whilst microvillar photoreceptors use the more widespread phosphoinositide cascade, characterized by the effector enzyme phospholipase C (PLC) and activation of nonselective cation channels, probably often belonging to the transient receptor potential (TRP) superfamily. Perhaps not surprisingly, the two classes of photoreceptors have in many respects functionally converged; however, there are several intriguing differences in performance. Most notably perhaps, vertebrate eyes usually solve the problems of absolute sensitivity, speed of response and dynamic range by using two classes of photoreceptors: rods, which can detect single photons with limited temporal resolution, but which saturate at moderate photon fluxes; and cones, which cannot detect single photons, but which respond rapidly and can light adapt to signal under the brightest daylight intensities (see Phototransduction in Rods and Cones). By contrast, many invertebrate photoreceptors not only detect single photons, they often do so more rapidly than rods and yet can still light adapt to signal in full sunlight, when photon fluxes per photoreceptor can exceed 10^6 effectively absorbed photons per second. This chapter attempts to describe the cellular and molecular mechanisms that underlie this performance, concentrating on the photoreceptors of the fruit fly *Drosophila,* which has become the preferred model of invertebrate phototransduction, primarily because of its enormous potential for genetic manipulation and analysis (reviewed in Montell, C., 1999; Minke, B. and Hardie, R. C., 2000; Hardie, R. C. and Raghu, P., 2001; Pak, W. L. and Leung, H. T., 2003). After introducing the structural and electrophysiological framework we consider the various molecular components and how they are regulated. We end by attempting to summarize our current understanding of the molecular strategies underlying the excitation and adaptation, and finally provide a brief overview of phototransduction mechanisms in some other invertebrate preparations.

1.05.2 Photoreceptor and Retinal Morphology

Rhodopsin is a transmembrane protein, and in order to maximize absorption of incident light most photoreceptors have evolved structures to increase the surface area of light-absorbing membrane. In vertebrate rods, these are the rod outer segments (ROS) consisting of stacks of internalized membranous disks. Many invertebrates, including arthropods and mollusks, utilize rhabdomeres, which consist of tightly packed arrays of microvilli. Rhabdomeres in *Drosophila* consist of ~30–50 000 microvilli, each 1–2 μm long and 60 nm in diameter (Figure 1). They develop from the apical surface of the cell to which they are attached by a narrow neck. Each microvillus contains ~1000 rhodopsin molecules closely packed in the microvillar membrane at a density of ~4000 μm^{-2}. Together, the microvilli form the rhabdomere, a 80- to100-μm-long and 1- to 2-μm-diameter tapering rod-like structure, which functions as a waveguide, trapping some 50% of the incident axial light at the wavelength of peak absorption (reviewed in Hardie, R. C., 1985).

Eight such photoreceptors are assembled in a so-called ommatidium behind each of the ~750 facets of the *Drosophila* compound eye. In cross section, the rhabdomeres form a precise hexagonal array with six

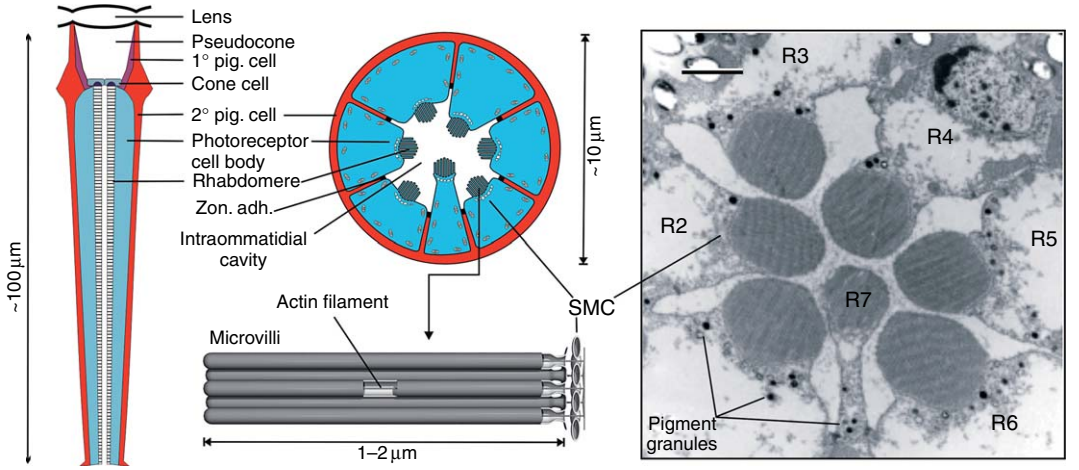

Figure 1 Photoreceptor and retinal morphology in *Drosophila*. Left: Schematic of ommatidium showing the photoreceptors with the microvillar rhabdomeres, surrounded by secondary pigment cells. Light is focussed on the rhabdomere tips by the overlying lens through the pseudocone. The pseudocone is filled with fluid secreted by the underlying cone cells (Semper cells), and surrounded by primary pigment cells. The schematic cross section shows the hexagonal array of rhabdomeres, projecting into the intraommatidial cavity. The central photoreceptor is R7 (an ultraviolet (UV) receptor), the rest are R1–6 cells. The eighth photoreceptor R8, whose rhabdomere is contiguous with that of R7, lies proximally in the ommatidium. The photoreceptors are connected by specialized junctions, called zonula adherens, or desmosomes, which separate the apical (medial) membrane of the cell from the basolateral membrane. The detailed schematic (below) shows how the rhabdomere is formed from tightly packed microvilli, with a system of submicrovillar cisternae (SMC) lining their base. Right: The electron micrograph shows the six R1–6 cells with large rhabdomeres and the central R7 cell; pigment granules can be seen close to the base of the rhabdomeres. Scale bar = 1 µm.

peripheral rhabdomeres (R1–6) all containing the same visual pigment (Rh1 with $\lambda_{max} = 480$ nm), and a central tiered rhabdomere (R7 in the distal two thirds of the ommatidium, R8 in the proximal third). R7 and R8 cells have a variety of visual pigments (λ_{max} ~340, 370, 440, and 510 nm), which subserve the fly's color vision. As far as is known, the basic mechanism of phototransduction is the same in the different classes of photoreceptors, and apart from the rhodopsins, there appear to be no cell-specific isoforms of the various component of the transduction cascade as is the case in vertebrate rods and cones (see Phototransduction in Rods and Cones). However, the majority of studies have been performed on the major class of photoreceptors, R1–6.

The rhabdomeres project toward the center of the ommatidium into a large extracellular space (the intraommatidial cavity), delimited by specialized junctions (desmosomes, or zonula adherens) between neighboring photoreceptors. Photoreceptors are derived from epithelial cells, and these junctions separate the apical (rhabdomere and stalks) membrane from the basolateral membrane, which forms the outer surface of the photoreceptor cluster (Figure 1). Unlike tight junctions, desmosomes do not represent a diffusion barrier between the intraommatidial cavity and the rest of the extracellular space (Chi, C. and Carlson, S. D., 1981). Completing the ommatidium are a number of accessory cells: four distal cone, or Semper cells, that form the floor of the fluid-filled transparent pseudocone, which forms the optical path between the rhabdomere tips and the facet lens; two primary pigment cells, which surround the distal ends of the photoreceptors and form the walls of the pseudocone, and 12 secondary and tertiary pigment cells, shared between ommatidia (Ready, D. F., 1989). Also referred to as pigmented glia, the pigment cells surround the photoreceptors, optically isolating the ommatidia over the depth of the retina. At the base of the retina, the R1–6 photoreceptors project short axons to the first neuropile (lamina), where they form histaminergic synapses with second-order cells, the large monopolar cells (Hardie, R. C., 1989; Sarthy, P.V., 1991). The microvilli contain no internal membranous structures; however, each contains a central F-actin filament. With appropriate fixation, the actin filament can be seen to be connected to the microvillar membrane via sidearms (see Figure 6), which may be formed by the class III unconventional myosin NINAC (Kumar, J. P. and Ready, D. F., 1995; Hicks, J. L. *et al.*, 1996). Closely apposed (10 nm) to the base of the microvilli, is an array of submicrovillar cisternae (SMC), which

are derived from smooth endoplasmic reticulum (ER). These have been considered to represent internal Ca^{2+} stores, and similar, more extensively developed structures in many arthropods (including bee and *Limulus*) mediate light-induced Ca^{2+} release (see Section 1.05.9, reviewed in Nasi, E. *et al.*, 2000). However, in *Drosophila* and many other Diptera, the SMC are much reduced in size with a very narrow lumen and it is questionable whether they perform any significant role in the release of Ca^{2+} (Section 1.05.6.1). They effectively form a fenestrated double-layered membranous curtain lining the bases of the microvilli and they may be more important as a site for PI recycling (Section 1.05.7), and also perhaps as a diffusion barrier or baffle between the rhabdomere and the rest of the cell.

The cell body contains numerous ~0.1 μm pigment granules, which migrate toward the rhabdomere in response to light, functioning as a cell autonomous pupil. Since the rhabdomere acts as a waveguide, a significant fraction of the light actually travels outside its perimeter (evanescent wave). The pupil pigment granules can therefore effectively bleed light from the rhabdomere, thereby attenuating up to 90–99% (Roebroek, J. G. H. and Stavenga, D. G., 1990) of the incident light. The pupil also significantly improves spatial resolution by narrowing the acceptance angle, whilst causing a blue shift in the spectral sensitivity (Hardie, R. C., 1979; Stavenga, D. G., 2004). Pupil pigment migration, which is intensity dependent, occurs over a time course of ~5 s following onset of illumination. The exact mechanism remains obscure, but it is Ca^{2+} dependent (Kirschfeld, K. and Vogt, K., 1980), and since it can be readily monitored with optical techniques in the intact animal, it can be used as an *in vivo* measure of photoreceptor performance and Ca^{2+} signaling (e.g., Hofstee, C. A. and Stavenga, D. G., 1996).

The immediately obvious function of the rhabdomeric structure is to provide the light capturing waveguide required for maximizing absorption whilst preserving spatial sensitivity. The parallel arrays of microvilli also provide the rhabdomere with an intrinsic dichroism, which forms the basis for the ability of arthropods and mollusks to detect and discriminate polarized light (Wehner, R., 1989). In addition, the microvillar structure is also the key to understanding many aspects of the photoreceptors' performance (see Section 1.05.8). All the major components of the transduction cascade, from rhodopsin to the light-sensitive channels are localized in the microvillus, and it seems likely that the immediate effect of single-photon absorption is more or less limited to activation of enzymes and channels in the microvillus where it was absorbed. This extreme compartmentalization is crucial for the rapid kinetics of the response to light, as it minimizes diffusional delays, and also greatly increases the effective concentration of molecular components and metabolic intermediates in the transduction cascade (see Section 1.05.8). For example, within the volume of one microvillus, just a single molecule represents a concentration of ~1 μM; whilst the average resting concentration of free Ca^{2+} (100–200 nM) would represent just one-quarter of a Ca^{2+} ion in solution at any one instant!

1.05.3 Electrophysiology

1.05.3.1 Invertebrate Photoreceptors Depolarize

Ever since the first photoreceptor intracellular recordings in the 1960s, it has been known that vertebrate photoreceptors hyperpolarize in response to light due to closing of cation channels, whilst most invertebrate ones depolarize. Under many conditions, this difference may be of minor functional significance, since both types of photoreceptors signal via graded potentials and under most situations are responding to fluctuations of intensity (contrast) around a mean background. However, there are important implications under certain conditions, such as the ability to detect single photons. In rods, there are ~10^4 channels open in the dark, and a large number need to be closed to make significant difference. Thus, a typical quantum bump in a vertebrate rod represents the closing of ~200 channels, generating a response of ~1 pA (see Phototransduction in Rods and Cones). By contrast, in microvillar photoreceptors the channels are closed in the dark, membrane resistance is at its highest, and only a few channels may need to be opened to generate a significant depolarization. Indeed, in *Drosophila* only ~15 channels are activated during a quantum bump (Henderson, S. R. *et al.*, 2000), generating a 10 pA current and a voltage response of ~1–2 mV in the intact eye (Wu, C. F. and Pak, W. L., 1978; Johnson, E. C. and Pak, W. L., 1986).

1.05.3.2 Voltage-Clamped Light-Induced Current

Because of their small size, intracellular recordings from *Drosophila* photoreceptors are technically challenging (see Section 1.05.3.4); however, it has also proved possible to record from single photoreceptors

using whole-cell patch clamp techniques from dissociated ommatidia of both pupae and young adults. This preparation, developed independently in two laboratories (Hardie, R. C., 1991a; 1991b; Ranganathan, R. *et al.*, 1991), allows isolation of the light-induced current (LIC) with excellent recording quality, whereby responses to single photons, single G proteins, and even single channels can be clearly resolved. This preparation, in combination with the molecular genetic potential of *Drosophila*, has been particularly important for recent advances in our mechanistic and quantitative understanding of phototransduction.

In the dark, photoreceptors have a resting potential of ~−70 to −80 mV, which is close to the potassium equilibrium potential (−85 mV) under standard recording conditions. The cells have a high input resistance (~2 GΩ) and a large capacitance (~60 pF), the majority (>80%) of which can be attributed to the surface area of the microvillar membrane. This results in a slow membrane time constant (12 ms for the dark-adapted (DA) values above), but intracellular recordings in the intact animal suggest that the membrane properties do not compromise the temporal resolution of even DA responses in the voltage domain, and may even be advantageous in filtering out high-frequency noise (Juusola, M. and Hardie, R. C., 2001).

An ongoing barrage of ~2 pA events at rates of 1–4 s^{-1} can be resolved in complete darkness (Figure 2), which is eliminated in mutants of the G protein α subunit and therefore probably represents activation of the cascade by spontaneous activation of single G proteins (Hardie, R. C. *et al.*, 2002). Recent evidence indicates that the rate is only kept this low by the presence of approximately twofold excess of G protein β subunits, and, the spontaneous dark noise is greatly increased in heterozygote mutations of Gβ when there are approximately equal numbers of β and α subunits (Elia, N. *et al.*, 2005). Much more rarely, random thermal rhodopsin isomerizations generate spontaneous quantum bumps at rates of less than 1 min^{-1} (Henderson, S. R. *et al.*, 2000).

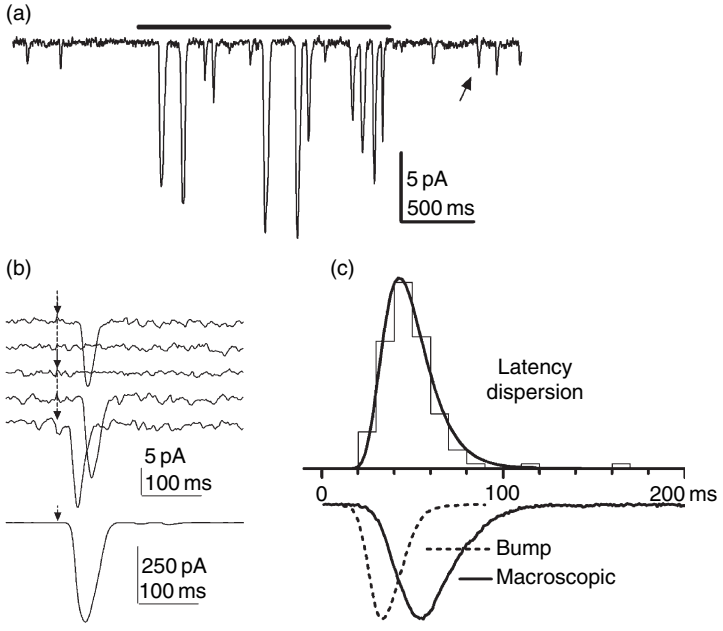

Figure 2 Quantum bumps. (a) Response of a whole-cell voltage-clamped photoreceptor to 2 s of dim illumination (~2 effectively absorbed photons per second, bar). In the dark, small ~2 pA events (e.g., arrow) are likely to represent spontaneous activation of single G proteins. Light induces a train of ~10 pA quantum bumps. (b) Responses to brief (1 ms) flashes (arrows), containing on average 0.5 effective photons. Some flashes induce no response (failures), others induce single quantum bumps with a variable latency; below, the macroscopic response of the same cell to a flash containing ~100 photons is broader than the individual quantum bumps. (c) Top: latency distribution (histogram) of quantum bumps elicited by brief flashes (as in (b)); below, normalized waveforms of quantum bump and macroscopic response. The smooth curve in the top trace, obtained by mathematically deconvolving the two waveforms, is an excellent fit to the latency distribution, confirming that the waveform of the macroscopic response represents the convolution of the bump latency distribution and bump waveform (Hardie, R. C; unpublished data; for further details, see Henderson, S. R. *et al.*, 2000).

With dim illumination individual quantum bumps can be clearly resolved (Figure 2). Strict adherence to Poisson statistics, as well as frequency of seeing curves, indicate that these represent responses to single-photon absorptions (Wu, C. F. and Pak, W. L., 1975; Henderson, S. R. *et al.*, 2000). The quantum bumps have a mean amplitude of ~10 pA (range ~2–20 pA) representing the simultaneous opening of ~15 channels. This is consistent with the opening of channels in a single microvillus, which, according to quantitative biochemical estimates in the larger fly *Calliphora*, should contain about 25 channels (Huber, A. *et al.*, 1996a). Quantum bumps have a duration (halfwidth) of ~20 ms and are generated with a characteristically variable latency of between ~20 and 100 ms (mean ~40–50 ms). Consequently, the waveform of the macroscopic response to brief flashes represents the convolution of the bump waveform and its latency dispersion. Unlike the situation in rods, voltage-clamped quantum bumps sum linearly over a large range, and the macroscopic response to brief flashes containing up to at least several hundred photons can be accurately reconstructed from the linear superposition of the underlying bumps (Henderson, S. R. *et al.*, 2000). The essential kinetic description of the DA flash response is thus embodied in the bump waveform and its latency distribution (Figure 2).

With longer steps of light, the bumps fuse to form a noisy maintained inward current, and as the intensity increases there is an increasingly rapid transition from peak to plateau representing the onset of light adaptation. At higher intensities this overshoots giving rise to what is effectively a damped oscillation (Figure 3(d)). Peak responses can greatly exceed 20 nA, but are not accurately voltage-clamped, whilst the steady-state plateau saturates at ~500 pA. Increments of intensity superimposed upon maintained backgrounds elicit responses with the classic features of light adaptation (Figure 4): gain is decreased as a function of background intensity, whilst the kinetics are significantly accelerated. In the current (voltage-clamped) domain, the shift of the response along the intensity (I) axis with light adaptation can simply be described as multiplicative reduction in gain (Gu, Y. *et al.*, 2005); in the voltage

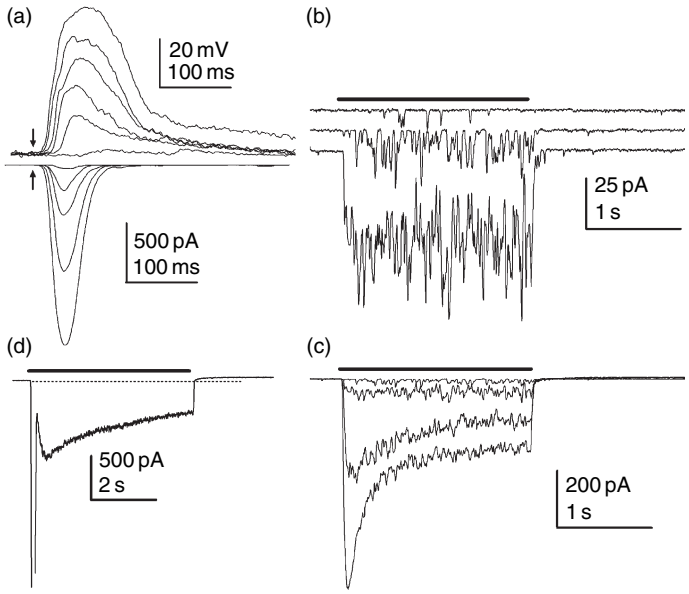

Figure 3 Whole-cell recordings of light responses in *Drosophila* photoreceptors. (a) Lower traces: Voltage-clamped responses recorded by whole-cell patch clamp from a dissociated ommatidium to brief (1 ms) flashes of increasing intensity (~5 to ~500 effective photons): responses in this range scale linearly with intensity. Upper family of traces: voltage recordings in current clamp mode from the same cell. (b–c) Responses to 2 s steps of light of increasing intensity (note different scales in (b) and (c)): bumps fuse to form noisy inward currents, which then show an increasingly rapid peak–plateau transition as intensity increases ((b): 3, 30, and 300 photons per second; (c) 30, 300, 3000, and 18 000 photons per second). This transition is a direct manifestation of light adaptation. (d) Response to a bright stimulus (3×10^5 photons per second), approximating daylight intensities: the peak response (>10 nA and off-scale) rapidly adapts, generating a notch before reaching a plateau that then slowly relaxes to the final steady-state level. After light off, there is a small outward current due to the electrogenic Na^+/K^+ ATPase (Hardie, R. C., unpublished data).

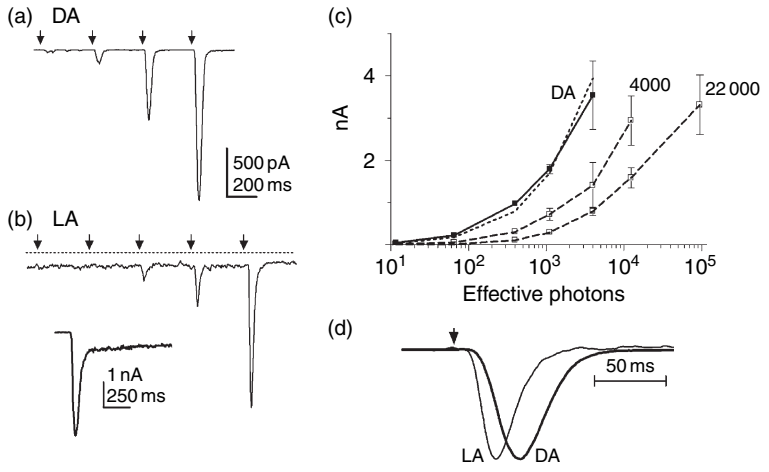

Figure 4 Light adaptation. (a) and (b) Voltage-clamped responses to brief (1 ms) flashes of increasing intensity in the dark, and the same flashes superimposed on a maintained background of ~22 000 effectively absorbed photons per second, generating a plateau response of ~150 pA (dotted line shows zero current). Inset shows the onset of the adapting light. (c) Response intensity functions from recordings, similar to those shown in (a) and (b), in dark-adapted (DA) and light-adapted (LA) states (intensity in effective photons per second). The DA response intensity function is accurately reproduced by simple linear scaling of a LA response intensity function (dotted line), indicating that light adaptation at this level can be simply described by a multiplicative reduction in gain. (d) Normalized flash responses of DA and LA responses show the acceleration in kinetics typical of light adaptation. Adapted from Gu, Y., Oberwinkler, J., Postma, M., and Hardie, R. C. 2005. Mechanisms of light adaptation in *Drosophila* photoreceptors. Curr. Biol. 15, 1228–1234, with permission.

domain, this translates into a more complex behavior (shifted $V/\log I$ functions, slope increasing with intensity) due to the passive and voltage-dependent properties of the membrane.

1.05.3.3 Potassium Channels

In the voltage domain, the overall response is further shaped by passive membrane properties, as well as a variety of voltage-sensitive conductances and electrogenic transporters. Dominant amongst these are at least four classes of potassium channels, which play important, though often subtle roles in shaping the voltage response.

1. A very rapidly activating and inactivating A current, I_A, encoded by the prototypical voltage-gated K^+ channel gene, *Shaker* (Hardie, R. C., 1991a; Hardie, R. C. *et al.*, 1991). The voltage operating range of this current is more negative (V_{50}act = −24 mV) than for other reported *Shaker* currents, though it can be shifted to a more positive range by serotonin (Hevers, W. and Hardie, R. C., 1995). Modeling and intracellular recordings from photoreceptors in the intact animal suggest that the voltage dependence of the so-called window current, representing the overlap of the steady-state activation and removal from inactivation voltage dependences, can effectively amplify voltage signals and thus results in a significant improvement in the information capacity (Niven, J. E. *et al.*, 2003). The *Shaker* channels are densely expressed on the outer (basolateral) membrane of the photoreceptors and are almost always encountered at high density in cell-attached patch recordings (Hardie, R. C., 1991a).
2. A slowly activating delayed rectifier, I_{Ks} (Hardie, R. C., 1991a), which is encoded by the *Shab* gene (Vahasoyrinki, M. *et al.*, 2006). Although generating similar sized currents to I_A, I_{Ks} channels are only very rarely encountered in cell-attached patch recordings, suggesting they have a different localization, possibly on the apical membrane. I_{Ks} has a more positive voltage operating range than I_A (V_{50} act = ~0 mV) and inactivates much more slowly with a time constant of ~1 s. This is the dominant maintained outward current at depolarized potentials, which would be predicted to counteract the depolarization and help prevent saturation. Interestingly, the *Shab* conductance is only expressed in R1–6, but not in R7 and R8 cells (Anderson, J. and Hardie, R. C., 1996).
3. A fast delayed rectifier, I_{Kf} with intermediate kinetics (inactivation $\tau \sim 50$ ms) and a slightly more negative operating range than I_A. From its properties, I_{Kf} is most likely encoded by *Shal*. This

conductance is found in R1–6, R7, and R8, but is not uniformly expressed, and is entirely lacking in some cells (Hardie, R. C., 1991a; Vahasoyrinki, M. *et al.*, 2006). One may speculate that it fine tunes the kinetics of the voltage output and may be expressed preferentially in certain eye regions with specific demands on temporal resolution.

4. A very slowly activating and noninactivating K current which has been revealed in *Sh;Shab* double mutants (Vahasoyrinki, M. *et al.*, 2006).

In addition, the photoreceptors may express two classes of Ca^{2+}-activated K channels (*Slo* and *Sk*), and preliminary data using intracellular voltage recording in the intact animal suggest that mutants lacking these channels have subtle defects in their peak-to-plateau transition (Wolfram, V., 2004).

1.05.3.4 Other Channels and Transporters

As well as K^+ channels, the photoreceptors also express a noninactivating voltage-gated Ca^{2+} conductance, which can be recorded in the cell body, but is presumably more important in synaptic release at the photoreceptor axon terminal (Hardie, R. C. and Mojet, M. H., 1995; Anderson, J. and Hardie, R. C., 1996). In addition, the photoreceptors exhibit inward rectification due to a hyperpolarization-activated chloride current (Hardie, R. C. and Minke, B., 1994b), recently characterized in detail by Ugarte G. *et al.* (2005), who suggest it is encoded by *clc-2*.

Finally, the photoreceptors express at least two electrogenic transporters:

1. A Na^+/K^+ ATPase, which is expressed predominantly on the basolateral surface of the cell away from the rhabdomere (Yasuhara, J. C. *et al.*, 2000). It generates an outward current (or afterhyperpolarization in the voltage domain) following bright stimulation (e.g., Figure 3) and can make a significant contribution to the depolarized plateau potential level (Jansonius, N. M., 1990).
2. An electrogenic Na^+/Ca^{2+} exchanger (*calx* gene), which is predominantly expressed in the microvillar membrane, and which can generate currents of up to ~100 pA (Hardie, R. C., 1995; Wang, T. *et al.*, 2005b). Belonging to the NCX family (Schwarz, E. M. and Benzer, S., 1997), it represents the dominant mechanism of Ca^{2+} extrusion, and plays an essential role in clearing the Ca^{2+} influx associated with the light-sensitive current (Wang, T. *et al.*, 2005b) (see also Section 1.05.6.1.2). A second, K^+-dependent Na^+/Ca^{2+} exchanger gene (NCKX) has also been reported to be expressed in the photoreceptors (Haug-Collet, K. *et al.*, 1999), but has not been detected electrophysiologically (Wang, T. *et al.*, 2005b).

1.05.3.5 Intracellular Recordings of Voltage Responses

Intracellular recordings of photoreceptors in the intact animal are demanding, and values for resting potential, and input resistance may often be underestimated due to the shunt resistance introduced by electrode penetration. The best recordings report resistances of up to ~200–500 MΩ, and resting potentials of ~−70 mV (Juusola, M. and Hardie, R. C., 2001). Apart from the shunt resistance, the difference between these values and values recorded in dissociated cells may also reflect the contribution from the axon terminal, which is severed during the dissociation. Thus, recent evidence suggests there is a significant depolarizing synaptic feedback at the receptor terminal, and when synaptic transmission was blocked by warming the temperature-sensitive *shibire* mutation, the photoreceptors hyperpolarized by a further 10–15 mV (Zheng, L. *et al.*, 2006). Responses to brief flashes show broadly similar kinetics to the LIC, but are slightly faster in rise time with a more skewed waveform; quantum bumps of ~1–2 mV can be resolved with dim illumination (Wu, C. F. and Pak, W. L., 1975; 1978). As in most arthropod photoreceptors, saturating responses reach ~70 mV, close to the reversal potential of the light-sensitive channels, with a maintained plateau of ~30 mV above resting potential. V/log I curves are sigmoidal, covering 4–5 log units of intensity with a log-linear region of ~2 log units.

Photoreceptors in wild type (WT) flies light adapt and continue responding to contrast fluctuations up until at least 10^6 effectively absorbed photons per second, equivalent to vision under the brightest daylight conditions. Contrast sensitivity and temporal resolution improve with light adaptation, allowing transmission of signals up to ~100 Hz (3 dB cutoff at 25 Hz) with an information capacity of ~200 bits per second at 25 °C (Juusola, M. and Hardie, R. C., 2001).

1.05.3.6 Electroretinogram

Extracellular electroretinogram (ERG) recordings can be made straightforwardly with an electrode placed on the surface of the cornea (Figure 5). The

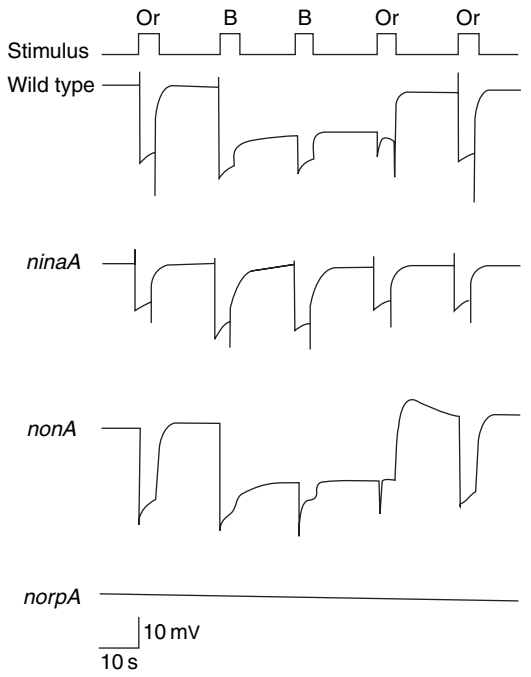

Figure 5 Electroretinogram (ERG) recordings. In a wild-type (WT) fly a 5 s pulse of orange light elicits a typical ERG with on and off transients and a maintained corneal negative component. At light off, the potential returns rapidly to baseline; however, a blue stimulus which converts >50% of R to M, creates a prolonged depolarizing afterpotential (PDA), whilst a second blue test flash elicits a much reduced (inactivated) response lacking the transients, and which is primarily mediated by the R7 cells. A subsequent orange stimulus, which reconverts M to R, terminates the PDA and restores sensitivity. In the *no inactivation no afterpotential* mutant, *ninaA*, there is no PDA and no loss of sensitivity (inactivation) to the second blue test flash. This is the classical *nina* phenotype found in a variety of mutants that have low levels of rhodopsin (*ninaA* encodes a chaperone required for rhodopsin folding and targeting). The *nonA* mutant lacks the on and off transients, but is otherwise normal, suggesting a defect in synaptic transmission. The *norpA* mutant (encoding PLC) has no detectable response. Reproduced with permission from Pak, W. L. 1995. *Drosophila* in vision research: the Friedenwald lecture. Invest. Ophthalmol. Vis. Sci. 36, 2340–2357.

ERG represents the summed activity of all the photoreceptors, and also higher-order neurons and glial cells. The sustained corneal negative component of the response is maximally ~20–30 mV. It is normally attributed to the photoreceptors, although experiments using a perfused preparation suggest caution in interpretation, since with bright light, slow components in particular may become dominated by depolarization of the pigmented glia (secondary pigment cells) by the build up of extracellular K^+ (Minke, B., 1982; Minke, B. and Selinger, Z., 1992). Nevertheless, it reflects indirectly at least the photoreceptor response and has been widely used as an easily recorded measure of photoreceptor output. The ERG also has rapid on (positive) and off (negative) transients, which reflect the activity of the second-order interneurons (large monopolar cells or LMCs) which have an amplified and transient response of inverted polarity due to sign-inverting synapses using the photoreceptor neurotransmitter, histamine, which activates histamine-gated chloride channels on the LMCs (Hardie, R. C., 1989).

1.05.4 Molecular Components of the Phototransduction Cascade

1.05.4.1 Strategies for Gene Discovery

The discovery and characterization of the molecular components of the transduction cascades in vertebrates and invertebrates (Figures 6 and 7) exploited two very different approaches. In vertebrates the ability to isolate ROS *en masse*, particularly from bovine retina, greatly facilitated the purification, and subsequent molecular identification of the elements of the cascade (see Phototransduction in Rods and Cones). In invertebrates, discovery relied in the first instance on classical forward genetic approaches in *Drosophila* to identify and positionally clones genes involved in phototransduction. The pioneers in this enterprise, starting in the late 1960s were Seymour Benzer (Hotta, Y. and Benzer, S., 1970) and Bill Pak (Pak, W. L. *et al.*, 1970). Benzer had a wider agenda, wanting to identify genes involved in vision generally, and thus isolated behavioral mutants defective in phototaxis. Pak was more focussed on the early events in vision and embarked upon a labor intensive, but ultimately rewarding electrophysiological screen to detect subtle defects using the readily recorded ERG.

At least 50 different complementation groups representing distinct genes were isolated. Some 30 of these had defects in the ERG transients and represent genes involved in synaptic transmission or responses of second-order neurons. Most of the remainder have turned out to be photoreceptor genes, many of which are directly involved in the transduction cascade (Table 1; reviewed in Pak, W. L., 1995; Pak, W. L. and Leung, H. T., 2003). A number of important genes were not discovered in these early screens, but were identified by molecular

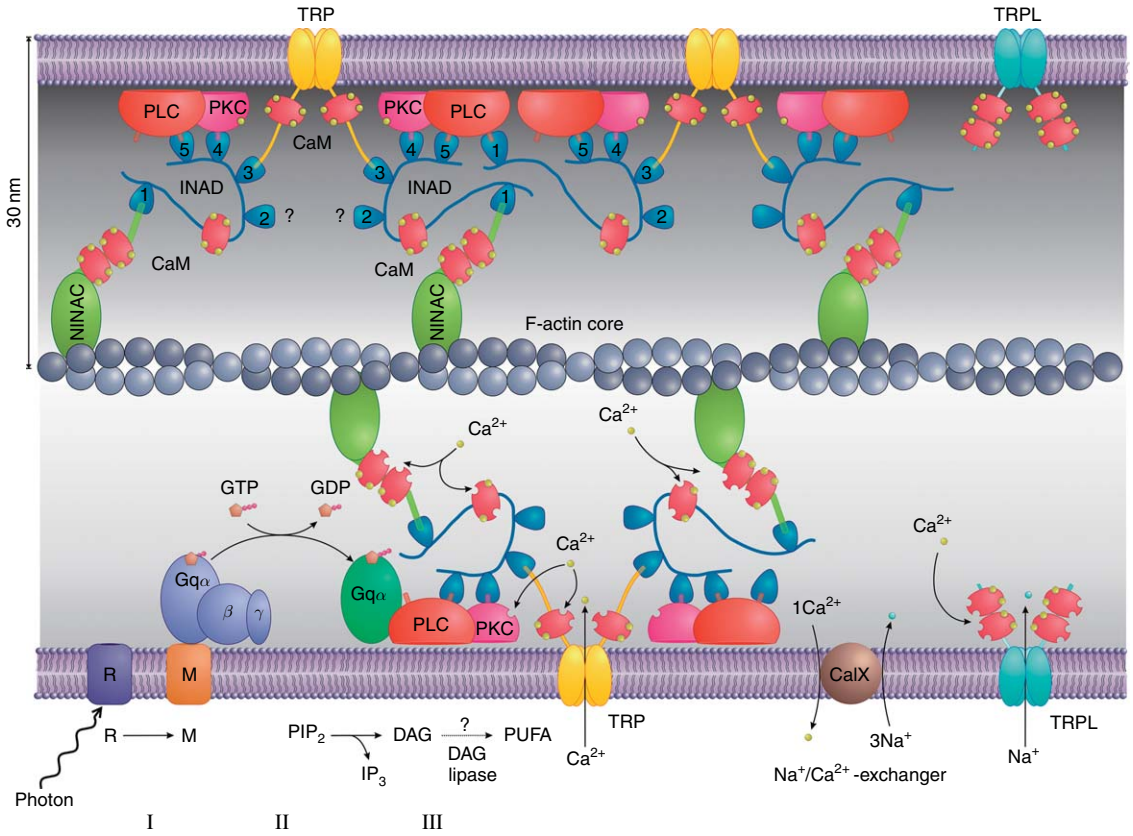

Figure 6 Overview of the phototransduction cascade in *Drosophila*. Lower half: (I) Photoisomerization of rhodopsin (R, encoded by *ninaE* gene) to metarhodopsin (M) activates G_q via GTP–GDP exchange, releasing the $G_q\alpha$ subunit (*Gαq* gene); (II) $G_q\alpha$ activates phospholipase C (PLC, *norpA* gene), generating $InsP_3$ and DAG from PIP_2. DAG is also a potential precursor for polyunsaturated fatty acids (PUFAs) via DAG lipase; although PUFAs can activate the channels, there is no direct evidence for this enzyme in the cascade. (III) Two classes of light-sensitive channels (*trp* and *trpl* genes) are activated by an unknown mechanism. TRP is primarily Ca^{2+} permeable; Ca^{2+} influx feeds back at multiple sites, including calmodulin (CaM), which itself has multiple targets, and PKC (see Section 1.05.6, Table 3). Ca^{2+} is extruded by the CalX Na^+/Ca^{2+} exchanger. All components drawn approximately to scale within a schematic microvillus. Upper half: Several components of the cascade, including TRP, protein kinase C (PKC, *inaC* gene), and PLC are assembled into a signaling complex by the scaffolding protein, INAD, which may be linked to the F-actin core via the NINAC class II myosin. The INAD protein contains five PDZ domains (1–5) joined by short linker regions. Each PDZ domain associates preferentially with different targets (Huber, A. *et al.*, 1996a; Shieh, B. H. and Zhu, M. Y., 1996; Chevesich, J. *et al.*, 1997; Tsunoda, S. *et al.*, 1997; Xu, X. Z. S. *et al.*, 1998). The precise composition of the native complex is uncertain as some PDZ domains are reported to bind at least two different targets, and there are several possibilities for multimerization: by homophilic interactions between INAD (PDZ domains 3 and 4) (Xu, X. Z. S. *et al.*, 1998); involvement of up to four TRP subunits and linkage of two INAD molecules via PLCβ which is reported to bind both PDZ1 and PDZ5 (van Huizen, R. *et al.*, 1998). Several of these scenarios are depicted in the figure. CaM binds to the linker region between PDZ1 and PDZ2 (Xu, X. Z. S. *et al.*, 1998) and also to NINAC, TRP, and TRPL.

approaches, such as subtractive hybridization and/or homology to vertebrate genes. Mutants of several these, including arrestin (Dolph, P. J. *et al.*, 1993), G protein (Scott, K. *et al.*, 1995), and the TRPL light-sensitive channels (Niemeyer, B. A. *et al.*, 1996), were generated in a second wave of mutagenesis based on antigenicity, that is, using antibodies to screen for mutants generated by random chemical mutagenesis lacking the proteins in question (see also Koundakjian, E. J. *et al.*, 2004).

1.05.4.2 Rhodopsin

The *n*o *i*nactivation *n*o *a*fterpotential E (*ninaE*) mutant was isolated by Pak and coworkers using the ERG screen (Figure 5). Even before it was cloned, it

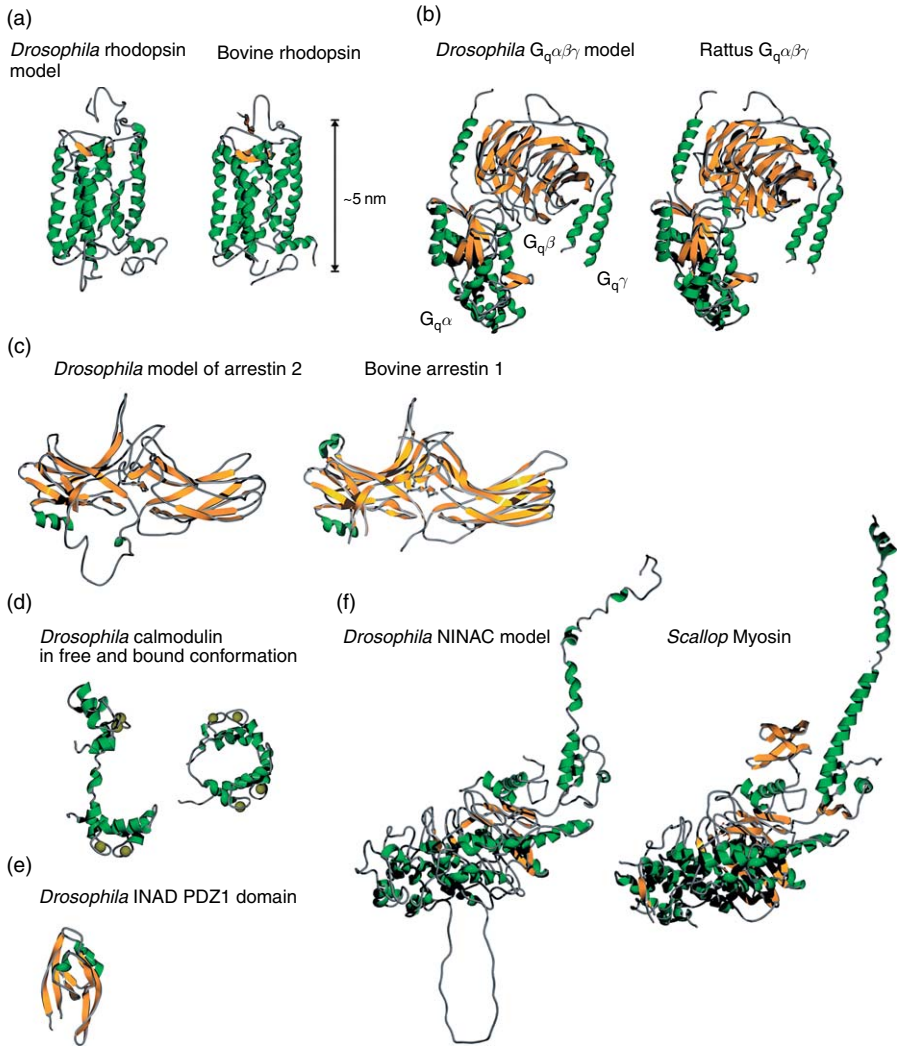

Figure 7 Molecular models of some key transduction proteins. Modeled protein structures of several proteins involved in fly phototransduction based on solved crystal structures of homologous proteins. (a) The solved structure of bovine rhodopsin (left structure, 1F88) was used to model *Drosophila* rhodopsin (*ninaE*). (b) Vertebrate (*Rattus*, 1GP2) G_q was used to model the structure of *Drosophila* G_q. (c) Bovine arrestin 1 (1G4R) was used to model the structure of *Drosophila* arrestin 2. (d) Structure of free and α-helix-bound *Drosophila* CaM (4CLN, 2BBN). (e) Structure of the first PDZ domain (PDZ1, 1IHJ) of *Drosophila* INAD, the other four PDZ domains have similar sizes (1IHJ). (f) Structure of single-headed scallop myosin (1B7T) used to model *Drosophila* NINAC. The models were generated using Geno3D (Geourjon, C. *et al.*, 2001; Combet, C. *et al.*, 2002). References: 1F88 (Palczewski, K. *et al.*, 2000); 1GP2 (Wall, M. A. *et al.*, 1995); 1G4R (Han, M. *et al.*, 2001); 1B7T (Houdusse, A. *et al.*, 1999); 4CLN (Taylor, D. A. *et al.*, 1991); 2BBN (Ikura, M. *et al.*, 1992); 1IHJ (Kimple, M. E. *et al.*, 2001).

was implicated as the gene encoding rhodopsin in R1–6 (Rh1) since it affected the visual pigment concentration in a gene dosage-dependent manner (Scavarda, N. J. *et al.*, 1983). It was cloned and sequenced a couple of years after vertebrate rhodopsin (O'Tousa, J. E. *et al.*, 1985), itself the first member of the G-protein-coupled receptor (GPCR) family, with the now classical seven transmembrane helix structure (Figure 7). Rh1 (*ninaE*) shares ~36% identity with bovine rhodopsin, including the lysine in the seventh transmembrane helix, which forms the covalent Schiff base linkage with the chromophore, and potential phosphorylation sites near the C-terminal. Six further genes with a similar *nina* mutant ERG phenotype are involved either in rhodopsin trafficking (*ninaA, calnexin*) (Baker, E. K. *et al.*, 1994; Rosenbaum, E. E. *et al.*, 2006), or chromophore production (*ninaB*, *ninaD*, *ninaG*, and *pinta*, see below).

Table 1 List of mutants of genes involved in *Drosophila* phototransduction, all of which have been cloned and sequenced

Mutant	*Protein*	*Function*
Excitation		
Gαq	G_q α subunit	Heterotrimeric G protein
Gβe	G_q β subunit	Heterotrimeric G protein
InaD	PDZ domain scaffolding protein	Signalplex scaffold
inaF	Novel	Required for TRP function
ninaE	Rhodopsin (Rh1)	Visual pigment
norpA	Phospholipase Cβ	Key effector enzyme
trp	TRP channel	Light-sensitive channel
trpl	TRPL channel	Light-sensitive channel
Deactivation and adaptation		
arr1	39-kDa arrestin1	Rhodopsin endocytosis
arr2	49-kDa arrestin 2	Rhodopsin deactivation
cam	Calmodulin	Ca^{2+}-dependent inactivation and Ca^{2+} buffer
inaC	Protein kinase C	Ca^{2+}-dependent inactivation
ninaC	Class III myosin kinase	CaM binding, response inactivation
rdgA	DAG kinase	Response termination, PIP_2 recycling
Phosphoinositide turnover		
cds	CDP–DAG synthase	PIP_2 recycling
laza	Lipid phosphate phosphohydrolase	DAG production from PA
rdgB	PITP	PIP_2 recycling
Calcium homeostasis		
calnexin	Calnexin	Rh1 chaperone and Ca^{2+} buffer
calphotin	Ca^{2+}-binding protein	Ca^{2+} buffer
calx	Na^+/Ca^{2+} exchanger	Ca^{2+} extrusion
Rhodopsin and chromophore biogenesis and pigment cycle		
ninaA	Peptidyl-prolyl *cis–trans* isomerase (cyclophilin)	Rh1 chaperone
ninaB	Dioxygenase	Chromophore synthesis
ninaD	Class B scavenger receptor	Chromophore synthesis (carotenoid uptake)
ninaG	Oxidoreductase	Chromophore synthesis
pintA	Retinoid-binding protein	Vitamin A uptake into pigment cells
rdgC	Rhodopsin phosphatase	Rhodopsin dephosphorylation
GPRK1	Rhodopsin kinase	Rhodopsin phosphorylation

Mutant genes have been classified according to their major function – excitation, deactivation, PI turnover, Ca^{2+} homeostasis, and visual pigment cycle and biogenesis (not mutually exclusive, though each gene listed only once). References in text.

An additional five *Drosophila* opsin genes, identified by homology to Rh1, account for the visual pigments of the ocelli (Rh2) and the various spectral classes of R7 (Rh3 and Rh4), and R8 (Rh5 and Rh6) (Feiler, R. *et al.*, 1992; Salcedo, E. *et al.*, 1999).

More than 60 invertebrate opsin genes have been cloned in the meantime (reviewed in Gärtner, W., 2000), and although recognizable as such they form a distinct subfamily from the majority of vertebrate opsins. An intriguing exception is melanopsin (Provencio, I. *et al.*, 1998), which appears to belong within the invertebrate opsin family, but is a vertebrate opsin found in a recently discovered novel class of intrinsically photosensitive retinal ganglion cells (ipRGCs). Melanopsin mediates a range of nonvisual responses such as circadian entrainment and the pupillary response (reviewed in Fu, Y. *et al.*, 2005). The ipRGCs also respond to light by depolarization, and at least in heterologous expression systems, melanopsin has been found to activate a G_q/PLC/TRP cascade as in invertebrates (Melyan, Z. *et al.*, 2005; Panda, S. *et al.*, 2005; Qiu, X. *et al.*, 2005).

1.05.4.2.1 Chromophore

Unusually, the chromophore of *Drosophila* opsin, as in most Diptera and a few other insect orders, is not retinal but a hydroxylated derivative, 11-*cis* 3-hydroxy retinal (Figure 8; Vogt, K. and Kirschfeld, K., 1984). Whilst this appears to function in an essentially identical manner to the more conventional 11-*cis* retinal, Diptera are remarkable in also using a second chromophore, 3-hydroxy retinol, that functions as a sensitizing or antenna pigment (Kirschfeld, K. and Franceschini, N., 1977). The

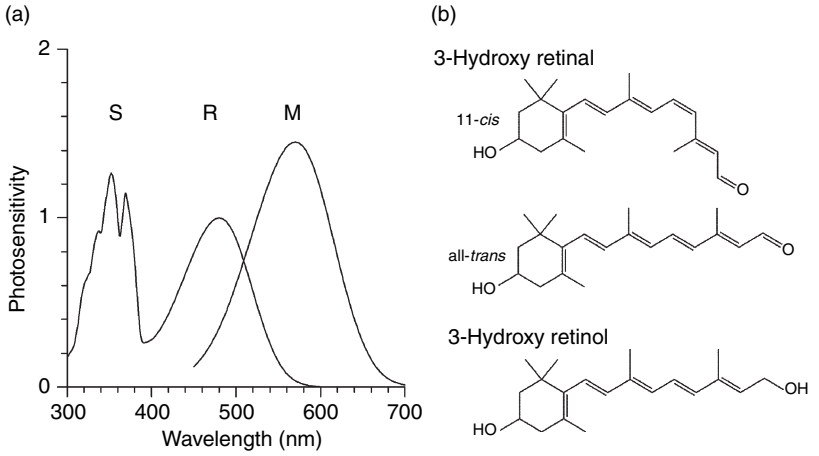

Figure 8 Chromophores and absorption spectra. Left: Idealized photosensitivity spectra of the Rh1 pigment system in *Drosophila* R1–6 cells, normalized to the rhodopsin (R) peak. Responses in the UV (300–400 nm) are primarily mediated by absorption of the sensitizing pigment (S: 3-hydroxy retinol), which transfers the energy of absorption to the chromophore proper (11-*cis* 3-hydryoxy retinal), which absorbs maximally at 480 nm in Rh1. Photoisomerization to all-*trans* 3-hydroxy retinal converts R to metarhodopsin (M), which absorbs maximally at 570 nm. The sensitizing pigment can also transfer energy to M, which is thus also effectively photoisomerized by UV light (not shown). Spectra based on rhodopsin nomograms (Govardovskii, V. I. *et al.*, 2000), combined with estimates of the sensitizing pigment spectrum. Right: Chemical structures of the chromophores of R and M (11-*cis* and all-*trans* 3-hydroxy retinal) and the sensitizing pigment (3-hydroxy retinol).

sensitizing pigment has a characteristic three-fingered absorption peak in the ultraviolet (peaks at ~330, 350, and 370 nm). It transfers the energy of an absorbed photon by fluorescence resonance energy transfer (FRET) to the chromophore proper, which then photoisomerizes exactly as if it had absorbed the photon directly (Kirschfeld, K. *et al.*, 1983). This rare biological example of FRET enhances quantum catch by extending the spectral sensitivity of the photoreceptors into the ultraviolet (Figure 8).

Recent biochemical and mutant analysis has identified several key genes required for chromophore production, including a class B scavenger receptor (*ninaD*), required for cellular uptake of dietary carotenoids (Kiefer, C. *et al.*, 2002), and a dioxygenase (*ninaB*), which cleaves the 40C carotenoids into the 20C chromophore precursor, vitamin A (all-*trans* retinol) (von Lintig, J. and Vogt, K., 2000; von Lintig, J. *et al.*, 2001). Whilst these stages take place outside the retina (Gu, G. *et al.*, 2004), uptake of vitamin A into the retina probably occurs first in the pigment cells, with the essential involvement of a recently identified retinal-binding protein, PINTA (Wang, T. and Montell, C., 2005). Finally, oxidization of the retinal ring to generate the hydroxylated 3-hydroxy retinal appears to take place in the photoreceptors via an oxidoreductase encoded by the recently discovered *ninaG* gene (Sarfare, S. *et al.*, 2005).

1.05.4.2.2 Invertebrate rhodopsins are bistable

Although *de novo* biosynthesis of chromophore from carotenoids is relatively complex, chromophore recycling following photoisomerization is much simpler than in vertebrates. Most invertebrate rhodopsins represent bistable, photointerconvertible pigment systems, whereby all-*trans* retinal can be directly reconverted to 11-*cis* by absorption of a second photon whilst still attached to the opsin. *Drosophila* Rh1, which has been extensively studied, absorbs maximally in the blue–green (480 nm), and on absorption of a photon, the 11-*cis* to all-*trans* isomerization leads to generation of a metarhodopsin (M) absorbing maximally at 570 nm (Figure 8). Metarhodopsin is thermostable, but can be photoisomerized back to the rhodopsin state (R) by absorption of a further photon. Such a bistable pigment system reaches a photoequilibrium determined by the spectral content of the illuminating light and the absorption spectra of the R and M states (reviewed in Hillman, P. *et al.*, 1983; Hardie, R. C., 1985; Stavenga, D. G., 1996). It is no coincidence that the screening pigments in the eye are transparent to long-wavelength (red) light – hence the red eye color

of most flies – and the red light diffusing through the eye reconverts M, ensuring that there is always a high fraction of R (reviewed in Hardie, R. C., 1986). Compared to the complex chromophore recycling of the vertebrate retina, this would appear to represent a much more efficient, rapid, and economical mechanism for pigment regeneration.

Under experimental conditions, however, particularly with white-eyed mutants lacking the screening pigments, or in biochemical preparations of purified photoreceptor membranes, it is possible to generate essentially any photoequilibrium simply by adjusting the wavelength of illumination. With blue light, which favors R → M conversion, up to ~80% of the pigment can be converted to the M form (it is not possible to create more than this as both R and M have second, overlapping photosensitivity peaks at short wavelengths due to β absorption peaks and sensitizing pigment). When flashes are delivered that result in more than ~20% of the pigment being converted to M, the photoreceptors develop a prolonged depolarizing afterpotential (PDA), that can last for several hours (Figure 5). This is because thermostable M remains active and capable of exciting the phototransduction cascade until it is inactivated by binding to arrestin (see Section 1.05.4.3.1). The photoreceptors contain only one arrestin molecule for every five rhodopsins, and thus, once more than 20% of the pigment exists in the M state, all arrestin is bound to M, and any further M molecules generated can no longer be inactivated. Although the PDA may last for several hours in *Drosophila*, it can be terminated at any time simply by delivering a bright long-wavelength (e.g., orange/red) flash, which inactivates M by reconverting it to R (Figures 5 and 9).

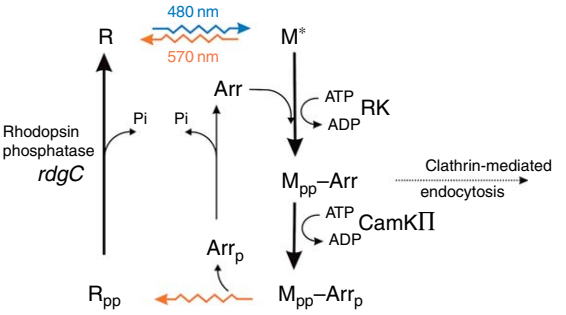

Figure 9 Visual pigment cycle in *Drosophila*. Photoisomerization of rhodopsin (R) by blue light (480 nm) generates active metarhodopsin (M^*). M^* is thermostable and continues to activate G_q until it binds arrestin (Arr). Arr2 is the dominant arrestin, but Arr1 can perform this function more slowly in its absence. M is also multiplely phosphorylated by rhodopsin kinase (RK), but this is not required for Arr2 binding and may even occur after Arr2 binding (Plangger, A. *et al.*, 1994). The M_{pp}–Arr state is a target for clathrin-mediated endocytosis, but this is inhibited by the CaMKII-dependent phosphorylation of Arr2 (Alloway, P. G. *et al.*, 2000; Kiselev, A. *et al.*, 2000b). Reconversion of M_{pp} to R_{pp} leads to the release of Arr_p. Finally, R_{pp} is dephosphorylated by the CaCaM-dependent rhodopsin phosphatase (encoded by *rdgC*) to recreate the ground state, R (Byk, T. *et al.*, 1993; Lee, S. J. and Montell, C., 2001).

1.05.4.3 Visual Pigment Cycle

1.05.4.3.1 Arrestins terminate active metarhodopsin

Arrestins are small soluble cytosolic proteins implicated in response termination and trafficking of most G-protein-coupled receptors. *Drosophila* photoreceptors express two arrestin isoforms: a 39 kDa protein (Arr1, originally called phosrestin 2) and 49 kDa Arr2 (or phosrestin 1). Arr2 is approximately fivefold more abundantly expressed than Arr1, and apart from Rh1 is the most abundant protein in the retina. As such, it was the only element of the cascade to be sequenced by protein purification and microsequencing (Yamada, T. *et al.*, 1990), whilst Arr1 was cloned by a subtractive hybridization strategy (Hyde, D. R. *et al.*, 1990). Both share ~40% identity with human arrestin, showing closer similarity to β-arrestins than the vertebrate visual arrestins (Figure 7). Mutants of both *arr1* and *arr2* genes were isolated by screening for loss of protein in Western blots (Dolph, P. J. *et al.*, 1993). As expected from its abundance, Arr2 is dominant with respect to inactivation of M. Thus *arr1* mutants have no overt physiological phenotype, though they undergo light-independent degeneration (Satoh, A. K. and Ready, D. F., 2005). By contrast, *arr2* mutants have a pronounced deactivation defect, with responses to brief flashes decaying slowly over 1–2 s (Figure 10). *arr2* mutants also enter a PDA state with much lower levels of illumination (Dolph, P. J. *et al.*, 1993). Although these phenotypes indicate that Arr2 binding to M is the dominant mechanism of M inactivation, Arr1 is also capable of binding to and inactivating M, since response deactivation in *arr1*;*arr2* double mutants lacking both arrestin isoforms is at least 10× slower than in *arr2* alone (Dolph, P. J. *et al.*, 1993). A recent study indicates that Arr1 also has a dedicated role in light-induced Rh1 endocytosis, a generic mechanism of receptor turnover found in most G-protein-coupled signaling cascades required for receptor turnover and cell maintenance (Satoh, A. K. and Ready, D. F., 2005).

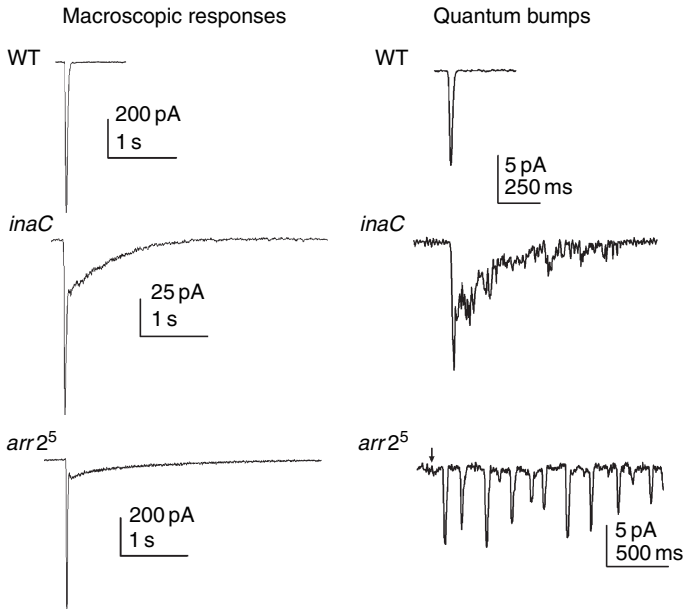

Figure 10 Responses in inactivation mutants. Left: Whole-cell voltage-clamped responses to brief (1 ms) flashes of light in wild type (WT) and two mutants (*inaC* and *arr2*^{5}) with defects in inactivation. Right: Quantum bumps elicited by single-photon absorptions in the same mutants. Macroscopically, both *inaC* and *arr2* mutants show a similar inactivation defect, with responses decaying over a period of 1–2 s. In the PKC mutant *inaC*, this defect is recapitulated in the bump waveform, and is due to a defect late in the transduction cascade (failure to inactivate PLC and the channels); however, in the arrestin 2 mutant (*arr2*^{5}) the defect manifests itself as a train of multiple bumps in response to a single absorbed photon, and represents a failure to terminate the activity of active metarhodopsin (Hardie, R. C., unpublished data; see also Hardie, R. C. *et al.*, 1993; Scott, K. *et al.*, 1997; Gu, Y. *et al.*, 2005).

1.05.4.3.2 Arrestin translocation

Light-induced translocation of components of the transduction cascade in both vertebrates and invertebrates has recently been appreciated as an important and widespread phenomenon, likely to be involved in long-term light and dark adaptation (reviewed in: Arshavsky, V. Y., 2003; Frechter, S. and Minke, B., 2006). In *Drosophila*, both arrestins, along with the G protein and the TRPL channel, have been reported to translocate in response to illumination. In DA cells most Arr2 is distributed throughout the cytosol, with only ~30% immunolocalized in the rhabdomeres, whilst Arr1 is only detectable in the cytosol; however, within 5 min of illumination by white or blue light, both Arr2 and Arr1 are predominantly localized in the rhabdomere (Lee, S. J. *et al.*, 2003; Satoh, A. K. and Ready, D. F., 2005). Arr2 remains in the rhabdomere during illumination, returning slowly (within 3 h) to the cytosol in the dark (Figure 11). The translocation of Arr2 into the rhabdomeres appears to have physiological consequences, as the ERG response to bright stimuli terminated more quickly in flies that had been preexposed to light to stimulate translocation (Lee, S. J. *et al.*, 2003). Arr1 translocation is more dynamic and transient, and even in continuous illumination Arr1 retreats from the rhabdomere within 30 min and is then found internalized in vesicles in association with Rh1 (Figure 11), indicative of a role in physiological Rh1 endocytosis (Satoh, A. K. and Ready, D. F., 2005).

Lee S. J. *et al.* (2003) found that Arr2 binds to PIP_3 *in vitro* (and less avidly to PIP_2), and that translocation was disrupted by neutralization of three basic residues in Arr2 required for this interaction (lysines 228, 231, and 257), or by genetic manipulation of PIP_3 metabolism. Lee S. J. and Montell C. (2004) also reported that translocation was disrupted in *ninaC* mutants (see Section 1.05.4.9) and proposed a model whereby Arr2 is transported by a NINAC myosin motor in PIP_3-enriched vesicles. However, a more recent study found that translocation of both Arr1 and Arr2 was unaffected by the *ninaC* mutation calling aspects of this model into question (Satoh, A. K. and Ready, D. F., 2005).

1.05.4.3.3 Rhodopsin kinase and phosphatase

In vertebrate rods, metarhodopsin inactivation is a two-stage process, whereby M must first be

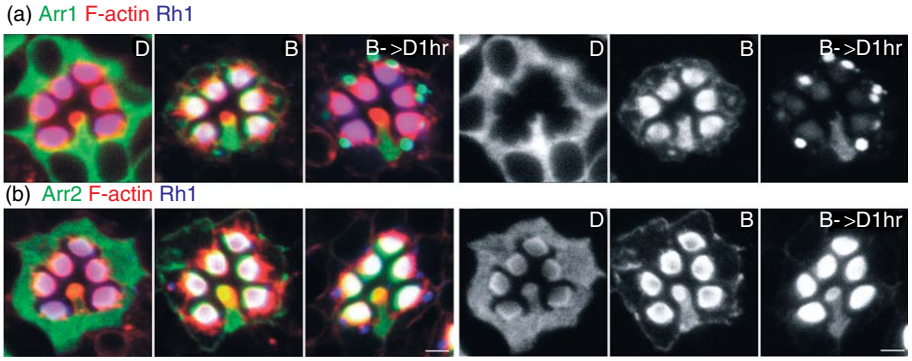

Figure 11 Translocation of arrestin. Immunostaining of Arr1 and Arr2 (green) in dark-adapted (D) retina, 5 min after illumination for 2 min by bright blue light (B), and 1 h after the same blue illumination (B > D 1 h). Sections are also stained for Rh1 (blue) and actin (red). The black and white image shows just the arrestin antibody staining. In the dark, all Arr1 is localized in the cytosol, whilst Arr2 is found in both cytosol and rhabdomere. Five minutes after illumination, both arrestins are found almost exclusively in the rhabdomeres. One hour later in the dark, Arr2 remains bound in the rhabdomeres, but Arr1 is now found predominantly in vesicles in the cell body, which also stain positive for Rh1. Images courtesy of Akiko Satoh and Don Ready (unpublished); see also Satoh A. K. and Ready D. F. (2005) for further details.

phosphorylated by a rhodopsin kinase (RK) before arrestin can bind and complete the inactivation (see Phototransduction in Rods and Cones). Unexpectedly, although fly rhodopsin is also multiplely phosphorylated at several serine residues in the C-terminal (Bentrop, J. and Paulsen, R., 1986; Byk, T. *et al.*, 1993), this appears not to be required for arrestin binding (Figure 9). Thus, transgenic flies in which the rhodopsin is replaced by a truncated version lacking the serine residues (*ninaE*$^{\Delta 356}$), or by a construct in which the serines have been individually mutated to alanine, show responses apparently normal in every respect including bump amplitude and waveform (Hardie, R. C., unpublished) and response inactivation (Vinos, J. *et al.*, 1997). The mutant Rh1 constructs also still bind Arr2 in biochemical assays (Kiselev, A. *et al.*, 2000a). Recently, Satoh A. K. and Ready D. F. (2005) reported that translocation of Arr1 and subsequent endocytosis of Arr1–Rh1 complexes was suppressed in these Rh1 phosphorylation mutants, suggesting that Rh1 phosphorylation may be specifically important for Rh1 binding to Arr1 (and/or its subsequent endocytosis) rather than Arr2.

A *Drosophila* G-protein-coupled receptor kinase (GPRK1) with homology to β-adrenergic receptor kinases has recently emerged as a strong candidate for RK. It is highly expressed in the photoreceptors where it associates with and phosphorylates rhodopsin (Lee, S. J. *et al.*, 2004). Interestingly, mutant flies expressing lower levels of GPRK1 had a significantly larger ERG responses, but without obvious response termination defects. Although responses were not measured at the single-cell level, at first sight this seems inconsistent with the lack of effect of the Rh1 phosphorylation site mutants on the response, which indicates that GPRK1 may also have a protein kinase-independent function.

After photoreisomerization from M to R, Arr2 is released from R, which must then be dephosphorylated before it can be used again (Figure 9). Dephosphorylation, which only takes place after Arr2 has been released, is mediated by a Ca^{2+} calmodulin (CaCaM)-dependent rhodopsin phosphatase encoded by the retinal degeneration C (*rdgC*) gene (Steele, F. R. *et al.*, 1992; Byk, T. *et al.*, 1993; Vinos, J. *et al.*, 1997; Lee, S. J. and Montell, C., 2001). *rdgC* mutants have a slow deactivation phenotype, but this may reflect a secondary defect, e.g., in Arr2 function, and is unlikely to be an immediate and direct consequence of the failure to dephosphorylate R, since by this stage in the rhodopsin cycle, the active M form should already have been inactivated by arrestin binding (Vinos, J. *et al.*, 1997). The original and most obvious phenotype of *rdgC* mutants, namely the severe light-dependent retinal degeneration, is suppressed by the truncated Rh1 phosphorylation site mutant *ninaE*$^{\Delta 356}$, and also by *arr2* mutations, suggesting that the accumulation of hyperphosphorylated M–Arr2 complexes may act as a trigger for apoptosis (Vinos, J. *et al.*, 1997; Kiselev, A. *et al.*, 2000a).

1.05.4.3.4 Arrestin phosphorylation

Both arrestin isoforms are themselves also phosphorylated in a light-dependent manner, and in fact Arr2 is

the major phosphoprotein revealed in proteomic analysis (Matsumoto, H. and Pak, W. L., 1984). It is also the most rapidly detectable phosphorylated protein in the eye, being phosphorylated by calmodulin-dependent kinase II (CaMKII) at a single serine residue (Ser^{366}) on a subsecond timescale following illumination (Matsumoto, H. and Pak, W. L., 1984; Matsumoto, H. *et al.*, 1994). Although it was originally speculated that CaMKII-dependent phosphorylation of Arr2 may be a necessary first step in the binding of arrestin to M, this seems not to be the case. Arr2 phosphorylation is prevented by mutating Ser^{366} to alanine ($Arr2^{S366A}$) or in the $arr2^{1}$ allele, in which the protein is truncated prior to this site (Alloway, P. G. and Dolph, P. J., 1999). However, Arr2 still binds normally to M in either of these mutants. The defect appears rather to be in the subsequent dissociation of Arr2 from rhodopsin after reconversion to R (Figure 9). Thus normally, Arr2 dissociates rapidly from M after it has been reconverted to R by long-wavelength light, but remains bound in $Arr2^{S366A}$ or $arr2^{1}$ (Alloway, P. G. and Dolph, P. J., 1999). Related to this, the phosphorylation also controls the subsequent trafficking of M–Arr2 complex, which become internalized by clathrin-mediated endocytosis if Arr2 fails to be phosphorylated (Kiselev, A. *et al.*, 2000a). This has the consequence that following light exposure, the non-phosphorylated mutant Arr2 becomes sequestered in stable complexes with phosphorylated rhodopsin, again triggering apoptosis and retinal degeneration. Before the onset of degeneration, it also results in a deactivation phenotype similar to an *arr2* hypomorph, presumably because there is no longer sufficient free Arr2 to inactivate M (Alloway, P. G. and Dolph, P. J., 1999; Alloway, P. G. *et al.*, 2000; Kiselev, A. *et al.*, 2000a).

In summary, it appears that, whilst having no direct role in the electrophysiological response, the rhodopsin and arrestin phosphorylation and dephosphorylation cycles (Figure 9) play vital, though still incompletely understood roles in rhodopsin turnover and photoreceptor maintenance and survival. Thus, as described above, *rdgC* mutants undergo light-dependent degeneration because of the accumulation of hyperphosphorylated metarhodopsin bound to arrestin. Since the *rdgC* rhodopsin phosphatase is dependent on the Ca^{2+} influx associated with the light response, hyperphosphorylated rhodopsin also accumulates in any mutants of the transduction cascade that block transduction, such as *norpA* (see below), and these mutants probably degenerate by a similar mechanism (Byk, T. *et al.*, 1993; Alloway, P. G. *et al.*, 2000; Kiselev, A. *et al.*, 2000a). Alloway P. G. *et al.* (2000) speculate that the clathrin-mediated endocytosis of M–Arr2 complexes may be a mechanism for removal of defective rhodopsin molecules, whilst Satoh A. K. and Ready D. F. (2005) suggest that Arr1 may play a scavenging role, binding phosphorylated M before it can accumulate in the lethal Arr2–M-p complexes. In support of this, they found that the light-independent degeneration in *arr1* mutants is actually rescued in the *arr1*;*arr2* double mutant.

1.05.4.4 Heterotrimeric G Protein

Heterotrimeric G proteins are holoenzymes composed of α, β, and γ subunits, with the α subunit bound to GDP in the (heterotrimeric) resting state (Figure 7). In common with all such G proteins, the G protein in the *Drosophila* phototransduction cascade is activated by interaction with the active receptor (M), which catalyzes the exchange of GDP for GTP on the α subunit, resulting in release of the active GTP-bound α subunit (Figure 6). The α subunit binds and activates its effector enzyme (in this case PLC), which then remains active until the GTP is hydrolyzed to GDP promoting dissociation of $G_q\alpha$ from PLC and its reassociation with $G\beta\gamma$.

Curiously, no mutants of any of the three G protein subunits were isolated in the early mutagenesis screens, but a strong candidate gene for the α subunit was identified amongst a collection of retinal genes identified by subtractive hybridization (Lee, Y. J. *et al.*, 1990). This G protein showed ~75% identity to mouse $G_q\alpha$, the isoform known to specifically couple to PLC. A role in transduction was indicated by showing it was localized in the rhabdomeres and by overexpressing a constitutively active form in the retina, which resulted in constitutive GTPase activity in the eye and suppression of the light response (Lee, Y. J. *et al.*, 1994). Definitive confirmation came with the characterization of a severe hypomorphic mutant *Gαq*, again isolated by screening for antigenicity, in which protein levels were reduced to <1%. Sensitivity to light in these mutants was reduced ~1000-fold (Figure 12), but this could be rescued in a dose-dependent manner by $G_q\alpha$ cDNA expressed under control of a heat-shock promoter (Scott, K. *et al.*, 1995).

The responses of *Gαq* mutants also appear to have a slow response deactivation (Figure 12); however, analysis of the underlying quantum bumps indicated, that this actually represents generation of bumps with delayed latencies, thereby substantially broadening the latency distribution. This can be readily

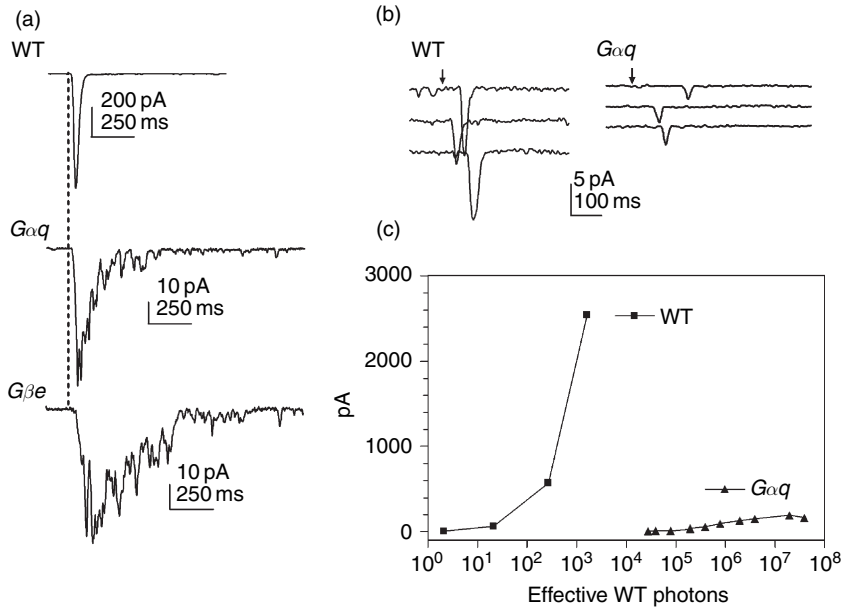

Figure 12 Responses in mutants of G_q. (a) Whole-cell voltage-clamped responses to brief (1 ms) flashes of light in wild type (WT), and in *Gαq* and *Gβe* mutants: (intensity for *Gαq* ~1000 times, and for Gβe ~100 times greater than for WT). Apart from the greatly reduced sensitivity, responses in both *Gαq* and *Gβe* show slow kinetics. For *Gαq* this is explained by delayed activation leading to longer bump latency (Scott, K. *et al.*, 1995), but in *Gβe* an additional defect in deactivation has been proposed (Dolph, P. J. *et al.*, 1994). (b) Individual quantum bumps elicited by dim flashes in *Gαq* are ~5× smaller than in WT. (c) Response intensity functions for WT and *Gαq* mutants: intensity expressed in effectively absorbed photons in WT photoreceptors. Adapted with permission from Hardie, R. C., Martin, F., Cochrane, G. W., Juusola, M., Georgiev, P., and Raghu, P. 2002. Molecular basis of amplification in *Drosophila* phototransduction. Roles for G protein, phospholipase C, and diacylglycerol Kinase. Neuron 36, 689–701; see also Dolph P. J. *et al.* (1994); Scott K. *et al.* (1995); Hardie R. C. *et al.* (2002).

understood by considering that one of the determinants of latency is the time taken for G protein to encounter the active M by diffusion in the microvillar membrane (see Section 1.05.8.2). Clearly, if the number of G proteins per microvillus is greatly reduced, then it will take longer on average for a G protein to encounter the single activated M in the microvillus (Scott, K. *et al.*, 1995).

Quantum bump amplitudes in *Gαq* (Scott, K. *et al.*, 1995), and also in hypomorphic PLC (*norpA*) mutants (Deland, M. C. and Pak, W. L., 1973; Cook, B. *et al.*, 2000), were originally reported to be the same as in WT, leading to the concept that amplification of the quantum bump was determined entirely downstream of PLC – that is, PLC activation serves only as a trigger for the quantum bump. However, it was subsequently found that quantum bumps were reduced by approximately fivefold in both these mutant backgrounds, indicating that G_q and PLC also contribute to the amplification process, and that normally activation of several G protein and PLC molecules is required to generate a full size quantum bump (Figures 12 and 13, Hardie, R. C. *et al.*, 2002). The discrepancy was attributed to the omission of ATP from the patch electrodes solution in earlier studies, resulting in artefactual amplification of the small bumps, probably as a consequence of reduced DAG kinase activity (Hardie, R. C. *et al.*, 2002) (see also Figure 16 and Section 1.05.5.1).

1.05.4.4.1 G protein β and γ subunits

A G protein β subunit that is expressed predominantly in the rhabdomeres has also been identified (Yarfitz, S. *et al.*, 1991; Yarfitz, S. L. *et al.*, 1994). Mutants (*Gβe*), subsequently isolated by screening for antigenicity, also show a greatly (~100-fold) decreased sensitivity to light (Dolph, P. J. *et al.*, 1994) as well as reduced light-induced GTPγS binding to retinae of cryosectioned heads (Yarfitz, S. L. *et al.*, 1994). Although this may indicate that Gβ is essential for effective coupling of $G_q\alpha$ with M, a recent study found that the majority of $G_q\alpha$ was mislocalized to the cytosol in *Gβe* mutants, i.e., the reduced sensitivity could in principle also be explained as consequence of G protein and rhodopsin being in separate cellular compartments (Elia, N. *et al.*, 2005). Interestingly, *Gβe* mutants also show a distinct

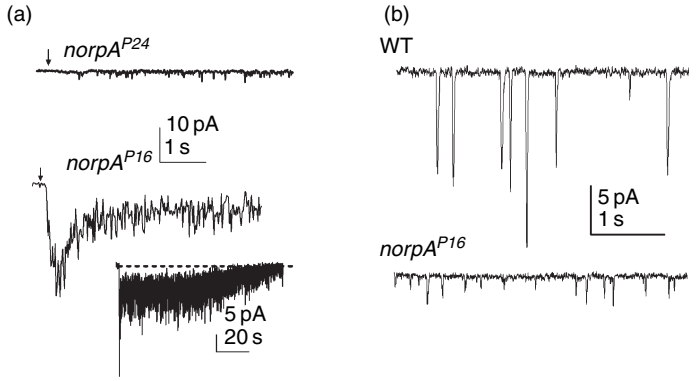

Figure 13 *norpA* mutant responses. (a) Whole-cell voltage-clamped responses to brief flashes of light (containing ~10^5 effectively absorbed photons) in the null PLC mutant *norpA*^{P24} and the severe hypomorph *norpA*^{P16}. Even in the supposedly null *norpA*^{P24}, a few ~1 pA bumps are elicited in response to bright illumination, whilst the same intensity elicits a small response in *norpA*^{P16} (these intensities would generate saturating responses in wild-type (WT) flies). Inset, on a slower timescale shows that the response in *norpA*^{P16} lasts for several minutes. (b) Quantum bumps in *norpA*^{P16} (recorded in the tail of a response to a weaker flash), are greatly reduced compared to WT (above). Adapted with permission from Hardie, R. C., Martin, F., Cochrane, G. W., Juusola, M., Georgiev, P., and Raghu, P. 2002. Molecular basis of amplification in *Drosophila* phototransduction. Roles for G protein, phospholipase C, and diacylglycerol Kinase. Neuron 36, 689–701.

deactivation defect, which is more severe than in $G\alpha q$ mutants (Figure 12), suggesting a distinct role for $G\beta$ in response termination (Dolph, P. J. *et al.*, 1994). There are no null or hypomorphic mutants of the G protein γ subunit; however, a dominant negative construct lacking the farnesylation site require for membrane anchoring also reduces light sensitivity as measured by ERG, presumably by sequestering $G\beta$ subunits away from the membrane (Schillo, S. *et al.*, 2004).

1.05.4.4.2 G_q translocation

Along with the arrestins (Section 1.05.4.3.2) and the TRPL channels (transient receptor potential-like translocation), G_q is one of three components of the *Drosophila* cascade that has been shown to translocate in response to illumination. In the dark, the majority of the G protein is found concentrated in the microvilli. However, following saturating illumination with blue light, ~50% of the $G_q\alpha$ is released from the membrane and moves out into the cell body over a time course of 50 min, returning to the rhabdomere slightly more slowly in the dark (Kosloff, M. *et al.*, 2003). Translocation was little affected by mutations in PLC, though curiously was largely blocked in mutants of the TRP channel. Like other G proteins, G_q is not a transmembrane protein, but can be anchored to the membrane by reversible palmitoylation of the α subunit, suggesting that depalmitoylation may be required to initiate the translocation (Kosloff, M. *et al.*, 2003). The return of $G_q\alpha$ in the dark was blocked in $G\beta e$ mutants, indicating that targeting to the microvillar membrane also requires $G\beta$ or, more likely, $G\beta\gamma$ with involvement of the farnesylation of the γ subunit in membrane anchoring.

1.05.4.5 Phospholipase C (NORPA)

Severe mutants of the *n*o *r*eceptor *p*otential *A* (*norpA*) gene have effectively no response to light, and were isolated independently by both the Pak and the Benzer groups (Hotta, Y. and Benzer, S., 1970; Pak, W. L. *et al.*, 1970). Although evidence had already implicated the PI cascade in invertebrate phototransduction (Brown, J. *et al.*, 1984; Fein, A. *et al.*, 1984; Inoue, H. *et al.*, 1985; Devary, O. *et al.*, 1987), the finding that *norpA* encoded a PI-specific PLC (Bloomquist, B. T. *et al.*, 1988) provided clear genetic evidence that PLC was the effector enzyme of the phototransduction cascade in *Drosophila* and represented a key milestone in the analysis of invertebrate phototransduction. Appropriate for its role, the NORPA protein was found to be highly enriched in the eyes and immunogold labeling showed it to be specifically localized to the rhabdomeres (Schneuwly, S. *et al.*, 1991). Although the obligatory control demonstrating that *norpA* cDNA could genetically rescue the mutant phenotype was not performed until much later (McKay, R. R. *et al.*, 1995); importantly, possible pleiotropic developmental effects of this mutation had already been effectively excluded by the availability of temperature-sensitive

alleles of *norpA* in which the light response was rapidly and reversibly abolished by warming to 35 °C (Deland, M. C. and Pak, W. L., 1973).

NORPA, one of the first PI-specific PLCs to be cloned, is clearly recognizable as a PLCβ isoform, which unlike PLCγ and PLCδ, are activated by interaction with heterotrimeric G proteins. Thus, NORPA has up to 60% identity with mammalian PLCβs in the conserved X and Y domains, which form the catalytic core of the enzyme and contains a C2 domain that may be involved in Ca^{2+}-dependent targeting to the membrane (reviewed in Pak, W. L., 1995). Interestingly, one of the vertebrate PLCβ isoforms (PLCβ4) is more closely related to NORPA than any other vertebrate PLC isoform and is predominantly expressed in the vertebrate cones (Ferreira, P. A. and Pak, W. L., 1994). Its role in vertebrate photoreceptors is not known, but may hint at some distant evolutionary common ancestral photoreceptor.

1.05.4.5.1 Phospholipase C is also a GTPase-activating protein

Numerous mutant alleles of the *norpA* gene have been isolated, which vary widely in their severity (Pearn, M. T. *et al.*, 1996). The most severe, such as $norpA^{P24}$, which has a 28-bp deletion resulting in a frameshift and a premature stop codon, have essentially no response to even saturating flashes (but see Figure 13 and Hardie, R. C. *et al.*, 2003) and no detectable protein. However, others such as $norpA^{P57}$ and $norpA^{P16}$ have residual protein and substantial responses to bright illumination. As well as a marked reduction in sensitivity, such hypomorphic alleles also have dramatically prolonged responses to light that can persist for many minutes, the time course increasing with the severity of the mutation (Figure 13, Scott, K. and Zuker, C. S., 1998; Cook, B. *et al.*, 2000). A combined electrophysiological and biochemical study indicated that this reflects the requirement for PLC to act as a GTPase-activating protein (GAP), essential to terminate the activity of $G_q\alpha$ subunit (Cook, B. *et al.*, 2000). With severely reduced PLC levels, it appears that $G_q\alpha$ subunits remain active indefinitely (for many minutes), before finally encountering and binding to a PLC molecule, only then initiating a cycle of bump generation, PLC inactivation, and response termination. GAP activity of the effector enzyme is a common feature in G protein signaling and as in vertebrate rods, such a mechanism is important in ensuring the fidelity of the response to light. Thus, firstly the G protein stays active until it has had the chance to activate its target (PLC), but then it is rapidly inactivated ensuring that only one bump is generated. Whether or not RGS proteins are also involved as GAP proteins, as in vertebrate photoreceptors, is not known.

1.05.4.5.2 Measuring phospholipase C activity

Light- and *norpA*-dependent PLC activity, generating DAG and $InsP_3$ from PIP_2 has directly been demonstrated in biochemical assays, using radiolabeled inositol or PIP_2 (Inoue, H. *et al.*, 1985; Devary, O. *et al.*, 1987; Toyoshima, S. *et al.*, 1990; Running Deer, J. L. *et al.*, 1995). Like other PLCs, *Drosophila* NORPA shows *in vitro* dependence on Ca^{2+}, both basal and light-activated PLC activity being increased in the range from 10 nm to 1 μM, and inhibited in the high micromolar range (Toyoshima, S. *et al.*, 1990; Running Deer, J. L. *et al.*, 1995).

The only available quantitative biochemical measurements come from squid, indicating that ~500 PIP_2 molecules can be hydrolyzed per absorbed photon (Szuts, E. Z., 1993). However, semiquantitative *in vivo* estimates of PIP_2 hydrolysis rates in *Drosophila* have recently been made using biosensors in the guise of PIP_2-sensitive inward rectifier ion channels (Kir2.1), genetically targeted to the rhabdomeres (Hardie, R. C. *et al.*, 2001; 2004). These channels are activated by PIP_2, and their open probability is simply related to PIP_2 concentration. When they replace the light-sensitive channels, they generate a constitutively active inward current maintained by the endogenous resting PIP_2 levels. This current is suppressed in an intensity-dependent manner by illumination, providing a rather direct *in vivo* measure of PIP_2 hydrolysis. The suppression of the Kir2.1 current by light indicated that PLC activity corresponded to rates of ~150% of the PIP_2 in the microvillus per second per effectively absorbed photon (Figure 14, Hardie, R. C. *et al.*, 2004). Interestingly, in complete darkness, a remarkably high basal PLC activity could also be readily resolved after blocking PIP_2 synthesis by ATP deprivation. Although ~1000× less than maximum light-induced rates, this was still sufficient to effectively deplete the rhabdomere of PIP_2 within 5–10 min (Figure 14).

Kir2.1 biosensors, in combination with manipulation of cytosolic Ca^{2+}, also allowed *in vivo* measurements of the Ca^{2+} dependence of basal and light-induced PLC activity. Broadly, these confirmed

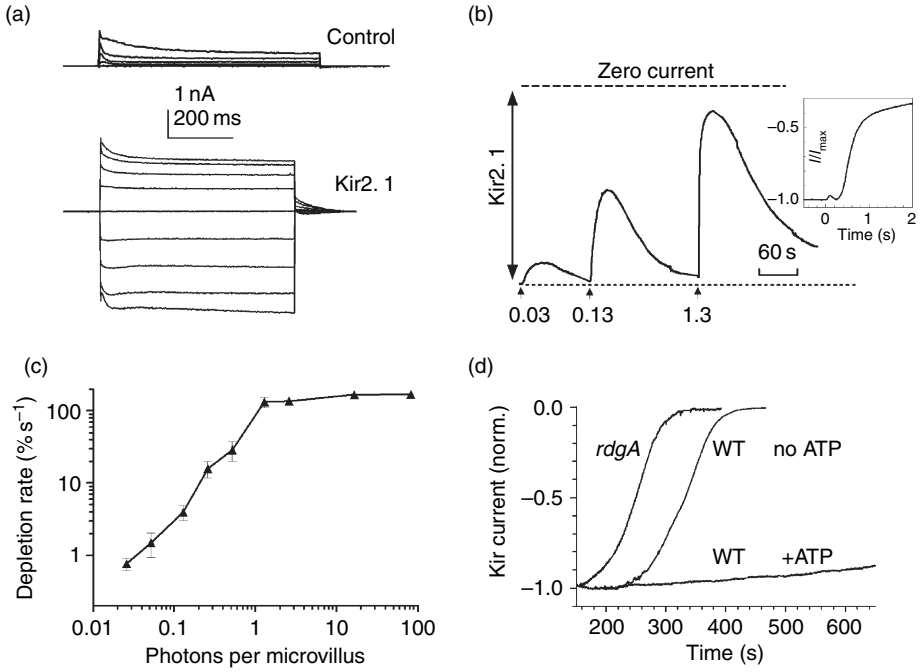

Figure 14 PIP_2 hydrolysis monitored with PIP_2 biosensor channels Kir2.1. Whole-cell recordings of inward K^+ currents in photoreceptors expressing the PIP_2-sensitive inwardly rectifying Kir2.1 channel. (a) Voltage steps (from −100 to −20 mV in 10 mV steps). In control cells, only outward K currents (mainly *Shaker* and *Shab*) are activated, but in cells expressing Kir2.1 large inwardly rectifying currents are seen at negative potentials. (b) When expressed in photoreceptors of *trpl*;*trp* double mutants, Kir2.1 is the only light-sensitive conductance in the cell. In the dark a large, ~1 nA constitutive current is activated by the prevailing PIP_2 levels (extent indicated by double arrow). Calibrated stimuli (0.03 etc., expressed in effectively absorbed photons per microvillus) suppress the current due to hydrolysis of PIP_2 by PLC: flashes containing one photon per microvillus deplete the entire rhabdomere of the majority of detectable PIP_2 within ~1 s (inset shows a response on a faster timescale). The Kir2.1 current is reactivated with a half time of ~60 s in the dark, representing the resynthesis of PIP_2. (c) Intensity response function of PLC activity – measured from the maximum slope of individual flash responses as in (b). Note that there is no Ca^{2+} influx associated with the light response in these experiments: under normal conditions, Ca^{2+} influx via TRP channels rapidly inhibits PLC activity, so that these rates of PLC activity will only be reached and briefly sustained during the latent period of the quantum bump (see Section 1.05.6.2). (d) Basal PLC activity monitored *in vivo* as a function of time after establishing the whole-cell configuration: a control (wild type (WT)) cell held in the dark with ATP in the patch pipette shows only very gradual rundown of the Kir2.1 current over 10 min. Without ATP however, the current decays to near zero within ~6 min. A similar behavior is seen in the *rdgA* mutant demonstrating ongoing basal PLC activity in this mutant as well. Adapted from Hardie, R. C., Gu, Y., Martin, F., Sweeney, S. T., and Raghu, P. 2004. *In vivo* light-induced and basal phospholipase C activity in *Drosophila* photoreceptors measured with genetically targeted phosphatidylinositol 4,5-bisphosphatesensitive ion channels (Kir2.1). J. Biol. Chem. 279, 47773–47782.

in vitro measurements; however, facilitation by Ca^{2+} was only noted in the range ~10–100 nM, and maximal activity appeared already to be reached at physiological resting levels of Ca^{2+} (Hardie, R. C., 2005). As discussed later (see Section 1.05.6.1.1), much higher concentrations (>50 μM) strongly inhibited PLC activity *in vivo*.

1.05.4.6 Light-Sensitive Channels *trp* and *trpl*

The *Drosophila* transient receptor potential mutant, *trp*, was first isolated as a spontaneously occurring mutation, in which the photoreceptor's response to light decayed to baseline during prolonged illumination (Cosens, D. J. and Manning, A., 1969; Minke, B. *et al.*, 1975). After the gene was positionally cloned (Montell, C. and Rubin, G. M., 1989), it was found to encode a novel transmembrane protein. Since mutants still had a light response, it was originally considered unlikely that TRP represented the light-sensitive channel. However, Hardie R. C. and Minke B. (1992) demonstrated that the Ca^{2+} selectivity of the light-sensitive current was reduced tenfold in *trp* mutants, leading to the proposal that it represented the major, Ca^{2+} selective component of

the light-sensitive current, and that a second, less Ca^{2+} permeable channel was responsible for the residual response in the *trp* mutant. At the same time, Phillips A. M. *et al.* (1992) reported the sequence of a second channel-like gene (TRP-like, or TRPL), now known to be responsible for this residual response (Niemeyer, B. A. *et al.*, 1996; Reuss, H. *et al.*, 1997). Both TRP and TRPL have been shown to be predominantly localized in the microvilli by immunogold labeling (Niemeyer, B. A. *et al.*, 1996), although as detailed below (see Section 1.05.4.6.4), TRPL may also be found in the cell body following translocation.

1.05.4.6.1 Structure of TRP and TRPL

The TRPL protein shares 40% identity to TRP and both sequences show structural similarity with the voltage-gated Ca^{2+} channel family with six transmembrane (TM) helices and a pore loop (Phillips, A. M. *et al.*, 1992). Unlike Ca^{2+} channel genes, which encode four such 6TM domains in a single peptide, the *trp* and *trpl* genes encode only one such domain, and consequently, like voltage-gated K channels or CNG channels, TRP channels are believed to be composed of homo- or heterotetramers. The identification of TRP as a PLC-regulated cation channel heralded the discovery of some 30 vertebrate isoforms, divided into seven subfamilies (TRPC, TRPV, TRPM, TRPML, TRPP, TRPA, and TRPN). They have remarkably diverse functions throughout the body, most notably, but by no means exclusively, in sensory transduction (reviewed in: Clapham, D. E., 2003; Montell, C., 2005; Ramsey, I. S. *et al.*, 2006).

Drosophila TRP and TRPL share closest homology with the vertebrate TRPC (*c*anonical TRP) subfamily, with similar overall topology, including four N-terminal ankyrin repeats (protein binding motifs) and a coiled-coil (CC) region in the N-terminal, and six transmembrane segments with a pore loop between S5 and S6 (Figure 15). The most highly conserved region is the so-called TRP domain, which is immediately adjacent to S6. In vertebrate TRPC1, part of this domain can serve as a binding site for a

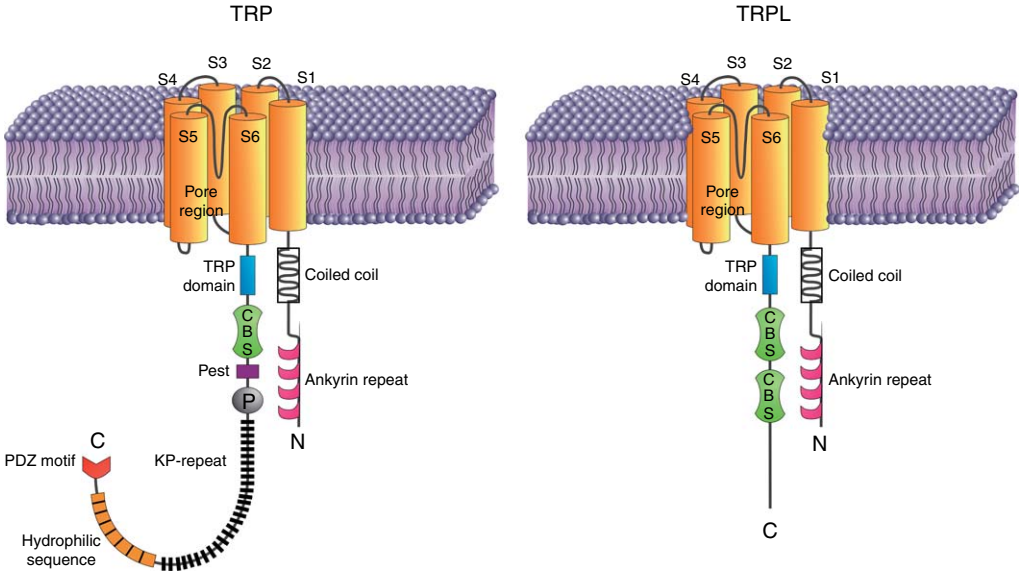

Figure 15 Structural features of the TRP and TRPL channel subunits. TRP and TRPL both belong to the overall superfamily of voltage-gated Ca^{2+}/Na^{+} and K^{+} channels and CNG channels; and represent subunits of tetrameric channels. Each subunit has six transmembrane helices (S1–S6), with a pore helix and pore loop between S5 and S6. The S4 helix lacks the positively charged residues characteristic of the voltage-gated members of the family. Their N-termini contain a coiled-coil region (CC) and four ankyrin repeats, which are potential protein–protein interaction domains. The most highly conserved region is the TRP domain adjacent to S6, with the motif EWKFAR found in all TRPC channels, and which is still recognizable in other TRP subfamilies. TRP has one, and TRPL, two CaM-binding sites (CBS) in the C-termini. TRP has an extended C-terminus with a PEST sequence, a proline-rich region with 29 KP repeats, multiple repeats of a hydrophilic eight to nine peptide sequence DKDKKP(A/G)D, and a PDZ domain binding motif in the last three amino acids required for binding to the INAD protein. Ser^{982} has been implicated as an *in vivo* PKC phosphorylation site (P) required for effective response termination (Popescu, D. C. *et al.*, 2006).

scaffolding protein, Homer, which is proposed to mediate interaction with $InsP_3$ receptor ($InsP_3R$) (Yuan, J. P. *et al.*, 2003). However, given that TRP channels are activated normally in the $InsP_3R$ null mutants in the photoreceptors (Section 1.05.5.1), the significance of this region in the *Drosophila* TRPs is not known. The rest of the C-terminal is rather divergent – both between TRP and TRPL and the vertebrate TRPCs – though all include one or more consensus CaM-binding domains (see Section 1.05.6.2.1). TRP has a conspicuously long C-terminal domain containing a proline-rich region, eight to nine peptide repeats of unknown function and a consensus PDZ-binding motif that binds to the scaffolding protein INAD (Section 1.05.4.8).

1.05.4.6.2 Channel properties

The properties of the native TRP- and TRPL-dependent currents *in vivo* have been characterized by exploiting null mutants of both genes to isolate the respective currents, providing characteristic biophysical fingerprints (Table 2; Reuss, H. *et al.*, 1997). TRP channels (isolated in *trpl* mutants) are highly selective for Ca^{2+} (P_{Ca}:P_{Na} ~100:1) and have a rather small single-channel conductance (~8 pS) with rapid kinetics (mean open time ~0.5 ms). TRP (but not TRPL) channels are completely blocked by micromolar levels of La^{3+}. TRPL channels, isolated in *trp* mutants are relatively nonselective (P_{Ca}:P_{Na}~4:1) with a conductance of 35 pS and slightly slower channel open times (1–2 ms). The only reported specific blocker is cinnamyl-dihidroxy-cyanocinnamate, with an IC_{50} of 1 μM (Chyb, S. *et al.*, 1999b). An interesting feature of the TRP channel is a pronounced voltage-dependent open channel block by physiological concentrations of Mg^{2+} (IC_{50} ~1 mM). The block is relatively weak around resting potential (−70 mV), but intensifies as the cell depolarizes. This means that the effective single-channel conductance should decrease as the cell depolarizes in response to light, and potentially would seem to be an elegant and economical mechanism for light adaptation (Hardie, R. C. and Mojet, M. H., 1995).

Both TRP and TRPL have also been expressed in heterologous expression systems, indicating that they encode bona fide channels (Vaca, L. *et al.*, 1994; Gillo, B. *et al.*, 1996; Hardie, R. C. *et al.*, 1997; Xu, X. Z. S. *et al.*, 1997). TRPL has been successfully expressed by many groups (Hu, Y. *et al.*, 1994; Harteneck, C. *et al.*, 1995; Gillo, B. *et al.*, 1996; Lan, L. *et al.*, 1996; Hardie, R. C. *et al.*, 1997), and its biophysical properties found to be indistinguishable from those of the native TRPL-dependent current isolated in *trp* mutants (Hardie, R. C. *et al.*, 1997; Chyb, S. *et al.*, 1999b). Together with the complete elimination of the native current by the *trpl* mutation (Niemeyer, B. A. *et al.*, 1996; Reuss, H. *et al.*, 1997), the close functional equivalence of native and heterologously expressed TRPL channels leaves little doubt as to their identification (Hardie, R. C. *et al.*, 1997). Although there is good evidence that TRPL can

Table 2 Biophysical properties of TRP and TRPL channels

A

Permeability ratios	*TRP (in trpl)*	*TRPL (in trp)*	*WT*
P_{Ca}:P_{Cs}	57	4.3	45.1
P_{Mg}:P_{Cs}	15.8	1.4	5.7
P_{Na}:P_{Cs}	1.27	0.84	1.16
P_{Li}:P_{Cs}	0.89	0.80	0.89

B

	γ (pS) (divalent free)	*γ (pS)*	*τ (ms)*	*IC_{50} Mg^{2+} (mM), 0 Ca^{2+}*	*IC_{50} Mg^{2+} (mM), 1.5 Ca^{2+}*	*La^{3+} block (10 μM)*
TRP (in *trpl*)	35	8	2, 0.2	0.28	1.3	Total
TRPL (in *trp*)	70	35	0.4	4	4	None

A: Permeability ratios (P_x:P_{Cs}) derived from bi-ionic reversal potential data. Values expressed with respect to internal Cs^+ (130 mM) and determined in respective mutants, i.e., TRPL channels measured in the *trp* mutant, TRP-dependent channels in *trpl*. Data from Reuss H. *et al.* (1997).

B: Estimates of single-channel characteristics and ion block. Single-channel conductances (γ, pS) derived from noise analysis in both divalent free and physiological Ringer's. Time constant (τ) refer to Lorentzian fits to power spectra. Mg^{2+} block has been determined only in WT (dominated by TRP channels) and *trp* mutant. Data from Hardie R. C. and Minke B. (1994b), Hardie R. C. and Mojet M. H. (1995), Hardie R. C. *et al.* (1997), Reuss H. *et al.* (1997), Raghu P. *et al.* (2000b), and Liu C. H. *et al.* (2007).

associate as a heteromultimer with TRP (Xu, X. Z. S. *et al.*, 1997), it seems questionable whether the *in vivo* light-sensitive TRPL-dependent conductance includes TRP subunits as well. Thus the WT light-sensitive conductance can readily be accounted for by the independent sum of TRP and TRPL, whilst blocking TRP channels with La^{3+} quantitatively mimics the effect of the *trp* mutation leaving TRPL channels indistinguishable from those found in *trp* mutants (Reuss, H. *et al.*, 1997). A third TRP homologue, TRPγ, has also been identified and found to be expressed in the photoreceptors (Xu, X. Z. S. *et al.*, 2000). TRPγ was also reported to form heteromultimers with TRPL (but not TRP) in expression systems and a dominant negative construct suppressed the TRPL-dependent light response *in vivo* suggesting that the native channels might also represent TRPL–TRPγ heteromultimers. However, unlike TRP and TRPL, recent evidence suggests that TRPγ is not particularly eye-enriched (Jors, S. *et al.*, 2006) and until a mutant is generated, its role remains uncertain.

By contrast, it has generally proved very difficult to express TRP, and the few published reports of its biophysical properties in expression studies (Vaca, L. *et al.*, 1994; Gillo, B. *et al.*, 1996; Xu, X. Z. S. *et al.*, 1997) do not closely match the properties of the *in vivo* TRP-dependent current (isolated in *trpl* mutants). This therefore raises the question of whether TRP actually represents a pore-forming channel subunit *in vivo*. This concern has recently been addressed by the identification of a unique aspartate residue (Asp^{621}) within the TRP pore region as the major determinant of Ca^{2+} permeation, most likely forming a ring of four such acidic residues in a tetramer, as in other Ca^{2+}-selective channels. Neutralizing Asp^{621} (to glycine) almost completely eliminated Ca^{2+} permeation *in vivo*, whilst more conservative substitutions resulted in intermediate ionic selectivities (Liu, C. H. *et al.*, 2007). Systematic alteration of pore properties by site-directed mutagenesis of the pore represents the most rigorous demonstration of channel identity, and thus these results conclusively demonstrate that TRP does indeed form a pore-forming subunit of the *Drosophila* light-sensitive channel *in vivo*.

1.05.4.6.3 *trp* and *trpl* phenotypes

Apart from the changes in permeation properties and pharmacology of block, both *trp* and *trpl* mutants have a number of intriguing secondary phenotypes. The original *trp* phenotype is the decay of the response to baseline during maintained illumination, associated with a complete loss of sensitivity that slowly recovers in the dark. After some debate, this now appears to be attributable to the complete loss of PIP_2 due to the failure of Ca^{2+}-dependent inhibition of PLC (see Figure 20 and Section 1.05.6.2). With weaker illumination, or brief flashes, responses in *trp* mutants are superficially similar to WT; however, they have about tenfold reduced sensitivity, their kinetics are slightly slower and fail to accelerate during light adaptation. Indeed, virtually all aspects of light adaptation are lacking, and the loss of response during light adaptation regimes is better described as exhaustion of the excitatory process (Minke, B., 1982). Whilst intracellular recordings originally suggested that quantum bumps were similar in WT and *trp*, the improved resolution of whole-cell recordings clearly showed a reduction in bump amplitude to ~3–4 pA (Niemeyer, B. A. *et al.*, 1996; Henderson, S. R. *et al.*, 2000). Given that the TRPL single-channel current is ~2 pA, this implies that bumps in *trp* usually consist of only one to two channel openings.

By contrast, quantum bumps and macroscopic flash responses in *trpl* mutants are almost indistinguishable from WT, and initially the only phenotypes found in whole-cell recordings of the LIC were changes in ionic selectivity and the complete block of the light response by La^{3+} (Niemeyer, B. A. *et al.*, 1996; Reuss, H. *et al.*, 1997). This suggests that the TRP channels make the dominant contribution to the WT light response, and it has been estimated that ~95% of the DA LIC in flash responses is attributable to TRP (Reuss, H. *et al.*, 1997). However, subsequent studies using prolonged illumination performed under more physiological conditions, using either the ERG or intracellular voltage recordings, revealed further distinct phenotypes. These include a reduced plateau potential, oscillations superimposed on the response and an impaired ability to light adapt to very dim background lights (Leung, H. T. *et al.*, 2000). With the possible exception of the reduced ability to light adapt (see Section 1.05.4.6.4), it remains unclear however, how these phenotypes relate to the known properties of the two channels. Leung H. T. *et al.* (2000) also reported an intriguing genetic interaction between *trpl*, *trp*, and a mutant of the scaffolding protein INAD (Section 1.05.4.8), $InaD^{P215}$, which has a point mutation disrupting its binding to TRP. Specifically, whilst *trpl* and $InaD^{P215}$ mutants have normal or near normal levels of TRP protein, the *trpl*,$InaD^{P215}$ double mutant has greatly reduced (<10%) levels of TRP and an even more profound loss of response, which could not be entirely

accounted for by the loss of protein. This suggests that when TRP is not bound to INAD, it requires TRPL in order to maintain TRP protein levels and to generate significant responses (Leung, H. T. *et al.*, 2000).

1.05.4.6.4 TRPL translocation

Another feature that distinguishes the TRPL from the TRP channel is that the former, like arrestin and G_q, also undergoes a massive light-induced translocation. Translocation of the TRPL protein out of the rhabdomere in response to illumination, and its return in the dark has been shown both by immunocytochemistry and by tracking an enhanced green fluorescent protein (eGFP)-tagged TRPL protein *in vivo* (Bahner, M. *et al.*, 2002; Meyer, N. E. *et al.*, 2006). In the larger fly *Calliphora*, translocation has also been confirmed by quantitative Western blotting of cytosolic and rhabdomeral fractions (Bahner, M. *et al.*, 2002). In *Drosophila*, at least 80% of eGFP-tagged TRPL leaves the rhabdomere during bright illumination with a halftime of 3.25 h, returning rather more quickly in the dark (halftime 1 h). The translocation mechanism appears to require operation of the full transduction cascade, being blocked in *Gαq*, *norpA*, and *trp* mutants, and also by removal of extracellular Ca^{2+}, whilst it is impaired in the *ninaC* and *arr2* mutants (Meyer, N. E. *et al.*, 2006). Importantly, whole-cell recordings confirmed the removal (and return) of functional TRPL channels from the rhabdomeres, assayed by their reversal potential and insensitivity to La^{3+}. One of the physiological consequences of the translocation of TRPL protein out of the rhabdomere following light exposure, namely an impaired inability to adapt to weak background lights, closely mimics one of the *trpl* mutant phenotypes (Section 1.05.4.6.3). A possible explanation for this is that the TRPL channel may be subject to more pronounced Ca^{2+}-dependent inactivation than the TRP channel, and that consequently low levels of Ca^{2+} influx associated with weak background illumination have more effect in inhibiting TRPL channels than TRP channels, and hence this cause less reduction in sensitivity when only TRP is present (Bahner, M. *et al.*, 2002).

1.05.4.7 INAF, a Novel Protein Required for TRP Function

The *inaF* gene encodes a small, highly eye-enriched protein with no homologies to other proteins in the databases and no predicted transmembrane domains. Null *inaF* mutants have substantially reduced (~10% of WT levels) TRP protein levels and a phenotype that resembles that of a *trp* null mutant, whilst TRPL channel function appears intact (Li, C. J. *et al.*, 1999). Interestingly, the residual TRP protein in *inaF* mutants is still localized to the rhabdomeres, yet the phenotype is as severe as in *trp* mutants in which there is no immunodetectable protein. Therefore, although the reduced levels of TRP protein may contribute to the phenotype, Li C. J. *et al.* (1999) suggest that the INAF protein may also have a direct regulatory role in TRP channel function.

1.05.4.8 Scaffolding Protein INAD

Along with translocation, one of the most intriguing recent developments in invertebrate photransduction has been the realization that not only are the molecular elements of the cascade highly compartmentalized within microvilli, but that several key proteins are also organized into a multimolecular signaling complex by a scaffolding protein, INAD (Figure 6). The first mutant allele of *InaD* ($InaD^{P215}$) was isolated by Pak and coworkers, and after it was cloned the gene was found to encode a protein with five so-called PDZ domains (Shieh, B. H. and Niemeyer, B., 1995; Shieh, B. H. and Zhu, M. Y., 1996; Chevesich, J. *et al.*, 1997; Tsunoda, S. *et al.*, 1997). PDZ domains are modules, which anchor a variety of protein targets, typically though not always by a short (three amino acids) C-terminal target sequence (see Figures 6 and 7). The final composition of the complex is still debated, but there is general agreement that a core set of three proteins TRP, PLC, and PKC, are bound to INAD in a stoichiometric (1:1:1:1) manner (Huber, A. *et al.*, 1996a; Tsunoda, S. *et al.*, 1997; Li, H. S. and Montell, C., 2000). Other reported targets include rhodopsin, the second ion channel (TRPL), NINAC (Section 1.05.4.9), which is a class III myosin that has been proposed to link the complex to the actin cytoskeleton, CaM, and the immunophilin FKBP59 (Montell, C., 1999; Goel, M. *et al.*, 2001; Huber, A., 2001). INAD can also form homophilic interactions with itself; together with the likelihood of linkage via TRP, which forms tetrameric channels, this in principle would provide the potential for extended complexes containing multiple channels and PLC molecules (Figure 6).

The precise functional role of the INAD complex (sometimes referred to as signalplex or transducisome) remains uncertain. It has been reasonably speculated

that tethering PLC and the channels together would minimize diffusional delays, thus contributing to the rapid kinetics. It has also been suggested that the INAD complex represents the molecular framework responsible for the quantum bump (Scott, K. and Zuker, C. S., 1998), but definitive evidence for this is lacking. The null $InaD^{1}$ mutant has greatly reduced sensitivity and quantum bumps are much reduced in size (Scott, K. and Zuker, C. S., 1998); however, this could simply reflect reduced levels of microvillar PLC since INAD is also required for targeting PLC to the microvillar membrane (Tsunoda, S. *et al.*, 2001). It is also possible to genetically disrupt specific INAD interactions; for example, the TRP channel's interaction with INAD can be disrupted by mutations either in the TRP-specific PDZ domain on the INAD protein (as in the original $InaD^{P215}$ mutation), or by mutation in the C-terminal PDZ-binding motif of the TRP protein (Li, H. S. and Montell, C., 2000). In either case, there is little, if any, defect in the kinetics or amplification of excitation, although there is a specific deactivation defect (quantum bumps terminate abnormally slowly) in the $InaD^{P215}$ mutant (Shieh, B. H. and Niemeyer, B., 1995; Henderson, S. R. *et al.*, 2000). Most recently, a similar deactivation defect, albeit measured in the ERG, was reported after engineering a point mutation of a key PKC phosphorylation site in the TRP protein, suggesting that the association of TRP with INAD and PKC (also a member of the signalplex) is critical for TRP phosphorylation (Popescu, D. C. *et al.*, 2006) (see also Section 1.05.6.2.2). Whether or not the proximity of PLC and TRP on a molecular scale is also essential for normal excitation, one of the vital roles of INAD is to maintain TRP and PLC and PKC in the microvillus in high concentrations (~100 copies per microvillus) and in stoichiometric relationship. In fact both TRP and INAD are essential for the long-term maintenance of the complexes in the rhabdomeres. Thus, whilst both TRP and INAD are initially correctly targeted to the rhabdomere in the absence of the other, over a period of days, TRP protein disappears from the rhabdomere in *InaD* mutants, whilst INAD protein is similarly destabilized in *trp* mutants (Tsunoda, S. *et al.*, 1997; Li, H. S. and Montell, C., 2000).

1.05.4.9 Myosin Kinase NINAC

The *ninaC* locus encodes two photoreceptor-specific class III myosins characterized by an N-terminus kinase domain followed by a myosin-like domain (Figure 7). A long form (174 kDa) is localized in the rhabdomeres, whilst a short cytosolic variant (132 kDa) is found only in the cell body (Montell, C. and Rubin, G. M., 1988). The rhabdomeric 174-kDa protein may be linked to the F-actin core of the microvillus (Hicks, J. L. *et al.*, 1996). *ninaC* null mutants or mutants lacking the rhabdomeric 174-kDa variant show defects in response termination and light adaptation, including an abnormally large steady-state plateau response (Porter, J. A. *et al.*, 1992; Porter, J. A. and Montell, C., 1993; Hofstee, C. A. *et al.*, 1996; Arnon, A. *et al.*, 1997a), and also undergo light-dependent retinal degeneration (Porter, J. A. *et al.*, 1992). The mechanistic basis for these phenotypes remains uncertain, though the deactivation defect can be attributed, at least in part, to its role as the major CaM-binding protein in the retina (Porter, J. A. *et al.*, 1993) (see Section 1.05.6.2.1). NINAC is also a phosphoprotein and an *in vitro* target for PKC and possibly other kinases. Targeted mutagenesis of two putative phosphorylation sites in NINAC resulted in an unusual ERG phenotype, with slow oscillations in the dark following a bright flash (Li, H. S. *et al.*, 1998). *ninaC* mutants have also been reported to be defective in a putative PKA-mediated modulation of response latency (Chyb, S. *et al.*, 1999a). More recently, *ninaC* mutants have been reported to show defects in the translocation of both arrestin (Lee, S. J. and Montell, C., 2004) (disputed by Satoh, A. K. and Ready, D. F., 2005) and the TRPL channels (Meyer, N. E. *et al.*, 2006), possible indicative of a motor function.

1.05.5 Messengers of Excitation

Genetic and other evidence have clearly established that fly phototransduction involves rhodopsin, G_q protein, and PLC, followed by activation of TRP and TRPL channels; however, the final steps of activation downstream of PLC, and in particular, the messenger of excitation are controversial and have still not been unequivocally resolved.

1.05.5.1 Evidence for Activation by Lipid Messengers

$InsP_3$ is the most familiar product of PIP_2 hydrolysis by PLC, and its major target is the $InsP_3R$ – an intracellular Ca^{2+} release channel found on internal Ca^{2+} stores. Although it was originally widely believed that $InsP_3$-induced Ca^{2+} release from the SMC was an essential step in excitation in

Drosophila, as appears to be the case, for example, in *Limulus* (see Section 1.05.9), most recent evidence suggests it plays no role. Firstly, neither $InsP_3$ nor Ca^{2+} has been found to activate the light-sensitive channels, even when released instantaneously by flash photolysis of caged precursors (Hardie, R. C., 1995; Hardie, R. C. and Raghu, P., 1998). Furthermore, although light induces a massive rise in cytosolic Ca^{2+}, this is almost entirely due to Ca^{2+} influx (see Section 1.05.6.1.1; Peretz, A. *et al.*, 1994; Ranganathan, R. *et al.*, 1994; Hardie, R. C., 1996b). Most importantly, all aspects of phototransduction appear to be completely normal in mutants of the only known $InsP_3R$ gene in *Drosophila* (Acharya, J. K. *et al.*, 1997; Raghu, P. *et al.*, 2000a). Although some pharmacological evidence has implicated the ryanodine receptor (RyR) in phototransduction in *Drosophila* (Arnon, A. *et al.*, 1997b), null mutants of the RyR again failed to shown any discernible phenotype (Sullivan, K. M. C. *et al.*, 2000).

By contrast, genetic evidence, particularly involving mutations of the *rdgA* gene encoding diacylgylcerol kinase (DGK), strongly implicates DAG in the excitatory pathway (Figure 16). The first indication was the finding that both TRP and TRPL channels were constitutively active in the dark in *rdgA* mutants, consistent with activation by build up of DAG by basal PLC activity (Raghu, P. *et al.*, 2000b). Recently, strong evidence for the requisite basal hydrolysis of PIP_2 by PLC has been

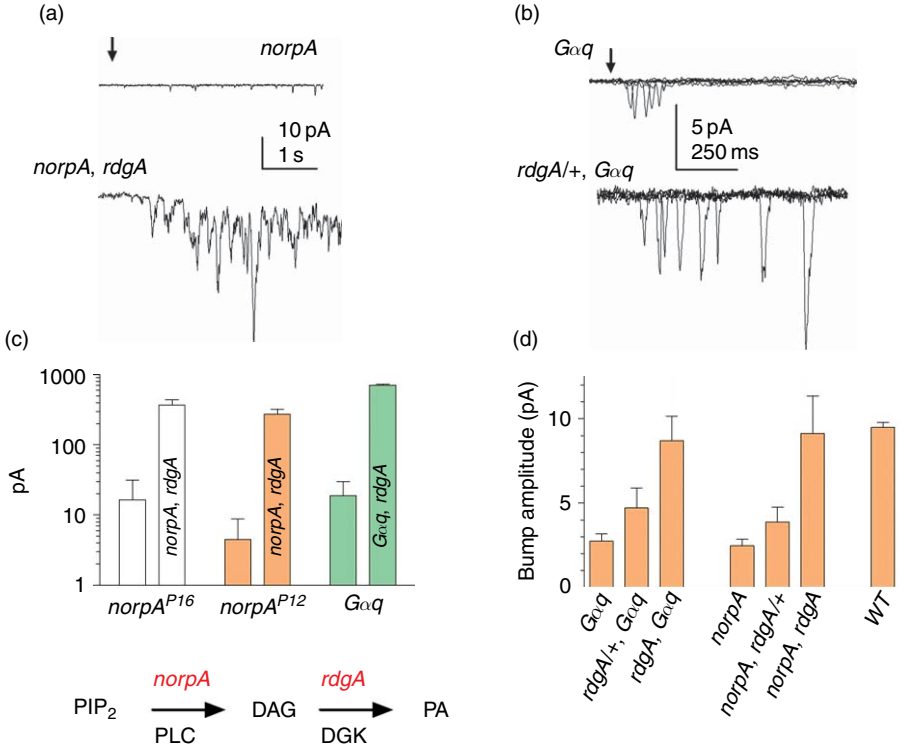

Figure 16 Genetic evidence for excitatory role of DAG. Mutations in DAG kinase (DGK, *rdgA* gene) greatly facilitate responses in PLC and *Gαq* hypomorphs. (a) A bright flash in a severe *norpA* hypomorph (*norpA*^{P12}) elicits no more than a few sporadic 1- to 2-pA bumps; in the double mutant *norpA*^{P12},*rdgA*^{1} the response to the same intensity is enhanced ~100-fold. (b) In a *Gαq* mutant, repeated flashes elicit small ~2-pA quantum bumps (traces superimposed); however, the bump amplitude is greatly increased even in a *rdgA*/+ heterozygote where the DGK levels are reduced by only ~50%. (c) Summary of averaged data (mean ± SEM) for macroscopic response amplitude in two *norpA* alleles (P12 and P16) and also the *Gαq* mutant (left bar, single mutant; right bar, in double mutant combination with *rdgA*) – note the logarithmic scale. (d) Summary of data on quantum bump amplitudes in *Gαq* and *norpA*^{P12}, showing dosage-dependent rescue by the *rdgA* mutation. Below: reference to the roles of PLC and DGK shows how the data can be readily interpreted if it is assumed that DAG is an excitatory messenger. Adapted with permission from Hardie, R. C., Martin, F., Cochrane, G. W., Juusola, M., Georgiev, P., and Raghu, P. 2002. Molecular basis of amplification in *Drosophila* phototransduction. Roles for G protein, phospholipase C, and diacylglycerol kinase. Neuron 36, 689–701.

obtained *in vivo* using the genetically targeted PIP_2 biosensor (Kir2.1 channel) in both WT and *rdgA* mutants (Figure 14 and Section 1.05.4.5.2). A second powerful argument is that DGK mutations massively facilitate the response to light in severe *norpA* or *Gαq* hypomorphs (Figure 16). In such mutants, bump amplitudes are reduced five- to tenfold (Figures 12 and 13) and the macroscopic response to light can be reduced 100- to 1000-fold. However, when combined with the *rdgA* mutation, responses are massively facilitated and quantum bump amplitudes restored to WT levels (Hardie, R. C. *et al.*, 2002). The possibility that pleiotropic effects of the *rdgA* mutation mediate such effects are effectively excluded by finding that even a ~50% knockdown of DGK activity in *rdgA*−/+ heterozygotes (themselves otherwise fully WT in behavior) is sufficient to substantially amplify responses in these PLC and G_q hypomorphic backgrounds (Figure 16, and Hardie, R. C. *et al.*, 2002).

The *Drosophila* TRP channels can also be activated by metabolic inhibition, and activate spontaneously for example in whole-cell recordings made without ATP in the electrode (Hardie, R. C. and Minke, B., 1994b; Agam, K. *et al.*, 2000). Whilst this has been taken as evidence of protein dephosphorylation – possibly of the channels themselves – contributing to their activation (Agam, K. *et al.*, 2000), a recent study found that activation by metabolic inhibition had an absolute requirement for PLC activity, and proposed that the primary mechanism was failure of DGK activity, combined with basal PLC activity, resulting in buildup of DAG (Hardie, R. C. *et al.*, 2004). An apparent additional requirement of Ca^{2+} inferred from the ability of high concentrations of BAPTA to block the spontaneous activation (Agam, K. *et al.*, 2004) may have been due to the suppression of PLC activity by low Ca^{2+} levels, and a previously unrecognized action of BAPTA as an inhibitor of PLC activity (Hardie, R. C., 2005).

Whilst DAG has been strongly implicated by these and other studies, and is now also widely accepted as an activator of several vertebrate TRPC channels (reviewed in: Hardie, R. C., 2003), at least two obstacles remain. Firstly the only data on DGK immunolocalization indicate that it is found predominantly in the SMC and not in the microvilli (Masai, I. *et al.*, 1997). However, the resolution was not sufficient to exclude presence at the base of the microvilli, which would potentially be sufficient to control DAG levels in the microvilli. Secondly, exogenous application of DAG either to photoreceptors or to heterologously expressed TRPL channels has little or no effect (Hardie, R. C., unpublished; Estacion, M. *et al.*, 2001). The only potential agonists yet found to activate the *Drosophila* channels are in fact poly- or monounsaturated fatty acids (PUFAs), such as arachidonic acid or linolenic acid. PUFAs activate TRPL channels in inside-out patches from heterologously expressed channels as well as both TRP and TRPL channels in whole-cell recordings from photoreceptors with an EC_{50} of ~10 μM (Chyb, S. *et al.*, 1999b). More recently, PUFAs, but not DAG have also been shown to activate the only other TRPC family member in *Drosophila*, namely TRPγ (Jors, S. *et al.*, 2006). PUFAs could in principle be released from DAG by DAG lipase or from phospholipids by PLA_2; however, to date there is no evidence for the existence of such enzymes in the transduction cascade in *Drosophila*. Although a mutation in a putative DAG lipase (rolling black out, *rbo*) recently described by Huang F. D. *et al.* (2004) did in fact result in a severe block in phototransduction, details of its phenotype, were not consistent with such a proposed role. Thus, *rbo* mutants were reported to show reduction in light-induced DAG production, interpreted as an apparent inhibition of PLC activity, whilst the mutant flies only stopped responding to light after continuous bright illumination.

One possible resolution to this problem is suggested by quantitative estimates of the rate of PIP_2 hydrolysis in the photoreceptors, again using the Kir2.1 channel as a PIP_2 biosensor. These measurements indicate that a single-photon absorption results in PLC activity at rates sufficient to hydrolyze all the PIP_2 (and probably also the PI and PIP reserve) in a single microvillus within less than 1 s (Figure 14; Hardie, R. C. *et al.*, 2001; 2004). Given that a single microvillus contains several thousand PI, PIP, and PIP_2 molecules, a simple calculation based on the surface area and volume of a microvillus suggests that, locally, DAG concentrations within the microvillus can be expected to reach near millimolar levels. DAG is notoriously insoluble and if the TRP channels respond to DAG levels in this concentration range, it may be experimentally impossible to apply exogenous DAG at such concentrations, whilst the more soluble PUFAs may act as surrogate, nonphysiological agonists on the same channels.

1.05.5.2 PIP_2 Depletion

In addition to mounting evidence for the role of DAG, recent studies have also raised the possibility that PIP_2 reduction may contribute to excitation.

The first indication was the finding that recombinant TRPL channels in inside-out patches, previously activated by application of exogenous PLCβ, could be inhibited by application of PIP_2 (Estacion, M. *et al.*, 2001). However, recordings of light-activated TRPL channel activity, isolated in *trp* mutants, suggest a different picture *in vivo*. In the *trp* mutant prolonged illumination leads to complete loss of PIP_2 in the microvillar membrane, because Ca^{2+} influx via the TRP channels appears to be required for inhibition of PLC activity (see Section 1.05.6.2), but under these conditions the remaining TRPL channels rapidly close and remain profoundly inactivated until PIP_2 is resynthesized (Hardie, R. C. *et al.*, 2001). This collapse of the response is consistent with a role for DAG in excitation, since the substrate for its generation is exhausted, but clearly contrary to what would be expected if PIP_2 depletion directly activated the channels. Interestingly, however, TRP channels behave rather differently. The Ca^{2+} influx required to prevent excessive PIP_2 hydrolysis by PLC can also be blocked by removing extracellular Ca^{2+}: under these conditions flashes of light which deplete a substantial fraction of PIP_2 usually result in a failure of the TRP channels to close after termination of the light flash. A similar failure in response termination can also be observed in mutants of the *rdgB* gene, which encodes an essential component of the PIP_2 recycling pathway (Vihtelic, T. S. *et al.*, 1993; Milligan, S. C. *et al.*, 1997; Hardie, R. C. *et al.*, 2001) (see Section 1.05.7 and Figure 17). Finally, when TRP channels are activated following ATP deprivation they remain active indefinitely, and long after all detectable PIP_2 has disappeared from the microvilli (Gu, Y. *et al.*, 2005). Since large amounts of DAG are also produced under all these conditions, activation cannot necessarily be attributed to PIP_2 depletion alone; however, a hypothesis worth further investigation is that channels may be activated by simultaneous generation of DAG and depletion of PIP_2. For example, the TRP protein (or associated proteins) might incorporate domains capable of binding PIP_2 and DAG (or PUFA); binding to PIP_2 would stabilize the closed state, whilst DAG/PUFA would stabilize the open state.

Further support for the roles of DAG and/or PIP_2 in excitation comes from recent studies of mutants (*laza*) of an eye-enriched phosphatidic acid phosphatase (PAP). More correctly referred to as lipid phosphate phosphohydrolase (LPP), this enzyme catalyzes the reverse reaction from DGK, namely PA to DAG (see Figure 17, Garcia-Murillas, I. *et al.*, 2006; Kwon, Y. and Montell, C., 2006). Analysis of *laza* mutants indicates that LPP acts antagonistically with DGK (*rdgA*) to regulate the levels of DAG and PA. Thus the normally slow response termination in the ERG of a hypomorphic *rdgA* mutant ($rdgA^3$) was accelerated in the $rdgA^3$; *laza* double mutant, but further slowed by overexpression of LPP using a WT *laza* transgene (Garcia-Murillas, I. *et al.*, 2006). Similarly, using an independently generated *laza* mutant, (Kwon, Y. and Montell, C., 2006) found that response amplitudes (measured by ERG) were reduced and response decay times accelerated in *laza* mutants. Similar genetic interactions between *laza* and *rdgA* were also seen in their retinal degeneration phenotypes – in that *laza* mutants suppress, and *laza* overexpression enhances degeneration in *rdgA* (Garcia-Murillas, I. *et al.*, 2006).

On the one hand, these results would appear to support a role for DAG in excitation and degeneration, since *laza* mutations would be expected to decrease DAG levels (at the expense of PA), whilst overexpression of LPP would increase DAG. However, Garcia-Murillas I. *et al.* (2006) also found that PI levels are reduced in *rdgA* mutants, particularly in combination with *laza* overexpression, due, not only to the involvement of PA as substrate for PI recycling (Section 1.05.7), but also because transcript levels of PI synthase, an essential enzyme for PIP_2 recycling were greatly reduced in these mutant backgrounds. Garcia-Murillas I. *et al.* (2006) also noted that whilst PA levels have been shown to be decreased in *rdgA* mutants (a finding which they confirm), DAG levels have been reported to remain unaltered (Inoue, H. *et al.*, 1989), and therefore interpret their results as support for the suggestion that the decrease in PIP_2 may underlie the degeneration, and possibly contribute to the excessive and prolonged activation of TRP channels.

In summary, there is little evidence to support a role for $InsP_3$ in excitation in *Drosophila*, whilst a number of recent studies have suggested that the alternative, membrane-delimited products of PLC activity (i.e., DAG, PUFAs, and PIP_2) are the relevant messengers of excitation. However, this area is still controversial and final resolution of the mechanism of excitation is likely to require, *inter alia*, identification and characterization of lipid-binding sites on the channel molecules, further biochemical analysis of light-induced lipid metabolism, and molecular identification and mutant analysis of any further gene products required for activation.

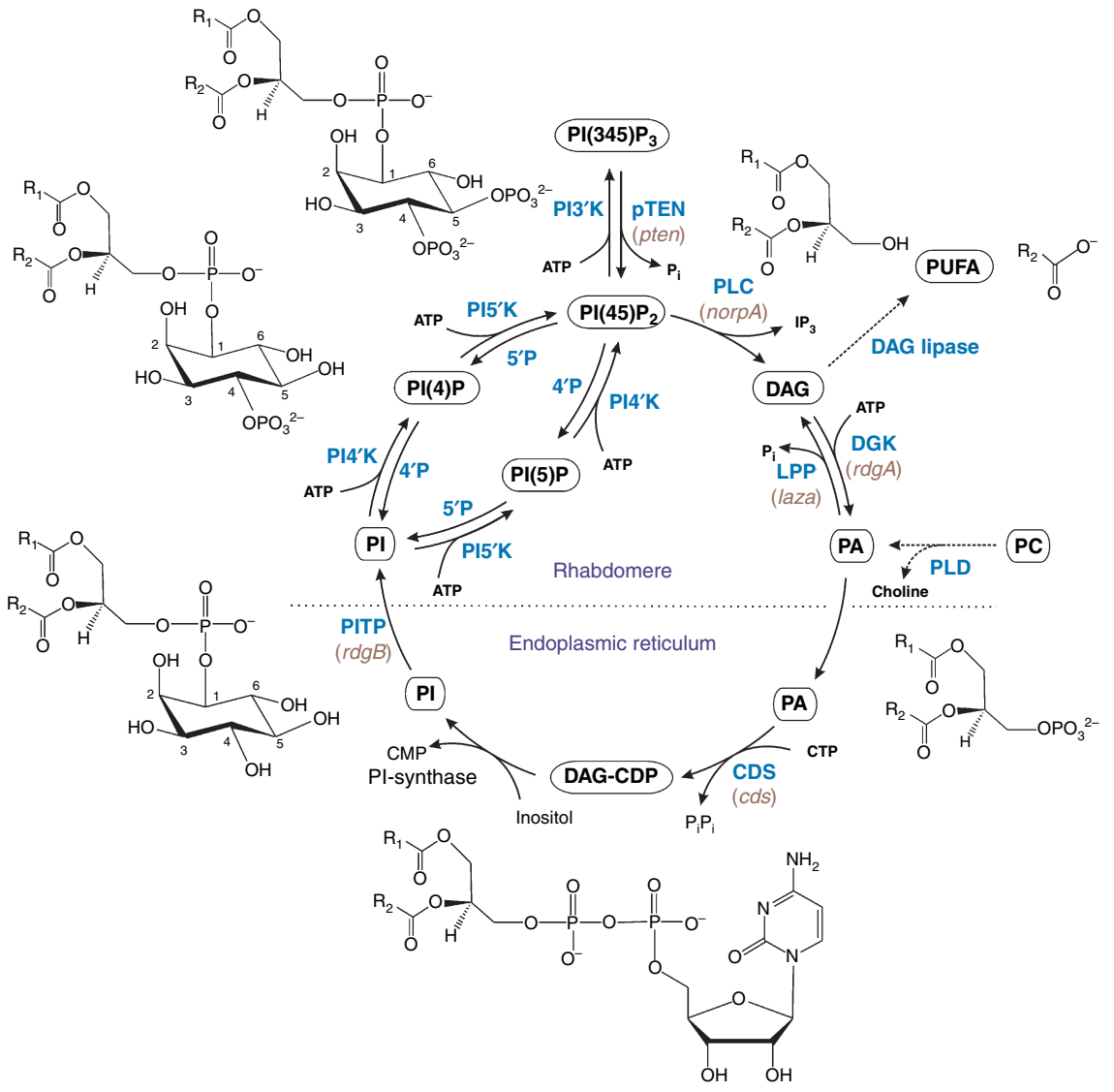

Figure 17 Phosphoinositide cycle. PIP_2 is hydrolyzed by PLC (*norpA* gene), generating diacylgylcerol (DAG) and $InsP_3$. DAG is converted to phosphatidic acid (PA) via DAG kinase (*rdgA*), the reverse reaction (PA to DAG) is catalyzed by LPP (*laza*); DAG may also be converted to PUFAs by a DAG lipase. PA can also be synthesized *de novo* by acylation of glycerophosphate and can be released from phosphatidylcholine (PC) by PLD. PA is combined with CTP to form CDP–DAG via CD synthase (*cds*) in the SMC. This in turn undergoes condensation with inositol to form to phosphatidylinositol (PI) via PI synthase. PI is transported back to the microvillar membrane by a PI transfer protein (*rdgB*). PI is converted to PIP_2 via sequential phosphorylation (PI kinase and PIP kinase) in the microvilli to reconstitute PIP_2. PIP_2 may also be further phosphorylated to PIP_3 via PI3′ kinase and reconverted via a PIP_3-specific lipid phosphatase (pTEN).

1.05.6 Ca^{2+}-Dependent Feedback and Mechanisms of Adaptation

Whilst current evidence argues that the primary agent of excitation is a membrane-delimited lipid messenger, the importance of Ca^{2+} influx via the channels as regulator of phototransduction and mediator of adaptation can hardly be overstated. This was graphically illustrated in some of the first whole-cell recordings from *Drosophila* photoreceptors investigating the effect of removing extracellular Ca^{2+} (Hardie, R. C. 1991b; Ranganathan, R. *et al.*, 1991). Both onset and offset kinetics are greatly slowed, quantum bump amplitudes are reduced about tenfold (Henderson, S. R. *et al.*, 2000), and the peak–plateau transition characteristic of light adaptation is largely abolished (Figure 18).

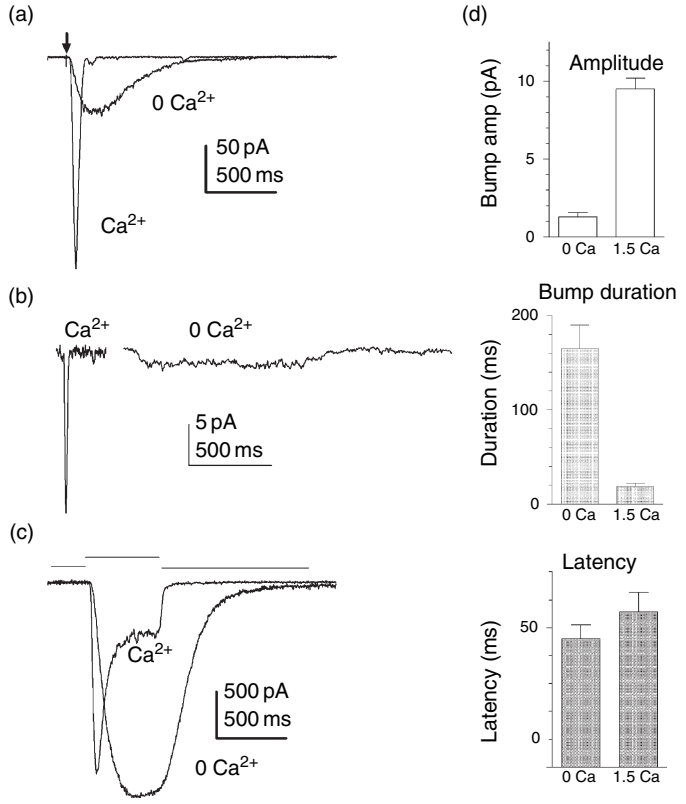

Figure 18 Ca^{2+}-dependent feedback. (a) Responses recorded in normal bath (Ca^{2+}) and after perfusing with EGTA-buffered Ca^{2+}-free Ringer (0 Ca^{2+}) reveal the profound influence of Ca^{2+} influx on the light response. Both rising and falling phases are greatly slowed down suggesting that Ca^{2+} influx mediates both positive and negative feedback. (b) This behavior is also seen at the level of the quantum bumps, which are greatly reduced in amplitude and prolonged in the absence of external Ca^{2+}. (c) Ca^{2+} influx is also essential for light adaptation: the peak-to-plateau transition during a 500 ms stimulus is eliminated in the absence of external Ca^{2+}. (d) Quantum bump parameters; amplitude, duration (half-width), and latency, measured in normal (1.5 mM Ca^{2+}) and Ca^{2+}-free bath. Note that the amplitude is reduced and the duration increased, but the latency is unaltered. For further details, see Henderson S. R. *et al.* (2000).

The mechanisms underlying this Ca^{2+}-dependent regulation are diverse and still not entirely understood, but they include both positive and negative feedback regulation, the latter in particular probably affecting most steps in the transduction cascade. Although Ca^{2+}-dependent positive feedback is arguably the most distinguishing feature of invertebrate phototransduction (in vertebrates, Ca^{2+}-dependent feedback is always operationally negative, see Phototransduction in Rods and Cones), there is little information on the underlying molecular mechanism(s) in *Drosophila*. Electrophysiologically, positive feedback is manifest as a about tenfold increase in the amplitude of the quantum bumps and an even larger increase in the absolute slope of the rising phase of the response. The feedback can be mimicked by cytosolic release of caged Ca^{2+}, which accelerates the light response with a submillisecond latency (Hardie, R. C., 1995). This would suggest that it acts at a very late stage in transduction – either on the channels themselves, and/or PLC which is facilitated by Ca^{2+} in the range from 10 nM to 1 μM (Running Deer, J. L. *et al.*, 1995) (see Sections 1.05.4.5.2 and 1.05.8.2 for further discussion).

1.05.6.1 Ca^{2+} Signals

Crucial to an understanding of Ca^{2+}-dependent feedback is an appreciation of the Ca^{2+} signals actually experienced by the photoreceptors during stimulation.

1.05.6.1.1 Ca^{2+} signals are dominated by Ca^{2+} influx

Ca^{2+} indicator dyes, including fluo-3, Ca orange, or INDO-1, loaded via the patch pipette reveal a massive and rapid light-induced rise in Ca^{2+} (Peretz, A.

et al., 1994; Ranganathan, R. *et al.*, 1994; Hardie, R. C., 1996b). Absolute estimates in *Drosophila*, made using ratiometric dyes indicate that Ca^{2+} concentration is ~160 nM in the dark, and can transiently reach light-induced values of ~50 μM, measured globally throughout the cell (Hardie, R. C., 1996b). The overwhelming majority of this signal derives from Ca^{2+} influx via the light-sensitive channels, since the Ca^{2+} signal is undetectable (Peretz, A. *et al.*, 1994; Ranganathan, R. *et al.*, 1994), or greatly reduced (Hardie, R. C., 1996b) when extracellular Ca^{2+} is removed. However, a small fluorescent signal, in principle representing a rise of ~20 nM free Ca^{2+}, can still be detected with bright illumination under optimal conditions in Ca^{2+}-free solutions (Hardie, R. C., 1996b; Cook, B. and Minke, B., 1999). Whilst this signal is clearly dependent on phototransduction (e.g., it is absent in *norpA* mutants), it was not significantly reduced in $InsP_3R$ mutants (Raghu, P. *et al.*, 2000a), but was eliminated in the absence of external Na^+ (Hardie, R. C., 1996b; Cook, B. and Minke, B., 1999). It therefore can even be questioned whether it represents release from internal stores; alternative possibilities might include release of buffered Ca^{2+} or a dye artefact induced by massive (bio)chemical changes and/or monovalent ion fluxes associated with responses under these conditions.

1.05.6.1.2 Ca^{2+} transients in the rhabdomeres

Notwithstanding the uncertainties concerning the origin and significance of the residual signal detected under Ca^{2+}-free conditions, the Ca^{2+} signal under physiological conditions is clearly predominantly mediated by Ca^{2+} influx via the TRP channels. TRPL channels are also permeable to Ca^{2+} and can sustain a reduced influx signal in *trp* mutants (Peretz, A. *et al.*, 1994; Hardie, R. C. 1996b) until they close following PIP_2 depletion. Both TRP and TRPL channels are localized along the length of the microvilli (Niemeyer, B. A. *et al.*, 1996), and spatial imaging of the Ca^{2+} influx in *Drosophila* also shows influx to be initially localized to the rhabdomeres (Ranganathan, R. *et al.*, 1994). Rather more accurate and informative Ca^{2+} imaging has been made in the larger fly *Calliphora*, using intracellular indicator dye-injection in the intact animal combined with imaging of the rhabdomeres through the fly's own optics (Oberwinkler, J. and Stavenga, D. G., 1998; 2000). By using a range of indicator dyes with different affinities, Ca^{2+} levels in the rhabdomeres were found transiently to reach values well in excess of 200 μM during bright illumination, before rapidly relaxing (within ~100 ms) to steady-state levels of maximally ~10 μM with the brightest illumination. Under light-adapted (LA) conditions, however, because of the reduction in gain associated with adaptation, incremental flashes generate greatly reduced inward currents and the Ca^{2+} transients in the microvilli now reached only ~50–100 μM (Figure 19). Whilst such measurements were made from the whole rhabdomere in *Calliphora*, theoretical considerations suggest that a similar situation should hold in *Drosophila*, and also that similar values are reached at the level of single microvilli in response to single-photon absorptions (Postma, M. *et al.*, 1999). In fact, the Ca^{2+} levels reached in single microvilli are probably even higher, since measurements will inevitably average the responses of both stimulated and unstimulated microvilli. The time course of the microvillar transients is also likely to be faster, as the measured responses will be smeared by the bump latency dispersion. Finally, the Ca^{2+} levels reached in individual microvilli in between photon absorptions in LA cells are likely to be lower than the measured steady-state level, again because this will represent the average of excited and unstimulated microvilli.

1.05.6.1.3 Ca^{2+} buffers and homeostasis

Invertebrate photoreceptors such as *Drosophila* experience more extreme Ca^{2+} levels than almost any other eukaryotic cells. There is relatively little information on how they cope with these levels, which probably reach a steady state of ~10 μM throughout the cell body during maintained illumination. However, appropriate regulation is vital not only for performance, but also because cell death and retinal degeneration rapidly result when levels are either too high or too low (e.g., Sahly, I. *et al.*, 1994; Alloway, P. G. *et al.*, 2000; Kiselev, A. *et al.*, 2000a; Raghu, P. *et al.*, 2000b; Yoon, J. *et al.*, 2000; Wang, T. *et al.*, 2005a; 2005b). By far, the dominant extrusion mechanism is a Na^+/Ca^{2+} exchanger (encoded by the *calx* gene), which is highly expressed in the microvillar membrane, where it can generate electrogenic Na^+/Ca^{2+} currents of at least 100 pA during Ca^{2+} extrusion. *calx* mutants show greatly reduced sensitivity to light, and response inactivation during continued illumination due to the Ca^{2+} overload, as well as severe and rapid light-dependent retinal degeneration due to Ca^{2+} cytotoxicity (Wang, T. *et al.*, 2005b).

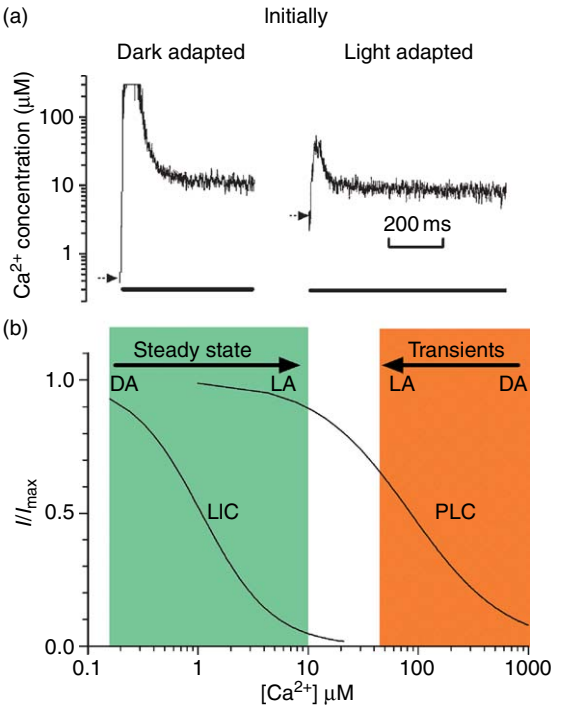

Figure 19 Ca^{2+} signals and adaptation strategy. (a) Ca^{2+} concentration measured in the rhabdomeres of the larger fly *Calliphora* in the intact animal using confocal imaging of the rhabdomeres via the intact optics. Cells were impaled with sharp intracellular microelectrodes containing the dye Oregon Green 5N. Left: In an initially dark adapted cell, Ca^{2+} rises from a submicromolar resting level (arrow) to values in excess of 200 μM (saturation level of the dye), before relaxing to a steady-state level of ~10 μM within ~200 ms. Right: In an initially light adapted cell, Ca^{2+} rises from an initial level of ~3 μM (arrow) to ~50 μM, relaxing now even more rapidly to a new steady state of 10 μM. (b) Based on these findings, as well as on detailed theoretical considerations, the global steady-state Ca^{2+} levels in the microvilli and cell body are believed to vary from ~150 nM in the dark to ~10 μM as background intensity is raised, whilst the transients experienced during incremental flashes (and at the level of microvilli, in response to single photons) vary from ~1 mM in dark adapted cells to ~50 μM in light-adapted cells. The curves show the Ca^{2+} dependence of the inhibition of the light-induced current and channels (LIC) with an IC_{50} of ~1 μM, and of PLC (IC_{50} ~75 μM) determined by manipulation of the Na^+/Ca^{2+} exchanger. This suggests that the gain during steady-state adaptation is primarily determined by the Ca^{2+}-dependent inhibition of TRP channels, whilst the transients experienced during the quantum bumps are sufficient to inhibit PLC, thereby preventing excessive PIP_2 hydrolysis. (a) Adapted with permission from Oberwinkler, J. and Stavenga, D. G. 2000. Calcium transients in the rhabdomeres of dark- and light-adapted fly photoreceptor cells. J. Neurosci. 20, 1701–1709. (b) Adapted with permission from Gu, Y., Oberwinkler, J., Postma, M., and Hardie, R. C. 2005. Mechanisms of light adaptation in *Drosophila* photoreceptors. Curr. Biol. 15, 1228–1234.

The cell body also contains Ca^{2+} stores, which can release enough Ca^{2+} to raise intracellular Ca^{2+} by a few 100 nM when their thapsigargin-sensitive Ca ATPase is inhibited. Although it is debatable whether the stores normally play any direct role in transduction, the Ca^{2+} released following application of thapsigargin or ionomycin is sufficient to facilitate responses to light recorded in Ca^{2+}-free solutions (Hardie, R. C., 1996a). The cell body and microvilli also contain a variety of Ca^{2+}-binding proteins that may function as Ca^{2+} buffers. Firstly, the microvilli have an unusually high level (~0.5 mM) of CaM (Porter, J. A. *et al.*, 1993), which may function as a buffer in addition to other roles described below (Section 1.05.6.2.1). Because of the high surface area-to-volume ratio in the microvillar lumen, low-affinity Ca^{2+} binding to negatively charged phospholipids may also be important. The cell body expresses at least two major Ca^{2+}-binding proteins, calphotin and calnexin. Calphotin is a novel Ca^{2+}-binding protein, which is enriched in the eye and found throughout a large, but distinct central region of the cell body. This region was also found to precipitate Ca oxalate, leading to speculation that it may represent a Ca^{2+}-sequestering sponge (Ballinger, D. G. *et al.*, 1993; Martin, J. H. *et al.*, 1993). Photoreceptors in *calphotin* mutants show severe developmental abnormalities, but calphotin's role as a buffer has not been further investigated (Yang, Y. and Ballinger, D., 1994). Calnexin is a molecular chaperone, and is required, along with the cyclophilin *ninaA* for Rh1 folding and targeting. However, it also appears to play a role as a Ca^{2+} buffer, since Ca^{2+} measurements reveal that abnormally high Ca^{2+} levels are reached during maintained illumination in *calnexin* mutants, whilst the photoreceptors also undergo light-dependent retinal degeneration that cannot be attributed to calnexin's role as a chaperone (Rosenbaum, E. E. *et al.*, 2006).

1.05.6.2 Ca^{2+}-Dependent Negative Feedback

Although a number of Ca^{2+}-dependent feedback targets have been identified in the transduction cascade (Table 3), until recently their respective contribution to light adaptation and response termination was rather poorly defined. A major advance in this respect was made recently by exploring the Ca^{2+} dependence of phototransduction by exploiting the properties of the Na^+/Ca^{2+} exchanger (CalX) to manipulate cytosolic Ca^{2+} in the microvilli (Gu, Y. *et al.*, 2005). The

Table 3 Molecular targets for Ca^{2+}-dependent feedback

Transduction protein	***Biochemical information***	***Function of feedback***
TRP	*In vivo* PKC substrate; contains CaM-binding site (CBS)	Ca^{2+}-dependent facilitation and inhibition
TRPL	*In vitro* PKC substrate; two CBS	Ca^{2+}-dependent inhibition
PLC (*norpA*)	Contains a Ca^{2+}-binding C2 motif. Inhibition is PKC dependent	Ca^{2+}-dependent regulation
INAD	*In vivo* PKC substrate; CBS	Unknown
Arrestin 2	CaMKII substrate	Prevents sequestration with M
Arrestin 1	CaMKII substrate	Unknown
Mediators (Ca^{2+}-dependent enzymes/binding protein)	***Substrates/binding partners***	***Function***
PKC (*inaC*)	TRP, INAD, NINAC	Ca^{2+}- (and DAG)-dependent inactivation
Rh phosphatase (*rdgC*)	CaCaM dependent	Rhodopsin dephosphorylation
CaMKII	Arr2 and Arr1	Pigment cycle
Calmodulin (*cam*)	TRP, TRPL, CaMKII, NINAC, INAD, RDGC	Ca^{2+}-dependent inactivation

Proteins reported to be subject to Ca^{2+}-dependent regulation. Protein targets have been separated into transduction proteins and mediators – i.e., Ca^{2+}-dependent enzymes and binding proteins. See text for further details and reference (Sections 1.05.6 and 1.05.8).

CalX exchanger, which is highly expressed in the microvilli (Wang, T. *et al.*, 2005b), belongs to the NCX family of exchangers, which have a stoichiometry of $3Na^+$:$1Ca^{2+}$, and as such should drive cytosolic Ca^{2+} toward an equilibrium determined by membrane voltage, the transmembrane Na^+ gradient and extracellular Ca^{2+}. By simply varying external Na^+, therefore, it is possible in principle to systematically manipulate cytosolic Ca^{2+} concentration to virtually any desired level. Using this approach it was shown that the LIC was sensitively inhibited by Ca^{2+} in the range 0.1–10 μM with an IC_{50} of ~1 μM Ca^{2+} (Gu, Y. *et al.*, 2005). Raising Ca^{2+} in this range in the dark also quantitatively mimicked the major features of light adaptation (gain reduction, parallel shift of V/log I curves and response acceleration). In marked contrast, PLC activity, monitored using the PIP_2 biosensor channels (Kir2.1), was completely unaffected over this range and was only inhibited by much higher Ca^{2+} levels (IC_{50} ~ 75 μM) indicating that the major features of light adaptation are mediated downstream of PLC (Figure 19, Gu, Y. *et al.*, 2005). An obvious target is the TRP channel that was also found to be inhibited by Ca^{2+} with an IC_{50} of ~1 μM. The very rapid time constant (1–2 ms) of Ca^{2+}-dependent inactivation of TRP, previously determined by applying hyperpolarizing voltage steps or by release of caged Ca^{2+}, suggests a direct mechanism, possibly with the involvement of CaM (Hardie, R. C. and Minke, B., 1994a; Hardie, R. C., 1995). These results thus suggested that the major features of light adaptation appear to be accounted for by Ca^{2+}-dependent inhibition of the light-sensitive channels, the final output stage of the transduction cascade.

Whilst apparently not directly contributing to light adaptation, the inhibition of PLC activity by higher levels of Ca^{2+}, which probably occur only during the Ca^{2+} transients, appears to be an essential mechanism to prevent depletion of PIP_2 during illumination. This inhibition fails not only in the absence of external Ca^{2+}, but also in *trp* mutants, apparently because the reduced Ca^{2+} influx through the less abundant, and less Ca^{2+}-permeable TRP channels is insufficient to generate the high Ca^{2+} levels required to inhibit PLC activity. The evidence for this again came from experiments using Kir2.1 biosensor channels to monitor PIP_2 hydrolysis (Figure 20): under normal conditions, illumination equivalent to bright daylight results in only very modest reductions of PIP_2 levels in the rhabdomere; however, in *trp* mutants even much weaker illumination results in hydrolysis of virtually all detectable PIP_2 (Hardie, R. C. *et al.*, 2001), with an intensity dependence similar to that of the *trp* decay phenotype (Hardie, R. C. *et al.*, 2004). The exhaustion of PLC substrate (PIP_2) due to failure of Ca^{2+}-dependent

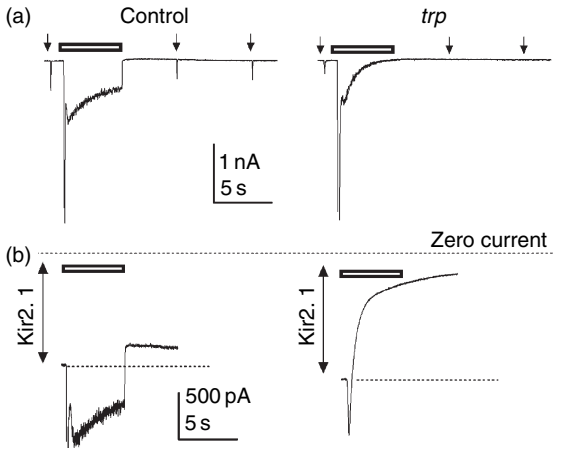

Figure 20 The *trp* decay phenotype is associated with depletion of PIP_2. (a) Whole-cell recordings of response in wild type (WT) (control) and *trp* mutant to a 5 s light stimulus (~30 000 photons per second). Whilst the WT response shows the typical peak–plateau transition due to light adaptation, the response in *trp* decays to baseline. Furthermore, responses to brief test flashes are completely eliminated following the decay in *trp*. (b) The same stimulus, now applied to WT and *trp* mutants expressing the PIP_2-sensitive Kir2.1 channel (see Figure 14). In both cases, the constitutive current of 1–2 nA (double arrows) indicates the response of Kir2.1 to prevailing dark levels of PIP_2. In the WT fly, following illumination there is only a minor reduction in the Kir2.1 current; however, in *trp* the Kir2.1 current is almost entirely suppressed, indicating hydrolysis of the majority of PIP_2. This suggests that Ca^{2+} influx via the TRP channel is required to inhibit PLC activity, and that failure of this inhibition leads to a catastrophic loss of PIP_2, accounting for the *trp* phenotype (Hardie, R. C. *et al.*, 2001).

inhibition of PLC activity thus provides a satisfying explanation for the long debated transient receptor potential *trp* phenotype, which had previously been attributed to depletion of intracellular Ca^{2+} stores (Cook, B. and Minke, B., 1999) or Ca^{2+}-/CaM-dependent inactivation of the TRPL channel (Scott, K. *et al.*, 1997).

The mechanism by which such high levels of Ca^{2+} inhibit PLC activity remains unsolved. Gu Y. *et al.* (2005) also found that PIP_2 levels were depleted by illumination in the PKC mutant *inaC* even more sensitively than is the case in the *trp* mutant, suggesting that the inhibition of PLC is PKC dependent (see Section 1.05.6.2.2).

1.05.6.2.1 Calmodulin

Effects of Ca^{2+} are often mediated by small Ca^{2+}-binding proteins (EF hand proteins), several of which have been implicated in feedback control in vertebrate rods and cones (see Phototransduction in Rods and Cones). In *Drosophila*, however, only one, the ubiquitously expressed CaM, has been implicated in phototransduction, where it acts on several target proteins (Table 3). CaM is highly localized in the microvilli, where it is expressed at unusually high levels (~0.5 mM), potentially enough to function as a Ca^{2+} buffer in addition to more direct roles (Porter, J. A. *et al.*, 1993). The major CaM-binding protein in the eye is the NINAC class III myosin (Section 1.05.4.9) (Porter, J. A. *et al.*, 1992), and the concentration of CaM in the microvilli is greatly reduced in *ninaC* mutants lacking the microvillar 174-kDa splice variant (Porter, J. A. *et al.*, 1993). These $ninaC^{\Delta 174}$ mutants also have a response deactivation defect and an abnormally large plateau response, which appears to be largely attributable to the reduced CaM level, since it can be mimicked in a mutant in which the CaM-binding site (CBS) alone has been deleted from the NINAC protein (Arnon, A. *et al.*, 1997a).

Further insight into CaM function has come from analysis of CaM hypomorphic mutants (*cam*) expressing less than 10% of the normal protein levels. *cam* mutants have even more pronounced defects in response termination than *ninaC*, and the kinetics of response termination no longer show an obvious dependence on external Ca^{2+} concentration (Scott, K. *et al.*, 1997). Closer examination revealed that the slow responses are predominantly a consequence of multiple bump trains in response to single-photon absorptions. Since these are similar to responses in *arr2* mutants (Figure 10), and are more or less abolished on a $G\alpha q$ mutant background, Scott K. *et al.* (1997) concluded that the defect was upstream of G protein and represented a defect in rhodopsin inactivation. They also found that the CaMKII phosphorylation of Arr2 was largely abolished in these flies. As discussed above (Arrestin Phosphorylation) however, Arr2 phosphorylation *per se* is not required for M inactivation by Arr2, so this result implies either an alternative role of CaM in M inactivation, or, as appears to be the case in the $Arr2^{S366A}$ mutant (which lacks the CaMKII phosphorylation site), that Arr2 in these flies becomes unavailable due to permanent sequestration in M–Arr2 complexes. As discussed in Rhodopsin Kinase and Phosphatase, another CaM target is rhodopsin phosphatase (encoded by *rdgC*), which is a Ca–CaM-dependent enzyme, though again the dephosphorylation of rhodopsin is not believed to impact directly upon the light response.

Both TRP and TRPL proteins also have one or more CBSs (Warr, C. G. and Kelly, L. E., 1996; Chevesich, J. *et al.*, 1997) and both channels are subject to Ca^{2+}-dependent inactivation (Hardie, R. C. and Minke, B., 1994a; Reuss, H. *et al.*, 1997; Scott, K. *et al.*, 1997). The TRP protein has one consensus CBS in the C-terminal; peptide fragments containing this region bind CaM in a Ca^{2+}-dependent manner *in vitro* (Chevesich, J. *et al.*, 1997), but the role of the TRP CBS has not been analyzed *in vivo*. *In vitro* studies indicate that one of the two CBS's in TRPL is conventional, binding CaM in a Ca^{2+}-dependent fashion, whilst the other (CBS2) binds the Ca^{2+}-free form of CaM, with dissociation occurring at high Ca^{2+} concentrations (>10 μM) (Warr, C. G. and Kelly, L. E., 1996). Warr C. G. and Kelly L. E. (1996) also found that CaM binding to the conventional CBS1 was modulated by both PKA and PKC phosphorylation *in vitro*. Scott K. *et al.* (1997) reported that transgenic flies expressing TRPL protein in which CBS1 had been deleted had abnormally long light responses with reduced Ca^{2+}-dependent inactivation.

1.05.6.2.2 Protein kinase C INAC

An eye-enriched PKC is a core member of the INAD signaling complex (Figure 6, Section 1.05.4.8), and is encoded by the *inaC* gene (Smith, D. P. *et al.*, 1991). The *inaC* PKC is a classical PKC with >50% identity to vertebrate PKC*β*s and PKC*α*s. Like them, it is presumed to be activated by a combination of DAG and Ca^{2+} via its two putative C1 domains (DAG binding) and one Ca^{2+}-binding C2 domain (reviewed in Shieh, B. H. *et al.*, 2002). INAC has at least two known *in vivo* substrates in the eye, namely the TRP channel and the INAD scaffolding protein (Huber, A. *et al.*, 1996b; 1998; Liu, M. *et al.*, 2000). The TRPL protein and the class III myosin NINAC have also been reported as *in vitro* targets for PKC phosphorylation (Warr, C. G. and Kelly, L. E., 1996; Li, H. S. *et al.*, 1998).

The *inaC* mutant has a specific deactivation defect, with flash responses showing a residual tail that decays slowly over 1–2 s (Figure 10) (Smith, D. P. *et al.*, 1991; Hardie, R. C. *et al.*, 1993). The deactivation phenotype is masked in recordings made in Ca^{2+}-free solutions (i.e., WT and *inaC* mutant responses are now similar), consistent with a defect in Ca^{2+}-dependent inactivation (Ranganathan, R. *et al.*, 1991). Although the deactivation defect in macroscopic responses resembles that in the *arr2* mutant, in *arr2* this results from each photon giving rise to a train of apparently normal bumps (Scott, K. *et al.*, 1997), whilst in *inaC* the defect occurs at the level of individual quantum bumps, which also show a similar waveform (Figure 10, Hardie, R. C. *et al.*, 1993). During sustained bright illumination, the response in *inaC* eventually decays to baseline, reminiscent of the *trp* phenotype (Hardie, R. C. *et al.*, 1993). Experiments using the Kir2.1 PIP_2 biosensor indicated that such responses are associated with a complete loss of PIP_2. This was interpreted as a requirement for PKC for the Ca^{2+}-dependent inhibition of PLC (Gu, Y. *et al.*, 2005). Failure to terminate PLC activity may thus explain the major features of the *inaC* phenotype:

1. the prolonged response, which could be interpreted as prolonged production of excitatory messenger (DAG and/or PIP2 reduction), and
2. the response decay with prolonged illumination due to PIP_2 depletion.

The mechanism by which PKC might inactivate PLC remains unclear, since PLC is not believed to be a direct substrate of PKC. However, since PLC is coupled to INAD in the signalplex, one possibility is that PLC activity could be modulated indirectly by the phosphorylation of INAD.

Recently, PKC was also shown to have an additional, and separable effect on the TRP channel. Popescu D. C. *et al.* (2006) identified a PKC phosphorylation site (Ser^{982}) on the TRP protein, and found that flies expressing TRP channels in which the site was mutated to alanine (TRP^{S982A}) showed a deactivation defect. This deactivation phenotype was less pronounced than that in an *inaC* null mutant, but was very similar to that observed in the $InaD^{P215}$ mutant, which has a point mutation in the PDZ domain responsible for binding TRP (Shieh, B. H. and Zhu, M. Y., 1996). This suggests that the association of TRP with INAD is required for its efficient phosphorylation by PKC. Despite this demonstration of PKC's role in TRP channel termination, it is important to note that the Ca^{2+}-dependent inhibition of the TRP channel is still essentially unaltered in *inaC* mutants (Gu, Y. *et al.*, 2005).

1.05.7 Phosphoinositide Metabolism

Maintenance of the substrate for PLC, PIP_2 is crucial to the functioning of the transduction cascade, as witnessed by the loss of all response when PIP_2 levels collapse, after failure of the Ca^{2+}-dependent inhibition of PLC in the *trp* mutant. PIP_2 recycling involves

a number of steps, summarized in Figure 17, which are believed to take place partly in the microvillar membrane and partly in the ER (i.e., the underlying SMC). Following complete depletion of PIP_2 in the rhabdomere by illumination in the *trp* or *trpl;trp* mutant, PIP_2 levels are restored with a halftime of ~60 s, as monitored either by Kir2.1 channels (see Figure 14), or by the time course for the recovery of the light response in the *trp* mutant (Hardie, R. C. *et al.*, 2001; Hardie, R. C. *et al.*, 2004). Indirect arguments suggest that the final steps in the microvilli (sequential phosphorylation of PI by PI and PIP kinases) are likely to be fast (seconds or subsecond), supplying PIP_2 essentially on demand (Hardie, R. C. *et al.*, 2001). This suggests that the rate-limiting step in recycling is likely to reside in a different part of the cycle, possibly slow transfer of lipids (e.g., PI) between the microvillar membrane and the ER, which form separate membrane containing compartments.

1.05.7.1 rdgA, Cytidine-5′-Diphosphate – Diacylglcerol Synthase, and Phosphatidylinositol Synthase

The first step in PI recycling after PIP_2 hydrolysis is the phosphorylation of DAG by DGK (encoded by *rdgA*) to form phosphatidic acid (PA), which also appears to be a key event in the termination of the light response (Section 1.05.5.1). As discussed in Section 1.05.5.2, the reverse reaction (dephosphorylation of PA to DAG) is catalyzed by LPP. The balance of activity between DGK and LPP appears to be crucial in determining the amount of PA available for PI recycling, and accordingly, *rdgA* mutants have significantly reduced PI and PIP_2 levels (Hardie, R. C. *et al.*, 2004; Garcia-Murillas, I. *et al.*, 2006). Recent evidence, suggests that PA derived from DAG is the major source of PA for PI recycling in the photoreceptors (Garcia-Murillas, I. *et al.*, 2006), but it may not be the only source. PA can be synthesized *de novo* (by acylation of glycerophosphate) and can also be generated by hydrolysis of phosphatidylcholine (PC) by the action of phospholipase D (PLD). Two recent studies of a *Drosophila* PLD mutant have suggested that PA derived from PC may also play a role in phototransduction and/or PI recycling (Lalonde, M. M. *et al.*, 2005; Kwon, Y. and Montell, C., 2006). However, an earlier biochemical study failed to find any evidence for involvement of PLD in PA synthesis in the *Drosophila* eye (Inoue, H. *et al.*, 1989).

PA is combined with CTP to form CDP–DAG by CDP–DAG synthase. A mutant in an eye-enriched isoform of this enzyme (*cds*) has a rather similar phenotype to *trp*, showing a loss of response after repeated stimulation, which could be restored by providing PIP_2 to the cell via the patch pipette (Wu, L. *et al.*, 1995). Strong evidence for essentially irreversible depletion of PIP_2 during continuous illumination was also provided by expressing the PIP_2 Kir2.1 biosensor channels in *cds* mutants (Hardie, R. C. *et al.*, 2002). In common with other mutants in the PI recycling pathway, *cds* mutants also undergo a light-dependent degeneration, which is rescued by the *norpA* (PLC) mutation PLC (Wu, L. *et al.*, 1995).

The next step in the PI cycle is the condensation of inositol and CDP–DAG to form phosphatidylinositol (PI) via the enzyme PI synthase. *Drosophila* contains only one PI synthase gene, and interestingly, its transcript levels are significantly reduced in the *rdgA* mutant and almost eliminated when LPP (*laza*) is overexpressed on the *rdgA* background (Garcia-Murillas, I. *et al.*, 2006). This suggests that PA, which is also severely reduced in these genetic backgrounds, may be a transcriptional regulator of this gene.

1.05.7.2 rdgB and Phosphatidylinositol Kinases

The reactions catalyzed by CDP–DAG synthase and PI synthase are presumed to take place in an ER compartment, probably the SMC. PI is then believed to be returned to the microvillar membrane by a PI transfer protein (PITP) encoded by the *rdgB* gene (Vihtelic, T. S. *et al.*, 1991; 1993), originally isolated as another light-dependent retinal degeneration mutant. Unlike previously characterized PITPs, which are soluble ~35 kDa proteins, RDGB protein is a 161kDa integral membrane protein. However its N-terminal has ~40% identity with the soluble PITP proteins, and in the meantime, mammalian homologues of *Drosophila rdgB* have been discovered, defining a new class (class II) of mammalian PITP proteins with similar topology (reviewed in Cockcroft, S., 2001).

Experiments with PIP_2 biosensors confirmed that PIP_2 recycling is effectively blocked in *rdgB* mutants (Hardie, R. C. *et al.*, 2001); however, there are indications that RDGB may have additional roles in the photoreceptors. For example, a point mutation in the PI transfer domain (T59E) restored PI transfer capability in an in *vitro* assay, but still resulted in a

dominant retinal degeneration phenotype, and in reduced levels of rhodopsin (Milligan, S. C. *et al.*, 1997). More generally, there is considerable evidence that mammalian *rdgB* homologues play multiple roles in membrane trafficking, including vesicle biogenesis and regulated exocytosis (Cockcroft, S., 2001; Allen-Baume, V. *et al.*, 2002).

Finally, PI must be sequentially phosphorylated by PI kinase and PIP kinase. There are several such kinases in the *Drosophila* genome, but which of them are involved in photoreceptors has yet to be unequivocally determined. The conventional route for PIP_2 synthesis would include phosphorylation of PI to PI(4)P by PI-4 kinase, followed by phosphorylation by a type I PIP kinase to PI(4,5) P_2. There are two type I PIP kinases in *Drosophila*, and one of these (*skittles*) has recently been implicated in the photoreceptors since *skittles* mutations were reported to enhance degeneration in *rdgA* (Garcia-Murillas, I. *et al.*, 2006).

1.05.8 Molecular Strategies of Quantum Bump Generation and Adaptation

As emphasized in the introduction, not only can *Drosophila* and other arthropod photoreceptors reliably detect single quanta of light with extremely fast response kinetics, but also they are able to light adapt over the full range of daylight light intensities. Although we do not yet fully understand the mechanism of channel activation and the precise mechanisms of Ca^{2+}-dependent regulation, our current knowledge of the transduction cascade allows us to draw some general conclusions about the strategies involved in achieving in this performance. At any one adaptational state the voltage-clamped macroscopic flash response is remarkably linear, simply representing the summation of the underlying quantum bumps (Figure 2, Henderson, S. R. *et al.*, 2000). The bumps themselves, however, are extremely nonlinear events with many of the characteristics of an action potential, including a threshold, positive and negative feedback and a refractory period. A key to understanding how these bumps are generated, and continue to be generated during light adaptation, is the extreme compartmentalization provided by the microvilli and possibly the ultrastructural organization of the INAD complex.

1.05.8.1 Compartmentalization and Local Signaling

The suggestion, that the signal transduction machinery driving single-photon responses is largely restricted to a single microvillus, dates back to observations that response saturation occurs at light levels equivalent to each microvillus absorbing just a single photon (Howard, J. *et al.*, 1987; Hochstrate, P. and Hamdorf, K., 1990). This is supported by the close congruence of the number of channels activated during a bump (~15) with biochemical estimates of the number (25) of TRP tetramers in a microvillus (Huber, A. *et al.*, 1996a). The restriction of activation to a single microvillus is also consistent with the relatively slow lateral diffusion expected in a membrane-delimited cascade, which is likely to prevent significant diffusion beyond the boundary of one microvillus during the relatively short latent period of the bump (Figure 21).

Each of the ~30–50 000 microvilli represents a tiny volume, ~1–2 μM in length and about 60 nm in diameter. The lumen of the microvillus is connected to the massive cell body via a narrow neck (Figure 1) allowing diffusional exchange of Ca^{2+}. The membrane of a single microvillus is densely packed with about 1000 rhodopsins, and contains only a limited number of the signal transduction components: estimated at about 50 G proteins, ~100 PLCs, ~25 TRP, and ~2 TRPL channels (Figure 21, Huber, A. *et al.*, 1996a). In *Drosophila* it is likely that only the G proteins and lipids are freely diffusible. In contrast, PLC and TRP channels are part of the INAD signaling complex (Figure 6, Section 1.05.4.8), which itself may be tethered to the cytoskeleton rendering it effectively immobile. Furthermore, by analogy to other arthropods (Goldsmith, T. H. and Wehner, R., 1977), it seems likely that rhodopsin itself is immobile on the timescale of transduction. Therefore G proteins are likely to act as diffusible shuttles that transduce the signal from the active M to the PLCs (Bahner, M. *et al.*, 2000). Importantly, a single rhodopsin can sequentially activate several G proteins, thereby amplifying the signal. The approximately fivefold reduction in bump amplitude in hypomorphic $G\alpha q$ mutants (Figure 12), where there is on average less than one G protein per microvillus, suggests that there may be five or so G proteins activated per rhodopsin, with an estimated minimal activation rate of 100–200 G proteins per second. After some delay, and at some distance from the activated rhodopsin, PLC molecules will be activated

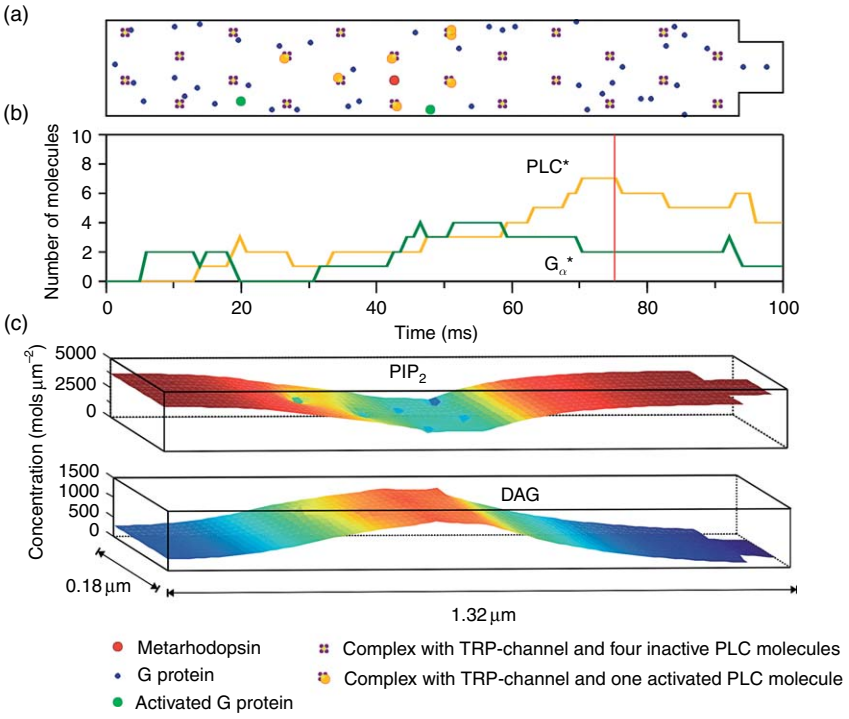

Figure 21 Stochastic modeling of the cascade. (a) Stochastic simulation (random walk encounter) of the membrane surface of a single microvillus, 75 ms after the absorption of a single photon. In the 75 ms since absorption of a single photon, the active metarhodopsin (red) has activated 10 G proteins, eight of which have encountered and activated a PLC (yellow), and two of which (green) are still freely diffusing in the membrane. Two PLCs have also already deactivated due to the PLC-activated GTPase activity of $G_q\alpha$. (b) Time course of the numbers of activated G proteins and PLC as a function of time after photon absorption. (c) Estimated levels of PIP_2 and DAG over the surface of the microvillus generated after 75 ms by the activated PLC molecules. The simulation has used best estimates of the numbers of G proteins (50) and PLC (100) in the microvillus and typical values for diffusion coefficients of G proteins and membrane lipids from the literature. Note that, whilst finite levels of DAG have already reached ~70% of the surface area of the microvillus, no significant diffusion beyond the microvillar boundaries has occurred by this time (Postma, M. and Hardie, R. C., unpublished). According to the model of positive feedback suggested in Section 1.05.8, once the first TRP channel opens (with relatively high DAG threshold), Ca^{2+} influx floods the microvillus within ~5 ms and facilitates activation of the remaining TRP channels to what were previously subthreshold levels of DAG (or derivative).

by $G_q\alpha$ subunits, and will start producing DAG, amplifying the signal further. DAG (or its derivative) will spread along the length of the microvillus and ultimately activate ~15 TRP channels (Figure 21).

1.05.8.2 Fast Nonlinear Response Kinetics

The high Ca^{2+} permeability of the TRP channels and the restricted luminal volume of the microvillus results in Ca^{2+} rising as high as 1 mM throughout the microvillus during a single-photon response (see Section 1.05.6.1.2, Figure 19, Postma, M. *et al.*, 1999; Oberwinkler, J. and Stavenga, D. G., 2000). This overwhelming Ca^{2+} rise is accompanied first by rapid facilitation, closely followed by complete inactivation of the current. Both the positive and negative feedback dominantly shape the waveform of the quantum bump (Figure 18).

The mechanism of facilitation is not known, but it is lacking in the *trp* mutant and therefore only appears to affect TRP channels. A plausible speculation is that it represents a Ca^{2+}-dependent shift in the affinity of the TRP channel for the active ligand, dramatically increasing its sensitivity, analogous perhaps to the shift in affinity to cGMP of the vertebrate CNG channels (Hsu, Y. T. and Molday, R. S., 1993). On this model, once the first channel opens, Ca^{2+} will flood the microvillus, thus further activating the TRP channels, which had been exposed to what were previously only subthreshold concentrations of the

excitatory lipid messenger (e.g., DAG). Another possibility is the facilitation of PLC by Ca^{2+} (Running Deer, J. L. *et al.*, 1995; Hardie, R. C., 2005).

Most of the components of the phototransduction cascade appear to be subject to Ca^{2+}-dependent inactivation (Section 1.05.6.2, Table 3). Firstly, Ca^{2+}-dependent inactivation of the light-sensitive channels TRP and TRPL, either directly, or via CaM (Section 1.05.6), terminates the LIC (Hardie, R. C. and Minke, B., 1994a; Gu, Y. *et al.*, 2005). Secondly, the Ca^{2+}- and PKC-dependent inhibition of PLC is crucial to prevent further production of DAG and depletion of PIP_2 (Hardie, R. C. *et al.*, 2001; Gu, Y. *et al.*, 2005). Finally, recent studies strongly suggest that inactivation of *Drosophila* metarhodopsin by Arr2 is also dependent on Ca^{2+} influx (Liu, C. H. *et al.*, in preparation). The requirement of Ca^{2+} influx for PLC and metarhodopsin inactivation has an elegant logic in that the upstream signals will only be terminated after the channels have been activated.

In summary, the key to fast response kinetics is a combination of the autocatalytic positive feedback loop caused by TRP channels leading to a massive Ca^{2+} influx in the restricted luminal volume of the microvillus, which then rapidly inactivates the cascade. Within 10–20 ms of the first channel opening, the single-photon response peaks and is then terminated with a time constant of about 8 ms. This contrasts with responses measured without Ca^{2+} influx, which peak at about 200 ms and have a decay time constant of about 200 ms with a about tenfold reduction in quantum bump amplitude (Figure 18, Henderson, S. R. *et al.*, 2000). In addition, two further important concepts need to be considered, namely quantum bump latency and the refractory period.

1.05.8.3 Quantum Bump Latency

After successful photon absorption, there is a finite delay before the response becomes apparent (e.g., Figure 2). This bump latency, with an average of ~45 ms, represents the time needed to open the first channel after photon absorption. Unlike vertebrate rods, which have rather invariant latencies, the bump latency in *Drosophila* is highly variable (20–100 ms), signifying on the one hand the stochastic nature of the phototransduction cascade, and on the other an effective threshold (and/or high cooperativity) for channel activation.

The stochastic variability in latency presumably originates from the low number of G proteins and PLC molecules activated during the latent period of the quantum bump. Indeed, stochastic modeling of the cascade, based on realistic diffusion coefficients for G protein and lipids can accurately model the latency and its variability (Postma, M. and Hardie, R. C. unpublished, Figure 21). Modeling also indicates that the latency should allow sufficient time for finite quantities of a putative lipid messenger of excitation to spread by lateral diffusion throughout most of the microvillus. This may help to ensure that the majority of the TRP channels in the microvillus are activated by the Ca^{2+}-dependent positive feedback once the first channel has opened.

As well as contributing to a large gain, such a locally saturated all-or-none response could also provide an excellent mechanism for ensuring reproducibility of the single-photon response, which over the cell has a coefficient of variance of ~0.4 (Henderson, S. R. *et al.*, 2000). The variability in even this relatively tight distribution may result from variability between microvilli, because single bumps repeatedly activated in the same microvillus are even more reproducible in amplitude (Scott, K. and Zuker, C. S., 1998). This performance may be achieved however, as a trade-off against the speed of the response, since the latency distribution is somewhat slower and broader than the quantum bump waveform, and hence represents a major constraint on the macroscopic response kinetics (Figure 2).

1.05.8.4 Refractory Period

Another potentially important consequence of the microvillar design is that the massive Ca^{2+} influx renders the microvillus inactive for a refractory period of about 100 ms. Only when the Ca^{2+} is cleared from the microvillus and the inactivation is removed will it be responsive again. Clearance of Ca^{2+} is predicted to occur very quickly (<100 ms) by a combination of diffusion into the cell body and the Na^+/Ca^{2+} exchanger, which acts very powerfully on the microvillus because of the high surface area-to-volume ratio.

An indication of this refractory period is provided by at least two lines of evidence. Firstly, when a carefully calibrated flash is delivered, just sufficient to activate every microvillus, then a second flash delivered immediately afterward is completely ineffective. However, when delivered after ~80 ms it can generate an additional response (Hochstrate, P. and Hamdorf, K., 1990). Secondly, in certain mutants (e.g., *arr2* and *cam*), activated metarhodopsin fails to

inactivate. In vertebrates, such mutants generate long-lasting quantum bumps that fail to terminate normally (Chen, J. *et al.*, 1995). However, in *Drosophila arr2* or *cam* mutants, single photons elicit a train of quantum bumps separated by an interbump interval of ~100 ms (e.g., Figure 10), but each quantum bump in the train terminates normally and is essentially indistinguishable from a WT bump (Scott, K. *et al.*, 1997). The interbump interval in such trains can thus be thought of as representing the refractory period during which activated rhodopsin can generate no response, but once this is over a second quantum bump can be generated again.

In a more conventional cascade such as in vertebrate rods, it is important that each and every stage of the transduction cascade is terminated rapidly, with the slowest step limiting the overall kinetics (see Phototransduction in Rods and Cones). However, a strictly localized refractory period can in principle mask the effect of any moderately slow termination reactions, as long as they are completed within the refractory period. This means that the off-response kinetics at the level of the electrophysiological response can be determined by very fast Ca^{2+}-dependent channel inactivation (time constant of <10 ms), whilst other steps such as metarhodopsin–arrestin binding, GTPase activity of the G protein and PIP_2 resynthesis could in principle afford to proceed more slowly, for example, 50–100 ms. Such a strategy could also reduce transducer noise associated with slower termination steps, which may be slow because of biophysical constraints, for example, slow binding or enzymatic reactions.

1.05.8.5 Adaptation

The microvillar design is also central to light adaptation, and in particular the ability of invertebrate photoreceptors to respond over the entire range of environmental intensities. With a refractory period of 100 ms (and probably less when light adapted), each individual microvillus should be able to generate quantum bumps at a rate of $\geq 10\,s^{-1}$. With ~45 000 microvilli in *Drosophila*, and more in the larger flies, this should allow the photoreceptors to process photon absorptions approaching $10^6\,s^{-1}$ – precisely the sorts of levels experienced under bright daylight conditions. This alone is not enough however, and to sustain such large photon fluxes without saturation, the light response needs to adapt by reducing gain. As in virtually all photoreceptors, this is achieved in the first instance by negative feedback regulation mediated primarily by Ca^{2+}, resulting in a progressive shifting of the intensity-response function curve, optimizing the dynamic range around the prevailing background light intensity. Early shot noise analysis in the 1970s and 1980s indicated that discrete quantum bumps continue to underlie the macroscopic response even under bright backgrounds, but that their amplitude and duration progressively decrease, giving rise to the adapting bump model of light adaptation, which still holds today (Wu, C. F. and Pak, W. L., 1978; Wong, F. *et al.*, 1980).

As discussed earlier (see Section 1.05.6.1), the microvillar design results in a distinction between

1. global steady-state Ca^{2+} levels, (~150 nm in the dark to maximally ~10 μM in the light), that are reached throughout the cell, including the unstimulated microvilli, and
2. the rapid microvillar transients, associated with each and every quantum bump that are maximally ~1 mM during the DA quantum bump, but only ~50–100 μM during the greatly attenuated LA quantum bumps (Figure 19).

In *Drosophila*, although Ca^{2+}-dependent feedback is found at virtually all stages of the cascade, our recent studies (see Section 1.05.6.2) suggest that the dominant mechanism for gain reduction during steady-state adaptation is the Ca^{2+}-dependent inhibition of the TRP (and TRPL) channels, which are inhibited with an IC_{50} of ~1 μM over a range that closely maps onto the global steady-state range of Ca^{2+} levels experienced during light adaptation (Figure 19). Although the mechanism is not fully understood, these relatively low concentrations of Ca^{2+} reduce the gain and shorten the duration of the quantum bump sufficiently to account for the major features of light adaptation, including the parallel shift of the response intensity function. By contrast, upstream activity of PLC appears not to be affected by these relatively low global Ca^{2+} levels, but importantly, it is inhibited over the range experienced during the rapid Ca^{2+} transients (Figure 19, Gu, Y. *et al.*, 2005).

This bipartite strategy (Ca^{2+}-dependent inhibition of channels by low global Ca^{2+} levels, and inhibition of upstream components such as PLC and M by rapid transients) can be seen as an effective solution for light adaptation, allowing for rapid response kinetics without exhausting the finite supply of PIP_2 required for phototransduction. Bump latency is a major determinant of response kinetics, and is itself critically dependent upon PIP_2 hydrolysis to generate sufficient lipid messenger to

overcome threshold for channel activation. Hence it is presumably important to maintain high PLC activity during light adaptation so as not to compromise latency. However, as shown by measurements with Kir2.1 PIP_2 biosensors (Figures 14 and 20), the rate of light-induced PLC activity in the microvilli is so high that it is sufficient to deplete the entire microvillus of PIP_2 in less than 1 s. The solution therefore is to rapidly terminate PLC activity by Ca^{2+} influx, but only after the bump has been initiated. The collapse of the light response due to exhaustion of PIP_2 in the *trp* mutant, or in Ca^{2+}-free bath, shows the disastrous consequences when this Ca^{2+}- (and PKC)-dependent inhibition fails (Figure 20).

Whilst accounting for many of the major features of light adaptation, this overview of adaptation is clearly an oversimplification. The overall output of the cell during adaptation is also influenced by many other factors, working on a variety of timescales. In particular, the description above has considered only the voltage-clamped LIC. In the physiologically relevant voltage domain, gain and kinetics will be further moderated by the passive and active (mainly voltage-dependent K^+ channels) properties of the membrane (Section 1.05.3.3); by the voltage-dependent Mg^{2+} block of the TRP channels, which reduces the effective single-channel conductance at depolarized membrane potentials (Section 1.05.4.6.2) and by synaptic feedback from higher-order interneurons (Zheng, L. *et al.*, 2006). As described in Section 1.05.2 every photoreceptor also has an autonomous pupil mechanism, whereby tiny pigment granules migrating toward the rhabdomere can reduce the effective light flux by up to two orders of magnitude. Photoreceptors in white-eyed mutants lacking this pupil saturate under bright illumination, indicating that this is an essential mechanism to avoid saturation under the brightest daylight intensities (Howard, J. *et al.*, 1987). Finally translocation of transduction components like G proteins (Section 1.05.4.4.2), TRPL channels (Section 1.05.4.6.4), and arrestin (Section 1.05.4.3.2), can fine-tune the gain and sensitivity during long-term adaptation.

1.05.9 Phototransduction Mechanisms in Other Invertebrates

1.05.9.1 Other Arthropods

It seems likely that all arthropod photoreceptors respond to light using a G_q-/PLC-based cascade resulting in a membrane depolarization. However, detailed information is restricted to relatively few preparations (notably *Limulus*, honeybee, crayfish, barnacle, and locust). Before the advent of molecular approaches, *Limulus* had been most extensively studied, and was the preferred preparation because of the large photoreceptors in the ventral eye, which allow stable intracellular recordings, and simultaneous impalement with several electrodes.

1.05.9.1.1 Limulus

In *Limulus* ventral photoreceptors, the role of $InsP_3$ as a messenger of excitation is well established. Injections of $InsP_3$ and Ca^{2+} itself both mimic the response to light (Brown, J. *et al.*, 1984; Fein, A. *et al.*, 1984; Bolsover, S. and Brown, J., 1985; Payne, R. *et al.*, 1986) and it is clear that $InsP_3$ activates $InsP_3$ receptors on the SMC, resulting in release of Ca^{2+} from intracellular stores which can raise free cytosolic Ca^{2+} to ~150 μM (Payne, R. *et al.*, 1986; Ukhanov, K. and Payne, R., 1995; Nasi, E. *et al.*, 2000). Despite compelling evidence for $InsP_3$ and Ca^{2+} as messengers of excitation in *Limulus*, the only substance that has been found to activate channels in excised patches from the microvillar membrane is cGMP (Bacigalupo, J. *et al.*, 1991). This has led to the proposal that generation of cGMP by a Ca^{2+}-dependent guanylate cyclase represents the final enzymatic component of the transduction cascade (Shin, J. *et al.*, 1993). Although there is no direct biochemical or molecular evidence for the presence of this enzyme, inhibitors of particulate guanylate cyclase severely attenuate the response to light (Garger, A. *et al.*, 2001), and a cGMP-gated ion channel has also recently been cloned from *Limulus*, which immunolocalizes to the microvillar membrane (Chen, F. H. *et al.*, 2001).

It has been suggested that this sequence of events accounts for the entire light response (Shin, J. *et al.*, 1993); however, a number of studies have reported that there may be three distinct classes of light-sensitive channels in *Limulus* (reviewed in: Nagy, K., 1991; Dorlochter, M. and Stieve, H., 1997; Nasi, E. *et al.*, 2000). These may correspond to three kinetic components of the light response that can be revealed by their differential recovery from light adaptation and distinct pharmacologies (Deckert, A. *et al.*, 1992; Nagy, K. *et al.*, 1993; Contzen, K. and Nagy, K., 1995; Nagy, K. and Contzen, K., 1997). This led to the suggestion that there may be parallel pathways involving three distinct G proteins, one operating via PLC and $InsP_3$, one via a guanylate cyclase, and one via adenylate cyclase (Dorlochter, M. and Stieve, H., 1997).

In an intriguing recent development, a *Limulus trp* homologue was cloned and found to be expressed in the ventral photoreceptors. Furthermore, the same authors found that a DAG analogue injected into the photoreceptors activate an inward current synergistically with Ca^{2+}, with electrical characteristics similar to the light-activated current (Bandyopadhyay, B. C. and Payne, R., 2004). This raises the possibility that at least one component of phototransduction in *Limulus* may be similar to *Drosophila*; i.e., a DAG-activated TRP channel. *Limulus* differs from *Drosophila* in that the light-induced current is essentially impermeable to Ca^{2+}, and therefore, the Ca^{2+}-dependent facilitation is provided by $InsP_3$-induced Ca^{2+} release, instead of Ca^{2+} influx as is the case in *Drosophila* (reviewed in Nasi, E. *et al.*, 2000).

Interestingly, quantum bumps in *Limulus* share many common features with those in *Drosophila*, including variable latency, low first stage (R-G) gain (Kirkwood, A. *et al.*, 1989), threshold, and positive and negative feedback by Ca^{2+}. However, there are also significant differences; firstly, the bump is mediated by several thousand channels spread over dozens of microvilli resulting in quantum bumps up to 4 nA in amplitude; secondly the Ca^{2+} originates primarily from Ca^{2+} release rather than influx. We can thus imagine that in *Limulus* the $InsP_3$ generated, initially in one microvillus, diffuses to the base of the microvillus where it releases Ca^{2+} from $InsP_3$-sensitive stores with sequential positive and negative feedback, probably being mediated by the bell-shaped Ca^{2+} sensitivity of the $InsP_3R$ (Payne, R. *et al.*, 1990). This results in a large, rapid, and relatively localized Ca^{2+} release signal, which can activate (possibly via GC) or facilitate ion channels over microvilli up to $\sim$2 μM distant from the release site.

1.05.9.1.2 Bee and crayfish

Bee photoreceptors have conspicuous and extensive SMC, which have functional $InsP_3$ receptors and also ryanodine receptors, which have been characterized in elegant studies using a permeabilized slice preparation (Baumann, O. and Walz, B., 1989; Walz, B. *et al.*, 1995). Whilst $InsP_3$-induced Ca^{2+} release almost certainly plays an important role in the bee, it is unknown whether the released Ca^{2+} is required for excitation or plays only roles in facilitation and adaptation, similar to the roles of Ca^{2+} influx in *Drosophila*. The large rhabdomeres in crayfish have been exploited for spectroscopic and biochemical measurements, but whilst it is clear that they have a G_q protein and PLC (Terakita, A. *et al.*, 1993) there is little data on downstream pathways. Intriguingly though, a recent report has detected PUFA production in crayfish eyes following long exposure to light, putatively via phospholipase A2 (Kashiwagi, T. *et al.*, 2000), which would release PUFAs from phosphatidylcholine. Apart from the evidence from *Limulus* there is very little evidence to suggest that cGMP plays a role in excitation in other arthropods.

1.05.9.2 Mollusks

Some of the most detailed biochemical characterizations of phototransduction in any microvillar photoreceptors have been performed in cephalopods such as the squid. Their large eyes, combined with a distinctive photoreceptor ultrastructure, whereby the microvillar membrane is separated from the rest of the cell, allows the isolation of large amounts of photoreceptive membrane in similar quantities to that available from mammalian preparations. Hence it was possible for example to extract and characterize squid rhodopsin some 50 years ago (Hubbard, R. and St. George, R. C. C., 1958). More recently, several groups have exploited this material to purify, characterize, and eventually clone and sequence several components of the cascade, including rhodopsin, G_q and PLCβ, along with a TRP homologue (Monk, P. D. *et al.*, 1996; Lott, J. S. *et al.*, 1999), which is likely to represent a light-sensitive channel. Quantitative biochemical experiments have demonstrated light-activated PLC activity (Szuts, E. Z., 1993); however, there is little or no indication as to whether $InsP_3$ or DAG (or indeed PIP_2) is the active messenger of excitation. The status and role of Ca^{2+} stores is also not clear, although (Walrond, J. P. and Szuts, E. Z., 1992) reported a system of submicrovillar tubules, which they suggested might be the equivalent of the SMC and function as Ca^{2+} stores.

Unfortunately, cephalopod photoreceptors have proved a difficult preparation for electrophysiology (but see Nasi, E. and Gomez, M. d. P., 1992) and the most detailed physiological studies of transduction in mollusks come from the scallops, *Pecten* and *Lima*. Remarkably, these bivalve mollusks have two distinct retinae with different types of photoreceptor: the proximal retina contains depolarizing microvillar photoreceptors, whilst the distal retina contains ciliary photoreceptors, which hyperpolarize. In keeping with the proposal that ciliary photoreceptors use cyclic nucleotide signaling pathways, the

light-sensitive channels in ciliary photoreceptors of the distal retina are cGMP-gated K^+ channels, and are probably activated by a cascade involving a G_o subclass of G protein and guanylate cyclase (Gomez, M. d. P. and Nasi, E., 1995; 2000). Uniquely amongst known photoreceptors, adaptation in these cells appears to be independent of Ca^{2+}, with sensitivity and kinetics of response completely unaffected by intracellular perfusion of 10 mM BAPTA (Gomez, M. d. P. and Nasi, E., 1997).

As in other microvillar photoreceptors, phototransduction in the proximal photoreceptors of *Lima* and *Pecten* is mediated by a PLC-based pathway, but once again the final mechanism of excitation is unclear (Nasi, E. *et al.*, 2000). There is clear evidence for light-induced release of Ca^{2+} from internal stores – presumably via $InsP_3$ – and $InsP_3$ injections have been reported to activate inward currents (Gomez, M. d. P. and Nasi, E., 1998). Since the light-sensitive channels (of which there are at least two classes) have only very limited permeability to Ca^{2+} (Gomez, M. d. P. and Nasi, E., 1996), the $InsP_3$ induced Ca^{2+} release is probably the major source of Ca^{2+} – whether it be for excitation, facilitation, or adaptation. In addition, DAG surrogates (phorbol esters), possibly acting via PKC, have also been reported to activate the light-sensitive channels (Gomez, M. d. P. and Nasi, E., 1998), whilst the most recent evidence has also suggested a direct role for PIP_2 depletion (Nasi, E. *et al.*, 2000; del Pilar Gomez, M. and Nasi, E., 2005).

1.05.9.3 Annelids

Leech photoreceptors, have a highly developed and extensive system of SMC, which have been shown to represent $InsP_3$-sensitive Ca^{2+} stores (Ukhanov, K. *et al.*, 2001). The photoreceptors have an unusual structure in which the microvilli enclose a large extracellular vacuole. This has been exploited by the development of a unique preparation of an inside-out cell, whereby the plasma membrane (but not the microvilli) is permeabilized, allowing unhindered intracellular perfusion of pharmacological agents, whilst an electrode can be inserted into the central vacuole to record conductance changes in the microvillar membrane. Using this preparation, it has been shown that Ca^{2+} can activate a depolarizing conductance with an EC_{50} of $\sim$1 μM. Agents that block $InsP_3$-induced Ca^{2+} release (such as heparin) block the plateau response to light, although a transient component appears relatively resistant to such agents (Walz, B. *et al.*, 2003).

1.05.10 Conclusion

Both vertebrate and invertebrate photoreceptors have been excellent models for our understanding of G-protein-coupled signaling. The bovine ROS preparation, in particular, was instrumental in the molecular identification of most of the key components of G protein-coupled signaling (see Phototransduction in Rods and Cones). *Drosophila* has been particularly important as a genetic model for PLC-based signaling, arguably the most widespread of the G-protein-coupled signaling cascades. The discovery of the TRP ion channel family was undoubtedly the most influential example of a novel signaling molecule discovered in this system, though others such as the RDGB family of PI transfer proteins, the NINAC class III myosin and the INAD scaffolding molecule also deserve mention. More than any other signal transduction cascade, phototransduction also lends itself to the most rigorous quantitative analysis, exemplified by the ability to analyze the responses to single photons. As such, the present detailed quantitative understanding of the molecular events underlying the photoresponse is unparalleled in other cellular signaling cascades.

Phototransduction in flies is often cited as the fastest known G-protein-coupled signaling cascade, and in the light-adapted state, some of the more rapidly flying Diptera can follow flickering stimuli at up to 300 Hz with 3 dB cutoffs greater than 100 Hz (Weckström, M. *et al.*, 1991). Remarkably, the same photoreceptors that sustain this performance under bright sunlight can still respond sensitively and rapidly to single photons in the dark. This is in marked contrast to vertebrates, which deploy two classes of photoreceptors to cover this range. Over 30 years of investigation, particularly in *Drosophila*, have now provided many of the answers as to how this performance is achieved. The key appears to be the extreme compartmentalization provided by the microvilli and possibly the INAD signaling complex. This minimizes diffusional delays, whilst allowing extremely rapid and highly localized Ca^{2+} transients, which accelerate the kinetics by sequential positive and negative feedback. There are nevertheless still important unanswered questions, the most pressing of which perhaps, are the exact mechanism of gating of the TRP channel, and how the dramatic facilitation by Ca^{2+} is achieved.

Although dipteran photoreceptors appear to outperform their vertebrate counterparts, their strategy

is not without costs. The main metabolic demand on any neuron is reestablishing the ionic gradients, which are required for electrical signaling and dissipated by every channel opening. The maximum potential LIC in *Drosophila* is probably in excess of 100 nA, and although this is never realized due to Ca^{2+}-dependent inhibition, peak responses of many tens of nanoamperes can be measured, and the steady-state voltage-clamped current during maintained illumination is ~500 pA. This contrasts with currents in vertebrate rods and cones, which are maximally only ~20–50 pA in the dark, and only progressively reduce during light.

Finally, although not comprehensively covered in this chapter, it has long been apparent that mutations in virtually any component of the cascade in *Drosophila* can result in retinal degeneration. In many, though by no means all cases, disturbances in Ca^{2+} homeostasis appear to be the underlying cause. Despite their distant evolutionary histories, the equivalent mutations in vertebrates also often result in hereditary retinal disease, or degenerative diseases in other systems. It is even possible to mimic a variety of human neurodegenerative diseases in the *Drosophila* eye, including Huntington's and Parkinson's disease by overexpressing the relevant mutant protein. Not only has the molecular genetic potential of *Drosophila* been decisive in enabling the analysis of the phototransduction cascade, but also similar strategies, such as genome saturating mutagenesis, can be applied to pursue the underlying molecular etiology of some of these devastating diseases (Bonini, N. M. and Fortini, M. E., 2003; Michno, K. *et al.*, 2005; Sang, T. K. and Jackson, G. R., 2005).

Acknowledgments

The authors' own work described in this chapter was supported by grants from the BBSRC, MRC, and the Wellcome Trust.

References

Acharya, J. K., Jalink, K., Hardy, R. W., Hartenstein, V., and Zuker, C. S. 1997. $InsP_3$ receptor is essential for growth and differentiation but not for vision in *Drosophila*. Neuron 18, 881–887.

Agam, K., von Campenhausen, M., Levy, S., Ben-Ami, H. C., Cook, B., Kirschfeld, K., and Minke, B. 2000. Metabolic stress reversibly activates the *Drosophila* light-sensitive channels TRP and TRPL *in vivo*. J. Neurosci. 20, 5748–5755.

Agam, K., Frechter, S., and Minke, B. 2004. Activation of the *Drosophila* TRP and TRPL channels requires both Ca^{2+} and protein dephosphorylation. Cell Calcium 35, 87–105.

Allen-Baume, V., Segui, B., and Cockcroft, S. 2002. Current thoughts on the phosphatidylinositol transfer protein family. FEBS Lett. 531, 74–80.

Alloway, P. G. and Dolph, P. J. 1999. A role for the light-dependent phosphorylation of visual arrestin. Proc. Natl. Acad. Sci. U. S. A. 96, 6072–6077.

Alloway, P. G., Howard, L., and Dolph, P. J. 2000. The formation of stable rhodopsin-arrestin complexes induces apoptosis and photoreceptor cell degeneration. Neuron 28, 129–138.

Anderson, J. and Hardie, R. C. 1996. Different photoreceptors within the same retina express unique combinations of potassium channels. J. Comp. Physiol. A 178, 513–522.

Arendt, D. 2003. Evolution of eyes and photoreceptor cell types. Int. J. Dev. Biol. 47, 563–571.

Arnon, A., Cook, B., Gillo, B., Montell, C., Sillinger, Z., and Minke, B. 1997a. Calmodulin regulation of light adaptation and store-operated dark current in *Drosophila* photoreceptors. Proc. Natl. Acad. Sci. U. S. A. 94, 5894–5899.

Arnon, A., Cook, B., Montell, C., Selinger, Z., and Minke, B. 1997b. Calmodulin regulation of calcium stores in phototransduction of *Drosophila*. Science 275, 1119–1121.

Arshavsky, V. Y. 2003. Protein translocation in photoreceptor light adaptation: a common theme in vertebrate and invertebrate vision. Sci. STKE 204, PE43.

Bacigalupo, J., Johnson, E. C., Vergara, C., and Lisman, J. E. 1991. Light-dependent channels from excised patches of *Limulus* ventral photoreceptors are opened by cGMP. Proc. Natl. Acad. Sci. U. S. A. 88, 7938–7942.

Bahner, M., Frechter, S., Da Silva, N., Minke, B., Paulsen, R., and Huber, A. 2002. Light-regulated subcellular translocation of *Drosophila* TRPL channels induces long-term adaptation and modifies the light-induced current. Neuron 34, 83–93.

Bahner, M., Sander, P., Paulsen, R., and Huber, A. 2000. The visual G protein of fly photoreceptors interacts with the PDZ domain assembled INAD signaling complex via direct binding of activated $G\alpha q$ to phospholipase $C\beta$. J. Biol. Chem. 275, 2901–2904.

Baker, E. K., Colley, N. J., and Zuker, C. S. 1994. The cyclophilin homolog NinaA functions as a chaperone, forming a stable complex in vivo with its protein target rhodopsin. EMBO J. 13, 4886–4895.

Ballinger, D. G., Xue, N., and Harshman, K. D. 1993. A *Drosophila* photoreceptor cell-specific protein, calphotin, binds calcium and contains a leucine zipper. Proc. Natl. Acad. Sci. U. S. A. 90, 1536–1540.

Bandyopadhyay, B. C. and Payne, R. 2004. Variants of TRP ion channel mRNA present in horseshoe crab ventral eye and brain. J. Neurochem. 91, 825–835.

Baumann, O. and Walz, B. 1989. Calcium- and inositol polyphosphate-sensitivity of the calcium-sequestering endoplasmic reticulum in the photoreceptor cells of the honeybee drone. J. Comp. Physiol. A 165, 627–636.

Bentrop, J. and Paulsen, R. 1986. Light-modulated ADP-ribosylation, protein phosphorylation and protein binding in isolated fly photoreceptor membranes. Eur. J. Biochem. 161, 61–67.

Bloomquist, B. T., Shortridge, R. D., Schneuwly, S., Pedrew, M., Montell, C., Steller, H., Rubin, G., and Pak, W. L. 1988. Isolation of putative phospholipase C gene of *Drosophila*, *norpA* and its role in phototransduction. Cell 54, 723–733.

Bolsover, S. and Brown, J. 1985. Calcium an intracellular messenger of light adaptation also participates in excitation of *Limulus* ventral photoreceptors. J. Physiol. (Lond.) 364, 381–393.

Bonini, N. M. and Fortini, M. E. 2003. Human neurodegenerative disease modeling using *Drosophila*. Annu. Rev. Neurosci. 10, 10.

Brown, J., Rubin, L., Ghalayini, A., Tarver, A. P., Irvine, R., Berridge, M., and Anderson, R. 1984. myo-inositol polyphosphate may be a messenger for visual excitation in *Limulus* photoreceptors. Nature 311, 160–163.

Byk, T., BarYaacov, M., Doza, Y. N., Minke, B., and Selinger, Z. 1993. Regulatory arrestin cycle secures the fidelity and maintenance of the fly photoreceptor cell. Proc. Natl. Acad. Sci. U. S. A. 90, 1907–1911.

Chen, F. H., Baumann, A., Payne, R., and Lisman, J. E. 2001. A cGMP-gated channel subunit in *Limulus* photoreceptors. Vis. Neurosci. 18, 517–526.

Chen, J., Makino, C. L., Peachey, N. S., Baylor, D. A., and Simon, M. I. 1995. Mechanisms of rhodopsin inactivation in vivo as revealed by a COOH- terminal truncation mutant. Science 267, 374–377.

Chevesich, J., Kreuz, A. J., and Montell, C. 1997. Requirement for the PDZ domain protein, INAD, for localization of the TRP store-operated channel to a signaling complex. Neuron 18, 95–105.

Chi, C. and Carlson, S. D. 1981. Lanthanum and freeze fracture studies on the retinular cell junction in the compound eye of the housefly. Cell Tissue Res. 214, 541–552.

Chyb, S., Hevers, W., Forte, M., Wolfgang, W. J., Selinger, Z., and Hardie, R. C. 1999a. Modulation of the light response by cAMP in *Drosophila* photoreceptors. J. Neurosci. 19, 8799–8807.

Chyb, S., Raghu, P., and Hardie, R. C. 1999b. Polyunsaturated fatty acids activate the *Drosophila* light-sensitive channels TRP and TRPL. Nature 397, 255–259.

Clapham, D. E. 2003. TRP channels as cellular sensors. Nature 426, 517–524.

Cockcroft, S. 2001. Phosphatidylinositol transfer proteins couple lipid transport to phosphoinositide synthesis. Semin. Cell Dev. Biol. 12, 183–191.

Combet, C., Jambon, M., Deleage, G., and Geourjon, C. 2002. Geno3D: automatic comparative molecular modelling of protein. Bioinformatics 18, 213–214.

Contzen, K. and Nagy, K. 1995. Current components stimulated by different G-proteins in *Limulus* ventral photoreceptor. NeuroReport 6, 1905–1908.

Cook, B., BarYaacov, M., BenAmi, H. C., Goldstein, R. E., Paroush, Z., Selinger, Z., and Minke, B. 2000. Phospholipase C and termination of G-protein-mediated signalling in vivo. Nat. Cell Biol. 2, 296–301.

Cook, B. and Minke, B. 1999. TRP and calcium stores in *Drosophila* phototransduction. Cell Calcium 25, 161–171.

Cosens, D. J. and Manning, A. 1969. Abnormal electroretinogram from a *Drosophila* mutant. Nature 224, 285–287.

Deckert, A., Nagy, K., Helricht, C. S., and Stieve, H. 1992. Three components in the light-induced current of the *Limulus* ventral photoreceptor. J. Physiol. (Lond.) 453, 69–96.

Deland, M. C. and Pak, W. L. 1973. Reversibly temperature sensitive phototransduction mutant of *Drosophila melanogaster*. Nat. New Biol. 244, 184–186.

Devary, O., Heichal, O., Blumenfeld, A., Cassel, D., Suss, E., Barash, S., Rubinstein, C. T., Minke, B., and Selinger, Z. 1987. Coupling of photoexcited rhodopsin to inositol phospholipid hydrolysis in fly photoreceptors. Proc. Natl. Acad. Sci. U. S. A. 84, 6939–6943.

Dolph, P. J., ManSonHing, H., Yarfitz, S., Colley, N. J., Running Deer, J., Spencer, M., Hurley, J. B., and Zuker, C. S. 1994. An eye-specific Gβ subunit essential for termination of the phototransduction cascade. Nature 370, 59–61.

Dolph, P. J., Ranganathan, R., Colley, N. J., Hardy, R. W., Socolich, M., and Zuker, C. S. 1993. Arrestin function in inactivation of G protein-coupled receptor rhodopsin *in vivo*. Science 260, 1910–1916.

Dorlochter, M. and Stieve, H. 1997. The *Limulus* ventral photoreceptor: light response and the role of calcium in a classic preparation. Prog. Neurobiol. 53, 451–515.

Elia, N., Frechter, S., Gedi, Y., Minke, B., and Selinger, Z. 2005. Excess of Gβe over Gqα in vivo prevents dark, spontaneous activity of *Drosophila* photoreceptors. J. Cell Biol. 171, 517–526.

Estacion, M., Sinkins, W. G., and Schilling, W. P. 2001. Regulation of *Drosophila* transient receptor potential-like (TRPL) channels by phospholipase C-dependent mechanisms. J. Physiol. 530, 1–19.

Feiler, R., Bjornson, R., Kirschfeld, K., Mismer, D., Rubin, G. M., Smith, D. P., Socolich, M., and Zuker, C. S. 1992. Ectopic expression of ultraviolet-rhodopsins in the blue photoreceptor cells of *Drosophila*: visual physiology and photochemistry of transgenic animals. J. Neurosci. Res. 12, 3862–3868.

Fein, A., Payne, R., Corson, D. W., Berridge, M. J., and Irvine, R. F. 1984. Photoreceptor excitation and adaptation by inositol 1,4,5-trisphosphate. Nature 311, 157–160.

Ferreira, P. A. and Pak, W. L. 1994. Bovine phospholipase C highly homologous to the NorpA protein of *Drosophila* is expressed specifically in cones. J. Biol. Chem. 269, 3129–3131.

Frechter, S. and Minke, B. 2006. Light-regulated translocation of signaling proteins in *Drosophila* photoreceptors. J. Physiol. (Paris) 99, 133–139.

Fu, Y., Liao, H. W., Do, M. T., and Yau, K. W. 2005. Non-image-forming ocular photoreception in vertebrates. Curr. Opin. Neurobiol. 15, 415–422.

Garcia-Murillas, I., Pettitt, T., Macdonald, E., Okkenhaug, H., Georgiev, P., Trivedi, D., Hassan, B., Wakelam, M., and Raghu, P. 2006. *lazaro* encodes a lipid phosphate phosphohydrolase that regulates phosphatidylinositol turnover during *Drosophila* phototransduction. Neuron 49, 533–546.

Garger, A., Richard, E. A., and Lisman, J. E. 2001. Inhibitors of guanylate cyclase inhibit phototransduction in *Limulus* ventral photoreceptors. Vis. Neurosci. 18, 625–632.

Gärtner, W. 2000. Invertebrate Visual Pigments. In: Molecular Mechanisms in Visual Transduction (*eds*. D. G. Stavenga, W. J. DeGrip, and E. N. Pugh), pp. 297–388. Elsevier.

Geourjon, C., Combet, C., Blanchet, C., and Deleage, G. 2001. Identification of related proteins with weak sequence identity using secondary structure information. Protein Sci. 10, 788–797.

Gillo, B., Chorna, I., Cohen, H., Cook, B., Manistersky, I., Chorev, M., Arnon, A., Pollock, J. A., Selinger, Z., and Minke, B. 1996. Coexpression of *Drosophila* TRP and TRP-like proteins in *Xenopus* oocytes reconstitutes capacitative Ca^{2+} entry. Proc. Natl. Acad. Sci. U. S. A. 93, 14146–14151.

Goel, M., Garcia, R., Estacion, M., and Schilling, W. P. 2001. Regulation of *Drosophila* TRPL channels by immunophilin FKBP59. J. Biol. Chem. 276, 38762–38773.

Goldsmith, T. H. and Wehner, R. 1977. Restrictions of rotational and translational diffusion of pigment in the membranes of a rhabdomeric photoreceptor. J. Gen. Physiol. 70, 453–490.

Gomez, M.d. P. and Nasi, E. 1995. Activation of light-dependent K^+ channels in ciliary invertebrate photoreceptors involves cGMP but not the IP_3/Ca^{2+} cascade. Neuron 15, 607–618.

Gomez, M.d. P. and Nasi, E. 1996. Ion permeation through light-activated channels in rhabdomeric photoreceptors – role of divalent-cations. J. Gen. Physiol. 107, 715–730.

Gomez, M.d. P. and Nasi, E. 1997. Light adaptation in *Pecten* hyperpolarizing photoreceptors insensitivity to calcium manipulations. J. Gen. Physiol. 109, 371–384.

Gomez, M.d. P. and Nasi, E. 1998. Membrane current induced by protein kinase C activators in rhabdomeric

photoreceptors: implications for visual excitation. J. Neurosci. 18, 5253–5263.
Gomez, M.d. P. and Nasi, E. 2000. Light transduction in invertebrate hyperpolarizing photoreceptors: possible involvement of a G_o-regulated guanylate cyclase. J. Neurosci. 20, 5254–5263.
Govardovskii, V. I., Fyhrquist, N., Reuter, T., Kuzmin, D. G., and Donner, K. 2000. In search of the visual pigment template. Vis. Neurosci. 17, 509–528.
Gu, Y., Oberwinkler, J., Postma, M., and Hardie, R. C. 2005. Mechanisms of light adaptation in *Drosophila* photoreceptors. Curr. Biol. 15, 1228–1234.
Gu, G., Yang, J., Mitchell, K. A., and O'Tousa, J. E. 2004. *Drosophila* NinaB and NinaD act outside of retina to produce rhodopsin chromophore. J. Biol. Chem. 279, 18608–18613.
Han, M., Gurevich, V. V., Vishnivetskiy, S. A., Sigler, P. B., and Schubert, C. 2001. Crystal structure of beta-arrestin at 1.9 A: possible mechanism of receptor binding and membrane translocation. Structure 9, 869–880.
Hardie, R. C. 1979. Electrophysiological analysis of the fly retina I comparative properties of R1–6 and R7 and R8. J. Comp. Physiol. A 129, 19–33.
Hardie, R. C. 1985. Functional organization of the fly retina. Prog. Sens. Physiol. 5, 1–79.
Hardie, R. C. 1986. The photoreceptor array of the dipteran retina. Trends Neurosci. 9, 419–423.
Hardie, R. C. 1989. A histamine-activated chloride channel involved in neurotransmission at a photoreceptor synapse. Nature 339, 704–706.
Hardie, R. C. 1991a. Voltage-sensitive potassium channels in *Drosophila* photoreceptors. J. Neurosci. 11, 3079–3095.
Hardie, R. C. 1991b. Whole-cell recordings of the light-induced current in *Drosophila* photoreceptors: evidence for feedback by calcium permeating the light sensitive channels. Proc. Roy. Soc. Lond. B 245, 203–210.
Hardie, R. C. 1995. Photolysis of caged Ca^{2+} facilitates and inactivates but does not directly excite light-sensitive channels in *Drosophila* photoreceptors. J. Neurosci. 15, 889–902.
Hardie, R. C. 1996a. Excitation of *Drosophila* photoreceptors by BAPTA and ionomycin: evidence for capacitative Ca^{2+} entry?. Cell Calcium 20, 315–327.
Hardie, R. C. 1996b. INDO-1 measurements of absolute resting and light-induced Ca^{2+} concentration in *Drosophila* photoreceptors. J. Neurosci. 16, 2924–2933.
Hardie, R. C. 2003. Regulation of TRP channels via lipid second messengers. Annu. Rev. Physiol. 65, 735–759.
Hardie, R. C. 2005. Inhibition of phospholipase C activity in *Drosophila* photoreceptors by 1,2-bis(2-aminophenoxy)ethane *N*,*N*,*N*′,*N*′-tetraacetic acid (BAPTA) and di-bromo BAPTA. Cell Calcium 38, 547–556.
Hardie, R. C. and Minke, B. 1992. The *trp* gene is essential for a light-activated Ca^{2+} channel in *Drosophila* photoreceptors. Neuron 8, 643–651.
Hardie, R. C. and Minke, B. 1994a. Calcium-dependent inactivation of light-sensitive channels in *Drosophila* photoreceptors. J. Gen. Physiol. 103, 409–427.
Hardie, R. C. and Minke, B. 1994b. Spontaneous activation of light-sensitive channels in *Drosophila* photoreceptors. J. Gen. Physiol. 103, 389–407.
Hardie, R. C. and Mojet, M. H. 1995. Magnesium-dependent block of the light-activated and *trp*-dependent conductance in *Drosophila* photoreceptors. J. Neurophysiol. 74, 2590–2599.
Hardie, R. C. and Raghu, P. 1998. Activation of heterologously expressed *Drosophila* TRPL channels: Ca^{2+} is not required and $InsP_3$ is not sufficient. Cell Calcium 24, 153–163.
Hardie, R. C. and Raghu, P. 2001. Visual transduction in *Drosophila*. Nature 413, 186–193.
Hardie, R. C., Gu, Y., Martin, F., Sweeney, S. T., and Raghu, P. 2004. *In vivo* light-induced and basal phospholipase C activity in *Drosophila* photoreceptors measured with genetically targeted phosphatidylinositol 4,5-bisphosphate-sensitive ion channels (Kir2.1). J. Biol. Chem. 279, 47773–47782.
Hardie, R. C., Martin, F., Chyb, S., and Raghu, P. 2003. Rescue of light responses in the *Drosophila* ''null'' phospholipase C mutant, *norpA*^{P24}, by the diacylglycerol kinase mutant, *rdgA*, and by metabolic inhibition. J. Biol. Chem. 278, 18851–18858.
Hardie, R. C., Martin, F., Cochrane, G. W., Juusola, M., Georgiev, P., and Raghu, P. 2002. Molecular basis of amplification in *Drosophila* phototransduction. Roles for G protein, phospholipase C, and diacylglycerol kinase. Neuron 36, 689–701.
Hardie, R. C., Peretz, A., Suss-Toby, E., Rom-Glas, A., Bishop, S. A., Selinger, Z., and Minke, B. 1993. Protein kinase C is required for light adaptation in *Drosophila* photoreceptors. Nature 363, 634–637.
Hardie, R. C., Raghu, P., Moore, S., Juusola, M., Baines, R. A., and Sweeney, S. T. 2001. Calcium influx via TRP channels is required to maintain PIP_2 levels in *Drosophila* photoreceptors. Neuron 30, 149–159.
Hardie, R. C., Reuss, H., Lansdell, S. J., and Millar, N. S. 1997. Functional equivalence of native light-sensitive channels in the *Drosophila trp*^{301} mutant and TRPL cation channels expressed in a stably transfected *Drosophila* cell line. Cell Calcium 21, 431–440.
Hardie, R. C., Voss, D., Pongs, O., and Laughlin, S. B. 1991. Novel potassium channels encoded by the *Shaker* locus in *Drosophila* photoreceptors. Neuron 6, 477–486.
Harteneck, C., Obukhov, A. G., Zobel, A., Kalkbrenner, F., and Schultz, G. 1995. The *Drosophila* cation channel Trpl expressed in insect Sf9 cells is stimulated by agonists of G-protein-coupled receptors. FEBS Lett. 358, 297–300.
Haug-Collet, K., Pearson, B., Webel, R., Szerencsei, R. T., Winkfein, R. J., Schnetkamp, P. P., and Colley, N. J. 1999. Cloning and characterization of a potassium-dependent sodium/calcium exchanger in *Drosophila*. J. Cell Biol. 147, 659–670.
Henderson, S. R., Reuss, H., and Hardie, R. C. 2000. Single photon responses in *Drosophila* photoreceptors and their regulation by Ca^{2+}. J. Physiol. (Lond.) 524, 179–194.
Hevers, W. and Hardie, R. C. 1995. Serotonin modulates the voltage dependence of delayed rectifier and *Shaker* potassium channels in *Drosophila* photoreceptors. Neuron 14, 845–856.
Hicks, J. L., Liu, X., and Williams, D. S. 1996. Role of the NINAC proteins in photoreceptor cell structure: ultrastructure of *ninaC* deletion mutants and binding to actin filaments. Cell Motil. Cytoskeleton 35, 367–379.
Hillman, P., Hochstein, S., and Minke, B. 1983. Transduction in invertebrate photoreceptors: role of pigment bistability. Physiol. Rev. 63, 668–772.
Hochstrate, P. and Hamdorf, K. 1990. Microvillar components of light adaptation in blowflies. J. Gen. Physiol. 95, 891–910.
Hofstee, C. A. and Stavenga, D. G. 1996. Calcium homeostasis in photoreceptor cells of *Drosophila* mutants *inaC* and *trp* studied with the pupil mechanism. Vis. Neurosci. 13, 257–263.
Hofstee, C. A., Henderson, S., Hardie, R. C., and Stavenga, D. G. 1996. Differential effects of NINAC proteins (p132 and p174) on light-activated currents and pupil mechanism in *Drosophila* photoreceptors. Vis. Neurosci. 13, 897–906.
Hotta, Y. and Benzer, S. 1970. Genetic dissection of the *Drosophila* nervous system by means of mosaics. Proc. Natl. Acad. Sci. U. S. A. 67, 1156–1163.

Houdusse, A., Kalabokis, V. N., Himmel, D., Szent-Gyorgyi, A. G., and Cohen, C. 1999. Atomic structure of scallop myosin subfragment S1 complexed with MgADP: a novel conformation of the myosin head. Cell 97, 459–470.

Howard, J., Blakeslee, B., and Laughlin, S. B. 1987. The intracellular pupil mechanism and the maintenance of photoreceptor signal: noise ratios in the blowfly *Lucilia cuprina*. Proc. R. Soc. Lond. B 231, 415–435.

Hsu, Y. T. and Molday, R. S. 1993. Modulation of the cGMP-gated channel of rod photoreceptor cells by calmodulin. Nature 361, 76–79.

Hu, Y., Vaca, L., Zhu, X., Birnbaumer, L., Kunze, D. L., and Schilling, W. P. 1994. Appearance of a novel Ca^{2+} influx pathway in Sf9 insect cells following expression of the transient receptor potential-like (*trpl*) protein of *Drosophila*. Biochem. Biophys. Res. Comm. 201, 1050–1056.

Huang, F. D., Matthies, H. J., Speese, S. D., Smith, M. A., and Broadie, K. 2004. Rolling blackout, a newly identified PIP_2–DAG pathway lipase required for *Drosophila* phototransduction. Nat. Neurosci. 7, 1070–1078.

Hubbard, R. and St. George, R. C. C. 1958. The rhodopsin system of the squid. J. Gen. Physiol. 41, 501–528.

Huber, A. 2001. Scaffolding proteins organize multimolecular protein complexes for sensory signal transduction. Eur. J. Neurosci. 14, 769–776.

Huber, A., Sander, P., Bahner, M., and Paulsen, R. 1998. The TRP Ca^{2+} channel assembled in a signaling complex by the PDZ domain protein INAD is phosphorylated through the interaction with protein kinase C (ePKC). FEBS Lett. 425, 317–322.

Huber, A., Sander, P., Gobert, A., Bahner, M., Hermann, R., and Paulsen, R. 1996a. The transient receptor potential protein (Trp), a putative store-operated Ca^{2+} channel essential for phosphoinositide-mediated photoreception, forms a signaling complex with NorpA, InaC and InaD. EMBO J. 15, 7036–7045.

Huber, A., Sander, P., and Paulsen, R. 1996b. Phosphorylation of the InaD gene product, a photoreceptor membrane protein required for recovery of visual excitation. J. Biol. Chem. 271, 11710–11717.

van Huizen, R., Miller, K., Chen, D. M., Li, Y., Lai, Z. C., Raab, R. W., Stark, W. S., Shortridge, R. D., and Li, M. 1998. Two distantly positioned PDZ domains mediate multivalent INAD–phospholipase C interactions essential for G protein-coupled signaling. EMBO J. 17, 2285–2297.

Hyde, D. R., Mecklenburg, K. L., Pollock, J. A., Vihtelic, T. S., and Benzer, S. 1990. Twenty *Drosophila* visual system cDNA clones: one is a homolog of human arrestin. Proc. Natl. Acad. Sci. U. S. A. 87, 1008–1012.

Ikura, M., Clore, G. M., Gronenborn, A. M., Zhu, G., Klee, C. B., and Bax, A. 1992. Solution structure of a calmodulin-target peptide complex by multidimensional NMR. Science 256, 632–638.

Inoue, H., Yoshioka, T., and Hotta, Y. 1985. A genetic study of inositol trisphosphate involvement in phototransduction using *Drosophila* mutants. Biochem. Biophys. Res. Commun. 132, 513–519.

Inoue, H., Yoshioka, T., and Hotta, Y. 1989. Diacylglycerol kinase defect in a *Drosophila* retinal degeneration mutant *rdgA*. J. Biol. Chem. 264, 5996–6000.

Jansonius, N. M. 1990. Properties of the sodium-pump in the blowfly photoreceptor cell. J. Comp. Physiol. A 167, 461–467.

Johnson, E. C. and Pak, W. L. 1986. Electrophysiological study of *Drosophila* rhodopsin mutants. J. Gen. Physiol. 88, 651–673.

Jors, S., Kazanski, V., Foik, A., Krautwurst, D., and Harteneck, C. 2006. Receptor-induced activation of *Drosophila* TRPgamma by polyunsaturated fatty acids. J. Biol. Chem. 281, 29693–29702.

Juusola, M. and Hardie, R. C. 2001. Light adaptation in *Drosophila* photoreceptors: I. Response dynamics and signaling efficiency at 25 degrees C. J. Gen. Physiol. 117, 3–25.

Kashiwagi, T., Meyer-Rochow, V. B., Nishimura, K., and Eguchi, E. 2000. Light activation of phospholipase A(2) in the photoreceptor of the crayfish (*Procambarus clarkii*). Acta Neurobiol. Exp. 60, 9–16.

Kiefer, C., Sumser, E., Wernet, M. F., and Von Lintig, J. 2002. A class B scavenger receptor mediates the cellular uptake of carotenoids in *Drosophila*. Proc. Natl. Acad. Sci. U. S. A. 99, 10581–10586.

Kimple, M. E., Siderovski, D. P., and Sondek, J. 2001. Functional relevance of the disulfide-linked complex of the N-terminal PDZ domain of InaD with NorpA. EMBO J. 20, 4414–4422.

Kirkwood, A., Weiner, D., and Lisman, J. E. 1989. An estimate of the number of G regulator proteins activated per excited rhodopsin in living *Limulus* ventral photoreceptors. Proc. Natl. Acad. Sci. U. S. A. 86, 3872–3876.

Kirschfeld, K. and Franceschini, N. 1977. Evidence for a sensitising pigment in fly photoreceptors. Nature 269, 386–390.

Kirschfeld, K. and Vogt, K. 1980. Calcium ions and pigment migration in fly photoreceptors. Naturwissenschaften 67, 516–517.

Kirschfeld, K., Feiler, R., Hardie, R., Vogt, K., and Franceschini, N. 1983. The sensitizing pigment in fly photoreceptors. Properties and candidates. Biophys. Struct. Mech. 10, 81–92.

Kiselev, A., Socolich, M., Vinos, J., Hardy, R. W., Zuker, C. S., and Ranganathan, R. 2000a. A molecular pathway for light-dependent photoreceptor apoptosis in *Drosophila*. Neuron 28, 139–152.

Kiselev, A., Sokolich, M., and Ranganathan, R. 2000b. Long-lived internalized phosphorylated Rh1 metarhodopsin/Arrestin-2/Clathrin complex mediates *Drosophila* photoreceptor cell apoptosis. *Drosophila*. Invest. Ophtalmol. Vis. Sci. 41, 4652B599.

Kosloff, M., Elia, N., Joel-Almagor, T., Timberg, R., Zars, T. D., Hyde, D. R., Minke, B., and Selinger, Z. 2003. Regulation of light-dependent G_q a translocation and morphological changes in fly photoreceptors. EMBO J. 22, 459–468.

Koundakjian, E. J., Cowan, D. M., Hardy, R. W., and Becker, A. H. 2004. The Zuker collection: a resource for the analysis of autosomal gene function in *Drosophila melanogaster*. Genetics 167, 203–206.

Kumar, J. P. and Ready, D. F 1995. Rhodopsin plays an essential structural role in *Drosophila* photoreceptor development. Development 121, 4359–4370.

Kwon, Y. and Montell, C. 2006. Dependence on the Lazaro phosphatidic acid phosphatase for the maximum light response. Curr. Biol. 16, 723–729.

Lalonde, M. M., Janssens, H., Rosenbaum, E., Choi, S. Y., Gergen, J. P., Colley, N. J., Stark, W. S., and Frohman, M. A. 2005. Regulation of phototransduction responsiveness and retinal degeneration by a phospholipase D-generated signaling lipid. J. Cell Biol. 169, 471–479.

Lan, L., Bawden, M. J., Auld, A. M., and Barritt, G. J. 1996. Expression of *Drosophila* TrpI cRNA in *Xenopus laevis* oocytes leads to the appearance of a Ca^{2+} channel activated by Ca^{2+} and Calmodulin, and by guanosine 5′[gamma-thio]triphosphate. Biochem. J. 316, 793–803.

Lee, S. J. and Montell, C. 2001. Regulation of the rhodopsin protein phosphatase, RDGC, through interaction with Calmodulin. Neuron 32, 1097–1106.

Lee, S. J. and Montell, C. 2004. Light-dependent translocation of visual arrestin regulated by the NINAC myosin III. Neuron 43, 95–103.

Lee, Y. J., Dobbs, M. B., Verardi, M. L., and Hyde, D. R. 1990. *dgq*: a *Drosophila* gene encoding a visual system-specific Galpha molecule. Neuron 5, 889–898.

Lee, Y. J., Shah, S., Suzuki, E., Zars, T., Oday, P. M., and Hyde, D. R. 1994. The *Drosophila dgq* gene encodes a Ga protein that mediates phototransduction. Neuron 13, 1143–1157.

Lee, S. J., Xu, H., Kang, L. W., Amzel, L. M., and Montell, C. 2003. Light adaptation through phosphoinositide-regulated translocation of *Drosophila* visual arrestin. Neuron 39, 121–132.

Lee, S. J., Xu, H., and Montell, C. 2004. Rhodopsin kinase activity modulates the amplitude of the visual response in *Drosophila*. Proc. Natl. Acad. Sci. U. S. A. 101, 11874–11879.

Leung, H. T., Geng, C., and Pak, W. L. 2000. Phenotypes of trpl mutants and interactions between the transient receptor potential (TRP) and TRP-like channels in *Drosophila*. J. Neurosci. 20, 6797–6803.

Li, H. S. and Montell, C. 2000. TRP and the PDZ protein, INAD, form the core complex required for retention of the signalplex in *Drosophila* photoreceptor cells. J. Cell Biol. 150, 1411–1422.

Li, C. J., Geng, C. X., Leung, H. T., Hong, Y. S., Strong, L. L. R., Schneuwly, S., and Pak, W. L. 1999. INAF, a protein required for transient receptor potential Ca^{2+} channel function. Proc. Natl. Acad. Sci. U. S. A. 96, 13474–13479.

Li, H. S., Porter, J. A., and Montell, C. 1998. Requirement for the NINAC kinase/myosin for stable termination of the visual cascade. J. Neurosci. 18, 9601–9606.

von Lintig, J. and Vogt, K. 2000. Filling the gap in vitamin A research. Molecular identification of an enzyme cleaving beta-carotene to retinal. J. Biol. Chem. 275, 11915–11920.

von Lintig, J., Dreher, A., Kiefer, C., Wernet, M. F., and Vogt, K. 2001. Analysis of the blind *Drosophila* mutant *ninaB* identifies the gene encoding the key enzyme for vitamin A formation *in vivo*. Proc. Natl. Acad. Sci. U. S. A. 98, 1130–1135.

Liu, M., Parker, L. L., Wadzinski, B. E., and Shieh, B. H. 2000. Reversible phosphorylation of the signal transduction complex in *Drosophila* photoreceptors. J. Biol. Chem. 275, 12194–12199.

Liu, C. H., Satoh, A. K., Postma, M., Ready, D. F., and Hardie, R. C. Ca^{2+} dependence of rhodopsin inactivation in *Drosophila* photoreceptors (in preparation).

Liu, C. H., Wang, T., Postma, M., Obukhov, A. G., Montell, C., and Hardie, R. C. 2007. *In vivo* identification and manipulation of the Ca^{2+} selectivity filter in the *Drosophila* transient receptor potential channel. J. Neurosci. 27, 604–615.

Lott, J. S., Wilde, J. I., Carne, A., Evans, N., and Findlay, J. B. C. 1999. The ordered visual transduction complex of the squid photoreceptor membrane. Mol. Neurobiol. 20, 61–80.

Martin, J. H., Benzer, S., Rudnicka, M., and Miller, C. A. 1993. Calphotin: a *Drosophila* photoreceptor cell calcium-binding protein. Proc. Natl. Acad. Sci. U. S. A. 90, 1531–1535.

Masai, I., Suzuki, E., Yoon, C. S., Kohyama, A., and Hotta, Y. 1997. Immunolocalization of *Drosophila* eye-specific diacylglycerol kinase, RdgA, which is essential for the maintenance of the photoreceptor. J. Neurobiol. 32, 695–706.

Matsumoto, H. and Pak, W. L. 1984. Light-induced phosphorylation of retina-specific polypeptides of *Drosophila in vivo*. Science 223, 184–186.

Matsumoto, H., Kurien, B. T., Takagi, Y., Kahn, E. S., Kinumi, T., Komori, N., Yamada, T., Hayashi, F., Isono, K., Pak, W. L., Jackson, K. W., and Tobin, S. L. 1994. Phosrestin I undergoes the earliest light-induced phosphorylation by a calcium/calmodulin-dependent protein kinase in *Drosophila* photoreceptors. Neuron 12, 997–1010.

McKay, R. R., Chen, D. M., Miller, K., Kim, S., Stark, W. S., and Shortridge, R. D. 1995. Phospholipase C rescues visual defect in norpA mutant of *Drosophila* melanogaster. J. Biol. Chem. 270, 13271–13276.

Melyan, Z., Tarttelin, E. E., Bellingham, J., Lucas, R. J., and Hankins, M. W. 2005. Addition of human melanopsin renders mammalian cells photoresponsive. Nature 433, 741–745.

Meyer, N. E., Joel-Almagor, T., Frechter, S., Minke, B., and Huber, A. 2006. Subcellular translocation of the eGFP-tagged TRPL channel in *Drosophila* photoreceptors requires activation of the phototransduction cascade. J. Cell Sci. 119, 2592–2603.

Michno, K., van de Hoef, D., Wu, H., and Boulianne, G. 2005. Demented flies? using *Drosophila* to model human neurodegenerative diseases. Clin. Genet. 67, 468–475.

Milligan, S. C., Alb, J. G., Elagina, R. B., Bankaitis, V. A., and Hyde, D. R. 1997. The phosphatidylinositol transfer protein domain of *Drosophila* retinal degeneration B protein is essential for photoreceptor cell survival and recovery from light stimulation. J. Cell Biol. 139, 351–363.

Minke, B. 1982. Light-induced reduction in excitation efficiency in the trp mutant of *Drosophila*. J. Gen. Physiol. 79, 361–385.

Minke, B. and Hardie, R. C. 2000. Genetic Dissection of *Drosophila* Phototransduction. In: Handbook of Biological Physics (*eds*. D. G. Stavenga, W. J. deGrip, and E. N. Pugh), Vol. 3, pp. 449–525. Elsevier.

Minke, B. and Selinger, Z. 1992. Intracellular Messengers in Invertebrate Photoreceptors Studied in Mutant Flies. In: Intracellular Messengers (*eds*. A. Boulton, G. Baker, and C. Talyor), pp. 517–563. The Humana Press.

Minke, B., Wu, C.-F., and Pak, W. L. 1975. Induction of photoreceptor noise in the dark in a *Drosophila* mutant. Nature 258, 84–87.

Monk, P. D., Carne, A., Liu, S. H., Ford, J. W., Keen, J. N., and Findlay, J. B. C. 1996. Isolation, cloning, and characterisation of a *trp* homologue from squid (*Loligo forbesi*) photoreceptor membranes. J. Neurochem. 67, 2227–2235.

Montell, C. 1999. Visual transduction in *Drosophila*. Annu. Rev. Cell Dev. Biol. 15, 231–268.

Montell, C. 2005. The TRP superfamily of cation channels. Sci. STKE 272, re3.

Montell, C. and Rubin, G. M. 1988. The *Drosophila ninaC* locus encodes two photoreceptor cell specific proteins with domains homologous to protein kinases and the myosin heavy chain head. Cell 52, 757–772.

Montell, C. and Rubin, G. M. 1989. Molecular characterization of *Drosophila trp* locus, a putative integral membrane protein required for phototransduction. Neuron 2, 1313–1323.

Nagy, K. 1991. Biophysical processes in invertebrate photoreceptors: recent progress and a critical overview based on *Limulus* photoreceptors. Q. Rev. Biophys. 24, 165–226.

Nagy, K. and Contzen, K. 1997. Inhibition of phospholipase C by U-73122 blocks one component of the receptor current in *Limulus* photoreceptor. Vis. Neurosci. 14, 995–998.

Nagy, K., Contzen, K., and Stieve, H. 1993. Two components of the receptor current are developed from distinct elementary signals in *Limulus* ventral nerve photoreceptor. Eur. Biophys. J. 22, 341–350.

Nasi, E. and Gomez, M.d. P. 1992. Light-activated ion channels in solitary photoreceptors of the scallop *Pecten irradians*. J. Gen. Physiol. 99, 747–769.

Nasi, E., Gomez, M.d. P., and Payne, R. 2000. Phototransduction Mechanisms in Microvillar and Ciliary Photoreceptors of Invertebrates. In: Handbook of Biological Physics (*eds*. D. G. Stavenga, W. J. deGrip, and E. N. Pugh), Vol. 3, pp. 389–448. Elsevier.

Niemeyer, B. A., Suzuki, E., Scott, K., Jalink, K., and Zuker, C. S. 1996. The *Drosophila* light-activated conductance is

composed of the two channels TRP and TRPL. Cell 85, 651–659.

Niven, J. E., Vahasoyrinki, M., Kauranen, M., Hardie, R. C., Juusola, M., and Weckstrom, M. 2003. The contribution of *Shaker* K^+ channels to the information capacity of *Drosophila* photoreceptors. Nature 421, 630–634.

Oberwinkler, J. and Stavenga, D. G. 1998. Light dependence of calcium and membrane potential measured in blowfly photoreceptors in vivo. J. Gen. Physiol. 112, 113–124.

Oberwinkler, J. and Stavenga, D. G. 2000. Calcium transients in the rhabdomeres of dark- and light-adapted fly photoreceptor cells. J. Neurosci. 20, 1701–1709.

O'Tousa, J. E., Baehr, W., Martin, R. L., Hirsh, J., Pak, W. L., and Applebury, M. L. 1985. The *Drosophila ninaE* gene encodes an opsin. Cell 40, 839–850.

Pak, W. L. 1995. *Drosophila* in vision research: the Friedenwald lecture. Invest. Ophthalmol. Vis. Sci. 36, 2340–2357.

Pak, W. L. and Leung, H. T. 2003. Genetic approaches to visual transduction in *Drosophila melanogaster*. Receptors Channels 9, 149–167.

Pak, W. L., Grossfield, J., and Arnold, K. S. 1970. Mutants of the visual pathway of *Drosophila melanogaster*. Nature 227, 518–520.

Palczewski, K., Kumasaka, T., Hori, T., Behnke, C. A., Motoshima, H., Fox, B. A., Le Trong, I., Teller, D. C., Okada, T., Stenkamp, R. E., Yamamoto, M., and Miyano, M. 2000. Crystal structure of rhodopsin: a G protein-coupled receptor. Science 289, 739–745.

Panda, S., Nayak, S. K., Campo, B., Walker, J. R., Hogenesch, J. B., and Jegla, T. 2005. Illumination of the melanopsin signaling pathway. Science 307, 600–604.

Payne, R., Corson, D. W., and Fein, A. 1986. Pressure injection of calcium both excites and adapts *Limulus* ventral photoreceptors. J. Gen. Physiol. 88, 107–126.

Payne, R., Flores, T. M., and Fein, A. 1990. Feedback inhibition by calcium limits the release of calcium by inositol trisphosphate in *Limulus* ventral photoreceptors. Neuron 4, 547–555.

Pearn, M. T., Randall, L. L., Shortridge, R. D., Burg, M. G., and Pak, W. L. 1996. Molecular, biochemical, and electrophysiological characterization of *Drosophila norpA* mutants. J. Biol. Chem. 271, 4937–4945.

Peretz, A., Suss-Toby, E., Rom-Glas, A., Arnon, A., Payne, R., and Minke, B. 1994. The light response of *Drosophila* photoreceptors is accompanied by an increase in cellular calcium: effects of specific mutations. Neuron 12, 1257–1267.

Phillips, A. M., Bull, A., and Kelly, L. E. 1992. Identification of a *Drosophila* gene encoding a calmodulin-binding protein with homology to the trp phototransduction gene. Neuron 8, 631–642.

del Pilar Gomez, M. and Nasi, E. 2005. A direct signaling role for phosphatidylinositol 4,5-bisphosphate (PIP_2) in the visual excitation process of microvillar receptors. J. Biol. Chem. 280, 16784–16789.

Plangger, A., Malicki, D., Whitney, M., and Paulsen, R. 1994. Mechanism of arrestin 2 function in rhabdomeric photoreceptors. J. Biol. Chem. 269, 26969–26975.

Popescu, D. C., Ham, A.-J. L., and Shieh, B.-H. 2006. Scaffolding protein INAD regulates deactivation of vision by promoting phosphorylation of transient receptor potential by rye protein kinase C in *Drosophila*. J. Neurosci. 26, 8570–8577.

Porter, J. A. and Montell, C. 1993. Distinct roles of the *Drosophila ninaC* kinase and myosin domains revealed by systematic mutagenesis. J. Cell Biol. 122, 601–612.

Porter, J. A., Hicks, J. L., Williams, D. S., and Montell, C. 1992. Differential localizations of and requirements for the two *Drosophila ninaC* kinase/myosins in photoreceptor cells. J. Cell Biol. 116, 683–693.

Porter, J. A., Yu, M., Doberstein, S. K., Pollard, T. D., and Montell, C. 1993. Dependence of calmodulin localization in the retina on the NINAC unconventional myosin. Science 262, 1038–1042.

Postma, M., Oberwinkler, J., and Stavenga, D. G. 1999. Does Ca^{2+} reach millimolar concentrations after single photon absorption in *Drosophila* photoreceptor microvilli? Biophys. J. 77, 1811–1823.

Provencio, I., Jiang, G. S., DeGrip, W. J., Hayes, W. P., and Rollag, M. D. 1998. Melanopsin: an opsin in melanophores, brain, and eye. Proc. Natl. Acad. Sci. U. S. A. 95, 340–345.

Qiu, X., Kumbalasiri, T., Carlson, S. M., Wong, K. Y., Krishna, V., Provencio, I., and Berson, D. M. 2005. Induction of photosensitivity by heterologous expression of melanopsin. Nature 433, 745–749.

Raghu, P., Colley, N. J., Webel, R., James, T., Hasan, G., Danin, M., Selinger, Z., and Hardie, R. C. 2000a. Normal phototransduction in *Drosophila* photoreceptors lacking an $InsP_3$ receptor gene. Mol. Cell Neurosci. 15, 429–445.

Raghu, P., Usher, K., Jonas, S., Chyb, S., Polyanovsky, A., and Hardie, R. C. 2000b. Constitutive activity of the light-sensitive channels TRP and TRPL in the *Drosophila* diacylglycerol kinase mutant, *rdgA*. Neuron 26, 169–179.

Ramsey, I. S., Delling, M., and Clapham, D. E. 2006. An introduction to trp channels. Annu. Rev. Physiol. 68, 619–647.

Ranganathan, R., Bacskai, B. J., Tsien, R. Y., and Zuker, C. S. 1994. Cytosolic calcium transients: spatial localization and role in *Drosophila* photoreceptor cell function. Neuron 13, 837–848.

Ranganathan, R., Harris, G. L., Stevens, C. F., and Zuker, C. S. 1991. A *Drosophila* mutant defective in extracellular calcium-dependent photoreceptor deactivation and rapid desensitization. Nature 354, 230–232.

Ready, D. F. 1989. A multifaceted approach to neural development. Trends Neurosci. 12, 102–110.

Reuss, H., Mojet, M. H., Chyb, S., and Hardie, R. C. 1997. In vivo analysis of the *Drosophila* light-sensitive channels, TRP and TRPL. Neuron 19, 1249–1259.

Roebroek, J. G. H. and Stavenga, D. G. 1990. On the effective optical density of the pupil mechanism in fly photoreceptors. Vision Res. 30, 1235–1242.

Rosenbaum, E. E., Hardie, R. C., and Colley, N. J. 2006. Calnexin is essential for rhodopsin maturation, Ca^{2+} regulation, and photoreceptor cell survival. Neuron 49, 229–241.

Running Deer, J. L., Hurley, J. B., and Yarfitz, S. L. 1995. G protein control of *Drosophila* photoreceptor phospholipase C. J. Biol. Chem. 270, 12623–12628.

Sahly, I., Schroder, W. H., Zierold, K., and Minke, B. 1994. Accumulation of calcium in degenerating photoreceptors of several *Drosophila* mutants. Vis. Neurosci. 11, 763–772.

Salcedo, E., Huber, A., Henrich, S., Chadwell, L. V., Chou, W. H., Paulsen, R., and Britt, S. G. 1999. Blue- and green-absorbing visual pigments of *Drosophila*: ectopic expression and physiological characterization of the R8 photoreceptor cell-specific Rh5 and Rh6 rhodopsins. J. Neurosci. 19, 10716–10726.

Sang, T. K. and Jackson, G. R. 2005. *Drosophila* models of neurodegenerative disease. NeuroRx 2, 438–446.

Sarfare, S., Ahmad, S. T., Joyce, M. V., Boggess, B., and O'Tousa, J. E. 2005. The *Drosophila* ninaG oxidoreductase acts in visual pigment chromophore production. J. Biol. Chem. 280, 11895–11901.

Sarthy, P. V. 1991. Histamine: a neurotransmitter candidate for *Drosophila* photoreceptors. J. Neurochem. 57, 1757–1768.

Satoh, A. K. and Ready, D. F. 2005. Arrestin1 mediates light-dependent rhodopsin endocytosis and cell survival. Curr. Biol. 15, 1722–1733.

Scavarda, N. J., Otousa, J., and Pak, W. L. 1983. *Drosophila* locus with gene-dosage effects on rhodopsin. Proc. Natl. Acad. Sci. U. S. A. 80, 4441–4445.

Schillo, S., Belusic, G., Hartmann, K., Franz, C., Kuhl, B., Brenner-Weiss, G., Paulsen, R., and Huber, A. 2004. Targeted mutagenesis of the farnesylation site of *Drosophila* Ggamma e disrupts membrane association of the G protein beta gamma complex and affects the light-sensitivity of the visual system. J. Biol. Chem. 279, 36309–36316.

Schneuwly, S., Burg, M. G., Lending, C., Perdew, M. H., and Pak, W. L. 1991. Properties of photoreceptor-specific phospholipase C encoded by the norpA gene of *Drosophila* melanogaster. J. Biol. Chem. 266, 24314–34319.

Schwarz, E. M. and Benzer, S. 1997. Calx, a Na–Ca exchanger gene of *Drosophila melanogaster*. Proc. Natl. Acad. Sci. U. S. A. 94, 10249–10254.

Scott, K. and Zuker, C. S. 1998. Assembly of the *Drosophila* phototransduction cascade into a signalling complex shapes elementary responses. Nature 395, 805–808.

Scott, K., Becker, A., Sun, Y., Hardy, R., and Zuker, C. 1995. G_q a protein function in vivo: genetic dissection of its role in photoreceptor cell physiology. Neuron 15, 919–927.

Scott, K., Sun, Y. M., Beckingham, K., and Zuker, C. S. 1997. Calmodulin regulation of *Drosophila* light-activated channels and receptor function mediates termination of the light response in vivo. Cell 91, 375–383.

Shieh, B. H. and Niemeyer, B. 1995. A novel protein encoded by the InaD gene regulates recovery of visual transduction in *Drosophila*. Neuron 14, 201–210.

Shieh, B. H. and Zhu, M. Y. 1996. Regulation of the TRP Ca^{2+} channel by INAD in *Drosophila* photoreceptors. Neuron 16, 991–998.

Shieh, B. H., Parker, L., and Popescu, D. 2002. Protein kinase C (PKC) isoforms in *Drosophila*. J. Biochem. (Tokyo) 132, 523–527.

Shin, J., Richard, E. A., and Lisman, J. E. 1993. Ca^{2+} is an obligatory intermediate in the excitation cascade of *Limulus* photoreceptors. Neuron 11, 845–855.

Smith, D. P., Ranganathan, R., Hardy, R. W., Marx, J., Tsuchida, T., and Zuker, C. S. 1991. Photoreceptor deactivation and retinal degeneration mediated by a photoreceptor-specific protein-kinase-C. Science 254, 1478–1484.

Stavenga, D. G. 1996. Insect retinal pigments: spectral characteristics and physiological functions. Prog. Retin. Eye Res. 15, 231–259.

Stavenga, D. G. 2004. Angular and spectral sensitivity of fly photoreceptors. III. Dependence on the pupil mechanism in the blowfly Calliphora. J. Comp. Physiol. A 190, 115–129.

Steele, F. R., Washburn, T., Rieger, R., and Otousa, J. E. 1992. *Drosophila* retinal-degeneration-C (Rdgc) encodes a novel serine threonine protein phosphatase. Cell 69, 669–676.

Sullivan, K. M. C., Scott, K., Zuker, C. S., and Rubin, G. M. 2000. The ryanodine receptor is essential for larval development in *Drosophila melanogaster*. Proc. Natl. Acad. Sci. U. S. A. 97, 5942–5947.

Szuts, E. Z. 1993. Concentrations of phosphatidylinositol 4,5-bisphosphate and inositol 1,4,5-trisphosphate within the distal segment of squid photoreceptors. Vis. Neurosci. 10, 921–929.

Taylor, D. A., Sack, J. S., Maune, J. F., Beckingham, K., and Quiocho, F. A. 1991. Structure of a recombinant calmodulin from *Drosophila melanogaster* refined at 2.2-A resolution. J. Biol. Chem. 266, 21375–21380.

Terakita, A., Hariyama, T., Tsukahara, Y., Katsukura, Y., and Tashiro, H. 1993. Interaction of GTP-binding protein Gq with photoactivated rhodopsin in the photoreceptor membranes of crayfish. FEBS Lett. 330, 197–200.

Toyoshima, S., Matsumoto, N., Wang, P., Inoue, H., Yoshioka, T., Hotta, Y., and Osawa, T. 1990. Purification and partial amino acid sequences of phosphoinositide-specific phospholipase C of *Drosophila* eye. J. Biol. Chem., 265, 14842–14848.

Tsunoda, S., Sierralta, J., Sun, Y. M., Bodner, R., Suzuki, E., Becker, A., Socolich, M., and Zuker, C. S. 1997. A multivalent PDZ-domain protein assembles signalling complexes in a G-protein-coupled cascade. Nature 388, 243–249.

Tsunoda, S., Sun, Y., Suzuki, E., and Zuker, C. 2001. Independent anchoring and assembly mechanisms of INAD signaling complexes in *Drosophila* photoreceptors. J. Neurosci. 21, 150–158.

Ugarte, G., Delgado, R., O'Day P, M., Farjah, F., Cid, L. P., Vergara, C., and Bacigalupo, J. 2005. Putative ClC-2 chloride channel mediates inward rectification in *Drosophila* retinal photoreceptors. J. Membr. Biol. 207, 151–160.

Ukhanov, K. and Payne, R. 1995. Light activated calcium release in *Limulus* ventral photoreceptors as revealed by laser confocal microscopy. Cell Calcium 18, 301–313.

Ukhanov, K., Mills, S. J., Potter, B. V., and Walz, B. 2001. $InsP_3$-induced Ca^{2+} release in permeabilized invertebrate photoreceptors: a link between phototransduction and Ca^{2+} stores. Cell Calcium 29, 335–345.

Vaca, L., Sinkins, W. G., Hu, Y., Kunze, D. L., and Schilling, W. P. 1994. Activation of recombinant trp by thapsigargin in Sf9 insect cells. Am. J. Physiol. Cell Physiol. 267, C1501–C1505.

Vahasoyrinki, M., Niven, J. E., Hardie, R. C., Weckstrom, M., and Juusola, M. 2006. Robustness of neural coding in *Drosophila* photoreceptors in the absence of slow delayed rectifier K^+ channels. J. Neurosci. 26, 2652–2660.

Vihtelic, T. S., Goebl, M., Milligan, S., O'Tousa, J. E., and Hyde, D. R. 1993. Localization of *Drosophila* retinal degeneration B, a membrane-associated phosphatidylinositol transfer protein. J. Cell Biol. 122, 1013–1022.

Vihtelic, T. S., Hyde, D. R., and Otousa, J. E. 1991. Isolation and characterization of the *Drosophila* retinal-degeneration-B (*rdgB*) gene. Genetics 127, 761–768.

Vinos, J., Jalink, K., Hardy, R. W., Britt, S. G., and Zuker, C. S. 1997. A G protein-coupled receptor phosphatase required for rhodopsin function. Science 277, 687–690.

Vogt, K. and Kirschfeld, K. 1984. The chemical identity of the chromophores of fly visual pigment. Z. Naturwiss. 71, 211–213.

Wall, M. A., Coleman, D. E., Lee, E., Iniguez-Lluhi, J. A., Posner, B. A., Gilman, A. G., and Sprang, S. R. 1995. The structure of the G protein heterotrimer Gi alpha 1 beta 1 gamma 2. Cell 83, 1047–1058.

Walrond, J. P. and Szuts, E. Z. 1992. Submicrovillar tubules in distal segments of squid photoreceptors detected by rapid freezing. J. Neurosci. 12, 1490–1501.

Walz, B., Baumann, O., Zimmermann, B., and Ciriacywantrup, E. V. 1995. Caffeine-sensitive and ryanodine-sensitive Ca^{2+}-induced Ca^{2+} release from the endoplasmic-reticulum in honeybee photoreceptors. J. Gen. Physiol. 105, 537–567.

Walz, B., Liebherr, H., and Ukhanov, K. 2003. Ca^{2+}-dependent and Ca^{2+} release-dependent excitation in leech photoreceptors: evidence from a novel ''inside-out'' cell model. Cell Calcium 34, 35–47.

Wang, T. and Montell, C. 2005. Rhodopsin formation in *Drosophila* is dependent on the PINTA retinoid-binding protein. J. Neurosci. 25, 5187–5194.

Wang, T., Jiao, Y., and Montell, C. 2005a. Dissecting independent channel and scaffolding roles of the *Drosophila* transient receptor potential channel. J. Cell Biol. 171, 685–694.

Wang, T., Xu, H., Oberwinkler, J., Gu, Y., Hardie, R. C., and Montell, C. 2005b. Light activation, adaptation, and cell survival functions of the Na^{+}/Ca^{2+} exchanger CalX. Neuron 45, 367–378.

Warr, C. G. and Kelly, L. E. 1996. Identification and characterization of two distinct calmodulin-binding sites in the TrpI ion-channel protein of *Drosophila* melanogaster. Biochem. J. 314, 497–503.

Weckström, M., Hardie, R. C., and Laughlin, S. B. 1991. Voltage-activated potassium channels in blowfly photoreceptors and their role in light adaptation. J. Physiol. (Lond.) 440, 635–657.

Wehner, R. 1989. Neurobiology of polarization vision. Trends Neursoci. 12, 353–359.

Wolfram, V. 2004. Impact of light history on processing of visual signals in *Drosophila* photoreceptors, Ph.D. thesis, Cambridge University, Ph.D. thesis.

Wong, F., Knight, B. W., and Dodge, F. A. 1980. Dispersion of latencies in photoreceptors of *Limulus* and the adapting-bump model. J. Gen. Physiol. 76, 517–537.

Wu, C. F. and Pak, W. L. 1975. Quantal basis of photoreceptor spectral sensitivity of *Drosophila melanogaster*. J. Gen. Physiol. 66, 149–168.

Wu, C. F. and Pak, W. L. 1978. Light-induced voltage noise in the photoreceptor of *Drosophila melanogaster*. J. Gen. Physiol. 71, 249–268.

Wu, L., Niemeyer, B., Colley, N., Socolich, M., and Zuker, C. S. 1995. Regulation of PLC-mediated signalling *in vivo* by CDP–diacylglycerol synthase. Nature 373, 216–222.

Xu, X. Z. S., Chien, F., Butler, A., Salkoff, L., and Montell, C. 2000. TRP gamma, a *Drosophila* TRP-related subunit, forms a regulated cation channel with TRPL. Neuron 26, 647–657.

Xu, X. Z. S., Choudhury, A., Li, X. L., and Montell, C. 1998. Coordination of an array of signaling proteins through homo- and heteromeric interactions between PDZ domains and target proteins. J. Cell Biol. 142, 545–555.

Xu, X. Z. S., Li, H. S., Guggino, W. B., and Montell, C. 1997. Coassembly of TRP and TRPL produces a distinct store-operated conductance. Cell 89, 1155–1164.

Yamada, T., Takeuchi, Y., Komori, N., Kobayashi, H., Sakai, Y., Hotta, Y., and Matsumoto, H. 1990. A 49-kilodalton phosphoprotein in the *Drosophila* photoreceptor is an arrestin homolog. Science 248, 483–486.

Yang, Y. and Ballinger, D. 1994. Mutations in calphotin, the gene encoding a *Drosophila* photoreceptor cell-specific calcium-binding protein, reveal roles in cellular morphogenesis and survival. Genetics 138, 413–421.

Yarfitz, S. L., Deer, J. L. R., Froelick, G., Colley, N. J., and Hurley, J. B. 1994. In situ assay of light-stimulated G protein activity in *Drosophila* photoreceptor G protein beta mutants. J. Biol. Chem. 269, 30340–30344.

Yarfitz, S., Niemi, G. A., McConnell, J. L., Fitch, C. L., and Hurley, J. B. 1991. A G beta protein in the *Drosophila* compound eye is different from that in the brain. Neuron 7, 429–438.

Yasuhara, J. C., Baumann, O., and Takeyasu, K. 2000. Localization of Na/K-ATPase in developing and adult *Drosophila melanogaster* photoreceptor. Cell Tissue Res. 300, 239–249.

Yoon, J., Ben-Ami, H. C., Hong, Y. S., Park, S., Strong, L. L., Bowman, J., Geng, C., Baek, K., Minke, B., and Pak, W. L. 2000. Novel mechanism of massive photoreceptor degeneration caused by mutations in the trp gene of *Drosophila*. J. Neurosci. 20, 649–659.

Yuan, J. P., Kiselyov, K., Shin, D. M., Chen, J., Shcheynikov, N., Kang, S. H., Dehoff, M. H., Schwarz, M. K., Seeburg, P. H., Muallem, S., and Worley, P. F. 2003. Homer binds TRPC family channels and is required for gating of TRPC1 by IP_3 receptors. Cell 114, 777–789.

Zheng, L., de Polavieja, G. G., Wolfram, V., Asyali, M. H., Hardie, R. C., and Juusola, M. 2006. Feedback network controls photoreceptor output at the layer of first visual synapses in *Drosophila*. J. Gen. Physiol. 127, 495–510.

Relevant Websites

http://flybase.bio.indiana.edu – Flybase: detailed information and annotation on all *Drosophila* genes and mutant phenotypes, including links to sequences, primary references, extensive stocklists and much more.

http://www.fruitfly.org – Home page for the Berkeley *Drosophila* Gene Project (BDGP). Definitive sequence and annotation for the *Drosophila* Genome. Plus P element-mediated mutagenesis on a scale unprecedented in metazoans.

http://geno3d-pbil.ibcp.fr – Pôle BioInformatique Lyonnais, Geno 3D.

1.06 Central Processing of Visual Information in Insects

H G Krapp, Imperial College London, London, UK

M Wicklein, University College London, London, UK

© 2008 Elsevier Inc. All rights reserved.

1.06.1	**Introduction**	132
1.06.1.1	Why Study Invertebrate Vision?	132
1.06.1.2	The Closed Loop of Action and Perception	132
1.06.1.3	Visually Induced Reflexes and Voluntary Movements: Inner-Loop and Outer-Loop Control	133
1.06.1.4	Goal of this Chapter	135
1.06.2	**Anatomy and Morphology of the Insect Brain**	135
1.06.2.1	General Organization	135
1.06.2.2	Lamina	136
1.06.2.3	Medulla	137
1.06.2.4	Lobula Complex	137
1.06.2.5	Projections to Other Parts of the Nervous System	138
1.06.2.6	Functional Anatomical Pathways	138
1.06.3	**Motion-Based Visual Information Processing**	139
1.06.3.1	Estimating Self-Motion Using Directional Motion Cues	139
1.06.3.1.1	Self-motion and optic flow	139
1.06.3.1.2	How does the visual system analyze directional motion?	142
1.06.3.1.3	Flies as model systems for directional motion processing	143
1.06.3.1.4	Self-motion estimation in other invertebrate species	158
1.06.3.1.5	Open questions	158
1.06.3.2	Responding to Motion from the Outside World – Visual Information Controlling the Outer Loop	159
1.06.3.2.1	Chasing females and prey	159
1.06.3.2.2	Discriminating small objects from the background	165
1.06.3.2.3	Distance control and looming detection	167
1.06.3.3	Image Segmentation – The Detection of Orientated Contours	173
1.06.4	**Exploiting Electromagnetic Properties of Light**	175
1.06.4.1	Processing of Color Information	175
1.06.4.1.1	Reasons for color vision	175
1.06.4.1.2	In what behavioral contexts is color vision used?	175
1.06.4.1.3	Visual pigments, photoreceptors, and filters	175
1.06.4.1.4	Receptor arrangement in the retina	176
1.06.4.1.5	Color perception	176
1.06.4.1.6	When does an animal have color vision?	176
1.06.4.1.7	Classifications of color vision	177
1.06.4.1.8	Behavioral tests for color vision	177
1.06.4.1.9	Neural mechanisms for color coding	177
1.06.4.2	Polarization Vision	179
1.06.4.2.1	Properties of polarized light	179
1.06.4.2.2	Adaptations to e-vector detection in the eye	179
1.06.4.2.3	Two theoretical models of e-vector detection	180
1.06.4.2.4	Neuronal mechanisms	181

1.06.5	**Ocelli – Visual Information Processing on the Fast Track**	182
1.06.5.1	Ocelli in Flies	182
1.06.5.2	The Functional Role of the Ocelli	182
1.06.5.3	Two Visual Mechanisms – One Motion Parameter	183
1.06.6	**Multisensory Integration and Sensorimotor Transformation**	184
1.06.6.1	Vision and Other Sense – Increasing the Reliability of Sensory Information	184
1.06.6.1.1	Multisensory contributions to inner-loop control	184
1.06.6.1.2	Multisensory contributions to outer-loop control	187
1.06.6.2	The Relationship between Sensory Systems and Motor Systems: Strategies of Sensorimotor Transformation	188
1.06.7	**Visual Cognition**	189
1.06.7.1	The Traditional View	189
1.06.7.2	Arguments for Cognitive Functions in Insects	189
1.06.7.3	Data Supporting Cognitive Functions	189
1.06.8	**Conclusions**	191
References		192

1.06.1 Introduction

1.06.1.1 Why Study Invertebrate Vision?

Invertebrates, in particular arthropods, have proven to be excellent model systems when it comes to studying visual information processing. This is because most arthropods show a behavioral repertoire that is mostly concerned with feeding, mating, and stability reflexes. At first glance this sounds rather boring, even though the motor tasks involved are in some cases performed at a level of speed and perfection beyond that of any vertebrate or manmade device. We will also see that some insects solve categorization and learning tasks that are complex enough for us to assume that these creatures possess cognitive capabilities. But still, why are invertebrates so successful in modern neuroscience even though their brains consist of only a tiny number of nerve cells compared to the number of nerve cells living in our own brain. The secret lies in the combination of a rigorous input–output analysis to assess the system's behavioral performance limit and a functional characterization of those identified cells and circuits underlying the studied behavior. The possibility to directly relate behavioral performance to neural activity facilitates finding conclusive answers to the question of how a given nervous system is functionally organized. Many fundamental principles in neuroscience, which turned out to apply across phyla, were actually first discovered in invertebrate model systems such as squid (e.g., Hodgkin, A. L. and Huxley, A. F. 1952), snail (e.g., Sweat, J. D and Kandel, E. R., 1989), horseshoe crab (e.g. Hartline, H. K. *et al.*, 1956), and beetle (Hassenstein, B. and Reichardt, W., 1953).

1.06.1.2 The Closed Loop of Action and Perception

The different processes taking place in the nervous system which underlie the control of behavior may be illustrated in an action–perception loop (Figure 1). Adaptive behavior relies on constantly sampling information from the environment. This is essential as behavior is always generated in relation to a given internal and environmental state. Therefore, successful behavioral control requires to identify and to distinguish between two different sources of information: First, information about the environment caused by external sources, for instance other animals. Second – when being active – information about how the animal is moving relative to its environment. Both aspects of information become the basis of any behavioral response, and as a long-range sense, vision plays a major role in it.

In invertebrates, arrays of thousands of specialized photoreceptor cells transduce local changes of photon flux into time-varying receptor signals. An account on the significance of the optics and the latest development in invertebrate phototransduction (Chapter Phototransduction in Microvillar Photoreceptors of Drosophila and Other Invertebrates) is given in earlier chapters. At the peripheral level the arrangement and functional structure of receptor cells already reflects on what the visual input to different regions of the eye might be used for in the context of behavioral control (Chapter Nocturnal Vision; Hardie, R. C. 1983; Stavenga, D. G. 1992). The next step is devoted to sensory processing mostly concerned with filtering,

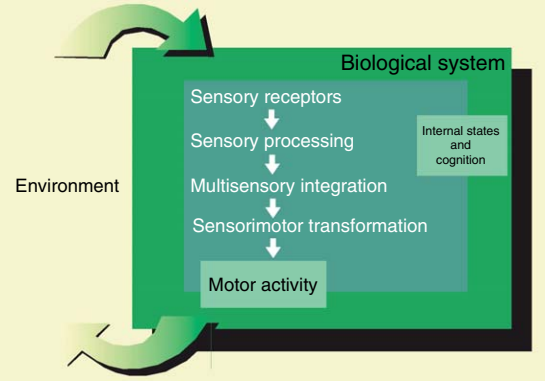

Figure 1 The action–perception loop. A bilogical system receives processes, and integrates sensory information before transforming the resulting signals into activity patterns controlling the motor system. Motor activity produces a behavior that changes the sensory environment, which is again sampled by the sensory receptors. The different steps of this action–perception loop may be modified depending on internal states or by higher cognitive functions. Such modifications may result in different behavioral patterns in response to one and the same sensory environment. Feedback loops may also be implemented at different levels to fine-tune the behavior.

refining, and encoding particular aspects of local sensory information. This step may be facilitated by taking into account internal models, or prior knowledge, of natural image statistics (van der Schaaf, A. and van Hateren, J. H., 1996) to optimize the extraction of behaviorally relevant information (Chapters Visual Ecology and Seeing in the Dark: Retinal Processing and Absolute Visual Threshold; Laughlin, S. B., 1981). In functional terms, the peripheral and the later central processing have fundamentally different purposes. Peripherally, it is important to gain detailed information about intensity and color distributions for each tiny patch of the visual scenery. It is like taking a photograph with a digital camera: bad optics in combination with low pixel resolution will not give you particularly good result. Similarly, whatever information visual systems loose in the periphery will never be retrieved at downstream stages.

A local sensory signal, equivalent to the color and the intensity of a single static pixel in a photograph, does not provide the animal with any evidence about its current behavioral state, whatsoever. Local signals are highly ambiguous since they lack any contextual information – unless they are meaningfully combined (e.g., Laughlin, S. B., 1999). Consequently, evidence of being in a state that requires a particular behavioral response is gained only by selective integration of local sensory signals. This task is commonly performed by populations of interneurons within each modality. In fact, in many modalities, different qualities, such as color or motion information in case of vision, may be processed and integrated in parallel anatomical pathways (see Section 1.06.2). The results are then combined with information from other senses to further increase the certainty of being in a distinct behavioral state. The final outcome of such multisensory integration is then transformed into activation patterns of motorneurons driving the muscles, which ultimately control the behavior.

Any behavioral response and its underlying neural processing take place under closed-loop conditions. Whilst executed, behavioral actions usually result in a continuously changing pattern of sensory inputs, which closes the action–perception loop. However, the sensory input does not entirely determine the behavioral output. Physiological parameters such as nutritional state and temperature may modify the operation of the nervous system at various levels so that one and the same sensory input pattern can result in different behavioral outputs. For instance, a hungry fly may land and search for food when it encounters a visual expansion pattern that indicates an approaching obstacle. Well-fed flies experiencing the very same pattern, on the other hand, may just fly past the obstacle to avoid collision (e.g., Srinivasan, M. V. and Zhang, S. W., 2000). This means that the neural machinery controlling the behavior does not entirely work in a deterministic way but may as well show a certain degree of context-dependent plasticity (e.g., Wolf, R. *et al.*, 1992; Heisenberg, M. and Wolf, R., 1993).

1.06.1.3 Visually Induced Reflexes and Voluntary Movements: Inner-Loop and Outer-Loop Control

In invertebrates, vision is involved in the control of several behaviors, which may be supported by differently organized neuronal pathways (e.g., rev.: Wehner, R., 1981). Flying insects in particular, not being able to use short-range senses such as touch and taste when airborne, heavily rely on vision in a variety of behavioral contexts. Vision is the key sense to identify and chase potential prey or mates, to detect, approach, and land on potential food sources in close range, to avoid collisions with obstacles in the environment, and for initiating escape responses. Insects also use visual information for estimating distance flown and navigation. Finally, invertebrates

generally use visual information to support two fundamental tasks: gaze and flight stabilization.

Gaze and flight stabilization should be distinguished from other visually guided behaviors since both operate very much like reflexes. The visually induced components of these reflexes are often referred to as optomotor responses (e.g., rev.: Heisenberg, M. and Wolf, R., 1993). But gaze and flight stabilization are under multimodal control. In Diptera – or two-winged flies – these reflexes depend, for instance, on the mechanosensory haltere system also (e.g., Nalbach, G., 1994; Sherman, A. and Dickinson, M. H., 2003; Bender, J. A. and Dickinson, M. H., 2006). The visual and mechanosensory components of gaze and flight control in insects are analog to the vestibulo-ocular, optokinetic, and postural reflexes in humans (rev.: Carpenter, R. H. S., 1988; Miles, F. A. and Wallman, J., 1993; Sparks, D. L., 2002). Across phyla they serve two essential functions: Postural control helps to maintain a stable attitude during locomotion – be it flying, swimming, or waking (rev.: Orlovsky, G. *et al.*, 1999). The stabilization of gaze keeps the retinal image in its default upright orientation, which is a necessary prerequisite for processing visual information, and simplifies the sensorimotor transformation (Miles, F. A. and Wallman, J., 1993).

In engineering terms, gaze and flight stabilization are governed by an inner-loop control system that is constantly in operation (Figure 2, dashed red line). No matter whether an insect chases another, performs a collision-avoidance maneuver, or is in cruising flight mode, gaze and flight need to be stabilized. For instance, when a gust of wind drifts a fly off course the optomotor response kicks in to support two fundamental tasks: (1) to maintain aerodynamic stability and (2) to compensate for the animal's deviation from its initial flight trajectory. This causes an interesting problem, which has been raised almost 60 years ago by von Holst E. and Mittelstaedt H. (1950). The control of visual reflexes and other visually guided behaviors has to interact, otherwise the animal would be trapped by its inner-loop control system (von Holst, E. and Mittelstaedt, H., 1950). What happens when the animal intends to fly a banked turn so that it can reach, say, an attractive landing site? As soon as the maneuver starts the inner-loop control should counteract the voluntary turn and the animal would never be able to reach the desired target location. The observation is, however, that insects have no problem at all to engage in maneuvers whose execution should be opposed by the optomotor reflexes (e.g.: Collett, T. S., 1980; Heisenberg, M. and Wolf, R., 1993).

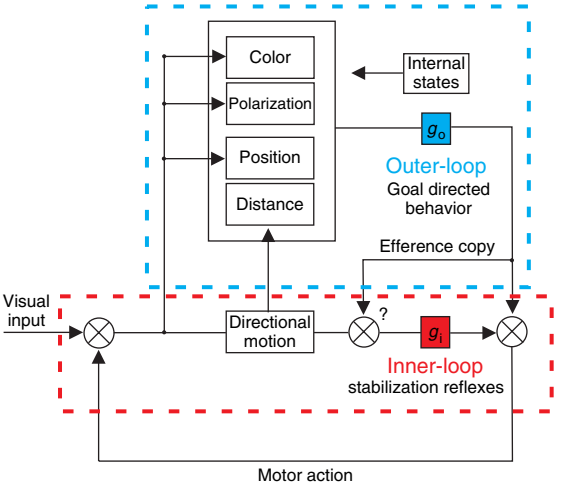

Figure 2 Inner-loop and outer-loop control. Inner-loop stabilization reflexes help an animal to keep its balance, or aerodynamic stability, and to maintain a default orientation of its eyes relative to the external world. Visual motion in particular is used in inner-loop control (dashed red frame). To perform any goal-directed behavior the inner-loop control has to be modified. Otherwise, inner-loop reflexes would immediately oppose voluntary action. Along the outer-loop (dashed blue frame) separate parallel pathways process and integrate different qualities of vision. Internal states of the animal may have an impact on outer-loop integration. The resulting signals are fed into the inner-loop control to modify its performance. If outer-loop and inner-loop dynamics greatly differ, the interaction between the loops would benefit from including an efference copy, which subtracts the expected consequences of any outer-loop action. At which stage, efference copy might effect the inner loop is not clear yet. g_i and g_o denote inner- and outer-loop gain. For further explanation see text. Inspired by Collett T. (1980).

Conceptually, this problem can be solved in two different ways either by disabling the reflex or by modifying its execution. The first solution could be the result of several, not necessarily mutually exclusive mechanisms. For instance, voluntary turns may be executed at such high speeds that the resulting retinal image velocities exceed the dynamic range of the motion vision system (rev.: Heisenberg, M. and Wolf, R., 1993). In this case a low gain in the optomotor response would simply be an inevitable consequence of the visual system's intrinsic properties. Classical reflex theory (e.g., Fulton, J. F., 1943) suggests another possible solution. Early hypotheses assumed that the visual processing of motion information or the resulting motor command may be inhibited whenever voluntary turns are performed.

These possibilities, though, had to be discarded after von Host E. and Mittelstaedt H. (1950) performed their classic experiments on the hoverfly showing that this is clearly not the case.

The second conceptual solution is reminiscent of the design of control systems in modern aircrafts. Like in flying insects an inner-loop control system that does not require pilot action is constantly maintaining the aircraft's attitude in conjunction with its aerodynamic stability by compensating for any deviations in roll, pitch, and yaw. During a voluntary banked turn the pilot due to joystick action simply changes the set point of the inner-loop control system. Such outer-loop control allows the pilot to perform intended flight maneuvers while keeping the inner-loop control active. In insects where there is no pilot the outer-loop control may be based on pathways processing, for instance, the retinal position of potential targets, information required during chasing flights.

The latter possibility was discussed as a follow-up model, one out of three possible ways of how the inner-loop optomotor pathway and an outer-loop pathway involved in chasing behavior may interact (Collett, T. S., 1980). Another possible interaction Collett T. S. (1980) put forward requires a copy of the motor command sent to the flight motor called an efference copy – an idea von Holst E. and Mittelstaedt H. introduced in their 1950 publication. An efference copy is a signal of the same amplitude but inverted in sign with respect to the reafferent sensory feedback that an animal's – or human's – own motor activity will cause. Voluntary movements during chasing could trigger an efference copy that cancels the visual feedback due to the animal's voluntary turns so that the inner-loop control will not generate an opposing optomotor response (Figure 2, blue dashed line).

Because an efference copy in a way predicts what the self-induced sensory feedback will be, it is conceptually similar to what is known as a forward model in human motor control. Any difference between the predicted feedback, the forward model, and the actual feedback may have two different reasons: Firstly, the mismatch was due to external factors in which case further correctional movements are required. Secondly, the motor program was not appropriately trained to achieve the goal. In the latter case the difference between actual feedback and forward model may be used to train the motor program for better future performance. In vertebrate motor control, forward models became quite popular as a concept (e.g., Wolpert, D. M. *et al.*, 1995) and were even associated with cognitive processes (Kawato, M., 1999; Wolpert, D. M. and Ghahramani, Z., 2000). The neural basis of forward models, however, has so far only been shown in a cerebellum-like area of the electric fish brain (rev.: Bell, C. C., 1989).

At which stage in the insect nervous system and how forward models or efferent copies modify visual information processing and the resulting motor output is not very well known yet either (Webb, B., 2004). Only in the context of gaze stabilization in locusts (Zaretsky, M. and Rowell, C. H., 1979) and attitude control in flies (Chan, W. P. *et al.*, 1998) some electrophysiological evidence hints at how the inner- and outer-loop control might interact.

1.06.1.4 Goal of this Chapter

The goal of this chapter is to complement the comprehensive account *Spatial Vision in Arthorpods* provided by Wehner R. (1981) in the *Handbook of Sensory Physiology*. We will confine ourselves to review a selection of examples where over the last decades an integrated approach of quantitative behavioral studies in combination with electrophysiology and modeling best illustrates neural mechanisms underlying visually guided behavior. Many of these studies have been successfully carried out in a variety of flying insects, namely flies. In Section 1.06.2, therefore, we will consider the general organization of the insect nervous system before outlining the control of behaviors involving vision – and, in some cases, other sensory mechanisms.

1.06.2 Anatomy and Morphology of the Insect Brain

1.06.2.1 General Organization

Here we will just give a short description of the neuronal organization of the insect brain to help readers of this chapter unfamiliar with insect brain anatomy to orient themselves with respect to structures and neurons discussed in more detail below. Detailed accounts on the anatomy and the structure of the optic lobes can be found in Strausfeld N. J. (1976; 1989) and Fischbach H. and Dittrich A. P. M. (1989). Strausfeld concentrates mainly on the housefly but also includes many other insects and invertebrates, whereas Fischbach and Dittrich focus only on *Drosophila*. There are also several detailed and interactive brain atlases available on the web (e.g., honeybee: http://www.neurobiologie.fu-berlin.de/

beebrain/; diptera: http://flybrain.neurobio.arizona.edu/). Here we concentrate mainly on the insect brain in which the general structure of the brain and optic lobes is conserved over different species.

The neural organization of the insect brain combines two design principles: single, identifiable neurons and multiple neurons arranged in a parallel architecture. The first principle is based on the existence of single neurons that are individually identifiable functional elements in sensory–motor routines and can be repeatedly and reliably identified due to their unique morphology and physiology. The H1 cell, for instance, that is found in the lobula plate of flies would be a famous example (see Section 1.06.3.1.3). Such identified neurons are characteristic of the invertebrate nervous system. Multiple neurons in a parallel architecture indicating higher-order integration are represented, for example, in the mushroom bodies (MBs). The MBs are central, prominent structures consisting of small, tightly packed, and parallelly arranged neurons called Kenyon cells.

In insects the nervous system is divided into a cephalic ganglion (brain), thoracic and abdominal ganglia, which may be fused. These ganglia are connected by interganglion tracts. The cephalic ganglion is the main area in which processing and integration of sensory information as well as higher-order functions such as learning and memory are performed. The thoracic ganglia contain most of the neuronal machinery responsible for the control of flight and leg muscles. All the ganglia and most notably the cephalic ganglion are subdivided into neuropil masses and connecting tracts. Most synapses and arborizations of neurons are situated in the neuropil masses. The cell bodies of the neurons are located in an outer rind that envelopes both the neuropil and the connecting tract regions. The cephalic ganglion can be easily divided into functional and anatomical distinct sensory and higher-order processing regions, with the olfactory and the optic lobes, the MBs, and central complex (CC) being prominent anatomical structures.

The visual system in insects consists of the retina and three nested optic lobe neuropils, lamina, medulla, and lobula complex. In Diptera, Lepidoptera, and Coleoptera, the lobula complex is divided into two neuropils, the lobula and the lobula plate. In all other insect groups these two neuropils are fused into the lobula or the lobula complex. Successive chiasmata link the lamina to the outer medulla and the inner medulla to the lobula complex (Figures 3 and 4).

The optic lobes of insects are retinotopically organized. The spatial relationship of information obtained

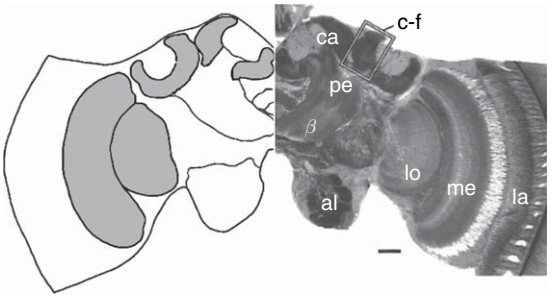

Figure 3 A frontal section of the bee brain is shown. The left side is a schematized drawing of the optic lobes and mushroom bodies (MBs), the right side shows an ethylgallate staining. Note the darker neuropil regions with clear columnar organization and the lighter colored chiasmata, fiber tracts, and cell body rind. al, antennal lobe; ca, calyx; la, lamina; lo, lobula; me, medulla; pe, peduncle; β, β-lobe of peduncle. Scale bars, 100 m. Adapted with permission from Ehmer, B. and Gronenberg, W. 2002. Segregation of visual input to the mushroom bodies in the honeybee (*Apis mellifera)*. J. Comp. Neurol. 451, 362–373.

at neighboring points in visual space is kept intact throughout processing in the optic lobes. The neuropils of the optic lobes are characterized by their columnar structure. Identical groups of cells, consisting of several different types of small-field neurons that are individually identifiable, are repeated for each visual sampling point. In the lamina these identical repeated groups of cells are called cartridges; in the medulla they are termed columns. This organization also implies that early processing of local information is repeated in each of the cartridges and columns. Preprocessing of local information is performed by different neurons or sets of neurons, which are identical in each of the columns. This columnar structure is intersected by several different planar networks of neurons, for example: (1) amacrin cells that provide local networks and (2) wide-field tangential cells that collect and process visual information from multiple columns and thus sample larger parts of the visual field. These neurons can access different types of preprocessed local information for each visual sampling point and relate it out to other visual areas in the optic lobes or central brain regions.

1.06.2.2 Lamina

The lamina, the first and the most peripheral of the three optic neuropils, receives retinotopic inputs from the retina. Each ommatidium provides receptor axons from the photoreceptors that are called short or long visual fibers depending on whether they terminate in

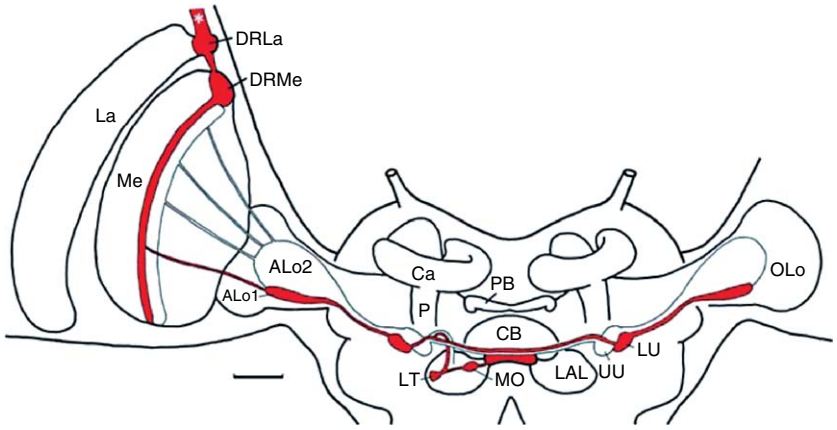

Figure 4 Schemata of the brain of the locust *Schistocerca gregaria* with its polarization vision pathways highlighted in red. ALo1-2, layers 1 and 2 of the anterior lobe of the lobula; Ca, calyces of the mushroom body (MB); CB, central body; DRLa, DRMe, dorsal rim areas in the lamina and medulla; La, lamina; LaL, lateral accessory lobe; Me, medulla; OLo, outer lobe of the lobula; P, pedunculus of the MB; PB, protocerebral bridge; UU, upper unit of the anterior optic tubercle. Adapted with permission from Homberg, U., Hofer, S., Pfeiffer, K., and Gebhardt, S. 2003. Organization and neural connections of the anterior optic tubercle in the brain of the locust, *Schistocerca gregaria*. J. comp. Neurol. 462, 415–30.

the lamina, short visual fibers, or in the outer medulla, long visual fibers. These axons from a single ommatidium form together with some second-order neurons a neuronal bundle, which is called a lamina cartridge. The lamina gives rise to monopolar cells. All monopolar cells from one lamina cartridge project together across the first optical chiasma into the corresponding column of the outer medulla. They are joined by the long visual fibers that pass through the same cartridge. Diptera are an exception to this type of organization. Flies possess a so-called neural supposition eye in which the R1–R6 photoreceptors (short visual fibers) of each ommatidium have different optical axis. Therefore they sample information at different points in visual space. However, six R1–R6 photoreceptors from different ommatidia share the same optical axis and thus sample the same point in space. The axons of these six photoreceptors converge onto a single optic cartridge in the lamina. Each lamina cartridge sends six neurons, five monopolar cells and one T basket cell, across the first optic chiasma to the medulla, together with the axons of R7 and R8 photoreceptors (long visual fibers) that also share the same optical alignment (Kirschfeld, K., 1967).

1.06.2.3 Medulla

The medulla is the second optical neuropil and can be divided into three regions, the outer, the inner medulla, and the serpentaine layer, which separates the outer and the inner medulla. Lamina monopolar cells and long visual fibers are the main inputs into the outer medulla. The chiasma between the lamina and the medulla is crossed but the retinotopy is conserved as mentioned above. Like the lamina, the inner and the outer medulla are characterized by a columnar structure. Several identified types of small-field neurons are repeated in each of the laminar cartridges and medullar columns. Centrifugal T cells, which are present in most species and comprise several distinct anatomical and functional subclasses, link the outer medulla to the inner medulla and the medulla to the lobula and the lobula plate. The serpentaine layer is characterized by large tangential neurons that collect and process information across several columns and project to the central brain.

1.06.2.4 Lobula Complex

The lobula plate receives retinotopic inputs from both the medulla and the lobula. The inputs are mainly small-field columnar neurons, such as various T, Tm, and Y cells from the medulla and the small-field columnar neurons, which connect the lobula with the lobula plate. The lobula plate houses large motion-sensitive tangential neurons that have been characterized both anatomically and physiologically in Diptera, Lepidoptera, and Orthoptera (see Sections 1.06.3.1 and 1.06.3.2).

The lobula in turn receives input from the medulla. The input is also retinotopic and consists mainly of small-field columnar neurons, similarly various T, Tm, and Y cells, and also receives inputs from the lobula plate via small-field columnar

neurons. The lobula consists mainly of columnar neurons, which are arranged in retinotopic arrays. Color processing seems to be one of the main features in the lobula (see Section 1.06.4.1), and neurons detecting orientations of lines have also been recorded there (see Section 1.06.3.3).

1.06.2.5 Projections to Other Parts of the Nervous System

The main output regions of the optic lobes are in the supra- and subesophageal ganglia. The dorsal protocerebrum receives terminals of neurons originating in the lobula plate. The ventrolateral protocerebrum is the main output area of the lobula. Both the dorsal and the ventrolateral protocerebra contain the dendrites of many descending neurons that connect to motor centers in the thoracic ganglion. Descending neurons are neurons that originate in the supra- or subesophageal ganglia and connect the brain to one or more thoracic and/or abdominal ganglia. Ascending neurons, on the other hand, are neurons with opposite polarity. The central body complex, the ventral or accessory lobes that are located on either side of the central body complex, and the MBs also receive input from the visual system (Figures 3 and 4).

The central complex CC is located in the center of the brain. It is a highly structured, columnar neuropil consisting of the protocerebral bridge (PB), the upper, and lower central body (CBU and CBL). The CC is connected to the motor centers in the thoracic ganglion and are thought to be involved in the spatial control of locomotion, and it might represent a general spatial organizer in the insect brain.

The MBs are paired structures located in both halves of the central brain region. They are divided into the main input region, the calyces and the peduncles, which show a highly parallel organization. They are composed of intrinsic neurons, the Kenyon cells. The MBs receive multisensory information and are thought to be important for multisensory integration, learning, and memory function. The MBs receive olfactory information through the calyces while other sensory information are received through the peduncles. Hymenoptera are an exception to this; here olfactory and visual information are received through the calyces.

1.06.2.6 Functional Anatomical Pathways

Similar to the above-mentioned principles of single individual neurons and multiple parallel neuron architecture, we can find two analog types of projection pathways. The first type supports mostly fast, reflex-like functions and comprises a single or very few neurons with just one or a few synapses between the neurons analyzing the visual input and the motor output regions.

A perfect example for a fast, small circuit pathway can be found in the locust (Section 1.06.3.2). Here the visual information that the locust uses to initiate escape or evasive flight maneuvers in response to approaching objects is processed in a lobula wide-field neuron, the lobula giant movement detector (LGMD). The output of the LGMD is transmitted to a descending neuron, the descending contralateral movement detector (DCMD), that projects to the motor centers in the thoracic ganglion. The visual information is thus transferred to motor neurons innervating leg and flight muscles. The synapse between the LGMD and the DCMD is a one to one synapse, for every spike in the LGMD a spike is generated in the DCMD, and thus there is no additional processing happening at this synapse (Section 1.06.3.2).

Projection pathways that are highly parallel and that might involve multiple synaptic transmissions between the sensor and the actor units are more indicative of higher-order integration. They are quite common in the visual system of invertebrates. Two good examples for such pathways are: (1) The polarization vision pathway. An up-to-date schemata of the understanding of this pathway is shown in Figure 4. (2) The projection of visual and chromatic information from the optic lobes to the MBs is another good example. In the medulla and the lobula of bees, several classes of color-opponent neurons have been characterized, which project through two tracts either to the MBs or to the contralateral optic lobe (see Section 1.06.4.1). These cells have receptive fields of varying size and so far no retinotopic organization has been found. Medulla and lobula outputs have been traced to the calyces, the main input area of the MBs. The outputs from the medulla comprise two different tracts, the anterior inferior and anterior superior optic tract, whereas neurons originating in the lobula use the lobula tract. All three tracts together contain roughly 400 neurons. The input into the MB calyces is not retinotopic except that it is segregated between the ventral and the dorsal halves of the visual field. Each input cell sends out multiple processes to different parts of the circumference of one of the calyces. The MBs comprise a large number, 340 000 in honeybees, of small,

parallelly arranged neurons, Kenyon cells, which originate in the calyces and run along the length of the MB peduncles. The color-sensitive medulla and lobula cells connect to these Kenyon cells. Here further processing takes place and the information is then relayed to other parts of the brain or to the thoracic ganglion and the motor output units. This example illustrates a much more complex pathway organization. Here we see a massive parallel organization of both the pre- and the postsynaptic components. Multiple synapses and multiple pre- and postsynaptic cells are involved in visual information processing and potentially in multisensory integration in the MBs. In this case lateral integration and complex processing of information might occur at each step of the pathway.

The organization of these two different pathways also highlights different principles of information processing. The LGMD integrates all these visual stimulus parameters required to sense an approaching object and, via the DCMD, transmits signals to various motor systems. Even though the DCMD also receives information from other modalities, the integrated information is used only in a specific context, evasive or escape behavior.

In contrast, the second example shows a more flexible way of visual information processing. A medulla cell can have color opponent properties. But, one color opponent cell is not sufficient for the bee to precisely identify the color of a stimulus and importantly whether this color is behaviorally relevant. The highly parallel organization of this pathway is perfectly well suited for the integration with other sensory information. Such architecture allows for a high degree of flexibility concerning further processing and motor output. Depending on the internal state of the animal, its prior experience and learning and information about the state of the world, the chromatic information may be used for widely different behavioral tasks.

1.06.3 Motion-Based Visual Information Processing

What is motion vision good for? Strictly speaking, motion, that is, relative motion between the eyes and the surroundings, is a necessary prerequisite for any visual perception. This might sound very strange but it is in fact just the consequence of the way photoreceptors work. Photoreceptors stimulated at a constant light level adapt. An image perfectly stabilized with respect to the retinal photoreceptor arrays will therefore result in the loss of any visual perception. Besides this phenomenon, there are many answers to the question, some of which are quite obvious from our everyday experience. When walking in a crowded place it is good to know whether we should better change our path to the left or to the right in order to avoid bumping into people. Or, when crossing a street knowing the direction the cars are driving in is essential for making it safely to the other side. But motion is also useful to make sense of the world in less intuitive ways. Relative motion allows visually oriented animals, including humans, to infer how far objects are away and breaks camouflage between motionless objects in front of a stationary background.

The analysis of directional motion, which is essential for the visual estimation of self-motion, is one of the most thoroughly investigated fields in insect vision. In this area, behavioral and neurophysiological experiments have been combined in a remarkably successful way. A couple of discoveries were made in this area during the past decade, which considerably improved our understanding of the neural basis of visually guided behavior. Comprehensive accounts on the computational aspects of vision, in general, may be found in some more specialized textbooks (e.g., Mallot, H. A., 2000).

1.06.3.1 Estimating Self-Motion Using Directional Motion Cues

Visual estimation of self-motion is a necessary requirement for an inner-loop control system to function. In this section we will focus on the significance of processing directional motion in the context of gaze and flight stabilization. At the end of this section we will also review recent evidence that directional motion vision may also play an important role in obtaining distance information useful to avoid collisions during flight in confined areas. The latter function could be seen as a potential basis for an outer-loop interacting with the flight-stabilizing inner loop (Figure 2). Most of our knowledge about the neural processing of directional motion comes from studies on various fly species – the model systems we will be concentrating on.

1.06.3.1.1 Self-motion and optic flow

To control gaze and flight in a closed-loop situation, animals constantly acquire information about their self-motion in space. This is where directional

motion vision comes into play. While moving through an otherwise stationary environment, animals experience panoramic retinal image shifts, optic flow fields. Optic flow fields result from relative movement between objects in the environment and the eyes. The structure of optic flow fields is intimately related to the way the animal moves, which is determined by the self-motion parameters, translation and rotation. Conversely, analyzing optic flow allows the animal to assess its self-motion parameters and to use this information for control purposes.

In the 1950s, Gibson J. J. (1950; 1958) already put forward the idea that optic flow provides a rich source of self-motion and distance information. Gibson's contributions, however, stayed at a rather qualitative level. Only later, Nakayama K. and Loomis J. M. (1974) as well as Koenderink J. J. and van Doorn A. J. (1987) introduced a formal description of optic flow that is incredibly useful to quantify self-motion-generated input to the visual system. Koenderink J. J. and van Doorn A. J. (1987) worked out a theoretical framework in vector notation – often referred to as **KvD** algorithm – which helped to develop ideas of how the visual system might be able to retrieve self-motion parameters from optic flow fields. They introduced an iterative least-square algorithm to estimate the self-motion parameters, i.e., the translation vector **T** and the rotation vector **R**, which best describe a field of noisy motion parallax vectors $\mathbf{p}_i$:

$$\mathbf{p}_i = \frac{\Delta \mathbf{d}_i}{\Delta t} = -(\mathbf{T} - (\mathbf{T}\cdot\mathbf{d}_i)\mathbf{d}_i)/D_i - (\mathbf{R}\times\mathbf{d}_i) \qquad [1]$$

with each $\mathbf{p}_i$ obtained at a defined direction in space $\mathbf{d}_i$. Equation [1] shows that each $\mathbf{p}_i$ is given by the linear sum of the translation- and rotation-induced contributions. It also shows that the translation-induced component depend not only on the magnitude of **T** but also on the distance D_i between the visual sensor and any visible object at directions $\mathbf{d}_i$. This confounding effect of distance and translational velocity causes a problem: Moving slowly past an object at close distance results in the same contribution to a given $\mathbf{p}_i$ as moving quickly past an object that is further away. There is no hope of recovering the actual translation vector **T** unless the distance D_i was explicitly known for each $\mathbf{d}_i$ and/or there was knowledge about the speed of translation $|\mathbf{T}|$.

Since this is usually not the case, Koenderink J. J. and van Doorn A. J. (1987) introduced the reduced nearness, $\mu_i = |\mathbf{T}|/D_i$, which allows for arbitrary combinations of speed and local distance resulting in the same reduced nearness. By doing so the **KvD** is confined to retrieve only the direction of translation **t** rather than both its direction and magnitude given by **T**. Taking this modification into account, eqn [1] can be rewritten as follows:

$$\mathbf{p}_i = -\mu_i(\mathbf{t} - (\mathbf{t}\cdot\mathbf{d}_i)\mathbf{d}_i) - (\mathbf{R}\times\mathbf{d}_i) \qquad [1a]$$

This equation provides the basis for a set of three coupled linear equations (Koenderink, J. J. and van Doorn, A. J. 1987) to obtain estimates of $\mathbf{R}'$, $\mathbf{t}'$, and $\boldsymbol{\mu}_i'$, Which produce estimates of the local parallax vectors $\mathbf{p}_i'$. The system then iterates the parameters to minimize the least-square error E between the measured and estimated local parallax vector.

$$E = <|| \mathbf{p}_i - \mathbf{p}_{i'} ||^2> = 0$$

where rectangular brackets denote the average across all n available directions $\mathbf{d}_i$. The iterative **KvD** algorithm theoretically requires only five directions at which local parallax vectors are measured to produce an estimate of the self-motion parameters. More directions increase the reliability with which the parameters can be estimated when applying the algorithm repetitively to noisy optic flow fields (Koenderink, J. J. and van Doorn, A. J., 1987). In that respect, insects such as fruitflies with 800 ommatidia per eye and dragonflies with nearly 30 000 ommatidia per eye (e.g., Land, M. F. and Nilsson, D. E., 2002) involved in estimating local motion direction are rather well equipped to solve the task. The short behavioral response time to visual stimuli, however, does not speak in favor of them applying an iterative algorithm to estimate self-motion. Therefore, based on the **KvD**, a one-shot estimator of self-motion parameters was proposed (Dahmen, H. *et al.*, 2001), which uses the following equations to estimate **t** and **R**:

$$\mathbf{t}' = -k[\mathbf{I} - \mathbf{M}_t/n]^{-1}\left[<\mu_i'\mathbf{p}_i> + R'\times<\mu_i'\mathbf{d}_i>\right] \qquad [2]$$

$$\mathbf{R}' = [\mathbf{I} - \mathbf{M}_r/n]^{-1}\left[<\mathbf{p}_i\times\mathbf{d}_i> + (\mathbf{t}'\times<\mu_i'\mathbf{d}_i>)\right] \qquad [3]$$

where k is a normalization factor chosen to grant $|\boldsymbol{t}'| = 1$, **I** stands for the 3×3 identity matrix, while $\mathbf{M}_t$ and $\mathbf{M}_r$ are 3×3 matrices containing the average of the dyadic products $\mu_i\mathbf{d}_i \otimes \mu_i\mathbf{d}_i$ and $\mathbf{d}_i \otimes \mathbf{d}_i$, respectively. These equations illustrate an important point in the context of estimating self-motion parameters from optic flow: The estimate of $\boldsymbol{t}$ also depends on $\boldsymbol{R}$ and vice versa as stated by the right-hand terms in eqns [2] and [3]. These apparent translation and rotation terms (Koenderink, J. J. and van Doorn, A. J., 1987; Dahmen, H. *et al.*, 2001) result

from ambiguities in local measurements of directional motion. A parallax vector $\mathbf{p}_i$ measured locally could have been caused by translation or rotation (Figure 5, gray areas in (b), (c), and (d)). But eqns [2] and [3] also suggest strategies of how to reduce these terms for a more reliable estimation of self-motion parameters – which, indeed, some insect visual systems seem to have adopted (Section 1.06.3.1.3).

As mentioned in the previous section, self-motion in space can be described in terms of translations **T** and rotations **R** referring to movements along and around the cardinal body axes (Figure 5(a)). Optic flow fields induced by translation have a different

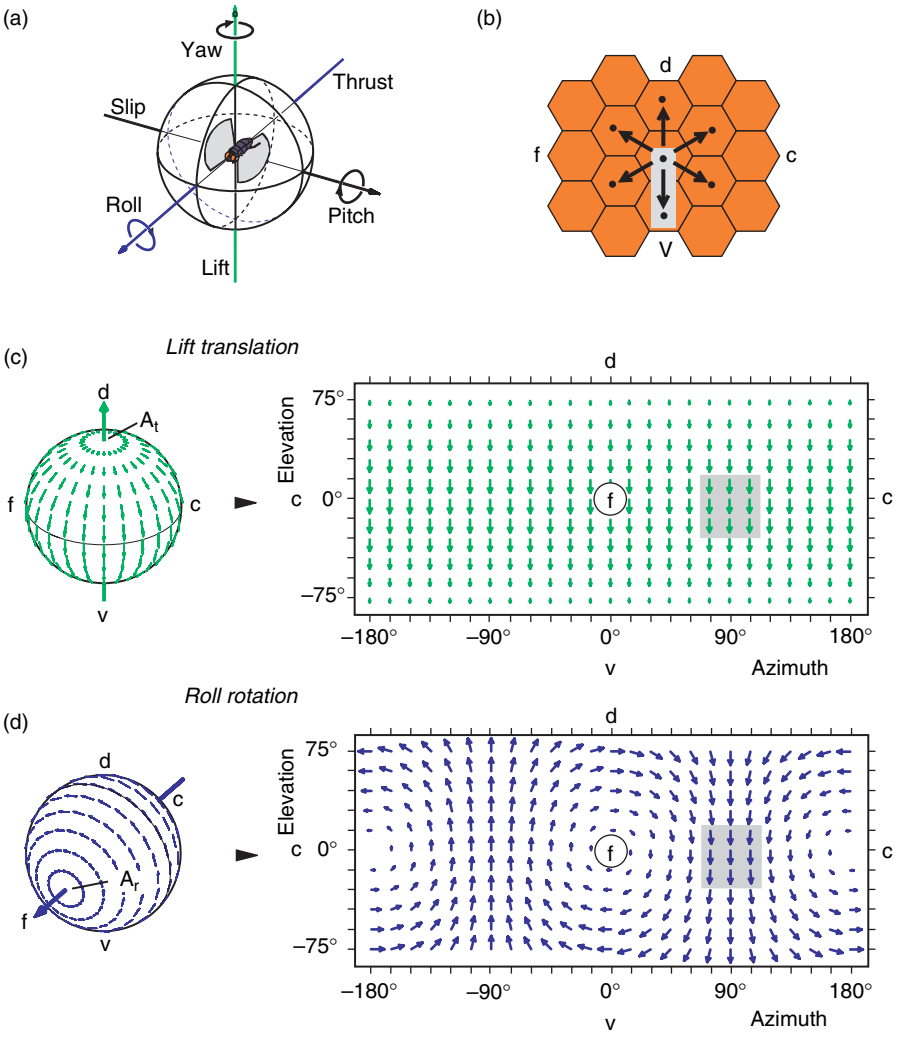

Figure 5 Self-motion and optic flow. (a) Self-motion can be described in terms of translation- and rotation-components along and around the cardinal body axes. (b) Small section of a compound eye sampling information in the lateral visual field of the right eye. In a first approximation, the direction of local retinal image shifts is analyzed along ommatidial rows within the hexagonal eye lattice (black arrows; f, frontal; c, caudal; d, dorsal; v, ventral). (c, d) Structural features of global optic flow generated during lift translation (c) and counter clockwise roll rotation (d) is presented on the surface of the visual unit sphere (left) and in a cylindrical projection (right), where *f* denotes the position directly in front of the animal. A_t in (c) and A_r in (d) indicate the axis of translation and rotation, respectively. Note the marked differences between translation- and rotation-induced optic flow at the global scale. But also note that at the local scale the direction of flow vectors is ambiguous. In the right visual field, around elevation = and azimuth = 90° (gray area), during lift translation and roll rotation, local flow vectors point in the same direction. For further explanation see text. Adapted from Krapp, H. G. and Hengstenberg, R. 1996. Estimation of self-motion by optic flow processing in single visual interneurons. Nature 384, 463–466; Krapp, H. G., Hengstenberg, B. and Hengstenberg, R. 1998. Dendritic structure and receptive-field organization of optic flow processing interneurons in the fly. J. Neurophysiol. 79, 1902–1917.

global structure than those induced by rotation. This becomes obvious when comparing optic flow fields occurring during upward movement along the vertical body axis (lift translation, Figure 5(c)) and during a rotation around the longitudinal body axis (roll rotation to the left, Figure 5(d)). Both flow fields were calculated using eqn [1a] assuming a unit distance to all objects in the visual world, which emphasizes the structural differences between rotational and translational flow fields.

The orientation and the length of each individual vector in Figures 5(c) and 5(d) indicate the direction and the relative magnitude of the retinal image shift at different positions within the spherical visual field. The positions are determined by two angles: the horizontal azimuth, φ, and the vertical elevation, θ, where azimuth = elevation = 0° defines the point directly in front of the animal (**f**, in Figures 5(c) and 5(d)). Negative and positive azimuths indicate positions in the left and the right visual hemisphere, respectively. Negative and positive elevations refer to positions below and above the horizon. Translation- and rotation-induced optic flow fields have in common that the direction of translation and the axis of rotation, respectively, define the location in the flow fields where no relative motion takes place and therefore the vectors disappear. From these flow field singularities the relative motion increases gradually and becomes maximum at the flow field equator. Two structural differences help to distinguish between translation- and rotation-induced flow fields: In a translation flow field the local velocity vectors are aligned along great circles connecting the two singularities in the field with one another. The vectors in the rotation flow field, instead, are aligned along parallel circles centered with the axis of rotation (Figure 5(c) and 5(d), spherical presentation). The second difference concerns the magnitude of local motion vectors. In translation-induced optic flow fields, the magnitude of local motion vectors depends on the distance between the eyes and the objects in the surroundings, which is not the case in a rotation-induced optic flow. We know the distance-dependence in translation flow fields from everyday experience: When sitting on a train, bushes close by rush past very quickly while trees and hills in the far distance hardly move at all.

Optic flow fields may be projected onto a 2D map of the visual field, which allows us to appreciate its complete structure including both visual hemispheres (Figure 5(c) and 5(d), right panels). This reduction from 3D spherical coordinates to two dimensions in a cylindrical projection, as it is used here, results in overemphasizing the dorsal and the ventral parts of the visual field. While on a sphere, the dorsal and the ventral pole areas consist only of a point, in the cylindrical projection these areas are expanded by factor of $1/\cos\theta$.

In whatever way optic flow is presented, globally, it is always easy to distinguish between translation- and rotation-induced optic flow fields – and thus to identify the self-motion that had caused them. However, both biological and technical systems analyzing directional motion work only locally (e.g., Bulthoff, H. *et al.*, 1989; Borst, A. and Egelhaaf, M., 1993; Barron, J. L. *et al.*, 1994). How directional selective motion detectors in biological systems work and what are the problems associated with local motion processing will be discussed in the next section.

1.06.3.1.2 How does the visual system analyze directional motion?

In the 1950s, Hassenstein and Reichardt carried out a number of behavioral experiments in the beetle *Chlorophanus viridis*. By means of a quantitative input–output analysis they derived a phenomenological model of an elementary movement detector (EMD, Hassenstein, B. and Reichard, W., 1953). This model captures the necessary and sufficient conditions to distinguish between motion in opposite directions. Its functional structure consist of (1) two spatially separated inputs, (2) an asymmetric processing of signals traveling along the two input channels where one signal is delayed in time, and (3) a nonlinear combination of the delayed and undelayed signal realized by a multiplication operation (rev.: Reichardt, W., 1961; 1987; Borst, A. and Egelhaaf, M., 1989). Such EMD responds to motion in its preferred direction with a positive output while motion in the opposite null direction does hardly render any output (Figure 6, upper panels). A fully directional-selective EMD is obtained by summing the outputs of two EMDs with opposite signs, one of which is arranged in a mirror-symmetric way. The summing unit then delivers a positive output when motion in the detector's preferred direction occurs and a negative output for motion in the opposite direction (Figure 6, lower panels). This generic model is also known as a correlation-type motion detector since it performs a spatiotemporal correlation of light intensities sampled at neighboring positions on the retina. Most of the motion detector schemes found across phyla are derivatives of the EMD but have different filters implemented at different processing stages. Borst A.

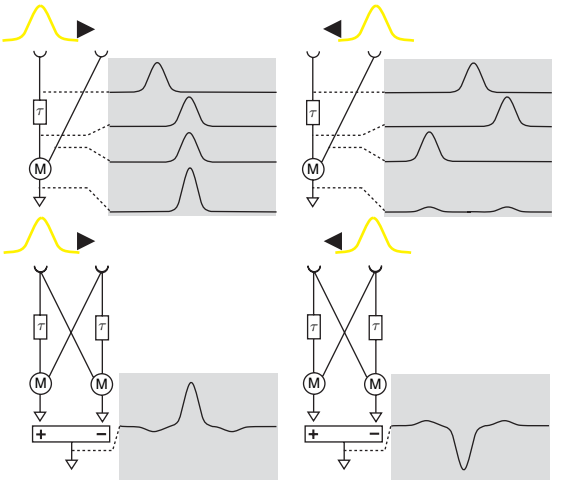

Figure 6 Elementary movement detectors (EMDs). Directional motion in biological systems is analyzed by EMDs, which receive input from and correlate light intensities at neighboring photoreceptors. *Upper left*, half-detector: A light stimulus moving from left-to-right (yellow Gaussian function) is sensed by the left input channel of an EMD first. Propagation of the signal in this channel is delayed by a period of time related to τ, the delay time constant of the EMD. If the time it takes the stimulus to reach the right input channel and the time the signal in the left channel is delayed are the same, both signals simultaneously arrive at the multiplication stage (M) and yield a strong output. *Upper right*: Motion in the opposite direction results in decorrelating the two input signals in time and consequently does not produce a strong output. *Lower left and right*: Subtracting the outputs from two mirror-symmetrical half-detectors results in fully directionally selective properties of the integrating stage. For further explanations see text. Adapted from Borst, A. and Egelhaaf, M. 1989. Principles of visual motion detection. Trends Neurosci. 12, 297–306.

and Egelhaaf M. (1993) provide a comprehensive comparison of different motion detector schemes that were derived either from experimental evidence obtained in different animal systems or from computer vision.

An inherent feature of the EMD is that its output depends not only on the direction and the velocity of visual motion but also on the properties of the visual scene such as contrast and its spatial frequency content (rev.: Buchner, E., 1984; Borst, A. and Egelhaaf, M., 1993). The EMD output depends in a bell-shaped manner on the ratio between the angular velocity at which a pattern of periodic light intensity fluctuations is moving and the pattern's spatial wavelength. Such contrast frequency, or temporal frequency dependence is fundamentally different from the output of another motion detector scheme, the gradient detector, which was originally derived from computer vision (e.g., rev.: Srinivasan, M. V., 1990). Gradient detectors also fulfill the three necessary and sufficient conditions required to analyze motion in a directional-selective way, but their output signals are linear in the velocity domain. Many behavioral and electrophysiological studies have been carried out in the past decades to decide what movement detector schemes different animals use (rev.: Buchner, E., 1984). Although there is good evidence suggesting flies to employ correlation-type motion detectors, bees, for instance, were found to use velocity information to solve many visually controlled tasks (rev.: Srinivasan, M. V. and Zhang, S. W., 2000). It is still an open question whether bees are capable of exploiting velocity information by using gradient detectors or by combining the outputs of correlation detectors tuned to different temporal frequencies – which were indeed found in crabs (Nalbach, H. O., 1989).

The basic structure of the EMD has been revised several times over the years to improve its predictive power (e.g., Clifford, C. W. *et al.*, 1997; Harris, R. A. *et al.*, 1999; Dror, R. O. *et al.*, 2001; Borst, A. *et al.*, 2003) and to investigate its potential of retrieving velocity information (e.g., Reichardt, W. *et al.*, 1988; Zanker, J. M. *et al.*, 1999; Dror, R. O. *et al.*, 2001). Recently in 2D EMD network models, more realistic assumptions about compound eye optics and gain control mechanisms (cf. section 1.06.3.1.3.(viii)) were implemented to overcome the detector's inherent pattern-dependent response properties (Lindemann, J. P. *et al.*, 2003; Shoemaker, P. A. *et al.*, 2005). In particular, when confronted with wide-field stimuli composed of naturalistic spatial frequency distributions (van der Schaaf, A. and van Hateren, J. H., 1996), some of the recent EMD networks performed extremely well to analyze dynamic motion sequences and to predict the activity in directional-selective interneurons (Heitwerth, J. *et al.*, 2005; Lindemann, J. P. *et al.*, 2005; Shoemaker, P. A. *et al.*, 2005).

1.06.3.1.3 Flies as model systems for directional motion processing

The fly is one of the most successful model systems in invertebrate vision and beyond. One of the reasons being that in this animal a variety of experimental approaches in combination with modeling the different processing stages along the visual pathways can be tightly linked to the performance of several visually guided behaviors (rev.: Egelhaaf, M. and Borst, A., 1993; Hausen, K., 1993; Egelhaaf, M. *et al.*, 2002). Not only is the anatomy of the fly

nervous system characterized in minute detail (Strausfeld, N. J., 1976) but also is it possible to investigate the physiological properties of individually identified neurons and neural populations. The extraordinary data body accumulated over the last couple of decades turned out to be an ideal prerequisite to address fundamental questions regarding peripheral and central visual processing and also to study general principles in motion detection, neural coding, mechanisms of adaptation, feature extraction, and, more recently, multimodal integration as well as sensorimotor transformation.

Different fly species are used in research on visual processing: (1) the fruitfly *Drosophila*, for its comparatively easy handling in behavioral experiments and the opportunity to apply neurogenetics to dissect the functional organization of the nervous system; (2) the housefly *Musca*, used in numerous behavioral experiments and several anatomical studies; (3) the blowflies *Calliphora* and *Lucilia*, which are sufficiently big to perform intra- and extracellular electrophysiology as well as optical imaging experiments on identified neurons and neural circuits; and (4) the hoverfly Eristalis, which, again, is accessible to electrophysiological studies.

Working on several different fly species was originally just a matter of practicality: the fruitfly was amenable to neurogenetics but electrophysiological studies were, in the early days, possible only in the bigger blowfly. There were some arguments about whether or not experimental evidence obtained in one species could be transferred straightaway to explain findings in others. Today, however, it becomes more and more obvious that a comparative approach allows us to discover both general principles in visual information processing and species-specific adaptations. For instance, the number of lobula plate tangential cells (LPTCs) constituting the vertical system (VS) (see below) (Hengstenberg, R. *et al.*, 1982), an identified population of visual interneurons, differs between species: While *Drosophila* employs only 6 VS cells, the housefly possesses 8 and *Calliphora* has got even 10 of these interneurons. This difference in terms of neuronal equipment seems to correlate with the complexity of the flight maneuvers the three species are required to control (O'Carroll, D.C. *et al.*, 1996; Buschbeck, E. K. and Strausfeld, N. J., 1997). We will get back to this point in a later section on the relationship between visual processing and motor control. For now, we will stay with LPTCs and discuss their role in processing directional motion information.

1.06.3.1.3.(i) Lobula plate tangential cells and the processing of directional motion Several years after Hassenstein B. and Reichardt W. (1953) derived the functional structure of an EMD the search for its neural correlate started. The input stages were obviously the ommatidia in the compound eye, which contain the photoreceptors sampling light intensities at neighboring locations in the visual field. But where was the multiplication stage located that is so crucial for the EMD to work? Despite a few attempts to identify the multiplication stage (e.g., locusts: Osorio, D., 1986), even today this question remains still unanswered. The summation stage, however, which establishes a fully opponent EMD, was found in the late 1960s and the 1970s. Groups at Caltech, USA, and at the Max-Planck-Institute für biologische Kybernetik in Tübingen, Germany, succeeded in recording the activity of LPTCs in blowflies (Bishop, L. G. *et al.*, 1968; Hausen, K., 1976; Hengstenberg, R., 1977). They found the LPTCs to respond to visual motion stimuli in a motion-sensitive and directional-selective way. In particular, studies at the Max-Planck-Institute in Tübingen over more than 30 years did result in a detailed description of the LPTC response properties. About 60 distinctly different LPTCs were anatomically identified (Hausen, K., 1993).

Most LPTCs possess extended dendritic input fields, which ramify within distinct and conserved parts of the retinotopically organized lobula plate (e.g., rev.: Hausen, K., 1984; 1993). On their dendrites these interneurons integrate the signals of hundreds or, in blowflies, even thousands of directional-selective small-field elements (e.g., Strausfeld, N. J., 1976; Bausenwein, B. and Fischbach, K. F., 1992). The responses of LPTCs when presented with local motion stimuli directly reflect the properties of EMDs (e.g., rev.: Hausen, K., 1984). Several different functional groups of LPTC were anatomically identified and electrophysiologically characterized:

(1) *Heterolateral LPTCs.* They integrate local motion signals obtained from one visual hemisphere and transmit this information via a thin axon to their target neurons in the contralateral part of the brain (e.g., Hausen, K., 1976). These LPTCs are regularly spiking neurons, which allow them to send information at high propagation speeds along the heterolateral pathways (e.g., Hausen, K., 1984; 1993). One of the most famous heterolateral LPTCs is the H1 cell (Hausen, K., 1976), which is used as a general model system to study neural spike coding (e.g., rev.: de Ruyter van Steveninck, R. R. *et al.*, 2001; Warzecha, A. and Egelhaaf, M., 2001).

Another example is the V1 cell (e.g., Hausen, K., 1984), which receives input from several identified VS cells and serves, for instance, as a model system in synaptic transmission and multisensory integration (e.g., Kurtz, R. *et al.*, 2001; Parsons, M. M. *et al.*, 2006).

Spiking LPTCs contribute to virtually all visually guided behaviors based on optic flow processing. Their central role results is due to the fact that only motion information combined from both visual hemisphere allows for an unambiguous distinction between rotation- and translation-induced optic flow (e.g., Krapp, H. G. *et al.*, 2001; rev.: Borst, A. and Haag, J., 2002). Binocular integration certainly takes place at the level of LPTC target neurons such as neck motor neurons (NMNs) and descending neurons (e.g., Gronenberg, W. *et al.*, 1995; Huston, S. J. and Krapp, H. G., 2003). Some tasks, however, require the computation of binocular motion information at the level of the lobula plate already, for instance, in the context of figure-ground discrimination (Egelhaaf, M., 1985a, and see below).

(2) *Output LPTCs.* They come in two distinctly different subpopulations, three horizontal system (HS) cells (Hausen, K., 1982) and ten VS cells (Pierantoni, R., 1976; Hengstenberg, R., 1982; Hengstenberg, R. *et al.*, 1982). The three HS cells, horizontal system north (HSN), horizontal system equatorial (HSE), and horizontal system south (HSS), sample visual information in the dorsal, the equatorial, and the ventral part of the ipsilateral visual field, respectively (Hausen, K., 1982). HSN and HSE receive additional rotation-specific input from the contralateral visual field mediated by heterolateral spiking LPTCs (Hausen, K., 1993; Krapp, H. G. *et al.*, 2001). The morphology of VS cells, numbered from VS1–VS10, is distinctly different from the HS cell morphology in that their main dendrites are not horizontally but vertically oriented. The VS1 main dendrite arborizes in the distal lobula plate and samples motion information within the frontal visual field, while the VS10 main dendrite ramifies in the proximal lobula plate receiving its retinotopic input from the caudal visual field (Krapp, H. G. *et al.*, 1998). Altogether the VS cell receptive fields cover the entire visual hemisphere.

The dendrites of VS and HS cells mostly ramify in four distinct directional input layers of the lobula plate. These layers convey information about vertical and horizontal motion presented in the equatorial visual field (Buchner, E. *et al.*, 1979). However, there are some exceptions: VS1, for instance, has got a second dendritic tree that arborizes in the most anterior directional input layer mediating horizontal back-to-front motion sensitivity (Hengstenberg, R. *et al.*, 1982; Hausen, K., unpublished). Furthermore, the proximal VS cells, VS7–VS10, possess dendritic side branches receiving input from the second most anterior input layer mediating horizontal front-to-back motion sensitivity. The HS cell dendrites also ramify within the second most anterior layer (Hausen, K., 1982; Hausen, K., unpublished; Hengstenberg, R. *et al.*, 1982).

When first discovered, the signals that output LPTCs generate were distinctly different from those of spiking heterolateral LPTCs. Motion in the neurons' preferred direction resulted in a depolarizing membrane potential shift while motion in the opposite null directions did hyperpolarize the cells. Pharmacological studies did show that VS and HS cells are equipped with ACh- and GABA receptors, which suggests these cells to receive input from the two mirror-symmetrical subunits of an EMD, one excitatory and the other one inhibitory (Brotz, T. M. and Borst, A., 1996). It is still debated, though, whether local input elements presynaptic to the LPTCs are already fully directional-selective (Douglass, J. K. and Strausfeld, N. J., 1995; Douglass, J. K. and Strausfeld, N. J., 1996).

On top of the graded response to preferred direction motion, superimposed spikelets of irregular amplitude were found (Hengstenberg, R., 1977). Later, the application of channel blockers did show that the irregular spikelets are in fact regular sodium spikes (Haag, J. and Borst, A., 1996). The small and irregular amplitudes of spikelets were concluded to be the result of a comparatively shallow resting potential in VS and HS cells. At about −50 mV resting potential, only a smaller fraction of sodium channels will contribute to a spike since not all channels would have completed the transition from the closed nonactivatable to the closed activatable state. The comparatively low input resistance mainly responsible for the shallow resting potential shortens the cells' time constant and thus increases its bandwidth (Haag, J. and Borst, A., 1996). The faster responses, however, also mean that the LPTCs are more expensive in terms of energy consumption (Laughlin, S. B., 2001). Meanwhile, most aspects of passive and active response properties in VS and HS cells could be explained by combining thorough electrophysiological experiments and compartmental modeling (Borst, A. and Haag, J., 1996; Haag, J. *et al.*, 1999; rev.: Borst, A. and Haag, J., 2002).

The axon terminals of VS and HS neurons ramify ipsilaterally within the ventrolateral protocerebrum where they make contact with their target neurons via mixed chemical–electrical synapses (Strausfeld, N. J., 1976; Strausfeld, N. J. and Bassemir, U. K., 1983;

Gauck, V. *et al.*, 1997). Their postsynaptic targets are mostly descending neurons (Gronenberg, W. and Strausfeld, N. J., 1990; Strausfeld, N. J. and Gronenberg, W., 1990) projecting to various motor neuropils in the thoracic ganglia and some motor neurons controlling the neck motor system (Gilbert, C. *et al.*, 1995; Gronenberg, W. *et al.*, 1995). The LPTC target area also contains output arborizations of afferent fibers from other sensory systems, such as the ocelli and the antennae, as well as from ascending neurons, which convey information from the thoracic neuropils (Strausfeld, N. J. and Seyan, H. S., 1985).

The functional significance of HS and VS LPTCs for visual stabilization reflexes was conclusively shown by a number of lesion experiments using different approaches. In *Drosophila*, the neurogenetic mutant omb^{H31} produces flies that do not develop HS and VS cells (Heisenberg, M. *et al.*, 1978). These mutants loose their inner-loop control, i.e., they fail in course and gaze stabilization tasks (Blondeau, J. and Heisenberg, M., 1982; Hengstenberg, R., 1995). But they remain capable of distinguishing object from background motion – indicating a separate neural pathway that may be used for outer-loop control, for instance, during chasing of small targets. Laser ablation and microsurgical lesion experiments in *Calliphora* larvae and adults, respectively, both causing dysfunction of the HS and VS led to similar results (Geiger, G. and Nässel, D. R., 1981; Hausen, K., and Wehrhahn, C., 1983).

(3) *Centrifugal LPTCs, CH cells.* These cells receive input at least at two different locations. First, with respect to the location of their cell body, they collect information from the ipsilateral protocerebrum where the terminals of output LPTCs arborize (rev.: Hausen, K., 1993). Second, they receive retinotopic input the HSE cell mediates to their contralateral arborizations in the lobula plate. Ultrastructural studies revealed colocalizations of input and output specializations on the extended contralateral arborizations of the CH cells (Gauck, V. *et al.*, 1997). Centrifugal cells generate graded membrane potential shifts without any superimposed sodium spikelets (rev.: Hausen, K., 1984). Their membrane potential fluctuations during visual stimulation reveal input from several spiking neurons causing distinctly different excitatory and inhibitory postsynaptic potentials (rev.: Hausen, K., 1984; Haag, J. *et al.*, 1999). Centrifugal cells are GABAergic and were shown to be key elements in an intrinsic lobula plate circuit involved in figure detection (FD; Egelhaaf, M., 1985c, and see below).

(4) *FD cells* (Egelhaaf, M., 1985b; rev.: Hausen, K. and Egelhaaf, M., 1989; Gauck, V. and Borst, A., 1999). The size dependence of FD cell responses is fundamentally different from that of all other LPTCs whose responses increase to a certain degree as the stimulus pattern size is increased. FD cells, instead, respond strongly to motion of small objects moving out of phase with wide-field background motion. As the size of the object increases the FD cell response decreases (Egelhaaf, M., 1985b). The way in which such small-field tuning is established could be demonstrated experimentally in case of the identified FD 1 cell. FD 1 receives input from the ventral centrifugal cell, VCH, also called a wide-field inhibitor. When the impact of the wide-field inhibitor was abolished either by applying GABA blockers or by laser-ablating the cell, FD 1 transformed into an ordinary, wide-field-tuned LPTC (Warzecha, A. K. *et al.*, 1993). Combined behavioral and electrophysiological experiments suggest FD cells to distinguish objects of potential interest from the background by using relative motion cues (Reichardt, W. and Poggio, T., 1976; Egelhaaf, M., 1985a; 1985b; 1985c).

1.06.3.1.3.(ii) HS and VS cells analyze self-motion-induced optic flow For many years HS and VS cells as well as heterolateral LPTCs were distinguished based on their predominant directional motion preferences, that is, horizontal front-to-back motion and vertical downward motion. In case of HS and VS cells, the overall orientation of their main dendritic branches within the different direction-specific input layers of the lobula plate also justified the distinction between horizontal and vertical cells. From the functional point of view, knowing both the horizontal and the vertical motion component at any location in the visual field would require only little additional computation to retrieve the exact direction of local motion.

Only in the mid-1990s, an alternative idea was put forward that would considerably simplify the extraction of self-motion parameter from optic flow fields. The hypothesis was that individual LPTCs were tuned to extract information about self-motion in a more specific way (Krapp, H. G. and Hengstengberg, R., 1996). To extract, for instance, the roll component of self-motion the local motion preferences within the receptive field of a VS cell should match the orientation of local velocity vectors in an optic flow field that is generated when the fly turns around is longitudinal body axis. Such a matched filter for particular self-motion components would get around the problem that local motion information is insufficient to infer what self-motion had caused it (Figure 7). This hypothesis assumed, however, that the distribution of local

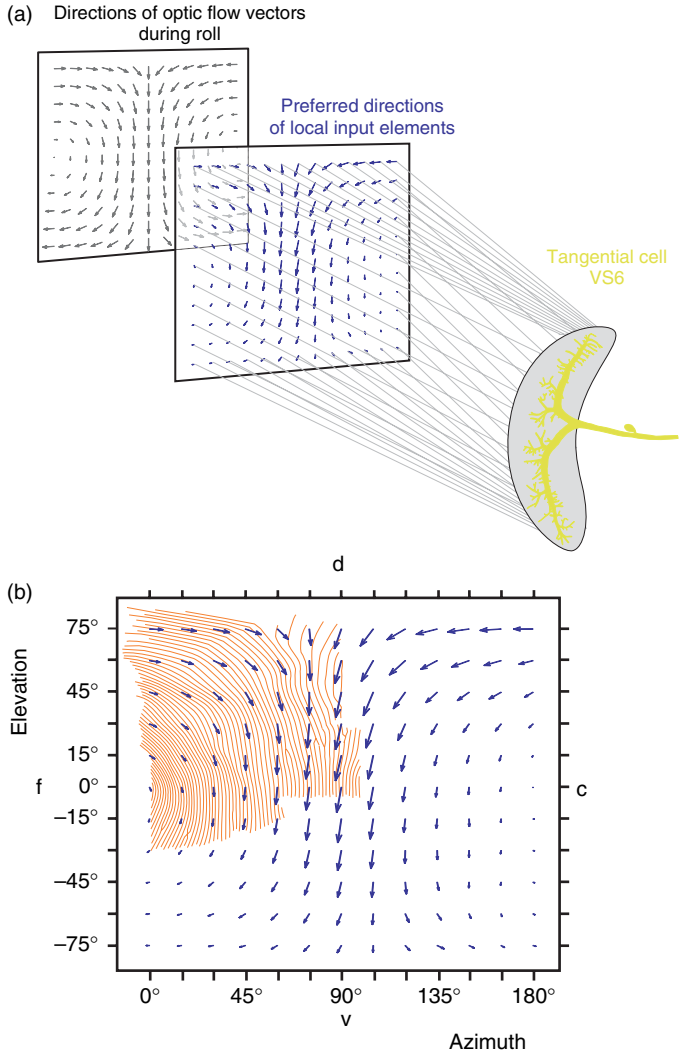

Figure 7 Lobula plate tangential cells (LPTCs) process optic flow. (a) To indicate roll rotation the VS6 cell selectively integrates the output of those local input elements whose preferred directions match the local orientation of velocity vectors in an optic flow field generated during roll. (b) The visual VS6 receptive field (same as in (a)) is shown in a cylindrical projection of the right visual hemisphere. The distribution of local preferred directions is indeed very similar to the vector distribution within a roll optic flow field (cf. Figure 5d, right half). Orange curved lines in the upper left quadrant give the course of ommatidial rows, the orientation of which is vertical in the eye equator (elevation = 0°). Note that these vertical rows are considerably distorted in the frontodorsal part of the eye and become almost horizontally oriented at most dorsal locations. Also note the striking similarity between the VS6 cell's local preferred directions and the local vertical row orientations in that area. This correlation reflects the anatomical arrangement of retinotopic inputs in the periphery at the most central level of directional motion processing, the lobula plate. For further explanation see text. Adapted from Egelhaaf, M., Kern, R., Krapp, H. G., Kretzberg, J., Kurtz, R. and Warzecha, A. K. 2002. Neural encoding of behaviourally relevant visual-motion information in the fly. Trends Neurosci. 25, 96–102.

motion preferences would gradually change in a position-dependent way altogether approximating the directional distribution of local velocity vectors within specific optic flow fields.

A detailed receptive field characterization using a local stimulation procedure (Krapp, H. G. and Hengstenberg, R., 1997) revealed that none of the LPTC receptive fields shows an isotropic distribution of local preferred directions. The results of several studies applying intracellular and extracellular recording techniques did indeed support the hypothesis that individual LPTCs are tuned to sense distinct self-motion components (Krapp, H. G. and Hengstenberg, R., 1996; Krapp, H. G. *et al.*, 1998;

rev.: Krapp, H. G. 2000; Krapp, H. G. *et al.*, 2001). Not only was the distribution of local preferred directions matches to estimate certain self-motion components. The local motion sensitivities within the receptive fields of some LPTCs were also adapted to optimize the distinction between rotation- and translation-induced optic flow (Figure 8). Analytical modeling did suggest that the decreased sensitivity to motion in the ventral receptive field of VS cells extracting the roll component is an optimal strategy to produce a response more or less independent of any superimposed translation flow (Franz, M. O. and Krapp, H. G., 2000). This makes perfect sense for a matched filter for roll rotation. Optic flow in the ventral visual field, where the distance to the visual structures is small, would be dominated by translation-induced flow that distorts the roll-specific flow vectors. In the dorsal visual field, however, the distances to visual structures are far greater, which means that the translation-induced optic flow is very small, if not zero (cf. eqn [1]. LPTCs estimating translation components show higher motion sensitivities in the ventral than in the dorsal visual field (Franz, M. and Krapp, H. G., 2000).

The anisotropic distribution of motion sensitivities within the receptive field of LPTCs suggests that the fly visual system makes assumptions about the average distance distribution usually encountered in the environment. Implementing prior knowledge is one measure to increase the reliability at which specific self-motion parameters can be extracted from optic flow (Dahmen, H. *et al.*, 2001).

1.06.3.1.3.(iii) Monocular and binocular integration of motion information From eqns [2] and [3] it follows that a reliable estimation of the self-motion parameters **R** and **t** will also benefit from an extended

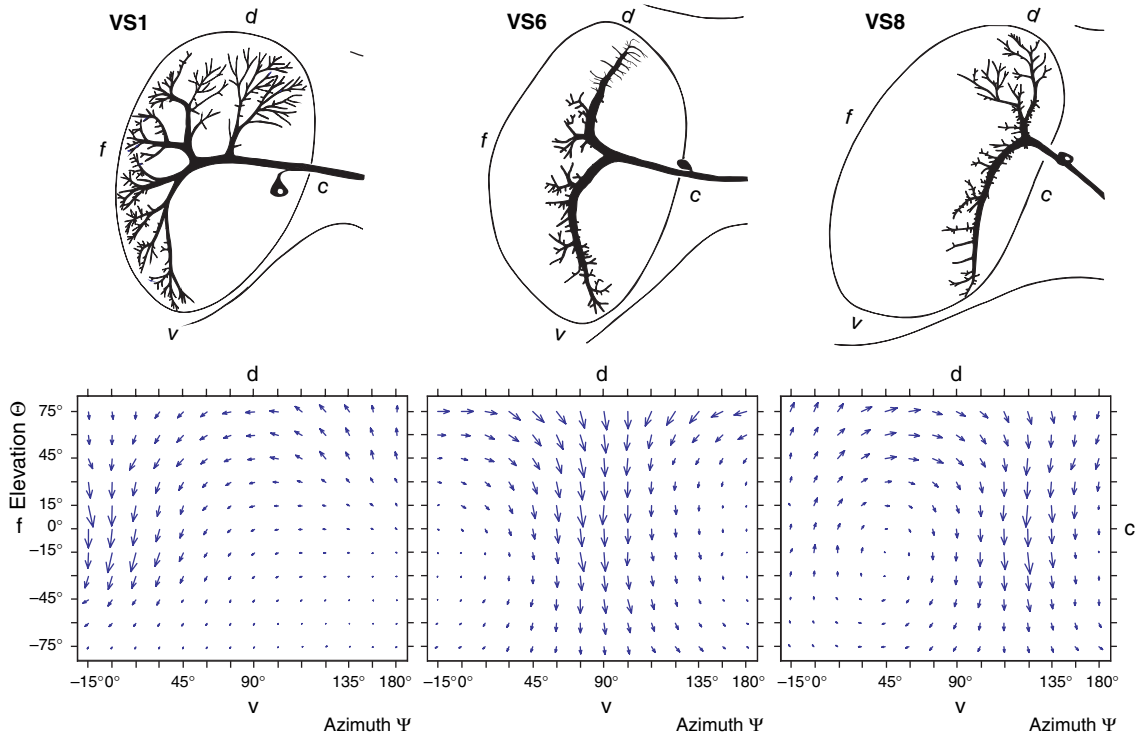

Figure 8 Vertical cells indicate self-rotations around horizontal body axes. Upper row of panels: The reconstructions from intracellular staining of individually identified tangential cells VS1, VS6, and VS8 drawn in the contours of the lobula plate. Lower row of panels: The visual receptive fields averaged across results obtained from at least five different flies per cell type. All receptive fields show a smooth transition of local motion preferences reminiscent of the directional gradient of velocity vectors in parts of or in an entire monocular rotation flow fields. Note that the location of the main vertical dendrite within the lobula plate corresponds to the positions where the respective cells are most sensitive to vertical downward motion within the visual field. In case of the VS1 cell the extent of its dendritic arborizations within the lobula plate is in agreement with the size and the location of the cells' receptive field, assuming a retinotopic input organization. This is not the case for VS6 and VS8. For further explanation see text. Adapted from Krapp, H. G. and Hengstenberg, R. 1996. Estimation of self-motion by optic flow processing in single visual interneurons. Nature 384, 463–466. Krapp, H. G., Hengstenberg, B. and Hengstenberg, R. 1988. Dendritic structure and receptive-field organization of optic flow processing interneurons in the fly. J. Neurophysiol. 79, 1902–1917.

area across which local flow measurements are taken. Ideally, to get rid of the apparent rotation and translation terms in these equations, measurements should be distributed in sufficient numbers and at locations so that $<\mathbf{d}_i>$ vanishes. In this case the apparent terms become zero, and **R** and **t** can be reliably estimated.

This consideration immediately explains why heterolateral elements are needed. Heterolateral elements establish a binocular receptive field. Interestingly, only a few LPTCs were found to have truly binocular receptive fields in the sense that they respond equally well to motion in either visual hemisphere. A prime example is the centrifugal cell VCH, the wide-field inhibitor of the FDI cell (Warzecha, A. K. *et al.*, 1993, and see above). In case of the figure detection circuit, binocular integration needs to take place at the level of the lobula plate to facilitate the specific action of the wide-field inhibitor, that is, the subtraction of wide-field background motion. Most of the output LPTCs, however, receive only weak, often quite variable contralateral input. The reason for this is not exactly clear but might be related to the internal physiological state of the individual fly. More substantial binocular integration takes place at the level of the neurons postsynaptic to the output LPTCs. This was shown for fly neck motor neurons and some descending neurons (e.g., Gronenberg, W. *et al.*, 1995; Huston, S. J. and Krapp, H. G., 2003). The most reasonable explanation is that binocular integration only at the level of the LPTC target neurons gives the system more flexibility. In combining the outputs of different LPTCs the target neurons' receptive field properties could be tuned more specifically to encode certain self-motions and to comply with the needs of the various motor systems they supply (Section 1.06.7.2). This strategy would significantly simplify the sensory motor transformation where information obtained in sensory coordinates has to be converted into signals controlling movements in motor coordinates (see Section 1.06.6).

Most of the heterolateral LPTCs themselves are sensitive to binocular motion. But again, as in output LPTCs the overall sensitivity is usually higher when motion stimuli are presented within the ipsilateral hemisphere. How the contralateral motion sensitivities are established is not exactly known as yet. The receptive field organization of these cells suggests, however, that direct or indirect mutual coupling takes place between heterolateral LPTCs from either side of the visual system (rev.: Borst, A. and Haag, J., 2002). Recent studies further developed earlier ideas of how network interactions among LPTCs may increase the neurons' flow field specificity (rev.: Hausen, K. 1993; Borst, A. and Haag, J., 2002; and see below).

1.06.3.1.3.(iv) Synaptic transmission: the VS–V1 synapse Combining motion information from either side of the visual field to increase optic flow specificity in LPTCs poses a couple of challenges. For instance, LPTCs receiving retinotopic input may be faster in integrating the signals than a heterolateral element would be able to integrate and transmit information from the contralateral eye. As a result there might be a time lag between ipsi- and contralateral optic flow information. How such synchronization issues are solved is currently unclear.

Another challenge concerns the synaptic signal transmission in heterolateral pathways. Assuming that the activity level in heterolateral and output LPTCs is related to rotation velocity in a similar way, ideally, their signals should be combined linearly. Graded chemical synapses, however, are known to involve several nonlinear processes, for example, the cooperative action of calcium on vesicle release (Dodge, F. A., Jr. and Rahamimoff, R., 1967; Smith, S. J. *et al.*, 1985).

Recent electrophysiological and optical imaging studies (Kurtz, R. *et al.*, 2001; Warzecha, A. K. *et al.*, 2003) did aim at characterizing the transfer properties of identified synapses between VS cells and the heterolateral LPTC, V1 (e.g., Hausen, K., 1984). The V1 cell receives input from four VS cells, VS1–VS4, as suggested by its receptive field organization (Krapp, H. G. and Hengstenberg, R., 1997; Krapp, H. G. *et al.*, 1998) and shown by means of simultaneous double recordings (Kurtz, R. *et al.*, 2001; Warzecha, A. K. *et al.*, 2003). The relationship between the spike rate in the postsynaptic V1 and both the membrane potential and the calcium concentration changes in individual presynaptic VS cells was found to be nearly linear. This finding suggests that the VS–V1 synaptic transmission operates in a linear range benefiting a meaningful integration of binocular motion information (ibid.). Laser ablation of individual VS cells led to the conclusion that VS2–VS4 transmit through chemical synapses while VS1 is electrically coupled to the V1 cell (Kalb, J. *et al.*, 2006). Kalb J. *et al.* (2006) conclude that the redundancy in the V1 input, that is, four VS cells contribute to the input, may increase the accuracy and the robustness of the heterolateral pathway in encoding self-motion information. Another possible reason, however, might be related to the time delay

issues in heterolateral pathways mentioned above. VS1–VS4 cells are tuned to slightly different preferred rotation axes (Krapp, H. G. *et al.*, 1998) and were found to be electrically coupled (e.g., Haag, J. and Borst, A., 2004). Both properties may improve the encoding of a dynamic self-motion sequence during a specific flight maneuvers rather than establishing a narrow static tuning to one particular rotation axis.

1.06.3.1.3.(v) How to explain the receptive field properties of LPTCs? When the detailed receptive field organization of LPTCs was discovered and their specific function in the context of optic flow processing became obvious (Krapp, H. G., 2000), one of the most intriguing questions to ask was: does such sophisticated distribution of local motion preferences depend on early visual experience? Classical deprivation experiments on kittens first showed that early visual experience is essential to properly develop the functional organization of the visual cortex (Hubel, D. H. and Wiesel, T. N., 1965). Despite the common preconception that the nervous system of most insects must be hardwired, several experiments did show a significant degree of plasticity in the developing fly visual system (behavior: Mimura, K., 1986; neuroanatomy: Barth, M. *et al.*, 1997; Rybak, J. and Meinertzhagen, I. A., 1997). Comparing the receptive field organization of the heterolateral LPTCs (V1 and H1) obtained in normally raised flies and in flies deprived of any visual input shows that the receptive field organization of the LPTCs is innate. This suggests that the adaptation to specific optic flow processing has happened on the phylogenetic timescale (Karmeier, K. *et al.*, 2001).

If not at all depending on visual experiences what determines the gradual changes of motion preferences within different parts of the receptive fields of the LPTCs? Hausen K. (1984) already pointed out that motion preferences of some LPTCs may be related to the anatomical organization of the compound eye. This comparison was probably inspired by earlier behavioral studies showing that directional motion information used for locomotor control in light-adapted flies correlates to 70% with the interactions of neighboring ommatidia along the hexagonal eye lattice (Buchner, E., 1976). Supporting evidence for a link between the orientation of the eye lattice and the processing of directional motion information came from electrophysiological studies also (Schuling, F. H. *et al.*, 1989). In a more recent study, the local orientation of ommatidial rows in the blowfly compound eye was determined for the frontodorsal quadrant of the eye (Petrowitz, R. *et al.*, 2000). A qualitative comparison revealed a remarkable correspondence between ommatidial row orientation and local motion preferences within monocular receptive fields of both HS cells and a subgroup of VS cells (Figure 7(b)); Egelhaaf, M. and Krapp, H. G., 1999; rev.: Egelhaaf, M. *et al.*, 2002). These findings suggests that the receptive field organization of some LPTCs may be explained directly from the geometrical arrangement of ommatidia in the hexagonal eye lattice. It is tempting to assume that the eye geometry, the most peripheral stage of the fly visual pathway, already serves as a filter that facilitates the processing of directional motion information in a task-specific way. Obviously, such adaptation to analyze optic flow would make sense only if it did not compromise the processing of visual information required for the control of other behaviors.

1.06.3.1.3.(vi) Lobula plate tangential cell network interactions Even though some of the local LPTC response properties could be directly understood from the eye geometry, there were still two open questions: Given that the LPTCs integrate local motion information in a retinotopic way, it should be possible to infer the size of the ipsilateral receptive field from the cells' dendritic arborization pattern within the lobula plate. While this is perfectly possible for the HS cells, several heterolateral LPTCs, and the centrifugal cells (Hausen, K., 1993; Krapp, H. G., 1995; Krapp, H. G. unpublished data; Krapp, H. G. *et al.*, 2001), the receptive field size of some VS cells is considerably larger than their dendritic arborization pattern suggests (Figure 8, cf. VS6 and VS8).

More recent electrophysiological studies solved this issue. By simultaneous intracellular recordings from pairs of VS cells, Haag J. and Borst A. (2004) were able to show that neighboring VS cells are coupled via electrical synapses. When injecting current into the most distal VS1 cell and measuring the membrane potential in increasingly more proximal VS cells, a monotonous decay of the coupling strength up to VS7/8 was found (Haag, J. and Borst, A., 2004). The coupling between VS1 and the most proximal VS9 and VS10 shows even a sign inversion. To explain the sign inversion, an ipsilateral spiking interneuron was suggested (ibid.). Further laser ablation experiments confirmed the ipsilateral coupling between VS cells (Farrow, K. *et al.*, 2005). Such ipsilateral network interactions (Figure 9) may indeed explain why proximal VS cells, which lack any dendritic arborization in the distal lobula plate, do nonetheless respond perfectly well to motion stimuli presented in the frontal visual

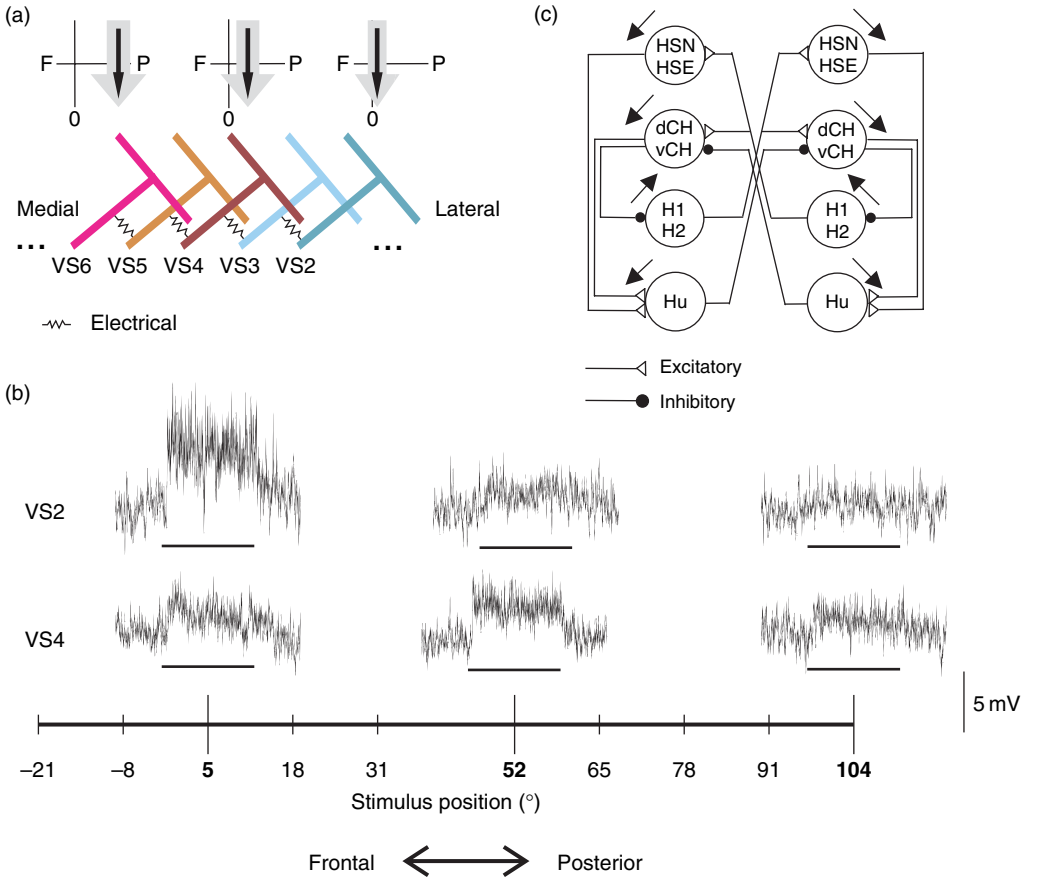

Figure 9 Network interactions between lobula plate tangential cells (LPTCs). (a) Simultaneous intracellular recordings from pairs of vertical system (VS) cells demonstrated ipsilateral network connections among VS neurons mainly mediated by electrical coupling. Broad gray arrows roughly indicate the extent of downward sensitivity within the VS cells receptive field at a center position given by the black arrow. (b) Simultaneous double recording of VS2 and VS4 shows that the activity induced by vertical downward motion depends on the position of the stimulus along the azimuth. If the stimulus is positioned in the frontal visual field, VS2 is stronger activated while VS4 responds stronger to downward motion at around 50° azimuth. Horizontal bars below intracellular traces, 1 s. For further explanations see text. Adapted from Farrow, K., Borst, A., Haag, J. 2005. Sharing receptive fields with your neighbors, tuning the vertical system cells to wide field motion. J. Neurosci. 25, 3985–3993. (c) Summary diagram showing heterolateral and ipsilateral network interactions among horizontal LPTCs. The interactions may be excitatory (open triangles) or inhibitory (filled circles) and all together are believed to increase the selectivity for sensing yaw rotation as opposed to thrust translation. H1, H2, and HU are spiking heterolateral cells, while HSE, HSN, dCH, and vCH respond to visual motion mainly by graded membrane potential shifts. For further explanation see text. Adapted from Haag and Borst 2001.

field. Together ipsilateral and heterolateral network interactions were thought to further increase the optic flow specificity in LPTCs (Haag, J. and Borst, A., 2001; rev.: Haag, J. and Borst, A., 2002; 2003; Farrow, K. *et al.*, 2005; 2006).

1.06.3.1.3.(vii) Robustness of encoding self-motion parameters A couple of years ago, much attention was paid to the nature of the neural code. In this context the fly spiking H1 cell did once again serve as a model system to study a fundamental issue in neuroscience. Different data analysis techniques, including information theory (Shannon, C. E. and Weaver, W., 1949), tried to solve the question as to whether rate coding or the exact timing of individual spikes is more important in information processing (de Ruyter van Steveninck, R. R. *et al.*, 1997; Warzecha, A. K. and Egelhaaf, M., 1999). Theoretical considerations in combination with outdoor electrophysiology led to the conclusion that the reliability of

reconstructing motion information in the fly visual system was limited only by photon noise (Lewen, G. D. *et al.*, 2001). Other groups, however, suggested noise in the neural circuits to determine the systems' accuracy (Warzecha, A. and Egelhaaf, M., 2001). While several studies aimed at deciding the coding question in one or the other way (rev.: de Ruyter van Steveninck, R. R. *et al.*, 2001; Warzecha, A. and Egelhaaf, M., 2001), it is still not clear what coding strategy the fly uses. The answer may come from studies on target neurons, which decode self-motion information that LPTCs provide. Eventually, more quantitative behavioral experiments are needed to test whether the exact timing of individual spikes in the fly motion vision pathway, affects the animals behavioral performance, which ultimately define the benchmark for neural coding.

The LPTC studies on the neural code were limited in that they focused only on one stimulus parameter, the yaw angular velocity. Recently, a question was raised more directly related to the function of LPTCs, which is the estimation of self-motion parameters. While angular velocity may be detected within a small patch of the receptive field, encoding self-motion parameters ideally involves the entire binocular visual space and requires selective integration of local motion information (see Section 1.06.3.1.3.(iii)). If individual LPTCs did encode particular self-motion components, as their local response properties suggest (Krapp, H. G. and Hengstenberg, R., 1996; rev.: Krapp, H. G., 2000), then each cell should prefer wide-field motion mimicking a specific self-motion of the animal. VS cells did indeed show a preference for wide-field motion patterns rotated around those axes predicted from the cells' local response properties (Karmeier, K. *et al.*, 2005). The tuning of the spiking V1 cell to its preferred rotation axis was robust even if the rotation flow field was superimposed with translation-induced optic flow (Karmeier, K. *et al.*, 2003).

But how quickly and accurately the entire population be able to encode any arbitrary rotation axis in the horizontal plane? Karmeier K. *et al.* (2005) addressed this question using Bayesian inference to estimate the rotation axis by considering the responses of all 10 VS cells and produced some interesting results: Considering the entire population shortens down the time interval over which the signals of the cells need to be integrated even if the intrinsic noise of the cells is correlated. Within less than 20 ms, the estimation error in determining the rotation axis is reduced to $<10^{\circ}$ (Karmeier, K. *et al.*, 2005). This time interval comes close to the consecutive time intervals of rotation and translation phases observed during semifree flight experiments in blowflies (Schilstra, C. and van Hateren, J. H., 1999). Another interesting aspect of the population code study concerns a question that has long been puzzling researchers in the field: Why using 10 VS cells to encode horizontal rotations when 2 VS cells would be sufficient from the theoretical point of view? The answer is partly that, given noise correlations and time constraints, a higher number means faster and more accurate estimations. Too many neurons, however, would result in higher energy consumption – a constraint inherent to sensory processing (Laughlin, S. B., 2001). Later we will discuss another explanation regarding the number of VS cells in Calliphora, which may be related to the efficiency of sensorimotor transformations (see Section 1.06.6.2).

1.06.3.1.3.(viii) Gain control and motion adaptation

All sensory systems share another common problem: Dynamic range matching. While the amplitude range of sensory stimuli often spans several orders of magnitude the dynamic response range within which a neuron can modulate its activity is drastically limited. A simple solution to this problem, for instance, scaling the input range, would work only in noise-free systems coding information in an ideal analog way. Neural systems, however, are everything but noise-free and at processing stages such as sensory transduction (see Chapter Phototransduction in Microvillar Photoreceptors of Drosophila and Other Invertebrates), synaptic transmission (see Section 1.06.3.1.3.(iv)), and signal propagation, discretization takes place. Even for image processing in semiconductor circuits, using the purest materials available, dynamic range compression is a serious issue. How do biological systems, built from proteins, fat, ions, and water, which – on top it – operate under permanent energy constraints (Laughlin, S. B., 2001) deal with this problem?

A general principle in sensory processing is to emphasize on significant changes in stimulus space by adapting the system's operating range. An efficient way of adaptation is to increase the sensitivity to a stimulus range where changes are most likely to occur. One possibility, for instance, would be high-pass filtering the signals to remove any DC signal components and thus to increase the gain on signal changes. In the peripheral visual system, such strategies were demonstrated at several stages (rev.: Laughlin, S. B. and Hardie, R. C., 1978; Laughlin, S.

B., 1989; Weckstrom, M. *et al.*, 1991; Land, M. F., 1997).

How about adaptation in LPTCs when processing wide-field motion stimuli? Flies reach translation velocities of up to 3 m s^{-1} (Taylor, G., personal communication) and may rotate at angular velocities exceeding 3000° per second. Without any measures of adaptation or gain control mechanisms, the output range of the LPTCs would be constantly at risk to saturate.

1.06.3.1.3.(viii).(a) Dendritic gain control In behavioral experiments on the housefly, Reichardt, W. *et al.* (1983) made an interesting observation when examining the intended yaw torque in response to stimulus patterns of different size rotated around the animal. First the fly increased its torque response with increasing pattern size. But beyond a certain size the response stayed at a plateau level that was dependent on pattern velocity: higher pattern velocities produced higher plateau levels (Figure 10(a)). The velocity dependence of the plateau levels obviously shows that the plateaus were not caused by an output saturation but, instead, a mechanism was in place that controlled the gain of the behavioral response (Reichardt. W. *et al.*, 1983). Based on their results, Reichardt W. *et al.* (1983) proposed two cells to receive the signals from all the EMDs activated during stimulation: a pool cell and an output cell, the latter of which controls the yaw torque. The integrated signal of the pool cell is then used to presynaptically inhibit all local elements connected to the output cell. Such shunting inhibition model requires the pool cell's output to be logarithmically compressed and an expansive gain at the site of the presynaptic inhibition. Altogether the model produces an invariant response with respect to the pattern size that scales with pattern velocity (ibid).

Later electrophysiological experiments on LPTCs provided an alternative explanation for the behavioral findings based on a biophysical model (Borst, A. *et al.*, 1995). The responses of EMD half-detectors were found to be less directional-selective than previously assumed. When challenged with preferred direction motion not only ACh-gated sodium channels changed their conductance resulting in a depolarization of an LPTC but also a fraction of GABA-gated chloride channels opened reducing the overall depolarization. The ratio of sodium and chloride channels activated did depend on pattern velocity (Figure 10(b)). The higher the pattern velocity, generally resulting in higher LPTC response amplitudes, the more chloride channels were activated effectively limiting the cell's

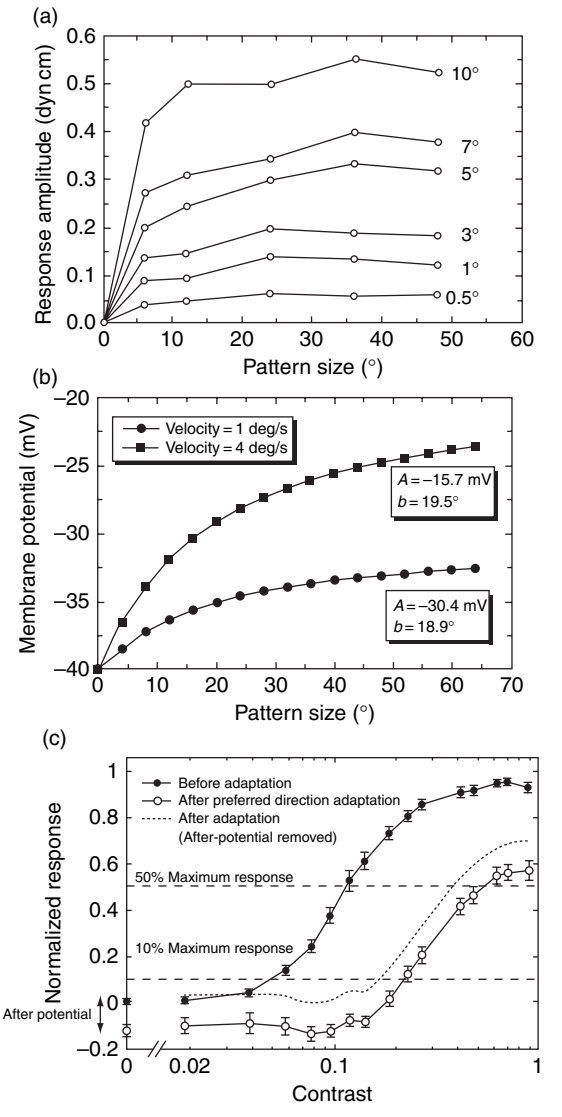

Figure 10 Gain control. (a) Output gain control in behavioral experiments on *Musca*. The response amplitude is plotted against the size of a moving background pattern oscillating at different amplitudes from 0.5° up to 10°. Beyond a certain pattern size the response stays a plateau level that depends on the respective pattern velocity. (b) Dendritic gain control simulations show similar results. The simulated membrane potential changes depend on pattern size in a qualitatively similar way. The velocity-dependent plateau responses were obtained by assuming differences in the ratio of excitatory and inhibitory conductances activated during directional motion stimuli presented at different speeds. For further explanation see text. Adapted from Borst, A. *et al.*, 1995, data in A from Reichardt, W., *et al.*, 1983. (c) Contrast gain function in the hoverfly before (filled circles) and after motion adaptation (open circles). Due to motion adaptation the contrast sensitivity function is shifted to the right, slightly compressed, and shifted downward by a hyperpolarizing afterpotential. For further explanation see text. Adapted from Harris, R. A., O'Carroll, D. C., Laughlin, S. B. 2000. Contrast gain reduction in fly motion adaptation. Neuron 28, 595–606.

output signal. Such dendritic gain control mechanism leads to a sublinear integration of local inputs and does not require the normalization of a pool cell (Borst, A. *et al.*, 1995). It was also found that dendritic integration in LPTCs depends on the spatial relationship of simultaneous inputs. Sublinear integration is more pronounced when local stimuli are presented in close proximity to one another while more distant stimuli produce almost a linear sum of the individual local responses (Haag, J. *et al.*, 1992). This phenomenon is nicely explained by the passive dendritic properties of the LPTCs in combination with the cell's extended dendritic morphology. Stimulus-induced opening of sodium channels results in the cell's depolarization but at the same time reduces its local input resistance. This attenuates the effect of further channel openings due to additional stimulation at neighboring locations. Since LPTCs are not electrotonically compact, additional stimulation that results in conductivity changes taking place further away or on different dendritic branches will not have such an attenuating effect. Altogether, the dendritic integration properties of LPTCs have two important functional consequences: (1) they prevent output saturation and (2) render the cells' responses to be mostly independent of the density of visual contrasts in a given environment.

1.06.3.1.3.(viii).(b) Contrast gain reduction Besides dendritic gain control, other mechanisms have been proposed to prevent LPTC output saturation or to increase the motion pathway's sensitivity to detect changes in image velocity. One idea was that the delay filter in the EMD may adapt to keep the doctor's sensitivity to velocity changes independent of the average image velocity it encounters (Maddess, T. and Laughlin, S. B., 1985; de Ruyter van Steveninck, R. R. *et al.*, 1986; Borst, A. and Egelhaaf, M., 1987). Later studies, however, did not confirm the presence of an adaptable time constant in the EMD (Harris, R. A. *et al.*, 1999). Another suggestion was that the H1 cell performs a dynamic adaptive rescaling of its input–output characteristics, which adjust the cell's sensitivity to the variance of the image velocities it is challenged with (Fairhall, A. L. *et al.*, 2001). The physiological mechanisms underlying such adaptation remain unknown, though.

A recent study by Harris R. A. *et al.* (2000) describes another way of coping with both dynamic range matching and preventing LPTC output saturation: contrast gain reduction. The contrast sensitivity function obtained from intracellularly recorded HSE cells in the hoverfly *Eristalis* was found to be transformed in three different ways after presenting strong adapting motion stimuli: (1) the contrast sensitivity function was shifted to the right – so that, after motion adaptation, higher contrasts were required to reach a certain response level. (2) The contrast sensitivity function was also shifted vertically because of the subtractive effect of an after hyperpolarization in the cell. And (3) the cell's output range was slightly compressed. The strongest of these effects by far resulted from a contrast gain reduction, which was found to be independent of the cell's activity level and, thus, nondirectional (Figure 10(c), Harris, R. A. *et al.*, 2000). There is no experimental evidence so far suggesting at which level along the motion detection pathway the contrast gain reduction operates. A sensible stage for the mechanism to kick in would be located before the two input signals are passed through the multiplication operation in the EMD (ibid), which causes an expensive relationship between image contrast and detector output (rev.: Buchner, E., 1984; Reichardt, W., 1987). The comparatively small subtractive effect of after-hyperpolarization is the only component whose magnitude depends on the direction of the adapting stimulus. The after-hyperpolarization might be caused by calcium accumulation in the cell, which results in an increase of calcium-dependent potassium conductances (Dürr, V. and Egelhaaf, M., 1999; Kurtz, R. *et al.*, 2001). Based on experimental and modeling studies, the latter adaptation measure has been proposed as a general mechanism applied in many species across phyla (e.g., Wang, X. J., 1998; Gabbiani, F. and Krapp, H. G., 2006).

In functional terms the work by Harris R. A. *et al.* (2000) is of particular significance regarding optic flow processing and the estimation of self-motion parameters. If the entire population of LPTCs is used to estimate self-motion parameters, all the cells are required to be in the same adaptational state. Nondirectional mechanisms would, in a first approximation, affect each LPTC of the population in about the same way (ibid).

1.06.3.1.3.(viii).(c) Local adaptation phenomena Besides one report in the 1980s (Maddess, T. and Laughlin, S. B., 1985), a few more recent studies addressed the spatial aspect of motion adaptation in spiking H1 and V1 cells. Neri P. and Laughlin S. B. (2005) found adapting stimuli moving in the antipreferred direction to increase the directional gain at a neighboring, but nonadapted position within the cells' receptive fields. This result did show that

local information about the adaptational state of the cell is spatially spread to other areas in the receptive field. Such mechanism could overcome the problem that visual scenes consisting of a patchy contrast distribution may result in an anisotropic adaptational state across the cell's receptive field. A related study on the local integration properties of LPTCs under different motion adaptation conditions (Neri, P., 2006) revealed evidence for a gain normalization mechanism previously proposed for motion-sensitive neurons in the primate visual system (Heeger, D. J. *et al*., 1996; Simoncelli, E. P. and Heeger, D. J., 1998).

Most of the physiological mechanisms underlying the spectrum of motion adaptation and gain control phenomena are not as yet understood. Nonetheless, it is obvious that any successful estimation of self-motion parameters the LPTCs perform critically depends on preventing the cells' output range from saturation and on a similar adaptational state of all members of the population.

1.06.3.1.3.(ix) Quantitative behavioral studies and electrophysiological replay experiments One of the major issues in studying motion-sensitive neurons is that most of the studies so far were carried out under laboratory conditions and using rather artificial motion stimuli. While such systems analysis approach revealed invaluable results regarding the functional organization of motion vision pathways, it does not allow us to directly infer their performance under natural conditions. Furthermore, electrophysiological experiments have to be performed under conditions where the animal is fully restrained and not able to move at all, otherwise, in particular stable intracellular recordings would not be possible. This, however, means that the action–perception loop (Figure 1) is not closed any more. The consequence is a situation for the animal that is fundamentally different from what it would experience under natural conditions. There are two key differences: (1) while in freely moving animals self-motion results in optic flow, within the entire 4pi visual field most laboratory stimuli were considerably smaller in size. (2) Many laboratory stimuli were designed to mimic particular movements of the animal. However, the actual combination of translation and rotation that a freely moving animal experiences in a specific visual environment was not very well defined. The latter point is particularly important since translation-induced optic flow depends on the distance between the animal's eyes and the visual objects in the surroundings (cf. eqn [1]).

Only a few years ago the so-called replay experiments (rev.: Heisenberg, M. and Wolf, R., 1993) were introduced into the combined behavioral, electrophysiological, and modeling research on insect vision (Kern, R. *et al*., 2000). Reply experiments partly address the limitations of artificial stimuli. They involve several steps: First, a video system monitors the trajectory of a freely moving animal in a well-defined visual environment. Second, from the animal's trajectory, the self-motion parameters are obtained, which – knowing the visual surroundings – are used to reconstruct the optic flow the animal has experienced. Finally, the reconstructed optic flow sequence is presented to animals during electrophysiological experiments while recording the activity of LPTCs and the resulting data may be correlated with the known self-motion parameters.

In a detailed behavioral analysis it was found that monocularly blinded flies walk along trajectories that balance translatory and rotatory optic flow (Kern, R. and Egelhaaf, M., 2000). This way the animals minimize the net difference between perceived retinal image shift over the left and the right eye to obtain an optomotor equilibrium (Götz, K. G., 1975). The first replay experiments used a computer monitor to present HSE cells with optic flow sequences reconstructed from average fly walking trajectories (Kern, R. and Egelhaaf, M., 2000). The electrophysiological results in combination with model simulations supported the conclusion that monocularly blinded flies try to keep their optomotor in equilibrium (Kern, R. *et al*., 2000). Further replay experiments were based on trajectories obtained from flies walking in an arena that contains obstacles. These experiments produced some interesting results regarding the coding of angular velocities in HSE cells. All angular velocities greater than $\pm 50^\circ$ per second changed the HSE membrane potential to the same level of depolarization/hyperpolarization, respectively. Within the intermediate range the HSE responses and the angular velocity were linearly related with an extremely steep slope. This result was found to be independent of the specific 3D layout of the surroundings (Kern, R. *et al*., 2001).

For further replay experiments, a highly sophisticated visual stimulator, flimax, was used (Lindemann, J. P. *et al*., 2003). Flimax consists of several thousand individually controllable light-emitting diodes (LEDs) altogether approximating about three quarters of the fly's spherical visual field. A spatial resolution below 1° per LED in combination with a fast control of light intensities made flimax (Lindemann, J. P. *et al*., 2003) more versatile than previous wide-field stimulation devices (e.g., Karmeier, K. *et al*., 2003).

Most recently another major finding was made in the context of processing optic flow information in fly LPTCs. Once again, quantitative behavioral experiments did build the foundation of a series of studies on new ideas about what parameters LPTCs encode. Using search coils small enough to be mounted on head and body of blowflies positioned in perpendicular magnetic fields, Schilstra C. and van Hateren J. H. (1998) monitored the animals' head and body movements at a continuous temporal resolution. This way an enormous body of semifree flight data was accumulated while the flies negotiated a cubicle of 0.4 m edge length (Figure 11(a)). A detailed analysis of the data produced not only the flight envelop of the insect but also a continuous monitor of the animals' head movements in space, which ultimately determine the optic flow it experiences. It was discovered that the flies generated a repetitive pattern of characteristic flight sequences: Short rapid saccades were followed by intervals of drifting translations, most likely the result of inertia, which were followed again by another saccade. The direction of the saccades was always away from the wall that was closest to the animal (van Hateren, J. H. and Schilstra, C., 1999). Like humans and many other visually oriented animals, flies keep their eyes aligned with the external horizon and also use fast head movements to minimize the time period during which rapid rotations cause motion blur and degrade visual processing (ibid).

Knowing head and body position at any point in time as well as the exact environmental layout allowed Kern R. *et al.* (2005) to model the fly movements in minute detail (Figures 11(b) and 11(c)). From these data, sequences of optic flow were calculated and, using flimax, were presented to flies in replay experiments while recording the activity of the HSE cell (Kern, R. *et al.*, 2005; van Hateren, J. H. *et al.*, 2005). A subsequent coherence analysis between the self-motion parameters and the HSE responses suggested that this cell serves to indicate not only yaw rotations around the vertical axis but also translation parameters. Depending on whether the sum or the difference of the HSE cell activities from the left and the right lobula plate was taken into account, either thrust or sideslip could be estimated as well (Figures 11(d) and 11(e)). This finding suggests a double function of the HSE cell: During saccadic flight intervals the neuron may encode yaw rotation while it indicates sideslip translation during the drift phases. A parsimonious model of the fly motion vision pathway did capture these new electrophysiological results (Kern, R. *et al.*, 2005).

That the HSE cells are also involved in assessing translation parameters opens up another possible way of exploiting optic flow: that is, to estimate relative distances – a notion that goes back to Gibson's J. J. (1950) accounts on the ecological aspects of optic flow. Comparing the activity level between HSE cells from both sides of the brain during translational drifts allows the animal to sense at which side objects in the visual field are closer. Based on this information the fly can decide in which direction the next saccadic turn should take place to avoid collision with any objects around (Kern, R. *et al.*, 2005; van Hateren, J. H. *et al.*, 2005). Because the magnitude of translational optic flow depends on distance (cf. eqn [1a]), the next turn should always be executed away from the side in which the HSE signal is stronger.

The other interesting conclusion is that flies seem to employ a strategy of active vision to assess distance information from optic flow. It is very likely that the motor program controlling such active vision mode changes depending on the given environment: Confined spaces need a higher frequency of saccades to avoid collision, while in open space when the fly performs cruising flights the saccade frequency may be significantly reduced. It would be very interesting to study the correlation between the fly's flight envelop depending on the distance distribution within the environment the animal is operating in.

An important prerequisite for such elegant active vision strategy to work one head movement. Only if the head is perfectly well stabilized relative to the surrounding by means of compensation for all rotational degrees of freedom a pure translation flow field is perceived useful for distance estimation. Blowflies compensate for roll rotations with a gain of nearly 1 employing a variety of sensory mechanisms (rev.: Hengstenberg, R., 1993, see Section 1.06.6.1). Pitch compensation also takes place but is limited by anatomical constraints (ibid). However, for obvious reasons the fly cannot compensate for massive body saccades about the yaw axis by means of head movements. A detailed analysis of the data obtained during semifree flight (van Hateren, J. H. and Schilstra, C. 1999; Schilstra, C. and van Hateren, J. H., 1999) shows flies to pursue a certain strategy when performing a body saccade around the yaw axis. By means of head movements the animals seem to actively minimize the time during which the head rotates in space. The rapid but shorter rotation phase means that the head is stabilized for a longer period of time to analyze the translation-induced component of optic flow, which are relevant to distance estimation. Minimizing the rotation phase is a

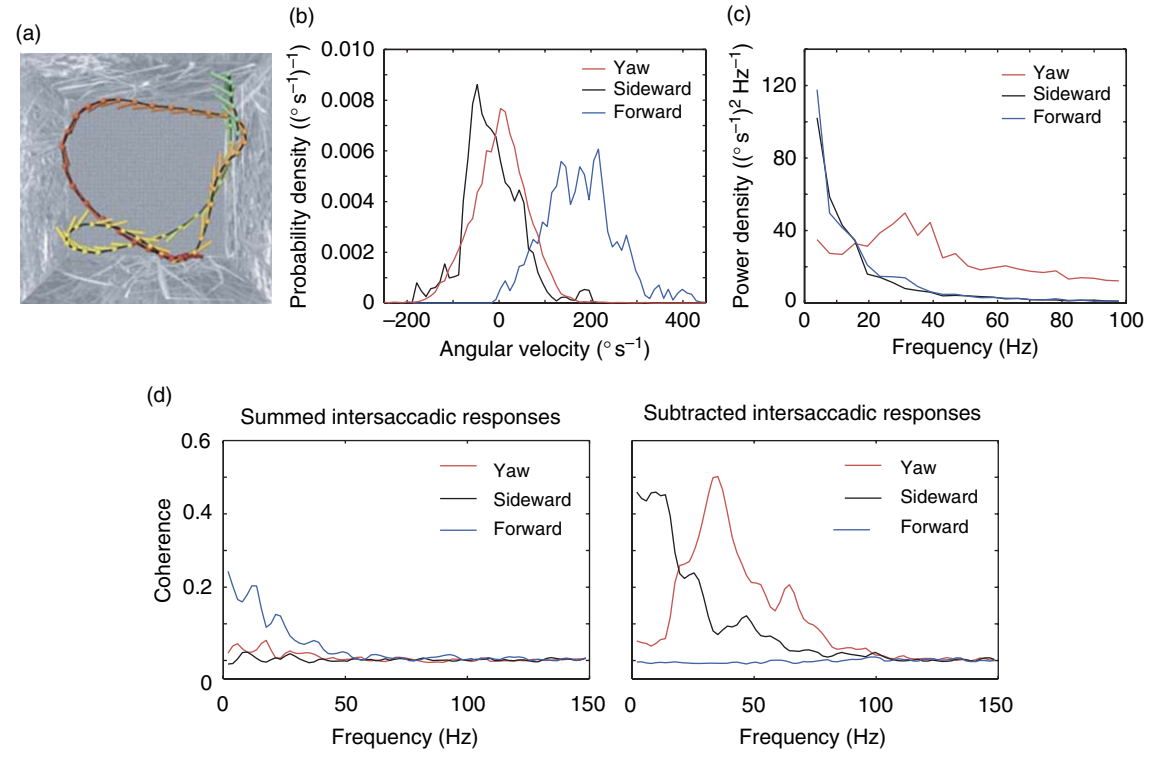

Figure 11 Electrophysiological reply experiments. (a) Reconstruction of a semifree flight trajectory of the blowfly Calliphora as seen from above when negotiating a cubicle of 0.4 m edge length. From such trajectories optic flow sequences were computed and used as stimuli in electrophysiological replay experiments. (b) Probability density of three different motion parameters computed from reconstructed trajectories, yaw (red), forward (blue), and sideslip (black). (c) The power density of the same three motion parameters plotted in the frequency domain. (d) The coherence between yaw rotation, forward translation, and sideslip components in reconstructed optic flow sequences and the responses of the HSE cell. The analysis was carried out for the time interval between two body saccader of the animal. If the activity obtained from the HSE cell in the left brain hemispheres is added to the activity of its counterpart in the right hemisphere the resulting signal shows coherence with forward translation in the low-frequency range (blue line, left panel). If the activity of the two HSE cells is subtracted the signal shows coherence with sideslip translation in the low-frequency range (black line, right panel) and with yaw rotation in the high-frequency range (red line, right panel). For further explanation see text. Adapted from Kern, R., van Hateren, J. H., Michaelis, C., Lindemann, J. P., and Egelhaaf, M. 2005. Function of a fly motion-sensitive neuron matches eye movements during free flight. PLoS Biol. 3, e171.

strategy that humans also apply in coordinated head and eye movements where vision is suppressed altogether (rev.: Carpenter, R. H. S., 1988).

The potential role of HS cells in analyzing translation flow was already discussed (e.g., rev.: Hausen, K., 1984; Krapp, H. G., 2000). The HSS cell, with its ventral receptive field suited to sense translation flow and not receiving rotation-specific contralateral input, was the ideal candidate for analyzing the translation flow in the context of estimating ground speed. However, studies on the distinctly different signal structure that HSE generates in response to approximated rotation and translation stimuli (Horstmann, W. *et al.*, 2000) anticipated as well a potential double function for the HSE cell. The distribution of motion preferences within the cell's receptive field also supports this idea: If analyzed in monocular animals the distribution shows a marked similarity to a translational optic flow field generated during an intermediate between forward motion, that is, thrust, and sideslip. In binocular animals, however, the local preferred directions of HSE and HSN cells, both of which receive rotation-specific contralateral input, reveal a distribution resembling an optic flow field that results from yaw rotation (Krapp, H. G. *et al.*, 2001). This point is interesting since it implies that the organization of local inputs seems to support the double function of the HSE cell. During yaw turns, the rotation flow better matches the cell's binocular receptive field organization. When translating, however, most of the rotation-specific

contralateral input is inhibited, which effectively converts the HSE into a monocular cell with a distribution of local inputs suitable to sense translation-induced optic flow.

In summary, several factors seem to contribute to the separation of rotation- and translation-induced optic flow underlying the double function of the HSE cell in the blowfly: (1) a particular flight pattern, active vision, which separates rotation from translation phases; (2) accurate gaze stabilization that keeps the head in its default orientation and minimizes the time intervals during which rapid rotation impair vision; and (3) the input organization of the HSE receptive field in combination with (4) the cell's differential signal structure. Together these factors allow the HSE to provide optic flow–derived information to be used in two different contexts. Responses during yaw rotations affect inner-loop flight and gaze stabilization while relative distance information may affect the outer-loop control to avoid collisions.

Experiments on freely flying *Drosophila* also suggest that flow field information is used to estimate the distance to the walls in a textured flight arena (e.g., Tammero, L. F. and Dickinson, M. H., 2002). Reconstructing the optic flow that the flies experienced just before they perform a saccade away from the arena wall revealed that pattern expansion seems to be the relevant motion cue. Unfortunately, virtually nothing is known about the neural circuits controlling collision avoidance saccades in *Drosophila* since electrophysiological studies on the central visual system in such a small fly are still extremely demanding. The receptive fields of interneurons involved in triggering the saccades may be differently organized than those of the HSE cells in the blowfly. So far only a few LPTCs have been characterized in the blowfly the receptive field organization of which suggests them to sense expansion patterns (Krapp, H. G. and Hengstenberg, R., 1996; Krapp, H. G. *et al.*, unpublished).

1.06.3.1.4 Self-motion estimation in other invertebrate species

The processing of optic flow information for inner-loop tasks – and also in the context of distance estimation – is obviously not confined to flies. Though not as exhaustive as the data body gathered in the fly visual system a few studies on wide-field directional-selective neurons were also performed in other arthropods. These studies are particularly interesting since they allow us to identify general principles and species-specific adaptations to optic flow processing. Directional-selective wide-field neurons were found in Hymenoptera (Ibbotson, M. R. 2001), Orthoptera (Kien, J., 1974; Gewecke, M *et al.*, 1990; Rind, F. C., 1990; Rind, F. C., 1990), Odonata (Olberg, R. M., 1986), and Lepidoptera (Collett, T. S. and Blest, A. D., 1966; Milde, J. J., 1993; Wicklein, M. and Varju, D., 1999). The presence of such neurons in a variety of insect species and in many vertebrates alike (Lappe, M., 2000) indicates that the analysis of optic flow is a common theme in visual information processing. Detailed information on the receptive field organization in wide-field optic flow neurons, however, is so far available only for a small number of flying insects other than blowflies (hoverflies: Straw, A. D. *et al.*, 2006; locusts: Wüstenberg, D. and Krapp, H. G., 2007) and crabs (Johnson, A. P. *et al.*, 2002).

1.06.3.1.5 Open questions

Our understanding of directional motion processing in insects has been significantly improved over the past three decades or so, thanks to the combination of quantitative behavioral experiments, electrophysiological, and modeling studies. In particular in the fly, key discoveries were made including the detailed organization of the LPTC receptive fields and their adaptation properties, the ipsilateral and heterolateral network interactions, as well as the suggested role of HS cells in estimating the distance to objects in the surroundings. These findings should help to refine our experimental efforts and to develop new concepts in visuomotor control. HS cells and probably VS cells, too, may contribute not only to inner-loop control tasks such as gaze and flight stabilization control, but also to collision avoidance, a typical outer-loop task. How does the fly nervous system integrate outer- and inner-loop control without compromising the respective function? Do flies use forward models or efference copies to tell apart rotation- and translation-induced LPTC signals? Where does the integration of visual information and signals from other sensory systems, also contributing to inner- and outer-loop control, take place? And finally, how is the information provided by LPTCs decoded at the next processing level to achieve an appropriate sensorimotor transformation?

From the methodological point of view, replay experiments were certainly an important step forward. Nonetheless, they still do not solve the problem that during replay experiments the animals are not in a natural closed-loop situation and have no access to information from sensory systems other than the compound eye (Kern, R. and Egelhaaf, M., 2000). Also, replay experiments depend strongly on

the availability of behavioral data obtained in freely moving animals. Current behavioral data may not reflect the entire range of self-motions that an animal would be able to perform if there were no spatial constraints. The greatest challenge for future research will be to design experimental approaches, which will allow us to record the activity in freely or at least in semifreely behaving animals. Some efforts on insects bigger than the fly are on its way to achieve this goal as electric circuits are now being miniaturized and radio transmission of sufficient bandwidth become available to log the data. But still, neural recording data will help us to further our understanding of general principles in visual information processing only if they are correlated with the sequences of optic flow that the animals experienced while moving.

1.06.3.2 Responding to Motion from the Outside World – Visual Information Controlling the Outer Loop

Inner-loop reflexes such as gaze and flight stabilization are meant to provide the basic requirements for any purposeful behavior, that is, to keep the retinal image in its default orientation, to facilitate sensory processing, and to maintain stable posture or locomotion. As mentioned earlier the systems controlling these two tasks need to be modified whenever the animal intends to perform a goal-directed task. Otherwise it would be trapped forever in its inner-loop reflexes. In the following we will outline a few examples of visually guided behaviors and their underlying neural processing, which, to be accomplished, require a modification of the inner-loop control. Many of these tasks exploit motion cues that are selectively integrated to support behaviors including object detection, chasing, preying, collision avoidance during swarming, escape, and landing.

Although any retinal image shift per definition has a direction, depending on the task the visual system may or may not require directional information to control it. For instance, stabilizing a target on the frontal retinal works perfectly well in a closed-loop situation when a sinusoidal transfer function relates the instantaneous retinal position to a turning response toward the target (e.g., Boeddeker, N. and Egelhaaf, M., 2003, see Section 1.06.3.2.1.(i)). A similar parsimonious strategy would also work to intercept a target. In this case, if a constant retinal target bearing is maintained by only adjusting thrust, interception eventually occurs (Collett, T. S., 1980; Olberg, R. M. *et al.*, 2000).

The benefit of any nondirectional detection mechanism is quite obvious: Computing the direction of motion always takes some extra time due to the delay filter in the EMD (see Section 1.06.3.1.2). Sensing and integrating nondirectional motion certainly works faster and is probably the default strategy when responses on the millisecond timescale are vital to survive. Interestingly, despite the obvious time constraints in controlling some of the behaviors mentioned above the visual system may combine directional and nondirectional motion information. In this section we will concentrate on a few selected examples where – at least partly – a specific behavior can be explained by its underlying neural mechanisms.

1.06.3.2.1 Chasing females and prey

Among flying insects, chasing comes in two behavioral contexts: mating and preying. In both cases the detection of comparatively small targets is required (see Section 1.06.3.2.3) followed by high-speed chasing maneuvers, which, if successful, culminate in mating or hitting prey.

1.06.3.2.1.(i) Chasing female flies In several insect species, chasing behavior is supported by conspicuous sexual dimorphisms (e.g., rev.: Land, M. F., 1997; Land, M. F. and Nilsson, D. E., 2002). Ommatidia arranged in the frontal to frontodorsal eye region of some male flies are equipped with bigger lenses (e.g., Stavenga, D. G. *et al.*, 1990) and sample the visual space at higher spatial resolution (e.g., Land, M. F. and Eckert, H., 1985). Male photoreceptors in that region are faster and significantly more efficient in detecting small moving objects (Hardie, R. C., 1983; Hornstein, E. P. *et al.*, 2000; Burton, B. G. *et al.*, 2001; Burton, B. G. and Laughlin, S. B., 2003). In the lobula, wide-field neurons integrate motion information in a sex-specific way. Individually identified male lobula giant (MLG) interneurons (Hausen, K. and Strausfeld, N. J., 1980) are either underdeveloped or even missing altogether in females. For obvious reasons there is massive evolutionary pressure on males to excel in a discipline that requires fitness in all departments and the results of which are so immediately turned into offspring, the hard currency of evolution.

There are two other points that should be mentioned before outlining in more detail what chasing

behavior in blowflies typically looks like. First, high-speed chasing in flies at close range purely depends on vision – no other long-range modality such as olfaction would be able to provide information quickly enough to control such aerobatic directional changes, which easily exceed angular velocities of 3000° per second. Second, chasing really needs to be efficient since it consumes energy spent not only on the flight motor but also on the sensory processing. Though the specialized photoreceptors in males, for instance, are way better tuned to the task than their female counterparts this comes at the cost of greater energy consumption (Laughlin, S. B., 2001; Burton, B. G. and Laughlin, S. B., 2003).

Early work suggested different control mechanisms being involved in chasing: A mechanism analog to the one controlling smooth pursuit eye movements in humans (Land, M. F. and Collett, T. S., 1974; Wehrhahn, C. *et al.*, 1982; Land, M. F., 1993) and a saccadic mechanism (Wagner, H., 1986) similar to the one that humans employ when trying to catch up with fast moving objects (e.g., Robinson, D. A., 1968; rev.: Carpenter, R. H. S., 1988). The analogy between eye movements in humans and chasing in flies is justified by their common function: Both human eye movements and chasing serve to stabilize a moving target on a certain retinal positions, that is, the fovea in humans and the area of highest spatial resolution concerned with chasing in flies, called the love spot. (Land, M. F. and Eckert, H., 1985).

In recent studies, male blowflies were video-taped while tracking dummy flies moved along a circular path. The observed trajectories did fall into two classes: Either the flies do catch the target (Figure 12(b), left) or the flies do not catch it but instead chase the target for several consecutive cycles (Figure 12(b), right). A detailed analysis of the data revealed a control system that takes into account the target's retinal position and size (Figure 12(a)). Whether the fly caught the target or not did depend on the speed and size of the dummy. Increasing the target speed or the size reduced the number of flights in which the male fly actually reached the dummy (Boeddeker, N. *et al.*, 2003).

Based on the experimental data a phenomenological model was derived, which, despite its parsimonious design, could explain the bistable distribution of chasing flights (Boeddeker, N. and Egelhaaf, M., 2003). Inputs to the model were retinal position and size of the target, which were transformed into two output variables, turning velocity and forward velocity, processed in two different

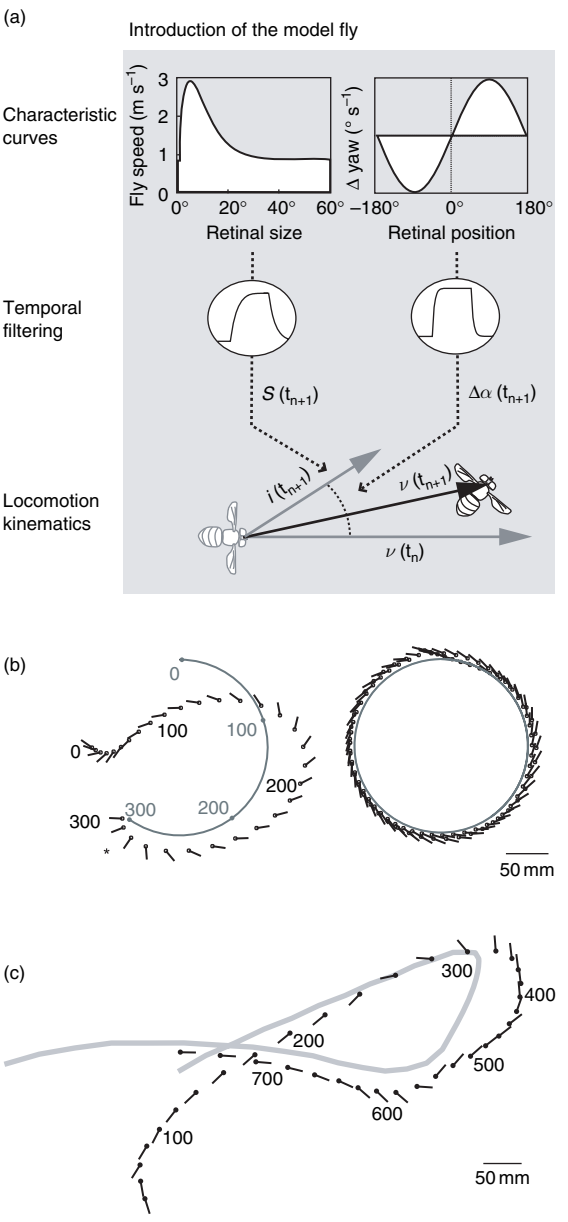

Figure 12 Chasing in male blowflies. (a) The relationship between thrust and yaw velocity, retinal size, and position of the target (upper panels), and the temporal filters (lower panels) used to model chasing flights in the blowfly *Lucilia*. The lower drawing illustrates the flight kinematics. (b) and (c) The model predicts chasing trajectories where the fly catches a dummy fly (b, left) and where it follows the target on a circular path for several consecutive rounds (b, right), but also situations where the leading fly performs more complex flight maneuvers (c). For further explanations see text. Adapted from Boeddeker, N. and Egelhaaf, M. 2003. Steering a virtual blowfly, simulation of visual pursuit. Proc. Biol. Sci. 270, 1971–1978; Boeddeker, N. and Egelhaaf, M. 2005. A single control system for smooth and saccade-like pursuit in blowflies. J. Exp. Biol. 208, 1563–1572.

pathways. (1) The thrust control did depend on retinal target size in a nonlinear way. For target sizes below 0.5° and above 20° the forward speed was set to a default value. In between it depended on the target size in an exponential way with a maximum thrust at about 5°. (2) The turning response of the fly toward the target was related to the target's retinal position by a sinus function with a zero crossings in front and behind the fly (Figure 12(a)).

The behavioral data suggested that the outputs of these pathways were differently delayed before affecting the flight trajectory, either due to latencies in neural processing or because of the low-pass properties of the motor system (Boeddeker, N. *et al.*, 2003). The delays were implemented by applying a 15-ms low-pass filter to the position-dependent and an 80-ms low-pass filter to the size-dependent motor commands, controlling rotation and forward velocity, respectively (Figure 12(a)).

The forces acting on flies flying under unsteady aerodynamic conditions (e.g., Dickinson, M. H. *et al.*, 1999; Ellington, C. P., 1999; Frye, M. A. *et al.*, 2003) in relation to its inertia were only approximated. The degree to which kinematics caused a difference between intended and actually flown velocities was a free parameter used to fit the model trajectories to those observed during the behavioral experiments.

In a follow-up account Boeddeker N. and Egelhaaf M. (2005) did show that their model also predicts features of male flies chasing females on a natural trajectory (Figure 12(c)). More realistic chasing flights did show a higher frequency of rapid, saccade-like turns even though saccadic turns were not explicitly implemented in the control structure. The saccade-like turns were interpreted as a consequence of different processing delays in the position and distance controller pathways in combination with the inertia of the chasing fly when applied to more complex trajectories of the leading fly (Boeddeker, N. and Egelhaaf, M., 2005).

The Boeddeker N. and Egelhaaf M. (2003; 2005) model is an excellent example to make an important point: Seemingly complex behavioral variants, either catching or pursuing a fly, are readily explained by a simple set of rules. When applying the rules under closed-loop conditions in an environment that approximates the laws of physics, two different behavioral outputs result. No explicit decision-making algorithm is required to produce either of the two behavioral traits. It is just a threshold angle on the retina in combination with a long time constant in the path of the control system computing forward velocity. This design also prevents the chasing fly from catching targets too big to be conspecific females – another useful feature for obvious reasons. And finally, the system's inherent properties nicely explain that during chases both saccade-like and smooth pursuit sections occur simply by approximating fly kinematics and without assuming a saccade controller (ibid). What the model does not take into account, however, is the question of how chasing control interacts with the inner-loop optomotor reflexes which some of the earlier studies did (e.g., Collett, T. S., 1980).

Casing behavior is meanwhile well characterized in several species and has inspired a number of models describing its possible control structure. How much do we know about the neural pathways controlling the behavior? Although sex-specific specializations at the level of the photoreceptors in the compound eye's love spot were conclusively demonstrated (e.g., Hornstein, E. P. *et al.*, 2000; Burton, B. G. *et al.*, 2001; Burton, B. G. and Laughlin, S. B., 2003), the underlying neural mechanisms working at more central stages are less well-known. The response properties of MLG interneurons (Hausen, K. and Strausfeld, N. J., 1980) and their postsynaptic targets conveying information to various motor systems were investigated only in a few studies (Gilbert, C. and Strausfeld, N. J., 1991; Gronenberg, W. and Strausfeld, N. J., 1991). Two MLG neurons, MLG1 and MLG2, seem to respond to motion in a directional-selective manner, though the electrophysiological data are mostly based on individual recordings. Other MLGs and their postsynaptic descending neurons were found to be sensitive to nondirectional motion of small objects (ibid). So far, our knowledge about the electrophysiological response properties of MLGs is in contrast to their solid neuroanatomical description. The latter includes the neurons' dendritic and terminal arborizations in parts of the lateral protocerebrum and different segments of the thoracic ganglia (ibid). By combining anatomical data and electrophysiological results, Gronenberg W. and Strausfeld N. J., (1991) proposed a putative circuit involved in chasing behavior. The model includes pathways devoted to the control of forward and yaw velocity – in a way supporting the design of the Boeddeker N. and Egelhaaf M. model (2003). Later studies confirmed directional-selective responses in MLG1 and MLG2 (Wachenfeld, A. and Hausen, K., 1994). Wachenfeld A. and Hausen K. (1994) suggested the function of these MLGs to be involved in controlling retinal target position during the chase

before the fly boosts its thrust for the final catch. This would mean that MLGs participate in both neural pathways Boeddeker N. and Egelhaaf M. (2003) suggest, though neither of these pathways explicitly requires directional motion information.

In summary, fly chasing remains an area where several questions still await answers. Besides the lack of conclusive electrophysiological data, one of the questions concerns the fundamental problem we already mentioned above that all motor control systems face: How does the system avoid being trapped in its inner-loop reflex control? Von Holst E. and Mittelstaedt H. (1950) put forward this question already more than 50 years ago. But in the work on insect vision, surprisingly few researchers did address this problem. Successful chasing behavior clearly requires the outer-loop control system to modify the operation of the inner-loop flight stabilization reflexes (e.g., Collett, T. S., 1980; rev.: Heisenberg, M. and Wolf, R., 1993; Chan, W. P., *et al.*, 1998). Switching off the reflexes altogether would be no viable option since to successfully complete any goal-directed behavior the control of posture and attitude are necessary prerequisites – as is gaze stabilization, without which none of the behaviors would work properly.

1.06.3.2.1.(ii) Catching prey on the fly – aerial predators' visual hunting strategies Prey catching during flight has been successfully investigated in dragonflies – for obvious reasons: Dragonflies of the family Aeschnidae possess an unbeatable number of 28 000 ommatidia per compound eye (Sherk, T. E., 1978), endowing these aerial predators with a – for insect standards – superb spatial resolution well below 1°. Most dragonflies show conspicuous anatomical specializations of their frontodorsal eyes designed to detect potential prey against the blue sky (e.g., Labhart, T. and Nilsson, D. E., 1995). The flight envelop of dragonflies, the combination of possible translations and rotations, is as impressive as is their peripheral visual system. Some species reach translation velocities of up to $10\,m\,s^{-1}$ and are capable of performing acrobatic flight maneuvers as spectacular as the Immelmann turn (Taylor, G., unpublished data). Its nearly perfect adaptation to aerial hunting makes the dragonfly a truly rewarding experimental model system to study the neural mechanisms underlying the detection and chasing of airborne prey.

Other than in the field of directional motion vision (see Section 1.06.3.1.2), the research on prey catching in dragonflies started with electrophysiological rather than behavioral observations. In the 1980s the response properties of descending neurons were investigated connecting protocerebral areas with different thoracic ganglia. These descending neurons could be grouped into multimodal large-field descending neurons, thought to mediate information about panoramic image shifts, and small-field descending neurons responding best to the movement of small visual stimuli. Because of their tuning to a certain visual feature, namely the movement of small objects, the latter group was termed target-selective descending neurons (TSDNs) (Olberg, R. M., 1986). Studies on cells in the dragonfly lobula complex, presynaptic to the descending neurons, revealed two types of feature detectors: small target-sensitive cells responding in a directional-selective way to motion and cells tuned to a specific orientation of a small elongated bar (O'Carroll, D. C., 1993). The response properties of small target-sensitive and bar-sensitive cells in the dragonfly did show a striking similarity to those of hypercomplex and simple cells in the mammalian visual cortex (O'Carroll, D. C., 1993; cf. Hubel, D. and Wiesel, T. N., 1962). This finding once again underlines similar principles in visual scene analysis across phyla when it comes to extracting specific features.

Further studies assessed the receptive field organization of TSDNs, probably the targets of lobula complex cells (Frye, M. A. and Olberg, R. M., 1995). Descending neurons of the medial dorsal tract and the dorsal intermediate tract were found to have receptive fields directed toward the frontal to frontolateral visual field above the external horizon (Figure 13(a)). Thus, these descending neurons most likely receive input from the compound eye region specialized for prey detection (Labhart, T. and Nilsson, D. E., 1995). The receptive field size of the TSDNs varied from about 40° to 90° in diameter. Some of them responded better to the motion of black squares of either 4° or 16° edge length, others were sensitive to both stimulus sizes. Most TSDNs were directionally selective. They preferred horizontal motion or vertical motion and, in some cases, intermediate components at certain locations within their receptive field (Frye, M. A. and Olberg, R. M., 1995).

Based on the electrophysiological data the TSDNs were hypothesized to play an important role in prey catching. It was not clear, though, which strategy dragonflies prefer during their aerial hunts. Collett T. S. and Land M. F. (1978) had earlier suggested two different strategies, which were observed in the general context of chasing behavior, tracking or intercepting

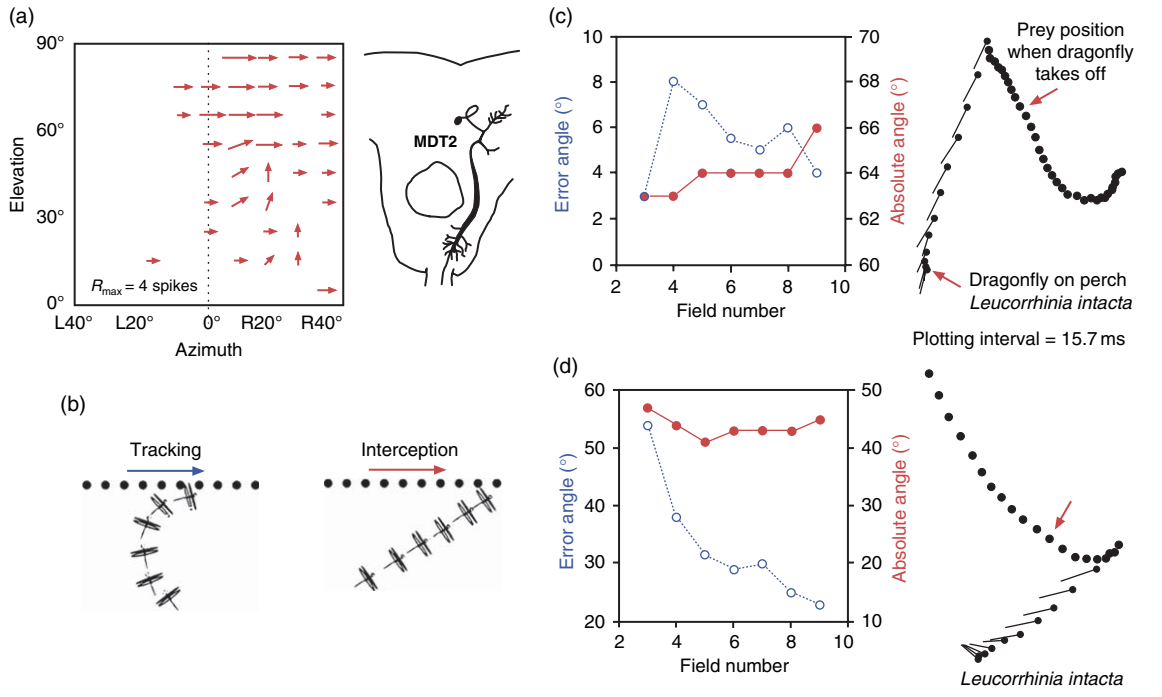

Figure 13 Target-selective neurons in the dragonfly. (a) Receptive field and reconstruction of the median dorsal tract neuron 2. The neuron responded in a directional-selective way to small black squares of 4° edge length presented in the frontal to frontolateral parts of the dorsal visual field (arrows, left panel). (b) When hunting dragonflies could either track or intercept potential prey (after Collett, T. S. and Land, M. F., 1978). For further explanation see text. (c, d) Dragonflies when detecting prey orient themselves toward the potential prey and approach nearly on a straight line. Left panels show the error angle (open blue symbols) and the absolute angle (filled red symbols) plotted against consecutive video frames (field number). The dragonflies achieve interception by adjusting thrust, so that the target's absolute angular position on the retina is kept constant. For further explanation see text. Redrawn from Frye, M. A. and Olberg, R. M. 1995. Visual receptive-field properties of feature detecting neurons in the dragonfly. J. Comp. Physiol. A Sens. Neural Behav. Physiol. 177, 569–576; Olberg, R. M., Worthington, A. H. and Venator, K. R. 2000. Prey pursuit and interception in dragonflies. J. Comp. Physiol. A 186, 155–162.

(Figure 13(b)). When tracking, the chasing animal aims to minimize the angle between its frontal visual field and the target's position on its retina. The result is a curved flight trajectory where the chasing animal spirals in on the target. Intercepting is controlled in a different way. In this case the retinal position of the target is kept constant by adjusting only the thrust, given the target position is within the frontolateral visual field. This strategy produces a fairly straight flight trajectory that eventually results in intercepting the target. Most insects track rather than intercept, whether it is tiger beetles hunting on the ground (Gilbert, C., 1997), male flies chasing females (e.g., Collett, T. S. and Land, M. F., 1975a; 1975b; Wagner, H., 1986; Land, M. F., 1993; Boeddeker, N. *et al.*, 2003), or honeybees tracking moving targets (Zhang, S. W. *et al.*, 1990).

A couple of years ago, Olberg R. M. *et al.* (2000) videotaped and quantified free-flight behavior in dragonflies to find out which strategy they employ during aerial hunts. Some dragonflies, such as *Erythemis simplicicollis* and *Leucorrhinia intacta*, are sit-and-wait predators. Most conveniently they select and keep a specific landing site to sit on when waiting for prey and return to it after they completed a hunting trip. Olberg R. M. *et al.* (2000) analyzed the behavior of these species in detail. Once potential prey appears in their visual field, the dragonflies perform some head movements and movements of the body, presumably to prepare for an appropriate take-off orientation, and then approach the prey on a straight trajectory (Figures 13(c) and 13(d)). In 97% of all attempts, the dragonflies were successful in catching the prey. This study quite clearly shows that dragonflies intercept rather than track their prey (Olberg, R. M. *et al.*, 2000). But it also raised the question of how dragonflies distinguish between big birds flying at greater distance and small insects flying past in close range, both of

which may assume the same angular size on the retina? The dragonflies took off only for small insects. The difference between the two situations was the distance and the angular velocity profile of the objects moving across the eye. The close-by prey generated a much more pronounced angular velocity peak on the dragonfly's eye than a distant bird did. This peak in perceived angular velocity was assumed to trigger the hunting flights (Olberg, R. M. *et al.*, 2000). Later work, however, suggests that the dragonfly might also use distance cues.

Further behavioral studies on *Libellula luctuosa* and *Sympetrum vicinum*, both perching hunters as well, demonstrated how accurately dragonflies are capable of discriminating between different target sizes (Olberg, R. M. *et al.*, 2005). Using glass beads of diameters between 0.5 and 0.8 mm as dummy prey revealed that both species would only launch a catching flight if the absolute size of the potential prey did not exceed the dragonflies' head diameter. Olberg R. M. *et al.* (2005) concluded that neither retinal size nor angular velocity of the target alone triggers takeoffs. Only within a preferred distance range a specific angular size initiated the behavior (ibid). What vision-based mechanism might underlie such discrimination task?

Two visual mechanisms potentially allow for distance estimation: motion parallax and stereopsis. Exploiting motion parallax to estimate distance is quite common (rev.: Srinivasan, M. V., 1993; Srinivasan, M. V., and Zhang, S. W., 2000). This possibility becomes immediately obvious from revisiting eqn [1] showing that the magnitude of the local parallax vectors, $\mathbf{p}_i$, is inversely proportional to the distance, D_i – but only for translational movements (Figure 14(c)). Therefore, it is not surprising that several insects actually perform so-called peering movements to induce motion parallax (e.g., locust: Wallace, G. K. 1959; Collett, T. S., 1978; grasshopper: Eriksson, E. S., 1980). The other mechanism, stereopsis, is based on the disparity between the different images seen by the two eyes. It requires an area of binocular overlap and sufficient spatial separation of the eyes – which makes it a common means of distance estimation in many vertebrates including humans (e.g., Rogers, B. and Graham, M., 1982). Despite the small separation of their eyes, even in insects, stereopsis was shown to be used for distance estimation, mainly in the context of preying (e.g., beetle: Bauer, T., 1981; mantis: Rossel, S. 1983; Walcher, F. and Kral, K., 1994, and – not too surprisingly – in dragonfly larvae: Baldus, K., 1926).

Adult dragonflies seem to combine motion parallax and stereopsis to estimate distance, which is a necessary condition for their ability to discriminate between different prey sizes (Olberg, R. M. *et al.*, 2005). How the perching dragonflies exactly perform peering movements to induce motion parallax while still sitting on the perch is not exactly clear yet. Head movements the animals perform upon prey detection usually have a strong rotational component and would therefore not allow for distance estimation (cf. eqn [1a], rotational term). If dragonflies, however, would compensate for the rotational component by simultaneously changing their body orientation, they could achieve a pure translation movement (rev.: Collett, T. *et al.*, 1993).

In summary, at least part of the exceptional dragonfly chasing behavior may be explained by the response

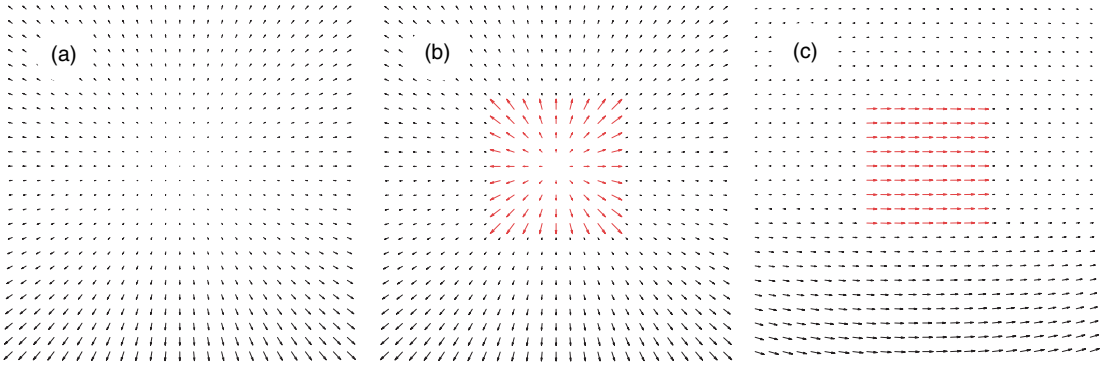

Figure 14 Further properties of translation-induced optic flow. (a) Translation-induced optic flow field, pure thrust, in an asymmetric environment with smaller distances to visual structures below the equator. A translation flow field has a focus of expansion, which, during pure translation, identifies the heading direction. (b) Same background flow field but with an object close in front. The object casts a looming pattern (red arrows) of object expansion, which is due to the closer distance to the object than to the background. (c) Side-wise translation induces motion parallax, which is also based on the difference between the distance to the object and to the background. All flow fields were computed using eqn [1].

properties of identified TSDNs (Olberg, R. M., 1986; O'Carroll, D.C., 1993; Frye, M. A. and Olberg, R. M., 1995). It is still not clear, though, how the different mechanisms involved in estimating distance and size of the potential prey work together with the animal's aerial intercepts to orchestrate all its actions resulting in a remarkable 97% of successful catches. Tough employing a different strategy to catch their prey, i.e., intercepting, they face the same problem as flies do when catching females: the inner- and outer-loop activity needs to be coordinated. There is also a need of conceptual and eventually mechanistic models, which integrate the different steps along the catching behavior with the inner-loop control of gaze and flight stability.

1.06.3.2.2 Discriminating small objects from the background

In dragonflies, takeoff is triggered by targets assuming retinal angles as small as 0.1° to 0.2° (Olberg, R. M. *et al.*, 2005). The smallest interommatidial angles, however, are only in the range of about 0.5° (Horridge, G. A., 1978). Small target detection is often supported by regional specializations of the eyes including anatomical and physiological adaptations. Photoreceptors in dragonflies, for instance, exploit the short wavelengths in the UV range (Laughlin, S. B., 1976; Laughlin, S. B., and McGinness, S. 1978; Labhart, T. and Nilsson, D. E., 1995; Yang, E. C. and Osorio, D., 1996), which increases spatial resolution in particular when targets are discriminated against the blue sky (rev.: Land, M. F. and Nilsson, D. E., 2002). Other flying insects, however, may operate in habitats composed of cluttered visual structure where the contrast between a potential target and the background is considerably reduced. What is the neural basis of such stunning target detection mechanisms?

Another good model system to demonstrate the remarkable ability to detect objects smaller than the compound eye's spatial resolution is the hoverfly *Eristalis*. These animals stabilize their flight to remain in a comfortable sunlit spot and defend this spot against any potential intruders – conspecific males or others – while waiting for females to pass by. Detecting a potential target triggers a sequence of events that starts with computing an interception course based on the target angular position and velocity on the hoverfly's retina (Collett, T. S., and Land, M. F., 1978). Hoverflies are less picky than dragonflies and can be easily persuaded to dart at targets, which do not fall into the size and speed range of conspecifics – in which case the effort will obviously remain unsuccessful given it was a female the hoverfly was after. Possible assumptions about size and speed of conspecifics were thought to be innate and, together with knowledge about its own speed, confine the animal's successful computation of intercept trajectories to other hoverflies (ibid). Once the trajectory is computed the outcome defines the magnitude of an initial rotation about the vertical axis, which sets the direction of the intersecting flight (ibid). The computation of the magnitude of this initial rotation and its execution are equivalent to the computation and the performance of catch-up saccades observed in primate eye movements (e.g., Robinson, D. A., 1973).

After the rotation the hoverflies perform a ballistic, open-loop acceleration along a straight path, which gets them close to the target. Then a closed-loop chasing controller takes over and governs the final flight sequence (Collett, T. S. and Land, M. F., 1978) which is probably comparable to the one blowflies employ (Boeddeker, N. and Egelhaaf, M., 2003, see Section 1.06.3.2.1).

The success of this behavior depends on an accurate detection of the target since target position is a critical parameter in the computation of the interception course. As mentioned, for hoverflies living in cluttered environments, this is a particularly challenging task. Recent electrophysiological studies discovered an extraordinary contrast sensitivity in small target motion detectors (STMDs) of the hoverfly lobula and lobula plate, which are tuned to the motion of tiny objects (Nordström, K. *et al.*, 2006).

Most STMDs were found to have receptive fields directed toward the frontal to frontolateral visual field above the eye equator (Nordström, K. *et al.*, 2006). Thus, at least part of the local elements STMDs receive signals from are supplied by the eye's bright zone (*Crysomiya*: van Hateren, J. H., *et al.*, 1989, *Eristalis*: Straw, A. D. *et al.*, 2006), which is equivalent to the love spot in *Musca* and *Calliphora* (rev: Land, M. F., 1997; Land, M. F. and Nilsson, D. E., 2002; see Section 1.06.3.2.1). This region is equipped with facets of increased diameter benefiting light capture (Straw, A. D. *et al.*, 2006). Also, like in *Musca* and *Calliphora*, pooling signals from all eight photoreceptors rather than only six in other eye regions increases the signal-to-noise ratio in the postsynaptic lamina cells (e.g., Franceschini, N. *et al.*, 1981; Hardie, R. C., 1983).

A detailed analysis revealed that most STMDs respond to motion of small objects in a directional-selective way (Nordström, K. *et al.*, 2006). Only a few nondirectional-selective STMDs were found as well (Figure 15). In some cases the motion stimuli were

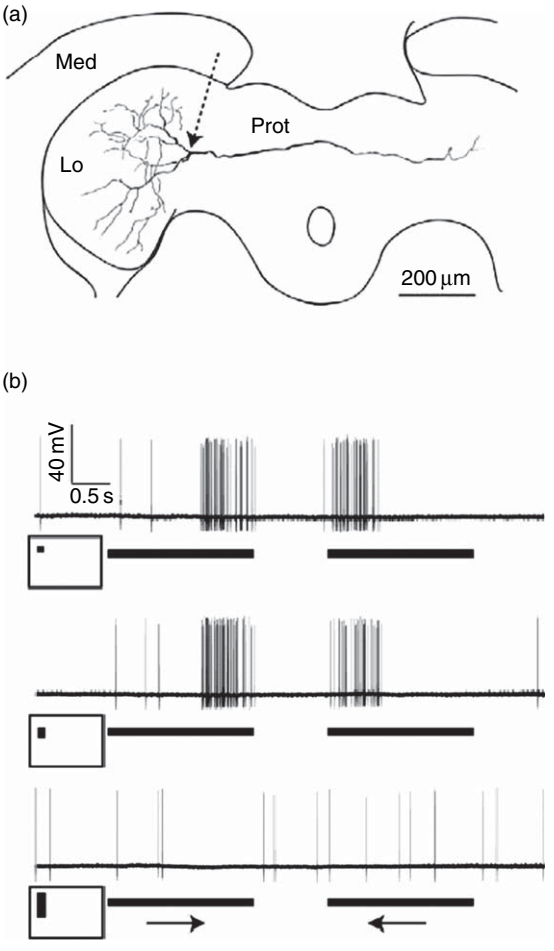

Figure 15 Small target detection in the hoverfly. (a) Reconstruction of a small target movement detector. (b) Intracellular recording traces. The neuron responds most strongly to nondirectional motion of a small bar of $0.8° \times 3.0°$ horizontal x vertical extent, respectively. For further explanation see text. Adapted from Nordström, K., Barnett, P. D. and O'Carroll, D. C. 2006. Insect detection of small targets moving in visual clutter. PLoS Biol. 4, e54.

much smaller than the smallest interommatidial angles measured in hoverflies (Straw, A. D. *et al.*, 2006). Taking into account the optical properties of the compound eye, objects as small as 0.2° in edge length and an effective contrast of only 12% did still produce significant responses in some STMDs (Nordström, K. *et al.*, 2006). Most STMDs did respond even if the object was presented on top of wide-field background motion, irrespective of whether the background was moving at a similar or at the same velocity as the object. Such extraordinary small-field tuning was suggested to depend on extreme contrast sensitivity and on at least two possible inhibitory mechanisms suppressing the response to wide-field motion: for one, a mechanism that involves local spatial inhibition acting at some stage along the peripheral pathway. And secondly, a feedback inhibition, also presynaptic to the STMDs, which may be provided by lobula plate wide-field cells (Nordström, K. *et al.*, 2006).

Studies on a subgroup of small-field STMDs (SF STMDs) in *Eristalis* whose receptive field sizes were only about 8° in diameter suggest that there are spatial limits for background motion-invariant responses (Barnett, P. D. *et al.*, 2007). The retinotopically organized SF STMDs show very similar response properties as their wide-field counterparts (Norström, K. *et al.*, 2006). However, they do not suppress wide-field background motion as efficiently if target and background move at similar or at the same velocity (Barnett, P. D. *et al.*, 2007). The results on both directional-selective and nondirectional-selective small-field and wide-field STMDs may be accounted for – at least partly – by a model for target detection (Higgins, C. M. and Pant, V., 2004). Originally based on the behavioral data obtained in housefly figure-ground discrimination (Reichardt, W. and Poggio, T., 1979), to establish small-field tuning the model incorporates presysnaptic shunting inhibition of local motion signals integrated by an output neuron that controls yaw torque (Reichardt, W. *et al.*, 1983, see Section 1.06.3.1.3.(viii)). The shunting inhibition signals provided by a pool cell are nondirectional-selective. For the model to explain the remarkable small-field tuning of STMDs the local input elements – either directional- or nondirectional-selective – require extreme contrast-sensitivity probably established by horizontal interactions at more peripheral stages (Barnett, P. D. *et al.*, 2007). The reduced invariance against background motion seems to suggest that the receptive field size of the pool cells providing the shunting inhibition signals correspond to the receptive field size of the respective STMDs.

Due to their specific properties, STMDs appear to be perfect candidates to mediate information about both the position and the motion direction of potential conspecifics appearing in the hoverfly's visual field. The way the detection and the subsequent chasing of the target links in with the hoverflies' inner-loop control that stabilizes gaze and flight, though, is yet unknown.

The discrimination between target and background motion is a common problem among visually oriented insects. The way the visual system solves such discrimination tasks, however, seems to depend on the given species. In the blowfly figure detection circuits, both

FD cells and its wide-field inhibitor respond to motion in a directional-selective way (Egelhaaf, M., 1985b, see Section 1.06.3.1.3). Also, the wide-field inhibitor of the FD1 cell has got a significantly more extended receptive field than the FD1 cell itself (Egelhaaf, M., 1985a; 1985b; Warzecha, A. K. *et al.*, 1993; Krapp, H. G. *et al.*, 2001). But most importantly, object motion has to be out of phase with background motion to efficiently activate the FD cells (Egelhaaf, M., 1985b), which is not a requirement for STMDs in hoverflies detecting small targets (see above). A neural circuit tuned to detect looming objects in locusts (Gabbiani, F. *et al.*, 2004, see Section 1.06.3.2.3.(ii)) needs to solve a similar problem. Its specificity to sense image expansion could be easily corrupted by self-motion-induced optic flow. In case of the locust, inhibitory feed-forward loops combined with a lateral inhibition network that acts on local-motion-sensitive inputs suppress responses to wide-field motion (e.g., Simmons, P. J. and Rind, F. C. 1992, see Section 1.06.3.2.3.(iii)).

1.06.3.2.3 Distance control and looming detection

Besides its role in estimating target size and controlling aerial chases (see Section 1.06.3.2.2), distance estimation plays an important role in a number of other visually guided outer-loop control tasks. We already mentioned its significance for avoiding collisions by integrating translation-induced optic flow in the blowfly where the underlying neural mechanism exploits directional wide-field motion (see Section 1.06.3.1.3.(ix)).

A special case of optic flow either due to an object approaching a stationary observer or due to an observer approaching a stationary object is image expansion. The key feature of image expansion is its inherent radial distribution of flow vectors all pointing outward from a singularity, which defines the approach direction. Image expansion is readily described by the translation term of the optic flow equation [1a], given a nonuniform distance distribution – which in natural environments always holds true. Let us assume an animal approaching a close-by object along a straight translation trajectory that sticks out from the background. In such case it will experience image expansion in two ways: (1) due to the animal's self-motion relative to the background an expansion pattern will be cast on its eyes (Figure 14(a)) and (2) because the object is closer to the animal than the background, the object will pop out of the optic flow pattern by generating local flow vectors of greater magnitude (Figure 14(b), red arrows). The other case, that is, the object is approaching a stationary observer, trivially results in only the object-included expansion pattern – since without self-motion no global optic flow is generated. Object-induced pattern expansion in either case is often referred to as looming stimulus. Looming stimuli contain sufficient visual information to estimate relative distance and to trigger a variety of behavioral responses in insects including landing in flies (e.g., Wagner, H., 1982), escape behavior in flies (e.g., Holmqvist, M. H. and Srinivasan, M. V., 1991), cockroaches (Camhi, J. M. and Levy, A., 1988), and locusts (Rind, F. C and Simmons, P. J., 1999; Gabbiani, F. *et al*, 2004), as well as controlling distance in the hovering hawkmoth (e.g., Farina, W. M. *et al.*, 1994). The potential role of pattern expansion for collision avoidance in freely flying *Drosophila* (Tammero, L. F. and Dickinson, M. H., 2002) we already mentioned in Section 1.06.3.1.3.(ix)

Here we will focus on hovering in hawkmoths and on the detection of looming objects in locusts to illustrate a couple of general principles in processing visual information used for outer-loop control. In both hawmoths and locusts, the activity of identified neural circuits and cells can be nicely linked to distinct and quantifiable behaviors. These animals are therefore ideal model systems to investigate task-specific neural computations – in case of the locust – down to the level of the underlying biophysical mechanisms.

1.06.3.2.3.(i) Distance control in hovering hawkmoths There are two well-studied systems in which the detection of change in distance between the animal and an object is investigated: landing and collision avoidance. Both behaviors require the detection of looming stimuli for the measurement of the change in distance and require information about object trajectory and velocity. Both result in a switch from one motor pattern, forward flight or sitting and feeding, to another, landing or avoidance behavior, respectively. The objective of the computation in both cases is to detect a change in distance and to find a threshold for the measured change to switch to a different motor pattern. In *Manduca sexta* (Sphingidae, Lepidoptera) we investigate a third behavioral paradigm that needs excellent detection and compensation for any change in distance, but here the context is distance control to a flower during feeding. *M. Sexta*, a hummingbird hawkmoth, flies rapidly, is highly maneuverable, and feeds while hovering in front of flowers. They have large superposition eyes, designed for optimal performance

under low-light conditions. The moths approach flowers fast, then decelerate several times, and finally stop precisely at a distance allowing them to insert the proboscis into the flower (Farina, W. M. *et al*., 1994). During this maneuver, the moths have to decide when to decelerate and to switch from forward flight to hovering. This can be viewed as a behavior analog to both landing and collision avoidance with respect to the requirements it poses for the visual system. But instead of landing on the blossom, the moths stay airborne and hover in front of the flower to reach the nectar with their long proboscis. To be able to successfully feed they have to maintain exact position in front of the flower even if it moves, irrespective of the direction of movement. The objective here is to detect the change in distance, monitor it, and maintain this fixed distance; this is in essence an optomotor control task and requires completely different mechanisms than landing or evasive maneuvers. The animal has to monitor both its approach and its retreat from the flower and has to compensate for the change to keep the distance stable. Time-to-collision networks like those proposed for the landing response or the escape response are concerned only with the approach of an object and are not designed to compute compensatory behavior. It is therefore interesting to investigate and to contrast the neuronal properties of these two different behavioral paradigms as the stimuli eliciting these behaviors are the same but the requirements for the execution of the appropriate motor patterns are quite different.

Looming stimuli can be detected in three principally different ways. The animal can detect the expansion/contraction flow field, the increase in object area, or the increase in object parameter or edge length. Wicklein M. and Strausfeld N. J. (2000) and Wicklein M. and Sejnowski T. J. (2001) designed and used a host of different stimuli with the goal to dissect these different detection mechanisms. They are using real, for example, expanding objects and simulated looming stimuli, e.g., rotating spirals and expanding/contracting bull's-eye patterns. These stimuli were designed to either provide stimulation to only one of the above mechanisms or have different temporal signatures for multiple mechanisms. Intracellular recordings in *M. sexta* identified two classes of wide-field spiking neurons that respond to looming or receding stimuli (Wicklein, M. and Strausfeld, N. J., 2000). These neurons do not habituate to repeated stimulation, which is in contrast to the LGMD but similar to fly optomotor neurons. The looming-sensitive neurons in the hawkmoth respond to both approach and retreat of an object and are able to distinguish between both. Two of the three above stated principally different mechanisms of looming detection are realized in the moth. Edge length detection (ELD) neurons, type 1 cells distinguish expansion from contraction on the base of changing perimeter length. These neurons are not sensitive to motion stimuli and respond only to stimuli in which the edge length of an object is increasing or decreasing. Flow field detection (FFD) neurons, type 2 cells, use motion cues to distinguish between expanding and contracting objects. Each FFD cell has a preferred and a null direction for both horizontal and vertical movement. So unlike the fly-motion-sensitive neurons the cells respond to both horizontal and vertical motion but distinguish for each motion orientation between a preferred and a null direction. Neurons with all four combinations of preferred directions, up-left, up-right, down-left, down right, have been found. Both ELD and FFDs neurons consist of two populations with opposing preferred directions for approach and retreat. One population responds with an increase in response strength to an expansion and a reduction of response strength when stimulated with a contracting stimulus; these cells are termed expansion cells. The other subset shows an increase in response strength when exposed to a contracting stimulus and shows a reduction in response strength when stimulated by an expanding stimulus. These cells are termed contraction cells. Both ELD and FFD neurons have front- to frontolateralal receptive fields and are wide-field neurons, with large up to 90° wide receptive fields. The two different cell classes also differ in their morphology and these differences can be used along side the physiological characterization of the neurons to identify a cell as ELD or FFD and set them apart from other neurons in the optic lobes that were already described in *M. sexta* (Milde, J. J., 1996; Rind, F. C. 1972). ELD neurons have arborizations in the innermost medulla layer, the outermost lobula layer, and throughout the lobula plate. They project to the posterior slope. FFD neurons have dense arborizations in the outermost layer of the medulla and in the ipsilateral or contralateral posterior slope; their cell bodies sit in a cluster between the calyces of the MBs.

Wicklein M. and Sejnowski. T. J. (2001) created a conceptual model for the ELD neurons and implemented this model in MATLAB taking the physiological and anatomical properties of the ELD neurons into account. As described above the input structure of the ELD neurons is divided between three neuropils, the medulla, the lobula, and the lobula plate. From anatomical studies we know that there has to be at least one

synapse between the outer medulla and the lobula or the lobula plate; this means that information that is present on the retina at the same time will arrive earlier at the medulla inputs, then at the inputs of the cell in the lobula and the lobula plate. This delay in input processing between different parts of the input arborizations in the ELD neuron is a main feature in the model and provides the model cell with the asymmetrical response characteristics seen in the recordings. To assess the validity of the model we tested both the model and the neurons with the same stimuli. The stimuli were presented to the input layer of the model, which projects to edge detectors whose output was summed spatially over the whole or parts of the input field, followed by a time derivative. The model behavior matched the neuronal behavior qualitatively well for a range of moving and looming stimuli.

Looming-sensitive neurons can be found throughout the animal kingdom including the nucleus rotundus of pigeons (Wang, Y. and Frost, B. J., 1992; Sun, H. and Frost, B. J., 1998), in the optic tectum of frogs (Arbib, M. A. and Liaw, J. S., 1995), and in area MSTd of primates (Duffy, C. J. and Wurtz, R. H., 1991; Tanaka, K. *et al.*, 1989). Recordings from single units in the primate MSTd have demonstrated neurons that discriminate between looming and antilooming, and between outward and inward spiral rotation (Graziano, M. S. *et al.*, 1994).

1.06.3.2.3.(ii) Detecting looming objects in locusts Like the fly in the context of directional motion vision, the locust is one of the most successful model systems in the context of looming detection. The reason for this is an impressive data body on the organization of its nervous system and many behavioral and electrophysiological studies on the control of movements in general (rev.: Burrows, M. 1996), and also in the context of various visuomotor control tasks (e.g., Reichert, H. and Rowell, C. H. F., 1986; Rowell, C. H. F., 1988; Eggers, A. *et al.*, 1991; Baader, A. *et al.*, 1992; Preiss, R., 1992; Robertson, R. M. and Reye, D. N., 1988; Spork, P. and Preiss, R., 1993; Santer, R. D. *et al.*, 2005; Santer, R. D. *et al.*, 2006).

An identified circuit consisting of the lobula gaint movement detector, LGMD, and its postsynaptic target neuron, the descending contralateral movement detector, DCMD, conveys information about approaching objects to the motor centers in the thoracic ganglia (Burrows, M. and Rowell, C. H. F., 1973). The response properties of the LGMD/DCMD have been extensively studied to address key issues of neuroscience including habituation, spike frequency adaptation, contrast- and shape-invariant neural responses, biophysical mechanisms underlying neural multiplication, and – more recently – the plasticity of visuomotor pathways (e.g., habituation: O'shea, M. and Rowell, C. H., 1975; Matheson, T. *et al.*, 2004; Gray, J. R., 2005; Guest, B. B. and Gray, J. R. 2006; spike frequency adaptation: Gabbiani, F. and Krapp, H. G., 2006; stimulus invariance: Simmons, P. J. and Rind, F. C., 1992; Gabbiani, F. *et al.*, 2001; neural multiplication: Hatsopoulos, N. *et al.*, 1995; Gabbiani, F. *et al.*, 1999; Gabbiani, F. *et al.*, 2002; plasticity: Rogers, S. M. *et al.*, 2007; rev.: Gabbiani, F. *et al.*, 2004).

The LGMD neuron has a conspicuous morphology (Figure 16(a)). It possesses three distinctly different dendritic input arborizations and a long axon along which action potentials are propagated toward its terminal ramifications in the lateral protocerebrum (Figures 16(a) and 16(b)). Each spike in the LGMD elicits, via a mixed chemical/electrical synapse exactly one spike in the postsynaptic DCMD (O'Shea, M. and Williams, J. L. 1974; Rind, F. C., 1984; Killmann, F. *et al.*, 1999). Attached to this faithful 1:1 transmission are two very useful properties of the circuit: Firstly, the LGMD can be easily identified even without intracellular staining as it is the only neuron that always generates a spike 1–2 ms before the DCMD fires a spike. Secondly, if only the spike frequency of the LGMD is of interest – as opposed to the neuron's intracellular membrane potential changes – this information is provided by extracellular DCMD recordings, easily kept stable for several hours.

As the LPTCs in the fly, the LGMD integrates thousands of local inputs. Its excitatory main dendrite spans the entire lobula and receives retinotopic input from local-motion-sensitive elements. Distal dendritic areas integrate signals obtained from the frontal visual field. The caudal visual field is mapped onto the proximal dendritic areas (O'Shea, M. and Williams, J. L. 1974). Two smaller dendritic fields receive nonretinotopic feed-forward inhibition – one activated by light-off and the other one by light-on stimuli, respectively (O'Shea, M. and Williams, J. L. 1974; Simmons, P. J. and Rind, F. C., 1992). A lateral inhibition network established between the arrays of local excitatory inputs is thought to be involved in local habituation to repetitive visual stimuli (O'shea, M. and Rowell, C. H., 1975). The integration properties of the LGMD proved to be highly sublinear and may play an important role in the neuron's invariant tuning to looming stimuli (Gabbiani, F. *et al.*, 2001; 2004;

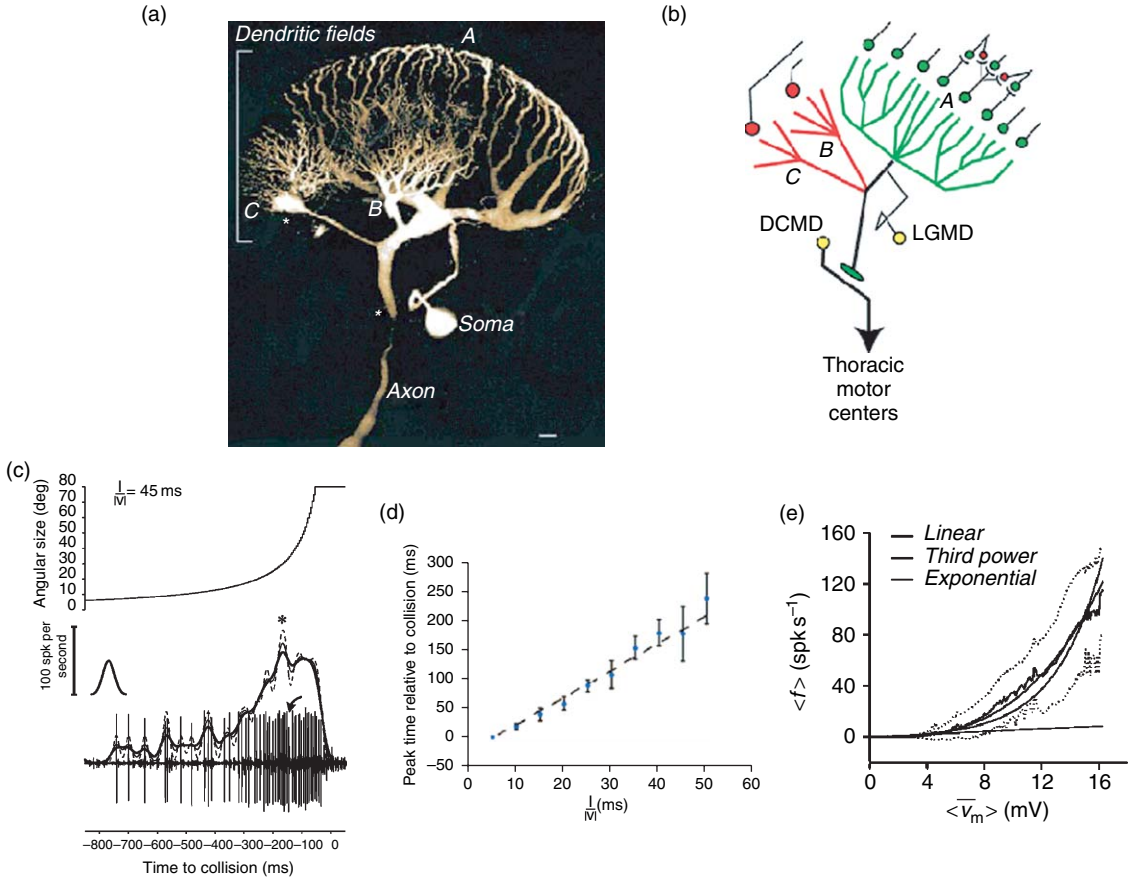

Figure 16 Detecting looming objects in the locust. (a) Two-photon confocal microscopic image of an lobula giant movement detector (LGMD) neuron in the locust. The neuron possesses three dendritic input arborizations, one excitatory (A) and two inhibitory fields (B and C), which receive retinotopic and nonretinotopic input, respectively. (b) Scheme of the LGMD and its target neuron, the descending contralateral movement detector (DCMD). (c) A looming stimulus (upper trace) induces an increase in LGMD/DCMD spiking activity that reaches a maximum close to the potential collision and then decays again. (d) The time of the peak activity is linearly related to the combined parameter l, absolute half-width of the stimulus, over v, the approach velocity of the looming object. This relationship suggests that the peak activity occurs at a certain time delay after the stimulus has exceeded a fixed angular threshold on the eye. (e) Relationship between spike rate and membrane potential changes in the LGMD neuron. The experimental data are best fitted with a third power law function, which is close to an exponential function. Such expansive nonlinear relationship was predicted by a model that describes the LGMD/DCMD responses over time as a function of retinal expansion velocity and retinal size of the looming object. For further explanation see text. Adapted from Gabbiani, F., Krapp, H.G., Koch, C. and Laurent, G. 2002. Multiplicative computation in a visual neuron sensitive to looming. Nature 420, 320–324; Gabbiani, F., Krapp, H.G. and Laurent, G. 1999. Computation of object approach by a wide-field, motion-sensitive neuron. J. Neurosci. 9, 1122–1141.

Krapp, H. G., and Gabbiani, F., 2005; Guest, B. B. and Gray, J. R., 2006).

Studies in the 1970s originally described the LGMD as an acridid movement detector responding briskly to any kind of motion presented in its extended receptive field (O'Shea, M. and Rowell, C. H., 1976; Rowell, C. H. and O'Shea, M., 1976; Rowell *et al.*, 1977). Further experiments revealed the neuron to respond particularly well to approaching objects, or looming stimuli (Schlotterer, G. R., 1977; Pinter, R. B. *et al.*, 1982). Objects directly approaching the eye did strongly activate the neuron independent of pattern contrast, while receding objects caused only weaker responses (Rind, F. C., 1990; Rind, F. C. and Simmons, P. J., 1992). Responses to wide-field motion were thought to be suppressed by mutual inhibition of separate pathways processing opposite contrast polarities (Simmons, P. J. and Rind, F. C., 1992). It was thought that the LGMD tracks object approaches by increasing its spike frequency as the looming object assumes an increasingly bigger angular size on the retina (Rind, F. C. and Simmons, P. J., 1992; Rind, F. C

and. Simmons, P. J., 1997). Based on a series of studies it was concluded that the LGMD neuron encodes the angular acceleration of an approaching object (e.g., rev.: Rind, F. C. and Simmons, P. J., 1999). A numerical model of the LGMD/DCMD circuit (Rind, F. C. and Bramwell, D. I., 1996) inspired the design of collision avoidance system implemented on a robot platform (Blanchard, M. *et al.*, 1999).

In the mid-1990s, the relationship between visual stimulus parameters and the neuron's response over time was studied more systematically. Hatsopoulos N. *et al.* (1995) realized that during a simulated object approach the LGMD activity reached a maximum and then steeply dropped – in most cases – while the stimulus was still expanding. The experimental data were fitted with a phenomenological model to describe the LGMD spike frequency in time. The model combined two visual parameters in a multiplicative way: the approaching object's change in angular size, $\mathrm{d}\theta/\mathrm{d}t$ and the instantaneous angular size, θ (Hatsopoulos, N. *et al.*, 1995). It predicted that for any given ratio between the absolute halfsize of an object, l, and the approach velocity, v, the neuron's peak response always occurs at a fixed time delay after the retinal projection of the object exceeds a certain angular threshold (ibid). Meanwhile, several studies by different groups working on the LGMD/DCMD circuit confirmed such relationship (Gabbiani, F. *et al.*, 1999; Gray, J. R. *et al.*, 2001; Matheson, T. *et al.*, 2004).

Such angular threshold computation or similar models involving a multiplication operation in the context of flight steering or escape behavior were also proposed for species including crabs (Schiff, W. 1965), pigeons (Sun, H. and Frost, B. J., 1998), frogs (Yamamoto, K. *et al.*, 2003), and fish (Preuss, T. *et al.*, 2006). This hints at a general principle in the detection of looming objects across phyla. Naturally, the question arises of how the proposed neural multiplication might be established in the nervous system? Even though the requirement of neural multiplication operations has been postulated for several sensory modalities – most notably in directional motion vision (see Section 1.06.3.1.2, rev.: Reichardt, W., 1987) and in auditory processing (Pena, J. L. and Konishi, M. 2001) – the underlying neural mechanisms are not yet completely understood (rev.: Gabbiani, F. *et al.*, 2004).

The model Hatsopoulos N. *et al.* (1995) put forward to describe the LGMD response over time, $r(t)$, is of the following form:

$$r(t) = \frac{\mathrm{d}\theta(t+\delta)}{\mathrm{d}t} \mathrm{e}^{(-\alpha\theta(t+\delta))} \qquad [4]$$

where $\mathrm{d}\theta(t+\delta)/\mathrm{d}t$ gives the expansion velocity of the approaching object at time t, plus the neural response delay δ, α is a coefficient, and $\theta(t+\delta)$ denotes the instantaneous angular size of the object at time $t+\delta$. The interpretation of the model is that during the early approach phase the expansion velocity term, $d\theta(t+\delta)/\mathrm{dt}$, dominates the LGMD spike frequency, which is, at later phases, strongly inhibited by the angular size term, $\theta(\mathrm{t}+\delta)$.

One way of performing a multiplication operation, used in analog very-large-scale integration (VLSI) circuits (Mead, C., 1989), is to take the logarithm of the input variables, sum them (eqn [5]), and backtransform the result by means of an exponentiation (eqn [6]).

$$\ln(r(t)) = \ln\left(\frac{\mathrm{d}\theta(t+\delta)}{\mathrm{d}t}\right) - \alpha\theta(t+\delta) \qquad [5]$$

With $a = \ln(\mathrm{d}\theta(t+\delta)/\mathrm{d}t)$ and $b = \alpha\theta(t+d)$ we may write:

$$r(t) = \mathrm{e}^{a-b} \qquad [6]$$

Assuming that, in a first approximation, the membrane potential of the LGMD corresponds to in a first approximation, to the sum of the integrated excitatory and inhibitory inputs, a–b, the required exponentiation could occur during the spike generation process (Gabbiani, F. *et al.*, 2002; 2004). Similar mechanisms have been proposed for simple and complex cells in cat primary visual cortex (Anderson, J. S. *et al.*, 2000) where the combination of synaptic noise and a linear threshold model results in an expansive nonlinearity when the neurons' membrane potential is transformed into a spike frequency (Carandini, M. and Ferster, D., 2000).

Recent experimental evidence suggests that the LGMD membrane potential is indeed transformed into a spike rate according to a third-order power law that comes close to an exponential function (Figure 16(e), Gabbiani, F. *et al.*, 2002). This finding is in agreement with the model proposed by Hatsopoulos N. *et al.* (1995).

Still, the question remains whether the inputs to the LGMD encode angular expansion velocity in logarithmic space and angular size in linear space, as eqn [5] implies. It has to be said that encoding velocity independent of size and encoding size independent of velocity is by no means a simple task in neural processing.

As far as the velocity-dependent excitatory inputs are concerned there is ample evidence for

logarithmic compression of the dynamic input range in the visual system (Laughlin, S. B., 1987). This includes the output of EMDs being logarithmically encoded in the velocity domain (Zanker, J. M. *et al.*, 1999). Together with a dendritic gain control mechanism as proposed for the fly LPTCs (Borst, A. *et al.*, 1995, see Section 1.06.3.1.3.(viii)), a size-independent logarithmic encoding of velocity might as well be a possible option for the LGMD. Furthermore, there is experimental evidence that the responses of local motion-sensitive elements presynaptic to the excitatory dendritic tree are indeed velocity-dependent (Krapp, H. G., and Gabbiani, F., 2005).

Regarding the size-dependent inhibitory input to the LGMD, so far, there is only indirect experimental evidence available (Gabbiani, F. *et al.*, 2005). If the forward inhibition is abolished using GABA antagonists, the peak firing rate of the LGMD neuron is delayed to occur closer to collision or even afterwards (Gabbiani, F. *et al.*, 2002). This result is compatible with the interpretation of the model: At later times during the approach, feed-forward inhibition, $-\alpha\theta(t+\delta)$ in eqn [5], dominates over the excitatory inputs, $\ln(\mathrm{d}\theta(t+\delta)/\mathrm{d}t)$, causing the firing rate to decrease and thus defines the timing of the LGMD peak response.

From a functional point of view the response properties of the LGMD neuron show some remarkable task-specific features which support its role in detecting approaching objects. The LGMD does not respond particularly well to optic flow as generated during self-motion (Simmons, P. J. and Rind, F. C., 1992). The lateral inhibition network acting on the excitatory input elements was suggested to prevent synaptic fatigue (O'Shea, M. and Rowell, C. H., 1976). Spike frequency adaptation shapes the activity pattern in the LGMD and may also prevent the LGMD output range from saturating (Gabbiani, F. and Krapp, H. G., 2006). The physiological process underlying this adaptation, that is, opening of calcium-dependent potassium channels, is readily explained by a model originally proposed for vertebrate neurons (Wang, X. J., 1998). Furthermore, the LGMD receptive field spans almost an entire visual hemisphere (Krapp, H. G. and Gabbiani, F., 2005) with an isotropic sensitivity profile to looming objects independent of the approach direction (Gabbiani, F. *et al.*, 2001; Rogers, S. M. *et al.*, 2004). Though such an extended receptive field does allow the animal only to detect whether an approach occurs from in front, left, or right it is sufficient to initiate adequate behavioral action. Correspondingly, behavioral experiments in freely moving locusts confronted with looming stimuli from different directions did not show a correlated relationship between approach direction and the direction of the escape jumps. The locusts' jumps were only away from, but not in a certain angular relationship relative to the direction of object approach (Santer, R. D. *et al.*, 2005). Open-loop experiments in tethered flying locusts suggest that in response to looming stimuli, different flight maneuvers, i.e., the initiation of evasive steering or gliding, depend on the level of spiking in the DCMD (Santer, R. D. *et al.*, 2006).

Recent studies on the LGMD/DCMD circuit in locusts addressed the question of how differences in behavioral states are related to differences in neural processing. In *Schistocerca gregaria*, a locust species that comes in two phases – one solitarious and one gregarious – the LGMD habituates to repeated stimuli in a phase-dependent way: In gregarious animals, which fly during daytime, and in swarms the LGMD habituates only mildly while in solitarious, which generally avoid conspecifics and fly during the night, the LGMD activity strongly habituates (Matheson, T. *et al.*, 2004). Another difference between the two phases is an overall lower spiking activity in solitarious animals. This difference was found to be compensated for by increasing the gain of an identified synapse between the DCMD and one of its target motor neurons that controls the activity in a leg muscle involved in the execution of escape jumps (Rogers, S. M *et al.*, 2007). The transition from behaviorally solitarious to gregarious locusts, which is usually caused by overpopulating a given area, partly occurs within several hours. This suggests that the differences between the functional properties of the LGMD/DCMD circuit in the two phases require intermediate-term neural plasticity.

Looming detection in locusts is an area where much progress has been made over the last couple of years. Not only in the sense that we now better understand the neural basis of specific visually guided behaviors in insects but also because several studies addressed questions of fundamental interest to neuroscience across species. One such principal question is: how do neurons multiply? Promising ideas have been put forward (Hatsopoulos, N. *et al.*, 1995), which were supported by experimental evidence (Gabbiani, F. *et al.*, 2002; rev.: Gabbiani, F. *et al.*, 2004). The key to further our understanding of the underlying biophysical mechanisms,

however, requires an approach that combines *in vivo* electrophysiology, compartmental modeling, and quantitative behavioral studies. A detailed compartmental model of the LGMD to investigate the neuron's passive integration properties has been recently presented (Peron, S. P. *et al.*, 2007) and awaits its extension to include active membrane properties. However, there is a lack of naturalistic stimulus sequences that capture the actual visual input a locust experiences in the wild, either during free flight or while sitting on the ground when an object approaches. Naturalistic stimulus sequences could be mapped onto the inputs of the compartmental model and/or may be used for stimulation during electrophysiological experiments to learn more about the LGMD's integration properties. Such replay experiments certainly do not solve all remaining problems but they might result in some new insights as they did in the research on directional motion vision of the fly (see Section 1.06.3.1.3.(ix)). It is important to keep in mind, however, that the results obtained from such replay experiments do not necessarily reflect the system's closed-loop behavior. Sensory mechanisms of other modalities not activated during such open-loop experiments may be required to gate or modify the responses of the LGMD.

In a recent study on freely moving locusts, not only escape jumps in response to looming stimuli but also the muscle activity during distinctly different preparatory phases immediately before the animals' takeoff were video monitored (Fotowat, H. and Gabbiani, F., in press). A correlation analysis of the behavioral and muscle recording data in combination with separate DCMD recordings produced the following results: the different preparatory phases before jumping always occur at a certain time before the impending collision. The starting point of most of the preparatory phases could be related to the different levels of DCMD spiking, which did consistently reflect the looming stimulus to exceed consecutive angular thresholds on the animal's retina. The fact that, during the entire sequence, the timing of reaching consecutive activity levels was independent of the kinematic parameter, $1/V$, is consistent with the model proposed (eqn [4]).

The experiments in freely walking animals (Santer, R. D. *et al.*, 2005; Gabbiani, F. personal communication) present an elegant approach to get around the problem of working on restrained animals. The situation for the animals is almost natural – except for the lack of realistic short-range air pressure changes, which an approaching predator would probably produce and which cockroaches also exploit for triggering their escape behavior (Camhi, J. M., 1993). The next step would ideally be to record neural and muscle activity in freely flying animals – either in combination with their immediate visual input using micro cameras or when the animals' trajectories and head movements are observed to reconstruct the visual input. Locusts, as apposed to flies, are big enough to handle a decent payload and indeed did carry amplifier and telemetric transmission gear for muscle recordings already in the mid-1990s (Fischer, H. *et al.*, 1996). It is probably just a matter of time until miniaturization of integrated electronic circuits, including micro cameras, will allow for neural recordings during flight.

1.06.3.3 Image Segmentation – The Detection of Orientated Contours

The segmentation of images is commonly associated with the ability to discriminate between contours of different orientation. Early work in mammals suggested simple and complex cells in areas V17, 18, and 19 to be involved (e.g., Hubel, D. H. and Wiesel, T. N., 1959). These cells are arranged in cortical columns and hypercolumns the proper development of which requires early visual experience (Hubel, D. H. and Wiesel, T. N. 1965).

Anatomical studies in insects have shown experience-dependent plasticity at different levels of the visual system (e.g., Barth, M., *et al.*, 1997, see Section 1.06.3.1.3.(v)). Besides ontogenetic plasticity during the development, insects perform remarkably well in learning tasks also, which require them to distinguish between visual cues such as object shape and size, edge and pattern orientation, as well as color (see Section 1.06.4.1). The classic experimental model system is the honeybee in which a remarkable data body on learning and memory based on visual cues has been accumulated since the work of von Frisch K. (1965) (rev.: Wehner, R., 1981; Srinivasan, M. V., 1994). The reason for honeybees to be different was partly attributed to the fact that these animals live in social aggregates. Honeybees are required to memorize the location. First, because they need to be able to find the food source again for themselves after they have returned to the hive. Second, they are required to communicate the yield and location of the food sources to their hive mates by means of the famous waggle dance (Esch, H. E. *et al.*, 2001).

Meanwhile, it becomes evident, however, that other insects not living in social aggregates and presumably lacking intraspecific communication also show the capability of learning and memory (see Section 1.06.7). Learning and memorizing is the second step following the identification of a relevant object in a particular context, for instance, feeding and requires the segmentation of the retinal input.

Behavioral studies recently showed that blowflies too are capable of distinguishing between differently oriented gratings and of memorizing those patterns that were rewarded during training sessions. Gratings tested against each other in these experiments were differently oriented by 90°, that is, horizontal versus vertical orientation, or oblique patterns tilted by 45° to the left versus right (Campbell, H. R., 2001; Campbell, H. R. and Strausfeld, N. J., 2001). The animals were even able to distinguish between orientation differences as small as 5° when they challenged with vertically and nearly vertically oriented patterns (Campbell, H. R. and Strausfeld, N. J., 2001).

Campbell H. R. and Strausfeld N. J. (2001) discussed several potential mechanisms, which may underlie the fly's orientation discrimination ability. Retinotopic template matching, suggested by earlier studies to be involved in distinguishing between different patterns in *Drosophila* learning experiments (Dill, M. *et al.*, 1993; Dill, M. and Heisenberg, M., 1995), was not required to accomplish the orientation discrimination task (Campbell, H. R., 2001). Although several parallel mechanisms based on directional motion cues could not be excluded for sure, a dedicated orientation-selective pathway was assumed that was inspired by a model on earlier pattern discrimination experiments in honeybees (Srinivasan, M. V., 1994; Chandra, B. C. S. *et al.*, 1998). The idea was that three orientation-selective channels at an angular spacing of 120° with a half-width orientation tuning of about 90° could account for the observed behavioral data (Campbell, H. R. and Strausfeld, N. J., 2001).

The neural correlate underlying orientation selectivity in insects is not very well-known. Some electrophysiological studies in honeybees (e.g., Yang, E.-C. and Maddess, T., 1997), dragonflies (O'Carroll, D.C., 1993), and earlier work in flies (McCann, G. D. and Dill, J. C., 1969) showed that insect nervous systems are endowed with orientation-selective neurons. However, a detailed description of the morphology and electrophysiological response properties of orientation-selective neurons was still missing.

Detailed anatomical studies (Strausfeld, N. J. and Okamura, J. Y., 2007) in connection with preliminary electrophysiological results (Okamura, J. Y. and Stausfeld, N. J., 2007) suggest that the optic glomeruli in the lateral protocerebrum of the fly are involved in the discrimination between differently oriented contours. The interconnectivity between individual optic glomeruli is somewhat reminiscent of the interconnectivity found among glomeruli of the antennal lobes processing olfactory and mechanosensory information. The optic glomeruli receive two sorts of inputs: (1) They receive input from columnar lobula complex neurons directed to specific glomeruli. The terminals of these neurons do not always directly contact any descending neurons but may connect to local interneurons, which set up an intrinsic network within each of the glomeruli. (2) The second type of inputs is provided by a class of wide-field neurons collecting information from both the lobula and the medulla (Strausfeld, N. J. and Okamura, J. Y., 2007).

Individual intracellular recordings from identified neurons connected to the glomeruli circuits seem to suggest these anatomical structures to be involved in the distinction between different contour orientations. Some neurons encountered had restricted dendritic fields in the lobula as well as in the lobula plate and, correspondingly, had small receptive fields. Together, these neurons build a population that covers the entire monocular visual field. Their response properties were somewhat heterogeneous, some responding in a directional-selective, some in an orientation-selective way or both. Four distinctly different morphological types were found. Individual specimens of each of the three classes were broadly tuned to specific orientations. Relay neurons in between the glomeruli and one local interneuron, instead, had a narrower orientation tuning (Okamura, J. Y. and Strausfeld, N. J., 2007).

The electrophysiological data presented in the latter study mark a first step and in combination with the solid anatomical data give a strong hint at which area in the insect brain might be dealing with pattern segmentation. A greater database obtained from repeated and systematic electrophysiological characterizations of the different cell types would be needed to obtain a conceptual model of how orientation-selectivity is actually established in the fly nervous system. Finally, the transfer function between the outputs of the optic glomeruli, which carry information relevant to outer-loop control, and

the neurons involved in maintaining postural stability needs to be determined.

1.06.4 Exploiting Electromagnetic Properties of Light

So far the visual mechanisms that we discussed, such as motion vision or detection of small objects, are coping with the detection of light intensity changes. The reason for this is that most of the reviewed mechanisms so far are driven by monochromatic contrast. In the next two sections we will investigate how invertebrates analyze and utilize properties arising from the electromagnetic nature of light: its spectral content and e-vector orientation. Color is intrinsic to light whereas polarization, patterns of e-vector orientation, arise only through scattering and reflection of light.

Visible light comprises just a part of the electromagnetic spectrum. The wavelengths that animals can detect are between 300 and 800 nm, while the far-infrared spectrum between 700 and 800 nm is visible only to few species. Most invertebrate trichromates possess a UV receptor, maximally sensitive to wavelengths around 350 nm, a blue receptor with maximal sensitivity around 450–480 nm, and a green receptor with maximal sensitivity around 500–550 nm (Kelber, A., 2006).

Polarized light arises from scattering of sunlight within the atmosphere and the hydrosphere and from reflection of light by shiny surfaces, such as water, leaves, scales, and cuticle (Horvath, G. and Varju, D., 2004). In contrast to color, polarized light has an intrinsic spatial component, the angle of polarization or e-vector orientation. This feature is exploited by invertebrates for navigational purposes (Wehner, R. and Labhart, T., 2006), as discussed in Polarization Vision. But first we will discuss the detection and the use of the chromatic information of light.

1.06.4.1 Processing of Color Information

A wide range of species in the animal kingdom and a host of invertebrates possess multiple types of photoreceptors and color vision (see tables 1 and 2 in Kelber, A. *et al.*, 2003). This is remarkable considering that an animal investing into color vision will have lowered absolute sensitivity and in many cases also lowered spatial resolution. Additionally the cost of neuronal processing and analysis of spectral information should act as an energetic constraint on the number of spectral receptor types (Laughlin, S. B., 2001). So the question arises: Why is color vision an evolutionary useful trait despite these obvious costs? Hence, why do so many animals possess color vision?

It is rather easy to convince oneself of the necessity of motion vision for any mobile animal, as it is clearly necessary to monitor ones motion in space, to steer a course, and to avoid collisions (see Sections 1.06.3.1 and 1.06.3.2). It is a bit harder to define a behavior that would be impossible to achieve without chromatic information and in which color vision is truly indispensable.

1.06.4.1.1 Reasons for color vision

One argument for color vision is that chromatic information is used for object detection and identification because the chromatic signature of objects should be more reliable for identification. The reason for this is that the spectral composition of the illumination varies less than the intensity (Kelber, A., 2006).

Campenhausen C. V. (1986) and Maximov V. V. (2000) argue that color vision evolved to filter out the large intensity differences between sunlit and shady spots and the flicker that they generate. The usefulness of knowing the color of light could have been an additional reason for color vision to evolve. One example for this is the detection of the solar and antisolar halves of the sky, which differ in the content of long-wavelength light. The identification of the solar half of the sky is useful for navigational purposes (see Section 1.06.4.2).

1.06.4.1.2 In what behavioral contexts is color vision used?

Bees, wasps, and butterflies foraging in a flower meadow would be one well-known example for a behavior that is undoubtedly mediated largely by color vision (Chittka, L. *et al.*, 1993). But other behaviors, both spontaneous and learned, such as mate recognition (Lepidoptera: Kelber, A., 1999a), camouflage (Lepidoptera: Starnecker, G., 1996), finding the correct food plant for oviposition (Lepidoptera: Kelber, A., 1999a), and nest finding (spiders: Peckham, G. W. and Peckham, E. G., 1894, hymenoptera: Steinmann, E. and Menzel, R., 1990) to name just a few, are also mediated at least in part by color vision (rev.: Kelber, A., 2006).

1.06.4.1.3 Visual pigments, photoreceptors, and filters

The relative likelihood of absorption of a photon defines the spectral sensitivity of a photoreceptor.

Once a photon is absorbed the electrical response of the photoreceptor is independent of the wavelength of the photon, which is called the principle of univariance (Rushton, W. A., 1965). This means that individual photoreceptors are color blind because the intensity of two visible spectra can always be adjusted to give equal receptor responses. Simply put, a green photoreceptor can be equally excited by a weak, low-intensity green light and a very intense blue light.

Visual pigments are G-protein-coupled receptors, which are composed of an opsin and a chromophore. The chromophore isomerizes when it absorbs a photon and this causes a confirmation change and activates phototransduction (Aidley, D. J., 1998). The chromophore and the opsin together specify the spectral sensitivity of the visual pigment. Retinal is the most common chromophore in the animal kingdom, but most insects use 3-hydroxyretinal. Usually a single photoreceptor cell contains one visual pigment, but there are exceptions to this rule. The swallowtail, for example, coexpresses two opsin genes in some of its photoreceptors (Kitamoto, J. *et al.*, 1998).

In invertebrates, the number of receptor types that are expressed is quite variable, ranging from a single spectral type in cephalopod molluscs (Messenger, J. B. 1981) to up to 16 different receptor types in stomatopod crustaceans (Cronin, T. W. and Marshall, N. J., 1989; Marshall, N. J., and Oberwinkler, J., 1999). Some spiders and crustaceans have two receptor types, but Salticidae (jumping spiders) may have four (Walla, P. *et al.*, 1996). Among insects, cockroaches and some ants have two receptor types, most bees and wasps have three, dragonflies and sawflies have four, and some flies and butterflies have five or more (rev.: Briscoe, A. and Chittka, L., 2001). In addition to the different spectral receptor types the sensitivity of photoreceptors can be changed in several ways by: (1) screening and sensitizing pigments; (2) diverse types of intraocular filters, cornea filters, and the filtering properties of distal receptor cells in tiered retinae; and (3) lateral filtering in single light-guiding rhabdoms in which several spectral receptors compete for photons (rev.: Kelber, A., 2006).

1.06.4.1.4 Receptor arrangement in the retina

The arrangement of photoreceptors in the eye has been studied intensely. In crustaceans and insects several different types of receptors can be found in a single ommatidium. Different receptor types can build a regular pattern in the retina or they can be randomly arranged. Examples for insects with randomly arranged retinae are *Papilio xuthus* (Arikawa, K. and Stavenga, D. 1997), the bumble bee (Späthe, J. and Briscoe, A. D., 2005), and the honeybee (Wakakuwa, M. *et al.*, 2005). As yet we do not understand what impact these different arrangements have on the neuronal coding of color vision.

Many animals have regionalized retinae where only parts of the eye are color-sensitive while other parts serve other functions like, for example, the polarization-sensitive dorsal rim area (DRA) in ants and locusts (see Section 1.06.4.2). In other species like some spiders and Stomadopods, only a small region of their visual fields is dedicated to sense color. In stomatopod eyes the color-sensitive area consists of only four rows of horizontal ommatidia (Marshall, N. J., 1988). Whereas in jumping spiders only the two principal eyes are color-sensitive and thus only a small area of their visual field can be analyzed for chromatic information (Land, M. F., 1985).

1.06.4.1.5 Color perception

In human vision, color has three distinct qualities, hue, saturation, and brightness. Hue and saturation are chromatic aspects of color. Brightness is the achromatic aspect of color; intensity-related cues are referred to as achromatic cues and the signal is an achromatic signal. Brightness describes how light or dark a stimulus is. Saturation describes how similar the color is to gray or white. A low saturation means the color is relatively close to gray or white, whereas a highly saturated color will be far removed from gray or white. Hue refers to color differences other than saturation and brightness and is described in terms of red, green, blue, etc. Hue and saturation are mediated by opponent mechanisms that involve the comparison of receptor outputs, while brightness involves only additive interactions.

1.06.4.1.6 When does an animal have color vision?

This is not a trivial question, because just the fact that an animal is in possession of multiple receptor types does not necessarily mean it is employing color vision. Each of the different receptor types could be used individually to drive a specific behavior. These behaviors would still be color blind and the corresponding channel would be an achromatic channel. In the honeybee, for example, single receptors are used for specific behavioral tasks and each of these channels is achromatic. In the bee, motion vision and high-resolution vision are based on the green receptor signal (Lehrer, M., 1994), polarization vision is based on the UV receptor

(Wehner, R., 1987), and all receptor types are pooled for phototaxis (Menzel, R., 1979). If more than one receptor type is used for a specific behavior and a ratio or difference of these receptor signals is computed this behavior is no longer color blind. In other words, if an animal possesses at least two spectrally distinct visual pigments in two different photoreceptors and compares their outputs, the result of this comparison, color opponency, is color sensitivity and will be largely independent of intensity. Therefore only if an animal can discriminate two lights of different spectral composition regardless of their relative intensity it is considered to employ color vision (Menzel, R., 1979; Neumeyer, C., 1991; DeValois, R. L. and DeValois, K. D., 1997).

1.06.4.1.7 Classifications of color vision

Color vision is classified as dichromatic, trichromatic, etc. depending on the number of lights required to match any spectral light. The number of colors that are needed to match any light cannot exceed the number of different spectral photoreceptors. But quite often it is lower than that, for example, humans do not use rods for color vision. For a trichromat, humans or bees, the intensities of the three primary spectra can match any light. Therefore in the case of trichromats, color can be specified by either the intensities of three known spectra required for a match or by the quantum catches of the three receptor types. A color can then be represented geometrically as a point in a color space whose dimensionality is given by the number of receptor types involved (3 for trichromats), which during color matching can be added positively or negatively. For a more detailed account of different color spaces see Kelber A. *et al.* (2003).

1.06.4.1.8 Behavioral tests for color vision

Lubock J. (1888) established that *Daphnia* sp. is color-sensitive and this was the first time that color vision was proven for an invertebrate. He tested *Daphnia*, which are positively phototactic, and found that they preferred light that was filtered with a yellow filter over the unfiltered light source. As the unfiltered light was higher in intensity at all wavelengths, he concluded that *Daphnia* has color vision preferring yellow over white light. Twenty-six years later, in 1914, von Frisch K. (1914) used associative learning with a food reward in the context of foraging to successfully demonstrate the use of achromatic and chromatic signals in honeybees. von Frisch's famous gray card experiment established irrevocably that bee's possess color vision. In that experiment the bees were trained to find and associate a food reward with a specific color. In the test that followed they had to choose between that color and many shades of gray. At least one of the gray shades should have been sufficiently similar in its achromatic signal to the trained color. If the bee discriminates the trained color successfully from all the gray shades, she must use color vision to complete the task, as she is not relying on achromatic cues. A huge body of data on bee color vision based on behavioral experiments is available (e.g., Kühn, A., 1927; von Helversen, O., 1972; Backhaus, W., 1991; Giurfa, M., *et al.*, 1995; Dyer, A. G. and Neumeyer, C., 2005; Wicklein, M. and Lotto, R. B. 2005; Späthe, J. *et al.*, 2006). A growing range of invertebrates were shown to have color vision when tested in different behavioral contexts and with different testing paradigms. One of the most astonishing results comes from night-flying hawkmoths who forage under starlight scotopic conditions under which humans are completely color blind. The moths use chromatic cues to find their flowers of choice (Kelber, A. *et al.*, 2002). Chapter Color in Invertebrate Vision gives a more detailed account of color vision under special conditions like low light levels. For a detailed list of invertebrates that were shown to have color vision see Kelber A. *et al.* (2003).

1.06.4.1.9 Neural mechanisms for color coding

Spectral opponency is the neural mechanism that has been found to code for hue contrast in primates and is also observed in invertebrates. Single receptors are detecting only quanta of light and cannot discriminate properties of light like its wavelength. They are color blind. Therefore output signals of multiple receptors that are tuned to different parts of the spectrum but observe the same visual area must be compared to get access to the spectral content. The same principle holds for the detection of polarization (see Section 1.06.4.2). Cells that compute such a comparison of different receptor outputs are called color-opponent neurons. Swihart C. A. (1971) was the first who found spectral-opponent neurons in insects. He recorded spectral-opponent neurons in the optic lobes and the protocerebrum of butterflies. Spectral opponency was also established in several other insect species including the locust (Osorio, D., 1986), the cockroach (Mote, M. I. and Rubin, L. J., 1981), and the honeybee (Kien, J. and Menzel, R., 1977a; 1977b; Hertel, H., 1980; Riehle, A. 1981; Hertel, H., *et al.*, 1987; Hertel, H. and Maronde, U.,

1987a; 1987b; Yang, E.-C. *et. al.*, 2004). In trichromates the three spectral inputs that arise from the photoreceptors in the retina are named according to their wavelength specificity as long – L, medium – M, and short – S wavelength receptors (Figure 17(b)). All spectral-opponent neurons recorded so far are characterized in principle by excitatory + and inhibitory − response patterns of the following kind: S + M − L−, S − M + L+, S + M − L+, or S − M + L− and the reverse combinations of these.

In insects and crustaceans, two anatomical types of photoreceptors are found, short or long visual fibers, which either terminate in the lamina, short visual fibers, or in the medulla, long visual fibers (see Section 1.06.2). In flies the long visual fibers constitute the chromatic pathway whereas the short visual fibers supply the achromatic motion-sensitive pathway. These two pathways are separated throughout the entire visual system (Strausfeld, N. J. and Lee, J. K., 1991). But flies seem to be an exception with this arrangement; in most insects and crustaceans both the short and long visual fibers contribute to the color pathway. For more details on different species see Kelber A. (2006).

The honeybee is the most thoroughly investigated invertebrate species for color vision and we will therefore use the honeybee to illustrate the principles of neuronal color coding (Figure 17(a)). Already at the first level of synaptic interaction in the lamina, separate pathways for achromatic contrast and spectral coding are formed. Four types of large monopolar cells (LMC) each with different input characteristics have been found. The first LMC is hyperpolarized by M and L receptor inputs and depolarized by the S receptor input. The second type of LMC is dominated by M receptor inputs and receives only weak L and S receptor inputs. The third LMC type receives only L receptor input. The forth and the last LMC type sums the inputs from all three receptor inputs and could represent a highly sensitive achromatic system (Menzel, R., 1974; Hertel, H. and Maronde, U., 1987a; 1987b). The outputs of all these LMCs are combined in the medulla with those of the S receptors that have long axons (long visual fibers) and project all the way to the medulla. Neurons recorded in the proximal medulla show spectral opponency similar to cells in the lobula and the protocerebrum. Two forms of opponency are found: (1) Tonic opponency, which seems to be the dominant form and can be found throughout the medulla, lobula, and the protocerebrum (Kien, J. and Menzel, R., 1977b; Hertel, H., 1980; Riehle, A., 1981; Hertel, H., *et al.*, 1987; Hertel, H., and Maronde, U., 1987b; Yang, E.-C. *et al.*, 2004). The neurons are excited or inhibited by a flash of monochromatic light in their sustained response. All combinations of L, M, and S receptor opponency possible as well as cells computing simple summations of two or all three receptor inputs have been recorded (Kien, J. and Menzel, R., 1977a; 1977b; Yang, E.-C. *et al.*, 2004). Interestingly the cells differ widely in their specific response patterns as well as in their receptive field size and structure. (2) ON/OFF or phasic opponency; this is observed much less frequently and seems to be present only in local neurons of the medulla. There two response patterns were found: S-OFF, M-ON, L-OFF, or S-ON and OFF, L-OFF (Hertel, H., 1980). The receptive fields of spectral-opponent neurons range from small, simple fields to large, complex receptive fields that can even

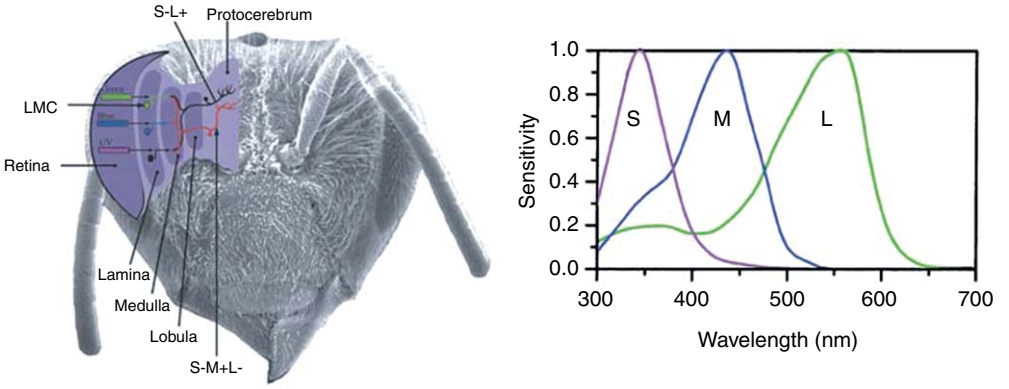

Figure 17 Color vision. (a) Scanning electron micrograph of a bee head. The inset shows a schematic depiction of the neuronal circuits involved in color vision. (b) Tuning curves of the S, M, and L receptors in the bee. Adapted from Chittka, L. and Raine, N. I. 2006. Recognition of flowers by pollinators. Curr. Opin. Plant Biol. 9, 428–435.

cover both eyes. But no center-surround spatial-opponent neurons like those observed in the vertebrate cortex have been found in the honeybee or any other invertebrate species so far. Spectral opponency neurons project mainly through two tracts: (1) the posterior optic commissure (POC), which runs between the left the and right visual hemisphere, and (2) the anterior optic commissure (AOC), which projects in a nonretinotopic manner to the MBs and the lateral protocerebrum (Hertel, H. and Maronde, U., 1987a; 1987b; Hertel, H. *et al.*, 1987; Ehmer, B. and Gronenberg, W., 2002). Anatomical data from Ehmer B. and Gronenberg W. (2002) were discussed in more detail in Section 1.06.2.

1.06.4.2 Polarization Vision

The ability to sense the polarization pattern of the sky and to make use of it for navigation is a trait shared by birds, fish, cephalopods, and arthropods (Horvath, G. and Varju, D., 2004). Polarization vision provides them with a powerful tool for a variety of orientation and navigation tasks or simply allows them to detect bodies of water in the case of some water-seeking insects (Schwind, R., 1984; 1991; Horvath, G. and Zeil, J., 1996; Kirska, G. *et al.*, 1998; Wildermuth, H. 1998). Many insects are able to use polarization vision for course control (flies: Wolf, R. and Heisenberg, M. 1980; von Philipsborn, A. and Labhart, T. 1990), as a global reference cue for the compass system in migratory species such as locusts (Mappes, M. and Homburg, U., 2004), and for foraging and homing in bees, ants, and fiddler crabs (Wehner, R., 1984; 1994; 1997; Zeil, J. and Layne, J. E., 2002; Wehner, R., and Srinivasan, M. V., 2003).

1.06.4.2.1 Properties of polarized light

Light can get polarized by scattering in air or water or when it reflects from surfaces. The polarization patterns created are different in each case and can be used to aid different behaviors (rev.: Wehner, R. and Labhart, T., 2006), e.g., light reflected from the surface of water bodies attracts water-seeking insects (Schwind, R., 1984). In this account we will concentrate on the situation created when light is scattered in air and its use for navigation. Here polarization vision is based on the detection of the polarization pattern that consists of concentrically arranged e-vectors around the sun that span the entire sky. These patterns vary systematically across the sky and depend on the sun's position. They are caused by the atmospheric scattering of sunlight. This scattering results in the partial plane polarization of sunlight. The prevailing oscillation plane e-vector is oriented orthogonal to an imaginary straight line between an observed point in the sky and the position of the sun (Figure 18(a)).

1.06.4.2.2 Adaptations to e-vector detection in the eye

von Frisch K. (1967) showed that only very small patches of sky of 10–15° wide are needed for insects to detect and orient toward polarization patterns.

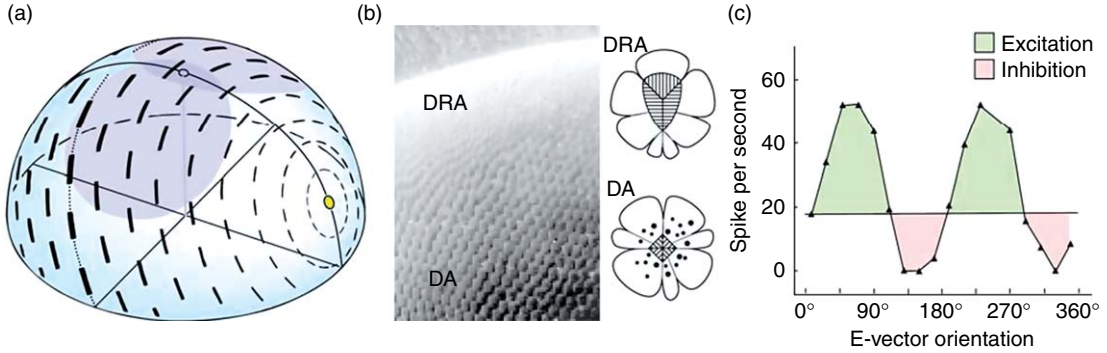

Figure 18 Polarization vision. (a) A representation of the polarization pattern observed at a sun elevation of 24°. The e-vector orientations are depicted as bars, their length and width indicate the degree of polarization. The shading represents the size and the location of the visual fields of polarization-sensitive interneurons (POL1 neurons) of the crickets. (b) Ommatidia in the specialized dorsal rim area (DRA) region of the field cricket are compared with regular ommatidia in the adjacent dorsal area (DA). Left: Scanning electron micrograph showing strongly reduced faceting in the DRA cornea. Right: Schematic representations of cross sections through ommatidia from both the DRA and the DA. (c) Polarization opponent response of a field cricket POL neuron. A strong modulation of spike frequency can be observed despite a low degree of polarization of 19%. Excitation is shown in green shading and inhibition in red shading. Adapted from Labhart, T. and Meyer, E. P. 2002. Neural mechanisms in insect navigation: polarization compass and odometer. Curr. Opin. Neurobiol. 12, 707–714.

Similarly new studies (Henze, M. J. and Labhart, T., 2006) revealed that crickets can detect and respond to changes in the direction of the e-vector in natural situations. They successfully tested the animals with very small areas of polarized light resembling the natural situation of either vegetation blocking big areas of the sky or when the sky is mostly covered by clouds. Even elliptical polarization as encountered in hazy conditions is sufficient for detection.

But how do animals detect polarization? Photoreceptors are detectors of quanta, therefore a single photoreceptor cannot disentangle the very different properties of light, such as spectral content and e-vector orientation. The output of differently tuned receptors must be compared to access the e-vector orientation or color as we have already seen in Section 1.06.4.1.

The eyes of insects are inherently sensitive to polarized light because rhodopsin, the photoreceptor molecule, is orientated parallel in the microvillar membranes. Therefore light with an e-vector parallel to the microvillus axis is absorbed maximally (Israelachvili, J. N. and Wilson, M., 1976). Many insect species possess a small polarization-sensitive DRA used for detecting the direction of polarization. In the DRA, each ommatidium contains two polarization-sensitive photoreceptors with microvilli oriented orthogonal to each other (Labhart, T. and Meyer, E. P., 1999; Homberg, U. and Paech, A., 2002, Figure 18(b)). The ommatidia in the DRA exhibit several specific adaptations aiding polarization vision. In each ommatidium the photoreceptors come in two sets with microvilli oriented at roughly 90° to each other, thus being sensitive to mutually orthogonal e-vectors and subserving polarization antagonism. Also the microvilli are well aligned enhancing polarization sensitivity. In many insects the receptive field size of the ommatidia in the DRA is increased and the DRA is mainly directed upward and contralaterally (Labhart, T. and Meyer, E. P., 1999).

In the remaining eye the microvillar orientation along the rhabdomer is misaligned. This reduces or completely abolishes polarization vision and results in better brightness and color vision, because it maximizes the capture of photons. The main problem for color vision caused by sensitivity to polarized light, the false color problem (Wehner, R. and Bernard, G. D., 1993; Kelber, A., 1999b), is discussed by Vorobyev in the chapter Color in Invertebrate Vision. Takemura S. Y. and Arikava K. (2006) found that swallowtails might use a different strategy to reduce or even completely remove polarization sensitivity. In this species the R5–R8 photoreceptors that express identical spectral sensitivity are interconnected in each ommatidia; the authors discuss this as a possible way of removing polarization sensitivity.

Thus it seems as if insects trade off polarization vision and quality of color and brightness vision by compartmentalization of the eye, using one small region, the DRA, for the specialized task of navigation by polarized light. Similarly in lycosid spiders, only the most ventral part of the prinicipal eyes contains two types of photoreceptors that have mutually orthogonal microvilli and a gnaphosid spider has at least one pair of secondary eyes that can be used for polarization vision (Dake, M. *et al.*, 1999; 2001).

Polarization vision itself is monochromatic. The polarization sensors in the DRA are all of the same spectral type but might be sensitive to a different wavelength in different species. For example, the polarization sensors in honeybees (Labhart, T., 1980), desert ants (Duelli, P. and Wehner, R., 1973; Labhart, T., 1986), flies (Hardie, R. C., 1984; von Philipsborn, A. and Labhart, T., 1990), and monarch butterflies (Sauman, I. *et al.*, 2005) are UV receptors. In crickets and locusts, polarization vision is mediated by blue receptors (Labhart, T. *et al.*, 1984; Herzman, D. and Labhart, T., 1989; Eggers, A. and Gewecke, M., 1993), and the DRA in cockchafers is dominated by green receptors (Labhart, T., *et al.*, 1992). This wavelength specificity of polarization vision renders the polarization vision system insensitive to changes in the spectral composition of the stimulus.

1.06.4.2.3 Two theoretical models of e-vector detection

Kirschfeld K. (1972) outlined two theoretical ways to determine the e-vector orientation. A single receptor must be able to rotate so that its microvilli would be in different orientations to the stimulus. The receptor would be maximally stimulated when it would be orientated parallel to the e-vector orientation and minimally stimulated when it would be orthogonal. The output would then be a sinusoidal modulation with a maximum for the orientation in which the microvilli are perfectly aligned with the e-vector. The only invertebrate species that could in principle use this method would be stomadopods, because they can rotated their eyes in the required manner (Land, M. F. *et al.*, 1990). The second possible way for e-vector detection would be to use several

receptors all of which exhibit a different e-vector tuning and to compare their outputs. This method requires that (1) at least three receptors of the same spectral type but with different e-vector orientation tuning would be combined and (2) all the photoreceptors involved in the task are aligned in a common reference system. None of these requirements is fulfilled in the polarization-sensitive regions of insects. Thus, both theoretical methods of e-vector detection can be rejected.

1.06.4.2.4 Neuronal mechanisms

The physiological properties of polarization-sensitive neurons have been studied using intracellular recordings in crickets and locusts, with some additional studies in desert ants and cockroaches. Recordings were performed either in the medulla of the optic lobes (cricket: Labhart, T., 1988; Labhart, T. *et al.*, 2001; Labhart, T. and Meyer, E. P., 2002) or at the level of the anterior optic tubercle and the CC (locust: Vitzthum, H. *et al.*, 2002; Pfeiffer, K. and Homberg, U., 2003). All polarization-sensitive interneurons (POL) neurons reported so far respond with tonic spiking activity when illuminated with polarized light. Two different response types of POL neurons have been found: polarization-opponent POL neurons and nonopponent POL neurons. Optic lobe neurons in locusts and cockroaches are nonopponent POL neurons. They are maximally excited by a particular and preferred e-vector and do not respond to e-vectors that are perpendicular to their individual preferred e-vector orientation. But they do not show polarization opponency and are sensitive to changes in light intensity (Homberg, U. and Wuerden, S., 1997; Loesel, R. and Homberg, U., 2001).

Polarization-opponent responses are encountered in optic lobe neurons in ants (Labhart, T. 2000), POL1 neurons in the cricket (Labhart, T. 1988; Labhart, T. and Petzold, J., 1993), and CC neurons in the locust (Vitzthum, H. *et al.*, 2002). The polarization-opponent responses correspond to the orientation of the two e-vector analyzers in each ommatidium. These analyzers are arranged perpendicular to each other and provide the antagonistic excitatory and inhibitory input to the next level of interneurons.

The POL1 neuron of the cricket is the best-studied example of this type. These neurons show sinusoidal spiking activity changes, which are induced by changes in the e-vector orientation and by including excitatory and inhibitory components (Figure 18(c)). The polarization-antagonism in these cells generates a differential signal. This enhances the e-vector contrast and at the same time renders the cells insensitive to changes in the variation of absolute light levels, to unpolarized light, and to chromatic contrast (Labhart, T. 1988; 1996; Labhart, T. and Petzold, J., 1993). Three physiologically different but anatomically identical bilateral pairs of POL1 neurons in the cricket medulla have been characterized. Their tuning differs according to the preferred e-vector orientation relative to the longitudinal body axis of the animal (Labhart, T. and Meyer, E. P., 2002; rev.: Wehner, R. and Labhart, T., 2006).

In the locust, most recordings focused on neurons in the lower unit of the anterior optic tubercle and the lower division of the CC (Vitzthum, H. *et al.*, 2002; Pfeiffer, K. and Homberg, U., 2003). These locust midbrain neurons differ in their physiological properties from polarization-sensitive POL1 neurons in the optic lobes of crickets. Locust midbrain neurons show polarization opponency but also respond to unpolarized light. The second difference regards the visual field of the locust midbrain neurons. Some of these cells not only receive binocular input, which is never seen in cricket POL1 neurons, but they can also have much larger receptive fields. Lastly the locust midbrain neurons respond to a continuum of e-vector orientations and cannot be classified into distinct physiological classes (rev.: Homberg, U., 2004). Recently Heinze S. and Homberg U. (2007) showed that polarization-sensitive tangential neurons, TB1 neurons, which were recorded in the PB, have arborizations in a single column in each hemisphere of the PB. The PB has eight columns in the left hemisphere L1–L8 and eight columns in the right hemisphere R1–R8. The TB1 arborizations in the left and the right hemisphere are always eight columns apart, for example, R1/L8 or R2/L7. Intracellular recordings showed that the pattern of columns with branching corresponded to the physiological properties of the cells. Each TB1 neuron showed polarization opponency and their e-vector tuning revealed a linear relation to the position of their arborizations. The range of tuning maxima corresponds to the whole range of e-vector orientations that are possible under natural conditions. This means that the TB1 neurons establish an e-vector map in the PB.

In addition, recordings were made from three columnar cell types that are potentially postsynaptic to the TB1 cells. They are, like the TB1 cells, polarization-sensitive and also reveal a spatial map of e-vector tuning albeit shifted to the TB1 map. This

spatial representation of the e-vector shows an extraordinary level of organization. It should allow the locust to compute its head orientation as long as the animal can distinguish the solar from the antisolar hemisphere of the sky. These neurons provide information about the sun's azimuth and therefore are similar to an internal 180° compass.

Over the day the polarization pattern in the sky is changing. So how do insects adjust for this time-dependent change? This is one of the main problems that still needs to be addressed for understanding the use of polarization vision. Some experimental data suggest that the CC and a specific part of the medulla, the accessory medulla, might play a central role in this timing issue (Homberg, U., 2004).

1.06.5 Ocelli – Visual Information Processing on the Fast Track

Besides the compound eye, many flying insects employ a second visual system, the ocelli, contributing to the inner-loop control of gaze and flight stabilization. In fact it was already noted very early that among insects there is a high degree of correlation between bearing wings and possessing an ocellar system (Kalmus, H., 1945). Due to their design in terms of optics, signal integration, and conductance velocity, the ocelli work faster than the compound eyes and thus cover a higher dynamic range of attitude changes. In that respect they complement the inner-loop-related functions of those pathways receiving input from the compound eyes. In the early 1980s, Goodman L. J. (1981) provided a comprehensive review on the structure and the function of ocellar systems in several insect species. Although most research on the ocellar system so far has been done in orthoptera, recent developments on the convergent processing of ocellar signals and compound-eye-mediated information came from studies in flies.

1.06.5.1 Ocelli in Flies

The ocelli in flies are a set of three small single-lens eyes, which seem to be well adapted to detect rotations in the manner of an artificial horizon (Wilson, M., 1978a; Taylor, C. P., 1981a; 1981b; Schuppe, H. and Hengstenberg, R., 1993; Stange, G. *et al.*, 2002). The retina of each ocellus is attached to the rear surface of the lens resulting in a highly blurred image at the level of the photoreceptors, which is composed only of low spatial frequencies. There is no evidence that the ocelli make use of any remaining image structure but only integrate light levels across their entire visual fields with the exception of the ocelli in dragonflies (Berry, R. *et al.*, 2006).

The anatomy of the fly ocellar system has been described in quite some detail (Nässel, D. R. and Hagberg, M., 1985). Attached to the retinae of the ocelli is a fused first-order neuropil from where three different types of interneurons project through the ocellar nerve to various areas in the brain and to the thoracic ganglia. The blowfly *Calliphora* has got 12 large inteneurons, L-neurons, which are particularly conspicuous because of their enormous axon diameter. The interneurons of the second type, 10 M-neurons, have intermediate axon diameters and the third type consists of a greater number of S-neurons having small axon diameters. L-neurons project to the posterior slope of the lateral protocerebrum where the axons of output LPTCs terminate (see Section 1.06.3.1.3.(i)). M-neurons dispatch information to many areas including the pro- and mesothoracic ganglia, the lateral protocerebrum, the lobula, and to the ventral medulla. The latter projection is interesting since columnar elements in the ventral medulla mediate information from the ventral visual field where brightness levels are not very high compared to those the ocelli face dorsally. S-neurons project to regions in the posterior slope also receiving input from antennal mechanosensory fibers (Nässel, D. R. *et al.*, 1984), which were implied in measuring air speed (Burkhardt, D. and Schneider, G., 1957).

1.06.5.2 The Functional Role of the Ocelli

Ocelli are particularly effective in sensing rotations of the animal, crucial for proper gaze stabilization (dragonflies: Stange, G. and Howard, J. 1979; Stange, G. 1981; locusts: Taylor, C. P., 1981a; 1981b). Behavioral experiments in flies show the ocelli to contribute only to gaze stabilization (Schuppe, H. and Hengstenberg, R., 1993; rev.: Hengstenberg, R., 1993) but anatomical evidence in combination with electrophysiological findings suggests them to also support the fly's attitude control (see below).

Compared to the neural processing performed on compound eye input in the context of directional motion analysis (rev.: Reichardt, W., 1987; Borst, A. and Egelhaaf, M., 1993), wiring up an ocellar-based rotation detector would be relatively straightforward. L-neurons integrate the outputs of ocellar

photoreceptors and code light intensity fluctuations in terms of graded membrane potential changes (Wilson, M., 1978b; Simmons, P. J. *et al.*, 1993; Simmons, P. J., 1999). Although the exact neural mechanism is unknown yet, directly comparing the outputs of L-neurons would be sufficient to build a rotation detector. The diameter of L-neuron axons, the largest in the fly nervous system (Nässel, D. R. and Hagberg, M., 1985; Simmons, P. J. *et al.*, 1993), results in a particularly fast signal propagation. Altogether, the functional adaptations suggested for the ocellar system would facilitate fast motor responses: In the locust, stimulation of the ocelli requires only half the time to elicit compensatory head movements than compound eye stimulation does (Taylor, C. P., 1981a).

Though faster, ocelli-induced motor responses in dragonflies are jerkier compared to responses the compound eye mediates (Taylor, C. P., 1981a), which might as well be a general trend across species. The integration of compound eye and ocellar outputs may establish a system that visually detects rotations by combining high speed with high precision. At which stage and how compound-eye-mediated self-motion information provided by LPTCs (see Section 1.06.3.1.3.(i)) and the ocelli signals may be integrated is by and large unknown.

Anatomical and electrophysiological evidence suggests descending neurons connecting to various motor centers in the thoracic ganglia to be a major stage of multimodal integration (dragonfly: e.g., Olberg, R. M., 1986; Frye, M. A. and Olberg, R. M., 1995; locust: e.g., Burrows, M. and Rowell, C. H. F., 1973; fly: Strausfeld, N. J. and Bassemir, U. K., 1983; Strausfeld, N. J. and Gronenberg, W., 1990). The dendritic input arborizations of fly descending neurons in the lateral protocerebrum overlap with output terminals of both LPTCs and L-neurons (Strausfeld, N. J., 1976; Strausfeld, N. J. and Bassemir, U. K., 1983). This implies information about specific rotations the LPTCs encode (Krapp, H. G. and Hengstenberg, R., 1996; Krapp, H. G. *et al.*, 1998; see Section 1.06.3.1.3.(i)) and ocellar information to converge at the multimodal descending neurons.

1.06.5.3 Two Visual Mechanisms – One Motion Parameter

A recent electrophysiological study shows, however, that the spiking activity in the heterolateral LPTC V1 (rev.: Hausen, K., 1984; Krapp, H. G. and Hengstenberg, R., 1997; Krapp, H. G. *et al.*, 2001) is modulated by ocellar input (Figure 19, Parsons, M. M. *et al.*, 2006). How this sensitivity to ocellar stimulation in the V1 cell is established has not been clarified yet. One possible explanation is based on the fact that descending neurons and the LPTC subgroup of VS cells presynaptic to the V1 cell are connected via mixed chemical/electrical synapses (Strausfeld, N. J., 1976). Ocellar inputs to the descending neurons may change

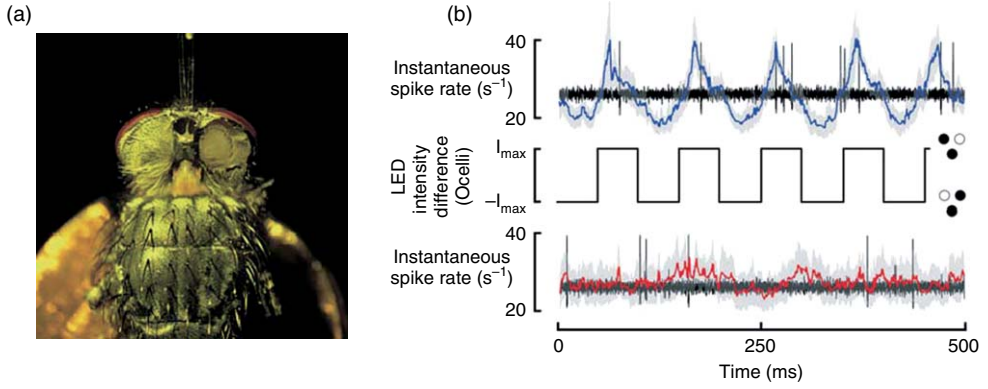

Figure 19 Ocellar-induced activity in lobula plate tangential cells (LPTCs). (a) Photograph taken from the rear of the fly showing the opened head capsule. Through the small hole in the middle the ocellar nerve connecting the ocellar neuropil, dorsal, with the protocerebrum. Through the hole on the right the lobula plate is exposed. (b) The upper panel shows an individual extracellular recording from the spiking V1 cell. Superimposed is the average response (blue line, $n = 563$, gray shaded area: $\pm$SEM) to alternating illumination of the left and right ocellus (middle trace). The ocellar stimulus clearly modulates the activity of the V1 cell. Cauterizing the ocellar nerve abolishes this effect. (red line, bottom panel). For further explanation see text. (a) Photograph courtesy of M. M. Parsons. (b) Adapted from Parsons, M. M., Krapp, H. G., and Laughlin, S. B. 2006. A motion-sensitive neurone responds to signals from the two visual systems of the blowfly, the compound eyes and ocelli. J. Exp. Biol. 209, 4464–4474.

the membrane potential in VS cells through the electrical synapses, which in turn modulate the activity in their postsynaptic target, the V1 cell (Parsons, M. M. *et al.*, 2006).

Such unusual pathway to establish the early convergence of compound eye and ocelli signals at the level of the LPTCs makes sense from the functional point of view: there is evidence from fly neck motor neurons recordings supplying the fly gaze stabilization system that LPTCs encode visual information in coordinates already adapted to the needs of the motor system (e.g., Huston, S. J., 2005; Huston, S. J. and Krapp, H. G., 2003). The impact of the ocellar signals on the LPTC activity could be interpreted as a weighting based on independent information about one and the same parameter: the animal's rotational self-motion. Recent studies show that the gradual modification of V1 cell activity by the ocelli follows a similar dependence on the mimicked rotation axis as the preferred axis tuning of the V1 cell upon wide-field motion stimulation of the compound eye. (Parsons, M. M., personal communication).

Behavioral experiments on the fly gaze stabilization system suggest that the contributions from the compound eye, the ocelli, and the mechanosensory halteres to compensatory head movements are scaled and then linearly combined (Hengstenberg, R., 1991; 1993). As far as the ocellar input is concerned these results were recently supported by an electrophysiological study on the integration properties of an individually identified descending neuron. In simultaneous double recordings it was found that the descending neuron indeed combines ocellar and LPTC signals in a linear way (Haag, J. *et al.*, 2007).

Even though our understanding of the functional organization of the ocellar system is certainly not yet complete the ocelli are a perfect model system to study a fundamental issue in neuroscience, multimodal integration (see Section 1.06.6). An ideal situation would be performing electrophysiological studies in behaving animals where the number of sensory mechanisms controlling distinct behavioral tasks is systematically reduced.

1.06.6 Multisensory Integration and Sensorimotor Transformation

From the previous section we know that visual systems in insects provide a great variety of information to the animals. Depending on the context in which particular aspects of visual information are needed, local signals may be selectively integrated to yield a parameter that can be used to support motor action. To successfully close the action–perception loop, however, nervous systems must solve two fundamental problems:

The first problem concerns the reliability of sensory information. Flies, for instance, when stabilizing their flight need to make sure that the information they have gathered reliably reflects changes in attitude, which require specific inner-loop reflex action. Another example concerns long-range localization of potential food sources – a behavioral trait that requires outer-loop control.

The second fundamental problem they cope with is the transformation of integrated sensory signals into patterns of motor commands, which generate an adequate behavior. In the following two subsections we will outline these problems by presenting a few selected examples and discuss potential strategies nervous systems have adopted to solve them.

1.06.6.1 Vision and Other Sense – Increasing the Reliability of Sensory Information

1.06.6.1.1 Multisensory contributions to inner-loop control

Local sensory signals are highly ambiguous. An activity change in a single photoreceptor could have been caused for many reasons. How the fly disambiguates local signals along its motion vision pathway to finally extract information about its self-motion was discussed in Section 1.06.3.1.3. On their own, however, not even the highly specific signals of the lobula plate tangential neurons LPTCs would be sufficient to guarantee perfect inner-loop attitude and gaze stabilization over the fly's entire flight envelope. Noisy signals as well as noisy processing within the visual system reduce the reliability at which the exact changes in flight attitude may be detected. At this end the evolution of the visual system has designed a couple of measures to overcome the noise problem by, for instance, implementing selective integration of local information, signal adaptation, and employing a population for sensing arbitrary rotations in space. What is the problem then?

The problem is that the fly's combination of possible translations and rotations, its flight envelop, drastically exceeds the dynamic range within which the visual system is able to reliably operate. Angular

velocities even higher than 3000° per second may still result in some responses in the LPTCs but their ability to indicate angular velocity changes and changes of the current rotation axis is greatly reduced in the high dynamic range. Also, the response delay within the directional motion pathway, i.e., the time it takes from onset of a stimulus until the first detectible change in LPTC activity, is greater than 20 ms. Compound-eye-mediated compensatory head movements require 30 ms to be executed. Such time delay might be too long for efficient inner-loop control when dealing with faster attitude changes. The dynamic range imitation is mostly given by the inherent properties of visual information processing, in general. The phototransduction mechanism in the periphery, though producing a high gain, is slow as it involves a cascade of biochemical processes (Chapter Phototransduction in Microvillar Photoreceptors of Drosophila and Other Invertebrates) each of which takes extra time to be completed. On top of it, processing directional motion requires additional time as we mentioned earlier already. As a result the visual system contributes most reliably to inner-loop control in the range of hundreds rather than thousands of degrees per second.

Self-motions at thousands of degrees per second are quicker and more reliably detected by mechanosensory systems. The fast response and sensitivity in mechanosensory systems is due to an immediate transduction mechanism. Physical forces directly open ion channels in a mechanoreceptor cell resulting in its immediate depolarization. In Diptera, during evolution the pair of hind wings, still present in more ancient species such as locusts and dragonflies, has turned into a powerful mechanosensory system, the halteres (Pringle, J. W. S., 1948). These tiny club-like structures move at the same frequency as the wings during flight but 180° out of phase. Halteres basically work like gyroscopes and by measuring Coriolis forces provide the animal with information about angular rotations (Nalbach, G., 1994; Nalbach, G. and Hengstenberg, R., 1994) within a higher dynamic range than LPTCs do. From the functional point of view halteres are equivalent to our vestibular system, which gives us information about fast postural changes and is heavily involved in controlling balance and gaze (e.g., rev.: Carpenter, R. H. S., 1988). Mostly due to the mechanosensory transduction mechanism, they employ both the vestibular system and the haltere system are not sensitive to slow attitude changes. The haltere system in flies performs best on angular rotations of a few thousand degrees per second and contributes strongly to gaze and flight stabilization. It is extremely fast as well. Haltere stimulation induces compensatory head movements within less than 10 ms.

The third sensory system that contributes to inner-loop control is the ocellar system (see Section 1.06.5). Even though depending on phototransduction, due to minimal processing and fast signal transduction the ocellar system has a comparatively short neural response delay of about 15 ms at the LPTCs level (Parsons, M. M. *et al*., 2006). As described in Section 1.06.5 the ocelli contribute to the phasic component of the dorsal light response, a postural reflex, that keeps the visual system aligned with the external horizon. Dorsal light responses are observed in a variety of lower vertebrates (von Buddenbrock, W., 1915; Meyer, D. L. and Bullock, T. H., 1977; rev.: Hengstenberg, R., 1993). This reflex has an additional tonic component, which, in flies, is mediated by the compound eye. The combined dorsal light reflex results in a behavioral output that is maximal for angular rotations at about 500° per second.

Using a behavioral paradigm Hengstenberg and colleagues systematically studied how the output of the different sensory mechanisms cooperate to support compensatory head movements in the fly (rev.: Hengstenberg, R., 1991; 1993). The major contribution of Hengstenberg's research was, firstly, to demonstrate that the dynamic ranges of the different mechanisms complement each other. And secondly, that in the fly the way the outputs from the different systems are combined seems to be surprisingly simple: The overall performance of compensatory head-roll movements is readily explained by the scaled sum of the outputs the different sensory mechanisms provide. (Figure 20, rev.: Hengstenberg, R., 1993). This result was true for both head movements as a function of time and as a function of angular velocity.

At least with respect to gaze stabilization, multisensory integration ensures that the entire dynamic range of attitude changes is covered by complementary sensory mechanisms. Each mechanism on its own has certain bandpass characteristics caused by the intrinsic properties of the respective sensory modality. At low angular velocities where the halteres do not respond above noise level, the ocelli and the compound eye take over. Conversely, the halteres provide reliable angular velocity information in a range too fast to be analyzed by any visual mechanism. Combining sensory mechanisms with overlapping and complementary dynamic ranges also benefits the reliability to detect changes in

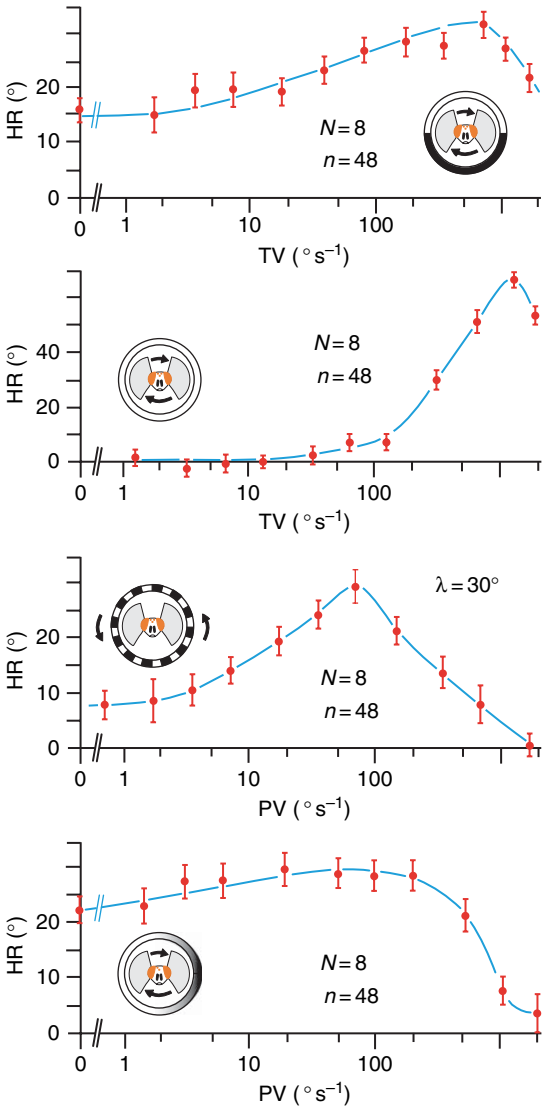

Figure 20 Multisensory integration in the gaze stabilization system of the blowfly. Different sensory systems contribute to compensatory head movements within different dynamic ranges. The head roll angel (HR) is plotted as a function of the angular velocity of the stimulus. In the top panel the total response is shown when the halteres, ocelli, and compound eyes contribute to the response. The second panel shows the haltere-mediated response, which peaks at about 1000° per second but hardly contributes to the low dynamic range. The third panel shows the contribution of directional motion mediated by the compound eye with a peak at about 100° per second. The phasic and tonic components of the dorsal light response, mediated by the ocelli and the compound eye, respectively, cover a wide range from DC stimulation up to stimulus velocities of about 500° per second (bottom panel). The overall performance of compensatory head roll (top panel) is very well explained by simply summing up the scaled outputs of the different sensory systems. TV, thorax velocity; PV, pattern velocity; λ, spatial wavelength of pattern. For further information see text. Redrawn from Hengstenberg, R. 1993. Multisensory Control in Insect Oculomotor Systems. In. Visual Motion and Its Role in the Stabilization of Gaze (*eds*. F.A. Miles and J. Wallman), pp. 5,285–298. Elsevier.

attitude: at whatever angular velocity a change in attitude occurs there will always be at least two independent mechanisms indicating it. This of course increases the reliability with which the magnitude of the change may be estimated.

Possible stages at which signals from the different sensory mechanisms may be integrated we mentioned in some of the previous sections already. In the ventrolateral protocerebrum the terminals of several classes of interneurons converge conveying

information from various sensory systems including the ocelli, the compound eyes, and the antennae (Strausfeld, N. J. and Bassemir, U. K., 1983; rev.: Strausfeld, N. J., 1976). In addition ascending neurons provide signals from the halteres and leg proprioceptors (rev.: Hengstenberg, R., 1991). Strong anatomical evidence suggests that descending neurons and neck motor neurons (NMNs) are among the prime target of multisensory integration. Consequently, descending neurons were found to respond to visual stimuli applied to the compound eyes and the ocelli (Gronenberg, W. and Strausfeld, N. J., 1990; Gronenberg, W. *et al.*, 1995; Haag, J. *et al.*, 2007) as well as mechanical stimulation of the halteres and other mechanoreceptors on the fly body (Gronenberg, W. and Strausfeld, N. J., 1990; Gronenberg, W. *et al.*, 1995). NMNs, which represent the final common pathway of the gaze stabilization system, also reflect multisensory integration. While some NMNs already respond to directional motion in small areas of the fly's visual field (Huston, S. J. and Krapp, H. G., 2003), others require visual wide-field stimulation (Milde, J. J. and Strausfeld, M. J., 1990, Huston, S. J., 2005). Huston S. J. (2005) studied the effect of combined haltere and compound eye stimulation on the response properties of NMNs. Intracellular recordings demonstrated a gating mechanism mediated by the halteres that enables visually induced spiking in NMNs. While visual stimulation alone only resulted in subthreshold excitatory postsynaptic potentials in some motor neurons, spiking was observed only when combined with haltere movements (Huston, S. J., 2005).

The evidence presented seems to be compatible with the common view that descending neurons and motor neurons are the sites of multisensory integration in the fly – most likely in the context of both gaze and flight stabilization. Recent findings suggest, however, that multisensory integration may take place even earlier in the motion vision pathway. Besides the results Parsons M. M. *et al.* (2006) provide on the modulation of the activity level in spiking LPTC V1 induced by ocellar stimulation (see Section 1.06.5) activity changes in the H1 cell upon air puffs delivered to the antennae and mechanical stimulation of the fly's abdomen were also observed (Laughlin, S. B., personal communication, Huston personal communication). In Section 1.06.6.2 we will discuss the potential significance of multisensory integration taking place already at the level of the LPTCs.

One of the next logical steps toward understanding the functional architecture of inner-loop control would be to create a conceptual model of multisensory gaze stabilization. It is still puzzling how several sensory mechanisms each of which operating best in a certain range of angular velocities and kicking in after different response delays manage to control the gaze without generating instabilities. Besides an anatomical description (Strausfeld, N. J., *et al.*, 1987) such model would require detailed knowledge about the dynamic and kinematic properties of the fly neck motor system, which – unfortunately – is not yet available.

1.06.6.1.2 Multisensory contributions to outer-loop control

In the previous section we outlined the significance of multisensory integration in the context of inner-loop control in flies where a fast and reliable response matters. Here we will give an example of how sensory information from different modalities may be combined for a specific outer-loop control task: long-range localization of attractive odor sources.

Recent experiments in freely flying *Drosophila* suggest that there is indeed a tight connection between anemotactic behavior, i.e., flying against with wind, olfaction, and vision. Without an odor presented in a wind tunnel experiment the flies show a trimodal trajectory distribution: a high proportion of trajectories is directed toward the wind but trajectories perpendicular to the wind direction induce two additional modes. The latter components may be explained by searching behavior while the dominant component indicates anemotaxis. Added odor abolishes the searching behavior and results in a focused average flight trajectory toward the odor source (Budick, S. A. and Dickinson, M. H., 2006). These findings imply that the combination of wind and odor facilitates steering maneuvers which keep the fly on a straight trajectory. This interpretation is supported by earlier experiments showing that *Drosophila* does compensate better for wide-field retinal image shifts when simultaneously presented with an attractive odor (Frye, M. A. and Dickinson, M. H., 2004).

These experiments in *Drosophila* demonstrates the importance of multimodal integration and also show that different sensory systems interact with each other to accomplish a goal-oriented behavior. How and where in the nervous system such integration is performed in *Drosophila* is not yet understood, though the involvement of MBs is likely as our next example implies.

1.06.6.2 The Relationship between Sensory Systems and Motor Systems: Strategies of Sensorimotor Transformation

Sensory signals are sampled in local coordinates, which are usually specified by the spatial arrangement and structural properties of the receptor cells. Mechanoreceptors, for instance, have a default activation plane defined by their functional morphology. Similarly, the neurons underlying the computation of directional motion correlate light intensities measured at neighboring ommatidia, which are arranged in the hexagonal lattice of the compound eye (see Section 1.06.3.1.2). Motor systems, however, employ coordinate systems defined by the pulling planes of the muscles. How is information obtained in various sensory coordinate systems transformed so that it is suitable to control movements in motor coordinates. In simple reflexes, for example, the knee jerk reflex, the sensory muscle spindle that measures changes in muscle length, is already aligned with the muscle it activates. In this case the sensorimotor transformation is basically inherent to the anatomical arrangement. Such coalignment was also shown in cases where different modalities use similar measuring axes to sense the same parameter but in complementary dynamic ranges. An example is the coalignment of the vestibular system and the preferred axes of visual neurons analyzing self-motions in pigeons (Wylie, D. R. *et al.*, 1998) and rabbits (Graf, W. *et al.*, 1983). But how the information is then transformed to control the respective motor plants is still unknown.

One possible way of achieving sensorimotor transformations involves an intermediate step that decomposes information encoded in sensory coordinates into independent components, which are then used to control the behavior. In the barn owl, for instance, Masino T. and Knudsen E. I. (1990) found that subsequent to the retinotopic code in the optic tectum and before the activation of the motor neurons, head movements are encoded in orthogonal components. Such an intermediate stage could be the target of different sensory modalities all of which sample information in their own local coordinate systems.

A possible approach to study sensorimotor transformations requires characterising the properties of neural elements at subsequent processing steps throughout a task-specific pathway. In the fly, electrophysiological experiments were performed on motor neurons innervating the animal's neck muscles controlling compensatory head movements (Strausfeld, N. J., *et al.*, 1987). These NMNs receive input from the lobula plate tangential cells (LPTCs) and from other sensory modalities (Milde, J. J., *et al.*, 1987, see Section 1.06.6.1.1). Based on the NMNs' responses to local directional motion their visual receptive fields could be characterized. Like LPTCs such as HS and VS cells, the NMNs show a distribution of local motion preferences and sensitivities that is similar to the structure of particular optic flow fields (Huston, S. J. and Krapp, H. G., 2003; Huston, S. J., 2005). From some recordings close to the neuromuscular junction, even the visual receptive fields of some neck muscles could be reconstructed. From the visual receptive fields the preferred rotation axis of each NMN was estimated as it was done previously for the VS and HS cells. Despite the fact that the NMN receptive fields show generally a higher degree of binocularity than the VS receptive fields do the preferred axis distributions of the two neural populations were correlated (Huston, S. J., 2005).

This finding has remarkable implications for the sensorimotor transformation in the fly gaze stabilization system. The fly seems not to employ an intermediate stage at which sensory information is decomposed into orthogonal components and then sent to the motor neurons as was suggested for the barn owl. Instead, information from the LPTC is merely combined from cells of both parts of the brain to increase the NMNs' specificity for particular self-rotations. Otherwise no obvious coordinate transformation seems to occur. This suggests that the population of output LPTCs already encodes visually derived information in a coordinate system that is closely related to the coordinate system the neck muscles use. Such simplified sensory motor transformation would be fast and – since no additional processing layer is required – also energy-efficient. The actual sensory motor transformation seems to take place already at the level of the LPTCs by selectively integrating local motion signals. The local preferred directions within the receptive fields of both LPTCs and NMNs reflect the organization of the local sensory coordinate system in the motion vision pathway. Their global properties, that is, their preferred self-motion axes, on the other hand, reflect the organization of the motor coordinate system. In particular the gaze stabilization system benefits from this computationally inexpensive conversion between sensory and motor coordinates. The neck motor system deals almost exclusively with rotational degrees of freedom to efficiently support visual processing. Rotation-

specific information that the population of LPTCs provides can therefore be used directly to control the gaze.

Such simplified sensorimotor transformation also makes sense in the context of multisensory integration. Once established a coordinate system compatible to the needs of the motor system can be used to integrate information about the same self-motion parameter but provided by other senses such as the halteres or the ocelli (see Section 1.06.6.1).

1.06.7 Visual Cognition

1.06.7.1 The Traditional View

The traditional way of thinking about arthropod or insect behavior and also the way we structured this chapter is to assume sets of mostly independent sensory–motor circuits, each of which is responsible for one particular task or behavior that the arthropod or insect is performing. For example, the visual flow field that is experienced during flight is used for flight stabilization. The information flow is thought to be mainly from the sensory input units vertically to the motor output sites, with little, if any, crosstalk with other sensory systems or other circuits that are processing information for different sensory–motor tasks. In most cases they are thought to consist of simple circuits of a few neurons or they can even be realized by single identified neurons.

Considering this traditional, widely held, and scientifically very well supported view of invertebrate processing, we should expect rather limited cognitive functions. Invertebrates should possess only specific adaptations to unchanging environmental conditions and behavioral tasks. But a closer inspection of sensory–motor circuits reveals substantial evidence for plasticity and cross talk between different control circuits as we discussed in earlier parts of this chapter. Additionally, invertebrates and insects in particular have adapted to all habitats and are evolutionarily extremely successful (Wilson, M. and Hölldobler, B., 1987). But this can only be explained if the insect brain is able to provide useful and adaptable solutions to a very wide range of ecologically relevant problems.

1.06.7.2 Arguments for Cognitive Functions in Insects

As more and more insects are studied in detail and in their natural habitats it becomes apparent that despite their relatively simple nervous systems, insects display a rich behavioral repertoire. Vision plays a major role in their ability to flexibly process information when adapting to their changing environment. As discussed above, the visual system of insects is characterized by a high temporal, though rather low spatial resolution compared to humans. This allows insects to analyze a variety of visual cues such as motion, color, and polarized light – to name just a few examples – in the context of outer-loop control, which they exploit to navigate, identify landmarks, and to detect mates or prey. But they are also capable of comparing current visual inputs to references previously stored in their memory. Thus, insects not only gather sensory information and use it in a predefined reflex-like way but also assess the information in a given behavioral context before they take appropriate action. In the following we will outline some experimental evidence for higher cognitive functions implemented in the insect brain.

1.06.7.3 Data Supporting Cognitive Functions

Two insect species are at the forefront of studies concerning more complex cognitive function, the fruit fly *Drosophila* and the honeybee. The honeybee can be studied in behavioral paradigms, which are akin to psychophysical tests in primates. They have a high capacity for learning in the context of foraging and navigation. Honeybees can be trained to perform rather complex tasks showing their impressive cognitive capacity. For example, honeybees can interpolate visual cues while navigating (Collett, T. S. and Baron, J., 1995). They can categorize and to a certain degree abstract visual information. This has been shown, for instance, by their ability to perceive and distinguish symmetrical from nonsymmetrical patterns (Giurfa, M., *et al.*, 1996) and by discriminating orientation during pattern recognition (van Hateren, J. H. *et al.*, 1990) or when learning flower-like patterns (Horridge, G. A. and Zhang, S. W., 1994). Bees can form sameness and difference concepts (Giurfa, M., *et al.*, 2001) by learning to solve delayed matching-to-sample tasks and delayed nonmatching-to sample' tasks (Figure 21). Bees exhibit associative recall during navigation (Zhang, S. W. *et al.*, 1999) and can even associate visual with olfactory information (Srinivasan, M. V., *et al.*, 1998). Bees were shown to learn contextual information (Collett, T. S. *et al.*, 1997) and are capable of communicating to their

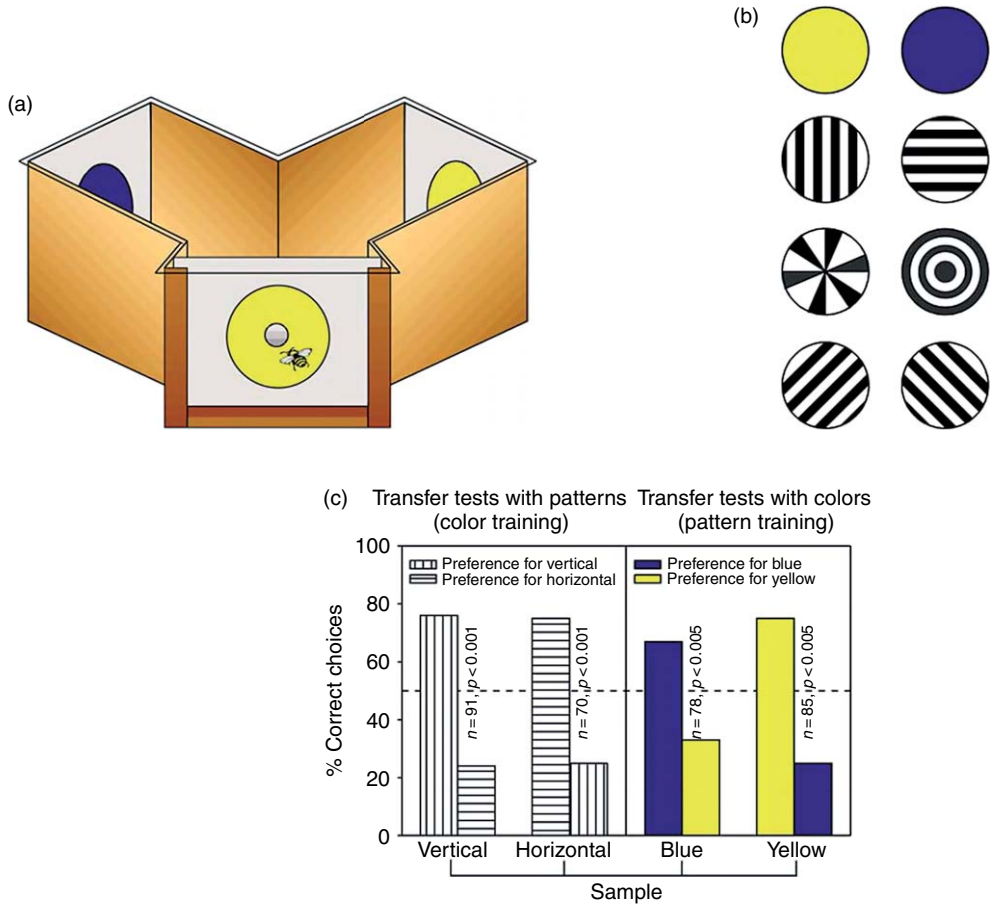

Figure 21 Visual cognition. (a) A y-maze is used for training and testing the bees in a delayed matching-to-sample procedure. This reveals whether bees can build a concept of sameness between stimuli, independent of which stimuli are used. Bees are presented with a sample and then with a set of stimuli including one stimulus that is identical to the sample. During training the bees are rewarded with sucrose solution if they always choose the stimulus that is identical to the sample despite the fact that the sample is regularly changed. The sample is presented at the entrance of the y-maze and the bees have to pass through the maze without being rewarded until they reach the back wall of the maze and choose the identical stimulus to the sample presented at the entrance. (b) Visual stimuli were used for training and testing the bees. In transfer test experiments, the bees were trained with colored disks and then tested with achromatic patterns that were novel to the bees and vice versa. (c) Performance levels of the bees in the transfer tests; the bees solved the problem for both transfer tests. Adapted with permission from Giurfa, M. 2003. Cognitive neuroethology: dissecting non-elemental learning in a honeybee brain. Curr. Opin. Neurobiol. 13, 726–735.

nest mates information about the location of a flower patch they have been visiting (von Frisch, K., 1967).

But honeybees are not alone in showing such capabilities. Fruit flies can perform associate (Wandell, S. and Quinn, W. G., 2001) and novelty learning (Dill, M. and Heisenberg, M., 1995) as well as contextual generalization (Liu, L. *et al.*, 1999). Next to behavioral, physiological, and molecular studies, which can be performed in bees as well, fruit flies permit genetic approaches also. All these techniques can be used to probe how complex cognitive functions are performed in the brain. Two examples for this are discussed here. Liu *et al.* (1999) show that individual flies can generalize their trained response to several other, different environmental contexts, in this case different lighting conditions. These changes in illumination did not affect the performance of the flies and this shows that context generalization guides this insect's learning. But when the authors eliminated the MBs, using three different techniques: (1) an *mbm* mutant lacking MBs, (2) selective pharmacological ablation using the cell poison hydroxyurea during the first larval stage, and (3) reverse genetic ablation by enhancer-driven tetanus toxin, they found that retention of the trained pattern was strictly bound to the context during learning. The

flies did not generalize to other contexts any more. Here the use of molecular techniques allows us to gain insights into the possible neuronal location of context generalization.

In another example the localization and the neuronal footprint of saliency and attention are probed. From behavioral tests it is apparent that insects apply different strategies depending on the salience of, and the attention toward, particular visual cues. Recent work by van Swinderen and Greenspan that combined a physiological and genetical approach gives the first physiological evidence on this cognitive function. They recorded local field potentials (LFPs) in the *Drosophila* brain and were able to show a change in the 20–30 Hz range of the LFP when visual stimuli presented to the fly were made more salient. The saliency levels were changed by combining the visual stimuli with an olfactory stimulus, heat, or through novelty. van Swinderen and Greenspan used saliency-inducing stimuli, which had been found to change the saliency of stimuli in behavioral experiments in *Drosophila* (olfaction: Guo, A. and Götz, K. G., 1997; heat: Wolf, R. and Heisenberg, M. 1991; orientation and shape: Mimura, K., 1982).

Insects are thus very suitable models for studying cognitive functions. They not only fulfill the criteria regarding the behavior complexity, but they are also amenable to quantitative experimental analysis. Most importantly, as apposed to vertebrates, insects lend themselves to molecular, genetical, and physiological studies of cognitive functions because of their well-characterized nervous system.

1.06.8 Conclusions

There is no doubt that over the past couple of years a great step forward has been made in understanding the processing of visual information in invertebrate, namely in insects. Several factors did contribute to this remarkable advance. Most of all it was the possibility to quantitatively describe the performance of specific behavioral tasks followed by a rigid characterization of the underlying neural circuits. Together, and in combination with analytical and numerical modeling, these approaches were tremendously successful in bridging the gap between neural processing and behavioral control. In addition, fundamental constraints were taken into account under which neural information processing takes place. The optimization of neural circuits was put into perspective by considering the cost of information in terms of energy consumption (Laughlin, S. B. *et al.*, 1998). It was also realized that visual information processing in insects is not confined to the laboratory environment but takes place in habitats where natural image statistics play an important role in tuning neural circuits to specific functions (Laughlin, S. B., 2001).

At the same time a promising trend has emerged challenging the traditional boundaries between different areas in neuroscience: General principles in sensory information processing are quantitatively linked more tightly to the kinematic and dynamic properties of the actual motor systems they control (Taylor, G. K. and Thomas, A. L., 2003). It is quite reasonable to assume that the operational constraints at the level of sensory and motor systems influence each other on a phylogenetic as well as on an ontogenetic timescales. Considering such parallel evolution may explain the functional organization of both systems more adequately compared to the classical attempt to understand their specific design principles in isolation.

A comprehensive understanding of visual information processing and its significance for the control of distinct behaviors also requires us to cross border between individual modalities and model systems. Multisensory integration, or – more technically – multisensor fusion, is another example. Studying the contributions that various modalities make toward the control of a specific behavior may help us to identify not only general principles in sensory information processing but also modality-specific adaptations. A similar rational motivates the comparison between the functional organization found in sensory systems of vertebrates and invertebrates.

Closely related to multisensory integration is the question of how visual information – or sensory information in general – is transformed into patterns of motor activity. The transformation was thought to takes place at descending neurons or at the motor neurons, also known as the final common pathway. Obviously, independent of the behavior that is controlled, both multisensory integration and sensorimotor transformation must have been completed at the motor neuron level the latest. In most species descending neurons and motor neurons show – unsurprisingly – highly complex response properties, which make them difficult to study. As a result, the actual transfer functions between sensory and motor neurons are mostly unknown. For the lack of experimental data, many models relate

sensory signals to the motor output only by approximating transfer functions and motor system properties. The predictive power of these models can be remarkably high in terms of explaining a specific behavior even if only one modality was considered to control it. Consequently, the question of how different behavioral tasks are actually coordinated and how they depend on the integration of multimodal information has – quite understandably – not been particularly popular over many years. The focus and the success in studying the neural circuits underlying individual aspects of visually guided behavior allow us now to proceed to the higher integrative systems level.

How are inner-loop reflexes and voluntary outer-loop modifications combined at the neuronal level to guarantee both flight stability and, for instance, a successful chasing flight? Does the insect visual system use efference copies to differentially read out optic flow information that lobula plate tangential cells provide during different flight phases? How is information obtained about different visual qualities and which is processed along separate pathways integrated to decide whether or not a particular flower should be approached? How is the continuous change in sun position compensated for in insects using polarized light patterns for navigation – and how does the polarization vision system modify inner-loop control? And finally – how are prior experience and cognitive aspects integrated to modify the neuronal processes underlying behavioral control?

This list of questions is far from being complete. In any case – how should we approach these questions? Besides further integrative experimental studies to specify, extend, and combine our existing models a test bed will be needed for their validation. The most rigorous test a model could be subjected to would be integrative hardware simulations. Such approach may be realized in a modular way, first testing simple control structures based on just one sensory modality. Then the hardware simulations may be increased in complexity by adding more modalities and the potential of including prior knowledge as well as plastic properties of the control circuits. It would be quite interesting to see what emergent features result as the level of integration is increased. Such system to test functional principles of sensory information processing discovered in insects may as well turn out to become a useful platform to assess the potential of small animals to address big questions in neuroscience.

Acknowledgments

This work was supported by funding from the BBSRC and EOARD to HGK.

References

Aidley, D. J. 1998. The Physiology of Excitable Cells, 4th edn. Cambridge University Press.

Anderson, J. S., Lampl, I., Gillespie, D. C., and Ferster, D. 2000. The contribution of noise to contrast invariance of orientation tuning in cat visual cortex. Science 290, 1968–1972.

Arbib, M. A. and Liaw, J. S. 1995. Sensorimotor transformations in the worlds of frogs and robots. Artif. Intell. 72, 53–79.

Arikawa, K. and Stavenga, D. 1997. Random array of colour filters in the eye of butterflies. J. Exp. Biol. 200, 2501–2506.

Baader, A., Schafer, M., and Rowell, C. H. F. 1992. The perception of the visual flow field by flying locusts – a behavioral and neuronal analysis. J. Exp. Biol. 165, 137–160.

Backhaus, W. 1991. Color opponent coding in the visual system of the honeybee. Vision Res. 31, 1381–1397.

Baldus, K. 1926. Experimentelle Untersuchung ueber die Entfernungslokalisation der Libellen (*Aeschna Cyanea*). J. Comp. Physiol. A 3, 475–505.

Barnett, P. D., Nordstrom, K., and O'Carroll, D. C. 2007. Retinotopic organization of small-field-target-detecting neurons in the insect visual system. Curr. Biol. 17, 1–10.

Barron, J. L., Fleet, D. J., and Beauchemin, S. S. 1994. Performance of optical flow techniques. Int. J. Comp. Vis. 12, 43–77.

Barth, M., Hirsch, H. V., Meinertzhagen, I. A., and Heisenberg, M. 1997. Experience-dependent developmental plasticity in the optic lobe of *Drosophila melanogaster*. J. Neurosci. 17, 1493–1504.

Bauer, T. 1981. Prey capture and structure of visual space of an insect that hunts by sight and on the littel layer (*Notiophilus biguttatus* F., Carabidae, Coleoptera). Behav. Ecol. Sociobiol. 8, 91–97.

Bausenwein, B. and Fischbach, K. F. 1992. Activity labeling patterns in the medulla of *Drosophila melanogaster* caused by motion stimuli. Cell Tissue Res. 270, 25–35.

Bell, C. C. 1989. Sensory coding and corollary discharge effects in mormyrid electric fish. J. Exp. Biol. 146, 229–253.

Bender, J. A. and Dickinson, M. H. 2006. A comparison of visual and haltere-mediated feedback in the control of body saccades in *Drosophila melanogaster*. J. Exp. Biol. 209, 4597–4606.

Bishop, L. G., Keehn, D. G., and McCann, G. D. 1968. Motion detection by interneurons of optic lobes and brain of the flies *Calliphora phaenicia* and *Musca domestica*. J. Neurophysiol. 31, 509–525.

Blanchard, M., Verschure, P. F., and Rind, F. C. 1999. Using a mobile robot to study locust collision avoidance responses. Int. J. Neural Syst. 9, 405–410.

Blondeau, J. and Heisenberg, M. 1982. The 3-dimensional optomotor torque system of *Drosophila-Melanogaster* – studies on wildtype and the mutant optomotor-blind H31. J. Comp. Physiol. 145, 321–329.

Boeddeker, N. and Egelhaaf, M. 2003. Steering a virtual blowfly, simulation of visual pursuit. Proc. Biol. Sci. 270, 1971–1978.

Boeddeker, N. and Egelhaaf, M. 2005. A single control system for smooth and saccade-like pursuit in blowflies. J. Exp. Biol. 208, 1563–1572.

Boeddeker, N., Kern, R., and Egelhaaf, M. 2003. Chasing a dummy target, smooth pursuit and velocity control in male blowflies. Proc. Biol. Sci. 270, 393–399.
Borst, A. and Egelhaaf, M. 1987. Temporal-modulation of luminance adapts time constant of fly movement detectors. Biol. Cybern. 56, 209–215.
Borst, A. and Egelhaaf, M. 1989. Principles of visual motion detection. Trends Neurosci. 12, 297–306.
Borst, A. and Egelhaaf, M. 1993. Detecting Visual Motion, Theory and Models. In: Visual Motion and Its Role in the Stabilization of Gaze. (*eds*. F. A. Miles and J. Wallman), pp. 5, 3–27. Elsevier.
Borst, A. and Haag, J. 1996. The intrinsic electrophysiological characteristics of fly lobula plate tangential cells, I. Passive membrane properties. J. Comput. Neurosci. 3, 313–336.
Borst, A. and Haag, J. 2002. Neural networks in the cockpit of the fly. J. Comp. Physiol. A Neuroethol. Sens. Neural Behav. Physiol. 188, 419–437.
Borst, A., Egelhaaf, M., and Haag, J. 1995. Mechanisms of dendritic integration underlying gain control in fly motion-sensitive interneurons. J. Comput. Neurosci. 2, 5–18.
Borst, A., Reisenman, C., and Haag, J. 2003. Adaptation of response transients in fly motion vision. II. Model studies. Vision Res. 43, 1309–1322.
Brenner, N., Strong, S. P., Koberle, R., Bialek, W., and de Ruyter van Steveninck, R. R. 2000. Synergy in a neural code. Neural Comput. 12, 1531–1552.
Briscoe, A. and Chittka, L. 2001. Insect color vision. Annu. Rev. Entomol. 46, 471–510.
Brotz, T. M. and Borst, A. 1996. Cholinergic and GABAergic receptors on fly tangential cells and their role in visual motion detection. J. Neurophysiol. 76, 1786–1799.
Buchner, E. 1976. Elementary movement detectors in an insect visual-system. Biol. Cybern. 24, 85–101.
Buchner, E. 1984. Behavioural Analysis of Spatial Vision in Insects. In: Photoreception and Vision in Invertebrates (*ed*. M. A. Ali), pp. 561–621. Plenum Press.
Buchner, E., Buchner, S., and Hengstenberg, R. 1979. 2-Deoxy-D-glucose maps movement-specific nervous activity in the second visual ganglion of *Drosophila*. Science 205, 687–688.
von Buddenbrock, W. 1915. Ueber das Vorhandensein des Lichtrueckenreflexes bei Insekten sowie bei dem Krebse Branchipus grubei. Sitz. Ber. Heidelberger Akad. Math. Kl. Abt. 5, 1–10.
Budick, S. A. and Dickinson, M. H. 2006. Free-flight responses of *Drosophila melanogaster* to attractive odors. J. Exp. Biol. 209, 3001–3017.
Bulthoff, H., Little, J., and Poggio, T. 1989. A parallel algorithm for real-time computation of optical flow. Nature 337, 549–555.
Burkhardt, D. and Schneider, G. 1957. Die Antennen von Calliphora als Anzeiger der Fluggeschwindigkeit. Z. Naturforsch. B 12, 139–143.
Burrows, M. 1996. The Neurobiology of an Insect Brain. Oxford University Press.
Burrows, M. and Rowell, C. H. F. 1973. Connections between descending visual interneurons and metathoracic motoneurons in locust. J. Comp. Physiol. 85, 221–234.
Burton, B. G. and Laughlin, S. B. 2003. Neural images of pursuit targets in the photoreceptor arrays of male and female houseflies *Musca domestica*. J. Exp. Biol. 206, 3963–3977.
Burton, B. G., Tatler, B. W., and Laughlin, S. B. 2001. Variations in photoreceptor response dynamics across the fly retina. J. Neurophysiol. 86, 950–960.
Buschbeck, E. K. and Strausfeld, N. J. 1997. The relevance of neural architecture to visual performance, phylogenetic conservation and variation in Dipteran visual systems. J. Comp. Neurol. 383, 282–304.
Camhi, J. M. 1993. Neural mechanisms of behaviour. Curr. Opin. Neurobiol. 3, 1011–1019.
Camhi, J. M. and Levy, A. 1988. Organization of a complex movement, fixed and variable components of the cockroach escape behaviour. J. Comp. Physiol. A 163, 317–328.
Campbell, H. R. 2001. Orientation discrimination independent of retinal matching by blowflies. J. Exp. Biol. 204, 15–23.
Campbell, H. R. and Strausfeld, N. J. 2001. Learned discrimination of pattern orientation in walking flies. J. Exp. Biol. 204, 1–14.
Campenhausen, C. V. 1986. Photoreceptors, lightness constancy and colour vision. Naturwissenschaften 76, 82–83.
Carandini, M. and Ferster, D. 2000. Membrane potential and firing rate in cat primary visual cortex. J. Neurosci. 20, 470–484.
Carpenter, R. H. S. 1988. Movements of the Eyes. Pion Limited.
Chan, W. P., Prete, F., and Dickinson, M. H. 1998. Visual input to the efferent control system of a fly's ''gyroscope''. Science 280, 289–292.
Chandra, B. C. S., Geetha, L., Abraham, V. A., Karnath, P., Thomas, K., *et al.* 1998. Uniform discrimination of pattern orientation by honeybees. Anim. Behav. 56, 1391–1398.
Chittka, L. and Raine, N. I. 2006. Recognition of flowers by pollinators. Curr. Opin. Plant Biol. 9, 428–435.
Chittka, L., Vorobyev, M., Shmida, A., and Menzel, R. 1993. Bee Colour Vision: The Optimal System for the Discrimination of Flower Colours with Three Spectral Photoreceptor Types. In: Advances in Life Sciences; Sensory Systems of Arthropods (*eds*. K. Wiese, *et al.*), pp. 211–218. Birkhäuser.
Clifford, C. W., Ibbotson, M. R., and Langley, K. 1997. An adaptive Reichardt detector model of motion adaptation in insects and mammals. Vis. Neurosci. 14, 741–749.
Collett, T. S. 1978. Peering – locust behavior pattern for obtaining motion parallax information. J. Exp. Biol. 76, 237–241.
Collett, T. S. 1980. Angular tracking and the optomotor response – an analysis of visual reflex interaction in a hoverfly. J. Comp. Physiol. 140, 145–158.
Collett, T. S. 1980. Some operating rules for the optomotor system of a hoverfly during voluntary flight. J. Comp. Physiol. 138, 271–282.
Collett, T. S. and Baron, J. 1995. Learn sensori-motor mappings in honeybees: interpolation and its possible relevance to navigation. J. Comp. Physiol. A 177, 287–298.
Collett, T. S. and Blest, A. D. 1966. Binocular, directionally selective neurones, possibly involved in the optomotor response of insects. Nature 212, 1330–1333.
Collett, T. S. and Land, M. F. 1975a. Visual control of flight behavior in hoverfly, *Syritta-Pipiens* l. J. Comp. Physiol. 99, 1–66.
Collett, T. S. and Land, M. F. 1975b. Visual spatial memory in a hoverfly. J. Comp. Physiol. 100, 59–84.
Collett, T. S. and Land, M. F. 1978. How hoverflies compute interception courses. J. Comp. Physiol. 125, 191–204.
Collett, T. S., Fauria, K., Dale, K., and Baron, J. 1997. Places and patterns a study of context learning in honeybees. J. Comp. Physiol. A 181, 343–353.
Collett, T., Nalbach, H. O., and Wagner, H. 1993. Visual stabilization in arthropods. Rev. Oculomot. Res. 5, 239–263.
Cronin, T. W. and Marshall, N. J. 1989. Multiple spectral classes of photoreceptors in the retinas of gonodactylid stomatopod shrimps. J. Comp. Physiol. A 166, 261–275.
Dacke, M., Doan, T. A., and O'Carroll, D. C. 2001. Polarized light detection in spiders. J. Exp. Biol. 204, 2481–2490.
Dacke, M., Nilsson, D.-E., Warrant, E. J., Blest, A. D., Land, M. F., and O'Carroll, D. C. 1999. Built-in polarizers form part of a compass organ in spiders. Nature 401, 470–473.
Dahmen, H., Franz, M. O., and Krapp, H. G. 2001. Extracting Egomotion from Optic Flow, Limits of Accuracy and Neural Matched Filters. In: Motion Vision. Computational, Neural,

and Ecological Constraints (*eds*. J. M. Zanker and J. Zeil), pp. 143–168. Springer.
DeValois, R. L. and DeValois, K. D. 1997. Neural Coding of Color. In: Readings on Color, (*eds*. A. Byrne and D. R. Hilbert), Vol. 2, pp. 93–140. MIT press.
Dickinson, M. H., Lehmann, F. O., and Sane, S. P. 1999. Wing rotation and the aerodynamic basis of insect flight. Science 284, 1954–1960.
Dill, M. and Heisenberg, M. 1995. Visual pattern memory without shape recognition. Philos. Trans. R. Soc. Lond. B Biol. Sci. 349, 143–152.
Dill, M., Wolf, R., and Heisenberg, M. 1993. Visual pattern recognition in *Drosophila* involves retinotopic matching. Nature 365, 751–753.
Dodge, F. A., Jr. and Rahamimoff, R. 1967. Co-operative action a calcium ions in transmitter release at the neuromuscular junction. J. Physiol. 193, 419–432.
Douglass, J. K. and Strausfeld, N. J. 1995. Visual motion detection circuits in flies, peripheral motion computation by identified small-field retinotopic neurons. J. Neurosci. 15, 5596–5611.
Douglass, J. K. and Strausfeld, N. J. 1996. Visual motion-detection circuits in flies, parallel direction- and non-direction-sensitive pathways between the medulla and lobula plate. J. Neurosci. 16, 4551–4562.
Dror, R. O., O'Carroll, D. C., and Laughlin, S. B. 2001. Accuracy of velocity estimation by Reichardt correlators. J. Opt. Soc. Am. A Opt. Image Sci. Vis. 18, 241–252.
Duelli, P. and Wehner, R. 1973. The spectral sensitivity of polarized light orientation in *Cataglyphis bicolour* (Formicidae, Hymenoptera). J. Comp. Physiol. 86, 37–53.
Duffy, C. J. and Wurtz, R. H. 1991. Sensitivity of MST neurons to optic flow stimuli. II. Mechanisms of response selectivity revealed by small-field stimuli. J. Neurophysiol. 65, 1346–1359.
Durr, V. and Egelhaaf, M. 1999. *In vivo* calcium accumulation in presynaptic and postsynaptic dendrites of visual interneurons. J. Neurophysiol. 82, 3327–3338.
Dyer, A. G. and Neumeyer, C. 2005. Simultaneous and successive colour discrimination in the honeybee (*Apis mellifera*). J. Comp. Physiol. A 191, 547–557.
Egelhaaf, M. 1985a. On the neuronal basis of figure-ground discrimination by relative motion in the visual-system of the fly. 1. Behavioral constraints imposed on the neuronal network and the role of the optomotor system. Biol. Cybern. 52, 123–140.
Egelhaaf, M. 1985b. On the neuronal basis of figure-ground discrimination by relative motion in the visual-system of the fly. 2. Figure-detection cells, a new class of visual interneurones. Biol. Cybern. 52, 195–209.
Egelhaaf, M. 1985c. On the neuronal basis of figure-ground discrimination by relative motion in the visual-system of the fly. 3. Possible input circuitries and behavioral significance of the Fd-cells. Biol. Cybern. 52, 267–280.
Egelhaaf, M. and Borst, A. 1993. A look into the cockpit of the fly, visual orientation, algorithms, and identified neurons. J. Neurosci. 13, 4563–4574.
Egelhaaf, M. and Krapp, H. G. 1999. Local Preferred Directions of Visual Wide Field Neurons and the Compound Eye Geometry of the Blowfly *Calliphora erythrocephala*. In: Göttingen Neurobiology Report, (*eds*. N. Elsner and U. Eysel), Vol.2, p. 440. Thieme.
Egelhaaf, M., Kern, R., Krapp, H. G., Kretzberg, J., Kurtz, R., and Warzecha, A. K. 2002. Neural encoding of behaviourally relevant visual-motion information in the fly. Trends Neurosci. 25, 96–102.
Eggers, A. and Gewecke, M. 1993. The Dorsal Rim Area of the Compound Eye and Polarization Vision in the Desert Locust (*Schistocerca gregaria)*. In: Sensory Systems of Arthropods (*eds*. K. Wiese, F. G. Gribakin, A. V. Popov, and G. Renninger), pp. 101–109. Birkhäuser.
Eggers, A., Preiss, R., and Gewecke, M. 1991. The optomotor yaw response of the desert locust, *Schistocerca-Gregaria*. Physiol. Entomol. 16, 411–418.
Ehmer, B. and Gronenberg, W. 2002. Segregation of visual input to the mushroom bodies in the honeybee (*Apis mellifera)*. J. Comp. Neurol. 451, 362–373.
Ellington, C. P. 1999. The novel aerodynamics of insect flight, applications to micro-air vehicles. J. Exp. Biol. 202, 3439–3448.
Eriksson, E. S. 1980. Movement prallax and distance perception in the grasshopper (*Phaulacridium vittatum* (Sjoestedt)). J. Exp. Biol. 86, 337–340.
Esch, H. E., Zhang, S., Srinivasan, M. V., and Tautz, J. 2001. Honeybee dances communicate distances measured by optic flow. Nature 411, 581–583.
Fairhall, A. L., Lewen, G. D., Bialek, W., and de Ruyter van Steveninck, R. R. 2001. Efficiency and ambiguity in an adaptive neural code. Nature 412, 787–792.
Farina, W. M., Varju, D., and Zhou, Y. 1994. The regulation of distance to dummy flowers during hovering flight in the hawk moth *Macroglossum stellatarum*. J. Comp. Physiol. A – Sens. Neural Behav. Physiol. 174, 239–247.
Farrow, K., Borst, A., and Haag, J. 2005. Sharing receptive fields with your neighbors, tuning the vertical system cells to wide field motion. J. Neurosci. 25, 3985–3993.
Farrow, K., Haag, J., and Borst, A. 2006. Nonlinear, binocular interactions underlying flow field selectivity of a motion-sensitive neuron. Nat. Neurosci. 9, 1312–1320.
Fischbach, K. F. and Dittrich, A. P. M. 1989. The optic lobe of *Drosophila melanogaster.* I. A golgi analysis of wild-type structure. Cell Tissue Res. 258, 441–475.
Fischer, H., Kautz, H., and Kutsch, W. 1996. A radiotelemetric 2-channel unit for transmission of muscle potentials during free flight of the desert locust, *Schistocerca gregaria*. J. Neurosci. Methods 64, 39–45.
Fotowat, H. and Gabbiani, F. Relation between the phases of sensory and motor activity during a looming-evoked multi-stage escape behavior. J. Neurosci.
Franceschini, N., Kirschfeld, K., and Minke, B. 1981. Fluorescence of photoreceptor cells observed in vivo. Science 213, 1264–1267.
Franz, M. O. and Krapp, H. G. 2000. Wide-field, motion-sensitive neurons and matched filters for optic flow fields. Biol. Cybern. 83, 185–197.
von Frisch, K. 1914. Der Farbensinn und Formensinn der Biene. Zoologische Jahrbuecher. Abteilung fuer allgemeine Zoologie und Physiologie der Tiere. 35, 1–188.
von Frisch, K. 1967. The Dance Language and Orientation of Bees. Harvard University Press.
Frye, M. A. and Dickinson, M. H. 2004. Motor output reflects the linear superposition of visual and olfactory inputs in *Drosophila*. J. Exp. Biol. 207, 123–131.
Frye, M. A. and Olberg, R. M. 1995. Visual receptive-field properties of feature detecting neurons in the dragonfly. J. Comp. Physiol. A Sens. Neural Behav. Physiol. 177, 569–576.
Frye, M. A., Tarsitano, M., and Dickinson, M. H. 2003. Odor localization requires visual feedback during free flight in *Drosophila melanogaster*. J. Exp. Biol. 206, 843–855.
Fulton, J. F. 1943. Physiology of the Nervous System. Oxford University Press.
Gabbiani, F. and Krapp, H. G. 2006. Spike-frequency adaptation and intrinsic properties of an identified, looming-sensitive neuron. J. Neurophysiol. 96, 2951–2962.
Gabbiani, F., Cohen, I., and Laurent, G. 2005. Time-dependent activation of feed-forward inhibition in a looming-sensitive neuron. J. Neurophysiol. 94, 2150–2161.

Gabbiani, F., Krapp, H. G., Hatsopoulos, N., Mo, C. H., Koch, C., and Laurent, G. 2004. Multiplication and stimulus invariance in a looming-sensitive neuron. J. Physiol. (Paris) 98, 19–34.

Gabbiani, F., Krapp, H. G., Koch, C., and Laurent, G. 2002. Multiplicative computation in a visual neuron sensitive to looming. Nature 420, 320–324.

Gabbiani, F., Krapp, H. G., and Laurent, G. 1999. Computation of object approach by a wide-field, motion-sensitive neuron. J. Neurosci. 19, 1122–1141.

Gabbiani, F., Mo, C., and Laurent, G. 2001. Invariance of angular threshold computation in a wide-field looming-sensitive neuron. J. Neurosci. 21, 314–329.

Gauck, V. and Borst, A. 1999. Spatial response properties of contralateral inhibited lobula plate tangential cells in the fly visual system. J. Comp. Neurol. 406, 51–71.

Gauck, V., Egelhaaf, M., and Borst, A. 1997. Synapse distribution on VCH, an inhibitory, motion-sensitive interneuron in the fly visual system. J. Comp. Neurol. 381, 489–499.

Geiger, G. and Nässel, D. R. 1981. Visual orientation behaviour of flies after selective laser beam ablation of interneurones. Nature 293, 398–399.

Gewecke, M., Kirschfeld, K., and Feiler, R. 1990. Identification of optic lobe neurons of locusts by video films. Biol. Cybern. 63, 411–420.

Gibson, J. J. 1950. The Perception of the Visual World. Houghton Mifflin.

Gibson, J. J. 1958. Visually controlled locomotion and visual orientation in animals. Br. J. Psychol. 49, 182–194.

Gilbert, C. 1997. Visual control of cursorial prey pursuit by tiger beetles (Cicindelidae). J. Comp. Physiol. A Sens. Neural Behav. Physiol. 181, 217–230.

Gilbert, C. and Strausfeld, N. J. 1991. The functional organization of male-specific visual neurons in flies. J. Comp. Physiol. A 169, 395–411.

Gilbert, C., Gronenberg, W., and Strausfeld, N. J. 1995. Oculomotor control in calliphorid flies, head movements during activation and inhibition of neck motor neurons corroborate neuroanatomical predictions. J. Comp. Neurol. 361, 285–297.

Giurfa, M. 2003. Cognitive neuroethology: dissecting non-elemental learning in a honeybee brain. Curr. Opin. Neurobiol. 13, 726–735.

Giurfa, M., Eichmann, B., and Menzel, R. 1996. Symmetry perception in an insect. Nature 382, 458–461.

Giurfa, M., Nunez, J., Chittka, L., and Menzel, R. 1995. Colour preferences of flower-naïve honeybees. J. Comp. Physiol. 177, 247–259.

Giurfa, M., Zhang, S., Jenett, A., Menzel, R., and Srinivasan, M. V. 2001. The concepts of 'sameness' and 'difference' in an insect. Nature 410, 930–933.

Goodman, L. J. 1981. The organization and physiology of the insect ocellar system. In: Invertebrate visual centres and behaviour II., VII/6C (*ed*. H. Autrum), pp. 201–286. Springer Verlag.

Götz, K. G. 1975. The optomotor equilibrium of the *Drosophila* navigation system. J. Comp. Physiol. A 99, 187–210.

Graf, W., McCrea, R. A., and Baker, R. 1983. Morphology of posterior canal related secondary vestibular neurons in rabbit and cat. Exp. Brain Res. 52, 125–138.

Gray, J. R. 2005. Habituated visual neurons in locusts remain sensitive to novel looming objects. J. Exp. Biol. 208, 2515–2532.

Gray, J. R., Lee, J. K., and Robertson, R. M. 2001. Activity of descending contralateral movement detector neurons and collision avoidance behaviour in response to head-on visual stimuli in locusts. J. Comp. Physiol. A 187, 115–129.

Graziano, M. S., Yap, G. S., and Gross, C. G. 1994. Coding of visual space by premotor neurons. Science 266, 1054–1057.

Gronenberg, W. and Strausfeld, N. J. 1990. Descending neurons supplying the neck and flight motor of Diptera, physiological and anatomical characteristics. J. Comp. Neurol. 302, 973–991.

Gronenberg, W. and Strausfeld, N. J. 1991. Descending pathways connecting the male-specific visual system of flies to the neck and flight motor. J. Comp. Physiol. A 169, 413–426.

Gronenberg, W., Milde, J. J., and Strausfeld, N. J. 1995. Oculomotor control in calliphorid flies, organization of descending neurons to neck motor neurons responding to visual stimuli. J. Comp. Neurol. 361, 267–284.

Guest, B. B. and Gray, J. R. 2006. Responses of a looming-sensitive neuron to compound and paired object approaches. J. Neurophysiol. 95, 1428–1441.

Guo, A. and Götz, K. G. 1997. Association of visual objects and olfactory cues in *Drosophila*. Learn. Mem. 4, 192.

Haag, J. and Borst, A. 2001. Recurrent network interactions underlying flow-field selectivity of visual interneurons. J. Neurosci. 21, 5685–5692.

Haag, J. and Borst, A. 2002. Dendro-dendritic interactions between motion-sensitive large-field neurons in the fly. J. Neurosci. 22, 3227–3233.

Haag, J. and Borst, A. 2003. Orientation tuning of motion-sensitive neurons shaped by vertical-horizontal network interactions. J. Comp. Physiol. A Neuroethol. Sens. Neural Behav. Physiol 189, 363–370.

Haag, J. and Borst, J. 1996. Amplification of high-frequency synaptic inputs by active dendritic membrane processes. Nature 379, 639–641.

Haag, J. and Borst, A. 2004. Neural mechanism underlying complex receptive field properties of motion-sensitive interneurons. Nat. Neurosci. 7, 628–634.

Haag, J., Egelhaaf, M., and Borst, A. 1992. Dendritic integration of motion information in visual interneurons of the blowfly. Neurosci. Lett. 140, 173–176.

Haag, J., Vermeulen, A., and Borst, A. 1999. The intrinsic electrophysiological characteristics of fly lobula plate tangential cells. III. Visual response properties. J. Comput. Neurosci. 7, 213–234.

Haag, J., Wertz, A., and Borst, A. 2007. Integration of lobula plate output signals by DNOVS1, an identified premotor descending neuron. J. Neurosci. 27, 1992–2000.

Hardie, R. C. 1983. Projection and connectivity of sex-specific photoreceptors in the compound eye of the male housefly (*Musca domestica)*. Cell Tissue Res. 233, 1–21.

Hardie, R. C. 1984. Properties of photoreceptors R7 and R8 in dorsal marginal ommatidia in the compound eyes of *Musca* and *Calliphora*. J. Comp. Physiol. A 154, 157–165.

Harris, R. A., O'Carroll, D. C., and Laughlin, S. B. 1999. Adaptation and the temporal delay filter of fly motion detectors. Vision Res. 39, 2603–2613.

Harris, R. A., O'Carroll, D. C., and Laughlin, S. B. 2000. Contrast gain reduction in fly motion adaptation. Neuron 28, 595–606.

Hartline, H. K., Wagner, H. G., and Ratliff, F. 1956. Inhibition in the eye of *Limulus*. J. Gen. Physiol. 39, 651–673.

Hassenstein, B. and Reichardt, W. 1953. Der Schluss von Reiz-Reaktions-Funktionen auf System-Strukturen. Z. Naturforsch. B 8, 518–524.

van Hateren, J. H. 1989. Photoreceptors, Optics, Theory, and Practics. In: Facets of Vision (*eds*. D. G. Stavenga and R. C. Hardie), pp. 74–89. Springer.

van Hateren, J. H. and Schilstra, C. 1999. Blowfly flight and optic flow. II. Head movements during flight. J. Exp. Biol. 202, 1491–1500.

van Hateren, J. H., Kern, R., Schwerdtfeger, G., and Egelhaaf, M. 2005. Function and coding in the blowfly H1 neuron during naturalistic optic flow. J. Neurosci. 25, 4343–4352.

van Hateren, J. H., Srinivasan, M. V., and Wait, P. B. 1990. Pattern recognition in bees: orientation discrimination. J. Comp. Physiol. A 167, 649–654.

Hatsopoulos, N., Gabbiani, F., and Laurent, G. 1995. Elementary computation of object approach by wide-field visual neuron. Science 270, 1000–1003.

Hausen, K. 1976. Functional characterization and anatomical identification of motion sensitive neurons in the lobula plate of the blowfly *Calliphora erythrocephala*. Z. Naturforsch. C 31, 629–633.

Hausen, K. 1982. Motion sensitive interneurons in the optomotor system of the fly. 1. The horizontal cells – structure and signals. Biol. Cybern. 45, 143–156.

Hausen, K. 1984. The Lobula-Complex of the Fly, Structure, Function and Significance in Visual Behaviour. In: Photoreception and Vision in Invertebrates (*ed*. M. A. Ali), pp. 523–559. Plenum Press.

Hausen, K. 1993. Decoding of Retinal Image Flow in Insects. In: Visual Motion and Its Role in the Stabilization of Gaze, 5 (*eds*. F. A. Miles and J. Wallman), pp. 203–235. Elsevier.

Hausen, K. and Egelhaaf, M. 1989. Neural Mechanisms of Visual Course Control in Insects. In: Facets of Vision (*eds*. R. C. Hardie and D. G. Stavenga), pp. 391–424. Springer.

Hausen, K. and Strausfeld, N. J. 1980. Sexually dimorphic interneuron arrangements in the fly visual-system. Proc. R. Soc. Lond. Ser. B Biol. Sci. 208, 57–71.

Hausen, K. and Wehrhahn, C. 1983. Microsurgical lesion of horizontal cells changes optomotor yaw responses in the blowfly *Calliphora erythrocephala*. Proc. R. Soc. Lond. Ser. B Biol. Sci. 219, 211–216.

Heeger, D. J., Simoncelli, E. P., and Movshon, J. A. 1996. Computational models of cortical visual processing. Proc. Natl. Acad. Sci. U. S. A. 93, 623–627.

Heinze, S. and Homberg, U. 2007. Maplike representation of celestrial e-vector orientations in the brain of an insect. Science 315, 995–997.

Heisenberg, M. and Wolf, R. 1993. The Sensory-Motor Link in Motion-Dependent Flight Control of Flies. In: Visual Motion and Its Role in the Stabilization of Gaze (*eds*. F. A. Miles and J. Wallman), pp. 5,265–283. Elsevier.

Heisenberg, M., Wonneberger, R., and Wolf, R. 1978. Optomotor-Blindh31 – *Drosophila* mutant of lobula plate giant neurons. J. Comp. Physiol. 124, 287–296.

Heitwerth, J., Kern, R., van Hateren, J. H., and Egelhaaf, M. 2005. Motion adaptation leads to parsimonious encoding of natural optic flow by blowfly motion vision system. J. Neurophysiol. 94, 1761–1769.

von Helversen, O. 1972. Zur spektralen Unterschiedsempfindlichkeit der Honigbiene. J. Comp. Physiol. 80, 439–472.

Hengstenberg, R. 1977. Spike responses of 'non-spiking' visual interneurone. Nature 270, 338–340.

Hengstenberg, R. 1982. Common visual response properties of giant vertical cells in the lobula plate of the blowfly *Calliphora*. J. Comp. Physiol. 149, 179–193.

Hengstenberg, R. 1991. Gaze control in the blowfly *Calliphora* – a multisensory two-stage integration process. Neuroscience 3, 19–29.

Hengstenberg, R. 1991. Stabilizing head movements in the blowfly *Calliphora*. Zool. Jahr. Abt. Allg. Zool. Physiol. Tiere 95, 297–304.

Hengstenberg, R. 1993. Multisensory Control in Insect Oculomotor Systems. In: Visual Motion and Its Role in the Stabilization of Gaze (*eds*. F. A. Miles and J. Wallman), pp. 5,285–298. Elsevier.

Hengstenberg, R. 1995. Gain Differences of Gaze-Stabilizing Head Movements, Elicited by Wide-Field Pattern Motion, Demonstrate in Wildtype and Mutant *Drosophila*, the Importance of HS-and VS-Neurons in the Third Visual Neuropil for the Control of Turning Behaviour. In: Nervous Systems and Behaviour (*eds*. M. Burrows, T. Matheson, P. L. Newland, and H. Schuppe). Proc. 4th Int. Cong. Neuroethol. p. 264. Thieme.

Hengstenberg, R., Hausen, K., and Hengstenberg, B. 1982. The number and structure of giant vertical cells (Vs) in the lobula plate of the blowfly *Calliphora erythrocephala*. J. Comp. Physiol. 149, 163–177.

Henze, M. J. and Labhart, T. 2006. Haze, Clouds and a Restricted Field of View: Can Crickets Make Use of Their Polarization Compass Under Unfavourable Sky Conditions? Proceedings of the 29th ECVP meeting, St. Petersburg, Russia.

Hertel, H. 1980. Chromatic properties of identified interneurons in the optic lobes of the bee. J.Comp. Physiol. 137, 215–231.

Hertel, H. and Maronde, U. 1987a. Processing of Visual Information in the Honey Bee Brain. In: The Neurobiology and Behavior of Honeybees (*eds*. R. Menzel and A. Mercer), pp. 141–157. Springer Verlag.

Hertel, H. and Maronde, U. 1987b. The physiology and morphology of centrally projecting interneurons in the honey bee brain. J. Exp. Biol. 133, 301–315.

Hertel, H., Schaefer, S., and Maronde, U. 1987. The physiology and morphology of visual commisures in the honeybee brain. J. Exp. Biol. 133, 283–300.

Herzmann, D. and Labhart, T. 1989. Spectral sensitivity and absolute threshold of polarization vision in crickets: a behavioural study. J. Comp. Physiol. A 165, 315–319.

Higgins, C. M. and Pant, V. 2004. An elaborated model of fly small-target tracking. Biol. Cybern. 91, 417–428.

Hodgkin, A. L. and Huxley, A. F. 1952. The dual effect of membrane potential on sodium conductance in the giant axon of *Loligo*. J. Physiol. 116, 497–506.

Holmqvist, M. H. and Srinivasan, M. V. 1991. A visually evoked escape response of the housefly. J. Comp. Physiol. A 169, 451–459.

von Holst, E. and Mittelstaedt, H. 1950. Das Reafferenzprinzip. Wechselwirkungen zwischen Zentralnervensystem und Peripherie. Naturwissenschaften 37, 464–476.

Homberg, U. 2004. In search of the sky compass in the insect brain. Naturwissenschaften 91, 199–208.

Homberg, U. and Paech, A. 2002. Ultrastructure and orientation of ommatidia in the dorsal rim area of the locust compound eye. Arthropod Struct. Dev. 30, 271–280.

Homberg, U. and Wuerden, S. 1997. Movement-sensitive, polarizationsensitive, and light-sensitive neurons of the medulla and accessory medulla of the locust, *Schistocerca gregaria*. J. Comp. Neurol. 386, 329–346.

Homberg, U., Hofer, S., Pfeiffer, K., and Gebhardt, S. 2003. Organization and neural connections of the anterior optic tubercle in the brain of the locust, *Schistocerca gregaria*. J. Comp. Neurol. 462, 415–30.

Hornstein, E. P., O'Carroll, D. C., Anderson, J. C., and Laughlin, S. B. 2000. Sexual dimorphism matches photoreceptor performance to behavioural requirements. Proc. Biol. Sci. 267, 2111–2117.

Horridge, G. A. 1978. The separation of visual axes in apposition compound eyes. Philos. Trans. R. Soc. Lond. B Biol. Sci. 285, 1–59.

Horridge, G. A. and Zhang, S. W. 1994. Pattern vision in honeybees (*Apis mellifera)*: fower-like patterns with no predominant orientation. J. Insect Physiol. 41, 681–688.

Horstmann, W., Egelhaaf, M., and Warzecha, A. K. 2000. Synaptic interactions increase optic flow specificity. Eur. J. Neurosci. 12, 2157–2165.

Horvath, G. and Varju, D. 2004. Polarized Light in Animal Vision: Polarization Patterns in Nature. Springer.

Horvath, G. and Zeil, J. 1996. Kuwait oil lakes as insect traps. Nature 379, 303–304.

Hubel, D. H. and Wiesel, T. N. 1959. Receptive fields of single neurones in the cat's striate cortex. J. Physiol. 148, 574–591.

Hubel, D. and Wiesel, T. N. 1962. Receptive fields, binocular interaction and functional architecture in the cat's visual cortex. J. Physiol 160, 106–154.

Hubel, D. H. and Wiesel, T. N. 1965. Binocular interaction in striate cortex of kittens reared with artificial squint. J. Neurophysiol. 28, 1041–1059.

Huston, S. J. 2005. Neural basis of a visuo-motor transformation in the fly. Ph.D. thesis, University of Cambridge.

Huston, S. J. and Krapp, H. G. 2003. The Visual Receptive Field of a Fly Motor Neuron. In: Göttingen Neurobiology Report 2003 (*eds*. N. Elsner and H. -U. Schnitzler), p. 483. Thieme.

Ibbotson, M. R. 2001. Evidence for velocity-tuned motion-sensitive descending neurons in the honeybee. Proc. Biol. Sci. 268, 2195–2201.

Israelachvili, J. N. and Wilson, M. 1976. Absorption characteristics of oriented photopigments in microvilli. Biol. Cybern. 21, 9–15.

Johnson, A. P., Horseman, B. G., Macauley, M. W. S., and Barnes, W. J. P. 2002. PC-based visual stimuli for behavioural and electrophysiological studies of optic flow field detection. J. Neurosci. Meth. 114, 51–61.

Kalb, J., Egelhaaf, M., and Kurtz, R. 2006. Robust integration of motion information in the fly visual system revealed by single cell photoablation. J. Neurosci. 26, 7898–7906.

Kalmus, H. 1945. Correlations between flight and vision, and particularly between wings and ocelli in insects. Proc. R. Entomol. Soc. Lond. [Biol] A 20, 84–96.

Karmeier, K., Krapp, H. G., and Egelhaaf, M. 2003. Robustness of the tuning of fly visual interneurons to rotatory optic flow. J. Neurophysiol. 90, 1626–1634.

Karmeier, K., Krapp, H. G., and Egelhaaf, M. 2005. Population coding of self-motion, applying bayesian analysis to a population of visual interneurons in the fly. J. Neurophysiol. 94, 2182–2194.

Karmeier, K., Tabor, R., Egelhaaf, M., and Krapp, H. G. 2001. Early visual experience and the receptive-field organization of optic flow processing interneurons in the fly motion pathway. Vis. Neurosci. 18, 1–8.

Kawato, M. 1999. Internal models for motor control and trajectory planning. Curr. Opin. Neurobiol. 9, 718–727.

Kelber, A. 1999a. Ovipositing butterflies use a red receptor to see green. J. Exp. Biol. 202, 2619–2630.

Kelber, A. 1999b. Why ''false colours'' are seen by butterflies. Nature 402, 251.

Kelber, A. 2006. Invertebrate Colour Vision. In: Invertebrate Vision (*eds*. E. Warrant and D. -E. Nilsson), pp. 250–290. Cambridge University Press.

Kelber, A., Balkenius, A., and Warrant, E. 2002. Scotopic colour vision in nocurnal hawkmoths. Nature 419, 922–925.

Kelber, A., Vorobyev, M., and Osorio, D. 2003. Animal colour vision-behavioural tests and physiological concepts. Biol. Rev. 78, 81–118.

Kern, R. and Egelhaaf, M. 2000. Optomotor course control in flies with largely asymmetric visual input. J. Comp. Physiol. A 186, 45–55.

Kern, R., van Hateren, J. H., Michaelis, C., Lindemann, J. P., and Egelhaaf, M. 2005. Function of a fly motion-sensitive neuron matches eye movements during free flight. PLoS Biol. 3, e171.

Kern, R., Lutterklas, M., and Egelhaaf, M. 2000. Neuronal representation of optic flow experienced by unilaterally blinded flies on their mean walking trajectories. J. Comp. Physiol. A 186, 467–479.

Kern, R., Petereit, C., and Egelhaaf, M. 2001. Neural processing of naturalistic optic flow. J. Neurosci. 21, RC139.

Kien, J. 1974. Sensory integration in the locust optomotor system. II. Direction selective neurons in the circumoesophageal connectives and the optic lobe. Vision Res. 14, 1255–1268.

Kien, J. and Menzel, R. 1977a. Chromatic properties of interneurons in the optic lobes of the bee. I. Broad band neurons. J. Comp. Physiol. 113, 17–34.

Kien, J. and Menzel, R. 1977b. Chromatic properties of interneurons in the optic lobes of the bee. II. Narrow band and colour opponent neurons. J. Comp. Physiol. 113, 35–53.

Killmann, F., Gras, H., and Schurmann, F. 1999. Types, numbers and distribution of synapses on the dendritic tree of an identified visual interneuron in the brain of the locust. Cell Tissue Res. 296, 645–665.

Kirschfeld, K. 1967. The projection of the optical environment on the screen of the rhabdomere in the compound eye of the *Musca*. Exp. Brain Res. 3, 248–270.

Kirschfeld, K. 1972. Die notwendige Anzahl von Rezeptoren zur Bestimmung der Richtung des elektrischen Vektors linear polarisierten Lichtes. Z. Naturforsch. 27c, 578–579.

Kirska, G., Horváth, G., and Andrikovics, S. 1998. Why do mayflies lay their eggs en masse on dry asphalt roads? Water-imitating polarized light reflected from asphalt attracts Ephemeroptera. J. Exp. Biol. 201, 2273–2286.

Kitamoto, J., Sakamoto, K., Ozaki, K., Mishina, Y., and Arikawa, K. 1998. Two visual pigments in a single photoreceptor cell: identification and histological localization of three mRNAs encoding visual pigment opsins in the retina of the butterfly *Papilio xuthus*. J. Exp. Biol. 201, 1255–1261.

Koenderink, J. J. and van Doorn, A. J. 1987. Facts on optic flow. Biol. Cybern. 56, 247–254.

Krapp, H. G. 1995. Repräsentation von Eigenbewegungen der Schmeissfliege *Calliphora erythrocephola* in VS-Neuronen des dritten visuellen Neuropils. Ph.D. thesis, Tübingen, University Tübingen.

Krapp, H. G. 2000. Neuronal matched filters for optic flow processing in flying insects. Int. Rev. Neurobiol. 44, 93–120.

Krapp, H. G. and Gabbiani, F. 2005. Spatial distribution of inputs and local receptive field properties of a wide-field, looming sensitive neuron. J. Neurophysiol. 93, 2240–2253.

Krapp, H. G. and Hengstenberg, R. 1996. Estimation of self-motion by optic flow processing in single visual interneurons. Nature 384, 463–466.

Krapp, H. G. and Hengstenberg, R. 1997. A fast stimulus procedure to determine local receptive field properties of motion-sensitive visual interneurons. Vision Res. 37, 225–234.

Krapp, H. G., Hengstenberg, R., and Egelhaaf, M. 2001. Binocular contributions to optic flow processing in the fly visual system. J. Neurophysiol. 85, 724–734.

Krapp, H. G., Hengstenberg, B., and Hengstenberg, R. 1998. Dendritic structure and receptive-field organization of optic flow processing interneurons in the fly. J. Neurophysiol. 79, 1902–1917.

Kühn, A. 1927. Über den Farbensinn der Bienen. Z. vergleichende Physiol. 5, 762–800.

Kurtz, R., Warzecha, A. K., and Egelhaaf, M. 2001. Transfer of visual motion information via graded synapses operates linearly in the natural activity range. J. Neurosci. 21, 6957–6966.

Labhart, T. 1980. Specialized photoreceptors at the dorsal rim of the honeybees compound eye – polarizational and angular sensitivity. J. Comp. Physiol. A. 141, 19–30.

Labhart, T. 1986. The electrophysiology of photoreceptors in different eye regions of the desert ant, Cataglyphis bicolour. J. Comp. Physiol. A. 158, 1–7.

Labhart, T. 1988. Polarization-opponent interneurones in the insect visual system. Nature 331, 435–437.

Labhart, T. 1996. How polarization-sensitive interneurones of crickets perform at low degrees of polarization. J. Exp. Biol. 199, 1467–1475.

Labhart, T. 2000. Polarization-sensitive interneurons in the optic lobe of the desert ant *Cataglyphis bicolor*. Naturwissenschaften 87, 133–136.
Labhart, T., Hodel, B., and Valenzuela, I. 1984. The physiology of the cricket's compound eye with particular reference to the anatomically specialized dorsal rim area. J. Comp. Physiol. A 155, 289–296.
Labhart, T. and Meyer, E. P. 1999. Detectors for polarized skylight in insects: a survey of ommatidial specializations in the dorsal rim area of the compound eye. Microsc. Res. Tech. 47, 368–379.
Labhart, T. and Meyer, E. P. 2002. Neural mechanisms in insect navigation: polarization compass and odometer. Curr. Opin. Neurobiol. 12, 707–714.
Labhart, T., Meyer, E. P., and Schenker, L. 1992. Specialized ommatidia for polarization vision in the compound eye of cockchafers, *Melolontha melolontha* (Coleoptera, Scarabaeidae). Cell Tissue Res. 286, 419–429.
Labhart, T. and Nilsson, D. E. 1995. The dorsal eye of the dragonfly *Sympetrum* – specializations for prey detection against the blue sky. J. Comp. Physiol. A – Sens. Neural Behav. Physiol. 176, 437–453.
Labhart, T. and Petzold, J. 1993. Processing of Polarized Light Information in the Visual System of Crickets. In: Sensory System of Arthropods. (*eds*. K. Wiese, F. Gribakin, A. V. Popov, and G. Renninger), pp. 158–168. Birkhäuser.
Labhart, T., Petzold, J., and Helbling, H. 2001. Spatial integration in polarization-sensitive interneurons of crickets: a survey of evidence, mechanisms and benefits. J. Exp. Biol. 204, 2423–2430.
Land, M. F. 1985. The Morphology and Optics of Spider Eyes. In: Neurobiology of Arachnids (*ed*. F. G. Barth), pp. 53–78. Springer.
Land, M. F. 1990. Direct observation of receptors and images in simple and compound eyes. Vision Res. 30, 1721–34.
Land, M. F. 1993. Chasing and pursuit in the dolichopodid fly *Poecilobothrus nobilitatus*. J. Comp. Physiol. A – Sens. Neural Behav. Physiol. 173, 605–613.
Land, M. F. 1997. Visual acuity in insects. Annu. Rev. Entomol. 42, 147–177.
Land, M. F. and Collett, T. S. 1974. Chasing behaviour of houseflies (*Fannia canicularis*). A description and analysis. J Comp Physiol 89, 331–357.
Land, M. F. and Eckert, H. 1985. Maps of the acute zones of fly eyes. J. Comp. Physiol. A – Sens. Neural Behav. Physiol. 156, 525–538.
Land, M. F. and Nilsson, D. E. 2002. Animal Eyes. Oxford University Press.
Lappe, M. (*ed*.) 2000. Neural Processing of Optic Flow. Academic Press.
Laughlin, S. B. 1976. The sensitivity of dragonfly photoreceptors and the voltage gain of transduction. J. Comp. Physiol. A 111, 221–247.
Laughlin, S. B. 1981. A simple coding procedure enhances a neuron's information capacity. Z. Naturforsch.C 36, 910–920.
Laughlin, S. B. 1987. Form and function in retinal processing. Trends Neurosci. 10, 478–483.
Laughlin, S. B. 1989. The role of sensory adaptation in the retina. J. Exp. Biol. 146, 39–62.
Laughlin, S. B. 1999. Visual motion, dendritic integration makes sense of the world. Curr. Biol. 9, R15–R17.
Laughlin, S. B. 2001. Energy as a constraint on the coding and processing of sensory information. Curr. Opin. Neurobiol. 11, 475–480.
Laughlin, S. B. and Hardie, R. C. 1978. Common strategies for light adaptation in the peripheral visual systems of fly and dragonfly. J. Comp. Physiol. A 128, 319–340.
Laughlin, S. B., de Ruyter van Steveninck, R. R., and Anderson, J. C. 1998. The metabolic cost of neural information. Nature Neurosci. 1, 36–41.
Laughlin, S. B. and McGinness, S. 1978. The structures of the dorsal and ventral regions of a dragonfly retina. Cell Tissue Res. 188, 427–447.
Lehrer, M. 1994. Spatial vision in the honeybee: the use of different cues in different tasks. Vision Res. 34, 2363–2385.
Lewen, G. D., Bialek, W., and de Ruyter van Steveninck, R. R. 2001. Neural coding of naturalistic motion stimuli. Network 12, 317–329.
Lindemann, J. P., Kern, R., van Hateren, J. H., Ritter, H., and Egelhaaf, M. 2005. On the computations analyzing natural optic flow, quantitative model analysis of the blowfly motion vision pathway. J. Neurosci. 25, 6435–6448.
Lindemann, J. P., Kern, R., Michaelis, C., Meyer, P., van Hateren, J. H., and Egelhaaf, M. 2003. FliMax, a novel stimulus device for panoramic and highspeed presentation of behaviourally generated optic flow. Vision Res. 43, 779–791.
Liu, L., Wolf, R., Ernst, R., and Heisenberg, M. 1999. Context generalization in *Drosophila* visual learning requires the mushroom bodies. Nature 400, 753–756.
Loesel, R. and Homberg, U. 2001. Anatomy and physiology of neurons with processes in the accessory medulla of the cockroach *Leucophaea maderae*. J. Comp. Neurol. 439, 193–207.
Lubock, J. 1888. On the Senses, Instincts and Intelligence of Animals with Special Reference to Insects. Kegan Paul.
Maddess, T. and Laughlin, S. B. 1985. Adaptation of the motion-sensitive neuron H-1 is generated locally and governed by contrast frequency. Proc. R. Soc. Lond. Ser. B Biol. Sci. 225, 251–275.
Mallot, H. A. 2000. Computational Vision, Information Processing in Perception and Visual Behaviour. MIT Press.
Mappes, M. and Homberg, U. 2004. Behavioral analysis of polarization vision in tethered flying locusts. J. Comp. Physiol. A. 190, 61–68.
Marshall, N. J. 1988. A unique colour and polarization vision system in mantis shrimps. Nature 333, 557–560.
Marshall, N. J. and Oberwinkler, J. 1999. The colourful world of the mantis shrimp. Nature 401, 873–874.
Masino, T. and Knudsen, E. I. 1990. Horizontal and vertical components of head movement are controlled by distinct neural circuits in the barn owl. Nature 345, 434–437.
Matheson, T., Rogers, S. M., and Krapp, H. G. 2004. Plasticity in the visual system is correlated with a change in lifestyle of solitarious and gregarious locusts. J. Neurophysiol. 91, 1–12.
Maximov, V. V. 2000. Environmental factors which may have led to the appearance of colour vision. Philos. Trans. R. Soc. Lond. B 355, 1239–1242.
McCann, G. D. and Dill, J. C. 1969. Fundamental properties of intensity, form, and motion perception in the visual nervous systems of *Calliphora phaenicia* and *Musca domestica*. J Gen. Physiol. 53, 385–413.
Mead, C. 1989. Analog VLSI and Neural Systems, Addison and Wesley.
Menzel, R. 1974. Spectral sensitivity of monopolar cells in the bee lamina. J. Comp. Physiol. 93, 337–346.
Menzel, R. 1979. Spectral Sensitivity and Color Vision in Invertebrates. In: Handbook of Sensory Physiology, Vol. VII 6A, Vision in Invertebrates (*ed*. H. Autrum), pp. 503–580. Springer.
Messenger, J. B. 1981. Comparative Physiology of Vision in Molluscs. In: Handbook of Sensory Physiology, Vol. VII, 6c (*ed*. H. Autrum), pp. 93–200. Springer.
Meyer, D. L. and Bullock, T. H. 1977. The hypothesis of sense-organ-dependent tonus mechanisms, history of a concept. Ann. N. Y. Acad. Sci. 290, 3–17.

Milde, J. J. 1993. Tangential medulla neurons in the moth *Manduca sexta* – structure and responses to optomotor stimuli. J. Comp. Physiol. A – Sens. Neural Behav. Physiol. 173, 783–799.

Milde, J. J., Seyan, H. S., and Strausfeld, N. J. 1987. The neck motor system of the fly *Calliphora erythrocephala.* 2. Sensory organization. J. Comp. Physiol. A – Sens. Neural Behav. Physiol. 160, 225–238.

Milde, J. J. and Strausfeld, N. J. 1990. Cluster organization and response characteristics of the giant fiber pathway of the blowfly *Calliphora erythrocephala*. J. Comp. Neurol. 294, 59–75.

Miles, F. A. and Wallman, J. 1993. Visual Motion and Its Role in the Stabilization of Gaze. Elsevier.

Mimura, K. 1982. Discrimination of some visual patterns in *Drosophila melanogaster*. J. Comp. Physiol. 146, 229.

Mimura, K. 1986. Development of visual pattern discrimination in the fly depends on light experience. Science 232, 83–85.

Mote, M. I. and Rubin, L. J. 1981. 'On' type interneurons in the optic lobe of *Periplaneta americana.* I. Spectral characteristics of response. J. Comp. Physiol. 141, 395–401.

Nakayama, K. and Loomis, J. M. 1974. Optical velocity patterns, velocity-sensitive neurons, and space perception, a hypothesis. Perception 3, 63–80.

Nalbach, H. O. 1989. 3 Temporal frequency channels constitute the dynamics of the optokinetic system of the crab, *Carcinus-Maenas* (L). Biol. Cybern. 61, 59–70.

Nalbach, G. 1994. Extremely non-orthogonal axes in a sense organ for rotation, behavioural analysis of the dipteran haltere system. Neuroscience 61, 149–163.

Nalbach, G. and Hengstenberg, R. 1994. The Halteres of the blowfly *Calliphora.* 2. 3-Dimensional organization of compensatory reactions to real and simulated rotations. J. Comp. Physiol. A Sens. Neural Behav. Physiol. 175, 695–708.

Nässel, D. R. and Hagberg, M. 1985. Ocellar interneurones in the blowfly *Calliphora erythrocephala* – morphology and central projections. Cell Tissue Res. 242, 417–426.

Nässel, D. R., Hogmo, O., and Hallberg, E. 1984. Antennal Receptors in the Blowfly *Calliphora erythrocephala*.1. the Gigantic Central Projection of the Pedicellar Campaniform Sensillum. J. Morphol. 180, 159–169.

Neri, P. 2006. Spatial integration of optic flow signals in fly motion-sensitive neurons. J. Neurophysiol. 95, 1608–1619.

Neri, P. and Laughlin, S. B. 2005. Global versus local adaptation in fly motion-sensitive neurons. Proc. Biol. Sci. 272, 2243–2249.

Neumeyer, C. 1991. Evolution of Colour Vision. In: Vision and Visual Dysfunction, (*ed*. J. Cronly-Dillon), Vol. 2, pp. 284–305. Macmillan.

Nordström, K., Barnett, P. D., and O'Carroll, D. C. 2006. Insect detection of small targets moving in visual clutter. PLoS Biol. 4, e54.

O'Carroll, D. C. 1993. Feature-detecting neurons in dragonflies. Nature 362, 541–543.

O'Carroll, D. C., Bidwell, N. J., Laughlin, S. B., and Warrant, E. J. 1996. Insect motion detectors matched to visual ecology. Nature 382, 63–66.

Okamura, J. Y. and Strausfeld, N. J. 2007. Visual system of calliphorid flies, motion- and orientation-sensitive visual interneurons supplying dorsal optic glomeruli. J. Comp Neurol. 500, 189–208.

Olberg, R. M. 1986. Identified target-selective visual interneurons descending from the dragonfly brain. J. Comp. Physiol. A Sens. Neural Behav. Physiol. 159, 827–840.

Olberg, R. M., Worthington, A. H., Fox, J. L., Bessette, C. E., and Loosemore, M. P. 2005. Prey size selection and distance estimation in foraging adult dragonflies. J. Comp. Physiol. A Neuroethol. Sens. Neural Behav. Physiol. 191, 791–797.

Olberg, R. M., Worthington, A. H., and Venator, K. R. 2000. Prey pursuit and interception in dragonflies. J. Comp. Physiol. A 186, 155–162.

Orlovsky, G., Deliagina, T. G., and Grillner, S. 1999. Neural control of locomotion. From mollusk to man. Oxford University Press.

O'Shea, M. and Rowell, C. H. 1975. Protection from habituation by lateral inhibition. Nature 254, 53–55.

O'Shea, M. and Rowell, C. H. 1976. The neuronal basis of a sensory analyser, the acridid movement detector system. II. response decrement, convergence, and the nature of the excitatory afferents to the fan-like dendrites of the LGMD. J. Exp. Biol. 65, 289–308.

O'Shea, M. and Williams, J. L. 1974. The anatomy and output connection of a locust visual interneuron; the lobula giant movement detector (LGMD). J. Comp. Physiol. A 91, 257–266.

Osorio, D. 1986. Ultraviolet sensitivity and spectral opponency in the locust. J. Exp. Biol. 122, 193–208.

Osorio, D. 1986. Directionally selective cells in the Locust medulla. J. Comp. Physiol. A Neuroethol. Sens. Neural. Behav. Physiol. 159, 841–847.

Parsons, M. M., Krapp, H. G., and Laughlin, S. B. 2006. A motion-sensitive neurone responds to signals from the two visual systems of the blowfly, the compound eyes and ocelli. J. Exp. Biol. 209, 4464–4474.

Peckham, G. W. and Peckham, E. G. 1894. The sense of sight in spiders with some observations of the colour sense. Trans. Wisconsin Acad. Sci. Arts Lett. 10, 231–261.

Pena, J. L. and Konishi, M. 2001. Auditory spatial receptive fields created by multiplication. Science 292, 249–252.

Peron, S. P., Krapp, H. G., and Gabbiani, F. 2007. Influence of electrotonic structure and synaptic mapping on the receptive field properties of a collision-detecting neuron. J. Neurophysiol. 97, 159–177.

Petrowitz, R., Dahmen, H., Egelhaaf, M., and Krapp, H. G. 2000. Arrangement of optical axes and spatial resolution in the compound eye of the female blowfly *Calliphora*. J. Comp. Physiol. A 186, 737–746.

Pfeiffer, K. and Homberg, U. 2003. Neurons of the Anterior Optic Tubercle of the Locust *Schistocerca gregaria* are Sensitive to the Plane of Polarized Light. In: The Neurosciences from Basic Research to Therapy (*eds*. N. Elsner and N. Zimmermann), pp. 567–568. Thieme.

von Philipsborn, A. and Labhart, T. 1990. A behavioral study of polarization vision in the fly *Musca domestica*. J. Comp. Physiol. 167, 737–743.

Pierantoni, R. 1976. O look into the cock-pit of a fly. Cell Tissue Res. 171, 101–122.

Pinter, R. B., Olberg, R. M., and Abrams, T. W. 1982. Is the locust DCMD a looming detector? J. Exp. Biol. 101, 327–331.

Preiss, R. 1992. Set point of retinal velocity of ground images in the control of swarming flight of desert locusts. J. Comp. Physiol. A Sens. Neural Behav. Physiol. 171, 251–256.

Preuss, T., Osei-Bonsu, P. E., Weiss, S. A., Wang, C., and Faber, D. S. 2006. Neural representation of object approach in a decision-making motor circuit. J. Neurosci. 26, 3454–3464.

Pringle, J. W. S. 1948. The gyroscopic mechanism of the halteres of Diptera. Philos. Trans. R. Soc. Lond. B Biol. Sci. 233, 347–385.

Reichardt, W. 1961. Autocorrelation, a Principle for the Evaluation of Sensory Information by the Central Nervous System. In: Sensory Communication (*ed*. W. A. Rosenblith), pp. 303–317. MIT Press.

Reichardt, W. 1987. Evaluation of optical motion information by movement detectors. J. Comp. Physiol. A 161, 533–547.

Reichardt, W. and Poggio, T. 1976. Visual control of orientation behaviour in the fly. Part I. A quantitative analysis. Q. Rev. Biophys. 9, 311–338.

Reichardt, W. and Poggio, T. 1979. Figure-ground discrimination by relative motion in the visual-system of the fly. 1. Experimental results. Biol. Cybern. 35, 81–100.

Reichardt, W., Egelhaaf, M., and Schlogl, R. W. 1988. Movement detectors provide sufficient information for local computation of 2-D velocity field. Naturwissenschaften 75, 313–315.

Reichardt, W., Poggio, T., and Hausen, K. 1983. Figure-ground discrimination by relative movement in the visual-system of the fly. 2. Towards the neural circuitry. Biol. Cybern. 46, 1–30.

Reichert, H. and Rowell, C. H. F. 1986. Neuronal circuits controlling flight in the locust – how sensory information is processed for motor control. Trends Neurosci. 9, 281–283.

Riehle, A. 1981. Colour opponent neurons of the honey bee in a hetero-chromatic flicker test. J. Comp. Physiol. 142, 81–88.

Rind, F. C. 1984. A chemical synapse between two motion detecting neurones in the locust brain. J. Exp. Biol. 110, 143–167.

Rind, F. C. 1990. A directionally selective motion-detecting neuron in the brain of the locust – physiological and morphological characterization. J. Exp. Biol. 149, 1–19.

Rind, F. C. and Bramwell, D. I. 1996. Neural network based on the input organization of an identified neuron signaling impending collision. J. Neurophysiol. 75, 967–985.

Rind, F. C. and Simmons, P. J. 1992. Orthopteran DCMD neuron, a reevaluation of responses to moving objects. I. Selective responses to approaching objects. J. Neurophysiol. 68, 1654–1666.

Rind, F. C. and Simmons, P. J. 1997. Signaling of object approach by the DCMD neuron of the locust. J. Neurophysiol. 77, 1029–1033.

Rind, F. C. and Simmons, P. J. 1999. Seeing what is coming, building collision-sensitive neurones. Trends Neurosci. 22, 215–220.

Robertson, R. M. and Reye, D. N. 1988. A local circuit interaction in the flight system of the locust. J. Neurosci. 8, 3929–3936.

Robinson, D. A. 1968. Eye movement control in primates. The oculomotor system contains specialized subsystems for acquiring and tracking visual targets. Science 161, 1219–1224.

Robinson, D. A. 1973. Oculomotor control system. Invest. Ophthalmol. 12, 164–166.

Rogers, B. and Graham, M. 1982. Similarities between motion parallax and stereopsis in human depth perception. Vision Res. 22, 261–270.

Rogers, S. M., Krapp, H. G., Burrows, M., and Matheson, T. 2007. Compensatory plasticity at an identified synapse tunes a visuomotor pathway. J Neurosci. 27, 4621–4633.

Rogers, S. M., Harston, G. W. J., Kilburn-Toppin, F., Matheson, T., and Krapp, H. G. 2004. Receptive field organisation of a collision-detecting visual interneurone in solitarious and gregarious locusts. Journal of Physiology 555P, PC130, University of Cambridge (2004).

Rossel, S. 1983. Binocular vision in the praying mantis. Experientia 39, 640.

Rowell, C. H. F. 1988. Mechanisms of flight steering in locusts. Experientia 44, 389–395.

Rowell, C. H. and O'shea, M. 1976. The neuronal basis of a sensory analyser, the acridid movement detector system. I. Effects of simple incremental and decremental stimuli in light and dark adapted animals. J. Exp. Biol. 65, 273–288.

Rushton, W. A. 1965. Visual adaptation. Proc. R. Soc. (Lond.) B 162, 22–46.

de Ruyter van Steveninck, R. R., Borst, A., and Bialek, W. 2001. Real-Time Encoding of Motion, Answerable Questions and Questionalbe Answers from the Fly Visual System. In: Motion Vision. Computational, Neural, and Ecological Constraints (*eds*. J. M. Zanker and J. Zeil), pp. 279–306. Springer.

de Ruyter van Steveninck, R. R., Lewen, G. D., Strong, S. P., Koberle, R., and Bialek, W. 1997. Reproducibility and variability in neural spike trains. Science 275, 1805–1808.

de Ruyter van Steveninck, R. R., Zaagman, W. H., and Mastebroek, H. A. K. 1986. Adaptation of transient responses of a movement-sensitive neuron in the visual system of the blowfly *Calliphora erythrocephala*. Biol. Cybern. 54, 223–236.

Rybak, J. and Meinertzhagen, I. A. 1997. The effects of light reversals on photoreceptor synaptogenesis in the fly *Musca domestica*. Eur. J. Neurosci. 9, 319–333.

Santer, R. D., Rind, F. C., Stafford, R., and Simmons, P. J. 2006. Role of an identified looming-sensitive neuron in triggering a flying locust's escape. J. Neurophysiol. 95, 3391–3400.

Santer, R. D., Simmons, P. J., and Rind, F. C. 2005. Gliding behaviour elicited by lateral looming stimuli in flying locusts. J. Comp. Physiol. A Neuroethol. Sens. Neural Behav. Physiol. 191, 61–73.

Sauman, I., Briscoe, A. D., Zhu, H., Shi, D., Froy, O., Stalleicken, J., Yuan, Q., Casselman, A., and Reppert, S. M. 2005. Connecting the navigational clock to sun compass input, in monarch butterfly brain. Neuron 46, 457–467.

van der Schaaf, A. and van Hateren, J. H. 1996. Modelling the power spectra of natural images, statistics and information. Vision Res. 36, 2759–2770.

Schiff, W. 1965. Perception of impending collision, a study of visually directed avoidant behavior. Psychol. Monogr. 79, 11–26.

Schilstra, C. and van Hateren, J. H. 1999. Blowfly flight and optic flow I. Thorax kinematics and flight dynamics. J. Exp. Biol. 202, 1481–1490.

Schlotterer, G. R. 1977. Response of locust descending movement detector neuron to rapidly approaching and withdrawing visual-stimuli. Can. J. Zool. (Revue Canadienne de Zoologie) 55, 1372–1376.

Schuling, F. H., Mastebroek, H. A. K., Bult, R., and Lenting, B. P. M. 1989. Properties of elementary movement detectors in the fly *Calliphora erythrocephala*. J. Comp. Physiol. A Sens. Neural Behav. Physiol. 165, 179–192.

Schuppe, H. and Hengstenberg, R. 1993. Optical-properties of the ocelli of *Calliphora erythrocephala* and their role in the dorsal light response. J. Comp. Physiol. A Sens. Neural Behav. Physiol. 173, 143–149.

Schwind, R. 1984. Evidence for true polarization vision based on a two-channel analyzer system in the eye of the water bug, *Notonecta glauca*. J. Comp. Physiol. 154, 53–57.

Shannon, C. E. and Weaver, W. 1949. The Mathematical Theory of Communication. The University of Illinois Press.

Sherk, T. E. 1978. Development of the compound eyes of dragonflies (Odonata). III. Adult compound eyes. J. Exp. Zool. 203, 61–80.

Sherman, A. and Dickinson, M. H. 2003. A comparison of visual and haltere-mediated equilibrium reflexes in the fruit fly *Drosophila melanogaster*. J. Exp. Biol. 206, 295–302.

Shoemaker, P. A., O'Carroll, D. C., and Straw, A. D. 2005. Velocity constancy and models for wide-field visual motion detection in insects. Biol. Cybern. 93, 275–287.

Simmons, P. J. 1999. The performance of synapses that convey discrete graded potentials in an insect visual pathway. J. Neurosci. 19, 10584–10594.

Simmons, P. J. and Rind, F. C. 1992. Orthopteran DCMD neuron, a reevaluation of responses to moving objects. II. Critical cues for detecting approaching objects. J. Neurophysiol. 68, 1667–1682.

Simmons, P. J., Jian, S., and Rind, F. C. 1993. Responses in-vivo to light signals by large, 2Nd-order ocellar neurons of the blowfly, *Calliphora erythrocephala*. J. Physiol. (Lond.) 473, 244.

Simoncelli, E. P. and Heeger, D. J. 1998. A model of neuronal responses in visual area MT. Vision Res. 38, 743–761.

Smith, S. J., Augustine, G. J., and Charlton, M. P. 1985. Transmission at voltage-clamped giant synapse of the squid, evidence for cooperativity of presynaptic calcium action. Proc. Natl. Acad. Sci. U. S. A. 82, 622–625.

Späthe, J. and Briscoe, A. D. 2005. Molecular characterization and expression of the UV opsin in bumblebees: three ommatidial subtypes in the retina and a new photoreceptor organ in the lamina. J. Exp. Biol. 208, 2347–2361.

Späthe, J., Tautz, J., and Chittka, L. 2006. Do honeybees detect colour targets using serial or parallel visual search? J. Exp. Biol. 209, 987–993.

Sparks, D. L. 2002. The brainstem control of saccadic eye movements. Nat. Rev. Neurosci. 3, 952–964.

Spork, P. and Preiss, R. 1993. Control of flight by means of lateral visual-stimuli in gregarious desert locusts, *Schistocerca-Gregaria*. Physiol. Entomol. 18, 195–203.

Srinivasan, M. V. 1990. Generalized gradient schemes for the measurement of two-dimensional image motion. Biol. Cybern. 63, 421–431.

Srinivasan, M. V. 1993. How insects infer range from visual motion. Rev. Oculomot. Res. 5, 139–156.

Srinivasan, M. V. 1994. Pattern-recognition in the honeybee – recent progress. J. Insect Physiol. 40, 183–194.

Srinivasan, M. V. and Zhang, S. W. 2000. Visual Navigation in Flying Insects. In: Neuronal Processing of Optic Flow (*ed*. M. Lappe), pp. 67–92. Academic Press.

Srinivasan, M. V., Zhang, S. W., and Zhu, H. 1998. Honeybees links sights to smells. Nature 396, 637–638.

Stange, G. 1981. The ocellar component of flight equilibrium control in dragonflies. J. Comp. Physiol. 141, 335–347.

Stange, G. and Howard, J. 1979. Ocellar dorsal light response in the dragonfly. J. Exp. Biol. 83, 351–355.

Stange, G., Stowe, S., Chahl, J. S., and Massaro, A. 2002. Anisotropic imaging in the dragonfly median ocellus, a matched filter for horizon detection. J. Comp. Physiol. A Neuroethol. Sens. Neural Behav. Physiol. 188, 455–467.

Starnecker, G. 1996. Colour preference for pupation sites of the butterfly larvea *Inachis io* and the significance of the pupation melanization reducing factor. Naturwissenschaften 83, 474–476.

Stavenga, D. G. 1992. Eye regionalization and spectral tuning of retinal pigments in insects. Trends Neurosci. 15, 213–218.

Stavenga, D. G., Kruizinga, R., and Leertouwer, H. L. 1990. Dioptrics of the facet lenses of male blowflies *Calliphora* and *Chrysomyia*. J. Comp. Physiol. A 166, 365–371.

Steinmann, E. and Menzel, R. 1990. Lernversuche mit der Einsiedlerbiene *Osmia rufa* (Linnaeus, 1758) (Hymenoptera, Apoidae). Mitt. Schweiz. Entomol. Ges. 63, 99–103.

Strausfeld, N. J. 1976. Atlas of an Insect Brain. Springer.

Strausfeld, N. J. and Bassemir, U. K. 1983. Cobalt-coupled neurons of a giant fibre system in Diptera. J. Neurocytol. 12, 971–991.

Strausfeld, N. J. and Gronenberg, W. 1990. Descending neurons supplying the neck and flight motor of Diptera, organization and neuroanatomical relationships with visual pathways. J. Comp. Neurol. 302, 954–972.

Strausfeld, N. J. and Lee, J. K. 1991. Neuronal basis for parallel visual processing in the fly. Vis. Neurosci. 7, 13–33.

Strausfeld, N. J. and Okamura, J. Y. 2007. Visual system of calliphorid flies, organization of optic glomeruli and their lobula complex efferents. J. Comp. Neurol. 500, 166–188.

Strausfeld, N. J. and Seyan, H. S. 1985. Convergence of visual, haltere, and prosternal inputs at neck motor neurons of *Calliphora erythrocephala*. Cell Tissue Res. 240, 601–615.

Strausfeld, N. J., Seyan, H. S., and Milde, J. J. 1987. The neck motor system of the fly *Calliphora erythrocephala.* 1. Muscles and motor. Neuron J. Comp. Physiol. A Sens. Neural Behav. Physiol. 160, 205–224.

Straw, A. D., Warrant, E. J., and O'Carroll, D. C. 2006. A ''bright zone'' in male hoverfly (*Eristalis tenax)* eyes and associated faster motion detection and increased contrast sensitivity. J. Exp. Biol. 209, 4339–4354.

Sun, H. and Frost, B. J. 1998. Computation of different optical variables of looming objects in pigeon nucleus rotundus neurons. Nat. Neurosci. 1, 296–303.

Sweatt, J. D. and Kandel, E. R. 1989. Persistent and transcriptionally-dependent increase in protein phosphorylation in long-term facilitation of *Aplysia* sensory neurons. Nature 339, 51–54.

Swihart, C. A. 1971. Colour discrimination by the butterfly, *Heliconius charitonius* Linn. Anim. Behav. 19, 156–164.

Takemura, S. Y. and Arikawa, K. 2006. Ommatidial type-specific interphotoreceptor connections in the lamina of the swallowtail butterfly, *Papilio xuthus*. J. Comp. Neurol. 494, 663–672.

Tammero, L. F. and Dickinson, M. H. 2002. Collision-avoidance and landing responses are mediated by separate pathways in the fruit fly, *Drosophila melanogaster*. J. Exp. Biol. 205, 2785–2798.

Tanaka, K., Fukada, Y., and Saito, H. A. 1989. Underlying mechanisms of the response specificity of expansion/contraction and rotation cells in the dorsal part of the medial superior temporal area of the macaque monkey. J. Neurophysiol. 62, 642–656.

Taylor, C. P. 1981a. Contribution of compound eyes and ocelli to steering of locusts in flight. 1. Behavioral-analysis. J. Exp. Biol. 93, 1–18.

Taylor, C. P. 1981b. Contribution of compound eyes and ocelli to steering of locusts in flight. 2. Timing changes in flight motor units. J. Exp. Biol. 93, 19–31.

Taylor, G. K. and Thomas, A. L. 2003. Dynamic flight stability in the desert locust *Schistocerca gregaria*. J. Exp. Biol. 206, 2803–2829.

Vitzthum, H., Muller, M., and Homberg, U. 2002. Neurons of the central complex of the locust *Schistocerca gregaria* are sensitive to polarized light. J. Neurosci. 22, 1114–1125.

Wachenfeld, A. and Hausen, K. 1994. The Role of Male-specific Visual Interneurons of the Mating Behaviour of the Blowfly, *Calliphora erythrocephala* (Meig.). In: Proc. 22nd Neurobiol. Conf (*eds*. N. Elsner and H. Breer), p. 440. Thieme.

Wagner, H. 1982. Flow-field variables trigger landing in flies. Nature 297, 147–148.

Wagner, H. 1986. Flight performance and visual control of flight of the free-flying housefly (*Musca-Domestica* L). 2. Pursuit of targets. Philos. Trans. R. Soc. Lond. Ser. B Biol. Sci. 312, 553–579.

Wakakuwa, M., Kurasawa, M., Giurfa, M., and Arikawa, K. 2005. The compound eye of the honeybee *Apis mellifera* is composed of three spectrally distinct types of ommatidia. Naturwissenschaften 92, 464–467.

Walcher, F. and Kral, K. 1994. Visual deprivation and distance estimation in the praying-mantis larva. Physiol. Entomol. 19, 230–240.

Walla, P., Barth, F. G., and Eguchi, E. 1996. Spectral sensitivity of single photoreceptors in the eyes of the Ctenid spider *Cupiennius salei*. Zool. Sci. 13, 199–202.

Wallace, G. K. 1959. Visual scanning in the desert locust (*Schistocerca gregaria* Forsk.). J. Exp. Biol. 36, 512–525.

Wandell, S. and Quinn, W. G. 2001. Flies, genes and learning. Annu. Rev. Neurosci. 24, 1283.

Wang, X. J. 1998. Calcium coding and adaptive temporal computation in cortical pyramidal neurons. J. Neurophysiol. 79, 1549–1566.
Wang, Y. and Frost, B. J. 1992. Time to collision is signalled by neurons in the nucleus rotundus of pigeons. Nature 356, 236–238.
Warzecha, A. K. and Egelhaaf, M. 1999. Variability in spike trains during constant and dynamic stimulation. Science 283, 1927–1930.
Warzecha, A. and Egelhaaf, M. 2001. Neuronal Coding of Visual Motion in Real-Time. In: Motion Vision. Computational, Neural, and Ecological Constraints (*eds*. J. M. Zanker and J. Zeil), pp. 239–277. Springer.
Warzecha, A. K., Egelhaaf, M., and Borst, A. 1993. Neural circuit tuning fly visual interneurons to motion of small objects. I. Dissection of the circuit by pharmacological and photoinactivation techniques. J. Neurophysiol. 69, 329–339.
Warzecha, A. K., Kurtz, R., and Egelhaaf, M. 2003. Synaptic transfer of dynamic motion information between identified neurons in the visual system of the blowfly. Neuroscience 119, 1103–1112.
Webb, B. 2004. Neural mechanisms for prediction, do insects have forward models? Trends Neurosci. 27, 278–282.
Weckstrom, M., Hardie, R. C., and Laughlin, S. B. 1991. Voltage-activated potassium channels in blowfly photoreceptors and their role in light adaptation. J. Physiol. 440, 635–657.
Wehner, R. 1981. Spatial Vision in Arthropods. In: Vision in Invertebrates, 7/6 C (*ed*. H. Autrum), pp. 287–616. Springer Verlag.
Wehner, R. 1984. Astronavigation in Insects. Annu. Rev. Entomol. 29, 277–298.
Wehner, R. 1987. 'Matched filters' – neural models of the external world. J. Comp. Physiol. 161, 511–531.
Wehner, R. 1994. The Polarization-Vision Project: Championing Organismic Biology. In: Neural Basis of Behavioural Adaptations (*eds*. K. Schildberger and N. Elsner), pp. 103–143. Fischer.
Wehner, R. 1997. The Ant's Celestial Compass System: Spectral and Polarization Channels. In: Orientation and Communication in Arthropods (*ed*. M. Lehrer), pp. 145–185. Birkhauser.
Wehner, R. and Bernhard, G. D. 1993. Photoreceptor twist: a solution to the false color problem. Proc. Natl. Acad. Sci. U. S. A. 90, 4132–4135.
Wehner, R. and Labhart, T. 2006. Polarization Vision. In: Invertebrate Vision (*eds*. E. Warrant and D. -E. Nilsson), pp. 291–348. Cambridge University Press.
Wehner, R. and Srinivasan, M. V. 2003. Path Integration in Insects. In: The Neurobiology of Spatial Behavior (*ed*. K. J. Jeffery), pp. 9–30. Oxford University Press.
Wehrhahn, C., Poggio, T., and Bulthoff, H. 1982. Tracking and chasing in houseflies (*Musca)* – an analysis of 3-D flight trajectories. Biol. Cybern. 45, 123–130.
Wicklein, M. and Lotto, R. B. 2005. Bees encode behaviorally significant spectral relationships in complex scenes to resolve stimulus ambiguity. Proc. Nat. Acad. Sci. U. S. A. 15, 16870–16874.
Wicklein, M. and Sejnowski, T. J. 2001. Perception of change in depth in the hummingbird hawkmoth *Manduca sexta* (Sphingidae, Lepidoptera). Neurocomputing 38–40, 1595–1602.
Wicklein, M. and Strausfeld, N. J. 2000. Organization and significance of neurons that detect change of visual depth in the hawk moth *Manduca sexta*. J. Comp. Neurol. 424, 356–376.
Wicklein, M. and Varju, D. 1999. Visual system of the European hummingbird hawkmoth *Macroglossum stellatarum* (Sphingidae, Lepidoptera), motion-sensitive interneurons of the lobula plate. J. Comp. Neurol. 408, 272–282.
Wildermuth, H. 1998. Dragonfly recognize the water of rendezvous and oviposition sites by horizontally polarized light: a behavioural field test. Naturwissenschaften 85, 297–302.
Wilson, M. 1978a. Functional organization of locust ocelli. J. Comp. Physiol. 124, 297–316.
Wilson, M. 1978b. Generation of graded potential signals in 2nd order cells of locust ocellus. J. Comp. Physiol. 124, 317–331.
Wilson, E. O. and Hölldobler, B. 1987. Causes of ecological success: the case of the ants. Ecology 56, 1–9.
Wolf, R. and Heisenberg, M. 1980. On the fine structure of yaw torque in visual flight orientation of *Drosophila melanogaster*. II. A temporally and spatially variable weighting function for the visual field (''visual attention''). J. Comp. Physiol. A 140, 69–80.
Wolf, R. and Heisenberg, M. 1991. Basic organization of operant behavior as revealed in *Drosophila* flight orientation. J. Comp. Physiol. 169, 699.
Wolf, R., Voss, A., Hein, S., and Heisenberg, M. 1992. Can a fly ride a bicycle? Phil. Trans. R. Soc. Lond. Ser. B Biol. Sci. 337, 261–269.
Wolpert, D. M. and Ghahramani, Z. 2000. Computational principles of movement neuroscience. Nat. Neurosci. 3 (Suppl.), 1212–1217.
Wolpert, D. M., Ghahramani, Z., and Jordan, M. I. 1995. An internal model for sensorimotor integration. Science 269, 1880–1882.
Wüstenberg, D. and Krapp, H. G. 2007. Self-motion estimation and flight control in blowflies and locusts: a comparative study. Proceeding of the 31st Goettingen Neurobiology Conference.
Wylie, D. R., Bischof, W. F., and Frost, B. J. 1998. Common reference frame for neural coding of translational and rotational optic flow. Nature 392, 278–282.
Yamamoto, K., Nakata, M., and Nakagawa, H. 2003. Input and output characteristics of collision avoidance behavior in the frog *Rana catesbeiana*. Brain Behav. Evol. 62, 201–211.
Yang, E. C. and Maddess, T. 1997. Orientation-sensitive neurons in the brain of the honey bee (*Apis mellifera)*. J. Insect Physiol. 43, 329–336.
Yang, E. C. and Osorio, D. 1996. Spectral responses and chromatic processing in the dragonfly lamina. J. Comp. Physiol. A Sens. Neural Behav. Physiol. 178, 543–550.
Yang, E.-C., Lin, H.-C., and Hung, Y.-S. 2004. Patterns of chromatic information processing in the lobula of the honeybee, *Apis mellifera* L. J. Insect Physiol. 50, 913–925.
Zanker, J. M., Srinivasan, M. V., and Egelhaaf, M. 1999. Speed tuning in elementary motion detectors of the correlation type. Biol. Cybern. 80, 109–116.
Zaretsky, M. and Rowell, C. H. 1979. Saccadic suppression by corollary discharge in the locust. Nature 280, 583–585.
Zeil, J. and Layne, J. E. 2002. Path Integration in Fiddler Crabs and Its Relation to Habitat and Social Life. In: Crustacean Experimental Systems in Neurobiology (*ed*. K. Wiese), pp. 227–247. Springer.
Zhang, S. W., Lehrer, M., and Srinivasan, M. V. 1999. Honeybee memory: navigation by associative grouping and recall of visual stimuli. Neurobiol. Learn. Mem. 72, 180–201.
Zhang, S. W., Wang, X. A., Liu, Z. L., and Srinivasan, M. V. 1990. Visual tracking of moving targets by freely flying honeybees. Vis. Neurosci. 4, 379–386.

Further Reading

Berry, R., Stange, G., Olberg, R., and van Kleef, J. 2006. The mapping of visual space by identified large second-order neurons in the dragonfly median ocellus. J. Comp. Physiol.

A – Neuroethol. Sens. Neural Behav. Physiol. 192, 1105–1123.
Farina, W. M. and Josens, R. B. 1994. Food source profitability modulates compensatory responses to a visual stimulus in the hawk moth *Macroglossum stellatarum*. Naturwissenschaften 81, 131–133.
Fraser Rowell, C. H. and O'Shea, M. 1976. Neuronal basis of a sensory analyser, the acridid movement detector system. III. Control of response amplitude by tonic lateral inhibition. J. Exp. Biol. 65, 617–625.
Fraser Rowell, C. H., O'Shea, M., and Williams, J. L. 1977. The neuronal basis of a sensory analyser, the acridid movement detector system. IV. The preference for small field stimuli. J. Exp. Biol. 68, 157–185.
Hallberg, E., Hogmo, O., and Nässel, D. R. 1984. Antennal receptors in the blowfly *Calliphora erythrocephala.* 2. Fine-structure of the large pedicellar campaniform sensillum. J. Morphol. 182, 115–123.
Robertson, R. M. 1991. Delayed excitatory connections in the flight system of the locust. J. Neurophysiol. 65, 1150–1157.
Rosenbaum, E. E., Hardie, R. C., and Colley, N. J. 2006. Calnexin is essential for rhodopsin maturation, Ca^{2+} regulation, and photoreceptor cell survival. Neuron 49, 229–241.
Solomon, P. R. and Moore, J. W. 1975. J. Comp. Physiol. Psychol. 89, 1192–1203.
Strausfeld, N. J. 1984. Functional Neuroanatomy of the Blowfly's Visual System. In: Photoreception and Vision in Invertebrates (*ed*. M. A. Ali), pp. 483–522. Plenum.
van Swinderen, B. and Greenspan, R. J. 2003. Saliency modulates 20–30 Hz brain activity in *Drosophila*. Nat. Neurosci. 6, 579–586.
Tu, M. S. and Dickinson, M. H. 1996. The control of wing kinematics by two steering muscles of the blowfly (*Calliphora vicina)*. J. Comp. Physiol. A 178, 813–830.
Wehner, R. 1992. Arthropods. In: Animal Homing (*ed*. F. Papi), pp. 45–144. Chapman and Hall.
Wehner, R. 2001. Polarization vision: a uniform sensory capacity? J. Exp. Biol. 204, 2589–2596.
Wehner, R. 2003. Desert ant navigation: how miniature brains solve complex tasks. J. Comp. Physiol. A 189, 579–588.
Wiesel, T. N. and Hubel, D. H. 1965. Extent of recovery from the effects of visual deprivation in kittens. J. Neurophysiol. 28, 1060–1072.

1.07 Color in Invertebrate Vision

M Vorobyev, University of Queensland, Brisbane, QLD, Australia

© 2008 Elsevier Inc. All rights reserved.

1.07.1	What Is Color Vision?	205
1.07.2	Color Vision and Color Blindness in Different Eye Types	206
1.07.3	Spectral Sensitivities of Invertebrate Photoreceptors	206
1.07.4	Color Vision in the Darkness	207
1.07.5	Interaction between Color and Polarization Vision	208
1.07.6	Spatial Resolution of Color Vision – Random Arrangement of Photoreceptors in Compound Eyes	208
1.07.7	Separation of Chromatic and Achromatic Vision	208
1.07.8	Why Color Vision?	209
References		209

Glossary

color Color is that aspect of visual perception by which an observer may distinguish differences between two structure-free fields of view of the same size and shape, such as may be caused by differnces in the spectral composition of the radiant energy concerned in the observation (Wyszecki, G., and Stiles, W.S., 1982).

1.07.1 What Is Color Vision?

What do we mean when we say that invertebrates have color vision? By definition, a human observer is assumed to have color vision if he can discriminate light stimuli of different spectral composition using cues other than their intensity (e.g., Wyszecki, G. and Stiles, W. S., 1982). Accordingly, we assume that an animal has color vision, if it can discriminate two light stimuli of different spectral composition (but equal in polarization) and continues to discriminate them when the intensity of the stimuli are varied, that is, these stimuli cannot be matched by adjusting their intensity. The first animals demonstrated to have color vision were invertebrates. Lubbock J. (1888) showed that a water flea *Daphnia*, which is positively phototactic, prefers yellow light to white light of a higher intensity. Some time later, von Frisch K. (1914) showed that honeybees could discriminate colored stimuli from various shades of gray. Since these pioneering studies, color vision has been demonstrated using behavioral experiments in a variety of invertebrates, including mites, spiders, crustaceans, and insects (for review see Kelber, A. *et al.*, 2003; Kelber, A., 2006).

Color vision is achieved by comparing the signals of photoreceptor cells sensitive to different parts of the spectrum. Anatomical and physiological studies show that the majority of invertebrates with eyes also have multiple spectral types of photoreceptors (Kelber, A. *et al.*, 2003). However, multiple spectral types of photoreceptors do not necessarily infer color vision – different spectral receptor types can be used for different purposes at different behaviors, giving receptor-specific (or wavelength-specific) behavior rather than color vision (Menzel, R., 1979). Receptor-specific behavior does not require the comparison of signals from different receptors and, therefore, is color blind. Animals that do have color vision can also show receptor-specific behavior in particular tasks. For example, a honeybee uses color vision for discriminating objects at close range (von Frisch, K. 1914, for reviews see Menzel, R., 1979; Menzel, R. and Backhaus, W., 1991), but it uses only a long-wavelength-sensitive photoreceptor for discriminating objects from far away and for motion vision (Srinivasan, M. V. and Lehrer, M., 1984; Giurfa, M. *et al.*, 1996; 1997). It is important to note that, while animals with multiple receptors can, in theory, be color blind in all behavioral contexts, such color blindness has not been revealed behaviorally in any animal so far tested.

1.07.2 Color Vision and Color Blindness in Different Eye Types

Eye design in invertebrates is diverse and gives rise to a variety of color-vision systems. Simple camera-type eyes, similar in plan to the vertebrate eye, are common in cephalopods and spiders. Compound eyes made up of many units called ommatidia are found in many insects and crustaceans (Land, M. F. and Nilsson, D.-E., 2002). The two types of eyes may coexist within the same animal, for example, insects have large compound eyes, which provide spatial, color, and polarization vision, and small camera-type eyes called ocelli. Ocelli detect overall illumination rather than form an image. Interestingly, physiology suggests that ocelli are capable of providing information about color without being able to resolve spatial details (Ruck, P., 1965; van Kleef, J. *et al.*, 2005). Usually, camera-type eyes have a better resolution than compound eyes (Land, M. F. and Nilsson, D.-E., 2002). The tiny (0.8 mm in diameter) camera-type eyes of the jumping spider *Portia fibriata* have an optical resolution only five times worse than ours and more than five times better than that of the best insect, a dragon fly (Land, M. F. and Nilsson, D.-E., 2002). These eyes allow spiders to locate prey with remarkable precision and provide spiders with a sense of color (Land, M. F., 1985; Nakamura, T. and Yamshita, S., 2000). The largest camera-type eyes are found among cephalopods (Land, M. F. and Nilsson, D.-E., 2002). While cephalopods have excellent spatial vision, they typically have only one type of visual pigment and, therefore, are color blind. The absence of color vision in cuttlefish and octopus has been questioned, because these animals can adjust body patterns, to match backgrounds consisting of differently colored natural objects, such as stones, sand, and algae. However, it appears that the match is achieved on the basis of brightness cues. When exposed to a background consisting of yellow and blue stones that are matched in brightness for cuttlefish eyes, cuttlefish ignore the difference in color (Marshall, N. J. and Messenger, J. B., 1996; Mathger, L. M. *et al.*, 2006) (Figure 1).

Surprisingly, the most sophisticated color vision may be associated with the low-resolution compound eyes of ancient marine crustaceans – mantis shrimps (stomatopoda). Mantis shrimps have 16 spectral types of photoreceptors, 12 of which are used for color vision including ultraviolet, the remaining four are used for spatial and polarization vision (Marshall, N. J., 1988; Cronin, T. W. and Marshall, N. J., 1989; Marshall, N. J. and Oberwinkler, J., 1999). The 12 types of spectrally different photoreceptors are located in a narrow strip across the eye – the midband – where photoreceptors used for color vision are combined in the top four rows of ommatidia (Figures 1 and 2). Each of these rows contains a ultraviolet (UV)-sensitive photoreceptor and two spectral types of photoreceptors sensitive in the visible range (Cronin, T. W. and Marshall, N. J., 1989; Marshall, N. J. and Oberwinkler, J., 1999). To be able to register colors of objects in the environment outside this very narrow strip, mantis shrimps move their eyes and scan midband photoreceptors over the image (Land, M. F. *et al.*, 1990). Such scans indeed allow shrimps to discriminate colored containers with food from gray containers of different shades (Marshall, N. J. *et al.*, 1996).

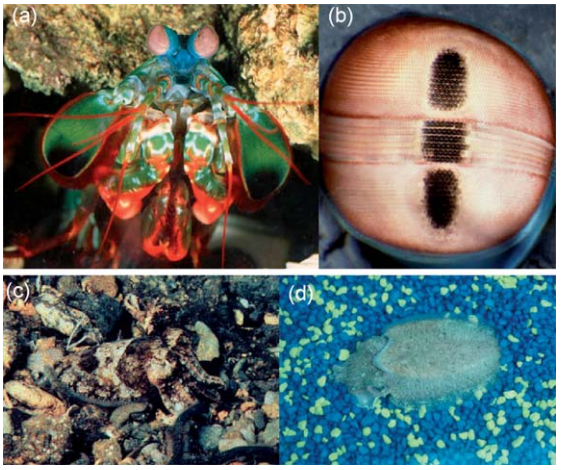

Figure 1 An animal with sophisticated color vision, mantis shrimp *Odontodactilus scyllarus* (a) and a color-blind cephalopod – cuttlefish *Sepia officinalis* (c, d). The frontal eye of a mantis shrimp (b) has a conspicuous stripe of facets – the midband. The four upper rows of the midband are specialized for color vision, its rows contain 12 spectral types of photoreceptors cells (Figure 2(b)). Color-blind cuttlefish is a master of camouflage – it matches texture, brightness, and color of the substrate – (c) but it fails to imitate the texture of yellow and blue gravel that is matched in brightness for the cuttlefish eye (Marshall, N. J. and Messenger, J. B., 1996). Photographs are courtesy of Justin Marshall and Roger T. Honlon.

1.07.3 Spectral Sensitivities of Invertebrate Photoreceptors

Visual pigments of all animals are constructed from a carotenoid chromophore bound to an opsin protein. In invertebrates, three types of chromophores are

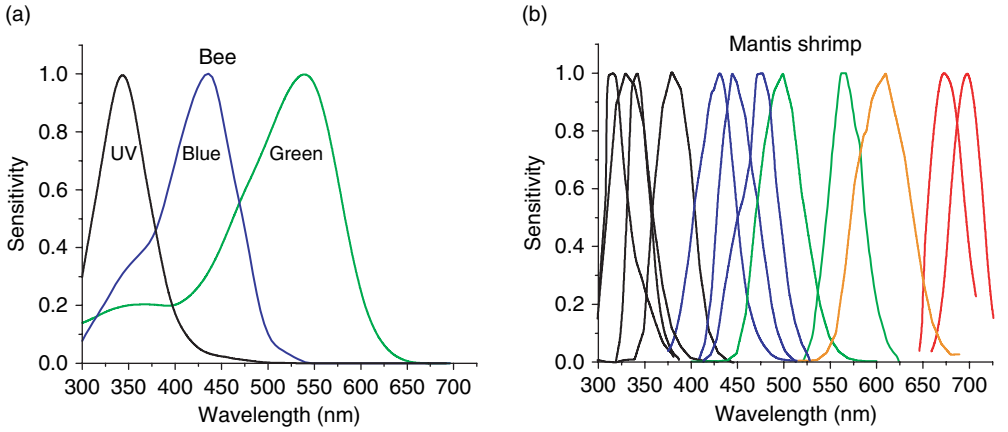

Figure 2 The spectral sensitivities of a honey bee, *Apis mellifera* (Menzel, R. and Backhaus, W., 1991) and of a mantis shrimp, *Neogonodactilus oesredii* (Marshall, N. J. and Oberwinkler, J., 1999). In a mantis shrimp, the narrowing of the spectral sensitivities is achieved by intrarhabdomal filtering.

found: (1) retinal, a chromophore found in terrestrial and marine vertebrates, is also found among cephalopods, crustaceans, and in insects such as bees and locusts; (2) 3,4-didehydroretinal, a chromophore typical of freshwater fish and amphibians, is present in several species of squid; (3) 3-hydroretinal, which is common in flies and butterflies (Vogt, K. and Kirschfeld, K., 1984). This chromophore is not found among vertebrates (for reviews see Kelber, A. *et al.*, 2003; Kelber, A., 2006). Generally, color vision is achieved by expressing different opsins in combination with the same chromophore to generate visual pigments with different sensitivities. However, some cephalopods, such as the firefly squid, *Watasenia scintitalis*, have three visual pigments probably derived from one opsin protein and three different chromophores (Seidowu, M. *et al.*, 1994). It remains unclear whether these visual pigments are used for color vision.

The spectral sensitivity of invertebrate photoreceptors often deviates substantially from the absorption spectrum of visual pigments. In the compound eyes of insects and crustaceans, rhabdomeric photoreceptors with different visual pigments are usually fused into a common light guide. This leads to mutual filtering of light and narrowing of receptor spectral sensitivity even in the absence of additional filtering pigments (Snyder, A. W. *et al.*, 1973). In the tired retina of the frontal eyes of a jumping spider, and in many insects and crustaceans, distal rhabdoms filter the light reaching the more proximal ones. However, the most prominent modification of spectral sensitivity is achieved by using additional pigments, which act as filters narrowing the spectral sensitivity, or transfer energy to the visual pigment, thus broadening the spectral sensitivity (for review see Douglas, R. H. and Marshall, N. J., 1999). The broad spectral sensitivity of the R1–R6 photoreceptors in the house fly is achieved by sensitizing pigment 3-hydroxyretinol (Vogt, K. and Kirschfeld, K. 1984). The same molecule serves as a screening pigment in a moth *Papilio*, where it narrows the spectral sensitivity (Arikawa, K. *et al.*, 1999). Perirhabdomal pigments change the spectral sensitivity of thin rhabdoms by lateral filtering. For example, the red perirhabomal pigment of *Papilio* shifts significantly the peak of the red pigment to the longer wavelength (Arikawa, K., 2003). In mantis shrimps, intrarhabdomal pigments create narrow spectral sensitivities, thus enabling color vision with 12 spectrally distinct photoreceptors. Interestingly, the spectral transmission of filters in the eyes of mantis shrimps changes as an adaptation to the light environment (Cronin, T. W. *et al.*, 2001).

1.07.4 Color Vision in the Darkness

In dim light, the signal-to-noise ratio of photoreceptor cells is low, which leads to an unreliability of color vision in darkness (for review see, Osorio, D. and Vorobyev, M., 2005). Accordingly, vertebrates use one spectral type of rods for scotopic vision and are color blind in dim light (but see Kelber, A. and Roth, L. S. V., 2006). However, invertebrates do not have a separate set of photoreceptors for nocturnal

and diurnal vision. Moreover, nocturnal insects, like hawkmoths, have several spectral types of photoreceptors in their eyes. It appears that nocturnal hawkmoths use color vision at light intensities where we use rod vision only (Kelber, A. *et al.*, 2002). To achieve reliable color discrimination, these insects must sum signals of many ommatidia and in doing so sacrifice spatial resolution. It remains unclear whether other insects that are active at night, such as nocturnal bees, retain their ability to discriminate colors in darkness.

1.07.5 Interaction between Color and Polarization Vision

The rhabdomeric photoreceptors of arthropods and mollusks are inherently polarization sensitive by virtue of their microvillar design (Land, M. F. and Nilsson, D.-E., 2002). Because a single polarization-sensitive photoreceptor cannot distinguish between the orientation of polarization and the spectral composition of light, the neural signals caused by changes in polarization cannot be distinguished from those caused by the change of spectral composition of light. Thus, polarization vision may be mixed with color vision inducing false colors, as has been shown for a butterfly *Papilio augeus* (Kelber, A., 1999). Because *Papilio*'s blue receptors are maximally sensitive to vertically polarized light, whereas green receptors are maximally sensitive to horizontally polarized light, the horizontally polarized light induces a sensation indistinguishable from green light. Papilio prefers to lay eggs on green surfaces to blue ones. It also prefers horizontal polarization to vertical polarization, indicating that polarization and color vision are mixed (Kelber, A., 1999). However, in the majority of insects and crustaceans, polarization vision is separated from color vision. In many insects, this is achieved by twisting photoreceptors along their longitudinal axis in such a way that microvilli of individual rhabdomers are not aligned (Wehner, R. and Bernard, G. D., 1992). For example, the honeybee eye is composed of twisted photoreceptors except for the uppermost dorsal rim of the eye (Wehner, R. *et al.*, 1975). In mantis shrimps, the polarization-sensitive parts of eye are spatially separated from the color-sensitive rows of the midband (Land, M. F. and Nilsson, D.-E., 2002) (see Figure 1).

1.07.6 Spatial Resolution of Color Vision – Random Arrangement of Photoreceptors in Compound Eyes

In our eyes, each photoreceptor cell samples a different point in the space. Since the receptive fields for color should include different spectral types of photoreceptor cells, the random distribution of cones in the human retina leads to a poor spatial resolution of chromatic vision (for review see Lee, B. B., 2004). However, because in compound eyes the rhabdomers are fused together into a common light guide, such eyes theoretically allow for higher spatial resolution of color vision, by virtue of locating all spectral types of receptors within each ommatidium. Early studies in the honeybee eye suggested that each ommatidium contains all three spectral types of photoreceptor (UV, blue, and green), indicating that insects have an eye design that optimizes the spatial resolution of color vision (Gribakin, F. G., 1969). This conclusion has been challenged recently by the discovery of a random arrangement of receptors with different spectral sensitivities first in a butterfly (Arikawa, K. and Stavenga, D., 1997) and later in the honeybee (Wakakuwa, M. *et al.*, 2005). Thus, it seems that the random arrangement of photoreceptors is a general pattern characteristic of insect color vision, predicting a significantly poorer resolution for color than for luminance vision.

1.07.7 Separation of Chromatic and Achromatic Vision

In humans, the chromatic aspects of color (hue and saturation) remain largely invariant when the intensity of a light stimulus varies. However, because color vision can be achieved by neural mechanisms that are sensitive to changes in light intensity (Brandt, R. and Vorobyev, M., 1997), animals that evolved color vision independently from the ancestors of humans can process color by neural mechanisms that do not permit separation of chromatic and achromatic vision. Therefore, invertebrates may have color vision that differs substantially from ours. Interestingly, behavioral experiments reveal striking similarities between color coding in bees and humans. Similar to humans, bees have three spectral receptor types, all of which are used for chromatic vision that is not sensitive to changes in stimulus intensity (Menzel, R., 1979; Menzel, R. and

Backhaus, W., 1991). Bees also have achromatic vision, which is mediated by their green receptor alone (for review see, Giurfa, M. and Vorobyev, M., 1997). In bees, as in humans, the spatial resolution of achromatic vision is better than that of chromatic vision. Bees detect and discriminate large stimuli (subtended angle >15°) on the basis of chromatic cues alone (Giurfa, M. *et al.*, 1996; 1997), whereas small stimuli (subtended angle <15°) are detected and discriminated on the basis of achromatic cues alone (Giurfa, M., and Vorobyev, M., 1998). Low spatial resolution may be a general feature of chromatic vision, because the signal-to-noise ratio can be improved by spatial summation of receptor signals. Indeed, comparisons of physiological recordings of receptor noise with behavioral thresholds shows that honeybees sum signals of individual photoreceptor cells to improve the signal-to-noise ratio (Vorobyev, M. *et al.*, 2001). The random arrangement of receptors may be a consequence of the low spatial resolution of chromatic vision, because there is no selective advantage in arranging all spectral receptor types within one ommatidium, if the receptive field for chromatic vision summates signals from many ommatidia. On the other hand, where receptors are arranged randomly in the retina, chromatic vision must utilize signals averaged over large areas. It remains unclear whether the separation of chromatic and achromatic vision is widespread among invertebrates.

1.07.8 Why Color Vision?

Color vision is useful for many tasks, and it is difficult to pinpoint one particular reason for the origin of color vision in animals (Vorobyev, M., 2004). However, two hypotheses explaining the origin of color vision have been widely discussed in the literature.

1. Color vision could have appeared as a general adaptation for seeing objects in conditions of patchy and changing illumination (Rubin, J. M. and Richards, W. A., 1982; Maximov, V. V., 2000). Since shadows yield strong variations in the intensity of illumination, achromatic vision is unreliable. Chromatic signals provide much more information about object material and can be used for reliable discrimination of objects from their backgrounds.
2. Color vision could have appeared as a specific adaptation for looking at colorful signals of plants and animals, which in turn could have coevolved with color vision. In the late nineteenth century, a prominent Canadian writer, Grant Allen, summed up the coevolution hypothesis for the origin of color vision in the following condensed formula: "Insects produce flowers. Flowers produce the colour-sense in insects. The colour-sense produces a taste for colour. The taste for colour produces butterflies and brilliant beetles" (Allen, G., 1879).

A number of studies of flower colors and insect vision have been inspired by this hypothesis of coevolution of flower colors and insect vision (e.g., Chittka, L. and Menzel, R., 1992). However, the analysis of spectral sensitivities of insects and crustaceans does not support this hypothesis (e.g., Vorobyev, M. and Menzel, R., 1999; Briscoe, A. D. and Chittka, L., 2001). In particular, it appears that the photoreceptors in flower foraging bees are practically identical to those in predatory wasps (Peitsch, D. *et al.*, 1992). Therefore, it is more likely that flowers exploited the preexisting color vision systems, which could have evolved for general tasks such as detection and identification of a variety of objects in conditions of patchy and changing illumination (Maximov, V. V., 2000; Vorobyev, M., 2004).

References

Allen, G. 1879. The Colour Sense. Its Origin and Development. Trubner.

Arikawa, K. 2003. Spectral organisation of the eye of a butterfly, *Papilio*. J. Comp. Physiol. A 189, 791–800.

Arikawa, K. and Stavenga, D. 1997. Random array of colour filters in the eyes of butterflies. J. Exp. Biol. 200, 2501–2506.

Arikawa, K., Mizuno, S., Scholten, D. G. W., Kinoshita, M., Seki, T., Kitamoto, J., and Stavenga, D. G. 1999. An ultraviolet absorbing pigment causes a narrow-band violet receptor and a single-peaked green receptor in the eye of the butterfly *Papilio*. Vis. Res. 39, 1–8.

Brandt, R. and Vorobyev, M. 1997. Metric analysis of increment threshold spectral sensitivity in the honeybee. Vis. Res. 37, 425–439.

Briscoe, A. D. and Chittka, L. 2001. Insect color vision. Annu. Rev. Entomol. 46, 471–510.

Chittka, L. and Menzel, R. 1992. The evolutionary adaptation of flower colors and insect pollinators color vision. J. Comp. Physiol. A 171, 171–181.

Cronin, T. W. and Marshall, N. J. 1989. A retina with at least ten spectral types of photoreceptors in a mantis shrimp. Nature 339, 137–140.

Cronin, T. W., Caldwell, R. L., and Marshall, J. 2001. Sensory adaptation: tunable colour vision in a mantis shrimp. Nature 411, 547–548.

Douglas, R. H. and Marshall, N. J. 1999. A Review of Vertebrate and Invertebrate Optical Filters. In: Adaptive Mechanisms of

Ecology of Vision (*eds*. S. Archer and J. Partrige), pp. 95–162. Kluwer Academic Publishers.
von Frisch, K. 1914. Der Farbensinn und Formensinn der Biene. Zool. Jabrb. Abt. Allg. Zool. Physiol. Tiere 35, 1–188.
Giurfa, M. and Vorobyev, M. 1997. The detection and recognition of colour stimuli by honeybees: performance and mechanisms. Israel J. Plant Sci. 45, 129–140.
Giurfa, M. and Vorobyev, M. 1998. The angular range of achromatic target detection by honeybees. J. Comp. Physiol. A 183, 101–110.
Giurfa, M., Vorobyev, M., Brandt, R., Posner, B., and Menzel, R. 1997. Discrimination of coloured stimuli by honeybees: alternative use of achromatic and chromatic signals. J. Comp. Physiol. A 180, 235–243.
Giurfa, M., Vorobyev, M., Kevan, P., and Menzel, R. 1996. Detection of coloured stimuli by honeybees: minimum visual angles and receptor specific contrasts. J. Comp. Physiol. A 178, 699–709.
Gribakin, F. G. 1969. Cellular basis of colour vision in the honey bee. Nature 223, 639–641.
Kelber, A. 1999. Why ''false colours'' are seen by butterflies. Nature 402, 251.
Kelber, A 2006. Invertebrate Color Vision. In: Invertebrate Vision (*eds*. E. J. Warrant and D. -E. Nilsson), pp. 250–290. Cambridge University Press.
Kelber, A. and Roth, L. S. V. 2006. Nocturnal colour vision – not as rare as we might think. J. Exp. Biol. 209, 781–788.
Kelber, A., Balkenius, A., and Warrant, E. J. 2002. Scotopic color vision in nocturnal hawkmoths. Nature 419, 922–925.
Kelber, A., Vorobyev, M., and Osorio, D. 2003. Animal colour vision – behavioural tests and physiological concepts. Biol. Rev. 78, 81–118.
van Kleef, J., James, A. C., and Stange, G. 2005. A spatiotemporal white noise analysis of photoreceptor response to UV and green light in the dragonfly median ocellus. J. Comp. Physiol. 126, 481–497.
Land, M. F. 1985. The Morphology and Optics of Spider Eyes. In: Neurobiology of Aracnids (*ed*. F. G. Barth), pp. 53–78. Springer.
Land, M. F. and Nilsson, D.-E. 2002. Animal Eyes. Oxford University Press.
Land, M. F., Marshall, N. J., Brownless, D., and Cronin, T. 1990. The eye movements of the mantis shrimp *Odontodactylus scyllarus* (Crustacea: Stomatopoda). J. Comp. Physiol. A 28, 1311–1328.
Lee, B. B. 2004. Paths of color in the retina. Clin. Exp. Optom. 87, 239–248.
Lubbock, J. 1888. On the Senses, Instincts and Intelligence of Animals with Special References to Insects. Kegal Paul.
Marshall, N. J. 1988. A unique color and polarization vision in mantis shrimps. Nature 333, 557–560.
Marshall, N. J. and Messenger, J. B. 1996. Color blind camouflage. Nature 382, 408–409.
Marshall, N. J. and Oberwinkler, J. 1999. The colourful world of the mantis shrimp. Nature 401, 873–874.
Marshall, N. J., Jones, J. P., and Cronin, T. W. 1996. Behavioural evidence for colour vision in stamatopod. J. Comp. Physiol. A 179, 473–481.
Mathger, L. M., Barbosa, A., Miner, S., and Hanlon, R. T. 2006. Color blindness and contrast perception in cuttlefish (*Sepia officinalis*) determined by a visual sensorimotor assay. Vis. Res. 11, 1746–1753.
Maximov, V. V. 2000. Environmental factors which may have led to the appearance of color vision. Phil. Trans. R. Soc. Lond. B 355, 1239–1242.
Menzel, R. 1979. Spectral Sensitivity and Color Vision in Invertebrates. In: Handbook of Sensory Physiology (*ed*. H. Autrum), Vol.VII, 6C, pp. 503–580.
Menzel, R. and Backhaus, W. 1991. Color Vision in Insects. In: The Perception of Colour (*ed*. P. Gouras), pp. 262–293.
Nakamura, T. and Yamshita, S. 2000. Learning and discrimination of colored papers in jumping spiders (Araneae, Salticidae). J. Comp. Physiol. A 186, 897–901.
Osorio, D. and Vorobyev, M. 2005. Photoreceptor spectral sensitivities in terrestrial animals: adaptations for seeing luminance and colour. Proc. R. Soc. Lond. B 272, 1745–1752.
Peitsch, D., Fietz, A., Hertel, H., Souza, J. D., Ventura, D., and Menzel, R. 1992. The spectral input systems of hymenopteran insects and their receptor-based colour vision. J. Comp. Physiol. A 170, 23–40.
Rubin, J. M. and Richards, W. A. 1982. Color vision and image intensities: when are changes material? Biol. Cybern. 45, 215–226.
Ruck, P. 1965. The components of the visual system of a dragonfly. J. Gen. Physiol. 49, 289–307.
Seidowu, M., Sugahara, M., Uchiyama, H., Hiraki, K., Hamanaka, T., Michnomae, M., Yoshihara, K., and Kito, K. 1994. On the three visual pigments in the retina of the firefly squid, *Wtasenia scintillans*. J. Comp. Physiol. A 166, 769–773.
Snyder, A. W., Menzel, R., and Laughlin, S. B. 1973. Structure and function of fused rhabdom. J. Comp. Physiol. 87, 99–135.
Srinivasan, M. V. and Lehrer, M. 1984. Temporal acuity of honeybee vision: behavioural studies using moving stimuli. J. Comp. Physiol. 155, 297–312.
Vogt, K. and Kirschfeld, K. 1984. Chemical identity of the chromophores of fly pigment. Naturwissenschaften 71, 211–213.
Vorobyev, M. 2004. Ecology and evolution of primate vision. Clin. Exp. Optom. 87, 230–239.
Vorobyev, M. and Menzel, R. 1999. Flower Advertisement for Insects. In: *Adaptive Mechanisms in the Ecology of Vision (eds*. S. Archer and J. Partrige), pp. 537–553. Kluwer Academic Publishers.
Vorobyev, M., Brandt, R., Peitsch, D., Laughlin, S. B., and Menzel, R. 2001. Colour thresholds and receptor noise: behaviour and physiology compared. Vis. Res. 41, 639–653.
Wakakuwa, M., Kurasawa, M., Giurfa, M., and Arikawa, K. 2005. Spectral heterogeneity of honeybee ommatidia. Naturwissenschaften 92, 464–467.
Wehner, R. and Bernard, G. D. 1992. Photoreceptor twist: a solution to the false-color problem. Proc. Natl. Acad. Sci. U. S. A. 90, 4132–4135.
Wehner, R., Bernard, G. D., and Geiger, E. 1975. Twisted and non-twisted rhabdoms and their significance for polarization detection in bee. J. Comp. Physiol. 104, 225–245.
Wyszecki, G. and Stiles, W. S. 1982. Color Science Concepts and Methods. Quantitative Data and Formulae, 2nd edn. Wiley.

1.08 Visual Ecology

T W Cronin, University of Maryland, Baltimore, MD, USA

© 2008 Elsevier Inc. All rights reserved.

1.08.1	**Introduction to Visual Ecology**	212
1.08.2	**The Visual Environment**	213
1.08.2.1	Properties of Light	213
1.08.2.2	Intensity and Duration of Light	213
1.08.2.3	Spectral Properties of Natural Light	214
1.08.2.4	Polarized Light in Nature	215
1.08.2.5	Natural Scenes	216
1.08.2.6	The Biological Visual Environment	216
1.08.3	**Visual Systems and Visual Evolution as Related to Visual Ecology**	217
1.08.3.1	Eye Design and Its Variation	217
1.08.3.2	Visual Optics	217
1.08.3.3	Receptor Arrays and Retinas	219
1.08.4	**Visual Function as Related to Visual Ecology**	221
1.08.4.1	Visual Sensitivity (Brightness Adaptation)	221
1.08.4.2	Spectral Sensitivity, Color Vision, and Ultraviolet Vision	222
1.08.4.3	Polarization Vision	228
1.08.4.4	Eye Movements	231
1.08.5	**The Role of Vision in Behavior**	232
1.08.5.1	Orientation	232
1.08.5.2	Predation and Its Avoidance	233
1.08.5.3	Visual Signaling	235
1.08.6	**Concluding Remarks**	239
References		239

Glossary

accommodation The process of focusing in an eye, normally producing a sharp image of an object at a given distance.

acute zone A region of a compound eye where ommatidia are aligned so as to sample the visual field unusually densely. Analogous to the fovea of a lens eye.

chromophore A molecule attached to a protein which gives it a color. In visual pigments, this is a derivative of vitamin A or a similar compound and is the component that gives the visual pigment the ability to absorb visible light and to initiate changes in the protein that ultimately generate a neural signal.

dark noise Refers to events that occur in photoreceptors that mimic the absorption of light but are caused by other processes, typically by thermal events in visual pigments.

dichroic The property of a substance or structure to absorb one plane of polarized light preferentially to others. Visual pigments are naturally dichroic, which is the basis of most polarized-light sensitivity.

dichromacy Refers to color-vision systems that have two spectral classes of photoreceptors.

dioptric apparatus The optical elements of an eye, typically consisting of apertures, pigment layers, lenses, and possibly mirrors.

F-number A measure of the light-gathering ability of an optical device, given as aperture divided by focal length. The lower the *F*-number, the brighter the image on the retina.

irradiance The amount of light falling on a surface, typically as photons per unit time and area.

lambda-max (λ_{max}) Refers to the wavelength of maximum absorption of light (typically by a visual pigment) or sensitivity to light (typically by a photoreceptor).

ommatidium The unit of a compound eye, consisting of a group of photoreceptors and associated optical and supporting elements.

opponent channel A neural output that is derived by subtracting two inputs. In vision, these can be spatially, spectrally, or polarizationally different inputs. Opponent channels tend to enhance contrast in the signal.
opsin The protein component of a visual pigment, which binds the chromophore. All opsins of animals arise from a common ancestor and have many functional similarities across species.
optokinesis A class of eye movements in which the eye smoothly follows a visual scene or field, with intermittent rapid movements in the opposite direction.
optokinetic nystagmus The saw-tooth-like movements generated during optokinesis, created by alternating smooth, slow movements and saccadic movements in the opposite direction.
refractive index Refers to the ability of a substance to bend, or refract, light. Given as the ratio of the speed of light in the substance to the speed of light in a vacuum.
photopic Refers to vision in bright light. In vertebrates, cones are responsible for photopic vision.
photopigment See 'visual pigment'.
polarization (of light) Refers to the property of a beam or ray of light that results from the orientations of electric vectors (*e*-vectors) of the photons making up the beam. If the *e*-vectors are all parallel, the beam is fully linearly polarized; if these vectors are random in orientation, the beam is depolarized; if the situation is intermediate to these extremes, the beam is partially linearly polarized.
radiance The amount of light arriving from a location, within a solid angle, given as photons per unit time, area, and steradian.
retina An array of photoreceptors arranged in a sheet, hemisphere, or line. The retina can include neural elements besides photoreceptors in many cases.
rhabdomeric photoreceptor Refers to a photoreceptor cell in which the visual pigment is found in a large number of microvilli. This is one of the two great classes of photoreceptors, found primarily in invertebrates; the other is the ciliary photoreceptor type, found mainly in vertebrates.
saccade A rapid eye movement. Saccades occur during some visual tracking, during fixation movements of eyes, during inspection of a scene, and during the flickback movement phase of optokinetic nystagmus.
scotopic Refers to vision in dim light. In vertebrates, rods are responsible for scotopic vision.
structural color A color that is produced by optical phenomena arising from the microstructure or nanostructure of an object or surface. Many violet, blue, and green colors of animals are structural in origin.
summation The adding together of neural elements to generate a stronger or more robust signal. In vision, receptor inputs can be summed from a greater retinal area (spatial summation) or over greater amounts of time (temporal summation).
tapetum A reflecting layer behind the retina or at the base of an ommatidium. It serves to increase the amount of light passing through the retina and also generates eyeshine.
tetrachromacy Refers to color-vision systems that have four spectral classes of photoreceptors.
trichromacy Refers to color-vision systems that have three spectral classes of photoreceptors.
veiling radiance The light introduced between an object and an eye viewing it by scattering, typically within fog or underwater. Veiling radiance produces a bright haze which obscures objects behind it.
visual ecology The study of the adaptations of eyes of animals for their required functions.
visual pigment The molecules in photoreceptor cells that absorb light and begin the process of vision. They are invariably built from a protein, opsin, plus a chromophore, a derivative of vitamin A or a similar compound. Also called photopigment.

1.08.1 Introduction to Visual Ecology

Visual ecology is the study of the adaptations of eyes of animals for their required functions. Visual ecologists are concerned with how animals use their eyes, with the environments where their vision takes place, and with the visual objects that these animals are particularly interested in. Obviously, the field is unusually integrative and multidisciplinary in its approach. It considers the properties of light

(including its sources, distribution, and temporal features), how light is modified as it transits environmental media, and how light is affected by objects and surfaces. It also notes the spatial, spectral, and polarizational reflectances of natural scenes and of objects within these scenes. Perhaps most importantly, visual ecologists must be expert vision scientists, as the field embraces visual optics, eye and retinal design, photoreceptor diversity and function, and visual processing. And since the ultimate goal of visual ecology is to understand how visual systems of animals meet their biological needs, the ecology and behavior of species must be considered. As can be seen, the field spans levels of study from the molecules and genes of vision and visual development to the ecological niches that animals occupy, and includes most aspects of biological science as well as biochemistry, physics, and computational modeling. Including so many areas of science, visual ecology is an unusually rewarding research area within visual science.

The questions that visual ecologists ask are among the oldest in biology: "Do other animals see things the way we do?," "Do animals have color vision?," "How can some animals see underwater, or at night?," and so forth. The field itself, however, was formally recognized only after 1979, when John Lythgoe published a rather small book called *The Ecology of Vision*. Lythgoe's viewpoints have withstood the test of time unusually well, and many of the issues he raised are still very active topics in the field. I suspect that the field's founding father would be delighted to see the vitality that visual ecological research has today. In fact, in a single chapter there is simply not sufficient space to cover the state of knowledge in any detail, so the focus here is on fundamentals and on particularly interesting and promising new areas of focus in the field.

I will begin with the properties of the stimulus light, its sources, spectra, and polarizational features, as well as its distribution in natural scenes and its special roles in biology. The discussion will then proceed to animal eyes, touching on eye evolution and design, visual optics, and retinal specializations. Next, I will cover how visual function is adapted, discussing specializations for increasing sensitivity, improving spectral sensitivity and color vision, enhancing polarization vision, and managing how eye movements are controlled. The final section of the chapter will be devoted to vision's role in the lives of animals, including how it functions in animal orientation, predation and predator avoidance, and visual signaling.

1.08.2 The Visual Environment

1.08.2.1 Properties of Light

Light is, of course, a form of electromagnetic energy, but deciding what part of the electromagnetic spectrum is properly called light is rather arbitrary. The spectral region seen by humans – visible light – by convention includes wavelengths from 400 to 700 nm (though humans can see outside this range in appropriate conditions). Visual systems of other animals respond to wavelengths from near 300 nm to beyond 750 nm. The dual nature of light, possessing properties of waves and particles, is critical to recognize when considering vision. The spectral region within which photoreceptors respond arises from light's wave properties, but the actual absorption events occur photon-by-photon and are thus quantal. Another wave property of light that can be important in vision is its polarization. So a complete description of light as a visual stimulus necessarily includes its intensity (the rate at which photons arrive), its spectrum (the distribution of these photons within the visual spectrum), and its polarization (generally, the fraction of photons that have electrical vectors that are aligned parallel to a particular plane).

1.08.2.2 Intensity and Duration of Light

Animals must cope with an astonishing range of light intensities. Just on the earth's surface, the variation from full sunlight to overcast night sky exceeds 10 log units; in the sea, light is further attenuated indefinitely, depending on the depth of overlying water. Given that light absorption in photoreceptors occurs photon-by-photon, light intensities should be given in quantal units, either as irradiance or as radiance. Irradiance is the measure of the amount of light falling on a surface, typically as photons per unit time and area, and is appropriate when considering the illumination of a scene. Radiance is the amount of light arriving from a location, within a solid angle, specified as photons per unit time and area and per unit steradian. It is used when considering the distribution of light in a scene, as in a region being visually imaged. When the spectral distributions of radiance or irradiance are being considered, a spectral unit (typically per nanometer) is also necessary to specify the spectral range within which bins of quanta are summed. Full sunlight irradiance is on the order of 10^{13} to 10^{14} photons $cm^{-2}\,s^{-1}\,nm^{-1}$ at 500 nm.

Irradiance varies with the location on the earth or in its waters, and it obviously also varies with time. The primary influences on temporal light variations are astronomical and are therefore predictable. These natural variations in lighting and their influences on vision and behavior have been nicely reviewed by McFarland W. N. (1986); the biological importance of diurnal, monthly, and seasonal patterns of illumination is well known and needs little further coverage here. Higher-frequency variations in lighting, caused by atmospheric conditions, surface waves (in water), wind effects on foliage, and so on, are recognized, but their effects on vision have not yet received much research attention (McFarland, W. N. and Lowe, E. R., 1983; Loew, E. R. and McFarland, W. N., 1990; Maximov, V. V., 2000; Cronin, T. W., 2006). Changes in irradiance with location in water (including depth) and under the forest canopy are associated with far more dramatic changes in the spectral content of light and will be covered in the next section.

1.08.2.3 Spectral Properties of Natural Light

Spectral variations that occur in natural illumination (Figure 1) are nearly as challenging to visual systems as those of intensity, and a huge literature exists on the topic of visual specialization for function in different spectral environments (touched on later in this chapter). The natural spectrum changes on the surface of the earth with time of day, sky state, and location (for instance, at various places within a forest). In water, these same influences also cause spectral shifts, but the spectrum of irradiance varies more dramatically with water quality, depth, and direction of illumination.

The whitening of the normally blue spectrum of the sky under clouds is widely recognized. Less well known is that the sky overhead becomes its bluest at twilight, when sunlight is scattered by 90°; simultaneously, the light from the direction of the sun becomes its reddest as it travels to the viewer through atmospheric dust, smoke, and haze. Thus, the relatively flat spectrum of daylight sharpens into two distinct peaks (Figure 1), in the blue and red, at twilight (Rozenberg, G. V., 1966; McFarland, W. N., 1986). As this is also a time of rapidly decreasing irradiance, it is likely that animals active at this time are specifically adapted to the spectral qualities of twilight.

Terrestrial animals move or fly around. If they are in open country, the light by which they see remains essentially constant, but this is not the case for forest-dwelling species. Here, the local illumination can vary on fine spatial and temporal scales, as animals move between deep shade and brighter patches of various sizes, lit by different parts of the sky. As the intensity

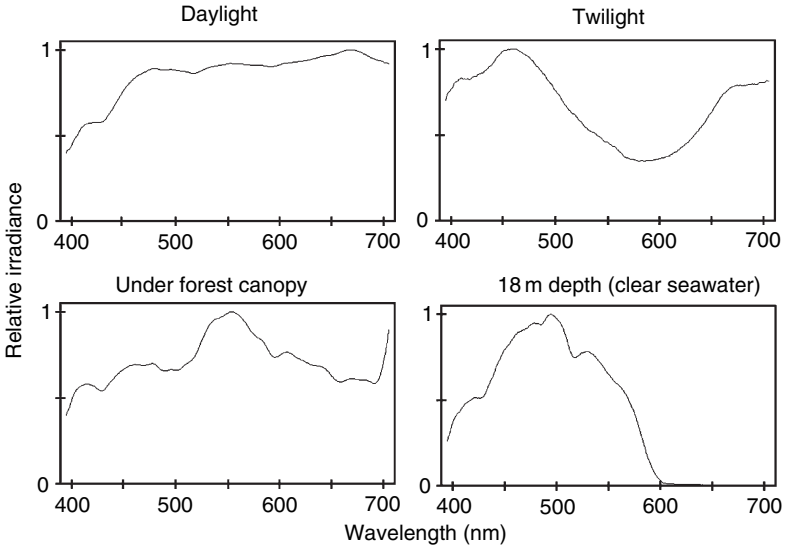

Figure 1 Typical irradiance spectra of light illuminating scenes viewed by animals, each normalized to its maximum. Top left: the daylight spectrum, which is spectrally broad and relatively flat. Top right: the spectrum at morning twilight, just at sunrise, showing the deep blue peak produced by scattering in the sky and the red peak produced by the passage of sunlight through a long atmospheric path when the sun is at the horizon. Bottom left: light in a Panamanian forest at midday, filtered by the forest canopy, showing the peak near 550 nm produced by chlorophyll in leaves. Bottom right: irradiance at 18 m depth in clear, coastal seawater, illustrating the removal of long wavelengths and the reduction in intensity at short wavelengths as light transits water.

changes, shifting contributions from direct sunlight (white), open sky (blue), and light transiting the canopy (green) produce an array of distinctive photic microenvironments (Endler, J. A., 1993; Chiao, C.-C. *et al*., 2000a). Animals can use such places for particular tasks depending on their appearance in them.

Underwater, the lighting situation is even more variable. There are still the diurnal variations in spectrum just described, at least near the surface, and lighting varies under aquatic vegetation much as it does in the forest (Cummings, M. E. and Partridge, J. C, 2001). Changes in spectral content produced by the water itself, however, probably have the greatest impact on aquatic species (reviews: Jerlov, N. G., 1976; Lythgoe, J. N., 1988; Loew, E. R. and McFarland, W. N., 1990). Water is a spectral filter, preferentially transmitting light near 475 nm, and the dissolved and suspended matter in natural waters increases the absorption of light and shifts its spectral distribution by up to 100 nm (or occasionally more) to longer wavelengths. Species that live in estuaries or other varying waters, that migrate between water types, or that change habitats with development, must cope with these variations. The filtering effects of water become increasingly critical at greater depths. Even in the clearest oceanic waters, which transmit light nearly as well as pure water does, light becomes dim and virtually monochromatic within a few hundred meters (Tyler, J. E. and Smith, R. C., 1970).

The relatively simple and predictable photic properties of water, particularly regarding the distribution of radiance and the transmitted spectrum, make it an ideal natural laboratory for investigations of visual design and function. Light is filtered as it enters water and again after it reflects from an object, and new light is scattered into the visual path, creating a unique, low-contrast, but optically well-defined visual environment (Figure 2). Much of the theory within visual ecology has been developed using aquatic systems and species, and the aquatic environment remains important for hypothesis generation and testing.

Figure 2 Reduction in color range and image contrast underwater produced by light absorption, background scattering, and veiling radiance. The upper photograph was taken of a school of squid, seen from a distance of about 3 m and at a depth of about 1 m in clear seawater. Note that scattering and absorption of light, even at this very shallow depth and relatively short viewing distance, produce a greenish-blue cast to the entire image and almost completely obscure both the squid and the coral beneath them. Color and brightness contrast were restored in the lower image to reproduce the approximate appearance of the scene to the photographer (the author) when the image was captured.

1.08.2.4 Polarized Light in Nature

The light produced by natural sources is weakly polarized at best, but polarized light is nevertheless abundant in nature (reviews: Waterman, T. H., 1981; 1984; Wehner, R., 2001). In the sky and underwater, scattering of incoming light produces partial linear polarization that varies with solar position and direction of view. Reflection of light from the air–water interface or from shiny surfaces (e.g., leaves, wet surfaces, animal skin, scales, or cuticle) also produces strong polarization in geometrically favorable circumstances. Terrestrial animals that detect polarized light, like insects, can use the reliable polarization patterns of the sky for navigation. On the other hand, for such animals, the chaotic and unpredictable pattern of polarized-light reflection can mask or taint the true colors of objects. Animals with polarization vision often employ special adaptations that eliminate polarization sensitivity in some spectral receptor classes to retain a form of color constancy (Wehner, R. and Bernard, G. D., 1993; Marshall, N. J. *et al*., 1999), or they may evaluate viewed objects using combined spectral and polarizational cues (Kelber, A., 2000;

Kelber, A. *et al.*, 2001). Light reflected from the surface of water presents a very strong polarization cue for many flying insects (Schwind, R., 1984; Schwind, R., 1991; Horváth, G. *et al.*, 1997).

The best-studied celestial polarization patterns are produced by scattered sunlight, and similar distributions of polarized light that appear in the sky when the moon is bright are useful to some nocturnal insects (see Gál, J. *et al.*, 2001; Dacke, M. *et al.*, 2003; 2004). Skylight polarization is exceptionally strong and stable at twilight (Figure 3), for about an hour before dawn and after sunset (Cronin, T. W. *et al.*, 2006). The polarization pattern of the twilight sky could be important for orienting both insects (Greiner, B. *et al.*, 2004) and vertebrates (Helbig, A. J., 1990).

Terrestrial scenes provide complex and shifting patterns of celestial polarization and reflections of polarized light from shiny objects, but the situation is almost always simpler underwater. Due to refraction at the air–water interface, illumination from the sky is within 46° of overhead at all times. The resulting light field is nearly horizontally polarized most of the time (Waterman, T. H, 1981; Cronin, T. W. and Shashar, N., 2001). Polarization under water is generally weaker than in the sky, and little polarization is produced by reflection from objects, as the refractive index gradient between water and most objects is less than in air. Despite this, polarization vision is common in aquatic animals, for reasons to be discussed later.

1.08.2.5 Natural Scenes

Natural scenes have special properties, quite different from those of either purely random or highly ordered geometric arrays. The relationships between the properties of natural scenes and the sensory systems are central to understanding sensory ecology. All natural stimuli exist within extended scenes (most obviously for visual, auditory, and chemical stimuli), and it is evident that environmental features of stimuli constrain the evolution of sensory systems (see Wehner, R., 1987). Understanding how spatial, temporal, and spectral properties of visual systems, as well as features of biological signaling, are molded by natural scenes requires appropriate descriptions of these scenes.

Natural visual scenes are scale invariant (Ruderman, D. L., 1994); their spatial properties are the same at any magnification. This result probably emerges from the presence of self-similar objects (e.g., trees, grass, and rocks) at all viewing distances and thus at all spatial scales (see Burton, G. J. and Moorhead, I. R., 1987; Ruderman, D. L. and Bialek, W., 1994). Common properties of visual systems, including sparse coding (Olshausen, B. A. and Field, D. J., 1996), lateral inhibition (Srinivasan, M. V. *et al.*, 1982; Laughlin, S. B., 1994), predictive coding (Srinivasan, M. V. *et al.*, 1982; Attick, J. J., 1992; Hosoya, T. *et al.*, 2005), and spatiotemporal processing (van Hateren, J. H., 1992; Laughlin, S. B. and Weckstrom, M., 1993; van Hateren, J. H., 1993), can be explained by natural scene properties. Later in the chapter, I will consider how scene spectral features have influenced the evolution of color vision. Current work on natural scenes includes research on how animals integrate themselves into these scenes for signaling and concealment.

1.08.2.6 The Biological Visual Environment

Even the simplest visual task must cope with many of the aspects of light and the visual environment

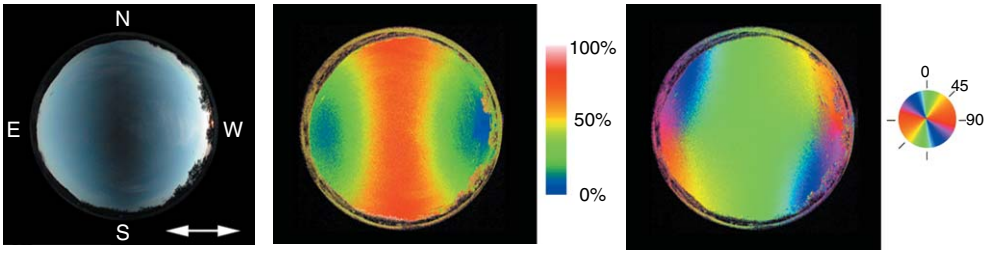

Figure 3 Polarization images of the clear sky at sunset near the autumnal equinox. All panels show the same celestial pattern. The left panel illustrates the appearance of the sky seen through a polarizer oriented E/W, and shows the strong N/S-oriented polarization as a dark band extending directly across the zenith. The middle panel is a false-color image illustrating the degree of polarization (% polarization), coded as in the key to the right. Note how strongly the N/S polarization band is polarized (~80%), with polarization falling in a symmetrical pattern toward the east and west. The right panel shows the *e*-vector angle (polarization angle) at each point in the sky, coded as illustrated in the key to the right. Again, note the extremely symmetrical pattern of polarization, with polarization in the N/S band all oriented parallel at about 0°.

presented above. This demands a lot from a visual system, as engineers have learned when designing even basic, artificial visual devices. Vision's evolution is influenced by the features of the physical and natural environment, but its function is biological. Thus, animals that inhabit similar habitats, even those active under very similar circumstances, require their visual systems to perform quite specific tasks, and similar animals often have different visual needs. Predators must track down their prey, while the prey strive to detect predators first. Bees and hummingbirds fly to flowers, but fruit bats and primates search trees for fruit. Navigating desert ants must find their way home in a featureless world, while forest ants have a superabundant set of visual cues to use to orient. Octopuses vary their appearance to disappear against backgrounds, while poisonous seaslugs in the same spot appear maximally conspicuous. Vision is involved in all these situations, and the huge diversity of visual systems and visual tasks motivate visual ecologists to attempt to understand how it all works.

1.08.3 Visual Systems and Visual Evolution as Related to Visual Ecology

1.08.3.1 Eye Design and Its Variation

Even a single photoreceptor cell provides useful information about the time of day or the passage of shadows, but complex eyes are needed if an animal requires far more than this. All eyes have two sets of functional components: a retina containing an array of photoreceptors that provide input into some sort of central or higher-order processor (or at least an effector) and a dioptric apparatus that controls how light reaches the retina by refraction, reflection, and/or absorption.

Eyes have apparently evolved independently a number of times, although it does seem possible that all eyes in existence today trace back to as few as two ancestral organs or cell masses (Oakley, T. H. and Cunningham, C. W., 2002; Nilsson, D.-E., 2005). There are about nine fundamentally different optical designs in modern eyes (Land, M. F., 1981; Land, M. F. and Nilsson, D.-E., 2002; Land, M. F., 2005;), divided into two main groups, simple (or single chambered) and compound. However, operating principles of eyes can be so divergent that it is often difficult to see how one type evolutionarily relates to another. Visual ecologists tend to not be so concerned with the evolutionary pathways that link eyes as with the evolutionary specializations that shape them for particular functions.

1.08.3.2 Visual Optics

The simplest eyes can hardly be said to have optics at all. Pigment-cup eyes consist of an invaginated retina backed by a layer of pigment, but they still provide a low-resolution representation of the outer world on the retina: objects to the left map to regions on the right side of the retina, and so forth. Though insensitive and incapable of much acuity, pigment-cup eyes give a basic sense of light's direction and change, and can mediate orientation or defensive behavior (Nordström, K. *et al.*, 2003; Land, M. F., 2003). Groups of pigment cups – perhaps the ancestors of today's highly evolved compound eyes – serve as detectors of approaching or passing objects (Nilsson, D.-E., 1994).

It is a surprisingly short distance from a pigment-cup eye to an optically excellent lens eye. Nilsson, D.-E. and Pelger, S. (1994) estimate that evolution could shape the change in less than a half-million years, even assuming quite weak selection. Good eyes based on spherical refracting lenses require a properly shaped gradient of refractive index from the center to the margin of the sphere (Land, M. F., 1981; 2005), but such eyes have turned up repeatedly, in quite disparate taxa. An unexpected example of this occurs in box jellyfish, animals that lack a central nervous system but nevertheless have eight optically excellent lens eyes of two types (Nilsson, D.-E. *et al.*, 2005). Strangely, even though each lens in these jellyfish eyes forms a sharp image, in life the retina is much closer to the lens than the focal plane. This produces severely underfocused images on the retina, perhaps suitable for sensing the overall light field while blurring out the shapes of small, floating objects.

Most animals with quality lens eyes, ranging from worms to octopuses to vertebrates, put the retina where it belongs, at the lens's plane of focus. These eyes all operate on the same fundamental optical principle, refracting light using spherical surfaces to produce the image. The most important differences among lens eyes relate to the medium in which they are used. The sudden change in refractive index when light enters ocular media from air means that in aerial vision the cornea, the outermost optical structure in a lens eye, normally has most of the refractive power used to form the image. In water, however, there is only a slight change in refractive index between water and the cornea, so the spherical lens, with its radial

refractive index gradient, is the major image-forming element. Eyes of amphibious animals must have special adaptations for effective use in both media; the functioning of amphibious lens eyes has been reviewed by Sivak J. G. (1988); see also the classic work on vertebrate eyes by Walls G. L. (1942), as well as Land M. F. and Nilsson D.-E. (2002).

The lens eyes of some deep-sea fishes show a particularly elegant functional modification. Due to refraction at the water's surface and further absorption as light travels down through the water column, sunlight in the deep sea is confined to an overhead patch perhaps 90° across. Predatory fishes look up into this window of light, searching for prey silhouetted against it and maximizing visual contrast by gathering as much light as possible. For optimal viewing in this limited visual field, they have discarded all but the central region of the retina; the resulting bullet-shaped eye is called a tubular eye (Warrant, E. J. *et al.*, 2003; Warrant, E. J., 2004; Figure 4). Despite its odd appearance, the tubular eye is functionally identical to any other fish eye;

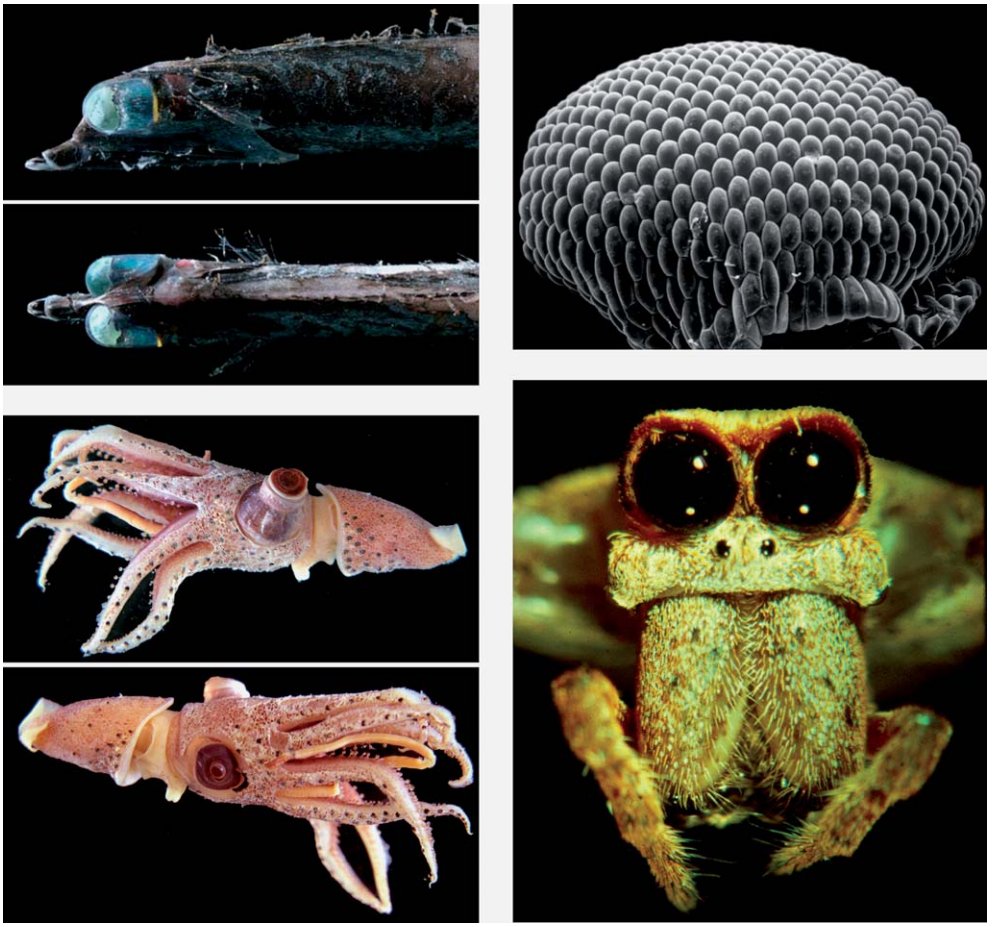

Figure 4 Eyes designed for visual function in conditions of very limited light. The left top panel pair shows the tubular eyes of the deep-sea fish *Stylephorus chordatus* in lateral and dorsal view. Photograph courtesy of E. A. Widder. Notice how the bullet-shaped tubular eyes face forward on the body axis, suggesting that the fish hunts while hanging vertically in the water. The lower panels show the asymmetrical eyes of the deep-sea squid *Histioteuthis* sp. The squid's right eye is also a tubular eye, functioning optically like that of *S. chordatus*, while the left eye is of normal size and has an extended visual field. The squid presumably hunts while swimming on its side, with the tubular eye directed upward (photographs by the author). The top panel on the right side shows the tubular compound eye of a euphausiid crustacean (probably *Nematoscelis*). The dorsal half of this eye, shown, has its ommatidia arranged to sample the same limited downwelling light field as seen by the tubular lens eyes of *S. chordatus* and *Histioteuthis*, revealing convergent optical design. The ventral half of each divided eye, not shown, is expanded to form a hemispheric field of view. Photograph courtesy of D. Pales. The lower right panel illustrates the lens eye of the spider *Dinopis subrufus*, which has an *F*-number of 0.6 (the lowest known for any lens eye), used for nocturnal hunting. Photograph courtesy of M. F. Land.

the only difference is that there is no retina present outside the central viewing area. Tubular eyes and their analogues also exist in a number of invertebrate deep-sea species (Figure 4).

Lens eyes have traditionally been likened to photographic cameras because their operating principles are so similar. Visual optics of other eye types are so diverse – and unfamiliar – that there is insufficient space in a review of this nature to describe them adequately. The best references to consult for more information are Land's and Nilsson's book, *Animal Eyes* (2002), and also Land's 1981 and 2005 reviews.

Compound eyes use a diverse and astonishingly complex assortment of optical principles to form images (Nilsson, D.-E., 1989), but these eyes are all built of an array of numerous, similar elements that sample space in a neatly geometrical pattern. With minor exceptions, they function analogously to other eye types, using a matrix of photoreceptor elements that correspond to points in visual space. It is convenient, therefore, to think of the receptor array as a retina and to consider how space is sampled as one would for any other retina, discussed in the next section.

1.08.3.3 Receptor Arrays and Retinas

As just suggested, retinas are generally made up of a geometrical array of photoreceptors that correspond to a similar array of spatial locations. The overlying optical elements govern how much light reaches each receptor and set a limit to visual resolution. While sensitivity and resolution are fairly constant across the retina in most eyes, they can vary considerably among receptors in some compound eye types. The visual ecological significance of retinal design arises from this sensory mapping of the external world. In a quite literal sense, retinal design informs us about the concerns and expectations of a species (see Wehner, R., 1987).

Few eyes sample visual space evenly, and those that do are generally simple in design or of very limited optical quality. Complex, image-forming eyes instead tend to use a disproportionate number of receptors to sample a relatively small portion of the whole visual field, so that it can be seen in extraordinary detail. The extended retinas of simple eyes normally control spatial sampling by varying the amount of neural convergence from receptors onto the neural elements that lead to the central nervous system (retinal ganglion cells in vertebrate eyes). A region of dense sampling often forms a depression in the retinal surface, and is therefore called a fovea (meaning pit). Compound eyes fine-tune sampling using variations in the angular spacing among adjacent units (each unit of a compound eye is called an ommatidium). When ommatidia are arranged so that the angular separation between neighbors is unusually small, this produces a region of elevated resolution termed an acute zone. Since acute zones of compound eyes are functionally equivalent to foveas of simple eyes, the term fovea is often generally used to designate any ocular region of high visual acuity (Figure 5).

In a given eye, the fovea might map to a single spot in the outside world, a common situation in animals with binocular vision. Or it might correspond to an extended location, such as the horizon; this is frequently seen in prey animals, especially in those that inhabit flat spaces such as plains or sand flats (reviewed in Cronin, T. W., 2005). Many species have multiple foveas in a single eye; for instance, vertebrates whose eyes face to the side almost always have one fovea sampling space in front of the head and another aimed laterally (Figure 5). The quality of vision in each fovea can vary according to the animal's needs. An interesting example is seen in raptors, aerial predators, where the extremely acute lateral fovea is used to detect and track prey. Since this part of the eye actually faces 45° to the flight path, the hunter spirals in as it attacks prey (Tucker, V. A., 2000). Invertebrate raptors, dragonflies, provide interesting analogues to this. Their compound eyes have a relatively weak acute zone aimed ahead plus a large, laterally extended one sampling the sky above and slightly in front of the direction of flight (Sherk, T. E., 1978). This permits them to image small flying prey against the bright sky background and to attack them with an upwardly swerving flight, while remaining relatively invisible below the intended prey, out of its best field of view.

Foveas in lens eyes by definition have little neural summation, and often contain unusually narrow, tightly packed photoreceptors. Thus, they are normally less sensitive to light than other retinal regions (this is why the most sensitive vision in humans is in the peripheral field). Acute zones of compound eyes, on the other hand, can combine sensitivity with acuity. In fact, in compound eye design these properties are linked because diffraction in the tiny corneal lenses limits spatial resolution (reviews: Snyder, A. W., 1979; Land, M. F., 1981). As neighboring ommatidial axes become more parallel, paradoxically the corneal facets must become larger to provide adequate resolution. This tends to flatten the surface of the compound eye and provides both improved acuity

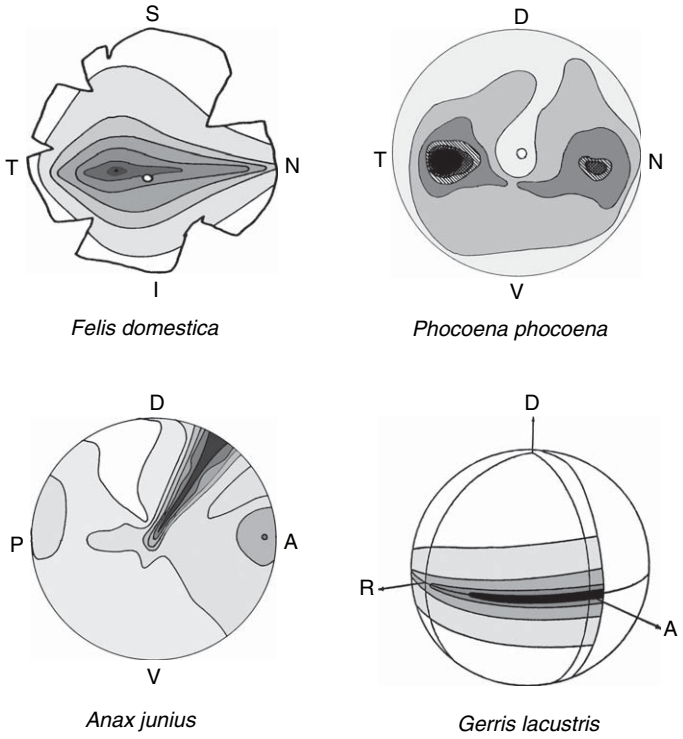

Figure 5 Sampling of the visual field by right eyes of vertebrates (top panels) and arthropods (bottom panels). Increasing density of fill indicates regions of increased acuity, sampled either by greater densities of ganglion cells in vertebrate retinas or by more tightly packed ommatidial arrays in compound eyes, but the coding does not indicate identical acuity values in the different panels. White circles near the centers of the vertebrate retinas show the location of the optic disk, where axons of retinal ganglion cells enter the optic nerve. Top left: The house cat, *Felis domestica* (after Land, M. F. and Nilsson, D.-E., 2002), illustrating the single central fovea and a suggestion of a horizontal visual band, or visual streak. Top right: Harbor porpoise *Phocoena phocoena* (after Mass, A. M. *et al.*, 1986), showing the two foveas, one directed forward and the other laterally. *Bottom left*: dragonfly *Anax junius* (after Sherk, T. E., 1978) to show the strip-shaped band of high acuity facing upward and forward, with a second smaller anterior acute zone. Bottom right: Visual fields of the waterstrider *Gerris lacustris* (after Land, M.F. and Nilsson, D.-E., 2002 using data from Dahmen, H., 1991). Note the extensive horizontal acute zone, representing the visual streak that samples the flat surface of the water on which *G. lacustris* lives. S, superior; I, inferior; T, temporal; N, nasal; D, dorsal; V, ventral; R, right. Reproduced from Cronin, T. W. 2005. The Visual Ecology of Predator-Prey Interactions. In: Ecology of Predator-Prey Interactions (*eds.* P. Barbosa and I. Castellanos), pp. 105–138. Oxford University Press, with permission.

and sensitivity at once. So the acute zone of a compound eye can have elevated sensitivity at no cost in resolution. For example, eyes of male blowflies, *Chrysomyia megacephala*, are specialized as dot detectors, having a very sensitive region looking overhead for the tiny silhouettes of female flies (van Hateren, J. H. *et al.*, 1989). Compound eyes also produce analogues of the horizontally extended foveas in eyes of vertebrates that live in flat terrain (see Walls, G. L., 1942). Fiddler crabs, denizens of sand flats, and waterstriders, who inhabit the flat surfaces of ponds and streams, both have compound eyes with acute zones that extend horizontally around the eye (Zeil, J. *et al.*, 1986; 1989; Dahmen, H., 1991). Their eyes are beautifully designed to pick out objects sitting on the level planes of their worlds (Figure 5).

The final word in this section is reserved for spiders, many of which have visual systems that combine features of both lens and compound eyes. Most spiders have eight lens eyes, aimed to cover the visual field with areas of both low and high resolution. Not only does this give excellent spatial coverage, but it also breaks up the world into different functional zones, some of which are monitored for suspicious events (like moving objects) while others are viewed in fine detail (Duelli, P., 1978; Land, M. F., 1985a; 1985b). Wolf spiders (Lycosidae) and jumping spiders (Salticidae), creatures that stalk their prey or make visually directed ambushes, have the highest-resolution vision of any terrestrial invertebrate (Land, M. F., 1985a), permitting unusually complex hunting and mating behavior.

1.08.4 Visual Function as Related to Visual Ecology

1.08.4.1 Visual Sensitivity (Brightness Adaptation)

Animals that use their eyes on the earth's surface during the day are provided with a wealth of photons for seeing, as something like 10^6 photons reach each photoreceptor per second (Land, M. F. and Nilsson, D.-E., 2002). This number is more than adequate for standard visual tasks, but still, only 1000 or so quanta arrive per millisecond, which limits signal quality in very fast-responding receptors. Human vision becomes barely possible on overcast, moonless nights, when the intensity is reduced by 10 orders of magnitude, providing the average receptor with a photon once every 10 000 s. Yet, under these conditions, and even more challenging ones in the deep sea, some animals see very well. How their visual systems achieve the required sensitivity is a classic question in visual ecology.

Vision starts with the photoconversion of a molecule of visual pigment, followed by the transduction of this event to initiate a neural signal. A single photon is sufficient to produce a usable change in photoreceptor membrane potential, but at this threshold vision is ruled by statistics. Not all photons are absorbed by visual pigments, not all absorptions activate the pigment, and not all activations lead to phototransduction. Furthermore, visual pigments can be activated in the dark by random thermal events; while these occurrences are rare, they become critically important near vision's threshold. Also, the photoreceptors must be fed with light, so light must enter and transit the optics of the eye, be properly collected and focused on the retina, and pass into the photoreceptor. Losses occur at every stage of this sequence. And ultimately, vision is a process that requires statistically distinct differences between photoreceptor signals both in time and in space, not just on catching the odd photon. Considering all that is required, it sometimes seems a wonder that animals see at all.

A photoreceptor's sensitivity to an extended scene increases with the area of the collecting aperture, the inverse of the focal length of the optics, the diameter and length of the receptor, and the density of visual pigment in the receptor (Land, M. F., 1981; Warrant, E. J. and Nilsson, D.-E., 1998; Warrant, E. J., 2004). Photopigment density is fairly consistent within phylogenetic taxa, with absorption ranging from 1% μm^{-1} to 3% μm^{-1} of receptor length. Animals can therefore increase sensitivity by increasing photoreceptor length and diameter and by making large eyes with big apertures but short focal lengths. Of course, all these adaptations have costs, and almost every improvement means that an animal must carry around and operate a bigger chunk of optical machinery.

Taking the *F*-number (aperture divided by focal length) of an eye is a simple way to estimate the image brightness on the retina – the smaller the *F*-number, the brighter the image. The dark-adapted human eye has a pupil diameter of about 8 mm and a focal length of 17 mm, giving an *F*-number near 2.1. Other vertebrate lens eyes reach minimal *F*-numbers near 1.25 in many fishes (see Land, M. F. and Nilsson, D.-E., 2002; Warrant, E. J. *et al.*, 2003) and similar or even lower values in nocturnal birds (Martin, G. R. *et al.*, 2004; Warrant, E. J., 2004). The minimum known *F*-number for a lens eye is 0.6, found in a nocturnal spider, *Dinopis subrufus* (Figure 4), and the best *F*-number of all, 0.25, is produced by the mirror eyes of a deep-sea ostracod (Land, M. F., 1981; Warrant, E. J., 2004). Interestingly, these record-breaking eyes are all extremely small and have relatively few photoreceptors, so their optical quality need not be perfect. Low *F*-numbers mean a bright retinal image, but there is a cost for vision in addition to the possible reduction in optical quality – the angular extent of the cone of light illuminating each receptor is broad, so light could fail to be trapped in the central receptor and even pass laterally between receptors.

Increasing photoreceptor diameter provides a larger area for light capture, but reduces the number of sampling points on the retina as a whole. On the other hand, photoreceptor length increases have little effect on spatial resolution. Another adaptation is to place a mirror layer, or tapetum, behind the neural retina to reflect transmitted light back through the receptor layer for a second chance at absorption. Tapetal layers are very common in nocturnal eyes of vertebrates (Walls, G. L., 1942), giving them their famous eyeshine. Among invertebrates, they occur in nocturnal spiders (Land, M. F., 1985a) and in the compound eyes of butterflies, moths, and marine crustaceans (Land, M. F., 1981). Another solution that effectively increases retinal thickness (if not receptor length) is to place photoreceptors in multiple layers. This is seen in many deep-sea fishes (Warrant, E. J. *et al.*, 2003; Warrant, E. J., 2004) and has recently been discovered in a nocturnal bird species, the oilbird *Steatornis caripensis* (Martin, G. R. *et al.*, 2004).

A final way to get more photons into photoreceptors is to decrease their reflective loss at the cornea. Compound eyes of many terrestrial arthropods use photonic solutions to enhance corneal transmission, covering each corneal facet with a lawn of tiny bumps termed corneal nipples by their discoverers (see Miller, W. H., 1979). These mimic the effect of a smooth transition in refractive index moving from air into the corneal matrix, increasing transmission while minimizing glare. Reflection suppression by corneal gratings has even been found in an extinct fly species (Parker, A. R. *et al.*, 1998).

The adaptations discussed so far are anatomical. Some are kludged together to make an optically limited eye of low resolution but with adequate sensitivity to meet the requirements of a small animal that must survive at night or in very dark water. Others are elegant fine tunings of optically outstanding ancestral eyes, as in deep-sea fishes or oilbirds. Ultimately, however, anatomical modifications reach their limits, and evolution then has only two ways out if a species must function in a darker world. The eye can increase in size, thereby providing a larger retina to hold bigger photoreceptors, or the visual system must turn to physiological solutions that improve sensitivity, using neural tactics to enhance vision that has reached terminal optical constraints (see Snyder, A. W. *et al.*, 1977; Laughlin, S. B., 1981; Warrant, E. J., 2004). Signals from individual receptors can be summed over time (effectively increasing integration time, thereby reducing temporal resolution), a process called temporal summation. Or the inputs from a number of adjacent receptors can be combined into a single neural signal (increasing collection area, reducing spatial acuity), termed spatial summation. Of course, spatial and temporal summation are commonly employed in unison, producing some appropriate compromise of decreased temporal or spatial acuity.

Integration times of photoreceptors often are adaptive for the ecological characteristics of species, as discussed earlier (see Laughlin, S. B. and Weckström, M., 1993), and they are commonly adjusted in individual receptor cells during the process of light or dark adaptation. It is also possible that higher-order neurons may accumulate photon signals over time, further increasing summation times (see Warrant, E. J. *et al.*, 1996). In some eyes, particularly compound eyes, individual photoreceptors alter their receptive field sizes during adaptation (e.g., Barlow, R. B., Jr. *et al.*, 1988). However, it is most common for receptors to be combined neurally, converging onto a single postsynaptic cell. Such cells extend horizontally in the retina, collecting inputs from a number of photoreceptors. An excellent example of this exists in the nocturnal bee, *Megalopta genalis*. Unlike almost all other bees, this unusual species flies under the rainforest canopy at twilight, well before sunrise or after sunset. It is capable of orienting itself in light intensities where human vision is impossible, and does this using a compound eye that is fundamentally the same as those of day-flying insects like honeybees. The immense increase in sensitivity required for this task is partially accomplished by extensive spatial summation, thought to be enabled by widely branched neurons onto which photoreceptors synapse (Warrant, E. J. *et al.*, 2004; Greiner, B. *et al.*, 2005). Theoretical analysis of summation suggests that visual function is surprisingly well maintained both spatially and temporally, even when sensitivity is improved by many orders of magnitude (Theobald, J. C. *et al.*, 2006). Some night-flying insects, for instance the hawkmoth, *Deilephila elpenor*, even maintain color vision in starlight intensities through the use of neural summation (Kelber, A. *et al.*, 2002).

1.08.4.2 Spectral Sensitivity, Color Vision, and Ultraviolet Vision

How the spectral sensitivities of photoreceptors should be tuned for best visual function is one of the oldest questions in visual ecology. If a photoreceptor is needed solely to catch available photons, then it seems obvious that its spectral sensitivity should somehow match the available spectrum of light (although, as will be seen shortly, even this may not be optimal). But vision is more than simple photon capture. It involves detecting the variations in light throughout a scene and sorting out the differences in light arriving from significant as opposed to insignificant sources (typically, objects vs. backgrounds). Thus, the fundamental requirement of a visual system is contrast detection. When the photic environment is nearly monochromatic (as in the deep sea), and everything is seen in a single spectral region, optimization of vision for sensitivity is equivalent to optimization for contrast. Most visual environments are far more spectrally complex (and often quite variable), and it is not often simple to predict how visual photoreceptors should be spectrally fit to visual tasks.

Photoreceptor spectral sensitivity is primarily determined by the spectral absorbance of the visual pigment it contains; typically, a single visual pigment class dominates in a given receptor class. All visual

pigments are derived from an opsin, a G-protein-coupled receptor protein, combined with a chromophore (either a retinaldehyde or a closely related derivative). Spectral tuning of the visual pigment results from interactions between charged amino acids in the chromophore-binding pocket of the opsin and the chromophore itself. Depending on opsin sequence, the wavelength of maximum absorption (λ_{max}) can range from near 300 nm, in the deep ultraviolet (UV), to beyond 600 nm, well into the red. There is also a chromophore-specific effect on λ_{max}: visual pigments that use 3,4-dehydroretinal as a chromophore (often termed A2 visual pigments) absorb at distinctly longer wavelengths than those with identical opsins bound to retinal itself (A1 visual pigments). Nevertheless, within each chromophore type the absorbance spectrum of the visual pigment is fully predictable, given the λ_{max} (Dartnall, H. J. A., 1953; Lipetz, L. E., and Cronin, T. W., 1988; Stavenga, D. G. *et al.*, 1993). This mathematical property makes it easy to model the potential performance of various visual pigments in any specified spectral environment, which has stimulated much recent work on the design of spectral sensitivity systems and the evolution of visual pigments and photoreceptors. The close and causally direct link between protein sequence, visual pigment absorbance, and (potentially) evolutionary history and current function make studies of visual ecology particularly attractive to sensory ecologists and evolutionary biologists.

The simplest spectral environments exist in the sea. Light near the surface has a broad spectrum, like light in the terrestrial world, but as depth increases the spectrum narrows rapidly, producing an asymptotic transmitted waveband that varies with water type and quality (Jerlov, N. G., 1976; Lythgoe, J. N., 1979; 1988). Modeling visual function in these simple spectral worlds is straightforward and generally successful in explaining the major visual pigment class of midwater and deep-sea animals (Lythgoe, J. N., 1972; Forward, R. B., Jr. *et al.*, 1988; Partridge, J. C., 1990; Marshall, N. J. *et al.*, 2003). The models predict that in seawater, the visual pigment maximum will move to shorter wavelengths as depth increases. Thus freshwater, amphibious, and shallow-water species have rod pigments that absorb maximally near or beyond 500 nm, and pigment λ_{max} decreases as the preferred foraging depth increases. This result even applies to animals like marine mammals, which commute to and from the surface to breathe (or, in the cases of pinnipeds, haul out onto beaches from time to time); their scotopic (dim light) photoreceptors are evidently adapted for best vision at the depth where each species searches for food (Fasick, J. I. and Robinson, P. R., 2000; Levenson, D. H. *et al.*, 2006).

Many species of animals that live in fresh water utilize the substantial spectral shifts available by changing chromophores on a single opsin. For example, exchanging retinal for 3,4-dehydroretinal shifts λ_{max} from 533 to 567 nm in crayfish (Zeiger, J. and Goldsmith, T. H., 1989). The use of A2 pigments should be favored in the relatively longer-wavelength freshwater (and even coastal marine) environments, which probably accounts for the presence of A2 types in many mysid (shrimplike crustaceans) species (Jokela-Määttä, M. *et al.*, 2005). In crayfish, and also many species of cold-blooded vertebrates inhabiting freshwater, changes of the chromophore occur seasonally, with the use of 3,4-dehydroretinal peaking in the winter (Bridges, C. D. B, 1972; Knowles, A. and Dartnall, H. J. A., 1977; Tsin, A. T. C. and Beatty, D. D., 1979; Suzuki, T. *et al.*, 1984; 1985). Since the use of A2 pigments is clearly appropriate in freshwater environments, the seasonality of the change between A1 and A2 visual pigments is interesting. A likely explanation is that the long-wavelength-absorbing forms are relatively unstable when warm and therefore are usable only in cold, wintry water (see Temple, S. E. *et al.*, 2006). This idea will be explored further later on.

While a ready explanation exists for the spectral positioning of visual pigments in many aquatic animals (especially those of low-light, or scotopic, receptor types), there is no simple way to account for the scotopic visual pigments of terrestrial species. Modeling invariably finds that in daylight, photon capture increases monotonically with visual pigment λ_{max} through at least 600 nm (Figure 6; see also Forward, R. B., Jr. *et al.*, 1988), suggesting that optimal visual pigments should have their maximum at 600 nm or even longer. But rod pigments of terrestrial vertebrates rarely peak beyond 500–505 nm, and the most sensitive receptors of terrestrial invertebrates have λ_{max} near 540 nm or less. The disparity between the predicted and the actual spectral locations is possibly explained by increasing thermal instability with greater λ_{max}. Activation energies of visual pigments decrease as λ_{max} increases, leading to rising levels of dark noise (Ala-Laurila, P. *et al.*, 2004). Given the immense number of visual pigment molecules in each photoreceptor cell, even very low rates of spontaneous activation mask the signals produced by rare photons near threshold. In fact, at low body temperatures, vertebrates like amphibians have

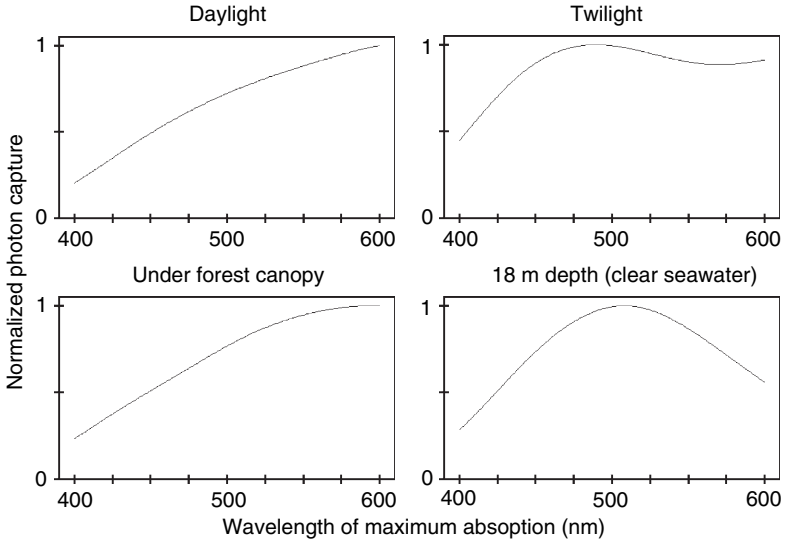

Figure 6 Relationship between photon capture and visual pigment λ_{max}, using template spectra developed by Stavenga D. G. *et al.* (1993) and assuming a total visual pigment absorbance of 0.75 in the photoreceptor. The modeling was done using the irradiance spectra portrayed in Figure 1, with panels arranged in the same arrangement. Note that generally photon capture increases with visual pigment maximum, with a small secondary maximum near 500 nm under the strongly spectrally biased illumination of twilight. The only exception is at depth in seawater, where the most effective visual pigment has its λ_{max} placed near the irradiance maximum due to the very narrow irradiance spectrum there.

significantly lower thresholds for light detection than do humans, a result of reduced random thermal isomerization of visual pigments in rods (Aho, A.-C. *et al.*, 1988). So the presence in dim-light receptors of visual pigments absorbing at unexpectedly short wavelengths likely results from the requirement to limit dark noise.

Only a few species of animals have just one photoreceptor class, and vertebrates are unusual in reserving a photoreceptor set (the rods) for use only in dim light. Besides their rods, nearly all vertebrate species possess at least two cone classes (Figure 7), and the huge majority of the invertebrates that have been studied have two or more spectral photoreceptor types. Figure 8 displays an assortment of color receptor sets, all from animals that are active in the daytime in brightly lit environments and that have been demonstrated to have true color vision. The diversity of both the number of spectral classes and the spectral placements of receptors is very impressive (and mildly disturbing).

The spectral positioning of receptor types in dichromatic color-vision systems (those with two color receptor classes) is well studied, and in many cases the design of these systems can be satisfactorily explained. Color vision is defined as the ability to discriminate among stimuli on the basis of their hue, independently of any other stimulus property (such as brightness or polarization). Thus, the ability to discriminate is fundamental to color vision, so modeling of dichromatic systems has generally proceeded on the assumption that

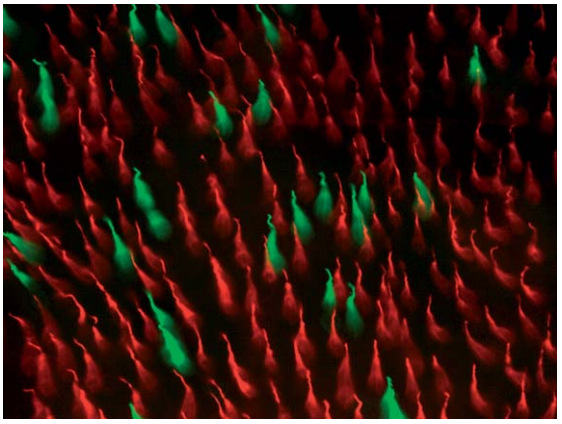

Figure 7 A region of the ventral retina of the chinchilla, showing the presence of two cone classes. Medium-wavelength absorbing cones are labeled with an antibody treatment that fluoresces red, while short-wavelength-absorbing cones are labeled with a green-fluorescing antibody. As in most mammals, only two cone classes are present, and medium-wavelength cones dominate. Photograph courtesy of L. Peichl.

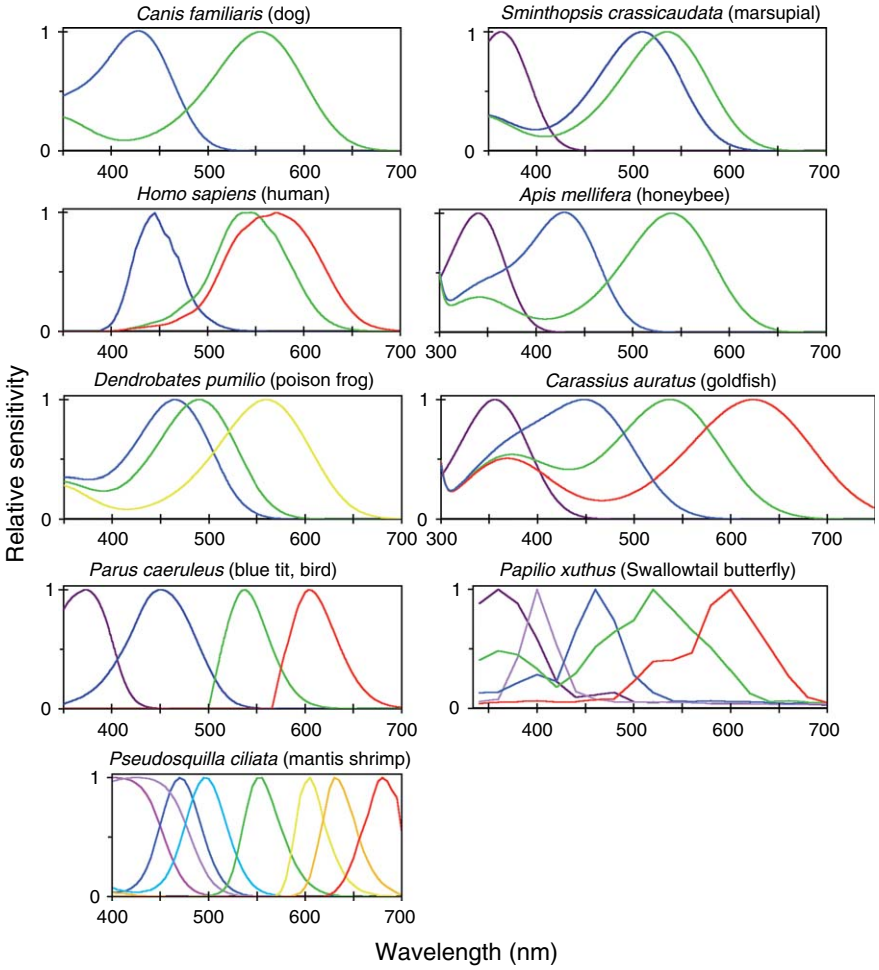

Figure 8 Color-vision systems of a variety of animals, all of which are active in the bright light of day either in terrestrial environments or in shallow water, and all of which have been demonstrated behaviorally to have true color vision. Note the extreme variability in receptor number and placement; even the three mammals that are illustrated near the top are quite different from each other. Data sources are as follows: *Canis familiaris* (visual pigments; Neitz, J. *et al.*, 1989); *Sminthopsis crassicaudata* (visual pigments; Arrese, C. A. *et al.*, 2002); *Homo sapiens* (spectral sensitivities; Stockman, A. *et al.*, 1993); *Apis mellifera* (visual pigments; Peitsch, D. *et al.*, 1992); *Dendrobates pumilio* (visual pigments; Siddiqi, A. *et al.*, 2004); *Carassius auratus* (visual pigments; Palacios, A. G. *et al.*, 1998); *Parus caeruleus* (computed sensitivities; Hart, N. S., 2001b); *Papilio xuthus* (spectral sensitivities; Arikawa, K., 2003); *Pseudosquilla ciliata* (computed sensitivities; Cronin, T. W. and Marshall, N. J., 1989).

the contributing pigment classes are spectrally placed to maximize the discriminability of objects likely to be viewed. A problem with this approach is that such objects have different sizes or probabilities of being in view, and they have different levels of biological significance. Initially, models were limited to relatively simple visual tasks, examining the performances of hypothetical pairs of cone types viewing pairs of spectra. In a pioneering study (Lythgoe, J. N. and Partridge, J. C., 1989), data were collected from objects in a typical forest (leaves and litter), and the cone pairs that provided the greatest variation in chromaticity (a measure of color value) of such objects correlated well with actual cone sets of arboreal mammals. This research team followed up with a more sophisticated approach that attempted to evaluate the ability of cone sets of animals in the relatively simple visual world of coastal water to discriminate objects in the foreground from a generalized background, either open water or an average spectrum of underwater plants. The best pairs of cone types were very similar to dichromatic sets found in common marine coastal fishes (Lythgoe, J. N. and Partridge, J. C., 1991).

More recently, technical advances have made it possible to examine spectral tuning of dichromatic color-vision systems with respect to the properties of entire scenes they are likely to view. Imaging spectroradiometry captures spectra of objects throughout a field of view, and the resulting data sets are free from bias concerning what objects to include in any analysis. Chiao C.-C. *et al.* (2000b) used this technique in a study of dichromatic vision in animals that inhabit temperate and tropical forests or that live on coral reefs in shallow marine waters. The optimal tuning systems they identified corresponded well with those of animals inhabiting either type of habitat. In a further analysis, they also found that the *in vivo* proportions of the two cone types were optimal for discrimination underwater by fish, but less than optimal for vision in forests by mammals (Chiao, C.-C. *et al.*, 2000b). The last result demonstrates that even in quite simple color-vision systems, spectral tuning is not the only factor controlling retinal design. Another wrinkle is that the proportions of receptor classes often vary across the retina, with many more short-wavelength-sensitive types occurring in the ventral than in the dorsal regions (Peichl, L., 2005). This could relate to spatiospectral properties of the visual field, but this has not been conclusively demonstrated.

The most complex receptor sets for which tuning has been successfully modeled are the trichromatic systems of honeybees and of Old World primates (like humans, see Figure 8). Both visual systems are used in day-active animals, but they are surprisingly different in their components, as honeybees have a receptor type responding deeply in the UV, lacked by primates, which in turn have a type that is tuned to wavelengths somewhat longer than the spectral range of bees. The spectral spacings of the two sets are also quite different.

The unusual features of human color vision (and of our anthropoid relatives) have received particular attention. The trichromatic color-vision systems of humans and Old World primates are nearly identical, based on sets of cone photoreceptors that are most sensitive in the blue (~425 nm), green (~535 nm), and yellow (~565 nm) (Mollon, J. D., 1989; Jacobs, G. H., 1993; Dulai, K. S. *et al.*, 1994; Shuye, S.-K. *et al.*, 1995; Jacobs, G. H., 1996). Vision in primates has been modeled using collections of spectra of objects that primates are known to favor, such as fruits or fresh foliage, as well as by examining the spectral and spatial properties of scenes likely to be of interest to primates. These studies confirm that primate color vision is highly adaptive for discriminating fruits from leaves, for discriminating ripe from unripe fruits, and also for discriminating young, nutritious leaves from older and less palatable ones (Mollon, J. D., 1989; Bowmaker, J. K. *et al.*, 1991; Osorio, D. and Vorobyev, M., 1996; Dominy, N. J. and Lucas, P. W., 2001; Regan, B. C. *et al.*, 2001; Párraga, C. A. *et al.*, 2002). Thus, primate color vision could have originated due to its advantages for locating palatable leaves, and this could have been followed by a lengthy coevolutionary sequence of fruit colors and tuning of color vision. Color vision of New World primates differs in important details from the human type; while the overall story is too lengthy and complex for this review, the references cited above should be sought for further information.

One disadvantage of devoting several receptor classes to color vision is that spatial acuity and color discrimination become entangled when adjacent receptors provide different signals – is the difference due to varying color or varying brightness in a scene? In primates, the 535 and 565 nm cone types provide information that is largely redundant for most classes of natural stimuli (but not the ones of special interest, noted above), reducing the ambiguity (Osorio, D. and Bossomaier, T. R. J., 1992; Nagle, M. G. and Osorio, D., 1993). Nevertheless, errors are not eliminated, and these clearly compromise spatial vision (Osorio, D. *et al.*, 1998; Regan, B. C. *et al.*, 2001).

An additional question concerning the design of primate color-vision systems is the means by which cone classes become correctly connected within the neural networks of the retina. Color vision could assemble nearly automatically by exploiting the spatial center-surround organization already in place. However, recent work suggests that this is not the case (Jusuf, P. R. *et al.*, 2006), so how new cone classes (such as the red receptors of Old World primates) become incorporated into preexisting color-vision systems is not currently understood. In Old World primates, color information is carried in two opponent channels, blue versus yellow (much like the original mammalian system) and red versus green. Spatiochromatic analysis of natural scenes indicates that these are entirely appropriate (Figure 9), with the red–green signals carrying the least informative (but potentially most biologically significant) signals (Ruderman, D. L. *et al.*, 1998; see also Buchsbaum, G. and Gottschalk, A., 1983).

The ecology of bee color vision has been examined using similar approaches. In a series of important papers, Lars Chittka and his coworkers proved that honeybee vision is optimal for discriminating among

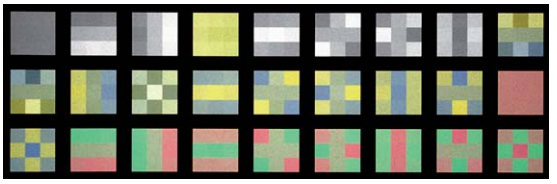

Figure 9 Spatial principal components of 3 × 3 pixels taken from multispectral images of natural scenes, and derived using the blue, green, and red sensitivities of the human eye using Stockman A. *et al.* (1993) sensitivities (see Figure 6) as described in Ruderman D. A. *et al.* (1998). Panels are arranged from left to right and top to bottom in order of decreasing contribution (eigenvalue). Note that all panels contain information from only a single visual channel (luminosity (gray), blue/yellow opponent, and red/green opponent), suggesting that the color channels of human color vision are well designed to optimize information analysis of natural scenes. Note also that the most significant components contain only luminosity, followed by blue/yellow (the typical mammalian color-vision system) and finally red/green (found only in primates). (See Ruderman, D. A. *et al.*, 1998 for further information.)

flowers (Chittka, L.and Menzel, R., 1992; Chittka, L. *et al.*, 1993). Paradoxically, however, the bee-type system is evolutionarily older than flower pollination (Chittka, L., 1996a), and trichromatic systems like those of bees are good for discriminating not only flowers, but also foliage, and thus have general utility to terrestrial insects (Chittka, L., 1996b; Briscoe, A. D. and Chittka, L., 2001). As in primates, the color classes of bee receptors work best in opponency to each other (Chittka, L. *et al.*, 1992; Chittka, L., 1996b).

There is good reason for animals like bees or primates, whose visual spectrum spans ~300 nm, to have a maximum of three receptor spectral classes. Visual pigment sensitivity spectra are fairly broad, so more than three receptor types provide no additional information (Barlow, H. B., 1982; Bowmaker, J. K., 1983). In fact, primates commonly become cone monochromats when they assume a nocturnal lifestyle (Jacobs, G. H., 1995), as do pinnipeds and cetaceans in the sea (Fasick, J. I. *et al.*, 1998; Peichl, L. *et al.*, 2001; Newman, L. A. and Robinson, P. R., 2005). But many animals, including vertebrates other than mammals, have a visual spectrum that exceeds 300 nm, commonly extending from 350 nm (in the UV) through 700 nm (Figure 8). Many such animals have four (or more) spectral receptor types, providing tetrachromatic color vision.

The great majority of bird species, and probably all passerines (perching birds), have four spectral classes of cones (Chen, D.-M. and Goldsmith, T. H., 1986; Jane, S. D. and Bowmaker, J. K., 1988; Hart, N. S., 2001a; 2001b). Surprisingly, terrestrial birds all have rather similar sets of photoreceptors – the major difference is the spectral peak of the shortest-wavelength receptor class, either in the violet or in the UV (Hart, N. S., 2001a; 2001b). However, there is some predictable variation in the abundances and distributions of the various cone sets (Hart, N. S., 2001a). The four cone types contribute to at least three opponent channels (UV/blue, blue/green, and green/red; see Goldsmith, T. H. and Butler, B. K., 2005). Modeling visual function in a 4D color-vision system is obviously tricky, and thus far has been tackled for relatively simple tasks (Vorobyev, M. *et al.*, 1998; Hart, N. S. and Vorobyev, M., 2005). However, this work shows that the colored oil droplets used as spectral filters in avian cone receptors improve color discrimination and possibly color constancy as well. In general, it appears that tetrachromacy in birds provides a basic visual competency that requires little tuning for species-specific tasks.

The spectrally most complicated color systems among vertebrates unexpectedly occur in fishes. Tetrachromacy in the lowly goldfish was recognized some time ago (Figure 8), although the visual ecology of the system is uninvestigated (Hawryshyn, C. W. and Beauchamp, R., 1985; Neumeyer, C., 1992). As of yet, the genetics underlying the complexity and the taxonomic distribution of receptor classes among fishes are not well understood, but recent work finds that the most ancient vertebrates already possessed a number of opsin genes available for future evolutionary elaboration (Collin, S. P. *et al.*, 2003; Trezise, A. E. O. and Collin, S. P., 2005). These have multiplied in modern cichlids, and perhaps other fishes, to as many as seven different cone opsins, expressed in different combinations among species (Parry, J. W. L. *et al.*, 2005). Sometimes, all seven appear in the retina (though some classes could be expressed only weakly). Ironically, even though modeling of color vision began with dichromatic fishes, the complexity found in many teleosts still evades explanation. The cichlids appear to customize their color vision, perhaps even at the level of individual animals, by selective expression of subsets of available opsin genes (Carleton, K. L. and Kocher, T. D., 2001; Parry, J. W. L. *et al.*, 2005), and this tactic for generating diversity in vision could be common in modern fishes (see also Fuller, R. C. *et al.*, 2004). Whether other animals, either vertebrates or invertebrates, have similar, genetically based tuning systems for color vision is unclear, but the extreme polymorphism within species makes it difficult to form generalizable hypotheses

about the functional basis of a given color-vision system. The visual ecology of cichlids and other fishes with similarly flexible visual systems (e.g., bluefin killifishes) is currently an active research area, and one that has real promise for providing insight from a rather different perspective than previous work.

While few (and perhaps no) vertebrates have more than four operational cone receptor classes, many invertebrates exceed this number of receptor types. Flies, for instance, have five classes (Hardie, R. C., 1986), although it is not clear that all five take part in color vision. On the other hand, the five spectral receptors of some species of swallowtail butterflies (Figure 8) clearly do contribute to high-quality color vision (Arikawa, K. *et al.*, 1987; Kinoshita, M. *et al.*, 1999). The current record-holders for spectral diversity, somewhat unexpectedly, are a group of marine crustaceans known as mantis shrimp, or (more formally) stomatopods (Figure 8). These creatures have up to 16 different visual pigments, with a minimum of eight classes devoted specifically to color vision (Marshall, N. J., 1988; Cronin, T. W. and Marshall, N. J., 1989; Cronin, T. W. *et al.*, 1994a; Marshall, N. J. *et al.*, 1996; Cronin, T. W. *et al.*, 2000). Mantis shrimps are able to pack so many receptor classes into a restricted spectral sensitivity range (~400 nm to a maximum of ~725 nm for the eight color classes), breaking the limit of three or four types, because the receptors are arranged uniquely, incorporating receptor-specific, photostable spectral filters and receptor tiering to narrow each receptor's spectral sensitivity (Marshall, N. J. *et al.*, 1991; Cronin, T. W. and Marshall, J., 2004). Mantis shrimps have two independent mechanisms for adjusting their visual systems to the specific photic environments they inhabit, ranging across species from the shallow waters of coral reefs to depths well over 100 m. Evolutionary tuning produces species-specific assemblages of visual pigments and photostable filters that provide a general fit to the local irradiance spectrum (Cronin, T. W. *et al.*, 1994a; 1996; 2000; Cronin, T. W. and Caldwell, R. L, 2002). The resulting spectral sensitivity functions are not necessarily fixed, however, as some mantis shrimp species can flexibly tune receptor sets to changing environmental conditions, in essence self-adjusting their visual systems to meet local requirements (Cronin, T. W. *et al.*, 2001; 2002; Cheroske, A. G. *et al.*, 2003; 2006). The functions of this complex and tunable color-vision system are not fully understood, providing a challenging problem for current and future visual ecologists.

As already noted, the visual spectrum of many animals extends into the UV, sampling wavelengths down to 350 nm or even shorter. While originally surprising, given the traditionally anthropocentric view of sensory physiology, UV photosensitivity turns out to be widespread among invertebrates and is found in all vertebrate classes (see Jacobs, G. H., 1992; Goldsmith, T. H., 1994). UV vision generally is incorporated seamlessly into color-vision systems, often adding a new opponent channel, as in birds. However, UV signals (discussed later in the chapter) are commonly involved in mate choice decisions, especially among vertebrates, so they do seem to have a special meaning in this sense (see Hunt, S. *et al.*, 2001).

Underwater, UV light is heavily scattered, but nevertheless is capable of penetrating at visually useful intensities to depths beyond 100 m (Frank, T. M. and Widder, E. A., 1996). Short-wavelength light thus can contribute to color vision and visual signaling in the sea (a concept that was long denied, a perception apparently originating from the observation that organic solutes in freshwater and coastal waters really do absorb UV light quite rapidly). The scattering of UV light in water provides a bright UV background, especially in shallow water, that can be exploited to enhance vision of nearby objects, making them stand out in silhouette (Figure 10). UV vision is common in shallow-water invertebrates (e.g., Cronin, T. W. *et al.*, 1994b) and fishes (Losey, G. S. *et al.*, 1999), where it is probably used to visualize objects that otherwise blend well into the underwater light field. UV vision should be particularly helpful for planktivores, which often feed by swimming up in the water column, attempting to spot their tiny prey against downwelling light.

1.08.4.3 Polarization Vision

As with UV sensitivity, humans are not sensitive to polarization properties of light and therefore tend to overlook the possibility that other animals may be sensitive to them. In reality, the huge majority of invertebrate species, and a number of vertebrates as well, sense and at least partially analyze light's polarization properties. The detection of polarized light is possible because the visual pigments of all animals are inherently dichroic (i.e., they absorb one orientation of polarized light preferentially over others). As the visual pigment molecules lie in the membranes of the receptor cell, the absorption axis of the chromophore extends roughly parallel to the membrane's surface. Membranes in rod and cone photoreceptors of vertebrates lie in stacks of planar structures, either

Green (490–560 nm) Ultraviolet (350–380 nm)

Figure 10 Images taken simultaneously at a depth of ~10 m on a site on the Great Barrier Reef, Australia through green-transmitting (Corning 4–64 filter, left) and ultraviolet-transmitting (Corning 7–60, right) glass filters. Note how the bright scattered background visible in the ultraviolet photograph silhouettes nearby fish and makes them far easier to see. The spectral ranges given beneath each panel are estimated from filter and lens transmission spectra and sensitivity of the film (Kodak Tri-X).

pancake-shaped disks (rods) or folded lamellae (cones) that are oriented perpendicular to the path of light, where the visual pigment molecules float freely (Cone, R. A., 1972). This arrays the chromophore dipoles orthogonally to incoming light, an advantage for capturing photons but a challenging situation for providing polarization sensitivity. The freely rotating visual pigments present a random array of absorbers with respect to their angular orientation, obviating polarization sensitivity (Figure 11, top left).

Nevertheless, a number of vertebrates display behaviors related to polarized light fields, and some show physiological responses to polarization features of a stimulus (reviews: Waterman, T. H., 1981; Hawryshyn, C. W., 1992; 2000; Horváth, G. and Varjú, D., 2004). In some species of anchovies, polarization sensitivity seems to be conferred by a set of specialized cone photoreceptors that lie on their sides, transverse to the optical axis of the eye and thus presenting their membranes parallel to light (Fineran, B. A. and Nichol, J. A. C., 1978; Novales Flamarique, N. and Harosi, F. I., 2002). There is also evidence that entopic phenomena may account for some cases of vertebrate polarization sensitivity; for instance, the visual sensation humans experience called Haidinger's Brush (see Minnaert, M., 1954). On the other hand, evidence from fish strongly suggests that some cone photoreceptors are polarization sensitive even when illuminated axially. Explanations require unusual optical phenomena in cones: graded-index-generated waveguide effects in elliptical cone inner segments (Rowe, M. P. *et al.*, 1994), grazing-incidence reflection in double-cone inner segments (Novales Flamarique, N. *et al.*, 1998), or tilted photoreceptive membranes (Roberts, N. W. *et al.*, 2004). Whether any, all, or none of these hypotheses will ultimately be accepted remains to be seen.

The situation in rhabdomeric photoreceptors of invertebrates like insects, crustaceans, or cephalopods is better understood. Their membranes are rolled into tiny tubes called microvilli that typically extend in groups from one margin of the receptor cell. In polarization-sensitive cells, all the microvilli are parallel, an anatomical arrangement diagnostic for polarization receptors. To permit polarization sensitivity, the absorption dipoles of visual pigment molecules also must be roughly parallel to the microvillar axis (Figure 11, top right). Unlike the freely moving visual pigments of rod and cone membranes, visual pigments in microvillar membranes are nearly immobilized within the microvillar membranes (Goldsmith, T. H., 1975; 1977; Goldsmith, T. H. and Wehner, R., 1977; Lillywhite, P. G., 1978; Doujak, F. E., 1984). Even reducing visual pigment concentration by 95% does not affect either the general alignment of the molecules or the polarization sensitivity of the receptor cell (Speck, M. and Labhart, T., 2001), implying that the molecules are well anchored, perhaps to cytoskeletal components such as the actin backbone or spectrin-like membrane proteins within the microvillus.

Ocular specializations can improve polarization sensitivity; an excellent example is the use of oriented mirrors or tapeta in spider eyes to direct light of a given polarization orientation to the appropriate receptors (Dacke, M. *et al.*, 1999; 2001). A variety of modifications can improve the polarization sensitivity of the microvillar receptors themselves (Figure 11), including extreme alignment and parallelism of microvilli throughout the receptor, thin layering of microvilli in

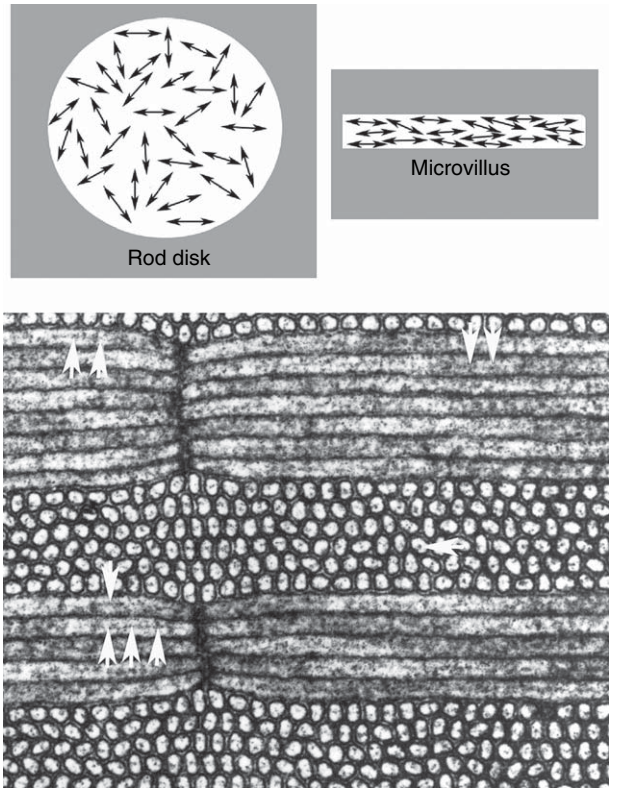

Figure 11 Top left: Schematic drawing of a rod disk as seen from the direction of approaching light *in vivo*. The double-headed arrows indicate the absorption dipoles of visual pigment molecules as they float in the membrane and freely rotate. Note that there is no preferred direction of orientation, so that all orientations of polarized light would be absorbed to similar amounts. Top right: Similar schematic of a microvillus, showing how the absorption dipoles tend to lie roughly parallel to the microvillar axis, providing an inherent preferential absorption to light with its electric vector polarized parallel to the microvillus. Bottom: Electron micrograph of polarization-sensitive photoreceptors of the mantis shrimp *Neogonodactylus oerstedii*, to show the alternating, orthogonal arrangements of microvilli in thin layers. The long, parallel microvilli extend parallel to the plane of the section, while the circular profiles are microvilli cut in cross section. The alternating layers are derived from different sets of photoreceptor cells, providing a two-axis polarizational analysis system. The white arrows show the actin cores of microvilli, which stabilize their structure. Photograph courtesy of C. A. King-Smith.

orthogonal polarization classes, and maximal dichroism of the receptor pigment itself (Snyder, A. W., 1973; Snyder, A. W. and Laughlin, S. B., 1975; Nilsson, D.-E. *et al.*, 1987). Polarization sensitivity can, of course, be further enhanced beyond the receptor level by post-receptoral processing (Saidel, W. M. *et al.*, 1983; Glantz, R. M., 2001). As noted earlier, the inherent polarization sensitivity of rhabdomeric photoreceptors can create stimulus ambiguity when spectral and polarizational features of a stimulus are mixed, so some invertebrate photoreceptors are structurally modified to destroy polarization sensitivity, while other species may evaluate viewed objects by combining spectral and polarizational cues.

Until recent years, polarization sensitivity throughout the animal kingdom was associated with behavioral tasks related to orientation or navigation. For example, honeybees have long been known to use patterns of polarization in the sky for travel between the hive and places of foraging, and many other insects orient themselves using celestial polarization cues (see reviews of Rossel, S., 1989 and Wehner, R., 2001). A similar capacity, using underwater light fields, could exist in salmonid fishes (Hawryshyn, C. W. and Bolger, A., 1991; Hawryshyn, C. W., 1992; 2003). Even some species of nocturnally migrating birds apparently calibrate their compasses using skylight polarization patterns, as they become disoriented when provided with a depolarized celestial pattern during twilight (Helbig, A. J., 1990). In another set of polarization-controlled orientation behaviors, water beetles and many other

insects recognize water surfaces by the horizontally oriented polarization reflected from them (Schwind, R., 1984; 1991), initiating responses that can bring about disaster when the polarization cue originates from artificial or oily flat surfaces (Horváth, G. and Zeil, J., 1996; Kriska, G. *et al.*, 1998). On the other hand, flying insects can use polarization to discriminate natural water surfaces from mirages or other virtual surfaces (Horváth, G. *et al.*, 1997). Finally, polarization vision plays roles in prey detection and in communication, topics to be covered later in the chapter.

1.08.4.4 Eye Movements

Eyes that produce quality images see only a portion of the visual world at any one time, and the region that is inspected in detail by the fovea (if present) is even smaller. So eyes must move to cover areas of interest, to follow objects in view that are themselves moving, to stabilize themselves in a moving panorama, and sometimes even to acquire visual information itself. Animals like humans, whose eyes are quite mobile within the head, are relatively uncommon; in most animals, the head itself does most of the moving that is responsible for shifts of gaze, and in many cases the animal as a whole makes the responsible movements. Engineers have paid special attention to how movements of the eyes are controlled, as the feedback channels and mechanisms of guidance can guide design of artificial, cybernetic systems. Eye movements also are interesting to visual ecologists, as the visual requirements of different species dictate different patterns of movement, which can give insight into visual needs and into the visual worlds these animals occupy.

Eye movements can be generally sorted into two general classes (Figure 12): those that stabilize the visual world or a portion of it and those that deliberately move the eye with respect to the world (see Land, M. F., 1995; 1999; Land, M. F. and Nilsson, D.-E., 2002). Perhaps the most fundamental eye-stabilizing behavior is optokinesis, in which the eye (or head, or body) turns in synchrony with a smoothly moving visual field. The field movement is most commonly generated by linear or angular movements of the animal itself, but can also be produced by steady flow as in natural waters. The compensatory behavior, called optokinetic nystagmus, involves an alternating series of smooth drifts of the eye to follow the visual field and quick returns in the reverse direction to permit further smooth drifts (Figure 12). During the saccadic return movement, the visual system is transiently blind. Optokinesis can be influenced by mechanical or vestibular inputs, or even by leg movements in crabs (Nalbach, H.-O.,

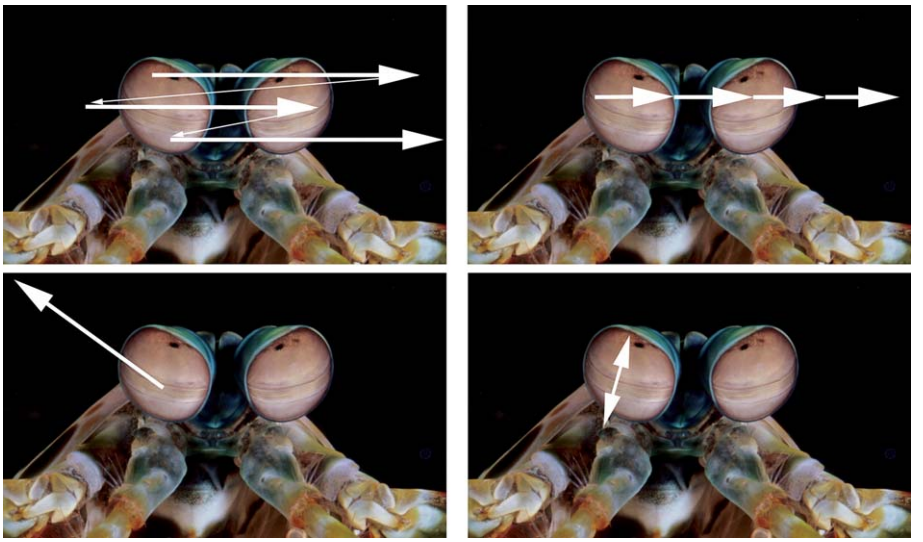

Figure 12 The major classes of eye movements, using the compound eyes of the mantis shrimp *Odontodactylus scyllarus* for illustration. The arrows show the direction and distance of movement. Top left: Optokinesis. The thin arrows represent the rapid returns occurring during optokinetic nystagmus. Top right: Saccadic tracking (for smooth tracking, only one long arrow would be drawn). Bottom left: Large fixation saccade. Bottom right: Scanning (note that the axis is perpendicular to the band of ommatidia forming the equator of the eye). Reproduced by permission of R. L. Caldwell.

1990), but its fine control is generally visual. This creates something of a paradox, as the movement itself is driven by the sliding of visual stimuli across the retina, and extremely high-gain systems required to minimize such slip are inherently unstable (see the original work on crustaceans by Horridge, G. A. and Sandeman, D. C., 1964). Nevertheless, visual control systems perform acceptably under natural conditions.

A second class of visual stabilizing movements involves tracking a small object moving within the larger visual field. This familiar visual task offers subtle but serious problems – the tracked object moves within the background field that normally serves to stabilize vision. Thus, the optokinetic system must be overcome during tracking, or retinal slip will instantly engage a countering response. Many animals switch effortlessly between optokinesis and visual tracking (consider the situation when you look out of the window of a moving vehicle, first letting the eye drift with the scene and then concentrating on a flying bird or other small, moving detail), but the control systems that permit this are by no means trivial (see Niven, J. E., 2006). Visual tracking can be smooth, driven either by the velocity of slip of the target on the retina (as in optokinesis) or by the angular displacement of the retinal location of the target from its desired fixation point (see Collett, T. S. and Land, M. F., 1975, for a classic study in hoverflies). Or it can be saccadic, occurring in a series of jumps reminiscent of the return phase in optokinetic nystagmus, but continuing in the direction of the target and following its movements in space (Figure 12). Praying mantises track prey smoothly against simple backgrounds but revert to a series of saccades when the background is spatially complex (Rossel, S., 1980). Or tracking may switch between smooth and saccadic eye movements with target position or speed (Cronin, T. W. *et al.*, 1988).

Of course, eye movements can be called upon to shift the visual field deliberately. At a minimum, if an animal wants to inspect particular locations in visual space without having a particular, moving target in mind, it still must escape optokinetic control; this is generally done by generating a saccade to the next fixation point. Many visual saccades occur simply because an animal wants to look here and there, perhaps checking for the presence of predators or to search for prey. Other visual shifts are smooth and continuous, and the visual system continues to operate throughout the movement. Peering behavior is a good example of this, where an animal like a praying mantis sways from side to side, generating relative motion flow between nearby objects and more distant ones and thereby gaining both absolute and relative depth information (Collett, T. S., 1978). Flying bees gain similar information as objects drift backward beneath their eyes at different angular velocities due to their different heights (Lehrer, M. *et al.*, 1988). In fact, much of their knowledge of space and its structure comes to bees via motion cues generated during flight (see Vladusich, T. *et al.*, 2005 for a recent report).

Slow visual scans make up a unique class of deliberate visual movements, found in only a few animals. We humans sometimes have the impression that we are scanning the environment, but this sort of visual behavior, which is common to many (if not most) animals, actually consists of a series of small saccades to stable fixation points. True scans are different; the speed of the eye's movement is relatively slow and is matched to the response time of individual receptors (Land, M. F., 1982; Land, M. F. *et al.*, 1990; Land, M. F., 1999). These movements occur in animals that have a linear retina consisting of a parallel array of a few rows of receptors, and the scans are perpendicular to its long axis translating the retina's view through visual space. In jumping spiders, the retinas of just the principal eyes (of four pairs, the ones with by far the best vision) sample a tiny region in front of an animal by scanning back and forth, looking for particular patterns signifying the presence of a potential mate (Land, M. F., 1999). Stomatopod crustaceans, whose eyes have both an extended and a linear retina, have to time share, alternating stabilizations or tracking movements and scans, which paint color and polarization information onto the extended visual field of the peripheral retina (Figure 12). This seems an awkward situation, and it requires an unusual system of driving muscles (Jones, J., 1994), but these mantis shrimps are fearful visual predators in shallow marine waters. There are many ways of seeing, and the fact that some animals have eye movements that seem awkward or inefficient probably means that we just do not understand them.

1.08.5 The Role of Vision in Behavior

1.08.5.1 Orientation

Little is needed for a photoreceptor organ to signal light's intensity and to provide basic information about the direction from which the light arrives (see Nilsson, D.-E. and Pelger, S., 1994). A simple pit lined with photoreceptive cells and backed with a layer of light-absorbing pigment can serve this task, or there may be various optical elaborations, but for many animals an eye need do no more than this: signal light's

intensity and general direction. Knowing these, daily activity patterns and orientation within a directional light field are possible. The vertical migratory behavior of plankton, reputedly the greatest rhythmic movement of life on earth, is mostly controlled by such simple eyes (Forward, R. B., Jr., 1976; Lenz, P. H. *et al.*, 1996). Even the multiple and optically advanced (but defocused) eyes of cubomedusans (Nilsson, D.-E. *et al.*, 2005) apparently serve only to permit station-keeping and obstacle avoidance among mangrove roots.

Of course, most animals larger than plankton, as well as some planktonic creatures, use more sophisticated orienting visual technologies. The widespread ability to use celestial polarization patterns, both during the day and at night, has already been remarked. Also noted earlier is the ability of many insects to orient to water surfaces using polarization reflections. These behaviors do not require particularly excellent eyes. In fact, celestial polarization orientation is generally provided by one area of each compound eye – the dorsal rim – that feeds three information channels produced by massive spatial integration (Rossel, S., 1989; Labhart, T. *et al.*, 2001). These extremely wide-field polarization sensors have the advantage of good performance even when much of the sky is obscured by canopy or clouds. In some species they can foster polarization orientation at nocturnal skylight intensities. Lacking compound eyes, some spider species use wide-field optical compasses, based on polarization detection, that are built from tiny simple eyes (Dacke, M. *et al.*, 1999; 2001).

Obviously, there are many other, and far more complicated, orienting and navigating strategies available to animals that use visual information, but discussing these would range well beyond the scope of this chapter and even beyond the usual borders of what constitutes visual ecology. An excellent and extensive literature exists on landmark navigation in animals, and navigating insects have often been considered as models upon which to base autonomous, artificial devices that evaluate landmarks, optical flow fields, and celestial polarization (see, for instance, Lambrinos, D., 2000). An unusual variant on landmark orientation has been found in forest-living ants, where the landmarks are actually patterns of light and foliage seen in the forest canopy (Hölldobler, B., 1980). Such a simple and elegant strategy should be ideal for many forest dwellers with small (or big) brains and eyes, but its use has not been identified in any other animal.

1.08.5.2 Predation and Its Avoidance

The conflict between predators and prey is nearly as ancient as life itself, and certainly predates the appearance of vision. The appearance of good visual organs, probably in the late pre-Cambrian, instantly accelerated the arms race between the two parties. In fact, early visual evolution likely initiated the rapid Cambrian explosion, when many new body plans and modes of life suddenly turn up in fossils (Parker, A. R., 1998; Land, M. F. and Nilsson, D.-E., 2002). Having good eyes benefited both predators and prey, but with vision progressing on both sides of the interaction, animals became evolutionarily obligated to ever-greater efficiency at both detecting others and escaping (or capturing) them. In reality, so many aspects of visual design relate to predation that only a superficial discussion is possible here. For a comprehensive recent review, see Cronin T. W. (2005).

Predators and prey have very asymmetrical interests. While the predator can usually survive a failed attempt to capture prey, a prey animal must always successfully evade its predator. Further, a predator need concentrate on only one prey at a time, while prey animals must detect every potential predator. Thus, eyes of prey generally have very extensive visual fields, most often sampled by eyes that are placed on the sides of the head. Foraging birds provide perfect examples. Woodcocks see almost the entire horizontal plane (Martin, G. R., 1994), and shoveler ducks view essentially the entire hemisphere above the horizon (Guillemain, M. *et al.*, 2002); both woodcocks and shovelers actually have binocular visual fields to front and rear. Prey animals that inhabit flat worlds, like plains animals, fish on the seabed, or animals living on mudflats, have their most acute vision right along the horizon. Such a specialization requires clustering of retinal ganglion cells along the equator of the eye in vertebrates, forming a visual streak (see Walls, G. L., 1942; Land, M. F. and Nilsson, D.-E., 2002). Compound eyes similarly can cluster their ommatidial axes near the horizontal plane, producing a different kind of visual streak. Fiddler crabs inhabit flat expanses of beach, and their compound eyes sample intensively along the horizon (Zeil, J. *et al.*, 1986; 1989; Land, M. F. and Layne, J. E., 1995). In fact, fiddler crabs live by a simple rule: if something in view breaks the line of the horizon or is above it, it is a predator.

Predators need not sample every point in the environment for the presence of prey, but it is certainly advantageous to spot prey and see them clearly at distances where the predator is still invisible. This

explains their frontally directed eyes, often with extensive binocular overlap for visual attention and distance estimation. These eyes can achieve outstanding spatial acuity, provided by foveas or acute zones that specialize in just a bit of the visual world (Figure 5). Some predators have double foveas in each eye, as noted earlier, one looking ahead and the other laterally. Searching birds rigorously stabilize the visual field on their retinas when stalking, holding the head steady as long as possible and then rapidly thrusting it forward to the next fixed position, no doubt to maximize the chance of spotting something (Cronin, T. W. *et al.*, 2005; Fujita, M., 2006). Tubular eyes, described earlier, expose their roles as prey detectors by their binocular visual fields and their concentration on a limited spatial region (Figure 4).

Localizing prey demands accurate depth measurement, too. Only a few vertebrate predators use true stereopsis, in which disparity between retinal images is used to generate a sense of depth, but monocular systems – especially accommodation – are widespread (Collett, T. S. and Harkness, L. I. K., 1982). Vertebrates from fish to mammals use focusing cues to range their attacks. Chameleons, famous for the robot-like movements of their turret eyes, use telephoto optics to form a large image with a shallow depth of focus, and thus can accommodate very accurately for distance measurements (Ott, M. and Schaeffel, F., 1985). Nearly identical optical engineering is found in the eyes of the sandlance, a piscine ambush predator (Pettigrew, J. D. *et al.*, 1999). Cuttlefish do not have telephoto eyes, but like the vertebrates to which they are often compared, they use accommodation to judge prey distance just before launching a tenticular attack (Schaeffel, F. *et al.*, 1999).

No matter what their calling, most animals benefit from being inconspicuous. This generally means looking like their surroundings or backgrounds – in other words, being camouflaged. In open water, the surroundings and background are the same, a spatially varying, but fully predictable, light field. Animals have found three ways to match this background: being transparent, reflecting downwelling light in the same spatial pattern as the background, or using bioluminescence to obliterate the silhouette they show from below (Nilsson, D.-E., 1997; Johnsen, S., 2001; 2002). These are all essentially contrast-reducing strategies, and they need not be perfect. Even a modest contrast decrease can significantly reduce visibility, providing a basis for the evolution of later, more sophisticated solutions (Land, M. F., 2000).

Camouflage more generally means dealing with a patterned background: fallen leaves and twigs, a pile of rocks, the trunk of a tree, and blotches on sand. The classic reference by H. B. Cott, *Adaptive Coloration in Animals* (1940), is still worth a good browse to review the stratagems used by animals. More recent work in visual ecology has examined how animals use system properties of vision and statistical features of natural scenes to generate effective camouflage. For example, spots and blotches used for crypsis are often outlined with a contrasting edge, tying into center-surround systems of edge enhancement and thereby verifying their presence as a background feature (Osorio, D. and Srinivasan, M. V., 1991). Some of the best model systems for examining biological camouflage are those that produce background matching on the spot, as used by flounders (Ramachandran, V. S. *et al.*, 1996) or cuttlefishes (Chiao, C.-C. *et al.*, 2005). The cues these animals use to create their nearly perfect patterns of concealment are not yet fully understood. The ability of cuttlefish to match backgrounds not only for spatial pattern but also for color is particularly puzzling, as the animals lack color vision (Marshall, N. J. and Messenger, J. B., 1996; Mäthger, L. M. *et al.*, 2006). Another surprising recent finding is that animals can use the same patterns and colors to be either conspicuous or cryptic, depending on how they allow themselves to be viewed. Forest-dwelling birds that display brilliant colors in patches of sun can become highly cryptic – nearly invisible – by moving a short distance away into the shade (Endler, J. A. and Théry, M., 1996). Similarly, the beautiful colors and patterns of reef fishes, obvious when seen from nearby, blend into the background of the coral reef at moderate distances (Marshall, N. J., 2000a; Marshall, N. J. and Vorobyev, M., 2003).

Color and pattern matching in camouflage are very difficult to break through, because natural selection shapes excellent matching very efficiently. The less-perfect systems available for hiding in midwater can be at least partially nullified, however. One solution to the problem has already been noted. Searching for reflective or transparent objects is improved using UV visual receptors that respond strongly to the background, scattered light, and allow prey to be visualized in silhouette (Figure 10). An alternative is to use polarization vision in the same way. The background light underwater is usually polarized, but animals either depolarize the light or reflect the light of different polarization. Squids and cuttlefish use their sensitive polarization vision to improve prey detection in such conditions (Shashar, N. *et al.*, 1998; 2000). It is

interesting to consider that, unlike the demonstrated benefits of polarization vision for predation in particular circumstances, color vision seems to be of little benefit to predators. This is probably true because the evolution of color camouflage is rapid and effective, quickly neutralizing improvements in color discrimination; polarization camouflage is a much more difficult evolutionary problem (and no example of polarization camouflage has ever been found). There is one case, though, where color vision is critically important to predators and that occurs when potential prey signal to predators that they are unpalatable or dangerous, so an attempt to consume them could have lethal consequences for the predator. These warning messages from prey to predator are known as aposematic signals, and these will be discussed in the next section.

1.08.5.3 Visual Signaling

As the earliest and simplest eyes gave way in many evolving lineages to more competent visual organs useful for orientation, predator detection, and other tasks like those discussed above, the improved vision also permitted new ways for animals to view other members of their own species. Visual signals must therefore have been used by many of the earliest animals that had complex body plans. In fact, the earliest well-preserved fossils of metazoans, from the Burgess Shale, already reveal evidence of functional color signals (Parker, A. R., 1998).

It seems obvious that visual systems of animals and the signals they view must coevolve (see Endler, J. A., 1992, 1993; Endler, J. A. and Basolo, A. L., 1998; Endler, J. A., 2000). Surprisingly few examples of coevolution of this type are documented, however. The only convincing cases of evolutionarily cooperative tuning of vision and signals are found in bioluminescent signaling systems, as in fireflies (Lall, A. B. *et al.*, 1998; Cronin, T. W. *et al.*, 2000) or deep-sea fish (Partridge, J. C. and Douglas, R. H., 1995; Douglas, R. H. *et al.*, 1999). A precise match between the single spectral channels in the eyes of these animals and the bioluminescent emissions of conspecifics is possible because the signaling environment is so simple. Essentially, there is little of visual interest in the dark surroundings of these signals, so it makes sense to shape vision to the signals and vice versa. In animals with a spectrally more complex – and typical – visual environment, visual systems (including color vision) are constrained by the need to carry out a variety of tasks; natural environmental properties limit evolutionary freedom. Even where there seems to be tuning of vision for special signaling tasks (e.g., species recognition, Bernard, G. D. and Remington, C. L., 1991; ovoposition, Kelber, A., 1999), there are so many spectral types of receptors present that it is difficult to make a case for strong selection on a particular class.

It therefore seems that the spectral mechanisms of most animals operate for many tasks, and are evolutionarily shaped by environments and fundamental properties of visual pigments and photoreceptor physiology. As noted before, the trichromatic visual system of honeybees probably appeared early in insect evolution, significantly predating the evolution of the flowers they pollinate (Chittka, L., 1996a; Briscoe, A. D. and Chittka, L., 2001). Bee vision is nonetheless nearly optimal for discriminating among flowers (Chittka, L., and Menzel, R., 1992; Chittka, L. *et al.*, 1993). The fitting of signals (in this case, flower colors) to preexisting visual systems (of insects) probably represents the typical evolutionary sequence. Similarly, the fruit colors that are well recognized and discriminated by the color-vision systems of primates with very diverse lifestyles and food preferences (Mollon, J. D., 1989; Osorio, D. and Vorobyev, M., 1996; Regan, B. C. *et al.*, 2001) imply that these colors were selected for their visibility to monkeys and apes. Birds, the canonical examples of colorful terrestrial vertebrates, fantastically diverse in their appearances, share very similar or even identical visual systems (Vorobyev, M. *et al.*, 1998; Hart, N. S., 2001a; 2001b). Looking at color vision and signals from a different perspective, the retinas of animals as different as birds and bees are so predictable that crab spiders hiding in flowers can match backgrounds (for crypsis) adaptively to become invisible to both avian predators and apian prey (Théry, M. and Casas, J., 2002). As a final example, a recent study that specifically examined the coevolution of signaling colors and color vision in stomatopod crustaceans found little evidence that vision was tuned to recognize signals (Chiao, C.-C. *et al.*, 2000c).

Visual ecological perspectives are of interest to almost anyone studying signals, but make up only a fraction of all studies of signal evolution. The general theory behind the evolution of signals, particularly visual signals, has been covered well by Endler J. A. (1992; 1993; 2000), and a recent book edited by Espmark Y. *et al.* (2000) discusses many current interests in the field of animal signals. Visual ecologists have concentrated on questions involving the function of the signal (information content), the nature of the signal (the underlying optics, pigment, and

structure), and particularly on the visual aspects of the signal (visual system of the viewer, environmental background, and lighting situation).

Animals signal to competitors that they are able to defend resources, to potential mates that they have the right stuff, and to potential predators that they are dangerous or toxic as prey. The ecological and social dynamics of such signaling appeal to evolutionary or behavioral biologists, but how the signals are tuned for best visibility and maximum visual impact obviously brings us back to sensory issues. The signals that appeal – or are even visible – to females can be explained by reference to their visual systems as well as to environmental backgrounds and lighting (Endler, J. A., 1991; Vorobyev, M. *et al.*, 1998; Siddiqi, A. *et al.*, 2004). Aposematic signals (warning colors) are unusually interesting in this regard, as they are the great exception to the general rule that color is irrelevant in predation. Here, the color is the signal (Sillen-Tullberg, B., 1985). In fact, the warning colors in some systems are so diverse and variable, as in the dart-poison frogs of the American tropics (Summers, K. *et al.*, 2003; Siddiqi, A. *et al.*, 2004), that the rule for a predator seems to be "don't eat any bright-colored frog"; the specific color (or pattern) expressed by the frog is perhaps irrelevant. Warning colors are so widely used that many predators innately avoid novel prey (Lindström, L. *et al.*, 2001).

Visual signals include many components: achromatic aspects, color pigments, structural colors, pattern, and movement. Of these, color and brightness have proven the easiest to analyze, but some work has begun on the meaning of pattern and on how movement ties into visual systems of intended receivers (see for instance Crook, A. C., 1997; Zeil, J. and Hemmi, J. M., 2006). Animal colors arise from an astonishing diversity of sources (Cott, H. B., 1940; Fox, D. L., 1976), pigments, either alone or in layers (including fluorescent ones), and structures, including interference reflectors, coherent scatterers, incoherent scatterers (see Prum, R. O. *et al.*, 1998; 2004), diffractive structures, and sophisticated photonic crystalline structures (Vukusic, P. and Sambles, J. R., 2003). The colors themselves carry information about the sender, because many pigments are thought to be costly to acquire and highly ordered structures probably signify that their builder is healthy and unusually free of parasites. The intensity and contrast of colors can be emphasized by adding fluorescent components emitting at wavelengths where the illumination itself is weak (Mäthger, L. M. and Denton, E. J., 2001; Arnold, K. E. *et al.*, 2002; Mazel, C. H. *et al.*, 2004; Figure 13). Some signals involve wavelengths that humans overlook, primarily in the UV, or provide polarization patterns invisible to humans and many other animals; these will be described further below. Making the signaling situation yet more complex, animals can change their appearances slowly or instantaneously, flashing their signals or making themselves inconspicuous (Lythgoe, J. N. and Shand, J., 1983; Shashar, N. *et al.*, 1996; Zeil, J. and Hemmi, J. M., 2006). And, as noted earlier, animals can change their appearances by moving into and out of varying lighting microenvironments as required.

Modeling how signals visually stimulate a given viewer under specific conditions of illumination and within specific visual environments has become

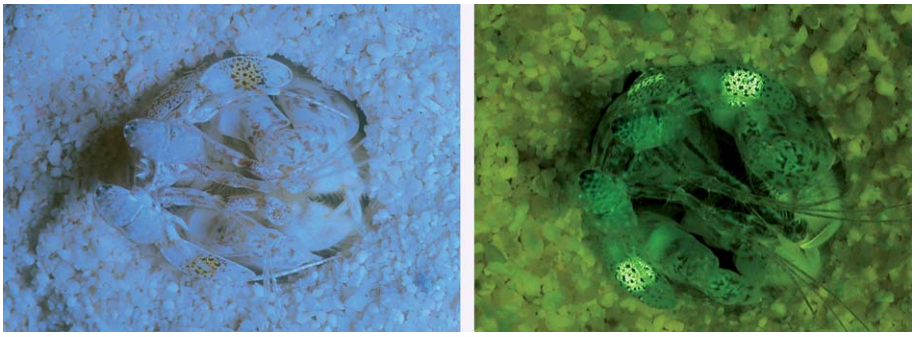

Figure 13 Fluorescent signaling in a mantis shrimp, *Lysiosquillina glabriuscula*. The left image shows a white-light-illuminated animal at its burrow entrance, while the right image shows the same animal illuminated with narrow-band blue light and photographed through a barrier filter that blocks the excitation light. Note how the yellow markings on the antennal scales (the flat plates extending to the right and left) look similar in both white (reflective) and blue (fluorescent excitation) illumination. Reproduced by permission of R. L. Caldwell.

routine. More recent approaches that have particular appeal involve attempts to recreate the appearances of signals as they might appear to a visual system of interest (e.g., Vorobyev, M. *et al.*, 1997; 2001; Marshall, N. J. and Vorobyev, M., 2003). The intent is not so much to enter the sensory world of an animal as to inspect the resulting images for guidance concerning which aspects of the signal seem special. A good example of this is illustrated in Figure 14, which shows the modeled appearance of a dart-poison frog as viewed by a human (to provide the appearance we see, for comparison), a bird (a model predator), and a conspecific frog (a potential mate). The patterns of coloration in these images suggest that the frog communicates with potential predators and with conspecifics using different signals aimed in different directions.

This section on the visual ecology of signals would not be complete without a mention of signals that animals use that we cannot see, based on patterns of reflectance of UV or polarized light. From one point of view, UV colors and patterns should be fundamentally similar to other color signals, although they do have the special property of being invisible to many visual systems. However, this is also true of very long-wavelength colors, specifically the reds, as they are also outside the spectral range of many mammals, insects, or other animals (Figure 8). UV signals frequently play critical roles in mate choice decisions by birds (Andersson, S. *et al.*, 1998; Bennett, A. T. D. *et al.*, 1996; 1997; review: Cuthill, I. C. *et al.*, 2000). UV patterns appear on the bodies of many reef fishes (Marshall, N. J., 2000b;

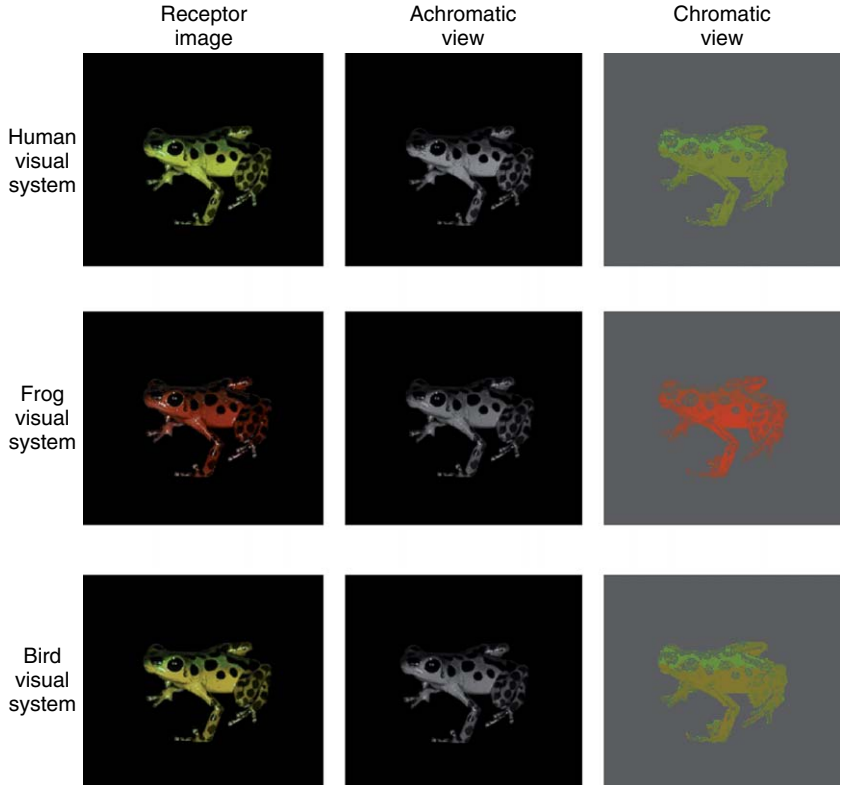

Figure 14 Reconstructed views of color signals in the dart-poison frog, *Dendrobates pumilio.* These images were derived by matching spectral reflectances to individual pixels of a digital photograph of the animal, using data obtained by Siddiqi A. *et al.* (2004). Each row of images portrays the computed view provided by the visual system indicated at the left, using the spectral sensitivities illustrated in Figure 6 (for the bird visual system, the modeling did not include the ultraviolet receptor class). The receptor image scales blue, green, and red pixel values to photon capture by the short-, medium-, and long-wavelength receptor classes of each species. Achromatic view shows photon capture only by the long-wavelength class (in birds, the double-cone class), which in each species approximates the intensity-only (luminosity) view. The chromatic view scales each pixel to a total intensity of 128 bits for the summed receptor channels, thus producing a roughly isoluminant image. Note that different color patterns are distinctive for the different visual systems; the human and bird are particularly sensitive to the dorsal green reflectance, while the frog system is most stimulated by the ventral yellow color.

Marshall, N. J. and Vorobyev, M., 2003), and have been demonstrated to be important in dominance interactions in damselfishes (Siebeck, U. E., 2004). It certainly seems possible that the high degree of structural or pigmentary integrity necessary to produce a good UV signal could be indicative of an animal's fitness, although this is not yet established.

Polarization signals have special features that differentiate them from typical color signals. For one thing, they are normally clearly visible only when viewed from the correct angle, so that linearly polarized light is reflected directly from the sender to the eye of the receiver. In butterflies, this should produce a flickering and presumably highly visible signal to conspecifics (Figure 15), and in fact, some tropical butterflies do use polarization reflections as mating signals (Sweeney, A. *et al.*, 2003). Most animals known to have polarization signals, however, live in the ocean. Here the use of polarization has very special advantages. First, unlike the case in air, few objects in water

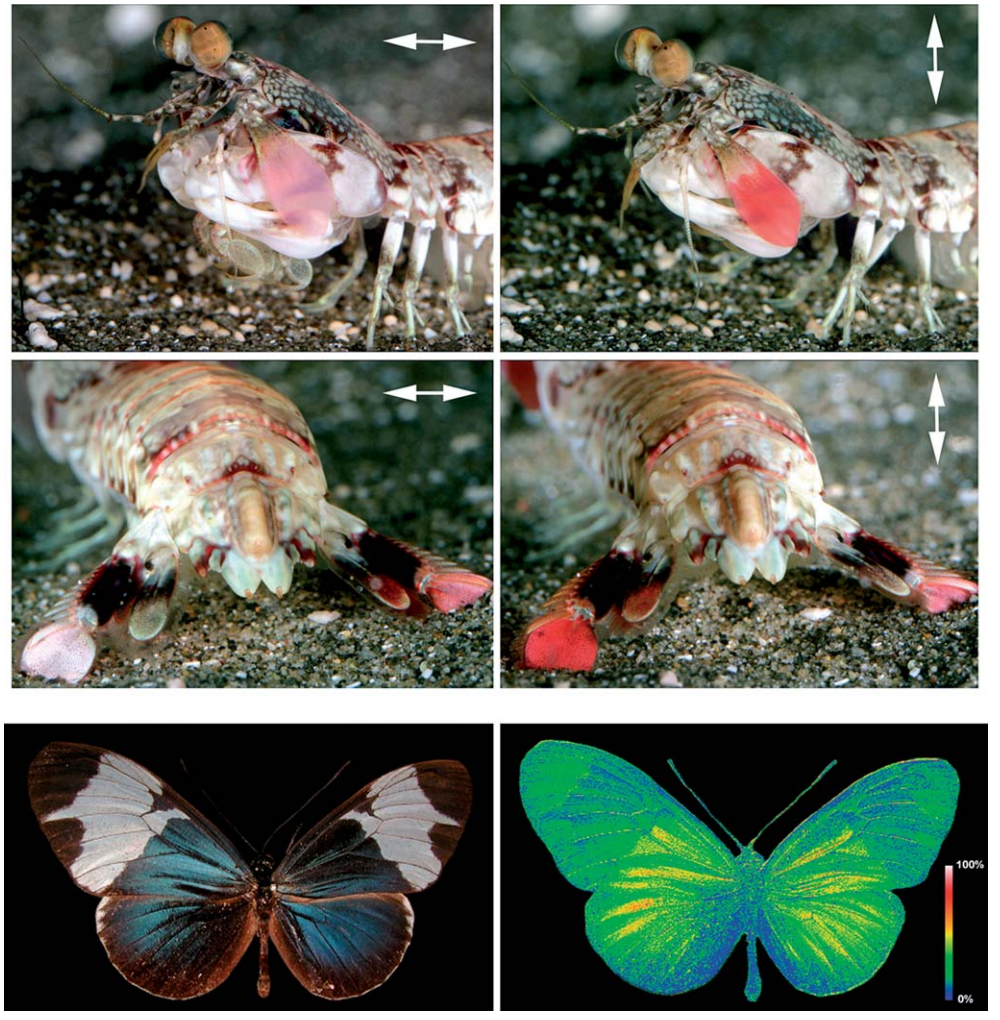

Figure 15 Polarization signals. Top image set: The stomatopod *Odontodactylus latirostris*, photographed through horizontal (left) and vertical (right) linear polarizers (direction of transmitted polarization is indicated by the double-headed arrows). Note the change in appearance of the antennal scale (upper two panels), the appendage extending down and to the animal's left, and of the uropod (lower two panels), the paddle-like appendage extending to the side. These appendages are displayed during mating or aggressive encounters, and the polarized reflections are thought to be intraspecific signals. Reproduced by permission of R. L. Caldwell. Bottom image pair: The tropical butterfly *Heliconius sappho*. The left panel shows a full-color image, while the right is an analyzed false-color image showing the percent polarization of reflected light (coded as indicated by the key). Note that the polarization pattern is quite unlike the color pattern. Photograph courtesy of J. Douglas.

reflect strongly polarized light, so a polarization signal should look distinctive when displayed. The second great advantage is that the relatively stable underwater lighting environment, where light arrives nearly always from overhead, produces a polarization reflection that is stable and constant over a range of depths. Signals based on color patterns are unreliable in water for this very reason; they change in appearance with changes in depth and water quality. Polarized-light signals are far more reliable. They are widely used by cephalopods, particularly squids and cuttlefishes (Shashar, N. *et al*., 1996; Shashar, N. and Hanlon, R. T., 1997). The other masters of underwater polarization communication are the mantis shrimps (Figure 15). These creatures have specialized polarization receptors in their compound eyes, and they use a wide diversity of polarization signals during mating and territorial interactions (Marshall, N. J. *et al*., 1999; Cronin, T. W. *et al*., 2003). It is reasonable to expect that biological signaling based on patterns of polarized light will turn out to be widespread among invertebrates, many of which are capable of good polarization vision.

1.08.6 Concluding Remarks

What other animals use their eyes for, and what they see, are questions that have interested humans since time immemorial. Today's visual ecologists have a varied and ever-changing set of tools to investigate animal vision and to begin to understand how animals get the information they need using their visual systems. Visual ecology provides the link between physiology and sensory biology and animal ecology, behavior, and social interactions. I have attempted to provide a feel for this vital and active field in this chapter, in the hope that this conveys some of the excitement experienced by researchers working on so many diverse topics stimulated by ideas on how animals view their worlds.

References

Aho, A.-C., Donner, K., Hydén, C., Larsen, L. O., and Reuter, T. 1988. Low retinal noise in animals with low body temperature allows high visual sensitivity. Nature 334, 340–350.

Ala-Laurila, P., Pahlberg, J., Koskelainen, A., and Donner, K. 2004. On the relation between the photoactivation energy and the absorbance spectrum of visual pigments. Vision Res. 44, 2153–2158.

Andersson, S., Örnborg, J., and Andersson, M. 1998. Ultraviolet sexual dimorphism and assortative mating in blue tits. Proc. Roy. Soc. Lond. B 265, 455–1450.

Arikawa, K. 2003. Spectral organization of the eye of a butterfly, *Papilio*. J. Comp. Physiol. A 189, 791–800.

Arikawa, K., Inokuma, K., and Eguchi, E. 1987. Pentachromatic visual system in a butterfly. Naturwissenschaften 74, 297–298.

Arnold, K. E., Owens, I. P. F., and Marshall, N. J. 2002. Fluorescent signaling in parrots. Science 295, 92.

Arrese, C. A., Hart, N. S., Thomas, N., Beazley, L. D., and Shand, J. D. 2002. Trichromacy in marsupials. Curr. Biol. 12, 657–660.

Attick, J. J. 1992. Could information theory provide an ecological theory of sensory processing? Network 3, 213–251.

Barlow, H. B. 1982. What causes trichromacy? A theoretical analysis using comb-filtered spectra. Vision Res. 22, 635–643.

Barlow, R. B., Jr., Powers, M. K., and Kass, L. 1988. Vision and Mating Behavior in *Limulus*. In: Sensory Biology of Aquatic Animals, (*eds*. J. Atema, R. R. Fay, A. N. Popper, and W. N. Tavolga), pp. 419–434. Springer.

Bennett, A. T. D., Cuthill, I. C., Partridge, J. C., and Lunau, K. 1997. Ultraviolet plumage colors predict mate preferences in starlings. Proc. Nat. Acad. Sci. U. S. A. 94, 8618–8621.

Bennett, A. T. D., Cuthill, I. C., Partridge, J. C., and Maier, E. J. 1996. Ultraviolet vision and mate choice in zebra finches. Nature 380, 433–435.

Bernard, G. D. and Remington, C. L. 1991. Color vision in *Lycaena* butterflies: spectral tuning of receptor arrays in relation to behavioral ecology. Proc. Nat. Acad. Sci. U. S. A. 88, 2783–2787.

Bowmaker, J. K. 1983. Trichromatic colour vision: why only three receptor channels? Trends Neurosci. 6, 41–43.

Bowmaker, J. K., Astell, S., Hunt, D. M., and Mollon, J. D. 1991. Photosensitive and photostable pigments in the retinae of Old World monkeys. J. Exp. Biol. 156, 1–19.

Bridges, C. D. B. 1972. The Rhodopsin–Porphyropsin Visual System. In: Handbook of Sensory Physiology, Vol.VII/I: The Photochemistry of Vision (*ed*. H. J. A. Dartnall), pp. 417–480. Springer.

Briscoe, A. D. and Chittka, L. 2001. The evolution of color vision in insects. Ann. Rev. Entomol. 46, 471–510.

Buchsbaum, G. and Gottschalk, A. 1983. Trichromacy, opponent colours coding and optimum colour information transmission in the retina. Proc. R. Soc. Lond. B 220, 89–113.

Burton, G. J. and Moorhead, I. R. 1987. Color and spatial structure in natural scenes. Applied Optics 26, 157–170.

Carleton, K. C. and Kocher, T. D. 2001. Cone opsin genes of African cichlid fishes: tuning spectral sensitivity by differential gene expression. Mol. Biol. Evol. 18, 1540–1550.

Chen, D.-M. and Goldsmith, T. H. 1986. Four spectral classes of cones in the retinas of birds. J. Comp. Physiol. A 159, 473–479.

Cheroske, A. G., Barber, P. H., and Cronin, T. W. 2006. Evolutionary variation in the expression of phenotypically plastic color vision in Caribbean mantis shrimps, genus *Neogonodactylus*. Mar. Biol. (in press).

Cheroske, A. G., Cronin, T. W., and Caldwell, R. L. 2003. Adaptive color vision in *Pullosquilla litoralis* (Stomatopoda, Lysiosquilloidea) associated with spectral and intensity changes in light environment. J. Exp. Biol. 206, 373–379.

Chiao, C.-C., Cronin, T. W., Osorio, D., and Marshall, J. 2000c. Eye design and color signaling in a stomatopod crustacean, *Gonodactylus smithii*. Brain Behav. Evol. 56, 107–122.

Chiao, C.-C., Kelman, E. J., and Hanlon, R. T. 2005. Disruptive body patterning of cuttlefish (*Sepia officinalis*) requires visual

information regarding edges and contrast of objects in natural substrate backgrounds. Biol. Bull. 208, 7–11.
Chiao, C.-C., Osorio, D., Vorobyev, M., and Cronin, T. W. 2000a. Characterization of natural illuminants in forests and the use of digital video data to reconstruct illuminant spectra. J. Opt. Soc. Am. A 17, 1713–1721.
Chiao, C.-C., Vorobyev, M., Cronin, T. W., and Osorio, D. 2000b. Spectral tuning of dichromats to natural scenes. Vision Res. 40, 3257–3271.
Chittka, L. 1996a. Does bee color vision predate the evolution of flower color? Naturwissenschaften 83, 136–138.
Chittka, L. 1996b. Optimal sets of color receptors and color opponent systems for coding of natural objects in insect vision. J. Theoret. Biol. 181, 179–196.
Chittka, L. and Menzel, R. 1992. The evolutionary adaptation of flower colors and the insect pollinators' color vision. J. Comp. Physiol. A 171, 171–181.
Chittka, L., Beier, W., Hertel, H., Steinmann, E., and Menzel, R. 1992. Opponent coding is a universal strategy to evaluate the photoreceptor inputs in hymenoptera. J. Comp. Physiol. A 170, 545–563.
Chittka, L., Vorobyev, M., Shmida, A., and Menzel, R. 1993. Bee Colour Vision – the Optimal System for the Discrimination of Flower Colours with Three Spectral Photoreceptor Types? In: Sensory Systems of Arthropods (*eds*. K. Wiese, F. G. Gribakin, A. V. Popov, and G. Renninger), pp. 211–218. Birkhauser.
Collett, T. S. 1978. Peering – a locust behavior pattern for obtaining motion parallax information. J. Exp. Biol. 76, 237–241.
Collett, T. S. and Harkness, L. I. K. 1982. Depth Vision in Animals. In: Analysis of Visual Behavior (*eds*. D. J. Ingle, M. A. Goodale, and R. J. W. Mansfield), pp. 111–176. MIT Press.
Collett, T. S. and Land, M. F. 1975. Visual control of flight behavior in the hoverfly, *Syritta pipiens* L. J. Comp. Physiol. 99, 1–66.
Collin, S. P., Knight, M. A., Davies, W. L., Potter, I. C., Hunt, D. M., and Trezise, A. E. O. 2003. Ancient colour vision: multiple opsin genes in the ancestral vertebrates. Curr. Biol. 13, R864–R865.
Cone, R. A. 1972. Rotational diffusion of rhodopsin in the visual receptor membrane. Nature 236, 39–43.
Cott, H. B. 1940. Adaptive Coloration in Animals. Methuen.
Cronin, T. W. 2005. Visual ecology of Predator–Prey Interactions. In: Ecology of Predator–Prey Interactions (*eds*. P. Barbosa and I. Castellanos), pp. 105–138. Oxford University Press.
Cronin, T. W. 2006. Vision in Water. In: Invertebrate Vision (*eds*. E. J. Warrant and D. E. Nilsson), pp. 211–249. Cambridge University Press.
Cronin, T. W. and Caldwell, R. L. 2002. Tuning of visual function in three mantis shrimp species that inhabit a range of depths. I. Visual pigments. J. Comp. Physiol. A 188, 187–197.
Cronin, T. W. and Marshall, N. J. 1989. A retina with at least ten spectral types of photoreceptors in a stomatopod crustacean. Nature 339, 137–140.
Cronin, T. W. and Marshall, J. 2004. The Unique Visual World of Mantis Shrimps. In: Complex Worlds From Simple Nervous Systems (*ed*. F. Prete), pp. 239–268. MIT Press.
Cronin, T. W. and Shashar, N. 2001. The linearly polarized light field in clear, tropical marine waters: spatial and temporal variation of light intensity, degree of polarization, and *e*-vector angle. J. Exp. Biol. 204, 2461–2467.
Cronin, T. W., Caldwell, R. L., and Erdmann, M. 2002. Tuning of visual function in three mantis shrimp species that inhabit a range of depths. II. Filter pigments. J. Comp. Physiol. A 188, 179–186.
Cronin, T. W., Caldwell, R. L., and Marshall, J. 2001. A deeper shade of red: colour vision tuned to habitat in a mantis shrimp. Nature 411, 547–548.
Cronin, T. W., Järvilehto, M., Weckström, M., and Lall, A. B. 2000. Tuning of photoreceptor spectral sensitivity in fireflies (Coleoptera: Lampyridae). J. Comp. Physiol. A 186, 1–12.
Cronin, T. W., Kinloch, M. R., and Olsen, G. H. 2005. Head-bobbing behavior in foraging whooping cranes favors visual fixation. Current Biology 15, R243–R244.
Cronin, T. W., Marshall, N. J., and Caldwell, R. L. 1996. Visual pigment diversity in two genera of mantis shrimps implies rapid evolution. J. Comp. Physiol. A 179, 371–384.
Cronin, T. W., Marshall, N. J., and Caldwell, R. L. 2000. Spectral tuning and the visual ecology of mantis shrimps. Phil. Trans. Roy. Soc. B 355, 1263–1267.
Cronin, T. W., Marshall, N. J., Caldwell, R. L., and Shashar, N. 1994a. Specialization of retinal function in the compound eyes of mantis shrimps. Vision Res. 34, 2639–2656.
Cronin, T. W., Marshall, N. J., Quinn, C. A., and King, C. A. 1994b. Ultraviolet photoreception in mantis shrimp. Vision Res. 34, 1443–1452.
Cronin, T. W., Nair, J. N., Doyle, R. D., and Caldwell, R. L. 1988. Ocular tracking of rapidly moving visual targets by stomatopod crustaceans. J. Exp. Biol. 138, 155–179.
Cronin, T. W., Shashar, N., Caldwell, R. L., Marshall, J., Cheroske, A. G., and Chiou, T.-H. 2003. Polarization vision and its role in biological signaling. Int. Comp. Biol. 43, 549–558.
Cronin, T. W., Warrant, E. J., and Greiner, B. 2006. Celestial polarization patterns during twilight. Appl. Opt. (in press).
Crook, A. C. 1997. Colour patterns in a coral reef fish. Is background complexity important? J. Exp. Mar. Biol. Ecol. 217, 237–252.
Cummings, M. E. and Partridge, J. C. 2001. Visual pigments and optical habitats of surfperch (Embiotocidae) in the California kelp forest. J. Comp. Physiol. A 187, 875–889.
Cuthill, I. C., Partridge, J. C., and Bennett, A. T. D. 2000. Avian UV Vision and Sexual Selection. In: Animal Signals: Signalling and Signal Design in Animal Communication (*eds*. Y. Espmark, T. Amundsen, and G. Rosenqvist), pp. 61–82. Tapir Press.
Dacke, M., Byrne, M. J., Scholtz, C. H., and Warrant, E. J. 2004. Lunar orientation in a beetle. Proc. R. Soc. Lond. B 271, 361–365.
Dacke, M., Doan, T. A., and O'Carroll, D. C. 2001. Polarized light detection in spiders. J. Exp. Biol. 204, 2481–2490.
Dacke, M., Nilsson, D.-E., Warrant, E., Blest, A. D., Land, M. F., and O'Carroll, D. C. 1999. Built-in polarizers form part of a compass organ in spiders. Nature 401, 470–473.
Dacke, M., Nilsson, D.-E., Scholtz, C. H., Byrne, M., and Warrant, E. J. 2003. Insect orientation to polarized moonlight. Nature 424, 33.
Dahmen, H. 1991. Eye specialization in waterstriders: an adaptation to life in a flat world. J. Comp. Physiol. A 169, 623–632.
Dartnall, H. J. A. 1953. The interpretation of spectral sensitivity curves. British Med. Bull. 9, 24–30.
Dominy, N. J. and Lucas, P. W. 2001. Ecological importance of trichromatic vision to primates. Nature 410, 363–366.
Douglas, R. H., Partridge, J. C., Dulai, K. S., Hunt, D. M., Mullineaux, C. W., and Hynninen, P. H. 1999. Enhanced retinal longwave sensitivity using a chlorophyll-derived photosensitiser in *Malacosteus niger*, a deep-sea dragon fish with far red bioluminescence. Vision Res. 17, 2817–2832.
Doujak, F. E. 1984. Electrophysiological measurement of photoreceptor membrane dichroism and polarization sensitivity in a grapsid crab. J. Comp. Physiol. A 154, 597–605.
Duelli, P. 1978. Movement detection in the posterolateral eyes of jumping spiders (*Evarcha arcuata*, Salticidae). J. Comp. Physiol. 124, 15–26.
Dulai, K. S., Bowmaker, J. K., Mollon, J. D., and Hunt, D. M. 1994. Sequence divergence, polymorphism and evolution

of middle-wave and long-wave visual pigment genes of great apes and old-world monkeys. Vision Res. 34, 2483–2491.
Endler, J. A. 1991. Variation in the appearance of guppy color patterns to guppies and their predators under different visual conditions. Vision Res. 31, 587–608.
Endler, J. A. 1992. Signals, signal conditions, and the direction of evolution. Am. Nat. 139, S125–S153.
Endler, J. A. 1993. Some general comments on the evolution and design of animal communication systems. Phil. Trans. R. Soc. Lond. B 340, 215–225.
Endler, J. A. 2000. Evolutionary Implications of the Interaction between Animal Signals and the Environment. In: Animal Signals: Signalling and Signal Design in Animal Communication (*eds*. Y. Espmark, T. Amundsen, and G. Rosenqvist), pp. 11–46. Tapir Press.
Endler, J. A. and Basolo, A. L. 1998. Sensory ecology, receiver biases and sexual selection. Trends Ecol. Evol. 13, 415–420.
Endler, J. A. and Théry, M. 1996. Interacting effects of lek placement, display behaviour, ambient light, and color patterns in three neotropical forest-dwelling birds. Am. Nat. 148, 421–452.
Espmark, Y., Amundsen, T., and Rosenqvist, G. 2000. Animal Signals: Signalling and Signal Design in Animal Communication. Tapir Press.
Fasick, J. I. and Robinson, P. R. 2000. Spectral-tuning mechanisms of marine mammal rhodopsins and correlations with foraging depth. Visual Neurosci. 17, 781–788.
Fasick, J. I., Robinson, P. R., Cronin, T. W., and Hunt, D. L. 1998. The visual pigments of the bottlenose dolphin (*Tursiops truncatus)*. Visual Neurosci. 15, 653–676.
Fineran, B. A. and Nicol, J. A. C. 1978. Studies on the photoreceptors of *Anchoa mitchilli* and *A. hepsetus* (Engraulidae) with particular reference to the cones. Phil. Trans. R. Soc. Lond. B 283, 25–60.
Forward, R. B., Jr. 1976. Light and diurnal vertical migration: photobehavior and photophysiology of plankton. Photochem. Photobiol. Rev. 1, 157–209.
Forward, R. B., Jr., Cronin, T. W., and Douglass, J. K. 1988. The visual pigments of crabs. II. Environmental adaptations. J. Comp. Physiol. A 162, 479–490.
Fox, D. L. 1976. Animal Biochromes and Structural Colors. University of California Press.
Frank, T. M. and Widder, E. A. 1996. UV light in the deep-sea: *in situ* measurements of downwelling irradiance in relation to the visual threshold sensitivity of UV-sensitive crustaceans. Mar. Freshwater Behav. Physiol. 27, 189–197.
Fujita, M. 2006. Head-bobbing and non-bobbing walking of black-headed gulls (*Larus ridibundus)*. J. Comp. Physiol. A 192, 481–488.
Fuller, R. C., Carleton, K. L., Fadool, J. M., Spady, T. C., and Travis, J. 2004. Population variation in opsin expression in the bluefin killifish, *Luciana goodei:* a real-time PCR study. J. Comp. Physiol. A 190, 147–154.
Gál, J., Horváth, G., Barta, A., and Wehner, R. 2001. Polarization of the moonlit clear night sky measured by full-sky imaging polarimetry at full moon: comparison of the polarization of moonlit and sunlit skies. J. Geophys. Res. 106(D19), 22647–22653.
Glantz, R. M. 2001. Polarization analysis in the crayfish visual system. J. Exp. Biol. 204, 2383–2390.
Goldsmith, T. H. 1975. The Polarization Sensitivity-Dichroic Absorption Paradox in Arthropod Photoreceptors. In: Photoreceptor Optics (*eds*. A. W. Snyder and R. Menzel), pp. 98–125. Springer.
Goldsmith, T. H. 1977. Membrane Adaptations of Visual Photoreceptors for the Analysis of Plane-Polarized Light. In: Research in Photobiology (*ed*. A. Castellani), pp. 651–658. Plenum.
Goldsmith, T. H. 1994. Ultraviolet receptors and color vision: evolutionary implications and a dissonance of paradigms. Vision Res. 34, 1479–1487.
Goldsmith, T. H. and Butler, B. K. 2005. Color vision of the budgerigar (*Melopsittacus undulatus)*: hue matches, tetrachromacy, and intensity discrimination. J. Comp. Physiol. A 191, 933–951.
Goldsmith, T. H. and Wehner, R. 1977. Restrictions of rotational and translational diffusion of pigment in the membranes of a rhabdomeric photoreceptor. J. Gen. Physiol. 70, 453–490.
Greiner, B., Ribi, W. A., and Warrant, E. J. 2004. Retinal and optical adaptations for nocturnal vision in the halictid bee *Megalopta genalis*. Cell Tissue Res. 316, 377–390.
Greiner, B., Ribi, W. A., and Warrant, E. J. 2005. A neural network to improve dim-light vision? Dendritic fields of first-order interneurons in the nocturnal bee *Megalopta genalis*. Cell Tissue Res. 322, 313–320.
Guillemain, M., Martin, G. R., and Fritz, H. 2002. Feeding methods, visual fields and vigilance in dabbling ducks (Anatidae). Funct. Ecol. 16, 522–529.
Hardie, R. C. 1986. The photoreceptor array of the dipteran retina. Trends Neurosci. 9, 419–423.
Hart, N. S. 2001a. Variations in cone photoreceptor abundance and the visual ecology of birds. J. Comp. Physiol. A 187, 685–698.
Hart, N. S. 2001b. The visual ecology of avian photoreceptors. Progr. Retinal Eye Res. 20, 675–703.
Hart, N. S. and Vorobyev, M. 2005. Modelling oil droplet absorption spectra and spectral sensitivities of bird cone photoreceptors. J. Comp. Physiol. A 191, 381–392.
Hateren, J. H.van. 1992. Real and optimal neural images in early vision. Nature 360, 68–70.
Hateren, J. H.van. 1993. Spatial, temporal, and spectral preprocessing for colour vision. Proc. Roy. Soc. Lond. B 251, 61–68.
Hateren, J. H.van, Hardie, R. C., Rudolph, A., Laughlin, S. B., and Stavenga, D. G. 1989. The bright zone, a specialized dorsal eye region in the male blowfly *Chrysomyia megacephala*. J. Comp. Physiol. A 164, 297–308.
Hawryshyn, C. W. 1992. Polarization vision in fish. Am. Sci. 80, 164–175.
Hawryshyn, C. W. 2000. Ultraviolet polarization vision in fishes: possible mechanisms for coding e-vector. Phil. Trans. R. Soc. Lond. B 355, 1187–1190.
Hawryshyn, C. W. 2003. Mechanisms of Ultraviolet Polarization Vision in Fishes. In: Sensory Processing in Aquatic Environments (*eds*. S. P. Collin and N. J. Marshall), pp. 252–265. Springer.
Hawryshyn, C. W. and Beauchamp, R. 1985. Ultraviolet photosensitivity in goldfish: an independent U.V. retinal mechanism. Vision Res. 25, 11–20.
Hawryshyn, C. W. and Bolger, A. 1991. Spatial orientation of rainbow trout: effects of the degree of polarisation of the polarised light field. J. Comp. Physiol. A 167, 691–697.
Helbig, A. J. 1990. Depolarization of natural skylight disrupts orientation of an avian nocturnal migrant. Experientia 46, 755–758.
Hölldobler, B. 1980. Canopy orientation: a new kind of orientation in ants. Science 210, 86–88.
Horridge, G. A. and Sandeman, D. C. 1964. Nervous control of optokinetic responses in the crab, *Carcinus*. Proc. Roy. Soc. Lond. B 161, 216–246.
Horváth, G. and Varjú, D. 2004. Polarized Light in Animal Vision. Springer.
Horváth, G. and Zeil, J. 1996. Kuwait oil lakes as insect traps. Nature 379, 303–304.
Horváth, G., Gál, J., and Wehner, R. 1997. Why are water-seeking insects not attracted by mirages? The polarization properties of mirages. Naturwissenschaften 84, 300–303.

Hosoya, T., Baccus, S. A., and Meister, M. 2005. Dynamic predictive coding by the retina. Nature 436, 71–77.
Hunt, S., Cuthill, I. C., Bennett, A. T. D., Church, S. C., and Partridge, J. C. 2001. Is the ultraviolet waveband a special communication channel in avian mate choice? J. Exp. Biol. 204, 2499–2507.
Jacobs, G. H. 1992. Ultraviolet vision in vertebrates. Amer. Zool. 32, 544–554.
Jacobs, G. H. 1993. The distribution and nature of colour vision among the mammals. Biol. Rev. 68, 413–471.
Jacobs, G. H. 1995. Variations in primate color vision: mechanisms and utility. Evol. Anthropol. 3, 196–205.
Jacobs, G. H. 1996. Primate photopigments and primate color vision. Proc. Nat. Acad. Sci. U. S. A. 93, 577–581.
Jane, S. D. and Bowmaker, J. K. 1988. Tetrachromatic colour vision in the duck (*Anas platyrhynchos L.*): microspectrophotometry of visual pigments and oil droplets. J. Comp. Physiol. A 162, 225–235.
Jerlov, N. G. 1976. Marine Optics, Elsevier.
Johnsen, S. 2001. Hidden in plain sight: the ecology and physiology of organismal transparency. Biol. Bull. 201, 301–318.
Johnsen, S. 2002. Cryptic and conspicuous coloration in the pelagic environment. Proc. Roy. Soc. Lond. B 269, 243–256.
Jokela-Määttä, M., Pahlberg, J., Lindström, M., Zak, P., Porter, M., Ostrovskii, M., Cronin, T., and Donner, K. 2005. Visual pigment absorbance and spectral sensitivity of *Mysis relicta* (Crustacea, Mysidae) in different light environments. J. Comp. Physiol. A 191, 1087–1097.
Jones, J. 1994. Architecture and composition of the muscles that drive stomatopod eye movements. J. Exp. Biol. 188, 317–331.
Jusuf, P. R., Martin, P. R., and Grünert, U. 2006. Random wiring in the midget pathway of primate retina. J. Neurosci. 26, 3908–3917.
Kelber, A. 1999. Ovipositing butterflies use a red receptor to see green. J. Exp. Biol. 202, 2619–2630.
Kelber, A. 2000. Why ''false'' colours are seen by butterflies? Nature 402, 251.
Kelber, A., Balkenius, A., and Warrant, E. J. 2002. Scotopic color vision in nocturnal hawkmoths. Nature 419, 922–924.
Kelber, A., Thunell, C., and Arikawa, K. 2001. Polarisation-dependent colour vision in *Papilio* butterflies. J. Exp. Biol. 204, 2469–2480.
Kinoshita, M., Shimada, N., and Arikawa, K. 1999. Colour vision, of the foraging swallowtail butterfly *Papilio xuthus*. J. Exp. Biol. 202, 95–102.
Knowles, A. and Dartnall, H. J. A. 1977. Habitat and Visual Pigments. In: The Eye; Vol. 2B, The Photobiology of Vision (*ed*. H. Davson), pp. 581–641. Academic Press.
Kriska, G., Horváth, G., and Andrikovics, S. 1998. Why do mayflies lay their eggs en masse on dry asphalt roads? Water-imitating polarized light reflected from asphalt attracts Ephemeroptera. J. Exp. Biol. 201, 2273–2286.
Labhart, T., Petzold, J., and Helbling, H. 2001. Spatial integration in polarization-sensitive interneurones of crickets: a survey of evidence, mechanisms and benefits. J. Exp. Biol. 204, 2423–2430.
Lambrinos, D., Möller, R., Labhart, T., Pfeifer, R., and Wehner, R. 2000. A mobile robot employing insect strategies for navigation. Robotics Autonomous Sys. 30, 39–64.
Lall, A. B., Strother, G. K., Cronin, T. W., and Seliger, H. H. 1988. Modification of spectral sensitivities by screening pigments in the compound eyes of twilight-active fireflies (Coleoptera: Lampyridae). J. Comp. Physiol. A 162, 23–33.
Land, M. F. 1981. Optics and Vision in Invertebrates. In: Handbook of Sensory Physiology, Vol. VII/6B, Invertebrate Visual Centers and Behavior (*ed*. H. Autrum), pp. 471–592. Springer.
Land, M. F. 1982. Scanning eye movements in a heteropod mollusc. J. Exp. Biol. 96, 427–430.
Land, M. F. 1985a. The Morphology and Optics of Spider Eyes. In: Neurobiology of Arachnids (*ed*. F. Barth), pp. 53–78. Springer.
Land, M. F. 1985b. Fields of view of the eyes of primitive jumping spiders. J. Exp. Biol. 119, 381–384.
Land, M. F. 1995. The Functions of Eye Movements in Animals Remote from Man. In: Eye Movement Research (*eds*. J. M. Findlay, R. W. Kentridge, and R. Walker), pp. 63–76. Elsevier.
Land, M. F. 1999. Motion and vision: why animals move their eyes. J. Comp. Physiol. A 185, 341–352.
Land, M. F. 2000. On the functions of double eyes in midwater animals. Phil. Trans. Roy. Soc. Lond. B 355, 1147–1150.
Land, M. F. 2003. The spatial resolution of the pinhole eyes of giant clams (*Tridacna maxima)*. Proc. Roy. Soc. Lond. B 270, 185–188.
Land, M. F. 2005. The optical structures of animal eyes. Curr. Biol. 15, R319–R323.
Land, M. F. and Layne, J. E. 1995. The visual control of behaviour in fiddler crabs. I. Resolution, thresholds, and the role of the horizon. J. Comp. Physiol. A 177, 81–90.
Land, M. F. and Nilsson, D-E. 2002. Animal Eyes. Oxford University Press.
Land, M. F., Marshall, N. J., Brownless, D., and Cronin, T. W. 1990. The eye-movements of the mantis shrimp *Odontodactylus scyllarus* (Crustacea: Stomatopoda). J. Comp. Physiol. A. 167, 155–166.
Laughlin, S. B. 1981. Neural principles in the Peripheral Visual Systems of Invertebrates. In: Handbook of Sensory Physiology, vol. VII/6B, Invertebrate Visual Centers and Behavior (*ed*. H. Autrum), pp. 133–280. Springer.
Laughlin, S. B. 1994. Matching coding, circuits, cells, and molecules to signals: general principles of retinal design in the fly's eye. Prog. Retinal Eye Res. 13, 165–196.
Laughlin, S. B. and Weckstrom, M. 1993. Fast and slow photoreceptors – a comparative study of the functional diversity of coding and conductances in the Diptera. J. Comp. Physiol. A 172, 593–609.
Lehrer, M., Srinivasan, M. V., Zhang, S. W., and Horridge, G. A. 1988. Motion cues provide the bee's visual world with a third dimension. Nature 332, 356–357.
Lenz, P. H., Hartline, D. K, Purcell, J. E., and Macmillan, D. L. 1996. Zooplankton: Sensory Ecology and Physiology. Gordon and Breach.
Levenson, D. H., Ponganis, P. J., Crognale, M. A., Deegan, J. F., II, Dizon, A, and Jacobs, G. H. 2006. Visual pigments of marine carnivores: pinnipeds, polar bear, and sea otter. J. Comp. Physiol. A (in press).
Lillywhite, P. G. 1978. Coupling between locust photoreceptors revealed by a study of quantum bumps. J. Comp. Physiol 125, 13–27.
Lindström, L., Alatalo, R. V., Lyytinen, A., and Mappes, J. 2001. Predator experience on cryptic prey affects the survival of conspicuous aposematic prey. Proc. R. Soc. Lond. B 268, 357–361.
Lipetz, L. E. and Cronin, T. W. 1988. Application of an invariant spectral form to the visual pigments of crustaceans: Implications regarding the binding of the chromophore. Vision Res. 28, 1083–1093.
Loew, E. R. and McFarland, W. N. 1990. The Underwater Visual Environment. In: The Visual System of Fish (*eds*. R. H. Douglas and M. B. A. Djamgoz), pp. 1–43. Chapman and Hall.
Losey, G. S., Cronin, T. W., Goldsmith, T. H., Hyde, D., Marshall, N. J., and McFarland, W. N. 1999. The UV visual world of fishes: a review. J. Fish Biol. 54, 921–943.
Lythgoe, J. N. 1972. The Adaptation of Visual Pigments to Their Photic Environment. In: Handbook of Sensory Physiology,

Vol.VII/I: The Photochemistry of Vision (*ed*. H. J. A. Dartnall), pp. 566–603. Springer.
Lythgoe, J. N. 1979. The Ecology of Vision. Clarendon.
Lythgoe, J. N. 1988. Light and Vision in the Aquatic Environment. In: Sensory Biology of Aquatic Animals (*ed*. J. Atema, R. R. Fay, A. N. Popper, and W. N. Tavolga), pp. 57–82. Springer.
Lythgoe, J. N. and Partridge, J. C. 1989. Visual pigments and the acquisition of visual information. J. Exp. Biol. 146, 1–20.
Lythgoe, J. N. and Partridge, J. C. 1991. The modeling of optimal visual pigments of dichromatic teleosts in green coastal waters. Vision Res. 31, 361–371.
Lythgoe, J. N. and Shand, J. 1983. Diel colour changes in the neon tetra, *Paracheirodon innesi*. Env. Biol. Fish. 8, 249–254.
Marshall, N. J. 1988. A unique colour and polarisation vision system in mantis shrimps. Nature 333, 557–560.
Marshall, N. J. 2000a. Communication and camouflage with the same ''bright'' colour in reef fishes. Phil. Trans. Roy. Soc. Lond. B 355, 1243–1248.
Marshall, N. J. 2000b. The Visual Ecology of Reef Fish Colours. In: Animal Signals: Signalling and Signal Design in Animal Communication (*eds*. Y. Espmark, T. Amundsen, and G. Rosenqvist), pp. 83–120. Tapir Press.
Marshall, N. J. and Messenger, J. B. 1996. Colour-blind camouflage. Nature 382, 408–409.
Marshall, N. J. and Vorobyev, M. 2003. Color Signals and Color Vision in Fishes. In: Sensory Processing in Aquatic Environments (*eds*. S. P. Collin and N. J. Marshall), pp. 194–222. Springer.
Marshall, N. J., Cronin, T. W., and Frank, T. N. 2003. Visual Adaptations in Crustaceans: Chromatic, Developmental, and Temporal aspects. In: Sensory Processing in the Aquatic Environment (*eds*. S. P. Collins and N. J. Marshall), pp. 343–372. Springer.
Marshall, N. J., Cronin, T. W., and Shashar, N. 1999. Behavioural evidence for polarization vision in stomatopods reveals a potential channel for communication. Curr. Biol. 9, 755–758.
Marshall, N. J., Jones, J. P., and Cronin, T. W. 1996. Behavioural evidence for color vision in stomatopod crustaceans. J. Comp. Physiol. A 179, 473–481.
Marshall, N. J., Land, M. F., King, C. A., and Cronin, T. W. 1991. The compound eyes of mantis shrimps (Crustacea, Hoplocarida, Stomatopoda). II. Colour pigments in the eyes of Stomatopod crustaceans: polychromatic vision by serial and lateral filtering. Phil Trans. R. Ser. B 334, 57–84.
Martin, G. R. 1994. Visual fields in woodcocks *Scolopax rusticola* (Scolopacidae; Charadriiformes). J. Comp. Physiol. A 174, 787–793.
Martin, G. R., Rojas, L. M., Ramirez, Y., and McNeil, R. 2004. The eyes of oilbirds (*Steatornis caripensis*): pushing at the limits of sensitivity. Naturwissenschaften 91, 26–29.
Mass, A. M., Supin, A. Y., and Severtsov, A. N. 1986. Topographic distribution of sizes and density of ganglion cells in the retina of a Porpoise, *Phocoena phocoena*. Aquatic Mammals 12, 95–102.
Mäthger, L. M. and Denton, E. J. 2001. Reflective properties of iridophores and fluorescent 'eyespots' in the loginid squid *Alloteuthis subulata* and *Loligo vulgaris*. J. Exp. Biol. 204, 2103–2118.
Mäthger, L. M., Barbosa, A., Miner, S., and Hanlon, R. T. 2006. Color blindness and contrast perception in cuttlefish (*Sepia officinalis*) determined by a visual sensorimotor assay. Vision Res. 46, 1746–1753.
Maximov, V. V. 2000. Environmental factors which may have led to the appearance of colour vision. Phil. Trans. R. Soc. Lond. B 355, 1239–1242.
Mazel, C. H., Cronin, T. W., Caldwell, R. L., and Marshall, J. 2004. Fluorescent enhancement of signaling in a mantis shrimp. Science 303, 51.
McFarland, W. N. 1986. Light in the sea – correlations with behaviors of fishes and invertebrates. Am. Zool. 26, 389–401.
McFarland, W. N. and Loew, E. R. 1983. Wave produced changes in underwater light and their relations to vision. Env. Biol. Fish 8, 173–184.
Miller, W. H. 1979. Ocular Optical Filtering. In: Handbook of Sensory Physiology, Vol. VII/6A, Invertebrate Photoreceptors, (*ed*. H. Autrum), pp. 69–143. Springer.
Minnaert, M. 1954. The Nature of Light and Colour in the Open Air. Dover.
Mollon, J. D. 1989. 'Tho' she kneel'd in the Place where they grew ....' J. Exp. Biol. 146, 21–38.
Nagle, M. G. and Osorio, D. 1993. The tuning of human photopigments may minimize red-green chromatic signals in natural conditions. Proc. R. Soc. Lond. B 252, 209–213.
Nalbach, H.-O. 1990. Multisensory control of eyestalk orientation in decapod crustaceans: an ecological approach. J. Crust. Biol. 10, 382–399.
Neitz, J., Geist, T., and Jacobs, G. H. 1989. Color vision in the dog. Vis. Neurosci. 3, 119–125.
Neumeyer, C. 1992. Tetrachromatic color vision in goldfish: evidence by color mixture experiments. J. Comp. Physiol. A 171, 639–649.
Newman, L. A. and Robinson, P. R. 2005. Cone visual pigments of aquatic mammals. Visual Neurosci. 22, 873–879.
Nilsson, D.-E. 1989. Optics and Evolution of the Compound Eye. In: Facets of Vision (*eds*. D. G. Stavenga and R. C. Hardie), pp. 30–73. Springer.
Nilsson, D.-E. 1994. Eyes as optical alarm systems in fan worms and ark clams. Phil. Trans. Roy. Soc. Lond. B 346, 195–212.
Nilsson, D.-E. 1997. Eye Design, Vision and Invisibility in Planktonic Invertebrates. In: Zooplankton: Sensory Ecology and Physiology (*eds*. P. H. Lenz, D. KHartline, J. E. Purcell, and D. L. Macmillan), pp. 149–162. Gordon and Breach.
Nilsson, D.-E. 2005. Photoreceptor evolution: ancient siblings serve different tasks. Curr. Biol. 15, R94–R96.
Nilsson, D.-E. and Pelger, S. 1994. A pessimistic estimate of the time required for an eye to evolve. Proc. R. Soc. Lond. B 256, 54–58.
Nilsson, D.-E., Gislén, L., Coates, M., Skogh, C., and Garm, A. 2005. Advanced optics in a jellyfish eye. Nature 435, 201–205.
Nilsson, D.-E., Labhart, T., and Meyer, E. 1987. Photoreceptor design and optical properties affecting polarization sensitivity in ants and crickets. J. Comp. Physiol. A 161, 645–658.
Niven, J. E. 2006. Visual motion: homing in on small target detectors. Curr. Biol. 16, R292–R294.
Nordström, K., Wallén, R., Seymour, J., and Nilsson, D.-E. 2003. A simple visual system without neurons in jellyfish larvae. Proc. R. Soc. Lond. B 270, 2349–2354.
Novales Flamarique, N. and Harosi, F. I. 2002. Visual pigments and dichroism of anchovy cones: a model system for polarization detection. Visual Neurosci. 19, 467–473.
Novales Flamarique, N., Hawryshyn, C. W., and Harosi, F. I. 1998. Double-cone internal reflection as a basis for polarization detection in fish. J. Opt. Soc. Am. A 15, 349–358.
Oakley, T. H. and Cunningham, C. W. 2002. Molecular phylogenetic evidence for the independent evolutionary origin of an arthropod compound eye. Proc. Nat. Acad. Sci. U. S. A. 99, 1426–1430.
Olshausen, B. A. and Field, D. J. 1996. Emergence of simple-cell receptive field properties by learning a sparse code for natural images. Nature 318, 607–609.

Osorio, D. and Bossomaier, T. R. J. 1992. Human cone-pigment spectral sensitivities and the reflectances of natural surfaces. Biol. Cybern. 67, 217–222.
Osorio, D. and Srinivasan, M. V. 1991. Camouflage by edge enhancement in animal coloration patterns and its implications for visual mechanisms. Proc. Roy. Soc. Lond. B 244, 81–85.
Osorio, D. and Vorobyev, M. 1996. Colour vision as an adaptation to frugivory in primates. Proc. R. Soc. Lond. B 263, 593–599.
Osorio, D., Ruderman, D. L., and Cronin, T. W. 1998. Estimation of errors in luminance signals encoded by primate retina resulting from sampling of natural images with red and green cones. J. Opt. Soc. Am. A 15, 16–22.
Ott, M. and Schaeffel, F. 1985. A negatively powered lens in the chameleon. Nature 373, 692–694.
Palacios, A. G., Varela, F. J., Srivastava, R., and Goldsmith, T. H. 1998. Spectral sensitivity of cones in the goldfish, *Carassius auratus*. Vision Res. 38, 2135–2146.
Parker, A. R. 1998. Colour in Burgess Shale animals and the effect of light on evolution in the Cambrian. Proc. Roy. Soc. Lond. B 265, 967–972.
Parker, A. R., Hegedus, Z., and Watts, R. A. 1998. Solar-absorber antireflector on the eye of an Eocene fly (45 Ma). Proc. R. Soc. Lond. B 265, 811–815.
Párraga, C. A, Troscianko, T., and Tolhurst, D. J. 2002. Spatiochromatic properties of natural images and human vision. Curr. Biol. 12, 483–487.
Parry, J. W. L., Carleton, K. L., Spady, T., Carboo, A., Hunt, D. M., and Bowmaker, J. K. 2005. Mix and match color vision: tuning spectral sensitivity by differential opsin gene expression in Lake Malawi cichlids. Curr. Biol. 15, 1734–1739.
Partridge, J. C. 1990. The Colour Sensitivity and Vision of Fishes. In: Light and Life in the Sea (*ed*. P. J. Herring, A. K. Campbell, M. Whitfield, and L. Maddock), pp. 167–184. Cambridge University Press.
Partridge, J. C. and Douglas, R. H. 1995. Far-red sensitivity of dragon fish. Nature 375, 21–22.
Peichl, L. 2005. Diversity of mammalian photoreceptor properties: adaptations to habitat and lifestyle? Anat. Record A 287A, 1001–1012.
Peichl, L., Günther Behrmann, G., and Kröger, R. H. H. 2001. For whales and seals the ocean is not blue: a visual pigment loss in marine mammals. Eur. J. Neurosci. 13, 1520–1528.
Peitsch, D., Fietz, A., Hertel, H., de Souza, J., Ventura, D. F., and Menzel, R. 1992. The spectral input systems of hymenopteran insects and their receptor-based colour vision. J. Comp. Physiol. A 170, 23–40.
Pettigrew, J. D., Collin, S. P., and Ott, M. 1999. Convergence of specialized behaviour, eye movements and visual optics in the sandlance (Teleostei) and the chameleon (Reptilia). Curr. Biol. 9, 421–424.
Prum, R. O., Cole, J. A, and Torres, R. H. 2004. Blue integumentary structural colours in dragonflies (Odonata) are not produced by incoherent Tyndall scattering. J. Exp. Biol. 207, 3999–4009.
Prum, R. O., Torres, R. H., Williamson, S, and Dyck, J. 1998. Coherent light scattering by blue feather barbs. Nature 396, 28–29.
Ramachandran, V. S., Tyler, C. W., Gregory, R. L, Rogers-Ramachandran, D., Duensing, S., Pillsbury, C., and Ramachandran, C. 1996. Rapid adaptive camouflage in tropical flounders. Nature 379, 815–818.
Regan, B. C., Julliot, C., Simmen, B., Viénot, F., Charles-Dominique, P., and Mollon, J. D. 2001. Fruits, foliage, and the evolution of primate colour vision. Phil. Trans. Roy. Soc. Lond. B 356, 229–283.
Roberts, N. W., Gleeson, H., Temple, S. E., Haimberger, T. J., and Hawryshyn, C. W. 2004. Differences in the optical properties of vertebrate photoreceptor classes leading to axial polarization sensitivity. J. Opt. Soc. Am. A 31, 335–345.
Rossel, S. 1989. Polarization Sensitivity in Compound Eyes. In: Facets of Vision (*eds*. D. G. Stavenga and R. C. Hardie), pp. 298–316. Springer.
Rossel, S. 1980. Foveal fixation and tracking in the praying mantis. J. Comp. Physiol. 139, 307–331.
Rowe, M. P., Engheta, N., Easter, S. S., Jr., and Pugh, E. N., Jr. 1994. Graded-index model of a fish double cone exhibits differential polarization sensitivity. J. Opt. Soc. Am. 11, 55–70.
Rozenberg, G. V. 1966. Twilight – A Study in Atmospheric Optics. Plenum.
Ruderman, D. L. 1994. The statistics of natural images. Network. Comp. Neural Sys. 5, 517–548.
Ruderman, D. L. and Bialek, W. 1994. Statistics of natural images: Scaling in the woods. Phys. Rev. Letters 73, 814–187.
Ruderman, D. L., Cronin, T. W., and Chiao, C.-C. 1998. Statistics of cone responses to natural images: implications for visual coding. J. Opt. Soc. Am. A 15, 2036–2045.
Saidel, W. M., Lettvin, J. Y., and McNichol, E. F. 1983. Processing of polarized light by squid photoreceptors. Nature 304, 534–536.
Schaeffel, F., Murphy, C. J., and Howland, H. C. 1999. Accommodation in the cuttlefish (*Sepia officinalis*). J. Exp. Biol. 202, 3127–3134.
Schwind, R. 1984. The plunge reaction of the backswimmer *Notonecta glauca*. J. Comp. Physiol. A 155, 319–321.
Schwind, R. 1991. Polarization vision in water insects and insects living on a moist substrate. J. Comp. Physiol. A 169, 531–540.
Shashar, N. and Hanlon, R. T. 1997. Squids (*Loligo pealii* and *Euprymna scolopes*) can exhibit polarized light patterns produced by their skin. Biol. Bull. 193, 207–208.
Shashar, N., Hanlon, R. T., and Petz, A. M. 1998. Polarization vision helps detect transparent prey. Nature 393, 222–223.
Shashar, N., Hagan, R., Boal, J. G., and Hanlon, R. T. 2000. Cuttlefish use polarization sensitivity in predation on silvery fish. Vision Res. 40, 71–75.
Shashar, N., Rutledge, P., and Cronin, T. W. 1996. Polarization vision in cuttlefish: a concealed communication channel? J. Exp. Biol. 199, 2077–2084.
Sherk, T. E. 1978. Development of the compound eyes of dragonflies (Odonata). III. Adult compound eyes. J. Exp. Zool. 203, 61–80.
Shuye, S.-K., Hewett-Emmett, D., Sperling, H. G., Hunt, D. M., Bowmaker, J. K., Mollon, J. D., and Li, W.-H. 1995. Adaptive evolution of color vision genes in higher primates. Science 269, 1265–1267.
Siddiqi, A., Cronin, T. W., Loew, E. R., Vorobyev, M., and Summers, K. 2004. Interspecific and intraspecific views of color signals in the strawberry poison frog, *Dendrobates pumilio*. J. Exp. Biol. 207, 2471–2485.
Siebeck, U. E. 2004. Communication in coral reef fish: the role of ultraviolet colour patterns in damselfish territorial behaviour. Anim. Behav. 68, 273–282.
Sillen-Tullberg, B. 1985. The significance of coloration per se, independent of background, for predator avoidance of aposematic prey. Anim. Behav. 33, 1382–1384.
Sivak, J. G. 1988. Optics of Amphibious Eyes in Vertebrates. In: Sensory Biology of Aquatic Animals (*eds*. J. Atema, R. R. Fay, A. N. Popper, and W. N. Tavolga), pp. 467–485. Springer-Verlag.
Snyder, A. W. 1973. Polarization sensitivity of individual retinula cells. J. Comp. Physiol. 83, 331–360.
Snyder, A. W. 1979. Physics of Vision in Compound Eyes. In: Handbook of Sensory Physiology, Vol. VII/6A,

Invertebrate Photoreceptors (*ed*. H. Autrum), pp. 225–313. Springer-Verlag.
Snyder, A. W. and Laughlin, S. B. 1975. Dichroism and absorption by photoreceptors. J. Comp. Physiol. 100: 101–116.
Snyder, A. W., Stavenga, D. G., and Laughlin, S. B. 1977. Information capacity of eyes. Vision Res. 17, 1163–1175.
Speck, M. and Labhart, T. 2001. Carotenoid deprivation and rhodopsin alignment in R1-6 photoreceptors of *Drosophila melanogaster*. Proc. Neurobiol. Conf. Goettingen 28, 514.
Srinivasan, M. V., Laughlin, S. B., and Dubs, A. 1982. Predictive coding: a fresh view of inhibition in the retina. Proc. R. Soc. Lond. B 216, 427–459.
Stavenga, D. G., Smits, R. P., and Hoenders, B. J. 1993. Simple exponential functions describing the absorbance bands of visual pigment spectra. Vision Res. 33, 1011–1017.
Stockman, A., MacLeod, D. I. A., and Johnson, N. E. 1993. Spectral sensitivities of the human cones. J. Opt. Soc. Am. A 10, 2491–2521.
Summers, K., Cronin, T. W., and Kennedy, T. 2003. Variation in spectral reflectance among populations of *Dendrobates pumilio*, the strawberry poison frog, in the Bocas del Toro Archipelago, Panama. J. Biogeography 30, 35–53.
Suzuki, T., Arikawa, K., and Eguchi, E. 1985. The effects of light and temperature on the rhodopsin–porphyropsin visual system of the crayfish, *Procambarus clarkii*. Zoological Sci. 2, 455–461.
Suzuki, T., Makino-Tasaka, M., and Eguchi, E. 1984. 3-Dehydroretinal (vitamin A_2 aldehyde) in crayfish eye. Vision Res. 24, 783–787.
Sweeney, A., Jiggins, C., and Johnsen, S. 2003. Polarized light as a mating signal in a butterfly. Nature 424, 31–32.
Temple, S. E., Plate, E. M., Ramsden, S., Haimberger, T. J., Roth, W.-M., and Hawryshyn, C. W. 2006. Seasonal cycle in vitamin A1/A2-based visual pigment composition during the life history of coho salmon (*Oncorhynchus kisutch*). J. Comp. Physiol. A 192, 301–313.
Theobald, J. C., Greiner, B., Wcislo, W. T., and Warrant, E. J. 2006. Visual summation in night-flying sweat bees: A theoretical study. Vision Res. 46, 2298–2309.
Théry, M. and Casas, J. 2002. Predator and prey views of spider camouflage. Nature 415, 133.
Trezise, A. E. O. and Collin, S. P. 2005. Opsins: evolution in waiting. Curr. Biol. 15, R794–R795.
Tsin, A. T. C. and Beatty, D. D. 1979. Scotopic visual pigment composition in the retinas and vitamins A in the pigment epithelium of the goldfish. Exp. Eye Res. 29, 15–26.
Tucker, V. A. 2000. The deep fovea, sideways vision and spiral flight paths in raptors. J. Exp. Biol. 203, 3745–3754.
Tyler, J. E. and Smith, R. C. 1970. Measurements of Spectral Irradiance Under Water. Ocean Series, 1. Gordon and Breach.
Vladusich, T., Hemmi, J. M., Srinivasan, M. V., and Zeil, J. 2005. Interactions of visual odometry and landmark guidance during food search in honeybees. J. Exp. Biol. 208, 4123–4135.
Vorobyev, M., Gumbert, A., Kunze, J., Giurfa, M., and Menzel, R. 1997. Flowers through insect eyes. Israel J. Plant Sci. 45, 93–102.
Vorobyev, M., Marshall, J., Osorio, D., Hempel de Ibarra, N., and Menzel, R. 2001. Colourful objects through animal eyes. Color Res. Appl. 26, S214–S217.
Vorobyev, M., Osorio, D., Bennett, A. T. D., Marshall, N. J., and Cuthill, I. C. 1998. Tetrachromacy, oil droplets and bird plumage colours. J. Comp. Physiol. A 183, 621–633.
Vukusic, P. and Sambles, R. H. 2003. Photonic structures in biology. Nature 424, 852–855.
Walls, G. L. 1942. The Vertebrate Eye and Its Adaptive Radiation. Cranbrook Institute of Science.
Warrant, E. J. 2004. Vision in the dimmest habitats on Earth. J. Comp. Physiol. A 190, 765–789.
Warrant, E. J. and Nilsson, D.-E. 1998. Absorption of white light in photoreceptors. Vision Res. 38, 195–207.
Warrant, E. J., Collin, S. P., and Locket, N. A. 2003. Eye Design and Vision in Deep-Sea Fishes. In: Sensory Processing in Aquatic Environments (*eds*. S. P. Collin and N. J. Marshall), pp. 303–322. Springer.
Warrant, E. J., Kelber, A., Gislén, A., Greiner, B., Ribi, W. A., and Wcislo, W. T. 2004. Nocturnal vision and landmark orientation in a tropical halictid bee. Curr. Biol. 14, 1309–1318.
Warrant, E., Porombka, T., and Kirchner, W. H. 1996. Neural image enhancement allows honeybees to see at night. Proc. R. Soc. Lond. B 263, 1521–1526.
Waterman, T. H. 1981. Polarization Sensitivity. In: Handbook of Sensory Physiology, vol. VII/6B, Invertebrate Visual Centers and Behavior (*ed*. H. Autrum), pp. 281–463. Springer.
Waterman, T. H. 1984. Natural Polarized Light and Vision. In: Photoreception and Vision in Invertebrates (*ed*. M. A. Ali), pp. 63–114. Plenum.
Wehner, R. 1987. ''Matched filters'' – neural models of the external world. J. Comp. Physiol. A 161, 511–531.
Wehner, R. 2001. Polarization vision – a uniform sensory capacity? J. Exp. Biol. 204, 2589–2596.
Wehner, R. and Bernard, G. D. 1993. Photoreceptor twist: a solution to the false-color problem. Proc. Natl. Acad. Sci. U. S. A. 90, 4132–4135.
Zeiger, J. and Goldsmith, T. H. 1989. Spectral properties of porphyropsin from an invertebrate. Vision Res. 29, 519–527.
Zeil, J. and Hemmi, J. M. 2006. The visual ecology of fiddler crabs. J. Comp. Physiol. A 192, 1–25.
Zeil, J., Nalbach, G., and Nalbach, H.-O. 1986. Eyes, eye stalks, and the visual world of semi-terrestrial crabs. J. Comp. Physiol. A 159, 801–811.
Zeil, J., Nalbach, G., and Nalbach, H.-O. 1989. Spatial Vision in a Flat World: Optical and Neural Adaptations in Arthropods. In: Neurobiology of Sensory Systems, (*eds*. R. N. Singh and N. Strausfeld), pp. 123–137. Plenum.

1.09 Mammalian Photopigments

J Carroll, Medical College of Wisconsin, Milwaukee, WI, USA

G H Jacobs, University of California, Santa Barbara, CA, USA

© 2008 Elsevier Inc. All rights reserved.

1.09.1	**Introduction**	247
1.09.2	**Structure of Photopigments**	247
1.09.2.1	Photoreceptor Structure	247
1.09.2.2	Protein Structure	248
1.09.2.3	Genetic Structure	249
1.09.3	**Photopigment Function**	251
1.09.3.1	Rod and Cone Specializations	251
1.09.3.2	Metabolic Support of Photoreceptors	252
1.09.4	**Diversity of Mammalian Photopigments**	252
1.09.4.1	Spectral Tuning of Photopigments	252
1.09.4.2	Nonrod, Noncone Opsins	254
1.09.4.3	Evolution of Mammalian Photopigments	255
1.09.5	**Photopigments and Mammalian Color Vision**	256
1.09.5.1	Photopigment Expression	256
1.09.5.2	The Mammalian Theme: Two Types of Cone Pigment	257
1.09.5.3	Evolutionary Loss of Mammalian S-Cone Pigments	258
1.09.5.4	Primate Cone Pigments and Color Vision	259
1.09.6	**Role of Photopigments in Human Retinal Disease**	261
1.09.6.1	Rhodopsin-Based Disorders	261
1.09.6.2	Cone Pigment-Based Disorders	261
1.09.6.2.1	Red-green color-vision defects	261
1.09.6.2.2	Blue cone monochromacy	262
1.09.6.2.3	Tritan color-vision defects	263
References		264

1.09.1 Introduction

The mammalian eye is a complex structure that has evolved to facilitate the extraction of information available in the photic environment. The process of seeing starts when light enters the eye through the pupil and reaches the photoreceptors at the back of the eye. These exquisitely specialized cells contain light-sensitive photopigments that absorb incident light and initiate the process of transducing light energy into a neural signal. Photons that are not absorbed by photopigments cannot contribute to sight, and so all higher-order visual analysis is conditioned by the successful execution of this fundamental step. This chapter examines the diverse family of mammalian photopigments by considering their structure, function, and evolution, as well as their role in color vision and in human retinal disease.

1.09.2 Structure of Photopigments

1.09.2.1 Photoreceptor Structure

The retinas of all mammals contain both rod and cone photoreceptors. In most mammals, rods greatly outnumber cones; in humans, for example, there are nearly 20 rods for every cone, but there are some mammalian lineages, such as the squirrels, in which cones are the predominant receptor type. Grossly, photoreceptors consist of an outer segment, an inner segment, and a synaptic terminal (Figure 1). The inner segment is the metabolic center of the photoreceptor, housing the nucleus, mitochondria, and other cellular machinery. Interposed between the inner and outer segments is the connecting cilium, a microtubule-based structure, through which all newly synthesized proteins (including photopigments) are transported from the inner segment to the outer segment. Visual

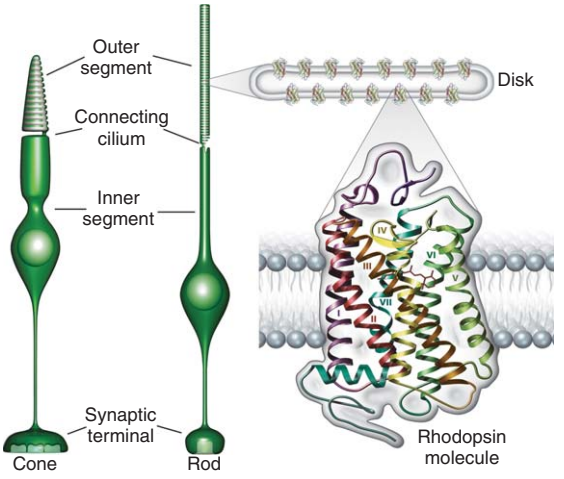

Figure 1 Basic structure of rod and cone photoreceptors. Both cells have an inner and outer segment, a cell body, and a synaptic terminal. The outer segment of both rods and cones consists of stacks of membranous disks. In cones, the disks are continuous with the plasma membrane of the cell, whereas in rods they are free-floating. The inset to the upper right illustrates the positioning of rhodopsin within the outer segment disk membranes, and the inset to the lower right is a magnified view of the molecule based on the rhodopsin crystal structure reported by Palczewski K. *et al.* (2000). Source: Figure adapted from WebVision, University of Utah reproduced with permission.

transduction takes place in the outer segment. The outer segment of both rods and cones consists of stacks of membranous disks – in cones, the disks are continuous with the plasma membrane of the cell, whereas in rods they are free-floating. Mammalian photopigments are integral membrane proteins located within the lipid membrane of these outer segment disks (see Figure 1). Photopigment is very abundant with some 100-million photopigment molecules being embedded throughout the outer segment of each rod and cone cell. It is estimated that photopigments represent about 90% of the protein molecules in the outer segment (Nathans, J., 1987; Rodieck, R. W., 1998; Filipek, S. *et al.*, 2003). Recent work suggests that photopigments either can exist as single molecules or can self-assemble into oligomeric complexes within the outer segment (Fotiadis, D. *et al.*, 2003; Filipek, S., 2005; Botelho, A. V. *et al.*, 2006). This higher-order arrangement appears in other members of the G-protein-coupled receptor (GPCR) protein family (see Angers, S. *et al.*, 2002; Park, P. S.-H. and Palczewski, K., 2005 and references therein). The functional consequences of assembly into higher-order structures are not completely understood, and with regard to photopigment oligomerization, there remains considerable controversy (Fotiadis, D. *et al.*, 2003; Botelho, A. V. *et al.*, 2006; Chabre, M. and Le Maire, M., 2006).

1.09.2.2 Protein Structure

Retinal photopigments consist of two parts: a protein (opsin) and a chromophore (in mammals, exclusively 11-*cis* retinal). The chromophore is covalently bound via a protonated Schiff base linkage with a specific lysine residue in the opsin (apoprotein) molecule (Wald, G., 1968). Opsins belong to the protein superfamily of GPCRs. GPCRs are the largest protein family known and serve to transduce extracellular signals (ligand binding) into intracellular signals (G-protein activation). All GPCRs share the structural motif of seven-transmembrane α-helical segments (for more detailed reviews see Okada, T. *et al.*, 2001; Menon, S. T. *et al.*, 2001). As depicted in Figure 1, about 50% of the opsin is within the bilipid membrane (Sakmar, T. P., 2003), while the C-terminal, N-terminal, and the short protein loops connecting the α-helices reside outside the membrane.

The photopigments in the mammalian outer retina can be placed into three main groups based on the wavelength of the maximum sensitivity (λ_{max}) of the pigment – rhodopsins, short-wavelength-sensitive (S) pigments, and long/middle-wavelength-sensitive (L/M) pigments. Mammalian rhodopsins typically have λ_{max} values of around 500 nm, whereas there is significant variation in the λ_{max} of the S and L/M pigments. As shown in Figure 2(a), mammalian S pigments have λ_{max} values that fall between about 360 nm and 445 nm, while mammalian L/M pigments have λ_{max} values between about 493 nm and 565 nm (Yokoyama, S., 1997; 1999; Ebrey, T. and Koutalos, Y., 2001). As described below, the exact amino acid sequence of the opsin determines the spectral differences between the photopigments.

For all mammals so far examined, the rhodopsin molecule is 348 amino acids in length, with a molecular mass of about 40 kDa. Mammalian S opsins vary in length from 346 to 350 amino acids, the human S opsin being 348 amino acids in length. L/M opsins are less variable, with most species (including humans) having L/M opsins that are 364 amino acids long. The additional length in the L/M opsins is found at the N-terminal where the conventional numbering of the protein starts. Thus, except for the N-terminal, all mammalian photopigments can be perfectly aligned. Given an amino acid position in one pigment, it is possible to identify the corresponding position in a pigment from either of the other two mammalian

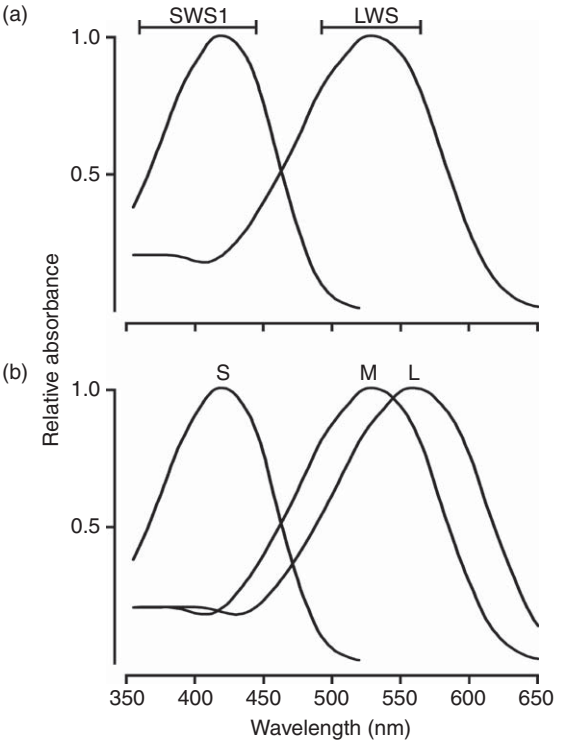

Figure 2 Spectral absorption curves for mammalian photopigments. (a) Mammalian SWS1 and LWS cone pigments have λ_{max} values that vary over wavelength ranges that are indicated by the extent of the horizontal bars (see text). (b) The photopigment complement found in most catarrhine (Old World) primates, conferring trichromatic color vision.

groups. The rule for the human pigments is to subtract 3 to identify the position in the S opsin that corresponds to a given position in rhodopsin or add 16 to find the corresponding position in the L/M opsins. The positions of all amino acids identified in this section are based on human rhodopsin numbering (Figure 3).

At the protein level, human rhodopsin is about 41% homologous with the S, M, and L opsins. The L and M pigments are about 96% homologous, though they show only 43% identity with the S pigment. The high homology between the L and M pigments arises as a result of their particular genetic origin (see Genetic Structure). There are a number of conserved residues that have important structural and functional roles for the photopigment, a few of which are mentioned here. The ϵ-amino group of a lysine residue in the seventh transmembrane domain (position 296) forms a Schiff base linkage with the aldehyde portion of retinal, providing the linkage between the opsin and the 11-*cis*-retinal chromophore. A glutamate residue at position 113 serves as the counterion for this linkage. A proline residue at position 291 appears critical in maintaining the binding pocket for the chromophore. Two cysteine residues (positions 110 and 187) form a disulfide bond that is critical for proper folding of the photopigment (Karnik, S. S. *et al.*, 1988). Disruption of this disulfide bond results in a complete loss of function of the associated photopigment, leading to retinitis pigmentosa (RP) when observed in rhodopsin (Richards, J. E. *et al.*, 1995), and to a red/green color-vision deficiency when observed in either an L or an M pigment (Winderickx, J. *et al.*, 1992; Kazmi, M. A. *et al.*, 1997; Jagla, W. M. *et al.*, 2002; Neitz, M. *et al.*, 2004).

Mammalian photopigments display a number of posttranslational modifications – the formation of a Schiff base linkage between 11-*cis* retinal and the lysine residue at position 296 mentioned above is one such modification. In addition, the N-terminal contains a number of carbohydrate attachment sites for glycosylation. A common posttranslational modification among rhodopsins is palmitoylation of cysteine residues at positions 322 and 323 (Figure 3), which may affect structural and functional roles such as membrane localization, protein stabilization, and receptor turnover (Ablonczy, Z. *et al.*, 2006). This palmitoylation appears to be absent from the mammalian cone opsins (Ostrer, H. *et al.*, 1998; Ablonczy, Z. *et al.*, 2006), though the functional consequence of this difference between mammalian rod and cone pigments remains to be determined. Finally, there is the potential for phosphorylation of serine and threonine residues on the C-terminus of the pigment molecule. For rhodopsin, this occurs primarily at positions 338 and 343, but other sites (e.g., 334 and 336) may also be involved (Hurley, J. B. *et al.*, 1998; Maeda, T. *et al.*, 2003).

1.09.2.3 Genetic Structure

Among mammals, a separate gene encodes each of the opsins found in rods and cones. The structure and length of mammalian opsin genes differs between species (Yokoyama, S. and Yokoyama, R., 2000). In humans, the gene encoding rhodopsin is 5.0 kilobase (kb) long and found on chromosome 3, while the gene encoding the S opsin is located on chromosome 7 and is 3.2 kb long. The rhodopsin and S-opsin genes each have four introns and five exons (Figure 4). As a result of their autosomal location, humans normally have two copies of each of these genes. In contrast, the L/M gene(s) are located on the X-chromosome. While most mammals have only a single L/M gene on the X-chromosome, most Old World primates (including

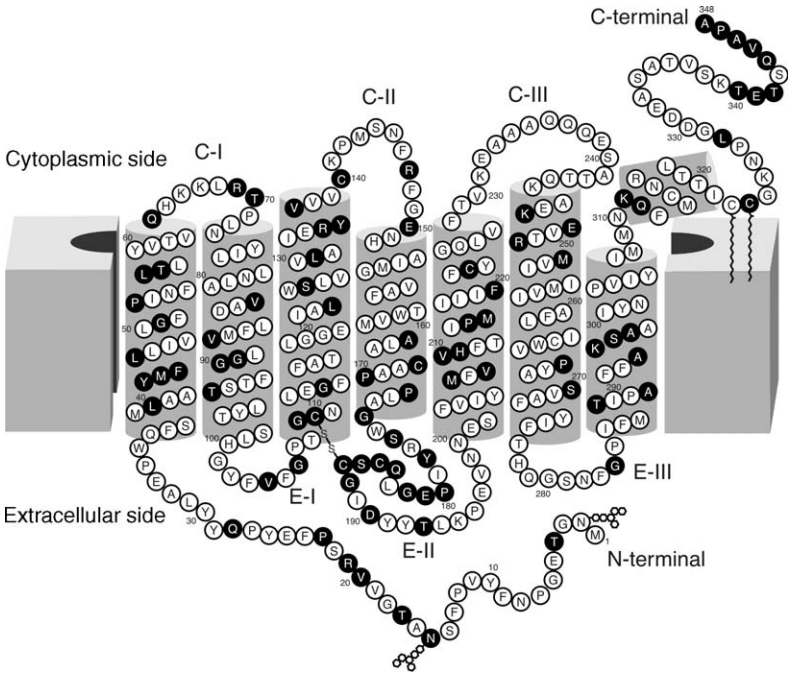

Figure 3 Two-dimensional model of human rhodopsin. Each circle represents a single amino acid, with 88 mutation sites identified by filled circles. Nearly every mutation has been associated with autosomal dominant retinitis pigmentosa (RP), while the others either cause congenital stationary night blindness (CSNB) or are believed to be benign. The α-helical transmembrane segments are connected by three cytoplasmic (interdiscal) and three extracellular (intradiscal) loops (indicated as C-I, E-1, etc.). The depicted secondary structure is based on the crystal structure reported by Palczewski, K., Kumasaka, T., Hori, T., Behnke, C. A., Motoshima, H., Fox, B. A., Letrong, I., Teller, D. C., Okada, T., Stenkamp, R. E., Yamamoto, M., and Miyano, M. 2000. Crystal structure of rhodopsin: A G-protein-coupled receptor. Science 289, 739–745 and is adapted from Stenkamp, R. E., Filipek, S., Driessen, C. A. G. G., Teller, D. C., and Palczewski, K. 2002. Crystal structure of rhodopsin: a template for cone visual pigments and other G protein-coupled receptors. Biochim. Biophys. Acta Biomembranes 1565, 168–182, with permission.

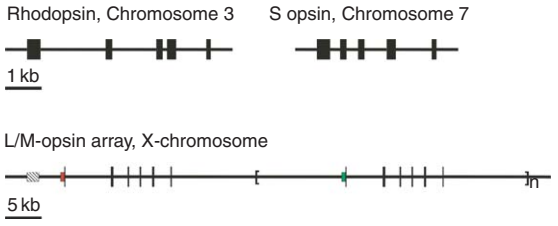

Figure 4 Schematic structure of the human opsin genes. Exons and introns are represented by vertical black boxes and horizontal lines, respectively. L and M genes reside in a head-to-tail tandem array, which is variable in gene number. The most common configuration among individuals with normal color vision is to have one L gene followed by one or more M genes. Each L or M gene is preceded by a proximal promoter (colored boxes), and the entire array has a single locus-control region (LCR) that is essential for the expression of genes from the array. Data on exon and intron lengths were taken from http://genome.ucsc.edu/cgi-bin/hgGateway (March 2006 build).

humans) possess both L and M genes. The physiological implications of having multiple pigments are covered below. In primates that have both the L and M genes on a single X-chromosome, they are located in a tandem array near the end of the long arm of the X-chromosome (Xq28) (Nathans, J. *et al.*, 1986b; Vollrath, D. *et al.*, 1988). This arrangement arose via a gene duplication event that is estimated to have occurred some 35 million years ago (Hunt, D. M. *et al.*, 1998). The selective expression of the L and M genes depends on a locus-control region (LCR) that is located about 3.5 kb upstream of the array (Wang, Y. *et al.*, 1992; Smallwood, P. M. *et al.*, 2002).

The L and M genes contain five introns each and six exons and are about 13.1 kb long (see Figure 4). Although the majority of humans have an intron 1 insert of about 2 kb in the L-pigment gene, about

35% of African-Americans lack this insert, while fewer than 1% of Caucasians have the shortened L-pigment gene (Jørgensen, A. L. *et al.*, 1990). There have been no reported phenotypic differences associated with having a shortened L-pigment gene. In individuals with normal color vision, it appears that the L gene is always the first gene in the X-chromosome tandem array. While there have been reports of individuals having L and M genes where the M gene is in the first position of the array, all had an accompanying color-vision deficiency due to other abnormalities in the array (Neitz, M. *et al.*, 2004; Ueyama, H. *et al.*, 2006).

As mentioned above, most mammals have only a single X-encoded photopigment gene. In some trichromatic primates, there is variability in the number of genes in this array. Among humans with normal color vision, the number of genes in the array varies from 2 (the minimum required to confer trichromacy) to as many as 9, with a mode of 3 (Drummond-Borg, M. *et al.*, 1989; Neitz, M. and Neitz, J., 1995; Neitz, M. *et al.*, 1995; Macke, J. P. and Nathans, J., 1997; Yamaguchi, T. *et al.*, 1997). Curiously, other trichromatic Old World primates show nowhere near this degree of variability in gene number (Onishi, A. *et al.*, 1999). The relevance of the variability in gene number for human color vision is not clear, especially given evidence suggesting that only the first two genes in the L/M array are significantly expressed (Hayashi, T. *et al.*, 1999).

The elucidation of the genetic basis for the mammalian photopigments has provided the opportunity to manipulate these genes so as to better understand the functional roles of the various pigments. For example, numerous rodent models expressing mutant rhodopsins have been used to examine the initial molecular mechanisms in human diseases involving analogous rhodopsin mutations (e.g., Hafezi, F. *et al.*, 2000; Jones, B. W. and Marc, R. E., 2005), while mice engineered to express a novel photopigment have been used to probe the evolutionary basis of color vision (Smallwood, P. M. *et al.*, 2003; Onishi, A. *et al.*, 2005; Jacobs, G. H. *et al.*, 2007).

1.09.3 Photopigment Function

The main business of the photoreceptor cells is to signal the capture of photons. As mentioned above, light serves as the ligand for the photopigments (GPCR), and absorption of light by the retinal chromophore causes an isomerization from the 11-*cis* to the all-*trans* form. The isomerization process is extraordinarily fast, occurring on a femtosecond time scale. Isomerization initiates a complex biochemical cascade that begins with conformational changes in the opsin protein that enable the associated G-protein (transducin) to bind to the cytoplasmic surface of the photopigment. This binding by the photopigment is regulated by discrete amino acids in the opsin portion of the pigment molecule. The end result of the subsequent steps in the cascade is a hyperpolarization of the cell in response to light. There are differences in some of the phototransduction proteins found in rods and cones, but the general process is the same for the two types of receptor (see Chapter Phototransduction in Rods and Cones for more detail). This section contrasts some of the functional properties of rods and cones.

1.09.3.1 Rod and Cone Specializations

Rod and cone photoreceptors have a number of important specializations that give them distinct functional properties. The primary advantage of having two classes of photoreceptor is to allow the visual system to function over a wide range of light intensities, about 11 orders of magnitude in the human eye. Rods are extremely sensitive – they are able to detect a single photon and thus work well at very low light intensities. Cones, on the other hand, are less sensitive and function best at higher light levels. Cones start to respond when they absorb light at a rate of about 3 photons/cone/s and continue to respond well for light intensities extending up to 1 000 000 photons per cone per second. In addition, cones respond more briskly to light, while rods have a more sluggish response. These physiological differences can be explained in part by the higher level of spontaneous activity in the cones; for example, L cones show about 10 000 times more frequent spontaneous isomerizations than do rods (Kefalov, V. *et al.*, 2003). The increased spontaneous activation in cones results in a high level of basal activity of the phototransduction components, thus reducing sensitivity while allowing a faster response recovery (Nikonov, S. *et al.*, 2000). Current evidence suggests that phototransduction cascade components downstream from the photopigment do not contribute significantly to the difference in rod versus cone sensitivity (Ma, J. *et al.*, 2001), though the issue is not entirely resolved. Studies on photoreceptor sensitivity have been done on various animal models (e.g., primate, African clawed frog, and tiger salamander), so it is likely that species differences have complicated our view

of rod and cone sensitivity. Moreover, there have been reports of differences in sensitivity between spectral subtypes of cone (Perry, R. J. and McNaughton, P. A., 1991; Makino, C. L. and Dodd, R. L., 1996), so variation in the opsin molecule itself may be contributing to the observed differences in sensitivity.

Another important difference between rods and cones is that at moderate light levels, rods reach a maximum response (saturate) and are thus unable to respond to continued increases in light intensity, while cones do not saturate under usual viewing conditions (though cones can be saturated with flash stimulation). The illumination levels at which rods saturate is quite low; for example, human rods are saturated under conditions of normal room illumination. This means that most of the time human vision is based on cone photoreceptors, which paradoxically comprise only 5% of the total number of photoreceptors in the human retina.

1.09.3.2 Metabolic Support of Photoreceptors

The photoreceptors of the human retina are the most metabolically active cells in the body. They rely heavily on the retinal pigment epithelium (RPE) for a great deal of their metabolic support. The RPE absorbs scattered light, transports metabolic byproducts from the subretinal space to the blood, delivers nutrients from the blood to the photoreceptors, and regenerates 11-*cis*-retinal (see Strauss, O., 2005 for a thorough review of the RPE). A normal rod cell sheds about 10% of its outer segment each day (Bok, D., 1985), and the RPE also performs the critical role of phagocytizing the shed photoreceptor material. The number of photoreceptors supported by a given RPE cell varies with retinal location – near the fovea as many as 15 cones are supported by one RPE cell, while in the periphery the total number of photoreceptors (rods + cones) supported by a single RPE cell may be as high as 40 or 50 (Snodderly, D. M. *et al.*, 2002). This topographical variation may have important consequences for the progression of various retinal degenerations. Recent advances in *in vivo* retinal imaging techniques (e.g., adaptive optics) make it possible to simultaneously image the cone and RPE mosaic in the living primate retina (Gray, D. C. *et al.*, 2006). These imaging techniques are likely to rapidly advance our understanding of the topographical relationship between the RPE/cone mosaics in normal and diseased retinas.

1.09.4 Diversity of Mammalian Photopigments

While mammalian photopigments have a number of structural and functional similarities, they are a diverse group of proteins. Of those pigments found in rods and cones, there is enormous variability in their spectral sensitivity. Recently, it has been discovered that photopigments exist in other cell types as well. In this section, we review what is known about the diversity among mammalian photopigments.

1.09.4.1 Spectral Tuning of Photopigments

As mentioned above, a common characteristic used to classify photopigments is the location of peak sensitivity (λ_{max}). Mammalian pigments have λ_{max} values ranging from about 360 to 565 nm, though all have an identical shape when plotted on a log-wavenumber axis. Since all mammalian photopigments employ the same chromophore (11-*cis*-retinal), the difference in λ_{max} between photopigments is attributed to the opsin portion of the photopigment. In particular, it is now known that a limited number of positions within the opsin molecule play major roles in spectrally tuning the pigment, a fact consistent with the observation that the λ_{max} values of vertebrate pigments tend to cluster at discrete spectral locations (Dartnall, H. J. A. and Lythgoe, J. N., 1965; Jacobs, G. H., 1998).

The chromophore 11-*cis*-retinal is joined to the opsin protein via a Schiff base linkage with a lysine residue at position 296 (human rhodopsin numbering) in the seventh transmembrane domain, while a glutamate at position 113 in the third transmembrane domain serves as the counterion to the protonated Schiff base. In solution, a protonated 11-*cis*-retinal Schiff base linkage absorbs maximally at about 440 nm. Deviations from this value are referred to as the opsin shift (Nakanishi, K. *et al.*, 1980) because the spectral shift is induced by the surrounding opsin protein. As described by Nathans, J. (1999), delocalization of the positive charge on the protonated Schiff base affects the spectral tuning of the pigment, with an increase in delocalization leading to a long-wavelength shift and a decrease in delocalization resulting in a shift toward the short wavelengths. This alteration of the charge distribution across the chromophore is accomplished through interactions between dipolar amino acid residues and the

chromophore (Kochendorfer, G. G. *et al.*, 1999; Lin, S. W. and Sakmar, T. P., 1999) and through a modulation of the interaction between the counterion (glutamate) and the protonated Schiff base.

Numerous amino acid residues within the opsin molecule have been implicated in spectral tuning of the mammalian cone photopigments. Among the L/M-cone pigments, five positions have been identified as major spectral tuning sites – 180, 197, 277, 285, and 308 (Yokoyama, S. and Radlwimmer, F. B., 1998). The S180A variants (mutants) are designated by the native amino acid residue and its position within the molecule followed by the substituted amino acid residue. For example, S180A refers to substitution of alanine for serine at position 180., H197Y, Y277F, T285A, and A308S substitutions shift the λ_{max} to shorter wavelengths by an estimated 7, 28, 7, 15, and 16 nm, respectively (Yokoyama, S. and Radlwimmer, F. B., 1999), although the magnitude of each individual substitution varies depending on the context. The tuning of S pigments is more complicated; at least nine positions within the opsin molecule are required to shift the absorption of rhodopsin from about 500 to 440 nm (Lin, S. W. *et al.*, 1988). Since the λ_{max} of the typical human S-cone pigment is about 420 nm, additional sites must also be involved. Additional sites have been shown to function synergistically to shift the λ_{max} to even shorter wavelengths, accounting for the observed λ_{max} of mouse ultraviolet (UV) pigments (Yokoyama, S. and Shi, Y., 2000). It should be noted that these *in vitro* studies can provide information about the effect of individual amino acid substitutions, but by themselves they offer only limited insight into the evolutionary origin of these changes.

Given their role in human trichromatic color vision, the L- and M-cone pigments have received particular attention. The number of amino acid differences between the human L- and M-cone pigments is highly variable, ranging from a minimum of 8 to a maximum of 18 (mode = 14) (Figure 5), though positions 277 and 285 account for the majority of the

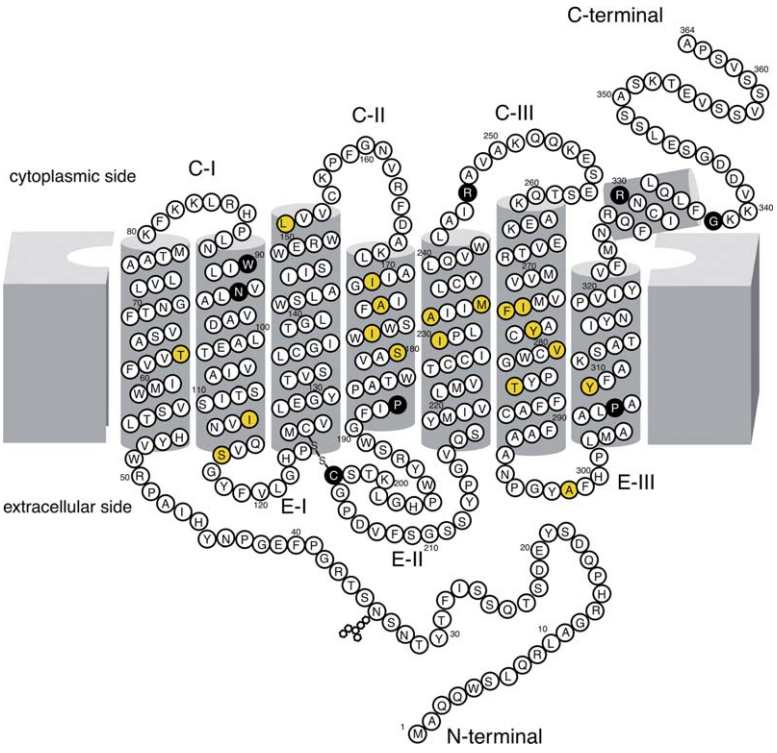

Figure 5 Two-dimensional model of the human L and M opsins. Each circle represents a single amino acid, with mutations associated with the loss of L- or M-pigment function shown as filled black circles. Filled yellow circles represent the dimorphic sites that can differ between the L and M pigments. A number of these sites have been shown to be involved in the spectral tuning of the pigments (see text). The amino acid identities at all 18 dimorphic sites are those of the presumed primordial L opsin (Deeb, S. S. *et al.*, 1994). Adapted from Stenkamp, R. E., Filipek, S., Driessen, C. A. G. G., Teller, D. C., and Palczewski, K. 2002. Crystal structure of rhodopsin: a template for cone visual pigments and other G protein-coupled receptors. Biochim. Biophys. Acta Biomembranes 1565, 168–182, with permission.

30 nm difference between L- and M-pigment λ_{max} (Neitz, M. *et al.*, 1991; Asenjo, A. B. *et al.*, 1994). In fact, with rare exception, positions 274, 275, 277, 279, 285, 298, and 309 all covary. That is, these sites vary between but not within the L and M photopigments, and thus the identity of these amino acid positions can be used to fairly reliably classify human L/M pigments as either L or M. The remaining 11 polymorphic positions show significant variation within the L- and M-pigment classes (Figure 6), and there is corresponding variability in the λ_{max} of human L- and M-cone pigments. Mutagenesis studies revealed that of these 11 sites, only positions 116, 180, 230, and 233 significantly affect the spectral tuning of the pigment (Asenjo, A. B. *et al.*, 1994). It thus becomes possible, given the sequence of a particular L or M pigment, to deduce its λ_{max}. Measurement of the spectral sensitivity of human dichromats possessing only a single L or M pigment, combined with analyses of their L- or M-pigment genes, suggests that, at least in humans, this practice is reliable (Sharpe, L. T. *et al.*, 1998; Carroll, J. *et al.*, 2002).

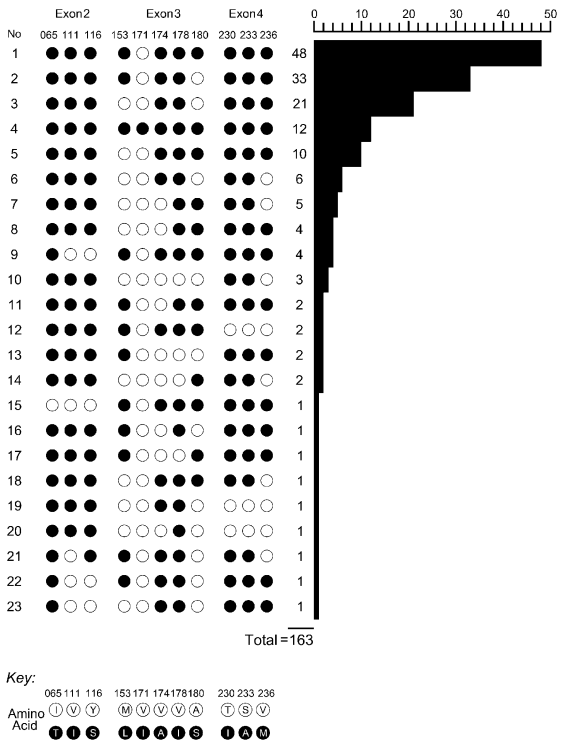

Figure 6 Variability in the human L-cone pigment observed among 163 males with normal color vision. Only the polymorphisms encoded by exons 2–4 vary within L and M pigments; that is, the identities of the seven polymorphic sites encoded by exon 5 covary and are thus used to classify a pigment as L or M. The key at the bottom indicates the amino acid identity of the polymorphic sites for the primordial M (top row) and L (bottom row) pigment. Accordingly, in the histogram, the filled circles represent primordial L-pigment amino acids, while open circles indicate primordial M-pigment amino acids. There has been significant intermixing of the L and M genes, resulting in this widespread variability in the L-cone pigment; for example, the presumed primordial L pigment is only the fourth most common variant. This degree of polymorphism among the L/M pigments appears to be unique to humans. Courtesy of J. Neitz and M. Neitz (unpublished data).

The spectral position of mammalian (indeed, all vertebrates) pigments appears to be nonrandom. While the clustering is a consequence of there being discrete amino acid positions that tune the spectrum, there is evidence that pigment positioning may also be driven by evolutionary considerations. For example, the λ_{max} of rhodopsin in the Mexican cavefish is shifted to longer wavelengths, and it has been suggested that this may reflect the visual requirements of life in a shallow freshwater environment (Yokoyama, S., 1997). Among the cottoid fish of Lake Baikal, as the depth of habitat increases, the λ_{max} of the pigments tend to decrease in line with the availability of ambient light at progressively deeper locations (Bowmaker, J. K. and Hunt, D. M., 2006) Likewise, the inferred rod pigment λ_{max} of the deep-diving elephant seal may be similarly adapted for vision in a marine environment, also being shifted toward shorter wavelengths (Levenson, D. H. *et al.*, 2006). Although these examples would seem to support the general view that photopigment positioning can be tuned in accord with environmental lighting, there is equally strong evidence to suggest that establishing such linkages will not be straightforward. For example, among the deep-diving pinnipeds, elephant seals may be unusual since many other species sharing these same habitats have rod pigments with the same spectral positioning as terrestrial mammals (Levenson, D. H. *et al.*, 2006). It seems likely that a much deeper understanding of the visual ecology of various mammalian lineages will be required in order to draw any tight connections between photic environments and photopigment positioning.

1.09.4.2 Nonrod, Noncone Opsins

Mammalian photopigments are not just restricted to the photoreceptor cells in the retina; in fact, they are not even restricted to retina. In recent years, a number of nonrod, noncone photopigments have been discovered (e.g., neuropsin, encephalopsin, RPE retinal G-protein-coupled receptor (RGR), peropsin, and melanopsin) (for recent reviews see

Foster, R. G. and Hankins, M. W., 2002; Kumbalasiri, T. and Provencio, T., 2005). Among vision scientists, melanopsin has received a great deal of attention as it has been linked to the process of circadian photoentrainment. Recently, it has been shown that melanopsin expression is restricted to a small subset of retinal ganglion cells (Hattar, S. *et al.*, 2002; Sollars, P. J. *et al.*, 2003). Indeed, these melanopsin-containing ganglion cells are intrinsically photosensitive (thus called ipRGCs), and they have been shown to play a role in activities like circadian photoentrainment, the pupillary light reflex, and regulation of the melatonin biosynthetic pathway. The response of melanopsin is much slower than that of the rod or cone opsins, so it is unlikely that these cells participate in most visual functions. There is a plethora of behavioral, physiological, and molecular data regarding the role of melanopsin, see Chapter Melanopsin Cells for more detail.

1.09.4.3 Evolution of Mammalian Photopigments

Over the past two decades, opsin gene sequences have been determined for many different species. Comparisons of these sequences can then be used to derive deductions about the evolution of photopigments. A consensus emerging from such comparisons is that all vertebrate photopigments fall into five paralogous groups (Hisatomi, O. and Tokunaga, F., 2002; Yokoyama, S., 2002). Figure 7 shows a vertebrate opsin family tree illustrated for a small sample of representative vertebrate species. Four of the opsin gene families (designated as LWS, Rh2, SWS2, and SWS1) specify photopigments typically expressed in cones, while the Rh1 derivatives are rod photopigments. An important insight emerging from this work is that rod pigments evolved only after all four of the cone pigment gene families were in place. The relative timing of the emergence of rod and cone photopigments is taken to imply that a capacity for daylight vision, including very likely some color vision, has been present throughout much of vertebrate history and that rod-mediated vision is a relatively more recent invention, perhaps arising coincident with the appearance of jawed vertebrates (Collin, S. P. *et al.*, 2003).

As illustrated in Figure 7, representatives from all four classes of cone opsin genes are present in some contemporary birds, fishes, and reptiles. Note however that the lone representative mammal in Figure 7

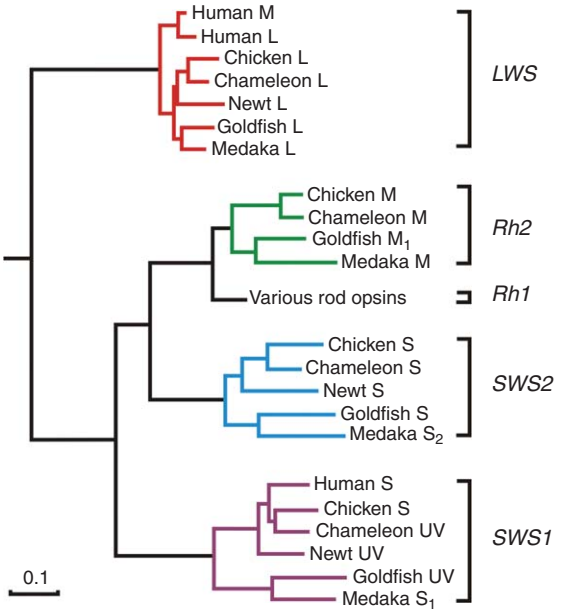

Figure 7 Phylogenetic relationship of some vertebrate opsins. The proposed relationships are inferred from comparison of published opsin gene sequences using the neighbor-joining method. Shown here are pigments from four cone opsin gene families and a single rod opsin gene family. Source: Jacobs, G. H. and Rowe, M. P. 2004. Evolution of vertebrate colour vision. Clin. Exp. Optom. 87, 206–216; reproduced with permission from Optometrists Association Australia.

(humans) draws cone pigments from only two of the four gene families (LWS and SWS1). That exclusivity seems true for all eutherian mammals. Early mammals are believed to have been strongly nocturnal, and it seems plausible that this phase of our photic history stimulated a number of alterations in mammalian retinas including, (a) average increases in rod/cone ratios, (b) loss of colored oil droplets from photoreceptors that remain characteristic of many other contemporary vertebrates, and (c) the disappearance of representative cone pigments from the Rh2 and SWS2 gene families (Jacobs, G. H. and Rowe, M. P., 2004). The latter change would imply that our early mammalian ancestors were limited to only two types of cone pigment, one absorbing maximally in the short wavelengths, the other in the middle to long wavelengths. Based on a comparison of the amino acid sites that are believed important for spectral tuning, the λ_{max} of the original mammalian LWS pigment has been inferred to have been at about 530 nm (Yokoyama, S. and Radlwimmer, F. B., 1999). From that point, subsequent divergences have spread the λ_{max} of mammalian pigments from this gene family across the middle- to long-wavelength

portion of the spectrum so as to yield values ranging from about 493 to 565 nm. Among early mammals, the short-wavelength pigment derived from the SWS1 gene family probably had maximum absorbance in the UV (Hunt, D. M. *et al.*, 2004). That spectral position has been retained in some contemporary mammals, but in many others, gene alterations have yielded pigments that are peak shifted toward the longer wavelengths. The result is that pigments found in contemporary mammals that are specified by genes in the SWS1 family span a range of λ_{max} values from about 360 to 445 nm.

Two groups of contemporary mammals differ significantly from this standard picture. First, many primate species have acquired a second LWS-based photopigment through processes detailed below, thus giving them a total of three types of cone pigment. Additionally, recent evidence suggests that some Australian marsupials have retained cone pigment representation from the Rh2 opsin gene family and so, like many primates, they too have a total of three types of cone pigment (Arrese, C. A. *et al.*, 2002). Why these marsupials have retained their Rh2 pigments while all other mammals have abandoned them is currently unknown.

1.09.5 Photopigments and Mammalian Color Vision

Except under limited circumstances, color vision reflects the operation of cones, and thus the emergence of color vision must be ultimately linked to the absorption of light by cone photopigments. Animals are said to have color vision if they can discriminate between lights of different spectral composition irrespective of their relative intensities (Jacobs, G. H., 1993; Kelber, A. *et al.*, 2003). Photoreceptors respond univariantly, providing a signal proportional to the number of photons captured by the resident pigment (thereby confounding wavelength and intensity), and thus an individual with only a single type of photoreceptor lacks color vision (Rushton, W. A. H., 1972). Such animals are classified as monochromatic. The dimensionality of color vision can be formally established through color matching, that is, determining by psychophysical measurement the number of lights of fixed spectral composition (so-called primaries), each independently adjustable in intensity, which are required to match in appearance any spectral light. If two primaries are required, the animal is said to be dichromatic; three confirms trichromacy, etc. The number of spectrally unique receptor types is compulsively linked to color-vision dimensionality in that there cannot be fewer receptor types than there are numbers of color-vision dimensions.

In light of this linkage between color vision and receptor types, knowledge about the number of cone photopigments present in any animal is frequently used to infer facts about color vision, for example, animals found to have two types of cone opsin genes are often described in the literature as being dichromatic. This is an obviously attractive strategy because it is almost always much easier to gain information about photopigments (or their genes) than it is to conduct direct studies of color-vision behavior. There are however some important additional assumptions that are required to make the inferential step between cone photopigment complement and color vision. First, the nervous system of the animal must be organized to allow signals from different cone types to be contrasted. Fortunately, the retinal pathways that permit such signal comparisons in mammalian retinas are largely conserved across the order (see Chapter Decomposing a Cone's Output (Parallel Processing)) and that commonality makes the inferential leap from the number of cone pigments to the dimensionality of color vision somewhat less risky. A second requirement is that the various cone pigment types have to be (at least to some extent) individually expressed in photoreceptors. The issue of photopigment expression is considered below. Finally, most procedures that allow the identification of the cone pigment types do not provide information about the relative numbers of cones containing each of the pigment types or about their distribution across the photoreceptor mosaic. Both of these features can greatly impact the quality of color vision, even as they may be without effect on the dimensionality of color vision. Clearly, learning the identity of the cone pigments in any given species is an important first step toward understanding its color-vision capacity, but it provides an incomplete picture.

1.09.5.1 Photopigment Expression

Photoreceptors respond univariantly. One consequence of this is that the expression of multiple cone pigments in each receptor will broaden the absorption spectrum for that receptor but will not allow the initiation of signals needed to support color vision. Consequently, the evolution of color

vision requires both the addition of spectrally unique photopigments and a mechanism for selective expression of the different types of photopigment. As mentioned above, among trichromatic mammals, the proximate mechanism that provides selective expression is an LCR located 3.5 kb upstream of the L/M-opsin gene array (see Figure 4). The LCR is presumed to act on the opsin gene promoter to activate gene transcription (Nathans, J. *et al.*, 1989; Wang, Y. *et al.*, 1992; Nathans, J. 1999; Smallwood, P. M. *et al.*, 2002).

Psychophysical studies of human color vision have long made clear that cone pigments must be selectively expressed, and, eventually, direct measurements made on primate cones provided evidence that, indeed, each cone contains only a single type of cone pigment (Dartnall, H. J. A. *et al.*, 1983; Schnapf, J. L. *et al.*, 1987). In recent years, however, it has been learned that the idea that any given cone must contain only a single type of photopigment does not hold for all mammals (for a recent review of this topic see Lukáts, A. *et al.*, 2005). So far, it appears that most of the species featuring cone pigment coexpression are rodents, but more may well be found as appropriate measurements are extended to include additional species. Interestingly, it has been shown that for some species (including primates), the coexpression profile in adulthood differs from that observed during development (Szél, Á. *et al.*, 1994; Xiao, M. and Hendrickson, A., 2000). The functional significance of this remains to be elucidated, although one possibility is that it is a remnant of the molecular processes of cone differentiation. Furthermore, in many species exhibiting coexpression in the adult retina, it appears to be incomplete in that not every cone coexpresses the two pigments to the same extent. A prominent example of such an arrangement is seen in the retina of the house mouse which features a topographic distribution pattern of the two pigment types, with M pigment more strongly expressed in the dorsal retina and UV pigment showing the reverse pattern (Applebury, M. L. *et al.*, 2000). Even though pigment coexpression is common in this retina, apparently some cones do express only a single pigment type (Haverkamp, S. *et al.*, 2005). The consequences that photopigment coexpression may have for vision are not well studied, but at least in the mouse, partial cone pigment coexpression does not eliminate the possibility for some limited color vision (Jacobs, G. H. *et al.*, 2004).

1.09.5.2 The Mammalian Theme: Two Types of Cone Pigment

Only two (SWS1 and LWS) of the four families of vertebrate cone opsin genes appear to have representation in eutherian mammals. A consequence is that with the exception of some primates, a group considered separately below, all other mammals express no more than two types of cone photopigment. One of these has peak sensitivity in the short wavelengths; the other is maximally sensitive to lights from the middle and long wavelengths (see Figure 2(a)). This provides the photopigment basis for dichromatic color vision. That capacity is believed to be widespread among mammals, although the reader should be cautioned that direct tests of color vision have been made on only a relatively small proportion of the some 4500 species of mammal. Details regarding the photopigment complements and color vision in the mammals that have been studied to date are summarized in a number of recent review papers which may be consulted for information about particular species (Jacobs, G. H., 1993; Yokoyama, S. and Radlwimmer, F. B., 1998; Ahnelt, P. K. and Kolb, H., 2000; Kelber, A. *et al.*, 2003; Peichl, L., 2005). We offer here a few summary observations on this photopigment theme.

Although the presence of two cone pigments is common in mammals, there are significant variations in the spectral positioning of these pigments. There are few generalizations to be gained from examination of the spectral placement of mammalian cone pigments, and likely most have exceptions. Most carnivores and ungulates studied so far have L/M pigments with λ_{max} values > 530 nm, while the corresponding pigments of most rodents have λ_{max} shorter than that value. The L/M pigments of marine mammals follow the pattern of terrestrial carnivores, while lagomorph L/M pigments seem similar to the rodents. Inferences drawn from studies of cone opsin genes suggest that some of the Chiroptera also have L/M-cone pigments positioned toward the longer wavelengths (Wang, D. *et al.*, 2004). Mammalian SWS1 pigments fall into two categories. A number of rodent species, including common laboratory animals such as mice and rats, have a UV pigment with a λ_{max} of about 360 nm (Jacobs, G. H. *et al.*, 1991). In all other mammalian groups, with the possible exception of some bats (Wang, D. *et al.*, 2004), the SWS1 pigments have been shifted into the visible, with associated λ_{max} values spread across the range from about 420 to

445 nm. Interestingly, some rodent species also have pigments in this latter interval.

As described above, the proximate reason for the variations in the spectral positioning of mammalian cone pigments rests on variations in a limited number of amino acid tuning sites in the opsin molecules. It is natural to assume that there are also adaptive reasons why particular animals or groups of animals have the pigments they do. As we noted above, if there are such reasons, they so far have defied easy understanding. Thus, mammals that occupy widely different photic habitats and natural histories often share their pigment positions in common. For example, the L/M pigment found in the deep-diving elephant seal has the same spectral absorption as the L/M pigments of domestic cats and goats (Levenson, D. H. *et al.*, 2006). It is not obvious how the presence of this same photopigment could be matched to seemingly disparate visual demands of all of these mammals. The absence of clear correlations between visual behavior and pigment positioning may obviously reflect a lack of a deep understanding of the visual ecology of these species, but among some invertebrates, phylogenetic relatedness better predicts pigment complement than does visual ecology (Briscoe, A. D. and Chittka, L., 2001), and that may well be the case here as well. Finally, quite beyond the issue of cone pigment positioning, there are significant variations across mammals in the relative numbers of cones and their retinal topography (Ahnelt, P. K. and Kolb, H., 2000). These factors will greatly influence the character of the visual message available to the downstream visual structures; thus, the mere fact that many mammals have two types of cone pigment provides only a relatively weak link to understanding how they see.

1.09.5.3 Evolutionary Loss of Mammalian S-Cone Pigments

A few years ago, the retinas of two types of primates (*Aotus*, the owl monkey and *Otolemur*, the bush baby) were shown to lack a population of functional S cones (Jacobs, G. H. *et al.*, 1996b). The absence of these cones was traced to the presence of deleterious mutational changes in the S-cone opsin genes that obviate pigment expression. Since that time, a variety of mammals have been shown to share a similar loss. The list of species so afflicted includes some prosimian primates, a number of rodents, some species from the family Procyonidae (raccoons, etc.), and apparently all marine mammals from the families Cetacea (dolphins and whales) and Pinnipedia (seals) (for complete listings see Peichl, L. and Moutairou, K., 1998; Peichl, L. *et al.*, 2001; Ahnelt, P. *et al.*; 2003; Levenson, D. H. and Dizon, A. 2003; Kawamura, S. and Kubotera, N., 2004; Levenson, D. H. *et al.*, 2006). There are probably still other species (so far, undetected) showing a similar loss.

As discussed below, some humans also lack S cones under circumstances that are traceable to mutational changes in their S-cone opsin genes. There is, however, an important difference between the losses of S cones in humans and in these other mammals – whereas the absence of S cones is rare among humans, S-cone loss is believed to be characteristic of all individuals in these other species. Although a species-wide loss of S-cone pigment could reflect the evolutionary occurrence of a neutral event, an alternative interpretation is that this loss represents an adaptive change that somehow increased the fitness of these animals.

Beyond the general thought that the absence of S cones might be adaptive, little progress has been made in understanding the circumstances surrounding this loss. In most mammalian retinas, S cones comprise only a very small proportion of all the cones. Partly because of that, the presence of S cones does not substantially increase an animal's ability to capture photons. Rather, because mammalian retinas contain a conserved neural pathway that allows for the comparison of signals from S cones and L/M cones, the presence of S cones provides information that facilitates the extraction of a dimension of color vision. The absence of S cones thus reduces normally dichromatic mammals to monochromacy.

It is not easy to see how abandoning an apparently low-cost color-vision capacity could prove adaptive. The first mammals found to lack S cones were nocturnal, and since color vision is only modestly useful under low-light conditions, it initially seemed possible that nocturnality and the loss of S cones might be linked (Jacobs, G. H. *et al.*, 1996b). That linkage now seems less certain as some additional mammals found to lack S cones are not strictly nocturnal; for example, whereas many species of *Aotus* monkey are strongly nocturnal at least one genus is cathemeral (i.e., behaviorally active under strongly photopic as well as scotopic conditions), yet all show mutational loss of S-cone opsin genes (Levenson, D. H. *et al.*, in press). Conversely, some very stringently nocturnal species (e.g., the tarsier – Hendrickson, A. *et al.*, 2000)

maintain a viable population of S cones. In sum, the loss of S cones triggered by opsin gene mutation represents a significant variation on the mammalian cone pigment theme. At the same time, the total extent of this loss and its evolutionary explanation remain to be determined.

1.09.5.4 Primate Cone Pigments and Color Vision

The idea that normal human color vision is trichromatic dates from the seventeenth century (Mollon, J. D., 2003), and by the early twentieth century, it had become clear that some nonhuman primate taxa share this capacity (Grether, W. F., 1939). Trichromacy was initially thought to reflect the physical properties of light, and it was not until the turn of the nineteenth century that the physiological basis of trichromacy was realized. This connection between primate trichromacy and the retinal presence of three classes of cone pigment was conclusively established with the first reports of direct measurements of both human and nonhuman primate cone pigments (Brown, P. K. and Wald, G., 1963; Marks, W. B. *et al.*, 1964). Subsequently, and particularly over the past two decades, much has been learned about the distribution and nature of primate color vision, its linkage to the cone pigments and to opsin genetics, and the evolution of these capacities. A brief summary of these issues follows.

As far as we now know, all catarrhine primates (Old World monkeys, apes, and humans) effectively share in common their acute trichromatic color-vision capacities (Jacobs, G. H. and Deegan, J. F. II, 1999). The reason why this is the case is that all members of this lineage have effectively the same cone photopigment complements (see Figure 2(b)) specified by X-chromosome (L/M pigments) and autosomal (S pigment) opsin genes, and they all share important organizational features of the afferent visual system. In the face of this commonality, an intriguing difference among the catarrhines is that polymorphic variations in the L/M-opsin genes are relatively common among humans (e.g., see Figure 6), resulting in the much-studied phenotypic variations in human color vision. Analogous polymorphisms are very rare among the nonhuman catarrhines; for example, only three of a sample of over 3000 macaque monkeys showed evidence for such variation (Onishi, A. *et al.*, 1999), an incidence that is vastly lower than that documented for Western European human populations. This difference has sometimes been explained as reflecting variations in the stringency of selective pressures against defective color vision for humans and other catarrhines; moreover, it could also reflect differences in the physical nature of the X-chromosome opsin gene arrays of these primates (Jacobs, G. H. and Williams, G. A., 2001).

The platyrrhine (New World) monkeys have been the focus of much attention because, unlike the catarrhines, cone pigment and color-vision polymorphism is rampant among New World monkeys (see Jacobs, G. H., in press for a review). Indeed, with the exceptions of only two genera, all platyrrhine monkeys have polymorphic color vision. The polymorphism is such that among the members of any given species, both dichromatic and trichromatic individuals are found with subvarieties in each of these dimensional categories. In the majority of such polymorphic species, six distinct color-vision phenotypes occur, three dichromatic types and three trichromatic types. These color-vision variations directly reflect polymorphisms in the X-chromosome opsin genes and the cone pigments they encode. An important feature of these polymorphisms, and an early key to their understanding, is that although female monkeys may be either trichromatic or dichromatic, all males are dichromats. That fact pointed to a fundamental difference between the X-chromosome opsin genes of catarrhines and platyrrhine primates. As described above, in catarrhines, the L- and M-opsin genes are situated in tandem array on the X-chromosome. By contrast, platyrrhines have only a single X-chromosome opsin gene, with allelic versions of this gene specifying different L and M pigments. A consequence is that males perforce have only a single L/M pigment and dichromatic color vision. Homozygous females have pigment complements like the males, but heterozygous females, through the agency of X-chromosome inactivation, have a receptor mosaic that features both L- and M-cone types, and that arrangement supports a trichromatic color-vision capacity.

A central question in the evolution of primate color vision has been whether the addition of a new L/M-pigment type suffices to immediately yield a new dimension of color vision, or whether subsequent nervous system reorganization would be required. A recent study involving a knock-in mouse designed to mimic the polymorphic photopigment arrangement seen in platyrrhine monkeys shows that even the murine visual system is sufficiently plastic that new color vision can emerge

from the simple addition of a new L/M pigment (Jacobs, G. H. *et al.*, 2007). This result supports the view that the addition of a new pigment in our primate ancestors probably immediately yielded new color vision and, with it, the benefits that accrue to such capacity.

There are a number of well-described variations on the polymorphic theme of platyrrhine color vision (Jacobs, G. H., in press). First, although all the platyrrhine L/M pigments have λ_{max} falling in the range from 530 to 560 nm, different sets of these pigments characterize different phenotypic subgroups. Second, although a total of three polymorphic L/M pigments are most common, some genera may have only two such pigment types, while one species is believed to harbor a total of five polymorphic L/M pigments. Third, as noted above, one genus of New World monkey (*Aotus*) features a mutational change in the S-opsin gene that reduces the cone pigment complement to one type, thus obviating the possibility of any color vision. Finally, and perhaps most surprising, the monkeys of one genus, *Alouatta* (the howler monkeys), resemble catarrhine primates in having both L- and M-opsin genes on their X-chromosome. This arrangement presumably arose from a gene duplication, although the duplication event in the howler monkey is distinct from that which occurred in the catarrhines as it includes the LCR in the duplicated segment. It is unclear how the presence of two LCRs affects the relative expression of the L and M genes. Electroretinogram (ERG) data does demonstrate the presence of functional L and M photopigments in howler monkeys setting the stage for all individuals to express two types of L/M pigment and, potentially, achieve trichromatic color vision (Jacobs, G. H. *et al.*, 1996a).

Relatively less is known about cone pigments and their visual concomitants in the third group of primates, the more primitive strepsirrhines. Based mainly on inferences drawn from cone opsin genes, three patterns can be discerned (Jacobs, G. H., 1996; Tan, Y. and Li, W.-H., 1999; Kawamura, S. and Kubotera, N., 2004). As described above, some species have S-cone opsin pseudogenes and apparently lack any L/M polymorphism and so, as is the case with *Aotus*, these primates also lack color vision. Another group of strepsirrhines, among which the ring-tailed lemur is a good example (Jacobs, G. H. and Deegan II, J. F., 2003), follows the standard mammalian pattern in having a functional S-cone pigment and a single type of L/M pigment providing them with the basis for dichromatic color vision. Finally, some (seemingly limited) number of diurnal strepsirrhines resemble the platyrrhines in having polymorphism in a single L/M-opsin gene so that heterozygous females have two types of L/M pigment and, potentially, trichromatic color vision while the males are uniformly dichromatic.

In recent years, comparative examinations of primate opsin genes have provided the basis for numerous discussions about the evolution of the primate cone pigments (see, e.g., Nathans, J. 1999; Surridge, A. K. *et al.*, 2003; Hunt, D. M. *et al.*, 2005). Although there is agreement on some issues, there is still considerable ambiguity concerning many of the details. Because all catarrhines share in common two highly homologous X-chromosome opsin genes, the step from the normal mammalian pattern (a single X-chromosome opsin gene) to the catarrhine norm involved a gene duplication event that must have occurred near the base of the catarrhine radiation, estimated at 30–35 million years ago (Nathans, J. *et al.*, 1986b), with the platyrrhine/catarrhine divergence dated as occurring before catarrhine gene duplication. X-chromosome opsin gene duplication also must have occurred in the ancestors of the only routinely trichromatic platyrrhine, the howler monkeys. However, comparative examination of the structure of the opsin gene arrays (see above) indicates that the duplication in howler monkeys occurred as an independent event at a time much later than the catarrhine duplication (Hunt, D. M. *et al.*, 1998).

The origins of the L/M-cone pigment polymorphisms remain uncertain. The genetic divergence between the L/M alleles of New World monkeys is considerably smaller than the divergence between the L/M genes of the catarrhines. This would suggest the platyrrhine polymorphisms arose after the catarrhine duplication event, but it has been noted that the process of gene conversion can obscure ancestral differences, and in such cases sequence comparisons can prove inconclusive (Hunt, D. M. *et al.*, 1998). Complicating the issue further is the recent discovery that some strepsirrhine species also feature L/M-gene polymorphisms. One interpretation of this latter discovery is that polymorphism may have been present before the emergence of catarrhines/platyrrhine lineages, perhaps arising relatively early in primate history. However, these events are ultimately resolved; the modern understanding of the linkages between primate opsin genes, cone pigments, and color vision can provide a unique window into our primate past.

1.09.6 Role of Photopigments in Human Retinal Disease

A well-studied feature of human photopigments is how small perturbations in photopigment structure can lead to visual loss. Two examples of this are the relationship between rhodopsin mutations and RP, and the relationship between disruptions in the cone opsins and color blindness.

1.09.6.1 Rhodopsin-Based Disorders

Due in part to its complexity, the human retina is extremely susceptible to disease with degenerations triggered by a variety of environmental and genetic insults. The pathway to blindness in hereditary retinal degenerations originates primarily from mutations in the genes encoding photoreceptor and RPE proteins. One of the most studied of the hereditary retinal degenerations involves rhodopsin. Rhodopsin defects are a common perpetrator of retinal disease accounting for nearly 30% of all cases of RP, while, in total, it is estimated that these cases represent 15% of all hereditary retinal degenerations. There are over 130 distinct rhodopsin mutants involving at least 88 sites within the molecule (data compiled from Zhang, F. *et al.*, 1998; Dryja, T. P. *et al.*, 2000; Sohocki, M. M. *et al.*, 2001; Horn, F. *et al.*, 2003; Stone, E. M., 2003; Schuster, A. *et al.*, 2005; Neidhardt, J. *et al.*, 2006; Retina International 2006; Sullivan, L. S. *et al.*, 2006). With rare exception (e.g., Macke, J. P. *et al.*, 1993; Dryja, T. P. *et al.*, 2000), each of these mutations has been associated with either RP or the condition called congenital stationary night blindness (CSNB). The mutation sites in rhodopsin that are currently known are shown in Figure 3.

The initial cellular mechanisms that enable a mutation in the rhodopsin molecule to lead to complete blindness vary. For example, the P23H mutation has been shown to cause misfolding and retention of the opsin in the endoplasmic reticulum, while mutations near the C-terminal region result in a properly folded opsin that is not then correctly transported to the outer segment. The different mutations have been classified according to their specific biochemical properties, though a number of mutants remain unclassified (see Mendes, H. F. *et al.*, 2005 for a detailed review). The fact that each of these mutations leads to the eventual loss of rod cells emphasizes the critical role of rhodopsin in maintaining cell viability. Moreover, in rhodopsin-knockout mice (rho −/−), rod outer segments fail to develop, suggesting a structural role for rhodopsin (Humphries, M. M. *et al.*, 1997). Indeed, Kumar J. P. and Ready D. F. (1995) have shown that rhodopsin-null alleles in *Drosophila* induce structural abnormalities well before those that are induced by mutants linked to adult degeneration, consistent with the idea that besides its role in phototransduction, rhodopsin is critical in the initial development of the intricate photoreceptor structure.

1.09.6.2 Cone Pigment-Based Disorders

As we have described, the majority of mammals have dichromatic color vision. Among trichromatic species like humans, individuals that have regressed from this norm are commonly called color blind. The most frequent forms of color blindness are inherited, and these most often result from disruptions in the genes encoding the cone photopigments. Usually, it is the absence of one of the three photopigment genes or a mutation in one of these genes that results in a nonfunctional photopigment, but there is one other form of inherited color blindness (called achromatopsia or rod monochromacy) that results from a defect in the components of the cone phototransduction cascade. For an extensive review on this latter disorder, see Hess R. F. *et al.* (1990). Here, we summarize what is known about the photopigment-based color-vision defects.

1.09.6.2.1 Red-green color-vision defects

Two main causes of inherited red-green color-vision deficiency have been identified. The most common cause is rearrangement of the L/M genes resulting either in the deletion of all but one visual pigment gene or in the production of a gene array in which the first two genes both encode a pigment of the same spectral class (Nathans, J. *et al.*, 1986a; Deeb, S. S. *et al.*, 1992; Jagla, W. M. *et al.*, 2002; Ueyama, H. *et al.*, 2003; Neitz, M. *et al.*, 2004). The second general cause is the introduction of an inactivating mutation in either the first or second gene in the array. The most prevalent inactivating mutation results in the substitution of arginine for cysteine at position 203 (C203R) in the L/M pigment (Winderickx, J. *et al.*, 1992; Bollinger, K. *et al.*, 2001; Neitz, M. *et al.*, 2004). Cysteine 203 forms an essential disulfide bond that is highly conserved among GPCRs (Sakmar, T. P., 2002). This mutation was first observed in blue cone monochromacy (BCM) (Nathans, J. *et al.*, 1989) where it was

shown to directly disrupt photopigment function (Kazmi, M. A. *et al.*, 1997). Interestingly, mutating the corresponding cysteine residue in human rhodopsin (position 187) causes autosomal dominant RP (Richards, J. E. *et al.*, 1995).

These two different causes of inherited color-vision defects might be expected to have different retinal phenotypes. It is thought that all photoreceptors destined to become L or M cones will express either the first or second gene in the X-chromosome array (Hayashi, T. *et al.*, 1999). In the case of gene rearrangements, all photoreceptors are expected to express a gene that encodes a functional pigment; however, in the case of the inactivating mutation, a fraction of the photoreceptors will express a pigment that is not functional and, in fact, may be deleterious to the viability of the cell. Recently, it was discovered that there are different retinal phenotypes among red-green color-blind individuals. Carroll, J. *et al.* (2005) found that in individuals having either a single-gene array, or an array in which the first two genes both encode a pigment of the same spectral class, the cone mosaic is normal in appearance. In contrast, in an individual in which one of the genes in the array encodes a pigment with an inactivating mutation, dramatic loss of healthy cones was observed, consistent with the hypothesis that cells expressing the mutant pigment degenerated (Carroll, J. *et al.*, 2004). To date, there have been eight missense mutations reported in the L/M opsins (see Figure 5): N94K, R330Q, and G338E (Ueyama, H. *et al.*, 2002), W90X (Wissinger, B. *et al.*, 2006), P187S (Neitz, M. *et al.*, 2004), R247X and P307L (Nathans, J. *et al.*, 1993), and C203R (Winderickx, J. *et al.*, 1992).

Color blindness can also arise due to promoter mutations within the L/M array, though this does not appear to be common. A mutation (A-71C) in the proximal promoter of the second gene in the array has been associated with both deutan and protan color-vision defects (Ueyama, H. *et al.*, 2003; Neitz, M. *et al.*, 2004). Although the mechanism through which this mutation acts is not entirely clear, it is believed that it either reduces or abolishes gene expression (Ueyama, H. *et al.*, 2003). Disruptions in the LCR can prohibit the expression of any gene in the array (Nathans, J. *et al.*, 1989), as occurs in some cases of BCM (see below).

Finally, an even rarer cause of color blindness results from a swap in gene order. In normal individuals, the array features an L gene followed by one or more M genes (Nathans, J. *et al.*, 1986b; Neitz, M. and Neitz, J., 1995). There are however three reported cases in which an M gene occurs in the first position, with an L gene downstream (Neitz, M. *et al.*, 2004; Ueyama, H. *et al.*, 2006). In all cases, this gene arrangement is associated with a protan defect. Neitz, M. *et al.* (2004) described a male with five genes in the L/M array, where the L gene was in the last position. Previous work has suggested that only the first two genes in the L/M array are significantly expressed (Hayashi, T. *et al.*, 1999), so the protan phenotype of this individual is not surprising. Ueyama, H. *et al.* (2006) described two unrelated males each with four genes in their L/M array. Both had an L gene in the second position of the array, but the L gene also had the A-71C promoter mutation, a change believed to preclude the expression of the associated gene. This also is consistent with the observed protan phenotype. In the absence of any other disruptions in the L/M array, one would predict that an array with an M gene in the first position and an L gene in the second position would confer normal color vision, though such cases have not yet been observed.

1.09.6.2.2 Blue cone monochromacy

BCM is a condition where L- and M-cone function is absent (Pokorny, J. *et al.*, 1979). As with the red-green defects, there are two main genetic causes of BCM, sometimes referred to as one-step or two-step mutations (Nathans, J. *et al.*, 1989; 1993), though both lead to the absence of functional L- and M-photopigment molecules. One-step mutations involve a deletion of essential cis-regulatory DNA elements needed for normal expression of the pigment genes. Two-step mutations involve a deletion of all but one of the X-chromosome visual pigment genes. This would normally confer a red-green dichromacy, but the one remaining gene contains a missense mutation (two-step mutation). It is also possible, though less common, for multiple genes in the array to contain the missense mutation (Nathans, J. *et al.*, 1993; Crognale, M. A. *et al.*, 2001). In both the one-step and two-step mechanisms, affected individuals have very poor visual acuity, myopia, nystagmus, and minimally detectable ERG responses. Due to the X-linked nature of the condition, female carriers are spared from a full manifestation of the associated defects, but they can show abnormal cone ERG amplitudes (Berson, E. L. *et al.*, 1986). One-step and two-step conditions may have important phenotypic differences in terms of the architecture of the cone mosaic in carriers. For the one-step mutations, the absence of an essential

enhancer means that the cone photoreceptors cannot transcribe an opsin gene from the affected X-chromosome. In contrast, for the two-step condition, there is a completely functional gene, but the encoded opsin has a deleterious amino acid substitution, and the photoreceptor is expected to produce the mutant opsin. Depending on the nature of the mutation, it may either reduce or abolish proper folding of the encoded protein, or the gene may be transcribed but the message may be immediately targeted for degradation, and these may in turn ultimately affect the viability of the cone or its neighboring cells. While both conditions will compromise the viability of the cone, they are likely to do so over different time scales.

1.09.6.2.3 Tritan color-vision defects

Tritan color-vision deficiency is an inherited autosomal dominant abnormality of S-cone function (Wright, W. D., 1952). The disorder exhibits incomplete penetrance, meaning that individuals with the same underlying mutation manifest different degrees of color-vision impairment, even within a sibship (Kalmus, H., 1955; Cole, B. L. *et al.*, 1966; Pokorny, J. *et al.*, 1981; Miyake, Y. *et al.*, 1985; Went, L. N. and Pronk, N., 1985). Mutations in the S-cone opsin gene, which encodes the protein component of the S-cone photopigment, have been identified, and they give rise to five different single amino acid substitutions that have only been found in affected individuals but not in unaffected control subjects (Figure 8): G79R and S214P (Weitz, C. J. *et al.*, 1992a), P264S (Weitz, C. J. *et al.*, 1992b), L56P (Gunther, K. L. *et al.*, 2006), and R283Q (Baraas, R. C. *et al.*, in press). Each substitution occurs at an amino acid position that lies in one of the transmembrane α-helices and is predicted to interfere with folding, processing, or stability of the encoded opsin. For example, one of the identified mutations (Weitz, C. J. *et al.*, 1992b) corresponds to an amino acid position at which a substitution in the rod pigment, rhodopsin, causes autosomal dominant retinal degeneration (Sheffield, V. C. *et al.*, 1991; Hwa, J. *et al.*, 1997).

A fundamental difference between S cones and L/M cones is the potential for dominant negative interactions between normal and mutant opsins. This is because each S cone expresses both autosomal copies of the S-opsin gene, whereas L and M cones each only

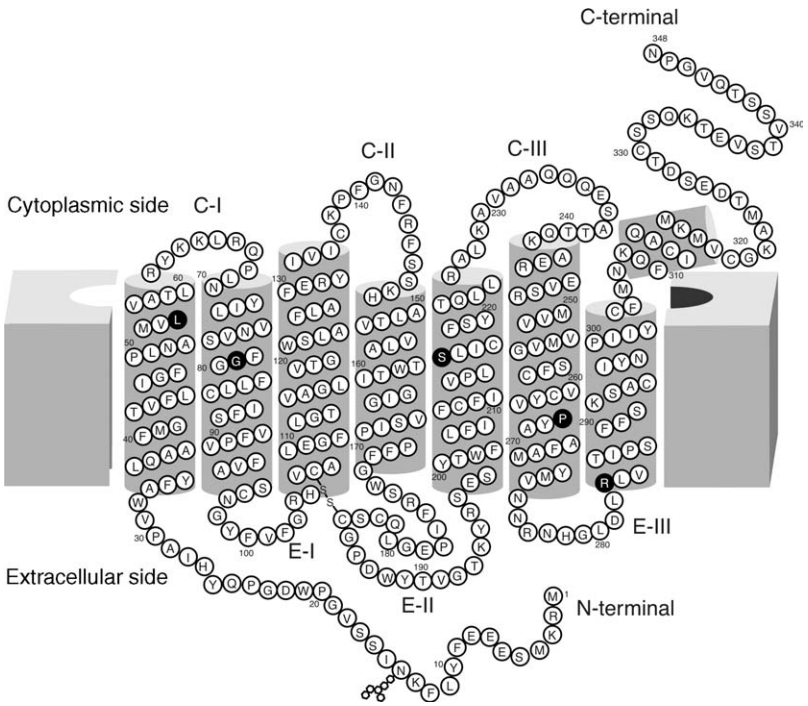

Figure 8 Two-dimensional model of human S opsin. Each circle represents a single amino acid, with tritan-causing mutations identified as filled circles. Adapted from Stenkamp, R. E., Filipek, S., Driessen, C. A. G. G., Teller, D. C., and Palczewski, K. 2002. Crystal structure of rhodopsin: a template for cone visual pigments and other G protein-coupled receptors. Biochim. Biophys. Acta Biomembranes 1565, 168–182, with permission.

expresses one opsin gene from the L/M array on the X-chromosome. Rod photoreceptors also express a rhodopsin gene from two autosomes, and for rhodopsin mutations underlying autosomal dominant RP, dominant negative interactions lead to the death of the photoreceptors and ultimately to the degeneration of the retina (see above). Curiously, tritan defects have not been reported to cause progressive retinal degeneration and are only slightly more rare than adRP; however, it has been suggested that the relative paucity of S cones compared to rods may be responsible for the absence of more general retinal degeneration (Weitz, C. J. *et al*., 1992a). Nevertheless, the structural homology between the S-cone opsin and rhodopsin, taken together with the similar molecular mechanisms underlying the defects, suggests that S cones themselves do degenerate in autosomal dominant tritan defects (Baraas, R. C., *et al*. 2007).

Acknowledgment

We thank K. Palczewski for assistance with photopigment diagrams, E. Kelly and P. Summerfelt for assistance in preparing the figures, M. Cheetham, T. Dryja, L. Sullivan, and D. Tait for assistance in compiling rhodopsin mutation data, and J. Neitz, M. Neitz, and T. Sakmar for helpful comments.

References

Ablonczy, Z., Kono, M., Knapp, D. R., and Crouch, R. K. 2006. Palmitylation of cone opsins. Vis. Res. 46, 4493–4501.

Ahnelt, P. K. and Kolb, H. 2000. The mammalian photoreceptor mosaic-adaptive design. Prog. Retin. Eye Res. 19, 711–777.

Ahnelt, P., Moutairou, K., Glösmann, M., and Kübber-Heiss, A. 2003. Lack of S-Opsin Expression In the Brush-Tailed Porcupine (*Atherurus africanus)* and Other Mammals. Is the Evolutionary Persistence of S-Cones a Paradox? In: Normal and Defective Colour Vision (*eds*. J. D. Mollon, J. Pokorny, and K. Knoblauch). Oxford University Press.

Angers, S., Salahpour, A., and Bouvier, M. 2002. Dimerization: An emerging concept for G protein-coupled receptor ontogeny and function. Annu. Rev. Pharmacol. Toxicol. 42, 409–435.

Applebury, M. L., Antoch, M. P., Baxter, L. C., Chun, L. L. Y., Kalk, J. D., Farhangfar, F., Kage, K., Krzystolik, M. G., Lyass, L. A., and Robbins, J. T. 2000. The murine cone photoreceptor: A single cone type expresses both S and M opsins with retinal spatial patterning. Neuron 27, 513–523.

Arrese, C. A., Hart, N. S., Thomas, N., Beazley, L. D., and Shand, J. 2002. Trichromacy in Australian marsupials. Curr. Biol. 12, 657–660.

Asenjo, A. B., Rim, J., and Oprian, D. D. 1994. Molecular determinants of human red/green color discrimination. Neuron 12, 1131–1138.

Baraas, R. C., Carroll, J., Gunther, K. L., Chung, M., Williams, D. R., Foster, D. H., and Neitz, M. 2007. Adaptive-optics retinal imaging reveals S-cone dystrophy in tritan color-vision deficiency. J. Opt. Soc. Am. A. 24, 1438–1446.

Berson, E. L., Sandberg, M. A., Maguire, A., Bromley, W. C., and Roderick, T. H. 1986. Electroretinograms in carriers of blue cone monochromatism. Am. J. Ophthalmol. 102, 254–261.

Bok, D. 1985. Retinal photoreceptor-pigment epithelium interactions. Friedenwald lecture. Invest. Ophthalmol. Vis. Sci. 26, 1659–1694.

Bollinger, K., Bialozynski, C., Neitz, J., and Neitz, M. 2001. The importance of deleterious mutations of M pigment genes as a cause of color vision defects. Color Res. Appl. 26, S100–S105.

Botelho, A. V., Huber, T., Sakmar, T. P., and Brown, M. F. 2006. Curvature and hydrophobic forces drive oligomerization and modulate activity of rhodopsin in membranes. Biophys. J. 91, 4464–4477.

Bowmaker, J. K. and Hunt, D. M. 2006. Evolution of vertebrate visual pigments. Curr. Biol. 16, R484–R489.

Briscoe, A. D. and Chittka, L. 2001. The evolution of color vision in insects. Annu. Rev. Entomol. 46, 471–510.

Brown, P. K. and Wald, G. 1963. Visual pigments in human and monkey retinas. Nature 200, 37–43.

Carroll, J., Neitz, M., Hofer, H., Neitz, J., and Williams, D. R. 2004. Functional photoreceptor loss revealed with adaptive optics: An alternate cause for color blindness. Proc. Natl. Acad. Sci. U. S. A. 101, 8461–8466.

Carroll, J., Neitz, M., and Neitz, J. 2002. Estimates of L:M cone ratio from ERG flicker photometry and genetics. J. Vis. 2, 531–542.

Carroll, J., Porter, J., Neitz, J., Williams, D. R., and Neitz, M. 2005. Adaptive optics imaging reveals effects of human cone opsin gene disruption. Invest. Ophthalmol. Vis. Sci. 46, ARVO E-Abstract 4564.

Chabre, M. and Le Maire, M. 2006. Monomeric G-protein-coupled receptor as a functional unit. Biochemistry 44, 9395–9403.

Cole, B. L., Henry, G. H., and Nathan, J. 1966. Phenotypical variations of tritanopia. Vis. Res. 6, 303–313.

Collin, S. P., Knight, M. A., Davies, W. L., Potter, I. C., Hunt, D. M., and Trezise, A. E. O. 2003. Ancient colour vision: Multiple opsin genes in ancestral vertebrates. Curr. Biol. 13, R864–R865.

Crognale, M. A., Nolan, J. B., Webster, M. A., Neitz, M., and Neitz, J. 2001. Color vision and genetics in a case of cone dysfunction syndrome. Color Res. Appl. 26, S284–S287.

Dartnall, H. J. A. and Lythgoe, J. N. 1965. The spectral clustering of visual pigments. Vis. Res. 5, 81–100.

Dartnall, H. J. A., Bowmaker, J. K., and Mollon, J. D. 1983. Human visual pigments: microspectrophotometric results from the eyes of seven persons. Proc. R. Soc. Lond. B 220, 115–130.

Deeb, S. S., Jørgensen, A. L., Battisti, L., Iwasaki, L., and Motulsky, A. G. 1994. Sequence divergence of the red and green visual pigments in great apes and humans. Proc. Natl. Acad. Sci. U. S. A. 91, 7262–7266.

Deeb, S. S., Lindsey, D. T., Hibiya, Y., Sanocki, E., Winderickx, J., Teller, D. Y., and Motulsky, A. G. 1992. Genotype-phenotype relationships in human red/green color-vision defects: molecular and psychophysical studies. Am. J. Hum. Genet. 51, 687–700.

Drummond-Borg, M., Deeb, S. S., and Motolsky, A. G. 1989. Molecular patterns of X chromosome-linked color vision genes among 134 men of European ancestry. Proc. Natl. Acad. Sci. U. S. A. 86, 983–987.

Dryja, T. P., Mcevoy, J. A., Mcgee, T. L., and Berson, E. L. 2000. Novel rhodopsin mutations Gly114Val and Gln184Pro in

dominant retinitis pigmentosa. Invest. Ophthalmol. Vis. Sci. 41, 3124–3127.
Ebrey, T. and Koutalos, Y. 2001. Vertebrate photoreceptors. Prog. Retin. Eye Res. 20, 49–94.
Filipek, S. 2005. Organization of rhodopsin in native membranes of rod cells – an old theoretical model compared to new experimental data. J. Mol. Model. 11, 385–391.
Filipek, S., Stenkamp, R. E., Teller, D. C., and Palczewski, K. 2003. G protein-coupled receptor rhodopsin: A prospectus. Annu. Rev. Physiol. 65, 851–879.
Foster, R. G. and Hankins, M. W. 2002. Non-rod, non-cone photoreception in the vertebrates. Prog. Retin. Eye Res. 21, 507–527.
Fotiadis, D., Liang, Y., Filipek, S., Saperstein, D. A., Engel, A., and Palczewski, K. 2003. Rhodopsin dimers in native disc membranes. Nature 421, 127–128.
Gray, D. C., Merigan, W. H., Wolfing, J. I., Gee, B. P., Porter, J., Dubra, A., Twietmeyer, T. H., Ahmad, K., Tumbar, R., Reinholz, F., and Williams, D. R. 2006. *In vivo* fluorescence imaging of primate retinal ganglion cells and retinal pigment epithelial cells. Opt. Expr. 14, 7144–7158.
Grether, W. F. 1939. Color vision and color blindness in monkeys. Comp. Psychol. Monogr. 29, 1–38.
Gunther, K. L., Neitz, J., and Neitz, M. 2006. A novel mutation in the short-wavelength-sensitive cone pigment gene associated with a tritan color vision defect. Vis. Neurosci. 23, 403–409.
Hafezi, F., Grimm, C., Simmen, B. C., Wenzel, A., and Remé, C. E. 2000. Molecular ophthalmology: an update on animal models for retinal degenerations and dystrophies. Br. J. Ophthalmol. 84, 922–927.
Hattar, S., Liao, H. W., Takao, M., Berson, D. M., and Yau, K. W. 2002. Melanopsin-containing retinal ganglion cells: architecture, projections, and intrinsic photosensitivity. Science 295, 1065–1070.
Haverkamp, S., Wässle, H., Duebel, J., Kuner, T., Augustine, G. J., Feng, G., and Euler, T. 2005. The primordial, blue-cone color system of the mouse retina. J. Neurosci. 25, 5438–5445.
Hayashi, T., Motulsky, A. G., and Deeb, S. S. 1999. Position of a 'green-red' hybrid gene in the visual pigment array determines colour-vision phenotype. Nat. Genet. 22, 90–93.
Hendrickson, A., Djajadi, H. R., Nakamura, L., Possin, D. E., and Sajuthi, D. 2000. Nocturnal tarsier retina has both short and long/medium-wavelength cones in an unusual topography. J. Comp. Neurol. 424, 718–730.
Hess, R. F. Sharpe, L. T. and Nordby K. (*eds.*) 1990. Night Vision: Basic, Clinical and Applied Aspects. Cambridge University Press.
Hisatomi, O. and Tokunaga, F. 2002. Molecular evolution of proteins involved in vertebrate phototransduction. Comp. Biochem. Physiol. B. 133, 509–522.
Horn, F., Bettler, E., Oliveira, L., Campagne, F., Cohen, F. E., and Vriend, G. 2003. GPCRDB information system for G protein-coupled receptors. Nucleic Acids Res. 31, 294–297.
Humphries, M. M., Rancourt, D., Farrar, G. J., Kenna, P., Hazel, M., Bush, R. A., Sieving, P. A., Sheils, D. M., Mcnally, N., Creighton, P., Erven, A., Boros, A., Gulya, K., Capecchi, M. R., and Humphries, P. 1997. Retinopathy induced in mice by targeted disruption of the rhodopsin gene. Nat. Genet. 15, 216–219.
Hunt, D. M., Cowing, J. A., Wilkie, S. E., Parry, J. W. L., Poopalasundaram, S., and Bowmaker, J. K. 2004. Divergent mechanisms for the tuning of shortwave sensitive visual pigments in vertebrates. Photochem. Photobiol. Sci. 3, 713–720.
Hunt, D. M., Dulai, K. S., Cowing, J. A., Julliot, C., Mollon, J. D., Bowmaker, J. K., Li, W.-H., and Hewett-Emmett, D. 1998. Molecular evolution of trichromacy in primates. Vis. Res. 38, 3299–3306.
Hunt, D. M., Jacobs, G. H., and Bowmaker, J. K. 2005. The Genetics and Evolution of Primate Visual Pigments. In: The Primate Visual System: A Comparative Approach (*ed*. J. Kremers). John Wiley and Sons, Ltd.
Hurley, J. B., Spencer, M., and Niemi, G. A. 1998. Rhodopsin phosphorylation and its role in photoreceptor function. Vis. Res. 38, 1341–1352.
Hwa, J., Garriga, P., Liu, X., and Khorana, H. G. 1997. Structure and function in rhodopsin; packing of the helices in the transmembrane domain and folding to a tertiary structure in the intradiscal domain are couples. Proc. Natl. Acad. Sci. U. S. A. 94, 10571–10576.
Jacobs, G. H. 1993. The distribution and nature of colour vision among the mammals. Biol. Rev. 68, 413–471.
Jacobs, G. H. 1996. Primate photopigments and primate color vision. Proc. Natl. Aca. 93(2), 577–581.
Jacobs, G. H. 1998. Photopigments and seeing – lessons from natural experiments: the Proctor lecture. Invest. Ophthalmol. Vis. Sci. 39, 2204–2216.
Jacobs, G. H. (in press) New World monkeys and color. Int. J. Primatol.
Jacobs, G. H. and Deegan, J. F., II 1999. Uniformity of colour vision in Old World monkeys. Proc. R. Soc. Lond. B. 266, 2023–2028.
Jacobs, G. H. and Deegan, J. F., II 2003. Diurnality and cone pigment polymorphism in strepsirrhines: Examination of linkage in *Lemur catta*. Am. J. Phys. Anthropol. 122, 66–72.
Jacobs, G. H. and Rowe, M. P. 2004. Evolution of vertebrate colour vision. Clin. Exp. Optom. 87, 206–216.
Jacobs, G. H. and Williams, G. A. 2001. The prevalence of defective color vision in Old World monkeys and apes. Color Res. Appl. 26, S123–S127.
Jacobs, G. H., Neitz, J., and Deegan, J. F., II 1991. Retinal receptors in rodents maximally sensitive to ultraviolet light. Nature 353, 655–656.
Jacobs, G. H., Neitz, M., Deegan, J. F., and Neitz, J. 1996a. Trichromatic colour vision in New World monkeys. Nature 382, 156–158.
Jacobs, G. H., Neitz, M., and Neitz, J. 1996b. Mutations in S-cone pigment genes and the absence of colour vision in two species of nocturnal primate. Proc. R. Soc. Lond. B 263, 705–710.
Jacobs, G. H., Williams, G. A., Cahill, H., and Nathans, J. 2007. Emergence of novel color vision in mice engineered to express a human cone photopigment. Science 315, 1723–1725.
Jacobs, G. H., Williams, G. A., and Fenwick, J. A. 2004. Influence of cone pigment coexpression on spectral sensitivity and color vision in the mouse. Vis. Res. 44, 1615–1622.
Jagla, W. M., Jägle, H., Hayashi, T., Sharpe, L. T., and Deeb, S. S. 2002. The molecular basis of dichromatic color vision in males with multiple red and green visual pigment genes. Hum. Mol. Genet. 11, 23–32.
Jones, B. W. and Marc, R. E. 2005. Retinal remodeling during retinal degeneration. Exp. Eye Res. 81, 123–137.
Jørgensen, A. L., Deeb, S. S., and Motulsky, A. G. 1990. Molecular genetics of X chromosome-linked color vision among populations of African and Japanese ancestry: High frequency of a shortened red pigment gene among Afro-Americans. Proc. Natl. Acad. Sci. U. S. A. 87, 6512–6516.
Kalmus, H. 1955. The familial distribution of congenital tritanopia, with some remarks on some similar conditions. Ann. Hum. Genet. 20, 39–56.
Karnik, S. S., Sakmar, T. P., Chen, H.-B., and Khorana, H. G. 1988. Cysteine residues 110 and 187 are required for the

formation of correct structure in bovine rhodopsin. Proc. Natl. Acad. Sci. U. S. A. 85, 8459–8463.
Kawamura, S. and Kubotera, N. 2004. Ancestral loss of short wave-sensitive cone visual pigment in lorsiform prosimians, contrasting with its strict conservation in other prosimians. J. Mol. Evol. 58, 314–321.
Kazmi, M. A., Sakmar, T. P., and Ostrer, H. 1997. Mutation of a conserved cysteine in the X-linked cone opsins causes color vision deficiencies by disrupting protein folding and stability. Invest. Ophthalmol. Vis. Sci. 38, 1074–1081.
Kefalov, V., Fu, Y., Marsh-Armstrong, N., and Yau, K.-W. 2003. Role of visual pigment properties in rod and cone phototransduction. Nature 425, 526–531.
Kelber, A., Vorobyev, M., and Osorio, D. 2003. Animal colour vision – behavioral tests and physiological concepts. Biol. Rev. 78, 81–118.
Kochendorfer, G. G., Lin, S. W., Sakmar, T. P., and Mathies, R. A. 1999. How color visual pigments are tuned. Trends Biochem. Sci. 24, 300–305.
Kumar, J. P. and Ready, D. F. 1995. Rhodopsin plays an essential structural role in Drosophila photoreceptor development. Development 121, 4359–4370.
Kumbalasiri, T. and Provencio, I. 2005. Melanopsin and other novel mammalian opsins. Exp. Eye Res. 81, 368–375.
Levenson, D. H. and Dizon, A. 2003. Genetic evidence for the ancestral loss of SWS cone pigments in mysticete and odontocete cetaceans. Proc. R. Soc. Lond. B Biol. Sci. 270, 673–679.
Levenson, D. H., Fernandez-Duque, E., Evans, S., and Jacobs, G. H. 2007. Mutational changes in S-cone opsin genes common to both nocturnal and cathemeral *Aotus* monkeys. Am. J. Primatol. 69, 757–765.
Levenson, D. H., Ponganis, P. J., Crognale, M. A., Deegan, II, J. F., Dizon, A., and Jacobs, G. H. 2006. Visual pigments of marine carnivores: Pinnipeds, polar bear, and sea otter. J. Comp. Physiol. A. 192, 833–843.
Lin, S. W. and Sakmar, T. P. 1999. Colour tuning mechanisms of visual pigments. Novartis Found. Symp. 224, 124–141.
Lin, S. W., Kochendoerfer, G. C., Carroll, K. S., Wang, D., Mathies, R. A., and Sakmar, T. P. 1988. Mechanisms of spectral tuning in blue cone visual pigment. J. Biol. Chem. 273, 24583–24591.
Lukáts, Á., Szabó, A., Röhlich, P., Vígh, B., and Szél, Á. 2005. Photopigment coexpression in mammals: comparative and developmental aspects. Histol. Histopathol. 20, 551–574.
Ma, J., Znoiko, S., Othersen, K. L., Ryan, J. C., Das, J., Isayama, T., Kono, M., Oprian, D. D., Corson, D. W., Cornwall, M. C., Cameron, D. A., Harosi, F. I., Makino, C. L., and Crouch, R. K. 2001. A visual pigment expressed in both rod and cone photoreceptors. Neuron 32, 451–461.
Macke, J. P. and Nathans, J. 1997. Individual variation in the size of the human red and green visual pigment gene array. Invest. Ophthalmol. Vis. Sci. 38, 1040–1043.
Macke, J. P., Davenport, C. M., Jacobson, S. G., Hennessey, J. C., Gonzalez-Fernandez, F., Conway, B. P., Heckenlively, J., Palmer, R., Maumenee, I. H., Sieving, P., *et al.* 1993. Identification of novel rhodopsin mutations responsible for retinitis pigmentosa: implications for the structure and function of rhodopsin. Am. J. Hum. Genet. 53, 80–89.
Maeda, T., Imanishi, Y., and Palczewski, K. 2003. Rhodopsin phosphorylation: 30 years later. Prog. Retin. Eye Res. 22, 417–434.
Makino, C. L. and Dodd, R. L. 1996. Multiple visual pigments in a photoreceptor of the salamander retina. J. Gen. Physiol. 108, 27–34.
Marks, W. B., Dobelle, W. H., and Macnichol, E. F. 1964. Visual pigments of single primate cones. Science 143, 1181–1183.
Mendes, H. F., Van Der Spuy, J., Chapple, J. P., and Cheetham, M. E. 2005. Mechanisms of cell death in rhodopsin retinitis pigmentosa: implications for therapy. Trends Mol. Med. 11, 177–185.
Menon, S. T., Han, M., and Sakmar, T. P. 2001. Rhodopsin: Structural basis of molecular physiology. Physiol. Rev. 81, 1659–1688.
Miyake, Y., Yagasaki, K., and Ichikawa, H. 1985. Differential diagnosis of congenital tritanopia and dominantly inherited juvenile optic atrophy. Arch. Ophthalmol. 103, 1496–1501.
Mollon, J. D. 2003. The Origins of Modern Color Science. In: The Science of Color 2nd edn. (*ed*. S. K. Shevell). Elsevier Science.
Nakanishi, K., Balogh-Nair, V., Arnaboldi, M., Tsujimoto, K., and Honig, B. 1980. An external point-charge model for bacteriorhodopsin to account for its purple color. J. Am. Chem. Soc. 102, 7945–7947.
Nathans, J. 1987. Molecular biology of visual pigments. Annu. Rev. Neurosci. 10, 163–194.
Nathans, J. 1999. The evolution and physiology of human color vision: insights from molecular genetic studies of visual pigments. Neuron 24, 299–312.
Nathans, J., Davenport, C. M., Maumenee, I. H., Lewis, R. A., Hejtmancik, J. F., Litt, M., Lovrien, E., Weleber, R., Bachynski, B., Zwas, F., Klingaman, R., and Fishman, G. 1989. Molecular genetics of human blue cone monochromacy. Science 245, 831–838.
Nathans, J., Maumenee, I. A., Zrenner, E., Sadowski, B., Sharpe, L. T., Lewis, R. A., Hansen, E., Rosenberg, P., Schwartz, M., Heckenlively, J. R., Traboulsi, E., Klingaman, R., Bech-Hansen, N. T., Larouche, G. R., Pagon, R. A., Murphy, W. H., and Weleber, R. G. 1993. Genetic heterogeneity among blue-cone monochromats. Am. J. Hum. Genet. 53, 987–1000.
Nathans, J., Piantanida, T. P., Eddy, R. L., Shows, T. B., and Hogness, D. S. 1986a. Molecular genetics of inherited variation in human color vision. Science 232, 203–210.
Nathans, J., Thomas, D., and Hogness, D. S. 1986b. Molecular genetics of human color vision: the genes encoding blue, green, and red pigments. Science 232, 193–202.
Neidhardt, J., Barthelmes, D., Farahmand, F., Fleischhauer, J. C., and Berger, W. 2006. Different amino acid substitutions at the same position in rhodopsin lead to distinct phenotypes. Invest. Ophthalmol. Vis. Sci. 47, 1630–1635.
Neitz, M., Carroll, J., Renner, A., Knau, H., Werner, J. S., and Neitz, J. 2004. Variety of genotypes in males diagnosed as dichromatic on a conventional clinical anomaloscope. Vis. Neurosci. 21, 205–216.
Neitz, M. and Neitz, J. 1995. Numbers and ratios of visual pigment genes for normal red-green color vision. Science 267, 1013–1016.
Neitz, M., Neitz, J., and Grishok, A. 1995. Polymorphism in the number of genes encoding long-wavelength sensitive cone pigments among males with normal color vision. Vis. Res. 35, 2395–2407.
Neitz, M., Neitz, J., and Jacobs, G. H. 1991. Spectral tuning of pigments underlying red-green color vision. Science 252, 971–974.
Nikonov, S., Lamb, T. D., and Pugh, E. N., Jr. 2000. The role of steady phosphodiesterase activity in the kinetics and sensitivity of the light-adapted salamander rod photoresponse. J. Gen. Physiol. 116, 795–824.
Okada, T., Ernst, O. P., Palczewski, K., and Hofmann, K. P. 2001. Activation of rhodopsin: new insights from structural and biochemical studies. Trends Biochem. Sci. 26, 318–324.
Onishi, A., Hasegawa, J., Imai, H., Chisaka, O., Ueda, Y., Honda, Y., Tachibana, M., and Shichida, Y. 2005. Generation of knock-in mice carrying third cones with spectral sensitivity different from S and L cones. Zool. Sci. 22, 1145–1156.

Onishi, A., Koike, S., Ida, M., Imai, H., Shichida, Y., Takenaka, O., Hanazawa, A., Komatsu, H., Mikami, A., Goto, S., Suryobroto, B., Kitahara, K., Yamamori, T., and Komatsu, H. 1999. Dichromatism in macaque monkeys. Nature 402, 139–140.

Ostrer, H., Pullarkat, R. K., and Kazmi, M. A. 1998. Glycosylation and palmitoylation are not required for the formation of the X-linked cone opsin visual pigments. Mol. Vis. 4, 28–32.

Palczewski, K., Kumasaka, T., Hori, T., Behnke, C. A., Motoshima, H., Fox, B. A., Letrong, I., Teller, D. C., Okada, T., Stenkamp, R. E., Yamamoto, M., and Miyano, M. 2000. Crystal structure of rhodopsin: A G-protein-coupled receptor. Science 289, 739–745.

Park, P. S.-H. and Palczewski, K. 2005. Diversifying the repertoire of G protein-coupled receptors through oligomerization. Proc. Natl. Acad. Sci. U. S. A. 102, 8793–8794.

Peichl, L. 2005. Diversity of mammalian photoreceptor properties: Adaptations to habitat and lifestyle? Anat. Rec. A 287A, 1001–1012.

Peichl, L. and Moutairou, K. 1998. Absence of short-wavelength sensitive cones in the retinae of seals (Carnivora) and African giant rats (Rodentia). Eur. J. Neurosci. 10, 2586–2594.

Peichl, L., Behrmann, G., and Kroger, R. H. H. 2001. For whales and seals the ocean is not blue: A visual pigment loss in marine mammals. Eur. J. Neurosci. 13, 1520–1528.

Perry, R. J. and McNaughton, P. A. 1991. Response properties of cones from the retina of the tiger salamander. J. Physiol. 433, 561–587; Erratum: J. Physiol. 436, p. 771.

Pokorny, J., Smith, V. C., and Verriest, G. 1979. Congenital Color Defects. In: Congenital and Acquired Color Vision Defects (*eds*. J. Pokorny, V. C. Smith, G. Verriest, and A. J. L. G. Pinckers). Grune and Stratton.

Pokorny, J., Smith, V. C., and Went, L. N. 1981. Color matching in autosomal dominant tritan defect. J. Opt. Soc. Am. 71, 1327–1334.

Retina International. 2006. *Mutations of the Rhodopsin gene,* Mutation Database http://www.retina-international.org/sci-news/rhomut.htm

Richards, J. E., Scott, K. M., and Sieving, P. A. 1995. Disruption of conserved rhodopsin disulfide bond by Cys187Tyr mutation causes early and severe autosomal dominant retinitis pigmentosa. Ophthalmology 102, 669–677.

Rodieck, R. W. 1998. The First Steps in Seeing. Sinauer Associates, Inc.

Rushton, W. A. H. 1972. Pigments and signals in colour vision. J. Physiol. (Lond.) 220, 1–31.

Sakmar, T. P. 2002. Structure of rhodopsin and the superfamily of seven-helical receptors: the same and not the same. Curr. Opin. Cell Biol. 14, 189–195.

Sakmar, T. P. 2003. Structure and Function of G-Protein Coupled Receptors: Lessons from the Crystal Structure Of Rhodopsin. In: Handbook of Cell Signaling (*eds*. R. Bradshaw and E. Dennis). Academic Press.

Schnapf, J. L., Kraft, T. W., and Baylor, D. A. 1987. Spectral sensitivity of human cone photoreceptors. Nature 325, 439–441.

Schuster, A., Weisschuh, N., Jägle, H., Besch, D., Janecke, A. R., Zierler, H., Tippmann, S., Zrenner, E., and Wissinger, B. 2005. Novel rhodopsin mutations and genotype-phenotype correlation in patients with autosomal dominant retinitis pigmentosa. Br. J. Ophthalmol. 89, 1258–1264.

Sharpe, L. T., Stockman, A., Jägle, H., Knau, H., Klausen, G., Reitner, A., and Nathans, J. 1998. Red, green, and red-green hybrid pigments in the human retina: correlations between deduced protein sequences and psychophysically measured spectral sensitivities. J. Neurosci. 18, 10053–10069.

Sheffield, V. C., Fishman, G. A., Beck, J. S., Kimura, A. E., and Stone, E. M. 1991. Identification of novel rhodopsin mutations associated with retinitis pigmentosa by GC-clamped denaturing gradient gel electrophoresis. Am. J. Hum. Genet. 49, 699–706.

Smallwood, P. M., Olveczky, B. P., Williams, G. L., Jacobs, G. H., Reese, B. E., Meister, M., and Nathans, J. 2003. Genetically engineered mice with an additional class of cone photoreceptors: Implications for the evolution of color vision. Proc. Natl. Acad. Sci. U. S. A. 100, 11706–11711.

Smallwood, P. M., Wang, Y. S., and Nathans, J. 2002. Role of a locus control region in the mutually exclusive expression of human red and green cone pigment genes. Proc. Natl. Acad. Sci. U. S. A. 99, 1008–1011.

Snodderly, D. M., Sandstrom, M. M., Leung, I. Y.-F., Zucker, C. L., and Neuringer, M. 2002. Retinal pigment epithelial cell distribution in central retina of Rhesus monkeys. Invest. Ophthalmol. Vis. Sci. 43, 2815–2818.

Sohocki, M. M., Daiger, S. P., Bowne, S. J., Rodriquez, J. A., Northrup, H., Heckenlively, J. R., Birch, D. G., Mintz-Hittner, H., Ruiz, R. S., Lewis, R. A., Saperstein, D. A., and Sullivan, L. S. 2001. Prevalence of mutations causing retinitis pigmentosa and other inherited retinopathies. Hum. Mutat. 17, 42–51.

Sollars, P. J., Smeraski, C. A., Kaufman, J. D., Ogilvie, M. D., Provencio, I., and Pickard, G. E. 2003. Melanopsin and non-melanopsin expressing retinal ganglion cells innervate the hypothalamic superchiasmatic nucleus. Vis. Neurosci. 20, 601–610.

Stenkamp, R. E., Filipek, S., Driessen, C. A. G. G., Teller, D. C., and Palczewski, K. 2002. Crystal structure of rhodopsin: a template for cone visual pigments and other G protein-coupled receptors. Biochim. Biophys. Acta Biomembranes 1565, 168–182.

Stone, E. M. 2003. Finding and interpreting genetic variations that are important to ophthalmologists. Transact. Am. Ophthalmol. Soc. 101, 437–484.

Strauss, O. 2005. The retinal pigment epithelium in visual function. Physiol. Rev. 85, 845–881.

Sullivan, L. S., Bowne, S. J., Birch, D. G., Hughbanks-Wheaton, D., Heckenlively, J. R., Lewis, R. A., Garcia, C. A., Ruiz, R. S., Blanton, S. H., Northrup, H., Gire, A. I., Seaman, R., Duzkale, H., Spellicy, C. J., Zhu, J., Shankar, S. P., and Daiger, S. P. 2006. Prevalence of disease-causing mutations in families with autosomal dominant retinitis pigmentosa: a screen of known genes in 200 families. Invest. Ophthalmol. Vis. Sci. 47, 3052–3064.

Surridge, A. K., Osorio, D., and Mundy, N. I. 2003. Evolution and selection of trichromatic vision in primates. Trends Ecol. Evol. 18, 198–206.

Szél, Á., Van Veen, T., and Röhlich, P. 1994. Retinal cone differentiation. Nature 370, 336.

Tan, Y. and Li, W.-H. 1999. Trichromatic vision in prosimians. Nature 402, 36.

Ueyama, H., Kuwayama, S., Imai, H., Tanabe, S., Oda, S., Nishida, S., Wada, A., Shichida, Y., and Yamada, S. 2002. Novel missense mutations in red/green opsin genes in congenital color-vision deficiencies. Biochem. Biophys. Res. Commun. 294, 205–209.

Ueyama, H., Li, Y.-H., Fu, G.-L., Lertrit, P., Atchaneeyasakul, L., Oda, S., Tanabe, S., Nishida, Y., Yamade, S., and Ohkubo, I. 2003. An A-71C substitution in a green gene at the second position in the red/green visual-pigment gene array is associated with deutan color-vision deficiency. Proc. Natl. Acad. Sci. U. S. A. 100, 3357–3362.

Ueyama, H., Tanabe, S., Muraki-Oda, S., Yamade, S., and Ohkubo, I. 2006. Protan color vision deficiency with a unique order of green-red as the first two genes of a visual pigment array. J. Hum. Genet. 51, 686–694.

Vollrath, D., Nathans, J., and Davis, R. W. 1988. Tandem array of human visual pigment genes at Xq28. Science 240, 1669–1672.
Wald, G. 1968. The molecular basis of visual excitation. Nature 219, 800–807.
Wang, D., Oakley, T., Mower, J., Shimmin, L. C., Yim, S., Honeycutt, R. L., Tsao, H., and Li, W.-H. 2004. Molecular evolution of bat color vision genes. Mol. Biol. Evol. 21, 295–302.
Wang, Y., Macke, J. P., Merbs, S. L., Zack, D. J., Klaunberg, B., Bennett, J., Gearhart, J., and Nathans, J. 1992. A locus control region adjacent to the human red and green visual pigment genes. Neuron 9, 429–440.
Weitz, C. J., Miyake, Y., Shinzato, K., Montag, E., Zrenner, E., Went, L. N., and Nathans, J. 1992a. Human tritanopia associated with two amino acid substitutions in the blue sensitive opsin. Am. J. Hum. Genet. 50, 498–507.
Weitz, C. J., Went, L. N., and Nathans, J. 1992b. Human tritanopia associated with a third amino acid substitution in the blue sensitive visual pigment. Am. J. Hum. Genet. 51, 444–446.
Went, L. N. and Pronk, N. 1985. The genetics of tritan disturbances. Hum. Genet. 69, 255–262.
Winderickx, J., Sanocki, E., Lindsey, D. T., Teller, D. Y., Motulsky, A. G., and Deeb, S. S. 1992. Defective colour vision associated with a missense mutation in the human green visual pigment gene. Nat. Genet. 1, 251–256.
Wissinger, B., Papke, M., Tippmann, S., and Kohl, S. 2006. Genotypes in blue cone monochromacy. Invest. Ophthalmol. Vis. Sci. 47. ARVO E-Abstract 4609.
Wright, W. D. 1952. The characteristics of tritanopia. J. Opt. Soc. Am. 42, 509–521.
Xiao, M. and Hendrickson, A. 2000. Spatial and temporal expression of short, long/medium, or both opsins in human fetal cones. J. Comp. Neurol. 425, 545–559.
Yamaguchi, T., Motulsky, A. G., and Deeb, S. S. 1997. Visual pigment gene structure and expression in the human retinae. Hum. Mol. Genet. 6, 981–990.
Yokoyama, S. 1997. Molecular genetic basis of adaptive selection: Examples from color vision in vertebrates. Annu. Rev. Genet. 31, 315–336.
Yokoyama, S. 1999. Molecular basis of color vision in vertebrates. Genes Genet. Syst. 74, 189–199.
Yokoyama, S. 2002. Molecular evolution of color vision in vertebrates. Gene 300, 69–78.
Yokoyama, S. and Radlwimmer, F. B. 1998. The ''five-sites'' rule and the evolution of red and green color vision in mammals. Mol. Biol. Evol. 15, 560–567.
Yokoyama, S. and Radlwimmer, F. B. 1999. The molecular genetics of red and green color vision in mammals. Genetics 153, 919–932.
Yokoyama, S. and Shi, Y. 2000. Genetics and evolution of ultraviolet vision in vertebrates. FEBS Lett. 486, 167–172.
Yokoyama, S. and Yokoyama, R. 2000. Comparative Molecular Biology of Visual Pigments. In: Molecular Mechanisms in Visual Transduction (*eds*. D. G. Stavenga, W. J. Degrip, and E. N. Pugh JR). Elsevier Science B. V.
Zhang, F., Zhang, Q., Shen, H., Li, S., and Xiao, X. 1998. Analysis of rhodopsin and peripherin/RDS genes in Chinese patients with retinitis pigmentosa. Yan Ke Xue Bao 14, 210–214.

Relevant Website

http://webvision.med.utah.edu – WebVision: The Organization of the Retina and Visual System, H. Kolb, E. Fernandez, R. Nelson (*eds.*).

1.10 Phototransduction in Rods and Cones

D-G Luo, Johns Hopkins University School of Medicine, Baltimore, MD, USA

V Kefalov, Washington University School of Medicine, St. Louis, MO, USA

K-W Yau, Johns Hopkins University School of Medicine, Baltimore, MD, USA

© 2008 Elsevier Inc. All rights reserved.

1.10.1	Introduction	270
1.10.2	Morphology of Rods and Cones	270
1.10.3	Light Response of Rods and Cones	271
1.10.4	Intensity–Response Relation	273
1.10.5	Kinetics of the Dim-Flash Response	276
1.10.6	The a-Wave of the Electroretinogram	277
1.10.7	Single-Photon Response	278
1.10.8	Pigment Noise	280
1.10.9	The cGMP-Gated, Light-Suppressible, Nonselective Cation Channel	281
1.10.10	Phototransduction Cascade	284
1.10.11	Background-Light Adaptation	289
1.10.12	Bleaching Adaptation	290
1.10.13	Dark Adaptation	291
1.10.14	Differences between Rods and Cones	291
1.10.15	Diseases	292
1.10.16	Parietal-Eye Photoreceptor in Lizards and a Possible Evolutionary Linkage to Rods and Cones	294
References		295

Glossary

background-light adaptation The process by which rod and cone photoreceptors change their response properties due to the presence of a steady background light. The photoreceptor becomes less sensitive to light, and the response also becomes faster.

bleaching The loss of color of the visual pigment due to the loss of its ability to absorb in the visible part of the spectrum. In the dark state, a holo pigment (opsin plus chromophore) absorbs light in a specific part of the visible spectrum. After absorbing a photon, the chromophore isomerizes and eventually separates (by hydrolysis) from the opsin. As a result, neither the chromophore nor the opsin absorbs in the visible spectrum anymore, until regeneration of the pigment.

bleaching adaptation The process by which rod and cone photoreceptors change their response properties when a significant fraction of their visual pigment content has lost the chromophore (see Chromophore) after light absorption (see Bleaching). Bleaching adaptation results from both loss of pigment due to bleaching and a mild activity of the opsin apoprotein.

chromophore A light-absorbing moiety. For visual pigments, the chromophore is 11-*cis*-retinaldehyde, which is a derivative of vitamin A (all-*trans*-retinol). It is covalently linked (via a Schiff base) to a lysine residue in the opsin apo-protein.

dark adaptation The process by which a photoreceptor recovers its sensitivity in darkness after exposure to a bleaching light.

electroretinogram An en-mass electrical recording from the retina of an animal or human eye. Different components reflecting the electrical activities of different types of retinal neurons can be identified in the electroretinogram. This is a very useful tool for clinical diagnosis of abnormal function in the retina.

parietal eye A primitive eye present in some lower vertebrates, especially lizard. It is an unpaired, midline organ on the forehead, not for acute vision (as the two lateral eyes) but most likely for detecting the passage of time during the day.

phototransduction The process by which light triggers an electrical response in retinal rod and cone photoreceptors.
single-photon response The response of a photoreceptor to a single absorbed photon. It is the fundamental building block of all light responses, containing precious information about the process of phototransduction.

1.10.1 Introduction

The physiology of rods and cones is conserved across animal species. Rods are extremely sensitive to light. The ingenious work of Hecht S. *et al.* (1942) has shown that these cells, when fully dark-adapted, are capable of signaling the absorption of a single photon. They mediate vision in dim light (scotopic vision). Cones, on the other hand, are less sensitive to light than rods, typically by two orders of magnitude under dark-adapted conditions. Moreover, whereas rods have only a limited ability to adapt to steady light, cones have a much higher adaptive ability. Accordingly, cones function in bright light (photopic vision). They also have faster response kinetics than rods, which makes them more suitable for the detection of motion. In addition, because there is typically more than one type of cone in the retina, each expressing a different photopigment, cones endow the animal with the ability of color vision. Most retinas are rod-dominant, but a minority of animal species, such as ground squirrel and chicken, have cone-dominant retinas. In the human retina, 95% or more of the photoreceptors are rods, but its center, the fovea, where acute vision occurs, has exclusively cones.

1.10.2 Morphology of Rods and Cones

Rods and cones are quite similar in structure (Cohen, A. I., 1987; Dowling, J. E., 1987; Rodieck, R. W., 1998). Each has an elongated outer segment, an inner segment, a cell body, and a synaptic terminal (Figure 1). Light traverses the entire thickness of the retina before being absorbed in the outer segment, where it triggers an electrical signal via a cascade of intracellular signaling events (visual transduction or phototransduction). The outer segment is actually a modified cilium that, during the development of the photoreceptor, has become highly expanded and convoluted so that the plasma membrane is folded upon itself hundreds of times (Steinberg, R. H. *et al.*, 1980). These so-called membranous disks, tightly stacked one on top of another and oriented perpendicular to the longitudinal axis of the outer segment, are densely embedded with the visual pigment, a transmembrane protein. Packed at a density as high as $30\,000\,\mu m^{-2}$ of membrane, there are altogether $\sim 10^8$ rod pigment (rhodopsin) molecules in a single mammalian rod. The number in an amphibian rod, such as that of toad, is tenfold even higher because of its larger outer segment. One convenient way to calculate the number of rhodopsin molecules in a rod outer segment is to simply multiply the volume of the outer segment by 3.5 mM, the effective pigment concentration (Harosi, F. I., 1975). The packing density of cone

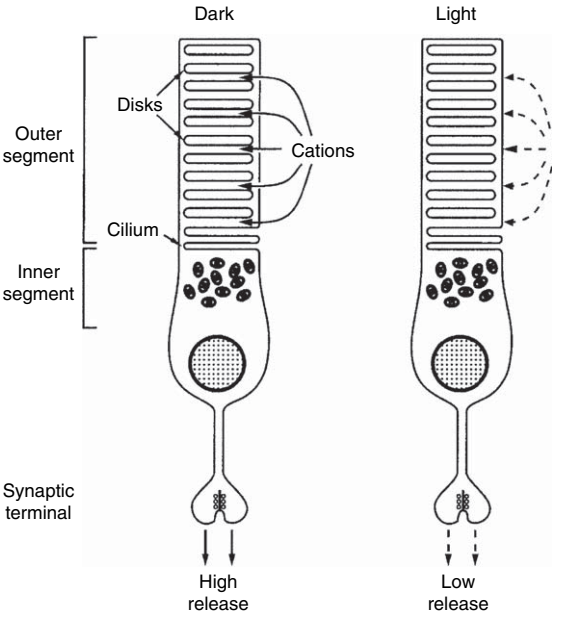

Figure 1 Diagram to show the overall morphology of a retinal rod photoreceptor and the behavior of its dark current in darkness and in the light (see text for details). Reproduced with permission from Yau, K.-W. 1994. Phototransduction mechanism in retinal rods and cones. The Friedenwald Lecture. Invest. Ophthalmol. Vis. Sci. 35, 10–32.

pigment in the membrane is similar. The disks are clearly designed for increasing the probability of absorption as a photon travels longitudinally through the outer segment. For example, the chance that a 500-nm photon (wavelength of maximum absorption for rhodopsin) will be absorbed upon longitudinally traversing a 15-μm-long mouse rod outer segment is almost 50%!

In rods, almost all of the disks (except for a small number at the base of the outer segment) are completely internalized, that is, no longer continuous with the plasma membrane. In cones, the disks do remain continuous with the plasma membrane (Cohen, A. I., 1987). These disks undergo continual renewal, with new disks being formed daily at the base of the outer segment (i.e., next to the inner segment) and a corresponding number shed at the tip, so that the total number remains more or less constant (La Vail, M. M., 1983). This renewal process may be important for removing any cumulative, harmful effects of photo-oxidation in the photoreceptors. It takes about 10 days for a mouse or rat rod to renew its entire outer segment.

Overlying the outer segments of rods and cones are the pigment epithelial cells. These cells serve multiple functions (Steinberg, R. H., 1985). One function is, by virtue of the melanin granules they contain, to absorb any light not absorbed by the rods and cones at a single pass, so as to prevent degradation of the visual image due to backscattering. A second function is to transport metabolites, ions, water, and other substances between the photoreceptors and the blood capillaries in the choriocapillaris on the opposite side of the pigment epithelium. Third, these cells contain the machinery critical for the regeneration of the visual pigment after the latter is bleached by light. Fourth, they phagocytize the shed disks at the tip of the outer segment.

1.10.3 Light Response of Rods and Cones

The membrane potential of rods and cones in darkness is at −30 to −35 mV. This potential is sufficiently depolarized to activate synaptic L-type Ca channels and trigger neurotransmitter (glutamate) release. Light produces a membrane hyperpolarization at the outer segment, which propagates electrotonically to the synaptic terminal and reduces the glutamate release. The response is graded with light so that the brighter the light, the larger is the membrane hyperpolarization and the greater the reduction in glutamate release. There are two types of bipolar cells, the second-order retinal throughput neurons receiving synaptic inputs from rods and cones. One type responds to light with a hyperpolarization (OFF-bipolar cell) and the other responds with a depolarization (ON-bipolar cell). OFF-bipolar cells use postsynaptic ionotropic glutamate receptors on their dendrites (so that the synapse is sign-preserving), whereas ON-bipolar cells use a metabotropic glutamate receptor (type 6) and a downstream second-messenger pathway (the details of which are still unclear; see Chapter Contributions of Bipolar Cells to Ganglion Cell Receptive Fields) that lead to a sign-inverting synapse.

The rod and cone responses to light are relatively slow, reflecting a second-messenger-mediated transduction mechanism (see Section 1.10.10). For example, amphibian rods at room temperature respond to a dim flash with a hyperpolarization that reaches a transient peak in approximately 1 s and takes another 1–3 s to subside (Figure 2(b)). The light response of mammalian rods (37 °C) is severalfold faster (Baylor, D. A., 1987). For a given animal species, cones are also up to severalfold faster than rods in response kinetics. The speed of the response dictates how rapidly a photoreceptor is capable of detecting image changes on the retina (temporal resolution), and therefore motion. Because cones have faster responses than rods, they are better motion detectors. On the other hand, the slower response of rods allows these cells to sum signals dispersed over time (temporal integration), thus enhancing the sensitivity in dim light especially for static images.

Historically, the photoreceptors of cold-blooded animals (fish, amphibians, and reptiles) have been favorite preparations for electrophysiological studies because of their large size and hardiness. The pioneering studies by Tomita and colleagues with sharp intracellular microelectrodes on fish first showed that retinal photoreceptors hyperpolarize to light and that this is due to a light-induced decrease in membrane conductance, presumably in the outer segment (Tomita, T., 1970). Subsequently, Hagins W. A. *et al.* (1970) used a linear array of three microelectrodes to map the current flow around the rod photoreceptors in the rat retina, demonstrating that a membrane current (the dark current) enters the rod outer segment and exits from the rest of the cell in darkness and that this current is suppressed by light (Figure 1). These findings corroborated those of Tomita and coworkers. With the advent of the suction-pipette recording method in the 1970s (Yau, K.-W. *et al.*,

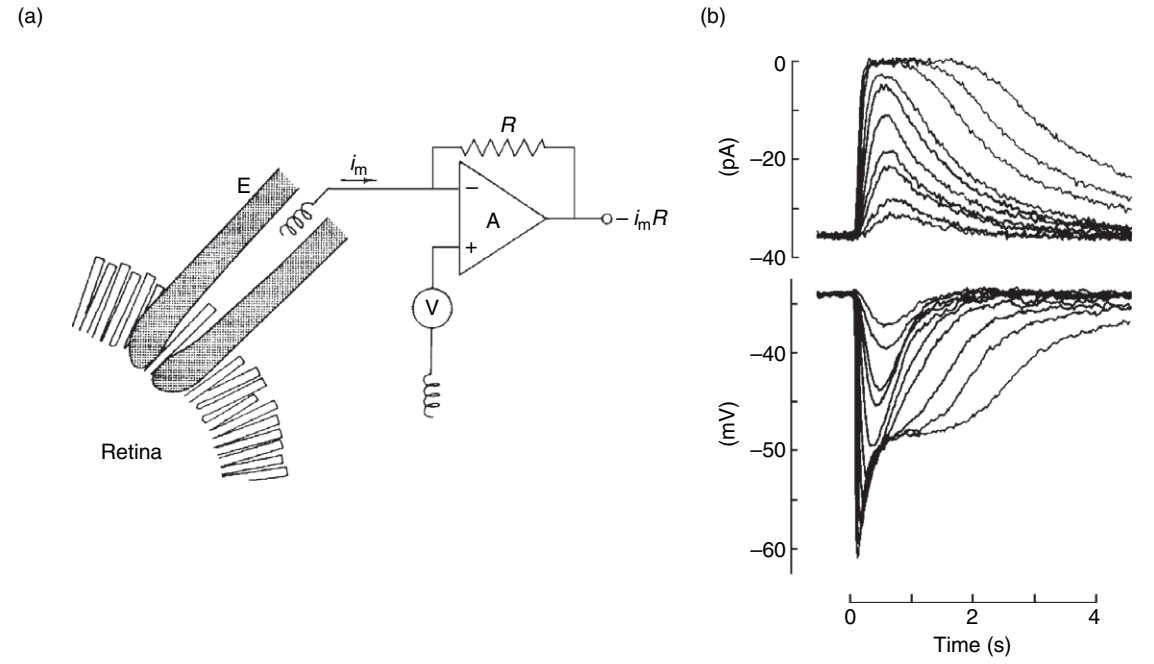

Figure 2 (a) The schematics of the suction-pipette method for recording from a photoreceptor. (a) Reproduced from Yau, K.-W., Lamb, T. D., and Baylor, D. A. 1977. Light-induced fluctuations in membrane current of single toad rod outer segments. Nature 269, 78–80. (b) Simultaneous current and voltage recordings from a salamander rod. (b) Reproduced with permission from Baylor, D. A., Matthews, G., and Nunn, B. J. 1984. Location and function of voltage-sensitive conductances in retinal rods of the salamander, Ambystoma tigrinum. J. Physiol. 354, 203–223.

1977), it has now become almost routine to record from the rods and cones of not just cold-blooded vertebrates, but also a variety of mammals, including humans. This recording method, inspired by the patch-clamp technique (Neher, E. and Sakmann, B., 1976), consists typically of drawing the outer segment of an isolated rod or cone, or an outer segment projecting from a fragment of retina, into a tight-fitting glass pipette filled with physiological extracellular solution and connected to a current-to-voltage transducer for recording membrane current (Figure 2(a)) (Baylor, D. A. *et al.*, 1979a; Schnapf, J. L. and McBurney, R. N., 1980). This method is simple, noninvasive, and stable, allowing continuous recordings without degradation for up to several hours.

Figure 2(b) shows simultaneous recordings from a salamander rod with a suction pipette and a sharp intracellular electrode (Baylor, D. A. *et al.*, 1984). In darkness, the membrane potential is −35 mV and there is a steady dark current of 20 pA entering the outer segment (it is conventional in the field of visual transduction to plot the membrane current flowing at the outer segment, with a negative sign to indicate inward current). In response to a light flash, the dark current transiently decreases and the membrane potential hyperpolarizes. With increasing flash intensity, the light response increases in a graded fashion until it saturates, corresponding to a complete suppression of the dark current (Hagins, W. A. *et al.*, 1970; Baylor, D. A. *et al.*, 1979a). Note that the current and voltage responses are similar in shape (as well as in kinetics, except that the voltage response reaches peak slightly earlier) with dim flashes but differ dramatically with bright flashes, in that the voltage response but not the current response shows a fast redepolarization from the peak hyperpolarization before settling to a plateau level. This transient nose in the voltage response, especially prominent in rods, reflects a hyperpolarization-activated cation current (I_h) carried by both Na^+ and K^+, with a reversal potential very roughly near 0 mV (Fain, G. L. and Lisman, J. E., 1981; Accili, E. A. *et al.*, 2002). The I_h current presumably also underlies the slightly earlier peak of the voltage response compared to that of the current response to dim light. This I_h current is situated at the inner segment and cell body. Because the light-sensitive conductance is the only ion conductance on the plasma membrane of the outer segment (Baylor, D. A. and Lamb, T. D., 1982), and

because it has an essentially flat current–voltage relation in the physiological voltage range (at least for the rod channel; see Section 1.10.9), the nose is not detected by the suction pipette (Baylor, D. A. *et al.*, 1979a). Some of these subtle properties were not anticipated when the suction-pipette method was first developed, but they have made the method tremendously useful for monitoring phototransduction in the outer segment, without much contamination by signals from other parts of the cell.

Another useful configuration of the suction-pipette method is to draw the cell body and inner segment of an isolated rod or cone photoreceptor into the suction pipette for recording (Figure 3(b)) (Yau, K.-W. *et al.*, 1981). Because current flows in a closed loop (dark current entering the outer segment through the light-sensitive conductance and exiting the rest of the cell through other conductances), the same current but of the opposite polarity is recorded in this configuration. This recording configuration has the advantage that the solution surrounding the outer segment can be changed selectively and rapidly, which turned out to be crucial for elucidating the mechanism of phototransduction. Being noninvasive, however, suction-pipette recording from a rod or cone does not allow internal dialysis of the cell, an often-useful manipulation. Internal dialysis can be achieved by another variant of the method, which consists of sucking the outer segment into the pipette and truncating the base of the outer segment for rods (Yau, K.-W. and Nakatani, K., 1985b), or the inner segment for cones (Nakatani, K. and Yau, K.-W. 1986; Rieke, F. and Baylor, D. A., 2000), situated outside the pipette in order to expose the interior of the recorded outer segment to the bath solution (Figure 3(c)). In this way, with the appropriate metabolites in the bath solution, the outer segment remains capable of transducing light for minutes or longer by virtue of the retained transduction proteins, most of which are transmembrane or peripheral membrane proteins rather than soluble. Depending on the question to be addressed, one recording configuration is more useful than another.

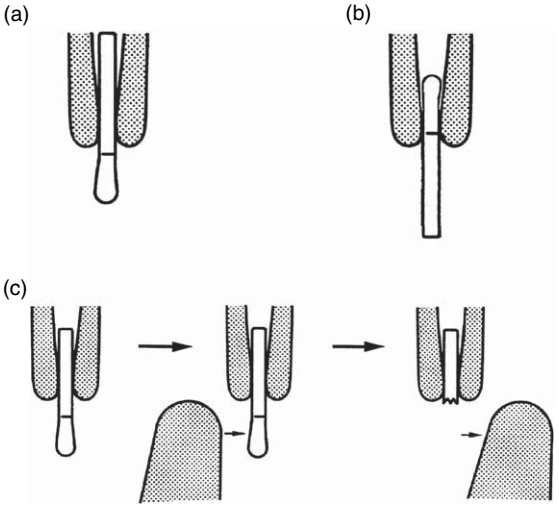

Figure 3 Three configurations of the suction-pipette recording method. (a) Outer segment inside the pipette. (b) Outer segment outside the pipette for perfusion purposes. (c) The truncated-outer-segment preparation.

Because of its usefulness, the suction-pipette method and its measured light responses will form the basis for all discussions to follow.

1.10.4 Intensity–Response Relation

In this chapter, we define a flash as a short-lasting light stimulus with a time duration that is negligible compared to the time course of the elicited response from the cell – with the flash preferably over before the response even becomes visible. In engineering terminology, a flash is an impulse, and the response to a flash is the impulse response. The advantage of the flash response is that, once it is known, the response to a more complex light stimulus (in intensity or duration) can be obtained by mathematically convolving the flash response with the light stimulus. The rigorous use of light flashes (typically 10–20 ms in duration) as defined above for studying retinal rods and cones was not adopted until Hodgkin A. L. and his disciples started using them routinely in the early 1970s (Baylor, D. A. and Hodgkin, A. L., 1973).

When the amplitude of the transient peak of the flash response is plotted against the corresponding flash intensity (the flash intensity–response relation at response peak), the relation can be described moderately well, especially for cold-blooded animals, by the Michaelis equation used in enzyme kinetics, namely, $R = R_{max}[I_F/(I_F + \sigma)]$, where R is the transient peak amplitude, R_{max} the saturated response amplitude (i.e., complete suppression of the dark current), I_F the flash intensity, and σ the half-saturating flash intensity (Figure 4(a)). The Michaelis equation is often called the rectangular hyperbola in vision research because, when plotted on coordinates of response versus log-intensity as commonly done, it assumes the shape of a rectangular hyperbola. The fact that the Michaelis equation provides a

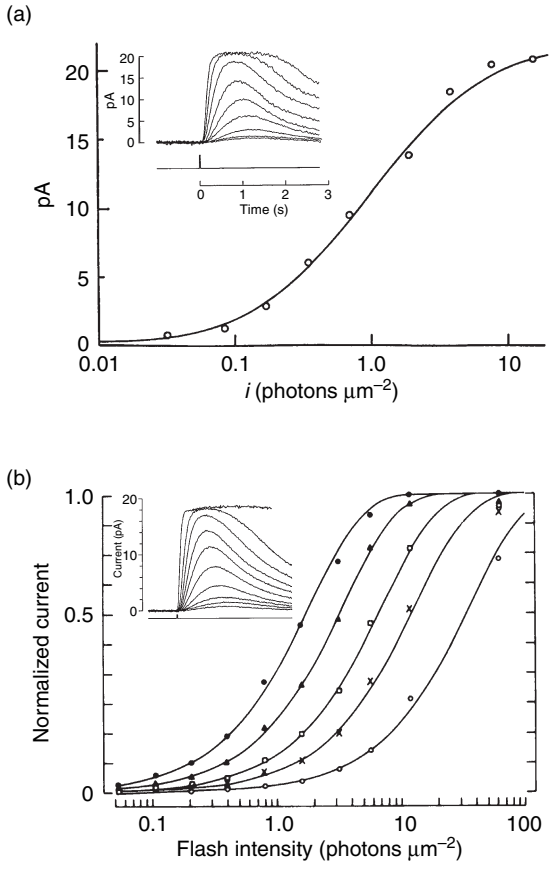

Figure 4 (a) Intensity–response relation at transient response peak of a toad rod recorded with the suction-pipette method. Outer segment inside the pipette. 500 nm, 20 ms flash (plane polarized transverse to the longitudinal axis of the outer segment) over the entire outer segment. Plot shows the transient peak response amplitude against incident flash intensity. The smooth curve is the Michaelis equation, with $\sigma = 1$ photon μm^{-2}. (b) Instantaneous flash intensity–response relation of a toad rod. Similar experimental conditions as in (a). The various symbols indicate the relation at different time instants on the rising phase of the flash response. The smooth curves are all drawn according to the saturating exponential function $1 - \exp(-I_F/\rho)$. This function is steeper than the Michaelis equation. (a) Reproduced with permission from Baylor, D. A., Lamb, T. D., and Yau, K.-W. 1979a. The membrane current of single rod outer segments. J. Physiol. 288, 589–611. (b) Reproduced with permission from Lamb, T. D., McNaughton, P. A., and Yau, K.-W. 1981. Spatial spread of activation and background desensitization in toad rod outer segments. J. Physiol. 319, 463–496.

moderately good fit to the flash intensity–response relation at response peak, together with the conceptual association of this equation with equilibrium binding, evoked early interest in interpreting the phototransduction mechanism according to a scheme of equilibrium binding between a second messenger and the light-suppressible conductance (Baylor, D. A. and Fuortes, M. G. F., 1970), especially in view of the prevailing Ca^{2+} hypothesis for phototransduction at the time (see Section 1.10.10). However, it later became clear that this approximate agreement between the Michaelis equation and the peak response–intensity relation is just accidental, with no deep implications about any simple mechanistic link between the two. Hodgkin and colleagues (Baylor, D. A. *et al.*, 1974) were again the first to point this out. For one thing, with increasing flash intensity, the transient peak of the response moves earlier in time; that is, the time between the flash and the transient peak of the response (or time-to-peak) gets shorter (Figure 2 or 4(a)). This speeding up of the response indicates that the decay phase of the response cuts into the rising phase progressively earlier with increasing flash intensity, an indication of active adaptation by the cell. Because the time-to-peak changes with increasing flash intensity, the intensity–response relation at transient peak is therefore not measured at a constant time, and any fit to the Michaelis equation (in which time is not a variable) has to be purely empirical. Hodgkin and colleagues (Baylor, D. A. *et al.*, 1974) first introduced the idea of an instantaneous intensity–response relation, meaning a relation measured at a fixed time instant after the flash (so that the time variable is removed), typically at an early time in the rising phase of the light response, before any active adaptation has set in. In this case, the flash intensity–response relation is better described by the saturating exponential function $R = R_{max}[1 - \exp(-I_F/\rho)]$, where the half-saturating flash intensity is given by $\rho(\log_e 2)$ (Figure 4(b)). This function is steeper than the Michaelis equation (Baylor, D. A. *et al.*, 1974; Lamb, T. D. *et al.*, 1981). It also bears a simple mechanistic interpretation, namely that each absorbed photon activates a spatially restricted domain on the outer segment, within which transduction essentially reaches saturation (i.e., all dark current within this domain is suppressed). While conceptually useful, this compartment model nonetheless should not be taken too literally. On the other hand, the idea of a fairly restricted spread of phototransduction elicited by the absorption of a photon is certainly valid and could be directly demonstrated (Lamb, T. D. *et al.*, 1981) with a light slit stimulating only a small longitudinal portion of the rod outer segment (see also Section 1.10.7).

If a long step (say, many seconds) instead of a flash of light is used for stimulation, the rod or cone response rises to a transient peak and then relaxes to a lower plateau level (Figure 5(a)). This response relaxation again reflects the progressive development of active adaptation by the cell to steady light (Baylor, D. A. *et al.*, 1979a; 1979b; 1980; Nakatani, K. and Yau, K.-W., 1988a). If the intensity–response relation (in this case often called the step intensity–response relation) is plotted at different fixed time points after the onset of light, the relation at early times after light onset is describable by the above saturating exponential function just as the instantaneous flash intensity–response relation, but it becomes progressively shallower with time (Nakatani, K. and Yau, K.-W. 1988a). In the plateau phase of the step response, the step intensity–response relation is shallower than even the Michaelis equation, being describable by a logarithmic rise (Figure 5(b); Nakatani, K. *et al.*, 1991) (see also Section 1.10.12).

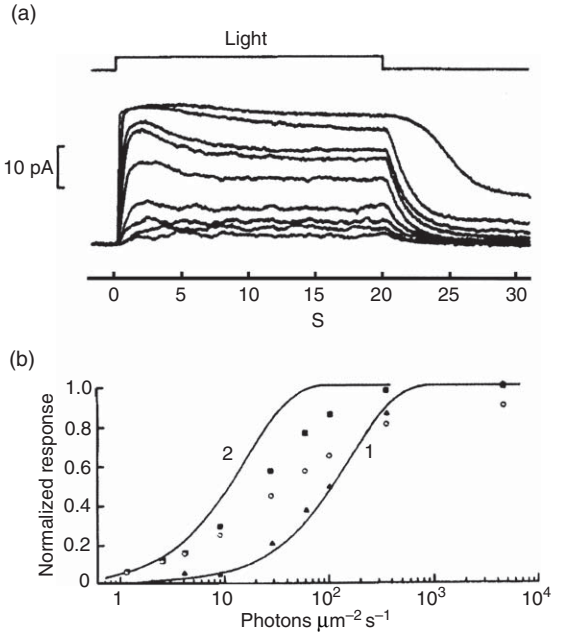

Figure 5 (a) Response family elicited by a light step of different intensities from a salamander rod. Similar experimental conditions as in Figure 4. Note the relaxation of the response at early times during the light step. (b) Step intensity–response families at different times of the response. Filled triangles: 0.4 s after light onset; filled squares: transient response peak; open circles: at plateau just before light off. Curves 1 and 2 are both drawn according to the saturating exponential function. Reproduced with permission from Nakatani, K. and Yau, K.-W. 1988a. Calcium and light adaptation in retinal rods and cones. Nature 334, 69–71.

The sensitivity of a rod or cone can be represented in two ways. One way is to simply use the value of σ (i.e., half-saturating flash intensity) as an indicator of sensitivity, with σ being inversely proportional to sensitivity. Sometimes, however, it is more informative to describe flash sensitivity as the transient peak amplitude of the response elicited by one absorbed photon in a weak flash (single-photon response). This latter parameter can be obtained from (and is only meaningful in) the linear range of the flash intensity–response relation by dividing the linear response amplitude by the calculated number of absorbed photons. The linear range refers to the foot of the intensity–response relation at low flash intensities such that doubling the intensity will exactly double the response, with negligible change in response kinetics (including negligible shift in the time-to-peak) (Baylor, D. A. and Hodgkin, A. L., 1973; Baylor, D. A. *et al.*, 1974). A linear foot of the intensity–response relation is implicit in the fitting by either the Michaelis equation or a saturating exponential function described above, because both are linear at low flash intensities (see Section 1.10.7 for more details). With suction-pipette recording, for which light is typically incident roughly at right angles to the longitudinal axis of the outer segment, the number of absorbed photons effected by a flash at low intensities is (assuming diffuse light that covers the entire outer segment) given by $I_F A_e$, where I_F is the number or equivalent number of incident photons per square micrometer contained in the flash at λ_{max} (the wavelength of maximal absorption for a given pigment), and A_e is the effective collecting area given by $A_e = 2.303(\pi d^2 L/4) Q_{isom} f \alpha$, where d and L are, respectively, the outer-segment diameter and length, Q_{isom} is the quantum efficiency of isomerization (equal to 0.67 for pigments containing 11-*cis*-retinal as chromophore), α is the axial optical density (in the neighborhood of 0.016 μm^{-1}), f is a factor equal to unity for plane-polarized light parallel to the membrane disks and equal to 0.5 with unpolarized light, and 2.303 is simply from $\log_e 10$ (Baylor, D. A. *et al.*, 1979b). For light that is incident along the outer-segment axis, as in situ in the eye, the number of absorbed photons is no longer directly proportional to the length of the light path in the outer segment because of self-screening by the pigment along the long light path. In this case, the percentage of absorbed photons is given by $1 - 10^{-\alpha L}$, where α is again the axial optical density as above and L the length of the outer segment. In this case, whether the light is unpolarized or plane-polarized makes no

difference. Finally, the single-photon response amplitude can also be estimated without the knowledge of the incident light intensity and the effective collecting area of the outer segment, by using variance analysis of the response amplitude, provided that the response lies in the linear range (Baylor, D. A. *et al.*, 1979b) (see Section 1.10.7). In principle, the same parameter can be resolved from the experimental response amplitude histogram derived from dim flashes, but, in practice, this is not an easy method unless the histogram is optimized in the experiment (Figure 9(b)).

If flash sensitivity is designated by S_F (in unit of picoamperes per photon), one can write the step sensitivity, S_S (defined as the steady response elicited by a continuous light causing one absorbed photon per second, and in unit of picoamperes per photon per second), as simply $S_S = S_F t_i$. Here t_i is the integration time of the (linear) response elicited by a dim flash, defined as $t_i = \int f(t)dt/f_p$, where $f(t)$ is the response profile of the single-photon response and f_p the amplitude of $f(t)$ at transient peak (Baylor, D. A. and Hodgkin, A. L., 1973). The integration time gives a measure of the effective lifetime of the dim-flash response. The mean steady response produced by a weak continuous light at intensity I_S (in units of absorbed photons per second at λ_{max}) is then $S_S I_S$. This relation holds, of course, only in the linear range of the intensity–response relation.

The above concepts and parameters, first introduced by Hodgkin and colleagues, have greatly facilitated the study of the physiology of rods and cones by providing a rigorous foundation.

1.10.5 Kinetics of the Dim-Flash Response

The kinetics of the dim-flash response provides empirical information about the underlying transduction mechanism. For example, the profile of the rod dim-flash response can generally be fitted by the convolution of a series of four linear delay stages (Figure 6(a); Baylor, D. A. *et al.*, 1979a). In other words, the foot of the response increases sigmoidally as the third power of time, and the final decline follows a single exponential. Depending on the cell, the time constants of the delay stages may be similar or different from each other, although such details are not necessarily very informative or precise, other than reflecting some variability from cell to cell in one or more of the underlying delay stages. One of several formal schemes compatible with the kinetics

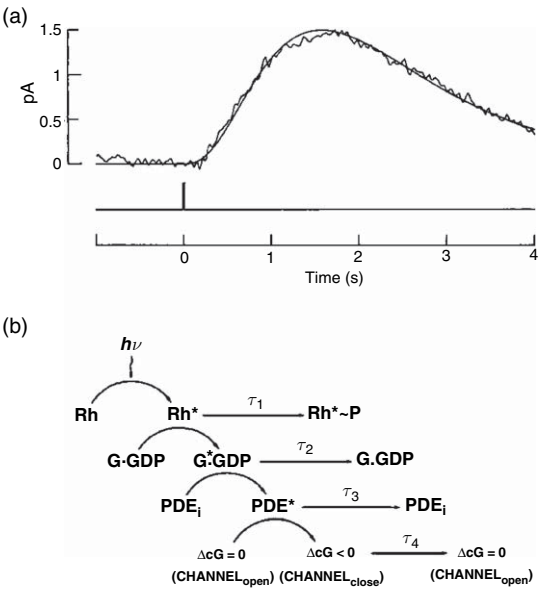

Figure 6 (a) Average dim-flash response from a toad rod. Smooth curve shows fit with a function corresponding to the convolution of four single-exponential decays. (b) Diagram showing a formal kinetic scheme that can describe the dim-flash response. The transduction components are inserted based on the underlying mechanism known much later. The states marked by '$*$' are active. The various τs indicate decay time constants. (a) Reproduced with permission from Baylor, D. A., Lamb, T. D., and Yau, K.-W. 1979a. The membrane current of single rod outer segments. J. Physiol. 288, 589–611. (b) Reproduced with permission from Yau, K.-W. 1994. Phototransduction mechanism in retinal rods and cones. The Friedenwald Lecture. Invest. Ophthalmol. Vis. Sci. 35, 10–32.

is shown in Figure 6(b) (Matthews, G. and Baylor, D. A., 1981; Yau, K.-W., 1994), so chosen because it happens to match more or less the underlying biochemistry subsequently worked out. For a linear system, the delay stages are commutative, that is, giving the same overall response profile regardless of their order in the cascade. Thus, the slowest step in the cascade, as reflected by the final exponential decay of the response, does not have to be the last step in the kinetic scheme at all. The scheme in Figure 6(b) is conceptual only, and not meant to be precise. With the underlying biochemistry now understood in great detail, a more precise formulation is realized (Pugh, E. N. and Lamb, T. D., 2000; Hamer, R. D. *et al.*, 2005).

Hodgkin and colleagues were the first to point out that when the light response is driven to saturation and beyond by an ever-increasing strong flash, the time of peeling off of the decline phase of the response from saturation is progressively delayed, with a duration

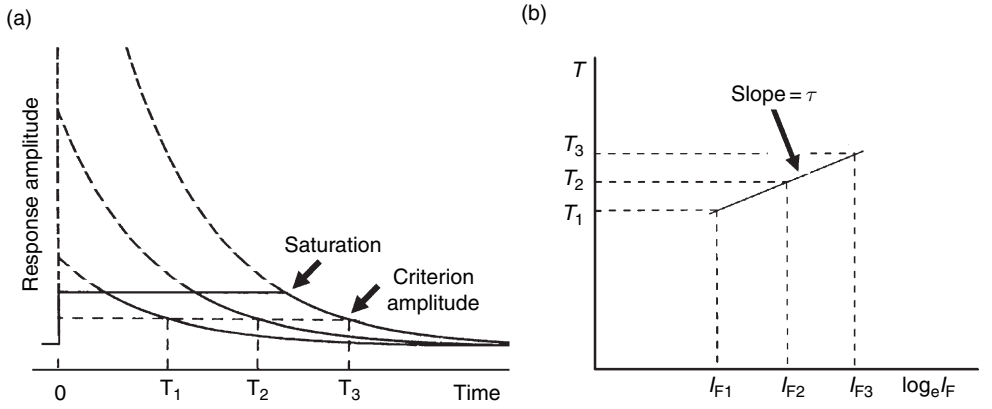

Figure 7 Diagram showing the concept of the Pepperberg time constant. (a) For simplicity, the response is taken to be a single-exponential-decline function (with time constant τ) that increases in amplitude in proportion to the flash intensity (I_F) and is subject to clipping by a saturation ceiling. Times T_1, T_2, etc. represent the progressive delay for the response to decay back to a criterion amplitude with increasing flash intensity. (b) Plot of T against $\log_e I_F$, with the slope giving τ.

that is proportional to the logarithm of the flash intensity (Baylor, D. A. *et al.*, 1974). The proportionality constant in fact corresponds to the time constant of the final exponential decay of the dim-flash response mentioned above. This idea was later popularized by Pepperberg D. R. *et al.* (1992), and the time constant has come to be referred to as the Pepperberg time constant or dominant time constant. This concept can be appreciated as follows. For simplicity, let us just consider a light response that obeys an underlying driving function, $AI_F \exp(-t/\tau)$, that is, one that has an amplitude proportional to the flash intensity, I_F, with a proportionality factor A and has a single-exponential decline with time constant τ, but the response is subject to a ceiling (saturation) that clips the would-be response beyond saturation (Figure 7). If we choose a constant criterion response amplitude at or below saturation, we have, if τ stays constant:

$$AI_F \exp\left(\frac{-t}{\tau}\right) = \text{constant}$$

or

$$t = \tau \log_e I_F + \text{constant}$$

Thus, in a plot of t against $\log_e I_F$, τ is simply equal to the slope.

1.10.6 The a-Wave of the Electroretinogram

The rod and cone photoresponses are detectable in the electroretinogram (ERG), a mass-recording from the retina with an electrode placed near the cornea of the intact eye (Berson, E. L., 1987). The ERG has several components, but the negative a-wave, which is one of the earliest components, reflects the activity of rods and cones (Figure 8). However, the a-wave does not provide the full-time profile of the photoreceptor response to light because the closely following b-wave of the ERG (which largely reflects the activity of ON-bipolar cells) cuts into and obscures the a-wave. The ERG nonetheless provides a very useful clinical tool for monitoring rod and cone function in human patients (Berson, E. L, 1993).

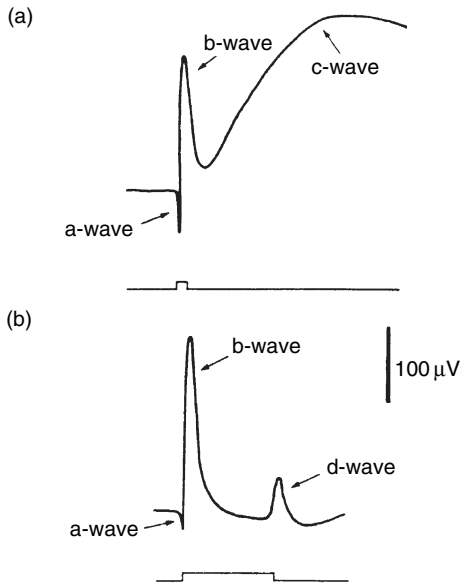

Figure 8 The electroretinogram (ERG). Electroretinographic recordings against time in response to a flash (a) and a step of light (b). Reproduced with permission from Dowling, J. E. 1987. The Retina: An Approachable Part of the Brain, Belknap.

1.10.7 Single-Photon Response

It was mentioned earlier that rods are so sensitive to light that they are capable of signaling the absorption of a single photon (Hecht, S. *et al.*, 1942). This rod single-photon response is quite large, corresponding to a transient reduction in the dark current by ~0.5–1 pA in both amphibians and mammals (Penn, R. D. and Hagins, W. A., 1972; Baylor, D. A. *et al.*, 1979b; Baylor, D. A. *et al.*, 1984). In the isolated rod, this current amplitude should produce a membrane hyperpolarization in the neighborhood of 1 mV (Fain, G. L., 1975; Detwiler, P. B. *et al.*, 1980; Schneeweis, D. M. and Schnapf, J. L., 1995). When this transient change in current triggered by a photon is 1 pA or higher, it is readily detectable with suction-pipette recording (Baylor, D. A. *et al.*, 1979b). For stimulation with very weak flashes so that no photons are absorbed in a good percentage of the trials, the single-photon response is visible as the elementary unit underlying the quantal fluctuations in the response amplitude (Figure 9(a)). For stimulation with a very weak step of light, the single-photon responses reveal themselves as the sporadic, randomly occurring quantum bumps in the dark current when the light is on (Figure 9(c)). With a dark

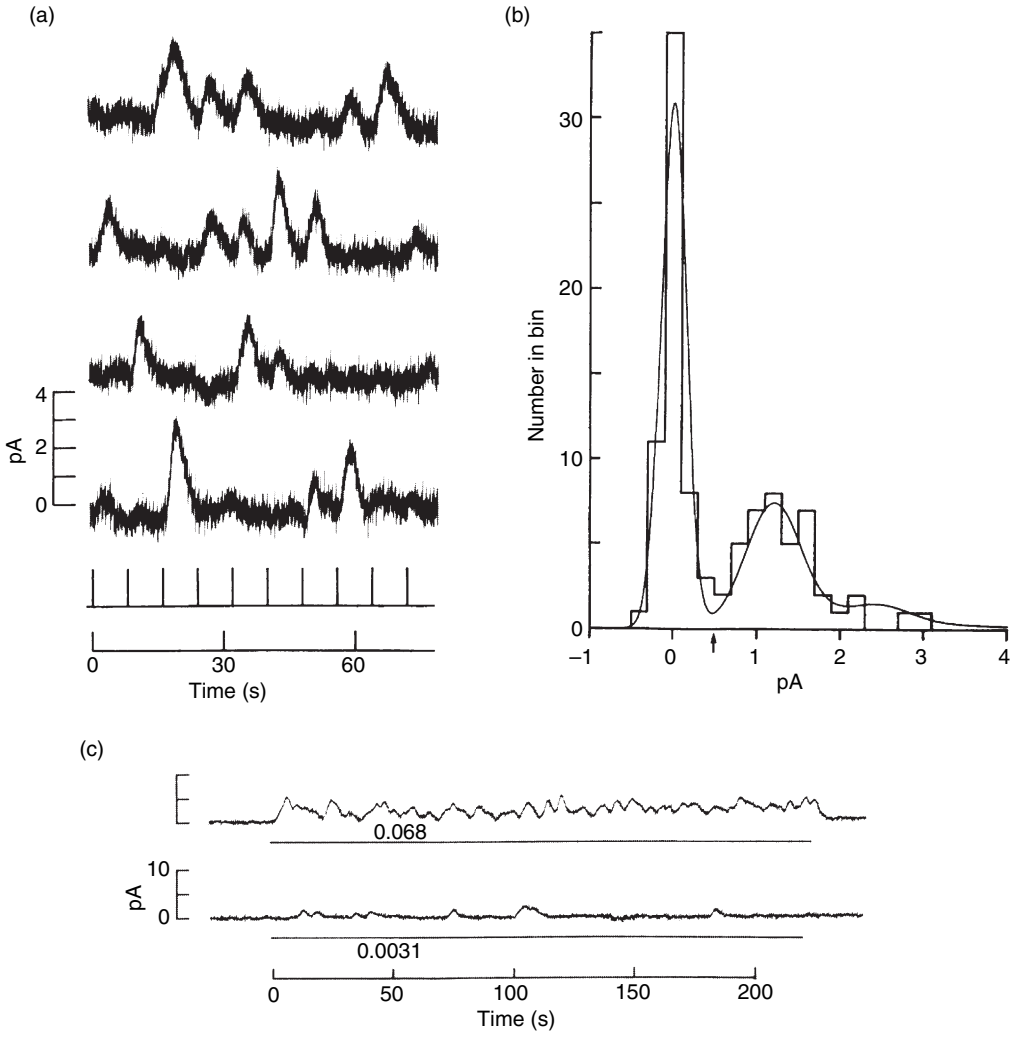

Figure 9 Single-photon responses recorded from toad rods. (a) Quantal fluctuations of a rod's responses to successive identical dim flashes. (b) Response amplitude histogram. The peak centered at 0 represents background noise; the peak centered near 1 pA represents the average response to a single absorbed photon. (c) Responses of a rod to a continuous dim light (timing given by horizontal line) at two different intensities (numbers above lines, in incident photons (500 nm) $\mu m^{-2} s^{-1}$). Reproduced with permission from Baylor, D. A., Lamb, T. D., and Yau, K.-W. 1979b. Responses of retinal rods to single photons. J. Physiol. 288, 613–634.

current in amphibian rods of typically ~20–40 pA, the single-photon response corresponds to about 3% of the maximum light response. In other words, as few as ~30 absorbed photons will elicit a half-maximum response from a rod. This large signal reflects the high amplification of the phototransduction mechanism in rods (see Section 1.10.10).

It was mentioned in Section 1.10.4 that the effect of an absorbed photon does not spread far along the outer segment (Lamb, T. D. *et al.*, 1981). Considering that the single-photon response in rods constitutes ~3% of the saturated response, the physical domain it occupies should be at least 2 μm along a toad or frog outer segment (~60 μm long). This minimum value corresponds to the situation where all dark current within the domain is suppressed (this is essentially the compartment model underlying the described saturating exponential function that fits the instantaneous flash intensity–response relation). The restricted spread is due largely to the tightly packed membranous disks, which constitute a barrier to longitudinal diffusion in the outer segment, thus confining the phototransduction event (Lamb, T. D. *et al.*, 1981). Radial diffusion, on the other hand, is relatively fast, so that phototransduction can be considered to be radially homogeneous (Lamb, T. D. *et al.*, 1981).

It was also mentioned in Section 1.10.4 that, at very low flash intensities, the response rises in direct proportion to (i.e., linearly with) flash intensity. In other words, the single-photon responses sum linearly when there are few of them occurring. It might not be immediately obvious why this linearity should be the case, considering that the phototransduction mechanism is intrinsically nonlinear (see Section 1.10.10). This linear foot is in fact the consequence of the spatially restricted domains occupied by individual single-photon responses. Thus, at very low intensities, when few photons are absorbed in an outer segment, the respective transduction domains are spatially isolated from each other (i.e., nonoverlapping). Consequently, the overall response is simply a linear sum of the responses contributed by the individual domains, hence a linear foot of the intensity–response relation. This linearity is independent of the intrinsic nonlinearities in the phototransduction process within each domain because under this condition it is simply the number of domains that matters. The linearity also makes the Poisson distribution applicable for analyzing the fluctuations in the responses elicited by identical dim flashes (much as what Bernard Katz and colleagues have first used for analyzing quantal release in synaptic transmission; del Castillo, J. and Katz, B., 1954). Essentially, the fluctuations are interpreted to result from the stochastic variations in the number of absorbed photons from flash trial to flash trial. As such, the single-photon response, which is the fundamental (or quantal) unit underlying the stochastic variations, can be evaluated from the ensemble variance/mean ratio of the response amplitude (variance analysis) (Baylor, D. A. *et al.*, 1979b). The advantage of this approach is that it does not require a priori knowledge of the mean number of absorbed photons resulting from a flash. When the probability of even one photon being absorbed in a flash is low, one obtains a response amplitude histogram as shown in Figure 9(b), which reveals the single-photon response as the first nonzero peak (provided that this amplitude is large enough to be well resolved from background noise). The overall amplitude histogram profile also obeys the Poisson distribution.

Within a given cell, the single-photon response is remarkably constant in both amplitude and kinetics from flash trial to flash trial – properties that make rods a very faithful photon counter at low intensities. How this constancy comes about was a question of great interest for years. If a photoactivated rhodopsin molecule is fully inactivated in a single molecular step, its active lifetime should be stochastic, that is, varying from rhodopsin molecule to rhodopsin molecule with an exponentially distributed time about some mean value (as observed, for example, for the open time of single ion-channel molecules with simple open–closed transitions in patch-clamp recordings). Along this line of thought, the amplitude and perhaps also the time course of the single-photon response should in principle vary substantially. The reason why this expected variability of the single-photon response is not observed has recently become better understood. It appears that photoactivated rhodopsin does not inactivate in a single molecular step and also that the time course of the single-photon response is not dominated by the inactivation of rhodopsin (i.e., its dominant time constant is not rhodopsin inactivation; see Section 1.10.10).

Finally, the single-photon response in cones is considerably (25–100 times) smaller than that in rods. This difference reflects a lower amplification in the transduction process in cones (with amplification defined here as the relative peak amplitude of the overall electrical signal triggered by an absorbed photon) (see Section 1.10.14). Most of the difference in sensitivity to incident light between dark-adapted rods and cones in fact comes from a difference in the

transduction amplification rather than in the photon-capturing ability, because the latter parameter is often well within a factor of 10 of each other between rods and cones. With the very small single-photon response in cones, the variance analysis described above is not useful for extracting its amplitude because the variance associated with the stochastic occurrence of quantal events is much smaller than the baseline noise in the dark current. Instead, light calibrations and cone outer-segment dimensions will have to be used for the estimate.

1.10.8 Pigment Noise

A visual-pigment molecule is composed of a protein moiety (opsin) and a covalently linked chromophore, the light-absorbing 11-*cis*-retinaldehyde (11-*cis*-retinal, also referred to as vitamin A_1 chromophore), which is a derivative of vitamin A (Wald, G., 1968; Thompson, D. A. and Gal, A., 2003; Blomhoff, R. and Blomhoff, H. K., 2006). Light acts by isomerizing 11-*cis*-retinal to all-*trans*-retinal, thereby activating the pigment. It takes substantial light energy to isomerize the pigment (Birge, R. R., 1990; Okada, D., *et al.*, 2001), so the latter is very stable in darkness. Nonetheless, simply for the fact that there are 10^8–10^9 pigment molecules in a rod (approximately tenfold fewer in cones), thermal isomerization is expected to occur spontaneously in darkness, albeit infrequently. These thermal events give rise to false signals that introduce noise to the system. Indeed, such events can be detected by suction-pipette recording (Baylor, D. A. *et al.*, 1980). In amphibian rods, the rate of spontaneous isomerization is about one event per minute per cell. Considering the large number of pigment molecules present in a cell, the corresponding rate constant is very low, about 10^{-12}–10^{-11} s^{-1} at room temperature. This gives a half-life of rhodopsin with respect to thermal isomerization of $\sim 10^3$ years at room temperature! Thus, rhodopsin is indeed very stable and ideal for the task of detecting dim light. The rate is not very different in mammalian rods, because, although the total amount of pigment per rod is about tenfold lower, the rate constant of thermal isomerization is about tenfold higher because of the difference in body temperature (room temperature versus 37 °C). Cone pigments, or at least the long-wavelength (red)-sensitive pigment with A_2 chromophore (11-*cis*-dehydroretinal), have a much higher tendency to isomerize thermally (Rieke, F. and Baylor, D. A., 2000; Kefalov, V. *et al.*, 2003). From the functional standpoint, this is not such a serious signal-to-noise problem because cones generally operate in bright light.

Another interesting difference between rod and cone pigments is that rod pigment, once formed from opsin and 11-*cis*-retinal, hardly dissociates except after isomerization of 11-*cis*-retinal to all-*trans*-retinal. Cone pigments, on the other hand, have some tendency to dissociate into opsin and 11-*cis*-retinal even in darkness, that is, without isomerization (Matsumoto, H. *et al.*, 1975; Kefalov, V. *et al.*, 2005). Consequently, a percentage of the pigment in cones appears to lack chromophore in darkness (Kefalov, V. *et al.*, 2005). Again, from the standpoint of photon capture, this may not matter much because cones function in bright light. Nonetheless, one implication of the dark dissociation of cone pigment but not of rhodopsin is that, after intense light, when rhodopsin and cone pigments are both bleached (i.e., the rod and cone opsins have dissociated from the isomerized all-*trans*-retinal), rod opsin will be able to outcompete cone opsin in acquiring free 11-*cis*-retinal recycled in the pigment epithelial cells, which is the primary site of retinoid turnover in the retina. Perhaps for this reason, cones appear to have acquired the ability of obtaining chromophore not just from the retinal pigment epithelium (the common source of 11-*cis*-retinal for both rods and cones) but also from another source apparently only available to cone cells (Mata, N. L. *et al.*, 2002), probably Müller glial cells (see also Section 1.10.10).

What good does it do to cone pigments to be dissociable in darkness? The answer lies perhaps not so much in the dissociation property itself as in the need for rapid recycling of cone pigments because they operate in bright-light conditions. This rapid recycling necessitates rapid dissociation of all-*trans*-retinal from the opsin so that the latter can quickly acquire 11-*cis*-retinal to become functional pigment again. The rapid dissociation of all-*trans*-retinal from cone opsins presumably requires a relatively open or loose chromophore-binding pocket in cone opsins. It is not unreasonable to think that such an open binding pocket unavoidably impacts the stability of the dark pigment as well, hence the dark dissociation. In other words, the molecular design for achieving rapid regeneration of bleached cone pigment may come with a price for the pigment in darkness. By the same token, rod pigment is extremely stable in darkness as discussed above, but apparently at the price of slow regeneration following a bleach.

Besides pigment noise, there is noise from the other steps of the phototransduction signaling cascade. These will be mentioned in Section 1.10.10. The functional implications of noise in light detection are discussed in a different chapter by another author (see Chapter Seeing in the Dark: Retinal Processing and Absolute Visual Threshold).

1.10.9 The cGMP-Gated, Light-Suppressible, Nonselective Cation Channel

The light-suppressible dark current entering the outer segments of rods and cones is now known to go through a nonselective cation channel that is opened (or gated) by cGMP (Fesenko, E. E. *et al.*, 1985; Yau, K.-W. and Nakatani, K., 1985b). When first discovered by Fesenko E. E. *et al.* (1985), the operation of this channel was highly surprising because, up till then, cyclic nucleotides (cAMP and cGMP) had been known (and thought) to act only indirectly on ion channels through cyclic nucleotide-dependent protein kinases. The cGMP-gated channel was thus a major discovery in the general context of ion channels. Even more importantly, the discovery provided a huge impetus to solving the phototransduction mechanism (see Section 1.10.10). Not long afterward, the discovery also helped solve the mechanism of olfactory transduction, which, remarkably, has turned out to involve an analogous signaling cascade and, in particular, a very similar cation channel (with cAMP acting as the second messenger gating the channel in this case) (Nakamura, T. and Gold, G. H., 1987). Rather atypical to ligand-gated channels, the cGMP-gated channel shows no desensitization to cGMP (the ligand). This property may be unusual, but it is functionally critical for phototransduction in rods and cones by allowing the channel to stay open and sustain a dark current in the presence of a steady concentration of free cGMP in the outer segment, and to close only in response to a decrease in the free cGMP concentration caused by light (see Section 1.10.10).

Rods and cones have molecularly distinct cGMP-gated channels, although these have broadly similar functional properties. These channels, together with the cAMP-activated channel mediating olfactory transduction in the olfactory receptor neurons of the nose, constitute the family of *c*yclic *n*ucleotide-*g*ated (CNG) channels (Finn, J. T. *et al.*, 1996; Kaupp, U. B. and Seifert, R., 2002; Craven, K. B. and Zagotta, W. N., 2006). The cGMP and cAMP designations refer only to the native ligand used by the respective cells for controlling the channel, and not to the intrinsic specific sensitivity of the channel to a particular cyclic nucleotide. Indeed, the cAMP-gated channel in olfaction is actually slightly more sensitive to cGMP than to cAMP, although cAMP is the native ligand at least in the nose (Nakamura, T. and Gold, G. H., 1987). The cGMP-gated channels in rods and cones are also sensitive to cAMP, though requiring over 100-fold higher concentrations of cAMP for the same effect.

A large amount of structure–function information is now available about the CNG channels. Briefly, this channel family comprises A (A1–A4) and B (B1 and B3; B2 does not exist in current terminology) subunits (Bradley, J. *et al.*, 2001; 2005). A-subunits can be viewed as principal subunits, and B subunits as accessory or modulatory subunits. When heterologously expressed, A1- to A3-subunits can form homomeric channels that are opened by cyclic nucleotides, but A4, as well as B1 and B3, cannot. The functional channel complex is a tetramer. The rod cGMP-gated channel is composed of three CNGA1 and one CNGB1 subunits (Weitz, D. *et al.*, 2002; Zheng, J. *et al.*, 2002; Zhong, H. *et al.*, 2002), while the cone cGMP-gated channel is reportedly composed of two CNGA3 and two CNGB3 subunits (Peng, C. *et al.*, 2004). The latter finding on the cone channel is rather surprising and perhaps best viewed as tentative, considering the fundamental difference in subunit symmetry from that of the rod channel.

The CNG channels are distant relatives of voltage-gated potassium channels (such as the Shaker K channel superfamily) with six transmembrane domains and a reentry hairpin between the fifth and sixth transmembrane domains forming part of the pore (Figure 10(a)) (for reviews, see Finn, J. T. *et al.*, 1996; Kaupp, U. B. and Seifert, R., 2002; Craven, K. B. and Zagotta, W. N., 2006). Although some of the molecular features of the voltage sensor (the so-called S4 domain) of the K channels are also present in the CNG channels (consisting of evenly spaced, positively charged amino acid residues in the fourth transmembrane domain), this sensor does not have the ability to gate CNG channels with voltage alone, that is, in the absence of cyclic nucleotide. The sensitivity of the CNG channels to cyclic nucleotides is conferred by a consensus cyclic nucleotide-binding site (similar in structure to that found in, for example, the cAMP-dependent protein kinase) situated in the cytoplasmic, C-terminal tail of the protein. With the site on each subunit binding a single cyclic nucleotide molecule, the functional channel complex therefore can bind four cyclic nucleotide molecules.

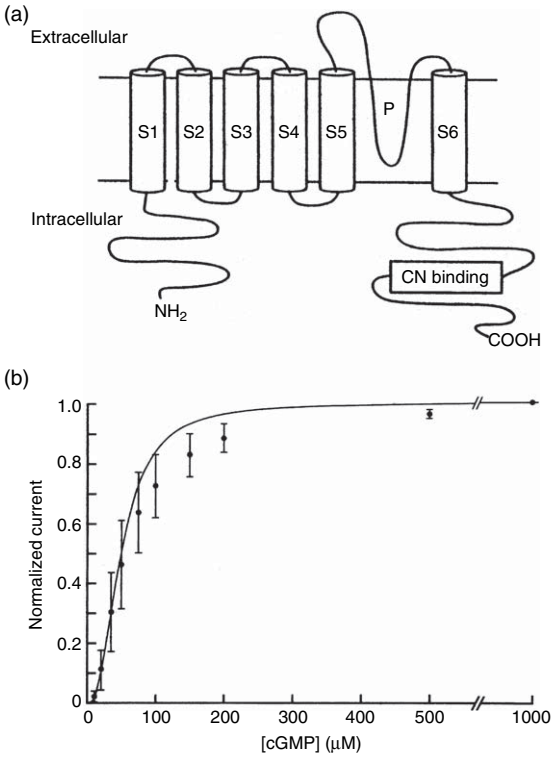

Figure 10 (a) Diagram showing the structure of one *c*yclic *n*ucleotide-*g*ated (CNG) channel subunit. P indicates pore region. "CN binding" indicates cyclic nucleotide-binding domain. (b) Dose–response relation of the rod cGMP-activated channel obtained from the truncated-rod-outer-segment preparation. Smooth curve is the Hill equation, with a coefficient of 2.4. (a) Reproduced with permission from Finn, J. T., Grunwald, M. E., and Yau, K.-W. 1996. Cyclic nucleotide-gated ion channels: an extended family with diverse functions. Annu. Rev. Physiol. 58, 395–426. (b) Reproduced with permission from Nakatani, K. and Yau, K.-W. 1988c. Guanosine 3′,5′-cyclic monophosphate-activated conductance studied in a truncated rod outer segment of the toad. J. Physiol. 731–753.

The channel complex has a very low or negligible probability of opening in the absence of cyclic nucleotide (depending on the particular complex), but the open probability increases dramatically when all, or nearly all, of the four sites are occupied (Picones, A. and Korenbrot, J. I., 1995; Ruiz, M. L. and Karpen, J. W., 1997). These facts explain the observed dose–response relation between channel opening and cyclic nucleotide concentration. For the native rod cGMP channel studied with excised membrane patches from the rod outer segment or with a truncated rod outer segment, this relation has a Hill coefficient of 2–3 (Figure 10(b); Yau, K.-W. and Nakatani, K., 1985b; Nakatani, K. and Yau, K.-W. 1988c). The same is true for the cone cGMP-gated channel (Haynes, L. W. and Yau, K.-W., 1985). The $K_{1/2}$ of activation is around 50 μM cGMP for both the rod and cone channels. There are some variations among studies in the Hill coefficient and the $K_{1/2}$ value for the rod channel (and probably the cone channel as well, although this channel has not been studied as extensively). This variability may be attributed to the channel population under study not being homogeneous, such as phosphorylated versus unphosphorylated (Gordon, S. E. *et al.*, 1992; Molokanova, E. *et al.*, 1997), and so on.

With the truncated-photoreceptor preparation (Figure 3(c)), it is possible to estimate the percentage of cGMP-gated channels that are open in darkness. It turns out that only of the order of 1% of the channels are open in darkness whether in the rod or in the cone, and, of course, this percentage only decreases in the light (Yau, K.-W. and Nakatani, K., 1985b; Nakatani, K. and Yau, K.-W., 1986; 1988c). Because cGMP binds and unbinds randomly and continuously, different channels open and close over time; however, the percentage of open channels stays at ~1% at a given time instant. Why are the channels present in such excess? The answer lies in the fact that, like any binding reaction, the approach to saturated binding is asymptotic (Figure 10(b)). Thus, if there were only as many cGMP-gated channels present on the membrane as the cell needs for sustaining a given dark current, a very high cGMP concentration would be necessary in order for all channels to be open. This scenario would conceivably introduce two problems. One is that a large decrease in free cGMP concentration would have to occur in the light in order for any substantial percentage of the open channels to close. The other is that cGMP is an important signaling messenger in cells, so it is probably inappropriate for the cell to maintain its free concentration beyond a certain level. Moreover, because the steady cGMP level represents a balance between steady synthesis and hydrolysis in darkness, a high steady cGMP concentration would also entail a high rate of steady hydrolysis, which is wasteful. In principle, to offset this, if the channel had a much lower $K_{1/2}$ value (i.e., a higher apparent affinity for cGMP), the required free cGMP concentration could be lowered considerably. However, a much lower $K_{1/2}$ would imply that the cGMP already bound to the channels at light onset would not necessarily dissociate rapidly even when the cytoplasmic free cGMP has decreased, thus making

phototransduction a slow process (Yau, K.-W. and Baylor, D. A., 1989; Yau, K.-W., 1994).

From the ~1% of channels open in darkness, and the dose–response relation mentioned above, the free cGMP concentration in the outer segment can be estimated to be around one to a few micromolar in darkness (Yau, K.-W. and Nakatani, K., 1985b; Nakatani, K. and Yau, K.-W., 1988c). The measured total concentration of cGMP in the outer segment is about 60 μM (Kilbride, P. and Ebrey, T. G., 1979). Thus, most of the cGMP is tightly bound, though not to the channels (see Section 1.10.10).

The cGMP-gated channel is a nonselective cation channel (Yau, K.-W. and Nakatani, K., 1984a; Hodgkin, A. L. *et al.*, 1985), passing not only Na^+ and K^+, but also Ca^{2+}, and perhaps Mg^{2+} (Yau, K.-W. and Nakatani, K., 1985a; Nakatani, K. and Yau, K.-W., 1988b; but see Chen, C. *et al.*, 2003). For the rod channel, 75–80% of the inward dark current at the outer segment is carried by Na^+, and about 15% by Ca^{2+} (Yau, K.-W. and Nakatani, K., 1985a; Nakatani, K. and Yau, K.-W., 1988b). For the cone channel, the percentage of dark current carried by Ca^{2+} may be as much as 30% (Perry, R. J. and McNaughton, P. A., 1991; Ohyama, T. *et al.*, 2000). There is probably not much K^+ efflux through the channel in darkness, but the exact amount is not known. In steady state in darkness, the Na^+ influx is balanced by an equal efflux via the Na^+ pump situated in the inner segment/cell body. The steady Ca^{2+} influx is balanced by an equal efflux at the outer segment via a Na^+/Ca^{2+} exchange mechanism that employs the inward-directing Na^+ electrochemical gradient to extrude Ca^{2+} (Yau, K.-W. and Nakatani, K., 1984b, 1985a; Nakatani, K. and Yau, K.-W., 1988c). Unlike the Na^+/Ca^{2+} exchanger found in most other tissues, the one on retinal photoreceptors also involves a K^+ efflux (Cervetto, L., *et al.*, 1989). Thus, it is really a $Na^+/Ca^{2+},K^+$ exchanger, with a stoichiometry of four Na^+ entering the cell for one Ca^{2+} and one K^+ leaving the cell, giving one net possible charge entering the cell for each Ca^{2+} leaving (Yau, K.-W. and Nakatani, K., 1984b; Cervetto *et al.*, 1989). The implication is that the outward-directing K^+ electrochemical gradient also helps the extrusion of Ca^{2+}. This stoichiometry endows the exchanger with the capability of pumping down the intracellular Ca^{2+} concentration to a very low level, in principle as low as 2 nM (Cervetto *et al.*, 1989), without even the consumption of ATP. The net entry of one positive charge per exchange cycle means that the exchanger is electrogenic, producing an inward membrane current that can be measured (Yau, K.-W. and Nakatani, K., 1984b). This electrogenicity has provided a great impetus to solving the phototransduction mechanism, by providing a convenient monitor of the intracellular free Ca^{2+} concentration (Yau, K.-W. and Nakatani, K., 1985a) (see Section 1.10.10). The steady influx of Na^+ through the cGMP-gated channels and through the $Na^+/Ca^{2+},K^+$ exchanger in darkness necessitates high activity of the Na^+ pump to maintain the Na^+ electrochemical gradient and imposes a heavy metabolic load on the rods and cones. Probably for this reason, there is a high concentration of mitochondria in the inner segment immediately next to the outer segment (Cohen, A. I., 1987; Dowling, J. E., 1987). Incidentally, on a per-gram basis, the retina is a tissue with one of the highest oxygen consumptions in the body – more than that of the brain (Anderson, B. and Saltzman, H. A., 1964; Ames, A., III, 1992).

One interesting property of the rod and cone cGMP-gated channels (and a property of CNG channels in general) is that, apart from being permeable to divalent cations (Ca^{2+} and Mg^{2+}), these channels are subject to partial blockage by them (Haynes, L. W. and Yau, K.-W., 1985; Haynes, L. W. *et al.*, 1986). One consequence of this (kinetically fast) blockage is that, under physiological ionic conditions, the channels have a very small effective single-channel current, which is in the femtoampere (10^{-15} A) instead of picoampere (10^{-12} A) range after low-pass filtering by the membrane time constant (Detwiler, P. B. *et al.*, 1982; Gray, P. and Attwell, D., 1985). This small effective single-channel current means that, for a given dark current (~20–40 pA), many more open channels are recruited (estimated to be 10^4, out of a total channel population of ~10^6 on the outer segment of rods and cones) (Yau, K.-W., 1994). The recruitment of a large number of effectively small open channels instead of a small number of large open channels reduces the quantization noise associated with the random opening and closing of channels in darkness and at the same time increases the reliability of the light signal by reducing its quantization as well (Yau, K.-W. and Baylor, D. A., 1989). With the background noise and the reliability of the signal each improved by the square root of the multiplication factor (100-fold) for the number of underlying channels, the overall signal-to-noise ratio of the light signal is effectively improved by as much as 100-fold. The blockage by external divalent cations also converts a roughly linear current–voltage relation of the cGMP-gated channel in the absence of

divalent cations into one that is highly rectifying. For the rod channel, the resulting current–voltage relation is such that the outward current rapidly increases with increasingly depolarized potentials (outward rectification), but the inward current is almost constant at voltages more negative than −35 mM, which is the physiological range of the membrane potential (Baylor, D. A. and Nunn, B. J., 1986). This flat current–voltage relation (like a constant-current generator) at physiological potentials helps the cell count/report absorbed photons with fidelity. The cone channel is, like the rod channel, outward-rectifying at positive potentials but is inward-rectifying at negative potentials (i.e., increasing inward current with increasing hyperpolarization) (Haynes, L. W. and Yau, K.-W., 1985). The functional benefit of the inward rectification at negative voltages is unclear; it may just be an inevitable feature associated with the higher permeability of the cone channel to divalent cations.

1.10.10 Phototransduction Cascade

The mechanism of phototransduction was a topic of intense dispute in the 1970s and early 1980s, centered on whether Ca^{2+} or cGMP was the true second messenger for the process, and in what manner. These competing ideas had come to be referred to as the Ca^{2+} hypothesis and the cGMP hypothesis, respectively (Miller, W. H., 1981). The dispute was finally settled in the mid-1980s, with the revelation that cGMP is the messenger for transduction and Ca^{2+} the messenger for light adaptation. The key findings leading to this resolution were the discoveries of the cGMP-gated channel (Fesenko, E. E. *et al.*, 1985; Yau, K.-W. and Nakatani, K., 1985b; Nakatani, K. and Yau, K.-W., 1988c) and of a light-induced decrease in the free Ca^{2+} concentration of the outer segment as revealed by the electrogenic $Na^+/Ca^{2+}/K^+$ exchanger (Yau, K.-W. and Nakatani, K., 1985a; Nakatani, K. and Yau, K.-W., 1988b), both entities described in the previous section. The details of the current picture of phototransduction are described below (Figure 11) (Burns, M. E. and Baylor, D. A., 2001; Arshavsky, V. Y. *et al.*, 2002; Chen, C.-K., 2005; Fu, Y. and Yau, K.-W., 2006). The tortuous path leading to the eventual solution of the problem can be found in a personal account (Yau, K.-W., 1994). In what follows, rod phototransduction is the basis for discussion because much more is known about it than about cone transduction. Qualitatively speaking, however, rod and cone transductions are very similar, although most proteins involved have distinct rod and cone isoforms. Some specific and important differences between rod and cone transductions will be briefly described in Section 1.10.14.

As mentioned earlier, a visual pigment is made up of opsin, which is a seven-transmembrane-helix protein and prototypical G-protein-coupled receptor (GPCR), covalently linked to a chromophore, which is 11-*cis*-retinal. Photoisomerization of 11-*cis*-retinal to all-*trans*-retinal unleashes spontaneous conformational changes in the opsin, leading eventually to the formation of the active intermediate, Meta II, within about 1 ms (Kandori, H. *et al.*, 2001). Essentially by diffusion on the disk membrane, Meta II collides and activates (Lamb, T. D., 1994; Calvert, P. D. *et al.*, 2000; Leskov, I. B. *et al.*, 2000) the peripheral membrane protein transducin, a heterotrimeric G protein (G_T, composed of α-, β-, and γ-subunits) with distinct isoforms in rod and cone photoreceptors. Meta II acts by catalyzing the exchange of GTP for GDP in the nucleotide-binding pocket of the α-subunit, $G_{T\alpha}$, and the consequent dissociation of $G_{T\alpha}GTP$ from $G_{T\beta\gamma}G_{T\alpha}GTP$ in turn stimulates a cGMP-phosphodiesterase (cGMP-PDE), another peripheral membrane protein, to increase the hydrolysis of cGMP. This enzyme is composed of two catalytic subunits (PDE$\alpha\beta$ in rods or two PDEα' in cones) and two inhibitory subunits (two PDEγ in rods and two PDEγ' in cones). $G_{T\alpha}GTP$ acts by binding to the inhibitory subunit (with a stoichiometry of one $G_{T\alpha}GTP$ for one PDEγ) and removing its inhibitory influence on a catalytic subunit. The resulting increase in PDE activity lowers the cytoplasmic level of free cGMP, and the cGMP-gated channels therefore close and produce a membrane hyperpolarization as the light response. The high amplification of phototransduction in rods described earlier, which allows these cells to signal single absorbed photons, arises in part from the fact that each rhodopsin molecule has a sufficiently long-lasting Meta-II state before inactivation sets in (see below) to be able to activate successively a substantial number of transducin molecules. Over the years, however, the estimate for the number of transducin molecules activated by one Meta-II molecule during the response has dwindled from an initial high of $\sim 10^3$ to a current number of perhaps 20 in a mouse rod (Krispel, C. M. *et al.*, 2006), still a substantial number nonetheless.

A very useful mathematical formulation, called the Lamb–Pugh model, was developed that very accurately describes the rising phase of the light response (Lamb, T. D. and Pugh, E. N., 1992).

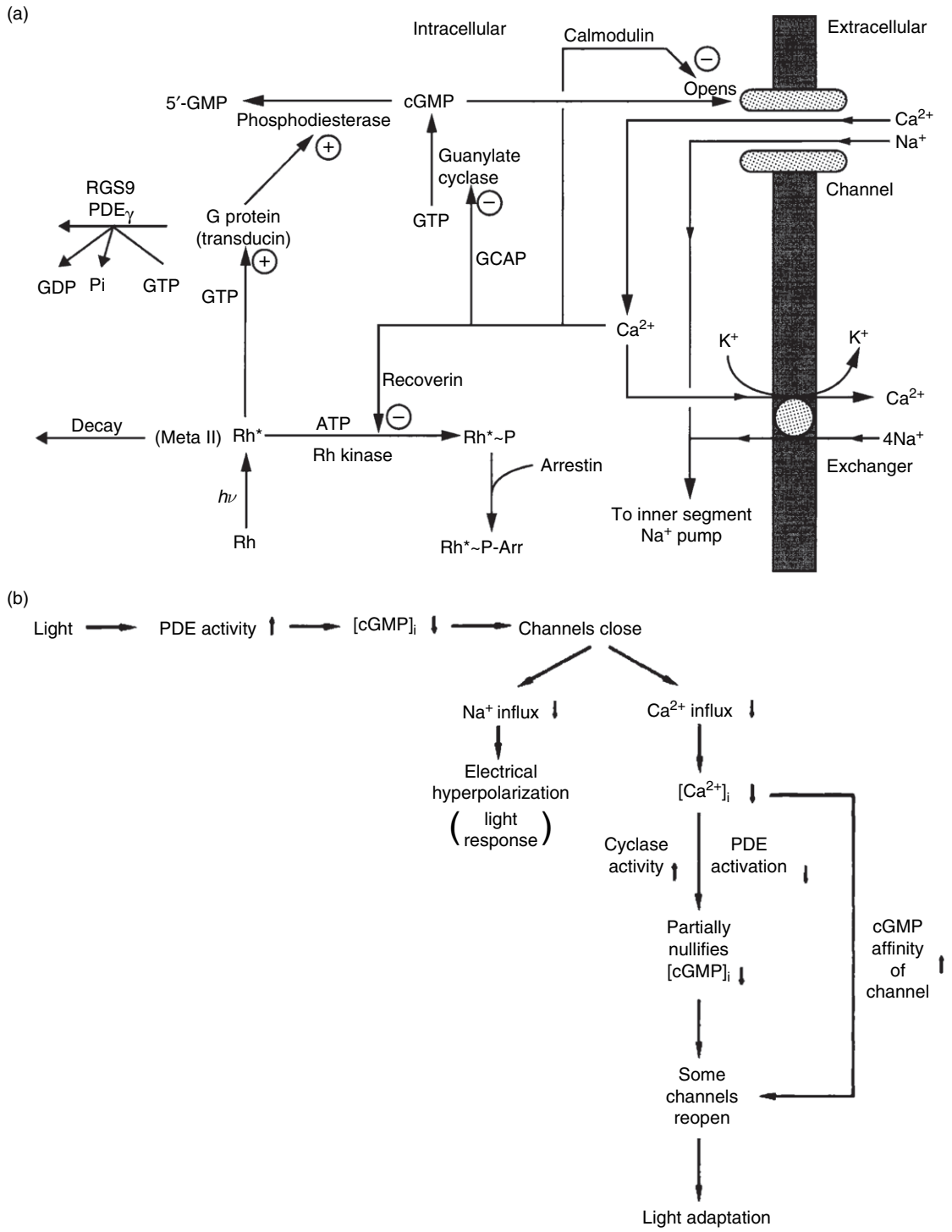

Figure 11 (a) Phototransduction mechanism underlying the light response in rods. GCAP, guanylate cyclase-activating protein; $h\nu$, photon; Rh, rhodopsin; Rh*, photoactivated rhodopsin; Rh*~P, phosphorylated form of rhodopsin; RGS9, regulator of G-protein-signaling isoform 9; PGE_γ, inhibitory (γ) subunit of the phosphodiesterase; +, stimulation or positive modulation; –, inhibition or negative modulation. In addition to RGS9, two other proteins not shown here (RG9P and $G_\beta 5$, see text) are also part of the GTPase-activating protein (GAP) complex. (b) Flow chart showing the sequence of events triggered by light in phototransduction. (a) Adapted with permission from Koutalos, Y. and Yau, K.-W. 1996. Regulation of light sensitivity in retinal rods. Trends in Neurosci. 19, 73–81. (b) Reproduced with permission from Yau, K.-W. 1994. Phototransduction mechanism in retinal rods and cones. The Friedenwald Lecture. Invest. Ophthalmol. Vis. Sci. 35, 10–32.

Ignoring the inactivation steps (see below) and making simplifying assumptions that are valid under most circumstances, the model arrives at the following Gaussian function, with a single free parameter, A, to describe the rising phase of the flash response:

$$F(t) = \exp\left(\frac{-\phi A(t - t_{\text{eff}})^2}{2}\right)$$

where Φ is the flash intensity, A the free parameter called the amplification constant of transduction, t time, and t_{eff} an effective delay time that lumps together several short delays in transduction. Once t_{eff} and A are appropriately chosen, the same value of A can predict a whole family of responses to flashes of different intensities. The parameter A embodies (and is indeed the multiplicative product of) the rate of PDE activation by a photon, the rate constant of cGMP hydrolysis by PDE, and the Hill coefficient of channel activation by cGMP. The above equation is equally applicable to single-cell recordings as to ERG recordings (Breton, M. E. *et al.*, 1994). It is especially useful for comparing the amplification gains of rods and cones from different animal species and also analyzing the light responses of rods and cones in disease conditions of humans or animal models.

The termination of phototransduction requires the inactivation of all active species in the signaling cascade (Burns, M. E. and Baylor, D. A., 2001; Arshavsky, V. Y. *et al.*, 2002; Chen, C.-K., 2005; Fu, Y. and Yau, K.-W., 2006). The shutoff of Meta II involves first the phosphorylation of multiple serine/threonine residues on its cytoplasmic C-terminus by a specific kinase (pigment kinase, which is a member of the GPCR kinase, or GRK, family; rhodopsin kinase is GRK1; see also Section 1.10.14), which partially stops its activity (Chen, J. *et al.*, 1995; Chen, C.-K. *et al.*, 1999; Mendez, A. *et al.*, 2000). This is followed by the binding of a protein called arrestin, also to its C-terminus, to cap the activity of Meta II (Xu, J. *et al.*, 1997). The downstream active species, $G_{T\alpha}GTP$, self-deactivates by its intrinsic GTPase activity, which hydrolyzes the bound GTP to GDP and consequently returns to its inactive $G_{T\alpha}GDP$ state to be ready for activation again after reassociation with $G_{T\beta\gamma}$. The GTPase activity of $G_{T\alpha}GTP$ is weak by itself, but in the native cell, this is enhanced by PDEγ, its substrate, together with a GTPase-activating protein (GAP) complex consisting of RGS9 (regulator of G-protein-signaling isoform 9), $G_{\beta 5}$ (another G protein β-subunit or a G protein β-subunit-like protein), and R9AP (RGS9-anchoring protein) (Tsang, S. H. *et al.*, 1998; Chen, C.-K. *et al.*, 2000; Krispel, C. M. *et al.*, 2003; Keresztes, G. *et al.*, 2004). When transducin deactivates, so does PDE by restoration of the inhibitory activity of PDEγ. The cytoplasmic free cGMP concentration then returns to the dark level because of the ongoing activity of the photoreceptor guanylate cyclase (GC), a cGMP-synthesizing enzyme. The closed cGMP-gated channels thus reopen. In short, as mentioned in a previous section, there is steady cGMP synthesis and hydrolysis in darkness, and a light flash simply transiently tips the balance toward hydrolysis (Hodgkin, A. L. and Nunn, B. J., 1988).

How is the pigment rejuvenated? The inactivated Meta II eventually decays to the intrinsically inactive Meta-III state, which then dissociates into opsin and free all-*trans*-retinal, a process called bleaching because neither component absorbs in the visible spectrum (Wald, G., 1968). Along the way, the opsin also loses its bound arrestin and is dephosphorylated by a generic kinase (protein phosphatase 2A). As for the all-*trans*-retinal, it is reduced to all-*trans*-retinol (-ol stands for alcohol) in the photoreceptor. All-*trans*-retinol diffuses, perhaps helped by the carrier protein IRBP (interphotoreceptor-matrix retinal-binding protein), from the photoreceptor to the pigment epithelial cell, where it is converted into all-*trans*-retinylester, then reisomerized by the isomerohydrolase enzyme RPE65 to 11-*cis*-retinol, and dehydrogenated to 11-*cis*-retinal before returning to the photoreceptor and recombining spontaneously with opsin to form the holopigment once more (Lamb, T. D. and Pugh, E. N., 2004; Jin, M. *et al.*, 2005; Moiseyev, G. *et al.*, 2005; Travis, G. H. *et al.*, 2006). Recently, it has become known that the cone-dominant retinas also possess a chromophore-regeneration mechanism, apparently available specifically to the cones (Mata, N. L. *et al.*, 2002). Presumably, this pathway takes place in the Müller cells, which is known to release the chromophore as 11-*cis*-retinol (Das, S. R. *et al.*, 1992). Cones are also known to be able to take up 11-*cis*-retinol directly, not necessarily just at the outer segment but also at other parts of the cell, and convert it to 11-*cis*-retinal for pigment regeneration (Jones, G. J. *et al.*, 1989). As pointed out in Section 1.10.8, this additional regeneration mechanism may be important in bright light, when cone pigment has to compete with rhodopsin for free 11-*cis*-retinal from the pigment epithelium but, being dissociable, may be outcompeted by the nondissociable rhodopsin acting as a huge sink of 11-*cis*-retinal (Kefalov, V. *et al.*, 2005; Travis, G. H., 2005).

Ca^{2+} has a critical role in active adaptation of the rod or cone to light. As mentioned in Section 1.10.9, there is in darkness a steady Ca^{2+} influx via the cGMP-gated channels and an equal Ca^{2+} efflux via a $Na^+/Ca^{2+},K^+$ exchanger both on the plasma membrane of the outer segment. In the light, the closure of CNG channels stops the Ca^{2+} influx, but the Ca^{2+} efflux through the exchanger continues, draining the free Ca^{2+} concentration in the outer segment. This Ca^{2+} decrease triggers multiple negative-feedback pathways to regulate phototransduction, producing active adaptation to light (Figure 11) (Koutalos, Y. and Yau, K.-W., 1996; Pugh, E. N. *et al.*, 1999). Perhaps the most convincing evidence for Ca^{2+}'s key role in adaptation is that, if Ca^{2+} in the rod outer segment is prevented from changing in the light, all signs of active adaptation disappear (Matthews, H. R. *et al.*, 1988; Nakatani, K. and Yau, K.-W., 1988a). One negative-feedback pathway triggered by the light-induced decrease in Ca^{2+} acts on the GC to enhance its activity, via Ca^{2+}-binding proteins called GC-activating proteins (GCAPs) (Koch, K.-W. and Stryer, L., 1988; Mendez, A. *et al.*, 2001; Burns, M. E. *et al.*, 2002). With no Ca^{2+} bound, the GCAPs facilitate the GC activity; with Ca^{2+} bound, however, the facilitating action of the GCAPs decreases. A second feedback pathway is thought to act, via a Ca^{2+}-binding protein called recoverin (also called S-modulin), on the pigment kinase that phosphorylates Meta II (Kawamura, S. and Murakami, M., 1991; Kawamura, S., 1993; Makino, C. L. *et al.*, 2004). It ultimately scales down the amount of PDE activity activated by a Meta-II molecule, presumably by speeding the phosphorylation of Meta II. A third pathway acts on the cGMP-gated channel, perhaps via Ca^{2+}-calmodulin, which binds to the channel and inhibits its opening by cGMP (Hsu, Y. T. and Molday, R. S., 1993; Chen, T.-Y. *et al.*, 1994; Nakatani, K. *et al.*, 1995). The binding site for the modulator on the rod channel has been localized to the cytoplasmic N-terminus of the single CNGB1 subunit in the channel complex (Grunwald, M. E. *et al.*, 1998; Weitz, D. *et al.*, 1998). Like calmodulin, GCAPs and recoverin are EF-hand-type Ca^{2+}-binding proteins. Of the three Ca^{2+}-mediated regulatory pathways, the one acting on GC is the most important for low and intermediate light levels (Koutalos, Y. *et al.*, 1995; Burns, M. E. *et al.*, 2002), above which the one decreasing PDE activity begins to kick in, becoming increasingly important with still higher light levels (Koutalos, Y. *et al.*, 1995). The regulatory pathway for the gating of the channel, on the other hand, is weak and of minimal importance. The same Ca^{2+} feedbacks exist in cones (Tamura, T. *et al.*, 1991), although the role of the feedback on channel gating and the identity of the Ca^{2+}-binding protein involved are still murky (Rebrik, T. I. and Korenbrot, J. I., 1998). Because cones adapt so much more effectively to light than do rods, there must be some quantitative differences between the two, albeit involving similar mechanisms.

Figure 11(b) provides a flowchart of the sequence of events triggered by light in the photoreceptor.

With the phototransduction mechanism now well understood, comments to several points raised earlier in this chapter are in order.

First, it was mentioned in Section 1.10.8 that there is in darkness a low level of spontaneous pigment isomerization activity, which introduces noise to the light-detection pathway. In addition to this so-called discrete noise (referring to the spontaneous quantum bumps, which are sporadic but large), there is a continuous noise that represents a steady rumble of the dark current (Baylor, D. A. *et al.*, 1980). In principle, this noise can originate either from the synthesizing or from the hydrolytic pathway of cGMP. It now appears that, at least in rods, most of the continuous noise comes from the latter, namely, constitutive rocking of the inhibitory γ-subunits on the catalytic $\alpha\beta$-subunits of the PDE, presumably giving rise to the basal activity of the enzyme (Rieke, F. and Baylor, D. A., 1996). Whether there is, additionally, constitutive transducin activity is still unclear. Nor is it clear whether the basal GC activity is associated with negligible noise. With respect to the cGMP-gated channel, because it has effectively a very small single-channel conductance (owing to the blockage by divalent cations mentioned in Section 1.10.9), the dark current associated with the open channels indeed has low noise, at least after low-pass filtering by the membrane time constant. Recently, it is reported that the PDE in cones is also noisy (Holcman, D. and Korenbrot, J. I., 2005).

Second, it was mentioned in Section 1.10.9 that only ~1% of the total cGMP content in the outer segment is free (Yau, K.-W. and Nakatani, K., 1985b; Nakatani, K. and Yau, K.-W., 1988c). Most of the cGMP turns out to be tightly bound to none other than noncatalytic sites on the catalytic subunits of the PDE, PDE$\alpha\beta$ (Arshavsky, V. Y. *et al.*, 1992). With a holo-PDE concentration of about 30 μM in the rod outer segment, and the PDEα and PDEβ each known to have one noncatalytic cGMP-binding site, just about all of the ~60 μM total cGMP is bound and not freely exchangeable with the cytosolic

cGMP, which is the pool relevant to channel gating. Apparently, the cGMP bound to PDEα and PDEβ acts allosterically on the respective catalytic sites to modulate the hydrolytic activity of the enzyme; the bound cGMP only comes off when the cytosolic cGMP decreases drastically in the light (Arshavsky, V. Y. *et al.*, 1992). Because the free pool of cGMP is very small, and the tight cGMP-binding sites on the PDE do not really function as a buffer, the large excess of unopen cGMP-gated channels in darkness present a potentially unstable situation. Any accidental metabolic surge in cGMP level will greatly increase the number of open channels (owing to the high Hill coefficient of channel activation) and flood the cell with Na^+ and Ca^{2+}, no doubt deleterious to the cell. From this standpoint, the negative-feedback pathways triggered by Ca^{2+} are not only important in the light, but they are equally important in darkness by stabilizing the cGMP level, safeguarding against such dangerous metabolic fluctuations and also helping signaling by reducing background noise (Nakatani, K. and Yau, K.-W., 1988b; Yau, K.-W., 1994; Burns, M. E. *et al.*, 2002).

Third, it was mentioned in Section 1.10.7 that the single-photon response is remarkably stereotypic from flash to flash. Long a puzzle, this observation has recently been intensively studied (Rieke, F. and Baylor, D. A., 1998; Whitlock, G. G. and Lamb, T. D., 1999; Field, G. D. and Rieke, F., 2002; Hamer, R. D. *et al.*, 2003) and may now be finally solved. The constancy of the single-photon response has two aspects: amplitude and duration. With respect to duration, it was long debated whether the decay of the response is dictated by the inactivation of rhodopsin or the deactivation of transducin ($G_{T\alpha}GTP$). It now appears that, at least in the mouse, the deactivation of transducin is in fact the dominant time constant (Krispel, C. M. *et al.*, 2006). Because each rhodopsin molecule activates many (estimated to be ~20) transducin molecules, the averaging over the decays of many transducin molecules can account for the constancy of the decay of the single-photon response (Krispel, C. M. *et al.*, 2006). As for the amplitude, rhodopsin decay is important. Here again, the multiphosphorylation of an active rhodopsin molecule (Mendez, A. *et al.*, 2000; Doan, T. *et al.*, 2006) may provide sufficient averaging to give an overall rather constant single-photon response amplitude.

And fourth, it was mentioned in Kinetics of the Dim-Flash Response that the kinetics of the dim-flash response can be described by a series of four linear stages. Based on the aforementioned, these stages can be schematically assigned as rhodopsin, transducin, phosphodoesterase, and cGMP-gated channel as shown in Figure 6(b). Again, the scheme is symbolic, not meant to be exact kinetically.

Several additional comments are in order. First of all, GPCRs, including visual pigments, have long been implicitly assumed to be monomers. This idea has begun to change in recent years when there is evidence that some synaptic metabotropic receptors are actually dimers (Kubo, Y. and Tateyama, M., 2005). The same appears true for some sensory GPCRs, such as taste receptors (Nelson, G. *et al.*, 2002; Xu, H. *et al.*, 2004). The idea of a monomer held firm for visual pigments, perhaps for the reason that all it takes is one photon to elicit a response. However, the tide is slowly changing even for vision, with some data suggesting that rhodopsin may be a dimer at least under some experimental conditions (Fotiadis, D. *et al.*, 2003; 2006). Strictly speaking, there is no incompatibility between the notion of a rhodopsin dimer and the single-photon response (or, more aptly, a linearity at the foot of the intensity–response relation of the photoreceptor) because all it may require for the rhodopsin dimer to be active is having one or the other rhodopsin monomer member in the dimer to capture a photon and isomerize. The unisomerized rhodopsin in the dimer may function purely as a passive partner, helping out but not physically catalyzing the GTP–GDP exchange.

Also, although the phototransduction process is extremely well understood, there are certain subtleties/-phenomena that remain to be fathomed. For example, although it is now firmly established that a simple imbalance between Ca^{2+} influx and efflux leads to a decline in the free Ca^{2+} concentration in the outer segment in the light, it appears that, under conditions of intense light, there may also be a transient release of Ca^{2+} into the cytosol from binding sites in the outer segment (Matthews, H. R. and Fain, G. L., 2001; 2002; 2003; Cilluffo, M. C. *et al.*, 2004; Leung, Y. T. *et al.*, 2006). The significance of this Ca^{2+} release is still far from clear. Another interesting observation is that mutant zebrafish cones with no functional transducin still have a small ability to produce a transient decrease in the inward current when illuminated with intense light (Brockerhoff, S. E. *et al.*, 2003). This latter point merits further investigation.

Finally, it is fair to say that phototransduction in rods and cones (especially rods) is by far the best-understood G-protein-mediated signaling pathway in the body. In fact, the advances in this field have often been used for understanding other G-protein signaling pathways. For

example, the high amplification of the rod transduction pathway – namely, a single active GPCR molecule in turn would activate a large number of downstream G-protein molecules – has been widely considered to be a dogma that applies to G-protein signaling in general. However, this generalization may not be too valid. In particular, recent work has indicated that an odorant receptor in the olfactory system, upon becoming active by binding a cognate ligand, has a very low probability of activating even a single G-protein molecule downstream (Bhandawat, V. *et al.*, 2005). Thus, most binding events are inconsequential. The reason is simple – namely, the ligand typically stays on the receptor for such a brief period that the receptor complex has scarcely little opportunity to encounter and activate even one G-protein molecule. Also, phosphorylation is unlikely the canonical deactivation mechanism for odorant receptors at the level of single-odorant-molecule binding, except possibly in the case of intense and prolonged stimulation (Bhandawat, V. *et al.*, 2005). Phototransduction is unique in that a photon disappears once absorbed by a pigment molecule. At the same time, the active Meta-II state of the rod or cone pigment remains essentially active continuously until inactivation by phosphorylation and arrestin-binding (the actual decay of Meta II to inactive Meta III is slow by comparison). With too little known quantitatively about the other GPCR pathways besides olfaction at present, it is too early to tell what (though most likely low) percentage of these pathways share the high amplification found in vision.

1.10.11 Background-Light Adaptation

Background-light adaptation is adaptation of the photoreceptor to a steady light – light that induces a significant response but not so bright that a substantial fraction of the pigment on the cell is bleached. The manifestation of background-light adaptation is a relaxation of the response to a steady light from a transient peak to a lower level soon after the onset of light (Figure 5(a)). As mentioned in Section 1.10.4, the step intensity–response relation reflects the development of background adaptation with time. At very early times after light onset, little or no adaptation is evident, with the instantaneous intensity–response relation following closely the saturating exponential function introduced in Section 1.10.4. At the transient peak of the response, however, the relation already deviates from this function, and it becomes progressively less steep at later times. At the plateau level, the relation shows a slow logarithmic rise (Nakatani, K. *et al.*, 1991).

A standard characterization of background-light adaptation is obtained by superposing incremental flashes on a steady background light in what is often called an increment-threshold experiment. In the presence of background light, the responses to incremental flashes show both a lower sensitivity and a shorter time-to-peak than those in darkness (i.e., without background light), with the shorter time-to-peak reflecting the increase in dominance of the inactivation of the response, which cuts into the rising phase at progressively earlier times (Baylor, D. A. *et al.*, 1979a; 1980). The dependence of flash sensitivity on background-light intensity is well described by the Weber–Fechner relation, $S_F = S_F^D I_o/(I_B + I_o)$, where S_F^D is flash sensitivity in the absence of background light, S_F flash sensitivity in the presence of background light with intensity I_B, and I_o a constant corresponding to the value of I_B that reduces S_F^D by half (Figure 12). This relation says that, for large I_B, $S_F \propto I_B^{-1}$. In vision, the significance of the $S_F \propto I_B^{-1}$ relation is that it allows the contrast sensitivity (i.e., the perception of light–dark contrast) to be independent of the ambient light intensity (Shapley, R. and Enroth-Cugell, C., 1984).

Mathematically, the plot of incremental flash sensitivity (the reciprocal of threshold) against background-light intensity is (approximately, by assuming no

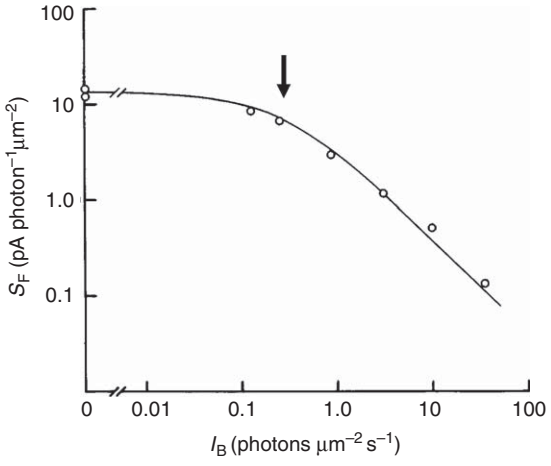

Figure 12 Incremental-flash-on-background-light experiment from a toad rod. Plot shows the dependence of flash sensitivity on background light intensity. Smooth curve is $S_F \propto 1/(I_B + I_o)$, with $I_o = 0.28$ photons (500 nm) μm^{-2} s^{-1} (arrow). Reproduced with permission from Baylor, D. J. A., Matthews, G., and Yau, K.-W. 1980. Two components of electrical dark noise in toad retinal rod outer segments. J. Physiol. 309, 591–621.

change in kinetics) nothing more than a plot of the slope of the step intensity–response relation at the plateau of the response against the steady-light intensity. Thus, the derivative of the saturating exponential function, $[1-\exp(-I_S/\rho)]$, introduced in Section 1.10.4 has the form $\exp(-I_S/\rho)$, which indeed describes the sensitivity-versus-background-intensity relation in the case of no active background adaptation (Matthews, H. R. *et al.*, 1988). Conversely, the integrated form of the Weber–Fechner relation, $\log_e(I+I_o)$ should fit the step intensity–response relation in the plateau phase of the response, which, as pointed out earlier, is roughly the case as well (Nakatani, K. *et al.*, 1991).

Like the Michaelis equation, the Weber–Fechner relation is mathematically simple, but, as in the case of the Michaelis equation, this just happens to be an approximately good fit. The underlying cellular mechanisms that give rise to the experimental observations are in fact quite complex, involving multiple active negative-feedback mechanisms mediated by a decrease in intracellular Ca^{2+} concentration during steady light, together with passive mechanisms such as the progressive saturation of the response and the basal phosphodiesterase activity in the presence of steady background light being already much higher than in darkness (Tamura, T. *et al.*, 1991; Koutalos, Y. *et al.*, 1995; Nikonov, S. *et al.*, 2000).

It had been thought for a long time that mammalian rods, unlike amphibian rods, do not adapt to background light. However, this is now known not to be the case (Tamura, T. *et al.*, 1989; Nakatani, K. *et al.*, 1991; Matthews, H. R., 1991; Tamura, T. *et al.*, 1991). Indeed, as a first approximation, mammalian and amphibian rods behave rather similarly (Nakatani, K. *et al.*, 1991). Moreover, the adaptation behavior of rods of the bush baby (galago), a strictly nocturnal primate, is very similar to that of the rods of the rhesus monkey, a diurnal primate (Tamura, T. *et al.*, 1991). Thus, it is as if the performance of rods were already optimized, and, when a natural habitat involves a broader range of light intensities, an animal simply adds cones of various extents to their retina. Finally, cones adapt to background light much more dramatically than rods, but the trigger is still Ca^{2+} (Nakatani, K. and Yau, K.-W., 1988a; Matthews, H. R. *et al.*, 1990).

1.10.12 Bleaching Adaptation

Bleaching adaptation is the desensitization that occurs in photoreceptors after a significant fraction of their pigment has been bleached by bright light. The physiological changes in photoreceptors induced by bleaching adaptation closely resemble those caused by background adaptation, discussed in Section 1.10.11 (Blakemore, C. B. and Rushton W. A. 1965; Cornwall, M. C. *et al.*, 1990). The bleaching of visual pigment by light is one mechanism by which photoreceptors change their sensitivity to bright illumination. During bleaching adaptation, the reduced level of photopigment decreases the probability of photon absorption, thus lowering photoreceptor sensitivity and increasing the range of light intensities to which the cell can respond. This loss of quantum catch is especially important for cones, which remain responsive in light bright enough to bleach up to 10^6 pigment molecules s^{-1} (Schnapf, J. L. *et al.*, 1990). Rods, in contrast, saturate in relatively dim backgrounds of less than 15 000 photons $rod^{-1}\,s^{-1}$ (Williams, T. P. *et al.*, 1998). Exposure of rods to still brighter light triggers another form of adaptation associated with the redistributions of transducin and arrestin in the photoreceptor that reduce the overall activity of the phototransduction cascade (see below).

An important feature of bleaching adaptation is that the observed decrease in sensitivity is much greater than would be expected simply from the decrease in the probability of photon capture due to reduced pigment content, either in situ in the retina (Campbell, F. W. and Rushton, W. A., 1955) or in isolated photoreceptors (Pepperberg, D. R. *et al.*, 1978; reviewed in Fain, G. L. *et al.*, 1996). It now appears that a large part of the decrease in sensitivity caused by bleaching actually comes from a finite, albeit weak, activity of opsin to activate the transduction process. This activity of free opsin has been demonstrated both in vitro (Okada, D. *et al.*, 1989; Surya, A. *et al.*, 1995) and in intact photoreceptors (Cornwall, M. C. and Fain, G. L., 1994; Fain, G. L. *et al.*, 2001). On a per-molecule basis, opsin has a very low ability to activate transduction, equivalent to 10^{-5}–10^{-7} that of Meta II (Cornwall, M. C. and Fain, G. L., 1994; Cornwall, M. C. *et al.*, 1995). However, in aggregate, the overall activity can still be substantial, especially if the percentage of bleached (bare) opsin is significant (say, 10% or more). This constitutive activity acts like steady background light to produce adaptation of the cell. The resulting desensitization is persistent in isolated photoreceptors, which have little 11-*cis*-retinal in them, and can only be reversed by the application of exogenous chromophore. The use of exogenous chromophore has also allowed the investigation of how, in the course of pigment regeneration, the initial noncovalent binding of

11-*cis*-retinal to opsin may affect the function of rods and cones. Interestingly, it is found that the initial bindings, noncovalently, of chromophore to rod and cone opsins have opposite effects (Kefalov, V. *et al.*, 2001). In rods, the constitutive activity of opsin is roughly doubled when chromophore binds noncovalently, whereas, in cones, noncovalent binding of chromophore already quenches free cone opsin activity completely (Kefalov, V. *et al.*, 2001). This property allows cones to recover from bleaching adaptation even faster than the actual regeneration of their pigment. In contrast, rod recovery from a bleach is delayed by the transient activation of opsin by noncovalently linked retinal.

The molecular mechanisms of some visual disorders can also be linked to the constitutive activity of mutant opsin similar in effect to bleaching adaptation. This idea, originally proposed by Fain G. L. and Lisman J. E. (1993), was recently confirmed by expressing in *Xenopus* rods mutant opsins with such a property that is linked to congenital night blindness (Jin, S. *et al.*, 2003).

Finally, early immunocytochemistry has suggested that $G_{T\alpha}$ can translocate from the outer segment to the inner segment of rods under light-adapted conditions (Brann, M. R. and Cohen, L. V., 1987). This phenomenon has been verified in recent years (Sokolov, M. *et al.*, 2002). Exposure to bright light induces translocation, of not only rod $G_{T\alpha}$ but also $GT_{\beta\gamma}$, out of the rod outer segment. Besides transducin, arrestin also translocates, but in the opposite direction, namely, to the outer segment from the rest of the cell. The idea has been proposed (Sokolov, M. *et al.*, 2002) that this en-mess translocation of transduction proteins serves the purpose of shutting down transduction – kind of an extreme form of light adaptation. However, the translocation can also be thought of as a protective mechanism against some forms of photodamage. The mechanisms by which the translocation occurs are still not understood. Two alternative proposals include passive diffusion driven by concentration gradients along the cell or active transport involving molecular motors (reviewed in Calvert, P. D. *et al.*, 2006). An interesting feature of transducin translocation is that there appears to be a steep threshold of light intensity below which transducin movement does not occur but above which massive translocation of transducin is observed (Sokolov, M. *et al.*, 2002). One possible explanation is that this threshold corresponds to the point where the ability of the cell to rapidly inactivate transducin becomes exhausted (Kerov, V. *et al.*, 2005).

1.10.13 Dark Adaptation

The recovery of sensitivity driven by pigment regeneration following bleaching is called dark adaptation. In order for dark adaptation to occur, the photoactivated pigment has to decay and the resulting free opsin has to regenerate with a fresh molecule of 11-*cis*-retinal supplied by the pigment epithelium. The so-called retinoid cycle involved in this process is complex, with some details only recently worked out. Because a large part of this process takes place in the pigment epithelium, dark adaptation is somewhat beyond the scope of this chapter. Recent reviews can be found elsewhere (Saari, J. C. 2000; Lamb, T. D. and Pugh, E. N., 2004).

1.10.14 Differences between Rods and Cones

As mentioned above, cones have a much lower sensitivity to light and faster response kinetics than rods, and they also adapt to light much more effectively. The mechanisms underlying these rod–cone differences in the context of a common phototransduction process are still an area of active research. It might be pointed out here that most, though not all, of the proteins involved in transduction have distinct isoforms in rods and cones, so some quantitative differences in the process between them are not surprising.

Considering that the activation of the visual pigment by light constitutes the first step of phototransduction, it is naturally the first place for scrutiny. One possible mechanism for the lower sensitivity and faster response kinetics of cones would be the well-known, significantly faster decay of the active Meta-II state of cone pigments. However, a direct comparison of the signaling properties of rod and cone pigments side by side in the same photoreceptor from transgenic animals has demonstrated that this is not the case (Kefalov, V. *et al.*, 2003). Thus, when expressed in rods, a cone pigment produces rod-like responses. By the same token, rhodopsin expressed in cones produces cone-like responses. The implication of this observation is that the decay of Meta II is not rate-limiting for the inactivation of pigment in intact cells, at least in dark-adapted conditions. Instead, the pigment is rapidly inactivated by rhodopsin kinase and arrestin. It is still possible, especially in cones, that the ability of the cell to inactivate the pigment will saturate under intense light,

rendering Meta-II decay dominant for the shutoff of the response. Because cone Meta II decays within several seconds (Wald, G. *et al.*, 1955; Okada, T. *et al.*, 1994), this will still allow cones to recover quickly from bright light. In rods, on the other hand, Meta II decays much more slowly and exists in equilibrium with the physiologically inactive Meta-III state (Heck, M. *et al.*, 2003), which has a lifetime of minutes and therefore rate-limits the overall recovery of rods from a bright bleaching light (Kolesnikov, A. V. *et al.*, 2003). Thus, while the visual pigments appear to play little role in the difference in light response properties between rods and cones in darkness or low light, this may not be the case in very bright light. In addition, cone pigments regenerate significantly more rapidly than rod pigments (Wald, G. *et al.*, 1955). Finally, as discussed in Section 1.10.8, the higher rate of thermal activation of red cone pigment compared to rhodopsin, as well as their dissociability, contributes to the lower sensitivity of red cones.

The visual pigments in both rods and cones are inactivated by phosphorylation by pigment kinase, or GRK, and the subsequent binding of arrestin. GRK exists as the rod-dominant GRK1 and the cone-dominant or cone-exclusive GRK7 (Ohguro, H. *et al.*, 1995; Tachibanaki, S. *et al.*, 2001; Weiss, E. R. *et al.*, 2001). The specific activity of GRK7 is over 10 times higher than that of GRK1 (Tachibanaki, S. *et al.*, 2005; Tachibanaki, S. *et al.*, 2007), implying a potentially faster cone pigment inactivation. In addition, in fish, the expression level of pigment kinase is tenfold higher in cones than in rods (Tachibanaki, S. *et al.*, 2005). The mouse represents an interesting and unusual case in that its rods and cones both express only GRK1 (Weiss, E. R. *et al.*, 2001). This simplicity has allowed the use of GRK1$^{-/-}$ mice, originally generated to investigate the role of phosphorylation in the shutoff of rod pigment (Chen, C.-K. *et al.*, 1999), to demonstrate that phosphorylation is also required for the proper inactivation of cone pigment (Lyubarsky, A. L. *et al.*, 2000). The same is true for GRK7 (Rinner, O. *et al.*, 2005). Rod arrestin is also shared between mouse rods and cones (Zhu, X. *et al.*, 2005). Interestingly however, the deletion of rod arrestin produces a dramatic delay in the shutoff of the rod response (Xu, J. *et al.*, 1997) but has no effect on the cone response (Lyubarsky, A. L. *et al.*, 2000). One possible explanation is that cone pigment is inactivated by a different, cone-specific arrestin identified recently (Zhu, X. *et al.*, 2002).

It is interesting that the RGS9 protein in the GAP complex involved in the deactivation of transducin is also present in much higher concentration in cones than in rods (Cowan, C. W. *et al.*, 1998; Zhang, X. *et al.*, 2003).

There are two isoforms of GC, GC1 and GC2, and two isoforms of GCAPs, GCAP1 and GCAP2 (each GCAP acts on both GCs). These proteins are present in both mouse rods and cones, although, more generally, the relative distributions of these proteins in rods versus cones, as well as the efficiencies of regulation of the cyclases by the GCAPs, appear to vary across species (reviewed by Gorczyca, W. A. and Sokal, I., 2002). The functional significance of the presence of two distinct isoforms of GCs and GCAPs in rod and cone photoreceptors is not presently understood, because their overall properties are not greatly different.

As discussed in Section 1.10.10, phototransduction in both rods and cones is subject to modulation by Ca^{2+}. During light, Ca^{2+} is extruded more rapidly from the cone outer segment than from the rod outer segment, at least partly because the much larger surface-to-volume ratio of the cone outer segment (Nakatani, K. and Yau, K.-W., 1989). The range of Ca^{2+} concentration change between darkness and light appears larger in cones than in rods (Sampath, A. P. *et al.*, 1999), possibly because of the higher fraction of dark current carried by Ca^{2+} (see Section 1.10.9) and the higher efficiency of the cone $Na^{+}/Ca^{2+},K^{+}$ exchanger NCKX2 compared to the rod exchanger NCKX1 (Korenbrot, J. I., 1995; Prinsen, C. F. *et al.*, 2000; Sheng, J. Z. *et al.*, 2000). Incidentally, the much larger surface area of the cone outer segment also speeds the release of all-*trans*-retinol from cones compared to rods following bleaching (Ala-Laurila, P. *et al.*, 2006).

1.10.15 Diseases

Rods and cones can be severely compromised by a variety of disease conditions, genetic or otherwise, that lead to their dysfunction or irreversible degeneration, causing a partial or complete loss of vision. In the past decade or two, tremendous advances have taken place in the understanding of many of these diseases, thanks to the revelations of the cellular and molecular details of rod and cone phototransductions. Because of the intimate relationship between the retinal pigment epithelium and the photoreceptors, the degeneration of the photoreceptors will also occur when the pigment epithelium malfunctions. Table 1 provides a fairly comprehensive list of the human diseases caused

Table 1 Photoreceptor's dysfunction resulting from gene mutations

Disease	*Symptom*	*Gene location*	*Protein*	*Reference*
Recessive retinitis pigmentosa	Retinal degeneration	3q22.1	Rhodopsin	Dryja, T. P. *et al.* (1990); Berson, E. L. (1993); Hartong, D. T. *et al.* (2006)
		4p16.3	Rod PDEβ (PDE6B)	Bowes, C. *et al.* (1990)
		4p12	CNGA1	Dryja, T. P. *et al.* (1995); Griffin, C. A. *et al.* (1993)
		16q13	CNGB1	Ardell, M. D. *et al.* (2000); Bareil, C. *et al.* (2001)
		5q33.1	Rod PDEα (PDE6A)	Dryja, T. P. *et al.* (1999); Pittler, S. J. *et al.* (1990)
		10q23.1	RPE-retinal G protein-coupled receptor (RGR)	Morimura, H. *et al.* (1999)
		4q32.1	Lecithin retinol acyltransferase (LRAT)	Ruiz, A. *et al.* (2001)
Dominant retinitis pigmentosa	Retinal degeneration	6p21.1	GCAP2	Sato, M. *et al.* (2005); Payne, A. M. *et al.* (1999)
Nougaret	Severe reduction in rod sensitivity, with mild reduction in cone sensitivity	3p21.31	Rod Tα (GNAT1)	Dryja, T. P. *et al.* (1996)
Oguchi	A stationary type of night blindness characterized by slow dark adaptation, the absence of visual loss	2q37.1	Rod arrestin	Fuchs, S. *et al.* (1995); Maw, M. A. *et al.* (1995)
		13q34	Rhodopsin kinase (GRK1)	Yamamoto, S. *et al.* (1997)
Dominant cone dystrophy	Progressive degeneration of cone photoreceptors, loss of visual acuity and color vision, and photophobia	6p21.1	GCAP1	Sokal, I. *et al.* (1998); Payne, A. M. *et al.* (1998)
Leber congenital amaurosis	Retinal degeneration	1p31.2	Retinal pigment epithelium-specific 65-kDa protein (RPE65)	Perrault, I. *et al.* (1999); Gu, S. *et al.* (1997); Marlhens, F. *et al.* (1997)
		17p13.1	GC1	Perrault, I. *et al.* (1996); Camuzat, A. *et al.* (1995)
Recessive achromatopsia	Color blindness	1p13.3	Cone Tα (GNAT2)	Aligianis, I. A. *et al.* (2002); Kohl, S. *et al.* (2002)
		8q21.3	CNGB3	Winick, J. D. *et al.* (1999); Milunsky, A. *et al.* (1999)
		2q11.2	CNGA3	Arbour, N. C. *et al.* (1997); Kohl, S. *et al.* (1998); Wissinger, B. *et al.* (1998)
Bradyopsia	Reduced ability to see moving objects with low contrast	17q24.1	RGS9	Nishiguchi, K. M. *et al.* (2004)
		19q13.12	R9AP	Nishiguchi, K. M. *et al.* (2004)
Recessive Stargardt disease	Age-related macular degeneration	1p22.1	ATP-binding cassette transporter (ABCR)	Allikmets, R. *et al.* (1997)
Fundus albipunctatus	Stationary night blindness	12q13.2	(11-*cis*-retinol dehydrogenase) RDH1 and 5	Cideciyan, A. V. *et al.* (2000); Nakamura, M. *et al.* (2000); Simon, A. *et al.* (1996); Yamamoto, H. *et al.* (1999)
Best's disease	Degeneration of the retinal fovea	11q13	Bestrophin	Marquardt, A. *et al.* (1998); Petrukhin, K. *et al.* (1998)

Refer to RetNet (see 'Relevant website') for a more complete database of retinal disease.

by mutations in known proteins in rods, cones, or the retinal pigment epithelium, along with their symptoms (for a complete list, see RetNet ('Relevant website' section)). The last one on the list, Best's disease, is caused by a protein named bestrophin, which recently has been found to be a hitherto unknown Ca^{2+}-activated chloride channel presumably involved in the transport function of the retinal pigment epithelium (Sun, S. *et al.*, 2002; Tsunenari, T. *et al.*, 2003; 2006). Because the fovea is so critical for everyday vision, any disease affecting this retinal region is particularly incapacitating to the patient.

1.10.16 Parietal-Eye Photoreceptor in Lizards and a Possible Evolutionary Linkage to Rods and Cones

The parietal (third) eye is quite unique to lizards (there is an analogous structure in amphibians called the frontal organ). It is situated on the forehead, in between the two regular (lateral) eyes. The exact function of this eye is still not entirely clear. The best suggestion so far is that it informs the animal about the passage of time in the course of the day by registering changes in the wavelength spectrum of the ambient light as the day progresses (Solessio, E. and Engbretson, G. A., 1993).

It resembles the two lateral eyes by having a cornea, a lens, and a retina (Eakin, R. M., 1973). The retina, however, has only photoreceptors, ganglion cells, and glial cells (i.e., no bipolar, horizontal, and amacrine cells). It is also opposite in orientation to the lateral-eye retina in that the photoreceptors face the front of the eye and are therefore the first neurons in the retina to encounter light. The photoreceptors have a well-formed outer segment, with orderly stacked disks. Electron microscopy indicates that the disks, like those in cones, are continuous with the plasma membrane (Eakin, R. M., 1973).

One very unusual feature of the parietal-eye photoreceptor is that each cell expresses two pigments (Su, C.-Y. *et al.*, 2006): the blue-sensitive pinopsin, first found in the light-sensitive chicken pineal gland (Okano, T. *et al.*, 1994; Max, M. *et al.*, 1995), and the green-sensitive parietopsin, an apparently ancient pigment not found in the lateral eyes. The coexistence of two pigments in a single cell fits with the physiology, which involves two antagonistic, cGMP-mediated phototransduction pathways in the same cell (Solessio, E. and Engbretson, G. A., 1993; Finn, J. T. *et al.*, 1997; Xiong, W.-H. *et al.*, 1998). One of these, best activated by blue light, is identical to that in rods and cones, consisting of cGMP-PDE stimulation, a decrease in cGMP concentration, closure of CNG channels, and a membrane hyperpolarization. The other, best activated by green light, consists of inhibition of the same PDE, an increase in cGMP concentration, opening of CNG channels, and a membrane depolarization. Thus, it appears that pinopsin activates the hyperpolarizing pathway and parietopsin the depolarizing pathway. Interestingly, transducin is not present in these cells. Instead, gustducin appears to take its role, coupling to pinopsin (Su, C.-Y. *et al.*, 2006). Although gustducin is not found in any other photoreceptor, it is nonetheless a close relative of transducin, with a similar protein sequence and function (McLaughlin, S. K. *et al.*, 1992; Hoon, M. A. *et al.*, 1995; He, W. *et al.*, 2002). G_o, on the other hand, appears to couple to parietopsin. G_o is more different from transducin and gustducin, although still belonging to the same subfamily of G proteins.

In vertebrates, the involvement of G_o in phototransduction is unique to the parietal-eye photoreceptor. However, in invertebrates, there is precedent for its involvement in vision, notably in the scallop hyperpolarizing photoreceptor, which is also of the ciliary type (i.e., with the photosensitive structure derived from a modified cilium) as rods, cones, pineal photoreceptors, and parietal photoreceptors. In this scallop photoreceptor, G_o is coupled to SCOP2, an apparently ancient pigment, to activate a cGMP-signaling pathway analogous, though not identical, to that in rods and cones (Kojima, D. *et al.*, 1997; Gomez, M. P. and Nasi, E., 2000). Thus, all evidence suggests that a G_o-mediated phototransduction pathway is ancient among ciliary photoreceptors. As such, the parietal-eye photoreceptor appears to be a living predecessor of rods and cones – a missing link between rods/cones and primitive ciliary photoreceptors. The notion is that a G_o-mediated phototransduction pathway existed in ciliary photoreceptors long ago, before vertebrates evolved from invertebrates. This pathway was retained in early vertebrates. In the course of evolution, however, a chromatically antagonistic, gustducin/transducin-mediated phototransduction pathway was added to the cells with the G_o-mediated pathway for the purpose of analyzing spectral information. This chromatic antagonism is retained by the parietal-eye photoreceptor to the present day. In parallel during evolution, the lateral eyes made their appearance over time but retained only the more recent gustducin/transducin-mediated pathway,

delegating the color opponency instead to downstream neurons – a good strategy because complex processing of color information is best provided by elaborate synaptic circuitry. As such, the chromatic opponency within a single parietal-eye photoreceptor represents a very primitive, simple form of color vision compared to, say, what goes on in the lateral-eye retina.

Incidentally, the parietal eye, like the two lateral eyes, develops as a protrusion of the diencephalon of the brain during embryogenesis (Eakin, R. M., 1973).

References

Accili, E. A., Proenza, C., Baruscotti, M., and DiFrancesco, D. 2002. From funny current to HCN channels: 20 years of excitation. News Physiol. Sci. 17, 32–37.

Ala-Laurila, P., Kolesniko, A. V., Crouch, R. K., Tsina, E., Shukolyukov, S. A., Govardovskii, V. I., Koutalos, Y., Wiggert, B., Estevez, M. E., and Cornwall, M. C. 2006. Visual cycle: Dependence of retinol production and removal on photoproduct decay and cell morphology. J. Gen. Physiol. 128, 153–169.

Aligianis, I. A., Forshew, T., Johnson, S., Michaelides, M., Johnson, C. A., Trembath, R. C., Hunt, D. M., Moore, A. T., and Maher, E. R. 2002. Mapping of a novel locus for achromatopsia (ACHM4) to 1p and identification of a germline mutation in the alpha subunit of cone transducin (GNAT2). J. Med. Genet. 39, 656–660.

Allikmets, R., Shroyer, N. F., Singh, N., Seddon, J. M., Lewis, R. A., Bernstein, P. S., Peiffer, A., Zabriskie, N. A., Li, Y., Hutchinson, A., Dean, M., Lupski, J. R., and Leppert, M. 1997. Mutation of the Stargardt disease gene (ABCR) in age-related macular degeneration. Science 277, 1805–1807.

Ames, A., III 1992. Energy requirements of CNS cells as related to their function and to their vulnerability to ischemia: a commentary based on studies on retina. Can. J. Physiol. Pharmacol. 70(Suppl.), S158–S164.

Anderson, B. and Saltzman, H. A. 1964. Retinal oxygen utilization measured by hyperbaric blackout. Arch. Ophthalmol. 72, 792–795.

Arbour, N. C., Zlotogora, J., Knowlton, R. G., Merin, S., Rosenmann, A., Kanis, A. B., Rokhlina, T., Stone, E. M., and Sheffield, V. C. 1997. Homozygosity mapping of achromatopsia to chromosome 2 using DNA pooling. Hum. Mol. Genet. 6, 689–694.

Ardell, M. D., Bedsole, D. L., Schoborg, R. V., and Pittler, S. J. 2000. Genomic organization of the human rod photoreceptor cGMP-gated cation channel beta-subunit gene. Gene 245, 311–318.

Arshavsky, V. Y., Dumke, C. L., and Bownds, M. D. 1992. Noncatalytic cGMP-binding sites of amphibian rod cGMP phosphodiesterase control interaction with its inhibitory gamma-subunits. A putative regulatory mechanism of the rod photoresponse. J. Biol. Chem. 267, 24501–24507.

Arshavsky, V. Y, Lamb, T. D., and Pugh, E. N., Jr. 2002. G proteins and phototransduction. Annu. Rev. Physiol. 64, 153–187.

Bareil, C., Hamel, C. P., Delague, V., Arnaud, B., Demaille, J., and Claustres, M. 2001. Segregation of a mutation in *CNGB1* encoding the beta-subunit of the rod cGMP-gated channel in a family with autosomal recessive retinitis pigmentosa. Hum. Genet. 108, 328–334.

Baylor, D. A. 1987. Photoreceptor signals and vision. The Proctor Lecture. Invest. Ophthalmol. Vis. Sci. 28, 34–49.

Baylor, D. A. and Fuortes, M. G. F. 1970. Electrical responses of single cones in the retina of the turtle. J. Physiol. 207, 77–92.

Baylor, D. A. and Hodgkin, A. L. 1973. Detection and resolution of visual stimuli by turtle photoreceptors. J. Physiol. 234, 163–198.

Baylor, D. A. and Lamb, T. D. 1982. Local effects of bleaching in retinal rods of the toad. J. Physiol. 328, 49–71.

Baylor, D. A. and Nunn, B. J. 1986. Electrical properties of the light-sensitive conductance of rods of the salamander *Ambystoma tigrinum*. J. Physiol. 371, 115–145.

Baylor, D. A., Hodgkin, A. L., and Lamb, T. D. 1974. The electrical response of turtle cones to flashes and steps of light. J. Physiol. 242, 685–727.

Baylor, D. A., Lamb, T. D., and Yau, K.-W. 1979a. The membrane current of single rod outer segments. J. Physiol. 288, 589–611.

Baylor, D. A., Lamb, T. D., and Yau, K.-W. 1979b. Responses of retinal rods to single photons. J. Physiol. 288, 613–634.

Baylor, D. A., Matthews, G., and Nunn, B. J. 1984. Location and function of voltage-sensitive conductances in retinal rods of the salamander, *Ambystoma tigrinum*. J. Physiol. 354, 203–223.

Baylor, D. J. A., Matthews, G., and Yau, K.-W. 1980. Two components of electrical dark noise in toad retinal rod outer segments. J. Physiol. 309, 591–621.

Baylor, D. A., Nunn, B. J., and Schnapf, J. L. 1984. The photocurrent, noise and spectral sensitivity of rods of the monkey *Macaca fascicularis*. J. Physiol. 357, 575–607.

Berson, E. L. 1987. Electrical Phenomena in the Retina. In: Adler's Physiology of the Eye (*eds*. R. A. Moses and W. M. Hart), pp. 506–567. Mosby.

Berson, E. L. 1993. Retinitis pigmentosa. The Friedenwald Lecture. Invest. Ophthalmol. Vis. Sci. 34, 1659–1676.

Bhandawat, V., Reisert, J., and Yau, K.-W. 2005. Elementary response of olfactory receptor neurons to odorants. Science 308, 1931–1934.

Birge, R. R. 1990. Photophysics and molecular electronic applications of the rhodopsins. Annu. Rev. Phys. Chem. 41, 683–733.

Blakemore, C. B. and Rushton, W. A. 1965. Dark adaption and increment threshold in a rod monochromat. J. Physiol. 181, 612–628.

Blomhoff, R. and Blomhoff, H. K. 2006. Overview of retinoid metabolism and function. J. Neurobiol. 66, 606–630.

Bowes, C., Li, T., Danciger, M., Baxter, L. C., Applebury, M. L., and Farber, D. B. 1990. Retinal degeneration in the rd mouse is caused by a defect in the beta subunit of rod cGMP-phosphodiesterase. Nature 347, 677–680.

Bradley, J., Frings, S., Yau, K.-W., and Reed, R. 2001. Nomenclature for ion channel subunits. Science 294, 2095–2096.

Bradley, J., Reisert, J., and Frings, S. 2005. Regulation of cyclic nucleotide-gated channels. Curr. Opin. Neurobiol. 15, 343–349.

Brann, M. R. and Cohen, L. V. 1987. Diurnal expression of transducin mRNA and translocation of transducin in rods of rat retina. Science 235, 585–587.

Breton, M. E., Schueller, A. W., Lamb, T. D., and Pugh, E. N., Jr. 1994. Analysis of ERG a-wave amplification and kinetics in terms of the G-protein cascade of phototransduction. Invest. Ophthalmol. Vis. Sci. 35, 295–309.

Brockerhoff, S. E., Rieke, F., Matthews, H. R., Taylor, M. R., Kennedy, B., Ankoudinova, I., Niemi, G. A., Tucker, C. L., Xiao, M., Cilluffo, M. C., Fain, G. L., and Hurley, J. B. 2003. Light stimulates a transducin-independent increase of

cytoplasmic Ca^{2+} and suppression of current in cones from the zebrafish mutant nof. J. Neurosci. 23, 470–480.
Burns, M. E. and Baylor, D. A. 2001. Activation, deactivation, and adaptation in vertebrate photoreceptor cells. Annu. Rev. Neurosci. 24, 779–805.
Burns, M. E., Mendez, A., Chen, J., and Baylor, D. A. 2002. Dynamics of cyclic GMP synthesis in retinal rods. Neuron 36, 81–91.
Calvert, P. D., Krasnoperova, N. V., Lyubarsky, A. L., Isayama, T., Nicolo, M., Kosaras, B., Wong, G., Gannon, K. S., Margolskee, R. F., Sidman, R. L., Pugh, E. N., Jr., Makino, C. L., and Lem, J. 2000. Phototransduction in transgenic mice after targeted deletion of the rod transducin alpha -subunit. Proc. Natl. Acad. Sci. U. S. A. 97, 13913–13918.
Calvert, P. D., Strissel, K. J., Schiesser, W. E., Pugh, En., Jr., and Arshavsky, V. Y. 2006. Light-driven translocation of signaling proteins in vertebrate photoreceptors. Trends Cell Biol. 16, 560–568.
Campbell, F. W. and Rushton, W. A. 1955. Measurement of the scotopic pigment in the living huming eye. J. Physiol. 130, 131–147.
Camuzat, A., Dollfus, H., Rozet, J. M., Gerber, S., Bonneau, D., Bonnemaison, M., Briard, M. L., Dufier, J. L., Ghazi, I., Leowski, C., Weissenbach, J., Frezal, J., Munnich, A., and Kaplan, J. 1995. A gene for Leber's congenital amaurosis maps to chromosome 17p. Hum. Mol. Genet. 4, 1447–1452.
Cervetto, L., Lagnado, L., Perry, R. J., Robinson, D. W., and McNaughton, P. A. 1989. Extrusion of calcium from rod outer segments is driven by both sodium and potassium gradients. Nature 337, 740–743.
del Castillo, J. and Katz, B. 1954. Quantal components of the end-plate potential. J. Physiol. 124, 560–573.
Chen, C.-K. 2005. The vertebrate phototransduction cascade: amplification and termination mechanisms. Rev. Physiol. Biochem. Pharmacol. 155, 101–121.
Chen, C.-K., Burns, M. E., He, W., Wensel, T. G., Baylor, D. A., and Simon, M. I. 2000. Slowed recovery of rod photoresponse in mice lacking the GTPase accelerating protein RGS9-1. Nature 403, 557–560.
Chen, C.-K., Burns, M. E., Spencer, M., Niemi, G. A., Chen, J., Hurley, J. B., Baylor, D. A., and Simon, M. I. 1999. Abnormal photoresponses and light-induced apoptosis in rods lacking rhodopsin kinase. Proc. Natl. Acad. Sci. U. S. A. 96, 3718–3722.
Chen, T.-Y., Illing, M., Molday, L. L., Hsu, Y. T., Yau, K.-W., and Molday, R. S. 1994. Modulation of the cGMP-gated channel of rod photoreceptor cells by calmodulin. Subunit 2 (or beta) of retinal rod cGMP-gated cation channel is a component of the 240-kDa channel-associated protein and mediates Ca(2+)-calmodulin modulation. Proc. Natl. Acad. Sci. U. S. A. 91, 11757–11761.
Chen, J., Makino, C. L., Peachey, N. S., Baylor, D. A., and Simon, M. I. 1995. Mechanisms of rhodopsin inactivation in vivo as revealed by a COOH-terminal truncation mutant. Science 267, 374–377.
Chen, C., Nakatani, K., and Koutalos, Y. 2003. Free magnesium concentration in salamander photoreceptor outer segments. J. Physiol. 553, 125–135.
Cideciyan, A. V., Haeseleer, F., Fariss, R. N., Aleman, T. S., Jang, G. F., Verlinde, C. L., Marmor, M. F., Jacobson, S. G., and Palczewski, K. 2000. Rod and cone visual cycle consequences of a null mutation in the 11-*cis*-retinol dehydrogenase gene in man. Vis. Neurosci. 17, 667–678.
Cilluffo, M. C., Matthews, H. R., Brockerhoff, S. E., and Fain, G. L. 2004. Light-induced Ca^{2+} release in the visible cones of the zebrafish. Vis. Neurosci. 21, 599–609.
Cohen, A. I. 1987. The Retina. In: Adler's Physiology of the Eye (*eds*. R. A. Moses and W. M. Hart), pp. 458–490. Mosby.
Cornwall, M. C. and Fain, G. L. 1994. Bleached pigment activates transduction in isolated rods of the salamander retina. J. Physiol. 480, 261–279.
Cornwall, M. C., Matthews, H. R., Crouch, R. K., and Fain, G. L. 1995. Bleached pigment activates transduction in salamander cones. J. Gen. Physiol. 106, 543–557.
Cornwall, M. C., Fein, A., and MacNichol, E. F., Jr. 1990. Cellular mechanisms that underlie bleaching and background adaption. J. Gen. Physiol. 96, 345–372.
Cowan, C. W., Fariss, R. N., Sokal, I., Palczewski, K., and Wensel, T. 1998. High expression levels in cones of RGS9, the predominant GTPase accelerating protein of rods. Proc. Natl. Acad. Sci. U. S. A. 95, 5351–5356.
Craven, K. B. and Zagotta, W. N. 2006. CNG and HCN channels: two peas, one pod. Annu. Rev. Physiol. 68, 375–401.
Das, S. R., Bhardwaj, N., Kjeldbye, H., and Gouras, P. 1992. Muller cells of chicken retina synthesize 11-cis-retinol. Biochem. J. 285, 907–913.
Detwiler, P. B., Conner, J. D., and Bodoia, R. D. 1982. Gigaseal patch clamp recordings from outer segments of intact retinal rods. Nature 300, 59–61.
Detwiler, P. B., Hodgkin, A. L., and McNaughton, P. A. 1980. Temporal and spatial characteristics of the voltage response of rods in the retina of the snapping turtle. J. Physiol. 300, 213–250.
Doan, T., Mendez, A., Detwiler, P. B., Chen, J., and Rieke, F. 2006. Multiple phosphorylation sites confer reproducibility of the rod's single-photon responses. Science 313, 530–533.
Dowling, J. E. 1987. The Retina: An Approachable Part of the Brain, Belknap.
Dryja, T. P., Finn, J. T., Peng, Y. W., McGee, T. L., Berson, E. L., and Yau, K.-W. 1995. Mutations in the gene encoding the alpha subunit of the rod cGMP-gated channel in autosomal recessive retinitis pigmentosa. Proc. Natl. Acad. Sci. U. S. A. 92, 10177–10181.
Dryja, T. P., Hahn, L. B., Reboul, T., and Arnaud, B. 1996. Missense mutation in the gene encoding the alpha subunit of rod transducin in the Nougaret form of congenital stationary night blindness. Nat. Genet. 13, 358–360.
Dryja, T. P., McGee, T. L., Reichel, E., Hahn, L. B., Cowley, G. S., Yandell, D. W., Sandberg, M. A., and Berson, E. L. 1990. A point mutation of the rhodopsin gene in one form of retinitis pigmentosa. Nature 343, 364–366.
Dryja, T. P., Rucinski, D. E., Chen, S. H., and Berson, E. L. 1999. Frequency of mutations in the gene encoding the alpha subunit of rod cGMP-phosphodiesterase in autosomal recessive retinitis pigmentosa. Invest. Ophthalmol. Vis. Sci. 40, 1859–1865.
Eakin, R. M. 1973. The Third Eye. University of California.
Fain, G. L. 1975. Quantum sensitivity of rods in the toad retina. Science 187, 838–841.
Fain, G. L. and Lisman, J. E. 1981. Membrane conductances of photoreceptors. Prog. Biophys. Mol. Biol. 37, 91–147.
Fain, G. L. and Lisman, J. E. 1993. Photoreceptor degeneration in vitamin A deprivation and retinitis pigmentosa: the equivalent light hypothesis. Exp. Eye Res. 57, 335–340.
Fain, G. L., Matthews, H. R., and Cornwall, M. C. 1996. Dark adaptation in vertebrate photoreceptors. Trends Neurosci. 19, 502–507.
Fain, G. L., Matthews, H. R., Cornwall, M. C., and Koutalos, Y. 2001. Adaptation in vertebrate photoreceptors. Physiol. Rev. 81(1), 117–151.
Fesenko, E. E., Kolesnikov, S. S., and Lyubarsky, A. L. 1985. Induction by cyclic GMP of cationic conductance in plasma membrane of retinal rod outer segment. Nature 313, 310–313.
Field, G. D. and Rieke, F. 2002. Mechanisms regulating variability of the single photon responses of mammalian rod photoreceptors. Neuron 35, 733–747.

Finn, J. T., Grunwald, M. E., and Yau, K.-W. 1996. Cyclic nucleotide-gated ion channels: an extended family with diverse functions. Annu. Rev. Physiol. 58, 395–426.

Finn, J. T., Solessio, E. C., and Yau, K.-W. 1997. A cGMP-gated cation channel in depolarizing photoreceptors of the lizard parietal eye. Nature 385, 815–819.

Fotiadis, D., Jastrzebska, B., Philippsen, A., Muller, D. J., Palczewski, K., and Engel, A. 2006. Structure of the rhodopsin dimer: a working model for G-protein-coupled receptors. Curr. Opin. Struct. Biol. 16, 252–259.

Fotiadis, D., Liang, Y., Filipek, S., Saperstein, D. A., Engel, A., and Palczewski, K. 2003. Atomic-force microscopy: rhodopsin dimers in native disc membranes. Nature 421, 127–128.

Fu, Y. and Yau, K.-W. 2007. Phototransduction in mouse rods and cones. Pflügers Arch. 454, 805–819 .

Fuchs, S., Nakazawa, M., Maw, M., Tamai, M., Oguchi, Y., and Gal, A. 1995. A homozygous 1-base pair deletion in the arrestin gene is a frequent cause of Oguchi disease in Japanese. Nat. Genet. 10, 360–362.

Gomez, M. P. and Nasi, E. 2000. Light transduction in invertebrate hyperpolarizing photoreceptors: possible involvement of a Go-regulated guanylate cyclase. J. Neurosci. 20, 5254–5263.

Gorczyca, W. A. and Sokal, I. 2002. GCAPs: Ca^{2+}-sensitive regulators of retGC. Adv. Exp. Med. Biol. 514, 319–332.

Gordon, S. E., Brautigan, D. L., and Zimmerman, A. L. 1992. Protein phosphatases modulate the apparent agonist affinity of the light-regulated ion channel in retinal rods. Neuron 9, 739–748.

Gray, P. and Attwell, D. 1985. Kinetics of light-sensitive channels in vertebrate photoreceptors. Proc. R. Soc. Lond. B Biol. Sci. 223, 379–388.

Griffin, C. A., Ding, C. L., Jabs, E. W., Hawkins, A. L., Li, X., and Levine, M. A. 1993. Human rod cGMP-gated cation channel gene maps to 4p12 → centromere by chromosomal in situ hybridization. Genomics 16, 302–303.

Grunwald, M. E., Yu, W.-P., Yu, H.-H., and Yau, K.-W. 1998. Identification of a domain on the beta-subunit of the rod cGMP-gated cation channel that mediates inhibition by calcium-calmodulin. J. Biol. Chem. 273, 9148–9157.

Gu, S., Thompson, D. A., Srikumari, C. R. S., Lorenz, B., Finckh, U., Nicoletti, A., Murthy, K. R., Rathmann, M., Kumaramanickavel, G., Denton, M. J., and Gal, A. 1997. Mutations in *RPE65* cause autosomal recessive childhood-onset severe retinal dystrophy. Nat. Genet. 17, 194–197.

Hagins, W. A., Penn, R. D., and Yoshikami, S. 1970. Dark current and photocurrent in retinal rods. Biophys. J. 10, 380–412.

Hamer, R. D., Nicholas, S. C., Tranchina, D., Lamb, T. D., and Jarvinen, J. L. 2005. Toward a unified model of vertebrate rod phototransduction. Vis. Neurosci. 22, 417–436.

Hamer, R. D., Nicholas, S. C., Tranchina, D., Liebman, P. A., and Lamb, T. D. 2003. Multiple steps of phosphorylation of activated rhodopsin can account for the reproducibility of vertebrate rod single-photon responses. J. Gen. Physiol. 122, 419–444.

Harosi, F. I. 1975. Absorption spectra and linear dichroism of some amphibian photoreceptors. J. Gen. Physiol. 66, 357–382.

Hartong, D. T., Berson, E. L., and Dryja, T. P. 2006. Retinitis pigmentosa. Lancet 368, 1795–1809.

Haynes, L. W. and Yau, K.-W. 1985. Cyclic GMP-sensitive conductance in outer segment membrane of catfish cones. Nature 317, 61–64.

Haynes, L. W., Kay, A. R., and Yau, K.-W. 1986. Single cyclic GMP-activated channel activity in excised patches of rod outer segment membrane. Nature 321, 66–70.

Hecht, S., Shlaer, S., and Pirenne, M. H. 1942. Energy, quanta, and vision. J. Gen. Physiol. 25, 819–840.

Heck, M., Schadel, S. A., Maretzki, D., Bartl, F. J., Ritter, E., Palczewski, K., and Hofmann, K. P. 2003. Signaling states of rhodopsin. Formation of the storage form, metarhodopsin III, from active metarhodopsin II. J. Biol. Chem. 278, 3162–3169.

He, W., Danilova, V., Zou, S., Hellekant, G., Max, M., Margolskee, R. F., and Damak, S. 2002. Partial rescue of taste responses of alpha-gustducin null mice by transgenic expression of alpha-transducin. Chem. Senses 27, 719–727.

Hodgkin, A. L. and Nunn, B. J. 1988. Control of light-sensitive current in salamander rods. J Physiol. 403, 439–471.

Hodgkin, A. L., McNaughton, P. A., and Nunn, B. J. 1985. The ionic selectivity and calcium dependence of the light-sensitive pathway in toad rods. J. Physiol. 358, 447–468.

Holcman, D. and Korenbrot, J. I. 2005. The limit of photoreceptor sensitivity: molecular mechanisms of dark noise in retinal cones. J. Gen. Physiol. 125, 641–660.

Hoon, M. A., Northup, J. K., Margolskee, R. F., and Ryba, N. J. 1995. Functional expression of the taste specific G-protein, alpha-gustducin. Biochem. J. 309, 629–636.

Hsu, Y. T. and Molday, R. S. 1993. Modulation of the cGMP-gated channel of rod photoreceptor cells by calmodulin. Nature 361, 76–79.

Jin, S., Cornwall, M. C., and Oprian, D. D. 2003. Opsin activation as a cause of congenital night blindness. Nat. Neurosci. 6, 731–735.

Jin, M., Li, S., Moghrabi, W. N., Sun, H., and Travis, G. H. 2005. Rpe65 is the retinoid isomerase in bovine retinal pigment epithelium. Cell 122, 449–459.

Jones, G. J., Crouch, R. K., Wiggert, B., Cornwall, M. C., and Chader, G. J. 1989. Retinoid requirements for recovery of sensitivity after visual-pigment bleaching in isolated photoreceptors. Proc. Natl. Acad. Sci. U. S. A. 86, 9606–9610.

Kandori, H., Shichida, Y., and Yoshizawa, T. 2001. Photoisomerization in rhodopsin. Biochemistry 66, 1197–1209.

Kaupp, U. B. and Seifert, R. 2002. Cyclic nucleotide-gated ion channels. Physiol. Rev. 82, 769–824.

Kawamura, S. 1993. Rhodopsin phosphorylation as a mechanism of cyclic GMP phosphodiesterase regulation by S-modulin. Nature 362, 855–857.

Kawamura, S. and Murakami, M. 1991. Calcium-dependent regulation of cyclic GMP phosphodiesterase by a protein from frog retinal rods. Nature 349, 420–423.

Kefalov, V., Estevez, M. E., Kono, M., Goletz, P. W., Crouch, R. K., Cornwall, M. C., and Yau, K.-W. 2005. Breaking the covalent bond–a pigment property that contributes to desensitization in cones. Neuron 46, 879–890.

Kefalov, V., Fu, Y., Marsh-Armstrong, N., and Yau, K.-W. 2003. Role of visual pigment properties in rod and cone phototransduction. Nature 425, 526–531.

Kefalov, V. J., Crouch, R. K., and Cornwall, M. C. 2001. Role of non-covalent binding of 11-cis-retinal to opsin in dark adaptation of rod and cone photoreceptors. Neuron 29, 749–755.

Keresztes, G., Martemyanov, K. A., Krispel, C. M., Mutai, H., Yoo, P. J., Maison, S. F., Burns, M. E., Arshavsky, V. Y., and Heller, S. 2004. Absence of the RGS9.Gbeta5 GTPase-activating complex in photoreceptors of the R9AP knockout mouse. J. Biol. Chem. 279, 1581–1584.

Kerov, V., Chen, D., Moussaif, M., Chen, Y. J., Chen, C. K., and Artemyev, N. O. 2005. Transducin activation state controls its light-dependent translocation in rod photoreceptors. J. Biol. Chem. 280, 41069–41076.

Kilbride, P. and Ebrey, T. G. 1979. Light-initiated changes of cyclic guanosine monophosphate levels in the frog retina measured with quick-freezing techniques. J. Gen. Physiol. 74, 415–426.

Koch, K.-W. and Stryer, L. 1988. Highly cooperative feedback control of retinal rod guanylate cyclase by calcium ions. Nature 334, 64–66.

Kohl, S., Baumann, B., Rosenberg, T., Kellner, U., Lorenz, B., Vadala, M., Jacobson, S. G., and Wissinger, B. 2002. Mutations in the cone photoreceptor G-protein alpha-subunit gene GNAT2 in patients with achromatopsia. Am. J. Hum. Genet. 71, 422–425.

Kohl, S., Marx, T., Giddings, I., Jagle, H., Jacobson, S. G., Apfelstedt-Sylla, E., Zrenner, E., Sharpe, L. T., and Wissinger, B. 1998. Total colourblindness is caused by mutations in the gene encoding the alpha-subunit of the cone photoreceptor cGMP-gated cation channel. Nat. Genet. 19, 257–259.

Kojima, D., Terakita, A., Ishikawa, T., Tsukahara, Y., Maeda, A., and Shichida, Y. 1997. A novel Go-mediated phototransduction cascade in scallop visual cells. J. Biol. Chem. 1997 272, 22979–22982.

Kolesnikov, A. V., Golobokova, E. Y., and Govardovskii, V. I. 2003. The identity of metarhodopsin III. Vis. Neurosci. 20, 249–265.

Korenbrot, J. I. 1995. Ca^{2+} flux in retinal rod and cone outer segments: differences in Ca^{2+} selectivity of the cGMP-gated ion channels and Ca^{2+} clearance rates. Cell Calcium 18, 285–300.

Koutalos, Y. and Yau, K.-W. 1996. Regulation of light sensitivity in retinal rods. Trends in Neurosci. 19, 73–81.

Koutalos, Y., Nakatani, K., and Yau, K.-W. 1995. The cGMP-phosphodiesterase and its contribution to sensitivity regulation in retinal rods. J. Gen. Physiol. 106, 891–921.

Krispel, C. M., Chen, D., Melling, N., Chen, Y. J., Martemyanov, K. A., Quillinan, N., Arshavsky, V. Y., Wensel, T. G., Chen, C. K., and Burns, M. E. 2006. RGS expression rate-limits recovery of rod photoresponses. Neuron 51, 409–416.

Krispel, C. M., Chen, C.-K., Simon, M. I., and Burns, M. E. 2003. Prolonged photoresponses and defective adaptation in rods of Gbeta5−/− mice. J. Neurosci. 23, 6965–6971.

Kubo, Y. and Tateyama, M. 2005. Towards a view of functioning dimeric metabotropic receptors. Curr. Opin. Neurobiol. 15, 289–295.

Lamb, T. D. 1994. Stochastic simulation of activation in the G-protein cascade of phototransduction. Biophys. J. 67, 1439–1454.

Lamb, T. D. and Pugh, E. N., Jr. 1992. A quantitative account of the activation steps involved in phototransduction in amphibian photoreceptors. J. Physiol. 449, 719–758.

Lamb, T. D. and Pugh, E. N., Jr. 2004. Dark adaptation and the retinoid cycle of vision. Prog. Retin. Eye Res. 23, 307–380.

Lamb, T. D., McNaughton, P. A., and Yau, K.-W. 1981. Spatial spread of activation and background desensitization in toad rod outer segments. J. Physiol. 319, 463–496.

La Vail, M. M. 1983. Outer segment disc shedding and phagocytosis in the outer retina. Trans. Ophthalmol. Soc. U. K. 103, 397–404.

Leskov, I. B., Klenchin, V. A., Handy, J. W., Whitlock, G. G., Govardovskii, V. I., Bownds, M. D., Lamb, T. D., Pugh, E. N., Jr., and Arshavsky, V. Y. 2000. The gain of rod phototransduction: reconciliation of biochemical and electrophysiological measurements. Neuron 27, 525–537.

Leung, Y. T., Fain, G. L., and Matthews, H. R. 2006. Simultaneous measurement of current and calcium in the UV-sensitive cones of zebrafish. J. Physiol. Nov 23 [Epub ahead of print].

Lyubarsky, A. L, Chen, C, Simon, M. I., and Pugh, E. N, Jr. 2000. Mice lacking G-protein receptor kinase 1 have profoundly slowed recovery of cone-driven retinal responses. J. Neurosci. 20, 2209–2217.

Makino, C. L., Dodd, R. L., Chen, J., Burns, M. E., Roca, A., Simon, M. I., and Baylor, D. A. 2004. Recoverin regulates light-dependent phosphodiesterase activity in retinal rods. J. Gen. Physiol. 123, 729–741.

Marlhens, F., Bareil, C., Griffoin, J. M., Zrenner, E., Amalric, P., Eliaou, C., Liu, S. Y., Harris, E., Redmond, T. M., Arnaud, B., Claustres, M., and Hamel, C. P. 1997. Mutations in RPE65 cause Leber's congenital amaurosis. Nat. Genet. 17, 139–141.

Marquardt, A., Stohr, H., Passmore, L. A., Kramer, F., Rivera, A., and Weber, B. H. 1998. Mutations in a novel gene, VMD2, encoding a protein of unknown properties cause juvenile-onset vitelliform macular dystrophy (Best's disease). Hum. Mol. Genet. 7, 1517–1525.

Mata, N. L., Radu, R. A., Ciemmons, R., and Travis, G. H. 2002. Isomerization and oxidation of vitamin A in cone-dominant retinas: a novel pathway for visual-pigment regeneration in daylight. Neuron 36, 69–80.

Matthews, H. R. 1991. Incorporation of chelator into guinea-pig rods shows that calcium mediates mammalian photoreceptor light adaptation. J. Physiol. 436, 93–105.

Matthews, G. and Baylor, D. A. 1981. The Photocurrent and Dark Current of Retinal Rods. In: Molecular Mechanisms of Photoreceptor Transduction. Current Topics in Membrane and Transport (*ed*. W. H. Miller), pp. 3–18. Academic.

Matthews, H. R. and Fain, G. L. 2001. A light-dependent increase in free Ca^{2+} concentration in the salamander rod outer segment. J. Physiol. 532, 305–321.

Matthews, H. R. and Fain, G. L. 2002. Time course and magnitude of the calcium release induced by bright light in salamander rods. J. Physiol. 542, 829–841.

Matthews, H. R. and Fain, G. L. 2003. The effect of light on outer segment calcium in salamander rods. J. Physiol. 552, 763–776.

Matthews, H. R., Fain, G. L., Murphy, R. L., and Lamb, T. D. 1990. Light adaptation in cone photoreceptors of the salamander: a role for cytoplasmic calcium. J. Physiol. 420, 447–469.

Matthews, H. R., Murphy, R. L., Fain, G. L., and Lamb, T. D. 1988. Photoreceptor light adaptation is mediated by cytoplasmic calcium concentration. Nature 334, 67–69.

Matsumoto, H., Tokunaga, F., and Yoshizawa, T. 1975. Accessibility of the iodopsin chromophore. Biochim. Biophys. Acta 404, 300–308.

Maw, M. A., John, S., Jablonka, S., Muller, B., Kumaramanickavel, G., Oehlmann, R., Denton, M. J., and Gal, A. 1995. Oguchi disease: suggestion of linkage to markers on chromosome 2q. J. Med. Genet. 32, 396–398.

Max, M., McKinnon, P. J., Seiderman, K. J., Barrett, R. K., Applebury, M. L., Takahashi, J. S., and Margolskee, R. F. 1995. Pineal opsin: a nonvisual opsin expressed in chick pineal. Science 267, 1502–1506.

McLaughlin, S. K., McKinnon, P. J., and Margolskee, R. F. 1992. Gustducin is a taste-cell-specific G protein closely related to the transducins. Nature 357, 563–569.

Mendez, A., Burns, M. E., Roca, A., Lem, J., Wu, L. W., Simon, M. I., Baylor, D. A., and Chen, J. 2000. Rapid and reproducible deactivation of rhodopsin requires multiple phosphorylation sites. Neuron 28, 153–164.

Mendez, A., Burns, M. E., Sokal, I., Dizhoor, A. M., Baehr, W., Palczewski, K., Baylor, D. A., and Chen, J. 2001. Role of guanylate cyclase-activating proteins (GCAPs) in setting the flash sensitivity of rod photoreceptors. Proc. Natl. Acad. Sci. U. S. A. 98, 9948–9953.

Miller, W. H. (*ed*.) 1981. Molecular Mechanisms of Photoreceptor Transduction. Current Topics in Membrane and Transport. Academic.

Milunsky, A., Huang, X. L., Milunskym, J., DeStefano, A. and Baldwin, C. T. 1999. A locus for autosomal recessive achromatopsia on human chromosome 8q. Clin. Genet. 56, 82–85.

Moiseyev, G., Chen, Y., Takahashi, Y., Wu, B. X., and Ma, J. X. 2005. RPE65 is the isomerohydrolase in the retinoid visual cycle. Proc. Natl. Acad. Sci. U. S. A. 102, 12413–12418.

Molokanova, E., Trivedi, B., Savchenko, A., and Kramer, R. H. 1997. Modulation of rod photoreceptor cyclic nucleotide-gated channels by tyrosine phosphorylation. J. Neurosci. 17, 9068–9076.

Morimura, H., Saindelle-Ribeaudeau, F., Berson, E. L., and Dryja, T. P. 1999. Mutations in RGR, encoding a light-sensitive opsin homologue, in patients with retinitis pigmentosa. Nat. Genet. 23, 393–394.

Nakamura, T. and Gold, G. H. 1987. A cyclic nucleotide-gated conductance in olfactory receptor cilia. Nature 325, 442–444.

Nakamura, M., Hotta, Y., Tanikawa, A., Terasaki, H., and Miyake, Y. 2000. A high association with cone dystrophy in fundus albipunctatus caused by mutations of the *RDH5* gene. Invest. Ophthalmol. Vis. Sci. 41, 3925–3932.

Nakatani, K. and Yau, K.-W. 1986. Light-suppressible, cyclic GMP-activated current recorded from a dialyzed cone preparation. ARVO Abstracts. Invest. Ophthalmol. Vis. Sci. 27, 300.

Nakatani, K. and Yau, K.-W. 1988a. Calcium and light adaptation in retinal rods and cones. Nature 334, 69–71.

Nakatani, K. and Yau, K.-W. 1988b. Calcium and magnesium fluxes across the plasma membrane of the toad rod outer segment. J. Physiol. 395, 695–729.

Nakatani, K. and Yau, K.-W. 1988c. Guanosine 3′,5′-cyclic monophosphate-activated conductance studied in a truncated rod outer segment of the toad. J. Physiol. 731–753.

Nakatani, K. and Yau, K.-W. 1989. Sodium-dependent calcium extrusion and sensitivity regulation in retinal cones of the salamander. J. Physiol. 409, 525–548.

Nakatani, K., Koutalos, K., and Yau, Y. 1995. Ca^{2+} modulation of the cGMP-gated channel of bullfrog retinal rod photoreceptors. J. Physiol. 484, 69–76.

Nakatani, K., Tamura, T., and Yau, K.-W. 1991. Light adaptation in retinal rods of the rabbit and two other nonprimate mammals. J. Gen. Physiol. 97, 413–435.

Neher, E. and Sakmann, B. 1976. Single-channel currents recorded from membrane of denervated frog muscle fibres. Nature 260, 799–802.

Nelson, G., Chandrashekar, J., Hoon, M. A., Feng, L., Zhao, G., Ryba, N. J. P., and Zuker, C. S. 2002. An amino-acid taste receptor. Nature 416, 199–202.

Nikonov, S., Lamb, T. D., and Pugh, E. N., Jr. 2000. The role of steady phosphodiesterase activity in the kinetics and sensitivity of the light-adapted salamander rod photoresponse. J. Gen. Physiol. 116, 795–824.

Nishiguchi, K. M., Sandberg, M. A., Kooijman, A. C., Martemyanov, K. A., Pott, J. W. R., Hagstrom, S. A., Arshavsky, V. Y., Berson, E. L., and Dryja, T. P. 2004. Defects in RGS9 or its anchor protein R9AP in patients with slow photoreceptor deactivation. Nature 427, 75–78.

Ohguro, H, Van Hooser, J. P., Milam, A. H., and Palczewski, K. 1995. Rhodopsin phosphorylation and dephosphorylation in vivo. J. Biol. Chem. 270, 14259–14262.

Ohyama, T., Hackos, D. H., Frings, S., Hagen, V., Kaupp, U. B., and Korenbrot, J. I. 2000. Fraction of the dark current carried by Ca(2+) through cGMP-gated ion channels of intact rod and cone photoreceptors. J. Gen. Physiol. 116, 735–754.

Okada, T., Ernst, O. P., Palczewski, K., and Hofmann, K. P. 2001. Activation of rhodopsin: new insights from structural and biochemical studies. Trends Biochem. Sci. 26, 318–324.

Okada, T., Matsuda, T., Kandori, H., Fukada, Y., Yoshizawa, T., and Shichida, Y. 1994. Circular dichroism of metaiodopsin II and its binding to transducin: a comparative study between meta II intermediates of iodopsin and rhodopsin. Biochemistry 33, 4940–4946.

Okada, D., Nakai, T., and Ikai, A. 1989. Transducin activation by molecular species of rhodopsin other than metarhodopsin II. Photochem. Photobiol. 49, 197–203.

Okano, T., Yoshizawa, T., and Fukada, Y. 1994. Pinopsin is a chicken pineal photoreceptive molecule. Nature 372, 94–97.

Payne, A. M., Downes, S. M., Bessant, D. A. R., Plant, C., Moore, T., Bird, A. C., and Bhattacharya, S. S. 1999. Genetic analysis of the guanylate cyclase activator 1B (*GUCA1B)* gene in patients with autosomal dominant retinal dystrophies. J. Med. Genet. 36, 691–693.

Payne, A. M., Downes, S. M., Bessant, D. A. R., Taylor, R., Holder, G. E., Warren, M. J., Bird, A. C., and Bhattacharya, S. S. 1998. A mutation in guanylate cyclase activator 1A (GUCA1A) in an autosomal dominant cone dystrophy pedigree mapping to a new locus on chromosome 6p21.1. Hum. Mol. Genet. 7, 273–277.

Peng, C., Rich, E. D., and Varnum, M. D. 2004. Subunit configuration of heteromeric cone cyclic nucleotide-gated channels. Neuron 42, 401–410.

Penn, R. D. and Hagins, W. A. 1972. Kinetics of the photocurrent of retinal rods. Biophys. J. 12, 1073–1094.

Pepperberg, D. R., Brown, P. K., Lurie, M., and Dowling, J. E. 1978. Visual pigment and photoreceptor sensitivity in the isolated skate retina. J. Gen. Physiol. 71, 369–396.

Pepperberg, D. R., Cornwall, M. C., Kahlert, M., Hofmann, K. P., Jin, J., Jones, G. J., and Ripps, H. 1992. Light-dependent delay in the falling phase of the retinal rod photoresponse. Vis. Neurosci. 8, 9–18.

Perrault, I., Rozet, J. M., Calvas, P., Gerber, S., Camuzat, A., Dollfus, H., Châtelin, S., Souied, E., Ghazi, I., Leowski, C., Bonnemaison, M., Paslier, D. L., Frézal, J., Dufier, J. L., Pittler, S., Munnich, A., and Kaplan, J. 1996. Retinal-specific guanylate cyclase gene mutations in Leber's congenital amaurosis. Nat. Genet. 14, 461–464.

Perrault, I., Rozet, J. M., Ghazi, I., Leowski, C., Bonnemaison, M., Gerber, S., Ducroq, D., Cabot, A., Souied, E., Dufier, J. L., Munnich, A., and Kaplan, J. 1999. Different functional outcome of RetGC1 and RPE65 gene mutations in Leber congenital amaurosis. Am. J. Hum. Genet. 64, 1225–1228.

Perry, R. J. and McNaughton, P. A. 1991. Response properties of cones from the retina of the tiger salamander. J. Physiol. 433, 561–587.

Petrukhin, K., Koisti, M. J., Bakall, B., Li, W., Xie, G., Marknell, T., Sandgren, O., Forsman, K., Holmgren, G., Andreasson, S., Vujic, M., Bergen, A. A., McGarty-Dugan, V., Figueroa, D., Austin, C. P., Metzker, M. L., Caskey, C. T., and Wadelius, C. 1998. Identification of the gene responsible for Best macular dystrophy. Nat. Genet. 19, 241–247.

Picones, A. and Korenbrot, J. I. 1995. Spontaneous, ligand-independent activity of the cGMP-gated ion channels in cone photoreceptors of fish. J. Physiol. 485, 699–714.

Pittler, S. J., Baehr, W., Wasmuth, J. J., McConnell, D. G., Champagne, M. S., vanTuinen, P., Ledbetter, D., and Davis, R. L. 1990. Molecular characterization of human and bovine rod photoreceptor cGMP phosphodiesterase alpha-subunit and chromosomal localization of the human gene. Genomics 6, 272–283.

Prinsen, C. F., Szerencsei, R. T., and Schnetkamp, P. P. 2000. Molecular cloning and functional expression of potassium-dependent sodium-calcium exchanger from human and chicken retinal cone photoreceptors. J. Neurosci. 20, 1424–1434.

Pugh, E. N., Jr. and Lamb, T. D. 2000. Phototransduction in Vertebrate Rods and Cones: Molecular Mechanisms of Amplification, Recovery and Light Adaptation. In: Handbook of Biological Physics, Vol. 3 In: Handbook of Biological Physics (*eds*. D. G. Stavenga, W. J. DeGrip, and E. N. Pugh Jr.), pp. 184–255. Elsevier: Amsterdam.

Pugh, E. N., Jr., Nikonov, S., and Lamb, T. D. 1999. Molecular mechanisms of vertebrate photoreceptor light adaptation. Curr. Opin. Neurobiol. 9, 410–418.

Rebrik, T. I. and Korenbrot, J. I. 1998. In intact cone photoreceptors, a Ca^{2+}-dependent, diffusible factor modulates the cGMP-gated ion channels differently than in rods. J. Gen. Physiol. 112, 537–548.

Rieke, F. and Baylor, D. A. 1996. Molecular origin of continuous dark noise in rod photoreceptors. Biophys. J. 71, 2553–2572.

Rieke, F. and Baylor, D. A. 1998. Origin of reproducibility in the responses of retinal rods to single photons. Biophys. J. 75, 1836–1857.

Rieke, F. and Baylor, D. A. 2000. Origin and functional impact of dark noise in retinal cones. Neuron 26, 181–186.

Rinner, O., Makhankov, Y. V., Biehlmaier, O., and Neuhauss, S. C. F. 2005. Knockdown of cone-specific kinase GRK7 in larval zebrafish leads to impaired cone response recovery and delayed dark adaptation. Neuron 47, 231–242.

Rodieck, R. W. 1998. The First Steps in Seeing. Sinauer.

Ruiz, M. L. and Karpen, J. W. 1997. Single cyclic nucleotide-gated channels locked in different ligand-bound states. Nature 389, 389–392.

Ruiz, A., Kuehn, M. H., Andorf, J. L., Stone, E., Hageman, G. S., and Bok, D. 2001. Genomic organization and mutation analysis of the gene encoding lecithin retinol acyltransferase in human retinal pigment epithelium. Invest. Ophthalmol. Vis. Sci. 42, 31–37.

Saari, J. C. 2000. Biochemistry of visual pigment regeneration: the Friedenwald lecture. Invest. Ophthalmol. Vis. Sci. 41, 337–348.

Sampath, A. P., Matthews, H. R., Cornwall, M. C., Bandarchi, J., and Fain, G. L. 1999. Light-dependent changes in outer segment free-Ca^{2+} concentration in salamander cone photoreceptors. J. Gen. Physiol. 113, 267–277.

Sato, M., Nakazawa, M., Usui, T., Tanimoto, N., Abe, H., and Ohguro, H. 2005. Mutations in the gene coding for guanylate cyclase-activating protein 2 (GUCA1B gene) in patients with autosomal dominant retinal dystrophies. Graefes. Arch. Clin. Exp. Ophthalmol. 243, 235–242.

Schnapf, J. L. and McBurney, R. N. 1980. Light-induced changes in membrane current in cone outer segments of tiger salamander and turtle. Nature 287, 239–241.

Schnapf, J. L., Nunn, B. J., Meister, M., and Baylor, D. A. 1990. Visual transduction in cones of the monkey Macaca fascicularis. J. Physiol. 427, 681–713.

Schneeweis, D. M. and Schnapf, J. L. 1995. Photovoltage of rods and cones in the macaque retina. Science 268, 1053–1056.

Shapley, R. and Enroth-Cugell, C. 1984. Visual adaptation and retinal gain controls. Prog. Retin. Res. 3, 263–346.

Sheng, J. Z., Prinsen, C. F., Clark, R. B., Giles, W. R., and Schnetkamp, P. P. 2000. Na(+)-Ca(2+)-K(+) currents measured in insect cells transfected with the retinal cone or rod Na(+)-Ca(2+)-K(+) exchanger cDNA. Biophys. J. 79, 1945–1953.

Simon, A., Lagercrantz, J., Bajalica-Lagercrantz, S., and Eriksson, U. 1996. Primary structure of human 11-*cis* retinol dehydrogenase and organization and chromosomal localization of the corresponding gene. Genomics 36, 424–430.

Sokal, I., Li, N., Surgucheva, I., Warren, M. J., Payne, A. M., Bhattacharya, S. S., Baehr, W., and Palczewski, K. 1998. GCAP1 (Y99C) mutant is constitutively active in autosomal dominant cone dystrophy. Mol. Cell 2, 129–133.

Sokolov, M., Lyubarsky, A. L., Strissel, K. J., Savchenko, A. B., Govardovskii, V. I., Pugh, E. N., Jr., and Arshavsky, V. Y. 2002. Massive light-driven translocation of transducin between the two major compartments of rod cells: a novel mechanism of light adaptation. Neuron 34, 95–106.

Solessio, E. and Engbretson, G. A. 1993. Antagonistic chromatic mechanisms in photoreceptors of the parietal eye of lizards. Nature 364, 442–445.

Steinberg, R. H. 1985. Interactions between the retinal pigment epithelium and the neural retina. Doc. Ophthalmol. 60, 327–346.

Steinberg, R. H., Fisher, S. K., and Anderson, D. H. 1980. Disc morphogenesis in vertebrate photoreceptors. J. Comp. Neurol. 190, 501–508.

Su, C.-Y., Luo, D.-G., Terakita, A., Shichida, Y., Liao, H.-W., Kazmi, M. A., Sakmar, T. P., and Yau, K.-W. 2006. Parietal-eye phototransduction components and their potential evolutionary implications. Science 311, 1617–1621.

Surya, A., Foster, K. W., and Knox, B. E. 1995. Transducin activation by the bovine opsin apoprotein. J. Biol. Chem. 270, 5024–5031.

Tachibanaki, S., Arinobu, D., Shimauchi-Matsukawa, Y., Tsushima, S., and Kawamura, S. 2005. Highly effective phosphorylation by G protein-coupled receptor kinase 7 of light-activated visual pigment in cones. Proc. Natl. Acad. Sci. U. S. A. 102, 9329–9334.

Tachibanaki, S., Tsushima, S., and Kawamura, S. 2001. Low amplification and fast visual pigment phosphorylation as mechanisms characterizing cone photoresponses. Proc. Natl. Acad. Sci. U. S. A. 98, 14044–14049.

Tachibanaki, S., Shimauchi-Matsukawa, Y., Arinobu, D., and Kawamura, S. 2007. Molecular mechanisms characterizing cone photoresponses. Photochem. Photobiol. 83, 19–26.

Tamura, T., Nakatani, K., and Yau, K.-W. 1989. Light adaptation in cat retinal rods. Science 245, 755–758.

Tamura, T., Nakatani, K., and Yau, K.-W. 1991. Calcium feedback and sensitivity regulation in primate rods. J. Gen. Physiol. 98, 95–130.

Thompson, D. A. and Gal, A. 2003. Vitamin A metabolism in the retinal pigment epithelium: genes, mutations, and diseases. Prog. Retin. Eye. Res. 22, 683–703.

Tomita, T. 1970. Electrical activity of vertebrate photoreceptors. Quart. Rev. Biophys. 3, 179–222.

Travis, G. H. 2005. DISCO! Dissociation of cone opsins: the fast and noisy life of cones explained. Neuron 46, 840–842.

Travis, G. H., Golczak, M., Moise, A. R., and Palczewski, K. 2006. Diseases caused by defects in the visual cycle: retinoids as potential therapeutic agents. Annu. Rev. Pharmacol. Toxicol. Sep. 12 [Epub ahead of print].

Tsang, S. H., Burns, M. E., Calvert, P. D., Gouras, P., Baylor, D. A., Goff, S. P., and Arshavsky, V. Y. 1998. Role for the target enzyme in deactivation of photoreceptor G protein in vivo. Science 282, 117–121.

Tsunenari, T., Nathans, J., and Yau, K.-W. 2006. Ca^{2+}-activated Cl- current from human bestrophin-4 in excised membrane patches. J. Gen. Physiol. 127, 749–754.

Tsunenari, T., Sun, H., Williams, J., Cahill, H., Smallwood, P., Yau, K.-W., and Nathans, J. 2003. Structure-function analysis of the bestrophin family of anion channels. J. Biol. Chem. 278, 41114–41125.

Wald, G. 1968. Molecular basis of visual excitation. Science 62, 230–239.

Wald, G., Brown, P. K., and Smith, P. H. 1955. Iodopsin. J. Gen. Physiol. 38, 623–681.

Weiss, E. R., Ducceschi, M. H., Horner, T. J., Li, A., Craft, C. M., and Osawa, S. 2001. Species-specific differences in expression of G-protein-coupled receptor kinase (GRK) 7 and GRK1 in mammalian cone photoreceptor cells: implications for cone cell phototransduction. J. Neurosci. 21, 9175–9184.

Weitz, D., Ficek, N., Kremmer, E., Bauer, P. J., and Kaupp, U. B. 2002. Subunit stoichiometry of the CNG channel of rod photoreceptors. Neuron 36, 881–889.

Weitz, D., Zoche, M., Muller, F., Beyermann, M., Korschen, H. G., Kaupp, U. B., and Koch, K.-W. 1998. Calmodulin controls the rod photoreceptor CNG channel through an unconventional binding site in the N-terminus of the beta-subunit. EMBO J. 17, 2273–2284.

Whitlock, G. G. and Lamb, T. D. 1999. Variability in the time course of single photon responses from toad rods: termination of rhodopsin's activity. Neuron 23, 337–351.

Williams, T. P., Webbers, J. P., Giordano, L., and Henderson, R. P. 1998. Distribution of photon absorption rates across the rat retina. J. Physiol. 508(Pt 2), 515–522.

Winick, J. D., Blundell, M. L., Galke, B. L., Salam, A. A., Leal, S. M., and Karayiorgou, M. 1999. Homozygosity mapping of the Achromatopsia locus in the Pingelapese. Am. J. Hum. Genet. 64, 1679–1685.

Wissinger, B., Jagle, H., Kohl, S., Broghammer, M., Baumann, B., Hanna, D. B., Hedels, C., Apfelstedt-Sylla, E., Randazzo, G., Jacobson, S. G., Zrenner, E., and Sharpe, L. T. 1998. Human rod monochromacy: linkage analysis and mapping of a cone photoreceptor expressed candidate gene on chromosome 2q11. Genomics 51, 325–331.

Xiong, W.-H., Solessio, E. C., and Yau, K.-W. 1998. An unusual cGMP pathway underlying depolarizing light response of the vertebrate parietal-eye photoreceptor. Nat. Neurosci. 1, 359–365.

Xu, J., Dodd, R. L., Makino, C. L., Simon, M. I., Baylor, D. A., and Chen, J. 1997. Prolonged photoresponses in transgenic mouse rods lacking arrestin. Nature 389, 505–509.

Xu, H., Staszewski, L., Tang, H., Adlet, E., Zoller, M., and Li, X. 2004. Different functional roles of T1R subunits in the heteromeric taste receptors. Proc. Natl. Acad. Sci. U. S. A. 101, 14258–14263.

Yamamoto, H., Simon, A., Eriksson, U., Harris, E., Berson, E. L., and Dryja, T. P. 1999. Mutations in the gene encoding 11-*cis* retinol dehydrogenase cause delayed dark adaptation and fundus albipunctatus. Nat. Genet. 22, 188–191.

Yamamoto, S., Sippel, K. C., Berson, E. L., and Dryja, T. P. 1997. Defects in the rhodopsin kinase gene in the Oguchi form of stationary night blindness. Nat. Genet. 15, 175–178.

Yau, K.-W. 1994. Phototransduction mechanism in retinal rods and cones. The Friedenwald Lecture. Invest. Ophthalmol. Vis. Sci. 35, 10–32.

Yau, K.-W. and Baylor, D. A. 1989. Cyclic GMP-activated conductance of retinal photoreceptor cells. Annu. Rev. Neurosci. 12, 289–327.

Yau, K.-W. and Nakatani, K. 1984a. Cation selectivity of light-sensitive conductance in retinal rods. Nature 309, 352–354.

Yau, K.-W. and Nakatani, K. 1984b. Electrogenic Na-Ca exchange in retinal rod outer segment. Nature 311, 661–663.

Yau, K.-W. and Nakatani, K. 1985a. Light-induced reduction of cytoplasmic free calcium in retinal rod outer segment. Nature 313, 579–582.

Yau, K.-W. and Nakatani, K. 1985b. Light-suppressible, cyclic GMP-sensitive conductance in the plasma membrane of a truncated rod outer segment. Nature 317, 252–255.

Yau, K.-W., Lamb, T. D., and Baylor, D. A. 1977. Light-induced fluctuations in membrane current of single toad rod outer segments. Nature 269, 78–80.

Yau, K.-W., McNaughton, P. A., and Hodgkin, A. L. 1981. Effect of ions on the light-sensitive current in retinal rods. Nature 292, 502–505.

Zhang, X., Wensel, T. G., and Kraft, T. W. 2003. GTPase regulators and photoresponses in cones of the eastern chipmunk. J. Neurosci. 23, 1287–1297.

Zheng, J., Trudeau, M. C., and Zagotta, W. N. 2002. Rod cyclic nucleotide-gated channels have a stoichiometry of three CNGA1 subunits and one CNGB1 subunit. Neuron 36, 891–896.

Zhong, H., Molday, L. L., Molday, R. S., and Yau, K.-W. 2002. The heteromeric cyclic nucleotide-gated channel adopts a 3A:1B stoichiometry. Nature 420, 193–198.

Zhu, X., Ma, B., Babu, S., Murage, J., Knox, B. E., and Craft, C. M. 2002. Mouse cone arrestin gene characterization: promoter targets expression to cone photoreceptors. FEBS Lett. 524, 116–122.

Zhu, X., Wu, K., Rife, L., Brown, B., and Craft, C. M. 2005. Rod arrestin expression and function in cone photoreceptors. Invest. Ophthalmol. Vis. Sci. 46, 1179.

Further Reading

Luo, D.-G., Su, C.-Y., and Yau, K.-W. 2007. Photoreceptors: Physiology. In: New Encyclopedia of Neuroscience (*ed*. L. R. Squire), Elsevier.

Sun, H., Tsunenari, T., Yau, K.-W., and Nathans, J. 2002. The vitelliform macular dystrophy protein defines a new family of chloride channels. Proc. Natl. Acad. Sci. U. S. A. 99, 4008–4013.

Relevant Website

http://www.sph.uth.tmc.edu/Retnet/ – RetNet. Retinal Information Network.

1.11 Mammalian Rod Pathways

E Strettoi, Neuroscience Institute, Pisa, Italy

© 2008 Elsevier Inc. All rights reserved.

1.11.1	Introduction	303
1.11.2	Additional Rod Pathways	308
1.11.3	How Could This Particular Synaptic Disposition Be Evolved?	309
1.11.4	Inherited Photoreceptor Degeneration: How Photoreceptor Death Affects the Architecture of the Rod and Cone Pathways	310
References		311

1.11.1 Introduction

Mammalian retinas are generally dominated by rods that normally constitute 90–97% of all the photoreceptors. Noticeable exceptions are few, purely diurnal animals (such as ground squirrels and three shrews, whose retinas are considered as cone-only), and highly specialized retinal areas, which include the area centralis of the cat, the visual streak of the rabbit, and the primate fovea. In these regions, cones represent the vast majority, if not the entire population, of photoreceptors. Given the fact that specialized, cone-enriched zones cover up a limited fraction of the retinal surface, even mammals which have evolved such dedicated areas are, in the end, rod dominated.

In most cold-blooded vertebrates, rods, and cones usually converge unto common second-order neurons; mammals, instead, exhibit multiple types of bipolar cells collecting information from cones, and one, single type of bipolar cell, entirely dedicated to gather signals from rods. The typical mammalian rod bipolar cell (Figure 1) is one of the best-characterized neurons of the central nervous system (CNS). It has been illustrated first by Santiago Ramón y Cajal, in his pioneering studies of Golgi-impregnated neurons and has a typical morphology, with a bushy, chandelier-like dendritic arborization, an ovoidal cell body, usually positioned at the outer aspect of the inner nuclear layer, a thin axon, and a stout axonal arborization, composed of large varicosities, which reach the deepest part of the inner plexiform layer (IPL), at the limit to ganglion cell bodies. In his handmade drawings of Golgi-stained retinas, Cajal represented the axonal endings of rod bipolar cells in close contact with the cell bodies of ganglion cells, postulating a direct pipeline conveying rod information to the final neurons projecting out of the retina. His discovery of two separate sets of bipolar cells, respectively, dedicated to cones and to rods, dictated enthusiastic words to his memories, reported in his biography *Recollections of My Life*:

> Observe how one variety of bipolar makes a contact through its ascending dendritic tuft with a group of terminal bulbs of the rods; while the axonic or deep process of the same cell, forming a warty foot, connects below with the body of a certain giant ganglionic neuron (Cajal, Santiago Ramón y, 1989).

Modern electron microscopy has discovered that the warty foot does not establish connections (synapses, totally unknown at Cajal's time) with ganglion cells. Indeed, synaptic contacts with cell bodies are rare in the retina, most of the connections being segregated in the two plexiform layers. But rod bipolar cells do not make connections with ganglion cell dendrites either: they utilize a chain of neurons ultimately leading to the confluence of rod- and cone-generated signals into common cohorts of ganglion cells.

This concept was totally illogical for Cajal's straightforward way of thinking (from which the concept of inhibition was entirely absent, for historical reasons): to him, separate rod and cone bipolar (CB) cells were "demanded by theory and guessed by rationale"; he could see no reason "why the ingenious expedient according to which nature has organized two classes of specific photoreceptor cells would be completely frustrated. . .." by mixing up rod and cone signals into a sole bipolar or, at a later stage of neural processing, into a common ganglion cell. We shall see later that the functional benefits of the ingenious expedient are indeed preserved, albeit the mixture of rod and cone pathways.

A close look at the very first synapse established in the outer plexiform layer (OPL) between rods and rod bipolar cells reveals that the terminal ending of

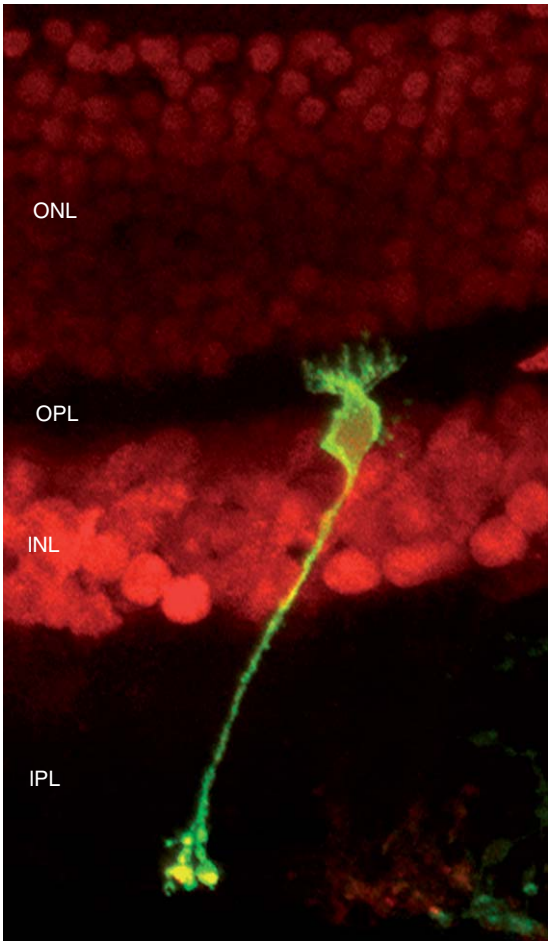

Figure 1 Rod bipolar cell of the mouse retina, individually labeled by a green fluorescent dye, in a vertical sections, in which cell nuclei have been stained with a red fluorescent molecule. The morphology of rod bipolar cells is highly conserved across various mammalian species. The body is ovoidal, the dendritic tree is chandelier shaped, and the axonal arbor is composed of several, large varicosities, which reach the deepest part of the IPL, close to the cell bodies of ganglion cells. For all the figures: GCL, ganglion cell layer; INL, inner nuclear layer; IPL, inner plexiform layer; ONL, outer nuclear layer; OPL, outer plexiform layer.

each dendrite of a rod bipolar cell penetrates deeply in the spherule, the synaptic terminal of a rod (Figure 2). The presynaptic membrane is marked by specialization named ribbons (R), a complex laminar sheet regulating the release of vesicles that fill the spherule cytoplasm. Opposed to each ribbon, a triad of processes is found: the two lateral elements originate from the axonal arborizations of horizontal cells (H in Figure 2); the central element of the triad is the dendrite of one rod bipolar cell (B). As a rule, a spherule makes contact with only one (or two) rod

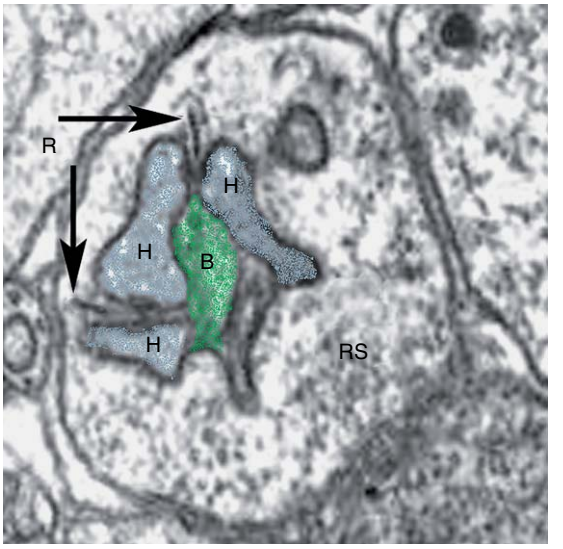

Figure 2 Electron micrograph of the synaptic terminal of a rod photoreceptor, termed spherule (RS). The cytoplasm is filled with synaptic vesicles; presynaptic sites are marked by dense ribbons (R). Postsynaptic processes are arranged in triads, in which lateral elements belong to horizontal cells (H, light blue processes) and the central element is the dendrite of a rod bipolar cell (B, green).

bipolar dendrites. This contact, named invaginated, is the only kind of synapse established by rod spherules. Unlike cone pedicles, therefore, in general rod spherules are not engaged in basal contacts.

At the postsynaptic site of the invagination, rod bipolar dendrites carry a retinal-specific type of metabotropic glutamate receptor, named mGluR6 (Ueda, Y. *et al.*, 1997). A high-resolution confocal image (Figure 3) shows terminal dendritic branches of rod bipolar cells (labeled green with antibodies against protein kinase C), decorated with clusters of red puncta, representing aggregates of mGluR6, exactly located at their tips. Each spherule contains one punctum, rarely two of them.

Figure 4 shows the profiles of rod spherules, labeled green with antibodies against the synaptic protein PSD95, encircling individual rod bipolar dendritic tips in the OPL. Via mGluR6, a graded hyperpolarization (representing the response triggered by light in rods) is transformed into a graded depolarization of postsynaptic rod bipolar cells. For that reason, invaginating synapses are called sign-inverting. Rod bipolars are depolarized by light stimuli that fall onto the center of their circular receptive fields: hence, they belong to the functional category of ON center neurons. As for ON center CB cells, rod bipolar cells are hyperpolarized by light

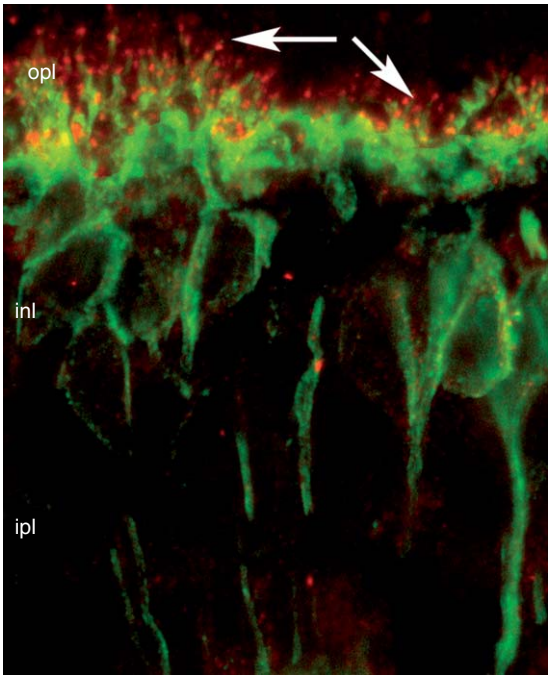

Figure 3 Confocal image of rod bipolar cells, labeled green by antibodies against protein kinase C, showing clusters of mGluR6 receptors on their dendritic tips (arrows, red labeling). This variety of glutamatergic receptor is almost unique to the retina.

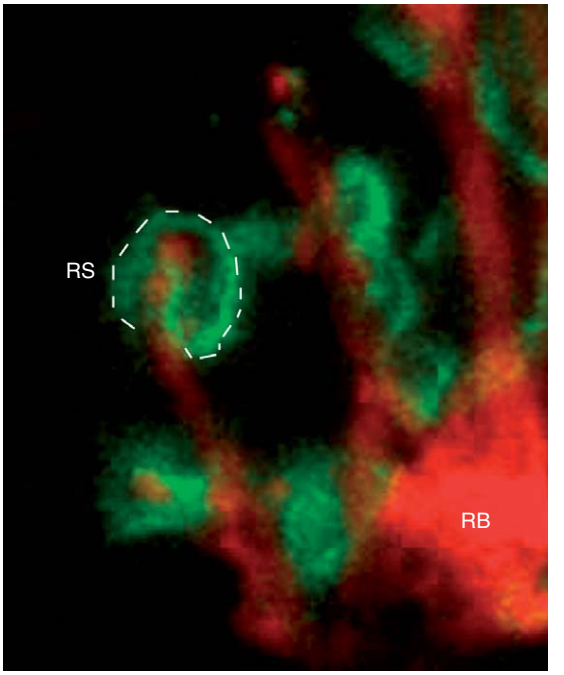

Figure 4 High-power confocal micrograph of rod spherules (RS), labeled green by antibodies against the synaptic protein PSD95. The profile of one spherule has been marked by a dashed line. Individual dendrites of rod bipolar (RB) cells (red staining) penetrate the spherules deeply, to receive ribbon synapses.

falling onto the annular area forming the periphery of their receptive fields. Therefore, they exhibit a typical OFF response at peripheral stimulation (Dacheux, R. F. and Raviola, E., 1986).

The number of rods converging upon a single rod bipolar cell varies greatly with the mammalian species and, within a species, with retinal eccentricity. In the periphery of a rabbit retina, where rods make up 97% of all photoreceptors, and dendritic arborizations of neurons are large, up to 80 rods converge upon a single bipolar cell. Near to the visual streak, dendritic trees become smaller, and the convergence is lower (about 60 rods for each bipolar). Regardless to retinal eccentricity, convergence in the rod pathway is usually higher than in the cone pathway. This contributes to the higher light sensitivity of the rod system, partially achieved through summation of inputs at postsynaptic level. Thus, the enormous amplification in individual rod photoreceptors (Baylor, D. A., *et al.*, 1979) and convergence within the rod bipolar pathway (Sterling, P. *et al.*, 1988), confer retinal ganglion cells, the retinal output neurons, a huge sensitivity: a cat ganglion cell can produce several extra spikes when one of the thousands of rods within its receptive field absorbs a single photon (Field, G. D. *et al.*, 2005).

All together, a rod spherule is less varied (in number of synaptic partners, as well as in types of synaptic contacts established), than a cone pedicle. Hence, if one had to limit the analysis of the rod pathway at the first synaptic station of the retina, the conclusion would be that there is neither scotopic contribution to the OFF channel nor parallel processing of signals generated in rods. This is not the case.

Both the OFF channel and the computation arising from parallel processing are opened to the rod pathway by means of an interposed, peculiar neuron, a small-field amacrine cell, named AII. AII amacrines were first described by Kolb H. (1979) in the cat retina. They are narrow-field neurons, with a typical, bistratified morphology (Figure 5). The outermost arborization is composed by round endings, called lobular appendages; the inner part is represented by a tangle of thin, elongated dendrites, with laterally oriented terminal tips. They are called tufted processes and occupy the innermost part of the IPL. Electron microscopy of serial sections has clearly demonstrated that AII amacrine cells are the main

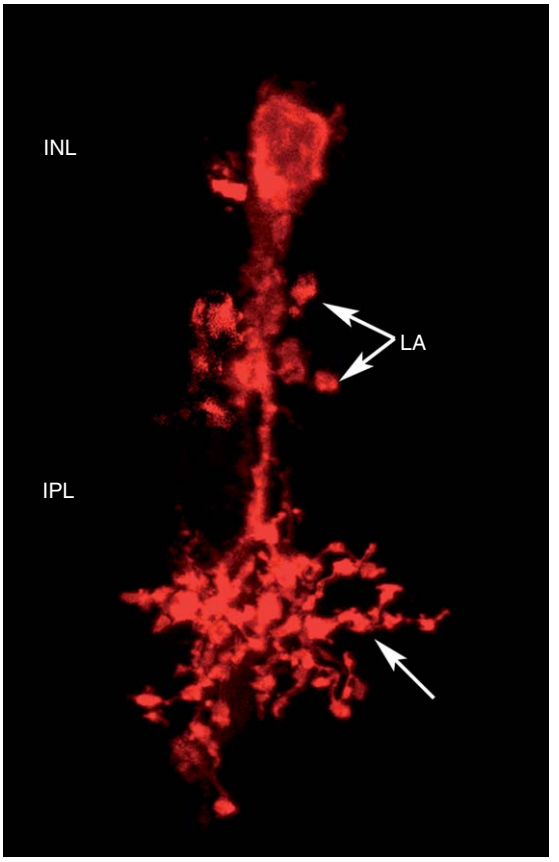

Figure 5 Single AII amacrine cell of the mouse retina. The typical bistratified morphology is clearly evident. Tufted processes receive synaptic inputs from rod bipolar cells in the innermost part of the inner plexiform layer (arrow), while lobular appendages (LA) establish output synapses in the outer half of the IPL.

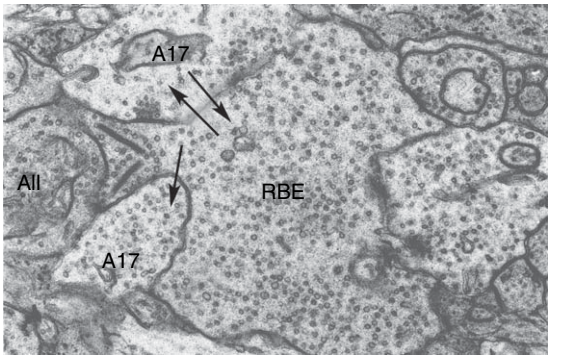

Figure 6 Electron micrograph of a rod bipolar axonal ending (RBE), with its typical synaptic arrangement. Two ribbon synapses are visible, with one dark dendrite, belonging to an AII amacrine cell, and two pale varicosities, filled with vesicles, belonging to A17 amacrine cells. One of them returns a reciprocal synapse onto the rod bipolar ending itself (arrow).

postsynaptic target of rod bipolar cells (Strettoi, E. *et al.*, 1992). The latter establish ribbon synapses (similar to those already found at photoreceptor synaptic terminals) in the deepest layer of the IPL with the tufted dendrites of AII amacrine cells.

A typical synaptic arrangement is depicted in Figure 6, in which a rod bipolar axonal ending establishes a dyad with two processes of different cytology. The dark, electron-dense dendrite, with few vesicles and a gray matrix, belongs to an AII amacrine cell. The other ending, filled with pale synaptic vesicles, belong to a wide-field amacrine, also known as A17. This is an indoleamine-accumulating amacrine and a gamma-aminobutyric acid (GABA)-releasing neuron. As for the AII, the major synaptic input to this cell is derived from rod bipolar cells; unlike AII amacrines, however, A17 cells are not projection neurons. Their function is exquisitely local, as they return feedback, inhibitory synapses onto the axonal endings of the rod bipolar itself (Sandell, J. H. *et al.*, 1989). Both AII and A17 amacrines respond to light with a graded depolarization, similar to that recorded in a rod bipolar cell. However, because of a feedback inhibitory loop created by A17 cells upon rod bipolar endings, AII responses become more transient that their rod bipolar input responses (Raviola, E. and Dacheux, R. F., 1987). Local feedback inhibition is a recurrent strategy of the CNS wiring diagram by which transient components of neuronal responses are enhanced.

If, then, the rod-generated signal cannot proceed further in the retinal pathway through A17 amacrines, it follows that the sole cell responsible for the progression of scotopic responses to the subsequent retinal synaptic station is represented by the AII amacrine. In fact, because of the peculiar, bistratified morphology of this interneuron, a dichotomy is generated in the rod pathway: each AII amacrine cell establishes sign-conserving gap junctions with the axonal endings of CB cells that ramify in the deepest layer of the IPL (or ON CBs; Figure 7); the lobular appendages of the same cell form sign-inverting, glycinergic synapses with OFF CBs, whose axons ramify in the outer half of the IPL.

Electrophysiology has demonstrated strong electrical coupling with symmetrical junction conductance between AII amacrine cells and various types of ON CB cells. However, signal transmission is more effective in the direction from AII amacrine cells to ON CB cells than in the other direction (Veruki, M. L. and Hartveit, E., 2002).

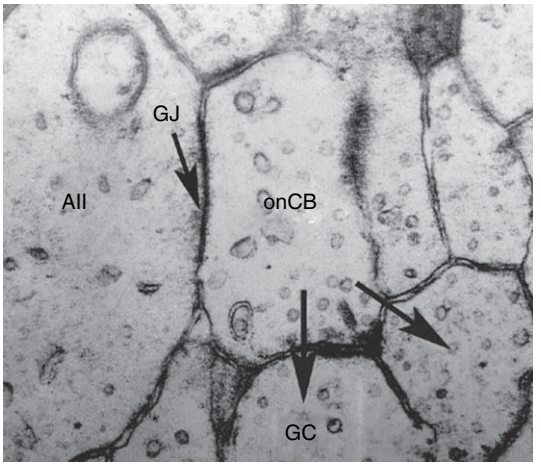

Figure 7 The primary dendrite of an AII amacrine cell establishes a large gap junction (GJ) with the axonal ending of a cone bipolar (CB) cell in the innermost part of the IPL (sublamina ON). In turn, the CB feeds a ribbon synapse to a ganglion cell (GC) dendrite. By this peculiar arrangement, the light response of an AII amacrine upon illumination (a graded depolarization) is transferred to the ON pathway of the retina, retaining its sign.

In the outer sublamina of the IPL, OFF CB cells receive a strong glycinergic input from the lobular appendages of AII amacrine cells; this input is preferentially based on the fast alpha1beta-containing channels (Ivanova, E. *et al.*, 2006). As a result, the depolarizing response generated by the fall of photons upon the central receptive field of a rod bipolar cell is first transformed into a more transient depolarizing response of AII amacrine cells, then split into the ON and the OFF channels, and finally fed into the cone pathway with great efficiency (Figure 8).

It is interesting to note that only few, direct synapses, are formed between AII amacrine cells and dendrites of ganglion cells. If some of these neurons had to collect a large number of AII amacrine inputs, they could be considered as mainly rod-dominated. However, physiology suggests that even in strongly rod-dominated, nocturnal animals, ganglion cells that are mostly rod-driven are encountered only rarely. Through AII amacrines, the largest part of the scotopic signal is infused directly into the cone pathway, in what is known as a piggyback arrangement. Further on, separate rod and cone pathways converge onto common ganglion cells. To our present knowledge, there are no privileged types of CB cells, either in the ON or in the OFF pathways, which establish connections with AII amacrine cells. Presumably, most of the ON CBs are engaged in gap junctions with the tufted processes of AII amacrines;

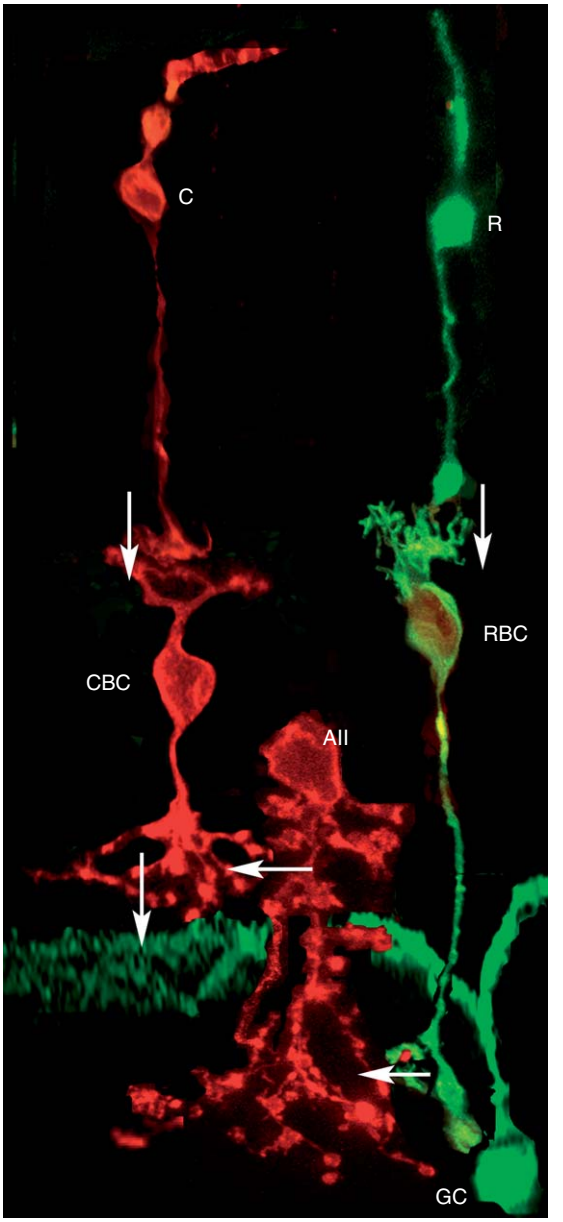

Figure 8 The rod pathway. Montage of neurons of the rod pathway stained individually by delivery of lipophilic, fluorescent dies, in the mouse retina. Rods (R) and cones (C) converge upon separate sets of bipolar cells. Because of rod bipolar (RB) cells make connections to AII amacrine cells and these, in turn, feed the information to cone bipolar (CB) cells, the rod pathway is a five-neuron chain. Direct connections to ganglion cells (GCs) are mostly established by means of chemical synapses between CB axonal endings and GC dendrites.

similarly, it is likely that most of the CB cells with axonal arbors in sublamina OFF are postsynaptic to AII lobular appendages. Thus, the role of information transfer of the scotopic signal from AII amacrines to

ganglion cells is almost entirely committed to the axonal arbors of ON and OFF CB cells. This transfer is operated through further sets of synaptic connections, represented by sign-conserving ribbon synapses, established between ON and OFF CB axonal endings and corresponding sets of ganglion cell dendrites, in the ON and OFF laminae of the IPL. These synapses use glutamate as a neurotransmitter.

A part of the rod pathway is summarized in Figure 9. This is a montage of mouse neurons, individually labeled with lipophilic, fluorescent dies delivered to retinal slices by a gun and propelled by helium gas. The images obtained are reminiscent of those achieved by means of classical Golgi impregnation.

There are several checkpoints in the piggyback arrangement described so far: first of all, CB cells return feedback synapses onto the lobular appendages of AII amacrine cells. This implies transfer of information from the cone to the rod system. Moreover, each AII amacrine receives profuse innervation from dopaminergic amacrine cells. These are rare, wide-field neurons (less than 600 of them in the retina of a mouse, which contains globally some 600 000 amacrine cells), with arborizations located in the outermost portion of the IPL (the sublamina 1). Dopamine, released in the dark, is a powerful modulator of gap junction permeability, and an overall regulator of retinal sensitivity to light. Dopamine controls many components of the retinal circuitry; it alters the gap junctional conductance between horizontal and amacrine cells, increases the responses of ionotropic glutamate receptors on bipolar cells, and ultimately affects the center-surround balance of ganglion cells. In several cases, dopamine action is mediated nonsynaptically, via a paracrine release of the neurotransmitter (Witkovsky, P., 2004).

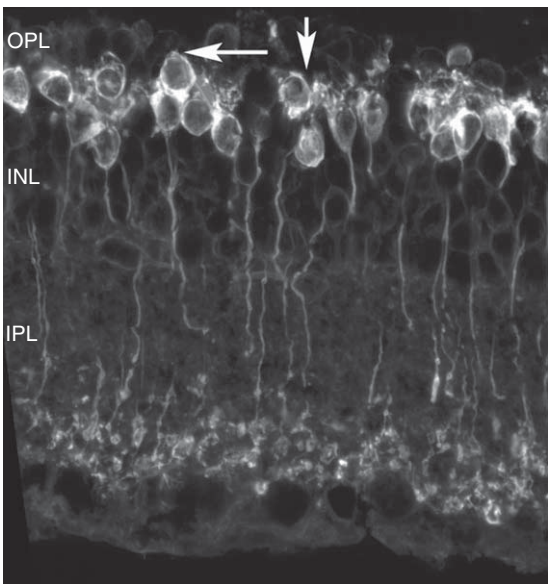

Figure 9 Vertical section of the retina of a mouse mutant in which photoreceptors have totally degenerated (rd10 mutant). In this and other mutations, rod bipolar cells retract their dendritic trees, which show an almost total secondary atrophy (arrows).

The AII amacrine is the nodal point where rod and cone, as well as ON and OFF pathways, intersect. Within scotopic levels of illumination, light stimuli hyperpolarize rods, eliciting a decrement in their glutamate release; this, in turn, depolarizes rod bipolar cells, causing the release of glutamate from their axonal endings onto the A17 amacrine cell and the AII amacrine cell. Glutamate excites the AII, causing at the same time: the release of glycine onto OFF CB cells, and thus the inhibition of OFF ganglion cells; the depolarization of ON CB cells via gap junctions, and thus the excitation of ON ganglion cells; the diffusion of the signal through the network of AIIs, also coupled through homologous gap junctions. In turn, AII responses are modified by inhibition from depolarized A17 amacrines through their feedback onto rod bipolar axonal endings. Thus, rod-generated signals produce inhibition of the OFF pathway and excitation of the ON pathway.

In bright light (photopic) conditions, AII amacrine cells receive inputs from both ON (through gap junctions) and OFF CBs (by means of conventional, chemical synapses). ON center responses are stronger and elicit glycine release from AII lobular appendages. In turn, these inhibit OFF CB cells. Moreover, because of the weaker coupling of gap junctions during bright light, the dissipation of cone signals through the AII network is limited, so that this can reach effectively ganglion cells. The net result is that the OFF channel is inhibited by the ON retinal channel and that high-acuity cone signals are preserved. In scotopic and photopic conditions, under the control of dopaminergic innervation, the AII amacrine cell operates as a switch from one input pathway to another, with high efficiency.

1.11.2 Additional Rod Pathways

Cone pedicles have thin, basal processes, named telodendria, that project horizontally to the OPL, forming small gap junctions with neighboring rod spherules and cone pedicles (Raviola, E. and Gilula, N. B., 1975). In

principle, such connections, that mix signals from photoreceptors of different sensitivity and different absorption spectra, appear to degrade visual perception, and particularly that of color. Physiology has shown in a long time that mammalian cones carry rod signals (Nelson, R., 1977), which appear as a slow hyperpolarization following the initial response to a brief flash of light. Although the utility of such an arrangement is still a matter of debate, through gap junctions with cones, rod signals can utilize the fast-tuned cone pathways to reach the IPL.

A novel family of connections has been identified recently in the outer retina of several mammalian species. Some OFF CB cells make symmetrical contacts with rod spherules and therefore collect direct input from rods (Hack, I. *et al.*, 1999; Tsukamoto, Y. *et al.*, 2001; Protti, D. A. *et al.*, 2005). Dendrites of such CBs appear to express ionotropic glutamate receptors at the site of apposition to rod spherules. Hence, besides the main pathway constituted by rod bipolars, AII amacrines, CBs, and ganglion cells, rod-generated signals can exit the retina through gap junctions between rods and cones as well as through this third pathway, using mixed cone–rod bipolar cells.

Although the alternative rod pathway was first discovered in the retina of rodents, anatomical evidence for direct connections between rods and OFF CB cells was later provided for the rabbit retina as well (Li, W. *et al.*, 2004). Electrophysiological recordings in the presence of drugs, capable of interfering with the scotopic transmission at various synaptic levels, demonstrated that around one-half of the ganglion cells in the rabbit retina receive off signals through a circuit that is independent of rod bipolar cells. In the mouse retina, however, a very low proportion of OFF signals carried in parallel to rod bipolar cells can be revealed, while no ganglion cells at all in the rat retina display off responses attributable to direct, flat contacts between rods and OFF CB cells as an alternative route (Protti, D. A. *et al.*, 2005). This suggest that the alternative rod pathway may be a common feature of the mammalian retina, but the relative importance and significance of this pathway differ between species. Noticeably, all the three rod pathways (both the classic and the two indirect ones) make use of CB axonal endings to gain access to ganglion cells.

1.11.3 How Could This Particular Synaptic Disposition Be Evolved?

A likely hypothesis is that the various rod pathways (and, particularly, the piggyback arrangement) have an evolutionary explanation: cone-mediated vision in bright light conditions evolved first, in parallel to color vision. This happened in ancestral vertebrates, with dim light vision appearing only after the evolution of the jawed vertebrates (Bowmaker, J. K., 1998). Hence, inner retinal circuitry was first shaped by cones: as each cone brings in a number of CB cells (ON, OFF, transient, sustained, etc.), one can postulate the hypothesis that the antique vertebrate retina was constituted by several types of CBs and cone-driven amacrine cells that shaped the responses of various types of ganglion cells.

When, later in evolution, rhodopsin appeared, as an effect of duplication of preexisting opsin genes, this pigment became segregated in a subtype of photoreceptor, the ancestor of a modern rod. The advantages of a dual retina were obvious: vertebrates could expand their life style to become partly nocturnal, colonizing additional habitats. To make the whole retinal network available to the newly evolved rods, it was not necessary to generate an additional inner retina. Useless duplication (with an undesirable increase in retinal thickness) was avoided introducing two novel interneurons: rod bipolar cells and AII amacrines. The first ensured retention of high sensitivity in the scotopic pathway by collecting information from a high number of rods. The second interneuron recruited the preexisting cone pathways, by establishing adequate connections with ON and OFF CB cells in the IPL. Through the evolution of this ingenious piggyback system, the whole neural network, previously reserved to cones, could be exploited by the newly evolved rods. Among other mechanisms, the switch in sensitivity of photopic versus scotopic pathways was ensured at inner retinal level by dopaminergic control of gap junction permeability.

This is somehow reflected in the fact that, contrary to the general belief, and as demonstrated by modern neuroanatomical techniques, CB cells largely outnumber rod bipolars, even in mammalians that are strongly rod dominated such as rodents. In these animals, cones are only 3% of all the photoreceptors (Jeon, C. J. *et al.*, 1998). Yet, CB cells are at least two times more numerous than rod bipolars. In a rabbit central retina, where cones are more abundant, CB cells outnumber rod bipolar cells by four to five times (Strettoi, E. and Masland, R. H., 1995). This is partly explained by the large converge of photoreceptors-to-bipolars characteristic of the rod system; however, part of it is accounted for the large variety of CB cells, acting in parallel and performing different types of computations (for instance, on temporal

properties) of the light-generated signals. Ultimately, the piggyback arrangement ensures the access of the scotopic signal to parallel processing, originally evolved in the cone system.

It is often underlined how AII amacrines are somewhat connotative of a mammalian retina; yet, cone-only retinas, or retinal areas from which rods are absent (such as the primate foveolar tip), lack AII amacrine cells completely. This also indicates that this cell evolved as a rod-system interneuron; in addition, a peculiarity of the AII is represented by the fact that this neuron belongs to the retinal vertical pathway more than to the horizontal, modulatory network, to which amacrine cells are traditionally assigned.

1.11.4 Inherited Photoreceptor Degeneration: How Photoreceptor Death Affects the Architecture of the Rod and Cone Pathways

A high number of mutations can occur in photoreceptors, with at least 100 of them affecting the rhodopsin gene alone (Mendes, H. F. *et al.*, 2005). The consequence is usually the progressive death of rods, followed by the secondary degeneration of cones, and subsequent blindness. These are the hallmarks of retinitis pigmentosa (RP), a family of inherited diseases characterized by progressive death of rods, initial loss of scotopic vision, secondary death of cones and, later, loss of all the effective sight. Many animal models of RP (Dalke, C. and Graw, J. 2005), and rodents in particular, are available to investigators to study this, otherwise rare, human disease, which affects 1 over 3500 individuals. These models have contributed invaluable tools to study the genetics as well as several biological aspects of this pathology, which is now well characterized in terms of symptoms and genetics.

Interestingly, very few investigators have been interested in understanding possible effects of photoreceptor degeneration upon other retinal cells, and particularly upon the neurons to which they are synaptically connected. This issue is however relevant for perspective therapies aimed at repairing the RP retina, and particularly for those approaches based on cellular transplantation (Lund, R. D. *et al.*, 2001) or implants of electronic devices (also known as silicon-retinal implants) (Loewenstein, J. I. *et al.*, 2004). Indeed, by examining the retina of various mouse mutants mimicking human RP, we detected secondary modifications of cells in the deeper retinal layers, and particularly in the neurons of the rod pathway described above (Marc, R. E. *et al.*, 2003). It appears that, concomitant to photoreceptor death, a stereotyped chain of events affects inner retinal cells, suggesting a close dependence of postsynaptic neurons from their afferent partners. The most striking feature is a dramatic regression of dendritic arbors in rod bipolar cells, associated to an abnormal localization and downregulation of the metabotropic glutamate receptor mGluR6.

Changes in horizontal cells are also quite striking. These neurons are connected to cones with their cell bodies and dendrites, and to rods by means of their axonal arborization. Both portions of the cells undergo a process of remodeling which follows photoreceptor death: ultimately, axonal endings loose their fine ramifications and grow enormously, covering the retina with a very loose mesh of processes. Later, the cell bodies become hypertrophic and loose the dendrites. After rod bipolar and horizontal cells, also CB cells start to show major anatomical changes; by the time that cone degeneration becomes complete, they retract their dendrites and show regressive changes similar to those described for rod bipolar cells. As reported above, CB cells are the most numerous interneurons of the mammalian retina. Their integrity is of clinical relevance, as they are a potential platform for therapeutic intervention.

Following abnormalities of their morphology, inner neurons retinas do eventually die out as a consequence of photoreceptor degeneration. Both rod bipolar and horizontal cells undergo a process of death that progresses slowly but continuously.

All together, these data point out clearly that the maintenance of a normal morphology, which include a dendritic tree and a normal complement of synaptic receptors, in second-order neurons, require the presence of viable photoreceptors. For this reason, RP cannot be considered as a pure photoreceptor disease: because it affects the very first neuronal type of a complex network of the CNS, RP should be considered a true central affection; thus, as any other neurological disorders, the whole network should be taken into account, rather than the affected cells only. This is a key concept when devising strategies aimed at restoring vision in RP: a timely intervention is required to precede widespread, adverse effects upon those neurons of the inner retina that represent the only network through which replaced photoreceptors or artificial implants can communicate with the visual part of the brain.

Acknowledgments

E. Strettoi is supported by the Italian National Research Council and by the NIH grant R01-EY 12654.

References

Baylor, D. A., Lamb, T. D., and Yau, K. W. 1979. Responses of retinal rods to single photons. J. Physiol. 288, 613–634.

Bowmaker, J. K. 1998. Evolution of colour vision in vertebrates. Eye 12(Pt 3b), 541–547.

Cajal Santiago Ramón y 1989. Recollections of My Life, 3rd edn. MIT Press.

Dacheux, R. F. and Raviola, E. 1986. The rod pathway in the rabbit retina: a depolarizing bipolar and amacrine cell. J. Neurosci. 6(2), 331–345.

Dalke, C. and Graw, J. 2005. Mouse mutants as models for congenital retinal disorders. Exp. Eye Res. 81(5), 503–512.

Field, G. D., Sampath, A. P., and Rieke, F. 2005. Retinal processing near absolute threshold: from behavior to mechanism. Annu. Rev. Physiol. 67, 491–514.

Hack, I., Peichl, L., and Brandstatter, J. H. 1999. An alternative pathway for rod signals in the rodent retina: rod photoreceptors, cone bipolar cells, and the localization of glutamate receptors. Proc. Natl. Acad. Sci. U. S. A. 96(24), 14130–14135.

Ivanova, E., Muller, U., and Wassle, H. 2006. Characterization of the glycinergic input to bipolar cells of the mouse retina. Eur. J. Neurosci. 23(2), 350–364.

Jeon, C. J., Strettoi, E., and Masland, R. H. 1998. The major cell populations of the mouse retina. J. Neurosci. 18(21), 8936–8946.

Kolb, H. 1979. The inner plexiform layer in the retina of the cat: electron microscopic observations. J. Neurocytol. 8(3), 295–329.

Li, W., Keung, J. W., and Massey, S. C. 2004. Direct synaptic connections between rods and OFF cone bipolar cells in the rabbit retina. J. Comp. Neurol. 474(1), 1–12.

Loewenstein, J. I., Montezuma, S. R., and Rizzo, J. F., III. 2004. Outer retinal degeneration: an electronic retinal prosthesis as a treatment strategy. Arch. Ophthalmol. 122(4), 587–596.

Lund, R. D., Kwan, A. S., Keegan, D. J., Sauve, Y., Coffey, P. J., and Lawrence, J. M. 2001. Cell transplantation as a treatment for retinal disease. Prog. Retin. Eye. Res. 20(4), 415–449.

Marc, R. E., Jones, B. W., Watt, C. B., and Strettoi, E. 2003. Neural remodeling in retinal degeneration. Prog. Retin. Eye Res. 22(5), 607–655.

Mendes, H. F., van der Spuy, J., Chapple, J. P., and Cheetham, M. E. 2005. Mechanisms of cell death in rhodopsin retinitis pigmentosa: implications for therapy. Trends Mol. Med. 11(4), 177–185.

Nelson, R. 1977. Cat cones have rod input: a comparison of the response properties of cones and horizontal cell bodies in the retina of the cat. J. Comp. Neurol. 172(1), 109–135.

Protti, D. A, Flores-Herr, N., Li, W., Massey, S. C., and Wassle, H. 2005. Light signaling in scotopic conditions in the rabbit, mouse and rat retina: a physiological and anatomical study. J. Neurophysiol. 93(6), 3479–3488.

Raviola, E. and Dacheux, R. F. 1987. Excitatory dyad synapse in rabbit retina. Proc. Natl. Acad. Sci. U. S. A. 84(20), 7324–7328.

Raviola, E. and Gilula, N. B. 1975. Intramembrane organization of specialized contacts in the outer plexiform layer of the retina. A freeze-fracture study in monkeys and rabbits. J. Cell. Biol. 65(1), 192–222.

Sandell, J. H., Masland, R. H., Raviola, E., and Dacheux, R. F. 1989. Connections of indoleamine-accumulating cells in the rabbit retina. J. Comp. Neurol. 283(2), 303–313.

Sterling, P., Freed, M. A., and Smith, R. G. 1988. Architecture of rod and cone circuits to the on-beta ganglion cell. J. Neurosci. 8(2), 623–642.

Strettoi, E. and Masland, R. H. 1995. The organization of the inner nuclear layer of the rabbit retina. J. Neurosci. 15, 875–888.

Strettoi, E., Raviola, E., and Dacheux, R. F. 1992 Synaptic connections of the narrow-field, bistratified rod amacrine cell (AII) in the rabbit retina. J. Comp. Neurol. 325(2), 152–168.

Tsukamoto, Y., Morigiwa, K., Ueda, M., and Sterling, P. 2001. Microcircuits for night vision in mouse retina. J. Neurosci. 21(21), 8616–8623.

Veruki, M. L. and Hartveit, E. 2002. Electrical synapses mediate signal transmission in the rod pathway of the mammalian retina. J. Neurosci. 22(24), 10558–10566.

Witkovsky, P. 2004. Dopamine and retinal function. Doc. Ophthalmol. 108(1), 17–40.

Further Reading

Gargini, C., Terzibasi, E., Mazzoni, F., and Strettoi, E. 2007. Retinal organization in the retinal degeneration 10 (rd10) mutant mouse: a morphological and ERG study. J. Comp. Neurol. 500(2), 222–238.

Mataruga, A., Kremmer, E., and Muller, F. 2007. Type 3a and type 3b OFF cone bipolar cells provide for the alternative rod pathway in the mouse retina. J. Comp. Neurol. 502(6), 1123–1137.

Ueda, Y., Iwakabe, H., Masu, M., Suzuki, M., and Nakanishi, S. 1997. The mGluR6 5′ upstream transgene sequence directs a cell-specific and developmentally regulated expression in retinal rod and ON-type cone bipolar cells. J. Neurosci. 17(9), 3014–3023.

1.12 Decomposing a Cone's Output (Parallel Processing)

H Wässle, Max-Planck-Institute for Brain Research, Frankfurt/Main, Germany

© 2008 Elsevier Inc. All rights reserved.

1.12.1	**Introduction**	313
1.12.2	**The Photoreceptor Synapse**	314
1.12.2.1	The Presynaptic Complex	314
1.12.2.2	The Postsynaptic Partners	316
1.12.2.3	Feedback from Horizontal Cells	316
1.12.3	**Morphological Types of Bipolar Cells**	317
1.12.3.1	Midget Bipolar Cells of the Primate Retina	318
1.12.3.2	Blue-Cone Bipolar Cells	320
1.12.3.3	Diffuse Bipolar Cells	321
1.12.3.4	Cone Contacts of Bipolar Cells	321
1.12.4	**Expression of Glutamate Receptors at Cone Pedicles**	322
1.12.4.1	Glutamate Receptor Subunits	322
1.12.4.2	ON-Bipolar Cell Glutamate Receptors	323
1.12.4.3	OFF-Bipolar Cell Glutamate Receptors	324
1.12.4.4	Horizontal Cell Glutamate Receptors	325
1.12.5	**Light-Evoked Responses of Bipolar Cells**	325
1.12.5.1	Temporal Transfer Characteristics	325
1.12.5.2	Spatial Transfer Characteristics	327
1.12.6	**Intensity-Response Function**	328
1.12.7	**Synaptic Contacts of Bipolar Cells in the Inner Plexiform Layer**	328
1.12.8	**Glutamate Receptors in the Inner Plexiform Layer**	330
1.12.8.1	α-Amino-3-Hydroxy-5-Methyl-4-Isoxazolepropionic Acid Receptor Subunits	330
1.12.8.2	Kainate Receptor Subunits	331
1.12.8.3	*N*-Methyl-D-Aspartate Receptor Subunits	331
1.12.8.4	Metabotropic Glutamate Receptors	331
1.12.8.5	Co-Stratification of Pre- and Postsynaptic Partners in the Inner Plexiform Layer	332
1.12.9	**Conclusions**	333
References		333

1.12.1 Introduction

It is well established that visual signals in the brain are processed in parallel, with contours, color, movement, stereopsis, and even more specific features such as facial expressions being processed in different brain areas (Casagrande, V. A. and Xu, X., 2004). The visual pathway from the eye to the brain is also organized into parallel streams, and fiber groups of the optic tract project to different subcortical areas such as the suprachiasmatic nucleus, the ventral and lateral geniculate complex, the pretectum, the superior colliculus, and the accessory optic nuclei. These brain areas have different roles in visual function and accordingly receive inputs from retinal ganglion cells (RGCs) which perfectly subserve such specific roles. For example, the suprachiasmatic nucleus, which regulates circadian rhythms, or the pretectum, which adjusts the pupil size, receive inputs from the recently discovered melanopsin-containing ganglion cells. They have intrinsic light responses in their dendrites and transmit a sustained light signal (Berson, D. M., 2003). Parallel routes can also be distinguished in the visual pathway that is commonly attributed to conscious vision, namely the projection from the eye through the lateral geniculate nucleus (LGN) to the visual cortex. Here, in primates, the parvocellular and magnocellular pathways are well established, and a third parallel tract is relayed in the intralaminar regions, the K-layers, of the geniculate (Hendry, S. H. and Reid, C., 2000).

Considerable processing and filtering of visual information occurs at the earliest stage of the mammalian visual system – the retina. In any mammalian retina there may well exist as many as 15 different ganglion cell types which cover the retina homogeneously with their dendritic fields. They represent 15 specific filters which encode in parallel different aspects of the image projected onto the retina. Ganglion cells receive specific inputs from bipolar and amacrine cells in the inner plexiform layer (IPL). The IPL is precisely stratified and the different ganglion cell types have their dendrites at specific levels within the IPL (Isayama, T. *et al.*, 2000; Sun, W. *et al.*, 2002; Dacey, D. M. *et al.*, 2003; Kong, J. H. *et al.*, 2005; Kim, T. J. and Jeon, C. J., 2006). The axons of bipolar cells, which transfer the light signals from the photoreceptors to the ganglion cells also terminate at distinct levels within the IPL (Ghosh, K. K. *et al.*, 2004). This suggests that the neurally encoded retinal image is different at different levels of the IPL, depending upon stratification of the various bipolar, amacrine, and ganglion cells (Roska, B. and Werblin, F., 2001). Bipolar cells provide the major excitatory drive for ganglion cells and their physiological signature, for instance OFF- or ON-light responses, is transferred onto ganglion cells. The physiological signature of bipolar cells in turn is defined by the glutamate receptors (GluRs) they express at their synaptic contacts with the cones. Parallel processing within the retina, therefore, begins already at the first synapse of the retina and here the molecular composition of GluRs represents the origin of the different channels (Wässle, H., 2004).

1.12.2 The Photoreceptor Synapse

1.12.2.1 The Presynaptic Complex

Cones respond to a light stimulus with a graded hyperpolarization and release their transmitter glutamate at a specialized synaptic terminal named cone pedicle. Transmitter release is high in darkness and is reduced by illumination of the cone. The cone pedicle is a giant synapse with multiple release sites and numerous postsynaptic partners (Figure 1). In the primate retina the cone pedicle increases from a diameter of approximately 4–5 µm close to the fovea to 8 µm diameter in peripheral retina. It contains between 20 and 50 presynaptic ribbons (Figures 1(c) and 1(e)), each of which is flanked by synaptic vesicles (Haverkamp, S. *et al.*, 2000; 2001). The synaptic terminal of rod photoreceptors, the rod spherule is smaller than the cone pedicle (~3 µm diameter) and contains one or two synaptic ribbons and release sites. The photoreceptor synaptic ribbon is a curved plate, ~30 nm thick, it extends ~200 nm into the cytoplasm and varies in length from 200 to 1000 nm. In rod spherules it is bent like a horseshoe (Figure 1(e)) and commonly cracks into two parts (Migdale, K. *et al.*, 2003). The ribbons are involved with the synaptic machinery of transmitter release and appear to represent a specialization of synapses, which have a sustained release of glutamate such as photoreceptors, bipolar cells, and auditory and vestibular hair cells (von Gersdorff, H., 2001; Heidelberger, R. *et al.*, 2005; Sterling, P. and Matthews, G., 2005). Proteins at the ribbon are just beginning to be identified and represent a specialization of the cytomatrix comparable and complementary to proteins present at the active zones of conventional synapses (tom Dieck, S. *et al.*, 2005; Deguchi-Tawarada, M. *et al.*, 2006). The proteins segregate into two compartments at the ribbon: a ribbon associated compartment including Piccolo, RIBEYE, CtBP1, RIM1, and the motor protein KIF3A, and an active zone compartment including RIM2, Munc 13-1, CAST1, and a calcium (Ca^{2+})-channel $\alpha 1$ subunit (Figure 1(b)). A direct interaction between the ribbon specific protein RIBEYE and bassoon seems to link the two compartments and is responsible for the integrity of the photoreceptor ribbon complex. In bassoon knockout mice the ribbons are no longer linked to the active zone and transmitter release is not possible (Dick, O. *et al.*, 2003). Fish deficient in RIBEYE lack an optokinetic response and have shorter synaptic ribbons in photoreceptors (Wan, L. *et al.*, 2005). The ribbons tether numerous synaptic vesicles (Usukura, J. and Yamada, E., 1987) and it has been suggested that they represent a conveyor belt transporting continuously synaptic vesicles toward the active zone (Gray, E. G. and Pease, H. L., 1971; Muresan, V. *et al.*, 1999). However, this is an oversimplification, because disruption of the actin cytoskeleton did not influence transmitter release (Heidelberger, R. *et al.*, 2002; Holt, M. *et al.*, 2004; Heidelberger, R. *et al.*, 2005). Ribbons, however, might serve as a platform along which vesicles can be primed for sustained release. Vesicles docked at the active zone probably represent the fast releasable pool. It has been estimated that a ribbon of a cone in the primate fovea has ~40 docking sites close to the active zone and 150 vesicles are packed along the ribbon (Sterling, P. and Matthews, G., 2005). The vesicles of all cones and of rods are loaded with glutamate through the vesicular glutamate transporter vGluT1 (Haverkamp, S.

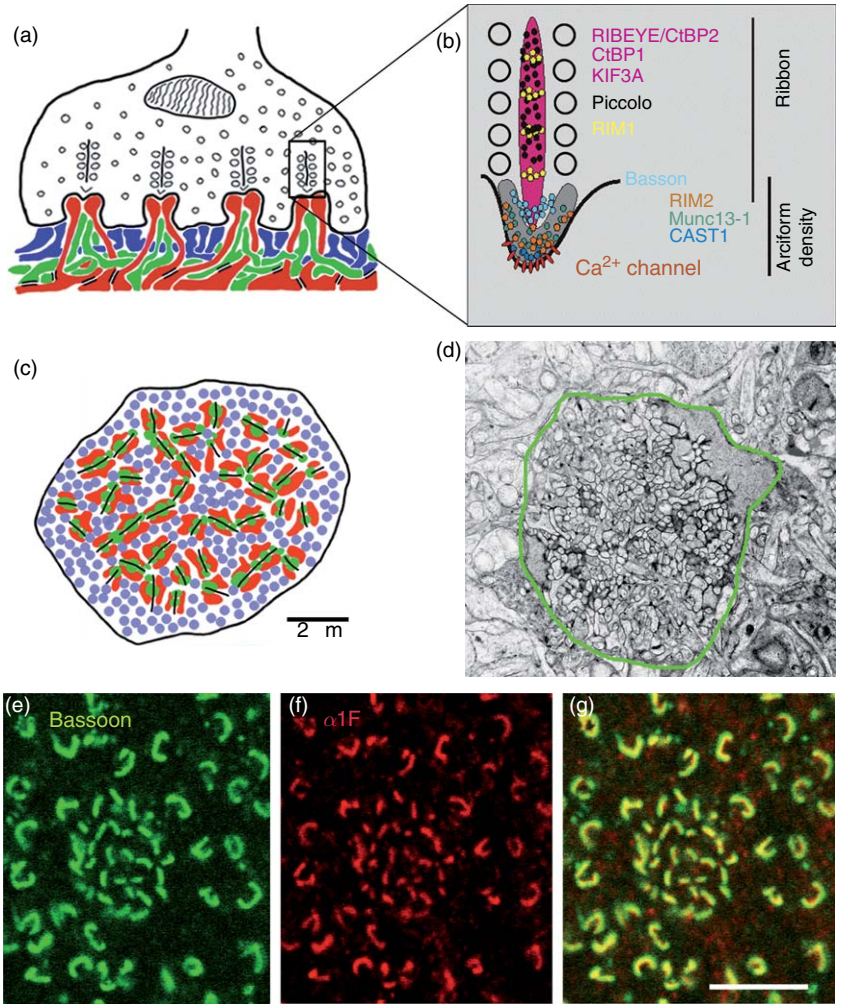

Figure 1 Structure of the cone pedicle, the synaptic terminal of cones. (a) Schematic vertical view of a cone pedicle. Four presynaptic ribbons are apposed to the invaginating dendrites of horizontal cells (red) and ON-cone bipolar cells (green). OFF-cone bipolar cell dendrites form contacts at the cone pedicle base (blue). (b) The presynaptic compartment is made up of the ribbon, the vesicles, and the arciform density. Adapted from tom Dieck, S., Altrock, W. D., Kessels, M. M., Qualmann, B., Regus, H., Brauner, D., Fejtova, A., Bracko, O., Gundelfinger, E. D., and Brandstätter, J. H. 2005. Molecular dissection of the photoreceptor ribbon synapse: physical interaction of Bassoon and RIBEYE is essential for the assembly of the ribbon complex. J. Cell Biol. 168, 825–836. The following proteins are associated with the ribbon: RIBEYE (Schmitz, F. *et al.*, 2000); CtBP1,2; KIF3A (Muresan, V. *et al.*, 1999); Piccolo; RIM1. The following proteins are associated with the arciform density: Bassoon; RIM2; Munc 13-1; CAST. The Ca^{2+} channels are inserted into the presynaptic membrane (Morgans, C. W. *et al.*, 2005). (c) Schematic horizontal view of a macaque monkey (primate) cone pedicle base. Ribbons (black lines), horizontal cell processes (red), and ON-cone bipolar cell dendrites (green) form a total of 40 triads. Numerous contacts of OFF-cone bipolar cells (blue) are found throughout the pedicle base. (d) Electron micrograph of a horizontal section taken underneath a primate cone pedicle (green outline). More than 500 individual processes contact this cone pedicle. (e–g) Fluorescence micrographs of a primate cone pedicle (center) surrounded by rod spherules, double labeled for bassoon (e) and the Ca^{2+} channel subunit α1F (f). Bassoon immunolabeling decorates the ribbons of the cone pedicle and the rod spherules (horseshoe-shaped). The superposition of (e) and (f) in (g) shows that the Ca^{2+} channels are in close vicinity of the synaptic ribbons. Scale bar = 5 μm.

et al., 2003; Johnson, J. *et al.*, 2003; Sherry, D. M. *et al.*, 2003). A subpopulation of approximately 10% of cones expresses vGluT2 in addition to vGluT1 (Fyk-Kolodziej, B. *et al.*, 2004; Wässle, H. *et al.*, 2006).

Exocytosis of the vesicles is finally triggered by voltage-gated Ca^{2+} channels clustered at the active zone. Immunostaining for the α1D and α1F subunits of L-type Ca^{2+} channels and Ca^{2+} entry have

been observed along the base of the ribbon (Figures 1(e)–1(g); Morgans, C. W., 2001; Wässle, H. *et al.*, 2003; Zenisek, D. *et al.*, 2003; 2004; tom Dieck, S. *et al.*, 2005). Mutations in the Ca^{2+} channel α1F result in impairment of the photoreceptor synaptic transmission and cause congenitory stationary nightblindness (Morgans, C. W. *et al.*, 2005). Ca^{2+} extrusion from the photoreceptor synaptic complex is mediated through the plasma membrane calcium ATPase (PMCA) localized along the sides of cone pedicles and rod spherules (Morgans, C. W. *et al.*, 1998; Duncan, J. L. *et al.*, 2006).

The potassium (K^+-) and Ca^{2+}-channels of cone pedicles and rod spherules can be modulated by several mechanisms which in turn also regulate the transmitter release. The metabotropic glutamate receptor 8 (mGluR8) at the photoreceptor synaptic terminals, acts as autoreceptor and upon glutamate binding the influx of Ca^{2+} is reduced (Koulen, P. *et al.*, 1999; 2005). Modulation of the voltage dependent Ca^{2+}-channels at the active zone is also a mechanism of horizontal cell feed back and will be discussed later. Cannabinoid receptors at cone pedicles regulate voltage-dependent K^+ currents (Struik, M. L. *et al.*, 2006). Finally, calcium extrusion modulates the amplitude and timing of transmission in cone pedicles and rod spherules (Duncan, J. L. *et al.*, 2006).

L- and M-cone pedicles are coupled to their immediate neighbors and to rod spherules through electrical synapses (gap junctions; Raviola, E. and Gilula, N. B., 1973) where connexin 36 is expressed. S-cone pedicles are only sparsely coupled (Tsukamoto, Y. *et al.*, 2001; Feigenspan, A. *et al.*, 2004; Hornstein, E. P. *et al.*, 2004; Li, W. and DeVries, H., 2004, O'Brien, J. J. *et al.*, 2004). This coupling allows the network to average out the uncorrelated noise in individual cones, and thereby to improve the response to a light stimulus (Lamb, T. D. and Simon, E. J., 1976). It also provides a route for the signal transfer from rod spherules to cone pedicles (see Mammalian Rod Pathways and Circuit Functions of Gap Junctions in the Mammalian Retina).

1.12.2.2 The Postsynaptic Partners

At the synaptic terminals of rods and cones, the light-evoked signals are transferred onto bipolar and horizontal cells (Figure 1(a)). Horizontal cells, of which there are between one and three types in mammalian retinas, provide lateral interactions in the outer plexiform layer (OPL). In the primate retina they are named H1 and H2 horizontal cells. Their dendritic tips are inserted into invaginations of the cone pedicle base which are formed at the ribbons. Two horizontal cell endings push up towards the ribbon and along the ribbon the two horizontal cells form a zone of contact between each other (Raviola, E. and Gilula, N. B., 1975).

Two kinds of bipolar cell contacts have been identified at cone pedicles: flat or basal contacts and invaginating contacts (Dowling, J. E. and Boycott, B. B., 1966). The dendritic tips of invaginating bipolar cells are inserted in between the two lateral horizontal cell dendrites, and this postsynaptic unit has been named a triad (Missotten, L., 1965). The dendritic tips of flat bipolar cells make numerous contacts at the cone pedicle base (Figures 1(a) and 1(c)).

Cone pedicles of the peripheral primate retina contain ~40 synaptic ribbons and invaginations, where they accommodate ~80 horizontal cell dendritic terminals (Figure 1(c)). L (red)- and M (green)-cones are connected to three or four H1 horizontal cells and make multiple contacts with every one of them. S (blue)-cones have only sparse, if any connections with H1 horizontal cells. L- and M-cones are also connected to three or four H2 horizontal cells, however, the number of contacts is smaller than with H1 cells. In contrast, S-cones have multiple contacts with H2 cells (Ahnelt, P. and Kolb, H., 1994). Cone pedicles of the peripheral primate retina accommodate ~80 dendritic tips of invaginating bipolar cells (Chun, M. H. *et al.*, 1996) and they are engaged in 200–300 flat contacts. Taken together, 400–500 synaptic contacts are found at individual cone pedicles (Figure 1(d)). Their details will be discussed later.

1.12.2.3 Feedback from Horizontal Cells

Horizontal cell dendrites are inserted as lateral elements into the invaginating contacts of cone pedicles (Figure 1(a)), and horizontal cell axon terminals form the lateral elements within rod spherules. Traditionally, it is assumed that horizontal cells release the inhibitory transmitter gamma-aminobutyric acid (GABA) and provide feedback inhibition at the photoreceptor synaptic terminal. As horizontal cells summate light signals from several cones, such feedback would cause lateral inhibition, through which a cone's light response is reduced by the illumination of neighboring cones. This mechanism is thought to enhance the response to the edges of visual stimuli and to reduce the response to areas of uniform brightness. However, the GABA-feedback model has recently been challenged because of the

lack of classical synapses from horizontal cells onto cones, the lack of GABA receptors on mammalian cones and the lack of GABA uptake into horizontal cells from the medium. Two alternative hypotheses of horizontal cell function have been proposed. One assumes that horizontal cell processes, which are inserted into cone pedicles and rod spherules, express connexins (hemigap junctions). Current that flows through the channels formed by the connexins changes the extracellular potential in the invaginations and thus shifts the activation curves of the cone pedicle Ca^{2+} channels. By this mechanism of electrical feedback, horizontal cells could modulate the glutamate release from cones and rods (Kamermans, M. *et al.*, 2001). The second hypothesis also postulates modulation of the Ca^{2+} channels that regulate the release of glutamate from cones; however, the mechanism responsible is a change in pH within the invagination, caused by voltage-dependent ion transport through the horizontal cell membrane (Hirasawa, H. and Kaneko, A., 2003). There is also evidence that light-dependent release of GABA from horizontal cells provides feed-forward inhibition of bipolar cell dendrites (Haverkamp, S. *et al.*, 2000; Duebel, J. *et al.*, 2006). Irrespective of their precise mode of action, horizontal cells sum light responses across a broad region, and subtract it from the local signal. Because horizontal cells are coupled through gap junctions (see Circuit Functions of Gap Junctions in the Mammalian Retina), their receptive fields can be much wider than their dendritic fields (Hombach, S. *et al.*, 2004).

1.12.3 Morphological Types of Bipolar Cells

Bipolar cells of the mammalian retina can be subdivided according to their morphology into many different types (Figure 2). Cajal S. R. Y. (1893) recognized rod bipolar (RB) cells as a separate type (Figure 2: RB). Their dendrites make invaginating contacts with rod spherules and their axons terminate in the innermost part of the IPL (see Mammalian Rod Pathways). Several types of cone bipolar cells have been recognized in different mammalian species. In the rabbit retina 13 types have been described from Golgi staining and single cell filling (Famiglietti, E. V., 1981; McGillem, G. S. and Dacheux, R. F., 2001; MacNeil, M. A. *et al.*, 2004). In the cat retina 8–10 different types of cone bipolar cells have been recognized (Famiglietti, E. V., 1981; Kolb, H. *et al.*, 1981; Cohen, E. D. and Sterling, P., 1990a; 1990b). In the ground squirrel seven different types have been described (West, R. W., 1976).

The diagram in Figure 2 compares the bipolar cells of the mouse and rat retinas with those of the peripheral macaque monkey retina. The nine putative cone bipolar cell types (labeled 1–9) and the RB cells of the mouse and rat retina are arranged according to the stratification level of their axon terminals in the IPL. The cells were drawn from vertical sections following intracellular injections (Euler, T. and Wässle, H., 1995; Hartveit, E., 1996; Ghosh, K. K. *et al.*, 2004; Pignatelli, V. and Strettoi, E., 2004). Immunocytochemical markers have been found for five bipolar cell types of the mouse retina (Haverkamp, S. *et al.*, 2003; illustrated in Figure 3). The type 7 and type 9 bipolar cells of the mouse retina have also been labeled in transgenic mouse lines by the expression of green fluorescent protein (GFP; Huang, L. *et al.*, 2003; Haverkamp, S. *et al.*, 2005). The cone contacts of the nine bipolar cell types of mouse and rat have not yet been analyzed in detail, however, they contact between five and 10 neighboring cone pedicles with one exception: type 9 has a wide dendritic tree that appears to be cone selective and it will be shown later that it contacts S-cones.

Rat and mouse retinas are considered to be rod dominated because only 1% of their photoreceptors are cones (Szél, A. *et al.*, 1993). However, the perspective changes if one examines the absolute number of cones. The cone density is between 8000 and 10 000 cones mm^{-2}, comparable to midperipheral cat, rabbit, and monkey retina. Consequently the types and retinal distributions of cone bipolar cells are closely similar between mammalian species. The bipolar cells of the monkey retina, shown schematically in Figure 2, where determined initially from Golgi stained whole mounts (Boycott, B. B. and Wässle, H., 1991). There is a striking similarity between mouse, rat, and monkey bipolar cells with respect to the shapes and stratification levels of their axons, however, there is also a clear difference; midget bipolar cells (flat midget bipolar, FMB; invaginating midget bipolar, IMB) are only found in the monkey retina. FMB and IMB cells have dendritic trees which contact a single cone (Polyak, S. L., 1941; Figure 2 and Figure 4(a)). Following the nomenclature of Polyak S. L. (1941), bipolar cells contacting several neighboring cone pedicles were named diffuse bipolar cells (DB1–DB6; Boycott, B. B. and Wässle, H. 1991; Figures 2 and 4(c)).

In summary these studies suggest that there are about 10 types of cone bipolar cells in the mammalian

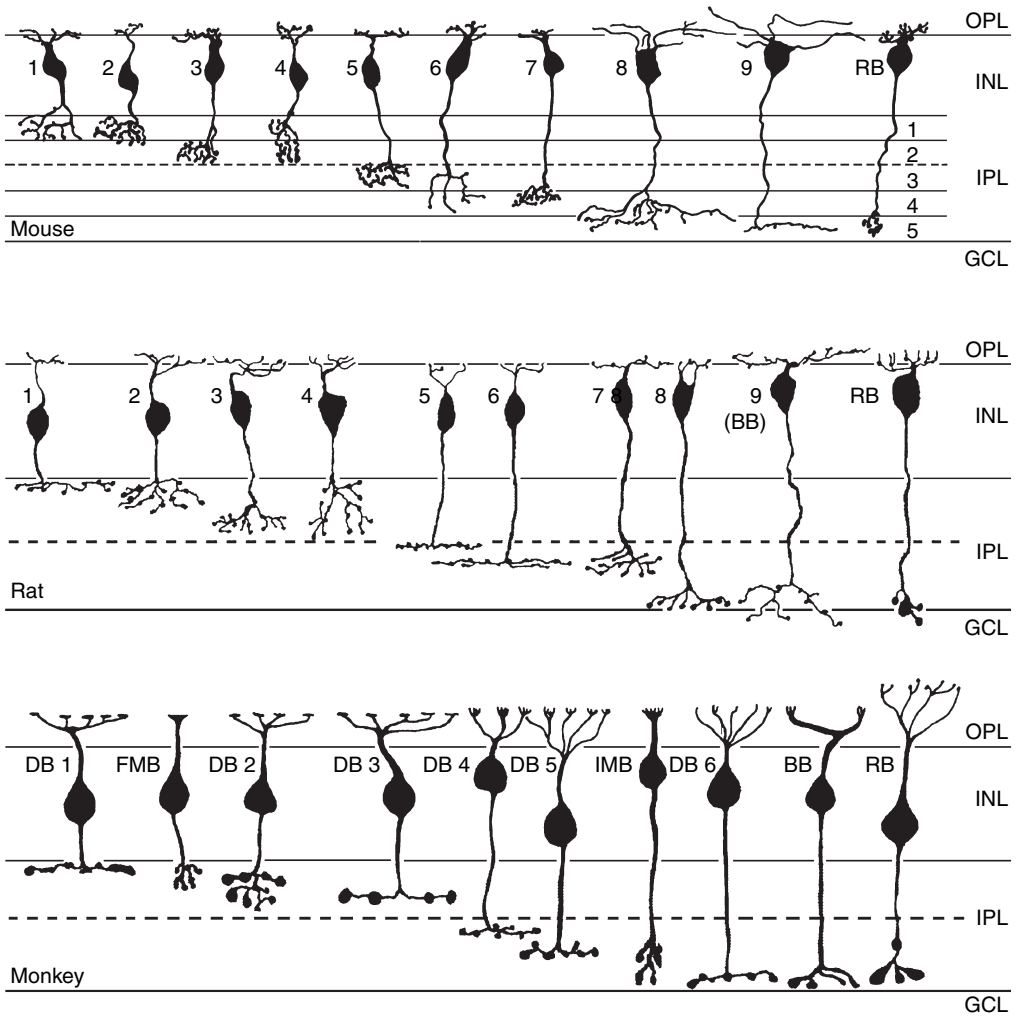

Figure 2 Schematic diagrams of bipolar cells of mouse, rat, and primate retina (Ghosh, K. K. *et al.*, 2004). The retinal layers are indicated (OPL, outer plexiform layer; INL, inner nuclear layer; IPL, inner plexiform layer; it can be subdivided into five sublaminas of equal width; GCL, ganglion cell layer). The bipolar cell types were named according to the level of stratification of their axon terminals in the IPL. The dashed horizontal lines dividing the IPL represent the border between the OFF- (upper) and the ON- (lower) sublayers. Bipolar cells with axons terminating above this line represent OFF bipolar cells, those with axons terminating below this line represent ON bipolar cells (DB, diffuse bipolar cells; FMB, flat midget bipolar cells; IMB, invaginating midget bipolar cells; BB, blue-cone bipolar cells; RB, rod bipolar cells).

retina and their major defining features are the shape and stratification of their axons in the IPL and in some instances their cone contacts in the OPL (Hopkins, J. M. and Boycott, B. B., 1996; 1997). The major functional subdivision of bipolar cells is into ON- and OFF-bipolar cells. ON-bipolar cells are depolarized by a light stimulus, OFF-bipolar cells are hyperpolarized by a light stimulus (Werblin, R. S. and Dowling, J. E., 1969; Kaneko, A., 1970). Their axons terminate at different levels (strata) within the IPL: OFF in the outer half, ON in the inner half (Euler, T. *et al.*, 1996; Hartveit, E., 1996; Euler, T. and Masland, R. H., 2000; Berntson, A. and Taylor, W. R., 2000). Superimposed on this ON/OFF dichotomy are four types of OFF and five types of ON-cone bipolar cells. We are just beginning to understand their functional roles (Freed, M. A., 2000).

1.12.3.1 Midget Bipolar Cells of the Primate Retina

Before discussing the function of midget bipolar cells, the distribution of cells across the retina (topography) has to be considered (Wässle, H. and Boycott, B. B.,

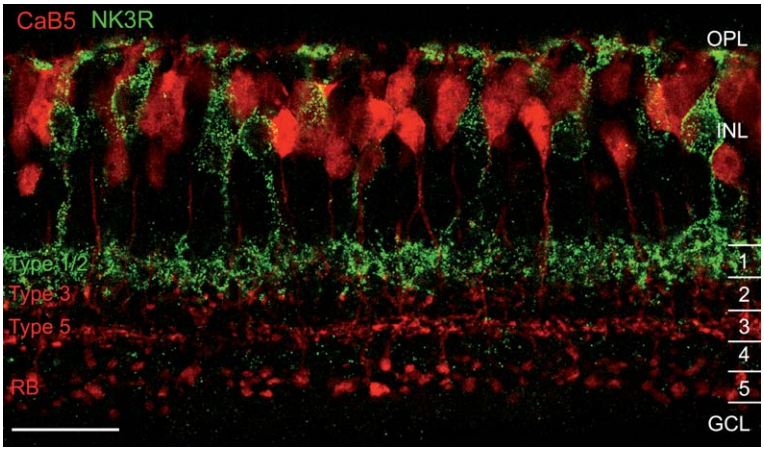

Figure 3 Immunocytochemical staining of mouse bipolar cells. Fluorescence micrograph of a vertical section through mouse retina double immunostained for the calcium-binding protein 5 (CaB5, red) and the neurokinin receptor 3 (NK3R, green). Three bipolar cell types (type 3, type 5 and RB express CaB5. Their axons terminate in the inner plexiform layer inner plexiform layer in sublamina 2, sublamina 3, and sublamina 5, respectively. Type 1/2 bipolar cells express NK3R and their axons are restricted to sublamina 1. GCL, ganglion cell layer; INL, inner nuclear layer; OPL, outer plexiform layer; RB, rod bipolar. Scale bar = 20 μm.

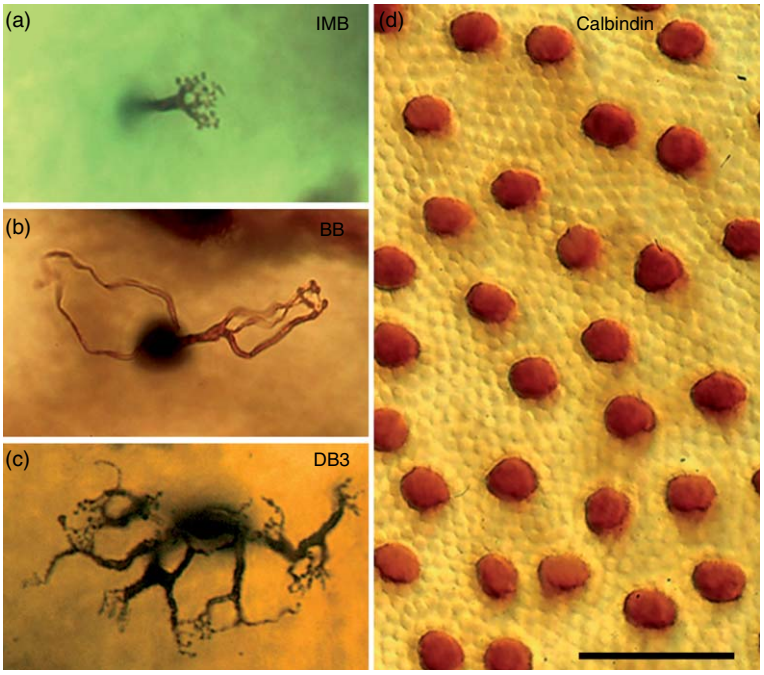

Figure 4 Bipolar cells and their cone contacts in the primate retina. Horizontal view of Golgi stained bipolar cells, with the plane of focus at their dendritic tips in the outer plexiform layer. (a) Dendritic tips of a invaginating midget bipolar cell (IMB). The micrograph in (d) shows the cone pattern (immunolabeled for the calcium-binding protein calbindin) at a comparable eccentricity, and the dendritic tips of the IMB cell in (a) are restricted in size to a single cone. (b) Dendritic branches of a blue-cone bipolar (RB) cell, which contact two widely spaced cones. Comparison with the cone pattern in (d) shows that this BB cell is cone-selective. (c) Dendritic branches of a diffuse bipolar cell (DB3) that would contact altogether nine neighboring cone pedicles. Scale bar = 20 μm.

1991). In the peripheral retina, there is a low density of cones, bipolar cells, and ganglion cells, whereas toward the center of the retina (the central area of cats, the visual streak of rabbits, or the fovea of primates) the density of these cells increases steeply. This results in greatly improved spatial resolution (visual acuity) at the fovea or central area. Concomitant with the increase in density, the cells' dendritic fields become smaller. During evolution, the spatial resolution of the primate eye and retina has been optimized. To achieve this, a high cone density and a low cone-to-RGC ratio have converged in the acuity pathway. The anatomic limits for this optimization are reached when each cone is connected through a midget bipolar cell to a midget ganglion cell, establishing a private line to the brain (Figures 4(a) and 4(d)). It has been suggested that only after this one-to-one connection in the central retina had evolved, 35 million years ago, did a subsequent mutation in the L-cone pigment create L- and M-cones of varying proportions at random spatial locations (Mollon, J. D. and Jordan, G., 1988; Mollon, J. D., 1989; Wässle, H. and Boycott, B. B., 1991; Boycott, B. B. and Wässle, H., 1999; Nathans, J., 1999). The midget system of the central retina was able to transmit this chromatic information to the brain where it could be used, for example to detect red fruit among green leaves. Recently it became possible to study the L-/M- and S-cone mosaics of the living human retina by the application of adaptive optics (Hofer, H. *et al.*, 2005). This revealed the irregular arrangement of L- and M-cones. Moreover it showed that the relative proportions of L- and M-cones greatly varied between human individuals (Roorda, A. and Williams, D. R., 1999). The midget system is able to transfer this irregular mosaic to the brain which apparently can compensate such variability, and color vision in human individuals is not affected by the different ratios of M- and L-cones (Neitz, J. *et al.*, 2002).

This midget theory of the evolution of trichromacy in primates has its basis in the general pattern of mammalian wiring. It is not necessary to postulate, in addition, specific mutations to change the cone selectivity of bipolar cells, the cone selectivity of GluRs, or the selectivity of ganglion cells (Calkins, D. J. and Sterling, P., 1999). It also explains why mammals other than primates have not evolved trichromacy: their cone bipolar cells sum the signals of several cones, and their RGCs sum the signals of many bipolar cells. A mutation that created M- and L-cones would be lost in this convergent network, which pools signals from many cones (Wässle, H., 1999). A recent transgenic mouse expressing human L- and M-opsins was not able to perform trichromatic color discrimination (Jacobs, G. H. *et al.*, 2004). However, in a further transgenic mouse where large patches of the cone mosaic expressed either L- or M-opsins trichromatic color discrimination was possible (Smallwood, P. M. *et al.*, 2003; Jacobs, G. H. *et al.*, 2007). The idea that trichromacy piggy-backs on the high acuity system of primates also postulates that the midget bipolar cells perform a double duty in visual signaling, acuity and trichromacy, an idea that has been promoted for some years (Ingling, C. R., Jr. and Martinez-Uriegas, E., 1983a; 1983b).

1.12.3.2 Blue-Cone Bipolar Cells

Placental mammals other than primates have only two types of cone: L-cones in which the visual pigment has an absorption maximum of greater than 500 nm and S-cones with an absorption maximum at less than 500 nm. They are, therefore, dichromats. In an evolutionary comparison of color pigments it has been estimated that the separation of the L- and S-cone pigments occurred more than 500 million years ago and thus represents the phylogenetically ancient, primordial color system (Mollon, J. D., 1989). The morphological substrate for the dichromatic color vision common to most placental mammals is the S-cone pathway (Calkins, D. J., 2001). Mariani A. P. (1983; 1984) described bipolar cells selective for S-cones in the macaque monkey retina. They have long, smoothly curved dendrites and contact between one and three cone pedicles (Figures 4(b) and 4(d)). Their axons terminate in rather large varicosities in the innermost part of the IPL, close to the ganglion cell layer (BB-cells in Figure 2). S-cone bipolar cells have been quantified by selective labeling with antibodies against cholecystokinin (CCK; Kouyama, N. and Marshak, D. W., 1992; Wässle, H. *et al.*, 1994). Their selective innervation of S-cones has been shown in old world and new world primates (Ghosh, K. K. *et al.*, 1997; Calkins, D. J. *et al.*, 1998), and it has been shown that they provide input to the inner tier of the dendritic tree of the small bistratified ganglion cells (Calkins, D. J. *et al.*, 1998). Small bistratified ganglion cells give blue-ON, yellow-OFF responses (Dacey, D. M. and Lee, B. B., 1994). In the retina of the ground squirrel light responses of a S-cone selective bipolar cell have been recorded and this bipolar cell was an ON-bipolar cell (Li, W. and DeVries, H., 2006).

Immunostaining with antisera specific for S-opsin has shown that S-cones constitute approximately 10% of the cones in most mammalian retinas (Szél, A. *et al.*,

1988; 1993). However, in some species S-cones have a very uneven topographical distribution across the retina and many cones express both L- and S-opsin (Glösmann, M. and Ahnelt, P. K., 1998; Applebury, M. L. *et al.*, 2000; Lukáts, A. *et al.*, 2005). So far only circumstantial evidence for the existence of S-cone selective bipolar cells in mammals other than primates has been presented (rabbit: Famiglietti, E. V., 1981; Jeon, C. J. and Masland, R. H., 1995; cat: Cohen, E. D. and Sterling, P., 1990a; 1990b; ground squirrel; West, R. W., 1976; rat: Euler, T. and Wässle, H., 1995; mouse: Ghosh, K. K. *et al.*, 2004; Pignatelli, V. and Strettoi, E., 2004). However, recently a transgenic mouse line could be studied, where Clomeleon, a genetically encoded fluorescence indicator, was expressed under the *thy1* promotor (Haverkamp, S. *et al.*, 2005). Clomeleon labeled ganglion cells, amacrine cells, and bipolar cells. Among the bipolar cells the S-cone-selective (blue cone) type could be identified, and the cone-selective contacts and the retinal distribution could be studied. The morphological details of the blue-cone bipolar cell match type 9 cells of rat and mice (Figure 2) and they are closely similar to the blue-cone bipolar cell of the primate retina (Figure 4(b)). It is interesting that in the ventral mouse retina, where most cones express both L- and S-opsin, blue-cone bipolar cells contact only those cones, which express S-opsin only, and they are the genuine blue cones of the mouse retina (Haverkamp, S. *et al.*, 2005).

1.12.3.3 Diffuse Bipolar Cells

Most bipolar cell types of the mammalian retina contact between five and seven neighboring cones (Figures 4(c) and 4(d)). Diffuse bipolar cells of the primate retina contact L- and M-cones in their dendritic field nonselectively (Boycott, B. B. and Wässle, H., 1991). They are, therefore, involved with the transfer of a luminosity signal, which is based on the combined sensitivity of L- and M-cones (Lee, B. B. *et al.*, 1990). Whether all diffuse bipolar cell types also contact S-cones is still a matter of discussion and it has been proposed that one type of diffuse bipolar cell avoids S-cones (Calkins, D. J. *et al.*, 1996). This type would be a good candidate to transfer a yellow (L-plus M-cone) signal into the IPL, where it could contact the outer tier of the dendritic tree of the small bistratified ganglion cells (Dacey, D. M. and Lee, B. B., 1994). Recordings from diffuse bipolar cells of the retina of the ground squirrel show that there are two groups of diffuse bipolar cells: one receives mixed input from S- and M-cones, while the other one receives an almost pure M-cone signal (Li, W. and DeVries, H., 2006).

1.12.3.4 Cone Contacts of Bipolar Cells

The cone pedicle has two kinds of synaptic specializations, which are occupied by bipolar cells: invaginating and flat contacts (Figure 1(a)). Reconstructions of Golgi-impregnated midget bipolar cells of the primate retina by serial electron microscopy (EM; Figure 5) showed a clear dichotomy: IMB cells made exclusively invaginating contacts, whereas FMB cells made only flat contacts (Kolb, H., 1970). Individual IMB cells make up to 25 contacts with a cone pedicle (Figure 5(a)), an FMB cell makes approximately 2.0–3.5 times that number of basal synapses (Hopkins, J. M. and Boycott, B. B., 1996; 1997). Most of the contacts of FMB cells are in the vicinity of the ribbons (Figure 5(b), triad associated, TA). Reconstructions of cone contacts of Golgi-impregnated diffuse bipolar cells by EM revealed that DB1, DB2, and DB3, which have their axon terminals in the outer IPL and are putative OFF bipolar cells, make exclusively basal junctions with the cone pedicle (Figure 5(c)). They always have TA and nontriad associated (NTA) contacts, the proportions varying according to the cell type, as does the average number of contacts per cone, which is between 10 and 20. Bipolar cells DB4, DB5, and DB6 have their axon terminals in the inner part of the IPL and are putative ON bipolar cells. They have an average of between four and eight invaginating synapses per cone pedicle. In addition they also form basal junctions, in a predominantly TA position (Hopkins, J. M. and Boycott, B. B., 1996; 1997). Thus, while the dichotomy invaginating = ON, flat = OFF holds for midget bipolar cells, it does not conform so clearly for diffuse bipolar cells. As discussed later, the type of synapse made by a bipolar cell at a cone pedicle, flat versus invaginating, is not the decisive feature; it is rather the GluR expressed there.

Recent results from the rodent and the rabbit retina have shown that some OFF-cone bipolar cells make also basal contacts with rod spherules and thus receive a direct input from rods (Hack, I. *et al.*, 1999; Tsukamoto, Y. *et al.*, 2001; Li, W. *et al.*, 2004; Protti, D. A. *et al.*, 2005). This represents a third route for the rod signal in addition to the RB cell circuit and the gap junctions between rods and cones (Volgyi, B. *et al.*, 2004).

The number of contacts per cone pedicle of a given diffuse bipolar cell varies across its dendritic field (Figure 5(c)). More contacts are made with cones in the center, and only few contacts are made

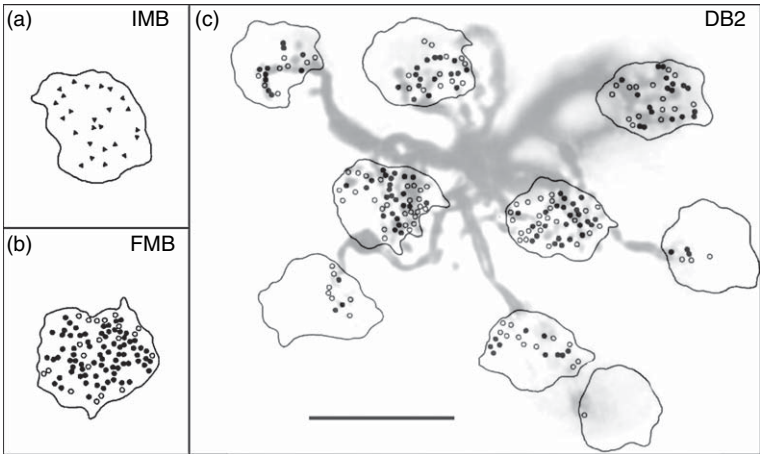

Figure 5 Cone contacts of bipolar cells of the primate retina. The cells were Golgi-stained and afterwards serially sectioned for electron microscopic analysis (Hopkins, J. M. and Boycott, B. B., 1996). (a) The 25 contacts of an invaginating midget bipolar cell are all invaginating. (b) The 97 contacts of a flat midget bipolar cell are all flat (●, triad associated; ○, nontriad associated). (c) reconstruction of the cone contacts of a diffuse bipolar cell DB2. The dendritic tree, as revealed by the Golgi staining, is inserted. This DB2 cell connects to nine cone pedicles, exclusively with flat contacts. Scale bar = 20 μm. Adapted from Boycott, B. B. and Wässle, H. 1999. Parallel processing in the mammalian retina: the Proctor Lecture. Invest. Ophthalmol. Vis. Sci. 40, 1313–1327.

with more peripheral cones, which predicts a Gaussian sensitivity profile. The dendrites of neighboring bipolar cells of a given type show different extents of overlap and their coverage factor is between one and four. This means that a cone pedicle may contact one to four bipolar cells of any given type. This is illustrated in Figure 6 for type 7 bipolar cells of a transgenic mouse line which expresses GFP under the control of the gustducin promotor (Huang, L. *et al.*, 2003). They were immunostained for GFP (Figure 6(a)) and their dendritic network (Figures 6(b) and 6(d)), cell bodies, and axon terminals (Figures 6(c) and 6(e)) are shown. The positions of cone pedicles are marked by the expression of GluR5 (Haverkamp, S. *et al.*, 2005). Analysis of individual bipolar cells in this network shows that bipolar cells contact approximately eight cone pedicles (convergence) and cone pedicles are innervated by approximately one bipolar cell (divergence). The cone density in this area is 13 000 mm^{-2}, the density of this bipolar cell type is 2000 mm^{-2}. Type 7 bipolar cells represent approximately 10% of the total cone bipolar cell population of the mouse retina. Some of the axon terminals are delineated by red circles in Figure 6(e) and it is obvious that they are precisely space filling, without any overlap. They are all within the same focal plane and therefore confined to a narrow stratum within the IPL (Figure 6(a)). This example shows the dendritic and axonal architecture of a defined bipolar cell type, and thus represents one of the parallel routes from the outer to the IPL.

1.12.4 Expression of Glutamate Receptors at Cone Pedicles

1.12.4.1 Glutamate Receptor Subunits

Molecular cloning has revealed a multiplicity of GluRs and receptor subunits. Ionotropic receptors are integral membrane proteins that form an ion channel. This channel, usually a nonselective cation channel, is made up of four subunits and opens upon glutamate binding. Three major groups of ionotropic GluRs can be distinguished: α-amino-3-hydroxy-5-methyl-4-isoxazolepropionic acid (AMPA), kainate, and *N*-methyl-D-aspartate (NMDA) receptors. They comprise the following subunits: AMPA (GluR1, GluR2, GluR3, GluR4); kainate (GluR5, GluR6, GluR7, KA-1, KA-2); NMDA (NR1, NR2A, NR2B, NR2C, NR2D and NR3A); further subunits are the orphan receptors δ1 and δ2. In addition multiple splice variants of the different subunits, have been identified, for example, the 10 splice variants of NR1 (Hollmann, M. and Heinemann, S., 1994; Dingledine, R. *et al.*, 1999; Kew, J. N. C. and Kemp, J. A., 2005). mGluRs belong to the family of receptors that have seven membrane-spanning domains and, when they

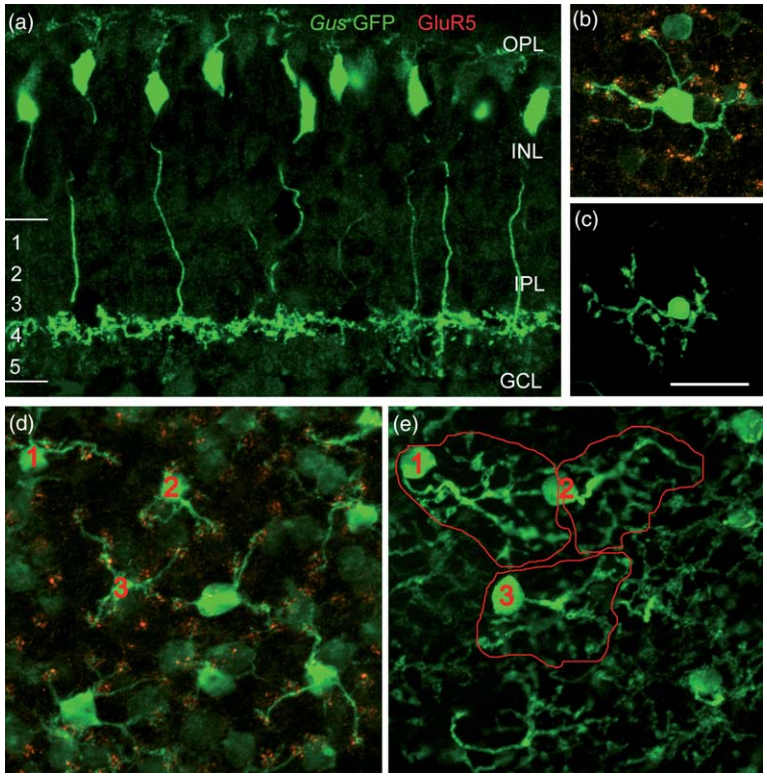

Figure 6 Array of type 7 bipolar cells of the mouse retina. The cells express green fluorescent protein (GFP) under the control of the α-gustducin promotor (Huang, L. *et al.*, 2003). (a) Fluorescence micrograph of a vertical section showing strong expression of GFP in type 7 bipolar cells their axon terminals in sublamina 3/4 of the inner plexiform layer (IPL). Faint expression can also be detected in some rod bipolar cell axon terminals in sublamina 5. (b, c) Horizontal view of the dendritic field and the axon terminal of an isolated type 7 bipolar cell. The dendrites in (b) contact all 12 cone pedicles within the dendritic field. They are labeled by the expression of the kainate receptor GluR5 (clusters of red dots). The axon terminal in (b) covers an area of $\sim$500 μm^2. (d, e) Horizontal view a patch of retina, where apparently all type 7 cells are labeled. Their dendritic trees in (d) contact an average number of 8.1 $\pm$ 1.3 ($n = 20$) cone pedicles (convergence). Dendritic fields of neighboring type 7 cells in this field show practically no overlap and, therefore, most cone pedicles are in contact with only one type 7 bipolar cell (divergence). The axon terminals of the type 7 bipolar cells in the IPL are space filling without much overlap (coverage of 1). This is indicated by the red outlines for three selected cells. GCL, ganglion cell layer; INL, inner nuclear layer; OPL, outer plexiform layer. Scale bar = 20 μm for (a), 17 μm for (b) and (c), 16 μm for (d) and (e).

bind glutamate, G protein, and second messenger systems are activated. So far eight different mGluRs have been identified (mGluR1–mGluR8). It is clear that a simple retinal scheme: glutamate released from photoreceptors acts on horizontal and bipolar cells and then, in turn glutamate released from bipolar cells activates amacrine and ganglion cells, can have any degree of complexity depending on the GluRs that are expressed.

1.12.4.2 ON-Bipolar Cell Glutamate Receptors

In a series of seminal experiments, Nakanishi and co-workers have cloned mGluR6, localized it with specific antibodies, and studied the function by gene directed (knockout) mutagenesis (Nomura, A. *et al.*, 1994; Masu, M. *et al.*, 1995). These experiments have shown that mGluR6 is expressed at the dendritic terminals of RB cells inserted into the rod spherules. In the mGluR6 knockout mouse, all ON-light responses were blocked (Masu, M. *et al.*, 1995; Renteria, R. C. *et al.*, 2003). Vardi N. *et al.* (1998) have shown that mGluR6 also is expressed in ON-cone bipolar cells at their invaginating, and occasionally flat, contacts with cone pedicles. Previous pharmacological studies had shown that light responses of all ON-bipolar cells are blocked by 2-aminophosphonobutyric acid (LAP-4; Slaughter, M. M. and Miller, R. F., 1981), a glutamate agonist at mGluR (group III) receptors (Pin, J. P. and Duvoisin, R., 1995). The signal cascade activated through

mGluR6 in ON-bipolar cells involves the G protein G alpha (o) (Dhingra, A. *et al.*, 2002; 2004), however, the membrane channel modulated by the cascade has not yet been identified (Nawy, S., 1999; Snellman, J. and Nawy, S., 2004). Recently a transgenic mouse was created, where the mGluR6 promotor drives the expression of GFP and all ON-bipolar cells were found to be labeled (Morgan, J. L. *et al.*, 2006). Taken together this shows that mGluR6 is the predominant GluR expressed in all ON-bipolar cells. However, it has to be emphasized that additional GluRs have been localized to them and their functions still need to be elucidated (Koulen, P. *et al.*, 1997; Vardi, N. *et al.*, 1998; Lo, W. *et al.*, 1998; Calkins, D. J., 2005). It is possible that they fulfill some modulatory roles in different ON bipolar cell types.

1.12.4.3 OFF-Bipolar Cell Glutamate Receptors

Immunocytochemical localization of GluR subunits to flat contacts of bipolar cells at the cone pedicle base has revealed a plethora of different GluRs. The AMPA receptor subunit GluR1 has exclusively been observed in flat contacts and has not been found in horizontal cell processes (Brandstätter, J. H., 2002). In retinas double labeled for the ribbon marker bassoon and for GluR1, GluR1 hot spots are located in close vicinity of the ribbons, suggesting a TA position (Figures 7(d)–7(f); Haverkamp, S. *et al.*, 2001). In the macaque monkey retina it was possible to compare the GluR1 expression of M/L- and S-cones. The same number of GluR1 hot spots was observed, however, they were more salient in S-cone pedicles (Haverkamp, S. *et al.*, 2001). Whether this represents a higher density of GluR1 expression at S-cones, or whether the hot spots are more closely packed at the smaller S-cone pedicles cannot be answered at present. Puller C. *et al.* (2007) could show that FMB cells of the primate retina express GluR1 at their contacts with cone pedicles. FMB cells have been shown to contact M/L- as well as S-cones in the macaque monkey retina (Klug, K. *et al.*, 2003). GluR1-labeled flat contacts have also been observed in the rodent

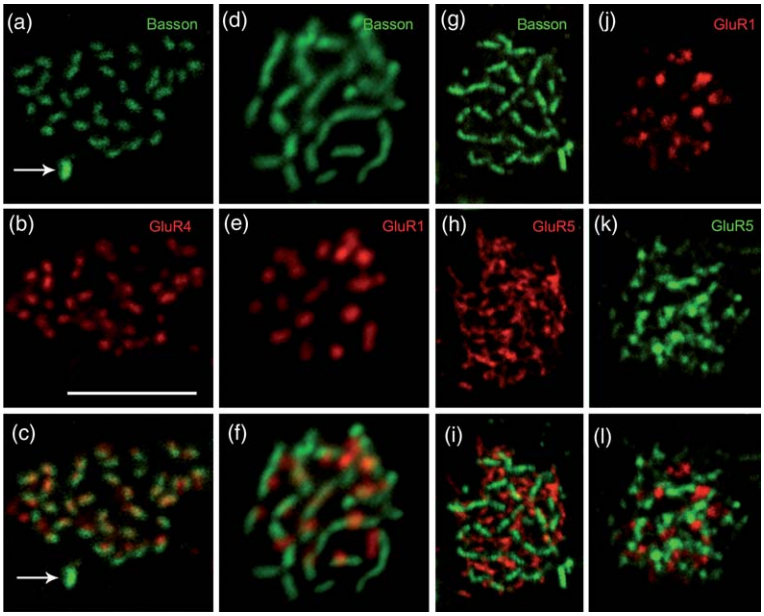

Figure 7 Horizontal confocal sections of cone pedicles of the primate retina that were double labeled for bassoon and glutamate receptor subunits (GluRs). (a) The ribbons of one cone pedicle and one rod spherule (arrow) are immunoreactive for bassoon (green). (b) GluR4 immunoreactive hot spots of the same section as in (a) (red). (c) Superposition of (a) and (b) shows that most of the GluR4 immunoreactive hot spots are in register with the ribbons. (d) Cone pedicle from the more central retina immunolabeled for bassoon. (e) GluR1 immunoreactive hot spots of the same section as in (d). (f) Superposition of (d) and (e) shows that GluR1 immunoreactive hot spots are associated, but not in perfect register, with the ribbons. (g) Cone pedicle immunolabeled for bassoon. (h) Same pedicle, immunolabeled for GluR5. (i) Superposition of (g) and (h) shows that GluR5 immunoreactive hot spots are found in between the ribbons. (j) and (k) Section through a cone pedicle that was double labeled for GluR1 ((j), red) and GluR5 ((k), green). (l) Superposition of (j) and (k) shows that GluR1 and GluR5 immunoreactive puncta are expressed at different synaptic contacts. Scale bar = 5 μm.

and cat retina (Qin, P. and Pourcho, R. G., 1999; Hack, I. *et al.*, 2001), however, the corresponding type of bipolar cell has not yet been identified.

The kainate receptor subunit GluR5 has also been observed in flat contacts and has not been found in horizontal cell processes. In retinas double labeled for the ribbon marker bassoon and for GluR5, the GluR5 hot spots are always displaced from the ribbons, suggesting a NTA position (Figures 7(g)–7(h)). When cone pedicles were double labeled for the AMPA receptor subunit GluR1 and the kainate receptor subunit GluR5 (Figures 7(j)–7(l)), the labeled hot spots did not coincide (Haverkamp, S. *et al.*, 2001). This suggests that they are expressed by two different types of OFF-cone bipolar cells. In retinas of primates, rodents, and ground squirrels there was a significant reduction of GluR5 hot spots at S-cone pedicles in comparison to M/L- and L-cone pedicles (Haverkamp, S. *et al.*, 2001; Li, W. and DeVries, H., 2004; Haverkamp, S. *et al.*, 2005). The OFF-cone bipolar cell expressing GluR5 makes, therefore, only sparse connections with S-cones. The kainate receptor subunit KA-2 has also been observed at bipolar cell flat contacts and not in horizontal cell processes (Brandstätter, J. H. *et al.*, 1997).

The GluR subunits GluR2, GluR2/3, GluR4, and GluR6/7 have also been localized to flat contacts of bipolar cells at the cone pedicle base, however, these subunits also decorated the processes of horizontal cells (Morigiwa, K. and Vardi, N., 1999). NMDA receptor subunits have not been observed at the flat contacts (Fletcher, E. L. *et al.*, 2000).

In conclusion: OFF-cone bipolar cells express at their flat contacts with cone pedicles the AMPA receptor subunits GluR1, GluR2, GluR2/3, and GluR4, they also express the kainate receptor subunits GluR5, GluR6/7, and KA-2. Therefore, different OFF-cone bipolar cell types can be connected to cone pedicles through AMPA receptors, or through kainate receptors. Further diversity is to be expected because AMPA and kainate receptors are composed of four subunits each, and different subunits can be combined to form the tetrameric receptor complex.

1.12.4.4 Horizontal Cell Glutamate Receptors

Horizontal cell dendrites of the primate retina express GluR hot spots at two postsynaptic locations: at the invaginating processes opposed to the presynaptic ribbons and at desmosomelike junctions between horizontal cell dendrites underneath the cone pedicle (Haverkamp, S. *et al.*, 2000). GluR2/3 and GluR4 clusters are found at the invaginating processes and at the desmosomelike junctions of all cone pedicles and these AMPA receptor subunits appear to constitute the dominant GluR expressed by horizontal cells (Figures 7(a)–7(c)). However, at M/L-cones pedicles horizontal cell dendrites also express the kainate receptor subunit GluR6/7. Since expression of GluR6/7 by horizontal cells was not observed at S-cone pedicles, the preferred target of H2 horizontal cells, it appears that only H1 horizontal cells express the GluR6/7 subunit (Haverkamp, S. *et al.*, 2001). The two horizontal types of the primate retina, therefore, not only have different shapes and cone contacts, but they express also different GluRs: H1 cells receive signals from cones through AMPA (GluR2/3, GluR4) and kainate (GluR6/7) receptors, H2 cells only through AMPA (GluR2/3, GluR4) receptors. Examination of GluR currents in horizontal cells from cultures human retina using whole-cell recordings showed that horizontal cells possess both AMPA and kainate receptors (Shen, W. *et al.*, 2004). Unfortunately the cells were not classified into H1 and H2 horizontal cells.

1.12.5 Light-Evoked Responses of Bipolar Cells

1.12.5.1 Temporal Transfer Characteristics

In the retinas of cold-blooded animals, especially the dogfish and the tiger salamander, the responses of bipolar cells to light have been studied extensively, contributing important results on the polarity (ON/OFF) and the time course (sustained/transient) of their responses, the currents involved, and the receptive field organization (Werblin, F. S., 1973; Kaneko, A. and Shimazaki, H., 1976; Saito, T. *et al.*, 1981; Saito, T. and Kujiraoka, T., 1982; Saito, T. *et al.*, 1985; Lasansky, A., 1992, Wu, S. M. *et al.*, 2000). Early recordings from intact mammalian retinas confirmed the ON/OFF dichotomy of cone bipolar cells (Nelson, R. *et al.*, 1981; Nelson, R. and Kolb, H., 1983) and showed that RB cells are ON-bipolar cells (Dacheux, R. F. and Raviola, E., 1986). Later, in patch clamp recordings from dissociated bipolar cells it was shown that RB cells express the metabotropic L-AP4 sensitive GluR, while cone bipolar cells express both ionotropic and metabotropic GluRs (Yamashita, M. and Wässle, H., 1991; de la Villa, P.

et al., 1995). Recordings from bipolar cells in rat retinal slices, together with a morphological identification of the cells and the application of glutamate agonists demonstrated that types 1, 2, 3, and 4 are OFF bipolar cells, while types 5, 6, 7, 8, 9, and RB cells are ON bipolar cells (Euler, T. *et al.*, 1996; Hartveit, E., 1996; 1997). In the retina of the ground squirrel dual recordings from synaptically connected cone pedicles and different bipolar cell types were performed (DeVries, S. H. and Schwartz, E. A., 1999; DeVries, S. H., 2000). The signal transfer between cones and OFF-cone bipolar cells was based on two different types of ionotropic GluRs: bipolar cell types b3 and b7 expressed kainate receptors, type b2 AMPA receptors. The three cell types showed substantial differences in their temporal properties as measured by their recovery from desensitization (Figures 8(e)–8(g)). Type b2 cells showed fast, b7

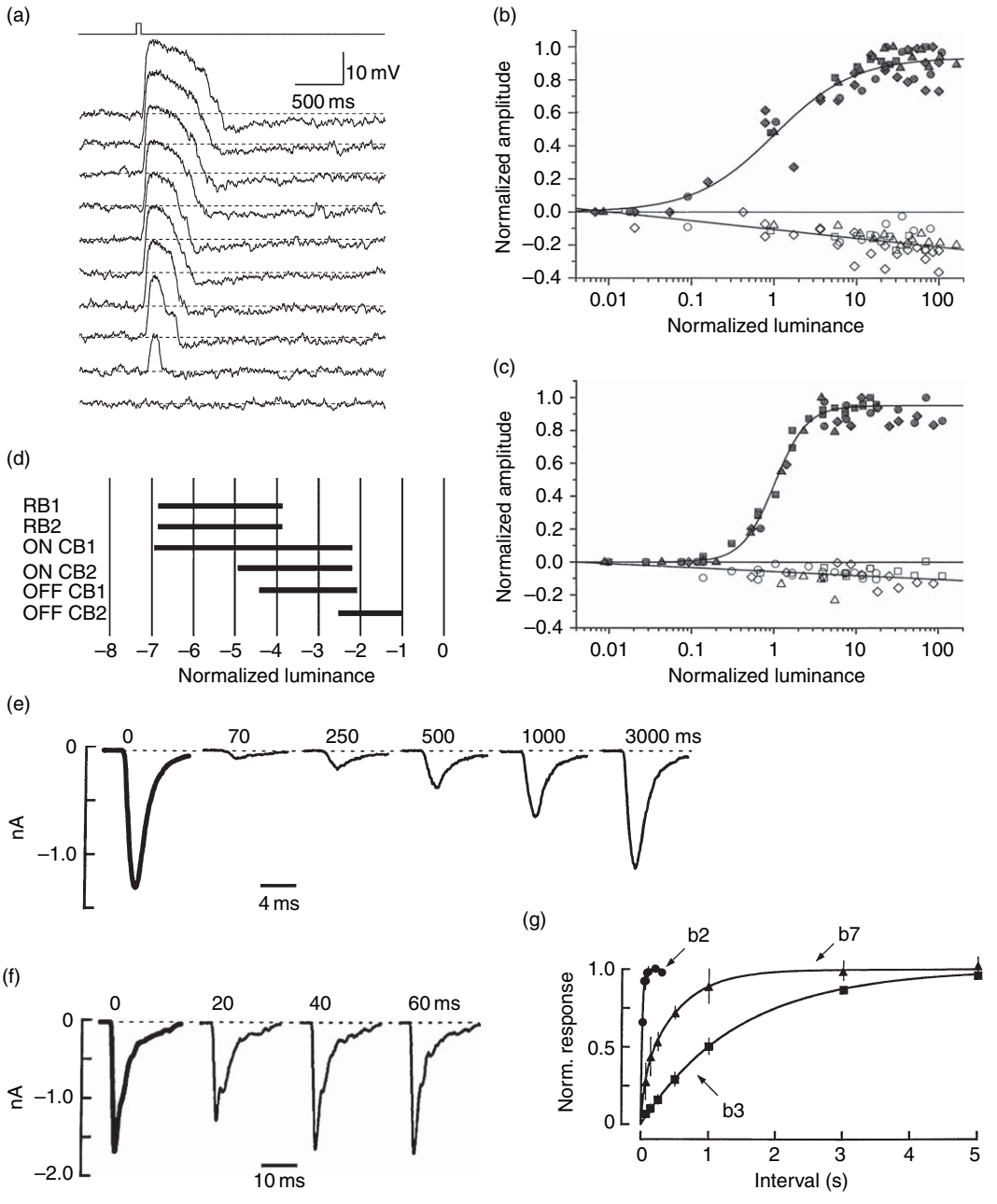

cells medium, and b3 cells show recovery. The rapidly recovering b2 cell AMPA receptors are well suited to signal transient components in the cone light response, whereas the slowly recovering b3 cell kainate receptors attenuate the transient components and consequently emphasize the steady (sustained) components. Further studies of the cone pedicle architecture of the retina of the ground squirrel showed that the b2 cells made TA contacts (DeVries, S. H. *et al.*, 2006) and consequently respond fast and transiently. The b3 and b7 cells made basal contacts further away from the triads (NTA) and glutamate released at the ribbons had a long way of diffusion, which resulted in smoothed and sustained responses of b3 and b7 cells. This shows that the cone to OFF bipolar synapse is an important locus in temporal processing. So far it has not yet been shown for the mammalian retina that the cone to ON bipolar synapse is also involved in temporal processing. However, Awatramani G. B. and Slaughter M. M. (2000) have shown that the cone to ON-bipolar synapse of the tiger salamander retina transduces either a sustained or a transient response.

In the rodent retina a specific expression of voltage-dependent sodium (Na^+) and K^+ channels was observed in retinal bipolar cells (Klumpp, D. J. *et al.*, 1995a; 1995b; Pan, Z. H. and Hu, H. J., 2000; Ma, Y. P. *et al.*, 2005). The presence of Na^+ channels in a subgroup of ON-cone bipolar cells accelerated their response kinetics and amplitudes. The results show that the expression of different GluRs at the cone pedicle base and the intrinsic, voltage-dependent Na^+- and K^+-channel shape the temporal transfer characteristic of the different bipolar cell types. Further temporal specificity is contributed by the expression of different voltage-dependent Ca^{2+}-channels at the bipolar cell output synapses (Protti, D. A. and Llano, I., 1998; Pan, Z. H., 2000; Protti, D. A. *et al.*, 2000). The transmitter release at the bipolar cells axon terminal is also controlled by the expression of hyperpolarization-activated and cyclic nucleotide-gated (HCN) channels. Different classes of bipolar cells have a different inventory of HCN channels, which are densely clustered at their axon terminals (Müller, F. *et al.*, 2003; Ivanova, E. and Müller, F., 2006).

1.12.5.2 Spatial Transfer Characteristics

Midget bipolar cells of the primate retina contact, up to an eccentricity of ~10 mm, as a rule, one cone pedicle, diffuse bipolar cells between five and 10 cone pedicles. Dacey D. M. *et al.* (2000) measured the receptive field profiles of midget and diffuse bipolar cells at ~10 mm eccentricity and observed for both cell types an antagonistic center/surround organization: ON center/OFF surround and OFF center/ON surround. The mean center diameter of midget bipolar cells was 42 µm, which would encompass ~5–10 cones. The mean center diameter of diffuse bipolar cells was 92 µm, which would suggest input from 20 to 30 cones. The basis for the apparently large receptive field center sizes is electrical coupling of neighboring cone pedicles (Raviola, E. and

Figure 8 Electrophysiological recordings from bipolar cells of the mouse (a–d) and of the retina of the ground squirrel (e–g). (a) Whole cell recordings of the light-evoked depolarizations of a rod bipolar (RB) cell in a slice preparation of the mouse retina (light stimulus 50 ms, Vrest = 43 m V, intensity stepwise increased from 0 cd m^{-2} at the bottom to 43.5 cd m^{-2} at the top trace). The light-evoked potential is a depolarization followed by a hyperpolarization. (b) Sensitivity curves of four intact RB cells sowing the normalized amplitude (V/V_{max}) of the light-evoked voltage responses as a function of the normalized (I/I_{50}) stimulus intensity (logarithmic axis). Each symbol represents one cell (filled symbols depolarization, open symbols hyperpolarization). (c) Sensitivity curves of four axotomized RB cells. Comparison with (b) shows that they are steeper. Adapted from Euler, T. and Masland, R. H. 2000. Light-evoked responses of bipolar cells in a mammalian retina. J. Neurophysiol. 83, 1817–1829. (d) Dynamic range of the light responses of two RB, two ON-cone bipolar, and two OFF diffuse bipolar cells of the mouse retina. The abscissa shows the normalized stimulus intensity (logarithmic units). The horizontal bars indicate for the light intensity range from threshold (5%) to saturation (95% of the maximum response) of the light-evoked excitatory currents. Adapted from Wu, S. M., Gao, F., and Pang, J. J. 2004. Synaptic circuitry mediating light-evoked signals in dark-adapted mouse retina. Vision Res. 44, 3277–3288. (e–g) Whole-cell currents elicited in three types of OFF-bipolar cells (b2, b3, b7) of the retina of the ground squirrel by the application of brief pulses (15 ms) of glutamate (2 mM) separated by variable intervals. (e) The average first response (thick line) and subsequent responses (thin lines) are shown for a b3 cell. The interpulse interval is given above each trace. (f) Recordings of glutamate responses of a b2 cell. The recovery from desensitization of this b2 cell is much faster than that of the b3 cell shown in (e). (g) Normalized peak response is plotted against interpulse interval (b2, $n = 5$; b3, $n = 9$; b7, $n = 5$). Type b2 bipolar cells show the fastest recovery ($\tau = 18$ ms), followed by b7 and b3 cells. Type b2 cells signal through α-amino-3-hydroxy-5-methyl-4-isoxazolepropionic acid (AMPA) receptors, b7 and b3 cells through two different kainate receptors. Adapted from DeVries, S. H. 2000. Bipolar cells use kainate and AMPA receptors to filter visual information into separate channels. Neuron 28, 847–856.

Gilula, N. B., 1973; Tsukamoto, Y. *et al.*, 1992; Hornstein, E. P. *et al.*, 2004; 2005). It is also possible, that neighboring bipolar cells are electrically coupled (Feigenspan, A. *et al.*, 2004; Han, Y. and Massey, S. C., 2005).

The mean diameter of the antagonistic surround of midget and diffuse bipolar cells was 467 µm and 743 µm, respectively. For midget bipolar cells, the surrounds are about the same as the receptive field diameters of macaque H1 horizontal cells (Dacey, D. M., 2000). The diffuse bipolar cell surrounds are consistently larger, suggesting in addition to the horizontal cell input an input at their axon terminal system from a wide field amacrine cell type.

1.12.6 Intensity-Response Function

RB cells have the lowest response threshold for light stimuli amongst mammalian bipolar cells (Figures 8(a)–8(d)). The mean threshold (defined as 5% of the maximum response) of mouse RB cells is 0.1 Rh^* rod^{-1} s^{-1} and their dynamic range is ~3.3 log units (Wu, S. M. *et al.*, 2004). This is more than 1 log unit wider than the rod photocurrent (Field, G. D. and Rieke, F., 2002). The light-evoked response of RB cells increases monotomically (Figure 8(a)) and follows a Hill function (Figure 8(b)) with a Hill coefficient of 1.07 ± 0.19 (Euler, T. and Masland, R. H., 2000) and 1.15 ± 0.11 (Berntson, A. and Taylor, W. R., 2000). Euler T. and Masland R. H. (2000) measured also the intensity–response function of RB cells which had lost their axons (axotomized). The dynamic range of the axotomized RB cells was reduced by more than 1 log unit and the Hill curve was much steeper (Hill coefficient 2.39 ± 0.84; Figure 8(c)). A comparable reduction of the dynamic range of RB cells was also observed when the cells were superfused with GABA antagonists. Both results show, that GABAergic inhibition at RB axon terminals can modulate the intensity-response function of RB cells. This conclusion is also supported by recent measurements of bipolar cells in $GABA_C$ receptor knockout mice (McCall, M. A. *et al.*, 2002).

The thresholds for light stimuli of ON-cone bipolar cells of the mouse retina are generally higher than those for RB cells (Wu, S. M. *et al.*, 2004). Different types of ON-cone bipolar cells exhibit different thresholds and dynamic ranges, and thus cover only a small range of light intensities (~2 log units). The full range of intensities transferred to the inner retina is therefore encoded by different bipolar cells types (Figure 8(d)).

1.12.7 Synaptic Contacts of Bipolar Cells in the Inner Plexiform Layer

The axons of bipolar cells terminate in the IPL in lobular swellings (Figure 9). Some bipolar cell types, such as DB3 and DB6 of the primate retina and type 7

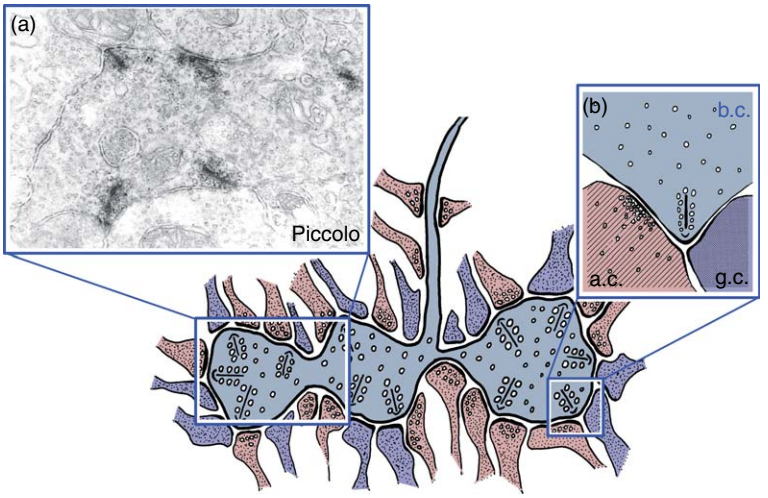

Figure 9 Synaptic output of bipolar cells in the inner plexiform layer. Schematic diagram of the axon terminal of a cone bipolar cell. It contains many presynaptic ribbons that are flanked by synaptic vesicles. (a) Electron micrograph of the axon terminal of a rod bipolar cell. Kindly provided by O. Dick. The five ribbons are marked by their expression of the ribbon associated protein piccolo. (b) Magnified view of a cone bipolar cell ribbon synapse (dyade). The presynaptic bipolar cell (b.c.) releases glutamate and the two postsynaptic partners (a.c., amacrine cell; g.c., ganglion cell) express two different sets of glutamate receptors. The amacrine cell in turn makes a synapse back onto the bipolar cell terminal (reciprocal synapse).

of the mouse retina keep their axon terminals within a narrow stratum (Figure 6; Chan, T. L. *et al.*, 2001; Jusuf, P. R. *et al.*, 2004; Lin, B. *et al.*, 2005). Hence their output will be restricted to the amacrine and ganglion cell dendrites they meet within that stratum. Other bipolar cells such as type 4 and type 6 of the mouse retina occupy with their axon terminals the complete OFF- or ON-sublamina, respectively (Ghosh, K. K. *et al.*, 2004). They are possible engaged in contacts with a wider variety of postsynaptic neurons. Midget bipolar cells of the primate retina represent a special case, because their axon terminals precisely match in width and depth the dendritic tops of midget ganglion cells, and they together form a densely interconnected glomerulus that can only be resolved by EM (Kolb, H. and Dekorver, L., 1991; Calkins, D. J. *et al.*, 1994; Jusuf, P. R. *et al.*, 2006). The axon terminals of neighboring bipolar cells of a given type usually tile the retina without much overlap in horizontal direction (RB cells: Young, H. M. and Vaney, D. I., 1991; midget cells: Wässle, H. *et al.*, 1994; calbindin bipolar cells of the rabbit: Massey S. C. and Mills S. L., 1996). Because of this basically onefold coverage the density of a given bipolar cell type is inversely proportional to the area occupied by the axon terminals (Figure 6(e)).

Bipolar cell axon terminals provide synaptic output through multiple ribbon synapses. The number of ribbon synapses made by midget bipolar cells of the macaque monkey retina ranged from nine to 48 (mean $\pm$ standard deviation 26.5 ± 9.3; Jusuf, P. R. *et al.*, 2006). An earlier report that this number differed between midget bipolar cells contacting M- or L-cones (Calkins, D. J. *et al.*, 1994) was not confirmed by Jusuf P. R. *et al.* (2006). The number of ribbon synapses made by RB cells of the rabbit retina was up to 30 compared to only 15 in the rat retina (Strettoi, E. *et al.*, 1990; Chun, M. H. *et al.*, 1993), which reflects the smaller size of RB axon terminals in rats (Figure 9(a)). The fine structure of the bipolar cell output synapses in the IPL was first described from EM by Missotten L. (1965). He identified the presynaptic ribbon surrounded by vesicles and the two postsynaptic elements. Dowling J. E. and Boycott B. B. (1966) named this synaptic arrangement a dyad. They recognized that one of the postsynaptic partners at cone bipolar cell dyads was usually a ganglion cell dendrite, while the other one was an amacrine cell process (Figure 9(b)). The amacrine cell process often made within about 0.5–1.0 µm of the dyad a conventional synapse back onto the bipolar cell axon terminal. This arrangement appears to be a reciprocal synapse and because most amacrine cells are inhibitory it is the structural correlate of negative feedback at the dyad. Bipolar cell axons receive in addition to reciprocal synapses also input from amacrine cells not related to the dyads (Sterling, P. and Lampson, L. A., 1986). In the case of RB cell dyads both postsynaptic partners are amacrine cells (AI and AII; Famiglietti, E. V. and Kolb, H., 1975; Kolb, H. and Famiglietti, E. V., 1976) and AI cells provide the reciprocal synapses (see Mammalian Rod Pathways).

The molecular composition of the presynaptic ribbon of bipolar cell dyads is similar to that of photoreceptor ribbons. RIBEYE, CtBP2, Kif3a, and Piccolo have all been localized to the bipolar cell ribbons (Muresan, V. *et al.*, 1999; Schmitz, F. *et al.*, 2000; tom Dieck, S. *et al.*, 2005; Deguchi-Tawarada, M. *et al.*, 2006; Jusuf, P. R. *et al.*, 2006) and this suggests that the mechanisms of glutamate release is also comparable to the photoreceptors synapses. Mb1-bipolar cells of the goldfish retina have a large, round axon terminal, and vesicle fusion, exocytosis, and endocytosis have been studied on this model system in great detail (von Gersdorff, H., 2001; Berglund, K. *et al.*, 2002; Heidelberger, R. *et al.*, 2002; Zenisek, D. *et al.*, 2000; Lagnado, L., 2003; Zenisek, D. *et al.*, 2003; Singer, J. H. *et al.*, 2004; Zenisek, D. *et al.*, 2004). The voltage signals that control neurotransmitter release from bipolar cells are graded with the intensity of the light stimulus and maintained according to the duration of the stimulus. These sustained signals stimulate a continuous cycle of vesicle exocytosis and endocytosis. The ribbon holds vesicles for exocytosis. The most direct evidence for this idea comes from the work of Zenisek D. *et al.* (2000) who used total internal reflection fluorescence microscopy (TIRF) to image individual vesicles in the synaptic terminal of Mb1-bipolar cells.

Glutamate release from bipolar cell terminals *a priori* depends upon the graded electrical response of the cell elicited by the light stimulus. However, it is also regulated by diverse feedback mechanisms acting at the dyad. (1) GABA or glycine released by the amacrine cells can feedback onto the bipolar cell terminal (Euler, T. and Masland, R. H., 2000; Shields, C. R. *et al.*, 2000; Matsui, K., *et al.*, 2001; Freed, M. A. *et al.*, 2003). (2) Bipolar cell terminals express mGluRs as autoreceptors that regulate voltage-dependent Ca^{2+}-channels (Awatramani, G. B. and Slaughter, M. M., 2001; Brandstätter, J. H. *et al.*, 1998; Palmer, M. J. *et al.*, 2003). (3) Bipolar cell axon

terminals express cannabinoid receptors, which regulate voltage-dependent K^+-channels (Fan, S. F. and Yazulla, S., 2005). (4) Synaptic vesicles release protons that inhibit Ca^{2+}-channels and thus inhibit locally the release (Hosoi, N. *et al.*, 2005).

1.12.8 Glutamate Receptors in the Inner Plexiform Layer

Bipolar cells release glutamate at their ribbon synapses (Tachibana, M., 1999) and the GluRs are clustered in the postsynaptic membranes adjacent to the ribbons. As a rule, only one member of the dyad expresses a given GluR subunit, which implies that the two postsynaptic partners express different GluRs (Hartveit, E. *et al.*, 1994; Qin, P. and Pourcho, R. G., 1996; Brandstätter, J. H. *et al.*, 1997; Qin, P. and Pourcho, R. G., 1999; Fletcher, E. L. *et al.*, 2000; Grünert, U. *et al.*, 2002). The postsynaptic clusters of GluRs appear as brightly immunofluorescent puncta when studied by light microscopy and their density and laminar distribution across the IPL differs for the different subunits (Figure 10).

1.12.8.1 α-Amino-3-Hydroxy-5-Methyl-4-Isoxazolepropionic Acid Receptor Subunits

The GluR1-immunoreactive puncta in the IPL have a stratified distribution and several bands of high and low expression can be recognized (Figure 10(a)). Some amacrine and ganglion cells are labeled extrasynaptically and GluR1 is probably expressed by a subset of these cell classes. GluR2/3-immunoreactive puncta occur at high density across the IPL with an increased density along the strata occupied by the dendrites of cholinergic amacrine cells (Figure 10(b)). The GluR4 subunit shows an even distribution of puncta across the OFF- and ON-sublamina of the IPL (Figure 10(c)). The GluR2/3 and the GluR4 subunits have been observed at the vast majority of bipolar cell ribbons in rabbit and primate retinas (Ghosh, K. K. *et al.*, 2001; Jusuf, P. R. *et al.*, 2006) which implies that at least one member of the dyad usually expresses an AMPA receptor. In the case of RB cells it has been shown that AII cells express the GluR2/3 and GluR4 subunits (Ghosh, K. K. *et al.*, 2001; Li, W. *et al.*, 2002). Physiological recordings from synaptically connected pairs of RB and AII cells have also shown

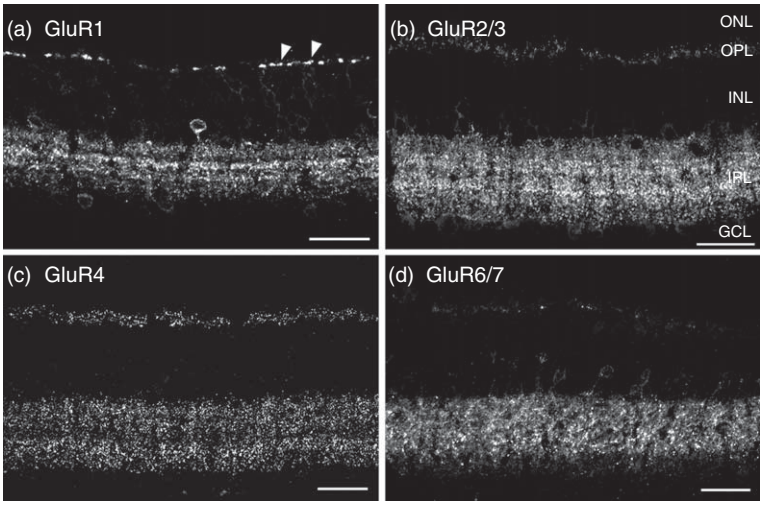

Figure 10 Expression of glutamate receptors (GluRs) in the inner plexiform layer (IPL) of the mouse retina. Confocal fluorescence micrographs of vertical sections that were immunolabeled for GluR subunits. (a) The GluR1 subunit is found extrasynaptically in bipolar, amacrine, and ganglion cells. The dashed line (arrowheads) in the outer plexiform layer (OPL) represents labeling of bipolar cell dendritic tips underneath cone pedicles. A punctate distribution representing synaptic clustering is found in the IPL. (b) The GluR 2/3 subunit shows punctate fluorescence in both the OPL and the IPL. (c) The GluR4 subunit is also found in synaptic hot spots both in the OPL and the IPL. The band of puncta in the OPL is rather wide in (b) and (c), suggesting that processes associated with rod spherules such as horizontal cell axon terminals are also labeled. (d) The kainate receptor subunit GluR 6/7 shows sparse label in the OPL, although many immunofluorescent puncta are present throughout the IPL. Scale bars = 25 μm. Adapted from Haverkamp, S. and Wässle, H. 2000. Immunocytochemical analysis of the mouse retina. J. Comp. Neurol. 424, 1–23.

that AMPA receptors mediate the signal transfer from RB to AII cells (Veruki, M. L. *et al.*, 2003; Singer, J. H. and Diamond, J. S., 2003).

1.12.8.2 Kainate Receptor Subunits

Immunoreactive puncta representing synaptic clusters of kainate receptor subunits KA2 and GluR6/7 have been found throughout the IPL (Figure 10(d); Qin, P. and Pourcho, R. G., 1996; Brandstätter, J. H. *et al.*, 1997; Qin, P. and Pourcho, R. G., 1999). Peng Y. W. *et al.* (1995) observed labeling of some amacrine and ganglion cells for GluR6/7, suggesting they both can express kainate receptors. Whole-cell recordings have shown that some amacrine cells express exclusively kainate receptors others express only AMPA receptors and many amacrine cells have a mixed population of GluRs (Dumitrescu, O. N. *et al.*, 2006). Kainate receptors were found to play only a minor role in generating the light-evoked synaptic currents of brisk sustained (X) type ganglion cells of the cat retina (Cohen, E. D., 2000). Synaptic clusters of the orphan receptor subunits $\delta 1/2$ have also been observed throughout the IPL (Brandstätter, J. H. *et al.*, 1997) postsynaptic to OFF-cone, ON-cone, and RB cells. However, in only one instance the postsynaptic partner was identified; the AI cell at RB cell terminals (Ghosh, K. K. *et al.*, 2001; Li, W. *et al.*, 2002). Unfortunately it is not yet known, which other GluR subunits, together with the $\delta 1/2$ subunits, constitute the GluR receptor channel of AI cells, however, kainate receptor subunits are the most probable candidates.

1.12.8.3 *N*-Methyl-D-Aspartate Receptor Subunits

Synaptic clusters of NMDA receptor NR1 subunits, which are a necessary constituent of all NMDA receptors, have been observed in the IPL, extending from the border of the amacrine cell layer to the innermost part of the IPL. There is a marked reduction of NMDA receptor clusters in the inner part of the IPL, where RB cells terminate (Fletcher, E. L. *et al.*, 2000; Kalloniatis, M. *et al.*, 2004), and signaling through NMDA receptors appears to have only a minor role in the signal transfer from RB cells to AI/AII cells (Boos, R. *et al.*, 1993; Singer, J. H. and Diamond, J. S., 2003; Veruki, M. L. *et al.*, 2003). The two subunits NR2A and NR2B have also a punctate distribution in the IPL; however, the density of puncta differs for the two subunits. Approximately four bands of higher density can be discerned for the NR2A subunit, in contrast to a prominent band in the center of the IPL in the case of the NR2B subunit. Only ~30% of the NR2A and NR2B clusters were found to coincide. These results suggest that there are at least three different types of postsynaptic NMDA receptor clusters in the IPL: those containing NR1/NR2A, NR1/NR2B, and only a small number composed of NR1/NR2A/NR2B.

NMDA receptors play an important role in the transfer of light signals from cone bipolar cells onto ganglion cells. This was first demonstrated in the retina of cold blooded animals (Mittman, S. *et al.*, 1990; Diamond, J. S. and Copenhagen, D. R., 1993; 1995; Matsui, K. *et al.*, 1998; Higgs, M. H. and Lukasiewicz, P. D., 1999). However, although light evoked, NMDA receptor mediated, postsynaptic currents were measured in these studies, spontaneous miniature postsynaptic currents (sEPSCs) lacked a NMDA receptor-mediated component. Light-evoked excitatory synaptic currents of brisk sustained (X) ganglion cells of the cat retina showed also a significant contribution from NMDAR (Cohen, E. D., 2000). In rat RGCs electrically evoked EPSCs recorded from ganglion cells were also mediated by both AMPA and NMDA receptors (Chen, S. and Diamond, J. S., 2002); however, sEPSCs were mediated solely by AMPA receptors. This problem was recently solved by the application of postembedding immunelectron microscopy: AMPA and NMDA receptors are both aggregated on ganglion cell dendrites postsynaptic to the bipolar cell ribbon. However, AMPA receptors are immediately adjacent to the ribbon and the glutamate release site, while NMDA receptors are found perisynaptically at some distance from the ribbon (Zhang, J. and Diamond, J. S., 2005). They are only activated during multivesicular, light-activated glutamate release and do not detect the small amount of glutamate released by the fusion of a single vesicle (Singer, J. H. *et al.*, 2004).

1.12.8.4 Metabotropic Glutamate Receptors

Of the eight different mGluR subtypes known presently, all but mGluR3 have been shown to be expressed and distinctly localized in the rodent retina (Tagawa, Y. *et al.*, 1999). They are clustered at the bipolar cell output synapses and EM has shown that they can occupy a pre- and/or postsynaptic position (Brandstätter, J. H. *et al.*, 1996; Koulen, P. *et al.*, 1996). Usually only one member of the dyad expresses a

given mGluR. The distribution of mGluR clusters across the IPL is different. The subtype mGluR2 for instance is enriched in two narrow bands of the IPL which coincide with the bands of the dendrites of cholinergic amacrine cells (Koulen, P. *et al.*, 1996). Postsynaptic clusters expressing the subtype mGluR7are enriched in four broad horizontal bands and show a reduced density along the cholinergic bands (Brandstätter, J. H. *et al.*, 1998). The different mGluR subtypes are unlikely to be involved with the direct signal transfer from bipolar cells onto the postsynaptic amacrine and ganglion cells. They are supposed to be modulators and it has been shown that $GABA_C$ receptors of RB cells are regulated down by mGluR1/5 agonists (Euler, T. and Wässle, H., 1998).

1.12.8.5 Co-Stratification of Pre- and Postsynaptic Partners in the Inner Plexiform Layer

Bipolar axons terminate at distinct levels within the IPL, and different types of amacrine and ganglion cells also keep their processes at specific levels within the IPL, which leads to the prediction that they also are engaged in mututal synaptic contacts (Figures 11(a)–11(d); Masland, R. H., 2001; Roska, B. and Werblin, F., 2001; Jusuf, P. R. *et al.*, 2004; Wässle, H., 2004; Lin, B. *et al.*, 2005; Coombs, J. *et al.*, 2006; Kim, T. J. and Jeon, C. J., 2006). However, this simple rule has only been verified in a few instances. Midget bipolar cells of the primate retina – both ON- and OFF-midget – contact midget ganglion cells and their axon terminal together with the ganglion cell dendrites form a kind of glomerulus (Kolb, H. and Dekorver, L., 1991; Calkins, D. J. *et al.*, 1994; Jusuf, P. R. *et al.*, 2006). Midget ganglion cells of the primate retina show sustained light responses and this predicts that midget bipolar cells also have sustained light responses.

Parasol ganglion cells of the primate retina also occur as OFF- and ON-pairs and their dendrites stratify in sublamina 2 and sublamina 4, respectively (Watanabe, M. and Rodieck, R. W., 1989; Dacey, D. M. and Packer, O. S., 2003; Dacey, D. M., 2004). OFF-parasol cells receive their major, excitatory input from DB3 bipolar cells (Calkins, D. J., 1999; Jacoby, R. A. *et al.*, 2000), ON-parasol cells from DB4/DB5 bipolar cells (Marshak, D. W. *et al.*, 2002). The DB3

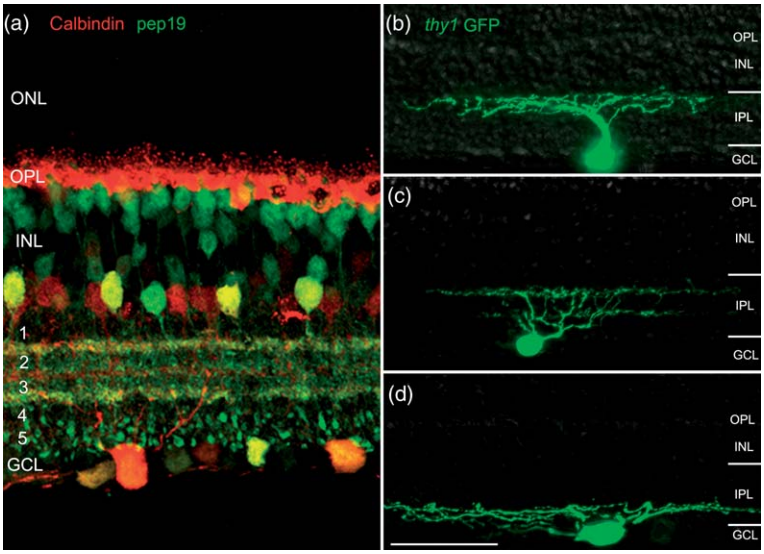

Figure 11 Stratification and functional subdivision of the inner plexiform layer (IPL). (a) Vertical section through a mouse retina that was double immunostained for calbindin (red) and for Pep 19 (green). Calbindin is expressed in horizontal, some amacrine, and some ganglion cells. Pep 19 labels rod bipolar (RB) cells, a subpopulation of cone bipolar, amacrine (among them the cholinergic amacrine cells) and ganglion cells. Their processes subdivide the IPL into distinct strata; among them are the OFF-(sublamina 1/2) and the ON-(sublamina 3/4) cholinergic strata. The axon terminals of RB cells terminate in stratum 4/5. Adapted from Haverkamp, S. and Wässle, H. 2000. Immunocytochemical analysis of the mouse retina. J. Comp. Neurol. 424, 1–23. (b) Vertical section through a transgenic mouse retina where ganglion cells express green fluorescent protein under the control of the thy1 promotor (Feng, G. *et al.*, 2000). This putative OFF (C2 type) ganglion cell stratifies in the outer IPL. (c) This bistratified (putative direction selective (DS)) cell stratifies at the same level as the cholinergic amacrine cells. This putative ON (A-type) ganglion cell stratifies in the inner IPL. Scale bar = 50 μm.

bipolar cell of the primate and the b2 cell of the ground squirrel are probably homologous types (DeVries, S. H., 2000). Since b2 cells receive their light signals through AMPA receptors, they have a high temporal transfer rate. This would be in accordance with the high flicker fusion frequency of parasol cells (Lee, B. B. *et al.*, 1988). Lin B. and colleagues (2005) studied the costratification of type 7 bipolar cell axon terminals and ganglion cell dendrites of the mouse retina. One monostratified ganglion cell and one bistratified cell tightly cofasciculate with the axon terminals of type 7 bipolar cells.

The small bistratified ganglion cells of the primate retina are the blue ON/yellow OFF ganglion cells (Dacey, D. M. and Lee, B. B., 1994). They have their inner dendritic tier in stratum 5 and their outer dendritic tier in stratum 1 of the IPL. The inner tier coincides with the axon terminal of blue-cone bipolar cells (BB in Figure 2), which provide the S-ON input. The outer tier collects synapses from DB2/DB3 bipolar cells and they provide the M- and L-OFF input (Calkins, D. J. *et al.*, 1998; Calkins, D. J., 2001). A further bistratified ganglion cell of the mammalian retina is the ON/OFF direction-selective (DS) ganglion cell (Amthor, F. R. *et al.*, 1989; Figure 11(c)). The inner and outer tier of its dendritic tree coincides with the level of stratification of ON- and OFF-cholinergic amacrine (Famiglietti, E. V., 1992) cells. Mouse cone bipolar cell axon terminals have been studied with respect to their costratification with the cholinergic strata (Ghosh, K. K. *et al.*, 2004; Pignatelli, V. and Strettoi, E., 2004), however, none of the nine types precisely coincided with the dendrites of cholinergic amacrine cells. In the rabbit retina it was shown that DS ganglion cells receive direct input from bipolar cells, however, the majority of their synaptic input is from amacrine cells (Dacheux *et al.*, 2003).Brown S. and Masland R. (1999) identified an ON-cone bipolar cell of the rabbit retina by its immunoreactivity for the carbohydrate epitope CD15 and demonstrated that CD15-positive bipolar cells axon terminals stratify within and slightly more distally of the ON-cholinergic band. In addition, they follow the pattern of the ON-cholinergic dendrites, and are, therefore, good candidates for providing synaptic input to the DS circuitry.

1.12.9 Conclusions

At least 10 different types of bipolar cells transfer the visual signals from the outer to the inner retina. RB cells are exclusively connected to rod spherules and they are involved with the transfer of scotopic signals. The major distinguishing anatomical feature of the different types of cone bipolar cells is the level of stratification of their axons in the IPL, where they preferentially contact those ganglion and amacrine cells which have their dendrites at the same level within the IPL. Some of the bipolar cells select certain types of cones, such as the midget bipolar cells of the primate retina or the blue-cone bipolar cells of most mammals and they transfer a chromatic signal into the IPL. However, most bipolar cells contact all cones, usually five to 10, within their dendritic field and they differ in their intrinsic properties. The major subdivision is into ON- and OFF-bipolar cells, and this is based on two different types of GluRs expressed at their dendrites: ionotropic GluRs in OFF-bipolars and mGluR6 in ON-bipolars. OFF-bipolar cells can be further subdivided according to the specific expression of AMPA or kainate receptors. The physiological consequences of this molecular diversity are different temporal resolution and possibly different threshold sensitivity. The axon terminals of bipolar cells in the IPL release glutamate at their output synapses. The release depends upon the intrinsic membrane properties of bipolar cells (HCN, K^+-, Na^+-, and Ca^{2+}-channels). It can also be modulated by the mGluR autoreceptors and possibly by other receptors, such as dopamine or cannabinoid receptors. Feedback from amacrine cells has been shown to regulate the bipolar cell intensity/response function. The postsynaptic partners of bipolar cells, amacrine, and ganglion cells also express different sets of GluRs, including NMDA receptors and mGluRs. How this molecular diversity is translated into the transfer of the light signal through the retina remains a challenging question.

References

Ahnelt, P. and Kolb, H. 1994. Horizontal cells and cone photoreceptors in human retina: A Golgi-electron microscopic study of spectral connectivity. J. Comp. Neurol. 343, 406–427.

Amthor, F. R., Takahashi, E. S., and Oyster, C. W. 1989. Morphologies of rabbit retinal ganglion cells with concentric receptive fields. J. Comp. Neurol. 280, 72–96.

Applebury, M. L., Antoch, M. P., Baxter, L. C., Chun, L. L. Y., Falk, J. D., Farhangfar, F., Kage, K., Krzystolik, M. G., Lyass, L. A., and Robbins, J. T. 2000. The murine cone photoreceptor: a single cone type expresses both S and M opsins with retinal spatial patterning. Neuron 27, 513–523.

Awatramani, G. B. and Slaughter, M. M. 2000. Origin of transient and sustained responses in ganglion cells of the retina. J. Neurosci. 20, 7087–7095.

Awatramani, G. B. and Slaughter, M. M. 2001. Intensity-dependent, rapid activation of presynaptic metabotropic glutamate receptors at a central synapse. J. Neurosci. 21, 741–749.

Berglund, K., Midorikawa, M., and Tachibana, M., 2002. Increase in the pool size of releasable synaptic vesicles by the activation of protein kinase C in goldfish retinal bipolar cells. J. Neurosci. 22, 4776–4785.

Berntson, A. and Taylor, W. R. 2000. Response characteristics and receptive field widths of on-bipolar cells in the mouse retina. J. Physiol. 524, 879–889.

Berson, D. M. 2003. Strange vision: ganglion cells as circadian photoreceptors. Trends Neurosci. 26, 314–320.

Boos, R., Schneider, H., and Wässle, H. 1993. Voltage- and transmitter-gated currents of AII-amacrine cells in a slice preparation of the rat retina. J. Neurosci. 13, 2874–2888.

Boycott, B. B. and Wässle, H. 1991. Morphological classification of bipolar cells of the primate retina. Eur. J. Neurosci. 3, 1069–1088.

Boycott, B. B. and Wässle, H. 1999. Parallel processing in the mammalian retina: the Proctor Lecture. Invest. Ophthalmol. Vis. Sci. 40, 1313–1327.

Brandstätter, J. H. 2002. Glutamate receptors in the retina: the molecular substrate for visual signal processing. Curr. Eye Res. 25, 327–331.

Brandstätter, J. H., Koulen, P., Kuhn, R., van der Putten, H., and Wässle, H. 1996. Compartmental localization of a metabotropic glutamate receptor (mGluR7): two different active sites at a retinal synapse. J. Neurosci. 16, 4749–4756.

Brandstätter, J. H., Koulen, P., and Wässle, H. 1997. Selective synaptic distribution of kainate receptor subunits in the two plexiform layers of the rat retina. J. Neurosci. 17, 9298–9307.

Brandstätter, J. H., Koulen, P., and Wässle, H. 1998. Diversity of glutamate receptors in the mammalian retina. Vision Res. 38, 1385–1397.

Brown, S. and Masland, R. 1999. Costratification of a population of bipolar cells with the direction-selective circuitry of the rabbit retina. J. Comp. Neurol. 408, 97–106.

Cajal, S. R. Y. 1893. La rétine des vertébrés. Cellule, 9, 119–257.

Calkins, D. J. 1999. Synaptic Organization of Cone Pathways in the Primate Retina. In: Color Vision: From Genes to Perception (*eds*. K. R. Gegenfurtner and L. T. Sharpe), pp. 163–179. Cambridge University Press.

Calkins, D. J. 2001. Seeing with S cones. Prog. Ret. Eye Res. 20, 255–287.

Calkins, D. J. 2005. Localization of ionotropic glutamate receptors to invaginating dendrites at the cone synapse in primate retina. Vis. Neurosci. 22, 469–477.

Calkins, D. J. and Sterling, P. 1999. Evidence that circuits for spatial and opponent color vision segregate at the first retinal synapse. Neuron 24, 313–321.

Calkins, D. J., Schein, S. J., Tsukamoto, Y., and Sterling, P. 1994. M and L cones in macaque fovea connect to midget ganglion cells by different numbers of excitatory synapses. Nature 371, 70–72.

Calkins, D. J., Tsukamoto, Y., and Sterling, P. 1996. Foveal cones form basal as well as invaginating junctions with diffuse ON bipolar cells. Vision Res. 36, 3373–3381.

Calkins, D. J., Tsukamoto, Y., and Sterling, P. 1998. Microcircuitry and mosaic of a blue–yellow ganglion cell in the primate retina. J. Neurosci. 18, 3373–3385.

Casagrande, V. A. and Xu, X. 2004. Parallel Visual Pathways: A Comparative Perspective. In: The Visual Neurosciences (*eds*. L. Chalupa and J. S. Werner), pp. 494–506. MIT Press.

Chan, T. L., Martin, P. R., Clunas, N., and Grünert, U. 2001. Bipolar cell diversity in the primate retina: morphologic and immunocytochemical analysis of a New World monkey, the marmoset Callithrix jacchus. J. Comp. Neurol. 437, 219–239.

Chen, S. and Diamond, J. S. 2002. Synaptically released glutamate activates extrasynaptic NMDA receptors on cells in the ganglion cell layer of rat retina. J. Neurosci. 22, 2165–2173.

Chun, M. H., Grünert, U., Martin, P. R., and Wässle, H. 1996. The synaptic complex of cones in the fovea and in the periphery of the macaque monkey retina. Vision Res. 36, 3383–3395.

Chun, M. H., Han, S. H., Chun, J. W., and Wässle, H. 1993. Electron microscopic analysis of the rod pathway of the rat retina. J. Comp. Neurol. 332, 421–432.

Cohen, E. D. 2000. Light-evoked excitatory synaptic currents of X-type retinal ganglion cells. J. Neurophysiol. 83, 3217–3229.

Cohen, E. D. and Sterling, P. 1990a. Demonstration of cell types among cone bipolar neurons of cat retina. Philos. Trans. R. Soc. Lond. B 330, 305–321.

Cohen, E. D. and Sterling, P. 1990b. Convergence and divergence of cones onto bipolar cells in the central area of the cat retina. Philos. Trans. R. Soc. Lond. B 330, 323–328.

Coombs, J., van der List, D., Wang, G. Y., and Calupa, L. M. 2006. Morphological properties of mouse retinal ganglion cells. Neuroscience 140, 123–136.

Dacey, D. M. 2000. Parallel pathways for spectral coding in primate retina. Ann. Rev. Neurosci. 23, 743–775.

Dacey, D. M. 2004. Origins of Perception: Retinal Ganglion Cell Diversity and the Creation of Parallel Visual Pathways. In: The Cognitive Neurosciences III (*eds*. M. S. Gazzaniga), pp. 281–301. MIT Press.

Dacey, D. M. and Lee, B. B. 1994. The 'blue-on' opponent pathway in primate retina originates from a distinct bistratified ganglion cell type. Nature 367, 731–735.

Dacey, D. M. and Packer, O. S. 2003. Colour coding in the primate retina: diverse cell types and cone-specific circuitry. Curr. Opin. Neurobiol. 13, 421–427.

Dacey, D. M., Packer, O. S., Diller, L., Brainard, D., Peterson, B., and Lee, B. 2000. Center surround receptive field structure of cone bipolar cells in primate retina. Vision Res. 40, 1801–1811.

Dacey, D. M., Peterson, B. B., Robinson, F. R., and Gamlin, P. D. 2003. Fireworks in the primate retina: *in vitro* photodynamics reveals diverse LGN-projecting ganglion cell types. Neuron 37, 15–27.

Dacheux, R. F. and Raviola, E. 1986. The rod pathway in the rabbit retina: a depolarizing bipolar and amacrine cell. J. Neurosci. 6, 331–345.

Dacheux, R. F., Chimento, M. F., and Amthor, F. R. 2003. Synaptic input to the on-off directionally selective ganglion cell in the rabbit retina. J. Comp. Neurol. 456, 267–278.

Deguchi-Tawarada, M., Inoue, E., Takao-Rikitsu, E., Inoue, M., Kitajima, I., Ohtsuka, T., and Takai, Y. 2006. Active zone protein CAST is a component of conventional and ribbon synapses in mouse retina. J. Comp. Neurol. 495, 480–496.

de la Villa, P., Kurahashi, T., and Kaneko, A. 1995. L-glutamate-induced responses and cGMP-activated channels in three subtypes of retinal bipolar cells dissociated from the cat. J. Neurosci. 15, 3571–3582.

DeVries, S. H. 2000. Bipolar cells use kainate and AMPA receptors to filter visual information into separate channels. Neuron 28, 847–856.

DeVries, S. H. and Schwartz, E. A. 1999. Kainate receptors mediate synaptic transmission between cones and ''Off'' bipolar cells in a mammalian retina. Nature 397, 157–160.

DeVries, S. H., Li, W., and Saszik, S. 2006. Parallel processing in two transmitter microenvironments at the cone photoreceptor synapse. Neuron 50, 735–748.

Dhingra, A., Faurobert, E., Dascal, N., Sterling, P., and Vardi, N. 2004. A retinal-specific regulator of G-protein signaling interacts with Gαo and accelerates an expressed metabotropic glutamate receptor 6 cascade. J. Neurosci. 24, 5684–5693.

Dhingra, A., Jiang, M., Wang, T. L., Lyubarsky, A., Savchenko, A., Bar-Yehuda, T., Sterling, P., Birnbaumer, L., and Vardi, N. 2002. Light response of retinal ON bipolar cells requires a specific splice variant of Gαo. J. Neurosci. 22, 4878–4884.

Diamond, J. S. and Copenhagen, D. R. 1993. The contribution of NMDA and non-NMDA receptors to the light-evoked input–output characteristics of retinal ganglion cells. Neuron 11, 725–738.

Diamond, J. S. and Copenhagen, D. R. 1995. The relationship between light-evoked synaptic excitation and spiking behaviour of salamander retinal ganglion cells. J. Physiol. 487, 711–725.

Dick, O., tom Dieck, S., Altrock, W. D., Ammermüller, J., Weiler, R., Garner, C. C., Gundelfinder, E. D., and Brandstätter, J. H. 2003. The presynaptic active zone protein bassoon is essential for photoreceptor ribbon synapse formation in the retina. Neuron 37, 775–786.

Dingledine, R., Borgs, K., Bowie, D., and Traynelis, S. F. 1999. The glutamate receptor ion channels. Pharmacol. Rev. 51, 7–61.

Dowling, J. E. and Boycott, B. B. 1966. Organisation of the primate retina: electron microscopy. Proc. R. Soc. Lond. B 166, 80–111.

Duebel, J., Haverkamp, S., Schleich, W., Feng, G., Augustine, G. J, Kuner, T., and Euler, T., 2006. Two-photon imaging reveals somatodendritic chloride gradient in retinal ON-type bipolar cells expressing the biosensor clomeleon. Neuron 49, 81–94.

Dumitrescu, O. N., Protti, D. S., Majumdar, S., Zeilhofer, H. U., and Wässle, H. 2006. Ionotropic glutamate receptors of amacrine cells of the mouse retina. Vis. Neurosci. 23, 79–90.

Duncan, J. L., Yang, H., Doan, T., Silverstein, R. S., Murphy, G. J., Nune, G., Liu, X., Copenhagen, D., Tempel, B. L., Rieke, F., and Krizaj, D. 2006. Scotopic visual signaling in the mouse retina is modulated by high-affinity plasma membrane calcium extrusion. J. Neurosci. 26, 7201–7211.

Euler, T. and Masland, R. H. 2000. Light-evoked responses of bipolar cells in a mammalian retina. J. Neurophysiol. 83, 1817–1829.

Euler, T. and Wässle, H. 1995. Immunocytochemical identification of cone bipolar cells in the rat retina. J. Comp. Neurol. 361, 461–478.

Euler, T. and Wässle, H. 1998. Different contributions of $GABA_A$ and $GABA_C$ receptors to rod and cone bipolar cells in a rat retinal slice preparation. J. Neurophysiol. 79, 1384–1395.

Euler, T., Schneider, H., and Wässle, H. 1996. Glutamate responses of bipolar cells in a slice preparation of the rat retina. J. Neurosci. 16, 2934–2944.

Famiglietti, E. V. 1981. Functional architecture of cone bipolar cells in mammalian retina. Vision Res. 21, 1559–1563.

Famiglietti, E. V. 1992. Dendritic costratification of on and on-off directionally selective ganglion-cell with starburst amacrine cells in rabbit retina. J. Comp. Neurol. 324, 322–335.

Famiglietti, E. V. and Kolb, H. 1975. A bistratified amacrine cell and synaptic circuitry in the inner plexiform layer of the retina. Brain Res. 84, 293–300.

Fan, S. F. and Yazulla, S. 2005. Reciprocal inhibition of voltage-gated potassium currents ((I) (K(v))) by activation of cannabinoid CB1 and dopamine D-1 receptors in ON bipolar cells of goldfish retina. Vis. Neurosci. 22, 55–63.

Feigenspan, A., Janssen-Bienhold, U., Hormuzdi, S., Monyer, H., Degen, J., Söhl, G., Willecke, K., Ammermüller, J., and Weiler, R. 2004. Expression of connexin36 in cone pedicles and OFF-cone bipolar cells of the mouse retina. J. Neurosci. 24, 3325–3334.

Feng, G., Mellor, R. H., Bernstein, M., Keller-Peck, C., Nguyen, Q. T., Wallace, M., Nerbonne, J. M., Lichtman, J. W., and Sanes, J. R. 2000. Imaging neuronal subsets in transgenic mice expressing multiple spectral variants of GFP. Neuron 28, 41–51.

Field, G. D. and Rieke, F. 2002. Nonlinear signal transfer from jouse rods to bipolar cells and implications for visual sensitivity. Neuron 34, 773–785.

Fletcher, E. L., Hack, I., Brandstätter, J. H., and Wässle, H. 2000. Synaptic localization of NMDA receptor subunits in the rat retina. J. Comp. Neurol. 420, 98–112.

Freed, M. A. 2000. Parallel cone bipolar pathways to a ganglion cell use different rates and amplitudes of quantal excitation. J. Neurosci. 20, 3956–3963.

Freed, M. A., Smith, R. G., and Sterling, P. 2003. Timing of quantal release from the retinal bipolar terminal is regulated by a feedback circuit. Neuron 38, 89–101.

Fyk-Kolodziej, B., Dzhagaryan, A., Qin, P., and Pourcho, R. G. 2004. Immunocytochemical localization of three vesicular glutamate transporters in the cat retina. J. Comp. Neurol. 475, 518–530.

Ghosh, K. K., Haverkamp, S., and Wässle, H. 2001. Glutamate receptors in the rod pathway of the mammalian retina. J. Neurosci. 21, 8636–8647.

Ghosh, K. K., Martin, P., and Grünert, U. 1997. Morphological analysis of the blue cone pathway in the retina of a new world monkey, the marmoset *Callithrix jacchus*. J. Comp. Neurol. 379, 211–225.

Ghosh, K. K., Bujan, S., Haverkamp, S., Feigenspan, A., and Wässle, H. 2004. Types of bipolar cells in the mouse retina. J. Comp. Neurol. 469, 70–82.

Glösmann, M. and Ahnelt, P. K. 1998. Coexpression of M- and S-opsin extends over the entire inferior mouse retina. Invest. Ophthalmol. Vis. Sci. 39, S1059.

Gray, E. G. and Pease, H. L. 1971. On understanding the organization of the retinal receptor synapses. Brain Res. 35, 1–15.

Grünert, U., Haverkamp, S., Fletcher, E. L., and Wässle, H. 2002. Synaptic distribution of ionotropic glutamate receptors in the inner plexiform layer of the primate retina. J. Comp. Neurol. 447, 138–151.

Hack, I., Frech, M., Dick, O., Peichl, L., and Brandstätter, J. H. 2001. Heterogeneous distribution of AMPA glutamate receptor subunits at the photoreceptor synapses of rodent retina. Eur. J. Neurosci. 13, 15–24.

Hack, I., Peichl, L., and Brandstätter, J. H. 1999. An alternative pathway for rod signals in the rodent retina: rod photoreceptors, cone bipolar cells, and the localization of glutamate receptors. Proc. Natl. Acad. Sci. U. S. A. 96, 14130–14135.

Han, Y. and Massey, S. C. 2005. Electrical synapses in retinal ON cone bipolar cells: subtype-specific expression of connexins. Proc. Natl. Acad. Sci. U. S. A. 102, 13313–13318.

Hartveit, E. 1996. Membrane currents evoked by ionotropic glutamate receptor agonists in rod bipolar cells in the rat retinal slice preparation. J. Neurophysiol. 76, 401–422.

Hartveit, E. 1997. Functional organization of cone bipolar cells in the rat retina. J. Neurophysiol. 77, 1716–1730.

Hartveit, E., Brandstätter, J. H., Sassoè-Pognetto, M., Laurie, D. J., Seeburg, P. H., and Wässle, H. 1994. Localization and developmental expression of the NMDA receptor subunit NR2A in the mammalian retina. J. Comp. Neurol. 348, 570–582.

Haverkamp, S. and Wässle, H. 2000. Immunocytochemical analysis of the mouse retina. J. Comp. Neurol. 424, 1–23.

Haverkamp, S., Ghosh, K. K., Hirano, A. A., and Wässle, H. 2003. Immunocytochemical description of five bipolar cell types of the mouse retina. J. Comp. Neurol. 455, 463–476.

Haverkamp, S., Grünert, U., and Wässle, H. 2000. The cone pedicle a complex synapse in the retina. Neuron 27, 85–95.

Haverkamp, S., Grünert, U., and Wässle, H. 2001. Localization of kainate receptors at the cone pedicles of the primate retina. J. Comp. Neurol. 436, 471–486.

Haverkamp, S., Wässle, H., Duebel, J., Kuner, T., Augustine, G. J., Feng, G., and Euler, T. 2005. The primordial, blue-cone color system of the mouse retina. J. Neurosci. 25, 5438–5445.

Heidelberger, R., Sterling, P., and Matthews, G. 2002. Roles of ATP in depletion and replenishment of the releasable pool of synaptic vesicles. J. Neurophysiol. 88, 98–106.

Heidelberger, R., Thoreson, W. B., and Witkovsky, P. 2005. Synaptic transmission at retinal ribbon synapses. Prog. Ret. Eye Res. 24, 682–720.

Hendry, S. H. and Reid, C. 2000. The koniocellular pathway in primate vision. Ann. Rev. Neurosci. 23, 127–153.

Higgs, M. H. and Lukasiewicz, P. D. 1999. Glutamate uptake limits synaptic excitation of retinal ganglion cells. J. Neurosci. 19, 3691–3700.

Hirasawa, H. and Kaneko, A. 2003. pH changes in the invaginating synaptic cleft mediate feedback from horizontal cells to cone photoreceptors by modulating Ca^{2+} channels. J. Gen. Physiol. 122, 657–671.

Hofer, H., Carroll, J., Neitz, J., Neitz, M., and Williams, D. R. 2005. Organization of the human trichromatic cone mosaic. J. Neurosci. 25, 9669–9679.

Hollmann, M. and Heinemann, S. 1994. Cloned glutamate receptors. Ann. Rev. Neurosci. 17, 31–108.

Holt, M., Cooke, A., Neef, A., and Lagnado, L. 2004. High mobility of vesicles supports continuous exocytosis at a ribbon synapse. Curr. Biol. 14, 173–183.

Hombach, S., Janssen-Bienhold, U., Söhl, G., Schubert, T., Büssow, H., Ott, T., Weiler, R., and Willecke, K. 2004. Functional expression of connexin57 in horizontal cells of the mouse retina. Eur. J. Neurosci. 19, 2633–2640.

Hopkins, J. M. and Boycott, B. B. 1996. The cone synapses of DB1 diffuse, DB6 diffuse and invaginating midget bipolar cells of a primate retina. J. Neurocytol. 25, 391–403.

Hopkins, J. M. and Boycott, B. B. 1997. The cone synapses of cone bipolar cells of primate retina. J. Neurocytol. 26, 313–325.

Hornstein, E. P., Verweij, J., and Schnapf, J. L. 2004. Electrical coupling between red and green cones in primate retina. Nat. Neurosci. 7, 745–750.

Hornstein, E. P., Verweij, J., Li, P. H., and Schnapf, J. L. 2005. Gap-junctional coupling and absolute sensitivity of photoreceptors in macaque retina. J. Neurosci. 25, 11201–11209.

Hosoi, N., Arai, I., and Tachibana, M. 2005. Group III metabotropic glutamate receptors and exocytosed protons inhibit L-type calcium currents in cones but not in rods. J. Neurosci. 25, 4062–4072.

Huang, L., Max, M., Margolskee, R. F., Su, H., Masland, R. H., and Euler, T. 2003. G protein subunit Gγ13 is coexpressed with Gαo, Gβ3, and Gβ4 in retinal ON bipolar cells. J. Comp. Neurol. 455, 1–10.

Ingling, C. R., Jr. and Martinez-Uriegas, E. 1983a. The relationship between spectral sensitivity and spatial sensitivity for the primate r-g X-channel. Vision Res. 23, 1495–1500.

Ingling, C. R., Jr. and Martinez-Uriegas, E. 1983b. The Spatio-Chromatic Signal of the r.g Channel. In: Colour-Vision: Physiology and Psychophysics (*eds*. J. D. Mollon and L. T. Sharpe), pp. 433–444. Academic Press.

Isayama, T., Berson, D. M., and Pu, M. 2000. Theta ganglion cell type of cat retina. J. Comp. Neurol. 417, 32–48.

Ivanova, E. and Müller, F. 2006. Retinal bipolar cell types differ in their inventory of ion channels. Vis. Neurosci. 23, 143–154.

Jacobs, G. H., Williams, G. A., and Fenwick, J. A. 2004. Influence of cone pigment coexpression on spectral sensitivity and color vision in the mouse. Vision Res. 44, 1615–1622.

Jacobs, G. H., Williams, G. A., Cahill, H., and Nathans, J. 2007. Emergence of novel color vision in mice engineered to express a human cone photopigment. Science 315, 442–454.

Jacoby, R. A., Wiechmann, A. F., Amara, S. G., Leighton, B. H., and Marshak, D. W. 2000. Diffuse bipolar cells provide input to OFF parasol ganglion cells in the macaque retina. J. Comp. Neurol. 416, 6–18.

Jeon, C. J. and Masland, R. H. 1995. A population of wide-field bipolar cells in the rabbit's retina. J. Comp. Neurol. 360, 403–412.

Johnson, J., Tian, N., Caywood, M. S., Reimer, R. J., Edwards, R. H., and Copenhagen, D. R. 2003. Vesicular neurotransmitter transporter expression in developing postnatal rodent retina: GABA and glycine precede glutamate. J. Neurosci. 23, 518–529.

Jusuf, P. R., Lee, S. C. S., and Grünert, U. 2004. Synaptic connectivity of the diffuse bipolar cell type DB6 in the inner plexiform layer of primate retina. J. Comp. Neurol. 469, 494–506.

Jusuf, P. R., Martin, P. R., and Grünert, U. 2006. Synaptic connectivity in the midget-parvocellular pathway of primate central retina. J. Comp. Neurol. 494, 260–274.

Kalloniatis, M., Sun, D., Foster, L., Haverkamp, S., and Wässle, H. 2004. Localization of NMDA receptor subunits and mapping NMDA drive within the mammalian retina. Vis. Neuroscience 21, 587–597.

Kamermans, M., Kraaij, D., and Spekreijse, H. 2001. The dynamic characteristics of the feedback signal from horizontal cells to cones in the goldfish retina. J. Physiol. 534, 489–500.

Kaneko, A. 1970. Physiological and morphological identification of horizontal, bipolar and amacrine cells in goldfish retina. J. Physiol. 207, 623–633.

Kaneko, A. and Shimazaki, H. 1976. Synaptic transmission from photoreceptors to bipolar and horizontal cells in the carp retina. Cold Spring Harb. Symp. Quant. Biol. 40, 537–546.

Kew, J. N. C. and Kemp, J. A. 2005. Ionotropic and metabotropic glutamate receptor structure and pharmacology. Psychopharmacology 179, 4–29.

Kim, T. J. and Jeon, C. J. 2006. Morphological classification of parvalbumin-containing retinal ganglion cells in mouse: single-cell injection after immunocytochemistry. Invest. Ophthalmol. Vis. Sci. 47, 2757–2764.

Klug, K., Herr, S., Ngo, I. Z., Sterling, P., and Schein, S. 2003. Macaque retina contains an S-cone OFF midget pathway. J. Neurosci. 23, 9881–9887.

Klumpp, D. J., Song, E. J., Ito, S., Sheng, M. H., Jan, L. Y., and Pinto, L. H. 1995a. The shaker-like potassium channels of the mouse rod bipolar cell and their contributions to the membrane current. J. Neurosci. 15, 5004–5013.

Klumpp, D. J., Song, E. J., and Pinto, L. H. 1995b. Identification and localization of K+ channels in the mouse retina. Vis. Neurosci. 12, 1177–1190.

Kolb, H. 1970. Organization of the outer plexiform layer of the primate retina: electron microscopy of Golgi-impregnated cells. Philos. Trans. R. Soc. Lond. B 258, 261–283.

Kolb, H. and Dekorver, L. 1991. Midget ganglion cells of the parafovea of the human retina: a study by electron microscopy and serial section reconstructions. J. Comp. Neurol. 303, 617–636.

Kolb, H. and Famiglietti, E. V. 1976. Rod and cone pathways in retina of cat. Invest. Ophthalmol 15, 935–946.

Kolb, H., Nelson, R., and Mariani, A. 1981. Amacrine cells, bipolar cells and ganglion cells of the cat retina: a Golgi study. Vision Res. 21, 1081–1114.

Kong, J. H., Fish, D. R., Rockhill, R. L., and Masland, R. H. 2005. Diversity of ganglion cells in the mouse retina: unsupervised

morphological classification and its limits. J. Comp. Neurol. 489, 293–310.
Koulen, P., Kuhn, R., Wässle, H., and Brandstätter, J. H. 1997. Group I metabotropic glutamate receptors mGluR1α and mGluR5a: localization in both synaptic layers of the rat retina. J. Neurosci. 17, 2200–2211.
Koulen, P., Kuhn, R., Wässle, H., and Brandstätter, J. H. 1999. Modulation of the intracellular calcium concentration in photoreceptor terminals by a presynaptic metabotropic glutamate receptor. Proc. Natl. Acad. Sci. U. S. A. 96, 9909–9914.
Koulen, P., Liu, J. Y., Nixon, E., and Madry, C. 2005. Interaction between mGluR8 and calcium channels in photoreceptors is sensitive to pertussis toxin and occurs via G protein beta gamma subunit signaling. Invest. Ophthalmol. Vis. Sci. 46, 287–291.
Koulen, P., Malitschek, B., Kuhn, R., Wässle, H., and Brandstätter, J. H. 1996. Group II and group III metabotropic glutamate receptors in the rat retina: distributions and developmental expression patterns. Eur. J. Neurosci. 8, 2177–2187.
Kouyama, N. and Marshak, D. W. 1992. Bipolar cells specific for blue cones in the macaque retina. J. Neurosci. 12, 1233–1252.
Lagnado, L. 2003. Ribbon synapses. Curr. Biol. 13, R631.
Lamb, T. D. and Simon, E. J. 1976. Power spectral measurements of noise in turtle retina. J. Physiol. 263, P103–P105.
Lasansky, A. 1992. Properties of depolarizing bipolar cell responses to central illumination in salamander retinal slices. Brain Res. 576, 181–196.
Lee, B. B., Martin, P. R., and Valberg, A. 1988. The physiological basis of heterochromatic flicker photometry demonstrated in the ganglion cells of the macaque retina. J. Physiol. 404, 323–347.
Lee, B. B., Pokorny, J., Smith, V. C., Martin, P. R., and Valberg, A. 1990. Luminance and chromatic modulation sensitivity of macaque ganglion cells and human observers. J. Opt. Soc. Am. A 7, 2223–2236.
Li, W. and DeVries, H. 2004. Separate blue and green cone networks in the mammalian retina. Nat. Neurosci. 7, 751–756.
Li, W. and DeVries, H. 2006. Bipolar cell pathways for color and luminance vision in a dichromatic mammalian retina. Nat. Neurosci. 9, 669–675.
Li, W., Keung, J. W., and Massey, S. C. 2004. Direct synaptic connections between rods and OFF cone bipolar cells in the rabbit retina. J. Comp. Neurol. 474, 1–12.
Li, W., Trexler, E. B., and Massey, S. C. 2002. Glutamate receptors at rod bipolar ribbon synapses in the rabbit retina. J. Comp. Neurol. 448, 230–248.
Lin, B., Jakobs, T. C., and Masland, R. H. 2005. Different functional types of bipolar cells use different gap-junctional proteins. J. Neurosci. 25, 6696–6701.
Lo, W., Molloy, R., and Hughes, T. E. 1998. Ionotropic glutamate receptors in the retina: moving from molecules to circuits. Vision Res. 38, 1399–1410.
Lukáts, A., Szabo, A., Röhlich, P., Vigh, B., and Szél, A. 2005. Photopigment coexpression in mammals: comparative and developmental aspects. Histol. Histopathol. 20, 551–574.
Ma, Y. P., Cui, J., and Pan, Z. H. 2005. Heterogeneous expression of voltage-dependent Na^+ and K^+ channels in mammalian retinal bipolar cells. Vis. Neurosci. 22, 119–133.
MacNeil, M. A., Heussy, J. K., Dacheux, R. F., Raviola, E., and Masland, R. H. 2004. The population of bipolar cells in the rabbit retina. J. Comp. Neurol. 472, 73–86.
Mariani, A. P. 1983. The neuronal organization of the outer plexiform layer of the primate retina. Int. Rev. Cytol. 86, 285–320.
Mariani, A. P. 1984. Bipolar cells in monkey retina selective for the cones likely to be blue-sensitive. Nature 308, 184–186.
Marshak, D. W., Yamada, E. S., Bordt, A. S., and Perryman, W. C. 2002. Synaptic input to an ON parasol ganglion cell in the macaque retina: a serial section analysis. Vis. Neurosci. 19, 299–305.
Masland, R. H. 2001. The fundamental plan of the retina. Nat. Neurosci. 4, 877–886.
Massey, S. C. and Mills, S. L. 1996. A calbindin-immunoreactive cone bipolar cell type in the rabbit retina. J. Comp. Neurol. 366, 15–33.
Masu, M., Iwakabe, H., Tagawa, Y., Miyoshi, T., Yamashita, M., Fukuda, Y., Sasaki, H., Hiroi, K., Nakamura, Y., Shigemoto, R., Takada, M., Nakamura, K., Nakao, K., Katsuki, M., and Nakanishi, S. 1995. Specific deficit of the ON response in visual transmission by targeted disruption of the mGluR6 gene. Cell 80, 757–765.
Matsui, K., Hasegawa, J., and Tachibana, M. 2001. Modulation of excitatory synaptic transmission by GABA(C) receptor-mediated feedback in the mouse inner retina. J. Neurophysiol. 86, 2285–2298.
Matsui, K., Hosoi, N., and Tachibana, M. 1998. Excitatory synaptic transmission in the inner retina: paired recordings of bipolar cells and neurons of the ganglion cell layer. J. Neurosci. 18, 4500–4510.
McCall, M. A., Lukasiewicz, P. D., Gregg, R. G., and Peachey, N. S. 2002. Elimination of the rho1 subunit abolishes GABA(C) receptor expression and alters visual processing in the mouse retina. J. Neurosci. 22, 4163–4174.
McGillem, G. S. and Dacheux, R. F. 2001. Rabbit cone bipolar cells: correlation of their morphologies with whole-cell recordings. Vis. Neurosci. 18, 675–685.
Migdale, K., Herr, S., Klug, K., Ahmad, K., Linberg, K., Sterling, P., and Schein, S. 2003. Two ribbon synaptic units in rod photoreceptors of macaque, human, and cat. J. Comp. Neurol. 455, 100–112.
Missotten, L. 1965. The Ultrastructure of the Human Retina. Editions Arscia.
Mittman, S., Taylor, W. R., and Copenhagen, D. R. 1990. Concomitant activation of two types of glutamate receptor mediates excitation of salamander retinal ganglion cells. J. Physiol. 428, 175–197.
Mollon, J. D. 1989. ''Tho' she kneel'd in that place where they grew''. The uses and origins of primate colour vision. J. Exp. Biol. 146, 21–38.
Mollon, J. D. and Jordan, G. 1988. Eine evolutionäre Interpretation des menschlichen Farbensehens. Die Farbe 35/36, 139–170.
Morgan, J. L., Dhingra, A., Vardi, N., and Wong, R. O. L. 2006. Axons and dendrites originate from neuroepithelial-like processes of retinal bipolar cells. Nat. Neurosci. 9, 85–92.
Morgans, C. W. 2001. Localization of the alpha(1F) calcium channel subunit in the rat retina. Invest. Ophthalmol. Vis. Sci. 42, 2414–2418.
Morgans, C. W., Bayley, P. R., Oesch, N. W., Ren, G., Akileswaran, L., and Taylor, W. R. 2005. Photoreceptor calcium channels: insight from night blindness. Vis. Neurosci. 22, 561–568.
Morgans, C. W., El Far, O., Berntson, A., Wässle, H., and Taylor, W. R. 1998. Calcium extrusion from mammalian photoreceptor terminals. J. Neurosci. 18, 2467–2474.
Morigiwa, K. and Vardi, N. 1999. Differential expression of ionotropic glutamate receptor subunits in the outer retina. J. Comp. Neurol. 405, 173–184.
Müller, F., Scholten, A., Ivanova, E., Haverkamp, S., Kremmer, E., and Kaupp, U. B. 2003. HCN channels are expressed differentially in retinal bipolar cells and concentrated at synaptic terminals. Eur. J. Neurosci. 17, 2084–2096.

Muresan, V., Lyass, A., and Schnapp, B. J. 1999. The kinesin motor KIF3A is a component of the presynaptic ribbon in vertebrate photoreceptors. J. Neurosci. 19, 1027–1037.

Nathans, J. 1999. The evolution and physiology of human color vision: insights from molecular genetic studies of visual pigments. Neuron 24, 299–312.

Nawy, S. 1999. The metabotropic receptor mGluR6 may signal through Go, but not phosphodiesterase, in retinal bipolar cells. J. Neurosci. 20, 4471–4479.

Neitz, J., Carroll, J., Yamauchi, Y., Neitz, M., and Williams, D. R. 2002. Color perception is mediated by a plasticneural mechanism that is adjustable in adults. Neuron 35, 783–792.

Nelson, R. and Kolb, H. 1983. Synaptic patterns and response properties of bipolar and ganglion cells in the cat retina. Vision Res. 23, 1183–1195.

Nelson, R., Kolb, H., Robinson, M. M., and Mariani, A. P. 1981. Neural circuitry of the cat retina: cone pathways to ganglion cells. Vision Res. 21, 1527–1536.

Nomura, A., Shigemoto, R., Nakamura, Y., Okamoto, N., Mizuno, N., and Nakanishi, S. 1994. Developmentally regulated postsynaptic localization of a metabotropic glutamate receptor in rat rod bipolar cells. Cell 77, 361–369.

O'Brien, J. J., Chen, X., MacLeish, P. R., and Massey, S. S. 2004. Connexin 36 forms gap junctions between telodendria of primae cones. Invest. Ophthalmol. Vis. Sci., 45, Assoc. Res. Vis. Ophthalmol. Meeting E Abstr, 1146.

Palmer, M. J., Taschenberger, H., Hull, C., Tremere, L., and von Gersdorff, H. 2003. Synaptic activation of presynaptic glutamate transporter currents in nerve terminals. J. Neurosci. 23, 4831–4841.

Pan, Z. H. 2000. Differential expression of high- and two types of low-voltage-activated calcium currents in rod and cone bipolar cells of the rat retina. J. Neurophysiol. 83, 513–527.

Pan, Z. H. and Hu, H. J. 2000. Voltage-dependent Na^+ currents in mammalian retinal cone bipolar cells. J. Neurophysiol. 84, 2564–2571.

Peng, Y. W., Blackstone, C. D., Huganir, R. L., and Yau, K. W. 1995. Distribution of glutamate receptor subtypes in the vertebrate retina. Neuroscience 66, 483–497.

Pignatelli, V. and Strettoi, E. 2004. Bipolar cells of the mouse retina: a gene gun, morphological study. J. Comp. Neurol. 476, 254–266.

Pin, J. P. and Duvoisin, R. 1995. Review: Neurotransmitter receptors I. The metabotropic glutamate receptors: structure and functions. Neuropharmacology 34, 1–26.

Polyak, S. L. 1941. The Retina. University of Chicago Press.

Protti, D. A. and Llano, I. 1998. Calcium currents and calcium signaling in rod bipolar cells of rat retinal slices. J. Neurosci. 18, 3715–3724.

Protti, D. A., Flores-Herr, N., and von Gersdorff, H. 2000. Light evokes Ca^{2+} spikes in the axon terminal of a retinal bipolar cell. Neuron 25, 215–227.

Protti, D. A., Flores-Herr, N., Li, W., Massey, S. C., and Wässle, H. 2005. Light signaling in scotopic conditions in the rabbit, mouse and rat retina: a physiological and anatomical study. J. Neurophysiol. 93, 3479–3488.

Puller, C., Haverkamp, S., and Grünert, U. 2007. OFF midget bipolar cells in the retina of the marmoset, callithrix jacchus, express AMPA receptors. J. Comp. Neurol. 502, 442–454.

Qin, P. and Pourcho, R. G. 1996. Distribution of AMPA-selective glutamate receptor subunits in the cat retina. Brain Res. 710, 303–307.

Qin, P. and Pourcho, R. G. 1999. Localization of AMPA-selective glutamate receptor subunits in the cat retina: a light- and electron-microscopic study. Vis. Neurosci. 16, 169–177.

Raviola, E. and Gilula, N. B. 1973. Gap junctions between photoreceptor cells in the vertebrate retina. Proc. Natl. Acad. Sci. U. S. A. 70, 1677–1681.

Raviola, E. and Gilula, N. B. 1975. Intramembrane organization of specialized contacts in the outer plexiform layer of the retina. A freeze-fracture study in monkeys and rabbits. J. Cell Biol. 65, 192–222.

Renteria, R. C., Copenhagen, D. R., Nakanishi, S., and Tian, N. 2003. ON responses in the retina of the mGluR6 knockout mouse. Invest. Ophthalmol. Vis. Sci. 44, Assoc. Res. Vis. Ophthalmol. Meeting E Abstr, 2073.

Roorda, A. and Williams, D. R. 1999. The arrangement of the three cone classes in the living human eye. Nature, 397, 520–522.

Roska, B. and Werblin, F. 2001. Vertical interactions across ten parallel, stacked representations in the mammalian retina. Nature 410, 583–587.

Saito, T. and Kujiraoka, T. 1982. Physiological and morphological identification of 2 types of on-center bipolar cells in the carp retina. J. Comp. Neurol. 205, 161–170.

Saito, T., Kondo, H., and Toyoda, J. I. 1981. Ionic mechanisms of two types of ON-center bipolar cells in the carp retina. II. The responses to annular illumination. J. Gen. Physiol. 78, 569–589.

Saito, T., Kujiraoka, T., Yonaha, T., and Chino, Y. 1985. Reexamination of photoreceptor-bipolar connectivity patterns in carp retina: HRP-EM and Golgi-EM studies. J. Comp. Neurol. 236, 141–160.

Schmitz, F., Königstorfer, A., and Südhof, T. C. 2000. RIBEYE, a component of synaptic ribbons: a protein's journey through evolution provides insight into synaptic ribbon function. Neuron 28, 857–872.

Shen, W., Finnegan, S. G., and Slaughter, M. M. 2004. Glutamate receptor subtypes in human retinal horizontal cells. Vis. Neurosci. 21, 89–95.

Sherry, D. M., Wang, M. M., Bates, J., and Frishman, L. J. 2003. Expression of vesicular glutamate transporter 1 in the mouse retina reveals temporal ordering in development of rod vs. cone and ON vs. OFF circuits. J. Comp. Neurol. 465, 480–498.

Shields, C. R., Tran, M. N., Wong, R. O. L., and Lukasiewicz, P. D. 2000. Distinct ionotropic GABA receptors mediate presynaptic and postsynaptic inhibition in retinal bipolar cells. J. Neurosci. 20, 2673–2682.

Singer, J. H. and Diamond, J. S. 2003. Sustained Ca^{2+} entry elicits transient postsynaptic currents at a retinal ribbon synapse. J. Neurosci. 23, 10923–10933.

Singer, J. H., Lassova, L., Vardi, N., and Diamond, J. S. 2004. Coordinated multivesicular release at a mammalian ribbon synapse. Nat. Neurosci. 7, 826–833.

Slaughter, M. M. and Miller, R. F. 1981. 2-amino-4-phosphonobutyric acid: a new pharmacological tool for retina research. Science 211, 182–185.

Smallwood, P. M., Ölveczky, B. P., Williams, G. L., Jacobs, G. H., Reese, B. E., Meister, M., and Nathans, J. 2003. Genetically engineered mice with an additional class of cone photoreceptors: Implications for the evolution of color vision. Proc. Natl. Acad. Sci. U. S. A., 100, 11706–11711.

Snellman, J. and Nawy, S. 2004. cGMP-dependent kinase regulates response sensitivity of the mouse ON bipolar cell. J. Neurosci. 24, 6621–6628.

Sterling, P. and Lampson, L. A. 1986. Molecular specificity of defined types of amacrine synapse in cat retina. J. Neurosci. 6, 1314–1324.

Sterling, P. and Matthews, G. 2005. Structure and function of ribbon synapses. Trends Neurosci. 28, 20–29.

Strettoi, E., Dacheux, R. F., and Raviola, E. 1990. Synaptic connections of rod bipolar cells in the inner plexiform layer of the rabbit retina. J. Comp. Neurol. 295, 449–466.

Struik, M. L., Yazulla, S., and Kamermans, M. 2006. Cannabinoid agonist WIN 55212-2 speeds up the cone response to light offset in goldfish retina. Vis. Neurosci. 23, 285–293.

Sun, W., Li, N., and He, S. 2002. Large-scale morphological survey of mouse retinal ganglion cells. J. Comp. Neurol. 451, 115–126.

Szél, A., Diamantstein, T., and Röhlich, P. 1988. Identification of the blue.sensitive cones in the mammalian retina by anti-visual pigment antibody. J. Comp. Neurol. 273, 593–602.

Szél, A., Röhlich, P., Mieziewska, K., Aguirre, G., and van Veen, T. 1993. Spatial and temporal differences between the expression of short- and middle-wave sensitive cone pigments in the mouse retina: a developmental study. J. Comp. Neurol. 331, 564–577.

Tachibana, M. 1999. Regulation of transmitter release from retinal bipolar cells. Prog. Biophys. Mol. Biol. 72, 109–133.

Tagawa, Y., Sawai, H., Ueda, Y., Tauchi, M., and Nakanishi, S. 1999. Immunohistological studies of metabotropic glutamate receptor subtype 6-deficient mice show no abnormality of retinal cell organization and ganglion cell maturation. J. Neurosci. 19, 2568–2579.

tom Dieck, S., Altrock, W. D., Kessels, M. M., Qualmann, B., Regus, H., Brauner, D., Fejtova, A., Bracko, O., Gundelfinger, E. D., and Brandstätter, J. H. 2005. Molecular dissection of the photoreceptor ribbon synapse: physical interaction of Bassoon and RIBEYE is essential for the assembly of the ribbon complex. J. Cell Biol. 168, 825–836.

Tsukamoto, Y., Masarachia, P., Schein, S., and Sterling, P. 1992. Gap junctions between the pedicles of macaque foveal cones. Vision Res. 32, 1809–1815.

Tsukamoto, Y., Morigiwa, K., Ueda, M., and Sterling, P. 2001. Microcircuits for night vision in mouse retina. J. Neurosci. 21, 8616–8623.

Usukura, J. and Yamada, E. 1987. Ultrastructure of the synaptic ribbons in photoreceptor cells of *Rana catesbeiana* revealed by freeze-etching and freeze-substitution. Cell Tiss. Res. 247, 483–488.

Vardi, N., Morigiwa, K., Wang, T. L., Shi, Y. J., and Sterling, P. 1998. Neurochemistry of the mammalian cone 'synaptic complex'. Vision Res. 38, 1359–1369.

Veruki, M. L., Morkve, S. H., and Hartveit, E. 2003. Functional properties of spontaneous EPSCs and non-NMDA receptors in rod amacrine (AII) cells in the rat retina. J. Physiol. 549, 759–774.

Volgyi, B., Deans, M. R., Paul, D. L., and Bloomfield, S. A. 2004. Convergence and segregation of the multiple rod pathways in mammalian retina. J. Neurosci. 24, 11182–11192.

von Gersdorff, H. 2001. Synaptic ribbons: versatile signal transducers. Neuron 29, 7–10.

Wan, L., Almers, W., and Chen, W. 2005. Two ribeye genes in teleosts: the role of ribeye in ribbon formation and bipolar cell development. J. Neurosci. 25, 941–949.

Wässle, H. 1999. A patchwork of cones. Nature 397, 473–475.

Wässle, H. 2004. Parallel processing in the mammalian retina. Nat. Neurosci. 5, 747–757.

Wässle, H. and Boycott, B. B. 1991. Functional architecture of the mammalian retina. Physiol. Rev. 71, 447–480.

Wässle, H., Grünert, U., Martin, P., and Boycott, B. B. 1994. Immunocytochemical characterization and spatial distribution of midget bipolar cells in the macaque monkey retina. Vision Res. 34, 561–579.

Wässle, H., Haverkamp, S., Grünert, U., and Morgans, C. W. 2003. The Cone Pedicle, the First Synapse in the Retina. In: The Neural Basis of Early Vision (*ed*. A. Kaneko), pp. 19–38. Springer.

Wässle, H., Regus-Leidig, H., and Haverkamp, S. 2006. Expression of the vesicular glutamate transporter vGluT2 in a subset of cones of the mouse retina. J. Comp. Neurol. 496, 544–555.

Watanabe, M. and Rodieck, R. W. 1989. Parasol and midget ganglion cells of the primate retina. J. Comp. Neurol. 289, 434–454.

Werblin, F. S. 1973. Control sensitivity in retina. Sci. Am. 228, 71–79.

Werblin, R. S. and Dowling, J. E. 1969. Organization of the mudpuppy, *Necturus maculosus*. II. Intracellular recording. J. Neurophysiol. 32, 339–355.

West, R. W. 1976. Light and electron microscopy of the ground squirrel retina: functional considerations. J. Comp. Neurol. 168, 355–378.

Wu, S. M., Gao, F., and Maple, B. R. 2000. Functional architecture of synapses in the inner retina: segregation of visual signals by stratification of bipolar cell axon terminals. J. Neurosci. 20, 4462–4470.

Wu, S. M., Gao, F., and Pang, J. J. 2004. Synaptic circuitry mediating light-evoked signals in dark-adapted mouse retina. Vision Res. 44, 3277–3288.

Yamashita, M. and Wässle, H. 1991. Responses of rod bipolar cells isolated from the rat retina to the glutamate agonist 2-amino-4-phosphonobutyric acid (APB). J. Neurosci. 11, 2372–2382.

Young, H. M. and Vaney, D. I. 1991. Rod-signal interneurons in the rabbit retina. 1. Rod bipolar cells. J. Comp. Neurol. 310, 139–153.

Zenisek, D., Davilla, V., Wan, L., and Almers, W. 2003. Imaging calcium entry sites and ribbon structures in two presynaptic cells. J. Neurosci. 23, 2538–2548.

Zenisek, D., Steyer, J. A., and Almer, W. 2000. Transport, capture and exocytosis of single synaptic vesicles at active zones. Nature, 406, 849–854.

Zenisek, D., Horst, N. K., Merrifield, C., Sterling, P., and Matthews, G. 2004. Visualizing synaptic ribbons in the living cell. J. Neurosci. 24, 9752–9759.

Zhang, J. and Diamond, J. S. 2005. Extrasynaptic location of NMDA receptors in ganglion cells of rat retina. Invest. Ophthalmol. Vis. Sci., 46, Assoc. Res. Vis. Ophthalmol. Meeting E Abstr. 5345.

1.13 Contributions of Horizontal Cells

R G Smith, University of Pennsylvania, Philadelphia, PA, USA

© 2008 Elsevier Inc. All rights reserved.

1.13.1	**Basic Circuit**	341
1.13.2	**Types of Horizontal Cells**	341
1.13.2.1	Morphology in Cat and Rabbit	341
1.13.2.2	Types in Primate and Other Species	342
1.13.2.3	Synaptic Inputs	342
1.13.2.4	Topology and Connectivity	343
1.13.2.5	Coupling	343
1.13.3	**Functional Properties**	343
1.13.3.1	Basic Light Response	343
1.13.3.2	Response Properties	343
1.13.3.3	Receptive Field	343
1.13.3.4	Feedback	344
1.13.3.5	Feedback Mechanisms	344
1.13.3.6	Ephaptic Feedback	344
1.13.3.7	Feedforward	345
1.13.3.8	Rod Horizontal Cell	345
1.13.4	**Function of Horizontal Cell Circuit**	345
1.13.4.1	Rationale for Outer Plexiform Layer: Noise Limits Information	345
1.13.4.2	A Spatiotemporal Bandpass Filter	345
1.13.4.3	Feedback Loop	346
1.13.4.4	Dynamic Modulation of Receptive Field	346
1.13.4.5	Contribution of Neuron Types	346
1.13.5	**Conclusion**	347
References		347

1.13.1 Basic Circuit

The horizontal cell receives synaptic input signals exclusively from photoreceptors and transmits back to them an inverted signal. This signal, called negative feedback, modulates the photoreceptors' release of neurotransmitter. The feedback signal is generated by a specialized synapse between the tip of the horizontal cell dendrite and the photoreceptor terminal. The exact nature of the synapse is unknown but there is convincing evidence for feedback mediated by gamma-aminobutyric acid (GABA), electrical conduction (ephaptic), and/or pH. There is also evidence for a GABAergic feedforward connection to bipolar cells. The horizontal cell's contribution to vision is important in two contexts:

1. its contribution to the ganglion cell receptive field and
2. its hypothesized noise-reducing function in the outer plexiform layer (OPL).

1.13.2 Types of Horizontal Cells

1.13.2.1 Morphology in Cat and Rabbit

Most vertebrates have at least two horizontal cell types (Figure 1). In cat and rabbit, two types process cone signals. One is larger (~250 μm) with a sparser dendritic tree, called type A or simply HA, and the other is smaller (~100 μm), with a more bushy dendritic tree, called type B or HB (Boycott, B. B. *et al.*, 1978). In addition, the HB has an axon ending in a large terminal, sometimes called HBAT (HB axon terminal), looking like an extensive but sparse dendritic tree, which receives synaptic connections from rods. The axon proceeds about 500 μm from the soma and is narrow (~0.3 μm) so the axon terminal's rod-driven signal is thought to be functionally independent from the soma's cone-driven signal, almost as if the axon terminal were a separate neuron (Golard, A. *et al.*, 1992). Most other mammals have two horizontal cell types very similar to those in cat and rabbit.

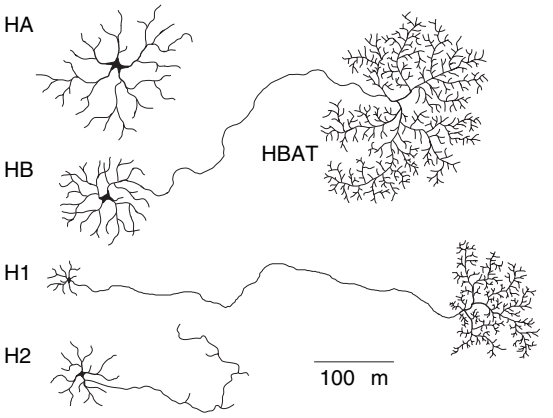

Figure 1 Two types of horizontal cell exist in most mammals. HA is larger, more sparse, with no axon. HB is smaller, and more bushy, with axon. In cat/rabbit, HA connects to ~200 cones, HB to ~100. The HB axon terminal (HBAT) connects to ~2000 rods, and is tethered to its parent HB by a ~400 μm axon, thought to be long and thin enough to maintain rod signal isolation. Two corresponding types H1, H2 exist in primate. They are proportionately smaller and connect to about tenfold fewer cones. The H2 has a sparse axon, which connects exclusively to S cones. An additional type, H3 (not illustrated) is similar to H1 but is 30% larger and more asymmetrical. Adapted from Boycott B. B. *et al.* (1978) and Kolb H. *et al.* (1992).

1.13.2.2 Types in Primate and Other Species

In primate, three anatomical types have been classified, types H1, H2, and H3, where H1 is smaller with a rod connecting axon, analogous to HB in cat (Kolb, H. *et al.*, 1992), and H2 is larger, analogous to HA in cat. Primate type H3 is similar to H1 except that H3 is larger, contacting 30% more cones with an asymmetrical dendritic field. Rat and mouse have only one horizontal cell type, analogous to the axon-bearing type HB in cat/rabbit, but this type appears to possess properties of both HA and HB (Peichl, L. and Gonzalez-Soriano, J., 1994; He, S. *et al.*, 2000). Other vertebrates (turtle, birds, and fishes) have several axonless horizontal cell types, some of which contact cone types seemingly indiscriminately, and others that make specific cone connections (Perlman, I. *et al.*, 2004).

1.13.2.3 Synaptic Inputs

Horizontal cell dendrites branch in the OPL just below the photoreceptor terminals and emanate very fine dendritic tips that contact the photoreceptors,

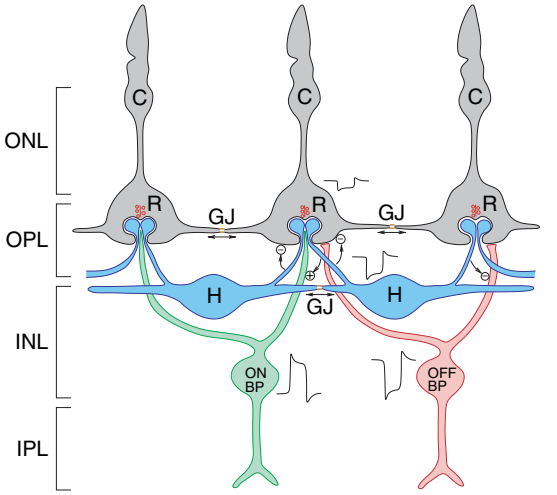

Figure 2 Schematic diagram of the outer retina showing the horizontal cell circuit. An array of cones (C) electrically coupled by gap junctions (GJ), provides input from ribbon synapse (R) to horizontal cells (H) and bipolar cells (ON BP, OFF BP). The triad is the association in the cone terminal between the ribbon and the dendritic processes from two horizontal cells and one ON bipolar cell. Horizontal cells exist in two or more types (not illustrated) and each type is electrically coupled by gap junctions (GJ). Response of cone to a flash of light is a small hyperpolarization, response of horizontal cell is a moderate hyperpolarization, response of OFF bipolar cell is a larger hyperpolarization, and response of ON bipolar cell (BP) is a larger depolarization. Feedback from horizontal cells to cones and feedforward to OFF bipolar cell is negative (arrow (−)), generating antagonistic surround. Feedforward from horizontal cells to ON bipolar cell is positive (arrow (+)), also generating an antagonistic surround in the ON bipolar because the bipolar's postsynaptic second messenger cascade inverts the signal it receives from cones. ONL, outer nuclear layer comprising photoreceptor (rod and cone) somas; OPL, outer plexiform layer where photoreceptors make synaptic connections to horizontal cells and bipolar cells; INL, inner nuclear layer comprising horizontal cell, bipolar cell, and amacrine cell somas; IPL, inner nuclear layer where bipolar cells and amacrine cells interconnect with ganglion cells. Diagram is not drawn to scale; elements of the triad feedback synapse are drawn larger in proportion to the neurons, and horizontal cells make synaptic connections with 100–200 cones.

where synaptic connections are made at a specialized synapse called a triad. This synapse, not fully understood, consists of an invagination formed in the photoreceptor membrane that contains dendritic tips of two horizontal cells and one or more bipolar cells (Figure 2). The horizontal cell processes are situated on either side of the presynaptic ribbon, which is a structure in the photoreceptor terminal involved in storage and release of vesicles (Parsons, T. D. and

Sterling, P., 2003). The synaptic output from photoreceptors is made at the ribbon synapse that releases vesicles containing the neurotransmitter glutamate. Postsynaptic glutamate receptors are located on the dendritic tips of horizontal cells and bipolar cells. The postsynaptic receptor on the horizontal cell is of the AMPA subtype (Morigiwa, K. and Vardi, N., 1999; Haverkamp, S. *et al.*, 2000; Pan, F. and Massey, S. C., 2007).

1.13.2.4 Topology and Connectivity

Horizontal cells exist in sufficient density that their dendrites are highly overlapped. HA and HB have a coverage factor of ~4 so each cone can potentially receive contacts from eight horizontal cells (Wassle, H. *et al.*, 1978b). Horizontal cells of most mammalian species, for example, the HA and HB in cat, receive connections from nearly all cones in their dendritic field (Kolb, H., 1977; Wassle, H. *et al.*, 1978a). The H1 of primate contacts most of the cones in its dendritic field, but mostly avoids S cones, and is analogous to HB with an axon collecting from rods. The H2 dendritic tree collects from all cone types and its axon collects specifically from S cones, and the H3 avoids S cones (Ahnelt, P. and Kolb, H., 1994). Therefore, horizontal cells cannot be the locus for color opponency in mammals (Dacey, D. M., 1996; Diller, L. *et al.*, 2004). In all vertebrates one horizontal cell type collects signals from rods; in mammals, this role is filled by the HBAT (see Section 1.13.3.8). Turtle, birds, and fishes have one luminosity type, one rod type, and two or more color-opponent types (see Chapter Vision in Birds).

1.13.2.5 Coupling

Most horizontal cells make connections only to their neighbors of the same type (homotypic) through gap junctions, which are electrical connections directly between the cytoplasm of one neuron and the next (Kolb, H., 1977). This electrical coupling broadens the receptive field and reduces noise. Type HA/H2 has strong coupling; type HB/H1 and its axon terminal have independent but weaker coupling. In most species, cones are also electrically coupled and are also interconnected to rods (Kolb, H., 1977; Smith, R. G. *et al.*, 1986; Hornstein, E. P. *et al.*, 2005). Coupling in horizontal cells and cones is modulated by light through dopamine released in the inner retina (DeVries, S. H. and Schwartz, E. A., 1989; Umino, O. *et al.*, 1991; Hampson, E. C. *et al.*, 1994; Baldridge, W. H. *et al.*, 1998; Xin, D. and Bloomfield, S. A., 1999; He, S. *et al.*, 2000; Witkovsky, P., 2004). The gap junctions between HAs are Cx50 type and between HBs the Cx57 type (O'Brien, J. J. *et al.*, 2006).

1.13.3 Functional Properties

1.13.3.1 Basic Light Response

Horizontal cells hyperpolarize to light, similar to photoreceptors, except that they have a greater response gain and adaptation (Wu, S. M., 1992). The HB/H1 has a cone-driven response in its soma and a rod response in its axon terminal. In addition, since rods and cones are interconnected, a rod signal is evident in cones and all cone-driven horizontal cells (Nelson, R., 1977). In turtle, fishes, and birds, color-opponent axonless types receive chromatic input from specific cone types. Their responses to color are complex because cones receive specific chromatic feedback from more than one horizontal cell type (Kamermans, M. *et al.*, 1991).

1.13.3.2 Response Properties

The light response of HA is fast, containing frequencies up to 100 Hz. The light response of HB is slower, containing frequencies up to 60 Hz. The receptive field of the HBAT is large and slowest at 30 Hz (Foerster, M. H. *et al.*, 1977). At high light intensities and contrasts, the light response may include a transient peak ($\tau \sim 50$–100 ms), derived from adaptation in the circuit but also from intrinsic properties. The biophysical properties of horizontal cells include several types of voltage-gated ion channel that amplify and shape its light response (Perlman, I. *et al.*, 1993; Aoyama, T. *et al.*, 2000), calcium-induced calcium release (Solessio, E. and Lasater, E. M., 2002), GABA release by vesicles and transporters (Schwartz, E. A., 2002; Hirano, A. A. *et al.*, 2005), and GABA autoreceptors, which are thought to amplify and lengthen its light response (Kamermans, M. and Werblin, F., 1992).

1.13.3.3 Receptive Field

In cat and rabbit, HA collects from ~200 cones and indirectly though gap junction coupling from several hundred more (Wassle, H. *et al.*, 1987a), and HB collects directly from ~100 cones. The receptive field size is modulated by dopamine and by light

(Lankheet, M. J. *et al.*, 1990; Hampson, E. C. *et al.*, 1994; He, S. *et al.*, 2000). Due to its robust electrical coupling, the receptive field of HA is large, under some conditions extending far (about tenfold) beyond its dendritic field (Lankheet, M. J. *et al.*, 1990). The electrical coupling of HB is weaker so its receptive field is smaller, not extending much beyond the dendritic field (Vaney, D. I., 1991). Receptive fields of primate H1, H2, H3 are much smaller than the analogous types in other mammals. The H2 receptive field is larger, collecting from ~20 cones, analogous to HA in cat. The H1 has a proportionately smaller receptive field not much larger than its dendritic field, collecting from ~10 cones, consistent with the receptive field surround of midget bipolar and ganglion cells (Packer, O. S. and Dacey, D. M., 2002) (see Chapter Contributions of Bipolar Cells to Ganglion Cell Receptive Fields).

1.13.3.4 Feedback

Horizontal cells provide negative feedback to cones (Baylor, D. A. *et al.*, 1971; Verweij, J. *et al.*, 2003; Tatsukawa, T. *et al.*, 2005) generating a cone surround. This feedback contributes to the surround in bipolar cells, and in some species horizontal cells are thought to be mainly responsible for the receptive field surround of ganglion cells such as the primate parasol cell (McMahon, M. J. *et al.*, 2004). Thus, surround feedback from horizontal cells is an important component of adaptation for all other neurons in the retina. In turtle and fishes, horizontal cell feedback generates color opponency in cones (Kamermans, M. *et al.*, 1991).

1.13.3.5 Feedback Mechanisms

Several mechanisms have been proposed for the feedback from horizontal cells to photoreceptors. Horizontal cells contain GAD, the synthetic enzyme for GABA (Vardi, N. *et al.*, 1994), and release GABA through a nonvesicular transporter mechanism (Schwartz, E. A., 2002). The classical feedback mechanism is that GABA released by horizontal cells modulates GABA-gated chloride channels in the photoreceptor membrane (Tachibana, M. and Kaneko, A., 1984; Wu, S. M., 1992; Dong, C. J. *et al.*, 1994; Liu, J. *et al.*, 2005). This mechanism has been found in several species (turtle, fishes, frog, and salamander), and may exist in some form in all vertebrates. An alternate mechanism has been proposed involving proton (pH) feedback from horizontal cells to the photoreceptor terminal (Hirasawa, H. and Kaneko, A., 2003; Tatsukawa, T. *et al.*, 2005). Another alternate mechanism, ephaptic (electrical) feedback has also been proposed (Byzov, A. L. and Shura-Bura, T. M., 1986; Kamermans, M. and Fahrenfort, I., 2004; McMahon, M. J. *et al.*, 2004).

1.13.3.6 Ephaptic Feedback

In the proposed ephaptic mechanism, the horizontal cell signal is relayed back to the cone terminal by the action of the current flow in the extracellular space of the photoreceptor terminal's invagination. When a remote spot of light hyperpolarizes the horizontal cell, current flow at cone terminals outside the spot increases from extracellular space into the horizontal cell's dendritic tip. This current causes a small negative shift in the voltage on the external surface of the cone's membrane in the invagination, which affects calcium channels in the membrane as a depolarization, thus generating negative feedback. The magnitude of the voltage shift depends on the electrical resistance of the extracellular space in the cone terminal's invagination. However, the opposite effect occurs at a cone terminal under a spot of light. In this case, light hyperpolarizes the cone terminal, reducing current flow into the horizontal cell's dendritic tip. This causes a positive shift in the voltage on the external surface of the cone's membrane, which appears to channels in the cone membrane as a hyperpolarization, generating positive feedback from a cone terminal back to itself. Horizontal cell dendrites also contain hemichannel gap junctions (i.e., connexin molecules), which are thought to be involved in the feedback because the application of carbenoxolone, a gap junction blocker, reduces the feedback signal (Kamermans, M. and Fahrenfort, I., 2004). This is also observed in animals where the gene encoding for the connexin molecule is knocked out. Because the hemichannels are not modulated by glutamate, the current through them shunts the glutamate-gated ion channels, reducing the gain of the light response, but shifting the balance in favor of negative feedback (Fahrenfort, I. *et al.*, 2005). In addition, the hemichannels may be modulated by voltage, complicating the mechanism (DeVries, S. H. and Schwartz, E. A., 1992). This postulated ephaptic feedback mechanism is controversial because it relies on a very narrow extracellular space in the cone terminal to produce a high resistance to the flow of current (Dmitriev, A. V. and Mangel, S. C., 2006).

1.13.3.7 Feedforward

There is also evidence for a direct GABAergic synaptic connection from horizontal cells to ON and OFF bipolar cells, enhancing their surround (Wu, S. M., 1992). Both ON and OFF bipolar types have GABA-A receptors on their dendrites (Vardi, N. and Sterling, P., 1994). For the ON bipolar cell, this implies a depolarizing chloride potential (see Figure 2) (Vardi, N. *et al.*, 2000; Duebel, J. *et al.*, 2006). Since the OFF bipolar cell dendritic tip is not directly adjacent to horizontal cell dendritic tips, to gate the GABA receptors located on OFF bipolar cell dendrites, the GABA released from horizontal cells would need to diffuse 1–2 μm (Vardi, N. and Sterling, P., 1994).

1.13.3.8 Rod Horizontal Cell

The HBAT in cat and rabbit receives input from 1000 to 2000 rods, most but not all in its field (Boycott, B. B. *et al.*, 1978; Pan, F. and Massey, S. C., 2007), with high gain and extensive electrical coupling, modulated like other horizontal cells by dopamine (Foerster, M. H. *et al.*, 1977; Vaney, D. I., 1993; Reitsamer, H. A. *et al.*, 2006), so it is ideally constructed to generate a smooth average rod signal at very low scotopic (starlight) backgrounds. Because the rod ribbon synapse is binary and transmits either a signal from one photon or none (Berntson, A. *et al.*, 2004), it is critically dependent on the tiny single photon signal to generate a discriminable slowing of glutamate release in a sea of thermal noise (Schein, S. and Ahmad, K. M., 2005). The single photon signal is only ~1 mV in amplitude so the rod terminal voltage must be regulated closely, within ~0.2 mV, to allow the binary synapse to function correctly (Berntson, A. *et al.*, 2004). Therefore, the HBAT seems likely to provide negative feedback, critical for modulating within the narrow voltage range the rod's release of glutamate. A feedback signal when summed with the rod's photon signal would traverse the rod→rod bipolar synapse, which has a nonlinear threshold on its postsynaptic side (van Rossum, M. C. and Smith, R. G., 1998; Field, G. D. *et al.*, 2005). Therefore, this feedback would generate a nonlinear surround, consistent with measurements of the ganglion cell hidden surround at low scotopic backgrounds (Wiesel, T. N. and Hubel, D. H., 1966; Barlow, H. B. and Levick, W. R., 1976).

1.13.4 Function of Horizontal Cell Circuit

1.13.4.1 Rationale for Outer Plexiform Layer: Noise Limits Information

A major problem facing the retina is that noise mixed with the visual signal limits information capacity (Barlow, H. B., 1981; Brenner, N. *et al.*, 2000; Abshire, P. A. and Andreou, A. G., 2001). The signal transmitted to the ganglion cell traverses two noisy ribbon synapses; one in the photoreceptor and the other in the bipolar cell. In daylight, the noise from the bipolar ribbon synapse is responsible for most of the noise recorded in the ganglion cell (Freed, M.A., 2000; van Rossum, M. C. *et al.*, 2003). To maximize the signal-to-noise (S/N) ratio in the ganglion cell, the OPL must modulate the photoreceptor signal to precisely set the synaptic gain, saturation, and basal release rate, and the horizontal cell is thought to provide the necessary feedback signal. But the feedback signal also contains noise (Freed, M. A. *et al.*, 2003), suggesting that horizontal cells are coupled to reduce it.

1.13.4.2 A Spatiotemporal Bandpass Filter

The horizontal cell is an essential part of the OPL circuit, which comprises a spatiotemporal bandpass filter and several adaptational mechanisms (Smith, R. G., 1995; van Hateren, H., 2005). The OPL removes the least essential signal components: the very high and very low frequencies, and the background light level. The remaining signal components therefore more fully modulate the photoreceptor signal's dynamic range. The horizontal cell generates a spatially low-pass response by collecting signals from an extended field of cones. The horizontal cell's output signal accumulates a temporal low-pass characteristic because it is filtered by the membrane time constants and synaptic delays in both photoreceptor and horizontal cell. This signal modulates glutamate release from photoreceptors through negative feedback, which removes low spatial and temporal frequencies. Current injected into the horizontal cell produces a similar effect to a light stimulus superimposed on the ganglion cell receptive field surround, directly implicating the horizontal cell's role (Mangel, S. C., 1991). The feedback prevents the photoreceptor's synaptic signal from saturating, which maximizes its sensitivity. The remaining signal transmitted to bipolar and ganglion cells is transient, spatially antagonistic, and contains mostly information about contrast (see Chapter Contributions of Bipolar Cells to

Ganglion Cell Receptive Fields). Thus, the OPL shapes the signal transmitted to ganglion cells to maximize their S/N ratio.

1.13.4.3 Feedback Loop

The negative feedback loop between photoreceptors and horizontal cell is important for the retina's ability to respond reliably under different lighting and physiological conditions. The negative feedback stabilizes the release rate of glutamate-filled vesicles by the ribbon synapse (Wu, S. M., 1992; Morgans, C. W., 2000). An increase in glutamate released by cones at dim intensities causes a stronger feedback signal from horizontal cells, leading to a partial restoration to the original level of release. The feedback is thought to have subtractive and divisive components, both of which contribute to adaptation. The feedback pathway from cone to horizontal cell includes a substantial (~10 ms) time delay, which at high frequencies (40–80 Hz) causes a 180° phase lag, inverting the feedback sign to positive. Therefore, the feedback loop can become unstable and oscillate, which occurs under some common conditions (e.g., low luminance, high contrast, opaque mask centered on receptive field; Foerster, M. H. *et al.*, 1977; Smith, V. C. *et al.*, 2001). Thus, to preserve stability, the loop gain (the product of the feedforward and feedback synaptic gains) must be limited. Because the feedforward synaptic gain from photoreceptors to horizontal cells is relatively strong (Belgum, J. H. and Copenhagen, D. R., 1988), the feedback gain must be weak (Smith, R. G., 1995; van Hateren, H., 2005).

1.13.4.4 Dynamic Modulation of Receptive Field

To reduce noise in the feedback signal, the horizontal cell collects a signal from many photoreceptors. The exact number is set by the conductance of its interconnecting gap junctions, which varies with background light intensity and stimulus contrast and shape (Lankheet, M. J. *et al.*, 1990; Reifsnider, E. S. and Tranchina, D., 1995; Xin, D. and Bloomfield, S. A., 1999). When measured with a bar flashed on and off at different positions, the HA receptive field is about tenfold larger then when measured with spots of different sizes centered on the receptive field (Lankheet, M. J. *et al.*, 1990). The explanation is that with a dark background, narrow spots or bars flashed at different positions do not adapt the retina much, dopamine remains at a low level, and gap junctions between horizontal cells remain open. But with the brighter light from a spot of increasing diameter, amacrine cells in the inner retina release dopamine, which closes gap junctions between horizontal cells (Baldridge, W. H. *et al.*, 1998; Xin, D. and Bloomfield, S. A., 1999). Electrical coupling is known to have a noise-reducing role (Lamb, T. D. and Simon, E. J., 1976; DeVries, S. *et al.*, 2002), suggesting the hypothesis that horizontal cell coupling is varied according to the need for noise reduction (Balboa, R. M. and Grzywacz, N. M., 2000). This is consistent with the noise properties of the retina because different background intensities generate different amounts of noise reflected in ganglion cell responses (Freed, M. A., 2000).

1.13.4.5 Contribution of Neuron Types

Receptive fields of the two types of horizontal cell have different profiles (Figure 3). The HA receptive field, when extended beyond the cell's dendritic field by gap junction coupling, is exponential in form (Bessel function) (Lamb, T. D. and Simon, E. J., 1976; Golard, A. *et al.*, 1992). The HB dendritic field is smaller, and coupling extends its receptive field less, so its receptive field is also smaller and more Gaussian. Because horizontal cells of both HA/H2 and HB/H1 feedback to the same cones, the surround passed on to the bipolar cell is likely to include contributions of both depending on the relative amplitude of their responses (Smith, R. G., 1995; Shen, Y. *et al.*, 2003) (Figure 2). Mixing of their receptive fields, each with a different spatial extent (Reifsnider, E. S. and Tranchina, D., 1995) may shape the bipolar cell surround to optimally filter and remove noise. The strength of feedback, and thus the depth of its contribution to the bipolar cell and ganglion cell surround, is limited to avoid oscillatory instability (Smith, R. G., 1995; van Hateren, H., 2005). But the contribution from inhibitory feedforward connections lacks this limitation and so may be deeper. The bipolar cell surround is also deepened by feedback from amacrine cells in the inner plexiform layer. The relative amplitude and extent of the surround components originating in horizontal versus amacrine cells is thought to vary dynamically according to background intensity and type of stimulus (Cook, P. B. and McReynolds, J. S., 1998; McMahon, M. J. *et al.*, 2004; Ichinose, T. and Lukasiewicz, P. D., 2005). Because wide-field amacrine cells extend farther, their surround contribution is shallower but wider (see Chapter Amacrine Cells).

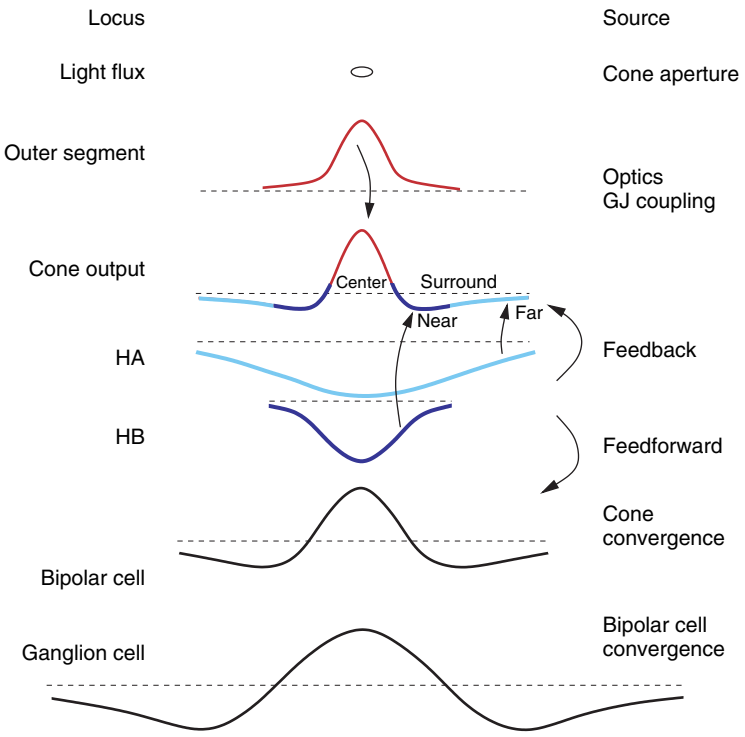

Figure 3 Horizontal cells contribute to receptive field surround of bipolar cell and ganglion cell. Left column: locus in different layers for measuring receptive field. Right column: source of changes between one layer and the next. When probed by a spot or bar at different locations, the cone receptive field has center surround organization. Top: center Gaussian component (~3 μm in primate and ~20 μm in cat) originates in cone aperture (~2 μm) and blur from the optics of the eye and gap junction coupling. Receptive field of horizontal cell is large because it collects directly from 100 to 200 cones, and indirectly from several hundred more through lateral coupling. Antagonistic surround in cone receptive field originates in feedback from HA (large) and HB (small) horizontal cells. HB feedback generates near surround, and HA feedback generates far surround. Profile of surround is a mixture of both the HA and the HB components and changes dynamically with stimulus. Receptive field center of bipolar cell (20–50 μm) is larger than cone center because the bipolar cell collects from several cones. Strength of bipolar surround is increased relative to the center by feedforward from horizontal cell and because the summed cone surrounds overlap more than the centers. Receptive field center of ganglion cell is wider (50–500 μm) because its dendritic field collects from many bipolar cells and its surround is stronger because the bipolar surrounds heavily overlap. Amacrine cells (not illustrated) provide additional surround feedback to bipolar cells and feedforward to ganglion cell. Receptive field profiles are normalized to same peak amplitude. Spatial extent of centers and surrounds is not drawn to scale.

1.13.5 Conclusion

Horizontal cells contribute to the ganglion cell receptive field surround through their feedforward and feedback connections. In this role, horizontal cells remove low spatial and temporal frequencies from the visual signal passed to the brain. In some species horizontal cells provide a color-opponent signal. But horizontal cells provide a more basic influence. The horizontal cell circuit computes a local average signal, which precisely regulates the photoreceptor's synaptic release thus preventing saturation, implying that the horizontal cell's function is to reduce noise and improve the quality of the ganglion cell signal.

References

Abshire, P. A. and Andreou, A. G. 2001. A communication channel model for information transmission in the blowfly photoreceptor. Biosystems 62, 113–133.

Ahnelt, P. and Kolb, H. 1994. Horizontal cells and cone photoreceptors in primate retina: a Golgi-light microscopic study of spectral connectivity. J. Comp. Neurol. 343, 387–405.

Aoyama, T., Kamiyama, Y., Usui, S., Blanco, R., Vaquero, C. F., and de la Villa, P. 2000. Ionic current model of rabbit retinal horizontal cell. Neurosci. Res. 37, 141–151.

Balboa, R. M. and Grzywacz, N. M. 2000. The role of early retinal lateral inhibition: more than maximizing luminance information. Vis. Neurosci. 17, 77–89.

Baldridge, W. H., Vaney, D. I., and Weiler, R. 1998. The modulation of intercellular coupling in the retina. Semin. Cell Dev. Biol. 9, 311–318.

Barlow, H. B. 1981. The Ferrier Lecture, 1980. Critical limiting factors in the design of the eye and visual cortex. Proc. R. Soc. Lond. B Biol. Sci. 212, 1–34.

Barlow, H. B. and Levick, W. R. 1976. Threshold setting by the surround of cat retinal ganglion cells. J. Physiol. 259, 737–757.

Baylor, D. A., Fuortes, M. G., and O'Bryan, P. M. 1971. Receptive fields of cones in the retina of the turtle. J. Physiol. 214, 265–294.

Belgum, J. H. and Copenhagen, D. R. 1988. Synaptic transfer of rod signals to horizontal and bipolar cells in the retina of the toad (*Bufo marinus*). J. Physiol. 396, 225–245.

Berntson, A., Smith, R. G., and Taylor, W. R. 2004. Transmission of single photon signals through a binary synapse in the mammalian retina. Vis. Neurosci. 21, 693–702.

Boycott, B. B., Peichl, L., and Wassle, H. 1978. Morphological types of horizontal cell in the retina of the domestic cat. Proc. R. Soc. Lond. B Biol. Sci. 203, 229–245.

Brenner, N., Bialek, W., and de Ruyter van Steveninck, R. 2000. Adaptive rescaling maximizes information transmission. Neuron 26, 695–702.

Byzov, A. L. and Shura-Bura, T. M. 1986. Electrical feedback mechanism in the processing of signals in the outer plexiform layer of the retina. Vision Res. 26, 33–44.

Cook, P. B. and McReynolds, J. S. 1998. Lateral inhibition in the inner retina is important for spatial tuning of ganglion cells. Nat. Neurosci. 1, 714–719.

Dacey, D. M. 1996. Circuitry for color coding in the primate retina. Proc. Natl. Acad. Sci. U. S. A. 93, 582–588.

DeVries, S. H. and Schwartz, E. A. 1989. Modulation of an electrical synapse between solitary pairs of catfish horizontal cells by dopamine and second messengers. J. Physiol. 414, 351–375.

DeVries, S. H. and Schwartz, E. A. 1992. Hemi-gap-junction channels in solitary horizontal cells of the catfish retina. J. Physiol. 445, 201–230.

DeVries, S., Qi, X.-F., Smith, R., Makous, W., and Sterling, P. 2002. Electrical coupling enhances contrast sensitivity of foveal cones. Curr. Biol. 12, 1900–1907.

Diller, L., Packer, O. S., Verweij, J., McMahon, M. J., Williams. D. R., and Dacey, D. M. 2004. L and M cone contributions to the midget and parasol ganglion cell receptive fields of macaque monkey retina. J. Neurosci. 24, 1079–1088.

Dmitriev, A. V. and Mangel, S. C. 2006. Electrical feedback in the cone pedicle: a computational analysis. J. Neurophysiol. 95, 1419–1427.

Dong, C. J., Picaud, S. A., and Werblin, F. S. 1994. GABA transporters and GABAC-like receptors on catfish cone- but not rod-driven horizontal cells. J. Neurosci. 14, 2648–2658.

Duebel. J., Haverkamp, S., Schleich, W., Feng, G., Augustine, G. J., Kuner, T., and Euler, T. 2006. Two-photon imaging reveals somatodendritic chloride gradient in retinal On-type bipolar cells expressing the biosensor Clomeleon. Neuron 49, 81–94.

Fahrenfort, I., Klooster, J., Sjoerdsma, T., and Kamermans, M. 2005. The involvement of glutamate-gated channels in negative feedback from horizontal cells to cones. Prog. Brain Res. 147, 219–229.

Field, G. D., Sampath, A. P., and Rieke, F. 2005. Retinal processing near absolute threshold: from behavior to mechanism. Annu. Rev. Physiol. 67, 491–514.

Foerster, M. H., van de Grind, W. A., and Grusser, O. J. 1977. Frequency transfer properties of three distinct types of cat horizontal cells. Exp. Brain Res. 29, 347–366.

Freed, M. A. 2000. Rate of quantal excitation to a retinal ganglion cell evoked by sensory input. J. Neurophysiol. 83, 2956–2966.

Freed, M. A., Smith, R. G., and Sterling, P. 2003. Timing of quantal release from the retinal bipolar terminal is regulated by a feedback circuit. Neuron 38, 89–101.

Golard, A., Witkovsky, P., and Tranchina, D. 1992. Membrane currents of horizontal cells isolated from turtleretina. J. Neurophysiol. 68, 351–361.

Hampson, E. C., Weiler, R., and Vaney, D. I. 1994. pH-gated dopaminergic modulation of horizontal cell gap junctions in mammalian retina. Proc. Biol. Sci. 255, 67–72.

van Hateren, H. 2005. A cellular and molecular model of response kinetics and adaptation in primate cones and horizontal cells. J. Vis. 5, 331–347.

Haverkamp, S., Grunert, U., and Wassle, H. 2000. The cone pedicle, a complex synapse in the retina. Neuron 27, 85–95.

He, S., Weiler, R., and Vaney, D. I. 2000. Endogenous dopaminergic regulation of horizontal cell coupling in the mammalian retina. J. Comp. Neurol. 418, 33–40.

Hirano, A. A., Brandstatter, J. H., and Brecha, N. C. 2005. Cellular distribution and subcellular localization of molecular components of vesicular transmitter release in horizontal cells of rabbit retina. J. Comp. Neurol. 488, 70–81.

Hirasawa, H. and Kaneko, A. 2003. pH changes in the invaginating synaptic cleft mediate feedback from horizontal cells to cone photoreceptors by modulating Ca^{2+} channels. J. Gen. Physiol. 122, 657–671.

Hornstein, E. P., Verweij, J., Li, P. H., and Schnapf, J. L. 2005. Gap-junctional coupling and absolute sensitivity of photoreceptors in macaque retina. J. Neurosci. 25, 11201–11209.

Ichinose, T. and Lukasiewicz, P. D. 2005. Inner and outer retinal pathways both contribute to surround inhibition of salamander ganglion cells. J. Physiol. 565, 517–535.

Kamermans, M. and Fahrenfort, I. 2004. Ephaptic interactions within a chemical synapse: hemichannel-mediated ephaptic inhibition in the retina. Curr. Opin. Neurobiol. 14, 531–541.

Kamermans, M. and Werblin, F. 1992. GABA-mediated positive autofeedback loop controls horizontal cell kinetics in tiger salamander retina. J. Neurosci. 12, 2451–2463.

Kamermans, M., van Dijk, B. W., and Spekreijse, H. 1991. Color opponency in cone-driven horizontal cells in carp retina. Aspecific pathways between cones and horizontal cells. J. Gen. Physiol. 97, 819–843.

Kolb, H. 1977. The organization of the outer plexiform layer in the retina of the cat: electron microscopic observations. J. Neurocytol. 6, 131–153.

Kolb, H, Linberg, K. A., and Fisher, S. K. 1992. Neurons of the human retina: a golgi study. J. Comp. Neurol. 318, 147–187.

Lamb, T. D. and Simon, E. J. 1976. The relation between intercellular coupling and electrical noise in turtle photoreceptors. J. Physiol. 263, 257–286.

Lankheet, M. J., Frens, M. A., and van de Grind, W. A. 1990. Spatial properties of horizontal cell responses in the cat retina. Vision Res. 30, 1257–1275.

Liu, J., Zhao, J. W., Du, J. L., and Yang, X. L. 2005. Functional GABA(B) receptors are expressed at the cone photoreceptor terminals in bullfrog retina. Neuroscience 132, 103–113.

Mangel, S. C. 1991. Analysis of the horizontal cell contribution to the receptive field surround of ganglion cells in the rabbit retina. J. Physiol. 442, 211–234.

McMahon, M. J., Packer, O. S., and Dacey, D. M. 2004. The classical receptive field surround of primate parasol ganglion cells is mediated primarily by a non-GABAergic pathway. J. Neurosci. 24, 3736–3745.

Morgans, C. W. 2000. Neurotransmitter release at ribbon synapses in the retina. Immunol. Cell Biol. 78, 442–446.

Morigiwa, K. and Vardi, N. 1999. Differential expression of ionotropic glutamate receptor subunits in the outer retina. J. Comp. Neurol. 405, 173–184.

Nelson, R. 1977. Cat cones have rod input: a comparison of the response properties of cones and horizontal cell bodies in the retina of the cat. J. Comp. Neurol. 172, 109–135.

O'Brien, J. J., Li, W., Pan, F., Keung, J., O'Brien, J., and Massey, S. C. 2006. Coupling between A-type horizontal cells is mediated by connexin 50 gap junctions in the rabbit retina. J. Neurosci. 26, 11624–11636.
Packer, O. S, and Dacey, D. M. 2002. Receptive field structure of H1 horizontal cells in macaque monkey retina. J. Vis. 2, 272–292.
Pan, F. and Massey, S. C. 2007. Rod and cone input to horizontal cells in the rabbit retina. J. Comp. Neurol. 500, 815–831.
Parsons, T. D. and Sterling, P. 2003. Synaptic ribbon. Conveyor belt or safety belt? Neuron 37, 379–382.
Peichl, L. and Gonzalez-Soriano, J. 1994. Morphological types of horizontal cell in rodent retinae: a comparison of rat, mouse, gerbil, and guinea pig. Vis. Neurosci. 11, 501–517.
Perlman, I., Kolb, H., and Nelson, R. 2004. Anatomy, Circuitry, and Physiology of Vertebrate Horizontal Cells. In: The Visual Neurosciences (*eds*. L. M. Chalupa and J. S. Werner), Vol. 1, p. 369. A Bradford Book, MIT Press.
Perlman, I., Sullivan, J. M., and Normann, R. A. 1993. Voltage- and time-dependent potassium conductances enhance the frequency response of horizontal cells in the turtle retina. Brain Res. 619, 89–97.
Reifsnider, E. S. and Tranchina, D. 1995. Background contrast modulates kinetics and lateral spread of responses to superimposed stimuli in outer retina. Vis. Neurosci. 12, 1105–1126.
Reitsamer, H. A., Pflug, R., Franz, M., and Huber, S. 2006. Dopaminergic modulation of horizontal-cell-axon-terminal receptive field size in the mammalian retina. Vision Res. 46, 467–474.
van Rossum, M. C. and Smith, R. G. 1998. Noise removal at the rod synapse of mammalian retina. Vis. Neurosci. 15, 809–821.
van Rossum, M. C., O'Brien, B. J., and Smith, R. G. 2003. Effects of noise on the spike timing precision of retinal ganglion cells. J. Neurophysiol. 89, 2406–2419.
Schein, S. and Ahmad, K. M. 2005. A clockwork hypothesis: synaptic release by rod photoreceptors must be regular. Biophys. J. 89, 3931–3949.
Schwartz, E. A. 2002. Transport-mediated synapses in the retina. Physiol. Rev. 82, 875–891.
Shen, Y., Zhang, A. J., and Yang, X. L. 2003. Uncoupling of horizontal cells alters the receptive fields of retinal bipolar cells. Neuroreport 14, 2159–2162.
Smith, R. G. 1995. Simulation of an anatomically defined local circuit: the cone-horizontal cell network in cat retina. Vis. Neurosci. 12, 545–561.
Smith, R. G., Freed, M. A., and Sterling, P. 1986. Microcircuitry of the dark-adapted cat retina: functional architecture of the rod–cone network. J. Neurosci. 6, 3505–3517.
Smith, V. C., Pokorny, J., Lee, B. B., and Dacey, D. M. 2001. Primate horizontal cell dynamics: an analysis of sensitivity regulation in the outer retina. J. Neurophysiol. 85, 545–558.
Solessio, E. and Lasater, E. M. 2002. Calcium-induced calcium release and calcium buffering in retinal horizontal cells. Vis. Neurosci. 19, 713–725.
Tachibana, M. and Kaneko, A. 1984. G-aminobutyric acid acts at axon terminals of turtle photoreceptors: difference in sensitivity among cell types. Proc. Natl. Acad. Sci. U. S. A. 81, 7961–7964.
Tatsukawa, T., Hirasawa, H., Kaneko, A., and Kaneda, M. 2005. GABA-mediated component in the feedback response of turtle retinal cones. Vis. Neurosci. 22, 317–324.
Umino, O., Lee, Y., and Dowling, J. E. 1991. Effects of light stimuli on the release of dopamine from interplexiform cells in the white perch retina. Vis. Neurosci. 7, 451–458.
Vaney, D. I. 1991. Many diverse types of retinal neurons show tracer coupling when injected with biocytin or neurobiotin. Neurosci. Lett. 125, 187–190.
Vaney, D. I. 1993. The coupling pattern of axon-bearing horizontal cells in the mammalian retina. Proc. Biol. Sci. 252, 93–101.
Vardi, N. and Sterling, P. 1994. Subcellular localization of GABAA receptor on bipolar cells in macaque and human retina. Vision Res. 34, 1235–1246.
Vardi, N., Kaufman, D. L., and Sterling, P. 1994. Horizontal cells in cat and monkey retina express different isoforms of glutamic acid decarboxylase. Vis. Neurosci. 11, 135–142.
Vardi, N., Zhang, L. L, Payne, J. A., and Sterling, P. 2000. Evidence that different cation chloride cotransporters in retinal neurons allow opposite responses to GABA. J. Neurosci. 20, 7657–7663.
Verweij, J., Hornstein, E. P., and Schnapf, J. L. 2003. Surround antagonism in macaque cone photoreceptors. J. Neurosci. 23, 10249–10257.
Wassle, H., Boycott, B. B., and Peichl, L. 1978a. Receptor contacts of horizontal cells in the retina of the domestic cat. Proc. R. Soc. Lond. B Biol. Sci. 203, 247–267.
Wassle, H., Peichl, L., and Boycott, B. B. 1978b. Topography of horizontal cells in the retina of the domestic cat. Proc. R. Soc. Lond. B Biol. Sci. 203, 269–291.
Wiesel, T. N. and Hubel, D. H. 1966. Spatial and chromatic interactions in the lateral geniculate body of the rhesus monkey. J. Neurophysiol. 29, 1115–1156.
Witkovsky, P. 2004. Dopamine and retinal function. Doc. Ophthalmol. 108, 17–40.
Wu, S. M. 1992. Feedback connections and operation of the outer plexiform layer of the retina. Curr. Opin. Neurobiol. 2, 462–468.
Xin, D. and Bloomfield, S. A. 1999. Dark- and light-induced changes in coupling between horizontal cells in mammalian retina. J. Comp. Neurol. 405, 75–87.

Further Reading

Smith, R. G. and Sterling, P. 1990. Cone receptive field in cat retina computed from microcircuitry. Vis. Neurosci. 5, 453–461.

Relevant Website

http://webvision.med.utah.edu – Webvision: The Organization of the Retina and Visual System.

1.14 Contributions of Bipolar Cells to Ganglion Cell Receptive Fields

M A Freed, University of Pennsylvania School of Medicine, Philadelphia, PA, USA

© 2008 Elsevier Inc. All rights reserved.

1.14.1	**Introduction**	351
1.14.2	**About 10 Types of Bipolar Cell**	352
1.14.3	**Bipolar Cells Contribute to Spatial Frequency Channels**	352
1.14.3.1	Receptive Field is a Convolution	352
1.14.3.2	Random Properties of Bipolar Array	352
1.14.3.3	Adaptive Properties of Bipolar Array	354
1.14.3.4	Contribution to Peak Contrast Sensitivity	355
1.14.3.5	Contribution to Contrast Threshold	355
1.14.4	**Bipolar Cells Contribute to Nonlinear Subunits**	355
1.14.4.1	Counter-Phased Grating Reveals Nonlinear Subunits	355
1.14.5	**Bipolar Cells May Initiate Temporal Frequency Channels**	356
1.14.5.1	Temporal Frequency Response of Bipolar Cells	356
1.14.5.2	A Bipolar Cell's Intrinsic Properties Modify Its Frequency Response	357
1.14.5.3	On and Off Bipolar Cells Initiate Matched Temporal Channels	357
1.14.6	**Contribution of Bipolar Cells to Information Encoding**	357
1.14.6.1	Contribution to Linear Responses	357
1.14.6.2	Contribution to Information Encoding	358
References		358

Glossary

contrast sensitivity The reciprocal of the contrast required to reach a criterion spike rate.

convolution A mathematical operation on two functions that determines how the shape of one is blurred by that of the other.

quantum The amount of transmitter packaged in a single vesicle.

1.14.1 Introduction

Every bipolar cell has an elongated cell body with dendrites at the top that contact photoreceptors and an axon terminal at the bottom that contacts amacrine and ganglion cells; thus it conveys information from the photoreceptor axon terminals (rod and cone) to ganglion cell dendrites in the inner plexiform layer (IPL).

Information is conveyed from bipolar cell to ganglion cell by chemical synapses that release glutamate in packets called quanta. Glutamate binds to receptors in the ganglion cell membrane and opens conductances for cations (mostly sodium (Na^+) and potassium (K^+)). Thus currents flow along dendrites until they reach the cell body and then the thin segment of the axon, where they charge up the membrane and initiate a spike. Because photoreceptors form a regular array across the retina, and transmit information through bipolar cells, the pattern of light across this array controls the pattern of glutamate quanta across ganglion cell dendrites, and thus controls the ganglion cell's spike transmission to the brain.

Bipolar cells constitute a set of parallel channels, each transmitting a different kind of information. Ganglion cells choose from among different bipolar cell types, sometimes relaying this information relatively unchanged, sometimes recombining information, and project this information to different

areas of the brain. This chapter focuses on how bipolar cells contribute to the ganglion cell's encoding of information about objects of different size (spatial frequency) and of different temporal properties.

1.14.2 About 10 Types of Bipolar Cell

There are about 9–13 types of bipolar cell, depending on the animal that end in distinct levels of the IPL (Boycott, B. B. and Wässle, H., 1991; Kolb, H. *et al.*, 1992; Ghosh, K. K. *et al.*, 2004; MacNeil, M. A. *et al.*, 2004; Pignatelli, V. and Strettoi, E., 2004). About half these types signal increases in contrast (On) and about half signal decreases in contrast (Off). On and Off bipolar cells can be aggregated into four basic groups that transmit different information. On and Off midget bipolar cells serve a perception of fine detail and may serve red/green opponency (Calkins, D. J. and Sterling, P., 1999; Martin, P. R., 1998; Dacey, D. M. and Packer, O. S., 2003). The On S bipolar cell contributes the blue component of blue/yellow opponency (Dacey, D. M. and Lee, B. B., 1994; Calkins, D. J. *et al.*, 1998; Calkins, D. J., 2001; Herr, S. *et al.*, 2003). The rod bipolar cell contributes sensitivity to very dim illumination (scotopic). On and Off diffuse bipolar cells contact multiple cones of mixed type and initiate temporal and spatial frequency channels. Unless otherwise stated, in the following discussion, bipolar cell will mean diffuse bipolar cell.

1.14.3 Bipolar Cells Contribute to Spatial Frequency Channels

1.14.3.1 Receptive Field is a Convolution

The eye's lens projects a receptive field onto the array of photoreceptors that is wired to a ganglion cell. The distribution of sensitivity across this receptive field looks like a Mexican hat; the hat's cross-section has been described as the difference of two Gaussians: one for the receptive field center, the other for the surround (Rodieck, R. and Stone, J., 1965; Enroth-Cugell, C. and Robson, J., 1966). It is this distribution that set a ganglion cell's spatial frequency selectivity.

To understand how a bipolar cell contributes to the ganglion cell's receptive field, consider a convolution model with two components (Figure 1(a)). First, bipolar receptive fields have a difference of Gaussians distribution of sensitivity and form a regularly spaced array. Second, the distribution of membrane area across the diameter of a dendritic tree is domed-shaped, and so too is the distribution of bipolar synapses, approximating a Gaussian weighting function (Kier, C. K. *et al.*, 1995). To combine these components, we convolve the bipolar receptive field center with the weighting function; we do the same for the bipolar receptive field surround. For either convolution, the result is a Gaussian. Furthermore, if σ_{bp} is a standard deviation for the bipolar receptive field (either center or surround) and σ_{dend} the standard deviation of the weighting function, then the standard deviation for the ganglion cell is $\sigma_{gc} = \sqrt{\sigma_{bp}^2 + \sigma_{dend}^2}$. It is significant that the standard deviation for the ganglion cell approximates the larger of the two component standard deviations.

The convolution model works out very differently for α and β cells of the cat retina and accurately predicts their sensitivity distributions (Freed, M. A. *et al.*, 1992; Figure 1(b)). In the area of central vision, both cells receive synapses from the same bipolar cell type that has a $\sigma_{bp\ center} \approx 20\,\mu m$, and $\sigma_{bp\ surround} \approx 130\,\mu m$. The α cell has a large dendritic arbor with $\sigma_{dend} \approx 50\,\mu m$. As a result of the convolution, the α center approximates its dendritic arbor, but its surround approximates the bipolar surround. The β cell has a small dendritic arbor with $\sigma_{dend} \approx 10\,\mu m$, and consequently its center and surround matches those of the bipolar cell.

The size of a ganglion cell's receptive field determines its spatial frequency selectivity, that is, its preference for stimuli of a particular size. Thus for large ganglion cells, selectivity is determined by the dendritic arbor, but for small ganglion cells selectivity is determined by the size of the bipolar receptive field. There is no evidence for a wide variety of bipolar receptive field sizes (Dacey, D. *et al.*, 2000), so they do not initiate spatial frequency channels; instead such channels result from ganglion cell dendritic trees.

1.14.3.2 Random Properties of Bipolar Array

Convolution models help us conceptualize the relation between dendritic tree size and receptive field size. But detailed mappings show that some ganglion cell sensitivity distributions are not smooth like a Gaussian but asymmetric and bumpy (Rodieck, R. and Stone, J., 1965; Peichl, L. and Wässle, H., 1979; Soodak, R. E. *et al.*, 1991; Brown, S. P. *et al.*, 2000). These bumps result from

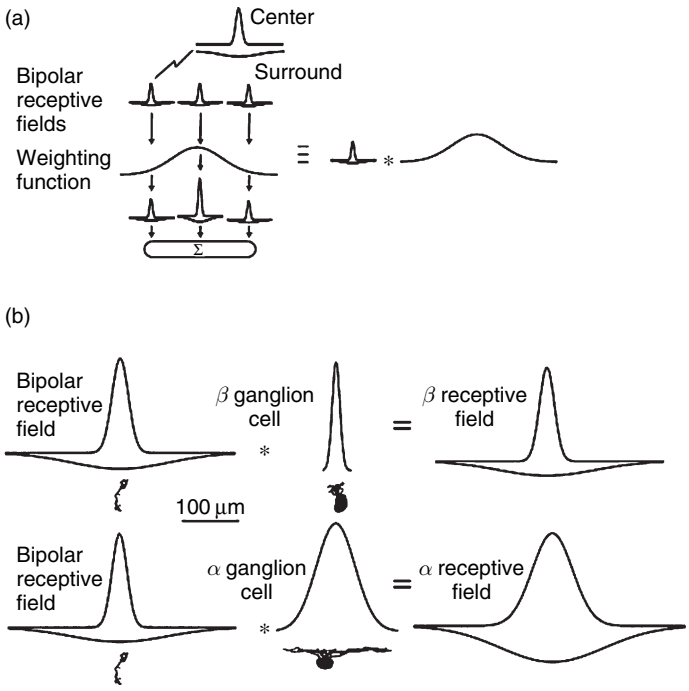

Figure 1 Contribution of bipolar cells to ganglion cell receptive field: convolution model. (a) Weighted summation. Bipolar receptive fields, each consisting of center and surround Gaussians, are scaled according to the local value of a weighting function, and then summed. This is identical to a convolution (∗) between receptive field and weighting function. (b) Convolution models of α- and β-cell receptive fields. The bipolar receptive field ($\sigma_{center} = 20$ mm; $\sigma_{surround} = 130$ μm) is convolved with a Gaussian that approximates the distribution of membrane across the α and β dendritic trees ($\sigma_{dend} \sim 50$ and 10 μm, respectively). As predicted by this model, the α receptive field center is enlarged and its surround is deepened but the β receptive field matches that of the bipolar cell. Adapted from Freed, M. A. and Sterling, P. 1988. The On-alpha ganglion cell of the cat retina and its presynaptic cell types. J. Neurosci. 8, 2303–2320; Kier, C. K., Buchsbaum, G., and Sterling, P. 1995. How retinal microcircuits scale for ganglion-cells of different size. J. Neurosci. 15, 7673–7683.

irregularities in the weighting function, which have several causes: bipolar cells form a somewhat disorderly array across the retina; not every bipolar cell in this array contacts a ganglion cell; the number of synapses each bipolar cell contributes varies (Freed, M. A. *et al.*, 1992). Further, some ganglion cells have large dendritic trees whose electrical structure may be complex: synapses at different loci in the dendritic tree may contribute different amounts of current to the spike initiation site at the axon's thin segment; spikes may be initiated throughout the dendritic tree (Velte, T. J. and Masland, R. H., 1999). Finally, ganglion cells receive amacrine input that the model does not account for. Thus a more complex model with an irregular weighting function that departs from a smooth Gaussian is necessary to explain the ganglion cells sensitivity distribution (Figure 2).

The sensitivity distribution across small receptive fields tends to be smoother than the distribution across larger receptive fields (Brown, S. P. *et al.*, 2000). This is probably because a small receptive field is the result of a small dendritic arbor: thus irregularities in the small weighting function are smoothed out by convolution with the larger bipolar receptive field. Some cells, such as the β cell of the cat retina, receive input from several overlapping bipolar cell arrays, which smoothes the weighting function.

Bumps can vary substantially from one ganglion cell to another of the same type. An extreme example is the bistratified blue/yellow ganglion cell, whose sensitivity distribution is sometimes dominated by a single S cone and sometimes by several S cones (Chichilnisky, E. J. and Baylor, D. A., 1999). This variability is probably due to variability in the strength of synaptic connections between a single S cone and several S bipolar cells (Schein, S. *et al.*, 2004). These bumps are not likely to be smoothed by the optics of the eye: the eye's blurring function is smaller than any of the receptive field components (<4 μm), and thus when convolved with these components, has little effect (Navarro, R. *et al.*, 1993). Such random irregularities are likely to be of

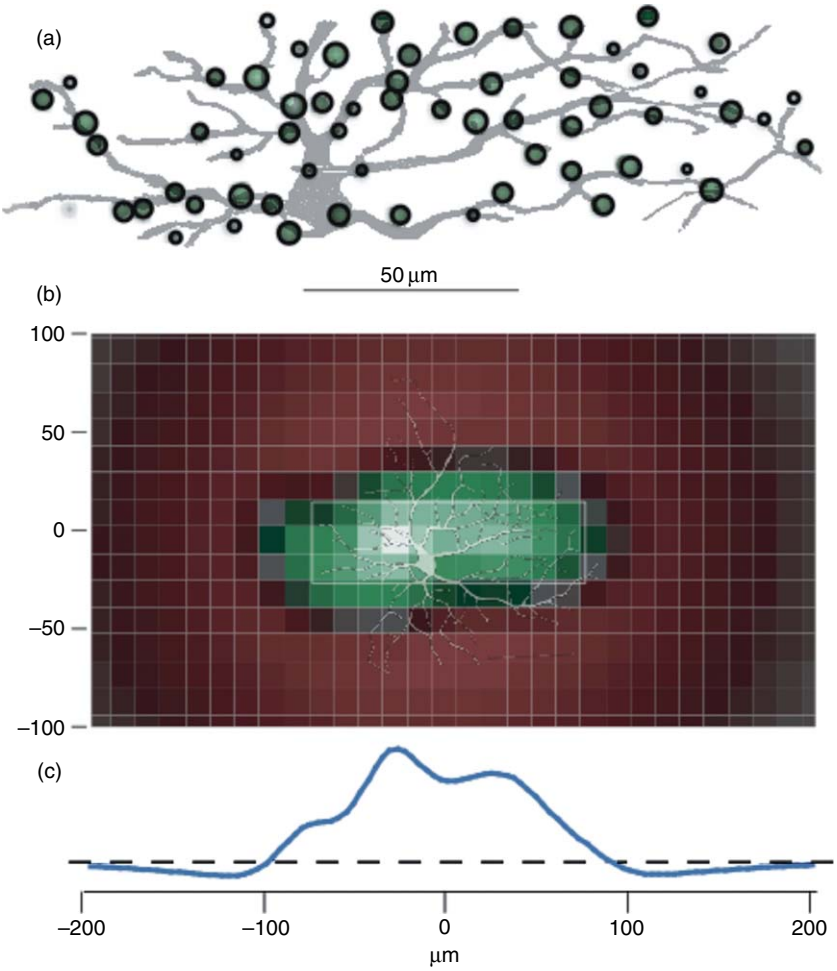

Figure 2 Contribution of bipolar cells to ganglion cell receptive field: detailed model. (a) A partial reconstruction of the dendritic arbor from ultra thin (80 nm) sections. An array of 74 diffuse cone bipolar cells of type b1 crossed the dendritic tree; the green disks represent 62 of these that synapsed on the α cell. Disk diameter is proportional to weighting, which is the product of the number of synapses and the effectiveness of each synapse at triggering a spike, as estimated from a compartmental model of the α cell. (b) Weighted summation of bipolar receptive fields: predicted α center is green (highest values are white), while the predicted surround is red. (c) A horizontal slice of the predicted receptive field. Bipolar cells outside the reconstructed region were omitted, but because the slice is centered on the region and parallel to it, this omission is inconsequential. The distribution of sensitivity shows asymmetry and bumps due to irregularities in the weighting function (compare to effect of smooth Gaussian weighting function in Figure 1). Adapted from Freed, M. A., Smith, R. G., and Sterling, P. 1992. Computational model of the on-alpha ganglion cell receptive field based on bipolar cell circuitry. Proc. Natl. Acad. Sci. U. S. A. 89, 236–240.

consequence to information decoding because the relationship between spike rate and the position or size of an object is inconsistent across ganglion cells.

1.14.3.3 Adaptive Properties of Bipolar Array

The bumps in a receptive field profile can adapt to a visual environment in order to increase sensitivity when the environment changes. During this adaptation, sensitivity changes within small subregions about the size of a bipolar cell receptive field, suggesting that adaptation is due to changes in bipolar cell sensitivity (Brown, S. P. and Masland, R. H., 2001; Baccus, S. A. and Meister, M., 2002; Hosoya, T. *et al.*, 2005). Bipolar cells are known to adapt and change sensitivity by an intrinsic mechanism that requires intracellular calcium (Shiells, R. A. and Falk, G., 1999; Rieke, F., 2001).

1.14.3.4 Contribution to Peak Contrast Sensitivity

The density of bipolar cell synapses on cellular membrane is $10\,\mu m^{-2}$ for α cells, about $30\,\mu m^{-2}$ for β cells of the cat retina. Furthermore, small β trees cover the retina about three times more densely with membrane than large α trees (Kier, C. K. *et al.*, 1995). Correspondingly, when peak contrast sensitivity is measured at the middle of the Gaussian receptive field center, cells with the smallest receptive fields (β) have about nine times higher peak contrast sensitivity than those with large receptive fields (α), suggesting that the number of bipolar synapses activated by a stimulus contributes to sensitivity. Smaller cells may have greater peak sensitivity for additional reasons: synaptic currents may have a shorter distance to reach the spike initiation site, which combined with a higher input resistance, would produce a larger voltage (O'Brien, B. J. *et al.*, 2002).

1.14.3.5 Contribution to Contrast Threshold

The total number of bipolar synapses should also set the lowest detectible contrast by setting the signal-to-noise ratio. This is because synaptic release is a Poisson process, for which the signal is the mean rate of quantal release n, and the noise is $\sqrt{n}$, so the signal-to-noise ratio is $\sqrt{n}$. By inference, ganglion cells that receive many bipolar cell synapses, presumably with a high mean rate n, provide a high signal-to-noise ratio. This inference appears to be true for at least one ganglion cell type: large β cells with many synapses have higher signal-to-noise ratios than small β cells with fewer synapses (Freed, M. A., 2000a). A study designed to test this inference for primate ganglion cells failed to confirm it, although this may have been due to a sinusoidal stimulus that increases and decreases synaptic noise every period, and thus shows no net difference (Croner, L. J. *et al.*, 1993).

1.14.4 Bipolar Cells Contribute to Nonlinear Subunits

1.14.4.1 Counter-Phased Grating Reveals Nonlinear Subunits

A counter-phased grating is an alternating series of light and dark bars: dark bars are exchanged for light bars and vice versa (Figure 3). If the grating is fine enough, many ganglion cells will fire at every exchange (Hochstein, S. and Shapley, R. M., 1976). This behavior, called frequency doubling has been attributed to an array of nonlinear subunits within the receptive field center and beyond. These subunits resemble, by their array and sensitivity to fine gratings, the array of bipolar cell receptive fields. Only subunits within the receptive field center persist when amacrine synapses are blocked, indicating that

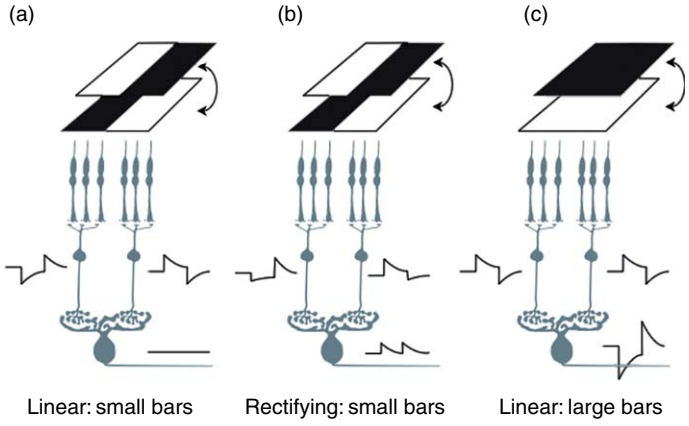

Figure 3 Contribution of bipolar cells to nonlinear subunits in the ganglion cell receptive field. (a) Linear responses, small bars: response to dark bar exchanging for light and response to light bar exchanging for dark are equal and opposite (the figure shows responses to a complete cycle of two exchanges). The result is no net ganglion cell response. (b) Rectifying responses, small bars: Response to dark bar exchanging for light is greater than response to light bar exchanging for dark: the result is a net response at each exchange. (c) Linear responses, large bars: for a large bar, the responses from the two bipolar cells are identical. The result is a large net response. Thus linear component of bipolar cell responses contributes selectivity to low spatial frequencies (≈ large bars) characteristic of ganglion cell's receptive field center and surround; rectifying response component contributes to sensitivity to high spatial frequencies (≈ small bars) characteristic of ganglion cells nonlinear subunits.

these subunits are transmitted through bipolar synapses on the ganglion cell; those beyond the center apparently require transmission by spiking amacrine cells, but may also originate, at least in part, in bipolar cells (Demb, J. B. *et al.*, 2001).

Rectifying and thus nonlinear bipolar cell responses are thought to contribute nonlinear subunits. A linear bipolar cell response would contribute sensitivity to low spatial frequencies characteristic of the receptive field center and surround (Figure 3). Because a given bipolar cell's response is never completely linear, the same bipolar cell could contribute to center, surround, and subunit in the ganglion cell receptive field. Subunits have at least one important consequence: a ganglion cell with a large receptive field can encode information about high spatial frequencies.

1.14.5 Bipolar Cells May Initiate Temporal Frequency Channels

1.14.5.1 Temporal Frequency Response of Bipolar Cells

Different types of ganglion cell have different temporal bandwidth, that is, respond to different ranges of temporal frequency. Bipolar cells show sustained and transient responses, corresponding to low and high frequencies. This suggests that bipolar cells initiate temporal frequency channels and impart their temporal tuning to ganglion cells. Yet the temporal tuning of only few bipolar types has been characterized.

In lieu of tuning curves for every bipolar cell type, it is tempting to infer each type's frequency response from the frequency response of ganglion cells that branch in the same stratum. But most bipolar types overlap several distinct frequency responses (MacNeil, M. A. *et al.*, 2004). It has been suggested that transient bipolar cells are in the middle of the IPL and sustained at the edges (Awatramani, G. B. and Slaughter, M. M., 2000; Roska, B. and Werblin, F., 2001), but it would be surprising if this were generally true because in some retinas a sustained (local edge) ganglion cell branches in the middle and a transient (α) ganglion cell branches at the edges (Rockhill, R. L. *et al.*, 2002).

A conceptual scheme shows how frequency channels, established by bipolar cells, may feed through different ganglion cell types to the brain (Figure 4). Narrowly tuned ganglion cells, selective for high or low frequencies, may select from narrowly tuned bipolar cells. Broadly tuned ganglion cells may select both high- and low-frequency bipolar cells. This scheme avoids the need for extra types of broadly tuned bipolar cells, which would require them to have greater bandwidth.

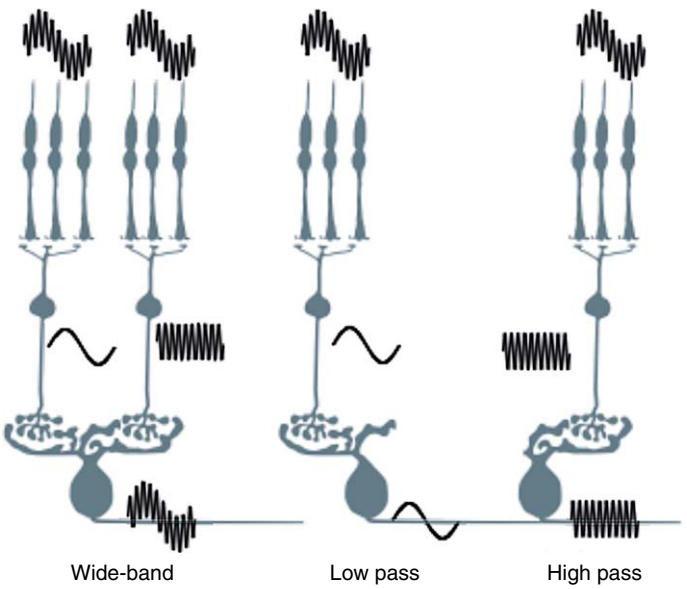

Figure 4 Contribution of bipolar cells to temporal frequency tuning of ganglion cells. Both high and low frequencies appear in the visual stimulus (shown here as a sum of sinusoids). The bipolar cell types decompose the signal into high and low frequencies. Wide-band ganglion cells receive synapses from both types of bipolar cell: low-pass and high-pass ganglion cells receive from low- and high-frequency bipolar cells, respectively.

1.14.5.2 A Bipolar Cell's Intrinsic Properties Modify Its Frequency Response

A bipolar cell's frequency tuning cannot be a function of the cones it contacts, because both sustained and transient diffuse bipolar cells contact the same cones. Instead, frequency tuning must be intrinsic to the bipolar cell or its synaptic interactions with amacrine cells. For example, all bipolar cells receive an inhibitory gamma-aminobutyric acid (GABA)ergic synapse from an amacrine cell, often the bipolar cell reciprocates with an excitatory glutamatergic synapse onto the amacrine cell, thus implementing a negative feedback loop. Some bipolar cells have $GABA_C$ receptors with slow kinetics that allow low frequencies to pass, others have $GABA_A$ that block low frequencies (Lukasiewicz, P. D. *et al.*, 1994; Euler, T. and Wassle, H., 1998; Freed, M. A. *et al.*, 2003). $GABA_B$ receptors modulate calcium currents and thus may alter release kinetics (Maguire, G. *et al.*, 1989).

Three different types of Off bipolar cell in the 13-lined ground squirrel use three distinct receptor types to sense glutamate release from the cone: two of the kainate type, one of the α-amino-3-hydroxy-5-methyl-4-isoxazoleproprionic acid (AMPA) type. All these receptors desensitize when continuously exposed to glutamate, but the AMPA receptor has the speediest recovery from desensitization (DeVries, S. H., 2000). Because cones release glutamate continuously in the dark, and presumably desensitize the receptor, and because light decreases release and allows recovery from desensitization, the AMPA receptors confer a speedier response to light, and thus sensitivity to higher frequencies.

Other intrinsic properties may modify the signal a bipolar cell transmits to a ganglion cell. Calcium channels within the axon terminal control release of glutamate onto a ganglion cells, may be either of transient (T) or sustained (L) properties, and may confer these properties to the ganglion cell (de la Villa, P. *et al.*, 1998; Pan, Z. H. *et al.*, 2001). Metabotropic autoreceptors on a bipolar cell sense its own glutamate release and modify release kinetics (Koulen, P. *et al.*, 1999).

1.14.5.3 On and Off Bipolar Cells Initiate Matched Temporal Channels

On and Off ganglion cells with similar morphology have similar response kinetics, with only small consistent differences (Chichilnisky, E. J. and Kalmar, R. S., 2002; Zaghloul, K. A. *et al.*, 2003). This is remarkable given that these responses come from different bipolar cells with entirely different mechanisms for transmitting signals. Transmission by On bipolar cells requires many steps: when glutamate from cones binds to its receptor, this initiates a multistep biochemical cascade that closes cation channels. Transmission by Off bipolar cells is simpler: when glutamate binds to its receptor, this closes a cation channel that is integral to the receptor. Despite the extra steps, On bipolar and ganglion cells are about as fast as Off cells (within 10 ms) and sometimes faster (Shiells, R. A. and Falk, G., 1994; Chichilnisky, E. J. and Kalmar, R. S., 2002; Zaghloul, K. A. *et al.*, 2003). Thus On and Off bipolar cells use different neural circuits and intrinsic mechanisms to initiate a set of approximately matched On and Off temporal channels.

1.14.6 Contribution of Bipolar Cells to Information Encoding

1.14.6.1 Contribution to Linear Responses

To ensure a spike train with adequate information entropy, spike rate must fluctuate up and down. But if synapses were to saturate, this would prevent fluctuation, and thus reduce information content. Bipolar cells prevent saturation at the synapse by releasing glutamate quanta at moderate rates. The dendritic tree of a medium-sized ganglion cell receives about 2000 bipolar synapses. During a just-maximal response to a high-contrast bar, these synapses collectively release about 40 000 quanta s^{-1} (Freed, M. A., 2000b; Freed, M. A. *et al.*, 2003). But a synapse releases only about 20 quanta s^{-1}. During more moderate responses to naturalistic stimuli, a synapse releases at even lower rate, only about 0.1 quanta s^{-1}, which is a quantum every 10 s (Freed, M. A., 2005)! In order to have an overlapping effect on the ganglion cell voltage quanta must be within an integration time of about 20 ms. Thus quanta at a synapse very rarely overlap, and the conductance at a synapse is kept well below the peak conductance caused by a quantum, about 100 pS. Such low conductances forestall saturation of the synapse's driving force, and thus enhance information encoding (Freed, M. A. *et al.*, 1992; Freed, M. A., 2000b). Interestingly, bipolar cell synapses can release quanta at tremendous rates for short periods of time when triggered electrically, but apparently do not operate this way under natural conditions (500 s^{-1}; von Gersdorff, H. and Matthews, G., 1994; von Gersdorff, H. *et al.*, 1996).

1.14.6.2 Contribution to Information Encoding

The amount of information that a ganglion cell sends to the brain is critically limited by variability in spike timing. The bipolar cell must therefore time glutamate release accurately to trigger spikes accurately. Indeed both quanta and spikes, when evoked by naturalistic stimuli, have about the same average temporal accuracy, 10 ms, and for some cells, spike accuracy, and by inference quantal accuracy, is as good as 1 ms (Berry, M. J. and Meister, M., 1998; Freed, M. A., 2005).

The random nature of quantal release reduces the reliability of chemical synapses. Even if an identical signal appeared repeatedly in the bipolar cell, the number of quanta that are released will be variable; thus the resulting count of triggered spikes will also be variable. Reproducibility can be expressed as the mean count over the standard deviation (of spikes or quanta). For a Poisson process such as quantal release, if the average count is n, then the reproducibility is $\sqrt{n}$. For ganglion cell spiking, reproducibility is greater (Troy, J. B. and Robson, J. G., 1992; Berry, M. J. *et al.*, 1997; van Steveninck, R. R. D. *et al.*, 1997).

An array of bipolar cells reduces spike variability by synchronizing release across many synapses whenever the visual stimulus matches bipolar cell tuning (i.e., the bipolar cell's spatiotemporal filter). This results in bursts of quanta that, for a moderate contrast, can include as many as 60 quanta and which average about 20 quanta (Freed, M. A., 2005). But a ganglion cell fires bursts of only one to six spikes (Berry, M. J. *et al.*, 1997; Koch, K. *et al.*, 2004), indicating that many quanta trigger few spikes. The advantage of triggering with multiple quanta can be calculated from their Poisson statistics. If a single quantum reliably triggered a single spike, then both would have a reproducibility of 1. But for an average burst size of 20, quanta have a reproducibility of 4.5. Thus many quanta triggering few spikes increases the reproducibility of the spike train.

References

Awatramani, G. B. and Slaughter, M. M. 2000. Origin of transient and sustained responses in ganglion cells of the retina. J. Neurosci. 20, 7087–7095.

Baccus, S. A. and Meister, M. 2002. Fast and slow contrast adaptation in retinal circuitry. Neuron 36, 909–919.

Berry, M. J. and Meister, M. 1998. Refractoriness and neural precision. J. Neurosci. 18, 2200–2211.

Berry, M. J., Warland, D. K., and Meister, M. 1997. The structure and precision of retinal spike trains. Proc. Natl. Acad. Sci. U. S. A. 94, 5411–5416.

Boycott, B. B. and Wässle, H. 1991. Morphological classification of bipolar cells of the primate retina. Eur. J. Neurosci. 3, 1069–1088.

Brown, S. P. and Masland, R. H. 2001. Spatial scale and cellular substrate of contrast adaptation by retinal ganglion cells. Nat. Neurosci. 4, 44–51.

Brown, S. P., He, S., and Masland, R. H. 2000. Receptive field microstructure and dendritic geometry of retinal ganglion cells. Neuron 27, 371–383.

Calkins, D. J. 2001. Seeing with S cones. Prog. Retin. Eye Res. 20, 255–287.

Calkins, D. J. and Sterling, P. 1999. Evidence that circuits for spatial and color vision segregate at the first retinal synapse. Neuron 24, 313–321.

Calkins, D. J., Tsukamoto, Y., and Sterling, P. 1998. Microcircuitry and mosaic of a blue-yellow ganglion cell in the primate retina. J. Neurosci. 18, 3373–3385.

Chichilnisky, E. J. and Baylor, D. A. 1999. Receptive-field microstructure of blue-yellow ganglion cells in primate retina. Nat. Neurosci. 2, 889–893.

Chichilnisky, E. J. and Kalmar, R. S. 2002. Functional asymmetries in On and Off ganglion cells of primate retina. J. Neurosci. 22, 2737–2747.

Croner, L. J., Purpura, K., and Kaplan, E. 1993. Response variability in retinal ganglion cells of primates. Proc. Natl. Acad. Sci. U. S. A. 90, 8128–8130.

Dacey, D., Packer, O. S., Diller, L., Brainard, D., Peterson, B., and Lee, B. 2000. Center surround receptive field structure of cone bipolar cells in primate retina. Vis. Res. 40, 1801–1811.

Dacey, D. M. and Lee, B. B. 1994. The 'blue-on' opponent pathway in primate retina originates from a distinct bistratified ganglion cell type. Nature 367, 731–735.

Dacey, D. M. and Packer, O. S. 2003. Colour coding in the primate retina: diverse cell types and cone-specific circuitry. Curr. Opin. Neurobiol. 13, 421–427.

de la Villa, P., Vaquero, C. F., and Kaneko, A. 1998. Two types of calcium currents of the mouse bipolar cells recorded in the retinal slice preparation. Eur. J. Neurosci. 10, 317–323.

Demb, J. B., Zaghloul, K., Haarsma, L., and Sterling, P. 2001. Bipolar cells contribute to nonlinear spatial summation in the brisk-transient (Y) ganglion cell in mammalian retina. J. Neurosci. 21, 7447–7454.

DeVries, S. H. 2000. Bipolar cells use kainate and AMPA receptors to filter visual information into separate channels. Neuron 28, 847–856.

Enroth-Cugell, C. and Robson, J. 1966. The contrast sensitivity of retinal ganglion cells of the cat. J. Physiol. (Lond.) 187, 517–552.

Euler, T. and Wassle, H. 1998. Different contributions of GABAA and GABAC receptors to rod and cone bipolar cells in a rat retinal slice preparation. J. Neurophysiol. 79, 1384–1395.

Freed, M. A. 2000a. Parallel cone bipolar pathways to a ganglion cell use different rates and amplitudes of quantal excitation. J. Neurosci. 20, 3956–3963.

Freed, M. A. 2000b. Rate of quantal excitation to a retinal ganglion cell evoked by sensory input. J. Neurophysiol. 83, 2956–2966.

Freed, M. A. 2005. Quantal encoding of information in a retinal ganglion cell. J. Neurophysiol. 94, 1048–1056.

Freed, M. A. and Sterling, P. 1988. The On-alpha ganglion cell of the cat retina and its presynaptic cell types. J. Neurosci. 8, 2303–2320.

Freed, M. A., Smith, R. G., and Sterling, P. 1992. Computational model of the on-alpha ganglion cell receptive field based on bipolar cell circuitry. Proc. Natl. Acad. Sci. U. S. A. 89, 236–240.

Freed, M. A., Smith, R. G., and Sterling, P. 2003. Timing of quantal release from the retinal bipolar terminal is regulated by a feedback circuit. Neuron 38, 89–101.

Ghosh, K. K., Bujan, S., Haverkamp, S., Feigenspan, A., and Wassle, H. 2004. Types of bipolar cells in the mouse retina. J. Comp. Neurol. 469, 70–82.

Herr, S., Klug, K., Sterling, P., and Schein, S. 2003. Inner S-cone bipolar cells provide all of the central elements for S cones in macaque retina. J. Comp. Neurol. 457, 185–201.

Hochstein, S. and Shapley, R. M. 1976. Linear and nonlinear spatial subunits in Y cat retinal ganglion cells. J. Physiol. (Lond.) 262, 265–284.

Hosoya, T., Baccus, S. A., and Meister, M. 2005. Dynamic predictive coding by the retina. Nature 436, 71–77.

Kier, C. K., Buchsbaum, G., and Sterling, P. 1995. How retinal microcircuits scale for ganglion-cells of different size. J. Neurosci. 15, 7673–7683.

Koch, K., McLean, J., Berry, M., Sterling, P., Balasubramanian, V., and Freed, M. A. 2004. Efficiency of information transmission by retinal ganglion cells. Curr. Biol. 14, 1523–1530.

Kolb, H., Linberg, K. A., and Fisher, S. K. 1992. Neurons of the human retina: a Golgi study. J. Comp. Neurol. 318, 147–187.

Koulen, P., Kuhn, R., Wassle, H., and Brandstatter, J. H. 1999. Modulation of the intracellular calcium concentration in photoreceptor terminals by a presynaptic metabotropic glutamate receptor. Proc. Natl. Acad. Sci. U. S. A. 96, 9909–9914.

Lukasiewicz, P. D., Maple, B. R., and Werblin, F. S. 1994. A novel GABA receptor on bipolar cell terminals in the tiger salamander retina. J. Neurosci. 14, 1202–1212.

MacNeil, M. A., Heussy, J. K., Dacheux, R. F., Raviola, E., and Masland, R. H. 2004. The population of bipolar cells in the rabbit retina. J. Comp. Neurol. 472, 73–86.

Maguire, G., Maple, B., Lukasiewicz, P., and Werblin, F. 1989. Gamma-aminobutyrate type B receptor modulation of L-type calcium channel current at bipolar cell terminals in the retina of the tiger salamander. Proc. Natl. Acad. Sci. U. S. A. 86, 10144–10147.

Martin, P. R. 1998. Colour processing in the primate retina: recent progress. J. Physiol. 513, 631–638.

Navarro, R., Artal, P., and Williams, D. R. 1993. Modulation transfer of the human eye as a function of retinal eccentricity. J. Opt. Soc. Am. A 10, 201–212.

O'Brien, B. J., Isayama, T., Richardson, R., and Berson, D. M. 2002. Intrinsic physiological properties of cat retinal ganglion cells. J. Physiol. 538, 787–802.

Pan, Z. H., Hu, H. J., Perring, P., and Andrade, R. 2001. T-type Ca(2+) channels mediate neurotransmitter release in retinal bipolar cells. Neuron 32, 89–98.

Peichl, L. and Wässle, H. 1979. Size, scatter and coverage of ganglion cell receptive field centres in the cat retina. J. Physiol. (Lond.) 291, 117–141.

Pignatelli, V. and Strettoi, E. 2004. Bipolar cells of the mouse retina: a gene gun, morphological study. J. Comp. Neurol. 476, 254–266.

Rieke, F. 2001. Temporal contrast adaptation in salamander bipolar cells. J. Neurosci. 21, 9445–9454.

Rockhill, R. L., Daly, F. J., MacNeil, M. A., Brown, S. P., and Masland, R. H. 2002. The diversity of ganglion cells in a mammalian retina. J. Neurosci. 22, 3831–3843.

Rodieck, R. and Stone, J. 1965. Analysis of receptive fields of cat retinal ganglion cells. J. Neurophysiol. 28, 833–849.

Roska, B. and Werblin, F. 2001. Vertical interactions across ten parallel, stacked representations in the mammalian retina. Nature 410, 583–587.

Schein, S., Sterling, P., Ngo, I. T., Huang, T. M., and Herr, S. 2004. Evidence that each S cone in macaque fovea drives one narrow-field and several wide-field blue-yellow ganglion cells. J. Neurosci. 24, 8366–8378.

Shiells, R. A. and Falk, G. 1999. A rise in intracellular Ca^{2+} underlies light adaptation in dogfish retinal 'on' bipolar cells. J. Physiol. 514, 343–350.

Shiells, R. A. and Falk, G. 1994. Responses of rod bipolar cells isolated from dogfish retinal slices to concentration-jumps of glutamate. Vis. Neurosci. 11, 1175–1183.

Soodak, R. E., Shapley, R. M., and Kaplan, E. 1991. Fine structure of receptive-field centers of X and Y cells of the cat. Vis. Neurosci. 6, 621–628.

Troy, J. B. and Robson, J. G. 1992. Steady discharges of X-retinal and Y-retinal ganglion cells of cat under photopic illuminance. Vis. Neurosci. 9, 535–553.

van Steveninck, R. R. D., Lewen, G. D., Strong, S. P., Koberle, R., and Bialek, W. 1997. Reproducibility and variability in neural spike trains. Science 275, 1805–1808.

Velte, T. J. and Masland, R. H. 1999. Action potentials in the dendrites of retinal ganglion cells. J. Neurophysiol. 81, 1412–1417.

von Gersdorff, H. and Matthews, G. 1994. Dynamics of synaptic vesicle fusion and membrane retrieval in synaptic terminals. Nature 367, 735–739.

von Gersdorff, H., Vardi, E., Matthews, G., and Sterling, P. 1996. Evidence that vesicles on the synaptic ribbon of retinal bipolar neurons can be rapidly released. Neuron 16, 1221–1227.

Zaghloul, K. A., Boahen, K., and Demb, J. B. 2003. Different circuits for On and Off retinal ganglion cells cause different contrast sensitivities. J. Neurosci. 23, 2645–2654.

1.15 Amacrine Cells

M Wilson, University of California, Davis, CA, USA

D I Vaney, The University of Queensland, Brisbane, QLD, Australia

© 2008 Elsevier Inc. All rights reserved.

1.15.1	Morphological Diversity	361
1.15.2	Neurochemical Diversity	361
1.15.3	Feedback and Feedforward Inhibition	363
1.15.4	Amacrine Cell Networks	364
1.15.5	Local Processing in Amacrine Cells	364
1.15.6	Neuromodulatory Functions	366
References		366

1.15.1 Morphological Diversity

By all measures, amacrine cells are the most diverse class of neurons in the retina and, in contrast to the other major classes of retinal neurons, no single statement adequately describes their structure or function. Both Cajal S. R. (1893) and Dogiel A. S. (1891) noted that the interneurons of the inner retina do not give rise to a classical axon, leading Cajal to name them amacrine cells, from the Greek *a-makrós-inos* meaning without long fiber. However, Cajal also recognized that some amacrine cells in the bird retina do give rise to a short intraretinal axon and these cells he called association amacrine cells, to distinguish them from amacrine cells proper. It has since become clear that there are numerous types of axon-bearing amacrine cells in the vertebrate retina (Vaney, D. I. *et al.*, 1988; Dacey, D. M., 1989; Famiglietti, E. V., 1992) and, in keeping with Cajal's broad view, the term amacrine cell now embraces all types of retinal interneurons that receive their synaptic input in the inner retina, including interplexiform cells (Vaney, D. I., 2003).

The input and output synapses of amacrine cells are typically located side by side on the dendrites, notwithstanding the minority of axon-bearing cells. Amacrine cells receive excitatory input from retinal bipolar cells and provide inhibitory output both to the dendrites of retinal ganglion cells and to the dendrites of other amacrine cells, as well as back to the axon terminals of bipolar cells. Thus, amacrine cells can modulate the activity of ganglion cells both postsynaptically, by inhibiting the ganglion cells directly, and presynaptically, by inhibiting the bipolar cells that provide the excitatory drive.

The mammalian retina has been conservatively estimated to contain about 30 morphological types of amacrine cells (Kolb, H. *et al.*, 1981; MacNeil, M. A. *et al.*, 1999; Figure 1). However, the recent identification of many novel types of axon-bearing amacrine cells, some represented by only a single example (Badea, T. C. and Nathans, J., 2004; Vaney, D. I., 2004; Lin, B. and Masland, R. H., 2006), indicates that more types remain to be characterized and that the number of distinct types of amacrine cells in the mammalian retina may well approach 50 or more (Vaney, D. I., 1990).

The numerous types of amacrine cells differ greatly in both their structure and cell density. At one extreme, the well-characterized AII amacrine cells account for over 10% of the amacrine cells and their narrow-field diffuse dendritic trees tile the retina with little overlap. At the other extreme, several types of axon-bearing amacrine cells account for only 0.1% of the amacrine cells, but their widely overlapping axonal fields, which may span ~10 mm of retina, create a very dense plexus. This is readily apparent for the dopaminergic amacrine cells, which were the first retinal neurons to be identified neurochemically (Häggendal, J. and Malmfors, T., 1965).

1.15.2 Neurochemical Diversity

Early histochemical and immunocytochemical studies highlighted the neurochemical diversity of the amacrine cells, with emphasis on the monoamine transmitters and neuropeptides (Brecha, N. *et al.*, 1979). However, virtually all amacrine cells contain elevated levels of glycine or GABA (Marc, R. E. *et al.*,

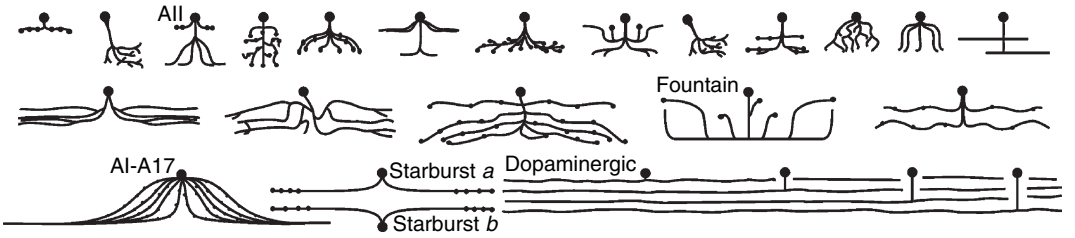

Figure 1 Diversity of amacrine cells in the mammalian retina. Schematic drawing of the different types of amacrine cells identified by MacNeil M. A. *et al*. (1999) using a photofilling technique in the rabbit retina. The cells are drawn as they would be seen in vertical section, with the somata in the inner nuclear layer and the dendrites in the inner plexiform layer. The multiple types of wide-field amacrine cells branching in each stratum are represented by a generic cell whose dendrites have been truncated. Labels mark specific types of amacrine cells referred to in the text. Masland, R. H. 2001. Neuronal diversity in the retina. Curr. Opin. Neurobiol. 11, 431–436.

1995), which may be colocalized with another neurotransmitter or neuromodulator. Most of the putative GABAergic cells express the GABA-synthesizing enzyme, glutamic acid decarboxylase, and most of the putative glycinergic cells express the plasma membrane glycine transporter, GlyT1. Although the glycinergic cells account for a small majority of amacrine cells in the mammalian retina (Figure 2), the inner plexiform layer is dominated by the processes of GABAergic amacrine cells, which usually have much more extensive dendritic trees than the glycinergic amacrine cells (Pourcho, R. G. and Goebel, D. J., 1983; Menger, N. *et al*., 1998). Correspondingly, the GABAergic cells account for 80–90% of the synapses made by all amacrine cells in the retina (Koontz, M. A. and Hendrickson, A. E., 1990; Marc, R. E. and Liu, W., 2000).

Both GABA and glycine are fast-acting inhibitory transmitters that gate closely related chloride-permeable channels. It is unclear why these amino acid transmitters are differentially distributed in the CNS, with GABA mediating most of the inhibition in the brain and glycine mediating most of the inhibition in the spinal cord. Uniquely within the CNS, the retina contains about equal numbers of GABAergic and glycinergic interneurons. An examination of the different roles of GABA and glycine in visual processing in the retina may cast light on why one or other of these inhibitory transmitters predominate in other parts of the CNS.

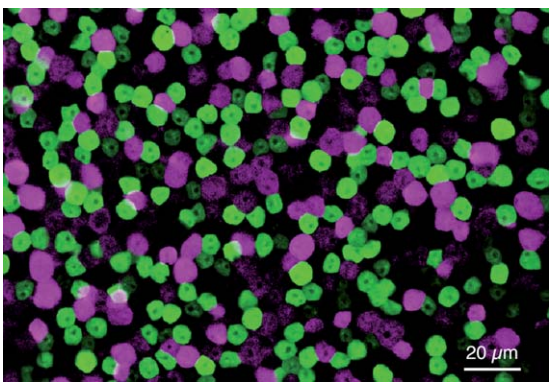

Figure 2 Almost all amacrine cells express glycine or GABA. Confocal fluorescence micrographs of a rabbit retinal wholemount immunolabeled for glycine (green) and GABA (magenta), with the focus on the amacrine sublayer of the inner nuclear layer (Wright, L. L. and Vaney, D. I., unpublished).

The glycinergic amacrine cells have small- or medium-field dendritic trees that typically occupy two or more strata of the inner plexiform layer and, therefore, can facilitate interactions between the parallel pathways established by the different types of cone bipolar cells (Pourcho, R. G. and Goebel, D. J., 1985). In other words, the glycinergic amacrine cells seem designed to mediate vertical inhibition in the retina (Roska, B. and Werblin, F., 2001). The GABAergic amacrine cells, by comparison, seem designed to mediate the lateral inhibition that has normally been attributed to amacrine cells, either via feedback inhibition of bipolar cells or via feedforward inhibition of ganglion cells and other amacrine cells (Roska, B. *et al*., 2000). Such a dichotomy does not appear to be rigid. The fountain amacrine cells, for example, are medium-field bistratified cells that contain GABA and probably substance P: their unusual morphological organization suggests that they receive input in the On sublamina and make output in the Off sublamina (MacNeil, M. A. *et al*., 1999; Wright, L. L. and Vaney, D. I., 1999).

Other neurotransmitters or neuromodulators expressed by amacrine cells are always colocalized with a fast-acting inhibitory transmitter, usually GABA but sometimes glycine, and the output synapses of these cells appear to be primarily

inhibitory. For example, the extensive synapses made by dopaminergic amacrine cells onto AII amacrine cells appear to be GABAergic, whereas the released dopamine diffuses to more distant receptors (Contini, M. and Raviola, E., 2003). Even the cholinergic starburst amacrine cells, which provided the definitive example of an excitatory amacrine cell, contain GABA (Vaney, D. I. and Young, H. M., 1988). Elegant dual-recording studies have shown that the inhibitory GABAergic inputs from starburst cells to each other and to retinal ganglion cells underlie the generation of direction selectivity in the retina (Fried, S. I. *et al.*, 2002; Lee, S. and Zhou, Z. J., 2006). Both GABA and acetylcholine may be released by starburst cells (O'Malley, D. M. *et al.*, 1992), but it remains an open question whether both transmitters are coreleased from the same synapses and under what circumstances.

Amacrine cells receive excitatory input from bipolar cells through ionotropic glutamate receptors; different amacrine types express distinct sets of NMDA, AMPA, and kainate receptors, which may be critical in shaping their temporal responses (Dumitrescu, O. N. *et al.*, 2006). Although the chemical synapses made by amacrine cells are primarily inhibitory, many types of amacrine cells also make excitatory electrical synapses through gap junctions. Different types of amacrine cells show different patterns of neuronal coupling (Vaney, D. I., 1994). Some types are homologously coupled to amacrine cells of the same type; others are heterologously coupled to amacrine cells of a different type or to specific types of retinal ganglion cells whose firing they help to synchronize (Mastronarde, D. N., 1989; Brivanlou, I. H. *et al.*, 1998).

1.15.3 Feedback and Feedforward Inhibition

Early physiological studies suggested that spatial visual processing takes place in the outer retina, through the actions of horizontal cells, and that temporal visual processing takes place in the inner retina, through the actions of amacrine cells (Werblin, F. S. and Dowling, J. E., 1969). However, recent work in amphibian and mammalian retinas makes it clear that the separate channels of temporal representation are first established in the outer retina (Awatramani, G. B. and Slaughter, M. M., 2000; DeVries, S. H., 2000). Conversely, although the receptive field surround is initially generated by horizontal cells in the outer retina (Mangel, S. C., 1991; McMahon, M. J. *et al.*, 2004), amacrine cells also make an important contribution in the inner retina (Cook, P. B. and McReynolds, J. S., 1998; Taylor, W. R., 1999).

One function of amacrine cells that has been closely investigated is their role in delivering inhibitory feedback to the axon terminals of bipolar cells. The transmitter used is GABA and both $GABA_A$ and $GABA_C$ receptors are thought to be involved. Pharmacological experiments and studies using $GABA_C$-knockout mice (McCall, M. A. *et al.*, 2002) show that the two receptor types have complementary functions. $GABA_A$ receptors activate quickly and provide fast and transient feedback while the intrinsically slower $GABA_C$ receptors mediate sustained inhibition (Vigh, J. and von Gersdorff, H., 2005; Eggers, E. D. and Lukasiewicz, P. D., 2006) and, in the case of goldfish, generate a standing current that regulates presynaptic excitability (Hull, C. *et al.*, 2006). In the mammalian retina, feedback to the rod bipolar cell is provided by a type of wide-field amacrine cell, termed the AI or A17 amacrine cell in the cat retina (Kolb, H. and Famiglietti, E. V., 1974). The effect of this feedback has been examined by recording from the bipolar cell body before and after inhibiting GABA receptors pharmacologically, or alternatively severing the bipolar cell axon terminal (Euler, T. and Masland, R. H., 2000). These experiments imply that feedback has a powerful ability to extend the dynamic range of the bipolar cell with respect to light intensity.

It is generally agreed that feedforward from amacrine cells to ganglion cells is a powerful inhibitory pathway, but there is disagreement concerning the receptors involved. Unlike the feedback pathway, where the reciprocal rod bipolar to A17 connection has proved very useful, the lack of an anatomically identifiable pair of connected cells has hampered the study of feedforward from amacrine cells. Lukasiewicz P. D. and Shields C. R. (1998) reported that $GABA_A$ receptors alone mediate inhibition to ganglion cells of the amphibian retina, but other studies suggested that there is also $GABA_C$ and $GABA_B$ input to ganglion cells (Zhang, J. and Slaughter, M. M., 1995; Shen, W. and Slaughter, M. M., 2001). As described by Zhang J. *et al.* (1997b), there are two separate $GABA_B$ receptors on salamander ganglion cells. Both the pharmacology of these two receptors and the signaling pathways they activate are different and, though they both reduce Ca^{2+} currents, one affects an N-type Ca^{2+} channel, whereas the other affects Ca^{2+} entry through L-type Ca^{2+} channels. Clearly, Ca^{2+} entry into ganglion cell dendrites, not only through the N- and L-type Ca^{2+} channels, but also through NMDA receptors and Ca^{2+}-permeable AMPA receptors, provides a mechanism for

integrating inputs. How these mechanisms work together and what role they play in vision is not yet clear.

1.15.4 Amacrine Cell Networks

Although inhibitory interactions in the retina are often represented as simple feedback or feedforward circuits, serial synapses between amacrine processes have long been recognized (Dowling, J. E. and Boycott, B. B., 1966; Dubin, M. W., 1970) In fact, a quantitative study of the synaptic connectivity of GABAergic amacrine cells in the goldfish retina indicated that the majority of amacrine cell circuitries are relatively complex, involving nested feedback, nested feedforward, and chains of inhibition (Marc, R. E. and Liu, W., 2000).

Connections between GABAergic and glycinergic amacrines can be inferred from a simple physiological experiment that measured the effects of a glycinergic antagonist (strychnine) or a GABAergic antagonist (picrotoxin) on the light-evoked currents in retinal ganglion cells of the mud puppy. As expected, each of these antagonists reduced the inhibitory current in a majority of ganglion cells. However, the inhibitory current was enhanced in almost one-third of the ganglion cells, indicating cross-inhibition between GABAergic and glycinergic feedforward pathways (Zhang, J. *et al.*, 1997a). Thus, in a minority of ganglion cells, the glycinergic antagonist produced disinhibition of the direct GABAergic input or the GABAergic antagonist produced disinhibition of the glycinergic input; all inhibitory current was blocked by the addition of both antagonists.

1.15.5 Local Processing in Amacrine Cells

Unlike the neurons of the outer retina, amacrine cells are capable of generating action potentials that can enhance transmitter release as evidenced, for example, by the observation that tetrodotoxin applied to the retina of goldfish suppresses a large fraction of spontaneous inhibitory postsynaptic currents (IPSCs) seen in amacrine cells (Watanabe, S. *et al.*, 2000). Transmitter release, however, does not require action potentials (Gleason, E. *et al.*, 1993; 1994; Bieda, M. C. and Copenhagen, D. R., 1999), and accumulating evidence suggests that input and output are very flexibly coupled in amacrine cells.

Three related features of amacrine cells are key to understanding how these neurons work. First, the input and output synapses of amacrine cells are frequently located in close proximity on the dendrites, unlike typical neurons where the synaptic output is segregated to the axon terminal. Second, amacrine cells perform at least some of their processing functions using cytoplasmic Ca^{2+} concentrations as the computing medium, rather than membrane voltage, as is predominantly the case in typical neurons. Third, individual amacrine cells comprise multiple processing units that are more or less independent; amacrine cells can operate in different modes, with processing units tightly or loosely coupled. These three characteristics and their interactions can be illustrated with a few examples.

Commonly, the two postsynaptic elements at the ribbon synapses of bipolar cells comprise a ganglion cell dendrite and an amacrine cell dendrite. In most instances, the identities of the postsynaptic elements are unknown; but, for the mammalian rod bipolar cell, it is well established that an AII amacrine cell takes the place of a ganglion cell, with the other postsynaptic element being an AI/A17 amacrine cell (Kolb, H. and Famiglietti, E. V., 1974). As already discussed, the A17 amacrine cell is reciprocally connected to the bipolar cell terminal, but only recently it has become clear that this GABAergic feedback loop can be entirely local. A similar example of local feedback is provided by the reciprocal connection of glutamatergic mitral cells and GABAergic granule cells of the olfactory bulb (Isaacson, J. S. and Strowbridge, B. W., 1998).

When voltage-gated Ca^{2+} channels are disabled pharmacologically, the A17 process is nevertheless still able to release GABA and hyperpolarize the bipolar terminal. This is possible because the glutamate released from the rod bipolar cell opens AMPA receptors that admit sufficient Ca^{2+} to promote transmitter release from the A17 varicosity (Chavez, A. E. *et al.*, 2006). An implication of this is that transmitter release needs only modest elevations in cytoplasmic Ca^{2+} concentration, as demonstrated in cultured amacrine cells (Frerking, M. *et al.*, 1997). A mechanism analogous to that in the A17 cell holds for the feedback from amacrine cells to the goldfish MB1 bipolar cells, except that Ca^{2+} entry into the amacrine cell process is mediated through NMDA receptors (Vigh, J. and von Gersdorff, H., 2005). Transmitter release is boosted by an additional step in the A17 amacrine cell: Ca^{2+} entering through

AMPA receptors leads to calcium-induced calcium release (CICR), a process by which Ca^{2+} sequestered in the endoplasmic reticulum is liberated into the cytoplasm.

The clearest example of local dendritic processing is provided by the starburst amacrine cells (Taylor, W. R. and Vaney, D. I., 2003). These radially symmetric cells receive input from bipolar cells over the whole dendritic tree but make synaptic output to ganglion cells only from the distal dendrites. The main targets of the starburst cells are direction-selective ganglion cells (DSGCs), which respond to image motion in a preferred direction (PD) but not the opposite null direction. The key mechanism underlying the directional responses is spatially offset inhibition, which arises from starburst cells located on the null side of the DSGC but not the preferred side. Thus, for each starburst cell, processes pointing in different directions would provide the null-direction inhibition to DSGCs with different PDs (Figure 3). Moreover, patch-clamp recordings from DSGCs have shown that this inhibition is already direction selective, reflecting the direction-selective Ca^{2+} responses measured in the distal dendrites of the starburst cells (Fried, S. I. *et al.*, 2002; Euler, T. *et al.*, 2002).

Such a scheme requires that the processes of starburst dendrites pointing in one direction be functionally isolated from those processes pointing in the other directions. There is no doubt that part of this isolation reflects the electroanatomy of the starburst cell, with long thin dendrites arising from a central shunting soma (Miller, R. F. and Bloomfield, S. A. 1983). However, it also seems possible that transmitter release from starburst cells, like that from A17 cells, is not rigidly tied to membrane voltage. It is well known that the null-direction inhibition is very long-lasting and a mechanism such as CICR would be ideal for generating the appropriate temporal characteristics.

Studies on cultured amacrine cells have shown that Ca^{2+} liberated from the endoplasmic reticulum plays a significant role in transmitter release, particularly long-lasting asynchronous release. In that instance, however, Ca^{2+} release from the endoplasmic reticulum is promoted by the entry of Ca^{2+} via voltage-gated channels (Warrier, A. *et al.*, 2005) and can give rise to substantial local differences in cytoplasmic Ca^{2+} in the absence of voltage differences (Hurtado, J. *et al.*, 2002). It is clear that Ca^{2+} events in amacrine cells can occur on a wide range of spatial scales and by a variety of underlying mechanisms

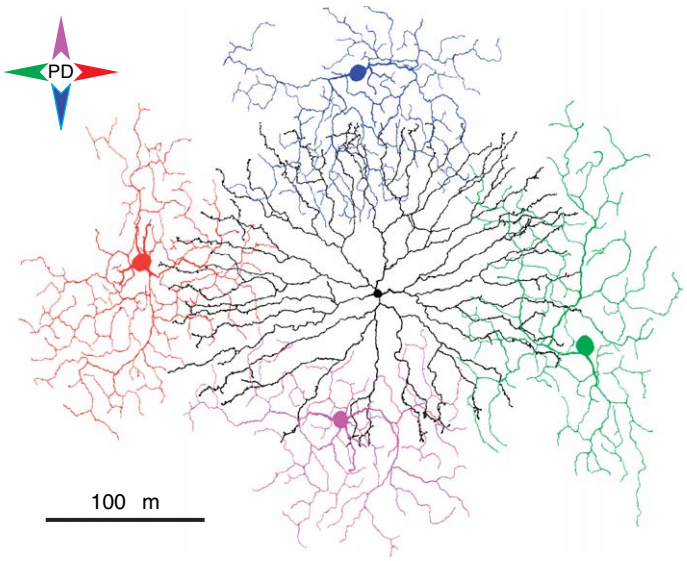

Figure 3 Local interactions of starburst amacrine cells. The rabbit retina contains four subtypes of On–Off direction-selective ganglion cells (DSGCs), whose preferred directions (PDs) are aligned with the cardinal ocular axes (colored dendritic trees and compass rose). Each DSGC receives asymmetric inhibitory input from starburst amacrine cells (black dendritic tree) located to the side of the DSGC first encountered by null-direction image motion: individual starburst cells provide null-direction inhibition to all subtypes of DSGCs. From Taylor, W. R. and Vaney, D. I. 2003. New directions in retinal research. Trends Neurosci. 26, 379–385.

(Azuma, T. *et al.*, 2004). Very likely these local and regional Ca^{2+} domains represent the dynamic functional subunits of these cells.

1.15.6 Neuromodulatory Functions

With the use of antibody staining, amacrine cells have been shown to contain a long list of peptides, such as vasointestinal peptide and substance P, that elsewhere in the nervous system are known to have roles in modulating neural function. Some amacrine cell types contain more than one peptide, for example, the enkephalin-, neurotensin-, and somatostatin-like immunoreactive (ENSLI) amacrine cells of the bird retina (Watt, C. B. *et al.*, 1985). Very little is known about the conditions under which peptides are released by amacrine cells or the function of these neuromodulators in retinal processing.

In addition to peptides, amacrine cells apparently use other signaling molecules including nitric oxide and endocannabinoids. Nitric oxide effects several distinct transient changes in the retina, including reducing the electrical coupling between horizontal cells. Studies on cultured amacrine cells have revealed an interesting and potentially important role in the inner retina: nitric oxide locally increases the cytoplasmic chloride concentration, in effect transiently converting inhibitory synapses to excitatory synapses (Hoffpauir, B. *et al.*, 2006). Recent work, also using cultured retinal neurons, has shown that endocannabinoids can increase the resting rate of transmitter release from amacrine cells (Warrier, A. and Wilson, M., 2007). Resting transmitter release is detectable in the intact retina as a continuous barrage of inhibitory input from amacrine cells (Watanabe, S. *et al.*, 2000), and it is likely that changes in the rate of resting release influence the voltage of other amacrine cells and perhaps ganglion cells.

References

Awatramani, G. B. and Slaughter, M. M. 2000. Origin of transient and sustained responses in ganglion cells of the retina. J. Neurosci. 20, 7087–7095.

Azuma, T., Enoki, R., Iwamuro, K., Kaneko, A., and Koizumi, A. 2004. Multiple spatiotemporal patterns of dendritic Ca^{2+} signals in goldfish retinal amacrine cells. Brain Res. 1023, 64–73.

Badea, T. C. and Nathans, J. 2004. Quantitative analysis of neuronal morphologies in the mouse retina visualized by using a genetically directed reporter. J. Comp. Neurol. 480, 331–351.

Bieda, M. C. and Copenhagen, D. R. 1999. Sodium action potentials are not required for light-evoked release of GABA or glycine from retinal amacrine cells. J. Neurophysiol. 81, 3092–3095.

Brecha, N., Karten, H. J., and Laverack, C. 1979. Enkephalin-containing amacrine cells in the avian retina: immunohistochemical localization. Proc. Natl. Acad. Sci. U. S. A. 76, 3010–3014.

Brivanlou, I. H., Warland, D. K., and Meister, M. 1998. Mechanisms of concerted firing among retinal ganglion cells. Neuron 20, 527–539.

Cajal, S. R. 1893. La rétine des vertebras. La Cellule 9, 119–257.

Chavez, A. E., Singer, J. H., and Diamond, J. S. 2006. Fast neurotransmitter release triggered by Ca influx through AMPA-type glutamate receptors. Nature 443, 705–708.

Contini, M. and Raviola, E. 2003. GABAergic synapses made by a retinal dopaminergic neuron. Proc. Natl. Acad. Sci. U. S. A. 100, 1358–1363.

Cook, P. B. and McReynolds, J. S. 1998. Lateral inhibition in the inner retina is important for spatial tuning of ganglion cells. Nat. Neurosci. 1, 714–719.

Dacey, D. M. 1989. Axon-bearing amacrine cells of the macaque monkey retina. J. Comp. Neurol. 284, 275–293.

DeVries, S. H. 2000. Bipolar cells use kainate and AMPA receptors to filter visual information into separate channels. Neuron 28, 847–856.

Dogiel, A. S. 1891. Ueber die nervösen Elemente in der Retina des Menschen. Arch. Mikrosk. Anat. 38, 317–344.

Dowling, J. E. and Boycott, B. B. 1966. Organization of the primate retina: electron microscopy. Proc. R. Soc. Lond. B Biol. Sci. 166, 80–111.

Dubin, M. W. 1970. The inner plexiform layer of the vertebrate retina: a quantitative and comparative electron microscopic analysis. J. Comp. Neurol. 140, 479–505.

Dumitrescu, O. N., Protti, D. A., Majumdar, S., Zeilhofer, H. U., and Wässle, H. 2006. Ionotropic glutamate receptors of amacrine cells of the mouse retina. Vis. Neurosci. 23, 79–90.

Eggers, E. D. and Lukasiewicz, P. D. 2006. Receptor and transmitter release properties set the time course of retinal inhibition. J. Neurosci. 26, 9413–9425.

Euler, T. and Masland, R. H. 2000. Light-evoked responses of bipolar cells in a mammalian retina. J. Neurophysiol. 83, 1817–1829.

Euler, T., Detwiler, P. B., and Denk, W. 2002. Directionally selective calcium signals in dendrites of starburst amacrine cells. Nature 418, 845–852.

Famiglietti, E. V. 1992. Polyaxonal amacrine cells of rabbit retina: PA2, PA3, and PA4 cells. Light and electron microscopic studies with a functional interpretation. J. Comp. Neurol. 316, 422–446.

Frerking, M., Borges, S., and Wilson, M. 1997. Are some minis multiquantal? J. Neurophysiol. 78, 1293–1304.

Fried, S. I., Münch, T. A., and Werblin, F. S. 2002. Mechanisms and circuitry underlying directional selectivity in the retina. Nature 420, 411–414.

Gleason, E., Borges, S., and Wilson, M. 1993. Synaptic transmission between pairs of retinal amacrine cells in culture. J. Neurosci. 13, 2359–2370.

Gleason, E., Borges, S., and Wilson, M. 1994. Control of transmitter release from retinal amacrine cells by Ca^{2+} influx and efflux. Neuron 13, 1109–1117.

Häggendal, J. and Malmfors, T. 1965. Identification and cellular localization of the catecholamines in the retina and choroid of the rabbit. Acta Physiol. Scand. 64, 58–66.

Hoffpauir, B., McMains, E., and Gleason, E. 2006. Nitric oxide transiently converts synaptic inhibition to excitation in retinal amacrine cells. J. Neurophysiol. 95, 2866–2877.

Hull, C., Li, G. L., and von Gersdorff, H. 2006. GABA transporters regulate a standing $GABA_C$ receptor-mediated current at a retinal presynaptic terminal. J. Neurosci. 26, 6979–6984.

Hurtado, J., Borges, S., and Wilson, M. 2002. Na^{+}-Ca^{2+} exchanger controls the gain of the Ca^{2+} amplifier in the dendrites of amacrine cells. J. Neurophysiol. 88, 2765–2777.
Isaacson, J. S. and Strowbridge, B. W. 1998. Olfactory reciprocal synapses: dendritic signaling in the CNS. Neuron 20, 749–761.
Kolb, H. and Famiglietti, E. V. 1974. Rod and cone pathways in the inner plexiform layer of cat retina. Science 186, 47–49.
Kolb, H., Nelson, R., and Mariani, A. 1981. Amacrine cells, bipolar cells and ganglion cells of the cat retina: a Golgi study. Vision Res. 21, 1081–1114.
Koontz, M. A. and Hendrickson, A. E. 1990. Distribution of GABA-immunoreactive amacrine cell synapses in the inner plexiform layer of macaque monkey retina. Vis. Neurosci. 5, 17–28.
Lee, S. and Zhou, Z. J. 2006. The synaptic mechanism of direction selectivity in distal processes of starburst amacrine cells. Neuron 51, 787–799.
Lin, B. and Masland, R. H. 2006. Populations of wide-field amacrine cells in the mouse retina. J. Comp. Neurol. 499, 797–809.
Lukasiewicz, P. D. and Shields, C. R. 1998. Different combinations of $GABA_A$ and $GABA_C$ receptors confer distinct temporal properties to retinal synaptic responses. J. Neurophysiol. 79, 3157–3167.
MacNeil, M. A., Heussy, J. K., Dacheux, R. F., Raviola, E., and Masland, R. H. 1999. The shapes and numbers of amacrine cells: matching of photofilled with Golgi-stained cells in the rabbit retina and comparison with other mammalian species. J. Comp. Neurol. 413, 305–326.
Mangel, S. C. 1991. Analysis of the horizontal cell contribution to the receptive field surround of ganglion cells in the rabbit retina. J. Physiol. 442, 211–234.
Marc, R. E. and Liu, W. 2000. Fundamental GABAergic amacrine cell circuitries in the retina: nested feedback, concatenated inhibition, and axosomatic synapses. J. Comp. Neurol. 425, 560–582.
Marc, R. E., Murry, R. F., and Basinger, S. F. 1995. Pattern recognition of amino acid signatures in retinal neurons. J. Neurosci. 15, 5106–5129.
Masland, R. H. 2001. Neuronal diversity in the retina. Curr. Opin. Neurobiol. 11, 431–436.
Mastronarde, D. N. 1989. Correlated firing of retinal ganglion cells. Trends Neurosci. 12, 75–80.
McCall, M. A., Lukasiewicz, P. D., Gregg, R. G., and Peachey, N. S. 2002. Elimination of the rho1 subunit abolishes $GABA_C$ receptor expression and alters visual processing in the mouse retina. J. Neurosci. 22, 4163–4174.
McMahon, M. J., Packer, O. S., and Dacey, D. M. 2004. The classical receptive field surround of primate parasol ganglion cells is mediated primarily by a non-GABAergic pathway. J. Neurosci. 24, 3736–3745.
Menger, N., Pow, D. V., and Wässle, H. 1998. Glycinergic amacrine cells of the rat retina. J. Comp. Neurol. 401, 34–46.
Miller, R. F. and Bloomfield, S. A. 1983. Electroanatomy of a unique amacrine cell in the rabbit retina. Proc. Natl. Acad. Sci. USA 80, 3069–3073.
O'Malley, D. M., Sandell, J. H., and Masland, R. H. 1992. Co-release of acetylcholine and GABA by the starburst amacrine cells. J. Neurosci. 12, 1394–1408.
Pourcho, R. G. and Goebel, D. J. 1983. Neuronal subpopulations in cat retina which accumulate the GABA agonist, (^{3}H)muscimol: a combined Golgi and autoradiographic study. J. Comp. Neurol. 219, 25–35.
Pourcho, R. G. and Goebel, D. J. 1985. A combined Golgi and autoradiographic study of (^{3}H)glycine-accumulating amacrine cells in the cat retina. J. Comp. Neurol. 233, 473–480.
Roska, B. and Werblin, F. 2001. Vertical interactions across ten parallel, stacked representations in the mammalian retina. Nature 410, 583–587.
Roska, B., Nemeth, E., Orzo, L., and Werblin, F. S. 2000. Three levels of lateral inhibition: a space-time study of the retina of the tiger salamander. J. Neurosci. 20, 1941–1951.
Shen, W. and Slaughter, M. M. 2001. Multireceptor GABAergic regulation of synaptic communication in amphibian retina. J. Physiol. 530, 55–67.
Taylor, W. R. 1999. TTX attenuates surround inhibition in rabbit retinal ganglion cells. Vis. Neurosci. 16, 285–290.
Taylor, W. R. and Vaney, D. I. 2003. New directions in retinal research. Trends Neurosci. 26, 379–385.
Vaney, D. I. 1990. The mosaic of amacrine cells in the mammalian retina. Prog. Retin. Eye Res. 9, 49–100.
Vaney, D. I. 1994. Patterns of neuronal coupling in the retina. Prog. Retin. Eye Res. 13, 301–355.
Vaney, D. I. 2003. Retinal Amacrine Cells. In: The Visual Neurosciences (*eds*. L. M. Chalupa and J. S. Warner), pp. 395–409. MIT Press.
Vaney, D. I. 2004. Type 1 nitrergic (ND1) cells of the rabbit retina: comparison with other axon-bearing amacrine cells. J. Comp. Neurol. 474, 149–171.
Vaney, D. I. and Young, H. M. 1988. GABA-like immunoreactivity in cholinergic amacrine cells of the rabbit retina. Brain Res. 438, 369–373.
Vaney, D. I., Peichl, L., and Boycott, B. B. 1988. Neurofibrillar long-range amacrine cells in mammalian retinae. Proc. R. Soc. Lond. B Biol. Sci. 235, 203–219.
Vigh, J. and von Gersdorff, H. 2005. Prolonged reciprocal signaling via NMDA and GABA receptors at a retinal ribbon synapse. J. Neurosci. 25, 11412–11423.
Warrier, A. and Wilson, M. 2007. Endocannabinoid signaling regulates spontaneous transmitter release from embryonic retinal amacrine cells. Vis. Neurosci. 24, 25–35.
Warrier, A., Borges, S., Dalcino, D., Walters, C., and Wilson, M. 2005. Calcium from internal stores triggers GABA release from retinal amacrine cells. J. Neurophysiol. 94, 4196–4208.
Watanabe, S., Koizumi, A., Matsunaga, S., Stocker, J. W., and Kaneko, A. 2000. GABA-mediated inhibition between amacrine cells in the goldfish retina. J. Neurophysiol. 84, 1826–1834.
Watt, C. B., Li, H. B., and Lam, D. M. 1985. The presence of three neuroactive peptides inpuatative glycinergic amacrine cells of an avian retina. Brain Res. 348, 187–191.
Werblin, F. S. and Dowling, J. E. 1969. Organization of the retina of the mudpuppy, Necturus maculosus. II. Intracellular recording. J. Neurophysiol. 32, 339–355.
Wright, L. L. and Vaney, D. I. 1999. The fountain amacrine cells of the rabbit retina. Vis. Neurosci. 16, 1145–1156.
Zhang, J. and Slaughter, M. M. 1995. Preferential suppression of the ON pathway by $GABA_C$ receptors in the amphibian retina. J. Neurophysiol. 74, 1583–1592.
Zhang, J., Jung, C. S., and Slaughter, M. M. 1997a. Serial inhibitory synapses in retina. Vis. Neurosci. 14, 553–563.
Zhang, J., Shen, W., and Slaughter, M. M. 1997b. Two metabotropic gamma-aminobutyric acid receptors differentially modulate calcium currents in retinal ganglion cells. J. Gen. Physiol. 110, 45–58.

Further Reading

Masland, R. H. 2001. The fundamental plan of the retina. Nat. Neurosci. 4, 877–886.
Taylor, W. R. and Vaney, D. I. 2002. Diverse synaptic mechanisms generate direction selectivity in the rabbit retina. J. Neurosci. 22, 7712–7720.

1.16 The P, M and K Streams of the Primate Visual System: What Do They Do for Vision?

E Kaplan, Mount Sinai School of Medicine, New York, NY, USA

© 2008 Elsevier Inc. All rights reserved.

1.16.1	**Introduction**	370
1.16.1.1	Parallel Processing: Visual Attributes, Labeled Lines, and Neuronal Streams	370
1.16.1.2	Classification of Cells into Types	370
1.16.2	**Properties of the M, P, and K Streams**	370
1.16.2.1	Anatomy	370
1.16.2.1.1	Numbers, density, and resolution	370
1.16.2.1.2	Size	371
1.16.2.1.3	Connectivity: inputs and projections	371
1.16.2.2	Physiology	372
1.16.2.2.1	Dynamics	372
1.16.2.2.2	Linearity of spatial summation; X–Y	372
1.16.2.2.3	Chromatic properties	373
1.16.2.2.4	Contrast gain	373
1.16.2.2.5	Spatial resolution	374
1.16.2.2.6	Extraclassical receptive field	374
1.16.2.3	Summary: The Properties of the Three Neuronal Streams	374
1.16.3	**How Solid Is the Parallel Streams Hypothesis?**	375
1.16.3.1	The World, the Mind, and the Brain: The Siren Lure of Parallel Functional Streams	375
1.16.3.2	Challenges to the Parallel Streams Hypothesis	375
1.16.3.2.1	Criteria for the validity of the parallel streams hypothesis	376
1.16.3.2.2	How homogeneous are the Three neuronal types?	376
1.16.3.2.3	Anatomy	376
1.16.3.2.4	Physiology	377
1.16.3.2.5	Psychophysics	377
1.16.3.3	The Need for Alternative Theories	377
1.16.3.3.1	Labeled lines, multiplexing, dynamical networks, and the modularity of functional organization	378
1.16.4	**Conclusions**	378
References		378

Glossary

parvocellular or P Designates tho midget retinal ganglion cells that project to the upper four layers of the primate lateral geniculate nucleus (LGN).

magnocellular or M Designates the large retinal ganglion cells that project to the bottom two layers of the primate LGN.

Koniocellular or K* Designates those retinal ganglion cells that project to the interlaminar spaces in the primate LGN.

1.16.1 Introduction

1.16.1.1 Parallel Processing: Visual Attributes, Labeled Lines, and Neuronal Streams

The notion that the visual world is analyzed in parallel by several neuronal types goes back to Hartline's surprising discovery of ON and OFF retinal ganglion cells (RGCs) (Hartline, H. K., 1940). The discovery of the X/Y dichotomy among cat RGCs (Enroth-Cugell, C. and Robson, J. G., 1966) provided another clear example of this parallelism, and analysis of the conduction velocity of optic nerve fibers reinforced the idea further (see Stone, J., 1983). The intense interest in the magno–parvo–koniocellular groups later on (see Kaplan, E. and Shapley, R. M., 1986; Kaplan, E. *et al.*, 1990; Lee, B. B., 1996; Kaplan, E., 2003) and the anatomical studies that established the segregation of these neuronal types from the retina through the lateral geniculate nucleus (LGN) to the visual cortex (Livingstone, M. S. and Hubel, D. H., 1984a; 1984b; Shipp, S. and Zeki, S., 1985; Livingstone, M. and Hubel, D., 1988) have all added further weight to the view that the world is being analyzed in parallel by several streams, and this hypothesis has become widespread in the visual neuroscience literature (e.g., Ungerleider, L. G. and Mishkin, M., 1982; Livingstone, M. and Hubel, D., 1988; Zeki, S., 1993; Callaway, E. M., 2005).

Visual attributes. In the physical world we find only space and time. Vision scientists, however, commonly organize the various combinations of spatiotemporal properties of the visual world into concepts such as color, size, motion, orientation, and texture. It is very tempting then to imagine that each aspect of the visual world is dealt with by a specialized neuronal population that is dedicated to the analysis of one (or a few) of these aspects of the visual environment: color and other surface properties could be scrutinized by the tonic, high-resolution parvocellular stream, motion could be detected and analyzed by the phasic, coarse magnocellular stream, and so forth. We must remember, however, that these organizing concepts are a figment of the vision scientist's imagination, and that – at this point – their existence or representation in the brain in any specific form is merely a hypothesis. We shall return to this issue later.

1.16.1.2 Classification of Cells into Types

An important first step in any scientific endeavor is to classify the objects under scrutiny, and then try to deduce from the properties of the different classes something about the role that they play in the system under study. The classification of neurons into various groups takes into account various aspects: morphology, connectivity, neurochemistry, and physiological properties, such as the spatial and dynamical properties of their receptive field (for visual neurons). Sometimes neurons are divided into classes along one dimension only, such as transient–sustained, simple–complex, or ON–OFF, and some properties tend to cluster together. For example, transient cells are large, ON cells synapse in a particular sublamina of the inner plexiform layer. Such clustering of properties often provides seductive hints about the possible role that a given population might play in the overall function of the system. For more information regarding classification criteria, and more references concerning cell typing and classification, see Rodieck R. W. and Brening R. K. (1983) and Troy J. and Shou J. (2002).

1.16.2 Properties of the M, P, and K Streams

Comprehensive comparisons of the properties of the three main streams (magnocellular, parvocellular, and koniocellular) can be found in Kaplan E. *et al.* (1990) and Kaplan E. (2003). The presentation here will therefore be brief, and we shall discuss the retina and LGN together. Our current knowledge of the various properties is summarized in Table 1.

1.16.2.1 Anatomy

1.16.2.1.1 Numbers, density, and resolution

Numbers. By far, the majority of the RGCs in the primate retina (~80%) are midget (Polyak, S. L., 1941) cells, which project to the parvocellular (upper four) layers of the LGN of primates (Goodchild, A. *et al.*, 1996). Because of their projection target, they are referred to as P cells. The much larger parasol (Polyak, S. L., 1941) cells project to the magnocellular (bottom two) layers of the LGN, and are thus called M cells. They account for ~10% of the RGCs (Leventhal, A. G. *et al.*, 1981; Perry, V. H. and Cowey, A., 1984). A population of small (but not midget) bistratified blue ON ganglion cells projects to the koniocellular layers, the thin interlaminar zones between the major layers of the LGN (Dacey, D. M. and Lee, B. B., 1994). In the LGN, the

Table 1 Properties of the P, M, and K neuronal streams

	Property	*P*	*M*	*K*
1	Clear spectral opponency	Yes (red-green)	No	Some (blue-yellow)
2	Response to light steps	Tonic	Phasic (transient)	Phasic; some sluggish
3	Luminance contrast gain	Low	High	Diverse (some high)
4	Receptive field size	Small	Large	Large
5	Spatial resolution of individual neurons	Similar to M	Similar to P	Diverse (some like M)
6	Retinal ganglion cell density (acuity of cell group)	High	Low	?
7	Retinal source	Midget RGCs	Parasol RGCs	Unknown (some blue-ON bistratified RGCs)
8	LGN projection target	Parvocellular	Magnocellular	Koniocellular (intercalated) layers
9	V1 projection target	Layer 4Cβ	Layer 4Cα	Layers 2–3, CO blobs, layer 1
10	Cell body size	Small	Large	Large/varied
11	Conduction velocity of retinal axons	Medium	High	Low/varied
12	Contrast sensitivity at scotopic luminance	Poor	Good	?
13	Linearity of spatial summation	Linear (X-like)	75% Linear, 25% Nonlinear (Y-like)	Linear (X-like)
14	Extraclassical receptive field effects	Weak	Strong	Intermediate (varied)
15	Number of cells (fraction of LGN population)	~1 000 000 (85%)	~70 000 (6%)	~100 000 (9%)

koniocellular cells comprise ~9% of the nucleus' population (Hendry, S. H. C. and Yoshioka, T., 1994; Hendry, S. H. C. and Reid, C. R., 2000). It is likely that other types of ganglion cells also project to the koniocellular layers, but these have not been identified yet.

Density and resolution. Although it was initially thought that the ratio of M and P RGCs varies with retinal eccentricity, more recent data indicated that the ratio remains essentially constant throughout the retina (Perry, V. H. and Cowey, A., 1984; Silveira, L. C. L. and Perry, V., 1991). Since the P cells are much more numerous and close to each other, the resolution with which they sample visual space is higher than that available to the more sparse M or bistratified cells. We note, however, that the greater contrast sensitivity of M cells (Contrast Gain) allows them to detect fine patterns (Blakemore, C. and Vital-Durand, F., 1986; Crook, J. M. *et al.*, 1988), although their sparse coverage of the retina prevents them from providing enough information for the identification of such patterns.

1.16.2.1.2 Size

On average, the receptive field diameters of M cells at all retinal eccentricities are approximately 2.5–3 times as large as those of P cells, which makes their receptive field area roughly 6–8 times larger (Croner, L. J. and Kaplan, E., 1995). This size advantage is responsible in large part for their increased sensitivity to luminance contrast (Kaplan, E. and Shapley, R. M., 1986, Contrast Gain). The link between size and contrast sensitivity (Enroth-Cugell, C. and Shapley, R. M., 1973b) is also seen in K cells. For example, the K cells in the LGN of owl monkeys are approximately as large as the M cells, and their contrast sensitivities are similar as well (Xu, X. *et al.*, 2001).

1.16.2.1.3 Connectivity: inputs and projections

Retina. The midget (P) cells receive their input from midget bipolar cells. Near the fovea, this input is private: each ganglion cell receives input from one bipolar cell, which, in turn, is driven by a single cone. This arrangement is required for maximal spatial resolution, and the resulting improved color-analyzing mechanism could be a beneficial by-product. Farther from the fovea, the dendritic trees become larger, and the midget cells receive input from several cones, reducing their chromatic selectivity. The parasol (M) cells receive input from diffuse bipolars (Boycott, B. B. and Wässle, H., 1991),

which collect input from several different cones, making them more sensitive but less suitable for chromatic analysis. The small bistratified cells receive their input from bipolars that synapse at both the upper and the lower portions of the inner plexiform layer, and their receptive field centers are driven by S (blue sensitive) cones (Dacey, D. M. and Lee, B. B., 1994).

LGN and V1. The main groups of RGCs project to distinct layers or compartments in the LGN and in V1. The four parvocellular layers of the LGN receive their input from the midget RGCs (P cells), but also from other ganglion cell types, including some with very large dendritic trees (Rodieck, R. W. and Watanabe, M., 1993). They project to layer 4Cβ of the primary visual cortex, V1. The two lower layers of the LGN (magnocellular) receive their input from the parasol cells, and project to layer 4Cα of V1. The koniocellular layers receive input from the small bistratified (blue ON) cells, and project directly to the cytochrome oxidase blobs found in layers 2 and 3 of V1 (Hendry, S. H. C. and Yoshioka, T., 1994; Yabuta, N. H. and Callaway, E. M., 1998a; 1998b).

Beyond V1. From V1 the various neuronal streams project to numerous higher brain areas (Felleman, D. J. and van Essen, D. C., 1991; Kaplan, E., 2003). The overall pattern of these projections stimulated the suggestion that they form two main functional streams, one (dorsal) that answers the question 'Where?', and the other (ventral) to explore 'What?' is out there (Ungerleider, L. G. and Mishkin, M., 1982). This theory combines a hierarchical flow of information with the notion of parallel processing of various visual attributes, and is in wide circulation today. As we shall argue below, the broad acceptance of its simplistic form rests on somewhat shaky ground, and is perhaps premature.

1.16.2.2 Physiology

Many of the physiological properties such as contrast gain, receptive field size, center-surround antagonism, and chromatic selectivity are directly related to the morphological properties reviewed above, and appear to be determined by the early circuitry of the outer retina (Dacey, D. *et al.*, 2000). Other properties, such as dynamics, are related to both the connectivity pattern and the biophysical repertoire (including ion channels, neurotransmitters, and receptors) of the neurons.

1.16.2.2.1 Dynamics

The difference between the temporal properties of M cells and those of P cells (Gouras, P., 1968) was the first physiological indication that the primate retina contains more than one homogeneous population of RGCs, something that the anatomists have known for some time. Gouras P. (1968) reported that the discharges of some RGCs were phasic, while others fired tonically. At the time, the projection pattern of these cells to the LGN layers was unknown, and only later it was determined that the phasic cells correspond to the anatomical cell type called parasol cells, which were found to project to the magnocellular layers of the LGN, while the tonic cells correspond to the midget RGCs, which project to the parvocellular layers of the LGN (Leventhal, A. G. *et al.*, 1981). Further study of the dynamical properties and the linearity of their temporal responses has shown that both M and P cells have nonlinear response properties, although these are more pronounced in the M population (Kaplan, E. and Shapley, R. M., 1989; Benardete, E. A. and Kaplan, E., 1997; 1999).

The fact that M cells are much more phasic than P cells has led to the hypothesis that they are specialized for the detection and analysis of motion, while the tonic P cells are thought to be used for the analysis of surface properties.

1.16.2.2.2 Linearity of spatial summation; X–Y

In the cat, Y RGCs are larger and more phasic than X cells (Enroth-Cugell, C. and Robson, J. G., 1966), and it was tempting to seek a homology between the X–Y classes of the cat retina and the P–M types in the primate retina (Dreher, B. *et al.*, 1976; Sherman, S. M. *et al.*, 1976). However, the initial attempts did not use the original classification approach that was used in the cat by Enroth-Cugell and Robson, who called X cells those cells that showed linear spatial summation within their receptive fields. When that same criterion was used, all P and most M cells turned out to be rather like cat X cells, and only a minority of M cells had significant nonlinear spatial summation (Kaplan, E. and Shapley, R., 1982; Levitt, J. B. *et al.*, 2001). We note that such a homology contributes little to any compelling determination of the role that these cell classes play in primate vision. It is reasonable, however, to postulate that the P/midget system is a later evolutionary specialization found in monkeys but not in cats.

1.16.2.2.3 Chromatic properties

P cells. The retinal connectivity pattern of these cells, which, near the fovea, provides each one with a private line from a single cone, endows them with both high spatial resolution and chromatic selectivity. The center region of the receptive field is obviously tuned to the same wavelength that the central cone prefers. Much controversy surrounded the chromatic selectivity of the surround mechanism of P cells' receptive fields. Early reports suggested that the surround of many P cells receives specific input from cones that are tuned to a wavelength different from that to which the center is tuned (Wiesel, T. N. and Hubel, D. H., 1966; De Monasterio, F. M. and Gouras, P., 1975), and the cells typically fall into one of two major groups: r-g and b-y cells (Derrington, A. M. *et al*., 1984). However, anatomical studies have shown that the horizontal cells, widely believed to mediate the surround response, receive promiscuous, nonspecific cone input (Boycott, B. B. *et al*., 1987). Further physiological measurements have demonstrated that for most of the P cells (and their recipient parvocellular LGN targets), the input to the surround is, functionally, rather selective (Reid, R. C. and Shapley, R. M., 1992). It is possible, in principle, that this chromatic selectivity is accomplished through some processing in the inner plexiform layer, but a detailed anatomical study of this possibility has failed to support it (Calkins, D. J. and Sterling, P., 1996). Thus the anatomical substrate for the chromatic selectivity of the surround of near-foveal P cells remains elusive. We note, however, that even a mixed cone input to the surround can still provide robust color vision capabilities (Paulus, W. and Kröger-Paulus, A., 1983; Lennie, P. *et al*., 1991).

M cells. Most of these cells receive combined L and M cone input to both center and surround of their receptive fields, with little contribution from S cones (Wiesel, T. N. and Hubel, D. H., 1966; Lee, B. B. *et al*., 1989). Other studies have found the magnocellular portion of the LGN to be both spatially and chromatically antagonistic (Derrington, A. M. *et al*., 1984). In a few magnocellular cells, the surround receives inhibitory input from L cones (Wiesel, T. N. and Hubel, D. H., 1966). The broad-band, nonselective nature of the responses of M cells motivated the suggestion that they are responsible for the color-blind luminance channel of psychophysics.

K cells. Some of these LGN cells have been shown to receive input from the small bistratified RGCs, which receive their excitatory input from S cones (Dacey, D. M. and Lee, B. B., 1994). They thus provide the cellular substrate for the blue ON channel. The chromatic properties of the other cells that project to the koniocellular layers of the LGN remain to be elucidated.

It appears that the major factor that determines the chromatic properties of the P, M, and K cells is the spatial characteristics of their receptive fields, rather than any specialized, genetically directed selectivity in the connectivity pattern between cones and ganglion cells. Evidence in support of this conclusion comes also from comparative studies (see, e.g., Yamada, E. S. *et al*., 1998; Blessing, E. *et al*., 2004).

1.16.2.2.4 Contrast gain

Contrast gain is the relative change in response for a given change in stimulus contrast. It is related to the size of the light collecting pool of the receptive field (Enroth-Cugell, C. and Shapley, R. M., 1973a; Croner, L. J. and Kaplan, E., 1995; Troy, J. and Shou, T., 2002; Blessing, E. *et al*., 2004), which, incidentally, also determines the light adaptation state of the cell, and thus its dynamics as well (Enroth-Cugell, C. and Shapley, R. M., 1973b). Since at any retinal eccentricity M cells are larger than P cells, their contrast gain to luminance stimuli is typically higher than that of the P cells around them (Kaplan, E. and Shapley, R. M., 1986; Croner, L. J. and Kaplan, E., 1995). This is especially true for low-contrast stimuli. At higher contrasts, the M cells' response increases at a rate that is rather similar to that of P cells (Figure 1).

The similar contrast gain of P and M cells at high contrasts suggests the possibility that in P cells there is only one mechanism that is responsible for the response, while in M cells two mechanisms are at work: one operates at low contrasts, and once that mechanism saturates (at intermediate contrasts), another mechanism, which might be common to both M and P cells, takes over. It is therefore unlikely that the contribution of the magnocellular population disappears at high contrasts (Rudvin, I. *et al*., 2000), because M cells continue to increase their response up to 100% contrast (Figure 1).

K cells tend to be more like M cells in several respects, including their contrast gain (Xu, X. *et al*., 2001). Note, however, that not only size but the number of input synapses and other factors can also influence contrast gain (Croner, L. J. and Kaplan, E., 1995).

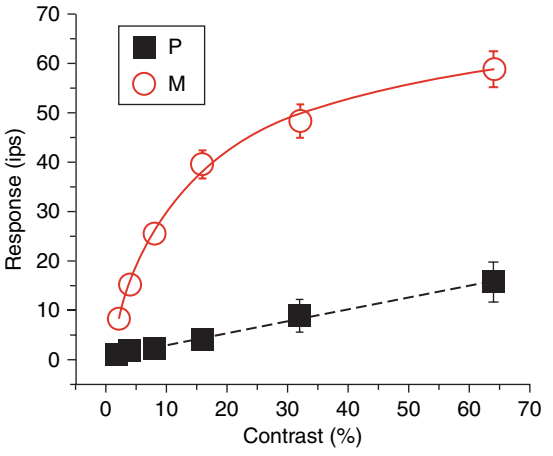

Figure 1 The contrast gain of M cells is higher than that of P cells for luminance stimuli. Shown are average responses of 28 P and 8 M retinal ganglion cells from one rhesus monkey as a function of luminance contrast. The stimulus was a drifting black-white sine wave grating of optimal spatial frequency for each cell, which modulated each cathode ray tube (CRT) pixel at 4 Hz. The smooth curves are the Michaelis–Menten equation, $y = ax/(b + x)$; error bars: ± 1 SEM. The half-saturation value, b, for the M (magnocellular projecting) ganglion cells, was 14%. Note the steeper slope (higher gain) at low contrasts for M cells (after Kaplan, E. and Shapley, R. M., 1986).

1.16.2.2.5 Spatial resolution

The high contrast gain of M cells is due, primarily, to their large receptive field. Because of their size, their density is low, and therefore they sample visual space rather sparely, which makes it impossible for them to identify fine patterns. Thus individual M cells can detect a fine drifting grating (Blakemore, C. and Vital-Durand, F., 1986; Crook, J. M. *et al.*, 1988), but the M system cannot determine whether it is drifting up or down. Despite their coarseness, the greater signal-to-noise ratio of M cell discharge suggests that they might contribute to hyperacuity performance (Rüttiger, L. and Lee, B., 2000; Rüttiger, L. *et al.*, 2002; Sun, H. *et al.*, 2004). For further details, see Kaplan E. (2003).

1.16.2.2.6 Extraclassical receptive field

We have detailed information about the classical receptive field (as originally defined for visual neurons by H. K. Hartline) of neurons in the early visual system of primates (for a review, see Kaplan, E., 1991). However, it is known that the response to a visual stimulus can be influenced by stimuli that fall far beyond that classical receptive field (see, e.g., Krüger, J., 1977). This is true for RGCs, LGN cells, and V1 neurons. The neural basis of these nonlinear effects is not firmly established, beyond the suspicion that, in the retina, amacrine cells are involved in mediating them. These effects have been investigated more completely in the New World primate, the common marmoset, than in the Old World primates like macaques (Felisberti, F. and Derrington, A., 2001; Solomon, S. G. *et al.*, 2002; Webb, B. S. *et al.*, 2002). In marmoset the nonclassical receptive field effects are mostly suppressive, and are more pronounced in the magnocellular layers of the LGN than in either parvocellular or koniocellular layers. The greater sensitivity of magnocellular neurons to stimulation beyond the classical receptive field was reported also by Felisberti F. and Derrington A. (2001) and by Webb B. S. *et al.* (2002), and might be related to the greater abundance of inhibitory interneurons in the magnocellular layers, compared with the parvocellular layers (Hámori, J. *et al.*, 1983). These findings suggest that cortical neurons might inherit much of their nonclassical receptive field properties from their subcortical inputs (see also Bonin, V. *et al.*, 2005).

1.16.2.3 Summary: The Properties of the Three Neuronal Streams

Table 1 summarizes the state of our current knowledge of the anatomical and physiological properties of the three main neuronal streams of the early primate visual system. Clearly, there are gaps in this summary view, and some of these gaps and their implications are taken up in the next section. Nevertheless, the clustering of properties listed in Table 1 has led to the hypothesis that links each of the three major streams to some distinct perceptual functions (Table 2). In the next section, we examine the validity of this hypothesis.

Table 2 The representation of the outside world in mind and brain

The visual world	*The mind's eye*	*The brain*
	Luminance	M?
	Motion, flicker	M,K?
	Hyperacuity, vernier	M?
$f(x, y, t, I, \lambda)$	Size	P,K?
	Color	P,K?
	Orientation	P?
	Texture	P,K?
	Depth	P?
	…	–
	…	–

The function in the left column describes the spatiotemporal distribution of light across the retina. x, y are retinal coordinates, t is time, I is intensity, and λ is wavelength.

1.16.3 How Solid Is the Parallel Streams Hypothesis?

Having briefly summarized the properties of the three major neuronal streams in the primate visual system (Table 1), and the prevalent view, which postulates a close, one-to-one correspondence between these streams and certain visual functions, we now raise some questions about the validity of such a view. This discussion should be viewed as a critical evaluation of the quality of the evidence in favor of the parallel streams hypothesis, the philosophical and psychological motivation for accepting it, and the possibility that some other design might be at work in the brain.

We note that the validity of the prevalent view is not only of purely academic interest, because, in addition to stimulating and directing many investigations of the brain and influencing the interpretation of experimental results, it has also inspired numerous computational models and simulations (e.g., Takács, B. *et al*., 1994; van Essen, D. and Andreson, C., 1995), and had a strong influence on machine vision.

1.16.3.1 The World, the Mind, and the Brain: The Siren Lure of Parallel Functional Streams

In the physical world, only space and time need to be specified in the description of any visual object or process (it is usually helpful to add wavelength and intensity as well). Vision scientists, however, typically organize the various manifestations of the visual world into certain visual attributes, such as color, motion, size, orientation, and texture. The extraction of each of these attributes from the spatiotemporal light distribution across the photoreceptor mosaic requires some neural computation and filtering. Conceptually, these attributes, which originated in psychological research on visual perception, can be viewed as similar to quantities such as pressure or heat in physics, which serve as shorthand global descriptions of the state of multitudes of atoms or molecules. The distinction between the physical, primary properties (left column of Table 2), and the perceptual, secondary properties (middle column of Table 2), is like the one made by John Locke in his *Essay Concerning Human Understanding* (1690).

From a belief in such a perceptual organization (of the secondary properties) it is but a small tempting step to assume that the brain organizes visual information in a similar fashion, and this assumption naturally leads to a search inside the brain for the physical footprints of these visual attributes. Vision scientists thus look for the neural representations of color, orientation, size, and motion in the brain. This quest often takes the form of a search for the brain area or neuronal population that is devoted to the analysis of a particular visual attribute. The three parallel domains of the physical, perceptual, and neuronal worlds are depicted schematically in Table 2.

We should bear in mind, however, that any notion of a specific organization of physical quantities into perceptual qualities is merely a theory. The association of distinct, segregated neuronal streams or populations with specific functional roles is, likewise, a (optional and inessential) corollary of the theory. Even if the world were, indeed, represented in our mind's eye along the dimensions of color, size, motion, etc., this representation could, in principle, be distributed across the neuronal network that comprises the visual system, and not lumped into functionally specific anatomical clusters or compartments. In addition, the attributes need not be represented by labeled lines or populations, but rather by the coordinated dynamical activity or temporal discharge patterns of the network. In other words, the representation of physical quantities in the brain need not be based on anatomy (cell location and connectivity) alone.

Economy of wires. An important advantage of clustering according to function is that, if extensive information exchange among members of a cluster is required (another hypothesis), clustering will reduce the length of the neuronal processes that will need to be created and maintained at high costs. Keeping the wires short has thus emerged as an important, perhaps even crucial, selective pressure on nervous systems (Mead, C., 1989; Cherniak, C., 1992; 1994; Chklovskii, D., 2000). Note, however, that we do not know what computational imperatives require interaction among functionally similar neurons, although some suggestions have been made (e.g., Somers, D. C. *et al*., 1995; Xiao, Y. *et al*., 2003).

1.16.3.2 Challenges to the Parallel Streams Hypothesis

We shall now sketch several reasons why the association of some neuronal populations with specific perceptual functions should be viewed with some caution. The argument rests on anatomical, physiological, and psychophysical findings. This sketch is

certainly incomplete at this time, and much work will be required to fill in the gaps in it.

1.16.3.2.1 Criteria for the validity of the parallel streams hypothesis

For a strict correspondence between distinct (anatomical) parts of the visual system and visual functions to hold, certain minimal criteria must be met:

1. *Homogeneity.* Each neuronal population that performs a distinct function should be homogeneous.
2. *Stream Isolation.* There should be no communication among the various parts that perform distinct functions.
3. *Perceptual Independence.* The perceptual functions should be distinct and independent of each other.
4. *Compatibility.* The properties of the neurons in each part should match the perceptual function that it is supposed to perform.

Note again that the parts (neuronal populations or streams) need not be physically segregated – functionally different neuronal clusters could, in principle, be mixed together, although such mixing could incur a high metabolic cost, because it is likely to increase the length of the nerve fibers in the brain.

As we shall see below, these criteria are not quite met by either the M, P, and K neuronal streams or the perceptual functions they are supposed to support.

1.16.3.2.2 How homogeneous are the Three neuronal types?

At the root of the proposed correlation between neuronal types and perceptual functions is the assumption that each neuronal population is relatively homogenous, at least along some dimension (our first criterion), and that most such types cover the entire visual space, in order to support the proposed function everywhere in the visual field. However, a simple one-to-one correspondence between perceptual tasks and neuronal types is impossible, since there are more perceptual aspects to cover than could be accounted for by the three main types that we have been discussing. This suggests that each group might have to take care of more than one perceptual task, perhaps by some specialized subtypes. The discovery of the koniocellular population (Hendry, S. H. C. and Yoshioka, T., 1994) and the melanopsin-containing RGCs (Berson, D., 2003) are but two recent examples of neuronal populations that were overlooked and were unknown in early studies (see also Watanabe, M. and Rodieck, R. W., 1989; Peterson, B. and Dacey, D., 1998; 1999; 2000; Calkins, D. *et al.*, 2005). How many more neuronal groups are awaiting discovery is unknown, and a function–structure correlation should probably wait until most of the distinct neuronal types have been described.

1.16.3.2.3 Anatomy

Several types of anatomical arguments provide reasons to reevaluate the prevalent view:

1. *Are there enough cell types for all the perceptual tasks?* The three major types in Table 1 are defined by (and derive their names from) the location of their cell bodies in the various compartments of the primate LGN. However, the RGCs that excite them are not monolithic types. The M cells come in at least two flavors: those that receive some amacrine input and those that receive three times as much amacrine input (Calkins, D. *et al.*, 1995). Note, however, that it is not yet established whether the different amount of amacrine input is related to the different degree of nonlinearity observed among M cells (Kaplan, E. and Shapley, R., 1982; Demb, J. *et al.*, 1999). The ganglion cells that project to the parvocellular layers also comprise several anatomical subtypes, some with tiny (midgets) and other with very large dendritic trees (Watanabe, M. and Rodieck, R. W., 1989), suggesting that they participate in diverse visual functions. Less is known about the koniocellular population, but it is likely that the blue-yellow bistratified cells that project to the K layers are not the only ganglion cells to do so. Further research will probably discover other types. We should also allow for the possibility that specialized subnetworks, distinguished primarily by their connectivity patterns rather than by their cell type, support various aspects of some perceptual tasks. Anatomical data in support of such a possibility have been reported recently for the visual cortex (Yoshimura, Y. *et al.*, 2005).
2. *Crosstalk among streams.* A different sort of argument against the simple correlation between neuronal types and visual function comes from anatomical evidence for crosstalk among the various streams (Malach, R., 1994; Malach, R. *et al.*, 1994; Sincich, L. and Horton, J., 2002; 2003; 2005). These anatomical connections violate our second required criterion, and they are likely to contribute to crosstalk among perceptual functions (see below).
3. *Lesion studies.* Some of the evidence for the hypothesis of separate functional streams comes from lesion studies, either on humans (Ungerleider, L.

G. and Mishkin, M., 1982) or on monkeys (Eskin, T. A. and Merigan, W. H., 1986; Merigan, W. H. and Maunsell, J. R. H., 1990; Logothetis, N. K. *et al.*, 1990; Merigan, W. H. and Maunsell, J. R. H., 1993). The interpretation of lesion studies suffers from both technical and conceptual difficulties. It is always difficult to be certain that the lesion is complete and specific, especially in human studies. In addition, examining the behavior or physiology of a lesioned brain can tell us not what the lesioned area does, but rather what the system can (or cannot) do without the missing area. These considerations reduce the weight that can be given to lesion-based evidence.

More specific arguments, based on detailed analysis of anatomical connections, and especially the relationship between the V1 to V2 pattern and the cytochrome oxidase compartments of V2 can be found in Horton J. and Sincich L. (2004) and Sincich L. and Horton J. (2005).

1.16.3.2.4 Physiology

The physiological literature contains several findings that pose difficulties for the parallel streams view. Below are a few examples:

1. In many brain areas, and especially in V1, most neurons are tuned to several stimulus parameters, although the tuning sharpness varies. This indicates that the neuronal discharge is modulated typically by more than one stimulus parameter at any given moment.
2. The proportion of cells in any given cortical (visual) area that are devoted exclusively to the presumed function of the area vary greatly among studies (Felleman, D. J. and van Essen, D. C., 1987). For example, in area V4, which is supposed to be the color area of the 'what?' stream (Shipp, S. and Zeki, S., 1985), only $\sim$ 20% of the cells show color selectivity or color opponency, on par with other cortical areas (Schein, S. J. *et al.*, 1982; Felleman, D. J. and van Essen, D. C., 1987).
3. Interactions between motion and chromatic signals have been documented in neurons of the macaque middle temporal area (MT), a cortical area that is believed to be dominated by M input (Dobkins, K. R. and Albright, T. D., 1994), and in magnetoencephalograhic (MEG) recordings from humans (Amano, K. *et al.*, 2004).
4. M cells have varying degrees of nonlinear spatial summation (Kaplan, E. and Shapley, R., 1982), perhaps representing the amount of amacrine synaptic input that they receive.

1.16.3.2.5 Psychophysics

The notion of segregation of function implies that the sensitivity for a given visual attribute should not be affected by the values or modulation of other attributes. For instance, color should be independent of luminance, or of the orientation or motion of the stimulus. However, despite initial reports that suggested perceptual segregation (e.g., Livingstone, M. S. and Hubel, D. H., 1987), there are now numerous psychophysical results that document significant interactions among these attributes (see, e.g., Switkes, E. *et al.*, 1988; Krauskopf, J. and Farell, B., 1990; Stoner, G. R. *et al.*, 1990; Cavanagh, P. and Anstis, S., 1991; Kooi, F. L. and De Valois, K. K., 1992; Sinha, P., 1995; Gegenfurtner, K. and Hawken, M., 1996; Nijhawan, R., 1997; Yantis, S. and Nakama, T., 1998; Giese, M., 1999; Clifford, C. W. G. *et al.*, 2003; Shabana, N. *et al.*, 2003).

In a way analogous to our previous argument regarding the heterogeneity of anatomical or physiological groupings, there is also evidence that (at least some) perceptual functions are not monolithic, and that they, too, depend on the interplay among several mechanisms (Gegenfurtner, K. and Hawken, M., 1996; Stockman, A. and Plummer, D., 2005). Thus it is unlikely that any of these complex functions is performed by a single neuronal population.

It is not known currently whether the interactions mentioned above are due to direct interactions among the various neuronal types/streams, or to top-down influences of the massive descending pathways that are ubiquitous in the brain, but it is likely that both contribute to the mutual influences among both streams and perceptual functions.

1.16.3.3 The Need for Alternative Theories

Our discussion here suggests that the experimental results in the literature do not yet provide sufficient constraints for the construction of a coherent view of how the outside world is represented in our brains, and, in particular, how visual objects are recognized by the combination of their visual attributes. It is clear that more experiments alone will not help. What we need are bolder theoretical approaches, anchored in the anatomy and physiology of the brain, but with sufficient distance from current views to allow for a fresh perspective. It is likely that computational simulations of large neuronal ensembles and circuits, of the

types that are beginning to emerge (McLaughlin, D. *et al.*, 2000; Omurtag, A. *et al.*, 2000a; 2000b; Giles, J., 2005), will play an important role in this quest.

1.16.3.3.1 Labeled lines, multiplexing, dynamical networks, and the modularity of functional organization

It is important to keep in mind the essential distinction between the notions of labeled lines and the anatomical clustering of cells according to the properties of their receptive fields. The two are, in principle, independent of one another: cells that perform a particular function may, or may not, cluster together in a given compartment or brain region. The ideas discussed above do not require or imply any connection between these two concepts.

The notion of labeled lines with distinct visual functions implies that the neurons in any given line will be tuned to only one visual parameter: color, orientation, speed of motion, etc. That means that if we modulate a stimulus along one dimension (say, change only its color), some neuronal population will respond, while others will ignore the modulation. However, as we noted above, the literature paints a different picture: most cortical neurons are tuned to many parameters, which means that most neurons will respond to most types of modulations (albeit to different degrees), and their discharge will therefore be ambiguous, because different combinations of stimulus parameters will produce similar firing rates or patterns. Interpreting the discharge pattern of the population, therefore, requires a coordinated computation that involves many neurons.

A heavily interconnected dynamical network like the brain might implement several distinct strategies to accomplish the tasks it faces. It is reasonable to assume that these strategies will depend on the task at hand, and therefore it could be that different functions rely on different strategies: in some cases, labeled lines and clustering might be advantageous, while in others, temporal discharge patterns could be more important (for a review, see Victor, J. D., 1999). Clearly, combinations of these, and other mechanisms, could be employed as well.

In the visual system there is a crucial factor that must be taken into account: the topographical representation of the world in the brain (Tootell, R. B. H. *et al.*, 1982). The topographic map forces the creation of cortical regions (hypercolumns) that must contain all the neuronal machinery that is required to handle whatever a region of visual space might present.

This means that all the streams should exist in each piece of cortex that represents a point in space. This mapping suggests that local interactions are, indeed, important in the visual cortex, and are probably responsible for the modular nature of the functional architecture of the cortex.

1.16.4 Conclusions

I have presented the prevalent view of a close correspondence between the major anatomical streams and visual functions, and raised some questions regarding the validity of such a theory. It is too early to present a coherent alternative to the parallel streams hypothesis. It might well be that further research will uncover a sufficiently large number of neuronal streams, each with exquisite selectivity for one or a few visual parameters. Many of the issues raised here could be settled by such a development, and the final picture will be similar, in principle, to the current three-way view, but with many more streams.

It is also possible that a deeper understanding of the temporal patterns of neuronal discharge across neural populations will reveal new ways in which the brain represents, encodes, and transforms physical attributes or their combinations. This means that neurons could, in principle, process different sorts of information at different times, depending on the context and the stimulus (see, e.g., Basole, A. *et al.*, 2003). Obviously, we should not ignore the clear differences among the neuronal types (Table 1). Discovering how these differences are employed in support of visual function remains a challenge. The future, no doubt, will continue to be exciting and surprising.

Acknowledgment

The author was supported by NIH grant EY016371.

References

Amano, K., Nihida, S., and Takeda, T. 2004. MEG responses for color-motion asynchrony. J. Vis. 4(8), 554a.

Basole, A., White, L., and Fitzpatrick, D. 2003. Mapping multiple features in the population response of visual cortex. Nature 423, 986–990.

Benardete, E. A. and Kaplan, E. 1997. The receptive field of the primate p retinal ganglion cell. I. Linear dynamics. Vis. Neurosci. 14, 169–185.

Benardete, E. A. and Kaplan, E. 1999. Dynamics of primate p retinal ganglion cells: responses to chromatic and achromatic stimuli. J. Physiol. (Lond.) 519, 775–790.

Berson, D. 2003. Strange vision: ganglion cells as circadian photoreceptors. Trends Neurosci. 26, 314–320.

Blakemore, C. and Vital-Durand, F. 1986. Effects of visual deprivation on the development of the monkey's lateral geniculate nucleus. J. Physiol. (Lond.) 380, 493–511.

Blessing, E., Solomon, S., Hashemi-Nezhad, M., Morris, B., and Martin, P. 2004. Chromatic and spatial properties of parvocellular cells in the lateral geniculate nucleus of the marmoset (*Callithrix jacchus)*. J. Physiol. (Lond.) 557(1), 229–249.

Bonin, V., Mante, V., and Carandini, M. 2005. The suppressive field of neurons in lateral geniculate nucleus. J. Neurosci. 25(47), 10844–10856.

Boycott, B. B. and Wässle, H. 1991. Morphological classification of bipolar cells of the primate retina. Eur. J. Neurosci. 3, 1069–1088.

Boycott, B. B., Hopkins, J. M., and Sperling, H. G. 1987. Cone connections of the horizontal cells of the rhesus monkeys retina. Proc. R. Soc. Lond. B 229, 345–379.

Calkins, D. J. and Sterling, P. 1996. Absence of spectrally specific lateral inputs to midget ganglion cells in primate retina. Nature 381(6583), 613–615.

Calkins, D., Sappington, R., and Hendry, S. 2005. Morphological identification of ganglion cells expressing the alpha subunit of type ii calmodulin-dependent protein kinase in the macaque retina. J. Comp. Neurol. (2), 194–209.

Calkins, D., Schein, S., Tsukamoto, Y., and Sterling, P. 1995. Ganglion Cell Circuits in Primate Fovea. In Color Deficiencies (*ed*. B. Drum), Vol. 12, pp. 267–274. Kluwer Publishing.

Callaway, E. M. 2005. Structure and function of parallel pathways in the primate early visual system. J. Physiol. 566, 13–19.

Cavanagh, P. and Anstis, S. 1991. The contribution of color to motion in normal and color-deficient observers. Vision Res. 31, 2109–2148.

Cherniak, C. 1992. Local optimization of neuron arbors. Biol. Cybern. 66, 503–510.

Cherniak, C. 1994. Component placement optimization in the brain. J. Neurosci. 14, 2418–2427.

Chklovskii, D. 2000. Optimal sizes of dendritic and axonal arbors in a topographic projection. J. Neurophysiol. 83, 2113–2119.

Clifford, C. W. G., Spehar, B., Solomon, S. G., Martin, P. R., and Zaidi, Q. 2003. Interactions between color and luminance in the perception of orientation. J. Vis. 3(2), 106–115.

Croner, L. J. and Kaplan, E. 1995. Receptive fields of p and m ganglion cells across the primate retina. Vision Res. 35, 7–24.

Crook, J. M., Lange-Malecki, B., Lee, B. B., and Valberg, A. 1988. Visual resolution of macaque retinal ganglion cells. J. Physiol. (Lond.) 396, 205–224.

Dacey, D. M. and Lee, B. B. 1994. The 'blue-on' opponent pathway in primate retina originates from a distinct bistratified ganglion cell type. Nature 367, 731–735.

Dacey, D., Packer, O., Diller, L., Brainard, D., Peterson, B., and Lee, B. 2000. Center surround receptive field structure of cone bipolar cells in primate retina. Vision Res. 40(14), 1801–1811.

De Monasterio, F. M. and Gouras, P. 1975. Functional properties of ganglion cells of the rhesus monkey retina. J. Physiol. (Lond.) 251, 167–195.

Demb, J., Haarsma, L., Freed, M., and Sterling, P. 1999. Functional circuitry of the retinal ganglion cell's nonlinear receptive field. J. Neurosci. 19, 9756–9767.

Derrington, A. M., Krauskopf, J., and Lennie, P. 1984. Chromatic mechanisms in lateral geniculate nucleus of macaque. J. Physiol. (Lond.), 357, 241–265.

Dobkins, K. R. and Albright, T. D. 1994. What happens if it changes color when it moves?: the nature of chromatic input to macaque visual area MT. J. Neurosci. 14, 4854–4870.

Dreher, B., Fukada, Y., and Rodieck, R. W. 1976. Identification, classification and anatomical segregation of cells with x-like and y-like properties in the lateral geniculate nucleus of old-world primates. J. Physiol. (Lond.) 258, 433–452.

Enroth-Cugell, C. and Robson, J. G. 1966. The contrast sensitivity of retinal ganglion cells of the cat. J. Physiol. (Lond.) 187, 517–552.

Enroth-Cugell, C. and Shapley, R. M. 1973a. Adaptation and dynamics of cat retinal ganglion cells. J. Physiol. (Lond.) 233, 271–309.

Enroth-Cugell, C. and Shapley, R. M. 1973b. Flux, not retinal illumination, is what cat retinal ganglion cells really care about. J. Physiol. (Lond.) 233, 311–326.

Eskin, T. A. and Merigan, W. H. 1986. Selective acrylamide-induced degeneration of color opponent ganglion cells in macaques. Brain Res. 378, 379–384.

van Essen, D. and Andreson, C. 1995. Information Processing Strategies in Primate Retina and Visual Cortex. In: Introduction to Neuronal and Electronic Networks (*eds*. S. Zornetzer, T. McKenna, C. Lau, and J. Davis), pp. 45–76. Academic Press.

Felisberti, F. and Derrington, A. 2001. Long-range interactions in the lateral geniculate nucleus of the new-world monkey, *Callithrix jacchus*. Vis. Neurosci. 18, 209–218.

Felleman, D. J. and van Essen, D. C. 1987. Receptive field properties of neurons in area V3 of macaque monkey extrastriate cortex. J. Neurophysiol. 57, 889–920.

Felleman, D. J. and van Essen, D. C. 1991. Distributed hierarchical processing in the primate cerebral cortex. Cereb. Cortex 1, 1–47.

Gegenfurtner, K. and Hawken, M. 1996. Perceived speed of luminance, chromatic and non-Fourier stimuli: influence of contrast and temporal frequency. Vision Res. 36, 1281–1290.

Giese, M. 1999. Evidence for multi-functional interactions in early visual motion processing. Trends Neurosci. 22(7), 287–290.

Giles, J. 2005. Blue brain boots up to mixed response. Nature 435, 720–721.

Goodchild, A., Ghosh, K., and Martin, P. 1996. Comparison of photoreceptor spatial density and ganglion cell morphology in the retina of human, macaque monkey, cat, and the marmoset *Callithrix jacchus*. J. Comp. Neurol. 366, 55–75.

Gouras, P. 1968. Identification of cone mechanisms in monkey ganglion cells. J. Physiol. (Lond.) 199, 533–547.

Hámori, J., Pasik, P., and Pasik, T. 1983. Differential frequency of p-cells and i-cells in magno-cellular and parvocellular laminae of monkey lateral geniculate nucleus. An ultrastructural study. Exp. Brain Res. 52, 57–66.

Hartline, H. K. 1940. The effects of spatial summation in the retina on the excitation of the fibers of the optic nerve. Am. J. Physiol. 130, 700–711.

Hendry, S. H. C. and Reid, C. R. 2000. The koniocellular pathway in primate vision. Annu. Rev. Neurosci. 23, 127–153.

Hendry, S. H. C. and Yoshioka, T. 1994. A neurochemically distinct third channel in the macaque dorsal lateral geniculate nucleus. Science 264, 575–577.

Horton, J. and Sincich, L. 2004. A New Foundation for the Visual Cortical Hierarchy, Ch. 17. pp. 233–243. MIY Press.

Kaplan, E. 1991. The Receptive Field Structure of Retinal Ganglion Cells in Cat and Monkey. In: The Neural Basis of Visual Function (*ed*. A. Leventhal), Vol. 4, pp. 10–40. Macmillan.

Kaplan, E. 2003. The M, P and K Pathways in the Primate Visual System. In: The Visual Neurosciences (*eds*. L. Chalupa and J. Werner), Vol. I, 481–494. MIT press.

Peterson, B. B. and Dacey, D. M. 1998. Morphology of human retinal ganglion cells with intraretinal axon collaterals. Vis. Neurosci. 15, 377–387.

Peterson, B. B. and Dacey, D. M. 1999. Morphology of wide-field, monostratified ganglion cells of the human retina. Vis. Neurosci. 16, 107–120.

Peterson, B. B. and Dacey, D. M. 2000. Morphology of wide-field bistratified and diffuse human retinal ganglion cells. Vis. Neurosci. 17, 567–578.

Kaplan, E. and Shapley, R. 1982. What controls information processing in the LGN? Soc. Neurosci. Abstr. 8(1), 405.

Kaplan, E. and Shapley, R. M. 1986. The primate retina contains two types of ganglion cells, with high and low contrast sensitivity. Proc. Natl. Acad. Sci. U. S. A. 83, 2755–2757.

Kaplan, E. and Shapley, R. M. 1989. Illumination of the receptive field surround controls the contrast gain of macaque p retinal ganglion cells. Soc. Neurosci. 15, 45–76.

Kaplan, E., Barlow, R. B., Renninger, G., and Purpura, K. 1990. Circadian rhythms in *Limulus* photoreceptors. II. Quantum bumps. J. Gen. Physiol. 96, 665–685.

Kooi, F. L. and De Valois, K. K. 1992. The role of color in the motion system. Vision Res. 32, 657–668.

Krauskopf, J. and Farell, B. 1990. Influence of colour on the perception of coherent motion. Nature 348, 328–331.

Krüger, J. 1977. Stimulus dependent colour specificity of monkey lateral geniculate neurones. Exp. Brain Res. 30, 297–311.

Lee, B. B. 1996. Receptive field structure in the primate retina. Vision Res. 36, 631–644.

Lee, B. B., Martin, P. R., and Valberg, A. 1989. Sensitivity of macaque retinal ganglion cells to chromatic and luminance flicker. J. Physiol. (Lond.) 414, 223–243.

Lennie, P., Haake, P., and Williams, D. 1991. The Design of Chromatically Opponent Receptive Fields. In: Computational Models of Visual Processing (*ed*. J. Movshon), pp. 71–82. MIT Press.

Leventhal, A. G., Rodieck, R. W., and Dreher, B. 1981. Retinal ganglion cell classes in the old world monkey: morphology and central projections. Science 213, 1139–1142.

Levitt, J. B., Schumer, R., Sherman, S. M., Spear, P. D., and Movshon, J. A. 2001. Visual properties of neurons in the LGN of normally reared and visually deprived macaque monkeys. J. Neurophysiol. 85, 2111–2129.

Livingstone, M. and Hubel, D. 1988. Segregation of form, color, movement, and depth: anatomy, physiology, and perception. Science 240, 740–749.

Livingstone, M. S. and Hubel, D. H. 1984a. Anatomy and physiology of a color system in the primate visual cortex. J. Neurosci. 4, 309–356.

Livingstone, M. S. and Hubel, D. H. 1984b. Specificity of intrinsic connections in primate primary visual cortex. J. Neurosci. 4, 2830–2835.

Livingstone, M. S. and Hubel, D. H. 1987. Psychophysical evidence for separate channels for the perception of form, color, movement and depth. J. Neurosci. 7, 3416–3468.

Logothetis, N. K., Schiller, P. H., Charles, E. R., and Hurlbert, A. C. 1990. Perceptual deficits and the activity of the color-opponent and broad-band pathways at isoluminance. Science 247, 214–217.

Malach, R. 1994. Cortical columns as devices for maximizing neuronal diversity. Trends Neurosci. 17(3), 101–104.

Malach, R., Tootell, R., and Malonek, D. 1994. Relationship between orientation domains, cytochrome oxidase stripes and intrinsic horizontal connections in squirrel monkey area V2. Cereb. Cortex 4, 151–165.

McLaughlin, D., Shapley, R., Shelley, M., and Wielaard, J. 2000. Models of neuronal dynamics in the visual cortex. Proc. Nat. Acad. Sci. U. S. A. 97, 8087–8092.

Mead, C. 1989. Analog VLSI and Neural Systems. Addison-Wesley.

Merigan, W. H. and Maunsell, J. R. H. 1990. Macaque vision after magnocellular lateral geniculate lesions. Vis. Neurosci. 5, 347–352.

Merigan, W. H. and Maunsell, J. H. R. 1993. How parallel are the primate visual pathways? Ann. Rev. Neurosci. 16, 369–402.

Nijhawan, R. 1997. Visual decomposition of colour through motion extrapolation. Nature 386, 66–69.

Omurtag, A., Kaplan, E., Knight, B. W., and Sirovich, L. 2000a. A population approach to cortical dynamics with an application to orientation tuning. Network: Comput. Neural Syst. 11, 1–14.

Omurtag, A., Knight, B. W., and Sirovich, L. 2000b. On the simulation of large populations of neurons. J. Comp. Neurosci. 8, 51–63.

Paulus, W. and Kröger-Paulus, A. 1983. A new concept of retinal colour coding. Vision Res. 23, 529–540.

Perry, V. H. and Cowey, A. 1984. Retinal ganglion cells that project to the superior colliculus and pretectum in the macaque monkey. Neuroscience 12, 1125–1137.

Polyak, S. L. 1941. The Retina. The University of Chicago Press.

Reid, R. C. and Shapley, R. M. 1992. Spatial structure of cone inputs to receptive fields in primate lateral geniculate nucleus. Nature 356, 716–718.

Rodieck, R. W. and Brening, R. K. 1983. Retinal ganglion cells: properties, types, genera, pathways and trans-species comparisons. Brain Behav. Evol. 23, 121–164.

Rodieck, R. W. and Watanabe, M. 1993. Survey of the morphology of macaque retinal ganglion cells that project to the pretectum, superior colliculus, and parvicellular laminae of the lateral geniculate nucleus. J. Comp. Neurol. 338, 289–303.

Rudvin, I., Valberg, A., and Kilavik, B. E. 2000. Visual evoked potentials and magnocellular and parvocellular segregation. Vis. Neurosci. 17, 579–590.

Rüttiger, L. and Lee, B. 2000. Chromatic and luminance contributions to a hyperacuity task. Vision Res., 40, 817–832.

Rüttiger, L., Lee, B., and Sun, H. 2002. Transient cells can be neurometrically sustained; the positional accuracy of retinal signals to moving targets. J. Vis. 2, 232–242.

Schein, S. J., Marrocco, R. T., and De Monasterio, F. M. 1982. Is there a high concentration of color-selective cells in area V4 of monkey visual cortex? J. Neurophysiol. 47, 193–213.

Shabana, N., Cornilleau Peres, V., Carkeet, A., and Chew, P. 2003. Motion perception in glaucoma patients: a review. Surv. Ophthalmol. 48(1), 92–106.

Sherman, S. M., Wilson, J. R., Kaas, J. H., and Webb, S. V. 1976. X- and y-cells in the dorsal lateral geniculate nucleus of the owl monkey (*Aotus trivirgatus*). Science 192, 475–477.

Shipp, S. and Zeki, S. 1985. Segregation of pathways leading from area V2 to areas V4 and V5 of macaque monkey visual cortex. Nature 315, 322–325.

Silveira, L. C. L. and Perry, V. 1991. The topography of magnocellular projecting ganglion cells (m-ganglion cells) in the primate retina. Neuroscience 40(1), 217–237.

Sincich, L. and Horton, J. 2002. Divided by cytochrome oxidase: a map of the projections from V1 to V2 in macaques. Science 295(5560), 1734–1737.

Sincich, L. and Horton, J. 2003. Independent projection streams from macaque striate cortex to the second visual area and middle temporal area. J. Neurosci. 23(13), 5684–5692.

Sincich, L. and Horton, J. 2005. The circuitry of v1 and v2: integration of color, form, and motion. Annu. Rev. Neurosci. 28, 303–326.

Sinha, P. 1995. Reciprocal Interactions Between Motion and Form Perception. AI Memo 1506, MIT.

Solomon, S. G., White, A. J. R., and Martin, P. R. 2002. Extraclassical receptive field properties of parvocellular, magnocellular, and koniocellular cells in the primate lateral geniculate nucleus. J. Neurosci. 22(1), 330–349.

Somers, D. C., Nelson, S. B., and Sur, M. 1995. An emergent model of orientation selectivity in cat visual cortex simple cells. J. Neurosci. 15, 5448–5465.

Stockman, A. and Plummer, D. 2005. Long-wavelength adaptation reveals slow, spectrally opponent inputs to the human luminance pathway. J. Vis. 5(9), 702–716.

Stone, J. 1983. Parallel Processing in the Visual System. Plenum.

Stoner, G. R., Albright, T. D., and Ramachandran, V. S. 1990. Transparency and coherence in human motion perception. Nature 344, 153–155.

Sun, H., Rüttiger, L., and Lee, B. 2004. The spatiotemporal precision of ganglion cell signals: a comparison of physiological and psychophysical performance with moving gratings. Vision Res. 44(1), 19–33.

Switkes, E., Bradley, A., and De Valois, K. K. 1988. Contrast dependence and mechanisms of masking interactions among chromatic and luminance gratings. J. Opt. Soc. Am A 5, 1149–1162.

Takács, B., Wegman, E., and Wechsler, H. 1994. Parallel Simulation of an Active Vision Model. Intel Supercomputer Users Group (ISUG), http://citeseer.ist.psu.edu/update/9175.

Tootell, R. B. H., Silverman, M. S., Switkes, E., and Valois, R. L. D. 1982. Deoxyglucose analysis of retinotopic organization in primate striate cortex. Science 218, 902–904.

Troy, J. and Shou, T. 2002. The receptive fields of cat retinal ganglion cells in physiological and pathological states: where we are after half a century of research. Prog. Ret. Eye Res. 21, 263–302.

Ungerleider, L. G. and Mishkin, M. 1982. Two Cortical Visual Systems. In: Analysis of Visual Behavior (*eds*. D. J. Ingle, M. A. Goodale, and R. J. W. Mansfield), pp. 549–586. MIT Press.

Victor, J. D. 1999. Temporal aspects of neural coding in the retina and lateral geniculate: a review. Exp. Brain Res. 57, 196–200.

Watanabe, M. and Rodieck, R. W. 1989. Parasol and midget cells of the primate retina. J. Comp. Neurol. 299, 434–454.

Webb, B. S., Tinsley, C. J., Barraclough, N. E., Easton, A., Parker, A., and Derrington, A. M. 2002. Feedback from V1 and inhibition from beyond the classical receptive field modulates the responses of neurons in the primate lateral geniculate nucleus. Vis. Neurosci. 19, 583–592.

Wiesel, T. N. and Hubel, D. H. 1966. Spatial and chromatic interactions in the lateral geniculate body of the rhesus monkey. J. Neurophysiol. 29, 1115–1156.

Xiao, Y., Wang, Y., and Felleman, D. J. 2003. A spatially organized representation of color in macaque area V2. Nature 421, 535–539.

Xu, X., Ichida, M. J., Allison, J. D., Boyd, J. D., Bonds, A. B., and Casagrande, V. A. 2001. A comparison of koniocellular, magnocellular and parvocellular receptive field properties in the lateral geniculate nucleus of the owl monkey (*Aotus trivirgatus*). J. Physiol. (Lond.) 531, 203–218.

Yabuta, N. H. and Callaway, E. M. 1998a. Cytochrome oxidase blobs and intrinsic horizontal connections of layer 2/3 pyramidal neurons in primate V1. Vis. Neurosci. 15, 1007–1027.

Yabuta, N. H. and Callaway, E. M. 1998b. Functional streams and local connections of layer 4C neurons in primary visual cortex of the macaque monkey. J. Neurosci. 18, 9489–9499.

Yamada, E. S., Marshak, D. W., Silveira, L. C. L., and Casagrande, V. A. 1998. Morphology of P and M retinal ganglion cells of the bush baby. Vision Res. 38(21), 3345–3352.

Yantis, S. and Nakama, T. 1998. Visual interactions in the path of apparent motion. Nature Neurosci. 1, 508–512.

Yoshimura, Y., Dantzker, J., and Callaway, E. 2005. Excitatory cortical neurons form fine-scale functional networks. Nature 433, 868–873.

Zeki, S. 1993. A Vision of the Brain. Blackwell Scientific Publications.

1.17 Neural Mechanisms of Natural Scene Perception

J L Gallant, Helen Wills Neuroscience Institute, Berkeley, CA, USA

R J Prenger, University of California, Berkeley, CA, USA

© 2008 Elsevier Inc. All rights reserved.

1.17.1	What Is a Natural Scene?	384
1.17.2	Luminance and Contrast	384
1.17.3	The Amplitude Spectrum and Scale Invariance	385
1.17.4	Optimal Basis Sets for Representing Natural Images	385
1.17.5	More Complex Spatial Properties	386
1.17.6	Temporal Statistics of Natural Images	388
References		389

Glossary

first-order statistics Mean luminance or contrast.

Gabor wavelet An oriented filter that is bandpass in both space and spatial frequency, similar in profile to a Gaussian-modulated sine wave.

higher-order statistics Statistical properties beyond second order. These are described by the Fourier phase spectrum rather than the amplitude spectrum.

information exploitation A theory that proposes the visual system should exploit signals that reliably indicate which structural elements are present in a scene.

natural image An image whose statistical properties (i.e., the distributions and joint distributions of pixel luminances) are representative of those encountered during natural vision.

natural scene See natural image.

redundancy reduction A theory that proposes the visual system should tend to ignore or reduce the influence of noninformative or redundant signals in the environment.

second-order statistics The Fourier amplitude or power spectrum.

sparse representation A set of filters designed so that a relatively small number of them is required to encode any specific natural image.

The ultimate purpose of the visual system is to create a useful internal representation of the complex, cluttered scenes that occur in the natural world. To solve this difficult computational problem humans and other primates have evolved a sophisticated visual system that consists of numerous distinct areas, embedded within a complex hierarchical and parallel network (Van Essen, D. C. and Gallant, J. L., 1994; Tootell, R. B. H. *et al.*, 2003). At the level of the peripheral photoreceptors natural images are represented as discretely sampled spatial images that vary continuously in time. Although these retinal images contain a vast amount of information about the external scene, most of this information is only implicit and cannot be extracted directly from the samples. At each successive stage of visual processing, each visual area performs a transformation that renders explicit some of the information represented only implicitly in the retinal image.

It has been argued that a maximally efficient visual system (i.e., one that minimizes computational load) should follow two general principles (Attneave, F., 1954; Laughlin, S., 1981; Atick, J. J. *et al.*, 1992; van Hateren, J. H., 1992; Field, D. J., 1994; Rieke, F. *et al.*, 1995; Zetzsche, C. and Krieger, G., 1999; Barlow, H. B., 2001). First, the visual system should tend to ignore or reduce the influence of noninformative or redundant signals in the environment (redundancy reduction). Second, the system should exploit signals that reliably indicate which structural elements are present in a scene (information exploitation). Given the hierarchical organization of the visual system, it

seems likely that peripheral stages focus most on relatively simple statistical stimulus properties, and more central stages focus on higher-order statistical regularities that are more difficult to extract from natural images. Even so, it is likely that each processing stage probably involves both redundancy reduction and signal exploitation.

The complimentary principles of redundancy reduction and signal exploitation suggest a potentially valuable and interesting strategy for investigating the visual system based on explicit consideration of the statistical structure of natural scenes (Field, D. J., 1993; 1994; Simoncelli, E. P. and Olshausen, B. A., 2001). Statistical regularities in natural images can be used as the basis for computational theories of optimal visual processing (Foldiak, P., 1990; Atick, J. J. *et al.*, 1992; Olshausen, B. A. and Field, D. J., 1996; Bell, A. J. and Sejnowski, T. J., 1997; van Hateren, J. H. and van der Schaaf, A., 1998; Simoncelli, E. P. and Schwartz, O., 1998); they can be used to test and interpret various theories of human vision (Dan, Y. *et al.*, 1996; Vinje, W. E. and Gallant, J. L., 2000; Sharpee, T. O. *et al.*, 2006); and they can be used as a powerful tool for investigating aspects of visual function about which little is currently known (David, S. V. *et al.*, 2006).

1.17.1 What Is a Natural Scene?

Researchers often distinguish between natural images and other stimuli that are not natural (e.g., sinusoidal gratings, white noise, etc.; Carandini, M. *et al.*, 2005; Rust, N. C. and Movshon, J. A., 2005). However, these two types of stimuli actually represent points on a continuum rather than discrete classes. Any image is natural to the extent that its statistical properties (i.e., the distributions and joint distributions of pixel luminances) are generated by the scenes we commonly encounter during natural vision (Field, D. J., 1987). According to this criterion some images, such as forests or meadows, are very natural; others, such as gratings or white noise, are relatively unnatural; still others, such as a cityscape or an interior scene, likely fall between these two extremes. Note that even the most unnatural scenes have some probability of appearing in the natural world. For example, one might acquire an image of a sinusoidal grating or white noise pattern while taking close-up photos of natural textured surfaces.

An understanding of the statistical properties of natural images and how the visual system exploits them provides insight into the function of known neural mechanisms and we can potentially predict yet undiscovered mechanisms (Field, D. J., 1987; Zhu, S. C. and Mumford, D., 1997; Simoncelli, E. P. and Olshausen, B. A., 2001). In the remainder of this chapter we review many of the known statistical properties of natural images: first-order spatial statistics of luminance and contrast, second-order spatial amplitude spectrum, higher-order statistical properties (insofar as they are known), and temporal statistics. For each property we review and discuss the various ways in which the visual system is optimized to reduce redundancy and exploit these statistical regularities.

1.17.2 Luminance and Contrast

The first-order spatial and temporal statistics of natural images describe the mean luminance values found across a large distribution of such images. The luminance of natural images can vary over several orders of magnitude, even within a single scene (van Hateren, J. H., 1993; Frazor, R. A. and Geisler, W. S., 2006). However, absolute luminance information is not a particularly useful measure for identifying specific image content. In accordance with the principle of redundancy reduction, many animals have evolved specialized neural machinery that compresses the luminance information in natural images (Fain, G. L. *et al.*, 2001). Nonlinear luminance gain control mechanisms are found in the photoreceptors of many insects (Laughlin, S. B., 1994; van Hateren, J. H., 1997), and in the mammalian retina (Fain, G. L. *et al.*, 2001) and lateral geniculate nucleus (LGN; Mante, V. *et al.*, 2005). Regardless of the species, these mechanisms convert the wide dynamic range of natural luminance signals into a more coarsely coded signal that still preserves critical information about relative luminance.

The local contrast in any natural image can also vary over a wide range. Local contrast is correlated with important structural features of natural scenes, such as edges, that are useful for scene segmentation (Marr, D. and Hildreth, E., 1980) and for guiding eye movements and attention (Reinagel, P. and Zador, A. M., 1999; Einhauser, W. *et al.*, 2006). However, local contrast gives little information about the specific features that are present in a scene. Therefore many animals have evolved a wide variety of nonlinear contrast gain control mechanisms that operate at both peripheral (Shapley, R. and Victor, J. D., 1979) and more central (Albrecht, D. G.

et al., 1984; Lennie, P. and Movshon, J. A., 2005) stages of visual processing. These mechanisms normalize contrast variation in order to minimize the computational resources necessary to represent and process natural visual images, and enhance the effective contrast of important features in a scene.

Although contrast is partially a function of luminance, in natural images these quantities are statistically independent (Mante, V. *et al.*, 2005; Frazor, R. A. and Geisler, W. S., 2006). The independence of luminance and contrast in natural images probably reflects the presence of specific structural elements whose higher-order statistics influence local contrast (Frazor, R. A. and Geisler, W. S., 2006). In order to remove redundant information about luminance and contrast while preserving potentially important information about the relationship between the two, the luminance and contrast gain control mechanisms in the mammalian visual system work independently (Mante, V. *et al.*, 2005).

The examples given here illustrate how visual systems exploit useful information in the simple first-order statistics of natural images while removing less informative and redundant information. Much of the information about the absolute magnitude of luminance and contrast is removed, while information about the variation of these quantities across each image is retained.

1.17.3 The Amplitude Spectrum and Scale Invariance

The second-order spatial statistics of natural images describe correlations between pairs of pixels. These relationships are summarized most conveniently by the amplitude spectrum. The amplitude spectrum of natural images has a characteristic 1/f profile (where f is spatial frequency; Field, D. J., 1987); low spatial frequencies tend to have the most power and power decreases at higher frequencies. Although natural images have a 1/f amplitude spectrum on average, the spectrum of any specific image may deviate somewhat. The 1/f profile reflects the fact that nearby pixels in a natural image tend to have similar luminance, but pixels far from one another tend to be less similar. This property is believed to reflect a fundamental scale invariance property of natural scenes (Field, D. J., 1994; Ruderman, D. L., 1997; Balboa, R. M. *et al.*, 2001; Lee, A. B. *et al.*, 2001).

Like luminance and contrast, the 1/f amplitude spectrum is a general property of natural images and gives little information about the specific content of a scene. In fact, theoretical studies suggest that a maximally efficient visual system should simply whiten the amplitude spectrum to remove the 1/f bias (Barlow, H. B., 1961; Atick, J. J., 1992; van Hateren, J. H., 1993; Dong, D. W. and Atick, J. J., 1995b). Whitening mechanisms have been found in both insects (Srinivasan, M. V. *et al.*, 1982) and mammals (Dan, Y. *et al.*, 1996). Psychophysical studies have shown that humans are remarkably insensitive to the power spectrum of natural images (Piotrowski, L. N. and Campbell, F. W., 1982; Tadmor, Y. and Tolhurst, D. J., 1993; Thomson, M. G. A. and Foster, D. H., 1997), suggesting that the human visual system also uses whitening to maximize information transmission during natural vision.

1.17.4 Optimal Basis Sets for Representing Natural Images

Several studies have sought to identify the optimal set of primitives (or basis functions) that could be used to represent natural scenes. The simplest primitives would be a set of linear filters that optimally describe any natural image according to some specific statistical criterion. In some of the earliest work on natural image statistics, Field D. J. (1987; 1994) argued that a sparseness criterion would provide an optimized representation of natural scenes. A sparse representation is one that contains a large number of filters selected such that a relatively small proportion of them is required to encode any specific scene. Thus, although a sparse representation requires many neurons, it minimizes overall metabolic costs (Laughlin, S. B. *et al.*, 1998). Others have argued that the best representation for natural scenes consists of linear filters whose responses to natural images are statistically independent (called independent components; Bell, A. J. and Sejnowski, T. J., 1997). However, the sparseness and independence criteria are closely related, and both produce filters that are spatially localized functions tuned to a limited range of orientations and spatial frequencies (Bell, A. J. and Sejnowski, T. J., 1997; Olshausen, B. A. and Field, D. J., 1997; Hyvarinen, A. and Hoyer, P., 2000; Willmore, B. *et al.*, 2000). These filters are known as Gabor wavelets (Daugman, J. G., 1988), and any natural image can be constructed from some combination of these Gabor wavelets.

If one goal of visual processing is to generate a sparse representation of natural scenes then we

would expect the early visual system to embody Gabor wavelets. Indeed, the Gabor wavelet model was used to describe receptive field organization in primary visual cortex even before the connection between Gabor wavelets and natural images was understood (Daugman, J., 1980; Daugman, J. G., 1988). Several studies have now demonstrated that the Gabor wavelet model provides a good description of how simple cells in primary visual cortex encode natural scenes (Smyth, D. *et al.*, 2003; David, S. V. *et al.*, 2004; Prenger, R. *et al.*, 2004; Felsen, G. *et al.*, 2005; Touryan, J. *et al.*, 2005).

1.17.5 More Complex Spatial Properties

Natural scenes possess a wealth of higher-order statistical information beyond luminance, contrast, and the amplitude spectrum (Field, D. J., 1987): by one estimate, the distribution of natural images has almost twice the structural regularity of a distribution of noise with the same power spectrum (Chandler, D. M. and Field, D. J., 2007). These higher-order statistical properties are captured in the phase spectrum, which describes the alignment of spatial frequencies within an image. The image structure described by the phase spectrum is critical for successful interpretation of natural scenes (Piotrowski, L. N. and Campbell, F. W., 1982; Tadmor, Y. and Tolhurst, D. J., 1993; Thomson, M. G. A. and Foster, D. H., 1997).

Several lines of evidence indicate that human perception and interpretation of natural scenes depends primarily on their higher-order statistics. An image that has a $1/f$ amplitude spectrum but no higher-order structure looks like a picture of wispy clouds and does not appear to contain any solid surfaces (see Figure 1). When a new image is constructed by combining the power spectrum of one image and the phase spectrum of another, perception is dominated by the phase spectrum, not the power spectrum (see Figure 1; Piotrowski, L. N. and Campbell, F. W., 1982; Tadmor, Y. and Tolhurst, D. J., 1993; Thomson, M. G. A. and Foster, D. H., 1997). Human contour detection and grouping performance have also been shown to reflect the co-occurrence statistics of contour elements found in natural scenes (Geisler, W. S. *et al.*, 2001), and these higher-order statistics are also critically dependent on information contained within the phase spectrum.

Although higher-order structure of natural scenes is critical for accurate perception of the world, relatively little is currently known about the neural mechanisms that are responsible for processing and interpreting this information. However, there is strong evidence that such mechanisms exist even in primary visual cortex. The diversity of neuronal responses observed in V1 during stimulation with natural images is much larger than would be expected if V1 neurons could be modeled perfectly as Gabor wavelets (Weliky, M. *et al.*, 2003; Felsen, G. *et al.*, 2005; Yen, S. C. *et al.*, 2007), and the Gabor wavelet model of V1 only predicts about half of the potentially explainable variance in natural visual responses (David, S. V. and Gallant, J. L., 2005).

One neural mechanism that is likely to play an important role in encoding complex structure in natural scenes is the nonclassical surround (nCRF; Wegmann, B. and Zetzsche, C., 1990; Vinje, W. E. and Gallant, J. L., 2000; 2002; Karklin, Y. and Lewicki, M. S., 2003; 2005). The nCRF is a region surrounding the classical receptive field (CRF) of each visual cortical neuron. Although stimuli falling in the nCRF do not elicit spikes directly, they modulate responses to stimuli occurring within the CRF. The predominant function of the nCRF is divisive normalization (Heeger, D. J. *et al.*, 1996), which probably reduces the influence of weak correlations amongst filters in the Gabor wavelet representation of natural scenes (Wegmann, B. and Zetzsche, C., 1990; Krieger, G. *et al.*, 1997; Simoncelli, E. P. and Schwartz, O., 1998; Thomson, M. G. A., 1999; Zetzsche, C. and Krieger, G., 1999; Schwartz, O. and Simoncelli, E. P., 2001). However, the nCRF also contains secondary mechanisms that likely exploit specific correlations between Gabor wavelets that reflect specific structural elements in natural scenes, such as edges and corners (Wegmann, B. and Zetzsche, C., 1990; Vinje, W. E. and Gallant, J. L., 2000; Schwartz, O. and Simoncelli, E. P., 2001; Zetzsche, C. and Rohrbein, F., 2001).

What about still more complex aspects of natural scenes? The primate visual system consists of a complex hierarchical network of numerous distinct visual areas (Van Essen, D. C. and Gallant, J. L., 1994; Tootell, R. B. H. *et al.*, 2003), and it is likely that these areas exploit more complex statistical regularities. Unfortunately little is currently known about the statistical structure of natural images beyond second order (Krieger, G. *et al.*, 1997; Thomson, M. G. A., 1999), so it is difficult to test this idea directly. The few studies that have investigated neural coding

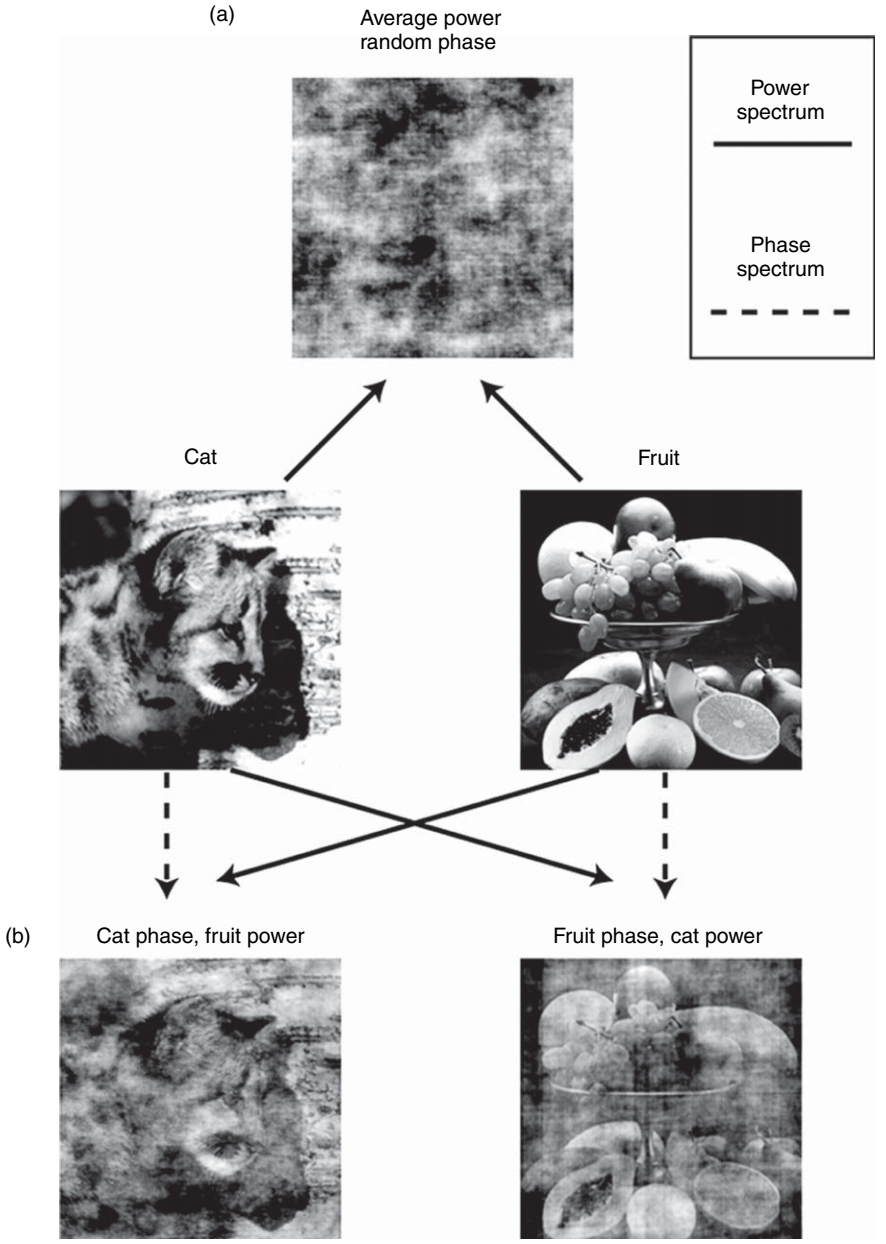

Figure 1 The phase spectrum largely determines the perception of structure in natural images, and the power spectrum has relatively little influence. (a) Two distinct images (a cat and a bowl of fruit, second row) are recombined by taking the Fourier transform of each image, discarding their phase spectra and averaging their power spectra (solid lines). The average power spectrum (not shown) is then combined with the phase spectrum of a sample of Gaussian white noise and inverse-Fourier transformed (top row). The resulting image appears as a wispy cloud and has no discernable structure. (b) The left panel shows the phase spectrum of the cat image (dotted line) combined with the power spectrum of the fruit bowl image (solid line). The right panel shows the phase spectrum of the fruit bowl image (dotted line) combined with the power spectrum of the cat image (solid line). In both cases the resulting images are dominated by the phase spectrum, not the power spectrum.

of natural images in extrastriate visual areas have focused on area V4 and the inferior-temporal complex. Studies using simple stimuli have suggested that V4 neurons are selective for complex shapes (Gallant, J. L. *et al.*, 1993; Pasupathy, A. and Connor, C. E., 1999; Gallant, J. L. *et al.*, 2000), and recent work confirms that these cells extract specific higher-order structure from natural scenes (David, S. V. *et al.*,

2006). Neurons downstream of V4 are also selective for complex features (Gross, C. G. *et al.*, 1972; Perrett, D. I. *et al.*, 1982; Desimone, R. *et al.*, 1984; Tanaka, K. *et al.*, 1991; Miyashita, M., 1993; Foldiak, P. *et al.*, 2003), but no study has yet linked complex feature tuning in these areas to the higher-order statistics of natural images. However, there is some evidence that the inferior temporal complex is optimized to encode natural scenes efficiently (Baddeley, R. *et al.*, 1997).

1.17.6 Temporal Statistics of Natural Images

Thus far we have discussed the spatial statistics of natural images, but these only describe the properties of still images taken by a stationary camera aimed at a stationary world. Real natural images are dynamic and change over time. Complete understanding of natural images also requires consideration of their temporal statistics: how their statistical properties change over time.

Many of the spatial statistics of natural images have analogous distributions in the temporal domain. For example, in certain regimes the temporal amplitude spectrum of natural images is 1/f (Dong, D. W. and Atick, J. J., 1995a; van Hateren, J. H. and van der Schaaf, A., 1996): low temporal frequencies tend to have the most power and power decreases at higher frequencies. Thus, natural images are temporally scale invariant. Because temporal scale invariance gives little information about the specific content of a scene, an efficient visual system should tend to whiten the temporal amplitude spectrum in order to reduce redundancy (Dong, D. W. and Atick, J. J., 1995b). Such temporal whitening mechanisms have been found in both insects and mammals (Dong, D. W. and Atick, J. J., 1995b; van Hateren, J. H. *et al.*, 2005).

One important property of natural images is that their spatial and temporal statistics are not separable (Dong, D. W. and Atick, J. J., 1995a). Theory suggests that this statistical regularity can be exploited by processing signals through multiple channels, some tuned to low spatial and high temporal frequencies, others tuned to high spatial and low temporal frequencies (Dong, D. W. and Atick, J. J., 1995b; van Hateren, J. H. and Ruderman, D. L., 1998). Separate, parallel pathways of this type have been found at many different stages of visual processing in mammals (Merigan, W. H. and Maunsell, J. H., 1993). One might speculate that this statistical property of natural images may have driven the development of separate ventral and dorsal streams in the mammalian visual system.

Some of the properties of neural coding in primary visual cortex that have been difficult to explain in terms of the spatial statistics of natural images might reflect the influence of temporal statistics. For example, although the sparseness criterion can explain the presence of Gabor wavelet filters in primary visual cortex, it cannot account for why many of these neurons are insensitive to spatial phase (Hubel, D. H., 1959). However, a different criterion that can exploit the statistical regularity of signals over time can account for phase invariance (Wiskott, L. and Sejnowski, T. J., 2002; Berkes, P. and Wiskott, L., 2005). This criterion, known as slow feature analysis, assumes that the visual system should be driven to represent those features in natural images that tend to change most slowly over time (because those features are most likely to represent important structural elements in natural scenes).

The temporal statistics of natural images are not determined entirely by the motion of objects in a scene; they are also influenced by saccadic eye movements and by the motion of the observer through the environment. Saccadic eye movements have a large effect on the temporal statistics of natural images, because they break long temporal correlations and introduce a substantial temporal transient after each saccade (David, S. V. *et al.*, 2004). The motion of the observer through the environment must also influence image statistics, though this has not yet been characterized.

Both the spatial and temporal statistics of natural images are stationary over long timescales. However, these statistics can change greatly from one moment to the next, due to changes in the scene itself, motion of the observer or eye movements. To maximize processing efficiency under such changing conditions the visual system should adapt to the prevailing statistical structure (Brenner, N. *et al.*, 2000). Dynamic adaptation in response to changes in stimulus statistics has now been observed at many different stages of visual processing: in the retina (Shapley, R. and Victor, J. D., 1979), LGN (Lesica, N. A. *et al.*, 2003; Lesica, N. A. and Stanley, G. B., 2004; Solomon, S. G. *et al.*, 2004), and even in the visual cortex (David, S. V. *et al.*, 2004; Sharpee, T. O. *et al.*, 2006). These pervasive adaptation effects allow the visual system to optimize both redundancy reduction and signal exploitation dynamically under changing conditions.

Acknowledgment

Preparation of the chapter was supported by the National Eye Institute.

References

Albrecht, D. G., Farrar, S. B., and Hamilton, D. B. 1984. Spatial contrast adaptation characteristics of neurones recorded in the cat's visual cortex. J. Physiol. 347, 713–739.

Atick, J. J. 1992. Could information theory provide an ecological theory of sensory processing? Network: Comput. Neural Syst. 3, 213–251.

Atick, J. J., Li, Z., and Redlich, A. N. 1992. Understanding retinal color coding from first principles. Neural Comput. 4, 559–572.

Attneave, F. 1954. Some informational aspects of visual perception. Psychol. Rev. 61, 183–193.

Baddeley, R., Abbott, L. F., Booth, M. C. A., Sengpiel, F., Freeman, R., Wakeman, E. A., and Rolls, E. T. 1997. Responses of neurons in primary and inferior temporal visual cortices to natural scenes. Proc. R. Soc. Lond. B 264, 1775–1783.

Balboa, R. M., Tyler, C. W., and Grzywacz, N. M. 2001. Occlusions contribute to scaling in natural images. Vision Res. 41, 955–964.

Barlow, H. B. 1961. Possible Principles Underlying the Transformation of Sensory Messages. In: Sensory Communication (*ed*. W. A. Rosenbluth), pp. 217–234. MIT Press.

Barlow, H. B. 2001. The exploitation of regularities in the environment by the brain. Behav. Brain Sci. 24, 602–607.

Bell, A. J. and Sejnowski, T. J. 1997. The ''independent components'' of natural scenes are edge filters. Vision Res. 37, 3327–3338.

Berkes, P. and Wiskott, L. 2005. Slow feature analysis yields a rich repertoire of complex cell properties. J. Vis. 5, 579–602.

Brenner, N., Bialek, W., and de Ruyter van Steveninck, R. 2000. Adaptive rescaling maximizes information transmission. Neuron 26, 695–702.

Carandini, M., Demb, J. B., Mante, V., Tolhurst, D. J., Dan, Y., Olshausen, B. A., Gallant, J. L., and Rust, N. C. 2005. Do we know what the early visual system does? J. Neurosci. 25, 10577–10597.

Chandler, D. M. and Field, D. J. 2007. Estimates of the information content and dimensionality of natural scenes from proximity distributions. J. Opt. Soc. Am. A 24, 922–941.

Dan, Y., Atick, J. J., and Reid, R. C. 1996. Efficient coding of natural scenes in the lateral geniculate nucleus: experimental test of a computational theory. J. Neurosci. 16, 3351–3362.

Daugman, J. 1980. Two-dimensional spectral analysis of cortical receptive field profiles. Vision Res. 20, 847–856.

Daugman, J. G. 1988. Complete discrete 2-D Gabor transforms by neural networks for image analysis and compression. IEEE Trans. Acoust. 36, 1169–1179.

David, S. V. and Gallant, J. L. 2005. Predicting neuronal responses during natural vision. Network 16, 239–260.

David, S. V., Vinje, B. V., and Gallant, J. L. 2004. Natural stimulus statistics alter the receptive field structure of V1 neurons. J. Neurosci. 24, 6991–7006.

David, S. V., Hayden, B. Y., and Gallant, J. L. 2006. Spectral receptive field properties explain shape selectivity in area V4. J. Neurophysiol. 96, 3492–3505.

Desimone, R., Albright, T. D., Gross, C. G., and Bruce, C. 1984. Stimulus-selective properties of inferior temporal neurons in the macaque. J. Neurosci. 4, 2051–2062.

Dong, D. W. and Atick, J. J. 1995a. Statistics of natural time-varying images. Network: Comput. Neural Syst. 6, 345–358.

Dong, D. W. and Atick, J. J. 1995b. Temporal decorrelation: a theory of lagged and nonlagged responses in the lateral geniculate nucleus. Network: Comput. Neural Syst. 6, 159–178.

Einhauser, W., Rutishauser, U., Frady, E. P., Nadler, S., Konig, P., and Koch, C. 2006. The relation of phase noise and luminance contrast to overt attention in complex visual stimuli. J. Vis. 6, 1148–1158.

Fain, G. L., Matthews, H. R., Cornwall, M. C., and Koutalos, Y. 2001. Adaptation in vertebrate photoreceptors. Physiol. Rev. 81, 117–151.

Felsen, G., Touryan, J., Han, F., and Dan, Y. 2005. Cortical sensitivity to visual features in natural scenes. PLoS Biol. 3, e342.

Field, D. J. 1987. Relations between the statistics of natural images and the response properties of cortical cells. J. Opt. Soc. Am. A 4, 2379–2394.

Field, D. J. 1993. Scale-Invariance and Self-Similar 'Wavelet' Transforms: an Analysis of Natural Scenes and Mammalian Visual Systems. In: Wavelets, Fractals, and Fourier Transforms (*eds*. M. Farge, J. C. R. Hunt, and J. C. Vascillicos), pp. 151–193. Clarendon Press.

Field, D. J. 1994. What is the goal of sensory coding? Neural Comput. 6, 559–601.

Foldiak, P. 1990. Forming Sparse Representations by Local Anti-Hebbian Learning. Biol. Cybern. 64, 165–170.

Foldiak, P., Xiao, D., Keysers, C., Edwards, R., and Perrett, D. I. 2003. Rapid serial visual presentation for the determination of neural selectivity in area STSa. Prog. Brain Res. 144, 107–116.

Frazor, R. A. and Geisler, W. S. 2006. Local luminance and contrast in natural images. Vision Res. 46, 1585–1598.

Gallant, J. L., Braun, J., and Van Essen, D. C. 1993. Selectivity for polar, hyperbolic, and Cartesian gratings in macaque visual cortex. Science 259, 100–103.

Gallant, J. L., Shoup, R. E., and Mazer, J. A. 2000. A human extrastriate cortical area functionally homologous to Macaque V4. Neuron 27, 227–235.

Geisler, W. S., Perry, J. S., Super, B. J., and Gallogly, D. P. 2001. Edge co-occurrence in natural images predicts contour grouping performance. Vision Res. 41, 711–724.

Gross, C. G., Rocha-Miranda, C. E., and Bender, D. B. 1972. Visual properties of neurons in inferotemporal cortex of the Macaque. J. Neurophysiol. 35, 96–111.

Heeger, D. J., Simoncelli, E. P., and Movshon, J. A. 1996. Computational models of cortical visual processing. Proc. Natl. Acad. Sci. U. S. A. 93, 623–627.

Hubel, D. H. 1959. Single unit activity in striate cortex of unrestrained cats. J. Physiol. 147, 226–238.

Hyvarinen, A. and Hoyer, P. 2000. Emergence of phase and shift invariant features by decomposition of natural images into independent feature subspaces. Neural Comput. 12, 1705–1720.

Karklin, Y. and Lewicki, M. S. 2003. Learning higher-order structures in natural images. Network 14, 483–499.

Karklin, Y. and Lewicki, M. S. 2005. A hierarchical Bayesian model for learning nonlinear statistical regularities in nonstationary natural signals. Neural Comput. 17, 397–423.

Krieger, G., Zetzsche, C., and Barth, E. 1997. Higher-Order Statistics of Natural Images and their Exploitation by Operators Selective to Intrinsic Dimensionality. In: Proceedings of the IEEE Signal Processing Workshop on Higher-Order Statistics, pp. 147–151. IEEE.

Laughlin, S. 1981. A simple coding procedure enhances a neuron's information capacity. Z. Naturforsch. C 36, 910–912.

Laughlin, S. B. 1994. Matching coding, circuits, cells, and molecules to signals – general-principles of retinal design in the flys eye. Prog. Retin. Eye Res. 13, 165–196.

Laughlin, S. B., Steveninck, d. R.v., and Anderson, J. C. 1998. The metabolic cost of neural information. Nat. Neurosci. 1, 36–41.

Lee, A. B., Mumford, D., and Huang, J. 2001. Occlusion models for natural images: a statistical study of a scale-invariant dead leaves model. Int. J. Comput. Vis. 41, 35–59.

Lennie, P. and Movshon, J. A. 2005. Coding of color and form in the geniculostriate visual pathway (invited review). J. Opt. Soc. Am. A Opt. Image Sci. Vis. 22, 2013–2033.

Lesica, N. A. and Stanley, G. B. 2004. Encoding of natural scene movies by tonic and burst spikes in the lateral geniculate nucleus. J. Neurosci. 24, 10731–10740.

Lesica, N. A., Boloori, A. S., and Stanley, G. B. 2003. Adaptive encoding in the visual pathway. Network 14, 119–135.

Mante, V., Frazor, R. A., Bonin, V., Geisler, W. S., and Carandini, M. 2005. Independence of luminance and contrast in natural scenes and in the early visual system. Nat. Neurosci. 8, 1690–1697.

Marr, D. and Hildreth, E. 1980. Theory of edge detection. Proc. R. Soc. Lond. B 207, 187–217.

Merigan, W. H. and Maunsell, J. H. 1993. How parallel are the primate visual pathways? Annu. Rev. Neurosci. 16, 369–402.

Miyashita, M. 1993. Inferior temporal cortex: where visual perception meets memory. Annu. Rev. Neurosci. 16, 245–263.

Olshausen, B. A. and Field, D. J. 1996. Emergence of simple-cell receptive field properties by learning a sparse code for natural images. Nature 381, 607–609.

Olshausen, B. A. and Field, D. J. 1997. Sparse coding with an overcomplete basis set: a strategy employed by V1? Vision Res. 23, 3311–3325.

Pasupathy, A. and Connor, C. E. 1999. Responses to contour features in macaque area V4. J. Neurophysiol. 82, 2490–2502.

Perrett, D. I., Rolls, E. T., and Caan, W. 1982. Visual neurons responsive to faces in the monkey temporal cortex. Exp. Brain Res. 47, 329–342.

Piotrowski, L. N. and Campbell, F. W. 1982. A demonstration of the visual importance and flexibility of spatial-frequency amplitude and phase. Perception 11, 337–346.

Prenger, R., Wu, M. C. K., David, S. V., and Gallant, J. L. 2004. Nonlinear V1 responses to natural scenes revealed by neural network analysis. Neural Netw. 17, 663–679.

Reinagel, P. and Zador, A. M. 1999. Natural scene statistics at the center of gaze. Network: Comput. Neural Syst. 10, 341–350.

Rieke, F., Bodnar, D. A., and Bialek, W. 1995. Naturalistic stimuli increase the rate and efficiency of information transmission by primary auditory afferents. Proc. R. Soc. Lond. B 262, 259–265.

Ruderman, D. L. 1997. Origins of scaling in natural images. Vision Res. 37, 3385–3398.

Rust, N. C. and Movshon, J. A. 2005. In praise of artifice. Nat. Neurosci. 8, 1647–1650.

Schwartz, O. and Simoncelli, E. P. 2001. Natural signal statistics and sensory gain control. Nat. Neurosci. 4, 819–825.

Shapley, R. and Victor, J. D. 1979. The contrast gain control of the cat retina. Vision Res. 19, 431–434.

Sharpee, T. O., Sugihara, H., Kurgansky, A. V., Rebrik, S. P., Stryker, M. P., and Miller, K. D. 2006. Adaptive filtering enhances information transmission in visual cortex. Nature 439, 936–942.

Simoncelli, E. P. and Schwartz, O. 1998. Modeling Surround Suppression in V1 Neurons with a Statistically-Derived Normalization Model. In: Neural Information Processing Systems 11 (*eds*. M. S. Kearns, S. A. Solla, and D. A. Cohn), 153–159. MIT Press.

Simoncelli, E. P. and Olshausen, B. A. 2001. Natural image statistics and neural representation. Annu. Rev. Neurosci. 24, 1193–1216.

Smyth, D., Willmore, B., Baker, G. E., Thompson, I. D., and Tolhurst, D. J. 2003. The receptive-field organization of simple cells in primary visual cortex of ferrets under natural scene stimulation. J. Neurosci. 23, 4746–4759.

Solomon, S. G., Peirce, J. W., Dhruv, N. T., and Lennie, P. 2004. Profound contrast adaptation early in the visual pathway. Neuron 42, 155–162.

Srinivasan, M. V., Laughlin, S. B., and Dubs, A. 1982. Predictive coding: a fresh view of inhibition in the retina. Proc. R. Soc. Lond. B 216, 427–459.

Tadmor, Y. and Tolhurst, D. J. 1993. Both the phase and the amplitude spectrum may determine the appearance of natural images. Vision Res. 33, 141–145.

Tanaka, K., Saito, H., Fukada, Y., and Moriya, M. 1991. Coding of visual images of objects in the inferotemporal cortex of the macaque monkey. J. Neurophysiol. 66, 170–189.

Thomson, M. G. A. 1999. Higher-order structure in natural scenes. J. Opt. Soc. Am. 16, 1549–1553.

Thomson, M. G. A. and Foster, D. H. 1997. Role of second- and third-order statistics in the discriminability of natural images. J. Opt. Soc. Am. A 14, 2081–2090.

Tootell, R. B. H., Tsao, D. Y., and Vanduffel, W. 2003. Neuroimaging weighs in: humans meet macaques in ''primate'' visual cortex. J. Neurosci. 23, 3981–3989.

Touryan, J., Felsen, G., and Dan, Y. 2005. Spatial structure of complex cell receptive fields measured with natural images. Neuron 45, 781–791.

Van Essen, D. C. and Gallant, J. L. 1994. Neural mechanisms of form and motion processing in the primate visual system. Neuron 13, 1–10.

van Hateren, J. H. 1992. A theory of maximizing sensory information. Biol. Cybern. 68, 23–29.

van Hateren, J. H. 1993. Spatial, temporal and spectral pre-processing for colour vision. Proc. Biol. Sci. 251, 61–68.

van Hateren, J. H. 1997. Processing of natural time series of intensities by the visual system of the blowfly. Vision Res. 37, 3401–3416.

van Hateren, J. H. and van der Schaaf, A. 1996. Temporal properties of natural scenes. Proc. SPIE 2657, 139–143.

van Hateren, J. H. and van der Schaaf, A. 1998. Independent component filters of natural images compared with simple cells in primary visual cortex. Proc. R. Soc. Lond. B 265, 359–366.

van Hateren, J. H. and Ruderman, D. L. 1998. Independent component analysis of natural image sequences yields spatio-temporal filters similar to simple cells in primary visual cortex. Proc. R. Soc. Lond. B 265, 2315–2320.

van Hateren, J. H., Kern, R., Schwerdtfeger, G., and Egelhaaf, M. 2005. Function and coding in the blowfly H1 neuron during naturalistic optic flow. J. Neurosci. 25, 4343–4352.

Vinje, W. E. and Gallant, J. L. 2002. Natural stimulation of the non-classical receptive field increases information transmission efficiency in V1. J. Neurosci. 22, 2904–2915.

Vinje, W. E. and Gallant, J. L. 2000. Sparse coding and decorrelation in primary visual cortex during natural vision. Science 287, 1273–1276.

Wegmann, B. and Zetzsche, C. 1990. Visual System Based Polar Quantization of Local Amplitude and Local Phase of Orientation Filter Outputs. In: Human Vision and Electronic Imaging: Models, Methods and Applications (*ed*. B. Rogowitz), pp. 306–317. SPIE.

Weliky, M., Fiser, J., Hunt, R. H., and Wagner, D. N. 2003. Coding of natural scenes in primary visual cortex. Neuron 37, 703–718.

Willmore, B., Watters, P. A., and Tolhurst, D. J. 2000. A comparison of natural-image-based models of simple-cell coding. Perception 29, 1017–1040.

Wiskott, L. and Sejnowski, T. J. 2002. Slow feature analysis: unsupervised learning of invariances. Neural Comput. 14, 715–770.

Yen, S. C., Baker, J., and Gray, C. M. 2007. Heterogeneity in the responses of adjacent neurons to natural stimuli in cat striate cortex. J. Neurophysiol. 97, 1326–1341.

Zetzsche, C. and Krieger, G. 1999. Nonlinear neurons and higher-order statistics: new approaches to human vision and electronic image processing. SPIE 3644, 2–33.

Zetzsche, C. and Rohrbein, F. 2001. Nonlinear and extra-classical receptive field properties and the statistics of natural scenes. Network: Comput. Neural Syst. 12, 331–350.

Zhu, S. C. and Mumford, D. 1997. Prior learning and Gibbs reaction-diffusion. IEEE Trans. Pattern Anal. Mach. Intell. 19, 1236–1250.

1.18 Seeing in the Dark: Retinal Processing and Absolute Visual Threshold

F Rieke, University of Washington, Seattle, WA, USA

© 2008 Elsevier Inc. All rights reserved.

1.18.1	**Introduction**	393
1.18.2	**Behavior**	393
1.18.2.1	Statistical Variations in Photon Absorption	394
1.18.2.2	Behavioral Estimates of Absolute Sensitivity and Dark Noise	395
1.18.2.3	Limitations to Behavioral Experiments	396
1.18.2.4	Constraints Imposed by Behavior	397
1.18.3	**Responses of Rod Photoreceptors to Single Photons**	397
1.18.3.1	Photon Capture	397
1.18.3.2	Amplification	397
1.18.3.3	Dark Noise	399
1.18.3.4	Reproducibility	400
1.18.4	**Retinal Readout of the Rod Signals**	403
1.18.4.1	Sparseness, Convergence, and Nonlinear Processing	404
1.18.4.2	Representing and Extracting Temporal Information	407
1.18.4.3	Extraction	407
1.18.4.4	Representation	408
1.18.4.5	Low Noise	410
1.18.5	**Summary**	410
References		411

1.18.1 Introduction

In starlight, only a few rod photoreceptors out of every 10 000 absorb photons during the ~200 ms integration time of rod signals. Yet this weak signal, embedded in noise arising in the remaining rods, can guide visual behavior. Understanding how vision under these conditions is possible provides an excellent opportunity to bring together biophysical studies of single molecules and synapses, computational studies of signal processing and neural coding, and behavioral studies of the overall system reliability.

Vision near absolute threshold requires that rods respond to single absorbed photons, that retinal synapses reliably transmit the resulting signals, and that the response to each absorbed photon is amplified to produce a noticeable change in ganglion cell spiking. Meeting these requirements challenges our understanding of several basic issues in neuroscience: sensory transduction, synaptic transmission, and neural coding. This chapter focuses on what is known about how these challenges are met and the general insights these studies have provided about neural function.

1.18.2 Behavior

The ability of human observers to detect absorption of a small number of photons has been appreciated for more than 100 years (reviewed by Field, G. D. *et al.*, 2005). It is clear from this long history of behavioral measurements that dark-adapted visual sensitivity approaches the limits set by the division of light into discrete photons and the consequent statistical fluctuations in photon absorption. This exquisite sensitivity imposes a set of constraints on the neural mechanisms responsible for detecting and processing signals from single-photon absorptions. This section briefly reviews behavioral measurements of absolute

sensitivity and describes the constraints that these measurements impose.

1.18.2.1 Statistical Variations in Photon Absorption

The physics of light itself imposes a key constraint on the reliability of rod vision. Figure 1 illustrates the impact of statistical fluctuations in photon absorption on the fidelity of signals in the rod photoreceptor array. Each pixel in the image represents, on a gray scale, the photon absorption rate in a single rod photoreceptor. Nominally constant light from an object in the visual scene will produce a time-varying rate of absorbed photons – for example, light that produces an average of five absorbed photons in 1 s will sometimes produce four, sometimes five, sometimes six absorbed photons. Similarly, these statistical fluctuations cause nominally homogeneous objects to produce spatially varying numbers of absorbed photons. The probability of obtaining n absorbed photons, given the mean number absorbed, follows Poisson statistics. A key property of Poisson statistics is that the variance in the event count is equal to the mean – thus the standard deviation of the number of absorbed photons is $\sqrt{m}$ for a mean of m.

Although Poisson fluctuations in photon absorption are present at all light levels, they have a particularly striking impact on the fidelity of inputs to the retina at low light levels. Thus in Figure 1 the mean number of absorbed photons in a single simulated rod is 1000 for the left panel, 10 for the middle panel, and 0.1 for the right panel. The histograms below the images show the distribution of the number of absorptions across rods. The impact of Poisson fluctuations increases as light levels fall. Assuming that each image in Figure 1 represents the photons absorbed in one 200 ms rod integration time, even the right panel is a factor of 100–1000 above absolute visual threshold and hence does not accurately capture how much the light inputs to the retina can vary. Poisson fluctuations in photon absorption such as those depicted in Figure 1 are unavoidable and impose a fundamental limit to visual fidelity that no imaging device can exceed.

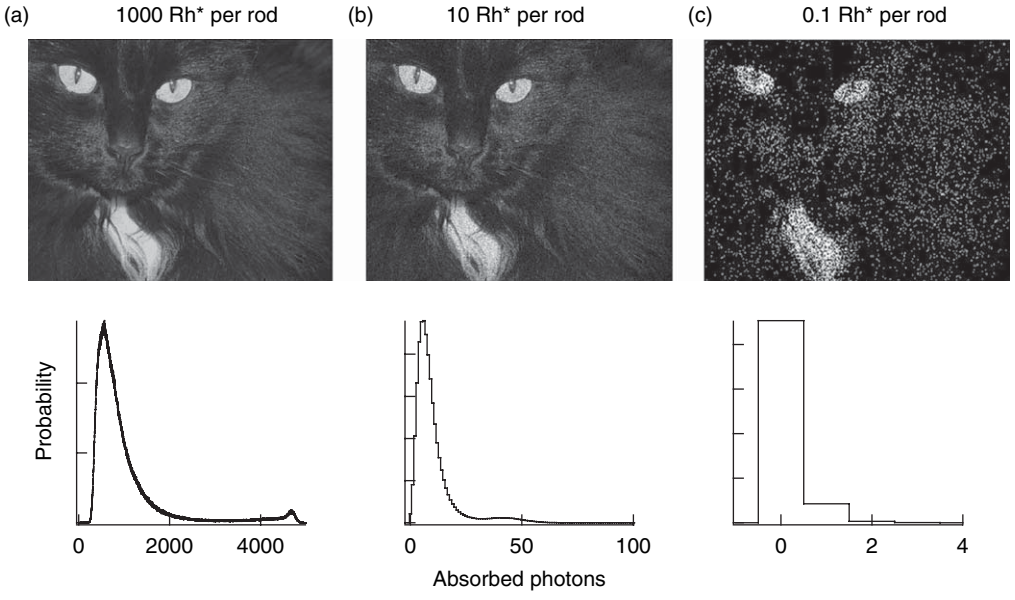

Figure 1 Simulation of Poisson fluctuations in the rod array. The top images represent the pattern of photon absorptions produced in a 2000 × 1500 array of rod photoreceptors in a single time period (e.g., a single 200 ms period corresponding to the integration time of the rod signals). Each pixel in the image corresponds to a single rod, with the gray scale encoding the number of absorbed photons (different gray scale for each image). The bottom histograms show the distributions of photon absorptions across simulated rods. The left panel is for a mean of 1000 photons per rod, the middle for 10 photons per rod, and the right for 0.1 photons per rod. The images were created in two steps. First, the pixel values of the original image were all scaled by a single constant so that the mean corresponded to the desired mean number of absorbed photons. Second, each pixel was replaced with a single sample from a Poisson distribution with a mean equal to the scaled pixel value from the first step.

1.18.2.2 Behavioral Estimates of Absolute Sensitivity and Dark Noise

How does the sensitivity of rod vision compare to limits imposed by the irreducible noise produced by Poisson fluctuations in photon absorption? Most behavioral experiments attempting to answer this question have used the frequency of seeing approach introduced by Hecht S. *et al.* (1942) and van der Velden H. A. (1946). The basic experiment is simple – on each trial a dark-adapted observer is asked to say 'yes' if he/she saw a flash, and the probability of seeing is plotted against the number of photons delivered to the cornea. Observers are cued at the beginning of the trial and are trained to a certain rate of false positive responses – that is, 'yes' responses when no flash was delivered. Such false-positive responses originate from noise within the visual system (see below). Figure 2(a) shows the measured frequency of seeing curve for one observer from the classic experiments of Hecht, Shlaer, and Pirenne.

Interpretation of experiments like that in Figure 2(a) would be simpler if we could convert the *x*-axis from the number of photons at the cornea to the number of photons absorbed within the rod photoreceptor array. However, the probability that a photon incident on the cornea is absorbed within the rod array is not well characterized even today. Hecht, Shlaer, and Pirenne instead estimated behavioral threshold from the variability in an observer's responses to a nominally fixed strength flash – for example, for the observer in Figure 2(a) a flash producing 90 photons at the cornea was seen ~50% of the time. Hecht, Shlaer, and Pirenne explained the broad range of flash strengths over which an observer generated variable responses based on two assumptions: the dominant source of noise was Poisson fluctuations in photon absorption and observers answered 'yes' only when more than a threshold number of photons were absorbed. Thus on some trials at a given flash strength, fewer than the threshold number of photons will be absorbed and the flash will go unseen, while on other trials the number absorbed will exceed the threshold and the flash will be seen. For a given threshold, the cumulative Poisson distribution predicts how the detection probability depends on the number of absorbed photons (Figure 2(b)). In particular, the width of the transition between seen and unseen flashes depends on threshold.

An advantage of the analysis described above is that the unknown probability that a photon at the cornea is absorbed in the rod array is naturally separated from the threshold by plotting the detection probability against the logarithm of the number of photons at the cornea as in Figure 2; in this case, the unknown absorption efficiency shifts the Poisson predictions along the *x*-axis while the shape is uniquely determined by the threshold (see Figure 3, right).

From the analysis described above, Hecht, Shlaer, and Pirenne concluded that the threshold for

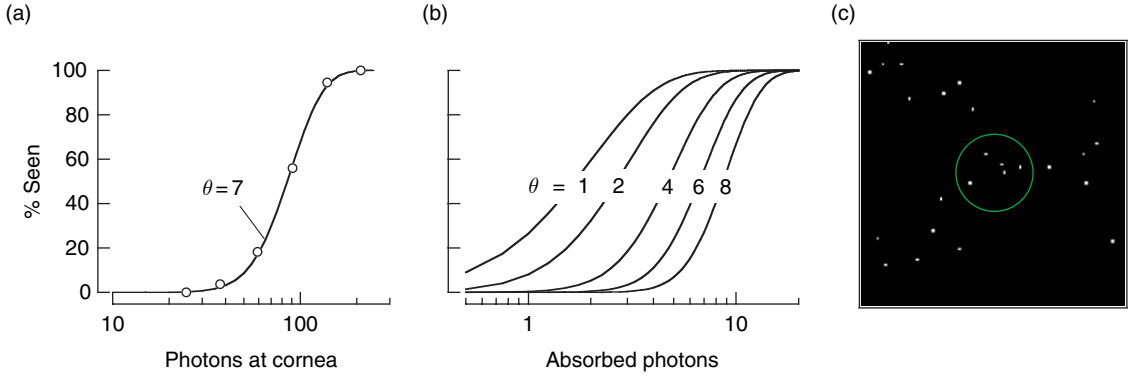

Figure 2 Frequency of seeing analysis. (a) Probability of yes response plotted against the mean number of photons delivered to the cornea for one observer from Hecht S. *et al.* (1942). (b) Theoretical frequency of seeing curves for different thresholds θ. Each point on each curve corresponds to a cumulative Poisson distribution for getting θ or more absorbed photons given the mean number of absorptions at each *x*-axis location. (c) Dark light and false positives. Simulated pattern of photon absorptions and photon-like noise events in the rod array. The green circle denotes the rods receiving incident photons. Internal noise in the visual system can be expressed as a rate of photon-like noise events in the rods (a dark light), shown here as a small subset of rods (e.g., those outside the green circle) generating photon-like responses though they did not absorb a photon. This dark light can be compared directly with real incident light, simplifying the estimates of the relationship between false positives and dark noise.

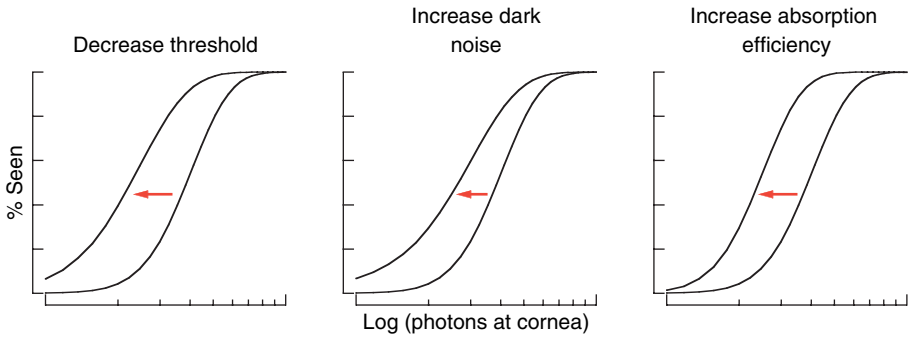

Figure 3 Ambiguities in fitting frequency of seeing curves. Predicted changes in frequency of seeing curves produced by changes in threshold (left), dark noise (middle), and absorption efficiency (right).

seeing was five to seven absorbed photons. Under the conditions tested, they also concluded that Poisson fluctuations were the dominant noise source producing variability in an observer's responses. Contemporary experiments by van der Velden H. A. (1946) concluded that the threshold was closer to two absorbed photons, leading to a speculation that the visual system detected coincident photon arrivals. The difference between these two estimates of threshold likely reflects differences in the rate of accepted false-positive responses from the observers (Marriot, F. H. *et al.*, 1959).

Subsequent experiments by Barlow H. B. (1956), Sakitt B. (1972), and Teich M. C. *et al.* (1982) allowed observers to adopt a less stringent criterion for detecting a flash, resulting in a higher (i.e., easily measurable) rate of false-positive responses. A non-zero false-positive rate indicated noise in addition to Poisson fluctuations in photon absorption, since no Poisson fluctuations are present on trials when no light is delivered. Hence the false-positive rate provides an estimate of noise within the visual system. It is convenient to express this noise as an equivalent background or dark light, which can be compared directly with true visual inputs (Figure 2(c)). Thus when the noise causes more than a threshold number of photon-like events, it also causes the perception of a flash – that is, a false-positive response. Assuming that the dark light and fluctuations in photon absorption are independent and additive, the dark light is easily incorporated into the fits to the frequency of seeing curves by adding a constant rate of photon-like events to those produced by the flash. The dark light estimated in these studies was approximately 0.01 equivalent photon-like events per rod per second. A second important finding in these studies was that observers could trade an increase in the rate of false-positive responses for a decreased threshold. This is consistent with the underlying neural signals that vary in a graded manner with the number of absorbed photons rather than signals that require a threshold number of photon absorptions to be produced.

1.18.2.3 Limitations to Behavioral Experiments

A key limitation to interpreting behavioral experiments on absolute visual sensitivity is that the fits to the frequency of seeing curves are not unique. In particular, changes in detection threshold, dark noise, and absorption threshold all produce similar (though not identical) changes in the shape of the frequency of seeing curves (Figure 3), and thus these parameters can trade against each other in fitting the data. For example, an increased threshold shifts the frequency of seeing curve to the right along the flash strength axis and makes it steeper (Figure 3, left), while an increase in dark noise has the opposite effect (Figure 3, middle). Absorption efficiency can similarly trade against other parameters (Figure 3, right). Plausible estimates of the absorption efficiency range from 0.05 to 0.3, producing a $\sim$ tenfold range in behavioral estimates of internal noise and detection threshold (Donner, K., 1992; Field, G. D. *et al.*, 2005).

The quantitative uncertainty in behavioral estimates of absolute sensitivity has a qualitative effect on how we view retinal processing. The low end of the behavioral estimates, as is often emphasized, is in good agreement with limits to sensitivity imposed by the rods (see below), implying that the remainder of the visual system operates effectively noiselessly and efficiently. If true, this is a strong constraint.

1.18.2.4 Constraints Imposed by Behavior

Despite the uncertainties in interpreting behavioral measures of absolute sensitivity, it is clear that a relatively small number of photons is required for detection and that Poisson fluctuations in photon absorption pose an important noise source limiting behavioral sensitivity. These observations serve to motivate a set of questions about phototransduction in the rod photoreceptors and the retinal processing of the resulting signals: How is the signal from a single activated rhodopsin molecule amplified in the rods and in the retinal circuitry? How does the retina maintain low noise so as not to swamp the single-photon responses? Are there mechanisms in the retinal circuitry that separate the signal of interest from noise that threatens to obscure them?

1.18.3 Responses of Rod Photoreceptors to Single Photons

Behavioral sensitivity unambiguously requires that rod photoreceptors detect a single absorbed photon since flashes producing much less than one photon absorbed per rod are detected. The rods perform this task admirably, with a performance that compares favorably with the best man-made room temperature light detectors. Understanding how this performance is achieved with components restricted to proteins and lipids has been a major achievement (see Chapter Phototransduction in Rods and Cones). As described below, the rods meet several functional requirements for reliable photon detection: (1) they efficiently capture incident photons; (2) they amplify the signals resulting from the activation of a single rhodopsin molecule by an absorbed photon to produce a macroscopic electrical response; (3) they maintain low dark noise; and (4) they generate near-identical responses to each absorbed photon.

1.18.3.1 Photon Capture

The first step in detecting single photons is capturing them. Rhodopsin is packed onto the surface of membrane disks in the rod outer segment at sufficiently high density to hinder protein diffusion on the disk (Pugh, E. N. and Lamb, T. D., 1993). This high density ensures that the majority (~70%) of photons that enter one end of the cylindrical outer segment are absorbed. Rhodopsin is a member of the G protein-coupled receptor family, and hence active rhodopsin catalyzes G protein activation. Rhodopsin is composed of two parts: a light-sensitive chromophore and the opsin protein that houses it (see Chapter Mammalian Photopigments). Absorption of a photon by the 11-*cis*-retinal chromophore produces an electronic excitation, which with high efficiency produces a *cis–trans* conformational change of the chromophore. The change in chromophore conformation in turn produces a change in the conformation of the opsin, rendering rhodopsin catalytically active. The steps between photon absorption and opsin activation occur with high efficiency – 60–70% of the absorbed photons lead to opsin activation (Dartnall, H. J. A., 1972; Baylor, D. A. *et al.*, 1979). The high rhodopsin content and high quantum efficiency of opsin activation together mean that 40–50% of the photons incident on the rod outer segment are converted into active rhodopsin molecules.

1.18.3.2 Amplification

As predicted by behavioral studies, rods generate discernable electrical responses to single absorbed photons (Baylor, D. A. *et al.*, 1979). In darkness, rods maintain a constant circulating current that flows into the outer segment and out of the inner segment. Light activates the phototransduction cascade and suppresses the current. Figure 4(a) shows the change in outer-segment membrane current of a primate rod in response to a repeated fixed-strength flash producing, on average, 0.5 effective photon absorptions (Rh^*). The rod responds to some flashes and fails to respond to others. The discreteness of the responses indicates an elementary response of ~2 pA in amplitude.

Two arguments indicate that the elementary response is produced by the absorption of a single photon rather than, for example, the coincident activation of two rhodopsin molecules or by an all-or-none response such as an action potential (Baylor, D. A. *et al.*, 1979). First, the trial-to-trial variations in the response are in good agreement with expectations from the Poisson statistics that govern photon absorption. Figure 4(b) (middle and right) plots histograms of the amplitudes of the responses to two different flash strengths measured in the same cell. The smooth curves show fits assuming that the number of photons absorbed obeyed Poisson statistics (Figure 4(b), left) and that the dark noise and noise in the elementary response were independent and additive. The key point is that the fits have been constrained so that the mean of the Poisson distribution used for the right panel is four times that used in

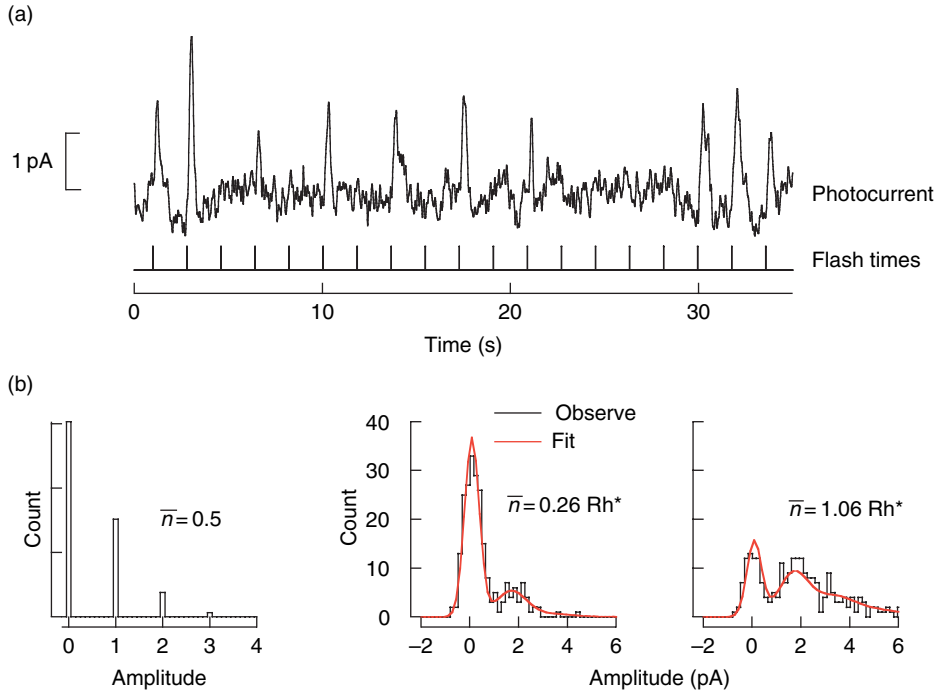

Figure 4 Rods respond to single photons. (a) Changes in the outer segment membrane current of a primate rod in response to a repeated fixed-strength flash. Currents were measured with a suction electrode. Flash timing is shown below the current record. This flash produced, on average, 0.5 Rh*. (b) Fits to amplitude histograms. Left panel shows the probability of 0, 1, and 2 absorbed photons calculated from a Poisson distribution with a mean of 0.5 absorbed photons per trial. The middle and right panels plot measured amplitude distributions for two different flash strengths that differ by a factor of 4. Peaks near 0 correspond to trials in which the cell failed to respond and the peak near 2 pA corresponds to the elementary responses. The smooth curves fit to the measured distributions are calculated assuming that the number of events per trial follows a Poisson distribution and that the noise in darkness and in the elementary response are independent and additive. The fits were constrained such that the means of the underlying Poisson distributions differed by a factor of 4, corresponding to the difference in flash strengths. Data from Greg Field.

the middle panel, corresponding to the fourfold difference in flash strengths used to collect two sets of responses. The scaling of the number of responses in the peaks centered at 0, 2, and 4 pA (corresponding to 0, 1, and 2 elementary responses) with flash strength is consistent with expectations from Poisson statistics and inconsistent with models in which the elementary response depends on more than one absorbed photon.

The second argument linking the rod's elementary response with activation of a single rhodopsin molecule comes from the agreement of different measures of a cell's ability to absorb incident photons. First, direct optical measures of the fraction of incident photons absorbed by the rod have been compared with measures of the number of elementary electrical events elicited by calibrated flashes (Baylor, D. A. *et al.*, 1979). These experiments indicate that 60–70% of the absorbed photons produce electrical responses, in good agreement with expectations from the quantum efficiency of rhodopsin activation. Second, the fraction of absorbed photons measured from the correspondence between calibrated photon flux (in photons per square micrometer) and elementary response probability agrees well with estimates from the rhodopsin density and the molecular absorption coefficient. Taken together, these arguments leave little doubt that the rod's elementary response corresponds to activation of a single molecule by absorption of a single photon.

Activation of a single rhodopsin molecule produces a macroscopic electrical response in the rod – on average a 1–2 pA reduction in current lasting for 200–300 ms in a primate rod (Baylor, D. A. *et al.*, 1984). This change in current produces a 1–2 mV hyperpolarization (Schneeweis, D. M. and Schnapf, J. L., 1995) and a decrease in transmitter release from the synaptic terminal. The amplification required to generate the single-photon response is nicely explained by the sequence of amplifying enzymatic reactions

that make up the transduction cascade (see Chapter Phototransduction in Rods and Cones). These events have been studied in detail using a combination of biochemical, molecular, and biophysical approaches. As a result, many of the events on phototransduction can be understood in quantitative detail (Pugh, E. N. and Lamb, T. D., 1993; Rieke, F. and Baylor, D. A., 1998a; Hamer, R. D. *et al.*, 2005). This work has made the rods the best understood of the many G protein cascades in biological systems. It also has had direct medical benefits, as we now understand the mechanisms and have potential treatments for several forms of stationary night blindness (Dryja, T. P., 2000).

The high amplification provided by the phototransduction process protects the single-photon response from noise introduced in downstream processing. The amplification in phototransduction, however, comes at the cost of a long-lasting single-photon response. This is an inevitable consequence of how second messenger cascades work: the underlying reactions require time to produce an amplified response even if they operate at or near the limit set by the rate of diffusional encounters between components (Pugh, E. N. and Lamb, T. D., 1993). The slow rod responses appear to have a considerable impact on behavior. For example, the temporal frequency at which flickering lights appear constant (flicker fusion frequency) for dark-adapted rod vision is 3–5 Hz, compared to 50–70 Hz for light-adapted cone vision (Hecht, S. and Verrijp, C. D., 1933). This difference is, at least in part, due to differences in the kinetics of the rod and cone light responses.

1.18.3.3 Dark Noise

Effective detection of single absorbed photons requires that the rods maintain low noise in darkness. The characteristics of the noise generated in the transduction process are important both functionally and mechanistically. Functionally, the properties of the noise generate testable predictions about the operation of downstream processing that aims to separate signal and noise; furthermore, noise generated in the rods is a potential source for the internal noise limiting behavioral sensitivity. Mechanistically, studies of rod noise have led to insights into the operation of the phototransduction cascade.

Figure 5 shows two sections of current recorded from a primate rod in complete darkness. Two sources of noise are apparent: occasional discrete events that have an amplitude and shape similar to the single-photon response and continuous variations in current. The discrete events originate from spontaneous activation of rhodopsin (Baylor, D. A. *et al.*, 1980). They occur once in every few hundred seconds in a primate rod at 37 °C (Baylor, D. A. *et al.*, 1984; Field, G. D. *et al.*, 2002 Neurosciences Abstract). This means that each of the 10^8 rhodopsin molecules in a primate rod activates spontaneously on average once or twice a millennium. The low rate of spontaneous activation is possible because visible photons carry considerable energy, and hence rhodopsin can be activated efficiently by 500 nm light while maintaining a large energy barrier for spontaneous activation. The temperature dependence of the rate of spontaneous activation indicates an energy barrier equal to about half the energy of a 500 nm photon (Baylor, D. A. *et al.*, 1980).

In principle, it would seem beneficial to pack more rhodopsin into the rod and capture more of the incident photons. Increasing the rod's rhodopsin content, however, would increase the rate of discrete noise events. Moreover, increasing the photon capture would require a large increase in rhodopsin content because of screening effects of other rhodopsin molecules – that is, ~70% of the incident photons are already captured and doubling the rhodopsin content would only increase this to ~90% at the cost of doubling the rate of discrete noise events. The rod's rhodopsin content comes close to optimizing the tradeoff between photon capture and discrete noise.

The continuous noise in the rod currents originates from spontaneous activation of an intermediate component (phosphodiesterase) within the phototransduction cascade (Rieke, F. and Baylor, D. A., 1996). Hence the kinetic properties of the continuous noise are determined by some of the same events that determine the kinetics of the single-photon response, and the continuous noise and single-photon response have similar (though not identical) temporal frequency content (Baylor, D. A. *et al.*, 1980; 1984). Although the continuous noise seems like an unnecessary evil, it in fact serves to keep the phototransduction cascade active in the dark, an important factor controlling the duration of the rod response (Hodgkin, A. L. and Nunn, B. J., 1988; Rieke, F. and Baylor, D. A., 1996; Nikonov, S. *et al.*, 2000). In particular, a decrease in spontaneous phosphodiesterase activation and continuous noise would slow the recovery of the single-photon response by increasing the time required for the transduction cascade to resynthesize second messengers depleted during the response (Rieke, F. and Baylor, D. A., 1996).

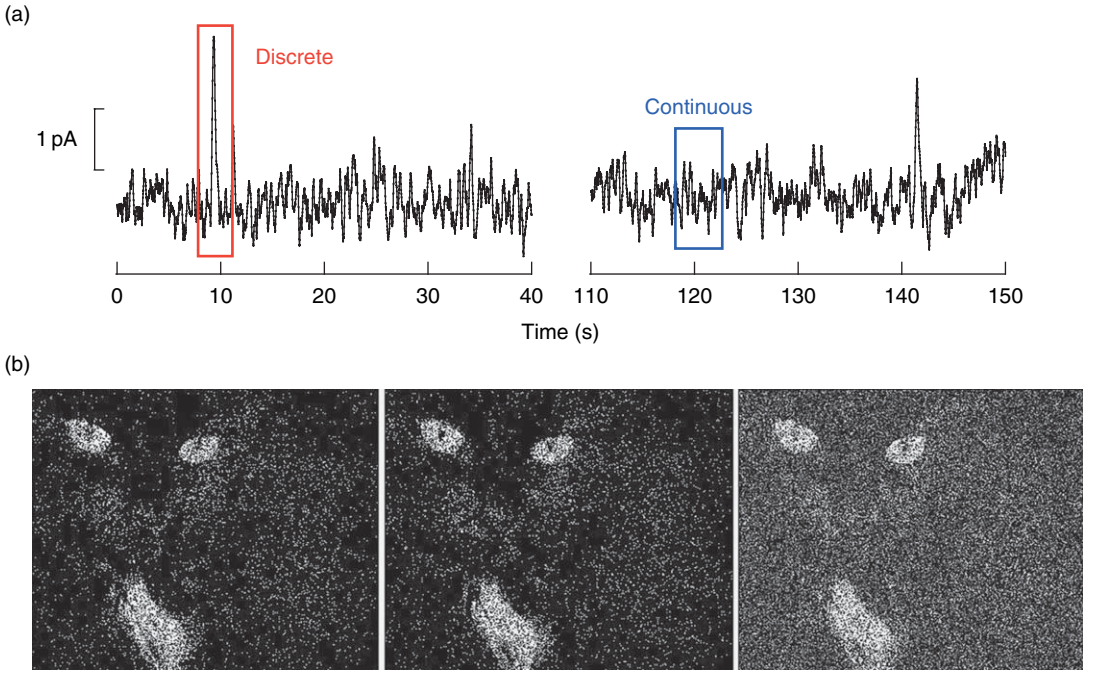

Figure 5 Dark noise and implications. (a) Two sections of dark record from a primate rod photoreceptor. Two sources of noise are apparent: continuous variations in baseline current and occasional discrete events. (b) Implications of dark noise for fidelity of signals in the rod array. The three images show the effects of Poisson fluctuations (left panel), Poisson fluctuations and discrete noise events (middle panel), and Poisson fluctuations and both discrete and continuous rod noise (right panel) on signals in the rod array. Simulations as in Figure 1. The mean number of absorbed photons per rod is 0.1 and the added noise is based on the measured noise in primate rods (discrete event probability of 0.001, continuous noise SD equal to 0.25 times single-photon response amplitude). Data from Greg Field.

Figure 5(b) illustrates the effect of dark noise on the fidelity of signals generated in the rod array. The left panel shows a simulation of the pattern of photon absorptions in the rod array for a mean of 0.1 Rh^* per rod (simulated as in Figure 1(c)). The middle panel includes discrete noise events at a probability of 0.001 per rod (corresponding to a discrete event rate of 0.005 per second and an integration time of 200 ms). Not surprisingly given the low probability of discrete events compared to incident photons, the discrete noise has little impact on the image. Except for light levels near absolute visual threshold (0.001–0.0001 Rh^* per rod per integration time), the impact of discrete noise events on the fidelity of signals in the rod array is small compared to Poisson variability in photon absorption. The right panel of Figure 5(b) shows a simulated pattern of signals in the rod array with both discrete and continuous noise added; at this intensity, continuous noise has a much more apparent effect on fidelity than discrete noise because it is present in every rod.

1.18.3.4 Reproducibility

Most signals controlled by single molecules vary considerably from one trial to the next. A familiar example is the charge flowing through an ion channel during its open time. Because the open–close transition for most ion channels is a memoryless, first-order process, the distribution of charge across multiple channel openings is exponential, with a coefficient of variation (CV; SD divided by mean) of 1. Rod responses to activation of single rhodopsin molecules show much smaller variability, with CVs of 0.25–0.35 for both the response amplitude and the area (Baylor, D. A. *et al.*, 1979; Rieke, F. and Baylor, D. A., 1998b; Whitlock, G. G. and Lamb, T. D., 1999; Field, G. D. and Rieke, F., 2002a; Doan, T. *et al.*, 2006). This reproducibility is interesting both functionally and mechanistically.

Reproducibility could permit the visual system to count absorbed photons by ensuring that responses to 0, 1, 2, etc., absorbed photons are separable. Indeed,

behavioral work suggests that dark-adapted humans can count photons (Sakitt, B., 1972), although other interpretations of the same data are possible because of the caveats raised above about behavioral estimates of absolute sensitivity (Donner, K., 1992; Field, G. D. *et al.*, 2005). Photon counting, however, is of questionable importance for visual function because of Poisson fluctuations in photon absorption – that is, a visual input producing an average of m absorbed photons will produce $m \pm \sqrt{m}$ on a single trial. The rod itself, because of reproducibility, would be capable of encoding finer gradations in light intensity.

Figure 6 compares the relative impact of Poisson fluctuations and variability in the single-photon response on signals encoded in the rod array. Figure 6(a) simulates the pattern of photon absorptions in the rod array at high light levels. Figure 6(b) is a discretized version of the image – that is, the simulated number of photons absorbed in each rod is an integer number, but Poisson fluctuations are absent. This pattern of photon absorptions is unphysical due to the lack of Poisson fluctuations, but it is useful in evaluating the relative impact of Poisson fluctuations and variability in the single-photon response since the two noise sources can be added independently. Figure 6(c) adds Poisson fluctuations in photon absorption to the image in Figure 6(b). Figure 6(d) adds variability in the single-photon response instead of Poisson fluctuations. Comparison of Figure 6(c) and (d) shows that Poisson fluctuations pose a much more severe limitation on the fidelity of the signal in the rod array than variability in the single-photon response. Only if the standard deviation of single-photon response was three to four times larger would response variability pose a limitation comparable to Poisson fluctuations. This argument applies across a wide range of mean light levels. Thus the rod appears overengineered for the task of counting incident photons.

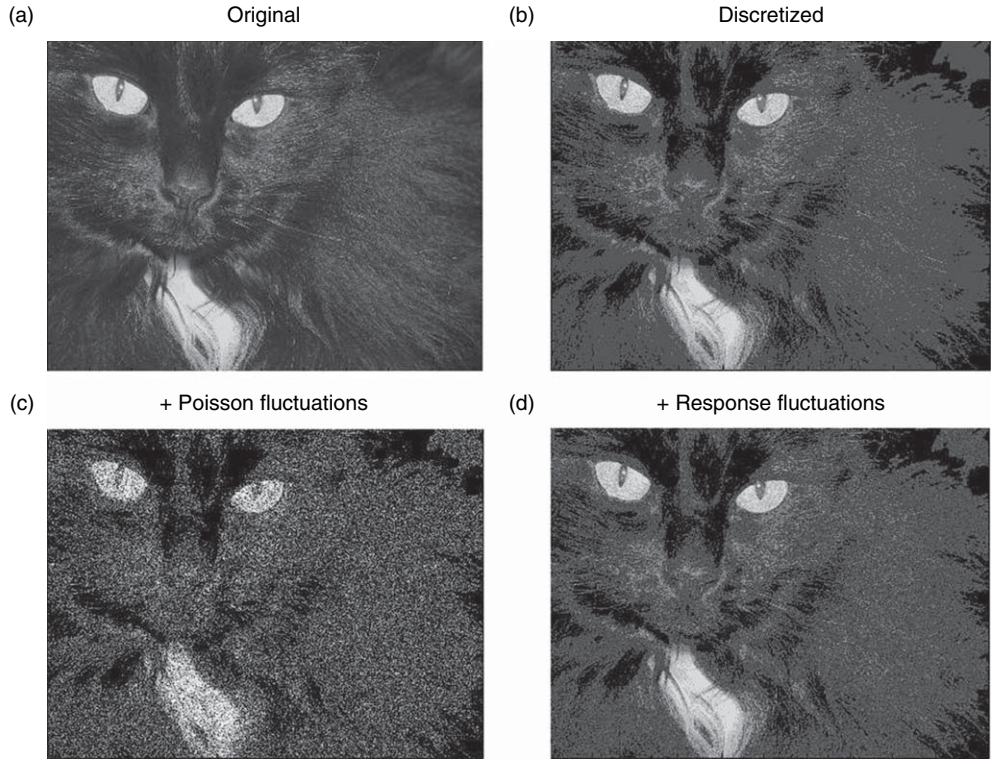

Figure 6 Reproducibility and photon counting. (a) Original image. (b) Discretized image in which the number of photons absorbed in each rod (i.e., pixel value) is an integer, with a mean of 2. (c) Image in (b) with Poisson fluctuations in photon absorption added. Each pixel in (b) was replaced by a sample from a Poisson distribution with appropriate mean. (d) Image in (b) with variability in rod's single-photon response added, assuming that the SD of the single-photon response was 0.25 times the mean. Thus each photon absorption from (b) was replaced by a sample from a Gaussian distribution with an SD of 0.25 and a mean of 1.

If photon counting is not an important consideration for rod vision, why are the rod responses reproducible? An alternative is that reproducibility is important for encoding the time of photon absorption rather than the photon count (Rieke, F. and Baylor, D. A., 1998a; 1998b; Field, G. D. and Rieke, F., 2002a). Figure 7 illustrates one test of this hypothesis. Figure 7(a) shows three individual single-photon responses recorded from a primate rod. The smooth curve in each case is a template formed from the average single-photon response; the template has been shifted along the *x*-axis to fit each single-photon response and the resulting time shift is used to estimate the apparent photon absorption time. The variability of the time shifts applied to the templates provides an estimate of the accuracy with which the photon arrival time is encoded by the single-photon response. Figure 7(b) shows a histogram of the resulting time shifts. The single-photon responses of primate rods permit estimation of the photon absorption time with a precision of ~50 ms, about 10% of the duration of the rod response (Field, G. D. *et al.*, 2002 Neurosciences Abstract). Both continuous noise and variability in the single-photon response contribute to the width of the histogram since both are present in the isolated single-photon responses. The impact of continuous noise alone can be determined by repeating this procedure using sections of dark record with added, identical single-photon responses; in this case all the variability in the responses is attributable to continuous noise. This results in the narrow histogram shown in Figure 7(b). Thus variability in the single-photon response, although small, still limits the temporal precision of the rod's single-photon response, and were reproducibility to fail temporal precision would suffer.

Reproducibility also raises an interesting molecular design question: how are the responses produced by single rhodopsin molecules controlled so that their variability is so much less than expected? Three mechanisms have been proposed: (1) saturation or compression that renders the measured current response insensitive to variations in rhodopsin's lifetime (Ramanathan, S. *et al.*, 2005); (2) feedback that reduces variability in rhodopsin's active lifetime (Whitlock, G. G. and Lamb, T. D., 1999); and (3) shutoff of a single rhodopsin molecule through a series of steps or transitions (Rieke, F. and Baylor, D. A., 1998b; Field, G. D. and Rieke, F., 2002a; Hamer, R. D. *et al.*, 2003). Each mechanism is capable of reducing variability in the single-photon response to measured levels. Direct evidence in favor of the

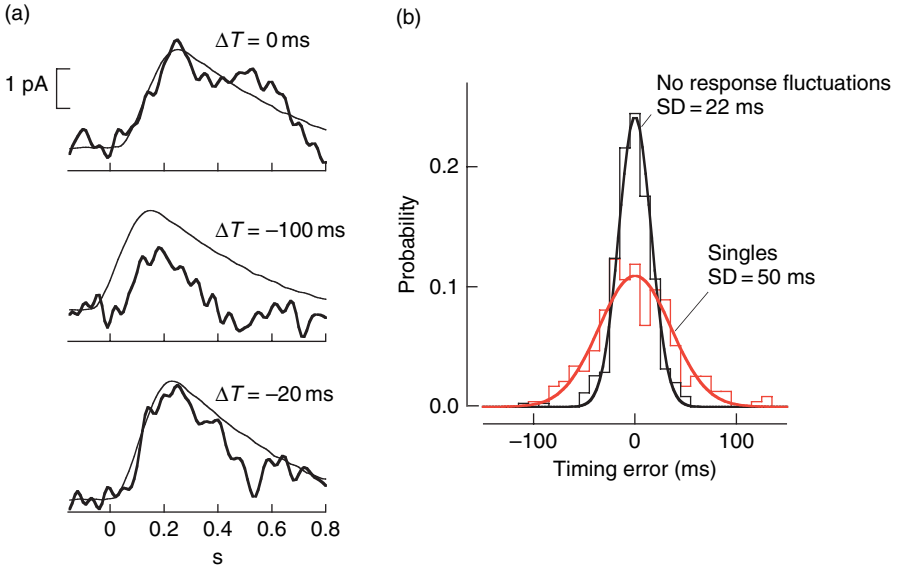

Figure 7 Reproducibility and temporal precision. (a) Three individual single-photon responses from a primate rod, each fit with a template to estimate temporal precision. Single-photon responses were identified from the responses to a repeated fixed-strength flash as in Figure 4. The template is the cell's average single-photon response. (b) Histograms of time shifts that provided best fits of the template to the single-photon responses as in (a). The red trace plots the histogram for identified single-photon responses. The black trace plots histogram for noise trials with added, deterministic single-photon response; this isolates the contribution of continuous noise to limiting temporal precision. Data from Greg Field.

multistep shutoff model comes from studying how response variability changed when rhodopsin was altered genetically (Doan, T. *et al.*, 2006). Variability of the single-photon response depends in a graded and systematic manner on the number of phosphorylation sites on rhodopsin – thus reproducibility is apparently produced by the shutoff of a single rhodopsin molecule through a series of steps, each provided by phosphorylation. This is a substantial departure from conventional models for the shutoff of single molecules. Rhodopsin is one of many G protein-coupled receptors; thus a similar strategy may decrease variability in signals controlled by other G protein cascades.

1.18.4 Retinal Readout of the Rod Signals

The elegance of photon detection by the rods would be wasted if not matched with an equally elegant readout circuit. To enable vision at low light levels, the retinal readout of signals in the rod array must meet three substantial challenges: (1) the circuitry must extract signals of relevance from the sparse pattern of photon absorptions created in the rod array; (2) the circuitry must extract and represent information about the timing of photon absorptions from the sluggish rod input signals; and (3) the circuitry must transmit and process rod signals while adding little noise.

Rod signals are conveyed across the mammalian retina through three pathways (Figure 8; see Chapter Mammalian Rod Pathways). The rod bipolar pathway is the dominant readout at low light levels (Deans, M. R. *et al.*, 2002; Volgyi, B. *et al.*, 2004) and is the focus of this section. In this pathway, rod signals are first transmitted to rod bipolar cells – a class of ON or depolarizing bipolar cell that receives only rod input. The synapse between rods and rod bipolar cells is an unusual sign-inverting glutamatergic synapse. Glutamate released from the rods in the dark activates metabotropic glutamate receptors on the rod bipolar dendrite, initiating a second messenger cascade that leads to closure of cationic channels. The decrease in glutamate release produced during the rod's hyperpolarizing light response decreases receptor activity, leading to channel opening and the production of an inward (depolarizing) current in the rod bipolar dendrites. The postsynaptic response in the rod bipolar is exceedingly rapid for one mediated by metabotropic receptors, and understanding how this cascade works is certain to be interesting. Signals in the rod bipolar are transmitted to AII amacrine cells through a more typical sign-conserving glutamatergic synapse that uses ionotropic receptors. AII amacrine cells contact ON cone bipolar cells through gap junctions and OFF cone bipolar cells through glycinergic synapses. Signals from the cone bipolar cells are then conveyed to ganglion cells. A key feature of the rod bipolar pathway is that rod and cone signals are mixed late

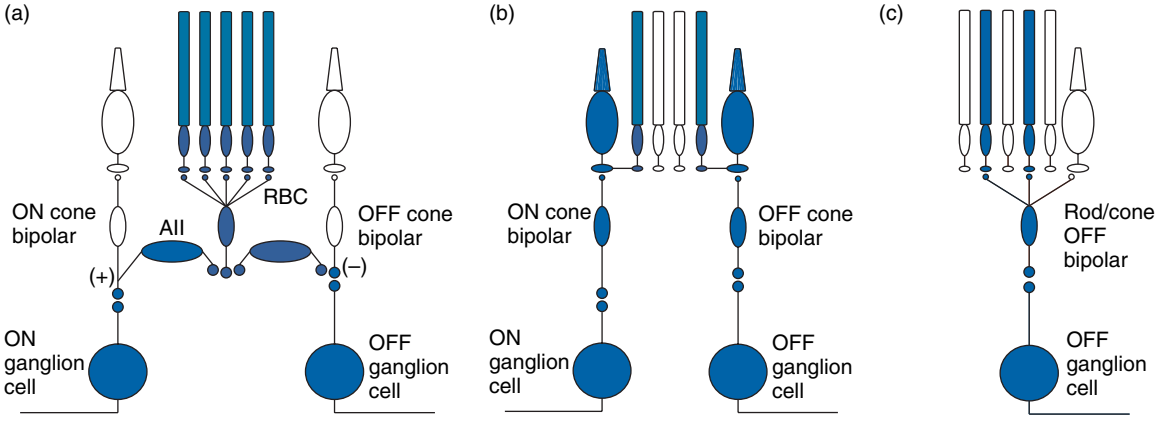

Figure 8 Pathways for rod signals in mammalian retina. (a) Rod bipolar pathway (Dacheux, R. F. and Raviola, E., 1986; Sterling, P. *et al.*, 1988). Rod signals are conveyed to ganglion cells through two dedicated cell types: rod bipolar cells and AII amacrine cells. Signals from the AII amacrine cells reach ganglion cells via ON and OFF cone bipolar cells. (b) Rod–cone pathway (Nelson, R., 1977; Schneeweis, D. M. and Schnapf, J. L., 1995). Rod signals reach cones through gap junctions and are conveyed across the cone circuitry to ganglion cells. (c) Rod–OFF cone bipolar pathway (Soucy, E. *et al.*, 1998; Hack, I. *et al.*, 1999; Tsukamoto, Y. *et al.*, 2001). Rod signals are transmitted to a class of OFF bipolar cell that receives mixed rod and cone input. AII, AII amacrine; RBC, Rod biopolar.

in retinal processing, unlike the other known pathways for rod signals in which this mixing occurs essentially immediately. Thus the rod bipolar pathway is unique in presenting multiple opportunities for rod-specific signal processing.

1.18.4.1 Sparseness, Convergence, and Nonlinear Processing

Rod vision at low light levels exemplifies a general problem: pooling of signals from an array of detectors under conditions where a small fraction of the detectors carry the signal of interest while all of the detectors generate noise. Cells throughout the nervous system face a similar issue when a small number of their converging inputs are active. This general issue is particularly tractable in the retina because the rod signal and the noise are well characterized and the relevant circuitry is well established.

Convergence is a dominant feature of rod signaling in the retina, with peripheral mammalian ganglion cells receiving input from thousands of rods. This convergence occurs in stages as signals traverse the rod bipolar pathway (Sterling, P. *et al.*, 1988): rod bipolar cells typically receive input from ~20 rods, AII amacrine cells receive input from ~500 rods via ~20 rod bipolar cells, and ganglion cells receive input from several AII amacrine cells via cone bipolar cells (Figure 9(a)). AII amacrine cells are coupled reciprocally through gap junctions, correlating signals among nearby cells (Famiglietti, E. V. J. and Kolb, H., 1975; Bloomfield, S. A. *et al.*, 1997). Signals also diverge in the circuitry: each rod contacts several rod bipolar cells, and each rod bipolar cell contacts several AII amacrine cells (Sterling, P. *et al.*, 1988; Migdale, K. *et al.*, 2003).

Corresponding to the convergence of rod signals, responses of cells late in the rod bipolar pathway saturate at lower light levels than cells early in the pathway (Pang, J. J. *et al.*, 2004; Dunn, F. A. *et al.*, 2006). Figure 9(b), top, shows families of flash responses from a mouse rod photoreceptor, a rod bipolar cell, an AII amacrine cell, and an ON ganglion cell. Each panel superimposes average responses to a series of flash strengths. The dependence of the response amplitude on flash strength for each cell type is summarized in Figure 8(b), bottom. The stimulus–response relations shift to the left for later stages in the pathway, with half-maximal flash strengths decreasing from ~10 Rh^* in the rods to ~1 Rh^* per rod in the rod bipolar cells and ~0.1 Rh^* per rod in AII amacrine and ganglion cells. Thus a flash of a given strength – for example, 0.1 Rh^* per rod – produces a larger fractional response in AII amacrine cells and ganglion cells than in the rods or rod bipolar cells.

The leftward shift of the stimulus–response relations in Figure 8(b) requires that the gain of signal transfer between cells in the rod bipolar pathway is well matched to the pattern of convergence, effectively boosting sparse single-photon responses in the rod array to create a measurable response in downstream cells. The high gain of signal transfer, together with the high gain of the phototransduction process itself, means that activation of a single rhodopsin molecule can produce a measurable change in the firing rate of a retinal ganglion cell. For example, a subset of cat ganglion cells appears to produce one to three extra action potentials when one of the thousands of rods within its receptive field absorbs a photon (Barlow, H. B. *et al.*, 1971; Mastronarde, D. N., 1983). While this high gain is essential for vision at absolute threshold, it threatens to saturate retinal responses at light levels in which only 1–2% of the rods absorb photons during the ~200 ms integration time of rod signals. Such saturation is prevented by adaptive mechanisms that decrease synaptic gain in the rod bipolar pathway (Dowling, J. E., 1963; Frishman, L. J. and Sieving, P. A., 1995; Dunn, F. A. *et al.*, 2006.

The discussion above neglects the noise that obscures the light responses of cells in the rod bipolar pathway. However, how noise is excluded, retained, or generated is central to understanding the relation between neural responses and behavior. Furthermore, noise is a key factor determining efficient strategies for retinal processing of the rod signals. Thus convergence of rod inputs creates an opportunity for downstream cells to achieve higher sensitivity than individual rods. Because of noise in the rod array, however, this opportunity would be squandered if the rod signals were simply averaged (Baylor, D. A. *et al.*, 1984; van Rossum, M. C. and Smith, R. G., 1998).

The sparse pattern of photon absorptions near visual threshold means that information about the visual inputs is carried in the responses of a small fraction (0.1–0.01%) of the rods. All of the rods, however, generate noise that threatens to obscure the responses of the few rods absorbing photons. The task facing the retina is like standing in the middle of a crowded stadium and trying to determine what a few of the thousands of people in the bleachers are yelling. Averaging responses under these

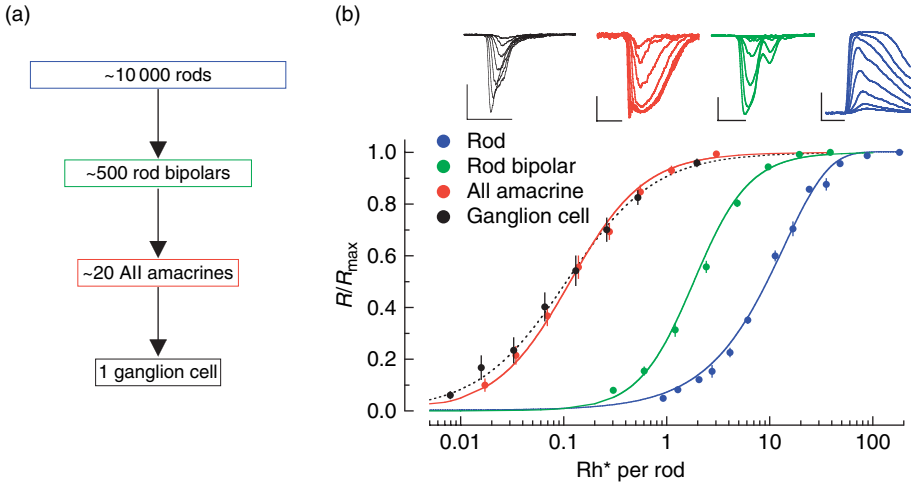

Figure 9 Convergence and stimulus–response relations for elements of rod bipolar pathway. (a) Schematic of convergence. (b) Top: Flash families for a single rod, rod bipolar, AII amacrine, and ON ganglion cell. Horizontal scale bars are 200 ms in each panel; vertical scale bars are 200 pA for the ganglion cell, 100 pA for the AII amacrine cell, 50 pA for the rod bipolar cell, and 5 pA for the rod. Bottom: Stimulus–response relations from flash families as in the top panels. Data from A. P. Sampath and Felice Dunn.

conditions is a disaster as it inextricably mixes signal and noise. A better strategy is to average only after first making a selection of signals from those people of potential interest (based on some prior criteria – for example, how loudly they are yelling) and discarding signals from the rest. This is the strategy the retinal readout adopts: the rod bipolar pathway selectively retains signals from those rods likely to be generating single-photon responses and discards noise from the remaining rods (Field, G. D. and Rieke, F., 2002b). This selective retention of signals of interest can dramatically improve visual sensitivity. To be effective, such a selection must occur prior to mixing of rod signals – that is, in the transmission of signals from the rod to the rod bipolar cell dendrite.

Responses likely to be generated by photon absorption can be selected by applying a threshold to the rod signals. Evidence for a thresholding nonlinearity at the rod-to-rod bipolar synapse comes from comparing light responses of rods and rod bipolar cells (Field, G. D. and Rieke, F., 2002b). Rods respond linearly to flashes producing up to ~5 Rh^* – for example, the rod response doubles when the flash strength is doubled (Baylor, D. A. *et al.*, 1984; Nakatani, K. *et al.*, 1991). Figure 10(a) illustrates this well-known linearity of the rod signals. The inset shows a flash family recorded from a mouse rod, with the thick traces showing responses to flashes producing <6 Rh^* on average. The amplitudes of the responses to dim flashes scale linearly with flash strength, as shown in the main panel of Figure 10(a). Rod bipolar cell responses depend supralinearly on flash strength for flashes producing 0.5–1 Rh^* per rod. For example, the response more than doubles when the flash strength is doubled (Figure 10(b)). This supralinear behavior can be explained if a small single-photon response in the rod fails to exceed a threshold required to generate a response in the rod bipolar, while a large single-photon response or a response to two photons exceeds threshold and is faithfully transmitted. Such a thresholding causes responses to flashes in which few or no rods absorb more than one photon to be attenuated relative to responses to flashes that produce a higher probability of two or more photon absorptions in single rods. As expected, this nonlinear transfer of signals eliminates much of the rod's continuous noise, so that the rod bipolar dark noise is much less than expected from a linear summation of ~20 rod inputs (Field, G. D. and Rieke, F., 2002b). Modeling of the rod-to-rod bipolar synapse (Berntson, A. *et al.*, 2004) and electroretinograms (Saszik, S. M. *et al.*, 2002) provide further evidence for a thresholding nonlinearity, although the fraction of excluded single-photon responses is not agreed upon.

In principle, several aspects of synaptic transmission could produce such a nonlinearity. In fact it appears to be produced by saturation within the second

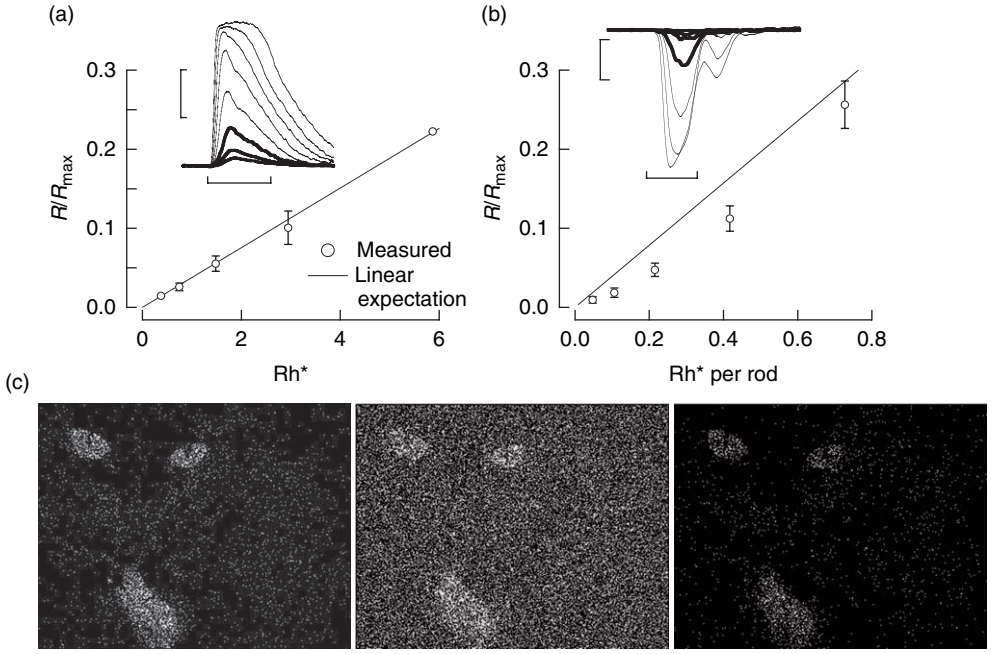

Figure 10 Thresholding nonlinearity at the rod-to-rod bipolar synapse. (a) Linearity of rod responses to dim flashes. Inset superimposes average rod responses to flashes producing an average of 0.75 to 100 Rh^*. Horizontal scale bar is 500 ms, vertical scale bar is 5 pA. (b) Supralinearity of rod bipolar responses. Inset superimposes average responses to flashes producing an average of 0.25 to 16 Rh^* per rod. Horizontal scale bar is 200 ms, vertical scale bar is 50 pA. (c) Simulation of effects of thresholding nonlinearity. (Left panel) Simulation of signals in rod array for an image producing a mean of 0.1 Rh^* per rod. (Right panel) The same image passed through a thresholding nonlinearity that discards all responses with an amplitude smaller than the mean single-photon response. Data from Greg Field and A. P. Sampath.

messenger cascade linking glutamate receptors to ion channels in the rod bipolar dendrite (Sampath, A. P. and Rieke, F., 2004). As a consequence, at most 1–2% of the transduction channels in the rod bipolar dendrites are open in the dark. This is an advantageous location. A nonlinearity located any later (e.g., by voltage-dependent conductances in the bipolar soma) would be ineffective in selectively retaining signals from rods generating single-photon responses because signals from different rods would already be mixed. A nonlinearity located earlier could fail to eliminate the noise generated within the bipolar – for example, noise inherent in the spontaneous activity of components of the rod bipolar transduction cascade, including channel noise.

Discarding a fraction of the rod's single-photon responses in transmission to the rod bipolar cell seems like a poor strategy to optimize sensitivity at low light levels. But this intuition is wrong. The likelihood that a given rod response is due to photon absorption as opposed to rod noise depends on light level. This dependence can be appreciated by considering the case of no incident light – in which case all rod responses are attributable to rod noise. In this extreme case, optimal processing means ignoring the rod signals altogether and instead relying on the prior information that no light is present – that is, under these conditions an optimally positioned thresholding nonlinearity should eliminate all rod responses. The low probability of photon absorption near absolute visual threshold introduces a strong prior probability (99.9% at 0.001 Rh^* per rod) that a rod is generating noise; the only single-photon responses that should be retained have an amplitude sufficiently large to overcome this prior probability because the likelihood that rod dark noise generates fluctuations of this amplitude is even smaller (i.e., less than 0.1% at 0.001 Rh^* per rod). This is analogous to seeing someone who looks like the president at your local supermarket. You have a strong bias that this is an unlikely event, and overcoming that bias would require substantial evidence (e.g., he installs wire taps in the supermarket intercom).

Figure 10(c) illustrates the effect of a thresholding nonlinearity on the fidelity of images in the rod array. The left panel shows a simulated pattern of photon

absorptions for an image producing an average of 0.05 Rh^* per rod. The middle panel simulates the resulting responses in the rod array – that is, with rod noise added. The right panel shows the effect of passing the rod responses through a thresholding nonlinearity that discards half of the rod's single--photon responses. The thresholding selectively preserves light signals in the rod array while discarding noise and hence substantially improves the fidelity of the image at the cost of eliminating half of the original responses. The impact of the thresholding nonlinearity on signal fidelity increases as light levels decrease; at light levels near absolute visual threshold (~0.0001 Rh^* per rod per integration time), the thresholding nonlinearity improves the signal-to-noise ratio of signals in the rod array by more than a factor of 100 (Field, G. D. and Rieke, F., 2002b).

An essentially identical issue arises at the synapse between rod bipolar and AII amacrine cells. AII amacrines receive converging input from the rod bipolars, and at visual threshold a small fraction (0.1–0.2% at 0.0001 Rh^* per rod per integration time) of the rod bipolars generate responses to photons absorbed within the pool of rods from which they receive input during the rod integration time. Meanwhile all of the rod bipolar cells generate intrinsic noise, which, if not removed before reaching the AII amacrine cell, could swamp the light responses. Thus a nonlinearity at the synapse between rod bipolar cells and AII amacrine cells could serve to remove noise intrinsic to the rod bipolar and faithfully transmit single-photon responses. This possibility has not been tested to date. In general, a repeated theme of nonlinear processing prior to convergence could enable sparse signals to be effectively transmitted through a neural circuit while rejecting noise introduced at each processing stage.

1.18.4.2 Representing and Extracting Temporal Information

Single-photon responses generated by the rods are slow – with a time-to-peak of ~200 ms and a duration of ~500 ms in mammalian rods (see Figure 7). Many critical computations, such as motion detection, rely on determining the relative timing of light inputs and thus require extracting temporal information from the rod responses. In the absence of noise, the low-pass temporal filtering provided by the rod phototransduction cascade could be undone to recover the exact times of photon absorptions. Rod noise makes recovery of the exact photon absorption times impossible, but still permits extraction of temporal information finer than the duration of the rod responses (Figure 7). This section summarizes what is known about how the retinal circuitry extracts temporal information from the rod responses and how accurately retinal ganglion cells represent this information.

1.18.4.3 Extraction

The rod-mediated dim flash responses of both amphibian (Ashmore, J. F. and Falk, G. 1980; Schnapf, J. L. and Copenhagen, D. R., 1982) and mammalian (Berntson, A. and Taylor, W. R., 2000; Euler, T. and Masland, R. H., 2000; Field, G. D. and Rieke, F., 2002b) bipolar cells are considerably briefer than those of the rods themselves. For example, Figure 11(a) compares dim flash responses of mouse rods and rod bipolar cells. The rod bipolar response reaches peak and recovers much more quickly than the rod response; in fact the bipolar response is nearly complete when the rod response reaches peak. The synaptic inputs to retinal ganglion cells evoked by dim flashes have kinetics similar to those of the rod bipolar responses (Field, G. D. *et al.*, 2005). Thus the synapse between rods and rod bipolar cells is a key determinant of the kinetics of rod-mediated signals in the retina.

The speeding of rod responses in transmission to rod bipolar cells has several consequences for the encoding of single-photon responses. First, the time of photon absorption is represented more explicitly in the briefer bipolar response as the synapse undoes some of the slowness of the rod transduction process. Second, the synapse transmits the most reliable part of the rod response – the rising phase – while suppressing the more variable recovery phase. Figure 11(b) illustrates the variability in the rod single-photon responses by superimposing 20 isolated single-photon responses and 20 responses to zero absorbed photons. Variability is small until roughly the response peak and then increases during the response recovery (Rieke, F. and Baylor, D. A., 1998a; 1998b; Field, G. D. and Rieke, F., 2002a). The increased late variability poses a particular threat for encoding the time course of continuous inputs, as the noise in the falling phase of the response to one photon absorption could obscure the response to a subsequent absorption. At low light levels, photons arrive rarely at a single rod, and hence the resulting responses are unlikely to overlap in time. However,

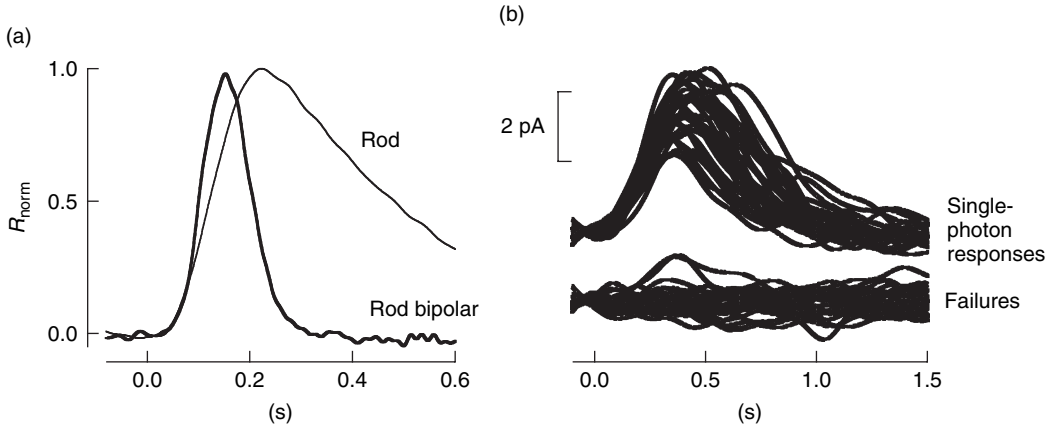

Figure 11 Extraction of temporal information in rod-to-rod bipolar signal transfer. (a) Average rod (thin trace) and rod bipolar (thick trace) responses to a weak flash. Responses have been normalized to facilitate comparison of their kinetics. (b) Variability of the single-photon responses is low during initial part of the response and increases during the response recovery. The top traces show 20 isolated single-photon responses from a mouse rod. The bottom traces show 20 isolated responses to 0 absorbed photons. Data from A. P. Sampath and Thuy Doan.

single-photon responses will often overlap in downstream cells that receive converging inputs from many rods. Eliminating or suppressing the falling phase of the rod's single-photon response in transmission to rod bipolar cells minimizes the impact of such temporal overlap on the fidelity with which continuous inputs are encoded.

In amphibians, the change in kinetics of rod-mediated responses in transmission to bipolar cells has been given a more solid theoretical and mechanistic basis. How should the rod responses be processed to estimate the photon absorption times? Low temporal frequencies have intrinsically lower temporal resolution and thus should be attenuated. High temporal frequencies are dominated by continuous noise, making these frequencies unreliable indicators of light inputs. Thus inferring temporal properties of the input signals involve filtering the rod responses with a band-pass filter matched to the signal and noise properties of the rod. This line of reasoning leads to a parameter-free prediction of the kinetics of the bipolar responses based solely on the measured rod signal and noise (Bialek, W. and Owen, W. G., 1990; Rieke, F. *et al.*, 1991). The measured bipolar responses are in good agreement with these predictions, indicating that the kinetics of signal transfer is matched to the temporal characteristics of the rod signal and noise.

Paired recordings from rods and synaptically connected bipolar cells in salamander retina directly showed the attenuation of low and high temporal frequencies at the rod-to-bipolar synapse (Armstrong-Gold, C. E. and Rieke, F., 2003). Thus modulations of the rod voltage at frequencies below 1 Hz or above 4 Hz were much less effective in producing postsynaptic responses than frequencies of 2–3 Hz. The attenuation of low temporal frequencies was apparent in the rate of excitatory postsynaptic currents measured in OFF bipolar cells, indicating that at least this part of the synaptic filtering was generated by presynaptic mechanisms.

1.18.4.4 Representation

How precisely do retinal ganglion cells encode changes in the photon absorption rate in the rods? Because they have access to signals from many rods, ganglion cells can in principle encode considerably more precise temporal information than individual rods. Two experimental approaches indicate that this is indeed the case.

One approach to estimate temporal precision is to determine the ability to discriminate between two possible flash times based on a single example of the ganglion cell spike response. Many examples of responses at the early and late time are used to learn how the ganglion cell responses differ between the two flash times. Then the most likely flash time is determined for a single response not used in the learning process. This process is repeated many times for different test responses and the percentage of correct discrimination determined. Temporal precision is defined as the time separation between the possible flash times resulting in a criterion level of

performance – for example, 75% correct discrimination. Not surprisingly, temporal precision in this discrimination task improves as flash strength increases. This dependence on flash strength means that it is not possible to give a single measure of temporal precision, unlike detection threshold, which lends itself to a unique definition. Nonetheless, the responses of both salamander and primate ganglion cells encode the flash time with a precision much finer than the duration of the rod response across a wide range of flash strengths (Chichilnisky, E. J. and Rieke, F., 2005; Field, G. D. *et al.*, 2003 Neurosciences Abstract; Uzzell *et al.*, 2003 Neurosciences Abstract). In both cases, flashes producing less than one Rh^* per rod (less than 0.01 Rh^* per rod in primate) are encoded with a temporal precision 10–30 times finer than the duration of the rod response.

A second approach to estimate temporal precision is to measure the similarity of different responses to a repeated stimulus. Figure 12 shows examples of the spike responses of a mouse ganglion cell to a repeated random stimulus with a mean intensity of 2.5 Rh^* per rod per second and a contrast of 50%. Each vertical tick in Figure 12(b) represents a single action potential, and each row shows the response to a single repetition of the stimulus. Figure 12(a) shows the average response of a single rod to the same stimulus. Figure 12(c) shows a short section of both rod and ganglion cell responses. The ganglion cell responses show strong similarity from one trial to the next; in particular they show similarity on a timescale much shorter than the modulations in the rod response, indicating that the temporal precision is much greater than might be expected from the slow rod inputs. Indeed, the standard deviation of the first spike time in bursts such as that in the bottom panel averages ~5 ms (range across events 2–10 ms) for these stimuli, ~3% of the correlation time of the rod response.

The temporal precision of ganglion cell responses is one of several examples of acuity beyond the naive

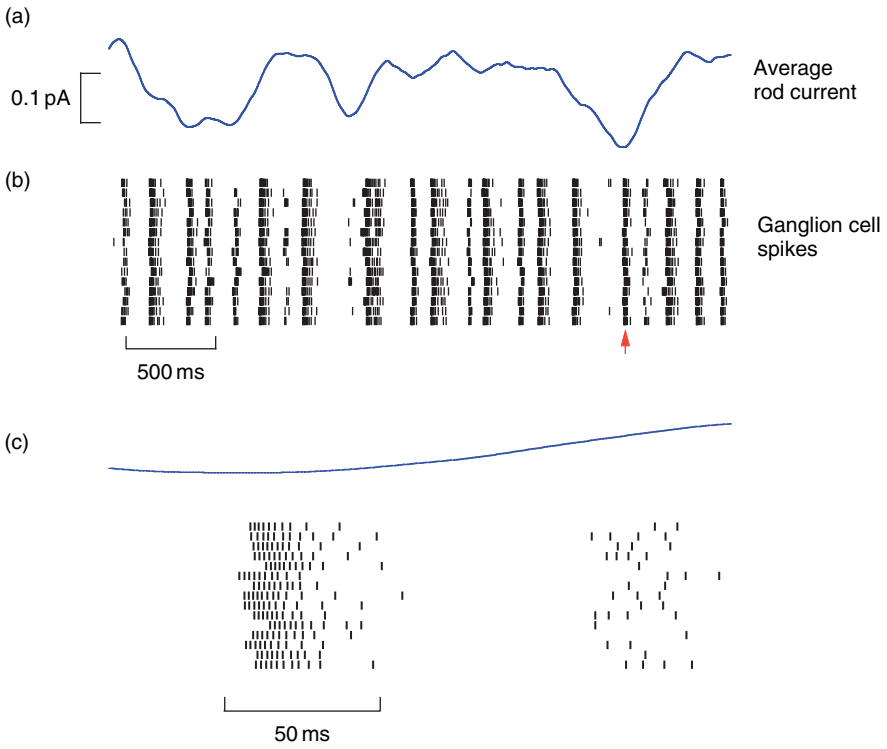

Figure 12 Temporal precision of ganglion cell responses to a repeated random stimulus with a mean of 2.5 Rh^* per rod per second. (a) Estimated average rod response to this stimulus. The rod response was generated by convolving the measured rod single-photon response with the random stimulus. Direct measurement of the average rod response is difficult because the low light level and the resulting large Poisson fluctuations in photon absorption would require averaging thousands of trials. (b) Several individual spike responses of an ON retinal ganglion cell to the same stimulus. (c) Section of rod (smooth line) and ganglion cells responses on expanded timescale. The burst of spikes on the left is marked by the red arrow in panel (b). Data from Gabe Murphy.

limits set by the sampling properties of the receptors. Other familiar examples are chromatic sensitivity, which exceeds expectations from the coarse spectral sensitivities of the cone photoreceptors, and spatial acuity, which exceeds expectations from the spacing between foveal cones. In each such instance, the true limit to acuity is set by the signal and noise properties of the receptor responses. We have an incomplete picture, however, of how effectively the retinal readout exploits the low noise of the rod signals to extract and represent temporal information – for example, how the temporal precision of retinal ganglion cells compares to that of the rods from which they receive input.

1.18.4.5 Low Noise

The high sensitivity of dark-adapted vision requires that noise introduced in each step of retinal processing is either small or is removed by subsequent processing. Two issues make the impact of synaptic noise (i.e., fluctuations in transmitter release or in the generation of postsynaptic currents) of particular importance at the rod-to-rod bipolar synapse. First, synaptic noise makes the task of separating single-photon responses from noise in the rod array more difficult; thus synaptic noise is an important factor in determining how much a thresholding nonlinearity at the rod-to-rod bipolar synapse can improve the fidelity of rod-mediated signals and in determining the best position of such a nonlinearity. Second, the presynaptic signal at this synapse is only ~1 mV (Schneeweis, D. M. and Schnapf, J. L., 1995), making reliable transmission challenging in the face of the expected statistical fluctuations in transmitter release.

Photon absorption produces a reduction or a pause in the ongoing transmitter release by the rod. Random pauses or slowing in release due to statistical fluctuations will mimic true photon events, producing a source of noise potentially limiting the visual sensitivity (Falk, G. and Fatt P., 1972). Rao-Mirotznik R. *et al.* (1998) argued that mammalian rods must maintain a dark release rate of at least $100\,s^{-1}$ to ensure that random pauses in release occur less often than thermal isomerization of rhodopsin in the rod outer segment. Their argument is based on two untested assumptions: (1) statistical fluctuations in release obey Poisson statistics and (2) release is completely suppressed for ~100 ms during the single-photon response. With these assumptions, dark release rates lower than $100\,s^{-1}$ lead to an unacceptably high rate of random, 100-ms pauses in release that mimic true single-photon responses.

Schein S. and Ahmad K. M. (2005; 2006) analyzed models for the rod output synapse that relax both of these assumptions. In particular, they explored how synaptic noise is affected by sub-Poisson variability in the release process and by partial rather than complete reductions in the release rate during the single-photon response. They argue that the reduction in release rate during the single-photon response is likely ~20% based on the voltage dependence of the rod Ca^2 channels and the ~1 mV hyperpolarization during the single-photon response. With this smaller signal, synaptic noise could be kept acceptably low for dark release rates near $100\,s^{-1}$, provided the release process is much more regular than a Poisson process. Such regularity in release could be produced, for example, by refractoriness at vesicle fusion sites or another process that effectively times the intervals between vesicle release events.

The above theoretical arguments focus on the criterion that synaptic noise introduces false photon-like noise events at a rate not higher than spontaneous rhodopsin activation. This criterion ensures that the impact of synaptic noise on the detection of dim lights is not greater than discrete noise in the rod outer segment currents. Although this is a convenient criterion, it is not unique. First, the comparison of rod noise with behavior or with retinal ganglion cell responses leaves open the possibility that significant noise is introduced in the retinal circuitry (see Section 1.18.2). This could relax the requirement on low noise at the synapse, though probably not enough to be consistent with Poisson fluctuations in release. Second, there is fortunately much more to vision than detecting the presence or the absence of dim lights. For example, as described above, rods and ganglion cells encode the timing of light inputs with high precision – a precision much finer than the ~100 ms integration times assumed for the studies described above. Maintaining sufficiently low synaptic noise to preserve information about the times of photon absorption would appear to pose a stringent requirement on the statistics of transmitter release.

1.18.5 Summary

The ability of human observers to detect the absorption of a few photons and the resulting activation of a few rhodopsin molecules is one of several examples

in which sensory performance approaches fundamental limits (reviewed by Bialek, W., 1987). Thus pheromone receptors can detect the binding of a few molecules to the receptors on their surface membrane (Leinders-Zufall, T. *et al.*, 2000), chemotactic bacteria can count molecules bound to receptors on their surface (Berg, H. C. and Purcell, E. M., 1977), and auditory hair cells can sense movements of their stereocilia less than the diameter of a hydrogen atom. These observations about the fidelity of sensory encoding provide a clear framework for studying how these systems work; they help pose precise questions, they provide a natural benchmark against which to evaluate our understanding, and they suggest that predictive, theoretical approaches based on optimization may be relevant. This line of reasoning has helped uncover how elegantly suited the rod photoreceptors are for the task of detecting incident photons (reviewed by Rieke, F. and Baylor, D. A., 1998a; 1998b; Burns, M. E. and Baylor, D. A., 2001). The challenges facing the retinal readout of the rod signals are no less daunting than those facing the rods themselves. We know much less, however, about how these challenges are met.

Acknowledgments

I thank Thuy Doan, Felice Dunn, Gabe Murphy, and Barry Wark for helpful comments and Thuy Doan, Felice Dunn, Greg Field, A. P. Sampath, and Gabe Murphy for experimental data for many of the figures. Support was provided by the NIH (EY-11850) and Howard Hughes Medical Institute.

References

Armstrong-Gold, C. E. and Rieke, F. 2003. Bandpass filtering at the rod to second-order cell synapse in salamander (*Ambystoma tigrinum*) retina. J. Neurosci. 23, 3796–3806.

Ashmore, J. F. and Falk, G. 1980. Responses of rod bipolar cells in the dark-adapted retina of the dogfish, *Scyliorhinus canicula*. J. Physiol. 300, 115–150.

Barlow, H. B. 1956. Retinal noise and absolute threshold. J. Opt. Soc. Am. 46, 634–639.

Barlow, H. B., Levick, W. R., and Yoon, M. 1971. Responses to single quanta of light in retinal ganglion cells of the cat. Vision Res. (Suppl. 3), 87–101.

Baylor, D. A., Lamb, T. D., and Yau, K. W. 1979. Responses of retinal rods to single photons. J. Physiol. 288, 613–634.

Baylor, D. A., Matthews, G., and Yau, K. W. 1980. Two components of electrical dark noise in toad retinal rod outer segments. J. Physiol. 309, 591–621.

Baylor, D. A., Nunn, B. J., and Schnapf, J. L. 1984. The photocurrent, noise and spectral sensitivity of rods of the monkey *Macaca fascicularis*. J. Physiol. 357, 575–607.

Berg, H. C. and Purcell, E. M. 1977. Physics of chemoreception. Biophys. J. 20, 193–219.

Berntson, A. and Taylor, W. R. 2000. Response characteristics and receptive field widths of on-bipolar cells in the mouse retina. J. Physiol. 524 (Pt 3), 879–889.

Berntson, A., Smith, R. G., and Taylor, W. R. 2004. Transmission of single photon signals through a binary synapse in the mammalian retina. Vis. Neurosci. 21, 693–702.

Bialek, W. 1987. Physical limits to sensation and perception. Annu. Rev. Biophys. Biophys. Chem. 16, 455–478.

Bialek, W. and Owen, W. G. 1990. Temporal filtering in retinal bipolar cells. Elements of an optimal computation? Biophys. J. 58, 1227–1233.

Bloomfield, S. A., Xin, D., and Osborne, T. 1997. Light-induced modulation of coupling between AII amacrine cells in the rabbit retina. Vis. Neurosci. 14, 565–576.

Burns, M. E. and Baylor, D. A. 2001. Activation, deactivation, and adaptation in vertebrate photoreceptor cells. Annu. Rev. Neurosci. 24, 779–805.

Chichilnisky, E. J. and Rieke, F. 2005. Detection sensitivity and temporal resolution of visual signals near absolute threshold in the salamander retina. J. Neurosci. 25, 318–330.

Dacheux, R. F. and Raviola, E. 1986. The rod pathway in the rabbit retina: a depolarizing bipolar and amacrine cell. J. Neurosci. 6, 331–345.

Dartnall, H. J. A. 1972. Photosensitivity. In: Handbook of Sensory Physiology, Vol. VII/1, Photochemistry of Vision (*ed*. H. J. A. Dartnall), pp. 122–145. Springer.

Deans, M. R. *et al.* 2002. Connexin36 is essential for transmission of rod-mediated visual signals in the mammalian retina. Neuron 36, 703–712.

Doan, T. *et al.* 2006. Multiple phosphorylation sites confer reproducibility of the rod's single-photon responses. Science 313, 530–533.

Donner, K. 1992. Noise and the absolute thresholds of cone and rod vision. Vision Res. 32, 853–866.

Dowling, J. E. 1963. Neural and photochemical mechanisms of visual adaptation in the rat. J. Gen. Physiol. 46, 1287–1301.

Dryja, T. P. 2000. Molecular genetics of Oguchi disease, fundus albipunctatus, and other forms of stationary night blindness: LVII Edward Jackson Memorial Lecture. Am. J. Ophthalmol. 130, 547–563.

Dunn, F. A. *et al.* 2006. Controlling the gain of rod-mediated signals in the mammalian retina. J. Neurosci. 26, 3959–3970.

Euler, T. and Masland, R. H. 2000. Light-evoked responses of bipolar cells in a mammalian retina. J. Neurophysiol. 83, 1817–1829.

Falk, G. and Fatt, P. 1972. Physical Changes Induced by Light in the Rod Outer Segment of Vertebrates. In: The Handbook of Sensory Physiology (*ed*. H. J. A. Dartnall), Vol. VII/1 pp. 200–244. Springer.

Famiglietti, E. V. J. and Kolb, H. 1975. A bistratified amacrine cell and synaptic circuitry in the inner plexiform layer of the retina. Brain Res. 84, 293–300.

Field, G. D. and Rieke, F. 2002a. Mechanisms regulating variability of the single photon responses of mammalian rod photoreceptors. Neuron 35, 733–747.

Field, G. D. and Rieke, F. 2002b. Nonlinear signal transfer from mouse rods to bipolar cells and implications for visual sensitivity. Neuron 34, 773–785.

Field, G. D., Sampath, A. P., and Rieke, F. 2005. Retinal processing near absolute threshold: from behavior to mechanism. Annu. Rev. Physiol. 67, 491–514.

Frishman, L. J. and Sieving, P. A. 1995. Evidence for two sites of adaptation affecting the dark-adapted ERG of cats and primates. Vision Res. 35, 435–442.

Hack, I., Peichl, L., and Brandstatter, J. H. 1999. An alternative pathway for rod signals in the rodent retina: rod photoreceptors, cone bipolar cells, and the localization of glutamate receptors. Proc. Natl. Acad. Sci. U. S. A. 96, 14130–14135.

Hamer, R. D. *et al.* 2003. Multiple steps of phosphorylation of activated rhodopsin can account for the reproducibility of vertebrate rod single-photon responses. J. Gen. Physiol. 122, 419–444.

Hamer, R. D. *et al.* 2005. Toward a unified model of vertebrate rod phototransduction. Vis. Neurosci. 22, 417–436.

Hecht, S. and Verrijp, C. D. 1933. The influence of intensity, color and retinal location on the fusion frequency of intermittent illumination. Proc. Natl. Acad. Sci. U. S. A. 19, 522–535.

Hecht, S., Shlaer, S., and Pirenne, M. H. 1942. Energy, quanta, and vision. J. Gen. Physiol. 25, 819–840.

Hodgkin, A. L. and Nunn, B. J. 1988. Control of light-sensitive current in salamander rods. J. Physiol. 403, 439–471.

Leinders-Zufall, T. *et al.* 2000. Ultrasensitive pheromone detection by mammalian vomeronasal neurons. Nature 405, 792–796.

Marriot, F. H., Morris, V. B., and Pirenne, M. H. 1959. The absolute visual threshold recorded from the lateral geniculate body of the cat. J. Physiol. 146, 179–184.

Mastronarde, D. N. 1983. Correlated firing of cat retinal ganglion cells. II. Responses of X- and Y-cells to single quantal events. J. Neurophysiol. 49, 325–349.

Migdale, K. *et al.* 2003. Two ribbon synaptic units in rod photoreceptors of macaque, human, and cat. J. Comp. Neurol. 455, 100–112.

Nakatani, K., Tamura, T., and Yau, K. W. 1991. Light adaptation in retinal rods of the rabbit and two other nonprimate mammals. J. Gen. Physiol. 97, 413–435.

Nelson, R. 1977. Cat cones have rod input: a comparison of the response properties of cones and horizontal cell bodies in the retina of the cat. J. Comp. Neurol. 172, 109–135.

Nikonov, S., Lamb, T. D., and Pugh, E. N. J. 2000. The role of steady phosphodiesterase activity in the kinetics and sensitivity of the light-adapted salamander rod photoresponse. J. Gen. Physiol. 116, 795–824.

Pang, J. J., Gao, F., and Wu, S. M. 2004. Light-evoked current responses in rod bipolar cells, cone depolarizing bipolar cells and AII amacrine cells in dark-adapted mouse retina. J. Physiol. 558, 897–912.

Pugh, E. N. and Lamb, T. D. 1993. Amplification and kinetics of the activation steps in phototransduction. Biochem. Biophys. Acta 1141, 111–149.

Ramanathan, S. *et al.* 2005. G-protein-coupled enzyme cascades have intrinsic properties that improve signal localization and fidelity. Biophys. J. 88, 3063–3071.

Rao-Mirotznik, R., Buchsbaum, G., and Sterling, P. 1998. Transmitter concentration at a three-dimensional synapse. J. Neurophysiol. 80, 3163–3172.

Rieke, F. and Baylor, D. A. 1996. Molecular origin of continuous dark noise in rod photoreceptors. Biophys. J. 71, 2553–2572.

Rieke, F. and Baylor, D. A. 1998a. Single-photon detection by rod cells of the retina. Rev. Mod. Phys. 70, 1027–1036.

Rieke, F. and Baylor, D. A. 1998b. Origin of reproducibility in the responses of retinal rods to single photons. Biophys. J. 75, 1836–1857.

Rieke, F., Owen, W. G., and Bialek, W. 1991. Optimal Filtering in the Salamander Retina. In: Advances in Neural Information Processing Systems (*eds*. D. Touretzky and J. Moody), pp. 377–383, Morgan kaufmann.

van Rossum, M. C. and Smith, R. G. 1998. Noise removal at the rod synapse of mammalian retina. Vis. Neurosci. 15, 809–821.

Sakitt, B. 1972. Counting every quantum. J. Physiol. 223, 131–150.

Sampath, A. P. and Rieke, F. 2004. Selective transmission of single photon responses by saturation at the rod-to-rod bipolar synapse. Neuron 41, 431–443.

Saszik, S. M., Robson, J. G., and Frishman, L. J. 2002. The scotopic threshold response of the dark-adapted electroretinogram of the mouse. J. Physiol. 543, 899–916.

Schein, S. and Ahmad, K. M. 2005. A clockwork hypothesis: synaptic release by rod photoreceptors must be regular. Biophys. J. 89, 3931–3949.

Schein, S. and Ahmad, K. M. 2006. Efficiency of synaptic transmission of single-photon events from rod photoreceptor to rod bipolar dendrite. Biophys. J. 91, 3257–3267.

Schnapf, J. L. and Copenhagen, D. R. 1982. Differences in the kinetics of rod and cone synaptic transmission. Nature 296, 862–864.

Schneeweis, D. M. and Schnapf, J. L. 1995. Photovoltage of rods and cones in the macaque retina. Science 268, 1053–1056.

Soucy, E. *et al.* 1998. A novel signaling pathway from rod photoreceptors to ganglion cells in mammalian retina. Neuron 21, 481–493.

Sterling, P., Freed, M. A., and Smith, R. G. 1988. Architecture of rod and cone circuits to the on-beta ganglion cell. J. Neurosci. 8, 623–642.

Teich, M. C. *et al.* 1982. Multiplication noise in the human visual system at threshold: 1. Quantum fluctuations and minimum detectable energy. J. Opt. Soc. Am. 72, 419–431.

Tsukamoto, Y., *et al.* 2001. Microcircuits for night vision in mouse retina. J. Neurosci. 21, 8616–8623.

van der Velden, H. A. 1946. The number of quanta necessary for the perception of light in the human eye. Opthalmologica 111, 321–331.

Volgyi, B. *et al.* 2004. Convergence and segregation of the multiple rod pathways in mammalian retina. J. Neurosci. 24, 11182–11192.

Whitlock, G. G. and Lamb, T. D. 1999. Variability in the time course of single photon responses from toad rods: termination of rhodopsin's activity. Neuron 23, 337–351.

1.19 Direction-Selective Cells

T Euler and S E Hausselt, Max-Planck-Institute for Medical Research, Heidelberg, Germany

© 2008 Elsevier Inc. All rights reserved.

1.19.1	**Direction-Selective Ganglion Cells**	413
1.19.2	**The Circuitry Underlying Retinal Direction Selectivity**	415
1.19.2.1	Pre- or Postsynaptic	415
1.19.2.2	Starburst Amacrine Cells	415
1.19.2.3	Pathways	417
1.19.2.3.1	Direction-Selective inhibition	417
1.19.2.3.2	Direction-Selective excitation	417
1.19.3	**Retinal Direction Selectivity Computation Mechanism(s)**	418
1.19.3.1	Computations Based on Network Interactions	418
1.19.3.1.1	Starburst cell networks	419
1.19.3.2	Computations Based on Intrinsic Properties	419
1.19.4	**Developmental Aspects**	419
1.19.5	**The Role of Direction-Selective Signals Originating in the Retina**	419
References		420

Glossary

direction-selective ganglion cell Certain type of retinal ganglion cell that codes the direction of image motion within its receptive field with its spike response.

direction selectivity/discrimination The ability of a neuronal network, a single neuron, or a subcellular compartment to detect and signal the direction of image motion.

global motion Motion of the whole visual field, as for example caused by head or body motion.

local motion Motion of an object relative to the background.

nonlinearity The behavior of a nonlinear system cannot be described as the sum of its parts.

null direction Direction of motion in which the response of a direction-selective cell is minimal.

preferred direction Direction of motion in which the response of a direction-selective cell is maximal.

starburst amacrine cell Retinal interneuron with a characteristic, radially symmetrical dendritic morphology that functionally participates in the propagation of Ca^{2+} waves in the developing retina and in the generation of direction selectivity in the mature retina. The synonym cholinergic amacrine cell is imprecise because other cholinergic amacrine cells exist in the retinas of at least some species.

1.19.1 Direction-Selective Ganglion Cells

Most of what we know about retinal direction selectivity (DS) comes from studies on rabbit retina, where direction-selective ganglion cells (DSGCs) (Figure 1(a)) were described first (Barlow, H. B. and Hill, R. M., 1963). Morphologically equivalent ganglion cell types have been found in a number of vertebrates (reviewed in Vaney, D. I. *et al.*, 2001), including primates (Yamada, E. S. *et al.*, 2005). Physiological recordings of DSGCs in species other than rabbits are rare; however, in cases where measurements were made, such as in mice (Weng, S. *et al.*, 2005) or turtles (Marchiafava, P. L., 1979; Borg-Graham, L. J., 2001), very similar functional properties have been found, suggesting the DS circuit to be present in all vertebrate retinas.

Two types of DSGCs can be distinguished (Figure 1(b); reviewed in Vaney, D. I. *et al.*, 2001; Taylor, W. R. and Vaney, D. I., 2003; Masland, R. H., 2004). In the rabbit, one type is the ON DSGC,

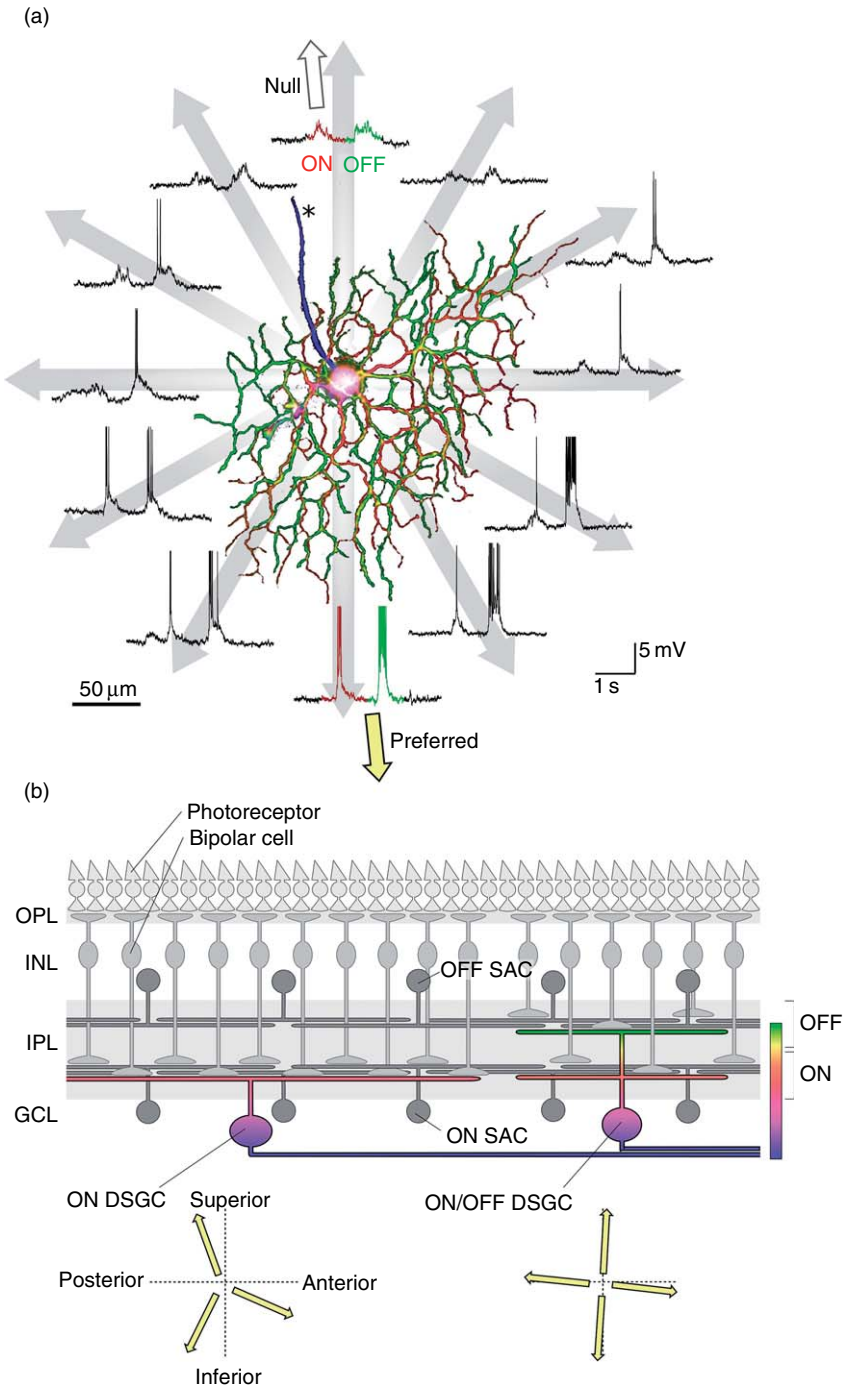

Figure 1 Direction-selective ganglion cells (DSGCs). (a) ON/OFF DSGC filled with fluorescent dye by microinjection (flat-mounted rabbit retina; pseudocolor codes for retinal depth). The cell is bistratified with dendrites ramifying in the ON (red) and OFF sublamina (green) of the inner plexiform layer (IPL). Axon (blue) is marked by asterisk. Electrical responses to a bright bar (300 μm wide, 1000 μm long) moving in 12 different directions on a dark background are shown. (b) Schematic diagram of a retinal cross-section. Only cells known to be directly involved in the DS circuitry are depicted; ON and ON/OFF DSGCs are color-coded for retinal depth (see (a)). Bottom: Preferred directions of the two types of DSGCs. GCL, ganglion cell layer; INL, inner nuclear layer; OPL, outer plexiform layer; SAC, starburst amacrine cell. Adapted from Oyster, C. W. and Barlow, H. B. 1967. Direction-selective units in rabbit retina: distribution of preferred directions. Science 155, 841–842.

which makes up less than 1% of all ganglion cells and is mainly found in the vicinity of the visual streak. Its monostratified dendritic arbor is in the inner half (ON sublamina) of the inner plexiform layer (IPL) and has a diameter between 300 and 800 µm. ON DSGCs respond to bright stimuli moving on a darker background, are sensitive to low-velocity motion (up to few degrees per second; $1^\circ \approx 150\,\mu m$ on an adult rabbit's retina), and comprise three functional subtypes, each preferring a distinct direction of motion (Figure 1(b), bottom). The second type is the ON/OFF DSGC, which accounts for more than 10% of all ganglion cells in rabbits and is found at all retinal eccentricities. It is bistratified, with one dendritic arborization in the OFF and the other in the ON sublamina. Tapping into both the ON and the OFF pathways allows this type of DSGC to detect objects that are brighter as well as objects that are darker than the background. The two arborizations, which are less than half the diameter of those of ON DSGCs, are not necessarily coextensive and can differ in size and shape (Oyster, C. W. *et al.*, 1993; Vaney, D. I., 1994), suggesting that the ON and OFF DS circuits work independently. ON/OFF DSGCs prefer higher velocities (up to $20^\circ\,s^{-1}$) than do the ON type; their functional subtypes prefer one of four different motion directions (Figure 1(b), bottom).

Each of the seven functional DSGC subtypes tiles the retinal surface in a territorial manner with little overlap (ON/OFF: Vaney, D. I., 1994; Amthor, F. R. and Oyster, C. W., 1995; ON: Buhl, E. H. and Peichl, L., 1986), such that information for any of the different preferred directions of motion is thought to be available at every retinal location (see Section 1.19.5). Since most research has focused on the ON/OFF DSGCs, in the following the term DSGC will refer to this type unless indicated otherwise.

1.19.2 The Circuitry Underlying Retinal Direction Selectivity

In one of the first models of retinal DS (Barlow, H. B. *et al.*, 1964), it was proposed that a DSGC receives delayed (or long-lasting) inhibitory input preferentially from interneurons displaced to the null side of its receptive field. An object moving in null direction would trigger this inhibition, which cancels out excitation by the object entering the DSGC's receptive field. While this model – in its original form – is not consistent with what we know today about the DS circuitry, it pointed out two of the three key properties of any detection circuit (Reichardt, W., 1961; reviewed in Borst, A. and Egelhaaf, M., 1989): a time delay (discussed in Section 1.19.3) and spatial asymmetry in the wiring. The third property is nonlinearity (see Section 1.19.3), which was not explicitly included in the original model (see also Masland, R. H., 2004).

There is ample functional evidence for asymmetrical wiring of the DS circuitry. For example, the preferred side of the DSGC's receptive field contains a zone in which motion elicits equivalent spiking responses for both preferred- and null-direction motion (Barlow, H. B. and Levick, W. R., 1965). The presence of this nondiscriminating zone indicates that synaptic input to DSGCs cannot be spatially symmetrical. Furthermore, recordings of pairs of DSGCs and neighboring starburst amacrine cells (SACs; see Section 1.19.2.2) revealed that DSGCs receive inhibitory inputs only from SACs located on the DSGCs' null side (Fried, S. I. *et al.*, 2002), indicating that DSGCs receive spatially offset inhibition. An anatomical correlate for such asymmetrical connectivity, however, has not yet been identified. In fact, it seems to be impossible to predict the preferred motion direction of a DSGC from its overall morphology (Amthor, F. R. *et al.*, 1984; Oyster, C. W. *et al.*, 1993; Yang, G. and Masland, R. H., 1994) or the distribution pattern of synaptic inputs (Jeon, C. J. *et al.*, 2002).

1.19.2.1 Pre- or Postsynaptic

The question whether DS is computed postsynaptically, that is, from non-DS excitatory and inhibitory inputs in the DSGCs themselves, or presynaptic to the DSGCs led to a long controversy (reviewed in Taylor, W. R. and Vaney, D. I., 2003; Masland, R. H., 2004). Progress toward answering this question has been made recently, when in a series of patch-clamp studies the synaptic inputs to DSGCs were found to be already direction-selective (Borg-Graham, L. J., 2001; Fried, S. I. *et al.*, 2002; Taylor, W. R. and Vaney, D. I., 2002). Stimuli moving in the preferred direction elicit more excitation and less inhibition in the DSGCs than stimuli moving in the null direction. Hence, motion direction is, at least in part, computed in interneurons presynaptic to the DSGCs.

1.19.2.2 Starburst Amacrine Cells

One type of interneuron that provides massive synaptic input to DSGCs and had been suggested to

participate in the computation of retinal DS in early studies (Masland, R. H. *et al.*, 1984a; Vaney, D. I. *et al.*, 1989; Borg-Graham, L. J. and Grzywacz, N. M., 1992) is the SAC (Figure 2(a); Masland, R. H. and Mills, J. W., 1979; Famiglietti, E. V., 1983).

SACs release two types of transmitters (Masland, R. H. *et al.*, 1984b; Brecha, N. *et al.*, 1988; Vaney, D. I. and Young, H. M., 1988): gamma-aminobutyric acid (GABA) and acetylcholine (ACh). There are OFF and ON SAC subtypes (Figure 2(c)), which – apart from their opposite response polarity – are considered functionally equivalent. The dendrites of both subtypes costratify with the respective arborizations of the ON/OFF DSGCs; the ON SAC also costratifies with the ON DSGC's arborization. Unlike most retinal neurons, SACs display extensive dendritic overlap (Tauchi, M. and Masland, R. H., 1984) and thus could provide input dedicated to each functional subtype of DSGC (see also Section 1.19.3.1). SACs feature a characteristic morphology (Famiglietti, E.

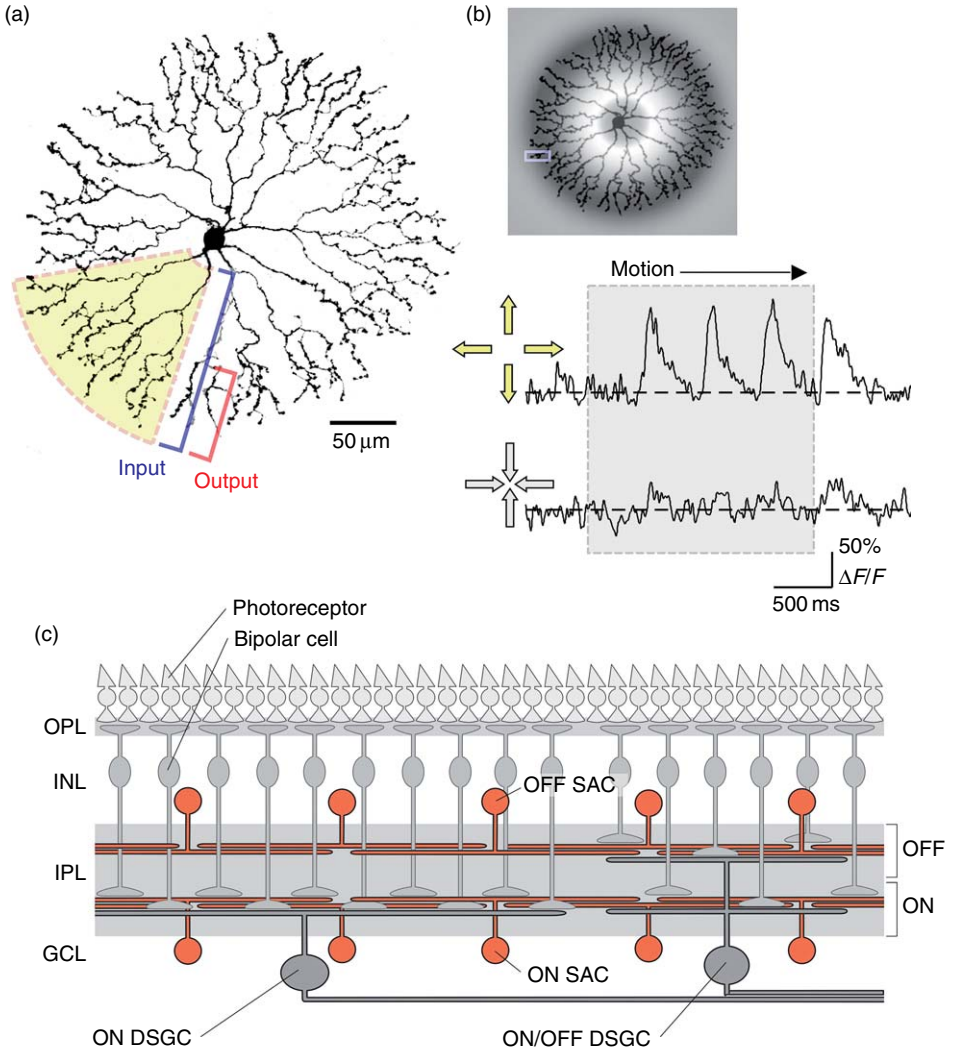

Figure 2 Starburst amacrine cells (SACs). (a) ON SAC filled with fluorescent Ca^{2+} indicator dye by microinjection (flat-mounted rabbit retina). Example for wedge-shaped dendritic sector (yellow) and radial distribution of input (blue) and output synapses (red) are indicated. (b) Top: Schematic representation of SAC with circular wave stimulus. *Bottom*: Dendritic Ca^{2+} response, recorded by two-photon fluorescence microscopy (Denk, W. *et al.*, 1990; light-blue box on cell image marks Ca^{2+}-imaging site), for centrifugal-motion (from soma to dendritic tips; upper trace) and centripetal-motion (from dendritic tips to soma; lower trace) of the circular wave stimulus. (c) Schematic diagram of a retinal cross-section; ON and OFF SACs are indicated (orange). DGSC, direction-selective ganglion cell; GCL, ganglion cell layer; INL, inner nuclear layer; IPL, inner plexiform layer; OPL, outer plexiform layer.

V., 1983; Tauchi, M. and Masland, R. H., 1984; Vaney, D. I., 1984), which is well conserved across species: four to six primary dendrites (sectors, Figure 2(a)) radiate from the soma before dividing into smaller branches. Each sector, unlike the whole cell, is strongly polarized anatomically and physiologically. Synaptic inputs from both bipolar and amacrine cells cover the whole length of the dendrite, but outputs are restricted to the distal part, which is decorated with bead-like varicosities (Famiglietti, E. V., 1991). Delayed rectifier K^+ channels are concentrated on the soma and proximal dendrite (Ozaita, A. *et al.*, 2004), which, in combination with the peculiar morphology, leads to an electrical isolation of the sectors from each other (Miller, R. F. and Bloomfield, S. A., 1983; Velte, T. J. and Miller, R. F., 1997). Hence, the sectors can be seen as largely independent processing units (Masland, R. H. *et al.*, 1984a; Vaney, D. I., 1990; Borg-Graham, L. J. and Grzywacz, N. M., 1992; Poznanski, R. R., 1992; Euler, T. *et al.*, 2002).

Massive ablation of SACs results in a selective loss of retinal DS (Yoshida, K. *et al.*, 2001; Amthor, F. R. *et al.*, 2002), and thus, it is commonly agreed that SACs are essential for DS. Optical measurements of light-stimulus-evoked Ca^{2+} signals (Denk, W. and Detwiler, P. B., 1999) in the dendrites of SACs suggest that these cells contribute directly to the directionally tuned input seen in DSGCs (Euler, T. *et al.*, 2002). These experiments showed that visual stimuli moving from the soma to the dendritic tips elicit larger Ca^{2+} responses in the dendritic tips than do those moving from the tips to the soma (Figure 2(b); Euler, T. *et al.*, 2002). That SACs' output synapses are located in the distal dendrites (Famiglietti, E. V., 1991) and transmitter release from SACs is Ca^{2+}-dependent (O'Malley, D. M. *et al.*, 1992; Zheng, J. J. *et al.*, 2004) is consistent with SACs providing directionally tuned synaptic output.

1.19.2.3 Pathways

The robust direction discrimination seen in DSGCs over wide contrast (Merwine, D. K. *et al.*, 1998) and velocity ranges (Oyster, C. W. *et al.*, 1972; Wyatt, H. J. and Daw, N. W., 1975) suggests that the underlying circuitry relies on multiple pathways and computational mechanisms (see also Section 1.19.3) to generate and enhance retinal DS signals (reviewed in Fried, S. I. *et al.*, 2005). For example, dendritic processing in DSGCs was found to contribute to DS by further sharpening directional tuning of synaptic inputs (Oesch, N. *et al.*, 2005). Support for multiple pathways also comes from the fact that both inhibitory and excitatory inputs to DSGCs are direction-selective (see Section 1.19.2.1).

1.19.2.3.1 Direction-Selective inhibition

Pharmacological block of $GABA_A$ receptors abolishes directional responses in DSGCs but leaves their light responsiveness intact (Wyatt, H. J. and Daw, N. W., 1976; Caldwell, J. H. *et al.*, 1978; Massey, S. C. *et al.*, 1997), indicating that the direction-selective inhibition of DSGCs is mediated by GABA. This GABAergic input is at least partially provided by SACs (see Section 1.19.2.2). DSGCs also receive inhibitory input from other, not identified amacrine cells (reviewed in Dacheux, R. F. *et al.*, 2003), which may provide additional DS inhibition. Unequivocal evidence for this, however, is lacking.

1.19.2.3.2 Direction-Selective excitation

DSGCs receive excitatory glutamatergic input from bipolar cells (Brandon, C., 1987; Famiglietti, E. V., 1991), which is directionally tuned (Fried, S. I. *et al.*, 2005). The underlying circuitry has not yet been identified. It is conceivable, though, that such tuning could arise from direction-dependent suppression of bipolar cell output by amacrine cells. SACs are a possibility, although SACs' output synapses onto bipolar cells appear to be rather sparse (Famiglietti, E. V., 1991; Yamada, E. S. *et al.*, 2003).

Since DSGCs possess ACh receptors and SACs are considered the main source of ACh in the retina, it is likely that SACs provide DSGCs with cholinergic input (reviewed in Vaney, D. I. *et al.*, 2001). Blocking ACh receptors in the presence of GABA antagonists reduces the DSGCs' response independent of motion direction (Chiao, C. C. and Masland, R. H., 2002), suggesting that cholinergic excitation affects DSGCs symmetrically and provides motion-sensitive but not direction-selective excitation (He, S. and Masland, R. H., 1997). On the other hand, blocking only cholinergic transmission reduces the directional tuning of inhibitory inputs to DSGCs (Fried, S. I. *et al.*, 2005), which may explain the finding that for certain stimuli, such as gratings, cholinergic blockers cause a decrease in ganglion cell DS (Grzywacz, N. M. *et al.*, 1998). Hence, complex interactions between the cholinergic and the GABAergic pathways clearly exist. Nonetheless, the functional role of cholinergic transmission for DS is not yet fully understood.

1.19.3 Retinal Direction Selectivity Computation Mechanism(s)

While a complete model of retinal DS that adequately incorporates the directionally tuned inhibitory and excitatory pathways is still lacking, some of the circuit's features and working principles are well understood. Direction-sensitive signals are generated presynaptic to DSGCs and appear to be enhanced by network interactions at several stages in the DS circuitry. In particular, spatially offset inhibition is a recurrent theme in the retinal DS circuit (discussed in Fried, S. I. *et al.*, 2005). While it is likely that SACs are a major, if not the main, source of DS signals, it is possible that additional DS arises somewhere else in the circuitry. The actual biophysical mechanism(s) by which DS is computed is still a matter of debate (reviewed in Vaney, D. I. *et al.*, 2001; Taylor, W. R. and Vaney, D. I., 2003).

In principle, a mechanism for detecting motion direction requires three key elements: a time delay, spatial asymmetry, and nonlinearity (Hassenstein, B. and Reichardt, W., 1956; Reichardt, W., 1961; reviewed in Borst, A. and Egelhaaf, M., 1989). A correlation-type direction detector, like the one shown in Figure 3, is the basis for most models of retinal DS. Nonetheless, the models differ greatly in the types of neurons recruited or in the biophysical mechanisms employed. The models listed in the following are not necessarily mutually exclusive; some may complement each other.

1.19.3.1 Computations Based on Network Interactions

One class of models is based on network interactions. In these models, nonlinearity is generated through the interaction of excitation and (shunting) inhibition (Koch, C. *et al.*, 1983; Borg-Graham, L. J. and Grzywacz, N. M., 1992). The required time delays are assumed to arise from electrical cable properties and/or synaptic interactions. In many models, the spatially displaced element is the SAC, with its role ranging from computing DS to simply relaying input to DSGCs.

Alternatively, other, not further specified amacrine cells are incorporated into some models. A general problem with this is that most neuron types tile the retina and, thus, are not numerous enough to provide the seven functional subtypes of DSGCs at each retinal location with adequate directional input (reviewed in Vaney, D. I. *et al.*, 2001). The lack of cells could, however, be compensated for by highly localized dendritic processing.

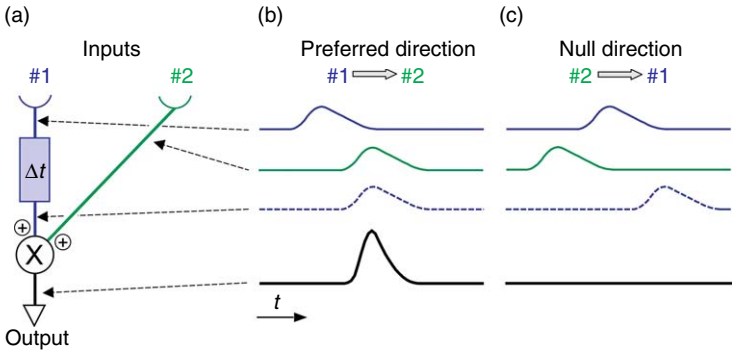

Figure 3 Model of a direction detector. (a) Simplified model of a correlation-type direction detector. This class of detectors was originally deduced from behavioral experiments on visual motion processing in insects (Reichardt, W., 1961). In the variant depicted here, light intensity is measured at two points (#1 and #2) in space, providing two excitatory (+) inputs. After input #1 has been delayed by a time interval (Δt), they are combined by a nonlinear operation (in this case, a multiplication; X). (b, c) Responses to preferred- (b) and null-direction motion (c) measured at different elements in the circuit. Due to the distance between the points of light measurement, the two input signals arrive at different time points (compare upper two traces). For preferred-direction motion (b), this temporal separation is compensated for by the delay applied to input #1 (third trace), such that at the multiplying stage, both inputs coincide (bottom trace). For null-direction motion (c), the temporal sequence of the inputs is reversed; the delay Δt increases the temporal shift between the inputs such that they do not coincide at the multiplying stage. This is just one possible variant of a correlation-type detector. Other variants combine excitatory and inhibitory inputs and/or use a different type of nonlinearity. The fixed time delay, which allows the detection of only a small range of motion velocities, can be replaced by a low-pass filter to broaden the velocity-tuning curve of the detector. (a) Adapted from Borst, A. and Egelhaaf, M. 1989. Principles of visual motion detection. Trends Neurosci. 12, 297–306.

1.19.3.1.1 Starburst cell networks

Ultrastructural (Millar, T. J. and Morgan, I. G., 1987) and functional data (Zheng, J. J. *et al.*, 2004) indicate that SACs form reciprocal synapses. In the mature retina, where GABAergic SAC interactions are prominent, this network has been implicated in the computation of DS (reviewed in Vaney, D. I. *et al.*, 2001). If an SAC is excited, it inhibits its neighbor. This in turn reduces the neighbor's GABA release and in effect enhances the first SAC's response. Such interaction can sharpen the DS difference in neighboring SAC dendrites pointing in opposite directions (Lee, S. and Zhou, Z. J., 2006). Nevertheless, since GABA receptor antagonists do not abolish DS in the dendritic Ca^{2+} signals (Euler, T. *et al.*, 2002) and in somatic voltage responses (Hausselt, S. E. *et al.*, 2007), it is unlikely that GABAergic SAC interactions are essential for dendritic DS in SACs.

1.19.3.2 Computations Based on Intrinsic Properties

The second class of models concentrates on intrinsic properties of SACs (e.g., Barlow, H. B., 1996; Gavrikov, K. E., *et al.*, 2003; Gavrikov, K. E., *et al.*, 2003; 2006; Tukker, J. J. *et al.*, 2004) and/or makes use of the fact that the dendritic sectors of SACs can be viewed as largely independent and polarized computational units (see Section 1.19.2.2). Each of the sectors is thought to code a different preferred direction, responding more strongly to motion from the soma toward the dendritic tips (centrifugal) than to motion from the tips toward the soma (centripetal) (Figures 2(a) and 2(b)).

Passive computational models predict that SAC dendrites generate weak DS signals simply by summation of inputs along the dendrite (reviewed in Tukker, J. J. *et al.*, 2004). Due to summation, motion from the soma to the dendritic tips evokes a larger signal in the dendritic tips, whereas motion from the dendrites to the soma evokes a larger signal in the soma. As the SACs' output synapses are located in the dendritic tips, motion from the soma to the dendritic tips would lead to a larger output signal to DSGCs. In this scenario, the threshold for transmitter release at the output synapse serves as the essential nonlinearity. The DS found in such passive models seems, however, small and too sensitive to stimulus parameters to explain the robust direction discrimination observed in DSGCs. Also, passive models predict a larger electrical signal at the soma for centripetal motion, which contradicts experimental observations (Peters, B. N. and Masland, R. H., 1996; Euler, T. *et al.*, 2002); Gavrikov, K. E., *et al.*, 2003.

To circumvent the deficits of passive models, voltage-gated channels have been incorporated to account for the nonlinearities that are differentially activated depending on the direction of motion (Borg-Graham, L. J. and Grzywacz, N. M., 1992). SACs possess a variety of suitable voltage-gated Ca^{2+} channels (Cohen, E. D., 2001; Kaneda, M. *et al.*, 2007) and possibly Na^{+} channels. Experimental data and modeling suggests that DS in SACs relies on a voltage difference between soma and (depolarized) distal dendrites that provides spatial asymmetry and leads to stronger activation of voltage-gated channels for motion from the soma toward the dendritic tips than for motion in opposite direction (Hausselt, S. E. *et al.*, 2007).

1.19.4 Developmental Aspects

So far no conclusive explanation of how the retinal DS circuitry arises during development has been presented. It is known, though, that this process does not require visual input, because the dendritic architecture of DSGCs and SACs is established before the retina responds to visual stimuli (Wong, R. O. and Collin, S. P., 1989; Wong, R. O. L., 1990) and DS responses in ganglion cells can be recorded at eye opening (Masland, R. H., 1977). SACs, which appear very early during development (Feller, M. B. *et al.*, 1996), might act as a scaffold for DSGCs as their dendrites are often surrounded by the dendrites of DSGCs in a fascicle (Vaney, D. I. and Pow, D. V., 2000; Stacy, R. C. and Wong, R. O. L., 2003). In the developing retina, the SAC network is dominated by excitatory cholinergic interactions and involved in generating activity waves (reviewed in Masland, R. H., 2005), which may participate in the generation of the DS circuitry.

1.19.5 The Role of Direction-Selective Signals Originating in the Retina

Considering the effort the retina puts into DS computation, it is surprising that the direction-selective neurons in the visual cortex probably recompute motion direction from nondirectional inputs (reviewed in Clifford, C. W. and Ibbotson, M. R., 2003). This seems to suggest that retinal DSGCs do not substantially contribute to cortical processing of motion and its

direction, but at the present time the exact role that retinal DS plays in higher vision is unknown.

It is known, however, that ablation of SACs, which abolishes retinal DS, results in a complete loss of the optokinetic reflex (Yoshida, K. *et al*., 2001; Amthor, F. R. *et al*., 2002), showing that DSGCs provide signals essential for the control of eye movement and gaze stabilization (reviewed in Vaney, D. I. *et al*., 2001). This is possibly the main task of ON DSGCs (Oyster, C. W. *et al*., 1972), because they prefer global motion, as caused by image slippage, and their preferred directions (Figure 1(b), bottom) correspond to the three axes of the semicircular canals in the inner ear. Moreover, ON DSGCs project to the accessory optic system (AOS) rather than to the superior colliculus (SC) and the lateral geniculate nucleus (LGN) like the majority of other ganglion cell types. ON/OFF DSGCs signal local motion (Wyatt, H. J. and Daw, N. W., 1975). They are attenuated by a synchronously moving background; thus, they are sensitive to motion contrast (Chiao, C. C. and Masland, R. H., 2003). The ON/OFF DSGCs' four preferred directions (Figure 1(b), bottom) are roughly aligned with the direction of apparent movement caused by contraction of the eye's rectus muscles (Oyster, C. W. and Barlow, H. B., 1967). The cells provide some input to the AOS and therefore contribute to the optokinetic system, likely for higher velocities. In addition, ON/OFF DSGCs send collaterals to the SC and the LGN and, therefore, may serve other visual functions, such as directing spatial attention to moving objects.

References

Amthor, F. R., Keyser, K. T., and Dmitrieva, N. A. 2002. Effects of the destruction of starburst-cholinergic amacrine cells by the toxin AF64A on rabbit retinal directional selectivity. Vis. Neurosci. 19, 495–509.

Amthor, F. R., Oyster, C. W., and Takahashi, E. S. 1984. Morphology of on-off direction-selective ganglion cells in the rabbit retina. Brain Res. 298, 187–190.

Barlow, H. B. 1996. Intraneuronal information processing, direction selectivity and memory for spatio-temporal sequences. Network Comput. Neural Syst. 7, 251–259.

Barlow, H. B. and Hill, R. M. 1963. Selective sensitivity to direction of movement in ganglion cells of the rabbit retina. Science 139, 412–414.

Barlow, H. B. and Levick, W. R. 1965. The mechanism of directionally selective units in rabbit's retina. J. Physiol. 178, 477–504.

Barlow, H. B., Hill, R. M., and Levick, W. R. 1964. Rabbit retinal ganglion cells responding selectively to direction and speed of image motion in the rabbit. J. Physiol. 173, 377–407.

Borg-Graham, L. J. 2001. The computation of directional selectivity in the retina occurs presynaptic to the ganglion cell. Nat. Neurosci. 4, 176–183.

Borg-Graham, L. J. and Grzywacz, N. M. 1992. A Model of the Directional Selectivity Circuit in Retina: Transformations by Neurons Singly and in Concert. In: Single Neuron Computation (*eds*. T. McKenna, S. F. Zornetzer, and J. L. Davis), pp. 347–375. Academic Press.

Borst, A. and Egelhaaf, M. 1989. Principles of visual motion detection. Trends Neurosci. 12, 297–306.

Brandon, C. 1987. Cholinergic neurons in the rabbit retina: dendritic branching and ultrastructural connectivity. Brain Res. 426, 119–130.

Brecha, N., Johnson, D., Peichl, L., and Wässle, H. 1988. Cholinergic amacrine cells of the rabbit retina contain glutamate decarboxylase and gamma-aminobutyrate immunoreactivity. Proc. Natl. Acad. Sci. U. S. A. 85, 6187–6191.

Buhl, E. H. and Peichl, L. 1986. Morphology of rabbit retinal ganglion cells projecting to the medial terminal nucleus of the accessory optic system. J. Comp. Neurol. 253, 163–174.

Caldwell, J. H., Daw, N. W., and Wyatt, H. J. 1978. Effects of picrotoxin and strychnine on rabbit retinal ganglion cells: lateral interactions for cells with more complex receptive fields. J. Physiol. 276, 277–298.

Chiao, C. C. and Masland, R. H. 2002. Starburst cells nondirectionally facilitate the responses of direction-selective retinal ganglion cells. J. Neurosci. 22, 10509–10513.

Chiao, C. C. and Masland, R. H. 2003. Contextual tuning of direction-selective retinal ganglion cells. Nat. Neurosci. 6, 1251–1252.

Clifford, C. W. and Ibbotson, M. R. 2003. Fundamental mechanisms of visual motion detection: models, cells and functions. Prog. Neurobiol. 68, 409–437.

Cohen, E. D. 2001. Voltage-gated calcium and sodium currents of starburst amacrine cells in the rabbit retina. Vis. Neurosci. 18, 799–809.

Dacheux, R. F., Chimento, M. F., and Amthor, F. R. 2003. Synaptic input to the on-off directionally selective ganglion cell in the rabbit retina. J. Comp. Neurol. 456, 267–278.

Denk, W. and Detwiler, P. B. 1999. Optical recording of light-evoked calcium signals in the functionally intact retina. Proc. Natl. Acad. Sci. U. S. A. 96, 7035–7040.

Denk, W., Strickler, J. H., and Webb, W. W. 1990. Two-photon laser scanning fluorescence microscopy. Science 248, 73–76.

Euler, T., Detwiler, P. B., and Denk, W. 2002. Directionally selective calcium signals in dendrites of starburst amacrine cells. Nature 418, 845–852.

Famiglietti, E. V. 1983. 'Starburst' amacrine cells and cholinergic neurons: mirror-symmetric on and off amacrine cells of rabbit retina. Brain Res. 261, 138–144.

Famiglietti, E. V. 1991. Synaptic organization of starburst amacrine cells in rabbit retina: analysis of serial thin sections by electron microscopy and graphic reconstruction. J. Comp. Neurol. 309, 40–70.

Feller, M. B., Wellis, D. P., Stellwagen, D., Werblin, F. S., and Shatz, C. J. 1996. Requirement for cholinergic synaptic transmission in the propagation of spontaneous retinal waves. Science 272, 1182–1187.

Fried, S. I., Münch, T. A., and Werblin, F. S. 2002. Mechanisms and circuitry underlying directional selectivity in the retina. Nature 420, 411–414.

Fried, S. I., Münch, T. A., and Werblin, F. S. 2005. Directional selectivity is formed at multiple levels by laterally offset inhibition in the rabbit retina. Neuron 46, 117–127.

Gavrikov, K. E., Dmitriev, A. V., Keyser, K. T., and Mangel, S. C. 2003. Cation-chloride cotransporters mediate neural

computation in the retina. Proc. Natl. Acad. Sci. U. S. A. 100, 16047–16052.
Gavrikov, K. E., Nilson, J. E, Dmitriev, A. V., Zucker, C. L., and Mangel, S. V. 2006. Dendritic compartmentalization of chloride cotransporters underlies directional responses of starburst amacrine cells in retina. Proc. Natl. Acad. Sci. U. S. A. 103, 18793–18798.
Grzywacz, N. M., Amthor, F. R., and Merwine, D. K. 1998. Necessity of acetylcholine for retinal directionally selective responses to drifting gratings in rabbit. J. Physiol. 512, 575–581.
Hassenstein, B. and Reichardt, W. 1956. Systemtheorische Analyse der Zeit-, Reihenfolgen- und Vorzeichenauswertung bei der Bewegungsperzeption des Rüsselkäfers Chlorophanus. Zeitschrift für Naturforschung 11b, 513–524.
Hausselt, S. E., Euler, T., Detwiler, P. B., and Denk, W. 2007. A dendrite-autonomous mechanism for direction selectivity in retinal starburst amacrine cells. PLoS Biol. 5(7), e185.
He, S. and Masland, R. H. 1997. Retinal direction selectivity after targeted laser ablation of starburst amacrine cells. Nature 389, 378–382.
Jeon, C. J., Kong, J. H., Strettoi, E., Rockhill, R., Stasheff, S. F., and Masland, R. H. 2002. Pattern of synaptic excitation and inhibition upon direction-selective retinal ganglion cells. J. Comp. Neurol. 449, 195–205.
Kaneda, M., Ito, K., Morishima, Y., Shigematsu, Y., and Shimoda, Y. 2007. Characterization of voltage-gated ionic channels in cholinergic amacrine cells in the mouse retina. J. Neurophysiol. 97(6), 4225–4234.
Koch, C., Poggio, T., and Torre, V. 1983. Nonlinear interactions in a dendritic tree: localization, timing, and role in information processing. Proc. Natl. Acad. Sci. U. S. A. 80, 2799–2802.
Lee, S. and Zhou, Z. J. 2006. The synaptic mechanism of direction selectivity in distal processes of starburst amacrine cells. Neuron 51(6), 787–799.
Marchiafava, P. L. 1979. The responses of retinal ganglion cells to stationary and moving visual stimuli. Vision Res. 19, 1203–1211.
Masland, R. H. 1977. Maturation of function in the developing rabbit retina. J. Comp Neurol. 175, 275–286.
Masland, R. H. 2004. Direction Selectivity in Retinal Ganglion Cells. In: The Visual Neurosciences (*eds*. L. M. Chalupa and J. S. Werner), pp. 451–462. MIT Press.
Masland, R. H. 2005. The many roles of starburst amacrine cells. Trends Neurosci. 28, 395–396.
Masland, R. H. and Mills, J. W. 1979. Autoradiographic identification of acetylcholine in the rabbit retina. J. Cell Biol. 83, 159–178.
Masland, R. H., Mills, J. W., and Cassidy, C. 1984a. The functions of acetylcholine in the rabbit retina. Proc. R. Soc. Lond. B Biol. Sci. 223, 121–139.
Masland, R. H., Mills, J. W., and Hayden, S. A. 1984b. Acetylcholine-synthesizing amacrine cells: identification and selective staining by using radioautography and fluorescent markers. Proc. R. Soc. Lond. B Biol. Sci. 223, 79–100.
Massey, S. C., Linn, D. M., Kittila, C. A., and Mirza, W. 1997. Contributions of GABAA receptors and GABAC receptors to acetylcholine release and directional selectivity in the rabbit retina. Vis. Neurosci. 14, 939–948.
Merwine, D. K., Grzywacz, N. M., Tjepkes, D. S., and Amthor, F. R. 1998. Non-monotonic contrast behavior in directionally selective ganglion cells and evidence for its dependence on their GABAergic input. Vis. Neurosci. 15, 1129–1136.
Miller, R. F. and Bloomfield, S. A. 1983. Electroanatomy of a unique amacrine cell in the rabbit retina. Proc. Natl. Acad. Sci. U. S. A. 80, 3069–3073.
Millar, T. J. and Morgan, I. G. 1987. Cholinergic amacrine cells in the rabbit retina synapse onto other cholinergic amacrine cells. Neurosci. Lett. 74, 281–285.
Oesch, N., Euler, T., and Taylor, W. R. 2005. Direction-selective dendritic action potentials in rabbit retina. Neuron 47, 739–750.
O'Malley, D. M., Sandell, J. H., and Masland, R. H. 1992. Co-release of acetylcholine and GABA by the starburst amacrine cells. J. Neurosci. 12, 1394–1408.
Oyster, C. W. and Barlow, H. B. 1967. Direction-selective units in rabbit retina: distribution of preferred directions. Science 155, 841–842.
Oyster, C. W., Amthor, F. R., and Takahashi, E. S. 1993. Dendritic architecture of ON-OFF direction-selective ganglion cells in the rabbit retina. Vision Res. 33, 579–608.
Oyster, C. W., Takahashi, E., and Collewijn, H. 1972. Direction-selective retinal ganglion cells and control of optokinetic nystagmus in the rabbit. Vision Res. 12, 183–193.
Ozaita, A., Petit-Jacques, J., Volgyi, B., Ho, C. S., Joho, R. H., Bloomfield, S. A., and Rudy, B. 2004. A unique role for Kv3 voltage-gated potassium channels in starburst amacrine cell signaling in mouse retina. J. Neurosci. 24, 7335–7343.
Peters, B. N., and Masland, R. H. 1996. Responses to light of starburst amacrine cells. J Neurophysiol. 75, 469–480.
Poznanski, R. R. 1992. Modelling the electrotonic structure of starburst amacrine cells in the rabbit retina: a functional interpretation of dendritic morphology. Bull. Math. Biol. 54, 905–928.
Reichardt, W. 1961. Autocorrelation, a principle for the evaluation of sensory information by the central nervous system. In: Sensory Communication (*ed*. W. A. Rosenblith), pp. 377–390. MIT Press and Wiley.
Stacy, R. C. and Wong, R. O. L. 2003. Developmental relationship between cholinergic amacrine cell processes and ganglion cell dendrites of the mouse retina. J. Comp. Neurol. 456, 154–166.
Tauchi, M. and Masland, R. H. 1984. The shape and arrangement of the cholinergic neurons in the rabbit retina. Proc. R. Soc. Lond. B Biol. Sci. 223, 101–119.
Taylor, W. R. and Vaney, D. I. 2002. Diverse synaptic mechanisms generate direction selectivity in the rabbit retina. J. Neurosci. 22, 7712–7720.
Taylor, W. R. and Vaney, D. I. 2003. New directions in retinal research. Trends Neurosci. 26, 379–385.
Tukker, J. J., Taylor, W. R., and Smith, R. G. 2004. Direction selectivity in a model of the starburst amacrine cell. Vis. Neurosci. 21, 611–625.
Vaney, D. I. 1984. 'Coronate' amacrine cells in the rabbit retina have the 'starburst' dendritic morphology. Proc. R. Soc. Lond. B Biol. Sci. 220, 501–508.
Vaney, D. I. 1990. The mosaic of amacrine cells in the mammalian retina. Prog. Retin. Eye Res. 9, 49–100.
Vaney, D. I. 1994. Territorial organization of direction-selective ganglion cells in rabbit retina. J. Neurosci. 14, 6301–6316.
Vaney, D. I. and Pow, D. V. 2000. The dendritic architecture of the cholinergic plexus in the rabbit retina: selective labeling by glycine accumulation in the presence of sarcosine. J. Comp. Neurol. 421, 1–13.
Vaney, D. I. and Young, H. M. 1988. GABA-like immunoreactivity in cholinergic amacrine cells of the rabbit retina. Brain Res. 438, 369–373.
Vaney, D. I., Collins, S. P., and Young, H. M. 1989. Dendritic relationships between Cholinergic Amacrine Cells and Direction Selective Retinal Ganglion Cells. In: Neurobiology of the Inner Retina (*eds*. R. Weiler and N. N. Osborn), pp. 157–168. Springer.
Vaney, D. I., He, S., Taylor, W. R., and Levick, W. R. 2001. Direction-Selective Ganglion Cells in the Retina. In: Motion Vision- Computational, Neural, and Ecological Constraint (*eds*. J. M. Zanker and J. Zeil), pp. 13–56. Springer.
Velte, T. J. and Miller, R. F. 1997. Spiking and nonspiking models of starburst amacrine cells in the rabbit retina. Vis. Neurosci. 14(6), 1073–1088.

Weng, S., Sun, W., and He, S. 2005. Identification of ON-OFF direction-selective ganglion cells in the mouse retina. J. Physiol. 562, 915–923.

Wong, R. O. L. 1990. Differential growth and remodelling of ganglion cell dendrites in the postnatal rabbit retina. J. Comp. Neurol. 294, 109–132.

Wong, R. O. and Collin, S. P. 1989. Dendritic maturation of displaced putative cholinergic amacrine cells in the rabbit retina. J. Comp. Neurol. 287, 164–178.

Wyatt, H. J. and Daw, N. W. 1975. Directionally sensitive ganglion cells in the rabbit retina: specificity for stimulus direction, size, and speed. J. Neurophysiol. 38, 613–626.

Wyatt, H. J. and Daw, N. W. 1976. Specific effects of neurotransmitter antagonists on ganglion cells in rabbit retina. Science 191, 204–205.

Yang, G. and Masland, R. H. 1994. Receptive fields and dendritic structure of directionally selective retinal ganglion cells. J. Neurosci. 14, 5267–5280.

Yamada, E. S., Bordt, A. S., and Marshak, D. W. 2005. Wide-field ganglion cells in macaque retinas. Vis. Neurosci. 22, 383–393.

Yamada, E. S., Dmitrieva, N., Keyser, K. T., Lindstrom, J. M., Hersh, L. B., and Marshak, D. W. 2003. Synaptic connections of starburst amacrine cells and localization of acetylcholine receptors in primate retinas. J. Comp. Neurol. 461, 76–90.

Yoshida, K., Watanabe, D., Ishikane, H., Tachibana, M., Pastan, I., and Nakanishi, S. 2001. A key role of starburst amacrine cells in originating retinal directional selectivity and optokinetic eye movement. Neuron 30, 771–780.

Zheng, J. J., Lee, S., and Zhou, Z. J. 2004. A developmental switch in the excitability and function of the starburst network in the mammalian retina. Neuron 44, 851–864.

1.20 Melanopsin Cells

I Provencio, University of Virginia, Charlottesville, VA, USA

© 2008 Elsevier Inc. All rights reserved.

1.20.1	Discovery of Melanopsin	423
1.20.2	Identification of Mammalian Melanopsin Homologs	424
1.20.3	Identification of Intrinsically Photosensitive Retinal Ganglion Cells	424
1.20.4	Functional Characterization of Intrinsically Photosensitive Retinal Ganglion Cells	426
1.20.5	Role of Intrinsically Photosensitive Retinal Ganglion Cells in Vision	427
1.20.6	Melanopsin-Activated Phototransduction	428
1.20.7	Conclusion	429
References		429

Glossary

circadian rhythm An endogenously generated biological rhythm with a period of about 24 h.

melanopsin The opsin-based photopigment of intrinsically photosensitive retinal ganglion cells.

nonvisual photophysiology Physiological responses to light that do not require the formation of images.

photoentrainment The synchronization of circadian rhythms to the daily light–dark cycle.

1.20.1 Discovery of Melanopsin

The discovery of the photopigment melanopsin has led to the identification of intrinsically photosensitive retinal ganglion cells (ipRGCs), a novel class of photoreceptor in the mammalian retina. This unique cell type plays a role in controlling many forms of light-regulated physiology that do not require the formation of images. Examples of such physiology include the synchronization of circadian rhythms to the day–night cycle (entrainment), the acute photoregulation of pineal melatonin synthesis, and the pupillary light reflex (PLR). Evidence is emerging that these melanopsin-based photoreceptors may also play a role in the regulation of the visual system proper (Dacey, D. M. *et al.*, 2005; Barnard, A. R. *et al.*, 2006).

Melanopsin was initially cloned from cultured dermal melanophores of *Xenopus laevis*. Melanophores are inherently photosensitive (Provencio, I. *et al.*, 1998). In the dark, melanosomes remain aggregated in a perinuclear domain giving the cells a blanched appearance. Upon illumination, the cells darken by distributing the melanosomes throughout the cytoplasm. This response is retinoid dependent suggesting the involvement of an opsin-based photopigment (Rollag, M. D., 1996). In an effort to identify such a photopigment, a *Xenopus* melanophore cDNA library was screened with a cocktail of probes derived from *Xenopus* rhodopsin and violet opsin nucleotide sequences (Provencio, I. *et al.*, 1998). This screen yielded a partial clone with a predicted amino acid sequence more similar to the opsins contained in rhabdomeric photoreceptors of invertebrates than the opsins of ciliary photoreceptors of vertebrates. A full-length clone was obtained and subsequently named melanopsin because of its derivation from melanophores. Expression of melanopsin transcripts in melanophores was verified by *in situ* hybridization studies (Provencio, I. *et al.*, 1998). These studies also demonstrated expression in several brain regions, iridial myocytes, and the retina. The retinal expression pattern was peculiar because it was restricted to the ganglion cell and inner nuclear layers which contain cells not previously believed to be photosensitive. This finding suggested that nonrod, noncone photoreceptors may be lurking in the vertebrate retina.

1.20.2 Identification of Mammalian Melanopsin Homologs

Using the nucleotide sequence information derived from amphibians, a chicken melanopsin homolog was identified (Chaurasia, S. S. *et al.*, 2005). Mammalian homologs were subsequently cloned from mice and humans using the chicken-derived sequence (Provencio, I. *et al.*, 2000). Both mammalian and non-mammalian versions share the molecular hallmarks common to all opsins such as a lysine residue in the predicted seventh transmembrane domain that is necessary for the covalent Schiff base linkage of the retinoid chromophore. As previously mentioned, melanopsins share greater amino acid similarity with rhabdomeric photoreceptor opsins than the visual opsins of vertebrates. Despite this invertebrate-like character, melanopsin homologs have not been found in true invertebrates, although, a melanopsin homolog has been identified in a cephalochordate (Koyanagi, M. *et al.*, 2005). In addition to the general similarity to rhabdomeric opsins, melanopsins also share individual molecular traits specific to rhabdomeric opsins. Most obvious among these is the aromatic residue in the third transmembrane domain (Provencio, I. *et al.*, 1998; 2000), a site in vertebrate rod and cone opsins that is occupied by an acidic residue which is necessary for salt-bridge formation with the protonated Schiff base (Kim, J. M. *et al.*, 2005).

In nonmammalian vertebrates, melanopsin is expressed in multiple tissues believed to be intrinsically photosensitive such as the pineal gland and areas of the deep brain (Provencio, I. *et al.*, 1998; Bellingham, J. *et al.*, 2002; Drivenes, O. *et al.*, 2003; Bailey, M. J. and Cassone, V. M., 2005; Chaurasia, S. S. *et al.*, 2005; Tomonari, S. *et al.*, 2005; Bellingham, J. *et al.*, 2006; Frigato, E. *et al.*, 2006). By contrast, the expression pattern in mammals is extremely restricted. In rodents, melanopsin expression is confined to 1–2% of retinal ganglion cells (RGCs; Hattar, S. *et al.*, 2002; Morin, L. P. *et al.*, 2003; Sollars, P. J. *et al.*, 2003; Hattar, S. *et al.*, 2006). Reverse transcriptase polymerase chain reaction (RT-PCR) of 26 human tissues revealed that melanopsin expression was limited to the retina (Provencio, I. *et al.*, 2000).

A second melanopsin gene has been identified in nonmammalian vertebrates (Bellingham, J. *et al.*, 2006). Based on synteny between the chicken and human genomes, it is clear that this second gene has been lost in mammals. Both genes appear capable of coding functional opsin proteins, however, the consequences of possessing two melanopsin genes remains to be determined.

1.20.3 Identification of Intrinsically Photosensitive Retinal Ganglion Cells

In the absence of rods and cones, visually blind mice homozygous for the *retinal degeneration* (*rd*) allele continue to photoregulate circadian locomotor rhythms in a manner indistinguishable from sighted controls (Foster, R. G. *et al.*, 1991). The spectral sensitivity for this response to light peaks in the blue wavelengths (480 nm; Yoshimura, T. and Ebihara, S., 1996; Hattar, S. *et al.*, 2003). The PLR in rodless, coneless (*rd*/*rd cl*) mice is also maximally sensitive to blue light (479 nm; Lucas, R. J. *et al.*, 2001). In humans, elevated nocturnal serum melatonin can be suppressed acutely by a pulse of light. Again, the spectral sensitivity of this response is maximal in the blue wavelengths (446–477 nm), a spectral domain not consistent with the well-characterized sensitivities of human rod and cone photoreceptors (Brainard, G. C. *et al.*, 2001; Thapan, K. *et al.*, 2001). Together, these findings suggested the existence of a nonrod, noncone class of photoreceptor that mediates these distinctly different nonvisual responses to light. Localization of melanopsin to a small set of RGCs pointed to a potentially novel photoreceptor class; the presence of a putative photopigment in RGCs implied that these cells are inherently photoreceptive. Berson D. M. *et al.* (2002) painstakingly proved this seemingly heretical implication to be the case.

The vast majority of melanopsin-containing RGCs project to the hypothalamic suprachiasmatic nuclei (SCN), a retinorecipient site and master circadian oscillator (Gooley, J. J. *et al.*, 2001; Hannibal, J. *et al.*, 2002a; Gooley, J. J. *et al.*, 2003; Morin, L. P. *et al.*, 2003; Sollars, P. J. *et al.*, 2003). Berson D. M. *et al.* (2002) retrogradely labeled SCN-projecting RGCs and recorded light-evoked membrane depolarizations from these cells even when they were pharmacologically deafferented; synaptic blockers were used to prevent signaling to those cells through rod or cone pathways. The intrinsic photosensitivity of these cells was shown unequivocally by the persistence of such light responses in labeled cells physically teased away from the RGC layer (Berson, D. M. *et al.*, 2002). Later studies confirmed that melanopsin does indeed confer photosensitivity upon ipRGCs (Lucas, R. J. *et al.*, 2003; Tu, D. C. *et al.*, 2005). Interestingly, like the action

spectra of circadian photoregulation and melatonin photosuppression, light responses in ipRGCs peak in the blue wavelengths (479 nm), thereby implicating this new class of melanopsin-based ganglion cell photoreceptor in the regulation of these nonvisual responses (Berson, D. M. *et al.*, 2002).

Unlike rods and cones that hyperpolarize in response to light, ipRGCs depolarize upon photic stimulation. Heterogeneity exists in these responses. The use of multielectroarrays (MEA) has facilitated the simultaneous recording from multiple ipRGCs (Tu, D. C. *et al.*, 2005). Using this tool, at least three electrophysiological phenotypes can be discriminated in neonates. Only two of these remain in adult mice (Table 1). No obvious distinguishing morphological characteristics correlate with these physiological phenotypes.

The onset of melanopsin expression occurs early in prenatal development in chickens, mice, and humans (Tarttelin, E. E. *et al.*, 2003; Tomonari, S. *et al.*, 2005). In mice, the number of ipRGCs at birth is at least fivefold greater than in the adult (Sekaran, S. *et al.*, 2005). There is also a general increase in sensitivity as ipRGCs mature. While ipRGCs can respond to light at birth (Hannibal, J. and Fahrenkrug, J., 2004), the responses are relatively insensitive and transient (Sekaran, S. *et al.*, 2005). Responses after the sixth postnatal day are around tenfold more sensitive and can persist after stimulus offset. Taken together, it has been unequivocally established that ipRGCs are the first light-sensitive cells to develop in the retina.

Adaptation, the dynamic regulation of sensitivity, is a hallmark of rods and cones that makes vision possible in light levels ranging from dim starlight to bright sunlight (Rodieck, R. W., 1998). The photic responses of ipRGCs and the behavioral outputs to which they contribute, such as pupillary constriction, are sustained in nature, suggesting that perhaps ipRGCs do not adapt. To the contrary, ipRGCs are capable of dark- and light-adaptation in response to lighting history (Wong, K. Y. *et al.*, 2005). Furthermore, adaptation occurs in the presence of pharmacologic synaptic blockers indicating that such an adjustment of sensitivity is an intrinsic property of ipRGCs and does not emerge from a network of communicating cells.

Table 1 Physiological phenotypes of intrinsically photosensitive retinal ganglion cells (ipRGCs; derived from Tu, D. C. *et al.*, 2005)

Type	*Sensitivity*[a]	*Termination*[b]
Type I[c]	$\sim 10^{12}$	~10 s
Type II	$>10^{13}$	~30 s
Type III	$\sim 10^{12}$	From 30 s to 2 min

[a] Half maximal response in photons s^{-1} cm^{-2} of 480 nm light.
[b] Amount of time after end of stimulus at which firing rate returns to baseline.
[c] Only observed in neonates (postnatal day 8).

The density of melanopsin RGCs is constant across the retinas of hamsters (Morin, L. P. *et al.*, 2003; Sollars, P. J. *et al.*, 2003) and mice (Lin, B. *et al.*, 2004), but rats and primates show a shallow density cline peaking in the superiotemporal (Hannibal, J. *et al.*, 2002a; Hattar, S. *et al.*, 2002) and parafoveal (Dacey, D. M. *et al.*, 2005) retinal domains, respectively. Electron microscopy confirms that melanopsin, like all opsin-based photopigments, is an integral membrane protein (Belenky, M. A. *et al.*, 2003). It is localized to the plasma membrane of the perikaryal, dendritic, and axonal domains of ipRGCs (Beaule, C. *et al.*, 2003; Provencio, I. *et al.*, 2002). Antimelanopsin immunoreactivity has been observed even in axon terminals within the SCN (Beaule, C. *et al.*, 2003). Dendritic immunoreactivity is spatially coincident with the receptive fields of ipRGCs, indicating the presence of functional photopigment out to the distal tips of dendrites (Berson, D. M. *et al.*, 2002).

Murine ipRGCs have relatively small cell bodies (~20 µm) that elaborate 2 or 3 primary dendrites which initially bifurcate within 50 µm of the cell body (Lin, B. *et al.*, 2004). Some somata are displaced into the inner aspect of the inner nuclear layer (Provencio, I. *et al.*, 2000; Hattar, S. *et al.*, 2002). Dendritic arbors are relatively sparse, having mean diameters of around 450 µm in mice (Lin, B. *et al.*, 2004) and 600 µm in rats (Warren, E. J. *et al.*, 2003), and are regularly tiled across the retina with substantial overlap (Lin, B. *et al.*, 2004). Pituitary adenylyl cyclase-activating peptide (PACAP) and glutamate are colocalized with melanopsin in ipRGCs (Hannibal, J. *et al.*, 2000; 2002a; 2004). The morphology of these cells is quite distinctive. Most striking are the regularly spaced varicosities that decorate the arbor, giving a rosary beads appearance (Hannibal, J. *et al.*, 2002a; Hattar, S. *et al.*, 2002; Provencio, I. *et al.*, 2002; Belenky, M. A. *et al.*, 2003; Panda, S. *et al.*, 2003; Sollars, P. J. *et al.*, 2003; Lin, B. *et al.*, 2004). The dendrites ramify into sublaminas S1 and S5 of the inner nuclear layer (Provencio, I. *et al.*, 2002; Belenky, M. A. *et al.*, 2003; Dacey, D. M. *et al.*, 2005). Whether each of these plexuses arises from a distinct subclass of ipRGCs or whether a single class is bistratified remains to be determined (Hattar, S. *et al.*, 2006; Figure 1).

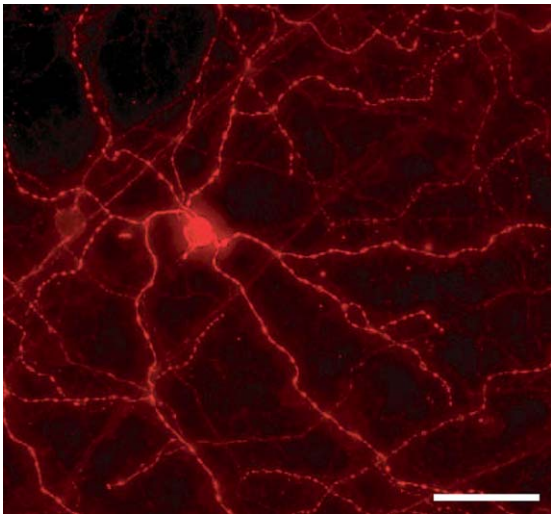

Figure 1 Scanning confocal photomicrograph of melanopsin immunopositive retinal ganglion cell seen in a flat-mounted mouse retina. Scale bar = 25 μm. Reproduced from Belenky, M. A., Smeraski, C. A., Provencio, I., Sollars, P. J., and Pickard, G. E. 2003. Melanopsin retinal ganglion cells receive bipolar and amacrine cell synapses. J. Comp. Neurol. 460, 380–393, with permission from John Wiley & Sons, Inc.

The principle central targets of ipRGCs are the SCN, the intergeniculate leaflet, the lateral habenula, and the olivary pretectal nucleus (Gooley, J. J. *et al.*, 2001; Hattar, S. *et al.*, 2002; Hattar, S. *et al.*, 2006; Figure 2). The secondary central targets are the subparaventricular zone, perisupraoptic nucleus, ventrolateral preoptic nucleus, ventral lateral geniculate nucleus, and superior colliculus (Gooley, J. J. *et al.*, 2003; Hattar, S. *et al.*, 2006). Also of note is the relative absence of ipRGC terminals in the rodent dorsal lateral geniculate nucleus (dLGN), a retinotopically mapped thalamic relay important in the construction of images (Hattar, S. *et al.*, 2006). This is in contrast to the primate brain where ipRGCs project to the dLGN (Dacey, D. M. *et al.*, 2005).

1.20.4 Functional Characterization of Intrinsically Photosensitive Retinal Ganglion Cells

The similarity between the spectral responses of ipRGCs (Berson, D. M. *et al.*, 2002) and the previously mentioned wavelength sensitivities of nonvisual responses to light (Yoshimura, T. and Ebihara, S., 1996; Brainard, G. C. *et al.*, 2001; Lucas, R. J. *et al.*, 2001; Thapan, K. *et al.*, 2001; Hattar, S. *et al.*, 2003) provides insight into the potential roles of this novel class of photoreceptor. In addition, many of the functions of the retinorecipient targets of ipRGCs have been well studied, thereby offering indirect clues to other potential functions of ipRGCs (Gooley, J. J. *et al.*, 2003; Morin, L. P. *et al.*, 2003; Hattar, S. *et al.*, 2006; Morin, L. P. and Allen, C. N., 2006). To directly establish the function of ipRGCs, three lines of melanopsin-null ($Opn4^{-/-}$) mice were independently generated (Hattar, S. *et al.*, 2002;

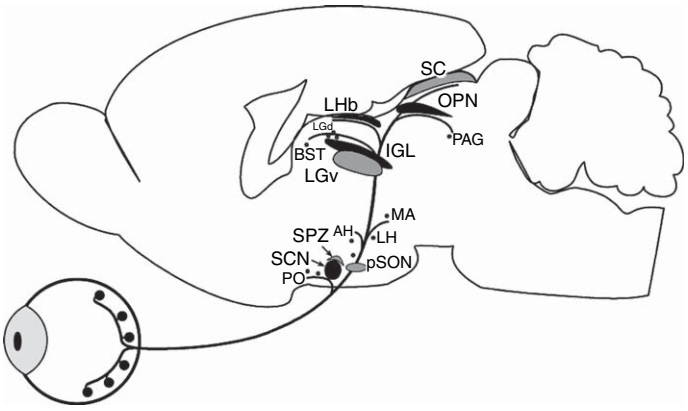

Figure 2 Central projections of intrinsically photosensitive retinal ganglion cells (ipRGCs). Principle targets are indicated in dark gray and secondary targets in light gray. Minor targets are indicated by dots. AH, anterior hypothalamic nucleus; BST, bed nucleus of the stria terminalis; IGL, intergeniculate leaflet; LGd, lateral geniculate nucleus, dorsal division; LGv, lateral geniculate nucleus, ventral division; LH, lateral hypothalamus; LHb, lateral habenula; MA, medial amygdaloid nucleus; OPN, olivary pretectal nucleus; PAG, periaqueductal gray; PO, preoptic area; pSON, perisupraoptic nucleus; SC, superior colliculus; SCN, suprachiasmatic nucleus; SPZ, subparaventricular zone. Reproduced from Hattar, S., Kumar, M., Park, A., Tong, P., Tung, J., Yau, K. W., and Berson, D. M. 2006 Central projections of melanopsin-expressing retinal ganglion cells in the mouse. J. Comp. Neurol. 497, 326–349, with permission from John Wiley & Sons, Inc.

Panda, S. *et al.*, 2002; Ruby, N. F. *et al.*, 2002). Surprisingly, all three mouse lines demonstrate that the loss of melanopsin does not cause profound deficits in circadian photoreception or other forms of nonvisual light detection. Under standard 12 h:12 h light–dark lighting conditions, these mice entrain their activity to the light–dark cycle just like wild-type littermates (Panda, S. *et al.*, 2002; Ruby, N. F. *et al.*, 2002). When housed in constant dark, and thereby isolated from temporal cues, $Opn4^{-/-}$ mice express rhythmic locomotor rhythms with circadian periods indistinguishable from $Opn4^{+/+}$ controls (Panda, S. *et al.*, 2002; Ruby, N. F. *et al.*, 2002). Only more sophisticated analyses, such as the circadian phase shifting effect to single pulses of light, reveal that these knockout mice exhibit some deficits. For example, at all irradiances tested, $Opn4^{-/-}$ mice show smaller light-induced phase shifts than melanopsin-intact mice. Additionally, the degree of circadian period lengthening observed in melanopsin-null mice maintained in constant light also was significantly blunted (Panda, S. *et al.*, 2002; Ruby, N. F. *et al.*, 2002). Like the regulation of circadian behavior, the PLR also is affected in significant but subtle ways. At nonsaturating irradiances, $Opn4^{-/-}$ mice do not differ from wild-type mice, however, at saturating irradiances, $Opn4^{-/-}$ mice fail to constrict the pupil fully (Hattar, S. *et al.*, 2003; Lucas, R. J. *et al.*, 2003; Panda, S. *et al.*, 2003).

The presence of residual responses in these animals suggests that rods and cones may, in the end, contribute to nonimage-forming photoreception. To address this possibility, melanopsin-null mice have been crossed with mice possessing functionally deficient rods and cones or missing the visual photoreceptors altogether (Hattar, S. *et al.*, 2003; Panda, S. *et al.*, 2003. The lack of functional rods, cones, and ipRGCs renders these animals visually and nonvisually blind; they behave as though they have been bilaterally enucleated. Unlike *rd* mice or mice only null for melanopsin, no responses to light could be recorded in these triple-knockout animals. Among the responses assessed were circadian photoentrainment, light-induced circadian phase shifting, acute light-evoked suppression of nocturnal activity (masking), constant-light circadian period lengthening, light-mediated suppression of the melatonin biosynthesis pathway, and the PLR (Hattar, S. *et al.*, 2003; Panda, S. *et al.*, 2003). Taken together, these data demonstrate the involvement of rods, cones, and ipRGCs in nonvisual photophysiology. The relative contributions of these photoreceptor classes to nonvisual light responses remains to be determined. The use of classical knockout strategies may not prove fruitful to this end. The impact of compensation elicited by the early developmental loss of melanopsin is difficult to quantify. Inducible knockout models should prove more useful in establishing the relative roles of rods, cones, and ipRGCs in nonvisual photoreception.

Melanopsin's role as a photopigment of nonvisual photoreceptors is perhaps best demonstrated by its presence in an obligate irradiance detector (Hannibal, J. *et al.*, 2002b). The eye of the blind mole rat (*Spalax* sp.) is atrophied and subcutaneous, thereby incapable of form vision (Cooper, H. M. *et al.*, 1993). Furthermore, anatomical and electrophysiological assessment of central visual structures also indicates an absence of a functional visual system. Like retinally degenerate mouse models, *Spalax* can entrain to daily light–dark cycles (Tobler, I. *et al.*, 1998; Avivi, A. *et al.*, 2001). The retina of Spalax only contains about 900 RGCs, but many of these cells contain melanopsin (Hannibal, J. *et al.*, 2002b). A long wavelength-sensitive (LWS) cone photopigment also has been cloned from *Spalax* retina (David-Gray, Z. K. *et al.*, 1999). The relative contributions to photoentrainment of the photoreceptive cells that harbor the LWS cone photopigment and the RGCs that express melanopsin remain to be determined.

1.20.5 Role of Intrinsically Photosensitive Retinal Ganglion Cells in Vision

Although little evidence exists suggesting that ipRGCs are involved in rodent vision, the situation in primates is quite different (Dacey, D. M. *et al.*, 2005). Melanopsin is expressed in giant RGCs which project to the lateral geniculate nucleus. The dendritic arbor diameters of these cells approach 1 mm and are the largest of the identified primate RGC classes. Only 3000 giant cells exist in the primate retina representing 0.2% of all RGCs. These cells are intrinsically photoreceptive, displaying a peak spectral sensitivity in the blue wavelengths (482 nm). Giant RGCs also are activated by rods and cones. Activation by cone pathways exhibit (L + M)-cone On S-cone Off chromatic opponency. Although relatively insensitive compared to rods and cones, the intrinsic photosensitivity of giant RGCs is highly correlated with the intensity of the stimulus,

thereby indicating precise irradiance coding. At irradiances subthreshold to the intrinsic sensitivity, giant cells receive irradiance-dependent information from rods and cones. Therefore, giant cells are capable of integrating and transmitting irradiance information across the entire dynamic range (scotopic, mesopic, and photopic) of the visual system (Dacey, D. M. *et al.*, 2005).

1.20.6 Melanopsin-Activated Phototransduction

The greater similarity of melanopsin to opsins of invertebrates than those of vertebrates has suggested that melanopsin may signal through a rhabdomeric-like phototransduction cascade through a $G\alpha_q/G\alpha_{11}$ G protein pathway (Arendt, D., 2003; Isoldi, M. C. *et al.*, 2005). Overexpression of melanopsin in amphibian dermal melanophores hypersensitizes them to light, indicating a prominent role for melanopsin in phototransduction (Rollag, M. D. *et al.*, 2000). As previously mentioned, *Xenopus* melanophores respond to light by dispersing their melanin granules, thereby increasing their optical density. This provides the experimentalist an easily quantifiable output. Melanophores can be cultured in the presence or absence of signaling inhibitors and these effects can be measured with a standard plate reader to gain insight into the potential signaling pathways involved (Rollag, M. D. *et al.*, 2000).

Melanosome dispersion in response to α-melanocyte-stimulating hormone is a well-studied cyclic AMP (cAMP)-dependent process (Nery, L. E. and Castrucci, A. M., 1997). However, light exposure does not increase intracellular cAMP in melanophores and inhibitors of adenylyl cyclase and protein kinase A have no effect on light-induced melanosome dispersion (Isoldi, M. C. *et al.*, 2005). Likewise, inhibitors of guanylyl cyclase and protein kinase G fail to have any effect on the melanophore light response. By contrast, inositol trisphosphate is elevated in response to light and inhibitors of phospholipase C (PLC) and protein kinase C (PKC) dramatically inhibit melanosome photodispersion. Furthermore, chelating intracellular calcium blocks the light response. These data, in concert with the observation that light causes a PKC-dependent phosphorylation of melanophore proteins indicate that melanopsin signals through a phosphoinositide pathway similar to the rhabdomeric photoreceptors of invertebrates (Isoldi, M. C. *et al.*, 2005). As previously mentioned, a second melanopsin gene has been discovered in nonmammalian vertebrates which seems to have been lost in mammals (Bellingham, J. *et al.*, 2006). Although, no opsins other than melanopsin are expressed in the melanophore cell line (Isoldi, M. C. *et al.*, 2005), it is unclear if one or both melanopsins are involved in initiating a phosphoinositide signaling cascade.

Melanopsin-initiated phototransduction, has also been studied by expressing the photopigment in cell lines (Koyanagi, M. *et al.*, 2005; Melyan, Z. *et al.*, 2005; Qiu, X. *et al.*, 2005). These heterologous systems provide many advantages for the study of photopigments, such as melanopsin, that have a very restricted tissue distribution. Primary among these benefits is the generation of many photopigment-expressing cells, providing sufficient material for biochemical studies. Typically, the cell lines used for heterologous expression are not inherently light-sensitive, thereby providing confidence that any light-evoked responses are attributable to the transfected photopigment. Melanopsin has been transiently expressed in several cell lines (Koyanagi, M. *et al.*, 2005; Melyan, Z. *et al.*, 2005; Qiu, X. *et al.*, 2005) and *Xenopus* oocytes (Panda, S. *et al.*, 2005). Some of these studies have shown that photoactivation of melanopsin promotes an intracellular increase in calcium (Melyan, Z. *et al.*, 2005; Qiu, X. *et al.*, 2005). Furthermore, studies using a human embryonic kidney cell line (HEK293-TRPC3) demonstrate that this rise in calcium is triggered by a phosphoinositide signaling cascade as in melanophores (Kumbalasiri, T. and Provencio, I., 2005). The basis of the photo-induced increase in intracellular calcium in melanopsin-transfected Neuro2A cells remains to be determined (Melyan, Z. *et al.*, 2005).

Heterologous expression of melanopsin has proven to be a useful approach to gain insight into the potential pathways of transduction. However, such a pharmacologic dissection has not been extended to mammalian ipRGCs. Experiments on the avian retina have been more productive. Contin M. A. *et al.* (2006) have shown that the light-induced suppression of melatonin production in chicken RGC cultures can be blocked through the use of inhibitors of phosphoinositide signaling or chelation of intracellular calcium. This study represents the first demonstration of a phosphoinositide phototransduction cascade in a vertebrate retina.

Melanopsin-initiated signaling through a $G\alpha_q/G\alpha_{11}$ pathway comports with melanopsin's rhabdomeric character (Arendt, D., 2003). Bistability is another characteristic of rhabdomeric opsin-based signaling. For example, *Drosophila* rhodopsins exhibit

a thermostable metastate and are capable of autonomously photoregenerating in the absence of a retinoid cycle (Hardie, R. C. and Raghu, P., 2001). Expression of amphioxus melanopsin in HEK293S cells has revealed a bistable spectral absorbance similar to squid rhodopsin; at neutral pH, irradiation with blue light generates a red-shifted photoproduct which can be reverted to the original spectral state by irradiation with orange light (Koyanagi, M. *et al.*, 2005). Other studies have also suggested a bistable nature of melanopsin (Fu, Y. *et al.*, 2005; Melyan, Z. *et al.*, 2005; Panda, S. *et al.*, 2005). Such a self-sufficient chromophore-handling strategy would be highly adaptive for photoreceptive cells not anatomically juxtaposed to a retinoid cycling tissue such as the retinal pigment epithelium.

1.20.7 Conclusion

The eye has been extensively studied for over a century. The relatively recent discovery of melanopsin-containing ipRGCs represents a novel photosensory system in the retina that has been literally overlooked. All future studies in retinal physiology must consider the potential contributions of this system.

References

Arendt, D. 2003. Evolution of eyes and photoreceptor cell types. Int. J. Dev. Biol. 47, 563–571.

Avivi, A., Albrecht, U., Oster, H., Joel, A., Beiles, A., and Nevo, E. 2001. Biological clock in total darkness: the Clock/MOP3 circadian system of the blind subterranean mole rat. Proc. Natl. Acad. Sci. U. S. A. 98, 13751–13756.

Bailey, M. J. and Cassone, V. M. 2005. Melanopsin expression in the chick retina and pineal gland. Brain Res. Mol. Brain Res. 134, 345–348.

Barnard, A. R., Hattar, S., Hankins, M. W., and Lucas, R. J. 2006. Melanopsin regulates visual processing in the mouse retina. Curr. Biol. 16, 389–395.

Beaule, C., Robinson, B., Lamont, E. W., and Amir, S. 2003. Melanopsin in the circadian timing system. J. Mol. Neurosci. 21, 73–89.

Belenky, M. A., Smeraski, C. A., Provencio, I., Sollars, P. J., and Pickard, G. E. 2003. Melanopsin retinal ganglion cells receive bipolar and amacrine cell synapses. J. Comp. Neurol. 460, 380–393.

Bellingham, J., Chaurasia, S. S., Melyan, Z., Liu, C., Cameron, M. A., Tarttelin, E. E., Iuvone, P. M., Hankins, M. W., Tosini, G., and Lucas, R. J. 2006. Evolution of melanopsin photoreceptors: discovery and characterization of a new melanopsin in nonmammalian vertebrates. PLoS Biol. 4, e254.

Bellingham, J., Whitmore, D., Philp, A. R., Wells, D. J., and Foster, R. G. 2002. Zebrafish melanopsin: isolation, tissue localisation and phylogenetic position. Brain Res. Mol. Brain Res. 107, 128–136.

Berson, D. M., Dunn, F. A., and Takao, M. 2002. Phototransduction by retinal ganglion cells that set the circadian clock. Science 295, 1070–1073.

Brainard, G. C., Hanifin, J. P., Greeson, J. M., Byrne, B., Glickman, G., Gerner, E., and Rollag, M. D. 2001. Action spectrum for melatonin regulation in humans: evidence for a novel circadian photoreceptor. J. Neurosci. 21, 6405–6412.

Chaurasia, S. S., Rollag, M. D., Jiang, G., Hayes, W. P., Haque, R., Natesan, A., Zatz, M., Tosini, G., Liu, C., Korf, H. W., Iuvone, P. M., and Provencio, I. 2005. Molecular cloning, localization and circadian expression of chicken melanopsin (Opn4): differential regulation of expression in pineal and retinal cell types. J. Neurochem. 92, 158–170.

Contin, M. A., Verra, D. M., and Guido, M. E. 2006. An invertebrate-like phototransduction cascade mediates light detection in the chicken retinal ganglion cells. FASEB J. 20, 2648–2650.

Cooper, H. M., Herbin, M., and Nevo, E. 1993. Ocular regression conceals adaptive progression of the visual system in a blind subterranean mammal. Nature 361, 156–159.

Dacey, D. M., Liao, H. W., Peterson, B. B., Robinson, F. R., Smith, V. C., Pokorny, J., Yau, K. W., and Gamlin, P. D. 2005. Melanopsin-expressing ganglion cells in primate retina signal colour and irradiance and project to the LGN. Nature 433, 749–754.

David-Gray, Z. K., Cooper, H. M., Janssen, J. W., Nevo, E., and Foster, R. G. 1999. Spectral tuning of a circadian photopigment in a subterranean 'blind' mammal (*Spalax ehrenbergi*). FEBS Lett. 461, 343–347.

Drivenes, O., Soviknes, A. M., Ebbesson, L. O., Fjose, A., Seo, H. C., and Helvik, J. V. 2003. Isolation and characterization of two teleost melanopsin genes and their differential expression within the inner retina and brain. J. Comp. Neurol. 456, 84–93.

Foster, R. G., Provencio, I., Hudson, D., Fiske, S., De Grip, W., and Menaker, M. 1991. Circadian photoreception in the retinally degenerate mouse (rd/rd). J. Comp. Physiol. A 169, 39–50.

Frigato, E., Vallone, D., Bertolucci, C., and Foulkes, N. S. 2006. Isolation and characterization of melanopsin and pinopsin expression within photoreceptive sites of reptiles. Naturwissenschaften 93, 379–385.

Fu, Y., Zhong, H., Wang, M. H., Luo, D. G., Liao, H. W., Maeda, H., Hattar, S., Frishman, L. J., and Yau, K. W. 2005. Intrinsically photosensitive retinal ganglion cells detect light with a vitamin A-based photopigment, melanopsin. Proc. Natl. Acad. Sci. U. S. A. 102, 10339–10344.

Gooley, J. J., Lu, J., Chou, T. C., Scammell, T. E., and Saper, C. B. 2001. Melanopsin in cells of origin of the retinohypothalamic tract. Nat. Neurosci. 4, 1165.

Gooley, J. J., Lu, J., Fischer, D., and Saper, C. B. 2003. A broad role for melanopsin in nonvisual photoreception. J. Neurosci. 23, 7093–7106.

Hannibal, J. and Fahrenkrug, J. 2004. Melanopsin containing retinal ganglion cells are light responsive from birth. Neuroreport 15, 2317–2320.

Hannibal, J., Hindersson, P., Knudsen, S. M., Georg, B., and Fahrenkrug, J. 2002a. The photopigment melanopsin is exclusively present in pituitary adenylate cyclase-activating polypeptide-containing retinal ganglion cells of the retinohypothalamic tract. J. Neurosci. 22, RC191.

Hannibal, J., Hindersson, P., Nevo, E., and Fahrenkrug, J. 2002b. The circadian photopigment melanopsin is expressed in the blind subterranean mole rat, Spalax. Neuroreport 13, 1411–1414.

Hannibal, J., Hindersson, P., Ostergaard, J., Georg, B., Heegaard, S., Larsen, P. J., and Fahrenkrug, J. 2004. Melanopsin is expressed in PACAP-containing retinal ganglion cells of the human retinohypothalamic tract. Invest. Ophthalmol. Vis. Sci. 45, 4202–4209.

Hannibal, J., Moller, M., Ottersen, O. P., and Fahrenkrug, J. 2000. PACAP and glutamate are co-stored in the retinohypothalamic tract. J. Comp. Neurol. 418, 147–155.

Hardie, R. C. and Raghu, P. 2001. Visual transduction in Drosophila. Nature 413, 186–193.

Hattar, S., Kumar, M., Park, A., Tong, P., Tung, J., Yau, K. W., and Berson, D. M. 2006. Central projections of melanopsin-expressing retinal ganglion cells in the mouse. J. Comp. Neurol. 497, 326–349.

Hattar, S., Liao, H. W., Takao, M., Berson, D. M., and Yau, K. W. 2002. Melanopsin-containing retinal ganglion cells: architecture, projections, and intrinsic photosensitivity. Science 295, 1065–1070.

Hattar, S., Lucas, R. J., Mrosovsky, N., Thompson, S., Douglas, R. H., Hankins, M. W., Lem, J., Biel, M., Hofmann, F., Foster, R. G., and Yau, K. W. 2003. Melanopsin and rod–cone photoreceptive systems account for all major accessory visual functions in mice. Nature 424, 76–81.

Isoldi, M. C., Rollag, M. D., Castrucci, A. M., and Provencio, I. 2005. Rhabdomeric phototransduction initiated by the vertebrate photopigment melanopsin. Proc. Natl. Acad. Sci. U. S. A. 102, 1217–1221.

Kim, J. M., Hwa, J., Garriga, P., Reeves, P. J., RajBhandary, U. L., and Khorana, H. G. 2005. Light-driven activation of beta 2-adrenergic receptor signaling by a chimeric rhodopsin containing the beta 2-adrenergic receptor cytoplasmic loops. Biochemistry 44, 2284–2292.

Koyanagi, M., Kubokawa, K., Tsukamoto, H., Shichida, Y., and Terakita, A. 2005. Cephalochordate melanopsin: evolutionary linkage between invertebrate visual cells and vertebrate photosensitive retinal ganglion cells. Curr. Biol. 15, 1065–1069.

Kumbalasiri, T. and Provencio, I. 2005. Melanopsin and other novel mammalian opsins. Exp. Eye Res. 81, 368–375.

Lin, B., Wang, S. W., and Masland, R. H. 2004. Retinal ganglion cell type, size, and spacing can be specified independent of homotypic dendritic contacts. Neuron 43, 475–485.

Lucas, R. J., Douglas, R. H., and Foster, R. G. 2001. Characterization of an ocular photopigment capable of driving pupillary constriction in mice. Nat. Neurosci. 4, 621–626.

Lucas, R. J., Hattar, S., Takao, M., Berson, D. M., Foster, R. G., and Yau, K. W. 2003. Diminished pupillary light reflex at high irradiances in melanopsin-knockout mice. Science 299, 245–247.

Melyan, Z., Tarttelin, E. E., Bellingham, J., Lucas, R. J., and Hankins, M. W. 2005. Addition of human melanopsin renders mammalian cells photoresponsive. Nature 433, 741–745.

Morin, L. P. and Allen, C. N. 2006. The circadian visual system, 2005. Brain Res. Brain Res. Rev. 51, 1–60.

Morin, L. P., Blanchard, J. H., and Provencio, I. 2003. Retinal ganglion cell projections to the hamster suprachiasmatic nucleus, intergeniculate leaflet, and visual midbrain: bifurcation and melanopsin immunoreactivity. J. Comp. Neurol. 465, 401–416.

Nery, L. E. and Castrucci, A. M. 1997. Pigment cell signalling for physiological color change. Comp. Biochem. Physiol. A Physiol. 118, 1135–1144.

Panda, S., Nayak, S. K., Campo, B., Walker, J. R., Hogenesch, J. B., and Jegla, T. 2005. Illumination of the melanopsin signaling pathway. Science 307, 600–604.

Panda, S., Provencio, I., Tu, D. C., Pires, S. S., Rollag, M. D., Castrucci, A. M., Pletcher, M. T., Sato, T. K., Wiltshire, T., Andahazy, M., Kay, S. A., Van Gelder, R. N., and Hogenesch, J. B. 2003. Melanopsin is required for non-image-forming photic responses in blind mice. Science 301, 525–527.

Panda, S., Sato, T. K., Castrucci, A. M., Rollag, M. D., De Grip, W. J., Hogenesch, J. B., Provencio, I., and Kay, S. A. 2002. Melanopsin (Opn4) requirement for normal light-induced circadian phase shifting. Science 298, 2213–2216.

Provencio, I., Jiang, G., De Grip, W. J., Hayes, W. P., and Rollag, M. D. 1998. Melanopsin: an opsin in melanophores, brain, and eye. Proc. Natl. Acad. Sci. U. S. A. 95, 340–345.

Provencio, I., Rodriguez, I. R., Jiang, G., Hayes, W. P., Moreira, E. F., and Rollag, M. D. 2000. A novel human opsin in the inner retina. J. Neurosci. 20, 600–605.

Provencio, I., Rollag, M. D., and Castrucci, A. M. 2002. Photoreceptive net in the mammalian retina. This mesh of cells may explain how some blind mice can still tell day from night. Nature 415, 493.

Qiu, X., Kumbalasiri, T., Carlson, S. M., Wong, K. Y., Krishna, V., Provencio, I., and Berson, D. M. 2005. Induction of photosensitivity by heterologous expression of melanopsin. Nature 433, 745–749.

Rodieck, R. W. 1998. The First Steps in Seeing. Sinauer.

Rollag, M. D. 1996. Amphibian melanophores become photosensitive when treated with retinal. J. Exp. Zool. 275, 20–26.

Rollag, M. D., Provencio, I., Sugden, D., and Green, C. B. 2000. Cultured amphibian melanophores: a model system to study melanopsin photobiology. Meth. Enzymol. 316, 291–309.

Ruby, N. F., Brennan, T. J., Xie, X., Cao, V., Franken, P., Heller, H. C., and O'Hara, B. F. 2002. Role of melanopsin in circadian responses to light. Science 298, 2211–2213.

Sekaran, S., Lupi, D., Jones, S. L., Sheely, C. J., Hattar, S., Yau, K. W., Lucas, R. J., Foster, R. G., and Hankins, M. W. 2005. Melanopsin-dependent photoreception provides earliest light detection in the mammalian retina. Curr. Biol. 15, 1099–1107.

Sollars, P. J., Smeraski, C. A., Kaufman, J. D., Ogilvie, M. D., Provencio, I., and Pickard, G. E. 2003. Melanopsin and non-melanopsin expressing retinal ganglion cells innervate the hypothalamic suprachiasmatic nucleus. Vis. Neurosci. 20, 601–610.

Tarttelin, E. E., Bellingham, J., Bibb, L. C., Foster, R. G., Hankins, M. W., Gregory-Evans, K., Gregory-Evans, C. Y., Wells, D. J., and Lucas, R. J. 2003. Expression of opsin genes early in ocular development of humans and mice. Exp. Eye Res. 76, 393–396.

Thapan, K., Arendt, J., and Skene, D. J. 2001. An action spectrum for melatonin suppression: evidence for a novel non-rod, non-cone photoreceptor system in humans. J. Physiol. 535, 261–267.

Tobler, I., Herrmann, M., Cooper, H. M., Negroni, J., Nevo, E., and Achermann, P. 1998. Rest-activity rhythm of the blind mole rat Spalax ehrenbergi under different lighting conditions. Behav. Brain Res. 96, 173–183.

Tomonari, S., Takagi, A., Akamatsu, S., Noji, S., and Ohuchi, H. 2005. A non-canonical photopigment, melanopsin, is expressed in the differentiating ganglion, horizontal, and bipolar cells of the chicken retina. Dev. Dyn. 234, 783–790.

Tu, D. C., Zhang, D., Demas, J., Slutsky, E. B., Provencio, I., Holy, T. E., and Van Gelder, R. N. 2005. Physiologic diversity and development of intrinsically photosensitive retinal ganglion cells. Neuron 48, 987–999.

Warren, E. J., Allen, C. N., Brown, R. L., and Robinson, D. W. 2003. Intrinsic light responses of retinal ganglion cells

projecting to the circadian system. Eur. J. Neurosci. 17, 1727–1735.

Wong, K. Y., Dunn, F. A., and Berson, D. M. 2005. Photoreceptor adaptation in intrinsically photosensitive retinal ganglion cells. Neuron 48, 1001–1010.

Yoshimura, T. and Ebihara, S. 1996. Spectral sensitivity of photoreceptors mediating phase-shifts of circadian rhythms in retinally degenerate CBA/J (rd/rd) and normal CBA/N (+/+)mice. J. Comp. Physiol. A 178, 797–802.

1.21 Blue-ON Cells

B B Lee, SUNY College of Optometry, New York, NY, USA

© 2008 Elsevier Inc. All rights reserved.

1.21.1	Introduction	433
1.21.2	Early Studies	433
1.21.3	Anatomical Substrate	434
1.21.4	Current Views of Cell Physiology	435
1.21.5	Other Cells with S-Cone Input	436
1.21.6	Conclusions	436
References		437

Glossary

tritan, tritanopia Tritanopia refers to the form of color blindness associated with absence of the short-wavelength cones. Such individuals are unable to distinguish colors that lie along a tritanopic confusion line in color space (along which only short-wavelength cone excitation varies). Individuals with normal color vision rely on short-wavelength cones to distinguish such colors. Stimuli that modulate along a tritan line are often used, psychophysically and physiologically, to isolate short-wavelength cone (colloquially blue–yellow) mechanisms.

1.21.1 Introduction

A cone with peak absorption in the short-wavelength region of the visible spectrum (400–500 nm), commonly termed the short-wavelenth (s) cone is common to most mammalian species (Jacobs, G. H., 1993) and presumably some form of blue–yellow color vision is present among them. However, there are only sparse reports on the physiology of these pathways in nonprimates. For example, cells with S-cone input have been reported in the cat retina (Cleland, B. G. and Levick, W. R., 1974) but little quantitative detail is available about their properties, or on blue–yellow discrimination ability in this (or other) species. Since blue–yellow color vision is thought to be phylogenetically ancient (Mollon, J. D., 1989), it is tempting to assume that blue-ON cell ganglion cell anatomy and physiology is similar in all mammals with S cones, but there is little or no evidence for this supposition.

Primates are the only mammals to possess full trichromatic vision, with middle-wavelength (M) and long-wavelength (L) cones as well as the S cone. The characteristics of the red–green color opponent pathway are discussed elsewhere in this volume. The blue–yellow opponent pathway forms a separate system, beginning in at least two ganglion cell classes, passing through the koniocellular layers of the lateral geniculate nucleus (LGN) to striate cortex. The best-studied of the ganglion cell classes is the small bistratified cell, which forms the main focus of this article. A more extensive overview of the S cones and their ganglion cell classes has been provided by Calkins D. J. (2001), and a complementary overview can be found in Dacey D. M. and Packer O. S. (2003).

1.21.2 Early Studies

Recordings from retinal ganglion cells and LGN neurons of the macaque (DeValois, R. L., 1971; Gouras, P. and Zrenner, E., 1981) revealed cells excited by lights of short wavelength and inhibited by lights through the rest of the spectrum. This would imply cells with excitatory input from S cones and inhibitory inputs from the other cone types. Such cells are colloquially known as blue-ON cells, and it has turned out that three other cell types have S-cone input, as described in a later section.

How far do these ganglion cells exclusively carry S-cone signals? Experiments using differential adaptation suggested that small S-cone inputs might be present to, for example, some red–green opponent cells (de Monasterio, F. M. *et al.*, 1975). However, it was unclear whether such an input, if present, played a significant role in cell responses under more neutral adaptation conditions. More sophisticated stimulus techniques, in which cell responses were measured to modulation around a neutral mean chromaticity, showed that S-cone inputs were not readily detected to ganglion classes other than those with major S-cone input (Derrington, A. M. *et al.*, 1984; Lee, B. B. *et al.*, 1987). These early measurements might not have detected weak inputs, but recently experiments using a more sensitive means for detecting S-cone input have shown that input to red–green opponent and parasol or magnocellular cells is very small indeed (Sun, H. *et al.*, 2006b), and that these cells must avoid S-cone input (Sun, H. *et al.*, 2006a). Thus, the blue-ON cell and a few other cell types carry exclusive responsibility for transmitting S-cone signals to the brain.

1.21.3 Anatomical Substrate

The small bistratified ganglion cell was described by Rodieck R. W. (1991) and Dacey D. M. (1993) provided strong anatomical evidence that it corresponded to the blue-ON cell. One inner dendritic layer ramifies close to the cell body, in the most vitreal stratum of the inner plexiform layer (IPL) near where the S-cone bipolar terminates (Kouyama, N. and Marshak, D. W., 1992). The outer layer of its dendrites ramifies in the outermost stratum of the IPL, is less dense and slightly smaller in diameter. A sketch of this arrangement in shown in Figure 1. The blue-ON circuitry is sketched, and the inner and outer dendritic trees of a small bistratified cell are shown. Overall dendritic tree size is slightly larger than parasol cells at the same eccentricity (Dacey, D. M., 1993). The small bistratified cell forms a single mosaic across the retina, suggesting a functionally homogenous cell class. One other feature is that there is electrotonic coupling to a small-field amacrine cell class. Physiological recordings from cells that were then stained with neurobiotin confirmed that these cells were members of the blue-ON class (Dacey, D. M. and Lee, B. B., 1994). One hypothesis as to the physiological basis of blue–yellow opponency is that excitatory S-cone input is received in the inner dendritic layer via the S-cone bipolar, and inhibitory input is received into the outer dendrites through some unidentified off diffuse bipolar. However, the basis of the opponency is likely to be more complicated. After blocking of the on pathways pharmacologically, not only is the blue-ON signal lost, but also most of the inhibitory response from the M and L cones (Dacey, D. M., 2000). It may be that some degree of blue–yellow opponency is already present in the blue-ON bipolar cell. In outer retina, the HII horizontal makes contact with both the S cones and the M and L cones (Dacey, D. M. *et al.*, 1996); all cone types hyperpolarize the cell. An opponent M,L-cone input could derive from horizontal cells to the S-cone bipolar and thence to the ganglion cell. Alternatively, the electrotonically coupled amacrine cell class may play a role. The relative weights of these contributions remain to be determined.

Since the proportion of S cones in the mosaic is small, the S-cone receptive field of the small bistratified cell must be nonuniform, in that only a few S cones can provide input. In elegant measurements using a multielectrode array so that local mapping of the inputs from S cones could be achieved, Chichilnisky E. J. and Baylor D. A. (1999) showed that small bistratified cells received major input from just one or two S cones, and that these inputs summed linearly. The punctate distribution of S cones must affect the response of such cells to spatial patterns; for example, drifting tritan gratings (just modulating the S cone) with a period length close to the field width would alias with the S-cone inputs. In any event, the results of Chichilnisky and Baylor form a basis for the psychophysical detectability of the S-cone mosaic (Williams, D. R. *et al.*, 1981).

The small bistratified cell was originally identified following injections of horseradish peroxidase in the parvocellular (PC) layers of the LGN (Watanabe, M. and Rodieck, R. W., 1989), and was assumed to be part of this afferent system. However, it is now clear that the intercalated, koniocellular layers of the LGN represent a separate system, and most if not all cells with S-cone input project to the cortex through this pathway (White, A. J. R. *et al.*, 1998; Szmajda, B. A. *et al.*, 2007). The earlier injections were not specific enough to make this distinction. This is consistent with the view that this pathway existed in mammals before the primate PC and magnocellular (MC) afferent pathways emerged. It now appears that this opponent color system terminates in a superficial layer of the cortex (Chatterjee, S. and Callaway, E. M., 2003), separately from the other systems.

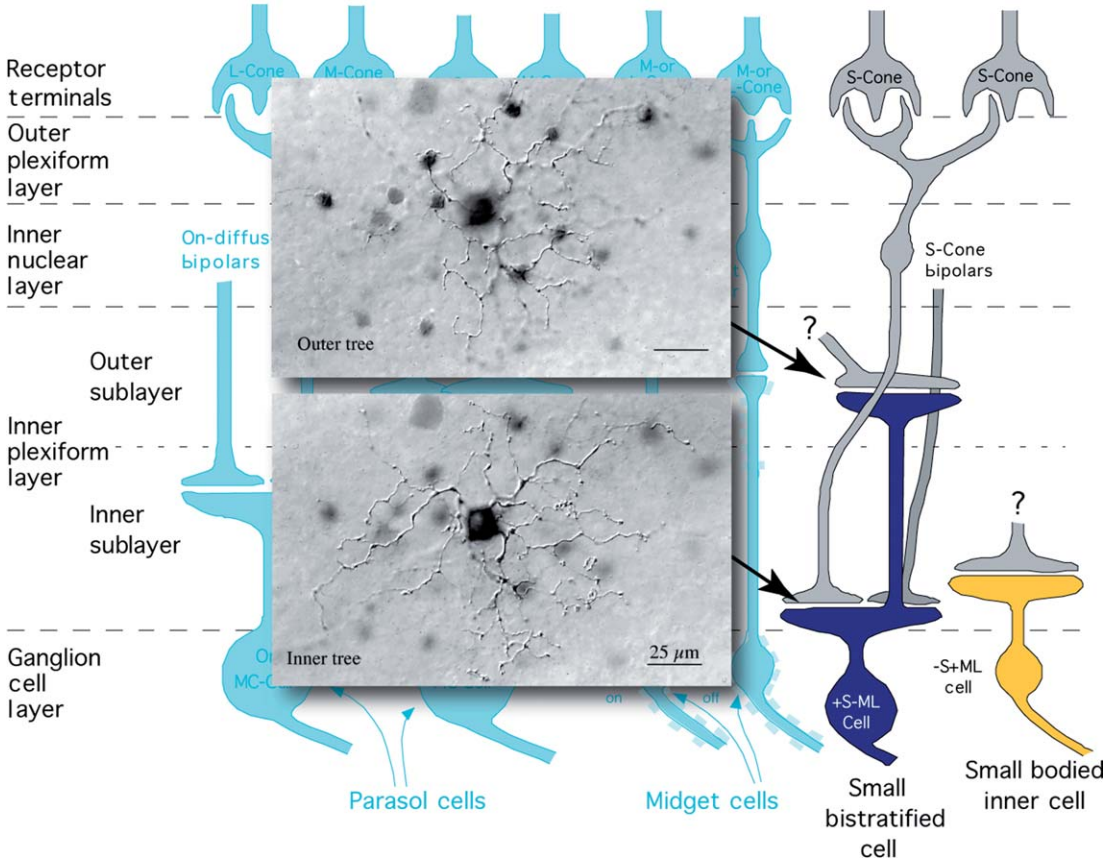

Figure 1 A sketch of blue-ON circuitry. The small bistratified cell has two layers of dendrites stratifying in the inner and outer strata of the inner plexiform layer. The micrographs show typical dendritic trees of the two strata, following neurobiotin staining after recording, viewed with different levels of focus in the retinal wholemount. In each, one layer of dendrites can be seen to be in focus, and the other blurred. The outer tree is sparser and smaller than the inner tree. The input to the inner tree is from the small-wavelength (S)-cone bipolar, the input to the outer tree is uncertain. There is also sketched the small field ganglion cell believed to correspond to the blue-OFF cell.

1.21.4 Current Views of Cell Physiology

It is well established that the blue-ON cell receives excitatory input from the S-cone and inhibitory input from the other two cone types. The L/M weighting of this inhibitory input may be random. One study specifically assessed this issue and found input from both L and M cones but with considerable variability (Smith, V. C. *et al.*, 1992), and other studies have also suggested combined input (Lee, B. B. *et al.*, 1987; Chichilnisky, E. J. and Baylor, D. A., 1999). As far as receptive field structure is concerned, the spatial extent of the antagonistic mechanisms is roughly coextensive (Solomon, S. G. *et al.*, 2005), as might be expected if the two layers of dendrites determined the extent of the opponent mechanisms. However, as noted above, the source of the M,L cone signal is still unsure.

Early studies of blue-ON cells found that their responses could be adequately described by linear combination of cone inputs (Derrington, A. M. *et al.*, 1984; Lee, B. B. *et al.*, 1987). Consistent with the linear model, the blue-ON cell underlies detection of S stimuli superimposed upon an achromatic background (Crook, J. M. *et al.*, 1987). However, psychophysical results associated with the S-cone system suggest some nonlinear features. In particular, immediately after exposure to strong yellow or blue adapting fields, sensitivity to S-cone increments is depressed; this is termed transient tritanopia (Mollon, J. D. and Polden,

P. G., 1980; Mollon, J. D. *et al.*, 1987), and appears to be due to the blue–yellow opponent system being driven into temporary saturation before it recovers with a time course of several seconds. This phenomenon appears to have a physiological basis at the ganglion cell level (Zrenner, E. and Gouras, P., 1981). It is unclear whether this is because it is easy to drive this color opponent system into saturation, since the S cone is spectrally well separated from the M and L cones, or whether it is because of some inherent nonlinearity of this pathway. The M and L cones are closer together spectrally, and it may be more difficult to provide for the red–green system such strong differential adaptation as can be achieved with the blue–yellow pathway. Physiologically however, midget, PC cells show similar effects (Yeh, T. *et al.*, 1996), although they have been difficult to detect psychophysically (Reeves, A., 1981). Van Hateren J. H. *et al.* (2002), when modeling blue-ON cell responses to natural scenes, found evidence for some kind of long-term adaptation effects, which were absent from midget, red–green opponent ganglion cells.

From early psychophysical measurements of S-cone modulation sensitivity it was concluded that this pathway had poor temporal resolution, with the speculation that the S cones themselves might have a sluggish response (Brindley, G. S. *et al.*, 1966). However, the impulse response of individual S cones is of similar duration to the impulse response of M and L cones (Schnapf, J. L. *et al.*, 1990), which would suggest a similar temporal chracteristic. Blue-ON ganglion cells respond up to a frequency of 30–40 Hz with tritan modulation, which is much higher than the frequency at which psychophysical detection of S-cone modulation fails (Yeh, T. *et al.*, 1995). There must therefore be low-pass filtering of the blue-ON cell signal at a central, cortical site, as is the case for PC cells and red–green modulation (Lee, B. B. and Dacey, D. M., 2007).

1.21.5 Other Cells with S-Cone Input

Despite early doubts as to the existence of cells with inhibitory S-cone input, their presence was eventually established in the macaque LGN (Valberg, A. *et al.*, 1986). They receive inhibitory input from the S cone, and some excitatory input from the other cone types, although in one recent study in the marmoset LGN (Szmajda, B. A. *et al.*, 2007) about half the cells in a small sample had no M,L-cone input. It is unclear whether this is a species difference; in the macaque, blue-OFF cells are generally excited by yellow light, and fill in Sloan's notch when chromatic targets are presented on an achromatic background (Crook, J. M. *et al.*, 1987), which suggests excitatory M,L-cone input. In the marmoset study, all cells were found in the koniocellular layers of the LGN, as expected.

The retinal origin of these cells is uncertain. Encounter rates of blue-ONs relative to blue-OFFs tend to be about 3:1 in the LGN (Derrington, A. M. *et al.*, 1984; Valberg, A. *et al.*, 1986; Szmajda, B. A. *et al.*, 2007, #2714), but encounter rates in the retina are lower (Lee, B. B. and Hao Sun, unpublished observations). This may account for early reports that ganglion cells with inhibitory S-cone input were not present (de Monasterio, F. M. and Gouras, P., 1975). Recently, Dacey D. M. and Packer. O. S. (2003) identified a small-field monostratified cell with inhibitory S-cone input (Figure 1), with its dendritic tree branching close to the S-cone-ON bipolar axonal arborization. However, how a sign inversion (how an S-cone-OFF response can be generated from an on signal in the bipolar cell) might be achieved remains unknown. Alternatively, based on reconstruction of electron micrographs it was proposed that a midget bipolar/midget ganglion cell pathway carries the blue-OFF signal (Klug, K. *et al.*, 2003). Receptive fields of blue-OFF cells are however larger than PC cells in the marmoset LGN, which makes this possibility less likely (Szmajda, B. A. *et al.*, 2007). Also, an immunocytochemical stain for off midget bipolar cells could found no S-cone contacts (Lee, S. C. *et al.*, 2005).

Physiologically, blue-OFF cells have type 2 (coextensive) receptive fields and a temporal response extending to 20–30 Hz (Yeh, T. *et al.*, 1995). Again it is likely that a central low-pass filter attenuates the frequency response.

A large bistratified cell also carries a blue-ON signal (Dacey, D. M. and Packer, O. S., 2003). This is a rare cell type and has not been extensively described. There are no indications from *in vivo* measurements of a dual blue-ON population, but it could be that these cells are very rarely encountered. S-cone inhibitory input is also present to the melanopsin containing ganglion cell (Dacey, D. M. *et al.*, 2005) but its contribution to color perception seems likely to be minimal.

1.21.6 Conclusions

Blue-ON cells correspond to the small bistratified ganglion cell type, but there are other ganglion cells with S-cone input which are likely to contribute to the blue–yellow channel of perception of color. This

is an evolutionary ancient system. Although to a first approximation cell responses can be described as a difference signal between S- and M,L-cone inputs, some features of this pathway are still poorly understood, in particular its characteristics during chromatic adaptation.

Acknowledgment

Preparation of this article was partially supported by NEI 13112.

References

Brindley, G. S., Du Croz, J. J., and Rushton, W. A. H. 1966. The flicker fusion frequency of the blue-sensitive mechanism of colour vision. J. Physiol. (Lond.) 183, 497–500.

Calkins, D. J. 2001. Seeing with S cones. Prog. Retin. Eye Res. 20, 255–287.

Chatterjee, S. and Callaway, E. M. 2003. Parallel colour-opponent pathways to primary visual cortex. Nature 426, 668–671.

Chichilnisky, E. J. and Baylor, D. A. 1999. Receptive-field microstructure of blue–yellow ganglion cells in primate retina. Nat. Neurosci. 2, 889–893.

Cleland, B. G. and Levick, W. R. 1974. Properties of rarely encountered types of ganglion cells in the cat's retina and an overall classification. J. Physiol. 240, 457–492.

Crook, J. M., Lee, B. B., Tigwell, D. A., and Valberg, A. 1987. Thresholds to chromatic spots of cells in the macaque geniculate nucleus as compared to detection sensitivity in man. J. Physiol. 392, 193–211.

Dacey, D. M. 1993. Morphology of a small field bistratified ganglion cell type in the macaque and human retina: is it the blue-ON cell? Vis. Neurosci. 10, 1081–1098.

Dacey, D. M. 2000. Parallel pathways for spectral coding in primate retina. Annu. Rev. Neurosci. 23, 743–775.

Dacey, D. M. and Lee, B. B. 1994. The blue-ON opponent pathway in primate retina originates from a distinct bistratified ganglion cell type. Nature 367, 731–735.

Dacey, D. M. and Packer, O. S. 2003. Colour coding in the primate retina: diverse cell types and cone-specific circuitry. Curr. Opin. Neurobiol. 13, 421–427.

Dacey, D. M., Lee, B. B., Stafford, D. M., Smith, V. C., and Pokorny, J. 1996. Horizontal cells of the primate retina: cone specificity without cone opponency. Science 271, 656–658.

Dacey, D. M., Liao, H. W., Peterson, B. B., Robinson, F. R., Smith, V. C., Pokorny, J., Yau, K. W., and Gamlin, P. D. 2005. Melanopsin-expressing ganglion cells in primate retina signal colour and irradiance and project to the LGN. Nature 433, 749–754.

de Monasterio, F. M. and Gouras, P. 1975. Functional properties of ganglion cells in monkey retina. J. Physiol. 251, 167–195.

Derrington, A. M., Krauskopf, J., and Lennie, P. 1984. Chromatic mechanisms in lateral geniculate nucleus of macaque. J. Physiol. 357, 241–265.

Devalois, R. L. 1971. Physiological basis of color vision. Die Farbe 20, 151–169.

Gouras, P. and Zrenner, E. 1981. Color coding in primate retina. Vision Res. 21, 1591–1598.

Jacobs, G. H. 1993. The distribution and nature of color vision among the mammals. Biol. Rev. 68, 413–471.

Klug, K., Herr, S., Ngo, I. T., Sterling, P., and Schein, S. 2003. Macaque retina contains an S-cone OFF midget pathway. J. Neurosci. 23, 9881–9887.

Kouyama, N. and Marshak, D. W. 1992. Bipolar cells specific for blue cones in the macaque retina. J. Neurosci. 12, 1233–1252.

Lee, B. B. and Dacey, D. M. 2007. Color Opponency in Retina, LGN. In: (*ed*. R. Masland).

Lee, S. C., Telkes, I., and Grunert, U. 2005. S-cones do not contribute to the OFF-midget pathway in the retina of the marmoset, *Callithrix jacchus*. Eur. J. Neurosci. 22, 437–447.

Lee, B. B., Valberg, A., Tigwell, D. A., and Tryti, J. 1987. An account of responses of spectrally opponent neurons in macaque lateral geniculate nucleus to successive contrast. Proc. R. Soc. B 230, 293–314.

Mollon, J. D. 1989. "Tho'she kneel'd in that place where they grew. . ." the uses and origins of primate colour vision. J. Exp. Biol. 146, 21–38.

Mollon, J. D. and Polden, P. G. 1980. A curiosity of light adaptation. Nature 286, 59–62.

Mollon, J. D., Stockman, A., and Polden, P. G. 1987. Transient tritanopia of a second kind. Vision Res. 27, 637–650.

de Monasterio, F. M., Gouras, P., and Tolhurst, D. J. 1975. Trichromatic colour opponency in ganglion cells of the rhesus monkey retina. J. Physiol. 251, 187–216.

Reeves, A. 1981. Transient desensitization of a red–green opponent site. Vision Res. 21, 1267–1277.

Rodieck, R. W. 1991. Which Cells Code for Color? In: From Pigments to Perception (*eds*. A. Valberg and B. B. Lee), pp. 88–93. Plenum.

Schnapf, J. L., Nunn, B. J., Meister, M., and Baylor, D. A. 1990. Visual transduction in cones of the monkey *Macaca fascicularis*. J. Physiol. 427, 681–713.

Smith, V. C., Lee, B. B., Pokorny, J., Martin, P. R., and Valberg, A. 1992. Responses of macaque ganglion cells to the relative phase of heterochromatically modulated lights. J. Physiol. 458, 191–221.

Solomon, S. G., Lee, B. B., White, A. J., Ruttiger, L., and Martin, P. R. 2005. Chromatic organization of ganglion cell receptive fields in the peripheral retina. J. Neurosci. 25, 4527–4539.

Sun, H., Smithson, H., Zaidi, Q., and Lee, B. B. 2006a. Do magnocellular and parvocellular ganglion cells avoid short-wavelength cone input. Vis. Neurosci. 23, 323–330.

Sun, H., Smithson, H., Zaidi, Q., and Lee, B. B. 2006b. Specificity of cone inputs to macaque ganglion cells. J. Neurophysiol. 95, 837–849.

Szmajda, B. A., Buzas, P., Fitzgibbon, T., and Martin, P. R. 2006. Geniculocortical rely of blue-off signals in the primate visual system. Proc. Natl. Acad. Sci. U. S. A. 103, 19512–19517.

Valberg, A., Lee, B. B., and Tigwell, D. A. 1986. Neurons with strong inhibitory S-cone inputs in the macaque lateral geniculate nucleus. Vision Res. 26, 1061–1064.

Van Hateren, J. H., Ruttiger, L., Sun, H., and Lee, B. B. 2002. Processing of natural temporal stimuli by macaque retinal ganglion cells. J. Neurosci. 22, 9945–9960.

Watanabe, M. and Rodieck, R. W. 1989. Parasol and midget ganglion cells of the primate retina. J. Comp. Neurol. 289, 434–454.

White, A. J. R., Goodchild, A. K., Wilder, H. D., Sefton, A. E., and Martin, P. R. 1998. Segregation of receptive field properties in the lateral geniculate nucleus of a New-World monkey, the marmoset, *Callithrix jacchus*. J. Neurophysiol. 80, 2063–2076.

Williams, D. R., Macleod, D. I. A., and Hayhoe, M. M. 1981. Punctate sensitivity of the blue-sensitive mechanism. Vision Res. 21, 1357–1375.

Yeh, T., Lee, B. B., and Kremers, J. 1995. The temporal response of ganglion cells of the macaque retina to cone-pecific modulation. J. Opt. Soc. Am. A 12, 456–464.

Yeh, T., Lee, B. B., and Kremers, J. 1996. The time course of adaptation in macaque ganglion cells. Vision Res. 36, 913–931.
Zrenner, E. and Gouras, P. 1981. Characteristics of the blue sensitive cone mechanism on primate retinal ganglion cells. Vision Res. 21, 1605–1609.

Relevant Website

http://www.biostr.washington.edu – Department of Biological Structure, University of Washington. Directory, Faculty, Dacey.

1.22 Mosaics, Tiling, and Coverage by Retinal Neurons

B E Reese, University of California, Santa Barbara, CA, USA

© 2008 Elsevier Inc. All rights reserved.

1.22.1	**Introduction**	440
1.22.2	**Retinal Mosaics**	440
1.22.2.1	Global Variations in the Distribution of Retinal Nerve Cell Types	440
1.22.2.2	Local Patterning in the Distribution of Retinal Nerve Cell Types	440
1.22.2.3	Assessing the Local Order of Retinal Nerve Cells	441
1.22.2.3.1	Nearest neighbor analysis	441
1.22.2.3.2	Voronoi-based analyses	443
1.22.2.3.3	Autocorrelation analysis and the density recovery profile	444
1.22.2.3.4	Packing factor analysis	445
1.22.2.4	Simulating the Distribution of Retinal Nerve Cells	446
1.22.2.5	Functional Implications of Regular Retinal Mosaics	446
1.22.3	**Dendritic Coverage**	448
1.22.3.1	Global Variation in Dendritic Field Size	448
1.22.3.1.1	Dendritic overlap and the coverage factor	448
1.22.3.2	Variation in Dendritic Overlap between Retinal Nerve Cell Types	448
1.22.3.2.1	Dendritic tiling and contact inhibition	448
1.22.3.2.2	Regulating dendritic overlap by homotypic interactions	451
1.22.3.2.3	Overlap unregulated by homotypic interactions?	452
1.22.3.3	Dendritic Coverage and Connectivity	452
1.22.4	**Conclusions**	453
References		453

Glossary

autocorrelogram Plot of the spatial position of all cells of a given type within the field relative to every other cell of the same type.

coverage factor The product of dendritic field area and cell density for a given cell type

cross-correlogram Plot of the spatial position of all cells of one type within the field relative to every other cell of a second type.

Delaunay segment Distance between any two cells that share a Voronoi border; the Delaunay triangulation of a population of cells is comprised of all such Delaunay segments between cells.

density recovery profile The spatial density of cells in the autocorrelogram as a function of distance from the origin.

effective radius The radius of the exclusion zone defined by the density recovery profile.

exclusion zone The region surrounding a cell where the probability of encountering a like-type cell is lower than the mean density for that cell-type.

packing factor Scale-independent measure describing the extent to which a mosaic of cells varies between a random distribution of points and a hexagonal lattice.

packing intensity The extent to which a population of cells covers the retinal surface by nonoverlapping fields with a size equal to the exclusion zone.

regularity index Scale-independent measure describing the variance within a population of nearest neighbor distances or other tessellation-based attributes (e.g., Voronoi domain area).

Voronoi domain Territory associated to a cell that is closer to that cell than to any other homotypic cell in the field.

1.22.1 Introduction

The visual field is sampled by a sheet of nerve cells composed of multiple types, each contributing uniquely to the postreceptoral processing of the visual signal. Each of these cell types is distributed across the retinal surface as a patterned array, extending dendrites that sample from the layer of afferent innervation within a plexiform layer. The morphological configuration of those dendrites and the extent to which they overlap one another are unique for each cell type, being associated with the functional contribution carried out by each population at every location across the retina. The present chapter will consider the extent to which such patterning and dendritic overlap are regulated in order to ensure a uniform coverage of the retinal surface.

1.22.2 Retinal Mosaics

1.22.2.1 Global Variations in the Distribution of Retinal Nerve Cell Types

The densities of different types of retinal neurons vary across the retinal surface in a manner that is both species- as well as cell-type specific. For example, ganglion and cone photoreceptor cell density in the primate retina both show a steep decline outside the perifoveal region, whereas dopaminergic and cholinergic amacrine cell density decline far less conspicuously as a function of eccentricity (Mariani, A. P. *et al.*, 1984; Perry, V. H. *et al.*, 1984; Curcio, C, A. *et al.*, 1990; Dacey, D. M., 1990; Rodieck, R. W. and Marshak, D. W., 1992). Figure 1 shows comparable results from the cat retina, in which the cell density profile as a function of eccentricity from the area centralis is unique for each cell type (Steinberg, R. H. *et al.*, 1973; Wässle, H. *et al.*, 1978; Hughes, A., 1981; Vaney, D. I. *et al.*, 1989). Other species, for example the rabbit, exhibit a visual streak rather than a single central area associated with the direction of gaze, in which cell densities are maximal along a horizontal strip of retina, falling off at different rates as a function of eccentricity for the different cell classes (Masland, R. H. *et al.*, 1984; Brecha, N. C. *et al.*, 1984; Massey, S. C. *et al.*, 1991; Mills, S. L. and Massey, S. C., 1991, 1994; Vaney, D. I. *et al.*, 1991; Young, H. M. and Vaney, D. I., 1991). Still other species like the mouse exhibit relatively minor changes in cell density across the retinal surface for most cell types (Jeon, C-J. *et al.*, 1998).

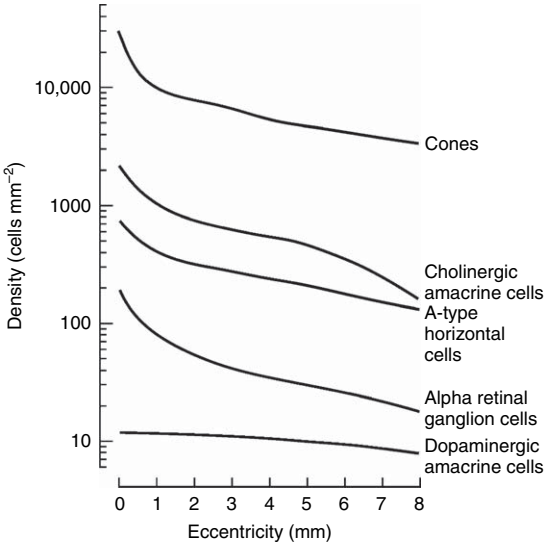

Figure 1 The density of different retinal cell types decreases as a function of increasing eccentricity in the cat's retina, but the rate of decline as a function of eccentricity is unique for each type of cell. Cones show the steepest decline outside the area centralis, while dopaminergic amacrine cell density shows relatively minor variation across the retina. Adapted from Vaney, D. I. 1985 The morphology and topographic distribution of AII amacrine cells in the cat retina. Proc. R. Soc. Lond. B. 224, 475–488, with permission from The Royal Society, London.

1.22.2.2 Local Patterning in the Distribution of Retinal Nerve Cell Types

The density of the somas of most retinal cell types is rarely so great as to crowd them together side-by-side. Where density is this great, the cells may approximate a hexagonal packing by virtue of this physical constraint of crowding circular profiles into a fixed space (Curcio, C. A. and Sloan, K. R., 1992). More commonly though, cell density is far lower than permitted by maximal packing. Under these circumstances, the distribution of a given type of cell still exhibits a degree of local order – the cells appear to be regularly arranged (Figure 2). The average intercellular spacing is typically large relative to the physical size of the cell bodies, yet this spacing is not imposed by any general physical constraint prohibiting somal positioning because cells of other type are positioned between these cells. Such regular arrays of nerve cells are commonly known as retinal mosaics because of the way they appear to tile the retinal surface uniformly, establishing territories of comparable size (Wässle, H. and Riemann, H. J., 1978). As we shall see, the notion of tiling has come to

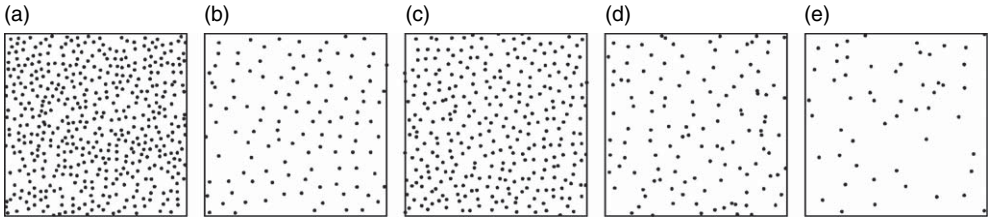

Figure 2 Local distribution of nerve cells for five different retinal cell types: (a) rod photoreceptors, (b) S cones, (c) B-type (axon-bearing) horizontal cells, (d) displaced cholinergic amacrine cells, and (e) dopaminergic amacrine cells. The images in (a) and (b) are from the ground squirrel retina, scaled identically, at local densities of approximately 12 000 cells mm^{-2} and 3000 cells mm^{-2} (Galli-Resta, L. *et al.*, 1999); those in (c–e) are from the mouse retina at varying magnifications, where average densities are 1600 cells mm^{-2}, 1400 cells mm^{-2}, and 36 cells mm^{-2} respectively (Raven, M. A. and Reese, B. E., 2002; Raven, M. A. *et al.*, 2003; Farajian, R. *et al.*, 2004). The mosaics of all five cell types differ from random distributions of cells. The average regularity indexes associated with these mosaics, derived from nearest neighbor analysis, are 6.0 (a), 5.5 (b), 4.9 (c), 3.3 (d), and 2.7 (e).

have a more specific meaning in association with the manner by which the dendritic fields associated with these cells distribute themselves relative to one another. For the moment, let us consider the means by which such arrays of retinal neurons can be objectively assessed for their orderliness.

1.22.2.3 Assessing the Local Order of Retinal Nerve Cells

1.22.2.3.1 Nearest neighbor analysis

The classic means of analyzing the regularity within such mosaics has been to measure the distance of each cell within the mosaic to its nearest neighboring cell (Wässle, H. and Riemann, H. J., 1978). While the absolute distance of such nearest neighbor measurements for a population of cells varies as a function of local density (Figure 3), when the variance in the population of nearest neighbor distances is taken into account by dividing the mean distance by the standard deviation, this ratio, commonly called the regularity index (Vaney, D. I. *et al.*, 1989) or conformity ratio (Cook, J. E., 1996), permits an appreciation of how the local order in a population is maintained across such variation in density.

Of course, such a ratio has no upper limit: as the variance in intercellular spacing approaches zero, say in association with a perfect square or hexagonal matrix, the ratio approaches infinity. In practice, a ratio of 5.0 or 6.0 is generally regarded as being regular (Figure 3), but little significance is generally attached to such differences. At the lower end of the scale, however, the ratio approaches the theoretical lower limit of 1.91 achieved by a population of infinitely small points that are randomly distributed within a field (Cook, J. E., 1996). Here, it is interesting to ask whether a population of cells is more regularly distributed than a random distribution, and most uses of the analysis have sought to determine only this. The distribution of nearest neighbor distances for the real population of cells is usually compared with that derived from a random distribution of points of identical density. That latter distribution approximates a Poisson distribution, while the distribution of nearest neighbor distances for many real mosaics approximates a Gaussian distribution (Figure 3). To the extent that a real mosaic more closely conforms to the latter, with a regularity index above 2.0, so the mosaic is said to be regular. Such a mosaic is sometimes qualified as 'highly' versus 'marginally' regular (e.g., Figure 2), depending on how different the mosaic is relative to random.

In some circumstances, retinal nerve cells may overlie one another where a nuclear layer is greater than a single cell thick. More often than not, cells of a given type are confined to a single stratum, even within a multicellular nuclear layer, so their physical size constrains them from getting closer to one another than the distance of an average soma size. For this reason, a more conservative comparison for addressing deviation from randomness would be with a random distribution of elements matched in density to the real population and assigned physical sizes drawn from the soma size distribution for that population (Figure 4, top). Such constrained random simulations maintain their generally Poisson characteristics (Raven, M. A. *et al.*, 2003), though they are truncated at the shortest distances, and consequently yield regularity indexes that differ substantially (particularly for higher density mosaics) from the theoretical value for a random distribution of points. For example, random simulations for the population

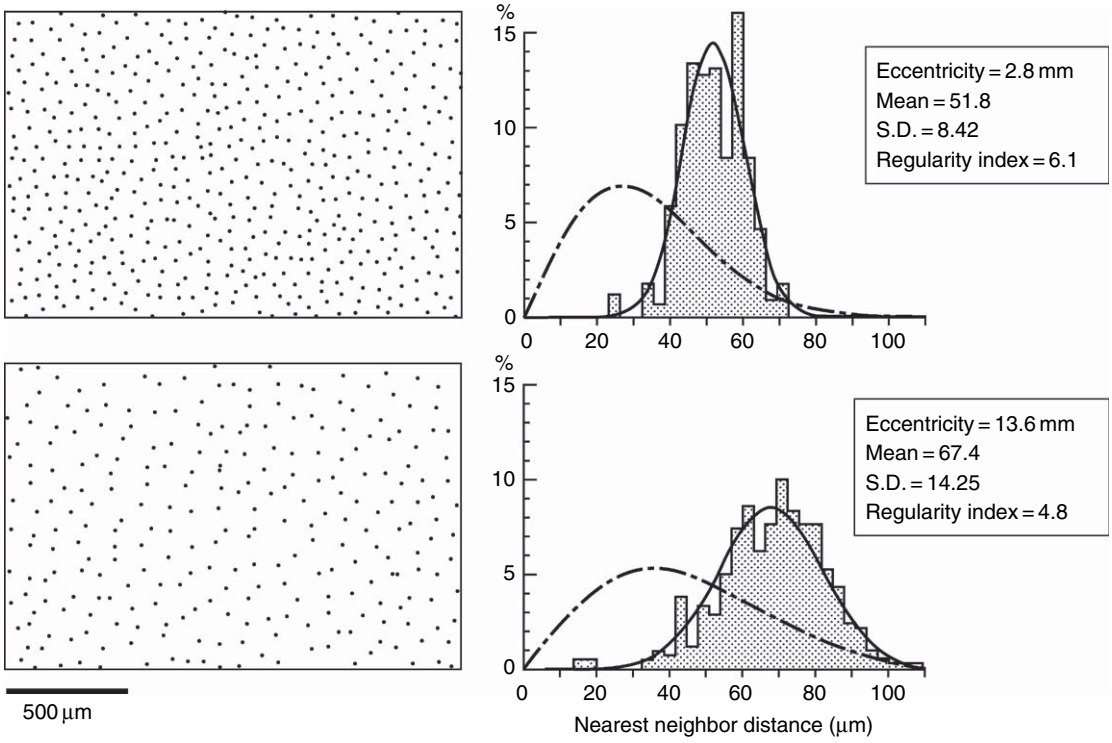

Figure 3 Mosaic of A-type (axonless) horizontal cells from the cat retina at two different eccentricities from the area centralis. As cell density declines with eccentricity, so the average intercellular spacing increases. The histograms show the nearest neighbor distances for these same fields; solid lines show the gaussian curve for a distribution with the same mean and standard deviation, while the broken lines show the Poisson distribution at identical density; this is the theoretical curve expected for a random distribution of points. Adapted from Wässle, H. and Riemann, H. J. 1978 The mosaic of nerve cells in the mammalian retina. Proc. R. Soc. Lond. B. 200, 441–461, with permission from The Royal Society, London.

of horizontal cells in the mouse retina generate regularity indexes derived from nearest neighbor analysis greater than 3.0 (Raven, M. A. and Reese, B. E., 2002), a value generally regarded as evidence of regularity. Real distributions of horizontal cells are still readily distinguishable from such random simulations, yielding regularity indexes around 5.0. Clearly, the physical constraint imposed by soma size will have an increasingly pronounced effect upon a random simulation as a function of its density. The regularity index then is less an objective yardstick for describing some feature of local order than it is a relative measure, and the magnitude of any difference from a random distribution will depend upon the assumptions defining the random simulation with which it is being compared.

One other criticism of the use of the nearest neighbor analysis is that it is dependent only upon relationships between each cell and its closest neighbor rather than factoring in relationships between all surrounding neighbors, and as such, will not discriminate between arrays that differ conspicuously in their spatial distribution. For example, a linear distribution of equally spaced points and a square matrix of cells with the same periodicity are identical in their nearest neighbor statistics, but only one distribution provides a uniform sampling across a two-dimensional surface. Within the retina, the ballroom dancers analogy provides an apt illustration of the point: nearest neighbor analysis will not discriminate between a pattern made up by pairs of dancers of low density versus pairs that fill the ballroom (Cook, J.E., 1996). Nearly random low-density distributions of cells occasionally yield high nearest neighbor regularity indexes for this reason (Raven, M. A. *et al.*, 2003). At higher densities, a regular array in which, for instance, every fifth cell is missing will not be discriminated from the intact array by nearest neighbor analysis. A few missing elements may reflect slight undersampling, and not perturb the nearest neighbor statistic significantly (Cook, J. E., 1996), but they may also be indicative of real biological

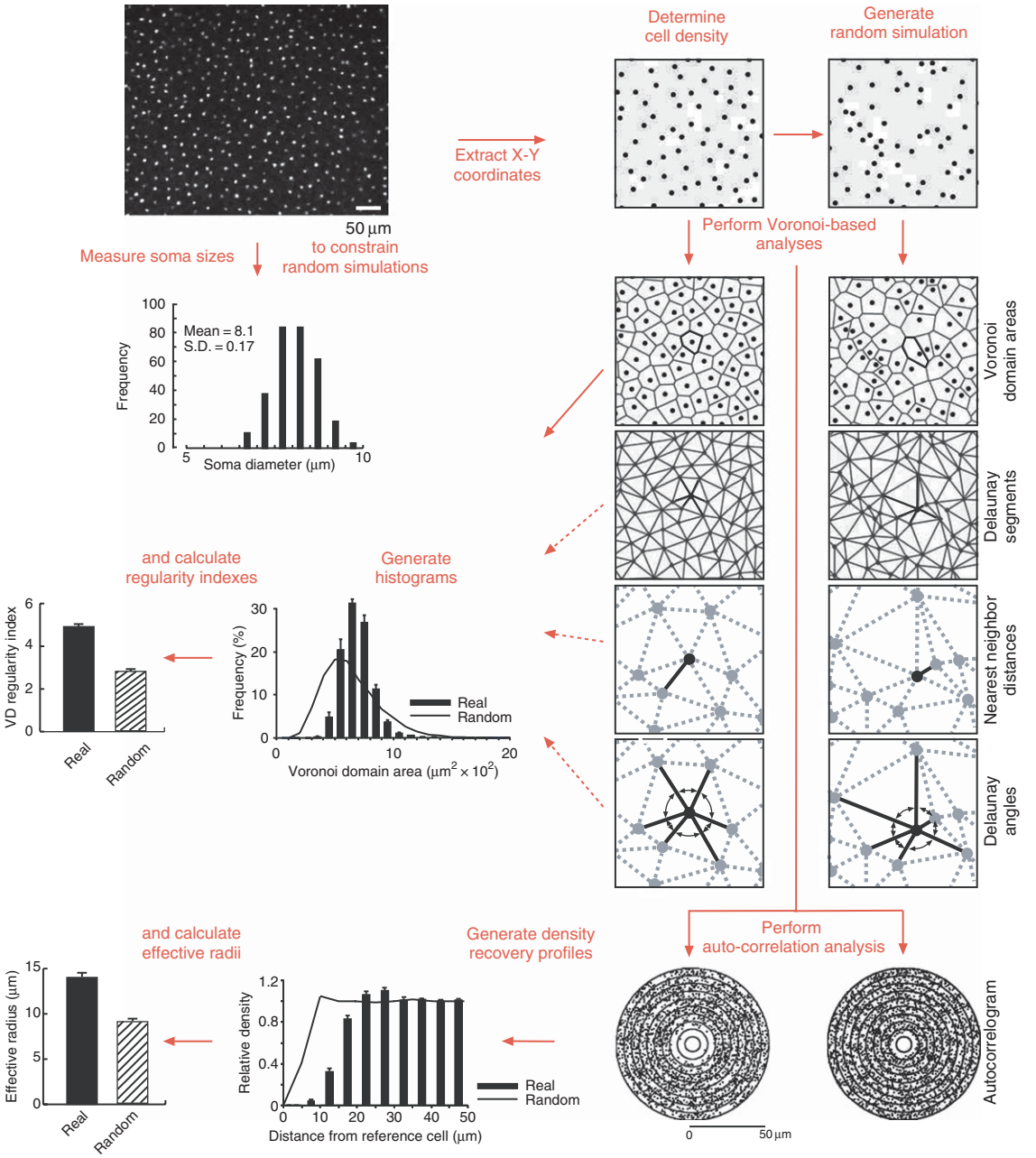

Figure 4 Assessing mosaic organization using Voronoi-based and autocorrelation analyses. Top: sample fields of cells (e.g., horizontal cells in the mouse retina) are analyzed for cell density and soma size, from which random simulations of cells matched in density and soma size are generated for comparison. Middle: from these real and random fields, Voronoi-based analyses are conducted and compared. Shown here are the Voronoi domain areas, the Delaunay segment lengths, the nearest neighbor distances (being the shortest Delaunay segment for each cell), and the Delaunay angles. These can be compared for the real and random simulations as frequency histograms or regularity indexes (only those for Voronoi domain areas are shown). Bottom: the autocorrelation analysis reveals the presence of an exclusion zone, the size of which can be estimated from the density recovery profile, termed the effective radius.

variation (Galli-Resta, L. *et al.*, 1999), and only a fuller analysis of the geometric relationships within the mosaic will allow a discrimination of such a difference.

1.22.2.3.2 Voronoi-based analyses

Other measures of mosaic order that take into consideration the relationship between each cell and all of its immediate neighbors have increasingly come

into favor (Shapiro, M. B. *et al.*, 1985; Ammermüller, J. *et al.*, 1993; Cellerino, A. *et al.*, 2000; Galli-Resta, L., 2000; Galli-Resta, L. and Novelli, E., 2000). Many of these are derived from Delaunay triangulation, connecting all of the cells to their immediate near neighbors (Figure 4, middle). Measuring the lengths of all Delaunay segments within a field, in both real samples and random simulations, is one such means to compare better their two-dimensional patterning, as is measuring the volumes of those triangles, or the angles defined by them. Another is to measure the Voronoi domain associated with each cell in the array, being the area within the plane of the array defining all points closer to each cell than to any other cell (and being identified by the intersections of all of the bisectors of the Delaunay segments). The reciprocal of the Voronoi domain area of a cell is therefore the local cellular density. The mosaic of Voronoi domains also has the attractive feature of approximating the tessellating nature of nonoverlapping dendritic fields (see further). All of these measures are related to one another but some prove more discriminating than others (Galli-Resta, L. *et al.*, 1999; Zhan, X. J. and Troy, J. B., 2000; Raven, M. A. *et al.*, 2003; Eglen, S. J. *et al.*, 2003b). Some researchers have used the coefficient of variation, being the ratio of the standard deviation of the Voronoi domain areas to the mean area, in an attempt to discriminate clustered, random, and regular arrays, either locally or across the retina (Curcio, C. A. and Sloan, K. R., 1992; Duyckaerts, C. and Godefroy, G., 2000; Palanza, L. *et al.*, 2005), this measure being the inverse of the Voronoi domain regularity index described in Figure 4. The general benefit of any of these analyses is that they encompass the geometric features of a two-dimensional array more thoroughly than does the nearest neighbor analysis.

1.22.2.3.3 Autocorrelation analysis and the density recovery profile

Still others have advocated the use of autocorrelation analysis and the density recovery profile derived from it, pioneered by Rodieck (Rodieck, R. W., 1991). The autocorrelogram of a field of cells is the plot of the position of all cells relative to every other cell, generated by placing the first cell in the array at the origin of the autocorrelogram and then plotting the position of all the other cells in the array relative to it, and then repeating this for each cell in the array. For a population that is distributed as a quasiregular lattice, that periodicity will reinforce itself and become more readily detectable as regions of high and low density at repeating intervals within the autocorrelogram. Most retinal mosaics do not contain such higher-order periodicity. Rather, the autocorrelogram usually reveals the presence of an exclusion zone at the origin (Figure 4, bottom), indicating that cells are less likely to be positioned near one another. Such exclusion zones have been taken as evidence for regularity in retinal mosaics (Cook, J. E., 1996; Rockhill, R. L. *et al.*, 2000) but it is not always the case that the presence of an exclusion zone, nor the size of it relative to soma size, reveals a regular mosaic (Galli-Resta, L. *et al.*, 1999; Raven, M. A. *et al.*, 2003), specifically, when packing intensity is low. (The packing intensity describes the extent to which the field is covered by nonoverlapping disks of a diameter associated with the average nearest neighbor distance within the field, being low for a field such as that in Figure 2(e)) (see Diggle, P. J., 2002).

Autocorrelation analysis, like the use of nearest neighbor and Voronoi analyses mentioned earlier, requires a consideration of the size of the cell body for cell types that are distributed in a single stratum, because the soma size itself defines an exclusion zone surrounding the position of each cell. The exclusion zones associated with real versus random arrays can be quantified and compared by constructing the density recovery profile derived from each autocorrelogram (Figure 4, bottom), being a histogram plotting the density of cells at increasing distances from the cell body, and from this, calculating the effective radius, being the radius of a cylinder with a volume equivalent to the empty region at the origin of the autocorrelogram (Rodieck, R. W., 1991). It should be obvious that the distribution of nearest neighbor distances for a field of cells overlaps with the initial slope of the density recovery profile. Consequently, the size of the effective radius is directly related to the mean nearest neighbor distance (Figure 5(a)) (Cook, J. E., 1996). Nearly all retinal mosaics that have been analyzed using this approach reveal the presence of such exclusion zones extending beyond the size of the cell body (Rockhill, R. L. *et al.*, 2000; Tyler, M. J. *et al.*, 2005). More often than not, the positioning of cells in such mosaics is independent of other mosaics in the retina, evidenced using cross-correlation analysis, including those that are either afferent to, or targets of the mosaic cells in question (but see Kouyama, N. and Marshak, D. W., 1997; Ahnelt, P. K. *et al.*, 2000). Together, those results have led to the conclusion that the rules governing cellular positioning within a

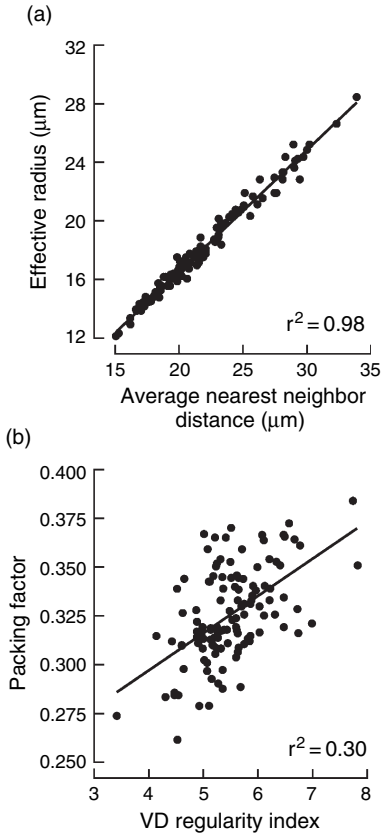

Figure 5 The scale-dependent effective radius is highly correlated with average nearest neighbor distance (a), the former measure being about 83% of the latter for the present dataset. The packing factor, like regularity index, is a scale-independent measure, but bears only a slight relationship to a field's regularity index derived from either nearest neighbor or Voronoi domain analysis (b). Data are from 121 fields of mouse horizontal cells drawn from four strains showing a twofold variation in horizontal cell density. From Raven, M. A., Stagg, S. B., and Reese, B. E. 2005a. Regularity and packing of the horizontal cell mosaic in different strains of mice. Vis. Neurosci. 22, 461–468.

mosaic involve interactions with only like-type neighbors (Reese, B. E. and Galli-Resta, L., 2002).

Because the detection of such an exclusion zone depends upon the size of the annuli used (the choice of which is influenced by the density of the cells in the field), an alternative is to plot a cumulative version of the density recovery profile (Ripley, B. D., 1976; Diggle, P. J., 2002), that is, the cumulative frequency histogram of intercellular distances between all cells within the array. This plot describes the fraction of intercellular distances that are above or below a given distance, and is compared with cumulative histograms for random simulations. The analysis is typically combined with Monte Carlo testing by generating 99 random simulations constrained by density and soma size to discern whether the real biological mosaic deviates from the envelop of the random simulations (Raven, M. A. *et al.*, 2003; Eglen, S. L. *et al.*, 2003b; Hofer, H. *et al.*, 2005). A reduction in the frequency of shorter intercellular distances (relative to random) is indicative of the presence of an exclusion zone, while an increase in the frequency of shorter intercellular distances is indicative of clustering of the cells. Such deviation from random can be determined by eye, or more objectively by a ranking test, in which the difference between the plot for each random simulation (and real distribution) and a Poisson distribution is calculated, and then ordered to allow the assignment of a p value to test for spatial randomness (Diggle, P. J.,1986). Such Monte Carlo analysis is particularly beneficial for analyzing small or single samples, not uncommon for rare specimens, but the inferences drawn from it are only as sound as that sample mosaic is truly representative of the population.

The tessellation-based analyses described above can discriminate between different spatial point patterns that have identical properties detected in the above correlation-based approaches, and so some have advocated the employment of both approaches in describing the distribution of retinal nerve cells (Shapiro, M. B. *et al.*, 1985; Raven, M. A. and Reese, B. E., 2002; Raven, M. A. *et al.*, 2003) as well as other means, for instance, quadrat analysis (Grieg-Smith, P., 1964), for addressing the longer-range spatial patterning present across a population (Tyler, M.J. *et al.*, 2005). The use of multiple approaches is particularly desired when seeking to model a retinal mosaic, as the model should replicate multiple features of the spatial distribution.

1.22.2.3.4 Packing factor analysis

For populations that do differ from random, the boundless regularity index as a descriptive statistic has its limitations in conveying a sense of the order within the mosaic. One alternative has been to describe how much the cells of a mosaic diverge from a regular lattice by examining the extent to which a lattice with known jitter can simulate the real mosaic (Shapiro, M. B. *et al.*, 1985; Curcio, C. A. and Sloan, K. R., 1992; Zhan, X. J. and Troy, J. B., 2000). A related descriptor has been to calculate the packing factor associated with the cells in a mosaic, it being the square of the ratio of the effective radius to the maximal radius permissible if a population of cells of identical density had been packed as a regular hexagonal matrix (Rodieck, R. W., 1991). Packing factor analysis provides an index that extends from zero (for a random point pattern) to

one (for perfect hexagonal packing), and as such, provides a sense along a finite continuum of where a mosaic is positioned. Like the regularity index, it is a scale-independent measure, allowing direct comparisons between mosaics across variation in density. But the packing factor is an index of packing, not regularity (e.g., square and hexagonal lattices have identical regularity indexes but differ in their packing), and exhibits only a weak correlation with regularity index (Figure 5(b)).

The relationships between nearest neighbor regularity index, Voronoi domain regularity index, effective radius, and packing factor across a twofold variation in density have recently been examined in a large sample of mosaic fields of horizontal cells in the mouse retina (Raven, M. A. *et al.*, 2005a). There, the correlation coefficient associated with the regularity index derived from a nearest neighbor analysis was always lower than that for the regularity index derived from the measure of Voronoi domain areas when correlated with any of the other features (density, packing factor, effective radius). Not surprisingly, the regularity indexes derived from nearest neighbor analysis and Voronoi domain analysis were positively correlated, but the fact that the former index is obtained by taking into account the relationship between each cell and only one of its neighbors produces a greater variance in the index that appears to be unrelated to the two-dimensional patterning of the mosaic.

1.22.2.4 Simulating the Distribution of Retinal Nerve Cells

Rather than model the mosaic upon a regular lattice that is distorted or jittered, others have sought to define the features that discriminate it best from a random distribution. Like a random simulation, most retinal mosaics yield autocorrelograms indicating that elements in the mosaic have no specific positional relationships beyond the stipulation that they do not encroach too closely upon one another, evidenced by the exclusion zone. In the case of the random mosaic, the size of the exclusion zone is defined by the soma size, while in the real mosaic, it is larger than this, being related to the average nearest neighbor distance. This, then, is the sole feature discriminating the autocorrelograms for these two conditions, despite the fact that the original mosaics are so qualitatively different with respect to the presence of patterning (Figure 4).

The minimal distance model is one such attempt to encapsulate this essence of the results derived from autocorrelation analysis. By specifying a minimal distance between the cells (the d_{min} rule, being some mean value and associated standard deviation) as they get added otherwise randomly to a simulation of given density (Figure 6, top), the simulated outcomes are often geometrically indiscriminable from their real mosaics (Figure 6, bottom). This approach has proven successful in replicating a variety of mosaics with great fidelity (Shapiro, M. B. *et al.*, 1985; Scheibe, R. *et al.*, 1995; Galli-Resta, L. *et al.*, 1997, 1999; Cellerino, A. *et al.*, 2000; Raven, M. A. *et al.*, 2003). Other variations on it have sought to encompass potential developmental mechanisms that might yield such minimal distance spacing rules, for instance, lateral inhibitory mechanisms that prevent cells of like-type from developing too close to one another (Cameron, D. A. and Carney, L. H., 2004; Tyler, M. J. *et al.*, 2005), selective cell-death mechanisms that eliminate neighboring cells of the same type (Eglen, S. J. and Willshaw, D.J., 2002), or mutual repulsion mechanisms that drive neighboring cells of the same type apart from one another (Eglen, S. J. *et al.*, 2000). Whatever the biological mechanism, or mechanisms, underlying it (Raven, M. A. *et al.*, 2005b), the minimal distance spacing rule provides a simple account of how homotypic interactions governing proximity can yield such biological patterning.

1.22.2.5 Functional Implications of Regular Retinal Mosaics

The assumed significance of such order in the distribution of various types of retinal nerve cell is that it ensures a relatively uniform contribution of each cell type in the local circuitry associated with visual analysis and so such patterning in retinal cell distributions has come to be taken for granted. Some examples, however, turn out to violate this expectation. For instance, the regularity in the patterning of rod photoreceptors in the ground squirrel's retina drops from 6.0 (e.g., Figure 2(a)) to approach 2.0 as rod density declines by about 80% from its peak value in the ventral retina (Galli-Resta, L. *et al.*, 1999); one would expect the rods to space themselves out as density declines to maintain a comparable order across such variation in density, as they generally do for other cell types. Rather, the rods maintain a fixed minimal spacing between themselves across variation in density, suggesting a developmental constraint upon their proximity rather than any functional constraint relating to

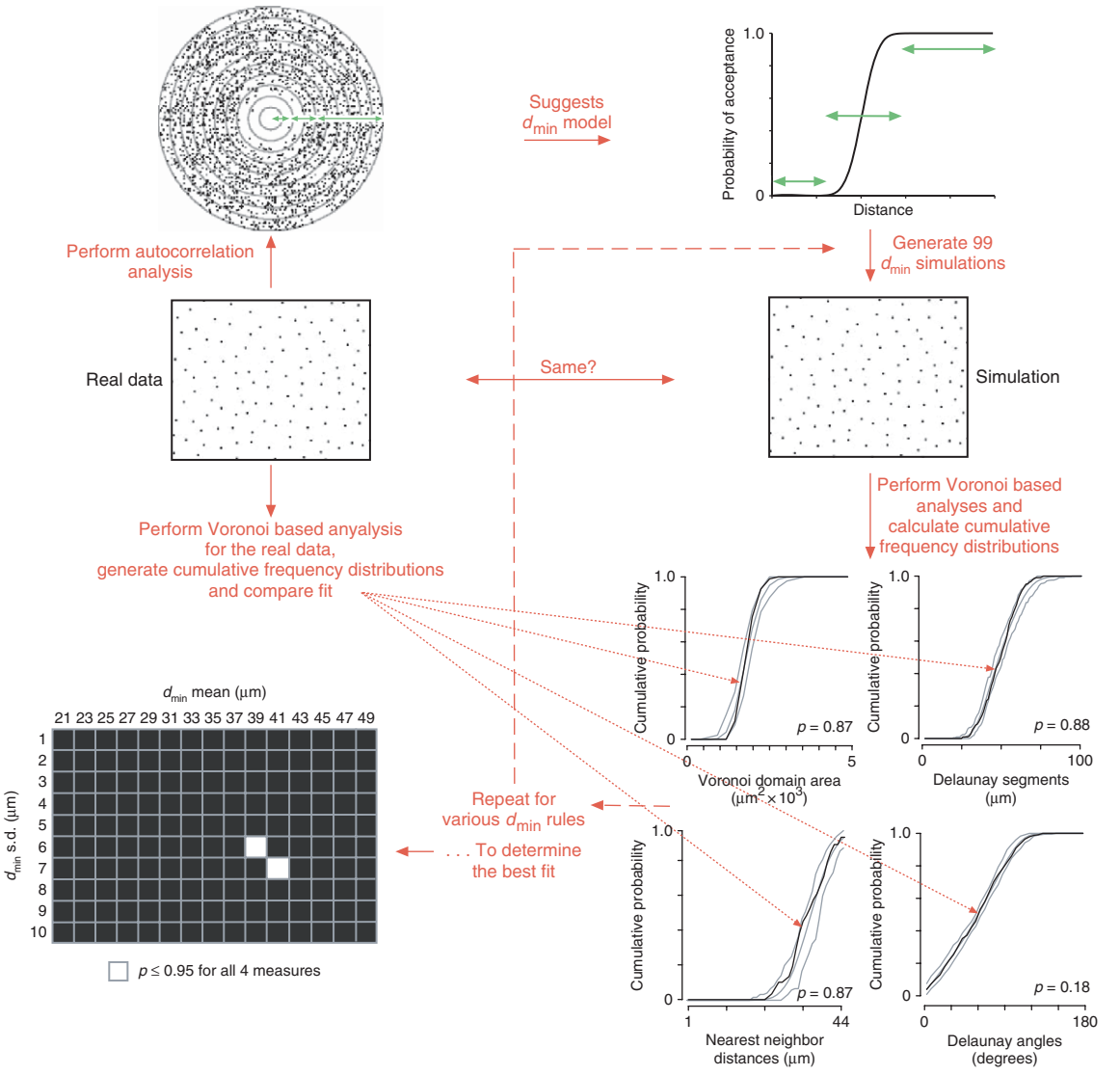

Figure 6 Modeling the mosaic using a minimal distance spacing rule. Top: the exclusion zone in the auto-correlogram indicates that neighboring cells avoid being positioned in close proximity. The minimal distance model (d_{min} model) stipulates a mean and standard deviation of minimal distances permissible in otherwise random simulations of cells generated sequentially. Ninety-nine simulations are generated, and each is compared with the original mosaic using Voronoi-based (or other) analyses. Bottom: a *p* value is assigned for the goodness of fit of the real mosaic relative to the simulations, shown here as cumulative frequency histograms, for each test. The entire process is repeated for slight variations in d_{min} mean and standard deviation (e.g., 150 d_{min} rules are shown for this example at lower left), to determine the best d_{min} rule simulating the mosaic. For the real mouse horizontal cell mosaic illustrated, only two d_{min} rules (39 ± 6 μm and 41 ± 7 μm) provided acceptable fits. Multiple fields are then tested, to examine the generality of the d_{min} rule, or to determine how it varies as a function of cell density or other features associated with the mosaic.

their orderliness (Reese, B. E. and Galli-Resta, L., 2002). The S cones in the ground squirrel's retina (Figure 2(b)), by contrast, show little variation in regularity across (a much smaller) variation in density, distributed in a pattern that is far more regular than achieved by random distributions, and assumed to reflect a greater functional benefit for photopic vision (Galli-Resta, L. *et al.*, 1999). But regularity in the S cone mosaic does not appear to confer any obvious functional benefit since other mammals show a striking variation in the extent to which S cone distributions deviate from random, particularly amongst the diurnal primates (deMonasterio, F. M. *et al.*, 1985; Ahnelt, P. K. *et al.*, 2000; Martin, P. R. *et al.*,

2000; Roorda, A. *et al.*, 2001). Whereas old world monkeys have regular distributions of S cones, the distribution in the human eye comes very close to being a random distribution (Martin, P. R. *et al.*, 2000; Roorda, A. *et al.*, 2001; Hofer, H. *et al.*, 2005) despite these species' comparable visual abilities.

The significance of such variation within photoreceptor mosaics remains to be determined. The contribution of photoreceptors to visual function is ultimately dependent upon their spatial distribution, given the punctate nature of their outer segments, but whether the critical feature is local density rather than patterning may depend upon the type of photoreceptor and the species in question. For other, postreceptoral, retinal cell types, their functional contribution to visual processing is associated with the distribution of their processes, and here, it is widely assumed that regular spacing between the cells increases the likelihood that the distribution of their processes will subserve the retinal surface uniformly. Indeed, the developmental constraints that produce such patterning in retinal neurons may also simplify the assembly of retinal connections during development (Galli-Resta, L., 2001), because such a population of cells may carry intrinsic instructions to grow a radially symmetric dendritic field of a specified size (Farajian, R. *et al.*, 2004; Lin, B. *et al.*, 2004). While this assumption may hold for some retinal cell types, it does not for many others where process growth is very much influenced by both homotypic neighbor-relationships and by relationships with afferents (Reese, B. E. *et al.*, 2005). These features associated with the morphology of the postreceptoral neurons, as they relate to retinal coverage, will be considered next.

1.22.3 Dendritic Coverage

1.22.3.1 Global Variation in Dendritic Field Size

Each type of postreceptoral retinal neuron exhibits its characteristic morphology across the retina, but with some variation in overall size as a function of the above global variations in cell density across eccentricity. Typically, the dendritic field of a given cell type increases with increasing eccentricity from the fovea, area centralis, or visual streak, coincident with the decline in density for that cell type. Figure 7 illustrates, for four different types of retinal cell, their increase in dendritic field size at progressively more eccentric locations upon the retina. Each displays unique morphological properties that remain discriminable as overall dendritic field size increases with eccentricity.

1.22.3.1.1 Dendritic overlap and the coverage factor

Figure 8(a) illustrates, for one such population, the A-type (axonless) horizontal cells in the cat retina, the change in dendritic field diameter as a function of eccentricity. Figure 8(b) shows the corresponding variation in A-type cell density across eccentricity (Wässle, H. *et al.*, 1978). That these two changes are related is made apparent by the fact that their product, dendritic field area × cell density (termed the coverage factor (Peichl, L. and Wässle, H., 1979)), is relatively constant across the retina (Figure 8(c)). These cells exhibit a constant dendritic overlap: on average, every location on the retina will be subserved by three to four dendritic fields for this cell type. A single cone pedicle, therefore (being the sole afferent to the horizontal cell dendrite), may contact up to four horizontal cells at every retinal locus. Similar trends hold for other retinal cell types, with dendritic field area increasing in proportion to the reduction in cell density, although a number of exceptions have been documented (Tauchi, M. and Masland, R. H., 1984; Mills, S. L. and Massey, S. C., 1991, 1994; Young, H. M. and Vaney, D. I., 1991; Wässle, H. *et al.*, 2000).

1.22.3.2 Variation in Dendritic Overlap between Retinal Nerve Cell Types

The coverage factor of a cell type is usually presumed to equal or exceed a value of 1, to ensure that no locations upon the retina are devoid of a contribution to the retinal circuitry by that cell type. But the coverage factors for different cell types differ markedly, ranging from 1 to >100, where such variation in field overlap is thought to reflect the distinct contributions of those different types of retinal cell to processing the retinal image.

1.22.3.2.1 Dendritic tiling and contact inhibition

A coverage factor of 1, then, indicates an average of one field overlying each location on the retinal surface, and coverages exceeding this slightly may indicate a consistent overestimate of the size of the dendritic field area. Of course, for circular dendritic field profiles to cover the retina completely, there must be some degree of overlap even if they are spaced as a regular hexagonal lattice, and so coverage factors in slight excess of 1 may simply reflect this

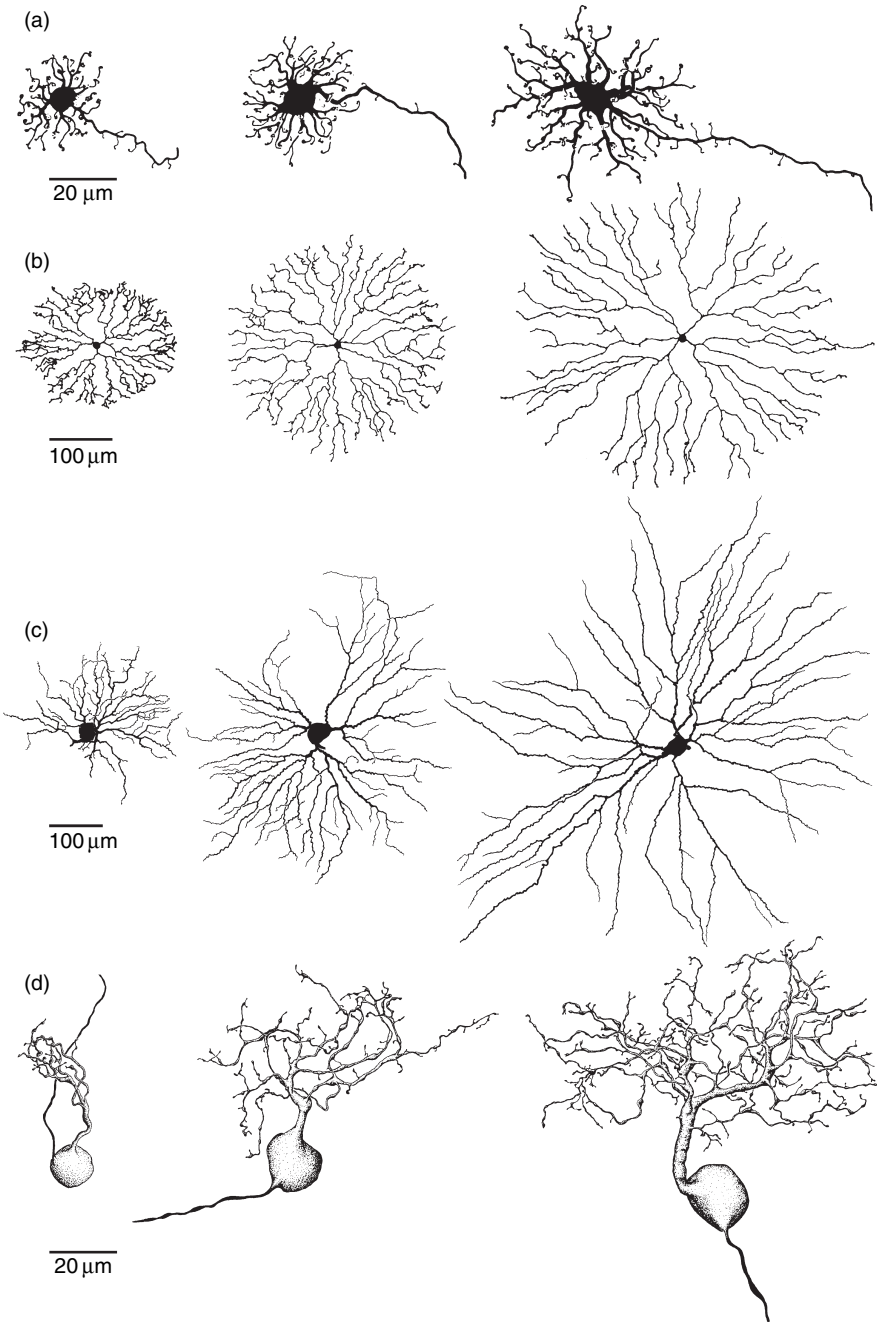

Figure 7 Increase in dendritic field size as a function of eccentricity: (a) H1 (axon-bearing) horizontal cells in the squirrel retina 1.7 mm, 4.3 mm, and 8.9 mm ventral to the visual streak; (b) cholinergic amacrine cells in the rabbit retina at the visual streak and 4 mm and 9 mm ventral to it; (c) alpha retinal ganglion cells in the cat retina 1 mm, 4 mm, and 10 mm from the area centralis; (d) midget retinal ganglion cells in the human retina at 2.5 mm, 6.5 mm, and 10 mm from the fovea. (a) Reprinted with permission of Wiley-Liss, Inc., a subsidiary of John Wiley & Sons, Inc. Linberg, K. A., Suemune, S, and Fisher, S. K. 1996. Retinal neurons of the California ground squirrel, *Spermophilus beecheyi*: a golgi study. J. Comp. Neurol. 365, 173–216. Copyright © 1996 John Wiley & Sons, Inc. (b) Reproduced from Tauchi, M. and Masland, R. H. 1984. The shape and arrangement of the cholinergic neurons in the rabbit retina. Proc. R. Soc. Lond. B 223, 101–119, with permission from The Royal Society, London. (c) Reprinted from Vision Res., Vol. 21, Kolb, H., Nelson, R., and Mariani, A., Amacrine cells, bipolar cells and ganglion cells of the cat retina, 1081–1114, Copyright 1981, with permission from Elsevier. (d) Reproduced from Dacey, D. M. 1993. The mosaic of midget ganglion cells in the human retina. J. Neurosci. 13, 5334–5355, Copyright 1993 by the Society for Neuroscience, with permission.

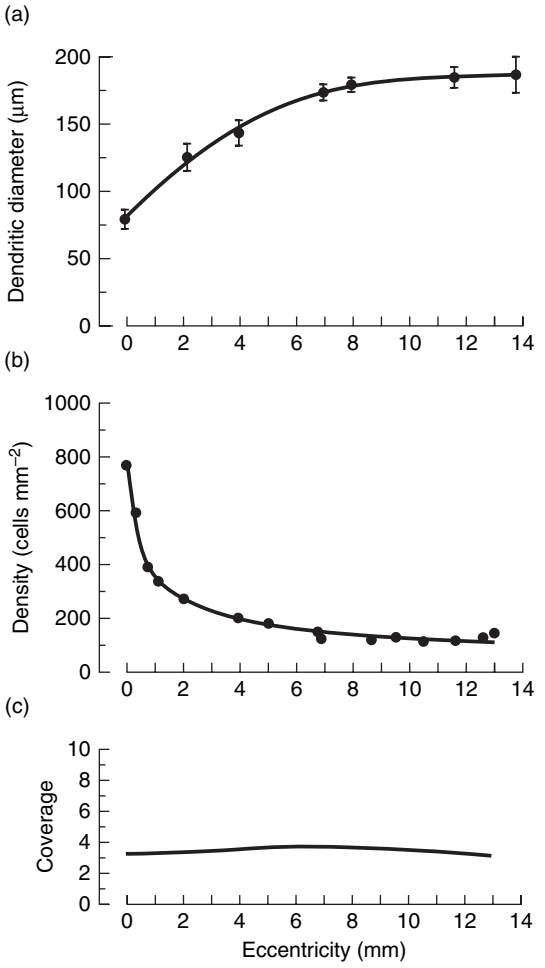

Figure 8 A-type (axonless) horizontal cell dendritic field diameter increases with eccentricity (a), while A-type cell density declines with eccentricity (b). The increase in dendritic field size compensates for the decline in density to maintain a constant dendritic coverage factor (dendritic field area × cell density) across the retinal surface (c). Adapted from Wässle, H., Peichl, L., and Boycott, B. B. 1978 Topography of horizontal cells in the retina of the domestic cat. Proc. R. Soc. Lond B. 203, 269–291, with permission from The Royal Society, London.

(Wässle, H. *et al.*, 1981b; Szmajda, B. A. *et al.*, 2005). Achieving a true uniform coverage of 1 requires a tiling of the retina by dendritic fields that extend right up to the boundary of the dendritic fields of adjacent cells, and by necessity cannot be circular profiles. That dendritic fields may modulate their growth in relation to the presence of neighboring homotypic dendritic fields had been suspected for some time, given the fact that they are often irregular rather than circularly symmetric around the soma. Consistent with this, the geometry of their dendritic

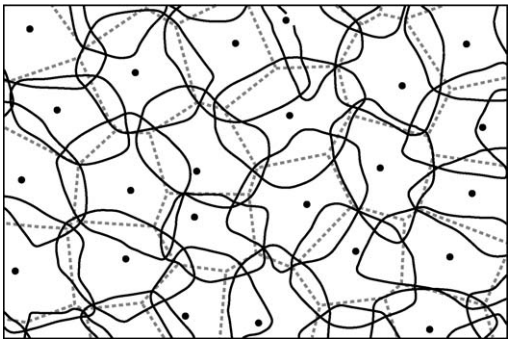

Figure 9 Mosaic of ON-alpha ganglion cell dendritic fields in the cat retina outlined in smooth contours to encircle the dendrites, plotted relative to their somatic positioning. The Voronoi domains associated with those somata are also illustrated, showing that dendritic field shape is constrained by proximity to homotypic neighbors. Adapted by permission from Macmillan Publishers Ltd: Nature, Wässle, H., Peichl, L., and Boycott, B. B. 1981c. Dendritic territories of cat retinal ganglion cells. Nature 292, 344–345, copyright 1981.

field shapes sometimes correlates with proximity to their Voronoi neighbors (Figure 9) (Wässle, C. *et al.*, 1981c). Dendritic field size and shape also undergo compensatory changes in response to early experimental manipulations that alter neighbor relationships (Perry, V. H. and Linden, R., 1982; Eysel, U. T. *et al.*, 1985; Kirby, M. A. and Chalupa, L. M., 1986). More recent studies eschewing the traditional means of estimating dendritic field size by constructing convex polygons or smooth closed outlines (Wässle, C. *et al.*, 1981c; 1989; Watanabe, M. and Rodieck, R. W., 1989) have attempted to assign precise concave profiles to the irregular boundaries associated with neighboring ganglion cell dendritic fields (Dacey, D. M., 1993; Szmajda, B. A. *et al.*, 2005), reporting the boundaries between adjacent midget retinal ganglion cells to be coincident, establishing minimal overlap, as should be expected for a perfect tiling of the retinal surface (Figure 10; see also Vaney, D. I., 1994; Amthor, F. R. and Oyster, C. W., 1995).

Given this evidence, the variation in dendritic field size across eccentricity might be thought to reflect active growth constrained by homotypic neighbor relationships, rather than a consequence of passive interstitial dendritic growth produced by greater expansion of the peripheral retina (Hitchcock, P. F. and Easter, S. S., 1986; Wong, R. O. L. and Collin, S. P., 1989; Rodieck, R. W. and Marshak, D. W., 1992). Likewise, while much of the published variation in dendritic field size for cells at a given eccentricity has been ascribed to differences in cell density along different retinal axes, a twofold variation in dendritic field

size is present even within the same patch of retina (Figure 10), consistent with the local variability in the size of Voronoi domains found in regular retinal mosaics (Figures 4 and 9). These studies support the notion that a simple developmental mechanism, that of contact-inhibition between the dendrites of homotypic neighbors, creates the tiling characteristic of such retinal mosaics.

1.22.3.2.2 Regulating dendritic overlap by homotypic interactions

For retinal mosaics with coverage factors greater than 1, it is unlikely that they require the same precision in their uniformity of coverage afforded by the above mechanism. Some cell types, for example, the horizontal cells (Figure 7(a)), have coverage factors in the region of 3–8 (Wässle, H. *et al.*, 1978; Mills, S. L. and Massey, S. C., 1994) that are reasonably (though not always) well preserved across marked variation in cell density. Such unchanging coverage could occur secondarily if dendritic growth was intrinsically specified, and passive (interstitial) growth driven by retinal expansion then diluted cell density in the more peripheral parts of the retina. This explanation cannot, however, account for the modulation of dendritic field size in horizontal cells in different strains of mice (Reese, B. E. *et al.*, 2005); there, in the absence of any appreciable variation in total retinal size, horizontal cell morphology is scaled accordingly to maintain constant coverage across a twofold variation in horizontal cell density between the strains (Figure 11). As predicted from these correlational studies, genetic manipulations that directly modulate horizontal cell density also produce corresponding changes in dendritic field size (Reese, B. E. *et al.*, 2006). These results are consistent with those considered above indicating that dendritic growth is constrained by homotypic neighbors, even if a simple contact-inhibition at the tips of dendrites is insufficient to explain the coverages obtained. The same may prove to be the case for some other cell types

Figure 10 Mosaic of ON-midget ganglion cell dendritic fields in the periphery of the human retina. Dendrites from adjacent cells share common boundaries without overlap, establishing a precise tiling of the retinal surface. Adapted from Dacey, D. M. 1993 The mosaic of midget ganglion cells in the human retina. J. Neurosci. 13, 5334–5355, Copyright 1993 by the Society for Neuroscience, with permission.

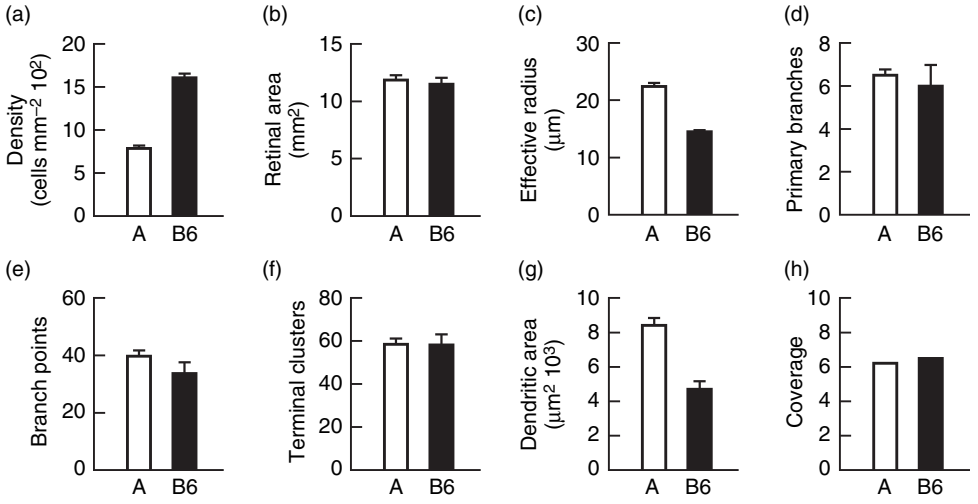

Figure 11 B-type (axon-bearing) horizontal cells in the C57BL/6J and A/J mouse retinas show a nearly twofold density difference (a) despite comparable retinal areas between the strains (b). They show a corresponding variation in the size of their effective radius, minimizing proximity between neighboring horizontal cells (c). These cells differentiate comparable dendritic morphologies (d–f), but modulate their overall dendritic field size (g) to maintain a constant dendritic coverage (h). Adapted from Reese, B. E., Raven, M. A., and Stagg, S. B. 2005 Afferents and homotypic neighbors regulate horizontal cell morphology, connectivity and retinal coverage. J. Neurosci. 25, 2167–2175, Copyright 2005 by the Society for Neuroscience, with permission.

with coverage factors in this range (Wässle, H. *et al.*, 1981a; Mills, S. L. and Massey, S. C., 1991; Vaney, D. I. *et al.*, 1991; Young, H. M. and Vaney, D. I., 1991).

1.22.3.2.3 Overlap unregulated by homotypic interactions?

Other types of retinal cell have coverage factors an order of magnitude greater than this. Perhaps the most widely studied is the cholinergic amacrine cell (Figure 7(b)), the coverage factor of which has been estimated to be as great as 70, depending upon the species (Tauchi, M. and Masland, R. H., 1984; Famiglietti, E. V., 1985; Schmidt, M. *et al.*, 1985; Voigt, T., 1986; Rodieck, R. W. and Marshak, D. W., 1992; Sandmann, D. *et al.*, 1997). Given such coverage, these cells should have ample opportunity to interact homotypically, particularly as their dendrites fasciculate together and exchange synaptic contacts (Tauchi, M. and Masland, R. H., 1985; Brandon, C., 1987; Lee, s. and Zhou, Z. J., 2006). Yet partially depleting this population of cells by 40% during early development, well before adult coverage is obtained, does not alter the dendritic field of the remaining cells, which continue to differentiate a normal adult morphology and size (Farajian, R. *et al.*, 2004). These cells behave as if their dendritic growth is controlled by cell-intrinsic mechanisms rather than by homotypic interactions. This strategy would seem increasingly likely for the various widefield amacrine cell types, where process growth is often vast, yet extremely sparse (Vaney, D. I., 1986, 2004; Dacey, D. M., 1990).

One would envision the need for precision in coverage to be related to retinal cell types associated with the creation of center-surround receptive fields employed in the transmission of the retinal image, rather than with other cell types modulating those radial pathways. Dopaminergic amacrine cells give rise to sparsely distributed dendritic and axon-like processes mostly restricted to a narrow stratum of the inner plexiform layer, yet dopamine acts upon receptors with a far broader distribution across the retina (Veruki, M. L. and Wässle, H., 1996) and its release is modulated extrasynaptically (Puopolo, M. *et al.*, 2001). Like retinal horizontal cells in the mouse, this cell class displays a large (threefold) variation in cell number between different strains (unpublished observations), but might establish a comparable functional contribution not by modulating field size in proportion to cell density, as in the case of the horizontal cells, but by modulating the release of dopamine (Puopolo, M. *et al.*, 2001). It is conceivable that the growth of the dopaminergic dendritic versus axonal processes is controlled independently, given their difference in estimated retinal coverage (3 vs. 300; Voigt, T. and Wässle, H., 1987; Dacey, D. M., 1990; see also Dacey, D. M., 1989), but a low coverage factor should not be taken to necessitate homotypic regulation of growth. Even certain classes of retinal ganglion cells with limited dendritic overlap may achieve their dendritic fields independent of neighbor-interactions, for instance, the melanopsin-containing ganglion cells that transmit information about the circadian variation in retinal luminance (Lin, B. *et al.*, 2004). Not surprisingly then, these very cell types have regularity indexes that are just marginally better, or no better, respectively, than matched random simulations (Raven, M. A. *et al.*, 2003; Semo, M. *et al.*, 2005). For the latter cell type, one might even conceive little benefit to having a minimal coverage of 1, since neither uniform nor complete retinal coverage would appear relevant for the detection of circadian changes in photic environment (see Chapter Melanopsin Cells). (In primates, at least, this cell type also receives synaptic input arising from photoreceptors in the outer retina, transmitting spatial information as well, and so may prove to be more regular in its cellular distribution and achieve a more uniform coverage than in other species; Dacey, D. M. *et al.*, 2005).

1.22.3.3 Dendritic Coverage and Connectivity

While the calculation of a coverage factor provides an index of the degree to which neighboring cells of the same type overlap one another, and may therefore intimate aspects of their functional contribution to retinal processing, coverage factors by themselves can be misleading, because the dendritic fields do not simply form overlapping blankets of processes of uniform density across the entire field. For instance, the density of higher order dendritic branching is not always uniform across the dendritic field (Figure 7(d)), such that regions of high- and low-branch frequency yield territories of dendritic clustering within the field of peripheral midget retinal ganglion cells in old world primates (Dacey, D. M., 1993). The significance of this clustering and its relationship to both afferent input and the sensitivity profile of the receptive field remain to be defined (Dacey, D. M., 1993; Brown, S. P. *et al.*, 2000; Jusuf, P. R. *et al.*, 2006) (see Chapter The P, M, and K Streams of the Primate Visual System: What Do They Do for Vision?). The cholinergic amacrine

cells, by contrast, are far more radially symmetrical in their dendritic morphology (Figure 7(b)) where an outer annulus of the field is defined by beaded presynaptic terminals, while synaptic inputs are formed throughout the field (Famiglietti, E. V., 1991). The processes of cholinergic amacrine cells fasciculate with one another within the inner plexiform layer yielding a lattice enclosing lacunae devoid of cholinergic processes (Tauchi, M. and Masland, R. H. 1985). There, they also fasciculate with the dendrites of direction-selective retinal ganglion cells, bestowing upon the latter their direction selectivity by virtue of the cholinergic dendrites being themselves directionally selective (Euler, T. *et al.*, 2002), releasing both GABA and acetylcholine to modulate different sets of directionally selective ganglion cells within a region of the cholinergic matrix (Taylor, W. R. and Vaney, D. I., 2003) (see Chapter Direction-Selective Cells). Indeed, given the local processing associated with different sectors of the dendritic field (Lee, S. and Zhou, Z. J., 2006), the functional coverage of this cell type may more closely approximate a factor of 2. The dendritic terminals of horizontal cells are punctate in their distribution within the dendritic field (Figure 7(a)) in association with their afferents, the cone pedicles (Ahnelt, P. and Kolb, H., 1994b). Furthermore, the number of dendritic terminal contacts per pedicle decreases as a function of increasing distance from the center of the dendritic field (Ahnelt, P. and Kolb, H., 1994a; Reese, B. E. *et al.*, 2005), so that, while each cone pedicle may be contacting an equivalent number of horizontal cells, its effect upon them is by no means equivalent. Horizontal cells are also electrically coupled via gap junctions, expanding their functional domain well beyond the limits of the dendritic field, and rendering the dendritic coverage factor functionally irrelevant in the coupled condition (Bloomfield, S. A. *et al.*, 1995; Packer, O. and Dacey, D. M., 2005) (see Chapter Contributions of Horizontal Cells). Finally, for those widefield amacrine cells that give rise to a few thin varicose processes extending for millimeters upon the retinal surface, while these cells have ample overlap evidenced by the crisscrossing of processes from adjacent cells, a simple calculation of their field area multiplied by cell density grossly overestimates the local density of processes upon the retinal surface (Dacey, D. M., 1990; Vaney, D. I., 2004) (see Chapter Amacrine Cells). Future studies integrating other measures of dendritic complexity and process density, for example, Sholl analysis (Sholl, D. A., 1953) in conjunction with cell density measures, would provide a richer appreciation of the retinal coverage of an individual cell type.

1.22.4 Conclusions

The positioning of a neuron within the plane of the retinal surface, like the distribution of its processes, is, for many types of retinal cell, dependent upon homotypic relationships. Other cell types show less obvious homotypic dependency, suggesting that the developmental mechanisms creating this patterning and process overlap are quite distinct. How these mosaics are assembled during development, and the nature of those cell intrinsic and environmental signals governing process outgrowth, target recognition and synapse formation are increasingly the focus of attention as we try to understand the construction of those features of the retinal circuitry that ultimately underlie the functional contribution of each cell type. Similar questions can be asked of neurons within the brain, where little is known about the constraints upon neuronal positioning in three dimensions, and even less about the coverage associated with their dendritic fields. As the biological and (more critically) software tools become available, the understanding of the three-dimensional spatial relationships between neurons will come to the forefront, enhancing our appreciation of the relationship between form and function at the population level.

Acknowledgment

Supported by the National Institutes of Health (EY-11087).

References

Ahnelt, P. and Kolb, H. 1994a. Horizontal cells and cone photoreceptors in primate retina: a golgi-light microscopic study of spectral connectivity. J. Comp. Neurol. 343, 387–405.

Ahnelt, P. and Kolb, H. 1994b. Horizontal cells and cone photoreceptors in human retina: a golgi-electron microscopic study of spectral connectivity. J. Comp. Neurol. 343, 406–427.

Ahnelt, P. K., Fernández, E, Martinez, O, Bolea, J. A., and Kübber-Heiss, A. 2000. Irregular S-cone mosaics in felid retinas. Spatial interaction with axonless horizontal cells, revealed by cross-correlation. J. Opt. Soc. Am. A. 17, 580–588.

Ammermüller, J., Möckel, W., and Rugan, P. 1993. A geometrical description of horizontal cell networks in the turtle retina. Brain Res. 616, 351–356.

Amthor, F. R. and Oyster, C. W. 1995. Spatial organization of retinal information about the direction of image motion. Proc. Nat'l. Acad. Sci. U. S. A. 92, 4002–4005.

Bloomfield, S. A., Xin, D., and Persky, S. E. 1995. A comparison of receptive field and tracer coupling size of horizontal cells in the rabbit retina. Vis. Neurosci. 12, 985–999.

Brandon, C. 1987. Cholinergic neurons in the rabbit retina: dendritic branching and ultrastructural connectivity. Brain Res. 426, 119–130.

Brecha, N. C., Oyster, C. W., and Takahashi, E. S. 1984. Identification and characterization of tyrosine hydroxylase immunoreactive amacrine cells. Invest. Ophthalmol. Vis. Sci. 25, 66–70.

Brown, S. P., He, S., and Masland, R. H. 2000. Receptive field microstructure and dendritic geometry of retinal ganglion cells. Neuron 27, 371–383.

Cameron, D. A. and Carney, L. H. 2004. Cellular patterns in the inner retina of adult zebrafish: quantitative analyses and a computational model of their formation. J. Comp. Neurol. 471, 11–25.

Cellerino, A., Novelli, E., and Galli-Resta, L. 2000. Retinal ganglion cells with NADPH-diaphorase activity in the chick form a regular mosaic with a strong dorsoventral asymmetry that can be modelled by a minimal spacing rule. Eur. J. Neurosci. 12, 613–620.

Cook, J. E. 1996. Spatial properties of retinal mosaics: An empirical evaluation of some existing measures. Vis. Neurosci. 13, 15–30.

Curcio, C. A. and Sloan, K. R. 1992. Packing geometry of human cone photoreceptors: variation with eccentricity and evidence for local anisotropy. Vis. Neurosci. 9, 169–180.

Curcio, C. A., Sloan, K. R., Kalina, R. E., and Hendrickson, A. E. 1990. Human photoreceptor topography. J. Comp. Neurol. 292, 497–523.

Dacey, D. M. 1989. Axon-bearing amacrine cells of the macaque monkey retina. J. Comp. Neurol. 284, 275–293.

Dacey, D. M. 1990. The dopaminergic amacrine cell. J. Comp. Neurol. 301, 461–489.

Dacey, D. M. 1993. The mosaic of midget ganglion cells in the human retina. J. Neurosci. 13, 5334–5355.

Dacey, D. M., Liao, H. W., Peterson, B. B., Robinson, F. R., Smith, V. C., Pokorny, J., Yau, K. W., and Gamlin, P. D. 2005. Melanopsin-expressing ganglion cells in primate retina signal colour and irradiance and project to the LGN. Nature. 433, 749–754.

deMonasterio, F. M., McCrane, E. P., Newlander, J. K., and Schein, S. J. 1985. Density profile of blue-sensitive cones along the horizontal meridian of macaque retina. Invest. Ophthalmol. Vis. Sci. 26, 289–302.

Diggle, P. J. 1986. Displaced amacrine cells in the retina of a rabbit: analysis of a bivariate spatial point pattern. J. Neurosci. Meth. 18, 115–125.

Diggle, P. J. 2002. Statistical analysis of spatial point patterns., 2nd edn. Edward Arnold.

Duyckaerts, C. and Godefroy, G. 2000. Voronoi tessellation to study the numerical density and the spatial distribution of neurones. J. Chem. Neuroanat. 20, 83–92.

Eglen, S. J. and Willshaw, D. J. 2002. Influence of cell fate mechanisms upon retinal mosaic formation: a modelling study. Development 129, 5399–5408.

Eglen, S. J., van Ooyen, A., and Willshaw, D. J. 2000. Lateral cell movement driven by dendritic interactions is sufficient to form retinal mosaics. Network- Comput. Neural. Syst. 11, 103–118.

Eglen, S. J., Raven, M. A., Tamrazian, E., and Reese, B. E. 2003b. Dopaminergic amacrine cells in the inner nuclear layer and ganglion cell layer comprise a single functional retinal mosaic. J. Comp. Neurol. 466, 343–355.

Euler, T., Detwiler, P. B., and Denk, W. 2002. Directionally selective calcium signals in dendrites of starburst amacrine cells. Nature 418, 845–852.

Eysel, U. T., Peichl, L., and Wässle, H. 1985. Dendritic plasticity in the early postnatal feline retina: quantitative characteristics and sensitive period. J. Comp. Neurol. 242, 134–145.

Famiglietti, E. V. 1985. Starburst amacrine cells: morphological constancy and systematic variation in the anisotropic field of rabbit retinal neurons. J. Neurosci. 5, 562–577.

Famiglietti, E. V. 1991. Synaptic organization of starburst amacrine cells in rabbit retina: analysis of serial thin sections by electron microscopy and graphic reconstruction. J. Comp. Neurol. 309, 40–70.

Farajian, R., Raven, M. A., Cusato, K., and Reese, B. E. 2004. Cellular positioning and dendritic field size of cholinergic amacrine cells are impervious to early ablation of neighboring cells in the mouse retina. Vis. Neurosci. 21, 13–22.

Galli-Resta, L. 2000. Local, possibly contact-mediated signalling restricted to homotypic neurons controls the regular spacing of cells within the cholinergic arrays in the developing rodent retina. Development 127, 1509–1516.

Galli-Resta, L. 2001. Assembling the vertebrate retina: global patterning from short-range cellular interactions. Neuroreport. 12, A103–A106.

Galli-Resta, L. and Novelli, E. 2000. The effects of natural cell loss on the regularity of the retinal cholinergic arrays. J. Neurosci. 20. RC60.

Galli-Resta, L., Resta, G., Tan, S-S., and Reese, B. E. 1997. Mosaics of islet-1 expressing amacrine cells assembled by short range cellular interactions. J. Neurosci. 17, 7831–7838.

Galli-Resta, L., Novelli, E., Kryger, Z., Jacobs, G. H., and Reese, B. E. 1999. Modelling the mosaic organization of rod and cone photoreceptors with a minimal-spacing rule. Eur. J. Neurosci. 11, 1461–1469.

Grieg-Smith, P. 1964. Quantitative Plant Ecology. 2nd edn. Butterworths.

Hitchcock, P. F. and Easter, S. S. 1986. Retinal ganglion cells in goldfish: a qualitative classification into four morphological types, and a quantitative study of the development of one of them. J. Neurosci. 6, 1037–1050.

Hofer, H., Carroll, J., Neitz, J., Neitz, M., and Williams, D. R. 2005. Organization of the human trichromatic cone mosaic. J. Neurosci. 25, 9669–9679.

Hughes, A. 1981. Population magnitudes and distribution of the major modal classes of cat retinal ganglion cell as estimated from HRP filling and a systematic survey of the soma diameter spectra for classical neurones. J. Comp. Neurol. 197, 303–339.

Jeon, C-J., Strettoi, E., and Masland, R. H. 1998. The major cell populations of the mouse retina. J. Neurosci. 18, 8936–8946.

Jusuf, P. R., Martin, P. R., and Grünert, U. 2006. Random wiring in the midget pathway of primate retina. J. Neurosci. 26, 3908–3917.

Kirby, M. A. and Chalupa, L. M. 1986. Retinal crowding alters the morphology of alpha ganglion cells. J. Comp. Neurol. 251, 532–541.

Kolb, H., Nelson, R., and Mariani, A. 1981. Amacrine cells, bipolar cells and ganglion cells of the cat retina. Vision Res. 21, 1081–1114.

Kouyama, N. and Marshak, D. W. 1997. The topographical relationship between two neuronal mosaics in the short wavelength-sensitive system of the primate retina. Vis. Neurosci. 14, 159–167.

Lee, S. and Zhou, Z. J. 2006. The synaptic mechanism of direction selectivity in distal processes of starburst amacrine cells. Neuron 51, 787–799.

Lin, B., Wang, S. W., and Masland, R. H. 2004. Retinal ganglion cell type, size, and spacing can be specified independent of homotypic dendritic contacts. Neuron 43, 475–485.

Linberg, K. A., Suemune, S, and Fisher, S. K. 1996. Retinal neurons of the California ground squirrel, *Spermophilus beecheyi*: a golgi study. J. Comp. Neurol. 365, 173–216.

Mariani, A. P., Kolb, H., and Nelson, R. 1984. Dopamine-containing amacrine cells of rhesus monkey retina parallel rods in spatial distribution. Brain Res. 322, 1–7.

Martin, P. R., Grünert, U., and Chan, T. L. 2000. Spatial order in short-wavelength-sensitive cone photoreceptors: a comparative study of the primate retina. J. Opt. Soc. Am. A 17, 557–567.

Masland, R. H., Mills, J. W., and Hayden, S. A. 1984. Acetylcholine-synthesizing amacrine cells: identification and selective staining by using radioautography and fluorescent markers. Proc. R. Soc. Lond. B 223, 79–100.

Massey, S. C., Blankenship, K., and Mills, S. L. 1991. Cholinergic amacrine cells in the rabbit retina accumulate muscimol. Vis. Neurosci. 6, 113–117.

Mills, S. L. and Massey, S. C. 1991. Labeling and distribution of AII amacrine cells in the rabbit retina. J. Comp. Neurol. 304, 491–501.

Mills, S. L. and Massey, S. C. 1994. Distribution and coverage of A- and B-type horizontal cells stained with Neurobiotin in the rabbit retina. Vis. Neurosci. 11, 549–560.

Packer, O. and Dacey, D. M. 2005. Synergistic center-surround receptive field model of monkey H1 horizontal cells. J. Vis. 5, 1038–1054.

Palanza, L., Jhaveri, S., Donati, S., Nuzzi, R., and Vercelli, A. 2005. Quantitative spatial analysis of the distribution of NADPH-diaphorase-positive neurons in the developing and mature rat retina. Brain Res. Bull. 65, 349–360.

Peichl, L. and Wässle, H. 1979. Size, scatter and coverage of ganglion cell receptive field centres in the cat retina. J. Physiol. 291, 117–141.

Perry, V. H. and Linden, R. 1982. Evidence for dendritic competition in the developing retina. Nature 297, 683–685.

Perry, V. H., Oehler, R., and Cowey, A. 1984. Retinal ganglion cells that project to the dorsal lateral geniculate nucleus in the macaque monkey. Neuroscience 12, 1101–1123.

Puopolo, M., Hochstetler, S. E., Gustincich, S., Wightman, R. M., and Raviola, E. 2001. Extrasynaptic release of dopamine in a retinal neuron: activity dependence and transmitter modulation. Neuron 30, 211–225.

Raven, M. A. and Reese, B. E. 2002. Horizontal cell density and mosaic regularity in pigmented and albino mouse retina. J. Comp. Neurol. 454, 168–176.

Raven, M. A., Stagg, S. B., and Reese, B. E. 2005a. Regularity and packing of the horizontal cell mosaic in different strains of mice. Vis. Neurosci. 22, 461–468.

Raven, M. A., Eglen, S. J., Ohab, J. J., and Reese, B. E. 2003. Determinants of the exclusion zone in dopaminergic amacrine cell mosaics. J. Comp. Neurol. 461, 123–136.

Raven, M. A., Stagg, S. B., Nassar, H., and Reese, B. E. 2005b. Developmental improvement in the regularity and packing of mouse horizontal cells: implications for mechanisms underlying mosaic pattern formation. Vis. Neurosci. 22, 569–573.

Reese, B. E. and Galli-Resta, L. 2002. The role of tangential dispersion in retinal mosaic formation. Prog. Ret. Eye Res. 21, 153–168.

Reese, B. E., Raven, M. A., and Stagg, S. B. 2005. Afferents and homotypic neighbors regulate horizontal cell morphology, connectivity and retinal coverage. J. Neurosci. 25, 2167–2175.

Reese, B. E., Poché, R. A., Raven, M. A., and Behringer, R. R. 2006. Partial depletion of the horizontal cell population in Lim1 conditional knock-out mice reveals afferent and homotypic control of dendritic morphology. ARVO Abs. S2778.

Ripley, B. D. 1976. The second-order analysis of stationary point processes. J. Appl. Probab. 13, 255–266.

Rockhill, R. L., Euler, T., and Masland, R. H. 2000. Spatial order within but not between types of retinal neurons. Proc. Natl. Acad. Sci. U. S. A. 97, 2303–2307.

Rodieck, R. W. 1991. The density recovery profile: a method for the analysis of points in the plane applicable to retinal studies. Vis. Neurosci. 6, 95–111.

Rodieck, R. W. and Marshak, D. W. 1992. Spatial density and distribution of choline acetyltransferase immunoreactive cells in human, macaque, and baboon retinas. J. Comp. Neurol. 321, 46–64.

Roorda, A., Metha, A. B., Lennie, P., and Williams, D. R. 2001. Packing arrangement of the three cone classes in primate retina. Vision Res. 41, 1291–1306.

Sandmann, D., Engelmann, R., and Peichl, L. 1997. Starburst cholinergic amacrine cells in the tree shrew retina. J. Comp. Neurol. 389, 161–176.

Scheibe, R., Schnitzer, J., Rohrenbeck, J., Wohlrab, F., and Reichenbach, A. 1995. Development of A-type (axonless) horizontal cells in the rabbit retina. J. Comp. Neurol. 354, 438–458.

Schmidt, M., Wässle, H, and Humphrey, M. 1985. Number and distribution of putative cholinergic amacrine cells in cat retina. Neurosci. Lett. 59, 235–240.

Semo, M., Munoz Llamosas, M., Foster, R. G., and Jeffery, G. 2005. Melanopsin (Opn4) positive cells in the cat retina are randomly distributed across the ganglion cell layer. Vis. Neurosci. 22, 111–116.

Shapiro, M. B., Schein, S. J., and deMonasterio, F. M. 1985. Regularity and structure of the spatial pattern of blue cones of macaque retina. J. Am. Stat. Assoc. 80, 803–814.

Sholl, D. A. 1953. Dendritic organization in the neurons of the visual and motor cortices of the cat. J. Anat. 87, 387–406.

Steinberg, R. H., Reid, M., and Lacy, P. L. 1973. The distribution of rods and cones in the retina of the cat (*Felis domesticus*). J. Comp. Neurol. 148, 229–248.

Szmajda, B. A., Grünert, U., and Martin, P. R. 2005. Mosaic properties of midget and parasol ganglion cells in the marmoset retina. Vis. Neurosci. 22, 395–404.

Tauchi, M. and Masland, R. H. 1984. The shape and arrangement of the cholinergic neurons in the rabbit retina. Proc. R. Soc. Lond. B 223, 101–119.

Tauchi, M and Masland, R. H. 1985. Local order among the dendrites of an amacrine cell population. J. Neurosci. 5, 2494–2501.

Taylor, W. R. and Vaney, D. I. 2003. New directions in retinal research. Trends NeuroSci. 26, 379–385.

Tyler, M. J., Carney, L. H., and Cameron, D. A. 2005. Control of cellular pattern formation in the vertebrate inner retina by homotypic regulation of cell-fate decisions. J. Neurosci. 25, 4565–4576.

Vaney, D. I. 1985. The morphology and topographic distribution of AII amacrine cells in the cat retina. Proc. R. Soc. Lond. B. 224, 475–488.

Vaney, D. I. 1986. Morphological identification of serotonin-accumulating neurons in the living retina. Science 233, 444–446.

Vaney, D. I. 1994. Territorial organization of direction-selective ganglion cells in rabbit retina. J. Neurosci. 14, 6301–6316.

Vaney, D. I. 2004. Type 1 nitrergic (ND1) cells of the rabbit retina: comparison with other axon-bearing amacrine cells. J. Comp. Neurol. 474, 149–171.

Vaney, D. I., Whitington, G. E., and Young, H. M. 1989. The morphology and topographic distribution of substance-P-like immunoreactive amacrine cells in the cat retina. Proc. R. Soc. Lond. B. 237, 471–488.

Vaney, D. I., Gynther, I. C., and Young, H. M. 1991. Rod-signal interneurons in the rabbit retina: 2. AII amacrine cells. J. Comp. Neurol. 310, 154–169.

Veruki, M. L. and Wässle, H. 1996. Immunohistochemical localization of dopamine D_1 receptors in rat retina. Europ J. Neurosci. 8, 2286–2297.

Voigt, T. 1986. Cholinergic amacrine cells in the rat retina. J. Comp. Neurol. 248, 19–35.

Voigt, T. and Wässle, H. 1987. Dopaminergic innervation of A II amacrine cells in mammalian retina. J. Neurosci. 7, 4115–4128.

Wässle, H. and Riemann, H. J. 1978. The mosaic of nerve cells in the mammalian retina. Proc. R. Soc. Lond. B. 200, 441–461.

Wässle, H., Peichl, L., and Boycott, B. B. 1978. Topography of horizontal cells in the retina of the domestic cat. Proc. R. Soc. Lond. B. 203, 269–291.

Wässle, H., Boycott, B. B., and Illing, R-B. 1981a. Morphology and mosaic of on- and off-beta cells in the cat retina and some functional considerations. Proc. R. Soc. Lond. B. 212, 177–195.

Wässle, H., Peichl, L., and Boycott, B. B. 1981b. Morphology and topography of on- and off-alpha cells in the cat retina. Proc. R. Soc. Lond. B. 212, 157–175.

Wässle, H., Peichl, L., and Boycott, B. B. 1981c. Dendritic territories of cat retinal ganglion cells. Nature 292, 344–345.

Wässle, H., Röhrenbeck, J., and Boycott, B. B. 1989. Horizontal cells in the monkey retina: cone connections and dendritic network. Europ. J. Neurosci. 1, 421–435.

Wässle, H., Dacey, D. M., Haun, T., *et al.* 2000. The mosaic of horizontal cells in the macaque monkey retina: with a comment on biplexiform ganglion cells. Vis. Neurosci. 17, 591–608.

Watanabe, M. and Rodieck, R. W. 1989. Parasol and midget ganglion cells of the primate retina. J. Comp. Neurol. 289, 434–454.

Wong, R. O. L. and Collin, S. P. 1989. Dendritic maturation of displaced putative cholinergic amacrine cells in the rabbit retina. J. Comp. Neurol. 287, 164–178.

Young, H. M. and Vaney, D. I. 1991. Rod-signal interneurons in the rabbit retina: 1. Rod bipolar cells. J Comp. Neurol. 310, 139–153.

Zhan, X. J. and Troy, J. B. 2000. Modeling cat retinal beta-cell arrays. Vis. Neurosci. 17, 23–39.

1.23 Circuit Functions of Gap Junctions in the Mammalian Retina

S C Massey, University of Texas Medical School, Houston, TX, USA

© 2008 Elsevier Inc. All rights reserved.

1.23.1	**Gap Junctions**	457
1.23.2	**Clinical Relevance**	458
1.23.3	**Functional Roles for Gap Junctions in the Retina**	459
1.23.3.1	Photoreceptors	459
1.23.3.1.1	Cone-to-cone coupling	459
1.23.3.1.2	Blue cones are not coupled to surrounding cones	460
1.23.3.1.3	Rod-to-cone coupling	460
1.23.3.1.4	Rod-to-rod coupling	461
1.23.3.2	Horizontal Cells	461
1.23.3.2.1	A-type horizontal cells and Cx50	462
1.23.3.2.2	B-type horizontal cells	463
1.23.3.2.3	Modulation	464
1.23.3.2.4	Horizontal cell feedback	464
1.23.3.3	AII Amacrine Cells/ON Cone Bipolar Cells, a Complex Heterocellular Network	464
1.23.3.3.1	AII/ON cone bipolar gap junctions	465
1.23.3.3.2	Physiology	466
1.23.3.4	Ganglion Cells	467
1.23.3.4.1	Alpha ganglion cells	467
1.23.3.4.2	ON/OFF directionally selective ganglion cells	468
1.23.3.4.3	Synchronized firing	468
1.23.4	**Conclusion**	469
References		469

1.23.1 Gap Junctions

Although chemical neurotransmission is the dominant means of communication between neurons, it is clear that electrical synapses, known as gap junctions, occur frequently and they are physiologically significant (Galarreta, M. and Hestrin, S., 2001). Gap junctions are named after the narrow gap between two closely apposed cell membranes. They are composed of two docked hemichannels, or connexons, each of which is built from six connexins surrounding a central pore (Figure 1). This pore forms an intercellular channel between the connected cells that allows the passage of ions and small molecules up to a molecular weight of approximately 1000. Each connexin spans the cell membrane four times. There are two extracellular loops, which are conserved and thought to be involved with docking between two adjacent cells to form a gap junction. In addition, there is one intracellular loop and both the N- and the C-terminals are cytoplasmic. These sites may be available for biochemical modulation. The intracellular loop and C-terminal sequences are commonly used to raise antibodies.

Approximately, 20 different connexins have been identified and this diversity is thought to underlie the functional properties of different gap junctions such as permeability, gating, voltage dependence, and modulation (Willecke, K. *et al.*, 2002; Menichella, D. M. *et al.*, 2003). In the retina, gap junctions in different cell types have distinct properties. For example, different gap junctions are selectively permeable to different dyes or tracers and they are differentially modulated by various signaling molecules such as cAMP and cGMP (Mills, S. L. and Massey, S. C., 1995; 2000). Thus, it appears multiple neuronal connexins are expressed in the mammalian retina and it has recently become clear that different cell types express specific neuronal connexins. Furthermore, gap junctions play specific and important functional roles in retinal circuitry.

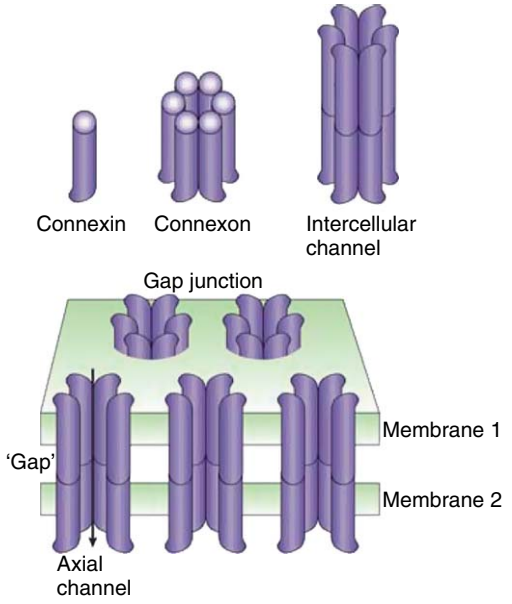

Figure 1 Gap junctions function as electrical synapses. They are constructed from membrane spanning proteins called connexins. Six connexins form a connexin, or hemichannel, and two connexins dock to form a gap junction, an intercellular pore between adjoining cells. Gap junctions are arranged in plaques, two-dimensional arrays that may contain many single channels. From Goodenough, D. A. and Paul, D. L. 2003. Beyond the gap: functions of unpaired connexin channels. Nat. Rev. Mol. Cell Biol. 4, 285–294.

From this family of twenty or so connexins, only four, Cx36, Cx45, Cx50, and Cx57 have so far been found in mammalian neurons and we will refer to these as neuronal connexins. Importantly, some additional homologs have been reported in fish retina (Shields, C. R. *et al.*, 2005; O'Brien, J. *et al.*, 2004). Connexin 36 is the dominant neuronal connexin and it is found in all cell types except horizontal cells (HCs) (Deans, M. R. and Paul, D. L., 2001; Feigenspan, A. *et al.*, 2001; Mills, S. L. *et al.*, 2001; Deans, M. R. *et al.*, 2002; Lee, E. J. *et al.*, 2003; Feigenspan, A. *et al.*, 2004). Recent data suggest that Cx50 and Cx57 are expressed in different types of HC (Massey, S. C. *et al.*, 2003; Hombach, S. *et al.*, 2004). In addition, Cx45 has also been found in mammalian retina in bipolar cells, amacrine cells, and ganglion cells (Guldenagel, M. *et al.*, 2000; Maxeiner, S. *et al.*, 2005).

Historically, gap junctions have been difficult to visualize. They are small and easily overlooked in electron micrographs but they present a distinctive profile in freeze–fracture preparations (Raviola, E. and Gilula, N. B., 1973; Kamasawa, N. *et al.*, 2006). Until recently, the connexin antibodies have been unreliable but this is rapidly improving. As the various neuronal connexins are identified and specific antibodies are developed, this may become the method of choice to identify gap junctions in neural networks.

The transfer of small tracers such as Neurobiotin can also reveal gap junction coupling and this type of experiment shows specific coupling patterns, often between cells of the same type, but also in complex heterocellular pathways such as the AII/cone bipolar network (Vaney, D. I., 1991). The use of other fluorescent dyes, particularly Lucifer Yellow, for visualizing coupled neurons must be interpreted very cautiously because many, or perhaps most, neuronal gap junctions do not pass Lucifer Yellow. A stunning exception to this rule is provided by A-type HCs in the rabbit retina, which are permeable to Lucifer Yellow. This also indicates that HC gap junctions are probably different from those of other retinal neurons (Dacheux, R. F. and Raviola, E., 1982). HCs in the fish retina also have gap junctions which pass Lucifer Yellow (Teranishi, T. *et al.*, 1983).

1.23.2 Clinical Relevance

Gap junctions also have potential clinical significance. Mutations in connexin genes underlie several genetic diseases including Charcot–Marie–Tooth disease, a peripheral myopathy due to demyelination, thought to result from the absence of Cx32 gap junctions which permit the diffusion of nutrients and metabolites in spiral structures (Menichella, D. M. *et al.*, 2003). Cx46 and Cx50 mutations cause congenital cataracts, Cx26 mutations are associated with deafness and Cx40 and Cx43 knockout mice have cardiac abnormalities (Willecke, K. *et al.*, 2002; Menichella, D. M. *et al.*, 2003). Given the prevalence of gap junctions in the retina, it seems likely that a connexin mutation could cause a visual defect, perhaps in the photoreceptor matrix or in rod pathways.

Gap junctions have also been implicated in photoreceptor degeneration via a mechanism known as the bystander effect. It has been proposed that dying rods transmit a signal to cones via gap junctions, spreading cell death in retinitis pigmentosa (Ripps, H., 2002; Cusato, K. *et al.*, 2003). In addition, in a model of cell death due to stroke, it has been suggested that one of the final terminal events is the opening of hemichannels in the cell membrane. This produces a profound

disruption of ionic balance, a ubiquitous component of ischemic neuronal death (Thompson, R. J. *et al.*, 2006).

1.23.3 Functional Roles for Gap Junctions in the Retina

Gap junctions are common in the central nervous system (CNS) but they seem to be particularly abundant in the retina. This may be the case because signal averaging and noise reduction are important strategies in the early steps of visual processing. Here, we will provide four examples from the retina where gap junctions appear to serve a specific function: photoreceptor coupling, HCs, the AII amacrine cell network, and ganglion cell coupling.

1.23.3.1 Photoreceptors

There are two kinds of photoreceptor in the mammalian retina. Cones support color vision under relatively bright conditions and, in central retina or the primate fovea, they are densely packed, to the exclusion of rods, to support the highest acuity. Rods are much more numerous, except in central retina, and they have increased sensitivity to function in low light conditions. There is an understandable tendency to think of rod and cone pathways as separate and distinct but in fact rod/cone coupling provides a pathway for substantial mingling of rod/cone signals.

1.23.3.1.1 Cone-to-cone coupling

Classic ultrastructural studies revealed small gap junctions between cones, as well as between cones and rods in mammals, including primate (Raviola, E. and Gilula, N. B., 1973; Kolb, H., 1977; Ahnelt, P. K. and Pflug, R., 1986; Tsukamoto, Y. *et al.*, 1992; Tsukamoto, Y. *et al.*, 2001). This is supported by tracer injections that show dye coupling between neighboring cones in several mammalian species (Hornstein, E. P. *et al.*, 2004; Li, W. and DeVries, S. H., 2004). At the base of each cone pedicle, there are fine processes, known as telodendria, which reach out to contact adjacent cones. In central retina, where the cone pedicles form a tightly packed array, the telodendria are necessarily short but in peripheral retina they extend further (Figure 2). The contact points between telodendria and adjacent cones are the sites of gap junctions with neighboring cone pedicles or intervening rod spherules.

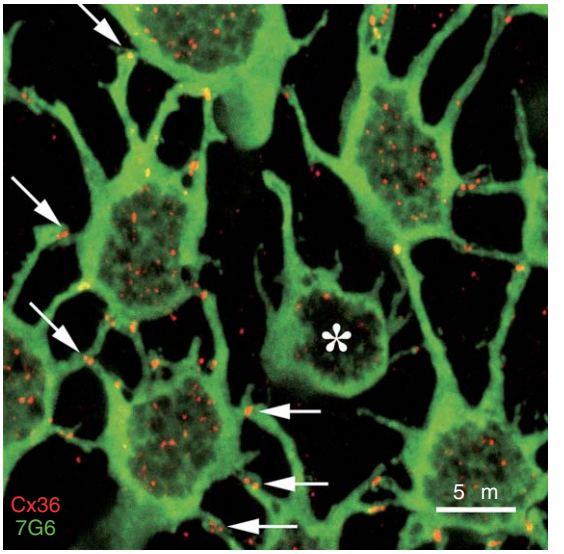

Figure 2 Connexin 36 gap junctions between the telodendria of cone pedicles, stained with an antibody against cone arrestin (7G6, green), in the outer plexiform layer of macaque retina. Some Cx36 gap junctions (red) at telodendrial contacts between adjacent cone pedicles are marked with arrows. The smaller cone pedicle, marked by an asterisk, is a blue cone pedicle with relatively few short telodendria. In contrast to red/green cones, the blue cone pedicles make few or no gap junctions with adjacent cones. Image courtesy of Jennifer O'Brien and Stephen C. Massey.

Small Cx36 plaques occur precisely at the contact points between telodendria and adjacent cones in the primate and ground squirrel retina (Figure 2) (Li, W. and DeVries, S. H., 2004). We have learned that this pattern, when Cx36 plaques occur at contact points, is diagnostic for gap junction labeling and similar to the pattern reported at dendritic crossings and intersections in the AII matrix (Mills, S. L. *et al.*, 2001). Thus, this result indicates that cone-to-cone coupling is mediated by Cx36 gap junctions and the network of telodendria forms the substrate for photoreceptor coupling. Punctate Cx36 labeling is found in the outer plexiform layer of all mammalian species and it is associated with cones (Feigenspan, A. *et al.*, 2004). The staining is fainter and the individual plaques are smaller than those on the AII matrix in the inner retina. A cluster of Cx36 labeling is also found under each cone pedicle, where incoming dendrites converge. Because HCs do not express Cx36, these gap junctions probably occur between bipolar cell dendrites before they contact the cone pedicle (Feigenspan, A. *et al.*, 2004).

Technically impressive dual recordings have established that adjacent cones in ground squirrel and

primate retina are electrically coupled (DeVries, S. H. *et al.*, 2002; Hornstein, E. P. *et al.*, 2004; Li, W. and DeVries, S. H., 2004). Coupling is bidirectional with a conductance of a few hundred picosiemens. Phototransduction is inherently noisy and cone-to-cone coupling improves the signal-to-noise ratio by correlating shared light-driven signals while random noise from each cone is reduced by averaging between adjacent cones across the network (DeVries, S. H. *et al.*, 2002). The small loss of spatial acuity as a result of coupling is apparently less than the optical blur of the eye. It has been calculated that cone-to-cone coupling results in a 70% increase in the signal-to-noise ratio.

1.23.3.1.2 Blue cones are not coupled to surrounding cones

Old World primates such as macaque are trichromatic with long, medium, and short wavelength-sensitive cones (red, green, and blue cones) (Baylor, D. A. *et al.*, 1987). It is not possible to discriminate morphologically between red and green cones but blue cones can be labeled with an antibody against blue cone opsin. Blue cones also have smaller pedicles with few telodendria (Figure 2) (Ahnelt, P. *et al.*, 1990). The ground squirrel, which has amenably large cones suitable for recording, and most other mammals have only green and blue cones. Red/green cones, in primate, or green cones in ground squirrel are dye coupled but the small minority of S cones, approximately 10%, are not coupled to the other cones. This has been directly confirmed by paired recordings which show that electrical coupling between red/green or green cones is bidirectional but, in both species, blue cones are isolated from surrounding cones (Hornstein, E. P. *et al.*, 2004; Li, W. and DeVries, S. H., 2004) The telodendria of blue cone pedicles are short and there are few or no Cx36 contacts with adjacent cone pedicles (Figure 2). These results are consistent: dual recording, dye coupling, and Cx36 labeling all indicate that blue cone pedicles are not coupled to the other cones. Cone-to-cone coupling leads to an increase in sensitivity but there is a concomitant loss in spectral discrimination. Calculations show this is minor between red and green cones because their spectral curves are so close together (Hornstein, E. P. *et al.*, 2004). Patchiness, or the random distribution of cones, may also minimize this loss (Hsu, A. *et al.*, 2000). Conversely, the blue absorption curve is far removed from the red/green curves. Thus, blue cones may be uncoupled to preserve spectral discrimination (Hsu, A. *et al.*, 2000; Hornstein, E. P. *et al.*, 2004; Li, W. and DeVries, S. H., 2004).

1.23.3.1.3 Rod-to-cone coupling

In EM preparations, small gap junctions have been observed between rod spherules and cone pedicles (Raviola, E. and Gilula, N. B., 1975; Smith, R. G. *et al.*, 1986). Cones and rods are also dye coupled (Hornstein, E. P. *et al.*, 2005). Thus, signals bearing a rod signature can be recorded in cones and in HCs that are exclusively connected with cones (Nelson, R., 1977; Schneeweis, D. M. and Schnapf, J. L., 1995; 1999; Hornstein, E. P. *et al.*, 2005). Furthermore, rod-to-cone transmission occurs at intensities when cone phototransduction can be expected to make a minimal contribution. In immunolabeled material, there are many Cx36 plaques around the perimeter of each cone pedicle, often on fine telodendria that do not reach adjacent cones (Figure 3). These gap junctions are aligned with the surrounding rod spherules and form the substrate for rod-to-cone coupling. It appears that almost every rod spherule is connected to a nearby cone pedicle. While the evidence for the expression of Cx36 in cones is convincing, the identity of the rod connexin is currently unknown. The extent of Cx36 expression in the outer nuclear layer (ONL) first suggested that both rods and cones could use Cx36 (Deans, M. R. *et al.*, 2002). However, in the mouse retina, Cx36 appears to be restricted to cones (Feigenspan, A. *et al.*, 2004) and at rod/cone gap junctions in the guinea pig retina, Cx36 labeling is located on the cone side of the gap junction (Lee, E. J. *et al.*, 2003). Thus, it is possible that rod-to-cone gap junctions are heterotypic with Cx36 only on the cone side.

Rod/cone coupling provides an alternative pathway for rod signals to enter cone pathways at intermediate light intensities such as twilight conditions (Smith, R. G. *et al.*, 1986). At threshold or starlight levels, the high-gain rod pathway via rod bipolar cells is operational. Around 30–100 rods have input to each rod bipolar cell, dependent on species, and this convergence means that only one or two rods need to absorb a photon to produce a threshold signal. If only a small number of rods are excited, then there will be insufficient signal to influence adjacent cones via gap junctions.

However, at light intensities above approximately 2.5 photons per rod, the rod bipolar cell response is saturated (Dunn, F. A. *et al.*, 2006). At these mesopic intensities, there is enough light to stimulate many rods simultaneously while the cone signals are still close to threshold. Thus, the combined rod signals may provide a substantial input to cones (Hornstein, E. P. *et al.*, 2005). At still higher light

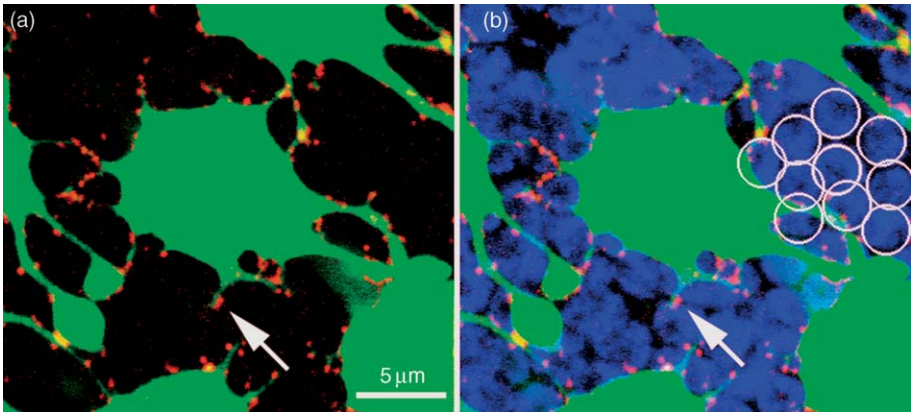

Figure 3 (a) A high-resolution image of cone pedicles, stained with an antibody against cone arrestin (green). Some of the telodendria are short and do not reach adjacent cone pedicles yet they still bear many small Cx36 plaques (red). (b) Same frame, showing rod spherules labeled with an antibody against the synaptic vesicle protein SV2B. Rod spherules appear as circular structures with a vesicle poor dark spot, often in the center, that corresponds to the synaptic invagination. Some examples of rod spherules are circled. Cx36 plaques on short telodendria are aligned with surrounding rod spherules and an example is marked with an arrow. These gap junctions are the substrate for rod/cone coupling. Image courtesy of Jennifer O'Brien and Stephen C. Massey.

intensities, the rod system is saturated but there is enough light to drive cones effectively. Thus, gap junctions between rods and cones are essential at intermediate light levels during the transition from rod-to-cone vision. It has long been suggested that rod/cone coupling should be variable so that at low light levels, the gap junctions are closed and single rod responses are not dissipated by the network (Smith, R. G. *et al.*, 1986).

1.23.3.1.4 Rod-to-rod coupling

Finally, in the mouse retina there are also gap junctions between rod spherules and tracer coupling has been reported between rods in the primate retina (Tsukamoto, Y. *et al.*, 2001; Hornstein, E. P. *et al.*, 2005). Under high scotopic conditions, this may improve performance in the high-gain rod pathway by delaying saturation of the rod bipolar cell response. However, rod-to-rod coupling may also increase the threshold for the very dimmest signals (Hornstein, E. P. *et al.*, 2005). If rod-to-rod gap junctions can also be modulated, then at threshold conditions they should be closed to maximize the response in a single rod. As more light is available, averaging between rods via open gap junctions would then be useful to extend the range of the rod pathway by preventing saturation of the rod bipolar response. There is no evidence yet that this occurs but it serves as an example for how gap junction plasticity can provide the best of both worlds in neural circuits.

1.23.3.2 Horizontal Cells

HCs are second-order, laterally extensive interneurons that provide negative feedback to cones in the outer retina and subtract a large, slow version of the visual scene. This is the basis for center surround antagonism, a common strategy in sensory systems, which helps to differentiate small, low-contrast signals against a common background (Wässle, H., 2004). HCs are much larger than cones and they are also famously connected via gap junctions into an extensively coupled network (Raviola, E. and Gilula, N. B., 1975; Kolb, H., 1977; Vaney, D. I., 1991; Mills, S. L. and Massey, S. C., 1994). Thus, the size of the receptive field far exceeds the extent of the dendritic field. This can be remarkable. For example, in the rabbit retina, the receptive field of A-type HCs is 20 times greater than the size of the dendritic field. Thus, the spatial extent of the feedback signal to cones is determined, in part, by the strength of coupling in the HC network (Dacheux, R. F. and Raviola, E., 1982; Bloomfield, S. A. *et al.*, 1995). In other words, the diameter of HC feedback can be changed according to factors, such as light adaptation, that modulate gap junction coupling between HCs. This is a good example of network plasticity and perhaps

the fundamental reason for gap junction coupling between HCs.

In the rabbit retina, there are two types of HC, which have different coupling properties (Dacheux, R. F. and Raviola, E., 1982; Mills, S. L. and Massey, S. C., 1994). Dye injections reveal that A-type HCs are extremely well coupled, allowing the passage of both Lucifer Yellow and Neurobiotin (Figure 4) (O'Brien, J. J. *et al.*, 2006). These are the only gap junctions in the rabbit retina that pass Lucifer Yellow. Dye injection of an A-type HC with Neurobiotin, which is much more permeable than Lucifer Yellow, yields thousands of dye-coupled A-type HCs in sheets that can stretch for millimeters across a wholemount retina. In contrast, B-type HCs are only permeable to Neurobiotin (Figure 4) (Vaney, D. I., 1993; Mills, S. L. and Massey, S. C., 1994). This immediately suggests that the two HC networks use different connexins.

1.23.3.2.1 A-type horizontal cells and Cx50

A-type HCs can be readily labeled either with an antibody against calbindin or, with more detail, by Neurobiotin injections. Double labeling with an antibody that recognizes Cx50 produced extensive labeling completely restricted to the A-type matrix (O'Brien, J. J. *et al.*, 2006) (Figure 5). The Cx50 labeling is coded green but in this image Cx50 plaques appears almost exclusively yellow because they only occur on A-type HC dendrites. Where large primary dendrites cross, there are often giant Cx50 plaques with irregular or polygonal shapes. The Cx50 plaque in the center of Figure 5 measures 63 μm^2 and must contain hundreds of thousands of gap junction channels. Cx50 channels have a high unitary conductance, 220 pS (Srinivas, M. *et al.*, 1999) so even if a large fraction of the gap junction channels are closed, our calculations suggest that the transjunctional resistance across such a giant plaque may be less than half a megaohm. The holes in the center of this plaque may indicate gap junction recycling and turnover. In addition, there are a large number of smaller Cx50 plaques spread throughout the A-type HC matrix including even the finest dendrites. Close inspection reveals that Cx50 plaques occur when dendrites cross or cofasciculate and this is the pattern expected for gap junction labeling. The numerous Cx50 plaques between the dendrites of A-type HC suggest that Cx50 gap junctions may adequately account for the remarkable coupling observed in this network.

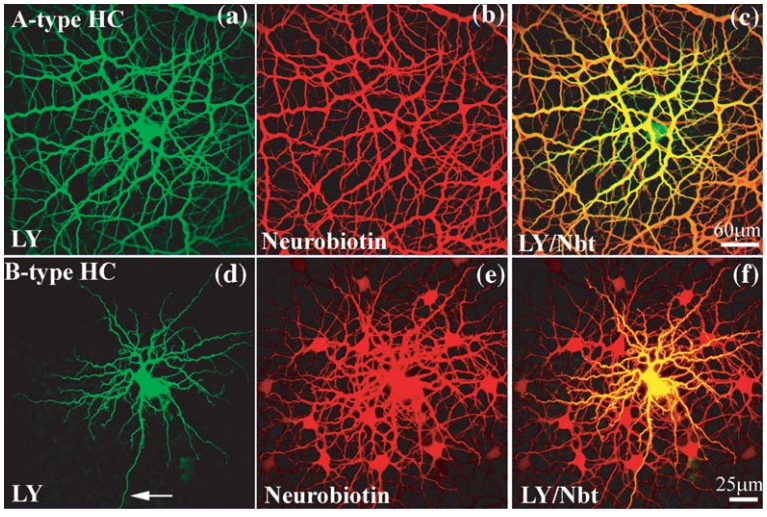

Figure 4 Differential tracer coupling of A- and B-type horizontal cells (HCs) in the rabbit retina. (a–c) A single A-type HC was filled with a combination of Lucifer Yellow and Neurobiotin. (a) Shows extensive Lucifer Yellow coupling (green) in this cell type. (b) Shows even greater Neurobiotin coupling (red). (c) Shows the overlay with double-labeled cells fading from yellow to orange because of the wider distribution of Neurobiotin. (d–f) A single B-type HC was filled with the same combination of Lucifer Yellow and Neurobiotin. (d) shows a single B-type HC filled with Lucifer Yellow (green), which indicates that Lucifer Yellow does not pass B-type HC gap junctions. The arrow indicates the axon of the injected cell. (e) Shows extensive Neurobiotin coupling (red) in B-type HCs. (f) Shows the overlay with numerous Neurobiotin coupled B-type HCs in red and a single double-labeled cell in the middle (yellow). From O'Brien, J. *et al*. 2006. Coupling between A-type HCs is mediated by connexin 50 in the rabbit retina. J. Neurosci. 26, 11624–11636.

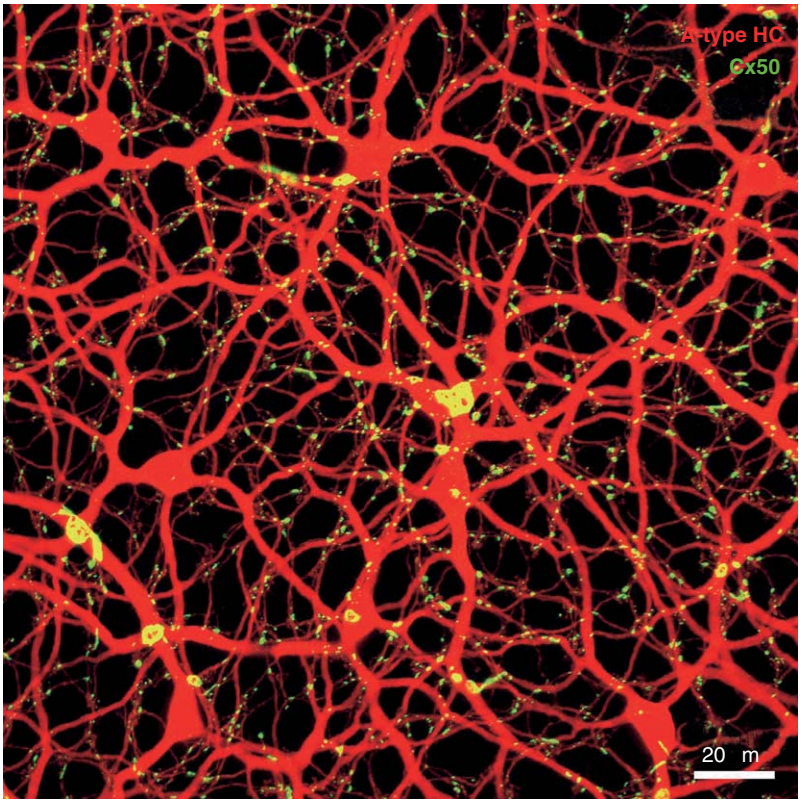

Figure 5 Connexin 50 labeling in the matrix of A-type horizontal cells (HCs) in the rabbit retina. A-type HCs were dye injected with Neurobiotin (red) and the Cx50 staining was coded green, but shows mostly as yellow due to colocalization. Essentially all the Cx50 labeling is on A-type HCs between adjacent or overlapping dendrites. There are numerous small Cx50 plaques among the finer dendrites as well as giant Cx50 plaques between major dendrites. The giant plaque in the center has an area of 63 μm^2 and must contain hundreds of thousands of gap junction channels. Courtesy of Jennifer O'Brien and Stephen C. Massey.

1.23.3.2.2 B-type horizontal cells

B-type HCs are axon-bearing cells in rabbit and cat retina. The somatic end of the cell has many fine, radially symmetrical dendrites, which form a dense meshwork and contact cone pedicles exclusively. The dendrites of B-type somas are also dye coupled, although less so than A-type HCs, since they pass less Neurobiotin and no Lucifer Yellow (Figure 4) (Vaney, D. I., 1993; Mills, S. L. and Massey, S. C., 1994). Presumably, this indicates the presence of different gap junctions in the two types of HC. The passage of Neurobiotin through the gap junctions between the somatic dendrites effectively prevents the diffusion of Neurobiotin along the axon. The tracer would rather spread through the network than pass along the narrow axon. In contrast, if the gap junctions are blocked using a gap junction antagonist such as meclofenamic acid, a complete fill of the axon and the axon terminal (AT) is obtained (Figure 6). Confocal analysis of this material confirms that the AT receives input exclusively from rods (Pan, F. and Massey, S. C., 2007).

The B-type AT is thought to be electrotonically isolated from the somatic dendrites because of the length and fine diameter of the axon, combined with the passive electrical properties of HCs (Nelson, R., 1977). However, evidence from dye injection indicates that the B-type ATs are independently coupled by gap junctions (Vaney, D. I., 1993; Pan, F. and Massey, S. C., 2007). Thus, in the outer retina of the rabbit, there are three independently coupled HC networks. Rats and mice are unusual among mammals in that they have only one type of HC, which is axon bearing and appears to be equivalent to the B-type HC of the rabbit (Peichl, L. and Gonzalez-Soriano, J., 1994).

In the mouse retina, axon-bearing HCs with the morphological appearance of B-type HCs express

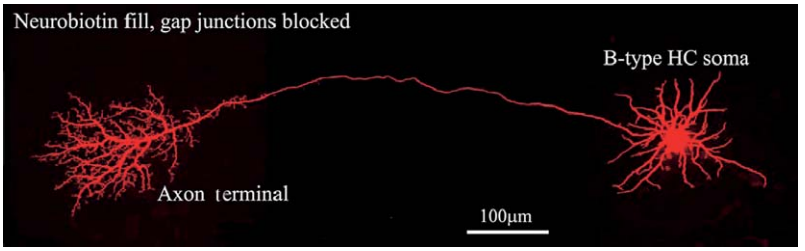

Figure 6 A single B-type horizontal cell (HCs) from the rabbit retina. This cell was filled with Neurobiotin while gap junction coupling was blocked with meclofenamic acid. Because coupling was blocked, the Neurobiotin passed down the axon and filled the axon terminal (AT) structure completely. B-type HCs are axon-bearing cells. The somatic dendrites receive input from cones while the AT structure receives input from approximately 1000 rods. Image courtesy of Feng Pan and Stephen C. Massey.

Cx57, and HC coupling was eliminated in the Cx57 knockout mouse (Peichl, L. and Gonzalez-Soriano, J., 1994; Hombach, S. *et al.*, 2004). This was a convincing demonstration because in the Cx57 knockout mouse, the injected HCs were single fills, including the AT. This results because coupling in the network was eliminated and dye passes along the axon instead of through the network. This is the same effect as when coupling is blocked with a gap junction antagonist (see Figure 6).

1.23.3.2.3 Modulation

Horizontal cell coupling appears to be affected by several neuromodulators including dopamine and nitric oxide (Teranishi, T. *et al.*, 1984; Hampson, E. C. *et al.*, 1994; Xin, D. and Bloomfield, S. A., 1999a; He, S. *et al.*, 2000). The effects of dopamine on goldfish HCs are particularly dramatic but this has been more difficult to demonstrate in the mammalian retina. It may be that there are additional factors to be uncovered in the mammalian retina. By inhibiting gap junction coupling, dopamine reduces the size of the receptive field. In addition, dopamine also increases the amplitude of the response to a small spot because the signals do not spread through the network. This suggests that HC coupling is plastic and that the strength and spatial properties of HC feedback can be modulated by light intensity or circadian processes (Teranishi, T. *et al.*, 1983).

1.23.3.2.4 Horizontal cell feedback

Despite the critical importance of HC feedback to photoreceptors in the outer retina, the exact mechanism by which this occurs remains unsolved. A large and convincing body of work suggests that feedback modulates the calcium current in photoreceptor terminals but the mechanism by which HCs control feedback is unknown (Kamermans, M. and Spekreijse, H., 1999). Classical neurotransmitters do not account for HC feedback and, in the absence of conventional candidates, electrical transmission via hemichannels has been proposed (Kamermans, M. *et al.*, 2001). The idea is that open hemichannels in the tips of HC dendrites pass a current that, in the restricted space of the cone pedicle invagination, can affect voltage-dependent calcium channels in the cone pedicle and thus influence glutamate release. In support of this hypothesis, carbenoxolone, a gap junction antagonist, also reduces HC feedback (Kamermans, M. *et al.*, 2001). However, carbenoxolone has also been shown to block calcium channels and thus may affect glutamate release from cones directly (Vessey, J. P. *et al.*, 2004). An alternative nonconventional mechanism for HC feedback involves the release of protons that may in turn modulate voltage-dependent calcium channels (DeVries, S. H., 2001). In support of this model, additional buffering reduced feedback but the mechanism controlling the release or uptake of protons is unknown (Vessey, J. P. *et al.*, 2005; Cadetti, L. and Thoreson, W. B., 2006). Regardless of which alternative is finally established, it seems likely that HC feedback is mediated by a novel mechanism.

1.23.3.3 AII Amacrine Cells/ON Cone Bipolar Cells, a Complex Heterocellular Network

Cone bipolar cells come in ON and OFF varieties that make direct connections with ganglion cells. In contrast, there is only one type of rod bipolar cell, which is connected to the AII amacrine cell. In turn, the AII splits the signals into ON and OFF pathways by connecting to OFF bipolar cells via glycinergic synapses and to ON bipolar cells via gap junctions. It is often said that the rod signals piggyback on the cone pathways. The heterocellular gap junctions with

ON bipolar cells are the conduits for the transfer of rod signals into the ON cone pathways (Strettoi, E. *et al.*, 1992; Strettoi, E. *et al.*, 1994; Bloomfield, S. A. and Dacheux, R. F., 2001).

The AII amacrine cell is the most numerous amacrine cell type in the mammalian retina. They are well coupled by prominent gap junctions that were described in the first morphological reports of AII amacrine cells (Famiglietti, E. V. and Kolb, H., 1975). The extent of coupling was dramatically confirmed by Neurobiotin injections, which yield a mosaic of AII amacrine cells and a large population of overlying ON cone bipolar cells (Figure 7) (Hampson, E. C. *et al.*, 1992; Mills, S. L. and Massey, S. C., 1995). The AIIs are all located in the amacrine cell layer, adjacent to the inner plexiform layer (IPL), while the bipolar cells have somas toward the top of the inner nuclear layer. The dye-coupled ON cone bipolar cells are made up from four to five morphological types so this is truly a complex heterocellular network (McGuire, B. A. *et al.*, 1984).

AII amacrine cells have a stout primary dendrite that tapers into the IPL. The top sublayer of the IPL contains a dense meshwork of dopaminergic dendrites, which are penetrated by the AII processes. When viewed in wholemount, it looks like there are holes in the dopaminergic plexus and each one contains an AII amacrine cell. The dopaminergic dendrites form a ring of varicosities around every AII amacrine cell. This is the motif of a major synaptic input and dopamine dramatically modulates coupling in the AII network via PKA (Hampson, E. C. *et al.*, 1992; Mills, S. L. and Massey, S. C., 1995). AII gap junctions are also modulated by light, with reduced coupling in dark or bright conditions and most coupling at intermediate light intensity (Bloomfield, S. A. and Volgyi, B., 2004). The exact details between dopamine levels, receptor subtypes, light modulation, circadian mechanisms, and other potential modulators have not yet been worked out. However, the input of dopamine, the dominant signal for light adaptation, to the AII network, a major intersection of rod and cone pathways, has clear functional significance.

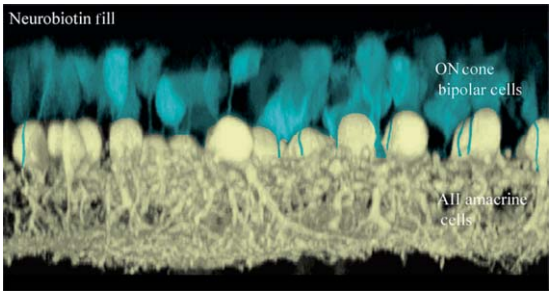

Figure 7 Three-dimensional reconstruction from a confocal series to show the heterocellular network of AII amacrine cells and ON cone bipolar cells in the rabbit retina. A single AII amacrine cell was filled with Neurobiotin. AII amacrine cells (beige) lie adjacent to the inner plexiform layer (IPL) and overlap extensively. ON cone bipolar cells (three to five types, blue) have cell bodies higher in the inner nuclear layer (INL) and they produce descending axons that are lost in the matrix of AII dendrites. Image courtesy of Brady Trexler and Stephen C. Massey.

It is well established that AII amacrine cells are coupled by Cx36 gap junctions (Feigenspan, A. *et al.*, 2001; Mills, S. L. *et al.*, 2001). Cx36 is predominantly expressed by AII amacrine cells and it occurs at dendritic crossings in the AII matrix. The Cx36 staining is punctate and we have learned that this type of labeling pattern is diagnostic for gap junction proteins. This indicates that AII/AII gap junctions are composed of homotypic, Cx36/Cx36 gap junctions. The level of Cx36 expression in AII amacrine cells is astonishing; the density is high and the Cx36 plaques are larger than other gap junctions in the IPL. So far, there have been few good examples to compare with. Now, as we start to uncover new coupling patterns, we find that the expression of connexins in other amacrine cell types is relatively meager. By comparison, the AII matrix has a heavy concentration of Cx36 gap junctions. This is suggestive of a special role for the AII network, which is unusually well coupled in all mammalian retinas.

1.23.3.3.1 AII/ON cone bipolar gap junctions

In addition to AII/AII gap junctions, Cx36 immunoreactivity occurs at AII/ON cone bipolar contacts (Figure 8). However, the AII/bipolar gap junctions have different properties than the AII/AII junctions. In early morphological work, it was noticed that the AII/bipolar gap junctions have an asymmetrical appearance (Strettoi, E. *et al.*, 1992; Wassle, H. *et al.*, 1995). Dye coupling studies with a series of biotinylated tracers related to Neurobiotin, show that the AII/bipolar gap junctions tend to exclude the high molecular weight compounds (Mills, S. L. and Massey, S. C., 1995; 2000). All else being equal, the size exclusion probably indicates that the AII/bipolar gap junction has a smaller unitary conductance than the AII/AII gap junctions. Furthermore, the two gap junction types have different pharmacological properties. The AII/AII gap junctions are preferentially closed by dopamine and cAMP analogs while the

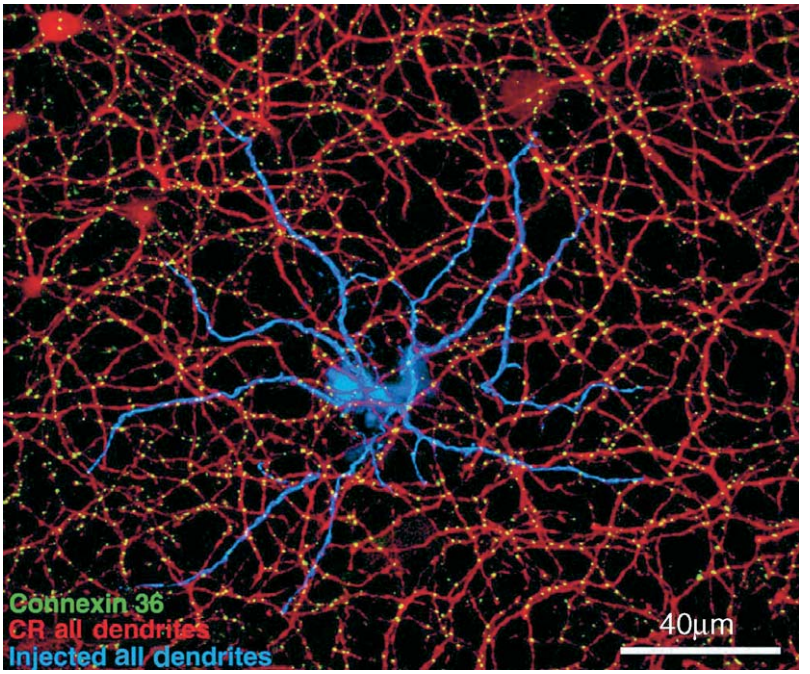

Figure 8 AII/AII gap junctions are Cx36/Cx36 in the rabbit retina. The fine dendrites of a single dye injected AII amacrine cell are shown in blue. The mosaic of surrounding AII amacrine cells was stained with an antibody against calretinin (red). Cx36 labeling is shown in green but appears mostly yellow due to colocalization with the AII matrix. Essentially, all the Cx36 plaques occur in the AII matrix, mostly at dendritic crossings. This is especially obvious where blue dendrites from the single dye injected AII cross red dendrites from neighboring AII amacrine cells. Image analysis shows there is a high probability of a Cx36 gap junction where AII dendrites cross. From Mills S. L. *et al*. 2001. Rod pathways in the mammalian retina use connexin36. J. Comp. Neurol. 436, 336–350, 2001.

AII/bipolar gap junctions respond better to NO donors and cGMP analogs (Mills, S. L. and Massey, S. C., 1995; Xin, D. and Bloomfield, S. A., 1999b). One explanation could be that the AII/bipolar gap junctions are heterotypic, with Cx36 on the AII side and a different connexin expressed in bipolar cells. This would be a heterotypic gap junction.

AII amacrine cells are glycinergic inhibitory interneurons and they express a glycine transporter. In contrast, bipolar cells are excitatory and use glutamate as a neurotransmitter. However, ON cone bipolar cells also contain substantial levels of glycine despite the fact that they do not express a glycine transporter (Cohen, E. and Sterling, P., 1986). The source of the glycine in bipolar cells is via the gap junction with AII amacrine cells. This was established by showing that the distribution of glycine can be changed by blocking gap junctions with carbenoxolone (Vaney, D. I. *et al*., 1998). In the presence of carbenoxolone, ON cone bipolar cells no longer accumulate glycine via the gap junctions with AII amacrine cells. In transgenic mice that express a Cx45 reporter, many amacrine cells and bipolar cells are labeled. Furthermore, in the Cx45 knockout, the labeling pattern for glycine was changed such that bipolar cells no longer contained glycine (Maxeiner, S. *et al*., 2005). In other words, in the Cx45 knockout, the gap junctions between bipolar cells and AII amacrine cells were blocked or absent. This strongly suggested that Cx45 plays a role at AII/bipolar gap junctions. Subsequently, double labeling with Cx36 and Cx45 showed the presence of punctate pairs with adjacent Cx36/Cx45 labeling and these structures were located at AII/bipolar cell contacts (Han, Y. and Massey, S. C., 2005; Dedek, K. *et al*., 2006). In summary, these results indicate that AII/bipolar cell gap junctions are heterotypic with Cx36/Cx45 gap junctions. There may be some variability among the bipolar cells because at least one specific bipolar subtype in the mouse retina expresses Cx36 (Han, Y. and Massey, S. C., 2005; Lin, B. *et al*., 2005).

1.23.3.3.2 Physiology

Paired recordings indicate that AII/AII gap junctions are bidirectional with a conductance in the range of 700 pS (Veruki, M. L. and Hartveit, E., 2002a). AII

amacrine cells are noisy neurons with a lot of spontaneous activity. This might be expected for a system that sits close to threshold so as to impart maximum sensitivity in low light conditions. Importantly, the gap junctions can synchronize action potentials between adjacent AII amacrine cells (Veruki, M. L. and Hartveit, E., 2002a; 2002b). This is consistent with the idea that gap junctions in the AII network serve the purpose of signal averaging and noise reduction in the high-gain rod bipolar pathway (Smith, R. G. and Vardi, N., 1995; Vardi N., and Smith, R. G., 1996).

Paired recordings also show that AII/bipolar gap junctions are bidirectional (Veruki, M. L. and Hartveit, E., 2002a). Under the right circumstances, Neurobiotin can also pass from AII amacrine cells to bipolar cells (Trexler, E. B. *et al.*, 2001; Veruki, M. L. and Hartveit, E., 2002b) and, of course, this is also the route for glycine (Vaney, D. I. *et al.*, 1998). This implies that electrical signals can pass, not only from the AII into bipolar cells but also from the cone pathways into the AII. When the rod bipolar input to the AII was blocked with a glutamate antagonist, there was a remaining light-driven signal with the characteristics of electrical input via the gap junctions with bipolar cells (Trexler, E. B. *et al.*, 2005). The idea of dual inputs to AII amacrine cells, via a chemical synapses with rod bipolar cells, and electrical synapses from ON cone bipolar cells was confirmed in experiments with transgenic mice. In the absence of rod bipolar inputs, the electrical input remained but it was eliminated in Cx36 knockout mice (Pang, J. J. *et al.*, 2007). Thus, AII amacrine cells may play a dual role in retinal circuitry: in dim light, they average rod bipolar signals for distribution to both ON and OFF cone bipolar cells while in bright conditions, input via gap junctions with ON bipolar cells may provide crossover inhibition to OFF cone bipolar cells.

Finally, in an elegant and important series of experiments, the Bloomfield lab has explored the physiological consequences of eliminating Cx36 gap junctions in a line of transgenic mice (Deans, M. R. *et al.*, 2002). In the wild-type mouse, ganglion cells show a variety of intensity response curves. This includes some ganglion cells that only respond at intensities above cone threshold. This implies that they receive input from an ON cone bipolar subtype that receives no rod input and is therefore not coupled to the AII network. However, in the Cx36 knockout there are significant changes. In particular, there is no rod-driven input to ON ganglion cells. At threshold intensities, rod signals pass through the high-gain rod bipolar pathway and through the AII/bipolar gap junctions and so to ON ganglion cells. But, in the Cx36 knockout, AII/AII and AII/ON bipolar coupling are eliminated. At intermediate intensities, the pathway is thought to pass via rod/cone coupling into the cone pathways. Rod/cone gap junctions depend on Cx36 expression in cones and are also eliminated in the Cx36 knockout. These experiments indicate that Cx36 is essential for processing rod-driven ON signals (Deans, M. R. *et al.*, 2002). This is the first time that a requirement for an electrical synapse has been demonstrated in a specific neuronal circuit in the mammalian CNS. The changes to OFF ganglion cell responses are more subtle. Rod-driven signals are still present in OFF pathways because there is no gap junction along this pathway. However, the sensitivity of rod-driven signals was reduced by a log unit, perhaps due to the absence of AII/AII coupling in the Cx36 knockout (Volgyi, B. *et al.*, 2004). This result is consistent with the idea that averaging in the AII network is necessary to provide maximum sensitivity in retinal circuits (Bloomfield, S. A. and Volgyi, B., 2004).

1.23.3.4 Ganglion Cells

Many ganglion cell types are also coupled. At first, this seems counterintuitive because coupling between adjacent cells of the same type would seem to spread the signals leading to a loss of spatial resolution. However, across many mammalian species including cat, rabbit, rodent, and primate, Neurobiotin injections reveal ganglion cell to ganglion cell coupling as well as coupling to one or more amacrine types. For example, in the rabbit, OFF α ganglion cells are coupled to surrounding OFF α ganglion cells and as many as a hundred amacrine cells (Hu, E. H. and Bloomfield, S. A., 2003). Of course, the cells are only visible after the Neurobiotin has been developed and often the dye-coupled cells are faintly labeled compared to the injected cell. Frequently, the coupled cells are wide-field amacrine cells but a complete description has not been possible in most cases. In a different approach, the use of a novel fluorescent nuclear tracer, Po-pro-1, which is gap junction permeable, has been used to make the somas of the coupled cells visible so they can be individually targeted (Hoshi, H. *et al.*, 2006). This method has confirmed that many of the coupled amacrine cells are wide-field axon-bearing types.

1.23.3.4.1 Alpha ganglion cells

α Ganglion cells are dye coupled but there is some variation across species. In the rodent retina, both

subtypes are coupled but in the rabbit retina only OFF α ganglion cells are coupled. This provides a useful test case to compare the effects of cell coupling: the spikes of ON α ganglion cells are not correlated whereas the spikes between neighboring OFF α ganglion cells are synchronized (DeVries, S. H., 1999; Hu, E. H. and Bloomfield, S. A., 2003). This indicates that electrical coupling via gap junctions underlies the correlated spikes in neighboring OFF α ganglion cells. In the rat retina, bidirectional electrical coupling between α ganglion cells resulted in precisely synchronized firing after current injection and electron microscopy revealed dendrodendritic Cx36 gap junctions at contact points between dye-coupled α ganglion cells (Hidaka, S. *et al.*, 2004). Most investigators have reported Cx36 at dendritic crossings between α ganglion cells but there is residual dye coupling between OFF α cells in the retina of the Cx36 knockout mouse (Schubert, T. *et al.*, 2005a; Volgyi, B. *et al.*, 2005). At least some of the ganglion cell to amacrine cell coupling is also Cx36 but other connexins are probably used at a subset of gap junctions. In the mouse retina, bistratified ganglion cells may be connected via Cx45 gap junctions because coupling is absent in the Cx45 knockout (Schubert, T. *et al.*, 2005b).

The common occurrence of electrical coupling among ganglion cell types has been independently confirmed by examining their biochemical signatures. Gap junctions with amacrine cells are thought to provide a route for metabolic coupling so that certain ganglion cells contain amacrine cell neurotransmitters such as GABA or glycine (Marc, R. E. and Jones, B. W., 2002). In addition, recording from the rabbit retina with a multielectrode array shows that 5/11 physiologically classified ganglion cells are coupled (DeVries, S. H., 1999). There is consistency between these different approaches such that OFF α ganglion cells in the rabbit retina are dye coupled, have synchronized firing, and contain GABA while ON α ganglion cells do not.

1.23.3.4.2 ON/OFF directionally selective ganglion cells

In the adult rabbit retina, there are four subtypes of ON/OFF directionally selective (ON/OFF DS) ganglion cells with orthogonal preferred stimulus directions. A subset of the ON/OFF DS ganglion cells, presumably responding to one of the four preferred axes, is dye coupled. These cells form a tiling pattern with a coverage factor close to one (Vaney, D. I., 1994). In contrast, other ON/OFF DS cells, presumably with different axes, overlie the coupled subtypes and their dendrites cofasciculate. The function of coupling in the ON/OFF DS cells is unknown but it may be related to development because coupling among all ON/OFF DS subtypes is much more prevalent in the neonatal retina (DeBoer, D. J. and Vaney, D. I., 2005).

1.23.3.4.3 Synchronized firing

Correlated firing patterns have been recorded between many ganglion cell types using a multielectrode array and it has been suggested that synchronized spikes could transmit additional information as a multineuronal code (Meister, M., 1996). Pairwise and adjacent interactions between primate parasol ganglion cells, most likely due to gap junction coupling, accounted for nearly all multineuronal firing patterns (Shlens, J. *et al.*, 2006). An alternative explanation is that synchronized firing delivers closely timed spikes to the lateral geniculate nuclei (LGN), which have a much higher probability of eliciting a postsynaptic spike (Usrey, W. M. *et al.*, 1998). Adjacent ON DS ganglion cells in the rabbit retina are dye coupled to many amacrine cells (Figure 9) and they also produced synchronous firing

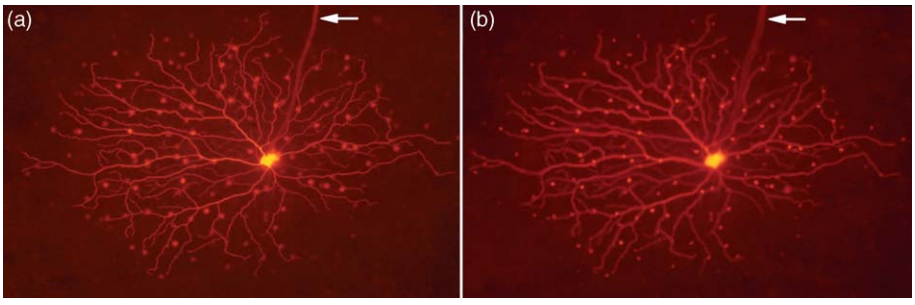

Figure 9 Dye coupling between amacrine cells and an ON directionally selective (ON DS) ganglion cell in the rabbit retina. A single ganglion cell with the morphology of an ON DS ganglion cell was filled with Neurobiotin. (a) Focus on the ON DS ganglion cell dendrites. (b) Focus on the cell bodies of numerous dye-coupled amacrine cells. Image courtesy of Stephen C. Massey.

patterns (Ackert, J. M. *et al*., 2006). These cells project to the accessory optic system and may play a role in image tracking or stabilizing the retinal image. The correlated firing of ON DS ganglion cells was also dependent on the direction of the stimulus: null axis stimuli generated fewer spikes that were not synchronized. This suggests that preferred axis motion not only generates more spikes but those from neighboring cells are also synchronized and thus much more likely to produce a postsynaptic response (Ackert, J. M. *et al*., 2006). This is in effect another form of signal averaging and noise reduction such that asynchronous signals are selectively filtered.

1.23.4 Conclusion

Gap junctions are common circuit elements in the mammalian retina and four different neuronal connexins have been identified. As in other regions of the CNS, Cx36 is the dominant connexin, serving AII coupling and photoreceptor coupling. Cx45 coupling is also found in certain amacrine and ganglion cells and heterotypic Cx36/Cx45 gap junctions are found between AII amacrine cells and cone bipolar cells. Cx50 and/or Cx57 appear to be responsible for HC coupling in the retina. There may be additional gap junction proteins still to be identified. Clear functional roles have been assigned to different gap junctions in stereotyped neuronal circuits. It seems that the signal averaging properties of gap junctions serve a vital noise reduction strategy in the early steps of vision. The modulation of gap junctions may also contribute to retinal plasticity. This is important because the retina is a self-adjusting neuronal network that continuously adapts to the visual input. Optimizing retinal function over a wide variety of conditions must have been associated with a high survival value over evolutionary time.

Acknowledgments

This research was supported by the National Eye Institute (NEI); Grant Numbers: EY 06515 (to S. C. M.) and EY 10608 (Vision Core Grant). Additional support was provided by an unrestricted grant from Research to Prevent Blindness to the Department of Ophthalmology and Visual Science. S. C. M. is the Elizabeth Morford Professor of Ophthalmology and Visual Science.

Thanks to past and present members of my lab who contributed time and figures including Feng Pan, Jennifer O'Brien, In-Beom Kim, Wei Li, and Brady Trexler.

References

Ackert, J. M., Wu, S. H., Lee, J. C., Abrams, J., Hu, E. H., Perlman, I., and Bloomfield, S. A. 2006. Light-induced changes in spike synchronization between coupled ON direction selective ganglion cells in the mammalian retina. J. Neurosci. 26, 4206–4215.

Ahnelt, P. K. and Pflug, R. 1986. Telodendrial contacts between foveolar cone pedicles in the human retina. Experientia 42, 298–300.

Ahnelt, P., Keri, C., and Kolb, H. 1990. Identification of pedicles of putative blue-sensitive cones in the human retina. J. Comp. Neurol. 293, 39–53.

Baylor, D. A., Nunn, B. J., and Schnapf, J. L. 1987. Spectral sensitivity of cones of the monkey *Macaca fascicularis*. J. Physiol. 390, 145–160.

Bloomfield, S. A. and Dacheux, R. F. 2001. Rod vision: pathways and processing in the mammalian retina. Prog. Retin. Eye Res. 20, 351–384.

Bloomfield, S. A. and Volgyi, B. 2004. Function and plasticity of homologous coupling between AII amacrine cells. Vision Res. 44, 3297–3306.

Bloomfield, S. A., Xin, D., and Persky, S. E. 1995. A comparison of receptive field and tracer coupling size of horizontal cells in the rabbit retina. Vis. Neurosci. 12, 985–999.

Cadetti, L. and Thoreson, W. B. 2006. Feedback effects of horizontal cell membrane potential on cone calcium currents studied with simultaneous recordings. J. Neurophysiol. 95, 1992–1995.

Cohen, E. and Sterling, P. 1986. Accumulation of (3H)glycine by cone bipolar neurons in the cat retina. J. Comp. Neurol. 250, 1–7.

Cusato, K., Zakevicius, J., and Ripps, H. 2003. An experimental approach to the study of gap-junction-mediated cell death. Biol. Bull. 205, 197–199.

Dacheux, R. F. and Raviola, E. 1982. Horizontal cells in the retina of the rabbit. J. Neurosci. 2, 1486–1493.

Deans, M. R. and Paul, D. L. 2001. Mouse horizontal cells do not express connexin26 or connexin36. Cell. Adhes. Commun. 8, 361–366.

Deans, M. R., Volgyi, B., Goodenough, D. A., Bloomfield, S. A., and Paul, D. L. 2002. Connexin36 is essential for transmission of rod-mediated visual signals in the mammalian retina. Neuron 36, 703–712.

DeBoer, D. J. and Vaney, D. I. 2005. Gap-junction communication between subtypes of direction-selective ganglion cells in the developing retina. J. Comp. Neurol. 482, 85–93.

Dedek, K., Schultz, K., Pieper, M., Dirks, P., Maxeiner, S., Willecke, K., Weiler, R., and Janssen-Bienhold, U. 2006. Localization of heterotypic gap junctions composed of connexin45 and connexin36 in the rod pathway of the mouse retina. Eur. J. Neurosci. 24, 1675–1686.

DeVries, S. H. 1999. Correlated firing in rabbit retinal ganglion cells. J. Neurophysiol. 81, 908–920.

DeVries, S. H. 2001. Exocytosed protons feedback to suppress the Ca^{2+} current in mammalian cone photoreceptors. Neuron 32, 1107–1117.

DeVries, S. H., Qi, X., Smith, R., Makous, W., and Sterling, P. 2002. Electrical coupling between mammalian cones. Curr. Biol. 12, 1900–1907.

Dunn, F. A., Doan, T., Sampath, A. P., and Rieke, F. 2006. Controlling the gain of rod-mediated signals in the mammalian retina. J. Neurosci. 26, 3959–3970.

Famiglietti, E. V., Jr. and Kolb, H. 1975. A bistratified amacrine cell and synaptic circuitry in the inner plexiform layer of the retina. Brain Res. 84, 293–300.

Feigenspan, A., Janssen-Bienhold, U., Hormuzdi, S., Monyer, H., Degen, J., Sohl, G., Willecke, K., Ammermuller, J., and Weiler, R. 2004. Expression of connexin36 in cone pedicles and OFF-cone bipolar cells of the mouse retina. J. Neurosci. 24, 3325–3334.

Feigenspan, A., Teubner, B., Willecke, K., and Weiler, R. 2001. Expression of neuronal connexin36 in AII amacrine cells of the mammalian retina. J. Neurosci. 21, 230–239.

Galarreta, M. and Hestrin, S. 2001. Electrical synapses between GABA-releasing interneurons. Nat. Rev. Neurosci. 2, 425–433.

Guldenagel, M., Sohl, G., Plum, A., Traub, O., Teubner, B., Weiler, R., and Willecke, K. 2000. Expression patterns of connexin genes in mouse retina. J. Comp. Neurol. 425, 193–201.

Hampson, E. C., Vaney, D. I., and Weiler, R. 1992. Dopaminergic modulation of gap junction permeability between amacrine cells in mammalian retina. J. Neurosci. 12, 4911–4922.

Hampson, E. C., Weiler, R., and Vaney, D. I. 1994. pH-gated dopaminergic modulation of horizontal cell gap junctions in mammalian retina. Proc. R. Soc. Lond. Ser B Biol. Sci. 255, 67–72.

Han, Y. and Massey, S. C. 2005. Electrical synapses in retinal ON cone bipolar cells: subtype-specific expression of connexins. Proc. Natl. Acad. Sci. U. S. A. 102, 13313–13318.

He, S., Weiler, R., and Vaney, D. I. 2000. Endogenous dopaminergic regulation of horizontal cell coupling in the mammalian retina. J. Comp. Neurol. 418, 33–40.

Hidaka, S., Akahori, Y. and Kurosawa, Y. 2004. Dendrodendritic electrical synapses between mammalian retinal ganglion cells. J. Neurosci. 24, 10553–10567.

Hombach, S., Janssen-Bienhold, U., Sohl, G., Schubert, T., Bussow, H., Ott, T., Weiler, R., and Willecke, K. 2004. Functional expression of connexin57 in horizontal cells of the mouse retina. Eur. J. Neurosci. 19, 2633–2640.

Hornstein, E. P., Verweij, J., and Schnapf, J. L. 2004. Electrical coupling between red and green cones in primate retina. Nat. Neurosci. 7, 745–750.

Hornstein, E. P., Verweij, J., Li, P. H., and Schnapf, J. L. 2005. Gap-junctional coupling and absolute sensitivity of photoreceptors in macaque retina. J. Neurosci. 25, 11201–11209.

Hoshi, H., O'Brien, J., and Mills, S. L. 2006. A novel fluorescent tracer for visualizing coupled cells in neural circuits of living tissue. J. Histochem. Cytochem. 54, 1169–1176.

Hsu, A., Smith, R. G., Buchsbaum, G., and Sterling, P. 2000. Cost of cone coupling to trichromacy in primate fovea. J. Opt. Soc. Am. A Opt. Image Sci. Vis. 17, 635–640.

Hu, E. H. and Bloomfield, S. A. 2003. Gap junctional coupling underlies the short-latency spike synchrony of retinal alpha ganglion cells. J. Neurosci. 23, 6768–6777.

Kamasawa, N., Furman, C. S., Davidson, K. G., Sampson, J. A., Magnie, A. R., Gebhardt, B. R., Kamasawa, M., Yasumura, T., Zumbrunnen, J. R., Pickard, G. E., Nagy, J. I., and Rash, J. E. 2006. Abundance and ultrastructural diversity of neuronal gap junctions in the OFF and ON sublaminae of the inner plexiform layer of rat and mouse retina. Neuroscience 142, 1093–1117.

Kamermans, M. and Spekreijse, H. 1999. The feedback pathway from horizontal cells to cones. A mini review with a look ahead. Vision Res. 39, 2449–2468.

Kamermans, M., Fahrenfort, I., Schultz, K., Janssen-Bienhold, U., Sjoerdsma, T., and Weiler, R. 2001. Hemichannel-mediated inhibition in the outer retina. Science 292, 1178–1180.

Kolb, H. 1977. The organization of the outer plexiform layer in the retina of the cat: electron microscopic observations. J. Neurocytol. 6, 131–153.

Lee, E. J., Han, J. W., Kim, H. J., Kim, I. B., Lee, M. Y., Oh, S. J., Chung, J. W., and Chun, M. H. 2003. The immunocytochemical localization of connexin 36 at rod and cone gap junctions in the guinea pig retina. Eur. J. Neurosci. 18, 2925–2934.

Li, W. and DeVries, S. H. 2004. Separate blue and green cone networks in the mammalian retina. Nat. Neurosci. 7, 751–756.

Lin, B., Jakobs, T. C., and Masland, R. H. 2005. Different functional types of bipolar cells use different gap-junctional proteins. J. Neurosci. 25, 6696–6701.

Marc, R. E. and Jones, B. W. 2002. Molecular phenotyping of retinal ganglion cells. J. Neurosci. 22, 413–427.

Massey, S. C., O'Brien, J. J., Trexler, E. B., Li, W., Keung, J. W., Mills, S. L., and O'Brien, J. 2003. Multiple neuronal connexins in the mammalian retina. Cell Commun. Adhes. 10, 425–430.

Maxeiner, S., Dedek, K., Janssen-Bienhold, U., Ammermuller, J., Brune, H., Kirsch, T., Pieper, M., Degen, J., Kruger, O., Willecke, K., and Weiler, R. 2005. Deletion of connexin45 in mouse retinal neurons disrupts the rod/cone signaling pathway between AII amacrine and ON cone bipolar cells and leads to impaired visual transmission. J. Neurosci. 25, 566–576.

McGuire, B. A., Stevens, J. K., and Sterling, P. 1984. Microcircuitry of bipolar cells in cat retina. J. Neurosci. 4, 2920–2938.

Meister, M. 1996. Multineuronal codes in retinal signaling. Proc. Natl. Acad. Sci. U. S. A. 93, 609–614.

Menichella, D. M., Goodenough, D. A., Sirkowski, E., Scherer, S. S., and Paul, D. L. 2003. Connexins are critical for normal myelination in the CNS. J. Neurosci. 23, 5963–5973.

Mills, S. L. and Massey, S. C. 1994. Distribution and coverage of A- and B-type horizontal cells stained with Neurobiotin in the rabbit retina. Vis. Neurosci. 11, 549–560.

Mills, S. L. and Massey, S. C. 1995. Differential properties of two gap junctional pathways made by AII amacrine cells. Nature 377, 734–737.

Mills, S. L. and Massey, S. C. 2000. A series of biotinylated tracers distinguishes three types of gap junction in retina. J. Neurosci. 20, 8629–8636.

Mills, S. L., O'Brien, J. J., Li, W., O'Brien, J., and Massey, S. C 2001. Rod pathways in the mammalian retina use connexin36. J. Comp. Neurol. 436, 336–350.

Nelson, R. 1977. Cat cones have rod input: a comparison of the response properties of cones and horizontal cell bodies in the retina of the cat. J. Comp. Neurol. 172, 109–135.

O'Brien, J. J., Li, W., Pan, F., Keung, J., O'Brien, J., and Massey, S. C. 2006. Coupling between A-type horizontal cells is mediated by connexin 50 gap junctions in the rabbit retina. J. Neurosci. 26, 11624–11636.

O'Brien, J., Nguyen, H. B., and Mills, S. L. 2004. Cone photoreceptors in bass retina use two connexins to mediate electrical coupling. J. Neurosci. 24, 5632–5642.

Pan, F. and Massey, S. C. 2007. Rod and cone input to horizontal cells in the rabbit retina. J. Comp. Neurol. 500, 815–831.

Pang, J. J., Abd-El-Barr, M. M., Gao, F., Bramblett, D. E., Paul, D. L., and Wu, S. M. 2007. Relative contributions of rod and cone bipolar cell inputs to AII amacrine cell light responses. J. Physiol. 580, 397–410.

Peichl, L. and Gonzalez-Soriano, J. 1994. Morphological types of horizontal cell in rodent retinae: a comparison of rat, mouse, gerbil, and guinea pig. Vis. Neurosci. 11, 501–517.

Raviola, E. and Gilula, N. B. 1973. Gap junctions between photoreceptor cells in the vertebrate retina. Proc. Natl. Acad. Sci. U. S. A. 70, 1677–1681.

Raviola, E. and Gilula, N. B. 1975. Intramembrane organization of specialized contacts in the outer plexiform layer of the retina. A freeze–fracture study in monkeys and rabbits. J. Cell. Biol. 65, 192–222.

Ripps, H. 2002. Cell death in retinitis pigmentosa: gap junctions and the 'bystander' effect. Exp. Eye Res. 74, 327–336.

Schneeweis, D. M. and Schnapf, J. L. 1995. Photovoltage of rods and cones in the macaque retina. Science 268, 1053–1056.

Schneeweis, D. M. and Schnapf, J. L. 1999. The photovoltage of macaque cone photoreceptors: adaptation, noise, and kinetics. J. Neurosci. 19, 1203–1216.

Schubert, T., Degen, J., Willecke, K., Hormuzdi, S. G., Monyer, H., and Weiler, R. 2005a. Connexin36 mediates gap junctional coupling of alpha-ganglion cells in mouse retina. J. Comp. Neurol. 485, 191–201.

Schubert, T., Maxeiner, S., Kruger, O., Willecke, K., and Weiler, R. 2005b. Connexin45 mediates gap junctional coupling of bistratified ganglion cells in the mouse retina. J. Comp. Neurol. 490, 29–39.

Shields, C. R., Klooster, J., Claassen, Y., Kamermans, M., Zoidl, G., and Dermietzel, R. 2005. Horizontal cell-specific expression of connexin 52.6 & connexin 55.5 in the zebrafish retina. Invest. Ophthalmol. Vis. Sci. 46, e-abstract 599.

Shlens, J., Field, G. D., Gauthier, J. L., Grivich, M. I., Petrusca, D., Sher, A., Litke, A. M., and Chichilnisky, E. J. 2006. The structure of multi-neuron firing patterns in primate retina. J. Neurosci. 26, 8254–8266.

Smith, R. G. and Vardi, N, 1995. Simulation of the AII amacrine cell of mammalian retina: functional consequences of electrical coupling and regenerative membrane properties. Vis. Neurosci. 12, 851–860.

Smith, R. G., Freed, M. A., and Sterling, P. 1986. Microcircuitry of the dark-adapted cat retina: functional architecture of the rod–cone network. J. Neurosci. 6, 3505–3517.

Srinivas, M., Costa, M., Gao, Y., Fort, A., Fishman, G. I., and Spray, D. C. 1999. Voltage dependence of macroscopic and unitary currents of gap junction channels formed by mouse connexin50 expressed in rat neuroblastoma cells. J. Physiol. (Lond.) 517, 673–689.

Strettoi, E., Dacheux, R. F., and Raviola, E. 1994. Cone bipolar cells as interneurons in the rod pathway of the rabbit retina. J. Comp. Neurol. 347, 139–149.

Strettoi, E., Raviola, E., and Dacheux, R. F. 1992. Synaptic connections of the narrow-field, bistratified rod amacrine cell (AII) in the rabbit retina. J. Comp. Neurol. 325, 152–168.

Teranishi, T., Negishi, K., and Kato, S. 1983. Dopamine modulates S-potential amplitude and dye-coupling between external horizontal cells in carp retina. Nature 301, 243–246.

Teranishi, T., Negishi, K., and Kato, S. 1984. Regulatory effect of dopamine on spatial properties of horizontal cells in carp retina. J. Neurosci. 4, 1271–1280.

Thompson, R. J., Zhou, N., and MacVicar, B. A. 2006. Ischemia opens neuronal gap junction hemichannels. Science 312, 924–927.

Trexler, E. B., Li, W., and Massey, S. C. 2005. Simultaneous contribution of two rod pathways to AII amacrine and cone bipolar cell light responses. J. Neurophysiol. 93, 1476–1485.

Trexler, E. B., Li, W., Mills, S. L., and Massey, S. C. 2001. Coupling from AII amacrine cells to ON cone bipolar cells is bidirectional. J. Comp. Neurol. 437, 408–422.

Tsukamoto, Y., Masarachia, P., Schein, S. J., and Sterling, P. 1992. Gap junctions between the pedicles of macaque foveal cones. Vision Res. 32, 1809–1815.

Tsukamoto, Y., Morigiwa, K., Ueda, M., and Sterling, P. 2001. Microcircuits for night vision in mouse retina. J. Neurosci. 21, 8616–8623.

Usrey, W. M., Reppas, J. B., and Reid, R. C. 1998. Paired-spike interactions and synaptic efficacy of retinal inputs to the thalamus. Nature 395, 384–387.

Vaney, D. I. 1991. Many diverse types of retinal neurons show tracer coupling when injected with biocytin or Neurobiotin. Neurosci. Lett. 125, 187–190.

Vaney, D. I. 1993. The coupling pattern of axon-bearing horizontal cells in the mammalian retina. Proc. R. Soc. Lond. Ser. B Biol. Sci. 252, 93–101.

Vaney, D. I. 1994. Territorial organization of direction-selective ganglion cells in rabbit retina. J. Neurosci. 14, 6301–6316.

Vaney, D. I., Nelson, J. C., and Pow, D. V. 1998. Neurotransmitter coupling through gap junctions in the retina. J. Neurosci. 18, 10594–10602.

Vardi, N. and Smith, R. G. 1996. The AII amacrine network: coupling can increase correlated activity. Vision Res. 36, 3743–3757.

Veruki, M. L. and Hartveit, E. 2002a. AII (Rod) amacrine cells form a network of electrically coupled interneurons in the mammalian retina. Neuron 33, 935–946.

Veruki, M. L. and Hartveit, E. 2002b. Electrical synapses mediate signal transmission in the rod pathway of the mammalian retina. J. Neurosci. 22, 10558–10566.

Vessey, J. P, Lalonde, M. R., Mizan, H. A., Welch, N. C., Kelly, M. E., and Barnes, S. 2004. Carbenoxolone inhibition of voltage-gated Ca channels and synaptic transmission in the retina. J. Neurophysiol. 92, 1252–1256.

Vessey, J. P., Stratis, A. K., Daniels, B. A., Da Silva, N., Jonz, M. G., Lalonde, M. R., Baldridge, W. H., and Barnes, S. 2005. Proton-mediated feedback inhibition of presynaptic calcium channels at the cone photoreceptor synapse. J. Neurosci. 25, 4108–4117.

Volgyi, B., Abrams, J., Paul, D. L., and Bloomfield, S. A. 2005. Morphology and tracer coupling pattern of alpha ganglion cells in the mouse retina. J. Comp. Neurol. 492, 66–77.

Volgyi, B., Deans, M. R., Paul, D. L., and Bloomfield, S. A. 2004. Convergence and segregation of the multiple rod pathways in mammalian retina. J. Neurosci. 24, 11182–11192.

Wässle, H. 2004. Parallel processing in the mammalian retina. Nat. Rev. Neurosci. 5, 747–757.

Wassle, H., Grunert, U., Chun, M. H., and Boycott, B. B. 1995. The rod pathway of the macaque monkey retina: identification of AII-amacrine cells with antibodies against calretinin. J. Comp. Neurol. 361, 537–551.

Willecke, K., Eiberger, J., Degen, J., Eckardt, D., Romualdi, A., Guldenagel, M., Deutsch, U., and Sohl, G. 2002. Structural and functional diversity of connexin genes in the mouse and human genome. Biol. Chem. 383, 725–737.

Xin, D. and Bloomfield, S. A. 1999a. Dark- and light-induced changes in coupling between horizontal cells in mammalian retina. J. Comp. Neurol. 405, 75–87.

Xin, D. and Bloomfield, S. A. 1999b. Comparison of the responses of AII amacrine cells in the dark- and light-adapted rabbit retina. Vis. Neurosci. 16, 653–665.

1.24 Plasticity of Retinal Circuitry

N Tian, Yale University, New Haven, CT, USA

D Copenhagen, University of California, San Francisco, CA, USA

© 2008 Elsevier Inc. All rights reserved.

1.24.1	**Visual Activity Regulates Synaptic Wiring in Developing Retina**	475
1.24.1.1	Visual Deprivation During Postnatal Development Modifies Dendritic Arborization Patterns and Visual Responses of Retinal Ganglion Cells	475
1.24.1.1.1	Dark rearing expands retinal ganglion cells receptive fields and dendritic coverage in turtle retina	475
1.24.1.1.2	Dark rearing retards developmental segregation of ON and OFF pathways in retinal ganglion cells	475
1.24.1.1.3	Molecular or genetic mechanisms mediating this activity-dependent developmental plasticity remain elusive	478
1.24.1.1.4	Light deprivation alters the normal developmental sequence of excitatory and inhibitory synaptic inputs to retinal ganglion cells	479
1.24.1.2	Visual Experience Regulates the Maturation of Amacrine Cell Processes	481
1.24.1.2.1	Visual experience controls development of serotonergic amacrine cells in chick retina	481
1.24.1.2.2	Visual deprivation reduces the number of detectable cholinergic amacrine cells and the extent of their processes in mouse retina	482
1.24.2	**Synaptic Circuitry Exhibits Plasticity in Response to Light and Dark Adaptation in Adult Retina**	482
1.24.2.1	Ambient Background Light Regulates Horizontal Cell Synapses and Gap Junction Coupling between Horizontal Cells	482
1.24.2.2	Light and Dark Conditions Modify the Morphology of Bipolar Cell Axons	483
1.24.2.3	Light and Dark Controls Gap Junction Coupling and Receptive Field Properties of Amacrine Cells	484
1.24.2.4	A Possible Mechanism by Which Light and Dark Could Regulate Synapse Strength Between Bipolar and Amacrine Cells	485
1.24.2.5	Light Can Regulate the Expression of α-Amino-3-Hydroxy-5-Methylisoxazole-4-Propionic Acid-Glutamate Receptors on Retinal Ganglion Cells	485
1.24.2.6	Light and Dark Adaptation Controls Receptive Field Organization of Retinal Ganglion Cells	485
1.24.3	**Survival Rewiring of Retinal Circuits**	486
1.24.3.1	Rewiring of Synaptic Connections in Outer Retina in Response to Photoreceptor Degeneration or Loss of Synaptic Signaling	486
1.24.3.2	Survival Plasticity of Retinal Wiring in Retinal Detachments	487
References		487

Glossary

plasticity State of being able to be reformed or refined. In the nervous system, plasticity refers to the modifiability of neuronal synaptic circuits. Plasticity is expressed as morphological and/or functional changes.

developmental plasticity Capability of neuronal circuits to be modified during initial maturation.

adaptive plasticity Ability of matured neuronal circuits to change functional status in response to alterations of environmental conditions.

compensatory plasticity Ability of neuronal circuits to make compensatory changes in structure or function in responding to pathological conditions and aging.

visual deprivation Conditions for animals in which normal visual stimuli are degraded or absent. These conditions could include lack of any light or selective absence of form, contrast or color.

dark rearing Conditions in which animals are housed in total darkness.

light adaptation Processes by which the visual system adjusts itself to increased ambient light. These processes include a reduced sensitivity of phototransduction in rods and cones, loss of functional photopigments in rods and cones (for very bright lights), changes in the gain of synaptic signal transfer and pupil constriction.

dark adaptation The process by which the visual system adjusts itself to decreased ambient lighting conditions. It is determined by the percentage of molecules of the rod photopigment, rhodopsin, that are bleached. Rhodopsin regenerates with a slow time course so that one would need 30–45 min to regenerate all bleached rhodopsin and regain sensitivity to dim light from a light adapted status.

RGC receptive field The area of visual field or retina over which an RGC can be activated, directly or indirectly.

RGC dendritic field The dendritic processes of RGCs extend laterally across the retina. The dendritic field is the physical area of retina encompassed by the usually circularly shaped 'tree' of all dendritic branches.

parallel synaptic pathway This term refers to specific synaptic structures carrying different aspects of neuronal perception in the nervous system. Many visual signals are processed by parallel synaptic pathways in visual system. For example, there are cells that respond to objects brighter than the background (increment of brightness or ON response) and the cells that respond to the objects darker than the background (decrement of brightness or OFF response), among bipolar and ganglion cells in the retina, cells in the lateral geniculate nucleus and visual cortex. These two types of visual signal are separated from each other after they are generated at the first synapses in the retina and do not come together again until the visual cortex is reached. Thus, there are clearly separated neuronal structures to process the two types of signal and little interaction between them along the way.

ionotropic glutamate receptor A class of membrane receptors that is activated by the neurotransmitter glutamate and are comprised of subunits that change their molecular configuration to allow charged ions to flow directly across cell walls. These are fast acting receptors that can be divided structurally and pharmacologically into three different classes: AMPA, Kainate, and NMDA receptors.

metabotropic glutamate receptor A class of membrane receptors that are activated by glutamate and are coupled to intracellular second messenger cascades. Glutamate binding to metabotropic receptors triggers this cascade. Glutamate binding to the mGluR6 metabotropic receptors of retinal ON bipolar cells results in the closure of cationic channels in the membrane with concomitant hyperpolarization.

bi-laminated RGC Retinal ganglion cell with dendritic processes that arborize in both sublaminae of the inner plexiform layer. The ganglion cells can receive synaptic inputs from both ON and OFF bipolar cells.

mono-laminated RGC Retinal ganglion cells with dendritic processes that arborize exclusively in one sublamina of the inner plexiform layer.

Plasticity in sensory, integrative, and motor pathways in the central nervous system (CNS) enables organisms to adapt to the environment and optimize performance under various physiological and pathological conditions. Although, neuronal circuits are for the most part hard wired, connectivity between neurons, synaptic structures and their basic behavior, and neuronal processing can be modified and refined. Plasticity is a commonly used term to denote the capability of neuronal systems, small circuits, and single cells to refine and modify their structure and behavior in response to environmental stimuli. In the visual system reorganization and refinement of neuronal pathways can take place during development or in mature animals including humans. The reorganization of the eye-specific ocular dominance columns in visual cortex in response to visual deprivation of one eye is a now classic example of plasticity during postnatal maturation. The adjustment of the gain of vestibular

ocular reflex (VOR) in response to new glasses is an example of plasticity in adults (Boyden, E. S. *et al.*, 2004).

Much of what we have learned about plasticity of synaptic wiring in sensory systems has been derived from studies in which functional and morphological changes have been documented in higher sensory centers of the brain. Little attention has been paid to plastic changes in retinal circuitry. It was commonly assumed previously that retinal synaptic circuitry matures early in development. Indeed, many aspects of synaptic signaling in retina reach maturity before the retina receive visual stimulation. Most of the morphological features of the retina and the expression of synthesizing enzymes, transporters, and receptors for neurotransmitters of retinal neurons resemble those in adult animals by the time of eye opening in mice, rats, rabbits, cats, and ferrets (Fisher, L. J., 1979; Greiner, J. V. and Weidman, T. A., 1981; Redburn, D. A. and Madtes, P., 1987; Pow, D. V. and Barnett, N. L., 2000; Sassoe-Pognetto, M. and Wässle, H., 1997; Johnson, J. *et al.*, 2003). Functionally, early experiments using rabbit retina showed that the size of retinal ganglion cell (RGC) receptive fields, RGC directional selectivity and light-evoked eye movements reached mature levels early during postnatal development (Daw, N. W. and Wyatt, H. J., 1974; Masland, R. H., 1977). However, recent and not so recent, studies have established that retinal circuitry is functionally and structurally malleable during postnatal development.

In this chapter we will discuss three types of plasticity in retinal circuitry. Our focus is on structural and functional modification of circuitry postsynaptic to rods and cones. Plasticity inherent in the structure and visual signaling of rods and cones has been well documented elsewhere (Dearry, A. and Burnside, B., 1986; Lamb, T. D. and Pugh, E. N., Jr., 2004). In the first two sections we will concentrate on changes in retinal circuitry induced by light itself. These will include alterations induced by visual deprivation during early postnatal maturation and short term changes in functional connectivity and activity of retinal circuitry evoked by background lighting conditions in adult retina, commonly termed light and dark adaptation. Finally, we will discuss alterations in synaptic morphology in retinas in which rods and cones degenerate or lose their visual signaling capabilities or in retinas in which genetic mutations lead to deficits in synaptic function.

1.24.1 Visual Activity Regulates Synaptic Wiring in Developing Retina

1.24.1.1 Visual Deprivation During Postnatal Development Modifies Dendritic Arborization Patterns and Visual Responses of Retinal Ganglion Cells

1.24.1.1.1 Dark rearing expands retinal ganglion cells receptive fields and dendritic coverage in turtle retina

A cogent example of how light deprivation can influence the receptive field sizes and structure of dendritic fields during early development was reported in turtle retina. Electrophysiologically recorded RGC receptive fields in dark-reared posthatched turtles can expand to twice the size of RGC receptive fields of adults raised in cyclic light (Sernagor, E. and Grzywacz, N. M., 1996). Analysis of dye-filled RGC dendritic arbors showed that dark rearing produced excessive growth of dendrites in the large-field RGCs of turtle, consistent with the larger receptive fields recorded in response to light patterns (Mehta, V. and Sernagor, E., 2006). While the effects of visual deprivation on RGC dendritic field coverage has not been reported in mammalian retina, during postnatal development visual inputs do regulate the laminar patterns of RGC dendritic arbors in the inner plexiform layer (IPL), and hence the relative proportions of exclusive inputs from the ON and OFF pathways.

1.24.1.1.2 Dark rearing retards developmental segregation of ON and OFF pathways in retinal ganglion cells

Separate parallel retinal synaptic pathways transmit signals about light increments (ON) and light decrements (OFF). The separation of ON and OFF pathways originates at the first synapse of the retina between photoreceptors and bipolar cells (Figure 1). In all vertebrate retinas, light stimulation hyperpolarizes the membrane potentials of photoreceptors (rods and cones) and decreases the synaptic release of glutamate from these cells. Glutamate released from photoreceptors activates ionotropic glutamate receptors on cone-driven OFF bipolar cells and depolarizes their membrane potentials. Glutamate activates a metabotropic glutamate receptors on the cone-driven ON bipolar cells and all rod-driven bipolar cells and thereby hyperpolarizes the membrane potentials of these cells (see Chapters Mammalian Rod Pathways and Contributions of Bipolar Cells to Ganglion Cell Receptive Fields for details). This sign

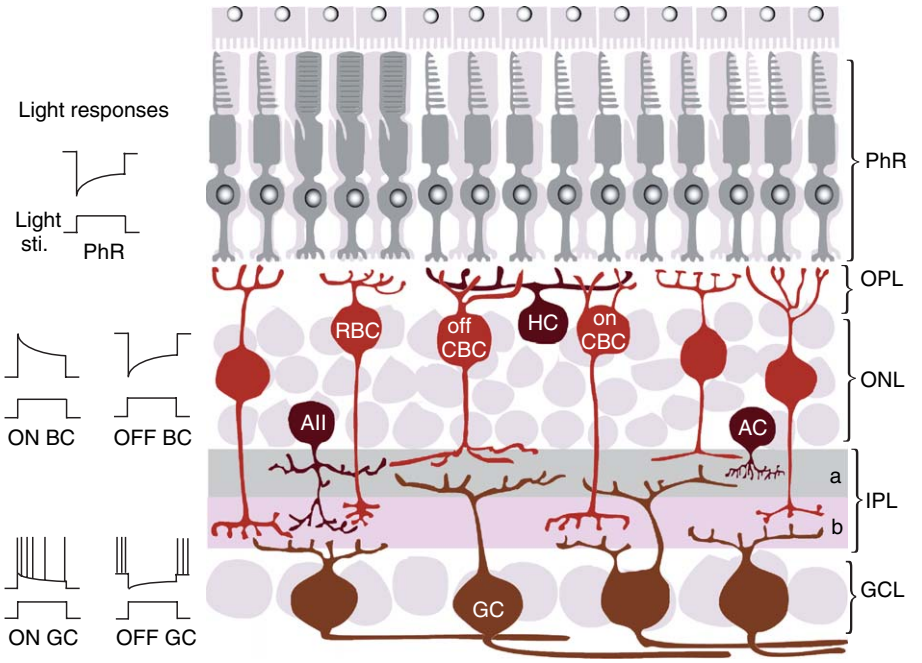

Figure 1 A schematic drawing of the principal anatomical components, synaptic connections, and representative light responses of ON–OFF pathways of mammalian retina. Photoreceptors (rods and cones) synapse with bipolar and horizontal cells (HCs) in the outer plexiform layer (OPL). ON and OFF signals are generated in the OPL by the activation of metabotropic and ionotropic glutamate receptors on the ON and OFF bipolar cells, respectively. All ON bipolar cell synapse with retinal ganglion cells (RGCs) in sublamina *b* and all OFF bipolar cell make synapses with RGCs in the sublamina *a* of inner plexiform layer (IPL). A subpopulation of RGCs receives synaptic inputs from both ON and OFF bipolar cells. Bipolar cells that receive rod inputs synapse with AII amacrine cells, which in turn make electrical synapse with cone-driven OFF bipolar cells and chemical synapse with cone-driven ON bipolar cells. Light responses in outer retinal neurons, such as photoreceptors, bipolar cells, and HCs, are graded potentials. In the inner retina RGCs and amacrine cells (ACs) typically signal more transient depolarization and action potentials. PhR, photoreceptor; GC, ganglion cell; OFF CBC, cone-driven OFF bipolar cell; ON CBC, cone-driven ON bipolar cell; RBC, rod-driven bipolar cell. Adapted from Xu, H. P. and Tian, N. 2004. Pathway-specific maturation, visual deprivation, and development of retinal pathway. Neuroscientist 10, 337–346, with permission from SAGE Publications Inc.

reversing and sign conserving action of glutamate on the ON and OFF bipolar cells, respectively, separates the increment and decrement luminance signals into ON and OFF pathways. At the level of synaptic inputs to RGCs the separation of ON and OFF pathways is preserved by the selectivity of the synaptic connections between bipolar and RGCs in distinct layers of the IPL. Despite the enormous diversity of the structural and functional properties among different subtypes of RGCs, all ON RGC dendrites ramify only in the sublamina *b* of the IPL and synapse with ON bipolar cells. In contrast, all OFF RGC dendrites ramify only in the sublamina *a* of the IPL and synapse with OFF bipolar cells (Famiglietti, E. V. and Kolb, H., 1976; Nelson, R. *et al.*, 1978). A subset of RGCs, the ON–OFF RGCs, ramify their dendrites in both sublaminas and signal both the onset and termination of light (Amthor, F. R. *et al.*, 1984). Thus, the ON and OFF pathways are maintained functionally and structurally separated.

Early in postnatal development, the dendrites of a large percentage of RGCs ramify diffusely throughout the IPL (Maslim, J. and Stone, J., 1988; Bodnarenko, S. R. *et al.*, 1995; 1999; Wang, G. Y. *et al.*, 2001; Diao, L. *et al.* 2004). With subsequent maturation, RGC dendrites are seen to be much more monostratified with most or all of the arbors restricted to sublamina *a* or *b*. This laminar refinement predicts there is an age-dependent decrease in the number of RGCs receiving synaptic inputs from both ON and OFF bipolar cells. Indeed, analysis of RGC dendritic arborization in mouse retina shows that whereas 53% of RGCs in postnatal (P)10-aged animals ramify in both sublamina *a* and *b* of IPL only 29% of mouse RGCs in P30-aged animals ramify in both sublaminas *a* and *b* (Tian, N. and Copenhagen, D. R., 2003). This developmental

pruning of RGC dendrites is one of the best examples of the maturational reorganization of neuronal synaptic circuitry (Wong, R. O. L. and Ghosh, A., 2002) and has been found in cats (Dann, J. F. *et al.*, 1988; Maslim, J. and Stone, J., 1988; Bodnarenko, S. R. *et al.*, 1995), ferrets (Bodnarenko, S. R. *et al.*, 1999), rabbits (Wong, R. O. L., 1990), rats (Yamasaki, E. N. and Ramoa, A. S., 1993), and mice (Bansal, A. *et al.*, 2000; Diao, L. *et al.*, 2004).

As a technical note, it should be mentioned that the morphological characterization of RGC dendritic patterns have been facilitated significantly by the availability of mouse lines in which green fluorscent protein (GFP) or yellow fluorscent protein (YFP) is driven by the Thy1 promoter (Feng, G. *et al.*, 2000). In line H of the Thy1-YFP-expressing mice, numerous YFP labeled RGCs are randomly distributed throughout the retina (Figure 2). Confocal microscopy of these individual cells in whole mounted retinas has allowed experimenters to classify the arborization patterns of the RGCs (Tian, N. and Copenhagen, D. R., 2003; Coombs, J. *et al.*, 2006). Figure 3 shows an example of two RGCs obtained from a Thy1-YFP retina. The inset shows the color coding scheme by which processes in sublamina *a* are colored green and processes in sublamina *b* and the ganglion cell layer are colored blue.

The developmental refinement of RGC dendritic arbors discussed above is reflected physiologically as an age-dependent decrease in the number of RGCs that respond with spikes at the onset and termination of a light. This maturational decline in the percentages of ON–OFF RGCs has been observed electrophysiologically in mouse, cat, and ferret retinas (Bisti, S. *et al.*, 1998; Wang, G. Y. *et al.*, 2001; Tian, N. and Copenhagen, D. R., 2003). These results serve to illuminate the observation that, because the ON and OFF sublaminas of the IPL are so well regulated, the retina proves to be one of the best places in the nervous system to directly link structural characteristics with functional responsiveness at the cellular level.

The activity-dependent developmental plasticity of mammalian retina is shown by the finding that light deprivation retards the maturational conversion of bilaminated RGC dendrites into monolaminated structures, and the consequent decline in the percentage of ON–OFF RGCs (Tian, N. and Copenhagen, D. R., 2003). Tian N. and Copenhagen D. R. (2003) compared the lamination patterns of RGCs in cyclic-reared mice to those in dark-reared mice. At P30, $53\% \pm 2.5\%$ of the RGCs were classified as bilaminated in the dark-reared mice versus $29\% \pm 3\%$ in cyclic light-reared mice. This difference was highly significant. The percentage of bilaminated cells in the P30 dark-reared animals was very close to the P10-aged mice raised in cyclic light ($53\% \pm 2.5\%$ vs. $53\% \pm 2.7\%$). These anatomical findings predicted that many more RGCs in the P30 dark-reared animals should be ON–OFF responsive RGCs. Multielectrode array recordings of light responses from RGCs verified this prediction. In the P27–30-aged mice raised in constant darkness, the percentage of ON–OFF RGCs was more than fourfold higher than age-matched cyclic light-reared mice. Moreover, the percentage of ON–OFF RGCs in the dark-reared mice at P27-30 was comparable to the

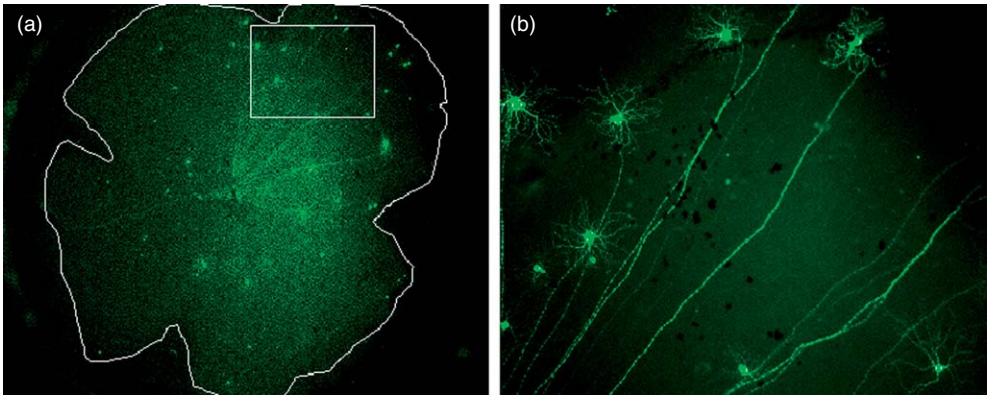

Figure 2 A small percentage of retinal ganglion cells (RGCs) are randomly labeled by YFP expression driven by Thy1 promoter in the H line of Thy1-YFP transgenic mouse. (a) A low magnified view from vitreal side of a flat-mounted retina harvested from a postnatal 30-aged Thy1-YFP-expressing mouse. (b) An enlarged view of the area indicated by the box in panel (a). Somata and dendrites are readily identifiable and the axons from individual RGCs cross the retina from each somata to the optic nerve head. Adapted from Tian, N. and Copenhagen, D. R. 2003. Visual stimulation is required for refinement of ON and OFF pathways in postnatal retina. Neuron 39, 85–96, with permission from Elsevier.

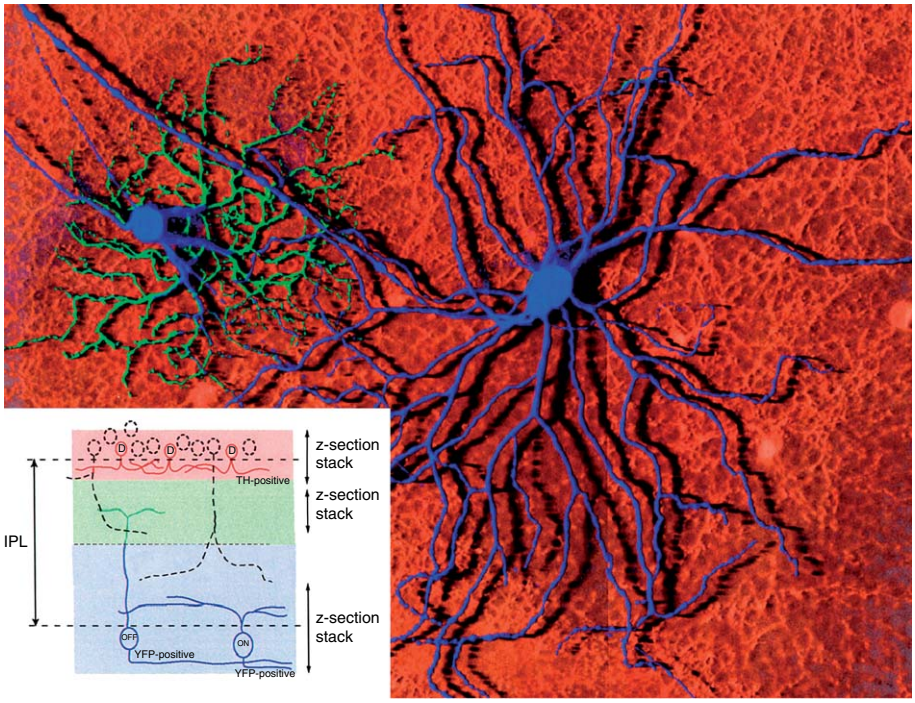

Figure 3 Dendritic ramification patterns of YFP-expression retinal ganglion cells (RGCs) in the inner plexiform layer (IPL) can be determined using confocal microscopy. Stacked image of two YFP-expressing RGCs from a postnatal 30-aged mouse retina. Red label denotes the immunolabeling pattern of TH-positive cells. These dopaminergic cells have their somata positioned at the inner nuclear layer (INL)/IPL border and their processes localized along the INL border of the IPL. TH-positive staining was used here as a marker for the distal edge of the IPL. The green processes show stacked images of YFP-expressing processes obtained from sequential z scans between the IPL/INL border to the middle of the IPL (see inset). The blue processes and somata show stacked images of YFP-expressing RGCs obtained from z scans from the middle of the IPL to the vitreal/RGC border. The OFF RGC is shown with monostratified dendrites (green) in sublamina *a* and a somata and axon (blue) in the proximal retina. The ON RGC has dendrites (blue) restricted exclusively to sublamina *b*.

percentage of ON–OFF RGCs at P10–12. These findings, which have been subsequently confirmed (Landi, S. *et al.*, 2007; Liu, X. *et al.*, 2007; Xu, H. P. and Tian, N., 2007) established that functionally and morphologically, retinal circuits are not hard-wired at birth and that the development of retinal wiring is influenced by visual inputs to the eye.

1.24.1.1.3 Molecular or genetic mechanisms mediating this activity-dependent developmental plasticity remain elusive

Chalupa L. M. and his colleagues concluded from intraocular injections of 2-amino-4-phosphonobutyric acid (APB), an agonist for class III metabotropic glutamate receptors, that glutamatergic signaling from ON bipolar cells, which exclusively express mGluR6, a class III receptor, played an important role in laminar refinement (Bodnarenko, S. R. and Chalupa, L. M., 1993; Bodnarenko, S. R. *et al.*, 1995). Based on the findings that the dendrites of more RGCs remained bilaminated in APB-treated eyes, they concluded that glutamatergic synaptic transmission from ON bipolar cells was important in laminar refinement. This conclusion is challenged by later results from mGluR6 knockout mice in which laminar stratification patterns appear normal (Tagawa, Y. *et al.*, 1999). One possibility that may reconcile these two different conclusions is that the membrane potential of the ON bipolar cells would be different in the two cases. In neither the APB nor mGluR6 mutant retinas should there be light responses in ON bipolar cells. However, in the APB-treated eyes, ON bipolar cells would be hyperpolarized. In mGluR6 mutant retinas ON bipolar cells would be depolarized. Further experiments will be needed to resolve this apparent inconsistency.

Chalupa L. M. *et al.* (1998) proposed two possible general synaptic mechanisms for the regulation of RGC dendritic stratification and the maturation of

the ON–OFF pathway. In the first model, they assumed that RGCs synapse functionally with only ON or OFF bipolar cells in early postnatal development, although the dendrites ramify in both the inner and outer IPL (Figure 4(a)). These asymmetrical inputs from ON or OFF bipolar cells could instruct those bilaminated RGCs to sever uninnervated dendrites during later postnatal development (Bodnarenko, S. R. *et al.*, 1995). If this were the case, one would expect to find RGCs stratified in both the inner and outer IPL but only respond to the onset or offset of light stimulation in early postnatal developing retina. Recent results obtained from simultaneous patch clamp and morphological recordings of ferret RGCs revealed that all RGCs with dendrites ramifying in both the inner and outer IPL responded to both the onset and offset of light in both young and adult animals, indicating that bilaminated RGCs are innervated by both ON and OFF bipolar cells (Wang, G. Y. *et al.*, 2001). Consistent with these results, intraocular injection of APB or light deprivation increased both the ON–OFF responsive and bilaminated RGCs in cat (Bodnarenko, S. R. and Chalupa, L. M., 1993; Bodnarenko, S. R. *et al.*, 1995; Bisti, S. *et al.*, 1998) and mouse (Tian, N. and Copenhagen, D. R., 2003) retina, respectively. Thus, it appears unlikely that an asymmetry of ON and OFF synaptic inputs is responsible for the elimination of exuberant processes in immature RGCs.

In the second model, it was assumed that synaptic transmission from bipolar cells triggers an intrinsic program in bilaminated RGCs leading to the retraction of one or another set of their dendritic processes (Figure 4(b)). This model relies on cell-specific intrinsic genetic programs that activate differential pruning of an individual cell's dendrites in either sublamina *a* or *b*. No molecular or genetic mechanisms that would mediate this selective pruning have been identified. Although the direct causal link between visual signaling and the molecular or genetic mechanisms that mediate selective proving has not been elucidated, brain-derived neurotrophic factor (BDNF) acting at TrkB receptors appears to play an important role in this proving (Landi, S. *et al.*, 2007; Liu, X. *et al.*, 2007).

1.24.1.1.4 Light deprivation alters the normal developmental sequence of excitatory and inhibitory synaptic inputs to retinal ganglion cells

In rodents, most of the molecular machinery required for synaptic transmission between retinal neurons develops during the time from birth until eye opening. Below we will focus on synaptic properties that reflect light-dependent regulation of the strength of synaptic inputs to RGCs after eye opening Specifically, the expression of glutamate *N*-methyl-D-aspartate (NMDA) receptors on RGCs and the rate of spontaneous excitatory and inhibitory

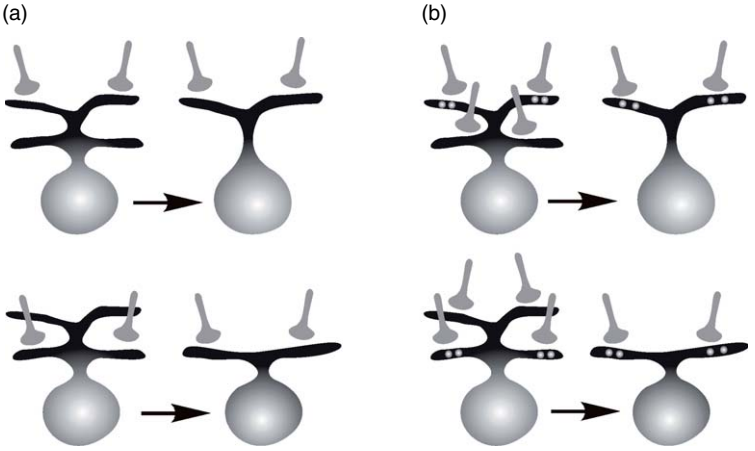

Figure 4 Schematic diagram illustrating possible mechanisms that underlying retinal ganglion cell (RGC) dendritic stratification. (a) Asymmetric afferent innervation model. RGC have their dendrites initially bi-laminated in both ON and OFF sublamina of inner plexiform layer and have asymmetric synaptic inputs. During development, dendrites that receive afferent inputs are maintained, whereas those do not receive afferent input are eliminated. (b) Intrinsic program model. Signal inputs from both ON and OFF bipolar cells trigger an intrinsic program in the bi-laminated RGCs, leading to elimination of the dendrites in either ON or OFF sublamina. Adapted from Xu, H. P. and Tian, N. 2004. Pathway-specific maturation, visual deprivation, and development of retinal pathway. Neuroscientist 10, 337–346, with permission from SAGE publications Inc.

synaptic inputs to RGCs are altered as a function of age after the time of eye opening in rodents. Light deprivation strongly influences all of these developmental events.

In mammalian retinas, neurogenesis and synaptogenesis follow similar maturational templates. During development, RGCs are the first neurons to differentiate, followed by cones, amacrine, and horizontal cells (HCs), and then rods, bipolar cells, and finally Müller cells. Morphologically identified conventional synapses between amacrine and ganglion cells in the IPL appear early during postnatal development. Cones and rods establish synaptic connectivity with horizontal and bipolar cells and then bipolar cells form ribbon synapses with amacrine and ganglion cells. At this time a synaptic link is completed that is necessary to elicit light responses in RGCs (Maslim, J. and Stone, J., 1986; Nishimura, Y. and Rakic, P., 1987). In rodents, the initial synaptic connections between amacrine and ganglion cells (conventional synapses) are established in the first postnatal week and the synaptic connections between bipolar and ganglion cells (ribbon synapses) begin forming around 10 days after birth (Fisher, L. J., 1979; Marquardt, T. and Gruss, P., 2002). Synapto-genesis continues for 2–3 weeks after the establishment of the synaptic connections from photoreceptor to RGCs (Figure 5(b)). In mice, the density of conventional synapses in the IPL rapidly increases in the second postnatal week from 85 synapses/1000 μm^3 at P3–10 to 223 synapses/1000 μm^3 around the time of eye opening (P11–15), which is very close to the adult level (250 synapses/1000 μm^3). The density of ribbon synapses in the IPL, in contrast, is low around the time of eye opening (45 synapses/1000 μm^3) and increase about 2.5-fold 3 weeks after eye opening to reach the adult level (113 synapses/1000 μm^3).

Physiologically, the percentage of rat RGCs having glutamate-activated NMDA receptor responses increases from birth until the time of eye opening after which this percentage, and the average amplitude of glutamate-induced NMDA currents, declines (Guenther, E. *et al.*, 2004). The percentage of RGCs with NMDA receptor-mediated responses in rats dark reared until P30 was almost double that of animals raised in cyclic light (96% vs. 47% in the cyclic-reared rats; Guenther, E. *et al.* 2004). Dark rearing appeared to delay the reduction in RGCs with NMDA receptor responses as the percentage dropped to 42% in those dark-reared animals that

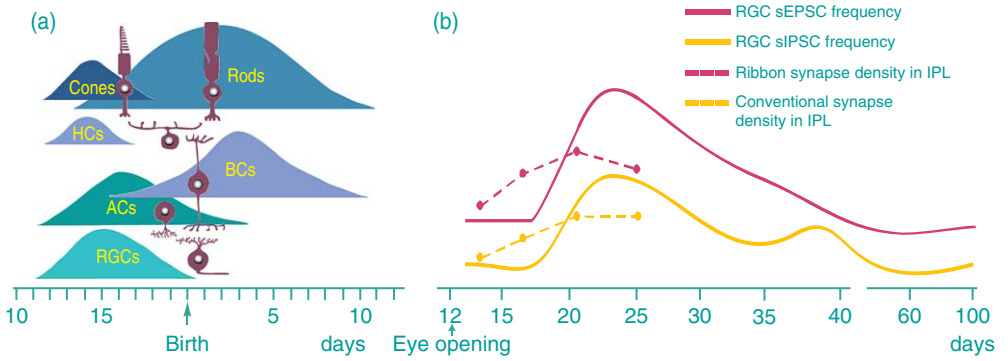

Figure 5 Neurogenesis and synaptogenesis in developing retina. (a) Neurogenesis in rodent retina begins before birth and is largely completed shortly after birth. There are roughly two waves in retinal neurogenesis. The differentiation of retinal ganglion cells (RGCs), horizontal cells (HCS), amacrine cells (ACS), and cones starts early during prenatal development and completes mostly before birth. The differentiation of rods and bipolar cells (BCS), however, starts shortly before birth and continues for 1–2 weeks after birth. (b) Synaptogenesis of mouse retina starts before eye opening and continues for several weeks after eye opening. The density of both ribbon and conventional synapse in inner plexiform layer reaches the peak at the age of postnatal 21 (modified from Fisher, L. J. 1979. Development of synaptic arrays in the inner plexiform layer of neonatal mouse retina. J. Comp. Neurol. 187, 359–372). The frequency of RGC spontaneous synaptic inputs increases with age and peaks around 2 weeks after eye opening (Tian, N. and Copenhagen, D. R., 2001). The curves show the relative cell populations, synaptic densities, and frequencies of spontaneous synaptic inputs as functions of time. The numbers indicate the prenatal and postnatal days of murine development. (Xu, H. P. and Tian, N., 2004) EPSC, excitatory postsynaptic current; IPL, inner plexiform layer; IPSC, inhibitory postsynaptic current. (a) Adapted from Young, R. W. 1985. Cell differentiation in the retina of the mouse. Anat. Rec. 212, 199–205. (b) Adapted from Tian, N. and Copenhagen, D. R. 2001. Visual deprivation alters development of synaptic function in inner retina after eye opening. Neuron 32, 439–443; and (Xu, H. P. and Tian, N., 2004); and Pathway-specific maturation, visual deprivation, and development of retinal pathway. Neuroscientist 10, 337–346.

were subsequently raised in cyclic light for 5 days. These findings demonstrate that the strength of glutamatergic inputs to RGCs can be regulated by light. Because NMDA receptors play such pivotal roles in both development and activity-dependent plasticity in other regions of the CNS, these light-dependent alterations of NMDA function are likely to be important for optimization of retinal functions.

The rate of vesicle-mediated spontaneous synaptic inputs into RGCs undergoes a maturational time-course that extends well past the time of eye opening; this maturational program is also regulated by visual inputs. After the time of eye opening the rates of spontaneous synaptic inputs from amacrine and bipolar cells onto RGCs continues to increase. In mouse retina, synaptic events associated with the random release of glutamate-filled vesicles from bipolar cells or gamma-aminobutyric acid (GABA)/glycine-filled vesicles from amacrine cells can be recorded in RGCs from about P7 (Johnson, J. *et al.*, 2003). Note that the glutamatergic events result from activation of α-amino-3-hydroxy-5-methylisoxazole-4-propionic acid (AMPA) receptors and not NMDA receptors. The rates of glutamate AMPA receptor-mediated spontaneous excitatory postsynaptic currents (sEPSCs) and GABA/glycine receptor-mediated spontaneous inhibitory postsynaptic currents (sIPSCs) remains constant for a few days after eye opening and then surge by four-fold around 2 weeks after eye opening. The rates of both sEPSCs and sIPSPs plateau by P60 (Figure 5(b)). The increase of the rate of RGC sEPSCs after eye opening might be partially attributed to a continuous increase of the number of synaptic contacts between bipolar and ganglion cells. The change in the rate of the RGC sIPSCs after eye opening, however, is more likely to reflect a change in the release probability of GABA/glycine of amacrine cells since the number of the conventional synapses in the IPL almost reaches the adult level at the time of eye opening.

Animals raised in darkness until P30 have significantly reduced rates of spontaneous RGC synaptic inputs. The frequencies of sEPSCs and sIPSCs fall to 35% and 48% of age-matched control animals raised in cyclic light/dark conditions, respectively (Tian, N. and Copenhagen, D. R., 2001). As with the NMDA-receptor-driven responses in RGCs, the rates of spontaneous events in dark-reared animals returned to those of cyclic light-reared mice after 6 days of cyclic light conditions. Dark rearing thus appears to delay the maturational increase in spontaneous synaptic inputs. Analysis of the amplitude and time-courses of the spontaneous synaptic currents strongly suggests that the suppression of RGC synaptic inputs induced by light deprivation does not influence the density of postsynaptic receptors or their single channel properties. Instead, it most likely reflects a reduction of the amount of glutamate released from presynaptic terminals (Tian, N. and Copenhagen, D. R., 2001) or the number of synaptic contacts. Future work will be required to determine how the release properties of amacrine and bipolar cells are regulated by visual inputs. Interestingly, even though the expression of NMDA receptors on RGCs and the release of vesicles are regulated by light, the peak expression of these two synaptic processes occurs at two different times. It is not known whether the developmental change in NMDA receptor expression regulates or triggers later occurring changes in release rates of glutamate and GABA/glycine.

1.24.1.2 Visual Experience Regulates the Maturation of Amacrine Cell Processes

Amacrine cells are interneurons in the inner retina. Amacrine cells extend their processes into different strata of the IPL where they can receive or transmit synaptic messages (see Masland, R. H., 2001; 2004, for an extensive structural analysis of amacrine cell classes and their processes, and Roska, B. and Werblin, F., 2001 for an example of the spatiotemporal processing served by amacrine cells). Using immunohistochemistry to identify structural arborization patterns of two classes of amacrine cell, separate groups have reported the development of serotonergic amacrine cells (Fosser, N. S. *et al.*, 2005) and cholinergic amacrine cells (Zhang, J. *et al.*, 2005) are influenced by visual stimulation.

1.24.1.2.1 Visual experience controls development of serotonergic amacrine cells in chick retina

In chicken retina, processes of serotoninergic (5-HT) amacrine cells arborize in two regions: an outer serotoninergic plexus is localized in the most distal layer of sublamina *a* of the IPL and an inner serotoninergic plexus is localized in the most proximal layers of sublamina *b* of the IPL. During postnatal development there is an age-dependent reduction in the number of processes in both the inner and the outer serotoninergic plexi, probably through developmental dendritic pruning. The serotonin amacrine cells of chicks raised in red-light from the time of hatching

had a significantly larger number of dendrites and varicosities. Thus, this change in 5HT amacrine cell dendritic arborization was interpreted as an inhibition of a visual activity-dependent dendritic pruning (Fosser, N. S. *et al.*, 2005). Although light seems to sculpt the serotonin amacrine cell processes, it is not known if the activity-dependent change in the morphology of serotonergic processes affects plasticity of visual functions in retina.

1.24.1.2.2 Visual deprivation reduces the number of detectable cholinergic amacrine cells and the extent of their processes in mouse retina

Visual activity reportedly modifies the maturation of mouse cholinergic amacrine cells during postnatal development (Zhang, J. *et al.*, 2005). In the vertebrate retina, cholinergic amacrine cells constitute a unique subpopulation of interneurons that contain acetylcholine and GABA and have processes confined to two narrow plexi in the IPL (Famiglietti, E. V., 1983; Vaney, D. I., 1984). Cholinergic amacrine cells mature relatively early in the retina. At birth, mouse cholinergic amacrine cells are already differentiated and their dendritic processes have projected specifically into the IPL. After birth, these cells undergo modest spatial rearrangement until 3 weeks after birth, which is characterized by the progressive increase of the thickness of the two cholinergic plexi and an increase of the space between the two plexi. Visual deprivation retarded the developmental processes occurring after eye opening, which resulted in thinner cholinergic plexi in the IPL, an interrupted mosaic of soma locations and reduced number of cholinergic immunoreactive cells. The effects induced by light deprivation could be reversed by returning the animals to normal dark/light conditions for 20–30 days (Zhang, J. *et al.*, 2005). In the adult retina, cholinergic amacrine cells synapse with bilaminated ON–OFF directional selective RGCs and mediate the directional selectivity of these RGCs (Famiglietti, E. V., 1991; Kittila, C. A. and Massey, S. C., 1997). In the immature retina, cholinergic synaptic transmission also plays an important role in mediating the spontaneous activity of RGCs during the early postnatal development before retina could respond to light (for review see Zhou, Z. J., 2001). Further study will be needed to determine whether visual deprivation affects these visual functions via the cholinergic amacrine cells.

1.24.2 Synaptic Circuitry Exhibits Plasticity in Response to Light and Dark Adaptation in Adult Retina

Visual stimulation regulates the refinement of retinal synaptic structures and functions in developing retina, a process which involves formation of new synapses and elimination of existing synapses and occurs over the course of days. In addition, visual stimulation can modify the strength and effectiveness of existing synapses in mature retina to alter the functional connectivity of retinal circuitry without any rewiring of the existing synaptic pathways. This process generally occurs in minutes and hours. We will term this type of plasticity as adaptive synaptic plasticity. Unlike the developmental synaptic plasticity, adaptive plasticity of synaptic wiring in mature retina is generally transitory and reversible and occurs at almost all level of retinal synaptic connections of many different species. We will first discuss microstructural changes and then cover functional alterations in synaptic connectivity and function.

1.24.2.1 Ambient Background Light Regulates Horizontal Cell Synapses and Gap Junction Coupling between Horizontal Cells

One of the most extensively studied examples of light-induced microstructural changes in retina is the transitory alteration of the synaptic processes linking photoreceptors and HCs. This has been documented primarily in fish retinas. Light can produce spinules, fingerlike protuberances of the HC dendritic membranes that project into the presynaptic terminals of photoreceptors. Spinulelike processes were first described in the rat hippocampus (Westrum, L. E. and Blackstad, T. W., 1962). In teleost retina, spinules are found in both outer plexiform layer (OPL) and IPL (Wagner, H. J., 1980; Dowling, J. E., 1987; Yazulla, S. and Studholme, K. M., 1992). They are most prominent on the dendritic terminals of HCs. During adaptation to brighter lights, numerous spinules arise from the terminal dendrites of HCs to invaginate the cone pedicles. Their presence may increase the contact area with the cone plasma membrane by up to 25% compared to the dark-adapted states. During dark adaptation, these spinules retract (Wagner, H. J., 1980).

The functional significance of HC spinules is still an open question. HCs are known to be involved in several different aspects of the visual process, such as

color signaling, spatial and temporal acuity, and the regulation of photoreceptor light sensitivity. It was suggested that HC spinules are the synaptic sites to generate biphasic chromatic responses in the retina. Support for this idea derives from the findings that the presence and absence of spinules is closely correlated with the development of biphasic chromatic responses in a class of cone HCs as well as the presence of color opponent responses in RGCs (see Wagner, H. J. and Djamgoz, M. B. A., 1993 for review). However, color-coding HCs are also present in other species that lack spinules completely (Simon, E. J., 1974), suggesting spinules might not be required for the chromatic signaling.

Both dopamine and glutamate are thought to act as neuromodulators to regulate spinule formation on HC dendrites, however multiple pathways may control their formation. The effect induced by light or exogenous dopamine on the spinule formation can be blocked most effectively by D1 antagonists (Kirsch, M. *et al.*, 1991; Behrens, U. D. *et al.*, 1992; Yazulla, S. *et al.*, 1996). Other studies suggested that dopamine receptor-associated mechanisms are probably not the only agents mediating the light-adaptive increase in spinule numbers since dopamine depletion or dopaminergic antagonists *in vivo* do not completely block the formation of spinules and the effect induced by dopamine is much weaker than that induced by light adaptation (Weiler, R. *et al.*, 1988; Kohler, K. *et al.*, 1990; Yazulla, S. *et al.*, 1996). Weiler R. *et al.* (1991) reported that activation of protein kinase C by phorbol esters promotes the formation of new HC spinules in dark-adapted animals, in retinas depleted of dopaminergic neurons and in synaptically isolated HCs, demonstrating that they have a direct action on the spinule-formation of these cells.

The dark-induced degradation of spinules may be controlled by glutamate released from photoreceptors. Glutamate or kainate application in isolated light-adapted retina effectively reduced the number of HC spinules to dark-adaptive levels (Weiler, R. *et al.*, 1988) probably through activation of AMPA receptors (Weiler, R. and Schultz, K., 1993). A more recent study suggested that calcium-influx through AMPA/kainite receptors during dark adaptation and subsequent activation of calmodulin-dependent protein kinase II (CaMKII) is an important step for spinule retraction (Schultz, K. *et al.*, 2004).

HCs have been found to be electrically coupled by gap junctions in virtually every vertebrate class studied. This coupling generally is between cells of the same subtype, that is, A-type HC to A-type HCs and B-type to B-type HCs in mammalian retina (see Webvision for details). Light adaptation regulates the conductance of intercellular gap junction coupling as revealed by the modulation of dye coupling from one injected cell to its neighbors and by the changes in receptive field size to light flashes. In rabbit retina, both A- and B-type HCs are uncoupled in the dark and receptive fields are relatively small. Increases of background illumination from roughly 0.25 log units above the threshold intensity for rods to approximately 1.5 log units above rod threshold resulted in increased dye coupling from an injected cell to its neighbors. Concomitantly, receptive fields enlarged. Further increases in background illumination reduced dye coupling and receptive field sizes to dark-adapted levels (Xin, D. and Bloomfield, S. A., 1999). Background light-induced changes in horizontal receptive field dimensions have been studied in nonmammalian retinas (Baldridge, W. H. and Ball, A. K., 1991). An extensive literature exists on the role of dopamine and other neuromodulators in regulating gap junctional conductance in both nonmammalian retina (see Witkovsky, P. and Dearry, A., 1992 for review) and mammalian retinas (see Witkovsky, P., 2004 for review).

1.24.2.2 Light and Dark Conditions Modify the Morphology of Bipolar Cell Axons

In the inner retina, bipolar cells are presynaptic to amacrine cells; amacrine cells, in turn, synapse back onto the bipolar terminals. In teleost retina, spinules evaginate from the terminals of the mixed rod–cone type of bipolar cell, and invaginate a substantial fraction of the presynaptic processes of amacrine cells. Yazulla S. and Studholme K. M. (1991) first described spinules on goldfish bipolar cell terminals in both sublaminas *a* and *b* of the IPL. Spinules of ON and OFF bipolar terminals responded oppositely to light and dark adaptation. Three-fold more of the mixed rod–cone ON bipolar terminals expressed spinules in the dark than in the light. In contrast, three-fold more OFF cone bipolar cells expressed spinules in the light versus the dark (Behrens, U. D. and Wagner, H. J., 1996).

Bipolar cells of mammals do not have spinules. However, mammalian rod ON bipolar cells also showed light/dark-related morphological changes at the surface of their synaptic terminals. Light-adapted axon terminals were round and smooth and exhibited more convexly curved synaptic membranes. In contrast, dark-adapted terminals had irregular contours, numerous dimples and a concave synaptic curvature (Behrens, U. D. *et al.*, 1998). Similar changes in

terminal morphology were observed in fish retinas (Yazulla, S. and Studholme, K. M., 1992; Behrens, U. D. and Wagner, H. J., 1996). Interestingly in rat retina, protein kinase C (PKC) immunoreactivity in light and dark was differentially localized in rod bipolar cells. In light-adapted rod bipolar cell axon terminals, PKC immunoreactivity was homogeneously distributed throughout the cytoplasm, whereas terminals from dark-adapted animals showed PKC immunoreactivity preferentially localized in the submembrane compartment and a reduced staining of the more central cytoplasm (Behrens, U. D. *et al.*, 1998).

1.24.2.3 Light and Dark Controls Gap Junction Coupling and Receptive Field Properties of Amacrine Cells

A large variety of amacrine cells provides both excitatory and inhibitory synaptic inputs to bipolar, ganglion as well as other amacrine cells (for review of subtypes see Webvision and Masland, R. H., 2001; 2004). AII amacrine cells, the most extensively studied amacrine cell in mammalian retina, connect rod-driven visual signals from rod bipolar cells to cone bipolar cells by forming glycinergic chemical synapses with OFF cone bipolar cells in sublamina *a* and gap junctional synapses with ON cone bipolar cells in sublamina *b* of the IPL (Famiglietti, E. V. and Kolb, H., 1975; Strettoi, E. *et al.*, 1992; 1994). AII amacrine cells also receive synaptic inputs from OFF cone bipolar cells (Strettoi, E. *et al.*, 1992; 1994; Sterling, P., 1995). This input accounts for nearly 40% of the chemical synaptic inputs from bipolar cells. Thus, AII amacrine cells receive and transmit both rod and cone signals. In addition, neighboring AII amacrine cells couple to each other through gap junctions (Famiglietti, E. V. and Kolb, H., 1975; Vaney, D. I., 1991; Strettoi, E. *et al.*, 1992). Intercellular coupling between AII amacrine cells can be modulated by background light. Coupling between AII amacrine cells and bipolar cells can be modulated by dopamine and nitric oxide (NO) released in the retina, both of which are regulated by light stimulation (see reviews of Witkovsky, P. and Dearry, A., 1992; Bloomfield, S. A., 2001).

By measuring the extent of neurobiotin found in neighboring neurons after injection into a single AII amacrine, Xin D. and Bloomfield S. A. (1997) demonstrated that there was dramatic increase in tracer coupling to both AII amacrine cells and cone bipolar following exposure to dim background lights. These dim background conditions increased the number of tracer labeled AII amacrine cells from 20, on average, in dark-adapted retinas to over 300 in dim backgrounds (Figure 6). As with HC tracer coupling

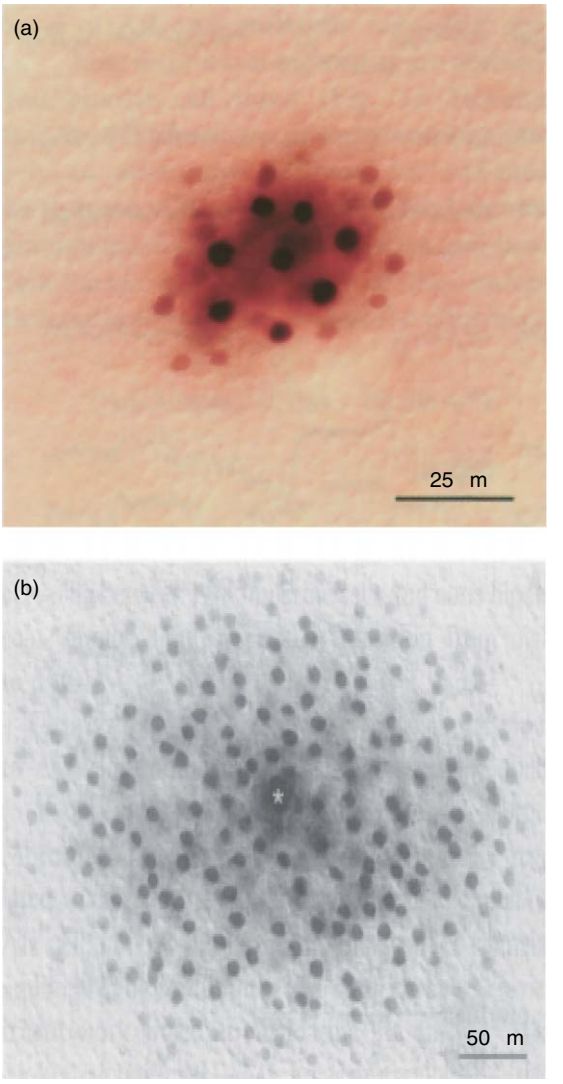

Figure 6 Light and dark controls gap junction coupling of AII amacrine cells. (a) Image of the tracer coupling pattern of AII amacrine cells in a dark-adapted retina following injection of neurobiotin into a single AII amacrine cell. The injected AII amacrine cell (center of the image) was well-coupled with seven surrounding AII amacrine cells to form an inner ring of eight darkly labeled AII amacrine cells and lightly coupled with other 10–15 more remote AII amacrine cells. (b) Image of tracer-coupled AII amacrine cells in a retina exposed to a log −5.5 intensity full-field illumination for 1 h prior to the injection of neurobiotin. The injected AII amacrine cell (star) was well coupled with many surrounding AII amacrine cells. Adapted from Bloomfield, S. A. 2001. Plasticity of AII amacrine cell circuitry in mammalian retina. Prog. Brain Res. 131, 185–200, with permission from Elsevier.

brighter backgrounds reduced the number of coupled cells back to the number found in dark-adapted retinas.

Background lights also regulated functional aspects of the receptive fields of the AII amacrine cells. In dark-adapted retina, AII amacrine cell receptive fields display a stereotypic ON-center-OFF-surround organization with a relatively small ON-center, extending only approximately 60–80 μm across the retina, and an OFF-surround extending 100–130 μm. The small receptive field of a dark-adapted AII amacrine cell reflects their narrow dendritic arbors and coupling to a relatively small group of neighboring AIIs. Dim background lights, which produced a so-called light-sensitized condition, increased the size of their ON-center and OFF-surround receptive fields. The ON-center receptive field measures approximately 6–7 times the size of the center receptive fields of AII amacrine cells in dark-adapted retinas. AII amacrine cells characterized in light-adapted retinas showed ON-center and OFF-center responses but did not display OFF-surround activity (Xin, D. and Bloomfield, S. A., 1999).

1.24.2.4 A Possible Mechanism by Which Light and Dark Could Regulate Synapse Strength Between Bipolar and Amacrine Cells

An activity-dependent modulation of the feedforward-feedback synapses between bipolar axon terminals and amacrine cell processes has been revealed in goldfish retina (Vigh, J. *et al.*, 2005). Although this modulation has not been shown to be regulated by light *per se*, this mechanism could easily control neurotransmitter output from bipolar cells under different lighting conditions. This recent study showed that synaptically released glutamate from goldfish Mb-type bipolar cell terminals activates mGluR1 receptors on amacrine cells. Activation of the mGluR1 receptors occurred only after bipolar cells were strongly depolarized briefly or depolarized for prolonged periods. Once mGluR1 was activated, it boosted the reciprocal negative feedback by enhancing GABA release from amacrine cells to the bipolar cells. Therefore, it was proposed that after prolonged stimulation reciprocal synapses between GABAergic amacrine cell and bipolar cells undergo an mGluR1-mediated long-term plasticity that lasts for several minutes. This mGluR1-mediated long-term potentiation of the GABAergic reciprocal feedback participates in downscaling the output of very active ON-type bipolar cells.

1.24.2.5 Light Can Regulate the Expression of α-Amino-3-Hydroxy-5-Methylisoxazole-4-Propionic Acid-Glutamate Receptors on Retinal Ganglion Cells

Background light is known to decrease the amplitude and sensitivity of light-evoked ganglion cell responses (Green, D. G. *et al.*, 1975; Green, D. G. and Powers, M. K., 1982). Although some of this desensitization and response compression reflects the behavior of photoreceptors, a significant component, particularly at dimmer intensities, is due to changes in the signaling properties of the inner retina (Green, D. G. and Powers, M. K., 1982). Given that the expression of AMPA-type glutamate receptors can be regulated by activity in cortical and hippocampal neurons (Malinow, R. and Malenka, R. C., 2002; Lu, H. C. *et al.*, 2003; Takahashi, T. *et al.*, 2003; Tomita, S. *et al.*, 2004), it is a intriguing idea that light adaptation could regulate glutamate receptor expression on retinal neurons (Thoreson, W. B. and Witkovsky, P., 1999). Xia Y. *et al.* (2006) reported that 8 hours or more of dark adaptation upregulated the rate of AMPA receptor cycling in ON RGCs. While net surface expression of AMPA receptors was not shown to be linked directly to changes in the amplitude and sensitivity of light-evoked responses, this study is a first step to demonstrate a light-dependent functional rewiring of synaptic inputs to retinal neurons that could be controlled by the trafficking of postsynaptic neurotransmitter receptors to locations opposite presynaptic release sites.

1.24.2.6 Light and Dark Adaptation Controls Receptive Field Organization of Retinal Ganglion Cells

Ganglion cell receptive field center sizes have been shown to increase with dark adaptation (Peichl, L. and Wassle, H., 1983; DeVries, S. H. and Baylor, D. A., 1997). Surround fields of RGCs become weaker with dark adaptation (Barlow, H. B. *et al.* 1957; Jensen, R. J., 1991; Muller, J. F. and Dacheux, R. F., 1997). It has been argued that the loss of surround fields in darkness is a tradeoff that allows greater spatial summation at the cost of reduced visual acuity. The cellular mechanisms responsible for these receptive field alterations have not been worked out. Interestingly, the decreased sensitivity of RGC surround fields with

dark adaptation is opposite to that of AII amacrine cells in which surrounds were more prominent in dark-adapted conditions. The dissimilarities underscore the idea that multiple activity-dependent mechanisms contribute to the functional structure of the receptive fields of retinal neurons.

1.24.3 Survival Rewiring of Retinal Circuits

Mature retinal synaptic circuits can show structural adjustments as a result of degenerative conditions or dysfunctions caused by the loss or mutation of key proteins in phototransduction or synaptic signaling pathways. This seemingly compensatory rewiring may or may not follow the original paths of the synaptic wiring of normal retina, but is nonetheless often considered a way that the retina readjusts itself to maintain some semblance of visual signaling.

Examples of this compensatory synaptic rewiring are the instances of the sprouting or rearrangement of synaptic connections between photoreceptors and bipolar cells in retinal degenerations or the sprouting of dendritic processes of second-order retinal neurons resulting from retinal detachments or loss of visual signaling from rods and cones. Although retinal rewiring under pathological conditions is not usually considered to be plasticity, this process is generally accompanied with changes in expression of specific proteins and/or transcriptional factors, which resemble the normal developmental processes. Neural remodeling that includes loss and sprouting of dendritic processes, degeneration of presynaptic structures and cellular reorganization has been extensively reviewed by others (Marc, R. E. *et al.*, 2003; Strettoi, E. *et al.*, 2003). Below, we will highlight some of the examples of synaptic rewiring in which new synaptic contacts are formed or in which new dendrites or axons sprout in a manner that suggests an attempt by the retina to either maintain former connections or search for new ones.

1.24.3.1 Rewiring of Synaptic Connections in Outer Retina in Response to Photoreceptor Degeneration or Loss of Synaptic Signaling

The extent and form of synaptic rewiring in the OPL seems to depend on the severity and time course of the degeneration of rods and cones. In mice with rapid rod and cone degeneration, such as *rd/rd*, rod bipolar dendrites are never fully formed (Strettoi, E. and Pignatelli, V., 2000; Strettoi, E. *et al.*, 2002). In these mice, rod bipolar dendritic processes retract and eventually disappear. Dendritic processes of rod-driven HCs in *rd/rd* mice also retract and vanish. However, these cells transiently sprout processes that reach into the inner retina and arborize. Cone bipolar cells progressively degenerate. In $crx^{-/-}$ mice, which have a slower rate of rod degeneration than *rd/rd* mice and have slower cone degeneration as well, rod and cone bipolar cells initially form dendritic processes in the OPL, but then these are degraded leading to loss of all dendrites and eventual bipolar cell death. HCs show the same morphological changes as in *rd/rd* mice but over a longer time period (Pignatelli, V. *et al.*, 2004).

In the P347L transgenic pig, a rhodopsin mutation that produces a prolonged degeneration and loss of rods but a slower and less severe loss of cones, rod bipolar cells are seen to extend dendritic processes to cone synaptic terminals (Peng, Y. W. *et al.*, 2000). The interpretation of the presence of these new processes, rarely seen in wild-type animals, is that the bipolar cells have tried to establish ectopic synaptic contact with surviving photoreceptors. The formation of similar ectopic synapses was observed in degenerative RCS rat retina, in which rods and cones develop normally initially and then there is a progressive loss of rods after about 3 weeks of age (Peng, Y. W. *et al.*, 2003). Therefore, the formation of ectopic synapses can be considered an activity-dependent rewiring of normally developed retina. Consistent with this idea, Haverkamp S. *et al.* (2006) found that cone bipolar cells form ectopic synapses with rods in a transgenic (*CNGA3*−/−) mouse model, which loses the function of cones with minimum loss of cone photoreceptors. In contrast, input-deprived rod bipolar cells form ectopic synapses with functional cones in *Rho*−/− mice, which loses the rod function without significant loss of rod photoreceptors. In addition, neither cone nor rod bipolar cells form ectopic synapses with inoperable cones or rods in the *CNGA3*−/−*Rho*−/− mouse. Sprouting of denditric processes from HCs and ON bipolar cells into the ONL and formation of ectopic synapses is also observed in mice lacking the essential synaptic protein bassoon in photoreceptors (Dick, O. *et al.*, 2003), and in mice with a mutant form of the calcium channel (α1f) that regulates exocytosis of glutamate from photoreceptors (Chang, B. *et al.*, 2006).

1.24.3.2 Survival Plasticity of Retinal Wiring in Retinal Detachments

Retinal detachment in mature animals triggers a reorganization of retinal circuits that include sprouting of bipolar and HC dendrites into the ONL. In experimental retinal detachments, rod bipolar cell processes grow into the ONL within 1 day. These outgrowing rod bipolar cell dendrites could persist in the ONL for a long time even after the detached retina was reattached (Lewis, G. P. *et al*., 1998; 2002; Fisher, S. K. and Lewis, G. P., 2003). Interestingly, most of these dendrites appear to remain connected to withdrawn rod terminals even though most of these dendrites have lost their deep synaptic invaginations. Thus, the outgrowth of rod bipolar cell dendrites appear to be target-directed. The synaptic terminals of both rods and cones, in contrast, change their morphology to appear more like synapses in immature retina (Erickson, P. A. *et al*., 1983; Linberg, K. A. and Fisher, S. K., 1990; Lewis, G. P. *et al*., 1998). Therefore, this remodeling of photoreceptor-bipolar cell synaptic connections might share the same underlying regulatory mechanisms for that of normal development. Upon reattachment of the detached retina, rod axons appear to regrow into the OPL and sometimes overshoot to growing into the inner retina (Fisher, S. K. and Lewis, G. P., 2003). This phenomenon has also been identified in early developing retina (Johnson, P. T. *et al*., 1999). The morphology of HCs also changes dramatically in the detached retina. Dendritic processes extend into the ONL and axonal-like processes may extend into proximal retina.

Little is known about the effect of retinal detachment on the inner retinal neurons. One recent study revealed that both gene expression and dendritic structure of RGCs are also affected in detached retina. The expression of both neurofilament protein and GAP43, a molecule associated with axon growth and targeted synaptogenesis during development, are upregulated in RGCs after detachment (Coblentz, F. E. *et al*., 2003). Thus, the effects of synaptic rewiring induced by retinal detachment extend across the entire neural network of the retina.

References

Amthor, F. R., Oyster, C. W., and Takahashi, E. S. 1984. Morphology of ON–OFF direction-selective ganglion cells in the rabbit retina. Brain Res. 298, 187–190.

Baldridge, W. H. and Ball, A. K. 1991. Background illumination reduces horizontal cell receptive-field size in both normal and 6-hydroxydopamine-lesioned goldfish retinas. Vis. Neurosci. 7, 441–450.

Bansal, A., Singer, J. H., Hwang, B. J., Xu, W., Beaudet, A., and Feller, M. B. 2000. Mice lacking specific nicotinic acetylcholine receptor subunits exhibit dramatically altered spontaneous activity patterns and reveal a limited role for retinal waves in forming ON and OFF circuits in the inner retina. J. Neurosci. 20, 7672–7681.

Barlow, H. B., Fitzhugh, R., and Kuffler, S. W. 1957. Change of organization in the receptive fields of the cat's retina during dark adaptation. J. Physiol. 137, 338–354.

Behrens, U. D. and Wagner, H. J. 1996. Adaptation-dependent changes of bipolar cell terminals in fish retina: effects on overall morphology and spinule formation in Ma and Mb cells. Vision Res. 36, 3901–3911.

Behrens, U. D., Kasten, P., and Wagner, H. J. 1998. Adaptation-dependent plasticity of rod bipolar cell axon terminal morphology in the rat retina. Cell Tissue Res. 294, 243–251.

Behrens, U. D., Wagner, H. J., and Kirsch, M. 1992. cAMP-mediated second messenger mechanisms are involved in spinule formation in teleost cone horizontal cells. Neurosci. Lett. 147, 93–96.

Bisti, S., Gargini, C., and Chalupa, L. M. 1998. Blockade of glutamate-mediated activity in the developing retina perturbs functional segregation of ON and OFF pathways. J. Neurosci. 18, 5019–5025.

Bloomfield, S. A. 2001. Plasticity of AII amacrine cell circuitry in mammalian retina. Prog. Brain Res. 131, 185–200.

Bodnarenko, S. R. and Chalupa, L. M. 1993. Stratification of ON and OFF ganglion cell dendrites depends on glutamate-mediated afferent activity in the developing retina. Nature 364, 144–146.

Bodnarenko, S. R., Jeyarasasingam, G., and Chalupa, L. M. 1995. Development and regulation of dendritic stratification in retinal ganglion cells by glutamate-mediated afferent activity. J. Neurosci. 15, 7037–7045.

Bodnarenko, S. R., Yeung, G., Thomas, L., and McCarthy, M. 1999. The development of retinal ganglion cell dendritic stratification in ferrets. Neuroreport 10, 2955–2959.

Boyden, E. S., Katoh, A., and Raymond, J. L. 2004. Cerebellum-dependent learning: the role of multiple plasticity mechanisms. Annu. Rev. Neurosci. 27, 581–609.

Chalupa, L. M., Jeyarasasingam, G., Snider, C. J., and Bodnarenko, S. R. 1998. Development of ON and OFF Retinal Ganglion Cell Mosaics. In: Development and Organization of the Retina: from Molecules to Function (*eds*. L. M. Chalupa and B. L. Finlay), pp. 77–89. Plenum.

Chang, B., Heckenlively, J. R., Bayley, P. R., Brecha, N. C., Davisson, M. T., Hawes, N. L., Hirano, A. A., Hurd, R. E., Ikeda, A., Johnson, B. A., McCall, M. A., Morgans, C. W., Nusinowitz, S., Peachey, N. S., Rice, D. S., Vessey, K. A., and Gregg, R. G. 2006. The nob2 mouse, a null mutation in Cacna1f: anatomical and functional abnormalities in the outer retina and their consequences on ganglion cell visual responses. Vis. Neurosci. 23, 11–24.

Coblentz, F. E., Radeke, M. J., Lewis, G. P., and Fisher, S. K. 2003. Evidence that ganglion cells react to retinal detachment. Exp. Eye Res. 76, 333–342.

Coombs, J., van der List, D., Wang, G. Y., and Chalupa, L. M. 2006. Morphological properties of mouse retinal ganglion cells. Neuroscience 140, 123–136.

Dann, J. F., Buhl, E. H., and Peichl, L. 1988. Postnatal dendritic maturation of alpha and beta ganglion cells in cat retina. J. Neurosci. 8, 1485–1499.

Daw, N. W. and Wyatt, H. J. 1974. Raising rabbits in a moving visual environment: an attempt to modify directional selectivity in the retina. J. Physiol. 240, 309–330.

Dearry, A. and Burnside, B. 1986. Dopaminergic regulation of cone retinomotor movement in isolated teleost retinas: I.

Induction of cone contraction is mediated by D2 receptors. J. Neurochem. 46, 1006–1021.
DeVries, S. H. and Baylor, D. A. 1997. Mosaic arrangement of ganglion cell receptive fields in rabbit retina. J. Neurophysiol. 78, 2048–2060.
Diao, L., Sun, W., Deng, Q., and He, S. 2004. Development of the mouse retina: emerging morphological diversity of the ganglion cells. J. Neurobiol. 61, 236–249.
Dick, O., tom Dieck, S., Altrock, W. D., Ammermuller, J., Weiler, R., Garner, C. C., Gundelfinger, E. D., and Brandstatter, J. H. 2003. The presynaptic active zone protein bassoon is essential for photoreceptor ribbon synapse formation in the retina. Neuron 37, 775–786.
Dowling, J. E. 1987. The Retina. Belknap Press.
Erickson, P. A., Fisher, S. K., Anderson, D. H., Stern, W. H., and Borgula, G. A. 1983. Retinal detachment in the cat: the outer nuclear and outer plexiform layers. IOVS 24, 927–942.
Famiglietti, E. V., Jr. 1983. ''Starburst'' amacrine cells and cholinergic neurons: mirror-symmetric on and off amacrine cells of rabbit retina. Brain Res. 261, 138–144.
Famiglietti, E. V. 1991. Synaptic organization of starburst amacrine cells in rabbit retina: analysis of serial thin sections by electron microscopy and graphic reconstruction. J. Comp. Neurol. 309, 40–70.
Famiglietti, E. V. and Kolb, H. 1975. A bistratified amacrine cell and synaptic circuitry in the inner plexiform layer of the retina. Brain Res. 84, 293–300.
Famiglietti, E. W. and Kolb, H. 1976. Structure basis for ON- and OFF-center responses in retinal ganglion cells. Science 194, 193–195.
Feng, G., Mellor, R. H., Bernstein, M., Keller-Peck, C., Nguyen, Q. T., Wallace, M., Nerbonne, J. M., Lichtman, J. W., and Sanes, J. R. 2000. Imaging neuronal subsets in transgenic mice expressing multiple spectral variants of GFP. Neuron 28, 41–51.
Fisher, L. J. 1979. Development of synaptic arrays in the inner plexiform layer of neonatal mouse retina. J. Comp. Neurol. 187, 359–372.
Fisher, S. K. and Lewis, G. P. 2003. Muller cell and neuronal remodeling in retinal detachment and reattachment and their potential consequences for visual recovery: a review and reconsideration of recent data. Vision Res. 43, 887–897.
Fosser, N. S., Brusco, A., and Rios, H. 2005. Darkness induced neuroplastic changes in the serotoninergic system of the chick retina. Dev. Brain Res. 160, 211–218.
Green, D. G. and Powers, M. K. 1982. Mechanisms of light adaptation in rat retina. Vision Res. 22, 209–216.
Green, D. G., Dowling, J. E., Siegel, I. M., and Ripps, H. 1975. Retinal mechanisms of visual adaptation in the skate. J. Gen. Physiol. 65, 483–502.
Greiner, J. V. and Weidman, T. A. 1981. Histogenesis of the ferretretina. Exp. Eye Res. 33, 315–332.
Guenther, E., Schmid, S., Wheeler-Schilling, T., Albach, G., Grunder, T., Fauser, S., and Kohler, K. 2004. Developmental plasticity of NMDA receptor function in the retina and the influence of light. FASEB J. 18, 1433–1435.
Haverkamp, S., Michalakis, S., Claes, E., Seeliger, M. W., Humphries, P., Biel, M., and Feigenspan, A. 2006. Synaptic plasticity in CNGA3–/– mice: cone bipolar cells react on the missing cone input and form ectopic synapses with rods. J. Neurosci. 26, 5248–5255.
Jensen, R. J. 1991. Involvement of glycinergic neurons in the diminished surround activity of ganglion cells in the dark-adapted rabbit retina. Vis. Neurosci. 6, 43–53.
Johnson, P. T., Williams, R. R., Cusato, K., and Reese, B. E. 1999. Rods and cones project to the inner plexiform layer during development. J. Comp. Neurol. 414, 1–12.
Johnson, J., Tian, N., Caywood, M. S., Reimer, R. J., Edwards, R. H., and Copenhagen, D. R. 2003. Vesicular neurotransmitter transporter expression in developing postnatal rodent retina: GABA and glycine precede glutamate. J. Neurosci. 23, 518–529.
Kirsch, M., Wagner, H. J., and Djamgoz, M. B. A. 1991. Dopamine and plasticity of horizontal cell function in the teleost retina: regulation of a spectral mechanism through D1-receptors. Vision Res. 31, 401–412.
Kittila, C. A. and Massey, S. C. 1997. Pharmacology of directionally selective ganglion cells in the rabbit retina. J. Neurophysiol. 77, 675–689.
Kohler, K., Kolbinger, W., Kurg-Isler, G., and Weiler, R. 1990. Endogenous dopamine and cyclic events in the fish retina. II: Correlation of retino motor movement, spinule formation, and connexon density of gap junctions with dopamine activity during light/dark cycles. Vis. Neurosci. 5, 417–428.
Lamb, T. D. and Pugh, E. N., Jr. 2004. Dark adaptation and the retinoid cycle of vision. Prog. Retin. Eye Res. 2, 307–380.
Landi, S., Cenni, M. C., Maffei, L., and Berardi, N. 2007. Environment enrichment effects on development of retinal ganglion cell dendritic stratification require retinal BDNF. PLOS ONE 2, e346.
Lewis, G. P., Charteris, D. G., Sethi, C. S., and Fisher, S. K. 2002. Animal models of retinal detachment and reattachment: identifying cellular events that may affect visual recovery. Eye 16, 375–387.
Lewis, G. P., Linberg, K. A., and Fisher, S. K. 1998. Neurite outgrowth from bipolar and horizontal cells after experimental retinal detachment. IOVS 39, 424–440.
Linberg, K. A. and Fisher, S. K. 1990. A burst of differentiation in the outer posterior retina of the eleven-week human fetus. Vis. Neurosci. 5, 43–60.
Liu, X., Grishanin, R. N., Tolwani, R. J., Renteria, R. C., Xu, B., Reichardt, L. F., and Copenhagen, D. R. 2007. Brain-derived neurotrophic factor and TrkB modulate visual experience-dependent refinement of neuronal pathways in retina. J. Neurosci. 27.
Lu, H. C., She, W. C., Plas, D. T., Neumann, P. E., Janz, R., and Crair, M. C. 2003. Adenylyl cyclase I regulates AMPA receptor trafficking during mouse cortical ''barrel'' map development. Nat. Neurosci. 6, 939–947.
Malinow, R. and Malenka, R. C. 2002. AMPA receptor trafficking and synaptic plasticity. Annu. Rev. Neurosci. 25, 103–126.
Marc, R. E., Jones, B. W., Watt, C. B., and Strettoi, E. 2003. Neural remodeling in retinal degeneration. Prog. Retin. Eye Res. 22, 607–655.
Marquardt, T. and Gruss, P. 2002. Generating neuronal diversity in the retina: one for nearly all. Trends Neurosci. 25, 32–38.
Masland, R. H. 1977. Maturation of function in the developing rabbit retina. J. Comp. Neurol. 175, 275–286.
Masland, R. H. 2001. Neuronal diversity in the retina. Curr. Opin. Neurobiol. 11, 431–436.
Masland, R. H. 2004. Neuronal cell types. Curr. Biol. 14, R497–R500.
Maslim, J. and Stone, J. 1986. Synaptogenesis in the retina of the cat. Brain Res. 373, 35–48.
Maslim, J. and Stone, J. 1988. Time course of stratification of the dendritic fields of ganglion cells in the retina of the cat. Dev. Brain Res. 44, 87–93.
Mehta, V. and Sernagor, E. 2006. Receptive field structure–function correlates in developing turtle retinal ganglion cells. Eur. J. Neurosci. 24, 787–794.
Muller, J. F. and Dacheux, R. F. 1997. Alpha ganglion cells of the rabbit retina lose antagonistic surround responses under dark adaptation. Vis. Neurosci. 14, 395–401.
Nelson, R., Famiglietti, E. V. J., and Kolb, H. 1978. Intracellular staining reveals different levels of stratification for ON- and OFF-center ganglion cells in cat retina. J. Neurophysiol. 41, 472–483.

Nishimura, Y. and Rakic, P. 1987. Synaptogenesis in the primate retina proceeds from the ganglion cells towards the photoreceptors. Neurosci. Res. Suppl. 6, S253–S268.
Peichl, L. and Wassle, H. 1983. The structural correlate of the receptive field centre of alpha ganglion cells in the cat retina. J. Physiol. 341, 309–324.
Peng, Y. W., Hao, Y., Petters, R. M., and Wong, F. 2000. Ectopic synaptogenesis in the mammalian retina caused by rod photoreceptor-specific mutations. Nat. Neurosci. 3, 1121–1127.
Peng, Y. W., Senda, T., Hao, Y., Matsuno, K., and Wong, F. 2003. Ectopic synaptogenesis during retinal degeneration in the royal college of surgeons rat. Neuroscience 119, 813–820.
Pignatelli, V., Cepko, C. L., and Strettoi, E. 2004. Inner retinal abnormalities in a mouse model of Leber's congenital amaurosis. J. Comp. Neurol. 469, 351–359.
Pow, D. V. and Barnett, N. L. 2000. Developmental expression of amino acid transporter 5: a photoreceptor and bipolar cell glutamate transporter in rat retina. Neurosci. Lett. 280, 21–24.
Redburn, D. A. and Madtes, P. 1987. GABA – its roles and development in retina. Prog. Ret. Eye Res. 6, 69–84.
Roska, B. and Werblin, F. 2001. Vertical interactions across ten parallel, stacked representations in the mammalian retina. Nature 410, 583–587.
Sassoe-Pognetto, M. and Wässle, H. 1997. Synaptogenesis in the rat retina: subcellular localization of glycine receptors, GABA(A) receptors, and the anchoring protein gephyrin. J. Comp. Neurol. 381, 158–174.
Schultz, K., Janssen-Bienhold, U., Gundelfinger, E. D., Kreutz, M. R., and Weiler, R. 2004. Calcium-binding protein caldendrin and CaMKII are localized in spinules of the carp retina. J. Comp. Neurol. 479, 84–93.
Sernagor, E. and Grzywacz, N. M. 1996. Influence of spontaneous activity and visual experience on developing retinal receptive fields. Curr. Biol. 6, 1503–1508.
Simon, E. J. 1974. Feedback loop between cones and horizontal cells in the turtle retina. Fed. Proc. 33, 1078–1082.
Sterling, P. 1995. Tuning retinal circuits. Nature 377, 676–677.
Strettoi, E. and Pignatelli, V. 2000. Modifications of retinal neurons in a mouse model of retinitis pigmentosa. Proc. Natl. Acad. Sci. U. S. A. 97, 11020–11025.
Strettoi, E., Dacheux, R. F., and Raviola, E. 1992. Synaptic connections of the narrow-field, bistratified rod amacrine cell (AII) in the rabbit retina. J. Comp. Neurol. 325, 152–168.
Strettoi, E., Dacheux, R. F., and Raviola, E. 1994. Cone bipolar cells as interneurons in the rod pathway of the rabbit retina. J. Comp. Neurol. 347, 139–149.
Strettoi, E., Pignatelli, V., Rossi, C., Porciatti, V., and Falsini, B. 2003. Remodeling of second-order neurons in the retina of rd/rd mutant mice. Vision Res. 43, 867–877.
Strettoi, E., Porciatti, V., Falsini, B., Pignatelli, V., and Rossi, C. 2002. Morphological and functional abnormalities in the inner retina of the rd/rd mouse. J. Neurosci. 22, 5492–5504.
Tagawa, Y., Sawai, H., Ueda, Y., Tauchi, M., and Nakanishi, S. 1999. Immunohistological studies of metabotropic glutamate receptor subtype 6-deficient mice show no abnormality of retinal cell organization and ganglion cell maturation. J. Neurosci. 19, 2568–2579.
Takahashi, T., Svoboda, K., and Malinow, R. 2003. Experience strengthening transmission by driving AMPA receptors into synapses. Science 299, 1585–1588.
Thoreson, W. B. and Witkovsky, P. 1999. Glutamate receptors and circuits in the vertebrate retina. Prog. Retin. Eye Res. 18, 765–810.
Tian, N. and Copenhagen, D. R. 2001. Visual deprivation alters development of synaptic function in inner retina after eye opening. Neuron 32, 439–443.
Tian, N. and Copenhagen, D. R. 2003. Visual stimulation is required for refinement of ON and OFF pathways in postnatal retina. Neuron 39, 85–96.
Tomita, S., Fukata, M., Nicoll, R. A., and Bredt, D. S. 2004. Dynamic interaction of stargazin-like TARPs with cycling AMPA receptors at synapses. Science 303, 1508–1511.
Vaney, D. I. 1984. ''Coronate'' amacrine cells in the rabbit retina have the ''starburst'' dendritic morphology. Proc. R. Soc. Lond. B Biol. Sci. 220, 501–508.
Vaney, D. I. 1991. Many diverse types of retinal neurons show tracer coupling when injected with biocytin or neurobiotin. Neurosci. Lett. 125, 187–190.
Vigh, J., Li, G. L., Hull, C., and von Gersdorff, H. 2005. Long-term plasticity mediated by mGluR1 at a retinal reciprocal synapse. Neuron 46, 469–482.
Wagner, H. J. 1980. Light-dependent plasticity of the morphology of horizontal cell terminals in cone pedicles of fish retinas. J. Neurocytol. 9, 573–590.
Wagner, H. J. and Djamgoz, M. B. A. 1993. Spinules: a case for retinal synaptic plasticity. Trends Neurosci. 16, 201–206.
Wang, G. Y., Liets, L. C., and Chalupa, L. M. 2001. Unique functional properties of ON and OFF pathways in the developing mammalian retina. J. Neurosci. 21, 4310–4317.
Weiler, R. and Schultz, K. 1993. Ionotropic non-N-methyl-D-aspartate agonists induce retraction of dendritic spinules from retinal horizontal cells. Proc. Natl. Acad. Sci. U. S. A. 90, 6533–6537.
Weiler, R., Kohler, K., and Janssen, U. 1991. Protein kinase C mediates transient spinule-type neurite outgrowth in the retina during light adaptation. Proc. Natl. Acad. Sci. U. S. A. 88, 3603–3607.
Weiler, R., Kohler, K., Kirsch, M., and Wagner, H. J. 1988. Glutamate and dopamine modulate synaptic plasticity in horizontal cell dendrites of fish retina. Neurosci. Lett. 87, 205–209.
Westrum, L. E. and Blackstad, T. W. 1962. An electron microscopic study of the stratum radiatum of the rat hippocampus (regio superior, CA 1) with particular emphasis on synaptology. J. Comp. Neurol. 119, 281–309.
Witkovsky, P. 2004. Dopamine and retinal function. Doc. Ophthalmol. 108, 17–40.
Witkovsky, P. and Dearry, A. 1992. Functional roles of dopamine in the vertebrate retina. Prog. Retin. Res. 11, 247–292.
Wong, R. O. L. 1990. Differential growth and remodelling of ganglion cell dendrites in the postnatal rabbit retina. J. Comp. Neurol. 294, 109–132.
Wong, R. O. L. and Ghosh, A. 2002. Activity-dependent regulation of dendritic growth and patterning. Nat. Rev. Neurosci. 3, 803–812.
Xia, Y., Carroll, R. C., and Nawy, S. 2006. State-dependent AMPA receptor trafficking in the mammalian retina. J. Neurosci. 26, 5028–5036.
Xin, D. and Bloomfield, S. A. 1997. Tracer coupling pattern of amacrine and ganglion cells in the rabbit retina. J. Comp. Neurol. 383, 512–528.
Xin, D. and Bloomfield, S. A. 1999. Comparison of the responses of AII amacrine cells in the dark- and light-adapted rabbit retina. Vis. Neurosci. 16, 653–665.
Xu, H. P. and Tian, N. 2004. Pathway-specific maturation, visual deprivation, and development of retinal pathway. Neuroscientist 10, 337–346.
Xu, H-P. and Tian, N. 2007. Retinal ganglion cell dendrites undergo a visual activity-dependent redistribution after eye opening. J. Comp. Neurol. 503, 244–259.
Yamasaki, E. N. and Ramoa, A. S. 1993. Dendritic remodelling of retinal ganglion cells during development of the rat. J. Comp. Neurol. 329, 277–289.
Yazulla, S. and Studholme, K. M. 1991. Glycine-receptor immunoreactivity in retinal bipolar cells is postsynaptic

to glycinergic and GABAergic amacrine cell synapses. J. Comp. Neurol. 310, 11–12.
Yazulla, S. and Studholme, K. M. 1992. Light-dependent plasticity of the synaptic terminals of Mb bipolar cells in goldfish retina. J. Comp. Neurol. 320, 521–530.
Yazulla, S., Lin, Z. S., and Studholme, K. M. 1996. Dopaminergic control of light-adaptive synaptic plasticity and role in goldfish visual behavior. Vision Res. 36, 4045–4057.
Young, R. W. 1985. Cell differentiation in the retina of the mouse. Anat. Rec. 212, 199–205.
Zhang, J., Yang, Z., and Wu, S. M. 2005. Development of cholinergic amacrine cells is visual activity-dependent in the postnatal mouse retina. J. Comp. Neurol. 484, 331–343.
Zhou, Z. J. 2001. The function of the cholinergic system in the developing mammalian retina. Prog. Brain Res. 131, 599–613.

Further Reading

Kohler, K. and Weiler, R. 1990. Dopaminergic modulation of transient neurite outgrowth from horizontal cells of the fish Retina is not mediated by cAMP. Eur. J. Neurosci. 2, 788–794.
Young, R. W. 1985. Cell differentiation in the retina of the mouse. Anat. Rec. 212, 199–205.

Relevant Website

http://webvision.med.utah.edu – Webvision: The Organization of the Retina and Visual System.

1.25 Retinal Ganglion Cell Types and Their Central Projections

D M Berson, Brown University, Providence, RI, USA

© 2008 Elsevier Inc. All rights reserved.

1.25.1	**Introduction**	491
1.25.2	**Ganglion Cell Types**	492
1.25.2.1	Morphological Classification	493
1.25.2.2	Physiological Classification	494
1.25.2.3	Structure–Function Correlations	494
1.25.2.4	Homologous Retinal Ganglion Cell Types in Mammalian Retinas	494
1.25.3	**A Survey of Some Conserved Ganglion Cell Types**	494
1.25.3.1	Melanopsin-Expressing Retinal Ganglion Cells	495
1.25.3.2	ON Direction-Selective Cells	497
1.25.3.3	Local Edge Detectors	499
1.25.3.4	ON–OFF Direction-Selective Cells	501
1.25.3.5	Alpha Cells	502
1.25.3.6	Beta Cells	505
1.25.4	**Retinofugal Projections and Their Origin in Specific Ganglion Cell Types**	506
1.25.4.1	Methods for Linking Retinofugal Projections to Retinal Ganglion Cell Types	506
1.25.4.2	Lateral Geniculate Complex and Dorsal Thalamus	507
1.25.4.3	Superior Colliculus	509
1.25.4.4	Accessory Optic System	511
1.25.4.5	Pretectal Region	511
1.25.4.6	Hypothalamic Region	512
1.25.4.7	Other Targets	513
References		513

Glossary

antidromic activation Induction of an action potential in a neuronal soma by triggering a spike in its axon and allowing it to propagate in a retrograde direction.

bistratified Having a dendritic arbor occupying two distinct levels of the inner plexiform layer.

costratification The arborization of the dendrites of two distinct cell types at the same level of the inner plexiform layer.

homologous cell types Cell types in different species sharing a common evolutionary origin.

monostratified Having a dendritic arbor restricted to a single level of the inner plexiform layer.

paramorphic pair A pair of neuronal cell types differing from one another mainly at the level of dendritic stratification, but otherwise more similar to one another than to other types.

retinal eccentricity Distance of a retinal location from the fovea or other site of maximum acuity.

retinal ganglion cell A neuron of the vertebrate retina that contributes an axon to the optic nerve.

1.25.1 Introduction

The eye communicates with the brain exclusively through the axons of retinal ganglion cells (RGCs). Since the seminal work of Ramon y Cajal in the late nineteenth century, it has been recognized that RGCs are remarkably heterogeneous in form, especially in the depth of stratification and the lateral spread of their dendrites in the plane of the retina. During the latter half of the twentieth century, single

unit recordings paved the way for an appreciation of the diversity these cells also exhibit in their functional properties. The emergence of anterograde and retrograde axoplasmic tract tracing methods revealed that retinofugal axons were distributed to a bewildering array of central visual targets and that individual retinorecipient targets received input from subsets of RGCs.

It has long been recognized that the structure, function, and central projections of RGCs are highly correlated. An enduring goal of visual neurobiologists has been to exploit these correlations to devise a comprehensive classification of ganglion cells and to reveal the unique roles of individual types in visual behavior and perception. For a comprehensive review of the intellectual roots and early history of this effort, the reader is referred to the excellent book by Stone J. (1983). In this chapter, an overview of more recent progress in this area has been presented. It is intended to serve as a bridge between the preceding chapters on selected RGC types, and the chapters to follow, which consider individual central visual nuclei and their functional roles.

Those courageous enough to make even a brief foray into the labyrinth of ganglion cell taxonomy quickly recognize that the literature in this area is large, unruly, and extraordinarily difficult to wrestle into coherency. There are wide disparities among studies in the empirical basis for classification, in the numbers of types defined, and in the properties and nomenclature applied to those types. This is true even within a single species and even when limiting consideration to only morphological or only physiological studies. The tenuous linkage between structural and functional observations further complicates the matter. Finally, only tentative steps have been made toward achieving the long-term goal of itemizing fully the RGC types providing input to each of the retinorecipient subnuclei of the brainstem and diencephalon. Much of the evidence in this area is fragmentary and defies generalization across mammalian orders.

Given the complexity, the focus in this chapter is on broad organizational principles and informative examples rather than a comprehensive itemization of the available data. The chapter begins with survey of some general principles of ganglion-cell taxonomy and of the evolution of techniques for characterizing and classifying these cells. It then describes a handful of RGC types that appear to be highly conserved across mammalian phylogeny and summarizes their salient characteristics. I will review the current state of knowledge about the range of central targets innervated by retinofugal axons, and relate these, where possible, to specific subtypes of RGCs.

1.25.2 Ganglion Cell Types

Before grappling with the complexities of individual ganglion cell types in diverse retinas, it is worth summarizing some general principles that have emerged from the work of the past several decades. These are covered in further detail in several fine reviews, theoretical manuscripts, and books (Rowe, M. H. and Stone, J., 1977; Wässle, H., 1982; Rodieck, R. W. and Brening, R. K., 1983; Stone, J., 1983; Wässle, H. and Boycott, B. B., 1991; Rodieck, R. W., 1998; Masland, R. H., 2001a). First, it now seems beyond question that mammalian retinas contain more than a dozen distinct types of RGCs. Any concerted effort at classification of these cells requires analysis of the systematic covariation of as many features of these cells as practical (Rowe, M. H. and Stone, J., 1977; Rodieck, R. W. and Brening, R. K., 1983; Rodieck, R. W., 1998). These have traditionally focused on structural and functional data, but future studies can be expected to incorporate genomic and proteomic analyses as well. In retinas with central retinal specializations (i.e., a fovea, area centralis, or visual streak), it is of particular importance to appreciate the enormous influence of retinal location (i.e., eccentricity), which, in turn, specifies local ganglion cell density. This density dictates the spatial precision or the grain of each type's representation by specifying how widely a member of that type deploys its dendrites across the retinal surface to sample the array of bipolar (and amacrine) cell inputs. In primate, cat, and rabbit retinas, cells of a single type exhibit radical eccentricity-dependent rescaling in the sizes of dendritic and receptive fields. In fact, this systematic variation in size within a type is often much greater than that between distinct types intermingled at a single retinal location.

There is broad consensus that the process of identifying biologically meaningful cell types consists of identifying, either implicitly or explicitly, clusters of points in multidimensional parameter space, with each point representing a single cell (Rowe, M. H. and Stone, J., 1977; Stone, J., 1983; Rodieck, R. W. and Brening, R. K., 1983; Rodieck, R. W., 1998). Types that are discovered according to these principles have proven, without any obvious exception, to form regular mosaics, with cells spaced from one another and

their dendritic field profiles arranged so as to efficiently tile the retinal surface (see Chapter Mosaics, Tiling and Coverage by Retinal Neurons for review).

1.25.2.1 Morphological Classification

Classification of RGCs by their structural features is most advanced in retinas of rabbit, cat, mouse, and primate, and this chapter thus focuses mainly on data from these species. The broad outlines of RGC taxonomy were established in early studies using Golgi, Nissl, and neurofibrillar stains (see Stone, J., 1983 for review). Progress accelerated significantly with the introduction of methods for intracellular dye filling. Initially this was achieved by iontophoresis through intracellular sharp electrodes in fixed or living tissue (e.g., Buhl, E. H. and Peichl, L., 1986; Dann, J. F. and Buhl, E. H., 1987; Dacey, D. M., 1989; Pu, M. L. and Amthor, F. R., 1990a; 1990b; Rodieck, R. W. and Watanabe, M., 1993). More recent innovations include the use of ballistic particle-mediated delivery of lipophilic fluorescent dyes or of genes coding for fluorescent proteins (e.g., Rockhill, R. L. *et al.*, 2002; Sun, W. *et al.*, 2002a; 2002b); various photofilling methods (e.g., Rockhill, R. L. *et al.*, 2002; Dacey, D. M. *et al.*, 2003); and the development of transgenic mouse strains in which marker proteins are expressed under the control of cell-type-specific promoters (Badea, T. C. and Nathans, J., 2004; Hattar, S. *et al.*, 2002; 2006; Kong, J. H. *et al.*, 2005; Coombs, J. *et al.*, 2006).

The two morphological parameters that have proven of the greatest power for RGC classification are the dendritic field size (when considered in association with eccentricity, as noted above) and the depth of stratification of dendrites within the inner plexiform layer (IPL). The latter parameter is typically quantified as a percentage of the distance between the inner and outer boundaries of the IPL, but distinctions between certain similar types require greater precision. This can be achieved by assessing the stratification of the RGC in relation to that of cells with well-established and narrow stratification in the same or adjoining sublayers (e.g., Famiglietti, E. V., 1992; Berson, D. M. *et al.*, 1998; Yamada, E. S. *et al.*, 2005). A particular useful fiducial marker of this sort is the paired bands of immunostaining for choline acetyltransferase (ChAT), with each band formed by dendrites of one of the two types of starburst amacrine cells (ON or OFF). Beyond dendritic stratification and field size, other useful parameters of dendritic structure include the number and density of branch points, branch angles, and various higher-order statistics capturing the architecture of the dendritic profile. The dimensions of the soma and thickness of the axon can be very informative for a few types, but for most others the overlap with other types on these measures is too great for them to be of much value.

Even with the application of powerful staining methods and quantitative morphometry in well-studied retinas, and despite years of concerted effort by many laboratories, no consensus exists about the precise number of structural RGC types or about the validity of many of the specific types proposed. This is partly because many of the studies conducted to date have been more descriptive than quantitative and have drawn upon a few examples of individual proposed types rather than a large sample obtained at many eccentricities. A few attempts have been made using objective cluster analysis to analyze multiparametric data sets on the full RGC population (Badea, T. C. and Nathans, J., 2004; Kong, J. H. *et al.*, 2005; Coombs, J. *et al.*, 2006). However, the collection and entry of large numbers of parameters for a large set of RGCs is extremely labor intensive, and most of the progress made to date has been made with less comprehensively quantitative approaches on large libraries of filled cells or by narrowing the scope to subpopulations of RGCs selected on the basis of cell size, retrolabeling from specific targets, or other distinctive features.

Many RGC types occur as paramorphic pairs (Famiglietti, E. V., Jr. and Kolb, H., 1976). These consist of two subtypes differing from one another in the stratification of their dendrites, but otherwise resembling one another far more than they do other RGC types. In such cases, one subtype arborizes in the outer (OFF) sublayer of the IPL and the other in the inner (ON) sublayer. Because their dendrites stratify in a relatively narrow plane within the IPL, these paramorphic types are said to be monostratified. Other ganglion cell types are monostratified but appear to lack a paramorphic partner. These may arborize in the ON sublayer, the OFF sublayer, or at the boundary between them. Still other types are broadly stratified or bistratified, with dendrites in both ON and OFF sublayers. Examples of all of these arrangements have been observed in every well-studied mammalian retina. Stratification is predictive of receptive-field center type, so that monostratified cells are generally known or presumed to be either ON or OFF center. In contrast,

monostratified RGCs stratifying at the ON/OFF sublayer border, as well as broadly stratified or bistratified RGCs, are known or presumed to have mixed ON–OFF receptive field centers.

1.25.2.2 Physiological Classification

The functional properties of RGCs have been most fully studied in cats, rabbits, and primates and attempts at systematic classification have progressed furthest in these species. Until very recently, functional information has come mainly from single-unit studies, with recordings made *in vivo* either intraocularly from the RGC somas or intracranially from their axons in the optic tract. The introduction of *in vitro* methods, and especially of the multielectrode array method, has greatly accelerated the rate at which recordings, especially of relatively rare types, can be obtained and has already been exploited to classify mammalian RGCs (Devries, S. H. and Baylor, D. A., 1997).

Most of the functional parameters that have been exploited in physiological classification efforts consist of various aspects of receptive-field organization. Among those most widely exploited are the size and sign (ON, OFF, or ON–OFF) of the receptive field center, the time course of response to a step in illumination (sustained or transient), and the linearity of spatial summation. Selectivity for stimulus wavelength, direction of motion, or orientation has often helped to identify specific RGC types. Biophysical properties such as peak firing rate (briskness), spike shape, and axonal conduction velocity have also proven useful in many cases, and the analysis of specific voltage-gated conductances may prove to be productive in intracellular studies (O'Brien, B. J. *et al.*, 2002).

1.25.2.3 Structure–Function Correlations

Cell types identified on the basis of morphological or physiological features alone far outnumber those for which both structure and function are known. When the form and function of single cells cannot be made directly, provisional associations can be made by exploiting well-established correlations between structural and functional features. For example, dendritic field areas are generally predictive of receptive field center sizes; dendritic stratification can be used to infer receptive-field center sign (ON, OFF, or ON–OFF); and axon caliber determines conduction velocity. Patterns of central projection can be used to indirectly link form and function because they can determined in anatomical experiments using retrograde labeling, and in physiological ones by antidromic activation. For central targets receiving input mainly from one or a few types, such correlations can be very informative. However, convincing linkages between form and function generally require intracellular recording followed by dye filling. The technical demands of such work are substantial and remain a significant impediment to developing a comprehensive integrative taxonomy.

1.25.2.4 Homologous Retinal Ganglion Cell Types in Mammalian Retinas

As efforts to devise robust classification schemes for RGCs have advanced in individual species, similarities between certain types in different species have encouraged the view that at least some of these types may be homologous, with lineages traceable to a common progenitor type in the last shared ancestor of the species in which the types are observed. In principle, some types might even be shared by all mammals or even by all vertebrates. Examples of types for which such homology might be obtained are discussed below. However, the evidence for such homologies is relatively scanty even in the clearest cases, and it is far from obvious how far this approach can be pushed. There is no help to be found in the fossil record. For extant retinas, the difficulty is partly that we lack sufficient data on enough cells in a large enough number of species. It may also be because homologous types have undergone such significant remodeling in the course of mammalian evolution that the common features are obscured. Finally, it is possible that entirely new RGC types have emerged independently during mammalian evolution, perhaps many times in multiple mammalian lineages. Efforts to seek equivalents of every known type across all mammals may thus be an exercise in futility.

1.25.3 A Survey of Some Conserved Ganglion Cell Types

Intensive work on ganglion cell classification has been ongoing for more than 30 years. There is thus a wealth of data concerning the structure, function, and projections of these cells in many mammalian species. Much of this information is qualitative or

fragmentary, and thus resists integration across observational domains (structure, function, and projection) and across species. A comprehensive survey of the literature relevant to individual species is beyond the scope of this chapter, and the reader is referred to Table 1 for a listing of selected papers on RGC types based on morphological, physiological, or combined structural and functional data. In this chapter, the focus is on a handful of types that most closely approach the ideal implicit in ganglion cell taxonomy, namely, types for which structure and function have been convincingly correlated and which have apparently been conserved in retinas of diverse mammalian orders.

1.25.3.1 Melanopsin-Expressing Retinal Ganglion Cells

The type most closely approaching this ideal is the melanopsin-expressing intrinsically photosensitive retinal ganglion cell (ipRGC). The salient characteristics of this type include their expression of the novel opsin melanopsin, their intrinsic photosensitivity, and their projections to brain regions mediating so-called nonimaging-forming visual functions. This cell type is the subject of the Chapter Melanopsin Cells, to which the reader is referred for details concerning their discovery, morphology, functional properties, and behavioral roles (see also Chapter The Suprachiasmatic Nucleus).

To summarize briefly, studies in rodents demonstrated that a rare population of ganglion cells (<2% of all RGCs) express melanopsin, project to the circadian pacemaker in the suprachiasmatic nucleus (SCN), and are intrinsically photosensitive (Provencio, I. *et al.*, 2000; 2002; Gooley, J. J. *et al.*, 2001; Berson, D. M. *et al.*, 2002; Hannibal, J. *et al.*, 2002; Hattar, S. *et al.*, 2002; Warren, E. J. *et al.*, 2003). These cells have a large, very sparsely branching dendritic arbor that stratifies narrowly in the outermost sublayer of the IPL (Berson, D. M. *et al.*, 2002; Hattar, S. *et al.*, 2002; Provencio, I. *et al.*, 2002; Hannibal, J. *et al.*, 2002; Coombs, J. *et al.*, 2006). This cell type appears highly conserved among mammals. It is present not only in several other rodents (blind mole rat: Hannibal, J. *et al.*, 2002; hamster: Sollars, P. J. *et al.*, 2003; Morin, L. P. *et al.*,

Table 1

Species	*Morphological types*	*Physiological types*	*Structure–function*
Primate	Yamada E. S. *et al.* (1996; 2005) Rodieck R. W. and Watanabe M., (1993) Watanabe M. and Rodieck R. W. (1989) Kolb H. Dacey D. M. (1993b) Dacey D. M. (1994) Dacey D. M. and Brace S. (1992) Dacey D. M. and Petersen M. R. (1992), Dacey *et al.* (2003), fire works Dacey D. M. (2004) Dacey D. M. *et al.* (2005) Kolb H. *et al.* (1992) Perry V. H. and Cowey A. (1981; 1984(?)) Peterson B. B. and Dacey D. M. (1999; 2000) Polyak S. L. (1941) Rodieck book? Silveira L. C. *et al.* (1994) Crook J. D. *et al.* (2007) Ghosh K. K. *et al.* (1996; 1997) Silveira L. C. *et al.* (1999)	Gouras P. (1969) Chapter "The P, M and K Streams of the Primate Visual System: What Do They Do for Vision?" Dacey D. M. *et al.* (2005) Lee B. B. *et al.* (2000) de Monasterio F. M. and Gouras P. (1975) de Monasterio F. M. *et al.* (1976) de Monasterio F. M. (1978a; 1978b) Schiller P. H. and Malpeli J. G. (1977)	Dacey D. M. (1993a) Dacey D. M. and Lee B. B. (1994) Dacey D. M. (2004) Dacey D. M. *et al.* (2005)

(*Continued*)

Table 1 (Continued)

Species	*Morphological types*	*Physiological types*	*Structure–function*
Cat	O'Brien B. J. *et al.* (2002) Berson D. M. *et al.* (1998; 1999), Isayama T. *et al.* (2000) Boycott B. B. and Wässle H. (1974) Stone J. (1983) Pu M. *et al.* (1994) Pu M. (1999) Dacey D. M. (1989) Famiglietti E. V. (1987) Kolb H. *et al.* (1981) Leventhal A. G. *et al.* (1980)	Stone J. (1983) Cleland B. G. and Levick W. R. (1974a; 1974b) Stone J. and Fukuda Y. (1974) Troy *et al.* (1989)	Stanford L. R. and Sherman S. M. (1984); Stanford L. R. (1987) Stone J. (1983) Fukuda Y. (1984) Saito H. A. (1983) Peichl L. and Wassle H. (1983) Pu M. *et al.* (1994)
Ferret	Vitek D. J. *et al.* (1985) Wingate R. J. *et al.* (1992)		
Rabbit	Pu M. L. and Amthor, F. R. (1990a; 1990b) Rockhill R. L. *et al.* (2002), van Wyk M. *et al.* (2006); ON–OFF DS papers Buhl E. H. and Peichl L. (1986) Famiglietti E. V. (1987; 1992a; 1992b; 2004; 2005) Peichl L. *et al.* (1987a) Roska B. *et al.* (2006) He S. and Masland R. H. (1998); Zhang J. *et al.* (2005)	Barlow H. B. and Hill R. M. (1963), Barlow H. B. *et al.* (1964) Caldwell J. H. and Daw N. W. (1978) Devries S. H. and Baylor D. A. (1997) Levick W. R. (1967) Oyster C. W. and Barlow H. B. (1967) Vaney D. I. *et al.* (1981a) Roska B. *et al.* (2001; 2006)	Amthor F. R. *et al.* (1984; 1989a; 1989b); He S. and Masland R. H. (1998); Roska B. and Werblin F. (2001); Roska B. *et al.* (2001; 2006) van Wyk M. *et al.* (2006) Bloomfield S. A. and Xin D. (1997) Jensen R. J. (1991) Ackert J. M. *et al.* (2006)
Mouse	Coombs J. *et al.* (2006) Badea T. C. and Nathans J. (2004) Kong J. H. *et al.* (2005) Sun W. *et al.* (2002b) Sun W. *et al.* (2006) Doi M. *et al.* (1995) Schubert T. *et al.* (2005) Provencio I. (2002?) Volgyi B. *et al.* (2005) Weng S. *et al.* (2005)	Stone C and Pinto L. H. (1993); Carcieri S. M. *et al.* (2003); Sagdullaev and McCall (2005)	Pang J. J. *et al.* (2003) Weng S. *et al.* (2005), Lucas *et al.*, (2003)
Rat	Huxlin K. R. and Goodchild A. K. (1997), Sun W. *et al.* (2002a), Perry V. H. (1979), Hannibal J. Hattar S. *et al.* (2002), Peichl L. (1989), Thanos S. (1988), Dann J. F. and Buhl E. H. (1987), Dreher B. *et al.* (1985)	Fukuda Y. (1977) Hale P. T. *et al.* (1979) Berson D. M. *et al.* (2002)	
Squirrel	Rivera N. and Lugo N. (1998) Linberg K. A. *et al.* (1996), West R. W. and Dowling J. E. (1972)		
Other	Dann J. F. and Buhl E. H. (1990), Moraes A. M. *et al.* (2000), Peichl L. (1991) Peichl L. (1992) Wilson P. D. and Condo G. J. (1985)		

2003) but also in strikingly similar form in the primate retina (giant RGCs; human: Provencio, I. *et al.*, 2000; Rollag, M. D. *et al.*, 2003; Dacey, D. M. *et al.*, 2005; macaque: Dacey, D. M. *et al.*, 2005; see also Pu, M., 1999 for relevant data in cat). It should be noted, however, that the primate retina has two subtypes of melanopsin-expressing RGCs. One of these corresponds closely in form to the rodent type already described, except that the cell body is usually displaced to the inner nuclear layer (Dacey, D. M. *et al.*, 2005). The second type has a dendritic arbor stratifying within the innermost IPL. This type, which is also intrinsically photosensitive (Dacey, D. M. *et al.*, 2005), appears to have an equivalent in mice, because melanopsin immunostaining marks two tiers of dendrites in the IPL, one corresponding to the rodent type already described and a second in the inner IPL (Provencio, I. *et al.*, 2002). This second plexus can be traced to a distinct population of more poorly stained cells in the ganglion cell layer (Castrucci, A. M., Berson, D. M., and Provencio, I., unpublished observations).

Behavioral studies have implicated these cells not only in circadian entrainment and the pupillary light reflex but also in the photic modulation of nocturnal melatonin levels and the acute suppression of activity by light in nocturnal rodents (see Chapter Melanopsin Cells). The functional properties of these cells appear well matched to these functional roles, with remarkably sustained responses to steady illumination that stably encode global light intensity (Berson, D. M. *et al.*, 2002).

The most comprehensive picture of the efferent projections of these cells comes from a mouse line genetically modified to express beta-galactosidase in the axons of melanopsin RGCs (Hattar, S. *et al.*, 2002; 2006). Similar data are available in rat using PACAP immunoreactivity as a marker for axons originating from melanopsin RGCs (Hannibal, J. and Fahrenkrug, J., 2004), though the interpretation of these patterns is complicated by the presence of PACAP immunopositive axons of nonretinal origin. Other experiments, combining retrolabeling with *in situ* hybridization or antimelanopsin immunolabeling, confirm several of the major projections of melanopsin RGCs (Gooley, J. J. *et al.*, 2003; Sollars, P. J. *et al.*, 2003; Hattar, S. *et al.*, 2002; Berson, D. M. *et al.*, 2002; Morin, L. P. *et al.*, 2003; Dacey, D. M. *et al.*, 2005; Hannibal, J. *et al.*, 2002). Individual targets are discussed in the section on retinofugal projections and are also reviewed in Chapters Melanopsin Cells, The Suprachiasmatic Nucleus, and Pupillary Control Pathways. To summarize briefly, two of the most prominent targets are the SCN and the intergeniculate leaflet, a division of the lateral geniculate nucleus (LGN) that has been implicated in circadian regulation. Another major target is the olivary pretectal nucleus, the critical brainstem relay for the pupillary light reflex. Minor axonal targets include the preoptic region, supraoptic nucleus of the hypothalamus, amygdala, and the ventral division of the lateral geniculate nucleus (LGNv). Most of these projections are implicated in reflexive physiological responses to light in such domains as sleep and neuroendocrine function. However, at least sparse projections have also been traced to the superior colliculus and dorsal division of the LGN (LGNd), two structures playing key roles in higher-resolution form vision or visuomotor behaviors (Morin, L. P. *et al.*, 2003; Dacey, D. M. *et al.*, 2005; Hattar, S. *et al.*, 2006).

1.25.3.2 ON Direction-Selective Cells

A second highly conserved cell type for which there is excellent structural, physiological, and behavioral information is the ON direction-selective RGC (ON-DS cell). These large-field monostratified cells (Figure 1) encode the direction of whole-field visual motion (retinal slip) and relay this signal to the accessory optic system (AOS) of the brainstem, which drives optokinetic responses. A synopsis of the close functional interrelationships between ON-DS cells and the optokinetic system is provided below (see Section 1.25.4.4).

The ON-DS cell was originally recognized and described in the rabbit retina, and it remains by far best characterized in this species. The original physiological description was made by Barlow H. B. *et al.* (1964). Oyster C. W. and Barlow H. B. (1967) demonstrated that these cells preferred slow stimulus velocities and were grouped into three subtypes, each with a characteristic preferred direction: superior temporal, inferior temporal, or temporonasal. The morphology of rabbit ON-DS cells is well established. Oyster C. W. *et al.* (1980) made initial morphological observations on presumptive ON-DS cells using retrograde labeling from the AOS. Buhl E. H. and Peichl L. (1986) provided a detailed description of the somadendritic architecture of these cells by making intracellular dye injections into RGCs retrolabeled from the medial terminal nucleus of the AOS. This labeled a single morphological cell type, with a large soma, and a large dendritic field stratifying almost entirely within the ON sublayer of the IPL. Dendrites exhibited moderate branching density and a space-filling structure (Figure 1).

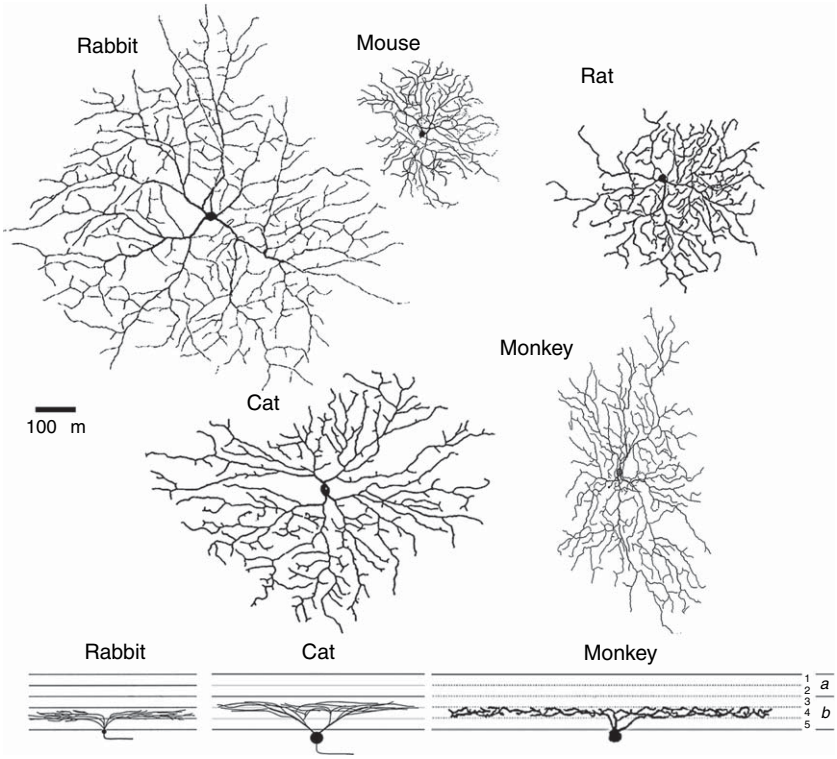

Figure 1 Morphology of known or presumed ON direction-selective (ON-DS) retinal ganglion cells in five mammalian species. Top panels show dendritic profiles as viewed in flatmounts. The rabbit and rat cells were dye-filled after retrograde labeling from the medial terminal nucleus of the accessory optic system. Rabbit RGCs with this morphology are known to be ON-DS cells physiologically (see text), and this was confirmed directly for the mouse cell illustrated. Cells with similar morphology are shown for cat and monkey retina. The contrast of some cells has been adjusted. Scale bar (=100 μm) applies to all of these profiles. Each of these types stratifies near the middle of the ON sublayer of the IPL, as shown below in schematic vertical sections. Panels have been resized and reoriented as needed for ready comparison. (Top panel, rabbit) From figure 2B of Buhl, E. H. and Peichl, L. 1986. Morphology of rabbit retinal ganglion cells projecting to the medial terminal nucleus of the accessory optic system. J. Comp. Neurol. 253(2), 163–174; and (top panel, rat) from figure 11 of Dann, J. F. and Buhl, E. H. 1987. Retinal ganglion cells projecting to the accessory optic system in the rat. J. Comp. Neurol. 262(1), 141–158; both © 1986, 1987 Alan R. Liss, Inc., reprinted with permission of Wiley-Liss, Inc., a subsidiary of John Wiley & Sons, Inc. (Top panel, mouse) From figure 2A of Sun, W., Deng, Q., Levick, W. R., and He, S. 2006. ON direction-selective ganglion cells in the mouse retina. J. Physiol. 576(Pt 1), 197–202, by permission of Wiley-Blackwell; © 2006 The Physiological Society. (Top panel, cat) Kappa cell from figure 1 of O'Brien, B. J., Isayama, T., Richardson, R., and Berson, D. M. 2002. Intrinsic physiological properties of cat retinal ganglion cells. J. Physiol. 538(Pt 3), 787–802, by permission of Wiley-Blackwell; © 2002 The Physiological Society. (Top panel, monkey) Recursive monostratified cell from figure 20.5 of Dacey, D. M. 2004. Origins of Perception: Retinal Ganglion Cell Diversity and the Creation of Parallel Visual Pathways. In: The Cognitive Neurosciences III (*ed.* M. S. Gazzaniga), pp. 281–301. MIT Press, by permission of MIT Press. (Bottom panel, rabbit) G10 type from figure 4 of Rockhill, R. L., Daly, F. J., MacNeil, M. A., Brown, S. P., and Masland, R. H. 2002. The diversity of ganglion cells in a mammalian retina. J. Neurosci. 22(9), 3831–3843. (Bottom panel, cat) Kappa cell, unpublished data: Isayama T., O'Brien B., and Berson D. (Bottom panel, monkey) Large moderate cell from figure 8 of Yamada, E. S., Bordt, A. S., and Marshak, D. W. 2005. Wide-field ganglion cells in macaque retinas. Vis. Neurosci. 22(4), 383–393. © 2005 Cambridge University Press.

Direct structure–function data confirming the identity of these cells as ON-DS cells was made by Amthor F. R. *et al.* (1989a) and later confirmed by He S. and Masland R. H. (1998) and Ackert J. M. *et al.* (2006). Several other purely morphological studies have elaborated the structural description of these cells, including their costratification and co-fasciculation with the dendrites of ON starburst cholinergic amacrine cells (Famiglietti, E. V., 1992 – ON-DS cells; Rockhill, R. L. *et al.*, 2002 – G10 cells; Dong, W. *et al.*, 2004; see also Yamada, E. S. *et al.*, 2005).

This ganglion cell type appears to be highly conserved in form and function in mammalian retinas, as does its role as the primary source of retinal input to AOS. As summarized in Figure 1, morphological types closely matching the rabbit ON-DS cells in branching

pattern and stratification have been observed in mouse (RG_{C1} of Sun, W. *et al.*, 2002b; 2006), rat (Dann, J. F. and Buhl, E. H., 1987), cat (kappa cell; O'Brien, B. J., *et al.* 2002 and unpublished observations), squirrel (G18; Linberg, K. A. *et al.*, 1996), and primate (recursive monostratified cell of Dacey, D. M., 2004; large moderate cell of Yamada, E. S. *et al.*, 2005). In several of these species, the apparent correspondence of these cell types to the rabbit ON-DS type has been strengthened by demonstrating that they can be labeled by retrograde transport from the AOS (rat: Dann, J. F. and Buhl, E. H., 1987) and by direct demonstration of ON-DS physiology (mouse: Sun, W. *et al.*, 2006). ON-DS cells have been encountered in extracellular surveys of cat ganglion cells (Stone, J. and Fukuda, Y., 1974). RGCs retrolabeled from the cat and monkey AOS, though incompletely characterized, are grossly similar to those in rabbits and rodents (Farmer, S. G. and Rodieck, R. W., 1982; Telkes, I. *et al.*, 2000). The functional properties of cells in the AOS are consistent with their input from ON-DS cells in the cat (Grasse, K. L. *et al.*, 1984), rat (van der Togt, C. *et al.*, 1993), and primate (Mustari, M. J. and Fuchs, A. F., 1989; Hoffmann, K. P. and Distler, C., 1989; see also Telkes, I. *et al.*, 2000).

Few projections outside of the accessory optic system have been documented for ON-DS ganglion cells. ON-DS cells preferring temporonasal motion project to the nucleus of the optic tract, a nucleus of the pretectal region closely linked to the AOS (Pu, M. L. and Amthor, F. R., 1990b; Gamlin, P. D., 2005). There is some evidence for a projection to the superior colliculus and LGNd (see below).

1.25.3.3 Local Edge Detectors

Another RGC type that appears highly conserved in mammalian retinas is a relatively small-field monostratified cell, arborizing near the boundary between the ON and OFF sublayers of the IPL, and having an ON–OFF receptive field center. The type is best characterized in the rabbit where it has been termed the local edge detector (LED), but apparently equivalent types have been described in primates, cats, and rodents.

The type was first described physiologically in rabbits by Levick W. R. (1967). His term "local edge detector" was intended to highlight the preference these cells exhibit for stimuli restricted to their small receptive field center and their poor responsiveness to large spots, full-field stimuli, or extended gratings. This selectivity has been attributed to the presence of a strong silent suppressive surround (Levick, W. R. 1967; van Wyk, M. *et al.*, 2006). Like ON–OFF-DS cells (see below), these cells respond well to both small light or dark spots, but unlike that type they exhibit no directional preference.

The morphology of rabbit local edge detectors was first characterized by Amthor F. R. *et al.* (1989a) on the basis of intracellular recording and dye filling, and has been confirmed by Roska B. *et al.* (2006) and van Wyk M. *et al.* (2006). A comprehensive analysis of this morphological type, which goes by various names, has been provided by Rockhill R. L. *et al.* (2002; G1 cell), Famiglietti E. V. (2005a; class IV, type 1, small tufted (IVst1) cell), and van Wyk M. *et al.* (2006; LED). They have the smallest dendritic field diameters of any rabbit ganglion cells. Their highly branched, tortuous dendrites rarely overlap one another (Figure 2). They form a monostratified arbor lying at or very near the boundary between the ON and OFF sublayers of the IPL, sandwiched between the ON and OFF tiers of the ON–OFF DS cell's dendritic arbor (and thus, by extension, between the inner and outer cholinergic bands) (Roska, B. *et al.*, 2006; van Wyk, M. *et al.*, 2006). In this position, these dendrites presumably collect synaptic inputs from both ON and OFF bipolar cell terminals stratifying near the ON/OFF sublaminar border.

Possible structural or functional equivalents of the rabbit LED have been encountered in a wide array of other mammalian retinas (Figure 2), although correlated structural and functional observations have yet to be made in most species. The picture is further complicated by the presence of multiple functional types with ON–OFF receptive field centers and several morphological types with relatively small, highly branched dendritic fields stratifying in mid-IPL.

Among the likely homologs of the LED type among other mammals, the best characterized is probably the zeta morphological type of cat retina (Berson, D. M. *et al.*, 1998; O'Brien, B. J. *et al.*, 2002). Except for the beta cell, these have the smallest dendritic field diameters of any cat RGCs, and their densely branched dendritic arbor is strikingly similar in form and stratification to the rabbit LED (Figure 2). Structure–function work indicates that this cell is, like the rabbit LED, an ON–OFF phasic type (O'Brien, B., Isayama, T., and Berson, D., unpublished observations). Cat ganglion cells with receptive fields resembling rabbit LEDs have been frequently encountered in physiological studies and have been referred to as ON–OFF phasic cells, and impressed-by-contrast cells as well as LEDs (Cleland, B. G. and Levick, W. R., 1974b; Stone, J. and Fukuda, Y., 1974; Troy *et al.*, 1989). A morphological type resembling the cat zeta cell has been described in the ferret,

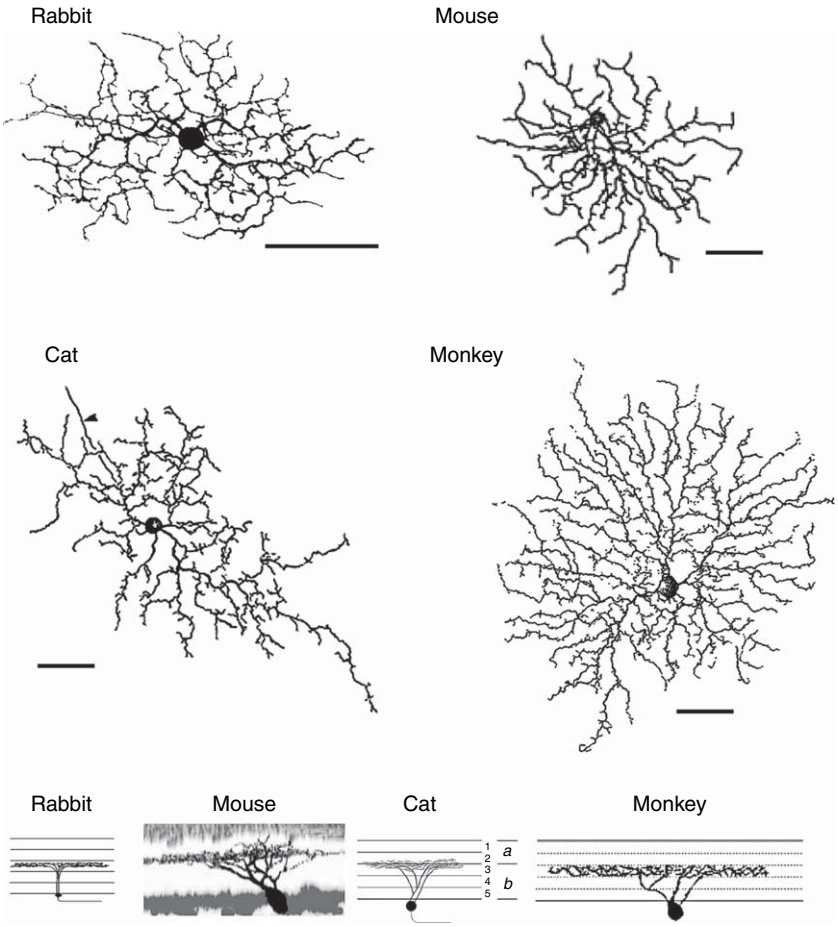

Figure 2 Morphology of ganglion cells of the local edge detector (LED) type in four mammalian retinas. Top panels show dendritic profiles as viewed in flatmounts. The contrast of some cells has been adjusted (and inverted for the rabbit cell) to promote comparisons. Each of these types stratifies near the boundary between the ON and OFF sublayers of the IPL, as shown below in digitally reconstructed or schematic vertical sections. Panels have been resized and reoriented as needed to facilitate comparison. Scale bars = 50 μm. The rabbit LED cell is taken from figure 2A of van Wyk, M., Taylor, W. R., and Vaney, D. I. 2006. Local edge detectors: a substrate for fine spatial vision at low temporal frequencies in rabbit retina. J. Neurosci. 26(51), 13250–13263. The cat RGC is a zeta cell, from figure 1G of Berson, D. M., Pu, M., and Famiglietti, E. V. 1998. The zeta cell: a new ganglion cell type in cat retina. J. Comp. Neurol. 399(2), 269–288. The mouse cell belongs to cluster 2 of Coombs, J., van der List, D., Wang, G. Y., and Chalupa, L. M. 2006. Morphological properties of mouse retinal ganglion cells. Neuroscience 140(1), 123–136, figure 2; © 2006 IBRO). The monkey RGC is a maze cell, from figure 7 of Rodieck, R. W. and Watanabe, M. 1993. Survey of the morphology of macaque retinal ganglion cells that project to the pretectum, superior colliculus, and parvicellular laminae of the lateral geniculate nucleus. J. Comp. Neurol. 338(2), 289–303; © 1993 Wiley-Liss, Inc., reprinted with permission of Wiley-Liss, Inc., a subsidiary of John Wiley & Sons, Inc. (Bottom panel, rabbit) G1 type from figure 4 of Rockhill, R. L., Daly, F. J., MacNeil, M. A., Brown, S. P., and Masland, R. H. 2002. The diversity of ganglion cells in a mammalian retina. J. Neurosci. 22(9), 3831–3843. (Bottom panel, mouse) Cluster 2 cell from figure 6 of Coombs, J., van der List, D., Wang, G. Y., and Chalupa, L. M. 2006. Morphological properties of mouse retinal ganglion cells. Neuroscience 140(1), 123–136. (© 2006, IBRO). (Bottom panel, cat) Zeta cell from figure 12 of Isayama, T., Berson, D. M., and Pu, M. 2000. Theta ganglion cell type of cat retina. J. Comp. Neurol. 417(1), 32–48. (Bottom panel, monkey) Narrow thorny cell from figure 8 of Yamada, E. S., Bordt, A. S., and Marshak, D. W. 2005. Wide-field ganglion cells in macaque retinas. Vis. Neurosci. 22(4), 383–393. © 2005 Cambridge University Press.

another carnivore (tight group of Wingate, R. J. *et al.*, 1992; see Berson, D. M. *et al.*, 1998 for details).

A strikingly similar monostratified type has been observed in primate retina by Rodieck R. W. and Watanabe M. (1993; their maze cell), although its level of stratification was not specified. The broad thorny cell illustrated by Dacey D. M. *et al.* (2003) appears to represent the same type and Dacey D. M.

(2004) reports preliminary evidence that this cell has a transient ON–OFF response to center stimulation. Yamada, E. S. *et al.* (2005) describe a cell type which they term narrow thorny and equate with the rabbit LED. This cell has an appropriate branching pattern and stratifies in the appropriate sublayer (between the ChAT bands). It should be noted, however, that they do not equate their cell with the maze cell of Rodieck R. W. and Watanabe M. (1993). Although the dendritic fields of all of these cell types are substantially larger than those of the midget and parasol cells, they nonetheless have among the smallest fields of any of the many RGCs that are neither midget nor parasol. ON–OFF phasic ganglion cells have been recorded extracellularly in macaque retina by Schiller P. H. and Malpeli J. G. (1977) and de Monasterio F. M. (1978).

In mice, several types of RGCs have small, highly branched dendritic fields and stratification near the interface between the ON and OFF sublayers of the IPL. These include the B2, B4, C4, and C5 types of Sun W. *et al.* (2002b), the M1 and M2 types of Coombs J. *et al.* (2006), cluster 1 cells of Kong J. H. *et al.* (2005), and clusters 1 and 2 of Badea T. C. and Nathans J. (2004). Similar types have been encountered in rat retina (RGB class of Huxlin, K. R. and Goodchild, A. K., 1997; B2 and perhaps B4 types of Sun, W. *et al.*, 2002a) and ground squirrels (G9 cells of Linberg, K. A. *et al.*, 1996). Some of these types, with denser, more highly overlapping dendritic profiles, may actually correspond less well to the rabbit LED than to the type 3 bistratified ganglion cell described in mouse by Schubert T. *et al.* (2005). This small-field type, like the cat theta cell (Isayama, T. *et al.*, 2000), to which it may be homologous, has such a densely branched dendritic arbor that its bistratification is difficult to discern on casual inspection. A compelling case for equivalence between any of these types and the LED is difficult because the differentiation among types is not as obvious in rodents as in the retinas of monkey, cat, or rabbit, and none of these studies used immunostaining of the ChAT plexuses or other fiducial markers for stratification. Nor is there any structure–function work on these types that would permit one to draw a equivalence based on physiological features. Nonetheless, it seems quite likely that cells analogous to the LED are present in rodent retina.

With respect to central projections, there is strong evidence for substantial contributions from this type to the retinocollicular projection, and conflicting evidence on their possible contribution to the retinogeniculate pathway. These outputs are considered more fully in Section 1.25.4.

1.25.3.4 ON–OFF Direction-Selective Cells

One of the best characterized types of RGC in any mammalian retina is a rabbit ganglion cell with an ON–OFF receptive field center and selectivity for the direction of stimulus motion. This ON–OFF DS cell, which has been definitively linked to a bistratified morphological type, is the focus in Chapter Direction-Selective Cells. The reader is referred to that chapter for information about the structure and function of this type and about current understanding of the synaptic basis of its directional preference.

Barlow H. B. and Hill R. M. (1963) provided the first functional description of these cells. Amthor F. R. *et al.* (1984; 1989a) used intracellular recording and dye filling to correlate this functional type with the type I bistratified morphological type, a finding that has been repeatedly confirmed (see Chapter Direction-Selective Cells). These cells have both somas and dendritic fields of intermediate size. A key structural feature is a clearly bistratified dendritic architecture, with an inner arbor costratifying with the cholinergic band in the ON sublayer of the IPL and the outer arbor costratifying with OFF cholinergic plexus (Famiglietti, E. V., 1992a).

Although nearly all the work on this cell type has been conducted in the rabbit retina, there is emerging evidence for the presence of homologous types in a variety of mammalian orders (Figure 3). In mice, an apparently homologous morphological type (RG_{D2} cell, Sun, W. *et al.*, 2002b; type 2 bistratified cell, Schubert, T. *et al.*, 2005) has recently been confirmed to be an ON–OFF DS type physiologically (Weng, S. *et al.*, 2005). In cat retina, ON–OFF DS cells have been encountered in extracellular recording surveys (Cleland, B. G. and Levick, W. R., 1974a; Stone, J. and Fukuda, Y., 1974), a bistratified morphological type with structural features strikingly similar to those of the rabbit type has been identified (Famiglietti, E. V., 1987, class IV, type 4; O'Brien, B. J. *et al.*, 2002, iota cell), and a preliminary structure/function correlation has made by recording and dye injection (O'Brien, B. J., Isayama, T., and Berson, D. M., unpublished observations). Similar morphological types have been reported in rat (RG_{D2} cell, Sun, W. *et al.*, 2002a), ground squirrel (G11; Linberg, K. A. *et al.*, 1996), and macaque (recursive monostratified cell of Dacey, D. M., 2004; multitufted cell of Yamada, E. S. *et al.*, 2005).

Remarkably little has been done to characterize the patterns of central projection of this cell type in any mammalian retina. However, there is at least

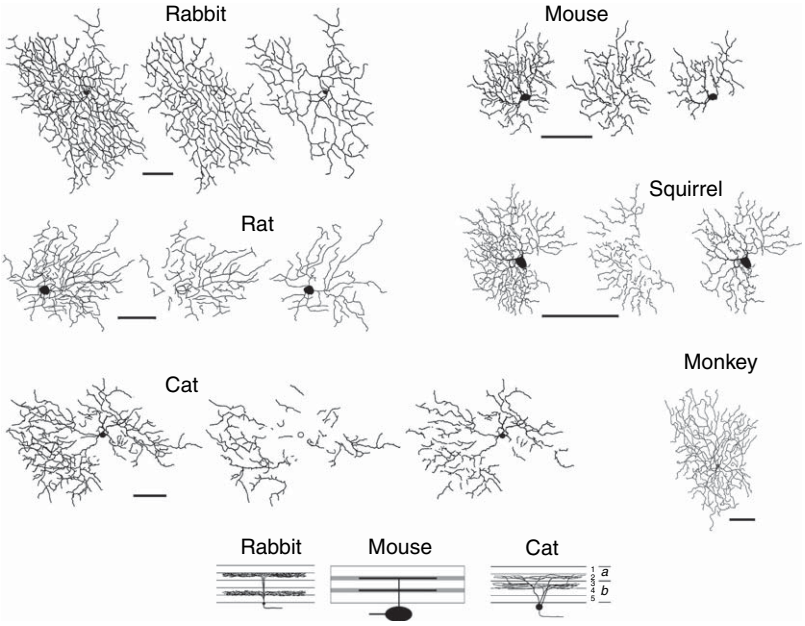

Figure 3 Morphology of known or presumed ON–OFF direction-selective (ON–OFF DS) retinal ganglion cells in six mammalian species. Top panels show dendritic profiles as viewed in flatmounts. Except for the monkey cell (lower right), each profile is shown three times. The leftmost is a representation of the entire profile, the middle shows only that part of the profile occupying the OFF sublayer of the IPL, and the right shows only the inner, ON arbor. The rabbit, mouse, and cat cells of this type have been physiologically confirmed to be ON–OFF DS cells physiologically (see text). The bistratified architecture of each of these types is shown below in schematic vertical sections. Shaded bands in mouse stratification drawing correspond to cholinergic plexuses. ON–OFF DS cell dendrites costratify with these ChAT bands in all species examined, though their positions relative to the boundaries of the IPL vary slightly among species (Famiglietti, E. V. 1987). Panels have been slightly edited to promote comparisons. Scale bars = 100 μm. (Top panel, rabbit) Derived from figure 12 of Vaney, D. I. 1994. Territorial organization of direction-selective ganglion cells in rabbit retina. J. Neurosci. 14(11 Pt 1), 6301–6316. (Top panel, mouse) Type 2 bistratified cell from figure 4 of Schubert, T., Maxeiner, S., Kruger, O., Willecke, K., and Weiler, R. 2005. Connexin 45 mediates gap junctional coupling of bistratified ganglion cells in the mouse retina. J. Comp. Neurol. 490(1), 29–39, © 2005 Wiley-Liss, Inc., reprinted with permission of Wiley-Liss, Inc., a subsidiary of John Wiley & Sons, Inc. (Top panel, rat) D2 cell from figure 1 of Sun, W., Li, N., and He, S. 2002a. Large-scale morphological survey of rat retinal ganglion cells. Vis. Neurosci. 19(4), 483–493, © 2002 Cambridge University Press. (Top panel, squirrel) Derived from drawing of G11 cell in figure 24 of Linberg, K. A., Suemune, S., and Fisher, S. K. 1996. Retinal neurons of the California ground squirrel, *Spermophilus beecheyi*: a Golgi study. J. Comp. Neurol. 365(2), 173–216, © 1996 Wiley-Liss, Inc., reprinted with permission of Wiley-Liss, Inc., a subsidiary of John Wiley & Sons, Inc. (Top panel, cat) Iota cell from O'Brien B., Isayama T., and Berson D. (unpublished data). (Top panel, monkey) Recursive bistratified cell from figure 20.5 of Dacey, D. M. 2004. Origins of Perception: Retinal Ganglion Cell Diversity and the Creation of Parallel Visual Pathways. In: The Cognitive Neurosciences III (*ed.* M. S. Gazzaniga), pp. 281–301. MIT Press, by permission of MIT Press. (Bottom panel, rabbit) G7 type from figure 4 of Rockhill, R. L., Daly, F. J., MacNeil, M. A., Brown, S. P., and Masland, R. H. 2002. The diversity of ganglion cells in a mammalian retina. J. Neurosci. 22(9), 3831–3843. (Bottom panel, mouse) Type 2 bistratified cell from figure 4 of Schubert, T., Maxeiner, S., Kruger, O., Willecke, K., and Weiler, R. 2005. Connexin 45 mediates gap junctional coupling of bistratified ganglion cells in the mouse retina. J. Comp. Neurol. 490(1), 29–39, © 2005 Wiley-Liss, Inc., reprinted with permission of Wiley-Liss, Inc., a subsidiary of John Wiley & Sons, Inc. (Bottom panel, cat) Iota cell from O'Brien B., Isayama T., and Berson D. (unpublished data).

circumstantial evidence for contributions to both the retinogeniculate and retinocollicular projections in a variety of species (see Section 1.25.4).

1.25.3.5 Alpha Cells

Alpha cells were originally described in cat retina by Boycott B. B. and Wässle H. (1974), where they are easily recognized by their extremely large cell bodies, thick axons, and large radiate dendritic fields (Figure 4). Presumed homologs of this cell type have been proposed in a larger number of mammalian species than for any other RGC type. This apparent consistency is deceptive, however, as several varieties of alpha-like cells have been recognized in rodent, rabbit, and primate retinas and there has been

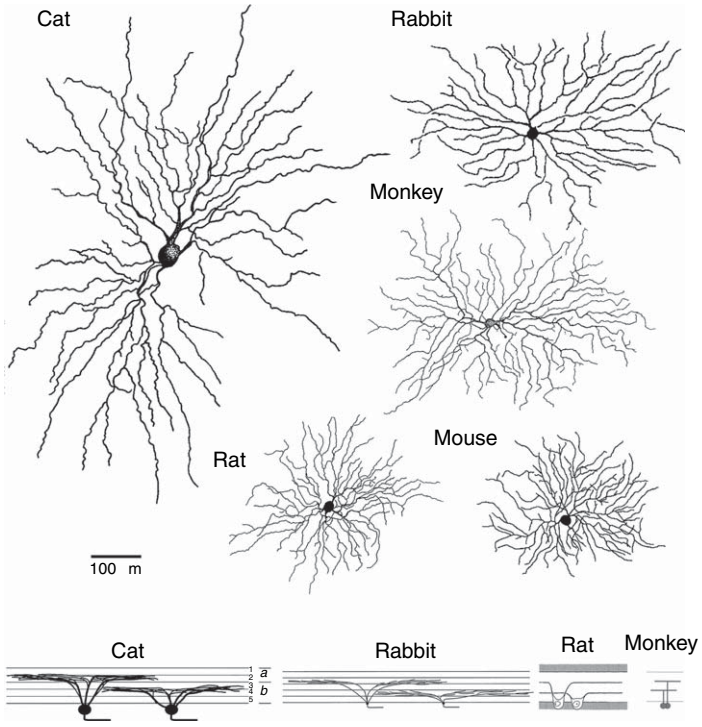

Figure 4 Morphology of alpha-like ganglion cells in five mammalian species. Top panels show dendritic profiles as viewed in flatmounts. Each of these types occurs as a paramorphic pair, with one subtype stratifying in the middle of the ON sublayer and the other in the middle of the OFF sublayer, as shown below in schematic vertical sections. Some panels have been modified slightly to promote comparison. Scale bars = 100 μm. (Top panel, rabbit) Alpha cell from figure 12 of Peichl, L., Buhl, E. H., and Boycott, B. B. 1987a. Alpha ganglion cells in the rabbit retina. J. Comp. Neurol. 263(1), 25–41, © 1987 Alan R. Liss, Inc., reprinted with permission of Wiley-Liss, Inc., a subsidiary of John Wiley & Sons, Inc. (Top panel, mouse) RG_{A2} cell from figure 1 of Sun, W., Li, N., and He, S. 2002b. Large-scale morphological survey of mouse retinal ganglion cells. J. Comp. Neurol. 451(2), 115–126, © 2002 Wiley-Liss, Inc., reprinted with permission of Wiley-Liss, Inc., a subsidiary of John Wiley & Sons, Inc. (Top panel, rat) RG_{A2} cell from figure 7C of Huxlin, K. R. and Goodchild, A. K. 1997. Retinal ganglion cells in the albino rat: revised morphological classification. J. Comp. Neurol. 385(2), 309–323, © 1997 Wiley-Liss, Inc., reprinted with permission of Wiley-Liss, Inc., a subsidiary of John Wiley & Sons, Inc. (Top panel, cat) Alpha cell from figure 10A of Berson, D. M., Isayama, T. and Pu, M. 1999. The eta ganglion cell type of cat retina. J. Comp. Neurol. 408(2), 204–219. (Top panel, monkey) Smooth monostratified cell from figure 20.5 of Dacey, D. M. 2004. Origins of Perception: Retinal Ganglion Cell Diversity and the Creation of Parallel Visual Pathways. In: The Cognitive Neurosciences III (*ed.* M. S. Gazzaniga), pp. 281–301. MIT Press, by permission of MIT Press. (Bottom panel, cat) Alpha cell from figure 12 of Isayama, T., Berson, D. M., and Pu, M. 2000. Theta ganglion cell type of cat retina. J. Comp. Neurol. 417(1), 32–48. (Bottom panel, rabbit) G11 type from figure 4 of Rockhill, R. L., Daly, F. J., MacNeil, M. A., Brown, S. P., and Masland, R. H. 2002. The diversity of ganglion cells in a mammalian retina. J. Neurosci. 22(9), 3831–3843. (Bottom panel, rat) Alpha cells from figure 6 of Peichl, L. 1989. Alpha and delta ganglion cells in the rat retina. J. Comp. Neurol. 286(1), 120–139, © 1989 Alan R. Liss, Inc., reprinted with permission of Wiley-Liss, Inc., a subsidiary of John Wiley & Sons, Inc. (Bottom panel, monkey) Smooth monostratified cell from figure 20.4A of Dacey, D. M. 2004. Origins of Perception: Retinal Ganglion Cell Diversity and the Creation of Parallel Visual Pathways. In: The Cognitive Neurosciences III (*ed.* M. S. Gazzaniga), pp. 281–301. MIT Press, by permission of MIT Press.

considerable controversy about which of these should be considered true homologs of the cat alpha cell.

Cat alpha cells comprise a paramorphic pair of subtypes, one ON and one OFF. Each subtype forms a regular mosaic that efficiently tiles the retina (Wässle, H. and Boycott, B. B., 1991; Chapter Mosaics, Tiling and Coverage by Retinal Neurons) and is narrowly monostratified near the middle of its respective sublamina, at approximately the same depth as the cholinergic plexuses (Vardi, N. *et al.*, 1989). Dendrites are relatively stout, branch at moderate density with acute branch angles, and overlap one another minimally. In their original report, Boycott B. B. and Wässle H. suggested a possible correspondence between alpha cells and Y cells, a physiological type of cat RGC distinguished by a

brisk, transient light response, fast axonal conduction velocity, and nonlinear spatial summation. This was quickly confirmed (Cleland, B. G. *et al*, 1975; Peichl, L. and Wässle, H., 1981; Saito, H. A., 1983; Fukuda, Y. *et al*., 1984; Stanford, L. R. and Sherman, S. M., 1984).

Paramorphically paired cell types with morphology resembling that of the cat alpha cells have been documented in marsupials, rodents, bats, carnivores, lagomorphs, ungulates, and primates (Perry, V. H., 1979; Vitek, D. J. *et al*., 1985; Peichl, L. *et al*., 1987a; Peichl, L., 1989; 1992; Dann, J. F. and Buhl, E. H., 1990; Wingate, R. J. *et al*., 1992; Huxlin, K. R. and Goodchild, A. K., 1997; Sun, W. *et al*., 2002a; 2002b). Figure 4 shows examples of such proposed homologs. Though nomenclature for these types has been variable (e.g., type I cells of Perry, V. H., 1979; RG_{A2} cells of Huxlin, K. R. and Goodchild, A. K., 1997 and Sun, W. *et al*., 2002a; 2002b), some have specifically referred to these morphological types as alpha cells (e.g., Perry, V. H. and Cowey, A., 1981; Peichl, L. *et al*., 1987a; 1987b; Peichl, L., 1989; 1991; 1992; Zhang, J. *et al*., 2005; Pang, J. J. *et al*., 2003). Structure–function data are lacking for many of these species, but at least some of these alpha-like forms do exhibit physiological properties broadly consistent with those of cat alpha (Y) cells (Amthor, F. R. *et al*., 1989b; Demb, J. B. *et al*., 1999; Pang, J. J. *et al*., 2003).

However, uncertainty about the implied homology with cat alpha cells has grown over the years, particularly in the better-studied species. For example, in the rat retina, Peichl L. (1989) initially described a single paramorphic pair of types with alpha-like morphology, but two subsequent studies suggest that the cells illustrated by Peichl comprise three types (Huxlin, K. R. and Goodchild, A. K., 1997; Sun, W. *et al*., 2002a). Two of these types form a paramorphic pair, termed RGA_2, that is arguably homologous to cat alpha cells. The third is an unpaired ON type, termed RGA1, characterized by a slightly larger, sparser dendritic profile that stratifies just beneath (i.e., vitread to) the presumed ON alpha homolog. A similar interpretation has been reported by at least one group in the mouse retina (Sun, W. *et al*., 2002b) but there appears to be no consensus on this point. For example, Coombs J. *et al*. (2006) consider their cluster M10 cells to be the probable mouse equivalent of alpha cells, but indicate that this type stratifies only in the ON sublayer and also equate them with the RG_{A1} cell of Sun W. *et al*. (2002b). Kong J. H. *et al*. (2005) suggest that mouse RGCs belonging to their clusters 10 and 11 comprise a paramorphic pair corresponding to the alpha cells, but also equate their cluster 11 with the RGA1 cells of Sun W. *et al*. (2002b) and offer their cluster 8 as an alternative candidate for the ON alpha homolog. To further complicate matters, Pang J. J. *et al*. (2003) found that mouse RGCs with large somas and alpha-like dendritic arbors consist of three functional types, two of which are OFF-center.

The uncertainty seems at least as great in the rabbit retina, as comprehensively reviewed by Famiglietti E. V. (2004) and Zhang J. *et al*. (2005). Several studies report a single paramorphic pair of alpha-like types (Peichl, L. *et al*., 1987a; Rockhill, R. L. *et al*., 2002; Zhang, J. *et al*., 2005), each of which exhibits a regular spacing of somata like those of other well-defined types (Peichl, L. *et al*., 1987a). However, Famiglietti recognizes no fewer than seven distinct morphological types among his type I and II classes, which resemble, more or less strongly, the alpha type, having relatively large somas and large, radiate dendritic fields. His type Ia2 and Ib2 form a paramorphic pair that appears to correspond best to the alpha cells described by Zhang J. *et al*. (2005). Interestingly, these two types apparently do not costratify with the ChAT bands as they do in the cat (Vardi, N. *et al*., 1989), arborizing instead just beneath those bands (Famiglietti, E. V., 2004; Zhang, J. *et al*., 2005). This may reflect differences among studies in the precision of laminar assignments, a real species difference in stratification of otherwise homologous types, or real differences that argue against true homology. Electrophysiological studies of rabbit retina have identified various types of brisk, large-field units likely to represent the functional equivalents of these alpha-like RGCs (Levick, W. R., 1967; Caldwell, J. H. and Daw, N. W., 1978; Vaney, D. I. *et al*., 1981a). The possible correspondences between these functional types and various alpha-like morphological types have been systematically evaluated by Famiglietti E. V. (2004). Structure–function studies show that at least some rabbit alpha-like cells have relatively transient, spatially nonlinear response properties resembling those of cat Y cells (Amthor, F. R. *et al*., 1989b; Jensen, R. J., 1991; Roska, B. *et al*., 2006).

The question of whether the primate retina contains a homolog of the alpha cell type remains controversial. The morphological cell type termed parasol by Polyak S. L. (1941) and referred to by others as Pα, A, or M (magnocellular-projecting) cells, has often been proposed as such a homolog

(e.g., Leventhal, A. G. *et al.*, 1981; Perry, V. H. and Cowey, A., 1981; Peichl, L., 1991). In favor of this proposed correspondence is the relatively large soma size of this type, its preferential staining by neurofibrillar methods, general features of its branching pattern and its projection to the LGNd, and its tracer coupling pattern (for details, see Peichl, L., 1991; Dacey, D. M. and Brace, S., 1992). Physiologically, these cells, like cat Y cells, exhibit transient light responses and high contrast sensitivity. On the other hand, parasol cells represent a larger fraction of the ganglion cell population than the do the alpha cells of cats or other species (~10% as compared to 1–4%). Also, though their dendritic fields are certainly larger than those of midget cells, they have smaller dendritic fields than most remaining ganglion cell types, whereas in most species alpha cells are among the largest-field types. Furthermore, many M (parasol) cells exhibit linear spatial summation, whereas Y (alpha) cells are nonlinear (Shapley, R. and Perry, V. H., 1986). Finally, in marked contrast to cat alpha cells, primate parasol cells contribute very little to the retinotectal projection (Leventhal, A. G. *et al.*, 1981; Rodieck, R. W. and Watanabe, M., 1993; see also Schiller, P. H. and Malpeli, J. G., 1977).

Recent studies have identified what may prove to be a better primate homolog of the alpha cell. Dacey D. M. (2004) describes a cell type he terms "smooth monostratified" (see Figure 4) which has the relatively coarse, smooth dendrites and radiate branching structure characteristic of alpha cells in other species. Both the cell body and the dendritic field are substantially larger than that of parasol cells and thus more reminiscent of alpha cells. Yamada E. S. *et al.* (2005) describe a similar type which they term "large radiate." They note that the dendrites of these cells minimally overlap one another and that their axons are relatively thick, again paralleling feature of cat alpha cells. Both groups agree that like alpha cells, this type comprises a paramorphic pair (Dacey, D. M., 2004; Yamada, E. S. *et al.*, 2005). One subtype costratifies with the dendrites of the ON starburst amacrines, and the other with the OFF starbursts (i.e., in register with the ChAT bands; Yamada, E. S. *et al.*, 2005). Recent evidence suggests that these cells share with cat alpha cells the same relative abundance (3% of all RGCs), nonlinear spatial summation, and prominent projections to both the LGN and superior colliculus (Dacey, D. M., 2004; Crook, J. D. *et al.*, 2007; and Dacey, D. M. personal communication). Thus, on many grounds, this type seems to match the alpha type much closely than does the parasol cell.

1.25.3.6 Beta Cells

This morphological type was first characterized, along with alpha cells, by Boycott B. B. and Wässle H. (1974). They suggested beta cells might be the morphological equivalent of the X cell, a brisk sustained physiological type exhibiting linear spatial summation (Stone, J., 1983). This was confirmed in structure–function work (Fukuda, Y. *et al.*, 1984; Saito, H. A., 1983; Stanford, L. R. and Sherman, S. M., 1984). The beta cells have the smallest receptive fields of all cat RGCs and project heavily to the LGNd. There is thus little doubt that they mediate the highest acuity vision of which cats are capable. Beta (X) cells apparently also innervate the pretectal region but lack any projection to the superior colliculus (Stone, J., 1983; Tamamaki, N. *et al.*, 1995).

Homologs of the beta cell are readily recognizable in other carnivores (ferret: Vitek, D. J. *et al.*, 1985; Wingate, R. J. *et al.*, 1992; dog and wolf: Peichl, L., 1992) and very similar morphological cell types have been documented in species belonging to other mammalian orders, including the flying fox (a variety of fruit bat; Dann, J. F. and Buhl, E. H., 1990) and the opossum (Wilson, P. D. and Condo, G. J., 1985; Moraes, A. M. *et al.*, 2000). On the other hand, it has been much more difficult to establish homologous types in some of the best-studied mammalian retinas. In primates, a RGC type variously termed midget, Pβ, B, or P (parvocellular projecting) has often been considered to be the likely primate equivalent of the beta cell, but there is no consensus on this point (for review, see Wässle, H. and Boycott, B. B., 1981; Shapley, R. and Perry, V. H., 1986; Peichl, L., 1991; Rodieck, R. W., 1988; 1998). Rodieck has noted the close morphological similarity of primate parasol and cat beta cells. Silveira L. C. *et al.* (1994) suggest that after normalizing for local density of each type, cat alpha and beta cells and primate parasol cells all strongly resemble one another, whereas midget cells stand alone. Shapley R. and Perry V. H. (1986) have pointed out that the primate magnocellular layers, to which parasol cells make the dominant input, contain many cells with X-like linear spatial summation and recordings recently made from identified parasol cells suggest that they exhibit far more linearity of spatial summation than previously recognized (Dacey, D. M., personal communication). A plausible alternative view, then, is that the parasol cell is the primate homolog of the beta cell, while the midget cells constitute a type unique to primates.

The situation is even less clear in rabbits and rodents. Neither have a clear morphological counterpart of the beta cell (Peichl, L. *et al.*, 1987a; Rockhill, R. L. *et al.*, 2002; Famiglietti, E. V., 2004; Sun, W. *et al.*, 2002a; 2002b; Kong, J. H. *et al.*, 2005; Coombs, J. *et al.*, 2006; Badea, T. C. and Nathans, J., 2004), though possible equivalents have been suggested on anatomical grounds (Fukuda, Y., 1977; Thanos, S., 1988; Rivera, N. and Lugo, N., 1998). In mouse retina, there is no physiological type that is distinguishable on the basis of its X-like linearity of spatial summation (Carcieri, S. M. *et al.*, 2003). In rabbits, receptive fields resembling those of cat X cells, with brisk sustained responses to light steps and linear spatial summation, have been encountered (X cells, Caldwell, J. H. and Daw, N. W., 1978; brisk sustained, Vaney, D. I. *et al.*, 1981a; brisk-sustained linear, Amthor, F. R. *et al.*, 1989b), but the distinction from rabbit Y-like cells is more difficult than in cat (see Famiglietti, E. V., 2004 for details). Structure–function data from Amthor F. R. *et al.* (1989b) and Roska B. *et al.* (2006) have linked this functional type mainly to a cell type with highly branched dendritic field of intermediate size. This morphological type, termed "beta" by Roska B. *et al.* (2006), appears to correspond to the G4 cell of Rockhill R. L. *et al.* (2002) and certain cells within class III of Famiglietti E. V. (2004). However, the equivalence of this type to cat beta cells on morphological grounds is far from clear, and the light responses of these cells appear far more transient than those of cat X (beta) cells. Famiglietti E. V. (2004) has argued that much larger-field cells within his class II may be the morphological equivalent of the brisk-sustained linear physiological type.

1.25.4 Retinofugal Projections and Their Origin in Specific Ganglion Cell Types

Retinofugal projections have been extensively explored in a large number of mammalian brains for many decades. The subnuclear organization of retinorecipient nuclei and the classification schemes for RGCs vary considerably from one species to the next. The literature on parallel retinofugal channels is thus too vast to be comprehensively covered in this chapter. The goal here is merely to survey the range of retinal targets, to summarize the main established functional roles of these nuclei, and to provide a brief synopsis of what is known about the types of RGCs that innervate them, with particular emphasis on the conserved types discussed above. Several of the major targets are the subject of separate chapters in this volume and their consideration here will be correspondingly brief.

1.25.4.1 Methods for Linking Retinofugal Projections to Retinal Ganglion Cell Types

The most complete surveys of retinofugal projections come from axon transport tracing experiments using the most sensitive available tracers, of which the most popular is the B subunit of cholera toxin. Such surveys are available for a wide variety of mammalian brains, including mouse (Godement, P. *et al.*, 1984; Miura, M. *et al.*, 1997; Hattar, S. *et al.*, 2006); rat (Levine, J. D. *et al.*, 1991; Hannibal, J. and Fahrenkrug, J., 2004); blind mole rat (Cooper, H. M. *et al.*, 1993); squirrel (Agarwala, S. *et al.*, 1989; Major, D. E. *et al.*, 2003); hamster (Pickard, G. E. and Silverman, A. J., 1981; Morin, L. P. and Blanchard, J. H., 1997; Ling, C. *et al.*, 1998; Johnson, R. F. *et al.*, 1988; Mikkelsen, J. D., 1992; Pickard, G. E. and Silverman, A. J., 1991; Reuss, S. and Decker, K., 1997; Youngstrom, T. G. *et al.*, 1991); cat (Matteau, I. *et al.*, 2003); and primates (Cooper, H. M. *et al.*, 1990; Mick, G. *et al.*, 1993; Costa, M. S. *et al.*, 1999; Abizaid, A. *et al.*, 2004). An additional source of information concerning retinal projections in mice comes from genetically modified strains in which specific subsets of RGCs have been induced to express marker proteins that are axonally distributed (Quina, L. A. *et al.*, 2005; Hattar, S. *et al.*, 2006).

Information about which specific morphological types of RGCs innervate these targets comes primarily from studies using retrograde transport. Typically this tracing method yields granular labeling within the soma and primary dendrites of RGCs. This can be used to obtain evidence about the size of the afferent RGCs, about their laterality of projection and topographic distribution, but only crude information about their dendritic structure. Beginning in the 1980s, methods were introduced for labeling cells by retrograde transport of fluorescent tracers, and for targeting the labeled cells for intracellular staining in fixed or living tissue. This innovation made it possible to reveal the full dendritic architecture of RGCs with known central projections (e.g., Buhl, E. H. and Peichl, L., 1986; Dann, J. F. and Buhl, E. H., 1987; Pu, M. L. and Amthor, F. R., 1990a; 1990b; Wingate, R. J. *et al.*, 1992; Rodieck, R. W. and Watanabe, M., 1993; Pu,

M. L. *et al.*, 1994). In a particularly powerful modification of this method, light has been used to induce the release of a retrograde fluorescent tracer from endocytotic vesicles in the soma into the cytosol. The dye diffuses freely within the cell, yielding smooth intracellular filling similar to that produced by intracellular dye injection (Dacey, D. M. *et al.*, 2003). In a few studies, inferences about the heterogeneity of RGCs innervating a particular central target have been made from a close examination of bulk-filled retinal afferents (e.g., Sachs, G. M. and Schneider, G. E., 1984). However, except in the case of intracellular recording from relatively large axons (e.g., Bowling, D. B. and Michael, C. R., 1980; Tamamaki, N. *et al.*, 1995), it has been difficult to link these arbor types to specific RGC classes.

For identifying physiological types of RGCs providing input to specific central nuclei, antidromic activation has been until very recently the method of choice. In some cases, orthodromic activation of postsynaptic targets by shocks to the optic pathway can be used to assess the conduction velocity of retinal afferents and thereby to draw inferences about the functional types of RGCs providing input. In a few targets, such as the LGNd and accessory optic system, where individual cells appear to receive inputs mainly from single RGC types, it has been possible to infer the RGC input population from postsynaptic visual response properties. This approach is impractical for many target nuclei in which postsynaptic properties can be significantly transformed by convergent input from multiple RGC types, extraretinal visual inputs and local circuits. By far the most powerful methods for linking specific functional types to outputs use retrograde transport of fluorescent tracers to label the afferent RGCs, which can then be targeted for *in vitro* recording. Though technically challenging, this approach has the added advantage of permitting intracellular dye injection or photofilling of recorded cells and thus a triple correlation between somadendritic structure, receptive field type, and central projection.

1.25.4.2 Lateral Geniculate Complex and Dorsal Thalamus

The lateral geniculate complex is the most prominent target of retinal projections in mammals. It consists of several distinct components. Of these, the best known and most thoroughly studied is the dorsal division (LGNd). The LGNd serves as the thalamic relay nucleus of the visual system routing retinal signals to the visual cortex. It thus plays an essential role in the cortical analysis of visual form and motion and in conscious visual perception. Chapter The Visual Thalamus provides an extensive review of the functional organization of the retinogeniculate projection. Of greatest relevance in the present context is that multiple ganglion cell types innervate the nucleus, that each type apparently terminates on a distinct set of LGNd neurons, and that these neurons are often segregated in separate sublaminae or subnuclei of the LGNd. In general, the available evidence suggests that many RGC types in a given species innervate the LGNd, but that not all do (e.g., Illing, R. B. and Wässle, H., 1981; Leventhal, A. G. *et al.*, 1981; 1985; Stone, J., 1983; Perry, V. H. and Cowey, A., 1984; Pu, M. L. and Amthor, F. R., 1990a; Wingate, R. J. *et al.*, 1995; Berson, D. M. *et al.*, 1998; 1999; Isayama, T. *et al.*, 2000; Dacey, D. M. *et al.*, 2003, Dacey, D. M., 2004). However, it is difficult to demonstrate definitively that an RGC type lacks a projection to the LGNd. This is because the retrograde tracers that are typically used to address such questions can label fibers passing through an injection site as well as axons terminating there. Some laminae of the LGNd lie so close to the optic tract that it is difficult to make tracer deposits there without involving passing retinofugal fibers.

As reviewed in detail in Chapter The Visual Thalamus, the most complete picture of the multiple functional components within the retinogeniculate pathway comes from work in primates and cats. In primates, the dominant retinal inputs to the parvocellular layers of the primate LGNd derives from midget (P) cells, that to the magnocellular layers comes mainly from the parasol (M) cells, while input to the koniocellular layers comes from a variety of widefield RGC types clearly distinct from midget and parasol cells (see Chapter The Visual Thalamus; Leventhal, A. G. *et al.*, 1981; Perry, V. H. *et al.*, 1984; Irvin, G. E. *et al.*, 1986; Casagrande, V. A., 1994; Dacey, D. M., 1994; 2004; White, A. J. *et al.*, 1998; Dacey, D. M. *et al.*, 2003; Hendry, S. H. and Reid, R. C., 2000; Shapley, R. and Perry, V. H., 1986; Calkins, D. J. *et al.*, 2005; Callaway, E. M., 2005). In cat, the large-celled A layers of the LGNd receive input exclusively from beta (X) and alpha (Y) cells, while the small-celled C layers and the medial interlaminar nucleus receive inputs mainly from alpha cells and from a variety of RGCs with small cell bodies and functional properties distinct from X and Y cells, which are sometimes grouped under the physiological designation W cells or the

morphological class gamma cells (Cleland, B. G. *et al.*, 1976; Wilson, P. D. *et al.*, 1976; Bowling, D. B. and Michael, C. R., 1980; Itoh, K. *et al.*, 1981; Sur, M. and Sherman, S. M., 1982; Stone, J., 1983; Sur, M. *et al.*, 1987; Berson, D. M. *et al.*, 1999; Isayama, T. *et al.*, 2000). A similar organization appears to apply to the ferret LGNd (Vitek, D. J. *et al.*, 1985; Wingate, R. J. *et al.*, 1992).

In mammals with poorly developed geniculate lamination, such as rodents and rabbits, the segregation among retinogeniculate channels is less obvious, but there is nonetheless diversity of the retinogeniculate pathway which is maintained to some degree in the properties of geniculate neurons (Hale, P. T. *et al.*, 1979; Dreher, B. *et al.*, 1985; Martin, P. R., 1986; Pu, M. L. and Amthor, F. R., 1990a). Latent laminar organization has been suggested in rodent and rabbit studies in which afferents from subsets of RGCs have been visualized by classical anatomical methods (Martin, P. R., 1986; Reese, B. E., 1988) or by molecular means (Brecha, N. *et al.*, 1987; Quina, L. A. *et al.*, 2005; Hattar, S. *et al.*, 2006).

Several of the highly conserved RGC types reviewed in the first part of this chapter appear to provide input to the LGNd. One of these is the ON–OFF DS type. LGNd relay cells with physiology closely matching that of ON–OFF DS ganglion cells have been encountered in various mammalian species (rabbit: Levick, W. R. *et al.*, 1969; cat: Cleland, B. G. *et al.*, 1976; Wilson, P. D. *et al.*, 1976; primate: Norton, T. T. and Casagrande, V. A., 1982; Irvin, G. E. *et al.*, 1986; Casagrande, V. A., 1994) and RGCs with bistratified morphology matching that of ON–OFF DS cells have been retrolabeled from the geniculate in rabbits (Pu, M. L. and Amthor, F. R., 1990a). There is some morphological evidence that the ON-center type of DS cells may also innervate the rabbit LGN (Pu, M. L. and Amthor, F. R., 1990a; Dacey, D. M., 2004). Alpha or alpha-like cells innervate the LGNd in cats (Illing, R. B. and Wässle, H., 1981; Stone, J., 1983; Leventhal, A. G. *et al.*, 1985), ferrets (Vitek, D. J. *et al.*, 1985; Wingate, R. J. *et al.*, 1992), rabbits (Pu, M. L. and Amthor, F. R., 1990a), and rats (Dreher, B. *et al.*, 1985). In primates, the LGNd receives input not only from the parasol cells, which have traditionally been considered homologous to the alpha cell, but also from the newly discovered alpha-like (smooth monostratified) cell which is a more likely homolog (Dacey, D. M., 2004; Crook, J. D. *et al.*, 2007). Beta (X) cells provide a major input to the LGNd in carnivores (e.g., Stone, J., 1983; Vitek, D. J. *et al.*, 1985; Wingate, R. J. *et al.*, 1992) and both midget and parasol cells of primates, which some have suggested as homologs of beta cells, likewise innervate the LGNd.

There is conflicting evidence on the question of whether the LED ganglion cell type innervates the LGNd. Several extensive morphological surveys of LGN-projecting RGCs in various mammalian species encountered few if any of this ganglion cell type (rabbit: Pu, M. L. and Amthor, F. R., 1990a; ferret: Wingate, R. J. *et al.*, 1992; macaque: Rodieck, R. W. and Watanabe, M., 1993; cat: Berson, D. M. *et al.*, 1998). However, it would be premature to exclude a projection to the geniculate, especially to the koniocellular or related layers, some of which are difficult to study with retrograde labeling methods due to the proximity of the optic tract. In macaque, the possibly homologous broad thorny type has been retrolabeled from the LGN (Dacey, D. M. *et al.*, 2003; Dacey, D. M., 2004), and de Monasterio F. M. (1978) was able to antidromically activate a few LED-like RGCs from the geniculate. LGN relay cells tend to closely resemble their RGC inputs in receptive-field organization, and geniculate cells with LED-like receptive fields have been encountered in many mammalian species (cat: Cleland, B. G. *et al.*, 1976; Wilson, P. D. *et al.*, 1976; bush baby: Norton, T. T. and Casagrande, V. A., 1982, Irvin, G. E. *et al.*, 1986; tree shrew: Holdefer, R. N. and Norton, T. T., 1995). Melanopsin-expressing RGCs have at most a very sparse and localized input to the LGNd in rodents (Hattar, S. *et al.*, 2002; 2006; Hannibal, J. and Fahrenkrug, J., 2004) but appear to have a more substantial projection to the primate LGNd (Dacey, D. M. *et al.*, 2005).

There are two other components of the geniculate complex that lack direct projections to the cortex and probably play little role in conscious vision. The first is the ventral division of the (LGNv), known in primates as the pregeniculate nucleus. This is a diencephalic region derived, like the zona incerta and thalamic reticular nucleus, from the embryonic ventral thalamus. The connectivity, neurochemistry, and physiological properties of the LGNv have been comprehensively reviewed by Harrington M. E. (1997). The nucleus is heavily interconnected with retinorecipient brain regions and receives input also from brainstem regions related to vestibular and oculomotor function. Visual receptive fields are large and light responses are typically dominated by sustained ON components. Relatively little is known about the ganglion cell types innervating this nucleus. In the cat, RGCs with small somas

which are clearly distinct from alpha and beta cells provide the dominant input (Leventhal, A. G. *et al.*, 1985). In rodents, melanopsin-expressing RGCs provide modest input to this nucleus (Hattar, S. *et al.*, 2002; 2006; Hannibal, J. and Fahrenkrug, J., 2004).

A second accessory component of the LGN complex is the intergeniculate leaflet (IGL), a thin sheet of neurons sandwiched between the LGNd and LGNv in rodents. The IGL is intimately interconnected with the SCN and is thought to contribute to mechanisms synchronizing circadian rhythms to environmental stimuli, both photic and nonphotic (Moore, R. Y. and Card, J. P., 1994; Harrington, M. E., 1997; Morin, L. P. and Blanchard, J. H., 1998). Mammals other than rodents lack an obvious IGL, although possibly homologous regions within primate pregeniculate nucleus and cat LGNv have been proposed based on patterns of connections and neurochemistry (Moore, R. Y., 1993; Pu, M. and Pickard, G. E., 1996; but see Chevassus-au-Louis, N. and Cooper, H. M., 1998). Many IGL neurons exhibit sustained ON responses that code light intensity (Harrington, M. E., 1997). This is in keeping with the observation that melanopsin-expressing RGCs, some with bifurcating projections to the SCN, provide most of the retinal input to this region (Pickard, G. E., 1985; Morin, L. P. *et al.*, 2003; Hattar, S. *et al.*, 2006).

Relatively sparse retinal projections have been traced to a number of regions of the dorsal thalamus other than the LGN complex. The most prominent of these lies just outside the LGNd in the pulvinar or lateral posterior nuclei (e.g., Berman, N. and Jones, E. G., 1977; Mizuno, N. *et al.*, 1982; Leventhal, A. G. *et al.*, 1980; Somogyi, G. *et al.*, 1981; Ling, C. *et al.*, 1998; Major, D. E. *et al.*, 2003). In the cat, the retinopulvinar projection arises almost exclusively from a single RGC type, the epsilon cell (Leventhal, A. G. *et al.*, 1980; Pu, M. *et al.*, 1994). This is a monostratified ON type with relatively large cell body, a large sparse dendritic field, and a sustained light response. In primates, a more diverse mix of RGC inputs to the pulvinar has been reported, apparently including some midget and parasol cells as well as other types (Cowey, A. *et al.*, 1994). Sparse input from optic fibers has also been reported in the vicinity of anterodorsal thalamic nuclei (Conrad, C. D. and Stumpf, W. E., 1975; Itaya, S. K. *et al.*, 1986; Cooper, H. M. *et al.*, 1993; Major, D. E. *et al.*, 2003) and the medial geniculate nucleus (Matteau, I. *et al.*, 2003).

1.25.4.3 Superior Colliculus

The superior colliculus is, aside from the LGN, the most prominent and well-studied target of retinofugal fibers. To summarize briefly, the superior colliculus is a laminated structure of the midbrain tectum. There is a topographically ordered and bilateral retinal projection to the superficial collicular layers, whereas the deeper layers translate spatiotopic visual and other sensory inputs into motor commands for reorienting the eyes and head. The retinal afferents to the superficial layers thus appear to serve, in part, as inputs elements in a visuomotor interface generating gaze shifts to visual targets of interest. Neurons of the superficial collicular layers also provide ascending visual input to the LGNd, pulvinar, and other thalamic visual nuclei. They thus provide a conduit distinct from the main retinogeniculostriate pathway by which retinal information can reach the visual cortex.

Ganglion cells innervating the superior colliculus are structurally and functionally heterogeneous in every mammalian species studied to date. Indeed, in rodents and rabbits it appears that nearly all RGCs innervate the colliculus (Chalupa, L. M. and Thompson, I., 1980; Vaney, D. I. *et al.*, 1981b; Linden, R. and Perry, V. H., 1983; Hofbauer, A. and Drager, U. C., 1985). In the cat, the fraction of all RGCs innervating the colliculus is closer to one half (Wässle, H. and Illing, R. B., 1980; Stein, J. J. *et al.*, 1995) while in primates the fraction is as low as one tenth (Perry, V. H. and Cowey, A., 1984). The smaller fractions of RGCs innervating cat and primate colliculus reflect the fact that a few very abundant RGC types make little if any contribution to this pathway. Specifically, most beta (X) cells in the cat and most midget (P) and parasol (M) cells in primates apparently lack collicular projections (e.g., Hoffmann, K. P., 1973; Cleland, B. G. and Levick, W. R., 1974b; Stone, J., 1983; Perry, V. H. and Cowey, A., 1984; Leventhal, A. G. *et al.*, 1985; Rodieck, R. W. and Watanabe, M., 1993; Tamamaki, N. *et al.*, 1995). In cats, it appears that virtually all ganglion cells other than beta cells innervate the superior colliculus (Stein, J. J. and Berson, D. M., 1995), and a variety of specific RGC types have been specifically shown to contribute in cats (Leventhal, A. G. *et al.*, 1985; Berson, D. M. *et al.*, 1998; 1999; Isayama, T. *et al.*, 2000), primates (Leventhal, A. G. *et al.*, 1981; Rodieck, R. W. and Watanabe, M., 1993; Dacey, D. M., 2004), ferrets (Vitek, D. J. *et al.*, 1985; Wingate, R. J. *et al.*, 1992), and squirrels (Rivera, N. and Lugo, N., 1998).

Most of the highly conserved RGC types reviewed earlier in this chapter contribute to the retinocollicular projection. This is particularly well documented for the alpha cell or its physiological equivalent, the Y or brisk-transient cell. This was first established in the cat visual system (Hoffmann, K. P. 1973; Cleland, B. G. and Levick, W. R., 1974b; Stone, J., 1983; Wässle, H. and Illing, R. B., 1980; Bowling, D. B. and Michael, C. R., 1980; Itoh, K. *et al.* 1981; Tamamaki, N. *et al.*, 1995) but has been confirmed in ferret (Vitek, D. J. *et al.*, 1985; Wingate, R. J. *et al.*, 1992), rat (Linden, R. and Perry, V. H., 1983; Dreher, B. *et al.*, 1985), mouse (Hofbauer, A. and Drager, U. C., 1985), hamster (Lau, K. C. *et al.*, 1992), and rabbit (Vaney, D. I. *et al.*, 1981a). As noted above (see Section 1.25.3.5), the absence of a substantial collicular projection from primate parasol cells led some to question whether they were homologous to the alpha cells of other mammals, and recent work has identified a distinct RGC type with features much more closely resembling those of cat alpha cells, including prominent collicular projections.

Few if any beta (X) cells contribute to the retinocollicular projection in cats or ferrets (e.g., Cleland, B. G. and Levick, W. R., 1974b; Stone, J. and Fukuda, Y., 1974; Wässle, H. and Illing, R. B., 1980; Stone, J., 1983; Leventhal, A. G. *et al.*, 1985; Wingate, R. J. *et al.*, 1992; Tamamaki, N. *et al.*, 1995). The same is true of primate midget and parasol cells (Schiller, P. H. and Malpeli, J. G., 1977; Leventhal, A. G. *et al.*, 1981; Perry, V. H. and Cowey, A., 1984; Rodieck, R. W. and Watanabe, M., 1993), both of which have been suggested as possible homologs of cat beta cells. Collicular projections have been reported for possible beta-cell homologs in the squirrel (Rivera, N. and Lugo, N., 1998) and for X-like cells in the rabbit (Vaney, D. I. *et al.*, 1981a), but the equivalence of these cells to beta cells is not firmly established.

Ganglion cells of the local edge detector (LED) type appear to make a major contribution to the retinocollicular projection. Cells of this receptive field type have been antidromically activated from the colliculus in cat (Cleland, B. G. and Levick, W. R., 1974a; Stone, J. and Fukuda, Y., 1974), rabbit (Vaney, D. I. *et al.*, 1981a), and primate (Schiller, P. H. and Malpeli, J. G., 1977). Studies combining retrograde labeling and dye filling have demonstrated collicular projections of RGCs with LED-like morphology in cat (Berson, D. M. *et al.*, 1998), ferret (Wingate, R. J. *et al.*, 1992), and primate (Rodieck, R. W. and Watanabe, M., 1993). The projection to the colliculus makes functional sense in that this structure generates gaze shifts to salient objects in the environment, and LEDs seem well suited for detecting object motion against a stable background while filtering out other sorts of image motion, such as translations due to gaze shifts or optic flow during locomotion.

Both types of DS cells also appear to contribute to the retinotectal projection. Input from ON–OFF DS cells to the colliculus were inferred from intracollicular recordings in the squirrel (Michael, C. R., 1972) and from antidromic activation of these cells from the superior colliculus in rabbits and cats (Cleland, B. G. and Levick, W. R., 1974a; Stone, J. and Fukuda, Y., 1974; Vaney, D. I. *et al.*, 1981a). Regarding the other directionally selective type, the ON-DS cell, Buhl E. H. and Peichl L. (1986) suggested on anatomical grounds that these cells lacked collicular projections and that most of the very rare RGCs without tectal projections (1%) were of this type. However, this conclusion appears to be at odds with the electrophysiological (Vaney, D. I. *et al.*, 1981a) and anatomical data (Peichl, L. *et al.*, 1987a), suggesting that ON-DS do contribute to the retinotectal projection. Melanopsin RGCs appear to provide at least a sparse input to the colliculus (Hattar, S. *et al.*, 2006; Morin, L. P. *et al.*, 2003).

Axons originating from different types of RGCs apparently terminate at different depths within the superficial collicular layers (Hoffmann, K. P., 1973; Marrocco, R. T., 1978; Itoh, K. *et al.*, 1981; Freeman, B. and Singer, W., 1983; Sachs, G. M. and Schneider, G. E., 1984; Hofbauer, A. and Drager, U. C., 1985; Berson, D. M., 1987; Mooney, R. D. and Rhoades, R. W., 1990). However, only the broad outlines of this arrangement have been explored to date. A remarkable degree of laminar segregation of optic afferents by functional or anatomical type has been documented in nonmammalian optic tectum (e.g., Maturana, H. R. *et al.*, 1960; Yamagata, M. *et al.*, 2006), and it would be of interest to learn whether a similar segregation holds for the dozen or more RGC types innervating the mammalian colliculus. The potential functional significance of this laminar arrangement of retinal afferents lies in its potential to route specific retinal signals to different populations of tectal cells with distinct output projections, since these output populations exhibit a parallel sublaminar organization (reviewed by May, P. J., 2005).

1.25.4.4 Accessory Optic System

The accessory optic system (AOS) consists of a scattered collection of small retinorecipient midbrain nuclei and the fascicles of optic fibers, termed accessory optic tracts, that innervate them. The AOS plays a key role in mechanisms of retinal image stabilization (for review, see Simpson, J. I., 1984; Giolli, R. A. *et al.*, 2005; Simpson, J. I. *et al.*, 1988a; 1988b). In particular, the AOS nuclei function as an essential conduit for whole-field retinal motion (retinal slip) signals that reach the vestibulocerebellum, through which they drive the slow phase of optokinetic nystagmus (for review, see Simpson, J. I. *et al.*, 1988c). This visuomotor reflex works complementarily and synergistically with signals from the vestibular semicircular canals to stabilize the retinal image during self-motion. Most mammals have three terminal nuclei of the accessory optic system (dorsal, lateral, and medial) which differ in their directional preferences for retinal whole-field motion (see Soodak, R. E. and Simpson, J. I., 1988; van der Togt, C. *et al.*, 1993). The nucleus of the optic tract (NOT), a component of the pretectal region, appears to be another element in this functional system (see below).

Retinal inputs to the AOS have been extensively studied by anterograde tracing methods in a wide variety of mammals, including primates, rodents, cats, and rabbits (Pickard, G. E. and Silverman, A. J., 1981; Weber, J. T., 1985; Cooper, H. M. *et al.*, 1990; Cooper, H. M. *et al.*, 1993; Miura, M. *et al.*, 1997; Pak, M. W. *et al.*, 1987; Ling, C. *et al.*, 1998; Telkes, I. *et al.*, 2000; Major, D. E. *et al.*, 2003; Matteau, I. *et al.*, 2003). There is overwhelming evidence that most, if not all, of this retinal input arises from a single type of RGC, the ON-DS cell. Oyster C. W. *et al.* (1972) noted that the directional selectivity and low-pass velocity tuning of ON-DS cells were well suited to the functional requirements of the optokinetic system. As noted above (see Section 1.25.3.2), Buhl E. H. and Peichl L. (1986) found that RGCs retrolabeled from the rabbit MTN formed a single morphological type, and structure–function studies by Amthor F. R. *et al.* (1989a) convincingly linked this anatomical type to the ON-DS receptive-field type.

Recordings from the accessory optic nuclei revealed large directionally selective receptive fields that could be easily assembled from convergent inputs from ON-DS RGCs (Soodak, R. E. and Simpson, J. I., 1988). Different directional preferences among the three AOS terminal nuclei suggested selective inputs from the three subtypes of ON-DS cells, which are themselves defined by their directional preferences (see above). In a remarkable insight, Simpson and colleagues observed that the preferred directions of each of the three ON-DS RGC subtypes and its associated AOS neurons was matched to the direction of retinal image motion that result when the head is rotated about the preferred axis of one of the three semicircular canals. This led Simpson and co-workers to conclude that the ON-DS/AOS network functions as "a visual system in vestibular coordinates," preprocessing visual motion signals to facilitate their seamless integration with vestibular representations of head rotation to drive gaze-stabilizing eye movements (Simpson, J. I. *et al.*, 1988b; 1988c).

1.25.4.5 Pretectal Region

The pretectum constitutes a collection of nuclei of the rostrodorsal brainstem lying just in front of the superior colliculus at the transition between midbrain and diencephalon. At least five distinct nuclei are recognized within this region: the NOT, olivary pretectal nucleus (OPN), and the anterior, medial, and posterior pretectal nuclei. These nuclei differ sharply from one another in inputs, outputs, and functional properties. Several of them constitute major targets of retinofugal axons and have been implicated in a variety of visuomotor reflexes, including optokinetic nystagmus (OKN) and the pupillary light reflex. Like the superior colliculus, the pretectum also gives rise to ascending projections to the visual thalamus, through which it may contribute to cortical visual mechanisms. For a thorough review of the relevant literature in this area, the reader is referred to Chapter Pupillary Control Pathways and to other key papers and reviews (Scalia, F., 1972; Scalia, F. and Arango, V., 1979; Clarke, R. J. and Ikeda, H., 1985; Pak, M. W. *et al.*, 1987; Gamlin, P. D., 2005; Simpson, J. I. *et al.*, 1988a; Trejo, L. J. and Cicerone, C. M., 1984; Weber, J. T., 1985).

Working out the types of RGCs providing input to the pretectal nuclei has been particularly difficult. This is attributable to the small size, complex boundaries and tight packing of retinorecipient pretectal nuclei. The problem is compounded by the fact that optic fibers within the brachium of the superior colliculus pass very near to or through these nuclei. Thus, RGCs retrolabeled or antidromically activated from the pretectal region may include some that merely send axons through the region *en route* to the

colliculus. Despite these impediments, strong evidence has been developed for inputs from specific RGC types to two pretectal nuclei, the NOT and the OPN.

At least a part of the NOT is closely associated with the accessory optic system (AOS), and is sometimes included with it (Gamlin, P. D., 2005). As just discussed, the AOS serves as a key link between the retina and brainstem circuits generating OKN. Cells in the NOT of many species have been shown to exhibit the same sort of directional preference for whole-field motion observed in cells of the AOS (see Gamlin, P. D., 2005 for review). In their preference for temporonasal slip, they most closely resemble the cells of the DTN, an AOS nucleus with which it is contiguous. The great majority of RGCs retrolabeled from the rabbit NOT have the morphology of the ON-DS type, though a few cells resembling ON–OFF DS cells were also labeled (Pu, M. L. and Amthor, F. R., 1990b). NOT cells functionally resembling neurons of the AOS appear segregated within the NOT, and other sectors of the nucleus exhibit distinctive properties and connections (Gamlin, P. D., 2005).

The olivary pretectal nucleus is an essential synaptic waystation in the neural circuit for the pupillary light reflex. As reviewed by Gamlin P. D. (2005 and Chapter Pupillary Control Pathways), the OPN receives direct retinal input and projects to the parasympathetic preganglionic nucleus mediating pupillary constriction. The dominant retinal input to the OPN appears to come from melanopsin RGCs (Hattar, S. *et al.*, 2002; 2006; Hannibal, J. and Fahrenkrug, J., 2004; Dacey, D. M. *et al.*, 2005; Gamlin, P. D. *et al.*, 2007), but other RGCs of unknown type appear to innervate this nucleus as well (Hattar, S. *et al.*, 2006). There are strong similarities between the melanopsin RGCs and OPN neurons in their tonic encoding of retinal irradiance (Clarke, R. J. and Ikeda, H., 1985; Berson, D. M. *et al.*, 2002; Dacey, D. M. *et al.*, 2005; Trejo, L. J. and Cicerone, C. M., 1984; Gamlin, P. D., 2005; Gamlin, P. D. *et al.*, 2007; see Chapter Pupillary Control Pathways). The persistence of pupillary responses when rod and cone photoreceptors are silenced pharmacologically or genetically is attributable to the intrinsic photosensitivity of the melanopsin RGCs (see Chapters Melanopsin Cells and Pupillary Control Pathways).

Beyond the OPN and the part of the NOT linked to the AOS, relatively little is known about the RGC types innervating the remaining pretectal nuclei. In cats, there is good evidence for inputs from both alpha (Y) and beta (X) cells (Cleland, B. G. and Levick, W. R., 1974b; Schoppmann, A. and Hoffmann, K. P., 1979; Bowling, D. B. and Michael, C. R., 1980; Stone, J., 1983; Leventhal, A. G. *et al.*, 1985; Koontz, M. A. *et al.*, 1985; Tamamaki, N. *et al.*, 1995). There is also clearly input to the pretectum from RGCs other than alpha or beta cells, judging from their small somata and slowly conducting axons (Schoppmann, A. and Hoffmann, K. P., 1979; Stone, J., 1983; Leventhal, A. G. *et al.*, 1985; Rodieck, R. W. and Watanabe, M., 1993; Perry, V. H. and Cowey, A., 1984; Koontz, M. A. *et al.*, 1985; Wingate, R. J. *et al.*, 1992; Young, M. J. and Lund, R. D., 1998). However, well-characterized RGC types have not yet been identified within this group.

1.25.4.6 Hypothalamic Region

The main target of the retinohypothalamic tract is the SCN, which is the master pacemaker for circadian rhythms. This pathway is essential for the resetting of circadian phase by light and, indirectly, for the photic regulation of pineal melatonin synthesis. Detailed information about SCN and the properties of its retinal input may be found in Chapters The Suprachiasmatic Nucleus and Melanopsin Cells, and in Section 1.25.3.1. To summarize, it is well established that the primary source of retinal input to the SCN derives from melanopsin-expressing ganglion cell photoreceptors, with a minor input from other as yet uncharacterized RGCs (Gooley, J. J. *et al.*, 2001; 2003; Berson, D. M. *et al.*, 2002; Hannibal, J. *et al.*, 2002; Hannibal, J. and Fahrenkrug, J., 2004; Hattar, S. *et al.*, 2002; 2006; Morin, L. P. *et al.*, 2003; Sollars, P. J. *et al.*, 2003).

Sparse retinal projections have been shown to reach a wide variety of hypothalamic targets other than the SCN in a wide variety of mammalian species (Johnson, R. F. *et al.*, 1988; Costa, M. S. *et al.*, 1999; Mick, G. *et al.*, 1993; Mikkelsen, J. D., 1992; Mikkelsen, J. D. and Serviere, J., 1992; Pickard, G. E. and Silverman, A. J., 1981; Reuss, S. and Decker, K., 1997; Youngstrom, T. G. *et al.*, 1991; Hattar, S. *et al.*, 2006; Leak, R. K. and Moore, R. Y., 1997; Hannibal, J. and Fahrenkrug, J., 2004; Levine, J. D. *et al.*, 1991; 1994; Abizaid, A. *et al.*, 2004). These include the preoptic region, supraoptic nucleus, lateral and anterior hypothalamic nuclei, subparaventricular zone, and retrochiasmatic area. The functional roles of these retinal outputs are obscure in many cases, but are likely to include modulation of sleep propensity,

neuroendocrine function, and circadian regulation. Melanopsin RGCs have been shown to contribute to many of these projections, although there are clearly also inputs from other unknown RGC types (Leak, R. K. and Moore, R. Y., 1997; Gooley, J. J. *et al.*, 2003; Hattar, S. *et al.*, 2006).

1.25.4.7 Other Targets

In addition to the sparse retinal projections to various dorsal thalamic nuclei noted above, weak retinal inputs have been detected in a variety of limbic, epithalamic, and brainstem sites. These include the amygdala, piriform cortex, bed nucleus of the stria terminalis, zona incerta, perihabenular region, periaqueductal gray, and dorsal raphe nuclei (Foote, W. E. *et al.*, 1978; Pickard, G. E. and Silverman, A. J., 1981; Cooper, H. M. *et al.*, 1993; Elliott, A. S. *et al.*, 1995; Qu, T. *et al.*, 1996; Morin, L. P. and Blanchard, J. H., 1998; Fite, K. V. *et al.*, 1999; 2003; Matteau, I. *et al.*, 2003; Hattar, S. *et al.*, 2006). In general, the ganglion cells from which these projections arise have been characterized only by retrograde transport, which does not permit identification of specific RGC types. However, at least some of these projections have been traced in part to melanopsin RGCs (Hattar, S. *et al.*, 2006), suggesting that these targets may participate in non-image-forming visual networks driving physiological responses to the presence or absence of daylight.

References

Abizaid, A., Horvath, B., Keefe, D. L., Leranth, C., and Horvath, T. L. 2004. Direct visual and circadian pathways target neuroendocrine cells in primates. Eur. J. Neurosci. 20(10), 2767–2776.

Ackert, J. M., Wu, S. H., Lee, J. C., Abrams, J., Hu, E. H., Perlman, I., and Bloomfield, S. A. 2006. Light-induced changes in spike synchronization between coupled ON direction selective ganglion cells in the mammalian retina. J. Neurosci. 26(16), 4206–4215.

Agarwala, S., Petry, H. M., and May, J. G., 3rd. 1989. Retinal projections in the ground squirrel (*Citellus tridecemlineatus*). Vis. Neurosci. 3(6), 537–549.

Amthor, F. R., Oyster, C. W., and Takahashi, E. S. 1984. Morphology of on–off direction-selective ganglion cells in the rabbit retina. Brain. Res. 298(1), 187–190.

Amthor, F. R., Takahashi, E. S., and Oyster, C. W. 1989a. Morphologies of rabbit retinal ganglion cells with complex receptive fields. J. Comp. Neurol. 280(1), 97–121.

Amthor, F. R., Takahashi, E. S., and Oyster, C. W. 1989b. Morphologies of rabbit retinal ganglion cells with concentric receptive fields. J. Comp. Neurol. 280(1), 72–96.

Badea, T. C. and Nathans, J. 2004. Quantitative analysis of neuronal morphologies in the mouse retina visualized by using a genetically directed reporter. J. Comp. Neurol. 480(4), 331–351.

Barlow, H. B. and Hill, R. M. 1963. Selective sensitivity to direction of movement in ganglion cells of the rabbit retina. Science 139, 412–414.

Barlow, H. B., Hill, R. M., and Levick, W. R. 1964. Retinal ganglion cells responding selectively to direction and speed of image motion in the rabbit. J. Physiol. 173, 377–407.

Berman, N. and Jones, E. G. 1977. A retino-pulvinar projection in the cat. Brain. Res. 134(2), 237–248.

Berson, D. M. 1987. Retinal W-cell input to the upper superficial gray layer of the cat's superior colliculus: a conduction-velocity analysis. J. Neurophysiol. 58(5), 1035–1051.

Berson, D. M., Dunn, F. A., and Takao, M. 2002. Phototransduction by retinal ganglion cells that set the circadian clock. Science 295(5557), 1070–1073.

Berson, D. M., Isayama, T., and Pu, M. 1999. The eta ganglion cell type of cat retina. J. Comp. Neurol. 408(2), 204–219.

Berson, D. M., Pu, M., and Famiglietti, E. V. 1998. The zeta cell: a new ganglion cell type in cat retina. J. Comp. Neurol. 399(2), 269–288.

Bloomfield, S. A. and Xin, D. 1997. A comparison of receptive-field and tracer-coupling size of amacrine and ganglion cells in the rabbit retina. Vis. Neurosci. 14(6), 1153–1165.

Bowling, D. B. and Michael, C. R. 1980. Projection patterns of single physiologically characterized optic tract fibres in cat. Nature 286(5776), 899–902.

Boycott, B. B. and Wässle, H. 1974. The morphological types of ganglion cells of the domestic cat's retina. J. Physiol. 240(2), 397–419.

Brecha, N., Johnson, D., Bolz, J., Sharma, S., Parnavelas, J. G., and Lieberman, A. R. 1987. Substance P-immunoreactive retinal ganglion cells and their central axon terminals in the rabbit. Nature 327(6118), 155–158.

Buhl, E. H. and Peichl, L. 1986. Morphology of rabbit retinal ganglion cells projecting to the medial terminal nucleus of the accessory optic system. J. Comp. Neurol. 253(2), 163–174.

Caldwell, J. H. and Daw, N. W. 1978. New properties of rabbit retinal ganglion cells. J. Physiol. 276, 257–276.

Calkins, D. J., Sappington, R. M., and Hendry, S. H. 2005. Morphological identification of ganglion cells expressing the alpha subunit of type II calmodulin-dependent protein kinase in the macaque retina. J. Comp. Neurol. 481(2), 194–209.

Callaway, E. M. 2005. Structure and function of parallel pathways in the primate early visual system. J. Physiol. 566(Pt 1), 13–19.

Carcieri, S. M., Jacobs, A. L., and Nirenberg, S. 2003. Classification of retinal ganglion cells: a statistical approach. J. Neurophysiol. 90(3), 1704–1713.

Casagrande, V. A. 1994. A third parallel visual pathway to primate area V1. Trends Neurosci. 17(7), 305–310.

Chalupa, L. M. and Thompson, I. 1980. Retinal ganglion cell projections to the superior colliculus of the hamster demonstrated by the horseradish peroxidase technique. Neurosci. Lett. 19(1), 13–19.

Chevassus-au-Louis, N. and Cooper, H. M. 1998. Is there a geniculohypothalamic tract in primates? A comparative immunohistochemical study in the circadian system of strepsirhine and haplorhine species. Brain Res. 805(1-2), 213–219.

Clarke, R. J. and Ikeda, H. 1985. Luminance and darkness detectors in the olivary and posterior pretectal nuclei and their relationship to the pupillary light reflex in the rat. I. Studies with steady luminance levels. Exp. Brain Res. 57(2), 224–232.

Cleland, B. G. and Levick, W. R. 1974a. Properties of rarely encountered types of ganglion cells in the cat's retina and an overall classification. J. Physiol. 240, 457–492.

Cleland, B. G. and Levick, W. R. 1974b. Brisk and sluggish concentrically organized ganglion cells in the cat's retina. J. Physiol. 240, 421–456.

Cleland, B. G., Levick, W. R., Morstyn, R., and Wagner, H. G. 1976. Lateral geniculate relay of slowly conducting retinal afferents to cat visual cortex. J. Physiol. 255(1), 299–320.

Conrad, C. D. and Stumpf, W. E. 1975. Direct visual input to the limbic system: crossed retinal projections to the nucleus anterodorsalis thalami in the tree shrew. Exp. Brain Res. 23(2), 141–149.

Coombs, J., van der List, D., Wang, G. Y., and Chalupa, L. M. 2006. Morphological properties of mouse retinal ganglion cells. Neuroscience 140(1), 123–136.

Cooper, H. M., Baleydier, C., and Magnin, M. 1990. Macaque accessory optic system: I. Definition of the medial terminal nucleus. J. Comp. Neurol. 302(2), 394–404.

Cooper, H. M., Herbin, M., and Nevo, E. 1993. Visual system of a naturally microphthalmic mammal: the blind mole rat, *Spalax ehrenbergi*. J. Comp. Neurol. 328(3), 313–350.

Costa, M. S., Santee, U. R., Cavalcante, J. S., Moraes, P. R., Santos, N. P., and Britto, L. R. 1999. Retinohypothalamic projections in the common marmoset (*Callithrix jacchus*): a study using cholera toxin subunit B. J. Comp. Neurol. 415(3), 393–403.

Cowey, A., Stoerig, P., and Bannister, M. 1994. Retinal ganglion cells labelled from the pulvinar nucleus in macaque monkeys. Neuroscience 61(W3), 691–705.

Crook, J. D., Peterson, B., and Dacey, D. 2007. Alpha-like ganglion cells of the primate retina. Association for Research in Vision and Ophthalmology annual meeting, Abstract #5943.

Dacey, D. M. 1989. Monoamine-accumulating ganglion cell type of the cat's retina. J. Comp. Neurol. 288(1), 59–80.

Dacey, D. M. 1993a. Morphology of a small-field bistratified ganglion cell type in the macaque and human retina. Vis. Neurosci. 10(6), 1081–1098.

Dacey, D. M. 1993b. The mosaic of midget ganglion cells in the human retina. J. Neurosci. 13(12), 5334–5355.

Dacey, D. M. 1994. Physiology, morphology and spatial densities of identified ganglion cell types in primate retina. Ciba Found Symp 184, 12–28; discussion 28–34, 63–70.

Dacey, D. M. 2004. Origins of Perception: Retinal Ganglion Cell Diversity and the Creation of Parallel Visual Pathways. In: The Cognitive Neurosciences III (*ed*. M. S. Gazzaniga), pp. 281–301. MIT Press.

Dacey, D. M. and Brace, S. 1992. A coupled network for parasol but not midget ganglion cells in the primate retina. Vis. Neurosci. 9(3-4), 279–290.

Dacey, D. M. and Lee, B. B. 1994. The 'blue-on' opponent pathway in primate retina originates from a distinct bistratified ganglion cell type. Nature 367(6465), 731–735.

Dacey, D. M., Liao, H. W., Peterson, B. B., Robinson, F. R., Smith, V. C., Pokorny, J., Yau, K. W., and Gamlin, P. D. 2005. Melanopsin-expressing ganglion cells in primate retina signal colour and irradiance and project to the LGN. Nature 433(7027), 749–754.

Dacey, D. M., Peterson, B. B., Robinson, F. R., and Gamlin, P. D. 2003. Fireworks in the primate retina: *in vitro* photodynamics reveals diverse LGN-projecting ganglion cell types. Neuron 37(1), 15–27.

Dann, J. F. and Buhl, E. H. 1987. Retinal ganglion cells projecting to the accessory optic system in the rat. J. Comp. Neurol. 262(1), 141–158.

Dann, J. F. and Buhl, E. H. 1990. Morphology of retinal ganglion cells in the flying fox (*Pteropus scapulatus*): a lucifer yellow investigation. J. Comp. Neurol. 301(3), 401–416.

de Monasterio, F. M. and Gouras, P. 1975. Functional properties of ganglion cells of the rhesus monkey retina. J. Physiol. 251(1), 167–195.

de Monasterio, F. M., Gouras, P., and Tolhurst, D. J. 1976. Spatial summation, response pattern and conduction velocity of ganglion cells of the rhesus monkey retina. Vision Res. 16(6), 674–678.

de Monasterio, F. M. 1978a. Properties of concentrically organized X and Y ganglion cells of macaque retina. J. Neurophysiol. 41(6), 1394–1417.

de Monasterio, F. M. 1978b. Properties of ganglion cells with atypical receptive-field organization in retina of macaques. J. Neurophysiol. 41(6), 1435–1449.

Demb, J. B., Haarsma, L., Freed, M. A., and Sterling, P. 1999. Functional circuitry of the retinal ganglion cell's nonlinear receptive field. J. Neurosci. 19(22), 9756–9767.

Devries, S. H. and Baylor, D. A. 1997. Mosaic arrangement of ganglion cell receptive fields in rabbit retina. J. Neurophysiol. 78(4), 2048–2060.

Doi, M., Uji, Y., and Yamamura, H. 1995. Morphological classification of retinal ganglion cells in mice. J. Comp. Neurol. 356(3), 368–386.

Dong, W., Sun, W., Zhang, Y., Chen, X., and He, S. 2004. Dendritic relationship between starburst amacrine cells and direction-selective ganglion cells in the rabbit retina. J. Physiol. 556(Pt 1), 11–17.

Dreher, B., Sefton, A. J., Ni, S. Y., and Nisbett, G. 1985. The morphology, number, distribution and central projections of Class I retinal ganglion cells in albino and hooded rats. Brain Behav. Evol. 26(1), 10–48.

Elliott, A. S., Weiss, M. L., and Nunez, A. A. 1995. Direct retinal communication with the peri-amygdaloid area. Neuroreport 6(5), 806–808.

Famiglietti, E. V. 1987. Starburst amacrine cells in cat retina are associated with bistratified, presumed directionally selective, ganglion cells. Brain Res. 413(2), 404–408.

Famiglietti, E. V. 1992a. Dendritic co-stratification of ON and ON–OFF directionally selective ganglion cells with starburst amacrine cells in rabbit retina. J. Comp. Neurol. 324(3), 322–335.

Famiglietti, E. V. 1992b. New metrics for analysis of dendritic branching patterns demonstrating similarities and differences in ON and ON–OFF directionally selective retinal ganglion cells. J. Comp. Neurol. 324(3), 295–321.

Famiglietti, E. V. 2004. Class I and class II ganglion cells of rabbit retina: a structural basis for X and Y (brisk) cells. J. Comp. Neurol. 478(4), 323–346.

Famiglietti, E. V. 2005a. ''Small-tufted'' ganglion cells and two visual systems for the detection of object motion in rabbit retina. Vis. Neurosci. 22(4), 509–534.

Famiglietti, E. V. 2005b. Synaptic organization of complex ganglion cells in rabbit retina: type and arrangement of inputs to directionally selective and local-edge-detector cells. J. Comp. Neurol. 484(4), 357–391.

Famiglietti, E. V., Jr. and Kolb, H. 1976. Structural basis for ON- and OFF-center responses in retinal ganglion cells. Science 194(4261), 193–195.

Farmer, S. G. and Rodieck, R. W. 1982. Ganglion cells of the cat accessory optic system: morphology and retinal topography. J. Comp. Neurol. 205(2), 190–198.

Fite, K. V., Birkett, M. A., Smith, A., Janusonis, S., and McLaughlin, S. 2003. Retinal ganglion cells projecting to the dorsal raphe and lateral geniculate complex in Mongolian gerbils. Brain Res. 973(1), 146–150.

Fite, K. V., Janusonis, S., Foote, W., and Bengston, L. 1999. Retinal afferents to the dorsal raphe nucleus in rats and Mongolian gerbils. J. Comp. Neurol. 414(4), 469–484.

Foote, W. E., Taber-Pierce, E., and Edwards, L. 1978. Evidence for a retinal projection to the midbrain raphe of the cat. Brain Res. 156(1), 135–140.

Freeman, B. and Singer, W. 1983. Direct and indirect visual inputs to superficial layers of cat superior colliculus: a current source-density analysis of electrically evoked potentials. J. Neurophysiol. 49(5), 1075–1091.

Fukuda, Y. 1977. A three-group classification of rat retinal ganglion cells: histological and physiological studies. Brain Res. 119(2), 327–334.

Fukuda, Y., Hsiao, C. F., Watanabe, M., and Ito, H. 1984. Morphological correlates of physiologically identified Y-, X-, and W-cells in cat retina. J. Neurophysiol. 52(6), 999–1013.

Gamlin, P. D. 2005. The pretectum: connections and oculomotor-related roles. Prog. Brain Res. 151, 379–405.

Gamlin, P. D., McDougal, D. H., Pokorny, J., Smith, V. C., Yau, K. W., and Dacey, D. M. 2007. Human and macaque pupil responses driven by melanopsin-containing retinal ganglion cells. Vision Res. 47(7), 946–954.

Ghosh, K. K., Goodchild, A. K., Sefton, A. E., and Martin, P. R. 1996. Morphology of retinal ganglion cells in a new world monkey, the marmoset *Callithrix jacchus*. J. Comp. Neurol. 366(1), 76–92.

Ghosh, K. K., Martin, P. R., and Grunert, U. 1997. Morphological analysis of the blue cone pathway in the retina of a New World monkey, the marmoset *Callithrix jacchus*. J. Comp. Neurol. 379(2), 211–225.

Giolli, R. A., Blanks, R. H., and Lui, F. 2005. The accessory optic system: basic organization with an update on connectivity, neurochemistry, and function. Prog. Brain Res. 151, 407–440.

Godement, P., Salaun, J., and Imbert, M. 1984. Prenatal and postnatal development of retinogeniculate and retinocollicular projections in the mouse. J. Comp. Neurol. 230(4), 552–575.

Gooley, J. J., Lu, J., Chou, T. C., Scammell, T. E., and Saper, C. B. 2001. Melanopsin in cells of origin of the retinohypothalamic tract. Nat. Neurosci. 4(12), 1165.

Gooley, J. J., Lu, J., Fischer, D., and Saper, C. B. 2003. A broad role for melanopsin in nonvisual photoreception. J. Neurosci. 23(18), 7093–7106.

Gouras, P. 1969. Antidromic responses of orthodromically identified ganglion cells in monkey retina. J. Physiol. 204(2), 407–419.

Grasse, K. L., Cynader, M. S., and Douglas, R. M. 1984. Alterations in response properties in the lateral and dorsal terminal nuclei of the cat accessory optic system following visual cortex lesions. Exp. Brain Res. 55(1), 69–80.

Hale, P. T., Sefton, A. J., and Dreher, B. 1979. A correlation of receptive field properties with conduction velocity of cells in the rat's retino-geniculo-cortical pathway. Exp. Brain Res. 35(3), 425–442.

Hannibal, J. and Fahrenkrug, J. 2004. Target areas innervated by PACAP-immunoreactive retinal ganglion cells. Cell Tissue Res. 316(1), 99–113.

Hannibal, J., Hindersson, P., Nevo, E., and Fahrenkrug, J. 2002. The circadian photopigment melanopsin is expressed in the blind subterranean mole rat, *Spalax*. Neuroreport 13(11), 1411–1414.

Harrington, M. E. 1997. The ventral lateral geniculate nucleus and the intergeniculate leaflet: interrelated structures in the visual and circadian systems. Neurosci. Biobehav. Rev. 21(5), 705–727.

Hattar, S., Kumar, M., Park, A., Tong, P., Tung, J., Yau, K. W., and Berson, D. M. 2006. Central projections of melanopsin-expressing retinal ganglion cells in the mouse. J. Comp. Neurol. 497(3), 326–349.

Hattar, S., Liao, H. W., Takao, M., Berson, D. M., and Yau, K. W. 2002. Melanopsin-containing retinal ganglion cells: architecture, projections, and intrinsic photosensitivity. Science 295(5557), 1065–1070.

He, S. and Masland, R. H. 1998. ON direction-selective ganglion cells in the rabbit retina: dendritic morphology and pattern of fasciculation. Vis. Neurosci. 15(2), 369–375.

Hendry, S. H. and Reid, R. C. 2000. The koniocellular pathway in primate vision. Annu. Rev. Neurosci. 23, 127–153.

Hofbauer, A. and Drager, U. C. 1985. Depth segregation of retinal ganglion cells projecting to mouse superior colliculus. J. Comp. Neurol. 234(4), 465–474.

Hoffmann, K. P. 1973. Conduction velocity in pathways from retina to superior colliculus in the cat: a correlation with receptive-field properties. J. Neurophysiol. 36(3), 409–424.

Hoffmann, K. P. and Distler, C. 1989. Quantitative analysis of visual receptive fields of neurons in nucleus of the optic tract and dorsal terminal nucleus of the accessory optic tract in macaque monkey. J. Neurophysiol. 62(2), 416–428.

Holdefer, R. N. and Norton, T. T. 1995. Laminar organization of receptive field properties in the dorsal lateral geniculate nucleus of the tree shrew (*Tupaiaglis belangeri*). J. Comp. Neurol. 358(3), 401–413.

Huxlin, K. R. and Goodchild, A. K. 1997. Retinal ganglion cells in the albino rat: revised morphological classification. J. Comp. Neurol. 385(2), 309–323.

Illing, R. B. and Wässle, H. 1981. The retinal projection to the thalamus in the cat: a quantitative investigation and a comparison with the retinotectal pathway. J. Comp. Neurol. 202(2), 265–285.

Irvin, G. E., Norton, T. T., Sesma, M. A., and Casagrande, V. A. 1986. W-like response properties of interlaminar zone cells in the lateral geniculate nucleus of a primate (*Galago crassicaudatus*). Brain Res. 362(2), 254–270.

Isayama, T., Berson, D. M., and Pu, M. 2000. Theta ganglion cell type of cat retina. J. Comp. Neurol. 417(1), 32–48.

Itaya, S. K., Van Hoesen, G. W., and Benevento, L. A. 1986. Direct retinal pathways to the limbic thalamus of the monkey. Exp. Brain Res. 61(3), 607–613.

Itoh, K., Conley, M., and Diamond, I. T. 1981. Different distribution of large and small retinal ganglion cells in the cat after HRP injections of single layers of the lateral geniculate body and the superior colliculus. Brain Res. 207(1), 147–152.

Jensen, R. J. 1991. Intracellular recording of light responses from visually identified ganglion cells in the rabbit retina. J. Neurosci. Methods 40(2–3), 101–112.

Johnson, R. F., Morin, L. P., and Moore, R. Y. 1988. Retinohypothalamic projections in the hamster and rat demonstrated using cholera toxin. Brain Res. 462(2), 301–312.

Kolb, H., Linberg, K. A., and Fisher, S. K. 1992. Neurons of the human retina: a Golgi study. J. Comp. Neurol. 318(2), 147–187.

Kolb, H., Nelson, R., and Mariani, A. 1981. Amacrine cells, bipolar cells and ganglion cells of the cat retina: a Golgi study. Vision Res. 21(7), 1081–1114.

Kong, J. H., Fish, D. R., Rockhill, R. L., and Masland, R. H. 2005. Diversity of ganglion cells in the mouse retina: unsupervised morphological classification and its limits. J. Comp. Neurol. 489(3), 293–310.

Koontz, M. A., Rodieck, R. W., and Farmer, S. G. 1985. The retinal projection to the cat pretectum. J. Comp. Neurol. 236(1), 42–59.

Lau, K. C., So, K. F., and Tay, D. 1992. Postnatal development of type I retinal ganglion cells in hamsters: a lucifer yellow study. J. Comp. Neurol. 315(4), 375–381.

Leak, R. K. and Moore, R. Y. 1997. Identification of retinal ganglion cells projecting to the lateral hypothalamic area of the rat. Brain Res. 770(1–2), 105–114.

Lee, B. B., Silveira, L. C., Yamada, E. S., Hunt, D. M., Kremers, J., Martin, P. R., Troy, J. B., and da Silva-Filho, M. 2000. Visual responses of ganglion cells of a New-World primate, the capuchin monkey, Cebus apella. J. Physiol. 528(Pt 3), 573–590.

Leventhal, A. G., Keens, J., and Tork, I. 1980. The afferent ganglion cells and cortical projections of the retinal recipient zone (RRZ) of the cat's pulvinar complex. J. Comp. Neurol. 194(3), 535–554.

Leventhal, A. G., Rodieck, R. W., and Dreher, B. 1981. Retinal ganglion cell classes in the Old World monkey: morphology and central projections. Science 213(4512), 1139–1142.

Leventhal, A. G., Rodieck, R. W., and Dreher, B. 1985. Central projections of cat retinal ganglion cells. J. Comp. Neurol. 237(2), 216–226.

Levick, W. R. 1967. Receptive fields and trigger features of ganglion cells in the visual streak of the rabbits retina. J. Physiol. 188(3), 285–307.

Levick, W. R., Oyster, C. W., and Takahashi, E. 1969. Rabbit lateral geniculate nucleus: sharpener of directional information. Science 165(894), 712–714.

Levine, J. D., Weiss, M. L., Rosenwasser, A. M., and Miselis, R. R. 1991. Retinohypothalamic tract in the female albino rat: a study using horseradish peroxidase conjugated to cholera toxin. J. Comp. Neurol. 306(2), 344–360.

Levine, J. D., Zhao, X. S., and Miselis, R. R. 1994. Direct and indirect retinohypothalamic projections to the supraoptic nucleus in the female albino rat. J. Comp. Neurol. 341(2), 214–224.

Linberg, K. A., Suemune, S., and Fisher, S. K. 1996. Retinal neurons of the California ground squirrel, *Spermophilus beecheyi*: a Golgi study. J. Comp. Neurol. 365(2), 173–216.

Linden, R. and Perry, V. H. 1983. Massive retinotectal projection in rats. Brain Res. 272(1), 145–149.

Ling, C., Schneider, G. E., and Jhaveri, S. 1998. Target-specific morphology of retinal axon arbors in the adult hamster. Vis. Neurosci. 15(3), 559–579.

Major, D. E., Rodman, H. R., Libedinsky, C., and Karten, H. J. 2003. Pattern of retinal projections in the California ground squirrel (*Spermophilus beecheyi*): anterograde tracing study using cholera toxin. J. Comp. Neurol. 463(3), 317–340.

Marrocco, R. T. 1978. Conduction velocities of afferent input to superior colliculus in normal and decorticate monkeys. Brain Res. 140(1), 155–158.

Martin, P. R. 1986. The projection of different retinal ganglion cell classes to the dorsal lateral geniculate nucleus in the hooded rat. Exp. Brain Res. 62(1), 77–88.

Masland, R. H. 2001a. The fundamental plan of the retina. Nat. Neurosci. 4(9), 877–886.

Matteau, I., Boire, D., and Ptito, M. 2003. Retinal projections in the cat: a cholera toxin B subunit study. Vis. Neurosci. 20(5), 481–493.

Maturana, H. R., Lettvin, J. Y., McCulloch, W. S., and Pitts, W. H. 1960. Anatomy and physiology of vision in the frog (*Rana pipiens*). J. Gen. Physiol. 43(6 Suppl.), 129–175.

May, P. J. 2005. The mammalian superior colliculus: laminar structure and connections. Prog. Brain Res. 151, 321–378.

Michael, C. R. 1972. Functional organization of cells in superior colliculus of the ground squirrel. J. Neurophysiol. 35(6), 833–846.

Mick, G., Cooper, H., and Magnin, M. 1993. Retinal projection to the olfactory tubercle and basal telencephalon in primates. J. Comp. Neurol. 327(2), 205–219.

Mikkelsen, J. D. 1992. Visualization of efferent retinal projections by immunohistochemical identification of cholera toxin subunit B. Brain Res. Bull. 28(4), 619–623.

Mikkelsen, J. D. and Serviere, J. 1992. Demonstration of a direct projection from the retina to the hypothalamic supraoptic nucleus of the hamster. Neurosci. Lett. 139(2), 149–152.

Miura, M., Dong, K., Ahmed, F. A., Okamura, H., and Yamadori, T. 1997. The termination of optic nerve fibers in the albino mouse. Kobe. J. Med. Sci. 43(3-4), 99–108.

Mizuno, N., Itoh, K., Uchida, K., Uemura-Sumi, M., and Matsushima, R. 1982. A retino-pulvinar projection in the macaque monkey as visualized by the use of anterograde transport of horseradish peroxidase. Neurosci. Lett. 30(3), 199–203.

Mooney, R. D. and Rhoades, R. W. 1990. Relationships between physiological and morphological properties of retinocollicular axons in the hamster. J. Neurosci. 10(9), 3164–3177.

Moore, R. Y. 1993. Organization of the primate circadian system. J. Biol. Rhythms 8 (Suppl.), S3–S9.

Moore, R. Y. and Card, J. P. 1994. Intergeniculate leaflet: an anatomically and functionally distinct subdivision of the lateral geniculate complex. J. Comp. Neurol. 344(3), 403–430.

Moraes, A. M., Oliveira, M. M., and Hokoc, J. N. 2000. Retinal ganglion cells in the South American opossum (*Didelphis aurita*). J. Comp. Neurol. 418(2), 193–216.

Morin, L. P. and Blanchard, J. H. 1997. Neuropeptide Y and enkephalin immunoreactivity in retinorecipient nuclei of the hamster pretectum and thalamus. Vis. Neurosci. 14(4), 765–777.

Morin, L. P. and Blanchard, J. H. 1998. Interconnections among nuclei of the subcortical visual shell: the intergeniculate leaflet is a major constituent of the hamster subcortical visual system. J. Comp. Neurol. 396(3), 288–309.

Morin, L. P., Blanchard, J. H., and Provencio, I. 2003. Retinal ganglion cell projections to the hamster suprachiasmatic nucleus, intergeniculate leaflet, and visual midbrain: bifurcation and melanopsin immunoreactivity. J. Comp. Neurol. 465(3), 401–416.

Mustari, M. J. and Fuchs, A. F. 1989. Response properties of single units in the lateral terminal nucleus of the accessory optic system in the behaving primate. J. Neurophysiol. 61(6), 1207–1220.

Norton, T. T. and Casagrande, V. A. 1982. Laminar organization of receptive-field properties in lateral geniculate nucleus of bush baby (*Galago crassicaudatus*). J. Neurophysiol. 47(4), 715–741.

O'Brien, B. J., Isayama, T., Richardson, R., and Berson, D. M. 2002. Intrinsic physiological properties of cat retinal ganglion cells. J. Physiol. 538(Pt 3), 787–802.

Oyster, C. W. and Barlow, H. B. 1967. Direction-selective units in rabbit retina: distribution of preferred directions. Science 155(764), 841–842.

Oyster, C. W., Simpson, J. I., Takahashi, E. S., and Soodak, R. E. 1980. Retinal ganglion cells projecting to the rabbit accessory optic system. J. Comp. Neurol. 190(1), 49–61.

Oyster, C. W., Takahashi, E., and Collewijn, H. 1972. Direction-selective retinal ganglion cells and control of optokinetic nystagmus in the rabbit. Vision Res. 12(2), 183–193.

Pak, M. W., Giolli, R. A., Pinto, L. H., Mangini, N. J., Gregory, K. M., and Vanable, J. W., Jr. 1987. Retinopretectal and accessory optic projections of normal mice and the OKN-defective mutant mice beige, beige-J, and pearl. J. Comp. Neurol. 258(3), 435–446.

Pang, J. J., Gao, F., and Wu, S. M. 2003. Light-evoked excitatory and inhibitory synaptic inputs to ON and OFF

alpha ganglion cells in the mouse retina. J. Neurosci. 23(14), 6063–6073.
Peichl, L. 1989. Alpha and delta ganglion cells in the rat retina. J. Comp. Neurol. 286(1), 120–139.
Peichl, L. 1991. Alpha ganglion cells in mammalian retinae: common properties, species differences, and some comments on other ganglion cells. Vis. Neurosci. 7(1-2), 155–169.
Peichl, L. 1992. Morphological types of ganglion cells in the dog and wolf retina. J. Comp. Neurol. 324(4), 590–602.
Peichl, L. and Wässle, H. 1983. The structural correlate of the receptive field centre of alpha ganglion cells in the cat retina. J. Physiol. 341, 309–324.
Peichl, L., Buhl, E. H., and Boycott, B. B. 1987a. Alpha ganglion cells in the rabbit retina. J. Comp. Neurol. 263(1), 25–41.
Peichl, L., Ott, H., and Boycott, B. B. 1987b. Alpha ganglion cells in mammalian retinae. Proc. R. Soc. Lond. B. Biol. Sci. 231(1263), 169–197.
Perry, V. H. 1979. The ganglion cell layer of the retina of the rat: a Golgi study. Proc. R. Soc. Lond. B. Biol. Sci. 204(1156), 363–375.
Perry, V. H. and Cowey, A. 1981. The morphological correlates of X- and Y-like retinal ganglion cells in the retina of monkeys. Exp. Brain Res. 43(2), 226–228.
Perry, V. H. and Cowey, A. 1984. Retinal ganglion cells that project to the superior colliculus and pretectum in the macaque monkey. Neuroscience 12(4), 1125–1137.
Perry, V. H., Oehler, R., and Cowey, A. 1984. Retinal ganglion cells that project to the dorsal lateral geniculate nucleus in the macaque monkey. Neuroscience 12(4), 1101–1123.
Peterson, B. B. and Dacey, D. M. 1999. Morphology of wide-field, monostratified ganglion cells of the human retina. Vis. Neurosci. 16(1), 107–120.
Peterson, B. B. and Dacey, D. M. 2000. Morphology of wide-field bistratified and diffuse human retinal ganglion cells. Vis. Neurosci. 17(4), 567–578.
Pickard, G. E. 1985. Bifurcating axons of retinal ganglion cells terminate in the hypothalamic suprachiasmatic nucleus and the intergeniculate leaflet of the thalamus. Neurosci. Lett. 55(2), 211–217.
Pickard, G. E. and Silverman, A. J. 1981. Direct retinal projections to the hypothalamus, piriform cortex, and accessory optic nuclei in the golden hamster as demonstrated by a sensitive anterograde horseradish peroxidase technique. J. Comp. Neurol. 196(1), 155–172.
Polyak, S. L. 1941. The retina Chicago University of Chicago Press.
Provencio, I., Rodriguez, I. R., Jiang, G., Hayes, W. P., Moreira, E. F., and Rollag, M. D. 2000. A novel human opsin in the inner retina. J. Neurosci. 20(2), 600–605.
Provencio, I., Rollag, M. D., and Castrucci, A. M. 2002. Photoreceptive net in the mammalian retina. This mesh of cells may explain how some blind mice can still tell day from night. Nature 415(6871), 493.
Pu, M. 1999. Dendritic morphology of cat retinal ganglion cells projecting to suprachiasmatic nucleus. J. Comp. Neurol. 414(2), 267–274.
Pu, M., Berson, D. M., and Pan, T. 1994. Structure and function of retinal ganglion cells innervating the cat's geniculate wing: an *in vitro* study. J. Neurosci. 14(7), 4338–4358.
Pu, M. and Pickard, G. E. 1996. Ventral lateral geniculate nucleus afferents to the suprachiasmatic nucleus in the cat. Brain Res. 725(2), 247–251.
Pu, M. L. and Amthor, F. R. 1990a. Dendritic morphologies of retinal ganglion cells projecting to the lateral geniculate nucleus in the rabbit. J. Comp. Neurol. 302(3), 675–693.
Pu, M. L. and Amthor, F. R. 1990b. Dendritic morphologies of retinal ganglion cells projecting to the nucleus of the optic tract in the rabbit. J. Comp. Neurol. 302(3), 657–674.
Qu, T., Dong, K., Sugioka, K., and Yamadori, T. 1996. Demonstration of direct input from the retina to the lateral habenular nucleus in the albino rat. Brain Res. 709(2), 251–258.
Quina, L. A., Pak, W., Lanier, J., Banwait, P., Gratwick, K., Liu, Y., Velasquez, T., O'Leary, D. D., Goulding, M, and Turner, E. E. 2005. Brn3a-expressing retinal ganglion cells project specifically to thalamocortical and collicular visual pathways. J. Neurosci. 25(50), 11595–11604.
Reese, B. E. 1988. 'Hidden lamination' in the dorsal lateral geniculate nucleus: the functional organization of this thalamic region in the rat. Brain Res. 472(2), 119–137.
Reuss, S. and Decker, K. 1997. Anterograde tracing of retinohypothalamic afferents with Fluoro-Gold. Brain Res. 745(1-2), 197–204.
Rivera, N. and Lugo, N. 1998. Four retinal ganglion cell types that project to the superior colliculus in the thirteen-lined ground squirrel (*Spermophilus tridecemlineatus*). J. Comp. Neurol. 396(1), 105–120.
Rockhill, R. L., Daly, F. J., MacNeil, M. A., Brown, S. P., and Masland, R. H. 2002. The diversity of ganglion cells in a mammalian retina. J. Neurosci. 22(9), 3831–3843.
Rodieck, R. W. 1988. The Primate Retina. In: Comparative Primate Biology (*ed*. H. D. Steklis), pp. 203–278, Liss.
Rodieck, R. W. 1998. The First Steps in Seeing. Sinauer Associates, Inc.
Rodieck, R. W. and Brening, R. K. 1983. Retinal ganglion cells: properties, types, genera, pathways and trans-species comparisons. Brain Behav. Evol. 23(3–4), 121–164.
Rodieck, R. W. and Watanabe, M. 1993. Survey of the morphology of macaque retinal ganglion cells that project to the pretectum, superior colliculus, and parvicellular laminae of the lateral geniculate nucleus. J. Comp. Neurol. 338(2), 289–303.
Rollag, M. D., Berson, D. M., and Provencio, I. 2003. Melanopsin, ganglion-cell photoreceptors, and mammalian photoentrainment. J. Biol. Rhythms. 18(3), 227–234.
Roska, B. and Werblin, F. 2001. Vertical interactions across ten parallel, stacked representations in the mammalian retina. Nature 410(6828), 583–587.
Roska, B., Molnar, A., and Werblin, F. S. 2006. Parallel processing in retinal ganglion cells: how integration of space-time patterns of excitation and inhibition form the spiking output. J. Neurophysiol. 95(6), 3810–3822.
Rowe, M. H. and Stone, J. 1977. Naming of neurons: classification and naming of cat retinal ganglion cells. Brain Behav. Evol. 14, 185–216.
Sachs, G. M. and Schneider, G. E. 1984. The morphology of optic tract axons arborizing in the superior colliculus of the hamster. J. Comp. Neurol. 230(2), 155–167.
Saito, H. A. 1983. Morphology of physiologically identified X-, Y-, and W-type retinal ganglion cells of the cat. J. Comp. Neurol. 221(3), 279–288.
Scalia, F. 1972. The termination of retinal axons in the pretectal region of mammals. J. Comp. Neurol. 145(2), 223–257.
Scalia, F. and Arango, V. 1979. Topographic organization of the projections of the retina to the pretectal region in the rat. J. Comp. Neurol. 186(2), 271–292.
Schiller, P. H. and Malpeli, J. G. 1977. Properties and tectal projections of monkey retinal ganglion cells. J. Neurophysiol. 40(2), 428–445.
Schoppmann, A. and Hoffmann, K. P. 1979. A comparison of visual responses in two pretectal nuclei and in the superior colliculus of the cat. Exp. Brain Res. 35(3), 495–510.

Schubert, T., Maxeiner, S., Kruger, O., Willecke, K., and Weiler, R. 2005. Connexin45 mediates gap junctional coupling of bistratified ganglion cells in the mouse retina. J. Comp. Neurol. 490(1), 29–39.

Shapley, R. and Perry, V. H. 1986. Cat and monkey retinal ganglion cells and their visual functional roles. Trends Neurosci. 9, 229–235.

Silveira, L. C., Lee, B. B., Yamada, E. S., Kremers, J., Hunt, D. M., Martin, P. R., and Gomes, F. L. 1999. Ganglion cells of a short-wavelength-sensitive cone pathway in New World monkeys: morphology and physiology. Vis. Neurosci. 16(2), 333–343.

Silveira, L. C., Yamada, E. S., Perry, V. H., and Picanco-Diniz, C. W. 1994. M and P retinal ganglion cells of diurnal and nocturnal New-World monkeys. Neuroreport 5(16), 2077–2081.

Simpson, J. I. 1984. The accessory optic system. Annu. Rev. Neurosci. 7, 13–41.

Simpson, J. I., Giolli, R. A., and Blanks, R. H. 1988a. The pretectal nuclear complex and the accessory optic system. Rev. Oculomot. Res. 2, 335–364.

Simpson, J. I., Leonard, C. S., and Soodak, R. E. 1988b. The accessory optic system of rabbit. II. Spatial organization of direction selectivity. J. Neurophysiol. 60(6), 2055–2072.

Simpson, J. I., Leonard, C. S., and Soodak, R. E. 1988c. The accessory optic system. Analyzer of self-motion. Ann. NY. Acad. Sci. 545, 170–179.

Sollars, P. J., Smeraski, C. A., Kaufman, J. D., Ogilvie, M. D., Provencio, I., and Pickard, G. E. 2003. Melanopsin and non-melanopsin expressing retinal ganglion cells innervate the hypothalamic suprachiasmatic nucleus. Vis. Neurosci. 20(6), 601–610.

Somogyi, G., Hajdu, F., Hassler, R., and Wagner, A. 1981. An experimental electron microscopical study of a direct retino-pulvinar pathway in the tree shrew. Exp. Brain Res. 43(3-4), 447–450.

Soodak, R. E. and Simpson, J. I. 1988. The accessory optic system of rabbit. I. Basic visual response properties. J. Neurophysiol. 60(6), 2037–2054.

Stanford, L. R. 1987. W-cells in the cat retina: correlated morphological and physiological evidence for two distinct classes. J. Neurophysiol. 57(1), 218–244.

Stanford, L. R. and Sherman, S. M. 1984. Structure/function relationships of retinal ganglion cells in the cat. Brain Res. 297(2), 381–386.

Stein, J. J. and Berson, D. M. 1995. On the distribution of gamma cells in the cat retina. Vis. Neurosci. 12(4), 687–700.

Stone, C. and Pinto, L. H. 1993. Response properties of ganglion cells in the isolated mouse retina. Vis. Neurosci. 10(1), 31–39.

Stone, J. 1983. Parallel Processing in the Visual System. The Classification of Retinal Ganglion Cells and its Impact on the Neurobiology of Vision. Plenum.

Stone, J. and Fukuda, Y. 1974. Properties of cat retinal ganglion cells: a comparison of W-cells with X- and Y-cells. J. Neurophysiol. 37(4), 722–748.

Sun, W., Deng, Q., Levick, W. R., and He, S. 2006. ON direction-selective ganglion cells in the mouse retina. J. Physiol. 576(Pt 1), 197–202.

Sun, W., Li, N., and He, S. 2002a. Large-scale morphological survey of rat retinal ganglion cells. Vis. Neurosci. 19(4), 483–493.

Sun, W., Li, N., and He, S. 2002b. Large-scale morphological survey of mouse retinal ganglion cells. J. Comp. Neurol. 451(2), 115–126.

Sur, M., Esguerra, M., Garraghty, P. E., Kritzer, M. F., and Sherman, S. M. 1987. Morphology of physiologically identified retinogeniculate X- and Y-axons in the cat. J. Neurophysiol. 58(1), 1–32.

Sur, M. and Sherman, S. M. 1982. Linear and nonlinear W-cells in C-laminae of the cat's lateral geniculate nucleus. J. Neurophysiol. 47(5), 869–884.

Tamamaki, N., Uhlrich, D. J., and Sherman, S. M. 1995. Morphology of physiologically identified retinal X and Y axons in the cat's thalamus and midbrain as revealed by intraaxonal injection of biocytin. J. Comp. Neurol. 354(4), 583–607.

Telkes, I., Distler, C., and Hoffmann, K. P. 2000. Retinal ganglion cells projecting to the nucleus of the optic tract and the dorsal terminal nucleus of the accessory optic system in macaque monkeys. Eur. J. Neurosci. 12(7), 2367–2375.

Thanos, S. 1988. Morphology of ganglion cell dendrites in the albino rat retina: an analysis with fluorescent carbocyanine dyes. J. Hirnforsch. 29(6), 617–631.

Trejo, L. J. and Cicerone, C. M. 1984. Cells in the pretectal olivary nucleus are in the pathway for the direct light reflex of the pupil in the rat. Brain Res. 300(1), 49–62.

van der Togt, C., van der Want, J., and Schmidt, M. 1993. Segregation of direction selective neurons and synaptic organization of inhibitory intranuclear connections in the medial terminal nucleus of the rat: an electrophysiological and immunoelectron microscopical study. J. Comp. Neurol. 338(2), 175–192.

van Wyk, M., Taylor, W. R., and Vaney, D. I. 2006. Local edge detectors: a substrate for fine spatial vision at low temporal frequencies in rabbit retina. J. Neurosci. 26(51), 13250–13263.

Vaney, D. I. 1994. Territorial organization of direction-selective ganglion cells in rabbit retina. J. Neurosci. 14(11 Pt 1), 6301–6316.

Vaney, D. I., Levick, W. R., and Thibos, L. N. 1981a. Rabbit retinal ganglion cells. Receptive field classification and axonal conduction properties. Exp. Brain Res. 44(1), 27–33.

Vaney, D. I., Peichl, L., Wassle, H., and Illing, R. B. 1981b. Almost all ganglion cells in the rabbit retina project to the superior colliculus. Brain Res. 212(2), 447–453.

Vardi, N., Masarachia, P. J., and Sterling, P. 1989. Structure of the starburst amacrine network in the cat retina and its association with alpha ganglion cells. J. Comp. Neurol. 288(4), 601–611.

Vitek, D. J., Schall, J. D., and Leventhal, A. G. 1985. Morphology, central projections, and dendritic field orientation of retinal ganglion cells in the ferret. J. Comp. Neurol. 241(1), 1–11.

Volgyi, B., Abrams, J., Paul, D. L., and Bloomfield, S. A. 2005. Morphology and tracer coupling pattern of alpha ganglion cells in the mouse retina. J. Comp. Neurol. 492(1), 66–77.

Warren, E. J., Allen, C. N., Brown, R. L., and Robinson, D. W. 2003. Intrinsic light responses of retinal ganglion cells projecting to the circadian system. Eur. J. Neurosci. 17(9), 1727–1735.

Wässle, H. 1982. In: Morphological Types and Central Projections of Ganglion Cells in the Cat Retina, (*eds*. N. Osborne and G. Chader). Pergamon.

Wässle, H. and Boycott, B. B. 1991. Functional architecture of the mammalian retina. Physiol. Rev. 71(2), 447–480.

Wässle, H. and Illing, R. B. 1980. The retinal projection to the superior colliculus in the cat: a quantitative study with HRP. J. Comp. Neurol. 190(2), 333–356.

Watanabe, M. and Rodieck, R. W. 1989. Parasol and midget ganglion cells of the primate retina. J. Comp. Neurol. 289(3), 434–454.

Weber, J. T. 1985. Pretectal complex and accessory optic system of primates. Brain Behav. Evol. 26(2), 117–140.

Weng, S., Sun, W., and He, S. 2005. Identification of ON–OFF direction-selective ganglion cells in the mouse retina. J. Physiol. 562(Pt 3), 915–923.

West, R. W. and Dowling, J. E. 1972. Synapses onto different morphological types of retinal ganglion cells. Science 178(60), 510–512.
White, A. J., Wilder, H. D., Goodchild, A. K., Sefton, A. J., and Martin, P. R. 1998. Segregation of receptive field properties in the lateral geniculate nucleus of a New-World monkey, the marmoset *Callithrix jacchus*. J. Neurophysiol. 80(4), 2063–2076.
Wilson, P. D. and Condo, G. J. 1985. beta-like ganglion cells in the retina of the North American opossum. Brain Res. 331(1), 155–159.
Wilson, P. D., Rowe, M. H., and Stone, J. 1976. Properties of relay cells in cat's lateral geniculate nucleus: a comparison of W-cells with X- and Y-cells. J. Neurophysiol. 39(6), 1193–1209.
Wingate, R. J., Fitzgibbon, T., and Thompson, I. D. 1992. Lucifer yellow, retrograde tracers, and fractal analysis characterise adult ferret retinal ganglion cells. J. Comp. Neurol. 323(4), 449–474.
Yamada, E. S., Bordt, A. S., and Marshak, D. W. 2005. Wide-field ganglion cells in macaque retinas. Vis. Neurosci. 22(4), 383–393.
Yamada, E. S., Silveira, L. C., Gomes, F. L., and Lee, B. B. 1996. The retinal ganglion cell classes of New World primates. Rev. Bras. Biol. 56 Su 1 Pt 2, 381–396.
Yamagata, M., Weiner, J. A., Dulac, C., Roth, K. A., and Sanes, J. R. 2006. Labeled lines in the retinotectal system: markers for retinorecipient sublaminae and the retinal ganglion cell subsets that innervate them. Mol. Cell. Neurosci. 33(3), 296–310.
Young, M. J. and Lund, R. D. 1998. The retinal ganglion cells that drive the pupilloconstrictor response in rats. Brain Res. 787(2), 191–202.
Youngstrom, T. G., Weiss, M. L., and Nunez, A. A. 1991. Retinofugal projections to the hypothalamus, anterior thalamus and basal forebrain in hamsters. Brain Res. Bull. 26(3), 403–411.
Zhang, J., Li, W., Hoshi, H., Mills, S. L., and Massey, S. C. 2005. Stratification of alpha ganglion cells and ON/OFF directionally selective ganglion cells in the rabbit retina. Vis. Neurosci. 22(4), 535–549.

Further Reading

Beckstead, R. M. and Frankfurter, A. 1983. A direct projection from the retina to the intermediate gray layer of the superior colliculus demonstrated by anterograde transport of horseradish peroxidase in monkey, cat and rat. Exp. Brain. Res. 52(2), 261–268.
Dacey, D. M. and Petersen, M. R. 1992. Dendritic field size and morphology of midget and parasol ganglion cells of the human retina. Proc. Natl. Acad. Sci. U. S. A. 89(20), 9666–9670.
DeVries, S. H. 1999. Correlated firing in rabbit retinal ganglion cells. J. Neurophysiol. 81(2), 908–920.
Masland, R. H. 2001. Neuronal diversity in the retina. Curr. Opin. Neurobiol. 11(4), 431–436.
Provencio, I., Jiang, G., De Grip, W. J., Hayes, W. P., and Rollag, M. D. 1998. Melanopsin: an opsin in melanophores, brain, and eye. Proc. Natl. Acad. Sci. U. S. A. 95, 340–345.
Taylor, W. R. and Vaney, D. I. 2003. New directions in retinal research. Trends Neurosci. 26(7), 379–385.
Wingate, R. J. and Thompson, I. D. 1995. Axonal target choice and dendritic development of ferret beta retinal ganglion cells. Eur. J. Neurosci. 7(4), 723–731.
Yoshida, K., Watanabe, D., Ishikane, H., Tachibana, M., Pastan, I., and Nakanishi, S. 2001. A key role of starburst amacrine cells in originating retinal directional selectivity and optokinetic eye movement. Neuron 30(3), 771–780.
Zeck, G. M., Xiao, Q., and Masland, R. H. 2005. The spatial filtering properties of local edge detectors and brisk-sustained retinal ganglion cells. Eur. J. Neurosci. 22(8), 2016–2026.
Zhao, H. and Rusak, B. 2005. Circadian firing-rate rhythms and light responses of rat habenular nucleus neurons *in vivo* and *in vitro*. Neuroscience 132(2), 519–528.

1.26 Pupillary Control Pathways

D H McDougal and P D R Gamlin, University of Alabama at Birmingham, Birmingham, AL, USA

© 2008 Elsevier Inc. All rights reserved.

1.26.1	**Advantages of a Mobile Pupil**	521
1.26.2	**Overview of the Pathways Controlling Pupil Diameter**	522
1.26.3	**Iris Musculature**	524
1.26.4	**Pupillary Light Reflex**	525
1.26.4.1	Description	525
1.26.4.2	Afferent Pathway	525
1.26.4.2.1	Intrinsically photosensitive retinal ganglion cells	526
1.26.4.2.2	Pretectal olivary nucleus	526
1.26.4.3	Efferent Pathway	528
1.26.4.3.1	The Edinger–Westphal nucleus	528
1.26.4.3.2	The ciliary ganglion	528
1.26.4.4	Sympathetic Influences on the Pupillary Light Reflex	528
1.26.5	**The Pupillary Near Response**	529
1.26.5.1	Description	529
1.26.5.2	Efferent Pathway of the Pupillary Near Response	529
1.26.5.3	Afferent Influences on the Pupillary Near Response	529
1.26.6	**Additional Cortical Influences on Pupillary Responses**	530
1.26.6.1	Visually Mediated Cortical Influences on Pupillary Behavior	531
1.26.6.2	Task-Evoked Pupillary Responses	531
1.26.7	**Influence of Alertness on Pupillary Behavior**	531
1.26.7.1	Arousal	532
1.26.7.2	Sleep	532
1.26.7.3	Ascending Neuromodulatory Systems	532
1.26.8	**Clinical Significance of Pupillary Abnormalities**	533
1.26.8.1	Dysfunctions in the Light Reflex Pathway	533
1.26.8.2	Dysfunctions in the Near Response Pathway	534
1.26.9	**Conclusion**	534
References		534

Glossary

accommodation A change in the refractive power of the crystalline lens of the eye.

miosis Pupillary constriction.

mydriasis Pupillary dilation.

1.26.1 Advantages of a Mobile Pupil

The normal human pupil can change diameter from 8 to 1.5 mm, which corresponds to approximately a 28-fold change in area. Thus, the movement of the iris can account for almost 1.5 log unit variation in retinal irradiance. Although the visual system can operate over a 10 log unit range of lighting levels through the process of adaptation, it can take several minutes for optimum sensitivity to return after an abrupt increase or decrease in retinal illumination. The rapid control of retinal irradiance by the iris allows the visual system to more quickly regain optimal sensitivity by dampening fast changes in ambient lighting levels and requiring less retinal adaptation to a given change in environmental lighting levels (Woodhouse, J. M. and Campbell, F. W., 1975; Hood, D. and Finkelstein, M., 1986).

However, changes in pupil size affect not only retinal illumination, but also diffraction, optical

aberrations, and depth of focus of the eye. These factors differentially affect visual performance, and given changing environmental lighting conditions and visual tasks, the nervous system continuously modulates pupil diameter for optimal visual performance.

The diffraction of light rays by an aperture is a major limiting factor in the resolution of an image in any optical system. The amount of disruption in image quality caused by diffraction at a circular aperture decreases as the size of the opening increases. Therefore, as pupil diameter increases, there is decreased degradation in retinal image quality caused by diffraction (Campbell, F. W. and Green, D. G., 1965; Fry, G. A., 1970; Charman, W. N., 1995). In contrast to diffraction, the image degrading effects of optical aberrations increase as aperture diameter increases. Therefore, as pupil diameter increases, the degradative effects of optical aberrations also increase and offset the benefits gained by reduced diffraction at larger pupil diameters (Liang, J. and Williams, D. R., 1997; Schwiegerling, J., 2000). Over the normal range of pupillary diameter, diffraction impacts image quality less than optical aberration, and the optimal pupil diameter is therefore approximately between 2 and 4 mm (Jenkins, T. C. A., 1963; Westheimer, G., 1964; Campbell, F. W. and Gubisch, R. W., 1966).

Along with diffraction and optical aberrations, defocus is an important determinant of retinal image quality. Although the iris does not refract or focus light, it influences the depth of field of the eye. Depth of field is the range of distance in depth in which objects appear to be in focus. For example, when one reads a book, the power of the crystalline lens of the eyes changes in order to bring the text on the page into focus through a process called accommodation. With the eyes accommodated on the book, all objects within a range in front of and behind the book will also appear in focus. This range is called the depth of field and is primarily dependent on both viewing distance and pupil diameter. When viewing distance is held constant, depth of field increases with decrease in pupil diameter, and therefore, pupil diameter can affect the focus of the retinal image (Marcos, S. *et al.*, 1999; Wang, B. and Ciuffreda, K. J., 2006).

Clearly, a mobile pupil allows the nervous system to optimize retinal irradiance, diffraction, ocular aberrations, and depth of focus despite differing conditions and visual tasks. For example, across a range of daylight (photopic) luminances, pupil size corresponds to that required for the highest visual acuity (Campbell, F. W. and Gregory, A. H., 1960), and the maximal information capacity of the retinal image (Laughlin, S. B., 1992; Hirata, Y. *et al.*, 2003). On the other hand, under low-light (scotopic) conditions in which poorer retinal image quality can be tolerated due to the lower resolution of rod photoreceptors, the pupil dilates sufficiently to maximize retinal illumination. Further evidence for the optimization of pupil diameter for differing visual tasks is evident in the pupillary near response (PNR). When viewing distance changes from far to near, the pupils constrict to increase the field of view and reduce retinal image defocus. This compensates for the decrease in effective field of view that naturally occurs when viewing distance decreases (see Section 1.26.5 for more details).

1.26.2 Overview of the Pathways Controlling Pupil Diameter

A summary diagram of the afferent, central, and efferent pathways controlling pupil diameter is shown in Figure 1. This figure shows the iris musculature innervated by autonomic efferents from both the parasympathetic and the sympathetic components of the ANS. A detailed description of the ANS is beyond the scope of this chapter but is provided by Hockman C. H. (1987) and Robertson D. (2004).

The parasympathetic component of the ANS innervates the sphincter pupillae muscle of the iris. The preganglionic parasympathetic fibers controlling the sphincter pupillae originate from neurons in the Edinger–Westphal nucleus (EW), the autonomic subdivision of the third cranial nerve nucleus, and travel via the third cranial nerve to the ciliary ganglion, which is located within the orbit of the eye (Figure 1). Within the ciliary ganglion, the preganglionic pupilloconstriction neurons form nicotinic, cholinergic synapses with the postganglionic neurons. The axons of these postganglionic neurons leave the ciliary ganglion to enter the eye via the short ciliary nerves and travel to the iris. Here they release acetylcholine, which acts on the muscarinic receptors of the sphincter pupillae (Figure 2) (Hockman, C. H., 1987; Loewenfeld, I. E. and Lowenstein, O., 1993; Oyster, C. W., 1999).

The sympathetic component of the ANS innervates the dilator pupillae muscle. The preganglionic

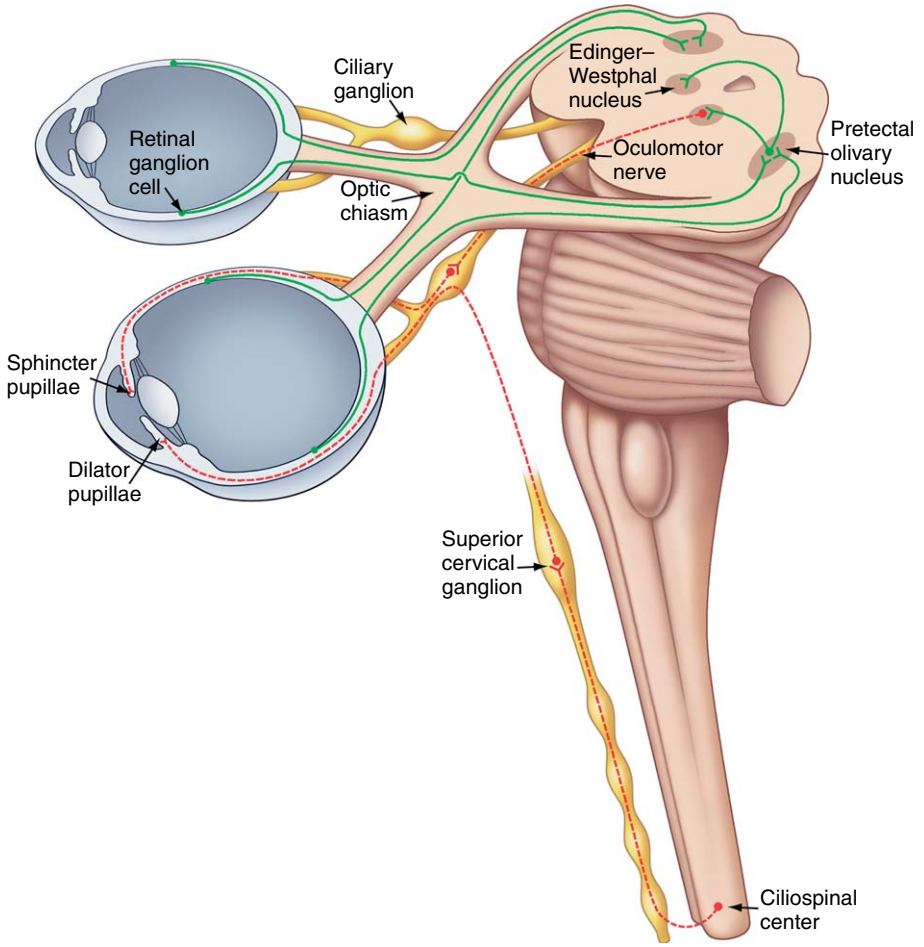

Figure 1 Anatomical drawing showing the direct and consensual pupillary light reflex pathways and the parasympathetic and sympathetic innervation of the iris in primates. The bilateral projection from the retina to the pretectum is also shown. The pretectal olivary nucleus (PON) receives input from the temporal retina of the ipsilateral eye and the nasal retina of the contralateral eye. The PON projects bilaterally to the Edinger–Westphal nucleus, which contains preganglionic parasympathetic pupilloconstriction neurons. The axons of these preganglionic neurons travel in the third cranial nerve to synapse upon postganglionic pupilloconstriction neurons in the ciliary ganglion. The axons of these postganglionic neurons leave the ciliary ganglion and enter the eye via the short ciliary nerves, and then travel through the choroid to innervate the sphincter muscle of the iris. The preganglionic sympathetic pupillodilation neurons are found at the C8-T1 segmental levels of the spinal cord. The axons of these neurons project from the spinal cord via the dorsal roots and enter the sympathetic trunk, and then project rostrally to the superior cervical ganglion where they synapse with the postganglionic neurons. These postganglionic neurons project from the superior cervical ganglion through the neck and carotid plexus and into the orbit of the eye. These fibers enter the eye either by passing through the ciliary ganglion and entering in the short ciliary nerves or by bypassing the ciliary ganglion and entering via the long ciliary nerves (for clarity, only one of these alternative pathways is shown). Upon entering the eye, these axons travel through the choroid and innervate the dilator muscle of the iris.

sympathetic neurons that control pupillary dilation are located in the C8-T1 segments of the spinal cord, a region termed the ciliospinal center of Budge (and Waller). The axons of these preganglionic neurons project to the sympathetic chain and travel in the sympathetic trunk to the superior cervical ganglion (Hockman, C. H., 1987; Kardon, R. H., 2005). Within the superior cervical ganglion, the preganglionic axons form nicotinic, cholinergic synapses with postganglionic pupillodilation neurons. The axons of these postganglionic neurons project from the superior cervical ganglion to the orbit, where they enter the eye via the short and long ciliary nerves and travel to the iris (Figure 1). Here they release norepinephrine, which acts on the adrenoreceptors of the dilator muscle (Figure 2).

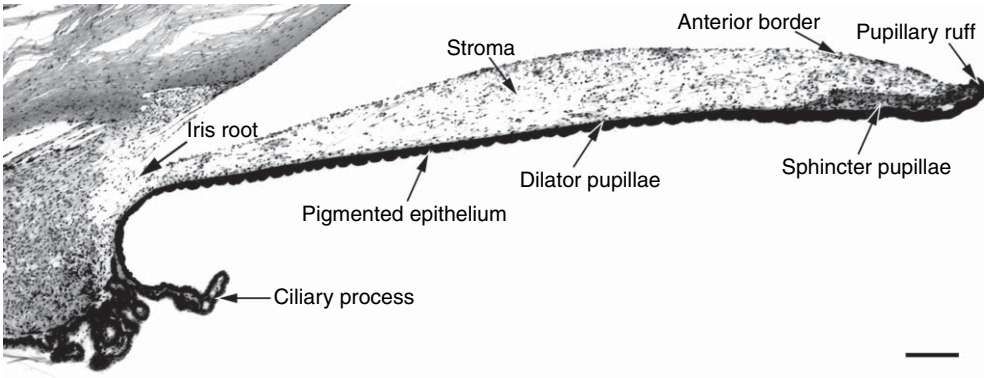

Figure 2 Low-power photomicrograph of a cross section of the macaque iris. Scale bar = 200 μm.

1.26.3 Iris Musculature

In a cross section of the iris, the sphincter pupillae can be seen as an annular band of smooth muscle (100—170 μm thick; 0.7–1.0 mm wide) encircling the pupil (Figure 2).

The sphincter, which is located in the posterior iris immediately anterior to the pigmented epithelium, interdigitates with the surrounding stroma and connects to dilator muscle fibers (see below). The smooth muscle cells of the sphincter are clustered in small bundles and are connected by gap junctions (Bron, A. J. *et al.*, 1997). These gap junctions ensure synchronized contraction of the sphincter muscle. The sphincter receives muscarinic, cholinergic innervation from the short ciliary nerves: postganglionic parasympathetic fibers arising from the ciliary ganglion. The m3 subtype of muscarinic receptor is the predominant receptor subtype expressed by smooth muscle cells of the sphincter pupillae. In the human iris, the m3 receptor subtype comprises 60–75% of the total number of expressed muscarinic receptors, whereas other muscarinic receptor subtypes (m1, m2, m4, and m5) are expressed at lower levels (5–10%) (Gil, D. W. *et al.*, 1997). Binding of acetylcholine to m3 receptors initiates a series of events leading to the activation of phospholipase C (PLC) via G proteins of the Gq family. Activated PLC generates inositol triphosphate (IP_3) and diacylglycerol (DAG) from phosphatidylinositol bisphosphate. The increase in IP_3 elicits the release of Ca^{2+} ions from the endoplasmic reticulum and the influx of extracellular Ca^{2+} ions. The resultant increase in intracellular free Ca^{2+} concentration produces muscle contraction (for review, see Eglen, R. M. *et al.*, 1996). Muscarinic receptor antagonists such as atropine, scopolamine, or tropicamide produce mydriasis, whereas agonists such as pilocarpine, bethanechol, metoclopramide, or oxotremorine produce miosis. The reversible cholinesterase inhibitor, physostigmine, also produces a marked miosis (for review, see Thompson, H. S., 1992).

The dilator pupillae is composed of radially oriented smooth muscle fibers that are myoepithelial in origin. Individual fibers are approximately 50 μm long and 5–7 μm wide. In the pupillary zone, dilator muscle processes fuse with the sphincter pupillae, while peripherally, their processes attach to the ciliary body. Contraction of the dilator muscle pulls the pupillary margin toward the ciliary body (Bron, A. J. *et al.*, 1997). The dilator receives adrenergic innervation from the long ciliary nerves: postganglionic sympathetic fibers arising from the superior cervical ganglion. The alpha 1a adrenoreceptor appears to be the predominant receptor subtype expressed by the smooth muscle cells of the dilator pupillae (Nakamura, S. *et al.*, 1999). Binding of norepinephrine to the alpha 1a adrenoreceptor, a G-protein-coupled receptor, produces muscle contraction through the same signaling cascade (PLC/IP_3) as that in the sphincter pupillae muscle.

Alpha-adrenoreceptor antagonists such as dapiprazole or thymoxamine produce miosis (Thompson, H. S., 1992), as does the more selective alpha 1a-adrenoreceptor antagonist, tamsulosin (Parssinen, O. *et al.*, 2006). The nonspecific adrenoreceptor agonist, phenylephrine, produces mydriasis. Mydriasis is also produced by hydroxyamphetamine and related drugs, which stimulate norepinephrine release from the postganglionic sympathetic nerve endings (Thompson, H. S., 1992).

1.26.4 Pupillary Light Reflex

1.26.4.1 Description

The pupillary light reflex (PLR) is the constriction of the pupil that is elicited by an increase in illumination of the retina. The direct PLR, present in virtually all vertebrates, is the constriction of the pupil in the same eye as that stimulated with light. The consensual PLR is the constriction of the pupil in the eye opposite to the eye stimulated with light. In mammals with laterally placed eyes, such as the rat and rabbit, the direct PLR is more pronounced than the consensual PLR. However, in those mammalian species with frontally placed eyes such as humans and monkeys, the direct and consensual PLR are essentially equal (Loewenfeld, I. E. and Lowenstein, O., 1993). An example of a human consensual PLR produced by two different wavelengths of light is shown in Figure 3.

The PLR has traditionally been divided into two separate pathways based on the clinical manifestations of the defects in this reflex. The afferent pathway is composed of both the retinal cells that project to the pretectum and their recipient neurons that project bilaterally to the EW (Figure 1). The efferent pathway is composed of the preganglionic pupilloconstriction fibers of the EW and their postganglionic recipient neurons in the ciliary ganglion, which project to the sphincter muscle of the iris (Figure 1).

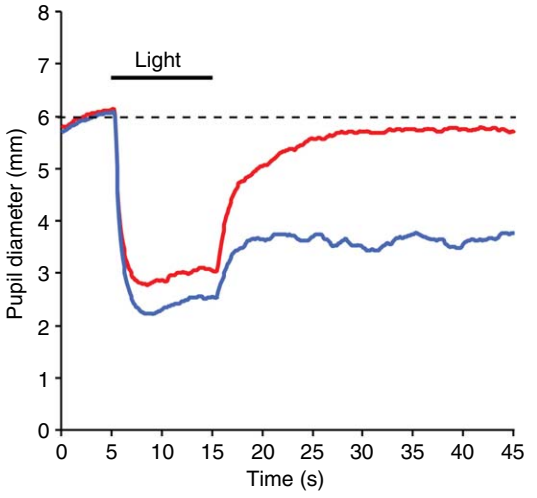

Figure 3 Pupilloconstriction elicited by a 10 s light stimulus of 493 nm wavelength light at 14.0 log quanta $cm^{-2} s^{-1}$ irradiance (blue trace), and 613 nm wavelength light at 14.1 log quanta $cm^{-2} s^{-1}$ irradiance (red trace). Note that a 473 nm stimulus, which effectively activates the intrinsic photoresponse of intrinsically photosensitive retinal ganglion cells (ipRGCs), drives a larger pupillary response than the 613 nm stimulus (red trace), which does not effectively activate the intrinsic photoresponse of ipRGCs at this irradiance level. Also note that the pupilloconstriction induced by the 473 nm light is maintained following stimulus offset.

1.26.4.2 Afferent Pathway

The first, centrally projecting, neurons in the afferent pathway of the PLR are retinal ganglion cells. It has recently been recognized that this reflex in rodents and primates is driven predominantly by a unique subset of intrinsically photosensitive retinal ganglion cells (ipRGCs) that project to the pretectal olivary nucleus (PON), a small nucleus in the pretectum; the pretectum is located in the dorsal lateral aspect of the midbrain at the level of the superior colliculus (Gamlin, P. D., 2005) (Figure 1). Early anatomical studies did not concentrate on the PON specifically, but instead examined all retinal projections to the pretectum, which contains five retinorecipient nuclei. Several of these early studies utilized tracers injected into the vitreous of the eye to anterogradely label all retinal ganglion cell projections to the pretectum. These studies found that the retinal projections to the pretectum were densest to the nucleus of the optic tract and PON and, in primates, were bilateral, with only a slightly denser contralateral component. In contrast, the retinal projection to the pretectum of rodents is predominantly contralateral and only exhibits a moderate ipsilateral component in cats. The ratio of crossed to uncrossed projections of the retinopretectal projections appears to correlate with the ratio of the direct to consensual PLR in mammals.

Other early anatomical studies used retrograde tracing to label pretectally projecting retinal ganglion cells by injecting the tracers into the pretectum. These studies are hard to interpret because fibers projecting to the superior colliculus were also often labeled. Retrograde labeling studies across several different species have found that pretectally projecting cells represented only a small percentage of the total population of ganglion cells (1–6%) and that these cells generally possess small or medium-sized cell bodies and can be classified morphologically as being gamma or W-like. Very few studies were able to successfully target injections exclusively to the PON, and therefore, it is unclear to what extent the retinal cells labeled in these studies actually participate in the PLR. However, an injection

centered on the PON in macaques gave rise to medium-sized labeled neurons, with a few coarse dendrites and extensive dendritic arbors (Perry, V. H. and Cowey, A., 1984). The morphology of these labeled cells is consistent with a newly described retinal cell type that has recently been shown to contribute significantly to the PLR.

1.26.4.2.1 Intrinsically photosensitive retinal ganglion cells

Prior to 2000, it was assumed that the PLR was driven by retinal ganglion cells that received light signals exclusively from rod and cone photoreceptors, which up to that time were the only known photoreceptive cells in the retina. Recent findings suggest that the PLR is driven by ipRGCs, which, unlike any other retinal ganglion cell class, are intrinsically photosensitive. The intrinsic photoresponse of ipRGCs is mediated by the photopigment melanopsin and has been shown to be well fit by a single pigment absorbance spectrum center at 482 nm. In addition to their intrinsic signal, it is clear that ipRGCs receive rod and cone inputs. In response to a pulse of light, intracellular recordings from this cell type show a characteristic transient burst of firing at stimulus onset, which rapidly decays to a plateau of sustained firing that often extends well past stimulus offset. The initial burst of firing is mediated by a rapidly adapting cone-mediated photoresponse and the sustained firing that follows is driven by the intrinsic response of these cells (Berson, D. M., 2003; Fu, Y. *et al.*, 2005).

ipRGCs project to the pretectum of rodents and primates, and it is clear that the confluence of photoreceptive signals impinging on this cell type has a significant impact on pupillary behavior. Several studies have examined the contribution of the separate photoresponses of ipRGCs to the PLR directly. These studies have demonstrated that the intrinsic photoresponse of ipRGCs is necessary but not sufficient to produce a normal PLR in both rodents and primates. Studies investigating the PLR of melanopsin-deficient mice ($Opn4^{-/-}$) have determined that these animals display a PLR, but the pupil fails to constrict maximally in bright lights. Rodents lacking both rod and cone photoreceptors due to retinal degeneration or transgenic manipulation also still display a PLR; however, the reflex has a higher irradiance threshold than normal. When rodless/coneless mice (rd/rdcl) are crossed with $Opn4^{-/-}$ mice to eliminate all potential photoreceptive inputs to ipRGCs, the PLR is completely absent (Berson, D. M., 2003; Fu, Y. *et al.*, 2005).

Recent studies in primates have also shown that the primate PLR is present in the absence of rod and cone input; however, the reflex has a higher retinal irradiance threshold than normal (Gamlin, P. D. *et al.*, 2007). Taken together, these results show that both the intrinsic photoresponse of ipRGCs and classical photoreceptor inputs provide signals of retinal irradiance that drive the PLR. There is evidence that the intrinsic photoresponse compensates for the rapid adaptation of cones and maintains pupilloconstriction during steady-state exposure at all photopic (daylight) illuminance levels. It is still unclear whether the influence of traditional photoreceptors on the PLR is mediated exclusively by the rod and cone inputs to ipRGCs or by other classes of retinal ganglion cells that may to project to the PON.

The intrinsic response of ipRGCs also includes an accumulative irradiance history signal, which can affect pupillary behavior in the absence of overt light stimulation. As noted above, recordings from ipRGCs have shown that these cells possess an ability to encode stimulus irradiance through an elevation of firing rate that extends beyond stimulus offset (Berson, D. M., 2003; Fu, Y. *et al.*, 2005). This sustained firing after stimulus offset appears to be a mechanism for encoding stimulus intensity, as the magnitude and duration of this sustained response varies linearly with stimulus intensity (Dacey, D. M. *et al.*, 2005). This cellular response also appears to influence pupillary responses. Studies of the human PLR have shown that bright light stimuli can produce a prolonged pupillary constriction that persists for up to 20 min, even when the subject is kept in complete darkness following stimulus presentation (Newsome, D. A., 1971; Alpern, M. and Ohba, N., 1972) (Figure 3). It has been determined that this phenomenon is mediated primarily by the intrinsic photoresponse of ipRGCs in primates including humans (Gamlin, P. D. *et al.*, 2007).

1.26.4.2.2 Pretectal olivary nucleus

The second neurons in the afferent pathway of the PLR are luminance neurons within the PON. PON luminance neurons are characterized by tonic firing rates that increase with increase in retinal illuminance.

In primates, these neurons exhibit a transient burst of activity followed by sustained tonic activity in response to increase in retinal illuminance (Figure 4). In addition, the tonic firing rate of these

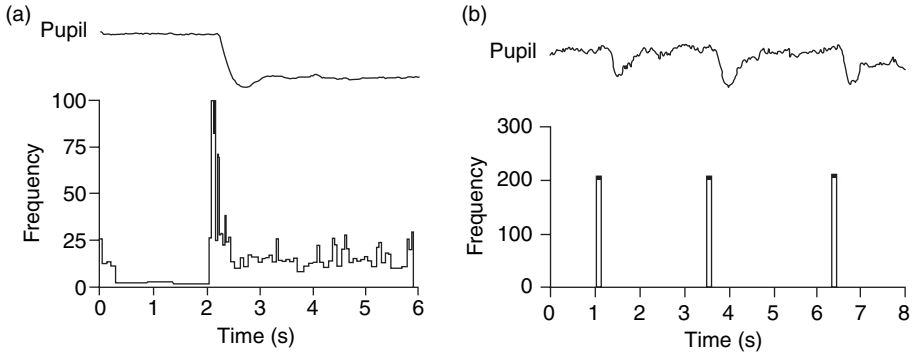

Figure 4 Luminance neurons in the pretectal olivary nucleus (PON) drive the pupillary light reflex. (a) The response of a single neuron is the PON in response to a 100-troland light stimulus. The pupillary response to the same light stimulus is shown in the trace above. (b) Electrical microstimulation at the level of the PON produces pupillary constriction, even in the absence of a light stimulus.

cells is proportional to retinal illuminance over at least a 3 log unit range of stimulus intensities in primates (Gamlin, P. D. *et al.*, 1995) and in rats (Clarke, R. J. and Ikeda, H., 1985b). Although it is clear that these luminance neurons receive inputs from ipRGCs and that the response characteristic of PON luminance neurons to increase in retinal illuminance is reminiscent of that of ipRGCs, it is possible that these neurons may receive input from other types of retinal ganglion cells. In addition to these retinal afferents, the PON also receives significant cortical, ventral thalamic, and midbrain inputs, which may also have a direct influence on the PLR or other pupillary movements. Owing to its importance in the PLR, the best-described efferent projection of the PON is to the EW. However, the PON has also been shown to have a variety of efferent connections that may influence pupillary behavior such as the hypothalamus, pons, and medulla (Gamlin, P. D., 2005).

Electrical microstimulation of the PON in rats and monkeys elicits pupilloconstriction at short latencies (Figure 4(b)), and lesions of the PON in rats produce deficits in pupillomotor function (Gamlin, P. D., 2005). These results provide strong support for models in which luminance neurons within the PON mediate the PLR.

Recently, the characteristics of PON neurons have been more closely examined in the alert primate. This study found that there were three classes of luminance cells in the PON that could be distinguished by their receptive field extent and location. Approximately 40% of the primate PON luminance neurons responded well to stimuli, whether they were presented in either the contralateral or the ipsilateral visual field. These neurons were classified as bilateral neurons. Approximately 30% of PON neurons responded only to stimuli presented in the contralateral visual field. These neurons were classified as contralateral neurons. Finally, 30% of PON neurons responded primarily to stimuli presented at or near the animal's fixation point. These neurons were classified as macular neurons. The mean firing rates of all classes of neurons increased with increase in stimulus size and luminance within their receptive fields. PON luminance neurons of the bilateral and contralateral classes possess very large receptive fields, which exceeded the sizes reported in cats and rats. In addition, while 84% of PON neurons are binocular in the primate, only 22% are reported to be binocular in cats. Thus, it is likely that PON neurons with such extensive, binocular receptive fields are unique to primates, and the existence of such neurons may also explain why the direct and consensual PLR are of comparable magnitudes in primates (Gamlin, P. D., 2005).

Although it has been firmly established that both the PON and the EW (see next section for details) play a critical role in the PLR, there is disagreement as to the route of connectivity between these two nuclei. Some studies propose both a direct connection between PON and EW and an indirect connection via the nucleus of the posterior commissure (NPC) in the rat and in primates, while other studies have reported only the indirect connection via NPC in the cat and tree shrew. A number of studies in primates, using several different tracing techniques, have reported only the direct connection between the PON and the EW (Gamlin, P. D., 2005). Further study will be required to definitively resolve this issue.

1.26.4.3 Efferent Pathway

The efferent leg of the PLR begins with preganglionic pupilloconstriction neurons of the EW that travel via the third cranial nerve to the ciliary ganglion (Figure 1). Within the ciliary ganglion, the preganglionic pupilloconstriction neurons synapse with the postganglionic pupilloconstriction neurons, and the axons of these postganglionic neurons leave the ciliary ganglion to enter the eye via the short ciliary nerves and travel to the iris.

1.26.4.3.1 The Edinger–Westphal nucleus

EW is a distinct nucleus of the midbrain, lying immediately dorsal to the oculomotor complex. It is located just slightly ventral and lateral to the cerebral aqueduct at the level of the superior colliculus (Figure 1). This nucleus was first described in a developmental study of human neuroanatomical material by Edinger L. (1885) and, a short time afterward, in a neuropathological study by Westphal C. (1887). Other early studies involving EW showed that pupilloconstriction could be evoked through the electrical stimulation of EW (Ranson, S. W. and Magoun, H. W., 1933) and determined the precise location of the preganglionic neurons within EW (Warwick, R., 1954). Since these pioneering studies, additional studies have clearly shown in many vertebrate classes that the EW contains the preganglionic neurons that synapse with the postganglionic fibers that innervate the iris sphincter. Further support for the course of the efferent parasympathetic pupillary pathway and the importance of the EW in pupilloconstriction come from electrical stimulation studies in the vicinity of EW that elicited pupilloconstriction in a variety of animal models (Gamlin, P. D., 2000).

The neurophysiology of EW pupilloconstriction neurons has not been extensively studied. This is due to the small size of EW and the small number of pupilloconstriction neurons present, reported to be as few as 10% of the total number of cells in EW (Gamlin, P. D., 2000). A study in cats found that pupilloconstrictor EW neurons displayed firing rates of approximately 8 spikes s^{-1} during maximal pupilloconstriction, but these neurons also displayed transient firing rates with light "on" of up to 28 spikes s^{-1}. A similar finding has been reported in primates, with a pupilloconstrictor neuron displaying a firing rate that ranged from 10 to 25 spikes s^{-1} with a burst-tonic response pattern (Gamlin, P. D., 2000). This firing pattern is similar to both ipRGCs and PON luminance neurons, and it has been postulated that the initial burst at stimulus onset in the pupilloconstriction cells of EW serves to overcome the sluggish nature of the iris musculature.

1.26.4.3.2 The ciliary ganglion

The ciliary ganglion is approximately 3 mm in size and located 2–3 mm posterior to the globe and lateral to the optic nerve. This ganglion contains the cell bodies of the postganglionic pupilloconstrictor neurons, which innervate the sphincter muscle of the iris. Although these neurons receive input primarily from the preganglionic pupilloconstrictor neurons of EW, there is evidence for additional neuronal inputs that may act to modulate this signal (May, P. J. and Warren, S., 1993). Therefore, the ciliary ganglion should not be considered only as a simple relay of preganglionic inputs from EW to the iris, but also as a site of potential neural integration (Gamlin, P. D., 2000).

1.26.4.4 Sympathetic Influences on the Pupillary Light Reflex

Although it is generally agreed that the parasympathetic pathway discussed above is the primary route of pupillary constriction associated with the PLR (Thompson, H. S., 1992; Loewenfeld, I. E. and Lowenstein, O., 1993; Kardon, R., 1995), there is evidence that light may also cause a reduction in the tone of the dilator muscle of the iris via the sympathetic pathway outlined in Figure 1 and thus enhance the PLR. Studies in cats have shown a light-induced inhibition of postganglionic pupillodilation fibers at the level of the long ciliary nerves (Nisida, I. *et al.*, 1960) and preganglionic pupillodilation fibers at the level of the cervical sympathetic nerve (Passatore, M. and Pettorossi, V. E., 1976). These studies found that the pupillodilation fibers were inhibited by light in an intensity-dependent manner, i.e., a more intense light brought about a greater inhibition in firing rate. These findings have not been replicated in primates, in which there is evidence that the sympathetic system plays a tonic role and does not contribute to the dynamics of the PLR (Clarke, R. J. *et al.*, 2003).

Other studies were undertaken to determine the route of the inhibitory light signal to the pupillodilation centers of the spinal cord. By determining the effects of selective lesions at various levels of the central nervous system (CNS) on the light-induced

inhibition of pupillodilation in the long ciliary nerves of cats, Okada H. *et al.* (1960) found that this light signal originated at the level of the pretectum, presumably from one of the retinorecipient nuclei contained within the pretectum. Further lesions in more caudal portions of the CNS suggested that the inhibitory light signal descended from the pretectum bilaterally to the pupillodilation centers of the spinal cord. A more recent series of anterograde labeling studies in the rat support these findings by demonstrating an anatomical connection between the PON and the pupillodilation center of the spinal cord (Klooster, J. and Vrensen, G. F. J. M., 1998).

It is not known whether the light-induced inhibitory signal is carried by pretectal neurons responding to an increase in light intensity, similar to the cells driving the parasympathetic pathway, although this would require an intervening sign-inverting synapse somewhere in the descending pathway. It is possible that the inhibition is a direct result of cells that decrease their firing in response to light. The existence of so-called darkness detector cells has been reported in the pretectum of rats. These cells show a reduction in firing rate in response to increase in retinal luminance (Clarke, R. J. and Ikeda, H., 1985a). Taken together, these findings suggest that the PLR is potentially augmented by a light-induced reduction in tone of the dilator muscle that occurs in conjunction with the increased tone of the sphincter muscle brought about by the parasympathetic pathway.

1.26.5 The Pupillary Near Response

1.26.5.1 Description

The PNR is a pupillary constriction associated with a change in viewing distance from far to near that occurs in primates including humans. When the eyes move from viewing an object at distance to viewing one at near (less than 20 ft away), three oculomotor responses occur. The eyes converge to bring the image of the object onto similar regions of each retina, the refractive power of the crystalline lens is adjusted to bring the image of the object into focus on the retina, and the iris constricts thus reducing the diameter of the pupil. These collective processes are classically referred to as the near response or the near triad.

1.26.5.2 Efferent Pathway of the Pupillary Near Response

The PNR is thought to be driven solely by an increased drive to the sphincter muscle of the iris via the parasympathetic efferent pathway (Kasthurirangan, S. and Glasser, A., 2005). Therefore, the neural control pathway of the PNR shares a common efferent pathway with the PLR, although the afferent inputs responsible for the PNR are more complex. These two reflexes appear to converge at the EW, since the activity of PON luminance neurons is not correlated with the pupil constriction that occurs during near viewing (Zhang, H. *et al.*, 1996). Furthermore, certain clinical neurological conditions are characterized by an intact PNR with the absence of the PLR (light-near dissociation) (Lowenstein, O., 1956).

It is generally accepted that preganglionic neurons in EW drive the PNR as well as the PLR. However, it has not been determined whether separate subpopulations of neurons exist in EW devoted exclusively to either the PLR or the PNR, or whether the same population of neurons drives pupillary constriction in both reflexes, although the latter seems most likely.

1.26.5.3 Afferent Influences on the Pupillary Near Response

Modern investigations into the afferent influences driving the PNR began in the late 1940s with the advent of infrared photographic recordings of the pupil during near viewing. This technique allowed researchers to measure the magnitude of the PNR in near darkness, thus eliminating any artifactual change in pupil diameter induced by decreased retinal illuminance originating from the constriction of the pupil during the response. The aim of these original investigations was to determine whether the PNR was driven primarily by ocular convergence or accommodation, the other two components of the near triad. Early studies found that the PNR was more closely associated with accommodation than with convergence (Fry, G. A., 1945; Knoll, H. A., 1949; Marg, E. and Morgan, M. W., 1949; Marg, E. and Morgan, M. W., 1950; Alpern, M. *et al.*, 1961). Later studies found a greater association with convergence (Backer, W. D. and Ogle, K. N., 1964) and even showed that the PNR could be totally absent during certain blur-driven accommodative responses (Stakenburg, M., 1991; Phillips, N. J. *et al.*, 1992). These conflicting results are likely a product of an

incomplete disassociation between the convergence and the accommodation system during these experiments, as these two systems have been shown to be highly interdependent.

A more modern view of the afferent influences of the PNR has recently emerged, in which the PNR is not seen as resulting from either accommodation or convergence alone, but as a separate output of the neural pathways that drive both accommodation and convergence. This view has followed an increase in the knowledge of the neural circuitry involved in all three oculomotor processes of the near triad. Experiments investigating the interaction between convergence and accommodation lead to the introduction of the dual-interaction model of convergence and accommodation (Semmlow, J. and Heerema, D., 1979; Hung, G. K. and Semmlow, J., 1980; Schor, C. M. and Narayan, V., 1982) (Figure 5). This model proposes that two neural controllers operate in the near triad: one that integrates stimuli for accommodation such as blur and the other that integrates stimuli driving convergence such as disparity between the images on the retinal of each eye (Mays, L. E. and Gamlin, P. D. R., 1995; Schor, M. and Ciuffreda, K. J. 1983).

It is now clear that the PNR is not driven exclusively by either the accommodation controller or the convergence controller, but actually by an interaction of the two controllers (Myers, G. A. and Stark, L., 1990; Takagi, M. *et al.*, 1993). These findings support the view that the outputs of the dual-interaction model drive the PNR in addition to accommodation and vergence (Figure 5). These findings also suggest that the three oculomotor components of the near triad share common afferent influences.

A number of brain areas play a role in controlling the near triad. These include cortical areas, such as extrastriate cortex, parietal cortex, frontal eye fields, as well as the cerebellum and the midbrain. Of particular interest to the PNR is the supraoculomotor area of the midbrain, which lies just dorsal and lateral to the oculomotor nucleus. The supraoculomotor area contains near response cells, which are modulated by both vergence and accommodation and which receive input from both the accommodation and the vergence controllers. These cells project to medial rectus motor neurons and thus contribute to vergence eye movements. It seems likely that these cells also project to EW and are responsible for carrying the signal from the accommodation and the convergence controllers to the preganglionic pupilloconstriction neurons (Schor, C. M. and Ciuffreda, K. J. 1983; Mays, L. E. and Gamlin, P. D. R., 1995; Gamlin, P. D. R., 2002).

1.26.6 Additional Cortical Influences on Pupillary Responses

In addition to cortical afferents mediating the PNR, the pupil is also influenced by both visual and nonvisual cortical regions. These afferents manifest themselves in small changes in pupil diameter measured during presentation of visual stimuli such as colored stimuli and gratings, as well as nonvisual stimuli such auditory tones, and even during higher-order cortical functions such as problem solving. These observations provide clear evidence that cortex exerts an influence on

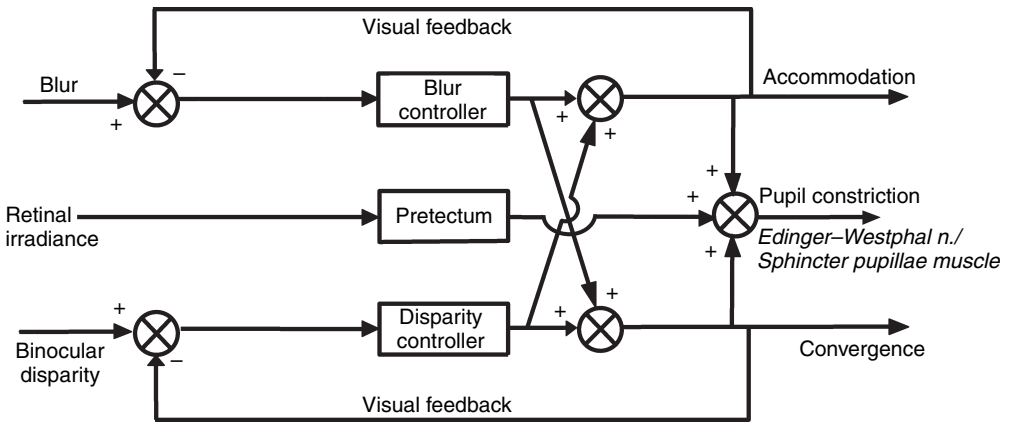

Figure 5 Schematic of the modified dual-interaction model that accounts for the pupillary near response component of the near response triad. This model indicates that the combined output of the accommodation controller and the convergence controller drives the pupillary near response.

pupillary behavior, which cannot be thought of as entirely reflexive in nature.

1.26.6.1 Visually Mediated Cortical Influences on Pupillary Behavior

Recent studies have shown that the pupil responds to complex aspects of visual stimuli such as color, motion, and texture. Slight pupillary constrictions have been shown to occur in both humans and macaques with the presentation of complex visual stimuli, even when the stimuli do not involve a change in viewing distance or retinal illuminance (Barbur, J. L., 1995; Gamlin, P. D. *et al.*, 1998). The three best-described stimulus attributes that produce this effect are color, spatial frequency, and apparent motion. It is clear from physiological and functional imaging studies that these stimulus characteristics are encoded in areas of visual cortex. Furthermore, when these cortically driven pupillary responses are assayed in human subjects with well-documented lesions to cortical areas involved in processing one or more of these stimulus characteristics, a deficit in the concurrent pupillary response is always observed (Barbur, J. L., 1995). In addition, Heywood C. A. and coworkers (1998) have demonstrated in macaques that lesions of rostral inferior temporal cortex but not V4 abolish pupillary responses to chromatically modulated gratings. These findings offer conclusive evidence of an influence of visual cortex on pupil diameter.

Studies have investigated the neural pathways by which visual cortex influences pupil diameter. Research utilizing patients with a well-defined neurological lesion of the midbrain has helped to elucidate one possible neural pathway involved in these responses. The neurological syndrome with which the patients were affected selectively affects the pretectum while sparing the EW. Therefore, the patient's pupils were unreactive to light but maintained a near response. These patients also maintained the pupillary responses to stimulus color and function, and therefore, it seems likely that this cortical influence is mediated by direct cortical inputs to EW (Wilhelm, B. J. *et al.*, 2002).

1.26.6.2 Task-Evoked Pupillary Responses

In the early 1960s, Hess E. H. and colleagues (Hess, E. H. and Polt, J. M., 1960; 1964; Hess, E. H., 1965) published a series of papers that reported modulations in human pupillary diameter associated with complex cognitive processes such as subjective attitudes or mental activity. Later studies failed to produce reliable replication of the findings relating pupillary dynamics to subjective attitudes, although the findings related to mental activity have been replicated and extensively studied. The small pupillary dilations associated with increased mental activity, or task-evoked pupillary responses (TEPRs), have now become a well-established tool of cognitive psychology. These pupillary responses are generally reported to vary in magnitude from 0.2 to 0.7 mm and have been shown to be an accurate reporter of cognitive load across such diverse functions as sensory perception, memory, language, and attention. TEPRs have been repeatedly shown to monotonically vary with the degree of mental activity required by a task as measured by other objective criteria such as reaction time and the extent of cortical activation indicated by positron emission tomography (PET) scan, and this has allowed TEPRs to be utilized successfully to empirically test theories of language processing and intelligence (Beatty, J. and Lucero-Wagoner, B., 2000).

Although the behavioral phenomenon of TEPRs has been extensively studied and quantified, much remains to be elucidated about the precise physiology that drives these responses. Very few, if any empirically driven theories have been developed to explain the neural pathways involved in these responses. It has been suggested that these pupillary responses may be driven by a neuromodulatory effect on pupillary control pathways mediated by noradrenergic projections from the locus coeruleus. The firing rate of neurons in this midbrain nucleus has been shown to correlate with both pupil diameter and task-related events (Aston-Jones, G. and Cohen, J. D., 2005).

1.26.7 Influence of Alertness on Pupillary Behavior

Since the muscles of the iris are controlled by the ANS, environmental or physiological conditions that cause changes in overall autonomic function can have a significant effect on pupillary behavior. Even though the environmental or physiological conditions that produce the change in autonomic tone may not have a direct influence on the visual system, they may still manifest themselves by affecting pupil diameter.

1.26.7.1 Arousal

Situations or stimuli that produce an emotional or a startle response often produce a profound pupillary dilation. This effect is mediated via the hypothalamus, the brain area responsible for the integration of autonomic function. This integration allows for the coordination of the various functions of the ANS and often leads to global changes in the balance between the sympathetic and the parasympathetic branch of the ANS. For example, an unexpected loud noise may produce a startle response that is characterized by increases in heart rate, respiratory rate, and pupil diameter; it is caused by a systemic increase in sympathetic tone mediated through the hypothalamus. This global increase in sympathetic tone can affect pupil diameter via activation of the pupillodilation centers of the spinal cord and inhibition of the pupilloconstriction neurons of EW. Neurons within the hypothalamus project to the preganglionic sympathetic pupillodilation neurons of the thoracic spinal cord. This direct effect of hypothalamic activation on pupil diameter can be shown through microstimulation of the posterior hypothalamus, which often causes rapid pupil dilation. Increase in sympathetic tone can also produce inhibition of pupilloconstriction neurons of EW via the influence of ascending neuromodulatory pathways (Yu, Y. and Koss, M. C., 2004) (see below for more details).

The hypothalamus is also the site at which autonomic function is regulated by the CNS via connections with the limbic system and cortical structures. The limbic system of the brain, which is responsible for emotions and short-term memory, has a direct connection to the hypothalamus and therefore can have significant effects on autonomic balance. Situations or stimuli that produce an intense emotional response are often accompanied by pupillary dilation, which is certainly mediated through limbic connections to the hypothalamus. In addition, cortical influences on the hypothalamus allow a wide variety of stimuli to affect autonomic tone and thus pupil diameter (Hockman, C. H., 1987; Loewenfeld, I. E. and Lowenstein, O., 1993).

1.26.7.2 Sleep

Sleep has a pronounced effect on the ANS, specifically a reduction in sympathetic outflow and an increase in parasympathetic outflow. Given this overall trend, it is not surprising that pupillary behavior during sleep is characterized by prolonged constriction of the pupil. It has been shown that sleep-induced pupillary constriction persists in animals with lesions of the preganglionic sympathetic pupillodilation fibers. This suggests that the sleep-induced pupillary changes are mediated by an activation of the preganglionic parasympathetic pupilloconstriction fibers of the EW. It should be noted that during some phases of sleep, particularly rapid eye movement (REM) sleep, the pupils tonically dilate at random intervals. This dilation mirrors the reversal of parasympathetic dominance with sympathetic dominance during the same intervals (Parmeggiani, P. L., 1984).

1.26.7.3 Ascending Neuromodulatory Systems

The ascending neuromodulatory systems of the midbrain and brainstem can have a variety of effects on pupillary behavior. These nuclei are the origin of neuromodulatory fibers, which release dopamine, norepinephrine, histamine, and serotonin at a number of brain areas implicated in pupillary control. These neuromodulatory systems appear to be critical in the regulation of sleep and arousal (Saper, C. B., *et al.*, 2005), as well as autonomic regulation (Boehm, S. and Kubista, H., 2002) and cortical plasticity (Gu, Q., 2002). In addition to these global neuromodulatory effects, all or some of which could have a profound influence on pupillary behavior, there is evidence for a direct inhibition of pupilloconstriction neurons in the EW by adrenergic neurons originating from the locus coeruleus in a number of animal models (Koss, M. C., 1986). This appears to be an addition mechanism for mydriasis produced by global sympathetic activation. Later studies in humans (Larson, M. D. and Talke, P. O., 2001) and rabbits (Yu, Y. and Koss, M. C., 2004) have failed to find that this direct noradrenergic inhibition of pupilloconstriction neurons, and it has been suggested that this effect is mediated by the dopaminergic neurons in these species (Yu, Y. and Koss, M. C., 2004). Drugs that agonize or antagonize these neuromodulatory neurotransmitters have been found to differentially affect pupillary behavior in a wide range of animal models and human studies. These differential effects are most likely due to the both interspecies variability in the projections of these neuromodulatory fibers (Gu, Q., 2002) and the differential activation of multiple brain areas implicated in pupillary behavior due to the extensive projections of these neuromodulators.

1.26.8 Clinical Significance of Pupillary Abnormalities

The PLR and PNR are commonly used clinical measures of visual and neurological functions. Due to the ease with which these responses can be elicited in a clinical setting, their assessment provides a rapid evaluation of certain critical brain functions. The varied nature of the brain areas that these reflexes traverse allows the clinician to assess retinal, midbrain, and autonomic functions concurrently with a few straightforward measurements of pupillary functions. This section will provide a broad overview of common pupillary dysfunctions and some of the clinical conditions indicated by each (see Kawasaki, A., 2005, for a more comprehensive review).

1.26.8.1 Dysfunctions in the Light Reflex Pathway

As previously stated, the PLR is driven by a simple, four-neuron reflex arc that passes out of the eye, via the optic nerve, to a series of midbrain nuclei, and back to the iris of the eye via the oculomotor nerve (Figures 1 and 6).

For diagnostic purposes, abnormalities of the pupil are traditionally classified as afferent or efferent defects. These divisions are based on whether the lesion involved occurs in the afferent of the efferent leg of the PLR. Afferent defects are indicative of conditions affecting the retina or optic nerve, whereas efferent defects are indicative of autonomic dysfunction or conditions affecting the oculomotor nerve.

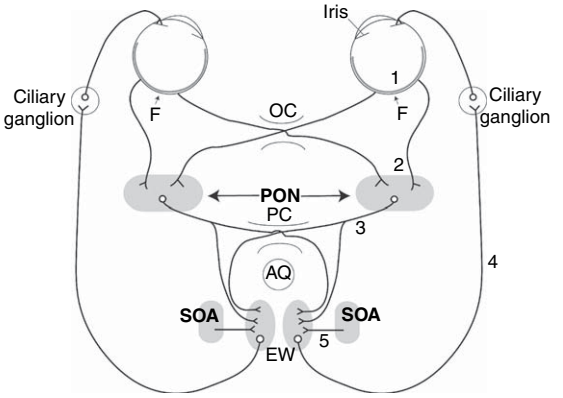

Figure 6 Schematic diagram of the direct and consensual pupillary light pathways in primates including humans. AQ, aqueduct; EW, Edinger–Westphal nucleus; F, fovea; OC, optic chiasm; PC, posterior commissure; PON, pretectal olivary nucleus; SOA, supraoculomotor area.

Afferent defects in the PLR are characterized by an asymmetry in the pupillary response between the two eyes in response to a brief flash of light (Thompson, H. S., 1992; Digre, K. B., 2005). This relative afferent pupillary defect (RAPD) is caused by a difference in the overall light sensitivity of one retina versus the other (Figure 6, pathway 1). When a light is presented to one eye, the neural impulses generated travel to each PON via the optic nerve and therefore generate both a direct and a consensual light response (Figure 6, pathway 2). If the magnitude of the pupillary response differs when the same light in shown in the other eye, this indicates a dysfunction in the visual pathway at the level of the retina or optic nerve in the eye with the lesser response, as the light is less efficient at generating a response in that eye. The presence of an RAPD is a primary symptom of acute disorders of the retina and optic tract, such as optic neuritis, retinal detachment, and retinal vein occlusion. An RAPD is also observed in many of the major diseases of the retina such as glaucoma and macular degeneration, although it is not the primary indicator of these conditions (Thompson, S. H. and Miller, N. R., 1998).

As stated previously, a significant portion of the neural pathway that drives the PLR is located in the midbrain, for example, EW and PON. This midbrain segment of the reflex allows the PLR to be used as a clinical assessment of overall midbrain function (Figure 6, pathway 3). Various midbrain lesions can produce abnormalities in the PLR, which are characterized by an absence or attenuation of the light reflex in one or both eyes, even when a constant, bright stimulus is used. Unless the lesion is small and localized to the pretectum or EW, the PLR deficits will present secondarily to other, more prominent neurological defects. This component of the reflex also allows the PLR to be used to evaluate overall brain function in unconscious or semiconscious patients. Not only does the PLR give a static measure of brain function in these patients, but it is also an important clinical tool used to assess the prognosis and progression of comatose patients and victims of severe head trauma (Thompson, S. H. and Miller, N. R., 1998).

Efferent defects of the PLR are most often characterized by a dissymmetry in the size of the two pupils under steady-state illumination, which is termed anisocoria. Since pupil diameter at any given time is determined by the relative activation of the iris sphincter and dilator muscles, if the relative drive on these two muscles is different in each eye, then anisocoria is produced. This unequal drive can

be caused by a specific lesion that blocks the outflow of neural impulses from EW to the sphincter, or from the superior cervical ganglion to the dilator muscle of one eye (Figure 6, pathway 4). More commonly, anisocoria is caused by a unilateral global dysfunction in either the sympathetic or the parasympathetic branch of the ANS. Therefore, the presence of anisocoria is indicative of disorders of the ANS such as familial dysautonomia and Horner's syndrome, as well as acute disturbances of ocular parasympathetic input such as those caused by basal meningitis and oculomotor nerve palsies (Thompson, S. H. and Miller, N. R., 1998).

1.26.8.2 Dysfunctions in the Near Response Pathway

The PNR is also regularly clinically utilized as a diagnostic tool. The PLR and PNR share a common efferent path from the midbrain to the iris, but due to differing afferent pathways, it is possible to retain one functional reflex in the absence of the other. This condition is called light-near dissociation and is a classic symptom of neurosyphilis (Lowenstein, O., 1956), although a variety of other conditions can also cause this phenomenon, e.g., multiple sclerosis (Loewenfeld, I. E., 1969), neurosarcoidosis (Poole, C. J., 1984), and diabetes mellitus (Dacso, C. C. and Bortz, D. L., 1989). The PNR is often assessed in conjunction with the PLR, as it provides insight into the source of any observed defects in the PLR (Digre, K. B., 2005). Modern neuroimaging techniques have shown the probable site of lesion that leads to the phenomenon of light-near dissociation can be localized to the periaqueductal gray (PAG) matter of the midbrain (Poole, C. J., 1984; Dacso, C.C. and Bortz, D. L., 1989). The PAG lies dorsal and lateral to EW, although the posterior to anterior extent of PAG is much more extensive than that of EW. It is likely that a lesion in the PAG interrupts fibers of passage from the PON to EW (Figure 6, pathway 3) while sparing the connection between SOA and EW (Figure 6, pathway 5). This would interrupt the afferent pathway of the PLR while maintaining the PNR afferents.

1.26.9 Conclusion

The neural regulation of pupil diameter allows for the adaptation of the optics of the eye to a variety of visual task and environmental conditions. This regulation is mediated by a variety of brain areas that have a variety of sensory inputs and functions. Although the control of pupil diameter is generally thought of as a simple reflexive process, the number and complexity of pupillary control pathways involved in the regulation of pupil diameter imparts an unexpected complexity that is only beginning to be appreciated and fully understood.

Acknowledgments

This work was supported by NIH grant EY09380 and the EyeSight Foundation of Alabama.

References

Alpern, M. and Ohba, N. 1972. The effect of bleaching and backgrounds on pupil size. Vision Res. 12, 943–951.
Alpern, M., Mason, G. L., and Jardinico, R. E. 1961. Vergence and accommodation. V. Pupil size changes associated with changes in accommodative vergence. Am. J. Ophthalmol. 52, 762–767.
Aston-Jones, G. and Cohen, J. D. 2005. An integrative theory of locus coeruleus-norepinephrine function: adaptive gain and optimal performance. Annu. Rev. Neurosci. 28, 403–450.
Backer, W. D. and Ogle, K. N. 1964. Pupillary response to fusional eye movements. Am. J. Ophthalmol. 58, 743–756.
Barbur, J. L. 1995. A Study of Pupil Response Components in Human Vision. In: Basic and Clinical Perspectives in Vision Research: A Celebration of the Career of Hisako Ikeda. (*eds*. J. G. Robbins *et al.*), pp. 3–18. Plenum.
Beatty, J. and Lucero-Wagoner, B. 2000. The Pupillary System. In: Handbook of Psychophysiology, 2nd ed. (*eds*. J. T. Cacioppo and L. G. Tassimary), pp. 142–162. Cambridge University Press.
Berson, D. M. 2003. Strange vision: ganglion cells as circadian photoreceptors. Trends Neurosci. 26, 314–320.
Boehm, S. and Kubista, H. 2002. Fine tuning of sympathetic transmitter release via ionotropic and metabotropic presynaptic receptors. Pharmacol. Rev. 54, 43–99.
Bron, A. J., Tripathi, R. C., Tripathi, B. J., and Wolff, E. 1997. Wolff's Anatomy of the Eye and Orbit. Chapman & Hall Medical.
Campbell, F. W. and Green, D. G. 1965. Optical and retinal factors affecting visual resolution. J. Physiol. 181, 576–593.
Campbell, F. W. and Gregory, A. H. 1960. Effect of size of pupil on visual acuity. Nature 187, 1121–1123.
Campbell, F. W. and Gubisch, R. W. 1966. Optical quality of the human eye. J. Physiol. 186, 558–578.
Charman, W. N. 1995. Optics of the Eye. In: Handbook of Optics (*ed*. M. Bass), pp. 24.3–24.54. McGraw-Hill.
Clarke, R. J. and Ikeda, H. 1985a. Luminance and darkness detectors in the olivary and posterior pretectal nuclei and their relationship to the pupillary light reflex in the rat. I. Studies with steady luminance levels. Exp. Brain Res. 57, 224–232.
Clarke, R. J. and Ikeda, H. 1985b. Luminance detectors in the olivary pretectal nucleus and their relationship to the pupillary light reflex in the rat. II. Studies using sinusoidal light. Exp. Brain Res. 59, 83–90.

Clarke, R. J., Zhang, H., and Gamlin, P. D. 2003. Characteristics of the pupillary light reflex in the alert rhesus monkey. J. Neurophysiol. 89, 3179–3189.

Dacso, C. C. and Bortz, D. L. 1989. Significance of the Argyll Robertson pupil in clinical medicine. Am. J. Med. 86, 199–202.

Dacey, D. M., Liao, H. W., Peterson, B. B., Robinson, F. R., Smith, V. C., Pokorny, J., Yau, K. W., and Gamlin, P. D. 2005. Melanopsin-expressing ganglion cells in primate retina signal colour and irradiance and project to the LGN. Nature 433, 749–754.

Digre, K. B. 2005. Principles and Techniques of Examination of the Pupil, Accommodation, and the Lacrimal System. Lippincott Williams & Wilkins.

Edinger, L. 1885. Ueber den verlauf der centralen hirnnervenbahnen mit demonstration von präparaten. Arch. Psychiatr. Nervenkr. 16, 858–859.

Eglen, R. M., Hegde, S. S., and Watson, N. 1996. Muscarinic receptor subtypes and smooth muscle function. Pharmacol. Rev. 48, 531–565.

Fry, G. A. 1945. The relation of pupil size to accommodation and convergence. Am. J. Optom. Arch. Am. Acad. Optom. 22, 451–465.

Fry, G. A. 1970. The optical performance of the human eye. Prog. Optics 8, 53–131.

Fu, Y., Liao, H. W., Do, M. T. H., and Yau, K. W. 2005. Non-image-forming ocular photoreception in vertebrates. Curr. Opin. Neurobiol. 15, 415–422.

Gamlin, P. D. 2000. Functions of the Edinger-Westphal Nucleus. In: Nervous Control of the Eye (*eds*. G. Burnstock *et al.*), pp. 117–154. Harwood Academic.

Gamlin, P. D. R. 2002. Neural mechanisms for the control of vergence eye movements. Ann. NY Acad. Sci. 956, 264–272.

Gamlin, P. D. 2005. The pretectum: connections and oculomotor-related roles. Prog. Brain Res. 151, 379–405.

Gamlin, P. D., McDougal, D. H., Pokomy, J., Smith, V. C., Yau, K. W., and Dacey, D. M. 2007. Human and macaque pupil responses driven by melanopsin-containing retinal ganglion cells. Vision Res. 47, 946–954.

Gamlin, P. D., Zhang, H., and Clarke, R. J. 1995. Luminance neurons in the pretectal olivary nucleus mediate the pupillary light reflex in the rhesus monkey. Exp. Brain Res. 106, 169–176.

Gamlin, P. D., Zhang, H., Harlow, A., and Barbur, J. L. 1998. Pupil responses to stimulus color, structure and light flux increments in the rhesus monkey. Vision Res. 38, 3353–3358.

Gil, D. W., Krauss, H. A., Bogardus, A. M., and Woldemussie, E. 1997. Muscarinic receptor subtypes in human iris-ciliary body measured by immunoprecipitation. Invest. Ophthalmol. Vis. Sci. 38, 1434–1442.

Gu, Q. 2002. Neuromodulatory transmitter systems in the cortex and their role in cortical plasticity. Neuroscience 111, 815–835.

Hess, E. H. 1965. Attitude and pupil size. Sci. Am. 212, 46–54.

Hess, E. H. and Polt, J. M. 1960. Pupil size as related to interest value of visual stimuli. Science 132, 349–350.

Hess, E. H. and Polt, J. M. 1964. Pupil size in relation to mental activity during simple problem solving. Science 143, 1190–1192.

Heywood, C. A., Nicholas, J. J., Lemare, C., and Cowey, A. 1998. The effect of lesions to cortical areas V4 or AIT on pupillary responses to chromatic and achromatic stimuli in monkeys. Exp. Brain Res. 122, 475–480.

Hirata, Y., Yamaji, K., Sakai, H., and Usui, S. 2003. Function of the pupil in vision and information capacity of retinal image. Syst. Comput. Jpn. 34, 48–57.

Hockman, C. H. 1987. Essentials of Autonomic Function: The Autonomic Nervous System: Fundamental Concepts from Anatomy, Physiology, Pharmacology, and Neuroscience for Students and Professionals in the Health Sciences. Thomas.

Hood, D. and Finkelstein, M. 1986. Sensitivity to Light. In: Handbook of Perception and Human Performance (*eds*. K. R. Boff *et al.*), pp. 5/1–5/66. Wiley.

Hung, G. K. and Semmlow, J. L. 1980. Static behavior of accommodation and vergence: computer simulation of an interactive dual-feedback system. IEEE Trans. Biomed. Eng. 27, 439–447.

Jenkins, T. C. A. 1963. Aberrations of the eye and their effects on vision: Part 2. Br. J. Physiol. Opt. 20, 161–201.

Kardon, R. 1995. Pupillary light reflex. Curr. Opin. Ophthalmol. 6, 20–26.

Kardon, R. H. 2005. Anatomy and Physiology of the Autonomic Nervous System. In Walshand Hoyt's Clinical Neuro-ophthalmology (*eds*. N. R. Miller, *et al.*), Vol. 3, pp. 649–714. Lippincott Williams & Wilkins.

Kasthurirangan, S. and Glasser, A. 2005. Characteristics of pupil responses during far-to-near and near-to-far accommodation. Ophthalmic Physiol. Opt. 25, 328–339.

Kawasaki, A. 2005. Disorders of Pupillary Function, Accommodation, and Lacrimation. In Walsh and Hoyt's Clinical Neuro-Ophthalmology (*eds*. N. R. Miller *et al*.), Vol. 3, pp. 739–805. Lippincott Williams & Wilkins.

Klooster, J. and Vrensen, G. F. J. M. 1998. New indirect pathways subserving the pupillary light reflex: projections of the accessory oculomotor nuclei and the periaqueductal gray to the Edinger–Westphal nucleus and the thoracic spinal cord in rats. Anat. Embryol. 198, 123–132.

Knoll, H. A. 1949. Pupillary changes associated with accommodation and convergence. Am. J. Ophthalmol. 26, 346–357.

Koss, M. C. 1986. Review article: pupillary dilation as an index of central nervous system alpha 2-adrenoceptor activation. J. Pharmacol. Methods 15, 1–19.

Larson, M. D. and Talke, P. O. 2001. Effect of dexmedetomidine, an alpha-adrenoceptor agonist, on human pupillary reflexes during general anaesthesia. Br. J. Clin. Pharmacol. 51, 27–33.

Laughlin, S. B. 1992. Retinal information capacity and the function of the pupil. Ophthalmic Physiol. Opt. 12, 161–164.

Liang, J. and Williams, D. R. 1997. Aberrations and retinal image quality of the normal human eye. J. Opt. Soc. Am. A 14, 2873–2883.

Loewenfeld, I. E. 1969. The Argyll Robertson pupil, 1869–1969: a critical survey of the literature. Surv. Ophthalmol. 14, 199–299.

Loewenfeld, I. E. and Lowenstein, O. 1993. The Pupil: Anatomy, Physiology, and Clinical Applications. Iowa State University Press.

Lowenstein, O. 1956. The Argyll Robertson pupillary syndrome; mechanism and localization. Am. J. Ophthalmol. 42, 105–121.

Marcos, S., Moreno, E., and Navarro, R. 1999. The depth-of-field of the human eye from objective and subjective measurements. Vision Res. 39, 2039–2049.

Marg, E. and Morgan, M. W. 1949. The pupillary near reflex. Am. J. Optom. 26, 183–198.

Marg, E. and Morgan, W. 1950. Further investigation of the pupillary near reflex. Am. J. Optom. 27, 217–225.

May, P. J. and Warren, S. 1993. Ultrastructure of the macaque ciliary ganglion. J. Neurocytol. 22, 1073–1095.

Mays, L. E. and Gamlin, P. D. R. 1995. Neuronal circuitry controlling the near response. Curr. Opin. Neurobiol. 5, 763–768.

Myers, G. A. and Stark, L. 1990. Topology of the near response triad. Ophthalmic Physiol. Opt. 10, 175–181.

Nakamura, S., Taniguchi, T., Suzuki, F., Akagi, Y., and Muramatsu, I. 1999. Evaluation of alpha1-adrenoceptors in the rabbit iris: pharmacological characterization and expression of mRNA. Br. J. Pharmacol. 127, 1367–1374.
Newsome, D. A. 1971. Afterimage and pupillary activity following strong light exposure. Vision Res. 11, 275–288.
Nisida, I., Okada, H., and Nakano, O. 1960. The activity of the ciliospinal centers and their inhibition in pupillary light reflex. Jpn. J. Physiol. 10, 73–84.
Okada, H., Nakano, O., Okamoto, K., Nakayama, K., and Nisida, I. 1960. The central path of the light reflex via the sympathetic nerve in the cat. Jpn. J. Physiol. 10, 646–658.
Oyster, C. W. 1999. The Iris and the Pupil. In: The Human Eye: Structure and Function (*ed*. C. W. Oyster), pp. 411–446. Sinauer Associates.
Parmeggiani, P. L. 1984. Autonomic Nervous System in Sleep. In: Sleep Mechanisms (*eds*. A. A. Borbély *et al.*), pp. 39–49. Springer-Verlag.
Parssinen, O., Leppanen, E., Keski-Rahkonen, P., Mauriala, T., Dugue, B., and Lehtonen, M. 2006. Influence of tamsulosin on the iris and its implications for cataract surgery. Invest. Ophthalmol. Vis. Sci. 47, 3766–3771.
Passatore, M. and Pettorossi, V. E. 1976. Efferent fibers in the cervical sympathetic nerve influenced by light. Exp. Neurol. 52, 66–82.
Perry, V. H. and Cowey, A. 1984. Retinal ganglion cells that project to the superior colliculus and pretectum in the macaque monkey. Neuroscience 12, 1125–1137.
Phillips, N. J., Winn, B., and Gilmartin, B. 1992. Absence of pupil response to blur-driven accommodation. Vision Res. 32, 1775–1779.
Poole, C. J. 1984. Argyll Robertson pupils due to neurosarcoidosis: evidence for site of lesion. Br. Med. J. 289, 356.
Ranson, S. W. and Magoun, H. W. 1933. The central path of the pupilloconstrictor reflex in response to light. Arch. Neurol. Psychiatry 30, 1193–1204.
Robertson, D. 2004. Primer on the Autonomic Nervous System. Academic Press.
Saper, C. B., Scammell, T. E., and Lu, J. 2005. Hypothalamic regulation of sleep and circadian rhythms. Nature 437, 1257–1263.
Schor, C. M. and Ciuffreda, K. J. 1983. Vergence Eye Movements: Basic and Clinical aspects. Butterworth.
Schor, C. M. and Narayan, V. 1982. Graphical analysis of prism adaptation, convergence accommodation, and accommodative convergence. Am. J. Optom. Phys. Opt. 59, 774–784.
Schwiegerling, J. 2000. Theoretical limits to visual performance. Surv. Ophthalmol. 45, 139–146.
Semmlow, J. and Heerema, D. 1979. The synkinetic interaction of convergence accommodation and accommodative convergence. Vision Res. 19, 1237–1242.
Stakenburg, M. 1991. Accommodation without pupillary constriction. Vision Res. 31, 267–273.
Takagi, M., Abe, H., Toda, H., and Usui, T. 1993. Accommodative and pupillary responses to sinusoidal target depth movement. Ophthalmic Physiol. Opt. 13, 253–257.
Thompson, H. S. 1992. The Pupil. In: Adler's Physiology of the Eye: Clinical Application (*eds*. F. H. Adler *et al.*), pp. 412–441. Mosby Year Book.
Thompson, S. H. and Miller, N. R. 1998. Disorders of Pupillary Function, Accommodation, and Lacrimation. In: Clinical Neuro-Ophthalmology (*eds*. N. R. Miller *et al.*), pp. 961–1018. Williams & Wilkins.
Wang, B. and Ciuffreda, K. J. 2006. Depth-of-focus of the human eye: theory and clinical implications. Surv. Ophthalmol. 51, 75–85.
Warwick, R. 1954. The ocular parasympathetic nerve supply and its mesencephalic sources. J. Anat. 88, 71–93.
Westheimer, G. 1964. Pupil size and visual resolution. Vision Res. 4, 39–45.
Westphal, C. 1887. Ueber einen Fall von chronischer progressiver Lähmung der Augenmuskeln (ophthalmoplegia externa) nebst Beschreibung von Ganglienzellengruppen in Bereiche des Oculomotoriuskerns. Arch. Psychiat. Nervenkr. 18, 846–871.
Wilhelm, B. J., Wilhelm, H., Moro, S., and Barbur, J. L. 2002. Pupil response components: studies in patients with Parinaud's syndrome. Brain 125, 2296–2307.
Woodhouse, J. M. and Campbell, F. W. 1975. The role of the pupil light reflex in aiding adaptation to the dark. Vision Res. 15, 649–653.
Yu, Y. and Koss, M. C. 2004. Alpha2-adrenoceptors do not mediate reflex mydriasis in rabbits. J. Ocul. Pharmacol. Ther. 20, 479–488.
Zhang, H., Clarke, R. J., and Gamlin, P. D. R. 1996. Behavior of luminance neurons in the pretectal olivary nucleus during the pupillary near response. Exp. Brain. Res. 112, 158–162.

Further Reading

Kardon, R. H. 2005. Anatomy and Physiology of the Autonomic Nervous System. In: Walsh and Hoyt's Clinical Neuro-Ophthalmology (*eds*. N. R. Miller *et al.*), pp. 649–714. Lippincott Williams & Wilkins.
Kawasaki, A. 2005. Disorders of Pupillary Function, Accommodation, and Lacrimation. In: Walsh and Hoyt's Clinical Neuro-Ophthalmology (*eds*. N. R. Miller *et al.*), pp. 739–805. Lippincott Williams & Wilkins.
Loewenfeld, I. E. and Lowenstein, O. 1993. The Pupil : Anatomy, Physiology, and Clinical Applications. Lowa State University Press.
Thompson, H. S. 1992. The Pupil. In: Adler's Physiology of the Eye: Clinical Application (*eds*. F. H. Adler *et al.*), pp. 412–441. Mosby Year Book.

1.27 The Suprachiasmatic Nucleus

G E Pickard and P J Sollars, Colorado State University, Fort Collins, CO, USA

© 2008 Elsevier Inc. All rights reserved.

1.27.1	**The Hypothalamic Suprachiasmatic Nucleus**	537
1.27.1.1	Molecular Components of the Suprachiasmatic Nucleus Circadian Oscillator	538
1.27.1.2	Suprachiasmatic Nucleus Neurons Express a Circadian Rhythm in Neural Activity	540
1.27.1.3	A Retinohypothalamic Tract Innervates the Suprachiasmatic Nucleus	541
1.27.1.4	The Retinohypothalamic Tract Arises from Intrinsically Photosensitive Ganglion Cells that Express Melanopsin	542
1.27.2	**Photic Entrainment of the Suprachiasmatic Nucleus**	542
1.27.2.1	Two Models of Photic Entrainment: Nonparametric versus Parametric	543
1.27.2.1.1	Nonparametric entrainment	543
1.27.2.1.2	Parametric entrainment	543
1.27.2.1.3	Entrainment in nature	544
1.27.2.2	Entrainment Confers Clock-Like Properties to the Suprachiasmatic Nucleus	545
1.27.2.3	Suprachiasmatic Nucleus Gating of the Light Response	546
1.27.3	**Serotonergic Modulation of Photic Input to the Suprachiasmatic Nucleus**	546
1.27.3.1	5-HT_{1B} Receptor-Mediated Inhibition of Retinohypothalamic Tract Input to the Suprachiasmatic Nucleus	547
1.27.4	**Anatomical Organization of the Suprachiasmatic Nucleus**	548
1.27.4.1	Suprachiasmatic Nucleus Divisions	549
1.27.4.2	Afferent and Efferent Connections	549
1.27.4.3	Suprachiasmatic Nucleus Regulation of Peripheral Oscillators	550
1.27.5	**Summary**	550
References		551

1.27.1 The Hypothalamic Suprachiasmatic Nucleus

In response to the ineluctable cycle of day and night, organisms have developed a self-sustaining clock-like mechanism that coordinates biological functions both with one another and with specific times of the day or night. Maynard Johnson was one of the first to describe clearly these clock-like properties in mammals. Under controlled conditions in the laboratory, he recorded the rest/activity behavior of feral mice maintained in either cyclic or constant lighting conditions. He noted that the 24 h rhythm of rest and activity evident under the day/night regimen persisted under conditions of constant light, free-running with a period of only approximately 24 h (Figure 1). This observation prompted him to conclude that "this animal has an exceptionally substantial and durable self-winding and self-regulating clock, the mechanism of which remains to be worked out" (Johnson, M. S., 1939). Although Johnson's account of the mouse rest/activity behavior with a period of ≈24 h under constant environmental conditions was a description of a behavioral circadian rhythm, it was not until 20 years later that Franz Halberg (1959) first used the term circadian (from the Latin circa "about" and dies "day").

Since that early account of a biological clock in the mouse, the identification of the hypothalamic suprachiasmatic nucleus (SCN) as the primary circadian oscillator in the mammalian brain and of the retinofugal pathways by which environmental day/night information is conveyed to the SCN have been firmly established (Klein, D. C. *et al.*, 1991). Remarkably, the retinal efferents that transmit environmental irradiance signals to the circadian clock in the SCN consist primarily of axons of a recently discovered novel class of mammalian photoreceptor, the intrinsically photosensitive retinal ganglion cell (ipRGC) (Berson, D. M., 2003).

In this review of the SCN, we begin with a brief account of the molecular mechanisms underlying circadian rhythm generation. Following that introduction, the discussion focuses primarily on the light input pathways to the SCN, the mechanisms by

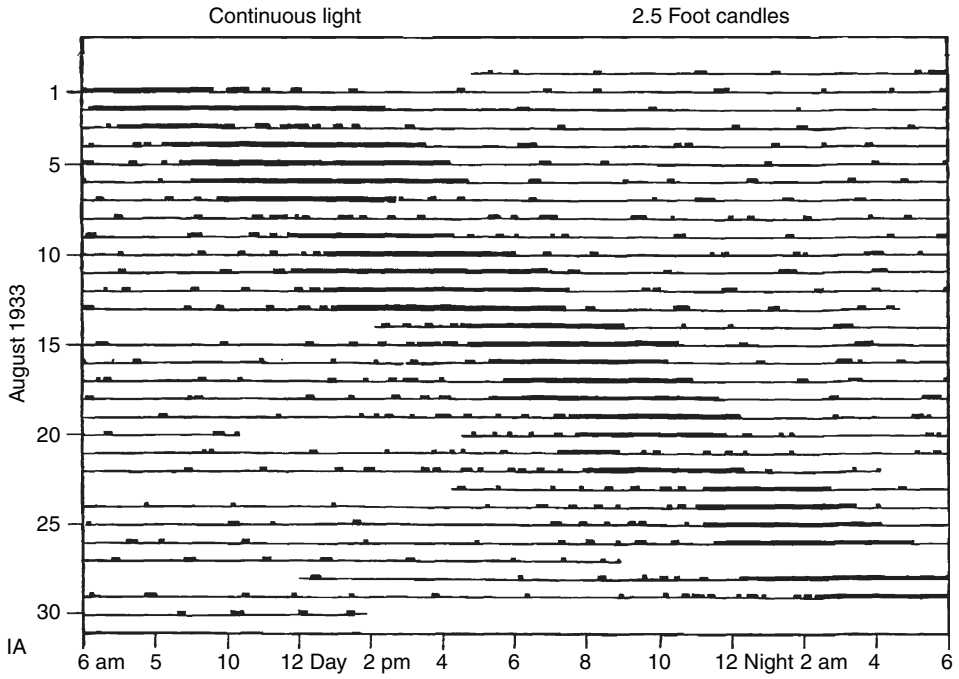

Figure 1 Activity record of a white-footed mouse (*Peromyscus leucopus*) maintained in dim constant light. Activity was recorded as the movement of a suspended cage traced onto smoked paper on a kymograph drum turned by a clockwork. Blocks of black represent cage movement corresponding to mouse activity. The record shows a well-defined circadian rhythm of activity with a period of approximately 24.7 h. Adapted from Johnson, M. S. 1939, Effect of continuous light on periodic spontaneous activity of white-footed mice (Peromyscus). J. Exp. Zool. 82, 315–328, with permission from John Wiley & Sons, Inc.

which these inputs entrain the SCN circadian oscillator to the environmental day/night cycle, and modulation of light input to the SCN by serotonergic afferents arising from the median raphe nucleus. We conclude with a brief summary of the anatomical organization of the SCN, its output pathways, and the role of the SCN in the regulation of peripheral clocks.

1.27.1.1 Molecular Components of the Suprachiasmatic Nucleus Circadian Oscillator

Insights into the molecular mechanisms of the circadian clock began with a mutagenesis screen conducted in the fruit fly that identified three mutant alleles of a single gene (*period*) that had the properties of either increasing or decreasing the circadian period or eliminating circadian rhythmicity altogether (Konopka, R. J. and Benzer, S., 1971). Following the discovery of the mammalian homolog of *Per* (Sun, Z. S. *et al.*, 1997; Tei, H. *et al.*, 1997), great strides have been made in defining the interlocking transcriptional/translational feedback loops that are believed to underlie the generation of circadian oscillations in SCN gene expression (Reppert, S. M. and Weaver, D. R., 2002; Lowrey, P. L. and Takahashi, J. S., 2004; Ko, C. H. and Takahashi, J. S., 2006).

At the core of the current working model of the SCN molecular clock are feedback loops involving positive and negative limbs. The transcription factors CLOCK and BMAL1 are believed to be the positive elements in the primary feedback loop. BMAL1 and CLOCK dimerize in the cytoplasm of SCN neurons, and following translocation to the nucleus, they initiate transcription of target genes of the negative feedback loop, including *period* (*Per1*, *Per2*, and *Per3*) and *cryptochrome* (*Cry1* and *Cry2*) by binding to E-box elements within enhancer and promoter sequences of these genes. The primary negative feedback loop results from the translocation of PER:CRY heterodimers back to the nucleus where they repress their own transcription by acting on the CLOCK:BMAL1 complex (Figure 2) (Ko, C. H. and Takahashi, J. S., 2006). Currently, *Bmal1* (also known as *Mop3*) is the only clock gene that appears to be essential for the generation of circadian oscillations in the SCN. *BMAL1*-null mice display arrhythmic locomotor

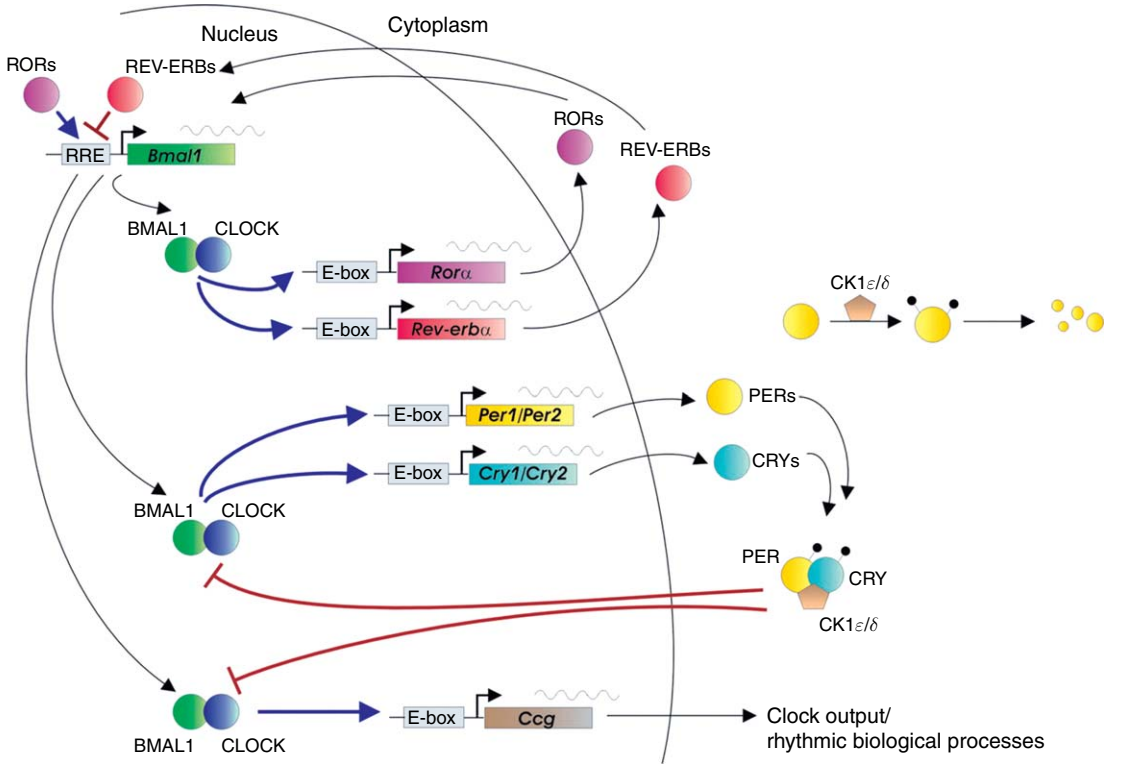

Figure 2 A network model of transcriptional–translational feedback loops that constitutes the mammalian circadian clock. CLOCK and BMAL1 form heterodimers and initiate transcription of *Per1*/*Per2* and *Cry1*/*Cry2*. Per:CRY heterodimers feedback to repress their own transcription. Adapted from Ko, C.H. and Takahashi, J.S. 2006, Molecular components of the mammalian circadian clock. *Hum. Mol. Genet.* 15, R271–R277, by permission of Oxford University Press.

activity immediately when transferred from day/night conditions into a constant dark environment, and the rhythmic expression of *Per1* and *Per2* in the SCN of these animals is abolished (Bunger, M. K. *et al.*, 2000). Two isoforms exist for all other known clock genes (e.g., *Per1* and *Per2*, *Cry1* and *Cry2*), and thus for example, *Per1*- and *Per2*-null mutants each exhibit only modest circadian phenotypes, whereas *Per1*/*Per2* double mutants are completely arrhythmic (Lowrey, P. L. and Takahashi, J. S., 2004).

The circadian behavior of animals with a mutated *clock* gene becomes arrhythmic in constant dark conditions after many days. Based on this gradual loss of rhythmic behavior in constant dark, it was believed initially that *clock* was an essential component of the core SCN molecular clock mechanism (Vitaterna, M. H. *et al.*, 1994). However, subsequent experiments revealed that behavioral circadian rhythmicity is actually retained in *clock* mutant mice when they are maintained under constant light conditions (Spoelstra, K. *et al.*, 2002). Spoelstra K. *et al.* (2002) point out that their new data raise two important questions:

1. Does behavioral arrhythmicity in a mutant mouse reflect an arrhythmic SCN pacemaker or a rhythmic pacemaker that has lost the ability to regulate a behavioral output?
2. Is CLOCK an essential component of the SCN molecular clock mechanism?

The first question was addressed when individual SCN neurons from homozygous *clock* mutant mice were analyzed *in vitro* and were shown to retain their ability to generate circadian rhythms in neural activity, indicating that the SCN is indeed rhythmic in these animals even though behavioral rhythmicity is lost in constant dark conditions (Nakamura, W. *et al.*, 2002). The essential role of CLOCK in circadian rhythm generation was tested by DeBruyne J. P. *et al.* (2006) who generated a *clock*-null mutant mouse; these mice express robust and sustained behavioral circadian rhythms in constant dark conditions, indicating that the CLOCK:BMAL1 heterodimer is not required for SCN circadian clock function. It seems likely that the transcription factor NPAS2, a closely related paralog of CLOCK, assumes the role

of CLOCK in these null mutant mice (DeBruyne, J. P. *et al.*, 2006). However, to date, NPAS2 mRNA has not been detected in the SCN and other possibilities should also be considered until there is evidence for NPAS2 in the SCN (Asher, G. and Schibler, U., 2006).

The period of the circadian oscillation is determined by many factors and is altered by several modulatory transcription factors. For example, *Rev-erbα*, a nuclear orphan receptor, represses the transcription of *BMAL1*, whereas *RORα* (retinoic acid-related orphan nuclear receptor alpha) activates *BMAL1* and alterations in these genes produce small but significant changes in period (Ko, C. H. and Takahashi, J. S., 2006). Post-translational modifications of core clock gene protein products are also clearly important in generating the period of the circadian oscillation observed in the SCN. Casein kinase I epsilon (*CKIε*) appears to be a key player in this process. A widely studied mutation in *CKIε*, the $CKI\varepsilon^{tau}$ mutant, has been shown to cause a loss of kinase function *in vitro*, and the homozygous tau mutant hamster has a circadian locomotor rhythm in constant dark conditions that is 4 h shorter than the period of the wild-type hamster (Lowrey, P. L. and Takahashi, J. S., 2004). Again, emphasizing the evolving nature of the current SCN clock model, Gallego M. *et al.* (2006) provide strong data indicating that $CKI\varepsilon^{tau}$ mutation is actually a highly specific gain-of-function mutation that increases the *in vivo* phosphorylation and degradation of Per1 and Per2. Thus, although impressive progress has been made in unraveling the molecular nature of the SCN circadian clock, there are additional inconsistencies and anomalous observations that do not fit the current clock model that must also be resolved before our understanding of the molecular underpinnings of circadian rhythm generation by SCN neurons is complete (Lakin-Thomas, P. L., 2006; Levi, F. and Schibler, U., 2007).

1.27.1.2 Suprachiasmatic Nucleus Neurons Express a Circadian Rhythm in Neural Activity

When the SCN is surgically isolated from the rest of the brain, rhythmic electrical activity within the hypothalamic island containing the SCN persists, whereas rhythms of multiunit activity in other brain regions that were rhythmic before the isolation of the SCN, as well as behavioral rhythms, are abolished (Inouye, S. I. T. and Kawamura, H., 1979; 1982). These early studies provided important data consistent with the interpretation that the SCN was a circadian oscillator. Recordings made from the SCN *in vitro* showed that the oscillations in neural activity in the hypothalamic island were indeed generated by SCN neurons. The spontaneous electrical activity of SCN neurons in a hypothalamic slice maintained *in vitro* is highest during the subjective day, similar to the time of peak firing of SCN multiunit activity recorded *in vivo* (Meijer, J. H. and Rietveld, W. J., 1989). Recordings from individual SCN neurons in dispersed cell cultures using multielectrode arrays provided definitive evidence that individual SCN neurons generate a rhythm in their rate of action potential firing and thus are competent circadian pacemakers (Welsh, D. K. *et al.*, 1995). The ionic mechanisms underlying rhythmic spontaneous action potential firing of SCN neurons remain to be definitively described (Pennartz, C. M. *et al.*, 2002; Jackson, A. C. *et al.*, 2004; Kononenko, N. I. *et al.*, 2004; Itri, J. N. *et al.*, 2005).

It is clear that the SCN displays circadian rhythms both in gene expression and in the rate of action potential firing. Recent studies at the single-cell level have shown that the phase of the molecular oscillation in SCN neurons is correlated with their action potential firing rate. Using a short-half-life green fluorescent protein (GFP) reporter of *Per1* with quantitative imaging and patch-clamp recording of SCN neurons in an *in vitro* slice preparation, Quintero J. E. *et al.* (2003) were able to define accurately the relationship between *Per1* gene expression and the neurophysiological output of individual SCN neurons. The precise interaction between molecular oscillations in SCN neurons and the membrane activities of these same cells is, however, unclear.

The work of Welsh D. K. *et al.* (1995) using dispersed SCN neurons in culture demonstrated that blockade of neuronal firing with the Na^+ channel blocker tetrodotoxin (TTX) did not affect the circadian rhythm in individual SCN cells, suggesting that neuronal firing was not an essential component of the cellular clock mechanism. However, it has been suggested that depolarization-activated ionic conductances in the membrane of clock neurons are required for circadian pacemaker function and molecular oscillations in core clock genes. By targeting specific clock neurons in *Drosophila* with K^+ channel variants that have a high open probability at resting membrane potential, Nitabach M. N. *et al.* (2002) made these clock cells electrically silent which rendered the flies behaviorally arrhythmic. Surprisingly,

the electrically silent clock cells also lost their molecular oscillations of PER (Nitabach, M. N. *et al.*, 2002). Similarly, Yamaguchi S. *et al.* (2003) have recently shown that TTX distorts synchrony among SCN neurons in an *in vitro* slice and also suppresses clock gene expression.

Calcium entry through voltage-gated Ca^{2+} channels is one likely candidate for transducing membrane electrical events to intracellular gene expression (van den Pol, A. N. and Obrietan, K., 2002). Indeed, blocking Ca^{2+} influx in SCN neurons *in vitro* abolishes the rhythmic expression of *Per1* (Lundkvist, G. B. *et al.*, 2005). However, Ikeda M. *et al.* (2003) reported a TTX-resistant circadian rhythm in cytosolic, but not nuclear Ca^{2+} concentration in SCN neurons transfected with a Ca^{2+}-sensitive fluorescent protein (cameleon). The rhythm in cytosolic Ca^{2+} appeared driven by the release of Ca^{2+} from ryanodine-sensitive Ca^{2+} stores and was also resistant to L-type voltage-gated Ca^{2+} channel blockers, suggesting that Ca^{2+} influx through the plasma membrane was not the primary mechanism responsible for the observed rhythm in cytosolic Ca^{2+} (Ikeda, M. *et al.*, 2003). To account for these conflicting data, Lundkvist G. B. *et al.* (2005) suggest that there may be two rhythmic systems affecting intracellular Ca^{2+} levels: one membrane-related electrical rhythm and one intracellular cytosolic Ca^{2+} rhythm. In either case, it seems as though it may be time to incorporate oscillations of intracellular Ca^{2+} into the cellular model of SCN circadian rhythm generation (Lundkvist, G. B. and Block, G. D., 2005).

1.27.1.3 A Retinohypothalamic Tract Innervates the Suprachiasmatic Nucleus

The visual system has played a prominent role in the study of mammalian circadian rhythms over the years. It was long known that in the absence of retinal efferent projections to the brain (e.g., following bilateral orbital enucleation), rhythmic behavior persists, expressing a free-running circadian period under light/dark conditions as if the eyeless animals were insensitive to the light (Richter, C. P., 1965). Thus, the early search for Johnson's self-regulating clock in mammals focused on structures in the brain that received retinal afferent fibers. However, systematic attempts to ablate all known retinorecipient structures caudal to the optic chiasm failed to generate the free-running circadian rhythms seen after removal of the eyes. This paradox was resolved following the introduction of autoradiography for the localization of anterogradely transported [^{3}H]-amino acids. Using this new tracing technique, two groups provided an unambiguous demonstration of a previously unknown bilateral retinal projection to the anterior hypothalamus terminating in the SCN located just dorsal to the optic chiasm (Hendrickson, A. E. *et al.*, 1972; Moore, R. Y. and Lenn, N. J., 1972). This was soon followed by the important observation that SCN ablation abolished circadian rhythms of drinking, locomotor activity, and hormone release (Moore, R. Y. and Eichler, V. B., 1972; Stephan, F. K. and Zucker, I., 1972). Based on this groundbreaking work, the SCN became the focus of intense investigation to establish its role as a biological clock. The retinal ganglion cells (RGCs) afferent to the SCN were then identified using retrograde tracing techniques, and it was determined that the retinohypothalamic tract (RHT) arose from a class of RGCs with sparsely branching dendrites and with axon collaterals that innervated the thalamic intergeniculate leaflet (IGL) (Pickard, G. E., 1980; 1982; 1985). The RHT has been described in every animal in which it has been investigated including primates and humans (Figure 3), and the RHT is now recognized as a common feature of the vertebrate visual system (Morin, L. P., 1994).

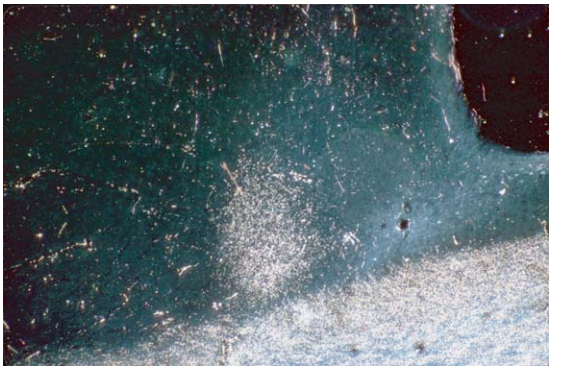

Figure 3 The retinohypothalamic tract (RHT) is a common feature of the mammalian visual system. In this dark-field photomicrograph, RHT processes terminating in the hypothalamic suprachiasmatic nucleus were labeled by a horseradish peroxidase (HRP) injection into the vitreous chamber of one eye of a pig-tailed macaque (*Macaca nemestrina*). The oval-shaped RHT terminal field is evident just above the optic chiasm near the midline, and just lateral to the third ventricle evident in the upper right of the photomicrograph. HRP anterograde tracing procedures were similar to those described by Pickard G. E. (1982).

1.27.1.4 The Retinohypothalamic Tract Arises from Intrinsically Photosensitive Ganglion Cells that Express Melanopsin

While it was evident from early studies that the RHT conveyed irradiance information to the SCN, it was not clear which retinal neurons relayed signals to the ganglion cells that gave rise to the RHT. It was reported that in mice with severe retinal degeneration caused by the *rd* gene, neither rods nor cones were required for entrainment of circadian behavior to the light/dark cycle, and the possibility was raised that cells other than rods or cones might be sensitive to light (Ebihara, S. and Tsuji, K., 1980; Foster, R. G. *et al.*, 1991). However, because some cone perikarya lacking outer segments but remaining immunoreactive for cone-opsin persist even in quite aged *rd/rd* mice, the possibility of RGCs being directly light sensitive was widely discounted. Foster and colleagues provided more definitive evidence that other retinal neurons may be light sensitive by using transgene constructs that eliminated virtually all rods and cones; the rodless/coneless mice remained capable of entraining their SCN circadian oscillator to the environmental day/night cycle (Freedman, M. S. *et al.*, 1999). Around this time, melanopsin was discovered, a novel mammalian opsin which localized to the inner retina (Provencio, I. *et al.*, 1998; 2000; Chapter Contributions of Horizontal Cells). Berson and co-workers ended the debate with their unambiguous demonstration that SCN-projecting RGCs were intrinsically photosensitive and expressed melanopsin (Berson, D. M. *et al.*, 2002; Hattar, S. *et al.*, 2002). The SCN is densely innervated by melanopsin RGCs (Hattar, S. *et al.*, 2002), and mice lacking rods, cones, and melanopsin fail to entrain to light/dark cycles, making it unlikely that additional opsins contribute to the entrainment process (Hattar, S. *et al.*, 2003; Panda, S. *et al.*, 2003).

It should be noted, however, that a small population (≈10–20%) of SCN-projecting RGCs in rodents do not appear to express melanopsin mRNA (rat; Gooley, J. J. *et al.*, 2003), nor melanopsin protein (golden hamster; Morin, L. P. *et al.*, 2003; Sollars, P. J. *et al.*, 2003). In genetically modified mice in which the *tau-lacZ* gene replaced the melanopsin gene *opn4* (Hattar, S. *et al.*, 2002), some retinal fibers and terminals in the SCN lack the reporter enzyme and thus would appear to arise from nonmelanopsin RGCs (Hattar, S. *et al.*, 2006). Little is currently known regarding the nonmelanopsin RGCs that send afferent fibers to the SCN. It was suggested early on, based on an analysis of the soma size of SCN-projecting RGCs in the golden hamster, that a large majority of RGCs afferent to the SCN had a soma size of about 100 μm^2, whereas an additional very small population of SCN-projecting RGCs was considerably larger (Pickard, G. E., 1982). The functional significance of two populations of RGC afferent to the SCN is unknown, and it remains to be determined whether individual SCN neurons receive input from both melanopsin and conventional RGCs or whether the input from each type of ganglion cell is segregated to specific SCN neurons.

Melanopsin-expressing RGCs are intrinsically photosensitive, yet their dendrites extend into the inner plexiform layer of the retina similar to conventional RGCs. Anatomical and physiological data indicate that rod and/or cone photoreceptors provide input to melanopsin RGCs. Ultrastructural work has shown that the somas and proximal dendrites of melanopsin RGCs located in the ganglion cell layer are postsynaptic to terminals containing ribbon synapses, indicating input from cone bipolar cells. Melanopsin ganglion cell dendrites receive GABAergic and non-GABAergic amacrine cell synapses along their entire length and also in S1 of the inner plexiform layer where most of the dendrites stratify (Belenky, M. A. *et al.*, 2003; Belenky, M. A. and Pickard, G. E., unpublished observations). Recordings from SCN-projecting RGCs in retinas maintained *in vitro* have shown that light can trigger synaptic currents in these cells via activation of ionotropic glutamate and GABA receptors (Perez-Leon, J. A. *et al.*, 2006). In addition, glutamate stimulates a rise in intracellular Ca^{2+} in isolated melanopsin RGCs maintained *in vitro*, and this effect is blocked by ionotropic glutamate receptor antagonists, providing an unambiguous demonstration of the presence of glutamate receptors on these cells (Hartwick, A. T. E., Sollars, P. J., and Pickard, G. E., unpublished observations). How the much faster rod/cone driven signals are integrated with the slow intrinsic light response in SCN-projecting melanopsin RGCs remains to be determined. Taken together, these data make it clear that the retinal circuits that provide irradiance signals to the SCN circadian oscillator are exceptionally complex.

1.27.2 Photic Entrainment of the Suprachiasmatic Nucleus

In mammals, unlike most other animals, retinal light perception and retinal efferent projections to the SCN have been shown to be required for photic

entrainment of circadian rhythms (Nelson, R. J. and Zucker, I., 1981). Campbell S. S. and Murphy P. J. (1998) challenged this long-established view when they reported that extraocular light stimulation (i.e., light on the back of the knee) shifts circadian rhythms of core body temperature and melatonin secretion in humans. Since that report, numerous studies have all failed to confirm extraocular effects of light on circadian rhythms in humans or other mammals (Lockley, S. W. *et al.*, 1998; Yamazaki, S. *et al.*, 1999; Eastman, C. I. *et al.*, 2000; Lushington, K. *et al.*, 2002; Wright, K. P. and Czeisler, C. A., 2002; Rüger, M. *et al.*, 2003). Based on the overwhelming evidence, it must be concluded that the effects of light on the SCN circadian oscillator in mammals require ocular light perception.

1.27.2.1 Two Models of Photic Entrainment: Nonparametric versus Parametric

Simply stated, entrainment of the SCN circadian oscillator to the day/night cycle means that the period of the endogenous SCN circadian oscillation becomes equal to that of the light/dark cycle (see below). Two different models have been proposed to explain the mechanisms by which the SCN circadian clock entrains to the day/night cycle, and these models refer to the nature of the action of light, whether discrete or phasic in the case of nonparametric entrainment, or continuous or tonic in the case of parametric entrainment (Daan, S., 1977). Large phase shifts in circadian behavior evoked by brief light pulses administered to animals in the dark provide the evidence for a nonparametric mechanism. The nonparametric model of entrainment therefore emphasizes instantaneous phase shifts (that reset the clock every day) evoked by light exposure at the dusk and/or dawn transitions of the day/night cycle. Changes in circadian period resulting from exposure to different constant light intensities provide evidence of tonic effects of light on the circadian pacemaker. Thus, the parametric model emphasizes gradual changes in circadian period during daylight exposure.

1.27.2.1.1 Nonparametric entrainment

The nonparametric model of entrainment has been derived primarily from the study of nocturnal rodents, although a similar phase-resetting mechanism exists in diurnal animals including humans. This model proposes that entrainment to the day/night cycle is accomplished by a daily resetting of the SCN such that the light-induced phase shift is equal in magnitude to the difference between the free-running period of the endogenous SCN oscillation and the period of the day/night cycle (i.e., typically 24 h but not restricted to this period). This mechanism is described empirically by the response of animals free-running under constant dark (DD) conditions and exposed briefly to light at different phases of the circadian cycle. The response of the SCN to brief light pulses is phase dependent: light exposure during the subjective day (i.e., the times when the animal would normally be exposed to daylight) has no effect on the phase of the free-running circadian rhythm. In contrast, light exposure early in the subjective night produces phase delays in circadian rhythms, whereas light exposure late in the subjective night results in phase advances. The phase response curve (PRC) to brief light pulses plots the amplitude of the phase shift as a function of the phase of the rhythm at the time of the light stimulation with the onset of wheel-running activity arbitrarily defined as circadian time (CT) 12 (Figure 4).

For nocturnal rodents, the PRC to light very accurately predicts the details of entrainment for short light pulses recurring once every 24 h (Pittendrigh, C. S. and Daan, S., 1976a). These pulses can be as brief as 1 s and as dim as 0.05 lux (DeCoursey, P. J., 1972; Earnest, D. J. and Turek, F. W., 1983). Circadian entrainment by the widely accepted nonparametric model of entrainment based on the PRC to light is critically dependent on phase shifts occurring at dusk and/or dawn as the portion of the circadian day sensitive to light is coincident with the twilight transitions in the day/night cycle.

1.27.2.1.2 Parametric entrainment

The discrete or nonparametric model of entrainment based on the PRC to brief light pulses is insufficient to predict circadian entrainment under all lighting conditions (Pittendrigh, C. S. and Daan, S., 1976b). Moreover, the SCN oscillator can be entrained to continuous dim light that rhythmically varies in intensity from 5 to 10 lux (with peak emission at 510 nm held constant) in the form of a sine wave with a 24 h period (Pickard, G. E., 1989). It is also well documented that the period of the free-running circadian activity rhythm of animals maintained under constant light conditions changes as a function of light intensity (Aschoff, J., 1960). The parametric model of entrainment, also called continuous or tonic, has been proposed to explain these types of observations. In its simplest form, this model states

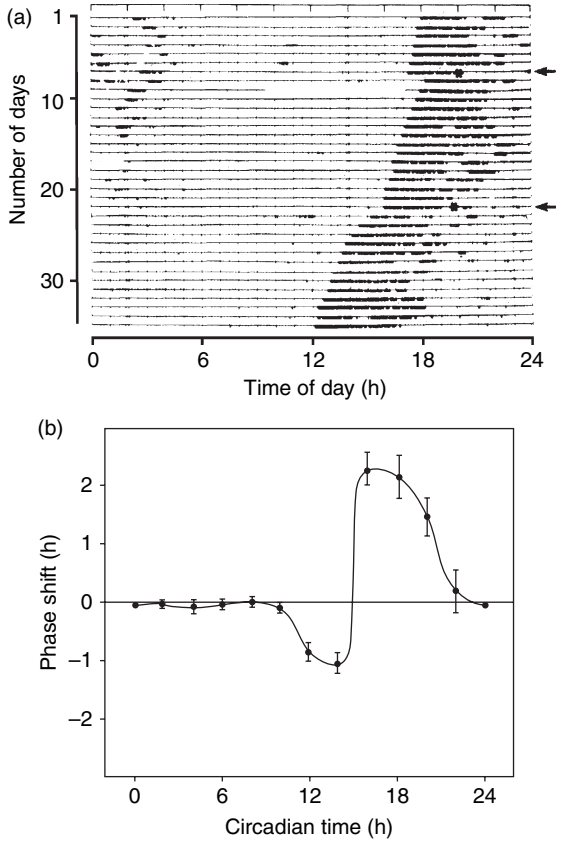

Figure 4 Effect of brief light pulses on the circadian rhythm of wheel-running activity of the golden hamster. (a) Wheel-running activity record of a hamster free-running in constant darkness illustrating the effect of exposure to 15 min of light on the days indicated by arrows and at the times indicated by asterisks. The first light pulse generated a phase delay and the second light pulse a phase advance in the onset of wheel-running activity. (b) A phase response curve to light showing the effects of light pulses presented at various times relative to hamster wheel-running onset defined as circadian time (CT) 12. Phase advances are plotted as positive and phase delays as negative phase shifts ($n = 6 \pm$ SD/time point). (a) Reproduced from Springer and J. Comp. Physiol, Vol. 106, 1976, pp. 253–266, A functional analysis of circadian pacemakers in nocturnal rodents. II. The variability of phase response curves, Daan, S. and Pittendrigh, C. S., with kind permission from Springer Science and Business Media. Reproduced from Takahashi, J. S. and Zatz, M. 1982. Regulation of circadian rhythmicity. *Science* 217, 1104–1111. Reprinted with permission from AAAS.

that the angular velocity or rate of motion of the clock mechanism changes proportionally to the intensity of light present. Thus, this model predicts that under entrainment to a light/dark cycle, the clock runs faster in light and slower in darkness. The modulation of angular velocity under the light and dark portions of the daily cycle would allow the SCN clock to continuously adjust its cycle length to that of the environment.

The ability of light to effect the period of the SCN circadian oscillator directly is perhaps most clearly demonstrated following entrainment to non-24 light/dark cycles and is observed as long-lasting after-effects on circadian period (Pittendrigh, C. S. and Daan, S., 1976a). For example, animals entrained to a 22 h light/dark cycle and then released to free-run in constant darkness initially have free-running periods only slightly greater than 22 h, and only after many (50–100) cycles in DD, does the free-running circadian period approach the endogenous circadian period of the SCN oscillator (Sollars, P. J. *et al.*, 2006a).

1.27.2.1.3 Entrainment in nature

Entrainment under natural photic conditions is likely based on both the nonparametric and the parametric effects of light on the SCN oscillator (Roenneberg, T. *et al.*, 2003), and of course under natural conditions, the exposure to light is quite different in day-active and night-active species. Observations of bats emerging from their caves support the nonparametric model of entrainment under natural conditions as the emergence time follows the time of sunset with a correlation to a narrow range of light intensities throughout the year (DeCoursey, G. and DeCoursey, P. J., 1964). In addition, observations of flying squirrels with access to dark nest boxes have shown that these nocturnal animals sample light at the dusk transition to entrain their SCN circadian system to the light/dark cycle (DeCoursey, P. J., 1986). Night-active golden hamsters living in a seminatural habitat containing a simulated burrow system entrain to the light/dark cycle but are exposed to light for very short amounts of time each day (Pratt, B. L. and Goldman, B. D., 1986). Thus, these limited data suggest that nocturnal animals under natural conditions experience very little light each day but that light at the dusk and dawn transitions is used for entrainment to the day/night cycle presumably via the nonparametric entrainment mechanism. Conversely, in a very carefully conducted field study in which the light environment for individual animals was measured with light-sensitive radio collar transmitters, Hut R. A. *et al.* (1999) reported that diurnal burrow-dwelling European ground squirrels observed under natural conditions never were above ground during twilight at dawn or at dusk. Thus, the animals were never

exposed to light during the portion of the circadian cycle (i.e., subjective night) when light phase shifts the SCN circadian oscillator (via the nonparametric mechanism). Yet these animals entrained to the day/night cycle, presumably in this case, via a continuous or parametric mechanism.

Although both nonparametric and parametric mechanisms may be used for entrainment, nocturnal animals may rely primarily on the dusk/dawn transitions to reset their circadian clocks each day (nonparametric effects), whereas burrow-dwelling diurnal animals appear to use only the parametric mechanism. For animals exposed to complete photoperiods (i.e., non-burrow-dwelling day-active animals), circadian entrainment is probably a combination of parametric and nonparametric mechanisms: by monitoring changes in ambient irradiance over the course of the day, the parametric mechanism would set the period of the endogenous pacemaker close to the 24 h period of the environmental day/night cycle while light at the dusk/dawn transitions coincident with early and/or late subjective night would also generate small daily phase shifts of the SCN circadian clock each day to fine-tune the period even more closely to 24 h.

The nonparametric model of entrainment has been used extensively to probe the cellular and molecular bases of the effects of light on the SCN primarily because the light stimulus and the behavioral responses are easily quantified and correlated with the cellular responses (see below). On the other hand, there is virtually nothing known regarding the cellular or molecular mechanisms underlying the parametric effect of light on the SCN because no convenient metric exists to analyze the modulation of the angular velocity of the SCN circadian oscillator.

It is interesting to speculate whether the two different entrainment mechanisms might be related to the two different populations of RGCs projecting to the SCN. The very sluggish irradiance-dependent responses of melanopsin RGCs to light may be better tuned to gradual changes in environmental lighting conditions, whereas the rod/cone input to the non-melanopsin SCN-projecting RGCs would seem better equipped to transmit signals elicited by short-duration light exposure. Considering the very slow response kinetics of melanopsin RGCs to light (Berson, D. M. *et al.*, 2002), it seems unlikely that these cells could contribute significantly to retinal input to the SCN during entrainment to daily 1 s light pulses. However, both the nonparametric (light-induced phase shifts) and the parametric (lengthening of circadian period in constant light) effects of light on the SCN circadian system are attenuated in melanopsin-knockout mice (Panda, S. *et al.*, 2002; Ruby, N. F. *et al.*, 2002).

1.27.2.2 Entrainment Confers Clock-Like Properties to the Suprachiasmatic Nucleus

The SCN circadian oscillator derives functional utility from its ability to be entrained to the 24 h environmental day/night cycle via input from the retina irrespective of whether a nonparametric or parametric mechanism is used. Entrainment provides a predictable and appropriate phase relationship to the day/night cycle, in effect enabling recognition of local time. The SCN circadian oscillator is thus said to function as a biological clock (Pittendrigh, C. S. and Daan, S., 1976b). Entrainment differs from simple synchronization to changes in the light/dark cycle. Entrainment is neither passive nor driven and therefore allows for great plasticity and adaptive potential. This plasticity is evidenced, for example, by the change in the phase angle of entrainment in the golden hamster that occurs with seasonal changes in day length (Elliott, J. A., 1976). Seasonal inversions of activity patterns have been described in normally nocturnal bats that become diurnal in the winter due to the availability of insects (Daan, S., 1981). Another example of plasticity in entrainment is the temporal partitioning that exists between two species of spiny mouse (*Acomys*). When coexisting in nature, the common spiny mouse (*Acomys cahirinus*) is nocturnal, whereas the golden spiny mouse (*Acomys russatus*) is diurnal. When the common spiny mouse is removed from the shared habitat, the golden spiny mouse becomes nocturnal; chemical signals released by *A. cahirinus* may alter the entrainment of *A. russatus* to the day/night cycle (Haim, A. and Rozenfeld, F. M., 1993; Shargal, E. *et al.*, 2000).

The establishment of an appropriate phase relationship between the environment and the circadian system allows the SCN to generate a temporal program whereby biological functions occur at specific times within the day/night cycle (Hastings, M. H. *et al.*, 2003). Alterations in SCN circadian function resulting from changes in the response of the SCN to RHT input or changes in SCN gene activity can result in altered phase relationships of daily oscillations in physiology, metabolism, or behavior with the day/night cycle. Such alterations in circadian function and the accompanying changes in phase have been associated with human disorders. Individuals

suffering from annual recurring depression or seasonal affective disorder (SAD) typically have phase-delayed circadian rhythms (Lewy, A. J. *et al.*, 1987); appropriately timed treatment with light can correct the alteration in phase and alleviate the depressive symptoms (Terman, M. and Terman, J. S., 2005). Individuals with advanced sleep phase syndrome (ASPS) regularly fall asleep in the early evening, whereas people with delayed sleep phase syndrome (DSPS) typically cannot fall asleep until early morning. These individuals may have an abnormality in one of the *Per* genes, resulting in an altered circadian period and hence an altered phase angle of entrainment of the sleep–wake cycle (Jones, C. R. *et al.*, 1999; Ebisawa, T. *et al.*, 2001; Toh, K. L. *et al.*, 2001; Archer, S. N. *et al.*, 2003).

1.27.2.3 Suprachiasmatic Nucleus Gating of the Light Response

Illumination of the retina evokes excitatory postsynaptic currents (EPSCs) in a subpopulation of SCN neurons. These responses have long latencies and are sustained (Meijer, J. H. and Schwartz, W. J., 2003), similar to the responses of ipRGCs to light (Berson, D. M., 2003). The light-induced EPSCs are the result of glutamate release from the RHT and are mediated by both ionotropic and metabotropic glutamate receptors. The location of light-responsive neurons in the SCN corresponds to the terminal field of the RHT primarily within the ventral and lateral aspects of the SCN, although species differences in the RHT terminal field exist and RHT fibers can be found throughout almost all of the SCN in many species (Hattar, S. *et al.*, 2006; Morin, L. P. and Allen, C. N., 2006). The excitatory response to NMDA is larger during the night than during the day, whereas AMPA/kainate-induced currents do not show a day/night difference (Pennartz, C. M. *et al.*, 2001; Michel, S. *et al.*, 2002). In addition to glutamate, most (if not all) SCN-projecting RGCs also synthesize pituitary adenylate cyclase-activating polypeptide (PACAP), which may act as a modulator of the glutamatergic input to the SCN (Hannibal, J., 2006).

Several reports from Obrietan and colleagues have provided evidence that the p42/p44 mitogen-activated protein kinase (MAPK) signal transduction pathway plays an important role in gating the responsiveness of the SCN to light. The MAPK pathway in the SCN is induced by light in a phase-restricted manner, couples light to transcriptional activation, and mediates light-induced phase shifts (Obrietan, K. *et al.*, 1998; Butcher, G. Q. *et al.*, 2002; Coogan, A. N. and Piggins, H. D., 2003; Dziema, H. *et al.*, 2003). MAPK activation is also triggered by glutamate and PACAP (Butcher, G. Q. *et al.*, 2005). The Ras-like G-protein Dexras1 also appears to be a critical factor in this process. *Dexras1*-null mice exhibit a restructured PRC to light at night and a loss of gating to photic resetting during the subjective day (Cheng, H.-Y. M. *et al.*, 2006). The exact mechanisms by which the SCN clock gates its response to light, shifting its phase during the subjective night but not during the subjective day, remain to be fully elucidated.

Investigation into the genes that might be involved in light-induced pacemaker resetting was initiated by the seminal observation that light induces a rapid and transient expression of the transcription factor c-Fos within the SCN during the same phases of the day/night cycle that light shifts the SCN circadian oscillation (Rea, M. A., 1989; Kornhauser, J. M. *et al.*, 1990). The *Per* genes (*Per1* and *Per2*) in the SCN are photoinducible with a phase dependence similar to that of light-induced behavioral phase shifts (Albrecht, U. *et al.*, 1997; Shigeyoshi, Y. *et al.*, 1997). Daan S. *et al.* (2001) offered an intriguing two-component molecular model for light-induced phase shifting in the SCN inspired by earlier work suggesting that *mPer1*-mediated phase advances and *mPer2* phase delays. However, a subsequent analysis of phase shift responses to light in mice lacking functional *Per* (*mPer1* and *mPer2*) or *Cry* (*mCry1* and *mCry2*) genes by Daan and co-workers revealed that all four genotypes of mice retain the capacity for both advancing and delaying responses to light, suggesting that neither *Per* nor *Cry* genes are associated specifically with light-induced phase advances or delays (Spoelstra, K. *et al.*, 2004). Thus, the molecular mechanisms underlying the biphasic response of the SCN to light remain to be determined.

1.27.3 Serotonergic Modulation of Photic Input to the Suprachiasmatic Nucleus

The SCN receives a robust serotonergic input arising from ascending projections of serotonin (5-HT) neurons in the mesencephalic median raphe nucleus. In an attempt to address the role of this dense monoaminergic projection to the SCN, it was determined early on that a 5-HT input to the SCN is not required for the generation of circadian activity rhythms (Block, M. and Zucker, I., 1976). This

finding resonates with the general theme outlined much later by Jacobs B. L. and Azmitia E. C. (1992) that 5-HT neurons do not play an essential role in physiological and behavioral processes but rather exert tonic modulatory influences on their targets. Since a substantial overlap exists between the distributions of the RHT and 5-HT terminal fields in the SCN, a modulatory influence of 5-HT on RHT input to the SCN was sought. Morin and colleagues were the first to demonstrate a modulatory role of 5-HT in the SCN; depletion of 5-HT within the SCN produced a small but significant change in the phase angle of entrainment of the circadian activity rhythm to the light/dark cycle and an augmentation of light-induced phase shifts, suggesting a tonic inhibitory influence of 5-HT on SCN responses to light (Smale, L. *et al.*, 1990; Morin, L. P. and Blanchard, J. H., 1991). However, at that time neither the 5-HT receptor subtype(s) mediating these effects nor their subcellular location within the SCN was known.

1.27.3.1 5-HT_{1B} Receptor-Mediated Inhibition of Retinohypothalamic Tract Input to the Suprachiasmatic Nucleus

There are at least 14 different 5-HT receptor subtypes grouped into several families, and as many as six 5-HT receptor subtypes have been described in the SCN including the 5-HT_{1A}, 5-HT_{1B}, 5-HT_{2A}, 5-HT_{2C}, 5-HT_{5A}, and 5-HT_7 (Belenky, M. A. and Pickard, G. E., 2001). Of these 5-HT receptor subtypes, activation of 5-HT_{1B} and 5-HT_7 receptors in the SCN attenuates light-induced responses (Morin, L. P., 1999). To date, the best-documented role for 5-HT in the SCN is its ability to modulate SCN sensitivity to light via presynaptic 5-HT_{1B} receptors located on RHT terminals. Bilateral enucleation reduces the number of 5-HT_{1B} binding sites in the SCN (Pickard, G. E. *et al.*, 1996; Manrique, C. *et al.*, 1999), and ultrastructural work has provided direct evidence for 5-HT_{1B} receptors on RHT terminals (Pickard, G. E. *et al.*, 1999). Activation of these presynaptic 5-HT_{1B} receptors *in vivo* attenuates (1) light-induced behavioral phase shifts in rodents (Pickard, G. E. *et al.*, 1996; Pickard, G. E. and Rea, M. A., 1997), (2) light-induced suppression of pineal melatonin (Rea, M. A. and Pickard, G. E., 2000), and (3) light-induced expression of several genes in the SCN (Pickard, G. E. *et al.*, 1996; Hayashi, S. *et al.*, 2001; Shimazoe, T. *et al.*, 2004). Moreover, 5-HT_{1B} receptor agonists applied to the SCN *in vitro* inhibit optic nerve-evoked glutamatergic EPSCs (Pickard, G. E. *et al.*, 1999; Smith, B. N. *et al.*, 2001), and these responses are eliminated in mice lacking functional 5-HT_{1B} receptors (Smith, B. N. *et al.*, 2001).

Based on substantial experimental evidence indicating that activation of 5-HT_{1B} presynaptic receptors on RHT terminals produces an inhibitory effect on RHT glutamate release and a subsequent reduction in photic input to the SCN, it might have been predicted that the circadian system of mice lacking functional 5-HT_{1B} receptors would show enhanced responses to light resulting from disinhibition. Indeed, 5-HT_{1B} receptor-knockout (KO) mice exhibit an exaggerated response to constant light treatment as evidenced by a greater lengthening of the free-running period compared with wild-type mice (Sollars, P. J. *et al.*, 2002). However, 5-HT_{1B} receptor-KO mice are actually less sensitive to light; they have reduced light-induced behavioral phase shifts and they show a reduction in light-induced Fos expression in the SCN (Sollars, P. J. *et al.*, 2006a; 2006b). The enhanced response of 5-HT_{1B} receptor-KO mice to constant light is apparently the result of a differential reduction in the effects of light in the early versus the late subjective night (Sollars, P. J. *et al.*, 2006a). Although it is clear that the SCN of 5-HT_{1B} receptor-KO mice has an attenuated response to light, it is not known with certainty why the circadian system responds in such a manner to the lack of 5-HT_{1B} presynaptic receptors. It has been suggested that increased GABAergic transmission in the SCN may contribute to this phenotype as 5-HT_{1B} receptors are also located presynaptically on GABA terminals in the SCN (Bramley, J. R. *et al.*, 2005), and loss of the 5-HT_{1B} receptor-mediated presynaptic inhibition in the 5-HT_{1B} receptor-KO mice could lead to increased GABA release.

Despite the considerable experimental evidence indicating that activation of 5-HT_{1B} presynaptic receptors on RHT terminals modulates photic input to the SCN, the role these receptors play in the entrainment process is only beginning to be understood. Mice lacking functional 5-HT_{1B} receptors entrain normally to standard laboratory 12L:12D conditions (Sollars, P. J. *et al.*, 2006a), but under these environmental lighting conditions, only a small daily light-induced phase delay is required for entrainment based on the nonparametric model of entrainment. When entrainment is examined under non-24-h light/dark cycles (T cycles), 5-HT_{1B}-KO mice show highly significant alterations in their phase angle of

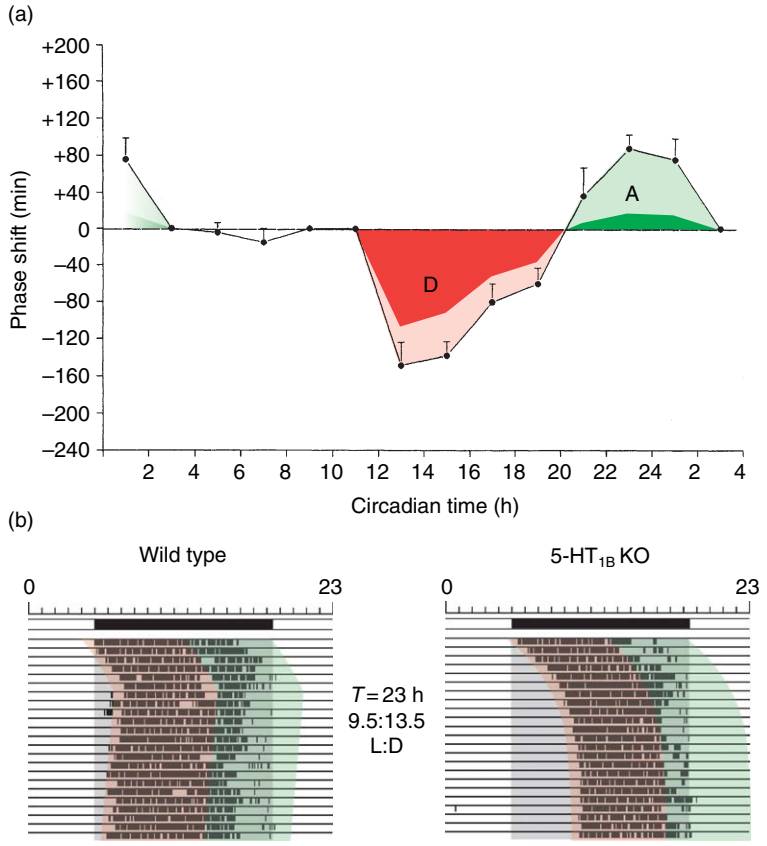

Figure 5 (a) A phase response curve (PRC) to light for a wild-type and a 5-HT_{1B}-knockout (KO) mouse. Wild-type (C57BL/6) mouse data (•—•) are redrawn from Schwartz and Zimmerman (1990) with the phase delay region (D) depicted as light red and the phase advance region (A) shown as light green. Light pulses were administered relative to activity onset designated as circadian time (CT) 12. Superimposed over the wild-type PRC in dark red and dark green is the predicted PRC for 5-HT_{1B} KO mice based on light-induced phase shifts observed at CT 16 and CT 23 from Sollars P. J. *et al.* (2006a). (b) Wheel-running activity records plotted in the standard manner, with each day's activity plotted beneath the previous day's activity, of a wild-type and a 5-HT_{1B}-KO mouse maintained in a 23 h short day light/dark cycle (9.5L:13.5D). Animals had been entrained to 12L:12D before being transferred to the 23-h short-day environment. The phase delay region (red) and phase advance region (green) are superimposed over the wheel-running data to illustrate the relationship between light and the late subjective night that is required for the 5-HT_{1B}-KO mouse entrain to the L:D cycle due to the reduced response of the suprachiasmatic nucleus (SCN) to retinohypothalamic tract (RHT) input. The greatly attenuated response of the 5-HT_{1B}-KO mouse to light in the late subjective night (a) requires that a greater portion of the late subjective night is coincident with the early morning light, resulting in a more delayed phase angle of entrainment (i.e., activity onset relative to lights off). The bar above the activity data and the gray-shaded region indicate the daily 13.5 h dark period. Reproduced from Sollars, P.J., Ogilvie, M.D., Simpson, A.M., and Pickard, G.E. 2006a. Photic entrainment is altered in the 5-HT_{1B} receptor knockout mouse. *J. Biol. Rhythms* 21, 21–32, with permision from SAGE publications.

entrainment, consistent with a reduction in the sensitivity of the SCN circadian system to light (Figure 5). Under short-day (winter-like) conditions, the phase angle of entrainment of 5-HT_{1B}-KO mice is phase delayed (i.e., the onset of wheel-running activity is initiated more than 4 h after lights off; Sollars, P. J. *et al.*, 2006a), similar to the phase-delayed circadian rhythms observed in SAD patients (Terman, M. and Terman, J. S., 2005). Various lines of clinical evidence point to a significant role for 5-HT in the pathophysiology of SAD and alterations in the function of 5-HT_{1B} receptors have been associated with depression-like states (Svenningsson, P. *et al.*, 2006).

1.27.4 Anatomical Organization of the Suprachiasmatic Nucleus

The SCN is composed of a heterogeneous group of about 8–10 000 very small neurons within a complex

neuropil containing a large variety of synapses. The dendritic arbors of SCN neurons are relatively simple with most cells having only two or three dendrites that branch very little. Dendrites in one region of the nucleus often reach into other parts of the SCN and are not always confined to the nucleus; axons enter the nucleus from all directions. Most SCN neurons are GABAergic and possess local collaterals innervating other neurons within the nucleus, thus forming a complex intra-SCN network that is important for the functional coordination of the unitary output of SCN circadian oscillations (van den Pol, A. N., 1991; Strecker, G. J. *et al.*, 1997; Liu, C. and Reppert, S. M., 2000).

1.27.4.1 Suprachiasmatic Nucleus Divisions

Several different neuroactive peptides have been localized within the SCN. Based primarily on the nonhomogenous distribution of these peptidergic neurons in the SCN, the nucleus can be subdivided into divisions: a ventrolateral region rich in vasoactive intestinal polypeptide (VIP) neurons and a dorsomedial region containing vasopressin (VP) neurons although most if not all of these neurons colocalize with GABA. This simplistic two-division organizational scheme based on chemoarchitecture has been replaced in recent years with the terms core and shell (Moore, R. Y., 1996). The SCN core/shell schema is described as a VIP neuron region that receives dense retinal and 5-HT afferents that is surrounded by a shell region containing VP neurons and receiving afferents from nonvisual cortical and subcortical regions (Moore, R. Y. *et al.*, 2002). In the core/shell organizational plan, RHT input is to the core and the core relays this photic information to the shell. However, Morin and colleagues have indicated that for a variety of reasons the core/shell terminology is problematic (including significant species variation) and perhaps a serious oversimplification of the complex organization of the mammalian SCN (Morin, L. P. and Allen, C. N., 2006; Morin, L. P. *et al.*, 2006; Morin, L. P., 2007). In addition, a one-way serial model of information transfer from a retinorecipient core to a critical locus for light-induced responses in clock cells located in the shell region (Yan, L. and Silver, R., 2002) is inconsistent both with the distribution of retinal fibers seen throughout much of the SCN in several species (Hattar, S. *et al.*, 2006) and with the reciprocal innervation reported between phenotypically defined SCN compartments (Daikoku, S. *et al.*, 1992; Romijn, H. J. *et al.*, 1997).

When maintained under cyclic lighting conditions, the left and right SCN function as a unitary circadian pacemaker due to the entraining influence of photic signals reaching each SCN, although a single SCN (right or left) is sufficient to drive circadian behavioral rhythms. In constant dark conditions, anatomical connections between the left and right suprachiasmatic nuclei may help keep the two sides in phase (Pickard, G. E., 1982). However, under conditions of constant light, some animals demonstrate a dissociation of the circadian activity rhythm into two components that initially have different circadian periods until an antiphase relationship is established between the two separate bouts of locomotor activity. This phenomenon is termed splitting, and although it was initially taken to provide the strongest evidence that the mammalian circadian pacemaker must be composed of multiple circadian oscillators, the SCN itself appears to regulate the split activity, with either side regulating one of the two bouts. This was first suggested because unilateral SCN ablation was found to abolish behavioral splitting (Pickard, G. E. and Turek, F. W., 1982). Further evidence consistent with the interpretation that splitting is the result of the oscillations of each SCN operating 180° out of phase was first shown in the asymmetrical distribution of glucose metabolism observed between the two SCN of animals demonstrating split behavioral rhythms (Figure 6) and more recently in the expression of *Per* and *Bmal1* in the two SCN in such animals (de la Iglesia, H. O. *et al.*, 2000).

1.27.4.2 Afferent and Efferent Connections

The best-studied afferent fiber inputs to the SCN are those of RGCs and 5-HT neurons of the median raphe (see above). The SCN also receives a bilateral input from the IGL interposed between the dorsal and the ventral lateral geniculate nuclei. The IGL relays both photic and nonphotic signals to the SCN via the geniculohypothalamic tract (GHT) and is necessary both for the change in free-running period typically seen when animals are maintained under constant lighting conditions (Pickard, G. E. *et al.*, 1987) and for activity-induced phase shifts of the SCN (Harrington, M. E., 1997). The SCN also receives another secondary visual input from the pretectal area. Additional afferents arise from the midline paraventricular nucleus of the thalamus,

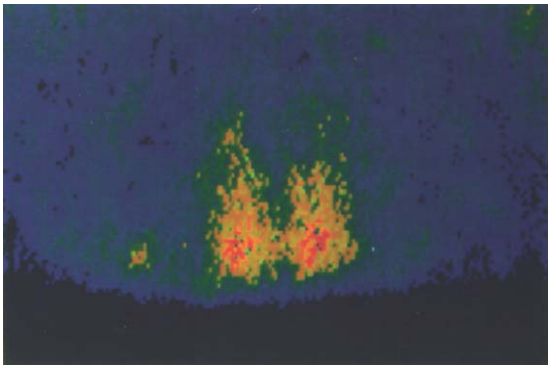

CT 14 Nonsplitter

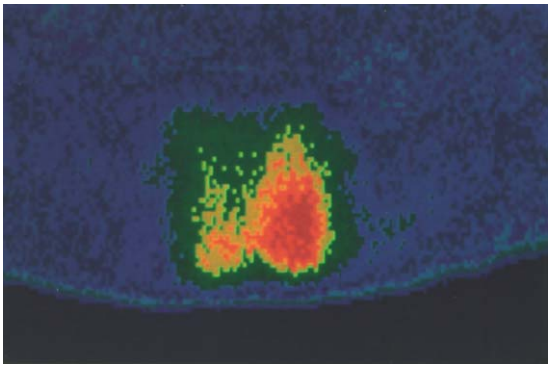

CT 14 Splitter

Figure 6 Autoradiographs of coronal brain sections through the suprachiasmatic nucleus (SCN) of a hamster that showed a single free-running bout of wheel-running activity in constant light (nonsplitter, upper panel) and of a hamster demonstrating a split activity rhythm in constant light (splitter, lower panel), following injection of 2-deoxy-D-[^{14}C] glucose at circadian time (CT) 14 (i.e., 2 h before activity onset). Note the asymmetrical density of label over the SCN in the splitter (Sollars, P. J., 1991).

limbic cortex, basal forebrain, and other hypothalamic nuclei (Moore, R. Y., 2002).

The majority of SCN efferent projections are to sites within the hypothalamus and preoptic area. SCN innervation of the dorsomedial hypothalamic nucleus participates in the regulation of the orexin/hypocretin system, which consolidates wakefulness (Aston-Jones, G. *et al.*, 2001). A major projection of the SCN is to the subparaventricular zone beginning at the caudal border of the SCN and terminating near the ventral border of the paraventricular nucleus of the hypothalamus. SCN projections outside the hypothalamus include a dorsally directed pathway to the bed nucleus of the stria terminalis and the midline paraventricular nucleus of the thalamus that relays SCN signals to the medial prefrontal cortex (Watts, A. G., 1991; Sylvester, C. M. *et al.*, 2002).

Connectivity studies using an alphaherpes virus as a transsynaptic tracer have been conducted with great success in recent years. The attenuated Bartha strain of pseudorabies virus (PRV Bartha) has been particularly useful since it carries a deletion in the unique short region of the genome that removes the coding sequences of several key genes that are required for the virus to spread in an anterograde direction. Thus, PRV Bartha is transported from the site of injection into brain parenchyma or after peripheral application along synaptically linked chains of neurons in only a retrograde direction (Pickard, G. E. *et al.*, 2002). The SCN is transsynaptically labeled after the injection of PRV Bartha into many different peripheral organs, providing evidence that the SCN is linked to a diverse set of sympathetic and parasympathetic motor pathways (Ueyama, T. *et al.*, 1999; Buijs, R. M. *et al.*, 2001; Smeraski, C. A. *et al.*, 2004).

1.27.4.3 Suprachiasmatic Nucleus Regulation of Peripheral Oscillators

Studies in *Drosophila* were once again instrumental in leading the way to a new understanding of the organization of a distributed circadian system. Using a luciferase reporter gene to monitor *Per* expression in isolated tissues maintained in vitro, many autonomous light-sensitive circadian clocks were found throughout the fly's body (Plautz, J. D. *et al.*, 1997). Clock genes are also expressed rhythmically in peripheral tissues in mammals including the liver, lung, and kidney although sustained circadian expression is dependent on signals from the SCN (Akhtar, R. A. *et al.*, 2002). However, it remains to be determined whether the loss of circadian oscillations in peripheral tissues is due to the loss of a driving signal from the SCN necessary to maintain these oscillations or whether it is because the component oscillators in peripheral tissues lose coordination resulting in the loss of temporal definition (Hastings, M. H. *et al.*, 2003). Analyses of circadian oscillations at the single-cell level may resolve this issue.

1.27.5 Summary

Considerable progress has been made in working out the functional organization of the SCN circadian system since Johnson M. S. (1939) first described the clock-like behavior of mice almost three-quarters of a century ago, yet unsurprisingly a considerable amount remains yet to be understood. Continued

rapid advances in molecular biology will continue to elucidate the underpinnings of circadian oscillation generation in the SCN. Further characterization of the retinal circuitry that provides irradiance signals to entrain the SCN oscillator, and the means by which it does so, will be aided both by knockout models and by techniques that isolate the photosensitive RGCs to examine their intrinsic properties. Still to be identified are the several specific pathways by which the SCN informs the rest of the brain and peripheral organs of the temporal structure required for the appropriately synchronous functioning of the whole animal. It is to be hoped that the combined results of these discoveries will ultimately lead to an alleviation of the pathophysiology associated with alterations in SCN circadian function thought to underlie or accompany a wide range of human conditions, both abnormal (as in a host of psychiatric and neurodegenerative diseases) and normal (as in aging, shift-work, and long-distance travel).

References

Akhtar, R. A., Reddy, A. B., Maywood, E. S., Clayton, J. D., King, V. M., Smith, A. G., Gant, T. W., Hastings, M. H., and Kyriacou, C. P. 2002. Circadian cycling of the mouse liver transcriptome, as revealed by cDNA microarray, is driven by the suprachiasmatic nucleus. Curr. Biol. 12, 540–550.

Albrecht, U., Sun, Z. S., Eichele, G., and Lee, C. C. 1997. A differential response of two putative mammalian circadian regulators, mper1 and mper2, to light. Cell 91, 1055–1064.

Archer, S. N., Robilliard, D. L., Skene, D. J., Smits, M., Williams, A., Arendt, J., and von Schantz, M. 2003. A length polymorphism in the circadian clock gene per3 linked to delayed sleep-phase syndrome and extreme diurnal preference. Sleep 26, 413–415.

Aschoff, J. 1960. Exogenous and endogenous components in circadian rhythms. Cold Spring Harb. Symp. Quant. Biol. 25, 11–28.

Asher, G. and Schibler, U. 2006. A CLOCK-less clock. Trends Cell Biol. 16, 547–549.

Aston-Jones, G., Chen, S., Zhu, Y., and Oshinsky, M. L. 2001. A neural circuit for circadian regulation of arousal. Nat. Neurosci. 4, 732–738.

Belenky, M. A. and Pickard, G. E., 2001. Subcellular distribution of 5-HT_{1B} and 5-HT_7 receptors in the mouse suprachiasmatic nucleus. J. Comp. Neurol. 432, 371–388.

Belenky, M. A., Smeraski, C. A., Provencio, I., Sollars, P. J., and Pickard, G. E. 2003. Melanopsin retinal ganglion cells receive bipolar and amacrine cell synapses. J. Comp. Neurol. 460, 380–393.

Berson, D. M. 2003. Strange vision: ganglion cells as circadian photoreceptors. Trends Neurosci. 26, 314–320.

Berson, D. M., Dunn, F. A., and Takao, M. 2002. Phototransduction by retinal ganglion cells that set the circadian clock. Science 295, 1070–1073.

Block, M. and Zucker, I. 1976. Circadian rhythms of rat locomotor activity after lesions of the midbrain raphe nuclei. J. Comp. Physiol. 109, 235–247.

Bramley, J. R., Sollars, P. J., Pickard, G. E., and Dudek, F. W. 2005. 5-HT_{1B} receptor-mediated presynaptic inhibition of GABA release in the suprachiasmatic nucleus. J. Neurophysiol. 93, 3157–3164.

Buijs, R. M., Chun, S. J., Nijima, A., Romijn, H. J., and Nagai, K. 2001. Parasympathetic and sympathetic control of the pancreas: a role for the suprachiasmatic nucleus and other hypothalamic centers that are involved in the regulation of food intake. J. Comp. Neurol. 431, 405–423.

Bunger, M. K., Wilsbacher, L. D., Moran, S. M., Clendenin, C., Radcliffe, L. A., Hogenesch, J. B., Simon, M. C., Takahashi, J. S., and Bradfield, C. A. 2000. *Mop3* is an essential component of the master circadian pacemaker in mammals. Cell 103, 1009–1017.

Butcher, G. Q., Dziema, H., Collamore, M., Burgoon, P. W., and Obrietan, K. 2002. The p42/44 mitogen-activated protein kinase pathway couples photic input to circadian clock entrainment. J. Biol. Chem. 277, 29519–29525.

Butcher, G. Q., Lee, B., Cheng, H. Y., and Obrietan, K. 2005. Light stimulates MSK1 activation in the suprachiasmatic nucleus via a PACAP-ERK/MAP kinase-dependent mechanism. J. Neurosci. 25, 5305–5313.

Campbell, S. S. and Murphy, P. J. 1998. Extraocular phototransduction in humans. Science 279, 396–399.

Cheng, H.-Y. M., Dziema, H., Papp, J., Mathur, D. P., Koletar, M., Ralph, M. R., Penninger, J. M., and Obrietan, K. 2006. The molecular gatekeeper dexras1 sculpts the photic responsiveness of the mammalian circadian clock. J. Neurosci. 26, 12984–12995.

Coogan, A. N. and Piggins, H. D. 2003. Circadian and photic regulation of phosphorylation of ERK1/2 and Elk-1 in the suprachiasmatic nuclei of the Syrian hamster. J. Neurosci. 23, 3085–3093.

Daan, S. 1977. Tonic and phasic effects of light in the entrainment of circadian rhythms. Ann. N. Y. Acad. Sci. 290, 51–59.

Daan, S. 1981. Adaptive Daily Strategies in Behavior. In: Handbook of Behavioral Neurobiology Biological Rhythms (*ed*. J. Aschoff), Vol. 4, pp. 275–298. Plenum.

Daan, S. and Pittendrigh, C. S. 1976. A functional analysis of circadian pacemakers in nocturnal rodents. II. The variability of phase response curves. J. Comp. Physiol. 106, 253–266.

Daan, S., Albrecht, U., van der Horst, G. T. J., Roenneberg, T., Wehr, T. A., and Schwartz, W. J. 2001. Assembling a clock for all seasons: are there M and E oscillators in the genes? J. Biol. Rhythms 16, 105–116.

Daikoku, S., Hisano, S., and Kagotani, Y. 1992. Neuronal associations in the rat suprachiasmatic nucleus demonstrated by immunoelectron microscopy. J. Comp. Neurol. 325, 559–571.

DeBruyne, J. P., Noton, E., Lambert, C. M., Maywood, E. S., Weaver, D. R., and Reppert, S. M. 2006. A clock shock: mouse CLOCK is not required for circadian oscillator function. Neuron 50, 465–477.

DeCoursey, P. J. 1972. LD ratios and the entrainment of circadian activity in a nocturnal and a diurnal rodent. J. Comp. Physiol. 78, 221–235.

DeCoursey, P. J. 1986. Light-sampling behavior in photoentrainment of a rodent circadian rhythm. J. Comp. Physiol. A 159, 161–169.

DeCoursey, G. and DeCoursey, P. J. 1964. Adaptive aspects of activity rhythms in bats. Biol. Bull. 126, 14–27.

Dziema, H., Oatis, B., Butcher, G. Q., Yates, R., Hoyt, K. R., and Obrietan, K. 2003. The ERK/MAP kinase pathway couples light to immediate early gene expression in the suprachiasmatic nucleus. Eur. J. Neurosci. 17, 1617–1627.

Earnest, D. J. and Turek, F. W. 1983. Effect of one second light pulses on testicular function and locomotor activity in the golden hamster. Biol. Reprod. 28, 557–565.

Eastman, C. I., Martin, S. K., and Herbert, M. 2000. Failure of extraocular light to facilitate circadian rhythm re-entrainment in humans. Chronobiol. Int. 17, 807–826.

Ebihara, S. and Tsuji, K. 1980. Entrainment of the circadian activity rhythm to the light cycle: effective light intensity for a Zeitgeber in the retinal degenerate C3H mouse and the normal C57BL mouse. Physiol. Behav. 24, 523–527.

Ebisawa, T., Uchiyama, M., Kajimura, N., Mishima, K., Kamei, Y., Katoh, M., Watanabe, T., Sekimoto, M., Shibui, K., Kim, K., *et al.* 2001. Association of structural polymorphisms in the human *period3* gene with delayed sleep phase syndrome. EMBO Rep. 2, 342–346.

Elliott, J. A. 1976. Circadian rhythms, and photoperiodic time measurement in mammals. Fed. Proc. 35, 2339–2346.

Foster, R. G., Provencio, I., Hudson, D., Fiske, S., DeGrip, W., and Menaker, M. 1991. Circadian photoreception in the retinally degenerate mouse (rd/rd). J. Comp. Physiol. A 169, 39–50.

Freedman, M. S., Lucas, R. J., Soni, B., von Shatz, M., Munoz, M., David-Gray, Z., and Foster, R. G. 1999. Regulation of mammalian circadian behavior by non-rod, non-cone, ocular photoreceptors. Science 284, 502–504.

Gallego, M., Eide, E. J., Woolf, M. F., Virshup, D. M., and Forger, D. B. 2006. An opposite role for tau in circadian rhythms revealed by mathematical modeling. Proc. Natl. Acad. Sci. U. S. A. 103, 10618–10623.

Gooley, J. J., Lu, J., Fischer, D., and Saper, C. B. 2003. A broad role for melanopsin in nonvisual photoreception. J. Neurosci. 23, 7093–7106.

Haim, A. and Rozenfeld, F. M. 1993. Temporal segregation in coexisting *Acomys* species: the role of odour. Physiol. Behav. 54, 1159–1161.

Halberg, F. 1959. Physiologic 24-hour periodicity in human beings and mice, the lighting regimen and daily routine. In: Photoperiodism and Related Phenomena in Plants and Animals (*ed*. R. B. Withrow), pp. 803–878. AAAS.

Hannibal, J. 2006. Roles of PACAP-containing retinal ganglion cells in circadian timing. Int. Rev. Cytol. 251, 1–39.

Harrington, M. E. 1997. The ventral lateral geniculate nucleus and the intergeniculate leaflet: interrelated structures in the visual and circadian systems. Neurosci. Biobehav. Rev. 21, 705–727.

Hastings, M. H., Reddy, A. B., and Maywood, E. S. 2003. A clockwork web: circadian timing in brain and periphery, in health and disease. Nat. Rev. Neurosci. 4, 649–661.

Hattar, S., Kumar, M., Park, A., Tong, P., Tung, J., Yau, K.-W., and Berson, D. M. 2006. Central projections of melanopsin-expressing retinal ganglion cells in the mouse. J. Comp. Neurol. 497, 326–349.

Hattar, S., Liao, H.-W., Takao, M., Berson, D. M., and Yau, K.-W. 2002. Melanopsin-containing retinal ganglion cells: architecture, projections, and intrinsic photosensitivity. Science 295, 1065–1070.

Hattar, S., Lucas, R. J., Mrosovsky, N., Thompson, S., Douglas, R. H., Hankins, M. W., Lem, J., Biel, M., Hofmann, F., Foster, R. G., and Yau, K.-W. 2003. Melanopsin and rod–cone photoreceptive systems account for all major accessory visual functions in mice. Nature 424, 76–81.

Hayashi, S., Ueda, M., Amaya, F., Matusda, T., Tamada, Y., Ibata, Y., and Tanaka, M. 2001. Serotonin modulates expression of VIP and GRP mRNA via the $5HT_{1B}$ receptor in the suprachiasmatic nucleus of the rat. Exp. Neurol. 171, 285–292.

Hendrickson, A. E., Wagoner, N., and Cowan, W. M. 1972. An autoradiographic and electron microscopic study of retinohypothalamic connections. Z. Zellforsch. 135, 1–26.

Hut, R. A., van Oort, B. E., and Daan, S. 1999. Natural entrainment without dawn and dusk: the case of the European ground squirrel (*Spermophilus citellus*). J. Biol. Rhythms 14, 290–299.

de la Iglesia, H. O., Meyer, J., Carpino, A., Jr., and Schwartz, W. J. 2000. Antiphase oscillation of the left and right suprachiasmatic nuclei. Science 290, 799–801.

Ikeda, M., Sugiyama, T., Wallace, C. S., Gompf, H. S., Yoshioka, T., Miyawaki, A., and Allen, C. N. 2003. Circadian dynamics of cytosolic and nuclear Ca^{2+} in single suprachiasmatic nucleus neurons. Neuron 38, 253–263.

Inouye, S. I. T. and Kawamura, H. 1979. Persistence of circadian rhythmicity in a mammalian hypothalamic ''island'' containing the suprachiasmatic nucleus. Proc. Natl. Acad. Sci. U. S. A. 76, 5962–5966.

Inouye, S. I. T. and Kawamura, H. 1982. Characteristics of a circadian pacemaker in the suprachiasmatic nucleus. J. Comp. Physiol. 146, 153–166.

Itri, J. N., Michel, S., Vansteensel, M. J., Meijer, J. H., and Colwell, C. S. 2005. Fast delayed rectifier potassium current is required for circadian neural activity. Nat. Neurosci. 5, 650–656.

Jackson, A. C., Tao, G. L., and Bean, B. P. 2004. Mechanisms of spontaneous firing in dorsomedial suprachiasmatic nucleus neurons. J. Neurosci. 24, 7985–7998.

Jacobs, B. L. and Azmitia, E. C. 1992. Structure and function of the brain serotonin system. Physiol. Rev. 72, 165–229.

Johnson, M. S. 1939. Effect of continuous light on periodic spontaneous activity of white-footed mice (Peromyscus). J. Exp. Zool. 82, 315–328.

Jones, C. R., Campbell, S. S., Zone, S. E., Cooper, F., DeSano, A., Murphy, P. J., Jones, B., Czajkowski, L., and Ptáček, L. J. 1999. Familial advanced sleep-phase syndrome: a short period circadian rhythm variant in humans. Nat. Med. 5, 1062–1065.

Klein, D. C., Moore, R. Y., and Reppert, S. M. 1991. Suprachiasmatic Nucleus: The Mind′s Clock. Oxford University Press.

Ko, C. H. and Takahashi, J. S. 2006. Molecular components of the mammalian circadian clock. Hum. Mol. Genet. 15, R271–R277.

Kononenko, N. I., Shao, L., and Dudek, F. E. 2004. Riluzole-sensitive slowing inactivating sodium current in rat suprachiasmatic nucleus neurons. J. Neurophysiol. 91, 710–718.

Konopka, R. J. and Benzer, S. 1971. Clock mutants of *Drosophila melanogaster*. Proc. Natl. Acad. Sci. U. S. A. 68, 2112–2116.

Kornhauser, J. M., Nelson, D. E., Mayo, K. E., and Takahashi, J. S. 1990. Photic and circadian regulation of *c-fos* gene expression in the hamster suprachiasmatic nucleus. Neuron 5, 127–134.

Lakin-Thomas, P. L. 2006. Transcriptional feedback oscillators: maybe, maybe not. J. Biol. Rhythms 21, 83–92.

Levi, F. and Schibler, U. 2007. Circadian rhythms: mechanisms and therapeutic implications. Annu. Rev. Pharmacol. Toxicol. 47, 593–628.

Lewy, A. J., Sack, R. L., Miller, S., and Hoban, T. M. 1987. Antidepressant and circadian phase-shifting effects of light. Science 235, 352–354.

Liu, C. and Reppert, S. M. 2000. GABA synchronizes clock cells within the suprachiasmatic nucleus. Neuron 25, 123–128.

Lockley, S. W., Skene, D. J., Thapan, K., English, J., Ribeiro, D., Haimov, I., Hampton, S., Middleton, B., von Schantz, M., and Arendt, J. 1998. Extraocular light exposure does not suppress plasma melatonin in humans. J. Clin. Endocrinol. Metab. 83, 3369–3372.

Lowrey, P. L. and Takahashi, J. S. 2004. Mammalian circadian biology: elucidating genome-wide levels of temporal organization. Annu. Rev. Genomics Hum. Genet. 5, 407–441.

Lundkvist, G. B. and Block, G. D. 2005. Role of neuronal membrane events in circadian rhythm generation. Methods Enzymol. 393, 623–642.

Lundkvist, G. B., Kwak, Y., Davis, E. K., Tei, H., and Block, G. D. 2005. A calcium flux is required for circadian rhythm generation in mammalian pacemaker neurons. J. Neurosci. 25, 7682–7686.

Lushington, K., Galka, R., Sassi, L. N., and Kennaway, D. J. 2002. Extraocular light exposure does not phase shift saliva melatonin rhythms in sleeping subjects. J. Biol. Rhythms 17, 377–386.

Manrique, C., Hery, F., Faudon, M., and Francois-Bellan, A. M. 1999. Indirect evidence for an association of 5-HT1B binding sites with retinal and geniculate axon terminals in the rat suprachiasmatic nucleus. Synapse 33, 314–323.

Meijer, J. H. and Rietveld, W. J. 1989. Neurophysiology of the suprachiasmatic circadian pacemaker in rodents. Physiol. Rev. 69, 671–707.

Meijer, J. H. and Schwartz, W. J. 2003. In search of the pathways for light-induced pacemaker resetting in the suprachiasmatic nucleus. J. Biol. Rhythms 18, 235–249.

Michel, S., Itri, J., and Colwell, C. S. 2002. Excitatory mechanisms in the suprachiasmatic nucleus: the role of AMPA/KA glutamate receptors. J. Neurophysiol. 88, 817–828.

Moore, R. Y. 1996. Entrainment Pathways and the Functional Organization of the Circadian Timing System. In: Hypothalamic Integration of Circadian Rhythms (*eds*. R. Buijs, A. Kalsbeek, H. J. Romijn, C. M. A. Pennartz, and M. Mirmiran), pp. 101–117. Elsevier.

Moore, R. Y. and Eichler, V. B. 1972. Loss of a circadian adrenal corticosterone rhythm following suprachiasmatic lesions in the rat. Brain Res. 42, 201–206.

Moore, R. Y. and Lenn, N. J. 1972. A retinohypothalamic projection in the rat. J. Comp. Neurol. 146, 1–14.

Moore, R. Y., Speh, J. C., and Leak, R. K. 2002. Suprachiasmatic nucleus organization. Cell Tissue Res. 309, 89–98.

Morin, L. P. 1994. The circadian visual system. Brain Res. Rev. 67, 102–127.

Morin, L. P. 1999. Serotonin and the regulation of mammalian circadian rhythmicity. Ann. Med. 31, 12–33.

Morin, L. P. 2007. SCN organization reconsidered. J. Biol. Rhythms 22, 3–13.

Morin, L. P. and Allen, C. N. 2006. The circadian visual system, 2005. Brain Res. Rev. 51, 1–60.

Morin, L. P. and Blanchard, J. H. 1991. Depletion of brain serotonin by 5,7-DHT modifies hamster circadian response to light. Brain Res. 566, 173–185.

Morin, L. P., Blanchard, J. H., and Provencio, I. 2003. Retinal ganglion cell projections to the hamster suprachiasmatic nucleus, intergeniculate leaflet, and visual midbrain: bifurcation and melanopsin immunoreactivity. J. Comp. Neurol. 465, 401–416.

Morin, L. P., Shivers, K.-Y., Blanchard, J. H., and Muscat, L. 2006. Complex organization of mouse and rat suprachiasmatic nucleus. Neuroscience 137, 1285–1297.

Nakamura, W., Honma, S., Shirakawa, T., and Honma, K. I. 2002. *Clock* mutation lengthens the circadian period without damping rhythms in individual SCN neurons. Nat. Neurosci. 5, 399–400.

Nelson, R. J. and Zucker, I. 1981. Absence of extra-ocular photoreception in diurnal and nocturnal rodents exposed to direct sunlight. Comp. Biochem. Physiol. A Physiol. 69, 145–148.

Nitabach, M. N., Blau, J., and Holmes, T. C. 2002. Electrical silencing of Drosophila pacemaker neurons stops the free-running circadian clock. Cell 109, 485–495.

Obrietan, K., Impey, S., and Storm, D. R. 1998. Light and circadian rhythmicity regulate MAP kinase activation in the suprachiasmatic nuclei. Nat. Neurosci. 1, 693–700.

Panda, S., Provencio, I., Tu, D. C., Pires, S. S., Rollag, M. D., Castrucci, A. M., Pletcher, M. T., Sato, T. K., Wiltshire, T., Andahazy, M., Kay, S. A., Van Gelder, R. N., and Hogenesch, J. B. 2003. Melanopsin is required for non-image-forming photic responses in blind mice. Science 301, 525–527.

Panda, S., Sato, T. K., Castrucci, A. M., Rollag, M. D., DeGrip, W. J., Hogenesch, J. B., Provencio, I., and Kay, S. A. 2002. Melanopsin (*Opn4*) requirement for normal light-induced circadian phase shifting. Science 298, 2213–2216.

Pennartz, C. M., de Jeu, M. T., Bos, N. P., Schaap, J., and Geurtsen, A. M. 2002. Diurnal modulation of pacemaker potentials and calcium current in the mammalian circadian clock. Nature 416, 286–290.

Pennartz, C. M., Hamstra, R., and Geurtsen, A. M. 2001. Enhanced NMDA receptor activity in retinal inputs to the rat suprachiasmatic nucleus during the subjective night. J. Physiol. (Lond.) 532, 181–194.

Perez-Leon, J. A., Warren, E. J., Allen, C. N., Robinson, D. W., and Brown, R. L. 2006. Synaptic inputs to retinal ganglion cells that set the circadian clock. Eur. J. Neurosci. 24, 1117–1123.

Pickard, G. E. 1980. Morphological characteristics of retinal ganglion cells projecting to the suprachiasmatic nucleus: a horseradish peroxidase study. Brain Res. 183, 458–465.

Pickard, G. E. 1982. The afferent connections of the suprachiasmatic nucleus of the golden hamster with emphasis on the retinohypothalamic projection. J. Comp. Neurol. 211, 65–83.

Pickard, G. E. 1985. Bifurcating axons of retinal ganglion cells terminate in the hypothalamic suprachiasmatic nucleus and the intergeniculate leaflet of the thalamus. Neurosci. Lett. 55, 211–217.

Pickard, G. E. 1989. Entrainment of the circadian rhythm of wheel-running activity is phase shifted by ablation of the intergeniculate leaflet. Brain Res. 494, 151–154.

Pickard, G. E. and Rea, M. A. 1997. TFMPP, a 5HT1B receptor agonist, inhibits light-induced phase shifts of the circadian activity rhythm and c-fos expression in the mouse suprachiasmatic nucleus. Neurosci. Lett. 231, 95–98.

Pickard, G. E. and Turek, F. W. 1982. Splitting of the circadian rhythm of activity is abolished by unilateral lesions of the suprachiasmatic nuclei. Science 215, 1119–1121.

Pickard, G. E., Ralph, M., and Menaker, M. 1987. The intergeniculate leaflet partially mediates the effects of light on circadian rhythms. J. Biol. Rhythms 2, 35–56.

Pickard, G. E., Smeraski, C. A., Tomlinson, C. C., Banfield, B. W., Kaufman, J., Wilcox, C. L., Enquist, L. W., and Sollars, P. J. 2002. Intravitreal injection of the attenuated pseudorabies virus PRV-Bartha results in infection of the hamster suprachiasmatic nucleus only by retrograde transsynaptic transport via autonomic circuits. J. Neurosci. 22, 2701–2710.

Pickard, G. E., Smith, B. N., Belenky, M., Rea, M. A., Dudek, F. E., and Sollars, P. J. 1999. 5-HT1B receptor-mediated presynaptic inhibition of retinal input to the suprachiasmatic nucleus. J. Neurosci. 19, 4034–4045.

Pickard, G. E., Weber, E. T., Scott, P. A., Riberdy, A. F., and Rea, M. A. 1996. 5HT1B receptor agonists inhibit light-induced phase shifts of behavioral circadian rhythms and expression of the immediate-early gene c-fos in the suprachiasmatic nucleus. J. Neurosci. 16, 8208–8220.

Pittendrigh, C. S. and Daan, S. 1976a. A functional analysis of circadian pacemakers in nocturnal rodents. I. The stability and lability of spontaneous period. J. Comp. Physiol. 106, 223–252.

Pittendrigh, C. S. and Daan, S. 1976b. A functional analysis of circadian pacemakers in nocturnal rodents. IV. Entrainment: pacemaker as clock. J. Comp. Physiol 106, 291–331.

Plautz, J. D., Kaneko, M., Hall, J. C., and Kay, S. A. 1997. Independent photoreceptive circadian clocks throughout Drosophila. Science 278, 1632–1635.

van den Pol, A. N. 1991. The Suprachiasmatic Nucleus: Morphological and Cytochemical Substrates for Cellular Interaction. In: Suprachiasmatic Nucleus: The Mind's Clock (*eds*. D. C. Klein, R. Y. Moore, and S. M. Reppert), pp. 17–50. Oxford University Press.

van den Pol, A. N. and Obrietan, K. 2002. Short circuiting the circadian clock. Nat. Neurosci. 5, 616–618.

Pratt, B. L. and Goldman, B. D. 1986. Activity rhythms and photoperiodism of Syrian hamsters in a simulated burrow system. Physiol. Behav. 36, 83–89.

Provencio, I., Jiang, G., DeGrip, W. J., Hayes, W. P., and Rollag, M. D. 1998. Melanopsin: an opsin in melanophores, brain and eye. Proc. Natl. Acad. Sci. U. S. A. 95, 340–345.

Provencio, I., Rodriguez, I. R., Jiang, G., Hayes, W. P., Moreira, E. F., and Rollag, M. D. 2000. A novel human opsin in the inner retina. J. Neurosci. 20, 600–605.

Quintero, J. E., Kuhlman, S. J., and McMahon, D. G. 2003. The biological clock nucleus: a multiphasic oscillator network regulated by light. J. Neurosci. 23, 8070–8076.

Rea, M. A. 1989. Light increases Fos-related protein immunoreactivity in the rat suprachiasmatic nuclei. Brain Res. Bull. 23, 577–581.

Rea, M. A. and Pickard, G. E. 2000. A 5-HT_{1B} receptor agonist inhibits light-induced suppression of pineal melatonin production. Brain Res. 858, 424–428.

Reppert, S. M. and Weaver, D. R. 2002. Coordination of circadian timing in mammals. Nature 418, 935–941.

Richter, C. P. 1965. Biological Clocks in Medicine and Psychiatry. Thomas, Springfield.

Roenneberg, T., Daan, S., and Merrow, M. 2003. The art of entrainment. J. Biol. Rhythms 18, 183–194.

Romijn, H. J., Sluiter, A. A., Pool, C. W., Wortel, J., and Buijs, R. M. 1997. Evidence from confocal fluorescence microscopy for a dense, reciprocal innervation between AVP-, somatostatin-, VIP/PHI-, GRP- and VIP/PHI/GRP-immunoreactive neurons in the rat suprachiasmatic nucleus. Eur. J. Neurosci. 9, 2613–2623.

Ruby, N. F., Brennan, T. J., Xie, X., Cao, V., Franken, P., Heller, H. C., and O'Hara, B. F. 2002. Role of melanopsin in circadian responses to light. Science 298, 2211–2213.

Rüger, M., Gordijn, M. C. M., Beersma, D. G. M., de Vries, B., and Daan, S. 2003. Acute and phase-shifting effects of ocular and extraocular light in human circadian physiology. J. Biol. Rhythms 18, 409–419.

Schwartz, W. J. and Zimmerman, P. 1990. Circadian timekeeping in BALB/c and C57 B1/6 inbred mouse strains. J. Neurosci. 10, 3685–3694.

Shargal, E., Kronfeld-Schor, N., and Dayan, T. 2000. Population biology and spatial relationships of coexisting spiny mice (*Acomys*) in Israel. J. Mammal. 81, 1046–1052.

Shigeyoshi, Y., Taguchi, K., Yamamoto, S., Takekida, S., Yan, l., Tei, H., Moriya, T., Shibata, S., Loros, J. J., Dunlap, J. C., and Okamura, H. 1997. Light-induced resetting of a mammalian circadian clock is associated with rapid induction of the mPer1 transcript. Cell 91, 1043–1053.

Shimazoe, T., Nakamure, S., Kobayashi, K., Watanabe, S., Miyasaka, K., Kono, A., and Funakoshi, A. 2004. Role of 5-HT_{1B} receptors in entrainment disorder of Otsuka Long Evans Tokushima fatty (OLETF) rats. Neuroscience 123, 201–205.

Smale, L., Michels, K. M., Moore, R. Y., and Morin, L. P. 1990. Destruction of the hamster serotonergic system by 5,7-DHT: effects on circadian rhythm phase, entrainment, and response to triazolam. Brain Res. 515, 9–19.

Smeraski, C. A., Sollars, P. J., Kaufman, J. D., Ogilvie, M. D., Enquist, L. W., and Pickard, G. E. 2004. Suprachiasmatic nucleus input to autonomic circuits identified by retrograde transsynaptic transport of pseudorabies virus from the eye. J. Comp. Neurol. 471, 298–313.

Smith, B. N., Sollars, P. J., Dudek, F. E., and Pickard, G. E. 2001. Serotonergic modulation of retinal input to the mouse suprachiasmatic nucleus mediated by 5-HT_{1B} and 5-HT_7 receptors. J. Biol. Rhythms 16, 25–38.

Sollars, P. J. 1991. Pacemaker autonomy in the suprachiasmatic nucleus: metabolic and transplantation studies. Ph.D. thesis, University of Oregon.

Sollars, P. J., Smeraski, C. A., Kaufman, J. D., Ogilvie, M. D., Provencio, I., and Pickard, G. E. 2003. Melanopsin and non-melanopsin expressing retinal ganglion cells innervate the hypothalamic suprachiasmatic nucleus. Vis. Neurosci. 20, 601–610.

Sollars, P. J., Ogilvie, M. D., Rea, M. A., and Pickard, G. E. 2002. 5-HT_{1B} receptor knockout mice exhibit an enhanced response to constant light. J. Biol. Rhythms 17, 428–437.

Sollars, P. J., Ogilvie, M. D., Simpson, A. M., and Pickard, G. E. 2006a. Photic entrainment is altered in the 5-HT_{1B} receptor knockout mouse. J. Biol. Rhythms 21, 21–32.

Sollars, P. J., Simpson, A. M., Ogilvie, M. D., and Pickard, G. E. 2006b. Light-induced Fos expression is attenuated in the suprachiasmatic nucleus of serotonin 1B receptor knockout mice. Neurosci. Lett. 401, 209–213.

Spoelstra, K., Oklejewicz, M., and Daan, S. 2002. Restoration of self-sustained circadian rhythmicity by the mutant *Clock* allele in mice in constant illumination. J. Biol. Rhythms 17, 520–525.

Spoelstra, K., Albrecht, U., van der Horst, G. T. J., Brauer, V., and Daan, S. 2004. Phase responses to light pulses in mice lacking functional *per* and *cry* genes. J. Biol. Rhythms 19, 518–529.

Stephan, F. K. and Zucker, I. 1972. Circadian rhythms in drinking behavior and locomotor activity of rats are eliminated by hypothalamic lesions. Proc. Natl. Acad. Sci. U. S. A. 69, 1583–1586.

Strecker, G. J., Wuaren, J.-P., and Dudek, F. E. 1997. $GABA_A$-mediated local synaptic pathways connect neurons in the rat suprachiasmatic nucleus. J. Neurophysiol. 78, 2217–2220.

Sun, Z. S., Albrecht, U., Zhuchenko, O., Bailey, J., Eichele, G., and Lee, C. C. 1997. RIGUI, a putative mammalian ortholog of the Drosophila period gene. Cell 90, 1003–1011.

Svenningsson, P., Chergui, K., Rachleff, I., Flajolet, M., Zhang, X., Yacoubi, M. E., Vaugeois, J.-M., Nomikos, G. G., and Greengard, P. 2006. Alterations in 5-HT_{1B} receptor function by p11 in depression-like states. Science 311, 77–80.

Sylvester, C. M., Krout, K. E., and Loewy, A. D. 2002. Suprachiasmatic nucleus projection to the medial prefrontal cortex: a viral transneuronal tracing study. Neuroscience 114, 1071–1080.

Takahashi, J. S. and Zatz, M. 1982. Regulation of circadian rhythmicity. Science 217, 1104–1111.

Tei, H., Okamura, H., Shigeyoshi, Y., Fukuhara, C., Ozawa, R., Hirose, M., and Sakaki, Y. 1997. Circadian oscillation of a mammalian homologue of the Drosophila period gene. Nature 389, 512–516.

Terman, M. and Terman, J. S. 2005. Light Therapy. In: Principles and Practice of Sleep Medicine, 4th edn. (*eds*. M. H. Kryger, T. Roth, and W. C. Dement), pp. 1424–1442. Elsevier.

Toh, K. L., Jones, C. R., He, Y., Eide, E. J., Hinz, W. A., Virshup, D. M., Ptácek, L. J., and Fu, Y.-H. 2001. An hPer2 phosphorylation site mutation in familial advanced sleep-phase syndrome. Science 291, 1040–1043.

Ueyama, T., Krout, K. E., Nguyen, X. V., Karpitskiy, V., Kollert, A., Mettenleiter, T. C., and Loewy, A. D. 1999. Suprachiasmatic nucleus: a central autonomic clock. Nat. Neurosci. 2, 1051–1053.

Vitaterna, M. H., King, D. P., Chang, A. M., Kornhauser, J. M., Lowrey, P. L., McDonald, J. D., Dove, W. F., Pinto, L. H., Turek, F. W., and Takahashi, J. S. 1994. Mutagenesis and mapping of a mouse gene, *Clock*, essential for circadian behavior. Science 264, 719–725.

Watts, A. G. 1991. The Efferent Projections of the Suprachiasmatic Nucleus: Anatomical Insights into the Control of Circadian Rhythms. In: Suprachiasmatic Nucleus: The Mind's Clock (*eds*. D. C. Klein, R. Y. Moore, and S. M. Reppert), pp. 77–106. Oxford University Press.

Welsh, D. K., Logothetis, D. E., Meister, M., and Reppert, S. M. 1995. Individual neurons dissociated from rat suprachiasmatic nucleus express independently phased circadian firing rhythms. Neuron 14, 697–706.

Wright, K. P., Jr. and Czeisler, C. A. 2002. Absence of circadian phase resetting in response to bright light behind the knee. Science 297, 571.

Yamaguchi, S., Isejima, H., Matsuo, T., Okura, R., Yagita, K., Kobayashi, M., and Okamura, H. 2003. Synchronization of cellular clocks in the suprachiasmatic nucleus. Science 302, 1408–1412.

Yamazaki, S., Goto, M., and Menaker, M. 1999. No evidence for extraocular photoreceptors in the circadian system of the Syrian hamster. J. Biol. Rhythms 14, 197–201.

Yan, L. and Silver, R. 2002. Differential induction and localization of mPer1 and mPer2 during advancing and delaying phase shifts. Eur. J. Neurosci. 16, 1531–1540.

1.28 The Visual Thalamus

S M Sherman, The University of Chicago, Chicago, IL, USA

© 2008 Elsevier Inc. All rights reserved.

1.28.1	**Introduction**	557
1.28.2	**Thalamic Cell Types**	558
1.28.3	**Cell Properties**	558
1.28.3.1	Properties of T-Type Ca^{2+} Channels	558
1.28.3.2	Properties of Burst and Tonic Firing	560
1.28.3.3	Hypothesis for Burst and Tonic Firing	561
1.28.4	**Circuit Properties**	561
1.28.4.1	Anatomical Features	562
1.28.4.2	Functional Features	562
1.28.5	**The Lateral Geniculate Nucleus**	564
1.28.5.1	Parallel Processing	564
1.28.5.1.1	The cat lateral geniculate nucleus	564
1.28.5.1.2	The monkey lateral geniculate nucleus	565
1.28.5.2	Laminar Relationships	565
1.28.5.2.1	Lateral geniculate nucleus	565
1.28.5.2.2	Visual cortex	566
1.28.6	**Drivers and Modulators**	566
1.28.7	**First- and Higher-Order Relays: The Lateral Geniculate Nucleus and Pulvinar**	569
1.28.7.1	Layer 5 Corticothalamic Inputs as Drivers	569
1.28.7.2	Branching of Driver Afferents to Thalamus	571
1.28.7.3	Role of Higher-Order Thalamic Relays in Corticocortical Processing	571
1.28.7.4	Overview	572
1.28.8	**Conclusions**	573
References		574

1.28.1 Introduction

The two major thalamic nuclei involved in visual processing are the lateral geniculate nucleus and the pulvinar. The lateral geniculate nucleus relays retinal input to the visual cortex, chiefly to the primary visual cortex. The pulvinar innervates most or all visual cortical areas, and what it is relaying has been something of a mystery, although this account makes the case that it is involved chiefly in relaying information between visual areas. Fortunately, most of the details regarding cell and circuit properties are common to thalamic relay nuclei, and so before considering these two visual relay nuclei in detail, it is worth standing back and considering some generally properties of thalamus.

The thalamus is a collection of adjacent nuclei located in the center of the brain. It is a paired structure, each side roughly the size of a walnut. Each of the various nuclei innervates one area of the cortex (unless otherwise specified, cortex use here refers to neocortex) or a small number of adjacent cortical areas. It is important to keep in mind that virtually all information reaching the cortex, and thus attentional and other cognitive levels, must first be relayed by thalamus. Also, as far as we know, every cortical area receives a thalamic projection.

Strictly speaking, thalamus has two broad divisions: dorsal thalamus and ventral thalamus. Dorsal thalamus includes the relay nuclei, namely, the bulk of thalamus in which neurons that project to the cortex are located. These relay nuclei can typically be distinguished by cytoarchitectonic criteria. Generally, homologous nuclei can be discerned across mammals, and so a lateral geniculate nucleus, which relays retinal information to the cortex, is known for all mammalian species so far

studied, but in some cases, identification of homologous nuclei across species remains elusive. The ventral thalamus includes as its chief component the thalamic reticular nucleus, which is a thin shell of neurons that lies generally lateral to the dorsal thalamus, like a shield, extending somewhat dorsally, ventrally, and anteriorly. These reticular cells do not project to the cortex but instead provide a gamma-aminobutyric acid (GABA)ergic, inhibitory input to relay cells of the dorsal thalamus. A minor component of the ventral thalamus is the ventral division of the lateral geniculate nucleus, whose cells project to other brainstem sites but not the cortex; the ventral division of the lateral geniculate nucleus is not considered further. For simplicity in what follows below, unless otherwise indicated, thalamus refers just to the dorsal thalamus, and lateral geniculate nucleus refers just to its dorsal division.

The main thalamic relays of visual information are the lateral geniculate nucleus and pulvinar. (Strictly speaking, this includes the lateral posterior nucleus and is often referred to as the lateral posterior/pulvinar complex, but for the sake of brevity, we shall refer to this simply as the pulvinar.) The main purpose of this chapter is to disabuse readers of the old notions about these thalamic nuclei: namely that the lateral geniculate nucleus is a simple, machine-like relay of retinal information to the primary visual cortex, and the pulvinar is a mysterious entity that innervates extrastriate visual areas and is somehow involved in attention (LaBerge, D. and Buchsbaum, M. S., 1990; Olshausen, B. A. *et al.*, 1993; Anderson, C. H. *et al.*, 2005; Van Essen, D. C., 2005). It is now clear that the complex cell and circuit functions of the thalamus, including the lateral geniculate nucleus, belie any simple relay functions. These thalamic nuclei act as gateways for information flow to the cortex, gateways that are dynamically modulated. Furthermore, we can now seriously consider a relatively new hypothesis for the function of pulvinar as a central element in information transfer between cortical areas involving a corticothalamocortical route. Related to this is the recent appreciation that, as noted above, while all thalamic relays share most basic cell and circuit functions, certain differences between the lateral geniculate nucleus and pulvinar identify them as members of two different kinds of relay found throughout thalamus.

1.28.2 Thalamic Cell Types

The thalamus consists of three basic cell types: relay cells, interneurons, and cells of the thalamic reticular nucleus (for details, see Sherman, S. M. and Guillery, R. W., 1996; 2006). Each of these may be further subdivided, but the complete classification of these cell types has yet to be done. Relay cells are glutamatergic, and the latter two cell types are GABAergic, providing a major inhibitory input to relay cells. Interneurons are located within the main dorsal thalamic relay nuclei, intermixed with relay cells, and the ratio of interneurons to relay cells is roughly 1:3. This ratio is similar throughout thalamus in all mammals with a peculiar exception. That is, outside of the lateral geniculate nucleus, the thalamus of rats and mice are essentially devoid of interneurons, but, curiously, the lateral geniculate nucleus in these animals does have a normal complement of interneurons (Arcelli, P. *et al.*, 1997). This is not a property of rodents, because hamsters, guinea pigs, squirrels, etc., have interneurons throughout thalamus (e.g., Arcelli, P. *et al.*, 1997). However, this point has been questioned recently by evidence that the lateral posterior nucleus of the rat has a substantial fraction of interneurons (Li, J. L. *et al.*, 2003).

1.28.3 Cell Properties

As we learn more about neurons throughout the central nervous system, it is clear that they possess a bewildering variety of voltage-gated ionic membrane conductances, and thalamic relay cells are no exception. The voltage-gated Na^+ conductance underlying the action potential is perhaps the best-known example. Other examples include various voltage-gated K^+ and Ca^{2+} conductances, and a more detailed listing can be found in Sherman S. M. and Guillery R. W. (1996; 2006). The presence of these conductances means that membrane voltage and its temporal pattern, which together determine whether and when each of these becomes activated, play an important role in relay cell excitability and thus the gating of information flow. While most of these conductances are ubiquitous to neurons everywhere, one in particular, a voltage-gated Ca^{2+} conductance that operates via T-type Ca^{2+} channels, is particularly important to relay cell function and relatively specific to thalamic neurons (for details, see Sherman, S. M. and Guillery, R. W., 1996; Sherman, S. M., 2001; Sherman, S. M. and Guillery, R. W., 2006).

1.28.3.1 Properties of T-Type Ca^{2+} Channels

Figure 1 shows the voltage and time dependency for the T channels (Jahnsen, H. and Llinás, R., 1984a; 1984b;

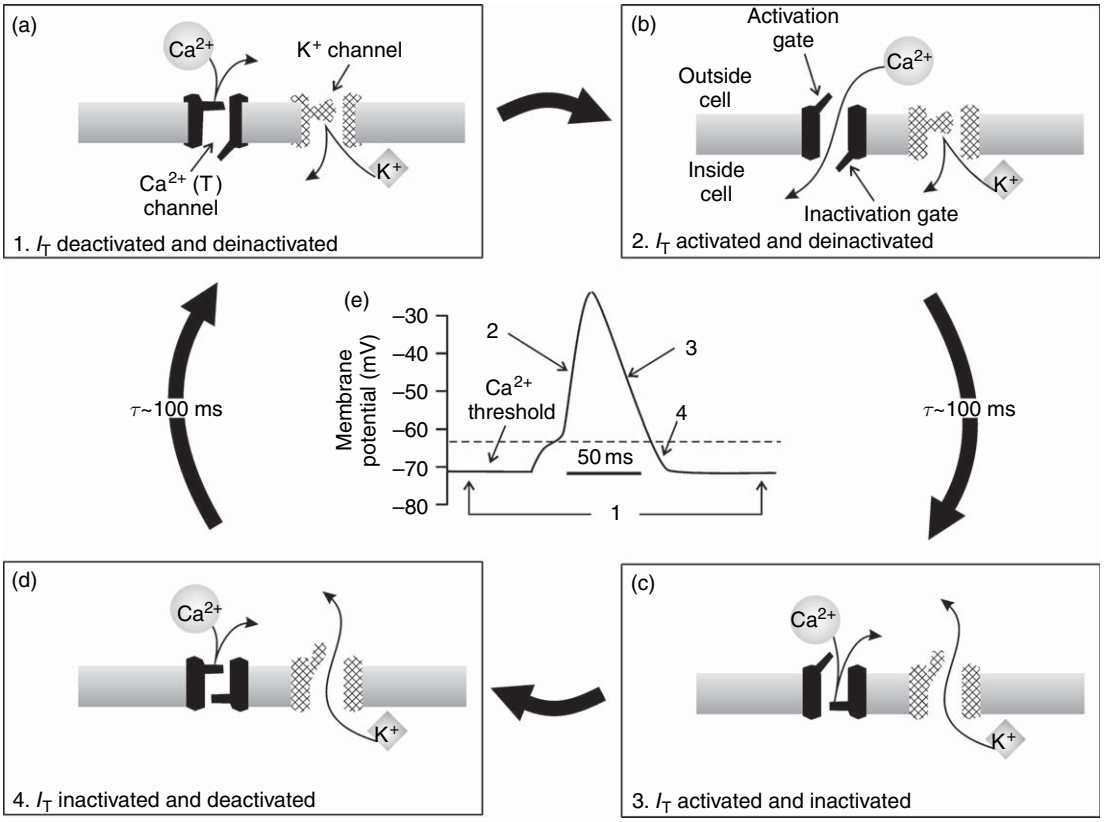

Figure 1 Schematized view of actions of voltage-dependent T (Ca^{2+}) and K^+ channels underlying low-threshold Ca^{2+} spike. Panels (a)–(d) show the sequence of channel events, and the central graph (e) shows the effects on membrane potential. The T channel has two voltage-dependent gates: an activation gate that opens with depolarization and closes at hyperpolarized levels and an inactivation gate that shows the opposite voltage dependency. The K^+ channel shown actually represents several such channels having a single gate that opens during depolarization; thus, these channels do not inactivate. (a) I_T deactivated and deinactivated. At a relatively hyperpolarized resting membrane potential (~70 mV), the activation gate of the T channel is closed, but the inactivation gate is open, and so the T channel is deactivated and deinactivated. The single gate for the K^+ channel is closed. (b) I_T activated and deinactivated. With sufficient depolarization to reach its threshold, the activation gate of the T channel opens, and Ca^{2+} flows into the cell. Thus, the T channel is activated and, for the time being, remains deinactivated. This further depolarizes the cell, providing the rise of the low-threshold spike. (c) I_T activated and inactivated. The inactivation gate of the T channel closes after being depolarized for roughly 100 ms (roughly, because closing of the channel is a complex function of voltage and time), and the K^+ channel also opens. Thus, the continued depolarization inactivates the T channel, although the activation gate remains open. These actions stop the influx of Ca^{2+} and allow the efflux of K^+, serving to repolarize the cell. (d) I_T inactivated and deactivated. Even though the initial resting potential is reached, the T channel remains inactivated, because it takes roughly 100 ms (roughly having the same meaning as above) of hyperpolarization to deinactivate it; thus, the T channel is inactivated and deactivated. It also takes a bit of time for the various K^+ channels to close. Note that the behavior of the T channel is qualitatively exactly like the Na^+ channel involved with the action potential, but with several quantitative differences: the T channel is slower to inactivate and deinactivate, and it operates in a more hyperpolarized regime.

Sherman, S. M., 2001; Sherman, S. M. and Guillery, R. W., 2006). These channels have two voltage gates, because they can be both activated and inactivated by voltage. At rest (roughly −70 mV), the inactivation gate is open, but the activation gate is closed; the channel is thus both deinactivated and deactivated (Figure 1(a)). Following depolarization to threshold for the activation gate (to roughly −65 mV), the activation gate opens and I_T is generated via entry of Ca^{2+} into the cell, leading to the upswing of the all-or-none Ca^{2+} spike; now, the T channel is activated and deinactivated (Figure 1(b)). This Ca^{2+} spike is often termed the low-threshold spike, because its activation threshold is hyperpolarized with respect to that for the action potential. After roughly 100 ms of depolarization, the T channel inactivates (control of the inactivation gate is a complex function of voltage and time (Jahnsen, H. and Llinás, R., 1984a; 1984b; Zhan, H. J. *et al.*, 1999) so that

the more depolarized (or hyperpolarized), the more quickly the gate closes (or opens), but the important point is that under normal conditions, roughly 100 ms is required for these actions) (Figure 1(c)), and this, combined with the activation of a slower series of K^+ conductances, repolarizes the neuron. However, the T channel remains inactivated (Figure 1(d)) for another 100 ms or so, after which time the original state shown in Figure 1(a) is returned. The two gates of the T channel have opposite voltage dependencies, but while the activation gate responds quickly to voltage change, the inactivation gate is slower, requiring roughly 100 ms of polarization change to open or close. Note that the roughly 100 ms of hyperpolarization needed to deinactivate the T channel provides a refractory period, limiting low-threshold Ca^{2+} spiking to 10 Hz.

Note also that this behavior of the T channel is qualitatively identical to that of the Na^+ channel underlying conventional action potentials, although there are two important quantitative differences: the regime of the voltage dependency of the T channel is 5–10 mV more hyperpolarized, and the inactivation kinetics of the T channel are much slower. Also, T channels are not found in the axons. The last point means that it is only action potentials that convey the information relayed to the cortex.

1.28.3.2 Properties of Burst and Tonic Firing

This behavior of T channels underlies the two very different response modes, tonic or burst, that are expressed by thalamic relay cells. How information is relayed to the cortex depends heavily on which response mode is in use (Sherman, S. M. 2001; Swadlow, H. A. and Gusev, A. G., 2001; MacLean, J. N. *et al.*, 2005; Bezdudnaya, T. *et al.*, 2006; Sherman, S. M. and Guillery, R. W., 2006). This is because the same input (e.g., an excitatory postsynaptic potential (EPSP) from retina) will evoke a very different response in the relay cell during tonic versus burst firing (Figures 2(a) and 2(b)). During tonic firing mode, the EPSP directly elicits action potentials, and so a larger EPSP elicits a higher firing rate, forming a fairly linear input/output relationship (Figure 2(c)). However, during bursting, the relationship is highly nonlinear, because the input or EPSP no longer directly elicits action potentials; instead, it elicits the low-threshold spike, which in turn elicits the action potentials, but because the low-threshold

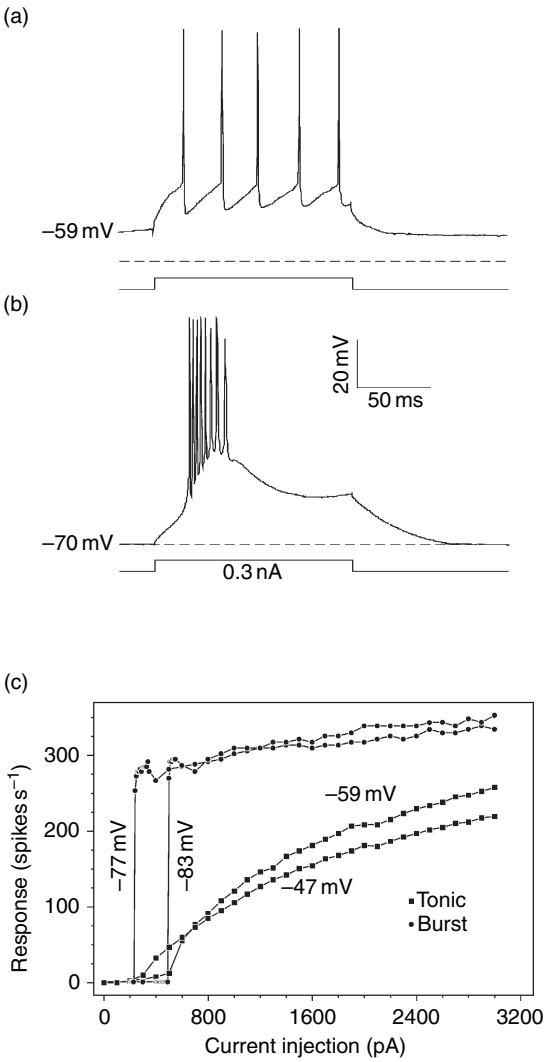

Figure 2 Properties of burst and tonic firing modes for relay cells of the lateral geniculate nucleus of the cat recorded intracellularly *in vitro*. (a, b) Voltage dependency of the low-threshold spike for one cell. Responses are shown to the same depolarizing current pulse administered intracellularly but from two different initial holding potentials. I_T is inactivated with relative depolarization (a), and the response is a succession of unitary action potentials for the duration of the suprathreshold stimulus. This is the *t*onic mode of firing. I_T is deinactivated with relative hyperpolarization (b), and the response is a low-threshold spike with eight action potentials riding its crest. This is the burst mode of firing. (c) Input–output relationship for another cell. The abscissa plots the amplitude of the depolarizing current pulse, and the ordinate plots the evoked firing frequency based on the first six action potentials of the response, since this cell usually exhibited six action potentials per burst in this experiment. The initial holding potentials are shown: −47 and −59 mV reflect tonic mode, whereas −77 and −83 mV reflect burst mode. Redrawn from Sherman, S. M. and Guillery, R. W. 2001. Exploring the Thalamus. Academic Press.

spike is all-or-none, a larger EPSP does not elicit a larger low-threshold spike or a higher firing.

The advantage for tonic firing is pretty clear: if the cortex is to faithfully reproduce the visual scene, the sort of nonlinear distortion seen during burst firing would hamper this process. While less obvious perhaps, there are at least two advantages for burst firing (Sherman, S. M., 2001; Swadlow, A. G. and Gusev, A. G., 2001; MacLean, J. N. *et al.*, 2005; Bezdudnaya, T. *et al.*, 2006; Sherman, S. M. and Guillery, R. W., 2006). First, because burst firing is associated with lower spontaneous activity but the burst itself represents a high rate of firing, burst firing has a higher signal-to-noise ratio and thus better stimulus detectability. Second, burst firing leads to a much greater postsynaptic response in the cortex. The second point follows from the nature of the thalamocortical synapse, which is a depressing synapse: the firing rate during tonic mode is sufficiently high to maintain the synapse in a depressed state, but the silent intervals before each burst (due to the requisite period of hyperpolarization needed to deinactivate I_T) completely relieves the synaptic depression. The overall implication is that, while tonic firing is better for stimulus reconstruction, burst firing is better for the detection of novel stimuli, and associated with this improved detectability is a much stronger cortical response.

1.28.3.3 Hypothesis for Burst and Tonic Firing

These properties of burst and tonic firing have led to the following hypothesis (Sherman, S. M., 2001). To the extent that burst firing is better for stimulus detection, it could be the mode more often seen when the information that the thalamic cell relays is not well attended to (due to drowsiness, attention directed elsewhere, etc.); under these conditions, the burst evoked by a novel stimulus would more likely get through to the cortex and be recognized as a signal than if the cell were firing tonically. In this sense, the burst is a sort of wake-up call that something has changed and that something should be attended to so that its importance can be evaluated. The idea here is not necessarily that bursting provides a stronger overall signal to the cortex than does tonic firing, but rather that bursting overcomes any disadvantage regarding stimulus detectability or cortical activation imposed by inattention. Once the burst activates cortical circuits, the relay cell would then switch to tonic firing so that the novel stimulus can be properly evaluated.

Several recent observations support this hypothesis (Weyand, T. G. *et al.*, 2001; Lesica, N. A. and Stanley, G. B., 2004; Alitto, H. J. *et al.*, 2005; Denning, K. S. and Reinagel, P., 2005). Both tonic and burst firing are seen in awake, behaving animals, including humans, with switching between modes. Bursting is seen relatively rarely in alert animals and more commonly in drowsy animals. Furthermore, recent receptive field studies of the lateral geniculate nucleus show that the type of visual stimulus most likely to evoke a burst is one that switches from inhibition to excitation, such as a dark region covering the receptive field of an on-center cell that is replaced by a bright spot. This indicates that the burst signals a significant change in the form of a novel stimulus just appearing. However, these observations, while supporting the hypothesis, do not constitute proof of its validity. Much more research will be needed to accept or reject the hypothesis.

1.28.4 Circuit Properties

Figure 3 schematically shows the main inputs to thalamic relay cells. The model used here is the lateral

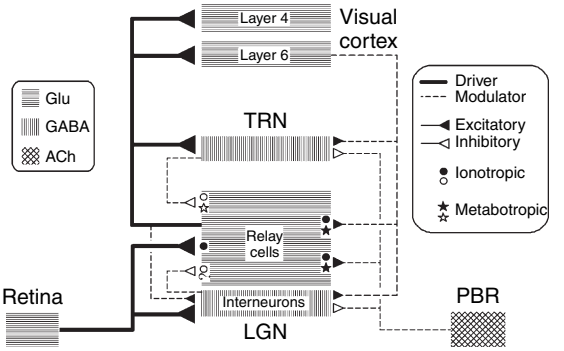

Figure 3 Schematic view of major circuit features of the lateral geniculate nucleus with related receptors present on relay cells. Other thalamic nuclei seem to be organized along the same pattern. The key to the left indicates the major transmitter systems involved. The retinal input activates only ionotropic receptors (circles), whereas all nonretinal inputs activate metabotropic receptors (stars) and often ionotropic receptors as well. The question mark related to input from interneurons indicates uncertainty whether metabotropic receptors are involved. Thick solid and thin dashed lines indicate driver and modulator inputs, respectively. Filled and open icons for synaptic terminals indicate excitatory and inhibitory inputs, respectively. ACh, acetylcholine; GABA, gamma-aminobutyric acid; Glu, glutamate; LGN, lateral geniculate nucleus; PBR, parabrachial region of the brainstem; TRN, thalamic reticular nucleus.

geniculate nucleus, because the circuitry shown here is essentially repeated throughout thalamus. For simplicity, certain pathways are omitted, but some that appear to be differentially distributed between the lateral geniculate nucleus and pulvinar are considered below. For details of these other inputs, see Sherman S. M. and Guillery R. W. (1996; 2006).

1.28.4.1 Anatomical Features

Figure 3 shows that retinal input is one of several to geniculate relay cells. Nonretinal input derives from local GABAergic sources (interneurons and reticular cells), layer 6 of the cortex, which provides a feedback, glutamatergic input, and from the brainstem, mostly from cholinergic cells in a midbrain area known as the parabrachial region. (Another term often applied to this area is pedunculopontine tegmental nucleus. We prefer parabrachial region, because, in many or most species, the cells that innervate thalamus from this area do not have a clear nuclear boundary, and they are found scattered around the brachium conjunctivum.) Thus, the main extrinsic, nonretinal inputs to geniculate relay cells derive from the cortex and brainstem. Note that the local, GABAergic inputs are also innervated by the same cortical and brainstem sources that innervate relay cells. Thus, these extrinsic inputs can affect relay cells directly or indirectly via local GABAergic circuitry.

1.28.4.2 Functional Features

Figure 3 makes clear that, while the retina may provide the main input relayed to the cortex, many nonretinal pathways innervate relay cells, presumably to modulate retinogeniculate transmission. All of these synapses onto relay cells are standard chemical synapses, meaning that they affect relay cells by releasing neurotransmitters that operate through various postsynaptic receptors on the relay cells. These receptors come in two main flavors: ionotropic and metabotropic. Figure 3 shows that a combination of ionotropic and metabotropic receptors is involved in postsynaptic responses of relay cells. Examples of the relevant ionotropic receptors are AMPA and NMDA for glutamate, nicotinic for acetylcholine, and the $GABA_A$ receptor. For metabotropic receptors, examples are various metabotropic glutamate receptors, various muscarinic receptors for acetylcholine, and the $GABA_B$ receptor.

Ionotropic and metabotropic receptors. Differences between ionotropic and metabotropic receptors are many, and only certain ones are considered here (for details, see Nicoll, R. A. *et al.*, 1990; Mott, D. D. and Lewis, D. V., 1994; Pin, J. P. and Duvoisin, R., 1995; Recasens, M. and Vignes, M., 1995; Brown, D. A. *et al.*, 1997; Conn, P. J. and Pin, J. P., 1997). Ionotropic receptors are simpler in construction and function, and the receptor protein itself usually contains the ion channel it controls. Typically, when transmitter binds to the ionotropic receptor, the receptor changes shape, thereby opening the ion channel. This, in turn, allows ions to flow down their electrochemical gradients, leading to an EPSP or IPSP. These ionotropic PSPs typically occurs with brief latencies (<1 ms) and durations (mostly over in 10 or a few tens of milliseconds). Metabotropic receptor functioning is more complicated, because the receptor is linked to ion channels via second messenger systems, which in thalamic relay cells usually involves a G protein and ultimately opens or closes K^+ channels. When K^+ channels open, K^+ flows out of the cell, producing an IPSP, and when K^+ channels close, leakage of K^+ is stopped, leading to an EPSP. One important difference with the activation of ionotropic receptors is that these PSPs related to metabotropic receptors typically have a long latency (~10 ms or so) and duration (hundreds of a millisecond to several seconds).

Figure 3 also shows the pattern of postsynaptic receptors associated with the various inputs onto relay cells. Note that retinal inputs activate only ionotropic receptors (mostly AMPA but also NMDA), whereas all nonretinal inputs activate metabotropic and often also ionotropic receptors. The fast EPSPs activated by retinogeniculate synapses means that for relatively high firing rates in the retinal afferent, it is possible to evoke a single, separate EPSP for each retinal action potential. Put another way, if retinogeniculate synapses activated metabotropic glutamate receptors, the resultant prolonged EPSPs would temporally summate at relatively low firing rates in the afferent; this would act like a low-pass temporal filter, and the result would be a loss of higher-frequency temporal information. Thus, the lack of metabotropic glutamate receptors associated with retinal input maximizes the faithful relay of temporal information. The nonretinal inputs, by activating metabotropic receptors, can achieve sustained changes in membrane potential and thus relay cell excitability, thereby modulating the gain of retinogeniculate transmission.

This pattern of receptors also has implications for the control of firing mode. Recall that to inactivate the T channel (i.e., to close the inactivation gate) requires 100 ms or so of sustained depolarization; likewise, to

deinactivate it (i.e., to open the inactivation gate) requires 100 ms or so of sustained hyperpolarization. This means that the fast EPSPs or inhibitory postsynaptic potentials (IPSPs) seen with ionotropic receptors are ill-suited to affect the inactivation gate; even action potentials, despite their amplitude, are terminated too quickly to effectively inactivate the T channel. In contrast, the sustained postsynaptic potentials of metabotropic receptors are ideally suited to inactivate or deinactivate T channels. It thus follows that retinal input by itself, with its fast EPSPs, is less likely to directly affect T channels. Even evoked action potentials are too fast to have much affect on the inactivation state of these channels.

This seems appropriate in the sense that burst or tonic firing is thought to be largely dependent on behavioral state (Sherman, S. M., 2001), and one would expect that to be mainly the function of the nonretinal inputs to relay cells that do not carry the main information to be relayed. Although visual stimuli can also affect firing rate, this, too, seems to be due to nonretinal afferents. That is, a visual stimulus that inhibits a geniculate cell for a sufficient time (e.g., a dark stimulus falling on the center of an on-center cell) can deinactivate the T channels, and when this stimulus is replaced by an excitatory one (e.g., a bright spot), a burst is evoked (Lesica, N. A. and Stanley, G. B., 2004; Alitto, H. J. *et al.*, 2005; Denning, K. S. and Reinagel, P., 2005). However, this is likely due to inhibitory circuits involving interneurons or reticular cells, or both, and perhaps also involving $GABA_B$ receptors, and is not likely to represent retinal inputs alone. Indeed, evidence exists (reviewed in Sherman, S. M. and Guillery, R. W., 1996; 2006) that metabotropic glutamate receptors activated from layer 6 of the cortex and muscarinic receptors activated from the parabrachial region produce long, slow EPSPs that inactivate the T channels and switch relay cells from burst to tonic firing mode. Likewise, activation of $GABA_B$ receptors from reticular inputs does the opposite: it produces a sustained inhibitory postsynaptic potential that switches firing modes from tonic to burst. Interneurons may also participate in this, but as indicated by the question mark in Figure 3, it is not yet known whether or not these inputs activate $GABA_B$ receptors on relay cells.

Role of parabrachial and cortical inputs. Figure 3 shows that increased activity in parabrachial inputs depolarizes relay cells directly. In addition, increased parabrachial activity inhibits reticular cells and interneurons, thereby disinhibiting relay cells. Thus, increased parabrachial activity results in more depolarized relay cells, which not only makes them more excitable, but also serves to activate their T channels, biasing relay cell responses to tonic mode. This is consistent with evidence that parabrachial neurons become more active and relay cells become less bursty with increasing vigilance, from slow-wave sleep through drowsiness to full attention (Steriade, M. and Contreras, D., 1995; Datta, S. and Siwek, D. F., 2002).

Understanding the consequence of the layer 6 cortical input is much more difficult. Figure 3 suggests that this input directly excites relay cells while it indirectly inhibits them, but in fact, the actual effect of this input depends on details of the circuit that are generally unknown. This is illustrated in Figure 4, which shows two variants of many possible for the relevant circuit. Figure 4(a) shows individual corticogeniculate axons innervating a reticular cell and a relay cell, with the reticular cell innervating the same relay cell. This is an example of feedforward inhibition. The consequence of increased corticogeniculate activity might be little or no net effect on the relay cell's membrane voltage (and T-channel inactivation or deinactivation) if the excitatory and inhibitory inputs are balanced. However, as pointed out by Chance F. S. *et al.* (2002), while this may not affect membrane voltage, the increased synaptic conductance among other factors will reduce relay cell excitability to other (i.e., retinal) inputs; thus, in the lateral geniculate nucleus, activation of this circuit would reduce the gain of retinogeniculate transmission.

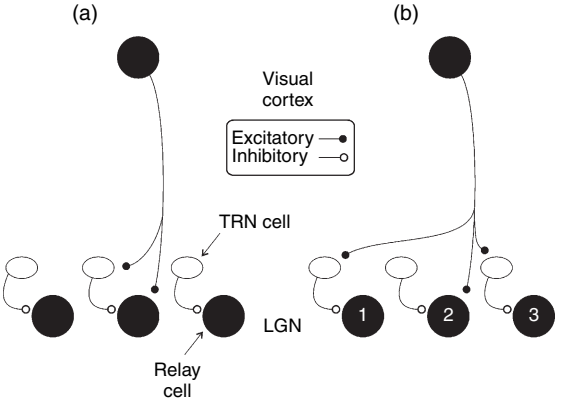

Figure 4 Two patterns among others possible for corticothalamic projection from layer 6 to cells of the thalamic reticular nucleus and geniculate relay cells. (a) Pattern of simple excitation and feedforward inhibition. (b) More complicated pattern in which activation of a cortical axon can excite some relay cells directly and inhibit others through activation of reticular cells. Further details in text. LGN, lateral geniculate nucleus; TRN, thalamic reticular nucleus.

The circuit of Figure 4(b) has very different consequences. Here, activation of the corticogeniculate axon purely excites one or a few relay cells (e.g., cell 2) and purely inhibits others (e.g., cells 1 and 3). Note that this circuit does not involve feedforward inhibition. Also, note that the final effect on relay cell membrane voltage is such that the activation of the corticogeniculate axon would promote tonic firing in cell 2 and burst firing in cells 1 and 3. This means that layer 6 increased corticogeniculate input can have very different and localized effects. Recent evidence is in support of this pattern (Wang, W. *et al.*, 2006). Figure 4 illustrates the importance of a much better understanding of these functional circuits at the single-cell level than we have at present. The example of Figure 4 includes just reticular cells, but one can easily imagine a similar circuit involving interneurons.

1.28.5 The Lateral Geniculate Nucleus

While the above sections describe properties that are applicable to the lateral geniculate nucleus, there are certain features of processing information that are specific to or more readily studied in this nucleus.

1.28.5.1 Parallel Processing

Relay cells in the lateral geniculate nucleus can be divided into at least three functional classes (Sherman, S. M., 1982; Shapley, R. and Lennie, P., 1985; Casagrande, V. A. and Norton, T. T., 1991; Hendry, S. H. C. and Reid, R. C., 2000; Casagrande, V. A. and Xu, X., 2004). Each of these geniculate classes represents a thalamic link in separate streams of retinogeniculocortical processing. That is, there are equivalent distinct classes of retinal ganglion cells that project to the lateral geniculate nucleus, and each retinal class seems to innervate a single class of geniculate relay cell to maintain separate, parallel streams of information to the cortex. In general, the receptive field properties that distinguish these cell types are similar for retina and the lateral geniculate nucleus, because geniculate receptive fields are essentially the same as their retinal inputs. These classes have been best studied in the cat, where they are called X, Y, and W cells, and in the monkey, where they are called parvocellular (P), magnocellular (M), and koniocellular (K). There appears to be a link in homology here between X and P cells, Y and M cells, and W and K cells. Homologies to these parallel cell classes have also been suggested for other species (Casagrande, V. A. and Norton, T. T., 1991; Van Hooser, S. D. *et al.*, 2003; Casagrande, V. A. and Xu, X., 2004).

1.28.5.1.1 The cat lateral geniculate nucleus

X and Y cells. X and Y cells are each a fairly homogeneous class, with both anatomical and receptive field correlates. Anatomically, retinal X cells are known as beta cells and Y cells as alpha cells (Boycott, B. B. and Wässle, H., 1974). Beta cells have smaller cell bodies with smaller dendritic arbors and thinner caliber axons. Similar relationships exist for geniculate X and Y cells (LeVay, S. and Ferster, D., 1977; Friedlander, M. J. *et al.*, 1981). Geniculate X cells have smaller cell bodies with thinner axons, and their dendritic arbors are elongated perpendicular to the geniculate laminar borders (see below for geniculate layers), whereas those of Y cells are organized into a roughly spherical shape. Also, X cells tend to have grape-like appendages near proximal dendritic branch points, whereas Y-cell dendrites are generally smooth. This is interesting, because these appendages on the X cells mark the postsynaptic target of the retinal inputs, whereas on Y cells, retinal inputs terminate directly onto proximal dendritic shafts (Wilson, J. R. *et al.*, 1984; Hamos, J. E. *et al.*, 1986).

The receptive fields of both cell types in retina and the lateral geniculate nucleus are organized into classic center/surround regions. There are roughly equal numbers of on- and off-center cells. However, X cells have smaller receptive fields and respond to higher spatial and lower temporal frequencies (Sherman, S. M., 1982; Shapley, R. and Lennie, P., 1985). These center/surround regions for both X and Y cells exhibit linear summation, but the Y cells, in addition, have small, nonlinear subunits in their receptive fields that produce a doubling response (i.e., a response to both onset and offset to both bright and dark spots) to visual stimuli (Enroth-Cugell, C. and Robson, J. G., 1966; Hochstein, S. and Shapley, R. M., 1976).

Based on receptive field properties, hypotheses have been developed for the distinct function of the X and Y pathways. X cells are thought to provide maximum acuity for detail vision, while Y cells are more important for motion detection and processing of low spatial frequencies (Sherman, S. M., 1985).

W cells. W cells remain a poorly understood cell group and probably represent a heterogeneous group with several distinct classes. However, for convenience and because the final classification and

functional correlates of W cells are lacking, they are considered together here (for further details of these cells, see Sherman, S. M., 1982; Berson, D. M. *et al*., 1998; 1999; Isayama, T. *et al*., 2000). Retinal W cells generally have small to medium-sized cell bodies with long, sparsely branched dendrites, but the morphological features of this group are so varied that any generality must be qualified. W cells so far described in the lateral geniculate nucleus have medium-sized cell bodies and dendritic arbors oriented parallel to the layers (Stanford, L. R. *et al*., 1983). The receptive fields of these cells, both in retina and in the lateral geniculate nucleus, are also quite varied but tend to be large and poorly responsive. Indeed, Cleland B. G. and Levick W. R. (1974) have named them sluggish; some have center/surround configuration, others have poorly defined borders with on/off responses throughout, some have directional selectivity, and some have some wavelength sensitivity. To date, there has not been much speculation regarding the function of the W pathway(s), and this remains a mystery.

1.28.5.1.2 The monkey lateral geniculate nucleus

P and M cells. In the retina (Rodieck, R. W., 1979; Leventhal, A. G. *et al*., 1981), P cells (called midget cells) are smaller than M cells (called parasol cells), and this size differential also holds in the lateral geniculate nucleus, as the names (Parvocellular and Magnocellular) imply. Their receptive fields both in retina and in the lateral geniculate nucleus have the classic center/surround configuration, but P cells have smaller receptive fields (Casagrande, V. A. and Norton, T. T., 1991; Hendry, S. H. C. and Reid, R. C., 2000; Casagrande, V. A. and Xu, X., 2004). M cells are much more sensitive to luminance contrast and moving stimuli, but, while M cells show no wavelength sensitivity, P cells show sensitivity for green and red wavelengths. One exception to this are owl monkeys, which are crepuscular, like cats, and, like cats, are thus not so reliant on color vision. For these animals, P cells show little wavelength sensitivity (O'Keefe, L. P. *et al*., 1998). As is the case for the cat, there has been much speculation concerning the role of these cell types in the monkey. Common suggestions are that P cells are important for color discrimination in monkeys with diurnal behavioral patterns, especially for red/green distinctions, and may also be involved in high acuity vision, whereas M cells provide for better luminance contrast sensitivity and are also important for motion detection (Casagrande, V. A. and Norton, T. T., 1991; Hendry, S. H. C. and Reid, R. C., 2000; Casagrande, V. A. and Xu, X., 2004).

K cells. Like W cells, K cells probably include many distinct cell classes, and also like W cells, are grouped together here, because their complete classification remains to be done. As the name (Koniocellular) implies, these are smaller than M or P cells in both the retina and the lateral geniculate nucleus. Not much is known of their receptive field properties, but some of these cells are thought to be responsible for yellow/blue wavelength discrimination. For a fuller account of K cells, see Martin P. R. *et al*. (1997), Martin P. R. (1998), Silveira L. C. L. *et al*. (1999), and Hendry S. H. C. and Reid R. C. (2000).

1.28.5.2 Laminar Relationships

1.28.5.2.1 Lateral geniculate nucleus

Layering is a constant feature of the lateral geniculate nucleus in all mammals so far studied. In some species (e.g., cats and monkeys), the layering is obvious, because cell-poor interlaminar zones exist to demarcate the layers. In other species (e.g., rats), such zones do not exist, so the layering is less obvious but still present. Each of these layers receives an input from one or the other eye. Geniculate laminar patterns vary greatly among species, but this ocular division between sets of layers seems to be one constant.

In addition to ocular dominance, the various cell types are distributed with varying levels of laminar specificity. In the cat, X and Y cells commingle in the dorsal two layers (called the A layers); the next ventral layer (layer C) has only Y cells; and the ventral few layers have only W cells (Sherman, S. M., 1982). In the rhesus monkey, P and M cells separate into four dorsal parvocellular layers and two ventral magnocellular layers. The K cells not only are found in all the interlaminar zones but also extend into the ventral regions of the parvocellular layers (Casagrande, V. A. and Norton, T. T., 1991; Hendry, S. H. C. and Reid, R. C., 2000; Casagrande, V. A. and Xu, X., 2004). In the mink and ferret, the A layers (containing commingled X and Y cells) further separate into sublayers containing only on- or off-center cells (LeVay, S. and McConnell, S. K., 1982; Stryker, M. P. and Zahs, K. R., 1983), and yet the closely related cat has these on- and off-center cells commingled in single layers. Figure 5 summarizes the laminar patterns for several representative mammalian species to illustrate the sort of bewildering variation present. Geniculate lamination does

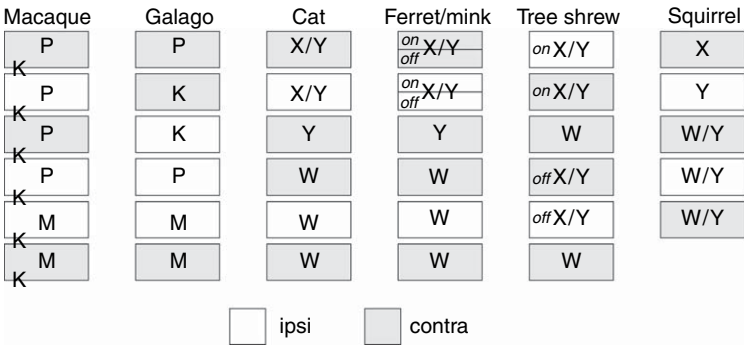

Figure 5 Schematic rendering of layers and distribution of cell types in the lateral geniculate nucleus of six different species (Kaas, J. H. *et al.*, 1972; Sherman, S. M. and Spear, 1982; Sherman, S. M., 1985; Casagrande, V. A. and Norton, T. T., 1991; Hendry, S. H. and Calkins, D. J., 1998; Van Hooser, S. D. *et al.*, 2003). The shaded boxes show layers innervated by the contralateral eye (contra), and the unshaded boxes show the input from the ipsilateral eye (ipsi). The X, Y, and W pathways are shown for the cat, the ferret/mink, the tree shrew, and the squirrel, and the magnocellular (M), parvocellular (P), and koniocellular (K) pathways are shown for the macaque and the galago. Where there is a clear segregation of on- and off-center (*on*, *off*) cells, this is also indicated. From Sherman, S. M. and Guillery, R. W. 2006. Exploring the Thalamus and its Role in Cortical Function, 2nd edn. MIT Press.

correlate with cell type, but the nature and extent of this correlation varies widely across species, and it is difficult to discern any special significance to these correlations.

1.28.5.2.2 Visual cortex

There is also a laminar correlation regarding the target zones of the various cell types (Ferster, D. and LeVay, S., 1978; Blasdel, G. G. and Lund, J. S., 1983; Humphrey, A. L. *et al.*, 1985; Casagrande, V. A. and Xu, X., 2004). In the cat, geniculate X-cell axons innervate the ventral part of layer 4, while those of Y cells innervate the upper part. Geniculate W cells mostly innervate layer 3. A similar arrangement holds for the monkey: P cells innervate the ventral half of layer 4 (sometimes called layer 4Cβ), M cells innervate the dorsal half of layer 4 (sometimes called 4Cα), and K cells mostly innervate layer 3. Thus, through the first stage of processing, the three parallel pathways are kept fairly independent, although what happens further centrally with regard to these pathways is not at all clear.

1.28.6 Drivers and Modulators

Figure 3 illustrates a fundamentally important point that is often overlooked: all inputs to geniculate relay cells are not equal. That is, the retinal input alone represents the main information actually relayed to the cortex. A consideration of receptive field properties helps demonstrate this fact, because the responses of the relay cell to visual stimulation identify the information relayed. It is clear that the receptive fields of geniculate relay cells are remarkably like those of their retinal afferents, having the same center/surround configuration and with only minor, subtle differences (reviewed in Sherman, S. M., 1985). Geniculate receptive fields do not closely match any other extrageniculate afferent: receptive fields of corticogeniculate afferents, which show selectivities for orientation and often direction typical of cortical cells (Gilbert, C. D., 1977), are quite different, and parabrachial inputs are not plausible sources of such clear center/surround properties. If it is the retinal input that provides the information to be relayed, then the nonretinal inputs must have another function. This, plus a number of morphological, pharmacological, and physiological differences that distinguish retinal and nonretinal afferents to relay cells, has led to the idea that these can be functionally divided: the retinal inputs are the drivers (so called because one of their properties is the very strong postsynaptic drive of their target relay cells; see Table 1), while all the nonretinal inputs are the modulators, the idea being that the driver input is the information-bearing input, while the modulators serve to modulate retinogeniculate transmission (Sherman, S. M. and Guillery, R. W., 1998; 2006). Modulation can take many forms, including, for example, the above-mentioned consequences of metabotropic receptor activation that lead to overall

Table 1 Drivers and modulators in lateral geniculate nucleus (LGN) plus layer 5 drivers

Criteria	*Retinal (driver)*	*Layer 5 to higher order (driver)*	*Modulator: layer 6*	*Modulator: PBR*	*Modulator: TRN and Int*
1	Determines relay cell receptive field	Determines relay cell receptive field[a]	Does not determine relay cell receptive field	Does not determine relay cell receptive field	Does not determine relay cell receptive field
2	Activates only ionotropic receptors	Activates only ionotropic receptors	Activates metabotropic receptors	Activates metabotropic receptors	TRN: activates metabotropic receptors; Interneuron: [b]
3	Large EPSPs	Large EPSPs	Small EPSPs	*b*	TRN: small IPSPs; Interneuron: [b]
4	Large terminals on proximal dendrites	Large terminals on proximal dendrites	Small terminals on distal dendrites	Small terminals on proximal dendrites	Small terminals; TRN: distal; Interneuron: proximal
5	Each terminal forms multiple contacts	Each terminal forms multiple contacts	Each terminal forms single contact	Each terminal forms single contact	Each terminal forms single contact
6	Little convergence onto target	Little convergence onto target[a]	Much convergence onto target	*b*	*b*
7	Very few synapses onto relay cells (∼5%)	Very few synapses onto relay cells (∼5%)	Many synapses onto relay cells (∼30%)	Many synapses onto relay cells (∼30%)	Many synapses onto relay cells (∼30%)
8	Often thick axons	Often thick axons	Thin axons	Thin axons	Thin axons
9	Glutamatergic	Glutamatergic	Glutamatergic	Cholinergic	GABAergic
10	Synapses show paired-pulse depression (high *p*)	Synapses show paired-pulse depression (high *p*)[a]	Synapses show paired-pulse facilitation (low *p*)	*b*	*b*
11	Well-localized, dense terminal arbors	Well-localized, dense terminal arbors	Well-localized, dense terminal arbors	Sparse terminal arbors	Well-localized, dense terminal arbors
12	Branches innervate subtelencephalic targets	Branches innervate subtelencephalic targets	Subcortically known to innervate thalamus only	*b*	Subcortically known to innervate thalamus only
13	Innervates dorsal thalamus but not TRN	Innervates dorsal thalamus but not TRN	Innervates dorsal thalamus and TRN	Innervates dorsal thalamus and TRN	TRN: both; Interneuron: dorsal thalamus only

[a]Very limited data to date.
[b]No relevant data available.
EPSP, excitatory postsynaptic potential; PBR, parabrachial region of the brainstem; TRN, thalamic reticular nucleus.

changes in relay cell excitability and that serve to control the tonic/burst transition. In addition, the circuit suggested by Figure 4(a) can operate to control the gain of retinogeniculate transmission.

Many properties distinguish drivers from modulators in thalamus, and the number will likely increase as we learn more about this issue. Table 1, which is not meant to be exhaustive, summarizes some important features (see also Sherman, S. M. and Guillery, R. W., 2006). Layer 5 drivers (the second column in Table 1) are considered below. The 13 criteria in Table 1, in a roughly decreasing order of importance, are as follows:

1. Drivers determine the main receptive field properties of the relay cell; modulators do not.
2. Drivers activate only ionotropic receptors; modulators activate metabotropic receptors as well.
3. Drivers evoke large EPSPs; modulators evoke smaller EPSPs or IPSPs.
4. Drivers form large terminals on proximal dendrites; modulators usually form small terminals throughout the dendritic arbor.
5. Each driver terminal forms multiple large synapses; each modulator terminal usually forms a single, small synapse.
6. Driver inputs show little convergence so that one or a small number of driver axons converge onto the postsynaptic target neuron; where evidence is available, modulator inputs show considerable convergence.
7. Driver inputs produce a small minority (~5%) of the synapses onto thalamic relays cells; many modulator inputs produce larger synaptic numbers (e.g., the cortical and parabrachial modulator inputs in Figure 3 each produces about 30% of the synapses).
8. Drivers have thick axons; modulators have thin axons.
9. Drivers are glutamatergic; modulators can use a variety of neurotransmitters.
10. Driver synapses show high release probability and paired-pulse depression, meaning that a given action potential is likely to result in transmitter release and that, with the initiation of a train of action potentials, there is a period after each evoked postsynaptic potential lasting for tens of a millisecond that the next one will be smaller (depressed); modulator synapses that have been tested so far show the opposite properties of low release probability and paired-pulse facilitation.
11. Driver terminal arbors are well localized with a dense array of terminals; modulator terminal arbors can be either well localized and dense or relatively poorly localized and sparse.
12. Branches of driver axons tend to innervate extrathalamic targets as well as thalamus (e.g., many or all retinogeniculate axons branch and also innervate midbrain targets); those modulator inputs so far tested innervate thalamus only.
13. Driver inputs innervate relay cells and interneurons in dorsal thalamus but do not innervate the thalamic reticular nucleus; modulator inputs innervate relay cells, interneurons, and reticular cells.

This driver/modulator distinction can be applied, not just to the lateral geniculate nucleus, but also to all thalamic relays for which sufficient information is available, such as the ventral portion of the medial geniculate nucleus (the primary auditory thalamic relay) and the ventral posterior nucleus (the primary somatosensory thalamic relay). The main point, again, is that not all anatomical pathways are functionally equivalent, acting in some sort of anatomical democracy, and if one is to understand the functional organization of the thalamus and what it is that is being relayed, one must identify and characterize the driver input. As we shall see, identifying the driver to the lateral geniculate nucleus is clear, but it is not so obvious for the pulvinar. An important possibility raised below is that this driver/modulator distinction may also apply outside of thalamus.

Regarding criterion 7 above, it may seem surprising at first that the main information to be relayed is responsible for such a small minority of synapses onto relay cells, but two factors may help explain this. First, despite the small number of inputs anatomically, these are especially powerful and effectively drive the relay cells. Second, if a relatively small but powerful number of synapses are needed to relay the basic information, many more, individually weaker synapses that can be combined in different ways are needed to provide a wide range of subtle modulatory effects.

One last point needs to be emphasized with respect to geniculate circuitry that should be considered when evaluating any circuits in the central nervous system. With anatomical information alone, such as numbers of synapses from subcortical sites, the number from the parabrachial region (~30%) is considerably greater than that from retina (5–10%). Such anatomical data in isolation might lead one to the mistaken conclusion that the parabrachial input is

the more important and thus represents the information being relayed, while the retinal input, being so small, performs some vague, lesser function that might not even merit inclusion in some schematic illustrations of geniculate circuitry. The key lesson here is that anatomical data, on their own, can be very misleading when trying to unravel functional circuits. With regard to information processing through thalamus, a most important issue is to identify what is being relayed, and to do so, it is potentially misleading to treat all pathways as equal: one must instead separately identify drivers from modulators. Look through any textbook on neuroscience, and perhaps even this volume, and you are likely to find examples of schematically illustrated circuits that are based on anatomy alone, as if all inputs were drivers in the sense the term has been used here. If the concept of drivers and modulators has validity beyond thalamus, many of these suggested circuits need to be reconsidered.

1.28.7 First- and Higher-Order Relays: The Lateral Geniculate Nucleus and Pulvinar

There are two ways to think about the function of the thalamus. One is to consider the properties of thalamic circuitry as they affect relay functions. For one example, how do the modulators affect retinogeniculate transmission? The other is to consider what it is that a thalamic nucleus is actually relaying. Put another way, we can define the function of lateral geniculate nucleus or the ventral posterior nucleus as relaying retinal or medial lemniscal information, respectfully. It is this latter aspect of thalamic functioning, which really boils down to identifying the driver input, that chiefly concerns us in this section.

1.28.7.1 Layer 5 Corticothalamic Inputs as Drivers

Identifying the function of a thalamic nucleus by identifying the driver input may seem obvious and trivial for well-studied relays like the lateral geniculate nucleus, but there are many other less-well-understood relays with unknown functions because, until recently, their driver inputs were undefined. Examples are the pulvinar and medial dorsal nucleus. We now know that a major source of driver input to thalamic relays like these is layer 5 of the cortex. This is illustrated in Figure 6.

First- and higher-order relays. Figure 6(a) illustrates key elements of this organization (details reviewed in Sherman, S. M. and Guillery, R. W., 2006). All thalamic nuclei receive a feedback corticothalamic projection from layer 6, and they also have inputs from the thalamic reticular nucleus; not shown for simplicity are inputs to relay cells from interneurons and the parabrachial region (Figure 3). However, while some thalamic nuclei relay subcortical driver inputs to the cortex (Figure 6(a)), others instead relay driver inputs that arise from cortical layer 5, and this appears to be feedforward (Figure 6(b); see Van Horn, S. C. and Sherman, S. M., 2004). We refer to the type of thalamic relay of Figure 6(a) as first order, because this is the first relay of a particular type of subcortical information (e.g., retinal) to the cortex, and that of Figure 6(b) as higher order, because this relays information already in the cortex but from one cortical area to another.

The lateral geniculate nucleus and pulvinar as first- and higher-order relays. Clearly, in this scheme, the lateral geniculate nucleus is a first-order nucleus. As noted above, examples of other first-order nuclei are the ventral posterior nucleus for somesthesis and the ventral (or lemniscal) portion of the medial geniculate nucleus for sounds. The pulvinar is mostly a higher-order nucleus. We say "mostly" here, because a small part of the pulvinar appears to relay driver information from the superior colliculus (Kelly, L. R. *et al.*, 2003), which would make this portion of the pulvinar first order. Examples of other higher-order thalamic nuclei are most of the posterior medial nucleus for somesthesia, most of the medial and dorsal (or nonlemniscal) portion of the medial geniculate nucleus for hearing, and the medial dorsal nucleus, which widely innervates the prefrontal cortex. Again, most here refers to the fact that some of these nuclei may contain first-order circuits: there is a spinothalamic zone of the posterior medial nucleus and an inferior collicular input to the nonlemniscal part of the medial geniculate nucleus. This possible complex organization of higher-order nuclei has to be clarified, and it will not be considered further here, but it does point up a potential shortcoming of classically defined, cytoarchitectonic boundaries for functional thalamic relays.

The key to this division of thalamic relays into first and higher order is the observation that the layer 5 inputs to relay cells have the same properties as do the subcortical drivers (e.g., retinal input to the lateral geniculate nucleus and medial lemniscal input to the ventral posterior nucleus). Support for

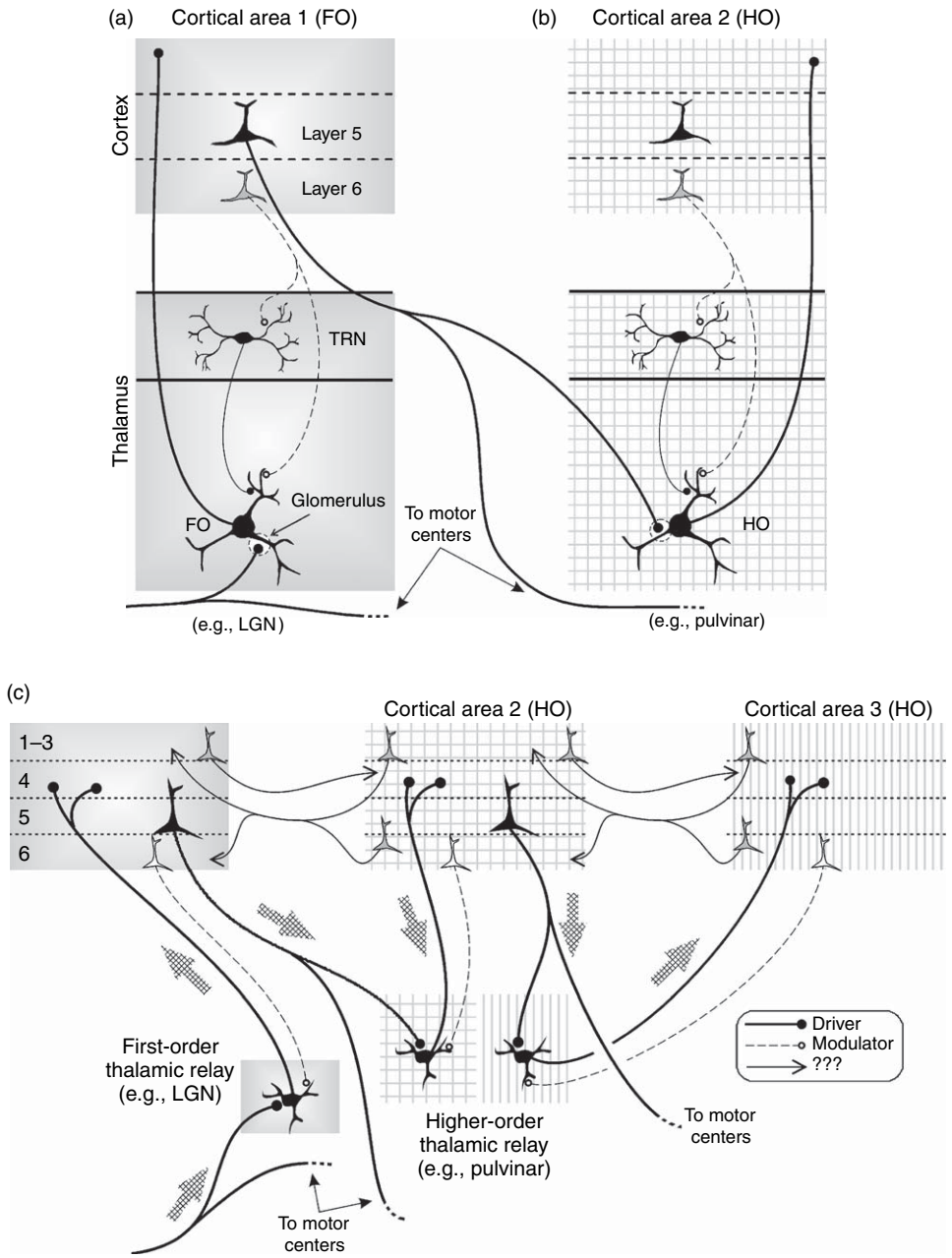

Figure 6 Schematic diagrams showing organizational features of first- and higher-order thalamic nuclei. (a, b) Distinction between first- and higher-order thalamic nuclei. A first-order nucleus (a) represents the first relay of a particular type of subcortical information to a first-order or primary cortical area. A higher-order nucleus (b) relays information from layer 5 of one cortical area to another. This relay can be between first- and higher-order cortical areas as shown or between two higher-order cortical areas. The important difference between them is the driver input, which is subcortical (a) for a first-order thalamic nucleus and from layer 5 of cortex (b) for a higher-order one. Note that all thalamic nuclei receive an input from layer 6 of cortex, which is mostly feedback, but higher-order nuclei in addition receive a layer 5 input from cortex, which is feedforward. (c) Role of higher-order thalamic nuclei in corticocortical communication. This involves a projection from layer 5 of cortex to a higher-order thalamic relay to another cortical area. As indicated, the role of the direct corticocortical projections, driver or modulator or other, is unclear. Note in (a)–(c) that the driver inputs, both subcortical and from layer 5, are typically from branching axons, the significance of which is elaborated in the text. FO, first order; HO, higher order; LGN, lateral geniculate nucleus; TRN, thalamic reticular nucleus. Redrawn from Sherman, S. M. 2005. Thalamic relays and cortical functioning. Prog. Brain Res. 149, 107–126.

this can be found in Table 1: note from the first two columns of Table 1 that the layer 5 input to higher-order relays matches retinogeniculate input on all criteria; in contrast, the second and third columns show that the corticothalamic inputs from layers 5 and 6 differ on all criteria (Reichova, I. and Sherman, S. M., 2004; Sherman, S. M. and Guillery, R. W., 2006; Lee, C. C. and Sherman, S. M., unpublished).

1.28.7.2 Branching of Driver Afferents to Thalamus

Figures 6(a) and 6(b) also shows that the driver inputs to both first- and higher-order relay cells are delivered mostly or wholly via branching axons, with one branch innervating thalamic relay cells and the other innervating extrathalamic targets in the brainstem and spinal cord that are generally motor in nature (Guillery, R. W., 2003; 2005; Sherman, S. M. and Guillery, R. W., 2006). For instance, most or all retinogeniculate axons branch to innervate the pretectum and/or superior colliculus, and, likewise, most or all layer 5 corticothalamic axons branch to innervate motor targets in the pons, midbrain, medulla, and sometimes even spinal cord. However, drivers do not branch to innervate the thalamic reticular nucleus. This is in contrast to most modulator inputs, which do branch to innervate the thalamic reticular nucleus but often have no extrathalamic targets. Limited data are consistent with a similar arrangement for relays of somatosensory and auditory information (reviewed in Guillery, R. W., 2003; 2005; Sherman, S. M. and Guillery, R. W., 2006), and so are not limited to the lateral geniculate nucleus and pulvinar. Guillery R. W. (2003; 2005) has described this feature of driver afferents and suggested what its functional significance might be; this is briefly outlined below.

One interpretation of this pattern of branching to innervate extrathalamic motor targets is that the information actually relayed by thalamus relates to motor commands, starting with first-order relays as perhaps quite crude commands that are constantly upgraded with further cortical processing and effected via higher-order layer 5 cortical outputs. If so, then even first-order sensory processing involves processing of motor commands, a notion that stands conventional views of early visual processing on its head. That is, conventionally, the primary visual cortex (V1) is generally viewed as a purely sensory structure, and this view seems at odds with the idea that V1 is processing motor information. Furthermore, as already noted, V1 (and, indeed all cortical areas so far studied) has a layer 5 projection that branches to innervate pulvinar and extrathalamic motor targets, so that even the corticofugal outputs of V1 have a motor tag according to this perspective. The conventional wisdom that V1 or any other visual, auditory, or somatosensory area is purely sensory is challenged by the observation that all of these areas have a motor output.

1.28.7.3 Role of Higher-Order Thalamic Relays in Corticocortical Processing

Figure 6(c) illustrates the suggested role played by higher-order thalamic relays. After initially reaching the cortex via a first-order relay, such as the lateral geniculate nucleus, information is then passed on to higher-order cortical areas through higher-order thalamic relays. This can involve a number of hierarchical levels of both cortical and thalamic processing. The obvious question raised here is: if the corticothalamocortical pathways involving higher-order thalamic nuclei represent a significant information route, what of the direct corticocortical projections? The answer, simply, is not yet available, but to help clarify the issue here, it is useful to consider three obvious hypotheses, among others.

One possibility is that all direct corticocortical pathways are modulators, in which case all information between cortical areas is relayed via the thalamus. One conclusion that could be drawn here is that all new information that reaches the cortex, whether originating from a subcortical source such as the retina or from another cortical area, benefits from a thalamic relay. That is, for the same reason that retinal information is relayed by the lateral geniculate nucleus and does not project directly to the visual cortex, information from one cortical area to another is relayed through thalamus. Benefits could include gating properties of the thalamus, the burst/tonic transition, etc.

One problem with this hypothesis is that higher-order relays such as the pulvinar may not have enough neurons to relay all of the requisite information needed for cortical processing. Although the pulvinar is the largest thalamic nucleus and dwarfs the lateral geniculate nucleus, Van Essen D. C. (2005) points out that pulvinar neurons may be insufficient in number to relay all information needed for corticocortical communication. A very small percentage of visual cortical neurons are represented by the layer 5 efferents that could provide the afferent link in the corticothalamocortical pathway (Callaway, E. M. and Wiser, A. K., 1996), and these numbers do not

seem to pose a limitation on the role of the pulvinar as a central relay structure between cortical areas. Unfortunately, we as yet have no answer to this general question, because we simply do not know the nature or neural coding of this information that is passed on, and our ignorance here is such that we cannot rule out the possibility that the small number of layer 5 efferent cells is sufficient to this task. It is also possible that the full extent of information processed in a cortical area requires an additional, corticocortical route, the case to which we now turn.

The second hypothesis is that the corticothalamocortical pathways involving higher-order thalamic nuclei serve a modulatory role with all information carried by direct corticocortical projections. For instance, Van Essen D. C. and co-workers (Olshausen, B. A. *et al.*, 1993; Anderson, C. H. *et al.*, 2005; Van Essen, D. C., 2005) have suggested that pulvinar projections to the cortex serve to regulate attentional responses, which, in turn, implies that these projections could act as modulators. However, evidence does exist that the relevant synapses in corticothalamocortical pathways – namely, the layer 5 corticothalamic projections and the higher-order thalamocortical projections – are drivers (Reichova, I. and Sherman, S. M., 2004) (Agmon, A. and Connors, B. W., 1991; Stratford, K. J. *et al.*, 1996; Castro-Alamancos, M. A. and Connors, B. W., 1997; Gil, Z. *et al.*, 1999; Lee, C. C. and Sherman, S. M., unpublished).

The third and final hypothesis is that the higher-order corticothalamocortical and direct corticocortical pathways represent two parallel, largely independent, and complementary routes of information flow. One example of this would be that the very large corticocortical projection handles all of the details of information that must be analyzed about the environment, and the corticothalamocortical projections inform the target cortical area about motor commands initiated by the source area. This is a more limited form of information but is essential, because higher-order cortical areas must maintain a real-time appreciation of how motor commands affect sensory processing. For example, higher-order visual cortical areas need to be able to factor in eye movements that cause the visual world to move on the retina and not view these as movement in the environment. This example of the limited sort of information carried by the corticothalamocortical pathways is consistent with the motor branches of the layer 5 axons described above.

Two further points need to be emphasized here. First, even if both pathways are involved in information flow, there is an important distinction to be made. Whatever information is carried by direct corticocortical connections, this remains in the cortex and is thus different in kind from information carried by the layer 5 outputs to higher-order thalamic nuclei, because as noted above, these layer 5 axons branch to carry the same information to various extrathalamic, subcortical targets. Second, even if some corticocortical projections carry information, the massive potential problem remains to determine which pathways are modulators and which are drivers. This assumes that the driver/modulator distinction makes sense for intracortical pathways, and some recent evidence suggests the plausibility of this. That is, Lee C. C. and Sherman S. M. (unpublished) have shown that, while both first- and higher-order thalamocortical inputs to layer 4 cells in mice have driver synaptic characteristics, intracortical layer 6 inputs to the same layer 4 cells have modulator characteristics. Identifying the subset of drivers among these direct corticocortical pathways, even if the subset proves to be small, along with a full appreciation of the corticothalamocortical pathways, would allow the creation of a more complete and accurate hierarchical scheme for cortical processing.

1.28.7.4 Overview

To help appreciate cortical processing according to the conventional view and how this departs from the alternative view offered here, Figure 7 shows schematically how different these are. In the conventional view, information is relayed by the thalamus to the sensory cortex and passes within the cortex to the sensorimotor and then to the motor cortex before an output is generated to motor centers (Figure 7(a)). This provides no specific role for most of thalamus, which we have defined as higher order, although there are suggestions that some of these thalamic nuclei could play a modulatory role related to attention (Olshausen, B. A. *et al.*, 1993; Anderson, C. H. *et al.*, 2005; Van Essen, D. C., 2005). The alternative view (Figure 7(b)) differs from the beginning, since initial information to be relayed via a first-order thalamic nucleus is a copy of information sent to motor structures. From the primary cortex, information can be relayed to other cortical areas via higher-order thalamic nuclei, and this continues through the various hierarchical stages. Also, these pathways involve layer 5 corticothalamic axons that branch to innervate extrathalamic motor structures. The role of direct corticocortical pathways remains unclear in this view, but it is plausible that there are

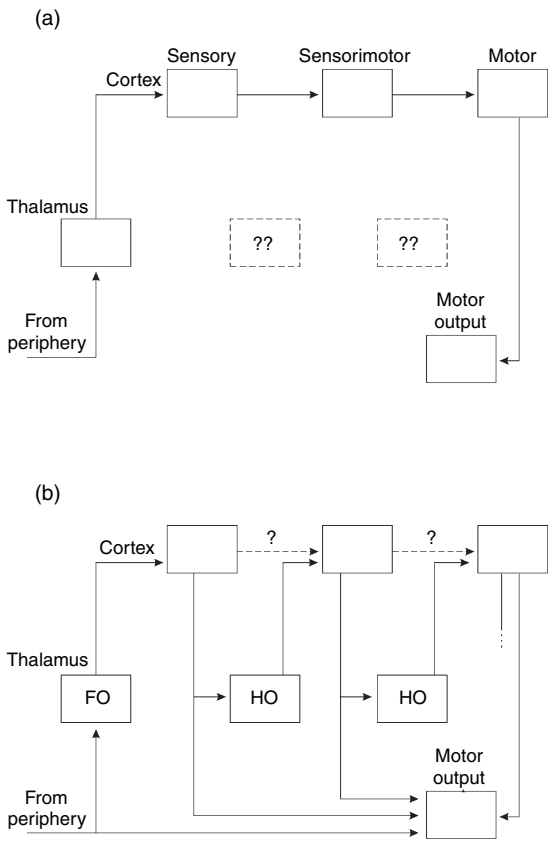

Figure 7 Comparison of conventional view (a) with the alternative view proposed here (b). The role of the direct corticocortical connections in (b) (dashed lines) is questioned (see text for details). FO, first order; HO, higher order. Further details in text. Reproduced from Sherman, S. M. 2005. Thalamic relays and cortical functioning. Prog. Brain Res. 149, 107–126.

two information routes operating independently and in parallel: one is the direct corticocortical route and the other the corticothalamocortical route.

It seems most likely that higher-order thalamic nuclei play an important and hitherto unappreciated role in corticocortical communication. Thus, thalamus is not there just to get information to the cortex in the first place but rather continues to play a role in further cortical processing of that information. What is less clear is the role of direct corticocortical pathways and their relationship to the corticothalamocortical pathways. If the driver/modulator has relevance for these pathways, and that is a major proviso, then it will be essential to identify which of these pathways, if any, are drivers. Only then can we have a clearer understanding of processing among the related cortical areas.

1.28.8 Conclusions

We have progressed from the days when the thalamus was seen as a dull, machine-like relay, providing interesting behaviors only during epilepsy or slow-wave sleep. To a large extent, this misconception grew out of the success of the receptive field approach to the study of sensory systems, particularly vision. Studies of the retina showed that receptive fields become increasingly complicated as one ascends synaptic hierarchies, leading ultimately to the classic center/surround receptive field of ganglion cells projecting to the lateral geniculate nucleus. This process continues across synaptic hierarchies in the cortex, providing cortical receptive fields with exquisite sensitivity to orientation, direction and speed of movement, spatial frequency, stereoscopic depth, etc. This receptive field elaboration in retina and the cortex is ultimately used to encode the sensory environment. The one synapse in the visual system across which no significant receptive field elaboration occurs is the retinogeniculate synapse, since the same basic center/surround organization is seen in retinal afferents and their target geniculate relay cells. This led to the notion that the lateral geniculate nucleus specifically and thalamus more generally represents an uninteresting, simple relay.

We can now turn that view on its head. Indeed, while the rest of the visual and other sensory systems can be ascribed to the same function – that is receptive field elaboration – the thalamus has a completely unique role to play in information processing. Recent appreciation of the complex cell and circuit properties of thalamus makes it clear that it is anything but simple and uninteresting in its functioning. These properties serve to regulate the flow of information to the cortex through mechanisms such as gain control of the retinogeniculate synapse (or equivalent for other nuclei) and the burst/tonic transition, functions that are probably just the tip of the iceberg. Furthermore, we can now see that thalamus is not there just to get information to the cortex but continues to play a significant role in corticocortical communication.

The challenge for students of the visual system is at least twofold. One is to gain a better appreciation of how and under what conditions information is affected before being relayed by the lateral geniculate nucleus or pulvinar to the cortex. The other is to address questions about the pulvinar. One of the great problems here is that we have no complete map of pulvinar that includes a full demarcation of what

regions of pulvinar innervate which regions of the cortex and which are innervated by each cortical area, with a separate mapping of layer 5 and 6 inputs. Given these variables and the presence of more than 30 visual cortical areas with which the pulvinar is involved, it may be that more than a hundred separate pulvinar regions remain to be discovered. This is a daunting task and should be seen as one of the major challenges for future studies of the visual system.

References

Agmon, A. and Connors, B. W. 1991. Thalamocortical responses of mouse somatosensory (barrel) *in vitro*. Neuroscience 41, 365–379.

Alitto, H. J., Weyand, T. G., and Usrey, W. M. 2005. Distinct properties of stimulus-evoked bursts in the lateral geniculate nucleus. J. Neurosci. 25, 514–523.

Anderson, C. H., Van Essen, D. C., and Olshausen, B. A. 2005. Directed Visual Attention and the Dynamic Control of Information Flow. In: Neurobiology of Attention (*eds*. L. Itti, G. Rees, and J. Tsotso), pp. 11–17. Elsevier.

Arcelli, P., Frassoni, C., Regondi, M. C., De Biasi, S., and Spreafico, R. 1997. GABAergic neurons in mammalian thalamus: a marker of thalamic complexity? Brain Res. Bull. 42, 27–37.

Berson, D. M., Isayama, T., and Pu, M. 1999. The eta ganglion cell type of cat retina. J. Comp. Neurol. 408, 204–219.

Berson, D. M., Pu, M., and Famiglietti, E. V. 1998. The zeta cell: a new ganglion cell type in cat retina. J. Comp. Neurol. 399, 269–288.

Bezdudnaya, T., Cano, M., Bereshpolova, Y., Stoelzel, C. R., Alonso, J. M., and Swadlow, H. A. 2006. Thalamic burst mode and inattention in the awake LGNd. Neuron 49, 421–432.

Blasdel, G. G. and Lund, J. S. 1983. Termination of afferent axons in macaque striate cortex. J. Neurosci. 3, 1389–1413.

Boycott, B. B. and Wässle, H. 1974. The morphological types of ganglion cells of the domestic cat's retina. J. Physiol. (Lond.) 240, 397–419.

Brown, D. A., Abogadie, F. C., Allen, T. G., Buckley, N. J., Caulfield, M. P., Delmas, P., Haley, J. E., Lamas, J. A., and Selyanko, A. A. 1997. Muscarinic mechanisms in nerve cells. Life Sci. 60, 1137–1144.

Callaway, E. M. and Wiser, A. K. 1996. Contributions of individual layer 2–5 spiny neurons to local circuits in macaque primary visual cortex. Vis. Neurosci. 13, 907–922.

Casagrande, V. A. and Norton, T. T. 1991. Lateral Geniculate Nucleus: A Review of its Physiology and Function. In: Vision and Visual Dysfunction (*ed*. A. G. Leventhal), pp. 41–84. MacMillan Press.

Casagrande, V. A. and Xu, X. 2004. Parallel Visual Pathways: A Comparative Perspective. In: The Visual Neurosciences (*eds*. L. M. Chalupa and J. S. Werner), pp. 494–506. MIT Press.

Castro-Alamancos, M. A. and Connors, B. W. 1997. Thalamocortical synapses. Prog. Neurobiol. 51, 581–606.

Chance, F. S., Abbott, L. F., and Reyes, A. 2002. Gain modulation from background synaptic input. Neuron 35, 773–782.

Cleland, B. G. and Levick, W. R. 1974. Brisk and sluggish concentrically organized ganglion cells in the cat's retina. J. Physiol. (Lond.) 240, 421–456.

Conn, P. J. and Pin, J. P. 1997. Pharmacology and functions of metabotropic glutamate receptors. Annu. Rev. Pharmacol. Toxicol. 37, 205–237.

Datta, S. and Siwek, D. F. 2002. Single cell activity patterns of pedunculopontine tegmentum neurons across the sleep-wake cycle in the freely moving rats. J. Neurosci. Res. 70, 611–621.

Denning, K. S. and Reinagel, P. 2005. Visual control of burst priming in the anesthetizedlateral geniculate nucleus. J. Neurosci. 25, 3531–3538.

Enroth-Cugell, C. and Robson, J. G. 1966. The contrast sensitivity of retinal ganglion cells of the cat. J. Physiol. (Lond.) 187, 517–552.

Ferster, D. and LeVay, S. 1978. The axonal arborizations of lateral geniculate neurons in the striate cortex of the cat. J. Comp. Neurol. 182, 923–944.

Friedlander, M. J., Lin, C.-S., Stanford, L. R., and Sherman, S. M. 1981. Morphology of functionally identified neurons in lateral geniculate nucleus of the cat. J. Neurophysiol. 46, 80–129.

Gil, Z., Connors, B. W., and Amitai, Y. 1999. Efficacy of thalamocortical and intracortical synaptic connections: quanta, innervation, and reliability. Neuron 23, 385–397.

Gilbert, C. D. 1977. Laminar differences in receptive field properties of cells in cat primary visual cortex. J. Physiol. (Lond.) 268, 391–421.

Guillery, R. W. 2003. Branching thalamic afferents link action and perception. J. Neurophysiol. 90, 539–548.

Guillery, R. W. 2005. Anatomical pathways that link action to perception. Prog. Brain Res. 49, 235–256.

Hamos, J. E., Van Horn, S. C., and Sherman, S. M. 1986. Synaptic circuitry of an individual retinogeniculate axon from a retinal Y-cell. Soc. Neurosci. 12, 1037.

Hendry, S. H. and Calkins, D. J. 1998. Neuronal chemistry and functional organization in the primate visual system. Trends Neurosci. 21, 344–349.

Hendry, S. H. C. and Reid, R. C. 2000. The koniocellular pathway in primate vision. Annu. Rev. Neurosci. 23, 127–153.

Hochstein, S. and Shapley, R. M. 1976. Linear and non-linear subunits in Y cat retinal ganglion cells. J. Physiol. (Lond.) 262, 265–284.

Kelly, L. R., Li, J., Carden, W. B., and Bickford, M. E. 2003. Ultrastructure and synaptic targets of tectothalamic terminals in the cat lateral posterior nucleus. J. Comp. Neurol. 464, 472–486.

Humphrey, A. L., Sur, M., Uhlrich, D. J., and Sherman, S. M. 1985. Projection patterns of individual X- and Y-cell axons from the lateral geniculate nucleus to cortical area 17 in the cat. J. Comp. Neurol. 233, 159–189.

Isayama, T., Berson, D. M., and Pu, M. 2000. Theta ganglion cell type of cat retina. J. Comp. Neurol. 417, 32–48.

Jahnsen, H. and Llinás, R. 1984a. Electrophysiological properties of guinea-pig thalamic neurones: an *in vitro* study. J. Physiol. (Lond.) 349, 205–226.

Jahnsen, H. and Llinás, R. 1984b. Ionic basis for the electroresponsiveness and oscillatory properties of guinea-pig thalamic neurones *in vitro*. J. Physiol. (Lond.) 349, 227–247.

Kaas, J. H., Guillery, R. W., and Allman, J. M. 1972. Some principles of organization in the dorsal lateral geniculate nucleus. Brain Behav. Evol. 6, 253–299.

LaBerge, D. and Buchsbaum, M. S. 1990. Positron emission tomographic measurements of pulvinar activity during an attention task. J. Neurosci. 10, 613–619.

LeVay, S. and Ferster, D. 1977. Relay cell classes in the lateral geniculate nucleus of the cat and the effects of visual deprivation. J. Comp. Neurol. 172, 563–584.

LeVay, S. and McConnell, S. K. 1982. ON and OFF layers in the lateral geniculate nucleus of the mink. Nature 300, 350–351.

Lesica, N. A. and Stanley, G. B. 2004. Encoding of natural scene movies by tonic and burst spikes in the lateral geniculate nucleus. J. Neurosci. 24, 10731–10740.
Leventhal, A. G., Rodieck, R. W., and Dreher, B. 1981. Retinal ganglion cell classes in the old world monkey: morphology and central projections. Science 213, 1139–1142.
Li, J. L., Wang, S. T., and Bickford, M. E. 2003. Comparison of the ultrastructure of cortical and retinal terminals in the rat dorsal lateral geniculate and lateral posterior nuclei. J. Comp. Neurol. 460, 394–409.
MacLean, J. N., Watson, B. O., Aaron, G. B., and Yuste, R. 2005. Internal dynamics determine the cortical response to thalamic stimulation. Neuron 48, 811–823.
Martin, P. R. 1998. Colour processing in the primate retina: recent progress. J. Physiol. 513, 631–638.
Martin, P. R., White, A. J., Goodchild, A. K., Wilder, H. D., and Sefton, A. E. 1997. Evidence that blue-on cells are part of the third geniculocortical pathway in primates. Eur. J. Neurosci. 9, 1536–1541.
Mott, D. D. and Lewis, D. V. 1994. The pharmacology and function of central GABAB receptors. Int. Rev. Neurobiol. 36, 97–223.
Nicoll, R. A., Malenka, R. C., and Kauer, J. A. 1990. Functional comparison of neurotransmitter receptor subtypes in mammalian central nervous system. Physiol. Rev. 70, 513–565.
O'Keefe, L. P., Levitt, J. B., Kiper, D. C., Shapley, R. M., and Movshon, J. A. 1998. Functional organization of owl monkey lateral geniculate nucleus and visual cortex. J. Neurophysiol. 80, 594–609.
Olshausen, B. A., Anderson, C. H., and Van Essen, D. C. 1993. A neurobiological model of visual attention and invariant pattern recognition based on dynamic routing of information. J. Neurosci. 13, 4700–4719.
Pin, J. P. and Duvoisin, R. 1995. The metabotropic glutamate receptors: structure and functions. Neuropharmacology 34, 1–26.
Recasens, M. and Vignes, M. 1995. Excitatory amino acid metabotropic receptor subtypes and calcium regulation. Ann. N. Y. Acad. Sci. 757, 418–429.
Reichova, I. and Sherman, S. M. 2004. Somatosensory corticothalamic projections: distinguishing drivers from modulators. J. Neurophysiol. 92, 2185–2197.
Rodieck, R. W. 1979. Visual pathways. Annu. Rev. Neurosci. 2, 193–225.
Shapley, R. and Lennie, P. 1985. Spatial frequency analysis in the visual system. Annu. Rev. Neurosci. 8, 547–583.
Sherman, S. M. 1982. Parallel Pathways in the Cat's Geniculocortical System: W-, X-, and Y-cells. In: Changing Concepts of the Nervous System (*eds*. A. R. Morrison and P. L. Strick), pp. 337–359.. Academic Press.
Sherman, S. M. 1985. Functional Organization of the W-, X-, and Y-Cell Pathways in the Cat: A Review and Hypothesis. In: Progress in Psychobiology and Physiological Psychology (*eds*. J. M. Sprague and A. N. Epstein), Vol. 11, pp. 233–314. Academic Press.
Sherman, S. M. 2001. Tonic and burst firing: dual modes of thalamocortical relay. Trends Neurosci. 24, 122–126.
Sherman, S. M. 2005. Thalamic relays and cortical functioning. Prog. Brain Res. 149, 107–126.
Sherman, S. M. and Guillery, R. W. 1996. The functional organization of thalamocortical relays. J. Neurophysiol. 76, 1367–1395.
Sherman, S. M. and Guillery, R. W. 1998. On the actions that one nerve cell can have on another: distinguishing ''drivers'' from ''modulators''. Proc. Natl. Acad. Sci. U. S. A. 95, 7121–7126.
Sherman, S. M. and Guillery, R. W. 2001. Exploring the Thalamus. Academic Press.
Sherman, S. M. and Guillery, R. W. 2006. Exploring the Thalamus and its Role in Cortical Function, 2nd edn. MIT Press.
Sherman, S. M. and Spear, P. D. 1982. Organization of visual pathways in normal and visually deprived cats. Physiol. Rev. 62, 738–855.
Silveira, L. C. L., Lee, B. B., Yamada, E. S., Kremers, J., Hunt, D. M., Martin, P. R., and Gomes, F. L. 1999. Ganglion cells of a short-wavelength-sensitive cone pathway in new world monkeys: morphology and physiology. Vis. Neurosci. 16, 333–343.
Stanford, L. R., Friedlander, M. J., and Sherman, S. M. 1983. Morphological and physiological properties of geniculate W-cells of the cat: a comparison with X- and Y-cells. J. Neurophysiol. 50, 582–608.
Steriade, M. and Contreras, D. 1995. Relations between cortical and thalamic cellular events during transition from sleep patterns to paroxysmal activity. J. Neurosci. 15, 623–642.
Stratford, K. J., Tarczy-Hornoch, K., Martin, K. A. C., Bannister, N. J., and Jack, J. J. B. 1996. Excitatory synaptic inputs to spiny stellate cells in cat visual cortex. Nature 582, 258–261.
Stryker, M. P. and Zahs, K. R. 1983. On and off sublaminae in the lateral geniculate nucleus of the ferret. J. Neurosci. 3, 1943–1951.
Swadlow, H. A. and Gusev, A. G. 2001. The impact of 'bursting' thalamic impulses at a neocortical synapse. Nat. Neurosci. 4, 402–408.
Van Essen, D. C. 2005. Corticocortical and thalamocortical information flow in the primate visual system. Prog. Brain Res. 149, 173–185.
Van Hooser, S. D., Heimel, J. A. F., and Nelson, S. B. 2003. Receptive field properties and laminar organization of lateral geniculate nucleus in the gray squirrel (*Sciurus carolinensis*). J. Neurophysiol. 90, 3398–3418.
Van Horn, S. C. and Sherman, S. M. 2004. Differences in projection patterns between large and small corticothalamic terminals. J. Comp. Neurol. 475, 406–415.
Wang, W., Jones, H. E., Andolina, I. M., Salt, T. E., and Sillito, A. M. 2006. Functional alignment of feedback effects from visual cortex to thalamus. Nat. Neurosci. 9, 1330–1336.
Weyand, T. G., Boudreaux, M., and Guido, W. 2001. Burst and tonic response modes in thalamic neurons during sleep and wakefulness. J. Neurophysiol. 85, 1107–1118.
Wilson, J. R., Friedlander, M. J., and Sherman, S. M. 1984. Fine structural morphology of identified X- and Y-cells in the cat's lateral geniculate nucleus. Proc. R. Soc. Lond. (Biol.) 221, 411–436.
Zhan, X. J., Cox, C. L., Rinzel, J., and Sherman, S. M. 1999. Current clamp and modeling studies of low threshold calcium spikes in cells of the cat's lateral geniculate nucleus. J. Neurophysiol. 81, 2360–2373.

Further Reading

Zhan, X. J., Cox, C. L., and Sherman, S. M. 2000. Dendritic depolarization efficiently attenuates low threshold calcium spikes in thalamic relay cells. J. Neurosci. 20, 3909–3914.

1.29 Functional Maps in Visual Cortex: Topographic, Modular, and Columnar Organizations

D J Felleman, University of Texas Medical School, Houston, TX, USA

© 2008 Elsevier Inc. All rights reserved.

1.29.1	**Topographic Maps in Macaque Visual Cortex**	578
1.29.2	**Functional Organization of Area V1: Anatomical Modules and Functional Maps**	578
1.29.2.1	Cytochrome Oxidase Modules	580
1.29.2.2	Ocular Dominance Maps	580
1.29.2.3	Orientation Maps	580
1.29.2.4	Hue Maps	580
1.29.2.5	Spatial Frequency and Direction Maps	582
1.29.2.6	Interrelationships Among V1 Functional Maps	582
1.29.2.7	Multiple Interdependent Feature Maps or One Spatiotemporal Energy Map?	583
1.29.3	**Modular Organization of Area V2**	583
1.29.3.1	Color, Hue, and Luminance-Change Maps	583
1.29.3.2	Contour Maps	584
1.29.3.3	Disparity and Motion Maps	585
1.29.4	**Modular Organization of Area V4**	585
1.29.4.1	V4 Functional Imaging	585
1.29.4.2	V4 Modular Cortical Connections	585
1.29.5	**Modular Organization of Area MT**	588
1.29.5.1	MT Single-Unit Mapping	588
1.29.5.2	MT Functional Maps	589
1.29.5.3	MT Functional Architecture and Projections	589
1.29.6	**Modular Organization of Inferotemporal Cortex**	589
1.29.6.1	Inferotemporal Areas	589
1.29.6.2	Inferotemporal Anatomical Modules and Connections	590
1.29.6.3	Inferotemporal Functional Imaging	590
1.29.6.4	Inferotemporal Functional Modules	590
1.29.7	**Summary and Conclusions**	591
References		591

Glossary

CO Cytochrome oxidase.
FST Floor of the superior temporal sulcus visual area (FSTd and FSTv subdivisions).
IT Inferotemporal cortex.
MST Middle superior temporal visual area.
MT Middle temporal visual area.
PITd Posterior inferotemporal dorsal visual area.
PITv Posterior inferotemporal ventral visual area.
TEad Anterior dorsal temporal visual area.
TEav Anterior ventral temporal visual area.
TEO Temporal occipital transitional visual area.
TEpd Posterior dorsal temporal visual area.
TEpv Posterior ventral temporal visual area.
V1 Primary visual cortex; striate cortex.
V2 Visual area 2.
V3 Visual area 3 (also known as V3d).
V3A Visual area V3A.
V4 Visual area 4.
VP Ventral posterior visual area (also known as V3v).

1.29.1 Topographic Maps in Macaque Visual Cortex

One of the defining features of visual cortical areas is a systematic representation of the visual field. Traditionally, microelectrode mapping has been used to determine the relationship between cortical location and receptive field position in the visual field. Cortical maps are described as first-order transformations of the visual field if adjacent points in visual space are mapped to adjacent loci in cortex (e.g., V1). In second-order transformations, the representation of visual space is often split along the representation of the horizontal meridian such that lower fields are generally represented in dorsal cortex and upper fields are represented in ventral cortex (e.g., V2 and V3/VP). Visual field sign has also been used to describe the topography of visual areas. This gradient description of topography is useful in describing the borders between areas that are sampled with low density or that have a somewhat complex internal organization (see Sereno, M. *et al.*, 1994). The topography of any given cortical area can be described by (1) its cortical magnification function (millimeter of cortex/degree of visual angle), (2) the degree of anisotropy of this magnification function (iso-polar vs. iso-eccentricity magnification factor), (3) the proportion of the visual field represented, (4) the topographic order of its representation (first or second order), and (5) its visual field sign.

Functional imaging offers a high-resolution method of topographic mapping in convoluted and buried cortex. In a now famous experiment, 2-deoxyglucose (2-DG) imaging of the topographic organization of macaque striate cortex allowed for precise measurements of cortical magnification factor and anisotropy (Tootell, R. B. H. *et al.*, 1988a; 1988b). In this 2-DG experiment, the monkey monocularly viewed a series of concentric rings and linking rays (Figure 1(a)) while 2-DG was infused. The labeled portions of V1 preferentially accumulated the 2-DG due to their metabolic demand. Figure 1(b) illustrates the representation of this stimulus pattern on an autoradiographic section of the flattened operculum of V1. This experiment provided a direct determination of the cortical magnification factor in foveal and parafoveal striate cortex.

More recently, functional magnetic resonance imaging (fMRI) has been widely applied to determine the topographic organizations and extents of many cortical areas (e.g., Brewer, A. A. *et al.*, 2002; Fize, D. *et al.*, 2003; Tootell, R. B. H. *et al.*, 2004). In general, phase encoding of MR signals, generated in response to sweeping checkerboard sectors or expanding/contracting rings, has become the *de facto* tool for topographic mapping of visual cortex in monkeys and humans (e.g., Sereno, M. I. *et al.*, 1995; DeYoe, E. A. *et al.*, 1996). The remaining portions of Figure 1 illustrate topographic mapping of large portions of macaque visual cortex using this fMRI paradigm. In these experiments, cortical voxels preferentially activated by different stimulus conditions are color coded by stimulus condition and illustrated on unfolded cortical surface maps (Figures 1(c)–1(g)) or on an inflated three-dimensional (3D) cortical surface (Figure 1(h)). In Figure 1(c), three maps are illustrated that indicate the representations of the vertical (blue) and horizontal (yellow) meridian (left panel); foveal (yellow), parafoveal (yellow), and peripheral (blue) visual fields (middle panel); and upper (blue) and lower (yellow) visual fields (right panel). These maps provide a compact representation of a large amount of topographic data and demonstrate that a large portion of occipital and parietal cortex is topographically organized. Figures 1(d)–1(g) illustrate more-detailed views of the representation of polar angle (Figures 1(d) and 1(f)) and eccentricity (Figures 1(e) and 1(g)) at posterior visual cortex (Figures 1(d) and (e)) and occipitotemporal cortex (Figures 1(f)–1(g)). Finally, Figure 1(h) illustrates the projection of these color-coded fMRI activations on a 3D surface reconstruction of the full left hemisphere that was illustrated in Figure 1(g). This method of topographic mapping has proven essential for linking functional activations to specific topographically organized visual areas and for the analysis of less well-understood portions of visual cortex.

1.29.2 Functional Organization of Area V1: Anatomical Modules and Functional Maps

A large number of functional parameters are mapped spatially within primary visual cortex, V1, including ocular dominance, orientation, and hue. Other parameters, such as spatial frequency, temporal frequency, and direction, may also be mapped within V1 of some species (e.g., direction of motion in ferret V1; e.g., Yu, H. *et al.*, 2005), but the evidence of the mapping in macaque monkeys is incomplete. Nevertheless, macaque primary visual cortex has proven to be a model system for understanding how

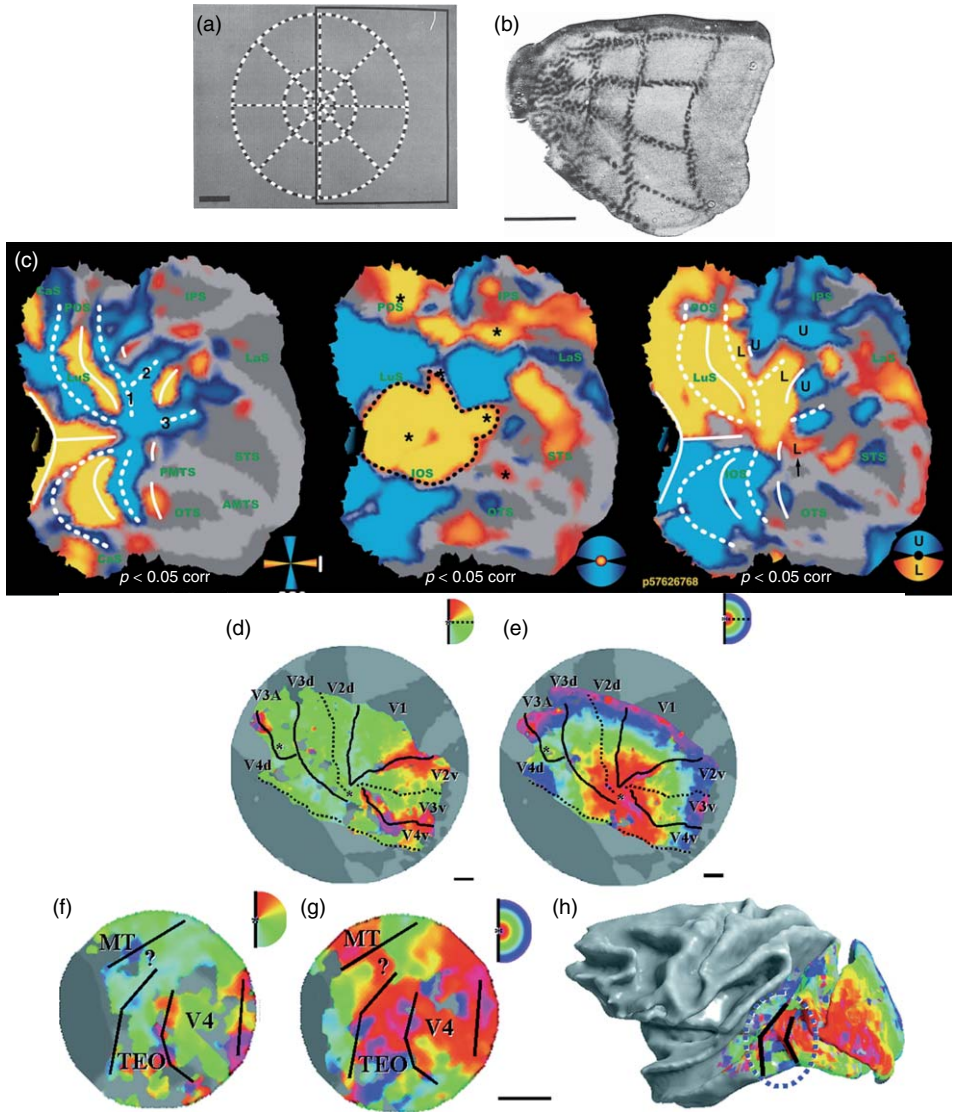

Figure 1 Topographic organization of visual cortex. (a) Visual stimulus of concentric circles and rays used on 2-deoxyglucose (2-DG) mapping of visual topography in macaque V1. From Tootell, R. B. H., Silverman, M. S., Hamilton, S. L., Switkes, E., and De Valois, R. L. 1988a. Functional anatomy of macaque striate cortex. V. Spatial frequency. J. Neurosci. 8, 1610–1624; Tootell R. B. H., Switkes, E., Silverman, M. S., and Hamilton S. L. 1988b. Functional anatomy of macaque striate cortex. II. Retinotopic organization. J. Neurosci. 8, 1531–1568; (figure 1). (b) 2-DG pattern in flattened macaque striate cortex resulting from visual stimulus shown in (a). From Tootell, R. B. H., Silverman, M. S., Hamilton, S. L., Switkes, E., and De Valois, R. L. 1988a. Functional anatomy of macaque striate cortex. V. Spatial frequency. J. Neurosci. 8, 1610–1624; Tootell, R. B. H., Switkes, E., Silverman, M. S. and Hamilton, S.L. 1988b. Functional anatomy of macaque striate cortex. II. Retinotopic organization. J. Neurosci. 8, 1531–1568; (figure 2). (c) Functional magnetic resonance imaging of visual topography displayed on unfolded cortical maps of macaque cortex. Left: Vertical (blue) and horizontal (yellow) median stimulation. Middle: Foveal (yellow), parafoveal (red), and peripheral (blue) stimulation. Right: Upper field (blue), upper field periphery (purple), lower field (yellow), and upper field periphery (red). From Fize, D., Vanduffel, W., Nelissen, K., Denys, K., Chef d'Hotel, C., Faugeras, O. and Orban, G. A. 2003. The retinotopic organization of primate dorsal V4 and surrounding areas: a functional magnetic resonance imaging study in awake monkeys. J. Neurosci. 23, 7395–7406; (figure 11A–D). (d) Representation polar angle in occipital areas V1, V2, V3, and V3A. From Brewer, A. A., Press, W. A., Logothetis, N. K. and Wandell, B. A. 2002. Visual areas in macaque cortex measured using functional magnetic resonance imaging. J. Neurosci. 22, 10416–10426; (figure 8a). (e) Representation of eccentricity in occipital areas V1, V2, V3, and V3A. From Brewer, A. A., Press, W. A., Logothetis, N. K. and Wandell, B. A. 2002. Visual areas in macaque cortex measured using functional magnetic resonance imaging. J. Neurosci. 22, 10416–10426. (figure 8b). Representation of polar angle (f) and eccentricity (g) in anterior occipital and posterior inferotemporal areas V4, MT, and TEO. From Brewer, A. A., Press, W. A., Logothetis, N. K. and Wandell, B. A. 2002. Visual areas in macaque cortex measured using functional magnetic resonance imaging. J. Neurosci. 22, 10416–10426. (figure 14a and b). (h) Partially unfolded surface representation of the functional activations observed in (d–g). From Brewer, A. A., Press, W. A., Logothetis, N. K. and Wandell, B. A. 2002. Visual areas in macaque cortex measured using functional magnetic resonance imaging. J. Neurosci. 22, 10416–10426; (figure 14c).

multiple, functional maps are represented within a single cortical sheet. These investigations have led to new theoretical considerations of the benefits and limitations of such multiparameter mapping within cerebral cortex (e.g., Swindale, N. V., 2000; Malach, R., 1994; Basole, A. *et al.*, 2003; Chklovskii, D. B. and Koulakov, A. A., 2004).

1.29.2.1 Cytochrome Oxidase Modules

Supragranular V1 is organized into cytochrome oxidase (CO)-dense blob and pale interblob regions (Figure 2(a); see Horton, J. C. and Hubel, D. H., 1981). These anatomically defined modules are also distinguished by distinct patterns of inputs from the lateral geniculate nucleus (e.g., Hendry, S. H. and Reid, R. C., 2000), distinct intracortical connections (e.g., Yabuta, N. H. and Callaway, E. M., 1998), distinct projections to extrastriate cortical areas (Sincich, L. C. and Horton, J. C., 2002; Xiao, Y. and Felleman, D. J., 2004), and different functional properties of their constituent neurons (e.g., Landisman, C. E. and Ts'o, D. Y., 2002b). Neurons within the CO blobs tend to lack orientation selectivity and many are color selective, with some displaying dual-opponent receptive fields (e.g., Livingstone, M. S. and Hubel, D. H., 1984), while other cells had color-opponent centers with broadband suppressive surrounds (modified type II; e.g., Ts'o, D. Y. and Gilbert, C. D., 1988). The discovery of CO blobs provided the first clear architectural feature of visual cortex that underlies a functional modular architecture.

1.29.2.2 Ocular Dominance Maps

Projections from the lateral geniculate nucleus are segregated within layer IV (layers IVCα, IVCβ, and IVA for LGN parvocellular and magnocellular inputs) and within layers II–III (for konicellular layer inputs). These inputs form a complex interdigitating 'zebra stripe'-like pattern that can be visualized using anatomical transneuronal transport of tracers following eye injection (e.g., LeVay, S. *et al.*, 1985), histochemical localization of downregulated CO activity following monocular enucleation (e.g., Horton, J. C. and Hocking, D. R., 1998), or by functional imaging of eye dominance domains using alternating monocular stimulation (e.g., Ts'o, D. Y. *et al.*, 1990; Xiao, Y. *et al.*, 1999; 2003). Figure 2b illustrates the V1 ocular dominance pattern in a differential imaging using optical recording of intrinsic cortical signals following alternating monocular stimulation of a multioriented luminance contrast stimulus. V1 is characterized by an alternative banding of ~0.5 mm wide zebra stripes that reflect the segregated projections of monocular inputs from alternating layers of the lateral geniculate nucleus. V1 ocular dominance stripes run roughly perpendicular to the V1–V2 border at which they then end abruptly since V2 is almost completely binocular.

1.29.2.3 Orientation Maps

Neurons located within the CO pale interblob regions tend to be orientation selective and adjacent neurons tend to prefer similar orientations. Furthermore, preferred orientation is mapped systematically across the cortical surface such that large iso-orientation domains that prefer similar orientations are arranged around pinwheel centers (singularities) and fractures in which preferred orientation changes rapidly. This systematic mapping of orientation and its relationship to the color-selective CO blobs is best demonstrated using functional imaging of intrinsic cortical signals (e.g., Bartfeld, E. and Grinvald, A., 1992; Blasdell, G. G., 1992) as illustrated in Figure 2(c). More recently, the visualization of orientation preference has been extended to the cellular level using *in vivo* dual-photon calcium imaging which demonstrated the precision of orientation preference extending up to the pinwheel centers which lack orientation tuning (e.g., Okhi, K. *et al.*, 2005).

1.29.2.4 Hue Maps

Although it has long been recognized that V1 CO blobs tend to contain a high proportion of color-selective cells, there has been little evidence for color differences between blobs (e.g., Landisman, C. E. and Ts'o, D. Y., 2002a; 2002b) or within individual blobs. Recently, however, intrinsic cortical imaging has demonstrated that the peak activation locus for individual hues shifts systematically within individual CO blobs (Figure 2(d); Xiao, Y. *et al.*, 2007). Although there is considerable overlap between the loci within blobs activated by specific hues, these data indicate that the first cortical representation of hue occurs at the level of V1 blobs. Furthermore, these data suggest that the perception of a specific hue is coded by the spatial locus of the peak neuronal population response.

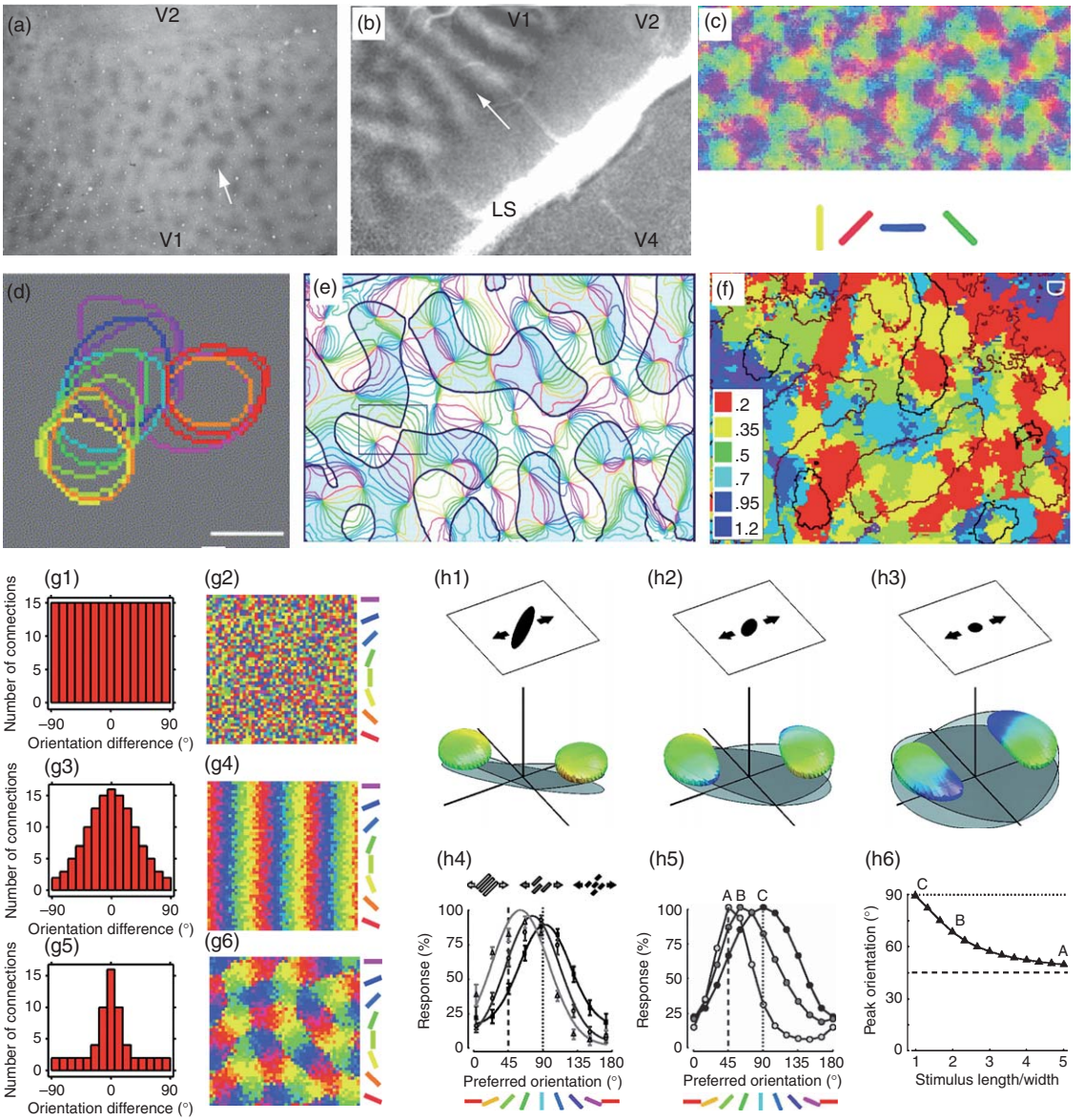

Figure 2 Functional maps and cortical modules in area V1. (a) Cytochrome oxidase blobs (arrow) in flattened macaque V1. (b) Differential intrinsic optical image of left and right eye monocular stimulation reveals the zebra-stripe-like pattern of dominance in macaque V1. V2 and V4 appear as homogeneous gray due to their complete intermixing of left and right eye signals. (c) Intrinsic optical imaging of activity induced by stimulation with four different orientations reveals an orientation selectivity map. From Landisman, C. E. and Ts'o, D. Y. 2002a. Color processing in macaque striate cortex: relationships to ocular dominance, cytochrome oxidase, and orientation. J. Neurophysiol. 87, 3126–3137; (figure 5). (d) Representation of statistically significant, peak cortical activity in response to isoluminant hue stimulation within a V1 blob. Scale: 100 μm. From Xiao, Y., Casti, A., Xiao, J., and Kaplan, E. 2007. Hue maps in primate striate cortex. NeuroImage. 35, 771–786; (figure 2a). (e) Interrelationship between ocular dominance (black contours) and orientation preference (colored contours) in cat V1. From Hübener, M., Shoham, D., Grinvald, A., and Bonhoeffer, T. 1977. Spatial relationships among three columnar systems in cat area 17. J. Neurosci. 17, 9270–9284; (figure 4). (f) Representation of spatial frequency preference in cat V1. From Issa, N. P., Trepel, C., and Stryker, M. P. 2000. Spatial frequency maps in cat visual cortex. J. Neurosci. 20, 8504–8514; (figure 6d). (g) Modeling of the effects of various distributions of orientation-specific connections (g1, g3, and g5) on the resultant orientation preference maps (g2, g4, and g6). From Chklovskii, D. B., and Koulakov, A. A. 2004. Maps in the brain: what can we learn from them? Annu. Rev. Neurosci. 27, 369–392; (figure 10). (h) The effects of varying stimulus length on the spatiotemporal energy distribution (h1–h3). Effects of varying stimulus length on the distribution of orientation-specific activations in cat V1. h4, experimental results. h5, modeling results (h6). Distribution of peak orientation activation as a function of stimulus length. From Mante, V., Carandini, M. 2005. Mapping of stimulus energy in primary visual cortex. J. Neurophysiol. 94, 788–798; (figure 5).

1.29.2.5 Spatial Frequency and Direction Maps

In addition to the systematic mapping of ocular dominance and orientation, V1 of some species also contains systematic maps of spatial frequency and direction of motion (e.g., Weliky, M. *et al.*, 1996; Hübener, M. *et al.*, 1997). Evidence for a columnar and tangential mapping of spatial frequency was first observed in macaque V1 using the 2-DG technique (Tootell, R. B. H. *et al.*, 1981; 1988a; 1988b). Subsequent optical imaging of spatial frequency preference in cat V1 has demonstrated highly ordered maps organized around pinwheels (e.g., Everson, R. M. *et al.*, 1998), continuous spatial frequency maps not organized around pinwheels (e.g., Figure 2(e); Issa, N. P. *et al.*, 2000), or binary spatial frequency maps that simply segregate domains preferring high and low spatial frequencies (e.g., Hübener, M. *et al.*, 1997; Shoham, D. *et al.*, 1997). Furthermore, on methodological grounds, Sirovich L. and Uglesich R. (2004) argued that all cat V1 cortical columns contain both high and low spatial frequency components and thus they are not spatially segregated across the cortical surface. The differences between these conclusions seem to be due to differences in experimental design and analysis largely concerning whether spatial frequency preference is determined across an average of all orientations or only at each pixel's preferred orientation.

1.29.2.6 Interrelationships Among V1 Functional Maps

The relationships among the retinotopic, orientation, ocular dominance, direction, color, and spatial frequency maps in V1 have received considerable experimental and theoretical attention (e.g., Hübener, M. *et al.*, 1997; Mante, V. and Carandini, M., 2005; Yu, H. *et al.*, 2005). In the original 'ice-cube' model of V1, microelectrode recording was used to support the view that each point image in V1 contained a regular progression of orientation slabs (Hubel, D. H. and Wiesel, T. N., 1977). With the advent of intrinsic signal optical imaging, it became possible to visualize the orientation map and to correlate its detailed structure of singularities, fractures, and iso-orientation domains to the coincident ocular dominance pattern (e.g., Hübener, M. *et al.*, 1997). Figure 2(f) supports the conclusion that in the cat, orientation singularities are generally located near the center of ocular dominance stripes and that iso-orientation contours intersect ocular dominance borders at right angles.

The specific relationships among retinotopic, orientation, ocular dominance, and spatial frequency maps were quantitatively examined in ferret V1, which provides the additional constraint of a distinct topographic anisotropy (Yu, H. *et al.*, 2005). When expressed as map feature gradients, previous modeling and experimental data from isotropic visual cortex supported the view that, when two maps interact, the steep gradient of one feature (e.g., ocular dominance) intersects with the low gradient of the other map feature (e.g., iso-orientation). However, in the topologically anisotropic ferret V1, the prediction of two maps intersecting at right angles is unexpected. Yet, the modeling and experimental data from anisotropic ferret V1 demonstrate that for any two maps, the highest gradient regions tend to avoid each other, but they tend not to intersect at right angles to each other (Yu, H. *et al.*, 2005).

In general, CO blobs (and thus hue maps) are centered within ocular dominance stripes (e.g., Bartfeld, E. and Grinvald, A., 1992). However, despite the view that blobs are generally nonoriented, orientation map singularities do not necessarily align with CO blobs (e.g., Landisman, C. E. and Ts'o D. Y., 2002a). Whereas maps of spatial frequency preference have been observed in cat and ferret V1 (e.g., Hübener, M. *et al.*, 1997; Yu, H. *et al.*, 2005), such maps have not been observed in macaque V1, and thus, their potential relationships to CO blobs, orientation maps, and the retinotopic map remain to be determined.

The above discussion of the relationships among the different functional maps suggests that V1 is organized to optimize uniform coverage of neuronal properties at each point image within cortex (e.g., Swindale, N. V., 2000). According to this view, the representations of visual space and feature maps are constrained by the opposing forces of the desirability for adjacent cortical loci to have similar receptive field properties (continuity) and by the desirability for all combinations of stimulus feature maps to be distributed uniformly over visual space (completeness). On theoretical groups, this coverage has been viewed as the consequence of the constraints imposed by dimension reduction.

What constrains the organization of cortical maps? One theory concerns the optimization of 'wiring' length such that neurons with similar receptive field properties (i.e., orientation) are interconnected with the minimal distance as constrained by retinotopic requirements. For example, modeling experiments

by Chklovskii D. B. and Koulakov A. A. (2004) demonstrated that nonbiased orientation connections predict a salt-and-pepper orientation map (Figures 2(g1)–2(g2)), whereas the orientation pinwheel pattern is a consequence of the restricted fan-out of local orientation connections (Figures 2(g5)–2(g6)).

1.29.2.7 Multiple Interdependent Feature Maps or One Spatiotemporal Energy Map?

According to the completeness constraint, a specific combination of stimulus features (as represented in the intersection of multiple, interdependent cortical maps) produces a unique cortical population response, thus supporting the view of a 'place code' for feature representation. The results of multiple optical imaging studies using extended sine wave gratings have supported this view (see above). However, experiments using iso-oriented line segments, varying in length, axis of motion, and speed, have critically challenged this view (Basole, A. *et al.*, 2003). For example, varying the lengths of the bar elements produced a systematic shift in the cortical activation pattern (Figure 2(h4)), a result that was not predicted from a simple orientation-specific activation pattern. Conversely, these experiments demonstrated that a specific cortical activation pattern could be produced by a range of stimuli differing in length, speed, and axis of motion. These results and subsequent modeling experiments (Mante, V. and Carandini, M., 2005) suggest that the cortical population response is better interpreted by a stimulus energy model in which cortical neurons filter the stimulus over restricted regions of 3D frequency space (orientation, spatial, and temporal frequency). According to this model, the reason that the cortical activation pattern varies with changes in iso-orientation bar length (or speed and axis of motion) is that these stimuli differ in their representations in 3D frequency space (Figure 2(h)).

1.29.3 Modular Organization of Area V2

Area V2, like area V1, has a modular architecture defined by the pattern of CO activity. Whereas V1 consists of an interdigitating array of CO blobs anchored to the centers of ocular dominance columns, V2 is characterized by a repeating triplet of CO stripes: CO-dense thick stripes, CO-dense thin stripes, and CO pale interstripes (Figure 3(a)). These stripe triplets, which number approximately 17 per hemisphere (Olavarria, J. F. and Van Essen, D. C., 1997), are oriented perpendicular to the V1 border, extending roughly 6–8 mm in length. Each V2 CO stripe compartment represents an arc of visual space that extends from the vertical to horizontal meridian (Roe, A. W. and Ts'o, D. Y., 1995). Visual space is represented smoothly within each of these CO compartments such that the transition from one stripe to another is characterized by an abrupt jump in receptive field position to re-represent the visual space previously represented (Roe, A. W. and Ts'o, D. Y., 1995). Overall, these V2 stripes can be distinguished by the stimulus parameters that are functionally mapped within their domains.

1.29.3.1 Color, Hue, and Luminance-Change Maps

V2 thin stripes have long been recognized to play an important role in color processing. Early single unit recording experiments identified a high concentration of color-selective cells in thin stripes (e.g., DeYoe, E. A. and Van Essen, D. C., 1985; Shipp, S. and Zeki, S., 1985; 2002), although subsequent studies failed to see large differences between stripe compartments (e.g., Levitt, J. B. *et al.*, 1994) except regarding the clustering of nonoriented, color-selective cells in thin stripes (Gegenfurtner, K. R. *et al.*, 1996). The functional clustering of color selectivity in thin stripes is best revealed in a differential 2-DG experiment that compared responses to isoluminant red-blue and luminance contrast gratings (Tootell, R. B. H. *et al.*, 2004; Figure 3(b)). In optical recording experiments, V2 thin stripes are preferentially activated in differential images in response to isoluminant red/green gratings versus luminance contrast gratings (Figure 3(c)). This result suggests that a preponderance of thin stripe neurons is selective for chromatic contrast, yet close examination of these images demonstrates that thin stripes contain both chromatic-selective (dark) and luminance-selective (bright) domains (Figure 3(d)). These domains are not selective for orientation in that chromatic or luminance gratings of different orientations activate nearly identical thin stripe loci. Within the chromatic-selective domain, individual isoluminance hue stimuli maximally activate restricted foci roughly 350 μm in diameter. Furthermore, the locations of peak activation foci shift systematically across the cortical surface, often in the order of perceptual color circle (Figure 3(e); Xiao, Y. *et al.*, 2003). Achromatic stimuli of varying luminance levels preferentially activate segregated luminance-change domains depending on whether

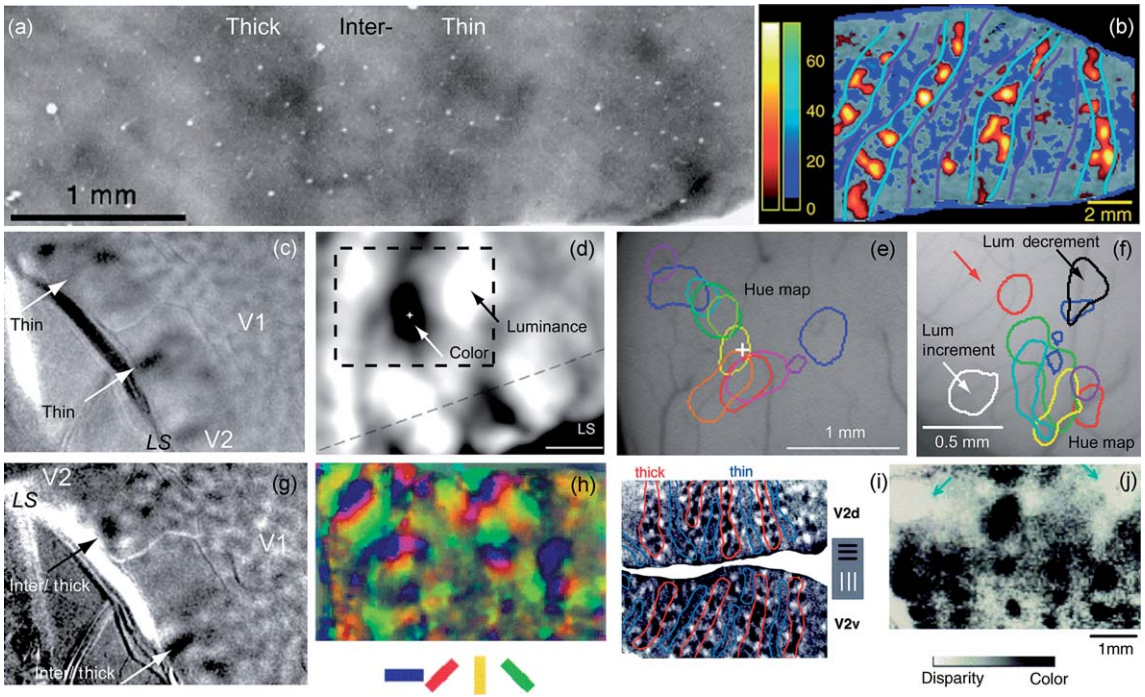

Figure 3 Functional maps and cortical modules in area V2. (a) Cytochrome oxidase thin, pale (interstripe), and thick stripes in flattened macaque V2. (b) Differential 2-deoxyglucose (2-DG) imaging of color-selective activation in flattened macaque V2. From Tootell, R. B. H., Nelissen, K., Vanduffel, W., and Orban, G. A. 2004. Search for color 'center(s)' in macaque visual cortex. Cereb. Cortex 14, 353–363; (figure 3k). (c) Color-preferring thin stripes (white arrows) in macaque V2 in differential intrinsic optical image of isoluminant red/green grating – luminance contrast grating stimulation. Color-preferring activity in V1 corresponds to cytochrome oxidase blobs. (d) High-magnification intrinsic optical image of color-preferring (white arrow) and luminance preferring (black arrow) domains in V2 thin stripe. From Xiao, Y., Wang, Y., and Felleman, D. J. 2003. Spatially organized representation of hue in macaque V2. Nature 421, 535–539; (figure 1b). (e) Optical recording of V2 thin stripe hue map in response to isoluminant hue stimulation. From Xiao, Y., Wang, Y., and Felleman, D. J. 2003. Spatially organized representation of hue in macaque V2. Nature 421, 535–539; (figure 1g). (f) Optical recording-derived contours of luminance increment-preferring (white arrow) and luminance decrement-preferring (black arrow) domains flanking the V2 thin stripe hue map. (g) Differential intrinsic optical image of orientation-specific (45–135°) activations in V2 thick/interstripes (white and black arrows). The gray area between these corresponds to the V2 thin stripe. (h) Preferred angle representation in V2 thick/interstripes from intrinsic optical recording responses to four orientations. From Ts'o, D. Y., Roe, A. W. and Gilbert, C. D. 2001. A hierarchy of the functional organization for color, form, and disparity in primate visual area V2. Vision Res. 41, 1333–1349; (figure 10b). (i) Differential 2-DG image of orientation-specific activation in dorsal (*upper panel*) and ventral (*lower panel*) V2. From Vanduffel, W., Tootell, R. B. H., Schoups, A. A. and Orban, G. A. 2002. The organization of orientation selectivity throughout macaque visual cortex. Cereb. Cortex 12, 647–662; (figure 7b). (j) Distribution of monocular and binocular domains of macaque V2 observed with optical recording. From Ts'o, D. Y., Roe, A. W. and Gilbert, C. D. 2001. A hierarchy of the functional organization for color, form, and disparity in primate visual area V2. Vision Res. 41, 1333–1349; (figure 3b).

the stimulus luminance is greater or less than the preceding background. Variations in the preceding background luminance demonstrate that the evoked optical activity represents the direction of luminance change rather than responses to a specific luminance (Wang *et al.*, 2007; Figure 3(f)).

1.29.3.2 Contour Maps

V2 thick and interstripes contain systematic maps of contour orientation. These V2 contour orientation domains are larger than those in V2 and appear to extend across thick and interstripe boundaries without clear functional borders. V2 orientation domains can be visualized in differential images of orthogonal orientation stimulation using optical recording of intrinsic cortical signals (e.g., Figure 3(g)) and a more complete pattern can be visualized using the vector sum representation of preferred orientation following stimulation with four (or more) orientations (e.g., Roe, A. W. and Ts'o, D. Y., 1995; Figure 3(h)). The full pattern of orientation selectivity in V2 is best seen

in a differential 2-DG experiment that demonstrates robust orientation-specific activity in thick and interstripes, but not in thin stripes (Figure 3(i); Vanduffel, W. *et al.*, 2002). It is interesting to note that V2 contour orientation maps appear to represent the orientation of object contours independent of the low-level feature that defines the contour. Specifically, V2 orientation maps appear nearly identical whether they are derived from luminance contrast or chromatic contrast contours. Similarly, illusory contours, defined by abutting lines, texture contrast, or motion contrast, also appear to activate similar V2 contour orientation domains (Dillenburger, B. C. *et al.*, 2006).

1.29.3.3 Disparity and Motion Maps

V2 thick stripes contain a large proportion of neurons selective for binocular disparity. Differential optical imaging for binocular versus monocular domains in macaques demonstrates disparity-selective domains that are largely, but not completely segregated from color selective domains (Figure 3(j); Ts'o, D. Y. *et al.*, 2001). Neurons centered within these obligatory-binocular compartments are selective for binocular disparity, while neurons near the borders with 'color' stripes are tuned for both color and binocular disparity. In general, the preferred orientations of neurons along 1–1.5 mm long penetrations in these obligatory-binocular stripes were highly consistent, but the preferred binocular disparity could shift systematically from near to far (e.g., Figure 7; Ts'o *et al.*, 2001). However, it remains to be determined whether this shift in preferred disparity is due to the electrode penetration crossing adjacent disparity columns or truly represents a systematic representation of disparity within a single 'disparity column'. Since thick stripes also contain orientation maps, it remains to be determined whether orientation and disparity are systematically represented in V2. Since V2 orientation domains are relatively large (e.g. 1–1.5 mm in width), it is reasonable to expect that preferred disparity is systematically represented within a submodular structure within each orientation domain.

1.29.4 Modular Organization of Area V4

Unlike areas V1 and V2, area V4 does not appear to contain a consistent pattern of CO staining, suggestive of an underlying functional modular architecture. However, functional imaging using optical recording and differential 2-DG visualization, segregated connections with V2 thin and interstripe modules, and anecdotal reports of single unit clustering suggest that V4 contains a functional architecture reminiscent of the thin and interstripe architecture of area V2.

1.29.4.1 V4 Functional Imaging

Functional imaging of hue, luminance, and orientation domains in V4 has proven to be considerably more difficult than in V1 or V2, due perhaps to the effects of anesthesia, intrinsic inhibition, or perhaps less segregation of neuronal properties. Nevertheless, optical imaging of intrinsic cortical signals has been successful in demonstrating V4 orientation modules in single differential images (Figure 4(a)) and in composite maps derived from the responses from four different orientations (Figure 4(b); Felleman, D. J. and Van Essen, D. C., 1991; Ghose, G. M. and Ts'o, D. Y., 1997). Often these orientation-specific responses appear segregated from color-specific activations (Figure 4(b)), while in other cases the orientation-selective responses extend across considerable portions of V4. This widespread pattern of orientation selectivity is more consistent with the pattern of differential orientation responses observed using 2-DG imaging (Figure 4(g); Vanduffel, W. *et al.*, 2002).

Differential optical recording of responses to isoluminant color and luminance contrast stimuli reveals punctuate activations in V4 that are larger than those in V1 (Figure 4(d)) and tend to partially overlap with orientation-specific foci (not shown). The variable size and inconsistent spacing and positions of V4 color activations are best observed in differential 2-DG studies (Figures 4(e) and 4(f)). These studies demonstrate that V4 modules preferentially activated by isoluminant color stimulation tend to be few in number and highly variable in size and thus reveal that the majority of ventral (Figure 4(e)) and dorsal (Figure 4(f)) V4 is not preferentially activated by color.

1.29.4.2 V4 Modular Cortical Connections

The segregation of V4 into functional domains dominated by orientation- or color-selective inputs is supported by studies of its inputs from the CO-defined stripes of V2. In early studies, it was observed that relatively large retrograde tracer injections into dorsal V4 could label either V2 thin or interstripes (but usually both; DeYoe, E. A. *et al.*, 1994; Felleman,

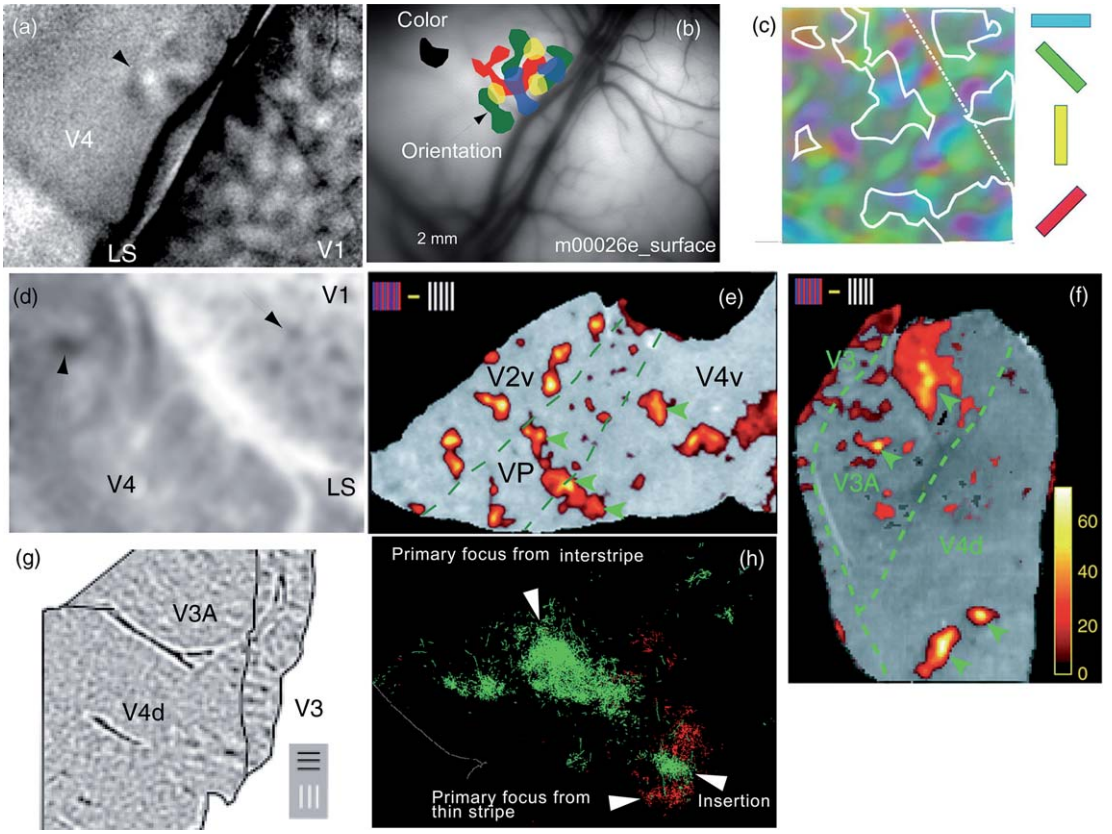

Figure 4 Functional imaging and cortical modules in area V4. (a) Optical recording of orientation-specific (45–135°) activation in area V4. (b) Surface projections of color-preferring (isoluminant red/green – luminance contrast gratings) and orientation map in area V4. (c) Orientation preference map in area V4 (left) and V2 (right). White contours represent S-zones that prefer small luminance stimuli and are suppressed with wide-field stimulation. From Ghose, G. M. Ts'o, D. Y. 1997. Form processing modules in primate area V4. J. Neurophysiol. 77, 2191–2196; (figure 3c). (d) Differential optical imaging of color-preferring foci (isoluminant red/green – luminance contrast gratings) in V4 (left) and V1 blobs (right). (e) Differential 2-deoxyglucose (2-DG) imaging of color-preferring foci in flattened ventral V4. From Tootell, R. B. H., Nelissen, K., Vanduffel, W. and Orban, G. A. 2004. Search for color 'center(s)' in macaque visual cortex. Cereb. Cortex 14, 353–363; (figure 4e). (f) Differential 2-DG imaging of color-preferring foci in flattened dorsal cortex. Area V4d contains few spatially restricted color foci while adjacent area V3A contains larger and more numerous color-preferring domains. From Tootell, R. B. H., Nelissen, K., Vanduffel, W. and Orban, G. A. 2004. Search for color 'center(s)' in macaque visual cortex. Cereb. Cortex 14, 353–363; (figure 5d). (g) Differential 2-DG imaging of orientation-specific activation in flattened dorsal cortex containing V4d, V3A, and V3. From Vanduffel, W., Tootell, R. B. H., Schoups, A. A. and Orban, G. A. 2002. The organization of orientation selectivity throughout macaque visual cortex. Cereb. Cortex 12, 647–662; (figure 12a). (h) Tangential reconstruction of V2 interstripe (green) and thin stripe (red) terminations in V4. From Xiao, Y., Zych, A., Felleman, D. J. 1999. Segregation and convergence of functionally defined V2 thin stripe and interstripe compartment projections to area V4 of macaques. Cereb. Cortex 9, 792–804; (figure 2h).

D. J. *et al.*, 1997). Furthermore, when paired injections separated by ~3 mm were made, cells labeled by the different tracers were sometimes found in the adjacent, segregated thin and interstripes. To visualize directly the size and segregation of this presumed V2 thin stripe and interstripe terminal domains in V4, distinguishable anterograde tracers were injected into adjacent V2 thin and interstripes following their functional characterization using optical imaging (Xiao, Y. *et al.*, 1999). These results indicated that V4 contains large (~12–20 mm^2) domains that receive input from either V2 thin or interstripes. Furthermore, within both the thin stripe and interstripe projection domains, small insertions of projection fields from the other stripe compartment were observed, perhaps providing the anatomical basis for functional interactions between these two cortical streams (Figure 4(h)). This modular

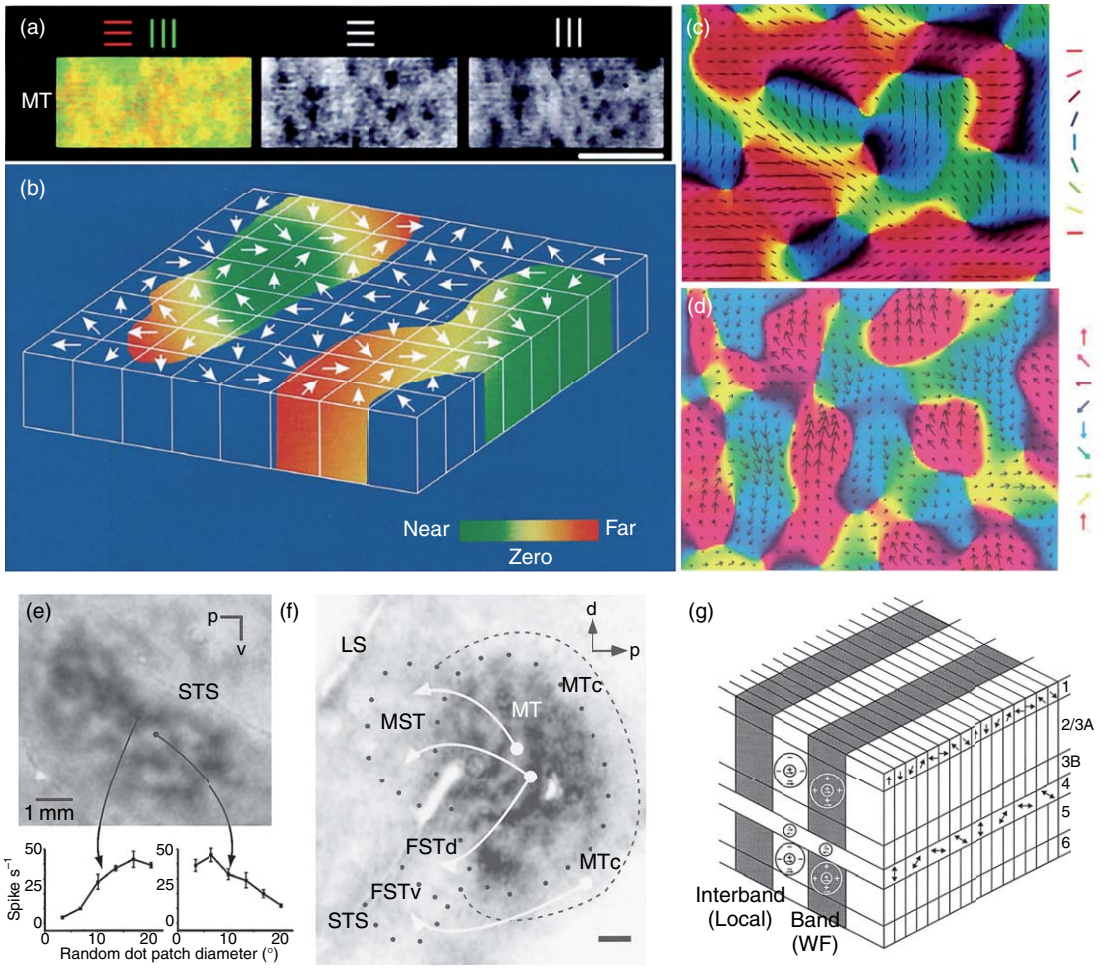

Figure 5 Functional imaging and cortical modules in area MT. (a) Differential (left) and single-condition (middle and right) 2-deoxyglucose (2-DG) imaging of orientation-specific activations in macaque area MT. From Vanduffel, W., Tootell, R. B. H., Schoups, A. A. and Orban, G. A. 2002. The organization of orientation selectivity throughout macaque visual cortex. Cereb. Cortex 12, 647–662; (figure 13). (b) Model of area MT direction of motion columns (arrows) and disparity modules (colors) in macaque area MT. From DeAngelis, G. C. Newsome, W. T. 1999. Organization of disparity-selective neurons in macaque area MT. J. Neurosci. 19, 1398–1415; (figure 18). (c) Orientation map derived from optical recording in owl monkey area MT. From Malonek, D., Tootell, R. B. H., Grinvald, A. 1994. Optical imaging reveals the functional architecture of neurons processing shape and motion in owl monkey area MT. Proc. R. Soc. Lond. B 258, 109–119; (figure 3c). (d) Direction of motion map derived from optical recording in owl monkey area MT. From Malonek, D., Tootell, R. B. H., Grinvald, A. 1994. Optical imaging reveals the functional architecture of neurons processing shape and motion in owl monkey area MT. Proc. R. Soc. Lond. B 258, 109–119; (figure 4c). (e) 2-Deoxyglucose (2-DG) image of surround-suppression architecture in owl monkey area MT. Dark regions do not show surround suppression while pale regions are suppressed by the movement of large (>10° stimuli). From Born, R. T. 2000. Center-surround interactions in the middle temporal visual area of the owl monkey. J. Neurophysiol. 84, 2658–2669; (figure 6a). (f) Cortical projections of MT wide-field and local processing modules. Wide-field modules (not suppressed by large stimuli; dark regions) project to ventral area MST and area FSTd while MT local processing modules (suppressed by large field stimuli; pale) project to dorsal portions of area MST. From Berezovskii, V. K. and Born, R. T. 2000. Specificity of projections from wide-field and local motion-processing regions within the middle temporal visual area of the owl monkey. J. Neurosci. 20, 1157–1169; (figure 12). (g) Model of functional architecture of owl monkey area MT. Bands of wide-field and local spatial summation intersect with axis of motion maps. From Born, R. T. 2000. Center-surround interactions in the middle temporal visual area of the owl monkey. J. Neurophysiol. 84, 2658–2669; (figure 15).

segregation of V2 thin and interstripe inputs, in conjunction with functional imaging evidence for segregated orientation and chromatic domains, suggests that V4 contains at least two functionally distinct modules that appear to maintain largely segregated processing of object surface and contour information.

1.29.5 Modular Organization of Area MT

Area MT is an extrastriate visual area that is characterized by preponderance of directional selectivity and is clearly implicated in perception of the direction of moving objects (e.g., Maunsell, J. H. and Van Essen, D. C., 1983; Newsome, W. T. *et al.*, 1989; Britten, K. H. *et al.*, 1992). In macaque monkeys, MT is buried in the posterior bank of the superior temporal sulcus and thus is not amenable to optical recording studies of columnar or modular organization. However, evidence for a modular organization of orientation preference was derived from a differential 2-DG imaging study that revealed irregular clusters of neurons with preferences for vertical or horizontal orientations (Figure 5(a); Vanduffel, W. *et al.*, 2002).

1.29.5.1 MT Single-Unit Mapping

Many single-unit recording studies have observed stretches of common direction preference attributed to iso-direction columns in macaque MT (e.g., Dubner, R. and Zeki, S. M., 1971). Furthermore, oblique penetrations across MT revealed smooth changes of preferred direction, punctuated by jumps of reversals of preferred direction, suggestive of an orderly map of direction (Albright, T. D. *et al.*, 1984). The resultant model of direction of motion modules in MT was subsequently expanded by DeAngelis G. C. and Newsome W. T. (1999), who demonstrated a columnar organization of binocular disparity tuning within MT such that regions of strong and weak disparity tuning are superimposed upon the direction preference map (Figure 5(b)).

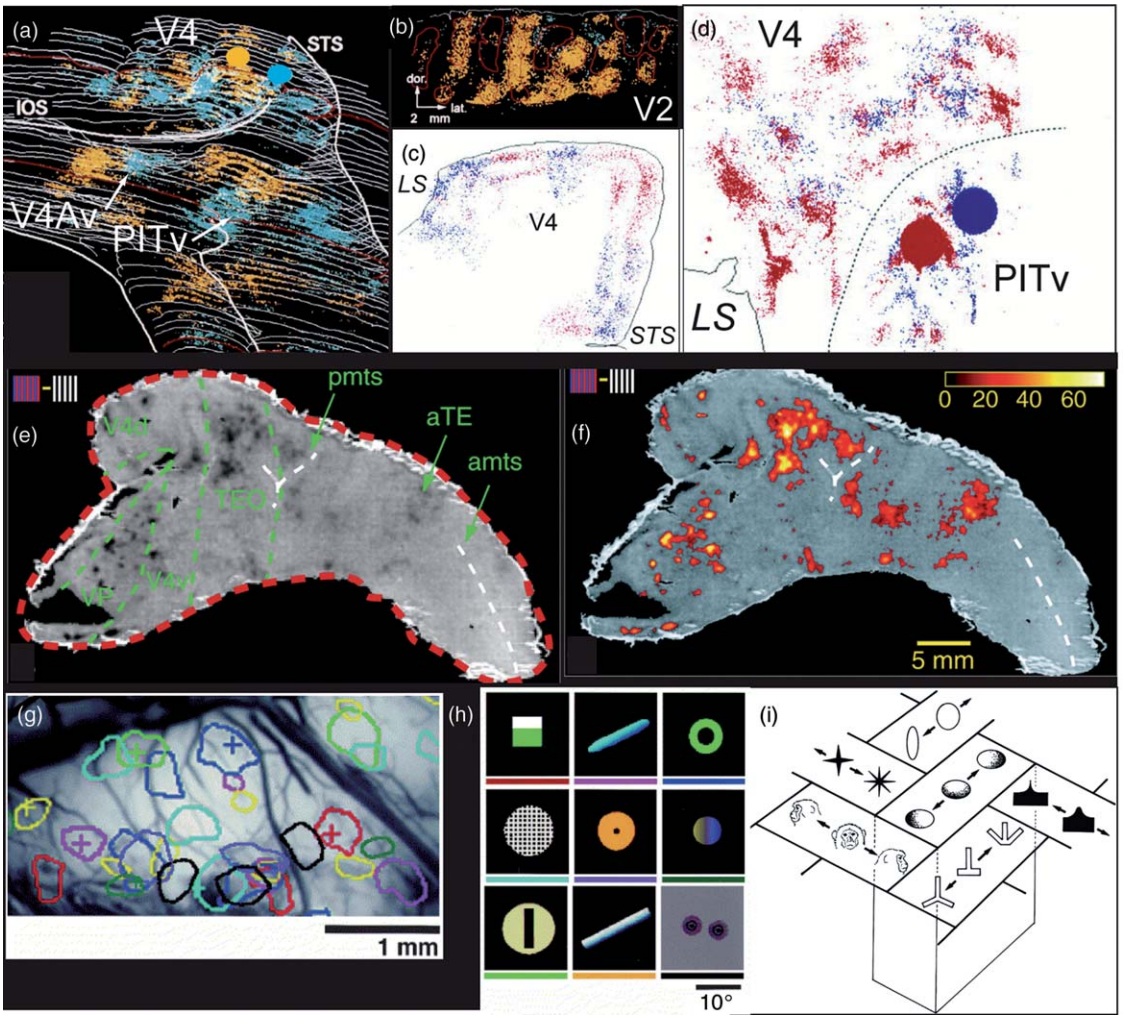

1.29.5.2 MT Functional Maps

Unlike in macaque monkeys, owl monkey MT is located on the exposed cortical surface and thus has been amenable to detailed analyses of orientation and direction maps. Neurons in owl monkey MT tend to be more highly tuned for orientation than their counterparts in macaque monkey MT. Consequently, it was not surprising to find a robust mapping of orientation in owl monkey MT that contained the characteristic pinwheel centers, iso-orientation domains, and orientation fractures (Malonek, D. *et al.*, 1994; Figure 5(c)). In addition, owl monkey MT contains an orderly map of preferred direction, characterized by long stretches of gradual direction change, pinwheels of rapid smooth change, and map fractures indicative of rapid breaks in direction change (Malonek, D. *et al.*, 1994; Figure 5(d)). Surprisingly, the functional map of orientation has larger response amplitude than the functional map of direction.

1.29.5.3 MT Functional Architecture and Projections

In owl monkeys, area MT is also characterized by a modular organization in which neurons with strong antagonistic surrounds are segregated from those that respond well to global motion stimuli (Born, R. T. and Tootell, R. B., 1992; Figure 5(e)). This modular architecture of surround antagonism is also reflected in the pattern of efferent connections such that neurons within the modules with strong surround antagonism project to area MST while neurons with weak surround antagonism project to areas MST and FSTd (Berezovskii, V. K. and Born, R. T., 2000; Figure 5(f)). The available evidence for the modular organization of area MT indicates that a comprehensive model of its functional architecture must include mapping of direction, orientation, and disparity (not shown), center–surround antagonism (local versus global motion processing), and efferent connectivity (Born, R. T. and Bradley, D. C., 2005; Figure 5(g)).

1.29.6 Modular Organization of Inferotemporal Cortex

1.29.6.1 Inferotemporal Areas

Inferotemporal cortex (IT) consists of a number of distinct subdivisions that have been distinguished on

Figure 6 Functional imaging and cortical modules in inferotemporal cortex. (a) Intrinsic and extrinsic connections following V4 retrograde tracer injections that labeled V2 interstripes (yellow injection and cells) or V2 thin stripes (blue injection and cells). Projections from area V4Av, PITv, and more anterior inferotemporal cortex are largely segregated from each other, suggestive of a modular organization that reflects the modular organization of area V2. From DeYoe, E. A., Felleman, D. J., Van Essen, D. C. and McClendon, E. 1994. Multiple processing streams in occipito-temporal visual cortex. Nature 371, 151–154; (figure 1a). (b) Pattern of projections arising from flattened V2 following retrograde tracer injections in panel (a). From DeYoe, E. A., Felleman, D. J., Van Essen, D. C. and McClendon, E. 1994. Multiple processing streams in occipito-temporal visual cortex. Nature 371, 151–154; (figure 1b). (c) Alternating, segregated modular projections across V4 on the prelunate gyrus and posterior bank of the STS following paired retrograde tracer injections into posterior inferotemporal area PITv. From Felleman, D.J., Xiao, Y. and McClendon, E. 1997. Modular organization of occipito-temporal pathways: cortical connections between areas V2, V4, and PITv in macaques. J. Neurosci. 17, 3185–3200; (figure 5a). (d) Segregated, modular projections from V4 to area PITv in a tangential reconstruction of anterior occipital-posterior inferotemporal cortex. From Felleman, D. J., Xiao, Y. and McClendon, E. 1997. Modular organization of occipito-temporal pathways: cortical connections between areas V2, V4, and PITv in macaques. J. Neurosci. 17, 3185–3200; (figure 5f). (e) Differential 2-deoxyglucose (2-DG) imaging of color-preferring modules in unfolded, ventral anterior occipital cortex and inferotemporal gyrus. Dashed green lines indicate the approximate borders between occipital areas V4d, VP, and V4v and inferotemporal areas TEO and anterior TE (aTE). From Tootell, R. B. H., Nelissen, K., Vanduffel, W., and Orban, G.A. 2004. Search for color 'center(s)' in macaque visual cortex. Cereb. Cortex 14, 353–363; (figure 7b). (f) Color-coded 2-DG t-map of color-selective activity from panel (e). Although areas VP, V4d, and V4v contain punctuate color-preferring modules, robust color modules are observed in area TEO and in several patches across middle and anterior TE. From Tootell, R. B. H., Nelissen, K., Vanduffel, W. and Orban, G. A. 2004. Search for color 'center(s)' in macaque visual cortex. Cereb. Cortex 14, 353–363; (figure 7c). (g) Optical imaging of object responses in dorsal anterior TE. Colored contours refer to cortical activations to stimuli (panel (h)) indicated by the same color underbar. Individual stimuli produce multiple cortical activations and different stimuli activate largely segregated portions of TE. From Wang, G., Tanifuji, M. and Tanaka, K. 1998. Functional architecture in monkey inferotemporal cortex revealed by in vivo optical imaging. Neurosci. Res. 32, 33–46; (figure 5). (i) Model of the modular organization of object representation in macaque anterior inferotemporal cortex. Different modules represent different object forms. However, adjacent modules may represent slight variations of a particular object type. From Tanaka, K. 2003. Columns for complex visual object features in the inferotemporal cortex: clustering of cells with similar but slightly different stimulus selectivities. Cereb. Cortex 13, 90–99; (figure 7).

the basis of cytoarchitecture (e.g., Brodmann, K., 1909; von Bonin, G. and Bailey, P., 1947; Lewis, J. W. and Van Essen, D. C., 2000), physiological properties (e.g., Baylis, G. C. *et al.*, 1987), behavioral effects following lesions (e.g., Buffalo *et al.*, 2005; Huxlin *et al.*, 2000), and cortical connections (e.g., Webster, M. J. *et al.*, 1994). Although the exact number of subdivisions or areas that comprise IT remains controversial, there is consensus that posterior subdivisions on the inferotemporal gyrus (ITG), area TEO (or PITv), and area PITd, within the adjacent lateral bank of the superior temporal sulcus, are anatomically and functionally distinct from the more anterior subdivisions. Anterior IT appears to consists of at least four (TEpd, TEpv, TEad, and TEav) and perhaps as many as eight subdivisions on the ITG and adjacent lateral bank of the superior temporal sulcus (e.g., Felleman, D. J. and Van Essen, D. C., 1991; Lewis, J. W. and Van Essen, D. C., 2000; Saleem, K. S. *et al.*, 2000).

Evidence for functional maps or modules within IT comes from several diverse experimental approaches. Posterior IT subdivisions, areas PITv and PITd, appear to be topographically organized based on electrophysiological mapping (e.g., Boussaovd *et al.*, 1991) and cortical connections with topographically organized occipital areas such as V2 and V4 (Van Essen, D. C. *et al.* 1990; 1992; Distler, C. *et al.* 1993). The remainder of IT does not appear to be topographically organized and contains neurons with relatively large receptive fields that almost always include the fovea (Baylis, G. C. *et al.*, 1987; Desimone, R. et al., 1984; Gochin, P. M. 1996).

1.29.6.2 Inferotemporal Anatomical Modules and Connections

Area PITv contains a modular organization that appears to be a continuation of the modular segregation of functional domains observed in areas V2 and V4. Although V4 does not contain an anatomical modular organization corresponding to the CO stripes of V2, it contains large segregated domains that receive input from either V2 thin or interstripes (Xiao, Y. *et al.*, 1999). Furthermore, paired retrograde tracer injections into V4 receive feedforward input from segregated thin and interstripe compartments of V2 and receive feedback projections from segregated modules in PITv (Figures 6(a) and 6(b); DeYoe, E. A. *et al.*, 1994). Similarly, paired retrograde tracer injections into PITv often label highly segregated, yet interdigitating modular domains in V4 (Figure 6(c); DeYoe, E. A. *et al.*, 1994; and Figure 6(d); Felleman, D. J. *et al.*, 1997). These results demonstrate that posterior IT (area PITv in particular) consists of segregated modules that appear to continue the functional segregation of neuronal populations involved in object surface and contour processing. It remains to be determined whether this functional segregation persists at higher levels of inferotemporal object processing or whether these anatomically distinct modules converge at higher levels to form a new functional architecture in anterior IT.

1.29.6.3 Inferotemporal Functional Imaging

The modular organization observed in area PITv on the basis of its segregated afferent connections with area V4 appears to be reflected in regional functional specializations. For example, differential 2-DG imaging, comparing functional activations to isoluminant chromatic versus luminance contrast stimulation, reveals a pattern of 2–3 mm wide hot spots in dorsal (foveal) PITv that are preferentially activated by chromatic stimuli (Tootell, R. B. H. *et al.*, 2004; Figures 6(e) and 6(f)). These foci appear larger and more selective for color than similar foci observed in area V4 and thus may represent the color area, corresponding to the most robust color-preferring domain in macaque visual cortex. Similarly, using fMRI in alert macaques, significant color activations were observed anterior to V4 in a region probably corresponding to area PITd (Conway, B. R. and Tsao, D. Y., 2006).

1.29.6.4 Inferotemporal Functional Modules

Neurons in posterior inferotemporal cortex, including areas PITv and perhaps CITv (TEO and posterior IT) appear selective for particular spatial configurations of relatively low level boundary contours (e.g., Brincat, and Connor, 2004; Pasupathy and Connor, 2001) whereas neurons in more anterior IT are selective for more complex stimuli (e.g., Tsunoda *et al.*, 2001). Furthermore, neurons in anterior IT appear to represent objects despite large variations in size, position, and features (e.g., Lueschow *et al.*, 1994; Sary *et al.*, 1993). Some IT neurons are selective for faces (e.g., Baylis, G. C. *et al.*, 1987; Tsao, D. Y. *et al.*, 2003; Tsao, D. Y. *et al.*, 2006), and although they tended to be encountered more frequently within the superior temporal sulcus, it was not until the application of fMRI mapping of functional specialization within IT was it appreciated that face cells are clustered in two or more IT subdivisions (e.g., Tsao, D. Y.

et al., 2006). Extensive microelectrode recording within IT has led investigators to propose a modular organization for objects within anterior IT in which clusters, roughly 0.5 mm in width, represented specific objects (e.g., Fujita, I. *et al.*, 1992; Tamura, H. *et al.*, 2005). This hypothesis was later confirmed using optical recording of intrinsic cortical signals (e.g., Wang, G. *et al.*, 1998), which demonstrated modular-specific activations (Figure 6(g)) that generalized across related object types (Figure 6(h)). The observation of relatively pure columnar representations of particular objects and the finding that similar objects are represented in adjacent columns led to a hypothesis of a modular organization of object representation within anterior portions of IT (Tanaka, K., 2003; Figure 6(i)). This model of IT implies that the representation of a given object is encoded by the activity of a complex combination of cortical columns or modules (Tsunoda, K. *et al.*, 2001).

1.29.7 Summary and Conclusions

Visual cortex of monkeys is characterized by functional maps and cortical modules that allow for the orderly representations of a large number of sensory attributes within a limited amount of cortical tissue. Most visual areas are topographically organized in that they contain a systematic representation of visual space. In some areas, such as V1, the representation of visual space is very precise and is only disrupted by the differential CO blob and interblob architecture that segregates color/brightness from orientation-specific processing. V1 contains simultaneous functional maps for visual topography, eye dominance, orientation, color/brightness, and perhaps spatial frequency. The topographic organization of area V2 is precise within each CO stripe compartment, but the overall topography is disrupted by functionally specific modules that segregate color/brightness, contour, and disparity processing. Area MT contains at least three functional maps that simultaneously represent visual topography, preferred direction of motion (and/or orientation), and binocular disparity. These functional maps also appear to be distributed across an additional modular system that segregates local from global motion processing, the result of which is distributed along two different efferent cortical streams. Area V4 and inferotemporal area PITv contain topographic maps of visual space, but less is known concerning how other visual attributes are represented. Both areas contain an anatomical modular architecture that appears to continue the anatomical and functional modularity observed within area V2 thin and interstripes. Thus, areas V4 and PITv appear to contain segregated functional modules that independently process object surface and contour information. These functional modules appear to converge at higher levels of IT where a modular organization of 3D object properties emerges. IT contains a modular representation of objects: columns represent specific object types and structurally similar objects appear to be represented within adjacent modules. Overall, these data demonstrate that visual cortical areas generally represent a number of stimulus attributes, simultaneously, and that anatomically and functionally defined modules provide mechanisms for efficient local computation and for efficient segregation of intercortical inputs and outputs.

References

Albright, T. D., Desimone, R., and Gross, C. G. 1984. Columnar organization of directionally selective cells in visual area MT of the macaque. J. Neurophysiol. 51, 16–31.

Bartfeld, E. and Grinvald, A. 1992. Relationships between orientation-preference pinwheels, cytochrome oxidase blobs, and ocular-dominance columns in primate striate cortex. Proc. Natl. Acad. Sci. U. S. A. 89, 11905–11909.

Basole, A., White, L. E., and Fitzpatrick, D. 2003. Mapping multiple features in the population response of visual cortex. Nature 423, 986–990.

Baylis, G. C., Rolls, E. T., and Leonard, C. M. 1987. Functional subdivisions of the temporal lobe neocortex. J. Neurosci. 7, 330–342.

Berezovskii, V. K. and Born, R. T. 2000. Specificity of projections from wide-field and local motion-processing regions within the middle temporal visual area of the owl monkey. J. Neurosci. 20, 1157–1169.

Blasdell, G. G. 1992. Differential imaging of ocular dominance and orientation selectivity in monkey striate cortex. J. Neurosci. 12, 3115–3138.

von Bonin, G. and Bailey, P. 1947. The Neocortex of *Macaca mulatta.* University of Illinois.

Born, R. T. 2000. Center-surround interactions in the middle temporal visual area of the owl monkey. J. Neurophysiol. 84, 2658–2669.

Born, R. T. and Bradley, D. C. 2005. Structure and function of visual area MT. Annu. Rev. Neurosci. 28, 157–189.

Born, R. T. and Tootell, R. B. 1992. Segregation of global and local motion processing primate middle temporal visual area. Nature 357, 497–499.

Brewer, A. A., Press, W. A., Logothetis, N. K., and Wandell, B. A. 2002. Visual areas in macaque cortex measured using functional magnetic resonance imaging. J. Neurosci. 22, 10416–10426.

Britten, K. H., Shadlen, M. N., Newsome, W. T., and Movshon, J. A. 1992. The analysis of visual motion: a comparison of neuronal and psychophysical performance. J. Neurosci. 12, 4745–4765.

Brodmann, K. 1909. Vergleichende lokalisationslehre der grosshirnrinde in ihren prinzipien dargestellt auf grund des zellenbaues. J.A. Barth.

Chklovskii, D. B. and Koulakov, A. A. 2004. Maps in the brain: what can we learn from them? Annu. Rev. Neurosci. 27, 369–392.

Conway, B. R. and Tsao, D. Y. 2006. Color architecture in alert macaque cortex revealed by fMRI. Cereb. Cortex 16, 1604–1613.

DeAngelis, G. C. and Newsome, W. T. 1999. Organization of disparity-selective neurons in macaque area MT. J. Neurosci. 19, 1398–1415.

DeYoe, E. A. and Van Essen, D. C. 1985. Segregation of efferent connections and receptive field properties in visual area V2 of the macaque. Nature 317, 58–61.

DeYoe, E. A., Carman, G. J., Bandettini, P., Glickman, S., Wieser, J., Cox, R., Miller, D., and Neitz, J. 1996. Mapping striate and extrastriate visual areas in human cerebral cortex. Proc. Natl. Acad. Sci. U. S. A. 93, 2382–2386.

DeYoe, E. A., Felleman, D. J., Van Essen, D. C., and McClendon, E. 1994. Multiple processing streams in occipito-temporal visual cortex. Nature 371, 151–154.

Dillenburger, B. C., Lu, H. D., Kaskan, P. M., and Roe, A. W. 2006. Real and illusory contour interactions in early visual cortex of the macaque monkey. Soc. Neurosci. Abstr. 640, 11.

Distler, C., Boursaovd, D., Derimone, R., and Ungerleider, L. G. 1993. Cortical connections of inferior area TEO in macaque monkeys. J. Comp. Neurd. 334, 125–150.

Dubner, R. and Zeki, S. M. 1971. Response properties and receptive fields of cells in an anatomically defined region of the superior temporal sulcus in the monkey. Brain Res. 35, 528–532.

Everson, R. M., Prashanth, A. K., Gabbay, M., Knight, B. W., Sirovich, L., and Kaplan, E. 1998. Representation of spatial frequency and orientation in the visual cortex. Proc. Natl. Acad. Sci. U. S. A. 95, 8334–8338.

Felleman, D. J. and Van Essen, D. C. 1991. Distributed hierarchical processing in the primate cerebral cortex. Cereb. Cortex 1, 1–47.

Felleman, D. J., Xiao, Y., and McClendon, E. 1997. Modular organization of occipito-temporal pathways: cortical connections between areas V2, V4, and PITv in macaques. J. Neurosci. 17, 3185–3200.

Fize, D., Vanduffel, W., Nelissen, K., Denys, K., Chef d'Hotel, C., Faugeras, O., and Orban, G. A. 2003. The retinotopic organization of primate dorsal V4 and surrounding areas: a functional magnetic resonance imaging study in awake monkeys. J. Neurosci. 23, 7395–7406.

Fujita, I., Tanaka, K., Ito, M., and Cheng, K. 1992. Columns for visual features of objects in monkey inferotemporal cortex. Nature 360, 343–346.

Gegenfurtner, K. R., Kiper, D. C., and Fenstemaker, S. B. 1996. Processing of color, form, and motion in macaque area V2. Vis. Neurosci. 13, 161–172.

Ghose, G. M. and Ts'o, D. Y. 1997. Form processing modules in primate area V4. J. Neurophysiol. 77, 2191–2196.

Hendry, S. H. and Reid, R. C. 2000. The konicellular pathway in primate vision. Annu. Rev. Neurosci. 23, 127–153.

Horton, J. C. and Hocking, D. R. 1998. Effect of early monocular enucleation upon ocular dominance columns and cytochrome oxidase activity in monkey and human visual cortex. Vis. Neurosci. 15, 289–303.

Horton, J. C. and Hubel, D. H. 1981. Regular patchy distribution of cytochrome oxidase staining in primary visual cortex of macaque monkey. Nature 292, 762–764.

Hubel, D. H. and Wiesel, T. N. 1977. Functional architecture of macaque monkey visual cortex (Ferrier Lecture). Proc. R. Soc. Lond. B 198, 1–59.

Hübener, M., Shoham, D., Grinvald, A., and Bonhoeffer, T. 1997. Spatial relationships among three columnar systems in cat area 17. J. Neurosci. 17, 9270–9284.

Issa, N. P., Trepel, C., and Stryker, M. P. 2000. Spatial frequency maps in cat visual cortex. J. Neurosci. 20, 8504–8514.

Landisman, C. E. and Ts'o, D. Y. 2002a. Color processing in macaque striate cortex: relationships to ocular dominance, cytochrome oxidase, and orientation. J. Neurophysiol. 87, 3126–3137.

Landisman, C. E. and Ts'o, D. Y. 2002b. Color processing in macaque striate cortex: electrophysiological properties. J. Neurophysiol. 87, 3138–3151.

LeVay, S., Connolly, M., Houde, J., and Van Essen, D. C. 1985. The complete pattern of ocular dominance stripes in the striate cortex and visual field of the macaque monkey. J. Neurosci. 5, 486–501.

Levitt, J. B., Kiper, D. C., and Movshon, J. A. 1994 Receptive fields and functional architecture of macaque V2. J. Neurophysiol. 71, 2517–2542.

Lewis, J. W. and Van Essen, D. C. 2000. Mapping of architectonic subdivisions in the macaque monkey, with emphasis on parieto-occipital cortex. J. Comp. Neurol. 428, 79–111.

Livingstone, M. S. and Hubel, D. H. 1984. Anatomy and physiology of a color system in the primate visual cortex. J. Neurosci. 4, 309–356.

Malach, R. 1994. Cortical columns as devices for maximizing neuronal diversity. Trends Neurosci. 17, 101–104.

Malonek, D., Tootell, R. B. H., and Grinvald, A. 1994. Optical imaging reveals the functional architecture of neurons processing shape and motion in owl monkey area MT. Proc. R. Soc. Lond. B 258, 109–119.

Mante, V. and Carandini, M. 2005. Mapping of stimulus energy in primary visual cortex. J. Neurophysiol. 94, 788–798.

Maunsell, J. H. and Van Essen, D. C. 1983. Functional properties of neurons in middle temporal visual area of the macaque monkey. I. Selectivity for stimulus direction, speed, and orientation. J. Neurophysiol. 49, 1127–1147.

Newsome, W. T., Britten, K. H., and Movshon, J. A. 1989. Neuronal correlates of a perceptual decision. Nature 341, 52–54.

Okhi, K., Chung, S., Ch'ng, Y. H., Kara, P., and Reid, R. C. 2005. Functional imaging with cellular resolution reveals precise micro-architecture in visual cortex. Nature 433, 597–603.

Olavarria, J. F. and Van Essen, D. C. 1997. The global pattern of cytochrome oxidase stripes in visual area V2 of the macaque monkey. Cereb. Cortex 5, 395–404.

Roe, A. W. and Ts'o, D. Y. 1995. Visual topography in primate V2: multiple representations across functional stripes. J. Neurosci. 15, 3689–3715.

Saleem, K. S., Suzuki, W., Tanaka, K., and Hashikawa, T. 2000. Connections between anterior inferotemporal cortex and superior temporal sulcus regions in the macaque monkey. J. Neurosci. 20, 5083–5101.

Sereno, M. I., Dale, A. M., Reppas, J. B., Kwong, K. K., Belliveau, V. W., Brady, T. J., Rosen, B. R., and Tootell, R. B. H. 1995. Borders of multiple visual areas in human revealed by functional magnetic resonance imaging. Science 268, 889–893.

Sereno, M., McDonald, C. T., and Allman, J. M. 1994. Analysis of retinotopic maps in extrastriate cortex. Cereb. Cortex 6, 601–620.

Shipp, S. and Zeki, S. 1985. Segregation of pathways leading from area V2 to areas V4 and V5 of macaque monkey visual cortex. Nature 315, 322–325.

Shipp, S. and Zeki, S. 2002. The functional organization of area V2, I: Specialization across stripes and layers. Vis. Neurosci. 19, 187–210.

Shoham, D., Hübener, M., Schulze, S., Grinvald, A., and Bonhoeffer, T. 1997. Spatio-temporal frequency domains and their relation to cytochrome oxidase staining in cat visual cortex. Nature 385, 529–533.

Sincich, L. C. and Horton, J. C. 2002. Divided by cytochrome oxidase: a map of the projections from V1 to V2 in macaques. Science 295, 1734–1737.
Sirovich, L. and Uglesich, R. 2004. The organization of orientation and spatial frequency in primary visual cortex. Proc. Natl. Acad. Sci. U. S. A. 101, 16941–16946.
Swindale, N. V. 2000. How many maps are there in visual cortex? Cereb. Cortex 10, 633–643.
Tamura, H., Kaneko, H., and Fujita, I. 2005. Quantitative analysis of functional clustering of neurons in the macaque inferior temporal cortex. Neurosci. Res. 52, 311–322.
Tanaka, K. 2003. Columns for complex visual object features in the inferotemporal cortex: clustering of cells with similar but slightly different stimulus selectivities. Cereb. Cortex 13, 90–99.
Tootell, R. B. H., Nelissen, K., Vanduffel, W., and Orban, G. A. 2004. Search for color 'center(s)' in macaque visual cortex. Cereb. Cortex 14, 353–363.
Tootell, R. B. H., Silverman, M. S., and De Valois, R. L. 1981. Spatial frequency columns in primary visual cortex. Science 214, 813–815.
Tootell, R. B. H., Silverman, M. S., Hamilton, S. L., Switkes, E., and De Valois, R. L. 1988a. Functional anatomy of macaque striate cortex. V. Spatial frequency. J. Neurosci. 8, 1610–1624.
Tootell, R. B. H., Switkes, E., Silverman, M. S., and Hamilton, S. L. 1988b. Functional anatomy of macaque striate cortex. II. Retinotopic organization. J. Neurosci. 8, 1531–1568.
Tsao, D. Y., Freiwald, W. A., Knutsen, T. A., Mandeville, J. B., and Tootell, R. B. H. 2003. Faces and objects in macaque cerebral cortex. Nat. Neurosci. 6, 989–995.
Tsao, D. Y., Freiwald, W. A., Tootell, R. B. H., and Livingstone, M. S. 2006. A cortical region consisting entirely of face-selective cells. Science, 311, 670–674.
Ts'o, D. Y. and Gilbert, C. D. 1988. The organization of chromatic and spatial interactions in the primate striate cortex. J. Neurosci. 8, 1712–1727.
Ts'o, D. Y., Frostig, R. D., Lieke, E. E., and Grinvald, A. 1990. Functional organization of primate visual cortex revealed by high resolution optical imaging. Science 249, 417–420.
Ts'o, D. Y., Roe, A. W., and Gilbert, C. D. 2001. A hierarchy of the functional organization for color, form, and disparity in primate visual area V2. Vision Res. 41, 1333–1349.
Tsunoda, K., Yamane, Y., Nishizaki, M., and Tanifuji, M. 2001. Complex objects are represented in macaque inferotemporal cortex by the combination of feature columns. Nat. Neurosci. 4, 832–838.
Vanduffel, W., Tootell, R. B. H., Schoups, A. A., and Orban, G. A. 2002. The organization of orientation selectivity throughout macaque visual cortex. Cereb. Cortex 12, 647–662.
Wang, G., Tanifuji, M., and Tanaka, K. 1998. Functional architecture in monkey inferotemporal cortex revealed by in vivo optical imaging. Neurosci. Res. 32, 33–46.
Webster, M. J., Bachevalier, J., and Ungerleider, L. G. 1994. Connections of inferior temporal areas TEO and TE with parietal and frontal cortex in macaque monkeys. Cereb. Cortex 4, 470–483.
Weliky, M., Bosking, W. H., and Fitzpatrick, D. 1996. A systematic map of direction preference in primary visual cortex. Nature 379, 725–728.
Xiao, Y. and Felleman, D. J. 2004. Projections from striate cortex (V1) to cytochrome oxidase thin stripes and interstripes of macaque V2. Proc. Natl. Acad. Sci. U. S. A. 101, 7147–7151.
Xiao, Y., Casti, A., Xiao, J., and Kaplan, E. 2007. Hue maps in primate striate cortex. NeuroImage. 35, 771–786
Xiao, Y., Wang, Y., and Felleman, D. J. 2003. Spatially organized representation of hue in macaque V2. Nature 421, 535–539.
Xiao, Y., Zych, A., and Felleman, D. J. 1999. Segregation and convergence of functionally defined V2 thin stripe and interstripe compartment projections to area V4 of macaques. Cereb. Cortex 9, 792–804.
Yabuta, N. H. and Callaway, E. M. 1998. Cytochrome-oxidase blobs and intrinsic horizontal connections of layer 2/3 pyramidal neurons in primate V1. Vis. Neurosci. 15, 1007–1027.
Yu, H., Farley, F. J., Jin, D. Z., and Sur, M. 2005. The coordinated mapping of visual space and response features in visual cortex. Neuron 47, 267–280.

Further Reading

Gattas, R., Nascimento-Silva, S., Soares, J. G. M., Lima, B., Jansen, A. K., Diogo, C. M., Farias, M. F., Marcondes, M., Botelho, E. P., Mariani, O. S., Azzi, J., and Fiorani, M. 2005. Cortical visual areas in monkeys: location, topography, connections, columns, plasticity, and cortical dynamics. Phil. Trans. R. Soc. B Published online, April 29, 2005.
Roe, A. W. 2003. Modular Complexity of Area V2 in the Macaque Monkey. In: The Primate Visual System (*eds*. J. Kaas and C. Collins). CRC Press.
Tamura, H. and Tanaka, K. 2001. Visual response properties of cells in the ventral and dorsal parts of the macaque inferotemporal cortex. Cereb. Cortex 11, 384–399.
Tanaka, K. 1997. Mechanisms of visual object recognition: monkey and human studies. Curr. Opin. Neurobiol. 7, 523–529.
Wang, Y., Xiao, Y., and Felleman, D. J. 2006. V2 thin stripes contain spatially organized representations of achromatic luminance change. Cereb. Cortex 17, 116–129.

1.30 Organization of Human Visual Cortex

R Rajimehr and R Tootell, Massachusetts General Hospital, Charlestown, MA, USA

© 2008 Elsevier Inc. All rights reserved.

1.30.1	**Introduction**	595
1.30.2	**Occipital Visual Areas**	595
1.30.2.1	Primary Visual Cortex	596
1.30.2.2	V2/V3/VP	598
1.30.2.3	V4/V8	598
1.30.2.4	V5 (Human MT+)	599
1.30.2.5	V3A/V3B	600
1.30.2.6	V7	601
1.30.3	**Ventral Stream Areas**	601
1.30.3.1	Lateral Occipital Complex	602
1.30.3.2	Fusiform Face Area	603
1.30.3.3	Parahippocampal Place Area	604
1.30.3.4	Extrastriate Body Area	604
1.30.4	**Dorsal Stream Areas**	604
1.30.4.1	Caudal Intraparietal Sulcus	605
1.30.4.2	Parieto-Occipital Cortex/V6	605
1.30.4.3	Parietal Reach Region	606
1.30.4.4	Anterior Intraparietal Area	606
1.30.4.5	Ventral Intraparietal Area	606
1.30.4.6	Lateral Intraparietal Area	606
1.30.4.7	Superior Parietal Lobule and Inferior Parietal Lobule	606
1.30.5	**Frontal Areas**	607
1.30.6	**Conclusions**	607
References		607

1.30.1 Introduction

The human visual system contains numerous visual areas that collectively occupy about 27% of the total extent of cerebral cortex (950 cm^2) (Van Essen, D. C., 2003). Typically, visual cortical areas can be identified by four main criteria: retinotopy, global functional properties, histology (cytoarchitecture and myeloarchitecture), and intercortical connectivity (Felleman, D. J. and Van Essen, D. C., 1991; Kaas, J. H., 1997; Tootell, R. B. *et al.*, 2003). Over the past decade, noninvasive neuroimaging methods, especially functional magnetic resonance imaging (fMRI), have greatly clarified the retinotopic organization and functional properties of the human visual system (Tootell, R. B. *et al.*, 1996; 1998b; 2003; Grill-Spector, K. and Malach, R., 2004). Several studies have also explored histological differences between human brain areas in postmortem specimens, but these data have been largely restricted to early visual areas (Horton, J. C. and Hedley-Whyte, E. T., 1984; Horton, J. C. *et al.*, 1990; Clarke, S., 1994a; 1994b; Tootell, R. B. and Taylor, J. B., 1995). More recently, anatomical MRI and diffusion tensor imaging (DTI) have revealed histological and connectional distinctions between areas as well (Conturo, T. E. *et al.*, 1999; Hagmann, P. *et al.*, 2003). Based on these criteria, human visual cortex can be tentatively parceled into more than a dozen distinct areas (Figure 1) (e.g., Tootell, R. B. *et al.*, 2003). In this chapter, we summarize our current understanding of visual cortical organization in humans. Visual areas will be classified and reviewed in four sections: occipital visual areas, ventral stream areas, dorsal stream areas, and frontal areas.

1.30.2 Occipital Visual Areas

The visual cortical hierarchy begins with occipital areas, which are involved in early visual processing. Topographic (retinotopic) mapping (Figure 2) is a

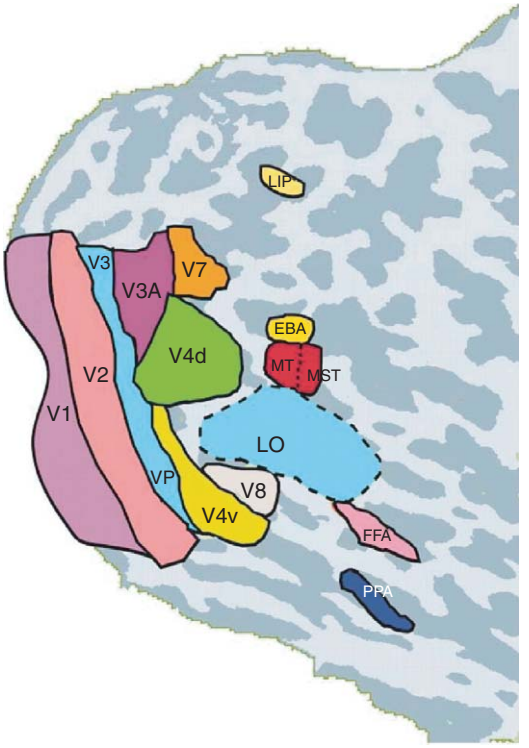

Figure 1 Map of reported areas in human visual cortex. Consensus is highest in lower-tier (generally, leftmost) areas; such areas tend to be evolutionarily more conserved, and the retinotopy is more easily resolved. Adapted from Tootell, R. B., Tsao, D., and Vanduffel, W. 2003. Neuroimaging weighs in: humans meet macaques in "primate" visual cortex. J. Neurosci. 23, 3981–3989.

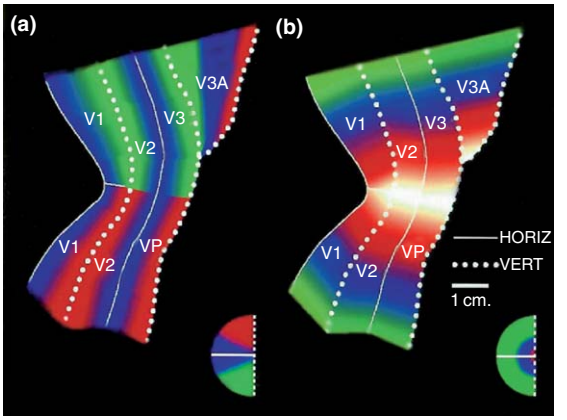

Figure 2 Principles of functional magnetic resonance imaging (fMRI) retinotopic mapping. (a) The polar angle retinotopy and (b) the eccentricity retinotopy. In (a), each of the red, blue, and green pseudocolor ranges represents retinotopically differentiable activation within a 60° subdivision of polar angle in the contralateral visual field (see *logo*, a). In (b), the red, blue, and green ranges correspond to activation within logarithmically equal subdivisions of the eccentricity range from 0.75 through ~15° in the visual field, centered at ~1.5° (red), 3.8° (blue), and 10.3° (green) (see *logo*, b). Adapted from Tootell, R. B., Mendola, J. D., Hadjikhani, N. K., Ledden, P. J., Liu, A. K., Reppas, J. B., Sereno, M. I., and Dale, A. M. 1997. Functional analysis of V3A and related areas in human visual cortex. J. Neurosci. 17, 7060–7078.

ubiquitous property of occipital visual areas in both human (Engel, S. A. *et al.*, 1994; Sereno, M. I. *et al.*, 1995; DeYoe, E. A. *et al.*, 1996; Engel, S. A. *et al.*, 1997a; Hadjikhani, N. K. *et al.*, 1998; Wandell, B. A., 1999; Tootell, R. B. and Hadjikhani, N. K., 2001) and non-human (Gattass, R. *et al.*, 1981; Van Essen, D. C., *et al.*, 1984; Gattass, R. *et al.*, 1988; Tootell, R. B. *et al.*, 1988; Brewer, A. A. *et al.*, 2002; Fize, D. *et al.*, 2003) primates. A visual cortical area is called retinotopic (or said to contain a retinotopic map) if nearby cortical regions receive inputs from nearby retinal regions. Mapping between the retina and the cortex can be best described as a log-polar transformation (Schwartz, E. L., 1977), in which standard axes in the retina are transformed into polar axes in the cortex: eccentricity (distance from fovea) and polar angle (angle from horizontal axis). The logarithmic component of the transformation accounts for the magnification of central representations in the cortex (Schwartz, E. *et al.*, 1985; Duncan, R. O. and Boynton, G. M., 2003).

Mapping the phase (angle) component of the retinotopic map reveals multiple horizontal and vertical meridian representations arranged in approximately parallel bands along the cortical surface. These vertical and horizontal meridian representations alternate and define the borders between mirror-symmetric retinotopic areas. Perpendicular to these bands lie isoeccentricity bands. In humans, the expanded foveal representation of low-level retinotopic areas converges in the occipital pole, in the confluent fovea. Flanking the confluent fovea, there are bands of parafoveal/peripheral representations present both ventrally and dorsally.

1.30.2.1 Primary Visual Cortex

Area V1 (also known as primary visual cortex, striate cortex, or Brodmann's area 17) is the human visual cortical area with the most well-defined anatomical boundaries (Brodmann, K., 1909; Holmes, G. and Lister, W. T., 1916; Von Economo, C. and Koskinas, G. N., 1925; Polyak, S. A., 1933; Stensaas, S. S. *et al.*, 1974). In primates, area V1 plays a critical role in early visual information processing, because most

visual information ultimately reaching the rest of visual cortex is first funneled through V1 (Felleman, D. J. and Van Essen, D. C., 1991). Presumably, this anatomically complicated routing task is partly why striate cortex is so markedly laminated. In fact, primate striate cortex has been anatomically subdivided into eleven identifiable laminar divisions (labeled 1, 2, 3, 4A, 4B, 4C alpha, 4C beta, 5A, 5B, 6A, and 6B) (Lund, J. S., 1988; Hendry, S. H. *et al.*, 1994) rather than the customary six layers described in most cortical areas. Sublamina 4C alpha receives most of the magnocellular input from the lateral geniculate nucleus (LGN) of thalamus, and sublamina 4C beta receives most of the input from the parvocellular LGN (Hubel, D. H. and Wiesel, T. N., 1972). The name striate cortex is derived from the *stria of Gennari*, a distinctive stripe that represents a dense concentration of myelinated fibers in cortical layer 4B. Recently, several groups have reported the in vivo detection of myelination patterns within the human V1 cortex using advanced MRI techniques (Barbier, E. L. *et al.*, 2002; Clare, S. and Bridge, H., 2005). Ocular dominance columns in human V1 have been also demonstrated by using multiple anatomical stains (Haseltine, E. C. *et al.*, 1979; Hitchcock, P. F. and Hickey, T. L., 1980; Horton, J. C. and Hedley-Whyte, E. T., 1984; Horton, J. C. *et al.*, 1990) and blood-oxygen-level dependent (BOLD)-based fMRI (Menon, R. S. *et al.*, 1997; Cheng, K. *et al.*, 2001).

The V1 is the largest known visual cortical area, and perhaps the largest cortical area, at least in macaques, where multiple cortical area boundaries are best known (Felleman, D. J. and Van Essen, D. C., 1991). In addition, one human fMRI study has estimated that neuronal receptive fields are smaller in V1, compared with those in higher-tier visual areas such as V2, V3/VP, V3A, and V4 (Smith, A. T. *et al.*, 2001).

It is well known that V1 normally extends over the depth and lips of the calcarine fissure. However, there is considerable individual variability in the size, location, and shape of V1, and even more variability in the shape of the calcarine fissure (Stensaas, S. S. *et al.*, 1974; Rademacher, J. *et al.*, 1993). Retinotopic lesion defects (Holmes, G. and Lister, W. T., 1916), electrically induced phosphenes (Penfield, W. *et al.*, 1954), and retinotopic maps in positron emission tomography (PET) (Fox, P. T. *et al.*, 1987) and fMRI (Engel, S. A. *et al.*, 1994; Sereno, M. I. *et al.*, 1995; DeYoe, E. A. *et al.*, 1996; Engel, S. A. *et al.*, 1997a; Tootell, R. B. *et al.*, 1998c) studies all confirm that human V1 has a well-defined topographic organization. Generally, the upper bank of the calcarine sulcus responds to the lower half of visual field, and the lower bank of the calcarine responds to the upper half of visual field. The horizontal meridian in the visual field is mapped onto the base of the calcarine sulcus, and the vertical meridian is represented rostrally at the border between V1 and V2. The central visual field activates the posterior tip of the calcarine sulcus, and the peripheral visual field activates anterior parts of the calcarine. Because of the cortical magnification factor (Engel, S. A. *et al.*, 1994; Sereno, M. I. *et al.*, 1995; Engel, S. A. *et al.*, 1997a), a large portion of V1 in the confluent fovea is devoted to the representation of small, central portion of visual field.

The correspondence between a given location in V1 and in the visual field is very precise: even the retinal blind spot is represented as a monocular region in V1 (Tootell, R. B. *et al.*, 1998c; Tong, F. and Engel, S. A., 2001). As one would predict from its location in the retina, the blind spot is located just inferior (superior in the visual field) to the cortical representation of the horizontal meridian, centered at the represented eccentricity near 15°.

The V1 has been generally considered as a feature preprocessing area where the neurons code for basic stimulus attributes, such as line orientation and motion direction. fMR-adaptation paradigms (Tootell, R. B. *et al.*, 1998c; Fang, F. *et al.*, 2005; Larsson, J. *et al.*, 2006; but see Boynton, G. M. and Finney, E. M., 2003) and pattern analysis of fMRI data (Kamitani, Y. and Tong, F., 2005; Haynes, J. D. and Rees, G., 2005) have confirmed that human V1 has strong first-order (luminance) orientation selectivity, as suggested by numerous studies in macaques (Hubel, D. H. and Wiesel, T. N., 1968). Recent fMRI studies also reveal the existence of asymmetric orientation sensitivity (including oblique effect and radial orientation bias) in human V1 cortex (Furmanski, C. S. and Engel, S. A., 2000; Sasaki, Y. *et al.*, 2006). Processing of first-order motion also originates in V1 (Smith, A. T. *et al.*, 1998; Seiffert, A. E. *et al.*, 2003; Nishida, S. *et al.*, 2003).

V1 also shows selectivity for stimulus color (Engel, S. A. *et al.*, 1997b) and spatial frequency (Tootell, R. B. *et al.*, 1998b). The systematic organization of spatial frequency preference in V1 is remarkably similar to that for retinotopic eccentricity (Tootell, R. B. *et al.*, 1998b).

One characteristic functional property of V1 is that its contrast response varies continuously and monotonically over contrasts greater than ~6% (Tootell, R. B. *et al.*, 1995b; Boynton, G. M. *et al.*,

1996). However, the contrast response in higher visual cortical areas (such as V3, MT, and LOC) is quite different, essentially saturated at contrasts higher than ~6% (Tootell, R. B. *et al.*, 1995b; 1998c; Avidan, G. *et al.*, 2002a).

Pathological damages to V1 usually lead to scotomas (e.g., hemianopia) restricted to corresponding regions of the visual field (Holmes, G., 1918). Interestingly, patients with scotomas are often able to make use of visual information presented to their scotomas, despite being unable to consciously perceive it – a phenomenon called blindsight (Stoerig, P. and Cowey, A., 1997).

1.30.2.2 V2/V3/VP

V2 (roughly, Brodmann's area 18) and V3 (even more roughly, Brodmann's area 19) are located adjacent to V1 and are part of extrastriate cortex, sometimes called the peristriate belt. As in V1, V2 and V3 have well-defined topographical (i.e., polar angle and eccentricity) representations of the contralateral visual hemifield (Engel, S. A. *et al.*, 1994; Sereno, M. I. *et al.*, 1995; DeYoe, E. A. *et al.*, 1996; Engel, S. A. *et al.*, 1997a). Each area has a dorsal part (V2d and V3d, above the calcarine fissure representing the lower visual field) and a ventral part (V2v and V3v/VP, below the calcarine representing the upper visual field). In macaques, there is an asymmetry in the size of V2v versus V2d; V2v is slightly wider than V2d (Olavarria, J. F. and Van Essen, D. C., 1997), but such an asymmetry has not been shown in humans.

A long-unresolved controversy in macaques is whether V3d and VP (ventral posterior area) are independent cortical areas (Burkhalter, A. *et al.*, 1986; Felleman, D. J. and Van Essen, D. C., 1987) or two parts of a common area V3 (Gattass, R. *et al.*, 1988; Lyon, D. C. and Kaas, J. H., 2001). Thus far, these two regions are functionally indistinguishable in the human fMRI data, supporting the latter model. In macaques, areas V3 and VP are unusually thin, relative to the width of their neighboring counterparts V2, V4v, and V3A (Felleman, D. J. and Van Essen, D. C., 1991). However, in humans, V3/VP are just as wide as these neighboring retinotopic areas (Tootell, R. B. *et al.*, 1997; Dougherty, R. F. *et al.*, 2003).

The border between V1 and V2 is the representation of vertical meridian, whereas the border between V2 and V3 is the representation of horizontal meridian. Thereby, V2 and V3 (likewise, V1 and V2) have mirror-symmetric visuotopic organizations. It has been suggested that this mirror-symmetric organization might be crucial for optimizing the wiring length of interareal connections (Van Essen, D. C., 1997). V1, V2, and V3 share a common foveal region (foveal confluence) near the occipital pole. Parafoveal and peripheral field stimuli are represented at increasingly anterior positions, in both ventral and dorsal cortex.

Functionally, V2 and V3 have many properties in common with V1. Cells are tuned to simple properties such as orientation, spatial frequency, and color. In macaques, the responses of many V2 neurons are also modulated by more complex properties, such as illusory contours and figure–ground relationships (von der Heydt, R. *et al.*, 1984; Zhou, H. *et al.*, 2000). FMRI suggests that human V2 may be relatively less sensitive to the illusory contours (Mendola, J. D. *et al.*, 1999) – but alternatively, this could be another case in which single units were simply not tested in the most activated areas (as measured by fMRI).

1.30.2.3 V4/V8

In ventral cortex, the border between V3v and V4v is defined by an upper vertical meridian. Currently, there is debate about what constitutes the anterior border of V4 (Figure 3) (Zeki, S. *et al.*, 1991; Hadjikhani, N. K. *et al.*, 1998; Wandell, B. A., 1999; Bartels, A. and Zeki, S., 2000; Wade, A. R. *et al.*, 2002; Tootell, R. B. *et al.*, 2003; Brewer, A. A. *et al.*, 2005). One proposal is that there is a complete hemifield representation, termed human V4 (hV4), adjacent and anterior to V3v, which might be complementary to the dorsal V3A representation (McKeefry, D. J. and Zeki, S., 1997; Kastner, S. *et al.*, 2001; Wade, A. R. *et al.*, 2002; Brewer, A. A. *et al.*, 2005). In contrast, Tootell and colleagues suggest that V4v has a quarter-field representation, and there is a separate area termed V8, consisting of a hemifield representation, which is located anterior to V4v and rotated relative to V4v (Hadjikhani, N. K. *et al.* 1998). In the V8 model, this area has its own representation of the fovea, quite distinct from the foveal representation in adjacent area V4v. All data place the human color-selective region well inferior to the topographic homologue of dorsal V4, which was the originally proposed site of color processing in macaques (e.g., Zeki, S. M., 1973; Zeki, S., 1980).

Clinical studies reveal that color vision loss (achromatopsia) is correlated with damage in the ventral occipito-temporal cortex (Pearlman, A. L. *et al.*, 1979; Damasio, A. *et al.*, 1980; Zeki, S. A.,

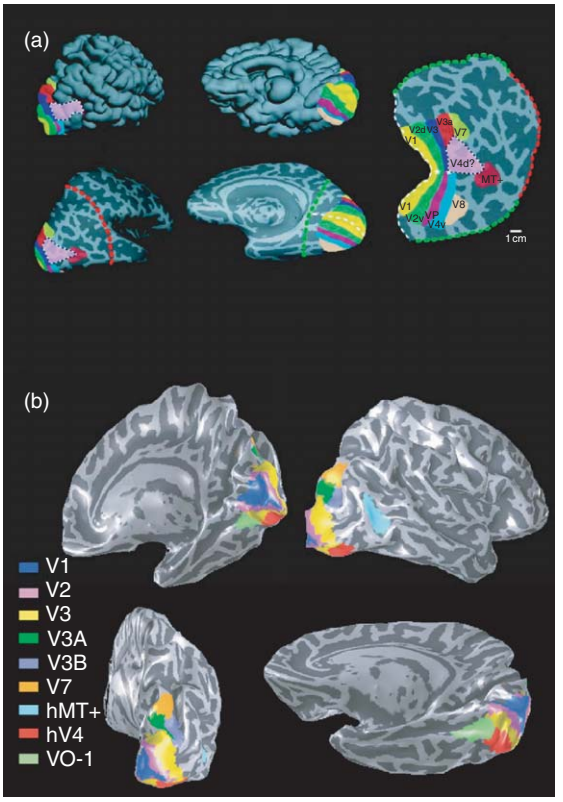

Figure 3 Two proposed models for the retinotopic organization of V4 in humans. The V8 model (a) specifies a quarter-field map, termed V4v, adjacent to the V3v. Anterior to V4v, the model proposes a rotated hemifield representation, termed V8. The hV4 (human V4) model (b) specifies a hemifield map, termed hV4, adjacent to the V3v. Anterior to hV4, the model proposes a cluster of hemifield maps in ventral occipital cortex (VO cluster). The region in the expected location of dorsal V4 (based on macaque V4d) has been assigned a variety of labels such as V4d-topo (a) or V3B (b). Several observations suggest that this region is functionally heterogeneous. (a) Adapted from Tootell, R. B. and Hadjikhani, N. K. 2001. Where is ''dorsal V4'' in human visual cortex? Retinotopic, topographic and functional evidence. Cereb. Cortex 11, 298–311. (b) Adapted from Wandell, B. A., Brewer, A. A., and Dougherty, R. F. 2005. Visual field map clusters in human cortex. Philos. Trans. R. Soc. Lond. B Biol. Sci. 360, 693–707, with permission.

1990). Neuroimaging studies have also shown regions in the vicinity of V4v (but not V4v itself) that respond more strongly to colored patterns than to luminance-defined patterns. These regions are referred to as V8 (Hadjikhani, N. K. *et al.*, 1998; Tootell, R. B. and Hadjikhani, N. K., 2001), the V4 complex (Lueck, C. J. *et al.*, 1989; McKeefry, D. J. and Zeki, S., 1997; Bartels, A. and Zeki, S., 2000), or the ventral occipital (VO) cluster (Wandell, B. A., 1999; Brewer, A. A. *et al.*, 2005). One study has reported that the cortical region V8 is also preferentially activated by color afterimages (Hadjikhani, N. K. *et al.*, 1998). In the V4-complex scheme, this area has been subdivided into two color-selective subdivisions: a posterior structure termed V4 and an anterior one termed V4 alpha (Beauchamp, M. S. *et al.*, 1999; Bartels, A. and Zeki, S., 2000). In the VO-cluster scheme, this cluster has two separate hemifield maps termed VO1 and VO2 (Brewer, A. A. *et al.*, 2005).

1.30.2.4 V5 (Human MT+)

Human MT+ (hMT+) is located at the temporo-parietal occipital junction (Watson, J. D. *et al.*, 1993; Tootell, R. B. *et al.*, 1995b). This region is a central motion-selective locus in the human brain and is a well-accepted homologue of the macaque motion-sensitive area called MT/V5 (Heeger, D. J. *et al.*, 2000; Rees, G. *et al.* 2000; Sereno, M. I. and Tootell, R. B., 2005). hMT+ is selectively activated by moving versus stationary stimuli and exhibits high contrast sensitivity (Tootell, R. B. *et al.*, 1995b). Consistent with psychophysical and electrophysiological findings, fMRI activity in this area decreases when moving color-varying stimuli are equated in luminance (Tootell, R. B. *et al.*, 1995b).

It has been reported that hMT+ contains two distinct subregions, as one might expect from studies of the corresponding region in nonhuman primates. The first subregion (putative hMT) has retinotopic organization but shows little response to peripheral ipsilateral stimulation, indicating smaller receptive fields (Dukelow, S. P. *et al.*, 2001; Huk, A. C. *et al.*, 2002). Conversely, the second subregion within hMT+ (putative human MST or MSTd) has no clear retinotopic organization but responds to peripheral stimuli in both the ipsilateral and contralateral visual hemifields, indicating larger receptive fields (Tootell, R. B. *et al.*, 1998d; Dukelow, S. P. *et al.*, 2001; Huk, A. C. *et al.*, 2002). Retinotopic organization and the relative position of these two subregions in hMT+ are similar to those in the macaque motion areas MT (middle temporal area) and MST (medial superior temporal area) (Gattass, R. and Gross, C. G., 1981; Albright, T. D. and Desimone, R., 1987; Maunsell, J. H. and Van Essen, D. C., 1987). In addition, Dukelow S. P. *et al.* (2001) have reported activity in the anterolateral subsection of the MT+ complex when subjects perform nonvisual pursuit of a self-generated somatosensory target in darkness, suggesting that this region receives extraretinal nonvisual signals,

and thereby corresponds to the human homologue of MSTl (lateral). Some evidence also suggests that there is a functional subregion within the hMT+, which selectively responds to particular radial and circular motion patterns (rather than simple translation) and thus may be involved in calculating optic flow (Morrone, M. C. *et al.*, 2000). Anteroventral to macaque MT/MST, there is another motion-selective area called fundus of the superior temporal sulcus (STS) (FST) (Erickson, R. G. and Dow, B. M., 1989). Currently, no study has reported a human homologue of macaque FST.

Several studies have shown that fMRI activity in hMT+ increases during the perceptual illusion of the motion aftereffect (Tootell, R. B. *et al.*, 1995a; He, S. *et al.*, 1998; Culham, J. C. *et al.*, 1999; Taylor, J. G. *et al.*, 2000; but see Huk, A. C. *et al.*, 2001). Because the motion aftereffect is direction specific, this indicates that hMT+ probably contains direction-selective neural populations, similar to findings in macaques (Maunsell, J. H. and Newsome, W. T. 1987; Britten, K. H. *et al.*, 1992; Salzman, C. D. *et al.*, 1992; Hegger, D. J. *et al.*, 1999). Furthermore, the activation within hMT+ increases linearly with the coherence of motion in random dot patterns (Rees, G. *et al.*, 2000), implying that this area has strong direction selectivity.

hMT+ seems to be mainly involved in global motion processing (Castelo-Branco, M. *et al.*, 2002). For example, hMT+ adapts to patterned motion, in contrast to lower visual areas, which adapt to component motion (Huk, A. C. and Heeger, D. J., 2002). Interestingly, human MT/MST is also activated by static images with implied motion (Kourtzi, Z. and Kanwisher, N., 2000a). Finally, activation of this area is enhanced when subjects attend to or track motion (Buchel, C. *et al.*, 1998; Culham, J. C. *et al.*, 1998).

Thus, converging evidence shows that hMT+ response properties parallel both the response properties of macaque single neurons (Rees, G. *et al.*, 2000) and perception (Muckli, L. *et al.*, 2002). This inference is further supported by clinical studies revealing that akinetopsia (the failure to perceive motion) is associated with lesions in the vicinity of hMT+ (see Zeki, S., 1991, for review).

Adjacent to hMT+, other motion-related cortical sites have been reported. Orban and colleagues described an area termed the kinetic-occipital area (KO) (Dupont, P. *et al.*, 1997; Van Oostende, S. *et al.*, 1997), which is located posterior to hMT+ and specializes in the processing of kinetic boundaries created by discontinuities in motion direction (but see Zeki, S. *et al.*, 2003; Tyler, C. W. *et al.*, 2006). Increasing evidence also suggests a distinct area specialized for perceiving biological motion. This hypothetical area is located within a small region on the posterior STS (STSp) (lateral and anterior to human MT/MST/KO) and is selectively activated during viewing of light-point-defined moving figures (Grossman, E. *et al.*, 2000; Vaina, L. M. *et al.*, 2001; Grossman, E. D. and Blake, R., 2002), but not by the random movement or inverted motion of the same dots that composed the light-point figures. This region is also activated by other types of biological motion such as movies of people walking (Pelphrey, K. A. *et al.*, 2003) or of hand, eye, or mouth movements (Puce, A. and Perrett, D., 2003), or perhaps even implied biological motion (see below).

1.30.2.5 V3A/V3B

After cortical visual areas V3 and V4 were identified and named in macaque monkeys, another region was discovered between them, named V3A (V3 accessory) (Van Essen, D. C. and Zeki, S. M., 1978; Zeki, S. M., 1978a; 1978b). fMRI studies in humans have also revealed a human homologue of V3A (Tootell, R. B. *et al.*, 1997; 1998a; Culham, J. C. *et al.*, 1998; Hasnain, M. K. *et al.*, 1998; Baseler, H. A. *et al.*, 1999; Boynton, G. M. *et al.*, 1999; Mendola, J. D. *et al.*, 1999; Somers, D. C. *et al.*, 1999; Sunaert, S. *et al.*, 1999; Wandell, B. A., 1999). As in macaques, human V3A is regarded as a cortical area that is entirely independent and distinct from its similarly named neighbor, V3, in terms of its retinotopy and functional properties (Tootell, R. B. *et al.*, 1997). Unlike other retinotopic areas in superior occipital cortex (i.e., V1d, V2d, and V3), human V3A has a distinctive, continuous map of the entire contralateral hemifield immediately anterior to area V3 (including a retinotopic representation of both lower and upper visual fields). The inferior vertical meridian is mapped posteriorly (bordering V3), and the superior vertical meridian is mapped at the anterior border of V3A (Tootell, R. B. *et al.*, 1997). The foveal representation is mapped inferiorly, and the periphery is mapped superiorly. In some cases, the V3A foveal representation is displaced from, and located superior to, the confluent foveal representations of V1, V2, V3, and VP (Tootell, R. B. *et al.*, 1997). These properties of human V3A are generally consistent with those described previously in macaque V3A (Tootell, R. B. *et al.*, 2003).

In both macaques and humans, V3A has large receptive fields (Gattass, R. *et al.*, 1988; Tootell, R. B. *et al.*, 1997), which are apparently involved in wide-field visual computations. Such calculations include the processing of binocular disparity (Backus, B. T. *et al.*, 2001; Tsao, D. Y. *et al.*, 2003b; Neri, P. *et al.*, 2004), and illusory contours (Mendola, J. D. *et al.*, 1999). Human V3A is moderately motion-selective, whereas human V3 is less so (Tootell, R. B. *et al.*, 1997; Braddick, O. J. *et al.*, 2001). As in hMT+, contrast sensitivity appears quite high in area V3A (Tootell, R. B. *et al.*, 1997).

Smith A. T. *et al.* (1998) have proposed that V3A (as defined by Tootell, R. B. *et al.*, 1997) may actually consist of two areas, V3A-proper and V3B. In this scheme, both V3A and V3B are located anterior to V3, but V3A borders the peripheral V3 representation, whereas V3B borders the foveal V3 representation. There is no correlate of proposed human area V3B in macaque cortex. Some studies have described a full contralateral hemifield representation in V3B (Press, W. A *et al.*, 2001; Wandell, B. A. *et al.*, 2005; Silver, M. A. *et al.*, 2005), while other groups have reported only a lower contralateral visual quadrant representation in this area (Smith, A. T. *et al.*, 1998; Dumoulin, S. O. *et al.*, 2003). Reportedly, V3B shares a parafoveal representation with V3A. It has motion and disparity specificity like V3A (Smith, A. T. *et al.*, 1998; Greenlee, M. W., 2000) and largely overlaps with the KO area (Zeki, S. *et al.*, 2003).

Tootell R. B. and Hadjikhani N. K. (2001) have discussed a topographic (rather than functional) homologue of macaque dorsal V4 (the V4d topologue), based on neighborhood relations among visual areas (i.e., anterior to V3A, posterior to hMT+, and superior to ventral V4) (Figure 3). V4d-topo incorporates both V3B and KO and hence responds selectively to kinetic motion boundaries. Unlike some previous reports in macaque V4d (Zeki, S. M., 1973; Zeki, S., 1980), human V4d-topo is not significantly color-selective (Tootell, R. B. and Hadjikhani, N. K., 2001).

1.30.2.6 V7

Anterior to V3A lies another representation of polar angle that includes both upper and lower visual fields and is mirror-symmetric to that in V3A. This area has been called V7 (Tootell, R. B. *et al.*, 1998a; 1998b; Tootell, R. B. and Hadjikhani, N. K., 2000; Press, W. A. *et al.*, 2001; Wandell, B. A. *et al.*, 2005; Tyler, C. W. *et al.*, 2005). V7 has a distinct foveal representation (Press, W. A. *et al.*, 2001), and it exhibits robust activity during spatial attention (Tootell, R. B. *et al.*, 1998a; Culham, J. C. *et al.*, 1998). This area may be homologous to the macaque dorsal prelunate (DP) area (Andersen, R. A. *et al.*, 1990; Tootell, R. B. *et al.*, 1998a).

Recently, more topographically organized areas have been reported adjacent and anterior to V7. These areas, labeled IPS1 and IPS2 (IPS: intraparietal sulcus), completely represent the contralateral hemifield and are separated from each other and from V7 by reversals in visual field orientation (Silver, M. A. *et al.*, 2005; Schluppeck, D. *et al.*, 2005). IPS1 and IPS2 are mainly activated during covert shifts of attention or saccadic eye movements (Silver, M. A. *et al.*, 2005; Schluppeck, D. *et al.*, 2005).

1.30.3 Ventral Stream Areas

Cortex anterior to V4 is generally considered part of the ventral (or 'what') processing stream (Ungerleider, L. G. and Mishkin, M., 1982; Mishkin, M. *et al.*, 1983). In macaque, this cortical region includes a cluster of inferotemporal areas that are implicated mainly in pattern recognition and form analysis (Tanaka, K., 1997; Desimone, R. and Ungerleider, L. G., 1989). Similarly, a complex of several subdivisions within human occipito-temporal cortex shows functional specialization in object representation and recognition (Figure 4), so that damage to these regions results in severe visual recognition deficit or agnosia (Farah, M., 1990). Nonetheless, the exact nature of representation in object-related areas is not yet understood. Functional imaging results in humans indicate that object recognition is mediated by both distributed and localized representations. For example, objects such as chairs can be distinguished based on the distributed and overlapping brain activity they elicit, even though no one claims a chair area in cortex (Haxby, J. V. *et al.*, 2001; Spiridon, M. and Kanwisher, N., 2002). However, there are reports of specialized regions in human cortex dedicated to the processing of particular categories such as faces (Kanwisher, N. *et al.*, 1997), places (Epstein, R. and Kanwisher, N., 1998), and body parts (Downing, P. *et al.*, 2001). Malach and colleagues have recently proposed that topographical organization of these specialized regions follows principles of eccentricity mapping (Levy, I. *et al.*, 2001; Malach, R. *et al.*, 2002; Hasson, U. *et al.*, 2002; 2003b; Levy, I. *et al.*, 2004). According to this model, different object categories have specific eccentricity biases (e.g., faces, letters,

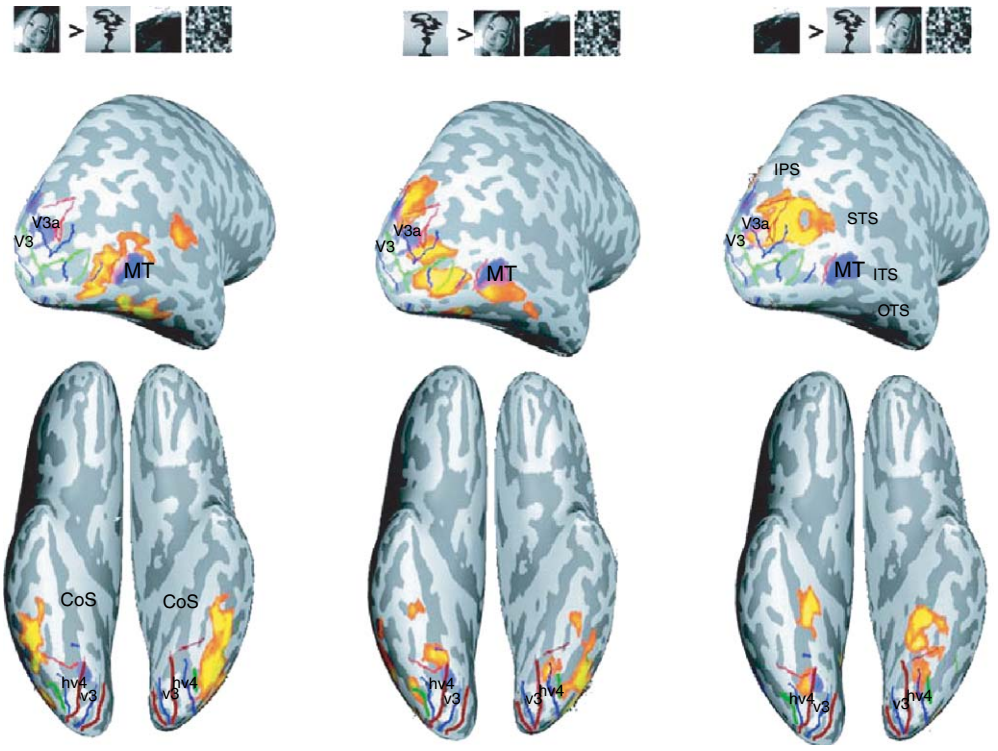

Figure 4 Face-, object-, and place-selective regions in the human brain displayed on an inflated cortical surface. Icons indicate the comparison done in the statistical tests. *Left*: Areas responding more strongly to faces than objects, places, or textures. *Center*: Areas responding more strongly to objects than faces, places, or textures. *Right*: Areas responding more strongly to places (scenes) than faces, objects, or textures. Yellow and orange indicate statistical significance. Colored lines indicate borders of retinotopic visual areas. Blue indicates area hMT+ that responds more strongly to moving versus stationary low-contrast gratings. Adapted from Grill-Spector, K. and Malach, R. 2004. The human visual cortex. Annu. Rev. Neurosci. 27, 649–677, with permission.

and words appear to be associated with central visual field bias, whereas buildings are associated with a peripheral one) (Figure 5). Another putative organizational rule for representation in high-order object areas is that different object categories are topographically represented based on shape-related differences (Fujita, I. *et al.*, 1992; Tanaka, K., 2003). Currently, no systematic investigation has addressed this possibility in human cerebral cortex.

1.30.3.1 Lateral Occipital Complex

Lateral occipital complex (LOC) is a complex of multiple areas in lateral occipital cortex that responds more strongly to a variety of object shapes, as compared with textures, noise patterns, scrambled objects, or scrambled Fourier phase information (which maintains the spatial frequency spectrum) (Malach, R. *et al.*, 1995; Grill-Spector, K. *et al.*, 1998b; 2001). These regions lie anterior and lateral to early retinotopic cortex. Based on fMRI data, the LOC can be divided into at least two putative subdivisions: a dorsal region (LO: lateral occipital) and a more ventral region (LOa: lateral occipital anterior) or pFs (posterior fusiform), along the posterior fusiform gyrus (Grill-Spector, K. *et al.*, 2001). fMRI results in LOC are generally consistent with earlier human PET studies, which had revealed selective activation of ventral and temporal regions associated with the recognition of objects (Haxby, J. V. *et al.*, 1991; Sergent, J. *et al.*, 1992; Kanwisher, N. *et al.*, 1996). This lateral occipital region can be strongly driven by ipsilateral as well as contralateral stimuli (Tootell, R. B. *et al.*, 1998d), and it may have a crude retinotopy (Larsson, J. *et al.*, 2006). The response in LOC is equivalent for familiar and unfamiliar shapes, so the response cannot be obviously accounted for in terms of matching to stored visual representations, or semantic/verbal coding of the stimuli (Malach, R. *et al.*, 1995; Kanwisher, N. *et al.*, 1996; Kanwisher, N., 2003).

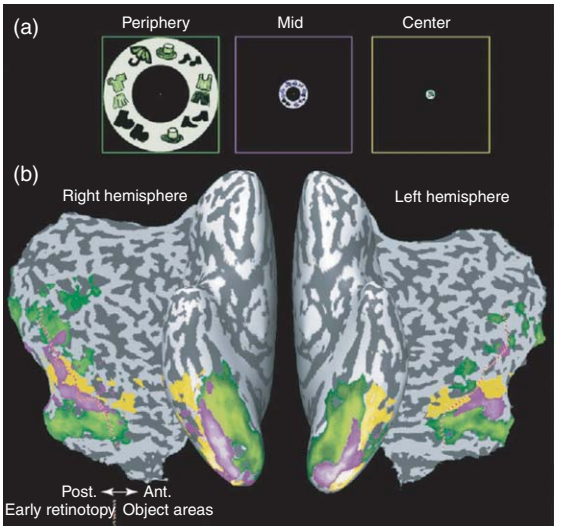

Figure 5 Eccentricity organization of human visual areas. The representations of center (yellow), mid (purple), and peripheral (green) visual field stimuli (a) are shown on a ventral view of the inflated hemispheres and on flattened cortical format (b). The eccentricity mapping is present even in the occipito-temporal cortex. Adapted from Malach, R., Levy, I., and Hasson, U. 2002. The topography of high-order human object areas. Trends Cogn. Sci. 6, 176–184, with permission.

Many studies have shown that the activation in object-selective cortex shows perceptual invariance. Object-selective regions in the ventral stream are activated when subjects view objects defined by luminance (Grill-Spector, K. *et al.*, 1998a), texture (Grill-Spector, K. *et al.*, 1998a; Kastner, S. *et al.*, 2000), motion (Grill-Spector, K. *et al.*, 1998a; Kriegeskorte, N. *et al.*, 2003), or depth cues (Kourtzi, Z. and Kanwisher, N., 2000b; 2001; Gilaie-Dotan, S. *et al.*, 2002), but not when subjects view textures, stationary dot patterns, coherently moving dots, or gratings defined by either motion or stereo. Other studies have shown that activation is independent of object format (photographs or line drawings) (Ishai, A. *et al.*, 2000) and that these regions are also activated when subjects perceive simple shapes created via illusory contours (Mendola, J. D. *et al.*, 1999; Stanley, D. A. and Rubin, N., 2003). Object-selective regions in the ventral stream represent shapes rather than contours or local features (Hasson, U. *et al.*, 2001; Kourtzi, Z. and Kanwisher, N., 2001; Andrews, T. J. *et al.*, 2002; Lerner, Y. *et al.*, 2002) and are more sensitive to the presentation of three-dimensional (3D) volumes relative to 2D shapes (Moore, C. and Engel, S. A., 2001; Kourtzi, Z. *et al.*, 2003a; Welchman, A. E. *et al.*, 2005). However, the unified perception of a global shape (or good Gestalt) may involve both LOC and lower visual areas (V1 and V2) (Murray, S. O. *et al.*, 2002; Altmann, C. F. *et al.*, 2003; Kourtzi, Z. *et al.*, 2003b). Interestingly, some regions within LO even show cross-modality convergence, with stronger activation to objects than textures, for both visually and haptically sensed objects (Amedi, A. *et al.*, 2001; James, T. W. *et al.*, 2002b).

fMR-adaptation paradigms (Grill-Spector, K. and Malach, R., 2001; Avidan, G. *et al.*, 2002b) have revealed more subtle aspects of LOC areas in invariant shape representations. Regions in the occipito-temporal sulcus (OTS) and fusiform gyrus (but not LO) show size and position invariance (Grill-Spector, K. *et al.*, 1999; 2001). In addition, two recent studies show some degree of viewpoint invariance for the representation of objects in ventral occipito-temporal (VOT) when using small rotation angles (James, T. W. *et al.*, 2002a; Vuilleumier, P. *et al.*, 2002; but see Grill-Spector, K. *et al.*, 1999).

Several studies have demonstrated a correlation between object perception and brain activation in lateral and ventral object areas such as LO (Grill-Spector, K. *et al.*, 2000; James, T. W. *et al.*, 2000; Bar, M. *et al.*, 2001; Avidan, G. *et al.*, 2002a; Kleinschmidt, A. *et al.*, 2002; Grill-Spector, K., 2003). In contrast, activity in lower-tier visual areas is not correlated with subjects' percepts in tasks requiring object recognition.

1.30.3.2 Fusiform Face Area

Neuroimaging studies have shown a specific region within the fusiform gyrus that is significantly more active when viewing faces (Sergent, J. and Signoret, J. L., 1992; Haxby, J. V. *et al.*, 1996) compared to other nonface stimuli such as objects (Kanwisher, N. *et al.*, 1997), letter strings (Puce, A. *et al.*, 1996), or houses (Tong, F. *et al.*, 2000). This area has been termed the fusiform face area (FFA) (Kanwisher, N. *et al.*, 1997). Human FFA appears to be topographically homologous to the macaque face patches located in the middle of the STS (Tsao, D. Y. *et al.*, 2003a; 2006). The FFA shows a higher response to upright than inverted faces (Yovel, G. and Kanwisher, N., 2005; but see Epstein, R. A. *et al.*, 2006), suggesting that upright faces are processed holistically in the FFA (see Tanaka, J. W. and Farah, M., 2003, for review). Holistic/configural aspects of face processing may be observed preferentially in the right FFA (Rossion, B. *et al.*, 2000; but see Yovel, G. and Kanwisher, N., 2004). Recently, fMR-adaptation paradigms have elegantly

revealed that the FFA contains subpopulations of neurons, which are selectively tuned to face identity (Rotshtein, P. *et al.*, 2005; Loffler, G. *et al.*, 2005).

FFA activation correlates well with successful face processing but not with successful object processing (Grill-Spector, K. *et al.*, 2004). Other experiments have also used bistable phenomena such as binocular rivalry (Tong, F. *et al.*, 1998), and the Rubin face-vase illusion (Hasson, U. *et al.*, 2001; Andrews, T. J. *et al.*, 2002) to show the correlation of FFA activation with different perceptual states.

Currently, there is debate whether the function of the FFA is truly specific to faces, or whether it instead involves a domain-general operation that could in principle be applied to other stimulus categories. Gauthier and colleagues have argued that the right FFA is an expertise center, responding better to any overtrained visual stimuli, including (but not limited to) faces (Tarr, M. J. and Gauthier, I., 2000). For instance, the FFA is reportedly activated by cars in car experts and by birds in bird experts (Gauthier, I. *et al.*, 2000a). The FFA is also more active when participants become expert at distinguishing computer-generated nonsense shapes known as greebles (Gauthier, I. *et al.*, 1999). These evidence led Tarr M. J. and Gautier I. (2000) to reinterpret the name FFA as the flexible fusiform area. Additional evidence that has challenged the role of FFA in face processing is apparently normal face-related fMRI activation in the FFA in congenital prosopagnosic individuals who are markedly impaired at face processing (Hasson, U. *et al.*, 2003a; Avidan, G. *et al.*, 2005; Behrmann, M. and Avidan, G., 2005).

Early studies of face-selective activation in the cortex have reported that, in addition to the FFA, other cortical areas are selectively active for faces, specifically in the STS and in the inferior and mid-occipital gyri (e.g., Kanwisher, N. *et al.*, 1997; Halgren, E. *et al.*, 1999; Haxby, J. V. *et al.*, 1999; Vaina, L. M. *et al.*, 2001), although in some studies these areas appeared to be less systematically activated (e.g., Kanwisher, N. *et al.*, 1997) or showed a weaker face-selective response (Gauthier, I. *et al.*, 2000b) than did the FFA. Gauthier I. *et al.* (2000b) termed the face-selective inferior occipital area that falls within the larger LOC region, the occipital face area (OFA).

1.30.3.3 Parahippocampal Place Area

The parahippocampal gyrus is a cortical region in the medial temporal lobe that surrounds the hippocampus and plays an important role in both spatial memory (Squire, L. R. and Zola-Morgan, S., 1991) and navigation (Aguirre, G. K. *et al.*, 1996; Maguire, E. A. *et al.*, 1996). The parahippocampal place area (PPA) is a subregion in posterior parahippocampal and anterior lingual cortex that responds preferentially to indoor/outdoor scenes and also to houses/buildings, but not to faces or objects (Epstein, R. and Kanwisher, N., 1998; Aguirre, G. K. *et al.*, 1998). It has been recently demonstrated that the PPA represents scenes in a viewpoint-specific manner (Epstein, R. *et al.*, 2003) and processes the spatial structure of the currently visible environment (Epstein, R. *et al.*, 1999). In addition, activity in the PPA correlates with the scene/house percept (Tong, F. *et al.*, 1998; but see Marois, R. *et al.*, 2004). The evidence for the PPA is supported by neuropsychological patients with topographic disorientation associated with damage in parahippocampal cortex (Habib, M. and Sirigu, A., 1987; Bohbot, V. D. *et al.*, 1998; Aguirre, G. K. and D'Esposito, M., 1999; Epstein, R. *et al.*, 2001).

Recently, Bar and colleagues have shown that the parahippocampal cortex mediates the representation and processing of familiar contextual associations in general, rather than places *per se* (Bar, M. and Aminoff, E., 2003; Bar, M., 2004), and therefore, this region is activated when people recognize highly contextual objects (e.g., a traffic light, houses).

1.30.3.4 Extrastriate Body Area

Downing P. *et al.* (2001) have described a distinct cortical region in humans that responds selectively to images of nonface body parts. This region is located in the lateral occipitotemporal cortex, adjacent to motion-selective MT/MST area, in or near region(s) reportedly activated by the perception of biological motion (Grossman, E. *et al.*, 2000). Peelen M. V. and Downing P. E. (2005) have also reported a fusiform region, so-called the fusiform body area (FBA), which is adjacent to and partially overlaps with the FFA and responds more strongly to headless bodies than to objects (see also Schwarzlose, R. F. *et al.*, 2005).

1.30.4 Dorsal Stream Areas

The human parietal lobes (excluding somatosensory regions) traditionally fall into the category of association cortex because of their complex and multimodal responses (see Zeki, S. M., 1993, for review). Regions of parietal cortex form a major component of the dorsal stream, which is involved in spatial

localization (the 'where' system) (Ungerleider, L. G. and Mishkin, M., 1982) and the control of action (the 'how' system) (Goodale, M. A. and Milner, A. D., 1992). Neuropsychological studies show that patients with parietal damage have attentional disorders (such as hemispatial neglect and simultanagnosia), spatial localization disorders, and sensorimotor coordination problems (Feinberg, T. E. and Farah, M. J., 1997). Single-neuron recordings in macaques also demonstrate numerous regions in parietal cortex that perform highly specialized spatial and sensorimotor functions (Andersen, R. A., 1989; Colby, C. L. and Goldberg, M. E., 1999). Recent neuroimaging studies have identified putative human homologues of macaque parietal regions (particularly regions in the IPS) (Figure 6) (Culham, J. C. and Kanwisher, N. G., 2001; Orban, G. A. *et al.*, 2004; 2006).

1.30.4.1 Caudal Intraparietal Sulcus

Monkey caudal intraparietal sulcus (cIPS) contains neurons selective for binocular disparity and 3D surface orientation and may provide information for the visual guidance of hand action (Sakata, H. *et al.*, 1997; 1998; 1999). Human neuroimaging has identified a region in the caudal end of the IPS that is activated during stereoscopic processing (Tsao, D. Y. *et al.*, 2003b), during object matching and grasping (Faillenot, I. *et al.*, 1997), as well as during discriminations of object size and surface orientation (Faillenot, I. *et al.*, 1999; Shikata, E. *et al.*, 2001). This area might be homologous to monkey cIPS.

1.30.4.2 Parieto-Occipital Cortex/V6

The anterior bank of the parieto-occipital (PO) sulcus of the macaque monkey (classically considered as part of Brodmann's area 19) contains two functionally distinct areas: a ventral, purely visual area, V6, and a dorsal area, V6A, containing visual neurons and neurons related to the control of reaching movements (Colby, C. L. *et al.*, 1988; Galletti, C. *et al.*, 1996; 2005). Macaque V6 contains a topographical representation of the contralateral (both upper and lower) visual field, up to an eccentricity of at least 80° (Galletti, C. *et al.*, 1999). Recent findings suggest that the likely

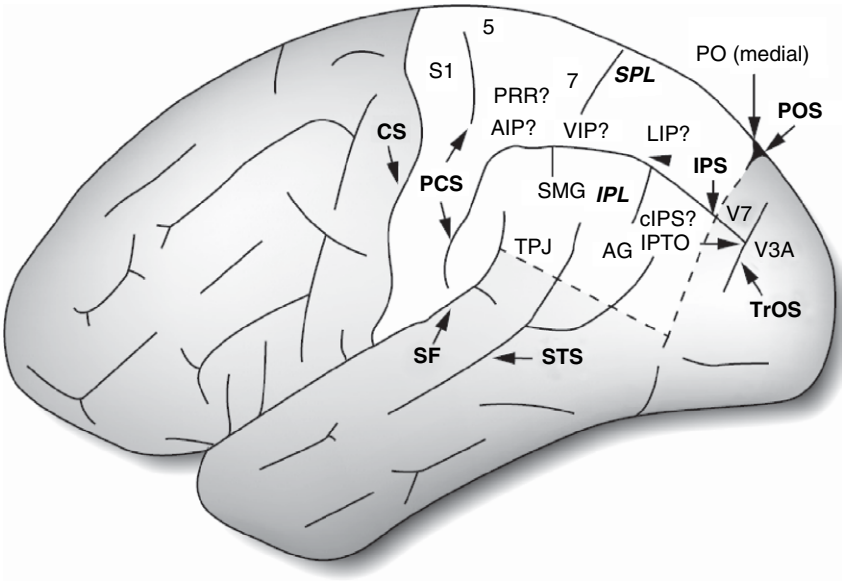

Figure 6 Dorsal stream areas in human parietal lobes. Major sulci, lobules, and functional or anatomical areas have been shown in the lateral view of human brain. Parietal boundaries are based on anatomical landmarks including central sulcus (CS), Sylvian fissure (SF), and parieto-occipital sulcus (POS). The intraparietal sulcus (IPS) divides the parietal lobe into the superior parietal (SPL) and inferior parietal (IPL) lobules. The IPS is located between the transverse occipital sulcus (TrOS near the POS) and the postcentral sulcus (PCS). Several human areas have been proposed to be putative human homologues of monkey areas in the anterior (AIP), ventral (VIP), medial (MIP), lateral (LIP), and caudal (cIPS) sections of the IPS, and also in the parieto-occipital (PO) region. Other areas without clear homologies include the supramarginal (SMG) and angular (AG) gyri, functional areas at the IPS/TrOS junction (IPTO), and the temporo-parietal junction (TPJ). Medial parietal areas have not been well characterized in humans. Adapted from Culham, J. C. and Kanwisher, N. G. 2001. Neuroimaging of cognitive functions in human parietal cortex. Curr. Opin. Neurobiol. 11, 157–163.

human homologue of the macaque V6 is also located in the parieto-occipital sulcus (anteromedial cuneus) (Dechent, P. and Frahm, J., 2003). Human V6 responds strongly to luminance flicker (Portin, K. and Hari, R., 1999; Vanni, S. *et al.*, 2001; Dechent, P. and Frahm, J., 2003). The topography of V6 has not yet been established in humans (Portin, K. and Hari, R., 1999; Dechent, P. and Frahm, J., 2003).

1.30.4.3 Parietal Reach Region

Monkey parietal reach region (PRR) includes both area V6A and the medial intraparietal area (MIP) (Galletti, C. *et al.*, 1997; Snyder, L. H. *et al.*, 1997; Galletti, C. *et al.*, 2003). Neuroimaging studies have also reported activation in the human IPS during reaching and pointing movements (Kertzman, C. *et al.*, 1997; Connolly, J. D. *et al.*, 2000). Reach activity has been reported anterior to saccade activity (Kawashima, R. *et al.*, 1996), whereas pointing-related activation seems to be more medial to a saccade-related region (Connolly, J. D. *et al.*, 2000). A reach-related region in the anterior IPS is modulated by eye position (Baker, J. T. *et al.*, 1999; DeSouza, J. F. X. *et al.*, 2000) and could be the human homologue of the monkey PRR (Andersen, R. A. *et al.*, 1985).

1.30.4.4 Anterior Intraparietal Area

Neurons in monkey anterior intraparietal area (AIP) are involved in fine grasping (Sakata, H. and Taira, M., 1994). The human anterior IPS is also activated during visually guided grasping (Faillenot, I. *et al.*, 1997; Binkofski, F. *et al.*, 1998; Shikata, E. *et al.*, 2003; Culham, J. C. *et al.*, 2003), although grasping activity appears to overlap with reach-related activity. This area is a probable human homologue of monkey AIP. Other studies have reported that this region is also activated by action observation (Iacoboni, M. *et al.*, 1999; Buccino, G. *et al.*, 2001; Muhlau, M. *et al.*, 2005), mental rotation (Bonda, E. *et al.*, 1995), cross-modal processing of object features (Grefkes, C. *et al.*, 2002), tactile manipulation of objects (Binkofski, F. *et al.*, 1999a; 1999b), and even by passive viewing of graspable objects, namely tools (Chao, L. L. and Martin, A., 2000).

1.30.4.5 Ventral Intraparietal Area

Monkey ventral intraparietal area (VIP) responds to motion in any sensory modality (Colby, C. L. *et al.*, 1993; Duhamel, J. R. *et al.*, 1998). Bremmer F. *et al.* (2001) have identified a region in the depth (fundus) of the human IPS that responds multimodally to visual, tactile, and auditory moving stimuli. They propose that this area might be the human equivalent of monkey area VIP. This region is also activated by 3D structure from motion (Orban, G. A. *et al.*, 1999; Vanduffel, W. *et al.*, 2002). In addition, human VIP may play a crucial role in the representation of quantity and number processing (Dehaene, S. *et al.*, 2003; Hubbard, E. M. *et al.*, 2005).

1.30.4.6 Lateral Intraparietal Area

Sereno M. I. *et al.* (2001) have identified a region of the posterior IPS that is thought to be homologous to monkey lateral intraparietal area (LIP) (Colby, C. L. *et al.*, 1996). This region is active when humans make visually guided saccades (Muri, R. M. *et al.*, 1996). Putative LIP contains a retinotopic map of saccade direction (Sereno, M. I. *et al.*, 2001), similar to macaque LIP (Ben Hamed, S. *et al.*, 2001). In addition, recent studies have shown that this region in the IPS is jointly activated by attending, pointing, and making saccades to peripheral targets (Astafiev, S. V. *et al.*, 2003). Another parallel between macaque and human area LIP is the involvement of these areas in spatial updating and representing the spatial location of targets in eye-centered coordinates (Medendorp, W. P. *et al.*, 2003; Merriam, E. P. *et al.*, 2003).

1.30.4.7 Superior Parietal Lobule and Inferior Parietal Lobule

The parietal lobe above the IPS and below the IPS is called superior parietal lobule (SPL) and inferior parietal lobule (IPL), respectively. Human SPL is believed to be homologous to area 7 in macaque cortex (Andersen, R. A., 1988). Human SPL and IPL (including the supramarginal gyrus) along with regions in the IPS, the postcentral sulcus, and the temporo-parietal junction are activated in attention-related tasks (Corbetta, M. *et al.*, 1993; 1998; Wojciulik, E. and Kanwisher, N., 1999; Donner, T. *et al.*, 2000; Corbetta, M. *et al.*, 2000; Hopfinger, J. B. *et al.*, 2000; Perry, R. J. and Zeki, S., 2000; Culham, J. C. *et al.*, 2001). So far, the precise role of these parietal regions in attention is a matter of substantial debate; however, several studies have strengthened the evidence that regions in parietal cortex (particularly SPL and in some cases IPL) are a source of attentional control signals (Kastner, S. *et al.*, 1999;

Shulman, G. L. *et al*., 1999; Corbetta, M., *et al*., 2000; Hopfinger, J. B. *et al*., 2000).

1.30.5 Frontal Areas

Felleman D. J. and Van Essen D. C. (1991) have classified macaque areas 8 (FEF: frontal eye field) and 46 as part of visual cortex. However, little is known about the visual properties of frontal and prefrontal cortical areas in humans. Recently, one study has shown that working memory-related areas in human dorsolateral prefrontal cortex contain a topological map of visual space (Hagler, D. J., Jr. and Sereno, M. I., 2006).

1.30.6 Conclusions

Over the past several decades, the intense and comprehensive study of visual cortical areas in monkeys and other mammals has resulted in what are arguably the best-understood regions of mammalian cortex. This body of work has formed the basis of well-informed models of how sensory information is processed on its way to higher-order integration.

Over most of that time span, very little was known about the workings of visual cortex in humans, except for a few hints from histology and neuropsychology about V1, and a few higher-order visual processing regions. However, with the advent of modern, non-invasive neuroimaging techniques, and with a more systematic comparison of information from macaques and humans, our understanding of human visual cortex is maturing nicely. The next few decades promise to be even more revealing.

References

Aguirre, G. K. and D'Esposito, M. 1999. Topographical disorientation: a synthesis and taxonomy. Brain 122, 1613–1628.

Aguirre, G. K., Detre, J. A., Alsop, D. C., and D'Esposito, M. 1996. The parahippocampus subserves topographical learning in man. Cereb. Cortex 6, 823–829.

Aguirre, G. K., Zarahn, E., and D'Esposito, M. 1998. An area within human ventral cortex sensitive to "building" stimuli: evidence and implications. Neuron 21, 373–383.

Albright, T. D. and Desimone, R. 1987. Local precision of visuotopic organization in the middle temporal area (MT) of the macaque. Exp. Brain. Res. 65, 582–592.

Altmann, C. F., Bulthoff, H. H., and Kourtzi, Z. 2003. Perceptual organization of local elements into global shapes in the human visual cortex. Curr. Biol. 13, 342–349.

Amedi, A., Malach, R., Hendler, T., Peled, S., and Zohary, E. 2001. Visuo-haptic object-related activation in the ventral visual pathway. Nat. Neurosci. 4, 324–330.

Andersen, R. A. 1988. The Neurobiological Basis of Spatial Cognition: Role of the Parietal Lobe. In: Spatial Cognition: Brain Bases and Development (*eds*. J. Stiles-Davis, M. Kritchevsky, and U. Bellugi), pp. 57–81. Erlbaum.

Andersen, R. A. 1989. Visual and eye movement functions of the posterior parietal cortex. Annu. Rev. Neurosci. 12, 377–403.

Andersen, R. A., Asanuma, C., Essick, G., and Siegel, R. M. 1990. Corticocortical connections of anatomically and physiologically defined subdivisions within the inferior parietal lobule. J. Comp. Neurol. 296, 65–113.

Andersen, R. A., Essick, G. K., and Siegel, R. M. 1985. Encoding of spatial location by posterior parietal neurons. Science 230, 456–458.

Andrews, T. J., Schluppeck, D., Homfray, D., Matthews, P., and Blakemore, C. 2002. Activity in the fusiform gyrus predicts conscious perception of Rubin's vase-face illusion. Neuroimage 17, 890–901.

Astafiev, S. V., Shulman, G. L., Stanley, C. M., Snyder, A. Z., Van Essen, D. C., and Corbetta, M. 2003. Functional organization of human intraparietal and frontal cortex for attending, looking, and pointing. J. Neurosci. 23, 4689–4699.

Avidan, G., Harel, M., Hendler, T., Ben-Bashat, D., Zohary, E., and Malach, R. 2002a. Contrast sensitivity in human visual areas and its relationship to object recognition. J. Neurophysiol. 87, 3102–3116.

Avidan, G., Hasson, U., Hendler, T., Zohary, E., and Malach, R. 2002b. Analysis of the neuronal selectivity underlying low fMRI signals. Curr. Biol. 12, 964–972.

Avidan, G., Hasson, U., Malach, R., and Behrmann, M. 2005. Detailed exploration of face-related processing in congenital prosopagnosia: 2. Functional neuroimaging findings. J. Cogn. Neurosci. 17, 1150–1167.

Backus, B. T., Fleet, D. J., Parker, A. J., and Heeger, D. J. 2001. Human cortical activity correlates with stereoscopic depth perception. J. Neurophysiol. 86, 2054–2068.

Baker, J. T., Donoghue, J. P., and Sanes, J. N. 1999. Gaze direction modulates finger movement activation patterns in human cerebral cortex. J. Neurosci. 19, 10044–10052.

Bar, M. 2004. Visual objects in context. Nat. Rev. Neurosci. 5, 617–629.

Bar, M. and Aminoff, E. 2003. Cortical analysis of visual context. Neuron. 38, 347–358.

Bar, M., Tootell, R. B., Schacter, D. L., Greve, D. N., Fischl, B., Mendola, J. D., Rosen, B. R., and Dale, A. M. 2001. Cortical mechanisms specific to explicit visual object recognition. Neuron 29, 529–535.

Barbier, E. L., Marrett, S., Danek, A., Vortmeyer, A., van Gelderen, P., Duyn, J., Bandettini, P., Grafman, J., and Koretsky, A. P. 2002. Imaging cortical anatomy by high-resolution MR at 3.0T: detection of the stripe of Gennari in visual area 17. Magn. Reson. Med. 48, 735–738.

Bartels, A. and Zeki, S. 2000. The architecture of the colour centre in the human visual brain: new results and a review. Eur. J. Neurosci. 12, 172–193.

Baseler, H. A., Morland, A. B., and Wandell, B. A. 1999. Topographic organization of human visual areas in the absence of input from primary cortex. J. Neurosci. 19, 2619–2627.

Beauchamp, M. S., Haxby, J. V., Jennings, J. E., and DeYoe, E. A. 1999. An fMRI version of the Farnsworth-Munsell 100-Hue test reveals multiple color-selective areas in human ventral occipitotemporal cortex. Cereb. Cortex 9, 257–263.

Behrmann, M. and Avidan, G. 2005. Congenital prosopagnosia: face-blind from birth. Trends Cogn. Sci. 9, 180–187.

Ben Hamed, S., Duhamel, J. R., Bremmer, F., and Graf, W. 2001. Representation of the visual field in the lateral

intraparietal area of macaque monkeys: a quantitative receptive field analysis. Exp. Brain Res. 140, 127–144.
Binkofski, F., Buccino, G., Posse, S., Seitz, R. J., Rizzolatti, G., and Freund, H.-J. 1999a. A fronto-parietal circuit for object manipulation in man: evidence from an fMRI-study. Eur. J. Neurosci. 11, 3276–3286.
Binkofski, F., Buccino, G., Stephan, K. M., Rizzolatti, G., Seitz, R. J., and Freund, H.-J. 1999b. A parieto-premotor network for object manipulation: evidence from neuroimaging. Exp. Brain Res. 128, 210–213.
Binkofski, F., Dohle, C., Posse, S., Stephan, K. M., Hefter, H., Seitz, R. J., and Freund, H.-J. 1998. Human anterior intraparietal area subserves prehension. Neurology 50, 1253–1259.
Bohbot, V. D., Kalina, M., Stepankova, K., Spackova, N., Petrides, M., and Nadel, L. 1998. Spatial memory deficits in patients with lesions to the right hippocampus and to the right parahippocampal cortex. Neuropsychologia 36, 1217–1238.
Bonda, E., Petrides, M., Frey, S., and Evans, A. 1995. Neural correlates of mental transformations of the body-in-space. Proc. Natl. Acad. Sci. U. S. A. 92, 11180–11184.
Boynton, G. M. and Finney, E. M. 2003. Orientation-specific adaptation in human visual cortex. J. Neurosci. 23, 8781–8787.
Boynton, G. M., Demb, J. B., Glover, G. H., and Heeger, D. J. 1999. Neuronal basis of contrast discrimination. Vision Res. 39, 257–269.
Boynton, G. M., Engel, S. A., Glover, G. H., and Heeger, D. J. 1996. Linear systems analysis of functional magnetic resonance imaging in human V1. J. Neurosci. 16, 4207–4221.
Braddick, O. J., O'Brien, J. M., Wattam-Bell, J., Atkinson, J., Hartley, T., and Turner, R. 2001. Brain areas sensitive to coherent visual motion. Perception 30, 61–72.
Bremmer, F., Schlack, A., Shah, N. J., Zafiris, O., Kubischik, M., Hoffmann, K., Zilles, K., and Fink, G. R. 2001. Polymodal motion processing in posterior parietal and premotor cortex: a human fMRI study strongly implies equivalencies between humans and monkeys. Neuron 29, 287–296.
Brewer, A. A., Liu, J., Wade, A. R., and Wandell, B. A. 2005. Visual field maps and stimulus selectivity in human ventral occipital cortex. Nat. Neurosci. 8, 1102–1109.
Brewer, A. A., Press, W. A., Logothetis, N. K., and Wandell, B. A. 2002. Visual areas in macaque cortex measured using functional magnetic resonance imaging. J. Neurosci. 22, 10416–10426.
Britten, K. H., Shadlen, M. N., Newsome, W. T., and Movshon, J. A. 1992. The analysis of visual motion: a comparison of neuronal and psychophysical performance. J. Neurosci. 12, 4745–4765.
Brodmann, K. 1909. Vergleichende Lokalisationslehre der Grosshirnrinde in ihren Prinzipien dargestellt auf Grund des Zellenbaues. Barth.
Buccino, G., Binkofski, F., Fink, G. R., Fadiga, L., Fogassi, L., Gallese, V., Seitz, R. J., Zilles, K., Rizzolatti, G., and Freund, H. J. 2001. Action observation activates premotor and parietal areas in a somatotopic manner: an fMRI study. Eur. J. Neurosci. 13, 400–404.
Buchel, C., Josephs, O., Rees, G., Turner, R., Frith, C. D., and Friston, K. J. 1998. The functional anatomy of attention to visual motion. A functional MRI study. Brain 121, 1281–1294.
Burkhalter, A., Felleman, D. J., Newsome, W. T., and Van Essen, D. C. 1986. Anatomical and physiological asymmetries related to visual areas V3 and VP in macaque extrastriate cortex. Vision Res. 26, 63–80.
Castelo-Branco, M., Formisano, E., Backes, W., Zanella, F., Neuenschwander, S., Singer, W., and Goebel, R. 2002. Activity patterns in human motion-sensitive areas depend on the interpretation of global motion. Proc. Natl. Acad. Sci. U. S. A. 99, 13914–13919.
Chao, L. L. and Martin, A. 2000. Representation of manipulable man-made objects in the dorsal stream. Neuroimage 12, 478–484.
Cheng, K., Waggoner, R. A., and Tanaka, K. 2001. Human ocular dominance columns as revealed by high-field functional magnetic resonance imaging. Neuron 32, 359–374.
Clarke, S. 1994a. Association and intrinsic connections of human extrastriate visual cortex. Proc. R. Soc. Lond. B Biol. Sci. 257, 87–92.
Clarke, S. 1994b. Modular organization of human extrastriate visual cortex: evidence from cytochrome oxidase pattern in normal and macular degeneration cases. Eur. J. Neurosci. 6, 725–736.
Clare, S. and Bridge, H. 2005. Methodological issues relating to in vivo cortical myelography using MRI. Hum. Brain Mapp. 26, 240–250.
Colby, C. L. and Goldberg, M. E. 1999. Space and attention in parietal cortex. Annu. Rev. Neurosci. 22, 319–349.
Colby, C. L., Duhamel, J. R., and Goldberg, M. E. 1993. Ventral intraparietal area of the macaque: anatomic location and visual response properties. J. Neurophysiol. 69, 902–914.
Colby, C. L., Duhamel, J. R., and Goldberg, M. E. 1996. Visual, presaccadic, and cognitive activation of single neurons in monkey lateral intraparietal area. J. Neurophysiol. 76, 2841–2851.
Colby, C. L., Gattass, R., Olson, C. R., and Gross, C. G. 1988. Topographical organization of cortical afferents to extrastriate visual area PO in the macaque: a dual tracer study. J. Comp. Neurol. 269, 392–413.
Connolly, J. D., Goodale, M. A., DeSouza, J. F. X., Menon, R. S., and Vilis, T. 2000. A comparison of frontoparietal fMRI activation during anti-saccades and anti-pointing. J. Neurophysiol. 84, 1645–1655.
Conturo, T. E., Lori, N. F., Cull, T. S., Akbudak, E., Snyder, A. Z., Shimony, J. S., McKinstry, R. C., Burton, H., and Raichle, M. E. 1999. Tracking neuronal fiber pathways in the living human brain. Proc. Natl. Acad. Sci. U. S. A. 96, 10422–10427.
Corbetta, M., Akbudak, E., Conturo, T. E., Snyder, A. Z., Ollinger, J. M., Drury, H. A., Linenweber, M. R., Petersen, S. E., Raichle, M. E., Van Essen, D. C., and Shulman, G. L. 1998. A common network of functional areas for attention and eye movements. Neuron 21, 761–773.
Corbetta, M., Kincade, J. M., Ollinger, J. M., McAvoy, M. P., and Shulman, G. L. 2000. Voluntary orienting is dissociated from target detection in human posterior parietal cortex. Nat. Neurosci. 3, 292–297.
Corbetta, M., Miezin, F. M., Shulman, G. L., and Petersen, S. E. 1993. A PET study of visuospatial attention. J. Neurosci. 13, 1202–1226.
Culham, J. C. and Kanwisher, N. G. 2001. Neuroimaging of cognitive functions in human parietal cortex. Curr. Opin. Neurobiol. 11, 157–163.
Culham, J. C., Brandt, S. A., Cavanagh, P., Kanwisher, N. G., Dale, A. M., and Tootell, R. B. 1998. Cortical fMRI activation produced by attentive tracking of moving targets. J. Neurophysiol. 80, 2657–2670.
Culham, J. C., Cavanagh, P., and Kanwisher, N. G. 2001. Attention response functions: characterizing brain areas using fMRI activation during parametric variations of attentional load. Neuron 32, 737–745.
Culham, J. C., Danckert, S. L., DeSouza, J. F., Gati, J. S., Menon, R. S., and Goodale, M. A. 2003. Visually guided grasping produces fMRI activation in dorsal but not ventral stream brain areas. Exp. Brain Res. 153, 180–189.
Culham, J. C., Dukelow, S. P., Vilis, T., Hassard, F. A., Gati, J. S., Menon, R. S., and Goodale, M. A. 1999. Recovery

of fMRI activation in motion area MT following storage of the motion aftereffect. J. Neurophysiol. 81, 388–393.
Damasio, A., Yamada, T., Damasio, H., Corbett, J., and McKee, J. 1980. Central achromatopsia: behavioral, anatomic, and physiologic aspects. Neurology 30, 1064–1071.
Dechent, P. and Frahm, J. 2003. Characterization of the human visual V6 complex by functional magnetic resonance imaging. Eur. J. Neurosci. 17, 2201–2211.
Dehaene, S., Piazza, M., Pinel, P., and Cohen, L. 2003. Three parietal circuits for number processing. Cognit. Neuropsychol. 20, 487–506.
Desimone, R. and Ungerleider, L. G. 1989. Neural mechanisms of visual processing in monkeys. In: Handbook of Neuropsychology, Vol. 2 (*eds*. F. Boller and J. Grafman), pp. 267–299. Elsevier.
Desouza, J. F. X., Dukelow, S. P., Gati, J. S., Menon, R. S., Andersen, R. A., and Vilis, T. 2000. Eye position signal modulates a human parietal pointing region during memory-guided movements. J. Neurosci. 20, 5835–5840.
DeYoe, E. A., Carman, G. J., Bandettini, P., Glickman, S., Wieser, J., Cox, R., Miller, D., and Neitz, J. 1996. Mapping striate and extrastriate visual areas in human cerebral cortex. Proc. Natl. Acad. Sci. U. S. A. 93, 2382–2386.
Donner, T., Kettermann, A., Diesch, E., Ostendorf, F., Villringer, A., and Brandt, S. A. 2000. Involvement of the human frontal eye field and multiple parietal areas in covert visual selection during conjunction search. Eur. J. Neurosci. 12, 3407–3414.
Dougherty, R. F., Koch, V. M., Brewer, A. A., Fisher, B., Modersitzki, J., and Wandell, B. A. 2003. Visual field representations and locations of visual areas v1|2|3 in human visual cortex. J. vis. 3(10), 586–598.
Downing, P., Jiang, Y., Shuman, M., and Kanwisher, N. A 2001. Cortical area selective for visual processing of the human body. Science 293, 2470–2473.
Duhamel, J. R., Colby, C. L., and Goldberg, M. E. 1998. Ventral intraparietal area of the macaque: congruent visual and somatic response properties. J. Neurophysiol. 79, 126–136.
Dukelow, S. P., DeSouza, J. F., Culham, J. C., van Den Berg, A. V., Menon, R. S., and Vilis, T. 2001. Distinguishing subregions of the human mt+ complex using visual fields and pursuit eye movements. J. Neurophysiol 86, 1991–2000.
Dumoulin, S. O., Baker, C. L., Jr., Hess, R. F., and Evans, A. C. 2003. Cortical specialization for processing first- and second-order motion. Cereb. Cortex 13, 1375–1385.
Duncan, R. O. and Boynton, G. M. 2003. Cortical magnification within human primary visual cortex correlates with acuity thresholds. Neuron 38, 659–671.
Dupont, P., De Bruyn, B., Vandenberghe, R., Rosier, A. M., Michiels, J., Marchal, G., Mortelmans, L., and Orban, G. A. 1997. The kinetic occipital region in human visual cortex. Cereb. Cortex 7, 283–292.
Engel, S. A., Glover, G. H., and Wandell, B. A. 1997a. Retinotopic organization in human visual cortex and the spatial precision of functional MRI. Cereb. Cortex 7, 181–192.
Engel, S. A., Rumelhart, D. E., Wandell, B. A., Lee, A. T., Glover, G. H., Chichilnisky, E. J., and Shadlen, M. N. 1994. fMRI of human visual cortex. Nature 369, 525.
Engel, S., Zhang, X., and Wandell, B. 1997b. Colour tuning in human visual cortex measured with functional magnetic resonance imaging. Nature 388, 68–71.
Epstein, R. and Kanwisher, N. A. 1998. cortical representation of the local visual environment. Nature 392, 598–601.
Epstein, R., DeYoe, E. A., Press, D. Z., Rosen, A. C., and Kanwisher, N. 2001. Neuropsychological evidence for a topographical learning mechanism in parahippocampal cortex. Cogn. Neuropsychol. 18, 481–508.
Epstein, R., Graham, K. S., and Downing, P. E. 2003. Viewpoint-specific scene representations in human parahippocampal cortex. Neuron 37, 865–876.
Epstein, R., Harris, A., Stanley, D., and Kanwisher, N. 1999. The parahippocampal place area: recognition, navigation, or encoding?. Neuron 23, 115–125.
Epstein, R. A., Higgins, J. S., Parker, W., Aguirre, G. K., and Cooperman, S. 2006. Cortical correlates of face and scene inversion: a comparison. Neuropsychologia. 44(7), 1145–1158.
Erickson, R. G. and Dow, B. M. 1989. Foveal tracking cells in the superior temporal sulcus of the macaque monkey. Exp. Brain. Res. 78, 113–131.
Faillenot, I., Decety, J., and Jeannerod, M. 1999. Human brain activity related to the perception of spatial features of objects. Neuroimage 10, 114–124.
Faillenot, I., Toni, I., Decety, J., Gregoire, M. C., and Jeannerod, M. 1997. Visual pathways for object-oriented action and object recognition: functional anatomy with PET. Cereb. Cortex 7, 77–85.
Fang, F., Murray, S. O., Kersten, D., and He, S. 2005. Orientation-tuned FMRI adaptation in human visual cortex. J. Neurophysiol. 94, 4188–4195.
Farah, M. 1990. Visual Agnosia: Disorders of Object Recognition and What They Tell Us about Normal Vision. MIT Press, Bradford Books.
Feinberg, T. E. and Farah, M. J. 1997. Behavioral Neurology and Neuropsychology. McGraw-Hill.
Felleman, D. J. and Van Essen, D. C. 1987. Receptive field properties of neurons in area V3 of macaque monkey extrastriate cortex. J. Neurophysiol. 57, 889–920.
Felleman, D. J. and Van Essen, D. C. 1991. Distributed hierarchical processing in the primate cerebral cortex. Cereb. Cortex 1, 1–47.
Fize, D., Vanduffel, W., Nelissen, K., Denys, K., Chef d'Hotel, C., Faugeras, O., and Orban, G. 2003. The retinotopic organization of primate dorsal V4 and surrounding areas: a functional magnetic resonance imaging study in awake monkeys. J. Neurosci. 23, 7395–7406.
Fox, P. T., Miezin, F. M., Allman, J. M., Van Essen, D. C., and Raichle, M. E. 1987. Retinotopic organization of human visual cortex mapped with positron-emission tomography. J. Neurosci. 7, 913–922.
Fujita, I., Tanaka, K., Ito, M., and Cheng, K. 1992. Columns for visual features of objects in monkey inferotemporal cortex. Nature 360, 343–346.
Furmanski, C. S. and Engel, S. A. 2000. An oblique effect in human primary visual cortex. Nat. Neurosci. 3, 535–536.
Galletti, C., Fattori, P., Battaglini, P. P., Shipp, S., and Zeki, S. 1996. Functional demarcation of a border between areas V6 and V6A in the superior parietal gyrus of the macaque monkey. Eur. J. Neurosci. 8, 30–52.
Galletti, C., Fattori, P., Gamberini, M., and Kutz, D. F. 1999. The cortical visual area V6: brain location and visual topography. Eur. J. Neurosci. 11, 3922–3936.
Galletti, C., Fattori, P., Kutz, D. F., and Battaglini, P. P. 1997. Arm movement-related neurons in the visual area V6A of the macaque superior parietal lobule. Eur. J. Neurosci. 9, 410–413.
Galletti, C., Gamberini, M., Kutz, D. F., Baldinotti, I., and Fattori, P. 2005. The relationship between V6 and PO in macaque extrastriate cortex. Eur. J. Neurosci. 21, 959–970.
Galletti, C., Kutz, D. F., Gamberini, M., Breveglieri, R., and Fattori, P. 2003. Role of the medial parieto-occipital cortex in the control of reaching and grasping movements. Exp. Brain Res. 153, 158–170.
Gattass, R. and Gross, C. G. 1981. Visual topography of striate projection zone (MT) in posterior superior temporal sulcus of the macaque. J. Neurophysiol. 46, 621–638.
Gattass, R., Gross, C. G., and Sandell, J. H. 1981. Visual topography of V2 in the macaque. J. Comp. Neurol. 201, 519–539.

Gattass, R., Sousa, A. P., and Gross, C. G. 1988. Visuotopic organization and extent of V3 and V4 of the macaque. J. Neurosci. 8, 1831–1845.

Gauthier, I., Skudlarski, P., Gore, J. C., and Anderson, A. W. 2000a. Expertise for cars and birds recruits brain areas involved in face recognition. Nat. Neurosci. 3, 191–197.

Gauthier, I., Tarr, M. J., Anderson, A. W., Skudlarski, P., and Gore, J. C. 1999. Activation of the middle fusiform ''face area'' increases with expertise in recognizing novel objects. Nat. Neurosci. 2, 568–573.

Gauthier, I., Tarr, M. J., Moylan, J., Skudlarski, P., Gore, J. C., and Anderson, W. A. 2000b. The fusiform ''face area'' is part of a network that processes faces at the individual level. J. Cogn. Neurosci. 12, 495–504.

Gilaie-Dotan, S., Ullman, S., Kushnir, T., and Malach, R. 2002. Shape-selective stereo processing in human object-related visual areas. Hum. Brain Mapp. 15, 67–79.

Goodale, M. A. and Milner, A. D. 1992. Separate visual pathways for perception and action. Trends Neurosci. 15, 20–25.

Greenlee, M. W. 2000. Human cortical areas underlying the perception of optic flow: brain imaging studies. Int. Rev. Neurobiol. 44, 269–292.

Grefkes, C., Weiss, P. H., Zilles, K., and Fink, G. R. 2002. Crossmodal processing of object features in human anterior intraparietal cortex: an fMRI study implies equivalencies between humans and monkeys. Neuron 35, 173–184.

Grill-Spector, K. 2003. The Functional Organization of the Ventral Visual Pathway and its Relationship to Object Recognition. In: Attention and Performance XX. Functional Brain Imaging of Visual Cognition (*eds*. N. Kanwisher and J. Duncan), pp. 169–193. Oxford University Press.

Grill-Spector, K. and Malach, R. 2001. fMR-adaptation: a tool for studying the functional properties of human cortical neurons. Acta Psychol. (Amst.) 107, 293–321.

Grill-Spector, K. and Malach, R. 2004. The human visual cortex. Annu. Rev. Neurosci. 27, 649–677.

Grill-Spector, K., Knouf, N., and Kanwisher, N. 2004. The fusiform face area subserves face perception, not generic within-category identification. Nat. Neurosci. 7, 555–562.

Grill-Spector, K., Kourtzi, Z., and Kanwisher, N. 2001. The lateral occipital complex and its role in object recognition. Vision Res. 41, 1409–1422.

Grill-Spector, K., Kushnir, T., Edelman, S., Avidan, G., Itzchak, Y., and Malach, R. 1999. Differential processing of objects under various viewing conditions in the human lateral occipital complex. Neuron 24, 187–203.

Grill-Spector, K., Kushnir, T., Edelman, S., Itzchak, Y., and Malach, R. 1998a. Cue-invariant activation in object-related areas of the human occipital lobe. Neuron 21, 191–202.

Grill-Spector, K., Kushnir, T., Hendler, T., Edelman, S., Itzchak, Y., and Malach, R. A. 1998b. sequence of object-processing stages revealed by fMRI in the human occipital lobe. Hum. Brain Mapp. 6, 316–328.

Grill-Spector, K., Kushnir, T., Hendler, T., and Malach, R. 2000. The dynamics of object-selective activation correlate with recognition performance in humans. Nat. Neurosci. 3, 837–843.

Grossman, E. D. and Blake, R. 2002. Brain areas active during visual perception of biological motion. Neuron 35, 1167–1175.

Grossman, E., Donnelly, M., Price, R., Pickens, D., Morgan, V., Neighbor, G., and Blake, R. 2000. Brain areas involved in perception of biological motion. J. Cogn. Neurosci. 12, 711–720.

Habib, M. and Sirigu, A. 1987. Pure topographical disorientation: a definition and anatomical basis. Cortex 23, 73–85.

Hadjikhani, N. K., Liu, A. K., Dale, A. M., Cavanagh, P., and Tootell, R. B. 1998. Retinotopy and color sensitivity in human visual cortical area V8. Nat. Neurosci. 1, 235–241.

Hagler, D. J., Jr., and Sereno, M. I. 2006. Spatial maps in frontal and prefrontal cortex. Neuroimage 29, 567–577.

Hagmann, P., Thiran, J. P., Jonasson, L., Vandergheynst, P., Clarke, S., Maeder, P., and Meuli, R. 2003. DTI mapping of human brain connectivity: statistical fibre tracking and virtual dissection. Neuroimage 19, 545–554.

Halgren, E., Dale, A. M., Sereno, M. I., Tootell, R. B., Marinkovic, K., and Rosen, B. R. 1999. Location of human face-selective cortex with respect to retinotopic areas. Hum. Brain Mapp. 7, 29–37.

Haseltine, E. C., DeBruyn, E. J., and Casagrande, V. A. 1979. Demonstration of ocular dominance columns in Nissl-stained sections of monkey visual cortex following enucleation. Brain Res. 176, 153–158.

Hasnain, M. K., Fox, P. T., and Woldorff, M. G. 1998. Intersubject variability of functional areas in the human visual cortex. Hum. Brain Mapp. 6, 301–315.

Hasson, U., Avidan, G., Deouell, L. Y., Bentin, S., and Malach, R. 2003a. Face-selective activation in a congenital prosopagnosic subject. J. Cogn. Neurosci. 15, 419–431.

Hasson, U., Harel, M., Levy, I., and Malach, R. 2003b. Large-scale mirror-symmetry organization of human occipito-temporal object areas. Neuron 37, 1027–1041.

Hasson, U., Hendler, T., Ben Bashat, D., and Malach, R. 2001. Vase or face? A neural correlate of shape-selective grouping processes in the human brain. J. Cogn. Neurosci. 13, 744–753.

Hasson, U., Levy, I., Behrmann, M., Hendler, T., and Malach, R. 2002. Eccentricity bias as an organizing principle for human high-order object areas. Neuron 34, 479–490.

Haynes, J. D. and Rees, G. 2005. Predicting the orientation of invisible stimuli from activity in human primary visual cortex. Nat. Neurosci. 8, 686–691.

Haxby, J. V., Gobbini, M. I., Furey, M. L., Ishai, A., Schouten, J. L., and Pietrini, P. 2001. Distributed and overlapping representations of faces and objects in ventral temporal cortex. Science 293, 2425–2430.

Haxby, J. V., Grady, C. L., Horwitz, B., Ungerleider, L. G., Mishkin, M., Carson, R. E., Herscovitch, P., Schapiro, M. B., and Rapoport, S. I. 1991. Dissociation of object and spatial visual processing pathways in human extrastriate cortex. Proc. Natl. Acad. Sci. U. S. A. 88, 1621–1625.

Haxby, J. V., Ungerleider, L. G., Clark, V. P., Schouten, J. L., Hoffman, E. A., and Martin, A. 1999. The effect of face inversion on activity in human neural systems for face and object perception. Neuron 22, 189–199.

Haxby, J. V., Ungerleider, L. G., Horwitz, B., Maisog, J. M., Rapoport, S. I., and Grady, C. L. 1996. Face encoding and recognition in the human brain. Proc. Natl. Acad. Sci. U. S. A. 93, 922–927.

He, S., Cohen, E. R., and Hu, X. 1998. Close correlation between activity in brain area MT/V5 and the perception of a visual motion aftereffect. Curr. Biol. 8, 1215–1218.

Heeger, D. J., Huk, A. C., Geisler, W. S., and Albrecht, D. G. 2000. Spikes versus BOLD: What does neuroimaging tell us about neuronal activity? Nat. Neurosci. 3, 631–633.

Hegger, D. J., Boynton, G. M., Demb, J. B., Seidemann, E., and Newrome, W. T. 1999. Motion opponency in visual cortex. J. Neurosci. 19(16), 7162–7174.

Hendry, S. H., Huntsman, M. M., Vinuela, A., Mohler, H., de Blas, A. L., and Jones, E. G. 1994. GABAA receptor subunit immunoreactivity in primate visual cortex: distribution in macaques and humans and regulation by visual input in adulthood. J. Neurosci. 14, 2383–2401.

von der Heydt, R., Peterhans, E., and Baumgartner, G. 1984. Illusory contours and cortical neuron responses. Science 224, 1260–1262.

Hitchcock, P. F. and Hickey, T. L. 1980. Ocular dominance columns: evidence for their presence in humans. Brain Res. 182, 176–179.
Holmes, G. 1918. Disturbances of vision by cerebral lesions. Brit. J. Ophthalmol. 2, 353–384.
Holmes, G. and Lister, W. T. 1916. Disturbances of vision from cerebral lesion with special reference to the cortical representation of the macula. Brain 39, 34–73.
Hopfinger, J. B., Buonocore, M. H., and Mangun, G. R. 2000. The neural mechanisms of top-down attentional control. Nat. Neurosci. 3, 284–291.
Horton, J. C. and Hedley-Whyte, E. T. 1984. Mapping of cytochrome oxidase patches and ocular dominance columns in human visual cortex. Philos. Trans. R. Soc. London Ser. B Biol. Sci. 304, 255–272.
Horton, J. C., Dagi, L. R., McCrane, E. P., and de Monasterio, F. M. 1990. Arrangement of ocular dominance columns in human visual cortex. Arch. Ophthalmol. 108, 1025–1031.
Hubbard, E. M., Piazza, M., Pinel, P., and Dehaene, S. 2005. Interactions between number and space in parietal cortex. Nat. Rev. Neurosci. 6, 435–448.
Hubel, D. H. and Wiesel, T. N. 1968. Receptive fields and functional architecture of monkey striate cortex. J. Physiol. (Lond.) 195, 215–243.
Hubel, D. H. and Wiesel, T. N. 1972. Laminar and columnar distribution of geniculo-cortical fibers in macaque monkey. J. Comp. Neurol. 146, 421–450.
Huk, A. C. and Heeger, D. J. 2002. Pattern-motion responses in human visual cortex. Nat. Neurosci. 5, 72–75.
Huk, A. C., Dougherty, R. F., and Heeger, D. J. 2002. Retinotopy and functional subdivision of human areas MT and MST. J. Neurosci. 22, 7195–7205.
Huk, A. C., Ress, D., and Heeger, D. J. 2001. Neuronal basis of the motion aftereffect reconsidered. Neuron 32, 161–172.
Iacoboni, M., Woods, R. P., Brass, M., Bekkering, H., Mazziotta, J. C., and Rizzolatti, G. 1999. Cortical mechanisms of human imitation. Science 286, 2526–2528.
Ishai, A., Ungerleider, L. G., Martin, A., and Haxby, J. V. 2000. The representation of objects in the human occipital and temporal cortex. J. Cogn. Neurosci. 12, 35–51.
James, T. W., Humphrey, G. K., Gati, J. S., Menon, R. S., and Goodale, M. A. 2000. The effects of visual object priming on brain activation before and after recognition. Curr. Biol. 10, 1017–1024.
James, T. W., Humphrey, G. K., Gati, J. S., Menon, R. S., and Goodale, M. A. 2002a. Differential effects of viewpoint on object-driven activation in dorsal and ventral streams. Neuron 35, 793–801.
James, T. W., Humphrey, G. K., Gati, J. S., Servos, P., Menon, R. S., and Goodale, M. A. 2002b. Haptic study of three-dimensional objects activates extrastriate visual areas. Neuropsychologia 40, 1706–1714.
Kaas, J. H. 1997. Theories of Visual Cortex Organization in Primates. In: Cerebral Cortex, Extrastriate Cortex in Primates, Vol. 12 (*eds*. K. S. Rockland, J. H. Kaas, and A. Peters), pp. 91–125. Plenum Press.
Kamitani, Y. and Tong, F. 2005. Decoding the visual and subjective contents of the human brain. Nat. Neurosci. 8, 679–685.
Kanwisher, N. 2003. The Ventral Visual Object Pathway in Humans: Evidence from fMRI. In: The Visual Neurosciences (*eds*. L. Chalupa and J. S. Werner), pp. 1179–1189. MIT Press.
Kanwisher, N., Chun, M. M., McDermott, J., and Ledden, P. J. 1996. Functional imaging of human visual recognition. Brain Res. Cogn. Brain Res. 5, 55–67.
Kanwisher, N., McDermott, J., and Chun, M. 1997. The fusiform face area: a module in human extrastriate cortex specialized for face perception. J. Neurosci. 17, 4302–4311.
Kastner, S., De Weerd, P., Pinsk, M. A., Elizondo, M. I., Desimone, R., and Ungerleider, L. G. 2001. Modulation of sensory suppression: implications for receptive field sizes in the human visual cortex. J. Neurophysiol. 86, 1398–1411.
Kastner, S., De Weerd, P., and Ungerleider, L. G. 2000. Texture segregation in the human visual cortex: a functional MRI study. J. Neurophysiol. 83, 2453–2457.
Kastner, S., Pinsk, M. A., De Weerd, P., Desimone, R., and Ungerleider, L. G. 1999. Increased activity in human visual cortex during directed attention in the absence of visual stimulation. Neuron 22, 751–761.
Kawashima, R., Naitoh, E., Matsumura, M., Itoh, H., Ono, S., Satoh, K., Gotoh, R., Koyama, M., Inoue, K., Yoshioka, S., and Fukuda, H. 1996. Topographic representation in human intraparietal sulcus of reaching and saccade. Neuroreport 7, 1253–1256.
Kertzman, C., Schwarz, U., Zeffiro, T. A., and Hallett, M. 1997. The role of posterior parietal cortex in visually guided reaching movements in humans. Exp. Brain Res. 114, 170–183.
Kleinschmidt, A., Buchel, C., Hutton, C., Friston, K. J., and Frackowiak, R. S. 2002. The neural structures expressing perceptual hysteresis in visual letter recognition. Neuron 34, 659–666.
Kourtzi, Z. and Kanwisher, N. 2000a. Activation in human MT/MST by static images with implied motion. J. Cogn. Neurosci. 12, 48–55.
Kourtzi, Z. and Kanwisher, N. 2000b. Cortical regions involved in perceiving object shape. J. Neurosci. 20, 3310–3318.
Kourtzi, Z. and Kanwisher, 2001. N. Representation of perceived object shape by the human lateral occipital complex. Science 293, 1506–1509.
Kourtzi, Z., Erb, M., Grodd, W., and Bulthoff, H. H. 2003a. Representation of the perceived 3-D object shape in the human lateral occipital complex. Cereb. Cortex 13, 911–920.
Kourtzi, Z., Tolias, A. S., Altmann, C. F., Augath, M., and Logothetis, N. K. 2003b. Integration of local features into global shapes: monkey and human FMRI studies. Neuron 37, 333–346.
Kriegeskorte, N., Sorger, B., Naumer, M., Schwarzbach, J., van den Boogert, E., Hussy, W., and Goebel, R. 2003. Human cortical object recognition from a visual motion flowfield. J. Neurosci. 23, 1451–1463.
Larsson, J., Landy, M. S., and Heeger, D. J. 2006. Orientation-selective adaptation to first- and second-order patterns in human visual cortex. J. Neurophysiol. 95, 862–881.
Lerner, Y., Hendler, T., and Malach, R. 2002. Object-completion effects in the human lateral occipital complex. Cereb. Cortex 12, 163–177.
Levy, I., Hasson, U., Avidan, G., Hendler, T., and Malach, R. 2001. Center-periphery organization of human object areas. Nat. Neurosci. 4, 533–539.
Levy, I., Hasson, U., Harel, M., and Malach, R. 2004. Functional analysis of the periphery effect in human building related areas. Hum. Brain Mapp. 22, 15–26.
Loffler, G., Yourganov, G., Wilkinson, F., and Wilson, H. R. 2005. fMRI evidence for the neural representation of faces. Nat. Neurosci. 8, 1386–1390.
Lueck, C. J., Zeki, S., Friston, K. J., Deiber, M. P., Cope, P., Cunningham, V. J., Lammertsma, A. A., Kennard, C., and Frackowiak, R. S. 1989. The colour centre in the cerebral cortex of man. Nature 340, 386–389.
Lund, J. S. 1988. Anatomical organization of macaque monkey striate visual cortex. Annu. Rev. Neurosci. 11, 253–288.
Lyon, D. C. and Kaas, J. H. 2001. Connectional and architectonic evidence for dorsal and ventral V3, and dorsomedial area in marmoset monkeys. J. Neurosci. 21, 249–261.
Maguire, E. A., Frackowiak, R. S. J., and Frith, C. D. 1996. Learning to find your way: a role for the human hippocampal region. Proc. R. Soc. Lond. B Biol. Sci. 263, 1745–1750.

Malach, R., Levy, I., and Hasson, U. 2002. The topography of high-order human object areas. Trends Cogn. Sci. 6, 176–184.

Malach, R., Reppas, J. B., Benson, R. R., Kwong, K. K., Jiang, H., Kennedy, W. A., Ledden, P. J., Brady, T. J., Rosen, B. R., and Tootell, R. B. 1995. Object-related activity revealed by functional magnetic resonance imaging in human occipital cortex. Proc. Natl. Acad. Sci. U. S. A. 92, 8135–8139.

Marois, R., Yi, D. J., and Chun, M. M. 2004. The neural fate of consciously perceived and missed events in the attentional blink. Neuron 41, 465–472.

Maunsell, J. H. and Newsome, W. T. 1987. Visual processing in monkey extrastriate cortex. Annu. Rev. Neurosci. 10, 363–401.

Maunsell, J. H. and Van Essen, D. C. 1987. Topographic organization of the middle temporal visual area in the macaque monkey: representational biases and the relationship to callosal connections and myeloarchitectonic boundaries. J. Comp. Neurol. 266, 535–555.

McKeefry, D. J. and Zeki, S. 1997. The position and topography of the human colour centre as revealed by functional magnetic resonance imaging. Brain 120, 2229–2242.

Medendorp, W. P., Goltz, H. C., Villis, T., and Crawford, J. D. 2003. Gaze-centered updating of visual space in human parietal cortex. J. Neurosci. 23, 6209–6214.

Mendola, J. D., Dale, A. M., Fischl, B., Liu, A. K., and Tootell, R. B. 1999. The representation of illusory and real contours in human cortical visual areas revealed by functional magnetic resonance imaging. J. Neurosci. 19, 8560–8572.

Menon, R. S., Ogawa, S., Strupp, J. P., and Ugurbil, K. 1997. Ocular dominance in human V1 demonstrated by functional magnetic resonance imaging. J. Neurophysiol. 77, 2780–2787.

Merriam, E. P., Genovese, G. R., and Colby, C. L. 2003. Spatial updating in human parietal cortex. Neuron 39, 361–373.

Mishkin, M., Ungerleider, L. G., and Macko, K. A. 1983. Object vision and spatial vision: two cortical pathways. Trends Neurosci. 6, 414–417.

Moore, C. and Engel, S. A. 2001. Neural response to perception of volume in the lateral occipital complex. Neuron 29, 277–286.

Morrone, M. C., Tosetti, M., Montanaro, D., Fiorentini, A., Cioni, G., and Burr, D. C. 2000. A cortical area that responds specifically to optic flow, revealed by fMRI. Nat. Neurosci. 3, 1322–1328.

Muckli, L., Kriegeskorte, N., Lanfermann, H., Zanella, F. E., Singer, W., and Goebel, R. 2002. Apparent motion: event-related functional magnetic resonance imaging of perceptual switches and States. J. Neurosci. 22, RC219.

Muhlau, M., Hermsdorfer, J., Goldenberg, G., Wohlschlager, A. M., Castrop, F., Stahl, R., Rottinger, M., Erhard, P., Haslinger, B., Ceballos-Baumann, A. O., Conrad, B., and Boecker, H. 2005. Left inferior parietal dominance in gesture imitation: an fMRI study. Neuropsychologia 43, 1086–1098.

Muri, R. M., Iba-Zizen, M. T., Derosier, C., Cabanis, E. A., and Pierrot-Deseilligny, C. 1996. Location of the human posterior eye fields with functional magnetic resonance imaging. J. Neurol. Neurosurg. Psychiatry 60, 445–448.

Murray, S. O., Kersten, D., Olshausen, B. A., Schrater, P., and Woods, D. L. 2002. Shape perception reduces activity in human primary visual cortex. Proc. Natl. Acad. Sci. U. S. A. 99, 15164–15169.

Neri, P., Bridge, H., and Heeger, D. J. 2004. Stereoscopic processing of absolute and relative disparity in human visual cortex. J. Neurophysiol. 92, 1880–1891.

Nishida, S., Sasaki, Y., Murakami, I., Watanabe, T., and Tootell, R. B. 2003. Neuroimaging of direction-selective mechanisms for second-order motion. J. Neurophysiol. 90, 3242–3254.

Olavarria, J. F. and Van Essen, D. C. 1997. The global pattern of cytochrome oxidase stripes in visual area V2 of the macaque monkey. Cereb. Cortex. 7, 395–404.

Orban, G. A., Claeys, K., Nelissen, K., Smans, R., Sunaert, S., Todd, J. T., Wardak, C., Durand, J. B., and Vanduffel, W. 2006. Mapping the parietal cortex of human and non-human primates. Neuropsychologia 44(13), 2647–2667.

Orban, G. A., Sunaert, S., Todd, J. T., Van Hecke, P., and Marchal, G. 1999. Human cortical regions involved in extracting depth from motion. Neuron 24, 929–940.

Orban, G. A., Van Essen, D., and Vanduffel, W. 2004. Comparative mapping of higher visual areas in monkeys and humans. Trends Cogn. Sci. 8, 315–324.

Pearlman, A. L., Birch, J., and Meadows, J. C. 1979. Cerebral color blindness: an acquired defect in hue discrimination. Ann. Neurol. 5, 253–261.

Peelen, M. V. and Downing, P. E. 2005. Selectivity for the human body in the fusiform gyrus. J. Neurophysiol. 93, 603–608.

Penfield, W., Jaspers, H., and McNaughton, F. 1954. Epilepsy and the functional anatomy of the human brain. Little Brown.

Pelphrey, K. A., Mitchell, T. V., McKeown, M. J., Goldstein, J., Allison, T., and McCarthy, G. 2003. Brain activity evoked by the perception of human walking: controlling for meaningful coherent motion. J. Neurosci. 23, 6819–6825.

Perry, R. J. and Zeki, S. 2000. The neurology of saccades and covert shifts in spatial attention: an event-related fMRI study. Brain 123, 2273–2288.

Polyak, S. A. 1933. Contribution to the cerebra representation of the retina. J. Comp. Neurol. 57, 541–617.

Portin, K. and Hari, R. 1999. Human parieto-occipital visual cortex: lack of retinotopy and foveal magnification. Proc. Biol. Sci. 266, 981–985.

Press, W. A., Brewer, A. A., Dougherty, R. F., Wade, A. R., and Wandell, B. A. 2001. Visual areas and spatial summation in human visual cortex. Vision Res. 41, 1321–1332.

Puce, A. and Perrett, D. 2003. Electrophysiology and brain imaging of biological motion. Philos. Trans. R. Soc. London Ser. B Biol. Sci. 358, 435–445.

Puce, A., Allison, T., Asgari, M., Gore, J. C., and McCarthy, G. 1996. Differential sensitivity of human visual cortex to faces, letter strings, and textures: a functional magnetic resonance imaging study. J. Neurosci. 16, 5205–5215.

Rademacher, J., Caviness, V. S., Jr., Steinmetz, H., and Galaburda, A. M. 1993. Topographical variation of the human primary cortices: implications for neuroimaging, brain mapping, and neurobiology. Cereb. Cortex. 3, 313–329.

Rees, G., Friston, K., and Koch, C. A 2000. Direct quantitative relationship between the functional properties of human and macaque V5. Nat. Neurosci. 3, 716–723.

Rossion, B., Dricot, L., Devolder, A., Bodart, J. M., Crommelinck, M., De Gelder, B., and Zoontjes, R. 2000. Hemispheric asymmetries for whole-based and part-based face processing in the human fusiform gyrus. J. Cogn. Neurosci. 12, 793–802.

Rotshtein, P., Henson, R. N., Treves, A., Driver, J., and Dolan, R. J. 2005. Morphing Marilyn into Maggie dissociates physical and identity face representations in the brain. Nat. Neurosci. 8, 107–113.

Sakata, H. and Taira, M. 1994. Parietal control of hand action. Curr. Opin. Neurobiol. 4, 847–856.

Sakata, H., Taira, M., Kusunoki, M., Murata, A., and Tanaka, Y. 1997. The TINS Lecture. The parietal association cortex in depth perception and visual control of hand action. Trends Neurosci. 20, 350–357.

Sakata, H., Taira, M., Kusunoki, M., Murata, A., Tanaka, Y., and Tsutsui, K. 1998. Neural coding of 3D features of objects for hand action in the parietal cortex of the monkey. Philos. Trans. R. Soc. Lond. B Biol. Sci. 353, 1363–1373.

Sakata, H., Taira, M., Kusunoki, M., Murata, A., Tsutsui, K., Tanaka, Y., Shein, W. N., and Miyashita, Y. 1999. Neural representation of three-dimensional features of manipulation objects with stereopsis. Exp. Brain Res. 128, 160–169.

Salzman, C. D., Murasugi, C. M., Britten, K. H., and Newsome, W. T. 1992. Microstimulation in visual area MT: effects on direction discrimination performance. J. Neurosci. 12, 2331–2355.

Sasaki, Y., Rajimehr, R., Kim, B. W., Ekstrom, L. B., Vanduffel, W., and Tootell, R. B. 2006. The radial bias: a different slant on visual orientation sensitivity in human and nonhuman primates. Neuron 51(5), 661–670.

Schluppeck, D., Glimcher, P., and Heeger, D. J. 2005. Topographic organization for delayed saccades in human posterior parietal cortex. J. Neurophysiol. 94, 1372–1384.

Schwartz, E. L. 1977. Spatial mapping in primate sensory projection: analytic structure and relevance to perception. Biol. Cybern. 25, 181–194.

Schwartz, E., Tootell, R. B., Silverman, M. S., Switkes, E., and De Valois, R. L. 1985. On the mathematical structure of the visuotopic mapping of macaque striate cortex. Science 227, 1065–1066.

Schwarzlose, R. F., Baker, C. I., and Kanwisher, N. 2005. Separate face and body selectivity on the fusiform gyrus. J. Neurosci. 25, 11055–11059.

Seiffert, A. E., Somers, D. C., Dale, A. M., and Tootell, R. B. 2003. Functional MRI studies of human visual motion perception: texture, luminance, attention and aftereffects. Cereb. Cortex 13, 340–349.

Sereno, M. I. and Tootell, R. B. 2005. From monkeys to humans: what do we now know about brain homologies? Curr. Opin. Neurobiol. 15, 135–144.

Sereno, M. I., Dale, A. M., Reppas, J. B., Kwong, K. K., Belliveau, J. W., Brady, T. J., Rosen, B. R., and Tootell, R. B. 1995. Borders of multiple visual areas in humans revealed by functional magnetic resonance imaging. Science 268, 889–893.

Sereno, M. I., Pitzalis, S., and Martinez, A. 2001. Mapping of contralateral space in retinotopic coordinates by a parietal cortical area in humans. Science 294, 1350–1354.

Sergent, J. and Signoret, J. L. 1992. Functional and anatomical decomposition of face processing: evidence from prosopagnosia and PET study of normal subjects. Philos. Trans. R. Soc. Lond. B Biol. Sci. 335, 55–61.

Sergent, J., Ohta, S., and MacDonald, B. 1992. Functional neuroanatomy of face and object processing. A positron emission tomography study. Brain 115(Pt. 1), 15–36.

Shikata, E., Hamzei, F., Glauche, V., Knab, R., Dettmers, C., Weiller, C., and Buchel, C. 2001. Surface orientation discrimination activates caudal and anterior intraparietal sulcus in humans: an event-related fMRI study. J. Neurophysiol. 85, 1309–1314.

Shikata, E., Hamzei, F., Glauche, V., Koch, M., Weiller, C., Binkofski, F., and Buchel, C. 2003. Functional properties and interaction of the anterior and posterior intraparietal areas in humans. Eur. J. Neurosci. 17, 1105–1110.

Shulman, G. L., Ollinger, J. M., Akbudak, E., Conturo, T. E., Snyder, A. Z., Petersen, S. E., and Corbetta, M. 1999. Areas involved in encoding and applying directional expectations to moving objects. J. Neurosci. 19, 9480–9496.

Silver, M. A., Ress, D., and Heeger, D. J. 2005. Topographic maps of visual spatial attention in human parietal cortex. J. Neurophysiol. 94, 1358–1371.

Smith, A. T., Greenlee, M. W., Singh, K. D., Kraemer, F. M., and Hennig, J. 1998. The processing of first- and second-order motion in human visual cortex assessed by functional magnetic resonance imaging (fMRI). J. Neurosci. 18, 3816–3830.

Smith, A. T., Singh, K. D., Williams, A. L., and Greenlee, M. W. 2001. Estimating receptive field size from fMRI data in human striate and extrastriate visual cortex. Cereb. Cortex 11, 1182–1190.

Snyder, L. H., Batista, A. P., and Andersen, R. A. 1997. Coding of intention in the posterior parietal cortex. Nature 386, 123–167.

Somers, D. C., Dale, A. M., Seiffert, A. E., and Tootell, R. B. 1999. Functional MRI reveals spatially specific attentional modulation in human primary visual cortex. Proc. Natl. Acad. Sci. U. S. A. 96, 1663–1668.

Spiridon, M. and Kanwisher, N. 2002. How distributed is visual category information in human occipito-temporal cortex? An fMRI study. Neuron 35, 1157–1165.

Squire, L. R. and Zola-Morgan, S. 1991. The medial temporal lobe memory system. Science 253, 1380–1386.

Stanley, D. A. and Rubin, N. 2003. fMRI activation in response to illusory contours and salient regions in the human lateral occipital complex. Neuron 37, 323–331.

Stensaas, S. S., Eddington, D. K., and Dobelle, W. H. 1974. The topography and variability of the primary visual cortex in man. J. Neurosurg. 40, 747–755.

Stoerig, P. and Cowey, A. 1997. Blindsight in man and monkey. Brain 120, 535–559.

Sunaert, S., Van Hecke, P., Marchal, G., and Orban, G. A. 1999. Motion-responsive regions of the human brain. Exp. Brain Res. 127, 355–370.

Tanaka, K. 1997. Columnar Organization in the Inferotemporal Cortex. In: Cerebral Cortex, Vol. 12, Extrastriate Cortex in Primates (*eds*. K. S. Rockland, J. H. Kaas, and A. Peters), pp. 469–495. Plenum Press.

Tanaka, K. 2003. Columns for complex visual object features in the inferotemporal cortex: clustering of cells with similar but slightly different stimulus selectivities. Cereb. Cortex 13, 90–99.

Tanaka, J. W. and Farah, M. 2003. The Holistic Representation of Faces. In: Perception of Faces, Objects and Scenes: Analytic and Holistic Processes (*eds*. M. A. Peterson and G. Rhodes), pp. 53–74. Oxford University Press.

Tarr, M. J. and Gauthier, I. 2000. FFA: a flexible fusiform area for subordinate level visual processing automatized by expertise. Nat. Neurosci. 3, 764–769.

Taylor, J. G., Schmitz, N., Ziemons, K., Grosse-Ruyken, M. L., Gruber, O., Mueller-Gaertner, H. W., and Shah, N. J. 2000. The network of brain areas involved in the motion aftereffect. Neuroimage 11, 257–270.

Tootell, R. B. and Hadjikhani, N. K. 2000. Attention-brains at work! Nat. Neurosci. 3, 206–208.

Tootell, R. B. and Hadjikhani, N. K. 2001. Where is ''dorsal V4'' in human visual cortex? Retinotopic, topographic and functional evidence. Cereb. Cortex 11, 298–311.

Tootell, R. B. and Taylor, J. B. 1995. Anatomical evidence for MT and additional cortical visual areas in humans. Cereb. Cortex 5, 39–55.

Tootell, R. B., Dale, A. M., Sereno, M. I., and Malach, R. 1996. New images from human visual cortex. Trends Neurosci. 19, 481–489.

Tootell, R. B., Hadjikhani, N. K., Hall, E. K., Marrett, S., Vanduffel, W., Vaughan, J. T., and Dale, A. M. 1998a. The retinotopy of visual spatial attention. Neuron 21, 1409–1422.

Tootell, R. B., Hadjikhani, N. K., Mendola, J. D., Marrett, S., and Dale, A. M. 1998b. From retinotopy to recognition: fMRI in human visual cortex. Trends Cognit. Sci. 2, 174–183.

Tootell, R. B., Hadjikhani, N. K., Vanduffel, W., Liu, A. K., Mendola, J. D., Sereno, M. I., and Dale, A. M. 1998c. Functional analysis of primary visual cortex (V1) in humans. Proc. Natl. Acad. Sci. U. S. A. 95, 811–817.

Tootell, R. B., Mendola, J. D., Hadjikhani, N. K., Liu, A. K., and Dale, A. M. 1998d. The representation of the ipsilateral visual field in human cerebral cortex. Proc. Natl. Acad. Sci. U. S. A. 95, 818–824.

Tootell, R. B., Mendola, J. D., Hadjikhani, N. K., Ledden, P. J., Liu, A. K., Reppas, J. B., Sereno, M. I., and Dale, A. M. 1997. Functional analysis of V3A and related areas in human visual cortex. J. Neurosci. 17, 7060–7078.

Tootell, R. B., Reppas, J. B., Dale, A. M., Look, R. B., Sereno, M. I., Malach, R., Brady, T. J., and Rosen, B. R. 1995a. Visual motion aftereffect in human cortical area MT revealed by functional magnetic resonance imaging. Nature 375, 139–141.

Tootell, R. B., Reppas, J. B., Kwong, K. K., Malach, R., Born, R. T., Brady, T. J., Rosen, B. R., and Belliveau, J. W. 1995b. Functional analysis of human MT and related visual cortical areas using magnetic resonance imaging J. Neurosci. 15, 3215–3230.

Tootell, R. B., Switkes, E., Silverman, M. S., and Hamilton, S. L. 1988. Functional anatomy of macaque striate cortex. II. Retinotopic organization. J. Neurosci. 8, 1531–1568.

Tootell, R. B., Tsao, D., and Vanduffel, W. 2003. Neuroimaging weighs in: humans meet macaques in ''primate'' visual cortex. J. Neurosci. 23, 3981–3989.

Tong, F. and Engel, S. A. 2001. Interocular rivalry revealed in the human cortical blind-spot representation. Nature 411, 195–199.

Tong, F., Nakayama, K., Moscovitch, M., Weinrib, O., and Kanwisher, N. 2000. Response properties of the human fusiform face area. Cogn. Neuropsych. 17, 257–279.

Tong, F., Nakayama, K., Vaughan, J. T., and Kanwisher, N. 1998. Binocular rivalry and visual awareness in human extrastriate cortex. Neuron 21, 753–759.

Tsao, D. Y., Freiwald, W. A., Knutsen, T. A., Mandeville, J. B., and Tootell, R. B. 2003a. Faces and objects in macaque cerebral cortex. Nat. Neurosci. 6, 989–995.

Tsao, D. Y., Freiwald, W. A., Tootell, R. B., and Livingstone, M. S. 2006. A cortical region consisting entirely of face-selective cells. Science 311, 670–674.

Tsao, D. Y., Vanduffel, W., Sasaki, Y., Fize, D., Knutsen, T. A., Mandeville, J. B., Wald, L. L., Dale, A. M., Rosen, B. R., Van Essen, D. C., Livingstone, M. S., Orban, G. A., and Tootell, R. B. 2003b. Stereopsis activates V3A and caudal intraparietal areas in macaques and humans. Neuron 39, 555–568.

Tyler, C. W., Likova, L. T., Chen, C. C., Kontsevich, L. L., Schira, M. M., and Wade, A. R. 2005. Extended concepts of occipital retinotopy. Curr. Med. Imaging Rev. 1, 319–329.

Tyler, C. W., Likova, L. T., Kontsevich, L. L., and Wade, A. R. 2006. The specificity of cortical region KO to depth structure. Neuroimage 30, 228–238.

Ungerleider, L. G. and Mishkin, M. 1982. Two Cortical Visual Systems. In: Analysis of Visual Behavior (*eds*. D. J. Ingle, M. A. Goodale, and R. J. W. Mansfield), pp. 549–586. MIT Press.

Vaina, L. M., Solomon, J., Chowdhury, S., Sinha, P., and Belliveau, J. W. 2001. Functional neuroanatomy of biological motion perception in humans. Proc. Natl. Acad. Sci. U. S. A. 98, 11656–11661.

Vanduffel, W., Fize, D., Peuskens, H., Denys, K., Sunaert, S., Todd, J. T., and Orban, G. A. 2002. Extracting 3D from motion: differences in human and monkey intraparietal cortex. Science 298, 413–415.

Van Essen, D. C. 1997. A tension-based theory of morphogenesis and compact wiring in the central nervous system. Nature 385, 313–318.

Van Essen, D. C. 2003. Organization of Visual Areas in Macaque and Human Cerebral Cortex. In: The Visual Neurosciences (*eds*. L. Chalupa and J. S. Werner), pp. 507–521. MIT Press.

Van Essen, D. C. and Zeki, S. M. 1978. The topographic organization of rhesus monkey prestriate cortex. J. Physiol. (Lond.) 277, 193–226.

Van Essen, D. C., Newsome, W. T., and Maunsell, J. H. 1984. The visual field representation in striate cortex of the macaque monkey: asymmetries, anisotropies, and individual variability. Vision Res. 24, 429–448.

Vanni, S., Tanskanen, T., Seppa, M., Uutela, K., and Hari, R. 2001. Coinciding early activation of the human primary visual cortex and anteromedial cuneus. Proc. Natl. Acad. Sci. U. S. A. 98, 2776–2780.

Van Oostende, S., Sunaert, S., Van Hecke, P., Marchal, G., and Orban, G. A. 1997. The kinetic occipital (KO) region in man: an fMRI study. Cereb. Cortex. 7, 690–701.

Von Economo, C. and Koskinas, G. N. 1925. Die Cytoarchitektonik der Hirnrinde des erwachsenen Menschen. Springer.

Vuilleumier, P., Henson, R. N., Driver, J., and Dolan, R. J. 2002. Multiple levels of visual object constancy revealed by event-related fMRI of repetition priming. Nat. Neurosci. 5, 491–499.

Wade, A. R., Brewer, A. A., Rieger, J. W., and Wandell, B. A. 2002. Functional measurements of human ventral occipital cortex: retinotopy and colour. Philos. Trans. R. Soc. Lond. B Biol. Sci. 357, 963–973.

Wandell, B. A. 1999. Computational neuroimaging of human visual cortex. Annu. Rev. Neurosci. 22, 145–173.

Wandell, B. A., Brewer, A. A., and Dougherty, R. F. 2005. Visual field map clusters in human cortex. Philos. Trans. R. Soc. Lond. B Biol. Sci. 360, 693–707.

Watson, J. D., Myers, R., Frackowiak, R. S., Hajnal, J. V., Woods, R. P., Mazziotta, J. C., Shipp, S., and Zeki, S. 1993. Area V5 of the human brain: evidence from a combined study using positron emission tomography and magnetic resonance imaging. Cereb. Cortex 3, 79–94.

Welchman, A. E., Deubelius, A., Conrad, V., Bulthoff, H. H., and Kourtzi, Z. 2005. 3D shape perception from combined depth cues in human visual cortex. Nat. Neurosci. 8, 820–827.

Wojciulik, E. and Kanwisher, N. 1999. The generality of parietal involvement in visual attention. Neuron 23, 747–764.

Yovel, G. and Kanwisher, N. 2004. Face perception: domain specific, not process specific. Neuron 44, 889–898.

Yovel, G. and Kanwisher, N. 2005. The neural basis of the behavioral face-inversion effect. Curr. Biol. 15, 2256–2262.

Zeki, S. M. 1973. Colour coding in rhesus monkey prestriate cortex. Brain Res. 53, 422–427.

Zeki, S. M. 1978a. Uniformity and diversity of structure and function in rhesus monkey prestriate visual cortex. J. Physiol. (Lond.) 277, 273–290.

Zeki, S. M. 1978b. The third visual complex of rhesus monkey prestriate cortex. J. Physiol. (Lond.) 277, 245–272.

Zeki, S. 1980. The representation of colours in the cerebral cortex. Nature 284, 412–418.

Zeki, S. A. 1990. century of cerebral achromatopsia. Brain 113(Pt. 6), 1721–1777.

Zeki, S. 1991. Cerebral akinetopsia (visual motion blindness). A review. Brain 114(Pt. 2), 811–824.

Zeki, S. 1993. The visual association cortex. Curr. Opin. Neurobiol. 3, 155–159.

Zeki, S., Perry, R. J., and Bartels, A. 2003. The processing of kinetic contours in the brain. Cereb. Cortex 13, 189–202.

Zeki, S., Watson, J. D., Lueck, C. J., Friston, K. J., Kennard, C., and Frackowiak, R. S. 1991. A direct demonstration of functional specialization in human visual cortex. J. Neurosci. 11, 641–649.

Zhou, H., Friedman, H. S., and von der Heydt, R. 2000. Coding of border ownership in monkey visual cortex. J. Neurosci. 20, 6594–6611.

2.01 Temporal Coherence: A Versatile Code for the Definition of Relations

W Singer, Max Planck Institute for Brain Research, Frankfurt, Germany

© 2008 Elsevier Inc. All rights reserved.

2.01.1	Synchrony as Tag of Relatedness	2
2.01.2	The Role of Oscillations in Adjusting Spike Timing	3
2.01.3	Feature Specific Binding by Gamma Phase-Dependent Spike Timing in Primary Visual Cortex	4
2.01.4	Mechanisms of Read-Out	5
2.01.5	The Duration of Synchronized Events	6
2.01.6	Synchrony and Feature Binding	6
2.01.7	Preattentive versus Attention-Dependent Grouping	7
2.01.8	Equivalence of Rate Codes and Temporal Codes	8
2.01.9	Conclusions	8

In the cerebral cortex the objects of perception are represented by the responses of groups of neurons which are tuned to rather complex combinations of the features that characterize a particular object. This coding strategy is a compromise between the option to represent objects by individual neurons that respond in a highly selective way only to a single object and the option to represent objects by very large assemblies of neurons each of which is tuned to only one of the many elementary features that constitute complex objects. The disadvantage of the first option is that it requires a very large number of representational units and cannot cope with the representation of novel objects. The disadvantage of the second option is that it requires an immense number of connections to assure flexible association of large numbers of neurons in ever changing constellations. Because the number of afferents that can effectively contribute to the selective recruitment of neurons into an assembly is limited by the dynamical range of the neurons, there is an upper limit for the degree of connectedness. Moreover, the two coding strategies differ with respect to processing speed. Less processing time is required to represent objects by individual specialized neurons than by dynamically configurated assemblies because the former can be realized in strictly feed-forward architectures while the latter requires cooperative interactions within reciprocally coupled networks. There is thus a tradeoff between different hardware constraints, versatility, and processing speed.

Analyses of the response properties of neurons encountered at the various levels of the processing hierarchy of sensory systems suggest the following sequence of processing steps. Neurons in the sensory organs encode in their responses very elementary, local properties and qualities of the components of perceptual objects and barely any relations. An exception is the retina of the eye. Unlike most other sensory organs it possesses a complex, multilayered network that permits, first, recombination of signals in convergent feed-forward architectures and, second, extensive lateral interactions that modulate responses in a context-dependent way. Thus, the rate-modulated output of ganglion cells does not only signal the presence of a local property of an object, in this case the brightness and spectral composition of a small part of its surface, but also the neighborhood relations of these particular features. Elaboration of truly feature-specific neurons occurs at the cortical level. As one proceeds along the cortical processing hierarchy, one encounters neurons that respond selectively to increasingly complex constellations of elementary features. It is commonly held that this increased selectivity is achieved by iterative recombination of feed-forward connections from lower- to higher-order neurons. If the thresholds of the respective higher-order neurons are adjusted such that they respond only if the full set of the feeding neurons is simultaneously active, they assume the function of conjunction detectors. Their responses signal not only the presence of certain sets of component features but also the way in which these features are related to each other. The latter information is implicitly encoded in the architecture of feed-forward connections that links selected sets of feeder neurons to higher-order conjunction detectors.

Several theoretical arguments suggest that these binding operations are complemented at each level of processing by additional mechanisms that permit flexible definition of relations among the responses of distributed neurons. Natural scenes, for example, usually contain a large number of different objects, the contours of which may be contiguous or partially occluded. A single border may be shared by several objects and features of occluding surfaces may appear as belonging to the occluded object. This introduces ambiguities that need to be resolved in order to channel appropriately sorted signals to the feed-forward circuits. Without such prior sorting it would be difficult to avoid accidental activation of conjunction specific neurons by features belonging to different objects and hence generation of false conjunctions. Thus, responses to contours belonging to the same object need to be grouped together for further joint processing and they need to be segregated from responses to other objects and the embedding background. This selection of groupable responses has to occur in a context-dependent way and hence requires dynamic routing of signals. Responses evoked by the features of individual objects need to be tagged as related in a way that assures their selective convergence on higher-order neurons. These grouping and routing operations must occur at early levels of the processing hierarchy because successful scene segmentation is a prerequisite for the later identification of individual objects. Context sensitive dynamic definition of relations is also required at the highest levels of processing where neurons are encountered that respond to very complex constellations of features, for example, the various components of a face, the mouth, the eyes, or the nose. This postulate follows from several arguments. First, neurons whose response properties are sufficiently complex and selective to encode only a single perceptual object are rare and seem to exist only for highly overlearned objects or objects of particular behavioral relevance. Second, it is inconceivable that novel objects can be represented by pre-established neurons because the required feed-forward architectures would have to be specified *a priori* to support formation of the appropriate conjunctions. Third, objects that are simultaneously encoded in different sensory modalities elicit responses in several different sensory systems, and these need to be related to each other in order to generate a comprehensive polymodal description of this object. These arguments suggest that objects not representable by individual neurons are encoded by assemblies of distributed neurons, each of which responds only to a particular aspect of the object. However, in assembly coding a relation-defining mechanism is indispensable because responses evoked by the same object need to be tagged as related in order to avoid false conjunctions. Therefore, neurons participating in assemblies need to convey two messages in parallel. First, whether the feature constellation for which they code is present and second, with which other neurons they cooperate in the representation of a particular perceptual object. It is commonly held that the presence of certain features is signaled by increase of discharge rate but it is still a matter of debate how the relatedness of responses is expressed.

2.01.1 Synchrony as Tag of Relatedness

Psychophysical and electrophysiological evidence indicates that attentional mechanisms play an important role in dynamic grouping operations both at the level where scene segmentation is accomplished as well as at higher levels where object identification is thought to occur. However, the mechanisms underlying these relation-defining grouping operations are still poorly understood. One proposal is that attentional mechanisms modulate the discharge rate of neurons and enhance the amplitude of responses to attended features. In this scenario the signature of relatedness is the concomitant enhancement of discharge frequency. Responses selected for combination in convergent feed-forward architectures or the formation of an assembly would be distinguished from all others by their higher discharge frequency. This interpretation has been challenged by the argument that response amplitude may be an ambiguous signature of relatedness because it depends on the match between stimulus and receptive field properties, requires long read-out times, and makes it difficult to segregate assemblies from one another that are simultaneously configurated within the same neuronal network. Therefore, it has been proposed that neurons use in addition to the well-established rate code a temporal code in order to express relations. This latter code should assure that responses tagged as related are processed jointly at subsequent stages, that is, are routed together into the appropriate feed-forward channels and/or are recognizable without ambiguity as originating from cells of the same assembly. Following the discovery that neurons in the primary visual cortex can synchronize their spike discharges with a precision in the millisecond

range, it has been proposed that the synchronization of responses could serve as the required tag of relatedness. One way to select subsets of responses for further joint processing and, thus, for binding them together is to selectively raise their saliency. Most models on the binding function of selective attention are based on such a mechanism but they usually assume that saliency is enhanced by rate increases. However, precise temporal synchronization of spike discharges is an equally efficient means to raise selectively the saliency of neuronal responses. The reason is that synchronized input to target neurons has a much stronger impact than temporally uncoordinated input. Simultaneously arriving excitatory postsynaptic potentials (EPSPs) summate much more effectively than temporally dispersed EPSPs, and this coincidence sensitivity of neurons is further augmented in cortical neurons by a number of specific mechanisms: (1) voltage-gated dendritic sodium and calcium conductances that amplify fast rising depolarizations of large amplitude, (2) the frequency adaptation of synaptic release and postsynaptic receptors which attenuates temporal summation of EPSPs, and (3) a dependence of firing threshold on the rising slope of depolarizations, favoring responses to fast rising depolarizations. These mechanisms increase selectively the impact of synchronous inputs, and they do so with a temporal resolution in the millisecond range. Thus, relations can be defined within narrow temporal windows (<10 ms), and hence different relations can be encoded within the same neuronal network with less ambiguity and in much more rapid alternation than if relations were expressed by joint rate increases.

The proposal that precise temporal synchrony is used as a tag of relatedness in neuronal processing agrees well with the temporal sensitivity of mechanisms supporting synaptic plasticity and Hebbian learning. Known mechanisms of synaptic plasticity exploit temporal correlations among the discharges of input connections and/or the discharges of inputs and those of the postsynaptic target cells. The temporal resolution of the mechanisms – spike timing-dependent plasticity is one example – that classify discharges as synchronous (asynchronous), that is, related (unrelated), and cause synapses to strengthen (weaken) also operate with a precision in the millisecond range. Thus, there is a perfect match between the signatures of relatedness used in signal processing and Hebbian learning. This cannot be otherwise because both processes have to rely on the same relation-defining code to avoid learning of false conjunctions.

2.01.2 The Role of Oscillations in Adjusting Spike Timing

Investigations of response synchronization in the visual system have revealed that precise synchronization of discharges is often associated with an oscillatory patterning of the neuronal responses. Because individual cells tend to skip cycles of these oscillations, they are rarely detectable in the spike trains of single cells but they are readily seen in data representing the responses of large populations of neurons, that is, in multiunit recordings or recordings of local field potentials (LFPs). *In vitro* experiments in cortical slices and simulation studies have in the meantime established causal relations between the two phenomena. The oscillatory patterning of the responses is mainly due to oscillations generated within the various pools of inhibitory interneurons that are coupled both through chemical and electrical synapses and capable of sustaining oscillatory activity patterns in different frequency bands. These oscillatory inhibitory inputs to pyramidal cells veto their discharges during the inhibitory troughs and favor discharges at the depolarizing peaks, thus causing synchrony in firing. These locally synchronized oscillatory responses can become synchronized over large distances due to reciprocal coupling of the oscillatory networks via excitatory corticocortical connections. It follows from this mechanism that the precision with which spikes can be synchronized increases with oscillation frequency. A relation exists also between oscillation frequency and the distance over which synchronization is maintained. Synchronization among remote groups of neurons or among large assemblies of neurons extending across different cortical areas tends to occur at lower oscillation frequencies than synchronization of local clusters of cells. The latter are often synchronized in the gamma-frequency band while long distance synchrony is more often supported by oscillations in the beta, alpha, and theta bands.

In addition to limiting discharges to the depolarizing phase of the oscillation cycle, which increases synchronous firing, the oscillatory modulation of the neurons' membrane potential has a second effect on spike timing that may be as important as the synchronization effect. As mentioned above, network oscillations are associated with rhythmic inhibition of pyramidal cells. Thus, an oscillation cycle consists of two phases: the depolarizing phase, during which the probability to respond to excitatory input increases progressively until the peak of the cycle is reached, and the hyperpolarizing phase, during

which cells are virtually refractory due to the shunting and hyperpolarizing effects of the inhibitory postsynaptic potential (IPSP) barrage. Therefore, weak inputs will be able to evoke spikes only late in the depolarizing phase while strong inputs will elicit discharges already during earlier segments of the depolarizing cycle. It follows that the phase in the oscillation cycle at which a neuron fires will depend on its excitatory drive and the relative phase at which two neurons fire will depend on the relation between their respective excitatory drives. Experimental evidence for this phenomenon of phase precession has been obtained both in the hippocampus and the neocortex. In the visual cortex the relative phase at which two multi-unit activities (MUAs) synchronize with the stimulus-induced gamma oscillations depends on the relative strength with which they are activated: when a stimulus is presented that activates one neuronal group strongly and another weakly, then the more strongly activated group fires slightly earlier in the gamma cycle than the more weakly activated group and vice versa. In view of the growing evidence that the precise timing of individual spikes matters, for example, as in spike timing-dependent plasticity, phase-dependent spike timing could be functionally relevant. As mentioned above, pyramidal cells can only respond within a narrow temporal window when the network engages in oscillations. Furthermore, pyramidal cell firing is a self-terminating process because pyramidal cells strongly excite interneurons and these feed back on the pyramidal cells, curtailing their firing. Thus, if a pyramidal cell does not fire sufficiently early in the gamma cycle, it will not be able to fire at all in that cycle. In other words, in each gamma cycle, there is a race among the pyramidal cells during which the most excited pyramidal cells will compete against the less excited ones. This winner-take-all mechanism could contribute to the selection and context-dependent routing of signals. Moreover, transforming the rate-coded amplitude of input signals into phase-defined spike times could be used very effectively to convert rate codes into temporal codes that, in turn, can then be used for the expression of relations.

Spike latency coding or spike rank order coding has been the core component in a class of computational models that perform object recognition with remarkable speed and computational efficiency. Changes in event-related potentials recorded from the scalp of human subjects asked to decide whether complex visual scenes contained an animal indicate that it takes the visual system as little as 150 ms to reach a decision. Given that it takes already about 50 ms for the image to activate the primary visual cortex, and given that there are multiple synapses between primary visual and inferotemporal cortex, it is highly unlikely that the luminance distribution of the retinal image was assessed solely by evaluating the average firing rates because this would require integration over too long time intervals. The alternative is that brightness values are encoded by the degree of phase precession of the first spikes in the responses and that further computations would be based on the relative spike latencies. Repetition of this coding strategy across the hierarchy of processing stages can support very rapid processing because it requires no temporal integration of rates. A necessary prerequisite for this processing strategy is that the respective next processing stage can decode the phase information. This can be achieved if it receives a copy of the temporal frame, that is, the oscillation cycle. Long-range synchronization of oscillations is now well established allowing distributed spike phase-based computations to operate on the same reference frame.

2.01.3 Feature Specific Binding by Gamma Phase-Dependent Spike Timing in Primary Visual Cortex

During states of focused attention and visual search, the networks in the visual cortex are entrained in internally generated oscillations in the beta and gamma-frequency range prior to any visual stimulation. In this case visual input can arrive at any phase within an ongoing gamma-band oscillation and response onset latencies should be determined not only by stimulus onset but also by the phase of ongoing rhythmic activity. This has been confirmed with recordings in primary visual cortex of anesthetized cats.

The crucial finding was that, across trials, neuronal responses had variable onset latencies with respect to stimulus presentation and part of this variability could be explained by the phase of the ongoing gamma-band activity at which visual stimulation was delivered. When visual stimulation happened to provide thalamic input to cortex during moments when inhibition faded, then latencies were short. Also in this case, the relative timing of spikes contained important information. The data showed that columns coding for related features (same or colinear orientation of contours), that tend to be grouped perceptually, oscillate with zero phase lag. This has the effect that the latencies of the first spikes

of cells responding to groupable features covary and are similar. Hence, these discharges are synchronized right from the beginning. Following the indications that synchronous firing serves to establish relations among distributed responses it has been proposed that this rapid synchronization of first spikes could support rapid feature binding and perceptual grouping.

Further support for this notion comes from multisite recordings in V1 of monkeys trained to freely inspect complex visual scenes. Shortly after the onset of fixation (40–100 ms) one observes a brief burst of highly synchronized high-frequency oscillations in the LFP that are precisely phase-locked across recording sites. These fixation-related oscillations are in turn associated with excess synchronization of spike discharges in the responses to the contours of the scene. As these oscillations occur also when the animal scans a blank screen, they are most likely due to corollary activity that is generated in anticipation of having to process new constellations of features once a new segment of the scene is fixated. In analogy to the effect of the spontaneous oscillations, this self-generated coherent activity could serve the read-out of grouping criteria residing in the network of tangential connection and the translation of these criteria into specific synchronization patterns. The saccade-related oscillations and the associated spike synchronization precede by several tens of milliseconds the peak of the neurons' rate responses which reach a maximum only around 100 ms after the eyes have come to rest. Grouping cues encoded in latency adjustments and spike synchronization would thus be available long before the changes in the neurons' discharge rate can be fully evaluated. Such rapid processing at early stages of the visual system appears desirable given that the animals changed gaze direction on average four to five times in a second. This implies that scene segmentation, the eventual resolution of ambiguities, the selection of signals for binding by convergence, and the subsequent dynamic grouping of neurons into object specific assemblies must have been accomplished within about 200 ms.

It should be noted that such a coding strategy may not apply for all processing streams. It has been demonstrated that spikes can be tightly locked to stimulus transients, for example, in visual area MT, an area of the dorsal visual stream while the above-mentioned synchronization phenomena were observed in recordings from cat area 17 and monkey area V1. Thus, it is conceivable that information conveyed by the magno (y) and the parvo (x) cellular pathways, respectively, is processed differently. The time stamps of external stimuli could be relayed undistortedly by the magnocellular system via rapidly conducting feed-forward loops to preserve precise timing information while the signals conveyed by the parvocellular system could be subject to internal timing mechanisms. In this case synchrony of spikes in the magnocellular system would signal temporal relations between external events while synchrony in the parvocellular system would signal – in the same format – relations between features that lack temporal structure and that are established by internal computations.

2.01.4 Mechanisms of Read-Out

The impact that an EPSP has on an oscillating target cell will depend crucially on the time of arrival relative to the gamma cycle. This time depends essentially on three variables: (1) the time of spike generation in the sending cell relative to its oscillation cycle, (2) the conduction delay between the sending and receiving cell, and (3) the phase relation between the oscillations of the sending and receiving network. Assuming fixed conduction delays, the effective gain of a given connection in oscillating networks can thus be modulated over a wide range (essentially from 0 to maximal) by adjusting the phase relations between the oscillating cell groups, the oscillation frequencies, and the phase at which spikes are emitted. Numerous studies on phase and frequency relations among oscillating cortical networks suggest the existence of mechanisms for the adjustment of phase-specific spike timing, of oscillation frequencies, and of phase relations among oscillating cell populations. Thus, the oscillatory patterning of neuronal activity offers a wide range of options to exploit the temporal domain for the dynamic routing of signals within the rigid network of fixed anatomical connections. This, in turn, can be used to support a large variety of functions that go beyond feature binding and polysensory integration such as sensory–motor coordination, attention-dependent selection of signals, dynamic association of the ever changing contents of working memory, and, through spike timing-dependent plasticity, the formation of long-term memories. All of these functions have been shown to be associated with oscillatory activity, in most cases in the high-frequency range of the beta and gamma band. These high-frequency oscillations appear to be particularly well suited for these functions because there

is a direct relation between the selectivity with which dynamic binding and routing can be accomplished and the oscillation frequency: as the frequency increases, the precision of spike timing increases and at the same time the network becomes more sensitive to small variations in spike timing.

2.01.5 The Duration of Synchronized Events

Early investigations of response synchronization were based mostly on conventional cross-correlation analysis of cell discharges and/or LFPs. This method reliably detects synchronous firing if it is sustained over prolonged periods of time but it fails if synchronous events occur only a few times in a response. Therefore, more sensitive measures have been developed that allow assessment of brief events of coincident firing. One of these methods, the unitary event analysis, uses statistical methods to identify single, nonaccidental incidences of coincident firing, the other (spike-field coherence), evaluates consistent phase relations between the discharges of individual neurons and LFP oscillations. Application of these methods to data obtained from conscious behaving animals has revealed that episodes of synchronized firing are often restricted to short epochs of particular behavioral sequences and may be as short as a few tens of milliseconds. This agrees with measurements of the minimal time required to segment scenes and identify objects. It was estimated that the grouping operations required for scene segmentation and object identification should not take more than 10–20 ms per processing stage. This implies that a substantial amount of information about the accomplished grouping must be encoded in the precise timing relations between individual discharges of distributed neurons. The reason is that not much information can be encoded in variations of discharge rates of individual cells, as they can generate only few spikes within such short time windows.

2.01.6 Synchrony and Feature Binding

Evidence from studies in the visual system suggests that response synchronization may be used throughout all processing stages, from the retina to the highest cortical areas, in order to establish relations among distributed responses, that is, to route responses into the appropriate feed-forward channels for binding by convergence and to tag responses of assembly members as related. In all cases synchronization probability reflects some of the Gestalt criteria that are used for scene segmentation and perceptual grouping. In the retina, ganglion cell responses synchronize with millisecond precision if evoked by continuous contours or coherent objects and there is evidence from studies on the escape response of frogs, that synchronicity of ganglion cell firing is actually carrying behaviorally relevant information. Retinal synchronization is associated with high-frequency oscillations (up to 90 Hz) and based on horizontal interactions within the network of coupled amacrin cells.

In the primary visual cortex synchrony is often associated, especially when it is observed over larger distances, with an oscillatory patterning of spike discharges in the gamma frequency range (30–60 Hz). At this processing stage, synchronization probability correlates well with elementary Gestalt rules. It is enhanced between responses evoked by continuous contours, by contours moving with the same speed in the same direction, by colinearly aligned contour segments, and by contours belonging to the same surface. It is maximal among responses evoked by coherent patterns such as regular gratings, and it is minimal or absent among responses to incoherent stimuli such as random dot patterns. In the cortex, long-distance synchronization of responses is mediated by the network of tangential horizontal connections, and if it occurs across the midline of the visual field, by callosal connections. One of the reasons why synchrony is stronger among responses to continuous or colinearly aligned contours or contours moving in the same direction is the anatomical anisotropy of these tangential connections. Those spanning larger distances connect preferentially columns with similar feature preference. Thus, elementary grouping criteria are implemented in the anisotropies of the network of tangential connections and translated into synchronization probability. In cats, such stimulus-specific synchronization phenomena have been observed both within and across different visual areas, both within and across hemispheres, and between the visual cortex and the superior colliculus. In primates, especially in conscious behaviorally trained animals, multisite recordings have been applied much less frequently and therefore less data are available on response synchronization. However, the results obtained from primary visual cortex closely resemble those obtained from cats – but oscillation frequencies tend to be higher and the distances over which synchrony

is observed tend to be shorter. In the motion sensitive area MT response synchronization was found to reflect the Gestalt rule of common fate which is one of the strongest binding cues for perceptual grouping. Presentation of two spatially overlapping bars moving in different directions led to the formation of two distinct assemblies of neurons whereby those responding to the same contour synchronized their discharges, while those responding to different contours, did not. In the inferior temporal cortex of the ventral processing stream, synchronization probability reflects the binding of neurons into assemblies representing individual objects. Neurons responding to the components of faces (eyes, nose, mouth, etc.) synchronized their responses when the arrangement of these components was such that the animals signaled having recognized a face while they did not synchronize when the components were scrambled or presented in a way that was judged by the animal as incompatible with the appearance of a normal face. Neither in the case of MT nor IT was it possible to distinguish between the various arrangements of the presented stimuli if only the discharge rate of the neurons was evaluated. This is compatible with the interpretation that discharge rate signals the presence of particular features while the correlations among the discharges of neurons indicate how these features are related to each other.

2.01.7 Preattentive versus Attention-Dependent Grouping

Grouping operations based on elementary Gestalt rules and the binding of the stereotyped feature constellations of highly familiar objects can occur preattentively. This automatic, attention-independent grouping is thought to be based on binding by convergence in fixed feedforward architectures. However, several arguments suggest that synchronization may also serve as a mechanism for automatic grouping. The synchronization of retinal responses cannot be influenced by attentional mechanisms as there are no efferent projections capable of conveying the required information. The fact that feature-specific response synchronization is readily observed in anesthetized preparations also suggests that binding through synchrony can occur preattentively. Interestingly (and this may turn out to be a feature distinguishing grouping by convergence from grouping by synchronization) grouping by synchrony – even if preattentive – is highly context dependent while grouping by convergence is not. Despite anesthesia, grouping by synchronization remains sensitive to the global configuration of stimuli. In cat areas 17 and 18 synchronization probability changes when variations in stimulus context require a change in grouping, and this reorganization of synchrony patterns occurs even if stimulus configurations are changed in a way that leaves the stimulus segments appearing within the aperture of the classical receptive fields of the recorded neurons unchanged.

In addition to this evidence for attention-independent grouping by synchrony, more recent results clearly indicate that synchronization is also highly susceptible to top-down, attention-dependent influences and that it plays an important role in attention-dependent response selection and binding. Various measures have been used to assess the influence of selective attention on neuronal synchrony: Correlations among spike discharges, spike-field coherence, correlations in phase locking between oscillatory field potentials, and finally, the amplitude and the phase locking of oscillatory responses in magnetencephalography (MEG) and electroencephalography (EEG) recordings. Because the amplitude of MEG and EEG signals depends to a crucial extent on the synchronicity of large populations of neurons, not only variations in phase locking but also in the power of oscillations can be taken as a measure of synchrony. These data indicate that focusing attention on a particular stimulus or on a particular modality increases the synchrony of responses in the neuronal networks that process the attended stimulus. Again, this enhanced synchronization is associated with and most likely caused by an oscillatory patterning of neuronal activity in the beta and especially in the gamma-frequency range. At the same time one observes a reduction of oscillatory activity in lower frequency bands (alpha, delta). Evidence also indicates that anticipation of a particular stimulus or a motor act is associated with the generation of oscillatory activity in the beta- and gamma-frequency band in cortical areas required for the processing of the stimulus or the execution of the task. For tasks involving sensory discrimination and motor responses this anticipatory synchronization can extend across widely distributed networks of cortical areas. This anticipatory modulation of oscillatory activity is usually not associated with major changes in the discharge activity of neurons, suggesting that it consists mainly of a synchronous pacing of excitability through oscillatory activity generated in the network of inhibitory interneurons. It has been proposed that this subthreshold modulation of excitability facilitates rapid synchronization of responses once stimuli are available, thereby enhancing

transmission across multiple cortical stages. Recent results from MEG studies in human subjects take this proposal one step further and suggest that the anticipatory induction of coherent oscillations across distributed cortical areas and executive structures facilitates selective routing of activity and rapid handshaking among the involved processing stages. However, at present, it is unknown which centers coordinate this attention- and task-dependent modulation. Thalamic nuclei such as the pulvinar, the nuclei of the basal forebrain, and the basal ganglia are candidates for the mediation of synchrony across widely distributed regions of the brain.

2.01.8 Equivalence of Rate Codes and Temporal Codes

In principle, synchronization could be used as an alternative mechanism to rate modulations in order to raise the saliency of responses. Experiments on binocular rivalry support this conjecture. In cat primary visual cortex the responses to the respective perceived stimulus differed from those to the suppressed stimulus because they were more synchronized and not because they were more vigorous. A similar conclusion is suggested by experiments on perceived brightness. If a small grating is superimposed on a large grating, the perceived contrast of the former increases with increasing orientation or phase offset between the two gratings. This effect is closely related to changes of neuronal responses in primary visual cortex. Neurons responding to the small grating increase their discharge rate but not their synchrony with increasing orientation offset while they increase the synchrony of their discharges but not the rate with increasing phase offset. This indicates that the saliency of responses can be enhanced either by increasing the rate or the synchronicity of discharges. The fact that the effects are perceptually indistinguishable illustrates nicely the complementarity of rate codes and temporal codes.

2.01.9 Conclusions

The data reviewed in this chapter suggest that sensory systems exploit two complementary ways to evaluate and represent relations between features of perceptual objects. One strategy consists of the generation of specialized neurons in feed-forward architectures that respond selectively to particular constellations of features. The discharge rate of these neurons encodes both the presence of particular features and the way in which they are related to each other. This coding strategy is fast but can encode only relations defined *a priori* by the convergence patterns of the feed-forward connections. As multisite recordings suggest, there is a second strategy that exploits the precise temporal relations between the discharges of distributed neurons to encode relations. This mechanism permits flexible and context-dependent definition of relations. It exploits the coincidence sensitivity of neurons and uses precise temporal synchronization of discharges as tag of relatedness. Interestingly, the same tag appears to be exploited by the mechanisms mediating use-dependent synaptic plasticity and associative learning. As synchronization enhances the impact of the synchronized responses, it appears to be used not only to define relations among distributed responses but also in a more general way to select responses for further processing, to raise their perceptual saliency, and to support selective routing of activity under the control of attentional mechanisms. Because temporal codes can only be assessed with multisite recordings and because these have a relatively short history, we are still at the beginning of understanding coding strategies based on the dynamic interactions among large numbers of neurons. It may turn out that precise synchronization is only one, albeit a very important signature of the many potentially significant dynamical states. Precisely timed phase offsets and sequences of patterns defined by specific temporal relations are likely to play an equally important role. To analyze these more complex patterns and to examine whether they contain information that can be related to behavior is one of the great challenges in future systems neurobiology.

Further Reading

Ariav, G., Polsky, A., and Schiller, J. 2003. Submillisecond precision of the input–output transformation function mediated by fast sodium dendritic spikes in basal dendrites of CA1 pyramidal neurons. J. Neurosci. 23, 7750–7758.

Arieli, A., Sterkin, A., Grinvald, A., and Aertsen, A. 1996. Dynamics of ongoing activity: explanation of the large variability in evoked cortical responses. Science 273, 1868–1871.

Azouz, R. and Gray, C. M. 2003. Adaptive coincidence detection and dynamic gain control in visual cortical neurons *in vivo*. Neuron 37, 513–523.

Burchell, T. R., Faulkner, H. J., and Whittington, M. A. 1998. Gamma frequency oscillations gate temporally coded afferent inputs in the rat hippocampal slice. Neurosci. Lett. 255, 151–154.

Castelo-Branco, M., Goebel, R., Neuenschwander, S., and Singer, W. 2000. Neural synchrony correlates with surface segregation rules. Nature 405, 685–689. Erratum in: Nature 2000; 407, 926.

Cook, E. P. and Maunsell, J. H. R. 2002. Attentional modulation of behavioral performance and neuronal responses in middle temporal and ventral intraparietal areas of macaque monkey. J. Neurosci. 22, 1994–2004.

Delorme, A. and Thorpe, S. J. 2001. Face identification using one spike per neuron: resistance to image degradations. Neural Netw. 14, 795–803.

Delorme, A. and Thorpe, S. J. 2003. Spike NET: an event-driven simulation package for modelling large networks of spiking neurons. Network 14, 613–627.

Engel, A. K., Fries, P., and Singer, W. 2001. Dynamic predictions: oscillations and synchrony in top-down processing. Nat. Rev. Neurosci. 2, 704–716.

Engel, A. K., König, P., and Singer, W. 1991. Direct physiological evidence for scene segmentation by temporal coding. Proc. Natl. Acad. Sci. U. S. A. 88, 9136–9140.

Engel, A. K., König, P., Kreiter, A. K., and Singer, W. 1991. Interhemispheric synchronization of oscillatory neuronal responses in cat visual cortex. Science 252, 1177–1179.

Fries, P. 2005. A mechanism for cognitive dynamics: neuronal communication through neuronal coherence. Trends Cogn. Sci. 9, 474–480.

Fries, P., Nirolic, D., and Singer, W. 2007. The gamma cycle. Trends Neurosci. (in press).

Fries, P., Neuenschwander, S., Engel, A. K., Goebel, R, and Singer, W. 2001. Rapid feature selective neuronal synchronization through correlated latency shifting. Nat. Neurosci. 4, 194–200.

Fries, P., Reynolds, J. H., Rorie, A. E., and Desiomone, R. 2001. Modulation of oscillatory neuronal synchronization by selective visual attention. Science 291, 1560–1563.

Fries, P., Schröder, J.-H., Roelfsema, P. R., Singer, W., and Engel, A. K. 2002. Oscillatory neuronal synchronization in primary visual cortex as a correlate of stimulus selection. J. Neurosci. 22, 3739–3754.

Gilbert, C. D. and Wiesel, T. N. 1989. Columnar specificity of intrinsic horizontal and corticocortical connections in cat visual cortex. J. Neurosci. 9, 2432–2442.

Gray, C. M. and Singer, W. 1989. Stimulus-specific neuronal oscillations in orientation columns of cat visual cortex. Proc. Natl. Acad. Sci. U. S. A. 86, 1698–1702.

Gray, C. M., König, P., Engel, A. K., and Singer, W. 1989. Oscillatory responses in cat visual cortex exhibit inter-columnar synchronization which reflects global stimulus properties. Nature 338, 334–337.

Hopfield, J. J. and Herz, A. V. 1995. Rapid local synchronization of action potentials: toward computation with coupled integrated-and-fire neurons. Proc. Natl. Acad. Sci. U. S. A. 92, 6655–6662.

König, P., Engel, A. K., Roelfsema, P. R., and Singer, W. 1995. How precise is neuronal synchronization? Neural Comput. 7, 469–485.

Kreiter, A. K. and Singer, W. 1996. Stimulus-dependent synchronization of neuronal responses in the visual cortex of the awake macaque monkey. J. Neurosci. 16, 2381–2396.

Logothetis, N. K., Pauls, J., Bulthoff, H. H., and Poggio, T. 1994. View-dependent object recognition by monkeys. Curr. Biol. 4, 401–414.

Löwel, S. and Singer, W. 1992. Selection of intrinsic horizontal connections in the visual cortex by correlated neuronal activity. Science 255, 209–212.

Markram, H. and Tsodyks, M. 1996. Redistribution of synaptic efficacy between neocortical pyramidal neurons. Nature 382, 807–810.

Markram, H., Lübke, J., Frotscher, M., and Sakmann, B. 1997. Regulation of synaptic efficacy by coincidence of postsynaptic APs and EPSPs. Science 275, 213–215.

Murthy, V. N. and Fetz, E. E. 1996. Oscillatory activity in sensorimotor cortex of awake monkeys: synchronization of local field potentials and relation to behavior. J. Neurophysiol. 76, 3949–3967.

Neuenschwander, S. and Singer, W. 1996. Long-range synchronization of oscillatory light responses in the cat retina and lateral geniculate nucleus. Nature 379, 728–733.

Phillips, W. A. and Singer, W. 1997. In search of common foundations for cortical computation. Behav. Brain Sci. 20, 657–722.

Pipa, G. and Grün, S. 2003. Non-parametric significance estimation of joint-spike events by shuffling and resampling. Neurocomputing 52–54, 31–37.

Roelfsema, P. R., Engel, A. K., König, P., and Singer, W. 1997. Visuomotor integration is associated with zero time-lag synchronization among cortical areas. Nature 385, 157–161.

Salinas, E. and Sejnowski, T. J. 2001. Correlated neuronal activity and the flow of neural information. Nat. Rev. Neurosci. 2, 539–550.

Schoffelen, J. M., Oostenveld, R., and Fries, P. 2005. Neuronal coherence as a mechanism of effective corticospinal interaction. Science 308, 111–113.

Singer, W. 1999. Neuronal synchrony: a versatile code for the definition of relations? Neuron 24, 49–65.

Tanaka, K. 1997. Mechanisms of visual object recognition: review of monkey and human studies. Curr. Opin. Neurobiol. 7, 523–529.

Thorpe, S., Fize, D., and Marlot, C. 1996. Speed of processing in the human visual system. Nature 381, 520–522.

Treisman, A. 1999. Solutions to the binding problem: progress through controversy and convergence. Neuron 24, 105–110.

Tsunoda, K., Yamane, Y., Nishizaki, M., and Tanifugi, M. 2001. Complex objects are represented in macaque inferotemporal cortex by the combination of feature columns. Nat. Neurosci. 4, 832–838.

VanRullen, R. and Thorpe, S. J. 2001. Rate coding versus temporal order coding: what the retinal ganglion cells tell the visual cortex. Neural Comput. 13, 1255–1283.

VanRullen, R. and Thorpe, S. J. 2002. Surfing a spike wave down the ventral stream. Vision Res. 42, 2593–2615.

Volgushev, M., Chistiakova, M., and Singer, W. 1998. Modification of discharge patterns of neocortical neurons by induced oscillations of the membrane potential. Neuroscience 83, 15–25.

von der Malsburg, C. 1999. The what and why of binding: the modeler's perspective. Neuron 24, 95–104.

Wang, D. L. 2005. The time dimension for scene analysis. IEEE Trans. Neural Netw. 16, 1401–1426.

Wespatat, V., Tennigkeit, F., and Singer, W. 2004. Phase sensitivity of synaptic modifications in oscillating cells of rat visual cortex. J. Neurosci. 24, 9067–9075.

Whittington, M. A., Doheny, H. C., Traub, R. D., LeBeau, F. E., and Buhl, E. H. 2001. Differential expression of synaptic and nonsynaptic mechanisms underlying stimulus-induced gamma oscillations *in vitro*. J. Neurosci. 21, 1727–1738.

Yuval-Greenberg, S. and Deouell, L. Y. 2007. What you see is not (always) what you hear: induced gamma band responses reflect cross-modal interactions in familiar object recognition. J. Neurosci. 27, 1090–1096.

2.02 High-Level Visual Processing

T Fukushima, H Kasahara, T Kamigaki, and Y Miyashita, The University of Tokyo School of Medicine, Tokyo, Japan

© 2008 Elsevier Inc. All rights reserved.

2.02.1	Introduction	11
2.02.2	Object Vision Pathway	11
2.02.3	Effects of Inferior Temporal Damage on Object Recognition	13
2.02.4	Stimulus Selectivity of Neurons in the Inferior Temporal Cortex	16
2.02.5	Invariance Properties of Inferior Temporal Neurons (Invariance With Respect to Position, Orientation and Size)	18
2.02.6	Viewpoint-Dependent and Viewpoint-Independent Responses in the Inferior Temporal Cortex	19
2.02.7	Columnar Organization of the Inferior Temporal Cortex	19
2.02.8	Plasticity of the Stimulus Selectivity of Neurons in the Inferior Temporal Cortex	20
2.02.9	Coding Schemes for Object Representation	22
2.02.10	Future Perspectives and Concluding Remarks	24
References		25

Glossary

binocular disparity Small differences in retinal position of an object between two eyes.

delayed matching-to-sample task In this task, a cue stimulus is presented at the beginning of a trial. After a delay, the subject is required to choose the cued stimulus from choice stimuli including distractors.

functional magnetic resonance imaging An imaging method to visualize the activated areas in the living brain during performance of cognitive tasks, usually used for human studies.

recognition memory An ability to judge whether an item was recently encountered or not, a type of long-term memory that includes an episodic aspect.

single-unit recording Extracellular recording of a single neuron using a microelectrode inserted in the living brain during performance of cognitive tasks, usually used for animal studies.

tachistoscopic presentation Very brief presentation of visual stimuli, say for 10 ms.

visual agnosia Impairments of visual object recognition usually following brain lesions.

2.02.1 Introduction

Visual object recognition is a goal of visual processing in the primate brain. Although we are able to quickly and effortlessly recognize the objects around us in everyday life, the underlying computation carried out by our visual system is not simple. The visual system must cope with a huge number of objects in the environment under various conditions. A single object can produce different retinal images as a result of differences in viewpoint or illumination, and the object may be obscured or partially occluded. Moreover, object recognition is not complete without linkage to knowledge about what the object is, so that the visual system must compare what it has just analyzed with previously stored memories or typical prototypes formed within the system. Such object recognition or high-level visual processing is thought to be subserved by the inferior temporal (IT) cortex. In this chapter, we argue primarily based on findings in animal studies using macaque monkeys.

2.02.2 Object Vision Pathway

Almost 30 visual areas have been identified in the cerebral cortex of the macaque monkey (Felleman, D. J. and

Van Essen, D. C., 1991; Van Essen, D. C. *et al.*, 1992). These areas comprise two main pathways for visual processing: the ventral pathway leads from the primary visual area (V1) to the IT cortex, while the dorsal pathway leads from V1 to the inferior parietal lobule (Ungerleider, L. G. and Mishkin, M., 1982; Desimone, R. and Ungerleider, L., 1989; Goodale, M. A. and Milner, A. D., 1992; Van Essen, D. C. and Gallant, J. L., 1994). Areas in the ventral pathway are thought to analyze what an object is (object vision pathway), while those of the dorsal pathway are thought to analyze where the object is and where it is going (spatial vision pathway).

The IT cortex is situated at the end of the ventral visual pathway. Via this pathway, retinal images are processed in areas V1, V2, and V4, after which the analyzed information is sent from V4 to the IT cortex (Figure 1(a)). More precisely, the posterior part of the

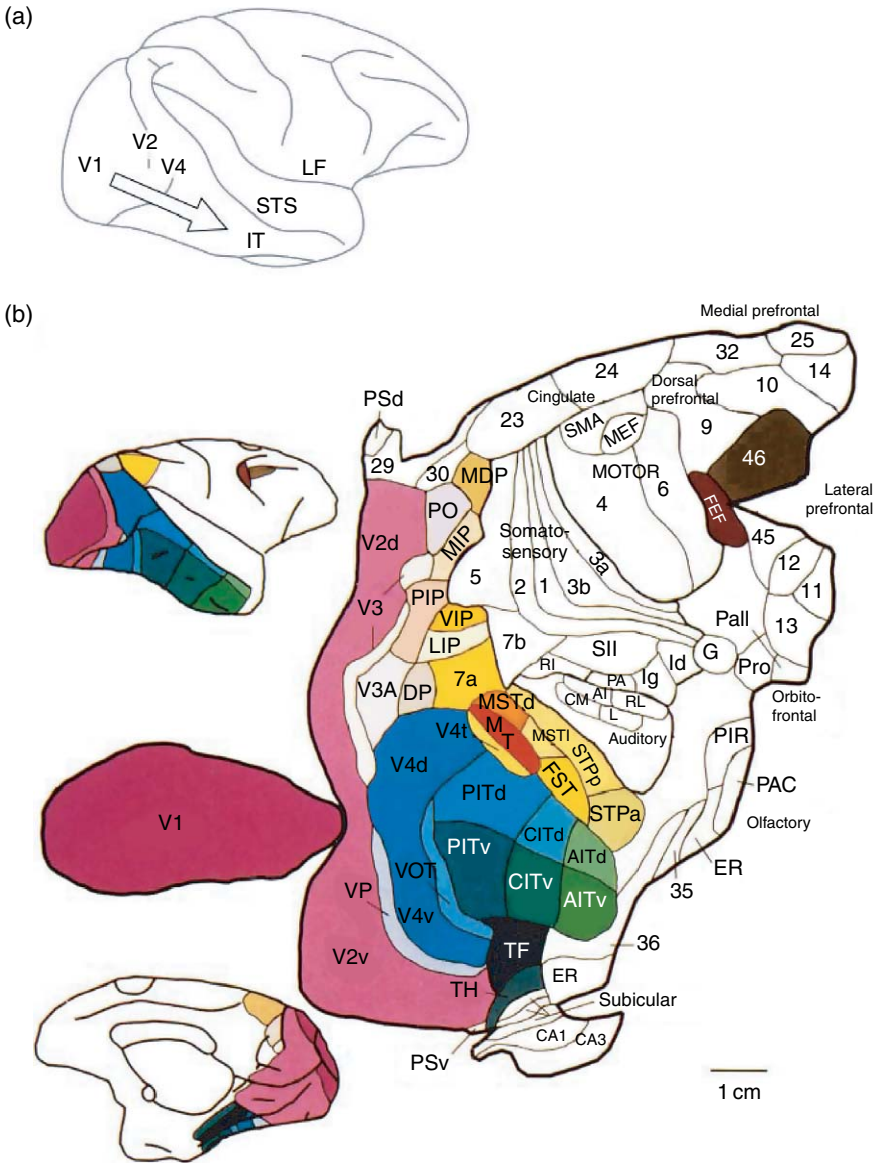

Figure 1 (a) Object vision pathway. A lateral view of a macaque brain is depicted. Arrow: Gross direction of the neuronal processing in the pathway. V1, V2, V4, areas V1, V2, V4; IT, inferior temporal cortex; LF, lateral fissure; STS, superior temporal sulcus. (b) Macaque flattened cortical map of a hemisphere (Felleman, D. J. and Van Essen, D. C., 1991). The IT cortex discussed in this chapter corresponds to areas PITd, PITv, CITd, CITv, AITd, AITv, and 36; area TEO within the IT cortex corresponds to PITd and PITv, while area TE corresponds to CITd, CITv, AITd, and AITv. Insets show lateral and medial views of the hemisphere. Reproduced from Felleman, D. J. and Van Essen, D. C. Distributed hierarchical processing in the primate cerebral cortex. Cereb. Cortex, 1991, Vol. 1, 1–47, by permission of Oxford University Press.

IT cortex (area TEO) receives projections from the prestriate areas V2, V3, and V4, as well as additional sparser projections from areas V3A, V4t, and MT (Distler, C. *et al.*, 1993; a macaque flattened cortical map is shown in Figure 1(b)). Within the IT cortex, the anterolateral part (area TE) receives forward projections from TEO, and the anteroventral part (area 36; A36) receives projections from TE and anterior TEO (Shiwa, T., 1987; Webster, M. J. *et al.*, 1991; Suzuki, W. A. and Amaral, D. G., 1994a; Saleem, K. S. and Tanaka, K., 1996). In addition, there are feedback projections from A36 to TE and TEO, and from TE to TEO (Webster, M. J. *et al.*, 1991; Distler, C. *et al.*, 1993). The IT cortex also receives projections from areas TF and TH in the parahippocampal cortex, from area TG at the temporal pole, and from areas FST at the fundus and STP at the dorsal bank of the superior temporal sulcus (STS; Shiwa, T., 1987; Webster, M. J. *et al.*, 1991; Martin-Elkins, C. L. and Horel, J. A., 1992; Saleem, K. S. *et al.*, 2000). The IT cortex, in turn, projects to the limbic systems, such as the amygdaloid nuclei (Herzog, A. G. and Van Hoesen, G. W., 1976; Iwai, E. and Yukie, M., 1987; Webster, M. J. *et al.*, 1991; McDonald, A. J., 1998) and the hippocampus via the entorhinal cortex (Van Hoesen, G. and Pandya, D. N., 1975; Insausti, R. *et al.*, 1987; Suzuki, W. A. and Amaral, D. G., 1994b; there also are direct routes to the hippocampus; Yukie, M. and Iwai, E., 1988; Rockland, K. S. and Van Hoesen, G. W., 1999). The IT cortex also projects to the ventrolateral and orbital prefrontal cortices (Barbas, H., 1988; Seltzer, B. and Pandya, D. N., 1989; Ungerleider, L. G. *et al.*, 1989; Petrides, M. and Pandya, D. N., 2002). Thus, the anatomical position of the IT cortex can be thought of as an interface between the visual cortices and the limbic systems and frontal lobe.

2.02.3 Effects of Inferior Temporal Damage on Object Recognition

The importance of the IT cortex for visual object recognition is known from both clinical studies in humans and lesion studies in monkeys. Human patients with right temporal lesions show an impaired ability to perform perceptual tasks in which the normal redundancy of visual stimuli is reduced by tachistoscopic presentation (Kimura, D., 1963) or by contrast exaggeration and contour elimination, such as in Mooney's Closure Faces Test (Figure 2(a); Milner, B., 1990). Patients with right temporal lesions also show markedly impaired recognition memory for

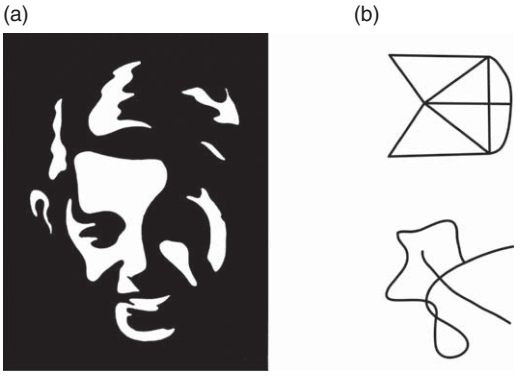

Figure 2 (a) An example face in the Mooney's Closure Faces Test (Milner, B., 1990). The stimuli used in the test are 44 incomplete faces, in which the contrasts are exaggerated and the contours are omitted. Within 30 s, the subjects have to discover the face and indicate the gender and approximate age of the person depicted. Patients who underwent right anterior temporal lobectomy for relief of focal epilepsy exhibited mildly impaired performance on this test. Milner also reported that right temporo-occipital lesions produced the most severe deficit in the test. (b) Examples of abstract line-drawings used in recognition memory tests (Kimura, D., 1963). Patients with right temporal excision performed more poorly on this test than patients with left temporal excision. Their inferior performance was due to the large number of false-positive responses. Upper: geometric design. Lower: nonsense design. (b) Reproduced from Kimura, D. 1963. Right temporal-lobe damage. Perception of unfamiliar stimuli after damage. Arch. Neurol 8, 264–271, the American Medical Association.

complex visual patterns, such as faces (Milner, B., 1968) and abstract line drawings (Figure 2(b); Kimura, D., 1963), which can not be easily encoded verbally. These deficits were found to be unrelated to the extent of hippocampal removal during temporal lobectomy (Milner, B., 1990), suggesting that the temporal neocortex itself may be critically involved in object perception and recognition memory.

Damage to the occipitotemporal area in the human brain often gives rise to certain types of visual agnosia (Humphreys, G. W. and Riddoch, M. J., 1987; Farah, M. J., 2004), including associative visual agnosia and prosopagnosia. Patients with associative visual agnosia have difficulty recognizing objects, which causes their daily life to be severely impaired (Rubens, A. B. and Benson, D. F., 1971; Brown, J. W., 1972; Humphreys, G. W. and Riddoch, M. J., 1987). These patients are not able to recognize objects presented visually until touching them (Figure 3(A)), even though they are able to describe the objects (e.g., a patient described a stethoscope as a long cord with a round thing at the end, while he mistakenly guessed it to be a watch). Furthermore,

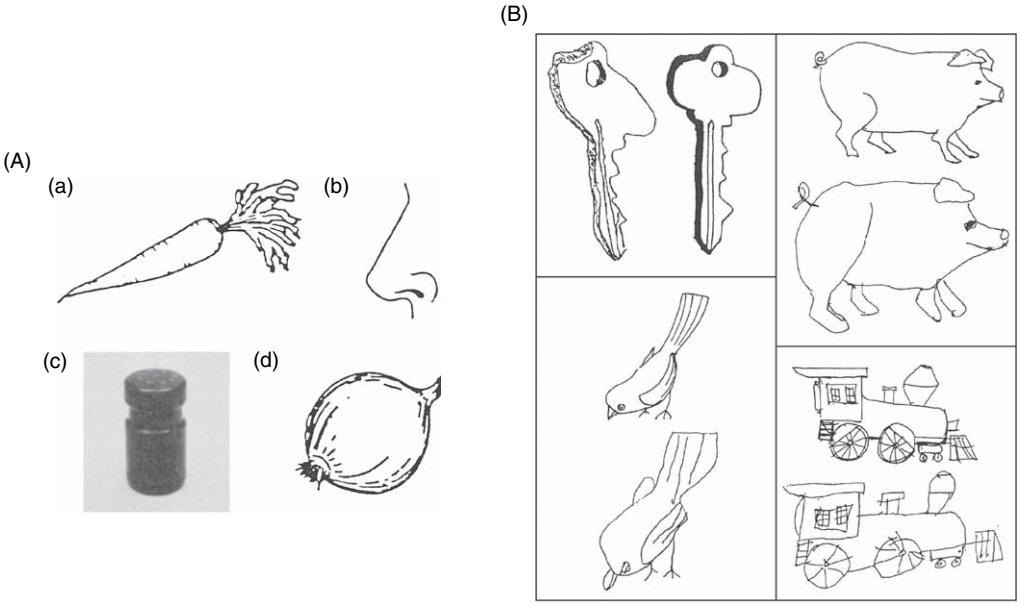

Figure 3 (A) Example of stimuli that an agnosic patient could not correctly identify (Humphreys and Riddoch, 1987). This patient spent a long time coming to his answers and seemed to guess the identity of objects by picking out a salient local feature, not by taking the object as a whole. (a) Line drawing of a carrot (the patient's response, "Some sort of a brush"); (b) line drawing of a nose ("A soup ladle"); (c) photograph of a pepper pot ("A stand containing three separate pans"); (d) line drawing of an onion ("A necklace of sorts"). (B) Copies of line drawings made by an associative visual agnosic (Rubens, A. B. and Benson, D. F., 1971). The line drawings on the right or top of the panels are samples. The patient did not recognize any of the objects in the pictures before or after copying them, although the copying performance was excellent. The patient's comments after copying were as follows: key (upper left), "I still don't know"; pig (upper right), "Could be a dog or any other animal"; bird (lower left), "Could be a beach stump"; locomotive (lower right), "A wagon or a car of some kind, the larger vehicle pulled by the smaller one." It should be noted that the patient drew the pictures rather slowly and in a line-by-line manner (Brown, J. W., 1972), perhaps suggesting impairment of shape perception (Farah, M. J., 2004). (A) Reproduced from Humphreys, G. W. and Riddoch, M. J. 1987. To See but not to See: a Case Study of Visual Agnosia, 1987, Lawrence Erlbaum Associates/Taylor & Francis Group. (B) Reproduced from Rubens, A. B. and Benson, D. F. 1971. Associative visual agnosia. Arch. Neurol. 24, 305–316, the American Medical Association.

without knowing what sample pictures indicate, they copy the pictures accurately (Figure 3(B)). These patients also are able to discriminate objects based on their visual features, but they are not able to classify them based on their category, such as clothing or food (but some patients can retain partial or crude information about the category or superordinate class to which an object belongs; McCarthy, R. A. and Warrington, E. K., 1990). Most patients with this type of agnosia have bilateral lesions, though many well-documented cases have either left or right unilateral occipitotemporal lesions (Levine, D. N., 1982; Farah, M. J., 2004).

Prosopagnosia is the inability to recognize faces, despite intact intellectual ability and even apparently intact visual recognition of most other stimuli (Humphreys, G. W. and Riddoch, M. J., 1987; Farah, M. J., 2004). When looking in a mirror, these patients even misjudge themselves to be an unfamiliar person staring at them. Prosopagnosia is known to often arise with bilateral occipitotemporal damage (Meadows, J. C., 1974; Damasio, A. R. *et al.*, 1982), while it was recently reported that some patients become prosopagnosic after unilateral right hemisphere damage (De Renzi, E. *et al.*, 1994; Wada, Y. and Yamamoto, T., 2001). Prosopagnosia suggests the existence of special neural mechanisms for face recognition. Consistent with that idea are the findings of functional magnetic resonance imaging (fMRI) studies, which revealed that different regions of the human occipitotemporal cortex are activated specifically in response to faces (fusiform face area), places (parahippocampal place area), or body parts (extrastriate body area; Kanwisher, N., 2003; but see also Haxby, J. V., 2004; Grill-Spector, K. *et al.*, 2006).

Another type of visual agnosia, apperceptive agnosia or perceptual categorization deficit, has been also known (Warrington, E. K., 1985; Farah, M. J., 2004). Patients with this disorder are unable to recognize common objects when viewed from unusual perspectives (Warrington, E. K. and Taylor, A. M., 1973) or illuminated from unusual directions (Warrington, E.

K., 1985). Although perceptual constancy across different viewing angles, which is cardinal for object recognition, appears to be impaired in these patients, the disorder probably does not affect object recognition proper but concerns an optional or subsidiary system that may boost the accuracy of object recognition (Warrington, E. K. and James, M., 1988; Farah, M. J., 2004). This is suggested by the fact that these patients are not impaired during usual situations in everyday life, as they are able to recognize objects from different perspectives, so far as they are ordinary. Thus these patients have not lost perceptual constancy across viewing angles. In actual fact, the brain lesions in apperceptive agnosia are not associated with the IT cortex, but with the right inferior parietal lobe (Warrington, E. K. and Taylor, A. M., 1973; McCarthy, R. A. and Warrington, E. K., 1990).

In monkeys, bilateral ablation of the IT cortex causes severe but selective deficits in their ability to learn tasks that require visual recognition of objects (Gross, C. G., 1973; Dean, P., 1976; Mishkin, M., 1982). IT lesions impair the retention of visual discriminations acquired prior to surgery as well as the acquisition of new visual discriminations following surgery (Gross, C. G., 1973). Although extensive and prolonged training might enable monkeys with IT lesions to eventually acquire new visual discriminations, it was revealed that these monkeys are able to solve tasks in abnormal ways. For instance, they may choose the target stimulus based on such visual properties as its position, size, brightness, or other local feature, but not based on its entire shape, *per se* (Iwai, E., 1985).

Monkeys with IT lesions also show an impaired ability to generalize visual stimuli. The normal visual system is able to recognize a given object consistently, even when that object appears in a different visual size (larger or smaller retinal image), in a different orientation (tilted or turned), or under different illumination. In monkeys with lesions of the IT cortex, however, early research revealed impairment of size constancy (Humphrey, N. K. and Weiskrantz, L., 1969; Ungerleider, L. G. *et al.*, 1977). More recently, it was reported that lesions in either the prestriate or anterior IT cortices impaired visual discrimination of objects transformed with respect to size, orientation, or illumination (Figure 4; Weiskrantz, L. and Saunders, R.

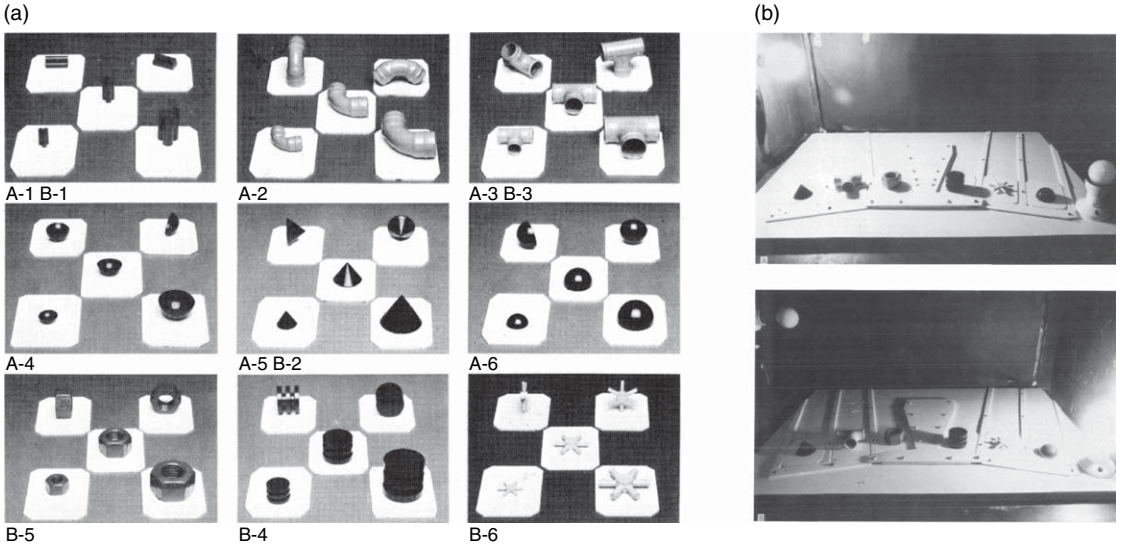

Figure 4 Photographs of example objects used in a visual discrimination task involving transformed objects (Weiskrantz, L. and Saunders, R. C., 1984). (a) Size and orientation transforms. The center object in each panel is the standard training object (not transformed). The two front objects are size transforms, while the back two are orientation transforms. The label for each panel indicates the order in which the transform set was presented to monkeys (see the original article). (b) Illumination transforms, shown with a six-choice apparatus. The illumination transforms were produced by turning off an ordinary overhead lamp in the test setting and turning on a side lamp situated to the left and above the objects (upper panel) or to the right (lower panel). After monkeys with cortical lesions completed discrimination learning of positive targets in the untransformed mode, they were tested in a retention test using untransformed and transformed objects. As compared with the unlesioned monkeys and those with parietal lesions, monkeys with prestriate or inferior temporal lesions showed an impaired ability to initially learn the untransformed objects (which is consistent with previous lesion studies) and then made more errors in the retention test when they were required to choose transformed positive targets. Reproduced from Weiskrantz, L. and Saunders, R. C. Impairments of visual object transforms in monkeys. Brain, 1984, Vol. 107, 1033–1072, by permission of Oxford University Press.

C., 1984). Furthermore, for the prestriate group, the more the lesion extended anteriorly into the IT region, the more severe was the transform deficit. These findings suggest that the more anterior part of the IT cortex may be concerned with formation and storage of an invariant representation, or prototype, of a visual object, which can be accessed during visual discrimination of transformed objects (Weiskrantz, L. and Saunders, R. C., 1984; Weiskrantz, L., 1990).

2.02.4 Stimulus Selectivity of Neurons in the Inferior Temporal Cortex

The response properties of IT neurons have been extensively investigated in electrophysiological studies of monkeys. Early evidence that IT neurons respond to visual stimuli came largely from experiments carried out by Gross and colleagues (Gross, C. G., 1973). They described the heterogeneous response properties of IT neurons as well as their large receptive fields. The visual responses of IT neurons vary depending on several stimulus parameters: direction and speed of movement, size, shape, contrast, and wavelength. The receptive fields of IT neurons cover both visual hemifields and almost always include the fovea: their median size is 418 degrees^2 with an interquartile range of 150–1410 degrees^2 (several recent studies argue that some neurons may have smaller receptive fields that span only a few degrees; Op De Beeck, H. and Vogels, R., 2000; Wang, Y. *et al.*, 2002; DiCarlo, J. J. and Maunsell, J. H., 2003; for a review, Fujita, I., 2002).

More specifically, several studies revealed selective responses within the IT cortex to complex objects, such as hands (Gross, C. G. *et al.*, 1972) and faces (Desimone, R. *et al.*, 1984; Rolls, E. T. and Baylis, G. C., 1986). Face-responsive temporal neurons were first identified in the fundus and the dorsal bank of the STS (Perrett, D. I. *et al.*, 1979; Bruce, C. *et al.*, 1981; Perrett, D. I. *et al.*, 1982; 1984), just adjacent to the IT cortex dorsally. Some of these face-responsive neurons in both areas exhibited different responses to different faces (Perrett, D. I. *et al.*, 1987; Hasselmo, M. E. *et al.*, 1989a; Young, M. P. and Yamane, S., 1992; Leopold, D. A. *et al.*, 2006), which suggests identity coding of faces in those areas. Indeed, the graded face-selective activities in IT neurons could reflect the physical properties of faces (e.g., distance between eyes, width from eyes to a hairline, and so on; Yamane, S. *et al.*, 1988; Young, M. P. and Yamane, S., 1992), or the structural differences between external face stimuli and an internal reference or prototype (Leopold, D. A. *et al.*, 2006). Recent macaque fMRI studies revealed multiple face-responsive areas in the STS (Logothetis, N. K. *et al.*, 1999; Tsao, D. Y. *et al.*, 2003; Pinsk, M. A. *et al.*, 2005). In addition, a later single-unit study demonstrated that most of the neurons in one face-responsive area showed a greater preference for faces than for other categories of objects, such as hands, bodies, and fruit (Figure 5; Tsao, D. Y. *et al.*, 2006).

Other complex two-dimensional figures can also be encoded by IT neurons. Miyashita Y. and Chang H. S. (1988) found anterior temporal cortical neurons that show highly selective responses to computer-generated colored fractal patterns (Miyashita, Y.

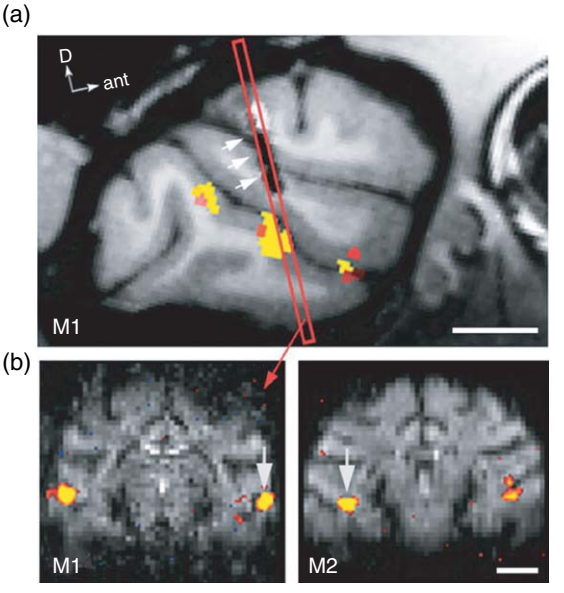

Figure 5 A face-responsive area identified by functional magnetic resonance imaging that was used for subsequent single-unit recording (Tsao, D. Y. *et al.*, 2006). (a) A semisagittal section through the right hemisphere of a monkey (M1) showing three face-selective patches along the superior temporal sulcus. Single-unit recordings in monkeys were performed in the middle patch; the red rectangle indicates a coronal slice through the middle patch. The three white arrows indicate the lesion caused by insertion of a guide tube for recording microelectrodes. (b) MION (monocrystalline iron oxide nanoparticle; a contrast agent) activation overlaid on raw echo-planar coronal images showing the middle face patches in monkeys (left, M1; right, M2). Arrows indicate the patches from which neuronal activity was recorded. The researchers reported that, out of 310 visually responsive neurons recorded from the middle patches in the monkeys, 302 (97%) were face selective. Scale bar = 1 cm. Reproduced from Tsao, D. Y., Freiwald, W. A., Tootell, R. B., and Livingstone, M. S. 2006. A cortical region consisting entirely of face-selective cells. Science 311, 670–674, with permission from the American Association for the Advancement of Science (AAAS).

et al., 1991) in monkeys trained to perform a delayed matching-to-sample (DMS) task. When the visual responses to a large set (usually 100) of fractal patterns were evaluated, it was found that individual neurons commonly responded well to only a small fraction of the stimulus set during the delay period (Figure 6(a)). That the optimal fractal patterns of the individual neurons showed no geometric similarity at all (Figure 6(b); Miyashita, Y., 1988) suggests associative encoding of visual stimuli by IT neurons (see a later section in this chapter).

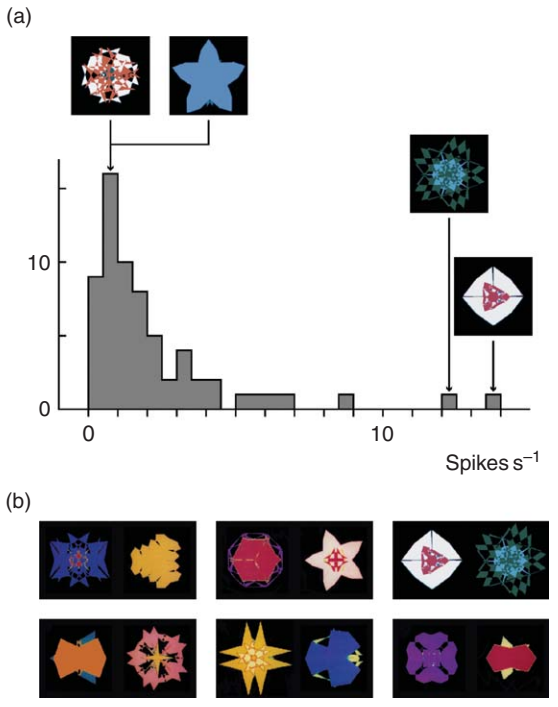

Figure 6 (a) Distribution of responses of a macaque inferior temporal (IT) neuron to 64 different colored fractal patterns (Miyashita, Y. and Chang, H. S., 1988). The monkey performed a delayed matching-to-sample task. For each fractal pattern, the neuronal discharges during the delay periods were averaged over more than four trials in which the fractal pattern was presented as a sample stimulus. The abscissa indicates response strength in terms of spike frequency, and the ordinate indicates the number of fractal patterns. Examples of the fractal patterns used are also shown in the panel with arrows indicating the neuronal responses they elicited. This neuron highly selectively responded to a few optimal stimuli (two examples are on the right-hand side) and only poorly to the others (the examples on the left-hand side). (b) Optimal fractal patterns of six neurons in the IT cortex (Miyashita, Y., 1988). These six pairs of fractal patterns elicited the two strongest delay discharges in six different IT neurons. Note that there is no similarity between the geometric patterns of the two optimal stimuli. (a) Adapted from Miyashita, Y. and Chang, H. S. 1988. Neuronal correlate of pictorial short-term memory in the primate temporal cortex. Nature 331, 68–70, with permission. (b) Adapted from Miyashita, Y. 1988. Neuronal correlate of visual associative long-term memory in the primate temporal cortex. Nature 335, 817–820, with permission.

Tanaka K. *et al.* (1991) used a unique reduction method to investigate the stimulus selectivity of neurons in area TE within the IT cortex. In a stepwise fashion, they removed ineffective or interfering features from an initial effective stimulus to obtain the simplest pattern to which an isolated neuron responded maximally. This reduction method revealed that the critical features to which individual IT neurons respond are more complex than simple bars or disks; they vary from moderately complex shapes, such as a spiny starlike shape or a striped triangle, to combinations of such shapes with color or texture (Figure 7). Moreover, neighboring IT neurons often preferred similar critical features, forming a columnar organization within the cortex (see a later section in this chapter).

Several recent studies showed that the responses of a number of IT neurons could be modulated by binocular disparity (Janssen, P. *et al.*, 1999; 2000; Uka, T. *et al.*, 2000; 2005; for a review, Orban, G. A. *et al.*, 2006). These IT neurons responded to disparity-defined three-dimensional shapes (Janssen, P. *et al.*,

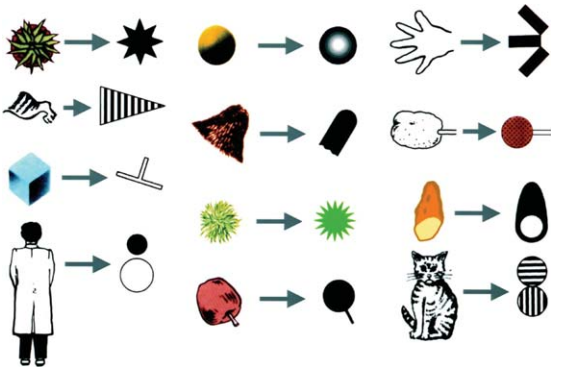

Figure 7 Examples of reductive determination of critical features for 12 neurons (Tanaka, K., 2003). The pictures to the left of the arrows represent the initial effective stimuli and those to the right of the arrows, the critical features determined using the reduction method. An original stimulus could undergo a different reductive process depending on the neuron tested. Note that the process of reducing the original complex stimuli is critically dependent on the experimenter's experience and intuition. Some of the critical features were moderately complex shapes, while others were combinations of such shapes with color or texture. Reproduced from Tanaka, K. Columns for complex visual object features in the inferotemporal cortex: clustering of cells with similar but slightly different stimulus selectivities. Cereb. Cortex, 2003, Vol. 13, 90–99, by permission of Oxford University Press.

1999; 2000) and exhibited selective activity in response to both binocular disparity and shape (Uka, T. *et al.*, 2000; 2005). These findings suggest that binocular disparity is utilized in the IT cortex to analyze and represent three-dimensional objects in the real world. Moreover, they are consistent with studies showing that monkeys with IT lesions have an impaired ability to discriminate between two disks of different physical sizes that are located at different distances from the monkeys (Humphrey, N. K. and Weiskrantz, L., 1969; Ungerleider, L. G. *et al.*, 1977).

2.02.5 Invariance Properties of Inferior Temporal Neurons (Invariance With Respect to Position, Orientation and Size)

The early discovery that IT neurons have large receptive fields was accompanied by the finding that IT neurons show considerable response invariance across retinal positions within those receptive fields (Gross, C. G., 1973). In addition to retinal translation, IT neurons also show varying degrees of response invariance when stimuli are transformed with respect to size, orientation, and other parameters. Several studies have shown that the relative preference of IT neurons for their optimal stimulus over several suboptimal stimuli is preserved over a wide range of stimulus sizes and positions (Sato, T. *et al.*, 1980; Schwartz, E. L. *et al.*, 1983; Tanaka, K. *et al.*, 1991; Lueschow, A. *et al.*, 1994; Ito, M. *et al.*, 1995), although the absolute responses of these neurons only rarely show invariance with respect to stimulus size or position. In addition, the shape selectivity of some IT neurons is maintained across the physical attributes that define the contours of the shape. For instance, the relative preferences of shape-selective neurons are unchanged whether the shapes are determined by differences in luminance, by the motion of dots, or by texture (Sáry, G. *et al.*, 1993; Tanaka, H. *et al.*, 2001). Furthermore, shape selectivity is preserved when visual stimuli are partially occluded (Kovács, G. *et al.*, 1995) or when shading and texture are removed altogether (Kovács, G. *et al.*, 2003). These results above were mainly obtained in the anterior part of the middle temporal gyrus.

In contrast, when IT neurons in the anterior part of inferior temporal gyrus (ITG) were tested in a DMS task using fractal patterns, an even higher degree of invariance was observed (Miyashita Y. and Chang H. S., 1988). Not only the relative stimulus selectivity, but also the absolute response levels, remained the same in the majority of tested neurons when sample pictures were manipulated by reducing their size, rotating them 90° clockwise, or transforming them from color to monochrome (Figure 8). These results, which demonstrate the invariance properties of IT neurons, support the hypothesis that the anterior portion of the IT cortex is involved in storing typical and invariant representations of visual objects (Weiskrantz, L. and Saunders, R. C., 1984; Weiskrantz, L., 1990). A similarly high degree of response invariance also was found in the face neurons located in the STS (Rolls, E. T. and Baylis, G. C., 1986; Perrett, D. I. *et al.*, 1987), which suggests that this region also may be concerned with invariant representation of objects.

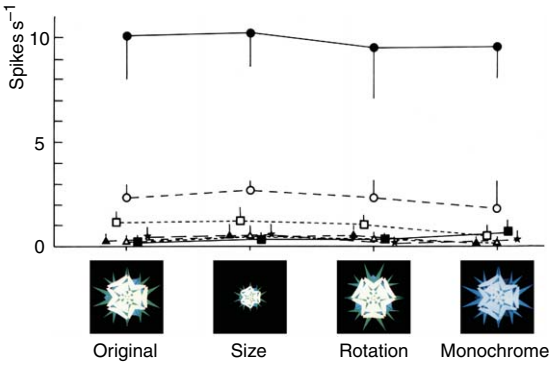

Figure 8 Invariance of the response of an inferior temporal neuron after transformation of the stimulus size, orientation or color (Miyashita, Y. and Chang, H. S., 1988). Original fractal patterns (original) were manipulated in the following way: (1) the size of the patterns was reduced by half (size), (2) the patterns were rotated by 90° in a clockwise direction (rotation), (3) colored patterns were transformed to monochrome by referring to a pseudo-color look up table (monochrome). In the figure, the averaged delay activities are plotted against stimulus transformation. This IT neuron fired during the delay after one particular fractal pattern (closed circles) but not after others (the other markers), irrespective of pattern size, orientation, or color. Similar response invariance also was observed in most of the neurons tested: size invariance was observed in 16 of 19 neurons, orientation invariance in five of seven neurons, and color invariance in 15 of 20 neurons. In the neurons that did not show response invariance, manipulation of the most effective pattern reduced or abolished delay activity. Closed circles: Responses to an original optimal fractal pattern and its transformed patterns; these are shown at the bottom of the figure. Error bars indicate standard deviations for four to 15 trials. The other markers: Responses to original suboptimal fractal patterns and their transformed patterns. Adapted from Miyashita, Y. and Chang, H. S. 1988. Neuronal correlate of pictorial short-term memory in the primate temporal cortex. Nature 331, 68–70, with permission.

2.02.6 Viewpoint-Dependent and Viewpoint-Independent Responses in the Inferior Temporal Cortex

Three-dimensional objects may cast different images on our retina, depending upon the viewing angle. For example, the appearance of a car is quite different when viewed from the front than when viewed from the side: from the front, the windshield, headlights, grille, and bumper stand out; from the side, two wheels, the doors, and the windows stand out. Thus, our perception is viewpoint dependent (front and side views of cars). However, we are able to recognize the object to be a car in both cases, even though the images of the car cast on our retina are quite different. Thus, our cognition is viewpoint independent (it is a car). Probably corresponding to such our perception and cognition, both viewpoint-dependent and -independent responses are found in the macaque IT cortex.

Using different views of visual stimuli, several studies have demonstrated that a large number of IT neurons respond only to limited views of specific objects, and that those neurons exhibit little or no response to nonpreferred objects, irrespective of the viewpoint (Hasselmo, M. E. *et al.*, 1989b; Logothetis, N. K. and Pauls, J., 1995; Logothetis, N. K. *et al.*, 1995; Booth, M. C. and Rolls, E. T., 1998). In contrast, viewpoint-invariant responses to preferred objects, that is, comparable activity favoring an optimal object at all viewing angles, are rarely observed in the IT cortex. It turns out that only a small percentage of neurons exhibit comparable responses to all views of an object, while showing little or no response to other objects, even after extensive discrimination training with the objects (Logothetis, N. K. and Pauls, J., 1995) or after several weeks of familiarization with the objects in the monkeys' home cages (Booth, M. C. and Rolls, E. T., 1998).

The existence of both viewpoint-dependent and viewpoint-independent responses in the IT cortex suggests that viewpoint invariance may have its start there. It would be natural to think that viewpoint invariance develops in the IT cortex through the convergence of viewpoint-dependent responses that are selective for both the object identity and the viewing angle. This is the same scheme that explains the emergence of complex cells from simple cells in V1 (Hubel, D. H. and Wiesel, T. N., 1962). Several proposed models of object recognition indeed include this convergent structure (Riesenhuber, M. and Poggio, T., 2002; Rolls, E. T. and Deco, G., 2002). An object representation that is invariant across viewpoints could be utilized for further processing, such as association with reward or punishment (Rolls, E. T. and Treves, A., 1998) or linkage with a memory about what the object indicates (Miyashita, Y. and Hayashi, T., 2000; Miyashita, Y., 2004). Furthermore, this invariant representation could be associated with prefrontal neuronal representations that are to be processed or manipulated for a task at hand (Goldman-Rakic, P. S., 1987; Hasegawa, I. *et al.*, 1998; Tomita, H. *et al.*, 1999; Fukushima, T. *et al.*, 2004; Ranganath, C. and D'Esposito M., 2005).

How then does the visual system make the convergent connections to realize viewpoint invariance, and how does the system learn that different appearances are of the same object viewed from different angles? A hypothesis comes from the fact that in our experience of the visual world, different views of an object are almost always presented in succession, transformed by the movement of the object or the observer. Therefore, temporal vicinity or successive presentation can be used as a clue to associate together these different images from different viewing angles (Földiák, P., 1991; Miyashita, Y., 1993; Rolls, E. T. and Deco, G., 2002). This hypothesis is experimentally underpinned by an electrophysiological study that showed long-term association of disparate fractal patterns in macaque IT neurons during a DMS task in which fractal samples in a stimulus set were always presented in the same order (Miyashita, Y., 1988). Single-unit recordings after overtraining on the task revealed that IT neurons exhibited correlated responses to sample patterns that were in close proximity to one another within the predetermined stimulus set (Figure 9). Guided by the close temporal proximity of the presented visual images, the IT neurons are thought to have learned associations between the images.

2.02.7 Columnar Organization of the Inferior Temporal Cortex

Similar to the somatosensory (Powell, T. P. and Mountcastle, V. B., 1959) and the primary visual (Hubel, D. H. and Wiesel, T. N., 1968) cortices, the macaque IT cortex is thought to have a columnar organization (Tanaka, K., 2003). The columns are comprised of neurons with similar response properties clustered vertically through the cortex from the pial surface to the white matter (Mountcastle, V. B.,

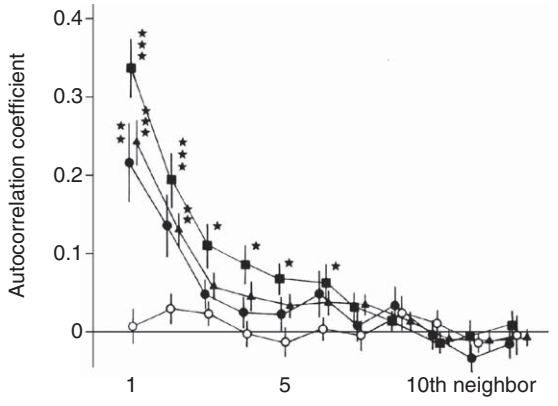

Figure 9 Stimulus–stimulus association among disparate fractal patterns in close proximity along a learned sample set (Miyashita, Y., 1988). Of 206 inferior temporal neurons recorded while monkeys performed a delayed matching-to-sample test, 57 exhibited shape-selective delay discharges. For each of those 57 neurons, autocorrelation coefficients for the responses to learned and new sample sets of fractal patterns were calculated, taking into account the serial position numbers (SPNs) of the sample stimuli, and were plotted against the distance between the SPNs used to calculate the coefficients. The correlation between neuronal responses were high for fractal patterns in close proximity within the learned set, but was nearly zero for both distantly positioned learned patterns and novel patterns. Closed and open circles, average autocorrelation coefficients for the learned and new stimulus sets in 17 neurons that were successfully tested with both sets; closed triangles, coefficients for the learned set in the 57 neurons; closed squares, coefficients for the learned set in the 28 neurons for which the nearest-neighbor correlation for the SPN was significant ($P < 0.05$) according to Kendall's test. Error bars are standard errors. Three vertical asterisks, $P < 0.001$; two vertical asterisks, $P < 0.01$; one asterisk, $P < 0.05$ versus the value for new stimulus list (Kolmogorov-Smirnov test). Reproduced from Miyashita, Y. 1988. Neuronal correlate of visual associative long-term memory in the primate temporal cortex. Nature 335, 817–820, with permission.

1997; Horton, J. C. and Adams, D. L., 2005). Early positive evidence of the columnar organization of the IT cortex came from several electrophysiological studies that suggested the clustering of IT neurons with similar response properties (Gochin, P. M. *et al.*, 1991; Fujita, I. *et al.*, 1992). In one study where functional relationship among IT neurons was investigated using simultaneous recording from multiple microelectrodes, neurons recorded on the same electrode (within about 100 μm) showed more similar stimulus selectivity and were more likely to show correlated discharge than those recorded on different electrodes spaced about 250–500 μm apart (Gochin, P. M. *et al.*, 1991).

In another study, a conventional approach (Powell, T. P. and Mountcastle, V. B., 1959; Hubel, D. H. and Wiesel, T. N., 1968) was used to investigate the columnar organization in the IT cortex (Fujita, I. *et al.*, 1992). The investigators inserted microelectrodes vertically or obliquely into the IT cortex and assessed the response properties of the neurons along the axis of the penetrations. Vertical penetrations revealed that neurons with similar selectivity span most of the cortical layers over distances of 0.7–2.1 mm, which suggests penetrations through single functional columns. In contrast, with oblique penetrations, the widths of clusters showing similar selectivity were shorter (0.2–0.7 mm); the preferred visual feature then changed to a different one after a gap of 0.4–1.0 mm, suggesting penetrations through multiple functional columns.

Recent optical imaging studies have provided further evidence of columnar organization within the IT cortex (Wang, G. *et al.*, 1996; 1998; Tsunoda, K. *et al.*, 2001). Presentation of complex visual stimuli modulated the intrinsic signals at multiple spots within the IT cortex (Figure 10). The size of the affected spots was 0.50 ± 0.13 mm along the longer axis and 0.35 ± 0.09 mm along the shorter axis (Tsunoda, K. *et al.*, 2001). Each spot was specific for a visual feature or a part of an object, and exhibited activation or inactivation in response to a variety of visual stimuli. This suggests that these columnar spots function as basic building blocks to construct neuronal representations of the real objects.

2.02.8 Plasticity of the Stimulus Selectivity of Neurons in the Inferior Temporal Cortex

Many of the studies summarized above show that large numbers of macaque IT neurons respond highly selectively to computer-generated geometrical stimuli (Miyashita, Y. and Chang, H. S., 1988; Sakai, K. and Miyashita, Y., 1991; Logothetis, N. K. *et al.*, 1995), even though these artificial stimuli were completely unfamiliar to the naive monkeys. Since it is highly unlikely that the IT cortex inherently contains neurons that are tuned to these artificial stimuli, the high degree of selectivity of the affected neurons for these computer-generated stimuli is thought to be newly acquired through repeated experience. Consistent with that idea, IT neurons have been shown to respond more selectively to some types of stimuli, including fractal patterns (Miyashita, Y., 1988; Sakai, K. and Miyashita, Y., 1994), batonlike stimuli

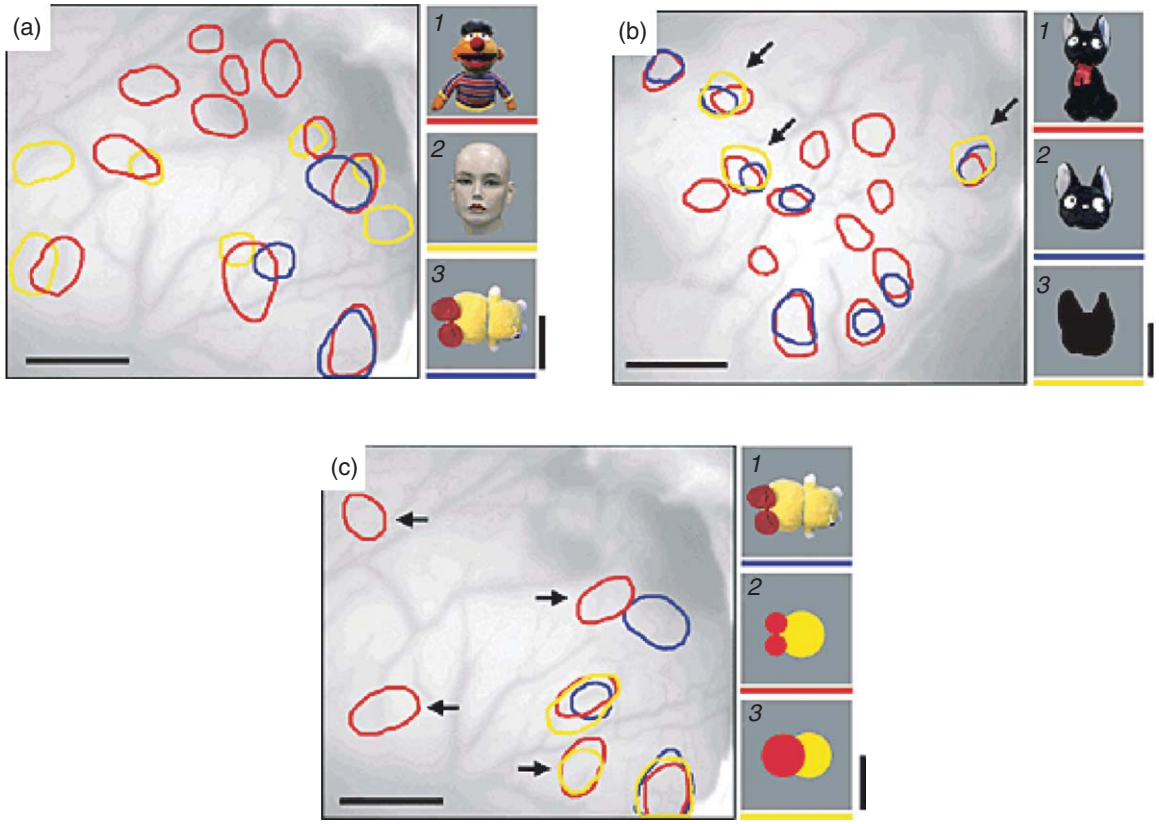

Figure 10 Intrinsic signal imaging in macaque area TE in the inferior temporal (IT) cortex (Tsunoda, K. *et al*., 2001). (a) Spatial patterns of the active spots elicited by three different complex objects. Each complex object elicited several active spots on the dorsal part of area TE in the macaque IT cortex. The outline colors of the spots denote the eliciting objects, which are shown to the right of the panel with colored bars below. Although the spatial patterns of the spots differed, parts of the spots were commonly activated by multiple objects. Activation within the common spots could reflect visual features common to the objects. For instance, the spot in the bottom right corner of the panel could represent a red circle which is common to the objects 1 and 3. (b) Spatial patterns of activation elicited by a complex object and its simplified versions (additive). Some of the spots activated by the initial complex object could not be activated by simplified versions of the object. In this panel, the head of the black cat (object 2) activated a subset of the spots activated by the whole black cat (object 1). Moreover, the silhouette of the head (object 3) activated only three spots (arrows). These results are consistent with the idea that each spot represents a simple visual feature and that a large number of spots are recruited to represent the whole object. (c) Spatial patterns of activation elicited by another object and its simplified versions (suppressive). In this case, some of the spots that were activated by simplified versions of initial complex objects could not be activated by the whole objects. In this panel, object 2 (two small red circles overlapping a large yellow circle) activated four additional spots (arrows) that were not activated by the whole object (object 1). This suggests that some of the spots representing a particular visual feature are suppressed when the feature is embedded within a complex object. Adapted by permission from Macmillan Publishers Ltd: Nature Neuroscience (Tsunoda, K., Yamane, Y., Nishizaki, M. and Tanifuji, M., Complex objects are represented in macaque inferotemporal cortex by the combination of feature columns. Nat Neurosci 4, 832-838, 2001), copyright 2001.

(Baker, C. I. *et al*., 2002), and animal-like stimuli (Freedman, D. J. *et al*., 2006), after training than before training. In addition, the proportion of neurons that selectively respond to moderately complex visual stimuli increases in the IT cortex of trained monkeys (Kobatake, E. *et al*., 1998). Visual experience also increases the similarity of the responses of nearby neurons to trained stimuli (Erickson, C. A. *et al*., 2000). When acquiring such stimulus selectivity through training, it was demonstrated that IT neurons become more specialized for the discrimination of relevant visual features (Sigala, N. and Logothetis, N. K., 2002). This plasticity within the IT cortex could underlie our ability to discriminate among familiar objects, for instance a bird-watcher's ability to distinguish a large number of birds.

Further evidence of plasticity within the IT cortex comes from the finding that some IT neurons can be

tuned to disparate visual images with no geometrical similarity by repeatedly presenting the images in close temporal proximity (Miyashita, Y., 1988), as is described in another section. This suggests that IT neuronal activity learns to reflect the temporal relationship between visual images through experience. A later study also showed that some IT neurons can encode semantic-like relationships between pairs of Fourier descriptor stimuli that are geometrically unrelated and have no other relationship to one another, except that they are operationally associated by the experimenters (Sakai, K. and Miyashita, Y., 1991). In this case, the experimenters trained monkeys on a pair-association (PA) task, which is a well-known neuropsychological test that is widely used to assess dysfunction of the medial temporal lobe memory system in humans (usually, the test is comprised of tens of word pairs). In the visual PA task for monkeys, after one member of a pair is presented as a cue stimulus, the monkeys are required to choose the other member of the pair. Single-unit recordings from the anterior part of the ITG made while the monkeys performed the task revealed that a population of neurons showed comparable or correlated responses to two Fourier descriptors arbitrarily paired in the task (Figure 11) and that they clustered within hot spots in the region. This correlated selectivity to paired visual stimuli develops while the subject is learning the relationship between the stimuli (Messinger, A. *et al.*, 2001). These correlated responses of single neurons could reflect a semantic-like linkage of one visual image to another, and might support object identification in the object vision pathway. Based on the plasticity of the stimulus selectivity in the IT cortex, visual long-term memories could be formed and stored there, probably through the medial temporal lobe memory system (Squire, L. R. and Zola-Morgan, S., 1991; Eichenbaum, H. and Cohen, N. J., 2001; Miyashita, Y., 2004).

2.02.9 Coding Schemes for Object Representation

What neuronal encoding is used in the IT cortex to represent objects? Considering that there are a huge number of natural objects, a one-to-one coding scheme, such as making use of grandmother cells or pontifical cells, would seem unlikely (Barlow, H. B., 1972; Rose, D., 1996). In actual brain, electrophysiological studies have shown that populations of IT neurons can exhibit graded responses to different objects (Komatsu, H. and Ideura, Y., 1993; Young, M. P. and Yamane, S., 1993; Booth, M. C. and Rolls, E. T., 1998). This suggests that the activity patterns of a population of responsive neurons could encode the identities of a variety of objects; this is referred to as sparse population coding (Young, M. P. and Yamane, S., 1992) or distributed encoding (Rolls, E. T. and Treves, A., 1998). Such distributed encoding by a population of neurons is reinforced by information theory (Rolls, E. T. and Treves, A., 1998). In adjoining cortices in the STS, the same coding scheme also has been suggested for face-selective neurons (Baylis, G. C. *et al.*, 1985; Rolls, E. T. and Treves, A., 1998).

Other aspects of neuronal encoding in the IT cortex also have been proposed. As mentioned in another section, the critical features that maximally activate individual IT neurons are moderately complex, but they are still too simple for a single neuron to specify a whole object in the real world (Tanaka, K. *et al.*, 1991). Consequently, multiple neurons with preferences for different visual features would be combined to represent an entire object (Tanaka, K., 1993). Consistent with this idea are the findings of recent optical-imaging studies in area TE of the IT cortex, which demonstrated that in some cases activation spots representing a complex object can be partially activated by components of that object (Figure 10(b); Tsunoda, K. *et al.*, 2001). However, one question raised by this coding scheme is how are objects discriminated in a neuronal representation when they share the same visual features or parts but in a different configuration? Simple convergence of the outputs of the feature-responsive IT neurons, which have moderate position invariance around the fovea, should not be able to discriminate such objects. This simple deduction based on the properties of IT neurons is known as an expression of binding problem in visual object recognition (Malsburg, C. v. d., 1995; Treisman, A., 1999). One possible way to resolve these embarrassing situations is to make use of temporal coding, as has been proposed in models (Malsburg, C. v. d., 1995) and sensory cortices (Singer, W., 1999). In the IT cortex, however, temporal coding was rather unclear, although several studies showed that IT neurons are capable of correlated discharges (Gochin, P. M. *et al.*, 1991; Gawne, T. J. and Richmond, B. J., 1993; Tamura *et al.*, 2004; Aggelopoulos, N. C. *et al.*, 2005). That said, a recent study tackled this issue and succeeded in showing that pairs of IT neurons exhibit more synchronous responses to facelike objects than to nonfacelike objects, both of which are comprised of the same parts (Hirabayashi, T. and Miyashita, Y., 2005).

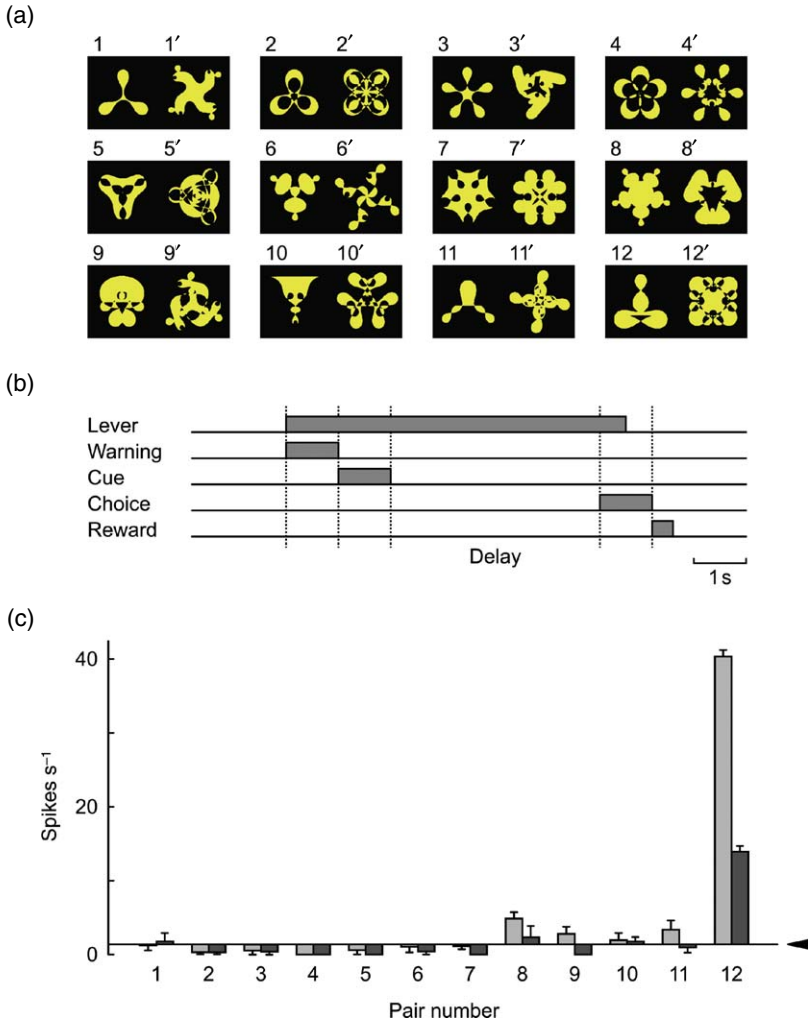

Figure 11 Associative coding of two disparate Fourier descriptors in the macaque anterior inferior temporal (IT) cortex (Sakai, K. and Miyashita, Y., 1991). (a) Twelve pairs of Fourier descriptors (pictures 1 and 1′ to 12 and 12′) were used as stimuli in a visual pair-association (PA) task for monkeys. This task was used to assess visual long-term memory. The monkeys learned to retrieve the other member of the pair when one member was presented as a cue stimulus. (b) Sequence of events in a trial in the visual PA task. Lever: Lever press by the monkey to initiate a new trial. Warning: Green square (1 s). Cue: One of 24 pictures serving as a cue stimulus (1 s). Delay: Green square (4 s). Choice: A choice of two stimuli, the paired associate of the cue and one from a different pair. Reward: Fruit juice reward for correctly touching the associate. (c) Responses of an IT neuron to the 12 pairs of Fourier descriptors. Mean discharge rates for each picture during the cue presentation period relative to the spontaneous discharge rate (denoted by arrowhead) are shown. Cue stimuli are labeled as pair number on the abscissa. For instance, in pair no. 1, the left bar indicates the response to picture 1, the right bar the response to picture 1′. The error bars indicate standard error of the mean. This neuron highly selectively responded to both pictures in pair no. 12, even though pictures 12 and 12′ (a) had no apparent geometrical similarity. Adapted from Sakai, K. and Miyashita, Y. 1991. Neural organization for the long-term memory of paired associates. Nature 354, 152–155, with permission.

Therefore, feature configuration within a whole object could be reflected in spike correlation among a subset of IT neurons.

Alternatively, it has been suggested that configurational information, that is, information about spatial arrangement of local parts, also is carried by IT neurons that have selectivity for complex visual stimuli (e.g., a black circle over a larger white circle, Figure 7, left-bottom). As a consequence, local visual features and their spatial relationship, which together comprise a visual entity, could be represented by a combination of IT neurons (Rolls, E. T. and Treves, A., 1998; Riesenhuber, M. and Poggio, T., 1999; Tanaka, K., 2003; Rousselet, G. A. *et al.*, 2004).

Supporting this is the finding that the responses of some IT neurons to preferred stimuli are influenced by the presence or relative position of neighboring stimuli (Sato, T., 1989; Miller, E. K. *et al.*, 1993; Missal, M. *et al.*, 1999; Aggelopoulos, N. C. and Rolls, E. T., 2005), i.e., the spatial relationship between objects can modulate stimulus-selective activity in IT neurons. Moreover, configurational selectivity was observed among IT neurons preferring stimuli with two local parts. Modifications of stimuli that altered the local parts with respect to color or shape but maintained their spatial relationship did not significantly change neuronal activity, while modification of the spatial relationship of the local parts markedly reduced neuronal activity (Tanaka, K. *et al.*, 1991; Yamane, Y. *et al.*, 2006). Thus, the configurational selectivity incorporated into feature-selective IT neurons may complement the representation of a whole object comprised of multiple local features.

2.02.10 Future Perspectives and Concluding Remarks

The critical role played by the IT cortex in visual object recognition has been well established by a large number of studies in both humans and monkeys. The neurons of the IT cortex, especially those in the anterior ITG, selectively respond to complex visual stimuli and exhibit response invariance with respect to the position, orientation, size, and viewing angle of an object. IT neurons with similar response properties cluster together within the cortex and form a columnar organization in which each column functions as a basic computational block to represent a complex whole object. Some IT neurons can encode novel multiple images through learning based on temporal proximity or on semantic-like relations. This associative property is thought to support the last stage of visual object recognition: identification of what the visual system analyzed along the object vision pathway.

Several different approaches could be used to our further understanding of the mechanism underlying visual object recognition. One possibility is back-engineering. If we could ultimately devise a neural network model that had the same potential for object recognition as a human, the model would provide us with very informative clues as to the details of the neural mechanism functioning in the actual brain. A number of models have been proposed in attempts to simulate some of the functions or behaviors of the visual system. Among those are the neocognitron (Fukushima, K., 1980), a hierarchical model for object recognition (Riesenhuber, M. and Poggio, T., 1999) and VisNet (Rolls, E. T. and Deco, G., 2002).

Another approach is to apply natural scenes to the examination of the visual system. A large number of studies of the IT cortex have focused on the neuronal properties revealed using a few concurrent stimuli with blank surrounds. This is remote from natural vision but is a rational way to control experimental conditions and precisely determine the properties of the responses of IT neurons to visual stimuli. However, the visual system normally works within a natural environment, where objects are cluttered in scenes and the eyes freely move, so that the actual behavior of IT neurons stimulated by natural scenes may differ from that stimulated by one or a few objects with blank surrounds. Indeed, it was recently reported that the responses of IT neurons to effective targets within natural scenes are strongly influenced by whether the subjects noticed the target objects during exploration of the scenes (Sheinberg, D. L. and Logothetis, N. K., 2001). In addition, the receptive fields of IT neurons tend to shrink when natural scenes are viewed (Rolls, E. T. *et al.*, 2003). Investigations making use of natural scenes would likely uncover some aspects of the response properties of IT neurons that are involved in the neuronal representation of cluttered multiple objects within scenes.

A third approach is the use of animal fMRI techniques, which could provide a more plausible means of associating the findings of animal experiments with human cognitive functions (Orban, G. A., 2002), including visual object recognition. Historically, animal experiments using cats and monkeys have provided us with a huge amount of information about the anatomies and functions of the visual cortices (Ungerleider, L. G. and Mishkin, M., 1982; Desimone, R. and Ungerleider, L., 1989; Goodale, M. A. and Milner, A. D., 1992; Van Essen, D. C. and Gallant, J. L., 1994). In contrast, a large number of human fMRI studies have brought extreme progress in the field of cognitive neuroscience for these one and a half decades. Now, fMRI techniques are being applied to animal studies (Stefanacci, L. *et al.*, 1998; Hayashi, T. *et al.*, 1999; Logothetis, N. K. *et al.*, 1999; for a review, Logothetis, N. K., 2003), enabling researchers to compare brain activation in monkeys with that in humans in a search for functional homologs in both

species (Nakahara, K. *et al*., 2002; Tsao, D. Y. *et al*., 2003; Koyama, M. *et al*., 2004). In addition, macroscopic detection of activated cortical regions in animal fMRI experiments enables fMRI-guided neurophysiological investigations (Figure 5; Kanwisher, N., 2006; Tsao, D. Y. *et al*., 2006). To clarify the neuronal mechanisms underlying visual object recognition, it would be greatly informative to record neuronal responses from cortical regions in the monkey that are known to be functionally as well as anatomically homologous to humans. It is anticipated that over the next several years, this last approach will prove to be an especially valuable means of obtaining significant clues to the higher neuronal processing behind visual object recognition, which our visual system so readily and efficiently performs.

References

Aggelopoulos, N. C., Franco, L., and Rolls, E. T. 2005. Object perception in natural scenes: encoding by inferior temporal cortex simultaneously recorded neurons. J. Neurophysiol. 93, 1342–1357.

Aggelopoulos, N. C. and Rolls, E. T. 2005. Scene perception: inferior temporal cortex neurons encode the positions of different objects in the scene. Eur. J. Neurosci. 22, 2903–2916.

Baker, C. I., Behrmann, M., and Olson, C. R. 2002. Impact of learning on representation of parts and wholes in monkey inferotemporal cortex. Nat. Neurosci. 5, 1210–1216.

Barbas, H. 1988. Anatomic organization of basoventral and mediodorsal visual recipient prefrontal regions in the rhesus monkey. J. Comp. Neurol. 276, 313–342.

Barlow, H. B. 1972. Single units and sensation: a neuron doctrine for perceptual psychology? Perception 1, 371–394.

Baylis, G. C., Rolls, E. T., and Leonard, C. M. 1985. Selectivity between faces in the responses of a population of neurons in the cortex in the superior temporal sulcus of the monkey. Brain Res. 342, 91–102.

Booth, M. C. and Rolls, E. T. 1998. View-invariant representations of familiar objects by neurons in the inferior temporal visual cortex. Cereb. Cortex 8, 510–523.

Brown, J. W. 1972. Aphasia, Apraxia, and Agnosia: Clinical and Theoretical Aspects. Charles C Thomas.

Bruce, C., Desimone, R., and Gross, C. G. 1981. Visual properties of neurons in a polysensory area in superior temporal sulcus of the macaque. J. Neurophysiol. 46, 369–384.

Damasio, A. R., Damasio, H., and Van Hoesen, G. W. 1982. Prosopagnosia: anatomic basis and behavioral mechanisms. Neurology 32, 331–341.

Dean, P. 1976. Effects of inferotemporal lesions on the behavior of monkeys. Psychol. Bull. 83, 41–71.

De Renzi, E., Perani, D., Carlesimo, G. A., Silveri, M. C., and Fazio, F. 1994. Prosopagnosia can be associated with damage confined to the right hemisphere – an MRI and PET study and a review of the literature. Neuropsychologia 32, 893–902.

Desimone, R., Albright, T., Gross, C. G., and Bruce, C. 1984. Stimulus-selective properties of inferior temporal neurons in the macaque. J. Neurosci. 4, 2051–2062.

Desimone, R. and Ungerleider, L. G. 1989. Neural Mechanisms of Visual Processing in Monkeys. In: Handbook of Neuropsychology (*eds*. F. Boller and J. Grafman), pp. 267–299. Elsevier.

DiCarlo, J. J. and Maunsell, J. H. 2003. Anterior inferotemporal neurons of monkeys engaged in object recognition can be highly sensitive to object retinal position. J. Neurophysiol. 89, 3264–3278.

Distler, C., Boussaoud, D., Desimone, R., and Ungerleider, L. G. 1993. Cortical connections of inferior temporal area TEO in macaque monkeys. J. Comp. Neurol. 334, 125–150.

Eichenbaum, H. and Cohen, N. J. 2001. From Conditioning to Conscious Recollection: Memory Systems of the Brain. Oxford University Press.

Erickson, C. A., Jagadeesh, B., and Desimone, R. 2000. Clustering of perirhinal neurons with similar properties following visual experience in adult monkeys. Nat. Neurosci. 3, 1143–1148.

Farah, M. J. 2004. Visual Agnosia, 2nd edn. MIT Press.

Felleman, D. J. and Van Essen, D. C. 1991. Distributed hierarchical processing in the primate cerebral cortex. Cereb. Cortex 1, 1–47.

Földiák, P. 1991. Learning invariance from transformation sequences. Neural Comput. 3, 194–200.

Freedman, D. J., Riesenhuber, M., Poggio, T., and Miller, E. K. 2006. Experience-dependent sharpening of visual shape selectivity in inferior temporal cortex. Cereb. Cortex 16, 1631–1644.

Fujita, I. 2002. The inferior temporal cortex: architecture, computation, and representation. J. Neurocytol. 31, 359–371.

Fujita, I., Tanaka, K., Ito, M., and Cheng, K. 1992. Columns for visual features of objects in monkey inferotemporal cortex. Nature 360, 343–346.

Fukushima, K. 1980. Neocognitron: a self organizing neural network model for a mechanism of pattern recognition unaffected by shift in position. Biol. Cybern. 36, 193–202.

Fukushima, T., Hasegawa, I., and Miyashita, Y. 2004. Prefrontal neuronal activity encodes spatial target representations sequentially updated after nonspatial target-shift cues. J. Neurophysiol. 91, 1367–1380.

Gawne, T. J. and Richmond, B. J. 1993. How independent are the messages carried by adjacent inferior temporal cortical neurons? J. Neurosci. 13, 2758–2771.

Gochin, P. M., Miller, E. K., Gross, C. G., and Gerstein, G. L. 1991. Functional interactions among neurons in the macaque inferior temporal cortex. Exp. Brain Res. 84, 505–516.

Goldman-Rakic, P. S. 1987. Circuitry of The Prefrontal Cortex and The Regulation of Behavior by Representational Memory. In: Handbook of Physiology, Sect. 1, Vol. V, Pt. 1 (*ed*. F. Plum), pp. 373–417. American Physiological Society.

Goodale, M. A. and Milner, A. D. 1992. Separate visual pathways for perception and action. Trends Neurosci. 15, 20–25.

Grill-Spector, K., Sayres, R., and Ress, D. 2006. High-resolution imaging reveals highly selective nonface clusters in the fusiform face area. Nat. Neurosci. 9, 1177–1185.

Gross, C. G. 1973. Visual Functions of Inferotemporal Cortex. In: Handbook of Sensory Physiology, Vol. VII, Pt. 3B (*ed*. R. Jung), pp. 451–482. Springer.

Gross, C. G., Rocha-Miranda, C. E., and Bender, D. B. 1972. Visual properties of neurons in inferotemporal cortex of the macaque. J. Neurophysiol. 35, 99–111.

Hasegawa, I., Fukushima, T., Ihara, T., and Miyashita, Y. 1998. Callosal window between prefrontal cortices: cognitive interaction to retrieve long-term memory. Science 281, 814–818.

Hasselmo, M. E., Rolls, E. T., and Baylis, G. C. 1989a. The role of expression and identity in the face-selective responses of

neurons in the temporal visual cortex of the monkey. Behav. Brain Res. 32, 203–218.
Hasselmo, M. E., Rolls, E. T., Baylis, G. C., and Nalwa, V. 1989b. Object-centered encoding by face-selective neurons in the cortex in the superior temporal sulcus of the monkey. Exp. Brain Res. 75, 417–429.
Haxby, J. V. 2004. Analysis of Topographically Organized Patterns of Response in fMRI Data: Distributed Representations of Objects in the Ventral Temporal Cortex. In: Functional Neuroimaging of Visual Cognition (*eds*. N. Kanwisher and J. Duncan), pp. 83–97. Oxford University Press.
Hayashi, T., Konishi, S., Hasegawa, I., and Miyashita, Y. 1999. Mapping of somatosensory cortices with functional magnetic resonance imaging in anaesthetized macaque monkeys. Eur. J. Neurosci. 11, 4451–4456.
Herzog, A. G. and Van Hoesen, G. W. 1976. Temporal neocortical afferent connections to the amygdala in the rhesus monkey. Brain Res. 115, 57–69.
Hirabayashi, T. and Miyashita, Y. 2005. Dynamically modulated spike correlation in monkey inferior temporal cortex depending on the feature configuration within a whole object. J. Neurosci. 25, 10299–10307.
Horton, J. C. and Adams, D. L. 2005. The cortical column: a structure without a function. Philos. Trans. R. Soc. Lond. B 360, 837–862.
Hubel, D. H. and Wiesel, T. N. 1962. Receptive fields, binocular interaction and functional architecture in the cat's visual cortex. J. Physiol. 160, 106–154.
Hubel, D. H. and Wiesel, T. N. 1968. Receptive fields and functional architecture of monkey striate cortex. J. Physiol. 195, 215–243.
Humphrey, N. K. and Weiskrantz, L. 1969. Size constancy in monkeys with inferotemporal lesions. Q. J. Exp. Psychol. 21, 225–238.
Humphreys, G. W. and Riddoch, M. J. 1987. To See but not to See: a Case Study of Visual Agnosia. Lawrence Erlbaum Associates.
Insausti, R., Amaral, D. G., and Cowan, W. M. 1987. The entorhinal cortex of the monkey: II. Cortical afferents. J. Comp. Neurol. 264, 356–395.
Ito, M., Tamura, H., Fujita, I., and Tanaka, K. 1995. Size and position invariance of neuronal responses in monkey inferotemporal cortex. J. Neurophysiol. 73, 218–226.
Iwai, E. 1985. Neuropsychological basis of pattern vision in macaque monkeys. Vision Res. 25, 425–439.
Iwai, E. and Yukie, M. 1987. Amygdalofugal and amygdalopetal connections with modality-specific visual cortical areas in macaques (*Macaca fuscata*, *M*. *mulatta*, and *M*. *fascicularis*). J. Comp. Neurol. 261, 362–387.
Janssen, P., Vogels, R., and Orban, G. A. 1999. Macaque inferior temporal neurons are selective for disparity-defined three-dimensional shapes. Proc. Natl. Acad. Sci. U. S. A. 96, 8217–8222.
Janssen, P., Vogels, R., and Orban, G. A. 2000. Selectivity for 3D shape that reveals distinct areas within macaque inferior temporal cortex. Science 288, 2054–2056.
Kanwisher, N. 2003. The Ventral Visual Object Pathway in Humans: Evidence from fMRI. In: The Visual Neurosciences (*eds*. L. Chalupa and J. Werner), pp. 1179–1189. MIT Press.
Kanwisher, N. 2006. Neuroscience. What's in a face? Science 311, 617–618.
Kimura, D. 1963. Right temporal-lobe damage. Perception of unfamiliar stimuli after damage. Arch. Neurol. 8, 264–271.
Kobatake, E., Wang, G., and Tanaka, K. 1998. Effects of shape-discrimination training on the selectivity of inferotemporal cells in adult monkeys. J. Neurophysiol. 80, 324–330.
Komatsu, H. and Ideura, Y. 1993. Relationships between color, shape, and pattern selectivities of neurons in the inferior temporal cortex of the monkey. J. Neurophysiol. 70, 677–694.
Kovács, G., Sary, G., Köteles, K., Chadaide, Z., Tompa, T., Vogels, R., and Benedek, G. 2003. Effects of surface cues on macaque inferior temporal cortical responses. Cereb. Cortex 13, 178–188.
Kovács, G., Vogels, R., and Orban, G. A. 1995. Selectivity of macaque inferior temporal neurons for partially occluded shapes. J. Neurosci. 15(3 Pt 1), 1984–1997.
Koyama, M., Hasegawa, I., Osada, T., Adachi, Y., Nakahara, K., and Miyashita, Y. 2004. Functional magnetic resonance imaging of macaque monkeys performing visually guided saccade tasks: comparison of cortical eye fields with humans. Neuron 41, 795–807.
Leopold, D. A., Bondar, I. V., and Giese, M. A. 2006. Norm-based face encoding by single neurons in the monkey inferotemporal cortex. Nature, 442, 572–575.
Levine, D. N. 1982. Visual Agnosia in Monkey and in Man. In: Analysis of Visual Behavior (*eds*. D. J. Ingle, M. A. Goodale, and R. J. W. Mansfield), pp. 629–670. MIT Press.
Logothetis, N. K. 2003. MR imaging in the non-human primate: studies of function and of dynamic connectivity. Curr. Opin. Neurobiol. 13, 630–642.
Logothetis, N. K., Guggenberger, H., Peled, S., and Pauls, J. 1999. Functional imaging of the monkey brain. Nat. Neurosci. 2, 555–562.
Logothetis, N. K. and Pauls, J. 1995. Psychophysical and physiological evidence for viewer-centered object representations in the primate. Cereb. Cortex 5, 270–288.
Logothetis, N. K., Pauls, J., and Poggio, T. 1995. Shape representation in the inferior temporal cortex of monkeys. Curr. Biol. 5, 552–563.
Lueschow, A., Miller, E. K., and Desimone, R. 1994. Inferior temporal mechanisms for invariant object recognition. Cereb. Cortex 4, 523–531.
Malsburg, C.v. d. 1995. Binding in models of perception and brain function. Curr. Opin. Neurobiol. 5, 520–526.
Martin-Elkins, C. L. and Horel, J. A. 1992. Cortical afferents to behaviorally defined regions of the inferior temporal and parahippocampal gyri as demonstrated by WGA-HRP. J. Comp. Neurol. 321, 177–192.
McCarthy, R. A. and Warrington, E. K. 1990. Cognitive Neuropsychology: A Clinical Introduction, Academic Press.
McDonald, A. J. 1998. Cortical pathways to the mammalian amygdala. Prog. Neurobiol. 55, 257–332.
Meadows, J. C. 1974. The anatomical basis of prosopagnosia. J. Neurol. Neurosurg. Psychiatry 37, 489–501.
Messinger, A., Squire, L. R., Zola, S. M., and Albright, T. D. 2001. Neuronal representations of stimulus associations develop in the temporal lobe during learning. Proc. Natl. Acad. Sci. U. S. A. 98, 12239–12244.
Miller, E. K., Gochin, P. M., and Gross, C. G. 1993. Suppression of visual responses of neurons in inferior temporal cortex of the awake macaque by addition of a second stimulus. Brain Res. 616, 25–29.
Milner, B. 1968. Visual recognition and recall after right temporal lobe excision in man. Neuropsychologia 6, 191–209.
Milner, B. 1990. Right Temporal-Lobe Contribution to Visual Perception and Visual Memory. In: Vision, Memory and the Temporal Lobe (*eds*. E. Iwai and M. Mishkin), pp. 43–53. Elsevier.
Missal, M., Vogels, R., Li, C. Y., and Orban, G. A. 1999. Shape interactions in macaque inferior temporal neurons. J. Neurophysiol. 82, 131–142.
Mishkin, M. 1982. A memory system in the monkey. Philos. Trans. R. Soc. Lond. B 298, 83–95.
Miyashita, Y. 1988. Neuronal correlate of visual associative long-term memory in the primate temporal cortex. Nature 335, 817–820.

Miyashita, Y. 1993. Inferior temporal cortex: where visual perception meets memory. Annu. Rev. Neurosci. 16, 245–263.
Miyashita, Y. 2004. Cognitive memory: cellular and network machineries and their top-down control. Science 306, 435–440.
Miyashita, Y. and Chang, H. S. 1988. Neuronal correlate of pictorial short-term memory in the primate temporal cortex. Nature 331, 68–70.
Miyashita, Y. and Hayashi, T. 2000. Neural representation of visual objects: encoding and top-down activation. Curr. Opin. Neurobiol. 10, 187–194.
Miyashita, Y., Higuchi, S., Sakai, K., and Masui, N. 1991. Generation of fractal patterns for probing the visual memory. Neurosci. Res. 12, 307–311.
Mountcastle, V. B. 1997. The columnar organization of the neocortex. Brain 120, 701–722.
Nakahara, K., Hayashi, T., Konishi, S., and Miyashita, Y. 2002. Functional MRI of macaque monkeys performing a cognitive set-shifting task. Science 295, 1532–1536.
Op De Beeck, H. and Vogels, R. 2000. Spatial sensitivity of macaque inferior temporal neurons. J. Comp. Neurol. 426, 505–518.
Orban, G. A. 2002. Functional MRI in the awake monkey: the missing link. J. Cogn. Neurosci. 14, 965–969.
Orban, G. A., Janssen, P., and Vogels, R. 2006. Extracting 3D structure from disparity. Trends Neurosci. 29, 466–473.
Perrett, D. I., Mistlin, A. J., and Chitty, A. J. 1987. Visual neurons responsive to faces. Trends Neurosci. 10, 358–364.
Perrett, D. I., Rolls, E. T., and Caan, W. 1979. Temporal lobe cells of the monkey with visual responses selective for faces. Neurosci. Lett. (Suppl 3), S358.
Perrett, D. I., Rolls, E. T., and Caan, W. 1982. Visual neurones responsive to faces in the monkey temporal cortex. Exp. Brain Res. 47, 329–342.
Perrett, D. I., Smith, P. A., Potter, D. D., Mistlin, A. J., Head, A. S., Milner, A. D., and Jeeves, M. A. 1984. Neurones responsive to faces in the temporal cortex: studies of functional organization, sensitivity to identity and relation to perception. Hum. Neurobiol. 3, 197–208.
Petrides, M. and Pandya, D. N. 2002. Comparative cytoarchitectonic analysis of the human and the macaque ventrolateral prefrontal cortex and corticocortical connection patterns in the monkey. Eur. J. Neurosci. 16, 291–310.
Pinsk, M. A., DeSimone, K., Moore, T., Gross, C. G., and Kastner, S. 2005. Representations of faces and body parts in macaque temporal cortex: a functional MRI study. Proc. Natl. Acad. Sci. U. S. A. 102, 6996–7001.
Powell, T. P. and Mountcastle, V. B. 1959. Some aspects of the functional organization of the cortex of the postcentral gyrus of the monkey: a correlation of findings obtained in a single unit analysis with cytoarchitecture. Bull. Johns Hopkins Hosp. 105, 133–162.
Ranganath, C. and D'Esposito, M. 2005. Directing the mind's eye: prefrontal, inferior and medial temporal mechanisms for visual working memory. Curr. Opin. Neurobiol. 15, 175–182.
Riesenhuber, M. and Poggio, T. 1999. Hierarchical models of object recognition in cortex. Nat. Neurosci. 2, 1019–1025.
Riesenhuber, M. and Poggio, T. 2002. Neural mechanisms of object recognition. Curr. Opin. Neurobiol. 12, 162–168.
Rockland, K. S. and Van Hoesen, G. W. 1999. Some temporal and parietal cortical connections converge in CA1 of the primate hippocampus. Cereb. Cortex 9, 232–237.
Rolls, E. T., Aggelopoulos, N. C., and Zheng, F. 2003. The receptive fields of inferior temporal cortex neurons in natural scenes. J. Neurosci. 23, 339–348.
Rolls, E. T. and Baylis, G. C. 1986. Size and contrast have only small effects on the responses to faces of neurons in the cortex of the superior temporal sulcus of the monkey. Exp. Brain Res. 65, 38–48.
Rolls, E. T. and Deco, G. 2002. Computational Neuroscience of Vision. Oxford University Press.
Rolls, E. T. and Treves, A. 1998. Neural Networks and Brain Function. Oxford University Press.
Rose, D. 1996. Some reflections on (or by?) grandmother cells. Perception 25, 881–886.
Rousselet, G. A., Thorpe, S. J., and Fabre-Thorpe, M. 2004. How parallel is visual processing in the ventral pathway? Trends Cogn. Sci. 8, 363–370.
Rubens, A. B. and Benson, D. F. 1971. Associative visual agnosia. Arch. Neurol. 24, 305–316.
Sakai, K. and Miyashita, Y. 1991. Neural organization for the long-term memory of paired associates. Nature 354, 152–155.
Sakai, K. and Miyashita, Y. 1994. Neuronal tuning to learned complex forms in vision. Neuroreport 5, 829–832.
Saleem, K. S., Suzuki, W., Tanaka, K., and Hashikawa, T. 2000. Connections between anterior inferotemporal cortex and superior temporal sulcus regions in the macaque monkey. J. Neurosci. 20, 5083–5101.
Saleem, K. S. and Tanaka, K. 1996. Divergent projections from the anterior inferotemporal area TE to the perirhinal and entorhinal cortices in the macaque monkey. J. Neurosci. 16, 4757–4775.
Sáry, G., Vogels, R., and Orban, G. A. 1993. Cue-invariant shape selectivity of macaque inferior temporal neurons. Science 260, 995–997.
Sato, T. 1989. Interactions of visual stimuli in the receptive fields of inferior temporal neurons in awake macaques. Exp. Brain Res. 77, 23–30.
Sato, T., Kawamura, T., and Iwai, E. 1980. Responsiveness of inferotemporal single units to visual pattern stimuli in monkeys performing discrimination. Exp. Brain Res. 38, 313–319.
Schwartz, E. L., Desimone, R., Albright, T. D., and Gross, C. G. 1983. Shape recognition and inferior temporal neurons. Proc. Natl. Acad. Sci. U. S. A. 80, 5776–5778.
Seltzer, B. and Pandya, D. N. 1989. Frontal lobe connections of the superior temporal sulcus in the rhesus monkey. J. Comp. Neurol. 281, 97–113.
Sheinberg, D. L. and Logothetis, N. K. 2001. Noticing familiar objects in real world scenes: the role of temporal cortical neurons in natural vision. J. Neurosci. 21, 1340–1350.
Shiwa, T. 1987. Corticocortical projections to the monkey temporal lobe with particular reference to the visual processing pathways. Arch. Ital. Biol. 125, 139–154.
Sigala, N. and Logothetis, N. K. 2002. Visual categorization shapes feature selectivity in the primate temporal cortex. Nature 415, 318–320.
Singer, W. 1999. Neuronal synchrony: a versatile code for the definition of relations? Neuron 24, 49–65, 111–125.
Squire, L. R. and Zola-Morgan, S. 1991. The medial temporal lobe memory system. Science 253, 1380–1386.
Stefanacci, L., Reber, P., Costanza, J., Wong, E., Buxton, R., Zola, S., Squire, L., and Albright, T. 1998. fMRI of monkey visual cortex. Neuron 20, 1051–1057.
Suzuki, W. A. and Amaral, D. G. 1994a. Perirhinal and parahippocampal cortices of the macaque monkey: cortical afferents. J. Comp. Neurol. 350, 497–533.
Suzuki, W. A. and Amaral, D. G. 1994b. Topographic organization of the reciprocal connections between the monkey entorhinal cortex and the perirhinal and parahippocampal cortices. J. Neurosci. 14(3 Pt 2), 1856–1877.
Tamura, H., Kaneko, H., Kawasaki, K., and Fujita, I. 2004. Presumed inhibitory neurons in the macaque inferior temporal cortex: visual response properties and functional interactions with adjacent neurons. J. Neurophysiol. 91, 2782–2796.

Tanaka, H., Uka, T., Yoshiyama, K., Kato, M., and Fujita, I. 2001. Processing of shape defined by disparity in monkey inferior temporal cortex. J. Neurophysiol. 85, 735–744.

Tanaka, K. 1993. Neuronal mechanisms of object recognition. Science 262, 685–688.

Tanaka, K. 2003. Columns for complex visual object features in the inferotemporal cortex: clustering of cells with similar but slightly different stimulus selectivities. Cereb. Cortex 13, 90–99.

Tanaka, K., Saito, H., Fukada, Y., and Moriya, M. 1991. Coding visual images of objects in the inferotemporal cortex of the macaque monkey. J. Neurophysiol. 66, 170–189.

Tomita, H., Ohbayashi, M., Nakahara, K., Hasegawa, I., and Miyashita, Y. 1999. Top-down signal from prefrontal cortex in executive control of memory retrieval. Nature 401, 699–703.

Treisman, A. 1999. Solutions to the binding problem: progress through controversy and convergence. Neuron 24, 105–125.

Tsao, D. Y., Freiwald, W. A., Knutsen, T. A., Mandeville, J. B., and Tootell, R. B. 2003. Faces and objects in macaque cerebral cortex. Nat. Neurosci. 6, 989–995.

Tsao, D. Y., Freiwald, W. A., Tootell, R. B., and Livingstone, M. S. 2006. A cortical region consisting entirely of face-selective cells. Science 311, 670–674.

Tsunoda, K., Yamane, Y., Nishizaki, M., and Tanifuji, M. 2001. Complex objects are represented in macaque inferotemporal cortex by the combination of feature columns. Nat. Neurosci. 4, 832–838.

Uka, T., Tanabe, S., Watanabe, M., and Fujita, I. 2005. Neural correlates of fine depth discrimination in monkey inferior temporal cortex. J. Neurosci. 25, 10796–10802.

Uka, T., Tanaka, H., Yoshiyama, K., Kato, M., and Fujita, I. 2000. Disparity selectivity of neurons in monkey inferior temporal cortex. J. Neurophysiol. 84, 120–132.

Ungerleider, L. G. and Mishkin, M. 1982. Two Cortical Visual Systems. In: Analysis of Visual Behavior (*eds*. D. J. Ingle, M. A. Goodale, and R. J. W. Mansfield), pp. 549–586. MIT Press.

Ungerleider, L. G., Gaffan, D., and Pelak, V. S. 1989. Projections from inferior temporal cortex to prefrontal cortex via the uncinate fascicle in rhesus monkeys. Exp. Brain Res. 76, 473–484.

Ungerleider, L. G., Ganz, L., and Pribram, K. H. 1977. Size constancy in rhesus monkeys: effects of pulvinar, prestriate, and inferotemporal lesions. Exp. Brain Res. 27, 251–269.

Van Essen, D. C., Anderson, C. H., and Felleman, D. J. 1992. Information processing in the primate visual system: an integrated systems perspective. Science 255, 419–423.

Van Essen, D. C. and Gallant, J. L. 1994. Neural mechanisms of form and motion processing in the primate visual system. Neuron 13, 1–10.

Van Hoesen, G. and Pandya, D. N. 1975. Some connections of the entorhinal (area 28) and perirhinal (area 35) cortices of the rhesus monkey. I. Temporal lobe afferents. Brain Res. 95, 1–24.

Wada, Y. and Yamamoto, T. 2001. Selective impairment of facial recognition due to a haematoma restricted to the right fusiform and lateral occipital region. J. Neurol. Neurosurg. Psychiatry 71, 254–257.

Wang, Y., Fujita, I., Tamura, H., and Murayama, Y. 2002. Contribution of GABAergic inhibition to receptive field structures of monkey inferior temporal neurons. Cereb. Cortex 12, 62–74.

Wang, G., Tanaka, K., and Tanifuji, M. 1996. Optical imaging of functional organization in the monkey inferotemporal cortex. Science 272, 1665–1668.

Wang, G., Tanifuji, M., and Tanaka, K. 1998. Functional architecture in monkey inferotemporal cortex revealed by *in vivo* optical imaging. Neurosci. Res. 32, 33–46.

Warrington, E. K. 1985. Agnosia: The Impairment of Object Recognition. In: Handbook of Clinical Neurology, Vol. 1 (45): Clinical Neuropsychology (*ed*. J. A. M. Frederiks), pp. 333–349. Elsevier.

Warrington, E. K. and James, M. 1988. Visual apperceptive agnosia: a clinico-anatomical study of three cases. Cortex 24, 13–32.

Warrington, E. K. and Taylor, A. M. 1973. The contribution of the right parietal lobe to object recognition. Cortex 9, 152–164.

Webster, M. J., Ungerleider, L. G., and Bachevalier, J. 1991. Connections of inferior temporal areas TE and TEO with medial temporal-lobe structures in infant and adult monkeys. J. Neurosci. 11, 1095–1116.

Weiskrantz, L. 1990. Visual Prototypes, Memory and the Inferotemporal Cortex. In: Vision, Memory and the Temporal Lobe (*eds*. E. Iwai and M. Mishkin), pp. 13–28. Elsevier.

Weiskrantz, L. and Saunders, R. C. 1984. Impairments of visual object transforms in monkeys. Brain 107, 1033–1072.

Yamane, S., Kaji, S., and Kawano, K. 1988. What facial features activate face neurons in the inferotemporal cortex of the monkey? Exp. Brain Res. 73, 209–214.

Yamane, Y., Tsunoda, K., Matsumoto, M., Phillips, A., and Tanifuji, M. 2006. Representation of the spatial relationship among object parts by neurons in macaque inferotemporal cortex. J. Neurophysiol. 96, 3147–3156.

Young, M. P. and Yamane, S. 1992. Sparse population coding of faces in the inferotemporal cortex. Science 256, 1327–1331.

Young, M. P. and Yamane, S. 1993. An Analysis at the Population Level of the Processing of Faces in the Inferotemporal Cortex. In: Brain Mechanisms of Perception and Memory: From Neuron to Behavior (*eds*. T. Ono, L. R. Squire, M. E. Raichle, D. I. Perrett, and M. Fukuda), pp. 47–70. Oxford University Press.

Yukie, M. and Iwai, E. 1988. Direct projections from the ventral TE area of the inferotemporal cortex to hippocampal field CA1 in the monkey. Neurosci. Lett. 88, 6–10.

2.03 Luminance Sensitivity and Contrast Detection

E Kaplan, The Mount Sinai School of Medicine, New York, NY, USA

© 2008 Elsevier Inc. All rights reserved.

2.03.1	**Overview**	30
2.03.2	**Introduction**	30
2.03.2.1	Sensitivity or Response Magnitude?	30
2.03.2.2	Why are Luminance and Contrast Sensitivities Important?	30
2.03.2.3	Adaptation to Luminance and Contrast	31
2.03.2.4	Spatiotemporal Selectivity: The Two-Scales Design	31
2.03.3	**Physiological Aspects**	32
2.03.3.1	Retina	32
2.03.3.1.1	Distal retina	32
2.03.3.1.2	Retinal ganglion cells	32
2.03.3.2	Lateral Geniculate Nucleus	33
2.03.3.3	Visual Cortex	33
2.03.3.3.1	Luminance	33
2.03.3.3.2	Contrast	33
2.03.3.3.3	Other measures of cortical activity	34
2.03.3.4	Contrast Gain	35
2.03.3.5	Contrast Gain Control	35
2.03.3.5.1	General considerations	35
2.03.3.5.2	Retina	35
2.03.3.5.3	Lateral geniculate nucleus	35
2.03.3.5.4	Visual cortex	36
2.03.3.5.5	Cellular basis of contrast adaptation in cortex	36
2.03.3.5.6	Contrast adaptation in parallel visual streams	36
2.03.3.6	Adaptation and Absolute Levels of Contrast and Luminance	37
2.03.3.7	Effects of Luminance Level on Contrast Sensitivity	37
2.03.4	**Psychophysical Aspects**	37
2.03.4.1	Steady State	37
2.03.4.1.1	Luminance	37
2.03.4.1.2	Contrast	37
2.03.4.1.3	Mach bands and other illusions	38
2.03.4.2	Dynamics	38
2.03.4.2.1	Cellular basis of the temporal contrast sensitivity function	38
2.03.4.3	Stimulus Parameters	39
2.03.4.4	Some Clinical Implications	39
2.03.4.5	From Neurons to Perception	40
2.03.5	**Conclusions**	40
References		40

Glossary

luminance Luminance refers to how bright something appears to us. It thus includes both the amount of light energy that arrives at the eye, and the sensitivity of the visual system to that light. It is measured in photometric units, such as candela m^{-2}.

contrast Contrast tells us how different is the luminance level at some point in space or time compared to some luminance reference, and is expressed as a ratio, often in percents. Spatial contrast refers to a comparison of some portion of

the visual field with another portion (e.g., the light bars of a grating compared with the dark ones), while temporal contrast refers to a comparison of some luminance level with a previous level at a given point in space. The Michelson contrast is defined as the ratio $C = (L_{max} - L_{min})/(L_{max} + L_{min})$, where L_{max} and L_{min} are the maximal and minimal luminance levels, respectively, and this form is the one used most often in vision science, although the Weber contrast $C = (L_{max} - L_{min})/L_{min}$ is sometimes used as well. In this chapter we shall limit ourselves to luminance contrast, and not discuss chromatic (isoluminant) contrast, in which the comparisons involve quantities that differ in their chromaticity.

contrast gain Contrast gain is the change in response elicited by a change in contrast. In considering neural responses it is the slope of the response versus contrast function (Kaplan, E. and Shapley, R. M., 1986; Croner, L. J. and Kaplan, E., 1995), and has units of impulses s^{-1} $\%^{-1}$ contrast. Contrast gain has also been called responsivity (Enroth-Cugell, C. *et al.*, 1983).

contrast gain control Contrast gain control is an adaptation of the visual system to the prevailing contrast. It has been also called contrast adaptation.

sensitivity Sensitivity is defined as the reciprocal of the minimal quantity of a given stimulus parameter that is required to produce a given response amplitude, typically a minimal (threshold) response. Thus contrast sensitivity is the contrast required to detect a stimulus, and is therefore expressed in units of contrast.

2.03.1 Overview

In this chapter we shall discuss why luminance and contrast are such important concepts in vision science. We shall survey the ways in which these two quantities are encoded and transmitted along the visual pathway from retina to cortex. We shall discuss briefly how these quantities interact in the visual system, what regulates our sensitivity to them, and describe some of the perceptual aspects of luminance and contrast sensitivities. The ways in which contrast sensitivity depends on spatial or temporal frequencies and on other aspects of the visual input are important and large topics, and will be described here only briefly.

2.03.2 Introduction

2.03.2.1 Sensitivity or Response Magnitude?

In general, it is more informative to measure sensitivity as a function of the relevant parameter under investigation (orientation, color, spatial frequency, etc.), rather than response magnitude. If the relationship between response magnitude and contrast is linear (as is the case for the parvocellular – but not the magnocellular – neurons in the primate retina and lateral geniculate nucleus (LGN)), than the two measures provide equivalent information. However, since in most cases that important relationship is nonlinear (showing logarithmic compression, expansive nonlinearity, threshold, or saturation), measuring sensitivity is preferable. In contrast, sensitivity measurements deal only with a limited portion of the dynamic range of the response, often near minimal responses or at threshold, while other measures explore more fully the range of stimuli and responses that the system encounters in the real world.

2.03.2.2 Why are Luminance and Contrast Sensitivities Important?

Luminance and contrast are central to the function of the visual system. Without light (luminance = 0) there can be no vision, and without contrast we can see no spatial or temporal patterns. The ability to respond to luminance is an essential first step in seeing, which makes possible all other visual processes. However, what is really important for making sense of the visual world is not the absolute, steady-state luminance level, but rather its temporal and spatial derivatives, namely, contrast. Contrast sensitivity is thus the beginning of pattern vision, and the mechanisms employed by the visual system to respond to contrast are fundamental for all subsequent visual analysis.

2.03.2.3 Adaptation to Luminance and Contrast

Light intensity at noon can be $\sim 10^{10}$ brighter than it is at midnight, and even in a snapshot of a given scene there is often a wide range of light intensities. This enormous dynamic range presents a special challenge to the visual system, which has several narrow bottlenecks with a rather limited dynamic range, including the synapse between photoreceptors and bipolar cells (Ashmore, J. F. and Falk, G., 1976; Ashmore, J. F. and Copenhagen, D. R., 1983), and the limited firing rates of retinal ganglion cells (RGCs) and cortical neurons. Special adaptive mechanisms are therefore required to reset the operating point, and thus allow the visual system to maintain its differential sensitivity over this huge range, which challenges even the most advanced human-made devices. This is true for both luminance and contrast, although the range of contrasts encountered in nature (especially under water) is typically much more limited than the range of luminance levels. We note that part of the adaptation process to luminance is photochemical (bleaching of the visual pigment), while adaptation to contrast is a neural process.

It is important to emphasize here that vision is a dynamical sense: steady-state measurements of sensitivity fail to account for the observed performance under normal visual situations, in which our gaze saccades rapidly from one fixation point to another. The dynamical influence of previous and neighboring stimuli is profound. However, the topic of adaptation is rather broad, and we shall touch upon it only briefly and incompletely here. One can find a comprehensive summary of luminance adaptation in the review by Shapley R. and Enroth-Cugell C. (1984). Contrast adaptation is discussed in Gardner J. L. *et al.* (2005), and further information can be found Baccus S. A. and Meister M. (2002). We shall touch briefly on contrast adaptation in Section 2.03.2.5.

2.03.2.4 Spatiotemporal Selectivity: The Two-Scales Design

To detect and respond to spatial or temporal contrast, the brain needs to compare the inputs from two or more points in space or time. Typically, one of the quantities that are being compared is some (weighted) average over space or time, while the other reflects a more restricted range of space or time. This two-scale strategy endows the detector with spatial or temporal selectivity: it responds best to some intermediate rate of change, and the response to changes at higher and lower rates is significantly lower. This is illustrated in Figure 1, in which the abscissa is labeled frequency, and could refer to either spatial or temporal frequency. In Figure 1 the inhibition subtracts from the effects of excitation, as in Rodieck's Difference of Gaussians (DOG) receptive field model (Rodieck, R. W., 1965). The mechanism sketched in Figure 1 is a linear one, but nonlinearities can alter the tuning (Shapley, R. M. and Victor, J. D., 1978).

The averaging of inputs across space or time allows the system to reject slow changes or gradients, and this rejection amounts to high-pass filtering or differentiation. The limitations imposed on the fine-scale component by optics, neural connectivity, or speed of reaction, bring about an unavoidable integration (low-pass filtering), which limits the performance at the high end of the frequency spectrum. Together, the high-pass and low-pass filters combine to form the band-pass filter shown in Figure 1. This two-scale antagonistic strategy is ubiquitous in the brain, and can be found in the retina, skin, ear, and visual cortex (Kuffler, S. W., 1953; Ratliff, F., 1965; von Békésy, G., 1967; Srinivasan, M. V. *et al.*, 1982; Somers, D. C. *et al.*, 1995). A more comprehensive, theoretical treatment of the way contrast signals and noise are processed and propagated in a (linear) neural network, can be found in Watson A. B. (1992) .

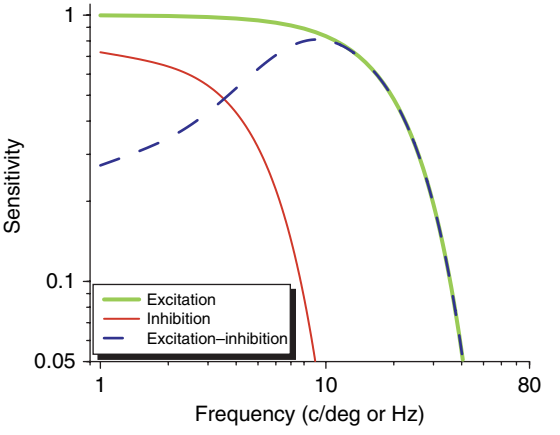

Figure 1 Spatial or temporal selectivity (dashed line) results from the antagonistic interplay of two processes that have very different spatial or temporal resolutions (scales), such as the center and surround of the receptive fields of retinal ganglion cells (Rodieck, R. W., 1965; Enroth-Cugell, C. and Robson, J. G., 1966). Note that both axes are logarithmic.

2.03.3 Physiological Aspects

2.03.3.1 Retina

The computations of both luminance and contrast begin in the retina, and reflect the spatiotemporal organization of the receptive field of each retinal neuron, that portion of the visual world to which each neuron is responsible (Hartline, H. K., 1940). The results of these computations are communicated to subsequent visual stages by the neural discharge of the RGCs.

2.03.3.1.1 Distal retina

The spectral sensitivity of the visual pigment in each retinal photoreceptor determines the probability that a photon of a given wavelength (energy) will be absorbed, and be given the chance to be converted into a neural signal. The luminosity function results from the convergence of the signals originating simultaneously in the various types of photoreceptors, and is therefore different from the spectral sensitivity function of any single class of photoreceptors.

A photoreceptor can respond only to temporal contrast, but not to spatial one, since spatial contrast requires a neural computation that compares the luminance at point A with that at point B. All such computations are, therefore, postreceptoral. (There are junctions among neighboring photoreceptors. However, they are all electrical (and therefore positive) and they appear to contribute very little to the receptors' signals; Schneeweis, D. M. and Schnapf, J. L., 1999.)

The horizontal cells, with their wide ranging dendritic trees, are an essential element of the antagonistic center-surround organization of bipolar and ganglion cells in the retina (Kuffler, S. W., 1953; Werblin, F. S. and Dowling, J. E., 1969). This organization, which pits the narrow center against the broad surround, is essential for the analysis of spatial contrast: it tunes each cell to respond best to spots of a particular size, or, equivalently, to some limited range of spatial frequencies. Some amacrine cells contribute to this tuning process by adding a second contribution to the surround component (Cook, P. B. and McReynolds, J. S., 1998; Kaplan, E. and Benardete, E., 2001).

2.03.3.1.2 Retinal ganglion cells

2.03.3.1.2.(i) Luminance The discharge of the RGCs is an encoded summary of all the processing done by the retina, and thus the effects of the luminance and contrast of the visual scene are embedded in that discharge.

The average, ambient luminance is registered only weakly in the discharge of most RGCs, except when the luminance changes relatively rapidly, when the change can modulate the discharge temporarily. In general, the center-surround antagonistic organization of receptive fields, together with the adapting mechanisms in the retina, keep the maintained discharge of the RGCs more or less constant over time, so that only a limited band of spatial and temporal frequencies of luminance modulation are allowed to influence the firing rate (Figure 1).

Although luxotonic units (neurons that can encode light intensity over a wide luminance range) have been reported in invertebrates (Kaplan, E. and Barlow, R. B., 1975) and in lower vertebrates (Yang, J. *et al.*, 2005), the situation in mammals is more complex, since most RGCs can vary their discharge over only a limited luminance range.

There are, however, some (rare) luminance units (Barlow, H. B. and Levick, W. R., 1969), which can change their maintained discharge monotonically over several log units of stimulus intensity. These might correspond to the recently discovered melanopsin-containing ganglion cells (Berson, D., 2003), which (in the monkey) change their maintained discharge over 8 log units of intensity, utilizing input from rods for scotopic (dim) light levels, and cone input plus their intrinsic melanopsin to respond to higher light levels (Dacey, D. M. *et al.*, 2005). They are involved in the regulation of the circadian rhythm, but since they also project to the LGN (among other targets), the information they provide is likely to be available to the visual cortex, and thus could contribute to the perception of luminance. Their influence on cortical physiology has not yet been explored.

2.03.3.1.2.(ii) Contrast Since contrast is what allows us to see patterns, the dependence of the discharge of visual neurons on it is of paramount importance, and this topic has, therefore, been investigated thoroughly. In general, it appears that the larger the receptive field center, the greater is the contrast gain (Kaplan, E. and Shapley, R. M., 1986; Croner, L. J. and Kaplan, E., 1995). Since the RGCs that project to the magnocellular layers (M cells) are larger than those that project to the parvocellular layers (P cells) at any given retinal eccentricity, they are also much more sensitive to luminance contrast (Kaplan, E. and Shapley, R. M., 1986): their contrast gain is higher. Because the maximum firing

rate of neurons is limited, M cells begin to saturate at much lower contrast than do the P cells, which show little or no sign of saturation at any contrast below 100%. The response versus contrast functions of both M and P cells are well fitted by the Hill equation (named after the English muscle physiologist A. V. Hill, who derived it empirically to describe the binding of oxygen to hemoglobin. The Michaelis–Menten equation of enzyme kinetics is a special case of the Hill equation, for which $n = 1$. In vision science this equation is sometimes referred to as the Naka–Rushton equation (Naka, K. I. and Rushton, W. A. H., 1966), or the hyperbolic tangent function):

$$R = R_{\max} \times C^n / \left(C^n + C_{50}^n\right) \quad [1]$$

in which R is the response, C is contrast, and C_{50} is the contrast at which the response reaches half its maximal amplitude, $R_{\max}$. For RGCs (and LGN cells), n is typically ~1. In the primate, the response of M cells reaches half $R_{\max}$ around 14% contrast, while the P cells' response shows almost no saturation (see figure 1 in Chapter The P, M and K Streams of the Primate Visual System: What Do They Do for Vision?).

Several other functions have been used to fit response versus contrast functions, but all share the basic characteristics of the Hill function: they are sigmoidal, with a steepening slope at low contrasts (an expansive nonlinearity), and a decreasing slope at higher contrasts (a compressive nonlinearity). These two end regions of the curve are connected by a more or less linear middle portion.

Luminance exerts a profound influence on the response to contrast, as expected from Weber's law (see Section 2.03.2.7): as luminance level increases, so does contrast gain (Purpura, K. *et al.*, 1988), at least in the scotopic–mesopic range. At very high luminance levels the effect on contrast gain becomes smaller. It is unclear how fast this adjustment takes place, but it is (at least in part) a neural process, rather than an effect of bleaching of visual pigments, and therefore it is likely to be fast.

2.03.3.2 Lateral Geniculate Nucleus

The responses of LGN neurons to changes in luminance and contrast are rather similar to those of their main excitatory input, the RGCs. In that respect, LGN neurons do function like relay cells, which transmit to the visual cortex the messages delivered to them by the RGCs, with only minor modifications due to dynamical differences and a stronger inhibitory (suppressive) surround (Hubel, D. H. and Wiesel, T. N., 1961; Levick, W. R. *et al.*, 1972; Kaplan, E. *et al.*, 1993; Bonin, V. *et al.*, 2005). A more complete description of how the response of LGN neurons in primates changes with spatial or temporal contrast can be found in two early studies (Kaplan, E. and Shapley, R. M., 1982; Derrington, A. M. and Lennie, P., 1984), and new information about LGN adaptation to luminance and contrast is reported in Mante V. *et al.* (2005), and summarized in Section 2.03.2.5.

2.03.3.3 Visual Cortex

2.03.3.3.1 Luminance

Most cortical neurons require a spatial pattern to be driven effectively, but approximately 25% of cortical units in primates do show luxotonic behavior (Kayama, Y. *et al.*, 1979) under Ganzfeld (diffuse, full field) stimulation. Some are photergic (respond to increased luminance), while the others are scotergic (respond to decreased luminance level). Other units are slowly adapting, namely: they respond temporarily to changes in luminance, but return gradually to their previous firing rate. Curiously, the luxotonic units are rather susceptible to the effects of anesthesia. Whether these neurons receive input from the melatonin-containing light sensitive RGCs has not yet been established. It is not known whether the neural mechanisms that provide information about the overall illumination are the same ones that tell us how bright an object (or a patterned stimulus) is.

A recent study used optical imaging to explore the representation of luminance in the primate cortex, and reported that the thin cytochrome oxydase stripes of V2 contain specialized regions that represent increments and decrements of luminance by the amplitude of their response to such luminance changes (Wang, K. H. *et al.*, 2006). These regions were of two complementary types: one responding to luminance increments, while the other responded to decrements. The input and output of these regions are yet to be determined.

2.03.3.3.2 Contrast

2.03.3.3.2.(i) Single units Visual cortex: one might expect stimulus contrast to be related to the firing rate of cortical neurons, with higher contrasts eliciting higher firing rates. This is, indeed, the case for many cells and many stimuli (e.g., Tolhurst, D. J.

et al., 1981; Albrecht, D. G. and Hamilton, D. B., 1982; Edwards, D. P. *et al.*, 1995). However, firing rate is not the only possible code of encoding contrast in the cortex. For example, Optican L. M. and Richmond B. J. (1987) reported that the temporal firing patterns of neurons in interior temporal cortex of alert monkeys contained information about both the luminance and the contrast of the stimulus. More recently, Reich D. *et al.* (2001) found that the temporal structure of the spike trains of neurons in primate V1 carried as much or more contrast-related information as did the mean firing rate, and that the temporally coded information was manifested most strongly in the latency to response onset. Other aspects of the responses (the transient, tonic, and off components) contributed relatively little additional information. Their results also showed that temporal coding can be used to distinguish subtle contrast differences, while firing rates were useful for coarser discriminations. This suggests that the temporal structure of neurons' responses could extend the dynamic range for contrast encoding in the primate visual system.

A thorough investigation of the dependence of cortical responses on stimulus contrast in mammals has been conducted by D. Albrecht, W. Geisler and their colleagues (Albrecht, D. G. and Hamilton, D. B., 1982; Albrecht, D. G. *et al.*, 1984; Albrecht, D. G. and Geisler, W. S., 1994). In general, most cortical neurons follow the Hill function (eqn. [1]) quite faithfully. On average, the exponent $n = 3$ (± 1.4), and $C_{50} = 25\%$ ($\pm 25\%$). If the stimulus is not the optimal one (e.g., a spot that is offset from the receptive field center, or a grating positioned in a suboptimal position on the receptive field), only the response amplitude is affected. The Hill function still applies for these suboptimal stimuli, but requires a change of scale (Albrecht, D. G. *et al.*, 2002).

The fact that the exponent (n) is much higher in cortex than in LGN or RGCs reflects the much narrower input range of cortical units, which typically go from threshold to saturation over a limited contrast range. The steep response versus contrast functions must be shifted along the contrast range to a new location as the ambient contrast changes. That is the business of contrast adaptation or contrast gain control (Ohzawa, I. *et al.*, 1985; see Section 2.03.2.5).

Because LGN magnocellular cells have a higher contrast gain than do parvocellular cells (Kaplan, E. and Shapley, R. M., 1986), and because the magnocellular and parvocellular inputs to the cortex are segregated, at least at the input layers (Blasdel, G. G. and Lund, J. S., 1983), it is possible to identify, physiologically, the M and P inputs to the cortex (Hawken, M. J. and Parker, A. J., 1984; Hawken, M. J. *et al.*, 1988; Edwards, D. P. *et al.*, 1995).

Response variability: it is worth noting that, like the response amplitude, the variability of the cortical response also increases with stimulus contrast, unlike what is seen in RGCs and LGN neurons (Tolhurst, D. J. *et al.*, 1981; Edwards, D. P. *et al.*, 1995).

2.03.3.3.3 Other measures of cortical activity

2.03.3.3.3.(i) Visual-evoked potentials Visual-evoked potentials (VEPs), which are recorded noninvasively from the unopened skull, reflect the activity of numerous cortical neurons. Nevertheless, the response versus contrast that one obtains in such a recording follows the same Hill function (eqn. [1]) that describes the responses of individual cells (Langheinrich, T. *et al.*, 2000). The exponent found was similar to what is found in single cells, although the C_{50} value was considerably higher. A recent study was able to relate the VEP responses elicited by multifocal stimulation in human to the response versus contrast functions recorded from individual neurons in monkey visual cortex, and show that, with some caveats, the VEP reflects a simple sum of the individual responses of the underlying neurons (Hood, D. C. *et al.*, 2006).

When nonlinear components of the VEP response are analyzed, it is possible to detect the distinct signatures of the magnocellular and parvocellular inputs to the cortex (Klistorner, A. *et al.*, 1997), namely the high contrast gain of the magnocellular cells at low contrast and the near-linear increase of parvocellular response with contrast (Kaplan, E. and Shapley, R. M., 1986).

2.03.3.3.3.(ii) Functional magnetic resonance imaging Like VEPs, the blood oxygen level detection (BOLD) response of functional magnetic resonance imaging (fMRI) obeys a modified version of Hill's function, with an added constant to the exponent of the numerator (Demb, J. B. *et al.*, 1997; Boynton, G. M. *et al.*, 1999). A recent study found that contrast adaptation resets the operating point of the response versus contrast function around the ambient contrast of the stimulus in areas V1, V2, and V3 of the human visual cortex (see below). Area hV4, in contrast, seems to rectify the contrast signal, and produces positive responses that ignore the sign of the contrast (Gardner, J. L. *et al.*, 2005). The

adjustment of the contrast gain took ~15 s. It is worth noting that these fMRI data from conscious humans are consistent with the electrophysiological results obtained from anesthetized cats and monkeys (Albrecht, D. G. and Hamilton, D. B., 1982; Ohzawa, I. *et al.*, 1985).

2.03.3.4 Contrast Gain

As mentioned above, contrast gain is the slope of the response versus contrast function, and has units of impulses s^{-1} $\%^{-1}$ contrast. In RGC and LGN neurons it is closely related to the size of the receptive field center, the region over which the cell integrates its dominant visual input (Croner, L. J. and Kaplan, E., 1995), and which determines its state of light adaptation (Enroth-Cugell, C. and Shapley, R. M., 1973). For cortical neurons, other mechanisms, such as input from the nonclassical receptive field (which, by definition, represents a nonlinear mechanism; the nonclassical receptive field is an area that extends beyond the boundaries of the classical receptive field, which, when stimulated alone, elicits no response, but in which such stimulation alters the responses to stimuli falling inside the boundaries of the classical receptive field), have a significant influence on the contrast gain. Some of these nonlinear effects, which are prominent in the cortex, originate – at least in part – in the retina (McIlwain, J. T., 1966; Krüger, J. and Fischer, B., 1973) and the LGN (Girardin, C. C. *et al.*, 2002).

2.03.3.5 Contrast Gain Control

2.03.3.5.1 General considerations

In order to squeeze the large dynamic range of the visual world through the narrow bottlenecks of its neural machinery, the visual system must adapt not only to the ambient luminance (see Section 2.03.2.7), but also to contrast. The topic of adaptation to ambient and dynamic contrast is a large and important one, and much recent experimental and theoretical work has been devoted to it, especially in connection with cortical mechanisms. It is described here only briefly, and a more complete discussion can be found in Section 2.03.1.3.

In general, the adapting mechanisms shape the spatiotemporal transfer function of the neurons at a particular level (retina, LGN, or cortex) in such a way that, as contrast (or luminance) increases, the transfer functions become more selective: sensitivity to low spatial and temporal frequencies decreases, while sensitivity to intermediate and high frequencies is either unaffected or increased, and the phase of the response is shifted. Thus the term contrast gain control is somewhat misleading, because this adaptation mechanism affects not only the gain, but also the temporal properties of the visual system (time constants and phase lags). This process can be accomplished either by linear means (e.g., subtraction, as in the DOG model of Rodieck), or by nonlinear processes, in which the response at a given frequency is divided or multiplied by some function of luminance or contrast.

Because the characteristics of the visual environment can change rapidly or slowly, the visual system has evolved several adapting mechanisms that have various time scales: some complete their work in milliseconds, while others span durations of seconds or minutes. It is likely that the great variety of cell types, neurotransmitters, and receptors is designed to accommodate this wide range of timescales.

It is important to point out here that adaptation to (spatial) contrast is different from light adaptation because it is pattern specific: adaptation to a stimulus of some orientation and spatial frequency will have little or no effect on the sensitivity to stimuli of different spatial characteristics (Movshon, J. A. and Lennie, P., 1979). This is especially apparent in the cortex, but has been demonstrated in the retina as well (Hosoya, T. *et al.*, 2005).

2.03.3.5.2 Retina

Early work has identified a retinal mechanism of adaptation to contrast, dubbed the Contrast Gain Control, which acts rapidly to adjust the (temporal) contrast sensitivity of RGCs, and to produce a phase shift in the response as contrast increases (Shapley, R. M. and Victor, J. D., 1978; Benardete, E. A. *et al.*, 1991). The spatial and dynamical properties of this mechanism suggest that it is mediated by an extensive network of amacrine cells. More recent work found two processes of retinal adaptation to contrast: fast (<0.1 s) and slow (~10 s; Chander, D. and Chichilnisky, E. J., 2001; Baccus, S. A. and Meister, M., 2002). The cellular basis of these processes remains to be established.

2.03.3.5.3 Lateral geniculate nucleus

The effects of contrast and luminance on LGN cells is roughly similar to their effects on RGCs. Recently, vision scientists have been paying more attention to the visual content of natural scenes, because it was thought, reasonably, that the visual system might

have evolved specialized mechanisms to deal with the visual world. Mante V. *et al.* (2005) have found that luminance and contrast vary independently in natural scenes, and that the actions of the adapting mechanisms (gain control) for luminance and for contrast are also independent, at least as they are expressed in the responses of LGN cells. It remains to be determined whether the same independence holds for subsequent stages in the visual system.

2.03.3.5.4 Visual cortex

Ohzawa I. *et al.* (1982; 1985) investigated the effect of ambient contrast on the response versus contrast function of cortical neurons. They found a contrast gain control mechanism that differs from the retinal one in several ways: it is slower (with a time constant of ~6 s, compared with a few milliseconds for the retinal mechanism), and appears to involve only the central discharge zone, while the retinal mechanism extends over a wide region. This mechanism is quite effective: contrasts as low as 3% can double the contrast threshold.

2.03.3.5.4.(i) Monocular versus binocular Anzai A. *et al.* (1995) found that contrast thresholds and slopes varied from cell to cell but, in general, binocular contrast thresholds were lower, and binocular slopes were steeper, than their monocular counterparts. Truchard A. M. *et al.* (2000) demonstrated that contrast gain reductions are made primarily at a monocular site, before the convergence of information from the two eyes takes place.

2.03.3.5.4.(ii) Contrast gain or response gain? We note that not only aspects of the stimulus can affect the sensitivity to contrast, but also the internal state of the observer. For example, attention can affect the response of cortical neurons to contrast, and such a modulation could reflect either a change in the effectiveness of the stimulus (changed effective contrast) or a different response amplitude due to a scaling effect of attention. In a recent study, the behavior of most neurons in V4 favored the hypothesis that attention increased significantly the effective contrast (Reynolds, J. H. *et al.*, 2000; Reynolds, J. H. and Chelazzi, L., 2004). Qualitatively similar results were obtained in neurons from the middle temporal (MT) area of primate by Cook E. P. and Maunsell J. H. R. (2004). For a discussion of the ways in which attention modulates neuronal responses in the visual cortex see Maunsell J. H. R. and Treue S. (2006).

2.03.3.5.5 Cellular basis of contrast adaptation in cortex

As in the retina, contrast is calculated across an extended region of cortex, and the result is used by the cortical contrast adaptation mechanisms to adjust the contrast gain of cortical units. The prevailing view is that this is accomplished by division, probably by shunting inhibition (Carandini, M. and Heeger, D. J., 1994; Carandini, M. and Ferster, D., 1997; Cavanaugh, J. R. *et al.*, 2002), but other mechanisms have been suggested, such as synaptic depression, either of intracortical synapses, or of the thalamocortical synapse (Carandini, M. *et al.*, 2002). Synaptic depression can exert a powerful influence on cortical dynamics (Chance, F. S. *et al.*, 1998), but there is still some doubt about its functional importance, because in recordings *in vivo* it is considerably less powerful than it appears in cortical slices (Sanchez-Vives, M. V. *et al.*, 2000). This topic is still being investigated by several groups, and it is likely that more than one mechanism will eventually be implicated.

It has been shown that the effect of contrast adaptation is to produce a sustained hyperpolarization in cortical neurons (Carandini, M. and Ferster, D., 1997; 2000; Sanchez-Vives, M. V. *et al.*, 2000), which reduces their firing rate without a significant change in their conductance.

A recent study, which used natural stimuli to explore how the stimulus ensemble shapes the receptive field properties of cortical neurons, found that contrast adaptation can be very slow (tens of seconds or more), and that it optimizes the spatiotemporal properties of the receptive field to maximize information transmission in the visual cortex (Sharpee, T. O. *et al.*, 2006). It appears, therefore, that several mechanisms, each with its own timescale, are marshaled in the service of this important adaptation process.

2.03.3.5.6 Contrast adaptation in parallel visual streams

In agreement with previous results (Benardete, E. A. *et al.*, 1992), Solomon S. G. *et al.* (2004) reported that contrast adaptation is profound in the magnocellular stream (beginning already in RGCs), but absent in the parvocellular or koniocellular stream. One interpretation of these results is that contrast adaptation requires summation of many inputs, and it is thus the larger receptive fields of the M stream (Gouras, P., 1968; Croner, L. J. and Kaplan, E., 1995) that endow them with greater ability to adapt to the ambient contrast. This difference between the various neuronal populations could be a quantitative rather than a

qualitative one: the tiny receptive field centers of the midget (P) ganglion cells allow little or no amacrine input, while the much larger centers of parasol (M) neurons can benefit from numerous such inputs.

2.03.3.6 Adaptation and Absolute Levels of Contrast and Luminance

Adaptation to luminance or contrast sacrifices the information about the absolute levels of these quantities. This is, again, a general theme in the nervous system: emphasize the change at the expense of the unchanging. We note, however, that some elements in the nervous system do seem to keep track of the absolute levels, and are thus immune to adaptation. Examples include the melanopsin-containing RGCs (Berson, D., 2003) and those cortical units that show no sign of contrast adaptation (Ohzawa, I. *et al.*, 1985).

2.03.3.7 Effects of Luminance Level on Contrast Sensitivity

Shakespeare already knew that a bright light makes a faint one more difficult to see, as Nerissa says in The Merchant of Venice "When the moon shone, we did not see the candle" (act 5, scene 1). In the nineteenth century, Weber determined experimentally that, at low and moderate intensities, the change in perceptual intensity is roughly proportional to the change in the stimulus: $dp = k \cdot dI/I$ (Weber's law, which is sometimes written simply as $dI/I = k$). At high intensities a saturation or compression sets in, and renders Weber's law invalid for these intensities.

If we integrate Weber's law we get Fechner's law: $p = k \cdot \log(I) + c$, which shows the well-known logarithmic compression of physical intensities when they are represented by the nervous system. In assuming a linear response at low intensities, the Weber–Fechner relationship does not account for the initial expanding nonlinearity that is often seen in visual neurons. This expansive nonlinearity has been proposed as one of the mechanisms that are used in the cortex to sharpen the tuning of cortical neurons (Albrecht, D. G. and Geisler, W. S., 1994), since it causes small responses to be amplified less than larger ones.

We note that the effect of ambient luminance on contrast sensitivity, as manifested in Weber's law, is a clear demonstration of adaptation at work.

2.03.4 Psychophysical Aspects

2.03.4.1 Steady State

2.03.4.1.1 Luminance

Can we tell how bright the world really is? Psychophysical experiments in humans, in which the stimuli provided no spatial cues (Gantzfeld), found that the sensation of brightness is graded over approximately 8 log units (Barlow, R. B. and Verrillo, R. T., 1976), suggesting that somewhere in the visual system there are neurons that encode luminance over several log units. This wide range is noteworthy, because each class of vertebrate photoreceptors (rods or cones) can vary its response to light over only ~4 log units (Fain, G. L. and Dowling, J. E., 1973; Dacey, D. M. *et al.*, 2005), although some invertebrate photoreceptors can encode light intensity over 10 log units (Kaplan, E. and Barlow, R. B., 1975). Thus it is likely that low luminance is encoded by rods, and higher luminance sensitivity results from the activity of cones and of the few specialized ganglion cells that contain melanopsin (Berson, D., 2003).

Perceptual brightness increases with luminance according to a power law: $B = k \times Lp$, where B is subjective brightness, L is luminance, and k and p are constants (Stevens, S. S., 1970). The exponent p has been found to be nearly one-third for brightness. Stevens has argued that the power law, which holds for all sensory modalities (each with its own distinctive exponent), is a more complete and faithful description of the relationship between perceptual magnitude and physical intensity than Fechner's much older logarithmic law (Stevens, S. S., 1961).

2.03.4.1.2 Contrast

Figure 2, in which contrast increases from top to bottom on the ordinate and spatial frequency increases from left to right on the abscissa, shows that we are most sensitive to intermediate spatial frequencies, with sensitivity to higher and lower frequency being much lower (Limitations of the printing process create distortion of the shape of the filter at high spatial frequencies in Figure 2). This forms a spatial band-pass filter, which is often called the contrast sensitivity function, and to the extent that we can think of the visual system in linear terms, we can imagine it to represent the envelope of many, much narrower, spatial filters, each with a peak at a slightly different spatial frequency, similar to the

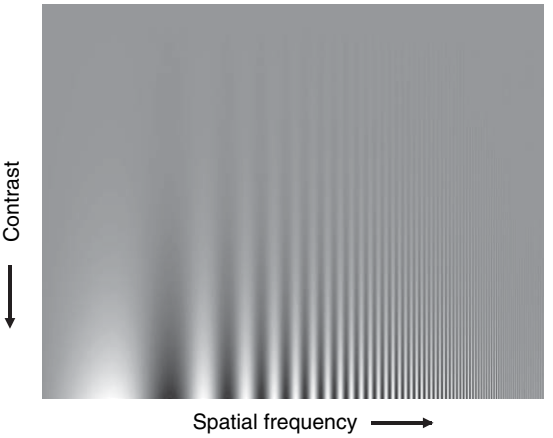

Figure 2 The (spatial) contrast sensitivity function. Contrast increases from top to bottom, and spatial frequency increases from left to right. From the appropriate distance, you can see that intermediate spatial frequencies can be seen at lower contrasts than either higher or lower spatial frequencies, creating an inverted U shaped function (for more information about this figure, which was created by J. Robson and F. Campbell, see: http://ohzawa-lab.bpe.es.osaka-u.ac.jp/ohzawa-lab/izumi/CSF/A_JG_RobsonCSFchart.html).

filter shown in Figure 1 (Campbell, F. W. and Robson, J. G., 1968). This is the origin of the notion, which was rather popular in the past, that the visual system might perform something akin to Fourier analysis on the visual world (e.g., Pollen, D. A. *et al.*, 1971; De Valois, K. K. *et al.*, 1979; Pollen, D. A. and Ronner, S. F., 1981). This idea, which relies entirely on linear mechanisms and interactions, had been criticized on theoretical grounds (e.g., Schwartz, E. L., 1980), and was mortally wounded by the discovery (Enroth-Cugell, C. and Robson, J. G., 1966) that the mammalian visual system includes a class of nonlinear neurons. That discovery, however, ushered in a new view of sensory information processing, which holds that information is processed by parallel neuronal populations, such as the M, P, and K streams, or the what and where streams (for a review, see Chapter The P, M and K Streams of the Primate Visual System: What Do They Do for Vision?), and by other considerations (e.g., Schwartz, E. L., 1980). In general, most visual neurons show some spatial tuning, which results from the antagonistic interplay of excitatory and inhibitory processes of quite different spatial scales (see Figure 1). The sharpness of this tuning increases as one moves from RGCs to LGN and primary visual cortex, at least for some classes of neurons.

2.03.4.1.3 Mach bands and other illusions

The notion that a spatial comparison of two antagonistic inputs of different scales will lead to tuning, and thus to an emphasis on intermediate and high frequencies at the expense of low ones, was already appreciated by E. Mach in the 1860s, when he realized that this could explain the enhancement of edges at light–dark borders (Mach Bands: Ratliff, F., 1965). In fact, Mach attempted to determine, from the width of the bright and dark bands, the extent of the retinal inhibitory influences that he surmised were responsible for that illusion. Neurophysiological experiments, carried out more than a century later, have confirmed his remarkable intuition (Enroth-Cugell, C. and Robson, J. G., 1966; Barlow, R. B. and Quarles, D. A., 1975).

A related illusion is the Craik-Obrien-Cornsweet illusion (for a demonstration, see Relevant Website Section), which is due, again, to the fact that we respond better to abrupt changes than to gradual ones.

2.03.4.2 Dynamics

We have seen that the visual system is more sensitive to change than to unchanging conditions. This is true not only in space but also in time: flicker is more visible than steady light. The human sensitivity to flicker at various frequencies, and its dependence on the ambient illumination (and on other stimulus parameters), has been the subject of intensive investigation since the 1950s (De Lange, H., 1958a; 1958b). The influence of the luminance level on the temporal contrast sensitivity function can be clearly seen in Figure 3: at low luminance levels the function is that of a low-pass filter. As luminance level increases, a band-pass filter emerges, rather similar to what we saw in the spatial domain (Figure 2). Both flicker sensitivity and the maximal flicker frequency that can be resolved (the critical fusion frequency) increase with luminance level.

2.03.4.2.1 Cellular basis of the temporal contrast sensitivity function

The function shown in Figure 3 reflects primarily the basic properties of photoreceptors, although several stimulus parameters (such as target size or retinal eccentricity) do influence the details of this important psychophysical function. The cellular basis that underlies it has been discovered in the primordial photoreceptors of the horseshoe crab, *Limulus* (Dodge, F. A. *et al.*, 1968) (*Limulus* is thought to be the oldest living creature on our planet, and fossils

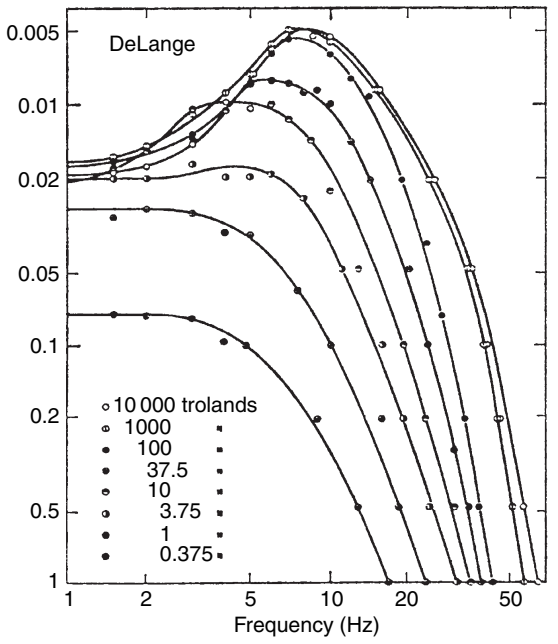

Figure 3 The human contrast sensitivity as a function of temporal frequency at several luminance levels. The axes are logarithmic. Contrast sensitivity and critical fusion frequency both increase with luminance level. Retinal illumination is given in trolands (luminance times the pupil area). Reproduced from De Lange, H. 1958a. Research into the dynamic nature of the human fovea–cortex systems with intermittent and modulated light. I. Attenuation characteristics with white and colored light. J. Opt. Soc. Am. 48, 777–784, with permission from the Optical Society of America.

with eyes remarkably like those of modern-day horseshoe crabs date back at least 300 million years). That study has demonstrated that light adaptation reduces the amplitude and duration of the quantal bumps, which are discreet responses to individual photons, and which sum up to produce the receptor's response to light. The major features of the De Lange celebrated function (the increased flicker sensitivity, the change from a low-pass to a band-pass behavior, and the decreased duration of temporal integration) have all been replicated in the individual photoreceptor, providing an impressive, and rare, link between biophysical processes and perceptual experience.

We can also relate the behavioral change in sensitivity depicted in Figure 3 to the contrast gain of visual neurons. As mentioned above, over a wide range of luminance, from scotopic levels up to high mesopic levels, as luminance increases, so does the contrast gain (Purpura, K. *et al.*, 1988).

2.03.4.3 Stimulus Parameters

As we have seen, contrast and luminance sensitivities are central to the process of vision. It is not surprising, therefore, that they are affected by most other aspects of the visual stimulus, such as size, retinal eccentricity, color, state of light or dark adaptation, and so on. A review of all these is outside the scope of this chapter, but comprehensive summaries of the early literature can be found in reviews by Blackwell H. R. (1972) and by Kelly D. H. (1972) and in the studies of Koenderink J. J. *et al.* (1978a; 1978b; 1978c; 1978d).

2.03.4.4 Some Clinical Implications

The growing appreciation of the importance of contrast sensitivity for vision has added new tests to the eye clinic, where letter charts (Pelli, D. G. *et al.*, 1988) and other devices are being used to supplement the venerable Snellen eye chart. The Snellen chart measures only acuity, the ability to see the highest spatial frequencies, but provides little information about the rest of the contrast sensitivity function (Figure 2). However, adequate contrast sensitivity across medium and low-spatial frequencies is essential for many visual tasks (Lennerstrand, G. and Ahlström, C. O., 1989).

Under certain pathological conditions, contrast sensitivity is compromised, and because of the crucial role that it plays in vision, such deterioration has serious consequences for the affected person. With age, a deterioration of the eye's optics (increased lens opacity, cataracts) increases glare which reduces the image contrast that is available to the retina. Aging thus causes a decrease in contrast sensitivity and an increase in the time to recover from glare, due to both optical and neural factors (Sloane, M. E. *et al.*, 1988; Sturr, J. F. *et al.*, 1988; Skeel, R. L. *et al.*, 2006), although under photopic conditions the optical factors appear to be dominant (Burton, K. B. *et al.*, 1993). In age related macular degeneration and drusen, contrast sensitivity is decreased at the peak and at the high-frequency end of the contrast sensitivity function (Kleiner, R. C. *et al.*, 1988). Other pathologies that affect contrast sensitivity at various spatial frequencies include retinitis pigmentosa (Alexander, K. R. *et al.*, 2004), dyslexia (Bednarek, D. B. and Grabowska, A., 2002, although this is highly controversial), amblyolpia (Bradley, A. and Freeman, R. D., 1981; Chino, Y. M. *et al.*, 1991; Asper, L. *et al.*, 2000), and glaucoma (Swindale, N. V. *et al.*, 1996; Raz, D.

et al., 2002; Altangerel, U. *et al.*, 2006). The cause of contrast sensitivity reduction in all of these is neural, rather than optical.

2.03.4.5 From Neurons to Perception

It is tempting to relate the results of neurophysiological experiments (usually done on anesthetized animals) to perception and psychophysics (usually studied in conscious humans). This is one of the major goals of neuroscience, and several partially successful attempts have been made (e.g., see Ratliff, F., 1965; Geisler, W. S., 1989), but its accomplishment is hampered by severe limitations, which include the following: (1) much of the analysis treats neurons and interactions as linear, while they are manifestly nonlinear (most response vs. contrast functions show nonlinearities, and the contrast gain control, especially in the cortex, is a nonlinear mechanism); (2) our knowledge of the wiring, biophysics, and neurochemistry of the brain is still far from complete; and (3) there are technical limitations in physiological experiments, which further restrict our knowledge base. For more on this important subject, see Olshausen B. A. and Field D. J. (2005).

2.03.5 Conclusions

The visual system is exquisitely sensitive to both spatial and temporal contrast, which it extracts from the visual scene by comparing the luminance at several points in space and time. It derives this sensitivity primarily from the antagonistic interplay of two processes that have two very different scales: one fine (fast) and the other coarse (slow). The system pays much less (direct) attention to luminance, although the luminance level does affect strongly the sensitivity to contrast. The brain has evolved an elaborate set of adaptive mechanisms, active at several stages along the path from retina to cortex, which adjust the sensitivity to contrast depending on both the ambient contrast and prevailing luminance. Thus luminance, contrast and adaptation all interact to permit the brain to focus on what is important in the visual scene: the new and unexpected.

Acknowledgments

The author was supported by NIH grants EY016371 and EY016224.

References

Albrecht, D. G. and Geisler, W. S. 1994. Visual cortex neurons in monkey and cat: contrast response nonlinearities and stimulus selectivity. Soc. Photo-Opt. Instrum. Eng. 2054, 12–31.

Albrecht, D. G. and Hamilton, D. B. 1982. Striate cortex of monkey and cat: contrast response function. J. Neurophysiol. 48, 217–237.

Albrecht, D. G., Farrar, S. B., and Hamilton, D. B. 1984. Spatial contrast adaptation characteristics of neurones recorded in the cat's visual cortex. J. Physiol. 347, 713–739.

Albrecht, D. G., Geisler, W. S., Frazor, R. B., and Crane, A. M. 2002. Visual cortex neurons in monkeys and cats: temporal dynamics of the contrast response function. J. Neurophysiol. 88, 889–914.

Alexander, K. R., Barnes, C. S., Fishman, G. A., Pokorny, J., and Smith, V. C. 2004. Contrast sensitivity deficits in inferred magnocellular and parvocellular pathways in retinitis pigmentosa. Invest. Ophthalmol. Vis. Sci. 45, 4510–4519.

Altangerel, U., Spaeth, G. L., and Steinmann, W. C. 2006. Assessment of function related to vision (afrev). Ophthalmic. Epidemiol. 13, 67–80.

Anzai, A., Bearse, M. A., Freeman, R. D., and Cai, D. 1995. Contrast coding by cells in the cat's striate cortex: monocular vs. binocular detection. Vis. Neurosci. 12, 77–93.

Ashmore, J. F. and Copenhagen, D. R. 1983. An analysis of transmission from cones to hyperpolarizing bipolar cells in the retina of the turtle. J. Physiol. 340, 569–597.

Ashmore, J. F. and Falk, G. 1976. Absolute sensitivity of rod bipolar cells in dark-adapted retina. Nature 263, 248–249.

Asper, L., Crewther, D., and Crewther, S. 2000. Strabismic amblyopia. Part 1. Psychophysics. Clin. Exp. Optom. 83, 49–58.

Baccus, S. A. and Meister, M. 2002. Fast and slow contrast adaptation in retinal circuitry. Neuron 36, 909–919.

Barlow, H. B. and Levick, W. R. 1969. Three factors limiting the reliable detection of light by retinal ganglion cells of the cat. J. Physiol. 200, 1–24.

Barlow, R. B. and Quarles, D. A. 1975. Mach bands in the lateral eye of. J. Gen. Physiol. 65, 709–730.

Barlow, R. B. and Verrillo, R. T. 1976. Brightness sensation in a ganzfield. Vision Res. 16, 1291–1297.

Bednarek, D. B. and Grabowska, A. 2002. Luminance and chromatic contrast sensitivity in dyslexia: the magnocellular deficit hypothesis revisited. Neuroreport 13, 2521–2525.

Benardete, E. A., Kaplan, E., and Knight, B. W. 1991. Contrast gain control in the primate retina. Soc. Neurosci. Abstr. 17, 394.

Benardete, E. A., Kaplan, E., and Knight, B. W. 1992. Contrast gain control in the primate retina: P cells are not x-like, some m cells are. Vis. Neurosci. 8, 483–486.

Berson, D. 2003. Strange vision: ganglion cells as circadian photoreceptors. Trends Neurosci. 26, 314–320.

Blackwell, H. R. 1972. Luminance Difference Threshold. In: Visual Psychophysics, Vol. VII/4 of Handbook of Sensory Physiology (*eds*. D. Jameson and L. M. Hurvich), Chap. 4, pp. 78–101. Springer.

Blasdel, G. G. and Lund, J. S. 1983. Termination of afferent axons in macaque striate cortex. J. Neurosci. 3, 1389–1413.

Bonin, V., Mante, V., and Carandini, M. 2005. The suppressive field of neurons in lateral geniculate nucleus. J. Neurosci. 25, 10844–10856.

Boynton, G. M., Demb, J. B., Glover, G. H., and Heeger, D. J. 1999. Neuronal basis of contrast discrimination. Vision Res. 39, 257–269.

Bradley, A. and Freeman, R. D. 1981. Contrast sensitivity in anisometropic amblyopia. Invest. Ophthalmol. Visual Sci. 21, 467–476.

Burton, K. B., Owsley, C., and Sloane, M. E. 1993. Aging and neural spatial contrast sensitivity: photopic vision. Vision Res. 33, 939–946.

Campbell, F. W. and Robson, J. G. 1968. Application of Fourier analysis to the visibility of gratings. J. Physiol. 197, 551–566.

Carandini, M. and Ferster, D. 1997. A tonic hyperpolarization underlying contrast adaptation in cat visual cortex. Science 276, 949–952.

Carandini, M. and Ferster, D. 2000. Membrane potential and firing rate in cat primary visual cortex. J. Neurosci. 20, 470–484.

Carandini, M. and Heeger, D. J. 1994. Summation and division by neurons in primate visual cortex. Science 264, 1333–1336.

Carandini, M., Heeger, D. J., and Senn, W. 2002. A synaptic explanation of suppression in visual cortex. J. Neurosci. 22, 10053–10065.

Cavanaugh, J. R., Bair, W., and Movshon, J. A. 2002. Nature and interaction of signals from the receptive field center and surround in macaque v1 neurons. J. Neurophysiol. 88, 2530–2546.

Chance, F. S., Nelson, S. B., and Abbott, L. F. 1998. Synaptic depression and the temporal response characteristics of v1 cells. J. Neurosci. 18, 4785–4799.

Chander, D. and Chichilnisky, E. J. 2001. Adaptation to temporal contrast in primate and salamander retina. J. Neurosci. 21, 9904–9916.

Chino, Y. M., Smith, E. L., Wada, H., Ridder, W. H., Langston, A. L., and Lesher, G. A. 1991. Disruption of binocularly correlated signals alters the postnatal development of spatial properties in cat striate cortical neurons. J. Neurophysiol. 65, 841–859.

Cook, E. P. and Maunsell, J. H. R. 2004. Attentional modulation of motion integration of individual neurons in the middle temporal visual area. J. Neurosci. 24, 7964–7977.

Cook, P. B. and McReynolds, J. S. 1998. Lateral inhibition in the inner retina is important for the spatial tuning of ganglion cells. Nat. Neurosci. 1, 714–719.

Croner, L. J. and Kaplan, E. 1995. Receptive fields of p and m ganglion cells across the primate retina. Vision Res. 35, 7–24.

Dacey, D. M., Liao, H. W., Peterson, B. B., Robinson, F. R., Smith, V. C., Pokorny, J., Yau, K. W., and Gamlin, P. D. 2005. Melanopsin expressing ganglion cells in primate retina signal colour and irradiance and project to the LGN. Nature 433, 749–754.

De Lange, H. 1958a. Research into the dynamic nature of the human fovea–cortex systems with intermittent and modulated light. I. Attenuation characteristics with white and colored light. J. Opt. Soc. Am. 48, 777–784.

De Lange, H. 1958b. Research into the dynamic nature of the human fovea–cortex systems with intermittent and modulated light. II. Phase shift in brightness and delay in color perception. J. Opt. Soc. Am. 48, 784–789.

De Valois, K. K., De Valois, R. L., and Yund, E. W. 1979. Responses of striate cortex cells to grating and checkerboard patterns. J. Physiol. 291, 483–505.

Demb, J. B., Boynton, G. M., and Heeger, D. J. 1997. Brain activity in visual cortex predicts individual differences in reading performance. Proc. Natl. Acad. Sci. U. S. A. 94, 13363–13366.

Derrington, A. M. and Lennie, P. 1984. Spatial and temporal contrast sensitivities of neurones in lateral geniculate nucleus of macaque. J. Physiol. 357, 219–240.

Dodge, F. A., Knight, B. W., and Toyoda, J. 1968. Voltage noise in Limulus visual cells. Science 160, 88–90.

Edwards, D. P., Purpura, K. P., and Kaplan, E. 1995. Contrast sensitivity and spatial frequency response of primate cortical neurons in and around the cytochrome oxidase blobs. Vision Res. 35, 1501–1523.

Enroth-Cugell, C. and Robson, J. G. 1966. The contrast sensitivity of retinal ganglion cells of the cat. J. Physiol. 187, 517–552.

Enroth-Cugell, C., Robson, J. G., Schweitzer-Tong, D. E., and Watson, A. B. 1983. Spatio-temporal interactions in cat retinal ganglion cells showing linear spatial summation. J. Physiol. 341, 279–307.

Enroth-Cugell, C. and Shapley, R. M. 1973. Adaptation and dynamics of cat retinal ganglion cells. J. Physiol. 233, 271–309.

Fain, G. L. and Dowling, J. E. 1973. Intracellular recordings from single rods and cones in the mudpuppy retina. Science 180, 1178–1180.

Gardner, J. L., Sun, P., Waggoner, R. A., Ueno, K., Tanaka, K., and Cheng, K. 2005. Contrast adaptation and representation in human early visual cortex. Neuron 47, 607–620.

Geisler, W. S. 1989. Sequential ideal-observer analysis of visual discriminations. Psych. Rev. 96, 267–314.

Girardin, C. C., Kiper, D. C., and Martin, K. A. 2002. The effect of moving textures on the responses of cells in the cat's dorsal lateral geniculate nucleus. Eur. J. Neurosci. 16, 2149–2156.

Gouras, P. 1968. Identification of cone mechanisms in monkey ganglion cells. J. Physiol. 199, 533–547.

Hartline, H. K. 1940. The receptive fields of optic nerve fibers. Am. J. Physiol. 130, 690–699.

Hawken, M. J. and Parker, A. J. 1984. Contrast sensitivity and orientation selectivity in lamina IV of the striate cortex of old world monkeys. Exp. Brain Res. 54, 367–372.

Hawken, M. J., Parker, A. J., and Lund, J. S. 1988. Laminar organization and contrast sensitivity of direction-selective cells in the striate cortex of the old world monkey. J. Neurosci. 8, 3541–3548.

Hood, D. C., Ghadiali, Q., Zhang, J. C., Graham, N. V., Wolfson, S. S., and Zhang, X. 2006. Contrast-response functions for multifocal visual evoked potentials: a test of a model relating v1 activity to multifocal visual evoked potentials activity. J. Vision 6, 580–593.

Hosoya, T., Baccus, S. A., and Meister, M. 2005. Dynamic predictive coding by the retina. Nature 436, 71–77.

Hubel, D. H. and Wiesel, T. N. 1961. Integrative action in the cat's lateral geniculate body. J. Physiol. 155, 385–398.

Kaplan, E. and Barlow, R. B. 1975. Properties of visual cells in the lateral eye of Limulus *in situ.* extracellular recordings. J. Gen. Physiol. 66, 303–326.

Kaplan, E. and Benardete, E. 2001. The Dynamics of Primate Retinal Ganglion Cells. In: Vision: From Neurons to Cognition, Vol. 134 of Progress in Brain Research (*eds*. C. Casanova and M. Ptito), pp. 1–18.

Kaplan, E., Mukherjee, P., and Shapley, R. M. 1993. Information Filtering in the Lateral Geniculate Nucleus. In: Contrast Sensitivity (*eds*. D. K. Lam and R. Shapley), pp. 183–200. MIT Press.

Kaplan, E. and Shapley, R. M. 1982. X and y cells in the lateral geniculate nucleus of macaque monkeys. J. Physiol. 330, 125–143.

Kaplan, E. and Shapley, R. M. 1986. The primate retina contains two types of ganglion cells, with high and low contrast sensitivity. Proc. Natl. Acad. Sci. U. S. A. 83, 2755–2757.

Kayama, Y., Riso, R. R., Bartlett, J. R., and Doty, R. W. 1979. Luxotonic responses of units in macaque striate cortex. J. Neurophysiol. 42, 1495–1517.

Kelly, D. H. 1972. Adaptation effects on spatiotemporal sine-wave thresholds. Vision Res. 12, 89–101.

Kleiner, R. C., Enger, C., Alexander, M. F., and Fine, S. L. 1988. Contrast sensitivity in age related macular degeneration. Arch. Ophthalmol. 106, 55–63.

Klistorner, A., Crewther, D. P., and Crewther, S. G. 1997. Separate magnocellular and parvocellular contributions from temporal analysis of the multifocal VEP. Vision Res. 37, 2161–2169.

Koenderink, J. J., Bouman, M. A., de Mesquita, A. E. B., and Slappendel, S. 1978a. Perimetry of contrast detection thresholds of moving spatial sine wave patterns. I. The near peripheral visual field (eccentricity 0°–8°). J. Opt. Soc. Am. 68, 845–849.

Koenderink, J. J., Bouman, M. A., de Mesquita, A. E. B., and Slappendel, S. 1978b. Perimetry of contrast detection thresholds of moving spatial sine wave patterns. II. The far peripheral visual field (eccentricity 0°–50°). J. Opt. Soc. Am. 68, 850–854.

Koenderink, J. J., Bouman, M. A., de Mesquita, A. E. B., and Slappendel, S. 1978c. Perimetry of contrast detection thresholds of moving spatial sine wave patterns. III. The target extent as a sensitivity controlling parameter. J. Opt. Soc. Am. 68, 854–860.

Koenderink, J. J., Bouman, M. A., de Mesquita, A. E. B., and Slappendel, S. 1978d. Perimetry of contrast detection thresholds of moving spatial sine wave patterns. IV. The influence of the mean retinal illuminance. J. Opt. Soc. Am. 68, 860–865.

Krüger, J. and Fischer, B. 1973. Dependence of surround effects on receptive field center illumination in cat retinal ganglion cells. Exp. Brain Res. 18, 304–315.

Kuffler, S. W. 1953. Discharge patterns and functional organization of mammalian retina. J. Neurophysiol. 16, 37–68.

Langheinrich, T., Tebartz, v., Lagreze, W. A., Bach, M., Lucking, C. H., and Greenlee, M. W. 2000. Visual contrast response functions in Parkinson's disease: evidence from electroretinograms, visually evoked potentials and psychophysics. Clin. Neurophysiol. 111, 66–74.

Lennerstrand, G. and Ahlström, C. O. 1989. Contrast sensitivity in macular degeneration and the relation to subjective visual impairment. Acta Ophthalmol. (Copenh.) 67, 225–233.

Levick, W. R., Cleland, B. G., and Dubin, M. W. 1972. Lateral geniculate neurons of cat: retinal inputs and physiology. Invest. Ophthalmol. 11, 302–311.

Mante, V., Frazor, R. A., Bonin, V., Geisler, W. S., and Carandini, M. 2005. Independence of luminance and contrast in natural scenes and in the early visual system. Nature Neurosci. 8, 1690–1697.

Maunsell, J. H. R. and Treue, S. 2006. Feature based attention in visual cortex. Trends Neurosci. 29, 317–322.

McIlwain, J. T. 1966. Some evidence concerning the physiological basis of the periphery effect in the cat's retina. Exp. Brain Res. 1, 265–271.

Movshon, J. A. and Lennie, P. 1979. Pattern selective adaptation in visual cortical neurones. Nature 278, 850–852.

Naka, K. I. and Rushton, W. A. H. 1966. S potentials from luminosity units in the retina of fish. J. Physiol. 185, 587–599.

Ohzawa, I., Sclar, G., and Freeman, R. D. 1982. Contrast gain control in the cat visual cortex. Nature 298, 266–268.

Ohzawa, I., Sclar, G., and Freeman, R. D. 1985. Contrast gain control in the cat's visual system. J. Neurophysiol. 54, 651–667.

Olshausen, B. A. and Field, D. J. 2005. How close are we to understanding v1? Neural Comput. 17, 1665–1699.

Optican, L. M. and Richmond, B. J. 1987. Temporal encoding of two-dimensional patterns by single units in primate inferior temporal cortex. III. Information theoretic analysis. J. Neurophysiol. 57, 162–178.

Pelli, D. G., Robson, J. G., and Wilkins, A. J. 1988. The design of a new letter chart for measuring contrast sensitivity. Clin. Vision Sci. 2, 187–199.

Pollen, D. A. and Ronner, S. F. 1981. Phase relationships between adjacent simple cells in the visual cortex. Science 212, 1409–1411.

Pollen, D. A., Lee, J. R., and Teylor, J. H. 1971. How does the striate cortex begin the reconstruction of the visual world? Science 173, 74–77.

Purpura, K., Kaplan, E., and Shapley, R. M. 1988. Background light and the contrast gain of primate P and M retinal ganglion cells. Proc. Natl. Acad. Sci. U. S. A. 85, 4534–4537.

Ratliff, F. 1965. Mach Bands: Quantitative Studies on Neural Networks in the Retina, Hoolden-Day.

Raz, D., Seeliger, M. W., Geva, A. B., Percicot, C. L., Lambrou, G. N., and Ofri, R. 2002. The effect of contrast and luminance on mferg responses in a monkey model of glaucoma. Invest. Ophthalmol. Vis. Sci. 43, 2027–2035.

Reich, D., Mechler, F., and Victor, J. 2001. Temporal coding of contrast in primary visual cortex: when, what, and why? J. Neurophysiol. 85, 1039–1050.

Reynolds, J. H. and Chelazzi, L. 2004. Attentional modulation of visual processing. Annu. Rev. Neurosci. 27, 611–647.

Reynolds, J. H., Pasternak, T., and Desimone, R. 2000. Attention increases sensitivity of v4 neurons. Neuron 26, 703–714.

Rodieck, R. W. 1965. Quantitative analysis of cat retinal ganglion cell response to visual stimuli. Vision Res. 5, 583–601.

Sanchez-Vives, M. V., Nowak, L. G., and McCormick, D. A. 2000. Membrane mechanisms underlying contrast adaptation in cat area 17 *in vivo*. J. Neurosci. 20, 4267–4285.

Schneeweis, D. M. and Schnapf, J. L. 1999. The photovoltage of macaque cone photoreceptors: adaptation, noise, and kinetics. J. Neurosci. 19, 1203–1216.

Schwartz, E. L. 1980. Computational anatomy and functional architecture of striate cortex: a spatial mapping approach to perceptual coding. Vision Res. 20, 645–669.

Shapley, R. and Enroth-Cugell, C. 1984. Visual Adaptation and Retinal Gain Controls. In: Progress in Retinal Research (*eds*. N. Osborne and G. Chader), pp. 263–346. Pergamon.

Shapley, R. M. and Victor, J. D. 1978. The effect of contrast on the transfer properties of cat retinal ganglion cells. J. Physiol. 285, 275–298.

Sharpee, T. O., Sugihara, H., Kurgansky, A. V., Rebrik, S. P., Stryker, M. P., and Miller, K. D. 2006. Adaptive filtering enhances information transmission in visual cortex. Nature 439, 936–942.

Skeel, R. L., Schutte, C., van Voorst, W., and Nagra, A. 2006. The relationship between visual contrast sensitivity and neuropsychological performance in a healthy elderly sample. J. Clin. Exp. Neuropsychol. 28, 696–705.

Sloane, M. E., Owsley, C., and Jackson, C. A. 1988. Aging and luminance-adaptation effects on spatial contrast sensitivity. J. Opt. Soc. Am. A 5, 2181–2190.

Solomon, S. G., Peirce, J. W., Dhruv, N. T., and Lennie, P. 2004. Profound contrast adaptation early in the visual pathway. Neuron 42, 155–162.

Somers, D. C., Nelson, S. B., and Sur, M. 1995. An emergent model of orientation selectivity in cat visual cortex simple cells. J. Neurosci. 15, 5448–5465.

Srinivasan, M. V., Laughlin, S. B., and Dubs, A. 1982. Predictive coding: a fresh view of inhibition in the retina. Proc. R. Soc. Lond. B 216, 427–459.

Stevens, S. S. 1961. To honor Fechner and repeal his law. Science 133, 80–86.

Stevens, S. S. 1970. Neural events and the psychophysical law. Science 170, 1043–1050.

Sturr, J. F., Church, K. L., and Taub, H. A. 1988. Temporal summation functions for detection of sine-wave gratings in young and older adults. Vision Res. 28, 1247–1253.

Swindale, N. V., Fendick, M. G., Drance, S. M., Graham, S. L., and Hnik, P. 1996. Contrast sensitivity for flickering and static letters and visual acuity at isoluminance in glaucoma. J. Glaucoma 5, 156–169.

Tolhurst, D. J., Movshon, J. A., and Thompson, I. D. 1981. The dependence of response amplitude and variance of cat

visual cortical neurones on stimulus contrast. Exp. Brain Res. 41, 414–419.
Truchard, A. M., Ohzawa, I., and Freeman, R. D. 2000. Contrast gain control in the visual cortex: monocular versus binocular mechanisms. J. Neurosci. 20, 3017–3032.
von Békésy, G. 1967. Mach band type lateral inhibition in different sense organs. J. Gen. Physiol. 50, 519–532.
Wang, K. H., Majewska, A., Schummers, J., Farley, B., Hu, C., Sur, M., and Tonegawa, S. 2006. *In vivo* two-photon imaging reveals a role of arc in enhancing orientation specificity in visual cortex. Cell 126, 389–402.
Watson, A. B. 1992. Transfer of contrast sensitivity in linear visual networks. Visual Neurosci. 8, 65–76.
Werblin, F. S. and Dowling, J. E. 1969. Organization of the retina of the mudpuppy. J. Neurophysiol. 32, 339–355.
Yang, J., Zhang, C., and Wang, S. R. 2005. Comparisons of visual properties between tectal and thalamic neurons with overlapping receptive fields in the pigeon. Brain Behav. Evol. 65, 33–39.

Relevant Website

http://www.michaelbach.de/ot/lum_cobc/index.html – Optical Illusions & Visual Penomenon by Michael Bach.

2.04 Lightness Perception and Filling-In

H Komatsu, National Institute for Physiological Sciences, Okazaki, Japan

© 2008 Elsevier Inc. All rights reserved.

2.04.1	Influence of Contrast on Perceived Brightness and Lightness	45
2.04.2	Neural Mechanisms of Brightness/Lightness Perception	47
2.04.3	Perceptual Filling-In	48
2.04.4	Neural Mechanisms of Filling-In	49
References		51

The main topic of this chapter is how our visual system processes the visual information related to the sense of brightness or lightness which is one of the most basic visual perception. The psychophysical and physiological findings on this topic will be summarized and recent advances on the understanding on the mechanisms of perceptual filling-in, which is closely related to the brightness/lightness perception, will be described.

At the outset, the difference among three related words should be clarified, namely, luminance, brightness, and lightness. All three are psychophysical measures of light intensity and are distinguished from physical measures such as light energy or number of quanta of light. Of the three, luminance is an objective measure of light intensity at a certain point in the visual field that can be measured by a device. The latter two, brightness and lightness, are both subjective measures of light intensity. Brightness refers to apparent light intensity of a stimulus in general or, more specifically, that of a light source. Lightness refers to the apparent surface reflectance which ranges between white and black.

2.04.1 Influence of Contrast on Perceived Brightness and Lightness

Perceived brightness of a stimulus depends on the light intensity coming from the stimulus to the eye, namely the luminance of the stimulus. When the luminance increases, the perceived brightness increases; their relationship obeys Stevens' law and can be represented by a power function. However, the perceived brightness of a stimulus patch is influenced by the surrounding stimuli. This is called brightness induction. When two stimuli with different luminance are placed next to each other, the difference in the perceived brightness between the two stimuli is often enhanced. This phenomenon is called brightness contrast. In Figure 1, each circle has the same shade of gray and the same luminance. However, because of the difference in the luminance of the surrounding region of each circle, the brightness of each circle appears different. This is an example of brightness induction. Brightness induction occurs across a considerably wide area in the visual field up to about 10° in visual angle (Yund, E. W. and Armington, J. C., 1975). Brightness induction can be generated by temporally changing surroundings. When the luminance of the surround is temporally modulated sinusoidally while keeping the luminance of the center patch constant, the brightness of the center patch appears temporally modulated in the opposite phase. Temporal characteristics of the brightness induction has been measured by changing the temporal frequency of the modulation of the surround. It was found that brightness induction occurs for the temporal frequency up to 1–4 Hz depending on the spatial frequency of the stimulus, but it did not occur for the faster modulation (De Valois, R. L. *et al.*, 1986; Rossi, A. F. and Paradiso, M. A., 1996). In contrast, we can easily perceive the flicker of the center patch over 10 Hz when the luminance of the patch itself is modulated. This indicates that the brightness induction requires extra processing, which is rather slow compared with the mechanism to detect luminance change at a certain position in the visual field.

There is tendency that lightness stays constant even when illumination changes. This is called lightness constancy. For example, when we read a newspaper, the letters look black and the paper looks white regardless of being under indoor illumination or in sunshine, even though the intensity of illumination is 100–1000 times stronger outdoors and

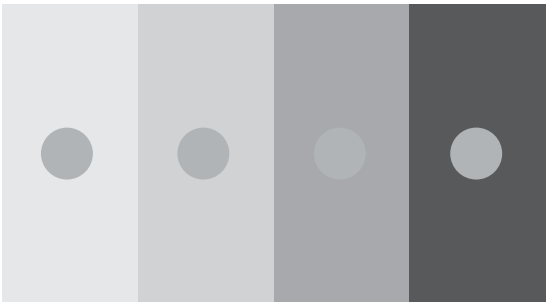

Figure 1 Brightness induction. The four circles have the same shade of gray and have the same luminance. However, because of the difference in the luminance of the background, they look to have different brightness.

the light reflected from the letter is enormously different. Wallach H. (1948) revealed that the luminance ratio between the surface and the surround region is the major factor determining the lightness of the surface. As long as the luminance ratio between the surface and surround is kept constant, the lightness of the surface stays constant even when the illumination changes. One remaining problem is that, according to this theory, only relative lightness can be determined. The visual system must somehow assign absolute value such as white or black to each surface. A simple heuristic mechanism is suggested in which white is assigned to the brightest surface in the scene (Gilchrist, A. *et al*., 1999).

The importance of the luminance ratio between the neighboring regions in lightness perception does not imply that lateral interaction between the neighboring region on the retinal image is the sole factor. Much evidence suggests that more complicated processes are involved. One example is shown in Figure 2, where the gray regions exist within black and white square-wave grating. Although the gray regions to the left and to the right have the same luminance, their brightness appears quite different. When we inspect the boundaries between the gray region and either the black or white stripes, for the gray region to the left, the boundary with the black stripe is longer than that with the white stripe, whereas for the gray region to the right, the opposite is true. If the amount of luminance contrast between the neighboring region is proportional to the boundary length, we can expect that the gray region at the left appears brighter that that at the right. However, contrary to expectations, the gray region at the right appears brighter than that at the left. This is discovered by White M. (1979) and is known as White's effect. One possible reason for such an effect is that

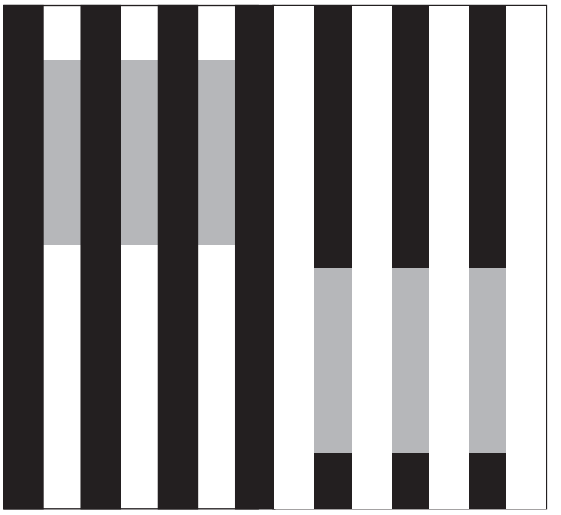

Figure 2 White's effect. Gray rectangles at the top left and bottom right have the same luminance, but appear to have quite different brightness.

when the boundaries between three regions form a T-junction, luminance contrast is mainly computed across the boundary between the regions that share the terminated edge of the T-junction (e.g., white and gray regions to the left; Moulden, B. and Kingdom, F., 1989; Todorovic, D., 1997).

Three-dimensional interpretation of the scene or tranparency also strongly influence on the lightness perception (Gilchrist, A. L., 1977; Adelson, E. H., 1993; Anderson, B. L. and Winawer, J., 2005). Gilchrist A. L. (1977) has shown by using a stimulus configuration shown in Figure 3(a), that luminance contrast is computed between regions on the same depth plane. In his setup, the horizontal plane contained a large white square and a small black trapezoidal tab that extended outward toward the subject. The vertical plane contained a large black square and a small white tab that extended upward. When the subject looked at the scene through a small hole, the scene looked like the one shown in Figure 3(b), and the right tab appeared to be on the same plane as the large white surface, and the left tab appeared to be on the same plane as the large black surface. In this situation, the right tab looked black, and the left tab looked white. In contrast, when the subject saw the scene binocularly, the three-dimensional structure of the scene was correctly perceived, and the right tab looked white and the left tab looked black. This result indicates that surface lightness perception is not determined by the surface luminance or the contrast on the retinal image, instead, it

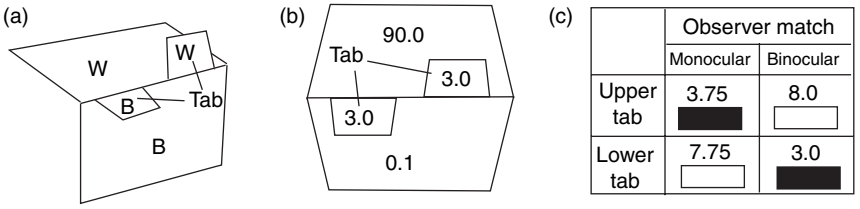

Figure 3 An experiment by Gilchrist A. L. (1977) that showed the three-dimensional perception of the scene strongly influences lightness perception. (a) Configuration of the stimulus used (B, black; W, white). (b) Monocular image of the scene with luminance of each region in foot-lamberts. (c) Average match of two tabs with Munsell swatch in monocular and binocular conditions. Adapted from Gilchrist, A. 1977. Perceived lightness depends on perceived spatial arrangement. Science 195, 185–187.

is determined after or at least in parallel with the analysis of depth structure of the scene or segmentation/grouping of the scene.

2.04.2 Neural Mechanisms of Brightness/Lightness Perception

Retinal ganglion cells and neurons in the lateral geniculate nucleus (LGN) have receptive fields with concentric center-surround organization. As a result of imbalance between the center and surround, these neurons can transmit luminance signals at low spatial frequency to the primary visual cortex (V1). These neurons include ON-type that increase the activity when the light intensity increases and OFF-type that decrease the activity. In V1, many neurons have orientation selectivity and respond well to the contrast at the border of the surface region, and they encode the magnitude of the contrast and some of them also encode the polarity of the contrast. A minority of V1 neurons respond to a uniform surface that covers the receptive field (surface-responsive neuron) and can transmit the information of the luminance of the surface. Thus, if we consider the population activity of V1 neurons, when we see a uniform surface, strong activity occurs at the position corresponding to the edge of the surface, and weak activity extends across the region corresponding to the interior of the surface (Friedman, H. S. *et al.*, 2003).

With regard to lightness perception, the properties of surface-responsive neurons are of particular interest because these neurons must carry signals concerning the visual attributes of the surface. Surface-responsive neurons include cells whose activity increases monotonically with either the increase or decrease of the surface luminance (Kayama, Y. *et al.*, 1979; Kinoshita, M. and Komatsu, H., 2001). Figure 4(a) shows an example of a surface-responsive V1 neuron that showed response increase with an increase in the surface luminance. It is also reported recently that some of surface-responsive neurons maximally responded at intermediate luminance (Peng, X. and Van Essen, D. C., 2005).

As was described in the previous section, perceived brightness/lightness of a surface region depends on the luminance contrast with the surrounding region. It has been shown that the responses of many surface-responsive neurons are modulated by changing the luminance of the surrounding region. Figure 4(b) shows the responses of the same neuron as in Figure 4(a) when the luminance of the surrounding annulus was changed while the luminance of the surface covering the receptive field was kept constant. Although the surrounding annulus is sufficiently away from the receptive field, the response of this neuron changed depending on the luminance of the annulus. The response change occurred in the direction consistent with the brightness induction. That is, this neuron increased activity with the luminance of the surface covering the receptive field increased (Figure 4(a)), and when the luminance of the surrounding annulus decreased (Figure 4(b)). In both cases, the perceived surface brightness on the receptive field increased. About two-thirds of the surface-responsive neurons studied by Kinoshita M. and Komatsu H. (2001) were influenced by the luminance of the surrounding annulus away from the receptive field, and about half of these showed responses that can qualitatively account for the brightness induction.

Paradiso and colleagues have shown that V1 neurons in cats exhibit response change when the luminance of the surround was temporally modulated while the luminance of the surface covering the receptive field was kept constant (Rossi, A. F. *et al.*, 1996; Rossi, A. F. and Paradiso, M. A., 1999). The same neurons also responded when the

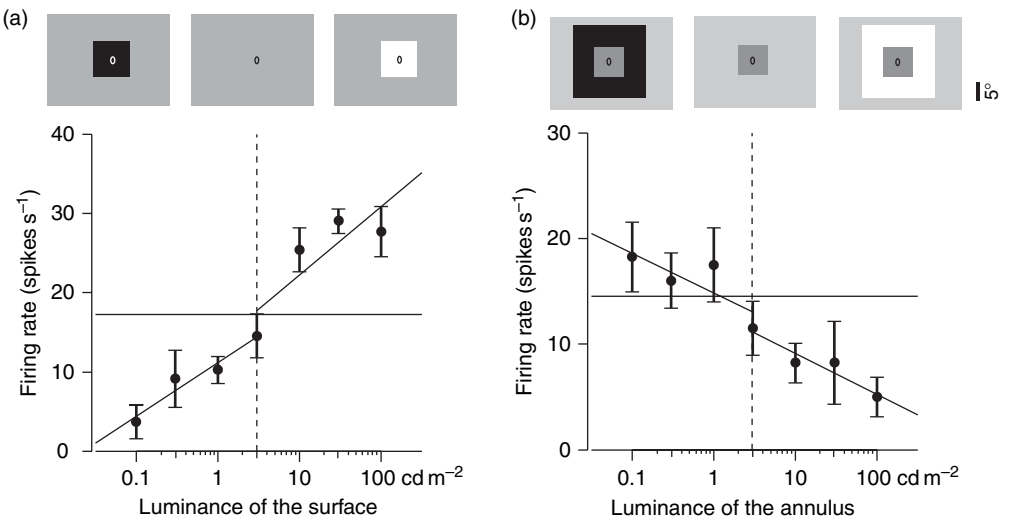

Figure 4 Responses of a surface-responsive V1 neuron when the luminance of the surface covering the receptive field (a) or the annulus apart from the receptive field (b) was changed. Schematic illustration of the stimulus is shown at the top, and a small oval is the receptive field. Adapted from Kinoshita, M. and Komatsu, H. 2001. Neural representation of the luminance and brightness of a uniform surface in the macaque primary visual cortex. J. Neurophysiol. 86, 2559–2570, used with permission.

luminance of the surface covering the receptive field was temporally modulated. In many neurons, the response change in these two conditions occurred in the opposite phase, but in both cases, it corresponded to the temporal change in the perceived brightness of the surface covering the receptive field. Even more interestingly, when the temporal frequency of the luminance change was increased, the response peaked at about 1 Hz and then decreased for the faster modulation of the surround luminance, whereas the responses still increased when the luminance of the surface covering the receptive field was modulated in higher temporal frequency. This is consistent with the lower cut-off in the brightness induction observed in psychophysical experiments (De Valois, R. L. *et al.*, 1986; Rossi, A. F. and Paradiso, M. A., 1996). These results indicate that response properties of some V1 neurons closely correlate with brightness induction. The same authors also conducted a similar test in LGN and the optic tract fibers, and found that only a few LGN neurons and no optic tract fibers correlated with the perceived brightness (Rossi, A. F. and Paradiso, M. A., 1999). This indicates that V1 is the first place where lateral interaction necessary for brightness induction takes place. In contrast, as is described in the previous section, various factors more complicated than the computation of luminance ratio between the neighboring regions is involved in the lightness perception, and neural processes related to such higher order computation have not been studied yet. In recent years, many studies have shown that responses of early visual areas such as V1 and V2 are influenced by higher order structure of the image such as the figure-ground organization or the three-dimensional structure of the scene (Zipser, K. *et al.*, 1996; Sugita, Y., 1999; Bakin, J. S. *et al.*, 2000; Zhou, H. *et al.*, 2000). We can conceive that this higher order information is combined with the simpler luminance and contrast information, and activities that can account for the complex properties of brightness/lightness perception are generated.

2.04.3 Perceptual Filling-In

As described above, perceived brightness of a region in the visual field is strongly influenced by the contrast at the edge of the region. It is important to realize that contrast information does not localize at the edge, instead it spreads across the entire region and influences the perceived brightness of the region. This fact can be clearly demonstrated by the Craik–O'Brien–Cornsweet illusion (Cornsweet, T., 1970) as shown in Figure 5. The luminance profile across this figure is shown at the bottom. It contains a sharp luminance change at two edges, one at the left one-third and the other at the right one-third of the figure where a large

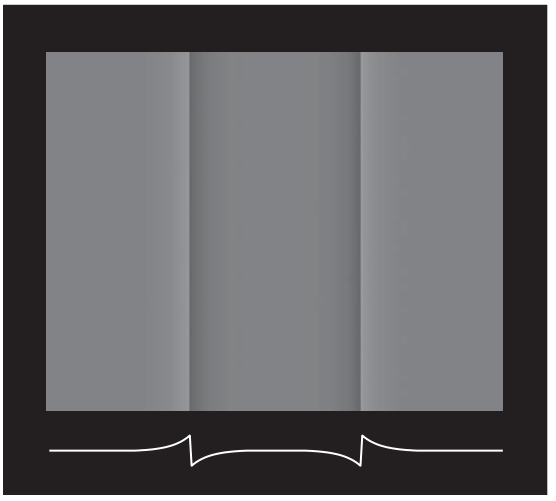

Figure 5 Craik–O'Brien–Cornsweet illusion. The luminance profile is shown below. There appears a wide dark band at the middle part although the luminances at the center & both right and left ends are the same.

contrast signal is generated in the cortex. At both sides of either edge, the luminance change is more gradual and the resulting contrast signal should be much weaker. The luminance at both ends of this figure is the same as that at the center of the figure, but the center looks much darker than the ends. This is because the contrast signal detected at the edges spreads across the regions at either side of the edges, and affects the perceived brightness of the regions.

Perceptual phenomenon like this is called filling-in, in which visual features, such as color, brightness, texture, and motion of the surrounding area are perceived in a certain part of the visual field even though these features are not physically present. The Craik–O'Brien–Cornsweet illusion demonstrates that at least two separate processes, one a contrast detection, the other a filling-in, operates as the underlying mechanisms for brightness perception to occur. In an ordinary situation in which visual stimulus physically exists, in addition to these two sorts of information, luminance information generated by the stimulus itself must be also taken into account as described in the previous section.

Perceptual filling-in is observed in various situations (Pessoa, L. *et al.*, 1998; Komatsu, H., 2006). One situation is when some regions of the visual field lack visual inputs because of an innate structure of the retina (blind spot) or circumscribed damage to some part of the retina or the visual system (scotoma). Even though there are no visual inputs within these regions in the visual field, we perceive as if the same visual features as the surrounding visual field exist within these regions. The second situation is when the contrast signal at the edge of an object is reduced as a result of steady fixation (Troxler effect) or stabilization of the retinal image. When this happens, the part of the visual field originally occupied by the object is filled-in with the visual features of the surround. Filling-in also occurs in certain figures without a need of prolonged fixation. One example of such illusion is the neon color spreading in which faint color spreads across a region enclosed by an illusory figures. Another example of filling-in that occurs without prolonged fixation is the Craik–O'Brien–Cornsweet illusion.

Filling-in should be considered as an essential part of normal surface perception rather than a special phenomenon. Paradiso M. A. and Nakayama K. (1991) demonstrated this by examining the spatiotemporal properties of masking of brightness perception. In their experiments, a large uniform disk was followed by a small mask such as a ring after a short interval of time (50–100 ms of stimulus-onset asynchorony). Suppression of the brightness occurred inside the mask where the brightness of the disk was blocked and that of the background was perceived. The latest time at which masking was effective was correlated with the distance between the edge of the disk stimulus and the contour of the mask. These results suggest that some process of filling-in occurs even when we see a uniform surface in the normal visual field.

Because filling-in requires lateral spread of visual information across a wide area in the visual field, horizontal connections in the visual cortex or feedback connection from higher areas to lower areas are thought to be responsible for filling-in. It should be noted, however, that filling-in includes processes more complicated than simple lateral spread of visual information. For example, Nakayama, K. *et al.*, (1990) have shown that neon-color spreading is strongly influenced by three-dimensional structure of the scene. Therefore, it may not be surprising that brightness/lightness perception is influenced by a higher order structure of the image if we consider that filling-in is critically involved in the underlying processes for brightness/lightness perception.

2.04.4 Neural Mechanisms of Filling-In

Mechanisms of filling-in are not well understood. Different types of filling-in may have different

underlying mechanisms. One extreme possibility is that visual system simply ignores the lack of information at a certain region in the visual field, and filling-in is a passive outcome of this. However, various observations suggest that some active processes are involved in the occurrence of filling-in. For example, it has been shown that removal of a stimulus that induced filling-in evokes an afterimage or aftereffect of the filled-in attributes (Ramachandran, V. S. and Gregory, R. L., 1991; Murakami, I., 1995). Without some active process, it is hard to understand why these events happen.

In recent years, attempts to study neural mechanisms of filling-in have been made, and neuron recordings from monkey visual cortex and functional magnetic resonance imaging (fMRI) experiments in human visual cortex were conducted. These experiments have employed a common strategy: they examined whether neurons are activated in the region of the retinotopic map of early visual areas that represented the interior of the surface where filling-in occurred. As described in the previous section, it is very likely that filling-in commonly occurs when we see an ordinary visual object in everyday life. However, in such an ordinary situation, it is hard to dissociate neuron activities evoked by the visual features present within the contour of object and those evoked by the lateral spread of contrast detected at the contour. In contrast, for the case of filling-in phenomena, neuron activities due to the lateral spread can be isolated because no visual features exist within the region under investigation. This strategy is conceptually the same as the one used to study neural representation of illusory contour; it has been shown that neurons in area V2 of monkey visual cortex are activated when illusory contour is perceived across the receptive field even though no contour is physically present (von der Heydt, R. *et al.*, 1984).

Several studies have been conducted to record neuronal activities related to filling-in at the blind spot (Fiorani, M. *et al.*, 1992; Komatsu, H. *et al.*, 2000; Matsumoto, M. and Komatsu, H., 2005). In monocular viewing, if the blind spot of the opened eye is covered by a surface with uniform color and brightness, the same color and brightness is perceived to fill in the blind spot even though there is no visual input in the blind spot (filling-in at the blind spot). Likewise, if a bar stimulus is presented across the blind spot, a complete bar is perceived (completion). It has been shown that, in these situations, some neurons located at the deep layer of V1 region that represented the visual field corresponding to the blind spot are activated. Response properties of these neurons are shown to be consistent with the characteristics of filling-in and completion at the blind spot. As there is no retinal input to this region in V1, neuron activities observed in these studies must be generated as a result of the lateral spread from the surrounding region. Neural responses related to the Craik–O'Brien–Cornsweet illusion were recorded by Roe A. W. and colleagues (2005). They examined neuron activities from the region corresponding to the visual field where brightness was induced, and found that neurons in the thin stripe of area V2 are activated. Neural responses related to the filling-in of dynamic texture stimulus within an empty region were examined by De Weerd, P. *et al.* (1995). They found that neurons in areas V2/V3 of monkeys having receptive fields in the empty region gradually increased activities with a time course similar to the occurrence of filling-in by the same stimulus in human subjects. These experiments show the possibility that lateral spread of neuron activities across the early visual areas such as V1, V2, or V3 are involved in the occurrence of these filling-in phenomena. In contrast, von der Heydt R. *et al.* (2003) failed to find neuron activities associated with the occurrence of filling-in of the Troxler effect in either V1 or V2.

Two different ideas about the neural mechanisms of filling-in have been proposed (Pessoa, L. *et al.*, 1998; Komatsu, H., 2006). One is the symbolic (or cognitive) theory. According to this theory, only the contrast information at the object contour is detected in the early visual area, and in the higher area, when object image is reconstructed based on this information, color and brightness at the interior of object are assigned. Another theory is the isomorphic theory. This theory assumes that two-dimensional array of feature sensitive neurons are activated in the early visual area are as a result of lateral spread of contrast signals detected at the border, and color and brightness at the interior of the object are represented by the activities of these neurons. The experiments described above suggest that, for some filling-in phenomena such as the Craik–O'Brien–Cornsweet illusion and texture filling-in, neuron activities occur in the visual areas as early as V2 in a manner consistent with the isomorphic theory. In contrast, the results of neural recordings about the Troxler effect is more consistent with the symbolic theory. With regard to the filling-in at the blind spot, the results appears not entirely consistent with either of

the above two theories because neural activation in V1 was observed mainly in deep layers. As an alternative possibility, Komatsu H. (2006) suggested that selective activation of neurons in deep layers of V1 that represent a particular spatial scale and that are sensitive to particular features may be important for filling-in at the blind spot.

Human fMRI experiments have also been conducted recently to study neuron activities related to filling-in. Studies examining filling-in at the blind spot (Tong, F. and Engel, S. A., 2001), neon-color spreading (Sasaki, Y. and Watanabe, T., 2004), and visual phantom illusion (Meng, M. *et al*., 2005) found activities related to filling-in in V1 region corresponding to the visual filed where filling-in occurred. In contrast, a study examining the Craik–O'Brien–Cornsweet illusion (Perna, A. *et al*., 2005) has observed activation only in higher visual areas.

Evidence is still too premature to identify precise neural mechanisms of filling-in, but observation of neural activities related to filling-in in early visual areas suggest that it is promising to study the functioning of neural networks in the early visual areas. At the same time, it should be noted that higher-order information strongly influences the filling-in, and neural interactions between higher and lower areas must be an important question to be pursued.

References

Adelson, E. H. 1993. Perceptual organization and the judgement of brightness. Science 262, 2042–2044.

Anderson, B. L. and Winawer, J. 2005. Image segmentation and lightness perception. Nature 434, 79–83.

Bakin, J. S., Nakayama, K., and Gilbert, C. D. 2000. Visual responses in monkey areas V1 and V2 to three-dimensional surface configurations. J. Neurosci. 20, 8188–8198.

Cornsweet, T. 1970. Visual Perception. Academic Press.

De Valois, R. L., Webster, M. A., De Valois, K. K., and Lingelbach, B. 1986. Temporal properties of brightness and color induction. Vision Res. 26, 887–897.

De Weerd, P., Gattass, R., Desimone, R., and Ungerleider, L. G. 1995. Responses of cells in monkey visual cortex during perceptual filling-in of an artificial scotoma. Nature 377, 731–734.

Fiorani, M. , Rosa, M. G. P., Gattas, R., and Rocha-Miranda, C. E. 1992. Dynamic surrounds of receptive fields in primate striate cortex: a physiological basis for perceptual completion?. Proc. Natl. Acad. Sci. U.S.A. 89, 8547–8551.

Friedman, H. S., Zhou, H., and von der Heydt, R. 2003. The coding of uniform colour figures in monkey visual cortex. J. Physiol. 548, 593–613.

Gilchrist, A., Kossyfidis, C., Bonato, E., Agostini, T., Cataliotti, J., Li, X., Spehar, B., Annan, V., and Economou, E. 1999. An anchoring theory of lightness perception. Psychol. Rev. 106, 795–834.

Gilchrist, A. L. 1977. Perceived lightness depends on perceived spatial arrangement. Science 195, 185–187.

Kayama, Y., Riso, R. R., Bartlett, J. R., and Doty, R. W. 1979. Luxotonic responses of units in macaque striate cortex. J. Neurophysiol. 42, 1495–1517.

Kinoshita, M. and Komatsu, H. 2001. Neural representation of the luminance and brightness of a uniform surface in the macaque primary visual cortex. J. Neurophysiol. 86, 2559–2570.

Komatsu, H. 2006. The neural mechanisms of perceptual filling-in. Nat. Rev. Neurosci. 7, 220–231.

Komatsu, H., Kinoshita, M., and Murakami, I. 2000. Neural responses in the retinotopic representation of the blind spot in the macaque V1 to stimuli for perceptual filling-in. J. Neurosci. 20, 9310–9319.

Matsumoto, M. and Komatsu, H. 2005. Neural responses in the macaque v1 to bar stimuli with various lengths presented on the blind spot. J. Neurophysiol. 93, 2374–2387.

Meng, M., Remus, D. A., and Tong, F. 2005. Filling-in of visual phantoms in the human brain. Nat. Neurosci. 8, 1248–1254.

Moulden, B. and Kingdom, F. 1989. White's effect: a dual mechanism. Vision Res. 29, 1245–1259.

Murakami, I. 1995. Motion aftereffect after monocular adaptation to filled-in motion at the blind spot. Vision Res. 35, 1041–1045.

Nakayama, K., Shimojo, S., and Ramachandran, V. S. 1990. Transparency: relation to depth, subjective contours, luminance, and neon color spreading. Perception 19, 497–513.

Paradiso, M. A. and Nakayama, K. 1991. Brightness perception and filling-in. Vision Res. 31, 1221–1236.

Peng, X. and Van Essen, D. C. 2005. Peaked encoding of relative luminance in macaque areas V1 and V2. J. Neurophysiol. 93, 1620–1632.

Perna, A., Tosetti, M., Montanaro, D., and Morrone, M. C. 2005. Neuronal mechanisms for illusory brightness perception in humans. Neuron 47, 645–651.

Pessoa, L., Thompson, E., and Noe, A. 1998. Finding out about filling-in: a guide to perceptual completion for visual science and the philosophy of perception. Behav. Brain Sci. 21, 723–748; discussion 748–802.

Ramachandran, V. S. and Gregory, R. L. 1991. Perceptual filling in of artificially induced scotomas in human vision. Nature 350, 699–702.

Roe, A. W., Lu, H. D., and Hung, C. P. 2005. Cortical processing of a brightness illusion. Proc. Natl. Acad. Sci. U.S.A. 102, 3869–3874.

Rossi, A. F. and Paradiso, M. A. 1996. Temporal limits of brightness induction and mechanisms of brightness perception. Vision Res. 36, 1391–1398.

Rossi, A. E. and Paradiso, M. A. 1999. Neural correlates of perceived brightness in the retina, lateral geniculate nucleus, and striate cortex. J. Neurosci. 19, 6145–6156.

Rossi, A. F., Rittenhouse, C. D., and Paradiso, M. A. 1996. The representation of brightness in primary visual cortex. Science 273, 1104–1107.

Sasaki, Y. and Watanabe, T. 2004. The primary visual cortex fills in color. Proc. Natl. Acad. Sci. U.S.A. 101, 18251–18256.

Sugita, Y. 1999. Grouping of image fragments in primary visual cortex. Nature 401, 269–272.

Todorovic, D. 1997. Lightness and junctions. Perception 26, 379–394.

Tong, F. and Engel, S. A. 2001. Interocular rivalry revealed in the human cortical blind-spot representation. Nature 411, 195–199.

von der Heydt, R., Peterhans, E., and Baumgartner, G. 1984. Illusory contours and cortical neuron responses. Science 224, 1260–1262.

von der Heydt, R., Friedman, H., and Zhou, H. 2003. Searching for the Neural Mechanisms of Color Filling-in. In: *Filling-in*

(eds. L. Pessoa and P. De Weerd), pp. 106–127. Oxford Univ Press.
Wallach, H. 1948. Brightness constancy and the nature of achromatic colors. J. Exp. Psychol. 38, 310–324.
White, M. 1979. A new effect of pattern on perceived lightness. Perception 8, 413–416.
Yund, E. W. and Armington, J. C. 1975. Color and brightness contrast effects as a function of spatial variables. Vision Res. 15, 917–929.
Zhou, H., Friedman, H. S., and von der Heydt, R. 2000. Coding of border ownership in monkey visual cortex. J Neurosci. 20, 6594–6611.
Zipser, K., Lamme, V. A. F., and Schiller, P. H. 1996. Contextual modulation in primary visual cortex. J. Neurosci. 15, 7376–7389.

Further Reading

Adelson, E. H. 2000. Lightness Perception and Lightness Illusion. In: *The New Cognitive Neuroscience (ed*. M. S. Gazzaniga), 2nd edn., pp. 339–351. MIT Press.

2.05 Nocturnal Vision

E Warrant, University of Lund, Lund, Sweden

© 2008 Elsevier Inc. All rights reserved.

2.05.1	**Introduction**	54
2.05.2	**What Is a Nocturnal Lifestyle?**	55
2.05.3	**Nocturnal Visual Scenes**	55
2.05.3.1	Light Intensity	55
2.05.3.2	Light Spectrum	56
2.05.3.3	Polarization	57
2.05.4	**Noise and the Reliability of Vision in Dim Light**	57
2.05.4.1	Sources of Visual Noise	57
2.05.4.2	A Trade-Off between Resolution and Sensitivity	58
2.05.5	**The Designs of Eyes and Their Sensitivity to Extended Scenes**	59
2.05.5.1	The Eyes of Arthropods and Vertebrates	59
2.05.5.2	The Optical Sensitivity of Eyes to Extended Scenes	60
2.05.6	**Vision and Visual Behavior in Nocturnal Arthropods**	60
2.05.6.1	Optical Adaptations for Increased Sensitivity in Arthropods	61
2.05.6.1.1	Spider camera eyes	61
2.05.6.1.2	Insect compound eyes	63
2.05.6.2	Neural Adaptations for Increased Sensitivity in Arthropods	64
2.05.6.2.1	Signal transduction in nocturnal arthropod photoreceptors	64
2.05.6.2.2	Spatial and temporal summation	65
2.05.6.3	Visual Behavior in Nocturnal Arthropods	67
2.05.6.3.1	Nocturnal navigation and homing	68
2.05.6.3.2	Nocturnal color vision	70
2.05.7	**Vision and Visual Behavior in Nocturnal Birds and Primates**	71
2.05.7.1	Optical Adaptations for Increased Sensitivity	72
2.05.7.2	Neural Adaptations for Increased Sensitivity	74
2.05.7.3	Visual Behavior in Nocturnal Birds and Primates	77
2.05.7.3.1	Vision versus other senses at night	77
2.05.7.3.2	Visual performance in dim light	78
2.05.7.3.3	Visually guided prey capture, locomotion, and navigation	80
2.05.8	**Conclusions**	82
References		82

Glossary

A Diameter of the aperture (pupil) (μm)
d Photoreceptor diameter (μm)
f Focal length (μm)
H Maximum spatial information capacity of the eye (bits sr^{-1})
i Number of discriminable intensity levels
I (λ) Quantal intensity of a natural radiance spectrum (photons nm^{-1})
k Absorption coefficient of the photoreceptor (μm^{-1})
l Photoreceptor length (μm)
L Ambient light intensity (photons μm^{-2} s^{-1} sr^{-1})
N Number of photons absorbed by a photoreceptor during one visual integration time (photons)
p Density of visual channels (channels μm^{-2})
R (λ) Normalized visual pigment absorption spectrum (nm^{-1})
S Optical sensitivity of the eye (μm^2 sr)
v Flight angular velocity (deg s^{-1})
w Minimum visible width of a black stripe (arc min)
Δt Visual integration time (s)
$\Delta\rho$ Acceptance angle (°)
κ Quantum efficiency of transduction

λ Wavelength of light (nm)
λ_1, λ_2 Wavelength limits for the integration in eqn [3] (nm)
ν Spatial frequency (cycles deg^{-1})
ν_{max} Maximum detectable spatial frequency (cycles deg^{-1})
τ Transmission of the eye's optics

2.05.1 Introduction

For day-active (or diurnal) animals, like ourselves, the visual sense is of paramount importance for orientation, food gathering, and the pursuit of suitable mates. This is hardly surprising since vision during the day is at its most reliable: the abundance of light enables diurnal visual systems to accurately code light intensity contrasts, the nuances of color, and, for those animals that can see it, the plane of polarized light. These reliable signals, in turn, allow diurnal animals a rich visual experience of their habitat and their daily life within it. But what of the multitude of animal species that have most or all of their activity confined to dim light, either in the vast darkness of the deep sea or under the mantle of night? What role, if any, does vision play for these animals?

From the outset, it is important to point out that the nocturnal visual world is essentially identical to the diurnal visual world. The contrasts of objects are identical and so (or nearly so) are their colors (Figure 1). The only distinguishing difference is the mean level of light intensity, which can be up to 11 orders of magnitude dimmer at night. It is this difference that severely limits the ability of imaging devices, such as eyes, to distinguish the colors and contrasts of the nocturnal world. Indeed, many animals, especially diurnal animals, distinguish very little at all. This is because vision in dim light is inherently unreliable. Why is this so? The basic answer is that visual signals in dim light are contaminated by visual noise. Part of this noise arises from the stochastic nature of photon arrival and absorption: each sample of absorbed photons (or signal) has a certain degree of uncertainty (or noise) associated with it. The relative magnitude of this uncertainty is greater at lower rates of photon absorption, and these quantum fluctuations set an upper limit to the visual signal-to-noise ratio (SNR) (Rose, A., 1942; De Vries, H., 1943). As light levels fall, the fewer the number of photons that are absorbed, the greater the noise relative to the

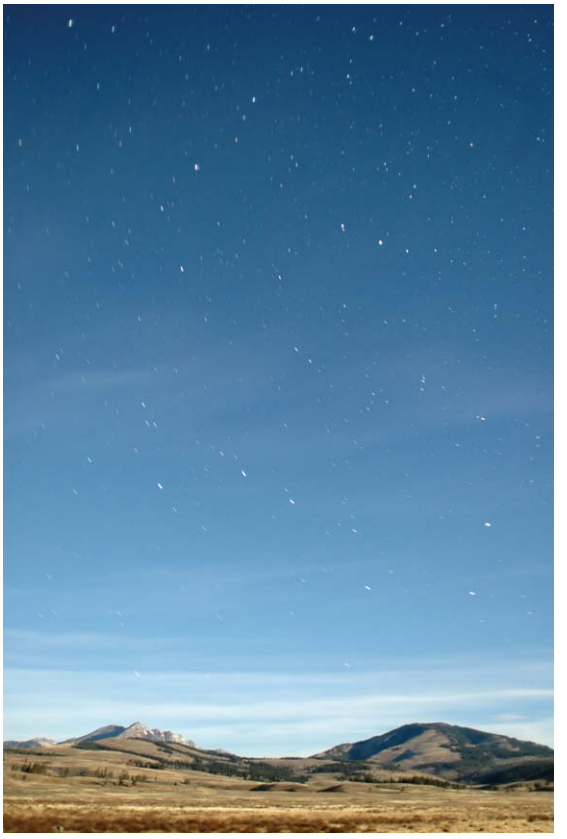

Figure 1 A nocturnal scene photographed with a long (148 s) exposure. This image was taken 3 h after sunset (20.34) on 18 October, 2005, in the northwestern part of Yellowstone National Park, looking north toward the Gallatin Mountain Range that lies between the Park and Bozeman, Montana. An almost full moon had recently risen on the eastern horizon. The scene appears as it would during the day (with the exception of the stars), because Rayleigh-scattered moonlight creates a blue sky and a similar illumination spectrum to sunlight (see Figure 3), only weaker (which the long camera exposure time integrates into a day-like image). Camera details: Nikon D70 digital SLR, Nikkor 20-mm lens, *f*/2.8, ISO 400. The image was very kindly supplied by Dr. Joseph A. Shaw of Montana State University and also appeared as part of a journal cover (Johnsen, S. *et al*., 2006).

signal and the less that can be seen. Signal reliability in dim light can thus be improved with an eye design of higher sensitivity to light.

It is now becoming apparent that the eyes of many nocturnal animals are indeed sufficiently sensitive to permit reliable vision in very dim light. Some animals even have sufficient visual sensitivity to distinguish colors, to detect faint movements, to learn visual landmarks, to orient to the faint polarization pattern produced by the moon, and to navigate using the constellations of stars in the sky. In this review, these impressive visual abilities, and the optical and neural strategies that animals have evolved to improve visual sensitivity, will be explored. Whereas other recent accounts have discussed nocturnal and deep-sea vision in general terms (Warrant, E. J. 2004; Warrant, E. J. and Locket, N. A., 2004; Warrant, E. J. 2006), here, for the sake of brevity, we concentrate on nocturnal vision and nocturnal visual behavior in two model animal groups, one vertebrate and one invertebrate: the birds and the arthropods. Even though most of our recent knowledge about nocturnal vision has been derived from these two groups, reference will also be made to other nocturnal animals (especially primates) where relevant. But before dealing with the animals themselves in detail, we will define what is meant by a nocturnal lifestyle and explore the illumination of nocturnal visual scenes.

2.05.2 What Is a Nocturnal Lifestyle?

For the purpose of answering this question, Martin G. R. (1990) very conveniently defined night as being the period of time between sunset and sunrise, and strictly nocturnal animals as those animals that execute all the waking activities of daily life during the same period of time. Thus, according to this definition, all animals that have only part of their waking activities during this period are not considered to be nocturnal, and this includes those active both night and day (referred to as cathemeral animals). In contrast, those active only for short periods of time during the dusk and dawn (i.e., crepuscular animals, including many species of dung beetles) are considered nocturnal. Despite being nocturnal, these animals may experience reasonably high light levels. As Martin carefully points out, this definition, whilst very convenient, does not imply anything about the light levels experienced by animals at night. As we will see below, even at one location and over a limited number of days, nocturnal light levels can vary over an enormous range. If one then adds the complications of latitude and time of year, then the variation is even greater: an animal in the polar summer experiences vastly brighter light levels at midnight than does an equatorial rainforest animal at the same longitude and moment in time.

Martin's definition of nocturnality is nonetheless very useful, and it is that which I adopt in this review: when discussing nocturnal vision, I will restrict my analysis to those species that are strictly nocturnal, that is, to those that carry out the waking activities of daily life entirely within the time interval between sunset and sunrise. I will nevertheless describe visual adaptations found in many diurnal species in order to highlight those found in nocturnal species.

2.05.3 Nocturnal Visual Scenes

2.05.3.1 Light Intensity

The intensity of light that reaches an eye in a natural setting depends on many factors (see Martin, G. R., 1990, for an excellent discussion). The first and most obvious of these is the time of day that the eye views the scene: at any one location, the transition from a bright sunny day to a clear night lit by a full moon brings with it a change in light intensity of around 5–6 orders of magnitude. If instead the night sky is clear and moonless, light levels are lower by a further 100 times (Lythgoe, J. N., 1979). Other factors that affect the intensity of natural light include the presence of clouds (which can reduce intensity by up to a factor of 10) and/or whether an animal is located under the closed canopy of a forest (which can reduce intensity by up to a factor of 100). Thus, the light intensity difference between an open sunny meadow on a clear summer day and the floor of a dense rainforest on a moonless and heavily overcast night could be up to 11 orders of magnitude (Martin, G. R., 1990; Figure 2). If we further use the Martin (1990) definition of night as the period of time between sunset and sunrise, then nocturnal light levels account for 8 of these 11 orders of magnitude. This clearly indicates that nocturnal animals (which in this definition also includes crepuscular animals) can experience an extremely wide range of light levels when compared with their diurnal relatives. As we shall see, this has led to the evolution of eyes that are specialized for different windows of nocturnal light intensity, with those adapted to dimmer light levels being considerably more sensitive.

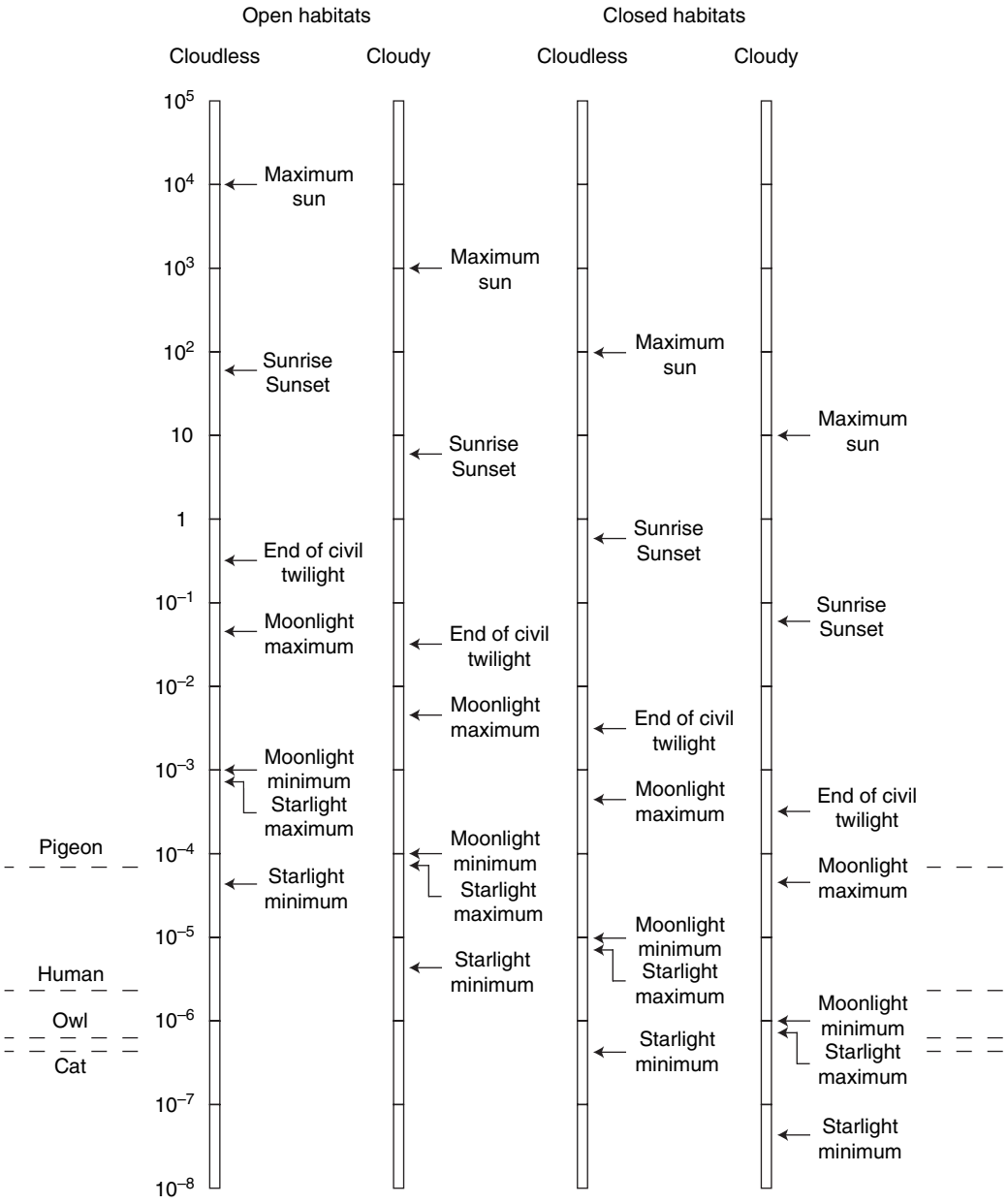

Figure 2 The luminance (in units of cd m^{-2}) of a natural substrate of leaf litter when illuminated by sunlight, moonlight, or starlight during cloudy and cloudless conditions. The luminance is shown for two habitat conditions: an open treeless field and beneath the closed canopy of a forest (which is considered here to reduce illumination by 100 times). Luminance is calculated assuming that the leaf litter substrate has an average reflectance of 25% and a fully overcast sky reduces illumination by a factor of 10. Dashed lines show absolute visual thresholds measured for pigeons, humans, tawny owls, and cats. Civil twilight is defined as the period during which the sun's disk is between the horizon and 6° below the horizon. Adapted with kind permission from Martin, G.R. 1990. Birds by Night. T. & A.D. Poyser.

2.05.3.2 Light Spectrum

Sunlight – the major source of light on earth – illuminates either directly, as during the day, or indirectly by reflection from the moon at night. The spectra of sunlight and moonlight, and the colors of objects seen under the two illuminations, are thus similar (Figure 3). However, on moonless starlit nights the spectrum is significantly red-shifted, a phenomenon that has implications for color vision at night (Johnsen, S. *et al.*, 2006).

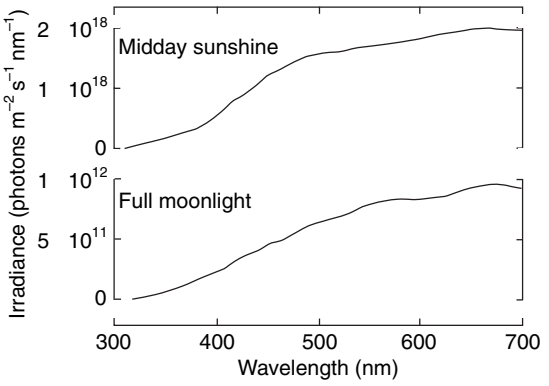

Figure 3 The irradiance spectra of sunlight and moonlight. The two spectra are similar, but moonlight is about a million times dimmer. Adapted from data given in Moon P. (1940) and Lythgoe J. N. (1979). From Warrant, E.J. 2004. Vision in the dimmest habitats on earth. J. Comp. Physiol. A. 190, 765–789.

2.05.3.3 Polarization

Due to the scattering of sunlight from particles in the atmosphere, the dome of the sky contains a circular pattern of polarized light centered on the sun, a pattern that many animals, especially invertebrates, are able to see and to use as a navigational compass cue. Within this pattern, the degree of polarization is greatest for light emitted from regions of the sky lying on a circular locus 90° from the sun (for review, see Waterman, T. H., 1981; Wehner, R., 1981), and the pattern moves with the sun during the course of the day. At sunset (or sunrise), when the sun is at the horizon, the polarization pattern is very simple, with the full sky emitting light polarized in a single direction. The degree of polarization is greatest across the zenith of the sky, up to 85% (Waterman, T. H., 1981; Cronin, T. W. *et al.*, 2006), the highest value attained during the day. Once the sun slips below the horizon, the degree of polarization declines, reaching negligible values at astronomical twilight when the sun is 18° below the horizon (Rozenberg, G. V., 1966).

For identical reasons, light from the moon also produces a circular pattern of polarized light, a fact we did not appreciate until recently (Gál, J. *et al.*, 2001). Apart from its intensity – which is a million times dimmer – the pattern of polarized light formed around the full moon is identical in structure to that formed around the sun. When the moon is in its first or last quarter, the pattern's intensity is a further 10 times dimmer.

2.05.4 Noise and the Reliability of Vision in Dim Light

2.05.4.1 Sources of Visual Noise

The greatest challenge for an eye that views a dimly illuminated scene is to absorb sufficient photons of light to reliably discriminate it (Laughlin, S. B., 1990). Because the arrival and absorption of photons is stochastic (and governed by Poisson statistics), quantum fluctuations set an upper limit to the visual SNR (Rose, A., 1942; De Vries, H., 1943). If we say that a photoreceptor absorbs N photons during one visual integration time, then it will experience an uncertainty – or photon shot noise – of $\sqrt{N}$ photons associated with this sample, that is, $N \pm \sqrt{N}$ photons (Rose, A., 1942; De Vries, H., 1943; Land, M. F., 1981; Warrant, E. J. and McIntyre, P. D., 1993; Warrant, E. J., 2004; 2006). This noise reduces the reliability of intensity discriminations and thereby the ability of the eye to distinguish contrast details in a scene. The SNR ($N/\sqrt{N} = \sqrt{N}$) thus improves with increasing photon catch, implying that photon shot noise, and contrast discrimination, is worse at lower light levels. This is the famous Rose–de Vries or square root law of visual detection at low light levels: the visual SNR, and thus contrast discrimination, improves as the square root of photon catch. As we shall see below, the eyes of nocturnal animals are usually adapted to capturing and absorbing as many photons as possible, thereby maximizing this SNR.

In addition to this external or extrinsic source of noise, there are also two internal or intrinsic sources of noise that further degrade visual discrimination by photoreceptors in dim light. The first of these, referred to as transducer noise, arises because photoreceptors are incapable of producing an identical electrical response, of fixed amplitude, latency, and duration, to each (identical) photon of absorbed light. This source of noise, originating in the biochemical processes leading to signal amplification, degrades the reliability of vision (Lillywhite, P. G. and Laughlin, S. B., 1979; Lillywhite, P. G., 1981; Laughlin, S. B. and Lillywhite, P. G., 1982). The second source of intrinsic noise, referred to as dark noise, arises because the biochemical pathways responsible for transduction are occasionally activated – even in perfect darkness (Barlow, H. B., 1956). These activations are due either to spontaneous conversion of rhodopsin to metarhodopsin or to spontaneous activation of G-protein-coupled steps in the transduction chain. Irrespective of their origin,

these activations produce dark events, electrical responses that are indistinguishable from those produced by real photons, and these are more frequent at higher retinal temperatures. At very low light levels, this dark noise can significantly contaminate visual signals. In insects and crustaceans, dark events are rare, only around 10 every hour at 25 °C (Lillywhite, P. G. and Laughlin, S. B., 1979; Dubs, A. *et al.*, 1981; Doujak, F. E., 1985). But in nocturnal toad rods, the rate is much higher – 360 per hour at 20 °C (Baylor, D. A. *et al.*, 1980) – and this sets the ultimate limit to visual sensitivity (Aho, A.-C. *et al.*, 1988; 1993).

2.05.4.2 A Trade-Off between Resolution and Sensitivity

Like the pixels of a digital camera, the density of detectors in an eye sets the finest spatial detail that can be reconstructed: more densely packed detectors can reconstruct finer details. This, however, is only true if the signals generated in neighboring detectors are significantly different. For a given eye radius, a greater density of smaller detectors means that each detector receives a smaller fraction of the available photons, and as we saw above, fewer photons lead to a noisier signal and a less reliable measurement of intensity. This leads in turn to fewer reliable levels of response to changes in intensity and thereby poorer contrast discrimination. In this case, the signals generated in neighboring detectors may not be significantly different, and the contrast differences inherent in the finer details may therefore remain unresolved. Thus, even though a greater density of smaller detectors has the potential for higher spatial resolution, the detectors risk being too insensitive to achieve it. This becomes more and more true as light levels fall.

This trade-off between resolution and sensitivity is nicely quantified by asking how much information can be extracted from a visual scene, that is, how many different pictures can be reconstructed by a matrix of visual channels (Snyder, A. W. *et al.*, 1977a; 1997b)? If there are p visual channels per unit solid angle of visual field, and each channel is capable of distinguishing i levels of intensity, then the maximum number of pictures that can be reconstructed is simply i^p. The natural logarithm of this number is the maximum spatial information capacity H of the eye (Snyder, A. W. *et al.*, 1977a; 1997b):

$$H = \ln i^p = p \ln i \qquad [1]$$

Equation [1] shows that a high amount of information can be extracted from a bright scene: the number of discriminable intensity levels (i) and the density of visual channels (p) can both be large. But as light levels fall, so too does the quantity of light captured by each channel. This in turn leads to an increase in the relative magnitude of the noise and a decline in both the SNR and the number of intensity levels that the channel can discriminate. The information capacity falls accordingly. One way of offsetting this loss is to somehow increase the amount of light reaching each visual channel. A common strategy is to decrease the density of channels and to widen their receptive fields, that is, to exchange spatial sampling density (reduced p) for an improved number of discriminable intensity levels (increased i).

Eyes with fewer channels, each having wider receptive fields and greater sensitivity, are a common feature of animals active in dim light. As we shall see below, specialized neural circuits may even perform spatial summation, the sole purpose of which is to increase sensitivity by coupling visual channels together to produce larger effective channels of lower density (Snyder, A. W., 1977; Laughlin, S. B., 1981a; Srinivasan, M. V. *et al.*, 1982; Laughlin, S. B., 1990; van Hateren, J. H., 1993; Warrant, E. J., 1999). In many animals, the trade-off between sampling density and signal levels may alter according to the ambient light intensity. For instance, some arthropods dark adapt by widening their rhabdoms and/or shortening their focal lengths at night (Leggett, L. M. W. and Stavenga, D. G., 1981; Williams, D. S., 1982; 1983; Nilsson, D.-E., 1989), while others experience migrations of screening pigments within the eye that widen the receptive fields of photoreceptors at night and narrow them again during the day (Autrum, H., 1981; Nilsson, D.-E., 1989; Land, M. F. and Osorio, D. C., 1990; Stavenga, D. G., 2004a; 2004b).

An unavoidable consequence of sacrificing spatial sampling density to improve the number of discriminable intensity levels is that vision becomes coarser. Reliable contrast discrimination becomes confined to a decreasing range of coarser image details as light levels fall, with all finer spatial details drowned by noise. The same information arguments apply to the resolution of contrasts in time. If a single photoreceptor views a moving object, then the photoreceptor's response will rise and fall as brighter and darker details of the object pass through the visual field. As the object moves faster, the ability of the photoreceptor to reliably code these contrast details declines due to the photoreceptor's finite response

speed (Srinivasan, M. V. and Bernard, G. D., 1975): the response of the photoreceptor is eventually too slow to collect sufficient light to support reliable contrast discrimination. The problem worsens as ambient light levels fall. The sufficient amount of light can only be collected from progressively slower objects. To compensate, vision generally slows down. This increases the SNR and improves contrast discrimination by suppressing photon noise at temporal frequencies that are too high to be reliably resolved (van Hateren, J. H., 1993). Just as in the spatial domain, reliable temporal contrast discrimination becomes confined to a decreasing range of slower image details as light levels fall, with all faster details drowned by noise. In other words, in terms of both space and time, the effects of noise confine vision to image details that are increasingly slower and coarser.

2.05.5 The Designs of Eyes and Their Sensitivity to Extended Scenes

2.05.5.1 The Eyes of Arthropods and Vertebrates

As the discussion above implies, the eyes of nocturnal animals are adapted both optically and neurally to capture as much of the available light as possible, thereby maximizing the amount of information that can be extracted from a dim nocturnal scene. This is equally true of compound eyes as of camera eyes, the two main eye designs we will deal with in this review (Figure 4).

Camera eyes (Figure 4(a)) have a retina that receives an image formed by an overlying lens and cornea. This eye design is possessed by all vertebrates, and also by many invertebrates, including cephalopods (squid and octopus) and arachnids (e.g., spiders, scorpions, and camel spiders). As we shall see below, the camera eyes of nocturnal vertebrates and arthropods are proportionately large and possess wide pupils, adaptations that maximize photon capture.

Compound eyes (Figures 4(b) and 4(c)) are chief organs of vision in most insects and crustaceans, and two major forms can be distinguished: apposition compound eyes (Figure 4(b)) and superposition compound eyes (Figure 4(c)). In apposition compound eyes (Figure 4(b)), each ommatidium is isolated from its neighbors by a sleeve of light-absorbing screening pigment, thus preventing light reaching the photoreceptive rhabdom from all but its own small corneal lens. This tiny lens – typically a few tens of micrometers across – represents the pupil of the apposition eye, and not surprisingly, this eye design is typical of insects and crustaceans living in bright habitats. Remarkable exceptions do exist, including nocturnal mosquitoes (Land, M. F. *et al.* 1997; 1999) and the nocturnal tropical halictid bee *Megalopta genalis* that we will discuss below. It is, however, the superposition eyes (Figure 4(c)) that are better known for their high sensitivity. In this eye design, typical of nocturnal insects and deep-sea crustaceans, the pigment sleeve is withdrawn, and a wide optically transparent area, the clear zone (*cz* in Figure 4(c)), is interposed between the lenses and the retina. This clear zone – and specially modified crystalline cones – allows light from a narrow region of space to be collected by a large number of ommatidia (comprising the superposition aperture) and to be focused onto a

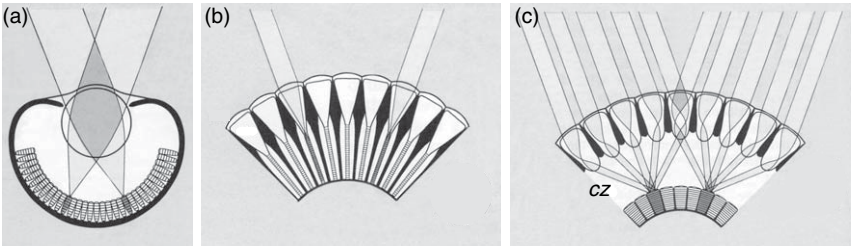

Figure 4 Three common eye designs. (a) A camera eye. Light is focused by the cornea (air only) and lens to form an image on the retina. (b) A focal apposition compound eye. Light reaches the photoreceptors exclusively from the small corneal lens located directly above. This eye design is typical of day-active insects. (c) A refracting superposition compound eye. A large number of corneal facets and bullet-shaped crystalline cones collect and focus light – across the clear zone of the eye (*cz*) – toward single photoreceptors in the retina. Several hundred, or even thousands, of facets service a single photoreceptor. Not surprisingly, many nocturnal arthropods have refracting superposition eyes, and benefit from the significant improvement in sensitivity. Courtesy of Dan-Eric Nilsson.

single rhabdom. Unlike the crystalline cones of most apposition eyes, those of superposition eyes have evolved refractive index gradients (in refracting superposition eyes), or reflecting surfaces (in reflecting superposition eyes), or a combination of both (in parabolic superposition eyes). These optical modifications allow as many as 2000 lenses to collect light for a single photoreceptor (as in some nocturnal moths). The width of this superposition aperture – which effectively acts as the pupil of the eye – is much larger than the width of a single corneal facet lens and represents a massive improvement in sensitivity.

2.05.5.2 The Optical Sensitivity of Eyes to Extended Scenes

The eyes of nocturnal animals, straining to see well in a dim extended world, are typically large relative to head size in order to maximize the area of the pupil and the sensitivity of the eye (Walls, G. L., 1942; Hughes, A., 1977). In addition to a large pupil, sensitivity to a dim extended scene is also improved by having visual channels with wide receptive fields. The wider the receptive field, the larger the region of the scene that the visual channel views, and the greater the number of photons it captures. Of course, spatial resolution is consequently compromised (Warrant, E. J. and McIntyre, P. D., 1992), but as we have implied above, this trade-off is typical of animals that view dim extended scenes.

These features of eyes are encapsulated in the Land sensitivity equation (Kirschfeld, K., 1974; Land, M. F., 1981), which describes the optical sensitivity S of an eye (in units of μm^2 sr) to an extended scene of broad spectral content (Warrant, E. J. and Nilsson, D.-E., 1998), as found in terrestrial habitats

$$S = \left(\frac{\pi}{4}\right)^2 A^2 \left(\frac{d}{f}\right)^2 \left(\frac{kl}{2.3 + kl}\right) \qquad [2]$$

Thus, good sensitivity to an extended scene results from a pupil of large area ($\pi A^2/4$), and photoreceptors each viewing a large solid angle ($\pi d^2/4f^2$ steradians) of visual space and absorbing a substantial fraction of the incident light ($kl/(2.3 + kl)$ for broad-spectrum light). Here A is the diameter of the pupil, f the focal length of the eye, and d and l the diameter and length of the photoreceptors, respectively. k is the peak absorption coefficient of the visual pigment. If all lengths have units of μm, then the unit of k is μm^{-1}. As recently pointed out by Stavenga D. G. (2003), the Land sensitivity equation, despite its great usefulness, does have some limitations, especially for photoreceptors behaving as waveguides and for certain eye designs of lower F-number.

A slightly more useful demonstration of sensitivity is to estimate the number of photons N that are absorbed by a photoreceptor from an extended scene during one integration time Δt. By calculating the number of absorbed photons, we can obtain an impression of the reliability of vision ($N \pm \sqrt{N}$), as well as the visual SNR ($\sqrt{N}$). N is obtained by multiplying the optical sensitivity of the eye S (μm^2 sr) with the intensity L (photons $\mu m^{-2} s^{-1} sr^{-1}$) of the light spectrum being viewed (Snyder, A. W., 1977; 1979; Warrant, E. J. and Nilsson, D.-E., 1998; Warrant, E. J., 1999; Kelber, A. *et al.*, 2002):

$$N = 1.13\left(\frac{\pi}{4}\right)\Delta\rho^2 A^2 \kappa \tau \Delta t \int \left(1 - e^{-kR(\lambda)l}\right) I(\lambda) d\lambda \qquad [3]$$

We have now replaced the solid angle of visual space viewed by a photoreceptor ($\pi d^2/4f^2$ steradians in eqn [2]) with the solid angular subtense of its (assumed) Gaussian receptive field ($\pi\Delta\rho^2/2.77 = 1.13\Delta\rho^2$, where $\Delta\rho$ is the angular half-width of the receptive field (or acceptance angle) in radians: Snyder, A. W., 1977; Laughlin, S. B. *et al.*, 1980). Other parameters in eqn [3] include the quantum efficiency of transduction κ and the transmission of the optics τ. The integral term describes the number of photons that will be absorbed by a photoreceptor viewing a radiance spectrum of quantal intensity $I(\lambda)$ with a resident visual pigment that has a normalized absorption spectrum $R(\lambda)$, where λ is wavelength. This integral is calculated between two wavelength limits: λ_1 and λ_2 (Warrant, E. J. and Nilsson, D.-E., 1998). λ_1 is set at 280 nm, the lowest wavelength likely to be seen by any animal (because the relative intensity of daylight below this wavelength is very low, and the internal structures of the eye absorb all wavelengths that are shorter). λ_2 is the wavelength at which the spectral sensitivity $R(\lambda)$ falls to 1% of its maximum at its long wavelength end. $R(\lambda)$ is given by the rhodopsin template of Stavenga D. G. *et al.* (1993). In this template, $\lambda_2 = 1.231\lambda_{max}$, where λ_{max} is the absorbance peak wavelength of the visual pigment.

2.05.6 Vision and Visual Behavior in Nocturnal Arthropods

The compound eyes and camera eyes of nocturnal arthropods – for example, insects, spiders, and crustaceans – are among the most sensitive found in the animal kingdom (Meyer-Rochow, V. B. and Nilsson,

H. L., 1998; Warrant, E. J., 2004; 2006). These eyes support an impressive repertoire of visual behaviors at night, including the ability to distinguish colors, to detect faint movements, to learn visual landmarks, to orient to the faint polarization pattern produced by the moon, and to navigate using the constellations of stars in the sky.

2.05.6.1 Optical Adaptations for Increased Sensitivity in Arthropods

As we discussed earlier (see Section 2.05.5.2), the optical structures of nocturnal eyes, irrespective of their type, are adapted for increased light capture in dim light. These adaptations are encapsulated in eqns [2] and [3]: larger eyes with larger pupils, having individual visual channels with large receptive fields, capture more of the available light. As we shall see, these are features of all nocturnal eyes, including arthropods.

2.05.6.1.1 Spider camera eyes

For their size, spiders have excellent vision, and many species – especially jumping spiders – have outstanding spatial resolution and the ability to distinguish color (Land, M. F., 1981; 1985). Their eyes are of the camera type, with well-developed corneal lenses that in many species can focus sharp aberration-free images on the underlying retina. This is also true of the large number of spiders with strict nocturnal activity, many of which are skillful visual hunters.

The nocturnal net-casting spider *Dinopis subrufus* is an excellent example (Figure 5(a); Blest, A. D. and Land, M. F., 1977). The posteromedial (PM) eyes of this formidable nocturnal hunter have lenses that can reach 1.4 mm in diameter, the largest known for a terrestrial arthropod, suggesting eyes with extreme sensitivity. This wide lens has a comparatively short focal length f, around 0.8 mm, which primarily improves sensitivity by widening the receptive fields of the visual channels (eqn [2]). The ratio of these two parameters – focal length f and lens diameter A – is frequently used to describe the light-gathering capacity of a lens. This ratio (f/A), known as the F-number, is also a useful and an easy metric for comparing the light-gathering capacities of different eyes (Warrant, E. J. and McIntyre, P. D., 1991), with a lower F-number indicating a brighter image (Table 1). *Dinopis* has an F-number of less than 0.6 (0.8/1.4), a much lower value than in the anteromedian (AM) eyes of the diurnal jumping spider *Phidippus johnsoni*, which have lenses of 0.38 mm diameter and an F-number of 2.0 (Land, M. F., 1981). The dark-adapted human eye has an

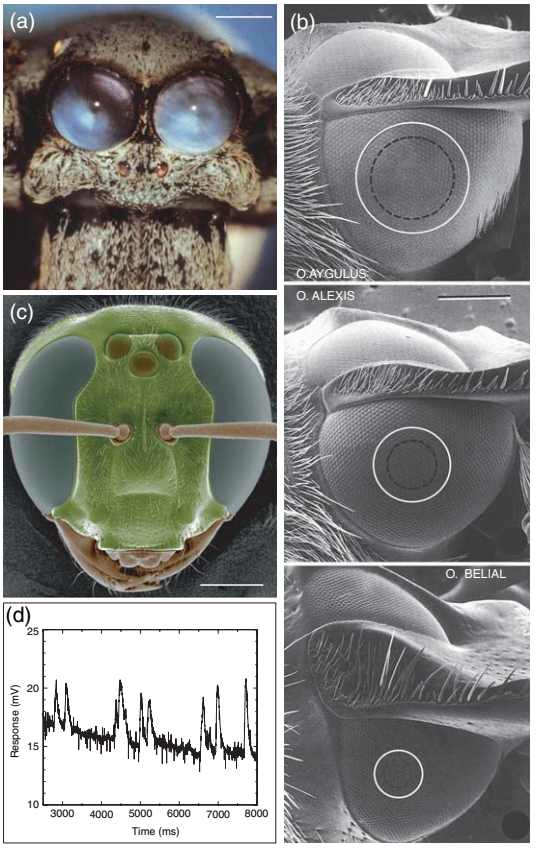

Figure 5 Nocturnal vision in arthropods. (a) The large posteromedial eyes of the nocturnal net-casting spider *Dinopis subrufus*, which have an F-number of 0.6. (b) The size of the superposition aperture in three species of onitine dung beetles: the nocturnal *Onitis aygulus* (upper panel), the crepuscular *Onitis alexis* (middle panel), and the diurnal *Onitis belial* (lower panel). The circular superposition aperture is indicated in white on the surface of each eye. The dashed circles refer to effective apertures, theoretically derived apertures in which each facet contributes light equally. In reality, facets near the edge of the aperture contribute less light than those near the center. Note how the superposition aperture is smaller in beetles from brighter habitats. (c) The head of the nocturnal halictid bee *Megalopta genalis* whose sensitive eyes allow them to forage at night. (d) Photoreceptor responses (bumps) to single photons of light in the nocturnal spider *Cupiennius salei*. Scale bar = 1 mm (a, c), 0.5 mm (a, d). (a) Adapted from Sinclair, S. 1985. How Animals See, Facts on File Publications. (b) From McIntyre, P.D. and Caveney, S. 1998. Superposition optics and the time of flight in onitine dung beetles. J. Comp. Physiol. A. 183, 45–60. (c) Scanning electron microscope image: Rita Wallén. (d) Pirhofer-Walzl, K., Barth, F.G., and Warrant, E.J. (in preparation).

F-number of around 2.1. Thus, the eyes of *Dinopis* are clearly constructed for high sensitivity.

The difference in optical sensitivity between these two spiders is not restricted to their lenses. Despite having similar focal lengths (~770 μm), their

Table 1 The *F*-numbers of eyes from nocturnal and diurnal animals

Species	*Animal*	*Activity*	*Eye*	*F-number*	*Reference*
Arthropods					
Dinopis subrufus	Net-casting spider	N	Cam[a]	0.58	1
Deilephila elpenor	Elephant hawkmoth	N	Sup	0.72	2
Ephestia kueniella	Meal moth	N	Sup	0.50	3
Onitis aygulus	Dung beetle	N	Sup	0.60	4
Megalopta genalis	Sweat bee	N	App	2.69	5
Phidippus johnsoni	Jumping spider	D	Cam[b]	2.02	6
Macroglossum stellatarum	Hummingbird hawkmoth	D	Sup[c]	0.70	7
Onitis belial	Dung beetle	D	Sup	1.09	4
Apis mellifera	European honeybee	D	App	3.30	5
Birds					
Elanus scriptus[d]	Letter-winged kite	N	Cam	0.98	8
Ninox novaeseelandiae[d]	Southern boobook owl	N	Cam	0.85	8
Speotyto cunicularia[d]	Burrowing owl	N	Cam	0.90	8
Tyto alba[d]	Barn owl	N	Cam	0.83	8
Strix aluco	Tawny owl	N	Cam	1.30	9
Strix aluco[e]	Tawny owl	N	Cam	0.78	10
Bubo virginianus[d]	Great horned owl	N/C	Cam	0.87	8
Nyctidromus albicollis[e]	Common pauraque	N/C	Cam	0.86	10
Charadrius wilsonia[e]	Wilson's plover	N	Cam	0.77	10
Steatornis caripensis	Oilbird	N	Cam	1.07	11
Steatornis caripensis[d]	Oilbird	N	Cam	0.86	8
Steatornis caripensis[e]	Oilbird	N	Cam	0.93	10
Nycticorax violaceus[e]	Yellow-crowned night heron	N/C	Cam	0.73	10
Rynchops niger[e]	Black skimmer	N[f]	Cam	0.93	10
Scolopax minor[e]	American woodcock	N[g]	Cam	1.15	8
Aegotheles cristatus[d]	Australian owlet-nightjar	N	Cam	0.88	8
Podargus strigoides[d]	Tawny frogmouth	N	Cam	0.87	8
Columba livia	Feral pigeon	D	Cam	1.40	8
Circus aeruginosus[d]	Marsh harrier	D	Cam	1.26	8
Falco berigora[d]	Brown falcon	D	Cam	1.07	8
Gymnorhina tibicen[d]	Australian magpie	D	Cam	1.12	8
Accipiter fasciatus[d]	Brown goskawk	D	Cam	1.04	8
Aquila audax[d]	Wedge-tailed eagle	D	Cam	1.16	8
Elanus notatus[d]	Black-shouldered kite	D	Cam	1.11	8
Collocalia spodiopygia[d]	White-rumped swiftlet	D	Cam	1.07	8
Primates[h]					
Aotus sp.	Owl monkeys	N	Cam	0.90	12
Cheirogaleus major	Dwarf lemur	N	Cam	0.69	12
Daubentonia madagascariensis	Aye-aye	N	Cam	0.76	12
Galago moholi	Lesser bushbaby	N	Cam	0.71	12
Galagoides demidoff	Demidoff's bushbaby	N	Cam	0.69	12
Loris tardigradus	Slender loris	N	Cam	0.72	12
Microcebus murinus	Lesser mouse lemur	N	Cam	0.69	12
Mirza coquereli	Giant mouse lemur	N	Cam	0.68	12
Nycticebus pygmaeus	Lesser slow loris	N	Cam	0.76	12
Perodicticus potto	Potto	N	Cam	0.71	12
Tarsius syrichta	Philippine tarsier	N	Cam	0.74	12
Cacajao rubicundus	Red uakari	D	Cam	1.25	12
Callithrix jacchus	Common marmoset	D	Cam	1.13	12
Cebus sp.	Capuchin monkey	D	Cam	1.18	12
Hylobates sp.	Gibbons	D	Cam	1.11	12

(*Continued*)

Table 1 (Continued)

Species	Animal	Activity	Eye	F-number	Reference
Lagothrix lagotricha	Common woolly monkey	D	Cam	1.20	12
Macaca radiata	Bonnet macaque	D	Cam	1.20	12
Saguinus midas	Red-handed tamarin	D	Cam	1.20	12
Theropithecus gelada	Gelada baboon	D	Cam	1.36	12

F-number, the ratio of focal length to aperture (pupil) diameter, is calculated for the dark-adapted state in selected species. N, nocturnal; D, diurnal; C, crepuscular; Cam, camera eye; Sup, superposition eye; App, apposition eye. Superscript letters: *a* = posterior medial (PM) eye; *b* = posterior medial (AL) eye; *c* = values taken from frontal eye; *d* = since values given by Pettigrew (reference 8) were mostly calculated using fixed material, posterior nodal distance was used instead of focal length (estimated as 0.6 × anteroposterior eyeball distance) and corneal diameter was used instead of pupil diameter. This may have led to lower absolute values than found by other authors (e.g., note the case of the oilbird), but relative comparisons between nocturnal and diurnal birds are still valid using this method; *e* = *F*-number calculated using Pettigrew's method, except using actual pupil diameter instead of corneal diameter; *f* = may be nocturnal and diurnal during the breeding season; *g* = nocturnal only in winter; *h* = *F*-numbers for all primates calculated using Pettigrew's method (see note corresponding to letter *d*) using data in reference 12. References: 1 = Blest A. D. and Land M. F. (1977); 2 = Warrant E. J. (unpublished); 3 = Cleary P. *et al*. (1977); 4 = McIntyre P. D. and Caveney S. (1998); 5 = Greiner B. *et al*. (2004a); 6 = Land M. F. (1969); 7 = Warrant E. J. *et al*. (1999); 8 = Pettigrew J. D. (1982); 9 = Martin G. R. (1994); 10 = references given in Rojas L. M. *et al.* (2004); 11 = Martin G. R. *et al*. (2004a; 2004b); 12 = Kirk E. C. (2006).

rhabdoms differ greatly in width: 20 μm in the dark-adapted *Dinopis* (Blest, A. D. and Land, M. F., 1977) but only 2 μm in *Phidippus* (Land, M. F., 1969; 1985). This tenfold difference means that the rhabdoms of *Dinopis* view solid angular regions of space that are about 100 times larger than those viewed by the rhabdoms of *Phidippus*. These large fields of view, together with their much wider lenses (1.4 vs. 0.4 mm), endow *Dinopis* with an optical sensitivity of 101 μm^2 sr, compared to just 0.038 μm^2 sr in *Phidippus* (eqn [2]). Thus, compared to *Phidippus*, *Dinopis* has clearly traded resolution for sensitivity. This difference in optical sensitivity between nocturnal and diurnal spiders is reflected in electrophysiological measurements of the number of axial photons (from a point source) that are required to generate a half-maximal response (called the PAQ_{50}) in the photoreceptors. In *Dinopis* PM eyes, $PAQ_{50} = 5 \times 10^5$ photons (Laughlin, S. B. *et al*., 1980), whereas in the posterolateral (PL) eyes of the diurnal jumping spider *Plexippus* $PAQ_{50} = 7 \times 10^{10}$ photons (Hardie, R. C. and Duelli, P., 1978). About 100 000 times more photons are required to generate a half-maximal response in the diurnal spider!

Even though *Phidippus* has an outstanding resolution for an animal of its size (Land, M. F., 1985), resolution in *Dinopis* is still impressive: electrophysiologically measured angular sensitivity functions in *Dinopis* have a half-width (i.e., acceptance angle $\Delta\rho$) of only 2.3° (Laughlin, S. B. *et al*., 1980), a value narrower than in nearly all nocturnal insects (which also generally have much lower sensitivity). The eyes of *Dinopis* are not only exquisitely sensitive, they also have excellent resolution, qualities that no doubt assist them during nocturnal hunting.

2.05.6.1.2 Insect compound eyes

Many of the same kinds of mechanisms used in camera eyes to improve sensitivity to a dim extended scene are also found in compound eyes. In apposition compound eyes (Figure 4(b)), each ommatidium is isolated from its neighbors by a sleeve of light-absorbing screening pigment, thus preventing light reaching the photoreceptors from all but its own small corneal lens. This tiny lens – typically a few tens of micrometers across – represents the pupil of the apposition eye, and not surprisingly, this eye design is typical of insects and crustaceans living in bright habitats. Remarkable exceptions do exist, including nocturnal mosquitoes (Land, M. F. *et al*., 1997; 1999) and the nocturnal tropical halictid bee *M. genalis* that we will discuss below.

However, it is the superposition design that is better adapted for vision in dim light. As we saw in The Eyes of Arthropods and Vertebrates, the superposition aperture plays a dominant role in setting the sensitivity of the eye, and its size is adapted to the light intensity that the eye normally encounters. This can be seen in the superposition eyes of dung beetles from the single genus *Onitis* (McIntyre, P. D. and Caveney, S., 1998; Figure 5(b)). Individual species fly in search of dung at different times of day. The superposition apertures of nocturnal species (width $A = 845$ μm in *O. aygulus*) are considerably larger than those of crepuscular species ($A = 655$ μm in *O. alexis*). These in turn are more than twice as large as those of diurnal species ($A = 309$ μm in *O. belial*). Moreover, the nocturnal species *O. aygulus* has huge contiguous rhabdoms (13 μm wide × 86 μm long) compared to the diurnal species *O. belial* where they are small (6.5 μm × 32 μm) and

widely spaced. And unlike *O. aygulus*, diurnal species like *O. belial* also have sheaths of screening pigment around their rhabdoms, which cuts down light flux even more (Warrant, E. J. and McIntyre, P. D., 1991). These differences are reflected in the sensitivities (S) of their eyes (eqn [2]): $S = 59\,\mu m^2\,sr$ in *O. aygulus* but only $1.5\,\mu m^2\,sr$ in *O. belial*.

The highly visual hawkmoths (Sphingidae) – which hover in front of flowers and suck nectar on the wing – all have superposition eyes and a well-developed tapetum, irrespective of whether they are nocturnal or diurnal. The remarkable superposition eyes of the diurnal hummingbird hawkmoth *Macroglossum stellatarum* have diffraction-limited optics, and local retinal acute zones that are unique for the superposition design (Warrant, E. J. *et al.*, 1999), and like honeybees, they also locate flowers using full trichromatic color vision (Kelber, A. and Hénique, U., 1999). Most hawkmoths, however, are active in dim light, such as the nocturnal elephant hawkmoth *Deilephila elpenor* Figure 9(a). The superposition aperture in the frontal eye region of *Deilephila* contains 947 facets, considerably more than the 340 facets found in *Macroglossum*. With a focal length of 675 μm, and photoreceptors of width 10.3 μm (Warrant, E. J., unpublished data), *Deilephila* achieves an optical sensitivity of $69\,\mu m^2\,sr$. In *Macroglossum*, on the other hand, the value is just over half of this – $38\,\mu m^2\,sr$ – a very high sensitivity for a diurnal eye (focal length 409 μm, rhabdom diameter 7.7 μm: Warrant, E. J. *et al.*, 1999). Since both hawkmoths have a similar receptive field size ($d/f \approx 1^\circ$), the better sensitivity in *Deilephila* is entirely due to its larger superposition aperture, a sensitivity that is sufficient to allow *Deilephila* to see color at night, the first animal known that can (Kelber, A. *et al.*, 2002; see Section 2.05.6.3.2).

Despite having apposition eyes, many bees (Greiner, B. *et al.*, 2004a; Warrant, E. J. *et al.*, 2004), wasps (Greiner, B., 2006), and ants (Menzi, U., 1987; Moser, J. C. *et al.*, 2004) have adopted nocturnal lifestyles to take advantage of reduced competition and predation. The Central American halictid bee *M. genalis* (Figure 5c) is an excellent example. This bee can visually learn and use landmarks for homing at night, an impressive feat considering the size and design of its eyes (Warrant, E. J. *et al.*, 2004). *Megalopta* is a facultatively social bee, with females living in groups of up to 10 in long bored-out sticks (Janzen, D. H., 1968; Arneson, L. and Wcislo, W. T., 2003; Wcislo, W. T. *et al.*, 2004). Each day, bees emerge twice from the nest to forage, each trip lasting up to about 35 min (Kelber, A. *et al.*, 2006). The first foraging trip begins up to an hour before dawn, and the second ends about 40 min after sunset, when light levels under the thick rainforest canopy are similar to starlight levels above. This behavior contrasts strongly with the European honeybee *Apis mellifera*, which is strictly day active. Not surprisingly, this contrast is also reflected in the structure and sensitivity of the eyes. Even though *Megalopta* has larger eyes and larger facets than in *Apis* (facets diameters up to 36 μm, compared to just 20 μm), the biggest difference between the two species lies in the size of the rhabdoms (Greiner, B. *et al.*, 2004a; Warrant, E. J. *et al.*, 2004). These have a width of only 2 μm in *Apis*, but in *Megalopta* they reach an extraordinary 8 μm, resulting in a receptive field of more than seven times greater solid angular extent. Similar adaptations are also found in the nocturnal wasp *Apoica pallens* (Greiner, B., 2006). These differences in receptive field and facet size allow *Megalopta* an optical sensitivity that is almost 30 times greater than in *Apis*: 2.7 versus $0.1\,\mu m^2\,sr$. Even though this is a significant improvement over *Apis*, sensitivity is still very modest compared to *Deilephila* ($69\,\mu m^2\,sr$) or *Dinopis* ($101\,\mu m^2\,sr$). This comparison shows up the inherent limitations of the apposition design for vision in dim light and begs the question – how can *Megalopta* nonetheless navigate using landmarks at night? The answer, we believe, lies in the optic lobe, a possibility we explore in Spatial and temporal summation.

2.05.6.2 Neural Adaptations for Increased Sensitivity in Arthropods

Arthropods are generally small animals and thus bear small eyes. Even though many nocturnal arthropods (especially nocturnal spiders) have considerable optical sensitivity, their small eyes on their own may still capture too few photons to support reliable vision. We have just highlighted this risk for the bee *M. genalis*. With only 30 times the optical sensitivity of its diurnal relatives, one might ask whether this is sufficient to explain its ability to see at night. The answer is probably no, and other mechanisms – particularly neural mechanisms – are likely to make up the short fall in sensitivity. Such mechanisms are already present at the level of the photoreceptors.

2.05.6.2.1 Signal transduction in nocturnal arthropod photoreceptors

Even if a nocturnal animal has very sensitive eyes that capture as many of the available photons as

possible, a reliable signal is only assured if each captured photon is transduced efficiently and reproducibly. This is the task of the photoreceptors, and signal reliability at this level depends on how ideal the receptors are as photodetectors. Even though arthropod photoreceptors are not perfectly ideal, suffering as we saw earlier from various sources of intrinsic noise, in many species they are nonetheless remarkably efficient.

Ever since the pioneering studies of Yeandle in the horseshoe crab *Limulus* in the late 1950s (Yeandle, S., 1958), we have known that photoreceptors can respond to single photons with small but distinct electrical responses known as bumps, responses found in both vertebrates and invertebrates (Figure 5(d)), both nocturnal and diurnal. Apart from the horseshoe crab, bumps have now been recorded from many invertebrates including insects (e.g., flies, locusts, and cockroaches; reviewed by Laughlin, S. B., 1990), crustaceans (e.g., Doujak, F. E., 1984), and spiders (e.g., Laughlin, S. B. *et al.*, 1980).

Despite this apparently remarkable sensitivity to single quanta of light, not all photons that strike the pupil of an eye are actually absorbed by the photoreceptors and lead to a bump. Due to reflections, screening pigments, waveguide effects, and visual pigment absorption efficiency, only a certain fraction of photons entering the pupil are transduced. In flies, the fraction is around 50% (Laughlin, S. B., 1990). In the shore crab *Leptograpsus variegatus*, it is 45% (Doujak, F. E., 1985) and in the locust *Locusta migratoria*, 59% (Lillywhite, P. G., 1977). In the nocturnal spider *D. subrufus*, the figure is likely to higher, around 74% (Blest, A. D., 1978; Laughlin, S. B. *et al.*, 1980). This capture efficiency is actually quite high: in vertebrates the figure tends to be somewhat lower, and in the cat it is probably below 25% (Barlow, H. B. *et al.*, 1971).

It has long been known that the bumps of nocturnal arthropods (e.g., those of nocturnal spiders: Laughlin, S. B. *et al.*, 1980) tend to be of much larger amplitude than those of diurnal species. Since there is (of course) no difference between photons available at night or during the day, larger bumps in nocturnal animals imply a higher transduction gain. The transduction gain sets the size of the response for a given step in stimulus intensity, an amplification mechanism that affects not only the amplitude of the response but also the amplitudes of any sources of noise. By itself, therefore, this photoreceptor amplification mechanism cannot provide an improvement in the visual SNR. However, recent work in nocturnal bees (Frederisken, R., Wcislo, W. T., and Warrant, E. J., in preparation) shows that the higher gain of nocturnal photoreceptors probably prepares the visual signal for a subsequent stage of neural processing, where spatial summation of signals from many converging photoreceptors may strongly enhance the signal but average out the noise (which is not correlated between photoreceptors). This summation, if it occurs, would thereby lead to a considerable improvement in the SNR (see next section), albeit at the cost of spatial resolution. Thus, even though an increased transduction gain (and large bumps) does not enhance visual reliability at the level of the photoreceptors *per se*, the enhancement probably manifests itself later as a result of spatial summation. How and where does this summation occur?

2.05.6.2.2 Spatial and temporal summation

Neural summation of light in space and time can significantly improve visual reliability in dim light (Snyder, A. W., 1977; Snyder, A. W. *et al.*, 1977a; 1977b; Laughlin, S. B., 1981a; 1990; Warrant, E. J., 1999). We have already mentioned summation in time above (see Section 2.05.4.2): when light gets dim, the visual systems of nocturnal animals can improve visual reliability by responding more slowly, either by having slower photoreceptors or by neurally integrating signals at a higher level in the visual system. But this only comes at a price: temporal summation can drastically degrade the perception of fast-moving objects, potentially disastrous for a fast-flying nocturnal animal that needs to negotiate obstacles! Not surprisingly, temporal summation is more likely to be employed by slowly moving animals.

Summation of photons in space can also improve image quality. Instead of each visual channel collecting photons in isolation (as in bright light), the transition to dim light could activate specialized laterally spreading neurons that couple the channels together into groups. Evidence of such neurons has been found in the first optic ganglion (lamina ganglionaris) of nocturnal cockroaches (Ribi, W. A., 1977), fireflies (Ohly, K. P., 1975), and hawkmoths (Strausfeld, N. J. and Blest, A. D., 1970), and these have been interpreted as an adaptation for spatial summation (Laughlin, S. B., 1981a). The nocturnal bee *M. genalis* also appears to have such neurons (Greiner, B. *et al.*, 2004b; 2005; Figure 6a). Each summed group – themselves now defining the

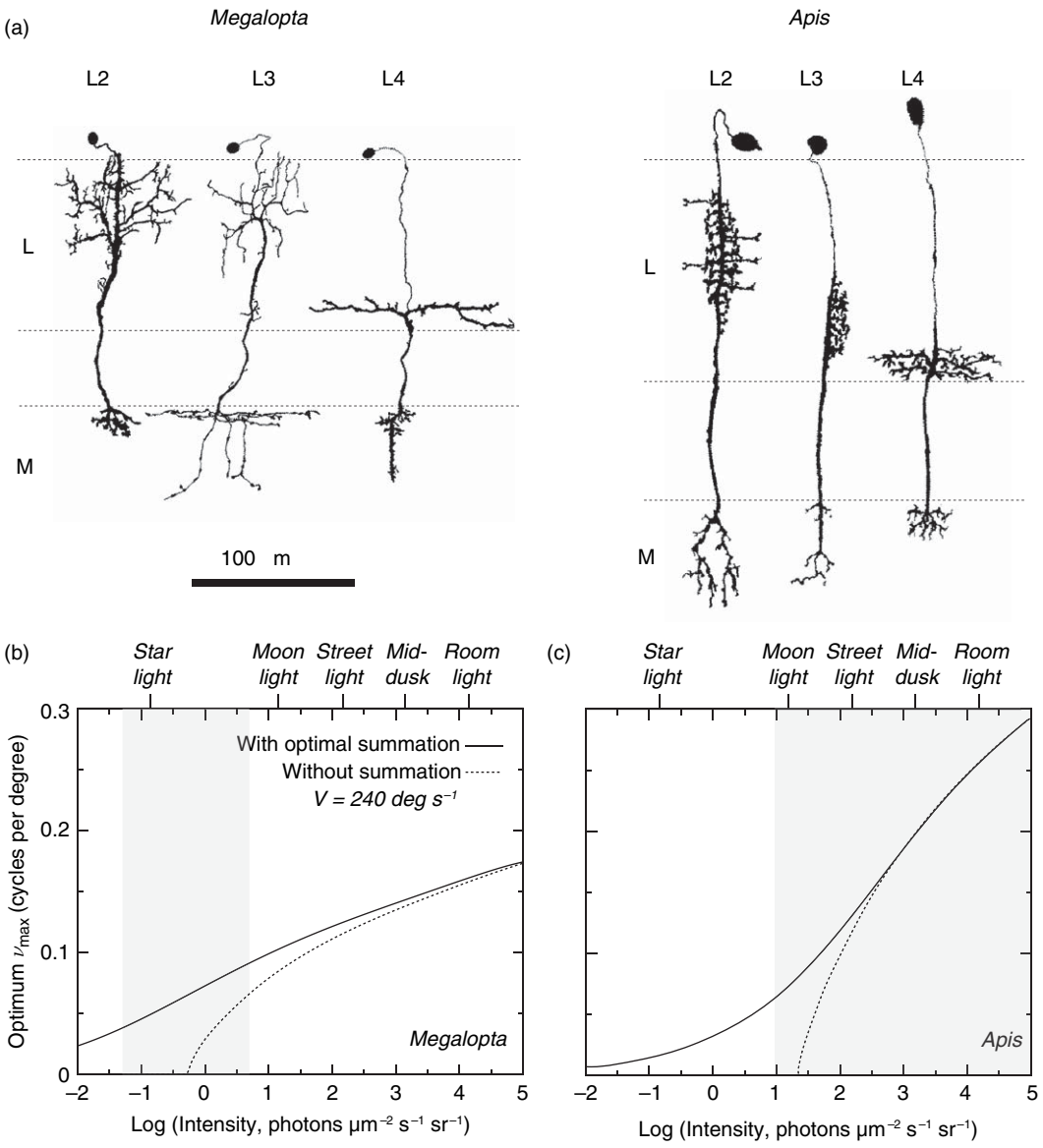

Figure 6 Spatial summation in nocturnal bees. (a) Comparison of the first-order interneurons – L-fiber types L2, L3, and L4 – of the *Megalopta genalis* female (left) and the worker honeybee *Apis mellifera* (right). Compared to the worker honeybee, the horizontal branches of L-fibers in the nocturnal halictid bee connect to a much larger number of lamina cartridges, suggesting a possible role in spatial summation. *L* = lamina, *M* = medulla. Reconstructions from Golgi-stained frontal sections. Adapted from Greiner B. *et al.* (2004b) and Ribi W. A. (1975). (b, c) Spatial and temporal summation modeled at different light intensities in *Megalopta genalis* (b) and *Apis mellifera* (c) for an image velocity of 240 °s^{-1} (measured from *Megalopta genalis* during a nocturnal foraging flight: Warrant, E. J. *et al.*, 2004). Light intensities are given for 540 nm, the peak in the bee's spectral sensitivity. Equivalent natural intensities are also shown. The finest spatial detail visible to flying bees (as measured by the maximum detectable spatial frequency, ν_{max}) is plotted as a function of light intensity. When bees sum photons optimally in space and time (solid lines), vision is extended to much lower light intensities (nonzero ν_{max}) compared to when summation is absent (dashed lines). Note that nocturnal bees can see in dimmer light than honeybees. Gray areas denote the light intensity window within which each species is normally active (although honeybees are also active at intensities higher than those presented on the graph).

channels – could collect considerably more photons over a much wider visual angle. The greatly enlarged receptive fields produced by this spatial summation result in a simultaneous and unavoidable loss of spatial resolution. Despite being much brighter, the image becomes necessarily coarser.

Spatial summation is likely to be widespread, as evidence from insects is now suggesting. Using

behavioral methods, Dubs A. *et al.* (1981) measured the threshold optomotor response of tethered flies that viewed a wide-field grating stimulus and in parallel recorded the rates of bump production at the same threshold intensity, both in the photoreceptors and in the first-order interneurons to which they connect. Using a point source centered in the field of view, the interneuron bump rate was found to be six times that of the photoreceptors – exactly the ratio expected, since six photoreceptors synapse onto one interneuron. However, when the point source was exchanged for the dim extended grating stimulus at threshold intensity, the interneuron bump rate increased to between 18 and 20 times the photoreceptor rate, implying that signals from several neighboring ommatidia were being summed at the interneuron (possibly via presynaptic summation between receptors). Spatial summation has also been found in the motion pathways that process the optomotor response in flies (Dvorak, D. and Snyder, A. W., 1978) and nocturnal hawkmoths (Warrant, E.J., O'Carroll, D. C., and Theobald, J. C., in preparation). In bright light, the elementary motion detectors of flies calculate motion by using signals generated in neighboring ommatidia. But as light levels fall, the elementary motion detectors calculate motion by comparing signals generated in successively more distant neighbors, up to two, three, or even four ommatidia apart (Pick, B. and Buchner, E., 1979). This increase in spatial summation is accompanied by a decrease in lateral inhibition (Srinivasan, M. V. and Dvorak, D. R., 1980).

Even though summation compromises spatial and temporal resolution, the gains in photon catch are so enormous that vision in dim light can be greatly improved. This is especially true in small eyes like those of arthropods. If a locust, an insect with apposition eyes, employs summation optimally, it has the potential to see reliably at light intensities up to 100 000 times dimmer than those in which they would normally become blind (Warrant, E. J., 1999). Like locusts, nocturnal bees would also benefit from optimal summation. Indeed, the wide lateral branches of its laminar monopolar cells L2, L3, and L4, which spread to 12, 11, and 17 lamina cartridges, respectively, are considerably wider than the homologous cells of *Apis*, which spread to 2, 0, and 4 cartridges, respectively (Greiner, B. *et al.*, 2004b; 2005; Figure 6(a)).

Even though their role in summation is yet to be shown, the morphologies of these cells in *Megalopta* are well suited to the task of summation. If one investigates the possible improvement afforded by optimal spatial and temporal summation using theoretical methods (Warrant, E. J., 1999), then both *Megalopta* (Figure 6(b)) and *Apis* (Figure 6(c)) are able to resolve spatial details in a scene at much lower intensities with summation than without it (Theobald, J. C. *et al.*, 2006). These theoretical results assume that both bees experience an angular velocity during flight of $240^{\circ}s^{-1}$, a value that has been measured from high-speed films of *Megalopta* flying at night. At the lower light levels where *Megalopta* is active, the optimum visual performance shown in Figure 6(b) is achieved with an integration time of about 30 ms and summation from about 12 ommatidia (or cartridges). This integration time is close to the photoreceptor's dark-adapted value (Warrant, E. J. *et al.*, 2004), and the extent of predicted spatial summation is very similar to the number of cartridges to which the L2 and L3 cells branch (Greiner, B. *et al.*, 2004b), thus strengthening the hypothesis that the lamina monopolar cells are involved in spatial summation.

Even in the honeybee *Apis*, summation can improve vision in dim light (Figure 6(c)). Interestingly, the Africanized race, *Apis mellifera scutellata*, and the closely related southeast Asian giant honeybee *Apis dorsata*, both forage during dusk and dawn, and even throughout the night, if a moon half-full or larger is present in the sky. Behavioral experiments show, however, that even the strictly day-active European honeybee is capable of seeing course habitat features, like large pale flowers, at moonlight intensities. This ability can be explained only if bees optimally sum photons over space and time (Warrant, E. J. *et al.*, 1996), and this is also revealed in Figure 6(c) (for an angular velocity of $240^{\circ}s^{-1}$). At the lower light levels where *Apis* is active, the optimum visual performance shown in Figure 6(c) is achieved with an integration time of about 18 ms and summation from about three or four cartridges. As in *Megalopta*, this integration time is close to the photoreceptor's dark-adapted value (Warrant, E. J. *et al.*, 2004), and the extent of predicted spatial summation is again very similar to the number of cartridges to which the L2 and L3 cells actually branch.

2.05.6.3 Visual Behavior in Nocturnal Arthropods

Arthropods clearly have many adaptations to increase sensitivity in dim light, and these allow nocturnal species to use vision to perform a number of important behavioral tasks.

2.05.6.3.1 Nocturnal navigation and homing

The nocturnal bee *M. genalis*, despite having eyes only 30 times as sensitive as those of a honeybee (see Section 2.05.6.1.2), is able to forage in a dark rainforest understory at night and return to its nest – a narrow hollowed-out stick in the undergrowth – without getting lost. This impressive feat is achieved visually. When *Megalopta* flies from its nest at night, it turns to face the nest entrance and begins to inspect the nest and other objects nearby in what is clearly an orientation flight (Figure 7(a)), a well-known phenomenon in diurnal bees such as the honeybee (Becker, L., 1958; Lehrer, M., 1996; Zeil, J. *et al.*, 1996; Capaldi, E. A. and Dyer, F. C., 1999). In honeybees, orientation flights are used to learn the arrangement of landmarks around the hive prior to departure, so that the hive entrance can be recognized and located upon return. Proof that *Megalopta* uses orientation flights to learn the arrangement of landmarks around the nest entrance was shown in a series of behavioral experiments (Figures 7(b) and 7(c); Warrant, E. J. *et al.*, 2004). Five nest sticks were placed beside one another on a small stand in the rainforest, and of these, only the middle nest was occupied (marked by a stars in Figures 7(b) and 7(c)). The bee left its nest at 18.48 (16 min after sunset), performed an orientation flight for a few seconds (presumably learning the spatial arrangement of the five nests), and then left (Figure 7(b), upper panel). While the bee was away, the positions of the bee's nest and an empty nest were swapped (Figure 7(b), lower panel). Upon return at 18.58, the bee flew without hesitation into the central unoccupied nest – the spatially correct nest – but after a couple of seconds flew out again. After resurveying the nests, the bee returned to the central nest, again immediately flying out. Presumably the aroma or some other feature of the nest was repellent to the bee, and it was not until the bee's actual nest was retuned to the central position that the bee ceased to reemerge. In a second experiment, a movable white card was instead used as a landmark – the bee's nest in this case remained in its original location. Prior to the bee's departure, the landmark was placed over the entrance of the central, occupied nest (Figure 7(c),

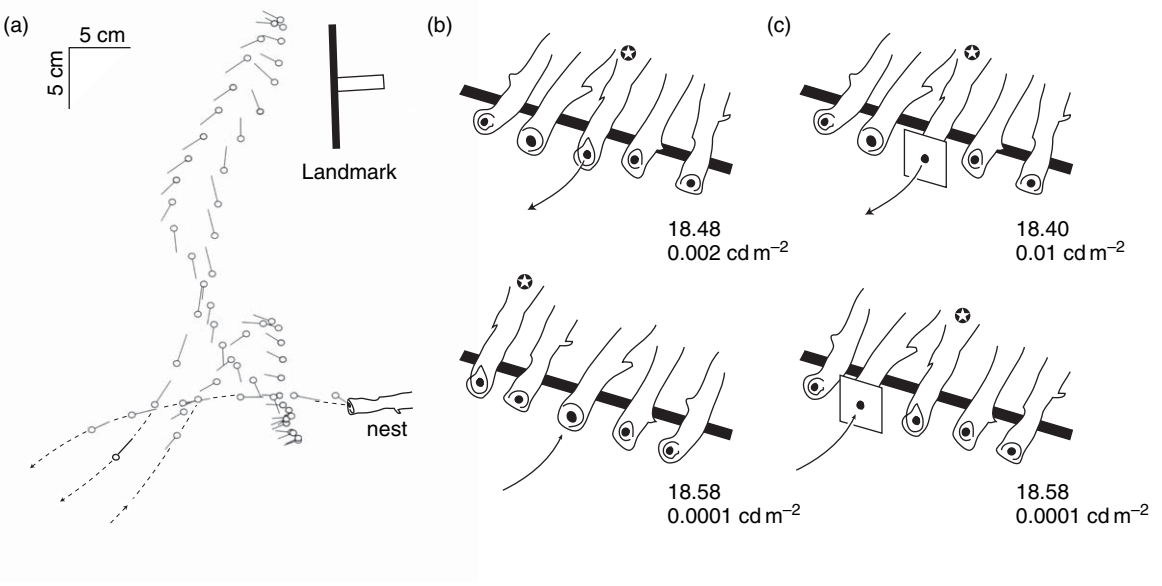

Figure 7 Nocturnal landmark orientation in the nocturnal halictid bee *Megalopta genalis*. (a) A typical nocturnal orientation flight, as seen from below. The bee leaves her nest and quickly returns to face the nest entrance. Flying in short arcs, she investigates the nest entrance and a neighboring landmark to learn their spatial arrangement before departing on her foraging trip. Each ball-and-stick represents the position of the head (ball) and body (stick) at 40 ms intervals. (b, c) Landmark learning. Bees leaving for a foraging trip learn the position of their nest relative to others (b) or learn the presence of a white square card attached to their nest (c). Upon return, bees enter the nest marked by the landmarks they have previously learned, not their actual nests (which are marked by stars). The rear side of the square card was attached to a Perspex cylinder that slipped neatly over the end of the nest stick to hold the card in place over the nest entrance. Times and light intensities at departure and return are also shown. From Warrant, E.J., Kelber, A., Gislén, A., Greiner, B., Ribi, W., and Wcislo, W.T. 2004. Nocturnal vision and landmark orientation in a tropical halictid bee. Curr. Biol. 14, 1309–1318.

upper panel). The bee departed its nest at 18.40, performed an orientation flight, and left. While the bee was away, the white card was placed over the entrance of a neighboring unoccupied nest. The bee returned at 18.58 and flew directly into the landmarked unoccupied nest (Figure 7(c), lower panel). As before, the bee flew out almost immediately, due to the foreign internal environment of the landmarked nest. This continued until the landmark was returned to the bee's actual nest, after which it no longer emerged. These two experiments show that *Megalopta* is capable of using landmarks at night to find their way home, an ability that can only be explained if these bees employ spatial and temporal summation at night (see Section 2.05.6.2.2). Similar abilities have now been found in the homing behavior of the giant nocturnal Indian carpenter bee *Xylocopa proximata* (Somanathan, H., Borges, R.M., Kelber, A., and Warrant, E.J., in preparation).

The sun, the moon, and the stars are well-known visual cues that help animals to navigate and to find their way home. Stars are point sources that vary considerably in their intensity from star to star. Eyes with greater sensitivity for point sources, that is, with wider pupils (eqns [2] and [3]), will see many more stars in the night sky than those with less sensitivity. The large 8 mm pupil of a dark-adapted human observer permits many thousands of stars to be seen, while for much smaller eyes and pupils, the number of visible stars will be a lot less. The apposition eyes of the shore crab – with corneal facet lenses 45 μm wide – will be limited to seeing the sky's 12 brightest stars (Doujak, F. E., 1985). Arthropods with superposition eyes, such as nocturnal moths, have the potential to see more stars, but as with the shore crab, the spatial resolving power of compound eyes may not be sufficient to accurately distinguish constellations. Nonetheless, the presence of a bright star, or a bright group of stars, within the visual field may act as a simple landmark during migration, as indeed seems to be the case for yellow underwing moths (Sotthibandhu, S. and Baker, R. R., 1979).

A more subtle landmark is the distinctive pattern of polarized light that is produced by the scattering of sunlight in the atmosphere. This pattern, symmetric around the sun and strongly visible to all animals with polarization vision, has long been known as a compass bearing that guides navigation in diurnal animals (Waterman, T. H., 1981; Wehner, R., 2001; Wehner, R. and Labhart, T., 2006). As we mentioned earlier (see Section 2.05.3.3), an identical but much dimmer pattern is also formed around the moon. Many animals have eyes of sufficient sensitivity to see the pattern and use it for navigation. One such animal is the crepuscular–nocturnal African dung beetle *Scarabaeus zambesianus* (Figure 8a; Dacke, M. *et al.*, 2003a; 2003b; 2004), whose dorsal superposition eyes (Figure 8(b)) have specialized polarization-sensitive regions (or dorsal rim areas (DRAs)) that analyze the polarization pattern of the moonlit night sky. The goal of this analysis is to help these beetles maintain a straight-line path while rolling a ball of dung away from the frenzied competition of the dung heap, the safest and most efficient route of escape. On moonlit nights (Figure 8(c)) *Scarabaeus* easily maintains a straight rolling path, whereas on moonless nights (Figure 8(d)) it cannot (on moonlit nights the moon's disk was obscured to ensure that it was unable to act as an orientation cue). This strongly suggests that polarized moonlight is the cue (Dacke, M. *et al.*, 2003a), a conclusion reinforced by experiments in which a UV-transmitting polarizing filter was placed directly over the rolling beetle (Figures 8(e) and 8(f)). With its transmission axis oriented perpendicularly to the dominant polarization direction of the moonlit night sky, the filter caused the beetle to turn by 90° (either to the left or to the right). Thus, *Scarabaeus*' small but very sensitive dorsal superposition eyes allow it to analyze the moon's dim polarization pattern and to orient with respect to it, the first animal known that can (Dacke, M. *et al.*, 2003a). Many other animals, notably nocturnally migrating insects and birds, may have a similar ability and utilize a celestial resource that until quite recently remained unknown. Nocturnal crickets, for instance, are prime candidates. Crickets have exquisite sensitivity to polarized light, with behavioral response thresholds occurring at even lower intensities than those of polarized moonlight (Herzmann, D. and Labhart, T., 1989; Labhart, T. *et al.*, 2001).

Another remarkable nocturnal navigator is the wandering spider *Leucorchestris arenicola* of southern Africa, a strictly nocturnal spider that prefers to leave its burrow in search of mates on moonless starlit nights (Nørgaard, T. *et al.*, 2003; Nørgaard, T., 2005; Nørgaard, T. *et al.*, 2006; 2007). Males search for females by leaving the burrow and meandering over large distances, often hundreds of meters. Nevertheless, they have no trouble finding their way home to the burrow. Careful experiments have ruled out olfactory and gravitational cues, leaving local visual landmarks, such as the shapes and locations of bushes, trees, and dunes in the vicinity of the

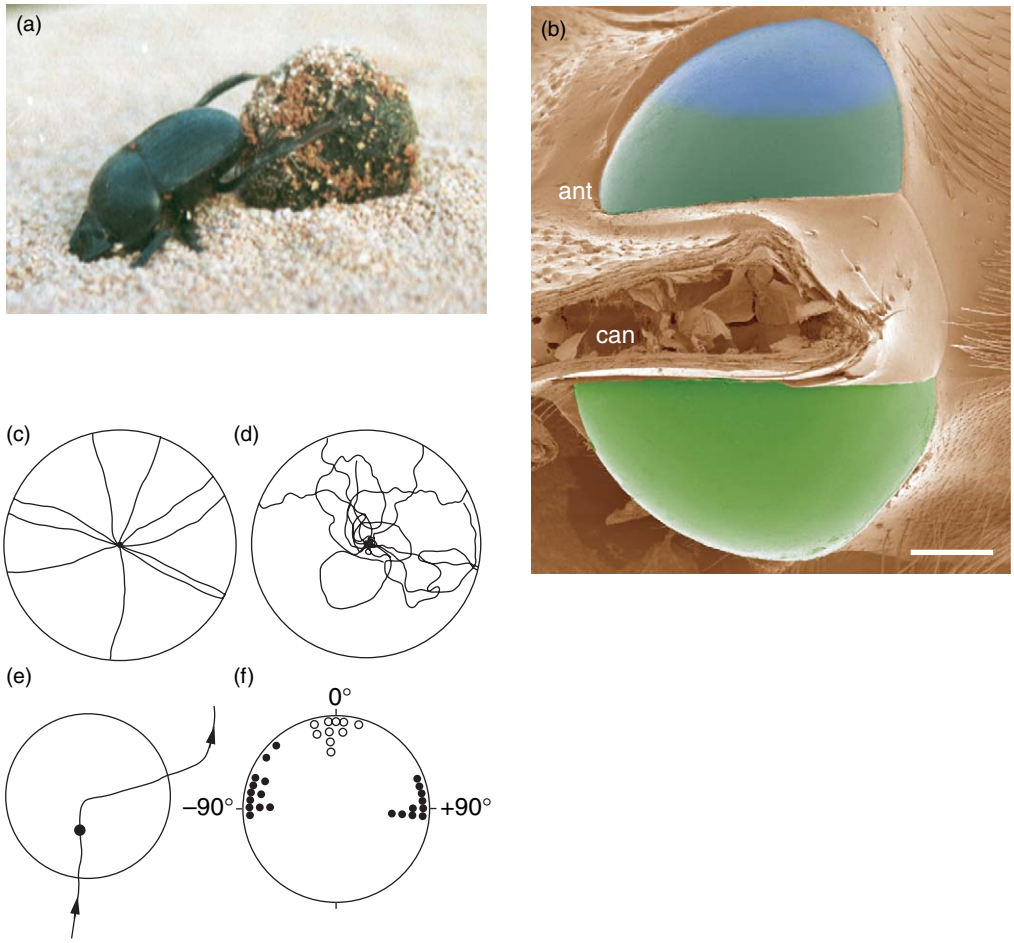

Figure 8 Polarization of moonlight and orientation in the dung beetle *Scarabaeus zambesianus*. (a) *Scarabaeus* rolling a ball of dung. (b) A false-color scanning electron micrograph of the left dorsal and ventral eyes. A canthus (*can*), here cut open to allow easier orientation, separates the two eyes. The blue region in the upper half of the dorsal eye indicates the dorsal rim area (or DRA), the region of the eye whose rhabdoms are specialized for the analysis of polarized light. In other parts of the dorsal eye, and throughout the ventral eye, the rhabdoms are unable to process polarized light (eye regions colored green). *ant* = anterior. Scale bar = 0.5 mm. (c) On a moonlit night, beetles orient along straight paths. (d) On moonless nights, beetles orient along random paths. (e) The change in direction (right turn, +70°) taken by a single rolling beetle when a perpendicularly polarizing filter is placed over the beetle at the position indicated by the *dot*. The beetle resumes its direction of travel on exposure to the open sky. The circle represents the extent of the 42 cm-diameter filter. (f) Average angles of turn made by 22 beetles when covered by the same filter as in E (filled circles, binned in 5° intervals): left turns, $-77° \pm 14.7°$; right turns, $87.9° \pm 9.3°$. Under a parallel polarizing filter, beetles did not deviate from their original direction (open circles). (a, c–f) Adapted from Dacke, M., Nilsson, D.-E., Scholtz, C.H., Byrne, M., and Warrant, E.J. 2003a. Insect orientation to polarized moonlight. Nature 424, 33. (b) Adapted from Dacke, M., Nordström, P., Scholtz, C.H. 2003b. Twilight orientation to polarised light in the crepuscular dung beetle *Scarabaeus zambesianus*. J. Exp. Biol. 106, 1535–1543.

burrow, as the most likely sensory basis for this homing behavior. However, spiders can sometimes return to the burrow using a bee-line trajectory. This suggests the use of path integration, a navigational mechanism that relies on celestial visual cues (such as polarized light), and which is known from diurnal insects such as the desert ant *Cataglyphis bicolor* (e.g., Wehner, R., 2003). Since polarized light information is not available when *Leucorchestris* is active, other cues must be responsible (such as the constellations of stars). Thus, even though vision is likely to drive homing behavior in *Leucorchestris*, this remains to be established with certainty.

2.05.6.3.2 Nocturnal color vision

As we mentioned above, the nocturnal world is just as rich in colors as the diurnal world (Figure 1), and we have recently begun to discover animals that have

sufficient visual sensitivity to distinguish them (Kelber, A. and Roth, L. S. V., 2006). The first such discovery was made in the nocturnal hawkmoth *D. elpenor* (which we discussed earlier). Like all hawkmoths so far investigated, *Deilephila* has three different spectral classes of photoreceptors, centered in the ultraviolet (350 nm), the violet (440 nm) and the green (525 nm) parts of the spectrum (Höglund, G. *et al.*, 1973; Schwemer, J. and Paulsen, R., 1973). The hummingbird hawkmoth *M. stellatarum* – *Deilephila*'s day-active cousin – has excellent trichromatic color vision based on these three spectral classes (Kelber, A. and Hénique, U., 1999; Kelber, A. *et al.*, 2003), and it has long been thought that *Deilephila* may also share this ability (Schlecht, P., 1979). After training *Deilephila* to associate a sugar reward with a blue disk (Kelber, A. *et al.*, 2002), the disk was placed within a series of other disks of equal size but of various shades of gray or of different colors (Figure 9(a)). These disks were placed on a uniform field of pale gray. With regard to the gray tones, these were deliberately made both lighter and darker in absolute brightness than the learned blue in order to test whether hungry moths use achromatic contrast cues, rather than color, to find the learned blue disk (Figures 9(b) and 9(c)).

The ability of trained *Deilephila* to distinguish the blue disk was tested in an arena illuminated by one of five intensities of broad-spectrum white light, ranging from 1 cd m^{-2} (mid-to-late dusk) to 10^{-4} cd m^{-2} (starlight). At all intensities, *Deilephila* discriminated the blue disk from all shades of gray with a choice frequency of at least 80%, even at starlight intensities (Figure 9(b)). When the training color was swapped to yellow, the results in starlight were similar (Figure 9(c)). Human observers, subjected to the same experimental conditions, succeeded in distinguishing the blue and yellow disks from the shades of gray only down to full-moon intensities (10^{-2} cd m^{-2}): at dimmer intensities light levels are too low for human color vision to function.

These results show that *Deilephila* is capable of discriminating colors in starlight, at light levels more than 100 times dimmer than the dimmest in which humans can do it. Using eqn [3], we can calculate the number of photons N absorbed by the green-, blue-, and UV-sensitive photoreceptors per integration time, when viewing the colored targets at the dimmest illuminating intensity (10^{-4} cd m^{-2}). Even though *Deilephila* has a very sensitive superposition eye, the photoreceptors only absorb between 1 and 16 photons per integration time for

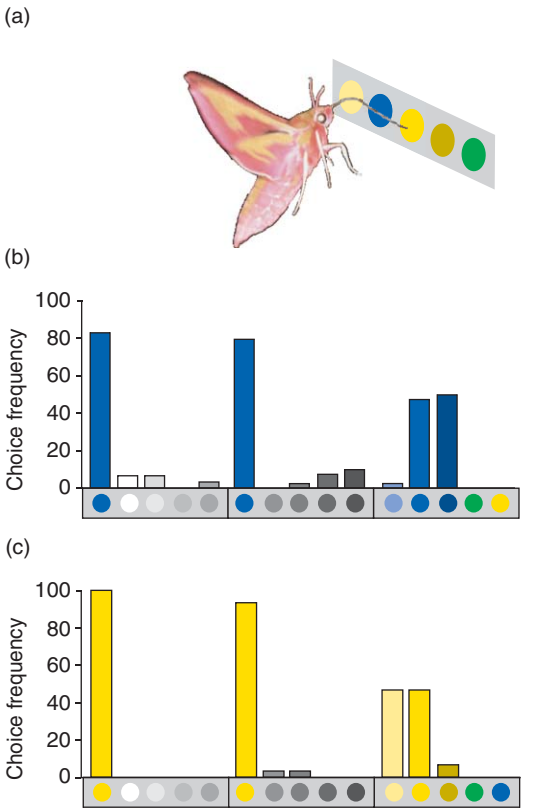

Figure 9 Color discrimination by the nocturnal hawkmoth *Deilephila elpenor.* In color discrimination experiments (a), the moth is required to choose a learned colored target from a selection of targets of various other colors. At starlight intensities, *Deilephila* is capable of discriminating a learned colored target (blue (b) or yellow (c)) from eight different shades of gray, but not from different shades of the same color. From Kelber, A., and Roth, L. S. V. 2006. Nocturnal colour vision – not as rare as we might think. J. Exp. Biol. 209, 781–788.

the gray shades and the various shades of blue (Kelber, A. *et al.*, 2002). This represents an *SNR* of between only 1 and 4 ($SNR = \sqrt{N}$, see above), which is insufficient to distinguish color reliably (Land, M. F., 1981). Once again we are left to conclude that *Deilephila*'s impressive visual performance can only be explained by spatial and temporal summation at higher levels in the visual system, a conclusion that future experimental work will no doubt verify.

2.05.7 Vision and Visual Behavior in Nocturnal Birds and Primates

Birds have excellent vision, with eyes that are considerably larger relative to body size than in most other animal groups (Walls, G. L., 1942; Martin, G. R.,

1994), an adaptation thought to be associated with rapid flight in bright environments. Diurnal birds that employ an active aerial visual hunting strategy, such as eagles, kites, hawks, and falcons, have even larger eyes for their body size than other birds (Brooke, M. *et al.*, 1999), which no doubt reflects their need for better spatial resolution. In birds, larger eyes are also accompanied by comparatively larger brains (Garamszegi, L. Z. *et al.*, 2002).

Even though most birds are diurnal, there are a considerable number of species that have become exclusively nocturnal (Martin, G. R., 1990). Many are flightless or nearly so and probably rely more on olfaction and mechanoreception, rather than on vision, for foraging. Well-known examples include the kiwis (*Apteryx* spp.), the night parrot, the ground parrot, and the kakapo, all endangered species from Australia or New Zealand. In contrast, actively flying species – including owls, frogmouths, nightjars, oilbirds, paurasques, the letter-winged kite, and various waterbirds – rely to a much greater degree on vision for orientation and feeding, and this is reflected in the size and design of their eyes. Like diurnal birds of prey, nocturnal flying birds generally have larger eyes for their body size than other birds (Brooke, M. *et al.*, 1999; Garamszegi, L. Z. *et al.*, 2002; Thomas, R. J. *et al.*, 2006; Hall, M. I. and Ross, C. F., 2007), an adaptation that has evolved in order to capture more light from a larger pupil (see Section 2.05.5.2), rather than to improve spatial resolution (a conclusion also drawn for the eyes of nocturnal primates: Kay, R. F. and Kirk, E. C., 2000; Kirk, E. C., 2004). Apart from their larger size, several other important adaptations have evolved within the eyes of nocturnal birds that enhance their sensitivity to light. Remarkably, one of these adaptations (found in the echolocating oilbird *Staetornis caripensis*) was, until very recently, known only from deep-sea fishes. For a fuller account of nocturnality in birds, the interested reader is referred to Martin's beautiful book on the subject (Martin, G. R., 1990).

In the discussion below, comparisons will also be made, where relevant, with nocturnal primates, another animal group whose members – lemurs, lorises, pottos, aye-ayes, bushbabies, tarsiers, and the owl monkey *Aotus* – have excellent nocturnal vision (for reasons similar to those we will outline below for birds).

2.05.7.1 Optical Adaptations for Increased Sensitivity

As we saw earlier, wider pupils, shorter relative focal lengths, and larger photoreceptors with wider receptive fields all improve photon capture N (eqn [3]) and increase sensitivity S (eqn [2]). These are common features of camera eyes in nocturnal vertebrates and are readily seen in the eyes of nocturnal birds (Hall, M. I. and Ross, C. F., 2007) and nocturnal primates (Kirk, E. C., 2004).

The camera eyes of nocturnal vertebrates are frequently constructed with a large, highly curved, and powerful cornea and a significantly thickened lens (especially in primates) that shortens the posterior nodal distance and shifts it closer to the retina than in a diurnal eye (Figure 10(c)). To achieve a focused image on the retina, this implies that the focal length f is relatively shorter in such an eye, and a shorter focal length leads to a lower F-number (see Section 2.05.6.1.1) and greater sensitivity (eqn [2]). As we discussed earlier, an eye of lower F-number (the ratio of focal length f to pupil diameter A) receives a brighter retinal image and is thus better adapted to vision in dim light. Indeed, a survey of F-numbers in nocturnal and diurnal birds and primates supports this principle: the eyes of nocturnal species have considerably lower F-number than those of diurnal species (Table 1; Pettigrew, J. D., 1982; Kirk, E. C., 2006).

The finite size of the vertebrate skull, and the demand for high sensitivity via a large pupil, has resulted in the evolution of very large eyes relative to head size in nocturnal animals (Walls, G. L., 1942; Brooke, M. *et al.*, 1999; Garamszegi, L. Z. *et al.*, 2002; Howland, H. C. *et al.*, 2004; Kirk, E. C., 2004; Thomas, R. J. *et al.*, 2006; Hall, M. I. and Ross, C. F., 2007). Nocturnal tarsiers and owl monkeys are excellent examples: in the latter, pupils can reach 2 cm in diameter. In tarsiers (Figure 10(a)), skillful hunters of nocturnal insects (Collins, C. E. *et al.*, 2005), the skull is dominated by enormous eye sockets (Figure 10(b)). Incredibly, each eye has a volume equal to that of the brain (Collins, C. E. *et al.*, 2005), and the eyes are believed to be the largest relative to body mass of any mammal (Polyak, S., 1957). Moreover, investigations of the brain reveal that the primary visual cortex (V1) of the tarsier *Tarsius spectrum* is unique among primates in that it occupies the largest proportion of the neocortex yet reported for this group (Collins, C. E. *et al.*, 2005). This finding no doubt reveals the importance of sensitive high-resolution vision for the tarsier's demanding predatory behavior and its locomotory habit of leaping from tree to tree.

Another common adaptation to life in dim light is an eye of tubular shape, and this is found in many nocturnal birds and deep-sea fishes (see Warrant, E. J. and Locket, N. A., 2004). The large forward-pointing eyes of owls are a good example (Figure 11a; Walls,

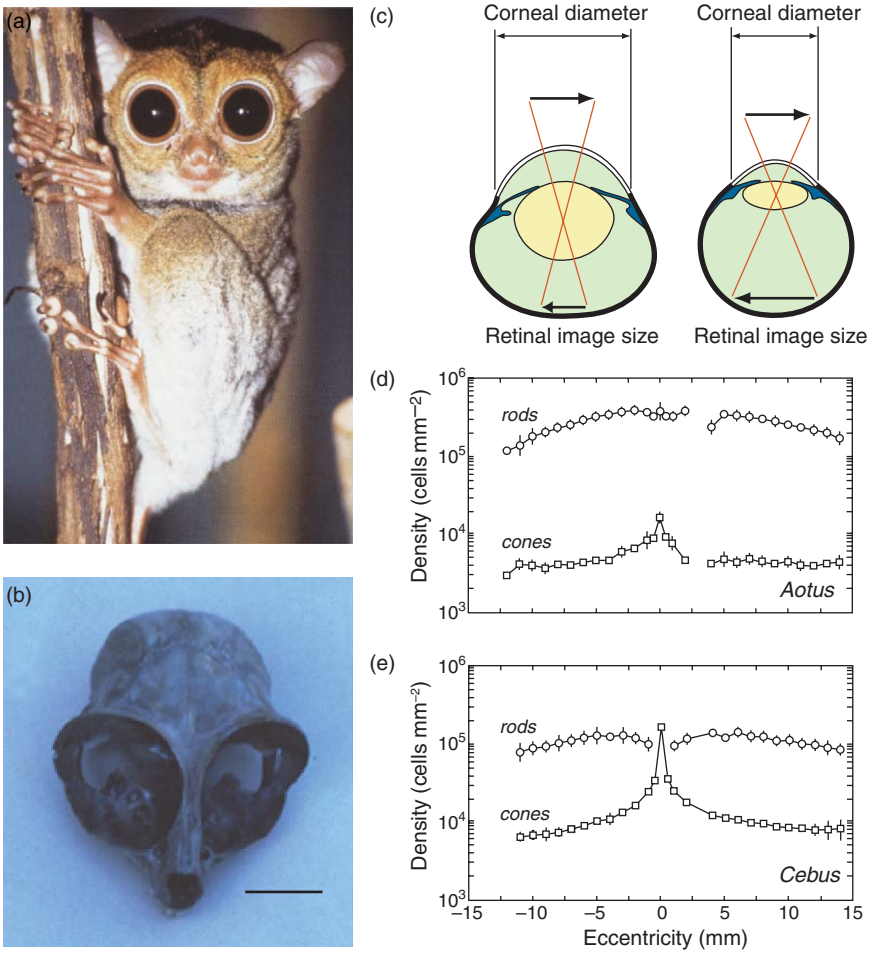

Figure 10 Nocturnal vision in primates. (a) The Western Tarsier *Tarsius bancanus*, whose huge eyes (each larger than its brain!) are likely to support excellent nocturnal vision. (b) The skull of a tarsier (*Tarsius* sp.), with huge eye sockets relative to head size. Scale bar = 10 mm. (c) A schematic comparison of eye morphology in the nocturnal bushbaby *Galago* (left) and the diurnal marmoset *Callithrix* (right). The larger corneal diameter of the bushbaby allows a larger pupil and greater sensitivity, while its thicker and more proximally placed lens shifts the posterior nodal point (roughly at the lens center) closer to the retina. This shortens the focal length, lowers the *F*-number, and increases sensitivity. It also leads to a smaller, and thus less well-resolved, image (as shown by the arrows). Redrawn with kind permission from Kirk E. C. (2004). (d and e) Photoreceptor densities as a function of retinal eccentricity in the nocturnal owl monkey *Aotus* (d) and the diurnal capuchin monkey *Cebus* (e). Note the larger rod density and lower cone density at all eccentricities in the owl monkey, and the great reduction of cones in its fovea. Nasal and temporal eccentricities are represented by positive and negative values, respectively (a) From Rowe, N. 1996. The Pictorial Guide to the Living Primates, Pogonias Press; used with kind permission of the photographer David Haring (Duke Lemur Center). (d, e) Adapted and redrawn with kind permission of Luiz Silveria from Yamada, E. S., Silveira, L. C. L., Perry, V. H., and Franco, E. C. S. 2001. M and P retinal ganglion cells of the owl monkey: morphology, size and photoreceptor convergence. Vision Res. 41, 119–131.

G. L., 1942; Martin, G. R., 1982; Murphy, C. J. *et al.*, 1985; Martin, G. R., 1994; Martin, G. R. and Katzir, G., 1999). A tubular form allows a portion of a larger (and thus more sensitive) spherical eye to fit onto a smaller head (Walls, G. L., 1942). This reduces the weight (payload) of the eye, and thus the energetic cost of maintaining visual function, while at the same time allowing a maximal pupil diameter (which improves sensitivity) and a comparatively longer focal length (which improves resolution). The price paid for this is a restricted visual field: the long tubular optics reduces the region of space from which light reaches the retina. In the tawny owl, the visual field of each eye has a width of 124°, about 40° less than in the more spherical eye of the European starling (Martin, G. R., 1984; 1986). Moreover, the more frontal placement of the owl's eyes (with a divergence angle of 55° that results in a binocular overlap of 48°) restricts the total field of vision to a frontal coverage of 200° width. In contrast, the

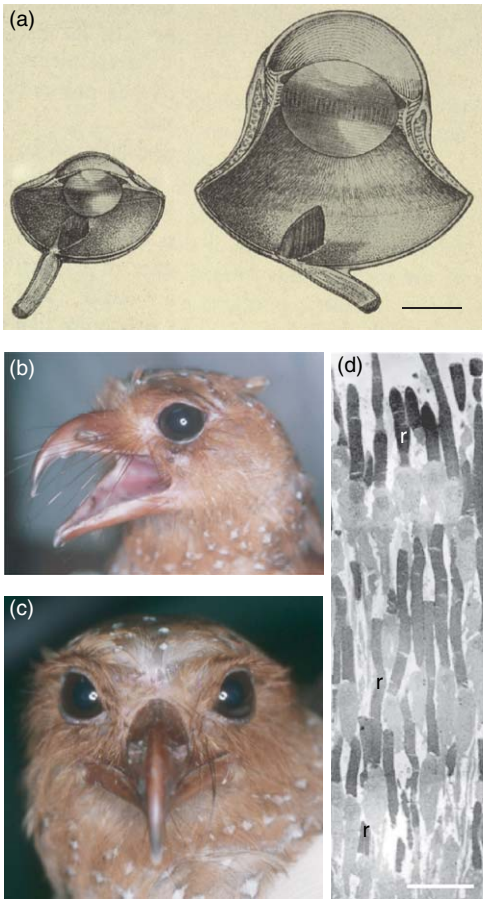

Figure 11 Nocturnal vision in birds. (a) Schematic cross-sections through the eyes of the diurnal swan *Cygnus olor* (left) and the nocturnal owl *Bubo bubo* (right). Note the large tubular form of the owl's eye and the more proximal position of the lens. Diagram adapted from Walls G. L. (1942). Side view (b) and frontal view (c) of the head of the oilbird *Steatornis caripensis*, showing the prominent eyes. Note the bird's rictal bristles in (b). (d) A section through the banked retina of the oilbird, showing the rod outer segments (*r*) arranged in three layers. Scales bar = 10 mm (a), 6 μm (d). (b–d) From Martin, G. R., Rojas, L. M., Ramirez, Y., and McNeil, R. 2004a. The eyes of oilbirds (*Steatornis caripensis*): pushing at the limits of sensitivity. Naturwissenschaften 91, 26–29, with the authors' kind permission.

starling, with more laterally placed eyes that diverge with an angle of 114°, has a total visual coverage of 328°. A binocular overlap similar to that of the owl can also be achieved by eye movements.

It should be stressed, however, that despite being common, large tubular eyes with narrow visual fields are not characteristic of nocturnal animals in general, including birds (Katzir, G. and Martin, G. R., 1998). For instance, the eyes of the nocturnal Caprimulgiformes, while being large relative to head size, are more conventionally shaped and placed laterally on the head. The oilbirds (Figures 11(b) and 11(c)) and common pauraques of South America are good examples (Martin, G. R. *et al.*, 2004a; 2004b), with narrow regions of frontal binocular overlap (25° and 38° wide, respectively) and a broad total visual coverage (around 270° in common pauraques). Despite having much smaller eyes than owls, these nocturnal birds still possess highly sensitive optics of low *F*-number (Table 1).

Because the eyes of nocturnal vertebrates are adapted to very low levels of light, their pupils tend to close very tightly during the day in order to protect the sensitive retina from overexposure to bright daylight. The vertical slit pupils of many nocturnal hunters, like the domestic cat, can almost completely close during the day (Walls, G. L., 1942; Ali, M. A. and Klyne, M. A., 1985). Interestingly, only one group of nocturnal birds – the skimmers – have a vertical slit pupil (Martin, G. R., 1990).

In addition to sensitive optics, many nocturnal animals also have a reflective layer within the retina, behind the photoreceptors – called the tapetum – that allows incident light to be reflected back through the retina. The tapetum thus allows a second chance for absorption of light that had not been absorbed during its first passage through the photoreceptors, thus effectively doubling the lengths of their outer segments. Despite this improvement in sensitivity, the unconstrained reflection provided by a flat tapetum can degrade spatial resolution (Walls, G. L., 1942; Munk, O., 1980; Nicol, J. A. C., 1989; Warrant, E. J. and McIntyre, P. D., 1991; Kirk, E. C. and Kay, R. F., 2004). This may be the reason why many nocturnal animals do not possess them: even though tapeta are common among the nocturnal Strepsirrhine primates (lemurs, lorises, bushbabies, pottos, and aye-ayes: Charles-Dominique, P., 1977), they are absent in the nocturnal Haplorhine primates (tarsiers and the owl monkey *Aotus*). Tapeta are also uncommon in the eyes of nocturnal birds, being found only in the eyes of some Caprimulgiformes, notably the nightjars (Nicol, J. A. C. and Arnott, H. J., 1974) and the common pauraque (Rojas, L. M. *et al.*, 2004).

2.05.7.2 Neural Adaptations for Increased Sensitivity

In the camera eyes of vertebrates, a common evolutionary response to a life in dim light has been a drastic change in the relative proportions of the rod and cone photoreceptors. The rods, responsible for

vertebrate vision in dim light, commonly dominate the retinae of both nocturnal and deep-sea vertebrates, and this is certainly the case for nocturnal birds and primates (Table 2). For instance, in the extreme case of the oilbird *S. caripensis*, there are 123 rods for every cone and one million rods per square millimeter (Martin, G. R. *et al.*, 2004a), the highest rod density recorded in any vertebrate and two-and-a-half times greater than the highest photoreceptor density recorded in a bird (380 000 cones mm^{-2} in the diurnal Brown Falcon *Falco berigora*; see Martin, G. R. *et al.*, 2004a). In other nocturnal birds, the ratio of rods to cones is much lower, but still high: in the barred owl *Strix varia* it is 10:1 and in the common pauraque *Nyctidromus albicolli* it is 5:1 (see Rojas, L. M. *et al.*, 2004; for other examples, see Table 2). In diurnal birds, the ratio is considerably lower, with the number of cones typically exceeding that of the rods: in the diurnal cattle egret *Bubulcus ibis*, the rod:cone ratio is 0.3:1 (Rojas, L. M. *et al.*, 1999a).

The same pattern can be found in primates (Figures 10(d) and 10(e); Table 2): at an eccentricity of 5 mm temporal of the fovea (−5 mm in Figures 10(d) and 10(e)), the density of rods in the nocturnal owl monkey *Aotus azarae* is about 60 times greater than the density of cones, while in the diurnal capuchin monkey *Cebus apella* the ratio is closer to 10:1 (Ogden, T. E., 1975; Wikler, K. C. and Rakic, P., 1990; Yamada, E. S. *et al.*, 2001; Silveira, L. C. L. *et al.*, 2001). Moreover, in *Cebus*, rods are absent altogether at the center of the fovea: instead, there is a massive peak in cone density, a characteristic of many diurnal vertebrates, including primates like ourselves. The situation is,

Table 2 Photoreceptor and convergence ratios in vertebrate eyes

Species	*Animal*	*Activity*	*Rods:cones*	*Rods:RGCs*	*Reference*
Birds				–	3
Strix varia	Barred owl	N	10:1	–	3
Rynchops niger	Black skimmer	N	5:1	–	3
Steatornis caripensis	Oilbird	N	123:1	–	3
Charadrius wilsonia	Wilson's plover	N[a]	1.3:1	–	3
Scolopax minor	American woodcock	N[b]	1.2:1	–	3
Bubo virginianus	Great horned owl	N/C	10.1–13:1	–	3
Nyctidromus albicollis	Common pauraque	N/C	5:1	–	3
Nycticorax violaceus	Yellow-crowned night heron	N/C	2.3:1	–	3
Ardea herodius	Great blue heron	C	0.6:1	–	2
Ajaia ajaja	Roseate spoonbill	C	0.9:1	–	2
Limnodromus griseus	Short-billed dowitcher	D/N	1.0:1	–	1,4
Himantopis himantopis	Black-winged stilt	D/N	1.1:1	–	1
Catoptrophorus semipalmatus	Willet	D/N	0.7:1	–	1
Bubulcus ibis	Cattle egret	D	0.3:1	–	2
Egretta tricolor	Tricolored egret	D	0.3:1	–	2
Eudocimus ruber ruber	American white ibis (scarlet)	D	0.3:1	–	2
Primates					
Otolemur garnettii	Greater bushbaby	N	–	307:1P[c]; 2135:1M[c]	5
Microcebus murinus	Lesser mouse lemur	N	90:1[d]	140:1[d]	6
Aotus azarae	Owl monkey	N	60:1[d]	900:1P[d]; 9000:1M[d]	7–11
Cebus apella	Capuchin monkey	D	10:1[d]	160:1P[d]; 1300:1M[d]	7–11
Macaca nemestrina	Pigtail macaque monkey	D	15.7:1[e]	320:1P[e]; 2000:1M[e]	12
Callithrix jacchus	Common marmoset	D	1.8:1[e]	320:1P[e]; 1000:1M[e]	12
Homo sapiens	Human	D	22:1[e]	200:1P[e]; 4000:1M[e]	12

The ratio of rods to cones was calculated from linear transects of the retina in birds (and are averages for the entire retina), and from photoreceptor densities in primates (i.e., this ratio is thus not directly comparable between birds and primates). RGC, retinal ganglion cell; N, nocturnal; D, diurnal; C, crepuscular; P, parvocellular RGC; M, magnocellular RGC. Superscript letters: *a* = may be nocturnal and diurnal during the breeding season; *b* = nocturnal only in winter; *c* = central retina (eccentricity 0 mm); *d* = eccentricity 5 mm temporal of the fovea; *e* = eccentricity 5 mm from the fovea (averaged from the temporal, upper and lower quadrants of the retina, and calculated using equations given in reference 11). References to original articles are given in 1 (Rojas, L. M. *et al.*, 1999a), 2 (Rojas, L. M. *et al.*, 1999b), and 3 (Rojas, L. M. *et al.*, 2004). Other references: 4 = Rojas L. M. *et al*. (1993); 5 = Yamada E. S. *et al*. (1998); 6 = Dkhissi-Benyahya O. *et al*. (2001); 7 = Silveira L. C. L. *et al*. (1994); 8 = Lima S. M. A. *et al*. (1996); 9 = Yamada E. S. *et al*. (2001); 10 = Silveira L. C. L. *et al*. (2001); 11 = Silveira L. C. L. *et al*. (2004); 12 = Goodchild A. K. *et al*. (1996) (and references therein).

however, quite different in *Aotus*. The large peak in foveal cone density seen in *Cebus* is missing in *Aotus* – the rods, absent in the central fovea of *Cebus*, dominate the fovea of *Aotus* (Figures 10(d) and 10(e)). Part of the reason for the great reduction of cones in the owl monkey *Aotus* is that it has lost two of the three classes of cones typical of diurnal primates like *Cebus*, or ourselves (Wikler, K. C. and Rakic, P., 1990). These three cone classes – short (S), medium (M), and long (L) wavelength sensitive – are responsible for the well-developed trichromatic color vision found in most diurnal Haplorhine primates. *Aotus* has lost its S-cone due to a defect in the S-class opsin gene (Wikler, K. C. and Rakic, P., 1990; Jacobs, G. H. *et al*., 1993; 1996), and the single remaining class is an M/L-cone with absorption peak at 543 nm. Loss of the S-cone has also occurred in the thick-tailed bushbaby *Otolemur crassicaudatus* (Deegan, J. F. and Jacobs, G. H., 1996; Jacobs, G. H. *et al*., 1996), implying that owl monkeys and bushbabies are monochromats. The nocturnal mouse lemur *Microcebus murinus* is similar to the owl monkey and bushbaby, although the S-cone is present, but in exceptionally low numbers (Dkhissi-Benyahya, O. *et al*., 2001). Although it is probable that owl monkeys, bushbabies, and possibly nocturnal lemurs have sacrificed color vision to achieve higher sensitivity, this does not imply that nocturnal color vision in other species is impossible. Indeed, as we saw above, it has recently been discovered in hawkmoths (Kelber, A. *et al*., 2002) and now also in nocturnal geckoes (Roth, L. S. V. and Kelber, A., 2004). And interestingly, it has been shown that tarsiers, unlike owl monkeys and bushbabies, have retained their S-cones (Hendrickson, A. *et al*., 2000), which even opens the possibility for dichromatic nocturnal color vision in a primate.

In oilbirds, the enormous rod:cone ratio (123:1) is due to a remarkable retinal adaptation, previously described only in deep-sea fishes (Warrant E. J. and Locket, N. A., 2004). As in deep-sea fishes, the rods of the oilbird are arranged in layers, one above the other, to create a so-called banked retina (Figure 11(d); Martin, G. R. *et al*., 2004a). In oilbirds, there are three such layers and their role is to increase the pathlength of light traveling through the retina, thus maximizing photon absorption. As a comparison, in the deep temporal foveae of the alepocephalid deep-sea fish *Bajacalifornia drakei*, there are no less than 28 layers of rod outer segments through which the incoming light must pass, although it is still unclear whether all layers are functional (Locket, N. A., 1985). Even though it remains unresolved as to whether banked retinae compromise spatial resolution, the increased sensitivity they undoubtedly afford represents a remarkable example of convergent evolution.

As we mentioned earlier, the photoreceptors of arthropods are capable of responding to single photons of light (see Section 2.05.6.2.1), and this is also the case for vertebrate rods (e.g., Baylor, D. A. *et al*., 1980; Rieke, F. and Baylor, D. A., 1998). Despite this apparent sensitivity, signal reliability in vertebrate photoreceptors – just as in invertebrate photoreceptors – is compromised in dim light due to various sources of noise (Donner, K., 1992), both intrinsic (dark noise and transducer noise) and extrinsic (photon shot noise). Capturing more light can lessen the deleterious effects of this noise, and as we have seen above, the optical structures of nocturnal eyes are adapted to do this. Neurally, however, just as in arthropods, there is no evidence that the rods of nocturnal vertebrates are intrinsically better at capturing and absorbing light than those of diurnal vertebrates. This can be seen in birds: the absorption coefficient of rods in the tawny owl is $0.039\,\mu m^{-1}$ (Bowmaker, J. K. and Martin, G. R., 1978), a value actually less than that found in diurnal chickens ($0.053\,\mu m^{-1}$: Bowmaker, J. K. and Knowles, A., 1977) and pigeons ($0.049\,\mu m^{-1}$: Bowmaker, J. K., 1977). There is, however, evidence that the rod-dominated retinae of some nocturnal birds respond more slowly (Rojas, L. M. *et al*., 1997; 1999a), and more sensitively, to stimulation with light than the cone-dominated retinae of diurnal birds. Measurements of the scotopic (dark-adapted, rod-mediated) electroretinogram (ERG) – and specifically the amplitude of the b-wave – suggest that in some groups of birds, the rods of nocturnal species are more sensitive to light than those of diurnal species (Rojas, L. M. *et al*., 1997; 1999a; 2004). However, in wading birds, this does not seem to be the case (Rojas, L. M. *et al*., 1999b).

Perhaps the greatest neural determinant of light capture, resolution, and sensitivity in a vertebrate camera eye is the extent of convergence (or summation), via the bipolar cells, of photoreceptor signals onto the underlying ganglion cells. In all vertebrate retinae, photoreceptors typically converge in large numbers onto single ganglion cells, the exact convergence ratio depending on the distance (eccentricity) from the center of the retina. The convergence ratio is lowest at the exact center of the retina. In the central foveae of diurnal anthropoid primates, signals

from a single cone photoreceptor are divided between two midget (parvocellular) ganglion cells, one OFF type and one ON type (Wässle, H. and Boycott, B., 1991). As one moves in any direction away from the fovea, the convergence ratio increases and, in the periphery of the retina, can become very great indeed, with large numbers of photoreceptor signals converging onto single ganglion cells.

The size of the converging photoreceptor pool, together with noise removal mechanisms in the photoreceptor–bipolar cell synapse (van Rossum, M. C. W. and Smith, R. G., 1998), sets the potential sensitivity of the receiving ganglion cell and the local spatial resolution (Hughes, A., 1977; Collin, S. P., 1999). A smaller photoreceptor pool builds a smaller and less-sensitive ganglion cell receptive field, and the density profile of ganglion cells across a retina reveals the trade-off between spatial resolution on the one hand and sensitivity to an extended source on the other. A denser packing of ganglion cells indicates a region of higher resolution where sensitivity has been sacrificed. For instance, in the central foveae of diurnal anthropoid primates, one cone supplies two ganglion cells, and the density of cones thus sets the local anatomical spatial resolution (which is also the highest achievable in the eye). As one moves away from the fovea, photoreceptor summation leads to a lower density of ganglion cells and lower spatial resolution, but higher sensitivity. Thus, one may expect vertebrates active in dim light to have a higher convergence ratio of photoreceptors (i.e., rods) to ganglion cells than found in diurnal vertebrates, and this is certainly the case (Hughes, A., 1977), even in the very center of the retina (Kirk, E. C. and Kay, R. F., 2004). The nocturnal domestic cat, for instance, has a higher convergence ratio and coarser vision than a human but are much more sensitive to light (Pasternak, T. and Merigan, W. H., 1981). The same can be said of nocturnal primates (Table 2): in the nocturnal owl monkey *Aotus*, the convergence ratios of rods to magnocellular and parvocellular ganglion cells at an eccentricity of −5 mm (Figures 10(d) and 10(e)) are around six to seven times greater than in the diurnal capuchin monkey *Cebus* (Silveira, L. C. L. *et al.*, 1994; Lima, S. M. A. *et al.*, 1996; Silveira, L. C. L. *et al.*, 2001; Yamada, E. S. *et al.*, 2001; Silveira, L. C. L. *et al.*, 2004). This is due to a significantly larger rod density (Figures 10(d) and 10(e)) and a much greater dendritic field size (and thus lower density) of bipolar cells (Dos Santos, S. N. *et al.*, 2005) and ganglion cells in *Aotus*. In fact, the magnocellular and parvocellular ganglion cells of *Aotus* have receptive field areas that are about four and six times larger (respectively) than those of *Cebus*, and this results in three times fewer ganglion cells (in total) within the eye. The largest area of difference is in the central (foveal) part of the retina, which in *Aotus* has fewer than 35% of the cones and fewer than 20% of the ganglion cells that are found centrally in *Cebus* (Silveira, L. C. L. *et al.*, 2004). However, despite having fewer ganglion cells, *Aotus* has a higher proportion of magnocellular cells than found in *Cebus*. This is commensurate with the presumed role of the magnocellular pathway, which is to mediate pattern vision at scotopic light levels (Yamada, E. S. *et al.*, 2001). Thus, the higher convergence ratios found in *Aotus* compared to *Cebus*, together with monochromacy, low ganglion cell densities (especially centrally), and a bias toward magnocellular processing, all suggest that the retinae of owl monkeys are adapted for coarser but more sensitive vision at very low light levels. This conclusion is reinforced by the structure of the lateral geniculate nucleus (LGN), the first relay station for information traveling from the eye to the visual cortex. In diurnal Haplorhine primates like ourselves, the LGN is divided into four large dorsal parvocellular layers (receiving inputs from the large proportion of parvocellular ganglion cells) and two smaller ventral magnocellular layers (receiving inputs from magnocellular ganglion cells). This dominance of the parvocellular division of the LGN in diurnal Haplorhine primates reflects their need for highly resolved foveal vision and color analysis during the day. In contrast, owl monkeys, tarsiers, and nocturnal Strepsirrhine primates (lorises, lemurs, and bushbabies) have only two parvocellular layers, which no doubt reflects their considerably less foveate retina and lack of color vision (Collins, C. E. *et al.*, 2005).

The same adaptational patterns are probably also found in nocturnal birds, but to my knowledge, no proper measurements have been made of convergence ratios and ganglion cell densities in this group.

2.05.7.3 Visual Behavior in Nocturnal Birds and Primates

2.05.7.3.1 Vision versus other senses at night

As mentioned above, some nocturnal birds are flightless, foraging for food on the forest floor (e.g., kiwis). Others are active flyers, frequently taking prey on the wing (e.g., owls). This difference in the lifestyles of birds has had a profound influence on the evolution

not only of their visual systems but also of their other sensory systems. The same is true of nocturnal primates: some groups (e.g., lorises) are slowly moving and capture slowly moving prey, while others (e.g., bushbabies and tarsiers) rapidly leap from tree to tree and capture fast-moving, and often flying, prey.

Since flightless foraging nocturnal birds potentially have less demanding visual requirements than their flying relatives, one might expect the energetic demands associated with extracting adequate visual information in dim light (Laughlin, S. B. *et al.*, 1998; Laughlin, S. B., 2001) to drive the evolution of regressed visual systems in these birds (Martin, G. R. *et al.*, 2007). In that case, other senses, such as olfaction and mechanoreception, could then take over the role of guiding the animal. This has indeed been a common evolutionary outcome in flightless nocturnal birds, the kiwis providing an excellent example. These birds have very small eyes relative to body mass (Brooke, M. *et al.*, 1999), with the smallest visual fields known for any bird and an optic tectum that is markedly reduced (Martin, G. R. *et al.*, 2007). In contrast, the olfactory and tactile senses of kiwis are greatly enhanced, with the long bill acting as a highly sensitive probe that the bird uses to search the leaf litter for food. The bill tip is covered in highly unusual mechanosensory pits, and in addition, two large nostrils open laterally at the same location (Martin, G. R. *et al.*, 2007). This nostril location is also very unusual for birds – most bird nostrils are located at the base of the bill. Information from this remarkable olfactory-tactile probe is processed within enlarged regions of the brain that are specialized for these sensory modalities (Martin, G. R. *et al.*, 2007). Many waterbirds, while wandering the mudflats and probing for submerged prey at night, also rely exclusively on tactile information collected by the bill, despite being visual feeders during the day (Robert, M. and McNeil, R., 1989; McNeil, R. *et al.*, 1992; 1993).

Even for actively flying nocturnal birds, the difficulties associated with seeing at night have not only resulted in enhanced visual sensitivity, but also in enhanced hearing (e.g., owls), olfaction (e.g., oilbirds), and touch (e.g., frogmouths). The oilbirds are especially interesting. Not only do these cave-dwelling birds apparently have enhanced olfactory abilities (Snow, D. W., 1961; Bang, B. G. and Wenzel, B. M., 1985; Martin, G. R., 1990), they also use echolocation to find their way around within the pitch-dark cave interior (see Martin, G. R., 1990). However, this echolocation is switched off upon leaving the cave at night, after which point vision and olfaction take over. Moreover, the oilbirds, like many nocturnal Caprimulgiformes, have long rictal bristles that project from the base of the beak (Figure 11(b)). These bristles are assumed to aid in the detection of food, for instance by bending when they come into contact with prey, thus providing a mechanosensory cue for guiding the beak, and triggering a peck.

Very similar conclusions can also be made for the nocturnal primates. After years of careful field studies in Gabon, Pierre Charles-Dominique P. (1977) provided our first and clearest picture of nocturnal behavior in African lorisines (the potto *Perodicticus potto* and Angwantibo *Arctocebus calabarensis*) and galagines (six species of bushbabies). His meticulous documentation of the feeding habits, locomotion, and social interactions of these nocturnal primates allowed him to assess the importance of vision, and the other senses, in their behavior. The lorisines slowly climb trees and traverse branches in the forest canopy and rely heavily on olfaction for capturing slow or sedentary insect prey. This is particularly true of the Angwantibo, which apparently sees rather poorly. The potto, whilst having better vision, also relies heavily on olfaction for capturing insect prey (Charles-Dominique, P., 1977). In contrast, bushbabies (just like tarsiers: Castenholz, A., 1984; Collins, C. E. *et al.*, 2005) are much more visually driven and rely on this sense to accurately leap from tree to tree in the dark and to locate and manipulate insect and vertebrate prey. Auditory localization of prey is also important (Charles-Dominique, P., 1977). Olfaction, whilst certainly useful, is of less importance in prey capture. Moreover, even though some nocturnal primates possibly use scent to mark preferred travel routes in the forest canopy, and to recognize conspecifics, it again seems that vision is the most important sense for selecting routes (Charles-Dominique, P., 1977; Wright, P. C., 1989) and possibly even for recognizing other members of the group (e.g., facial feature recognition in the owl monkey: Bearder, S. K. *et al.*, 2006).

Thus, despite having large and sensitive eyes, flying nocturnal birds and leaping nocturnal primates rely on all of their senses to survive. Nevertheless, considerable information is gained visually, and much of their behavior is visually driven. How well do nocturnal birds and primates actually see?

2.05.7.3.2 Visual performance in dim light

Whilst many anecdotal field observations exist attesting to the visual prowess of nocturnal birds

(especially owls) and primates, exceedingly few studies have been made to behaviorally measure visual performance in dim light quantitatively.

Apart from a few inconclusive earlier studies (Hecht, S. and Pirenne, M. H., 1940; Dice, D. L., 1945; Lindblad, J., 1967), Fite K. V. (1973) and Martin and colleagues (Martin, G. R. and Gordon, I. E., 1974a; 1974b; Martin, G. R., 1974, 1977) were the first and, to my knowledge, only investigators that have reliably measured dim-light visual performance in nocturnal birds (contrast sensitivity has been measured in barn owls, but not at scotopic light levels: Ghim, M. M. and Hodos, W., 2006). Behavioral methods, based on training birds to associate food with a visual stimulus, were used to measure absolute sensitivity in the tawny owl (Martin, G. R., 1977) and scotopic visual acuity in the great horned owl (Fite, K. V., 1973). Their results reveal that these owls, despite their nocturnal habits and large eyes, have only 2.2 times greater absolute sensitivity and four times greater threshold visual acuity (Figure 12) than humans.

These small differences in performance between owls and humans are probably explained on the basis of differences in the optics and sizes of their eyes

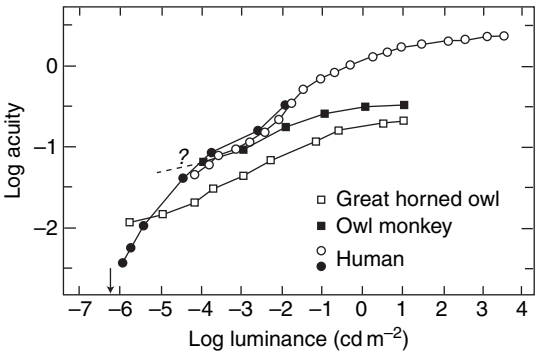

Figure 12 Visual acuity in nocturnal vertebrates. The visual acuity of the human (circles), the great horned owl *Bubo virginianus* (open squares), and the owl monkey *Aotus trivirgatus* (filled squares) as a function of luminance. At each intensity, acuity is calculated from the minimum angular width w (in minutes of arc) of a stripe, from a uniform black-and-white square-wave grating, that is just visible to the observer. Acuity $= \log w^{-1}$. The arrow marks the absolute visual threshold of the tawny owl (see Figure 2). Adapted and redrawn with kind permission from Martin G. R. (1990), with data for the owl monkey taken from Jacobs G. H. (1977b). Jacobs G. H. (1977b) also published acuity data for humans that indicate slightly poorer performance at the dimmest light levels than the human data presented here (by about 0.3 log units of acuity) – his owl monkeys outperformed his human observers at 10^{-4} cd m^{-2} and could presumably continue to so even at dimmer intensities (dashed line).

(Martin, G. R., 1990). Humans and tawny owls have eyes of similar axial length (25 and 28.5 mm, respectively), but the owl has a significantly larger pupil (13.3 vs. 8 mm, fully dark adapted). This endows the tawny owl with a lower F-number (1.3 vs. 2.13: Table 1), and thereby a retinal image that is $(2.13/1.3)^2 = 2.7$ times brighter than in humans, an improvement in optical sensitivity entirely consistent with the 2.2 times greater absolute sensitivity measured behaviorally. The greater acuity of the great horned owl is certainly partly due to its more sensitive eyes (also of much lower F-number than the human eye: Table 1). However, the owl's much larger axial eye length (38.7 mm), and correspondingly longer focal length, must also play a part. The difference in axial eye length suggests that an object imaged on the owl's retina would be about 1.5 times larger than the image formed on a human retina. Moreover, the deep convexiclivate foveal pit of the great horned owl (Fite, K. V., 1973) may also have telephoto properties that magnify the image in the retina, thereby improving acuity further (as is known for diurnal birds of prey: Snyder, A. W. and Miller, W. H., 1978).

To my knowledge, absolute sensitivity has never been measured behaviorally in a nocturnal primate (although spectral thresholds, which are not the same thing, have been measured in the owl monkey *Aotus trivirgatus*: Jacobs, G. H., 1977a). However, acuity measurements have been made, and these are comparable to those made in the great horned owl. In the owl monkey, visual acuity is higher than that in the great horned owl at all intensities (Jacobs, G. H., 1977b) and even exceeds that of humans at the lowest intensities (Figure 12), suggesting that compared to many nocturnal vertebrates, *Aotus* probably has excellent night vision. Spatial resolution has also been measured in the bushbaby *Galago crassicaudatus*, but not at scotopic light levels (Langston, A. *et al.*, 1986).

What do the above measures of absolute sensitivity and threshold visual acuity in nocturnal birds and primates tell us about their visual abilities relative to other animals? First, examination of Figure 2 reveals that the absolute sensitivity of the tawny owl would allow it to see without difficulty under all levels of natural nocturnal illumination in open habitats, but in closed habitats (like woodland) it would be facing difficulties, particularly on overcast nights. The situation is slighter better for the nocturnal domestic cat, and slightly worse for humans. Diurnal pigeons, with their small and insensitive eyes, would be

unable to see well in all but the brightest nocturnal habitats. Second, at threshold, and at a distance of 1 m, the acuity of the great horned owl would prevent it seeing high-contrast objects smaller than about 3 cm in diameter (Martin, G. R., 1990). At a viewing distance of 10 m, the minimum visible size would be 29 cm! For the much lower contrasts of objects found in natural habitats (Laughlin, S. B., 1981b; Vu, T. Q. *et al.*, 1997), these minimum sizes would be considerably larger.

These results suggest that the retinas of owls and humans are equally sensitive and that the modest enhancements in visual performance found in owls are due to optical differences alone. This conclusion at first seems surprising. Humans are considered diurnal animals with poor night vision, whilst owls are thought to be quintessential nocturnal hunters. Indeed, many species of owls fly in cluttered woodland environments at night when light levels are extremely low (Figure 2), even capturing their prey on the forest floor from the air. How can the above measurements of visual performance be reconciled with these observations? The answer lies in an examination of their predation strategies in the wild.

2.05.7.3.3 Visually guided prey capture, locomotion, and navigation

As we saw in Figure 2, nocturnal light levels can vary over many orders of magnitude, being brightest in open habitats with cloudless, moonlit skies and dimmest under a forest canopy illuminated by a moonless but overcast sky. As we mentioned above, even a diurnal pigeon is probably able to see reasonably well on the brightest nights, so it is not surprising that many nocturnal birds and primates, adapted for vision in dim light, are able to do so as well. But seeing well enough to visually capture prey, or to move through the forest, may restrict some nocturnal animals to the brighter nocturnal light levels, thus restricting the types of habitats where these animals can live. It may also restrict the range of methods they can adopt for locomotion or to capture prey. Those animals that live in the dimmest nocturnal habitats may be forced to give up on vision altogether and rely on other senses. As we will see, all these scenarios have evolved among nocturnal birds (Martin, G. R., 1990) and primates (Wright, P. C., 1978; Bearder, S. K. *et al.*, 2006).

Because the world under a closed forest canopy is about 100 times dimmer than an open field or an intertidal mudflat (Figure 2), it is not surprising to find that many nocturnal birds, due to insufficient sensitivity, are restricted to hunt prey visually in open habitats. All of the nocturnal Charadriiformes – particularly the coursers, stone-curlews, and thick-knees – inhabit open habitats with sparse and/or short vegetation in the vicinity of water, with good visibility and no barriers to walking and running, their chief locomotory method for detection and pursuit of prey (Martin, G. R., 1990). Despite their large eyes, hearing no doubt plays an important role in their detection of prey (mostly larger insects and other invertebrates). Among the Caprimulgiformes, nightjars (Martin, G. R., 1990) and pauraques (Martin, G. R. *et al.*, 2004b) also restrict hunting to open habitats, or above the forest canopy. Unlike coursers, stone-curlews, and thick-knees, the nightjars and pauraques hunt prey on the wing, taking insects from the air. The nightjars do this by trawling the air ahead for insects, in much the same way that a whale trawls for plankton. They achieve this with an extraordinarily large gape, a gape that is afforded by specialized skull adaptations that allow the beak to open to a much greater extent than in other birds (Buhler, P., 1970). The nightjar beak is also richly endowed with rictal bristles, suggesting that tactile cues may also alert the bird to collisions with insects (thereby triggering prey capture behavior). A wide gape and rictal bristles are also characteristics of the common pauraque (Martin, G. R. *et al.*, 2004b). Thus, in nightjars and pauraques, even though vision is probably important for flight orientation, it may play a lesser role in prey capture. Nevertheless, both birds have large eyes, and both are known to take insects from below, indicating that, silhouetted against the night sky, a large flying insect may be a reliable visual target (Martin, G. R. *et al.*, 2004b). Many Strigiformes (owls) are also open-habitat hunters. Good examples include the snowy owl, the short-eared owl, and the African marsh owl (Martin, G. R., 1990). These owls prefer open country devoid of trees, tend to be nonsedentary, and are active in brighter light levels, typically hunting during the day or in twilight. They hunt by visually scanning the landscape for potential prey from an elevated vantage point (or perch), a strategy that probably requires the higher light levels found in open crepuscular habitats.

In contrast to life in an open habitat, life under the closed canopy of a forest is particularly challenging for nocturnal animals that use vision for locomotion and prey capture. As we mentioned above, many nocturnal primates (such as the potto *Perodicticus potto* and the Angwantibo *Arctocebus calabarensis*) reduce

their dependence on vision by moving very slowly and relying on other senses, such as olfaction and hearing, for capturing prey (Charles-Dominique, P., 1977). However, others clearly have excellent nocturnal vision. Tarsiers and bushbabies move through the dark nocturnal forest by deftly leaping from tree to tree and, like owl monkeys, follow familiar routes, suggesting the visual recognition of learned landmarks (Charles-Dominique, P., 1977; Wright, P. C., 1978). Moreover, vision plays an important role in prey capture (Charles-Dominique, P., 1977; Castenholz, A., 1984). Interestingly, however, many nocturnal primates reveal activity levels that are correlated to moonlight levels. The nightly wanderings of owl monkeys, lemurs, and bushbabies through the forest canopy are longer for more intense levels of moonlight. On moonless nights, these animals move very little at all. However, this reduction in travel distance on the darkest nights is more likely due to predation risk rather than to limitations in visual sensitivity (Wright, P. C., 1978; Donati, G. *et al.*, 2001; Bearder, S. K. *et al.*, 2006).

The difficulties of living and hunting under a dark forest canopy are similar for nocturnal birds, especially if hunting also involves flight. Frogmouths and potoos (Caprimulgiform birds) and various species of owls (Strigiform birds) fall into this category. Most pounce on prey (typically invertebrates and small rodents) from an elevated perch, and many are sedentary and solitary in their habits. And all need to deal with life in the forest understory, which is not only very dim, but also spatially complex, with many obstacles to flight and orientation. Like the nightjar, the tawny frogmouth *Podargus strigoides* has a wide gape and a beak surrounded by rictal bristles and takes prey by pouncing upon them from an elevated perch or by chasing them along the ground (Martin, G. R., 1990). Despite its large eyes, it is not known what role (if any) vision plays in this behavior. Hearing may also be important, and the presence of rictal bristles also suggests a role for mechanoreception.

Not all owls that frequent forests also hunt there (Martin, G. R., 1990). Many species only roost in the forest but restrict their hunting to open areas away from forests where light levels are higher. Good diurnal–crepuscular examples include the great gray owl, the hawk owl, and the pygmy owl, while nocturnal-crepuscular examples include the long-eared owl, Tengmalm's owl, the eagle owl, and the barn owl (Martin, G. R., 1990). There are, however, a number of strictly nocturnal species that not only roost in the forest, but like frogmouths and potoos, also hunt there. These include the tawny owl, the ural owl, the barred owl, and the spotted owl, all perch-and-swoop hunters in the dark understory. As we discussed above, these owls must perform this hunting behavior in light levels at or below the minimum they can detect (Figure 2). How do they manage then to fly and capture prey in the forest at night? Part of the answer lies in their exquisite hearing: many owls, notably the long-eared owl, the barn owl, and the barred owl, are capable of locating and capturing prey in total darkness, guided only by the sounds of the prey as it moves through the leaf litter (Payne, R. S. and Drury, W. H., 1958; Payne, R. S., 1962; 1971). In other words, owls are capable of flying blind and herein lies the key to how they cope with the dark nocturnal forest habitat. To be able to fly blind, owls must know their surroundings intimately, otherwise crashes with trees (and injuries) would be inevitable. This would require owls to spend long periods in the same habitat, learning the locations of trees and other obstacles. Not surprisingly then, it turns out that the more strictly nocturnal species of owls are also those species which are most territorial and most sedentary (Martin, G. R., 1990). The tawny owl, the ural owl, the barred owl, and the spotted owl – the most strictly nocturnal forest dwellers – all have small territories that are vigorously defended, and they never leave these territories throughout their entire lives. Tawny owls can have territories as small as 16 Ha, depending on this territory for all prey that it eats throughout its life (which may be up to 5 years: Martin, G. R., 1990). To capture this prey, it is very likely that these owls learn the spatial layout of trees and bushes within their territories, allowing them to fly blind for short distances through the forest after hearing their prey. Their eyes may be sensitive enough to detect coarser high-contrast details in their habitat that aid longer flights within the territory (such as gaps in the forest canopy), but it is probably the spatial memory of local obstacles within the territory that ultimately guides nocturnal flight (Martin, G. R., 1990). Such a phenomenal memory task, while overwhelming for humans, is not unknown for birds – many species have remarkable memory (see MacPhail E. M., 1986, for a review). However, developing a spatial memory such as this requires that the owl remains within its territory, and this is precisely what it does. However, whether such a strategy explains the unusual nocturnal hunting prowess of owls remains to be demonstrated.

2.05.8 Conclusions

The colors and contrasts of the nocturnal world are just as rich as those found in the diurnal world, and many animals – both vertebrates and invertebrates – have evolved visual systems to exploit this abundant information. Via a combination of highly sensitive optical eye designs, and unique alterations in the morphology, circuitry, and physiology of the retina and higher visual centers, nocturnal animals are capable of advanced and reliable vision at night. They can see color and negotiate dimly illuminated obstacles while flying or leaping through the forest understory. They can also navigate using learned terrestrial landmarks, the constellations of stars, or the dim pattern of polarized light formed around the moon. Nevertheless, the enormous span of intensities found at night forces many animals to restrict their visual activities to brighter nocturnal light levels, such as those experienced in an open and/or moonlit habitat. However, many other nocturnal animals – such as owls, bushbabies, and tarsiers – are active in the very dimmest habitats, flying, leaping, and capturing prey in extremely little light. Many owls, it seems, have dispensed with vision altogether, relying on hearing and a small and well-known territory to fly blind through the forest in pursuit of prey. But tarsiers, bushbabies, and owl monkeys, even on the darkest nights, apparently rely on vision to execute the daily tasks of life. Exactly how well they see is still an open question, and a fascinating and fruitful avenue for future research.

Acknowledgments

I wish to thank Dan-Eric Nilsson, Almut Kelber, Graham Martin, Chris Kirk, David Haring, and Luiz Silveira for graciously allowing me to reproduce their figures in this review. I am also extremely grateful for the ongoing support of the Swedish Research Council (Vetenskapsrådet) and the Royal Physiographic Society of Lund.

References

Aho, A.-C., Donner, K., Hydén, C., Larsen, L. O., and Reuter, T. 1988. Low retinal noise in animals with low body temperature allows high visual sensitivity. Nature 334, 348–350.

Aho, A.-C., Donner, K., Helenius, S., Larsen, L. O., and Reuter, T. 1993. Visual performance of the toad (*Bufo bufo)* at low light levels, retinal ganglion cell responses and prey-catching accuracy. J. Comp. Physiol. A 172, 671–682.

Ali, M. A. and Klyne, M. A. 1985. Vision in Vertebrates. Plenum.

Arneson, L. and Wcislo, W. T. 2003. Dominant-subordinate relationships in a facultatively social, nocturnal bee, *Megalopta genalis* (Hymenoptera, Halictidae). J. Kansas Entomol. Soc. 76, 183–193.

Autrum, H. 1981. Light and Dark Adaptation in Invertebrates. In: Handbook of Sensory Physiology (*ed*. H. Autrum), Vol. VII/6C, pp. 1–91. Springer.

Bang, B. G. and Wenzel, B. M. 1985. Nasal Cavity and Olfactory System. In: Form and Function in Birds (*eds*. A. S. King and J. McLelland), Vol. 3, pp. 195–225. Academic Press.

Barlow, H. B. 1956. Retinal noise and absolute threshold. J. Opt. Soc. Am. 46, 634–639.

Barlow, H. B., Levick, W. R., and Yoon, M. 1971. Responses to single quanta of light in retinal ganglion cells of the cat.. Vision Res. 11, 87–101.

Baylor, D. A., Matthews, G., and Yau, K.-W. 1980. Two components of electrical dark noise in toad retinal rod outer segments. J. Physiol. 309, 591–621.

Bearder, S. K., Nekaris, K. A. I., and Curtis, D. J. 2006. A re-evaluation of the role of vision in the activity and communication of nocturnal primates. Folia Primatol. 77, 50–71.

Becker, L. 1958. Untersuchungen über das Heimfindevermögen der Bienen. Z. Vergl. Physiol. 41, 1–25.

Blest, A. D. 1978. Rapid synthesis and destruction of photoreceptor membrane by a dinopid spider – daily cycle. Proc. R. Soc. Lond. B. 200, 463–483.

Blest, A. D. and Land, M. F. 1977. The physiological optics of *Dinopis subrufus*, a fish lens in a spider. Proc. R. Soc. Lond. B. 196, 197–222.

Bowmaker, J. K. 1977. The visual pigments, oil droplets and spectral sensitivity of the pigeon. Vision Res. 17, 1129–1138.

Bowmaker, J. K. and Knowles, A. 1977. The visual pigments and oil droplets of the chicken retina. Vision Res. 17, 755–764.

Bowmaker, J. K. and Martin, G. R. 1978. Visual pigments and colour vision in a nocturnal bird, *Strix aluco* (Tawny Owl). Vision Res. 18, 1125–1130.

Brooke, M., de, L., Hanley, S., and Laughlin, S. B. 1999. The scaling of eye size with body mass in birds. Proc. R. Soc. Lond. B. 266, 405–412.

Buhler, P. 1970. Schademorphologie und Kiefermechanik der Caprimulgidae (Aves). Z. Morph. Tiere. 66, 337–399.

Capaldi, E. A. and Dyer, F. C. 1999. The role of orientation flights on homing performance in honeybees. J. Exp. Biol. 202, 1655–1666.

Castenholz, A. 1984. The Eye of *Tarsius*. In: Biology of Tarsiers (*ed*. C. Niemitz), pp. 303–318. Gustav Fischer Verlag.

Charles-Dominique, P. 1977. Ecology and Behaviour of Nocturnal Primates (*trans.* R. D. Martin), Columbia University Press.

Cleary, P., Deichsel, G., and Kunze, P. 1977. The superposition image in the eye of *Ephestia kühniella*. J. Comp. Physiol. 119, 73–84.

Collin, S. P. 1999. Behavioural Ecology and Retinal Cell Topography. In: Adaptive Mechanisms in the Ecology of Vision (*eds*. S. N. Archer, M. B. A. Djamgoz, E. R. Loew, J. C. Partridge, and S. Vallerga), pp. 509–535. Kluwer Academic Publishers.

Collins, C. E., Hendrickson, A., and Kaas, J. H. 2005. Overview of the visual system of *Tarsius*. Anatom. Rec. A. 287A, 1013–1025.

Cronin, T. W., Greiner, B., and Warrant, E. J. 2006. Celestial polarization patterns during twilight. App. Opt. 45, 5582–5589.

Dacke, M., Byrne, M., Scholtz, C. H., and Warrant, E. J. 2004. Lunar orientation in a beetle. Proc. R. Soc. Lond. B. 271, 361–365.

Dacke, M., Nilsson, D.-E., Scholtz, C. H., Byrne, M., and Warrant, E. J. 2003a. Insect orientation to polarized moonlight. Nature 424, 33.

Dacke, M., Nordström, P., and Scholtz, C. H. 2003b. Twilight orientation to polarised light in the crepuscular dung beetle *Scarabaeus zambesianus*. J. Exp. Biol. 106, 1535–1543.

Deegan, J. F. and Jacobs, G. H. 1996. Spectral sensitivity and photopigments of a nocturnal prosimian, the bushbaby (*Otolemur crassicaudatus*). Am. J. Primat. 40, 55–66.

De Vries, H. 1943. The quantum character of light and its bearing upon threshold of vision, the differential sensitivity and visual acuity of the eye. Physica 10, 553–564.

Dice, D. L. 1945. Minimum intensities of illumination under which owls can find dead prey by sight. Am. Nat. 79, 384–416.

Dkhissi-Benyahya, O., Szel, A., Degrip, W. J., and Cooper, H. M. 2001. Short and mid-wavelength cone distribution in a nocturnal Strepsirrhine primate (*Microcebus murinus*). J. Comp. Neurol. 438, 490–504.

Donati, G., Lunardini, A., Kappeler, P. M., and Borgognini Tarli, S. M. 2001. Nocturnal activity in the cathemeral red-fronted lemur (*Eulemur fulvus rufus)*, with observations during a lunar eclipse. Am. J. Primatol. 53, 69–78.

Donner, K. 1992. Noise and the absolute thresholds of cone and rod vision. Vision Res. 32, 853–866.

Dos Santos, S. N., Dos Reis, J. W. L., Silva Filho, M.da, Kremers, J., and Silveira, L. C. L. 2005. Horizontal cell morphology in nocturnal and diurnal primates: a comparison between owl monkey (*Aotus)* and capuchin monkey (*Cebus*). Vis. Neurosci. 22, 405–415.

Doujak, F. E. 1984. Electrophysiological measurement of photoreceptor membrane dichroism and polarization sensitivity in a Grapsid crab. J. Comp. Physiol. A. 154, 597–605.

Doujak, F. E. 1985. Can a shore crab see a star? J. Exp. Biol. 166, 385–393.

Dubs, A., Laughlin, S. B., and Srinivasan, M. V. 1981. Single photon signals in fly photoreceptors and first order interneurons at behavioural threshold. J. Physiol. 317, 317–334.

Dvorak, D. and Snyder, A. W. 1978. The relationship between visual acuity and illumination in the fly *Lucilia sericata*. Z. Naturforsch. C. 33, 139–143.

Fite, K. V. 1973. Anatomical and behavioural correlates of visual acuity in the great horned owl. Vision Res. 13, 219–230.

Gál, J., Horváth, G., Barta, A., and Wehner, R. 2001. Polarization of the moonlit clear night sky measured by full-sky imaging polarimetry at full moon: comparison of the polarization of moonlit and sunlit skies. J. Geophys. Res. 106, 22647–22653.

Garamszegi, L. Z., Møller, A. P., and Erritzøe, J. 2002. Coevolving avian eye size and brain size in relation to prey capture and nocturnality. Proc. R. Soc. Lond. B. 269, 961–967.

Ghim, M. M. and Hodos, W. 2006. Spatial contrast sensitivity of birds. J. Comp. Physiol. A. 192, 523–534.

Goodchild, A. K., Ghosh, K. K., and Martin, P. R. 1996. Comparison of photoreceptor spatial density and ganglion cell morphology in the retina of human, macaque monkey, cat, and the marmoset *Callithrix jacchus*. J. Comp. Neurol. 366, 55–75.

Greiner, B. 2006. Visual adaptations in the night-active wasp *Apoica pallens*. J. Comp. Neurol. 495, 255–262.

Greiner, B., Ribi, W. A., and Warrant, E. J. 2004a. Retinal and optical adaptations for nocturnal vision in the halictid bee *Megalopta genalis*. Cell Tissue Res. 316, 377–390.

Greiner, B., Ribi, W. A., and Warrant, E. J. 2004b. Neuronal organisation in the first optic ganglion of the nocturnal bee *Megalopta genalis*. Cell Tissue Res. 318, 429–437.

Greiner, B., Ribi, W. A., and Warrant, E. J. 2005. A neural network to improve dim-light vision? Dendritic fields of first-order interneurons in the nocturnal bee *Megalopta genalis*. Cell Tissue Res. 323, 313–320.

Hall, M. I. and Ross, C. F. 2007. Eye shape and activity in birds. J. Zool. 271, 437–444.

Hardie, R. C. and Duelli, P. 1978. Properties of single cells in posterior lateral eyes of jumping spiders. Z. Naturforschung. C. 33, 156–158.

Hateren, J. H.van 1993. Spatiotemporal contrast sensitivity of early vision. Vision Res. 33, 257–267.

Hecht, S. and Pirenne, M. H. 1940. The sensibility of the nocturnal long-eared owl in the spectrum. J. Gen. Physiol. 23, 709–717.

Hendrickson, A., Djajadi, H. R., Nakamura, L., Possin, D. E., and Sajuthi, D. 2000. Nocturnal tarsier retina has both short and long/medium-wavelength cones in an unusual topography. J. Comp. Neurol. 424, 718–730.

Herzmann, D. and Labhart, T. 1989. Spectral sensitivity and absolute threshold of polarization vision in crickets, a behavioral study. J. Comp. Physiol. A. 165, 315–319.

Höglund, G., Hamdorf, K., and Rosner, G. 1973. Trichromatic visual system in an insect and its sensitivity control by blue light. J. Comp. Physiol. 86, 265–279.

Howland, H. C., Merola, S., and Basarab, J. R. 2004. The allometry and scaling of the size of vertebrate eyes. Vision Res. 44, 2043–2065.

Hughes, A. 1977. The Topography of Vision in Mammals of Contrasting Life Style: Comparative Optics and Retinal Organisation. In: Handbook of Sensory Physiology, (*ed*. F. Crescitelli), Vol. VII/5, pp. 613–756. Springer.

Jacobs, G. H. 1977a. Visual capacities of the owl monkey (*Aotus trivirgatus*). I. Spectral sensitivity and color vision. Vision Res. 17, 811–820.

Jacobs, G. H. 1977b. Visual capacities of the owl monkey (*Aotus trivirgatus*). II. Spatial contrast sensitivity. Vision Res. 17, 821–825.

Jacobs, G. H., Deegan, J. F., Neitz, J., Crognale, M. A., and Neitz, M. 1993. Photopigments and color vision in the nocturnal monkey, *Aotus*. Vision Res. 33, 1773–1783.

Jacobs, G. H., Neitz, M., and Neitz, J. 1996. Mutations in S-cone pigment genes and the absence of colour vision in two species of nocturnal primate. Proc. R. Soc. Lond. B. 263, 705–710.

Janzen, D. H. 1968. Notes on nesting and foraging behavior of *Megalopta* (Hymenoptera, Halictidae) in Costa Rica. J. Kansas Ent. Soc. 41, 342–350.

Johnsen, S., Kelber, A., Warrant, E. J., Sweeney, A. M., Widder, E. A., Lee, R. L., and Hernandez-Andres, J. 2006. Twilight and nocturnal illumination and its effects on color perception by the nocturnal hawkmoth *Deilephila elpenor*. J. Exp. Biol. 209, 789–800.

Katzir, G. and Martin, G. R. 1998. Visual fields in the black-crowned night heron *Nycticorax nycticorax*: nocturnality does not result in owl-like features. Ibis. 140, 157–162.

Kay, R. F. and Kirk, E. C. 2000. Osteological evidence for the evolution of activity pattern and visual acuity in primates. Am. J. Physic. Anthrop. 113, 235–262.

Kelber, A. and Hénique, U. 1999. Trichromatic colour vision in the hummingbird hawkmoth, *Macroglossum stellatarum*. J. Comp. Physiol. A. 184, 535–541.

Kelber, A. and Roth, L. S. V. 2006. Nocturnal colour vision – not as rare as we might think. J. Exp. Biol. 209, 781–788.

Kelber, A., Balkenius, A., and Warrant, E. J. 2002. Scotopic colour vision in nocturnal hawkmoths. Nature 419, 922–925.

Kelber, A., Balkenius, A., and Warrant, E. J. 2003. Colour vision in diurnal and nocturnal hawkmoths. Integr. Comp. Biol. 43, 571–579.

Kelber, A., Warrant, E. J., Pfaff, M., Wallén, R., Theobald, J. C., Wcislo, W., and Raguso, R. 2006. Light intensity limits the foraging activity in nocturnal and crepuscular bees. Behav. Ecol. 17, 63–72.

Kirk, E. C. 2004. Comparative morphology of the eye in primates. Anatom. Rec. A. 281A, 1095–1103.

Kirk, E. C. 2006. Eye morphology in cathemeral lemurids and other mammals. Folia Primatol. 77, 27–49.

Kirk, E. C. and Kay, R. F. 2004. The Evolution of High Visual Acuity in the Anthropoidea. In: Anthropoid Origins: New Visions (*eds*. C. F. Ross and R. F. Kay), pp. 539–602. Kluwer Academic/Plenum Publishers.

Kirschfeld, K. 1974. The absolute sensitivity of lens and compound eyes. Zeitschrift für Naturforschung 29C, 592–596.

Labhart, T., Petzold, J., and Helbling, H. 2001. Spatial integration in polarization-sensitive interneurones of crickets, a survey of evidence, mechanisms and benefits. J. Exp. Biol. 204, 2423–2430.

Land, M. F. 1969. Structure of the principal eyes of jumping spiders. (Salticidae, Dendryphantinae) in relation to visual optics. J. Exp. Biol. 51, 443–470.

Land, M. F. 1981. Optics and Vision in Invertebrates. In: Handbook of Sensory Physiology (*ed*. H. Autrum), Vol VII/6B, pp. 471–592. Springer.

Land, M. F. 1985. The Morphology and Optics of Spider Eyes. In: Neurobiology of arachnids (*ed*. F. G. Barth), pp. 53–78. Springer.

Land, M. F. and Osorio, D. C. 1990. Waveguide modes and pupil action in the eyes of butterflies. Proc. R. Soc. Lond. B. 241, 93–100.

Land, M. F., Gibson, G., and Horwood, J. 1997. Mosquito eye design, conical rhabdoms are matched to wide aperture lenses. Proc. R. Soc. Lond. Ser. B. 264, 1183–1187.

Land, M. F., Gibson, G., Horwood, J., and Zeil, J. 1999. Fundamental differences in the optical structure of the eyes of nocturnal and diurnal mosquitoes. J. Comp. Physiol. A. 185, 91–103.

Langston, A., Casagrande, V. A., and Fox, R. 1986. Spatial resolution of the galago. Vision Res. 26, 791–796.

Laughlin, S. B. 1981a. Neural Principles in the Peripheral Visual Systems of Invertebrates. In: Handbook of Sensory Physiology, Vol VII/6B (*ed*. H. Autrum), pp. 133–280. Springer.

Laughlin, S. B. 1981b. A simple coding procedure enhances a neuron's information capacity. Z. Naturforsch. 36C, 910–912.

Laughlin, S. B. 1990. Invertebrate Vision at Low Luminances. In: Night Vision (*eds*. R. F. Hess, L. T. Sharpe, and K. Nordby), pp. 223–250. Cambridge University Press.

Laughlin, S. B. 2001. The Metabolic Cost of Information – A Fundamental Factor in Visual Ecology. In: Ecology of Sensing (*eds*. F. G. Barth and A. Schmid), pp. 170–185. Springer.

Laughlin, S. B. and Lillywhite, P. G. 1982. Intrinsic noise in locust photoreceptors. J. Physiol. 332, 25–45.

Laughlin, S. B., Blest, A. D., and Stowe, S. 1980. The sensitivity of receptors in the posterior median eye of the nocturnal spider *Dinopis*. J. Comp. Physiol. 141, 53–65.

Laughlin, S. B., de Ruyter van Steveninck, R. R., and Anderson, J. C. 1998. The metabolic cost of neural information. Nat. Neurosci. 1, 36–41.

Leggett, L. M. W. and Stavenga, D. G. 1981. Diurnal changes in angular sensitivity in crab photoreceptors. J. Comp. Physiol. 144, 99–109.

Lehrer, M. 1996. Small-scale navigation in the honeybee, active acquisition of visual information about the goal. J. Exp. Biol. 199, 253–261.

Lillywhite, P. G. 1977. Single photon signals and transduction in an insect eye. J. Comp. Physiol. 122, 189–200.

Lillywhite, P. G. 1981. Multiplicative intrinsic noise and the limits to visual performance. Vision Res. 21, 291–296.

Lillywhite, P. G. and Laughlin, S. B. 1979. Transducer noise in a photoreceptor. Nature 277, 569–572.

Lima, S. M. A., Silveira, L. C. L., and Perry, V. H. 1996. Distribution of M ganglion cells in diurnal and nocturnal New-World monkeys. J. Comp. Neurol. 368, 538–552.

Lindblad, J. 1967. I Ugglemarker, Bonniers.

Locket, N. A. 1985. The multiple bank rod foveae of *Bajacalifornia drakei*, an alepocephalid deep-sea teleost. Proc. R. Soc. Lond. B. 224, 7–22.

Lythgoe, J. N. 1979. The Ecology of Vision, Clarendon Press.

MacPhail, E. M. 1986. Animal memory: past, present and future. Quart. J. Exp. Psychol. 38B, 349–364.

Martin, G. R. 1974. Colour vision in the tawny owl (*Strix aluco*). J. Comp. Physiol. Psych. 86, 133–141.

Martin, G. R. 1977. Absolute visual threshold and scotopic spectral sensitivity in the tawny owl *Strix aluco*. Nature 268, 636–638.

Martin, G. R. 1982. An owl's eye – schematic optics and visual performance in *Strix aluco* L. J. Comp. Physiol. 145, 341–349.

Martin, G. R. 1984. The visual fields of the tawny owl, *Strix aluco* L. Vision Res. 24, 1739–1751.

Martin, G. R. 1986. The eye of a Passeriforme bird, the European Starling (*Sturnus vulgaris)*: eye movement amplitude, visual fields and schematic optics. J. Comp. Physiol. A. 159, 545–557.

Martin, G. R. 1990. Birds by Night. T. & A.D. Poyser.

Martin, G. R. 1994. Form and Function in the Optical Structure of Bird Eyes. In: Perception and Motor Control in Birds: An Ecological Approach (*eds*. M. N. O. Davies and P. R. Green), pp. 5–34. Springer.

Martin, G. R and Gordon, I. E. 1974a. Increment-threshold spectral sensitivity in the tawny owl (*Strix aluco*). Vision Res. 14, 615–621.

Martin, G. R and Gordon, I. E. 1974b. Acuity in the tawny owl (*Strix aluco*). Vision Res. 14, 1393–1397.

Martin, G. R. and Katzir, G. 1999. Visual field in short-toed eagles *Circaetus gallicus* and the function of binocularity in birds. Brain Behav. Evol. 53, 55–66.

Martin, G. R., Rojas, L. M., Ramirez, Y., and McNeil, R. 2004a. The eyes of oilbirds (*Steatornis caripensis)*: pushing at the limits of sensitivity. Naturwissenschaften 91, 26–29.

Martin, G. R., Rojas, L. M., Ramirez, Y., and McNeil, R. 2004b. Binocular vision and nocturnal activity in oilbirds (*Steatornis caripensis)* and pauraques (*Nyctidromus albicollis)*: Caprimulgiformes. Ornitol. Neotrop. 15 (Suppl.), 233–242.

Martin, G. R., Wilson, K.-J., Wild, J. M., Parsons, S., Kubke, M. F., and Corfield, J. 2007. Kiwi forego vision in the guidance of their nocturnal activities. PLoS ONE, 2, e198. doi: 10.1371/journal.pone.0000198.

McIntyre, P. D. and Caveney, S. 1998. Superposition optics and the time of flight in onitine dung beetles. J. Comp. Physiol. A. 183, 45–60.

McNeil, R., Drapeau, P., and Goss-Custard, J. D. 1992. The occurrence and adaptive significance of nocturnal habits in waterfowl. Biol. Rev. 67, 381–419.

McNeil, R., Drapeau, P., and Pierotti, R. 1993. Nocturnality in Colonial Waterbirds: Occurrence, Special Adaptations, and Suspected Benefits. In: Current Ornithology, (*ed*. D. M. Power), Vol. 10, pp. 187–246. Plenum.

Menzi, U. 1987. Visual adaptation in nocturnal and diurnal ants. J. Comp. Physiol. A. 160, 11–21.

Meyer-Rochow, V. B. and Nilsson, H. L. 1998. Compound Eyes in Polar Regions, Caves and the Deep-Sea. In: Atlas of Arthropod Sensory Receptors (*eds*. E. Eguchi and Y. Tominaga), pp. 134–155. Springer.

Moon, P. 1940. Proposed standard solar-radiation curves for engineering use. J. Franklin. Inst. 230, 583–617.

Moser, J. C., Reeve, J. D., Bento, J. M. S., Della Lucia, T. M. C., Cameron, R. S., and Heck, N. M. 2004. Eye size and behaviour of day- and night-flying leafcutting ant alates. J. Zool. 264, 69–75.

Munk, O. 1980. Hvirveldyrøjet: Bygning, funktion og tilpasning, Berlingske Forlag.

Murphy, C. J., Evans, H. E., Howland, and H.C 1985. Towards a schematic eye for the great horned owl. Fortschr. Zool. 30, 703–706.

Nicol, J. A. C. 1989. The Eyes of Fishes, Oxford University Press.

Nicol, J. A. C. and Arnott, H. J. 1974. Tapeta lucida in the eyes of goatsuckers (Caprimulgidae). Proc. R. Soc. Lond. B. 187, 349–352.

Nilsson, D.-E. 1989. Optics and Evolution of the Compound Eye. In: Facets of Vision (*eds*. D. G. Stavenga and R. C. Hardie), pp. 30–73. Springer.

Nørgaard, T. 2005. Nocturnal navigation in *Leucorchestris arenicola* (Araneae, Sparassidae). J. Arach. 33, 533–540.

Nørgaard, T., Henschel, J. R., and Wehner, R. 2003. Long-distance navigation in the wandering desert spider *Leucorchestris arenicola*: can the slope of the dune surface provide a compass cue? J. Comp. Physiol. A. 189, 801–809.

Nørgaard, T., Henschel, J. R., and Wehner, R. 2006. The night-time temporal window of locomotor activity in the Namib Desert long-distance wandering spider, *Leucorchestris arenicola*. J. Comp. Physiol. A. 192, 365–372.

Nørgaard, T., Henschel, J. R., and Wehner, R. 2007. Use of local cues in the night-time navigation of the wandering desert spider *Leucorchestris arenicola* (Araneae, Sparassidae). J. Comp. Physiol. A. 193, 217–222.

Ogden, T. E. 1975. The receptor mosaic of *Aotes trivirgatus*: distribution of rods and cones. J. Comp. Neurol. 163, 193–202.

Ohly, K. P. 1975. The neurons of the first synaptic regions of the optic neuropil of the firefly, *Phausius splendidula* L. (Coleoptera). Cell Tissue Res. 158, 89–109.

Pasternak, T. and Merigan, W. H. 1981. The luminance dependence of spatial vision in the cat. Vision Res. 21, 1333–1339.

Payne, R. S. 1962. How the barn owl locates prey by hearing. Living Bird 1, 151–159.

Payne, R. S. 1971. Acoustic localization of prey by barn owls (*Tyto alba*). J. Exp. Biol. 54, 535–573.

Payne, R. S. and Drury, W. H. 1958. Marksman of the darkness. Nat. Hist. (N. Y.) 67, 316–323.

Pettigrew, J. D. 1982. A note on the eyes of the letter-winged kite. *Elanus scriptus.* Emu. 82 (Suppl.), 305–308.

Pick, B. and Buchner, E. 1979. Visual movement detection under light- and dark-adaptation in the fly, *Musca domestica*. J. Comp. Physiol. A. 134, 45–54.

Polyak, S. 1957. The Vertebrate Visual System. The University of Chicago Press.

Ribi, W. A. 1975. The first optic ganglion of the bee I. Correlation between visual cell types and their terminals in the lamina and medulla. Cell. Tissue Res. 165, 103–111.

Ribi, W. A. 1977. Fine structure of the first optic ganglion (lamina) of the cockroach *Periplaneta americana*. Tissue Cell 9, 57–72.

Rieke, F. and Baylor, D. A. 1998. Origin of reproducibility in the responses of retinal rods to single photons. Biophys. J. 75, 1836–1857.

Robert, M. and McNeil, R. 1989. Comparative day and night feeding strategies of shorebird species in a tropical environment. Ibis. 131, 69–79.

Rojas, L. M., McNeil, R., Cabana, T., and Lachapelle, P. 1997. Diurnal and nocturnal visual function in two tactile foraging water birds: the American white ibis and the black skimmer. The Condor 99, 191–200.

Rojas, L. M., McNeil, R., Cabana, T., and Lachapelle, P. 1999a. Diurnal and nocturnal visual capabilities in shore birds as a function of their feeding strategies. Brain. Behav. Evol. 53, 29–43.

Rojas, L. M., McNeil, R., Cabana, T., and Lachapelle, P. 1999b. Behavioural, morphological and physiological correlates of diurnal and nocturnal vision in selected wading bird species. Brain. Behav. Evol. 53, 227–242.

Rojas, L. M., Ramirez, Y., McNeil, R., Mitchell, M., and Marin, G. 2004. Retinal morphology and electrophysiology of two caprimulgiformes birds: the cave-living and nocturnal Oilbird (*Steatornis caripensis)* and nocturnally foraging common pauraque (*Nyctidromus albicollis)*: Brain. Behav. Evol. 64, 19–33.

Rojas, L. M., Tai, S., and McNeil, R. 1993. Comparison of rod/cone ratio in three species of shore birds having different nocturnal foraging strategies. The Auk. 110, 141–145.

Rose, A. 1942. The relative sensitivities of television pickup tubes, photographic film and the human eye. Proc. Inst. Radio Eng. (New York), 30, 293–300.

Rossum, M. C. W.van and Smith, R. G. 1998. Noise removal at the rod synapse of mammalian retina. Vis. Neurosci. 15, 809–821.

Roth, L. S. V. and Kelber, A. 2004. Nocturnal colour vision in geckos. Proc. R. Soc. Lond. B. 271 (Suppl.), S485–S487.

Rowe, N. 1996. The Pictorial Guide to the Living Primates, Pogonias Press.

Rozenberg, G. V. 1966. Twilight: A Study in Atmospheric Optics, Plenum Press.

Schlecht, P. 1979. Colour discrimination in dim light: an analysis of the photoreceptor arrangement of the moth *Deilephila*. J. Comp. Physiol. 129, 257–267.

Schwemer, J. and Paulsen, R. 1973. Three visual pigments in *Deilephila elpenor* (Lepidoptera, Sphingidae). J. Comp. Physiol. 86, 215–229.

Silveira, L. C. L., Saito, C. A., Lee, B. B., Kremers, J., Silva Filho, M. da, Kilavik, B. E., Yamada, E. S., and Perry, V. H. 2004. Morphology and physiology of primate M- and P-cells. Prog. Brain Res. 144, 21–46.

Silveira, L. C. L., Yamada, E. S., Franco, E. C. S., and Finlay, B. L. 2001. The specialization of the owl monkey retina fro night vision. Colour Res. Appl. 26, S118–S122.

Silveira, L. C. L., Yamada, E. S., Perry, V. H., and Picanco-Diniz, C. W. 1994. M and P retinal ganglion cells of diurnal and nocturnal New-World monkeys. NeuroReport 5, 2077–2081.

Sinclair, S. 1985. How Animals See, Facts on File Publications.

Snow, D. W. 1961. The natural history of the oilbird, *Steatornis caripensis*, in Trinidad. 1. General behaviour and breeding habits. Zoologica 46, 27–48.

Snyder, A. W. 1977. Acuity of compound eyes, physical limitations and design. J. Comp. Physiol. 116, 161–182.

Snyder, A. W. 1979. Physics of Vision in Compound Eyes. In: Handbook of Sensory Physiology (*ed*. H. Autrum), Vol VII/6A, pp. 225–313. Springer.

Snyder, A. W. and Miller, W. H. 1978. Telephoto lens system of falconiform eyes. Nature 275, 127–129.

Snyder, A. W., Laughlin, S. B., and Stavenga, D. G. 1977b. Information capacity of eyes. Vision Res. 17, 1163–1175.

Snyder, A. W., Stavenga, D. G., and Laughlin, S. B. 1977a. Spatial information capacity of compound eyes. J. Comp. Physiol. 116, 183–207.

Sotthibandhu, S. and Baker, R. R. 1979. Celestial orientation by the large yellow underwing moth, *Noctua pronuba* L. Anim. Behav. 27, 786–800.

Srinivasan, M. V. and Bernard, G. D. 1975. The effect of motion on visual acuity of the compound eye, a theoretical analysis. Vision Res. 15, 515–525.

Srinivasan, M. V. and Dvorak, D. R. 1980. Spatial processing of visual information in the movement-detecting pathway of the fly. J. Comp. Physiol. 140, 1–23.

Srinivasan, M. V., Laughlin, S. B., and Dubs, A. 1982. Predictive coding, a fresh view of inhibition in the retina. Proc. R. Soc. Lond. B. 216, 427–459.

Stavenga, D. G. 2003. Angular and spectral sensitivity of fly receptors. II. Dependence on facet lens F-number and rhabdomere type in *Drosophila.* J. Comp. Physiol. A. 189, 189–202.

Stavenga, D. G. 2004a. Angular and spectral sensitivity of fly receptors. III. Dependence on the pupil mechanism in the blowfly *Calliphora*. J. Comp. Physiol. A. 190, 115–129.

Stavenga, D. G. 2004b. Visual acuity of fly photoreceptors in natural conditions – dependence on UV sensitizing pigment and light-controlling pupil. J. Exp. Biol. 207, 1703–1713.

Stavenga, D. G., Smits, R. P., and Hoenders, B. J. 1993. Simple exponential functions describing the absorbance bands of visual pigment spectra. Vision Res. 33, 1011–1017.

Strausfeld, N. J. and Blest, A. D. 1970. Golgi studies on insects. I. The optic lobes of Lepidoptera. Phil. Trans. R. Soc. Lond. B. 258, 81–134.

Theobald, J. C., Greiner, B., Wcislo, W. T., and Warrant, E. J. 2006. Visual summation in night-flying sweat bees: a theoretical study. Vision Res. 46, 2298–2309.

Thomas, R. J., Székely, T., Powell, R. F., and Cuthill, I. C. 2006. Eye size, foraging methods and the timing of foraging in shorebirds. Funct. Ecol. 20, 157–165.

Vu, T. Q., McCarthy, S. T., and Owen, W. G. 1997. Linear transduction of natural stimuli by dark-adapted and light-adapted rods of the salamander, *Ambystoma tigrinum*. J. Physiol. 505. 1, 193–204.

Walls, G. L. 1942. The Vertebrate Eye and Its Adaptive Radiation, The Cranbrook Press.

Warrant, E. J. 1999. Seeing better at night, life style, eye design and the optimum strategy of spatial and temporal summation. Vision Res. 39, 1611–1630.

Warrant, E. J. 2004. Vision in the dimmest habitats on earth. J. Comp. Physiol. A. 190, 765–789.

Warrant, E. J. 2006. The Sensitivity of Invertebrate Eyes to Light. In: Invertebrate Vision (*eds*. E. J. Warrant and D. -E. Nilsson), pp. 83–126. Cambridge University Press.

Warrant, E. J. and Locket, N. A. 2004. Vision in the deep sea. Biol. Rev. 79, 671–712.

Warrant, E. J. and McIntyre, P. D. 1991. Strategies for retinal design in arthropod eyes of low F-number. J. Comp. Physiol. A. 168, 499–512.

Warrant, E. J. and McIntyre, P. D. 1992. The Trade-Off Between Resolution and Sensitivity in Compound Eyes. In: Nonlinear Vision: Determination of Neural Receptive Fields, Function, and Networks (*eds*. R. B. Pinter and B. Nabet), pp. 391–421. CRC Press.

Warrant, E. J. and McIntyre, P. D. 1993. Arthropod eye design and the physical limits to spatial resolving power. Prog. Neurobiol. 40, 413–461.

Warrant, E. J. and Nilsson, D.-E. 1998. Absorption of white light in photoreceptors. Vision Res. 38, 195–207.

Warrant, E. J., Bartsch, K., and Günther, C. 1999. Physiological optics in the hummingbird hawkmoth, a compound eye without ommatidia. J. Exp. Biol. 202, 497–511.

Warrant, E. J., Kelber, A., Gislén, A., Greiner, B., Ribi, W., and Wcislo, W. T. 2004. Nocturnal vision and landmark orientation in a tropical halictid bee. Curr. Biol. 14, 1309–1318.

Warrant, E. J., Porombka, T., and Kirchner, W. H. 1996. Neural image enhancement allows honeybees to see at night. Proc. R. Soc. Lond. B. 263, 1521–1526.

Wässle, H. and Boycott, B. 1991. Functional architecture of the mammalian retina. Vision Res. 30, 1897–1911.

Waterman, T. H. 1981. Polarization Sensitivity. In: Handbook of Sensory Physiology (*ed*. H. Autrum), Vol. VII/6B, pp. 281–469. Springer.

Wcislo, W. T., Arneson, L., Roesch, K., Gonzalez, V., Smith, A., and Fernandez, H. 2004. The evolution of nocturnal behaviour in sweat bees, *Megalopta genalis* and *M. ecuadoria* (Hymenoptera, Halictidae): an escape from competitors and enemies?. Biol. J. Linnean Soc. 83, 377–387.

Wehner, R. 1981. Spatial Vision in Arthropods. In: Handbook of Sensory Physiology (*ed*. H. Autrum), Vol. VII 6C, pp. 287–616. Springer.

Wehner, R. 2001. Polarization vision – a uniform sensory capacity? J. Exp. Biol. 204, 2589–2596.

Wehner, R. 2003. Desert ant navigation: how miniature brains solve complex tasks. J. Comp. Physiol. A. 189, 579–588.

Wehner, R. and Labhart, T. 2006. Polarisation Vision. In: Invertebrate Version (*eds*. E. J. Warrant and D.-E. Nilsson), pp. 291–347. Cambridge University Press.

Wikler, K. C. and Rakic, P. 1990. Distribution of photoreceptor subtypes in the retina of diurnal and nocturnal primates. J. Neurosci. 10, 3390–3401.

Williams, D. S. 1982. Ommatidial structure in relation to turnover of photoreceptor membrane in the locust. Cell Tissue Res. 225, 595–617.

Williams, D. S. 1983. Changes of photoreceptor performance associated with the daily turnover of photoreceptor membrane in the locust. J. Comp. Physiol. 150, 509–519.

Wright, P. C. 1978. Home range, activity pattern and agonistic encounters of a group of night monkeys (*Aotus trivigatus*) in Peru. Folia Primatol. 29, 43–55.

Wright, P. C. 1989. The nocturnal primate niche in the new world. J. Hum. Evol. 18, 635–658.

Yamada, E. S., Marshak, D. W., Silveira, L. C. L., and Casagrande, V. A. 1998. Morphology of P and M retinal ganglion cells of the bushbaby. Vision Res. 38, 3345–3352.

Yamada, E. S., Silveira, L. C. L., Perry, V. H., and Franco, E. C. S. 2001. M and P retinal ganglion cells of the owl monkey: morphology, size and photoreceptor convergence. Vision Res. 41, 119–131.

Yeandle, S. 1958. Evidence of quantized slow potentials in the eye of *Limulus*. Am. J. Ophthalmol. 46, 82–87.

Zeil, J., Kelber, A., and Voss, R. 1996. Structure and function of learning flights in bees and wasps. J. Exp. Biol. 199, 245–252.

2.06 Spectral Sensitivity

A Stockman and L T Sharpe, University College London, London, UK

© 2008 Elsevier Inc. All rights reserved.

2.06.1	**Introduction**	88
2.06.1.1	Univariance and Trichromacy	88
2.06.1.2	Color Matching Functions	89
2.06.1.3	Dichromacy and Monochromacy	90
2.06.2	**Cone Spectral Sensitivities**	91
2.06.2.1	Historical Overview	91
2.06.2.2	Cone Spectral Sensitivity Measurements	92
2.06.2.3	From Cone Spectral Sensitivities to Color Matching Functions	92
2.06.2.4	Rod Spectral Sensitivity Measurements	93
2.06.3	**Achromatic and Chromatic Spectral Sensitivity**	94
2.06.3.1	Achromatic Luminous Efficiency	94
2.06.3.1.1	Scotopic luminous efficiency	94
2.06.3.1.2	Photopic Luminous Efficiency	94
2.06.3.1.3	Mesopic Luminous Efficiency	95
2.06.3.2	Chromatic Spectral Sensitivity	95
2.06.4	**Other Factors that Influence Spectral Sensitivity**	95
2.06.4.1	Photopigment Variability and Anomalous Trichromacy	96
2.06.4.2	Lens Pigment	96
2.06.4.3	Macular Pigment	96
2.06.4.4	Photopigment Optical Density	97
2.06.4.5	Changes with Eccentricity	97
2.06.5	**Conclusions**	97
References		97

Glossary

achromatic Perceptually, devoid of hue or colorless. The nonchromatic dimension of a visual stimulus; including neutral grays, white, and black.

anomalous trichromacy A type of color blindness, in which one of the three cone pigments is altered in its spectral sensitivity, but trichromacy is not fully impaired.

chromatic Perceived as having hue or being colored (blue, green, yellow, red, purple, etc.). The hue and saturation dimensions of a visual stimulus.

color match A perceptual match between pairs or mixtures of lights with different spectral power distributions (which are therefore metamers).

color matching function (CMF) $\bar{x}(\lambda), \bar{y}(\lambda)$, and $\bar{z}(\lambda)$. Tristimulus values, usually defined for an equal-energy spectrum locus.

Commission Internationale de l'Éclairage (CIE; or International Commission on Illumination) An organization that recommends international standards of color and lighting.

cone fundamentals Cone spectral sensitivities: $\bar{l}(\lambda), \bar{m}(\lambda),$ and $\bar{s}(\lambda)$ in color matching function (CMF) notation. These are the CMFs that would result if imaginary primaries could be used that uniquely stimulated the three cones.

dichromacy A type of color blindness in which one of the three normal cone pigments is missing and color vision is reduced to two dimensions, so that any test light can be matched with a mixture of only two independent primary lights. There are three kinds of dichromacy: protanopia (lacking the L-cones), deuteranopia (lacking the M-cones), and tritanopia (lacking the S-cones).

large-field or 10-deg matches Color matches for centrally viewed, circular fields subtending 10-deg diameter of visual angle.

mesopic Light levels at which both rods and cones operate.

monochromacy A type of color blindness, in which two or all three of the cone pigments are

missing and color and lightness vision is reduced to a single dimension, so that any test light can be matched with a single primary light. At night, when only the rods are functioning, normal observers are monochromats.

photometry The measurement and quantification of the luminous efficiency of lights. It is intended to be independent of color.

photopic Light levels at which only cones operate.

photopic luminous efficiency function Photometric measure of the efficiency or effectiveness as a function of wavelength under photopic, rod-free conditions: $V(\lambda)$ or $\bar{y}(\lambda)$.

photoreceptors The light-sensitive receptors, lying on the rear surface of the eye or retina, which transduce photons into electrical signals. Morphologically and physiologically, they can be distinguished as either rods, responsible for our achromatic night vision, or cones, responsible for our chromatic daytime vision.

primary lights R, G, B. The three independent primaries (real or imaginary) to which the test light is matched (actually or hypothetically), when defining color-matching functions. They must be independent in the sense that no combination of any two can match the third.

scotopic Light levels at which only rods operate.

small-field or 2-deg matches Color matches for centrally viewed, circular fields subtending 2-deg diameter of visual angle.

trichromacy The ability of normal observers to match test lights with a mixture of three independent primary lights, one of which may have to be added to the test light to complete the match.

tristimulus values *R*, *G*, *B*, the amounts of the three primaries required to match a given stimulus.

univariance The output of a photoreceptor varies unidimensionally according only to the rate of photon absorption.

visual angle The angle subtended by an object in the external field at the effective optical center of the eye: $\theta = 2\tan^{-1}([x/2]/d)$ where x is the dimension of the object that is of interest (e.g., height, width, or diameter) and d is the distance of the object from the eye.

2.06.1 Introduction

Vision is initially limited by the transduction properties of the light-sensitive photoreceptors in the eye, and in particular by their spectral sensitivities. In most observers with normal color vision, there are four photoreceptor classes: three types of cone photoreceptors, which are referred to as long-, middle-, and short-wavelength-sensitive (L, M, and S), according to the part of the visible spectrum in which they are most sensitive, and a single type of rod photoreceptor. A knowledge of the spectral sensitivities of these photoreceptors is essential for the understanding and modeling of visual function. Rods, which are more sensitive than cones, mediate vision at night when photons are relatively scarce, whereas cones mediate color vision during the day when photons are abundant. Those conditions under which the rods and the cones operate alone are known as scotopic and photopic, respectively, while those under which they operate jointly are known as mesopic (see Figure 1).

2.06.1.1 Univariance and Trichromacy

Photoreceptors are essentially sophisticated photon counters, the outputs of which vary according to the number of photons that they absorb (e.g., Stiles, W. S., 1948; Mitchell, D. E. and Rushton, W. A. H., 1971). Although the probability that a photon is absorbed by a photoreceptor varies substantially with wavelength (defining its spectral sensitivity), the effect of an absorbed photon is independent of wavelength. Thus, it is impossible to tell whether a change in the output of a single photoreceptor is due to a change in light intensity, or due to a change in wavelength. Color and intensity are confounded, so that the output of an individual photoreceptor is effectively color blind or monochromatic. By extension, normal photopic human vision, which depends on the outputs of three different classes of photoreceptor, is a trichromatic or trivariant system. A behavioral consequence of trichromacy is that observers can match a test light of any spectral composition to a mixture of just three primary lights, as illustrated in Figure 2.

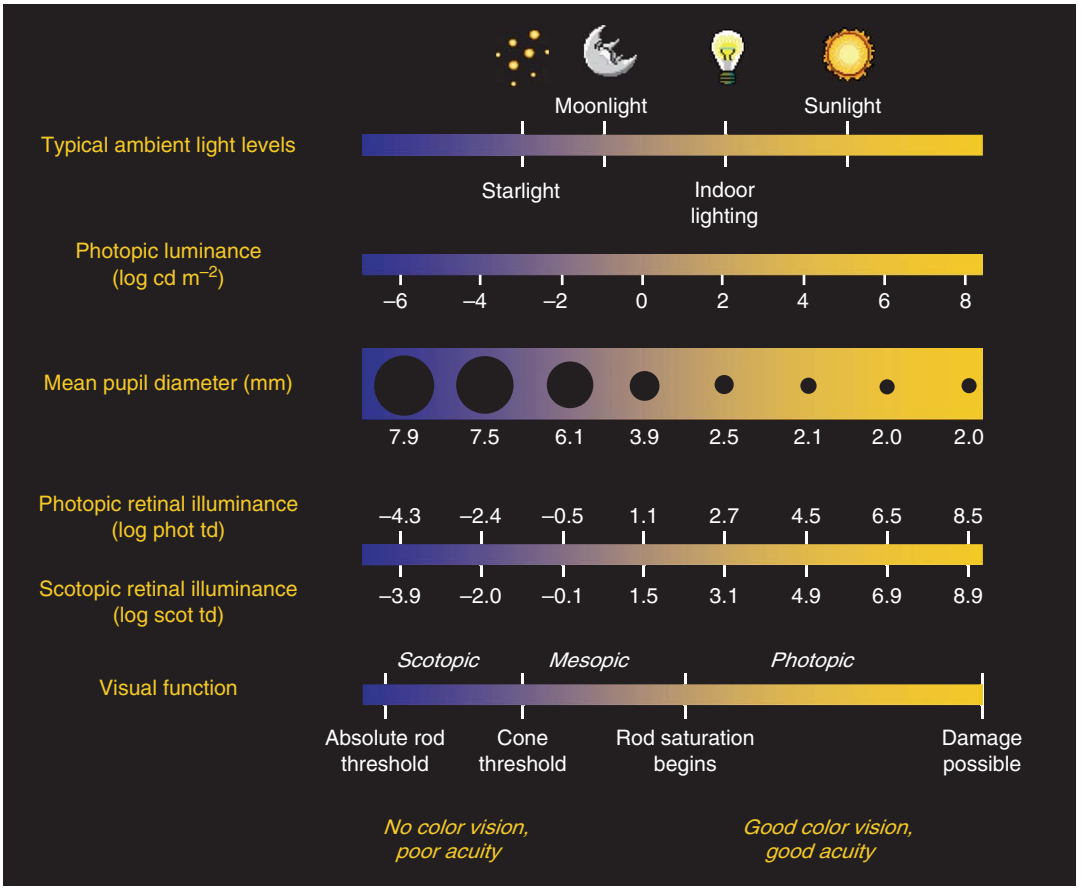

Figure 1 Illumination levels. Typical ambient light levels are compared with photopic luminance (log cd. m^{-2}), mean pupil diameter (mm), photopic and scotopic retinal illuminance (log photopic and scotopic tds, respectively), and visual function. The scotopic, mesopic, and photopic regions are defined according to whether rods alone, rods and cones, or cones alone operate. The conversion from photopic to scotopic values assumes a white standard CIE D_{65} illumination. Figure based in part on the design of Hood, D. C. and Finkelstein, M. A. 1986. Sensitivity to Light. In: Handbook of Perception and Human Performance (*eds*. K. Boff, L. Kaufman, and J. Thomas), pp. 5–1–5–66. Wiley.

2.06.1.2 Color Matching Functions

Because normal human photopic vision is trichromatic, the color of a light can be defined by just three variables: the intensities of three specially chosen primary lights that match it. Figure 2 shows examples of the $\bar{r}(\lambda)$, $\bar{g}(\lambda)$, and $\bar{b}(\lambda)$ color matching functions (CMFs) for red–green–blue (RGB) primaries of 645, 526, and 444 nm. Each CMF defines the amount of that primary required to match monochromatic targets of equal energy. CMFs can be determined without any knowledge of the underlying cone spectral sensitivities. The only restriction on the choice of primary lights is that they must be independent – in the sense that no two will match the third.

CMFs can be linearly transformed to any other set of real primary lights, and, as illustrated in Figure 2, to imaginary primary lights, such as the all-positive X, Y, and Z primaries favored by the CIE to define international lighting standards, or to the L, M and S cone fundamental primaries, which are physiologically relevant. The three cone fundamental primaries (or Grundempfindungen – fundamental sensations) are the three imaginary primary lights that would uniquely stimulate each of the three cones to yield $\bar{l}(\lambda)$, $\bar{m}(\lambda)$, and $\bar{s}(\lambda)$, or the L-, M-, and S-cone spectral sensitivity functions. For convenience and precision, cone spectral sensitivities are usually defined in terms of transformed CMFs (see Section 2.06.2.3), rather than as raw sensitivity measurements (like those shown in Figure 3, below). Notice that for the R, G, and B primaries, one of the CMFs is negative over the region of the spectrum where three primaries are required, which indicates that

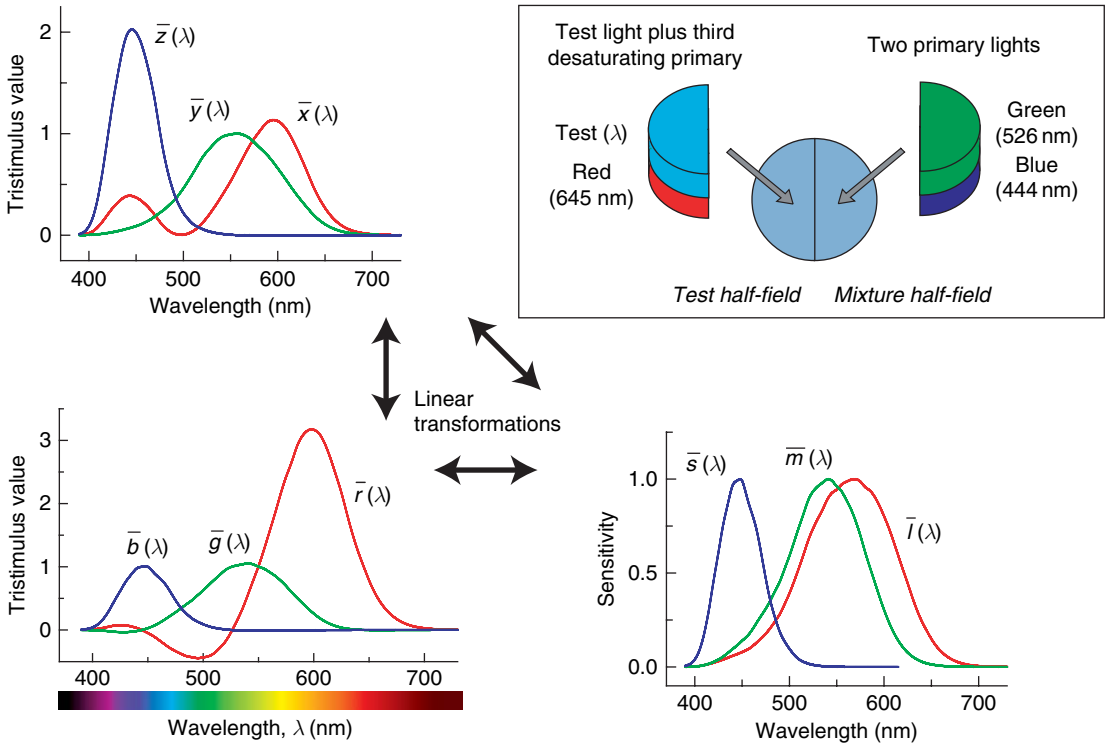

Figure 2 Upper right inset: Maximum saturation method of color matching using spectral lights. A monochromatic test field of wavelength, λ, is matched to a mixture of red (645 nm), green (526 nm), and blue (444 nm) monochromatic primary lights, one of which, as in this example, may have to be added to the test field to complete the match. The amounts of each of the three primaries required to match monochromatic lights spanning the visible spectrum are known as the red, $\bar{r}(\lambda)$, green, $\bar{g}(\lambda)$, and blue, $\bar{b}(\lambda)$ color matching function (CMFs; red, green, and blue lines, respectively) shown in the lower left panel. A negative sign means that that primary must be added to the target to complete the match. CMFs can be linearly transformed from one set of primaries to another. Also illustrated here are CMFs for the imaginary X, Y, and Z primaries (top left) and the cone fundamental L, M, and S primaries (bottom right). The CMFs are transformations of the Stiles W. S. and Burch J. M. (1959) 10-deg CMFs. The fundamentals are the 10-deg cone fundamentals of Stockman A. and Sharpe L. T. (2000).

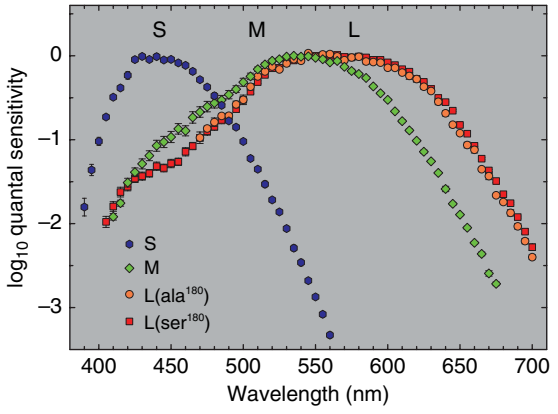

Figure 3 Mean spectral sensitivity data. L-cone data from 17 L(ser^{180}) subjects (red squares), five L(ala^{180}) subjects (orange circles), and M-cone data from nine L1M2/L2M3 protanopes (green diamonds) measured by Sharpe L. T. *et al.* (1998); and S-cone data from five normals and three blue-cone monochromats (blue hexagons) measured by Stockman A. *et al.* (1999).

the primary in question has to be added to the test light in order to complete the match. This does not violate the trichromatic principle, but simply reflects the fact that real primaries excite more than one cone type (see Figures 3 and 4), with the result that no triad of such primaries can completely enclose the three-dimensional space of physically realizable colors. For a further discussion about colorimetry, and its link to the cone fundamentals, see Stockman A. and Sharpe L. T. (1999) and Stockman A. (2003).

2.06.1.3 Dichromacy and Monochromacy

Some people have reduced forms of normal trichromat color vision. Dichromats, who lack one of the three cone photoreceptor types and can therefore match test lights to a mixture of just two primary lights, fall into three classes: protanopes, deuteranopes, and tritanopes, who lack the L-, M-, and S-cones,

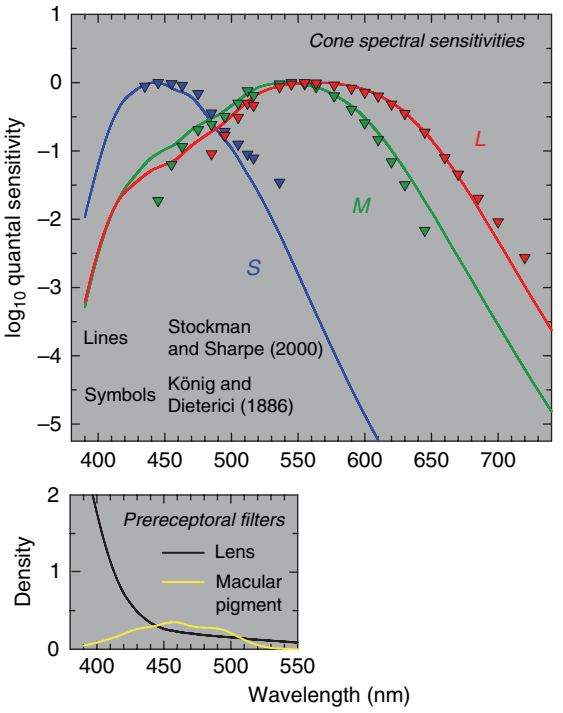

Figure 4 S-, M-, and L-cone 2-deg spectral sensitivity estimates of Stockman A. and Sharpe L. T. (2000), based on linear transformations of the Stiles W. S. and Burch J. M. (1959) 10-deg RGB color matching function (CMFs), determined by the mean spectral sensitivity data shown in Figure 3 as a guide, (colored lines) compared with the historical estimates of König A. and Dieterici C. (1886) (colored triangle). The lower inset shows the mean macular density spectrum for a 2-deg field (yellow line) based on measurements by Bone R A. *et al.* (1992), and the mean lens density spectrum of van Norren D. and Vos J. J. (1974) slightly adjusted by Stockman A. *et al* (1999) (black line).

respectively. Most estimates of the cone spectral sensitivities (see below) depend on the use of dichromats and the assumption – known as the loss, reduction, or König hypothesis – that their remaining cone classes are normal (Maxwell, J. C., 1860; König, A. and Dieterici, C., 1886). This approach now has a much firmer foundation, since it is possible to use molecular genetics to select those dichromats who truly conform to the reduction hypothesis (Nathans, J. *et al.*, 1986a; 1986b). Appropriate selection is important, because some red–green or X-linked dichromats have an LM-hybrid cone photopigment with a spectrally shifted spectral sensitivity, while others have multiple cone photopigments (LM-hybrid plus normal) with slightly different spectral sensitivities. If an individual has an LM-hybrid and a normal photopigment that differ sufficiently from one another, that person will usually retain some (reduced) trichromacy and be classed as an anomalous trichromat (see Section 2.06.4.1).

Monochromats can match test lights to just one primary light. In principle, they can lack two of the three cone types (S-, M-, and L-cone monochromats) or all three of them (rod monochromats, or complete achromats). S-cone (or blue-cone) monochromats (Blackwell, H. R. and Blackwell, O. M., 1957; 1961) are particularly useful for measuring S-cone spectral sensitivity (see Section 2.06.2.2). For an extended discussion of color deficiencies and their molecular origins, see Sharpe L. T. *et al.* (1999).

2.06.2 Cone Spectral Sensitivities

Since the establishment of trichromatic color theory (e.g., Young, T., 1802; von Helmholtz, H. L. F., 1852; Maxwell, J. C., 1855), a central goal of color science has been the accurate determination of the three cone spectral sensitivities, $\bar{l}(\lambda)$, $\bar{m}(\lambda)$, and $\bar{s}(\lambda)$. Studies of human cone spectral sensitivity have encompassed many fields of inquiry, including fundus reflectometry (e.g., Rushton, W. A. H., 1965), microspectrophotometry (e.g., Dartnall, H. J. *et al.*, 1983), suction electrode recordings (e.g., Schnapf, J. L. *et al.*, 1987; Kraft, T. W. *et al.*, 1998), electroretinography (e.g., Neitz, J. *et al.*, 1995), and absorption spectroscopy (Oprian, D. D. *et al.*, 1991; Merbs, S. L. and Nathans, J., 1992a; 1992b; Asenjo, A. B. *et al.*, 1994). Our primary focus will be visual psychophysics, which provides the most extensive and accurate *in vivo* spectral sensitivity data.

2.06.2.1 Historical Overview

Arguably, the first plausible psychophysical estimates of $\bar{l}(\lambda)$, $\bar{m}(\lambda)$, and $\bar{s}(\lambda)$ were obtained by König A. and Dieterici C. (1886; see Figure 4). Since then, many other estimates have been made, notably those by Bouma P. J. (1942), Judd D. B. (1945; 1949), Wyszecki G. and Stiles W. S. (1967), Vos J. J. and Walraven P. L. (1971), Vos J. J. (1978), Estévez O. (1979), Vos J. J. *et al.* (1990), and Stockman A. *et al.* (1993a). These have been discussed elsewhere (e.g., Parsons, J. H., 1924; Boring, E. G., 1942; Le Grand, Y., 1968; Stockman, A. and Sharpe, L. T., 1999). Until recently, the estimates by Smith V. C. and Pokorny J. (1975) have been widely used in science and research as a *de facto* standard. Newer estimates by Stockman A.

and Sharpe L. T. (2000) have been proposed as a new CIE standard for physiologically relevant fundamental primaries.

2.06.2.2 Cone Spectral Sensitivity Measurements

Although the cone fundamentals can be estimated by comparing dichromatic and normal color matches (Maxwell, J. C., 1855; 1856), the most straightforward method is to measure the cone spectral sensitivities directly. Because the three cone types peak in sensitivity in different parts of the spectrum, and their spectral sensitivities overlap extensively, spectral sensitivity measurements reflect the activity of more than one cone type. The isolation of the response of a single cone type over substantial regions of the spectrum requires special procedures to favor the wanted cone type and disfavor the two unwanted ones; or it requires the use of dichromats or monochromats, who lack one or two of the cone types. A now classical approach is to use selective chromatic adaptation (e.g., Stiles, W. S., 1939; 1978) and to present a target of variable wavelength on a larger adapting or background field of a second wavelength (or mixture of wavelengths) that selectively suppresses the sensitivities of the two unwanted cone types. However, cone isolation in normal observers becomes increasingly difficult as the wavelength of the target approaches the wavelength of the background, because any advantage gained by the background's selective suppression of the unwanted cone types is offset by the target selectively favoring detection by the unwanted cone types. Complete isolation can be achieved, but only if the selective sensitivity losses due to adaptation by the background exceed the selective effect of the target (e.g., King-Smith, P. E. and Webb, J. R., 1974; Eisner, A. and MacLeod, D. I. A., 1981; Stockman, A. and Mollon, J. D., 1986; Stockman, A. *et al.*, 1993a). Data obtained in normals can be effectively used to complement and verify much more easily isolated cone spectral sensitivity data measured in monochromats and dichromats who lack one or two of the three normal cone types (for such comparisons, see figures 3–5 of Stockman, A. and Sharpe, L. T., 2000). Now that the approach of using data from color deficient observers to model normal color vision has a firm molecular genetic foundation, it is in many ways the more preferable approach.

With the S-cones disadvantaged or suppressed, L- and M-cone spectral sensitivities can be directly measured in deuteranopes who lack M-cone function and in protanopes without L-cone function. Figure 3 shows the mean spectral sensitivity data obtained from seventeen single-gene L(ser^{180}) deuteranopes with serine at position 180 of their L-cone photopigment opsin gene (red squares), from five single-gene L(ala^{180}) deuteranopes with alanine at position 180 (orange circles), and from nine L1M2/L2M3 protanopes (green diamonds). For further details, see Sharpe, L. T. *et al.*, 1998; Stockman, A. and Sharpe, L. T., 2000. The two mean L-cone functions, which are separated by ~2.7 nm in λ_{max} (Sharpe, L. T. *et al.*, 1998), reflect the two commonly occurring L-cone photopigment polymorphisms (see Section 2.06.4.1). An overall L-cone mean was also derived (not shown) to reflect the proportions of the two polymorphic variants in the population (Stockman, A. and Sharpe, L. T., 2000). This was used to determine the mean L-cone fundamentals (see Section 2.06.2.3).

S-cone spectral sensitivity is most easily measured throughout the spectrum in S-cone monochromats (e.g., Blackwell, H. R. and Blackwell, O. M., 1961; Grützner, P., 1964; Alpern, A. *et al.*, 1965; Alpern, M. *et al.*, 1971; Daw, N. W. and Enoch, J. M., 1973; Smith, V. C. *et al.*, 1983; Hess, R. F. *et al.*, 1989). In defining a mean S-cone spectral sensitivity, Stockman A. *et al.* (1999) measured S-cone spectral sensitivities in three blue-cone monochromats known to lack L- and M-cones on genotypical as well as phenotypical grounds, and combined them with S-cone data from normals obtained at short and middle wavelengths on an intense yellow background field that selectively adapted the M- and L-cones. Their mean S-cone function is shown in Figure 3 (blue hexagons).

2.06.2.3 From Cone Spectral Sensitivities to Color Matching Functions

Although the cone spectral sensitivities could be defined as the direct sensitivity measurements shown in Figure 3, it is customary to define them in terms of linear combinations of a set of CMFs, which are – in principle at least – more precise. All that is required is to find the linear combinations of $\bar{r}(\lambda)$, $\bar{g}(\lambda)$, and $\bar{b}(\lambda)$ that best fits each cone spectral sensitivity, as defined above, allowing adjustments in the densities of prereceptoral filtering and photopigment optical density in order to account for differences in the mean densities between different populations (these factors are age- and race-dependent and highly variable between individuals) and to account for differences in retinal area (because the filtering densities change with retinal eccentricity; see Section 2.06.4).

The significance of the best-fitting linear combination can be stated formally. When an observer matches the test and mixture fields in a color matching experiment, the two fields are matched for each of his or her three cones types. The match, in other words, is a match at the level of the cones, thus:

$$\begin{aligned}\bar{l}_R\bar{r}(\lambda)+\bar{l}_G\bar{g}(\lambda)+\bar{l}_B\bar{b}(\lambda)&=\bar{l}(\lambda)\\ \bar{m}_R\bar{r}(\lambda)+\bar{m}_G\bar{g}(\lambda)+\bar{m}_B\bar{b}(\lambda)&=\bar{m}(\lambda)\\ \bar{s}_R\bar{r}(\lambda)+\bar{s}_G\bar{g}(\lambda)+\bar{s}_B\bar{b}(\lambda)&=\bar{s}(\lambda)\end{aligned} \quad [1]$$

where $\bar{l}_R, \bar{l}_G$, and $\bar{l}_B$ are, respectively, the L-cone sensitivities to the R, G, and B primary lights, and similarly $\bar{m}_R, \bar{m}_G$, and $\bar{m}_B$ and $\bar{s}_R, \bar{s}_G$, and $\bar{s}_B$ are the analogous M- and S-cone sensitivities. Since the S-cones are insensitive in the red, it can be assumed that $\bar{s}_R$ is effectively zero for a long-wavelength R primary. There are therefore eight unknowns required for the linear transformation:

$$\begin{pmatrix}\bar{l}_R & \bar{l}_G & \bar{l}_B\\ \bar{m}_R & \bar{m}_G & \bar{m}_B\\ 0 & \bar{s}_G & \bar{s}_B\end{pmatrix}\begin{pmatrix}\bar{r}(\lambda)\\ \bar{g}(\lambda)\\ \bar{b}(\lambda)\end{pmatrix}=\begin{pmatrix}\bar{l}(\lambda)\\ \bar{m}(\lambda)\\ \bar{s}(\lambda)\end{pmatrix} \quad [2]$$

Because we are only concerned about the relative shapes of $\bar{l}(\lambda), \bar{m}(\lambda)$, and $\bar{s}(\lambda)$, the eight unknowns collapse to just five:

$$\begin{pmatrix}\bar{l}_R/\bar{l}_B & \bar{l}_G/\bar{l}_B & 1\\ \bar{m}_R/\bar{m}_B & \bar{m}_G/\bar{m}_B & 1\\ 0 & \bar{s}_G/\bar{s}_B & 1\end{pmatrix}\begin{pmatrix}\bar{r}(\lambda)\\ \bar{g}(\lambda)\\ \bar{b}(\lambda)\end{pmatrix}=\begin{pmatrix}k_l\bar{l}(\lambda)\\ k_m\bar{m}(\lambda)\\ k_s\bar{s}(\lambda)\end{pmatrix} \quad [3]$$

where the absolute values of $k_l\left(1/\bar{l}_B\right), k_m(1/\bar{m}_B)$, and $k_s(1/\bar{s}_B)$ remain unknown, but are typically chosen to scale three functions in some way: for example, so that $k_l\bar{l}(\lambda), k_m\bar{m}(\lambda)$, and $k_s\bar{s}(\lambda)$ peak at unity. The five unknowns in Eqn. (3), $\bar{l}_R/\bar{l}_B, \bar{l}_G/\bar{l}_B, \bar{m}_R/\bar{m}_B, \bar{m}_G/\bar{m}_B$, and $\bar{s}_G/\bar{s}_B$, can then be estimated by directly fitting CMFs to the Stockman A. and Sharpe L. T. (1999) cone spectral sensitivity data shown in Figure 3. The transformation matrix for the Stiles W. S. and Burch J. M. (1959) 10-deg RGB CMFs, on which the Stockman A. and Sharpe L. T. (2000) cone fundamentals are based, is:

$$\begin{pmatrix}2.846201 & 11.092490 & 1\\ 0.168926 & 8.265895 & 1\\ 0 & 0.010600 & 1\end{pmatrix} \quad [4]$$

This transformation is illustrated in Figure 2. The transformation matrix given in eqn [4] multiplied by the CMFs (which are in energy units) yields cone fundamentals in energy units. To convert to quantal units multiply by λ^{-1}. The values of k_l, k_m, and k_s in eqn [3] depend on the desired normalization and on the units (energy or quanta). More details can be found in Stockman A. *et al.* (1999) and in Stockman A. and Sharpe L. T. (2000).

Figure 4 shows the current 2-deg estimates of Stockman A. and Sharpe L. T. (2000) (colored lines) compared with the much earlier estimates obtained 120 years ago by König A. and Dieterici C. (1886) (colored triangles). The Stockman A. and Sharpe L. T. 2-deg estimates are based on a transformation of the Stiles W. S. and Burch J. M. (1959) 10-deg CMFs given by eqn [4] adjusted to 2-deg by correcting for changes in photopigment optical density and macular pigment density (for details, see Stockman, A., and Sharpe, L. T., 2000). These 10-deg CMFs, which were measured in 49 subjects from approximately 390 to 730 nm (and in nine subjects from 730 to 830 nm), were chosen as the basis of the 2-deg cone fundamentals because they are the most secure set of existing color matching data, and are available as individual as well as mean data.

2.06.2.4 Rod Spectral Sensitivity Measurements

Because there is only a single type of rod photoreceptor, rod spectral sensitivity is achromatic and univariant and may be measured by any method that excludes detection being mediated by the less sensitive cones (e.g., scotopic luminance levels should be used). It is identical with scotopic luminous efficiency (see Section 2.06.3.1.1 and Figure 5).

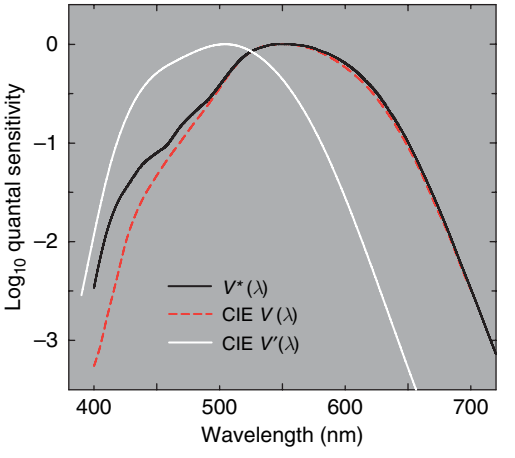

Figure 5 The Commission Internationale de l'Eclairage (CIE) scotoptic $V'(\lambda)$ (white line) and 1924 photopic $V(\lambda)$ (red dashed line) functions. The recent, photopic luminous efficiency function, $V*(\lambda)$, proposed by Sharpe L. T. *et al.* (2005) is shown by the black line.

2.06.3 Achromatic and Chromatic Spectral Sensitivity

When spectral sensitivity is measured under most practical conditions, it will inevitably involve detection by more than one photoreceptor type. Such spectral sensitivities are potentially complex, since they typically reflect interactions that occur between photoreceptor signals in different postreceptoral channels. One simplification has been to measure the spectral sensitivity of achromatic or luminance mechanisms (or luminous efficiency) separately from those of chromatic ones.

2.06.3.1 Achromatic Luminous Efficiency

Luminous efficiency is a measure of spectral sensitivity that might be described as a measure of apparent intensity. It is actually defined as the effectiveness of lights of different wavelength in specific matching or detection tasks. The term was introduced by the International Lighting Commission (CIE) to provide a psychophysical or perceptual analog of radiance, called luminance. Luminous efficiency has been defined for scotopic, photopic, and mesopic illumination levels.

2.06.3.1.1 Scotopic luminous efficiency

Scotopic luminous efficiency is comparatively straightforward, since it depends on the activity of a single univariant photoreceptor type, the rods. Thanks to univariance, scotopic luminous efficiency fulfils the basic requirement of any system of photometry that the luminous efficiency of any mixture of lights is the sum of the efficiencies of the components of the mixture; otherwise known as Abney's Law (Abney, W. d. W. and Festing, E. R., 1886; Abney, W. d. W., 1913). Figure 5 shows the scotopic CIE 1951 $V'(\lambda)$ function (white line), which is based on original data from Crawford B. H. (1949) and Wald G. (1945).

2.06.3.1.2 Photopic Luminous Efficiency

Photopic luminous efficiency, $V(\lambda)$, is complicated by the fact that there are considerable differences between the efficiency functions obtained by different measurement procedures and criteria, which include heterochromatic flicker photometry (HFP) or minimum flicker, a version of minimum flicker called heterochromatic modulation photometry (HMP), direct heterochromatic brightness matching, step-by-step brightness matching, minimally distinct border (MDB), minimum motion, color matching, absolute threshold, increment threshold, visual acuity, and critical flicker frequency (for reviews, see Wagner, G. and Boynton, R. M., 1972; Wyszecki, G. and Stiles, W. S., 1982; Lennie, P. *et al.*, 1993; Stockman, A. and Sharpe, L. T., 1999).

Although $V(\lambda)$ is often treated as if it were comparable to the spectral sensitivity of a univariant photoreceptor, it is not: it depends on the activity of more than one photoreceptor type. Thus, unlike $V'(\lambda)$, additivity is not inevitable, but requires the adoption of special tasks, the performance of which is supposed to depend on an additive luminance mechanism. Such tasks include HFP, in which continuously alternating lights of different wavelength are matched in luminance to minimize the perception of flicker, and MDB, in which the relative intensities of the two half fields is set so that the border between them appears minimally distinct (e.g., Sperling, H. G., 1958; Wagner, G. and Boynton, R. M., 1972). The generality of such luminous efficiency functions are severely limited, however, since their spectral sensitivities are strongly dependent on chromatic adaptation (e.g., De Vries, H., 1948; Eisner, A. and MacLeod, D. I. A., 1981; Stockman, A. *et al.*, 1993b). In other words, the shapes of measured luminous efficiency functions vary with the adapting condition, even though functions like $V(\lambda)$ and $V^*(\lambda)$ (see below) have a fixed shape.

Nevertheless, a luminous efficiency function is of practical use in many applications, especially for conditions that are similar to those under which the function was defined (e.g., neutral adaptation). Unfortunately, however, the standard CIE photopic 1924 $V(\lambda)$ function is seriously in error. It is a speculative hybrid function, artificially smoothed, and dubiously constructed from divergent data measured under very different procedures at several laboratories (Wyszecki, G. and Stiles, W. S., 1982). The CIE $V(\lambda)$ function shown in Figure 5 as the dashed red line substantially underestimates luminous efficiency at short wavelengths. Attempts to improve it (Judd, D. B., 1951; Vos, J. J., 1978) have been less than satisfactory (Stockman, A. and Sharpe, L. T., 1999; 2000), and have been little used outside vision science laboratories.

Recently, Sharpe L. T. *et al.* (2005) have proposed a new luminous efficiency function, $V^*(\lambda)$, which is based on experimentally determined 25-Hz, 2-deg

diameter, HFP data from 40 observers of known genotype, taking into account the polymorphism of the L-cone photopigment. $V^*(\lambda)$ defines luminance for a reproducible, phase of natural daylight (CIE standard illuminant D_{65} adaptation), while being a linear combination of the Stockman A. and Sharpe L. T. (2000) M- and L-cone fundamentals. The $V^*(\lambda)$ function (black line) is shown in Figure 5. In terms of the Stockman A. and Sharpe L. T. (2000) M- and L-cone quantal fundamentals normalized to unity peak, the quantal $V^*(\lambda) = [1.891\bar{l}(\lambda) + \bar{m}(\lambda)]/2.80361$; whereas, in terms of the Stockman A. and Sharpe L. T. (2000) M- and L-cone energy fundamentals normalized to unity peak, the energy-based $V^*(\lambda) = [1.98065\bar{l}_e(\lambda) + \bar{m}_e(\lambda)]/2.87091$. The different weights and scaling factors simply reflect the different unity normalizations in quantal and energy units. Note that these constants define $V^*(\lambda)$, which was determined for adaptation to the D_{65} daylight standard; different adaptation conditions would lead to different constants and different efficiency functions.

2.06.3.1.3 Mesopic Luminous Efficiency

Mesopic luminous efficiency has been measured in several laboratories using a variety of methods (e.g., Walters, H. V. and Wright, W. D., 1943; Kinney, J. A. S., 1958; Palmer, D. A., 1968; Kokoschka, S., 1972; Yaguchi, H. and Ikeda, M., 1984; Nakano, Y. and Ikeda, M., 1986; Sagawa, K. and Takeichi, K., 1986; Viénot, F. and Chiron, F., 1992; He, Y. *et al.*, 1998). The main challenge of mesopic photometry is to characterize how the luminous efficiency changes between the scotopic and photopic levels. The modeling, however, has proven to be difficult, since the relationship between mesopic luminous efficiency and $V(\lambda)$ and $V'(\lambda)$ is complex and nonlinear. Such complexities are inevitable because of the substantial and often rapid changes in the spatial and temporal properties of the visual system that accompany the transition from scotopic to photopic vision. These are caused not only by the change from rod to cone photoreceptors, but also by changes between the different postreceptoral pathways through which the rod and cone signals are transmitted. For a recent review, see Stockman A. and Sharpe L. T., 2006.

2.06.3.2 Chromatic Spectral Sensitivity

Spectral sensitivities measured under conditions that are not specially chosen to yield additive data typically reflect the interaction of complex processes. Generally the shape of the sensitivity curve becomes broader and has pronounced notches and humps (e.g., Stiles, W. S. and Crawford, B. H., 1933; Sperling, H. G. and Harwerth, R. S., 1971; King-Smith, P. E. and Carden, D., 1976; Kranda, K. and King-Smith, P. E., 1979; Thornton, J. E. and Pugh, E. N., Jr., 1983; Kalloniatis, M. and Sperling, H. G., 1990). These characteristics can be accounted for by detection being mediated by chromatic, cone-opponent mechanisms in addition to achromatic ones. Thus, the so-called Sloan's notch (Sloan, L. L., 1928) occurs at target wavelengths at which the target produces the same chromatic signal as the background, so that it cannot be detected by the chromatic mechanism, and is instead detected by a less sensitive achromatic one; by contrast, the humps correspond to target wavelengths at which the target produces a large chromatic signal with respect to the background (e.g., Ingling, C. R., Jr., 1969; Sperling, H. G. and Harwerth, R. S., 1971; King-Smith, P. E. and Carden, D., 1976; Kranda, K. and King-Smith, P. E., 1979; Thornton, J. E. and Pugh, E. N., Jr., 1983; Kalloniatis, M. and Sperling, H. G., 1990; Calkins, D. J. *et al.*, 1992).

Chromatic detection is treated further in Chapter Chromatic Detection and Discrimination. By replotting these types of spectral sensitivity data in cone contrast space, the importance of detection by chromatic and luminance mechanisms becomes much clearer (e.g., Stromeyer, C. F., III *et al.*, 1985; Kalloniatis, M. and Sperling, H. G., 1990; Chaparro, A. *et al.*, 1995; Eskew, R. T. *et al.*, 1999). Spectral sensitivity measurements are now of little value in studying chromatic mechanisms, which are better studied using more complex stimuli that produce chromatic modulations (e.g., modulations of opposite signs in the M- and L-cones). It should be noted, however, that the production of these complex stimuli is still critically dependent on a precise knowledge of the underlying cone spectral sensitivities.

2.06.4 Other Factors that Influence Spectral Sensitivity

Several other factors influence spectral sensitivities and color matches. The most important ones arise from individual differences among observers, and so should be taken into account when trying to predict the spectral sensitivities of an individual from standard or mean functions. Some of them vary with retinal position, and so should be considered when

trying to predict the spectral sensitivities for retinal areas or retinal positions that differ from the centrally viewed 2-deg or 10-deg areas used to obtain the standard functions.

2.06.4.1 Photopigment Variability and Anomalous Trichromacy

There is now clear molecular genetic, psychophysical, and electroretinographic evidence that the M- and L-cone photopigments can vary in spectral position between observers (for a review, see Sharpe, L. T. *et al.*, 1999), thus confirming earlier evidence for such shifts (e.g., Alpern, M. and Pugh, E. N., Jr., 1977; Dartnall, H. J. A. *et al.*, 1983; MacLeod, D. I. A. and Webster, M. A., 1983; Alpern, M., 1987; Webster, M. A. and MacLeod, D. I. A., 1988). These shifts are caused by the inheritance of hybrid LM or ML cone photopigment opsin genes, which are fusion genes produced by intragenic crossing over, containing the coding sequences of both L- and M-cone pigment genes. Both *in vitro* and *in vivo* measurements of the absorbance spectrum peaks of the hybrid pigments reveal a wide range of possible anomalous pigments lying between the normal L- and M-cone pigments. Rather than a continuous distribution, there is a clustering of LM hybrid pigments having their peak absorbances within about 8 nm of the peak absorbance of the normal M-cone pigment and a clustering of ML hybrid pigments having their peak absorbances within about 12 nm of the peak absorbance of the normal L-cone pigment (see table 1 of Stockman, A. *et al.*, 2000). Smaller shifts occur within the normal population, because of different polymorphisms (commonly occurring allelic differences) of the M- and L-cone photopigment opsin genes. The two common polymorphic variants of the L-cone photopigment (which have either alanine or serine at position 180 of the L photopigment opsin gene) differ in spectral position by 2.7 nm or more. The same polymorphic variation occurs in the M-cone photopigment, with a similar shift in spectral sensitivity, but the serine variant is rather rare (see Sharpe, L. T. *et al.*, 1999).

Hybrid LM and ML pigments in people with otherwise normal photopigments result in anomalous trichromacy. Individuals with a hybrid LM pigment replacing one of the two polymorphic variants of the normal L cone pigment are known as protanomalous trichromats; whereas those with a hybrid ML pigment replacing one of the two polymorphic variants of the normal M cone pigment are known as deuteranomalous trichromats. The color vision deficits of anomalous trichromats are usually less severe than those of dichromats, but there is considerable variability among individuals. In general, the smaller the separation between the spectral sensitivities of the normal and anomalous hybrid pigments, the poorer the anomalous trichromat's color discrimination (for more details, see Sharpe, L. T. *et al.*, 1999). Anomalous trichromacy can sometimes arise in individuals lacking either the normal L- or M-cone photopigment because of photopigment optical density differences between photoreceptors containing ostensibly the same remaining L- or M-cone photopigment (Neitz, J. *et al.*, 1999).

2.06.4.2 Lens Pigment

Light is brought into focus on the retina by the cornea and the pigmented crystalline lens. The pigment in the lens absorbs light mainly of short wavelengths (see lower inset of Figure 4, black line). Individual differences in lens pigment density can be large with a range of approximately $\pm 25\%$ of the mean density in young observers (<30 years old; see van Norren, D. and Vos, J. J., 1974). Since lens density increases with the age of the observer (e.g., Crawford, B. H., 1949; Said, F. S. and Weale, R. A., 1959; Pokorny, J. *et al.*, 1988), the variability in the general population is even larger. A two-factor model has been proposed to account for changes in lens density spectrum with age (Pokorny, J. *et al.*, 1988; Xu, J. *et al.*, 1997). Stockman, A. *et al.* (1999) have proposed a slightly adjusted version of the mean lens density spectrum of van Norren D. and Vos J. J. (1974) that is consistent with the Stockman A. and Sharpe L. T. (2000) cone fundamentals.

2.06.4.3 Macular Pigment

Before reaching the photoreceptor, light must pass through the ocular media, including, at the fovea, the macula lutea, which contains macular pigment. This pigment also absorbs light mainly of short wavelengths (see lower inset of Figure 4, yellow line). Individual differences in its density can also be large with a range of peak density from 0.0 to *c.* 1.2 at 460 nm (Wald, G., 1945; Bone, R. A. and Sparrock, J. M. B., 1971; Pease, P. L. *et al.*, 1987). The density of the pigment changes with retinal location; tending to become more transparent with eccentricity. It is

wholly or largely absent by a retinal eccentricity of 10 deg (e.g., Bone, R. A. *et al.*, 1988). Stockman A. and Sharpe L. T. (2000) have proposed a mean macular density spectrum based on measurements by Bone R. A. *et al.* (1992) that is consistent with their cone fundamentals.

2.06.4.4 Photopigment Optical Density

The axial optical density of the photopigment in the receptor outer segment varies between individuals. Estimates of photopigment optical density vary considerably depending to a large extent on the method used to estimate them, but all estimates show sizeable individual differences (e.g., Terstiege, H., 1967; Miller, S. S., 1972; King-Smith, P. E., 1973b, 1973a; Smith, V. C. and Pokorny, J., 1973; Alpern, M., 1979; Burns, S. A. and Elsner, A. E., 1993; Berendschot, T. T. J. M. *et al.*, 1996). Decreases in photopigment optical density result in a narrowing of cone spectral sensitivity curves, which cause corresponding changes to their linear transformations, the CMFs. Any corrections are most easily applied to the cone fundamentals rather than the CMFs. For further details and the relevant equations, see Stockman A. and Sharpe L. T. (1999), eqns [9]–[12].

2.06.4.5 Changes with Eccentricity

Macular pigment and photopigment optical density both decline with eccentricity. Consequently, cone spectral sensitivities, which are defined for centrally viewed 2- or 10-deg diameter fields, must be adjusted in order to predict accurately color matches for other viewing conditions – either for different field sizes or for different viewing angles.

One additional complication is that the S-cones are absent in approximately the central 25 min diameter of vision, so that in that region color matches become tritanopic (e.g., König, A., 1894; Thomson, L. C. and Wright, W. D., 1947; Willmer, E. N., 1950; Williams, D. R. *et al.*, 1981). The small-field tritanopic effect may also occur with steady fixation of parafoveal fields (Hartridge, H., 1945; Thomson, L. C. and Wright, W. D., 1947). The exclusion of the S-cones from the very central fovea is usually attributed to the need to counteract the deleterious effects of light scattering and axial chromatic aberration on spatial resolution, which cause blurring and/or defocus particularly at short wavelengths (but see McClellan, J. S. *et al.*, 2002). For most practical purposes, small field tritanopia can be largely ignored, however, because its influence on color matching and discrimination is mitigated by the blur introduced by the optics of the eye and constant microsaccades (Bedford, R. E. and Wyszecki, G., 1958; McCree, K. J., 1960).

2.06.5 Conclusions

A precise knowledge of the spectral sensitivity of the human rod and cone photoreceptors is central to our understanding and modeling of vision and visual function in normals and individuals with color vision deficiencies. For the rods, spectral sensitivity and luminous efficiency are identical and both are defined by the CIE 1951 $V'(\lambda)$ function. For the cones, the 2-deg and 10-deg cone fundamentals, and the associated lens and macular pigment and photopigment templates, of Stockman A. and Sharpe L. T. (2000), and the photopic luminous efficiency functions of Sharpe L. T. *et al.* (2005) provide a consistent set of standard functions with which to model human vision. These functions, and others, can be downloaded from the Color and Vision Research Laboratories' website.

Acknowledgments

Thanks to Rhea Eskew for comments. Supported by The Wellcome Trust and Fight for Sight.

References

Abney, W.d.W. 1913. Researches in Colour Vision. Longmans, Green.

Abney, W.d.W. and Festing, E. R. 1886. Colour photometry. Philos. Trans. R. Soc. Lond. 177, 423–456.

Alpern, A., Lee, G. B., and Spivey, B. E. 1965. Pi1 cone monochromatism. Arch. Ophthalmol. 74, 334–337.

Alpern, M. 1979. Lack of uniformity in colour matching. J. Physiol. 288, 85–105.

Alpern, M. 1987. Variation in the Visual Pigments of Human Dichromats and Normal Human Trichromats. In: Frontiers of Visual Science: Proceedings of the 1985 symposium, ed. Committee on Vision NRC, pp. 169–193. National Academy Press.

Alpern, M., Lee, G. B., Maaseidvaag, F., and Miller, S. S. 1971. Colour vision in blue-cone 'monochromacy'. J. Physiol. 212, 211–233.

Alpern, M. and Pugh, E. N., Jr. 1977. Variation in the action spectrum of erythrolabe among deuteranopes. J. Physiol. 266, 613–646.

Asenjo, A. B., Rim, J., and Oprian, D. D. 1994. Molecular determinants of human red/green color discrimination. Neuron 12, 1131–1138.

Bedford, R. E. and Wyszecki, G. 1958. Wavelength discrimination for point sources. J. Opt. Soc. Am. 48, 129–135.

Berendschot, T. T. J. M., van der Kraats, J., and van Norren, D. 1996. Foveal cone mosaic and visual pigment density in dichromats. J. Physiol. 492, 307–314.
Blackwell, H. R. and Blackwell, O. M. 1957. Blue mono-cone monochromacy: a new color vision defect. J. Opt. Soc. Am. 47, 338–341.
Blackwell, H. R. and Blackwell, O. M. 1961. Rod and cone receptor mechanisms in typical and atypical congenital achromatopsia. Vision Res. 1, 62–107.
Bone, R. A., Landrum, J. T., and Cains, A. 1992. Optical density spectra of the macular pigment *in vivo* and *in vitro*. Vision Res. 32, 105–110.
Bone, R. A., Landrum, J. T., Fernandez, L., and Tarsis, S. L. 1988. Analysis of the macular pigment by HPLC: retinal distribution and age study. Invest Ophthalmol Vis. Sci. 29, 843–849.
Bone, R. A. and Sparrock, J. M. B. 1971. Comparison of macular pigment densities in the human eye. Vision Res. 11, 1057–1064.
Boring, E. G. 1942. Sensation and Perception in the History of Psychology. Appleton-Century-Crofts.
Bouma, P. J. 1942. Mathematical relationship between the colour vision system of trichromats and dichromats. Physica 9, 773–784.
Burns, S. A. and Elsner, A. E. 1993. Color matching at high luminances: photopigment optical density and pupil entry. J. Opt. Soc. Am. A 10, 221–230.
Calkins, D. J., Thornton, J. E., and Pugh, E. N., Jr. 1992. Monochromatism determined at a long-wavelength/middle-wavelength cone-antagonistic locus. Vision Res. 13, 2349–2367.
Chaparro, A., Stromeyer, C. F., III, Chen, G., and Kronauer, R. E. 1995. Human cones appear to adapt at low light levels: Measurements on the red–green detection mechanism. Vision Res. 35, 3103–3118.
Crawford, B. H. 1949. The scotopic visibility function. Proc. Physic. Soc. Lond. B 62, 321–334.
Dartnall, H. J. A., Bowmaker, J. K., and Mollon, J. D. 1983. Human visual pigments: microspectrophotometric results from the eyes of seven persons. Proc. R. Soc. Lond. B 220, 115–130.
Daw, N. W. and Enoch, J. M. 1973. Contrast sensitivity, Westheimer function and Stiles-Crawford effect in a blue cone monochromat. Vision Res. 13, 1669–1680.
De Vries, H. 1948. The luminosity curve of the eye as determined by measurements with the flicker photometer. Physica 14, 319–348.
Eisner, A. and MacLeod, D. I. A. 1981. Flicker photometric study of chromatic adaptation: selective suppression of cone inputs by colored backgrounds. J. Opt. Soc. Am. 71, 705–718.
Eskew, R. T., McLellan, J. S., and Giulianini, F. 1999. Chromatic Detection and Discrimination. In: Color Vision: From Genes to Perception (*eds*. K. Gegenfurtner and L. T. Sharpe), pp. 345–368. Cambridge University Press.
Estévez, O. 1979. On the Fundamental Database of Normal and Dichromatic Color Vision. Amsterdam University.
Grützner, P. 1964. Der normale Farbensinn und seine abweichungen. Ber. Deut. Ophthalmol. Gesell. 66, 161–172.
Hartridge, H. 1945. The change from trichromatic to dichromatic vision in the human retina. Nature 155, 657–662.
He, Y., Bierman, A., and Rea, M. S. 1998. A system of mesopic photometry. Light Res. Technol. 30, 175–181.
Hess, R. F., Mullen, K. T., Sharpe, L. T., and Zrenner, E. 1989. The photoreceptors in atypical achromatopsia. J. Physiol. 417, 123–149.
Hood, D. C. and Finkelstein, M. A. 1986. Sensitivity to Light. In: Handbook of Perception and Human Performance (*eds*. K. Boff, L. Kaufman, and J. Thomas), pp. 5-1–5-66. Wiley.
Ingling, C. R., Jr. 1969. A tetrachromatic hypothesis for human color vision. Vision Res. 9, 1131–1148.
Judd, D. B. 1945. Standard response functions for protanopic and deuteranopic vision. J. Opt. Soc. Am. 35, 199–221.
Judd, D. B. 1949. Standard response functions for protanopic and deuteranopic vision. J. Opt. Soc. Am. 39, 505.
Judd, D. B. 1951. Report of U.S. Secretariat Committee on Colorimetry and Artificial Daylight. In: Proceedings of the Twelfth Session of the CIE, Stockholm, Technical Committee No. 7 edn., pp. 1–60. Bureau Central de la CIE.
Kalloniatis, M. and Sperling, H. G. 1990. The spectral sensitivity and adaptation characteristics of cone mechanisms under white light adaptation. J. Opt. Soc. Am. A 7, 1912–1928.
King-Smith, P. E. 1973a. The optical density of erythrolabe determined by a new method. J. Physiol. 230, 551–560.
King-Smith, P. E. 1973b. The optical density of erythrolabe determined by retinal densitometry using the self-screening method. J. Physiol. 230, 535–549.
King-Smith, P. E. and Carden, D. 1976. Luminance and opponent-color contributions to visual detection and adaptation and to temporal and spatial integration. J. Opt. Soc. Am. 66, 709–717.
King-Smith, P. E. and Webb, J. R. 1974. The use of photopic saturation in determining the fundamental spectral sensitivity curves. Vision Res. 14, 421–429.
Kinney, J. A. S. 1958. Spectral sensitivity of the eye to spectral radiation at scotopic, mesopic, and photopic intensity levels. J. Opt. Soc. Am. 45, 507–514.
Kokoschka, S. 1972. Untersuchungen zur mesopischen Strahlungsbewertung. Die Farbe 21, 39–112.
König, A. 1894. Über den menschlichen Sehpurpur und seine Bedeutung fur das Sehen. Acad. Wissen. Sitzung. 30, 577–598.
König, A. and Dieterici, C. 1886. Die Grundempfindungen und ihre Intensitäts-Vertheilung im Spectrum. Sitzung. Akad. Wissen. Berl. 1886, 805–829.
Kraft, T. W., Neitz, J., and Neitz, M. 1998. Spectra of human L cones. Vision Res. 38, 3663–3670.
Kranda, K. and King-Smith, P. E. 1979. Detection of colored stimuli by independent linear systems. Vision Res. 19, 733–745.
Le Grand, Y. 1968. Light, Colour and Vision. Chapman and Hall.
Lennie, P., Pokorny, J., and Smith, V. C. 1993. Luminance. J. Opt. Soc. Am. A 10, 1283–1293.
MacLeod, D. I. A. and Webster, M. A. 1983. Factors Influencing the Color Matches of Normal Observers. In: Colour Vision: Physiology and Psychophysics (*eds*. J. D. Mollon and L. T. Sharpe), pp. 81–92. Academic Press.
Maxwell, J. C. 1855. Experiments on colours, as perceived by the eye, with remarks on colour-blindness. Trans. R. Soc. Edin. 21, 275–298.
Maxwell, J. C. 1856. On the theory of colours in relation to colour-blindness. A letter to Dr. G. Wilson. Trans. R. Scot. Soc. Arts 4, 394–400.
Maxwell, J. C. 1860. On the theory of compound colours and the relations of the colours of the spectrum. Philos. Trans. R. Soc. Lond. 150, 57–84.
McClellan, J. S., Marcos, S., Prieto, P. M., and Burns, S. A. 2002. Imperfect optics may be the eye's defence against chromatic blur. Nature 417, 174–176.
McCree, K. J. 1960. Small-field tritanopia and the effects of voluntary fixation. Opt. Acta (Lond.) 7, 317–323.
Merbs, S. L. and Nathans, J. 1992a. Absorption spectra of human cone pigments. Nature 356, 431–432.
Merbs, S. L. and Nathans, J. 1992b. Absorption spectra of the hybrid pigments responsible for anomalous color vision. Science 258, 464–466.
Miller, S. S. 1972. Psychophysical estimates of visual pigment densities in red–green dichromats. J. Physiol. 223, 89–107.
Mitchell, D. E. and Rushton, W. A. H. 1971. Visual pigments in dichromats. Vision Res. 11, 1033–1043.

Nakano, Y. and Ikeda, M. 1986. A model for brightness perception at mesopic levels. Kogaku (Jap. J. Opt.) 15, 295–302.

Nathans, J., Piantanida, T. P., Eddy, R. L., Shows, T. B., and Hogness, S. G. 1986a. Molecular genetics of inherited variation in human color vision. Science 232, 203–210.

Nathans, J., Thomas, D., and Hogness, S. G. 1986b. Molecular genetics of human color vision: the genes encoding blue, green and red pigments. Science 232, 193–202.

Neitz, M., Neitz, J., and Jacobs, G. H. 1995. Genetic basis of photopigment variations in human dichromats. Vision Res. 35, 2095–2103.

Neitz, J., Neitz, M., and Shevell, S. K. 1999. Trichromatic color vision with two spectrally distinct photopigments. Nat. Neurosci. 2, 884–888.

Oprian, D. D., Asenjo, A. B., Lee, N., and Pelletier, S. L. 1991. Design, chemical synthesis, and expression of genes for the three human color vision pigments. Biochemistry (Mosc.) 30, 11367–11372.

Palmer, D. A. 1968. Standard observer for large-field photometry at any level. J. Opt. Soc. Am. 58, 1296–1299.

Parsons, J. H. 1924. An Introduction to Colour Vision, 2nd edn. Cambridge University Press.

Pease, P. L., Adams, A. J., and Nuccio, E. 1987. Optical density of human macular pigment. Vision Res. 27, 705–710.

Pokorny, J., Smith, V. C., and Lutze, M. 1988. Aging of the human lens. Appl. Opt. 26, 1437–1440.

Rushton, W. A. H. 1965. A foveal pigment in the deuteranope. J. Physiol. 176, 24–37.

Sagawa, K. and Takeichi, K. 1986. Spectral luminous efficiency functions in the mesopic range. J. Opt. Soc. Am. A 3, 71–75.

Said, F. S. and Weale, R. A. 1959. The variation with age of the spectral transmissivity of the living human crystalline lens. Gerontologia 3, 213–231.

Schnapf, J. L., Kraft, T. W., and Baylor, D. A. 1987. Spectral sensitivity of human cone photoreceptors. Nature 325, 439–441.

Sharpe, L. T., Stockman, A., Jagla, W., and Jägle, H. 2005. A luminous efficiency function, $V^*(\lambda)$, for daylight adaptation. JOV 5, 948–968.

Sharpe, L. T., Stockman, A., Jägle, H., Knau, H., Klausen, G., Reitner, A., and Nathans, J. 1998. Red, green, and red–green hybrid photopigments in the human retina: correlations between deduced protein sequences and psychophysically-measured spectral sensitivities. J. Neurosci. 18, 10053–10069.

Sharpe, L. T., Stockman, A., Jägle, H., and Nathans, J. 1999. Opsin Genes, Cone Photopigments, Color Vision and Colorblindness. In: Color Vision: From Genes to Perception (*eds*. K. Gegenfurtner and L. T. Sharpe), pp. 3–51. Cambridge University Press.

Sloan, L. L. 1928. The effect of intensity of light, state of adaptation of the eye, and size of photometric field on the visibility curve. Psychol. Monogr. 38, 1–87.

Smith, V. C. and Pokorny, J. 1973. Psychophysical estimates of optical density in human cones. Vision Res. 13, 1119–1202.

Smith, V. C. and Pokorny, J. 1975. Spectral sensitivity of the foveal cone photopigments between 400 and 500 nm. Vision Res. 15, 161–171.

Smith, V. C., Pokorny, J., Delleman, J. W., Cozijnsen, M., Houtman, W. A., and Went, L. N. 1983. X-linked incomplete achromatopsia with more than one class of functional cones. Invest. Ophthalmol. Vis. Sci. 24, 451–457.

Sperling, H. G. 1958. An Experimental Investigation of the Relationship Between Colour Mixture and Luminous Efficiency. In: Visual Problems of Colour, Volume 1, pp. 249–277. Her Majesty's Stationery Office.

Sperling, H. G. and Harwerth, R. S. 1971. Red–green cone interactions in increment-threshold spectral sensitivity of primates. Science 172, 180–184.

Stiles, W. S. 1939. The directional sensitivity of the retina and the spectral sensitivity of the rods and cones. Proc. R. Soc. Lond. B 127, 64–105.

Stiles, W. S. 1948. The Physical Interpretation of the Spectral Sensitivity Curve of the Eye. In: Transactions of the Optical Convention of the Worshipful Company of Spectacle Makers, pp. 97–107. Spectacle Maker's Company.

Stiles, W. S. 1978. Mechanisms of Colour Vision. Academic Press.

Stiles, W. S. and Burch, J. M. 1959. NPL colour-matching investigation: final report (1958). Opt. Acta (Lond.) 6, 1–26.

Stiles, W. S. and Crawford, B. H. 1933. The liminal brightness increment as a function of wave-length for different conditions of the foveal and parafoveal retina. Proc. R. Soc. Lond. B 113, 496–530.

Stockman, A. 2003. Colorimetry. In: The Optics Encyclopedia: Basic Foundations and Practical Applications (*eds*. T. G. Brown, K. Creath, H. Kogelnik, M. A. Kriss, J. Schmit, and M. J. Weber), pp. 207–226. Wiley-VCH.

Stockman, A., MacLeod, D. I. A., and Johnson, N. E. 1993a. Spectral sensitivities of the human cones. J. Opt. Soc. Am. A 10, 2491–2521.

Stockman, A., MacLeod, D. I. A., and Vivien, J. A. 1993b. Isolation of the middle- and long-wavelength sensitive cones in normal trichromats. J. Opt. Soc. Am. A 10, 2471–2490.

Stockman, A. and Mollon, J. D. 1986. The spectral sensitivities of the middle- and long-wavelength cones: an extension of the two-colour threshold technique of W S. Stiles. Perception 15, 729–754.

Stockman, A. and Sharpe, L. T. 1999. Cone Spectral Sensitivities and Color Matching. In: Color vision: From Genes to Perception (*eds*. K. Gegenfurtner and L. T. Sharpe), pp. 53–87. Cambridge University Press.

Stockman, A. and Sharpe, L. T. 2000. Spectral sensitivities of the middle- and long-wavelength sensitive cones derived from measurements in observers of known genotype. Vision Res. 40, 1711–1737.

Stockman, A. and Sharpe, L. T. 2006. Into the twilight zone: the compexities of mesopic vision and luminous efficiency. Ophthal. Physiol. Opt. 26, 225–239.

Stockman, A., Sharpe, L. T., and Fach, C. C. 1999. The spectral sensitivity of the human short-wavelength cones. Vision Res. 39, 2901–2927.

Stockman, A., Sharpe, L. T., Merbs, S., and Nathans, J. 2000. Spectral Sensitivities of Human Cone Visual Pigments Determined *In Vivo* and *In Vitro*. In: Vertebrate Phototransduction and the Visual Cycle, Part B Methods in Enzymology, (*ed*. K. Palczewski), Vol. 316, pp. 626–650. Academic Press.

Stromeyer, C. F., III, Cole, G. R., and Kronauer, R. E. 1985. Second-site adaptation in the red–green chromatic pathways. Vision Res. 25, 219–237.

Terstiege, H. 1967. Untersuchungen zum Persistenz- und Koeffizientesatz. Die Farbe 16, 1–120.

Thomson, L. C. and Wright, W. D. 1947. The colour sensitivity of the retina with the central fovea of man. J. Physiol. 105, 316–331.

Thornton, J. E. and Pugh, E. N., Jr. 1983. Red/green color opponency at detection threshold. Science 219, 191–193.

van Norren, D. and Vos, J. J. 1974. Spectral transmission of the human ocular media. Vision Res. 14, 1237–1244.

Viénot, F. and Chiron, F. 1992. Brightness matching and flicker photometric data obtained over the full mesopic range. Vision Res. 32, 533–540.

von Helmholtz, H. L. F. 1852. On the theory of compound colours. Philos. Mag. Ser. 44, 519–534.

Vos, J. J. 1978. Colorimetric and photometric properties of a 2-deg fundamental observer. Color Res. Appl. 3, 125–128.
Vos, J. J., Estévez, O., and Walraven, P. L. 1990. Improved color fundamentals offer a new view on photometric additivity. Vision Res. 30, 936–943.
Vos, J. J. and Walraven, P. L. 1971. On the derivation of the foveal receptor primaries. Vision Res. 11, 799–818.
Wagner, G. and Boynton, R. M. 1972. Comparison of four methods of heterochromatic photometry. J. Opt. Soc. Am. 62, 1508–1515.
Wald, G. 1945. Human vision and the spectrum. Science 101, 653–658.
Walters, H. V. and Wright, W. D. 1943. The spectral sensitivity of the fovea and parafovea in the Purkinje range. J. Opt. Soc. Am. 45, 507–514.
Webster, M. A. and MacLeod, D. I. A. 1988. Factors underlying individual differences in the color matches of normal observers. J. Opt. Soc. Am. A 5, 1722–1735.
Williams, D. R., MacLeod, D. I. A., and Hayhoe, M. M. 1981. Foveal Tritanopia. Vision Res. 19, 1341–1356.
Willmer, E. N. 1950. Further observations on the properties of the central fovea in colour-blind and normal subjects. J. Physiol. 110, 422–446.
Wyszecki, G. and Stiles, W. S. 1967. Color Science: Concepts and Methods, Quantitative Data and Formulae. Wiley.
Wyszecki, G. and Stiles, W. S. 1982. Color Science: Concepts and Methods, Quantitative Data and Formulae. Wiley.
Xu, J., Pokorny, J., and Smith, V. C. 1997. Optical density of the human lens. J. Opt. Soc. Am. A 14, 953–960.
Yaguchi, H. and Ikeda, M. 1984. Mesopic luminous-efficiency functions for various adapting levels. J. Opt. Soc. Am. A 1, 120–123.
Young, T. 1802. On the theory of light and colours. Philos. Trans. R. Soc. Lond. 92, 20–71.

Relevant Website

http://www.curl.org – Color and Vision Research Laboratories, Institute of Opthalmology, UCL.

2.07 Chromatic Detection and Discrimination

R T Eskew Jr., Northeastern University, Boston, MA, USA

© 2008 Elsevier Inc. All rights reserved.

2.07.1	**Introduction**	102
2.07.2	**Definitions and Representations**	103
2.07.2.1	Cone Signals and Spaces	103
2.07.2.2	Psychophysical Color Mechanisms	103
2.07.3	**Methods**	105
2.07.4	**Chromatic Mechanisms**	105
2.07.4.1	Cardinal Mechanisms	105
2.07.4.2	R and G Mechanisms	106
2.07.4.3	B and Y Mechanisms	108
2.07.4.4	I and D Mechanisms	110
2.07.4.5	Higher-Order Mechanisms	111
2.07.5	**Conclusions**	114
References		114

Glossary

cardinal axes Color directions defined by an exchange of L- and M-cone excitations at constant luminance, an S-cone excitation direction, and a luminance direction.

cardinal mechanisms Bipolar chromatic mechanisms that are stimulated in isolation by colored stimuli varying along the three cardinal axes. Generally referred to as red–green, blue–yellow, and luminance mechanisms.

classical mechanisms Six unipolar chromatic mechanisms, R (red), G (green), B (blue), Y (yellow), I (increment), and D (decrement). When arranged in pairs (R/G, B/Y, I/D) these are similar to the cardinal mechanisms.

chromatic mechanism A psychophysical construct, based upon a linear or nonlinear combination of cone signals. The inputs to a mechanism are assumed to have undergone cone-specific adaptation; the outputs are univariant and labeled-line.

cone excitation A number representing the quantal or energy catch of an L, M, or S cone.

cone contrast A dimensionless number representing the relative quantal or energy catch of an L, M, or S cone, for example $\Delta L/L$. The numerator represents a change in quantal catch due to a stimulus modulation, the denominator represents the quantal catch to which the cone is adapted.

cone contrast space A color space with axes representing the cone contrasts produced by a stimulus modulation. The origin represents the mean or prevailing illumination; stimulus directions are normally specified by vectors in the three-dimensional space or planes within it, and strengths by the cone contrast vector length (or, alternatively, root mean square).

chromatic bandwidth A measurement of the region of color space to which a mechanism is sensitive. Normally measured by use of field methods.

cone opponency A type of combination of cone inputs to a chromatic mechanism, in which two of the signals have opposing effects within a single mechanism. Compare with *color opponency*.

color opponency A perceptual or phenomenological opposition of color, in which the possible outputs of a color mechanism have two qualitatively different and nonoverlapping (mutually exclusive) ranges, for example, red and green. Compare with *cone opponency*.

cone-specific adaptation Adaptation to light that acts on the signals generated by a single class of cone photoreceptor.

detection contour A set of thresholds measured in a plane of some color space, such as cone excitation or cone contrast space.

DKL (Derrington Krauskopf Lennie) space A version of a cone excitation space in which the axes are aligned with the three cardinal mechanism

axes. Often parameterized in spherical coordinates, with the origin representing the adapting field; stimulus modulations are represented by the azimuth for the angle in the equiluminant plane, elevation for the projection onto the luminance axis, and stimulus strength being represented by the radial coordinate.

field methods Indirect psychophysical methods in which a test chromaticity is fixed, but an auxiliary stimulus such as masking noise is varied to determine the spectral sensitivity of the mechanism detecting the test.

first-site adaptation See cone-specific adaptation.

higher-order mechanism A chromatic mechanism tuned to an intermediate color direction, in-between the directions of the cardinal or classical mechanisms.

labeled line The idea, going back to Müller's Law of Specific Nerve Energies, that the activity of a mechanism is labeled such that its quality (e.g., red versus green) can be identified.

mechanism vector A triplet of three numbers that specify the relative amounts of L-, M-, and S-cone signals that are combined within a linear chromatic mechanism. The three weights may be all of the same sign (a nonopponent mechanism) or one or two may be negative (a cone opponent mechanism). The vector points in the direction of maximum responsivity in cone excitation or cone contrast space.

null plane The plane that goes through the origin of cone excitation or cone contrast space and contains stimuli that have no effect upon a linear chromatic mechanism. For a linear, bipolar mechanism these are the only stimuli to which the mechanism does not respond. For a unipolar mechanism the null plane is the boundary of the half of cone space to which the mechanism does not respond.

off-axis looking When multiple chromatic mechanisms have overlapping sensitivities in color space, a mechanism that is not tuned exactly to the test color direction (and is thus off-axis) may have the highest signal-to-noise ratio and therefore determine performance. Analogous to off-frequency listening in hearing.

second-site desensitization Adaptation that occurs at the output of a chromatic mechanism, and so acts upon a combined signal from more than one cone class.

test methods Psychophysical methods in which the chromaticity of a test is varied and spectral sensitivity is measured directly.

2.07.1 Introduction

Color vision begins with the encoding of light by the three classes of cone photoreceptor. In the modern approach to the study of chromatic detection and discrimination, the major thrust is to understand what computations are performed by the remainder of the visual system on the signals generated by the cones. Starting no later than the bipolar cells (Dacey, D. *et al.*, 2000), signals may be recombined so that they resemble a subtraction of the signals from different cone classes. By the late 1970s the picture that had emerged (Lennie, P. and D'Zmura, M., 1988) is that, at least by the time the signals reach the lateral geniculate nucleus (LGN), these cone-opponent signals are carried by three pathways or mechanisms: one opponent mechanism signaling a red–green difference, another opponent mechanism for a blue–yellow difference, and a third that carries a summed signal representing achromatic or brightness information. There were good reasons to accept this view: opponent computations like these create efficient representations of color (Buchsbaum, G. and Gottschalk, A., 1983), would help the visual system distinguish changes in surface materials from shadow boundaries (Rubin, J. M. and Richards, W. A., 1988), can explain much data from chromatic detection and discrimination experiments (Boynton, R. M., 1979), and also seemed to be consistent with phenomenological and psychophysical studies of color appearance (Hurvich, L. M. and Jameson, D., 1957), which can be described along color opponent red–green, blue–yellow, and bright-dark dimensions.

However, difficulties in describing both chromatic detection and color appearance within a single framework have led more recent theorists to propose a recoding of lower-level mechanisms suitable for detection to higher-level ones suitable for color

appearance (e.g., Guth, S. L., 1991; De Valois, R. L. and De Valois, K., 1993). The present treatment focuses on detection and discrimination, but even here complications – reviewed below – have arisen (Krauskopf, J. *et al.*, 1986a; Krauskopf, J., 1999). Over the past 20 years the textbook picture of three opponent detection mechanisms has been shown to be incorrect in many of its aspects. Consensus on a computable alternative theory has not yet emerged.

2.07.2 Definitions and Representations

2.07.2.1 Cone Signals and Spaces

To begin to understand how cone signals are transformed by the brain to serve color discrimination, one must first usefully represent the photoreceptor signals that are produced by visual stimuli. A representation employed in both psychophysics and physiology is that of cone excitations: lights are denoted by three numbers that are proportional to the quantal (or energy) catch rates in L-, M-, and S-cones. To represent test modulations above and below an adapting background field, the three excitations created by the adapting field (L_a, M_a, S_a) are subtracted from the excitations created by the test modulation to make local cone excitation coordinates ($\Delta L = L_{test}$-L_a, $\Delta M = M_{test}$-M_a, $\Delta S = S_{test}$-S_a). The influential DKL color space used by Derrington A. M. *et al.* (1984) is a linear transformation of these three coordinate axes, so that they no longer lie along the cone excitation directions but are along ΔL-ΔM, ΔS, and luminance axes (see Section 35.4.3.1). Spherical coordinates are often used, with the azimuth specifying the angle in the equiluminant plane (axes ΔL-ΔM, ΔS) and elevation specifying the projection onto the luminance axis. Because the axes of cone excitation space are scaled arbitrarily with respect to each other, many psychophysicists normalize the units along the axes to threshold values in order to define angles and distances.

An alternative to using cone excitations is to use cone contrasts, created by dividing the local cone excitation coordinates (e.g., ΔL) by the cone excitation produced by the adapting field (e.g., $\Delta L/L_a$ or simply $\Delta L/L$). By dividing out the background, cone contrasts approximately account for adaptation within the cones and within pathways before different cone signals are combined (Normann, R. A. and Perlman, I., 1979; Valeton, J. M., 1983; Valeton, J. M. and van Norren, D., 1983; MacLeod, D. I. A. *et al.*, 1992; MacLeod, D. I. A. and He, S., 1993). Accounting for first-site, cone-specific adaptation regularizes some data (see below) and helps to focus attention on neural computations that occur later in the system. Cone contrasts are dimensionless, and need not be further normalized.

2.07.2.2 Psychophysical Color Mechanisms

The nature and number of psychophysical color mechanisms is now in much dispute, as summarized below. One reason for this disagreement may be the lack of clear definitions of what is meant by the term mechanism. Explicit definition of the mechanism concept is particularly important when comparing psychophysics and physiology. At some level, a mechanism must be a neuron, but a neuron need not be a mechanism.

A chromatic detection mechanism is here defined as a fixed (relative) combination of cone signals which is correlated with the observer's behavior in detection and discrimination experiments. Mechanisms are stochastically independent at threshold. There is no need to require mechanisms to be orthogonal in any particular color space. The signals are combined in the mechanism postreceptorally, meaning that first-site, cone-specific adaptation has already occurred. This cone-specific adaptation is approximated by use of cone contrasts here, but other models of that adaptation could easily be substituted. Manipulations such as masking or habituation, or facilitation due to pedestals or edges (Eskew, R. T., 1989; Cole, G. R. *et al.*, 1990; Eskew, R. T. *et al.*, 1991; Gowdy, P. D. *et al.*, 1999b), which act at the mechanism output, change overall sensitivity but not chromatic tuning.

Two additional assumed properties of mechanisms make strong predictions about chromatic discrimination, thereby making the definition of mechanism more specific and testable. First, univariance implies that when two stimuli are detected by one and only one mechanism, there is some relative intensity at which the two stimuli cannot be discriminated from one another. Second, the labeled line assumption (Graham, N. V. S., 1989; Watson, A. B. and Robson, J. G., 1981) implies that when two stimuli are detected by different mechanisms, they must be discriminable from one another at all relative intensities. These discrimination assumptions have important implications. For example, since red and green stimuli, and S-increment and S-decrement

stimuli, can be discriminated from one another at detection threshold, (Krauskopf, J. *et al.*, 1986a; Mullen, K. T. and Kulikowski, J. J., 1990; Eskew, R. T. *et al.*, 2001), these stimuli are detected by different mechanisms, by definition. While the cone inputs may act antagonistically within the mechanism (they may be cone-opponent), the mechanism cannot be color-opponent in the traditional sense, because qualitatively different outputs must be associated with different mechanisms, according to these two assumptions. Although there are cells at early levels of the visual system that have bipolar responses, the responses of later cells that are the substrate for psychophysical mechanisms must be rectified in some way. Empirical evidence in support of the unipolar nature of psychophysical chromatic mechanisms is summarized below.

Consistent with the behavior of many cells in the LGN (Derrington, A. M. *et al.*, 1984), chromatic mechanisms are often modeled as quasi-linear combinations of cone signals, as shown in Figure 1. For example, for a green mechanism G,

$$G = \gamma P\left(w_L\frac{\Delta L}{L} + w_M\frac{\Delta M}{M} + w_S\frac{\Delta S}{S}\right) + N(0,\sigma)$$
$$= \gamma P(\mathbf{w}_G \cdot \mathbf{v}) + N(0,\sigma) \quad [1]$$

where

$$\mathbf{w}_G = (w_L w_M w_S), \quad \mathbf{v} = \begin{pmatrix} \Delta L/L \\ \Delta M/M \\ \Delta S/S \end{pmatrix}$$

and

$$P(x) = \begin{cases} x & x > 0 \\ 0 & x \le 0 \end{cases}$$

G is the number representing the mechanism response (crudely, an amount of greenness); $\mathbf{v}$ represents the stimulus by the vector of cone contrasts it produces; $\mathbf{w_G}$ is a unit-length vector of weights, each of which might be positive or negative; and γ is a positive number representing the gain of the mechanism. P is a half-wave rectification function (see below) that restricts the response to a single polarity; this nonlinearity is not present in traditional models, but the mechanism definition above and data summarized below require it. N refers to the probability density of a stochastic process, with zero mean and standard deviation σ, that is added to the mechanism in order to model all of the noise sources that corrupt its signal, viz., quantum light fluctuations, neural noises in cone-independent pathways, and neural noises at stages after cone signals have been combined.

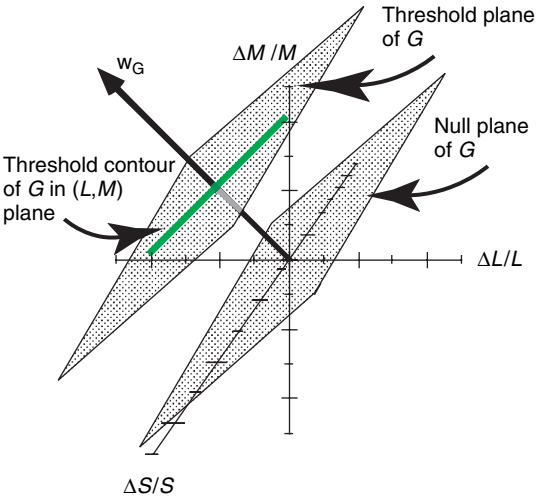

Figure 1 The mechanism vector $\mathbf{w_G}$ (straight arrow) for the G mechanism depicted in three-dimensional cone contrast space. The plane through the origin is the null plane; all stimuli in that plane, and all stimuli on the side of that plane opposite the mechanism vector, produce no response in the mechanism. The threshold plane contains all the stimuli producing a threshold-level response; the intersection of the threshold plane with the L,M plane of cone contrast space is the detection contour shown by the thick green line. Adapted from Eskew R. T., Jr., McLellan J. S., and Giulianini F. 1999. Chromatic Detection and Discrimination. In: Color Vision: from Genes to Perception (*eds*. K. Gegenfurtner and L. T. Sharpe), pp. 345–368. Cambridge University Press, figure 18.2, with permission.

The vector of weights $\mathbf{w}_G$ is the mechanism vector, with components that may be interpreted in signal/noise or d' units (Eskew, R. T. *et al.*, 1999). The mechanism vector points in the direction of maximum responsivity in cone contrast space. The response of this hypothetical half-wave linear mechanism (Giulianini, F. and Eskew, R. T., 2007) to any stimulus vector $\mathbf{v}$ is proportional to the projection of $\mathbf{v}$ onto the mechanism vector, in half of the color space, and zero in the other half (due to the rectification function, P). The linearity implies that stimuli that produce a constant response lie in planes in three-dimensional cone contrast space, or in lines in two-dimensional space, that are at right angles to the mechanism vector, since those regions have a constant projection onto the mechanism vector (Figures 1 and 2). A linear mechanism has a null plane that divides its two response polarities

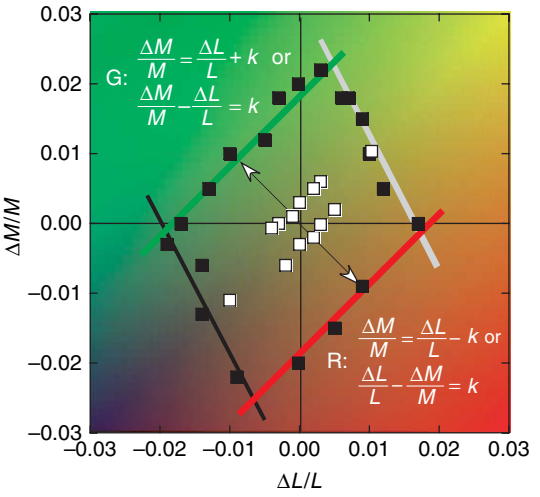

Figure 2 A detection contour measured in the (L,M) plane. The background color gradient roughly suggests the color of the test at that point in the plane. The tests were Gaussian blobs, flashed for 200 ms. The open symbols show unmasked detection, with typical long flanks of slope 1. Flickering random colored rings were superimposed over the test region for the measurements represented by the filled symbols; this noise color direction is indicated by the double-headed arrow. The double arrow also represents the G and R mechanism vectors. The noise shifts the G and R detection contours outward, without changing their shapes. Sensitivity to the 45° and 225° tests is unchanged, because these are detected by I and D which are largely unaffected by this noise. Adapted from Giulianini F. and Eskew R. T., Jr. 1998. Chromatic masking in the (ΔL/L, ΔM/M) plane of cone-contrast space reveals only two detection mechanisms. Vis. Res. 38, 3913–3926, Figure 3a, with permission.

(Derrington, A. M. *et al.*, 1984); half-wave linear mechanisms have a null volume bounded by this plane. Explicitly including rectification in the mechanism definition pushes the physiological substrate of the mechanism back into the cortex, where cells responses are rectified (De Valois, R. L. and De Valois, K., 1993) – and where that substrate is surely to be found, rather than in retina or LGN. It is worth noting that from a computational perspective, rectification can improve contrast coding in noisy neurons (von der Twer, T. and MacLeod, D. I. A., 2001).

2.07.3 Methods

Two classes of procedures, with a venerable history (Stiles, W. S., 1978), have been widely used to study detection mechanisms. In test methods, weak stimuli of various chromaticities are presented, without significantly altering the adapting state of the system, and sensitivity to the tests is measured. Field methods involve a fixed test stimulus, with steady or habituating-flicker fields, or added visual noise, used to alter the state of the system; the goal is to use changes in test threshold as a marker for sensitivity to the field stimuli.

A useful way to define stimulus strengths, including thresholds, is the vector length of a stimulus in cone contrast space, $|v| = \sqrt{(\Delta L/L)^2 + (\Delta M/M)^2 + (\Delta S/S)^2}$. This is the natural metric to use to characterize a linear (or half-wave linear) mechanism, and a measure based upon squared vector length, cone contrast energy (Chaparro, A. *et al.*, 1993) is especially useful for comparing mechanisms. Other measures are useful for this purpose too, particularly those based upon models of ideal chromatic observers (see Geisler, W. S., 1989; Sekiguchi, N. *et al.*, 1993; Brainard, D. H., 1996). It is not generally possible to compare mechanism sensitivities using cone excitation values, due to their arbitrary scaling.

2.07.4 Chromatic Mechanisms

2.07.4.1 Cardinal Mechanisms

The first six mechanisms reviewed below, arranged in three opposing pairs, are often referred to as cardinal mechanisms (Krauskopf, J. *et al.*, 1982a). This naming scheme refers to mechanisms, not by the color directions that best stimulate them, but by the color directions that isolate them (Knoblauch, K., 1995; Eskew, R. T. *et al.*, 1999) – that is, the cone modulations that would leave the other mechanisms unstimulated. Krauskopf J. *et al.* (1982) argued that these were: (1) an L–M axis where L- and M-cone excitation is exchanged at equal luminance and equal S-cone excitation; (2) an S-cone axis where S cones are modulated at equal luminance and unchanging |L–M|; and (3) a luminance axis. However, even ignoring the issues raised by studies of higher order color mechanisms (see Section 35.4.5), there are several problems with this model. First, the use of the S-cone axis to designate a mechanism may lead the unwary to believe, incorrectly, that this mechanism gets no input from L and M cones (the correct implication would be that the *other* mechanisms get no S-cone input). Second, there may in fact be a small S-cone input to the red and green detection mechanisms (see Section 35.4.2) contrary to the cardinal axis scheme. Third, it is now clear that the achromatic flicker mechanism gets L−M as well as S-cone inputs (see Section 35.4.4), also contrary to this scheme. Finally, as discussed below, psychophysical

mechanisms are unipolar (red rather than red/green). To avoid confusion, the term classical rather than cardinal will be used here for the unipolar R, G, B, Y, I, and D mechanisms (see next sections).

2.07.4.2 R and G Mechanisms

The best understood chromatic detection mechanisms receive oppositely signed inputs from L and M cones, are very sensitive to low- and medium-temporal and spatial frequencies, and generate percepts of orangey–red and bluish–green at and near threshold. Following convention, these mechanisms will be referred to as R and G, for red and green, although the percepts they create are certainly not unique hues (De Valois, R. L. and De Valois, K., 1993; De Valois, R. L. *et al.*, 1997; Wuerger, S. M. *et al.*, 2005). There is some evidence, collected using test methods, that one or both of these mechanisms receive a very small S-cone input (Boynton, R. M. *et al.*, 1983; Eskew, R. T. and Kortick, P. M., 1994; Stromeyer, C. F. *et al.*, 1998), and some evidence, collected using field methods, against that input (Krauskopf, J. *et al.*, 1982; Mollon, J. D. and Cavonius, C. R., 1987; Stromeyer, C. F. and Lee, J., 1988). It may be that a sensitive minority of relevant cells receive S-cone input (e.g., Derrington, A. M. *et al.*, 1984), but these cells are too desensitized by S-cone habituation or masking to contribute in the field procedures, leaving the cells without S-cone input to determine sensitivity; test methods would tap these sensitive cells and show an S-cone input (Stromeyer, C. F. and Lee, J., 1988). If so, this would imply multiple R and G mechanisms with very similar spectral tuning, since the S-cone weight is small at best.

R and G have been shown to be remarkably linear combinations of L- and M-cone contrasts using both test and field methods. The high sensitivities of R and G make it easy to isolate them with weak test stimuli in the (L, M) chromatic plane, and their threshold contours are remarkably straight (see Figures 2 and 3). This linearity is not only seen with very weak

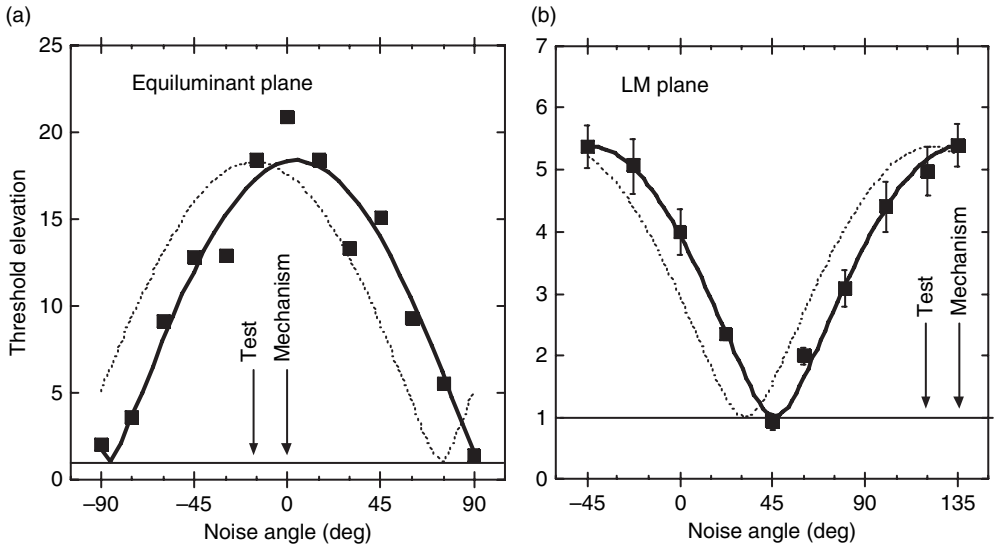

Figure 3 Threshold elevations plotted against the color angle of the masking noise in two different planes of cone contrast space, compared to the direction pointed to by the mechanism vectors $\mathbf{w_R}$ and $\mathbf{w_G}$ in these planes. (a) The test was a 1 cycle per degree equiluminant grating, with equal and opposite contrasts, at color directions of –16° and 164°. Only half of the symmetric data are shown. In this plane, the R and G mechanism directions are 0° and 180°, respectively. Replotted from Figure 4 of Sankeralli M. J. and Mullen K. T. 1997. Postreceptoral chromatic detection mechanisms revealed by noise masking in three-dimensional cone contrast space. J. Opt. Soc. Am. A 14, 2633–2646, with permission. Observer MJS. (b) The test was a green, equiluminant Gaussian blob (120° color direction). In this plane $\mathbf{w_G}$ points in the 135° direction, where the L and M contrasts are of equal magnitude and opposite sign. Adapted from Figure 4 of Giulianini, F. and Eskew, R. T., Jr. 1998. Chromatic masking in the (ΔL/L, ΔM/M) plane of cone-contrast space reveals only two detection mechanisms. Vis. Res. 38, 3913–3926, with permission. Observer F6. In both (a) and (b), the thick curve represents the best fit of $\sqrt{1+q\mathrm{Cos}^2(\alpha-\alpha_0)}$ (see eqn [2]). The dotted curve shows the same function shifted laterally to make the peak coincide with the test, illustrating that masking is aligned with the R and/or G mechanism directions, not the test direction. For both (a) and (b), the function applied in the original papers differs slightly from the correct one shown here.

signals; the contours remain straight (and of unity slope in the L,M plane) even when the use of noise (Giulianini, F. and Eskew, R. T., 1998; Stromeyer, C. F. *et al.*, 1999), chromatic adaptation (Chaparro, A. *et al.*, 1995), or tiny (Chaparro, A. *et al.*, 1994) or very brief (Eskew, R. T. *et al.*, 1994) test spots raises thresholds substantially. Giulianini F. and Eskew R. T. (2007) demonstrated linearity in G even when noise raised threshold by 20-fold (in one observer).

The mechanism vector for R is very close to $\mathbf{w}_R = (1, -1, 0)/\sqrt{2}$ (normalized to unit length) and, for G, $\mathbf{w}_G = -\mathbf{w}_R$, neglecting the possible small S-cone input. The equal and opposite L and M weights in both R and G mean that at threshold, the size of the difference between the L and M-cone signals $\left|\frac{\Delta L}{L} - \frac{\Delta M}{M}\right|$ is constant (Figures 2 and 3). Individual differences (in color normal observers) in these weights are very small (reviewed in Eskew, R. T. *et al.*, 1999). Thus, although observers differ widely in the relative numbers of L and M cones in their retinas (Hofer, H., *et al.*, 2005), these numbers are apparently not an important determinant of the strength of cone contrast inputs to R and G (except, of course, near the limit of protanopia or deuteranopia; see Chapter Spectral Sensitivity).

The symmetry of cone weights of R and G means their threshold planes or lines are parallel (Figure 2) and therefore no light can stimulate both of them; taken as a pair, these two cone-opponent mechanisms act very much like a color-opponent bipolar linear mechanism, with a null plane (where neither responds) that contains the equichromatic axis (the axis of lights with the same chromaticity as the adapting field). However, habituating to sawtooth modulations of chromaticity can selectively elevate thresholds for reddish or greenish stimuli (Krauskopf, J. *et al.*, 1986a; Krauskopf, J. and Zaidi, Q., 1986). Sankeralli M. J. and Mullen K. T. (2001) used unipolar tests and quick flashes of unipolar (e.g., red or green) noise and showed that masking was almost entirely restricted to the cases where the test and noise had the same polarity. These findings are consistent with other results that R and G are separate mechanisms in the fovea at threshold (Gowdy, P. D. *et al.*, 1999a; 1999b), as well as with models such as that of De Valois R. L. and De Valois K. (1993). This empirical evidence buttresses the use of the univariance and labeled line assumptions in the definition of mechanism (Section 35.2.2). The evidence outlined above indicates that R and G are linear except for this rectification.

A field method may be used to study this linearity, by adding dynamic noise of various chromaticities to a white background field. The theory of noise masking (Burgess, A. and Barlow, H. B., 1983; Legge, G. E. *et al.*, 1987; Pelli, D. G., 1990), in which test contrast energy is related to noise power, leads to the expectation that the squared threshold elevation is linear with the squared-cosine of the angle between the noise vector at α and the mechanism vector $\mathbf{w}$ at α_0,

$$(c/c_0)^2 = 1 + q'(\mathbf{r}\cdot\mathbf{w})^2 = 1 + q\,\mathrm{Cos}^2(\alpha - \alpha_0) \qquad [2]$$

where $\mathbf{r}$ is the vector of noise, c is the threshold with noise and c_0 without it, and q and q' are constants that account for stimulus parameters as well as the rectification in eqn [1]. The chromatic masking bandwidth (half-width at half-height) of Eqn. (2) is 45°, or about 56.5° if the square root is taken of both sides (not the 60° of a cosine). Figure 3 shows that threshold elevations for stimuli detected by R or G follow this relationship closely (Sankeralli, M. J. and Mullen, K. T., 1997; Giulianini, F. and Eskew, R. T., 1998), consistent with linear detection. Note that the maximum masking is not obtained at the test direction; rather, the maximum is at the mechanism direction α_0 (the direction that $\mathbf{w}$ points) in both of these planes of color space (see section 35.4.5).

Figure 4 shows R and G thresholds collected on green, red/green–neutral (yellow), and deep red adapting fields (Chaparro, A. *et al.*, 1995). The detection contours have unit slope in all conditions, indicating that the use of cone contrasts has adequately accounted for different first-site adaptations produced by the three fields. In comparison, the same data plotted in local cone excitation coordinates (right) show substantial variation in slope with adapting chromaticity. Because the pairs of cone contrast contours are parallel to the equichromatic axis (at 45°) on all three field colors, neither mechanism will respond to radiance modulations (such as, approximately, shadows), regardless of the prevailing chromatic conditions. Both the R and G thresholds are higher on the red fields, indicating postreceptoral, second-site desensitization of the combined cone signal. This desensitization means the criterion signal k must be larger on the red field for both G and R; that both mechanisms are desensitized suggests the locus of second-site desensitization is prior to the rectification that splits early bipolar signals into unipolar mechanisms.

R and G are more sensitive than achromatic mechanisms (and, presumably, B and Y; see below),

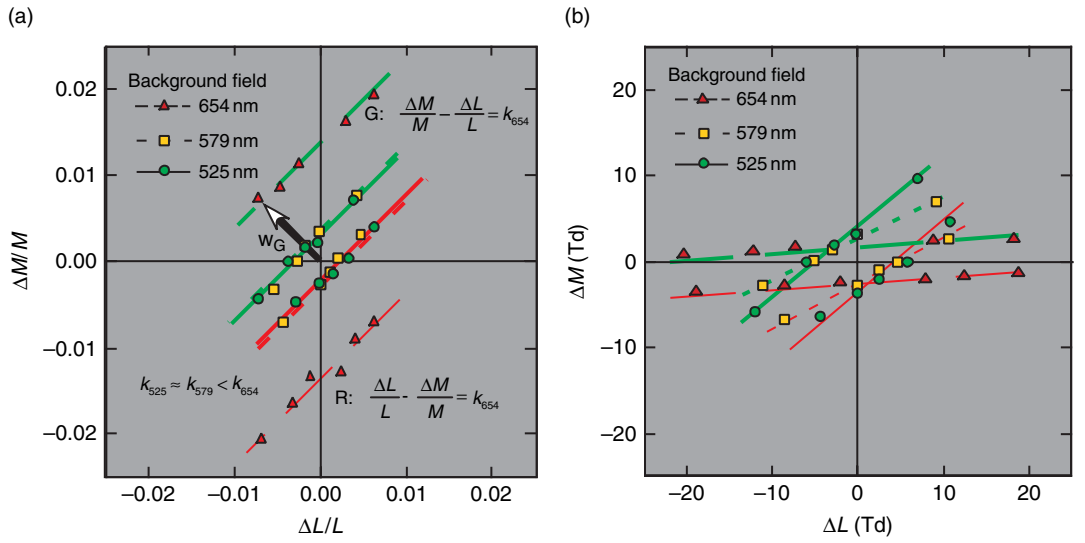

Figure 4 (a) Thresholds measured on three chromatic adapting fields (525, 579, and 654 nm), plotted in cone contrast space. The upper lines represent the G mechanism; the lower lines, R. On the red field, the magnitude of the threshold-level response (k) is largest, but the contour slope is 1.0 in all cases. The heavy arrow depicts the G mechanism vector, at a polar angle of 135° where the L and M contrast weights are of equal magnitude and opposite sign. (b) The same data as in (a) but plotted in local cone excitation coordinates. Without using the contrast variables to account for first-site, cone-specific adaptation, the detection contour slopes vary with field color. Adapted from Chaparro A., Stromeyer C. F., 3rd, Chen G., and Kronauer R. E. 1995. Human cones appear to adapt at low light levels: measurements on the red–green detection mechanism. Vis. Res. 35, 3103–3118, figures 2 and 4, with permission.

even at the shortest flash durations (Eskew, R. T. *et al.*, 1994) and for very tiny spots (Chaparro, A. *et al.*, 1994). Even when R or G is compared with the increment achromatic mechanism using spot sizes and durations that are optimal for each mechanism, R/G is about seven times more sensitive in contrast energy terms (Chaparro, A. *et al.*, 1993). In cone contrast space, the vast majority of the chromatic volume will be detected by R or G except at high temporal frequencies (>15 Hz), for reasonably bright adapting conditions (Stromeyer, C. F. *et al.*, 1987).

The sensitivity of R and G is highest in the central fovea and falls off rapidly with eccentricity (Mullen, K. T., 1991; Stromeyer, C. F. *et al.*, 1992; Mullen, K. T. and Kingdom, F. A., 2002). Dating at least back to Abney W. d. W. (1897), data has suggested that sensitivity to green falls off more rapidly with eccentricity than other colors, including red (for historical reviews, see Parsons, J. H., 1915; Boring, E. G., 1942). More recent studies confirm this peripheral asymmetry (Moreland, J. D. and Cruz, A., 1959; Conners, M. M. and Kelsey, P. A., 1961; Abramov, I. *et al.*, 1991). It is now clear that the loss of sensitivity to green is postreceptoral: there are losses in sensitivity to L-cone decrements as well as M-cone increments (and their combinations), compared to L-cone increments and M-cone decrements (and their combinations; Stromeyer, C. F. *et al.*, 1992; Newton, J. R. and Eskew, R. T., 2003; Sakurai, M. and Mullen, K. T., 2006). Whether (Hagstrom, S. A. *et al.*, 1998) or not (Deeb, S. S. *et al.*, 2000) there is variation in the relative L- and M-cone number with eccentricity is not relevant. The site of the asymmetry is most naturally attributable to double-opponent cells in the cortex (Hubel, D. H. and Wiesel, T. N., 1968; Gouras, P., 1974; Michael, C. R., 1978; Livingstone, M. S. and Hubel, D. H., 1984; Tootell, R. B. *et al.*, 1988; Gegenfurtner, K. R., 2003; Lennie, P. and Movshon, J. A., 2005), which have the type of correlation between cone type and increment/decrement polarity that seems called for, but since these cells are often studied with red–green gratings and many of them respond to equichromatic stimuli as well as red–green ones (e.g., Johnson, E. N. *et al.*, 2001) the actual locus of this asymmetry is unknown.

2.07.4.3 B and Y Mechanisms

The central panel of Figure 5 shows detection data collected in the equiluminant plane with a Gabor patch test (which, since it contains tests of two symmetric polarities, produces a set of symmetric

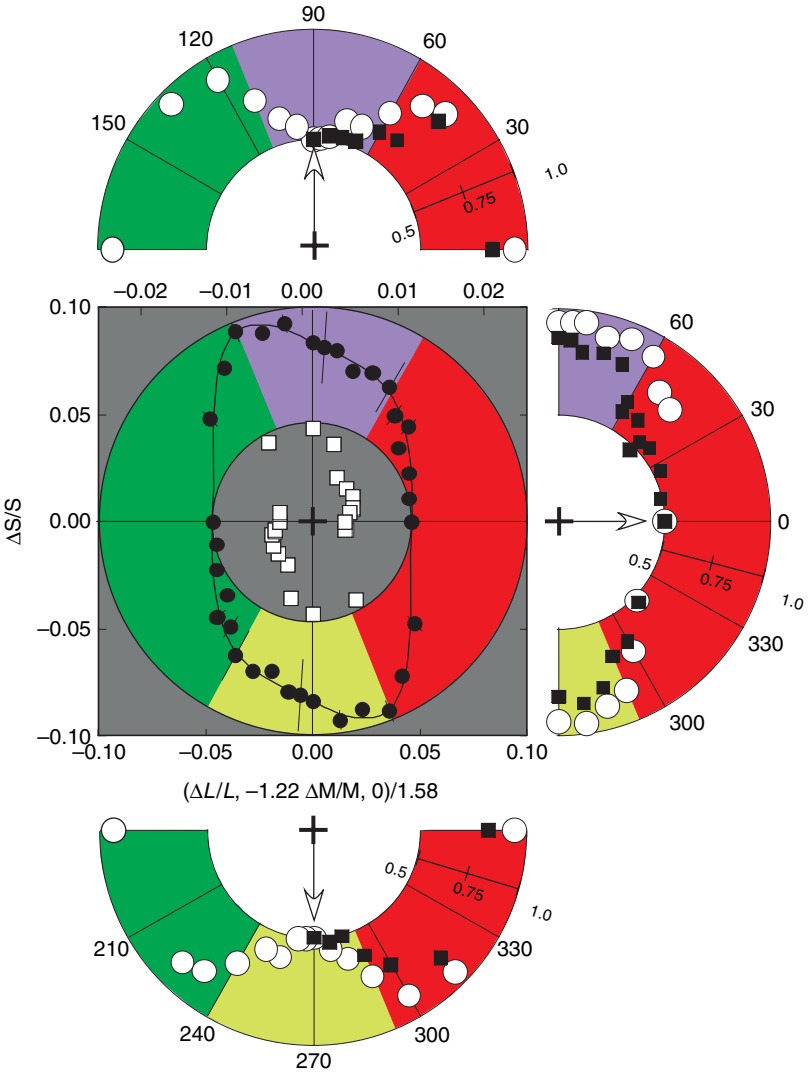

Figure 5 The center square panel shows detection thresholds for Gabor patches with (filled symbols) or without (open symbols) red/green masking noise (0°/180° color direction). Note that the horizontal scale is expanded for the no-noise thresholds represented by the open symbols, as shown on the top axis. The weighting constants on the L-M contrast axis result from using unit-length basis vectors in the equiluminant plane. Data are symmetric about the origin due to the symmetric stimuli. The solid black line fitted to the masked thresholds represents probability summation among four symmetric unipolar linear mechanisms. The three arcs are polar plots, with the angular coordinate referring to the same stimuli, at the same angles, as in the detection data. The radial coordinate gives the discriminability (0.5–1.0) of the given test color angle with the standard color angle indicated by the arrow. Solid symbols are data, open symbols are predictions of a Bayesian classifier model that takes the outputs of the four mechanisms fitted to the detection data as its inputs. All the parameter fitting was done in estimating the detection model; the discrimination predictions are made with no free parameters. Colored regions indicate bands of poorly discriminated stimuli, and are redrawn on the detection plot for comparison. Adapted from Figure 4 of Eskew, R. T., Jr., Newton, J. R., and Giulianini, F. 2001. Chromatic detection and discrimination analyzed by a Bayesian classifier. Vis. Res. 41, 893–909, with permission, observer JRN; the greenish indiscriminability region was taken from model fit and data from other observers.

thresholds). The open symbols make up a pure test method detection contour. Thresholds along the vertical, S cone, axis are about 10 times higher than those along the horizontal, red/green axis (top horizontal axis scale), consistent with the long-established insensitivity of S-cone detection (Stiles, W. S., 1949). This insensitivity means that it is very difficult to use direct, test methods alone to isolate and study the B and Y mechanisms. The filled symbols show a repetition of the experiment with red/green masking

noise added (along the horizontal axis direction), which expands the contour horizontally (and, to a lesser extent, vertically – S-cone detection here is not independent of modulations along the R/G direction). The smooth contour is a fit of a probability summation model based upon symmetric R and G, and B and Y mechanisms; the long straight segments represent isolated mechanisms (B, R, Y, and G going clockwise from top). Even after R and G have been desensitized by the noise, they still dominate the detection contour. In this particular set of data it appears that the detection contour at top and bottom, representing B and Y, is reasonably linear over its limited extent; in other data it is more difficult to tell (Eskew, R. T. *et al.*, 2001).

Sankeralli M. J. and Mullen K. T. (1997) added static one-dimensional noise to raise thresholds of S-cone gratings. The threshold elevations were roughly consistent with the (linear) cosine model. Sankeralli M. J. and Mullen K. T. found evidence that the L- and M-cone inputs to the mechanisms responsible for S-cone detection had roughly equal magnitudes and were both opposite in sign to the S-cone weight. Mullen K. T. and Kingdom F. A. (2002) found sensitivity to S-cone gratings to decrease less sharply with eccentricity than to R/G gratings.

However, these studies used S-cone gratings with both incremental and decremental components. Like R and G, S increments can be masked independently of S decrements and vice versa (Sankeralli, M. J. and Mullen, K. T., 2001), but whereas (in the fovea) R and G are remarkably symmetric (opposite cone weights, identical sensitivity), this is not so for S-cone detection. Thresholds may be higher for S increment than S decrement spots (Vassilev, A. *et al.*, 2003), transient adapting flashes and pedestal masks raise S increment more than S decrement thresholds (Shapiro, A. G. and Zaidi, Q., 1992; Zaidi, Q. *et al.*, 1992; Vingrys, A. J. and Mahon, L. E., 1998), and also the long-wave inputs differ as a function of S-cone polarity (Shinomori, K. *et al.*, 1999; McLellan, J. S. and Eskew, R. T., 2000), meaning that – even if each were half-wave linear – their mechanism vectors (Figure 1) would not be opposite one another. McLellan J. S. and Eskew R. T. measured action spectra for transient tritanopia (Stiles, W. S., 1949; Pugh, E. N. and Mollon, J. D., 1979) using S increment and decrement tests. The function for S increment tests is shifted to longer-wavelengths, suggesting a relatively greater L-cone input to B than to Y. Both action spectra are too narrow to be any linear combination of L and M signals, consistent with results of Giulianini F. and Eskew R. T. (2007) who used a noise superposition test to show that both B and Y are nonlinear. Cortical cells with substantial S-cone inputs have been reported to be significantly nonlinear (Cottaris, N. P. and De Valois, R. L., 1998; Horwitz, G. D. *et al.*, 2005).

S-ON signals are carried in at least two distinctly different pathways, and S-OFF in at least one other (Dacey, D. M. and Lee, B. B., 1994; Klug, K. *et al.*, 2003; see review by Dacey, D. M. and Packer, O. S., 2003). Given these differences in anatomy it is not surprising that the L- and M-cone inputs that oppose S increment and S decrement signals would differ. Indeed, Solomon S. G. and Lennie P. (2005) have recently reported an asymmetry in L and M-cone opposition to S increments and decrements in LGN cells.

2.07.4.4 I and D Mechanisms

The letters I and D stand for increment and decrement. These mechanisms are thought to be isolated by cone modulations along the main diagonal of three-dimensional cone contrast space, the equichromatic direction, where the three cones are modulated in the same proportion to their background quantal catches. Together these mechanisms are usually called the luminance mechanism, but that term is avoided here because of the confusion it causes with photometric luminance, and to be parallel with the terms used for the other mechanisms above. There is little doubt that I and D are distinct mechanisms as defined above (Krauskopf, J., 1980; Krauskopf, J. *et al.*, 1982; Bowen, R. W. *et al.*, 1989; Tyler, C. W. *et al.*, 1992; Bowen, R. W. and Wilson, H. R., 1994; Bowen, R. W., 1997).

These mechanisms are of relatively low sensitivity except at high temporal frequencies, and they are therefore often studied using 12 Hz or faster flicker (or motion). Because flicker contains both incremental and decremental contrasts, it cannot be used psychophysically to study I and D separately, and the results, depending on conditions, might represent the more sensitive of I or D or some mixture of the two. Despite this important limitation, flicker experiments have made important contributions.

For example, it is now abundantly clear that I/D receives a spectrally opponent, L−M signal in addition to the additive L + M signal postulated in the textbook models (Lindsey, D. T. *et al.*, 1986; Swanson, W. H. *et al.*, 1987; Stromeyer, C. F. *et al.*, 1997; Stockman, A. and Plummer, D. J., 2005; Stockman, A. *et al.*, 2005), and analogously to the magnocellular

ganglion cells that are often hypothesized to underlie flicker detection (Smith, V. C. *et al.*, 1992; Lennie, P. *et al.*, 1993). In Stockman's model (Stockman, A. and Plummer, D. J., 2005; Stockman, A. *et al.*, 2005), fast L and fast M signals are combined with slow L and slow M signals. The slow, opponent inputs (sL and sM) and fast, nonopponent inputs (fL and fM) have relative magnitudes and temporal phases that depend upon the chromaticity to which the observer is adapted, so under some adapting conditions (e.g., high-intensity red fields) the slow inputs are of opposite sign to the fast ones and in other conditions (e.g., lower-intensity red fields) the slow inputs have the same signs as the fast ones. Direct comparisons show no phase shifts between L- and M-cone signals in R/G under the same conditions in which they are found in I/D (Stromeyer, C. F. *et al.*, 1997). Besides inducing phase shifts, chromatic adapting fields can cause suppression of signal amplitudes (Eisner, A. and MacLeod, D. I. A., 1981; Stromeyer, C. F. *et al.*, 1987; Tsujimura, S. *et al.*, 1999). In addition to these complicated L- and M-cone inputs, there is a slow S-cone input to I or D or both (Stockman, A. *et al.*, 1991). These extra inputs are not, in general, directly observable on chromatically neutral fields.

The luminance mechanism is generally believed to be a linear combination of cone signals, because photometric matches approximately obey Abney's Laws – i.e., they are additive (Wyszecki, G. and Stiles, W. S., 1982). Such tests have generally been performed only with relatively high flicker frequencies, and under conditions where the observer's state of adaptation changes with the wavelengths of the stimuli. However, flicker or motion thresholds taken under constant adaptation conditions also appear to result from linear cone combinations (Stromeyer, C. F. *et al.*, 1987; 1995), with most evidence obtained at higher temporal frequencies. When a fixed chromatic noise is used to help isolate I and D, detection contours for flashes in the L,M plane appear reasonably straight (Giulianini, F. and Eskew, R. T., 1998), over the very limited range of L/M ratios that can be studied with this test method. When Sankeralli M. J. and Mullen K. T. (1997) used a field method, by superimposing various noises on an achromatic grating, they described the threshold elevations with the cosine relationship (eqn [2]); however, in fact the fit to the data in the L,M plane of cone contrast space was much worse than the corresponding ones for R/G (e.g., Figure 3(a)), suggesting significant nonlinearities of cone combination in I/D.

Most of these studies used flicker or gratings, and since those results reflect some mixture of two mechanisms they do not bear on the symmetry of I and D. Moreover, nonlinearities might be hidden behind the envelope of the most-sensitive of the two mechanisms. The linearity of cone combinations in I and D, at least at low-temporal frequencies, is not well established.

2.07.4.5 Higher-Order Mechanisms

In an extremely influential paper, Krauskopf J. and colleagues (1986a) found evidence for what they termed higher-order color mechanisms, conceived of as recombinations of signals from the cardinal mechanisms, and tuned to intermediate color directions (such as orange or blue–green). The summary above has already indicated that, as Krauskopf J. and colleagues concluded 20 years ago, the textbook picture of three bipolar, linear mechanisms is incorrect. Although the pair of R and G mechanisms comes close to being such a mechanism (because of their linearity, symmetrical cone weights, and equal sensitivity), the other possible pairs are dissimilar from bipolar mechanisms.

Evidence for higher-order mechanisms has been obtained from studies of detection (Krauskopf, J. *et al.*, 1986a; Gegenfurtner, K., and Kiper, D., 1992; D'Zmura, M. and Knoblauch, K., 1998; Lindsey, D. T., and Brown, A. M., 2004), classification images (Bouet, R. and Knoblauch, K., 2004; Hansen, T. and Gegenfurtner, K. R., 2005), first-order discrimination (Krauskopf, J. *et al.*, 1986a; Krauskopf, J. and Gegenfurtner, K., 1992; Zaidi, Q. and Halevy, D., 1993; Li, A. and Lennie, P., 1997; Hansen, T. and Gegenfurtner, K. R., 2006), and second-order (texture) discrimination (Goda, N. and Fujii, M., 2001). Other tasks providing such evidence include visual search (D'Zmura, M., 1991; Monnier, P. and Nagy, A. L., 2001; Nagy, A. L. and Thomas, G., 2003), spatial alignment (McGraw, P. V. *et al.*, 2004; McKeefry, D. J. *et al.*, 2004), detection of Glass patterns (Wilson, J. A. and Switkes, E., 2005), motion coherence (Krauskopf, J. *et al.*, 1996), tilt aftereffect (Flanagan, P. *et al.*, 1990), and color appearance (Krauskopf, J. *et al.*, 1986b; Webster, M. A. and Mollon, J. D., 1991; 1994; Mizokami, Y. *et al.*, 2004). However, after 20 years of these and other studies, no higher-order mechanism has yet been isolated and characterized the way that R and G have been, and much is still unclear. The key issue, of course, is whether there are more than the six mechanisms described above, or whether

the unipolar, asymmetric, and nonlinear aspects of some of these mechanisms suffice to explain the results that have been attributed to additional mechanisms.

Using noise masking in the chromatic plane in which only L and M cones are modulated, Li A. and Lennie P. (1997) and Giulianini F. and Eskew R. T. (1998) found evidence for only four mechanisms (R, G, I, and D, in the present terminology). In particular, maximal masking was not generally obtained along a given stimulus (noise) direction, as might be expected if there were many different mechanisms, but rather along the mechanism directions of R and G (Figure 3); this result does not agree with Gegenfurtner K. and Kiper D.'s (1992) innovative early study. Stromeyer C. F. *et al.* (1999) offered a compelling alternative account of Gegenfurtner K. and Kiper D.'s results based upon spatial phase interactions between grating stimulus components, but recently Hansen T. and Gegenfurtner K. R. (2006) used a stimulus consisting of discrete checks (designed to minimize such interactions) and still obtained maximal masking in the test direction.

Most of the other experiments on higher-order mechanisms were conducted in an equiluminant plane, in an attempt to silence I and D. However, as noted above, the linearity of I/D is not well established, and if these mechanisms are nonlinear they may not be silent in any given plane. Furthermore, it is well established that these mechanisms receive a spectrally opponent signal (Stockman, A. *et al.*, 2005) at least under some conditions. Therefore it is not always clear whether one should compare results collected in the equiluminant plane against a model with four (R, G, B, and Y) or six (plus I and D) mechanisms. Another justification for using the equiluminant plane is that it includes the S-cone axis, and it is plausible that multiple, higher order mechanisms would get input from multiple, S-cone pathways (Dacey, D. M. and Packer, O. S., 2003).

How many mechanisms have been found in the equiluminant plane? In a detection experiment using noise masking of Gabor patches, Eskew R. T. *et al.* (2001), were able to account for detection contours using only four mechanisms (R, G, B, and Y), independent of the noise color direction: noises at four different color angles produced maximum masking at the classical R/G and B/Y directions, but not at intermediate noise directions (Figure 5, central panel, shows data from one noise condition). In addition, these authors used a discrimination procedure to test the model based upon these four mechanisms: pairs of threshold-level stimuli (in the presence of the noise), were presented in random order to the observer, who had to pick the designated standard color pairs (because these were Gabor patches, the discrimination was of a color at a particular spatial phase). The logic is based upon the two discrimination assumptions (see Section 35.3.2.2): if and only if the two stimuli are detected by the same mechanism will two threshold-level stimuli be indiscriminable. The three arcs in Figure 5 represent discrimination data (filled squares) and model predictions (open circles) in polar coordinates. Within each arc, the angular coordinate represents the angle of the stimulus (same angles as in the central panel of detection data), and the radial coordinate represents the proportion of tests that were discriminable from the standard. Three standards are shown (arrows). Consider the right-hand arc, with a standard stimulus represented along the 0°/180°, red–green horizontal axis. The observer was unable to discriminate this standard from tests lying between about 300° and 60°; these angles have been colored red. In contrast, tests lying above 60° (purple) or below 300° (yellow) were readily discriminable from the standard. Taken together with other data not shown here, the results of this experiment suggest only four spectral bands of indiscriminable stimuli.

These results are consistent with earlier work. Using monochromatic increment lights in the Rayleigh spectral region, Calkins D. J. *et al.* (1992) found only three bands of indiscriminable stimuli (detected by R, G, and I, presumably), up to 0.7 log units above threshold. At threshold, across the entire visible spectrum, Mullen K. T. and Kulikowski J. J. (1990) also found evidence for a limited number of indiscriminable spectral bands (four or five, with the fifth corresponding to violet and possibly indicating an S-cone input to R). Neither result is consistent with the existence of a large number of (labeled line) mechanisms.

The open circles in Figure 5 represent predicted discriminability based upon a Bayesian classifier that takes, as its input, the responses of R, G, B, and Y. Discrimination performance is generally, and unsurprisingly, slightly lower for the inefficient human than the efficient Bayesian classifier. However, Krauskopf J. *et al.* (1986a) interpreted a similarly sized discrepancy in discrimination performance as representing detection by multiple mechanisms, thus leading to imperfect discrimination (in essence, thresholds are lowered by probability summation among mechanisms but discrimination is made

more difficult). The size of the discrepancy needing explanation suggests the difficulty of settling this vexed issue.

D'Zmura M. and Knoblauch K. (1998) used two masking noise components, one aligned with the test color direction and the other perpendicular to it. These two noise components were summed to make a fanlike sector of noise, centered on the test color direction, which was varied in width by altering the amplitude of the orthogonal noise component. If the test were detected by a linear mechanism tuned to the test direction, the noise sector width would have no effect (because the orthogonal noise has no effect). Some of the four chosen test directions (e.g., orange) were selected to simultaneously stimulate two classical mechanisms, which would result in an increase in masking with increasing noise sector width. Yet the clear result was that the amount of masking was independent of sector width for all four test directions, which would be very difficult to explain with only classical mechanisms even if they are assumed to be nonlinear and asymmetric. D'Zmura and Knoblauch interpreted their findings to mean there must be a large number of linear mechanisms tuned to various directions.

Recently Hansen T. and Gegenfurtner K. R. (2006) used a field method in the equiluminant plane. With a single noise vector, maximal masking was obtained at each test direction rather than the expected classical mechanism direction (unlike Figure 3), consistent with detection by multiple mechanisms tuned to various directions, and the tuning function was narrower than the cosine predicted by linear cone combination. This nonlinearity was attributed to off-axis looking, shifting between multiple mechanisms that have overlapping sensitivities (see also D'Zmura, M. and Knoblauch, K., 1998). With noises consisting of two vectors that were symmetrically disposed about the test direction (to defeat off-axis looking), cosine (linear) tuning curves were obtained. In these conditions, however, maximal masking was not always obtained at the test direction.

On the one hand, off-axis looking between linear mechanisms may produce narrow, spuriously nonlinear tuning curves; on the other hand, the noise masking stimuli typically available for field method experiments in the equiluminant plane, which are sharply limited in contrast power, may produce spurious linearity due to weak inputs (Giulianini, F. and Eskew, R. T., 2007). The interplay of these two factors might account for some of the differences between studies on higher-order color mechanisms.

Krauskopf J. and Gegenfurtner K. (1992) measured pedestal discrimination contours, by presenting four 36 min. diameter disks around a central fixation spot, all on a 10° steady white adapting field. Three of the four disks had the same chromaticity, one of them was different, and the observer's task was to select that one (a four spatial alternative forced-choice task). In other words, three pedestal stimuli were presented along with a fourth stimulus that consisted of the (vector) sum of the pedestal plus a test; the discrimination of the odd disk is equivalent to detection of the test in the presence of a pedestal. Krauskopf J. and Gegenfurtner K. varied the chromaticity of the pedestal in the equiluminant plane. Data are shown in Figure 6.

Krauskopf J. and Gegenfurtner K. argued that if discrimination was based solely on mechanisms tuned to the cardinal axes (the axes of the graph), the discrimination contours should be oriented with their long axis parallel to the closest cardinal axis,

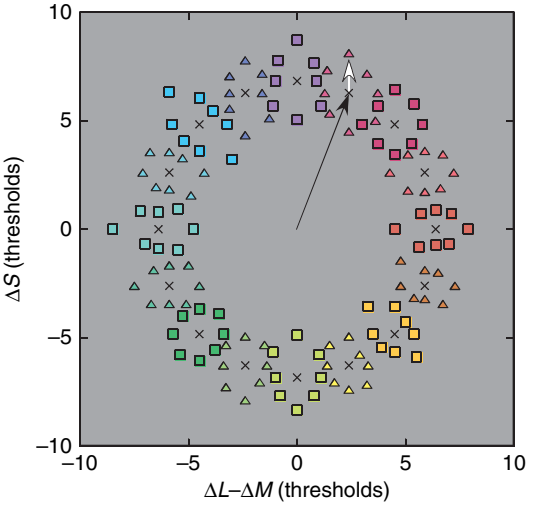

Figure 6 Pedestal discrimination thresholds. The center of the plot represents the white monitor background. Excursions along the two cardinal axes are represented along the horizontal and vertical axes, each scaled in units of the threshold for detection (with no pedestal). One pedestal vector is illustrated by the black arrow; to it is added an S-cone increment test (white arrow). The x represent the tips of all of the pedestal vectors; the distance to each symbol from the x represents the amount of test modulation required to discriminate test + pedestal from pedestal alone. Discriminations around each pedestal are coded with different shapes and colors for clarity; the color of each set of symbols very roughly represents the color of the pedestal alone. Adapted from Figure 14 of Krauskopf J. and Gegenfurtner K. 1992. Color discrimination and adaptation. Vis. Res. 32, 2165–2175, with permission.

because the pedestal masking would occur primarily in that direction. For the pedestals that are equidistant from the two axes (45°, 135°, 225°, and 315°) the contour should be roughly circular. In contrast, if there are higher-order mechanisms tuned to many directions in color space all the contours should be of similar shapes with their long axis pointed at the origin, since each pedestal would mask maximally and equally in its own color direction, the same logic as in some noise masking experiments discussed above. As Figure 6 shows, most of the sets of thresholds would be well described by the cardinal axes account, but two of the pedestals (at 135° and 315°) are more like the higher-order one.

Only a handful of studies have explicitly tried to estimate the number of higher-order mechanisms. Zaidi Q. and Halevy D.'s (1993) model of dynamic chromatic discrimination required more than four, and Goda N. and Fujii M.'s (2001) texture discrimination model required five or seven depending on observer. Hansen T. and Gegenfurtner K. R. (2006) tested models with four, eight, and 16 mechanisms and found that four mechanisms could not account for their results, and 16 provided a better fit than eight. However, Giulianini F. and Eskew R. T. (2007) showed that the same model failed to account for noise masking of S-cone increment or decrement tests in the three principal planes of cone contrast space.

In summary, a substantial number of studies have found evidence against the textbook model of three, bipolar, linear chromatic mechanisms. Some of these studies have provided evidence that there are more than the six, unipolar mechanisms reviewed above. None of these higher-order mechanisms has been isolated and characterized, and there is disagreement as to their number and nature. Partly the issue may be that different mechanisms come into play for different tasks, yet there is controversy even for the detection and simple discrimination tasks emphasized here.

2.07.5 Conclusions

Two detection mechanisms, R and G, have been very well characterized. The other four classical mechanisms (B, Y, I, and D) are less well understood. If there are higher-order detection mechanisms in addition to these six, it seems likely that these will cover some of the same chromatic territory that was attributed to B and Y above, as the peculiarities of S-cone pathways and performance suggest.

The cortical neurons that have been studied electrophysiologically undoubtedly have more diverse chromatic tuning than do LGN neurons (Gegenfurtner, K. R., 2003; Lennie, P. *et al*., 1990; Lennie, P. and Movshon, J. A., 2005), and this increased variability has often been taken to support the existence of higher-order psychophysical color mechanisms. However, given that no particular neuron can yet be identified with a color mechanism, and it is not even clear which cortical areas are most relevant, caution would seem to be called for. Until the psychophysics is better understood, it will be difficult to interpret the ever-increasing knowledge of the behavior of single visual neurons.

Since a large number of different lights – not to mention surfaces – can be discriminated in color, there must be different neurons at some level of the brain that are tuned to many different color directions, at least at the moment the discrimination is made. The question is only whether their behavior can be characterized as consistent with a well-defined psychophysical mechanism.

Acknowledgments

Thanks to Charles Stromeyer and Karl Gegenfurtner for providing the data in Figure 3 and 6, respectively. Preparation of this chapter was supported by NIH EY09712.

References

Abney, W.d. W. 1897. The sensitiveness of the retina to light and color. Philos. Trans. R. Soc. Lond. A 190, 155–195.

Abramov, I., Gordon, J., and Chan, H. 1991. Color appearance in the peripheral retina: effects of stimulus size. J. Opt. Soc. Am. A 8, 404–414.

Boring, E. G. 1942. Sensation and Perception in the History of Experimental Psychology. Irvington.

Bouet, R. and Knoblauch, K. 2004. Perceptual classification of chromatic modulation. Vis. Neurosci. 21, 283–289.

Bowen, R. W. 1997. Isolation and interaction of ON and OFF pathways in human vision: contrast discrimination at pattern offset. Vis. Res. 37, 185–198.

Bowen, R. W., Pokorny, J., and Smith, V. C. 1989. Sawtooth contrast sensitivity: decrements have the edge. Vis. Res. 29, 1501–1509.

Bowen, R. W. and Wilson, H. R. 1994. A two-process analysis of pattern masking. Vis. Res. 34, 645–657.

Boynton, R. M. 1979. Human Color Vision. Holt, Rinehart, and Winston.

Boynton, R. M., Nagy, A. L., and Olson, C. X. 1983. A flaw in equations for predicting chromatic differences. Color Res. Appl. 8, 69–74.

Brainard, D. H. 1996. Cone Contrast and Opponent Modulation Color Spaces. In: Human Color Vision, 2nd ed. (*eds*. P. K. Kaiser and R. M. Boynton), Optical Society of America.

Buchsbaum, G. and Gottschalk, A. 1983. Trichromacy, opponent colours coding and optimum colour information transmission in the retina. Proc. R. Soc. Lond. B 220, 89–113.

Burgess, A. and Barlow, H. B. 1983. The precision of numerosity discrimination in arrays of random dots. Vis. Res. 23, 811–820.

Calkins, D. J., Thornton, J. E., and Pugh, E. N., Jr. 1992. Monochromatism determined at a long-wavelength/middle-wavelength cone-antagonistic locus. Vis. Res. 32, 2349–2367.

Chaparro, A., Stromeyer, C. F., 3rd, Chen, G., and Kronauer, R. E. 1995. Human cones appear to adapt at low light levels: measurements on the red–green detection mechanism. Vis. Res. 35, 3103–3118.

Chaparro, A., Stromeyer, C. F., 3rd, Huang, E. P., Kronauer, R. E., and Eskew, R. T., Jr. 1993. Colour is what the eye sees best. Nature 361, 348–350.

Chaparro, A., Stromeyer, C. F., 3rd, Kronauer, R. E., and Eskew, R. T., Jr. 1994. Separable red–green and luminance detectors for small flashes. Vis. Res. 34, 751–762.

Cole, G. R., Stromeyer, C. F., 3rd, and Kronauer, R. E. 1990. Visual interactions with luminance and chromatic stimuli. J. Opt. Soc. Am A 7, 128–140.

Conners, M. M. and Kelsey, P. A. 1961. Shape of the red and green color zone gradients. J. Opt. Soc. Am. 51, 874–877.

Cottaris, N. P. and De Valois, R. L. 1998. Temporal dynamics of chromatic tuning in macaque primary visual cortex. Nature 395, 896–900.

D'Zmura, M. 1991. Color in visual search. Vis. Res. 31, 951–966.

D'Zmura, M. and Knoblauch, K. 1998. Spectral bandwidths for the detection of color. Vis. Res. 38, 3117–3128.

Dacey, D. M. and Lee, B. B. 1994. The 'blue-on' opponent pathway in primate retina originates from a distinct bistratified ganglion cell type. Nature 367, 731–735.

Dacey, D. M. and Packer, O. S. 2003. Colour coding in the primate retina: diverse cell types and cone-specific circuitry. Curr. Opin. Neurobiol. 13, 421–427.

Dacey, D., Packer, O. S., Diller, L., Brainard, D., Peterson, B., and Lee, B. 2000. Center surround receptive field structure of cone bipolar cells in primate retina. Vis. Res. 40, 1801–1811.

De Valois, R. L. and De Valois, K. 1993. A multi-stage color model. Vis. Res. 33, 1053–1065.

De Valois, R. L., De Valois, K. K., Switkes, E., and Mahon, L. 1997. Hue scaling of isoluminant and cone-specific lights. Vis. Res. 37, 885–897.

Deeb, S. S., Diller, L. C., Williams, D. R., and Dacey, D. M. 2000. Interindividual and topographical variation of L:M cone ratios in monkey retinas. J. Opt. Soc. Am. A 17, 538–544.

Derrington, A. M., Krauskopf, J., and Lennie, P. 1984. Chromatic mechanisms in lateral geniculate nucleus of macaque. J. Physiol., 357, 241–265.

Eisner, A. and MacLeod, D. I. A. 1981. Flicker photometric study of chromatic adaptation: selective suppression of cone inputs by colored backgrounds. J. Opt. Soc. Am. 71, 705–717.

Eskew, R. T., Jr. 1989. The gap effect revisited: slow changes in chromatic sensitivity as affected by luminance and chromatic borders. Vis. Res. 29, 717–729.

Eskew, R. T., Jr. and Kortick, P. M. 1994. Hue equilibria compared with chromatic detection in 3D cone contrast space. Invest. Ophthalmol. Vis. Sci. 34, 1555 (Abstract).

Eskew, R. T., Jr., McLellan, J. S., and Giulianini, F. 1999. Chromatic Detection and Discrimination. In: Color Vision: from Genes to Perception (*eds*. K. Gegenfurtner and L. T. Sharpe), pp. 345–368. Cambridge University Press.

Eskew, R. T., Jr., Newton, J. R., and Giulianini, F. 2001. Chromatic detection and discrimination analyzed by a Bayesian classifier. Vis. Res. 41, 893–909.

Eskew, R. T., Jr., Stromeyer, C. F., 3rd, and Kronauer, R. E. 1994. Temporal properties of the red–green chromatic mechanism. Vis. Res. 34, 3127–3137.

Eskew, R. T., Jr., Stromeyer, C. F., 3rd, Picotte, C. J., and Kronauer, R. E. 1991. Detection uncertainty and the facilitation of chromatic detection by luminance contours. J. Opt. Soc. Am. A, 8, 394–403.

Flanagan, P., Cavanagh, P., and Favreau, O. E. 1990. Independent orientation-selective mechanisms for the cardinal directions of colour space. Vis. Res. 30, 769–778.

Gegenfurtner, K. R. 2003. Cortical mechanisms of colour vision. Nat. Rev. Neurosci. 4, 563–572.

Gegenfurtner, K. R. and Kiper, D. C. 1992. Contrast detection in luminance and chromatic noise. J. Opt. Soc. Am. 9, 1880–1888.

Geisler, W. S. 1989. Sequential ideal-observer analysis of visual discriminations. Psychol. Rev. 96, 267–314.

Giulianini, F. and Eskew, R. T., Jr. 1998. Chromatic masking in the (ΔL/L, ΔM/M) plane of cone-contrast space reveals only two detection mechanisms. Vis. Res. 38, 3913–3926.

Giulianini, F. and Eskew, R. T., Jr. 2007. Theory of chromatic noise masking applied to testing linearity of S-cone detection mechanisms. J. Opt. Soc. Am. A. In press.

Goda, N. and Fujii, M. 2001. Sensitivity to modulation of color distribution in multicolored textures. Vis. Res. 41, 2475–2485.

Gouras, P. 1974. Opponent-colour cells in different layers of foveal striate cortex. J. Physiol. 238, 583–602.

Gowdy, P. D., Stromeyer, C. F., 3rd, and Kronauer, R. E. 1999a. Detection of flickering edges: absence of a red–green edge detector. Vis. Res. 39, 4186–4191.

Gowdy, P. D., Stromeyer, C. F., 3rd, and Kronauer, R. E. 1999b. Facilitation between the luminance and red–green detection mechanisms: enhancing contrast differences across edges. Vis. Res. 39, 4098–4112.

Graham, N. V. S. 1989. Visual Pattern Analyzers. Oxford University Press.

Guth, S. L. 1991. Model for color vision and light adaptation. J. Opt. Soc. Am. A, 8, 976–993.

Hagstrom, S. A., Neitz, J., and Neitz, M. 1998. Variations in cone populations for red–green color vision examined by analysis of mRNA. Neuroreport, 9, 1963–1967.

Hansen, T. and Gegenfurtner, K. R. 2005. Classification images for chromatic signal detection. J. Opt. Soc. Am. A 22, 2081–2089.

Hansen, T. and Gegenfurtner, K. R. 2006. Higher level chromatic mechanisms for image segmentation. J. Vis. 6, 239–259.

Hofer, H., Carroll, J., Neitz, J., Neitz, M., and Williams, D. R. 2005. Organization of the human trichromatic cone mosaic. J. Neurosci. 25, 9669–9679.

Horwitz, G. D., Chichilnisky, E. J., and Albright, T. D. 2005. Blue–yellow signals are enhanced by spatiotemporal luminance contrast in macaque V1. J. Neurophysiol. 93, 2263–2278.

Hubel, D. H. and Wiesel, T. N. 1968. Receptive fields and functional architecture of monkey striate cortex. J. Physiol. 195, 215–243.

Hurvich, L. M. and Jameson, D. 1957. An opponent-process theory of color vision. Psychol. Rev. 64, 384–404.

Johnson, E. N., Hawken, M. J., and Shapley, R. 2001. The spatial transformation of color in the primary visual cortex of the macaque monkey. Nat. Neurosci. 4, 409–416.

Klug, K., Herr, S., Ngo, I. T., Sterling, P., and Schein, S. 2003. Macaque retina contains an S-cone OFF midget pathway. J. Neurosci. 23, 9881–9887.

Knoblauch, K. 1995. Dual Bases in Dichromatic Color Space. In: Colour Vision Deficiencies XII (*ed*. B. Drum). Kluwer Academic. pp.165-176.

Krauskopf, J. 1980. Discrimination and detection of changes in luminance. Vis. Res. 20, 671–677.

Krauskopf, J. 1999. Higher Order Color Mechanisms. In: Color Vision: from Genes to Perception (*eds*. K. R. Gegenfurtner and L. T. Sharpe). Cambridge University Press. pp. 303-316.

Krauskopf, J. and Gegenfurtner, K. 1992. Color discrimination and adaptation. Vis. Res. 32, 2165–2175.

Krauskopf, J. and Zaidi, Q. 1986. Induced desensitization. Vis. Res. 26, 759–762.

Krauskopf, J., Williams, D. R., and Heeley, D. W. 1982. Cardinal directions of color space. Vis. Res. 22, 1123–1131.

Krauskopf, J., Williams, D. R., Mandler, M. B., and Brown, A. M. 1986a. Higher order color mechanisms. Vis. Res. 26, 23–32.

Krauskopf, J., Wu, H. J., and Farell, B. 1996. Coherence, cardinal directions and higher-order mechanisms. Vis. Res. 36, 1235–1245.

Krauskopf, J., Zaidi, Q., and Mandler, M. B. 1986b. Mechanisms of simultaneous color induction. J. Opt. Soc. Am. A 3, 1752–1757.

Legge, G. E., Kersten, D., and Burgess, A. E. 1987. Contrast discrimination in noise. J. Opt. Soc. Am. A 4, 391–404.

Lennie, P. and D'Zmura, M. 1988. Mechanisms of color vision. Crit. Rev. Neurobiol. 3, 333–400.

Lennie, P. and Movshon, J. A. 2005. Coding of color and form in the geniculostriate visual pathway (invited review). J. Opt. Soc. Am. A 22, 2013–2033.

Lennie, P., Krauskopf, J., and Sclar, G. 1990. Chromatic mechanisms in striate cortex of macaque. J. Neurosci. 10, 649–669.

Lennie, P., Pokorny, J., and Smith, V. C. 1993. Luminance. J. Opt. Soc. Am. A, 10, 1283–1293.

Li, A. and Lennie, P. 1997. Mechanisms underlying segmentation of colored texture. Vis. Res. 37, 83–97.

Lindsey, D. T., and Brown, A. M. 2004. Masking of grating detection in the isoluminant plane of DKL color space. Vis. Neurosci. 21, 269–273.

Lindsey, D. T., Pokorny, J., and Smith, V. C. 1986. Phase-dependent sensitivity to heterochromatic flicker. J. Opt. Soc. Am. A 3, 921–927.

Livingstone, M. S. and Hubel, D. H. 1984. Anatomy and physiology of a color system in the primate visual cortex. J. Neurosci. 4, 309–356.

MacLeod, D. I. A. and He, S. 1993. Visible flicker from invisible patterns. Nature 361, 256–258.

MacLeod, D. I. A., Williams, D. R., and Makous, W. 1992. A visual nonlinearity fed by single cones. Vis. Res. 32, 347–363.

McGraw, P. V., McKeefry, D. J., Whitaker, D., and Vakrou, C. 2004. Positional adaptation reveals multiple chromatic mechanisms in human vision. J. Vis. 4, 626–636.

McKeefry, D. J., McGraw, P. V., Vakrou, C., and Whitaker, D. 2004. Chromatic adaptation, perceived location, and color tuning properties. Vis. Neurosci. 21, 275–282.

McLellan, J. S. and Eskew, R. T., Jr. 2000. ON and OFF S-cone pathways have different long-wave cone inputs. Vis. Res. 40, 2449–2465.

Michael, C. R. 1978. Color vision mechanisms in monkey striate cortex: dual-opponent cells with concentric receptive fields. J. Neurophysiol. 41, 572–588.

Mizokami, Y., Paras, C., and Webster, M. A. 2004. Chromatic and contrast selectivity in color contrast adaptation. Vis. Neurosci. 21, 359–363.

Mollon, J. D. and Cavonius, C. R. 1987. The Chromatic Antagonisms of Opponent Process Theory are not the Same as those Revealed in Studies of Detection and Discrimination. In: Colour Vision Deficiencies VIII (*ed*. G. Verriest), pp. 473–483. Junk.

Monnier, P. and Nagy, A. L. 2001. Uncertainty, attentional capacity and chromatic mechanisms in visual search. Vis. Res. 41, 313–328.

Moreland, J. D. and Cruz, A. 1959. Colour perception with the peripheral retina. Opt. Acta 6, 117–151.

Mullen, K. T. 1991. Colour vision as a post-receptoral specialization of the central visual field. Vis. Res. 31, 119–130.

Mullen, K. T. and Kingdom, F. A. 2002. Differential distributions of red–green and blue–yellow cone opponency across the visual field. Vis. Neurosci. 19, 109–118.

Mullen, K. T. and Kulikowski, J. J. 1990. Wavelength discrimination at detection threshold. J. Opt. Soc. Am. A 7, 733–742.

Nagy, A. L. and Thomas, G. 2003. Distractor heterogeneity, attention, and color in visual search. Vis. Res. 43, 1541–1552.

Newton, J. R. and Eskew, R. T., Jr. 2003. Chromatic detection and discrimination in the periphery: a postreceptoral loss of color sensitivity. Vis. Neurosci. 20, 511–521.

Normann, R. A. and Perlman, I. 1979. The effects of background illumination on the photoresponses of red and green cones. J. Physiol. 286, 491–507.

Parsons, J. H. 1915. An Introduction to the Study of Colour Vision. Cambridge University Press.

Pelli, D. G. 1990. The Quantum Efficiency of Vision. In: Vision: Coding and Efficiency (*ed*. C. Blakemore), pp. 3–24. Cambridge University Press.

Pugh, E. N., Jr. and Mollon, J. D. 1979. A theory of the $\pi 1$ and $\pi 3$ color mechanisms of Stiles. Vis. Res. 19, 293–312.

Rubin, J. M. and Richards, W. A. 1988. Color Vision: Representing Material Categories. In: Natural Computation (*ed*. W. A. Richards). pp. 194–213. MIT Press.

Sakurai, M. and Mullen, K. T. 2006. Cone weights for the two cone-opponent systems in peripheral vision and asymmetries of cone contrast sensitivity. Vis. Res. 46, 4346–4354.

Sankeralli, M. J. and Mullen, K. T. 1997. Postreceptoral chromatic detection mechanisms revealed by noise masking in three-dimensional cone contrast space. J. Opt. Soc. Am. A 14, 2633–2646.

Sankeralli, M. J. and Mullen, K. T. 2001. Bipolar or rectified chromatic detection mechanisms? Vis. Neurosci. 18, 127–135.

Sekiguchi, N., Williams, D. R., and Brainard, D. H. 1993. Efficiency in detection of isoluminant and isochromatic interference fringes. J. Opt. Soc. Am. A 10, 2118–2133.

Shapiro, A. G. and Zaidi, Q. 1992. The effects of prolonged temporal modulation on the differential response of color mechanisms. Vis. Res. 32, 2065–2075.

Shinomori, K., Spillmann, L., and Werner, J. S. 1999. S-cone signals to temporal OFF-channels: asymmetrical connections to postreceptoral chromatic mechanisms. Vis. Res. 39, 39–49.

Smith, V. C., Lee, B. B., Pokorny, J., Martin, P. R., and Valberg, A. 1992. Responses of macaque ganglion cells to the relative phase of heterochromatically modulated lights. J. Physiol. 458, 191–221.

Solomon, S. G. and Lennie, P. 2005. Chromatic gain controls in visual cortical neurons. J. Neurosci. 25, 4779–4792.

Stiles, W. S. 1949. Increment thresholds and the mechanisms of colour vision. Doc. Ophthalmol. 3, 138–165.

Stiles, W. S. 1978. Mechanisms of Colour Vision. Academic Press.
Stockman, A. and Plummer, D. J. 2005. Spectrally opponent inputs to the human luminance pathway: slow +L and –M cone inputs revealed by low to moderate long-wavelength adaptation. J. Physiol. 566, 77–91.
Stockman, A., MacLeod, D. A., and DePriest, D. D. 1991. The temporal properties of the human short-wave photoreceptors and their associated pathways. Vis. Res. 31, 189–208.
Stockman, A., Plummer, D. J., and Montag, E. D. 2005. Spectrally opponent inputs to the human luminance pathway: slow +M and –L cone inputs revealed by intense long-wavelength adaptation. J. Physiol. 566, 61–76.
Stromeyer, C. F., 3rd., Chaparro, A., Rodriguez, C., Chen, D., Hu, E., and Kronauer, R. E. 1998. Short-wave cone signal in the red–green detection mechanism. Vis. Res. 38, 813–826.
Stromeyer, C. F., 3rd., Chaparro, A., Tolias, A. S., and Kronauer, R. E. 1997. Colour adaptation modifies the long-wave versus middle-wave cone weights and temporal phases in human luminance (but not red–green) mechanism. J. Physiol. 499, 227–254.
Stromeyer, C. F., 3rd, Cole, G. R., and Kronauer, R. E. 1987. Chromatic suppression of cone inputs to the luminance flicker mechanism. Vis. Res. 27, 1113–1137.
Stromeyer, C. F., 3rd, Kronauer, R. E., Ryu, A., Chaparro, A., and Eskew, R. T., Jr. 1995. Contributions of human long-wave and middle-wave cones to motion detection. J. Physiol. 485, 221–243.
Stromeyer, C. F., 3rd and Lee, J. 1988. Adaptational effects of short wave cone signals on red–green chromatic detection. Vis. Res. 28, 931–940.
Stromeyer, C. F., 3rd, Lee, J., and Eskew, R. T., Jr. 1992. Peripheral chromatic sensitivity for flashes: a post-receptoral red–green asymmetry. Vis. Res. 32, 1865–1873.
Stromeyer, C. F., 3rd, Thabet, R., Chaparro, A., and Kronauer, R. E. 1999. Spatial masking does not reveal mechanisms selective to combined luminance and red–green color. Vis. Res. 39, 2099–2112.
Swanson, W. H., Ueno, T., Smith, V. C., and Pokorny, J. 1987. Temporal modulation sensitivity and pulse-detection thresholds for chromatic and luminance perturbations. J. Opt. Soc. Am. A 4, 1992–2005.
Tootell, R. B., Silverman, M. S., Hamilton, S. L., De Valois, R. L., and Switkes, E. 1988. Functional anatomy of macaque striate cortex. III. Color. J. Neurosci. 8, 1569–1593.
Tsujimura, S., Shioiri, S., Hirai, Y., and Yaguchi, H. 1999. Selective cone suppression by the L-M- and M-L-cone-opponent mechanisms in the luminance pathway. J. Opt. Soc. Am. A 16, 1217–1228.
Tyler, C. W., Chan, H., and Liu, L. 1992. Different spatial tunings for ON and OFF pathway stimulation. Ophthal. Physiol. Opt. 12, 233–240.
Valeton, J. M. 1983. Photoreceptor light adaptation models: an evaluation. Vis. Res. 23, 1549–1554.
Valeton, J. M. and van Norren, D. 1983. Light adaptation of primate cones: an analysis based on extracellular data. Vis. Res. 23, 1539–1547.
Vassilev, A., Mihaylova, M. S., Racheva, K., Zlatkova, M., and Anderson, R. S. 2003. Spatial summation of S-cone ON and OFF signals: effects of retinal eccentricity. Vis. Res. 43, 2875–2884.
Vingrys, A. J. and Mahon, L. E. 1998. Color and luminance detection and discrimination asymmetries and interactions. Vis. Res. 38, 1085–1095.
von der Twer, T. and MacLeod, D. I. A. 2001. Optimal nonlinear codes for the perception of natural colours. Network, 12, 395–407.
Watson, A. B. and Robson, J. G. 1981. Discrimination at threshold: labelled detectors in human vision. Vis. Res. 21, 1115–1122.
Webster, M. A. and Mollon, J. D. 1991. Changes in colour appearance following post-receptoral adaptation. Nature 349, 235–238.
Webster, M. A. and Mollon, J. D. 1994. The influence of contrast adaptation on color appearance. Vis. Res. 34, 1993–2020.
Wilson, J. A. and Switkes, E. 2005. Integration of differing chromaticities in early and midlevel spatial vision. J. Opt. Soc. Am. A 22, 2169–2181.
Wuerger, S. M., Atkinson, P., and Cropper, S. 2005. The cone inputs to the unique-hue mechanisms. Vis. Res. 45, 3210–3223.
Wyszecki, G. and Stiles, W. S. 1982. Color Science: Concepts and Methods, Quantitative Data and Formulae, 2nd edn. Wiley.
Zaidi, Q. and Halevy, D. 1993. Visual mechanisms that signal the direction of color changes. Vis. Res. 33, 1037–1051.
Zaidi, Q., Shapiro, A., and Hood, D. 1992. The effect of adaptation on the differential sensitivity of the S-cone color system. Vis. Res. 32, 1297–1318.

2.08 Color Appearance

D H Foster, University of Manchester, Manchester, UK

© 2008 Elsevier Inc. All rights reserved.

2.08.1	**Specifying and Describing Color**	119
2.08.1.1	The Color Signal and Spectral Sampling	119
2.08.1.2	Tristimulus Values	120
2.08.1.3	Related Colors	120
2.08.1.4	CIELAB Color Space	122
2.08.2	**Illuminant and Viewing Media**	122
2.08.2.1	Color Constancy	123
2.08.2.2	Separating Illuminant and Reflectance Spectra	123
2.08.2.3	Relational Color Constancy	123
2.08.3	**Sensory and Perceptual Cues**	124
2.08.3.1	Estimating the Illuminant	125
2.08.3.2	Color Contrast and Variance	125
2.08.3.3	Spatial Ratios of Cone Excitations	125
2.08.4	**Measuring Perceived Surface Color**	126
2.08.4.1	Color Naming and Scaling	126
2.08.4.2	Setting Unique Hues	126
2.08.4.3	Achromatic Adjustment	126
2.08.4.4	Asymmetric Color Matching	127
2.08.4.5	Discriminating Illuminant from Reflectance Changes	127
2.08.5	**Levels of Color Constancy**	127
2.08.5.1	Dual Representations	127
2.08.5.2	Role of Task and Stimulus	127
2.08.6	**Color Appearance in Natural Environments**	128
2.08.6.1	Colors of Natural Surfaces	128
2.08.6.2	Discriminating and Identifying Natural Surfaces	128
2.08.7	**Physiological Mechanisms**	128
2.08.7.1	Processing in Retina and Lateral Geniculate Nucleus	128
2.08.7.2	Cortical Processing	129
2.08.7.3	Inherited Color-Vision Deficiency	129
References		130

2.08.1 Specifying and Describing Color

Because of the importance of color measurement in the materials, printing, electronic imaging, and lighting industries, a large technical vocabulary has evolved based on international agreement. Recommendations of the Commission Internationale de l'Eclairage (CIE) concerning colorimetry and a color-appearance model are available in two technical reports (CIE, 2004a; 2004b). Colorimetric terms and formulas are introduced here only as they are needed, and the specification of color appearance with reference to proprietary color-order systems is not discussed (e.g., see Wyszecki, G. and Stiles, W. S., 1982; Hunt, R. W. G., 1998; Fairchild, M. D., 2005).

2.08.1.1 The Color Signal and Spectral Sampling

The light reflected from an illuminated scene or emitted by an electronic display system produces a stimulus to the human eye consisting of a distribution of spectral radiance $c(\lambda)$ over wavelength λ at each point in the field of view. For reflected light, this color signal $c(\lambda)$ (Buchsbaum, G. and Gottschalk, A., 1983) is

the wavelength-by-wavelength product of an illuminant spectrum $E(\lambda)$ and the spectral reflectance $R(\lambda)$ at each point in the scene; that is, $c(\lambda) = E(\lambda)R(\lambda)$, in suitable radiometric units. Figure 1, first column, shows the normalized spectrum $E_1(\lambda)$ of light from the sun (second row) illuminating a flower stamen with spectral reflectance $R_1(\lambda)$ (third row), giving the color signal $c_1(\lambda) = E_1(\lambda)R_1(\lambda)$ (fourth row).

The color signal, imaged onto the retina, is normally sampled by the long-, medium-, and short-wavelength-sensitive cone photoreceptors with spectral sensitivities $L(\lambda)$, $M(\lambda)$, and $S(\lambda)$, respectively (Figure 1, fifth row). The corresponding cone excitations l_1, m_1, and s_1, are obtained by integrating the product of $c_1(\lambda)$ with, in turn, $L(\lambda)$, $M(\lambda)$, and $S(\lambda)$ over wavelength λ.

If any two spectra, for example $c_2(\lambda)$ and $c_3(\lambda)$ in Figure 1 (second and third columns, fourth row), produce triplets (l_2, m_2, s_2) and (l_3, m_3, s_3) of excitations at a point that are the same, then they are visually indistinguishable, for after absorption all information about their spectral origins is lost (Naka, K. I. and Rushton, W. A. H., 1966). But as is evident here, identical triplets do not imply identical color signals: $c_2(\lambda)$ and $c_3(\lambda)$ are different functions of λ. In general, color signals need more than three numbers to specify them, experimentally about eight with natural scenes (Nascimento, S. M. C. *et al.*, 2005b). This ambiguity – of different spectra producing the same cone excitations, and therefore the same color information – is known as metamerism (Wyszecki, G. and Stiles, W. S., 1982; Hunt, R. W. G., 1998). Metamerism can arise from differences in illuminant spectra or reflectance spectra or other viewing factors, and it sets a limit, even under constant viewing conditions, on how well color can be used to represent the spectral properties of surfaces.

2.08.1.2 Tristimulus Values

With just three classes of cones in the normal eye, the colors of stimuli could be specified by triplets of cone excitations, as in Figure 1, but for historical reasons, the established system of colorimetry is instead based on color-matching functions $\bar{r}(\lambda)$, $\bar{g}(\lambda)$, and $\bar{b}(\lambda)$, which represent the amounts, sometimes negative, of three monochromatic, primary lights needed to match a monochromatic light of constant radiant power at each wavelength λ (Wright, W. D., 1928–1929; Guild, J., 1931). For computational convenience, these color-matching functions – standardized internationally in 1931 by the CIE – were transformed to a new set of functions $\bar{x}(\lambda)$, $\bar{y}(\lambda)$, and $\bar{z}(\lambda)$ with non-negative values and with $\bar{y}(\lambda)$ equated to $V(\lambda)$, the daylight luminance sensitivity of the eye. An arbitrary color signal $c(\lambda)$ in this system is specified by a triplet of tristimulus values X, Y, and Z, obtained by integrating the product of $c(\lambda)$ with, in turn, $\bar{x}(\lambda)$, $\bar{y}(\lambda)$, and $\bar{z}(\lambda)$ over wavelength λ (for details, e.g., see Wyszecki, G. and Stiles, W. S., 1982; Fairchild, M. D., 2005).

The parallel between the calculation of tristimulus values X, Y, Z and of cone excitations l, m, s is not accidental: the functions $\bar{x}(\lambda)$, $\bar{y}(\lambda)$, $\bar{z}(\lambda)$ are a linear transformation of the cone spectral sensitivities $L(\lambda)$, $M(\lambda)$, $S(\lambda)$, and the tristimulus values X, Y, Z are the same linear transformation of the cone excitations l, m, s.

A two-dimensional chromaticity space with coordinates (x, y) can be derived from tristimulus values X, Y, Z by normalizing; that is, $x = X/(X + Y + Z)$ and $y = Y/(X + Y + Z)$. In this space, the spectral colors form a horseshoe-shaped arc around the point (1/3, 1/3) representing a white with constant radiant power across the spectrum. But the distance between a pair of points, 1 and 2 say, defined by the Euclidean formula $[(x_1 - x_2)^2 + (y_1 - y_2)^2]^{1/2}$ gives a poor guide to the perceived color difference between the corresponding stimuli, which varies according to where the pair of points lies in the space and the orientation of the line joining them. This chromaticity space is perceptually nonuniform; so also is the space of tristimulus values X, Y, Z (Wyszecki, G. and Stiles, W. S., 1982).

2.08.1.3 Related Colors

Although the tristimulus values X, Y, Z of a light (or cone excitations l, m, s) are sufficient to specify the color of a light, and the coordinates (x, y) its chromaticity, they do not describe its appearance: its hue, saturation, lightness, and so on. For example, a monochromatic light of 590 nm, which has chromaticity coordinates $x = 0.575$, $y = 0.424$, appears orange when viewed in isolation in a dark field but brown if surrounded by a brighter, white light.

In natural viewing, colors are normally perceived in relation to each other, as part of a larger scene, and are technically termed related colors (Fairchild, M. D., 2005). Canonical examples of related colors include, in addition to brown, the colors olive green, khaki, and navy blue. Any system for representing color appearance must therefore include some information about the context of the color.

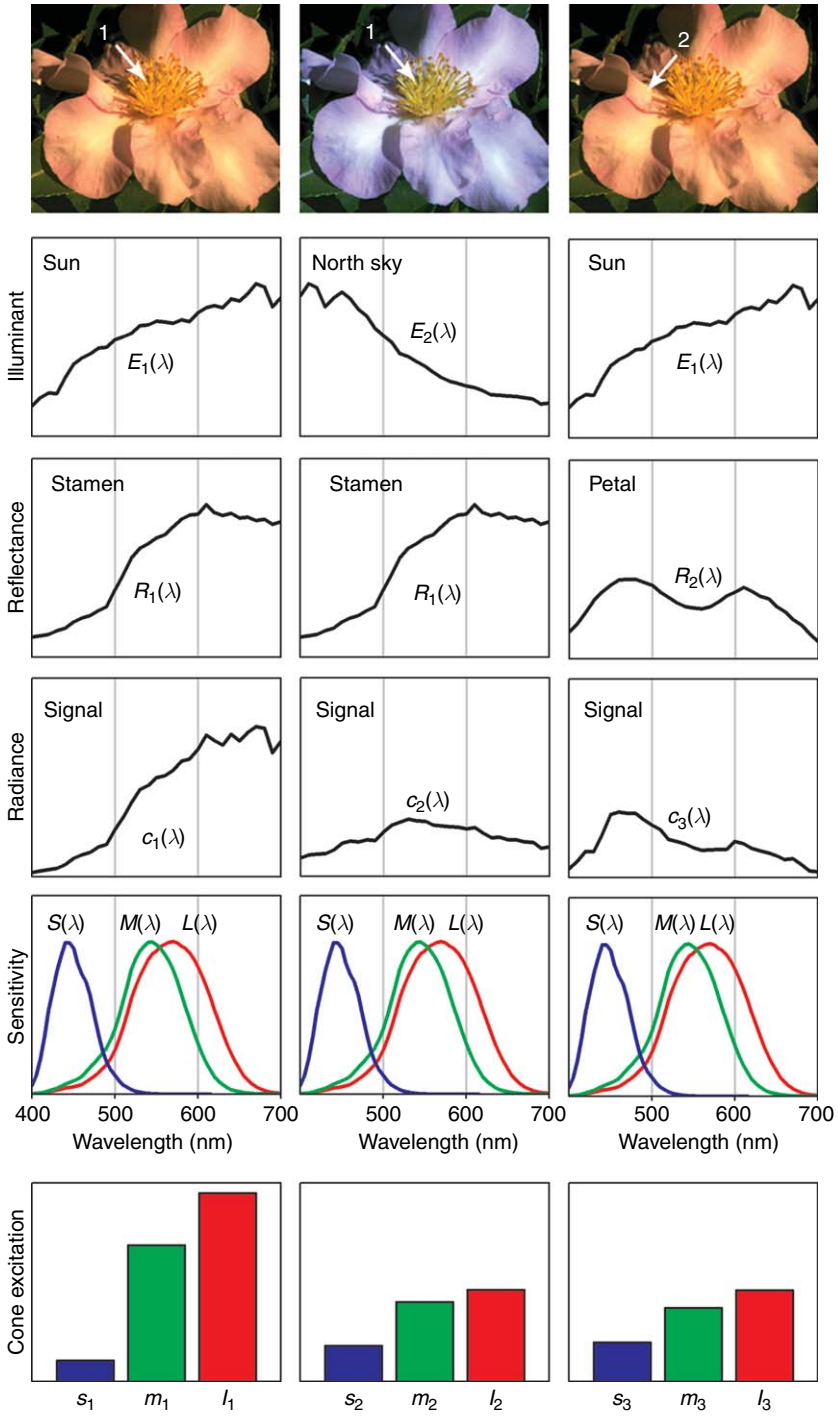

Figure 1 Two areas of a flower under different colored illuminations and the resulting pattern of cone excitations. The spectral reflectance $R_1(\lambda)$ of the stamen (1) under light with spectrum $E_1(\lambda)$ from the sun (correlated color temperature 4000 K) gives a color signal $c_1(\lambda)$ with greatest power at long wavelengths (first column) but a much more even distribution $c_2(\lambda)$ (second column) under a light with spectrum $E_2(\lambda)$ from the north sky (correlated color temperature 25 000 K). As a result, there are marked differences in the triplet of cone excitations (l_1, m_1, s_1) and (l_2, m_2, s_2) (bottom row). By contrast, the spectral reflectance $R_2(\lambda)$ of the petal (2) under sunlight (column 3) gives a different color signal $c_3(\lambda)$ but an almost identical pattern of cone excitations (l_3, m_3, s_3), showing how the effects of illuminant and reflectance spectra may be indistinguishable at a point.

2.08.1.4 CIELAB Color Space

An effect of context is abstracted in CIELAB color space with the specification of a reference white (Wyszecki, G. and Stiles, W. S., 1982; Fairchild, M. D., 2005). This space, defined by the CIE in 1976, has coordinates (L^*, a^*, b^*), which, for a given color, are calculated as follows. First, the tristimulus values X, Y, Z of the color are normalized against the tristimulus values X_n, Y_n, Z_n of the reference white to give X/X_n, Y/Y_n, Z/Z_n. A cube-root transformation is then applied to represent a sensory compression of the response, that is, $(X/X_n)^{1/3}$, $(Y/Y_n)^{1/3}$, $(Z/Z_n)^{1/3}$. Finally, a numerical scaling is applied to $(Y/Y_n)^{1/3}$ to give the coordinate L^* and other numerical scalings applied to the differences $(X/X_n)^{1/3} - (Y/Y_n)^{1/3}$ and $(Y/Y_n)^{1/3} - (Z/Z_n)^{1/3}$ to give the coordinates a^* and b^*, respectively. The coordinate L^* defines a lightness axis, a^* a redness–greenness axis, and b^* a yellowness–blueness axis. Values of L^* range from 0 for black to 100 for a perfectly diffusing white (and possibly >100 for specular reflecting surfaces).

Although not intended as a color-appearance system, some color-appearance attributes can be obtained from L^*, a^*, b^* by defining relative colorfulness or chroma C^*_{ab} as $(a^{*2} + b^{*2})^{1/2}$ and hue h_{ab} as an angle $\tan^{-1}(b^*/a^*)$, in degrees, to form a cylindrical coordinate system (Fairchild, M. D., 2005). Saturation is the colorfulness of area judged in proportion to its brightness.

Figure 2 shows some example CIELAB cylindrical coordinates (L^*, C^*_{ab}, h_{ab}) from a natural scene. The hue angles (third coordinate) of the red and orange petals are 50° and 69°, that is, between the reddish end of the a^* axis and yellowish end of the b^* axis and the hue angle of the purple flower is −57°, that is, between the reddish end of the a^* axis and the bluish end of the b^* axis. The chroma of the points on all three flowers is moderate to high, ranging from 37 to 102, but the chroma of the gray sphere inserted in the scene is low, just 7, although a truly neutral surface would have zero chroma. The flowers and sphere all have similar lightnesses, ranging from 46 to 72.

Figure 2 CIELAB cylindrical color coordinates of points in the image of a natural scene under daylight. The lightness, chroma, and hue angle (in degrees) of each point are indicated.

In CIELAB space, the color difference, denoted by ΔE^*_{ab}, between a pair of stimuli, 1 and 2, say, defined by the Euclidean distance formula $[(L^*_1 - L^*_2)^2 + (a^*_1 - a^*_2)^2 + (b^*_1 - b^*_2)^2]^{1/2}$, is perceptually more uniform than the Euclidean distance formula in the untransformed X, Y, Z space, but large nonuniformities remain. CIELAB space is also designed for viewing scenes under a standardized daylight illuminant, and the device of dividing the tristimulus values of a color by the tristimulus values of a reference white is only partly successful in accommodating changes in the illuminant (Terstiege, H., 1972; Fairchild, M. D., 2005).

Since the introduction of CIELAB space, progressively more accurate and comprehensive color-difference formulas and color-appearance models have been developed for colorimetric applications (Hunt, R. W. G., 1998; Fairchild, M. D., 2005). Thus, the non-Euclidean CIE color-difference formula CIEDE2000 (Luo, M. R. *et al.*, 2001) largely corrects the perceptual nonuniformities of the Euclidean formula in CIELAB space. A subsequent color-appearance model CIECAM02 (Li, C. J. and Luo, M. R., 2005) that takes into account simple surround conditions provides formulas for transforming from CIE tristimulus values to correlates of the perceptual attributes of lightness, brightness, chroma, saturation, colorfulness, and hue, and also an approximately Euclidean distance formula for uniform color differences (Luo, M. R. *et al.*, 2006).

2.08.2 Illuminant and Viewing Media

The influence of context on color appearance may be interpreted as a consequence of our visual experience, of seeing colored surfaces surrounded by other colored surfaces in the natural environment (Judd, D. B., 1940). Here the color appearance of an object may serve as a cue to its identity or condition: the greenness of grass, the redness of ripe fruit. But this is

possible only if color appearance correctly represents in some way surface color – the visual correlate of spectral reflectance – within the limits of metamerism (Section 2.08.1.1).

2.08.2.1 Color Constancy

As noted in Section 2.08.1.1, the color signal $c(\lambda)$ reaching the eye is the wavelength-by-wavelength product of the illuminant spectrum $E(\lambda)$ and the spectral reflectance $R(\lambda)$ at each point in the scene. As a representative of surface reflectance, this color signal is confounded with the properties of the illuminant, for example, whether it has more radiant power at long wavelengths (Figure 1, first column, second row) than at short wavelengths (Figure 1, second column, second row), affecting the resulting triplet of cone excitations l, m, s (bottom row).

Yet in everyday experience, the color appearance of surfaces seems fairly stable. As T. Young (1807) pointed out, a sheet of writing paper appears to retain its whiteness whether illuminated by the yellow light of a candle or by the red light of a fire. This stability is summarized in the notion of color constancy: the constant appearance of object or surface color despite changes in the color of the illumination, and, in modern usage, in scene composition and configuration (Maloney, L. T., 1999). Color constancy is a complex phenomenon (Foster, D. H., 2003; Smithson, H. E., 2005), with a long history of analysis, attracting contributions from G. Monge (1789), T. Young (1807), and H. von Helmholtz (1867), and later by Land, E. H. (1959a; 1959b). But it has proved an elusive phenomenon to quantify, for the stability of color appearance seems to vary with the methods used to measure it, as explained later.

2.08.2.2 Separating Illuminant and Reflectance Spectra

How, in principle, can the confounding effect of the spectrum of the illumination on a scene be eliminated from the color signal at the eye? Suppose that the cone excitations l_0, m_0, s_0 corresponding directly to the illuminant $E(\lambda)$ were available, for example, by reflection from a perfectly diffusing white surface somewhere in the scene. Then an approximately unbiased estimate of a surface color might be obtained by normalizing the excitations l, m, s from the light reflected from this surface against l_0, m_0, s_0, to give l/l_0, m/m_0, s/s_0 (cf. Section 2.08.1.4). In this way, if the illuminant contained an excessive radiant power at long wavelengths, the relatively large value of l would be reduced by the relatively large value of l_0. These scaled cone excitations would be uniquely linked to surface color within the scene, again within the limits of metamerism (Section 2.08.1.1).

This scaling hypothesis was formulated by J. von Kries (1905) to describe the adaptation of the eye to colored lights, albeit not necessarily globally (Ives, H. E., 1912; Smithson, H. E., 2005). Although better known for its role in modeling color constancy, the hypothesis also provided a powerful experimental technique for estimating the spectral sensitivities of the three cone types from color-matching measurements (Wyszecki, G. and Stiles, W. S., 1982).

Formally, von Kries scaling constitutes a diagonal matrix transformation of cone responses (Terstiege, H., 1972; Worthey, J. A. and Brill, M. H., 1986; Brainard, D. H. and Wandell, B. A., 1992), but in practice the extent of the chromatic adaptation provided by this scaling is restricted. Thus, full perceptual compensation for the illuminant occurs only with unsaturated lights. With saturated lights, perceptual compensation is usually incomplete (Judd, D. B., 1940): the red safelight of the photographic darkroom never appears white (Ives, H. E., 1912).

Despite limited experimental evidence, many models of color constancy, including the multiplication rule used in Land's so-called retinex models (Land, E. H., 1959a; 1959b; 1986), assumed implicitly that the formalism of the scaling hypothesis applies also to lights reflected from surfaces. When tested more directly, it was found that the ratios l/l_0, m/m_0, s/s_0 of cone excitations from reflected lights – and not just from those surfaces where one was white – are indeed almost independent of the illuminant (Foster, D. H. and Nascimento, S. M. C., 1994). If cone responses are first transformed so that they are spectrally sharper, for example, by cone-opponent interactions (Foster, D. H. and Snelgar, R. S., 1983; Finlayson, G. D. *et al.*, 1994b), then the independence is even better (Finlayson, G. D. *et al.*, 1994a).

2.08.2.3 Relational Color Constancy

If the eye does not adapt completely to the illumination on part or all of a scene, then color appearance ought to be affected, and, in turn, judgments of surface color. But not all judgments that appear to involve color constancy involve complete chromatic adaptation. For example, in the natural world, surfaces are often seen partly in direct light and partly in shadow, but the shadowed region appears to have the

Figure 3 Images of a natural scene containing a test sphere (bottom left in each image) under different illuminations. In the upper left and right images, the illuminant is north sky light (correlated color temperature 25 000 K) and sunlight (4000 K), respectively, and the sphere is covered with gray paint. In the lower left image, the illuminant is sunlight and the sphere is covered with blue–gray paint. In the lower right image, the illuminant is a mixture of sunlight and north sky light (6500 K), and the sphere is covered with gray paint.

same surface color as the unshadowed region, even though it is simultaneously seen to be less bright and generally more blue (Arend, L. E. *et al.*, 1991). This apparently paradoxical separation of percepts was identified by Georg Christoph Lichtenberg in 1793 in a letter to Johann Wolfgang von Goethe thus: "In ordinary life we call white, not what looks white, but what would look white if it was set out in pure sunlight" (Joost, U. *et al.*, 2002, p. 302).

To make effective surface-color judgments in these conditions, an observer could use the perceived color relations between parts of a scene. For example, in Figure 3, in the upper left and upper right images of a scene, the color of the light reflected from the sphere in the bottom left corner is clearly different; nevertheless, it is possible to decide that the sphere has the same surface color by comparing it with, for example, the nearby leaves. By contrast, in the lower left image, although the color of the light reflected from the sphere is the same as in the upper left image, it is possible to decide that the sphere has a different, bluish, surface color, again by comparing it with nearby leaves. In the upper left and upper right images, the perceived relations between the colors are preserved; in the upper left and lower left images, they are not (the lower right image is discussed in Section 2.08.4.4).

Relational color constancy refers to the constancy of perceived color relations under illuminant changes, or other viewing conditions (Foster, D. H. and Nascimento, S. M. C., 1994), and has an operational interpretation described later (Section 2.08.4.5). It is distinct from the phenomenon of related colors, which requires other colors for their perception.

Notice that the comparisons just described may be made simultaneously with fixed gaze, or sequentially by moving the eye from one image to the other (Cornelissen, F. W. and Brenner, E., 1995), or with fixed gaze and the illumination on the scene changing, or any combination of these. Although some chromatic adaptation does take place with these images, either locally or globally, or both, it is insufficient to eliminate the perceived differences in illumination.

2.08.3 Sensory and Perceptual Cues

If color constancy is achieved partly or wholly by scaling cone responses – or their transforms – to compensate for the color of the illumination on a scene, then information about the illuminant is required. But the illuminant itself may not be visible; for example, the light may come from behind the observer, and there may be no designated perfectly diffusing white surface in the scene from which the corresponding cone excitations l_0, m_0, s_0 representing the illuminant can be derived. Other strategies are needed to obtain the required information.

2.08.3.1 Estimating the Illuminant

In natural scenes, there are several indirect cues to illuminant color (Maloney, L. T., 2002). One is the spatial average of the colors in the scene, estimated visually by global mechanisms or by local mechanisms combined with eye movements (D'Zmura, M. and Lennie, P., 1986), or both. If the color gamut of the surfaces is sufficiently large, then their average should be chromatically neutral (the gray-world hypothesis: Evans, R. M., 1946/1951; Buchsbaum, G., 1980; Land, E. H., 1986), and any bias away from neutral should represent the illuminant color. Another indirect cue is the color of the highest-luminance surface in the scene. As it reflects the most light, it is most likely to be white or specular, and therefore any bias should represent the illuminant color (the bright-is-white hypothesis: Land, E. H. and McCann, J. J., 1971; Gilchrist, A. *et al.*, 1999). These two cues normally covary, but when pitted against each other, the spatial-average cue seems to dominate the highest-luminance cue, except when the scene has few surfaces (Linnell, K. J. and Foster, D. H., 2002).

Mutual illumination (Bloj, M. G. *et al.*, 1999) and specularities with nonuniform surfaces (Yang, J. N. and Maloney, L. T., 2001) may also be used to infer the scene illuminant, and, over a limited region, luminance-color correlations (Golz, J. and MacLeod, D. I. A., 2002; Granzier, J. J. M. *et al.*, 2005) may be used in a similar way.

2.08.3.2 Color Contrast and Variance

The cues to the scene illuminant provided by the spatial average and the brightest surface or specularity represent two spatial extremes in sampling the visual environment. The influence of more intermediate-range sampling is found in the classical color-contrast or chromatic-induction effects whereby the hue of a stimulus is shifted away from that of a surround field. These effects may be interpreted as local illuminant compensation (Hurlbert, A. and Wolf, K., 2004), being limited to about 1° of visual angle from the point of gaze (Brenner, E. *et al.*, 2003, see also Barbur, J. L. *et al.*, 2004), although some modulatory effects on color appearance may extend to 10° of visual angle (Wachtler, T. *et al.*, 2001).

Other spatial factors influencing color appearance in variegated scenes include differences in texture, which weaken chromatic-contrast induction (Hurlbert, A. and Wolf, K., 2004), and chromatic variation in a background field: areas appear more vivid and richly colored against low-contrast, gray surrounds than against high-contrast, multicolored surrounds (Brown, R. O. and MacLeod, D. I. A., 1997; Shevell, S. K. and Wei, J., 1998; Brenner, E. and Cornelissen, F. W., 2002; Brenner, E. *et al.*, 2003).

2.08.3.3 Spatial Ratios of Cone Excitations

Unlike color constancy, relational color constancy (Section 2.08.2.3) does not require an estimate of the illuminant on the scene. In fact, the spatial ratios of cone excitations generated in response to light reflected from pairs of surfaces or groups of surfaces may provide sufficient cue to the stability or otherwise of surface color. As already noted (Section 2.08.2.2), such ratios have the property of being almost exactly invariant under changes in illuminant, both with artificial scenes of colored papers (Foster, D. H. and Nascimento, S. M. C., 1994) and with natural scenes (Nascimento, S. M. C. *et al.*, 2002), as illustrated in Figure 4 for long-, medium-, and short-wavelength cones in turn.

In theory, temporal ratios of cone excitations may also be calculated with similar effect. Eye movements back and forth across an edge separating different surfaces could define a ratio signal over recent time that, like spatial ratios, is almost exactly invariant under changes in illuminant. In making surface-color matches across two simultaneously presented Mondrian-like images, experimental observers switch gaze between test and reference surfaces with increasing frequency just before a match is made (Cornelissen, F. W. and Brenner, E., 1995). Spatial (and temporal) ratios may also be calculated across postreceptoral combinations (Zaidi, Q. *et al.*, 1997); across spatial averages of cone excitations (Amano, K. and Foster, D. H., 2004); and across the two eyes, suggesting the involvement of binocularly driven processes (Nascimento, S. M. C. and Foster, D. H., 2001; Barbur, J. L. *et al.*, 2004; see also Section 2.08.7.2).

The invariance or otherwise of these ratios may explain performance in several color-vision tasks (Westland, S. and Ripamonti, C., 2000; Ripamonti, C. and Westland, S., 2003; Foster, D. H. *et al.*, 2001b), including asymmetric color matching (Tiplitz Blackwell, K. and Buchsbaum, G., 1988). The calculation of ratios is a general device, which need not be restricted to primate or indeed vertebrate vision (Section 2.08.7). Bumblebees appear to make similar calculations to encode contrast relations between distinct elements of complex scenes (Lotto, R. B. and Wicklein, M., 2005).

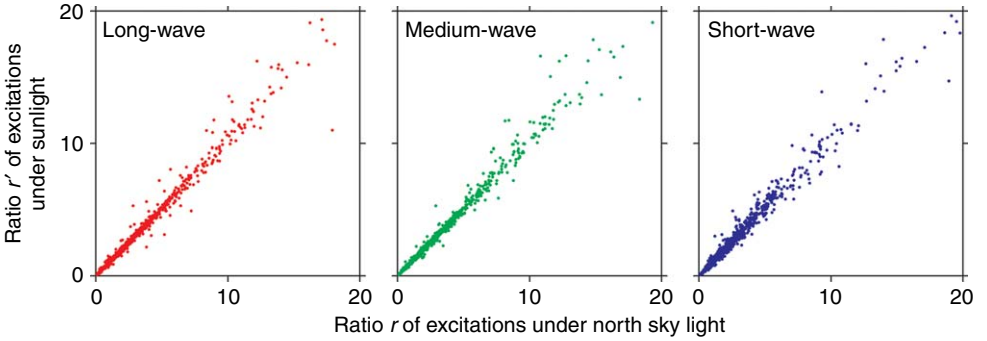

Figure 4 Scatterplot of ratios of cone excitations for long-, medium-, and short-wavelength-sensitive cones. Each point represents a pair of ratios r and r' of excitations in a cone class produced by light from a pair of surfaces drawn at random from a set of 25 natural scenes under, respectively, north sky light and sunlight, with correlated color temperatures 25 000 K and 4000 K. The mean deviation of pairs of ratios from equality is about 5% (see Foster, D. H. and Nascimento, S. M. C., 1994; Nascimento, S. M. C. *et al*., 2002). Number of points in each graph is approximately 2400.

As illustrated earlier (Section 2.08.2.3, Figure 3), the cue provided by spatial cone-excitation ratios, unlike the scaling of cone responses defined by von Kries adaptation, has the advantage that it allows the separation of judgments about the stability of surface colors from judgments about the color of the illumination, which, environmentally, may be equally important (Jameson, D. and Hurvich, L. M., 1989).

2.08.4 Measuring Perceived Surface Color

Given that with one cue or another it is possible to estimate surface color from the light reflected from a scene, how is the ability to make this estimate assessed experimentally in the laboratory? There are four main methods of measurement, each of which is limited in different ways (Foster, D. H., 2003).

2.08.4.1 Color Naming and Scaling

The most direct approach to measuring color constancy is to test the consistency of color naming under different lights. Although certain color terms are basic (Berlin, B. and Kay, P., 1969; Uchikawa, K. and Boynton, R. M., 1987), observers may be given a free choice; for example, if they call an intense yellow surface cadmium yellow under one illuminant, do they use the same name under a different illuminant? In practice, however, even when the illuminant is constant, observers use the same name for other shades of intense yellow. The problem is that there are many more distinguishable surface colors, perhaps more than two million (Pointer, M. R. and Attridge, G. G., 1998), than can be named accurately or consistently.

It is possible to increase the precision of color naming by adjoining a numerical scale, although the system is then no longer purely categorical (Foster, D. H., 2003). For example, observers may be asked to judge how red, green, blue, and yellow a test patch appears on a fixed scale of numbers (Schultz, S. *et al*., 2006).

2.08.4.2 Setting Unique Hues

In contrast with color names in general, the so-called unique hues red, green, blue, and yellow can be set by an experimental observer precisely (Valberg, A., 1971). Surface-color judgments under different illuminants may then be measured by finding a color setting that excludes the other hues: a yellow test stimulus, for example, is set so that it is neither reddish nor greenish (Arend, L. E., 1993; Shevell, S. K. and Wei, J., 1998). But the method is necessarily limited to these four hues.

2.08.4.3 Achromatic Adjustment

Setting a color to neutral is the logical intersection of setting unique hues: a white or gray test surface is adjusted so that it appears neither reddish nor greenish nor bluish nor yellowish. Although used to measure color constancy, achromatic adjustment strictly records only the observer's estimate of local illuminant color. But by measuring the bias of this estimate, it may be used to probe the effects of scene

structure such as local chromatic context (Brainard, D. H., 1998; Kraft, J. M. and Brainard, D. H., 1999) and to reveal the role of memory in surface-color judgments (Smithson, H. and Zaidi, Q., 2004; Hansen, T. *et al.*, 2006).

2.08.4.4 Asymmetric Color Matching

Color naming and setting unique hues both involve color identification, but asymmetric color matching does not. Rather, it simply requires a match to be made between a test and a reference surface under different lights (Wyszecki, G. and Stiles, W. S., 1982). For example, with the lower left and right images of Figure 3, an experimental observer would adjust the color of the (initially gray) test sphere in the right scene under the mixture of sunlight and north sky light so that it appears to have the same color as the (blue) sphere in the left scene under sunlight. The scenes may be viewed simultaneously or sequentially. This surface-color match is also referred to as a paper match (Arend, L. and Reeves, A., 1986), owing to its association with test samples taken from the Munsell Book of Color (Munsell Color Corporation, 1976).

Color matching ensures only the equivalence of two stimuli, not necessarily that they produce the same color percepts (Foster, D. H., 2003). In principle, observers need judge merely whether the relation between the color of one surface in the scene and the color of one or more others is the same as when the scene is viewed under a different illuminant; in other words, whether relational color constancy holds (Section 2.08.2.3). Estimating the illuminant seems to be unnecessary, as reliable surface-color matches are possible with minimalist scenes of just two surfaces, which provide little information about the illuminant (Tiplitz Blackwell, K. and Buchsbaum, G., 1988; Arend, L. E. *et al.*, 1991; Amano, K. and Foster, D. H., 2005).

2.08.4.5 Discriminating Illuminant from Reflectance Changes

A completely operational approach to measuring surface-color perception is to ask observers to distinguish between illuminant and surface-reflectance changes in a scene (Craven, B. J. and Foster, D. H., 1992; Nascimento, S. M. C. and Foster, D. H., 1997; Zaidi, Q., 2001). Performance in one such task has been found to be fast, accurate, and effortless, suggesting the spatially parallel detection of deviations from constancy in spatial cone-excitation ratios over the visual field (Foster, D. H. *et al.*, 2001b).

2.08.5 Levels of Color Constancy

The methods of measuring surface-color perception outlined in Section 2.08.4 vary in the kinds of information they provide. For accurate results, it is important to have a criterion that refers implicitly or explicitly to surface color; otherwise, other aspects of color appearance may determine performance.

2.08.5.1 Dual Representations

When experimental observers are asked to match a test surface for hue and saturation (e.g., the sphere in the upper left and right images of Figure 3), the level of color constancy obtained is much poorer than when they are asked to make a paper match. One explanation (Arend, L. and Reeves, A., 1986) of these different levels has been based on the roles played by two kinds of constancy process, which have already been mentioned (Section 2.08.2).

In one process, the eye becomes accustomed to the new illuminant with both light adaptation (von Kries, J., 1905; Whittle, P., 1996) and contrast adaptation (Webster, M. A. and Mollon, J. D., 1995; Brown, R. O. and MacLeod, D. I. A., 1997). Mechanisms with multiple time courses may be involved (Fairchild, M. D. and Reniff, L., 1995; Rinner, O. and Gegenfurtner, K. R., 2000). As hue and saturation are preserved under the change in illuminant, a paper that looks unique yellow under direct sunlight would continue to look unique yellow under, say, the greenish light reflected or transmitted beneath a tree. In the other process there is little opportunity for this adaptation, as when the eye moves over a scene patterned by light and shade (Zaidi, Q. *et al.*, 1997). Hue and saturation change when the illuminant changes, but they are interpreted as resulting from constant surface colors – constant spectral reflectances – under varying illumination. The paper that looks unique yellow under direct sunlight would in fact look greenish-yellow under a tree but be clearly identifiable as yellow paper. The differences in the completeness of these two processes affect the level of color constancy achieved in the two kinds of task (Bäuml, K.-H., 1999; Logvinenko, A. D. and Maloney, L. T., 2006).

2.08.5.2 Role of Task and Stimulus

On a continuous scale in which perfect color constancy is 1 and perfect inconstancy 0 (Arend, L. E. *et al.*, 1991), average levels of constancy have, depending on task

and stimulus, been reported as 0.79–0.87 for asymmetric color matching in computer-simulated images of flat Mondrian-like patterns of different colored Munsell papers (Bäuml, K.-H., 1999; Foster, D. H. *et al.*, 2001a); 0. 61 for asymmetric matching of real Munsell papers (Brainard, D. H. *et al.*, 1997) and 0.82 for achromatic adjustment of a test surface in an array of real Munsell papers (Brainard, D. H., 1998); 0.83 for achromatic adjustment of a test surface in a three-dimensional geometric tableau (Kraft, J. M. and Brainard, D. H., 1999); 0.70 for hue scaling of a test patch in a computer-simulated three-dimensional geometric tableau (Schultz, S. *et al.*, 2006); and 0.86 for asymmetric matching of a test object in a real three-dimensional geometric tableau (de Almeida, V. M. N. *et al.*, 2004) and 0.80 for discriminating illuminant from reflectance changes with similar stimuli (Nascimento, S. M. C. *et al.*, 2005a).

These constancy indices represent sometimes large variations across individual observers and stimuli, but systematic stimulus effects are identifiable. For example, with images of rural and urban scenes, 70% of the total variance in constancy indices can be explained by a combination of spatially averaged differences in spatial cone-excitation ratios, chroma, and hue (Foster, D. H. *et al.*, 2006a). Interestingly, three-dimensional scenes and natural scenes seem to provide no special advantage over flat and artificial scenes in eliciting high levels of constancy.

2.08.6 Color Appearance in Natural Environments

The abstract geometric displays used in laboratory measurements of color appearance usually have large, uniformly distributed color gamuts. By contrast, surfaces in natural scenes have smaller, more biased gamuts.

2.08.6.1 Colors of Natural Surfaces

The distribution of chromaticities of surfaces in natural scenes is dominated by browns, greens, and blues, from earth, vegetation, and sky (Hendley, C. M. and Hecht, S., 1949; Burton, G. J. and Moorhead, I. R., 1987; Osorio, D. and Bossomaier, T. R. J., 1992; Webster, M. A. and Mollon, J. D., 1997). More detailed analysis of these spectra suggests that the spectral positions of the long- and medium-wavelength-sensitive pigments (Figure 1) are optimal for primates discriminating ripe fruit or young leaves against a background of mature foliage (Sumner, P. and Mollon, J. D., 2000; Dominy, N. J. and Lucas, P. W., 2001; Lucas, P. W. *et al.*, 2003), but color vision is also important more generally for identifying objects and surfaces in variegated environments (Chiao, C.-C. *et al.*, 2000; Osorio, D. and Vorobyev, M., 2005). The fact that metamerism (Section 2.08.1.1) is rare in natural scenes (Foster, D. H. *et al.*, 2006b) suggests the sufficiency of trichromatic vision, that is, more cone classes are unnecessary.

2.08.6.2 Discriminating and Identifying Natural Surfaces

How well does color appearance allow us to identify objects in natural scenes under different illuminants? Performance depends not only on color constancy but also on other factors, such as the number of different colored surfaces present that might act as distractors. For example, if just two surfaces are sampled, there is little risk of confusion with a change in lighting: their color appearance will generally be different, and this difference will persist when the illuminant changes. But as the number of surfaces increases, the risk of confusion increases.

The success of color-appearance models (Sections 2.08.1.4 and 2.08.2.2) in predicting object identification in natural scenes under different illuminants can be quantified in a quite general way by applying methods from information theory (Cover, T. M. and Thomas, J. A., 1991). For any particular model, the magnitude of the information preserved from a scene varies surprisingly little from scene to scene, suggesting that the sensory coding of surface color in natural scenes can be optimized independent of viewing direction for any particular range of illuminants (Foster, D. H. *et al.*, 2004).

2.08.7 Physiological Mechanisms

Color appearance is the product of multiple stages of processing in the visual system (Walsh, V., 1999; Hurlbert, A. and Wolf, K., 2004), but its precise neural basis remains unresolved, partly because of different experimental criteria used to assess it, as indicated earlier.

2.08.7.1 Processing in Retina and Lateral Geniculate Nucleus

Significant chromatic adaptation takes place retinally. Microelectrode recordings from monkey horizontal

cells have shown that, consistent with the von Kries scaling hypothesis, adaptation is cone-specific at moderate light levels, although it is also incomplete and necessarily spatially local (Lee, B. B. *et al.*, 1999). Recordings from goldfish, which can make color-constant judgments (Neumeyer, C. *et al.*, 2002), have indicated that cone synaptic gains are modulated by the horizontal cell network in such a way that the ratios of cone outputs are almost invariant with the illuminant spectrum (Kraaij, D. A. *et al.*, 1998; Kamermans, M. *et al.*, 1998). Normalizing shifts in chromatic sensitivity have also been found in monkey parvocellular lateral geniculate neurons and their retinal afferents (Creutzfeldt, O. D. *et al.*, 1991).

A retinal contribution has also been revealed in humans by functional magnetic resonance imaging (Wade, A. R. and Wandell, B. A., 2002) and in subjective reports of color-induction in hemianopia (Pöppel, E., 1986).

2.08.7.2 Cortical Processing

A potential basis for the cortical calculation of spatial cone-excitation ratios is provided by double-opponent cells, which have been found in area V1 of the monkey visual cortex and which are sensitive to spatial chromatic contrast (Conway, B. R., 2001; Conway, B. R. and Livingstone, M. S., 2006). These cells are probably different from those cells in V1 that respond strongly to homogenous colored patches on large backgrounds (Wachtler, T. *et al.*, 2003) and which may contribute to chromatic-induction effects found in humans (Wachtler, T. *et al.*, 2001), including, the effect of colored patches remote from the test stimulus (Section 2.08.3.2).

Asymmetric color matching and color naming by patients with lesions higher than V1 also suggest that chromatic-contrast effects are calculated in area V1 or lower (Hurlbert, A. and Wolf, K., 2004). One patient with cerebral achromatopsia, despite being unable to match or name surface colors, was found able to discriminate changes in spatial cone-excitation ratios with simple scenes, but not with complex ones, suggesting a failure of integrative processes over the visual field (Hurlbert, A. C. *et al.*, 1998; see also Kentridge, R. W. *et al.*, 2004; Barbur, J. L. *et al.*, 2004).

Reminiscent of Land's experiments with Mondrian-like displays (Land, E. H., 1959a), cells in area V4 of the monkey visual cortex have been found to respond to a red patch when an entire multicolored Mondrian pattern was illuminated by long-, medium- and short-wavelength lights, but not with long-wavelength light alone (Zeki, S., 1980). Conversely, with lesions to V4, monkeys experience difficulty in identifying a colored surface under different illuminants (Walsh, V. *et al.*, 1993), and patients with lesions to the lingual and fusiform gyri, which include part of putative human area V4, have deficits in surface-color perception (Kennard, C. *et al.*, 1995; Clarke, S. *et al.*, 1998). Color constancy can also be selectively impaired after circumscribed unilateral lesions in parieto-temporal cortex (Rüttiger, L. *et al.*, 1999).

2.08.7.3 Inherited Color-Vision Deficiency

The abnormalities of inherited color-vision deficiency are evident on traditional clinical color-vision testing. Yet red-green dichromats, protanopes and deuteranopes, who have, respectively, no long- and medium-wavelength-sensitive pigments (Deeb, S. S., 2004), are able to identify surface colors under a fixed illuminant (Cole, B. L. *et al.*, 2006). They can also make achromatic settings (Rüttiger, L. *et al.*, 2001) and discriminate reflectance changes from illuminant changes with Mondrian-like patterns under different illuminants (Baraas, R. C. *et al.*, 2004), although their performance, and that of tritanopes (Foster, D. H. *et al.*, 2003), who have no short-wavelength-sensitive pigment, may be more variable and poorer than that of normal controls.

Deuteranomalous trichromats, whose medium-wavelength-sensitive pigment is replaced by a pigment closer to the long-wavelength-sensitive pigment (Deeb, S. S., 2004), can discriminate random reflectance changes from illuminant changes in natural scenes about as well as normal trichromats can (Baraas, R. C. *et al.*, 2006). Protanomalous trichromats, whose long-wavelength-sensitive pigment is replaced by a pigment closer to the medium-wavelength-sensitive pigment, perform somewhat less well.

The reasons for these variations in performance are incompletely understood. Possible explanatory factors include the influence of rod signals at lower light levels; the availability of cues from spatial ratios of cone excitations or of opponent combinations of cone excitations with altered spectral coverage; differences between stimuli based on natural and artificial reflectance spectra; and, for dichromats, the direction in chromaticity space of the loci of indistinguishable colors relative to the direction of the illuminant change. In general, however, individuals with color-vision deficiency may be less disadvantaged in judging natural surface colors than might be expected from clinical color-vision data.

Acknowledgment

This work was partly supported by the Engineering and Physical Sciences Research Council.

References

Amano, K. and Foster, D. H. 2004. Colour constancy under simultaneous changes in surface position and illuminant. Proc. R. Soc. Lond. B 271, 2319–2326.

Amano, K. and Foster, D. H. 2005. Minimalist surface-colour matching. Perception 34, 1009–1013.

Arend, L. and Reeves, A. 1986. Simultaneous color constancy. J. Opt. Soc. Am. A 3, 1743–1751.

Arend, L. E. 1993. How much does illuminant color affect unattributed colors? J. Opt. Soc. Am. A 10, 2134–2147.

Arend, L. E., Jr, Reeves, A., Schirillo, J., and Goldstein, R. 1991. Simultaneous color constancy: papers with diverse Munsell values. J. Opt. Soc. Am. A 8, 661–672.

Baraas, R. C., Foster, D. H., Amano, K., and Nascimento, S. M. C. 2004. Protanopic observers show nearly normal color constancy with natural reflectance spectra. Vis. Neurosci. 21, 347–351.

Baraas, R. C., Foster, D. H., Amano, K., and Nascimento, S. M. C. 2006. Anomalous trichromats' judgments of surface color in natural scenes under different daylights. Vis. Neurosci. 23, 629–635.

Barbur, J. L., de Cunha, D., Williams, C. B., and Plant, G. 2004. Study of instantaneous color constancy mechanisms in human vision. J. Electron. Imaging 13, 15–28.

Bäuml, K.-H. 1999. Simultaneous color constancy: how surface color perception varies with the illuminant. Vision Res. 39, 1531–1550.

Berlin, B. and Kay, P. 1969. Basic Color Terms. University of California Press.

Bloj, M. G., Kersten, D., and Hurlbert, A. C. 1999. Perception of three-dimensional shape influences colour perception through mutual illumination. Nature 402, 877–879.

Brainard, D. H. 1998. Color constancy in the nearly natural image. 2. Achromatic loci. J. Opt. Soc. Am. A 15, 307–325.

Brainard, D. H. and Wandell, B. A. 1992. Asymmetric color matching: how color appearance depends on the illuminant. J. Opt. Soc. Am. A 9, 1433–1448.

Brainard, D. H., Brunt, W. A., and Speigle, J. M. 1997. Color constancy in the nearly natural image. 1. Asymmetric matches. J. Opt. Soc. Am. A 14, 2091–2110.

Brenner, E. and Cornelissen, F. W. 2002. The influence of chromatic and achromatic variability on chromatic induction and perceived colour. Perception 31, 225–232.

Brenner, E., Ruiz, J. S., Herráiz, E. M., Cornelissen, F. W., and Smeets, J. B. J. 2003. Chromatic induction and the layout of colours within a complex scene. Vision Res. 43, 1413–1421.

Brown, R. O. and MacLeod, D. I. A. 1997. Color appearance depends on the variance of surround colors. Curr. Biol. 7, 844–849.

Buchsbaum, G. 1980. A spatial processor model for object colour perception. J. Frank. Instit. 310, 1–26.

Buchsbaum, G. and Gottschalk, A. 1983. Trichromacy, opponent colours coding and optimum colour information transmission in the retina. Proc. R. Soc. Lond. B 220, 89–113.

Burton, G. J. and Moorhead, I. R. 1987. Color and spatial structure in natural scenes. Appl. Opt. 26, 157–170.

Chiao, C.-C., Vorobyev, M., Cronin, T. W., and Osorio, D. 2000. Spectral tuning of dichromats to natural scenes. Vision Res. 40, 3257–3271.

CIE 2004a. Colorimetry. 3rd edn. CIE Central Bureau.

CIE 2004b. A colour appearance model for colour management systems: CIECAM02. CIE Central Bureau.

Clarke, S., Walsh, V., Schoppig, A., Assal, G., and Cowey, A. 1998. Colour constancy impairments in patients with lesions of the prestriate cortex. Exp. Brain Res. 123, 154–158.

Cole, B. L., Lian, K.-Y., Sharpe, K., and Lakkis, C. 2006. Categorical color naming of surface color codes by people with abnormal color vision. Optom. Vis. Sci. 83, 879–886.

Conway, B. R. 2001. Spatial structure of cone inputs to color cells in alert macaque primary visual cortex (V-1). J. Neurosci. 21, 2768–2783.

Conway, B. R. and Livingstone, M. S. 2006. Spatial and temporal properties of cone signals in alert macaque primary visual cortex. J. Neurosci. 26, 10826–10846.

Cornelissen, F. W. and Brenner, E. 1995. Simultaneous colour constancy revisited: an analysis of viewing strategies. Vision Res. 35, 2431–2448.

Cover, T. M. and Thomas, J. A. 1991. Elements of Information Theory. John Wiley & Sons.

Craven, B. J. and Foster, D. H. 1992. An operational approach to colour constancy. Vision Res. 32, 1359–1366.

Creutzfeldt, O. D., Crook, J. M., Kastner, S., Li, C.-Y., and Pei, X. 1991. The neurophysiological correlates of colour and brightness contrast in lateral geniculate neurons.1. Population analysis. Exp. Brain Res. 87, 3–21.

D'Zmura, M. and Lennie, P. 1986. Mechanisms of color constancy. J. Opt. Soc. Am. A 3, 1662–1672.

de Almeida, V. M. N., Fiadeiro, P. T., and Nascimento, S. M. C. 2004. Color constancy by asymmetric color matching with real objects in three-dimensional scenes. Vis. Neurosci. 21, 341–345.

Deeb, S. S. 2004. Molecular genetics of color-vision deficiencies. Vis. Neurosci. 21, 191–196.

Dominy, N. J. and Lucas, P. W. 2001. Ecological importance of trichromatic vision to primates. Nature 410, 363–366.

Evans, R. M. 1946/1951. Method for correcting photographic color prints. USA Patent No. 2,571,697.

Fairchild, M. D. 2005. Color appearance models. John Wiley & Sons.

Fairchild, M. D. and Reniff, L. 1995. Time-course of chromatic adaptation for color-appearance judgments. J. Opt. Soc. Am. A 12, 824–833.

Finlayson, G. D., Drew, M. S., and Funt, B. V. 1994a. Color constancy: generalized diagonal transforms suffice. J. Opt. Soc. Am. A 11, 3011–3019.

Finlayson, G. D., Drew, M. S., and Funt, B. V. 1994b. Spectral sharpening: sensor transformations for improved color constancy. J. Opt. Soc. Am. A 11, 1553–1563.

Foster, D. H. 2003. Does colour constancy exist? Trends Cogn. Sci. 7, 439–443.

Foster, D. H. and Nascimento, S. M. C. 1994. Relational colour constancy from invariant cone-excitation ratios. Proc. R. Soc. Lond. B 257, 115–121.

Foster, D. H. and Snelgar, R. S. 1983. Test and field spectral sensitivities of colour mechanisms obtained on small white backgrounds: action of unitary opponent-colour processes? Vision Res. 23, 787–797.

Foster, D. H., Amano, K., and Nascimento, S. M. C. 2001a. Colour constancy from temporal cues: better matches with less variability under fast illuminant changes. Vision Res. 41, 285–293.

Foster, D. H., Amano, K., and Nascimento, S. M. C. 2003. Tritanopic colour constancy under daylight changes? In: Normal and defective colour vision (*eds*. J. D. Mollon,

J. Pokorny, and K. Knoblauch), pp. 218–224. Oxford University Press.
Foster, D. H., Amano, K., and Nascimento, S. M. C. 2006a. Color constancy in natural scenes explained by global image statistics. Vis. Neurosci. 23, 341–349.
Foster, D. H., Amano, K., Nascimento, S. M. C., and Foster, M. J. 2006b. Frequency of metamerism in natural scenes. J. Opt. Soc. Am. A 23, 2359–2372.
Foster, D. H., Nascimento, S. M. C., and Amano, K. 2004. Information limits on neural identification of colored surfaces in natural scenes. Vis. Neurosci. 21, 331–336.
Foster, D. H., Nascimento, S. M. C., Amano, K., Arend, L., Linnell, K. J., Nieves, J. L., Plet, S., and Foster, J. S. 2001b. Parallel detection of violations of color constancy. Proc. Natl. Acad. Sci. U. S. A. 98, 8151–8156.
Gilchrist, A., Kossyfidis, C., Bonato, F., Agostini, T., Cataliotti, J., Li, X. J., Spehar, B., Annan, V., and Economou, E. 1999. An anchoring theory of lightness perception. Psychol. Rev. 106, 795–834.
Golz, J. and MacLeod, D. I. A. 2002. Influence of scene statistics on colour constancy. Nature 415, 637–640.
Granzier, J. J. M., Brenner, E., Cornelissen, F. W., and Smeets, J. B. J. 2005. Luminance-color correlation is not used to estimate the color of the illumination. J. Vis. 5, 20–27.
Guild, J. 1931. The colorimetric properties of the spectrum. Philos. Trans. R. Soc. Lond. A 230, 149–187.
Hansen, T., Olkkonen, M., Walter, S., and Gegenfurtner, K. R. 2006. Memory modulates color appearance. Nat. Neurosci. 9, 1367–1368.
Hendley, C. M. and Hecht, S. 1949. The colors of natural objects and terrains, and their relation to visual color deficiency. J. Opt. Soc. Am. 39, 870–873.
Hunt, R. W. G. 1998. Measuring Colour. Fountain Press.
Hurlbert, A. and Wolf, K. 2004. Color contrast: a contributory mechanism to color constancy. Prog. Brain Res. 144, 147–160.
Hurlbert, A. C., Bramwell, D. I., Heywood, C., and Cowey, A. 1998. Discrimination of cone contrast changes as evidence for colour constancy in cerebral achromatopsia. Exp. Brain Res. 123, 136–144.
Ives, H. E. 1912. The relation between the color of the illuminant and the color of the illuminated object. Trans. Illum. Engin. Soc. 7, 62–72.
Jameson, D. and Hurvich, L. M. 1989. Essay concerning color constancy. Annu. Rev. Psychol. 40, 1–22.
Joost, U., Lee, B. B., and Zaidi, Q. 2002. Lichtenberg's letter to Goethe on ''Färbige schatten'' – commentary. Color Res. Appl. 27, 300–303.
Judd, D. B. 1940. Hue saturation and lightness of surface colors with chromatic illumination. J. Opt. Soc. Am. 30, 2–32.
Kamermans, M., Kraaij, D. A., and Spekreijse, H. 1998. The cone/horizontal cell network: a possible site for color constancy. Vis. Neurosci. 15, 787–797.
Kennard, C., Lawden, M., Morland, A. B., and Ruddock, K. H. 1995. Colour identification and colour constancy are impaired in a patient with incomplete achromatopsia associated with prestriate cortical lesions. Proc. R. Soc. Lond. B 260, 169–175.
Kentridge, R. W., Heywood, C. A., and Cowey, A. 2004. Chromatic edges, surfaces and constancies in cerebral achromatopsia. Neuropsychologia 42, 821–830.
Kraaij, D. A., Kamermans, M., and Spekreijse, H. 1998. Spectral sensitivity of the feedback signal from horizontal cells to cones in goldfish retina. Vis. Neurosci. 15, 799–808.
Kraft, J. M. and Brainard, D. H. 1999. Mechanisms of color constancy under nearly natural viewing. Proc. Natl. Acad. Sci. U. S. A. 96, 307–312.
Land, E. H. 1959a. Color vision and the natural image. Part I. Proc. Natl. Acad. Sci. U. S. A. 45, 115–129.
Land, E. H. 1959b. Color vision and the natural image. Part II. Proc. Natl. Acad. Sci. U. S. A. 45, 636–644.
Land, E. H. 1986. Recent advances in Retinex Theory. Vision Res. 26, 7–21.
Land, E. H. and McCann, J. J. 1971. Lightness and retinex theory. J. Opt. Soc. Am. 61, 1–11.
Lee, B. B., Dacey, D. M., Smith, V. C., and Pokorny, J. 1999. Horizontal cells reveal cone type-specific adaptation in primate retina. Proc. Natl. Acad. Sci. U. S. A. 96, 14611–14616.
Li, C. J. and Luo, M. R. 2005. Testing the robustness of CIECAM 02. Color Res. Appl. 30, 99–106.
Linnell, K. J. and Foster, D. H. 2002. Scene articulation: dependence of illuminant estimates on number of surfaces. Perception 31, 151–159.
Logvinenko, A. D. and Maloney, L. T. 2006. The proximity structure of achromatic surface colors and the impossibility of asymmetric lightness matching. Percept. Psychophys. 68, 76–83.
Lotto, R. B. and Wicklein, M. 2005. Bees encode behaviorally significant spectral relationships in complex scenes to resolve stimulus ambiguity. Proc. Natl. Acad. Sci. U. S. A. 102, 16870–16874.
Lucas, P. W., Dominy, N. J., Riba-Hernandez, P., Stoner, K. E., Yamashita, N., Loria-Calderon, E., Petersen-Pereira, W., Rojas-Duran, Y., Salas-Pena, R., Solis-Madrigal, S., Osorio, D., and Darvell, B. W. 2003. Evolution and function of routine trichromatic vision in primates. Evolution 57, 2636–2643.
Luo, M. R., Cui, G., and Li, C. 2006. Uniform colour spaces based on CIECAM02 colour appearance model. Color Res. Appl. 31, 320–330.
Luo, M. R., Cui, G., and Rigg, B. 2001. The development of the CIE 2000 colour-difference formula: CIEDE2000. Color Res. Appl. 26, 340–350.
Maloney, L. T. 1999. Physics-Based Approaches to Modeling Surface Color Perception. In: Color Vision: From Genes to Perception (*eds*. K. R. Gegenfurtner and L. T. Sharpe), pp. 387–416. Cambridge University Press.
Maloney, L. T. 2002. Illuminant estimation as cue combination. J. Vis. 2, 493–504.
Monge, G. 1789. Memoire sur quelques phénomènes de la vision. Ann. Chim. 3, 131–147 (commentary and translation by R. G. Kuehni. 1997. Color Res. Appl. 1922, 1199–1203).
Munsell Color Corporation 1976. Munsell Book of Color – Matte Finish Collection. Munsell Color Corporation.
Naka, K. I. and Rushton, W. A. H. 1966. S-potentials from colour units in the retina of fish (*Cyprinidae)*. J. Physiol. (Lond.) 185, 536–555.
Nascimento, S. M. C. and Foster, D. H. 1997. Detecting natural changes of cone-excitation ratios in simple and complex coloured images. Proc. R. Soc. Lond. B 264, 1395–1402.
Nascimento, S. M. C. and Foster, D. H. 2001. Detecting changes of spatial cone-excitation ratios in dichoptic viewing. Vision Res. 41, 2601–2606.
Nascimento, S. M. C., de Almeida, V. M. N., Fiadeiro, P. T., and Foster, D. H. 2005a. Effect of scene complexity on colour constancy with real three-dimensional scenes and objects. Perception 34, 947–950.
Nascimento, S. M. C., Ferreira, F. P., and Foster, D. H. 2002. Statistics of spatial cone-excitation ratios in natural scenes. J. Opt. Soc. Am. A 19, 1484–1490.
Nascimento, S. M. C., Foster, D. H., and Amano, K. 2005b. Psychophysical estimates of the number of spectral-reflectance basis functions needed to reproduce natural scenes. J. Opt. Soc. Am. A 22, 1017–1022.
Neumeyer, C., Dörr, S., Fritsch, J., and Kardelky, C. 2002. Colour constancy in goldfish and man: influence of surround size and lightness. Perception 31, 171–187.

Osorio, D. and Bossomaier, T. R. J. 1992. Human cone-pigment spectral sensitivities and the reflectances of natural surfaces. Biol. Cybern. 67, 217–222.
Osorio, D. and Vorobyev, M. 2005. Photoreceptor spectral sensitivities in terrestrial animals: adaptations for luminance and colour vision. Proc. R. Soc. Lond. B 272, 1745–1752.
Pointer, M. R. and Attridge, G. G. 1998. The number of discernible colours. Color Res. Appl. 23, 52–54.
Pöppel, E. 1986. Long-range color-generating interactions across the retina. Nature 320, 523–525.
Rinner, O. and Gegenfurtner, K. R. 2000. Time course of chromatic adaptation for color appearance and discrimination. Vision Res. 40, 1813–1826.
Ripamonti, C. and Westland, S. 2003. Prediction of transparency perception based on cone-excitation ratios. J. Opt. Soc. Am. A 20, 1673–1680.
Rüttiger, L., Braun, D. I., Gegenfurtner, K. R., Petersen, D., Schönle, P., and Sharpe, L. T. 1999. Selective colour constancy deficits after circumscribed unilateral brain lesions. J. Neurosci. 19, 3094–3106.
Rüttiger, L., Mayser, H., Sérey, L., and Sharpe, L. T. 2001. The color constancy of the red–green color blind. Color Res. Appl. 26, S209–S213.
Schultz, S., Doerschner, K., and Maloney, L. T. 2006. Color constancy and hue scaling. J. Vis. 6, 1102–1116.
Shevell, S. K. and Wei, J. 1998. Chromatic induction: border contrast or adaptation to surrounding light? Vision Res. 38, 1561–1566.
Smithson, H. and Zaidi, Q. 2004. Colour constancy in context: roles for local adaptation and levels of reference. J. Vis. 4, 693–710.
Smithson, H. E. 2005. Sensory, computational and cognitive components of human colour constancy. Philos. Trans. R. Soc. Lond. B 360, 1329–1346.
Sumner, P. and Mollon, J. D. 2000. Catarrhine photopigments are optimized for detecting targets against a foliage background. J. Exp. Biol. 203, 1963–1986.
Terstiege, H. 1972. Chromatic adaptation: a state-of-the-art report. J. Color Appear. 1, 19–23 (cont. 40).
Tiplitz Blackwell, K. and Buchsbaum, G. 1988. Quantitative studies of color constancy. J. Opt. Soc. Am. A 5, 1772–1780.
Uchikawa, K. and Boynton, R. M. 1987. Categorical color perception of Japanese observers: comparison with that of Americans. Vision Res. 27, 1825–1833.
Valberg, A. 1971. Method for precise determination of achromatic colours including white. Vision Res. 11, 157–160.
von Helmholtz, H. 1867. In: Handbuch der Physiologischen Optik, vol. II, 1st edn., Leopold Voss. Translation 3rd edition (Helmholtz's Treatise on Physiological Optics, 1909) (*ed*. J. P. C. Southall), Optical Society of America. 1924, pp. 286–287. Republished by Dover Publications, 1962.
von Kries, J. 1905. Die Gesichtsempfindungen. In: Handbuch der Physiologie des Menschen (*ed*. W. Nagel), pp. 109–282. Vieweg und Sohn.
Wachtler, T., Albright, T. D., and Sejnowski, T. J. 2001. Nonlocal interactions in color perception: nonlinear processing of chromatic signals from remote inducers. Vision Res. 41, 1535–1546.
Wachtler, T., Sejnowski, T. J., and Albright, T. D. 2003. Representation of color stimuli in awake macaque primary visual cortex. Neuron 37, 681–691.
Wade, A. R. and Wandell, B. A. 2002. Chromatic light adaptation measured using functional magnetic resonance imaging. J. Neurosci. 22, 8148–8157.
Walsh, V. 1999. How does the cortex construct color? Proc. Natl. Acad. Sci. U. S. A. 96, 13594–13596.
Walsh, V., Carden, D., Butler, S. R., and Kulikowski, J. J. 1993. The effects of V4 lesions on the visual abilities of macaques: hue discrimination and color constancy. Behav. Brain Res. 53, 51–62.
Webster, M. A. and Mollon, J. D. 1995. Color constancy influenced by contrast adaptation. Nature 373, 694–698.
Webster, M. A. and Mollon, J. D. 1997. Adaptation and the color statistics of natural images. Vision Res. 37, 3283–3298.
Westland, S. and Ripamonti, C. 2000. Invariant cone-excitation ratios may predict transparency. J. Opt. Soc. Am. A 17, 255–264.
Whittle, P. 1996. Perfect von Kries contrast colours. Perception 25 (supplement), 16.
Worthey, J. A. and Brill, M. H. 1986. Heuristic analysis of von Kries color constancy. J. Opt. Soc. Am. A 3, 1708–1712.
Wright, W. D. 1928–1929. A re-determination of the trichromatic coefficients of the spectral colours. Trans. Opt. Soc. 30, 141–164.
Wyszecki, G. and Stiles, W. S. 1982. Color Science: Concepts and Methods, Quantitative Data and Formulae. Wiley.
Yang, J. N. and Maloney, L. T. 2001. Illuminant cues in surface color perception: tests of three candidate cues. Vision Res. 41, 2581–2600.
Young, T. 1807. A Course of Lectures on Natural Philosophy and the Mechanical Arts, Volume I, Lecture XXXVIII. Joseph Johnson.
Zaidi, Q. 2001. Color constancy in a rough world. Color Res. Appl. 26, S192–S200.
Zaidi, Q., Spehar, B., and DeBonet, J. 1997. Color constancy in variegated scenes: role of low-level mechanisms in discounting illumination changes. J. Opt. Soc. Am. A 14, 2608–2621.
Zeki, S. 1980. The representation of colours in the cerebral cortex. Nature 284, 412–418.

2.09 Motion Detection Mechanisms

B Krekelberg, Rutgers University, Newark, NJ, USA

© 2008 Elsevier Inc. All rights reserved.

2.09.1	**Introduction**	133
2.09.1.1	Computations	134
2.09.1.2	Algorithms	134
2.09.1.3	Implementations	134
2.09.2	**Research on Motion**	135
2.09.3	**Space–Time Correlation**	136
2.09.3.1	The Reichardt Detector	136
2.09.3.2	Behavioral Evidence	137
2.09.3.2.1	Facilitation	137
2.09.3.2.2	Reverse-Phi	137
2.09.3.2.3	Phase invariance	138
2.09.3.2.4	Pattern dependence	138
2.09.3.3	Physiological Evidence	139
2.09.3.3.1	Facilitation and suppression	139
2.09.3.3.2	Reverse-phi	140
2.09.3.3.3	Nonlinear interactions	141
2.09.3.3.4	Shunting inhibition	141
2.09.4	**Space–Time Orientation**	143
2.09.4.1	The Motion Energy Model	143
2.09.4.2	Behavioral Evidence	144
2.09.4.3	Physiological Evidence	144
2.09.4.3.1	Input from the lateral geniculate nucleus	145
2.09.4.3.2	Linear summation	147
2.09.4.3.3	Motion opponency	148
2.09.5	**Space–Time Gradients**	149
2.09.5.1	Behavioral Evidence	150
2.09.5.2	Physiological Evidence	150
2.09.6	**Conclusion**	151
References		152

> Like beauty and color, motion is in the eye of the beholder.

2.09.1 Introduction

The physical phenomenon, motion, can easily be defined as an object's change in position over time. An animal that can detect moving predators, prey, and mates has a clear survival advantage and this evolutionary pressure has presumably led to the development of neural mechanisms sensitive to motion. However, the combined effect of evolutionary circumstance, conflicting demands on the perceptual apparatus, and limitations of biological hardware have led to motion detection mechanisms that are far from perfect. A neural motion detection mechanism may not respond appropriately to all kinds of changes in position, and it may respond to some inputs that are not changes in position at all. It is in this sense that I subscribe to the quote from Watson A. B. and Ahumada A. J. (1985) at the start of this chapter; (the percept of) motion is constructed by the beholder's imperfect mechanisms for the detection of (physical) motion. The goal of this chapter is first to elucidate the principles that the brain relies on to detect motion. But second, to point out that strict adherence to those principles is quite rare, and that imperfect implementations are the rule, rather than the exception.

Research into motion detection mechanisms is strongly model-driven. Many studies are guided by particular views of the computations that are needed to detect motion; they aim to uncover the algorithms used by the brain, and describe the details of the neural implementations (Marr, D., 1982). Before delving into the details of motion detection mechanisms, a brief view of motion detection along these lines will be given.

2.09.1.1 Computations

Three views of the computations required for motion detection have emerged. The first states that a motion detector must compute whether the presence of light at one position is followed by light at another position. To detect motion, light has to be detected at both positions and times, and then compared. In the second view of motion, it is a continuous process of change. This view states that a moving object traces out an oriented light distribution in space–time. To detect motion, this orientation needs to be measured. The third view starts from the observation that motion can only be observed when there is both a temporal and a spatial change in light intensity. To detect motion, both need to be measured and compared. Each of these views suggests a different emphasis on algorithms that are relevant to compute motion (Figure 1).

2.09.1.2 Algorithms

The computations required by the first view can be performed by detecting light in the first position, delaying the signal, and multiplying it with the signal arising from the (undelayed) signal arising from the detector in the second position. This algorithm essentially performs a space–time autocorrelation. The computations of the second view require an estimate of space–time slant. This can be done by convolving the image with filters that are oriented in space–time. The computations of the third view require the estimation of both the spatial and temporal gradients in light intensity of an image. In abstract terms, such gradients can be determined by convolving the image with appropriate (differentiating) filters. The motion signal is then given by the ratio of the temporal and spatial gradients. Each of these algorithms requires different neural hardware for its implementation.

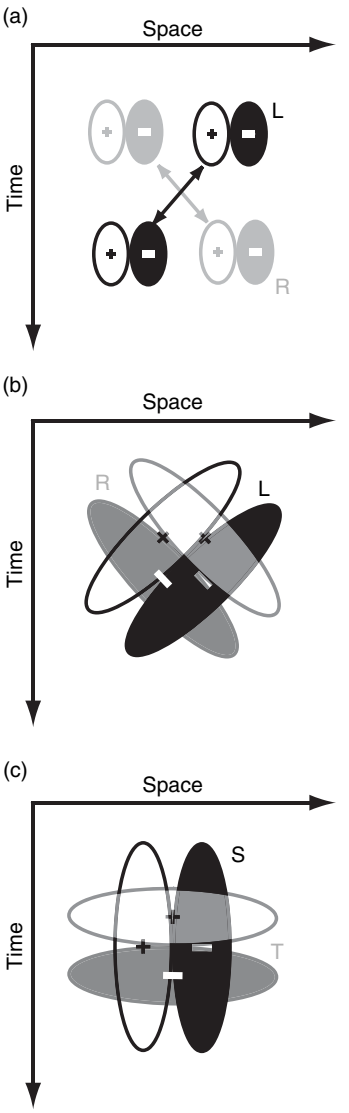

Figure 1 Three views of motion detection. (a) The Reichardt detector makes use of sensors that are displaced in space and time with respect to each other. By multiplying their outputs (indicated by the arrows), one can create a rightward (R) or leftward (L)-selective detector. (b) The motion energy detector uses overlapping sensors that are sensitive to rightward (R) or leftward (L) space–time slant. (c) The gradient detector uses overlapping detectors, sensitive to either spatial (S) or temporal (T) change. Adapted from Johnston, A. and Clifford, C. W. 1995b. A unified account of three apparent motion illusions. Vision Res. 35, 1109–1123.

2.09.1.3 Implementations

In the space–time correlation view, temporal delays and multiplication are the essential ingredients to detect motion. While temporal delays are part and

parcel of neural responses, typical synapses only add or subtract input signals, and multiplication of two signals is not as straightforward. Much of the research at the implementation level is therefore devoted to understanding if and how neurons can perform a multiplication. In the space–time orientation view, neurons' space–time receptive fields (RFs) must be slanted. Research in this tradition therefore concentrates on measuring detailed properties of space–time RFs. In the space–time gradient view, neurons' space–time response maps should match those of differentiating filters. Research in this tradition looks for such properties in visual neurons.

The three views of motion detection (correlation, orientation, and gradients) will be used as the skeleton to organize this chapter. It should be noted, however, that they are not mutually exclusive or even entirely independent. In fact, under some assumptions about the visual input, the detectors based on the three views become formally identical at their output levels (Adelson, E. H. and Bergen, J. R., 1985; van Santen, J. P. and Sperling, G., 1985; Bruce, V. *et al.*, 2003). On the other hand, these formal proofs should not be misconstrued to imply that the three computations, algorithms, and implementations are all the same. Behavioral methods may not be able to distinguish among some of the models because they only have access to the output of the motion detection mechanisms. But, as will be seen, neurophysiological methods can gain access to intermediate steps in the computations that are distinct.

The goal is to present some of the salient evidence that either provides support for one of the models or allows us to distinguish among the correlation, orientation, or gradient models. At the same time, however, it is important to realize that the brain may not perform any of these computations perfectly. Such imperfections may have arisen from competing constraints during the evolution of the visual system, or the limitations of biological hardware. As such, imperfections may be a nuisance in a model of motion detection, but in fact, they can be instructive in the larger view of the organization of the brain.

Sections 2.09.3, 2.09.4, and 2.09.5 review the literature on correlation, orientation, and gradient models, respectively. Before delving into the literature, however, some of the methods and terminology that have proven useful in the study of motion detection are discussed.

2.09.2 Research on Motion

Motion mechanisms can be studied by comparing the (behavioral or neural) response to a stimulus moving in one direction with that same stimulus moving in another direction. For direction-selective neurons, this is often reduced to responses to a stimulus moving in the preferred and the opposite, antipreferred direction. Many studies use sinusoidal gratings as the stimulus. The reason for using gratings is that, as long as a neuron (or mechanism) is well described as a linear system, the response to sinusoidal gratings can be used to predict the response to an arbitrary stimulus (Movshon, J. A. *et al.*, 1978a; 1978b). This Fourier analysis is only truly applicable to linear systems, which neurons in general and direction-selective neurons in particular are not. Nevertheless, the Fourier method has proven to be useful and much of the terminology in the field is derived from it.

To study the internal mechanisms of a motion detector, a sinusoidal grating may not always be the best choice. Although somewhat counterintuitive at first, even moving stimuli may not be the optimal stimuli to study motion mechanisms. The reason for this is that any motion mechanism worth considering would predict that motion in the preferred direction evokes a larger response than motion in the antipreferred direction. Hence, finding such responses does not tell us much about the internal mechanisms of the detector.

Many studies use flashed stimuli to characterize the response of motion detection mechanisms. A single flash by definition does not contain a motion signal, but nevertheless, it often activates motion detectors (and therefore may even appear to move). The minimal true motion signal is generated by two successive flashes. Thus, by comparing the response of a motion detector to two successive flashes with the response evoked by those same flashes presented in isolation, the motion-specific response properties can be extracted.

A further elaboration of this technique leads to the white noise analysis of nonlinear systems identification (Marmarelis, P. Z. and Marmarelis, V. Z., 1978). In this approach, the stimulus is a noisy pattern whose intensity varies rapidly and randomly. This can be viewed as a stimulus with multiple flashes occurring at the same time. Given enough time, all possible patterns will be presented to the detector, the responses to all possible patterns will be recorded, and the complete input–output relationship can be determined. In the finite

time available for an experiment this situation can of course only be approximated. Typically these approximations take into account the first-order response (response to a flash at a particular position) and the second-order response (interaction between two flashes separated in space and time).

With these methods it is possible to measure the properties that have proven to be useful to describe motion detection mechanism and that will recur throughout this chapter:

Direction selectivity (DS). The property that a mechanism (e.g., a neuron) responds differently when a stimulus moves in one direction than when that stimulus moves in the opposite direction.

Space–time response map or space–time RF. The response at time t to a flash presented at time zero at some position x. Because only one-dimensional motion will be considered, the space–time response map is two-dimensional.

Space–time interaction map. The response enhancement observed for a stimulus presented at ($t1$, $x1$), when another stimulus has already been presented at ($t2$, $x2$). This is a four-dimensional map. Often, however, the relative rather than the absolute time and position of the flashes matter. In such cases, the interaction map becomes two-dimensional and represents the enhancement in the response to a flash caused by the presentation of another flash dt earlier and at a distance of dx.

In the sections that follow, these measures of the internal properties of a motion detector will be used extensively to characterize experimental data, and to distinguish between models.

2.09.3 Space–Time Correlation

The study of the neural mechanisms of motion detection started in earnest with work on insects by Hassenstein, Reichardt, and Varju, in the early 1950s. Considering the faceted eyes of insects, it is natural to view motion as the detection of successive activation of neighboring ommatidia.

2.09.3.1 The Reichardt Detector

Hassenstein B. and Reichardt W. (1956) proposed the first formal model of motion detection on the basis of careful observations of the behavior of the beetle (*Chlorophanus viridis*). When placed in a moving environment, this beetle has the instinctive reaction to turn with the motion of the environment. Presumably it does this to keep moving in a direction that is constant with respect to the environment. Later studies have made use of similar optomotor responses in houseflies, blow flies, and locusts to gain access to their percept of motion.

By putting the beetle on a Y-globe (or *Spangenglobus*, in German), and surrounding it by a cylinder marked with vertical patterns, Hassenstein B. and Reichardt W. (1956) were able to quantify the beetle's motion percept (Figure 2). For instance, when they first presented a bright (+1) bar such that its light hit a specific ommatidium and then another bright bar to stimulate the nearest ommatidium to the left, the beetle turned toward the left. When a dark (−1) bar was followed by a dark bar on the left, the beetle also turned to the left. But, when a bright (+1) bar followed a dark (−1) bar on the left, the beetle turned to the right. From these key observations, they concluded that a simple algebraic multiplication of the contrasts of the visual patterns could underlie the motion response.

Figure 2 A beetle on a Spangenglobus. The beetle is glued to the black pole which holds it stationary in space. When it is lowered onto the y-maze globe, it instinctively grabs it and starts walking along the ridges. When it comes to a y-junction, it must make a decision to go right or left. This decision can be influenced by presenting motion in the environment (© Freiburger Universitaetsblaetter)

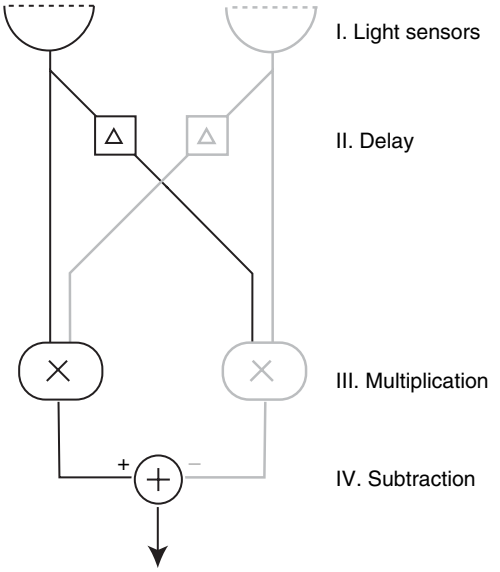

Figure 3 The (Hassenstein-) Reichardt detector. The light sensors represent the beetle's ommatidia. Signals from two neighboring ommatidia (I) are multiplied at stage III. One of the two input signals, however, is first delayed (II). The output of the multiplication stage in black is selective for rightward motion. This selectivity is enhanced in the last stage (IV) by subtracting the output of a leftward-selective subunit (in gray) from that of the rightward-selective subunit.

Additionally, they found that, for any given two-bar sequence, the optomotor response was strongest when there was about 250 ms between the two stimuli. A simple model that captures these properties is shown in Figure 3.

The first stage represents the input from two neighboring ommatidia. At the second stage, the input from one location is delayed. The third stage implements the multiplication that Hassenstein B. and Reichardt W. (1956) observed to underlie the beetle's behavior. This is an essential nonlinear operation, without which no DS could be generated in the time-averaged signal (Poggio, T. and Reichardt, W., 1973; 1981). To create a signal whose average value indicates the direction of motion, this stage can also average the signal over time. Finally, the output of a leftward-selective motion detector is subtracted from that of a rightward detector in the fourth stage. This subtraction greatly improves the selectivity of the detector (Borst, A. and Egelhaaf, M., 1990). The result is a single-valued output that is positive for rightward motion and negative for leftward motion. It could be imagined that such a number is fed straight into a motor control system to generate the beetle's following response. Formally, it can be shown that the output of this stage is the autocorrelation of the input signal (Reichardt, W., 1961). In other words, the detector determines how much a signal in one location is like the signal at a later time at a position to the right. If this autocorrelation is positive, motion is to the right; if it is negative motion is to the left.

2.09.3.2 Behavioral Evidence

The Reichardt detector makes some very specific and sometimes counterintuitive predictions about motion perception that have been tested in detail. A few of these will be highlighted here.

2.09.3.2.1 Facilitation

When a stimulus jumps from one position to the next and increases its contrast at the same time, the Reichardt model predicts that the motion signal is proportional to the product of the prejump and postjump contrast. As long as stimulus contrast is small enough, this is indeed the case in many insects (Reichardt, W., 1961; McCann, G. D. and MacGinitie, G. F., 1965; Buchner, E., 1984). For higher contrasts, however, further increases in contrast no longer strengthen the motion signal. Hence, a complete model should incorporate some kind of saturation or normalization of the response for high contrast.

van Santen J. P. and Sperling G. (1984) investigated this issue in humans and showed that, at least at low contrast, the motion signal indeed increased as the product of prejump and postjump contrasts. This clearly argues in favor of facilitation and even suggests that this facilitation takes the form of a multiplication. More recent experiments, however, show that perception is affected differently depending on whether the prejump or postjump stimulus contrast is increased (Morgan, M. J. and Chubb, C., 1999). Neither of these effects would be expected in a pure Reichardt detector, but may be explained by adding noise sources and contrast normalization mechanisms to the motion detector (Solomon, J. A. *et al.*, 2005).

2.09.3.2.2 Reverse-Phi

The multiplication in the Reichardt model ensures that motion detection does not depend on the polarity of the contrast of a moving object (dark objects lead to the same motion signals as bright objects). At

the same time, however, the multiplication causes a reversal of motion direction for stimuli whose contrast changes polarity. This inversion of motion direction with an inversion of contrast polarity during a motion step is called reverse-phi and has been observed behaviorally in insects (Reichardt, W., 1961; Buchner, E., 1984), nonhuman primates (Krekelberg, B. and Albright, T. D., 2005) and humans (Anstis, S. M., 1970; Anstis, S. M. and Rogers, B. J., 1975). This behavioral evidence suggests that the pathways detecting bright (On) and dark (Off) onsets interact within the motion system and that this interaction has the signature of a multiplication.

Behavioral evidence in humans, however, suggests that the On and Off systems are not treated as symmetrically as envisaged in the Reichardt model. For instance, the direction of motion in a sequence of dark and bright flashes requires a much longer interstimulus interval to be detectable than a sequence of flashes of the same polarity (Wehrhahn, C. and Rapf, D., 1992). Moreover, the reverse-phi phenomenon is found for eccentric presentations, but is much reduced near the fovea or when the distance between the observer and the stimulus is increased (Lu, Z. L. and Sperling, G., 1999).

2.09.3.2.3 Phase invariance

The Reichardt detector determines the autocorrelation of an input signal. Because the autocorrelation does not depend on the starting phase of the signal, this implies that for any arbitrary pattern (that can be described as the sum of sinusoidal gratings), replacing one of the component gratings by a phase-shifted grating does not change the output of the detector. This prediction has been confirmed at the behavioral level in the beetle. Reichardt took two (essentially arbitrary) spatial patterns and constructed a first visual stimulus by simple addition of the patterns, and a second visual stimulus by adding the patterns with a spatial phase shift. When a beetle was confronted with these two visual stimuli, its walking behavior on the Spangenglobus was identical (Reichardt, W., 1961).

2.09.3.2.4 Pattern dependence

While the phase of gratings does not affect the output of the detector, other properties, such as the spatial frequency, do. This shows that the Reichardt detector is not ideal; its output is not the same for every visual stimulus with the same velocity. While suboptimal from the viewpoint of an ideal motion detector, this does provide another counterintuitive prediction of the Reichardt model. To be precise, the model predicts that for every speed the detector responds only weakly to the lowest spatial frequencies, climbs to a maximum, and then declines for higher spatial frequencies. Optomotor responses in many insects are consistent with this prediction (Buchner, E., 1984).

A more extreme case of mistaken velocity arises from spatial aliasing for high spatial frequencies. When a rightward Reichardt detector is stimulated with a rightward moving grating whose spatial period is smaller than twice the distance between the input channels it will evoke a negative (i.e., leftward) response. While this is clearly an undesirable property for a motion detector, the behavior of the blowfly actually matches this (Zaagman, W. H. *et al.*, 1976). In other insects, the relationship between the behavioral inversion and receptor spacing is not as clean, although this may be understood by assuming that the detector receives input from more than one neighboring ommatidium (McCann, G. D. and MacGinitie, G. F., 1965; Thorson, J., 1966b).

Human visual motion perception is also spatial frequency dependent in a manner that is consistent with the Reichardt model (Burr, D. C. and Ross, J., 1982; Smith, A. T. and Edgar, G. K., 1990). The inversion of the perceived direction of motion that is observed at high spatial frequencies in insects, however, is not observed in human behavior (van Santen, J. P. and Sperling, G., 1984). The simplest way to modify the Reichardt model such that the spatial aliasing no longer occurs is to remove the affected high spatial frequencies from the input at an early stage. van Santen J. P. and Sperling G. (1984) proposed the extended Reichardt model, which has such prefilters and removes the spatial aliasing behavior (see flow-chart in Figure 4). The presence of the prefilters reflects the fact that the elementary light sensors that provide input to the motion detectors are not point sensors, but have an (overlapping) spatial extent.

Interestingly, the pattern dependence in the Reichardt detector arises only at the last subtraction stage. The so-called half-detectors' response to a moving pattern is almost independent of its spatial frequency. In other words, they are velocity tuned and not spatiotemporal frequency tuned (Zanker, Z. M. *et al.*, 1999). But, as pointed out above, the motion selectivity of such half-detectors is weak (Borst, A. and Egelhaaf, M., 1990). In a biological system, it seems likely that the subtraction of a leftward and

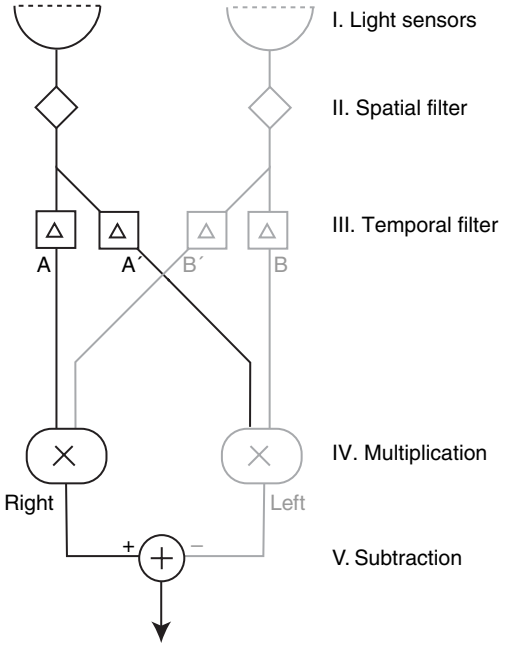

Figure 4 The extended Reichardt model. Light falling on the retina is spatially (II) and temporally filtered (III). The outputs of the four filters are then pairwise multiplied (stage IV). As in the standard Reichardt detector, the rightward-selective subunit (black) is combined with a mirror symmetric leftward-selective subunit (gray), at stage V.

rightward half-detector may not be perfect. This would have the effect of creating detectors that trade-off motion selectivity (fully symmetric subtraction at stage IV) against pattern invariance (no subtraction of opposite motion detectors).

2.09.3.3 Physiological Evidence

Many physiological studies have looked for and found neural response properties consistent with the Reichardt detector. Figure 5 shows what the model predicts for experiments that measure the space–time response map by presenting single flashes at various positions in a neuron's RF. The first four space–time response maps represent recordings from neurons at stage III of the extended Reichardt model (indicated by A, B, A′, and B′ in Figures 4 and 5). The defining property of these space–time RFs is that they are not oriented in space–time; they are well described as the product of a spatial and a temporal profile. This separability is also observed at stage IV; here both the left and the rightward subunit are predicted to have the same response to flashed stimuli. As a result, the complete detector, which subtracts the outputs of left and right detectors, gives no response at all to single flashes.

2.09.3.3.1 Facilitation and suppression

As can be seen from Figure 5, an ideal Reichardt detector should not respond at all to a single flashed bar. With an ingenious device that allowed them to flash a light on individual photoreceptors of the fly's eye while recording extracellularly from an identified direction-selective neuron (H1) in the optic lobe, Franceschini N. *et al.* (1989) provided evidence for this property. Single flashes, whether dark or bright, did not evoke a response in the H1 neuron. Such clean Reichardt behavior is rare; typically, motion detectors

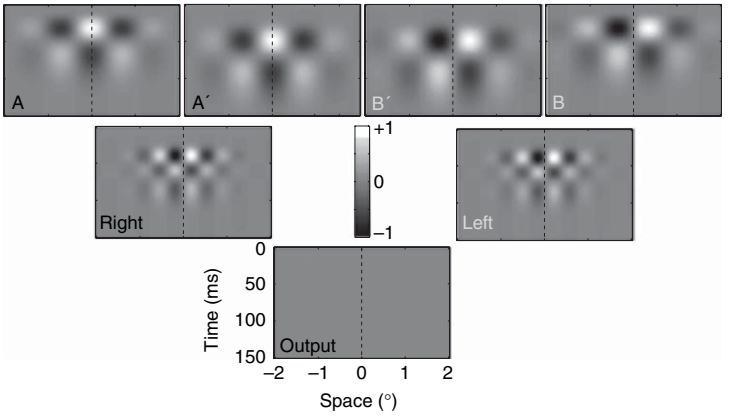

Figure 5 One flash space–time response maps of the Reichardt model. Each of these plots shows the response of a stage in the extended Reichardt model to the presentation of a single bright flashed stimulus. Time after the stimulus runs down the vertical axis, the position of the stimulus relative to the receptive field center, is on the horizontal axis. Pixels brighter than the gray zero level (see scale bar at center), represent an increase in the activity, dark pixels represent a decrease in activity. Within the linear model, such a decrease in firing after the presentation of a bright bar is equivalent to an increase in firing after the presentation of a dark bar. The labels in the lower left corner of each space–time response map refer to the labels in Figure 5.

will respond vigorously to a single flash (Borst, A. and Egelhaaf, M., 1990). No major modification of the model is required to explain this. For instance, some level of spontaneous activity in the multiplication stage would suffice to allow a strong input to always evoke a significant response. Alternatively, the subtraction of the left and right subunit outputs may not be perfect. For instance, instead of calculating R-L, the detector may calculate R-βL, where $0 < \beta < 1$ (Borst, A. and Egelhaaf, M., 1990).

The essential prediction of the Reichardt detector is that the response to two successive flashes – displaced in the preferred direction – is larger than that to two successive flashes displaced in the antipreferred direction. In other words, by comparing two-flash apparent motion in the preferred and antipreferred direction, one should observe facilitation and suppression of the neural response, respectively. Model calculations for this facilitation (bright) and suppression (dark) are shown for a rightward Reichardt motion detector in Figure 6.

Franceschini N. *et al.* tested this in the H1 neuron of the fly. When two successive flashes to separate photoreceptors simulated preferred motion, the second flash evoked a strong response (Franceschini, N. *et al.*, 1989). Presenting these flashes in the opposite order, simulating antipreferred motion, however, evoked no response or, in a cell with a large spontaneous firing rate, a suppression of the firing rate. This is consistent with the regions of facilitation (white) and suppression (black) around the origin of the interaction map in Figure 6. This was confirmed by Borst A. and Egelhaaf M. (1990) who recorded interaction maps for the fly H1 neuron. At low contrast, the preferred direction flashes showed clear facilitation, while the antipreferred direction flashes showed suppression. The suppression was evident also at high contrast, but the facilitation disappeared. The latter may be explained by a saturation process: if the individual flashes evoke a strong response, their combination in the preferred direction may not lead to any further enhancements because the response is already near the maximum and saturates. This, again, shows an imperfection in the neural motion detector. While the Reichardt detector predicts a quadratic increase of the response with contrast, real neurons do not have an infinite range and will saturate at some contrast level (Ibbotson, M. R. *et al.*, 1999). This is not a difficult property to incorporate into the model, but uncertainty about the shape of the contrast response function for all systems provides additional obstacles to the creation of a quantitative model.

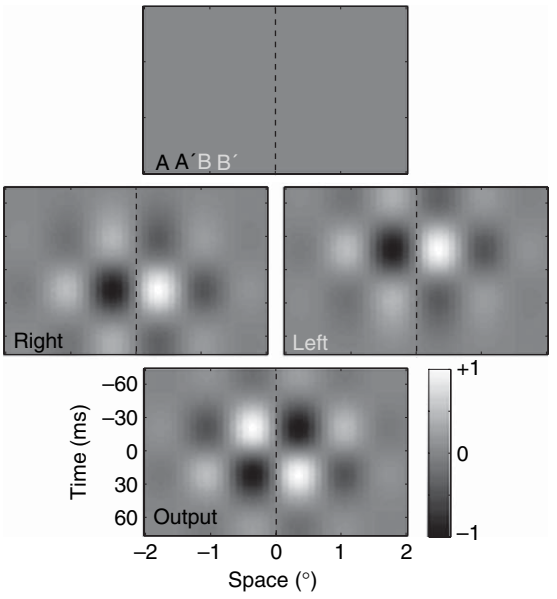

Figure 6 Two-flash space–time interaction maps of the extended Reichardt model. These interaction maps show which part of the response to two successive flashes is not expected based on the linear summation of the response to the two flashes presented in isolation. The time between the two flashes is on the vertical axis, the distance between the flashes on the horizontal axis. Bright pixels show a facilitating interaction, dark pixels a suppressive interaction.

In the rabbit retina, the main effect underlying DS appears to be a suppression for the antipreferred direction (Barlow, H. B. and Hill, R. M., 1963; Barlow, H. B. *et al.*, 1964; Amthor, F. R. and Grzywacz, N. M., 1993; Fried, S. I. *et al.*, 2002), with a smaller contribution from facilitation for two flashes presented in the preferred direction (Grzywacz, N. M. and Amthor, F. R., 1993; Taylor, W. R. and Vaney, D. I., 2002; Fried, S. I. *et al.*, 2005). This has led to the so-called veto model. In this model, the activity of a second flash, presented in the antipreferred direction, is inhibited (vetoed) by the presentation of the first flash. The requirements for this model are very similar to those of the Reichardt model. Notably, the first flash must be able to evoke suppression at a later time (i.e., a delay is needed). Later work has shown that a multiplicative nonlinearity may implement this veto mechanism (Torre, V. and Poggio, T., 1978; see Section 2.09.3.3.4).

2.09.3.3.2 Reverse-phi

The Reichardt model predicts that an inversion of the contrast of a two-flash stimulus leads to an inversion of directional preference.

Franceschini N. *et al.* (1989) investigated this by stimulating individual photoreceptors and found that there is more facilitation between flashes of the same contrast polarity than between flashes of opposite polarity. Thus they argue for some level of separation between the On and Off pathways. A later study, however, showed clear evidence of reverse-phi in the fly H1 cell: suppression is observed when a bright–dark two-flash stimulus is presented in the preferred direction, and facilitation is seen for a bright–dark two-flash stimulus presented in the anti-preferred direction (Egelhaaf, M. and Borst, A., 1992). While not entirely resolved, the discrepancy between these two studies may have been due to response saturation at the high contrasts used in the earlier studies. Alternatively, it could be due to the small sample size of the earlier studies (Franceschini, N. *et al.*, 1989; Horridge, G. A. and Marcelja, L., 1991) and the fact that there is considerable inter-fly variability between H1 neuron responses (Egelhaaf, M. and Borst, A., 1992).

In vertebrates a segregation of pathways processing brightness increments (On) and brightness decrements (Off) is already found at the first synapse; between photoreceptors and bipolar cells (Kuffler, S. W., 1953). The behavioral reverse-phi phenomenon, however, shows that the motion system must recombine these pathways at some stage. Indeed, the reverse-phi property has been observed in primary visual cortex (cat: Emerson, R. C. *et al.*, 1987; monkey: Livingstone, M. S. and Conway, B. R., 2003), subcortical motion pathways in marsupials (Ibbotson, M. R. and Clifford, C. W., 2001), and the cortical middle temporal area in the monkey (Livingstone, M. S. *et al.*, 2001; Krekelberg, B. and Albright, T. D., 2005).

2.09.3.3.3 Nonlinear interactions

The multiplication of two signals is the essential nonlinearity that creates DS in the Reichardt detector (Poggio, T. and Reichardt, W., 1973; 1981). Such a quadratic nonlinearity predicts that a sinusoidal input signal will lead to output signals that vary at the fundamental as well as the second harmonic frequency. To be specific, for a moving grating sliding over the detector, one can split the response of the detector into three terms. The first is time independent and changes sign with the direction of motion, the second term modulates at the temporal frequency of the stimulus, and the third term modulates at twice the frequency of the stimulus (Egelhaaf, M. *et al.*, 1989).

In an ideal Reichardt detector the oscillations in one subunit precisely cancel those in the other subunit. But, of course, precise cancellation is a mathematical abstraction that is not truly expected in biological hardware. When stimulated with a moving grating, direction-selective horizontal cells (HS) in the blowfly show oscillations. Nearly 90% of the signal was found at or below the second harmonic frequency. This shows that the nonlinearity in the HS motion detector is indeed close to second-order. Moreover, as predicted by the Reichardt model, the oscillations at the fundamental (stimulus) frequency depended strongly on the direction of the stimulus, but the frequency-doubled responses did not (Egelhaaf, M. *et al.*, 1989). This confirms that the Reichardt model provides a good description of the directional properties exhibited by the HS neuron, with the addition that the subtraction of the subunit outputs is not perfect. Typically, the gain of the antipreferred subunit is on the order of 0.9. This makes the motion detector suboptimal, because the equal subtraction of the two subunits maximizes DS (Borst, A. and Egelhaaf, M., 1990). Moreover, this imbalance will also cause vigorous responses to flickering patterns that do not move, but whose luminance is modulated over time. This is found for many motion sensitive neurons both in invertebrate (Egelhaaf, M. *et al.*, 1989) and vertebrate systems (Churan, J. and Ilg, U. J., 2002).

Interestingly, however, such imperfectly balanced and therefore suboptimal motion detection units have a reduced dependence on the spatial frequency of the stimulus. In fact, the response of a single subunit is tuned for velocity, and not temporal frequency (Zanker, Z. M. *et al.*, 1999). This suggests that some visual systems could use imperfect subunit subtraction (stage V, Figure 4) to trade-off optimal DS against spatial frequency dependence. One price to pay for imperfect subunit subtraction, however, is that in such a detector the direction-selective signal rides on top of a large nondirection-selective component. It is not clear under which circumstances the advantage of reduced spatial frequency dependence could outweigh this disadvantage of high energetic cost and reduced signal-to-noise.

2.09.3.3.4 Shunting inhibition

The Reichardt detector makes use of multiplication. This is a decidedly nonlinear mechanism and does not fit easily with the standard integrate and fire view of a neuron. When one takes a closer look at the biophysics of realistic neurons, however,

multiplicative nonlinearities appear to be possible by a mechanism called shunting inhibition (Thorson, J., 1966a; 1966b; Torre, V. and Poggio, T., 1978).

Consider a model neuron with an excitatory channel and inhibitory channel. The reversal potential for the excitatory channel is typically much larger than the resting potential; this provides the depolarizing current flow of an excitatory input. The reversal potential of the inhibitory channel, however, is assumed to be slightly above the resting potential. The two channels are organized such that preferred motion leads to temporally nonoverlapping activation of the channels. For a two-flash preferred direction stimulus this arrangement will lead to a depolarizing current from the excitatory channel as well as a depolarizing current from the inhibitory channel. In other words, the response to a two-flash sequence is somewhat higher than that to a one-flash sequence. Note, however, that this effect is a simple linear summation, and no difference is expected between the sum of the response to two single flashes and the response to two flashes, i.e. there is no nonlinear facilitation in this shunting inhibition model. While this may account for the limited facilitation found in direction-selective cells in the rabbit retina (Barlow, H. B. and Hill, R. M., 1963; Barlow, H. B. *et al.*, 1964), it is not a good model of the nonlinear facilitation observed in insects (Borst, A. and Egelhaaf, M., 1990).

When motion in the antipreferred direction is presented to the model shunting neuron, the excitatory and inhibitory conductances are activated at the same time. Under these circumstances the inhibitory channel essentially creates a large hole in the membrane. Any current flow caused by the simultaneous activation of excitatory channels will simply seep out through this hole. In other words, this so-called shunting inhibitory channel can veto nearby excitatory currents. A formal analysis shows that the efficacy of the veto is proportional to the product of the excitatory and inhibitory conductances (Torre, V. and Poggio, T., 1978). Hence, the suppressive part of the motion mechanism is similar to the multiplicative nonlinear element in Reichardt's original model. This example relies on a simplified model neuron, but Koch C. *et al.* (1983) developed a model that incorporates the spatial extent of the dendritic tree and the relative positioning of excitatory and shunting inhibition channels. They confirmed that shunting inhibition can lead to the desired veto-effect, but found that it will only veto excitatory input if the inhibitory conductance is located between the excitatory input and the soma. It should be noted, however, that in such a model with biophysically realistic assumptions the pure quadratic nonlinearity as envisaged in the Reichardt model is difficult to implement with shunting inhibition (Grzywacz, N. M. and Koch, C., 1987).

The shunting inhibition model provides a possible mechanism to implement a multiplicative nonlinearity, but what is the evidence that shunting inhibition is actually used in neural systems? Many direction-selective neurons contain gamma-aminobutyric acid (GABA) activated chlorine channels whose reversal potential is close to the resting potential. In other words, the GABAergic synapse could function as a shunt. Indeed, shunting inhibition has been demonstrated directly in cat visual cortex (Borg-Graham, L. J. *et al.*, 1998; Hirsch, J. A. *et al.*, 1998). Moreover, when GABAergic synapses are inactivated pharmacologically, DS in many systems is greatly reduced (fly: Schmid, A. and Bülthoff, H., 1988; rabbit: Ariel, M. and Daw, N. W., 1982; cat: Sillito, A. M., 1977). However, one should be cautious in interpreting this as evidence in favor of the shunting inhibition model. There are many stages in the Reichardt model that require some kind of inhibition. For instance, the subtraction stage (IV in Figure 3, V in Figure 4), subtracts the outputs of the two subunits. This subtraction removes nondirection-selective components from the subunits and helps create a strongly direction-selective motion detector (Borst, A. and Egelhaaf, M., 1990). If GABAergic synapses underlie this subtraction, then GABA antagonists would be expected to decrease DS, no matter how the multiplicative interaction were implemented.

In the fly, a clever experiment was done to distinguish such linear GABA-dependent contributions from nonlinear GABA-dependent contributions to DS. The crucial idea behind this experiment is that the multiplicative nonlinearity introduces higher harmonics in the output signal of the detector. The subtraction of the two subunits of the Reichardt detector, however, removes those components. In other words, by determining whether GABA agonists decrease or increase the higher harmonics, one can determine whether they affect the multiplicative or subtractive element of the Reichardt detector. Egelhaaf M. *et al.* (1990) showed that while GABA application decreased the overall DS of the H1 cell, the power of the second harmonic frequency increased nearly tenfold. This clearly shows that, if the H1 cell is indeed well-described by the Reichardt model, its multiplicative stage in the fly H1 cell is unlikely to be implemented with GABAergic shunting inhibition.

2.09.4 Space–Time Orientation

The view of motion as the successive activation of two detectors by the same feature may work well as the basis for the study of insect vision, and some artificial motion detection systems. In contrast, for vertebrates – and humans in particular – the distribution of detectors is nearly continuous and it is unclear which features need to be matched across which periods of time and between which detectors. Adelson E. H. and Bergen J. R. (1985) formulated a view of motion that deals with such problems and side-steps the correspondence problems associated with feature matching. They noted that a single bar, moving along a horizontal trajectory, can be represented as a slanted pattern in a space–time diagram (Figure 7(a)). Rightward slant implies rightward motion, and leftward slant leftward motion. Moreover, the slant angle in the pattern corresponds to the speed of the motion. The slant does not depend on the shape or features of the moving object; hence the correspondence problem essentially vanishes.

Moreover, in this view of motion, there is no fundamental difference between continuous motion and apparent motion. Figure 7(b) shows the space–time diagram that corresponds to the apparent motion that a bar in a modern neurophysiological experiment would typically trace out on a computer screen. A detector that detects the space–time slant corresponding to continuous motion would also respond to the slant associated with apparent motion. This is an appealing property of this view of motion; not only does it provide an intuitive explanation of the perceptual phenomenon of apparent motion (and hence why movies generate a sense of motion); it also validates the use of (apparent) motion on computer screens to study motion detection (Watson, A. B. *et al.*, 1986).

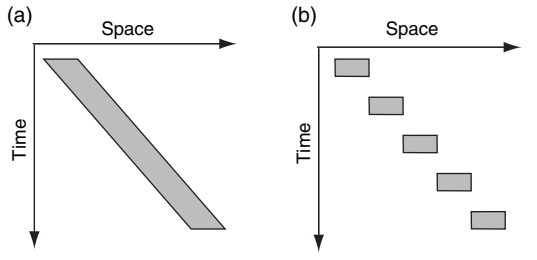

Figure 7 Motion as space–time orientation. (a) When a bar moves smoothly rightward over time, it traces out an oriented trapezoid in a space–time plot. (b) When that same bar jumps from one place to the next (apparent motion), the space–time orientation is still clearly visible.

2.09.4.1 The Motion Energy Model

Adelson E. H. and Bergen J. R. developed a multistage spatiotemporal filtering model that could detect space–time slant with neurophsyiologically realistic building blocks. The flow diagram of this so-called energy model is shown in Figure 8.

Each stage in this filtering model serves a specific purpose. The first stage collects light; it represents the photoreceptor input. The second stage filters the image spatially, with one of two spatial filters, shown in panel (b). In this particular example, the spatial filters are odd and even Gabor functions. The third stage filters the image temporally, using the filters shown in panel C. One filter's response is slower than the other, thus allowing the comparison of images at different times.

At the fourth stage, inputs from two separate pathways are summed linearly. In this particular example, the spatial and temporal filters were carefully chosen such that the fourth stage of the model would lead to slanted space–time filters. These particular filters are said to be in quadrature relationship (one filter reaches its peak when the other goes through zero; Watson, A. B. and Ahumada, A. J., 1985). While this relationship leads to the best sensitivity to motion, the only features that are essential to create space–time slant are the presence of a fast and a slow temporal filter, and spatial filters that prefer flashes in slightly different positions in space. Neurons at this stage modulate their response in a direction-selective manner, but their time-averaged response is independent of direction. This is a very general finding; a linear model cannot generate a time-averaged direction-selective output (Poggio, T. and Reichardt, W., 1973; 1981). Stage V represents the only nonlinear element in the motion energy model; it creates a signal whose time average is direction selective. At this point in the model the average response is direction selective, but the response of the neuron still depends on the position of the moving stimulus in the cell's RF. This so-called phase dependence is removed in stage VI by adding two detectors with slightly different spatial properties. Based on psychophysical data obtained in humans, Adelson E. H. and Bergen J. R. added the seventh stage to the model. At this stage, the rightward motion energy is subtracted from the leftward motion

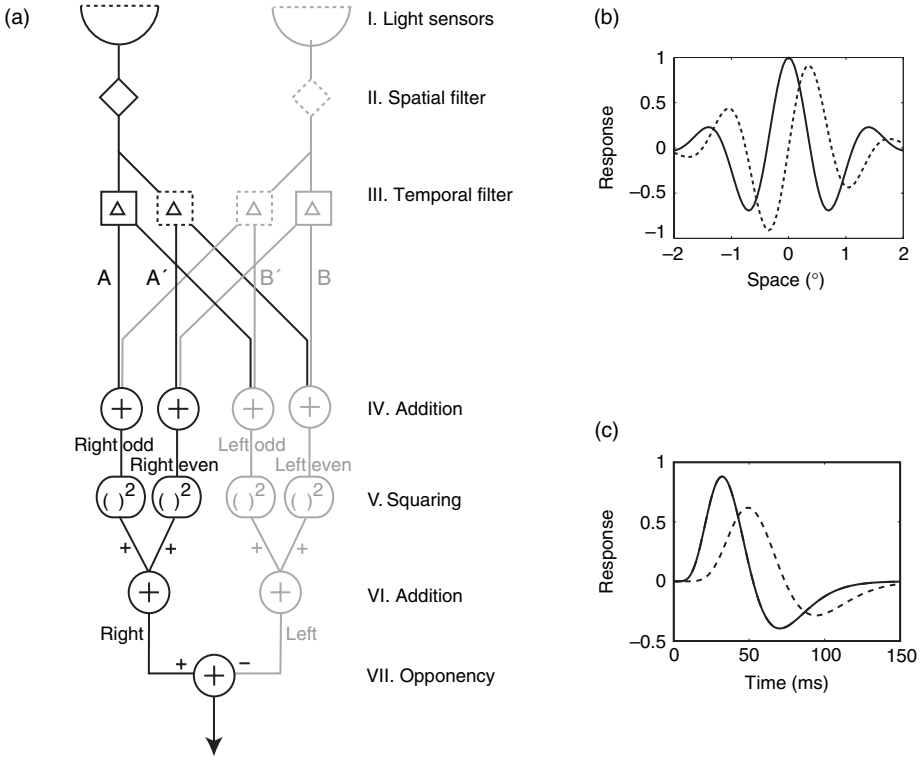

Figure 8 The motion energy model. (a) A chart of the signal flow in the model. In black are the components of the rightward-selective subunit, in gray the mirror symmetric leftward-selective unit. The diamonds at level II indicate spatial filtering with the filters shown in panel (b). Similarly, the temporal filtering of stage III uses the filters of panel (c). (b) Even (solid line) and odd (dashed line) spatial filters. (c) Fast (solid line) and delayed (dashed line) temporal filters.

energy to provide a single-valued output that represents the perceived direction. Positive values correspond to rightward motion, negative values to leftward motion.

The name motion energy arises from a consideration of the model in Fourier terms. In a Fourier spectrogram of the luminance distribution, opposite quadrants represent motion in the same directions. Hence, to create a detector that responds to rightward motion (quadrants I and III), one first has to remove the DC components along the spatial and temporal frequency axes. Stages II and III do this. Stage IV then selectively removes signal components from quadrants II and IV. Finally, the squaring operation of stage V measures the power or energy present in the remaining signal.

2.09.4.2 Behavioral Evidence

Given the different components in the model, it may be somewhat surprising that – at the output level – the (extended) Reichardt detector and the motion energy model are in fact identical (Adelson, E. H. and Bergen, J. R., 1985; van Santen, J. P. and Sperling, G., 1985). As only the output of the whole detector is typically observable behaviorally, psychophysical experiments cannot distinguish between these two models. This implies that the evidence cited in favor of the Reichardt detector in Section 2.09.3.2 equally supports the motion energy detector.

The internal algorithms of the detectors – how they reach their conclusion – however, are fundamentally different. Physiological methods can probe that internal implementation of motion detection mechanisms and are discussed in the next section.

2.09.4.3 Physiological Evidence

Simulations of the motion energy model make specific predictions about the properties of cells at various stages in the model. Figure 9 shows the predicted space–time response maps as assessed with one-flash stimuli. First, note that the structure of the motion–energy model at stage III (Figure 8) is identical to that of the Reichardt detector at stage III (Figure 4). Hence, the motion energy model also

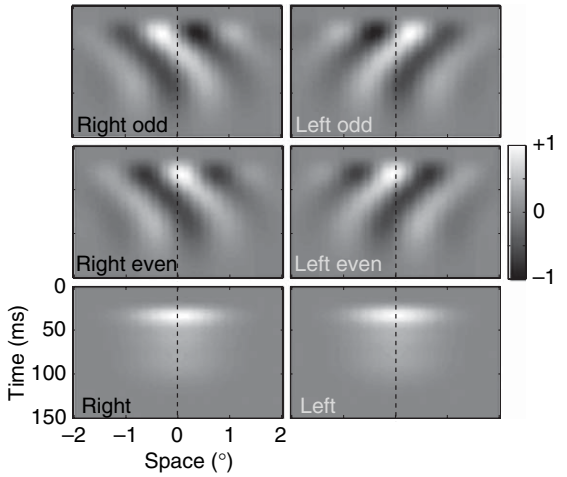

Figure 9 One-flash space–time response maps of the motion energy model. This figure follows the conventions of Figure 5. The space–time response maps of stage III of the motion energy model (A, B, A′, B′), are identical to those of the Reichardt model shown in Figure 6 and are not repeated here.

predicts the existence of cells with space–time response maps as shown for A, B, A′, and B′ in Figure 5. At stage IV, however, the models diverge. Figure 9 shows the characteristic slanted response maps expected at stages IV and VI of the motion energy model.

The various stages of the motion energy model can be mapped quite naturally onto the visual system of cats and primates. I will review the evidence for the various stages in sequence.

2.09.4.3.1 Input from the lateral geniculate nucleus

In cats and primates, few retinal or lateral geniculate nucleus (LGN) cells are direction selective, but many cells in primary visual cortex are (Hubel, D. H. and Wiesel, T. N., 1959; 1962). Hence, much of the research guided by the motion energy model has been devoted to determining whether a linear summation of the output of appropriate LGN cells can lead to a direction-selective response in the cortex.

Cai D. *et al.* (1997) probed cat LGN RFs with single flashes. They showed that the space–time RFs were typically not slanted. The space–time response maps resembled the outputs at stage III (A, B) shown in Figure 5. Note, however, that even though these LGN space–time response maps were not slanted, they were are also not separable. That is, their space–time response map could not be written as the product of a spatial impulse response function and a temporal impulse response function. For the discussion of motion detection, however, I will ignore this and approximate them by separable functions. Qualitatively this is a good approximation.

Stage IV of the motion energy model requires inputs that are delayed with respect to each other. In the LGN of the cat, the lagged and nonlagged cell classes seem to fulfill this prediction quite well (Mastronarde, D. N., 1987a; 1987b; Saul, A. B. and Humphrey, A. L., 1990; Cai, D. *et al.*, 1997). Primate LGN also has classes of cells that are delayed with respect to each other; the magnocellular cells typically give fast, transient responses, while parvocellular cells respond with a later sustained firing rate (Marrocco, R. T., 1976; Schiller, P. H. and Malpeli, J. G., 1978).

In the spatial domain, the inputs to the motion detector also need to be shifted; either in phase, or in space. A shift in phase, combining an odd and an even symmetric cell whose spatial RFs are in so-called quadrature, would be optimal (Figure 8(b)). Most cells in the LGN, however, have even symmetric spatial RFs; hence it will be difficult to construct an optimal motion detector from combining LGN cells. The motion energy detector, however, can also function with two RFs that are shifted spatially. Because LGN cells have RFs covering the whole visual field and because neighboring LGN cells are organized in a retinotopic fashion, collecting input from two LGN cells with slightly shifted spatial inputs should be relatively straightforward.

Given that appropriate input neurons exist in both cat and primate LGN, what is the evidence that these actually provide the input to the direction-selective cells of primary visual cortex? Certainly, both lagged and nonlagged cells project to the cortex, and simple cells – especially those in layer 4B – contain subregions of the RF in which response properties mimic those of LGN lagged cells and other subregions that match properties of nonlagged cells (Saul, A. B. and Humphrey, A. L., 1992). Moreover, some direction-selective (DS) simple cells have been shown to receive monosynaptic inputs from lagged LGN cells (Alonso, J. M. *et al.*, 2001). However, this does not necessarily mean that all DS cells must receive their input directly from the LGN. The alternative hypothesis is that the LGN projects to non-DS simple cells and these provide the input to DS simple cells.

There is evidence that at least some DS cells follow this indirect route. Peterson M. R. *et al.* (2004) recorded from pairs of monosynaptically

connected simple cells; one was DS, the other was not. For each cell in such a pair, they determined the space–time response map and then subtracted the RF of the non-DS cell from the RF of the DS cell. Given the linearity assumptions of the motion energy model, this should result in the RF of the missing second-input neuron. Peterson M. R. *et al.* show examples of DS simple cells in which the non-DS simple cell provides the late-input component. Because such a DS simple cell receives its delayed input from another simple cell, it does not have to rely on a lagged LGN cell. This shows that a direct input from lagged LGN cells is not necessary for DS.

Using these same methods, Peterson M. R. *et al.* also showed that there is a range of time delays between the two inputs of DS cells, and most are much smaller than predicted by the original motion energy model. In the original model, the inputs were in temporal quadrature (Figure 8(c)). While this relationship produces an optimal detector (Watson, A. B. and Ahumada, A. J., 1985), it is not necessary to create moderate DS. Taken together the evidence from the cat suggests that DS simple cells receive both direct lagged and nonlagged LGN input as well as input from other (non-DS) simple cells. The temporal delay between these inputs varies considerably across cells.

In monkey V1, De Valois and colleagues (De Valois, R. L. and Cottaris, N. P., 1998; De Valois, R. L. *et al.*, 2000) investigated the source of the input signals of DS simple cells by determining the temporal profile of the response in V1 simple cells. According to the motion energy model, this temporal profile should consist of the sum of two components; one delayed with respect to the other (Figure 8(c)). To extract these components, De Valois R. L. *et al.* used principal components analysis. First, they looked at non-DS cells. These cells typically had only a single significant component and there were two clearly distinct subsets. One set of cells had a profile with a short latency and a biphasic temporal profile; the other set had a longer latency and a monophasic profile. Then, they determined the response profiles of direction-selective cells. These cells had two significant input components, one matched the early biphasic profile, and the other matched the late monophasic profile of the non-DS cells. This strongly suggests that DS cells become direction selective by linear summation of the output of cells from the two distinct classes of non-DS simple cells (or their LGN inputs). Interestingly, the delay between the two temporal profiles corresponds closely to temporal quadrature, which suggests that these motion detectors are better optimized than those in the cat (Peterson, M. R. *et al.*, 2004). In the spatial domain, the relationship between the inputs was more varied and the optimal spatial quadrature relationship between the two inputs is expected to be rare.

The two temporal profiles observed in V1 simple cells correspond quite closely to the response properties of two anatomically identifiable subclasses of LGN cells. Magnocellular cells have short latencies and transient biphasic responses. Parvocellular cells have longer latencies and typically a monophasic sustained response. Hence, the view that arises from this work is that magnocellular and parvocellular LGN cells each have their own non-DS simple cell targets in V1. Other simple cells then sum the input from these non-DS simple cells to generate DS in the linear manner envisaged by the motion energy model.

This is controversial because anatomical, lesion, and psychophysical studies have all been used to argue that motion is processed by the magnocellular stream. Anatomical evidence shows that layer IVcα of V1 – where many DS cells are found – mainly receives magnocellular input (Blasdel, G. G. and Fitzpatrick, D., 1984). The counter argument is that there is also evidence showing strong vertical interactions within a column; hence even if the parvocellular properties cannot reach DS cells after crossing one synapse, they can after two. Second, lesion studies have been interpreted as showing a selective involvement of the magnocellular pathway in motion perception (Merigan, W. H. and Maunsell, J. H., 1993), but there are counter examples. Two studies have recorded from V1 cells while reversibly inactivating magnocellular and/or parvocellular layers in the LGN (Malpeli, J. G. *et al.*, 1981; Nealey, T. A. and Maunsell, J. H., 1994). These studies showed that many DS simple cells receive input from both classes of LGN neurons and that DS is often only abolished when both magnocellular and parvocellular inputs have been silenced. While this shows that a contribution of parvocellular cells to motion detection is certainly likely, it remains unlikely that the roles of the magnocellular and parvocellular cells in motion detection are as symmetric as in the de Valois model. For instance, lesions of the magnocellular layers of the LGN have a greater influence on the responses of direction-selective cells in the middle temporal area (Maunsell, J. H. *et al.*, 1990).

2.09.4.3.2 Linear summation

The previous section shows that signals with appropriate temporal and spatial shifts find their way into V1 simple cells. The next question is how these nondirection-selective inputs are combined. The motion energy model predicts linear summation of inputs.

Many studies using extracellular recordings from cat simple cells support this view. In a typical experiment, the RF of a neuron is mapped with one kind of stimulus (single flashes, stationary gratings) and then the response to another kind of stimulus (drifting sine wave gratings, or two successive flashes) is predicted based on the assumption of linear response properties. Qualitatively this was already done in the first studies of simple cells in the cat visual cortex (Hubel, D. H. and Wiesel, T. N., 1959) and found to account for the direction preference of some, but certainly not all cells. In later studies these statements have become more precise. It was found that the RF determined with flashes could predict quite well when a moving bar elicited the largest response (i.e., when moving from an Off to an On region). Other features, in particular the small response for motion in the antipreferred direction could not be predicted from linear superposition and various schemes of nonlinear lateral facilitation and inhibition were proposed (Goodwin, A. W. *et al.*, 1975; Emerson, R. C. and Gerstein, G. L., 1977a; 1977b; Ganz, L. and Felder, R., 1984). All of these studies, however, used extracellular recordings and they could not distinguish between nonlinear synaptic integration and nonlinear spike generation. Hence, these results left the possibility that all observed nonlinearities were in fact due to spike generation nonlinearities (Movshon, J. A. *et al.*, 1978b).

A new wave of studies in the late 1980s tested the linear model. Although the authors sometimes differed in their conclusions, with the benefit of hindsight their datasets actually appear quite similar. Most measured space–time response maps were slanted and corresponded with the motion energy model (Figure 9), but not with the separable response maps predicted by the Reichardt detector (Figure 5). These slanted space–time RF maps could usually predict the preferred direction of a cell, but underestimated the magnitude of the directional preference (Mclean, J. and Palmer, L. A., 1989; Tolhurst, D. J. and Dean, A. F., 1991; Reid, R. C. *et al.*, 1987; 1991; Baker, C. L., Jr., 2001). Albrecht D. G. and Geisler W. S. (1991) resolved this discrepancy by realizing that nonlinearities unrelated to DS itself, could nevertheless affect the predictions of the linear model. One nonlinearity they had recently measured was the contrast dependence of the neural response. They proposed a neural model in which linear summation of the inputs is followed by half-wave rectification and an exponential nonlinearity. The exponent of this nonlinearity could be derived from the contrast response function of the neuron. With this model, they could explain nearly 80% of the magnitude of the DS of simple cells and later studies have confirmed this (DeAngelis, G. C. *et al.*, 1993). While this model still leaves ~20% to be explained, this does not necessarily mean that the 20% are due to nonlinearities essential to the generation of DS. Instead this could be due to other contrast-related nonlinearities such as gain control (Heeger, D. J., 1992).

To really answer the question whether DS is based on linear summation, one needs to bypass the spike-generation nonlinearity. Jagadeesh B. *et al.* (1993; 1997) did this by recording intracellularly from cat simple cells. Their data provide clear evidence for three aspects of the motion energy model. First, DS simple cells sum their non-DS inputs linearly. This was shown by predicting the membrane potentials evoked by moving gratings from the linear superposition of the potentials evoked by stationary contrast modulated gratings. This prediction was highly accurate. Second, Jagadeesh B. *et al.* showed that the DS of the spike record (i.e. what would have been measured in extracellular recordings) was about three times larger than that observed in the intracellular recordings. This directly confirms the role of the spike-generation nonlinearity as an amplifier of DS (Albrecht, D. G. and Geisler, W. S., 1991; McLean, J. *et al.*, 1994). Third, they showed that nearly all of the membrane potential could be explained by the summation of inputs from only two subunits. These subunits had nonoriented space–time response maps (Kontsevich, L. L., 1995; Jagadeesh, B. *et al.*, 1997).

In a further test of the linear model, Priebe N. J. and Ferster D. (2005) measured separate space–time response maps of excitatory and inhibitory conductances in DS cat simple cells for bright and dark bars. First, all four response maps were clearly slanted; showing that both excitation and inhibition were direction selective for both dark and bright bars. Second, the slant in the excitatory and inhibitory maps was the same. Hence excitation and inhibition preferred the same direction of motion. This argues strongly against a vetolike mechanism for DS in these

cells, because such a model would predict an opposite direction preference for the inhibition. Third, when and wherever the excitation was maximal, inhibition was minimal. This suggests that DS is derived in a push–pull fashion; a bright bar in an On region of the RF evokes a depolarization (push) and a dark bar at the same position evokes a hyperpolarization (pull). When a stimulus moves across a RF, the pushes and pulls are evoked at different times and sum linearly. Finally, a nonlinear spike-generation mechanism removes subthreshold modulations and amplifies the relatively weak DS in the membrane potential (by a factor of 2–3; just above the squaring nonlinearity of the motion energy model). Together this creates a spike signal whose time-average is strongly direction selective (Priebe, N. J. and Ferster, D., 2005).

In the monkey, tests of the motion energy model have followed a similar path. Extracellular recordings showed slanted space–time response maps for DS simple cells (De Valois, R. L. and Cottaris, N. P., 1998; Livingstone, M. S., 1998; De Valois, R. L. *et al.*, 2000; Conway, B. R. and Livingstone, M. S., 2003). As explained above for cat simple cells, this is evidence against a Reichardt model. As was the case for cat simple cells, the space–time response map could predict the preferred direction of a cell, but it underestimated the magnitude of the DS (Conway, B. R. and Livingstone, M. S., 2003). To date, no intracellular recordings have been performed to determine whether the spike-generation nonlinearity underlies the enhancement of DS as it does in the cat (Jagadeesh, B. *et al.*, 1993).

2.09.4.3.3 Motion opponency

In the final step of the motion energy model, the output of a leftward motion-selective unit is subtracted from that of a rightward motion-selective unit. Behavioral evidence in humans shows that such an opponent stage must be present in the brain (Stromeyer, C. F. *et al.*, 1984). Given the description of DS simple cells in the previous section, it seems natural to ask whether complex cells, which are thought to combine input from multiple simple cells, implement this opponent stage of motion processing.

To test this hypothesis, Emerson R. C. *et al.* (1992) measured space–time interaction maps in cat complex cells. These maps show the nonlinear facilitation or suppression that one flash causes in the response of a second flash. Up until the squaring stage of the motion energy model, no nonlinear interactions are predicted, but at stage VI, simulations show that the

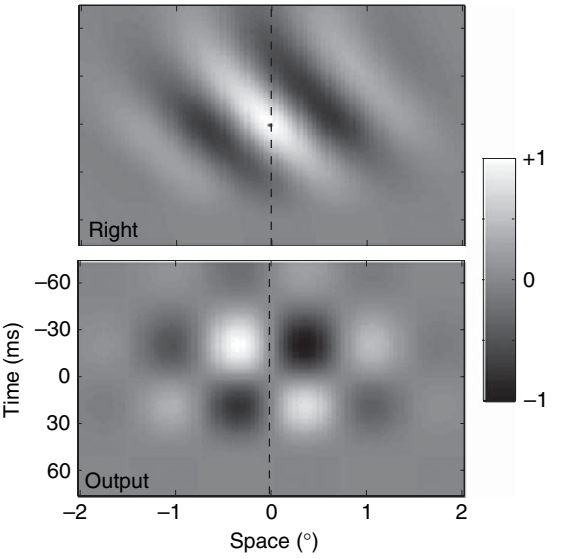

Figure 10 Two-flash space–time interaction maps in the motion energy model. This figure follows the conventions of Figure 6.

interaction maps should be slanted (Figure 10). At the opponent stage of the detector, on the other hand, the interaction maps should be separable (remember that the opponent stage is formally identical to the output of the Reichardt model, which has separable interaction maps at all stages). The evidence shows, however, that cat complex cells have slanted spatiotemporal interaction maps (Emerson, R. C. *et al.*, 1992; Touryan, J. *et al.*, 2002), which is incompatible with the motion-opponent stage. Moreover, in a direct test of motion opponency, van Wezel R. J. *et al.* (1996) demonstrated that complex cell responses are suppressed by a stimulus moving in the antipreferred direction, but this suppression is far from complete ($\sim$ 50%). In fact, the response to a stimulus consisting of two directions of motion is often well described by the average of the responses to the two directions of motion presented separately. These data suggest that complex cells are best described by stage VI of the motion energy model.

Macaque complex cells also have slanted interaction maps and, when combined with a squaring nonlinearity, account reasonably well for the DS to grating stimuli (Gaska, J. P. *et al.*, 1994; Livingstone, M. S., 1998; Conway, B. R. and Livingstone, M. S., 2003). As in the cat, this shows that they are well described by stage VI of the motion energy model but not the opponent stage. In agreement with this, macaque V1 cells also show

incomplete suppression for stimuli containing two opposing directions (Qian, N. and Andersen, R. A., 1994). Somewhat surprisingly, macaque complex cells not only have slanted interaction maps, but also slanted space–time response maps (Conway, B. R. and Livingstone, M. S., 2003). This is not expected in the motion energy model (Figure 9), although an imbalance between the subunits could cause this kind of response.

Finally, Livingstone M. S. (1998) showed that many macaque V1 complex cells had a spatially offset inhibitory zone on the null side of the RF. Such a zone is not expected in the motion energy model, but is reminiscent of the veto model of DS in the retina (Barlow, H. B. *et al.*, 1964). To recap, in the latter view a stimulus moving into the RF from the null side, produces a delayed inhibition that removes the fast excitation produced when the stimulus is in the center of the RF. Livingstone M. S. and Conway B. R. (1998; 2003) speculated that such delayed asymmetric inhibition could arise from an asymmetric dendritic tree. If such a tree has slow inhibitory inputs near the soma, and fast excitatory inputs on the asymmetric dendritic tree, then a stimulus moving in the antipreferred direction (from soma to dendrites) would evoke overlapping excitation and inhibition and therefore lead to little activation. For a stimulus moving from the dendrites toward the soma, on the other hand, the excitatory input would reach the soma and evoke spikes before the somatic inhibition could stop it. Anderson J. C. *et al.* (1999) investigated this hypothesis by a combination of physiology, anatomical reconstruction of single neurons, and modeling. First, they showed that the asymmetry of a dendritic tree did not predict cells' preferred direction. Second, their compartmental model showed that the delays that can be generated within a typical single dendritic tree were too short to explain sensitivity to slow motion. This suggests that the contribution of asymmetric inhibition to DS in the monkey is small.

The main projection area of DS complex cells in the macaque is the middle temporal area. Many of these cells reduce their response below the spontaneous firing rate when stimulated in the antipreferred direction (Maunsell, J. H. and Van Essen, D. C., 1983; Albright, T. D., 1984). While this shows the presence of some opponent mechanisms, there is no clear evidence for an opponent stage as it is postulated in the motion energy model. First, space–time interaction maps in MT are slanted, and not space–time separable (Livingstone, M. S. *et al.*, 2001; Pack, C. C. *et al.*, 2006). Second, even in MT the suppression of the response to a preferred stimulus by an antipreferred stimulus is far from complete (Snowden, R. J. *et al.*, 1991; Qian, N. and Andersen, R. A., 1994). Rather than a linear subtraction of opponent responses, the interaction of multiple directions of motion may be described more accurately as a (nonlinear) competition among multiple spatial and temporal frequency components (Krekelberg, B. and Albright, T. D., 2005).

When considering how MT cells can be constructed from their V1 (and LGN: Nassi, J. J. *et al.*, 2006) inputs, it is important to keep in mind that some motion tuning properties change considerably between V1 and MT. This is the case even if we consider only MT component cells and not the even more complex MT pattern cells (see Chapter Cortical Mechanisms for the Integration of Visual Motion). For instance, MT cells are much more invariant to changes in the stimulus pattern (Albright, T. D., 1992), MT cells integrate motion over longer periods of time (Mikami, A. *et al.*, 1986), the preferred speed of MT cells is typically higher than that of V1 cells (Mikami, A. *et al.*, 1986; Churchland, M. M. *et al.*, 2005), and MT cells are more speed-tuned than temporal frequency-tuned (Perrone, J. A. and Thiele, A., 2001; Priebe, N. J. *et al.*, 2003; Perrone, J. A., 2006; Priebe, N. J. *et al.*, 2006). It is difficult to see how such differences can arise from the simple linear operations envisaged in the motion energy model. The issues concerning speed tuning may be resolved in a model by Perrone and Thiele. In this model, MT cells combine inputs from typical transient and sustained V1 cells in a nonlinear manner, which generates sensitivity to higher speeds and speed tuning that is invariant to stimulus pattern (Perrone, J. A. and Thiele, A., 2001; 2002; Perrone, J. A., 2005). Some of the features of this model (e.g., using transient V1 cells to estimate temporal stimulus gradients) are similar to space–time gradient models; the next section discusses such models in detail.

2.09.5 Space–Time Gradients

Models building on the principle of space–time gradients start from the observation that spatial and temporal change must coincide in an image to produce motion. This insight leads to a measure of

velocity in an image (I) that is defined as the ratio of the temporal and spatial change:

$$V(x, t) = \frac{(\partial I/\partial t)}{(\partial I/\partial x)}$$

Mathematically, this measure defines the true velocity at every point in space and time. This is quite different from the outputs of the Reichardt and motion energy detector, which do not signal the same velocity for every spatial pattern (see Section 2.09.3.2.4). Moreover, because a contrast change will affect both the numerator and the denominator of the gradient model, the velocity estimate does not depend on the contrast of the image. In other models, such contrast-invariance is commonly built-in after motion estimation by processes of normalization and gain control (Heeger, D. J., 1992). Mathematically, therefore, this model truly is a better estimator of velocity. The question is, however, whether this estimate is used by the brain.

The biggest challenge for the model is that velocity becomes ill-defined in regions where the spatial gradient is zero. A number of solutions have been proposed to circumvent this problem. For instance, one can first find regions with spatial change (edges) and only then determine the ratio in a second processing stage (Marr, D. and Ullman, S., 1981). Other alternatives are to include higher-order spatiotemporal derivatives – one of which will likely be nonzero (Johnston, A. *et al.*, 1992), or to pool velocity estimates over space – the estimate will be well defined for at least some positions (Heeger, D. J. and Simoncelli, E. P., 1994).

The elementary computation required in this model is differentiation. While at first somewhat difficult to imagine, differentiation is easy to implement with simple neural elements. Consider a standard On center neuron. Its output can be described as the weighted sum of its inputs. If we assume the RF is a bell-shaped function (for instance a Gaussian), we can write its output as G^*I, the weighted sum of the image with the RF. The gradient model requires outputs that are related to dI/dx, for instance G^*dI/dx. Because this neuron's output is linear, the order of the weighted sum and differentiation operations does not matter: $G^*dI/dx = dG/dx^*I$. In other words an output proportional to the derivative of the image can be obtained from a simple linear neuron whose RF is shaped like the derivative of a bell-shaped function. Higher-order derivatives can be computed using increasingly complex RF structures (Koenderink, J. J. and Van Doorn, A. J., 1987). Looking at the spatial filters in the motion energy model (Figure 8) they are reasonably well described as each other's derivatives. The same is true for the temporal filters. In other words, the motion energy model implicitly relies on spatial and temporal derivatives. By reformulating the models, it can actually be shown that some variants of the gradient models are formally equivalent to motion energy models (Heeger, D. J. and Simoncelli, E. P., 1994; Bruce, V. *et al.*, 2003).

2.09.5.1 Behavioral Evidence

Given that some gradient schemes are formally equivalent to correlation and energy schemes for restricted classes of stimuli, it is difficult to distinguish among these schemes using behavioral methods. In line with this, Johnston A. *et al.* (1992) have demonstrated that many motion phenomena that have been interpreted in favor of the space–time correlation or orientation schemes, such as reverse-phi, are also found in their variant of the gradient scheme.

An attractive property of the gradient model, which is not found in the other schemes, is that it accounts quite naturally for some second-order motion percepts (Johnston, A. and Clifford, C. W., 1995a; Johnston, A. *et al.*, 1999; Benton, C. P. *et al.*, 2001). Correlation or energy-based schemes need to hypothesize a separate rectification stage for the processing of second-order motion (Chubb, C. and Sperling, G., 1988; Cavanagh, P. and Mather, G., 1989; Chubb, C. and Sperling, G., 1989).

In a perfect gradient model, the velocity estimate does not depend on the spatial frequency of the visual pattern. As discussed in Section 2.09.3.2.4, however, both insect and human motion perception do depend on the stimulus pattern. Similarly, the gradient model predicts no stimulus contrast dependence, but behavioral data in humans clearly show a strong effect of contrast on speed estimates (Thompson, P., 1982; Krekelberg, B. *et al.*, 2006b). It is not clear whether an imperfect implementation of the gradient scheme could account for these known imperfections in motion perception.

2.09.5.2 Physiological Evidence

Johnston A. (1992) has proposed a biologically plausible way to implement the gradient scheme in the

biological hardware of primary visual cortex. Johnston's solution to the problem of ill-defined velocities in image regions without luminance change is to determine a series expansion of the image. The best least-squares estimate of the velocity is then given by:

$$V = T/S$$

$$T = \frac{\partial^2 I}{\partial x^2}\frac{\partial^2 I}{\partial x \partial t} + \frac{\partial^3 I}{\partial x^3}\frac{\partial^3 I}{\partial^2 x \partial t} + \cdots + \frac{\partial^n I}{\partial x^n}\frac{\partial^n I}{\partial^{n-1} x \partial t}$$

$$S = \frac{\partial^2 I}{\partial x^2}\frac{\partial^2 I}{\partial x^2} + \frac{\partial^3 I}{\partial x^3}\frac{\partial^3 I}{\partial x^3} + \cdots + \frac{\partial^n I}{\partial x^n}\frac{\partial^n I}{\partial x^n}$$

Each term in T and S can be implemented with differentiating filters of second and higher order. Figure 11 shows a few representative examples of the space–time response maps that this gradient model would require. Just as the response maps of the Reichardt detector, none of these are oriented in space–time. Clearly, there is no lack of such simple cells in primary visual cortex (Livingstone, M. S. 1998; Conway, B. R. and Livingstone, M. S., 2003) and they could provide the input to a gradient motion detector. Hence, in principle, the required filters seem to be present in visual cortex. However, as discussed in Section 2.09.4.3.2, many direction-selective simple and complex cells have space–time oriented response maps; those cells match the components of the motion–energy model, but they do not seem to have a place in the gradient model.

The gradient model has not received as much physiological attention as the other models. The reason for this may be that the behavioral evidence suggests that motion perception is not as perfect as the gradient model predicts. In the fly, however, the gradient model was explicitly compared to the Reichardt detector and the data clearly speak in favor of the latter. To wit, both the spike output (Egelhaaf, M. *et al.*, 1989) and dendritic calcium concentrations (Haag, J. *et al.*, 2004) of the direction-selective fly H1 neuron show clear nondirection-selective modulations that follow the intensity modulations of the input. Moreover, both response measures are tuned for a particular temporal frequency and not a true velocity (Pattern dependence; see Section 2.09.3.2.4). These imperfections in the H1 neuron indicate that it does not use the gradient scheme to detect motion. Similarly, it has been shown that the speed tuning of neurons in the macaque middle temporal area strongly depend on contrast (Krekelberg, B. *et al.*, 2006b) and it is known that these neurons are closely linked to the animal's speed percept (Liu, J. and Newsome, W. T., 2005; Krekelberg, B. *et al.*, 2006a). This contrast dependence would not be expected in a motion detection mechanism that relies on the ratio of spatial and temporal gradients.

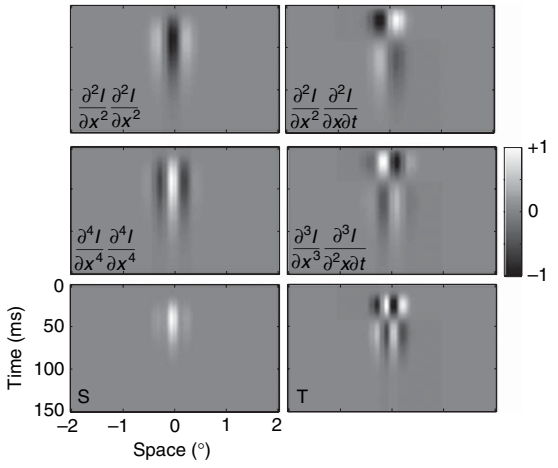

Figure 11 One-flash space–time response maps of the gradient model. This figure shows some of the differentiating filters that are required in the gradient model of Johnston, A. *et al.* (1992). Conventions as in Figure 5.

2.09.6 Conclusion

While motion itself is not a complicated phenomenon, motion detection by neural systems certainly is. The reason is that motion can be detected in so many different ways. Many of those detection mechanisms will not be perfect, but they may be good enough for a particular purpose. For instance, while the gradient model may balk at the imperfections of a motion energy detector, such details may not be important when deciding whether to stay put or flee an approaching predator. This view of motion detection – as a problem with many good but suboptimal solutions – suggests a less absolutist approach to the study of motion mechanisms.

Simulations of a perfect Reichardt, motion energy, or gradient-based model may appear to make strict and testable predictions, but small deviations from the ideal model can lead to significant changes in those predictions. The first factor to consider here is noise. Estimating RF properties such as space–time response maps and interaction maps with extracellular recordings is time consuming and even then results in relatively noisy estimates. For instance, a significant amount of noise could make the separable space–time

response map of a Reichardt detector look like the slanted space–time response map of the motion energy detector. Figure 1 illustrates the basic space–time filtering properties of the three models in a similar format. Without much difficulty, the motion energy filters can be seen as a blurred version of the Reichardt filters. Similarly, with enough measurement noise, the filters of the gradient scheme would be indistinguishable from those of the motion energy model. This shows that, due to their low signal-to-noise and the confounding influence of the unknown spike-generation nonlinearity, extracellular recordings alone may not be enough to really distinguish among these models. At the very least it shows that a small number of positive examples for a given model will not be enough to accept it. Intracellular recordings – with their ability to bypass the spike-generation nonlinearity – have revealed a surprising degree of linearity in the early stages of motion detection. It would be very interesting to see what these methods can reveal about later stages of motion detection such as the motion opponent responses in complex cells in the cat and cells in the middle temporal area of the macaque.

Apart from measurement noise, the possibility of an imperfect implementation of a motion detection scheme should also be taken into account. These imperfections sometimes lead to testable predictions (Borst, A. and Egelhaaf, M., 1990), but they can also blur the lines between the models. For Figure 12, I simulated an (extended) Reichardt detector that receives its input not from odd and even Gabor spatial filters (as in Figure 4), but from two even Gabor functions with a small spatial shift. The interaction map at the level of the leftward motion subunit shows elements that are oriented in space–time, one of the supposedly identifying markers of the motion energy model. Certainly, the space–time slant of this simulated imperfect Reichardt detector is much less clear than that of Figure 10, as well as that measured in detail in a complex cell in the cat (Emerson, R. C. *et al.*, 1992), but it shows that the lines between the models are not as clear as one might like.

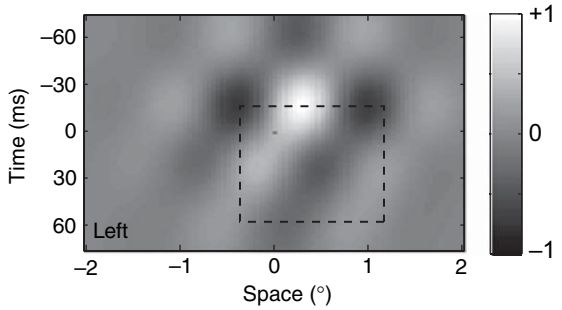

Figure 12 An imperfect Reichardt model. This space–time interaction map was calculated from an extended Reichardt detector in which the two spatial inputs are both even symmetric, but they are shifted such that the spatial receptive fields still have significant overlap. This overlap creates space–time slant in the area indicated by the dashed rectangle. Conventions as in Figure 6.

One can look at this issue from a quite different point of view. For the neuroscientist, models that are difficult to distinguish are a problem; they make the scientific story harder to follow and the conclusion less forceful. From the point of view of the brain, however, multiple models with similar prerequisites may be advantageous. Consider Figure 1 again; it shows that once the essential filters for a Reichardt detector are in place, building a motion energy detector should be relatively easy. Similarly, a slightly different combination of the same filters used for the motion energy detector could function as a gradient model. This suggests that the brain may not use motion detection mechanisms based exclusively on correlation, orientation, or gradients. Instead, multiple mechanisms could contribute at the same time and side-by-side. Although such mixing of multiple mechanisms does not appeal to the modeler with a keen eye for mathematical beauty, it may be the ugly reality of the perception of motion.

Acknowledgments

I gratefully acknowledge the support of the Charles and Johanna Busch Memorial Fund at Rutgers, The State University of New Jersey and thank Michael Ibbotson and Richard van Wezel for their helpful comments on the manuscript.

References

Adelson, E. H. and Bergen, J. R. 1985. Spatiotemporal energy models for the perception of motion. J. Opt. Soc. Am. A 2, 284–299.

Albrecht, D. G. and Geisler, W. S. 1991. Motion selectivity and the contrast-response function of simple cells in the visual cortex. Vis. Neurosci. 7, 531–546.

Albright, T. D. 1984. Direction and orientation selectivity of neurons in visual area MT of the macaque. J. Neurophysiol. 52, 1106–1130.

Albright, T. D. 1992. Form-cue invariant motion processing in primate visual cortex. Science 255, 1141–1143.

Alonso, J. M., Usrey, W. M., and Reid, R. C. 2001. Rules of connectivity between geniculate cells and simple cells in cat primary visual cortex. J. Neurosci. 21, 4002–4015.

Amthor, F. R. and Grzywacz, N. M. 1993. Inhibition in On–Off directionally selective ganglion cells of the rabbit retina. J. Neurophysiol. 69, 2174–2187.

Anderson, J. C., Binzegger, T., Kahana, O., Martin, K. A., and Segev, I. 1999. Dendritic asymmetry cannot account for directional responses of neurons in visual cortex. Nat. Neurosci. 2, 820–824.

Anstis, S. M. 1970. Phi movement as a subtraction process. Vision Res. 10, 1411–1430.

Anstis, S. M. and Rogers, B. J. 1975. Illusory reversal of visual depth and movement during changes of contrast. Vision Res. 15, 957–961.

Ariel, M. and Daw, N. W. 1982. Pharmacological analysis of directionally sensitive rabbit retinal ganglion cells. J. Physiol. 324, 161–185.

Baker, C. L., Jr. 2001. Linear filtering and nonlinear interactions in direction-selective visual cortex neurons: a noise correlation analysis. Vis. Neurosci. 18, 465–485.

Barlow, H. B. and Hill, R. M. 1963. Selective sensitivity to direction of movement in ganglion cells of the rabbit retina. Science 139, 412–414.

Barlow, H. B., Hill, R. M., and Levick, W. R. 1964. Retinal ganglion cells responding selectively to direction and speed of image motion in the rabbit. J. Physiol. 173, 377–407.

Benton, C. P., Johnston, A., Mcowan, P. W., and Victor, J. D. 2001. Computational modeling of non–Fourier motion: further evidence for a single luminance-based mechanism. J. Opt. Soc. Am. A Opt. Image Sci. Vis. 18, 2204–2208.

Blasdel, G. G. and Fitzpatrick, D. 1984. Physiological organization of layer 4 in macaque striate cortex. J. Neurosci. 4, 880–895.

Borg-Graham, L. J., Monier, C., and Fregnac, Y. 1998. Visual input evokes transient and strong shunting inhibition in visual cortical neurons. Nature 393, 369–373.

Borst, A. and Egelhaaf, M. 1990. Direction selectivity of blowfly motion-sensitive neurons is computed in a two-stage process. Proc. Natl. Acad. Sci. U S A 87, 9363–9367.

Bruce, V., Green, P. R., and Georgeson, M. A. 2003. Visual Perception: Physiology, Psychology and Ecology. Taylor & Francis, Inc.

Buchner, E. 1984. Behavioural Analysis of Spatial Vision in Insects. In: Photoreception and Vision in Invertebrates (*ed*. M. A. Ali). Plenum.

Burr, D. C. and Ross, J. 1982. Contrast sensitivity at high velocities. Vision Res. 22, 479–484.

Cai, D., Deangelis, G. C., and Freeman, R. D. 1997. Spatiotemporal receptive field organization in the lateral geniculate nucleus of cats and kittens. J. Neurophysiol. 78, 1045–1061.

Cavanagh, P. and Mather, G. 1989. Motion: the long and short of it. Spat. Vis 4, 103–129.

Chubb, C. and Sperling, G. 1988. Drift-balanced random stimuli: a general basis for studying non-Fourier motion perception. J. Opt. Soc. Am. A 5, 1986–2007.

Chubb, C. and Sperling, G. 1989. Two motion perception mechanisms revealed through distance-driven reversal of apparent motion. Proc. Natl. Acad. Sci. U S A 86, 2985–2989.

Churan, J. and Ilg, U. J. 2002. Flicker in the visual background impairs the ability to process a moving visual stimulus. Eur J. Neurosci. 16, 1151–1162.

Churchland, M. M., Priebe, N. J., and Lisberger, S. G. 2005. Comparison of the spatial limits on direction selectivity in visual areas MT and V1. J. Neurophysiol. 93, 1235–1245.

Conway, B. R. and Livingstone, M. S. 2003. Space–time maps and two-bar interactions of different classes of direction-selective cells in macaque V-1. J. Neurophysiol. 89, 2726–2742.

De Valois, R. L. and Cottaris, N. P. 1998. Inputs to directionally selective simple cells in macaque striate cortex. Proc. Natl. Acad. Sci. U S A 95, 14488–14493.

De Valois, R. L., Cottaris, N. P., Mahon, L. E., Elfar, S. D., and Wilson, J. A. 2000. Spatial and temporal receptive fields of geniculate and cortical cells and directional selectivity. Vision Res. 40, 3685–3702.

Deangelis, G. C., Ohzawa, I., and Freeman, R. D. 1993. Spatiotemporal organization of simple-cell receptive fields in the cat's striate cortex. II. Linearity of temporal and spatial summation. J. Neurophysiol. 69, 1118–1135.

Egelhaaf, M. and Borst, A. 1992. Are there separate On and Off channels in fly motion vision? Vis. Neurosci. 8, 151–164.

Egelhaaf, M., Borst, A., and Pilz, B. 1990. The role of GABA in detecting visual motion. Brain Res. 509, 156–160.

Egelhaaf, M., Borst, A., and Reichardt, W. 1989. Computational structure of a biological motion-detection system as revealed by local detector analysis in the fly's nervous system. J. Opt. Soc. Am. A 6, 1070–1087.

Emerson, R. C. and Gerstein, G. L. 1977a. Simple striate neurons in the cat. I. Comparison of responses to moving and stationary stimuli. J. Neurophysiol. 40, 119–135.

Emerson, R. C. and Gerstein, G. L. 1977b. Simple striate neurons in the cat. II. Mechanisms underlying directional asymmetry and directional selectivity. J. Neurophysiol. 40, 136–155.

Emerson, R. C., Bergen, J. R., and Adelson, E. H. 1992. Directionally selective complex cells and the computation of motion energy in cat visual cortex. Vision Res. 32, 203–218.

Emerson, R. C., Citron, M. C., Vaughn, W. J., and Klein, S. A. 1987. Nonlinear directionally selective subunits in complex cells of cat striate cortex. J. Neurophysiol. 58, 33–65.

Franceschini, N., Riehle, A., and Le Nestour, A. 1989. Directionally Selective Motion Detection by Insect Neurons. In: Facets of Vision (*eds*. D. G. Stavenga and R. C. Hardie), pp. 360–390. Springer.

Fried, S. I., Munch, T. A., and Werblin, F. S. 2002. Mechanisms and circuitry underlying directional selectivity in the retina. Nature 420, 411–414.

Fried, S. I., Munch, T. A., and Werblin, F. S. 2005. Directional selectivity is formed at multiple levels by laterally offset inhibition in the rabbit retina. Neuron 46, 117–127.

Ganz, L. and Felder, R. 1984. Mechanism of directional selectivity in simple neurons of the cat's visual cortex analyzed with stationary flash sequences. J. Neurophysiol. 51, 294–324.

Gaska, J. P., Jacobson, L. D., Chen, H. W., and Pollen, D. A. 1994. Space–time spectra of complex cell filters in the macaque monkey: a comparison of results obtained with pseudowhite noise and grating stimuli. Vis. Neurosci. 11, 805–821.

Goodwin, A. W., Henry, G. H., and Bishop, P. O. 1975. Direction selectivity of simple striate cells: properties and mechanism. J. Neurophysiol. 38, 1500–1523.

Grzywacz, N. M. and Amthor, F. R. 1993. Facilitation in On–Off directionally selective ganglion cells of the rabbit retina. J. Neurophysiol. 69, 2188–2199.

Grzywacz, N. M. and Koch, C. 1987. Functional properties of models for direction selectivity in the retina. Synapse 1, 417–434.

Haag, J., Denk, W., and Borst, A. 2004. Fly motion vision is based on Reichardt detectors regardless of the signal-to-noise ratio. Proc. Natl. Acad. Sci. U. S. A. 101, 16333–16338.

Hassenstein, B. and Reichardt, W. 1956. Systemtheoretische Analyse der Zeit-, Reihenfolgen und Vorzeichenauswertung bei der Bewegungsperzeption des Russelkaefers Chlorophanus. Z. Naturforsch. 11B, 513–524.

Heeger, D. J. 1992. Normalization of cell responses in cat striate cortex. Vis. Neurosci. 9, 181–197.

Heeger, D. J. and Simoncelli, E. P. 1994. Model of Visual Motion Sensing. In: Spatial Vision in Humans and Robots (*eds*. L. Harris and M. Jenkin), pp. 367–392. Cambridge University Press.

Hirsch, J. A., Alonso, J. M., Reid, R. C., and Martinez, L. M. 1998. Synaptic integration in striate cortical simple cells. J. Neurosci. 18, 9517–9528.

Horridge, G. A. and Marcelja, L. 1991. A test for multiplication in insect directional motion detectors. Philos. Trans. R. Soc. Lond. B Biol. Sci. 331, 199–204.

Hubel, D. H. and Wiesel, T. N. 1959. Receptive fields of single neurones in the cat's striate cortex. J. Physiol. 148, 574–591.

Hubel, D. H. and Wiesel, T. N. 1962. Receptive fields, binocular interaction and functional architecture in the cat's visual cortex. J. Physiol. 160, 106–154.

Ibbotson, M. R. and Clifford, C. W. 2001. Interactions between On and Off signals in directional motion detectors feeding the not of the wallaby. J. Neurophysiol. 86, 997–1005.

Ibbotson, M. R., Clifford, C. W., and Mark, R. F. 1999. A quadratic nonlinearity underlies direction selectivity in the nucleus of the optic tract. Vis. Neurosci. 16, 991–1000.

Jagadeesh, B., Wheat, H. S., and Ferster, D. 1993. Linearity of summation of synaptic potentials underlying direction selectivity in simple cells of the cat visual cortex. Science 262, 1901–1904.

Jagadeesh, B., Wheat, H. S., Kontsevich, L. L., Tyler, C. W., and Ferster, D. 1997. Direction selectivity of synaptic potentials in simple cells of the cat visual cortex. J. Neurophysiol. 78, 2772–2789.

Johnston, A. and Clifford, C. W. 1995a. Perceived motion of contrast-modulated gratings: predictions of the multi-channel gradient model and the role of full-wave rectification. Vision Res. 35, 1771–1783.

Johnston, A. and Clifford, C. W. 1995b. A unified account of three apparent motion illusions. Vision Res. 35, 1109–1123.

Johnston, A., Benton, C. P., and McOwan, P. W. 1999. Induced motion at texture-defined motion boundaries. Proc. R. Soc. Lond. B Biol. Sci 266, 2441–2450.

Johnston, A., McOwan, P. W., and Buxton, H. 1992. A computational model of the analysis of some first-order and second-order motion patterns by simple and complex cells. Proc. R. Soc. Lond. B Biol. Sci. 250, 297–306.

Koch, C., Poggio, T., and Torre, V. 1983. Nonlinear interactions in a dendritic tree: localization, timing, and role in information processing. Proc. Natl. Acad. Sci. U. S. A. 80, 2799–2802.

Koenderink, J. J. and Van Doorn, A. J. 1987. Representation of local geometry in the visual system. Biol. Cybern. 55, 367–375.

Kontsevich, L. L. 1995. The nature of the inputs to cortical motion detectors. Vision Res. 35, 2785–2793.

Krekelberg, B. and Albright, T. D. 2005. Motion mechanisms in macaque MT. J. Neurophysiol. 93, 2908–2921.

Krekelberg, B., Van Wezel, R. J., and Albright, T. D. 2006a. Adaptation in macaque MT reduces perceived speed and improves speed discrimination. J. Neurophysiol. 95, 255–270.

Krekelberg, B., Van Wezel, R. J., and Albright, T. D. 2006b. Interactions between speed and contrast tuning in the middle temporal area: implications for the neural code for speed. J. Neurosci. 26, 8988–8998.

Kuffler, S. W. 1953. Discharge patterns and functional organization of mammalian retina. J. Neurophysiol. 16, 37–68.

Liu, J. and Newsome, W. T. 2005. Correlation between speed perception and neural activity in the middle temporal visual area. J. Neurosci. 25, 711–722.

Livingstone, M. S. 1998. Mechanisms of direction selectivity in macaque V1. Neuron 20, 509–526.

Livingstone, M. S. and Conway, B. R. 2003. Substructure of direction-selective receptive fields in macaque V1. J. Neurophysiol. 89, 2743–2759.

Livingstone, M. S., Pack, C. C., and Born, R. T. 2001. Two-dimensional substructure of MT receptive fields. Neuron 30, 781–793.

Lu, Z. L. and Sperling, G. 1999. Second-order reversed phi. Percept. Psychophys. 61, 1075–1088.

Malpeli, J. G., Schiller, P. H., and Colby, C. L. 1981. Response properties of single cells in monkey striate cortex during reversible inactivation of individual lateral geniculate laminae. J. Neurophysiol. 46, 1102–1119.

Marmarelis, P. Z. and Marmarelis, V. Z. 1978. Analysis of Physiological Systems: The White–Noise Approach. Plenum.

Marr, D. 1982. Vision: A Computational Investigation into the Human Representation and Processing of Visual Information. W. H. Freeman.

Marr, D. and Ullman, S. 1981. Directional selectivity and its use in early visual processing. Proc. R. Soc. Lond. B Biol. Sci 211, 151–180.

Marrocco, R. T. 1976. Sustained and transient cells in monkey lateral geniculate nucleus: conduction velocites and response properties. J. Neurophysiol. 39, 340–353.

Mastronarde, D. N. 1987a. Two classes of single-input X-cells in cat lateral geniculate nucleus. I. Receptive-field properties and classification of cells. J. Neurophysiol. 57, 357–380.

Mastronarde, D. N. 1987b. Two classes of single-input X-cells in cat lateral geniculate nucleus. II. Retinal inputs and the generation of receptive-field properties. J. Neurophysiol. 57, 381–413.

Maunsell, J. H. and Van Essen, D. C. 1983. Functional properties of neurons in middle temporal visual area of the macaque monkey. I. Selectivity for stimulus direction, speed, and orientation. J. Neurophysiol. 49, 1127–1147.

Maunsell, J. H., Nealey, T. A., and Depriest, D. D. 1990. Magnocellular and parvocellular contributions to responses in the middle temporal visual area (MT) of the macaque monkey. J. Neurosci. 10, 3323–3334.

McCann, G. D. and MacGinitie, G. F. 1965. Optomotor response studies of insect vision. Proc. R. Soc. Lond. B Biol. Sci. 163, 369–401.

Mclean, J. and Palmer, L. A. 1989. Contribution of linear spatiotemporal receptive field structure to velocity selectivity of simple cells in area 17 of cat. Vision Res. 29, 675–679.

Mclean, J., Raab, S., and Palmer, L. A. 1994. Contribution of linear mechanisms to the specification of local motion by simple cells in areas 17 and 18 of the cat. Vis. Neurosci. 11, 271–294.

Merigan, W. H. and Maunsell, J. H. 1993. How parallel are the primate visual pathways? Annu. Rev. Neurosci. 16, 369–402.

Mikami, A., Newsome, W. T., and Wurtz, R. H. 1986. Motion selectivity in macaque visual cortex. II. Spatiotemporal range of directional interactions in MT and V1. J. Neurophysiol. 55, 1328–1339.

Morgan, M. J. and Chubb, C. 1999. Contrast facilitation in motion detection: evidence for a Reichardt detector in human vision. Vision Res. 39, 4217–4231.

Movshon, J. A., Thompson, I. D., and Tolhurst, D. J. 1978a. Receptive field organization of complex cells in the cat's striate cortex. J. Physiol. 283, 79–99.

Movshon, J. A., Thompson, I. D., and Tolhurst, D. J. 1978b. Spatial summation in the receptive fields of simple cells in the cat's striate cortex. J. Physiol. 283, 53–77.

Nassi, J. J., Lyon, D. C., and Callaway, E. M. 2006. The parvocellular LGN provides a robust disynaptic input to the visual motion area MT. Neuron 50, 319–327.
Nealey, T. A. and Maunsell, J. H. 1994. Magnocellular and parvocellular contributions to the responses of neurons in macaque striate cortex. J. Neurosci. 14, 2069–2079.
Pack, C. C., Conway, B. R., Born, R. T., and Livingstone, M. S. 2006. Spatiotemporal structure of nonlinear subunits in macaque visual cortex. J. Neurosci. 26, 893–907.
Perrone, J. A. 2005. Economy of scale: a motion sensor with variable speed tuning. J Vis. 5, 28–33.
Perrone, J. A. 2006. A single mechanism can explain the speed tuning properties of MT and V1 complex neurons. J. Neurosci. 26, 11987–11991.
Perrone, J. A. and Thiele, A. 2001. Speed skills: measuring the visual speed analyzing properties of primate MT neurons. Nat. Neurosci. 4, 526–532.
Perrone, J. A. and Thiele, A. 2002. A model of speed tuning in MT neurons. Vision Res. 42, 1035–1051.
Peterson, M. R., Li, B., and Freeman, R. D. 2004. The derivation of direction selectivity in the striate cortex. J. Neurosci. 24, 3583–3591.
Poggio, T. and Reichardt, W. 1973. Considerations on Models of movement detection. Kybernetik 13, 223–227.
Poggio, T. and Reichardt, W. 1981. Characterization of Nonlinear Interactions in the Fly's Visual System. In: Theoretical Approaches in Neurobiology (*eds*. W. Reichardt and T. Poggio), pp. 64–84. MIT Press.
Priebe, N. J. and Ferster, D. 2005. Direction selectivity of excitation and inhibition in simple cells of the cat primary visual cortex. Neuron 45, 133–145.
Priebe, N. J., Cassanello, C. R., and Lisberger, S. G. 2003. The neural representation of speed in macaque area MT/V5. J. Neurosci. 23, 5650–5661.
Priebe, N. J., Lisberger, S. G., and Movshon, J. A. 2006. Tuning for spatiotemporal frequency and speed in directionally selective neurons of macaque striate cortex. J. Neurosci. 26, 2941–2950.
Qian, N. and Andersen, R. A. 1994. Transparent motion perception as detection of unbalanced motion signals. II. Physiology. J. Neurosci. 14, 7367–7380.
Reichardt, W. 1961. Autocorrelation, a Principle for the Evaluation of Sensory Information by the Central Nervous System. In: Sensory Communication (*ed*. W. A. Rosenblith). pp. 303–317. MIT Press.
Reid, R. C., Soodak, R. E., and Shapley, R. M. 1987. Linear mechanisms of directional selectivity in simple cells of cat striate cortex. Proc. Natl. Acad. Sci. U. S. A. 84, 8740–8744.
Reid, R. C., Soodak, R. E., and Shapley, R. M. 1991. Directional selectivity and spatiotemporal structure of receptive fields of simple cells in cat striate cortex. J. Neurophysiol. 66, 505–529.
Saul, A. B. and Humphrey, A. L. 1990. Spatial and temporal response properties of lagged and nonlagged cells in cat lateral geniculate nucleus. J. Neurophysiol. 64, 206–224.
Saul, A. B. and Humphrey, A. L. 1992. Evidence of input from lagged cells in the lateral geniculate nucleus to simple cells in cortical area 17 of the cat. J. Neurophysiol. 68, 1190–1208.
Schiller, P. H. and Malpeli, J. G. 1978. Functional specificity of lateral geniculate nucleus laminae of the rhesus monkey. J. Neurophysiol. 41, 788–797.
Schmid, A. and Bülthoff, H. 1988. Using neuropharmacology to distinguish between excitatory and inhibitory movement detection mechanisms in the fly. *Calliphora erythrocephala*. Biol. Cybern. 59, 71–80.
Sillito, A. M. 1977. Inhibitory processes underlying the directional specificity of simple, complex and hypercomplex cells in the cat's visual cortex. J. Physiol. 271, 699–720.
Smith, A. T. and Edgar, G. K. 1990. The influence of spatial frequency on perceived temporal frequency and perceived speed. Vision Res. 30, 1467–1474.
Snowden, R. J., Treue, S., Erickson, R. G., and Andersen, R. A. 1991. The response of area MT and V1 neurons to transparent motion. J. Neurosci. 11, 2768–2785.
Solomon, J. A., Chubb, C., John, A., and Morgan, M. 2005. Stimulus contrast and the Reichardt detector. Vision Res. 45, 2109–2117.
Stromeyer, C. F., 3rd., Kronauer, R. E., Madsen, J. C., and Klein, S. A. 1984. Opponent-movement mechanisms in human vision. J. Opt. Soc. Am. A 1, 876–884.
Taylor, W. R. and Vaney, D. I. 2002. Diverse synaptic mechanisms generate direction selectivity in the rabbit retina. J. Neurosci. 22, 7712–7720.
Thompson, P. 1982. Perceived rate of movement depends on contrast. Vision Res. 22, 377–380.
Thorson, J. 1966a. Small-signal analysis of a visual reflex in the locust. I. Input parameters. Kybernetik 3, 41–53.
Thorson, J. 1966b. Small-signal analysis of a visual reflex in the locust. II. Frequency dependence. Kybernetik 3, 53–66.
Tolhurst, D. J. and Dean, A. F. 1991. Evaluation of a linear model of directional selectivity in simple cells of the cat's striate cortex. Vis. Neurosci. 6, 421–428.
Torre, V. and Poggio, T. 1978. A synaptic mechanism possibly underlying directional selectivity to motion. Proc. R. Soc. Lond. (Biol.) 202, 409–416.
Touryan, J., Lau, B., and Dan, Y. 2002. Isolation of relevant visual features from random stimuli for cortical complex cells. J. Neurosci. 22, 10811–10818.
van Santen, J. P. and Sperling, G. 1984. Temporal covariance model of human motion perception. J. Opt. Soc. Am. A 1, 451–473.
van Santen, J. P. and Sperling, G. 1985. Elaborated Reichardt detectors. J. Opt. Soc. Am. A 2, 300–321.
van Wezel, R. J., Lankheet, M. J., Verstraten, F. A., Maree, A. F., and Van De Grind, W. A. 1996. Responses of complex cells in area 17 of the cat to bi-vectorial transparent motion. Vision Res. 36, 2805–2813.
Watson, A. B. and Ahumada, A. J. 1985. Model of human visual-motion sensing. J. Opt. Soc. Am. A Optics Image Sci. (Washington) 2, 322–342.
Watson, A. B., Baker, C. L., Jr., and Farrell, J. E. 1986. Window of visibility: a psychophysical theory of fidelity in time-sampled visual motion displays. J. Opt. Soc. Am. A 3, 300–307.
Wehrhahn, C. and Rapf, D. 1992. On- and Off-pathways form separate neural substrates for motion perception: psychophysical evidence. J. Neurosci. 12, 2247–2250.
Zaagman, W. H., Mastebroek, H. A., Buyse, T., and Kuiper, J. W. 1976. Receptive field characteristics of a directionally selective movement detector in the visual system of the blowfly. J. Comp. Physiol. A 116, 39–50.
Zanker, J. M., Srinivasan, M. V., and Egelhaaf, M. 1999. Speed tuning in elementary motion detectors of the correlation type. Biol. Cybern. 80, 109–116.

2.10 Cortical Processing of Visual Motion

C H McCool and K H Britten, University of California, Davis, CA, USA

© 2008 Elsevier Inc. All rights reserved.

2.10.1	**Introduction**	157
2.10.2	**Local Motion Mechanisms: V1**	158
2.10.2.1	Simple Cells and Linear Motion Mechanisms	158
2.10.2.2	Nonlinear Motion Mechanisms	160
2.10.2.3	Complex Cells and Motion Energy	161
2.10.2.4	Circuitry Underlying Local Motion Processing	162
2.10.2.5	The Spatial Scale of Local Motion Operations	163
2.10.2.6	Extrastriate Local Motion Processing	164
2.10.3	**Medium Scale Motion Processing: Area MT**	165
2.10.3.1	Anatomy and Connections	165
2.10.3.2	Physiological Properties and Functional Organization	166
2.10.3.3	Motion Integration: The Aperture Problem	167
2.10.3.4	Integration for Speed Perception	169
2.10.3.5	The Problem with Integration: Segmentation Is Needed Too	169
2.10.3.6	The Effect of Contrast	170
2.10.3.7	Relating MT to Perception	171
2.10.3.8	Adaptation	172
2.10.3.9	Attention and Memory	173
2.10.3.10	Human MT	174
2.10.4	**Global Motion**	175
2.10.4.1	What Is Optic Flow?	175
2.10.4.2	Area Medial Superior Temporal	176
2.10.4.3	Extraretinal Inputs	177
2.10.4.4	Relating Media Superior Temporal Area to Perception	179
2.10.4.5	Other Areas with Optic Flow Responses	179
2.10.4.6	Higher Motion Areas in Cat Visual Cortex	180
2.10.5	**Conclusion**	181
References		181

2.10.1 Introduction

Motion is one of the most important submodalities of vision, and specialized mechanisms to analyze movement are ubiquitous among visual creatures. Perceptually, there is good evidence that motion is a primary visual attribute like color, even though it is not directly available on the sensory epithelium as color is. Motion requires calculation, which makes the neural substrates of motion analysis particularly fruitful for study. The history of the study of motion analysis has benefited from a synergy between computational, physiological, and perceptual approaches.

Visual motion arises from the independent motion of objects in the visual environment or from the motion of the observer or a receptor surface – the retina, and frequently from both at once. Figure 1 shows a typical visual scene for a moving observer. This scene contains a multiplicity of moving objects, each with many contours. But all the retina receives is a complex time- and space-varying luminance pattern, from which we must reconstruct the physical causes, in order to generate appropriate behavior. This is not as simple as it first appears, for at least a couple of reasons. First and foremost, motion occurs in three dimensions, and the retina reduces this to a two-dimensional image. Second, other factors besides object motion can lead to time-varying luminance patterns on the retina – most notably changes in illumination – and the visual system must distinguish these from the real thing. Last, occlusion of one object by another or transparent motion can leave

Figure 1 Soccer World Cup 2006. Shows multiple objects, which move in three dimensions for the typical observer.

very complex patterns of local motions on the retina. So, the problem for motion analysis, as for many other visual calculations, is to take this raw, often ambiguous local data and calculate (or infer, as Helmholtz emphasized) the object and scene motions. It is not yet known how the visual system accomplishes this, but many parts of this problem are becoming fairly well understood. It is becoming increasingly clear that numerous operations at both local and global levels are happening in parallel at different levels of the motion system.

Most theoretical accounts of motion analysis are hierarchical in nature, and it comes as little surprise that there is also a hierarchy for processing motion in the cortex of primates – which is the focus of this chapter. In our description of the biology of motion processing, we will follow the functional logic of this hierarchy, which starts at a small spatial scale and ends at a large (global) spatial scale. Our point of view will be dominated by the physiology, but we will attempt to draw parallels to anatomy and computation whenever possible.

Not surprisingly, the central pathway implicated in motion analysis is also arranged hierachically. This pathway consists of a number of connected cortical areas, beginning in primary visual cortex. The defining property of these areas is the presence of directional selectivity. All areas in the figure have cells that signal the direction of moving stimuli in their firing rates, though in some of these areas only a fraction of neurons display this property. What we are emphasizing here, though, is the progressive change in the spatial scale of motion processing, from very local operations early in the cortical hierarchy through to very large-scale representations at the highest levels of the system. As we follow this pathway, we will attempt to capture what is known of the operations at each level, while also describing what remains unknown.

2.10.2 Local Motion Mechanisms: V1

2.10.2.1 Simple Cells and Linear Motion Mechanisms

Motion processing begins with local operations that detect the progression of image contrast across space and time. Local feature motion is best portrayed in a space–time diagram, of which several examples are shown in Figure 2.

What stands out in these figures is the presence of space–time orientation. Just as the analysis of stationary contours requires matched, orientation-selective receptive fields (RFs), the analysis of local motion requires RFs that are oriented in space and time (Poggio, T. and Reichardt, W., 1973; Borst, A. and Egelhaaf, M., 1989). Neurons with this property have been found early in the visual systems of a wide range of species, including insects (Egelhaaf, M. and Borst, A., 1993; Srinivasan, M. V. *et al.*, 1999; Ibbotson, M. R., 2001), birds (Frost, B. J. *et al.*, 1990; Wolf-Oberhollenzer, F. and Kirschfeld, K., 1994), reptiles (Fleishman, L. J., 1986; Wilke, S. D. *et al.*, 2001), fish (Wartzok, D. and Marks, W. B., 1973), and of course mammals (Ibbotson, M. R. *et al.*, 1994; Taylor, W. R. and Vaney, D. I., 2002). Motion processing in rabbits is particularly well studied, as they possess numerous

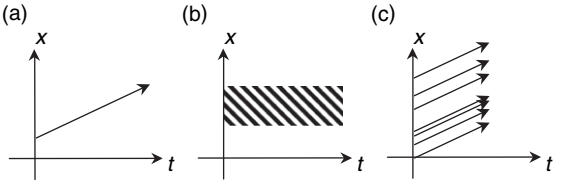

Figure 2 Space–time diagrams plotting an object's equation of motion $x(t)$, which is its spatial location as a function of time. (a) This diagram gives a visual picture of a bar's motion, with each point on the line representing both a location (collapsed across y) and a time. The straight line illustrated represents uniform motion, i.e., the object is moving at a constant speed. The slope of the line is equal to the velocity of the object at that moment. This object is moving rightward along x. (b) Space–time diagram for a moving grating, and (c) a coherently moving dot field.

direction-selective retinal ganglion cells (Barlow, H. B. *et al.*, 1964; Barlow, H. B. and Levick, W. R., 1965). As we focus on cortical mechanisms, this subject is outside our scope, and the reader is referred to recent reviews on the subject (Taylor, W. R. and Vaney, D. I., 2003; Poznanski, R. R., 2005).

In the well-studied geniculocortical pathway of the monkey, local motion detectors are first prominent in area V1, so we will focus on this area first. David Hubel and Torsten Wiesel (1962) recorded responses from striate neurons during the presentation of visual stimuli (moving bars of light) to the RF. In 1981, they won a Nobel Prize for their description of cells in V1 that respond preferentially to particular orientations or directions of movement. An example of a V1 simple cell, selective for both orientation and direction (DS), is shown in Figure 3. This cell is a simple cell, as evidenced by the distinct subregions of the RF responsive to bright and dark stimuli (green and red, respectively).

One key proposal from the work of Hubel D. H. and Wiesel T. N., which has largely been supported by decades of experimental testing, is the presence of a processing hierarchy through primary visual cortex. It is self-evident that RFs such as that shown in Figure 3 must be constructed from simpler (nonoriented) precursors. The key property evident in this RF is its slant, which can be phrased more accurately as space–time inseparability. What this term captures is that the temporal dynamics of the cell depend on the spatial location; this is what gives the slant to the RF. This property could emerge, in principle, from simpler subunits either in the direct input from the LGN or from other cortical neurons.

Figure 4 places the neuron shown in Figure 3 into a hierarchy of processing. Figure 4(a) shows an example of a nondirectional and nonorientation-tuned LGN neuron, which is quite similar to the RF of the nondirectional (space–time separable) simple cell in Figure 4(b). The similarity of the two RFs is allowed by the fact that these figures collapse across the two dimensions of space, concealing the orientation selectivity of the simple cell in Figure 4(b).

Numerous experiments have tested the adequacy of such linear mechanisms for producing the directional responses of simple cells to moving stimuli. In general, the approach is to use the superposition of successive stationary stimuli to predict the response to a moving stimulus (Reid, R. C. *et al.*, 1987; McLean, J. and Palmer, L. A., 1989; Reid, R. C. *et al.*, 1991; Jagadeesh, B. *et al.*, 1993; Livingstone, M. S., 1998). McLean J. and Palmer L. A. (1989) and Reid R. C. *et al.* (1991) found that the slant in the spatiotemporal RF correlated well with the DS and speed tuning of the cells. Thus, for these neurons, simple linear mechanisms can produce a good account of their directionality. However, while the linear mechanisms predicted the sign of the directionality and the speed tuning rather well, there was typically an underestimation of the magnitude of the directionality of the cells. Specifically, the response to motion in the nonpreferred direction seemed to be suppressed below the linear prediction (Reid, R. C. *et al.*, 1987).

The neuronal circuitry underlying the space–time inseparable RF remains unknown, but at least two

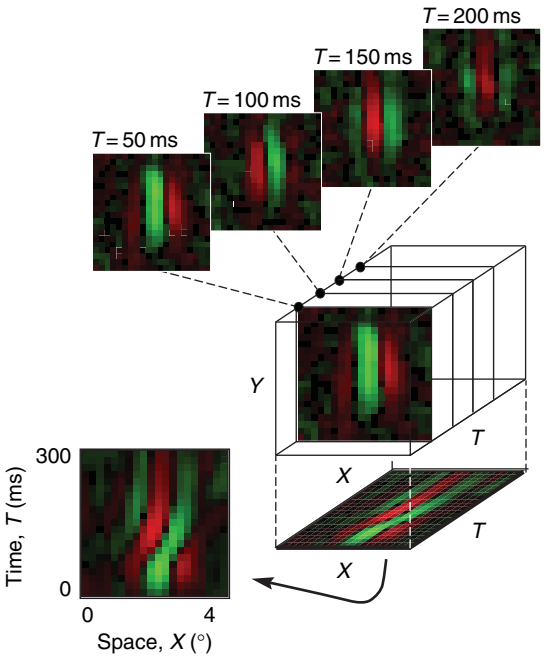

Figure 3 Example of a neuron tuned for orientation in both space and time. The map is formed by presenting white noise stimuli, and averaging to reveal what locations and times effectively trigger spiking. This procedure reveals the linear RF of a visual neuron. The horizontal axis is space (0–4°), vertical axis is time (0–300 ms), going backward in time. Time zero is at the bottom. This cell prefers leftward motion, because of the slant of the subregions in space and time. A contour or grating moving from right to left will first trigger long-latency responses, which can then sum with the shorter-latency responses from points farther to the left, if the stimulus is moving at a speed matched to the slant of the RF. See Reid, R. C., Soodak, R. E., and Shapley, R. M. 1991. Directional selectivity and spatiotemporal structure of receptive fields of simple cells in cat striate cortex. J. Neurophysiol. 66, 505–529. Copyright DeAngelis, G. C., Ohzawa, I., and Freeman, R. D. 1993. Spatiotemporal organization of simple-cell receptive fields in the cat s striate cortex. I. General characteristics and postnatal development. J. Neurophysiol. 69, 1091–1117.

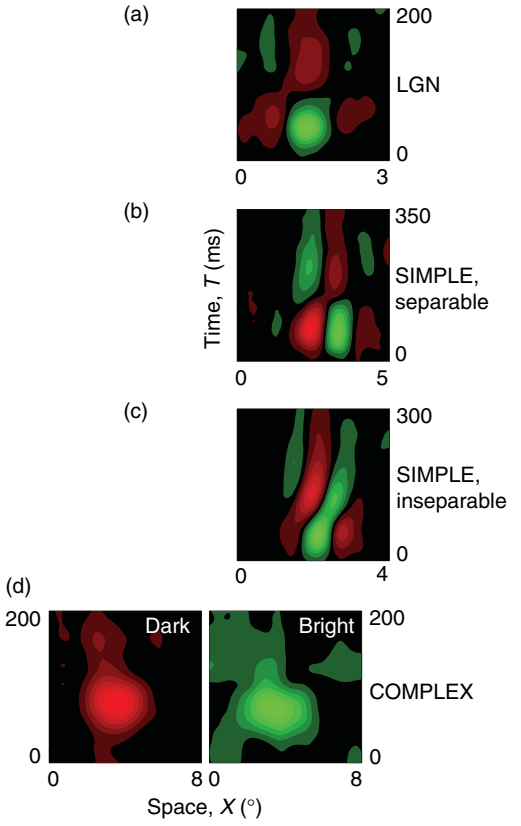

Figure 4 Spatiotemporal receptive field (RF) profiles (*X–T* plots) for neurons in the lateral geniculate nucleus (LGN) and V1 of the cat. The RF has been collapsed along the *Y*-axis. Subregions shown in green and red represent excitation to bright (ON) and dark (OFF) stimuli, respectively. (a) An *X–T* profile for a typical ON center *X*-cell from the LGN. The center and surround reverse sign at T > 50 ms. (b) An *X–T* profile for a simple cell with a space–time separable, not directionally selective, RF. For *T* > 100 ms, each subregion reverses polarity, so that the ON subregion is now on the left. (c) The same simple cell for which two-dimensional spatial profiles are shown in Figure 3, with a clearly inseparable *X–T* profile. Note how the spatial arrangement of ON and OFF subregions (i.e., the spatial phase of the RF) changes gradually with time. Note that the subregions are tilted in the space–time domain. The directional selectivity of this cell is leftward. (d) *X–T* profiles are shown for a complex cell. Responses to bright and dark stimuli are shown separately because these regions overlap extensively. From DeAngelis, G. C., Ohzawa, I., and Freeman, R. D. 1995. Receptive-field dynamics in the central visual pathways. Trends Neurosci. 18, 451–458.

possibilities exist. For both, there is a need to provide input to the directional cell from inputs that are slightly offset in space, with one slightly delayed in time relative to the other. Neurons tuned for different speeds could be constructed by employing inputs separated by different amounts in space and time. Theory suggests that if two inputs are in use – and most models are built this way to be tractable – they should be arranged in spatial and temporal quadrature (Watson, A. B. and Ahumada, A. J., Jr., 1983), which is a formalism for a quarter-cycle offset in both space and time.

Saul A. B. and Humphrey A. L. (1990) have identified two classes of X cells in the LGN of the cat, termed lagged and nonlagged, which have slightly different response latencies, close to this theoretical ideal. They have proposed that these two classes provide the necessary input timing delays to produce directional simple cells in striate cortex.

Another circuit possibility for directional simple cells is that the space–time inseparable RF is constructed from cortical inputs with suitable spatial and temporal separation, rather than directly from geniculate inputs. In monkeys, there is less agreement that separate populations of lagged and nonlagged LGN neurons exist. However, magnocellular (M) and parvocellular (P) LGN neurons might supply appropriate timing differences to subpopulations of V1 neurons (De Valois, R. L. *et al.*, 2000; Conway, B. R. and Livingstone, M. S., 2003). The fast biphasic responses of the (M) V1 cells and the slower monophasic responses of the P V1 cells differ in temporal phase by about a quarter of a cycle and could underlie direction selectivity. Direction selective V1 simple cells could combine the signals from subpopulations of non-DS V1 cells, which differ in their origins, either (M) or (P). In a similar vein, it has been argued that (M) neurons are not all purely transient, that some show sustained responses, and these could combine together to produce direction selectivity (Saul, A. B. *et al.*, 2005). In addition, a pair of separable (nondirectional) simple cell RFs might have even- and odd-symmetry (approximate spatial quadrature) and different temporal delays, to provide the correct inputs. One specific proposal is illustrated in Figure 5. Note the relatively rapid dynamics of the right-hand input, and the spatial phase difference between the two (Peterson, M. R. *et al.*, 2004).

2.10.2.2 Nonlinear Motion Mechanisms

While the linear, oriented RFs of simple cells can be directionally selective, the bulk of directional neurons are not well described by such simple models. Three broad classes of nonlinearity have been proposed, and direct evidence for each of the three has been found. First, divisive nonlinearity can be used to veto responses to nonpreferred motion. This sort of

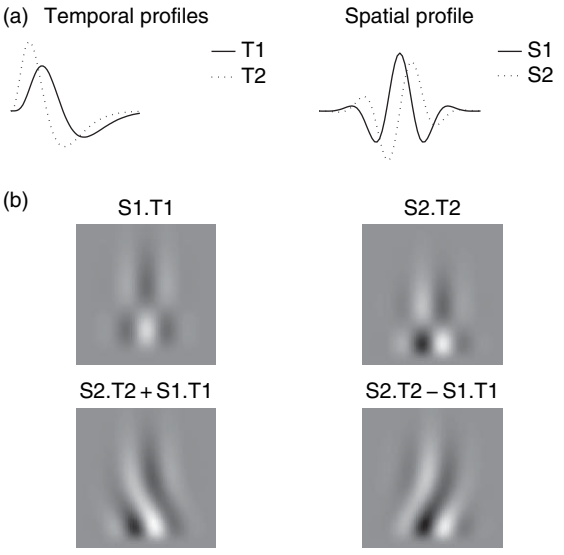

Figure 5 (a) Spatial (S1, S2) and temporal (T1, T2) filters that can be combined to produce (b) a linear motion sensor. The first stage of the linear motion sensor consists of spatiotemporal filters, each of which is the product of one of the two spatial filters and one of the two temporal filters. Space–time plots of the spatiotemporal sensitivity profiles of the two filters are shown in the upper part of (b), labeled S1, T1 and S2, T2. From Derrington, A. M., Allen, H. A., and Delicato, L. S. 2004. Visual mechanisms of motion analysis and motion perception. Annu. Rev. Psych. 55, 181–205.

operation appears to underlie the directionally selective responses of rabbit retinal ganglion cells (Hildreth, E. C. and Koch, C., 1987). Second, multiplicative operations can be used to facilitate preferred direction responses. This kind of model is consistent with the well-studied directional responses underlying optomotor responses in insects (Borst, A. and Egelhaaf, M., 1989; Egelhaaf, M. and Borst, A., 1993), and is mathematically described by a correlation operation (Hassenstein, B. and Reichardt, W., 1956). Last, a squaring operation is at the heart of motion energy models for directionality. Because this kind of operation is commonly related to the responses of directionally selective complex cells in cortex, we will primarily focus on this last class of model.

2.10.2.3 Complex Cells and Motion Energy

The defining feature of a complex cell, which differentiates it from a simple cell, is the absence of distinct RF subregions (see Figure 4(d)). For a grating stimulus, simple cell responses depend on the spatial phase of the stimulus, so that maximum response occurs when the bright parts of the stimulus are aligned with the on-region of the RF. In contrast, complex cells do not have RF subregions, making them insensitive to the phase of the stimulus, and they will respond to an appropriately oriented bar or grating anywhere within the RF.

Importantly, where simple cells linearly combine local responses, complex cells do so nonlinearly (Hubel, D. H. and Wiesel, T. N., 1962; Movshon, J. A. *et al.*, 1978). One significant nonlinearity is rectification – responses to both increments and decrements of illumination, leading to frequency-doubled responses to sinusoidally modulated stimuli, and approximately constant (DC) responses to drifting gratings. However, this is less important for directionality than nonlinear interactions between multiple stimuli within an RF. Direction selectivity is not evident in the appearance of the complex cell RF as it is in a simple cell, and is only revealed by experiments where two stimuli are allowed to interact within the RF. Such a second-order RF is obtained by probing the nonlinear interactions between two bars as they occur in relatively different positions and times within the RF. Figure 6 illustrates the regions in the RF where the responses depart from the expected linear sum of the first-order responses, and reveals both suppressive and facilitatory interactions. The second-order RFs are elongated, and oriented spatiotemporally, with the slope matching the cell's preferred direction and speed.

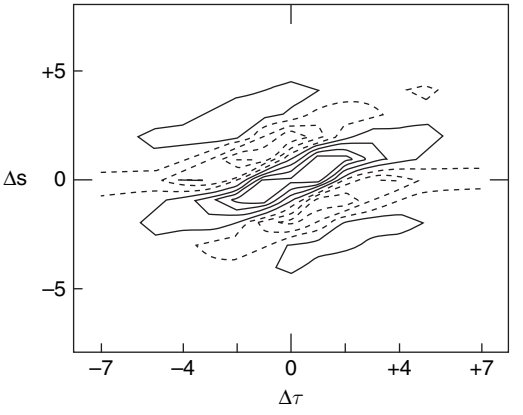

Figure 6 A second-order (nonlinear) receptive field profile, obtained from a mapping experiment with two bars present: a reference bar and a test bar. The responses to the test bar are plotted relative to what they would be absent the presence of the reference bar. The dashed contour lines denote negative regions of the interaction. From Emerson, R. C., Citron, M. C., Vaughn, W. J., and Klein, S. A. 1987. Nonlinear directionally selective subunits in complex cells of cat striate cortex. J. Neurophysiol. 58, 33–65.

Generally, this sort of RF is consistent with the predictions of a family of related motion models (Adelson, E. H. and Bergen, J. R., 1985; Heeger, D. J., 1987; Watson, A. B., 1987), all of which contain essential nonlinearities. The most commonly used is the motion energy model of Adelson E. H. and Bergen J. R. (1985), whose structure is illustrated in Figure 7. Its predictions, however, converge with those of Reichardt-style correlation models under most circumstances (van Santen, J. P. H. and Sperling, G., 1985). Where correlation models and motion energy models have been tested head-to-head (Emerson, R. C. *et al.*, 1992), the data tend to favor the motion energy model.

As is the case for directional simple cells, direct evidence for the local circuit that bestows directionality on DS complex cells is scant. This is unfortunate, since the various models make explicit (if somewhat abstract) predictions for cortical wiring, which are subject to direct experimental test. This is supported by the finding that simple cells in layer 4 project strongly to complex cells in layers 2 and 3 (Pollen, D. A. and Ronner, S. F., 1981; Field, D. J. and Tolhurst, D. J., 1986; Martinez, L. M. and Alonso, J. M., 2001). Many of these simple cells demonstrate the necessary range of spatial phases to produce quadrature pairs and motion energy detection.

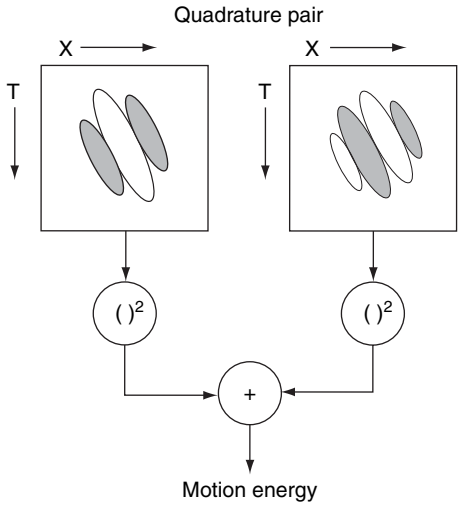

Figure 7 Simplified motion energy model. Note that one receptive field is odd-symmetric while the other is even. The outputs of the filters are squared and then added together to produce the motion energy. Each filter is phase dependent, with rightward direction selectivity. In comparison, the motion energy is phase invariant, with rightward direction selectivity. Reprinted from Adelson, E. H. and Bergen, J. R. 1985. Spatio-temporal energy models for the perception of motion. J. Opt. Soc. Am. A 2, 284–299.

2.10.2.4 Circuitry Underlying Local Motion Processing

The M pathway, as it arises from the LGN, is specially designed to be sensitive to moving stimuli. The parasol ganglion cells in the retina carry high contrast sensitivity, temporally acute, yet spatially coarse information to the M layers of the LGN (Enroth-Cugell, C. and Robson, J. G., 1966; Leventhal, A. G. *et al.*, 1981). This M information enters V1 in a segregated manner by synapsing in layer 4C. The most direct route this information can take through V1 is very short, via a monosynaptic connection between layer 4Cα and spiny stellate neurons in layer 4B that project directly to dorsal visual areas, particularly MT (Sawatari, A. and Callaway, E. M., 2000; Yabuta, N. H. *et al.*, 2001). Apart from this route, the transmission and integration of M information becomes more complex. In particular, while the input to the spiny stellate cells in layer 4B appear dominated by an M pathway connection from layer 4Cα, large pyramidal cells in layer 4B, which receive mixed M and P input also project to MT, though indirectly (Yabuta, N. H. *et al.*, 2001). This provides more sensitivity to form and color information then the M pathway alone could, and helps the animal to see what is moving.

In addition, M cells in layer 4Cα make synapses in layer 2/3 in conjunction with many color and form sensitive P cells, resulting in some degree of convergence (Lund, J. S. and Boothe, R. G., 1975; Callaway, E. M. and Wiser, A. K., 1996). Also, M cells project to layer 6 and synapse onto local type Iα cells and larger Meynert cells (Briggs, F. and Callaway, E. M., 2001). Layer 6 is one of the more directionally selective layers, and these cells may encode very specific columnar orientation and direction information (Hawken, M. J. *et al.*, 1988; Ringach, D. L. *et al.*, 1997). Though the local nature of their processes may be spatially restricted, the type Iα cells could synergistically work with the Meynert cells, which have broader dendritic fields, and may sum directional information across greater spatial distances, and project directly to area MT (Valverde, F., 1985). These α cells also provide feedback connections to layer 4Cα and may modify the inputs of this layer. Finally, layer 5 projects to the superior colliculus and the pulvinar, which has many directionally

selective neurons and provides an alternative route to area MT (Bender, D. B., 1982; Maunsell, J. H. R. and Van Essen, D. C., 1983a; Krubitzer, L. A. and Kaas, J. H., 1990; Dumbrava, D. *et al.*, 2001).

Complex cells, which often show strong direction selectivity, are found in greater numbers in layers 4B, 2/3, 5 and 6, all layers with strong M input (Hubel, D. H. and Wiesel, T. N., 1968; Hubel, D. H. *et al.*, 1976; Michael, C. R., 1981). Direction selectivity appears to emerge in neurons in upper layer 4 and layer 6 (Hubel, D. H. and Wiesel, T. N., 1968; Hubel, D. H. *et al.*, 1976; Michael, C. R., 1981; Blasdel, G. G. and Fitzpatrick, D., 1984; Livingstone, M. and Hubel, D., 1984; Hawken, M. J. *et al.*, 1988; Leventhal, A. G. *et al.*, 1995).

It was once believed that P and M inputs remained largely segregated in V1, which would enable outputs to separate areas or compartments to retain their characteristics (Livingstone, M. S. and Hubel, D., 1988). Instead, as Figure 8 illustrates, it now appears that P, M, and koniocellular inputs to V1 become mixed before their output to V2 (Sincich, L. C. and Horton, J. C., 2005) but see (Briggs, F. and Callaway, E. M., 2005). The functional consequences

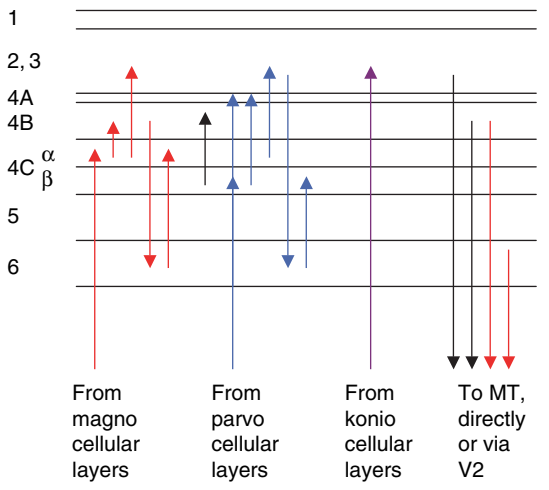

Figure 8 The segregation and integration of magno, parvo, and konio pathways through V1. The connections dominated by a class of input, magno (red), parvo (blue), or konio (purple) are drawn to highlight the segregation of signals in V1 and to MT. In addition, connections that integrate magno, parvo, and konio signals on the way to MT are illustrated in black. Most of the output from layer 2/3 goes to area V2, where it is further mixed, with some continuing to MT from there. A direct connection from the koniocellular layers in lateral geniculate nucleus to MT has also been described.

of this anatomical mixing are still unclear, however. Blocking responses in the M layers of the LGN nearly eliminates responses in MT (Maunsell, J. H. *et al.*, 1990), suggesting that the outputs from V1 toward MT remain largely unmixed. In contrast, substantial S-cone input appears evident in the chromatic sensitivity of both M LGN (Chatterjee, S. and Callaway, E. M., 2002) and in MT responses. Since S-cone inputs are dominant in the koniocellular pathway, this suggests a selective mixing of koniocellular and M signals; the consequences of this mixing for directional selectivity remain mysterious. Last, there is yet another opportunity for crosstalk between the parallel pathways in both feedback from higher cortical areas (e.g., V4) and in connections with accessory subthalamic nuclei, such as the pulvinar.

2.10.2.5 The Spatial Scale of Local Motion Operations

The spatial extent of directional selectivity has long been a fruitful platform for directly relating physiological and anatomical properties to perceptual phenomena. Motion psychophysics has a long history of quantifying the limits of perception, and this can be quantitatively related to the properties of different cortical areas. Examination of the spatial limits of direction discrimination provided one of the early uses of random noise displays, or kinematograms (random dot kinematograms). These are useful tools because they isolate local, or short-range motion mechanisms, which are perceptually very distinct from long-range apparent motion (Braddick, O. J., 1980). When a field of dots is displaced from one frame to the next, and if it exceeds a certain critical distance, then the direction of the displacement becomes perceptually ambiguous. This critical distance (D_{max}) was originally estimated to be about 15 arc minutes for central vision (Braddick, O., 1974). This corresponds fairly well with the dimensions of V1 RFs in the fovea. Furthermore, D_{max} scales with retinal eccentricity in a manner consistent with the scaling of RF sizes in V1 (Baker, C. L., Jr., and Braddick, O. J., 1982; 1985). This correspondence was directly examined by Mikami A. *et al.* (1985), and found to be remarkably precise.

These results are normally interpreted in the context of the Reichardt correlation model (Hassenstein, B. and Reichardt, W., 1956), illustrated in Figure 9. This class of models is conceptually the easiest to relate to

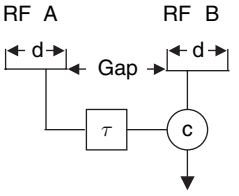

Figure 9 The Reichardt unidirectional bilocal correlation detector. The correlator (c) has delayed (τ) input from the detector at receptive field (RF) A and direct input from the detector at RF B. The psychophysically measured limits of motion detection can place meaningful values on both the size of the gap and the time delay (τ) between the detectors. Adapted from van den Berg, A. V. and van de Grind, W. A. 1989. Reaction times to motion onset and motion detection thresholds reflect the properties of bilocal motion detectors. Vision Res. 29, 1261–1266.

psychophysical measurements because the distance between the two local luminance-sensitive elements will directly predict the spatial limits of directionality; it fails when the extent of the displacement exceeds the distance between the detectors. Formal testing of the limits of perception in the context of this kind of model has proven very revealing (van den Berg, A. V. and van de Grind, W. A., 1989; van de Grind, W. A. *et al.*, 1992). From this whole body of work, a strong case can be made that directionally selective neurons in V1 are the primary, limiting location where the direction of object contours is calculated.

Another means to examine the spatial properties of motion processing is in the frequency domain. Because of the nature of Fourier analysis, the actual locations of the detectors are obscured, but their underlying filter properties are highlighted. Again, because these filter properties have been extensively studied in cortex, one can make quantitative comparisons between physiology and psychophysics.

Directionally selective neurons in V1 (and V2) prefer a wide range of spatial and temporal frequencies, but with a bias toward lower spatial frequencies and higher temporal frequencies (Foster, K. H. *et al.*, 1985). Under nonpreferred temporal frequencies, direction selectivity is reduced or even reversed in V1 (Saul, A. B. and Humphrey, A. L., 1992). Likewise, motion perception can reverse at high (or low) temporal frequency (Purves, D. *et al.*, 1996). This occurs because motion discrimination is band-pass for temporal frequency (Derrington, A. M. and Henning, G. B., 1993; Gegenfurtner, K. R. and Hawken, M. J., 1995), which matches perception with tuning properties in V1. Importantly, the timing properties of lagged and nonlagged cells in LGN are affected by temporal frequency in a manner consistent with these changes in direction selectivity.

2.10.2.6 Extrastriate Local Motion Processing

While V1 (Van Essen, D. C. and DeYoe, E. A., 1995) assumes legitimate importance as the first site of directional computations in cortex, motion processing occurs in a large number of connected cortical areas. The so-called motion system of dorsal extrastriate cortex is illustrated in Figure 10. The diagram indicates both hierarchical (serial) and parallel organization in this pathway. Connections from V1 fan out to multiple areas as they ascend the cortical processing hierarchy. Despite this fact, the literature of motion processing emphasizes only three areas, connected in series: V1, MT, and MST. However, the parallel ascending pathways to higher areas no doubt have considerable importance, though they have yet received very little study.

The most obvious change that occurs as one ascends the hierarchy is of RF size. This can be approximated as a doubling of RF diameter with each level beyond V1. Thus, V2 RFs are approximately twice the

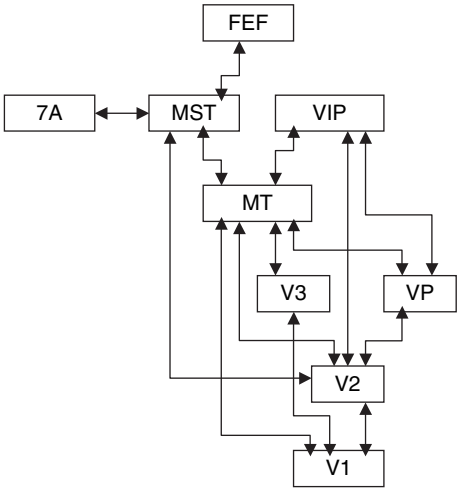

Figure 10 Major cortical areas in the motion system or pathway. Connection arrows are double headed to represent reciprocal connectivity between areas. Connections between the dorsal motion processing system and the ventral object-processing pathway exist, but are not illustrated here for clarity. These are the primary known connections; others may also exist. FEF, frontal eye feilds; MST, middle superior temporal area; MT, middle temporal area; VIP, ventral intraparietal area; VP, ventral posterior area.

dimensions of V1, V3 are around four times the dimensions, and MT about eight times the dimensions. This increase in spatial scale arises because of the pattern of divergent and convergent connections between connected cortical areas (Van Essen, D. C. *et al.*, 1986; Maunsell, J. H. R. and Van Essen, D. C., 1987; Amir, Y. *et al.*, 1993).

The functional relationship between these areas is probably best revealed by the increasing prevalence of direction selectivity. Direction selectivity is found in about 15% of V2 cells, and these occur mainly in the thick stripes (Levitt, J. *et al.*, 1994). Tracer studies show that roughly two-thirds of all V2 input comes from V1 (Sincich, L. C. and Horton, J. C., 2003). Layer 4B is one of the main inputs to the thick stripes in V2, and predominantly carries motion signals via a M stream (Shipp, S. and Zeki, S., 2002). However, there is evidence that novel response properties emerge in V2 as well. It is also the first area where a significant number of cells show directional responses to so-called second-order motion stimuli (Leventhal, A. G. *et al.*, 1998). These stimuli contain motion defined not by moving luminance contrast, but by the motion of regions defined by changes of contrast, flicker, or other higher-order image properties. The motion of such stimuli is highly visible to human observers, but do not trigger directional responses in either linear motion filters or in motion energy filters.

Strong direction selectivity occurs in 40% of area V3 cells, making it second only to MT in motion sensitivity. Area V3 receives both M- and P-dominated inputs, and projects to both MT and V4. While more than half the cells show some direction selectivity, most of the cells in layer 4, receiving V1 and V2 input, do not have such directional responses. Therefore, it is hypothesized that directional selectivity is developed *de novo* within V3 (Gegenfurtner, K. R. *et al.*, 1997). By studying the responses of directional cells to plaid patterns, Gegenfurtner K. R. and colleagues (1997) found that many V3 cells respond to the pattern motion of a plaid stimulus, much as area MT does. In addition, many motion responsive cells were also color sensitive, and respond directionally to isoluminant moving gratings. The significant integration of motion and color signals in V3 would be of practical use in dynamic form processing.

Regarding the function of area V3, differences between the neuronal properties and cytoarchitecture of areas V3d (also called DM) and V3v suggest that they constitute separate functional areas (Rosa, M. G. and Manger, P. R., 2005). Because of this, these areas may be redesignated, with area V3v becoming the newly redefined V3. V3d has a separate topographic representation of the visual field and appears much more directionally selective than V3v. More thorough research into this area's function in motion processing is required, but preliminary studies indicate a role in integrating motion signals, possibly for dynamic form analysis and figure-ground segregation (Felleman, D. J. and Van Essen, D. C., 1987; Gegenfurtner, K. R. *et al.*, 1997; Zeki, S. *et al.*, 2003).

Finally, both V2 and V3 receive extensive reciprocal connections with motion processing area MT (Van Essen, D. C. and DeYoe, E. A., 1995), which probably provides important feedback to functionally influence these earlier areas in their analysis of moving stimuli, whether defined by luminance (first order) or contrast (second order).

2.10.3 Medium Scale Motion Processing: Area MT

2.10.3.1 Anatomy and Connections

MT stands for middle temporal, the location where it was originally discovered in the owl monkey (Allman, J. M. and Kaas, J. H., 1971). Allman J. M. and Kaas J. H. (1971) found a retinotopically organized area that responded best to moving bars. At the same time, Dubner R. and Zeki S. M. (1971) discovered the homolog in the macaque monkey, located on the posterior bank of the superior temporal sulcus, which they named V5. Following this, many studies confirmed the location of MT as a well-defined area with dense myelination, receiving direct input from V1, and containing a high concentration of direction-selective neurons (Van Essen, D. C. *et al.*, 1981; Maunsell, J. H. R. and Van Essen, D. C., 1983b; Albright, T. D. *et al.*, 1984). Since its original discovery, this area has attracted tremendous interest and is probably better understood than any other extrastriate visual area. This interest arises from a number of factors, chief among them being the vigor and homogeneity of its directional responses.

As seen in Figure 11, MT lies near the middle of the dorsal stream and integrates inputs from a large number of areas. The cortical connections to MT are well understood, and come from V1, V2, V3, V3A, VP, V3d, and PIP (Maunsell, J. H. R. and Van Essen, D. C., 1983a; Felleman, D. and Van Essen, D., 1991). The most important input into MT, however, is from layer 4B of V1, as illustrated by the thickest arrow. This input is highly specialized, containing large diameter

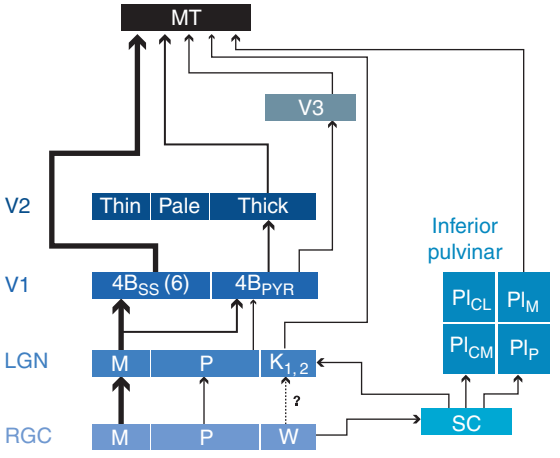

Figure 11 Major routes into MT in the manner of Felleman D. and Van Essen D. (1991). Line thickness is roughly proportional to the magnitude of the inputs. The thickest lines represent the direct cortical pathway emphasized in the text. The pathways shown omit a number of known feed-forward cortical inputs that appear lesser in magnitude (V3A, VP, PIP) as well as many subcortical inputs. The precise nature of the retinal inputs to K1,2 is not known, though their response properties are W-like in the galago Irvin, G. E., Norton, T. T., Sesma, M. A., and Casagrande, V. A. 1986. W-like response properties of interlaminar zone cells in the lateral geniculate nucleus of a primate (*Galago crassicaudatus*). Brain Res. 362, 254–270. $4B_{SS}$, spiny stellate neurons in layer 4B; $4B_{PYR}$, pyramidal neurons in layer 4B; LGN, lateral geniculate nucleus; M, magnocellular stream; P, parvocellular stream; K, koniocellular layers of LGN; PI_{CL}, central lateral nucleus of the inferior pulvinar; PI_{CM}, central medial nucleus of the inferior pulvinar; PI_{M}, medial nucleus of the inferior pulvinar; PI_{P}, posterior nucleus of the inferior pulvinar; RGC, retinal ganglion cells; SC, superior colliculus; VP, ventral posterior area. From Born, R. T. and Bradley, D. C. 2005. Structure and function of visual area MT. Annu. Rev. Neurosci. 28, 157–189.

axons (up to 3μm), which form multiple synapses onto an MT neuron (Rockland, K. S., 1989). Physiologically, the majority of these MT-projecting neurons are directionally selective complex cells (Movshon, J. A. and Newsome, W. T., 1996). In addition to its cortical connections, MT receives input from subcortical areas: the superior colliculus, inferior pulvinar, and a small subset of koniocellular neurons in the LGN (Stepniewska, I. *et al.*, 1999; Sincich, L. C. *et al.*, 2004).

2.10.3.2 Physiological Properties and Functional Organization

The defining property of MT is its directional selectivity. Approximately 80–90% of MT neurons are strongly directionally selective. Figure 12 shows the response of a typical single MT neuron to a bar moving through its RF. Tuning bandwidths average about 50–60° by most estimates (half-width at half-height, or the nearly equivalent sigma of a fit Gaussian (Maunsell, J. H. R. and Van Essen, D. C., 1983b; Albright, T. D. *et al.*, 1984; Britten, K. H. *et al.*, 1996). The neuron in Figure 12 is also typical in that it is inhibited by motion in a direction opposite to its preferred direction (often called the null direction). This inhibition is not found in all MT neurons, and is typically weaker than preferred direction excitation (Snowden, R. J. *et al.*, 1991; Britten, K. H. *et al.*, 1993; Qian, N. and Andersen, R. A., 1995). This push–pull kind of response is termed motion opponency and is potentially important in motion adaptation (below).

Motion direction in MT is organized in columns, like orientation in V1, and this can be seen in Figure 13. Neurons with very similar direction preferences occur together in columns, which progressively vary in their tuning from one another by a small amount or occasionally by 180° (Albright, T. D., 1984). Binocular disparity, for which MT neurons are also selective, is also organized in columns in MT (DeAngelis, G. C. and Newsome, W. T., 1999). These columns for binocular disparity appear not to be systematically arranged with respect to the direction columns, but instead form a separate, independent pattern.

MT RFs are approximately 10 times larger in diameter than those in V1, and their size scales proportionately with eccentricity. Despite this larger area, however, the directional calculations appear to occur on a small scale, much more like the dimensions of their V1 afferents. Several laboratories have measured the responses of MT neurons to apparent motion sequences as the spatial and temporal interval between the stimuli was varied (Mikami, A. *et al.*, 1986; Churchland, M. M. *et al.*, 2005). In all of these experiments, it was evident that MT cells were directional over spatial intervals much smaller than the dimensions of the RF of the MT cell, and more similar to those of V1 afferents. These observations, together with the direct observations that MT-projecting V1 cells are themselves directional (Movshon, J. A. and Newsome, W. T., 1996), strongly make the case that MT inherits its directionality from earlier structures, rather than calculating it *de novo*.

MT cells are tuned for speed as well as for direction, though the tuning is often quite broad (Maunsell, J. H. R. and Van Essen, D. C., 1983b). The speed tuning of cells in MT are either low-pass, preferring slow speeds, well tuned for intermediate speeds, or broadly tuned (Maunsell, J. H. R. and Van Essen, D. C., 1983b; Lagae, L. *et al.*, 1993).

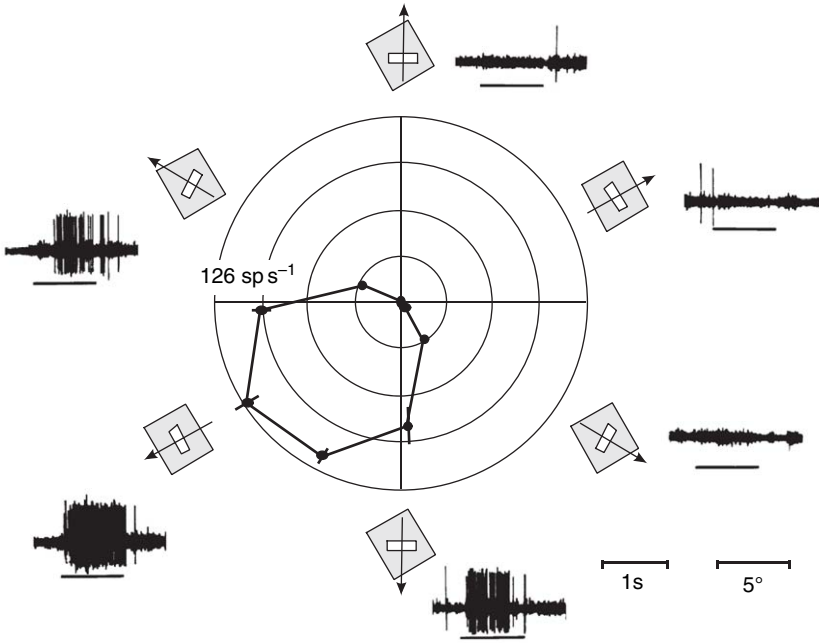

Figure 12 Tuning of a directionally selective cell in MT. Illustrated is the pattern of data typically obtained in studies of direction selectivity. The polar plot displays the magnitude of the cell's response to eight directions of motion. Also depicted are the neural spiking responses for six of the motion directions. The speed of the movement is approximately 5° s^{-1}. The neuron's preferred direction is down and to the left. From Maunsell, J. H. R. and Van Essen, D.C. 1983b. Functional properties of neurons in the middle temporal visual area (MT) of the macaque monkey: I. Selectivity for stimulus direction, speed and orientation. J. Neurophysiol. 49, 1127–1147.

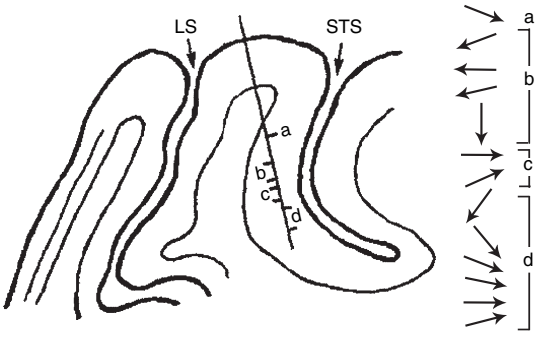

Figure 13 Oblique penetration through MT (modified from figure 3 of Dubner, R. and Zeki, S. M. 1971. Response properties and receptive fields of cells in an anatomically defined region of the superior temporal sulcus. Brain Res. 35, 528–532) showing the shifts in preferred direction indicative of the direction columns subsequently demonstrated by Albright T. D. *et al.* 1984).

There is a systematic, if not extremely precise, relationship between speed preference and RF location, with more foveal neurons preferring slower speeds, and more peripheral ones, faster speeds. In general, response latencies are decreased as speed is increased (Raiguel, S. E. *et al.*, 1999). MT firing rates appear to be correlated with speed perception (Priebe, N. J. and Lisberger, S. G., 2004; Liu, J. and Newsome, W. T., 2005). Last, the response dynamics of MT neurons, which are typically fast, also carry a covert signal of target acceleration (Lisberger, S. G. and Movshon, J. A., 1999).

2.10.3.3 Motion Integration: The Aperture Problem

The small scale of directional neurons' RFs in V1 causes each neuron to see only a small part of a moving object. The orientation selectivity of a V1 neuron additionally means that each neuron can detect only the component of velocity at right angles to the edge; the component parallel to the edge is invisible. This is frequently referred to as the aperture problem because the RF is like a small window through which the cell sees the motion in the world, as illustrated in Figure 14. To represent the actual motion of an object, these local estimates of individual object boundaries must be combined in some way. The history of this problem has been a good example of the cross-fertilization of theory, psychophysics, and physiology in neuroscience.

The problem is fairly straightforward – the retinal motion of an object is represented by a two-

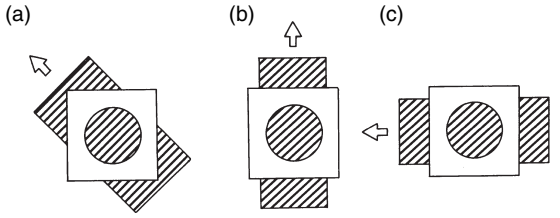

Figure 14 Because of the aperture problem, the local motion in each of the apertures is the same even though the true motion of the grating differs. Reprinted from Movshon, J. A., Adelson, E. H., Gizzi, M. S., and Newsome, W. T. 1985. The Analysis of Moving Visual Patterns. In: Study Group on Pattern Recognition Mechanisms (*eds*. C. Chagas, R. Gattass, and C. Gross), pp. 117–151. Pontifica Academia Scientiarum.

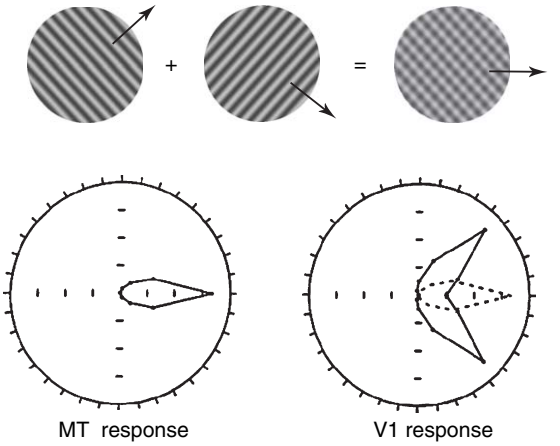

Figure 15 Responses in MT and V1 to pattern motion stimulus (the moving plaid). 20% of MT cells are selective to the plaid motion, 40% respond to component motion, and 40% are intermediate.

dimensional vector, yet each V1 (or other equally fine-grained directional neurons) can only estimate a single dimension. To estimate the actual velocity of an object with multiple contours, one must be able to integrate the different vectors corresponding to individual moving contours. Plaid stimuli make a good tool to probe this integration process, since one can superimpose multiple single vectors to study integration at either a perceptual or physiological level. Perceptually, subjects integrate the motions of each component of a plaid very well, under a variety of conditions (Levinson, E. and Sekuler, R., 1975; Adelson, E. H. and Movshon, J. A., 1983).

There are several theoretical possibilities as to exactly how the individual vectors are combined to extract the true object velocity. The veridical answer is provided by a method known as intersection of constraints, but this is a bit complex to implement physiologically (Movshon, J. A. *et al*., 1985). A weighted vector-average solution will produce a good approximation to the correct motion under most real-world situations, and perceptual experiments show that the visual system often makes the mistakes predicted by this approach, when views are brief or when reduced contrast or added noise weakens the image (Stone, L. S. *et al*., 1990; Yo, C. and Wilson, H. R., 1992). More recently, a Bayesian solution has been proposed, which is both physiologically plausible and consistent with perception in a variety of test situations (Weiss, Y., 2000).

At the physiological level, it is clear that some MT neurons integrate multiple directions of motion in such plaid stimuli, as illustrated in Figure 15. When tested with a plaid containing two different directions, such pattern direction-selective neurons respond maximally when the plaid pattern is moving in their preferred direction, but this is a stimulus in which neither component of the plaid is so moving. Another fraction of MT cells responds in a component direction-selective manner, like V1 cells, and another fraction is intermediate (Movshon, J. A. *et al*., 1985).

There is one other possible mechanism for computing the true plaid motion. Because of their small RFs, cells in V1 are unable to signal the true motion of a contour, and so V1 has generally been regarded as incapable of carrying true motion information for plaid patterns. However, a subpopulation of V1 neurons, called end-stopped cells, are capable of signaling motion independently of the contour (Pack, C. C. *et al*., 2003). These cells respond only to the endpoints of the contour, and would thus be sensitive to the true motion of the object.

While many of the accounts of how pattern motion is perceived are fairly abstract and theoretical, some have been phrased in more biological terms, directly testable by physiological experiments in area MT. An earlier model of the integration of inputs by MT neurons (Simoncelli, E. P. and Heeger, D. J., 1998) incorporated a specific pattern of projection from V1 to MT, followed by a modest nonlinearity in MT. This model provided a good account of pattern direction selectivity in MT, as well as other phenomena. More recently, an elaboration of this model has been formed and directly tested (Rust, N. C. *et al*., 2006) and, by subtle cell-to-cell changes in the pattern of connections into and within MT, could account not only for pattern direction selectivity itself, but also for the range of cell responses from component- to pattern-direction selective.

2.10.3.4 Integration for Speed Perception

It is less intuitively obvious that integration is also useful for correctly estimating the speed of moving objects. The reason is that individual features of a moving object, even if they are all moving in the same direction, have different spatial scales and thus will activate multiple populations of V1 afferents sensitive to different spatial frequencies. When an object with multiple spatial frequencies moves with a single velocity, the spatial and temporal frequencies in the object will be correlated, with a constant of proportionality capturing the speed of motion. This relationship is illustrated in Figure 16. A long-standing question is to what extent MT cells integrate their multiple inputs so as to encode a single speed. MT neurons have the opportunity to integrate in this way, since their spatial and temporal bandwidths are substantially larger than those in V1 (Movshon, J. A. *et al.*, 1988). When tested with multiple combinations of spatial and temporal frequencies, many MT cells have a slant in their joint tuning, indicating a preference for a single velocity, irrespective of the exact spatial and temporal frequency composition (Movshon, J. A. *et al.*, 1985; Perrone, J. A. and Thiele, A., 2001; Priebe, N. J. *et al.*, 2003). The extent of this slant, however, varied considerably across cells, and a substantial minority of MT cells was not evidently tuned for a single speed, consistent with broad tuning for speed. Interestingly, however, V1 complex cells are often slanted as much as MT cells (Priebe, N. J. *et al.*, 2006), so it is not clear this property is entirely formed *de novo* in MT. However, these measurements were made with single gratings, and the effects of summation in MT were more apparent when compound stimuli containing multiple spatial frequencies were used. In order to account for the measured speed selectivity of MT neurons to such stimuli, a modest summation nonlinearity is required (Priebe, N. J. *et al.*, 2003). While not modeled in exactly the same way, it is likely that this summation nonlinearity is closely related to that employed by Rust N. C. *et al.* (2006) to account for plaid direction selectivity. Thus, qualitatively similar summation is important in how MT solves two distinct, important problems requiring integration of multiple inputs. This suggestion still needs to be made explicit with a larger-scale theoretical account, however.

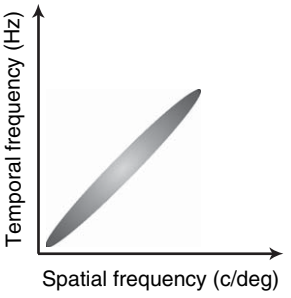

Figure 16 The spatial and temporal frequencies in a single moving object are proportional, with higher spatial frequencies being modulated at higher temporal frequencies. The slope of this relationship is the speed of the object.

2.10.3.5 The Problem with Integration: Segmentation Is Needed Too

Although integration appears vital for solving the aperture problem and might be used by the motion system for speed perception, it has a problem. It would be detrimental to our perception of the world if our visual system integrated the motions from two independent objects in the same part of the visual scene. The solution to this problem is segmentation, a mechanism that separates the signals from different objects that are to be analyzed separately.

Opposing motions from two objects in the same space usually occur on different planes of depth, otherwise they would collide. Motions that occur at different depths modulate MT responses. Many neurons in MT are tuned for depth, and responses to the preferred motion are less suppressed by nonpreferred motion when it occurs at a different depth (Qian, N. and Andersen, R. A., 1994; Bradley, D. C. *et al.*, 1995).

About half of the cells in MT, especially in the supragranular layers, are likely to possess antagonistic surrounds. A surround is a spatial region that extends well beyond the classical RF and suppresses the neuron's response when a stimulus is large enough to activate it (Lagae, L. *et al.*, 1989). These surrounds are also directional, and suppress most actively for stimuli moving in the cell's preferred direction, and least for motion in the opposite direction. The surrounds in MT cells are frequently very irregular in shape, sometimes only encompassing a small fraction of the perimeter of the RF center (Xiao, D. K. *et al.*, 1995). Surrounds in MT are clearly important in segmenting multiple motions in the image.

Many neurons in MT have antagonistic surrounds that modulate the response to a central stimulus.

A surround stimulus that moves in a direction, speed, and/or depth that differs from the central stimulus will cause the least suppression (Allman, J. M. *et al.*, 1985; Xiao, D. K. *et al.*, 1997; Bradley, D. C. and Andersen, R. A., 1998).

In contrast to these antagonistic surrounds, reinforcing surrounds, which prefer motion in the same direction as the center, have also been described (Allman, J. M. *et al.*, 1985; Tanaka, K. *et al.*, 1986). These different types of surrounds, preferring the same or opposite direction, appear to be columnarly organized in owl monkey (Born, R. T., 2000). It seems reasonable that this organization separates the important functions of wide-field and object motion processing.

Surrounds even show the ability to switch between integration and segmentation. When the motion signal is weak, say because the contrast is low, the visual system integrates to increase its sensitivity (Tadin, D. *et al.*, 2003). Under low contrast conditions, some MT neurons actually fire more to a large stimulus that includes the normally suppressive surround, as illustrated in Figure 17 (Pack, C. C. *et al.*, 2005).

Color also appears to be a useful segmentation cue in MT. Croner L. J. and Albright T. D. (1999) found that, like human observers, individual neurons in MT are better able to discriminate motion direction when the motion signal is a different color than the noise.

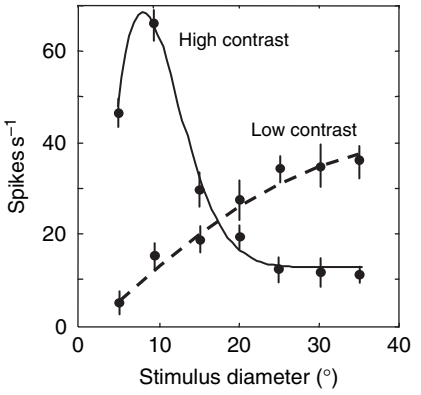

Figure 17 Center-surround interactions in MT. Effect of contrast on center-surround interactions for one MT neuron. When tested with high-contrast random dots (RMS, root-mean-square contrast 9.8 cd m^{-2}) the neuron responded optimally to a circular dot patch 10° in diameter and was strongly suppressed by larger patterns. The same test using a low-contrast dot pattern (0.7 cd/m^2) revealed strong area summation with increasing size. Reprinted from Pack, C. C., Hunter, J. N., and Born, R. T. 2005. Contrast dependence of suppressive influences in cortical area MT of alert macaque. J. Neurophysiol. 93, 1809–1815.

2.10.3.6 The Effect of Contrast

Contrast is a primary attribute of any visual stimulus, and its effects on motion perception and physiology have been extensively studied. The most conspicuous change in motion perception at low contrast is a decrease in perceived speed (Thompson, P., 1982; Thompson, P. and Stone, L. S., 1997), although this effect paradoxically reverses if the spatial frequency is high enough (Thompson, P. *et al.*, 2006). This result has guided a large number of studies exploring the effect of varying contrast at all levels of the motion system. The goal is to identify the important loci that limit the perception of speed, based on where the physiologically observed effects of contrast are most consistent with the perceptual phenomena. The problem is that one needs a good model as to how any candidate neuronal population supports the perception of speed, and as of now, the experimental results have not clearly pointed to a single model.

Neurons at all levels of the visual system give graded, monotonically increasing responses to rising contrast. M neurons have considerably steeper contrast-response functions than P neurons (Derrington, A. M. and Lennie, P., 1984). Also, neurons in MT have substantially steeper contrast-response functions than those of neurons in V1 (Sclar, G. *et al.*, 1990). Therefore, at any level of the motion system, the primary effect of reducing contrast will be to reduce firing rates, but this will be by differing amounts for different populations.

In V1, reducing contrast lowers both preferred spatial and temporal frequency (Holub, R. A. and Morton-Gibson, M., 1981; Albrecht, D. G., 1995; Carandini, M. *et al.*, 1997; Sceniak, M. P. *et al.*, 2002). At the cell's preferred temporal frequency, reducing contrast acts to decrease the neuron's preferred spatial frequency. And likewise, at the preferred spatial frequency, reduced contrast decreases the preferred temporal frequency. In addition, recent findings show that most V1 cells, regardless of their directionality, have reduced speed tuning under lowered contrast (Livingstone, M. and Conway, B. R., 2006). This effect was well correlated with differences in the space–time slant of the RF with different contrasts.

In MT, the situation is more complicated. Three laboratories have measured MT responses to either random-dot (Pack, C. C. *et al.*, 2005; Krekelberg, B. *et al.*, 2006) or grating (Priebe, N. J. *et al.*, 2003; Priebe, N. J. and Lisberger, S. G., 2004) stimuli as contrast is varied. All agree on only one finding, that overall, firing rates are lower at lower contrast. Priebe and

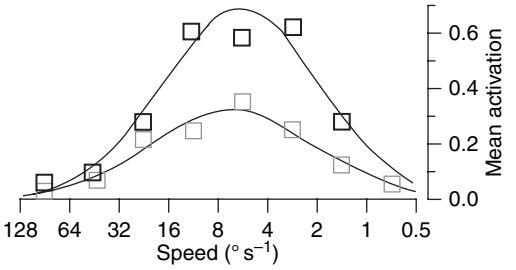

Figure 18 Population response in MT for gratings of high or low contrast. The figure summarizes the population response as a function of the preferred speeds of the neurons (x axis). Black and gray symbols and curves show the population codes for contrasts of 32% and 8%, respectively. Symbols show averages of neural responses binned according to preferred speed and curves show Gaussian fits to the symbols. Lowered contrast reduced the neural response, but did not shift the population response. Adapted from Priebe, N. J., Cassanello, C. R., and Lisberger, S. G. 2003. The neural representation of speed in macaque area MT/V5. J. Neurosci. 23, 5650–5661.

Lisberger (Priebe, N. J. *et al.*, 2003; Priebe, N. J. and Lisberger, S. G., 2004) examined both perceptual and physiological effects of changing spatial frequency and contrast. In these experiments, contrast had the expected effects of reducing perceived speed, but did not systematically change the distribution of responses in MT (Figure 18). This would appear to call into question any simple model where the distribution of activity in MT directly supports the perception of speed. However, a fairly standard vector average model of how the population codes for speed can be reconciled with these data if you add an additional feature that lowers the overall speed estimate as the population response drops. This is not very different from a Bayesian prior assumption of low speed, which was also used in the interpretation of plaids by Weiss Y. *et al.* (2002).

When random-dot stimuli are employed with varying contrast, the effects on speed tuning are more pronounced. Lowering the contrast of dots profoundly shifts speed-tuning functions to lower values. This is particularly true for neurons that prefer higher speeds in the first place (Pack, C. C. *et al.*, 2005; Krekelberg, B. *et al.*, 2006). While at first glance this might appear consistent with perception, it is actually backwards. As contrast is lowered, neurons preferring higher speeds become relatively more active, and a vector average would predict a higher speed percept. The same thing would be true for the other main class of readout models, which extract speed from a ratio between the activities of a high-speed and a low-speed subpopulation (Perrone, J. A., 2006; Thompson, P. *et al.*, 2006). While the authors reject both these simple models, they also do not attempt to employ the Bayesian idea that allowed the grating responses to be consistent with perception. Because the effects on the population are different in magnitude for the two classes of stimuli, it is not yet clear that a single model will work for both, but this has not yet been tried.

2.10.3.7 Relating MT to Perception

Area MT has become a favored target for experiments designed to quantitatively relate neuronal responses to perception. There is now a large body of work from several laboratories testing the hypothesis that MT is both necessary and sufficient for motion perception. Necessity is best established using lesion methods (Schiller, P. H. *et al.*, 1987; Newsome, W. T. and Paré, E. B., 1988), and these experiments show that MT is necessary for normal motion sensitivity, but also clearly suggest that other areas contribute as well. Even after large MT lesions, substantial perceptual abilities remain.

Sufficiency is somewhat more difficult to demonstrate, and relies on correlation between neuronal and perceptual performance. A large number of experiments of this sort have been performed, testing the relationship between neuronal spiking activity in MT and performance on a variety of tasks (Britten, K. H. *et al.*, 1992; Thiele, A. *et al.*, 1999; Dodd, J. V. *et al.*, 2001; Uka, T. and DeAngelis, G. C., 2001; Grunewald, A. *et al.*, 2002; Krug, K. *et al.*, 2004; Liu, J. and Newsome, W. T., 2005). On direction discrimination between opposed alternatives when limited by noise, the average MT cell had thresholds nearly equal to the monkeys'. When the alternatives were made closer together, MT performance dropped relative to the monkeys and only the best neurons showed performance similar to that of the monkey (Dodd, J. V. *et al.*, 2001; Purushothaman, G. and Bradley, D. C., 2005). Last, in the discrimination of small speed differences, again, only the best neurons showed performance equivalent to what the monkey could do (Liu, J. and Newsome, W. T., 2005).

Another demonstration of the correlation between MT activity and perception comes from the discovery of a trial-by-trial correlation between neuronal discharge and monkey choices, when both are measured at the same time. This kind of correlation does not suggest sufficiency, but instead suggests that the neurons might be contributing to the signals that

support performance. The first such observation (Logothetis, N. K. and Schall, J. D., 1990) was not entirely encouraging. In a study of binocular motion rivalry, MT signals were frequently associated with the percept, but this association was approximately as often in the expected direction (higher rates when the animal reported preferred direction motion) as in the opposite. More recently, such correlations have been described in the context of difficult perceptual choices, and most of these experiments reveal a preponderance of the more intuitively sensible positive correlations. This association is commonly described using a metric termed the choice probability (Britten, K. H. *et al.*, 1996). Significant choice probabilities have now been observed in MT in the context of a number of motion-related tasks, including direction discrimination (Britten, K. H. *et al.*, 1996; Purushothaman, G. and Bradley, D. C., 2005), cylinder rotation judgment (Dodd, J. V. *et al.*, 2001; Parker, A. J. *et al.*, 2002), and speed discrimination (Liu, J. and Newsome, W. T., 2005). Figure 19 illustrates choice probability for the cylinder rotation judgment.

Perhaps the most direct evidence linking MT to perception comes from electrical microstimulation experiments. While lesion experiments cannot distinguish a direct, causal role from an indirect, supporting role in perception, microstimulation can directly support a causal role in perception. Newsome's group has documented this kind of involvement in direction discrimination (Salzman, C. D. *et al.*, 1990; 1992; Salzman, C. D. and Newsome, W. T., 1994; Newsome, W. *et al.*, 1995) as well as in speed discrimination (Liu, J. and Newsome, W. T., 2005). They found that microstimulating a cluster or column of similarly tuned MT neurons biased the animal's decisions in favor of the direction of motion encoded by the stimulated neurons.

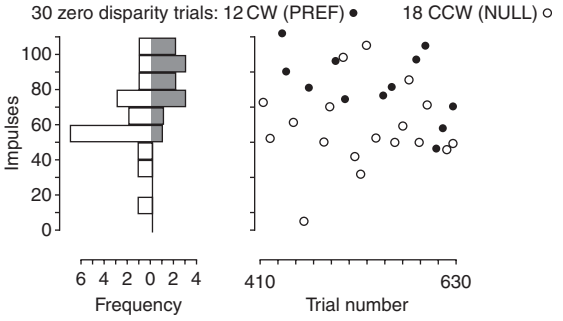

Figure 19 Trial-by-trial correlation between neuronal response and behavioral choice for a single cell in an ambiguous cylinder rotation task (zero disparity). The uppermost plots illustrate the neuronal responses for trials in which the animal chose CW (PREF) rotation or CCW (NULL) rotation. Higher firing rates (impulses) were correlated with CW (PREF) choices. The choice probability for this cell was high, 0.79, based on the separation of the distributions as can be seen in the scatterplot. The distribution of choice probabilities, bottom panel, shows a mean choice probability of 0.67, ranging from 0.35 to 0.98. Adapted from Dodd, J. V., Krug, K., Cumming, B. G., and Parker, A. J. 2001. Perceptually bistable three-dimensional figures evoke high choice probabilities in cortical area MT. J. Neurosci. 21, 4809–4821, figures 3 and 5.

Taken together, this body of evidence forms one of the strongest sets of data linking a specific cortical area to perception. It suggests, furthermore, that the same neuronal signals contribute to many aspects of motion discrimination. However, one must be careful not to over-interpret these data as well. In particular, it is tempting to suggest that MT is the only, or a single dominant player in motion perception, and nothing in this body of work supports this conclusion. Likewise, it is now clear that MT is not completely specialized for motion perception. An extensive series of studies from the laboratory of DeAngelis and colleagues has documented that MT is extensively involved in judgments of stereoscopic depth as well (DeAngelis, G. C. *et al.*, 1998; Uka, T. and DeAngelis, G. C., 2004; 2006). Therefore, it would be unwise to make too strong a claim that MT is completely specialized for motion analysis. It is also potentially revealing that the quantitative details of the relationship between neuronal activity and perception varies widely from task to task, which suggests that the readout mechanisms by which such signals inform perception are not fixed but are instead malleable and context dependent.

2.10.3.8 Adaptation

Neural adaptation is the change in neuronal responses due to preceding stimulation of the cell. Because adaptation effects are often profound at both the neural and perceptual levels, it has been widely used as a tool to probe the neuronal signals underlying perception. Motion adaptation, in particular, has a long and influential history, because of the vivid motion aftereffect (MAE), or waterfall illusion (Wohlgemuth, A., 1911; Krekelberg, B. *et al.*, 2006). One unusual aspect of this phenomenon is that, unlike many other adaptation phenomena, it results in a positive percept – motion is visible where none is present on the retina. This has led to a large literature reporting both positive (facilitatory) and negative neuronal effects at all levels of the motion system. While detailed examination of this complex and often contradictory literature is beyond the scope of

this chapter, one can safely say that there is no clear consensus yet as to the critical neuronal changes underlying the MAE.

Perceptually, the MAE can be extremely local, suggesting a critical locus early in the motion system, and there is good supporting evidence from both cat and monkey physiology experiments (Verstraten, F. A. *et al.*, 1999; Freeman, T. C. *et al.*, 2003; Blaser, E. *et al.*, 2005) of directionally selective adaptation effects as early as V1. However, there is clear evidence from perceptual experiments of specific adaptation to complex (global) motion patterns as well (Regan, D. and Beverly, K., 1978; Snowden, R. J. and Milne, A. B., 1997), which presumably points to additional changes late in the motion system. These have not been explored in physiology experiments, and this clearly is an important future direction.

Perhaps the most compelling physiology experiments come from work in MT. In experiments using only two directions of motion (preferred and antipreferred), substantial decrements in activity following preferred direction motion adaptation have been observed (Petersen, S. E. *et al.*, 1985; Van Wezel, R. J. and Britten, K. H., 2002), consistent with the biases seen in motion perception. In a recent study, adaptation reduced the activity of neurons with tuning similar to the adapting stimulus, narrowed the tuning curve, and importantly, shifted the tuning of cells with nearby preferred directions toward the adapted direction (Kohn, A. and Movshon, J. A., 2004). These attractive shifts in tuning and narrowed bandwidths resulted in nearby directions of motion eliciting a greater difference in neural response and therefore an effect that was perceptually repulsive. Thus, the neuronal results appear consistent with the perceptual effects, and probably arise from local inhibitory interactions between neurons tuned to different directions in MT or prior structures.

In a related set of experiments using different speeds, rather than different directions, Van Wezel R. J. and colleagues (Krekelberg, B. *et al.*, 2006), found that adaptation to a particular speed reduces the firing rate for neurons tuned for nearby speeds while narrowing their tuning curves. This is again consistent with the perceptual effects of adaptation on speed identification and discrimination. So, overall, a fairly good case is developing that MT is one important locus supporting adaptation at the perceptual level, but again, these preceding experiments do not allow one to conclude that MT is the critical locus, and more work is needed at other locations in the motion system.

2.10.3.9 Attention and Memory

Visual perception depends not only on retinal information, but also on cognitive or top-down information. Such cognitive contributions to vision include directed attention for selecting behaviorally relevant stimuli in visual scenes as well as remembered associations of visual stimuli. Neuroscientists have long sought correlates of such high-level, cognitive phenomena, and the motion system of cortex is a good example of the success of this endeavor.

One form of directed attention operates as a kind of spotlight, to spatially select the most important locations in the visual scene for processing (Treisman, A. M. and Gelade, G., 1980). Another, related form of attention is directed toward particular visual features (e.g., a particular color or motion direction) irrespective of where they appear in space. This form of attention may be useful in the integration of low-level attributes for the perception of coherent objects (Treisman, A. M. and Gelade, G., 1980; Wolfe, J. M. and Bennett, S. C., 1997). Many studies have shown that attention can be directed to a spatial location independent of the eye fixation location (Posner, M. I., 1980; Desimone, R. *et al.*, 1985).

The seminal observation of attention-related effects in MT comes from Treue S. and Maunsell J. H. (1999). In this experiment, a monkey was instructed to attend to one of two independently moving dots and respond to a small speed change; responses to speed changes of the other stimulus were not rewarded. This caused substantial modulation, so that the firing rate was much higher (~80%) when the attended dot was moving in the preferred direction than if the unattended dot was doing so. The two situations were designed to be retinally identical, and only the attentional state of the animal caused the modulation. In this experiment, both spatial- and feature-based attention might contribute, since the dots were in different locations and also were moving in different directions.

Recent experiments allow us to dissociate the magnitude of purely spatial- and feature-based attention effects in MT. Purely spatial attention effects were measured in the experiments of Seidemann E. and Newsome W. T. (1999), in which a monkey was cued to attend to one of two patches of dots, one of which was within the RF. When the directions of the two were the same, spatial attention alone would modulate responses, and when it was directed within the RF of the cell, modulation of about 9% was observed. Conversely, Treue and colleagues have measured the

modulatory effects of attending to different directions, while keeping spatial attention fixed, and found slightly larger effects of 12–20% (Treue, S. and Martínez Trujillo, J. C., 1999; Martinez-Trujillo, J. C. and Treue, S., 2004). In these experiments, the attended stimulus was often as far as 20° from the RF under study, suggesting that feature-based attentional modulation can cross large distances in cortex.

Subsequent work has further expanded our understanding of the phenomenology of attentional modulation. The modulation by either spatial- or feature-based attention appears to be dominantly a multiplicative change in response magnitude (a gain change; Motter, B. C., 1993; McAdams, C. J. and Maunsell, J. H., 1999). The finding (Womelsdorf, T. *et al.*, 2006) that spatial attention can actually shift the RF of MT neurons toward the attended location while shrinking the RF around it, is consistent with the spotlight view of spatial attention. However, these shifts were modest in magnitude, relative to the diameter of the RF.

Quantitative comparison of the magnitude of attentional modulation in MT in a related task (Cook, E. P. and Maunsell, J. H., 2002b) indicated that the magnitudes of the neuronal changes in MT were insufficient to explain the simultaneously measured behavioral performance benefits. Interestingly, directional neurons in area VIP had the opposite problem – attentional modulations larger than those seen behaviorally. This also helps to reinforce the view that signals supporting performance on such discrimination or detection tasks are pooled from multiple cortical areas.

These experiments (and others not mentioned here) certainly help to constrain the mechanisms underlying attentional modulation, but do not directly lead to a circuit-level hypothesis as to how the changes take place, or where the attentional control signals arise. These are challenges for the next generation of attention experiments.

Neurons in MT also carry information about the remembered direction for a memory delay task. Pasternak and colleagues recorded the activity of MT neurons during the delay in a motion discrimination memory task (Bisley, J. W. *et al.*, 2004). They found that many neurons fired during the delay period, especially near the end before the test stimulus would appear. Furthermore, the neurons' firing rates differed with respect to the motion direction of the remembered stimulus. Again, this is strong evidence for the presence of signals concerning the cognitive context being present in the firing rates of MT neurons. It would be parsimonious to suggest that these might be a consequence of the same top-down signals responsible for directed attention, but this has not been directly tested.

2.10.3.10 Human MT

Human MT was one of the first areas identified using functional magnetic resonance imaging (fMRI) techniques, which noninvasively image the blood flow changes in the human brain that are consequent to local neuronal activity. While low in spatial and temporal resolution, the method allows one to ask questions regarding human brain function that cannot be addressed in animal experiments.

Human MT is usually localized using fMRI by repeatedly presenting a coherently moving dot stimulus followed by a motionless dot stimulus to the subject. The activity resulting from the stationary stimuli is subtracted from the trials containing the moving stimuli, leaving behind only the motion-induced activity, as can be seen in Figure 20 (Deutsch, C. K. *et al.*, 2000).

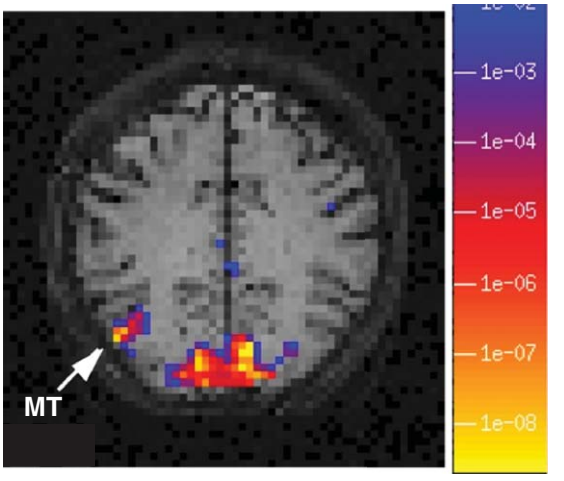

Figure 20 Functional magnetic resonance imaging (fMRI) image showing relative levels of activation in both MT and V1 while the subject was looking at dot motion. Patches of activation are defined as activity to the moving dots minus activity to static dots. The flame scale to the right shows the amount of functional activation. The most common imaging technique, blood oxygen level-dependent fMRI, measures change in local deoxyhemoglobin to indirectly measure neuronal activity. Reprinted from Deutsch, C. K., Oross, S., DiFiore, A., and McIlvane, W. J. 2000. Measuring brain activity correlates of behavior: a methodological overview. Exp. Anal. Hum. Behav. Bull. 36–42.

Since many motion responsive areas are localized in this task, putative MT in humans is often called hMT to highlight the difference. hMT or the MT complex in humans probably includes some of the areas near MT in monkeys, such as MST. It is likely that these motion areas in humans are the evolutionary homologs of those found in monkeys, but this idea is still unproven because of the difficulty of doing the necessary anatomical and physiological experiments in human subjects.

Still, much has been learned about human MT that supports its similarity to macaque MT. The area is retinotopically organized and responds best to motion-based stimuli. Much like the firing rate of MT cells in macaque, the degree of MT activation in humans depends on the coherence of the motion signal and is contrast sensitive, both important features of area MT (Tootell, R. B. *et al.*, 1995; Rees, G. *et al.*, 2000). In addition, Smith and colleagues (Smith, A. T. *et al.*, 1998) have shown that human MT is strongly activated by both first- and second-order motion. Human MT is also speed gradient sensitive (Martinez-Trujillo, J. C. *et al.*, 2005).

These studies have been vital to indicating the strong functional homology between human and macaque MT. In contrast with these similarities, it seems as though humans have more motion sensitive regions than the macaque, including area V3A and parts of the intraparietal sulcus (Orban, G. A. *et al.*, 2003). In addition, the relationship between the blood oxygen level-dependent fMRI population response and single-neuron physiology is becoming clearer (Rees, G. *et al.*, 2000).

Finally, hMT has been shown to activate vigorously even in the absence of visual motion (Culham, J. C. *et al.*, 1999; Kourtzi, Z. and Kanwisher, N., 2000). Studies measuring hMT activation as a result of the mental imagery of rotation support its role in motion perception, and the idea that mental imagery engages similar neural networks as direct perception (Cohen, M. S. *et al.*, 1996).

2.10.4 Global Motion

When we move through the world, a large-scale pattern of image motion results. This motion was called optic flow by J. J. Gibson (1950), and moving organisms use it for navigation and visual guidance of trajectory. The problems of how optic flow appears on the retina, how this pattern is processed in the brain, and how our trajectory is perceived have been the focus of considerable effort. The field shows the benefits of the interaction between theory, perceptual studies, and physiological approaches.

2.10.4.1 What Is Optic Flow?

The terminology used in the literature can be confusing, since optic flow, retinal flow, global motion, and wide-field motion are all used, with sometimes overlapping and sometimes distinct meanings. However, the patterns of motion themselves are fairly straightforward, with helpful regularities. Any observer trajectory produces a physical pattern of movement vectors simply from geometrical optics, and this is what Gibson originally termed optic flow. The projection of this pattern on the retina is technically referred to as retinal flow, which incorporates the independent movements of the eye. However, the use of the term optic flow for this retinal pattern is now widespread, and we will adopt it as well. For normal forward motion, the pattern of motion that results contains expansion across the frontal field of vision. The direction of the movement, or the destination, is a point at the center of the expansion. Gibson termed this point the focus of expansion, and theorized that it is used by the visual system to determine the heading, or path along which observer movement occurs. The exact pattern of motion surrounding this focus of expansion is also influenced by the depth structure of the scene: distant points result in lower speeds and nearby points result in high speeds, though both velocity vectors radiate directly from the focus of expansion. Where depth discontinuities happen at the edges of occluding objects, there are abrupt changes in the velocity on either side of the boundary (Figure 21).

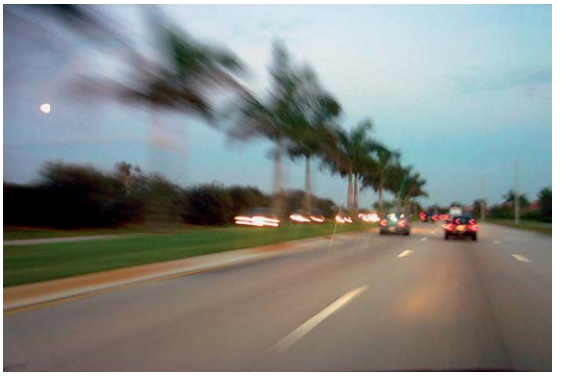

Figure 21 Example of expanding optic flow pattern, possibly seen while driving.

The pattern of motion is also affected by anything that causes the angle of gaze to shift over time. Most commonly, this would be head or eye movements causing rotations of the gaze direction even as one's trajectory remains on a straight line. This will superimpose an additional vector pattern on the pattern produced by the motion, which complicates the image considerably. If one is tracking an object in the scene – a common occurrence – the focus of expansion will no longer be at our direction of heading, but will instead be centered on the object we are tracking. If, however, we are tracking some independently moving object, there will often be no focus of expansion at all, so any method that simply tracks the focus of expansion will fail.

Perceptual experiments on optic flow have been closely guided by the foregoing theoretical considerations, but the history of physiological experiments on cortical mechanisms have been more guided by a reductionist desire to break down complex motion patterns into simple ones that can be parametrically varied for neuronal tuning measurements, making direct comparison difficult at times. In this account, we will focus on the physiology, while attempting to relate these results to the underlying theory whenever possible.

2.10.4.2 Area Medial Superior Temporal

Many cortical areas respond to optic flow, including the ventral intraparietal area (VIP), superior temporal polysensory area, area 7A and MT. However, the first area in which optic flow signals were discovered in monkey cortex, the medial superior temporal area (MST), has received by far the most attention. Area MST adjoins MT on the cortical surface and receives dense feed-forward input from MT (Boussaoud, D. *et al.*, 1990; 1992). Like MT, it is recognizable in histological sections as a densely myelinated region. MST can be further divided into two subregions, which differ in their connectivity and in their response properties. The distal subdivision of the MST (MSTd) tends to respond better to very large stimuli, while neurons in the lateral subdivision, MSTl, often show poor responses to such stimuli and better responses to small stimuli (Tanaka, K. *et al.*, 1986). This distinction is quantitative, however, and neurons in both places show many common properties, including large RFs and a preponderance of directionally selective responses. RFs in MST are many times larger than those in MT; some of them cover the entire visual field. Unlike in MT, there appears to be no relationship between RF size in MSTd and eccentricity (Orban, G. A., 1997). MSTd RFs cover a broad range of sizes, usually very large, at all eccentricities. These RFs also tend to be more elliptical than MT and often extend into the ipsilateral visual field (Duffy, C. J. and Wurtz, R. H., 1991).

The visual responses of MST neurons (most studies have focused on MSTd) are more complex than those of earlier levels of the motion system. Most MST neurons are selective for direction, and generally prefer faster speeds than does MT (Tanaka, K. and Saito, H., 1989). But what is most distinctive about MST is the selectivity for nonuniform motion patterns. A substantial fraction of MST neurons are selective for complex motion patterns, such as expansions, contractions or rotations (Saito, H. *et al.*, 1986; Duffy, C. J. and Wurtz, R. H., 1991; Graziano, M. S. A. *et al.*, 1994). Most MST cells, however, have a mixture of selectivities, including both for simple translation as well as for some combination of selectivity for rotation or radial motion (Duffy, C. J. and Wurtz, R. H., 1991). The latter can be well characterized using a spiral space, which represents different combinations of radial and rotary motion (spirals) as an angle in two-dimensional space. This is shown in Figure 22(a), which illustrates a single MST neuron responding to a family of such stimuli. It is clear that the cell is not tuned to a cardinal axis (pure rotation or contraction), but to a spiral stimulus that is a mixture of contraction and clockwise rotation, as in Figure 22(b), When one examines the population of neurons in MST, all possible directions are tiled by these responses, but there is a clear overabundance of expansion-selective neurons (Graziano, M. S. A. *et al.*, 1994). This has been viewed as good evidence for a role of MST in the analysis of optic flow during self-motion, since motion is usually forward, and expansion will thus be more common in natural viewing than contraction. Additional evidence supporting such a role for expansion-preferring cells in MST is that their responses are usually tuned for a particular location of the focus of expansion (Duffy, C. J. and Wurtz, R. H., 1995).

However, it is possible that even neurons not specifically tuned for expansion might have a role in the analysis of self-motion. Several models of heading perception (Lappe, M. and Rauschecker, J. P., 1993; Ben Hamed, S. *et al.*, 2003) rely on signals that are sigmoidally tuned for different headings. To examine this physiologically, researchers have turned to a more natural class of stimuli that simulate linear translations in particular directions in three-dimensional space,

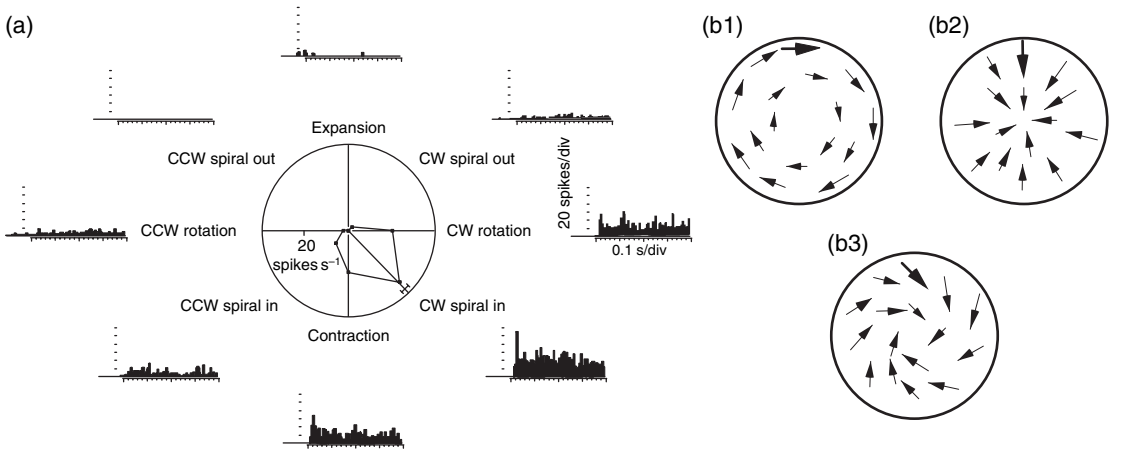

Figure 22 (a) The complex motion tuning of an example MST cell. This cell is tuned to clockwise contracting spiral. The radius represents the response magnitude. In the perimeter are the response histograms, summed over 10 trials. The dashed line marks the onset of the visual stimulus. CW, clockwise; CCW, counterclockwise. (b) Schematic drawings of spiral space random dot stimuli, for rotation (1), contraction (2), and spiral (3). Reprinted from Graziano, M. S. A., Andersen, R. A., and Snowden, R. J. 1994. Tuning of MST neurons to spiral motions. J. Neurosci. 14, 54–67.

usually through a random cloud of points. Such a stimulus is shown in Figures 23(a) and 23(b). Using such a stimulus, one can directly examine the tuning of neurons for heading, irrespective of the exact visual components of the pattern to which the cell is responding and observe tuning functions such as that shown in Figure 23(c). This neuron is clearly very informative about small changes of heading direction, especially near directly ahead where its firing rate changes most rapidly. This is also the region of heading directions to which observers are most accurate in estimation of their heading.

2.10.4.3 Extraretinal Inputs

In addition to its well-characterized motion responses, MST is the first area on the motion system to conspicuously represent nonvisual attributes. These include the position and velocity of the eyes (Sakata, H. *et al.*, 1983; Squatrito, S. and Maioli, M. G., 1997), as well as vestibular signals (Gu, Y. *et al.*, 2006). It is clear that MST is intimately involved in the generation of pursuit eye movements, since lesions to MST have deleterious effects on pursuit (Dursteler, M. R. *et al.*, 1987) and since microstimulation of MST can transiently interfere with ongoing pursuit. There are two classes of functional interpretation to the mixture of such extraretinal signals with visual motion signals. First, motion is the dominant signal supporting smooth pursuit, so having explicit motor signals mixed in with sensory signals might play a role in feedback correction of pursuit. Second, and not exclusively, ongoing eye movements distort and bias the optic flow signals upon which heading perception is based, so having direct access to such extraretinal signals might allow the neural representation of heading to be stable in the face of such interference.

Evidence for this latter view comes from experiments measuring MST heading tuning in the presence of eye and head movements (Bradley, D. C. *et al.*, 1996; Page, W. K. and Duffy, C. J., 1999; Shenoy, K. V. *et al.*, 1999; Britten, K. H. and Van Wezel, R. J., 2002). In such experiments, it has been found that MST neurons can partially or completely compensate for ongoing eye and head movements, producing a fairly stable representation of heading. One example of such stability is shown in Figure 23(c). This shows tuning with the eyes stationary, as well as in the presence of smooth pursuit to an independent target moving at $10^\circ\,s^{-1}$. Such pursuit might be expected to shift the focus of expansion by up to 60° in space, yet clearly the tuning functions of this cell are nearly unaffected by the pursuit. This suggests that MST can compensate quite well for ongoing eye movements, though the mechanism by which eye movement signals and visual signals are combined remains an open question.

MST also contains neurons that fire during pursuit or when the target temporarily disappears, while

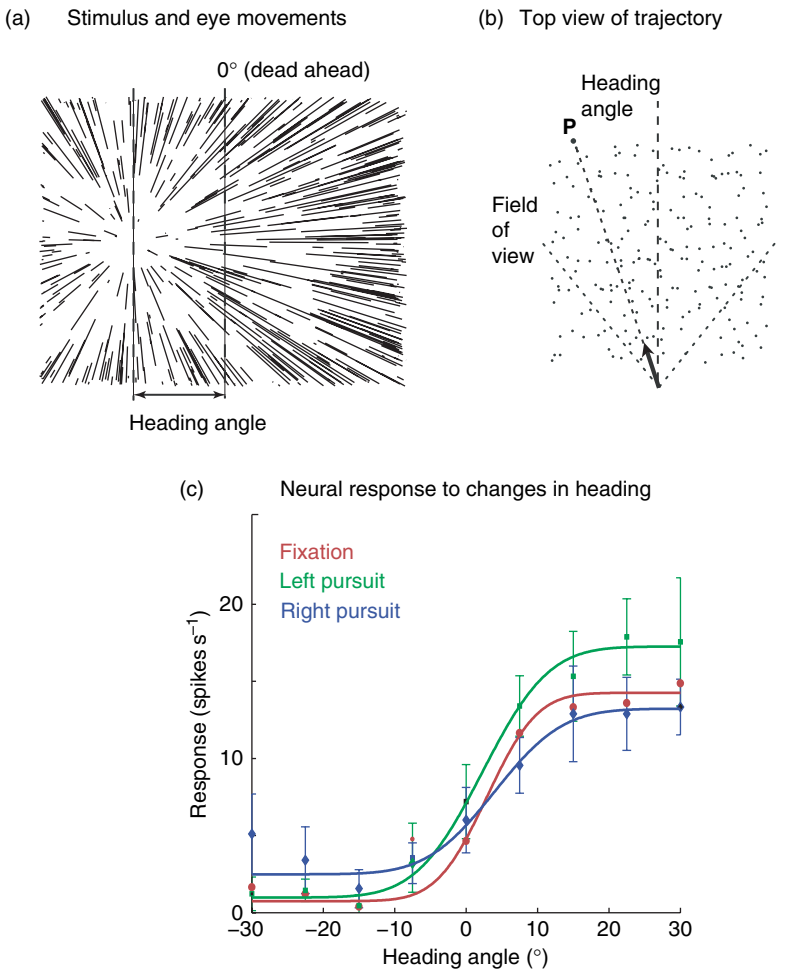

Figure 23 (a) The simulated geometry of the virtual trajectory of the animal with respect to the stimulus, as seen from above. The arrows are approximately to scale and illustrate large heading angles. Note that the cloud of points contains simulated depth. (b) Appearance of left and right heading stimuli, as seen from the observer's perspective. The length of each line shows the speed of each dot, which is inversely proportional to its simulated depth. The vertical dashed line corresponds to a heading of zero, directly ahead of the subject. The heading corresponds to the center of radial expansion, in the absence of eye movements. (c) Sigmoid function of neuronal response to changes in heading angle. This cell prefers rightward heading and shows increased firing rate to more rightward heading angles. This cell also shows excellent response stability in the presence of pursuit eye movements.

others only fire for moving stimuli in the absence of eye movements (Komatsu, H. and Wurtz, R., 1988; Newsome, W. *et al.*, 1988; Komatsu, H. and Wurtz, R., 1989; Erickson, R. G. and Their, P., 1991). In combination, these cells would be capable of differentiating between real motion in the world and motion that results from self-movement. These pursuit neurons could aid in optic flow processing by signaling the speed of the eye movement (Lappe, M., 1998; Ben Hamed, S. *et al.*, 2003). Direct measurements of population responses in MST, however, find that by whatever mechanism, the focus of expansion tuning is maintained in the presence of eye movements (Page, W. K. and Duffy, C. J., 1999).

Another source of relevant extraretinal inputs arises from the vestibular system. These are useful in locomotion because the vestibular system is capable of providing additional information about both linear and angular acceleration, which might help to augment heading signals or help to compensate for head rotations. In the dark, many MST neurons respond robustly to both circular and linear accelerations (Page, W. K. and Duffy, C. J., 1999; Gu, Y. *et al.*, 2006). Several things are interesting about these

signals. First, the tuning of where maximal response occurs under visual and vestibular stimulation is often very divergent. Second, when visual and vestibular inputs are combined, the responses do not appear to reflect a linear sum of these inputs, but instead a visual dominance. This is most evident when the precision of heading signals is compared under visual stimulation alone and combined visual/vestibular stimulation (Gu, Y. *et al.*, 2006). The use of such inputs to visual cortex in the guidance of locomotion is an exciting new area of research, and much remains to be understood about it.

2.10.4.4 Relating Media Superior Temporal Area to Perception

The presence of such optic flow signals suggests a role for MST in the perception of movement or of self-motion from optic flow. Several stronger lines of evidence support this suggestion more directly. MST is clearly involved with simple direction discrimination, from the experiments of Celebrini S. and Newsome W. T. (1995). The entire suite of observations that allowed the Newsome group to conclude that MT was directly involved in a direction discrimination task were replicated nearly identically in MST, showing that MST has at least as strong a role in simple direction discrimination as does MT. It is worth emphasizing that this task involved the discrimination of pattern motion on a scale of 10–40° in size, clearly not global in a strict sense. Therefore, it is clear that MST contributes essential information to medium-scale motion perception as well, and is not specialized for truly global motion.

In a related series of experiments, Heuer H. W. and Britten K. H. (2004) simultaneously recorded neuronal and behavioral responses to spiral space stimuli, to be able to ask how well MST supported performance on such discriminations. Interestingly, the results of this study supported a weaker relationship between MST activity and behavior on this class of discriminations. Neuronal sensitivity was on average much lower than was behavioral sensitivity, and choice probabilities were weak or nonexistent. Clearly, MST is not specialized for complex pattern motion over translational motion, and if anything is more involved in simpler motion judgments.

Consistent with this view, and with the idea that translational motion is a useful indicator of horizontal heading direction, Britten K. H. and Van Wezel R. J. (2002) microstimulated MST while an animal performed a heading discrimination task. Microstimulation of columns of MST cells biased the animal's response toward the heading direction preferentially encoded by the stimulated cells. Interestingly, the results were both larger and more systematic when the animal was engaged in pursuit eye movements. The results support a role for MST in the perception of self-motion from optic flow and the determination of heading during eye movements. Furthermore, since the sites stimulated in these experiments were not tuned for expansion, but instead for optic flow with a horizontal component, it supports the use of simpler motion components in discriminating heading, as suggested by recent population-based models (Lappe, M. and Rauschecker, J. P., 1993; Ben Hamed, S. *et al.*, 2003).

2.10.4.5 Other Areas with Optic Flow Responses

Area MST is not the only structure to respond to optic flow signals. Area 7A, in the parietal lobe, receives input from MST and VIP and also responds to optic flow patterns (Read, H. L. and Siegel, R. M., 1997; Siegel, R. M. and Read, H. L., 1997). In addition to being tuned for directions of optic flow, some cells in area 7A respond selectively to a class of optic flow stimuli, such as all radial motion (expansion and contraction). Also, optic flow responses in 7A are modulated by the position of the eyes (Read, H. L. and Siegel, R. M., 1997).

Area VIP, in the ventral intraparietal sulcus, receives feed-forward connections from MT and in turn projects to area 7A. Like MST and area 7A, many cells in VIP are tuned for optic flow patterns, most preferring expansion over contraction (72%; Bremmer, F. *et al.*, 2000; 2002). Furthermore, individual cell's response magnitudes are modulated by the location of the focus of expansion; thus, the population is capable of encoding the animal's heading. VIP also contains a large number of directionally selective neurons, and neuronal activity has been documented to be correlated with both choice and reaction time in a motion-onset-detection task (Cook, E. P. and Maunsell, J. H., 2002a).

Though VIP has many similarities with MST, with both encoding the direction of heading, there are differences that specify each area's particular role in optic flow processing. For VIP, the area's neurons respond to visual, vestibular, and tactile stimuli; MST lacks these somatosensory inputs. This has led to the suggestion that VIP may have the important function of encoding object movement in

near-extrapersonal space (Duhamel, J. R. *et al.*, 1998; Cooke, D. F. and Graziano, M. S., 2003; Graziano, M. S. and Cooke, D. F., 2006). If this suggestion is correct, as seems likely, then it is probable that VIP signals are used on both near-field and far-field tasks, and is not completely specialized for any single task.

Many areas contain a subset of neurons that have a significant response to optic flow stimuli, including motor cortex, area 5, and area PEc in the dorsal pathway and area STPa in the ventral pathway. In the motor cortex, neurons respond selectively to one type of optic flow stimuli (Merchant, H. *et al.*, 2001). In area PEc, in the dorsal portion of the superior parietal lobe, cells are responsive to optic flow and are selective for the location of the focus of expansion with respect to the fovea (Raffi, M. *et al.*, 2002). This selectivity could encode the heading direction of the animal.

Finally, area STPa, the anterior part of the superior temporal polysensory area, receives input from motion processing stream areas MST and 7A and from object processing area TEO. Neurons in this area show a selectivity for object motion, with most cells only responding to movements of objects in the world, rather than optic flow caused by self-motion (Hietanen, J. K. and Perrett, D. I., 1996a; 1996b). In addition, the area has direction preferences biased toward expansion with upward and downward motion stimuli. Since STPa responds best to the motion of external objects and prefers radial expansion, this suggests an involvement in the processing of looming stimuli.

2.10.4.6 Higher Motion Areas in Cat Visual Cortex

In the cat visual system, there are many cortical areas involved in processing motion. Compared with the monkey, the cat visual system appears much simpler, containing fewer extrastriate areas (Payne, B. R., 1993). The posteromedial lateral suprasylvian (PMLS) region has a preponderance of direction selective cells and is strongly reciprocally interconnected with area 18, a V2 homolog. Cells in these areas are also speed tuned (Price, N. S. *et al.*, 2006). As discussed earlier in this chapter, the directional responses in both these areas might very well arise from the input of lagged and nonlagged X and Y cells (Saul, A. B. and Humphrey, A. L., 1990; Mastronarde, D. N. *et al.*, 1991).

The cat homolog for motion processing area MT is the lateral suprasylvian visual area (LS; Zeki, S., 1974), and the two have very similar connectivity, retinotopy, and direction-selective responses. Area LS, like MT, has RFs with very large silent surrounds that have a preferred direction opposite that of the RF center. These surrounds are inhibitory for motion in the same direction as the center. Possibly, these cells are used to differentiate between the cat shifting its gaze, where image motion is uniform and activates the surround, and its locomotion, which would cause an optic flow field with many different directions.

When Sherk H. *et al.* (1997) compared LS cells' responses under these two different kinds of image motion, they found many cells responded better to the optic flow, most showing very little suppression, and 20% responded better to the optic flow than to RF center stimulation. However, LS is quite heterogeneous, with cells that prefer large-field frontoparallel motion, optic flow with a strong bias for expansion, or small moving bars (Kim, J. N. *et al.*, 1997). Surprisingly, during large field optic flow movies, the preferred direction of the cell was modified. Many cells responded robustly to the optic flow stimulus even though the direction of motion in the RF was orthogonal to the cell's preference (Mulligan, K. *et al.*, 1997; Sherk, H. *et al.*, 1997).

It is probably significant that one-fifth of cells in LS are selective for disparity, and many are selective for motion in depth (Toyama, K. and Kozasa, T., 1982; Toyama, K. *et al.*, 1986). Furthermore, bilateral lesions of area LS results in permanent deficits in direction discrimination and the perception of structure from motion (Rudolph, K. K. and Pasternak, T., 1996), demonstrating that LS plays a role in integrating motion signals.

The exact homolog of area MST in the cat remains unknown, and thus optic flow processing appears distributed. To begin with, area 18 contains a subset of cells selective for motion in depth (Cynader, M. and Regan, D., 1978). These neurons might be useful during locomotion, though this is dubious since most of these preferred motion away from the animal. There is another population of neurons in area 18, with large RFs showing directional selectivity for large fields of moving dots. Many of these RFs are in the lower visual field and respond best to downward motion, consistent with the visual stimulation during locomotion. Also, as in the monkey, these cells are part of a network that projects to the cerebellum, which is involved in the ongoing guidance of motor activity.

2.10.5 Conclusion

The motion system in visual cortex has been a very fruitful target of study over the years, as the work on this chapter has attempted to show. It has been studied from a variety of perspectives, and clearly much has been learned. However, almost equally striking is how much remains to be learned. One of the most obvious lacks is perhaps central to the entire system: we do not yet know the circuit on which directional selectivity in cortex is based. While good models exist, and even a good sketch of V1 circuitry up to the loci where directional cells appear, the synaptic basis of directionality remains shrouded in mystery.

Similar ignorance of local circuits becomes even more salient as one moves away from V1; we have a much better grip on the phenomenology than we do on the mechanisms. For instance, while we can say with certainty that MT cells integrate across space, spatial frequency, and temporal frequency, we do not know whether this happens monosynaptically from afferent connections, indirectly through multiple feed-forward pathways, or even laterally from other MT cells. As in the case of the V1 circuit questions, the difficulty of critical experiments should not forbid the attempt. It is possible that with the improvement of high-resolution *in vivo* imaging methodologies, such questions will become more tractable in the near future.

Large-scale questions also remain about the relation between structure and function in the motion system. While this pathway, and particularly area MT, has been a fertile proving ground for experiments that relate the firing of cortical neurons quantitatively to perception, there are suggestions that this work is far from complete. Specifically, this line of investigation has clearly suggested that the perception of motion is a widely shared function. Nonetheless, most experiments have looked at single areas. We also have little idea how the perceptual readout of these many areas works, or how the multiple signals are combined in the service of awareness or visually guided behavior. This is a set of questions that existing techniques will probably be very adequate to address.

Oddly, there also seems to be a dearth of theory in the analysis of cortical motion mechanisms, despite the extensive theory associated with motion perception. In part, this is related to a lack of data to support more biologically realistic, structural models of motion processing, and in part it probably stems from theorists' desires to develop more elegant mathematical models. But in any case, the field clearly appears to be at a stage where more crosstalk between theory and experimental test would be of direct and immediate benefit.

As this brief and incomplete list shows, there is at least no worry that the book on cortical motion is now closed, and it is exciting to think that the next 20 years might provide as many important insights as has the last two decades.

References

Adelson, E. H. and Movshon, J. A. 1983. The perception of coherent motion in two-dimensional patterns. ACM Siggraph and Sigart Interdisciplinary Workshop on Motion: Representation and Perception:11–16. Toronto.

Adelson, E. H. and Bergen, J. R. 1985. Spatio-temporal energy models for the perception of motion. J. Opt. Soc. Am. A 2, 284–299.

Albrecht, D. G. 1995. Visual cortex neurons in monkey and cat: effect of contrast on the spatial and temporal phase transfer functions. Vis. Neurosci. 12, 1191–1210.

Albright, T. D. 1984. Direction and orientation selectivity of neurons in visual area MT of the macaque. J. Neurophysiol. 52, 1106–1130.

Albright, T. D., Desimone, R., and Gross, C. G. 1984. Columnar organization of directionally selective cells in visual area MT of macaques. J Neurophysiol 51, 16–31.

Allman, J. M. and Kaas, J. H. 1971. A representation of the visual field in the caudal third of the middle temporal gyrus of the owl monkey (*Aotus trivirgatus*). Brain Res. 31, 85–105.

Allman, J. M., Meizin, F., and McGuinness, E. 1985. Direction and velocity-specific responses from beyond the classical receptive field in the middle temporal visual area (MT). Perception 14, 105–126.

Amir, Y., Harel, M., and Malach, R. 1993. Cortical hierarchy reflected in the organization of intrinsic connections in macaque monkey visual cortex. J. Comp. Neurol. 334, 19–46.

Baker, C. L., Jr. and Braddick, O. J. 1982. Does segregation of differently moving areas depend on relative or absolute displacement? Vision Res. 22, 851–856.

Baker, C. L., Jr. and Braddick, O. J. 1985. Eccentricity-dependent scaling of the limits for short-range apparent motion perception. Vision Res. 25, 803–812.

Barlow, H. B. and Levick, W. R. 1965. The mechanism of directionally selective units in rabbit's retina. J. Physiol. 178, 477–504.

Barlow, H. B., Hill, R. M., and Levick, W. R. 1964. Retinal ganglion cells responding selectively to direction and speed of image motion in the rabbit. J. Physiol. 173, 377–407.

Ben Hamed, S., Page, W., Duffy, C., and Pouget, A. 2003. MSTd neuronal basis functions for the population encoding of heading direction. J. Neurophysiol. 90, 549–558.

Bender, D. B. 1982. Receptive-field properties of neurons in the macaque inferior pulvinar. J. Neurophysiol. 48, 1–17.

Bisley, J. W., Zaksas, D., Droll, J. A., and Pasternak, T. 2004. Activity of neurons in cortical area MT during a memory for motion task. J. Neurophysiol. 91, 286–300.

Blasdel, G. G. and Fitzpatrick, D. 1984. Physiological organization of layer 4 in macaque striate cortex. J. Neurosci. 4, 880–895.

Blaser, E., Papathomas, T., and Vidnyanszky, Z. 2005. Binding of motion and colour is early and automatic. Eur. J. Neurosci. 21, 2040–2044.

Born, R. T. 2000. Center-surround interactions in the middle temporal visual area of the owl monkey. J. Neurophysiol. 84, 2658–2669.

Born, R. T. and Bradley, D. C. 2005. Structure and function of visual area MT. Annu. Rev. Neurosci. 28, 157–189.

Borst, A. and Egelhaaf, M. 1989. Principles of motion detection. Trends Neurosci. 12, 297–306.

Boussaoud, D., Desimone, R., and Ungerleider, L. G. 1992. Subcortical connections of visual areas MST and FST in macaques. Vis. Neurosci. 9, 291–302.

Boussaoud, D., Ungerleider, L. G., and Desimone, R. 1990. Pathways for motion analysis: cortical connections of the medial superior temporal and fundus of the superior temporal visual areas in the macaque. J. Comp. Neurol. 296, 462–495.

Braddick, O. 1974. A short-range process in apparent motion. Vision Res. 14, 519–527.

Braddick, O. J. 1980. Low level and high level processes in apparent motion. Phil. Trans. R. Soc. Lond. B 290, 137–151.

Bradley, D. C. and Andersen, R. A. 1998. Center-surround antagonism based on disparity in primate area MT. J. Neurosci. 18, 7552–7565.

Bradley, D. C., Qian, N., and Andersen, R. A. 1995. Integration of motion and stereopsis in middle temporal cortical area of macaques. Nature 373, 609–611.

Bradley, D. C., Maxwell, M., Andersen, R. A., Banks, M. S., and Shenoy, K. V. 1996. Mechanisms of heading perception in primate visual cortex. Science 273, 1544–1547.

Bremmer, F., Duhamel, J. R., Ben Hamed, S., and Graf, W. 2000. Stages of self-motion processing in primate posterior parietal cortex. Int. Rev. Neurobiol. 44, 173–198.

Bremmer, F., Duhamel, J. R., Ben Hamed, S., and Graf, W. 2002. Heading encoding in the macaque ventral intraparietal area (VIP). Eur. J. Neurosci. 16, 1554–1568.

Briggs, F. and Callaway, E. M. 2001. Layer-specific input to distinct cell types in layer 6 of monkey primary visual cortex. J. Neurosci. 21, 3600–3608.

Briggs, F. and Callaway, E. M. 2005. Laminar patterns of local excitatory input to layer 5 neurons in macaque primary visual cortex. Cereb. Cortex 15, 479–488.

Britten, K. H. and Van Wezel, R. J. 2002. Area MST and heading perception in macaque monkeys. Cereb. Cortex 12, 692–701.

Britten, K. H., Shadlen, M. N., Newsome, W. T., and Movshon, J. A. 1992. The analysis of visual motion: a comparison of neuronal and psychophysical performance. J. Neurosci. 12, 4745–4765.

Britten, K. H., Shadlen, M. N., Newsome, W. T., and Movshon, J. A. 1993. Responses of neurons in macaque MT to stochastic motion signals. Vis. Neurosci. 10, 1157–1169.

Britten, K. H., Newsome, W. T., Shadlen, M. N., Celebrini, S., and Movshon, J. A. 1996. A relationship between behavioral choice and the visual responses of neurons in macaque MT. Vis. Neurosci. 13, 87–100.

Callaway, E. M. and Wiser, A. K. 1996. Contributions of individual layer 2-5 spiny neurons to local circuits in macaque primary visual cortex. Vis. Neurosci. 13, 907–922.

Carandini, M., Heeger, D. J., and Movshon, J. A. 1997. Linearity and normalization in simple cells of the macaque primary visual cortex. J. Neurosci. 17, 8621–8644.

Celebrini, S. and Newsome, W. T. 1995. Microstimulation of extrastriate area MST influences performance on a direction discrimination task. J. Neurophys. 73, 437–448.

Chatterjee, S. and Callaway, E. M. 2002. S cone contributions to the magnocellular visual pathway in macaque monkey. Neuron 35, 1135–1146.

Churchland, M. M., Priebe, N. J., and Lisberger, S. G. 2005. Comparison of the spatial limits on direction selectivity in visual areas MT and V1. J. Neurophysiol. 93, 1235–1245.

Cohen, M. S., Kosslyn, S. M., Breiter, H. C., DiGirolamo, G. J., Thompson, W. L., Anderson, A. K., Brookheimer, S. Y., Rosen, B. R., and Belliveau, J. W. 1996. Changes in cortical activity during mental rotation. A mapping study using functional MRI. Brain 119, 89–100.

Conway, B. R. and Livingstone, M. S. 2003. Space–time maps and two-bar interactions of different classes of direction-selective cells in macaque V-1. J. Neurophysiol. 89, 2726–2742.

Cook, E. P. and Maunsell, J. H. 2002a. Dynamics of neuronal responses in macaque MT and VIP during motion detection. Nat. Neurosci. 5, 985–994.

Cook, E. P. and Maunsell, J. H. 2002b. Attentional modulation of behavioral performance and neuronal responses in middle temporal and ventral intraparietal areas of macaque monkey. J. Neurosci. 22, 1994–2004.

Cooke, D. F. and Graziano, M. S. 2003. Defensive movements evoked by air puff in monkeys. J. Neurophysiol. 90, 3317–3329.

Croner, L. J. and Albright, T. D. 1999. Segmentation by color influences responses of motion-sensitive neurons in the cortical middle temporal visual area. J. Neurosci. 19, 3935–3951.

Culham, J. C., Dukelow, S. P., Vilis, T., Hassard, F. A., Gati, J. S., Menon, R. S., and Goodale, M. A. 1999. Recovery of fMRI activation in motion area MT following storage of the motion aftereffect. J. Neurophysiol. 81, 388–393.

Cynader, M. and Regan, D. 1978. Neurones in cat parastriate cortex sensitive to the direction of motion in three-dimensional space. J. Physiol. 274, 549–569.

De Valois, R. L., Cottaris, N. P., Mahon, L. E., Elfar, S. D., and Wilson, J. A. 2000. Spatial and temporal receptive fields of geniculate and cortical cells and directional selectivity. Vision Res. 40, 3685–3702.

DeAngelis, G. C. and Newsome, W. T. 1999. Organization of disparity-selective neurons in macaque area MT. J. Neurosci. 19, 1398–1415.

DeAngelis, G. C., Cumming, B. G., and Newsome, W. T. 1998. Cortical area MT and the perception of stereoscopic depth. Nature 394, 677–680.

DeAngelis, G. C., Ohzawa, I., and Freeman, R. D. 1993. Spatiotemporal organization of simple-cell receptive fields in the cat s striate cortex. I. General characteristics and postnatal development. J. Neurophysiol. 69, 1091–1117.

DeAngelis, G. C., Ohzawa, I., and Freeman, R. D. 1995. Receptive-field dynamics in the central visual pathways. Trends Neurosci. 18, 451–458.

Derrington, A. M. and Lennie, P. 1984. Spatial and temporal contrast sensitivities of neurones in lateral geniculate nucleus of macaque. J. Physiol. 357, 219–240.

Derrington, A. M. and Henning, G. B. 1993. Detecting and discriminating the direction of motion of luminance and colour gratings. Vision Res. 33, 799–811.

Derrington, A. M., Allen, H. A., and Delicato, L. S. 2004. Visual mechanisms of motion analysis and motion perception. Annu. Rev. Psych. 55, 181–205.

Desimone, R., Schein, S. J., Moran, J., and Ungerleider, L. G. 1985. Contour, color and shape analysis beyond the striate cortex. Vision Res. 25, 441–452.

Deutsch, C. K., Oross, S., DiFiore, A., and McIlvane, W. J. 2000. Measuring brain activity correlates of behavior: a methodological overview. Exp. Anal. Hum. Behav. Bull. 36–42.

Dodd, J. V., Krug, K., Cumming, B. G., and Parker, A. J. 2001. Perceptually bistable three-dimensional figures evoke high choice probabilities in cortical area MT. J. Neurosci. 21, 4809–4821.

Dubner, R. and Zeki, S. M. 1971. Response properties and receptive fields of cells in an anatomically defined region of the superior temporal sulcus. Brain Res. 35, 528–532.

Duffy, C. J. and Wurtz, R. H. 1991. Sensitivity of MST neurons to optic flow stimuli. I. A continuum of response selectivity of large-field stimuli. J. Neurophysiol. 65, 1329–1345.
Duffy, C. J. and Wurtz, R. H. 1995. Response of monkey MST neurons to optic flow stimuli with shifted centers of motion. J. Neurosci. 15, 5192–5208.
Duhamel, J. R., Colby, C. L., and Goldberg, M. E. 1998. Ventral intraparietal area of the macaque: congruent visual and somatic response properties. J. Neurophysiol. 79, 126–136.
Dumbrava, D., Faubert, J., and Casanova, C. 2001. Global motion integration in the cat's lateral posterior-pulvinar complex. Eur. J. Neurosci. 13, 2218–2226.
Dursteler, M. R., Wurtz, R. H., and Newsome, W. T. 1987. Directional pursuit deficits following lesions of the foveal representation within the superior temporal sulcus of the macaque monkey. J. Neurophysiol. 57, 1262–1287.
Egelhaaf, M. and Borst, A. 1993. Movement detection in arthropods. Rev. Oculomot. Res. 5, 53–77.
Emerson, R. C., Bergen, J. R., and Adelson, E. H. 1992. Directionally selective complex cells and the computation of motion energy in cat visual cortex. Vision Res. 32, 203–218.
Emerson, R. C., Citron, M. C., Vaughn, W. J., and Klein, S. A. 1987. Nonlinear directionally selective subunits in complex cells of cat striate cortex. J. Neurophysiol. 58, 33–65.
Enroth-Cugell, C. and Robson, J. G. 1966. The contrast sensitivity of retinal ganglion cells of the cat. J. Physiol. 187, 517–552.
Erickson, R. G. and Their, P. 1991. A neuronal correlate of spatial stability during periods of self-induced visual motion. Exp. Brain Res. 86, 608–616.
Felleman, D. and Van Essen, D. 1991. Distributed hierarchical processing in the primate cerebral cortex. Cereb. Cortex 1, 1–47.
Felleman, D. J. and Van Essen, D. C. 1987. Receptive field properties of neurons in area V3 of macaque monkey extrastriate cortex. J. Neurophys. 57, 889–920.
Field, D. J. and Tolhurst, D. J. 1986. The structure and symmetry of simple-cell receptive-field profiles in the cat's visual cortex. Proc. R. Soc. Lond. B 228, 379–400.
Fleishman, L. J. 1986. Motion detection in the presence and absence of background motion in an Anolis lizard. J. Comp. Physiol. 159, 711–720.
Foster, K. H., Gaska, J. P., Nagler, M., and Pollen, D. A. 1985. Spatial and temporal frequency selectivity of neurones in visual cortical areas V1 and V2 of the macaque monkey. J. Physiol. 365, 331–363.
Freeman, T. C., Sumnall, J. H., and Snowden, R. J. 2003. The extra-retinal motion aftereffect. J. Vis. 3, 771–779.
Frost, B. J., Wylie, D. R., and Wang, Y. C. 1990. The processing of object and self-motion in the tectofugal and accessory optic pathways of birds. Vision Res. 30, 1677–1688.
Gegenfurtner, K. R. and Hawken, M. J. 1995. Temporal and chromatic properties of motion mechanisms. Vision Res. 35, 1547–1563.
Gegenfurtner, K. R., Kiper, D. C., and Levitt, J. B. 1997. Functional properties of neurons in macaque area V3. J. Neurophysiol. 77, 1906–1923.
Gibson, J. J. 1950. Perception of the Visual World. Houghton-Mifflin.
Graziano, M. S. and Cooke, D. F. 2006. Parieto-frontal interactions, personal space, and defensive behavior. Neuropsychologia 44, 2621–2635.
Graziano, M. S. A., Andersen, R. A., and Snowden, R. J. 1994. Tuning of MST neurons to spiral motions. J. Neurosci. 14, 54–67.
Grunewald, A., Bradley, D. C., and Andersen, R. A. 2002. Neural correlates of structure-from-motion perception in macaque V1 and MT. J. Neurosci. 22, 6195–6207.
Gu, Y., Watkins, P. V., Angelaki, D. E., and DeAngelis, G. C. 2006. Visual and nonvisual contributions to three-dimensional heading selectivity in the medial superior temporal area. J. Neurosci. 26, 73–85.
Hassenstein, B. and Reichardt, W. 1956. Systemtheoretische Analyse der Zeit-, Reihenfolgen-, und Vorzeichenauswertung bei der Bewgungsperzeption des Russelkafers Chlorophanus. Z. Naturforsch B 11, 513–524.
Hawken, M. J., Parker, A. J., and Lund, J. S. 1988. Laminar organization and contrast sensitivity of direction-selective cells in the striate cortex of the old world monkey. J. Neurosci. 8, 3541–3548.
Heeger, D. J. 1987. Model for the extraction of image flow. J Opt Soc Am A 4, 1455–1471.
Heuer, H. W. and Britten, K. H. 2004. Optic flow signals in extrastriate area MST: comparison of perceptual and neuronal sensitivity. J. Neurophysiol. 91, 1314–1326.
Hietanen, J. K. and Perrett, D. I. 1996a. A comparison of visual responses to object- and ego-motion in the macaque superior temporal polysensory area. Exp. Brain Res. 108, 341–345.
Hietanen, J. K. and Perrett, D. I. 1996b. Motion sensitive cells in the macaque superior temporal polysensory area: response discrimination between self-generated and externally generated pattern motion. Behav. Brain Res. 76, 155–167.
Hildreth, E. C. and Koch, C. 1987. The analysis of visual motion: from computational theory to neuronal mechanisms. Ann. Rev. Neurosci. 10, 477–533.
Holub, R. A. and Morton-Gibson, M. 1981. Response of Visual Cortical Neurons of the cat to moving sinusoidal gratings: response-contrast functions and spatiotemporal interactions. J. Neurophysiol. 46, 1244–1259.
Hubel, D. H. and Wiesel, T. N. 1962. Receptive fields, binocular interaction and functional architecture in the cat visual system. J. Physiol. Lond. 160, 106–154.
Hubel, D. H. and Wiesel, T. N. 1968. Receptive fields and functional architecture of monkey striate cortex. J. Physiol. Lond. 195, 215–243.
Hubel, D. H., Wiesel, T. N., and LeVay, S. 1976. Functional architecture of area 17 in normal and monocularly deprived macaque monkeys. Cold Spring Harb. Symp. Quant. Biol. 40, 581–589.
Ibbotson, M. R. 2001. Evidence for velocity-tuned motion-sensitive descending neurons in the honeybee. Proc. Biol. Sci. 268, 2195–2201.
Ibbotson, M. R., Mark, R. F., and Maddess, T. L. 1994. Spatiotemporal response properties of direction-selective neurons in the nucleus of the optic tract and dorsal terminal nucleus of the wallaby, Macropus eugenii. J. Neurophysiol. 72, 2927–2943.
Irvin, G. E., Norton, T. T., Sesma, M. A., and Casagrande, V. A. 1986. W-like response properties of interlaminar zone cells in the lateral geniculate nucleus of a primate (*Galago crassicaudatus*). Brain Res. 362, 254–270.
Jagadeesh, B., Wheat, H. S., and Ferster, D. 1993. Linearity of summation of synaptic potentials underlying direction selectivity in simple cells of the cat visual cortex. Science 262, 1901–1904.
Kim, J. N., Mulligan, K., and Sherk, H. 1997. Simulated optic flow and extrastriate cortex. I. Optic flow versus texture. J. Neurophysiol. 77, 554–561.
Kohn, A. and Movshon, J. A. 2004. Adaptation changes the direction tuning of macaque MT neurons. Nat. Neurosci. 7, 764–772.
Komatsu, H. and Wurtz, R. 1988. Relation of cortical areas MT and MST to pursuit eye movements. I. Localization and visual properties of neurons. J. Neurophysiol. 60, 580–603.
Komatsu, H. and Wurtz, R. H. 1989. Modulation of pursuit eye movements by stimulation of cortical areas MT and MST. J. Neurophysiol. 62, 31–47.

Kourtzi, Z. and Kanwisher, N. 2000. Activation in human MT/MST by static images with implied motion. J. Cogn. Neurosci. 12, 48–55.

Krekelberg, B., Van Wezel, R. J., and Albright, T. D. 2006. Interactions between speed and contrast tuning in the middle temporal area: implications for the neural code for speed. J. Neurosci. 26, 8988–8998.

Krubitzer, L. A. and Kaas, J. H. 1990. Cortical connections of MT in four species of primates: areal, modular, and retinotopic patterns. Vis. Neurosci. 5, 165–204.

Krug, K., Cumming, B. G., and Parker, A. J. 2004. Comparing perceptual signals of single V5/MT neurons in two binocular depth tasks. J. Neurophysiol. 92, 1586–1596.

Lagae, L., Raiguel, S., and Orban, G. A. 1993. Speed and direction selectivity of macaque middle temporal neurons. J. Neurophys. 69, 19–39.

Lagae, L., Gulyas, B., Raiguel, S., and Orban, G. A. 1989. Laminar analysis of motion information processing in macaque V5. Brain Res. 496, 361–367.

Lappe, M. 1998. A model of the combination of optic flow and extraretinal eye movement signals in primate extrastriate visual cortex. Neural model of self-motion from optic flow and extraretinal cues. Neural Netw. 11, 397–414.

Lappe, M. and Rauschecker, J. P. 1993. A neural network for the processing of optic flow from ego-motion in man and higher mammals. Neural Comput. 5, 374–391.

Leventhal, A. G., Rodieck, R. W., and Dreher, B. 1981. Retinal ganglion cell classes in the Old World monkey: morphology and central projections. Science 213, 1139–1142.

Leventhal, A. G., Wang, Y., Schmolesky, M. T., and Zhou, Y. 1998. Neural correlates of boundary perception. Vis. Neurosci. 15, 1107–1118.

Leventhal, A. G., Thompson, K. G., Liu, D., Zhou, Y., and Ault, S. J. 1995. Concomitant sensitivity to orientation, direction, and color of cells in layers 2, 3, and 4 of monkey striate cortex. J. Neurosci. 15, 1808–1818.

Levinson, E. and Sekuler, R. 1975. The independence of channels in human vision selective for direction of movement. J. Physiol. Lond. 250, 347–366.

Levitt, J., Kiper, D., and Movshon, A. 1994. Receptive fields and functional architecture of macaque V2. J. Neurophysiol. 71, 2517–2542.

Lisberger, S. G. and Movshon, J. A. 1999. Visual motion analysis for pursuit eye movements in area MT of macaque monkeys. J. Neurosci. 19, 2224–2246.

Liu, J. and Newsome, W. T. 2005. Correlation between speed perception and neural activity in the middle temporal visual area. J. Neurosci. 25, 711–722.

Livingstone, M. S. 1998. Mechanisms of direction selectivity in macaque V1. Neuron 20, 509–526.

Livingstone, M. and Conway, B. R. 2006. Contrast affects speed tuning, space-time slant, and receptive-field organization of simple cells in macaque V1. J. Neurophysiol. 97, 849–857.

Livingstone, M. and Hubel, D. 1988. Segregation of form, color, movement, and depth: anatomy, physiology, and perception. Science 240, 740–749.

Livingstone, M. S. and Hubel, D. H. 1984. Anatomy and physiology of a color system in the primate visual cortex. J. Neurosci. 4, 309–356.

Logothetis, N. K. and Schall, J. D. 1990. Binocular motion rivalry in macaque monkeys: eye dominance and tracking eye movements. Vision Res. 30, 1409–1419.

Lund, J. S. and Boothe, R. G. 1975. Interlaminar connections and pyramidal neuron organization in the visual cortex, area 17, of the macaque monkey. J. Comp. Neurol. 159, 305–334.

Martinez-Trujillo, J. C. and Treue, S. 2004. Feature-based attention increases the selectivity of population responses in primate visual cortex. Curr. Biol. 14, 744–751.

Martinez-Trujillo, J. C., Tsotsos, J. K., Simine, E., Pomplun, M., Wildes, R., Treue, S., Heinze, H. J., and Hopf, J. M. 2005. Selectivity for speed gradients in human area MT/V5. Neuroreport 16, 435–438.

Martinez, L. M. and Alonso, J. M. 2001. Construction of complex receptive fields in cat primary visual cortex. Neuron 32, 515–525.

Mastronarde, D. N., Humphrey, A. L., and Saul, A. B. 1991. Lagged Y cells in the cat lateral geniculate nucleus. Vis. Neurosci. 7, 191–200.

Maunsell, J. H., Nealey, T. A., and DePriest, D. D. 1990. Magnocellular and parvocellular contributions to responses in the middle temporal visual area (MT) of the macaque monkey. J. Neurosci. 10, 3323–3334.

Maunsell, J. H. R. and Van Essen, D. C. 1983a. The connections of the middle temporal visual area (MT) and their relationship to a cortical hierarchy in the macaque monkey. J. Neurosci. 3, 2563–2586.

Maunsell, J. H. R. and Van Essen, D. C. 1983b. Functional properties of neurons in the middle temporal visual area (MT) of the macaque monkey: I. Selectivity for stimulus direction, speed and orientation. J. Neurophysiol. 49, 1127–1147.

Maunsell, J. H. R. and Van Essen, D. C. 1987. Topographic organization of the middle temporal visual area in the macaque monkey: representational biases and the relationship to callosal connections and myeloarchitectonic boundaries. J. Comp. Neurol. 266, 535–555.

McAdams, C. J. and Maunsell, J. H. 1999. Effects of attention on orientation-tuning functions of single neurons in macaque cortical area V4. J. Neurosci. 19, 431–441.

McLean, J. and Palmer, L. A. 1989. Contribution of linear spatiotemporal receptive field structure to velocity selectivity of simple cells in area 17 of cat. Vision Res. 29, 675–679.

Merchant, H., Battaglia-Mayer, A., and Georgopoulos, A. P. 2001. Effects of optic flow in motor cortex and area 7a. J. Neurophysiol. 86, 1937–1954.

Michael, C. R. 1981. Columnar organization of color cells in monkey's striate cortex. J. Neurophysiol. 46, 587–604.

Mikami, A., Newsome, W. T., and Wurtz, R. H. 1986. Motion selectivity in macaque visual cortex: II. Spatio-temporal range of directional interactions in MT and V1. J. Neurophysiol. 55, 1328–1339.

Motter, B. C. 1993. Focal attention produces spatial selective processing in visual cortical areas V1, V2, and V4 in the presence of competing stimuli. J. Neurophysiol. 70, 909–919.

Movshon, J. A. and Newsome, W. T. 1996. Visual response properties of striate cortical neurons projecting to area MT in macaque monkeys. J. Neurosci. 16, 7733–7741.

Movshon, J. A., Thompson, I. D., and Tolhurst, D. J. 1978. Receptive field organization of complex cells in the cat's striate cortex. J. Physiol. Lond. 283, 79–99.

Movshon, J. A., Adelson, E. H., Gizzi, M. S., and Newsome, W. T. 1985. The Analysis of Moving Visual Patterns. In: Study Group on Pattern Recognition Mechanisms (*eds*. C. Chagas, R. Gattass, and C. Gross), pp. 117–151. Pontifica Academia Scientiarum.

Movshon, J. A., Newsome, W. T., Gizzi, M. S., and Levitt, J. B. 1988. Spatio-temporal tuning and speed sensitivity in macaque visual cortical neurons. Invest. Opth. Vis. Sci. Suppl. 29, 327.

Mulligan, K., Kim, J. N., and Sherk, H. 1997. Simulated optic flow and extrastriate cortex. II. Responses to bar versus large-field stimuli. J. Neurophysiol. 77, 562–570.

Newsome, W., Shadlen, M., Zohary, E., Britten, K., and Movshon, J. 1995. Visual Motion: Linking Neuronal Activity to Psychophysical Performance. In: The Cognitive Neurosciences (*ed*. M. Gazzaniga), pp. 401–414. MIT Press.

Newsome, W. T. and Paré, E. B. 1988. A selective impairment of motion perception following lesions of the middle temporal visual area (MT). J. Neurosci. 8, 2201–2211.

Newsome, W. T., Wurtz, R. H., and Komatsu, H. 1988. Relation of cortical areas MT and MST to pursuit eye movements. II. Differentiation of retinal from extraretinal inputs. J. Neurophysiol. 60, 604–620.

Orban, G. A. 1997. Visual Processing in Macaque Area MT/V5 and its Satellites (MSTd and MSTv). In: Cerebral Cortex (*eds*. K. S. Rockland, J. H. Kaas, and A. Peters), pp. 359–434. Plenum.

Orban, G. A., Fize, D., Peuskensm, H., Denys, K., Nelissen, K., Sunaert, S., Todd, J., and Vanduffel, W. 2003. Similarities and differences in motion processing between the human and macaque brain: evidence from fMRI. Neuropsychologia 41, 1757–1768.

Pack, C. C., Hunter, J. N., and Born, R. T. 2005. Contrast dependence of suppressive influences in cortical area MT of alert macaque. J. Neurophysiol. 93, 1809–1815.

Pack, C. C., Livingstone, M. S., Duffy, K. R., and Born, R. T. 2003. End-stopping and the aperture problem: two-dimensional motion signals in macaque V1. Neuron 39, 671–680.

Page, W. K. and Duffy, C. J. 1999. MST neuronal responses to heading direction during pursuit eye movements. J. Neurophysiol. 81, 596–610.

Parker, A. J., Krug, K., and Cumming, B. G. 2002. Neuronal activity and its links with the perception of multi-stable figures. Philos. Trans. R. Soc. Lond. B 357, 1053–1062.

Payne, B. R. 1993. Evidence for visual cortical area homologs in cat and macaque monkey. Cereb. Cortex 3, 1–25.

Perrone, J. A. 2006. A single mechanism can explain the speed tuning properties of MT and V1 complex neurons. J. Neurosci. 26, 11987–11991.

Perrone, J. A. and Thiele, A. 2001. Speed skills: measuring the visual speed analyzing properties of primate MT neurons. Nat. Neurosci. 4, 526–532.

Petersen, S. E., Baker, J. F., and Allman, J. M. 1985. Direction-specific adaptation in area MT of the owl monkey. Brain Res. 346, 146–150.

Peterson, M. R., Li, B., and Freeman, R. D. 2004. The derivation of direction selectivity in the striate cortex. J. Neurosci. 24, 3583–3591.

Poggio, T. and Reichardt, W. 1973. Considerations on models of movement detection. Kybernetik 13, 223–227.

Pollen, D. A. and Ronner, S. F. 1981. Phase relationships between adjacent simple cells in the visual cortex. Science 212, 1409–1411.

Posner, M. I. 1980. Orienting of attention. Q. J. Exp. Psychol. 32, 3–25.

Poznanski, R. R. 2005. Biophysical mechanisms and essential topography of directionally selective subunits in rabbit's retina. J. Integr. Neurosci. 4, 341–361.

Price, N. S., Crowder, N. A., Hietanen, M. A., and Ibbotson, M. R. 2006. Neurons in V1, V2, and PMLS of cat cortex are speed tuned but not acceleration tuned: the influence of motion adaptation. J. Neurophysiol. 95, 660–673.

Priebe, N. J. and Lisberger, S. G. 2004. Estimating target speed from the population response in visual area MT. J. Neurosci. 24, 1907–1916.

Priebe, N. J., Cassanello, C. R., and Lisberger, S. G. 2003. The neural representation of speed in macaque area MT/V5. J. Neurosci. 23, 5650–5661.

Priebe, N. J., Lisberger, S. G., and Movshon, J. A. 2006. Tuning for spatiotemporal frequency and speed in directionally selective neurons of macaque striate cortex. J. Neurosci. 26, 2941–2950.

Purushothaman, G. and Bradley, D. C. 2005. Neural population code for fine perceptual decisions in area MT. Nat. Neurosci. 8, 99–106.

Purves, D., Paydarfar, J. A., and Andrews, T. J. 1996. The wagon wheel illusion in movies and reality. Proc. Natl. Acad. Sci. U. S. A. 93, 3693–3697.

Qian, N. and Andersen, R. A. 1994. Transparent motion perception as detection of unbalanced motion signals. II Physiology. J. Neurosci. 14, 7367–7380.

Qian, N. and Andersen, R. A. 1995. V1 responses to transparent and nontransparent motions. Exp. Brain Res. 103, 41–50.

Raffi, M., Squatrito, S., and Maioli, M. G. 2002. Neuronal responses to optic flow in the monkey parietal area PEc. Cereb. Cortex 12, 639–646.

Raiguel, S. E., Xiao, D. K., Marcar, V. L., and Orban, G. A. 1999. Response latency of macaque area MT/V5 neurons and its relationship to stimulus parameters. J. Neurophysiol. 82, 1944–1956.

Read, H. L. and Siegel, R. M. 1997. Modulation of responses to optic flow in area 7a by retinotopic and oculomotor cues in monkey. Cereb. Cortex 7, 647–661.

Rees, G., Friston, K., and Koch, C. 2000. A direct quantitative relationship between the functional properties of human and macaque V5. Nat. Neurosci. 3, 716–723.

Regan, D. and Beverly, K. 1978. Illusory motion in depth: after-effect of adaptation to changing size. Vision Res. 18, 209–212.

Reid, R. C., Soodak, R. E., and Shapley, R. M. 1987. Linear mechanisms of directional selectivity in simple cells of cat striate cortex. Proc. Natl. Acad. Sci. U. S. A. 84, 8740–8744.

Reid, R. C., Soodak, R. E., and Shapley, R. M. 1991. Directional selectivity and spatiotemporal structure of receptive fields of simple cells in cat striate cortex. J. Neurophysiol. 66, 505–529.

Ringach, D. L., Hawken, M. J., and Shapley, R. 1997. Dynamics of orientation tuning in macaque primary visual cortex. Nature 387, 281–284.

Rockland, K. S. 1989. Bistratified distribution of terminal arbors of individual axons projecting from area V1 to middle temporal area (MT) in the macaque monkey. Vis. Neurosci. 3, 155–170.

Rosa, M. G. and Manger, P. R. 2005. Clarifying homologies in the mammalian cerebral cortex: the case of the third visual area (V3). Clin. Exp. Pharmacol. Physiol. 32, 327–339.

Rudolph, K. K. and Pasternak, T. 1996. Lesions in cat lateral suprasylvian cortex affect the perception of complex motion. Cereb. Cortex 6, 814–822.

Rust, N. C., Mante, V., Simoncelli, E. P., and Movshon, J. A. 2006. How MT cells analyze the motion of visual patterns. Nat. Neurosci. 9, 1421–1431.

Saito, H., Yukie, M., Tanaka, K., Hikosaka, K., Fukada, Y., and Iwai, E. 1986. Integration of direction signals of image motion in the superior temporal sulcus of the macaque monkey. J. Neurosci. 6, 145–157.

Sakata, H., Shibutani, H., and Kawano, K. 1983. Functional properties of visual tracking neurons in posterior parietal association cortex of the monkey. J. Neurophysiol. 49, 1364–1380.

Salzman, C. D. and Newsome, W. T. 1994. Neural mechanisms for forming a perceptual decision. Science 264, 231–237.

Salzman, C. D., Britten, K. H., and Newsome, W. T. 1990. Cortical microstimulation influences perceptual judgements of motion direction. Nature 346, 174–177.

Salzman, C. D., Murasugi, C. M., Britten, K. H., and Newsome, W. T. 1992. Microstimulation in visual area MT: effects on direction discrimination performance. J. Neurosci. 12, 2331–2355.

Saul, A. B. and Humphrey, A. L. 1990. Spatial and temporal response properties of lagged and non-lagged cells in the cat lateral geniculate nucleus. J. Neurophysiol. 64, 206–224.

Saul, A. B. and Humphrey, A. L. 1992. Evidence of input from lagged cells in the lateral geniculate nucleus to simple cells in cortical area 17 of the cat. J. Neurophysiol. 68, 1190–1208.

Saul, A. B., Carras, P. L., and Humphrey, A. L. 2005. Temporal properties of inputs to direction-selective neurons in monkey V1. J. Neurophysiol. 94, 282–294.

Sawatari, A. and Callaway, E. M. 2000. Diversity and cell type specificity of local excitatory connections to neurons in layer 3B of monkey primary visual cortex. Neuron 25, 459–471.

Sceniak, M. P., Hawken, M. J., and Shapley, R. 2002. Contrast-dependent changes in spatial frequency tuning of macaque V1 neurons: effects of a changing receptive field size. J. Neurophysiol. 88, 1363–1373.

Schiller, P. H., Sandell, J. H., and Maunsell, J. H. 1987. The effect of frontal eye field and superior colliculus lesions on saccadic latencies in the rhesus monkey. J. Neurophysiol. 57, 1033–1049.

Sclar, G., Maunsell, J. H. R., and Lennie, P. 1990. Coding of image contrast in central visual pathways of the macaque monkey. Vision Res. 30, 1–10.

Seidemann, E. and Newsome, W. T. 1999. Effect of spatial attention on the responses of area MT neurons. J. Neurophysiol. 81, 1783–1794.

Shenoy, K. V., Bradley, D. C., and Andersen, R. A. 1999. Influence of gaze rotation on the visual response of primate MSTd neurons. J. Neurophys. 81, 2764–2786.

Sherk, H., Mulligan, K., and Kim, J. N. 1997. Neuronal responses in extrastriate cortex to objects in optic flow fields. Vis. Neurosci. 14, 879–895.

Shipp, S. and Zeki, S. 2002. The functional organization of area V2, I: specialization across stripes and layers. Vis. Neurosci. 19, 187–210.

Siegel, R. M. and Read, H. L. 1997. Analysis of optic flow in the monkey parietal area 7a. Cereb. Cortex 7, 327–346.

Simoncelli, E. P. and Heeger, D. J. 1998. A model of neuronal responses in visual area MT. Vision Res. 38, 743–761.

Sincich, L. C. and Horton, J. C. 2003. Independent projection streams from macaque striate cortex to the second visual area and middle temporal area. J. Neurosci. 23, 5684–5692.

Sincich, L. C. and Horton, J. C. 2005. The circuitry of V1 and V2: integration of color, form, and motion. Annu. Rev. Neurosci. 28, 303–326.

Sincich, L. C., Park, K. F., Wohlgemuth, M. J., and Horton, J. C. 2004. Bypassing V1: a direct geniculate input to area MT. Nat. Neurosci. 7, 1123–1128.

Smith, A. T., Greenlee, M. W., Singh, K. D., Kraemer, F. M., and Hennig, J. 1998. The processing of first- and second-order motion in human visual cortex assessed by functional magnetic resonance imaging (fMRI). J. Neurosci. 18, 3816–3830.

Snowden, R. J. and Milne, A. B. 1997. Phantom motion after effects – evidence of detectors for the analysis of optic flow. Curr. Biol. 7, 717–722.

Snowden, R. J., Treue, S., Erickson, R. G., and Andersen, R. A. 1991. The response of area MT and V1 neurons to transparent motion. J. Neurosci. 11, 2768–2785.

Squatrito, S. and Maioli, M. G. 1997. Encoding of smooth pursuit direction and eye position by neurons of area MSTd of macaque monkey. J. Neurosci. 17, 3847–3860.

Srinivasan, M. V., Poteser, M., and Kral, K. 1999. Motion detection in insect orientation and navigation. Vision Res. 39, 2749–2766.

Stepniewska, I., Qi, H. X., and Kaas, J. H. 1999. Do superior colliculus projection zones in the inferior pulvinar project to MT in primates? Eur. J. Neurosci. 11, 469–480.

Stone, L. S., Watson, A. B., and Mulligan, J. B. 1990. Effect of contrast on the perceived direction of a moving plaid. Vision Res. 30, 1049–1067.

Tadin, D., Lappin, J. S., Gilroy, L. A., and Blake, R. 2003. Perceptual consequences of centre-surround antagonism in visual motion processing. Nature 424, 312–315.

Tanaka, K. and Saito, H. 1989. Analysis of motion of the visual field by direction, expansion/contraction and rotation cells clustered in the dorsal part of the medial superior temporal area of the Macaque monkey. J. Neurophysiol. 62, 626–641.

Tanaka, K., Hikosaka, H., Saito, H., Yukie, Y., Fukada, Y., and Iwai, E. 1986. Analysis of local and wide-field movements in the superior temporal visual areas of the macaque monkey. J. Neurosci. 6, 134–144.

Taylor, W. R. and Vaney, D. I. 2002. Diverse synaptic mechanisms generate direction selectivity in the rabbit retina. J. Neurosci. 22, 7712–7720.

Taylor, W. R. and Vaney, D. I. 2003. New directions in retinal research. Trends Neurosci. 26, 379–385.

Thiele, A., Distler, C., and Hoffmann, K. P. 1999. Decision-related activity in the macaque dorsal visual pathway. Eur. J. Neurosci. 11, 2044–2058.

Thompson, P. 1982. Perceived rate of movement depends on contrast. Vision Res. 22, 377–380.

Thompson, P. and Stone, L. S. 1997. Contrast affects flicker and speed perception differently. Vision Res. 37, 1255–1260.

Thompson, P., Brooks, K., and Hammett, S. T. 2006. Speed can go up as well as down at low contrast: implications for models of motion perception. Vision Res. 46, 782–786.

Tootell, R. B., Reppas, J. B., Kwong, K. K., Malach, R., Born, R. T., Brady, T. J., Rosen, B. R., and Belliveau, J. W. 1995. Functional analysis of human MT and related visual cortical areas using magnetic resonance imaging. J. Neurosci. 15, 3215–3230.

Toyama, K. and Kozasa, T. 1982. Responses of Clare-Bishop neurones to three dimensional movement of a light stimulus. Vision Res. 22, 571–574.

Toyama, K., Komatsu, Y., and Kozasa, T. 1986. The responsiveness of Clare-Bishop neurons to motion cues for motion stereopsis. Neurosci. Res. 4, 83–109.

Treisman, A. M. and Gelade, G. 1980. A feature-integration theory of attention. Cognit. Psychol. 12, 97–136.

Treue, S. and Martínez Trujillo, J. C. 1999. Feature-based attention influences motion processing gain in macaque visual cortex. Nature 399, 575–579.

Treue, S. and Maunsell, J. H. 1999. Effects of attention on the processing of motion in macaque middle temporal and medial superior temporal visual cortical areas. J. Neurosci. 19, 7591–7602.

Uka, T. and DeAngelis, G. C. 2001. Contribution of MT neurons to depth discrimination. I. Comparison of neuronal and behavioral sensitivity. Soc. Neurosci. Abstr. p. 680.612.

Uka, T. and DeAngelis, G. C. 2004. Contribution of area MT to stereoscopic depth perception: choice-related response modulations reflect task strategy. Neuron 42, 297–310.

Uka, T. and DeAngelis, G. C. 2006. Linking neural representation to function in stereoscopic depth perception: roles of the middle temporal area in coarse versus fine disparity discrimination. J. Neurosci. 26, 6791–6802.

Valverde, F. 1985. The Organizing Principles of the Primary Visual Cortex in the Monkey. In: Cerebral Cortex 3 (*eds*. A. Peters and E. G. Jones), pp. 207–257. Plenum Press.

van de Grind, W. A., Koenderink, J. J., and van Doorn, A. J. 1992. Viewing-distance invariance of movement detection. Exp. Brain Res. 91, 135–150.

van den Berg, A. V. and van de Grind, W. A. 1989. Reaction times to motion onset and motion detection thresholds reflect the properties of bilocal motion detectors. Vision Res. 29, 1261–1266.

Van Essen, D. C. and DeYoe, E. A. 1995. Concurrent Processing in the Primate Visual Cortex. In: The Cognitive Neurosciences (*ed*. Michael S Gazzaniga), pp. 383–400. MIT Press.

Van Essen, D. C., Maunsell, J. H. R., and Bixby, J. L. 1981. The middle temporal visual area in the macaque:

myeloarchitecture, connections, functional properties and topographic representation. J. Comp. Neurol. 199, 293–326.
Van Essen, D. C., Newsome, W. T., Maunsell, J. H., and Bixby, J. L. 1986. The projections from striate cortex (V1) to areas V2 and V3 in the macaque monkey: asymmetries, areal boundaries, and patchy connections. J. Comp. Neurol. 244, 451–480.
van Santen, J. P. H. and Sperling, G. 1985. Elaborated Reichardt detectors. J. Opt. Soc. Am. 2, 300–321.
Van Wezel, R. J. and Britten, K. H. 2002. Motion adaptation in area MT. J. Neurophysiol. 88, 3469–3476.
Verstraten, F. A., van der Smagt, M. J., Fredericksen, R. E., and van de Grind, W. A. 1999. Integration after adaptation to transparent motion: static and dynamic test patterns result in different aftereffect directions. Vision Res. 39, 803–810.
Wartzok, D. and Marks, W. B. 1973. Directionally selective visual units recorded in optic tectum of the goldfish. J. Neurophysiol. 36, 588–604.
Watson, A. B. 1987. Efficiency of a model human image code. J. Opt. Soc. Am. A 4, 2401–2417.
Watson, A. B. and Ahumada, A. J., Jr. 1983. A Look at Motion in the Frequency Domain. In: Motion: Perception and Representation (*ed*. J. K. Tsotsos), pp. 1–10. Association for Computing Machinery.
Weiss, Y. 2000. Correctness of local probability in graphical models with loops. Neural Comput. 12, 1–41.
Weiss, Y., Simoncelli, E. P., and Adelson, E. H. 2002. Motion illusions as optimal percepts. Nat. Neurosci. 5, 598–604.
Wilke, S. D., Thiel, A., Eurich, C. W., Greschner, M., Bongard, M., Ammermuller, J., and Schwegler, H. 2001. Population coding of motion patterns in the early visual system. J. Comp. Physiol. 187, 549–558.
Wohlgemuth, A. 1911. On the aftereffect of seen movement. Br. J. Psychol. Monogr.Suppl. No. 1 1–117.
Wolf-Oberhollenzer, F. and Kirschfeld, K. 1994. Motion sensitivity in the nucleus of the basal optic root of the pigeon. J. Neurophysiol. 71, 1559–1573.
Wolfe, J. M. and Bennett, S. C. 1997. Preattentive object files: shapeless bundles of basic features. Vision Res. 37, 25–43.
Womelsdorf, T., Anton-Erxleben, K., Pieper, F., and Treue, S. 2006. Dynamic shifts of visual receptive fields in cortical area MT by spatial attention. Nat. Neurosci. 9, 1156–1160.
Xiao, D. K., Marcar, V. L., Raiguel, S. E., and Orban, G. A. 1997. Selectivity of macaque MT/V5 neurons for surface orientation in depth specified by motion. Eur. J. Neurosci. 9, 956–964.
Xiao, D. K., Raiguel, S., Marcar, V., Koenderink, J., and Orban, G. A. 1995. Spatial heterogeneity of inhibitory surrounds in the middle temporal visual area. Proc. Natl. Acad. Sci. U. S. A. 92, 11303–11306.
Yabuta, N. H., Sawatari, A., and Callaway, E. M. 2001. Two functional channels from primary visual cortex to dorsal visual cortical areas. Science 292, 297–300.
Yo, C. and Wilson, H. R. 1992. Perceived direction of moving two-dimensional patterns depends on duration, contrast and eccentricity. Vision Res. 32, 135–147.
Zeki, S., Perry, R. J., and Bartels, A. 2003. The processing of kinetic contours in the brain. Cereb. Cortex 13, 189–202.
Zeki, S. M. 1974. Functional organization of a visual area in the posterior bank of the superior temporal sulcus of the rhesus monkey. J. Physiol. 236, 549–573.

2.11 Cortical Mechanisms for the Integration of Visual Motion

C C Pack, McGill University School of Medicine, Montreal, PQ, Canada

R T Born, Harvard Medical School, Boston, MA, USA

© 2008 Elsevier Inc. All rights reserved.

2.11.1	Introduction – Visual Motion	192
2.11.2	The Correspondence Problem	192
2.11.3	Motion Noise	192
2.11.4	The Aperture Problem	193
2.11.5	Measurement of Motion in the Primate Brain	194
2.11.6	Receptive Fields for Measuring Motion	194
2.11.7	A Note on Terminology	195
2.11.8	The Middle Temporal Area of the Visual Cortex	196
2.11.9	Tiling: The Simplest Model	196
2.11.10	Tiling and Motion Noise	197
2.11.11	A Problem for the Tiling Model	198
2.11.12	Conceptual Approaches to Solving the Aperture Problem	198
2.11.13	Plaids	198
2.11.14	Plaid Physiology	199
2.11.15	Integrationist Models	200
2.11.16	The Intersection of Constraints, or Fourier-Plane, Model	202
2.11.17	Other Integrationist Models	204
2.11.18	Challenges to Integrationist Models	204
2.11.19	Intersection of Constraints, Vector Average, or Feature Tracking?	205
2.11.20	Dynamics of 1D and 2D Computations	206
2.11.21	Bar-Field Physiology	206
2.11.22	Physiological Evidence for Early 2D Motion Signals	208
2.11.23	Selective Motion Integration	211
2.11.24	Theoretical Considerations: Redundancy Reduction	211
2.11.25	Selectionist Models	212
2.11.26	Hybrid Models	213
2.11.27	Future Challenges	213
2.11.28	Final Thoughts	214
References		215

Glossary

adaptation Neural process by which the response to a constant stimulus decreases over time.

aperture problem Ambiguity of the true velocity of 1D features (such as lines or edges) sampled through spatially delimited windows. See Section 2.11.4.

barber pole A visual stimulus consisting of a 1D grating moving behind a rectangular aperture. Though the predominant motion energy is in the direction perpendicular to the grating's stripes, the perceived direction of motion is parallel to the long axis of the aperture. This motion illusion was one of the first demonstrations that terminators are powerful motion cues. See Section 2.11.19 and Figure 9(a).

Bayesian model A class of models that use Bayes' theorem for inverting conditional probabilities to incorporate prior knowledge of the world into the intrepretation of sensory data. In a typical Bayesian model of some visual function, one wishes to calculate the probability of occurrence of a particular visual stimulus, *S*, based on some

evidence variable, E, such as a measurement derived from a noisy image or a noisy neural response (written as $p[S/E]$, or the probability of S given E). Typically one has a measure of the inverse probability ($p[E/S]$, the probability of measurement E given stimulus S) and makes use of the prior likelihood of that particular stimulus ($p[S]$) to produce a better estimate, called the posterior probability, of the stimulus that produced the evidence.

bistable Ambiguous visual stimuli that may be seen in either of two mutually exclusive configurations; common non-motion examples are the Necker cube or face-vase illusion.

center-surround opponency: A receptive property in which the neuron's response to a preferred stimulus decreases as the size of the stimulus increases.

coherence/transparency Two mutually exclusive possible perceptual experiences when viewing a moving plaid pattern. Coherence refers to the situation in which the pattern appears to move as a single rigid entity; transparency, to the situation in which the two component gratings appear to slide over one another independently, creating the impression that the nearer surface is partially transparent.

component/pattern prediction Two possible predictions of a neuron's direction tuning curve in response to a 2D plaid stimulus, based on its tuning curve to a 1D grating stimulus; see Sections 2.11.14 and Figure 4.

correspondence problem Problem in determining, for two images that are separated in space and/or time, which image elements belong to the same features. See Section 2.11.2 and Figure 1.

cross-correlation Mathematical technique for determining the degree to which two images are similar; of the two images are snapshots in time, cross-correlation can be used to detect motion; see also correspondence problem; see Section 2.11.6 and Figures 1 and 2.

differentiation Mathematical operation for calculating the rate of change of one variable, x, with respect to another variable, y. The result of the operation is referred to as the **derivative** of x with respect to y. If x represents the position of an object and y is time, differentiation yields the velocity of the object.

end-stopping Receptive property in which responses to extended contours are suppressed by inhibitory zones lying outside the central activating region along the axis of the cell's preferred orientation; see Section 2.11.22 and Figure 10.

extrastriate Regions of visual cortex beyond primary visual cortex (V1).

feature tracking Strategy for solving the aperture problem by locating corresponding 2D features, such as corners of objects or the intersections of plaids, in successive image frames and then calculating their direction of motion; see Section 2.11.19; See also, selectionist model.

frequency domain Shorthand for spatiotemporal frequency domain, a coordinate system for specifying visual motion in terms of two dimensions of spatial frequency (the frequency of a sinusoidal modulation of image intensity of each dimension of 2D space) and one of temporal frequency (the modulation of image intensity over time); the frequency domain representation can be related to the more familiar coordinates of x, y, and t by taking the Fourier transform of the space–time coordinates. Any visual motion sequence (i.e., a movie) can be decomposed into a series of pure sinusoidal gratings (ω_x, ω_y, and ω_t) of differing amplitudes and phases in the same way that complex sounds can be broken down into sums of pure tones (a pure tone being the auditory equivalent of a sinusoidal grating). Because any local sample from a rigidly moving object is constrained to lie on a plane in the spatiotemporal frequency domain, this coordinate system has been used to characterize the receptive fields of neurons that solve the aperture problem. See Figure 6; see also F-plane model.

F-plane model Short for Fourier-plane model. Refers to a class of computational models in which pattern selectivity is created by summing the responses of neurons whose spatiotemporal frequency receptive fields all lie on a single plane in spatiotemporal frequency space; the F-plane model actually represents the power spectrum of the space–time image, as it discards the phase component. See Section 2.11.16 and Figure 6. See also frequency domain.

hypercomplex Term used by Hubel D. H. and Wiesel T. N. (1965) to refer to the receptive fields of neurons that did not respond to extended contours; see also end-stopping and Figure 10.

hypersurface A technical term from differential geometry used to generalize the notion of a curve into multiple dimensions; in the present context it is used to describe the set of points that define the

image intensity as a function of two spatial dimensions (x, y) and one temporal dimension (t).

integrationist model A class of computational model of motion integration that integrates all 1D motion signals to determine the 2D direction of motion; see Section 2.11.15.

intersection of constraints (IOC) Method for computing 2D motion by combining measurements from two or more 1D samples; see Section 2.11.16 and Figure 6.

layers (of cortex) Cut in cross section, the cerebral is a laminar structure, typically consisting of six layers visible with histological stains for cell bodies (such as Nissl stain); neurons whose cell bodies occupy different layers have different patterns of inputs and outputs.

masking Phenomenon in which one visual stimulus impairs the ability to detect another visual stimulus.

motion after-effect (MAE) Visual illusion in which prolonged adaptation to motion in one direction causes a subsequently viewed stationary scene to appear to contain motion in the opposite direction.

motion opponency A receptive field property in which null direction motion causes a reduction in the neuron's response.

MT The middle temporal visual area; also known as V5.

multistable Ambiguous visual stimuli that can be seen in one of several (more than two) mutually exclusive configurations.

nonlinear Any mathematical operation, such as squaring, for which the operation on the sum of two or more inputs is not the same as the sum of the operation's results on the individual inputs; that is, for a linear operation, f, it must be true that $f(a+b) = f(a) + f(b)$. If this relationship does not hold, the operation is nonlinear.

nonlinear systems identification A method for deriving a model of a system based on the relationship between input and output. Often applied to the study of receptive field structure; See Section 2.11.6 and Figure 2.

normalization In the present context it refers to the operation of dividing the output of a given visual filter by the sum of the outputs of all such filters.

plaid Visual motion stimulus created by superimposing two drifting sinusoidal gratings. See Section 2.11.13 and Figure 4.

plaid test Method of classifying visual neurons by comparing responses to both 1D gratings and 2D plaids. See Section 2.11.14 and Figure 4.

preferred/null direction Direction of motion that produces the best/worst response of a given neuron

receptive field The region of visual space in which visual stimuli can alter the firing rate of a neuron; the definition also includes other features of the visual stimulus required, such as the direction of motion, or the temporal pattern of inputs.

retinal disparity Difference in the relative positions produced by a single image on the retinas of the two eyes; such disparity can be used to determine the relative depth (distance from the fixation plane) of the object.

Riemann tensor Mathematical operation used to measure the curvature of a hypersurface.

segmentation The process of determining which image elements belong together.

selectionist model A class of computational model of motion integration that first filters out motion signals emanating from 1D features and thus selectively combines motion signals arising from 2D features; see Section 2.11.25.

sinusoidal grating A visual stimulus in which the intensity of the image is modulated by a sine function along one dimension; if I is a 2D image with the horizontal dimension indexed by x and the vertical dimension by y, the function $I = \sin(\omega x)$ would produce a vertically oriented sinusoidal grating of spatial frequency ω.

T-junction An image feature in the configuration of the letter T generally produced by a near surface occluding a far one.

type I plaid A visual plaid stimulus whose component gratings have directions that lie on opposite sides of the IOC resultant; see Figures 7(a) and 7(b). See also plaid.

type II plaid visual plaid stimuli whose component gratings have directions that lie on the same side of the IOC resultant; See Figure 7(c). See also plaid.

vector sum/average Method for combining two 2D velocity vectors, which have both a direction and a magnitude (speed), to obtain a single velocity vector; geometrically this is done by placing the tail of one vector to the head of the other and drawing a line from the tail of the first to the head of the second, yielding the sum; to obtain the average, the magnitude of the vector sum is scaled by dividing its length by the sum of the lengths of the two

individual vectors. Both methods yield a velocity vector having the same direction. See Figure 7.

V1 Primary visual cortex, the first stage of visual processing in the cerebral cortex and the first stage at which direction selectivity appears; also known as area 17 and striate cortex.

winner-take-all Mathematical operation which, given two or more inputs, produces an output equal to the strongest input, ignoring the weaker ones.

2.11.1 Introduction – Visual Motion

At the level of the retina, visual motion occurs whenever something in the environment moves, or whenever the observer moves or rotates his or her eye. Thus visual motion is a fundamental aspect of our interactions with the world around us. Because retinal image motion has multiple possible causes, it is both computationally challenging and richly informative, serving many functions besides the detection of moving objects. The pattern of image motion created by self-motion, for example, can be used to recover depth and to detect object boundaries as well as to aid in orienting to the environment. It is also useful in guiding eye movements that serve to stabilize images on the retina for high-acuity form vision. However, because movement is a feature that distinguishes many items of great behavioral relevance – potential predators, prey, and mates – the detection of object motion is particularly important.

The latter function will be the focus of this review. In particular, we will address the difficult problem of how information from elementary motion detectors is combined in order to provide accurate representations of the motion of objects. To consider the mechanisms by which brains achieve this integration, we will draw from two sources of data: (1) psychophysical experiments, mainly from humans, and (2) microelectrode recordings from neurons in early cortical motion processing regions of the monkey (and other mammals) – particularly the primary visual cortex (V1) and the middle temporal area (MT). The data will lead us to a discussion of general theoretical approaches as well as specific computational models of motion integration.

2.11.2 The Correspondence Problem

To see why motion integration is necessary, it is first helpful to consider some general problems associated with the basic, low-level detection of motion. Figure 1 shows a pair of successive snapshots of a scene containing the motion of a rigid object. Superimposed on the second panel is the motion that was measured at each point by simply finding pixels in the second image whose luminance corresponded closely to nearby luminances in the first image. There are of course more sophisticated ways to measure motion, and some of them will be discussed in subsequent sections. Although it is apparent that the figure in the pair of images moved from right to left, many of the motion vectors point in other directions. The confusion stems from the fact that many of the pixels in each image have the same luminance, and there is no obvious way to match the individual pixels in the first frame to those in the second frame. This problem is often called the correspondence problem (Ullman, S., 1979), and it renders the computation of velocity difficult for both biological and artificial visual systems.

One might propose that the correspondence problem could be solved both easily and efficiently if one used fewer pixels. That is, if each pixel were the size of the moving figure, then one could imagine a motion algorithm that simply matched the mean luminance of the figure in the first frame to that of the figure in the second frame. The problem with this type of solution is that it requires a visual system that has rather low acuity, which in turn runs the risk of combining motions from separate objects into one measurement. Thus the necessity for high-acuity vision tends to complicate the measurement of quantities that require correspondence between two or more images. Stereo vision and motion are the best-studied examples of such computations. For simplicity we will initially ignore the problem of multiple moving objects and return to this difficulty in later sections.

2.11.3 Motion Noise

Figure 1 also contains a number of motion vectors (purple arrows) that do not correspond to any

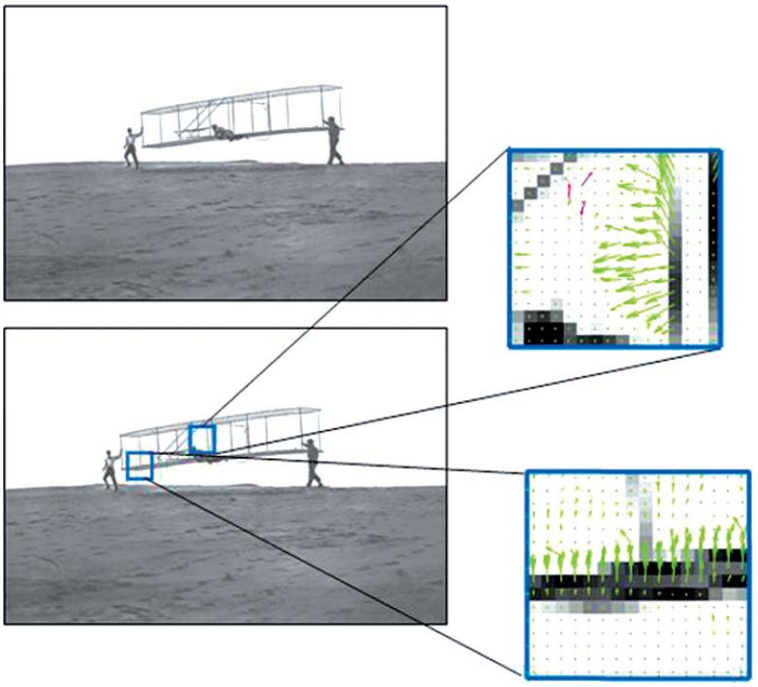

Figure 1 Orville Wright being launched by Dan Tate and his brother Wilbur, in an attempt to fly the Wright Glider in 1902. The green arrows show the average motion vector found between frame 1 (top) and frame 2 (bottom) in a small region of space around each pixel. Purple arrows indicate motion vectors that do not appear to result from the motion of the Glider, which turned out to be unfit for flight. Adapted from a public-domain image on www.first-to-fly.com.

particular object in the scene. These are false matches, in which the luminance of a pixel in the second frame happened to correspond to the luminance of a nearby pixel in the first frame. Such false matches are inevitable when dealing with inputs that are corrupted by noise, jitter, or local image correlations. The visual system possesses at least two mechanisms for reducing such noise in natural images: directional opponency and local pooling. The former has been characterized in early visual areas (Snowden, R. J. *et al.*, 1991; Qian, N. and Andersen, R. A., 1994) and is manifested as a suppression of the response to nearby stimuli moving in opposite directions. Since many sources of motion noise have equal motion energy in all directions, subtracting opposite directions of motion is an efficient way to reduce their contribution. Another way to reduce noise is to pool local measurements over some region of the visual field to produce something like an average of the different local motion vectors (Lisberger, S. G. and Ferrera, V. P., 1997; Recanzone, G. H. *et al.*, 1997; Britten, K. H. and Heuer, H. W., 1999) In fact, direction opponency is a special case of highly localized vector averaging, since the average of two vectors of equal magnitude and opposite direction is zero. It is clear that the visual system possesses mechanisms for pooling across both visual space and velocity space, and these mechanisms pose interesting problems for models of motion integration.

2.11.4 The Aperture Problem

A special case of the correspondence problem occurs when the stimulus contains extended edges or contours, as is almost always the case in natural viewing. As can be seen in Figure 1, when the stimulus consists locally of a single moving edge, the correspondence problem leads to a series of measurements indicating motion vectors perpendicular to the edge's orientation. This is a straightforward consequence of the fact that the parallel component of the actual velocity contains no time-varying information. As a result incorrect measurements will occur whenever an edge that is more than one pixel in length moves in a direction that is not perpendicular to the orientation of the edge. More generally, any motion detector will make similar errors when measuring the motion of a contour that extends beyond its field of view. Consequently, this

problem is often referred to as the aperture problem (Marr, D., 1982), as the limited field of view constitutes a kind of aperture. As it turns out, neurons in the early stages of the primate visual cortex have extremely limited fields of view, so the aperture problem is an important issue in understanding biological vision.

2.11.5 Measurement of Motion in the Primate Brain

The primate visual cortex is an example of a system that has both very high acuity and excellent sensitivity to motion. Both of these properties can be observed at the level of individual neurons. Each neuron in the early stages of the primate visual system responds to stimulation over a very small part of the visual field. In visual neurophysiology, this limited field of view is called the receptive field (RF), and most V1 RFs are smaller than the width of one's thumbnail held at arm's length. It is useful to think of RFs as pinholes (or apertures) through which neurons view the outside world. Their job is to measure certain aspects of the visual world that occur within the pinhole, and they are largely oblivious to events that occur outside this small region. Within any part of the visual cortex, neurons are found whose RFs collectively tile the whole of visual space. In addition to having a spatially delimited RF, each neuron has a limited range of visual stimuli to which it will respond. Some neurons are tuned to the shape of the stimulus, some to the color, and others are tuned to the motion that occurs within their RF. Here we focus on neurons that are selectively responsive to motion, predominantly those in V1 and MT.

2.11.6 Receptive Fields for Measuring Motion

Any system that measures motion must be sensitive to the parts of the visual image that change position over time. That is, any two separate measurements of the position of a moving object will reveal that it has changed position by a certain amount (Δx and Δy) during the interval (Δt) between the two measurements. If the measurements are accurate, these quantities (Δx, Δy, Δt) describe the velocity of the object. Such a measurement is sometimes called a second-order calculation, because it requires a conjunction of two snapshots, separated in space and time.

Second-order measurements are, both intuitively and mathematically (Poggio, T. and Reichardt, W., 1973), the minimal way to compute motion, since a single snapshot cannot meaningfully be said to contain motion. Over the last few decades, researchers have accumulated a great deal of evidence suggesting that this minimal model is actually sufficient to account for the responses of motion-sensitive neurons (Reichardt, W., 1961; Emerson, R. C. *et al.*, 1987; Emerson, R. C. *et al.*, 1992) and certain aspects of human motion perception (Adelson, E. H. and Bergen, J. R., 1985). Such second-order models are equivalent to the better-known motion-energy and Reichardt models (Adelson, E. H. and Bergen, J. R., 1985; Courellis, S. H. and Marmarelis, V. Z., 1992).

A variety of methods have been used to characterize the second-order behavior of V1 neurons, including recently an engineering technique known as nonlinear systems identification (Wiener, N., 1958). The technique is outlined in Figure 2, which shows a sequence of stimuli that were displayed on a computer monitor, which was viewed by an alert macaque monkey. The stimulus was simply a pair of spots, one black and one white, which changed position at random on each refresh of the monitor. The first frame shows the position of the spots at one point in this sequence, and the second frame shows that, a moment later, they changed position, in this case both moving to the right. The dotted squares show the positions occupied by the spots on the previous frame, and the arrows indicate the displacements of the spots from the first to the second frame.

There are four such displacements, corresponding to the four possible ways to match the spots on the first and second frames (white-to-white, white-to-black, black-to-white, black-to-black). Below these two frames is shown the cross-correlation of frame one and frame two. The cross-correlation is a simple statistical way of showing the motion energy that occurs between the frames (van Santen, J. P. and Sperling, G., 1985; Courellis, S. H. and Marmarelis, V. Z., 1992). It shows the amount of motion that occurred at a fixed temporal interval (Δt) in a plane defined by the coordinates (Δx, Δy). In other words, it shows all of the motion vectors that can be found in the two-frame sequence.

The spiking activity of a hypothetical V1 neuron that is sensitive to these motion vectors (e.g., direction-selective) is displayed above the stimulus sequence. To determine which motion vectors the neuron prefers, we average all of the cross-correlations that preceded the spike by a reasonable neuronal latency τ. This procedure allows us to

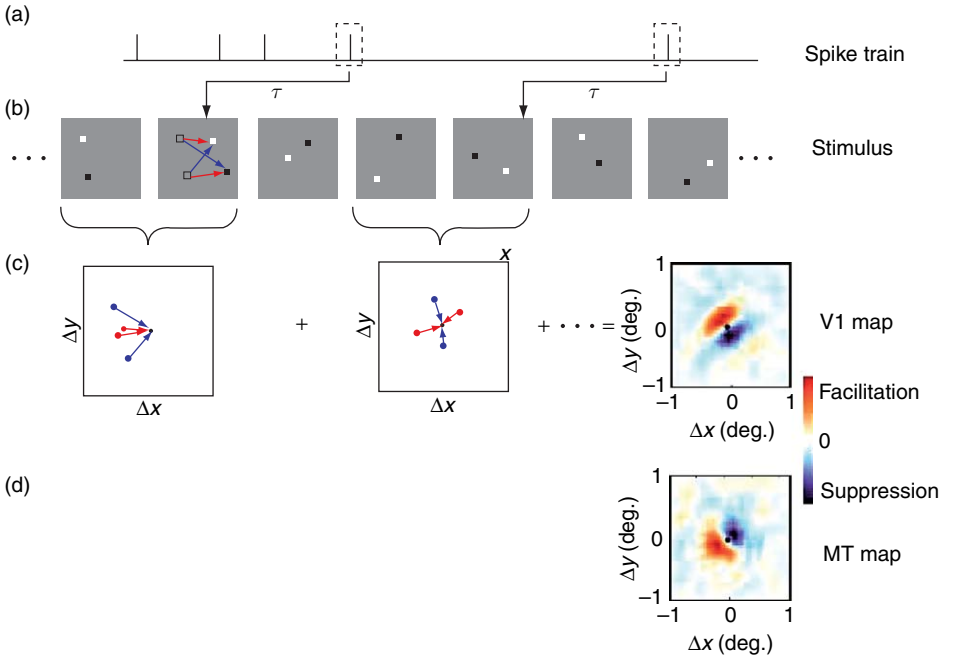

Figure 2 Reverse correlation method. (a) A hypothetical spike train produced by a neuron in response to the mapping stimulus shown in (b). Each time a spike occurs we look back in time by an amount (τ) that corresponds to the latency of the neuron. The stimulus in (b) is a pair of spots that change position randomly on each monitor refresh. Between any two stimulus frames, there are four motion signals, which can be computed by cross-correlating the two images. (c) Displacement maps, corresponding to cross-correlations between pairs of frames, with the origin corresponding to instances in which a spot appeared in the same position twice in a row. The spike-triggered cross-correlations are summed together to produce a map of the average motion vector that led to a spike. A map for an actual V1 cell is shown in the right-most column of (c). (d) A map obtained in the same way for an middle temporal (MT) cell.

characterize the selectivity of the neuron for the velocity parameters Δx, Δy, and Δt.

Such a picture for a V1 neuron is shown on the right side of Figure 2(c). The image shows the response of the neuron as a function of different values of Δx, Δy at a fixed Δt equal to 16 ms, with a neuronal latency of $\tau = 58$ ms. The neuron's response was facilitated for motion sequences down and to the right (bright orange), and suppressed for motion signals up and to the left (dark blue). We will refer such a map as a subunit to indicate that it captures a portion of the neuron's response properties, in this case the second-order selectivity for motion.

2.11.7 A Note on Terminology

The fact that the motion in a stimulus is a second-order property of the input has led to some confusion in the literature. It is common, particularly in theoretical papers, to refer to direction-selective V1 neurons as being linear. Taken literally this would be a contradiction in terms, and it is generally meant as a kind of shorthand to indicate that the neuron's RF acts as a linear spatial filter that works in parallel with a nonlinear mechanism for generating direction selectivity. Some of these models will be discussed below.

Beyond the nonlinear mechanisms that determine direction selectivity, it is generally acknowledged that additional nonlinearities are necessary to account for the behavior of visual neurons. That is, any linear combination of the output of a group of direction-selective neurons will not lead to correct estimates of stimulus velocity. We will discuss the evidence for the possible nonlinearities used by the visual cortex in some detail.

Finally, the use of the term second-order to describe the behavior of direction-selective neurons refers to the statistical order of the computation, and should not be confused with the psychophysical phenomenon called second-order motion, which is a separate concept that will not be discussed in this review.

2.11.8 The Middle Temporal Area of the Visual Cortex

MT has been the subject of intense study since it was first discovered in 1971 (Dubner, R. and Zeki, S. M., 1971). MT neurons receive most of their input from the primary visual cortex (V1), but unlike V1 neurons, they are almost without exception selective for motion direction. Neurons in the MT are also on average more tuned to retinal disparity than V1 neurons, but less tuned to stimulus shape, color, and texture (Born, R. T. and Bradley, D. C., 2005).

Perhaps the most obvious physiological difference between V1 and MT neurons is the RF size. Although the retinotopic arrangement of RFs is similar in the two areas, MT RFs are roughly 10 times the diameter of V1 RFs at any given retinal eccentricity (Albright, T. D. and Desimone, R., 1987). Thus, one might expect that MT neurons could respond to a much larger range of spatial displacements (Δx, Δy) than V1 neurons at a comparable eccentricity. In fact, previous work, using larger stimuli and long display times, has shown that MT neurons do respond better to high speeds than V1 neurons (Mikami, A. *et al.*, 1986; Churchland, M. M. *et al.*, 2005).

Stimuli identical to those used in V1 have been used to compute motion subunits for a large number of MT neurons (Livingstone, M. S. *et al.*, 2001; Pack, C. C. *et al.*, 2003a; Pack, C. C. *et al.*, 2006). An example MT subunit is shown in Figure 2(d). This neuron's response was facilitated for motion sequences up and to the right (bright orange), and suppressed for motion signals down and to the left (blue). However, other than suggesting a different preferred motion direction, the structure of this map is identical to that shown for the V1 neuron in Figure 2(c). That is, the MT neuron responds to roughly the same range of spatial displacements as the V1 neuron.

A systematic study of the subunits in V1 and MT found that the result shown in Figure 2(d) holds for every MT neuron tested: The spatial range over which the MT subunits measure motion is the same as in V1, despite the difference in RF sizes and velocity preferences between the two areas. On average, the optimal spatial displacement in MT is about 0.25°, roughly one-fiftieth the size of the RFs. Nearly identical spatial scales are found in V1 (Pack, C. C. *et al.*, 2003a; Churchland, M. M. *et al.*, 2005; Pack, C. C. *et al.*, 2006), suggesting that the MT subunits represent inputs from V1.

2.11.9 Tiling: The Simplest Model

Given these observations on the MT subunits, a simple model for motion integration by an MT neuron is a tiling model, in which large MT RFs simply sum the outputs of spatially distributed V1 neurons sharing a common preferred direction, with no interactions among the subunits. This model is supported by experiments in which the subunits are mapped at multiple points in an MT RF (Figure 3). The subunits are nearly identical at each point, a finding that held true for all the neurons examined in this way (Pack, C. C. *et al.*, 2006).

Although this is the simplest possible model for how MT RFs may be wired up, the behavior of such a neuron may, in fact, be quite complex. It depends to a large extent on how smart the inputs from V1 are. This will be an important theme that recurs throughout the ensuing discussion: How many of the seemingly more sophisticated motion processing properties of MT neurons are simply inherited from the V1 inputs?

There is a long history in visual electrophysiology of higher-order RF properties first being discovered in an extrastriate visual area, only to be re-discovered in V1 upon closer inspection. There are at least two good reasons why this occurs. First, as we have already seen for MT, extrastriate RFs tend to be much larger than those in V1, and this makes tests with more complex stimuli practically easier to conduct. For example, the miniature eye movements present during fixation are of a similar size to V1 RFs, and this makes many measurements, such as the nonlinear systems identification techniques described above, much more

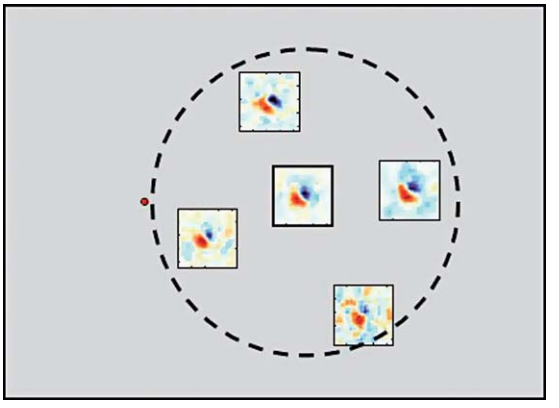

Figure 3 The result of performing the mapping procedure shown in Figure 2 at multiple points within an MT receptive field. The dot shows the fixation point, and the dashed circle shows the estimated extent of the receptive field.

technically challenging. Second, V1 is an incredibly heterogeneous visual area, containing, in essence, all of the basic visual information that it subsequently distributes to a multitude of more specialized extrastriate areas. This means that the neurons that form the principal driving input to a given extrastriate area might constitute only a tiny, and highly homogeneous, fraction of the neurons in V1, thus making comparisons of average properties between V1 and any extrastriate area difficult at best. This is clearly the case for MT, whose V1 inputs are very different from V1 as a whole: they originate mainly from a single sublayer (4B, with a small minority also coming from the so-called solitary cells of Meynert found at the border between layers 5 and 6; Maunsell, J. H. and van Essen, D. C., 1983; Shipp, S. and Zeki, S., 1989), are highly direction selective, respond over a wide range of temporal and spatial frequencies, and are very sensitive to stimulus contrast (Movshon, J. A. and Newsome, W. T., 1996). However, because they constitute such a small fraction of the total V1 population, it has been difficult to characterize very many of them in precise detail and thus to know the true nature of MT's inputs.

Given the above considerations, one way to proceed would be to start with the conceptually simple tiling model and ask what it can explain, and, perhaps more interestingly, what it might explain given certain properties of V1 neurons that have been widely documented and which are quite likely to be properties of the V1 neurons projecting to MT.

2.11.10 Tiling and Motion Noise

As noted above, one benefit of summation across many subunits within a larger RF (i.e., spatial pooling) is an improved signal-to-noise ratio. MT neurons are indeed remarkably good at detecting weak motion signals embedded in noise. In some cases the sensitivity of single MT neurons exceeds the perceptual sensitivity of the animal measured simultaneously (Newsome, W. T. *et al.*, 1989; Britten, K. H. *et al.*, 1992). In order to account for ability of MT neurons to pool many V1 inputs fully, one probably would have to add some kind of divisive normalization (Heuer, H. W. and Britten, K. H., 2002), which appears common to most cortical circuitry (Carandini, M. *et al.*, 1997), in order to compensate for the limited dynamic range of neural spiking. This can also account for the observation that when two small targets move in different directions within a single MT RF (in the absence of attentional influences) the neural response represents the average of the two motion vectors (Lisberger, S. G. and Ferrera, V. P., 1997; Recanzone, G. H. *et al.*, 1997). More on this idea below.

With respect to noise reduction, there appears to be a subtractive interaction between subunits tuned to opposite directions of motion; however, it is also possible that opponent processing is inherited from V1. Andersen and colleagues examined directional interactions in both V1 and MT using two superimposed fields of random dots moving in opposite directions (Snowden, R. J. *et al.*, 1991; Qian, N. and Andersen, R. A., 1994) . In one important study, they compared the amount of suppression produced by the null-direction dot field under conditions in which the two dot fields contained paired dots (i.e., for every dot moving in the preferred direction, there was an immediately adjacent dot moving in the null direction) versus two random dot fields that were spatially unpaired. They found, on average, more suppression to paired dot fields in MT than in V1 and concluded that it was likely that MT performed additional subunit subtraction for purposes of noise reduction (Qian, N. and Andersen, R. A., 1994). However, although the population averages were different, some V1 neurons were as suppressed by paired opponent motion as those in MT (compare figures 4 and 14 of Qian, N. and Andersen, R. A., 1994). Furthermore, the V1 cells most strongly suppressed by paired null motion were also the most strongly direction-selective (see figure 15 of Qian, N. and Andersen, R. A., 1994), a hallmark of the V1 neurons known to project to MT (Movshon, J. A. and Newsome, W. T., 1996). It is thus quite possible that the directional opponency seen in MT neurons is passively inherited from the highly specialized subset of V1 neurons that serve as its inputs. Indeed, it would seem to make sense to perform this very local comparison at a stage where RFs are small. Insofar as this is the case, the tiling model may be sufficient to account for most of the exceptional noise immunity of MT neurons. A certain degree of motion opponency is implicit in the subunits, as seen in the negative response to null-direction motion (Figures 2(c) and 2(d)). However, many models posit an additional opponency stage that subtracts the outputs of individual subunits preferring opposite motion directions (Courellis, S. H. and Marmarelis, V. Z., 1992).

2.11.11 A Problem for the Tiling Model

The tiling model simply sums the outputs of V1 neurons that share a common subunit structure, which in turn predicts the motion vectors to which the neurons will be responsive, and, as we have seen, provides improved motion integration under noisy conditions. The aperture problem, however, guarantees that many of these motion vectors will not just be randomly incorrect, but rather systematically biased (Figure 1(b)). In this case, simply adding them up will not yield the correct stimulus velocity. Rather, the visual system needs to process the motion signals in such a way as to overcome the limitations imposed by the errors that are implicit in the input. This issue lies at the heart of our remaining discussion of motion integration.

2.11.12 Conceptual Approaches to Solving the Aperture Problem

In its most basic form, the problem consists of recovering a two-dimensional (2D) velocity based on measurements that have been rendered one-dimensional (1D) by the existence of edges in the visual world and the small RFs of neurons in the brain. This necessitates some comparison of two or more motion measurements made at edges having different orientations. General approaches to the solution can be divided into two categories that differ primarily according to the stage at which the comparison occurs. In the first category of models, which includes what has become the standard model (Heeger, D. J. *et al*., 1996; Simoncelli, E. P. and Heeger, D. J., 1998), the first stage, assigned to V1 neurons, is relatively unintelligent: it nonselectively extracts only 1D motion signals which are then combined nonlinearly, at the second stage, assigned to MT, that recovers 2D velocity. Because these models combine all local 1D signals to compute the final velocity, we refer them as integrationist models.

In contrast, a second category of models places the comparison between orientations in V1, by way of known mechanisms such as end-stopping that suppress 1D motion signals in favor of motion signals emanating from 2D features. These features are just regions of the image where multiple orientations can be found locally. The second stage then simply averages the stage-one outputs to compute the final 2D velocity, an operation that can be accounted for by the tiling concept. Because the essential strategy of these models is to first select regions of the image where 2D motion measurements are most reliable and then to combine only these in the final computation, we refer to them as selectionist models.

The two categories of models are not mutually exclusive, and in many cases they make similar predictions. In the following paragraphs, we will review the psychophysical and physiological evidence supporting these different approaches, and then consider in more detail some of the computational models that have been put forth to embody them.

2.11.13 Plaids

The initial evidence for the two-stage, integrationist models came from psychophysical and physiological experiments using visual plaids (Adelson, E. H. and Movshon, J. A., 1982; Movshon, J. A. *et al*., 1985). Visual plaids are usually constructed by superimposing two, circularly windowed, sinusoidal (1D) gratings that are rotated with respect to each other (Figure 4). When the gratings are of similar spatial frequency and contrast, the resulting percept is generally of motion in a single direction, a condition referred to as coherence, with the resulting direction being the pattern (2D) direction, as distinguished

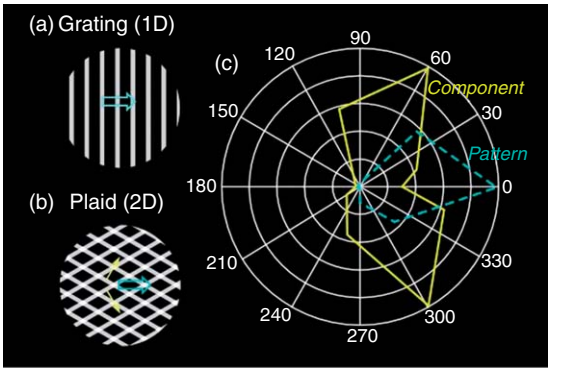

Figure 4 Plaid test for single neurons. The neuron's direction tuning curve to a one-dimensional (1D) grating stimulus (a) is used to make two predictions for the tuning curve to a two-dimensional (2D) plaid (b) in which the two components are rotated ±60° with respect to the original grating. Two predictions for an MT neuron are shown in (c) and consist of the pattern prediction (dashed curve), which is identical to that obtained with the 1D grating, and the component prediction (solid curve), which is obtained by summing two copies of the grating tuning curve that have been rotated ±60°.

from the different component (1D) directions of the two gratings comprising the plaid.[1]

In a series of psychophysical experiments, Movshon and colleagues tested the effects of masking (Adelson, E. H. and Movshon, J. A., 1982) and adaptation (Movshon, J. A. *et al.*, 1985) on human observers' tendencies to perceive coherent motion in plaids. Given the evidence that neurons in striate cortex responded optimally to contours of a particular orientation (Hubel, D. H. and Wiesel, T. N., 1962), they set out to find perceptual evidence for an orientation-selective 1D stage prior to the stage at which coherence was computed. In one experiment, they used 1D dynamic noise (oriented, flickering bars of various widths) to mask the plaids. They reasoned that, if the first-stage filtering was in fact orientation-selective, then the mask should interfere with the perception of coherence when it was parallel to one of the component gratings. In contrast, if the first stage was not orientation-selective, but rather a kind of blob-tracking mechanism that signaled the direction of the plaid's intersections, the effect of the mask would either not depend on its orientation or perhaps would be greatest when it was perpendicular to the direction of pattern motion. They found that the 1D masks were only effective when oriented within 20° of one of the component gratings, in agreement with an orientation-selective first stage.

In a second experiment, they examined the effects of adaptation on the subjects' abilities to both detect the presence of a moving stimulus and to perceive coherence of the plaid pattern. The premise of this experiment was that detection thresholds are a signature of early processing, such as that found in V1 and characterized psychophysically by orientation- and direction-selective adaptation (Sekuler, R. W. and Ganz, L., 1963), whereas the coherence thresholds reflected later stages of motion processing. Any differences in the adaptability of these two measures would be evidence for separate processing stages. Further, by testing for cross-adaptation, that is, effects of adapting with a 1D grating on the perception of a 2D plaid (and vice versa), they might uncover further evidence for an orientation-selective early stage. To see the logic of this, imagine a horizontal grating moving upwards as the adapting stimulus and an upward-moving coherent plaid (whose components move obliquely: up-left and up-right), as the test stimulus. If the earliest stage codes direction of motion, irrespective of orientation, then we might expect to find considerable cross-adaptation for these stimuli, because they both appear to be moving upwards. If, however, the early stage is both orientation- and direction-selective, then we would expect little cross-adaptation since such a stage would see only the components of the plaid, neither of which is horizontal or moving directly upwards. The results revealed little evidence for cross-adaptation of detection thresholds (see figure 7 of Movshon, J. A. *et al.*, 1985), but considerable cross-adaptation for coherence thresholds (see figure 8 of Movshon, J. A. *et al.*, 1985), both consistent with a two-stage model in which the early (detection) stage consists of filters that are tuned to both orientation and direction of motion.

Subsequent psychophysical experiments further supported the two-stage model of Adelson E. H. and Movshon J. A. (1982). In one experiment, Welch L. (1989) measured speed discrimination (Weber fractions) for gratings and plaids. Because the pattern and the components of a plaid move at different speeds (pattern speed is always faster than component speed, according to the cosine rule given below) and because discrimination performance varies with the baseline speed, Welch was able to ask which of the two speeds better predicted discrimination performance for plaids. The answer was clearly that the component speed, not the pattern speed, predicted discrimination performance (Welch, L., 1989). In another experiment, Derrington A. and Suero M. (1991) used the motion after-effect (MAE) to reduce the perceived speed of one of the components of a plaid stimulus. When they did this, they found that the perceived direction of the plaid, after adaptation, deviated in the direction of the nonadapted component. The deviation could be nulled by reducing the speed of the nonadapted component to match the perceived speed of the adapted component (Derrington, A. and Suero, M., 1991). Both results suggested that the visual system first estimated the motion of the plaid's components before combining them to generate the percept of pattern motion.

2.11.14 Plaid Physiology

Based on the psychophysical results with plaids, Movshon and colleagues used these same visual stimuli to characterize direction-selective neurons of the visual cortex. They recorded from both V1 and MT in anesthetized monkeys and from the homologous areas (area 17 and lateral suprasylvian cortex, respectively) in anesthetized cats. This allowed the authors to assess directly whether neurons in a given area tended to respond to the direction of the 1D

components or the 2D patterns, since, for any given stimulus these moved in different directions.

The physiological version of the plaid test was performed as follows (Figure 4). The direction-tuning curve of the neuron was first determined using a 1D sinusoidal grating, and this tuning curve was then used to make two predictions about the shape of the same cell's tuning curve to a plaid stimulus. Insofar as the cell sees only the 1D components of the plaid, its direction tuning curve should be bi-lobed (Figure 4, solid yellow line), with the peak of each lobe corresponding to the direction of plaid motion that places one of the component's direction of motion in the cell's preferred direction. For example, suppose a neuron prefers rightward motion to the grating stimulus. When tested with the plaid stimulus, the neuron's response is plotted as a function of the direction of the pattern motion. For a 120° plaid, when the pattern is moving to the right, neither of the grating components is moving in the preferred direction. However, for plaid pattern directions of either +60° or −60°, one or the other component grating will be moving in the cell's preferred direction. In contrast, if the cell sees pattern motion, the plaid-derived direction tuning curve is predicted to be identical to that obtained with the grating.[2] By correlating the actual tuning curve obtained to a plaid with each of the two predictions, the authors were able to quantify the extent to which a given neuron was responding to the direction of motion of the 1D components or the 2D pattern.

The results, like the plaid psychophysics, supported their two-stage model, and did so more directly. The investigators found that the majority of the neurons in cat area 17 and monkey V1 were of the component type (59 of 69 cells, 85%) with the remaining 10 neurons falling in the unclassed zone, corresponding to neurons for which neither prediction was significantly better than the other. Importantly, none of the neurons were classified as pattern-type. The results from macaque MT neurons were somewhat different: while a majority of the neurons were still classified as either component (40%) or unclassed (35%), a significant minority were characterized as pattern (25%). Thus V1 neurons appeared to see only the 1D motion (as predicted by the aperture problem) while at least some of those in MT were able to combine the 1D measurements into a representation of 2D velocity. This result clearly supported models of the integrationist type.

2.11.15 Integrationist Models

Accepting for the moment the notion that V1 neurons respond only to the 1D motion components, the challenge raised by the experiments of Movshon and colleagues is to explain how an MT neuron can have inputs that are component-selective and an output that is pattern-selective. An extremely simple explanation is depicted in Figure 5. Here three model MT

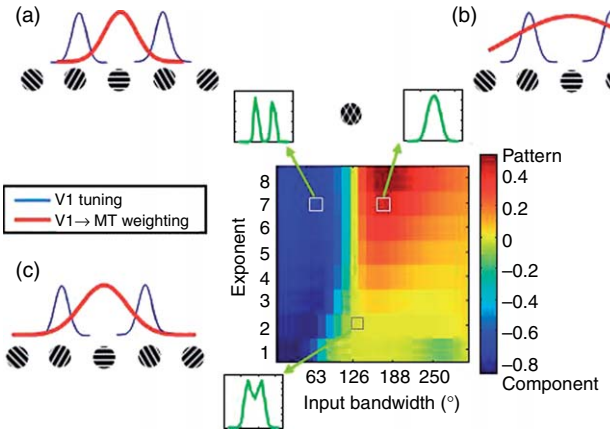

Figure 5 Three examples of hypothetical primary visual cortex (V1) tuning curves and middle temporal (MT) weighting functions. The blue tuning curves show the responses of V1 neurons to the component gratings in a plaid moving upward, which is the preferred direction of the simulated MT neuron. The red curves show the function that weights the output of the V1 neurons in the projection to MT. The central panel shows how tuning for pattern motion is affected by different bandwidths of the weighting function and different output nonlinearities. The green tuning curves show specific examples of simulated neuronal tuning to plaid patterns. The simulated plaid contained components moving in direction separated by 120°. Simulated V1 tuning bandwidth was 27° (Albright, T. D. 1984). The range of exponents was taken from DeAngelis, G. C. *et al.* (1993).

neurons receive inputs from a group of component-selective V1 neurons. For each neuron each V1 input is weighted by a Gaussian function (red curve) centered on the MT neuron's preferred direction, which in each case is upward. In Figure 5(a) the Gaussian function is sufficiently narrow that the V1 responses to the component gratings (blue curves) receive little weight when the plaid moves in the MT neuron's preferred direction. The result is a bi-lobed tuning curve (green) typical of a neuron that is classified as a component-selective. In contrast the tuning width of the MT neuron in Figure 5(b) is sufficiently large that the neuron responds to both of the plaid gratings simultaneously when the pattern direction is the same as the preferred direction of the MT neuron. The summed response to the two components is then greater than when either of the component gratings is moving in the preferred direction. In essence the MT neuron is blurring or averaging the motion inputs, so that the component directions no longer appear to be visible to it. As mentioned above, this kind of blurring is thought to have a role in eliminating motion noise, which is likely to be randomly distributed over space (Qian, N. and Andersen, R. A. 1994).

Note that the hypothetical neuron shown in Figure 5(b) would not yet meet the definition of pattern selectivity given by Movshon J. A. *et al.* (1985). The reason is that such neurons are defined as exhibiting responses that cannot be predicted from a linear combination of the responses to the components. For the neuron shown in Figure 5(b), the response to the plaid is still a linear sum of the response to the component gratings, and thus would not be considered a true pattern-selective neuron.

Nevertheless, the existence of a response peak in the pattern direction suggests that the tuning-width explanation may be a reasonable place to start. To determine if this type of explanation can be brought into line with the results of the plaid experiments, we can equip the hypothetical MT neuron with some standard nonlinearities that are known to influence the responses of all neurons. For instance, neurons have a threshold for firing spikes, and so input causing depolarization of the postsynaptic membrane that does not reach this threshold cannot be observed in the spiking activity. Furthermore, the spiking response of a neuron is generally not a linear function of its input, but rather an expansive nonlinear function. These are two uncontroversial nonlinearities that have been observed many times (Carandini, M. and Ferster, D., 2000). We will therefore consider how they might influence the responses of MT neurons to plaid stimuli.

We simulated a population of MT neurons with different bandwidths, thresholds, and expansive nonlinearities.[3] Each neuron was then classified according to a pattern index (Stoner, G. R. and Albright, T. D., 1992; Pack, C. C. *et al.*, 2001) that captured how well it conformed to the pattern prediction, taking into account the overlap between the component and pattern predictions. The central panel in Figure 5 shows the results, with red pixels corresponding to neurons that would statistically be considered pattern-selective, and blue corresponding to component-selective. As expected, increasing the bandwidth was necessary but not sufficient for generating pattern selectivity (Figure 5, bottom rows). However, when a large bandwidth was combined with either a high firing threshold (not shown) or a sharply accelerating nonlinearity, pattern selectivity emerged. Indeed using a range of parameters similar to that observed in V1 studies (e.g., DeAngelis, G. C. *et al.*, 1993) produces a distribution of component and pattern selectivities that is not unlike the distribution seen in anesthetized macaque MT. In this model, pattern and component neurons are identical, except that the former have broader tuning bandwidths than the latter (Figure 5, top rows). This can be seen clearly by comparing Figures 5(a) and 5(b), which have exactly the same nonlinearities, but differ radically in their component/pattern classification.

The nonlinearities used in the simple model described above are routinely observed in real neurons, and hence have become standard features of neural models. For example the model of Simoncelli E. P. and Heeger D. J. (1998), which will be described in more detail below, uses similar nonlinearities in its implementation of an intersection of constraints (IOC) rule to compute pattern motion. However, as we have shown here the IOC part of the model is not strictly necessary to produce pattern selectivity, although it presumably plays an important role in modeling other types of data. The strong prediction of the hypothesis shown in Figure 5 is that the pattern index would correlate on a cell-by-cell basis with each neuron's tuning bandwidth. This appears to be the case, since pattern neurons were observed to have substantially broader tuning than component neurons (Albright, T. D., 1984).[4]

A recent model has built upon a similar approach to model MT neurons, and reached a similar conclusion. Rust N. C. *et al.* (2006) developed a model in which component and pattern cells differed in tuning

bandwidth, but had similar nonlinearities. However, to model pattern cells realistically, it was necessary to add two additional features. The first was an inhibitory influence of V1 neurons on MT neurons with different preferred directions. This allowed the model to use lower (and probably more realistic) exponents than those used in the model shown in Figure 5. The second addition was strong surround suppression at the level of V1. This feature of the model is similar to the central mechanism of many selectionist models, which will be described in a subsequent section of this chapter.

2.11.16 The Intersection of Constraints, or Fourier-Plane, Model

As for the tuning-width model above, in the model proposed by Simoncelli E. P. and Heeger D. J. (1998) each V1 subunit sees only the small slice of space-time orthogonal to its preferred orientation (Figure 6), that is, it is tuned to a relatively narrow range of spatial and temporal offsets for contours of a given orientation, and it cannot discern exactly how a particular $\Delta x/\Delta t$ combination arose. Thus the model's V1 outputs suffer from the aperture problem.

The aperture problem is solved at the second stage, where MT cells collect inputs from many V1 component cells each of whose orthogonal, 1D speed measurement is consistent with a given 2D velocity. Conceptually, one can think of each 1D measurement as being consistent with a number of possible 2D velocities, all of which must fall on a line in velocity space (Figure 7, dashed lines). The intersection of any two of these constraint lines (provided the 1D measurements were made at edges having different orientations and belonging to the same object) provides the solution. As a result, this type of model is often referred to as an intersection of constraints, or IOC, model.

To see better how the IOC calculation might be carried out by a neuron, we consider an example MT cell that is to be tuned for true 2D velocity upwards at $10^\circ\ s^{-1}$ (Figure 6(a)). Such a cell would receive excitatory inputs from a family of horizontally oriented V1 cells with upwards direction preferences but with different combinations of preferred spatial and temporal offsets ranging from spatially fine subunits, say an optimal Δx of 0.1° and a Δt of 10 ms, to spatially coarser subunits, such as one with optimal values of a Δx of 1° and a Δt of 100 ms – all consistent with a speed of $10^\circ\ s^{-1}$ perpendicular to their horizontal orientation. In addition, this same MT cell would receive excitatory drive from additional $\Delta x/\Delta t$ families of V1 cells tuned to different orientations/directions but corresponding to slower preferred orthogonal speeds, according to a cosine relationship: $S_{V1} = S_{MT} * \cos(\theta_{V1} - \theta_{MT})$, where S_{MT} and θ_{MT} are the desired preferred speed and direction of the MT neuron, and S_{V1} and θ_{V1} are the corresponding directional preferences of the oriented V1 inputs. Thus, the entire range of possible orientation–velocity relationships is described by a circle in velocity space (Figure 6(b)). For our example, MT neuron, the optimal Δx's and Δt's of the family of inputs preferring right oblique orientations and upright motion would all have preferred orthogonal speeds of $7^\circ\ s^{-1}$, and, similarly, the preferred orthogonal speed of the

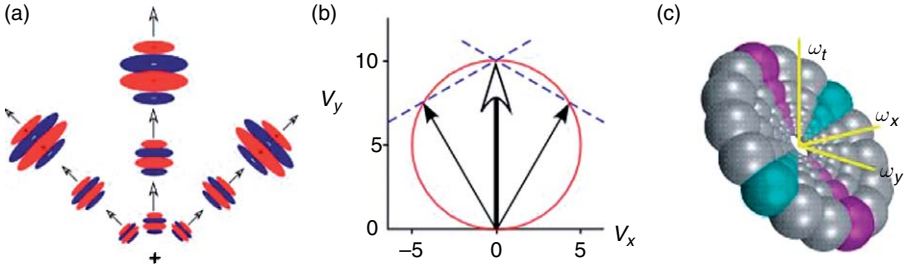

Figure 6 Integrationist model of pattern direction selectivity in middle temporal (MT) proposed by Simoncelli E. P. and Heeger D. J. (1998). (a) Partial collection of primary visual cortex (V1) inputs to a pattern cell tuned to a velocity of $10^\circ\ s^{-1}$ upwards. Each subunit corresponds to the receptive field of a V1 complex cell. (b) Velocity–space representation of the intersection of constraints (IOC) calculation. Any one-dimensional (1D) velocity measurement (solid arrows) is consistent with a range of two-dimensional (2D) velocities falling along a constraint line (dashed lines) perpendicular to its motion vector. For two such measurements made at different orientations, the 2D velocity is given by the point of intersection of the two constraint lines. Conversely, all 1D velocities consistent with a given 2D velocity (hollow arrow) fall on a circle in velocity space. (c) The frequency–space representation of the model depicted in (a). See text for additional details. (a,c) Adapted from figures 2D and 3B of Simoncelli, E. P. and Heeger, D. J. 1998. A model of neuronal responses in visual area MT. Vision Res. 38, 743–761.

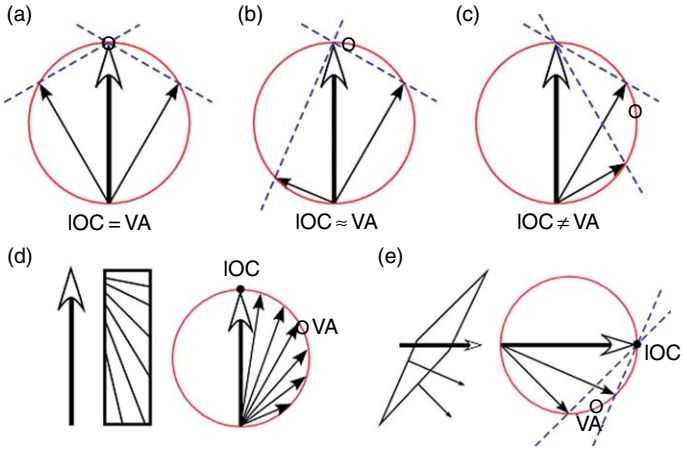

Figure 7 Velocity–space representations of different, multicomponent motion stimuli. (a) Symmetric plaids of the kind used by Adelson E. H. and Movshon J. A. (1982) in which the intersection of constraints (IOC) and vector average (VA) produce identical directions. (b) Asymmetric type I stimuli in which the two components move at different speeds. For most such stimuli, the IOC and VA yield approximately the same direction of motion, though the VA is not always perfectly accurate. (c) Type II stimuli in which the one-dimensional (1D) velocities of the two components both lie on the same side of the resultant. For these stimuli, the IOC and VA directions are quite different. (d) Type II barber poles used by Rubin N. and Hochstein S. (1993) along with the velocity–space representation of the component motion vectors. (e) Thin rhombus from Weiss, Y. *et al*. (2002), which, at low contrasts, appears to move in the VA direction.

vertically oriented V1 inputs to this cell would be $0° \text{ s}^{-1}$. The range of Δx's and Δt's within each family of V1 inputs at a given orientation confers upon the model MT cell true speed tuning (i.e., independent of the spatial composition of the stimulus) and the different families at different orientations/directions allow MT cells to solve the aperture problem and respond to the pattern direction of a plaid.

While the velocity–space construction used above is conceptually useful, in practice the model is implemented in the spatiotemporal frequency domain (Figure 6(c)). In the first stage, the Fourier-transformed visual stimulus is multiplied by the frequency-space representations of oriented Gabor filters whose output is half-squared (i.e., the negative values are clipped off and the result is squared) and normalized to produce a measure of motion energy (Adelson, E. H. and Bergen, J. R., 1985) orthogonal to the orientation of the Gabor. When plotted in the three-dimensional space comprised of two dimensions of spatial frequency (ωx and ωy) and one of temporal frequency (ωt), the selectivity of a given model V1 neuron appears as a pair of localized blobs positioned symmetrically about the origin, and the different spatial scales of the filters (corresponding to the $\Delta x/\Delta t$ families described above) fall along a line passing through the origin. In this frequency space the locus of points corresponding to a unique 2D velocity describes a plane, so a given MT cell just sums up all of the spatiotemporal blobs within the plane consistent with its particular preferred direction and speed. The plane of blobs in Figure 6(c) thus comprises the responses of V1 neurons representing eight different orientations/directions at five different spatial scales. Because the model MT neurons in stage two can be thought of as planar templates in frequency space, the IOC model has also been referred to as the Fourier-plane, or F-plane, model (Born, R. T. and Bradley, D. C., 2005).

This model has been highly successful in accounting for, not only the original plaid data that motivated it, but a number of other known MT properties, such as responses to random dots embedded in noise (Newsome, W. T. *et al*., 1989; Britten, K. H. *et al*., 1992). Subsequently, further support for this type of model came from Okamoto H. *et al*. (1999), who showed that component MT neurons have bimodal direction tuning for dots moving at high speeds, while pattern cells have bimodal tuning for bars moving at slow speeds. Both of these results are direct predictions of the F-plane model (Simoncelli, E. P. *et al*., 1996), although they are also consistent with other types of integrationist models (Kawakami, S. and Okamoto, H., 1996; Albright, T. D., 1984). The F-plane model also predicts bimodal responses in MT pattern cells for stimuli composed of overlapping dot fields, a prediction that was recently confirmed (Bradley, D. C. *et al*., 2005). Finally a direct test of the F-plane model in MT

found a population of cells that demonstrated the spatiotemporal selectivity predicted by the model (Perrone, S. A. and Thiele, A., 2001). However, these cells turned out not to be pattern cells when tested with plaids (Priebe, N. J. *et al.* 2003), as described below (see Section 2.11.18 Challenges to Integrationist Models).

2.11.17 Other Integrationist Models

There are a number of other models whose basic structure is very similar to that of the IOC model described above in that they all first indiscriminately calculate local, 1D measures of motion and then combine them nonlinearly to yield the IOC solution at a subsequent stage of the model. One source of relatively minor differences is the nature of the elementary motion detectors used at the first stage. Perhaps the most popular method is the motion energy model of Adelson E. H. and Bergen J. R. (1985), which was used by Heeger and colleagues in the model detailed above (Heeger, D. J., 1987) as well as by Grzywacz, N. M. and Yuille, A. L. (1990). Other methods include the gradient constraint method of Limb J. O. and Murphy J. A. (1975), used in the model of Fennema C. and Thompson W. (1979), and those based on scalar motion sensors described by Watson, A. B. and Ahumada, A. J. (1985) and used in the motion integration model of Ogata M. and Sato T. (1991). Similarly, the IOC calculation at the second stage can be realized in a variety of ways. We have already seen two of them in the form of the velocity–space construction, also used by Sereno M. E (1993) and Albright T. D. (1984) and the F-plane template implementation by Heeger D. J. (1987). Another way of calculating the intersection of constraint lines is to use the inverse Hough transform, and this has been featured in several other integrationist models (Fennema, C. and Thompson, W., 1979; Ogata, M. and Sato, T., 1991; Kawakami, S. and Okamoto, H., 1996). The details of these models are important – they affect the models' performance in comparison to human observers and how well it describes the response properties of neurons in V1 and MT, and they also are critical for evaluating the model's biological plausibility in terms of computations that can be carried out by neural circuits – but they are beyond the scope of this review. The issue of greater concern is to see to what extent they are consistent with the existing psychophysical and physiological data, and to compare them with models of a fundamentally different kind.

2.11.18 Challenges to Integrationist Models

As mentioned above, indirect evidence for the F-plane model comes from experiments that have confirmed the model's predictions on bimodal direction tuning. However, these same findings are predicted by other models, so they do not constitute a direct test of any particular hypothesis. A more decisive test of the F-plane model would involve stimulating MT neurons with gratings of different spatial and temporal frequencies, and measuring the extent to which neuronal responses display velocity invariance. That is, according to the F-plane model pattern-selective neurons should be selective for velocity in a manner that is largely independent of the spatiotemporal composition of the stimulus. This experiment has been done by Priebe N. J. *et al.* (2003), who found that true velocity tuning is rare in MT and, more importantly, it does not correlate in any obvious way with the pattern-component categorization (Priebe, N. J. *et al.*, 2003). In fact, velocity selectivity as hypothesized by the F-plane model is no more common in MT than in V1 (Priebe, N. J. *et al.*, 2006), suggesting that it is not related to the computation of pattern motion. Similar findings on velocity tuning were found using bars (Mikami, A. *et al.*, 1986) and small spots (Pack, C. C. *et al.*, 2006). The F-plane model thus does not appear to be consistent with the finding that the vast majority of MT neurons are capable of accurately encoding motion direction despite large changes in the spatiotemporal components that comprise the stimulus (Pack, C. C. and Born, R. T., 2001).

To the extent that integrationist models do not account for the MT data, it is useful to examine some of the models' underlying assumptions. Perhaps the strongest of these hypotheses is the notion of a purely linear first stage that measures only 1D spatial frequency components. This concept has often proven useful in vision modeling, but it is important to keep in mind its status as an approximation to the real behavior of V1 neurons. Real neurons at all stages of visual processing have a variety of nonlinear responses, some of which may be important to the integration of motion signals. A second category of models, which we call selectionist models, examines the extent to which these early nonlinearities might contribute to motion integration. Before considering

the models themselves, we will review some of the issues that motivated their conception.

2.11.19 Intersection of Constraints, Vector Average, or Feature Tracking?

The early experiments on the perception of plaid motion used component gratings whose orthogonal 1D velocities were symmetrically placed on either side of the resultant 2D pattern velocity, producing so-called symmetric type I plaids (Figure 7(a)). For such symmetrical stimuli, a simple average (or sum) of the two 1D vectors will produce a resultant vector with the same direction (though a different speed) as that produced by the IOC computation. For simplicity, we will refer to this type of computation as the vector average (VA). The experiments of Adelson E. H. and Movshon J. A. (1982) could not distinguish between these two computations. Furthermore, their stimuli contained potentially trackable 2D features, in the form of the bright blobs formed at the intersections of the two gratings. Such features could be detected by a simple operation that detects luminance maxima (Bowns, L., 1996). And since these 2D features always move in the pattern direction, this strategy cannot be easily distinguished from an IOC. While the adaptation and masking experiments (Adelson, E. H. and Movshon, J. A., 1982) argued against a feature-tracking strategy for plaids composed of sinusoidal gratings, we will see below that other, more salient, features can dramatically affect perception.

While symmetric plaids cannot distinguish between an IOC (or feature-based) computation and a VA, other stimuli can be constructed in which the component velocities either straddle the resultant asymmetrically (asymmetric type I; Figure 7(b)) or both lie to the same side of the resultant (type II; Figure 7(c)). In terms of probing the nature of the second-stage computation, type II stimuli are particularly interesting, because the perceived direction predicted by an IOC can be very different from that predicted by a VA (Figure 7(c)). In this case, the IOC computation produces the veridical direction of pattern (or object) motion, whereas the VA is inaccurate. As such it would seem to make sense for the visual system to use the IOC. Surprisingly, however, human observers misperceive the direction of motion of such stimuli under certain conditions, and they do so in the direction predicted by the VA. This was found, for example, for type II plaids of low contrast or those viewed for brief durations (Yo, C. and Wilson, H. R., 1992), for modified, type II, barber pole stimuli (Rubin, N. and Hochstein, S., 1993; Figure 7(d)), for multiple line segments each presented within a separate aperture (Mingolla, E. *et al.*, 1992), and for a thin, rhombus at low contrast (Weiss, Y. *et al.*, 2002; Figure 7(e)). For all of the above stimuli, there was a consistent direction of rigid translational motion that an IOC computation recovers. The fact that this direction was not perceived argues strongly that the visual system does not always use an IOC calculation.

Further evidence against a strict IOC computation came from experiments in which type I and type II plaids were compared with respect to their ability to interfere with the perception of a test pattern moving in the IOC resultant direction (Ferrera, V. P. and Wilson, H. R., 1987) and with respect to direction discrimination thresholds (Ferrera, V. P. and Wilson, H. R., 1990). In both sets of experiments, type II plaids behaved very differently from their type I counterparts. In particular, the type II plaids were much less effective at masking, being no more effective than their 1D component that was nearest to the resultant direction (Ferrera, V. P. and Wilson, H. R., 1987), and they yielded much higher direction discrimination thresholds that were also biased towards the direction of motion of their components (Ferrera, V. P. and Wilson, H. R., 1990). To explain their psychophysical results, Wilson and colleagues (1992) suggested a type of integrationist model, in which a VA of Fourier and nonFourier motion components is computed.

Some of these same experiments also revealed that 2D features, such as dots or line endings, had a powerful effect on the perceived motion of visual patterns. In the experiments of Rubin N. and Hochstein S. (1993), using dashed, instead of solid, lines to construct the modified barber pole stimulus dramatically changed the perceived direction of motion from the VA to veridical. In another series of experiments, they added variable numbers of randomly placed dots to the regions between the solid lines and found that even a single dot was sufficient for observers to report the true direction of pattern motion. Mingolla E. *et al.* (1992) found a similar transition from a VA of the isolated 1D elements to the true direction of pattern motion when they added 2D features such as small rectangles defining the line segment's endpoints. Finally, the classic barber pole illusion, originally described by Wallach (Wallach, H., 1935; Wuerger, S. *et al.*, 1996), is a powerful demonstration of the ability of the motion of 2D features to influence perception. In this case, the

features are the angular endings of the windowed grating, often referred to as terminators. Despite the fact that the 1D component contributes much more motion energy, the prevailing direction of 2D terminator motion along the long axis of the aperture dominates the percept.

The barber pole illusion might seem to indicate that the 1D motion signals are completely ignored by the visual system, but this is clearly not the case. The influence of 1D motion can be seen in the phenomenon of capture (Castet, E. *et al.*, 1999), which refers to the greater probability of perceiving motion in the terminator direction as the direction of the 1D signals approaches it more nearly. Other evidence for an active competition between 1D and 2D motion signals is the multistability of barber pole stimuli, which refers to the possibility of seeing one of three modal directions (long axis, short axis, or perpendicular to contour) during single brief observations (Castet, E. *et al.*, 1999) and to the fact that the perceived direction alternates randomly during prolong viewing (Wallach, H., 1935). The multistability is particularly apparent when the 2D signals are weakened by rendering them extrinsic[5] (Castet, E. *et al.*, 1999), suggesting mechanisms for computing the salience of 2D features (Shimojo, S. *et al.*, 1989).

2.11.20 Dynamics of 1D and 2D Computations

In the context of the competition between 1D contours and 2D features, perhaps the simplest way to probe motion integration psychophysically is to construct a stimulus that consists entirely of line segments moving in a direction that is not perpendicular to their orientation. As for barber poles, the contour motion is in a different direction than the motion of the line-segments' ends. This kind of stimulus was first used in psychophysical experiments by Lorençeau J. *et al.* (1993), who demonstrated that humans perceive the motion of such stimuli inaccurately when viewed for brief durations or when the lines were of low contrast. Importantly, these inaccurate percepts were not randomly wrong, but rather were systematically biased in the direction perpendicular to the edges of the line segments, as predicted by the aperture problem. This result was thus similar to those obtained with type II plaids (Yo, C. and Wilson, H. R., 1992), and strongly suggested an interesting temporal dynamic from an early VA of 1D signals to a more veridical percept at later times, produced by either an IOC or feature-based computation.

2.11.21 Bar-Field Physiology

The stimuli used by Lorençeau J. *et al.* (1993) can be readily adapted to neurophysiological experiments, and they can test many of the same hypotheses that have been addressed with plaid stimuli. Indeed from the point of view of models with a purely linear first stage, the tilted bar stimulus is simply a plaid with multiple component gratings. A crucial difference is that the tilted bar stimulus contains spatial frequency components that move in the direction of the pattern as a whole. These components always have substantially lower amplitude than the components that move perpendicular to the orientation, so under this hypothesis any neuron that accurately measures their motion must have nonlinear response properties.[6]

The response of MT neurons to tilted bar stimuli has been measured using an experimental design that dissociated stimulus orientation from direction of motion. The bars moved in one of eight directions, and on different trials they were tilted at angles of 45°, 90°, or 135° with respect to the motion direction. The 90° tilt condition served as a measure of the baseline direction tuning of each neuron, since in this case the local measurements perpendicular to the orientation were by definition correct. For the 45° and 135° conditions, local measurements would be expected to be inaccurate, and so these stimuli provided a different way to probe the ability of MT neurons to overcome the aperture problem.

Figure 8 shows the experimental results. The early responses in MT showed substantial biases for motion perpendicular to edge orientation, as would be predicted from the simple tiling model described previously. In contrast, the later responses were almost completely independent of stimulus orientation for nearly every neuron in the population.

This result differs from what one would expect based on the plaid experiments (Movshon, J. A. *et al.*, 1985). In particular, the existence of component neurons has been interpreted to mean that a substantial fraction of MT neurons have responses that can be modeled based solely on linear spatial frequency channels. This is clearly not the case for the vast majority of neurons in the Pack C. C. and Born R. T. (2001) study[7] and indeed other studies have found that all MT neurons exhibit nonlinear behavior in response to even modest stimulus manipulations (Stoner, G. R.

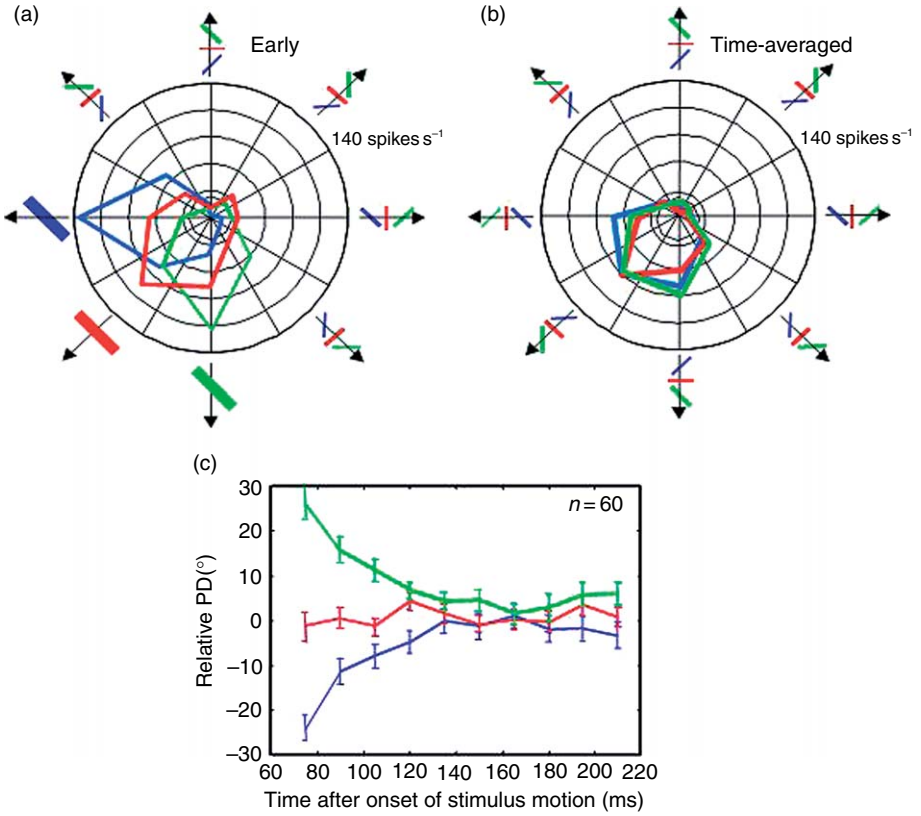

Figure 8 Response of middle temporal (MT) neurons to the bar field stimulus. (a) For a single MT neuron, the early part of the response depends on both the orientation and direction of the bar field. This neuron responds best whenever the bar has a left-oblique orientation and a leftward or downward motion component, indicating that it sees only the component of motion perpendicular to the bars. (b) The later part of the response depends only on the motion direction. (c) The transition from orientation-dependent responses to purely motion-dependent responses is evident in the population of 60 MT neurons. PD, preferred direction.

and Albright, T. D., 1992; Pack, C. C. *et al.*, 2004; Krekelberg, B. and Albright, T. D., 2005). This is not to say that linear models are incorrect – the hypothesis of linearity is after all just a way of representing the stimulus, and the responses are clearly related to the stimulus. Rather the results indicate that linear models are not sufficient to account for the behavior of MT cells, even if one grants that they may provide an accurate description of V1 outputs.

The results with bar fields did not distinguish between integrationist and selectionist models, since both would be expected to measure motion direction accurately. However, they did provide an impetus for looking for such differences in V1. This proves critical for distinguishing between the two types of models, because selectionist models would predict that selectivity for the motion of 2D features should be found in V1, while integrationist models predict that only 1D motion is represented at the first stage. Further motivation to look for a representation of 2D feature motion in V1 came from psychophysical experiments, which strongly suggested that the motion of terminators is calculated at a very fine spatial scale (Power, R. P. and Moulden, B., 1992; Kooi, F. L., 1993). A particularly dramatic illustration of this is that the barber pole illusion is completely abolished by cutting small notches in the aperture so that the direction of local terminator motion becomes the same as that of the 1D contours (Figure 9(a)).

A similar effect was seen for MT neurons in conscious monkeys (Pack, C. C. *et al.*, 2004). These investigators demonstrated that MT neurons reveal an effect similar to that of the barber pole illusion: their directional responses were dominated by the motion of the 2D terminators and not by that of the 1D contours. In fact, by testing neurons with barber poles of different aspect ratios, they were able to show that, as a population, MT neurons compute the VA of

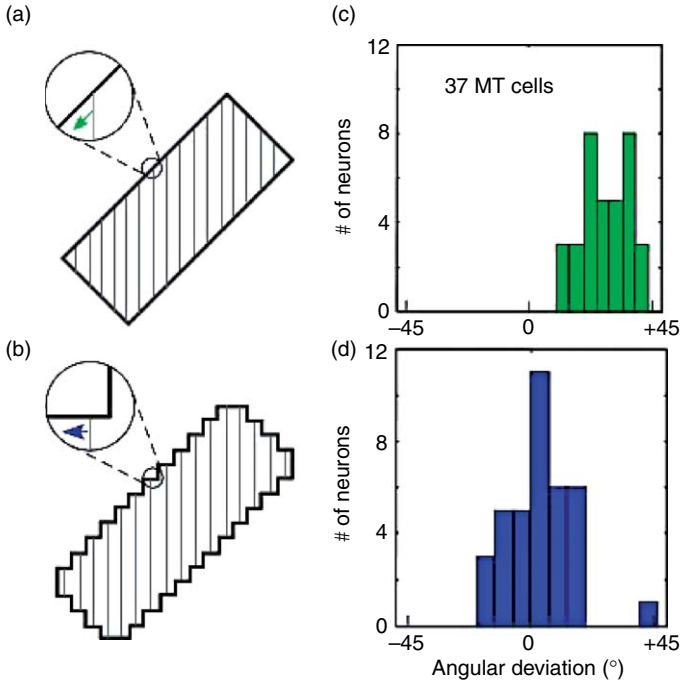

Figure 9 Effect of aperture shape on the responses of middle temporal (MT) cells. In the standard barber pole illusion (a), the dominant perceived direction of motion is parallel to the long edge of the aperture – in this case, down and to the left. Cutting notches in the aperture (b) abolishes the illusion, such that the perceived direction is now to the left, in the same direction as the one-dimensional grating. The notches have the same effect on MT cells (c) and (d). For normal barber poles (c), the direction vectors of the MT population are deviated from the grating direction toward the direction of motion of the terminators on the long axis of the aperture. (d) Cutting notches in the aperture eliminates this deviation, and the MT population now shifts back to the direction of grating motion. Adapted from figure 8 of Pack, C.C., Gartland, A.J., and Born, R.T. 2004. Integration of contour and terminator signals in visual area MT of alert macaque. J. Neurosci. 24, 3268–3280.

the two directions of terminators – those along the short and long edges of the aperture – weighted according to their relative frequencies, with little influence of the 1D signals.[8] This was measured as a deviation in the neuron's preferred direction away from the 1D and towards the 2D direction of motion (Figure 9(a)).When notches were cut in the barber poles (emulating the psychophysical experiment of Kooi F. L. (1993)) the MT population response collapsed back to the 1D direction, just as for the percept (Figure 9(b)). The most striking aspect of this result was the relative dimensions of the features: the barber poles were scaled to nearly fill the center of the MT RFs, making them, on average, 6–10° along the long axis of the aperture, while the indentations that abolished the barber pole effect were only 0.4° in length, less than one-tenth the size of the MT RF's linear dimensions. In fact, at the eccentricities tested, the indentation's dimensions were much more closely matched to RF sizes in V1 (Van Essen, D. C. *et al.*, 1984).

Similar results were also obtained with plaid stimuli. In this experiment, Majaj N. J. *et al.* (2007) first characterized MT cells using the plaid test, but with versions of plaids that were a fraction of the size of the MT RF. They next tested the same neurons with pseudoplaids that had been, in effect, pulled apart so that the two component gratings were now side-by-side instead of overlapping, yet both still well within the RF center. The effect of this manipulation was always to make the cell's direction tuning curve less patternlike, suggesting again that the 2D computation is performed locally at a spatial scale smaller than that of MT RFs.

2.11.22 Physiological Evidence for Early 2D Motion Signals

The first physiological evidence for 2D motion signals early in the cortical motion pathways had already been provided by Hubel D. H. and Wiesel T. N. (1965) who described neurons that were both direction-selective and end-stopped (or hypercomplex in their original nomenclature; Figure 10). The

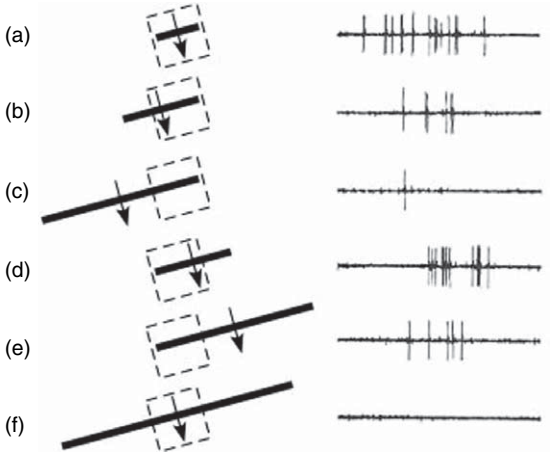

Figure 10 An end-stopped, direction-selective cell recorded by Hubel D. H. and Wiesel T. N. (1965). The neuron responds to a short bar, just covering its activating region (a), and to longer bars whose endpoints are centered over the activating region (b)–(e), but gives no response to a long bar centered over its activating region (f). Adapted from figure 17 of Hubel, D. H. and Wiezel, T. N. 1965. Receptive fields and functional architecture in two nonstriate visual areas (18 and 19) of the Cat. J. Neurophysiol. 28, 229–289.

cell responds preferentially to motion downwards (and slightly to the right), giving no response to the opposite direction of movement. Moreover, the cell is completely silent to any bar longer than the cell's tiny activating region. Such a neuron would appear to be a perfect candidate for providing 2D motion signals.[9] However, as Hubel D. H. and Wiesel T. N. only tested motion orthogonal to the orientation of the (very short) bar, they were not able to rigorously test the neuron's relative immunity to the aperture problem, nor did they demonstrate true 2D direction selectivity for line endings.

Both of these properties were subsequently demonstrated for neurons in striate cortex of alert monkeys by Pack C. C *et al.* (2003b). Figure 11a shows the RF of an end-stopped, direction-selective V1 neuron, as mapped with small spots identical to those shown in Figure 2. In this case the analysis reveals the parts of visual space to which the neuron responds (i.e., the RF). Figure 11(d) shows the same neuron's second-order subunit.[10] calculated using exactly the same method as that shown in Figure 2. Neither map shows any characteristic that would distinguish the neuron from the standard notion of a direction-selective complex cell.

Based on these maps, one can generate predictions of the same neuron's response to a second stimulus, in which the small spots were replaced with two long bars, one white and one black. In this experiment, the bars matched the neuron's preferred orientation, and were substantially longer than the RF shown in

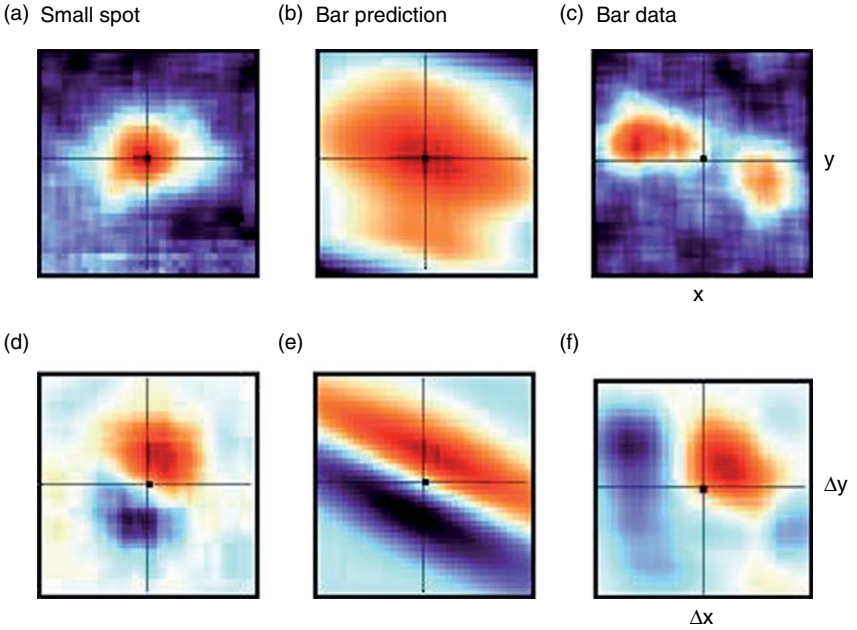

Figure 11 Subunit structure for a direction-selective, end-stopped primary visual cortex (V1) neuron. (a) The map of the receptive field obtained with small spots. (b) The predicted response to long bars flashed at different positions near the receptive field. (c) The actual map obtained with long bars. (d)–(f) As in (a)–(c), but the maps and predictions are for two-frame displacements of the long bars.

Figure 11(a). Otherwise the experiment was identical to the first one, with the bars changing position at random on each frame. The predictions, computed using convolution integrals, are shown in Figures 11(b) and 11(e). Not surprisingly, the long bar has the effect of stretching both maps along the bar's axis of orientation. This is what would be expected if the neuron viewed the long bar as simply a collection of spots like those used to generate the original maps.

The actual data, obtained using a variant of the analysis shown in Figure 2, is shown in Figures 11(c) and 11(f). The map of responses to individual bar positions, shown in Figure 11(c), reveals a characteristic signature of end-stopping: two hot spots with an intervening cold zone, which gives the maps the appearance of a dumb-bell (Figure 11(c)). One can view this map as depicting the parts of the bar to which the neuron responds best, and the two hot spots as indicating that the neuron only responses to the endpoints of the bar. The response to the center of the bar is suppressed by the mechanism that generates end-stopping, with the result that the neuron is essentially a detector of 2D features. This confirms that end-stopped neurons respond to the endpoints of long bars as was previously shown by Hubel D. H. and Wiesel T. N. (1965). In the study of Pack C. C. *et al.* (2003), the presence of end-stopping was also verified by the standard method of sweeping bars of various lengths across the RF and measuring the response of the neuron.

The data for the second-order subunit also showed a striking departure from the linear prediction shown in Figure 11(e). Rather than being smeared along the axis of bar orientation, the map shows a discrete region of activation which suggests a preference for roughly the same range of velocities as when the cell was stimulated with small spots. The cell was likely to fire an action potential in response to any two-bar sequence proceeding from up-right to down-left, corresponding to a preferred direction of 225°. This closely matched the preferred direction in the map obtained with spots, as well as the preferred direction obtained by a conventional direction tuning curve using swept bars or drifting random dots. The similarity of all three measures presumably reflects the neuron's selectivity to the bar's endpoints, because the motion of these 2D features are not influenced by the aperture problem. That this representation was truly independent of the 1D motion signals generated by the bar was shown by generating additional second-order maps using long bars that were rotated ±45° from the cell's preferred orientation. In all cases, the preferred direction indicated by the second-order map changed little, if at all.

It has not been shown that the type of end-stopped, direction-selective V1 neuron described above actually projects to MT, so it is possible that MT neurons receive only 1D motion signals from nonend-stopped cells and must use an IOC or VA to recover the 2D motion *de novo*. This seems unlikely, however, based on the known properties of neurons in 4B, which, in terms of numbers of neurons, provide over 90% of the V1 input to MT (Maunsell, J. H. and van Essen, D. C., 1983; Shipp, S. and Zeki, S., 1989). It is well established that layer 4B has a great proportion of highly direction-selective neurons (Dow, B. M., 1974; Blasdel, G. G. and Fitzpatrick, D., 1984; Livingstone, M. S. and Hubel, D. H., 1984; Hawken, M. J. *et al.*, 1988), and that most of these neurons also exhibit strong suppressive surrounds, including end-stopping (Sceniak, M. P. *et al.*, 2001). While these previous studies did not identify any of the recorded neurons as projecting to MT, it highly likely that many of them did, as the MT-projecting neurons are the largest neurons in layer 4B (Sincich, L. C. and Horton, J. C., 2003) and thus more likely to be sampled by a microelectrode than their smaller neighbors (Towe, A. L. and Harding, G. W., 1970; Humphrey, D. R. and Corrie, W. S., 1978; Lemon, R., 1984). In sum, it is highly likely that the bulk of the V1 inputs to MT originating from layer 4B are both direction-selective and strongly surround suppressed.

The finding of 2D motion selectivity in end-stopped cells suggests a reasonable explanation for the responses to bar fields in MT, but it remains unclear to what extent end-stopping can account for the observed responses to plaids. Theoretically the possibility makes sense, since most macaque V1 neurons are strongly end-stopped, and such neurons respond poorly to stimuli that contain only one orientation (Jones, H. E. *et al.*, 2001; Sceniak, M. P. *et al.*, 2001). For these neurons the component gratings in a plaid stimulus would not elicit strong responses, but the points near the intersections of the two gratings contain multiple orientations and thus might elicit stronger responses. These points move in the direction of the plaid pattern, so a simple explanation for the responses of pattern-selective MT neurons is that they receive input from V1 neurons that are themselves biased toward pattern selectivity.

Unfortunately, the end-stopping hypothesis is somewhat difficult to test with plaids, because pattern selectivity is typically defined with respect to predictions based on the responses to individual gratings.

Because a grating is defined as having only one orientation, a neuron that (by whatever mechanism) responded only to multiple orientations would be untestable by this method. In other words, a neuron that was pattern selective to the exclusion of component response would be unclassifiable. Consequently there is a bias inherent in all plaid studies towards overestimating the percentage of neurons that respond only to motion components.

Evidence against the idea of a pattern-selective projection from V1 to MT comes from Movshon J. A. and Newsome W. T. (1996), who found that V1 neurons that were identified as projecting to MT were all classified as component-type. However, the data consisted of only 12 neurons, half of which were from layer 6 where neurons appear specialized to provide 1D motion signals (Gilbert, C. D., 1977; Sceniak, M. P. *et al.*, 1999) but which provides a tiny fraction of MT's V1 input (<10%), and the degree of surround suppression present in these neurons was not reported.

The situation is further complicated by recent studies that have reported the existence of pattern-selective neurons in V1 (Tinsley, C. J. *et al.*, 2003; Guo, K. *et al.*, 2004). One group has found that, in macaque monkeys, general anesthesia appears to abolish these pattern responses (Guo, K. *et al.*, 2004). This is interesting because other groups have found that nonlinearities responsible for contextual surround effects are reduced by anesthesia (Lamme, V. A. *et al.*, 1998) and for stimuli of low contrast (Levitt, J. B. and Lund, J. S., 1997; Polat, U. *et al.*, 1998; Kapadia, M. K. *et al.*, 1999; Sceniak, M. P. *et al.*, 1999; Anderson, J. S. *et al.*, 2001; Cavanaugh, J. R. *et al.*, 2002), both of which characterized the physiological recordings of Movshon J. A. *et al.* (2003). This finding is also consistent with reports that, in MT, general anesthesia has the effect of reducing the sensitivity to pattern motion for both bar fields and certain types of plaids (Pack, C. C. *et al.*, 2001; but see Movshon, J. A. *et al.* 2003).

2.11.23 Selective Motion Integration

Integrationist models are useful for combining visual motion signals across 2D space, but a significant difficulty arises when multiple objects are present in 3D space. In this case it does not make sense to integrate across them, as they may be moving in different directions. A particularly elegant example is the case of a moving plaid stimulus, in which the two component gratings are located at different depths from the observer. Psychophysical work has shown that observers naturally segmented the two gratings to form a noncoherent percept when the depth ordering is defined by transparency (Stoner, G. R. and Albright, T. D., 1990), binocular disparity (Stoner, G. R. and Albright, T. D., 1998), surface segmentation (Trueswell, J. C. and Hayhoe, M. M. 1993; Stoner, G. R. and Albright, T. D., 1996), or occlusion (Lorençeau, J. and Shiffrar, M., 1992; McDermott, J. and Adelson, E. H. 2004). Correlates of selective motion integration based on depth segmentation were subsequently found in MT (Stoner, G. R. and Albright, T. D., 1992; Duncan, R. O. *et al.*, 2000; Thiele, A. and Stoner, G. 2003; Pack, C. C. *et al.*, 2004) and in area posteromedial lateral suprasylvian cortex (PMLS) of the cat (Castelo-Branco, M. *et al.*, 2000). These observations suggest that motion signals are identified early in visual processing and selected for integration based in part on their relative depths.

2.11.24 Theoretical Considerations: Redundancy Reduction

Another important source of motivation for selectionist models was a line of thinking, dating back to Attneave F. (1954) and Barlow H. (1961), which considered the goal of early sensory processing to be a reduction in redundancy of the primary sensory information, using principles developed by Claude Shannon in his seminal work on information theory (Shannon, C. E., 1948; Shannon, C. E. and Weaver, W., 1963). One of the important ideas that emerged from this field was the notion that regions of the image that were uniform in space and time were highly redundant and should be ignored in favor of regions of change. From this perspective, features of retinal RFs can be thought of as performing the mathematical operation of differentiation of the image luminance function with respect to various parameters, including: (1) visual space, observed as the RF property known as center-surround opponency (Kuffler, S. W., 1953; Hartline, H. K. and Ratliff, F., 1957), (2) time, manifest as adaptation (Hartline, H. K., 1941), (3) space–time, seen as sensitivity to movement (Hassenstein, B. and Reichardt, W., 1956; Reichardt, W., 1961; Barlow, H. B. and Levick, W. R., 1965), and iv) chromaticity, as evidenced by color opponency (Svaetichin, G. and MacNichol, E. F., Jr., 1959). Likewise, once a representation of the local orientation of contours has been performed by the cortex (Hubel, D. H. and Wiesel, T. N., 1962), one can construct a derivative for

orientation with respect to visual space, an operation which would identify regions of high curvature or other 2D features, which, as it turns out, are highly informative about shape (Attneave, F., 1954; Hubel, D. H. and Livingstone, M. S., 1987; Dobbins, A. *et al.*, 1989). In addition, as described above, such a representation can be further elaborated upon to compute the motion of 2D features and thus solve the aperture problem (Pack, C. C. *et al.*, 2003b). This is the basic approach of many selectionist models.

2.11.25 Selectionist Models

The theoretical considerations of forming efficient representations, combined with the psychophysical and physiological observations demonstrating the potency of the motion of terminators, have yielded a variety of models that we term selectionist. The central idea behind these models is that not all local motion vectors are treated equally. Rather, regions of redundant (and ambiguous) 1D motion vectors, such as those emanating from edges, are filtered out or, put another way, highly informative regions, such as those emanating from corners or line-endings, are selected prior to integration.

A key distinguishing feature of these models is how they have implemented the selection process. One approach, championed by Barth and colleagues (Zetzsche, C. and Barth, E., 1990; Barth, E., 2000) uses a geometric formulation of the luminance function as a hypersurface, and the operation of selecting regions of curvature (as measured by the Riemann tensor), to effectively model the kind of end-stopped, direction selective cells shown in Figures 10 and 11 and thus directly represent 2D velocity. The important point about these models is that they have spatial filters that respond selectively to image regions that contain multiple orientations. There are many ways to design such an operator, but as pointed out by Barth and colleagues all of them must involve nonlinear operations, the simplest nonlinearity being multiplication (Zetzsche, C. and Barth, E., 1990).

Along these lines, Skottun B. C. (1998; 1999) developed neuronal models that simply multiply the responses of orientation-tuned linear filters to arrive at selectivity for 2D features. This operation is sufficient to reproduce many of the results on both end-stopping (Skottun, B. C., 1998) and plaid tuning (Skottun, B. C., 1999). The multiplication operation is used for mathematical convenience, but in principle it could be approximated by any number of the standard nonlinearities known to affect neuronal responses (Tal, D. and Schwartz, E. L., 1997).

Another important model was put forward by Nowlan S. J. and Sejnowski T. J. (1995), and it is selectionist in spirit, even though the selective calculation is nominally performed at the MT stage of the model. In their case, the nonlinear step selects regions of change in local motion vectors by simulating MT neurons with suppressive surrounds (Allman, J. *et al.*, 1985). Such neurons are inhibited when motion is in the same direction in both center and surround, so they respond poorly, if at all, to the motion of 1D contours. This selectivity network then retinotopically gates a second, parallel integration network that pools the motion signals from the selected regions (Figure 12). Thus, for example, for a moving square, MT neurons in the selection network having RF centers overlying the contours respond weakly because there are similar directions of motion in both their RF centers and surrounds.

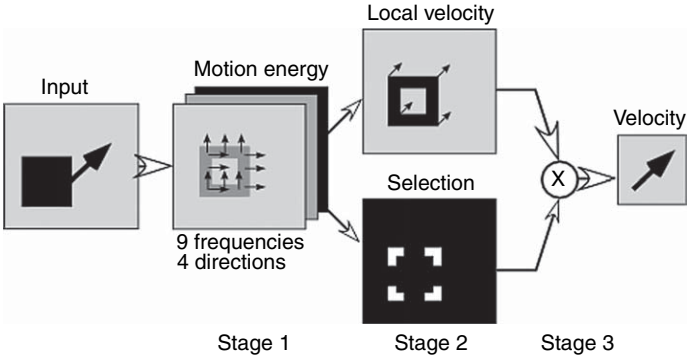

Figure 12 Selectionist model proposed by Nowlan S. J. and Sejnowski T. J. (1995). See text for details. Adapted from figure 2 of Nowlan, S. J. and Sejnowski, T. J. 1995. A selection model for motion processing in area MT of primates. J. Neurosci. 15, 1195–1214.

Surround-inhibited neurons with RF centers positioned at the corners are not effectively suppressed, resulting in a selection of these regions for pooling by the integration network, effectively producing feature tracking. The same logic allows the model to effectively track the motion of 2D intersections in plaid stimuli.

2.11.26 Hybrid Models

Thus the selectionist category of models can be thought of as instantiating a kind of feature tracking, whereas the integrationist models implement an IOC computation. The perceptual data, however, suggest that a single computational strategy will not suffice: under some circumstances, an IOC or feature-tracking rule seems to be in effect, whereas for others, a VA best describes the integration process. This lack of parsimony has motivated computational modelers to seek more general descriptions that can better accommodate the variety of behaviors. A notable recent effort by Weiss Y. *et al.* (2002) essentially embeds many of the features of the IOC calculation in a Bayesian model. The Bayesian calculation involves weighting the first-stage inputs according to the uncertainty associated with the local motion measurement, with the result that 2D features strongly influence the velocity–space calculation in the second stage. Because the velocity–space constraints are subject to noise, the constraint lines are more or less fuzzy depending on the contrast of the stimulus. The stimulus-based evidence is multiplied by a second probability distribution that a priori favors slow speeds (a symmetrical 2D Gaussian centered about the origin in velocity space) in order to obtain the posterior probability in favor of a given 2D object velocity.

These properties endow the model with a rather intuitively appealing behavior that explains much of the existing psychophysical data (Weiss, Y. and Adelson, E. H., 1998). The two key observations are, (1) that the VA percept tends to dominate in conditions where the stimulus-based evidence is relatively weak (low contrast, short duration, or a narrow range of component orientations), and (2) the velocity predicted by the VA is always slower than that of the IOC. The model's behavior can be understood in terms of the relative influence of the prior favoring slow speeds. When the stimulus-based evidence is strong, the prior has little effect and the result is essentially an IOC. When the stimulus-based evidence is weak, the likelihood functions are dim and fuzzy, and the prior has a relatively large effect, pushing the result towards a slower speed, which approaches the VA.

In a related study, Stocker A. A. and Simoncelli E. P. (2006) used a speed discrimination task to estimate the slowness prior and the likelihood functions at different speeds and contrasts for individual observers. Their measurements revealed significant differences between the measured functions and those assumed by the model of Weiss Y. *et al.* (2002). For example, the slowness prior was not well described by a Gaussian, but rather flattened out at higher speeds, and the inverse relationship between the width of the likelihood function and stimulus contrast was different for different observers. It will be important to test whether such differences can be used to better account for individual performance on other motion integration tasks, such as those used by Weiss Y. *et al.* (2002).

Weiss Y. *et al.* (2002) did not hypothesize a physiological basis for the model's computations, but many of the phenomena reported are also consistent with physiological properties of end-stopped V1 cells. End-stopping (and nonlinear contextual effects in general) is weak or nonexistent for stimuli of low contrast (Levitt, J. B. and Lund, J. S., 1997; Polat, U. *et al.*, 1998; Sceniak, M. P. *et al.*, 1999) and takes time to manifest itself in the neuronal response (Pack, C. C. *et al.*, 2003b). Under such circumstances, the local velocity measurements made in V1 are essentially 1D, as postulated by integrationist models, although the perceived direction is more similar to a VA than an IOC. For high-contrast stimuli end-stopping is effective, allowing 1D motion signals to be filtered out, thus emphasizing the veridical velocity of 2D features. Both of these observations are at least qualitatively consistent with the Bayesian computation described by Weiss Y. *et al.* (2002).

2.11.27 Future Challenges

While there has been much speculation about the role of various direction-selective neurons in motion integration and the solution to the aperture problem (Albright, T. D., 1984; Movshon, J. A. *et al.*, 1985; Pack, C. C. *et al.*, 2003b), there has been a complete lack of experiments in which these neural signals are directly compared to perceptual reports. For example, while Pack C. C. *et al.* (2003b) demonstrated that end-stopped, direction-selective neurons in V1

could, in principle, provide faithful 2D velocity measurements of features, there is no direct evidence that such neurons are actually used by perceptual systems (or even that these neurons project to MT, though, statistically, many are likely to do so). Similarly, the evidence that V1 neurons projecting to MT provide only 1D motion information (Movshon, J. A. and Newsome, W. T., 1996) cannot be considered definitive given the small sample size, the considerable oversampling of layer 6 neurons, which are known to prefer long bars (Gilbert, C. D., 1977; Sceniak, M. P. *et al.*, 2001), and the aforementioned shortcomings of the plaid test for character-izing end-stopped neurons. What is needed is a demonstration of which neurons are actively contributing to a given percept at a given time. Such evidence would need to consist of trial-by-trial correlations between the activity of these neurons and the choices of the monkey on a suitable perceptual task (Parker, A. J. and Newsome, W. T., 1998). For example, if pattern cells are important for the perception of coherent motion, then, for ambiguous plaid stimuli for which the animal may report either coherence or transparency, one would expect pattern cells to fire at higher rates during trials on which the animal reports coherence. An inverse relationship would be predicted for component cells. Such measures of choice probability (Britten, K. H. *et al.*, 1996) would strongly support the proposed roles of these neurons. Furthermore, insofar as there is spatial clustering of pattern or component neurons in MT or some other visual structure, microstimulation experiments could be used to attempt to bias an animal's reports in predictable ways, as has been done for perceived direction of motion in random dot displays (Salzman, C. D. *et al.*, 1990; 1992).

Both a challenge and a potential boon to studies linking neurophysiology to percepts of motion integration is the fact that many of the stimuli used to study it are perceptually bi- or even multistable. This is true of both plaids (Stoner, G. R. and Albright, T. D., 1996; Hupé, J. M. and Rubin, N., 2003) and barber poles (Rubin, N. and Hochstein, S., 1993; Castet, E. *et al.*, 1999). For example, prolonged viewing of plaid stimuli produces spontaneous perceptual transitions between coherence and transparency (Hupé, J. M. and Rubin, N., 2003), and this is true even for plaids whose intersection luminance values are not consistent with transparency (see Relevant Websites section). Such phenomena argue for an active, ongoing competition amongst local motion cues and will present future models with challenges similar to those encountered by models of binocular rivalry (Leopold, D. A. and Logothetis, N. K., 1999). Furthermore, the plaid multistability (Hupé, J. M. and Rubin, N., 2003) and the profound influence of shape and occlusion cues on the integration of motion (Lorençeau, J. and Shiffrar, M., 1992; Lorençeau, J. and Alais, D., 2001), underline the fact that integration and segmentation are tightly linked, even at early stages of visual processing.

In fact, relatively few motion models address the complications that arise when the visual input contains multiple objects. In such cases motion integration appears to be influenced by a mechanism that performs segmentation, presumably to avoid integrating over multiple objects or surfaces (Shimojo, S. *et al.*, 1989). The segmentation system has proven difficult to model, in part because it is influenced by nonmotion cues, especially perceived depth as defined by retinal disparity, T-junctions, or transparency. Most segmentation models involve the explicit detection of motion boundaries based on depth cues, along with the smoothing of motion signals across individual objects or surfaces (Nowlan, S. J. and Sejnowski, T. J., 1995; Koechlin, E. *et al.*, 1999; Lidén, L. and Pack, C., 1999; Bulthoff, H. *et al.*, 1989; Grossberg, S. *et al.*, 2001; Bayerl, P. and Neumann, H., 2004).

The smoothing in these models is often accomplished by a winner-take-all interaction of motion signals across networks of neurons with small RFs. This process is motivated by the perceptual observation that objects appear to move rigidly, despite the presumed diversity in local motion measurements. That is, each part of an object appears to move in the same direction, even when small RFs are reporting different velocities. However, evidence for this kind of smoothing process in V1 has not been found (Pack, C. C. *et al.*, 2004), even for stimuli that should engage the perceptual winner-take-all mechanism. In fact for barber-pole stimuli the responses in MT can be estimated with reasonable precision based on a local end-stopping procedure observable at the level of individual V1 neurons (Pack, C. C. *et al.*, 2004). However, neither the V1 nor the MT responses appear to be entirely consistent with perceptual observations, suggesting that it may make sense to start the search for neural correlates of percep-tual smoothing in regions of the cortex beyond V1 and MT.

2.11.28 Final Thoughts

As we have tried to emphasize, the existing evidence suggests that under some circumstances observers

perceive motion that is consistent with the standard integrationist model (Simoncelli, E. P. and Heeger, D. J., 1998). In contrast, there are many exceptions in the psychophysical literature, and the results of physiological tests of the model have been equivocal at best.

Evidence for 2D feature selectivity in V1 has been found in a few studies, although it is not clear how this selectivity influences MT responses. In this regard a significant problem is the lack of a standard selectionist model that can be meaningfully compared to the standard integrationist model. While many selectionist models exist, they tend to be substantially more complicated than the integrationist models discussed here, and as a result the predictions are less clear, rendering a detailed comparison problematic. Thus an important avenue for future research will be the development of a standard selectionist model. There is no reason why this cannot be done, since as we have pointed out many of the core computations are the same in both types of models.

Endnotes

[1] (Under certain conditions, such as when the components are configured to simulate transparent occlusion, even plaids with identical components can fail to cohere (Stoner *et al.*, 1990).)

[2] Even though the pattern direction would be the same as the grating direction under the plaid prediction, there is no good reason why the tuning curves should be identical. They are, after all, quite different stimuli with different perceptual properties. Nevertheless, it is an intuitively simple way to set up the test.

[3] The model's response to a component grating moving in direction d is given by

$$\left[\left[\left[\sum_i g(p_i - d)h(P - p_i)\right] - \theta\right]^+\right]^n$$

where g is a Gaussian function that describes the ith V1 neuron's direction tuning as a function of preferred direction p_i, h is another Gaussian that weights V1 inputs according to the MT neuron's preferred direction P, and θ is a threshold.

[4] The MT neurons described in Albright T. D. (1984) were categorized as belonging to type I or type II, the latter having broader tuning than the former. It was subsequently shown that these two categories corresponded to component and pattern neurons, respectively (Rodman, H. R. and Albright, T. D., 1989). The same explanation, based on differences in tuning bandwidths, also applies to the observed differences in orientation tuning preferences between pattern and component neurons (Rodman, H. R. and Albright, T. D., 1989).

[5] Extrinsic terminators are created by using binocular disparity or other occlusion cues to indicate that the grating endings are accidents of occlusion (Shimojo, S. *et al.*, 1989) and therefore not likely to belong to the moving object. Two distinguish the two types of terminators (those belonging to an object versus those that are created by occlusion) psychophysicists refer to intrinsic and extrinsic terminators, respectively. This classification, though useful, is undoubtedly too simple. Experiments by Castet E. *et al*. (1999) indicate that there may be different degrees of extrinsicness.

[6] An alternative possibility is that a linear neuron could be selective for the high spatial frequencies found near the endpoints of the moving edge. However, this does not appear to be the case for MT neurons, which generally prefer low spatial frequencies.

[7] It has often been argued that the time course observed in this experiment constitutes evidence for linear responses in MT, since the motion components moving in the global stimulus direction are low in amplitude, and hence might be expected to have longer latencies. While it is entirely possible that the 2D features are processed more slowly than 1D features, the stronger hypothesis of linearity merely begs the question of why the low-amplitude component dominates the neuronal response.

[8] Since the direction of the 1D grating motion was always 45° from the direction of either set of terminators, these experiments did not test for the influence of grating direction (capture) found psychophysically by Castet E. *et al*. (1999).

[9] Another compelling example of such a neuron is shown in one of Hubel and Wiesel's now-classic movies (see Relevant Website section).

[10] Technically, both types of maps are second-order subunits, since the response to the individual spots is independent of contrast. To avoid confusion we continue to refer only to the motion maps (Figures 11(c) and 11(f)) as second-order subunits.

References

Adelson, E. H. and Bergen, J. R. 1985. Spatiotemporal energy models for the perception of motion. J. Opt. Soc. Am. A 2, 284–299.

Adelson, E. H. and Movshon, J. A. 1982. Phenomenal coherence of moving visual patterns. Nature 300, 523–525.

Albright, T. D. 1984. Direction and orientation selectivity of neurons in visual area MT of the macaque. J. Neurophysiol. 52, 1106–1130.

Albright, T. D. and Desimone, R. 1987. Local precision of visuotopic organization in the middle temporal area (MT) of the macaque. Exp. Brain Res. 65, 582–592.

Allman, J., Miezin, F., and McGuinness, E. 1985. Direction- and velocity-specific responses from beyond the classical receptive field in the middle temporal visual area (MT). Perception 14, 105–126.

Anderson, J. S., Lampl, I., Gillespie, D. C., and Ferster, D. 2001. Membrane potential and conductance changes underlying length tuning of cells in cat primary visual cortex. J. Neurosci. 21, 2104–2112.

Attneave, F. 1954. Some informational aspects of visual perception. Psychol. Rev. 61, 183–193.

Barlow, H. 1961. Possible Principles Underlying the Transformation of Sensory Messages. In: Sensory Communication (*ed*. W. A. Rosenblith), pp. 217–234. MIT Press.

Barlow, H. B. and Levick, W. R. 1965. The mechanism of directionally selective units in rabbit's retina. J. Physiol. (Lond.) 178, 477–504.

Barth, E. 2000. A geometric view on early and middle level visual coding. Spat. Vis. 13, 193–199.

Bayerl, P. and Neumann, H. 2004. Disambiguating visual motion through contextual feedback modulation. Neural Comput. 16, 2041–2066.

Blasdel, G. G. and Fitzpatrick, D. 1984. Physiological organization of layer 4 in macaque striate cortex. J. Neurosci. 4, 880–895.

Born, R. T. and Bradley, D. C. 2005. Structure and function of visual area MT. Annu. Rev. Neurosci. 28, 157–189.

Bowns, L. 1996. Evidence for a feature tracking explanation of why type II plaids move in the vector sum direction at short durations. Vision Res. 36, 3685–3694.

Bradley, D. C., Goyal, M. S., and Scott, B. B. 2005. Pattern Velocity Computation by Primate MT Neurons. Program No. 136.9. 2005, Abstract Viewer/Itinerary Planner, Washington, DC: Society for Neuroscience.

Britten, K. H. and Heuer, H. W. 1999. Spatial summation in the receptive fields of MT neurons. J. Neurosci. 19, 5074–5084.

Britten, K. H., Newsome, W. T., Shadlen, M. N., Celebrini, S., and Movshon, J. A. 1996. A relationship between behavioral choice and the visual responses of neurons in macaque MT. Vis. Neurosci. 13, 87–100.

Britten, K. H., Shadlen, M. N., Newsome, W. T., and Movshon, J. A. 1992. The analysis of visual motion: a comparison of neuronal and psychophysical performance. J. Neurosci. 12, 4745–4765.

Bulthoff, H., Little, J., and Poggio, T. 1989. A parallel algorithm for real-time computation of optical flow. Nature 337, 549–555.

Carandini, M. and Ferster, D. 2000. Membrane potential and firing rate in cat primary visual cortex. J. Neurosci. 20, 470–484.

Carandini, M., Heeger, D. J., and Movshon, J. A. 1997. Linearity and normalization in simple cells of the macaque primary visual cortex. J. Neurosci. 17, 8621–8644.

Castelo-Branco, M., Goebel, R., Neuenschwander, S., and Singer, W. 2000. Neural synchrony correlates with surface segregation rules. Nature 405(6787), 685–689.

Castet, E., Charton, V., and Dufour, A. 1999. The extrinsic/intrinsic classification of two-dimensional motion signals with barber-pole stimuli. Vision Res. 39, 915–932.

Cavanaugh, J. R., Bair, W., and Movshon, J. A. 2002. Nature and interaction of signals from the receptive field center and surround in macaque V1 neurons. J. Neurophysiol. 88, 2530–2546.

Churchland, M. M., Priebe, N. J., and Lisberger, S. G. 2005. Comparison of the spatial limits on direction selectivity in visual areas MT and V1. J. Neurophysiol. 93, 1235–1245.

Courellis, S. H. and Marmarelis, V. Z. 1992. Nonlinear Functional Representations for Motion Detection and Speed Estimation Schemes. In: Nonlinear Vision (*eds*. B. Nabet and R. B. Pinter), pp. 91–108. CRC Press.

DeAngelis, G. C., Ohzawa, I., and Freeman, R. D. 1993. Spatiotemporal organization of simple-cell receptive fields in the cat's striate cortex. II. Linearity of temporal and spatial summation. J. Neurophysiol. 69, 1118–1135.

Derrington, A. and Suero, M. 1991. Motion of complex patterns is computed from the perceived motions of their components. Vision Res. 31, 139–149.

Dobbins, A., Zucker, S. W., and Cynader, M. S. 1989. Endstopping and curvature. Vision Res. 29, 1371–1387.

Dow, B. M. 1974. Functional classes of cells and their laminar distribution in monkey visual cortex. J. Neurophysiol. 37, 927–946.

Dubner, R. and Zeki, S. M. 1971. Response properties and receptive fields of cells in an anatomically defined region of the superior temporal sulcus in the monkey. Brain Res. 35, 528–532.

Duncan, R. O., Albright, T. D., and Stoner, G. R. 2000. Occlusion and the interpretation of visual motion: perceptual and neuronal effects of context. J. Neurosci. 20, 5885–5897.

Emerson, R. C., Bergen, J. R., and Adelson, E. H. 1992. Directionally selective complex cells and the computation of motion energy in cat visual cortex. Vision Res. 32, 203–218.

Emerson, R. C., Citron, M. C., Vaughn, W. J., and Klein, S. A. 1987. Nonlinear directionally selective subunits in complex cells of cat striate cortex. J. Neurophysiol. 58, 33–65.

Fennema, C. and Thompson, W. 1979. Velocity determination in scenes containing several moving objects. Comp. Graph. Image Process. 9, 301–315.

Ferrera, V. P. and Wilson, H. R. 1987. Direction specific masking and the analysis of motion in two dimensions. Vision Res. 27, 1783–1796.

Ferrera, V. P. and Wilson, H. R. 1990. Perceived direction of moving two-dimensional patterns. Vision Res. 30, 273–287.

Gilbert, C. D. 1977. Laminar differences in receptive field properties of cells in cat primary visual cortex. J. Physiol. 268, 391–421.

Grossberg, S., Mingolla, E., and Viswanathan, L. 2001. Neural dynamics of motion integration and segmentation within and across apertures. Vision Res. 41, 2521–2553.

Grzywacz, N. M. and Yuille, A. L. 1990. A model for the estimate of local image velocity by cells in the visual cortex. Proc R Soc Lond B Biol Sci. 239(1295), 129–161.

Guo, K., Benson, P. J., and Blakemore, C. 2004. Pattern motion is present in V1 of awake but not anaesthetized monkeys. Eur. J. Neurosci. 19, 1055–1066.

Hartline, H. K. 1941. The neural mechanisms of vision. Harvey Lectures Ser. 37, 39.

Hartline, H. K. and Ratliff, F. 1957. Inhibitory interaction of receptor units in the eye of Limulus. J. Gen. Physiol. 40, 357–376.

Hassenstein, B. and Reichardt, W. 1956. Systemtheoretische analyse der zeit-, reihenfolgen- und vorzeichenauswertung bei der bewegungsperzeption des rüsselkäfers, Chlorophanus. Z. Naturforsch. Teil. B 11, 513–524.

Hawken, M. J., Parker, A. J., and Lund, J. S. 1988. Laminar organization and contrast sensitivity of direction-selective cells in the striate cortex of the Old World monkey. J. Neurosci. 8, 3541–3548.

Heeger, D. J. 1987. Model for the extraction of image flow. J. Opt. Soc. Am. A 4, 1455–1471.

Heeger, D. J., Simoncelli, E. P., and Movshon, J. A. 1996. Computational models of cortical visual processing. Proc. Natl. Acad. Sci. U. S. A. 93, 623–627.

Heuer, H. W. and Britten, K. H. 2002. Contrast dependence of response normalization in area MT of the rhesus macaque. J. Neurophysiol. 88, 3398–3408.

Hubel, D. H. and Livingstone, M. S. 1987. Segregation of form, color, and stereopsis in primate area 18. J. Neurosci. 7, 3378–3415.

Hubel, D. H. and Wiesel, T. N. 1962. Receptive fields, binocular interaction and functional architecture in the cat's visual cortex. J Physiol 160, 106–154.

Hubel, D. H. and Wiezel, T. N. 1965. Receptive fields and functional architecture in two nonstriate visual areas (18 and 19) of the cat. J. Neurophysiol. 28, 229–289.

Humphrey, D. R. and Corrie, W. S. 1978. Properties of pyramidal tract neuron system within a functionally defined subregion of primate motor cortex. J. Neurophysiol. 41, 216–243.

Hupé, J. M. and Rubin, N. 2003. The dynamics of bi-stable alternation in ambiguous motion displays: a fresh look at plaids. Vision Res. 43, 531–548.

Jones, H. E., Grieve, K. L., Wang, W., and Sillito, A. M. 2001. Surround suppression in primate V1. J. Neurophysiol. 86, 2011–2028.

Kapadia, M. K., Westheimer, G., and Gilbert, C. D. 1999. Dynamics of spatial summation in primary visual cortex of alert monkeys. Proc. Natl. Acad. Sci. U. S. A. 96, 12073–12078.

Kawakami, S. and Okamoto, H. 1996. A cell model for the detection of local image motion on the magnocellular pathway of the visual cortex. Vision Res. 36, 117–147.

Koechlin, E., Anton, J. L., and Burnod, Y. 1999. Bayesian inference in populations of cortical neurons: a model of motion integration and segmentation in area MT. Biol. Cybern. 80, 25–44.

Kooi, F. L. 1993. Local direction of edge motion causes and abolishes the barberpole illusion. Vision Res. 33, 2347–2351.

Krekelberg, B. and Albright, T. D. 2005. Motion mechanisms in macaque MT. J. Neurophysiol. 93, 2908–2921.

Kuffler, S. W. 1953. Discharge patterns and functional organization of mammalian retina. J. Neurophysiol. 16, 37–68.

Lamme, V. A., Zipser, K., and Spekreijse, H. 1998. Figure-ground activity in primary visual cortex is suppressed by anesthesia. Proc. Natl. Acad. Sci. U. S. A. 95, 3263–3268.

Lemon, R. 1984. Methods for Neuronal Recording in Conscious Animals, Wiley.

Leopold, D. A. and Logothetis, N. K. 1999. Multistable phenomena: changing views in perception. Trends Cogn. Sci. 3, 254–264.

Levitt, J. B. and Lund, J. S. 1997. Contrast dependence of contextual effects in primate visual cortex. Nature 387, 73–76.

Lidén, L. and Pack, C. 1999. The role of terminators and occlusion cues in motion integration and segmentation: a neural network model. Vision Res. 39, 3301–3320.

Limb, J. O. and Murphy, J. A. 1975. Estimating the velocity of moving images in television signals. Comp. Graph. Image Process. 4, 311–327.

Lisberger, S. G. and Ferrera, V. P. 1997. Vector averaging for smooth pursuit eye movements initiated by two moving targets in monkeys. J. Neurosci. 17, 7490–7502.

Livingstone, M. S. and Hubel, D. H. 1984. Specificity of intrinsic connections in primate primary visual cortex. J. Neurosci. 4, 2830–2835.

Livingstone, M. S., Pack, C. C., and Born, R. T. 2001. Two-dimensional substructure of MT receptive fields. Neuron 30, 781–793.

Lorençeau, J. and Alais, D. 2001. Form constraints in motion binding. Nat. Neurosci. 4, 745–751.

Lorençeau, J. and Shiffrar, M. 1992. The influence of terminators on motion integration across space. Vision Res. 32, 263–273.

Lorençeau, J., Shiffrar, M., Wells, N., and Castet, E. 1993. Different motion sensitive units are involved in recovering the direction of moving lines. Vision Res. 33(9), 1207–1217.

Majaj, N. J., Carandini, M., and Movshon, J. A. 2007. Motion integration by neurons in macaque MT is local, not global. J. Neurosci. 27, 366–370.

Marr, D. 1982. Vision. W.H. Freeman & Co.

Maunsell, J. H. and van Essen, D. C. 1983. The connections of the middle temporal visual area (MT) and their relationship to a cortical hierarchy in the macaque monkey. J. Neurosci. 3, 2563–2586.

McDermott, J. and Adelson, E. H. 2004. The geometry of the occluding contour and its effect on motion interpretation. J. Vis. 4(10), 944–954.

Mikami, A., Newsome, W. T., and Wurtz, R. H. 1986. Motion selectivity in macaque visual cortex. II. Spatiotemporal range of directional interactions in MT and V1. J. Neurophysiol. 55, 1328–1339.

Mingolla, E., Todd, J. T., and Norman, J. F. 1992. The perception of globally coherent motion. Vision Res. 32, 1015–1031.

Movshon, J. A. and Newsome, W. T. 1996. Visual response properties of striate cortical neurons projecting to area MT in macaque monkeys. J. Neurosci. 16, 7733–7741.

Movshon, J. A., Adelson, E. H., Gizzi, M. S., and Newsome, W. T. 1985. The Analysis of Moving Visual Patterns. In: Pattern Recognition Mechanisms (*eds*. C. Chagas, R. Gattass, and C. Gross), pp. 117–151. Vatican Press.

Movshon, J. A., Albright, T. D., Stoner, G. R., Majaj, N. J., and Smith, M. A. 2003. Cortical responses to visual motion in alert and anesthetized monkeys. Nat. Neurosci. 6, 3 (reply by Pack, C. C., Berezovskii, V. K. and Born, R. T., pp. 3–4).

Newsome, W. T., Britten, K. H., and Movshon, J. A. 1989. Neuronal correlates of a perceptual decision. Nature 341, 52–54.

Nowlan, S. J. and Sejnowski, T. J. 1995. A selection model for motion processing in area MT of primates. J. Neurosci. 15, 1195–1214.

Ogata, M. and Sato, T. 1991. Motion perception model with interaction between spatial frequency channels. Syst. Comput. Jap. 22, 30–39.

Okamoto, H., Kawakami, S., Saito, H., Hida, E., Odajima, K., Tamanoi, D., and Ohno, H. 1999. MT neurons in the macaque exhibited two types of bimodal direction tuning as predicted by a model for visual motion detection. Vision Res. 39(20), 3465–3479.

Pack, C. C. and Born, R. T. 2001. Temporal dynamics of a neural solution to the aperture problem in visual area MT of macaque brain. Nature 409, 1040–1042.

Pack, C. C., Berezovskii, V. K., and Born, R. T. 2001. Dynamic properties of neurons in cortical area MT in alert and anaesthetized macaque monkeys. Nature 414, 905–908.

Pack, C. C., Born, R. T., and Livingstone, M. S. 2003a. Two-dimensional substructure of motion and stereo interactions in primary visual cortex of alert macaque. Neuron 37, 525–535.

Pack, C. C., Conway, B. R., Born, R. T., and Livingstone, M. S. 2006. Spatiotemporal structure of nonlinear subunits in macaque visual cortex. J. Neurosci. 26, 893–907.

Pack, C. C., Gartland, A. J., and Born, R. T. 2004. Integration of contour and terminator signals in visual area MT of alert macaque. J. Neurosci. 24, 3268–3280.

Pack, C. C., Livingstone, M., Duffy, K., and Born, R. T. 2003b. End-stopping and the aperture problem: two-dimensional motion signals in macaque V1. Neuron 39, 671–680.

Parker, A. J. and Newsome, W. T. 1998. Sense and the single neuron: probing the physiology of perception. Annu. Rev. Neurosci. 21, 227–277.

Perrone, J. A. and Thiele, A. 2001. Speed skills: measuring the visual speed analyzing properties of primate MT neurons. Nat. Neurosci. 4(5), 526–532.

Poggio, T. and Reichardt, W. 1973. Considerations on models of movement detection. Kybernetik 13, 223–227.

Polat, U., Mizobe, K., Pettet, M. W., Kasamatsu, T., and Norcia, A. M. 1998. Collinear stimuli regulate visual responses depending on cell's contrast threshold. Nature 391, 580–584.

Power, R. P. and Moulden, B. 1992. Spatial gating effects on judged motion of gratings in apertures. Perception 21, 449–463.

Priebe, N. J., Cassanello, C. R., and Lisberger, S. G. 2003. The neural representation of speed in macaque area MT/V5. J. Neurosci. 23, 5650–5661.

Priebe, N. J., Lisberger, S. G., and Movshon, J. A. 2006. Tuning for spatiotemporal frequency and speed in directionally selective neurons of macaque striate cortex. J. Neurosci. 26, 2941–2950.

Qian, N. and Andersen, R. A. 1994. Transparent motion perception as detection of unbalanced motion signals. II. Physiology. J. Neurosci. 14, 7367–7380.

Recanzone, G. H., Wurtz, R. H., and Schwarz, U. 1997. Responses of MT and MST neurons to one and two moving objects in the receptive field. J. Neurophysiol. 78, 2904–2915.

Reichardt, W. 1961. Autocorrelation, a Principle for the Evaluation of Sensory Information by the Central Nervous System. In: Sensory Communications (*ed*. W. A. Rosenblith), pp. 303–318. Wiley.
Rodman, H. R. and Albright, T. D. 1989. Single-unit analysis of pattern-motion selective properties in the middle temporal visual area (MT). Exp. Brain Res. 75(1), 53–64.
Rubin, N. and Hochstein, S. 1993. Isolating the effect of one-dimensional motion signals on the perceived direction of moving two-dimensional objects. Vision Res. 33, 1385–1396.
Rust, N. C., Mante, V., Simoncelli, E. P., and Movshon, J. A. 2006. How MT cells analyze the motion of visual patterns. Nat. Neurosci. 9, 1421–1431.
Salzman, C. D., Britten, K. H., and Newsome, W. T. 1990. Cortical microstimulation influences perceptual judgements of motion direction. Nature 346, 174–177.
Salzman, C. D., Murasugi, C. M., Britten, K. H., and Newsome, W. T. 1992. Microstimulation in visual area MT: effects on direction discrimination performance. J. Neurosci. 12, 2331–2355.
Sceniak, M. P., Hawken, M. J., and Shapley, R. 2001. Visual spatial characterization of macaque V1 neurons. J. Neurophysiol. 85, 1873–1887.
Sceniak, M. P., Ringach, D. L., Hawken, M. J., and Shapley, R. 1999. Contrast's effect on spatial summation by macaque V1 neurons. Nat. Neurosci. 2, 733–739.
Sekuler, R. W. and Ganz, L. 1963. Aftereffect of seen motion with a stabilized retinal image. Science 139, 419–420.
Sereno, M. E. 1993. Neural Computation of Pattern Motion. MIT Press.
Shannon, C. E. 1948. A mathematical theory of communication. Bell Syst. Tech. J. 27, 379–423.
Shannon, C. E. and Weaver, W. 1963. The Mathematical Theory of Communication. University of Illinois Press.
Shimojo, S., Silverman, G. H., and Nakayama, K. 1989. Occlusion and the solution to the aperture problem for motion. Vision Res. 29, 619–626.
Shipp, S. and Zeki, S. 1989. The organization of connections between areas V5 and V1 in macaque monkey visual cortex. Eur. J. Neurosci. 1, 309–332.
Simoncelli, E. P. and Heeger, D. J. 1998. A model of neuronal responses in visual area MT. Vision Res. 38, 743–761.
Simoncelli, E. P., Bair, W. D., Cavanaugh, J. R., and Movshon, J. A. 1996. Testing and refining a computational model of neuronal responses in area MT. Investigative Ophthalmology and Visual Science 37, 916.
Sincich, L. C. and Horton, J. C. 2003. Independent projection streams from macaque striate cortex to the second visual area and middle temporal area. J. Neurosci. 23, 5684–5692.
Skottun, B. C. 1998. A model for end-stopping in the visual cortex. Vision Res. 38, 2023–2035.
Skottun, B. C. 1999. Neuronal responses to plaids. Vision Res. 39, 2151–2156.
Snowden, R. J., Treue, S., Erickson, R. G., and Andersen, R. A. 1991. The response of area MT and V1 neurons to transparent motion. J. Neurosci. 11, 2768–2785.
Stocker, A. A. and Simoncelli, E. P. 2006. Noise characteristics and prior expectations in human visual speed perception. Nat. Neurosci. 9, 578–585.
Stoner, G. R. and Albright, T. D. 1992. Neural correlates of perceptual motion coherence. Nature 358, 412–414.
Stoner, G. R. and Albright, T. D. 1996. The interpretation of visual motion: evidence for surface segmentation mechanisms. Vision Res. 36(9), 1291–1310.
Stoner, G. R. and Albright, T. D. 1998. Luminance contrast affects motion coherency in plaid patterns by acting as a depth-from-occlusion cue. Vision Res. 38(3), 387–401.
Svaetichin, G. and MacNichol, E. F., Jr. 1959. Retinal mechanisms for chromatic and achromatic vision. Ann. N. Y. Acad. Sci. 74, 385–404.
Tal, D. and Schwartz, E. L. 1997. Computing with the leaky integrate-and-fire neuron: logarithmic computation and multiplication. Neural Comput. 9, 305–318.
Thiele, A. and Stoner, G. 2003. Neuronal synchrony does not correlate with motion coherence in cortical area MT. Nature 421(6921), 366–370.
Tinsley, C. J., Webb, B. S., Barraclough, N. E., Vincent, C. J., Parker, A., and Derrington, A. M. 2003. The nature of V1 neural responses to 2D moving patterns depends on receptive-field structure in the marmoset monkey. J. Neurophysiol. 90, 930–937.
Towe, A. L. and Harding, G. W. 1970. Extracellular microelectrode sampling bias. Exp. Neurol. 29, 366–381.
Trueswell, J. C. and Hayhoe, M. M. 1993. Surface segmentation mechanisms and motion perception. Vision Res. 33(3), 313–328.
Ullman, S. 1979. The Interpretation of Visual Motion, MIT Press.
Van Essen, D. C., Newsome, W. T., and Maunsell, J. H. 1984. The visual field representation in striate cortex of the macaque monkey: asymmetries, anisotropies, and individual variability. Vision Res. 24, 429–448.
van Santen, J. P. and Sperling, G. 1985. Elaborated Reichardt detectors. J. Opt. Soc. Am. A 2, 300–321.
Wallach, H. 1935. Uber visuell wahrgenommene Bewegungsrichtung. Psychol. Forsch. 20, 325–380.
Watson, A. B. and Ahumada, A. J. 1985. Model of human visual-motion sensing. J Opt Soc Am A. 2(2), 322–341.
Weiss, Y. and Adelson, E. H. 1998. Slow and smooth: a Bayesian theory for the combination of local motion signals in human vision. AI Memo 1624.
Weiss, Y., Simoncelli, E. P., and Adelson, E. H. 2002. Motion illusions as optimal percepts. Nat. Neurosci. 5, 598–604.
Welch, L. 1989. The perception of moving plaids reveals two motion-processing stages. Nature 337, 734–736.
Wiener, N. 1958. Nonlinear Problems in Random Theory. MIT Press.
Wuerger, S., Shapley, R., and Rubin, N. 1996. ''On the visually perceived direction of motion'' by Hans Wallach: 60 years later. Perception 25, 1317–1367.
Yo, C. and Wilson, H. R. 1992. Perceived direction of moving two-dimensional patterns depends on duration, contrast and eccentricity. Vision Res. 32, 135–147.
Zetzsche, C. and Barth, E. 1990. Fundamental limits of linear filters in the visual processing of two-dimensional signals. Vision Res. 30, 1111–1117.

Further Reading

Bradley, D. C., Qian, N., and Andersen, R. A. 1995. Integration of motion and stereopsis in middle temporal cortical area of macaques. Nature 373, 609–611.

Relevant Websites

http://www.cns.nyu.edu/~hupe/plaid_demo/demo_plaids.html

http://viperlib.york.ac.uk/scripts/Portweb.dll?field=filename&op=matches&value=HypercomplexCortCell250.mpg&template=main_record&catalog=protol

2.12 Optic Flow

W H Warren, Brown University, Providence, RI, USA

© 2008 Elsevier Inc. All rights reserved.

2.12.1	**Introduction**	220
2.12.2	**The Optic Flow Field**	220
2.12.2.1	Translational Component	220
2.12.2.2	Rotational Component	221
2.12.2.3	Combined Translation and Rotation	221
2.12.3	**Perception of Self-Motion**	222
2.12.3.1	Perception of Translational Heading	222
2.12.3.2	Perception of Rotation	223
2.12.3.3	Decomposing Translation and Rotation	223
2.12.3.4	Retinal Flow Theories	223
2.12.3.5	Extraretinal Theories	224
2.12.3.6	Perception of Heading During Rotation	224
2.12.3.7	Simulated Rotation	224
2.12.3.8	The Path of Self-Motion	225
2.12.3.9	The Optic Flow Illusion	226
2.12.3.10	Extraretinal Signals	227
2.12.4	**Toward an Integrated View**	227
2.12.4.1	Functional Level	227
2.12.4.2	Neural Level	227
2.12.4.3	Conclusion	228
References		228

Glossary

curl The local rate of rotatory flow at a point in the flow field.

deformation (def) The local rate of shear along two orthogonal axes at a point in the flow field.

differential motion Motion parallax between points at different depths within a local neighborhood of the visual field.

divergence (div) The local rate of expansion at a point in the flow field.

expansion Informally refers to a radial flow. Technically, the rate of expansion is characterized by the divergence (div). Note that the highest rate of expansion (maximum div) is not at the focus of expansion, where div is zero.

extraretinal signals Efferent, proprioceptive, or vestibular signals that are produced by eye or head movements.

focus of expansion (FOE) The fixed point at the center of a radial flow pattern. The divergence at the focus of expansion is zero.

heading The observer's instantaneous direction of translation. If the observer is traveling on a straight path, the heading direction coincides with the path direction; if traveling on a curved path, the heading direction is tangent to the path.

lamellar flow A pattern of parallel or laminar flow, in which the vector directions are parallel and of equal magnitude. Sometimes called translational motion or planar motion.

motion parallax Relative motion between environmental points at different depths produced by observer translation. Local motion parallax or differential motion, is defined within a neighborhood of the visual field ($\sim 15^{\circ}$), global motion parallax may be distributed widely across the visual field.

optic array The pattern of light reflected from environmental surfaces to a point of observation. (More generally, the volume of light reflected from surfaces to all potential points of observation, filling the medium.)

optic flow The motion pattern produced at an eye that is moving relative to environmental surfaces. The eye may be moving with respect to stationary

surfaces, or surfaces may be moving with respect to a stationary eye.
path The observer's trajectory over time.
radial flow A flow pattern in which the velocity vectors radiate, expand, or diverge outward from a focus of expansion.
retinal flow The optic flow pattern projected onto the surface of the retina. Whereas optic flow is purely radial, retinal flow can have an added rotational component due to eye rotation.
rotary flow A flow pattern that rotates around a fixed point. Sometimes called rotational motion. The rate of rotary flow is the curl.
rotational component The component of retinal flow produced by observer rotation, a solenoidal flow pattern. Observer yaw or pitch generates a lamellar flow pattern, roll or torsion about the line of sight generates a rotary flow pattern.
self-motion Movement of the observer. Instantaneously described as the sum of a translation and a rotation, each having a direction and a speed.
solenoidal flow A flow field without sources or sinks (such as a focus of expansion or contraction).
time-to-contact The time remaining before a moving observer hits an environmental surface (or vice versa).
translational component The component of retinal flow produced by observer translation, a radial flow pattern.

2.12.1 Introduction

When an observer moves through the environment, a pattern of motion is generated at the eye known as optic flow. The term was introduced by Gibson J. J. (1950) in order to generalize Helmholtz's notion of motion parallax to a motion field produced by the surrounding environment. The concept played a key role in the development of Gibson J. J.'s (1979) ecological approach to perception, which emphasizes the richness of information available in natural environments and the biological function of vision in guiding adaptive behavior. Optic flow provides a primary example of a higher-order variable that both specifies complex environmental relations and can reciprocally be used to control action. In particular, flow patterns contain information about the observer's self-motion, time-to-contact with objects (Pepping, G. J. and Grealy, M. L., 2007), the motions of other objects (Burr, this volume), and the three-dimensional (3D) shape and layout of environmental surfaces (Todd, J. T., 1995; Domini, F. and Caudek, C., 2003; Siegel, R. M. this volume) and are used to control locomotion (Warren, W. H. and Fajen, B. R., 2004). In this chapter, I focus on human perception of self-motion from optic flow; the neural basis for the detection of flow patterns is reviewed in depth elsewhere (Duffy, C. J., 2004; Raffi, M. and Siegel, R. M., 2004; see Chapter Cortical Processing of Visual Motion).

2.12.2 The Optic Flow Field

Optic flow is the pattern of motion produced at an eye that is moving relative to environmental surfaces. It is commonly represented by an instantaneous velocity field, in which each vector corresponds to the optical motion of a point in the environment. (This is only a partial description because it leaves out such properties as optical acceleration, optical trajectories, dynamic occlusion, and so on.) Given that any rigid motion can be instantaneously decomposed into a translation and a rotation, it follows that the flow pattern projected on the moving retina has two corresponding components: a translational component of radial flow due to translation of the observer (Figure 1(a)) and a rotational component of solenoidal flow due to rotation of the observer (Figure 1(b)). The problem I consider is how the visual system can determine self-motion from such flow patterns.

2.12.2.1 Translational Component

Translation of the eye on a straight path generates a radial flow pattern (Figures 1(a) and 2(a)), in which the vectors radiate outward from a focus of expansion in the direction of travel or heading and converge to a focus of contraction in the opposite direction. The radial pattern formed by the directions of the vectors depends solely on the observer's direction of travel and is independent of the distance of environmental

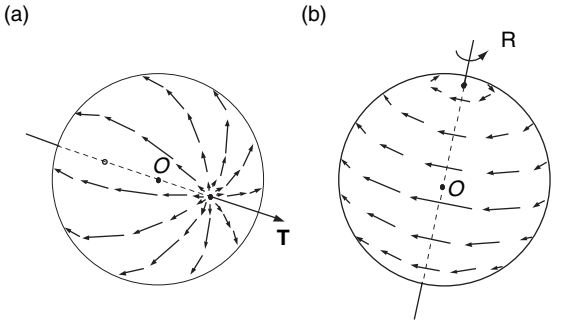

Figure 1 The retinal flow field, as projected on a sphere that moves with the eye; vectors correspond to the optical velocity of a point in the environment. (a) Translational component due to observer translation along the axis, with a focus of expansion in the direction of travel and a focus of contraction at the opposite pole. (b) Rotational component due to eye rotation about the axis, yielding solenoidal flow without sources or sinks. Reprinted from Warren, W. H. 1998. The State of Flow. In: High-Level Motion Processing (*ed*. T. Watanabe), p. 315. MIT Press, copyright 1998 by MIT Press.

surfaces. Hence, it uniquely specifies the current heading direction. On the other hand, the magnitude of each vector depends on its visual angle from the focus of expansion, the observer's speed of travel, and the distance of the corresponding point in the environment. Thus, flow magnitudes carry information about relative depth and are also correlated with the observer's heading.

In principle, determining heading from the radial flow pattern is straightforward. Any pair of vectors can be triangulated to determine their common point of origin, and doing so for many pairs yields a reliable estimate of the focus of expansion. The flow field is thus highly redundant and supports a robust heading estimate in the presence of noise, although biases result if the focus itself is not in view. This suggests a process of spatial integration in which heading is determined by pooling over many vectors in a flow pattern.

2.12.2.2 Rotational Component

When the observer rotates via either an eye or head movement, the resulting retinal flow pattern is solenoidal, that is, without sources or sinks (Figure 1(b)). Specifically, yaw or pitch of the observer generates a lamellar or parallel flow pattern (Figure 2(b)), whereas roll about the line of sight generates a rotary flow pattern. The rotational component of flow is

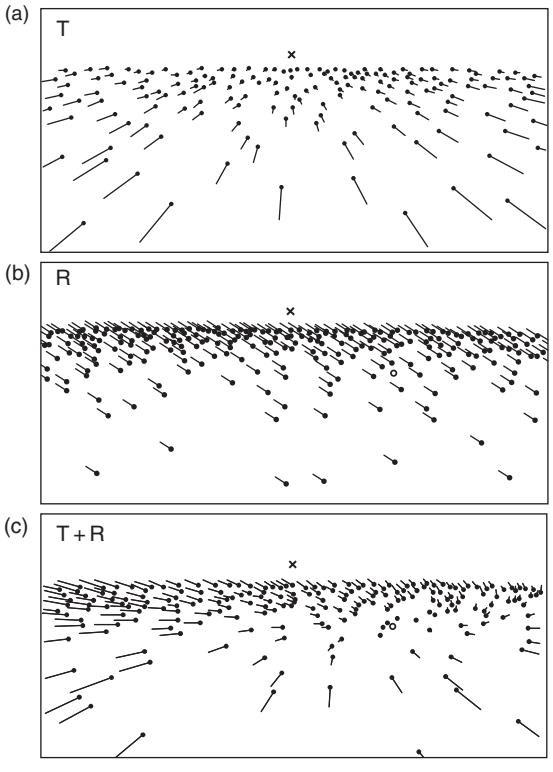

Figure 2 The rotation problem. (a) Translational component of retinal flow for a ground plane due to travel toward the X, yielding a radial flow pattern. (b) Rotational component of retinal flow due to eye rotation about a diagonal axis, yielding lamellar flow in the opposite direction. (c) Retinal flow during combined translation and rotation, due to travel toward the X while pursuit tracking the O on the ground plane. The flow field in (c) is the vector sum of those in (a) and (b). Reprinted from Warren, W. H. and Hannon, D. J. 1990. Eye movements and optical flow. J. Opt. Soc. Am. A 7, 160, copyright 1990 by Optical Society of America.

independent of distance and carries information about the observer's rotation. In particular, the vector directions depend entirely on the axis of rotation, and hence specify the observer's rotation direction. The vector magnitudes depend on their visual angle from the rotation axis and the speed of rotation, and hence specify the observer's rotation rate. Spatial integration over the flow pattern would thus permit the determination of the direction and speed of observer rotation.

2.12.2.3 Combined Translation and Rotation

When the eye is translating, the direction of heading is specified by the radial pattern of optic flow. But the

optic flow must be detected by a moving eye in a moving head, and observer rotation alters the flow pattern on the retina. When the eye is simultaneously translating and rotating, the retinal flow pattern is the vector sum of the corresponding translational and rotational components (Figure 2(c)). A pursuit eye movement induced by fixating a point in the environment, for example, annihilates the focus of expansion in the heading direction and creates a new singularity at the fixation point, as illustrated in Figure 2(c). How, then, can the visual system disentangle the translational and rotational components of retinal flow to recover the instantaneous heading direction? This has come to be known as the rotation problem in heading perception.

It is worth noting that the flow pattern on the retina is usually radial. About 60% of the time, walkers exhibit travel gaze fixation, in which the gaze direction is fixed relative to the heading direction, without pursuit movements (Patla, A. E. and Vickers, J. N. 1997; 2003). However, the rest of the time they tend to fixate obstacles, targets on the ground, or the locomotor goal, often inducing pursuit rotations.

Fortunately, as long as the environment has 3D structure, the retinal flow contains sufficient information to solve the rotation problem in principle. Specifically, observer translation is specified by the motion parallax between points at different depths, whereas observer rotation is specified by the common lamellar motion across the visual field. But with little depth structure, as in the case of a frontal plane with a small field of view, there is little motion parallax and a pseudofocus of expansion appears at the fixation point (Figure 3). Extraretinal signals about eye and head movements could also be used to determine the rotation and contribute to recovering observer translation.

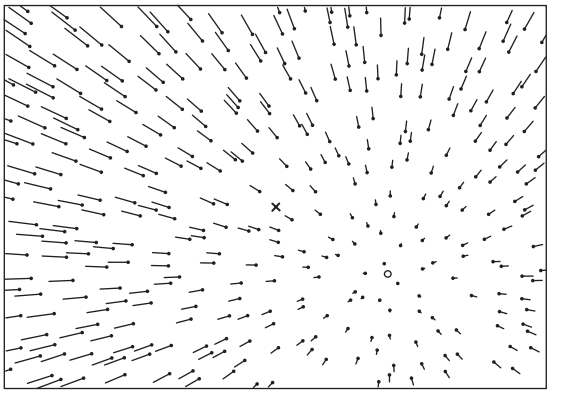

Figure 3 Special case of a frontal plane. Retinal flow during translation toward the X while rotating about a diagonal axis to track the O, yielding a pseudofocus of expansion at the fixation point. With a small field of view, there is little motion parallax across the display because the distance of the surface from the eye changes very little. Reprinted from Warren, W. H. and Hannon, D. J. 1990. Eye movements and optical flow. J. Opt. Soc. Am. A 7, 160. copyright 1990 by Optical Society of America.

2.12.3 Perception of Self-Motion

We now turn from the properties of the flow field to consider empirical data on perceiving self-motion.

2.12.3.1 Perception of Translational Heading

Psychophysical results demonstrate that heading can be perceived from radial optic flow patterns with an accuracy better than 1° of visual angle (Warren, W. H. *et al.*, 1988). In such experiments, participants view random-dot displays of radial flow with either stationary or free fixation and judge the direction of self-motion. Consistent with the independence of radial flow from distance, heading accuracy is comparable with different 3D scenes, including a ground plane, a frontal plane, or a cloud of dots. It remains high when the vector magnitudes are randomized, leaving only the radial pattern, but not when vector directions are randomized (Warren, W. H. *et al.*, 1991a). Consistent with the notion of spatial integration, heading judgments improve with the number of dots in the display (Warren, W. H. *et al.*, 1988) and are robust to added noise in vector directions (Warren, W. H. *et al.*, 1991a). Moreover, judgments of motion direction in displays of radial, rotary, and lamellar flow improve as the area of coherent motion increases, indicative of spatial summation over visual angles up to 72° (Burr, D. C. *et al.*, 1998).

The psychophysical evidence suggests that there are independent neural mechanisms sensitive to radial, rotary, and lamellar flow, either at the single-cell or at the population level. Judgments of expansion in spiral flow patterns that combine radial and rotary motions are comparable to those for radial flow patterns alone (and vice versa) (Freeman, T. C. and Harris, M. G., 1992; Barraza, J. F. and Grzywacz, N. M., 2005), and the same holds for combinations of radial or rotary motion with lamellar motion (Kappers, A. M. L. *et al.*, 1994; 1996; Te Pas, S. F. *et al.*, 1996).

These behavioral data cohere with the results from single-cell recordings in primate visual cortex. The dorsal medial superior temporal area (MSTd) contains cells selective for expansion/contraction, rotary flow, and lamellar flow (Saito, H. *et al.*, 1986); a majority of cells respond to two or three of these individual patterns (Duffy, C. J. and Wurtz, R. H., 1991a), and there is evidence for intermediate units tuned to spiral flow (Graziano, M. S. A. *et al.*, 1994). Such cells have large receptive fields up to 65° in diameter, exhibit stronger responses to larger flow patterns, and are position invariant, consistent with spatial integration of local motions (Tanaka, K. and Saito, H., 1989; Duffy, C. J. and Wurtz, R. H., 1991b; Lagae, L. *et al.*, 1994). Moreover, 90% of expansion units have receptive fields with a preferred focus of expansion (Duffy, C. J. and Wurtz, R. H., 1995; Raiguel, S. *et al.*, 1997), and microstimulation in MSTd biases the heading judgments of macaque monkeys (Britten, K. H. and Wezel, R. J. A. v., 1998). Although some expansion cells prefer an increasing speed gradient from center to periphery (Duffy, C. J. and Wurtz, R. H., 1997), eliminating the speed gradient has a far smaller impact on a cell's response than eliminating the radial pattern of directions (Tanaka, K. *et al.*, 1989). These results suggest a distributed coding of the focus of expansion in MSTd, although further processing of optic flow takes place higher in the dorsal pathway, including the ventral intraparietal area (VIP), area 7a, and the superior temporal polysensory area (STPa).

In sum, the evidence indicates that the direction of heading can be accurately perceived from radial flow patterns, and neural substrates for the extraction of radial, rotary, and lamellar flow appear to be present in the primate visual system.

2.12.3.2 Perception of Rotation

The psychophysical data on the perception of observer rotation come largely from the literature on circular (yaw) vection, a visual illusion of self-motion produced by a striped drum rotating about a stationary observer. As expected from the flow field analysis, the perceived speed of complete vection closely corresponds to that of the visual display over a wide range, up to a saturation velocity of about $120° s^{-1}$ (Brandt, T. *et al.*, 1973). Surprisingly, however, perceived speed also increases with the perceived distance of the display (Wist, E. R. *et al.*, 1975), contrary to the independence of the flow magnitude from distance. However, yaw rotation may be partially perceived as lateral translation of the observer, due to the similarity of the flow patterns generated with a 2D surface; tests of a 3D display with motion parallax are required. To my knowledge, there are no data on the perceived direction (axis) of self-rotation.

It is suggestive that most MSTd cells respond to lamellar motion, with large receptive fields, direction selectivity, and broad tuning to the overall speed of motion (Saito, H. *et al.*, 1986; Tanaka, K. and Saito, H., 1989; Orban, G. A. *et al.*, 1995). Moreover, many of these cells also encode pursuit eye movements, with a preferred pursuit direction that is on average opposite the preferred flow direction (Komatsu, H. and Wurtz, R. H., 1988). These characteristics are appropriate for the detection of flow patterns produced by eye or head rotation.

2.12.3.3 Decomposing Translation and Rotation

When one walks on a straight path while making a pursuit eye movement, the eye is simultaneously translating and rotating, and the retinal flow pattern corresponds to the sum of these two components (Figure 2). How might the visual system decompose this complex flow pattern to recover the observer's instantaneous heading and self-rotation? There are two general approaches to this problem, one relying on the information in retinal flow and the other on extraretinal signals about eye and head rotation.

2.12.3.4 Retinal Flow Theories

It has been shown formally that the retinal flow pattern for a 3D scene contains sufficient information to recover the translational heading during rotation. This is possible in principle because a rotation simply adds a constant to the flow field, leaving the motion parallax intact. There are roughly five classes of retinal flow theories, which will be briefly described: discrete, differential, subtractive, local motion parallax, and template models (see Hildreth, E. C. and Royden, C. S., 1998; Warren, W. H., 1998; Lappe, M. *et al.*, 1999 for reviews).

Initially, several discrete models proved that observer translation and rotation can be computed from the motions of a minimum number of points in two successive images (Prazdny, K., 1980; Longuet-Higgins, H. C., 1981; Tsai, R. Y. and Huang, T. S., 1981). At the same time, a class of differential models showed that self-motion and surface slant can be determined from spatial derivatives of the flow field

such as divergence, curl, and deformation, as well as lamellar motion (Koenderink, J. J. and van Doorn, A. J., 1975; Longuet-Higgins, H. C. and Prazdny, K., 1980; Koenderink, J. J. and van Doorn, A. J., 1981; Waxman, A. M. and Ullman, S., 1985). However, these theories rely on precise measurements of a few points and are highly vulnerable to noise, or assume surface smoothness, casting doubt on their biological plausibility (see also Kappers, A. M. L. *et al.*, 1996).

A third class of theories first estimates the rotational component from the lamellar flow, and then subtracts it from the flow pattern to determine the translational component (Perrone, J. A., 1992). Koenderink J. J. (1986) noted that observer rotation during translation can be estimated by independently integrating the global flow about three orthogonal axes, and there is evidence for such a system in the rabbit (Simpson, J. I. *et al.*, 1981).

A complementary class of theories determines the translational component from local motion parallax, also known as differential motion (Longuet-Higgins, H. C. and Prazdny, K., 1980; Rieger, J. H. and Lawton, D. T., 1985; Lappe, M. and Rauschecker, J. P., 1993; Cutting, J. E., 1996; Royden, C. S. 1997). Differential motion is due to depth differences within a local neighborhood in the flow field and can be represented by a difference vector. Remarkably, the set of difference vectors once again forms a radial pattern centered on the heading and is invariant to rotation. The rotation problem can thus be solved quite elegantly if there is sufficient 3D structure in the scene.

Finally, a fifth class is based on templates for the set of flow patterns generated by possible combinations of observer translation and rotation (Perrone, J. A. and Stone, L. S., 1994; Beintema, J. A. and van den Berg, A. V., 1998; Perrone, J. A. and Stone, L. S., 1998). Each such template is selective for a complex motion pattern, rather than for an elementary flow component. Due to depth variation in the environment, however, the space of possible flow patterns is very large and must be constrained, for example, by assuming fixation of a point attached to the scene. These analyses demonstrate that it is theoretically possible to determine the observer's translation and rotation from the retinal flow pattern alone.

2.12.3.5 Extraretinal Theories

In contrast, the extraretinal approach proposes that efferent or proprioceptive signals about the rotational velocity of the eye and head are used to estimate the observer's rotation (Royden, C. S. *et al.*, 1994; Banks, M. S. *et al.*, 1996); interestingly, vestibular signals seem not to play a role (Crowell, J. A. *et al.*, 1998). In principle, the rotational component can then be subtracted from the retinal flow pattern in order to determine the instantaneous translational heading.

One possible implementation uses extraretinal velocity signals to subtract the rotational component at the level of MSTd, thereby shifting the preferred focus of expansion within the retinal receptive field. This implies head-centric expansion cells in MSTd that fully compensate for eye rotation. A related model realizes a least-squares solution to the rotation problem in the connection weights from MT to MSTd, augmented by extraretinal signals that modulate MSTd responses (Lappe, M., 1998). The model implies sigmoidal tuning curves and a population code for heading at the level of MSTd. Alternatively, MSTd cells might serve as templates for combinations of radial and lamellar flow, with extraretinal velocity signals modulating their response gain to create a heading map in a separate neural layer (Beintema, J. A. and van den Berg, A. V., 1998). This implies the existence of gain fields and head-centric expansion cells elsewhere in the dorsal pathway. A fourth possibility is a recurrent basis function network, with separate input layers that code oculocentric flow signals, head-centric vestibular signals, and extraretinal eye position signals, which are recurrently connected to a multisensory layer such as MSTd (Pouget, A. *et al.*, 2002; Fetsch, C. R. *et al.*, 2007). This model implies gain fields and a continuum of intermediate reference frames in MSTd, without convergence on common head-centric units.

2.12.3.6 Perception of Heading During Rotation

The empirical question at hand is whether humans can in fact perceive their instantaneous heading during an eye rotation on the basis of retinal flow alone, or whether extraretinal signals are necessary. The evidence, though still controversial, points to the conclusion that the visual system exploits both types of solutions.

2.12.3.7 Simulated Rotation

The rotation problem has been investigated using displays that simulate the retinal flow corresponding to a pursuit rotation, while the eye is actually

stationary (see Figure 2(c)); any extraretinal signal thus indicates zero rotation. Initially, Warren W. H. and Hannon D. J. (1988; 1990) reported heading thresholds better than 1.5° during both simulated and real eye rotation (for rotation rates $<1° s^{-1}$), as long as there was 3D structure in the scene, consistent with retinal flow theories based on motion parallax. With a frontal plane of dots, on the other hand (Figure 3), heading judgments were only accurate during real eye movements, consistent with extraretinal theories. Yet Grigo A. and Lappe M. (1999) reported accurate judgments during simulated rotation with a larger field of view, presumably due to global motion parallax from the periphery (Grigo, A. and Lappe, M., 1999). Subsequent research also supported some version of a retinal flow theory (Cutting, J. E. *et al.*, 1992; van den Berg, A. V. 1993; 1996; Stone, L. S. and Perrone, J. A., 1997; Wang, R. F. and Cutting, J. E., 1999).

However, when Banks, M. S. and his colleagues (Royden, C. S. *et al.*, 1992; 1994; Banks, M. S. *et al.*, 1996) tested higher rotation rates ($1–5 s^{-1}$), they found large heading errors of up to 15° in the simulated rotation condition, contrary to retinal flow theories. Whether the visual system can determine the direction of heading from retinal flow was thus cast into doubt.

2.12.3.8 The Path of Self-Motion

There is, however, a known ambiguity in the retinal flow: the same instantaneous velocity field can be produced by translation on a straight path plus a rotation, or by travel on a circular path (Figure 4). The retinal velocity field by itself is thus insufficient to distinguish straight and curved paths of self-motion, which is known as the path ambiguity.

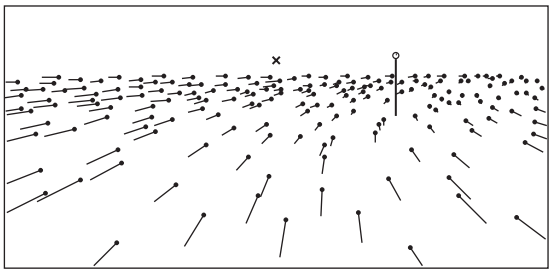

Figure 4 The path ambiguity. The same retinal velocity field can be produced by combined translation toward X while rotating about a vertical axis to track O, or by travel on a circular path to the right. Reproduced from Li, L. and Warren, W. H. 2000. Perception of heading during rotation: Sufficiency of dense motion parallax and reference objects. Vis. Res. 40, 3873, copyright 2000 by Elsevier Ltd.

(Theoretically, the ambiguity can be resolved by considering accelerative components of the flow or element trajectories over time, but the evidence suggests that the visual system is not sufficiently sensitive to these properties (Warren, W. H. *et al.*, 1991a; Ehrlich, S. M. *et al.*, 1998; Paolini, M. *et al.*, 2000).) Although the simulated rotation paradigm was intended to assess the perception of instantaneous heading (the tangent to the path at any moment), participants often reported seeing a curved path of self-motion, and their heading errors were consistent with this report (Royden, C. S., 1994). It thus appears that errors during simulated rotation were likely due to the path ambiguity, together with a tendency to judge the path of self-motion instead of the instantaneous heading, rather than evidence of the visual system's inability to decompose translation and rotation.

If the retinal flow is ambiguous, how might the visual system determine the path of self-motion? On an extraretinal approach (Banks, M. S. *et al.*, 1996), velocity signals can be used to subtract eye and head rotation from the retinal flow field; if the residual flow pattern has a rotational component, it is attributed to a curved path. However, this approach assumes accurate extraretinal signals, whereas their gain is believed to be significantly less than one (Wertheim, A. H., 1987). Moreover, the residual flow pattern may still need to be decomposed into translational and rotational components in order to estimate the curvature of that path (Ehrlich, S. M. *et al.*, 1998). On the other hand, once the path ambiguity is resolved, it is possible that the current path may be determined directly from the curved optic flow pattern (Lee, D. N. and Lishman, R., 1977; Warren, W. H. *et al.*, 1991b; Kim, N.-G. and Turvey, M. T., 1998).

Alternatively, the path ambiguity might be resolved by determining the object-relative heading, that is, heading, with respect to reference objects in the environment. (Li, L. and Warren, W. H., 2000). Specifically, if the instantaneous heading remains fixed relative to objects in the scene over time, then the observer is on a straight path, whereas if the heading drifts over reference objects, then the observer is on a curved path, and rate of drift corresponds to path curvature. Most previous research used sparse random-dot displays without reference objects that could be tracked over time. But when one or more distinct objects are added to a display containing textured surfaces, path errors remain below 4° (at $7° s^{-1}$) (Cutting, J. E. *et al.*, 1997; Li, L. and Warren,

W. H., 2000). This is also the case for active steering to a target during simulated rotation (Li, L. and Warren, W. H., 2002). Thus, with distinct reference objects and motion parallax from textured surfaces, the retinal flow solution tends to dominate the extraretinal solution.

Nevertheless, simulated rotation is a cue conflict condition, and hence features of the display or task can bias the observer toward one path or the other. Extraretinal signals indicate that the eye is not rotating, so the retinal flow pattern indicates the observer is on a curved path; yet the object-relative heading remains fixed in the scene, indicating that the observer must be on a straight path. Consistent with this analysis, when participants are told they are traveling on a straight path, errors remain below 4° (at 5° s^{-1}), whereas when they are told they are on a curved path, errors rise to 12° (Li, L. and Warren, W. H., 2004). Thus, the visual system has the capacity to recover observer translation from the retinal flow alone.

In sum, results from the simulated rotation paradigm indicate that both extraretinal and retinal flow solutions contribute to the perception of self-motion.

2.12.3.9 The Optic Flow Illusion

A second paradigm that bears on the decomposition of retinal flow is known as the optic flow illusion (Duffy, C. J. and Wurtz, R. H., 1993). When a transparent plane of laterally moving dots is superimposed on a plane of radially moving dots (Figure 5), the perceived location of the focus of expansion shifts in the direction of the lateral motion. This phenomenon suggests that the visual system uses the global lamellar flow to estimate eye rotation and compensates by shifting the perceived focus of expansion in the opposite direction (Duffy, C. J. and Wurtz, R. H., 1993; Lappe, M. and Rauschecker, J. P., 1995; Pack, C. and Mingolla, E., 1998).

However, the illusion can also be explained by motion-opponent operators that extract the local differential motion between the lamellar and radial flow patterns (Royden, C. S. and Conti, D. M., 2003). Such operators could be the basis for recovering heading from local motion parallax (Royden, C. S., 1997), and also account for biases in perceived heading induced by a moving object in the scene (Warren, W. H. and Saunders, J. A., 1995; Royden, C. S. and Hildreth, E. C., 1996; Royden, C. S., 2002). When local parallax is eliminated by presenting nonoverlapping flow patterns, the focus of expansion shifts only 17% as

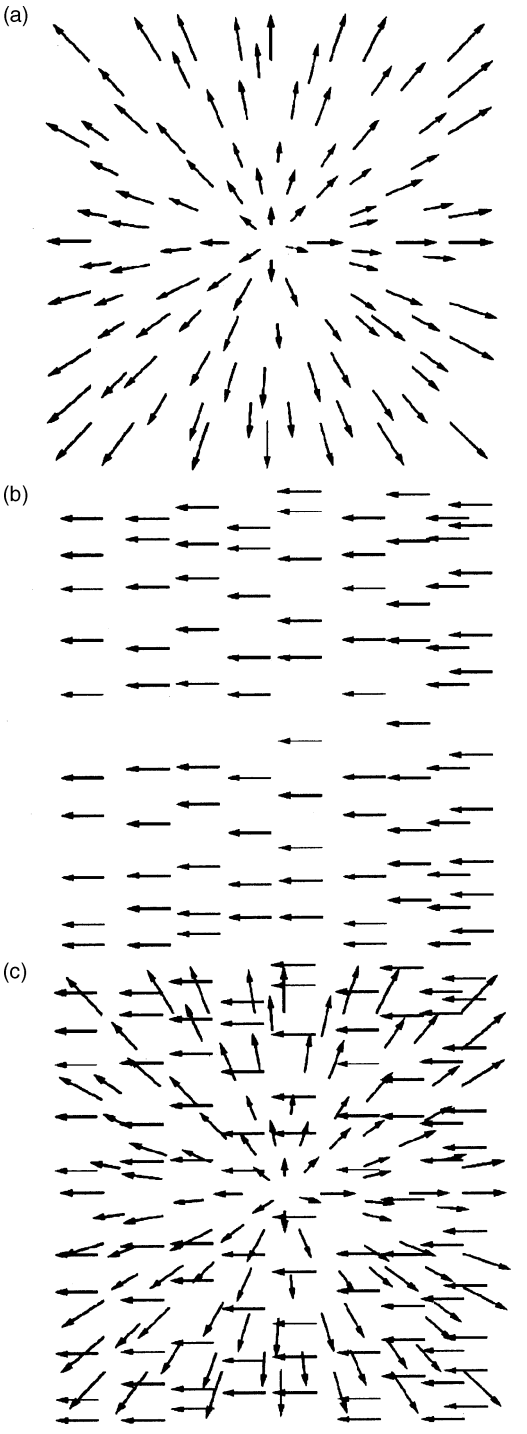

Figure 5 The optic flow illusion. (a) Radial flow pattern with a focus of expansion for one plane of dots. (b) Lamellar flow pattern to the left for second plane of dots. (c) Superimposed radial and lamellar flow patterns, which yield a perceived focus of expansion shifted to the left. Reproduced from Royden, C. S. and Conti, D. M. 2003. A model using MT-like motion-opponent operators explains an illusory transformation in the optic flow field. Vis. Res. 43, 2811, copyright 2003 by Elsevier.

far, but nonetheless a residual illusion persists (Duijnhouwer, J. *et al.*, 2006). It thus appears that both local motion parallax and global lamellar mechanisms are involved in decomposing the retinal flow. The lamellar motion might be extracted by large-field lamellar cells or by motion-opponent units with large surrounds.

2.12.3.10 Extraretinal Signals

The simulated rotation paradigm demonstrated that extraretinal signals contribute to the estimate of observer rotation. But work by Crowell J. A. and Anderson R. A. (2001) indicates that they do so in a particular way. When the retinal flow corresponds to a 3D scene (e.g., contains motion parallax), the rotational component is determined solely from the lamellar flow. Extraretinal signals merely indicate whether or not the eye is moving and serve to gate the interpretation of the lamellar flow as either being due to an eye rotation or to a curved path of self-motion. When the retinal flow does not contain motion parallax, observer rotation is determined from extraretinal signals, but is underestimated by nearly 50%. This implies that full pursuit compensation must also depend on the lamellar flow.

Moreover, extraretinal signals only begin to play a role 500 ms after the onset of flow, prior to which heading judgments are based solely on the retinal flow (Grigo, A. and Lappe, M., 1999). Given that fixation duration is normally 300–500 ms, this implies that ordinarily the visual system determines heading primarily from retinal flow.

2.12.4 Toward an Integrated View

2.12.4.1 Functional Level

The picture of self-motion perception that emerges from the psychophysical literature looks something like the following. First, observer translation is determined from motion parallax in the retinal flow field, which depends on 3D structure in the scene. The visual system appears to extract both local differential motion and global motion parallax, and this information seems sufficient to recover the instantaneous direction of heading.

Second, observer rotation is determined from the common lamellar motion in the retinal flow. The visual system appears to extract large-field lamellar flow that corresponds to eye rotation. This rotation estimate is subtracted from the retinal flow to contribute to the recovery of the translational component, as evidenced by the residual optic flow illusion.

Third, extraretinal signals similarly contribute to the recovery of observer translation, but in a limited way. When the retinal flow contains motion parallax, the rotational component is determined from lamellar flow, and extraretinal signals merely specify whether it should be attributed to eye rotation or a curved path. In the absence of motion parallax, the rotational component is estimated from extraretinal signals, but with low gain and only after 500 ms.

Finally, the path of self-motion appears to be based on the object-relative heading over time. A heading direction that is fixed in the scene specifies a straight path, whereas a heading that shifts with respect to environmental objects specifies a curved path.

2.12.4.2 Neural Level

The neural support for these functions remains contested, given that evidence can be found for competing theories. Consistent with local motion parallax theories, a majority of cells in area MT possess bilateral motion-opponent receptive fields (Allman, J. *et al.*, 1985; Xiao, D.-K. *et al.*, 1997) and project to MSTd. Expansion cells in MSTd could detect the radial pattern of difference vectors, and their response is enhanced when motion parallax is added to a radial flow display (Upadhyay, U. D. *et al.*, 2000). On the other hand, consistent with template theories, many MSTd cells respond to combinations of radial, rotary, and/or lamellar flow rather than constituting a simple heading map.

Extraretinal theories gain support from the finding that the preferred focus of expansion in most MSTd cells shifts within the retinal receptive field during a pursuit eye movement, partially compensating for the pursuit (Bradley, D. C. *et al.*, 1996; Shenoy, K. V. *et al.*, 1999; 2002; Lee, B. *et al.*, 2007). Such findings appear to be consistent with a heading map in MSTd. However, the shifts undercompensate for pursuit, although full compensation might occur with motion parallax in the display. Nevertheless, the population response seems to exhibit full pursuit compensation (Page, W. K. and Duffy, C. J., 1999), consistent with Lappe M.'s (1998) model. Alternatively, these partial shifts can also be interpreted as evidence of intermediate oculocentric and head-centric reference frames in MSTd, without convergence on head-centric units, consistent with a recurrent basis function network (Fetsch, C. R. *et al.*, 2007).

But recently, head-centric expansion cells have been identified in primate area VIP that exhibit full pursuit compensation with motion parallax in the display (Zhang, T. *et al*., 2004). This is consistent both with an extraretinal contribution and with determining rotation from lamellar flow in 3D displays. Such a VIP heading map is expected from the gain field model of pursuit compensation (Beintema, J. A. and van den Berg, A. V., 1998; van den Berg, A. V. and Beintema, J. A., 2000), and gain modulation of flow responses has been observed in MSTd and area 7a (Bremmer, S. *et al*., 1997; Read, H. L. and Siegel, R. M., 1997; Shenoy, K. V. *et al*., 1999).

Finally, neurons in area STPa respond to both optic flow and object boundaries in their receptive fields (Anderson, K. C. and Siegel, R. M., 1999). This suggests a possible site for the detection of object-relative heading.

2.12.4.3 Conclusion

In sum, current evidence indicates that the visual system exploits redundant information for robust perception of self-motion. Translational heading is determined from local and global motion parallax in the retinal flow pattern, whereas observer rotation is determined from lamellar motion and extraretinal signals and contributes to the estimate of instantaneous translation. The path of self-motion may be determined from the heading relative to environmental objects over time. These functions are carried out in a distributed dorsal network that integrates information in a head-centric heading map. Precisely how they are implemented across multiple cortical areas is a matter of ongoing investigation.

References

Allman, J., Miezin, F., and McGuinness, E. 1985. Direction- and velocity-specific responses from beyond the classical receptive field in the middle temporal visual area (MT). Perception 14, 105.

Anderson, K. C. and Siegel, R. M. 1999. Optic flow selectivity in the anterior superior temporal polysensory area, STPa, of the behaving monkey. J. Neurosci. 19, 2681.

Banks, M. S., Ehrlich, S. M., Backus, B. T., and Crowell, J. A. 1996. Estimating heading during real and simulated eye movements. Vis. Res. 36, 431.

Barraza, J. F. and Grzywacz, N. M. 2005. Parametric decomposition of optic flow by humans. Vis. Res. 45, 2481.

Beintema, J. A. and van den Berg, A. V. 1998. Heading detection using motion templates and eye velocity gain fields. Vis. Res. 38, 2155.

Bradley, D. C., Maxwell, M., Andersen, R. A., Banks, M. S., and Shenoy, K. V. 1996. Mechanisms of heading perception in primate visual cortex. Science 273, 1544.

Brandt, T., Dichgans, J., and Koenig, E. 1973. Differential effects of central versus peripheral vision on egocentric and exocentric motion perception. Exp. Brain Res. 16, 476.

Bremmer, S., Ilg, U. J., Thiele, A., Distler, C., and Hoffman, K. P. 1997. Eye position effects in monkey cortex. 1. Visual and pursuit-related activity in extrastriate areas MT and MST. J. Neurophysiol. 77, 944.

Britten, K. H. and Wezel, R. J. A. v. 1998. Electrical micro stimulation of cortical area MST biases heading perception in monkeys. Nat. Neurosci. 1, 59.

Burr, D. C., Morrone, M. C., and Vaina, L. M. 1998. Large receptive fields for optic flow detection in humans. Vis. Res. 38, 1731.

Crowell, J. A. and Andersen, R. A. 2001. Pursuit compensation during self-motion. Perception 30, 1465.

Crowell, J. A., Banks, M. S., Shenoy, K. V., and Andersen, R. A. 1998. Visual self-motion perception during head turns. Nat. Neurosci. 1, 732.

Cutting, J. E. 1996. WayfInding from multiple sources of local information in retinal flow. J. Exp. Psychol. Hum. Percept. Perform. 22, 1299.

Cutting, J. E., Springer, K., Braren, P. A., and Johnson, S. H. 1992. Wayfinding on foot from information in retinal, not optical, flow. J. Exp. Psychol. Gen. 121, 41.

Cutting, J. E., Vishton, P. M., Fluckiger, M., Baumberger, B., and Gerndt, J. D. 1997. Heading and path information from retinal flow in naturalistic environments. Percept. Psychophys. 59, 426.

Domini, F. and Caudek, C. 2003. 3-D structure perceived from dynamic information: A new theory. Trends Cogn. Sci. 7, 444.

Duffy, C. J. 2004. The Cortical Analysis of Optic Flow. In: The Visual Neurosciences, (*eds*. L. M. Chalupa and J. S. Werner), Vol. II p. 1260. MIT Press.

Duffy, C. J. and Wurtz, R. H. 1991a. Sensitivity of MST neurons to optic flow stimuli. 1. A continuum of response selectivity to large-field stimuli. J. Neurophysiol. 65, 1329.

Duffy, C. J. and Wurtz, R. H. 1991b. Sensitivity of MST neurons to optic flow stimuli. II. Mechanisms of response selectivity revealed by small-field stimuli. J. Neurophysiol. 65, 1346.

Duffy, C. J. and Wurtz, R. H. 1993. An illusory transformation of optic flow fields. Vis. Res. 33, 1481.

Duffy, C. J. and Wurtz, R. H. 1995. Response of monkey MST neurons to optic flow stimuli with shifted centers of motion. J. Neurosci. 15, 5192.

Duffy, C. J. and Wurtz, R. H. 1997. Medial superior temporal area neurons respond to speed patterns in optic flow. J. Neurosci. 17, 2839.

Duijnhouwer, J., Beintema, J. A., van den Berg, A. V., and van Wezel, R. J. A. 2006. An illusory transformation of optic flow fields without local motion interations. Vis. Res. 46, 439.

Ehrlich, S. M., Beck, D. M., Crowell, J. A., Freeman, T. C. A., and Banks, M. S. 1998. Depth information and perceived self-motion during simulated gaze rotations. Vis. Res. 38, 3129.

Fetsch, C. R., Wang, S., Gu, Y., DeAngelis, G. C., and Angelaki, D. E. 2007. Spatial reference frames of visual, vestibular, and multimodal heading signals in the dorsal subdivision of the medial superior temporal area. J. Neurosci. 27, 700.

Freeman, T. C. and Harris, M. G. 1992. Human sensitivity to expanding and rotating motion: Effects of complementary masking and directional structure. Vis. Res. 32, 81.

Gibson, J. J. 1950. Perception of the Visual World. Houghton Mifflin.

Gibson, J. J. 1979. The Ecological Approach to Visual Perception. Houghton Mifflin.
Graziano, M. S. A., Andersen, R. A., and Snowden, R. J. 1994. Tuning of MST neurons to spiral motions. J. Neurosci. 14, 54.
Grigo, A. and Lappe, M. 1999. Dynamical use of different sources of information in heading judgments from retinal flow. J. Opt. Soc. Am. A 16, 2079.
Hildreth, E. C. and Royden, C. S. 1998. Computing Observer Motion from Optical Flow. In: High-Level Motion Processing (*ed*. T. Watanabe), p. 269. MIT Press.
Kappers, A. M. L., te Pas, S. F., and Koenderink, J. J. 1996. Detection of divergence in optical flow fields. J. Opt. Soc. Am. A 13, 227.
Kappers, A. M. L., van Doom, A. J., and Koenderink, J. J. 1994. Detection of vorticity in optical flow fields. J. Opt. Soc. Am. A 11, 48.
Kim, N.-G. and Turvey, M. T. 1998. Visually perceiving heading on circular and elliptical paths. J. Exp. Psychol. Hum. Percept. Perform. 24, 1690.
Koenderink, J. J. 1986. Optic flow. Vis. Res. 26, 161.
Koenderink, J. J. and van Doom, A. J. 1975. Invariant properties of the motion parallax field due to the movement of rigid bodies relative to an observer. Opt. Acta (Lond.). 22, 737.
Koenderink, J. J. and van Doom, A. J. 1981. Exterospecific component of the motion parallax field. J. Opt. Soc. Am. 71, 953.
Komatsu, H. and Wurtz, R. H. 1988. Relation of cortical areas MT and MST to pursuit eye movements. III. Interaction with full-field visual stimulation. J. Neurophysiol. 60, 621.
Lagae, L., Maes, H., Raiguel, S., Xiao, D.-K., and Orban, G. A. 1994. Responses of Macaque STS neurons to optic flow components: A comparison of areas MT and MST. J. Neurophysiol. 71, 1597.
Lappe, M. 1998. A model of the combination of optic flow and extraretinal eye movement signals in primate extrastriate visual cortex: Neural model of self-motion from optic flow and extraretinal cues. Neural Netw. 11, 397.
Lappe, M. and Rauschecker, J. P. 1993. A neural network for the processing of optic flow from ego-motion in man and higher mammals. Neural Comput. 5, 374.
Lappe, M. and Rauschecker, J. P. 1995. An illusory transformation in a model of optic flow processing. Vis. Res. 35, 1619.
Lappe, M., Bremmer, F., and van den Berg, A. V. 1999. Perception of self-motion from visual flow. Trends Cogn. Sci. 3, 329.
Lee, D. N. and Lishman, R. 1977. Visual control of locomotion. Scand. J. Psychol. 18, 224.
Lee, B., Pesaran, B., and Andersen, R. A. 2007. Translation speed compensation in the dorsal aspect of the medial superior temporal area. J. Neurosci. 27, 2582.
Li, L. and Warren, W. H. 2000. Perception of heading during rotation: Sufficiency of dense motion parallax and reference objects. Vis. Res. 40, 3873.
Li, L. and Warren, W. H. 2002. Retinal flow is sufficient for steering during simulated rotation. Psychol. Sci. 13, 485.
Li, L. and Warren, W. H. 2004. Path perception during rotation: influence of instructions, depth range, and dot density. Vis. Res. 44, 1879.
Longuet-Higgins, H. C. 1981. A computer algorithm for reconstructing a scene from two projections. Nature 293, 133.
Longuet-Higgins, H. C. and Prazdny, K. 1980. The interpretation of a moving retinal image. Proc. R. Soc. Lond. B 208, 385.
Orban, G. A., Lagae, L., Raiguel, S., Xiao, D., and Maes, H. 1995. The speed tuning of middle superior temporal (MST) cell responses to optic flow components. Perception 24, 269.
Pack, C. and Mingolla, E. 1998. Global induced motion and visual stability in an optic flow illusion. Vis. Res. 38, 981.
Page, W. K. and Duffy, C. J. 1999. MST neuronal responses to heading direction during pursuit eye movements. J. Neurophysiol. 81, 596.
Paolini, M., Distler, C., Bremmer, F., Lappe, M., and Hoffman, K. P. 2000. Responses to continuously changing optic flow in area MST. J. Neurophysiol. 84, 730.
Patla, A. E. and Vickers, J. N. 1997. Where and when do we look as we approach and step over an obstacle in the travel path? Neuroreport 8, 3661.
Patla, A. E. and Vickers, J. N. 2003. How far ahead do we look when required to step on specific locations in the travel path during locomotion? Exp. Brain Res. 148, 133.
Pepping, G. J. and Grealy, M. L. (*ed*.) 2007 Closing the Gap: The Scientific Writings of David N. Lee, Erlbaum.
Perrone, J. A. 1992. Model for the computation of self-motion in biological systems. J. Opt. Soc. Am. A 9, 177.
Perrone, J. A. and Stone, L. S. 1994. A model of self-motion estimation within primate extrastriate visual cortex. Vis. Res. 34, 2917.
Perrone, J. A. and Stone, L. S. 1998. Emulating the visual receptive-field properties of MST neurons with a template model of heading estimation. J. Neurosci. 18, 5958.
Pouget, A., Deneve, S., and Duhamel, J. R. 2002. A computational perspective on the neural basis of multisensory spatial representations. Nat. Rev. Neurosci. 3, 741.
Prazdny, K. 1980. Egomotion and relative depth map from optical flow. Biol. Cybern. 36, 87.
Raffi, M. and Siegel, R. M. 2004. Multiple cortical representations of optic flow processing. In: Optic Flow and Beyond (*eds*. L. M. Vaina, S. A. Beardsley, and S. K. Rushton), p. 3. Kluwer.
Raiguel, S., van Hulle, M. M., Xiao, D.-K., Marcar, V. L., Lagae, L., and Orban, G. A. 1997. Size and shape of receptive fields in the medial superior temporal area (MST) of the macaque. Neuroreport 8, 2803.
Read, H. L. and Siegel, R. M. 1997. Modulation of responses to optic flow in area 7a by retinotopic and oculomotor cues in monkey. Cereb. Cortex 7, 647.
Rieger, J. H. and Lawton, D. T. 1985. Processing differential image motion. J. Opt. Soc. Am. A 2, 354.
Royden, C. S. 1994. Analysis of misperceived observer motion during simulated eye rotations. Vis. Res. 34, 3215.
Royden, C. S. 1997. Mathematical analysis of motion-opponent mechanisms used in the determination of heading and depth. J. Opt. Soc. Am. A 14, 2128.
Royden, C. S. 2002. Computing heading in the presence of moving objects: A model that uses motion-opponent operators. Vis. Res. 42, 3043.
Royden, C. S. and Conti, D. M. 2003. A model using MT-like motion-opponent operators explains an illusory transformation in the optic flow field. Vis. Res. 43, 2811.
Royden, C. S. and Hildreth, E. C. 1996. Human heading judgments in the presence of moving objects. Percept. Psychophys. 58, 836.
Royden, C. S., Banks, M. S., and Crowell, J. A. 1992. The perception of heading during eye movements. Nature 360, 583.
Royden, C. S., Crowell, J. A., and Banks, M. S. 1994. Estimating heading during eye movements. Vis. Res. 34, 3197.
Saito, H., Yukie, M., Tanaka, K., Hikosaka, K., Fukada, Y., and Iwai, E. 1986. Integration of direction signals of image motion in the superior temporal sulcus of the Macaque monkey. J. Neurosci. 6, 145.
Shenoy, K. V., Bradley, D. C., and Andersen, R. A. 1999. Influence of gaze rotation on the visual response of primate MSTd neurons. J. Neurophysiol. 81, 2764.

Shenoy, K. V., Crowell, J. C., and Andersen, R. A. 2002. Pursuit speed compensation in cortical area MSTd. J. Neurophysiol. 88, 2630.

Simpson, J. I., Graf, W., and Leonard, C. 1981. The Coordinate System of Visual Climbing Fibers to the Flocculus. In: Progress in Oculomotor Research (*eds*. A. F. Fuchs and W. Becker), p. 475. Elsevier.

Stone, L. S. and Perrone, J. A. 1997. Human heading estimation during visually simulated curvilinear motion. Vis. Res. 37, 573.

Tanaka, K. and Saito, H. 1989. Analysis of motion of the visual field by direction, expansion/contraction, and rotation cells clustered in the dorsal part of the medial superior temporal area of the Macaque monkey. J. Neurophysiol. 62, 626.

Tanaka, K., Fukada, Y., and Saito, H. 1989. Underlying mechanisms of the response specificity of expansion/ contraction and rotation cells in the dorsal part of the medial superior temporal area of the Macaque monkey. J. Neurophysiol. 62, 642.

Te Pas, S. F., Kappers, A. M. L., and Koenderink, J. J. 1996. Detection of first-order structure in optic flow fields. Vis. Res. 36, 259.

Todd, J. T. 1995. The Visual Perception of Three-Dimensional Structure from Motion. In: Perception of Space and Motion (*eds*. W. Epstein and S. Rogers), p. 201. Academic Press.

Tsai, R. Y. and Huang, T. S. 1981. Estimating three-dimensional motion parameters of a rigid planar patch. IEEE Transactions on Acoustics, Speech and Signal Processing ASSP-29, 1147.

Upadhyay, U. D., Page, W. K., and Duffy, C. J. 2000. MST responses to pursuit across optic flow with motion parallax. J. Neurophysiol. 84, 818.

van den Berg, A. V. 1993. Perception of heading. Nature 365, 497.

van den Berg, A. V. 1996. Judgements of heading. Vis. Res. 36, 2337.

van den Berg, A. V. and Beintema, J. A. 2000. The mechanism of interaction between visual flow and eye velocity signals for heading perception. Neuron 26, 747.

Wang, R. F. and Cutting, J. E. 1999. Where we go with a little good information. Psychol. Sci. 10, 71.

Warren, W. H. 1998. The State of Flow. In: High-Level Motion Processing (*ed*. T. Watanabe), p. 315. MIT Press.

Warren, W. H. and Fajen, B. R. 2004. From Optic Flow to Laws of Control. In: Optic Flow and Beyond (*eds*. L. Vaina, S. Beardsley, and S. K. Rushton), p. 307. Kluwer.

Warren, W. H. and Hannon, D. J. 1988. Direction of self-motion is perceived from optical flow. Nature 336, 162.

Warren, W. H. and Hannon, D. J. 1990. Eye movements and optical flow. J. Opt. Soc. Am. A 7, 160.

Warren, W. H. and Saunders, J. A. 1995. Perception of heading in the presence of moving objects. Perception 24, 315.

Warren, W. H., Blackwell, A. W., Kurtz, K. J., Hatsopoulos, N. G., and Kalish, M. L. 1991a. On the sufficiency of the velocity field for perception of heading. Biol. Cybern. 65, 311.

Warren, W. H., Mestre, D. R., Blackwell, A. W., and Morris, M. W. 1991b. Perception of circular heading from optical flow. J. Exp. Psychol. Hum. Percept. Perform. 17, 28.

Warren, W. H., Morris, M. W., and Kalish, M. 1988. Perception of translational heading from optical flow. J. Exp. Psychol. Hum. Percept. Perform. 14, 646.

Waxman, A. M. and Ullman, S. 1985. Surface structure and 3D motion from image flow: a kinematic analysis. Int. J. Robtics Res. 4, 72.

Wertheim, A. H. 1987. Retinal and extraretinal information in movement perception: how to invert the Filehne illusion. Perception 16, 289.

Wist, E. R., Diener, H. C., Dichgans, J., and Brandt, T. 1975. Perceived distance and the perceived speed of self-motion: Linear vs. angular velocity? Percept. Psychophys. 17, 549.

Xiao, D.-K., Raiguel, S., Marcar, V., and Orban, G. A. 1997. The spatial distribution of the antagonistic surround of MT /V5 neurons. Cereb. Cortex 7, 662.

Zhang, T., Heuer, H. W., and Britten, K. H. 2004. Parietal area VIP neuronal responses to heading stimuli are encoded in head-centric coordinates. Neuron 42, 993.

2.13 Biological Motion Perception

N F Troje, Queen's University, Kingston, ON, Canada

© 2008 Elsevier Inc. All rights reserved.

References 236

Glossary

biological motion Here, we use this term to refer to general motion of an animal or a human as compared to non-animate object motion. The usage of this term, however, varies in the literature. Some authors use it only in connection with the perception of point-light displays.

point-light displays An animation which shows only a number of small dots moving as if attached to the major joints or other parts of the body of a human or animal. Point-light displays convey a vivid percept of a moving figure and are a striking demonstration of the visual systems ability of perceptual organization.

superior temporal sulcus (STS) A prominent sulcus in the upper part of the temporal lobe of the primate brain.

double dissociation A double dissociation between two functions A and B exists when function A is not required for function B, and function B is not required for function A. The concept of a double dissociation is central to neuropsychological methodology.

periventricular leukomalacia (PVL) PVL occurs in fetuses and newborns and is particularly frequent in prematurely born neonates. It is caused by a lack of oxygen or blood flow to the periventricular area of the brain, which results in the death or loss of white matter brain tissue.

Down syndrome Down syndrome (or trisomy 21) is a genetic disorder caused by the presence of an extra instance of the 21st chromosome. The condition is characterized by a combination of differences in body structure and impaired cognitive disabilities.

brain imaging This term is used for a number of methods that allow researchers to watch the awake, functioning brain at work by imaging areas that are more active during a certain task than others. Among the most common methods are positron emission tomography (PET) and functional magnetic resonance imaging (fMRI).

A little more than 30 years ago, the Swedish psychologist Johansson G. (1973; 1976) fascinated the vision science community with an arresting demonstration of the organizational efficiency of the human visual system: he attached small light bulbs to the major joints of a human figure dressed entirely in black. Filming the movement of that figure created a highly reduced display that consisted only of a small number of white dots moving against a black background. Yet, it created the vivid and immediate percept of a human figure in action. Only 10 dots and 150 ms of display time were sufficient for a human observer to perceptually organize the dots into a fully coherent, articulated shape of a human figure, implicating the involvement of a highly specialized perceptual process. Today, we call Johansson's phenomenon biological motion perception, and the point-light displays he first used to demonstrate it have become recognized as a very effective research tool for studying the mechanisms upon which it is based. A demonstration of point-light displays and their potential to convey information about a walking person can be found at the website of The Bio Motion Lab.

The functional significance of this fascinating phenomenon lies in the vitally important ability to detect and to adequately interpret the movements of another animal. The other animal might be a predator, potential prey, or of one's own kind. If the latter is the case, it might be a potential mate, a rival, or

Box 1

Point-light displays in current research typically depict the motion of the main joints of a human body in terms of small dots. Johansson G. (1973) had already started to replace actively light-emitting light bulbs with patches of passively reflecting material. Particularly with the advent of broad availability of video technology, it became easy to process the recorded material such that only the reflections would be visible as bright dots on a uniformly black background. Today, many laboratories employ three-dimensional (3D) motion capture technology to create stimuli for biological motion research (Figure 1). Such systems provide the digitized 3D trajectories of small markers that are attached to an actor's body. The data can in turn be rendered into typical point-light displays. In contrast to older film and video technology, the enormous advantage of motion capture technology lies in its access to the motion data themselves, rather than just the final visual display. The same motion data can now be displayed from any viewpoint and individual trajectories can be displaced, inverted, or otherwise manipulated before turning them into a stimulus. Dots can be connected to create stick figures or they can be used to animate 3D computer graphics characters. The time series of marker locations can also be used as input for biomechanical models designed to retrieve the true joint locations and other anatomical landmarks inside the body from the markers attached to its surface, as well as moments and forces acting on the body. Finally, they also provide valuable input for computational models of human biological motion processing.

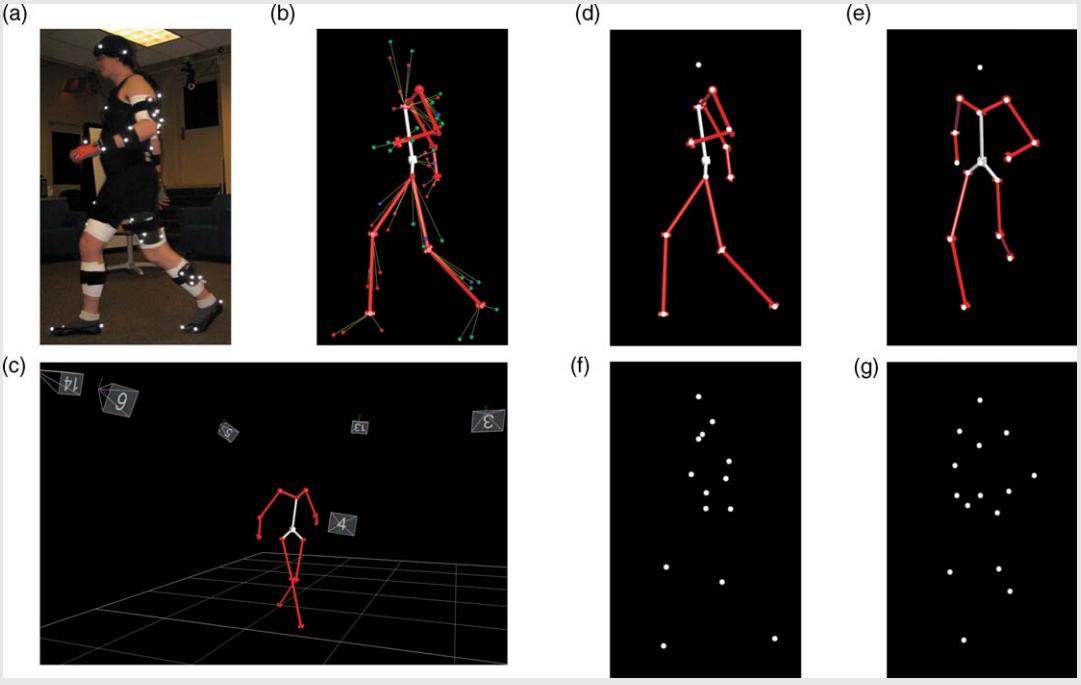

Figure 1 For optical motion capture, a person is attached with a number of retroreflective markers to his body (a). An array of high-speed video cameras tracks the markers and reconstructs their trajectories in three-dimensional space (c). These marker trajectories are then used as input for a biomechanical model (b) that computes the movements of anatomical landmarks, such as the major joints of the body (d). These are then displayed in terms of point-light displays (e). Because the underlying biomechanical model is inherently three dimensional, similar displays can be created from other viewpoints (f and g).

maybe a particular individual that we depend on, for instance, a parent or an offspring. Visual motion plays a major role in identifying another living creature and can inform the observer about its actions and intentions. Humans are highly social animals. Not surprisingly, this is reflected in many specializations of our sensory systems, such as the ability to comprehend speech, to recognize faces, and – the topic of this chapter – to retrieve information from the way a person moves.

Signatures contained in biological motion patterns identify the agent as an animal or human figure (Mather, G. and West, S., 1993) and reveal its actions (Dittrich, W. H., 1993). They are sufficient to

recognize a familiar person (Cutting, J. E. and Kozlowski, L. T., 1977; Troje, N. F. *et al.*, 2005; Westhoff, C. and Troje, N. F., 2007) and to attribute socially relevant attributes such as sex, age, mental states, actions, and intentions to unfamiliar individuals (Barclay, C. D. *et al.*, 1978; Mather, G. and Murdoch, L., 1994; Runeson, S., 1994; Dittrich, W. H. *et al.*, 1996; Blakemore, S. J. and Decety, J., 2001; Pollick, F. E. *et al.*, 2001; Troje, N. F., 2002a; 2002b). Research into the cues that convey this information unveils a rich composition of configural, anthropometric features, on the one hand, and kinematic features such as speed and spectral composition of the point-light trajectories, on the other hand (Pollick, F. E. *et al.*, 2001; Troje, N. F., *et al.*, 2005; Westhoff, C. and Troje, N. F., 2007). If pit against one another, the information provided by kinematic features clearly dominates the role of static features (Mather, G. and Murdoch, L., 1994; Troje, N. F., 2002a).

The ability to perceive biological motion arises early in life. Four-month-old infants stare at human motion sequences for longer durations than they will at the same number of dots undergoing random motions (Fox, R. and McDaniel, C., 1982; Bertenthal, B., 1993), and event-related potential (ERP) studies imply that the brain areas involved are similar to the ones found in adults (Jokisch, D. *et al.*, 2005; Reid, V. M. *et al.*, 2006). On the other hand, however, children show a number of fundamental differences in the way they perceive biological motion and keep improving their ability to retrieve the shape of a moving body until they reach adult levels of performance at about the age of 5 (Pavlova, M. *et al.*, 2001).

In the adult brain, multiple areas are involved in biological motion processing (for comprehensive reviews, see Allison, T. *et al.*, 2000; Puce, A. and Perrett, D. I., 2003). Recording from single cells in macaque cortex, Oram M. W. and Perrett D. I. (1994) first identified structures in the upper bank of the superior temporal sulcus (STS) as selectively responsive to human form and motion. A number of more recent brain imaging studies corroborate this finding and show that the posterior part of STS (STSp) is particularly active when looking at point-light displays of an upright human walker (Bonda, E. *et al.*, 1996; Grossman, E. D. *et al.*, 2000; Grossman, E. D. and Blake, R., 2002; Grossman, E. D. *et al.*, 2004; Peuskens, H. *et al.*, 2005). While STSp is clearly responsive to biological motion, it is not clear how specific this area is. Stimuli such as faces (Grossman, E. D. and Blake, R., 2002), speech (Beauchamp, M. S., 2005), the sound of footsteps (Bidet-Caulet, A. *et al.*, 2005), and visual motion confined to specific limbs, the eyes, or mouth (Grezes, J. *et al.*, 1998; Puce, A. *et al.*, 1998) also result in STSp activation. Besides STSp, other areas have been identified that are responsive to biological motion. They involve the ventral surface of the temporal lobe (Vaina, L. M. *et al.*, 2001), the fusiform gyrus (Beauchamp, M. S. *et al.*, 2002), and the fusiform face area (Grossman, E. D. and Blake, R., 2002; Peelen, M. V. and Downing, P. E., 2005). For all these areas, it is rather unclear if they respond specifically to human motion or if they are triggered generally by biological motion. Only very few imaging studies have contrasted representations of humans versus nonhumans, and none of these has used standard biological motion point-light displays (Downing, P. E. *et al.*, 2001; Buccino, G. *et al.*, 2004). More research is required to characterize and understand the neuronal circuits involved in the perception of biological motion.

Given the complexity and sophistication of biological motion perception, it is not surprising that it is susceptible to failure. Case studies with brain-lesioned patients demonstrate a double dissociation between general motion perception and the ability to see and interpret biological motion (Vaina, L. M. *et al.*, 1990; McLeod, P. *et al.*, 1996). Specific deficits in the ability to perceive and adequately interpret biological motion patterns have also been described in the context of a number of different disorders. Autistic children have been demonstrated to show deficits in biological motion perception (Blake, R. *et al.*, 2003; Dakin, S. and Frith, U., 2005), which is consistent with the finding that they also show STS abnormalities (Waiter, G. D. *et al.*, 2004). Patients suffering from periventricular leukomalacia (PVL), which is often present in children born prematurely, have been described to be compromised in their ability to perceive biological motion (Pavlova, M. *et al.*, 2003; 2005; 2006a; 2006b). Impairments in biological motion perception have also been described in schizophrenic patients (Kim, J. *et al.*, 2005) and in children with Down syndrome (Virji-Babul, N. *et al.*, 2006).

In many respects, the information contained in biological motion and our ability to exploit it resembles the phenomenology of face recognition (see Chapter Face Recognition). For instance, both visual domains are highly susceptible to a pronounced inversion effect: if a point-light stimulus (or a face) is turned upside down, perception is strongly impaired (Sumi, S., 1984; Pavlova, M. and Sokolov, A., 2000). For faces, there is convincing evidence that the inversion effect is caused by an impairment of mechanisms

responsible for assessing the details of the spatial configuration of facial features (Farah, M. J. *et al.*, 1995; Maurer, D. *et al.*, 2002), and the same has been implied to be the case for biological motion (e.g., Proffitt, D. R. and Bertenthal, B. I., 1990; Dittrich, W. H., 1993; Reed, C. L. *et al.*, 2003; Troje, N. F., 2003).

A number of debates have arisen concerning the mechanisms that serve the complex visual abilities involved with biological motion perception. One of them concerns the question to what extent biological motion perception is driven by global, conceptual information processing and to what extent it is determined by local, low-level motion processing. While some authors think that local motion is sufficient (e.g., Mather, G. *et al.*, 1992), others clearly demonstrate global effects (e.g., Neri, P. *et al.*, 1998). Another dispute that is connected to the question about the role of local versus global information (Thornton, I. M. *et al.*, 1998) concerns the contributions of attentional mechanisms (Cavanagh, P. *et al.*, 2001; Thornton, I. M. *et al.*, 2002) and the role of learning (Grossman, E. D. *et al.*, 2004; Hiris, E. *et al.*, 2005; Jastorff, J. *et al.*, 2006). Finally, there are seemingly contradictory findings about how well biological motion can be processed in the visual periphery (Thompson, B. *et al.*, in press; Ikeda, H. *et al.*, 2005). Here, we want to argue that these controversies can be resolved only if we acknowledge that biological motion is not a single phenomenon but consists of a number of different aspects that have to be distinguished carefully – both conceptually and experimentally. Typical paradigms used in biological motion research such as detecting a point-light walker in a mask or deriving the direction into which the walker is facing might address very different processing stages and are therefore not interchangeable but may address very different processing stages.

The majority of biological motion research focuses on the impressive ability to organize the individual dots of a point-light display into the coherent structure of a human body. Here, we will refer to this as the structure-from-motion aspect of biological motion perception. In general, such a focus is not explicitly intended but results from a standard task widely used in biological motion research: the detection of a point-light walker that is masked by superimposing it with multiple scrambled walkers. Scrambled walkers are derived from veridical, coherent point-light walkers by adding a random but constant offset to the location of the single trajectories. This manipulation disrupts the structure of the display but leaves the local motion of the individual dots intact. The only difference between a display that consists only of a mask of scrambled walkers and the one that embeds a coherent walker in this mask is the presence of the coherent structure of the single walker. A similar focus also characterizes large parts of the brain imaging literature. Here, brain activity in response to intact biological motion is often contrasted with responses to scrambled motion – a contrast that once again reduces biological motion perception to its structure-from-motion aspect.

In a recent study by Troje N. F. and Westhoff C. (2006), it was shown that scrambled biological motion of humans and animals, even though devoid of any structural information, still carries information about the direction in which a walker was facing (Figure 2). Interestingly, observers can exploit this information only if the stimulus is presented upright. Since the locations of the individual dot trajectories are random in a scrambled biological motion display, the information about the direction as well as the corresponding inversion effect must be contained in local dot trajectories. In fact, it could be shown that the critical information is carried by the motion of a human's or animal's feet. The dependence on orientation is hypothesized to be due to inherent expectations about the direction of gravitational acceleration, an assumption corroborated by earlier findings on the role of heuristics about gravity in the perception of biological motion (Runeson, S., 1994; Jokisch, D. and Troje, N. F., 2003; Shipley, T. F., 2003) and nonanimate motion (Pittenger, J. B., 1985; Watson, J. S. *et al.*, 1992). Troje N. F. and Westhoff C. (2006) suggest that the sensitivity to the dynamics of the feet reflects its potential role as a visual invariant for the nonspecific detection of an animal in the visual environment.

I want to conclude this chapter by pointing out that biological motion perception is not just a single phenomenon. In order to fully understand and appreciate its rich and fascinating phenomenology, we have to distinguish between a number of different processing levels:

1. *Life detection.* Troje N. F. and Westhoff C. (2006) identified the ballistic movements of the limps of a terrestrial animal to provide an invariant that our visual system uses to spot an animal in the visual environment independent of its particular shape. The cue seems to work well not only for foveal vision but also in the visual periphery (Thompson, B. *et al.*, in press) and probably directs attention to an event of potentially vital significance. The

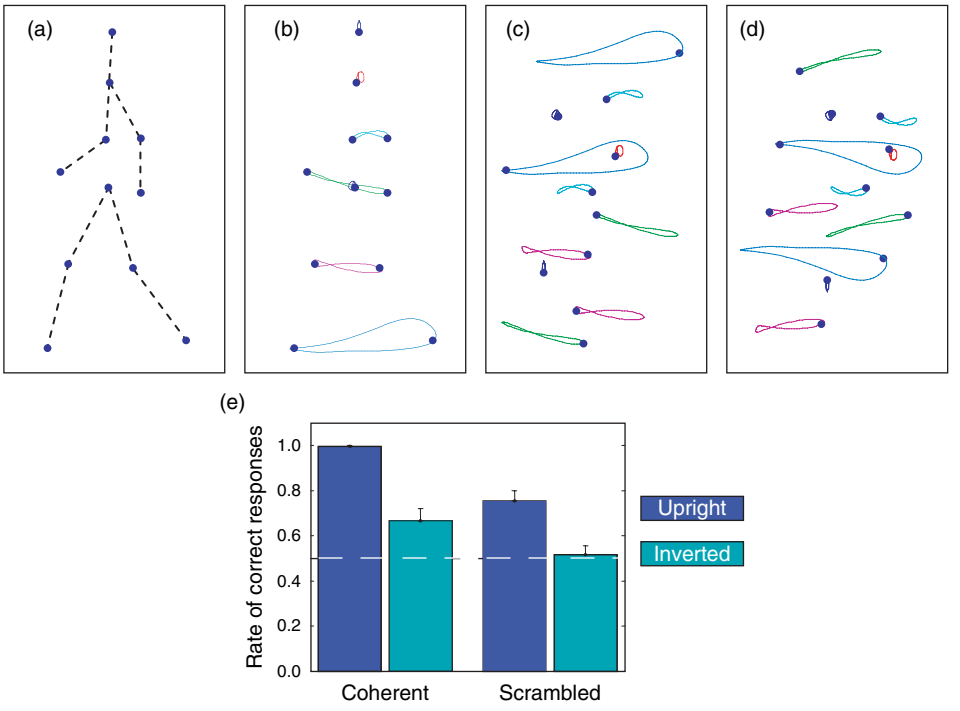

Figure 2 Scrambled biological motion is derived from normal, coherent biological motion (a and b) by randomly offsetting the trajectories of the individual dots (c). This disrupts the structure of the human figure. Yet, if asked in which direction 'this odd creature' is facing, observers are still quite accurate. Only if the scrambled point-light display is turned upside down (d), performance drops to chance level (e). The dashed lines that show the articulation of the individual dots (a) and the solid lines that illustrate their trajectories (b, c, and d) are not shown in the experiment. Visit http://www.biomotionlab.ca/Demos/scrambled.html for an interactive animation that demonstrates the stimuli. For experimental details, see Troje N. F. and Westhoff C. (2006).

underlying visual filter mechanism is expected to be evolutionary old and shared by other animals as well. Behavioral experiments on visually naive, newly hatched chicks suggest that they use the same cue to identify the object of filial imprinting and they even show the same inversion effect (Vallortigara, G. *et al.*, 2005; Vallortigara, G. and Regolin, L., 2006).

2. *Structure-from-motion.* Once a living creature is detected, its movements can be used to perceptually organize it into a coherent, articulated body structure, resulting in 'basic level' (Rosch, E., 1988) agent recognition (e.g., is this a human, a cat, or a bird?). In contrast to the early 'life detection' stage, this mechanism does not work very well in the visual periphery (Ikeda, H. *et al.*, 2005), it probably requires attention (Cavanagh, P. *et al.*, 2001; Thornton, I. M. *et al.*, 2002), and it is susceptible to learning and individual experience (Jastorff, J. *et al.*, 2006). It is also subject to an inversion effect, which, however, is independent of the one operating on the 'life detection' mechanism and rather related to the orientation dependency of configural processing observed in face recognition. The relation between the two mechanisms for life detection and for structure-from-motion retrieval might be similar to the relation between two processes in the development of face recognition suggested by Morton J. and Johnson M. H. (1991). These authors suggested that an innate system guides attention to face-like patterns, while a second mechanism is responsible for learning about the detailed characteristics of faces required for individual face recognition.
3. *Action recognition.* On this level, structural and kinematic information is integrated into a system that classifies and categorizes the action. Efficient classification on this level is expected to be invariant to the particular agent, viewing conditions, and the style of the action. As yet, we know rather little about this processing level. More research is required to understand which features define a

particular action. Some interesting ideas may come from recent work on general event perception (e.g., Zacks, J. M., 2004). Given the ease with which the human visual system categorizes actions, the difficulty to experimentally and theoretically identify action-specific invariants is surprising – and probably related to the harsh contrast between human 'basic' level (Rosch, E., 1988) object classification and the lack of good computational models for it.

4. *Style recognition.* Once both agent and action are identified, pattern recognition at a 'subordinate' level (Rosch, E., 1988) helps retrieve further information about the details of both. For instance, once we know we are confronted with a human walker (let's say, rather than a hunting tiger), we are able to use motion as a source of information about individual identity, gender, age, emotional state, personality traits, and as a complex means for signaling and communications. Depending on the particular property, the results of initial data processing required to characterize and isolate diagnostic features might eventually feed into different neuronal circuits, and in that respect 'style recognition' might not be due to a single mechanism but to several. Yet, at least from a computational point of view, it is very likely that all of them share certain processing principles (Troje, N. F., 2002a; 2002b).

Adopting this multilevel view has important implications for understanding biological motion perception. It resolves many of the above-mentioned debates (local vs. global, role of attention and learning, foveal vs. peripheral vision) in a canonical way. Furthermore, it generates new hypotheses about the development of biological motion perception, both ontogenetically and evolutionarily. It also has implications concerning the role of impaired biological motion perception in disorders that affect social competence and the complex sensory basis of communicative behavior.

Before I finish this short review on biological motion perception, I want to point out that it is by no means comprehensive. Much more work has been done in all the areas that I tried to cover here. In addition, there are topics that I did not address at all. One of them refers to the large field of computational models for human motion recognition. Some of the models are explicitly biologically motivated, trying to incorporate information we have about the physiology of biological motion perception (e.g., Giese, M. A. and Poggio, T., 2003). On the other hand, there is a large body of work conducted in the fields of computer vision and machine learning that approaches biological motion perception as a pattern recognition problem. Another area that I did not even try to address given the limited scope of this chapter is the interesting question of understanding biological motion in the context of human interaction. Concepts such as simulation theory, common-coding theory (Prinz, W., 1997), the direct-matching hypothesis (Rizzolatti, G. *et al.*, 2001), and particularly the discovery of mirror neurons in the monkey brain (Gallese, V. *et al.*, 1996; Rizzolatti, G. *et al.*, 1996) provide an interesting basis for speculations about how the behavior between two interacting people becomes coupled and coordinated (Decety, J. and Grezes, J., 1999; Blakemore, S. J. and Decety, J., 2001). The perception of social contingency and the mechanisms through which it determines our own actions in social situations probably has to be considered a fifth level in the above proposed taxonomy of levels of biological motion perception.

References

Allison, T., Puce, A., and McCarthy, G. 2000. Social perception from visual cues: role of the STS region. Trends Cogn. Sci. 4(7), 267–278.

Barclay, C. D., Cutting, J. E., and Kozlowski, L. T. 1978. Temporal and spatial factors in gait perception that influence gender recognition. Percept. Psychophys. 23, 145–152.

Beauchamp, M. S. 2005. See me, hear me, touch me: multisensory integration in lateral occipital-temporal cortex. Curr. Opin. Neurobiol. 15(2), 145–153.

Beauchamp, M. S., Lee, K. E., Haxby, J. V., and Martin, A. 2002. Parallel visual motion processing streams for manipulable objects and human movements. Neuron 34(1), 149–159.

Bertenthal, B. 1993. Perception of Biomechanical Motions by Infants: Intrinsic Image and Knowledge-Based Constraints. In: Visual Perception and Cognition in Infancy (*ed*. C. Granrud), pp. 175–214. Erlbaum.

Bidet-Caulet, A., Voisin, J., Bertrand, O., and Fonlupt, P. 2005. Listening to a walking human activates the temporal biological motion area. Neuroimage 28(1), 132–139.

Blake, R., Turner, L. M., Smoski, M. J., Pozdol, S. L., and Stone, W. L. 2003. Visual recognition of biological motion is impaired in children with autism. Psychol. Sci. 14(2), 151–157.

Blakemore, S. J. and Decety, J. 2001. From the perception of action to the understanding of intention. Nat. Rev. Neurosci. 2(8), 561–567.

Bonda, E., Petrides, M., Ostry, D., and Evans, A. 1996. Specific involvement of human parietal systems and the amygdala in the perception of biological motion. J. Neurosci. 16(11), 3737–3744.

Buccino, G., Lui, F., Canessa, N., Patteri, I., Lagravinese, G., Benuzzi, F., *et al.* 2004. Neural circuits involved in the recognition of actions performed by nonconspecifics: an FMRI study. J. Cogn. Neurosci. 16(1), 114–126.

Cavanagh, P., Labianca, A. T., and Thornton, I. M. 2001. Attention-based visual routines: sprites. Cognition 80(1–2), 47–60.

Cutting, J. E. and Kozlowski, L. T. 1977. Recognizing friends by their walk: gait perception without familiarity cues. Bull. Psycho. Soc. 9(5), 353–356.
Dakin, S. and Frith, U. 2005. Vagaries of visual perception in autism. Neuron 48(3), 497–507.
Decety, J. and Grezes, J. 1999. Neural mechanisms subserving the perception of human actions. Trends Cogn. Sci. 3(5), 172–178.
Dittrich, W. H. 1993. Action categories and the perception of biological motion. Perception 22(1), 15–22.
Dittrich, W. H., Troscianko, T., Lea, S. E. G., and Morgan, D. 1996. Perception of emotion from dynamic point-light displays represented in dance. Perception 25(6), 727–738.
Downing, P. E., Jiang, Y., Shuman, M., and Kanwisher, N. 2001. A cortical area selective for visual processing of the human body. Science 293(5539), 2470–2473.
Farah, M. J., Tanaka, J. W., and Drain, H. M. 1995. What causes the face inversion effect? J. Exp. Psychol. Hum. Percept. Perform. 21(3), 628–634.
Fox, R. and McDaniel, C. 1982. The perception of biological motion by human infants. Science 218(4571), 486–487.
Gallese, V., Fadiga, L., Fogassi, L., and Rizzolatti, G. 1996. Action recognition in the premotor cortex. Brain 119, 593–609.
Giese, M. A. and Poggio, T. 2003. Neural mechanisms for the recognition of biological movements. Nat. Rev. Neurosci. 4(3), 179–192.
Grezes, J., Costes, N., and Decety, J. 1998. Top-down effect of strategy on the perception of human biological motion: a PET investigation. Cogn. Neuropsychol. 15(6–8), 553–582.
Grossman, E. D. and Blake, R. 2002. Brain areas active during visual perception of biological motion. Neuron 35(6), 1167–1175.
Grossman, E. D., Blake, R., and Kim, C. Y. 2004. Learning to see biological motion: brain activity parallels behavior. J. Cogn. Neurosci. 16(9), 1669–1679.
Grossman, E. D., Donnelly, M., Price, R., Pickens, D., Morgan, V., Neighbor, G., *et al.* 2000. Brain areas involved in perception of biological motion. J. Cogn. Neurosci. 12(5), 711–720.
Hiris, E., Krebeck, A., Edmonds, J., and Stout, A. 2005. What learning to see arbitrary motion tells us about biological motion perception. J. Exp. Psychol. Hum. Percept. Perform. 31(5), 1096–1106.
Ikeda, H., Blake, R., and Watanabe, K. 2005. Eccentric perception of biological motion is unscalably poor. Vision Res. 45(15), 1935–1943.
Jastorff, J., Kourtzi, Z., and Giese, M. A. 2006. Learning to discriminate complex movements: biological versus artificial trajectories. J. Vis. 6, 791–804.
Johansson, G. 1973. Visual perception of biological motion and a model for its analysis. Percept. Psychophys. 14(2), 201–211.
Johansson, G. 1976. Spatio-temporal differentiation and integration in visual motion perception. Psychol. Res. 38, 379–393.
Jokisch, D. and Troje, N. F. 2003. Biological motion as a cue for the perception of size. J. Vis. 3(4), 252–264.
Jokisch, D., Daum, I., Suchan, B., and Troje, N. F. 2005. Structural encoding and recognition of biological motion: evidence from event-related potentials and source analysis. Behav. Brain Res. 157(2), 195–204.
Kim, J., Doop, M. L., Blake, R., and Park, S. 2005. Impaired visual recognition of biological motion in schizophrenia. Schizophr. Res. 77(2–3), 299–307.
Mather, G. and Murdoch, L. 1994. Gender discrimination in biological motion displays based on dynamic cues. Proc. R. Soc. Lon. Ser. B 258, 273–279.
Mather, G. and West, S. 1993. Recognition of animal locomotion from dynamic point-light displays. Perception 22(7), 759–766.
Mather, G., Radford, K., and West, S. 1992. Low-level visual processing of biological motion. Proc. R. Soc. Lond. B Biol. Sci. 249(1325), 149–155.
Maurer, D., Grand, R. L., and Mondloch, C. J. 2002. The many faces of configural processing. Trends Cogn. Sci. 6(6), 255–260.
McLeod, P., Dittrich, W., Driver, J., Perrett, D., *et al.* 1996. Preserved and impaired detection of structure from motion by a ''motion-blind'' patient. Vis. Cogn. 3(4), 363–391.
Morton, J. and Johnson, M. H. 1991. CONSPEC and CONLERN: a two-process theory of infant face recognition. Psychol. Rev. 98(2), 164–181.
Neri, P., Morrone, M. C., and Burr, D. C. 1998. Seeing biological motion. Nature 395(6705), 894–896.
Oram, M. W. and Perrett, D. I. 1994. Responses of anterior superior temporal polysensory (STPa) neurons to ''biological motion'' stimuli. J. Cogn. Neurosci. 6(2), 99–116.
Pavlova, M. and Sokolov, A. 2000. Orientation specificity in biological motion perception. Percept. Psychophys. 62(5), 889–899.
Pavlova, M., Krageloh-Mann, I., Sokolov, A., and Birbaumer, N. 2001. Recognition of point-light biological motion displays by young children. Perception 30(8), 925–933.
Pavlova, M., Marconato, F., Sokolov, A., Braun, C., Birbaumer, N., and Krageloh-Mann, I. 2006a. Periventricular leukomalacia specifically affects cortical MEG response to biological motion. Ann. Neurol. 59(2), 415–419.
Pavlova, M., Sokolov, A., Birbaumer, N., and Krageloh-Mann, I. 2006b. Biological motion processing in adolescents with early periventricular brain damage. Neuropsychologia 44(4), 586–593.
Pavlova, M., Sokolov, A., Staudt, M., Marconato, F., Birbaumer, N., and Krageloh-Mann, I. 2005. Recruitment of periventricular parietal regions in processing cluttered point-light biological motion. Cereb. Cortex 15(5), 594–601.
Pavlova, M., Staudt, M., Sokolov, A., Birbaumer, N., and Krageloh-Mann, I. 2003. Perception and production of biological movement in patients with early periventricular brain lesions. Brain 126(Pt 3), 692–701.
Peelen, M. V. and Downing, P. E. 2005. Selectivity for the human body in the fusiform gyrus. J. Neurophysiol. 93(1), 603–608.
Peuskens, H., Vanrie, J., Verfaillie, K., and Orban, G. A. 2005. Specificity of regions processing biological motion. Eur. J. Neurosci. 21(10), 2864–2875.
Pittenger, J. B. 1985. Estimation of pendulum length from information in motion. Perception 14(3), 247–256.
Pollick, F. E., Paterson, H. M., Bruderlin, A., and Sanford, A. J. 2001. Perceiving affect from arm movement. Cognition 82(2), B51–B61.
Prinz, W. 1997. Perception and action planning. Eur. J. Cogn. Psychol. 9, 129–154.
Proffitt, D. R. and Bertenthal, B. I. 1990. Converging operations revisited: assessing what infants perceive using discrimination measures. Percept. Psychophys. 47(1), 1–11.
Puce, A. and Perrett, D. I. 2003. Electrophysiology and brain imaging of biological motion. Philos. Trans. R Soc. Lond. B Biol. Sci. 358, 435–445.
Puce, A., Allison, T., Bentin, S., Gore, J. C., and McCarthy, G. 1998. Temporal cortex activation in humans viewing eye and mouth movements. J. Neurosci. 18(6), 2188–2199.
Reed, C. L., Stone, V. E., Bozova, S., and Tanaka, J. 2003. The body-inversion effect. Psychol. Sci. 14(4), 302–308.
Reid, V. M., Hoehl, S., and Striano, T. 2006. The perception of biological motion by infants: an event-related potential study. Neurosci. Lett. 395(3), 211–214.

Rizzolatti, G., Fadiga, L., Gallese, V., and Fogassi, L. 1996. Premotor cortex and the recognition of motor actions. Cogn. Brain Res. 3(2), 131–141.
Rizzolatti, G., Fogassi, L., and Gallese, V. 2001. Neurophysiological mechanisms underlying the understanding and imitation of action. Nat. Rev. Neurosci. 2(9), 661–670.
Rosch, E. 1988. Principles of Categorization. In: Readings in Cognitive Science (*eds*. A. Collins and E. E. Smith), pp. 312–322. Morgenkaufmann.
Runeson, S. 1994. Perception of Biological Motion: The Ksd-Principle and the Implications of a Distal Versus Proximal Approach. In: Perceiving Events and Objects (*eds*. G. Jansson, W. Epstein, and S. S. Bergström), pp. 383–405. Erlbaum.
Shipley, T. F. 2003. The effect of object and event orientation on perception of biological motion. Psychol. Sci. 14(4), 377–380.
Sumi, S. 1984. Upside-down presentation of the Johansson moving light-spot pattern. Perception 13(3), 283–286.
Thompson, B., Hansen, B. C., Hess, R. F., and Troje, N. F. Peripheral vision; good for biological motion, bad for breaking camouflage. J. Vision. (in press).
Thornton, I. M., Pinto, J., and Shiffrar, M. 1998. The visual perception of human locomotion. Cogn. Neuropsychol 15, 535–552.
Thornton, I. M., Rensink, R. A., and Shiffrar, M. 2002. Active versus passive processing of biological motion. Perception 31(7), 837–853.
Troje, N. F. 2002a. Decomposing biological motion: a framework for analysis and synthesis of human gait patterns. J. Vis. 2(5), 371–387.
Troje, N. F. 2002b. The Little Difference: Fourier Based Synthesis of Gender-Specific Biological Motion. In: *Dynamic Perception* (*eds*. R. Würtz and M. Lappe), pp. 115–120. Aka Press.
Troje, N. F. 2003. Reference frames for orientation anisotropies in face recognition and biological-motion perception. Perception 32(2), 201–210.
Troje, N. F. and Westhoff, C. 2006. The inversion effect in biological motion perception: evidence for a ''life detector''? Curr. Biol. 16(8), 821–824.
Troje, N. F., Westhoff, C., and Lavrov, M. 2005. Person identification from biological motion: effects of structural and kinematic cues. Percept. Psychophys. 67(4), 667–675.
Vaina, L. M., Lemay, M., Bienfang, D. C., Choi, A. Y., and Nakayama, K. 1990. Intact ''biological motion'' sand ''structure from motion'' perception in a patient with impaired motion mechanisms: a case study. Vis. Neurosci. 5(4), 353–369.
Vaina, L. M., Solomon, J., Chowdhury, S., Sinha, P., and Belliveau, J. W. 2001. Functional neuroanatomy of biological motion perception in humans. Proc. Natl. Acad. Sci. U. S. A. 98(20), 11656–11661.
Vallortigara, G. and Regolin, L. 2006. Gravity bias in the interpretation of biological motion by inexperienced chicks. Curr. Biol. 16(8), R279–R280.
Vallortigara, G., Regolin, L., and Marconato, F. 2005. Visually inexperienced chicks exhibit spontaneous preference for biological motion patterns. PLoS Biol. 3(7), e208.
Virji-Babul, N., Kerns, K., Zhou, E., Kapur, A., and Shiffrar, M. 2006. Perceptual-motor deficits in children with Down syndrome: implications for intervention. Downs Syndr. Res. Pract. 10(2), 74–82.
Waiter, G. D., Williams, J. H., Murray, A. D., Gilchrist, A., Perrett, D. I., and Whiten, A. 2004. A voxel-based investigation of brain structure in male adolescents with autistic spectrum disorder. Neuroimage 22(2), 619–625.
Watson, J. S., Banks, M. S., von Hofsten, C., and Royden, C. S. 1992. Gravity as a monocular cue for perception of absolute distance and/or absolute size. Perception 21(1), 69–76.
Westhoff, C. and Troje, N. F. 2007. Kinematic cues for person identification from biological motion. Percept. Psychophys. 69, 241–253.
Zacks, J. M. 2004. Using movement and intentions to understand simple events. Cogn. Sci. 28, 979–1008.

Relevant Website

http://www.biomotionlab.ca – The Bio Motion Lab.

2.14 Transparency and Occlusion

B L Anderson, University of New South Wales, Sydney, NSW, Australia

© 2008 Elsevier Inc. All rights reserved.

2.14.1	The Computation of Transparency	239
2.14.2	Anchoring Perceived Transmittance	242
2.14.3	Scission and the Perception of Lightness	243
References		244

Glossary

transparency The property of objects, surfaces, and media that allows for the transmission of light.
lightness The proportion of light reflected by a surface.
occlusion The interruption of the optical projection of a more distant object by a nearer object.
scission The decomposition of an image into multiple surfaces or causes along the same line of sight.
transmittance The proportion of light that passes through an object.

One of the great computational challenges in recovering scene structure from images arises from the fact that some surfaces in a scene are partially obscured by nearer surfaces or media. Both occluding and transparent surfaces interrupt the projection of more distant surfaces, and may be considered two ends of a continuum. Occluding surfaces completely obscure the surfaces that they occlude, whereas transparent surfaces only partially obscure the surfaces they overlay. The degree to which a transparent surface obscures an underlying surface depends on its transmittance (i.e., the proportion of light that it lets through of the underlying layer). Thus, when the transmittance is zero, the near surface is an opaque occluder; when it is greater than zero, some light of the underlying layer is transmitted. In order for the visual system to recover scene structure in contexts in which the transmittance of a near layer falls between zero and one, it must decompose the image into a layered representation that specifies the presence of multiple surfaces (or a surface and intervening media) along the same line of sight. This form of decomposition has been termed scission.

In addition to the relationship between transparency and occlusion, the physical transformations induced by transparent surfaces are intimately related to the physical transformations that are caused by changes in illumination. This suggests the possibility that the scission that underlies the perception of transparency may also underlie the separation of illumination from surface reflectance, and hence, the computation of surface lightness and/or color. Thus, the topic of transparency is intimately related to two apparently distinct domains: the computation of occlusion relationships and the computation of surface lightness. In this chapter, I will describe some recent evidence that reveals the intimate relationship between scission and the perception of surface opacity, lightness, and depth, and the impact this research has on theoretical frameworks in vision more broadly.

2.14.1 The Computation of Transparency

The topic of transparency emerged as a fundamental area of vision research with the seminal work of the Italian psychologist Metelli F. (1970; 1974a; 1974b). Metelli developed a model of transparency based on the physical setup he used to generate of transparent images – namely, a disk with a missing sector (episcotister) that rotated in front of a two-toned background (see Figure 1). Metelli derived a simple set of equations that described the relationship between the reflectance of the underlying background surfaces,

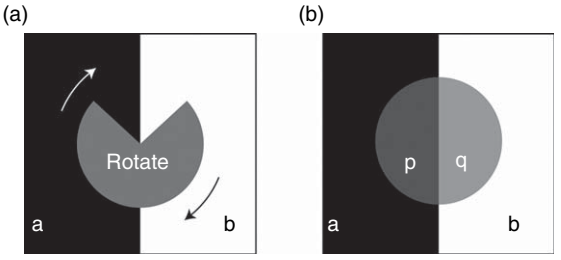

Figure 1 A schematic of Metelli's episcotister setup that served as the basis of his model of transparency. (a) An opaque disk with a missing sector subtending angle α is rotated over a two-toned background. When spun rapidly, it produces a percept similar to that depicted in (b). Note that the transparent surface appears to possess a particular opacity and color (here, an achromatic lightness).

the transmittance of the transparent filter (i.e., the size of the missing sector), and the reflectance of the transparent layer. Metelli argued that perceived transparency was well predicted by the physical constraints that must be satisfied to produce a transparent surface, and thus, embraced an inverse optics approach to modeling visual perception. In particular, Metelli used his episcotister display to derive a physical model for the transmittance (α) and reflectance (t) of the transparent surface, which was just a weighted sum of the contributions of the light transmitted from the underlying layer and that reflected by the episcotister:

$$p = \alpha a + (1-\alpha)t \quad [1]$$

$$q = \alpha b + (1-\alpha)t \quad [2]$$

where p is the region containing the transparent layer that overlaps background a; q is the region containing the transparent layer that overlaps background b; and α is the transmittance of the transparent layer (i.e., the proportion of the size of the holes in the episcotister). These equations can be solved to derive separate expressions for the transmittance and reflectance of the transparent surface:

$$\alpha = (p-q)/(a-b) \quad [3]$$

$$t = (aq-bp)/(a+q-b-p) \quad [4]$$

To make physical sense, α is restricted to be between 0 and 1, which imposes two basic constraints on the images that are consistent with transparency: the luminance difference between the regions of transparency $(p-q)$ must have the same sign as the luminance difference between the regions in plain view $(a-b)$ (to ensure that α is positive); and the magnitude of the luminance difference of the regions of transparency $(p-q)$ must be less than or equal to the luminance difference of the surface in plain view $(a-b)$; (to insure that the transmittance falls between 0 and 1). Perhaps the most salient restriction of the applicability of these equations is that they can only be used to describe transparent filters containing a uniform reflectance and transmittance. They make no predictions of displays containing unbalanced transparent filters or media, that is, forms of transparency that are not uniform in reflectance and/or transmittance. Note that Metelli's model is a purely generative model, that is, his equations described the (simplified) physics of his episcotister display. Thus, the issue of whether such equations could be used to predict when, whether, and how transparency was perceived is an issue that required psychological experimentation.

Nearly three decades of research into transparency perception seemed to provide compelling evidence that Metelli's model successfully predicted when transparency was and was not perceived (Metelli, F., 1974a; 1974b; 1985; Metelli, F. *et al.*, 1985; Gerbino, W. *et al.*, 1990; Kasrai, R. and Kingdom, F., 2001). However, we have recently argued that that this apparent success stems from the particular methodologies employed to assess his model. Although Metelli derived separate expressions for the transmittance and reflectance of a transparent surface, until recently, no experiments assessed whether these expressions accurately captured human perception of transparent surfaces. Rather, most experiments typically required observers to adjust (or otherwise judge) the luminance of a test patch in a display until it appeared to form a uniform transparent filter; they did not measure whether Metelli's equations could quantitatively predict the perceived transmittance and reflectance of a transparent filter.

To provide a more direct quantitative test of Metelli's model, we (Singh, M. and Anderson, B. L., 2002) recently performed a number of experiments to directly assess whether his equations correctly predicted the perception of transparency. In these experiments, observers were required to separately match the transmittance and reflectance of a transparent filter. Observers viewed displays containing a central sine wave grating surrounded by a higher contrast sine wave grating of the same frequency, orientation, and phase. To enhance the perception of transparency, binocular disparity was added to the edges of the central patch, giving rise to a clear

percept of a homogeneous transparent filter lying on top of a high-contrast grating. Metelli's model predicts that the perceived transmittance of a transparent filter should only depend on the ratio of luminance differences (i.e., the luminance range) of the regions of transparency to the regions in plain view (see eqn [3]). In one of our experiments, the luminance range of the region in plain view (the high-contrast grating) and the luminance difference of the region of transparency was held constant; only the mean luminance of the region of transparency was varied. Observers adjusted the luminance range of a matching pattern to match the perceived transmittance of the transparent filter with varying mean luminance values. In this experiment, the luminance range of the region of transparency and the region in plain view are constant, so Metelli's equations predict that the transmittance settings in this experiment should be independent of mean luminance. This was not at all what was observed experimentally. Rather, observer's matches are very strongly dependent on the mean luminance of the transparent region (see Figure 2). In particular, observers significantly underestimate the transmittance of light filters, and systematically overestimate the transmittance of dark filters.

The results of this experiment reveal that human observers are not simply inverting the physics of transparency to compute the properties of transparent surfaces. The theoretical importance of this finding should not be underestimated, as one of the main theoretical views of visual processing assumes that the visual system extracts the properties of the world by performing computations that invert the image formation process. These results on the perception of transparency provide a striking example where human observers have a very clear sense of a surface property (the transmittance of a transparent layer) that almost always generates the physically incorrect answer. Why, then, does the visual system err in this manner? What information is the visual system using to compute these properties that causes it to give such incorrect responses? One of the main problems with Metelli's model is that it assumes that

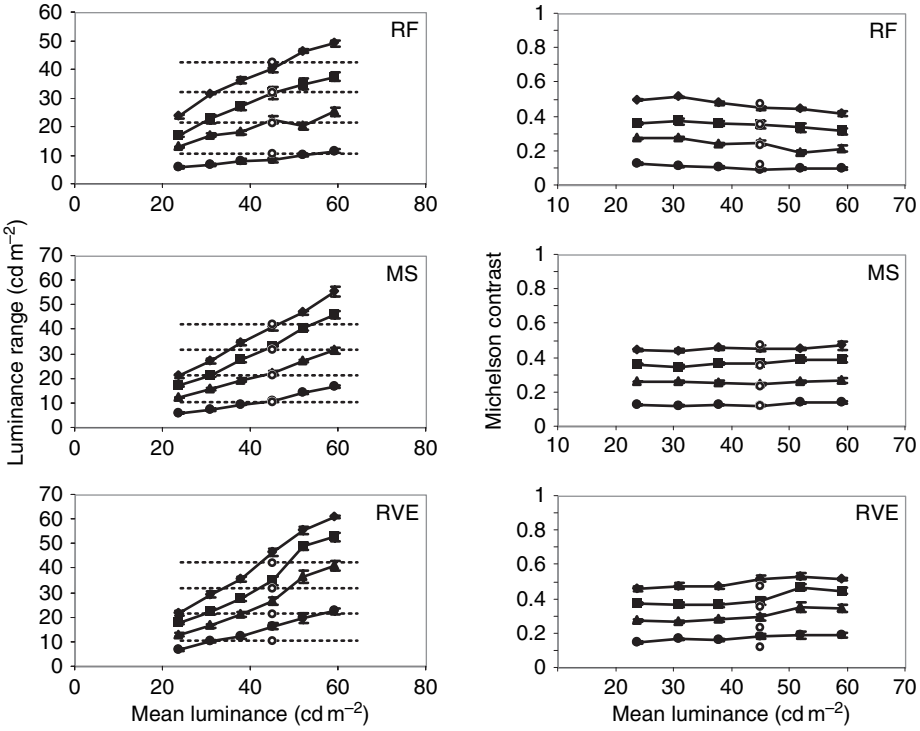

Figure 2 Results from the Singh M. and Anderson B. L. (2002) transmittance matching experiment for three observers (RF, RVE, and MS). Observers adjusted the perceived opacity of a matching pattern to the opacity of a target patch that varied in mean luminance. The open circles depict when the mean luminance of the target and match were identical; the dashed lines in the figure on the left correspond to the predictions of Metelli's model. The right-hand figure reveals that the data are independent of mean luminance when plotted in terms of Michelson contrast, showing that observers rely on contrast when matching the opacity of transparent filters.

transmittance is computed on the basis of the ratio of luminance differences between the regions of transparency and the regions in plain view. (Strictly speaking, Metelli's model is formulated on the basis of reflectance differences. However, Gerbino, W. *et al.* (1990) showed that Metelli's equations could be rewritten as difference in luminance values, and that the form of these equations were identical to eqns [1]–[4].) However, the earliest stages of cortex have little access to raw luminance values. Rather, the information about image structure seems to be largely transformed into a contrast code. Indeed, when the data from this experiment are plotted in terms of Michelson contrast, it becomes evident that the visual system uses contrast to scale the transmittance of a transparent surface, even though this yields the physically incorrect answer. In our sinusoidal displays, Michelson contrast provides a good measure of perceived contrast, so works well in accounting for perceived contrast in our displays. However, Michelson contrast fails to provide an adequate measure of contrast in more complex spatial patterns containing, for example, random patches of achromatic surfaces. Despite these shortcomings, recent work has shown that observer's transparency judgments can be well described by the perceived contrast of images (Robillotto, R. *et al.*, 2002; Robillotto, R. and Zaidi, Q., 2004), suggesting that transparency computations are indeed based on some measure of image contrast.

In sum, there is now clear evidence that the visual system uses the relative contrast of image regions to compute the opacity of transparent surfaces. In what follows, I will consider the implications that this discovery has had in understanding when the decomposition into a layered representation is initiated, and the consequences that this decomposition can have on not just the properties of the transparent surface, but the underlying surface as well.

2.14.2 Anchoring Perceived Transmittance

In addition to the quantitative failures of Metelli's model, it was also not easily generalized to a variety of naturally occurring forms of transparency. Metelli's model only described conditions of balanced transparency, that is, conditions where the transmittance and reflectance of the transparent layer is uniform. However, many naturally occurring forms of transparency – such as that induced by smoke and fog – are typically unbalanced, particularly in transmittance. Clearly, a more general framework is needed to understand the wide variety of ways that transparent surfaces and media can transform image structure. How does the visual system determine whether a scene is in plain view or viewed through a transparent layer or medium when the properties of the transparent layer vary continuously?

If image contrast is the currency through which the properties of transparent surfaces are computed, then any general theory of transparency perception will have to use image contrast as one of main ingredients in the computation of transparency. However, all natural scenes generate variations in image contrast, and the properties of the underlying surfaces are unknown. So how can the visual system determine whether a given image arose from a scene in plain view or a higher contrast scene viewed through a (contrast reducing) transparent layer? The image data is always consistent with both possibilities, so something is needed to understand how the visual system determines when transparency is and is not perceived. I have recently proposed that the visual system employs a transmittance anchoring principle to determine when transparency is (and is not) inferred (Anderson, B. L., 1999; 2003a). The intuitive content of this principle is that the visual system assumes the fewest surfaces necessary to account for the image data. More specifically, it states that the visual system treats the highest contrast region along surfaces and contours as transmittance anchors that are in plain view. All other contrast values along such contours and/or surfaces are compared to this anchor region, and decreases in contrast along surfaces are used to infer the presence of transparency. More specifically, this theory asserts that if there are reductions in contrast along surfaces or contours that are geometrically continuous, then scission is initiated and transparency is perceived. The magnitude of the contrast reduction is used to compute the transmittance of the overlying (transparent) layer (in proportion to this reduction; i.e., the greater the contrast reduction, the more opaque the transparent surface will appear). In the limit, where the contrast of the underlying surface goes to zero, the transmittance of the overlying surface goes to zero, and the near layer becomes an occluder. Note also that if a change in mean luminance occurs without a corresponding reduction in contrast, that such transformations are consistent with a change in illumination, and hence, would be correctly predicted to appear in plain view in both regions of the image.

Thus, the contrast relationships along surfaces and contours could be used to provide information about both transparent media and changes in illumination.

We have recently shown that this theory correctly predicts the perception of transparency in both balanced displays, as well as spatially inhomogeneous media (Anderson, B. L. *et al.*, 2006). In addition, we have shown that transmittance anchoring also has a temporal component: if the contrast of a texture is modulated in time, the highest contrast region in the spatiotemporal sequence is treated as a region in plain view, and the spatiotemporal reductions in contrast appear as the intrusion of transparent media. Thus, the transmittance anchoring principle appears to provide a foundation on which to predict when transparency is and is not perceived, and the perceived transmittance of the transparent layer.

2.14.3 Scission and the Perception of Lightness

The decomposition of an image region into multiple layers can also have a significant impact on perceived lightness. In the preceding, I have focused on how variations in image contrast can be used to determine whether transparent surfaces are present, and if so, how the opacity of the transparent layer is computed. However, when multiple surfaces are present along the same line of sight, the visual system must also compute properties of the underlying surface, such as its lightness. Given the close relationship between the physical transformations induced by transparent surfaces and the transformations induced by changes in illumination, there is good *a priori* reasons to suspect that a process of scission may play a critical role in the perception of surface lightness. Although a number of authors have suggested the possibility that scission may play a critical role in lightness perception (Anderson, B. L., 1997; Bergström, S. S., 1977; Gilchrist, A. L., 1977; 1979; Adelson, E. H., 1993), such authors have questioned whether an explicit decomposition actually underlies lightness perception. More recently, we have been developing a new paradigm that explicitly reveals the role that scission can play in the perception of surface lightness (Anderson, B. L., 1999; 2003a; 2003b; Anderson, B. L. and Winawer, J., 2005). Traditional lightness studies typically employ homogeneous targets to be judged and measure the effect different contexts have on their perceived lightness or brightness. In such paradigms, it can often be difficult to determine whether scission is occurring, and if so, whether it is playing any causal role in the perceived lightness of a figure. However, in the paradigm we have developed, if scission occurs, it is phenomenologically very explicit, and the effects it has on perceived lightness can be directly experienced.

To see the role that scission can play in lightness perception, consider the image depicted in Figure 3. This figure appears to contain white chess pieces viewed through dark smoke, and black chess pieces viewed through white fog. However, the image regions containing the chess pieces in the top and bottom of the image are actually absolutely identical; the only difference between the top and bottom images is the overall lightness of the surrounds. These images were carefully constructed to satisfy the constraints of transparency. In the top image, all of the boundaries separating the chess pieces from the surround are lighter inside the chess pieces than outside (so that the boundary separating the regions has the same contrast polarity), whereas the opposite polarity holds for the bottom figure. In addition to the shift in polarity between the top and bottom figure, there are also significant differences in the way the magnitude of contrast varies along the borders separating the chess pieces and their surrounds in the two images. Consider, for example, the king in the two images. In the top figure, the greatest

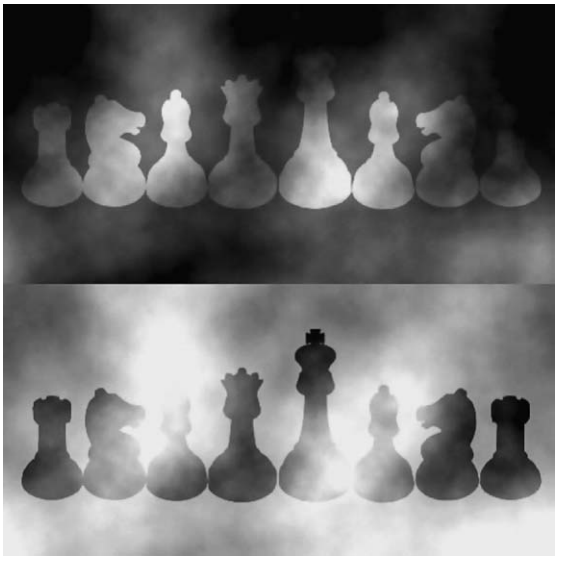

Figure 3 A figure demonstrating the role of scission on perceived lightness. The textures in the chess pieces on the top and bottom are identical; the only difference in the two images is the luminance distributions in the surrounds. From Anderson, B. L. and Winawer, J. 2005. Image segmentation and lightness perception. Nature 434, 79–83.

contrast between the king and the surround occurs along the bottom right of the piece, whereas the lowest contrast occurs along the top. Thus, the transmittance anchoring principle states that the bottom right of this figure should appear in plain view, which is white; whereas the reductions in contrast that occurs along the boundaries separating the king from its surround should signal the presence of a transparent medium that varies in opacity (being most opaque where the contrast of the boundary is lowest, which here, occurs along the top of the king). A similar analysis holds for the bottom figure, except now the polarity and magnitude relationships are reversed. In this image, the highest contrast region along the border separating the king from its surround occurs along its top, and hence, the transmittance anchoring principle predicts that this portion of the king (which is dark) should appear in plain view, and lower contrast regions along the contour should appear partially obscured by transparent media. In the bottom image, the lowest contrast region of the king-surround border occurs along the lower right of the image, and thus, the opacity of the transparent layer should be greatest in this region. This is consistent with what observers report.

In sum, the perception of transparency and lightness in Figure 3 reveals the close relationship between the perception of transparency, occlusion, and lightness. The perception of transparency involves the decomposition of an image into multiple layers, and the properties of the layers depend critically on exactly how luminance is partitioned between them. There is a growing body of data suggesting that the contrast relationships that occur along surfaces and contours play a critical role in determining when scission is initiated, as well as determining how surface properties such as lightness and opacity are attributed to the layers that are formed when this decomposition occurs. Such results reveal severe limitations on inverse optics models of perception, since the computation of properties such as the transmittance of transparent surfaces are almost always physically incorrect. Moreover, there is currently no single measure of image contrast that adequately captures perceived contrast in arbitrary images, which impedes the ability to predict the precise conditions that lead to scission and the quantitative consequences that scission should have on perceptual experience. It is therefore of critical importance to develop a measure of contrast that actually captures the human experience of contrast, so that it can be used to develop and assess theories of transparency perception. Finally, although phenomena such as those depicted in Figure 3 reveal that scission can have a dramatic effect on perceived lightness, more research is needed to determine if an explicit decomposition of images into layers is responsible for the perception of lightness (and color) in all images.

References

Adelson, E. H. 1993. Perceptual organization and the judgment of brightness. Science 262, 2042–2044.

Anderson, B. L. 1997. A theory of illusory lightness and transparency in monocular and binocular images. Perception 26, 419–453.

Anderson, B. L. 1999. Stereoscopic surface perception. Neuron 26, 919–928.

Anderson, B. L. 2003a. The role of occlusion in the perception of depth, lightness, and opacity. Psychol. Rev. 110, 762–784.

Anderson, B. L. 2003b. The role of perceptual organization in White's illusion. Perception 32, 269–284.

Anderson, B. L. and Winawer, J. 2005. Image segmentation and lightness perception. Nature 434, 79–83.

Anderson, B. L., Singh, M., and Meng, J. 2006. The perceived opacity of inhomogeneous surfaces and media. Vision Res. 46, 1982–1995.

Bergström, S. S. 1977. Common and relative components of reflected light as information about the illumination, colour, and three-dimensional form of objects. Scand. J. Psychol. 18, 180–186.

Gerbino, W., Stultiens, C. I., Troost, J. M., and de Weert, C. M. 1990. Transparent layer constancy. J. Exp. Psychol. Human Percept. Perform. 16, 3–20.

Gilchrist, A. L. 1977. Perceived lightness depends on perceived spatial arrangement. Science 195, 185–187.

Gilchrist, A. L. 1979. The perception of surface blacks and whites. Sci. Am. 240, 112–123.

Kasrai, R. and Kingdom, F. 2001. Precision, accuracy, and range of perceived achromatic transparency. J. Opt. Soc. Am. A 18, 1–11.

Metelli, F. 1970. An algebraic development of the theory of perceptual transparency. Ergonomic 13, 59–66.

Metelli, F. 1974a. Achromatic Color Conditions in the Perception of Transparency. In: Perception: Essays in Honor of J. J. Gibson (*eds*. R. B. MacLeod and H. L. Pick), pp. 95–116. Cornell University Press.

Metelli, F. 1974b. The perception of transparency. Sci. Am. 230, 90–98.

Metelli, F., Da Pos, O., and Cavedon, A. 1985. Balanced and unbalanced, complete and partial transparency. Percept. Psychophys. 38, 354–366.

Robillotto, R. and Zaidi, Q. 2004. Perceived transparency of neutral density filters across dissimilar backgrounds. J. Vis. 4, 183–195.

Robillotto, R., Khang, B., and Zaidi, Q. 2002. Sensory and physical determinants of perceived achromatic transparency. J. Vis. 2, 388–403.

Singh, M. and Anderson, B. L. 2002. Perceptual assignment of opacity to translucent surfaces: the role of image blur. Perception 31, 531–552.

2.15 Three-Dimensional Shape: Cortical Mechanisms of Shape Extraction

G A Orban, K.U. Leuven Medical School, Leuven, Belgium

© 2008 Elsevier Inc. All rights reserved.

2.15.1	**Introduction**	247
2.15.2	**The Visual Ecology and Perception of Three-Dimensional Shape**	247
2.15.2.1	Orders of Depth	247
2.15.2.2	Cues for Three-Dimensional Shape and Stimuli	249
2.15.2.3	Human Perception of Three-Dimensional Shape	249
2.15.2.4	Monkey Perception of Three-Dimensional Structure	250
2.15.3	**The Extraction of Three-Dimensional Shape from Motion**	251
2.15.3.1	Single-Cell Studies	251
2.15.3.1.1	Area MT/V5	251
2.15.3.1.2	Beyond MT/V5	252
2.15.3.2	Human Imaging Studies	253
2.15.3.2.1	Human MT/V5+	253
2.15.3.2.2	V3A and parietal regions	256
2.15.3.2.3	Lateral occipital sulcus and ventral regions	257
2.15.3.2.4	Cue combination	257
2.15.3.3	Monkey Functional Magnetic Resonance Imaging Studies	257
2.15.3.3.1	MT/V5 and satellites	257
2.15.3.3.2	Other cortical regions	259
2.15.4	**The Extraction of Three-Dimensional Shape from Disparity or Stereo (Three-Dimensional SFS)**	262
2.15.4.1	Single-Cell Studies	262
2.15.4.1.1	Higher-order disparity selectivity in TEs, part of the inferotemporal complex	262
2.15.4.1.2	Exquisite coding of three-dimensional shape from disparity by TEs neurons	265
2.15.4.1.3	The invariance of three-dimensional shape selectivity in TEs	266
2.15.4.1.4	Selectivity of caudal intraparietal neurons for first-order disparity	267
2.15.4.1.5	Three-dimensional shape from disparity selectivity in other cortical regions	268
2.15.4.2	Imaging Studies	268
2.15.5	**Extraction of Three-Dimensional Shape from Static Monocular Cues**	268
2.15.5.1	Single-Cell Studies	268
2.15.5.2	Imaging Studies: Need for Two-Dimensional Shape Controls	269
2.15.6	**Conclusions**	269
References		270

Glossary

CIP caudal intraparietal region. Located posteriorly on the lateral bank of the intraparietal sulcus (IPS) in the monkey.

correspondence problem To determine for each pixel in the pattern of one eye the matching pixel of the pattern in the other eye.

DIPSA Dorsal intraparietal sulcus anterior region in humans: located rostrally in the parietal part of the IPS, near junction with postcentral sulcus. Located posterior to human anterior intraparietal (hAIP) and anterior to the dorsal intraparietal sulcus medial (DIPSM). Originally defined as a motion-sensitive region.

DIPSM Dorsal intraparietal sulcus medial region in humans: located caudally on the horizontal or parietal part of the IPS, rostral from the

parieto-occipito intraparietal sulcus (POIPS). Originally defined as a motion-sensitive region.

disparity Difference in position relative to the fovea of retinal images in the two eyes. The differences can occur in the horizontal and vertical directions. Given the horizontal separation between the two eyes, the horizontal disparity differs between points at different distance from the fixation point (which projects onto the fovea).

FST Fundus of the superior temporal region, another satellite of MT/V5 in monkeys.

functional magnetic resonance imaging (fMRI) Imaging technique visualizing the hemodynamic responses in different parts of the brain (typically in voxels a few millimeters on the side). In humans, fMRI uses the BOLD (brain oxygen level-dependent) effect based on the paramagnetic properties of hemoglobin. In monkeys, a contrast agent is used: MION (monocrystalline iron oxide nanoparticle) or a very similar product, Sinerem (Guerbet, France). While BOLD reflects three variables: blood volume and flow and oxygen extraction, MION depends only on blood volume. This latter signal is not only much stronger than the BOLD effect (a factor five), but also reaches a maximum in the middle cortical layers, while BOLD peaks in the most superficial layers.

hAIP Human homolog of monkey anterior intraparietal (AIP) region. Identified by grasping movements.

hMT/V5+ Human homolog of MT/V5, supposedly includes the homologs of the MT/V5 satellites (as indicated by the +).

ITG Inferior temporal gyrus (human cortex).

LOC Lateral occipital complex. Despite its name most of this object or two-dimensional (2D) shape processing region is located ventral and anteroventral to hMT/V5+.

LOS Lateral occipital sulcus region: shape processing region posterior to hMT/V5+, was originally included in the definition of lateral occipital complex (LOC), but subsequently removed.

MSTd Medial superior temporal region, dorsal part, satellite of MT/V5 in monkey.

MT Area in the monkey; originally defined as V5, located caudally in the lower bank of the superior temporal sulcus (STS).

OTS Occipitotemporal sulcus separates inferior temporal gyrus (ITG) from fusiform gyrus in humans.

POIPS Parieto-occipito intraparietal sulcus region in humans, located at the junction of parieto-occipital sulcus and intraparietal sulcus (IPS), dorsal from the ventral intraparietal sulcus (VIPS). Originally defined as a motion-sensitive region.

Stereogram Stimuli presented to the two eyes to produce an impression of depth. Random-dot stereograms (RDSs) were introduced to study stereoscopic processing without contamination of edges or shape. Part of the pixels in the random-dot pattern of one eye is moved laterally over a small distance in the pattern of the other eye to induce a horizontal disparity. Thus, in a RDS each pixel of the random-dot pattern in one eye has a match in that of the other eye. When the pixels in the pattern of one eye are reversed in contrast all pixels in one eye are matched by one of opposite contrast in the other eye, yielding an anticorrelated RDS. If the pixels of the pattern of eye have a random relationship to those of the pattern in the other eye, the RDS is decorrelated. The coherence of the RDS is manipulated by changing the percentage of pixels that have a match in the other eye: a standard RDS has 100% coherence, a decorrelated RDS has 0% coherence.

TEs Small part of TE, the anterior part of the inferotemporal cortex, located in the lower bank of the superior temporal sulcus (STS) of the monkey.

Tilt and slant Basic parameters of three-dimensional (3D) surface orientation: tilt is the direction in which the surface is angled away from the frontoparallel plane (or equivalently the orientation of the axis around which the surface has been rotated) and the slant indicates how much it is angled away from the frontoparallel surface.

VIPS Ventral intraparietal sulcus region in humans, located in the bottom of the occipital part of the IPS, just dorsal of V3A. Originally defined as a motion-sensitive region.

2.15.1 Introduction

For years the combination of single-cell recording and psychophysics were considered the golden avenue to unravel sensory processing (LaMotte, R. H. and Mountcastle, V. B., 1975; Westheimer, G., 1979). This led to a number of studies in awake monkeys, in which, for a given stimulus dimension, perceptual performance, usually a discrimination threshold, was compared to single-cell encoding performance. Well-known examples are coarse and fine direction discrimination (Britten, K. H. *et al.*, 1992; Purushothaman, G. and Bradley, D. C., 2005), fine orientation discrimination (Vogels, R. and Orban, G. A., 1990), or disparity discrimination (Uka, T. and DeAngelis, G. C., 2003). Some of these studies have pursued the parallelism beyond the simple encoding of a stimulus dimension, investigating the neuronal basis of cognitive components of discrimination tasks such as decision processes (Shadlen, M. N. and Newsome, W. T., 2001) or temporal comparison of successive stimuli (Orban, G. A. and Vogels, R., 1998). These studies relied on anatomy to pinpoint the successive steps of processing to be investigated with single-cell recording. The correct choice is far from evident as most cortical regions project to many target areas and selecting the one involved in a particular cognitive component of a task generally involves a great deal of guesswork. Hence, progress has been slow.

Direct study of the sensory processing in the human brain became possible in the early 1990s with the development of functional magnetic resonance imaging (fMRI). This technique visualizes the cortical regions engaged by discrimination tasks (Sunaert, S. *et al.*, 2000; Faillenot, I. *et al.*, 2001; Shikata, E. *et al.*, 2001; Claeys, K. *et al.*, 2004), or even regions simply involved in the passive processing of different visual stimuli (Tootell, R. B. *et al.*, 1995; Hadjikhani, N. *et al.*, 1998; Sunaert, S. *et al.*, 1999; Bartels, A. and Zeki, S., 2000; Kourtzi, Z. and Kanwisher, N., 2000; Backus, B. T. *et al.*, 2001; Denys, K. *et al.*, 2004). Furthermore, with the advent of fMRI in awake monkeys (Vanduffel, W. *et al.*, 2001; Nakahara, K. *et al.*, 2002), direct links can be established between human fMRI and single-cell studies in the monkey. First, comparing fMRI responses in the two species allows the investigator to advance the question of homology, or at least functional equivalence, between cortical regions in the two species. Second, comparing the fMRI responses and the single-cell responses in the awake monkey allows derivation of the fMRI signature of the neuronal property under investigation, or the reverse. The macroscopic view provided by monkey fMRI is a useful complement to the detailed description of the activity of a single neuron, out of the billions of neurons contributing to a given function, provided by single-cell recording. In fact, the monkey fMRI technique represents a golden scouting opportunity for finding cortical areas engaged in a given type of processing. These areas can then be targeted by more specific, but also more labor-intensive techniques, such as single-cell recording, electrical stimulation, or inactivation studies. This promises to accelerate the progress of monkey studies.

The triad of systems neuroscience techniques – single-cell recording and fMRI in awake monkey and human fMRI – has been applied to the question of extracting three-dimensional (3D) shape from the motion cue. Hence this chapter endeavors, for the first time, to integrate the results from the three techniques addressing the same question. Although efforts have also been directed towards the extraction of 3D shape from other cues such as stereo, texture, and shading (Janssen, P. *et al.*, 2002; Tsutsui, K. *et al.*, 2002; Georgieva, S. *et al.*, 2003a; 2003b; 2005; Durand, J. B. *et al.*, 2007), less progress has been achieved so far. Hence, the overview will have to be much more limited for these other cues.

2.15.2 The Visual Ecology and Perception of Three-Dimensional Shape

2.15.2.1 Orders of Depth

Although the processing of depth and 3D shape has a common origin in the loss of the third dimension at the level of retinal transduction and is based on similar cues, these two perceptual aspects have to be sharply distinguished. Depth is a property of space and 3D shape a property of objects. In order to distinguish 3D-shape processing from simple depth processing, it is useful to remember the different orders of depth (Figure 1). Zero-order depth corresponds to fronto-parallel planes at different distances from the observer or from the fixation plane. For the disparity cue this corresponds to a stimulus with constant disparity, provided the stimuli are sufficiently small and sufficiently close to the median plane (Howard, I. P. and Rogers, B., 2002). While absolute disparity references a fronto-parallel plane to the fixation point, relative disparity (Howard, I. P.

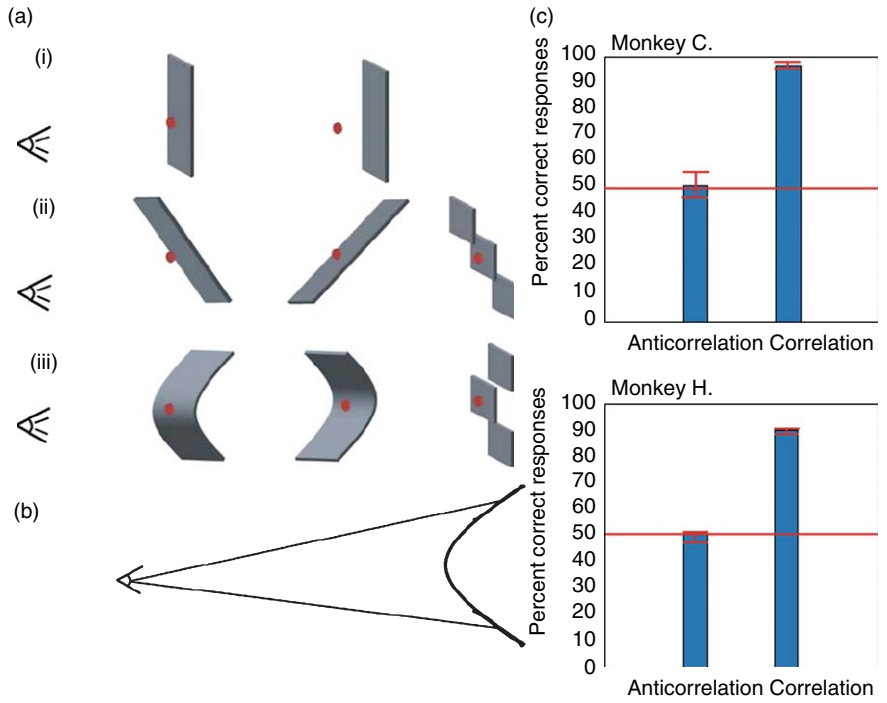

Figure 1 Orders of depth and monkey perception. (a) 3D surfaces (side view) at different positions from the fixation point (red dot), seen from the left (eye icon) portraying variations in different depth orders: zero order (i), first order (ii) and second order (iii). Approximations by zero order are indicated in (b) and (c). Notice that in the first and second-order disparity stimuli presented on computer screens, disparity also changed in discrete steps, but these steps were very small (2 minarc). (b) Viewing of curved surface with an indication of tilted planes (dark lines) giving rise to disparity gradients. (c) Percent correct responses of monkeys C and H for distinguishing between convex and concave surfaces in anticorrelated RDS and correlated RDS. With kind permission from Orban, G. A., Janssen, P., and Vogels, R. 2006b. Extracting 3D structure from disparity. Trends Neurosci. 29, 466–473.

and Rogers, B., 1995) references it to another reference plane in depth. First-order depth refers to planar surfaces tilted in depth; for disparity this corresponds to a linear gradient of disparity. For motion it corresponds to a linear gradient in speed (Gibson, J. J., 1950), for texture to gradients in size, foreshortening, and density (Hillis, J. M. *et al.*, 2004). Finally, second-order depth corresponds to surfaces curved in depth, for example, a surface with a constant, nonzero value of the second-spatial derivative of disparity. This second derivative can be taken in either the horizontal or vertical direction, yielding a horizontally or vertically curved surface, respectively. Again, for motion and texture, curvature in depth corresponds to second-order derivatives in speed or any of the three texture cues. Note that a higher-order depth input can be approximated by steps in a lower-depth order.

In the case of disparity it is well known that the second-spatial derivative is independent of the distance from the observer (Figure 1) and hence is an intrinsic property of the object (Rogers, B. and Cagenello, R., 1989). First-order disparity can either be intrinsic to an object that is bound by tilted planes, or extrinsic as it can represent the overall orientation of an object in space. Thus second-order depth, and to some extent first-order depth, capture rather well local aspects of 3D shape (Koenderink, J. J., 1990), but more global aspects also contribute to 3D-shape processing especially from texture and shading (Todd, J. T., 2004; Todd, J. T. *et al.*, 2005).

At this point it is worth remembering that 3D structure can also be a property of the visual environment, something sometimes referred to as the 3D layout of the environment. This 3D structure of the visual scene is a critical aspect for, for example, walking or climbing. Since most of the stimuli used in the reported investigations were relatively small, they relate mainly to processing of the 3D shape of objects. This latter processing is critical for grasping and manipulating objects (Watt, S. J. and Bradshaw, M. F., 2003) and in some instances for identification

or categorization (e.g., balls vs. disks). Thus in this review 3D structure is the more general term. For small stimuli, 3D structure and 3D shape will be used interchangeably.

2.15.2.2 Cues for Three-Dimensional Shape and Stimuli

The main cue for 3D shape is the stereo cue which allows the complete recovery of 3D shape including its sign (convex vs. concave curvatures). This cue can be carried by surfaces or edges. Examples of the latter are the images of elongated objects tilted or curved in depth (Sakata, H. *et al.*, 1998) as well as the multiple connected random lines, images of wireframe objects or paperclips (Edelman, S. and Bülthoff, H., 1992; Orban, G. A. *et al.*, 1999). In experimental settings, surfaces in depth are frequently portrayed by random-dot stereograms (RDS, Julesz, B., 1971). Given the two-dimensional (2D) shape selectivity of most IT neurons (Gross, C. G. *et al.*, 1972) we (Janssen, P. *et al.*, 1999) have frequently used a special type of random stereogram enclosed in a 2D shape. Such bounded surfaces can be characterized by a texture inside the boundary and the boundary, both of which carry depth information. So-called solid figure stereograms (Shikata, E. *et al.*, 1996), by contrast, only carry depth information at the boundaries.

Motion is also a potent cue for 3D structure (Gibson, J. J., 1950). When the observer is moving the motion parallax will provide information about the layout of the environment (Rogers, B. and Graham, M. E., 1979). When the observer is stationary different parts of a moving object will move at different speeds if they are at different distances from the eye. Both aspects of linear motion parallax can be unified in optic flow, which arises from the relative movement between the observer and the environment and provides not only information about motion of the observer or the environment but also about the 3D layout of the environment. Linear parallax differs from another type of motion parallax: the kinetic depth effect (Wallach, H. and O'Connell, D. N., 1953), in which vivid 3D structure is perceived when portraying an object that rotates around a frontal axis.

3D shape can also be recovered from a wide range of cues other than motion and disparity (Norman, J. F. *et al.*, 2004), such as occlusion, shading, and specular highlights, as well as texture. Shading and texture require surface stimuli either bounded surfaces, that is, portraying objects, such as the randomly deformed spheres introduced by Todd J. T. *et al.* (1997), or unbounded surfaces, that is, portraying the environment. Occlusion characterizes, by definition, bounded surfaces, including silhouettes. In edge-type stimuli, static monocular cues include perspective for the first-order case and closure based on T-junctions, portraying a volume, for example, a polyhedron, bounded by edges (Orban, G. A. *et al.*, 1999) for the second-order case.

2.15.2.3 Human Perception of Three-Dimensional Shape

Stereo and motion are two powerful cues for 3D shape perception. Motion sequences with three or more views and binocular displays with both horizontal and vertical disparities allow in theory a complete and unambiguous determination of the object 3D shape. Stereo does specify the sign of the curvature (convex and concave). Motion, however, does so under perspective projection, but not under orthographic projection (Braunstein, M. L., 1977). The neuronal processing of these two cues is quite distinct. This probably explains why humans are more sensitive for stereo than for motion parallax in detecting corrugations in depth (Rogers, B. J. and Graham, M. E., 1979; Bradshaw, M. F. and Rogers, B. J., 1999). Texture is a less powerful cue for 3D shape and the shading cue has strong inherent limitations (Belhumeur, P. N. *et al.*, 1999). Yet all of these cues allow fine distinction to be made between different shapes (Norman, J. F. *et al.*, 2004). In particular, these four cues, including shading, allow sensitive distinctions between different values of the shape index (Figure 2), provided the visual information is presented in patches of at least 3–4° in diameter (Phillips, F. and Todd, J. T., 1996). This index, based on the ratio of curvatures along two orthogonal lines, captures the local 3D shape (Howard, I. P. and Rogers, B. J., 2002). Further studies have shown that at a more local level (around a point of the surface) curvedness and shape index may not be represented independently, while slant and tilt are (Norman, J. F. *et al.*, 2006).

Three cues – stereo, motion, and texture – support qualitatively correct 3D shape perception: the perceived 3D shape correlates with the 3D shape of the depicted surfaces (e.g., Sperling, G. *et al.*, 1990 for the motion cue). Correlations are also high between observers or across multiple sessions of a given observer. Thus observers correctly perceive the pattern of

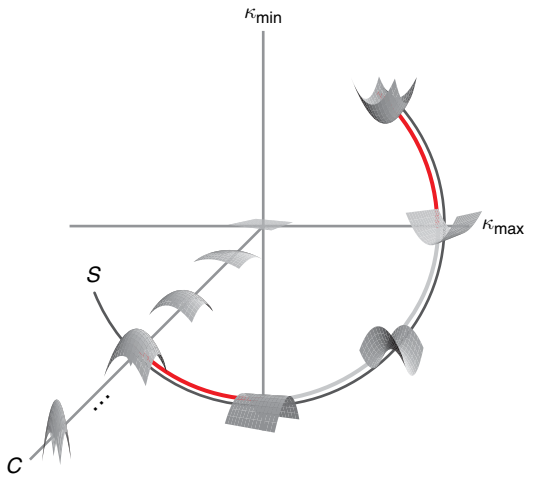

Figure 2 Shape index (S) and curvedness (C) defined from two orthogonal single curvatures (κ_{min} and κ_{max}). With kind permission adapted from Norman, J. F., Todd, J. T., Norman, H. F., Clayton, A. M., and McBride, T. R. 2006. Visual discrimination of local surface structure: slant, tilt, and curvedness. Vision Res. 46, 1057–1069.

concavities and convexities of 3D objects. Yet, there is mounting evidence that the metric aspect of 3D shape is not well perceived. Even for motion and disparity cues, the 3D shape perceived is different from the physically specified structure (the slope of the line expressing perceived depth as a function of veridical depth is significantly different from unity) and varies considerably depending on experimental conditions (Todd, J. T. and Norman, J. F., 2003). For motion or stereo the amount of perceived depth or magnitude of the relief deviates from the real values by up to 30–40% and this deviation depends on distance or the task. For the less powerful texture cue (Todd, J. T. *et al.*, 2004) the magnitude of the relief is strongly underestimated (up to 75%). Thus the processing of these three cues allows the building of a representation of 3D shape that is correct up to a stretch factor, that is, one that is related to the real 3D shape by an affine stretch transformation. The representation built up from the shading cue is of a different nature, however, since the correlation of perceived shape between observers or between tasks for a given observer can be close to zero. Subsequent analyses have revealed that most of the perceptual variance could be removed by an affine shearing transformation in depth rather than a simple stretching (Koenderink, J. J. *et al.*, 2001).

The obvious answer to the lack of reliability of single cues is to combine their information. But even under conditions where the full complement of cues is available, the metric structure is still perceived inaccurately (Todd, J. T. and Norman, J. F., 2003). This raises the issue whether the cues are combined at all. Recent studies (Knill, D. C. and Saunders, J. A., 2003; Hillis, J. M. *et al.*, 2004) have indeed indicated that at least for slant judgments, cues are combined according to an optimal rule which follows Bayses' rule: the cues are weighted according to their reliability. Similar combination rules have also been demonstrated for judgments combining inputs from different senses (Ernst, M. O. and Banks, M. S., 2002). Not only are 3D shape cues combined, it has been argued that within the sense of vision, the fusion of cues is mandatory and that individual cues cannot be accessed by perception (Hillis, J. M. *et al.*, 2002). This would imply that at higher levels, 3D shape is represented in a cue invariant manner.

2.15.2.4 Monkey Perception of Three-Dimensional Structure

Since many of the studies reviewed involve monkeys rather than human subjects, it is important to ascertain whether or not monkeys perceive 3D shape from the various cues and how similar their perception is to that of human subjects.

Siegel R. M. and Andersen R. A. (1988; 1990) provided evidence that monkeys perceived 3D structure from motion (SFM) and that their perception is relatively similar to that of humans. They used a task in which subjects have to signal the change from an unstructured to a structured display, where structure can be an optic flow component (expansion, or rotation) or 3D shape. Reaction times were longer and the amount of structure needed was larger for the 3D shape than the flow components suggesting more complex processing was necessary for performing the 3D task. This conclusion was also supported by the longer point lifetime (timepoint remains visible) and the larger number of points in the display required in the 3D task. These lifetime and number-of-points thresholds were relatively similar for the two species. The stimulus used in this 3D task, a rotating transparent cylinder, was also used in another task, sometimes referred to as a 3D shape discrimination task (Bradley, D. C. *et al.*, 1998; Dodd, J. V. *et al.*, 2001). The stimulus is bistable, given the ambiguity of motion parallax, and the monkey simply has to indicate whether the dots on the front surface appear to move to the right or left. While this task requires the distinction between two surfaces in depth it is not clear whether it requires analysis of

the shape of the front or back surfaces. Hence, it is more correctly considered an order in depth task (Born, R. T. and Bradley, D. C., 2005).

Monkeys can make a distinction between convex and concave 3D surfaces specified by disparity (Figure 1; Janssen, P. *et al.*, 2003). This judgment depends on stereo coherence just as in humans (Liu, Y. *et al.*, 2002). As in humans, this perception vanishes when correlated stereograms are replaced by anticorrelated (see Glossary) stereograms (Figure 1; Janssen, P. *et al.*, 2003).

Finally, there is also indirect evidence that monkeys perceive 3D shape from texture. After training in matching two stereo-specified planar 3D surfaces, monkeys can match a texture-specified slanted planar surface with a stereo-specified surface (Tsutsui, K. *et al.*, 2002). Similarly, monkeys trained to distinguish convex from concave surfaces specified by both stereo and texture can make similar distinctions when the stereo cue reliability is strongly compromised by reducing its coherence. However, the discrimination performance, while significantly different from random choice, was relatively weak and much lower (in % correct) than that of humans (Liu, Y. *et al.*, 2002).

2.15.3 The Extraction of Three-Dimensional Shape from Motion

The extraction of 3D SFM has been studied at multiple levels in the monkey using single-cell recording and fMRI. Furthermore the same fMRI paradigms have been used in humans and awake monkeys allowing direct functional comparison. We will follow the historical order in which the relevant experiments were performed, starting with single-cell recording.

2.15.3.1 Single-Cell Studies

Most studies have used linear speed gradients, the direction of which corresponds to the tilt of a 3D surface (direction in which a 3D surface is angled away from a fronto-parallel plane). In MT/V5 studies these gradients have been superimposed onto fields of translating dots, in medial superior temporal dorsal part (MSTd) studies onto flow components.

2.15.3.1.1 Area MT/V5

Initially, two alternative views have been proposed as mechanisms for the detection of speed gradients: hotspots in the receptive field (RF) itself (Treue, S. and Andersen, R. A., 1996) or a surround-based mechanism (Xiao, D. K. *et al.*, 1995). Subsequent work has indicated that the main mechanism is surround based. In anesthetized monkeys, about 50% (27/57) of MT/V5 neurons were selective for the direction of the speed gradient (Figure 3) and different neurons were tuned to different tilts (Xiao, D. K. *et al.*, 1997a). This tilt selectivity critically depended on the surround since all of the selective neurons had antagonistic surrounds and the selectivity was strongly reduced when the surround was masked (Figure 3). Further studies (Xiao, D. K. *et al.*, 1997b) showed that the majority of MT/V5 neurons have nonhomogeneous antagonistic surrounds, as predicted by computational models (Baracas, G. T. and Albright, T. D., 1996; Gautama, T. and Van Hulle, M. M., 2001). Figure 4 illustrates the stimuli used to map the excitatory RF (ERF, A), to unmask the presence of a surround (spatial summation test, B) and to map the spatial distribution of the surround effects either coarsely (in one of eight directions around the ERF, C) or in detail (same spacing as excitatory mapping, D). The neuron in Figure 4 had a strong surround effect (F) which arose from an antagonistic region located above the ERF (G and H). Such unimodal surrounds allow the neuron to compute a spatial derivative of speed (thus a gradient) provided the inhibitory surround influence is itself speed dependent. In many MT/V5 neurons this is indeed the case, as shown in Figure 5. This MT/V5 neuron had a strongly asymmetric surround but only when the stimuli in the surround moved at the same or faster speed than the dots moving over the ERF.

These studies in anesthetized monkeys have been replicated recently by Nguyenkim J. D. and DeAngelis G. C. (2004) in awake monkeys by using large stimuli involving the surround, similar to those used by Xiao D. K. *et al.* (1997a). These authors confirmed the selectivity of MT/V5 neurons for speed gradients (Figure 6) and provided an important control test: the selectivity for the speed gradient is invariant with respect to the average speed in the display. Furthermore, they showed that MT/V5 neurons are frequently selective for disparity gradients and occasionally even texture gradients, but to a lesser degree than for speed gradients. Furthermore, the selectivity for the three cues combined reflected largely that for the speed gradients (Nguyenkim, J. D., personal communication). Although the optimal tilt for the different gradients was not always congruent, Nguyenkim J. D. and DeAngelis G. C. (2004) obtained evidence for increased selectivity when cues were combined.

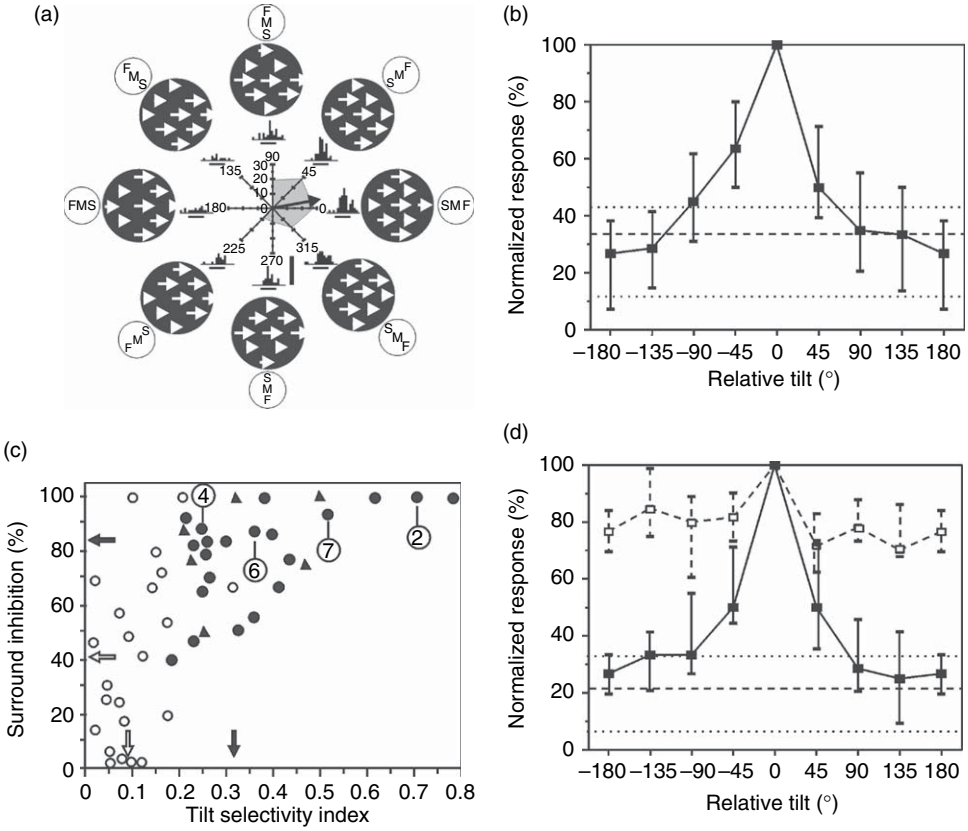

Figure 3 Selectivity of MT/V5 neurons for speed gradients corresponding to tilt in depth of 3D planar surfaces. (a) Tuning of neuron 8228 plotting net firing rate as a function of tilt direction. For each tilt the poststimulus time histogram (vertical bar 50 spikes s^{-1}) and speed gradient is shown pictorially or schematically (S, slow; M, medium; F, fast). (b) Average tuning for 27 selective neurons. (c) Plot of surround strength (in %) as a function of selectivity for tilt (SI): filled symbols, selective neurons; arrows, medians for selective (filled) and nonselective (open) neurons; numbers refer to example neurons in Xiao D. K. *et al.* (1997a). (d) Tuning curve of seven selective neurons with surround in view (full lines) or masked (dotted lines). In (b) and (d) the horizontal lines indicate the median and quartiles of responses to a fronto-parallel surface of same size as gradients (25.6°). With kind permission from Xiao, D. K., Marcar, V. L., Raiguel, S. E., and Orban, G. A. 1997a. Selectivity of macaque MT/V5 neurons for surface orientation in depth specified by motion. Eur. J. Neurosci. 9, 956–964.

The selectivity of MT/V5 neurons for disparity gradients might similarly be surround based as MT/V5 neurons also have surround effects in the disparity domain (Bradley, D. C. and Andersen, R. A., 1998). Nguyenkim J. D. and DeAngelis G. C. (2003), however, provided evidence that they rather arose from heterogeneities in the RF. This latter finding further suggests that the selectivity for disparity gradients does reflect spatial variations in position disparity rather than orientation disparity. That the gradient selectivity for disparity arises from the RF, while that for speed arises from interaction between the surround and the RF might reflect the difference in coding of speed and disparity at this level. Speed tuning of MT/V5 neurons is rather coarse (Maunsell, J. H. R. and Van Essen, D. C., 1983a; Lagae, L. *et al.*, 1993; Priebe, N. J. *et al.*, 2003) while that of disparity is finer (Maunsell, J. H. R. and Van Essen, D. C., 1983b; DeAngelis, G. C. and Uka, T., 2003). Hence, to capture a given value of a gradient a larger distance may be required for speed than disparity, explaining the need to resort to RF surround interactions to extract speed gradients.

Finally, one study reported an impairment of SFM perception after lesion of MT/V5 (Andersen, R. A. *et al.*, 1996), indicating that this area is a critical component of the 3D shape from motion extraction pathway.

2.15.3.1.2 Beyond MT/V5

Selectivity for speed gradients has also been documented in MSTd, a region receiving input from MT/V5 and which is know to process optic flow

(Ungerleider, L. G. and Desimone, R., 1986; Saito, H. *et al.*, 1986; Duffy, C. J. and Wurtz, R. H., 1991, Lagae, L. *et al.*, 1994; Graziano, M. S. *et al.*, 1994). Duffy C. J. and Wurtz R. H. (1997) noted that the speed gradients superimposed on flow components significantly affected the firing of MSTd neurons in awake monkeys. Sugihara H. *et al.* (2002) superimposed speed gradients onto rotatory flow, producing rotating planes with various 3D orientations. A substantial fraction (43/97) of MSTd neurons were selective for the tilt of the speed gradient. Selectivity for slant (the amount by which the 3D surface is angled away from the fronto-parallel plane) was also observed in nearly half the MSTd neurons.

In the anterior superior temporal polysensory (STPa) area, neurons are also selective for optic flow components (Anderson, K. C. and Siegel, R. M., 2005; Nelissen, K. *et al.*, 2006), and a fraction of them are selective for 3D SFM (Anderson, K. C. and Siegel, R. M., 2005). These authors used a transparent sphere similar to the hollow cylinder used in the perceptual experiments of Siegel R. M. and Andersen K. C. (1990). While this stimulus is characterized by second-order speed variations, it does not allow parameters describing the surface to be easily manipulated. A number of STPa neurons responded at the onset of 3D SFM and some of these were selective for the axis or rotation and were size invariant.

2.15.3.2 Human Imaging Studies

2.15.3.2.1 Human MT/V5+

It is generally accepted that human MT/V5+ (hMT/V5+) represents the homolog of monkey MT and its satellites, including MSTd (Zeki, S. *et al.*, 1991; Tootell, R. B. *et al.*, 1995; DeYoe, E. A. *et al.*, 1996; Orban, G. A. *et al.*, 2004). Hence, the single-cell results reviewed above predict that hMT/V5+ should be involved in extracting 3D SFM. This was the hypothesis tested by our initial imaging study (Orban, G. A. *et al.*, 1999). hMT/V5+ was indeed more active when subjects viewed rotating random lines portraying a 3D shape than when they saw the same lines translating at uniform speed. In fact, the dimensionality of structure and rigidity of the shape were manipulated independently in this experiment and the stronger magnetic resonance response to 3D compared to 2D structure held up for both rigid and nonrigid shapes (Figure 7). Several controls were performed, as illustrated in Figures 7(c)–7(e). hMT/V5+ activation by 3D SFM exceeded that of various 2D controls in which low-level motion factors such as speed or range of directions were manipulated, that of a 2D control to which attention of the subject was attracted and that evoked by a combination of 3D shape and motion (moving polyhedra, using the closure cue for 3D shape).

The rotating random-line stimuli used in Orban G. A. *et al.* (1999) still contained two perceptual aspects which both could have caused the hMT/V5+ activation: motion of the lines along 3D trajectories and a 3D shape. These two stimulus aspect are nondissociable in dynamic 3D SFM displays and, hence, we had to resort to an active experiment, in which we asked subjects to pay attention to one of the two aspects. Thus, in the Peuskens H. *et al.* (2004) study subjects faced randomly deformed 3D spheres rotating around near-vertical axes and made three same–different judgments: about the 3D shape, the axis of rotation (pattern of 3D motion), or the texture on the surface of the sphere (Figure 8). In addition, in two lower control conditions they detected the dimming of central or peripheral parts of the objects. hMT/V5+ was significantly more active when subjects made 3D shape or 3D motion judgments than when they made the texture judgments, indicating that hMT/V5+ is indeed processing features related to 3D shape, extracted from motion.

Finally, one could argue that the random-line stimuli were very different from the stimuli used in the single-cell studies (Xiao, D. K. *et al.*, 1997a). To ensure the generality of the hMT/V5+ activation by 3D SFM we (Orban, G. A. *et al.*, 2006a) again tested passive subjects with random lines portraying the sides of a randomly oriented cube and random dots portraying a sphere rotating around a vertical axis. In addition to dimensionality of structure (3D vs. 2D) and lines versus dots, we manipulated a third factor: transparency. hMT/V5 displayed a significant main effect for 3D compared to 2D structure in the 3×2 design, as well as in each of the four 2×2 subdesigns (for opaque and transparent surfaces, for dot and lines surfaces), confirming the generality of its engagement by 3D shape extraction (see also Vanduffel, W. *et al.*, 2002). This does not mean that these other factors had no effect on the activation of hMT/V5+ by 3D shape stimuli compared to 2D shapes. This differential activation was stronger for opaque than for transparent stimuli and also for random lines than random-dot stimuli (Figure 9).

The activation of hMT/V5+ by SFM was confirmed by Kriegeskorte N. *et al.* (2003) using a SFM stimulus (on-surface SFM) derived from a technique initially developed by Perotti V. J. *et al.* (1996): hMT/

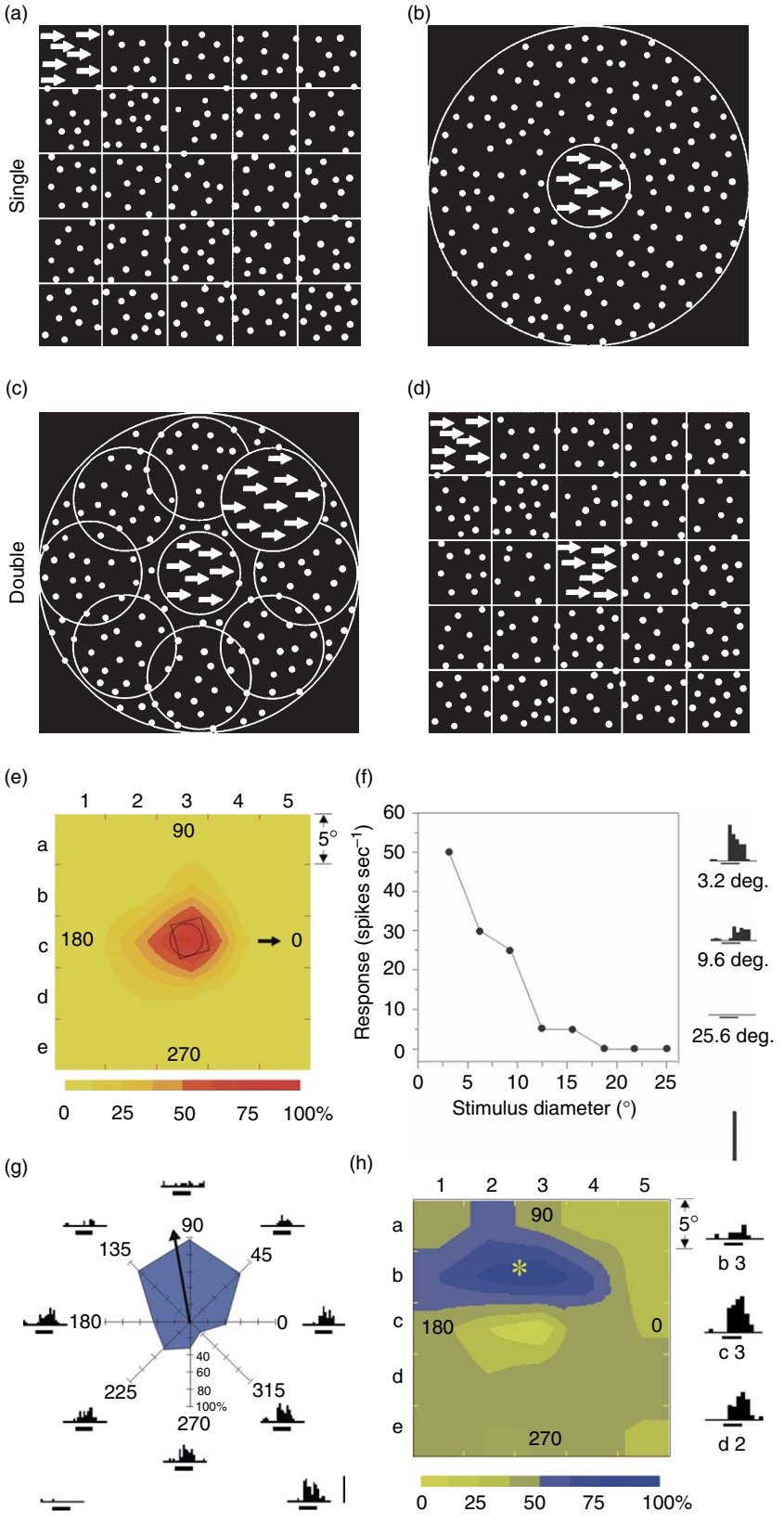
(a)
(b)
Single
(c)
(d)
Double
(e)
1 2 3 4 5
a
b
c
d
e
90
180
0
270
5°
0 25 50 75 100%
(f)
Response (spikes sec⁻¹)
60
50
40
30
20
10
0
0 5 10 15 20 25
Stimulus diameter (°)
3.2 deg.
9.6 deg.
25.6 deg.
(g)
90
135
45
180
0
225
315
270
40
60
80
100%
(h)
1 2 3 4 5
a
b
c
d
e
90
180
0
270
5°
b 3
c 3
d 2
0 25 50 75 100%

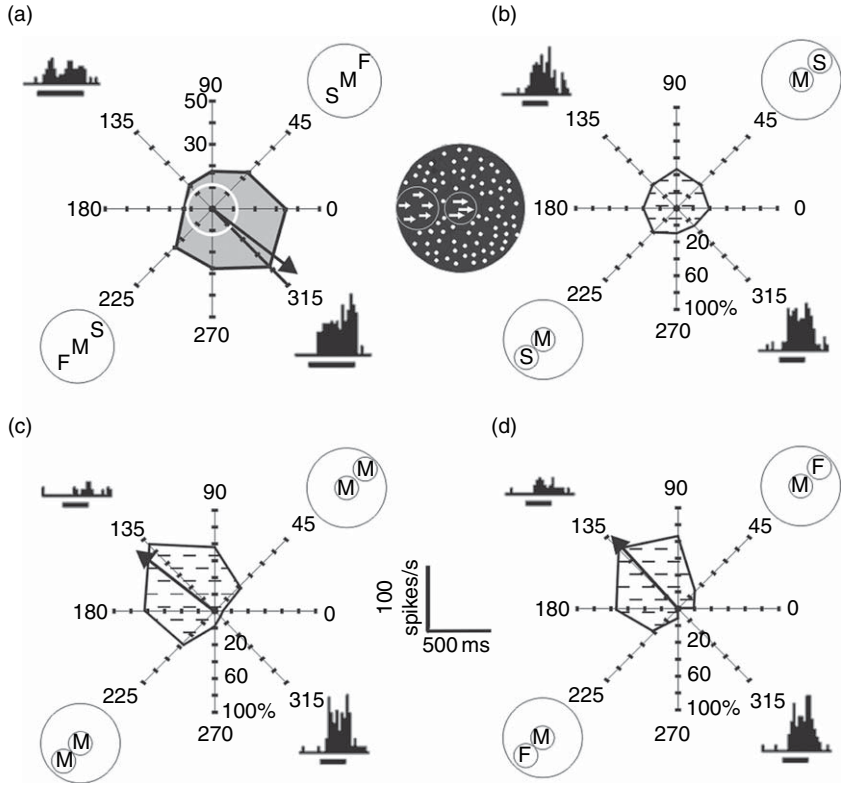

Figure 5 Speed dependence of surround effects in MT/V5 neurons. Tilt tuning of neuron 8207 (a) and the asymmetry of the surround tested at three relative speeds: slower than center (b), same speed as center (c), and faster than center (d). Same conventions as Figures 3 and 4; With kind permission from Xiao, D. K., Marcar, V. L., Raiguel, S. E., and Orban, G. A. 1997a. Selectivity of macaque MT/V5 neurons for surface orientation in depth specified by motion. Eur. J. Neurosci. 9, 956–964.

V5+ was significantly more active in on-surface SFM when the implicit object was moving (as in classical SFM) than when it was stationary, even if these two flow fields were extremely similar. This study also confirmed another conclusion drawn from our studies: stimulus differences affect the level of hMT/V5+ activation by SFM stimuli. These stimulus effects may explain why two studies (Paradis, A. L. *et al.*, 2000 and Murray, S. O. *et al.*, 2003) did not observe hMT/V5+ activation by SFM stimuli: both studies used transparent random-dots stimuli which are less effective in driving hMT/V5+. Furthermore, both used scrambled dots as a control rather than uniformly translating stimuli. Scrambled dots activate hMT/V5 much more than uniformly translating dots (Figure 9), because they contain many more motion directions. Their effect might be similar to flickering dots which also activate MT/V5+ strongly (Figure 7A). Had these flickering stimuli been used as controls rather than static stimuli, hMT/V5+ might never have been discovered!

These experiments show that hMT/V5+ is involved in the extraction of 3D shape from motion for a wide variety of displays, but the exact degree of the activation by 3D shape stimuli, relative to control stimuli, does depend on the particular stimulus conditions.

Figure 4 Asymmetry of surrounds of MT/V5 neurons. (a–d) Stimulus diagrams for 2D position test (a), spatial summation test (b), surround asymmetry test (c), and surround mapping test (d). Arrows indicate moving dots, surround mapping in C and D required two stimuli. (e–h) Results of the four tests for MT/V5 neuron 7916. (e, h) Color maps of excitation (red) and suppression (blue). In (f) and (g) response is plotted as a function of stimulus diameter (f) or test position of the stimulus in surround (g). In (f)–(h), sample peristimulus time histograms (PSTHs) are shown, including complete and no surround stimulation in (g). Arrow in (g) points to strongest suppression in surround which matches a similar indication by the asterisk in (h). With kind permission from Xiao, D. K., Raiguel, S., Marcar, V., and Orban, G. A. 1997b. The spatial distribution of the antagonistic surround of MT/V5 neurons. Cereb. Cortex 7, 662–677.

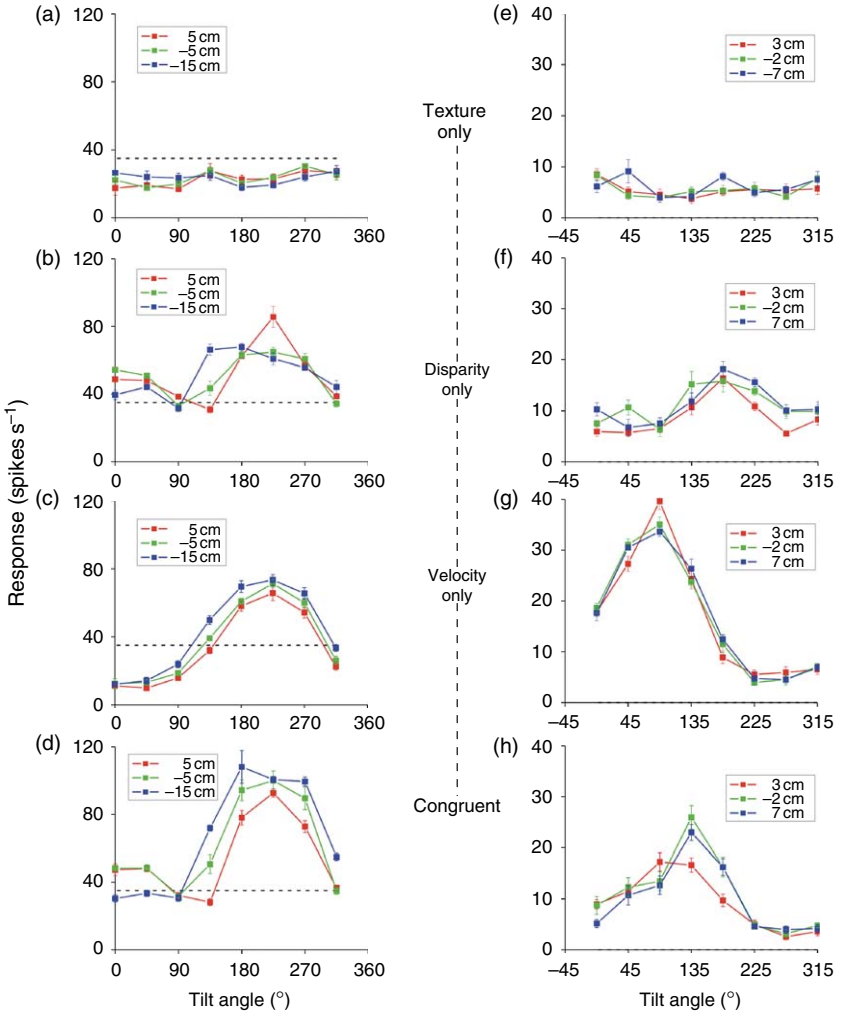

Figure 6 Tilt selectivity of two MT/VR neurons in awake monkey for three cues and their combination (Nguyenkim, J. D. and DeAngelis, G. C., 2004). Tilt tuning curves at three different mean depths (relative to fixation point, color coded) in the texture only condition (a and e), the disparity only condition (b and f), the speed only condition (c and g), and the congruent condition (d and h). The stimulus parameters for the neuron in a–d were: direction of motion 135°, speed of motion 32 cm s^{-1}, aperture diameter 24 cm, eccentricity 3.4 cm, slant 65°; for the neuron in (e)–(h): direction 0°, speed 8.4 cm s^{-1}, aperture diameter 28 cm, eccentricity 10.9 cm, slant 65°. At the distance from the screen used 1 cm = 1°. With kind permission from Nguyenkim J. D. (2005).

2.15.3.2.2 V3A and parietal regions

In each of the four studies (Orban, G. A. *et al.*, 1999; Vanduffel, W. *et al.*, 2002; Peuskens, H. *et al.*, 2004; Orban, G. A. *et al.*, 2006a) mentioned above, 3D SFM also engaged parietal regions near the intraparietal sulcus (IPS). In the passive experiments, V3A (referred to as transverse intraparietal sulcus (TRIPS) in Orban, G. A. *et al.*, 1999) and four IPS regions were activated by 3D SFM stimuli (Figure 10): the ventral intraparietal sulcus (VIPS) region in the occipital part of the IPS, just dorsal of region V3A; the parieto-occipito intraparietal sulcus (POIPS) region at the junction of the IPS and parietal occipital sulcus; the dorsal intraparietal sulcus medial (DIPSM) region (referred to as DIPSL in Orban, G. A. *et al.*, 1999), and the dorsal intraparietal sulcus anterior (DIPSA) region in the horizontal or dorsal part of IPS (for homology of these regions with macaque IPS regions see Orban, G. A. *et al.*, 2006a). These four parietal regions are also motion sensitive, just as hMT/V5+ is (Sunaert, S. *et al.*, 1999) and differ in the part of the visual field they represent: DIPSM and DIPSA represent the central visual field, POIPS the peripheral part, and VIPS both (Orban, G. A. *et al.*, 2006a). In the active experiment (Peuskens, H. *et al.*, 2004), DIPSM was active when subjects made same-different judgments about 3D shape, while DIPSA was active both when they made both

3D shape and 3D motion judgments. This latter activity was part of a wider, more anterior activation centered in the human anterior intraparietal (hAIP) region (Binkofski, F. *et al.*, 1999).

Parietal activations were also observed by Paradis A. L. *et al.* (2000), Murray S. O. *et al.* (2003), and Kriegeskorte N. *et al.* (2003). In fact, according to stereotaxic coordinates, the region defined as mid-lateral parietal cortex by Murray S. O. *et al.* (2003) and as IPS by Kriegeskorte N. *et al.* (2003) is close to DIPSA, underscoring its involvement in 3D SFM. The region near the occipito-parietal junction described by Paradis A. L. *et al.* (2000) might correspond to VIPS and POIPS which both respond relatively well to opaque random-dot 3D stimuli compared to scrambled dots (table 1 of Orban, G. A. *et al.*, 2006a).

2.15.3.2.3 Lateral occipital sulcus and ventral regions

Finally, a number of middle occipital and ventral, occipitotemporal regions are also engaged by 3D SFM. The activation of the region between V3/V3A and hMT/V5+, which we refer to as lateral occipital sulcus (LOS) (following the original Malach, R. *et al.*, 1995 study), was observed in all our passive and active studies (Orban, G. A. *et al.*, 1999; Vanduffel, W. *et al.*, 2002; Peuskens, H. *et al.*, 2004; Orban, G. A. *et al.*, 2006a). It may include the region referred to as SLO by Murray S. O. *et al.* (2003).

Some studies have indicated that ventral V3 might have been engaged by SFM: Vanduffel, W. *et al.* (2002), in which retiotopic regions were mapped, Orban G. A. *et al.* (1999), where it probably corresponds to the collateral sulcus region, and Paradis A. L. *et al.* (2000), who described a similar region as the occipitotemporal junction. The activation of V2 and V3 by 3D SFM might depend on the stimuli used, and was stronger with the random lines at right angles (Vanduffel, W. *et al.*, 2002) than at random angles (Orban, G. A. *et al.*, 1999, main experiment).

Finally subparts of 0LO complex might be engaged by 3D SFM, in particular the region immediately ventral to the hMT/V5+ complex (Figure 10). This region has been described as Fus/inferior temporal gyrus (ITG) in Orban G. A. *et al.* (1999), posterior ITG in Peuskens H. *et al.* (2004), and mid-occipitotemporal sulcus (OTS) in Orban G. A. *et al.* (2006a). It is a candidate region for cue convergence, as static monocular 3D shape cues also activate this region (Georgieva, S. *et al.*, 2003a; 2003b), as well as 3D structure from stereo (Figure 11) and tactile 3D shape cues (Amedi, A. *et al.*, 2001; James, T. W. *et al.*, 2002). Kriegeskorte N. *et al.* (2003) demonstrated a 3D SFM activation of the fusiform face area (FFA) when face stimuli but not when random stimuli were presented. This raises the possibility that other parts of lateral occipital (LO) might be activated by meaningful stimuli portrayed by 3D SFM. Alternatively, this 3D shape processing might be restricted to faces, as these seem to be processed in a separate manner (Kanwisher, N. *et al.*, 1997; Tsao, D. Y. *et al.*, 2006).

2.15.3.2.4 Cue combination

Most 3D shape imaging studies have so far used single cues. A notable exception is Welchman A. E. *et al.* (2005), who studied the combination of disparity and perspective cues in slant. These authors report specific effects of cue combination in hMT/V5+ and lateral occipital complex (LOC). The rebound from adaptation effects were larger for the two cues combined than for single cue. Although the interpretation of fast adaptation magnetic resonance techniques is far from straightforward (Sawamura, H. *et al.*, 2006), this might indicate greater selectivity for combined cues. We have observed negative interactions between 3D shape cues: the differential effect of 3D SFM was larger for 2D stimuli than for 3D shape stimuli whether the 3D shape was created by the closure cue, as in the Orban G. A. *et al.* (1999) control experiment (Figure 7F) or by disparity (Figure 7F; Figure 11). This reduced activation is compatible with narrower tuning curves, that is, stronger selectivity. Interestingly, this effect disappeared when the two cues were in conflict (Figure 7F).

2.15.3.3 Monkey Functional Magnetic Resonance Imaging Studies

2.15.3.3.1 MT/V5 and satellites

The three fMRI studies using monkeys that have investigated the monkey cortical regions engaged in 3D SFM (Sereno, M. E. *et al.*, 2002; Vanduffel, W. *et al.*, 2002; Nelissen, K. *et al.*, 2006), all three report a strong activation of MT/V5 and the fundus of the superior temporal (FST) by 3D shape from motion stimuli compared to various controls. In particular, the MT/V5 3D SFM activation (Figure 12) has been obtained in a large number of animals (>10 monkeys), for a wide range of stimulus conditions (different types of random lines, random-dots surfaces) and in different animal states (anesthetized and awake monkeys, various levels of attention to the fixation target). This MT/V5 activation is therefore a robust link between the single-cell studies (Xiao, D. K. *et al.*, 1997a; Nguyenkim, J. D. and

DeAngelis, G. C., 2004) and the human activation of the MT/V5 complex (Orban, G. A. *et al.*, 1999; Vanduffel, W. *et al.*, 2002; Kriegeskorte, N. *et al.*, 2003), even if the exact same stimuli have yet to be tested in the two types of experiments.

In general, the hMT/V5 complex is described as including the homologs of the MST subparts, but in the case of 3D SFM it is important to stress the inclusion of the FST homolog in the complex. It is unclear why so little MSTd activation by 3D

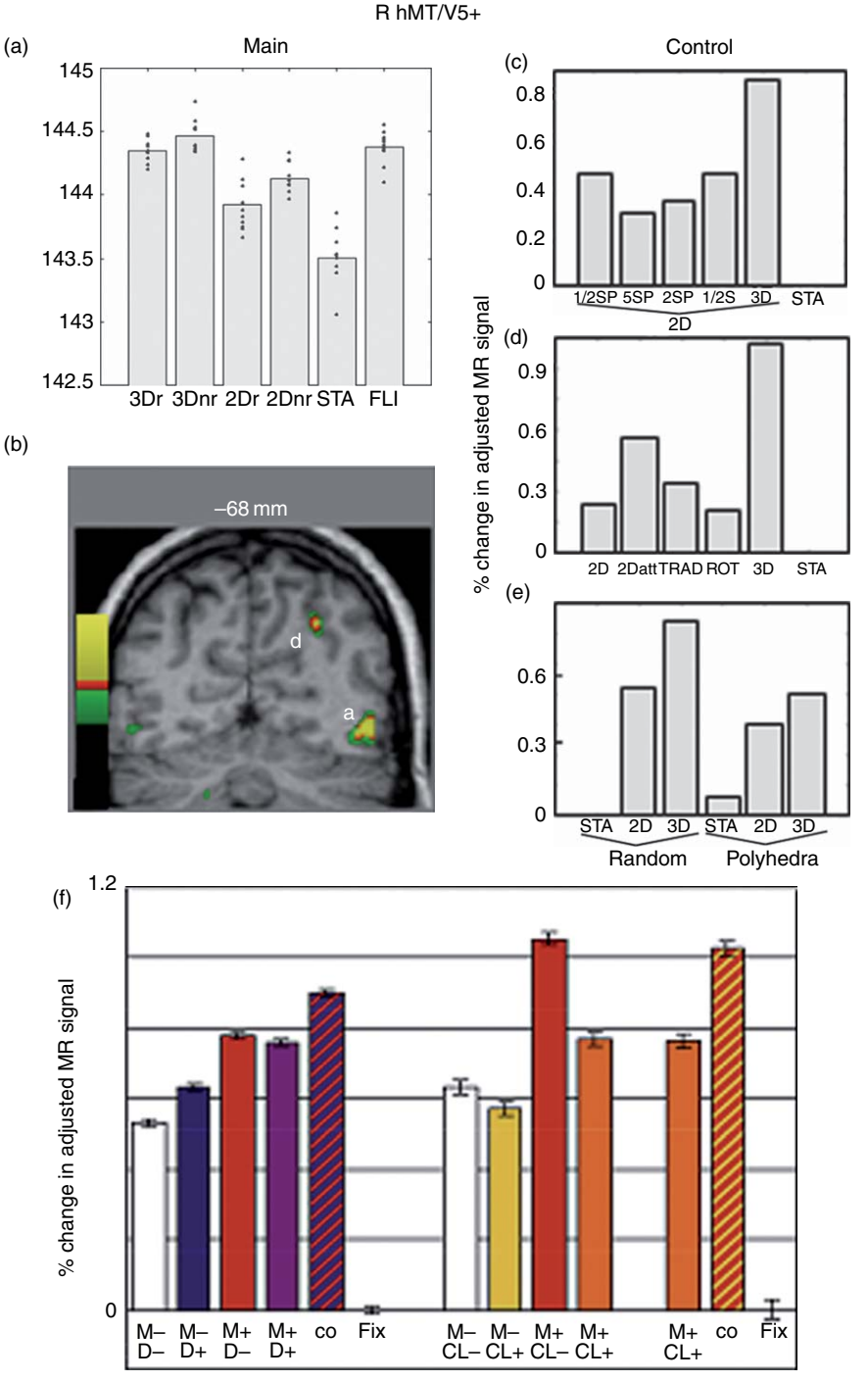

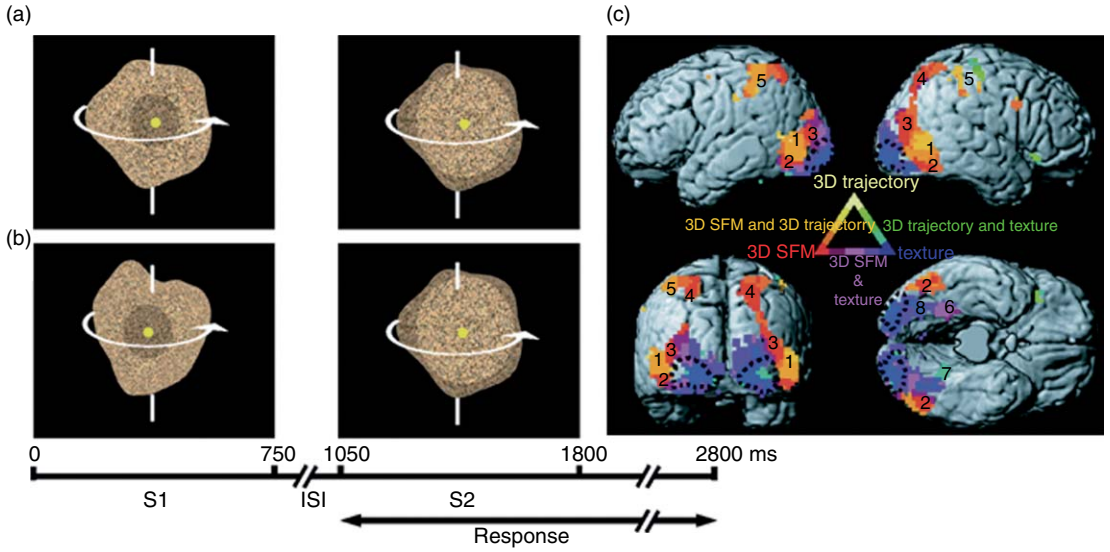

Figure 8 Distinguishing between 3D shape from motion and 3D motion pattern: (a–b) schematic representation of two texture trials: same trial (a) and different trial (b). Stimulus 1 and 2 show the central and peripheral dimming, respectively. The timing of the stimulus presentations and response period are indicated. The vertical line indicates the axis of rotation, slanted in the Z direction (outside the plane of the figure). Notice that the stimuli were identical in all five conditions (3 discrimination and 2 dimming detection conditions), only the aspect to which the subjects were instructed to pay attention was manipulated. (c) Activation patterns rendered on a standard brain (random effects, $P < 0.001$ uncorrected) Color scale indicates relative activation in the three different conditions: attention to 3D shape from motion (red), to axis of rotation (3D motion pattern, pale yellow), or to texture (blue). Dotted line indicates regions in which spatial attention had an effect. Numbers denote local maxima in regions significant at $P < 0.05$ (corrected for multiple comparisons): 1: hMT/V5+, 2: inferior temporal gyrus (ITG), 3: lateral occipital sulcus (LOS), 4: posterior intraparietal sulcus (IPS), 5: anterior IPS, 6: right collateral sulcus, 7: left middle lingual gyrus, 8: right posterior collateral sulcus with kind permission from Peuskens, H., Claeys, K. G., Todd, J. T., Norman, J. F., Van Hecke, P., and Orban, G. A. 2004. Attention to 3-D shape, 3-D motion and texture in 3-D structure from motion displays. J. Cogn. Neurosci. 16, 665–682.

SFM stimuli has been observed so far in the monkey fMRI studies. One possibility is the need to superimpose the speed gradients onto flow components.

2.15.3.3.2 Other cortical regions

Both in awake (Vanduffel, W. *et al.*, 2002) and anesthetized monkeys (Sereno, M. E. *et al.*, 2002) V2 and V3 are activated by 3D SFM stimuli. Whether or

Figure 7 Differential activation of right hMT/V5+ by 3D rotation displays compared to 2D translation displays: A–E data from Orban, G. A. *et al.* (1999); F data from Peuskens, H. *et al.* (personal communication); (a) activity profile of right hMT/V5+ from the main experiment. Adjusted magnetic resonance (MR) signal (resulting from proportional scaling), averaged over 11 subjects, is plotted for the six conditions of the main experiment: 3D rigid (3Dr), 3D nonrigid (3Dnr), 2D rigid (2Dr), 2D nonrigid (2Dnr), static (STA), and flickering (FLI) displays. The dots indicate individual responses. The profile is that of the most significant voxel at 52, −62, −4. Notice that in right hMT/V5+, the difference between 3Dr and 2Dnr is still significant ($z = 3.01$). (b) Single subject SPM showing the difference between viewing of 3Dr and 3Dnr displays and viewing of similar 2D displays in subject 3. Voxels reaching different levels of activation (yellow: $P < 0.05$, corrected; red: $P < 0.2$, corrected; green: $P < 0.001$, uncorrected) are shown on a coronal section at −68. Maximum Z score was 7.19 in this subject. The letters indicate the regions reaching statistical significance ($P < 0.05$, corrected for multiple comparisons): right hMT/V5+ (a), right ventral intraparietal sulcus (VIPS) (d). (c–e) Activity profiles of right hMT/V5+, obtained in control experiment 1, rigid case (c); control experiment 2 (d); and control experiment 3 (e). The percent change in adjusted MR signal, relative to viewing static displays, averaged over two (c) or three (d and e) subjects, is plotted for the different conditions: 2Dr with half the standard speed (1/2SP), with standard speed (SSP), with double speed (2SP), and with half-size (1/2S); 3Dr and STA in (C); 2Dr, 2Dr with attention (2Datt), rotation in the fronto-parallel plane (ROT), trajectory-in-depth (TRAD), 3Dr, and STA in (d); and random lines, static in 2D and 3D motion and polyhedra, static in 2D and 3D motion in (e). (f) Activity profiles (plotting MR signal changes relative to fixation) in an experiment in which two cues were combined: motion (M) and disparity (D) in left profile and motion (M) and closure (Cl) in right profile: Co: conflict between the two cues, + and − cue present, absent respectively; M–corresponds to translating lines and M+ to rotating lines. With kind permission from Orban, G. A., Sunaert, S., Todd, J. T., Van Hecke, P., and Marchal, G. 1999. Human cortical regions involved in extracting depth from motion. Neuron 24, 929–940.

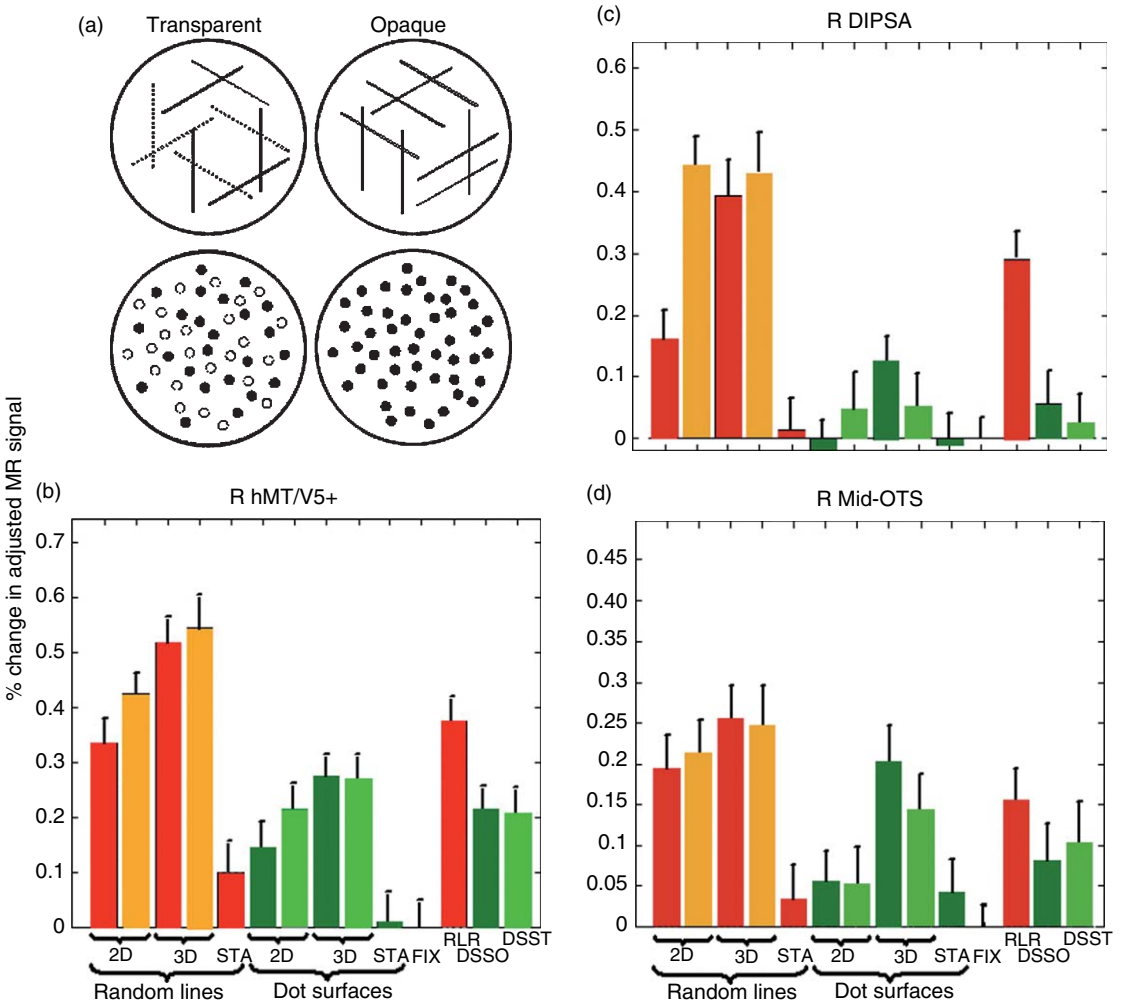

Figure 9 3D SFM: interaction with transparency in displays. (a) line and dot displays that undergo 3D rotation or 2D translation. The nine random (position and orientation) lines and 720 random (position) dots (lifetime 30 frames) moved at 3° s^{-1} in a circular aperture (9.9 diameter) in the center of the display. Lines (average projected length 4.5°) were constrained to lie on the faces of a randomly oriented cube centered in the aperture. Dots were constrained to lie on the surface of a sphere of the same diameter as the aperture. Lines and dots either rotated in depth around a vertical axis or translated in the plane. Open circles and stippled lines indicated lines and dots located on the back of the 3D object and moved in the opposite direction with respect to those on the front of the object. (b–d) Activity profiles of h MT/V5+ (b), DIPSA (c), and mid-OTS (d) in right hemisphere: the % magnetic resonance signal change (group of six subjects) compared to fixation is plotted for the 14 conditions analyzed. Red/orange bars indicate line surfaces, green bars are dot surfaces; opaque conditions are in red and dark green, transparent conditions in orange and light green. STA, stationary; FIX, fixation; RLR, random lines rotating in the image plane; DSSO, dot surfaces scrambled (vertical positions of dot trajectories) opaque; and DSST dot surfaces scrambled (vertical positions of dot trajectories) transparent (appear as a cloud of dots randomly distributed in a volume). Vertical bars indicate standard error of mean. With kind permission from Orban, G. A., Claeys, K., Nelissen, K., Smans, R., Sunaert, S., Todd, J., Wardak, C., Durand, J. B., and Vanduffel, W. 2006a. Mapping the parietal cortex of human and nonhuman primates. Neuropsychologia 44, 2647–2667.

not this activation, limited to the stimulus edges, reflects the location in depth of the whole stimulus (Bakin, J. S. *et al.*, 2000) is unclear.

There is less agreement about the involvement of other cortical regions: Sereno M. E. *et al.* (2002) described further temporal activation sites in the lower and upper bank of the superior temporal sulcus (STS), beyond FST, which were not observed in the Vanduffel W. *et al.* (2002) study, as well as an anterior middle temporal sulcus (AMTS) activation, which might correspond to the weak TE activation observed by Vanduffel W. *et al.* (2002). In humans, random-dot stimuli were relatively more effective than random-line stimuli in occipitotemporal regions, and this

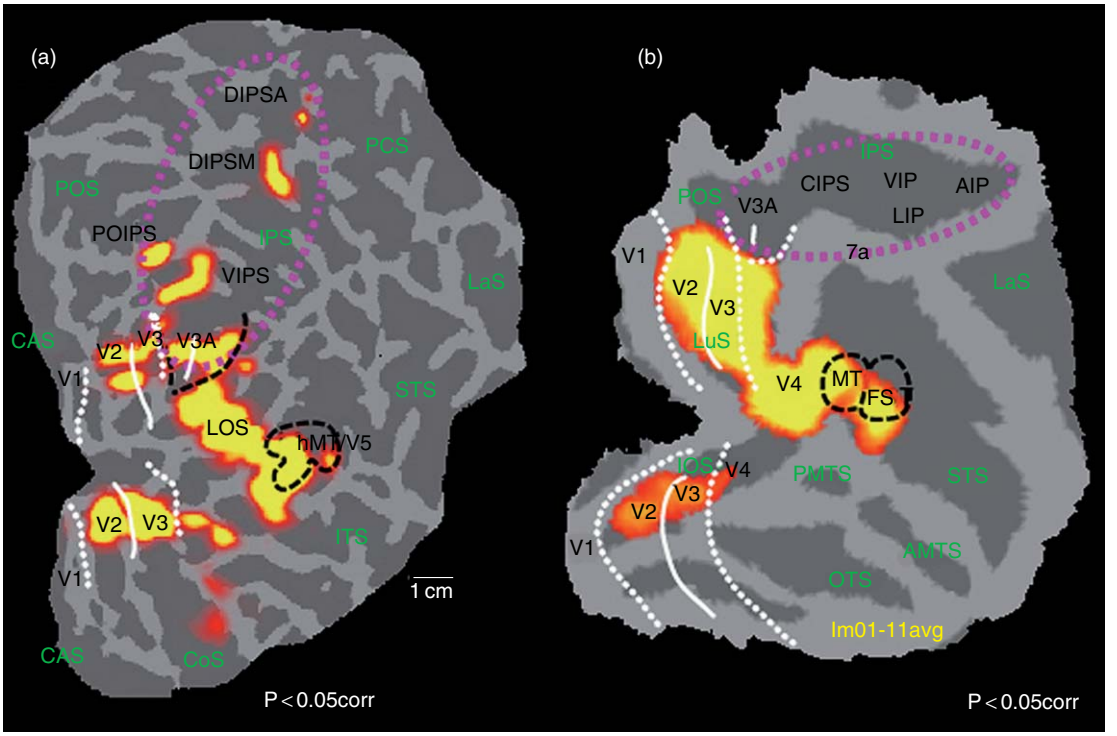

Figure 10 3D SFM network of human and monkey compared. SPMs for the subtraction viewing of 3D rotating lines minus viewing of 2D translating lines ($P < 0.05$, corrected for multiple comparisons) of a single human (a) and monkey (M4: b) subject projected on the posterior part of the flattened right hemisphere. White stippled and full lines: vertical and horizontal meridian projections (from separate retinotopic mapping experiments); black stippled lines: motion responsive regions from separate motion localizing tests; purple stippled lines region of interspecies difference encompassing V3 and intraparietal sulcus (IPS). AMTS, anterior middle temporal sulcus; CAS, calcarine sulcus; CoS, collateral sulcus; DIPSA, dorsal intrapatietal sulcus anterior; DIPSM, dorsal intraparietal sulcus medial; IOS, inferior occipital sulcus; ITS, inferior temporal sulcus; LaS, lateral sulcus; LOS, lateral occipital sulcus; LuS, lunate suclus; OTS, occipitotemporal sulcus; PCS, postcentral sulcus; PMTS, posterior middle temporal sulcus; POIPS, parieto-occipito intraparietal sulcus; POS, parieto-occipital sulcus; STS, superior temporal sulcus; VIPS, ventral intraparietal sulcus. Adapted from Vanduffel, W., Fize, D., Peuskens, H., Denys, K., Sunaert, S., Todd, J. T., and Orban, G. A. 2002. Extracting 3D from motion: differences in human and monkey intraparietal cortex. Science 298, 413–415. With kind permission from Orban, G. A., Fize, D., Peuskens, H., Denys, K., Nelissen, K., Sunaert, S., Todd, J., and Vanduffel, W. 2003. Similarities and differences in motion processing between the human and macaque brain: evidence from fMRI. Neuropsychologia 41, 1757–1768.

stimulus difference might explain the discrepancies between the two studies, as might the more stringent criterion used by Vanduffel W. *et al.* (2002) ($P < 0.05$ corrected for multiple comparisons).

Vanduffel W. *et al.* (2002) described an important species difference between monkey and human IPS, with the former being much less sensitive to 3D SFM than its human counterpart. Out of three monkeys tested in the original study, only one animal (M3) had a weak ($P < 0.001$ uncorrected for multiple comparisons) 3D SFM activation in what was described as VIP, but might also correspond to ventral LIP (Orban, G. A. *et al.*, 2006a). Subsequent testing of two more monkeys, both of whom had relatively weak stereopsis, disclosed a significant ($P < 0.05$ corrected for multiple comparisons) activation of the anterior lateral bank by 3D SFM in these two animals (Orban, G. A. *et al.*, 2006a). This activation might correspond to the activation described as LIP by Sereno M. E. *et al.* (2002). Yet these latter authors described several additional activation sites in and near the monkey IPS (multiple LIP sites, POJ, LOP) which were not observed in the Vanduffel W. *et al.* (2002) study. In this case stimulus differences are a less likely explanation, since random lines drive monkey parietal regions well (Vanduffel, W. *et al.*, 2002) and in human imaging random-line stimuli, as used by Vanduffel W. *et al.* (2002), engage the IPS 3D SFM regions more than random-dot stimuli do (Figure 9).

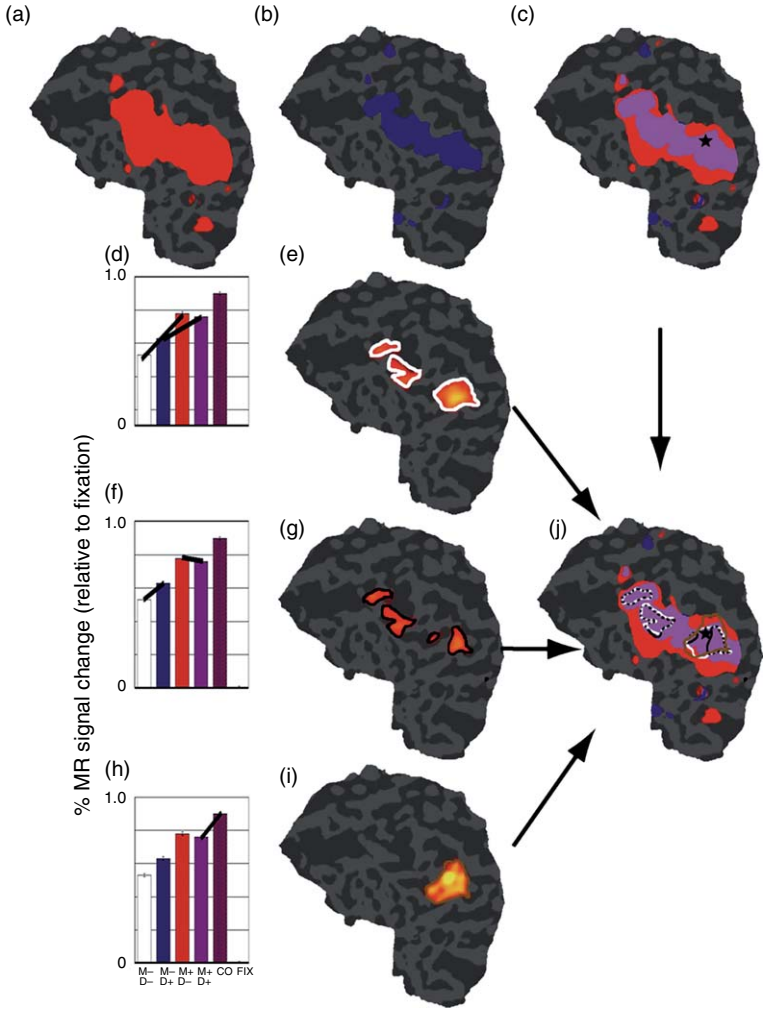

Figure 11 Combination of motion and stereo in the extraction of 3D shape (random-line stimuli, Peuskens, H., personal communication). SPMs (group, $n = 6$) plotting voxels significant ($P < 0.05$ corrected for multiple comparisons) in the single effect of 3D SFM (a), of 3D SFS (b), in the cue interaction in the motion regions (e), the cue interaction in the disparity regions (g) and in the subtraction cue conflict minus cue agreement (i) on the flattened hemisphere of the six subjects. The single effect SPMs are superimposed in c, and further combined with the outlines of interaction and conflict regions in (j). The activity profiles (plotting magnetic resonance signal changes relative to fixation) of right hMT/V5+ (asterisk) are plotted to illustrate the negative effect of stereo on the motion cue (d), the negative effect of motion on the stereo cue (f), and the conditions used to calculate the conflict effect (black lines in (h)).

2.15.4 The Extraction of Three-Dimensional Shape from Disparity or Stereo (Three-Dimensional SFS)

2.15.4.1 Single-Cell Studies

Neuronal selectivity for higher-order disparity has been documented mainly in two cortical regions: the caudal part of the lateral bank of IPS, caudal intraparietal (CIP), explored by Sakata and his collaborators and a small region in lower bank of the STS, TEs, explored by our group. Since much more information is available about TE neurons, the TE regions will be reviewed first and then CIP will then be compared to it (for reviews see Sakata, H. *et al.*, 2005; Orban, G. A. *et al.*, 2006b).

2.15.4.1.1 Higher-order disparity selectivity in TEs, part of the inferotemporal complex

The Janssen P. *et al.* (1999) study, reporting that a fraction of inferotemporal (IT) neurons were selective for 3D shape defined by disparity, was not only the first study to report selectivity for second-order

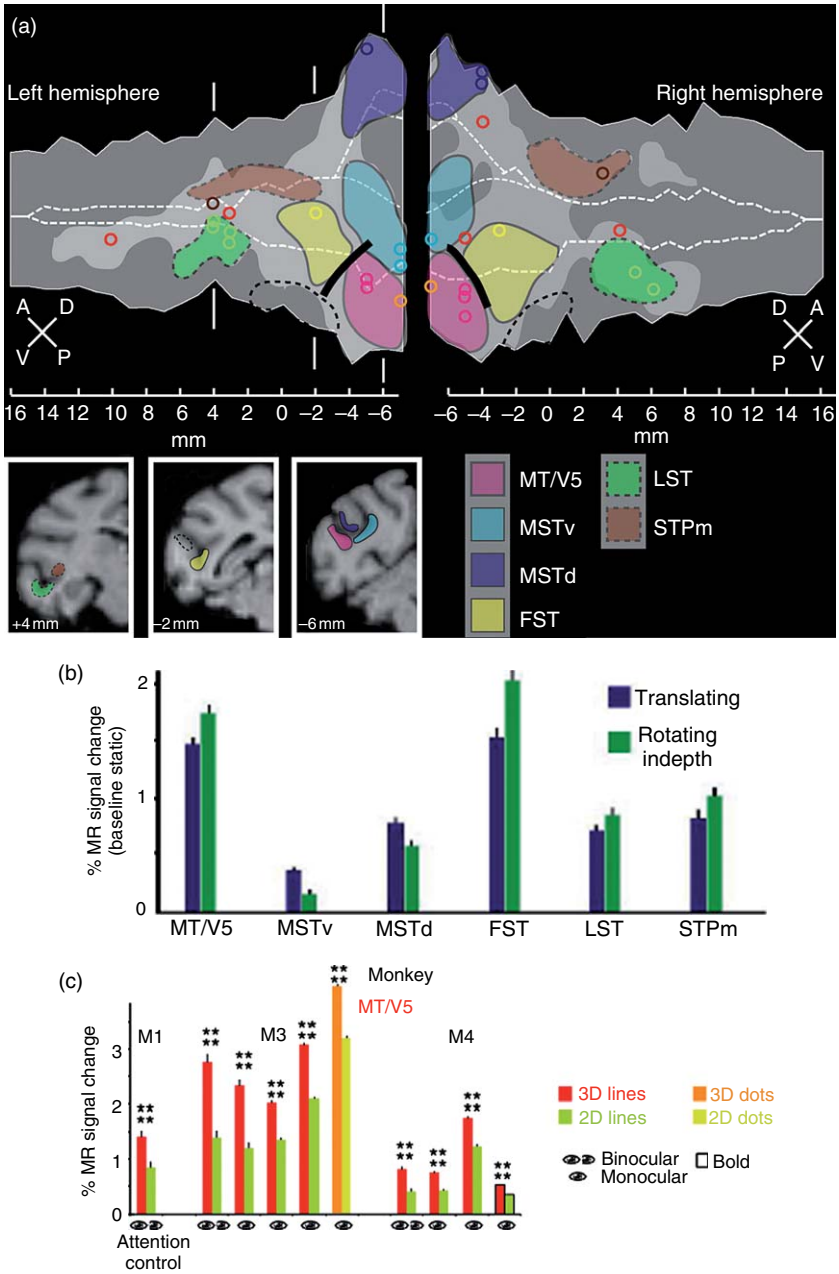

Figure 12 Monkey MT/V5 engaged by 3D SFM: (a) Overview of motion-responsive regions within the left and right STS. Boundaries of six motion-responsive regions are shown: MT/V5 (pink), MSTv (cyan), MSTd (blue), fundus of the superior temporal (FST) (yellow), STPm (brown), and LST (green). Boundaries that are less certain are indicated by dashed lines. The light gray overlay indicates the motion-responsive cortex identified with five motion contrasts. Colored circles correspond to SPM local maxima. The black solid line indicates the location of the VM representation that forms the border between areas MT/V5 and FST. The dashed black line indicates the region giving strong responses to static shapes, probably corresponding to (part of) TEO. At the bottom, three coronal sections (at -6, -2, and $+4$ mm, respectively, to the interaural plane) show the locations of the different regions: MT/V5, MSTv, and MSTd at level -6 mm; FST at -2 mm; and LST and STPm at $+4$ mm to the interaural plane. A, anterior; D, dorsal; P, posterior; V, ventral. (b) Magnetic resonance response profiles of the six STS motion regions: percentage of MR signal changes for random lines translating or rotating in depth compared with stationary control. Group data of three monkeys (M1, M3, and M5) are shown. (c) Activity profiles of area MT/V5. The different profiles for each animal are derived from a separate experiment. Each profile represents the average % signal change from the two hemispheres relative to the static control condition. Significance levels ($^{**} = P < 0.05$ corrected) are indicated for the right and left hemisphere (lower symbols) separately. ATT–: negative attention (high-acuity fixation task); black outline bold measurement rather than monocrystalline iron oxide nanoparticle (MION) measurement; vertical lines: standard error of means. With kind permission from Nelissen, K., Vanduffel, W., and Orban, G. A. 2006. Charting the lower superior temporal region, a new motion-sensitive region in monkey superior temporal sulcus. J. Neurosci. 26, 5929–5947 (a, b) and Vanduffel, W., Fize, D., Peuskens, H., Denys, K., Sunaert, S., Todd, J. T., and Orban, G. A. 2002. Extracting 3D from motion: differences in human and monkey intraparietal cortex. Science 298, 413–415 (c).

disparity stimuli, but it was also the first to report disparity selectivity as such in the ventral stream. Indeed, stereo was classically associated with the dorsal stream (Ungerleider, L. G. and Mishkin, M., 1982; Van Essen, D. C. *et al.*, 1992), although lesion studies had indicated some involvement of the ventral stream in stereoscopic processing (Cowey, A. and Gross, C. G., 1970; Ptito, A. *et al.*, 1991). Many subsequent studies have confirmed that stereo is processed in the ventral stream (Uka, T. *et al.*, 2000; Hinkle, D. A. and Connor, C. E., 2001; 2002; Watanabe, M. *et al.*, 2002; Tanabe, S. *et al.*, 2004; Hegdé, J. and Van Essen, D. C., 2005a; 2005b; Tanabe, S. *et al.*, 2005; Uka, T. *et al.*, 2005). The demonstration of higher-order selectivity was provided by showing that the selectivity for curved surfaces of opposite sign (convex and concave) did not depend on the position in depth of the surfaces. This position invariance criterion is reminiscent of the test used by Lagae L. *et al.* (1994) to demonstrate higher-order motion selectivity of MST neurons.

Subsequent studies (Janssen, P. *et al.*, 2000a) indicated that neurons selective for 3D shape defined by disparity (3D shape from disparity, 3D SFD) were not scattered throughout IT, but were concentrated in a small region in the rostral part of the lower bank of the STS. This region (Figure 13), labeled TEs, houses many 3D SFD selective neurons, in contrast to the convexity of IT. The two parts of IT also differ in their degree of binocular summation, which is stronger in TEs than in lateral TE (Janssen, P. *et al.*, 2000a). Since the anatomical connectivity of this lower STS region is also different from the remainder of the convexity (Saleem, K. S. *et al.*, 2000; Luppino, G., 2005), we (Janssen, P. *et al.*, 2000a) proposed that TEs is a separate cortical region linked to the IPS.

Finally, TEs neurons were shown to be endowed with another higher-order property which had been frequently postulated but never observed: the rejection of false matches such as those in anticorrelated stereograms (Janssen, P. *et al.*, 2003). In contrast to V1 neurons (Cumming, B. G. and Parker, A. J., 1997), TEs neurons, which are selective for 3D shape depicted by correlated RDS, do not respond selectively to anticorrelated RDS. In this respect anticorrelated RDS are similar to decorrelated RDS which also evoke no differential response from TEs neurons (Figure 14). Thus at the level of TEs what has been referred to as the stereo correspondence problem (Marr, D. and Poggio, T., 1979) is solved. This need not imply that it has not already been solved at some earlier level. Recent results suggest that the false matches are greatly reduced in V4 (Tanabe, S. *et al.*, 2004), but not in V2 (Allouni, A. K. *et al.*, 2005).

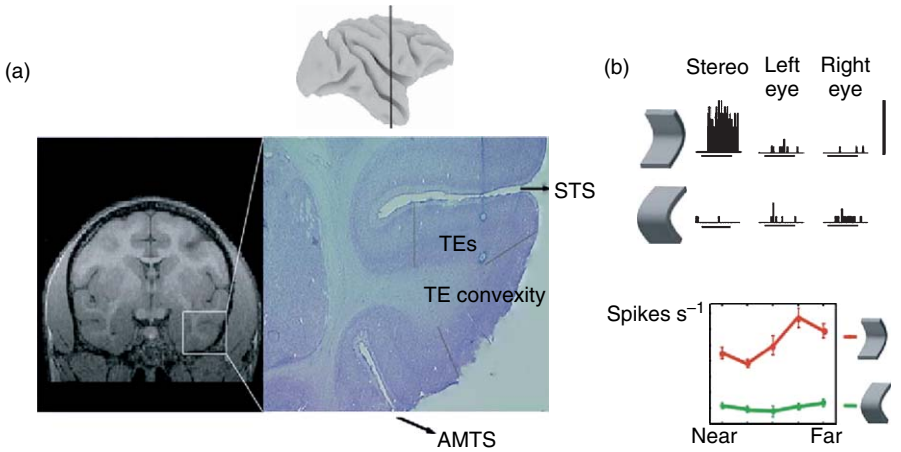

Figure 13 Defining characteristics and localization of higher-order disparity selective neurons in inferotemporal cortex. (a) Localization of recording on a magnetic resonance (MR) image (coronal section at level indicated) and histological section (monkey H); (b) Peristimulus time histograms (PSTHs) indicating responses to stereo and monocular stimuli and curves plotting average net responses to curved surfaces as a function of position in depth (1° range). Horizontal line indicates stimulus duration (300 ms) and vertical bar 90 spikes s^{-1}. Adapted from Janssen, P., Vogels, R., and Orban, G. A. 2000a. Selectivity for 3D shape that reveals distinct areas within macaque inferior temporal cortex. Science 288, 2054–2056. AMTS, anterior middle temporal sulcus; STS, superior temporal sulcus. The approximative locations of TFs and the convexity of TE are indicated. With kind permission from Orban, G. A., Janssen, P., and Vogels, R. 2006b. Extracting 3D structure from disparity. Trends Neurosci. 29, 466–473.

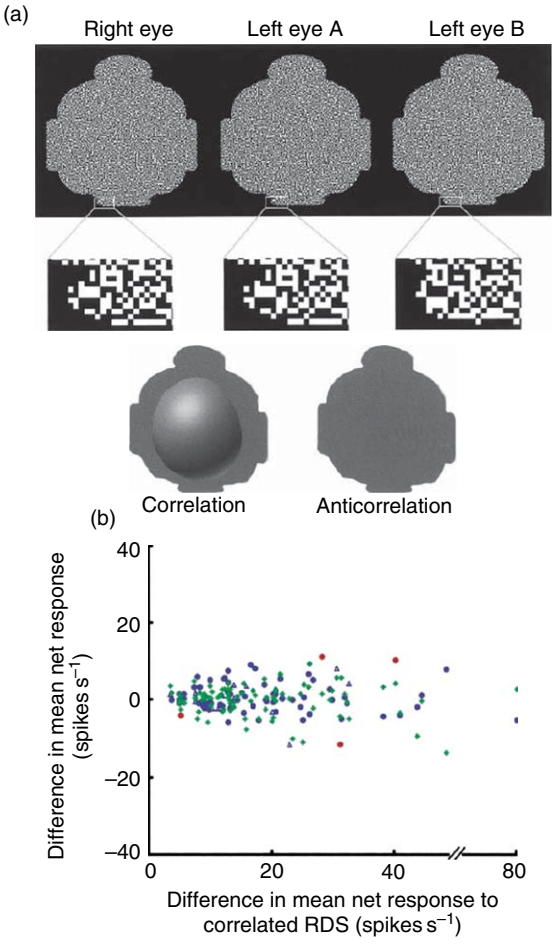

Figure 14 Rejection of false matches by TEs neurons. (a) Stimuli. The top row shows the monocular images for a correlated (right eye and left eye A) and an anticorrelated (right eye and left eye B) RDS in the correlation/anticorrelation test. The second row illustrates for zero disparity the inverted contrast polarity in the anticorrelated RDS (left and right panel) compared to the correlated RDS (left and middle panel). The bottom row shows a schematic illustration of the perceived 3D structure. (b) Population Analysis. Scatterplot of difference in mean net response to the anticorrelated (blue, circles: higher-order neurons; triangles: zero-order neurons) and decorrelated (green) RDSs plotted as a function of the difference in mean net response to the correlated RDS. Red circles: four neurons with significant response modulation to the anticorrelated RDS. With kind permission from Janssen, P., Vogels, R., Liu, Y., and Orban, G. A. 2003. At least at the level of inferior temporal cortex, the stereo correspondence problem is solved. Neuron 37, 693–701.

2.15.4.1.2 Exquisite coding of three-dimensional shape from disparity by TEs neurons

In the initial studies we emphasized the selectivity of TEs neurons for second-order disparity stimuli (Janssen, P. *et al.*, 1999; 2000a). In fact, TEs houses neurons selective for all three orders of depth signaled by disparity. Figure 15 shows an example of zero-order, first-order, and second-order disparity-selective neurons. The defining criterion for a higher-order neuron was a selectivity which did not reverse at any position in depth. This criterion supposes that vergence eye movements of the monkey are controlled. Generally we only recorded the position of only one eye, but we have shown that this suffices to detect vergence eye movements, provided enough trials are averaged (Janssen, P. *et al.*, 2000b). Furthermore, a number of higher-order neurons were recorded while we monitored positions of both eyes (Janssen, P. *et al.*, 2001). Thus, we were able to demonstrate the validity of our definition of higher-order neurons. In the initial study, this criterion was implemented by the requirement that the response to the preferred shape at its optimal position exceeds the response to the nonpreferred shape at any position (Janssen, P. *et al.*, 1999). Subsequently, this requirement was quantified by an index comparing the best position for the nonpreferred shape to the worst position of the preferred shape (Janssen, P. *et al.*, 2000b). The ratio of these responses did not exceed a factor of 2 in higher-order neurons and was generally smaller than 1.5. For the cell in Figure 15A the ratio exceeded 5. A simple disparity test with fronto-parallel surfaces sufficed to confirm that this cell was zero order: the cell was a near neuron (Poggio, G. F. and Fischer, B., 1977). First-order neurons were position-in-depth invariant and responded as well to the 3D shapes as to a planar 3D surface tilted in depth (Figure 15(b)). In the Liu Y. *et al.* (2004) study, these neurons were shown to be tuned for the tilt (3D orientation) in depth. Finally, second-order neurons were invariant for position in depth and responded selectively to shapes curved in depth but not to first-order stimuli (Figure 15(c)). In about half of them, the first-order approximation, a wedge, evoked a significantly weaker response than the original curved stimulus (Figure 15(c)). In the other half, this approximation was as effective as that stimulus. Note that zero-order approximations were effective in only a few higher-order neurons, as in Figure 15(b).

It is worthwhile emphasizing the exquisite sensitivity of TEs neurons for small changes in 3D structure. The difference between curved stimuli and their linear approximations is only one example. Most neurons remained selective for the sign of curvature up to the smallest amplitude of depth variation (0.03°) tested. In addition, most neurons

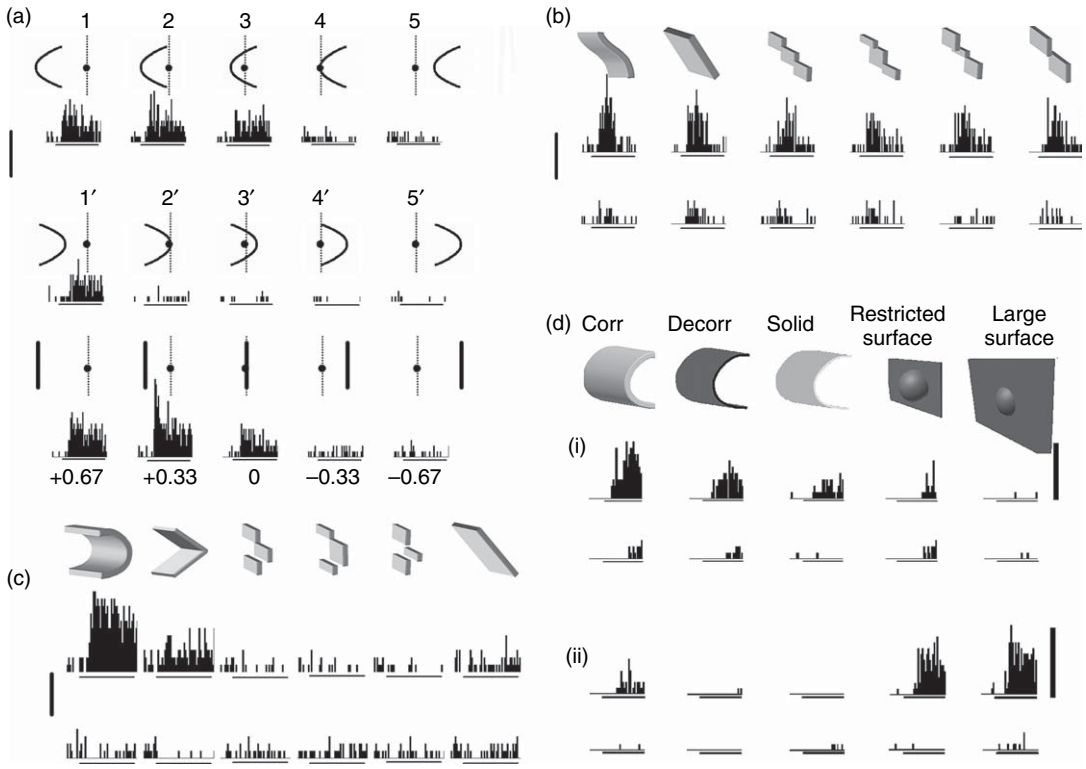

Figure 15 Types of TEs neurons. (a–c) Peristimulus time histograms (PSTHs) indicating average responses of zero-order (a), first-order (b), and second-order (c) selective neurons. (d) Responses of TEs neurons selective for the 3D shape of the edges of surfaces (i) and of texture inside the edges (ii). The horizontal lines below the PSTH indicate stimulus duration. In A all stimuli are indicated above the corresponding PSTHs, in B–D only the preferred stimulus polarity is shown. Vertical bars indicate 60 spikes s^{-1} (a), 30 spikes s^{-1} (b, c), and 65 spikes s^{-1} (d). corr, correlated; decorr, decorrelated. With kind permission of Orban, G. A., Janssen, P., and Vogels, R. 2006b. Extracting 3D structure from disparity. Trends Neurosci. 29, 466–473.

were sensitive to differences in the amplitude of depth variation in convex or concave stimuli. Their response usually decreased monotonically with decreasing amplitude, but in some cases was tuned to a preferred amplitude.

Selectivity for curvature of 3D surfaces could reflect selectivity for the 3D shape of either the edges or the texture pattern inside the edges. In fact, TEs neurons can be selective for both components of the surface stimuli (Janssen, P. *et al.*, 2001). The neuron in the top part of Figure 15D retains its selectivity with decorrelated RDS and solid stereograms in which only the boundary carries depth information, while losing it when the edges are removed in the doubly curved stimuli. This neuron was thus selective for the 3D shape of the edges. The neuron in the bottom part of Figure 15(d) reacted in exactly the opposite way and was selective for the 3D shape of the texture inside the edges. In the same study, we also showed that TEs neurons can encode the orientation of the 3D curvature and can, in all likelihood, combine selectivity for orthogonally oriented curvatures as captured by the shape index (Figure 2) of Koenderink J. J. (1990).

2.15.4.1.3 The invariance of three-dimensional shape selectivity in TEs

The 3D shape selectivity was found to be invariant for changes in fronto-parallel position and in size (Janssen, P. *et al.*, 2000b), as has been observed for 2D shape selectivity (Schwartz, E. L. *et al.*, 1983; Ito, M. *et al.*, 1995; Logothetis, N. K. and Sheinberg, D. L., 1996; Tanaka, K., 1996; Vogels, R. and Orban, G. A., 1996; Vogels, R., 1999). The invariance for fronto-parallel position complements the invariance for position in depth already reported in the first study (Janssen, P. *et al.*, 1999), defining a region in 3D space in which TEs neurons maintain their 3D shape selectivity.

The 2D shape selectivity of IT neurons has been shown to be cue invariant (Sáry, Gy. *et al.*, 1993; Tanaka, K. *et al.*, 2001). In the same way, the 3D

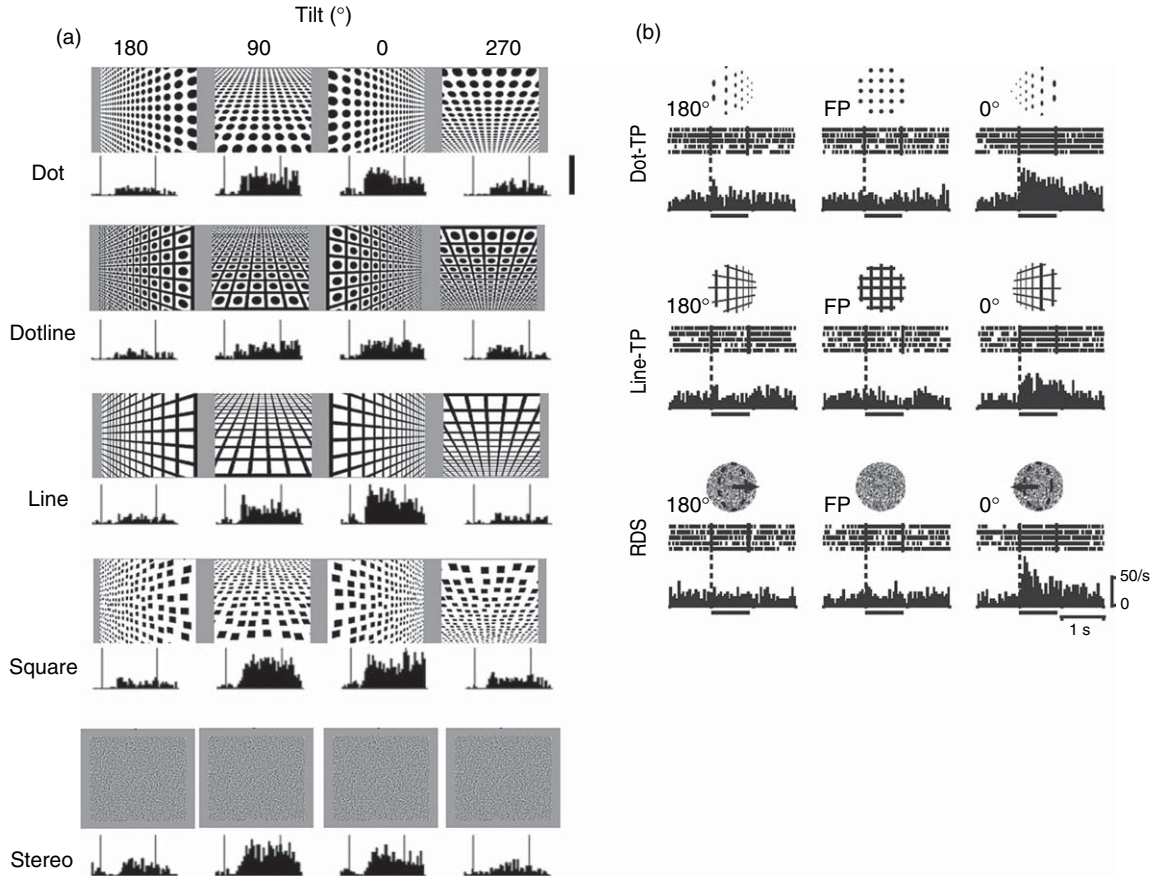

Figure 16 Average responses of TEs (a) and CIP (b) neurons to planar surfaces tilted in depth defined by disparity or different types of texture. Data from Liu Y. *et al.* (2004) and of Tsutsui K. *et al.* (2002). Stimulus duration is indicated by vertical lines in a and horizontal line in b; vertical bar in A indicates 87 spikes s^{-1}. Textures in A not drawn to size (about 7° in diameter and enclosed in a 2D shape, to match well-known shape selectivity of IT neurons). With kind permission from Orban, G. A., Janssen, P., and Vogels, R. 2006b. Extracting 3D structure from disparity. Trends Neurosci. 29, 466–473.

shape selectivity of TEs neurons has also been shown to be depth-cue invariant. We opted for a comparison of selectivity for the disparity and texture cues (see below). TEs neurons are selective for tilt specified by disparity but also those specified by texture gradients (Liu, Y. *et al.*, 2004), and preferred tilt is similar for the two cues (Figure 16A). In addition, the selectivity for tilt specified by texture was shown to be invariant for texture type, for slant and for binocular versus monocular presentations.

2.15.4.1.4 Selectivity of caudal intraparietal neurons for first-order disparity

Shikata E. *et al.* (1996) reported that neurons in the caudal part of the lateral bank of IPS were selective for the tilt of stereoscopic surfaces. This caudal region has been referred to as cIPS (Sakata, H. *et al.*, 1997), CIP (Taira, M. *et al.*, 2000), or posterior LIP (Nakamura, H. *et al.*, 2001) and probably corresponds to pIPS as defined by Denys K. *et al.* (2004) and to LOP as defined by Lewis J. W. and Van Essen D. C. (2000). Although that initial study established the disparity selectivity of the CIP neurons, it is only in Taira M. *et al.* (2000) that the higher-order nature of the selectivity was established by showing invariance for changes in the fixation distance. It has been reported in abstract form that CIP neurons have also solved the correspondence problem (Katsuyama, N. *et al.*, 2004). Importantly, Tsutsui K. *et al.* (2001) have demonstrated that inactivation of CIP interferes with judgments about surface tilt.

So far, only first-order selectivity has been demonstrated in CIP, although second-order selectivity has also been suggested to be present

(Katsuyama, N. *et al.*, 2005). Cue convergence has been documented for CIP neurons, for the combination of texture and disparity (Tsutsui, K. *et al.*, 2002, Figure 16(b)), as well as for perspective and disparity (Tsutsui, K. *et al.*, 2001).

Finally, CIP neurons, rather than being selective for the orientation in depth of surfaces (surface orientation selective), can be selective for the orientation in 3D of elongated stimuli (axis orientation selective, Sakata, H. *et al.*, 1998).

2.15.4.1.5 Three-dimensional shape from disparity selectivity in other cortical regions

V1 neurons display no higher-order disparity selectivity (Nienborg, H. *et al.*, 2004) and are selective for anticorrelated RDS as well as for correlated RDS (Cumming, B. G. and Parker, A. J., 1997). Thus, most properties of TEs and CIP neurons reflect processing beyond V1. V4 provides input to IT, and V4 neurons are selective for the orientation in depth of elongated stimuli (Hinkle, D. A. and Connor, C. E., 2002) but not for surfaces curved in depth (Hegdé, J. and Van Essen, D. C., 2005). Thus, either TEs neurons acquire their higher-order selectivity through local connections in TEs or TEO, or TEs receives its selective input from IPS. Indeed it has been suggested that selectivity for 3D orientation is a property of neurons along the lateral bank of IPS (Nakamura, H. *et al.*, 2001). The selectivity of anterior intraparietal (AIP) neurons for real objects supposedly supports their role in the control of grasping (Murata, A. *et al.*, 2000). Whether or not this selectivity is based on a selectivity for 3D shape is presently investigated (Durand, J. B. *et al.*, 2006).

Some 3D orientation selectivity, based on disparity has been reported for MT/V5 neurons (see above), which also have intermediate properties with respect to responses to aRDS (Nguyenkim, J. D. and DeAngelis, G. C., 2003; Krug, K. *et al.*, 2004). Nguyenkim J. D. and DeAngelis G. C. (2003) reported that the preferred tilt of MT/V5 neurons, specified by disparity did not depend on slant. Thus the origin of higher-order disparity selectivity and the extent of this selectivity throughout the visual system remain unclear. The stronger selectivity in CIP and TEs compared to MT/V5, however, suggests that MT/V5 represents one of the early stages of 3D shape and 3D surface orientation extraction.

2.15.4.2 Imaging Studies

Very few studies so far have been specifically devoted to the extraction of 3D shape from stereo, although several studies in human and monkeys are currently ongoing in our group (Janssen, P. *et al.*, 2002; Durand, J. B. *et al.*, 2006a; 2006b). Tsao D. Y. *et al.* (2003) used a large checkerboard stimulus with random disparity levels in the different checks as a first-pass stimulus for 3D structure. In both species these authors observed an activation in V3A and the abutting posterior part of the IPS. In monkeys this activation included CIP. Welchman A. E. *et al.* (2005) tested for selectivity for slant defined by disparity in early retinotopic regions as well as hMT/V5+ and LOC. These authors failed to observe a significant rebound from adaptation for changes in slant defined by disparity in any of the regions studied. Preliminary data (Figure 11) suggest that similar human cortical regions are engaged by 3D SFS and 3D SFM.

2.15.5 Extraction of Three-Dimensional Shape from Static Monocular Cues

2.15.5.1 Single-Cell Studies

The difficulty in demonstrating a selectivity of single IT neurons for first- or second-order gradients of texture concerns the need to provide a control for simple texture or pattern selectivity of these neurons (Tanaka, K. *et al.*, 1991). Hence we adopted the strategy to study the invariance of TEs neurons for first- and second-order gradients specified by both disparity and texture. The initial study was done with single curved surfaces (Liu, Y. *et al.*, 2002) for which TEs neurons show limited selectivity in the texture case. We subsequently switched to linear texture gradients to which TEs neurons are much more sensitive and were able to show cue invariant processing by TEs of disparity and texture gradients (Liu, Y. *et al.*, 2004, see above). These authors showed that the preferred tilt specified by texture did not depend on slant, suggesting that slant and tilt are separable, in agreement with psychophysical results (Norman, J. F. *et al.*, 2006). For CIP neurons, Tsutsui K. *et al.* (2002) likewise demonstrated selectivity for tilt to texture gradients combined with selectivity of disparity gradients.

For shading little is know about neuronal processing, although Hanazawa A. and Komatsu H. (2001)

demonstrated that a number of V4 neurons are selective for the direction of illumination, a critical step for the extraction of 3D shape from shading (Khang, B. G. *et al.*, 2003; Koenderink, J. J. *et al.*, 2004).

2.15.5.2 Imaging Studies: Need for Two-Dimensional Shape Controls

Three studies (Humphrey, G. K. *et al.*, 1997; Taira, M. *et al.*, 2001; Kourtzi, Z. *et al.*, 2003) have been devoted the extraction of 3D shape from shading with conflicting results, some emphasizing early retinotopic regions, others LOC or IPS regions. All three studies suffer from the lack of controls for 2D shape sensitivity as all 3D-shape stimuli also contain clear 2D-shape elements and adaptation effects or discrimination might be based on these spurious 2D cues rather than the 3D percept.

In an effort to locate the regions involved in extracting texture gradients Shikata E. *et al.* (2001) investigated 3D orientation discrimination, but in this case also 2D controls were lacking, perhaps because the 2D shape selectivity of parietal cortex (Denys, K. *et al.*, 2004) had not been appreciated well enough. The extent to which these 2D cues also contributed to the change in perspective effects documented by Welchman A. E. *et al.* (2005) in hMT/V5 and LOC is unclear.

2.15.6 Conclusions

The veil that has long covered the extraction of 3D shape from the retinal inputs has only begun to be lifted. An important step in this direction is the recognition that 3D shape and depth are different perceptual entities. With the availability of monkey fMRI the pace of progress should accelerate (Durand, J. B. *et al.*, 2007).

The extraction of 3D SFM exemplifies the strength of the triadic approach in which the same perceptual/cognitive process is probed by single-cell recording, and by fMRI in awake monkeys and humans. Indeed all three experimental strategies underscore the contribution of MT/V5 and its human homolog to the 3D SFM, even though the stimuli used in the three approaches were not identical. Furthermore, even if the homology is generally accepted at the level of the MT/V5 complex, the detailed homology between MT/V5 and each of its satellites in two species has still to be worked out (Huk, A. C. *et al.*, 2002; Nelissen, K. *et al.*, 2006). This approach may document further species differences in addition to that documented in the primate IPS (Vanduffel, W. *et al.*, 2002). Although both humans and monkeys perceive 3D structure form motion similarly (Siegel, R. M. and Andersen, R. A., 1990), human IPS processes 3D SFM much more extensively than its monkey counterpart. We have proposed that this is due to the much wider use of tools in humans than in monkeys. This view has received support recently from the study of Stout D. and Chaminade T. (2007).

The neuronal mechanisms unraveled so far clearly indicate that 3D shape is not represented as a 3D map, underscoring the distinction between depth and 3D shape. Rather the primate brain has evolved mechanisms to extract the linear- and second-order gradients in speed and disparity from the retinal images. The direct encoding of these first- and second-order derivatives is one of the main conclusions that can be derived from the studies performed so far. In the case of speed gradients in MT/V5 the encoding of gradients involves the surround. Whether this will turn out to be a general mechanism or not remains an open question. Indeed the coding by speed is relatively coarse (Orban, G. A., 1997) and a mechanism based solely in the ERF cannot capture enough of the speed variation to be sensitive. Other neural encoding mechanisms such as those of disparity are finer (Poggio, G. F. and Fischer, B., 1977) and hence a purely excitatory mechanism might suffice.

A third conclusion that can be derived from the data available is that 3D shape is processed both by the ventral and dorsal stream, in agreement with the double behavioral use of 3D shape in identification/categorization and in guidance of action, in particular grasping. How different these dorsal and ventral representations of 3D shape are remains an open question and will require a direct comparison of neuronal populations in both streams.

Another question which has hitherto received insufficient attention is the distinction between the processing of the 3D shape of objects and the 3D layout of the environment. In the studies performed so far widely different stimulus sizes have been used. The interaction between the extraction of 3D structure and size will have to be studied much more systematically to dissociate these two aspects of 3D structure.

Acknowledgments

The work described in parts of this chapter was supported by GOA 2000/11, GOA 2005/18, IUAP P5/04, EU grants Insight2 and Insight2+, FWO G0151.04. The author is indebted to Dr. J. T. Todd and Dr. S. Raiguel for comments on an earlier draft and Dr. G. DeAngelis for commenting on an earlier version of the draft and providing Figure 6.

References

Allouni, A. K., Thomas, O. M., Solomon, S. G., Krug, K., and Parker, A. J. 2005. Local and global binocular matching in V2 of the awake macaque. Soc. Neurosci. Abstr. 510.8.

Amedi, A., Malach, R., Hendler, T., Peled, S., and Zohary, E. 2001. Visuo-haptic object-related activation in the ventral visual pathway. Nat. Neurosci. 4, 324–330.

Anderson, K. C. and Siegel, R. M. 2005. Three-dimensional structure-from-motion selectivity in the anterior superior temporal polysensory area, STPa, of the behaving monkey. Cereb. Cortex 15, 1299–1307.

Andersen, R. A., Bradley, D. C., and Shenoy, K. V. 1996. Neural mechanisms for heading and structure from motion perception. Cold Spring Harbar Symp. Quant. Biol. 61, 15–25.

Backus, B. T., Fleet, D. J., Parker, A. J., and Heeger, D. J. 2001. Human cortical activity correlates with stereoscopic depth perception. J. Neurophysiol. 86, 2054–2068.

Bakin, J. S., Nakayama, K., and Gilbert, C. D. 2000. Visual responses in monkey areas V1 and V2 to three-dimensional surface configurations. J. Neurosci. 20, 8188–8198.

Baracas, G. T. and Albright, T. D. 1996. Contribution of area MT to perception of three-dimensional shape: a computational study. Vis. Res. 36, 869–887.

Bartels, A. and Zeki, S. 2000. The architecture of the colour centre in the human visual brain: new results and a review. Eur. J. Neurosci. 12, 172–193.

Belhumeur, P. N., Kriegeman, D. J., and Yuille, A. L. 1999. The bas-relief ambiguity. Int. J. Comp. Vision 35, 33–44.

Binkofski, F., Buccino, G., Posse, S., Seitz, R. J., Rizzolatti, G., and Freund, H. 1999. A fronto-parietal circuit for object manipulation in man: evidence from an fMRI study. Eur. J. Neurosci. 11, 3276–3286.

Born, R. T. and Bradley, D. C. 2005. Structure and function of visual area MT. Ann. Rev. Neurosci. 28, 157–189.

Bradley, D. C. and Andersen, R. A. 1998. Center-surround antagonism based on disparity in primate area MT. J. Neurosci. 18, 7552–7565.

Bradley, D. C., Chang, G. C., and Andersen, R. A. 1998. Encoding of three-dimensional structure-from-motion by primate area MT neurons. Nature 392, 714–717.

Bradshaw, M. F. and Rogers, B. J. 1999. Sensitivity to horizontal and vertical corrugations defined by binocular disparity. Vision Res. 39, 3049–3056.

Braunstein, M. L. 1977. Perceived direction of rotation of simulated three-dimensional patterns. Percept. Psychophys. 21, 553–557.

Britten, K. H., Shadlen, M. N., Newsome, W. T., and Movshon, J. A. 1992. The analysis of visual motion: a comparison of neuronal and psychophysical performance. J. Neurosci. 12, 4745–4765.

Claeys, K., Dupont, P., Cornette, L., Sunaert, S., Van Hecke, P., De Schutter, E., and Orban, G. A. 2004. Color discrimination involves ventral and dorsal stream visual areas. Cereb. Cortex 14, 803–822.

Cowey, A. and Gross, C. G. 1970. Effects of foveal prestriate and inferotemporal lesions on visual discriminations. Exp. Brain Res. 11, 128–144.

Cumming, B. G. and Parker, A. J. 1997. Responses of primary visual cortical neurons to binocular disparity without depth perception. Nature 389, 280–283.

DeAngelis, G. C. and Uka, T. 2003. Coding of horizontal disparity and velocity by MT neurons in the alert macaque. J. Neurophysiol. 89, 1094–1111.

Denys, K., Vanduffel, W., Fize, D., Nelissen, K., Peuskens, H., Van Essen, D., and Orban, G. A. 2004. The processing of visual shape in the cerebral cortex of human and nonhuman primates: a functional magnetic resonance imaging study. J. Neurosci. 24, 2551–2565.

DeYoe, E. A., Carman, G. J., Bandettini, P., Glickman, S., Wieser, J., Cox, R., Miller, D., and Neitz, J. 1996. Mapping striate and extrastriate visual areas in human cerebral cortex. Proc. Natl. Acad. Sci. U. S. A. 93, 2382–2386.

Dodd, J. V., Krug, K., Cumming, B. G., and Parker, A. J. 2001. Perceptually bistable three-dimensional figures evoke high choice probabilities in cortical area MT. J. Neurosci. 21, 4809–4821.

Duffy, C. J. and Wurtz, R. H. 1991. Sensitivity of MST neurons to optic flow stimuli. I. A continuum of response selectivity to large-field stimuli. J. Neurophysiol. 65, 1329–1345.

Duffy, C. J. and Wurtz, R. H. 1997. Medial superior temporal area neurons respond to speed patterns in optic flow. J. Neurosci. 17, 2839–2851.

Durand, J. B., Nelissen, K., Joly, O., Wardak, C., Todd, J. T., Norman J. F., Georgieva, S., Janssen, P., Raiguel, S., Vanduffel, W., and Orban, G. A. 2006. A postero-anterior gradient for visual 3D shape processing in the IPS: fMRI evidence from awake monkeys. Soc. Neurosci. Abstr. 504.1.

Durand, J.-B., Nelissen, K., Joly, O., Wardak, C., Todd, J. T., Norman, J. F., Janseen, P., Vanduffel, W., and Orban, G. A. 2007. Anterior regions of monkey parietal cortex process visual 3D shape. Neuron (in press).

Edelman, S. and Bülthoff, H. 1992. Orientation dependence in the recognition of familiar and novel views of 3D objects. Vision Res. 32, 2385–2400.

Ernst, M. O. and Banks, M. S. 2002. Humans integrate visual and haptic information in a statistically optimal fashion. Nature 415, 429–433.

Faillenot, I., Sunaert, S., Van Hecke, P., and Orban, G. A. 2001. Orientation discrimination of objects and gratings compared: an fMRI study. Eur. J. Neurosci. 13, 585–596.

Gautama, T. and Van Hulle, M. M. 2001. Function of center-surround antagonism for motion in visual area MT/V5: a modeling study. Vision Res. 41, 3917–3930.

Georgieva, S., Todd, J., Peeters, R., and Orban, G. 2003a. Cortical regions involved in extracting 3D shapes from shading. J. Vision 3, 508.

Georgieva, S., Todd, J., Peeters, R., and Orban, G. A. 2005. Functional neuroanatomy for the processing of 3D shape from shading and texture in humans. Soc. Neurosci. Abstr. 768.6.

Georgieva, S. S., Todd, J., Nelissen, K., Vanduffel, W., Peeters, R., and Orban, G. A. 2003b. Cortical regions involved in extracting 3D shape from shading: a human and monkey fMRI study. Soc. Neurosci. Abstr. 819.19.

Gibson, J. J. 1950. The perception of visual surfaces. Am. J. Psychol. 63, 367–384.

Graziano, M. S., Andersen, R. A., and Snowden, R. J. 1994. Tuning of MST neurons to spiral motions. J. Neurosci. 14, 54–67.

Gross, C. G., Rocha-Miranda, C. E., and Bender, D. B. 1972. Visual properties of neurons in inferotemporal cortex of the macaque. J. Neurophysiol. 35, 96–111.

Hadjikhani, N., Liu, A. K., Dale, A. M., Cavanagh, P., and Tootell, R. B. 1998. Retinotopy and color sensitivity in human visual cortical area V8. Nat. Neurosci. 1, 235–241.

Hanazawa, A. and Komatsu, H. 2001. Influence of the direction of elemental luminance gradients on the responses of V4 cells to textured surfaces. J. Neurosci. 21, 4490–4497.

Hegdé, J. and Van Essen, D. C. 2005a. Stimulus dependence of disparity coding in primate visual area V4. J. Neurophysiol. 93, 620–626.

Hegdé, J. and Van Essen, D. C. 2005b. Role of primate visual area V4 in the processing of 3-D shape characteristics defined by disparity. J. Neurophysiol. 94, 2856–2866.

Hillis, J. M., Ernst, M. O., Banks, M. S., and Landy, M. S. 2002. Combining sensory information: mandatory fusion within, but not between, senses. Science 298, 1627–1630.

Hillis, J. M., Watt, S. J., Landy, M. S., and Banks, M. S. 2004. Slant from texture and disparity cues: optimal cue combination. J. Vision 4, 967–992.

Hinkle, D. A. and Connor, C. E. 2001. Disparity tuning in macaque area V4. Neuroreport 12, 365–369.

Hinkle, D. A. and Connor, C. E. 2002. Three-dimensional orientation tuning in macaque area V4. Nat. Neurosci. 5, 665–670.

Howard, I. P. and Rogers, B. 1995. Binocular Vision and Stereopsis. Oxford University Press.

Howard, T. P. and Rogers, B. J. *(eds.)* 2002. Seeing in Depth I. Porteous.

Huk, A. C., Dougherty, R. F., and Heeger, D. J. 2002. Retinotopy and functional subdivision of human areas MT and MST. J. Neurosci. 22, 7195–7205.

Humphrey, G. K., Goodale, M. A., Bowen, C. V., Gati, J. S., Vilis, T., Rutt, B. K., and Menon, R. S. 1997. Differences in perceived shape from shading correlate with activity in early visual areas. Curr. Biol. 7, 144–147.

Ito, M., Tamura, H., Fujita, I., and Tanaka, K. 1995. Size and position invariance of neuronal responses in monkey inferotemporal cortex. J. Neurophysiol. 73, 218–226.

James, T. W., Humphrey, G. K., Gati, J. S., Servos, P., Menon, R. S., and Goodale, M. A. 2002. Haptic study of three-dimensional objects activates extrastriate visual areas. Neuropsychologia 40, 1706–1714.

Janssen, P., Pareto, D., Peuskens, H., Sunaert, S., Vogels, R., and Orban, G. A. 2002. Higher-order disparity sensitive regions in human cortex? An fMRI study. Soc. Neurosci. Abstr. 56.11.

Janssen, P., Vogels, R., and Orban, G. A. 1999. Macaque inferior temporal neurons are selective for disparity-defined three-dimensional shapes. Proc. Natl. Acad. Sci. U. S. A. 96, 8217–8222.

Janssen, P., Vogels, R., and Orban, G. A. 2000a. Selectivity for 3D shape that reveals distinct areas within macaque inferior temporal cortex. Science 288, 2054–2056.

Janssen, P., Vogels, R., and Orban, G. A. 2000b. Three-dimensional shape coding in inferior temporal cortex. Neuron 27, 385–397.

Janssen, P., Vogels, R., Liu, Y., and Orban, G. A. 2001. Macaque inferior temporal neurons are selective for three-dimensional boundaries and surfaces. J. Neurosci. 21, 9419–9429.

Janssen, P., Vogels, R., Liu, Y., and Orban, G. A. 2003. At least at the level of inferior temporal cortex, the stereo correspondence problem is solved. Neuron 37, 693–701.

Julesz, B. 1971. Foundations of Cyclopean Perception, p. 406. University Chicago Press.

Kanwisher, N., McDermott, J., and Chun, M. M. 1997. The fusiform face area: a module in human extrastriate cortex specialized for face perception. J. Neurosci. 17, 4302–4311.

Katsuyama, N., Naganuma, T., Sakata, H., and Taira, M. 2004. Representation of 3D curvature in the caudal intraparietal (CIP) area of macaque. Soc. Neurosci. Abstr. 751.11.

Katsuyama, N., Yamashsita, A., Sawada, K., Tsutsui, K., and Taira, M. 2005. Architectonic structures and 3D-selective neurons in the caudal intraparietal area of Japanese macaque (*Macaca fuscata*). Soc. Neurosci. Abstr. 510.6.

Khang, B. G., Koenderink, J. J., and Kappers, A. M. L. 2003. Perception of surface reflectance of 3-D geometrical shapes: influence of the lighting mode. Perception 32, 1311–1324.

Knill, D. C. and Saunders, J. A. 2003. Do humans optimally integrate stereo and texture information for judgments of surface slant? Vision Res. 43, 2539–2558.

Koenderink, J. J. (*ed*.) 1990. Solid Shape. The MIT Press.

Koenderink, J. J., van Doorn, A. J., and Pont, S. C. 2004. Light direction from shad(ow)ed random Gaussian surfaces. Perception 33, 1405–1420.

Koenderink, J. J., van Doorn, A. J., Kappers, A. M., and Todd, J. T. 2001. Ambiguity and the 'mental eye' in pictorial relief. Perception 30, 431–448.

Kourtzi, Z. and Kanwisher, N. 2000. Cortical regions involved in perceiving object shape. J. Neurosci. 20, 3310–3318.

Kourtzi, Z., Erb, M., Grodd, W., and Bulthoff, H. H. 2003. Representation of the perceived 3-D object shape in the human lateral occipital complex. Cereb. Cortex 13, 911–920.

Kriegeskorte, N., Sorger, B., Naumer, M., Schwarzbach, J., van den Boogert, E., Hussy, W., and Goebel, R. 2003. Human cortical object recognition from a visual motion flowfield. J. Neurosci. 23, 1451–1463.

Krug, K., Cumming, B. G., and Parker, A. J. 2004. Comparing perceptual signals of single V5/MT neurons in two binocular depth tasks. J. Neurophysiol. 92, 1586–1596.

Lagae, L., Maes, H., Raiguel, S., Xiao, D., and Orban, G. A. 1994. Responses of macaque STS neurons to optic flow components: a comparison of areas MT and MST. J. Neurophysiol. 71, 1597–1626.

Lagae, L., Raiguel, S., and Orban, G. A. 1993. Speed and direction selectivity of macaque middle temporal neurons. J. Neurophysiol. 69, 19–39.

LaMotte, R. H. and Mountcastle, V. B. 1975. Capacities of humans and monkeys to discriminate vibratory stimuli of different frequency and amplitude: a correlation between neural events and psychological measurements. J. Neurophysiol. 38, 539–559.

Lewis, J. W. and Van Essen, D. C. 2000. Corticocortical connections of visual, sensorimotor, and multimodal processing areas in the parietal lobe of the macaque monkey. J. Comp. Neurol. 428, 112–137.

Liu, Y., Vogels, R., and Orban, G. A. 2002. The effect of texture depth cue on the disparity selectivity of macaque inferior temporal neurons. Soc. Neurosci. Abstr. 56.13.

Liu, Y., Vogels, R., and Orban, G. A. 2004. Convergence of depth from texture and depth from disparity in macaque inferior temporal cortex. J. Neurosci. 24, 3795–3800.

Logothetis, N. K. and Sheinberg, D. L. 1996. Visual object recognition. Ann. Rev. Neurosci. 19, 577–621.

Luppino, G. 2005. Organization of the Posterior Parietal Lobe and of Parietofrontal Connections. In: From Monkey Brain to Human Brain: A Fyssen Foundation Symposium (Bradford Books) (*eds*. S. Dehaene, J. R. Duhamel, M. D. Hauser, and G. Rizzolatti), pp. 235–252. The MIT Press.

Malach, R., Reppas, J. B., Benson, R. R., Kwong, K. K., Jiang, H., Kennedy, W. A., Ledden, P. J., Brady, T. J., Rosen, B. R., and Tootell, R. B. 1995. Object-related activity revealed by functional magnetic resonance imaging in human occipital cortex. Proc. Natl. Acad. Sci. U. S. A. 92, 8135–8139.

Marr, D. and Poggio, T. 1979. A computational theory of human stereo vision. Proc. R. Soc. Lond. B. Biol. Sci. 204, 301–328.

Maunsell, J. H. R. and Van Essen, D. C. 1983a. Functional properties of neurons in middle temporal visual area of the macaque monkey. I. Selectivity of stimulus direction, speed, and orientation. J. Neurophysiol. 49, 1127–1147.

Maunsell, J. H. R. and Van Essen, D. C. 1983b. Functional properties of neurons in middle temporal visual area of the macaque monkey. II. Binocular interactions and sensitivity to binocular disparity. J. Neurophysiol. 49, 1148–1167.

Murata, A., Gallese, V., Luppino, G., Kaseda, M., and Hideo, S. 2000. Selectivity for the shape, size, and orientation of objects for grasping in neurons of monkey parietal area AIP. J. Neurophysiol. 83, 2580–2601.

Murray, S. O., Olshausen, B. A., and Woods, D. L. 2003. Processing shape, motion and three-dimensional shape-from-motion in the human cortex. Cereb. Cortex 13, 508–516.

Nakahara, K., Hayashi, T., Konishi, S., and Miyashita, Y. 2002. Functional MRI of macaque monkeys performing a cognitive set shifting task. Science 295, 1532–1536.

Nakamura, H., Kuroda, T., Wakita, M., Kusunoki, M., Kato, A., Mikami, A., Sakata, H., and Itoh, K. 2001. From three-dimensional space vision to prehensile hand movements: the lateral intraparietal area links the area V3A and the anterior intraparietal area in macaques. J. Neurosci. 21, 8174–8187.

Nelissen, K., Vanduffel, W., and Orban, G. A. 2006. Charting the lower superior temporal region, a new motion-sensitive region in monkey superior temporal sulcus. J. Neurosci. 26, 5929–5947.

Nguyenkim, J. D. and DeAngelis, G. C. 2003. Disparity-based coding of three-dimensional surface orientation by macaque middle temporal neurons. J. Neurosci. 23, 7117–7128.

Nguyenkim, J. D. and DeAngelis, G. C. 2004. Macaque MT neurons are selective for 3D surface orientation defined by multiple cues. Soc. Neurosci. Abstr. 368.12.

Nienborg, H., Bridge, H., Parker, A. J., and Cumming, B. G. 2004. Receptive field size in V1 neurons limits acuity for perceiving disparity modulation. J. Neurosci. 24, 2065–2076.

Norman, J. F., Todd, J. T., and Orban, G. A. 2004. Perception of three-dimensional shape from specular highlights, deformations of shading, and other types of visual information. Psychol. Sci. 15, 565–570.

Norman, J. F., Todd, J. T., Norman, H. F., Clayton, A. M., and McBride, T. R. 2006. Visual discrimination of local surface structure: slant, tilt, and curvedness. Vision Res. 46, 1057–1069.

Orban, G. A. 1997. Visual Processing in Macaque Area MT/V5 and Its Satellites (MSTd and MSTv). In: Cerebral Cortex, Vol. 12, Extrastriate Cortex in Primates (*eds*. K. S. Rockland, J. H. Kaas, and A. Peters), pp. 359–434. Plenum.

Orban, G. A. and Vogels, R. 1998. The neuronal machinery involved in successive orientation discrimination. Prog. Neurobiol. 55, 117–147.

Orban, G. A., Claeys, K., Nelissen, K., Smans, R., Sunaert, S., Todd, J., Wardak, C., Durand, J. B., and Vanduffel, W. 2006a. Mapping the parietal cortex of human and non-human primates. Neuropsychologia 44, 2647–2667.

Orban, G. A., Fize, D., Peuskens, H., Denys, K., Nelissen, K., Sunaert, S., Todd, J., and Vanduffel, W. 2003. Similarities and differences in motion processing between the human and macaque brain: evidence from fMRI. Neuropsychologia 41, 1757–1768.

Orban, G. A., Janssen, P., and Vogels, R. 2006b. Extracting 3D structure from disparity. Trends Neurosci. 29, 466–473.

Orban, G. A., Sunaert, S., Todd, J. T., Van Hecke, P., and Marchal, G. 1999. Human cortical regions involved in extracting depth from motion. Neuron 24, 929–940.

Orban, G. A., Van Essen, D., and Vanduffel, W. 2004. Comparative mapping of higher visual areas in monkeys and humans. Trends Cogn. Sci. 8, 315–324.

Paradis, A. L., Cornilleau-Pérès, V., Droulez, J., Van de Moortele, P. F., Lobel, E., Berthoz, A., Le Bihan, D., and Poline, J. B. 2000. Visual perception of motion and 3-D structure from motion: an fMRI study. Cereb. Cortex 10, 772–783.

Perotti, V. J., Todd, J. T., and Norman, J. F. 1996. The visual perception of rigid motion from constant flow fields. Percept. Psychophys. 58, 666–679.

Peuskens, H., Claeys, K. G., Todd, J. T., Norman, J. F., Van Hecke, P., and Orban, G. A. 2004. Attention to 3-D shape, 3-D motion and texture in 3-D structure from motion displays. J. Cogn. Neurosci. 16, 665–682.

Phillips, F. and Todd, J. T. 1996. Perception of local three-dimensional shape. J. Exp. Psychol. Hum. Percept. Perform. 22, 930–944.

Poggio, G. F. and Fischer, B. 1977. Binocular interaction and depth sensitivity in striate and prestriate cortex of behaving rhesus monkey. J. Neurophysiol. 40, 1392–1405.

Priebe, N. J., Cassanello, C. R., and Lisberger, S. G. 2003. The neural representation of speed in macaque area MT/V5. J. Neurosci. 23, 5650–5661.

Ptito, A., Zatorre, R. J., Larson, W. L., and Tosoni, C. 1991. Stereopsis after unilateral anterior temporal lobectomy. Dissociation between local and global measures. Brain 114, 1323–1333.

Purushothaman, G. and Bradley, D. C. 2005. Neural population code for fine perceptual decisions in area MT. Nat. Neurosci. 8, 99–106.

Rogers, B. and Cagenello, R. 1989. Disparity curvature and the perception of thee-dimensional surfaces. Nature 339, 135–137.

Rogers, B. J. and Graham, M. E. 1979. Motion parallax as an independent cue for depth perception. Perception 8, 125–134.

Saito, H., Yukie, M., Tanaka, K., Hikosaka, K., Fukada, Y., and Iwai, E. 1986. Integration of direction signals of image motion in the superior temporal sulcus of the macaque monkey. J. Neurosci. 6, 145–157.

Sakata, H., Taira, M., Kusunoki, M., Murata, A., and Tanaka, Y. 1997. The TINS Lecture The parietal association cortex in depth perception and visual control of hand action. Trends Neurosci. 20, 350–357.

Sakata, H., Taira, M., Kusunoki, M., Murata, A., Tanaka, Y., and Tsutsui, K. 1998. Neural coding of 3D features of objects for hand action in the parietal cortex of the monkey. Philos. Trans. R. Soc. Lond. B. Biol. Sci. 353, 1363–1373.

Sakata, H., Tsutsui, K., and Taira, M. 2005. Toward an understanding of the neural processing for 3D shape perception. Neuropsychologia 43, 151–161.

Saleem, K. S., Suzuki, W., Tanaka, K., and Hashikawa, T. 2000. Connections between anterior inferotemporal cortex and superior temporal sulcus regions in the macaque monkey. J. Neurosci. 20, 5083–5101.

Sáry, Gy., Vogels, R., and Orban, G. A. 1993. Cue-invariant shape selectivity of macaque inferior temporal neurons. Science 260, 995–997.

Sawamura, H., Orban, G. A., and Vogels, R. 2006. Selectivity of neuronal adaptation does not match response selectivity: a single-cell study of the fMRI adaptation paradigm. Neuron 49, 307–318.

Schwartz, E. L., Desimone, R., Albright, T. D., and Gross, C. G. 1983. Shape recognition and inferior temporal neurons. Proc. Natl. Acad. Sci. U. S. A. 80, 5776–5778.

Sereno, M. E., Trinath, T., Augath, M., and Logothetis, N. K. 2002. Three-dimensional shape representation in monkey cortex. Neuron 33, 635–652.

Shadlen, M. N. and Newsome, W. T. 2001. Neural basis of a perceptual decision in the parietal cortex (area LIP) of the rhesus monkey. J. Neurophysiol. 86, 1916–1936.

Shikata, E., Hamzei, F., Glauche, V., Knab, R., Dettmers, C., Weiller, C., and Buchel, C. 2001. Surface orientation discrimination activates caudal and anterior intraparietal sulcus in humans: an event-related fMRI study. J. Neurophysiol. 85, 1309–1314.

Shikata, E., Tanaka, Y., Nakamura, H., Taira, M., and Sakata, H. 1996. Selectivity of the parietal visual neurones in 3D orientation of surface of stereoscopic stimuli. Neuroreport 7, 2389–2394.

Siegel, R. M. and Andersen, R. A. 1988. Perception of three-dimensional structure from motion in monkey and man. Nature 331, 259–261.

Siegel, R. M. and Andersen, R. A. 1990. The perception of structure from visual motion in monkey and man. J. Cogn. Neurosci. 2, 306–319.

Sperling, G., Dosher, B., and Landy, M. S. 1990. How to study the kinetic depth effect experimentally. J. Exp. Psychol. 16, 445–450.

Stout, D. and Chaminade, T. 2007. The evolutionary neuroscience of tool making. Neuropsychologia 45, 1091–1100.

Sugihara, H., Murakami, I., Shenoy, K. V., Andersen, R. A., and Komatsu, H. 2002. Response of MSTd neurons to simulated 3D orientation of rotating planes. J. Neurophysiol. 87, 273–285.

Sunaert, S., Van Hecke, P., Marchal, G., and Orban, G. A. 1999. Motion-responsive regions of the human brain. Exp. Brain Res. 127, 355–370.

Sunaert, S., Van Hecke, P., Marchal, G., and Orban, G. A. 2000. Attention to speed of motion, speed discrimination, and task difficulty: an fMRI study. Neuroimage 11, 612–623.

Taira, M., Nose, I., Inoue, K., and Tsutsui, K. 2001. Cortical areas related to attention to 3D surface structures based on shading: an fMRI study. Neuroimage 14, 959–966.

Taira, M., Tsutsui, K. I., Jiang, M., Yara, K., and Sakata, H. 2000. Parietal neurons represent surface orientation from the gradient of binocular disparity. J. Neurophysiol. 83, 3140–3146.

Tanabe, S., Ta kahiro, D., Umeda, K., and Fujita, I. 2005. Disparity-tuning characteristics of neuronal responses to dynamic random-dot stereograms in macaque visual area V4. J. Neurophysiol. 94, 2683–2699.

Tanabe, S., Umeda, K., and Fujita, I. 2004. Rejection of false matches for binocular correspondence in macaque visual cortical area V4. J. Neurosci. 24, 8170–8180.

Tanaka, K., Saito, H., Fukada, Y., and Moriya, M. 1991. Coding visual images of objects in the inferotemporal cortex of the macaque monkey. J. Neurophysiol. 66, 170–189.

Todd, J. T. 2004. The visual perception of 3D shape. Trends Cogn. Sci. 8, 115–121.

Todd, J. T. and Norman, J. F. 2003. The visual perception of 3-D shape from multiple cues: are observers capable of perceiving metric structure? Percept. Psychophys. 65, 31–47.

Todd, J. T., Norman, J. F., Koenderink, J. J., and Kappers, A. M. 1997. Effects of texture, illumination, and surface reflectance on stereoscopic shape perception. Perception 26, 807–822.

Todd, J. T., Oomes, A. H., Koenderink, J. J., and Kappers, A. M. 2004. The perception of doubly curved surfaces from anisotropic textures. Psychol. Sci. 15, 40–46.

Todd, J. T., Thaler, L., and Dijkstra, T. M. 2005. The effects of field of view on the perception of 3D slant from texture. Vision Res. 45, 1501–1517.

Tootell, R. B., Reppas, J. B., Kwong, K. K., Malach, R., Born, R. T., Brady, T. J., Rosen, B. R., and Belliveau, J. W. 1995. Functional analysis of human MT and related visual cortical areas using magnetic resonance imaging. J. Neurosci. 15, 3215–3230.

Treue, S. and Andersen, R. A. 1996. Neural responses to velocity gradients in macaque cortical area MT. Vis. Neurosci. 13, 797–804.

Tsao, D. Y., Freiwald, W. A., Tootell, R. B., and Livingstone, M. S. 2006. A cortical region consisting entirely of face-selective cells. Science 311, 670–674.

Tsao, D. Y., Vanduffel, W., Sasaki, Y., Fize, D., Knutsen, T. A., Mandeville, J. B., Wald, L. L., Dale, A. M., Rosen, B. R., Van Essen, D. C., Livingstone, M. S., Orban, G. A., and Tootell, R. B. H. 2003. Stereopsis activates V3A and caudal intraparietal areas in macaques and humans. Neuron 39, 555–568.

Tsutsui, K., Jiang, M., Yara, K., Sakata, H., and Taira, M. 2001. Integration of perspective and disparity cues in surface-orientation-selective neurons of area CIP. J. Neurophysiol. 86, 2856–2867.

Tsutsui, K., Sakata, H., Naganuma, T., and Taira, M. 2002. Neural correlates for perception of 3D surface orientation from texture gradient. Science 298, 409–412.

Uka, T. and DeAngelis, G. C. 2003. Contribution of middle temporal area to coarse depth discrimination: comparison of neuronal and psychophysical sensitivity. J. Neurosci. 23, 3515–3530.

Uka, T., Tanaka, H., Yoshiyama, K., Kato, M., and Fujita, I. 2000. Disparity selectivity of neurons in monkey inferior temporal cortex. J. Neurophysiol. 84, 120–132.

Uka, T., Tanabe, S., Watanabe, M., and Fujita, I. 2005. Neural correlates of fine depth discrimination in monkey inferior temporal cortex. J. Neurosci. 25, 10796–10802.

Ungerleider, L. G. and Desimone, R. 1986. Cortical connections of visual area MT in the macaque. J. Comp. Neurol. 248, 190–222.

Ungerleider, L. G. and Mishkin, M. 1982. Two Cortical Visual Systems. In: Analysis of Visual Behavior (*eds*. D. J. Ingle, M. A. Goodale, and R. J. W. Mansfield), pp. 549–586. The MIT Press.

Van Essen, D. C., Anderson, C. H., and Felleman, D. J. 1992. Information processing in the primate visual system: an integrated systems perspective. Science 255, 419–423.

Vanduffel, W., Fize, D., Mandeville, J. B., Nelissen, K., Van Hecke, P., Rosen, B. R., Tootell, R. B. H., and Orban, G. A. 2001. Visual motion processing investigated using contrast agent-enhanced fMRI in awake behaving monkey. Neuron 32, 565–577.

Vanduffel, W., Fize, D., Peuskens, H., Denys, K., Sunaert, S., Todd, J. T., and Orban, G. A. 2002. Extracting 3D from motion: differences in human and monkey intraparietal cortex. Science 298, 413–415.

Vogels, R. 1999. Categorization of complex visual images by rhesus monkeys. Part 2: single-cell study. Eur. J. Neurosci. 11, 1239–1255.

Vogels, R. and Orban, G. A. 1990. How well do response changes of striate neurons signal differences in orientation: a study in the discriminating monkey. J. Neurosci. 10, 3543–3558.

Vogels, R. and Orban, G. A. 1996. Coding of Stimulus Invariances by Inferior Temporal Neurons. In: Progress in Brain Research: Extrageniculostriate Mechanisms Underlying Visually-Guided Orientation Behavior, Vol. 112 (*eds*. M. Norita, T. Bando, and B. Stein), pp. 195–211. Elsevier.

Wallach, H. and O'Connell, D. N. 1953. The kinetic depth effect. J. Exp. Psychol. 45, 205–217.

Watanabe, M., Tanaka, H., Uka, T., and Fujita, I. 2002. Disparity-selective neurons in area V4 of macaque monkeys. J. Neurophysiol. 87, 1960–1973.

Watt, S. J. and Bradshaw, M. F. 2003. The visual control of reaching and grasping: binocular disparity and motion parallax. J. Exp. Psychol. Hum. Percept. Perform. 29, 404–415.
Welchman, A. E., Deubelius, A., Conrad, V., Bülthoff, H. H., and Kourtzi, Z. 2005. 3D shape perception from combined depth cues in human visual cortex. Nat. Neurosci. 8, 820–827.
Westheimer, G. 1979. The spatial sense of the eye. Proctor lecture. Invest. Ophthalmol. Vis. Sci. 18, 892–912.
Xiao, D. K., Marcar, V. L., Raiguel, S. E., and Orban, G. A. 1997a. Selectivity of macaque MT/V5 neurons for surface orientation in depth specified by motion. Eur. J. Neurosci. 9, 956–964.
Xiao, D. K., Raiguel, S., Marcar, V., and Orban, G. A. 1997b. The spatial distribution of the antagonistic surround of MT/V5 neurons. Cereb. Cortex 7, 662–677.
Xiao, D. K., Raiguel, S., Marcar, V., Koenderink, J., and Orban, G. A. 1995. Spatial heterogeneity of inhibitory surrounds in the middle temporal visual area. Proc. Natl. Acad. Sci. U. S. A. 92, 11303–11306.
Zeki, S., Watson, J. D., Lueck, C. J., Friston, K. J., Kennard, C., and Frackowiak, R. S. 1991. A direct demonstration of functional specialization in human visual cortex. J. Neurosci. 11, 641–649.

Further Reading

Orban, G. A. Higher order visual processing in macaque extrastriate cortex. Physiol. Reviews in press.
Parker, A. J. 2007. Binocular depth perception and the cerebral cortex. Nat. Neurosci. Reviews 8, 379–391.
Tanaka, K. 1996. Inferotemporal cortex and object vision. Ann. Rev. Neurosci. 19, 109–139.

Relevant Websites

http://www.kuleuven.be/neuro – Laboratorium voor Neuro- en Psycholysiologie, K. U. Leuven Medical School.
http://www.sciencemag.org/cgi/content/full/298/5592/413/DC1

2.16 Visual Search

J M Wolfe, Brigham and Women's Hospital & Harvard Medical School, Cambridge, MA, USA

J Reynolds, The Salk Institute for Biological Studies, San Diego, CA, USA

© 2008 Elsevier Inc. All rights reserved.

2.16.1	**What is Visual Search?**	275
2.16.1.1	Detection Under Conditions of Location Uncertainty	275
2.16.1.2	The Binding Problem and Limits on Object Recognition	275
2.16.2	**How Do We Study Visual Search?**	276
2.16.2.1	Real Time Methods	276
2.16.2.2	Accuracy Methods	277
2.16.2.3	Neurophysiological, Lesion and Microstimulation Studies of the Neural Mechanisms that Mediate Visual Search	277
2.16.3	**What Determines the Efficiency of Visual Search**	277
2.16.3.1	Feature Guidance	277
2.16.3.2	Other Factors	278
2.16.4	**Modeling Visual Search**	278
2.16.4.1	Signal Detection Approaches	278
2.16.4.2	Physiological Approaches	278
2.16.4.3	Biased Competition	278
2.16.4.4	Two-Stage Models	279
2.16.4.5	Feature Integration Theory	279
2.16.4.6	Guided Search	279
2.16.5	**Memory in Visual Search**	279
2.16.6	**Terminating Unsuccessful Searches**	279
2.16.7	**Conclusion**	280
References		280

2.16.1 What is Visual Search?

The world presents the visual system with more information than it can process at any one time. In response, the visual system and other sensory systems have selective processes that restrict full analysis to a subset of the available input. If an observer wants to deploy visual processing resources to some item that is not the current object of attention, the observer will need to search for that item. Even when the observer has no particular top-down goal, the limited resources of the visual system must be deployed in some manner in response to the current stimulus situation. Research on visual search examines the ways in which visual system uses attentional mechanisms to find something in a world filled with other things.

Attention is a broad term that covers a variety of different selective operations in vision and elsewhere. Two specific examples can illustrate the range of uses of attention in visual search.

2.16.1.1 Detection Under Conditions of Location Uncertainty

Imagine a clock face arrangement of 12 disks of visual noise. You are asked to find a signal (e.g., an oriented blob) embedded in the noise. The whole display is presented very briefly. If you are told that the signal, if present, will be at the 7 o'clock position, you will be better at detecting that signal than if you are uncertain about the location. This will be true even though the visual stimulus is identical in the two cases. Apparently, the ability to direct attention to a subset of the stimuli changes the detectability of the target (Palmer, J. *et al.*, 2000).

2.16.1.2 The Binding Problem and Limits on Object Recognition

In most cases, the visual stimuli of interest are more complex than simple signals in noise. Often they are

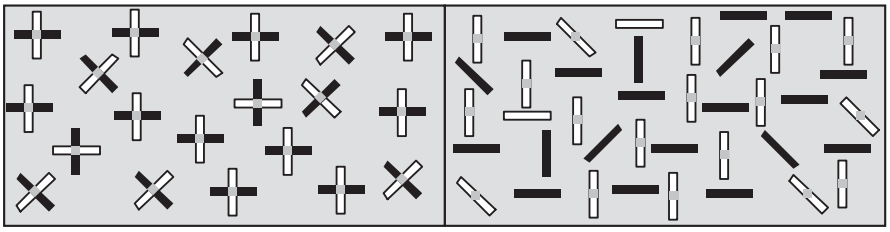

Figure 1 Search for the black vertical lines is harder on the left than on the right.

objects needing to be recognized. As a general rule, attention needs to select an object before that object can be identified. Attention is required because most objects have multiple attributes (e.g., the colors, shapes, and orientations of several parts and the relationship between those parts). In the absence of attention, those attributes cannot be bound together in a manner that permits unambiguous identification. This is known as the binding problem (Treisman, A., 1996; von der Malsburg, C., 1981). Figure 1 provides a demonstration.

It is relatively hard to find the plus with black vertical and white horizontal arms on the left (there are two of them) because there are other items that are black and white and vertical and horizontal in the figure. Without attention, the correct binding of color to orientation is not available. It is easier to find either black vertical or white horizontal on the right of the figure because the black vertical items are the only items with the properties, black and vertical. It would be even easier if the target was the only black or the only vertical item (see below). Figure 1 may also illustrate this point in another way. Look at the right panel of the figure and then return to this paragraph. Did you see a white bar, tilted to the right? If you are sure you did, you may have experienced an illusory conjunction of features (see Treisman, A., 1996). There are white objects and right tilted objects, but no white objects tilted to the right. Illusory conjunctions can be described as binding errors, perhaps reflecting the fact that color and orientation (in this example) are processed in different parts of the visual system and need to be bound to a single object, one attended object at a time.

2.16.2 How Do We Study Visual Search?

The choice of methods with which to study visual search depends on the question under study and the stimulus used. Searches with large detailed images require eye movements, as do most real-world searches. Measurements of those eye movements can give useful information about the progress of the search (Zelinsky, G. J. and Sheinberg, D. L., 1997). Voluntary, saccadic eye movements occur at a rate of about 3–4 Hz. Covert attentional deployments can be separated from the point of fixation and can occur at a faster rate. Many visual search tasks use stimuli large enough to render eye movements unnecessary or they present stimuli for a period brief enough to render voluntary eye movements impossible. Under these circumstances, the primary measures of search performance are derived from reaction time (RT) data and/or accuracy data.

2.16.2.1 Real Time Methods

In typical RT studies, observers search for a target item among a variable number of distractor items under the instruction to respond as quickly and accurately as possible. The primary interest is in the relationship of RT to set size, the number of items in the display. The slope of the RT × set size function is a measure of search efficiency, the rate with which items can be processed. In a search for a target defined by a single basic feature (e.g., a red target among green distractors), slope will be near zero, as if all items are processed in a single step. If no basic feature information distinguishes a simple target from distractors and if the items are large enough to be resolved without requiring eye movements, search slopes will typically fall in the range of 20–40 μs per item on trials when the target is present and a bit more than twice that when the target is absent. Going from that slope to an estimate of items processed per second requires assumptions about, for example, whether search samples the display with or without replacement (see below) or whether we have the attentional capacity to attend to more than one item at a time (Cavanagh, P. and Alvarez, G. A., 2005). Search slopes can be much steeper if items are hard to identify (e.g., a random complex target shape

among similar distractor shapes). If each item must be fixated, slopes will reflect the slow rate of eye movements (3–4 s^{-1}).

2.16.2.2 Accuracy Methods

In RT tasks, stimuli are typically visible until response, and errors are typically held to 5–10%. False alarm errors are very rare. Accuracy methods typically use brief presentations and/or degraded/masked stimuli in order to force observers to respond on the basis of incomplete information. This creates patterns of errors that are amenable to analysis by various decision theory methods. RT and accuracy methods often produce converging results but the different stimulus conditions sometimes lead to different conclusions about underlying mechanisms of search. For example, effects of reentrant feedback will be hard see with brief, masked stimuli (Di Lollo, V. *et al*., 2000).

2.16.2.3 Neurophysiological, Lesion and Microstimulation Studies of the Neural Mechanisms that Mediate Visual Search

Electrophysiological studies in humans and nonhuman primates have helped characterize the neural mechanisms that mediate visual search. The N2pc component of the event-related potential (ERP) has been an effective measure of the temporal dynamics of attention. Positron emission tomography (PET) and functional magnetic resonance imaging (fMRI) have been used to identify a frontoparietal network of regions active in search. These studies are complemented by microstimulation studies in nonhuman primates that have implicated the frontal eye fields (FEF) in the allocation of spatial attention (Moore, T. and Fallah, M., 2001). Studies in nonhuman primates have found that selection of a target from among distracters is strongly impaired when extrastriate visual areas V4, TEO, and MT are lesioned (Schiller, P., 1993; De Weerd, P. *et al*., 1999). Single-unit recording studies have found that neurons in these and other visual cortical areas are more responsive to stimuli that appear at an attended location (for a review, see Reynolds, J. H. and Chelazzi, L., 2004). There is also evidence that these areas are modulated by nonspatial forms of attention. For example, Chelazzi L. *et al*. (1993) trained monkeys to perform a visual search task in which the target was presented and then, after a brief pause, a search array appeared. They found that, during the pause period, the baseline firing rate of neurons in area TEO was elevated whenever the monkey prepared to search for a target that contained the neuron's preferred features. Then, when the search array appeared, the response to the array was initially undifferentiated, but over time separated out, with higher firing rates observed on trials when the monkey was searching for the preferred stimulus. This elevated firing rate occurred in the absence of knowledge about where the target would appear in the array, so it illustrates a spatially nonselective, feature-selective signal that is posited by the guided search model. Evidence for feature-based attentional signals has also been found in areas V4 and MT. Feature-based attentional modulation has also been observed in human subjects using fMRI (reviewed in Reynolds, J. H. and Chelazzi, L., 2004). The view that has emerged from these studies is that the frontoparietal network that is active during search is the source of spatial and nonspatial descending control signals that modulate the responses of neurons in the visual cortices, causing them to enhance processing of visual targets while suppressing processing of irrelevant distracters.

2.16.3 What Determines the Efficiency of Visual Search

2.16.3.1 Feature Guidance

As noted above, some visual search tasks are highly efficient, with attention directed to the target item with little or no distraction from other items. A limited number of stimulus attributes seem to be able to guide attention to targets. These include obvious attributes such as color and size as well as less obvious attributes such as a variety of depth cues. Some important features of the stimulus (e.g., intersection type) fail to attract attention. Similarly, even though they are very interesting to the visual system, stimuli like faces and letters do not seem to guide attention (though this remains a contentious point). The set of guiding attributes probably numbers 12–18 (Wolfe, J. M. and Horowitz, T. S., 2004).

Even if a target is defined by a guiding feature, search will be efficient only if a variety of other conditions are met. Search efficiency declines as the similarity of targets and distractors increases. Thus, search for 0° (vertical) among 30° distractors is typically efficient while search for 0° among 10° is not. Search efficiency declines as the heterogeneity of the distractors increases. Thus, search for green among yellow is trivial. Search for green among yellow, red,

blue, etc. is less efficient. For purposes of guidance, attributes appear to be coarsely and, perhaps, categorically coded. For example, a target tilted 10° to the right of vertical will be easier to find among distractors tilted 50° to the left and 50° to the right of vertical than among distractors tilted 70° to the right and 30° to the left. In both cases, distractors are 40° and 60° different from the target but in the first case, the target is uniquely steep. It is not uniquely steep in the second case because the 30° items are also steep.

2.16.3.2 Other Factors

Targets can be identified by conjunctions of features. Thus, search can be very efficient for targets that are red and vertical among distractors that are red and horizontal or green and vertical. Most real world search items are conjunctively defined. Your shoes will be defined as search items by their color, size, and so on. Search will be reasonably efficient even in the presence of other objects of similar color or size. Certainly, you will not need to examine every object in the scene as a candidate shoe. In general, you seem to be able to specify one feature per attribute. Thus, search is inefficient if the target is red and yellow and distractors are red–blue and blue–yellow.

As search stimuli become more complex, other factors come into play. For example, scene properties guide the deployment of attention given enough time. Thus, we do not search for people in places that will not support people, for example, the middle of the ceiling (Torralba, A. *et al.*, 2006). It is also possible to search in some ordered manner (e.g., left to right) though, again, this requires time.

2.16.4 Modeling Visual Search

2.16.4.1 Signal Detection Approaches

Visual search can be modeled as a signal detection problem with multiple noise sources. Rather than determining if a particular item is signal or noise, the observer must determine if a signal is present in a whole display. When a few, relatively simple stimuli are presented briefly, signal detection models have proven fruitful. Here observers typically make a two-alternative forced-choice response to a stimulus that can be quite precisely characterized (Verghese, P., 2001). Matters become more complicated when search stimuli remain visible until the observer responds. Now, from the vantage point of decision theory, search becomes a series of decisions. When an observer attends to an item, the observer decides if that item is the target. In signal detection terms, the observer will decide if the signal generated by that item exceeds a target criterion value. If the item is deemed to be the target, the observer responds positively and ends the trial. However, if the signal does not exceed the target criterion, the observer must make a second decision about whether to continue searching or quit with a negative response. This negative response would be made if some other signal exceeds a second, quitting criterion. The complexity of this situation has restricted most signal detection models to the more tractable, brief exposure condition.

2.16.4.2 Physiological Approaches

From a physiological point of view, a central issue is how neurons that might respond to many stimuli in many locations (e.g., inferotemporal cortex neurons) and come to have their activity dominated by one stimulus in one location. Early models had a feedforward structure where early visual processes were not influenced by attention. Attention served as a gate or filter permitting some stimuli to reach later stages. More recent modeling, based on the accumulation of more recent data, proposes that attentional effects can feedback on to the earliest stages of visual cortical processing (Reynolds, J. H. and Chelazzi, L., 2004).

2.16.4.3 Biased Competition

Desimone and Duncan's Biased Competition model is illustrative. When activity from more than one stimulus converges on the same neurons, a competition results that will be won, at least temporarily, by one of the contenders. That victory influences other visual areas so that one stimulus will tend to emerge as the currently favored or attended item. Other theories differ in many details but many share the general notion that the same neural network can settle into multiple states, depending on top-down and bottom-up, stimulus-driven factors.

Experimental evidence has revealed several types of attentional effects on the responses of single neurons. Attention can boost the signal. It can act to exclude noise. The tuning of a receptive field might be changed (e.g., sharpening the tuning for orientation) or the spatial extent of a receptive field might shift or shrink to exclude all but the attended item.

2.16.4.4 Two-Stage Models

In two-stage models, a distinction is made between processing that occurs before the effects of selective attention and processing that comes after. In their early formulations, these models assumed that before and after referred to anatomical location as well as temporal order. As in physiological modeling, more recent versions of these theories have allowed for the possibility of feedback or reentrant processing that would make it possible for one anatomical location to participate in both preattentive and attentive processing of stimuli.

2.16.4.5 Feature Integration Theory

The most influential two-stage model has been Anne Treisman's Feature Integration Theory. It proposed that a limited set of basic features (e.g., color, size, etc.) could be processed in parallel across the visual field. Any operation that required the binding together of two or more of these features would require attention to a single item or, perhaps, a small group of items. Thus, preattentive processes could distinguish a red line from a green one but attention would be required to distinguish a red vertical line from green vertical and red horizontal lines (Treisman, A. and Gelade, G., 1980).

2.16.4.6 Guided Search

Feature Integration Theory was parent to a family of subsequent models. Many of these include the concept of guided search. In guided search, the information gathered about basic features can be used to guide attention toward likely targets. Thus, if an observer is looking for a red letter T, attention will be guided to red letters and not wasted on letters that could never be the target (Wolfe, J. M., 1994). In two-stage modeling, critical questions include the nature of the stimulus attributes that can be processed prior to attentional selection as discussed earlier. Some attributes, like color and orientation clearly fall into the preattentive category. The more interesting and problematic cases are complex and/or learned classes of stimuli like faces and letters.

All models must resolve issues about the nature of selection. What is selected? If objects are selected, how are objects parsed from the background prior to selection? What are the limits on selection? Can more than one item be selected at one time? What does selection do? Does it enhance processing? Does it enable different types of processing?

2.16.5 Memory in Visual Search

Since visual search tasks are typically extended in time, the role of memory becomes an issue. Does the visual system use what has happened in the search so far in order to determine what will happen next? In models that propose that attention is directed from one item to the next in series, the question is whether previously attended items can be resampled during the same search. Classic two-stage models assumed that search proceeded without replacement. Research on the phenomenon of inhibition of return showed that it was harder to get attention and/or the eyes to return to a previously attended/fixated item than it was to move attention or the eyes to a new, unattended item. However, later research showed that inhibition of return was limited to only a few items and several lines of experiments produced data consistent with sampling with replacement – a random deployment of attention without regard to the prior history of search. Current consensus suggests that visual search uses only a very modest memory to limit the revisiting of previously attended items (Horowitz, T. S. and Wolfe, J. M., 2005).

2.16.6 Terminating Unsuccessful Searches

All visual searches must come to an end. Successful searches are easy to understand. Search ends when the target is found. More problematic is the case of unsuccessful search. When does the search end if the target is not found? Models that propose serial selection of items have a simple answer. Search ends when all items have been selected and rejected. However, this only works if observers have perfect memory for attended and rejected items and, as noted above, it is quite clear that this is not the case. Instead, search must end when the observer deems that he has searched for long enough. It proves to be difficult to produce a satisfying definition of long enough. It may be based on elapsed time or on some search metric such as the proportion of items rejected (regardless of whether they have been inadvertently rejected more than once). At present, this has proven to be one of the more recalcitrant problems in visual search.

2.16.7 Conclusion

The problem of unsuccessful searches provides an opportunity to revisit the question of why anyone should care about the mechanics of visual search. As noted at the outset, search is a ubiquitous visual behavior because of limits on visual processing capacity. From a more practical point of view, understanding search is important because our civilization has a knack for creating very difficult artificial search tasks and then insisting that they be done very well. Airport baggage screening and routine medical screening (e.g., mammography) are examples. The stimuli are complex. The targets are rare, so most searches will be unsuccessful. Errors, especially misses, can be a matter of life and death. Advances in the understanding of search may make it possible to design such tasks for greater success.

References

Cavanagh, P. and Alvarez, G. A. 2005. Tracking multiple targets with multifocal attention. Trends Cogn. Sci. 9, 349–354.

Chelazzi, L., Miller, E. K., Duncan, J., and Desimone, R. 1993. A neural basis for visual search in inferior temporal cortex. Nature 363, 345–347.

De Weerd, P., Peralta, M. R., 3rd, Desimone, R., and Ungerleider, L. G. 1999. Loss of attentional stimulus selection after extrastriate cortical lesions in macaques. Nat. Neurosci. 2, 753–758.

Di Lollo, V., Enns, J. T., and Rensink, R. A. 2000. Competition for consciousness among visual events: the psychophysics of reentrant visual processes. J. Exp. Psychol. Gen. 129, 481–507.

Horowitz, T. S. and Wolfe, J. M. 2005. Visual Search: The Role of Memory for Rejected Distractors. In: Neurobiology of Attention (*eds*. L. Itti, G. Rees, and J. Tsotsos), pp. 264–268. Academic Press/Elsevier.

Moore, T. and Fallah, M. 2001. Control of eye movements and spatial attention. Proc. Natl. Acad. Sci. U. S. A. 98, 1273–1276.

Palmer, J., Verghese, P., and Pavel, M. 2000. The psychophysics of visual search. Vision Res. 40, 1227–1268.

Reynolds, J. H. and Chelazzi, L. 2004. Attentional modulation of visual processing. Annu. Rev. Neurosci. 27, 611–647.

Schiller, P. 1993. The effects of V4 and middle temporal (MT) lesions on visual perfromance in the rhesus monkey. Vis. Neurosci. 10, 717–746.

Torralba, A., Oliva, A., Castelhano, M. S., and Henderson, J. M. 2006. Contextual guidance of eye movements and attention in real-world scenes: the role of global features on object search. Psychol. Rev. 113, 766–786.

Treisman, A. 1996. The binding problem. Curr. Opin. Neurobiol. 6, 171–178.

Treisman, A. and Gelade, G. 1980. A feature-integration theory of attention. Cogn. Psychol. 12, 97–136.

Verghese, P. 2001. Visual search and attention: a signal detection approach. Neuron 31, 523–535.

von der Malsburg, C. 1981. The Correlation Theory of Brain Function. Max-Planck-Institute for Biophysical Chemistry.

Wolfe, J. M. 1994. Guided Search 2.0: a revised model of visual search. Psychon. Bull. Rev. 1, 202–238.

Wolfe, J. M. and Horowitz, T. S. 2004. What attributes guide the deployment of visual attention and how do they do it? Nat. Rev. Neurosci. 5, 495–501.

Zelinsky, G. J. and Sheinberg, D. L. 1997. Eye movements during parallel/serial visual search. J. Exp. Psychol. Hum. Percept. Perform. 23, 244–262.

2.17 Object-Based Attention

M J Valdés-Sosa, V Rodríguez, and J Iglesias, Cuban Center for Neuroscience, Habana, Cuba

Published by Elsevier Inc.

2.17.1	Surface-Based Attentional Selection	282
2.17.2	Neural Basis of Surface-Based Attention	284
2.17.3	Neural Basis of Competitive Interactions	285
2.17.4	Neural Integration of Competition	286
2.17.5	Neural Control Signals (Bias Inducers)	287
2.17.6	Other Approaches to Object-Based Attention	288
2.17.7	Unanswered Questions	288
References		288

Glossary

event-related potential (ERP) Voltage fluctuations recorded at the scalp that represent the activity of large neural populations time-locked to measurable events.

Gabor patches Image modified by a filter impulse response defined by a harmonic function multiplied by a Gaussian function.

object-token An episodic trace containing information about the relationship between object features, possibly enriched by object-related knowledge from long-term memory, and addressed via location codes.

single-unit recording Refers to the use of an electrode to record the electrophysiological activity (action potentials) of a single neuron.

Although visual scenes are full of numerous locations, features, and objects, only a small portion of this rich information influences action and memory systems or reaches awareness (Desimone, R. and Duncan, J., 1995; Duncan, J., 2006). Diverse stimuli compete for what we know as visual attention. In previous chapters, attentional selection of spatial locations and features has been examined. However, in natural scenes objects of interest (e.g., a predator observed by its prey) can rapidly change location and specific visual features (such as presented shape and shading). The relevant objects can also be in close visual proximity to, or partially overlapped by irrelevant distracters. In these situations it makes sense to monitor the object itself, not the location or the changeable features of the object. These ecological considerations suggest that competition between objects as distinct entities (and not just a sequence of locations or disconnected features) is a fundamental aspect of visual attention. This conclusion is supported by the experimental evidence reviewed in this chapter. This does not imply that we are not capable of selectively attending to locations or features (which we can), it just means that there are important visual tasks that require attention to objects as wholes.

Given that objects exist in space and have characteristic features, for the goals of this chapter it is necessary to demonstrate in any experiment that it is the object and not only its location or features that are being selected by attention. This has been achieved using three approaches (Valdes-Sosa, M. *et al.*, 1998b; O'Craven, K. *et al.*, 1999; Valdes-Sosa, M. *et al.*, 2000). The first tack is to graphically superimpose distinct objects in order to impede spatial selection. Under these conditions detecting or remembering a stimulus is much better for events related to attended, than to unattended, objects (Neisser, U. and Becklen, R., 1975; Rock, I. and Gutman, D., 1981). Studies using superimposed stimuli have also found that it is easier to divide attention between two features on one object, than

to do so for two features of different objects, even when the two objects are in intimate spatial proximity (Duncan, J., 1984; Vecera, S. P. and Farah, M., 1994; Lavie, N. and Driver, J., 1996; Behrmann, M. *et al.*, 1998). This pattern of results cannot, therefore, be attributed to the time required to shift attention from the location of one stimulus to the location of the other. This is incompatible with the classical spotlight metaphor for spatial attention. However, in the above mentioned experiments the competing objects did not completely overlap, and the findings could therefore be explained by a hybrid mechanism whereby the selection of spatial locations is guided by objects (Vecera, S. P. and Farah, M., 1994).

The second approach is to pit the influence of object organization within visual scenes against spatial proximity. Dividing spatial attention is more difficult for locations farther apart (Egly, R. and Homa, D., 1991), but this spatial effect can be overruled when separate stimuli are perceived as part of the same object (Bundesen, C. and Pedersen, L. F., 1983; Driver, J. and Baylis, G. C., 1989; Kramer, A. F. and Jacobson, A., 1991; Driver, J. *et al.*, 1992). Further, attention spreads more readily between locations within a three-dimensional surface than among points in a different surface, even if they are spatially closer together (reviewed in Nakayama, K. *et al.*, 1995). It is also easier to shift attention between sites within the same figure than between parts of different figures, even for equivalent distances (Egly, R. and Homa, D., 1991; Valdes-Sosa, M. *et al.*, 2004).

The third method is to move the objects in order to dissociate them from a fixed location. Object-based effects have been inferred (Tipper, S. P. *et al.*, 1991; 1994) from the observation that attention can follow the stimuli, instead of being glued to a location. For example, Kahneman D. *et al.* (1992) have shown object-based priming effects: the facilitation in recognition of specific letters by repetition is larger if the repeats are presented within the same moving objects.

Taken together, these experiments provide psychophysical evidence for object-based attention not easily explained by implicit spatial- or feature-based selection. However, modifications of theories about spatial- or feature-based attention could also explain part of the findings. As mentioned above, a flexible attentional spotlight that follows the silhouette of objects would guarantee selection of partially overlapping objects. In the following section we present a situation in which these types of selection are precluded.

2.17.1 Surface-Based Attentional Selection

In this chapter we concentrate on research involving selective attention to one of two superimposed transparent surfaces. This stimulus configuration offers several advantages for understanding object-based attention and has been studied recently with multiple approaches including psychophysical (Valdes-Sosa, M. *et al.*, 1998b; 2000; Rodriguez, V. *et al.*, 2002; Reynolds, J. H. *et al.*, 2003), electrophysiological (Pinilla, T. *et al.*, 2001; Khoe, W. *et al.*, 2005; Rodriguez, V. and Valdes-Sosa, M., 2006), functional magnetic resonance imaging (fMRI; O'Craven, K. *et al.*, 1999; Serences, J. T. *et al.*, 2004), and monkey single-unit experiments (Fallah, M. *et al.*, 2007; Wanning, A. *et al.*, 2007).

Transparency arises when more than one surface lies along a line of sight. Transparent motion is created when different visual patterns (say two sets of dots, or an image of a face and of a house) move in distinct directions within the same region of visual space (see examples in Figure 1). This creates the illusion of two surfaces (or objects) sliding across each other. Each surface is a distinct entity or object-token (Kahneman, D. *et al.*, 1992), and its individuality is preserved by over time and space (Blazer, E. *et al.*, 2000; Valdes-Sosa, M. *et al.*, 2000).

Transparency is ideal for isolating object-based attention since it combines the three approaches outlined above. A spatial spotlight of attention would find it difficult to select only one of the surfaces: it would tend to encompass both or neither. This is especially true for the sliding dots situation. The dots that define two different surfaces are densely intermingled, thus precluding selection of one surface's dots via spatial attention. Finally, stimulus elements are not fixed in location.

Several studies have shown that it is possible to selectively attend to one of two transparent surfaces. Specifically, with sliding dots (Figure 1(a)) is easier to divide attention between the direction and speed of motion of the same surface than between identical attributes for different surfaces (Valdes-Sosa, M. *et al.*, 1998b), which is also true for direction of motion and shape of the moving elements (Rodriguez, V. *et al.*, 2002). Note that since the overlap between the two surfaces is very complete, this data can not be explained by a spotlight of attention, and moreover cannot be explained by object-guided spatial selection.

In one study using transparent surfaces (Valdes-Sosa, M. *et al.*, 2000), subjects discriminated brief

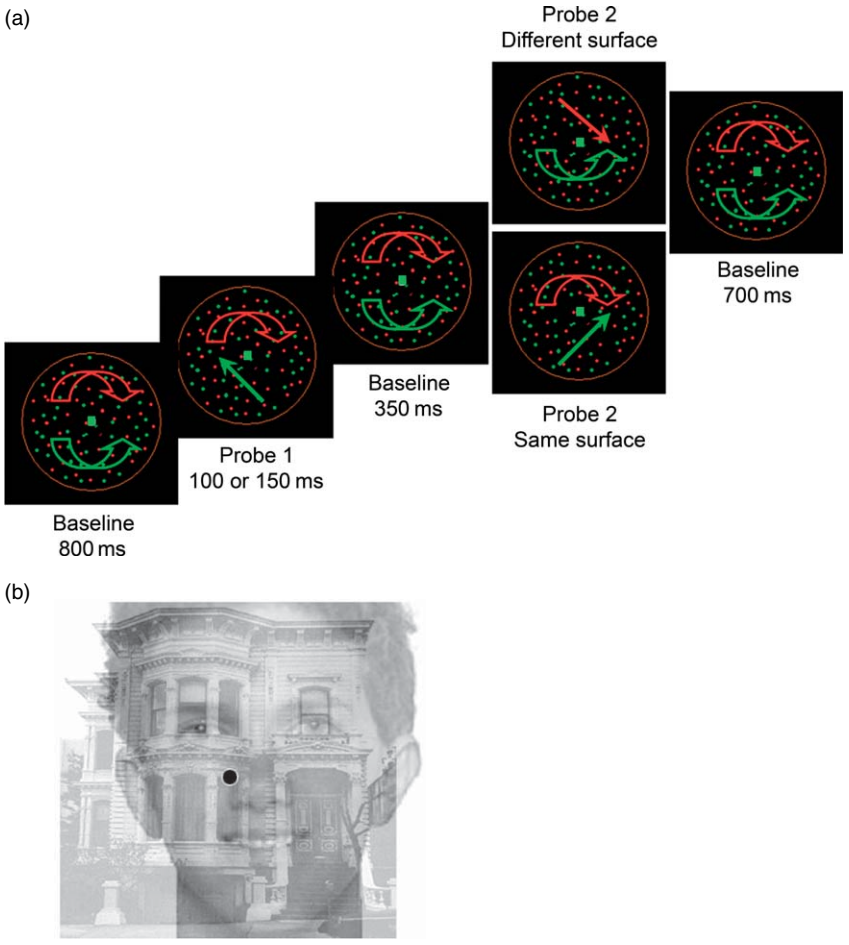

Figure 1 Two experimental designs using transparency for studying object-based attention. (a) Transparent surfaces used by Valdés-Sosa M. *et al.* (1998a; 1998b; 2000), generated by rotating two sets of dots (one red, the other green) in opposite directions. Subjects had to report the direction of two brief changes in the direction of motion of one surface (the second event affected either the same or a different surface than the first, defining two types of trial). (b) Stimuli used by O'Craven K. *et al*. (1999), which consisted in a face transparently superimposed on a house, one moving and the other stationary. Subjects were asked to attend to the face, the house or the motion. (b) Adapted from O'Craven, K., Downing, P. E., and Kanwisher, N. G. 1999. fMRI evidence for objects as the units of attentional selection. Nature 401, 584–587, with permission from Macmillan Publishers Ltd.

changes in the direction of motion of the surfaces. A set of green and a set of red dots rigidly rotated in opposite directions (Figure 1(a)). Subsequently the dots from one surface briefly underwent a translation (T1). This induced the illusion that the surface defined by one pattern of dots suddenly heads in another direction, and rapidly returns to its original motion. After an additional period of rotation, either the same or the other surface underwent another change in direction (T2). Observers reported the direction taken by both targets (T1 and T2). The surface affected by T1 was cued in advance by the color of the fixation point (an endogenous cue for attention), whereas the surface affected by T2 was unpredictable (see two types of trials in Figure 1(a)). Note that T1 itself could attract attention to the surface (this acting as an exogenous cue for attention).

The direction of the first translation (T1) was discriminated accurately under all conditions (Figure 2(a)). Performance was also high for the second translation (T2) if it involved the same surface as T1. In sharp contrast, observers were unable to discriminate T2 when it involved the other surface from T1 and the delay between the two events was short (in the example of Figure 2(a) about 400 ms). Not only is discrimination affected, but it is also difficult to merely detect the T2 motion (Pinilla, T. *et al.*, 2001). Thus, it takes time to shift attention from

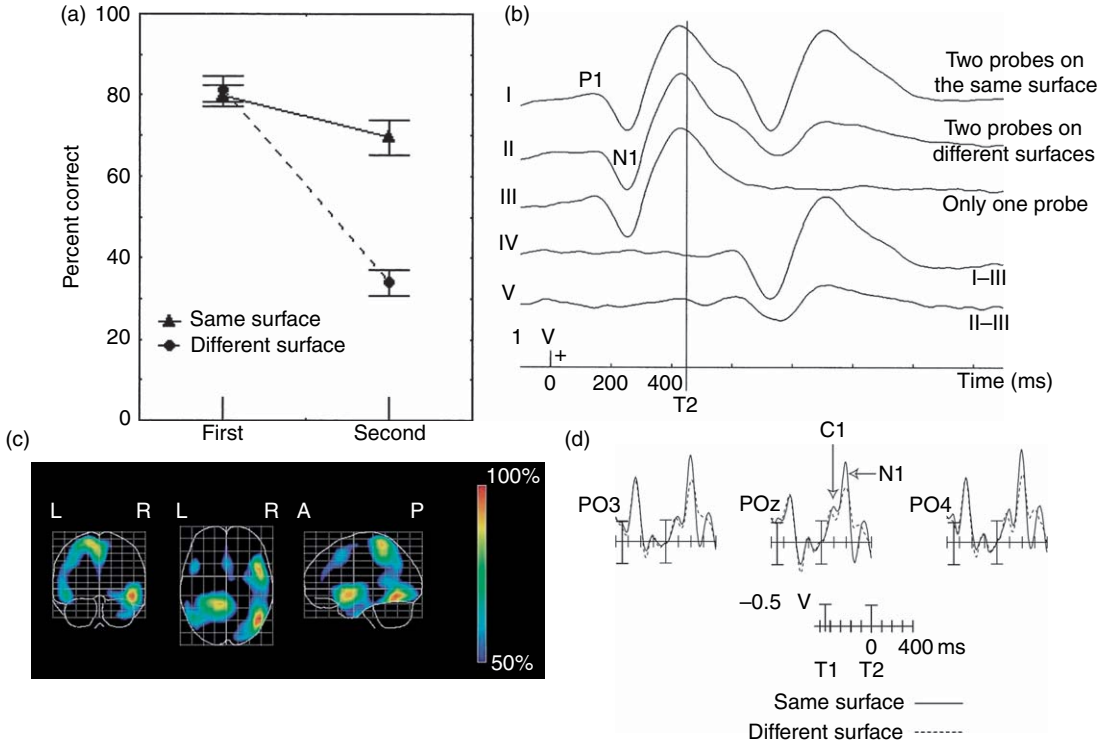

Figure 2 Neural basis of surface-based attention. (a) Attentional interference in the paradigm of Figure 1(a). Response accuracy as a function of the two events: lines represent either same – or different – surface trials. (b) Grand average event-related potentials (ERPs) elicited by the events in Figure 1(a) from a posterior temporal electrode for same- (I) and different-surface (II) trials. Below, difference waveforms (IV–V) which isolate response to second event. (c) Current source density modeling for N200 attentional effect. The largest current sources were found at visual extrastriate areas (posterior right middle-temporal and lateral occipito-temporal gyri). (d) Attentional effect on the grand average ERPs obtained by Khoe W. *et al*. (2005) in a modified sliding-dots paradigm. (a, b) Reprinted from Pinilla, T., Cobo, A., Torres, K., and Valdes-Sosa, M. 2001. Attentional shifts between surfaces: effects on detection and early brain potentials. Vision Res. 41, 1619–1630, with permission from Elsevier. (c) Adapted from Rodriguez, V. and Valdes-Sosa, M. 2006. Sensory suppression during shifts of attention between surfaces in transparent motion. Brain Res. 1072, 110–118, with permission from Elsevier. (d) Adapted from Khoe, W., Mitchell, J. F., Reynolds, J. H., and Hillyard, S. A. 2005. Exogenous attentional selection of transparent superimposed surfaces modulates early event-related potentials. Vision Res. 45, 3004–3014, with permission from Elsevier.

one surface to another even though they occupy the same region of visual space. Similar results have also been evinced with pairs of superimposed Gabor patches that change orientation, spatial frequency, and color (Blazer, E. *et al*., 2000).

Selective attention for transparent surfaces is not only incompatible with spatial selection. It cannot be explained by the feature selection. The set of possible directions of translation for T1 and T2 were the same for both surfaces, hence motion direction was not the basis of selection. And though color possibly guides attention in these experiments, it is not indispensable, since the between-surface attentional interference is still found when the two surfaces have the same color (Rodriguez, V. *et al*., 2002; Mitchell, J. F. *et al*., 2003).

Further work has shown that these surface-based effects can be found in the absence of endogenous precueing (and thus volitional control of attention), since changes in one surface will automatically attract attention to it (Rodriguez, V. *et al*., 2002; Mitchell, J. F. *et al*., 2003). In contrast, another study (Lopez, M. *et al*., 2004) has shown that endogenous – in absence of exogenous – cueing also enables surface-based selection, so both types of biases can influence in object-based attention.

2.17.2 Neural Basis of Surface-Based Attention

Recent research on the neural basis of attention has been guided by the Biased (or Integrated) Competition model (Desimone, R. and Duncan, J., 1995; Duncan, J., 2006). This model has three basic

ideas; (1) Neural representations of objects compete, with activation of one representation leading to suppression of others; (2) This competition can be biased by stimulus (exogenous) factors like salience or by top-down (endogenous) signals from task context, such as the subjects goals; (3) Despite a disperse cortical representation with different object features and properties coded across multiple brain areas, competition is integrated: dominance in one brain site boosts responses to the same object in other sites. We review evidence on the neural basis of surface-based attention within this framework.

2.17.3 Neural Basis of Competitive Interactions

Considerable effort has been devoted to establishing the brain sites where attentional competition is played out, that is where the unattended inputs are filtered out and where the attended inputs are boosted. In fact, different types of visual attention could operate at different stages of visual processing (Treue, S. and Maunsell, J., 1996; Luck, S. J. *et al.*, 1997; Chelazzi, L. *et al.*, 1998; Duncan, J., 2006). Here we consider this question for visual surfaces which has been studied event-related potentials (ERPs), fMRI, and single-unit recordings in monkeys.

ERPs are voltage fluctuations (recorded at the scalp) that are driven by the activity of large neural populations time-locked to measurable events. Different components of the ERP arise from distinct cortical sites (Hillyard, S. A. and Anllo-Vento, L., 1998). ERPs triggered by the motion-direction changes (T1 and T2) in the sliding-dot paradigm described above were recorded when the time interval between the two events was held at about 400 ms, in other words at a timing when it was difficult to shift attention between the two surfaces (Pinilla, T. *et al.*, 2001). Both the responses contained a negative wave known as N200 (Figure 3), which reflects motion processing (Kuba, M. and Kubova, Z., 1992; Bach, M. and Ullrich, D., 1994; Torriente, I. *et al.*, 1999). This wave begins at about 180 ms after stimulus onset.

The N200 elicited by T2 was significantly reduced when the translations involved different surfaces, relative to when they involved the same surface (Figure 2(b)).This suggests that when attention is allocated to one surface, this reduces the neural response evoked by the translation of the other surface. In experiment just described, it was not possible to find an effect on the earlier P1 component (which

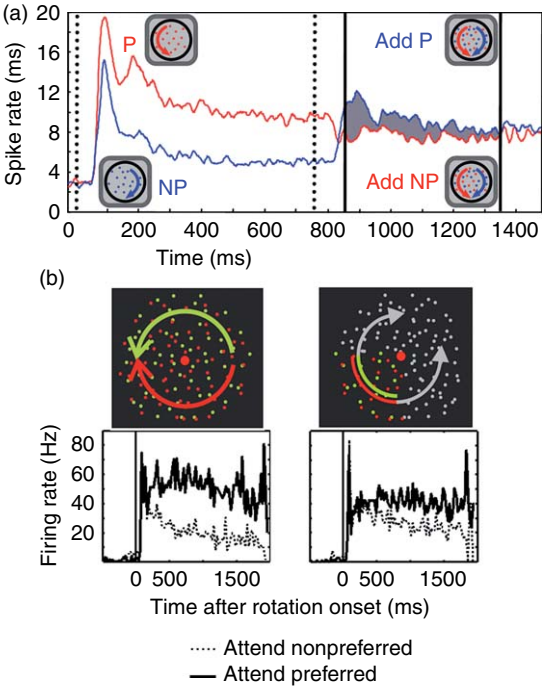

Figure 3 Surface-based attentional effects on unit activity in monkeys. (a) Population average responses in V4 obtained by Fallah M. *et al*. (2007). Red line indicates the response when the nonpreferred surface appeared last, and blue line when the preferred surface appeared last (the last surface attracts attention). (b) Response modulation of an MT neuron (Wanning, A. *et al*., 2007) during the rotation of two transparent surfaces while monkeys selectively attended the cued surface. To the left the surfaces had different colors during all the trial; to the right the surfaces were only colored in a small part of the display. In both cases the neuron responded more to motion in the preferred direction when it was attended. (a) Adapted from Fallah, M., Stoner, G. R., and Reynolds, J. H. 2007. Stimulus-specific competitive selection in macaque extrastriate visual area V4. Proc. Natl. Acad. Sci. U. S. A. 104, 4165–4169 with permission from PNAS. (b) Reprinted from Wanning, A., Rodriguez, V., and Freiwald, W. A. 2007. Attention to surfaces modulates motion processing in extrastriate area MT. Neuron 54, 639–651, with permission.

is clearly modulated by spatial attention). This seems to suggest that surface attention takes place later than spatial selection, but probably does not apply to all situations since when the observer's perceptual load and the time required to sustain attention on one surface is increased, both the N200 and P1 are reduced more than what is typical for spatial selection, with the virtual suppression of both components (Valdes-Sosa, M. *et al.*, 1998a).

The N200 attentional-effect seems to originate from reduced activity of neural generators in visual extrastriate cortex, possibly involving MT

(Rodriguez, V. and Valdes-Sosa, M., 2006), a visual cortical area specialized in motion processing (Albright, T. *et al.*, 1984; Figure 2(c)).The reduction of N200 for unattended surfaces has also been described by Khoe W. *et al.* (2005), who also found smaller P1 and C1 (that peaks at about 92 ms after stimulus onset; Figure 2(d)).This last wave originates in primary visual cortex, suggesting that surface-based attention may influence processing at this early stage (Mitchell, J. F. *et al.*, 2004).

Although the temporal resolution of ERPs is good, localization of their neural sources is not precise. fMRI, despite its slow temporal response, has more spatial resolution. Hence it is reassuring that when observing two transparent surfaces, one due to translating dots and the other to expanding dots, fMRI activity is reduced in V1 when attention was directed to the expanding surface, a less effective stimulus for V1 than translation (Watanabe, K. *et al.*, 1998). This reinforces the idea that attention can modulate activity in the earliest stages of cortical visual processing.

Additional information has been obtained from single-units recordings in awake monkeys. Fallah *et al.* (2007) adapted the paradigm developed for human studies (Valdes-Sosa, M. *et al.*, 1998b; Reynolds, J. H. *et al.*, 2003) for use with monkey observers, while recording in V4, a cortical area specialized for form and color processing. They delayed the onset of one of the surfaces in time relative to the other surface (see Figure 3(a)), taking advantage of the fact that attention is drawn to a newly appearing stimulus (Yantis, S. and Jonides, J., 1984; Yantis, S. and Egeth, H. E., 1997; Gottlieb, J. P. *et al.*, 1998). This is an example of stimulus-driven (or exogenous) attentional capture (Mitchell, J. F. *et al.*, 2003). V4 neurons selective for the color of the attended surface responded strongly, while responses of neurons selective for the unattended stimulus were suppressed. Neuronal responses were driven preferentially by the delayed surface (Figure 3(a)), a difference that resulted from both an increase in response upon addition of the preferred-color surface and a decrease in response upon addition of the nonpreferred-color surface.

Furthermore, Wanning A. (2007) demonstrated a surface-based effects in macaque monkeys performing an attention-demanding direction discrimination task, in a paradigm closer to the one originally employed in humans (Valdes-Sosa, M. *et al.*, 2000). They trained two macaque monkeys to selectively attend one of two overlapping transparent surfaces by matching its color with the fixation spot, a form of goal-driven (or endogenous) attentional control while recording in MT. After a period of reversing rotations, the two surfaces underwent simultaneous translations in different directions. The monkeys reported with a saccade the direction of this translation for the attended surface. Motion selectivity was observed during the rotations and translations, one direction eliciting a robust response and the others a poor response. The MT neurons were driven more by motion in the attended surface than in the nonattended surface for both rotations and translations (Figure 3(b)). This surface-based effect survived when the difference in color between surfaces was removed (Figure 3(b)).

Taken together ERP, fMRI, and single-unit studies indicate that competition between these surfaces is played out at early stages of visual processing (certainly involving extrastriate areas and with weaker evidence for V1), beginning very shortly after stimulus onset.

2.17.4 Neural Integration of Competition

As mentioned above, attention to one attribute of an object – or surface – can entail some degree of obligatory attention to other attributes of the same object (for psychophysical evidence see Duncan, J. *et al.*, 1994; Egly, R. *et al.*, 1994; He, Z. J. and Nakayama, K., 1995; Duncan, J. and Nimmo-Smith, M. I., 1996). In a seminal experiment (O'Craven, K. *et al.*, 1999) observers viewed a sequence of superimposed pairs of semitransparent images (one face and one house, Figure 1(b)). One image was stationary while the other oscillated. In each block observers judged whether an object of one class (house or face) was repeated while ignoring the other class. Responses in FFA (a visual area responding preferentially to faces) and in PPA (a visual area responding preferentially to scenes or houses) were enhanced when attention was directed towards its preferred object type relative to when directed towards the other class (Figure 4(a)).

While providing additional support for object-based attention, this experiment evinced integration of responses from different visual extrastriate areas. Even though motion was ignored in this experiment, activity in the area sensitive to motion (MT+) increased when the attended object was moving relative to when the unattended object was moving (Figure 4(b)). This is consistent with the integrated competition-model: neurons coding features of the attended object assume dominance throughout distributed brain networks (see also Mitchell, J. F. *et al.*, 2004).

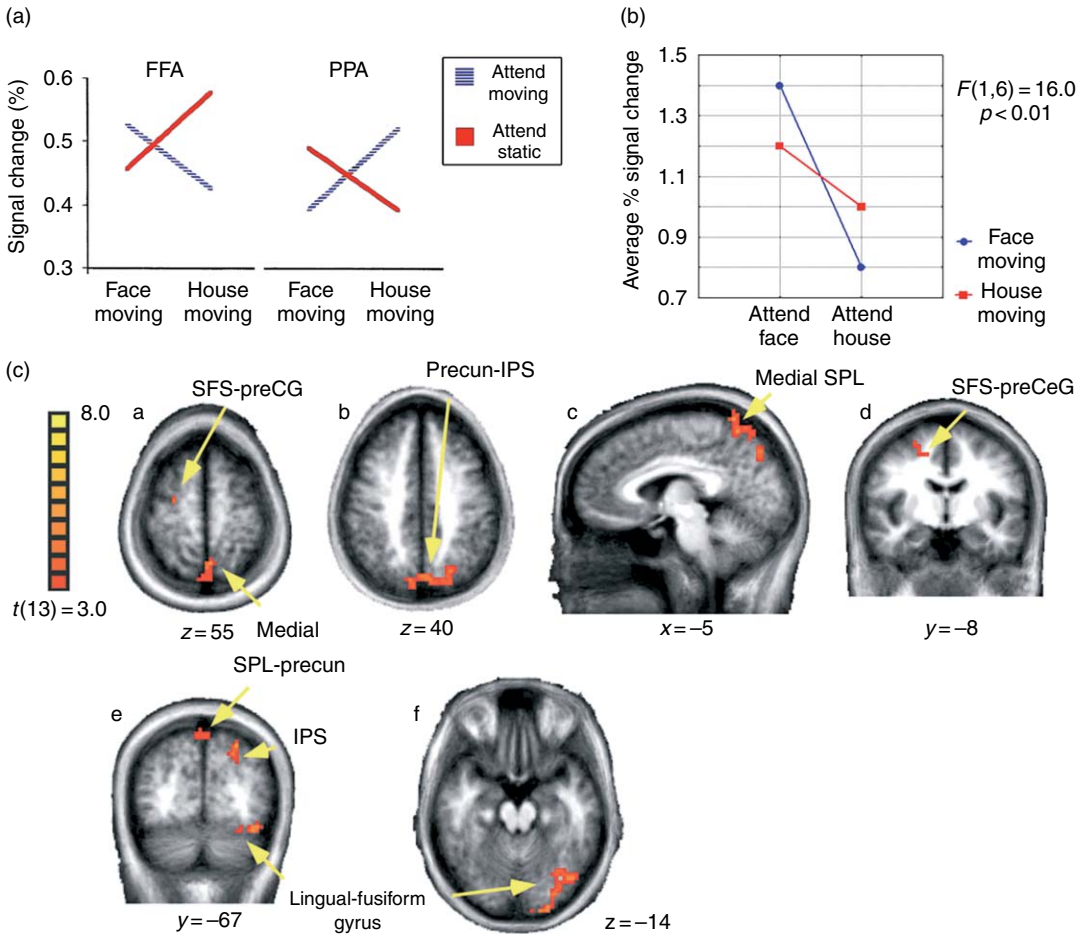

Figure 4 Results obtained by O'Craven K. *et al*. (1999) and Serences J. T. *et al*. (2004) using a transparent superimposition of a house and a face in a functional magnetic resonance imaging (fMRI) design. (a) Means of the peak evoked responses in the fusiform face area (FFA, a visual area responding preferentially to faces) and parahippocampal place area (PPA, a visual area responding preferentially to scenes or houses) as a function of task (attend moving or attend static) and stimulus (face moving or house moving). Magnetic resonance responses were greater to the task-irrelevant attribute of the attended object than to the irrelevant attribute of the unattended object, as predicted by object-based theories of attention motion. (b) Pattern of results in middle temporal/middle superior temporal areas (MT/MST). The signal change was greater when subjects attended to the face or house when they were moving than when they were stationary. (c) Regions exhibiting a greater BOLD response to shift as compared to hold targets in Serences J. T. *et al*. (2004) study. Significant activations were found in right superior frontal sulcus (SFS)–precentral gyrus (PreCeG) and medial superior parietal lobe (SPL)–precuneus (a), left intraparietal sulcus (IPS) (b), medial SPL–precuneus (c), right SFS–PreCeG (d), left IPS (e) and left lingual–fusiform gyrus (f) motion. (a) Adapted from O'Craven, K., Downing, P. E., and Kanwisher, N. G. 1999. fMRI evidence for objects as the units of attentional selection. Nature 401, 584–587, with permission from Macmillan Publishers Ltd. (b) Based on data from O'Craven, K., Downing, P. E., and Kanwisher, N. G. 1999. fMRI evidence for objects as the units of attentional selection. Nature 401, 584–587. (c) Adapted from Serences, J. T., Schwarzbach, J., Courtney, S. M., Golay, X., and Yantis, S. 2004. Control of object-based attention in human cortex Cereb. Cortex 14, 1346–1357, with permission from Oxford University Press.

2.17.5 Neural Control Signals (Bias Inducers)

We have seen stimulus factors (like the sudden onset of a surface or object luminance) can bias competition in favor of one surface. Top-down, endogenous, signals like task instructions (e.g., look out for the red surface) also can tip the balance in favor of one object.

One study of endogenous signals with transparent surfaces (Serences, J. T. *et al*., 2004) has built on the face/house design previously described (O'Craven, K.

et al., 1999). In this case, the stream of superimposed house/face pairs were periodically (1/s) morphed so each object was changed into another exemplar of its class. Attention was directed to either the house or the face stream as the observer searched for particular memorized faces or houses. Some targets signaled that attention should remain on the attended stream; other targets signaled that attention should be shifted to the other stream.

In the superior parietal lobe (SPL) there was a transient increase in fMRI activity during switch trials (both face-to-house and house-to-face) that was absent during trials where attention was maintained on the same stream (Figure 4(c)). Studies of shifts of spatially based attention show equivalent results in the SPL suggesting that endogenous control signals operate similarly for different types of attentional selection. If this is the case then evidence for sustained control signals should be found for object-based attention in frontal and inferior parietal lobe, as has been the case for space-based attention (Corbetta, M. and Shulman, G. L., 2002; Serences, J. T. *et al.*, 2004).

2.17.6 Other Approaches to Object-Based Attention

In this review we have concentrated on studies of object-based attention that superimposed transparent surfaces to preclude spatial selection. We suspect that the strong perceptual rivalry set up between competing surfaces (akin to binocular rivalry) has assisted in reaping clear attentional effects with different experimental tools. The other approaches to study object-based attention have not been reviewed because of limited space. However, we mention a promising series of studies that take advantage of the greater ease observers have in shifting attention between sites within the same figure than between parts of different figures in a design originally described by Egly R. *et al.* (1994; see also Valdes-Sosa, M. *et al.*, 2004). Several groups (He, X. *et al.*, 2004; Martinez, A. *et al.*, 2006; 2007) have shown that stimuli related to irrelevant parts of an attended object are associated with larger N1 (but not P1) components than any part of an unattended object (i.e., attention spreads to all parts of cued object). fMRI activity within the lateral occipital complex is also modulated by this object-based spread of attention (Mueller, N. G. and Kleinschmidt, A., 2003; Martinez, A. *et al.*, 2006; 2007). Further study is needed to establish the relationship between this type of object-based effect and that found for transparent motion. Nonetheless, the former effects are compatible with object-guided spatial selection. This is consistent with the smaller N1 found for irrelevant relative to relevant locations within the attended object. In contrast, results with transparent motion cannot be explained by object-guided spatial selection.

2.17.7 Unanswered Questions

Despite solid evidence that object-based attention exists, and successful first steps in understanding its neural basis, there are several fundamental but poorly understood issues that require work in the future. Perhaps the most puzzling of these issues is how the integration of object codes is achieved. This is also known as the binding problem. Further discussion of this important issue is not possible here (readers are referred to Roskies, A. L., 1999; Hommel, B., 2004). Among other issues that need to be examined are the relative time course of different attentional mechanisms (endogenous versus exogenous; space-, feature- and object-based attention). Finally, the involvement of V1 (primary visual cortex) in object-based attention should be further examined, given the tantalizing evidence (mentioned in the chapter) that surface-based attention modulates the activity of this area, evidence which contrasts with previous findings ruling out this modulation for spatial attention (Martinez, A. *et al.*, 1999).

References

Albright, T., Desimone, R., and Gross, C. G. 1984. Columnar organization of directionally selective cells in visual area MT of the macaque. J. Neurophysiol. 51, 16–31.

Bach, M. and Ullrich, D. 1994. Motion adaptation governs the shape of motion-evoked cortical potentials. Vision Res. 34, 1541–1547.

Behrmann, M., Zemel, R. S., and Mozer, M. C. 1998. Object-based attention and occlusion: evidence from normal participants and a computational model. J. Exp. Psychol. 24, 1011–1036.

Blazer, E., Pylyshyn, Z. W., and Holcombe, A. 2000. Tracking an object through feature space. Nature 408, 196–199.

Bundesen, C. and Pedersen, L. F. 1983. Color segregation and visual search. Percept. Psychophys. 33, 487–493.

Chelazzi, L., Duncan, J., Miller, E. K., and Desimone, R. 1998. Responses of neurons in inferior temporal cortex during memory-guided visual search. J. Neurophysiol. 80, 2918–2940.

Corbetta, M. and Shulman, G. L. 2002. Control of goal-directed and stimulus-driven attention in the brain. Nat. Rev. Neurosci. 3, 201–215.

Desimone, R. and Duncan, J. 1995. Neural mechanisms of selective visual attention. Annu. Rev. Neurosci. 18, 193–222.

Driver, J. and Baylis, G. C. 1989. Movement and visual attention: the spotlight metaphor breaks down. J. Exp. Psychol. Hum. Percept. Perform. 15, 448–456.

Driver, J., Baylis, G. C., and Rafal, R. D. 1992. Preserved figure-ground segregation and symmetry perception in visual neglect. Nature 360, 73–75.

Duncan, J. 1984. Selective attention and the organization of visual information. J. Exp. Psychol. Gen. 113, 501–517.

Duncan, J. 2006. EPS Mid-Career Award 2004: brain mechanisms of attention. Q. J. Exp. Psychol. 59, 2–27.

Duncan, J. and Nimmo-Smith, M. I. 1996. Objects and attributes in divided attention: surface and boundary systems. Percept. Psychophys. 58, 1076–1084.

Duncan, J., Ward, R., and Shapiro, K. L. 1994. Direct measurement of attentional dwell time in human vision. Nature 369, 313–315.

Egly, R. and Homa, D. 1991. Reallocation of visual attention. J. Exp. Psychol. Hum. Percept. Perform. 17, 142–159.

Egly, R., Driver, J., and Rafal, R. D. 1994. Shifting visual attention between objects and locations: evidence from normal and parietal lesion subjects. J. Exp. Psychol. Gen. 123, 161–177.

Fallah, M., Stoner, G. R., and Reynolds, J. H. 2007. Stimulus-specific competitive selection in macaque extrastriate visual area V4. Proc. Natl. Acad. Sci. U. S. A. 104, 4165–4169.

Gottlieb, J. P., Kusunoki, M., and Goldberg, M. E. 1998. The representation of visual salience in monkey parietal cortex. Nature 391, 481–483.

He, X., Fan, S., Zhou, K., and Chen, L. 2004. Cue validity and object-based attention. J. Cogn. Neurosci. 16, 1085–1097.

He, Z. J. and Nakayama, K. 1995. Visual attention to surfaces in three-dimensional space. Proc. Natl. Acad. Sci. U. S. A. 92, 11155–11159.

Hillyard, S. A. and Anllo-Vento, L. 1998. Event-related brain potentials in the study of visual selective attention. Proc. Natl. Acad. Sci. U. S. A. 95, 781–787.

Hommel, B. 2004. Event files: feature binding in and across perception and action. Trends Cogn. Sci. 8, 494–500.

Kahneman, D., Treisman, A. M., and Gibbs, B. J. 1992. The reviewing of object files: object-specific integration of information. Cognit. Psychol. 24, 175–219.

Khoe, W., Mitchell, J. F., Reynolds, J. H., and Hillyard, S. A. 2005. Exogenous attentional selection of transparent superimposed surfaces modulates early event-related potentials. Vision Res. 45, 3004–3014.

Kramer, A. F. and Jacobson, A. 1991. Perceptual organization and focused attention: the role of objects and proximity in visual processing. Percept. Psychophys. 50, 267–284.

Kuba, M. and Kubova, Z. 1992. Visual evoked potentials specific for motion onset. Doc. Ophthalmol. 80, 83–89.

Lavie, N. and Driver, J. 1996. On the spatial extent of attention in object-based visual selection. Percept. Psychophys. 58, 1238–1251.

Lopez, M., Rodriguez, V., and Valdes-Sosa, M. 2004. Two-object attentional interference depends on attentional set. Int. J. Psychophysiol. 53, 127–134.

Luck, S. J., Chelazzi, L., Hillyard, S. A., and Desimone, R. 1997. Neural mechanisms of spatial selective attention in areas V1, V2 and V4 of macaque visual cortex. J. Neurophysiol. 77, 24–42.

Martinez, A., Anllo-Vento, L., Sereno, M. I., Frank, L. R., Buxton, R. B., Dubowitz, D. J., Wong, E. C., Hinrichs, H., Heinze, H. J., and Hillyard, S. A. 1999. Involvement of striate and extrastriate visual cortical areas in spatial attention. Nat. Neurosci. 2, 364–369.

Martinez, A., Teder-Salejarvi, W. A., and Hillyard, S. A. 2007. Spatial attention facilitates selection of illusory objects: evidence from event-related brain potentials. Brain Res. 1139, 143–152.

Martinez, A., Teder-Salejarvi, W., Vazquez, M., Molholm, S., Foxe, J. J., Javitt, D. C., Di Russo, F., Worden, M. S., and Hillyard, S. A. 2006. Objects are highlighted by spatial attention. J. Cogn. Neurosci. 18, 298–310.

Mitchell, J. F., Stoner, G. R., and Reynolds, J. H. 2004. Object-based attention determines dominance in binocular rivalry. Nature 429, 410–413.

Mitchell, J. F., Stoner, G. R., Fallah, M., and Reynolds, J. H. 2003. Attentional selection of superimposed surfaces cannot be explained by modulation of the gain of color channels. Vision Res. 43, 1323–1328.

Mueller, N. G. and Kleinschmidt, A. 2003. Dynamic interaction of object- and space-based attention in retinotopic visual areas. J. Neurosci. 23, 9812–9816.

Nakayama, K., He, Z. J., and Shimojo, S. 1995. Visual Surface Representation: A Critical Link Between Lower-Level and Higher-Level Vision. MIT Press.

Neisser, U. and Becklen, R. 1975. Selective looking: attending to visually specified events. Cogn. Psychol. 7, 480–494.

O'Craven, K., Downing, P. E., and Kanwisher, N. G. 1999. fMRI evidence for objects as the units of attentional selection. Nature 401, 584–587.

Pinilla, T., Cobo, A., Torres, K., and Valdes-Sosa, M. 2001. Attentional shifts between surfaces: effects on detection and early brain potentials. Vision Res. 41, 1619–1630.

Reynolds, J. H., Alborzian, S., and Stoner, G. R. 2003. Exogenously cued attention triggers competitive selection of surfaces. Vision Res. 43, 59–66.

Rock, I. and Gutman, D. 1981. The effect of inattention on form perception. J. Exp. Psychol. Hum. Percept. Perform. 7, 275–285.

Rodriguez, V. and Valdes-Sosa, M. 2006. Sensory suppression during shifts of attention between surfaces in transparent motion. Brain Res. 1072, 110–118.

Rodriguez, V., Valdes-Sosa, M., and Freiwald, W. A. 2002. Dividing attention between form and motion during transparent surface perception. Brain Res. Cogn. Brain Res. 13, 187–193.

Roskies, A. L. 1999. The binding problem. Neuron 24, 7–9.

Serences, J. T., Schwarzbach, J., Courtney, S. M., Golay, X., and Yantis, S. 2004. Control of object-based attention in human cortex Cereb. Cortex 14, 1346–1357.

Tipper, S. P., Driver, J., and Weaver, B. 1991. Object-centred inhibition of return of visual attention. Q. J. Exp. Psychol. A 43, 289–298.

Tipper, S. P., Weaver, B., Jerreat, L. M., and Burak, A. L. 1994. Object-based and environment-based inhibition of return of visual attention. J. Exp. Psychol. Hum. Percept. Perform. 20, 478–499.

Torriente, I., Valdes-Sosa, M., Ramirez, D., and Bobes, M. A. 1999. Visual evoked potentials related to motion-onset are modulated by attention. Vision Res. 39, 4122–4139.

Treue, S. and Maunsell, J. 1996. Attentional modulation of visual motion processing in cortical areas MT and MST. Nature 382, 539–541.

Valdes-Sosa, M., Bobes, M. A., Rodriguez, V., and Pinilla, T. 1998a. Switching attention without shifting the spotlight: object-based attentional modulation of brain potentials. J. Cogn. Neurosci. 10, 137–151.

Valdes-Sosa, M., Bobes, M. A., Rodriguez, V., Acosta, Y., Perez, A., Iglesias, J., and Borrego, M. 2004. The Influence of Scene Organization on Attention: Psychophysics and

Electrophysiology. In: Attention and Performance XX: Functional Brain Imaging of Visual Cognition (*eds*. N. Kanwisher and J Duncan), pp. 321–344. Oxford University Press.

Valdes-Sosa, M., Cobo, A., and Pinilla, T. 1998b. Transparent motion and object-based attention. Cognition 66, 13–23.

Valdes-Sosa, M., Cobo, A., and Pinilla, T. 2000. Attention to object files defined by transparent motion. J. Exp. Psychol. Hum. Percept. Perform. 26, 488–505.

Vecera, S. P. and Farah, M. 1994. Does visual attention select objects or locations? J. Exp. Psychol. Gen. 123, 146–160.

Wanning, A., Rodriguez, V., and Freiwald, W. A. 2007. Attention to surfaces modulates motion processing in extrastriate area MT. Neuron 54, 639–651.

Watanabe, K., Harner, A. M., Miyauchi, S., Sasaki, Y., Nielsen, M., Palomo, D., and Mukai, I. 1998. Task-dependent influences of attention on the activation of human primary visual cortex. Proc. Natl. Acad. Sci. U. S. A. 95, 11489–11492.

Yantis, S. and Egeth, H. E. 1997. Visual attention: control, representation, and time course. Annu. Rev. Physiol. 48, 269–297.

Yantis, S. and Jonides, J. 1984. Abrupt visual onsets and selective attention: evidence from visual search. J. Exp. Psychol. Hum. Percept. Perform. 10, 601–621.

2.18 Visual Attention and Saccadic Eye Movements

T Moore, K M Armstrong, and R J Schafer, Stanford University School of Medicine, Stanford, CA, USA

© 2008 Elsevier Inc. All rights reserved.

2.18.1	Introduction: Active Vision – Saccadic Eye Movements and Visual Perception	291
2.18.2	Visual Representations and the Guidance of Saccadic Eye Movements	292
2.18.3	Psychophysical Links between Covert Spatial Attention and Saccade Preparation	293
2.18.4	Evidence of Oculomotor Involvement in Spatial Attention	294
2.18.4.1	Attention Deficits Following Brain Damage	294
2.18.4.2	Neurophysiological Correlates of Attention in Saccade-Related Brain Structures	295
2.18.4.3	Driving Attention	295
2.18.5	Conclusions	296
References		296

2.18.1 Introduction: Active Vision – Saccadic Eye Movements and Visual Perception

Unlike a camera, which passively and instantaneously captures light onto film or a sensor, the primate visual system extracts information from the environment actively and sequentially. Under natural circumstances, behaviorally relevant visual targets draw a viewer's attention, which is typically shifted overtly by way of a saccadic eye movement (saccade). Saccades are the rapid shifts in the direction of gaze that are used to position the tiny portion of the retina with the highest spatial acuity, called the fovea, onto targets of interest. The repositioning of the fovea via saccades occurs about four to five times per second and represents the most crucial of visually guided behaviors. It is apparent from our remarkable ability to read text, hit a pitched baseball, or scan for a familiar face in a crowd that the goal of the saccadic system is more than simply to move the eyes randomly across the visual scene. Indeed, over the past 30 years or so, neurophysiological and psychophysical evidence has revealed the extensive interconnectedness of the saccadic system and the visual and cognitive machinery of the brain.

Considerable evidence demonstrates that saccadic eye movements both reflect and influence the perception of visual stimuli. For example, the Muller–Lyer illusion (Figure 1) is well known to have a robust effect on the judgment of the lengths of two lines. In the illusion, lines feathered with outward-going segments at the ends (top) tend to appear longer than those feathered with inward-going segments (bottom) despite the fact that both lines are of equal length. Interestingly, when subjects freely view the two lines and make voluntary saccades while judging their lengths, the metrics of the individual saccades used to scan the lines are different, and reflect the perceptual illusion. Saccades made between endpoints of the line mistakenly perceived to be longer have greater amplitudes. This observation, made originally by Yarbus A. L. (1967), reveals the tight coupling between the perception of visual stimulus features and the movement commands issued to target them.

More recently, Kowler and colleagues have investigated the correlation between the metrics of saccades and perception by comparing the perceived centers of complex visual targets to the landing points of the saccades required to visually acquire the objects (Vishwanath, D. and Kowler, E., 2003). While isolated saccades were influenced by local object features more than was perception, the perceived centers of the visual objects and the landing points of naturalistic scanning saccades were remarkably similar. Other investigators have found that saccades made to targets that evoke a strong perception of visual motion robustly influence saccade metrics. For example, saccades made to fields of coherently drifting dots are strongly biased in the direction of the perceived motion, despite the fact that the aperture itself is stationary (Moore, T. *et al.*, 2001; Gross, C. G. *et al.*, 2004; Xiao, Q. *et al.*, 2006).

Saccades not only reflect visual perception but also appear to shape and enhance it. He P. and

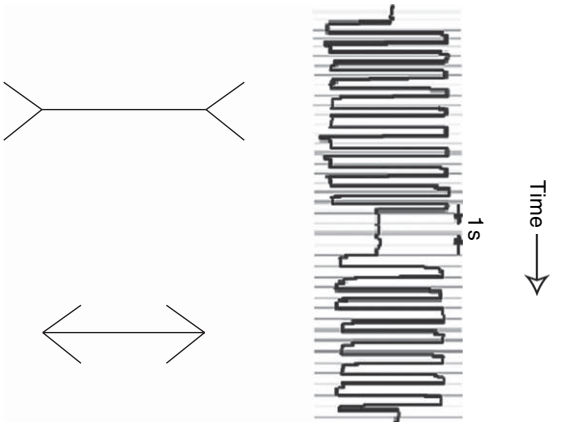

Figure 1 The influence of a visual illusion on the metrics of saccades. Left: An example of the Muller–Lyer illusion is shown in which two equally long horizontal lines appear to be of different lengths due to the direction of attached line segments. Subjects were instructed to judge the lengths of the lines while eye movements were recorded. Right: The traces show the horizontal position of a subject's gaze during saccades made between the ends of the two illusory stimuli. Note that the amplitude (left-to-right) of the top set of saccades is greater than that of the bottom set, which correspond to the top and bottom Muller–Lyer stimuli, respectively.

Kowler E. (1992) examined the effect of saccades on human perception of polygonal patches of texture patterns presented foveally against a differently textured background. They found that the ability to accurately determine the size and shape of the target polygonal patch was improved when the subject was allowed to saccade freely, despite the fact that individual texture elements were easily identifiable under fixation alone. This benefit of saccades on perception supports previous reports of such improvement, such as the enhancement that accompanies saccades when counting scattered visual targets (Kowler, E. and Steinman, R. M., 1977). While some studies indicate that the saccadic and visual–perceptual representations are not completely identical and can be influenced independently (e.g., Aglioti, S. *et al.*, 1995), the relationship between them clearly suggests overlapping mechanisms.

2.18.2 Visual Representations and the Guidance of Saccadic Eye Movements

The links between perception and saccades suggest that the representation of a stimulus in visual cortex might be involved not only in determining the way in which the stimulus is perceived but also in helping the saccadic system specify an appropriate eye movement to foveate the stimulus. Most of what is understood about how the visual world is represented by neurons within the primate brain is derived from studies of the macaque visual system. The macaque visual cortex is composed of a large array of separate maps of the visual field (Felleman, D. J. and Van Essen, D. C., 1991). These maps can be divided into two distinct sets or processing streams, one ventral and one dorsal (Ungerleider, L. G. and Mishkin, M. 1982) (Figure 2(a)). Early electrophysiological studies of monkey parietal cortex, within the dorsal stream, found single neurons that exhibited bursts of activity immediately prior to the execution of saccades to visual targets (Hyvarinen, J. and Poranen, A., 1974; Mountcastle, V. B. *et al.*, 1975). Mountcastle V. B. *et al.* (1975) described these cells as part of "a command apparatus for operation of the . . . eyes within immediate extrapersonal space." Later, Andersen and colleagues described the saccade-related activity in parietal cortex as being "involved in the transformations of visual information for the planning of saccadic eye movements" (Barash, S. *et al.*, 1991). Rather than a motor signal or a visual signal, the activity was interpreted as serving a role in transforming visual representations into visually guided saccadic eye movement commands. More recent evidence has confirmed that although some visual areas of parietal cortex are clearly involved in representing the behavioral relevance, or salience, of visual targets (Gottlieb, J. P. *et al.*, 1998; Bisley, J. W. and Goldberg, M. E., 2003; Ipata, A. E. *et al.*, 2006), the activity of parietal neurons is nonetheless predictive of the goal and time of initiation of saccades (Ipata, A. E. *et al.*, 2006).

Evidence of an accompanying role of ventral stream visual areas in the programming of saccades began with the early observations of Fischer and Boch, who conducted studies of area V4 neurons in monkeys trained to make saccades to visual targets (Fischer, B. and Boch R., 1981; Boch, R. and Fischer, B., 1983). They found that the visual responses of neurons in area V4 are enhanced prior to saccades made to visual targets appearing in a neuron's receptive field (RF). Chelazzi L. *et al.* (1993) subsequently showed that the activity of neurons in inferior temporal cortex is also enhanced when a visual stimulus was chosen as the target of a saccade. The enhancement of visual activity of ventral visual cortical neurons has also been described during free viewing of natural scenes. Gallant J. L. *et al.* (1998) pioneered the study of visual cortical representations in freely viewing monkeys. During free viewing, monkeys are

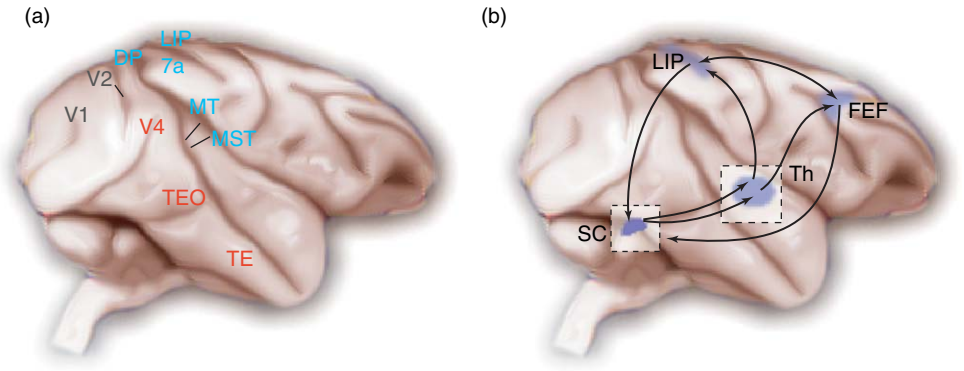

Figure 2 Visual cortical areas and visuosaccadic structures of the macaque monkey brain. (a) Some of the many separate visual areas within cortex. Labels in red denote some of the ventral stream visual areas, while labels in blue show some in the dorsal stream. (b) The principal structures involved in the programming and execution of visually guided saccades and their connections, namely, the lateral intraparietal area (LIP), the frontal eye field (FEF), and the superior colliculus (SC). Forward projections from the SC to the LIP and the FEF are via thalamic nuclei (labeled Th), namely, the pulvinar and mediodorsal nucleus, respectively. The dotted box surrounds the two subcortical structures, SC and Th.

permitted to scan large field displays with saccades. Because the majority of visual RFs in cortex are fixed to a particular retinal location, saccades shift the RFs from one location to the next every time a saccade is made. Gallant J. L. *et al.* (1998) recorded from single neurons in visual areas V1, V2, and V4 during free viewing and found that nearly half of the neurons had activity that was modulated during eye movements, even if one accounted for the physically shifting RFs. Similarly, Sheinberg D. L. and Logothetis N. K. (2001) investigated perisaccadic activity in inferior temporal cortex using a free-viewing paradigm in which a monkey was instructed to find a visual target embedded within a natural scene. During this task, many neurons within the temporal cortex were found to become active just prior to a saccade that targeted an RF stimulus, but not prior to saccades that would target stimuli outside of the RF.

Moore T. *et al.* (1998) followed up on the studies of Fischer B. and Boch R. (1981) and found that the presaccadic enhancement of V4 visual responses is selective for the features of the saccade target, just as is the initial response of the target in the RF, and thus demonstrated that the enhancement itself contained both visual and motor information. Thus, for example, presaccadic enhancement is greatest prior to saccades to targets presented at a particular V4 neuron's preferred orientation. To address the significance of the presaccadic signals in V4, Moore T. (1999) examined the metrics of saccades made to targets of varying orientation and found that saccades on trials with more robust presaccadic activity were more faithfully distributed along the axis of orientation than were saccades on trials with weaker activity. Thus, similar to what is more well established within the dorsal visual stream, neurons in the ventral stream appear to play at least some role in the preparation of saccades.

To summarize, neurophysiological evidence to date reveals an interaction of visual representations with saccade plans that is distributed throughout visual cortex. This evidence suggests that the parameters of visual stimuli and the parameters of saccades are specified simultaneously via those interactions every time a particular stimulus is targeted, thus providing the basic machinery for visual exploration during the overt orienting of attention (Moore, T. *et al.*, 2003). Next, we consider a similar basis for covert orienting.

2.18.3 Psychophysical Links between Covert Spatial Attention and Saccade Preparation

Early physiologists and theorists of cognition hypothesized that the mechanisms controlling eye movements must exert an influence on visual perception (von Helmholtz, H., 1866/1962) and might provide the basis for some aspects of visual attention (Ferrier, D., 1890; Ribot, T. H., 1980). Numerous modern psychophysical studies have revealed evidence linking selective attention and the preparation of saccades. Generally, this evidence suggests one or both of two possibilities: that visual spatial attention influences saccade preparation and that saccade preparation influences the deployment of visual spatial attention. The most classic

demonstration of the influence of directed attention on saccades was provided by Rizzolatti G. *et al.* (1987). In this study, the authors examined how covert attention perturbed saccade trajectories. Subjects were instructed to initiate saccades to a location in one half of the visual field according to cues presented in the other half. The cues could be presented in one of several locations in the cued half of the visual field. The authors found that saccade trajectories were systematically deviated according to the location of the covertly attended (i.e., cued) location. Thus, the deployment of covert attention can perturb saccade programming. The above observation and similar findings from other investigators (e.g., Kowler, E. *et al.*, 1995) are frequently cited as evidence for what is commonly referred to as the premotor theory of attention, a more modern incarnation of the early hypothesis of an oculomotor basis of attention (e.g., Ferrier, D., 1876).

To address the role of saccade preparation in the deployment of attention, Hoffman J. E. and Subramaniam B. (1995) had subjects make saccades to a location while also detecting visual targets presented prior to the eye movement. These authors found that target detection was typically best at the location of planned saccades and that subjects were unable to completely dissociate the attended and saccade locations. These results suggest that the preparation of saccades to a location deploys attention to that location. Deubel H. and Schneider W. X. (1996) found similar results and concluded that a single mechanism must drive the selection of objects for perceptual processing and the information needed to drive the appropriate saccadic response.

Although these psychophysical studies provide a sound rationale for the hypothesis that oculomotor and attentional circuits have a common neural substrate, they cannot rule out the alternative view that these are two distinct and independent systems. In recent years, neurophysiological studies have taken a more direct approach to this problem by perturbing neural signals within oculomotor structures and examining the effects of those perturbations on spatial attention. These structures include the frontal eye field (FEF) and the superior colliculus (SC), both having a known role in the programming and triggering of saccades. The approach of directly manipulating signals in these areas addresses the causal relationship between neural activity in oculomotor circuits and shifts of spatial attention.

2.18.4 Evidence of Oculomotor Involvement in Spatial Attention

2.18.4.1 Attention Deficits Following Brain Damage

One source of evidence for an involvement of the saccadic system in visual spatial attention comes from the cognitive impairments that ensue when areas of the brain that control eye movements are damaged. The earliest evidence comes from the nineteenth-century physiologist Sir David Ferrier (1890) mentioned above. Perhaps Ferrier's most noteworthy discovery was that electrical stimulation of a region within frontal cortex could elicit contraversive, conjugate movements of the eyes (Ferrier, D., 1876). This region later became known as the frontal eye field and is known to play a crucial role in the planning and execution of visually guided saccades (Bruce, C. J. *et al.*, 1985; Schall, J. D. and Hanes, D. P., 1993; Tehovnik, E. J. *et al.*, 2000). Ferrier also performed a series of lesion experiments in monkeys in order to localize functions within specific brain regions. Following lesions of frontal cortex, including the FEF, he observed that monkeys were impaired in their ability to voluntarily direct gaze toward objects, a deficit he described as tantamount to a "loss of the faculty of attention." He went on to propose that "the power of attention is intimately related to the volitional movements of the head and eyes." His early finding that frontal cortical lesions disrupt attention and eye movements was corroborated by later lesion studies in which unilateral ablations were performed in a restricted region of frontal cortex, corresponding approximately to the FEF (Welch, K. and Stuteville, P., 1958). These studies reported deficits in monkeys' ability to orient and respond to salient objects (food and frightening stimuli) in the contralateral visual field. Latto R. and Cowey A. (1971) were the first to quantify these visual deficits by training monkeys to release a lever in response to a flash of light presented at different locations throughout the visual field and examining how performance on this task was affected by lesions to the FEF. They found that unilateral FEF removal transiently impaired performance in the contralateral visual field. The animals were not blind, as they could still respond correctly on a fraction of trials; however, they were far more likely to fail to respond to stimuli presented in

the affected hemifield than elsewhere. Latto R. and Cowey A. (1971) suggested that the FEF might normally modulate the visual system according to eye position and that this could explain the fact that such small lesions were able to produce such pronounced deficits.

More recently, studies have used reversible pharmacological inactivation to temporarily disrupt neural activity in a number of structures with known roles in the control of saccades, including the FEF (Wardak, C. *et al.*, 2006), the SC (McPeek, R. M. and Keller, E. L., 2004), and the lateral interparietal area (LIP) (Wardak, C., *et al.*, 2002). Generally, inactivation of these structures increases the time it takes an animal to initiate saccades to visual targets appearing in the affected part of space (Hikosaka, O. and Wurtz, R. H., 1986; Lynch, J. C. and Mclaren, J. W., 1989; Sommer, M. A. and Tehovnik, E. J., 1997). In addition, the inactivation also impairs performance on attention-demanding tasks in the affected part of visual space when other distracting stimuli are present. Performance on tasks without an attentional demand, such as those using a single visual stimulus, is not affected. Thus, to date there is good evidence that brain structures involved in controlling visually guided saccades also play a causal role in directing visuospatial attention.

2.18.4.2 Neurophysiological Correlates of Attention in Saccade-Related Brain Structures

The deficits following lesions and reversible inactivation of saccade-related structures suggest that neurons in these areas are critically involved in the allocation of attention across space. Evidence from recording studies that monitor the activity of single neurons in different saccade-related areas is consistent with this interpretation. Early studies showed that the responses of SC neurons to visual stimuli are enhanced only when those stimuli are used as targets for saccades (Goldberg, M. E. and Wurtz, R. H., 1972). Subsequently, similar results of a dependence of enhanced visual activity were obtained in the FEF (Goldberg, M. E. and Bushnell, M. C., 1981). However, recent studies involving more sophisticated covert attention paradigms have found that neurons in the FEF and the SC exhibit attention-related modulation that is not tied specifically to saccade initiation (Ignashchenkova, A. *et al.*, 2004; Thompson, K. G. *et al.*, 2005) similar to what is observed in LIP (Bushnell, M. C. *et al.*, 1981) and throughout extrastriate visual cortex (Reynolds, J. H. and Chelazzi, L., 2004).

2.18.4.3 Driving Attention

The results from recording and lesion studies suggest that spatial attention is driven by neural activity from saccade-related structures. If this is the case, then it should be possible to direct attention by driving neural activity within these structures. Recent studies have used electrical microstimulation to test the hypothesis that saccade-related circuits play a causal role in driving attention to particular locations in the visual field. While it had long been known that microstimulation of the FEF and the SC can elicit saccades, Moore T. and Fallah M. (2001) were the first to examine the effect of microstimulation on visual attention. They found that when they stimulated sites within the FEF using currents that were too low to evoke a saccade, they could nonetheless enhance monkeys' ability to detect changes in a visual target. Importantly, the improvements observed with microstimulation were dependent on the target of attention being positioned at the location to which suprathreshold microstimulation would shift the monkey's gaze (Moore, T. and Fallah, M., 2001; 2004). Thus, it appeared that by increasing the likelihood that the monkey would foveate a location in visual space, the microstimulation also enhanced the animal's ability to process visual events there. Subsequently, two other studies reported similar enhancements in visual spatial attention following subthreshold microstimulation of the SC (Cavanaugh, J. and Wurtz, R. H., 2004; Muller, J. R. *et al.*, 2005). In both cases, the performance-enhancing effects of microstimulation were spatially dependent as in the FEF studies.

The effect of electrical microstimulation of the FEF and the SC on visual spatial attention performance suggests that during stimulation, visual representations of spatially correspondent stimuli are enhanced compared to those of stimuli at other locations. As mentioned earlier, a wealth of evidence has established that correlates of visual attention can be observed throughout much of macaque visual cortex (Reynolds, J. H. and Chelazzi, L., 2004): visual responses to RF stimuli are typically enhanced when a monkey is trained to covertly attend to them. Thus, one might expect that microstimulation of the FEF or the SC will likewise result in the enhancement of the responses of visual cortical neurons to RF stimuli. This was the hypothesis posed by Moore T. and

Armstrong K. M. (2003), who paired FEF microstimulation with single-neuron recording in extrastriate area V4. Specifically, they studied the impact of subthreshold microstimulation of FEF sites on the visual responses of V4 neurons with RFs that were either overlapping or nonoverlapping with the spatial location represented at the FEF site. They found that following very brief trains of FEF stimulation (20–50 ms) visual responses were enhanced at overlapping locations in the visual field, whereas they were suppressed at nonoverlapping locations. Furthermore, this attention-like modulation was greatest when there was another distracter stimulus presented outside of the V4 neuron's RF. A subsequent study also found that FEF microstimulation can alter the structure of V4 RFs and can bias V4 responses in favor of one of two RF stimuli (Armstrong, K. M. *et al.*, 2006). These changes in V4 responses are very similar to what has been observed in the same area during voluntary attention (Moran, J. and Desimone, R., 1985; Reynolds, J. H. *et al.*, 1999). Together, the above results suggest that microstimulation of oculomotor structures drives covert attention and its correlates in visual cortex and that indeed, as speculated by Latto R. and Cowey A. (1971), visual spatial attention seems to be driven by feedback from the oculomotor system onto visual cortical areas, and this feedback influence may exist in order to modulate processing according to eye movement plans.

In summary, recent neurophysiological work has directly addressed and found much evidence of a role of saccade mechanisms in directing covert visual spatial attention. This evidence appears to support the conclusion that the neural mechanisms of covert and overt spatial attention are identical with respect to the influence of the saccade plan on visual representations. Although it is clear that some different mechanisms must be in effect when attention is directed overtly, that is, when planned movements are triggered and shifts in gaze are actually carried out (Awh, E. *et al.*, 2006), than when it is directed covertly, recent results suggest that those differences are less important than the similarities.

2.18.5 Conclusions

Unlike the passive camera, the primate visual system extracts information from the environment actively and sequentially by way of saccadic eye movements. Every saccade must accurately position targets of interest onto the fovea where visual acuity is greatest, and this takes place four to five times per second. We have described the psychophysical and physiological evidence of highly interconnected mechanisms for visual perception and saccade preparation. This evidence includes correlates of saccade planning within visual cortex as well as changes in visual cortical signals following perturbations of saccade representations and thus argues for a reciprocal relationship between the coding of visual features and of saccade metrics. Furthermore, recent evidence suggests that this reciprocal interaction serves as the basis for covert spatial attention.

References

Aglioti, S., DeSouza, J. F., and Goodale, M. A. 1995. Size-contrast illusions deceive the eye but not the hand. Curr. Biol. 5, 679–685.

Armstrong, K. M., Fitzgerald, J. K., and Moore, T. 2006. Changes in visual receptive fields with microstimulation of frontal cortex. Neuron 50, 791–798.

Awh, E., Armstrong, K. M., and Moore, T. 2006. Visual and oculomotor selection: links, causes and implications for spatial attention. Trends Cogn. Sci. 10, 124–130.

Barash, S., Bracewell, R. M., Fogassi, L., Gnadt, J. W., and Andersen, R. A. 1991. Saccade-related activity in the lateral intraparietal area. I. Temporal properties; comparison with area 7a. J. Neurophysiol. 66, 1095–1108.

Bisley, J. W. and Goldberg, M. E. 2003. Neuronal activity in the lateral intraparietal area and spatial attention. Science 299, 81–86.

Boch, R. and Fischer, B. 1983. Saccadic reaction times and activation of the prelunate cortex: parallel observations in trained rhesus monkeys. Exp. Brain Res. 50, 201–210.

Bruce, C. J., Goldberg, M. E., Bushnell, M. C., and Stanton, G. B. 1985. Primate frontal eye fields. II. Physiological and anatomical correlates of electrically evoked eye movements. J. Neurophysiol. 54, 714–734.

Bushnell, M. C., Goldberg, M. E., and Robinson, D. L. 1981. Behavioral enhancement of visual responses in monkey cerebral cortex. I. Modulation in posterior parietal cortex related to selective visual attention. J. Neurophysiol. 46, 755–772.

Cavanaugh, J. and Wurtz, R. H. 2004. Subcortical modulation of attention counters change blindness. J. Neurosci. 24, 11236–11243.

Chelazzi, L., Miller, E. K., Duncan, J., and Desimone, R. 1993. A neural basis for visual search in inferior temporal cortex. Nature 363, 345–347.

Deubel, H. and Schneider, W. X. 1996. Saccade target selection and object recognition: evidence for a common attentional mechanism. Vis. Res. 36, 1827–1837.

Felleman, D. J. and Van Essen, D. C. 1991. Distributed hierarchical processing in the primate cerebral cortex. Cereb. Cortex 1, 1–47.

Ferrier, D. 1876. Functions of the Brain. Smith, Elder and Co.

Ferrier, D. 1890. Cerebral Localisation, p. 151. Smith, Elder and Co.

Fischer, B. and Boch, R. 1981. Enhanced activation of neurons in prelunate cortex before visually guided saccades of trained rhesus monkeys. Exp. Brain Res. 44, 129–137.

Gallant, J. L., Connor, C. E., and Van Essen, D. C. 1998. Neural activity in areas V1, V2 and V4 during free viewing of natural scenes compared to controlled viewing. Neuroreport 9, 85–90.

Goldberg, M. E. and Bushnell, M. C. 1981. Behavioral enhancement of visual responses in monkey cerebral cortex. II. Modulation in frontal eye fields specifically related to saccades. J. Neurophysiol. 46, 773–787.

Goldberg, M. E. and Wurtz, R. H. 1972. Activity of superior colliculus in behaving monkey. II. Effect of attention on neuronal responses. J. Neurophysiol. 35, 560–574.

Gottlieb, J. P., Kusunoki, M., and Goldberg, M. E. 1998. The representation of visual salience in monkey parietal cortex. Nature 391, 481–484.

Gross, C. G., Moore, T., and Rodman, H. R. 2004. Visually guided behavior after V1 lesions in young and adult monkeys and its relation to blindsight in humans. Prog. Brain Res. 144, 279–294.

He, P. and Kowler, E. 1992. The role of saccades in the perception of texture patterns. Vis. Res. 32, 2151–2163.

von Helmholtz, H. 1866/1962. Treatise on Physiological Optics, Vol. 2. (trans. J. P. L. Southall). Dover.

Hikosaka, O. and Wurtz, R. H. 1986. Saccadic eye movements following injection of lidocaine into the superior colliculus. Exp. Brain Res. 61, 531–539.

Hoffman, J. E. and Subramaniam, B. 1995. The role of visual attention in saccadic eye movements. Percept. Psychophys. 57, 787–795.

Hyvarinen, J. and Poranen, A. 1974. Function of the parietal associative area 7 as revealed from cellular discharges in alert monkeys. Brain 97, 673–692.

Ignashchenkova, A., Dicke, P. W., Haarmeier, T., and Thier, P. 2004. Neuron-specific contribution of the superior colliculus to overt and covert shifts of attention. Nat. Neurosci. 7, 56–64.

Ipata, A. E., Gee, A. L., Gottlieb, J., Bisley, J. W., and Goldberg, M. E. 2006. LIP responses to a popout stimulus are reduced if it is overtly ignored. Nat. Neurosci. 9, 1071–1076.

Kowler, E. and Steinman, R. M. 1977. The role of small saccades in counting. Vis. Res. 17, 141–146.

Kowler, E., Anderson, E., Dosher, B., and Blaser, E. 1995. The role of attention in the programming of saccades. Vis. Res. 35, 1897–1916.

Latto, R. and Cowey, A. 1971. Visual field defects after frontal eye-field lesions in monkeys. Brain Res. 30, 1–24.

Lynch, J. C. and McLaren, J. W. 1989. Deficits of visual attention and saccadic eye movements after lesions of parietooccipital cortex in monkeys. J. Neurophysiol. 61, 74–90.

McPeek, R. M. and Keller, E. L. 2004. Deficits in saccade target selection after inactivation of superior colliculus. Nat. Neurosci. 7, 757–763.

Moore, T. 1999. Shape representations and visual guidance of saccadic eye movements. Science 285, 1914–1917.

Moore, T. and Armstrong, K. M. 2003. Selective gating of visual signals by microstimulation of frontal cortex. Nature 421, 370–373.

Moore, T. and Fallah, M. 2001. Control of eye movements and spatial attention. Proc. Natl. Acad. Sci. U. S. A. 98, 1273–1276.

Moore, T. and Fallah, M. 2004. Microstimulation of the frontal eye field and its effects on covert spatial attention. J. Neurophysiol. 91, 152–162.

Moore, T., Armstrong, K. M., and Fallah, M. 2003. Visuomotor origins of covert spatial attention. Neuron 40, 671–683.

Moore, T., Rodman, H. R., and Gross, C. G. 2001. Recovery of Visual Function Following Damage to Striate Cortex in Monkeys. In Out of Mind: Varieties of unconscious processing (*eds*. B. de Gelder, E. Dettaan, and C. Heywood), pp. 35–51. Oxford: Oxford University Press.

Moore, T., Tolias, A. S., and Schiller, P. H. 1998. Visual representations during saccadic eye movements. Proc. Natl. Acad. Sci. U. S. A. 95, 8981–8984.

Moran, J. and Desimone, R. 1985. Selective attention gates visual processing in the extrastriate cortex. Science 229, 782–784.

Mountcastle, V. B., Lynch, J. C., Georgopoulos, A., Sakata, H., and Acuna, C. 1975. Posterior parietal association cortex of the monkey: command functions for operations within extrapersonal space. J. Neurophysiol. 38, 871–908.

Muller, J. R., Philiastides, M. G., and Newsome, W. T. 2005. Microstimulation of the superior colliculus focuses attention without moving the eyes. Proc. Natl. Acad. Sci. U. S. A. 102, 524–529.

Reynolds, J. H. and Chelazzi, L. 2004. Attentional modulation of visual processing. Annu. Rev. Neurosci. 27, 611–647.

Reynolds, J. H., Chelazzi, L., and Desimone, R. 1999. Competitive mechanisms subserve attention in macaque areas V2 and V4. J. Neurosci. 19, 1736–1753.

Ribot, T. H. 1890. The Psychology of Attention, pp. 29–71, Open Court Publishing.

Rizzolatti, G., Riggio, L., Dascola, I., and Umilta, C. 1987. Reorienting attention across the horizontal and vertical meridians: evidence in favor of a premotor theory of attention. Neuropsychologia 25, 31–40.

Schall, J. D. and Hanes, D. P. 1993. Neural basis of saccade target selection in frontal eye field during visual search. Nature 366, 467–469.

Sheinberg, D. L. and Logothetis, N. K. 2001. Noticing familiar objects in real world scenes: the role of temporal cortical neurons in natural vision. J. Neurosci. 21, 1340–1350.

Sommer, M. A. and Tehovnik, E. J. 1997. Reversible inactivation of macaque frontal eye field. Exp. Brain Res. 116, 229–249.

Tehovnik, E. J., Sommer, M. A., Chou, I. H., Slocum, W. M., and Schiller, P. H. 2000. Eye fields in the frontal lobes of primates. Brain Res. Brain Res. Rev. 32, 413–448.

Thompson, K. G., Biscoe, K. L., and Sato, T. R. 2005. Neuronal basis of covert spatial attention in the frontal eye field. J. Neurosci. 25, 9479–9487.

Ungerleider, L. G. and Mishkin, M. 1982. Two Cortical Visual Systems. In Analysis of Visual Behavior (*eds* D. J. Ingle, M. A. Goodale, and R. J. W. Mausfield), pp. 549–586. MIT Press.

Vishwanath, D. and Kowler, E. 2003. Localization of shapes: eye movements and perception compared. Vis. Res. 43, 1637–1653.

Wardak, C., Ibos, G., Duhamel, J. R., and Olivier, E. 2006. Contribution of the monkey frontal eye field to covert visual attention. J. Neurosci. 26, 4228–4235.

Wardak, C., Olivier, E., and Duhamel, J. R. 2002. Saccadic target selection deficits after lateral intraparietal area inactivation in monkeys. J Neurosci. 22(22), 9877–9884.

Welch, K. and Stuteville, P. 1958. Experimental production of unilateral neglect in monkeys. Brain 81, 341–347.

Xiao, Q., Barborica, A., and Ferrera, V. P. 2006. Radial motion bias in macaque frontal eye field. Vis. Neurosci. 23, 49–60.

Yarbus, A. L. 1967. Eye Movement and Vision. Plenum Press.

2.19 Saliency

J Gottlieb, Columbia University, New York, NY, USA

© 2008 Elsevier Inc. All rights reserved.

2.19.1	Introduction	299
2.19.2	Stimulus and Task-Related Factors in Early Vision	299
2.19.3	Behavioral Salience in Higher-Order Attention-Related Areas	301
2.19.4	Summary	302
References		302

2.19.1 Introduction

The term salience (or saliency) has an easy intuitive definition. We say that an object is salient if it is easily noticed or appears to jump out at us from the surround. Salient objects are those that attract our attention automatically, apparently with little effort on our part.

Since the time of William James, psychologists have recognized that attention may be captured in stimulus-driven manner (i.e., may be attracted to certain objects by virtue of their intrinsic physical properties alone) or may be deployed in voluntary fashion (i.e., may be allocated to objects that are known to be significant in a specific context). Recast in different terms, this means that saliency is determined both by stimulus-related and by task- or observer-related factors. Stimulus-related factors define the physical conspicuity of an object, that is, the contrast between the physical properties of the object and those of the surrounding environment. A red apple is salient in a pile of green apples because its color contrasts strongly with that of the surround; the same apple is not salient in a pile of other red apples because its color is no longer unique in this context. Task- or observer-related factors describe the state (goal, expectations, action plans) of the observer. In an elegant series of experiments, Mack A. and Rock I. (2000) illustrated the distinction between physical conspicuity and attentional weight. Mack and Rock showed that human observers may fail to notice even objects that are highly conspicuous if these objects are entirely unexpected and unrelated to an ongoing task, a phenomenon so striking that it was labeled inattentional blindness. Both physical conspicuity and behavioral state determine the subjective salience of a given object in a given context.

Just as physical and behavioral factors come into play in our intuitive notion of saliency, these factors continuously interact in visual areas of the brain. Physical conspicuity strongly influences neural activity starting in the retina and through higher-order visual areas. Behavioral factors also influence neuronal responses, and these influences become progressively stronger in higher-order visual and visuomotor association areas that link visual percepts with behavior. The attentional weight of an object is computed in the brain through continuous interactions among lower and higher-level visual representations.

2.19.2 Stimulus and Task-Related Factors in Early Vision

Starting at the earliest levels of the visual system the brain preferentially encodes loci of luminance contrast in the visual input. Many bipolar cells and ganglion cells in the retina as well as neurons in the lateral geniculate nucleus and primary visual cortex (V1) respond not to absolute levels of illumination but rather to luminance contrast within their spatial receptive field. These neurons have antagonistic center-surround organization, with ON-center cells preferring stronger light intensity in the receptive field center and weaker intensity in the surround, and OFF-center neurons preferring the opposite gradient. Neurons in V1 have elongated receptive fields and respond optimally for contrast edges of specific orientation, thus encoding contours or edges that segment the visual input into objects or surfaces.

In these early visual areas sensitivity to contrast is not generally thought of in terms of physical conspicuity, but rather as a strategy for compressing visual information or for efficient visual encoding. For instance, to encode a uniformly lit shape it is more parsimonious to represent the boundary of the shape

(which contains multiple, possibly abruptly changing orientations) than to represent the shape's interior, which contains essentially redundant (uniform) luminance information. Loci of high contrast are highly informative in the initial encoding of a visual scene. The fact that high-contrast loci also tend to attract attention may reflect an adaptation of the visual system to give priority processing to features that are most useful in interpreting the visual input.

Converging evidence from neurophysiological and psychophysical studies shows that elementary computations that extract informative visual features are not carried out in an encapsulated early vision system. Instead, these computations continuously interface with behavioral systems, and they are both influenced by and in turn influence mechanisms of voluntary attention.

A first line of evidence for this idea is the finding that, while elementary visual computations in early visual areas are to some extent automatic, these computations can nevertheless be influenced by attention. The interacting role of automatic and voluntary processes is best illustrated by an experiment by Charles Gilbert and his colleagues in primary visual cortex (V1) of the monkey. In this experiment, Li W *et al.* (2006) tested the responses of V1 neurons to linear contours embedded within uniform texture backgrounds in monkeys. Backgrounds were composed of randomly oriented line segments, while contours were formed by aligning a small number of these line segments along a collinear, straight path. The monkey's task was to detect the presence of a continuous contour. Even though V1 neurons have small receptive fields that typically encompass only one line segment, neurons were influenced by the broader visual group of which that segment was a part: firing rates were higher if the line segment inside the receptive field was part of a continuous contour than if it was part of the noisy background texture. Further, when the saliency of the contour was manipulated by changing the number of aligned elements or the spacing between these elements V1 responses increased in proportion to the salience (detectability) of the contour. To see to what extent these responses depended on top-down attention (on the monkey's explicit strategy of looking for the contour), Li W. *et al.* (2006) also probed V1 responses in condition in which monkeys performed a different discrimination task while a (now task-irrelevant) contour appeared in the receptive field. V1 neurons continued to signal the presence and salience of this contour but had lower overall firing rates relative to the attended condition.

This experiment makes three important points. First, although V1 neurons are exquisitely tuned for local visual features, their responses reflect processes of contour integration and grouping that pull out salient contours on a larger spatial scale. Second, contour integration occurs to some extent automatically, regardless of explicit behavioral strategy. This is consistent with findings that sensitivity to contrast and local orientation is robust even in anesthetized animals, and thus that it is, to some extent, a hard-wired property of early visual representations. However, contour integration is facilitated by voluntary or top-down attention showing that voluntary factors can impact the extraction of visual features even at early stages of visual processing.

Consistent with the findings of Li W. *et al.* (2006), psychophysical studies confirm that the detection of even the most elementary visual features requires some amount of attention. The paradigmatic easy visual task is pop-out detection – the ability to detect a unique, highly conspicuous element in a uniform background (i.e., a red apple in a pile of green apples). Initially pop-out detection was proposed to be accomplished by automatic feature extraction mechanisms in early visual areas, and to operate without the need for directed attention. However, Ken Nakayama and his colleagues showed that pop-out detection performance declines dramatically if subjects simultaneously perform a very demanding letter identification task (Joseph, J. S. *et al.*, 1997). In line with the findings of Mack A. and Rock I. (2000), even the detection of a highly salient object commands some attentional resources. The attentional requirements of a pop-out task are very low, so that, to effectively influence performance on this task a very difficult competing task had to be used. Nevertheless, when an appropriate challenge is applied it becomes clear that even a simple task such as pop-out detection demands attention.

A final line of evidence from neurophysiological recordings confirms the idea that a visible object makes automatic demands on a limited pool of neuronal resources by virtue of its presence, or intrinsic salience alone. Single neuron recordings in monkeys and functional magnetic imaging in human subjects show that in extrastriate visual cortex the neural representations of multiple objects compete, so that neurons show lower, not higher, firing rates as more objects are added to a display. In areas V2 and V4 (which lie at somewhat higher levels than area V1)

neural responses to two simultaneously presented visual stimuli interact, so that the information that neurons transmit about the features of each object is corrupted in the presence of other objects. These competitive interactions occurred in the absence of voluntary attention, showing that they can be triggered merely by the intrinsic salience of a visual entity. The mere presence of an object in the field of view can command neural resources, and these resources become increasingly significant when the object is selected by voluntary, top-down attention.

In sum, no sharp border exists in the brain between processes reflecting physical conspicuity and those reflecting attentional weight. Aspects of the visual input that are perceived as salient are preferentially encoded starting in the retina and primary visual cortex and become attentional attractors. The extraction of these salient entities is in part automatic and in part dependent on top-down attention. The entities created by early visual mechanisms – objects, boundaries and surfaces – pose intrinsic demands, automatically competing for a pool of limited neuronal representations.

2.19.3 Behavioral Salience in Higher-Order Attention-Related Areas

While neurons in striate and extrastriate cortex show the influence of behavioral state, these top-down effects are thought to originate outside the visual system itself, in higher-order visual association areas in the frontal and parietal lobes. Unilateral damage to frontal and parietal cortex in humans produces spatial neglect (or its milder form, extinction), a deficit in noticing and reacting to task-relevant objects in the region of space opposite to the affected hemisphere. Neglect has both sensory and motor manifestations and reflects a complex failure of linking sensory representations with conscious perception and overt behavior. The exact areas in the human brain whose damage produces neglect and the homologues of these areas in monkeys are not known with certainty. However, converging evidence suggests that in the monkey a parietal area, the lateral intraparietal area (LIP), and a frontal area, the frontal eye field (FEF), are critically important for spatial attention (Thompson, K. G. *et al.*, 2005; Gottlieb, J., 2007).

The LIP and FEF receive strong converging inputs from dorsal and ventral stream extrastriate areas and in turn send feedback to these areas. Consistent with these anatomical connections, LIP and FEF neurons have visual responses and circumscribed receptive fields similar to neurons in extrastriate areas. However, responses in LIP and FEF differ from those in extrastriate cortex in two important ways. First, LIP and FEF neurons are not strongly feature selective, but provide primarily information about the location of a selected object. Second, behavioral influences on neuronal activity in LIP and FEF are stronger and more multifaceted than those in extrastriate cortex.

Although they receive visual inputs, LIP and FEF neurons do not respond to most objects they encounter during viewing of complex visual scenes, but selectively encode the locations of objects that are physically conspicuous or that become relevant to an immediate goal. Conspicuous objects are encoded regardless of their specific visual features (e.g., their color or motion) and likewise, task-relevant objects are encoded regardless of the specific task for which they are relevant (for instance, whether they are designated as targets for a perceptual discrimination or for overt action). Thus, these areas appear to construct a relatively abstract salience representation that keeps track of a wide variety of objects that are likely to attract attention. Such integrated salience maps may be an efficient computational strategy for controlling the moment-by-moment allocation of attention.

The range of behavioral modulations in LIP and FEF is exceptionally broad and includes (but is probably not limited to) information about behavioral context or strategy, the expectation of reward and the prediction of the location and timing of task events. Modulations related to behavioral context filter visual inputs according the likelihood that these inputs are relevant to immediate behavior. For example, when monkeys search for a specific target in a cluttered display, FEF neurons respond strongest to the search target, more weakly to a distractor that is physically similar to the target and weakest to distractors that share the fewest features with the target. Similarly, LIP neurons respond more strongly to a salient visual transient if that transient is expected to mark the location of a search target than if it is not. The expectation of reward also modifies LIP and FEF responses so that targets expected to yield higher rewards elicit stronger responses than those expected to give lower payoffs. LIP and FEF neurons predict the expected location of a task-relevant target and LIP neurons are modulated

dynamically according to the monkeys' prediction of the timing of task events. Finally, prolonged training with a constant target can give rise to enduring modifications in visual sensitivity of attention-related areas in humans as well as monkeys, suggesting that connections between visual and attention-related areas are modifiable with experience.

These far-ranging behavioral effects suggest that the LIP and FEF interact with multiple behavioral systems including systems related to memory, temporal estimation, or reward estimation, and integrate information from these systems into a topographically organized signal of behavioral salience. This signal can guide the spatial allocation of attention based on a synthesis of immediate task demands. One way in which this signal is likely to act is by biasing the competition for neural responses in feature-selective visual areas (Reynolds, J. H. *et al.*, 2004). By virtue of feedback from LIP and FEF, task-relevant objects win the competition for neural representation in visual areas and consequently, are encoded and perceived more clearly relative to task-irrelevant distractors. Thus, attention-related areas can be seen as gateways that modulate the quality of visual perception according to a synthesis of immediate behavioral demands.

Simultaneously with their impact on visual processing attention-related areas are also instrumental in linking selected visual input with overt behavior (movement). Initially the LIP and FEF were thought to be specific for saccades – rapid eye movements with which primates scan their environment – and which are most closely related to visual attention. However, it is now recognized that these areas contribute to a wider array of actions including both ocular and skeletal movements and movements that are directly target or that are indirectly instructed by visual stimuli. The links between LIP and FEF and overt movement are bidirectional. In the forward direction, the salience representations in these areas influence motor planning by selecting objects relevant for action and facilitating motor orienting (e.g., with an eye movement) toward a task-relevant target. In the backward direction, salience responses in LIP and FEF are in turn influenced by motor planning. Thus, the preparation of an eye or limb movement become ingredients of salience – a means by which selection-for-perception can be coordinated with immediate motor output. The LIP and FEF therefore implement a complex, dynamic coordination between the perceptual selection of task-relevant targets and the planning of appropriate actions related to those targets.

2.19.4 Summary

Determining the salience, or potential importance, of various objects is one of the key operations of the brain. This determination is a multilevel process that depends on continuous feedforward and feedback interactions among multiple levels of visual representation. Elementary salient features of the visual input are extracted by hardwired circuitry at the earliest stages of visual processing. From the earliest stages, however, neural representations are also influenced by top-down information regarding the state of the observer. Top-down signals appear to be forged in higher-order visual association areas that bind sensory information with input from multiple behavioral, including motor, systems. Thus the construction of salience is an active process that depends on continuous interactions among sensory, behavioral and motor systems and may allow coherent, coordinated control of perception and action.

References

Gottlieb, J. 2007. Salience representations for perception, action and cognition. Neuron. 53, 9–16.

Joseph, J. S., Chun, M. M., and Nakayama, K. 1997. Attentional requirements in a 'preattentive' feature search task. Nature 387, 805–807.

Li, W., Piech, V., and Gilbert, C. D. 2006. Contour saliency in primary visual cortex. Neuron 50, 951–962.

Mack, A. and Rock, I. 2000. Inattentional Blindness, MIT Press.

Reynolds, J. H. and Chelazzi, L. 2004. Attentional modulation of visual processing. Annu. Rev. Neurosci. 27, 611–647.

Further Reading

Thompson, K. G. and Bichot, N. P. 2005. A visual salience map in the primate frontal eye field. Prog. Brain Res. 147, 251–262.

2.20 Perceptual Learning

W Li and C D Gilbert, The Rockefeller University, New York, NY, USA

© 2008 Elsevier Inc. All rights reserved.

2.20.1	**Introduction**	304
2.20.2	**Psychophysical Studies on Perceptual Learning**	306
2.20.2.1	Time Course of Perceptual Learning	306
2.20.2.2	Specificity of Perceptual Learning	307
2.20.2.3	Perceptual Learning and Contextual Interaction	308
2.20.2.4	Perceptual Learning and Top-Down Influences	310
2.20.2.5	Section Summary	311
2.20.3	**Cortical Mechanisms of Perceptual Learning**	311
2.20.3.1	Implications from Psychophysical Studies	311
2.20.3.2	Implications from Lesion-Induced Cortical Plasticity	312
2.20.3.3	Changes in Early Sensory Cortex Associated with Perceptual Learning	312
2.20.3.3.1	Changes in cortical maps associated with discrimination training	313
2.20.3.3.2	Changes in response properties of neurons associated with discrimination training	314
2.20.3.3.3	Changes in neuronal responsiveness associated with discrimination and detection training	317
2.20.3.3.4	Shift of cortical representation of a learned stimulus with training on visual search	318
2.20.3.3.5	Changes in temporal properties of neuronal responses	318
2.20.3.4	Section Summary	318
2.20.4	**Theories and Models about Perceptual Learning**	320
2.20.5	**Cellular and Molecular Basis**	321
2.20.6	**Concluding Remarks**	322
References		323

Glossary

classical receptive field (CRF) The CRF, also referred to as the minimum responsive field, is the receptive field mapped with a simple stimulus for which the sensory neuron is most selective. Stimuli placed outside the CRF alone usually do not evoke any response from the neuron, but when combined with other stimuli located in the CRF, they can significantly modulate neuronal responses, a phenomenon known as contextual modulation. The modulatory regions outside the CRF constitute the so-called nonclassical receptive field.

contextual modulation/interaction In perception, the term refers to various perceptual phenomena whereby the percept of a stimulus can be modified by the stimulus context within which the stimulus appears. In visual processing, it refers to an alteration of neuronal responses by contextual stimuli placed outside the classical receptive field.

cortical recruitment The reorganization of the cortical representation of the sensory surface, which can be induced by perceptual learning. Cortical recruitment usually results in an expansion of the cortical area representing the trained sensory surface by recruiting adjacent cortical areas representing untrained surfaces.

perceptual learning The unconscious improvement of perceptual ability with practice in simple discrimination and detection tasks.

top-down influences The modulation of perception or sensory processing by higher-order cognitive functions, like selective attention and expectation.

2.20.1 Introduction

Early investigation into the mechanisms of learning reflected the current philosophical trends. From the perspective of modern neuroscience, it is a commonsense notion that we assimilate all kinds of knowledge by interacting with the physical world. Until the seventeenth century, however, it was still a received doctrine that humans have native ideas stamped upon the mind from the very first being, and that we retrieve or derive our knowledge from an innate repository of ideas and principles. This idea was originally represented in the Platonic dialogues, which reflected the Socratic idea that learning is a recovery of lost knowledge that can be achieved by deductive reasoning (known as the Platonic doctrine of recollection). English philosopher John Locke attacked this notion in his essay (Locke, J., 1689), in which he likened the human mind to a blank slate, initially void of any ideas, and subsequently imprinted by ideas or knowledge obtained from an individual's experiences. Locke described perception as "the first and simplest idea we have from reflection," in which "the mind is, for the most part, only passive; and what it perceives, it cannot avoid perceiving." In his essay, Locke also reasoned that "the ideas we receive by sensation are often, in grown people, altered by the judgment, without our taking notice of it." Locke's concept here is a primitive form of the contemporary idea that our past experiences influence our perception.

Along similar lines, in the nineteenth century German physicist and physiologist Helmholtz H. (1866) interpreted perception as nothing more than our subjective ideas about external objects derived from the stimulation of our sensory organs; for Helmholtz, perception is a form of unconscious inference made by the mind. Given the psychical and creative nature of perception, Helmholtz observed that "the judgment of the senses may be modified by experience and by training derived under various circumstances, and may be adapted to the new conditions. Thus, persons may learn in some measure to utilize details of the sensation which otherwise would escape notice and not contribute to obtaining any idea of the object." This concept is exactly what we call perceptual learning today. By summarizing the writings of his contemporaries, American psychologist William James posed a theory of the neural basis of skill learning. James compared the formation of habits and skills to the plastic changes of materials, and attributed these behavioral changes to the plasticity of the brain (James, W., 1890). According to James, plasticity "means the possession of a structure weak enough to yield to an influence, but strong enough not to yield all at once." He stated that "our nervous system grows to the modes in which it has been exercised ... Habit diminishes the conscious attention with which our acts are performed ... The more of the details of our daily life we can hand over to the effortless custody of automatism, the more our higher powers of mind will be set free for their own proper work." A more contemporary representation of the idea of nervous system plasticity is found in the work of polish physiologist Jerzy Konorski (for a review on Konorski's work see Zielinski, K., 2006). Konorski distinguished plasticity from excitability as "an independent property of the functioning of higher nervous activity," "by virtue of which certain permanent functional transformations arise in particular systems of neurons as the result of appropriate stimuli or their combinations" (Konorski, J., 1948).

Among the experimental psychologists in the early twentieth century who contributed profoundly to our understanding of learning, Edward Thorndike (a student of James) was one of the most influential. By timing how fast cats were able to escape from a specially designed cage by trial-and-error, Thorndike proposed the law of effect governing behavioral learning, which states that "of several responses made to the same situation, those which are accompanied or closely followed by satisfaction to the animal will, other things being equal, be more firmly connected with the situation, so that, when it recurs, they will be more likely to recur" (Thorndike, E. L., 1911). Another important contribution by Thorndike to our understanding of the learning mechanisms comes from his studies on the transfer of learning. In the history of educational psychology there was a theory – the doctrine of formal discipline – which holds that the mind is like muscle: learning of a difficult disciplinary subject such as Latin can strengthen one's cognitive power in general and can therefore facilitate the learning of any other difficult subject. This doctrine was challenged by Thorndike's theory of identical elements, whereby the transfer of learning from one task to another can only occur insofar as the two tasks share common elements. This theory applies to very simple discrimination tasks, like judging the areas of geometric shapes (Thorndike, E. L. and Woodworth, R. S., 1901a; 1901b; 1901c). At about the same time, Russian physiologist Ivan Pavlov discovered a

different type of associative learning – classical conditioning (Pavlov, I. P., 1927). Based on the innate reflex that animals possess to certain stimuli (i.e., their unconditioned response to an unconditioned stimulus; e.g., salivation to favorite food), a new reflex (a conditioned response) can be formed in such a way that a neutral stimulus (conditioned stimulus, e.g., bell) that repeatedly precedes the unconditioned stimulus will eventually evoke the same response by itself. These earlier studies on associative learning inspired behaviorists like the American psychologist, Skinner B. F. (1938) and Konorski J. (1948) who made significant contributions to our understanding of instrumental learning (also known as operant conditioning, instrumental conditioning or type II conditioning), in which an animal's behavior is shaped by the consequences (e.g., reward and punishment) of past behavior, as stated by Thorndike's law of effect.

Learning is always associated with the formation and retention of certain forms of memory, which can be retrieved either consciously or unconsciously. The conscious form of memory, such as the recollection of previously seen objects and experienced events, is referred to as declarative memory or explicit memory, which is often acquired with a single exposure. The unconscious form of memory, which includes acquired habits and improved motor and perceptual skills, is called nondeclarative memory or implicit memory, which usually results from repeated experience. This classification of memory, which is based on the nature of memories and the involved brain structures (Figure 1), has been widely adopted throughout the study of learning and memory since the 1980s (for reviews see Schacter, D. L. *et al.*, 1993; Squire, L. R. *et al.*, 1993; Squire, L. R. and Zola, S. M., 1996; Squire, L. R., 2004; Squire, L. R. *et al.*, 2004). Whereas declarative memory is based in the medial temporal lobe, implicit memory can involve any area of the neocortex or cerebellum.

Much of what we know about learning and memory comes from studies on patients with specific damage to certain brain areas. The most famous case is patient HM, who has been used as a subject for 50 years (for review on HM see Corkin, S., 2002). HM's bilateral medial temporal lobes, including the hippocampal formation, were resected in an attempt to relieve his severe epilepsy (Scoville, W. B. and Milner, B., 1957). After the surgery, HM was no longer able to form any new explicit long-term memory, but the memories formed before the surgery were largely spared, despite partial retrograde amnesia. This suggests that the brain structures that store explicit memories are different from those that encode them. Moreover, despite HM's inability to form any long-term explicit memory, he is able to acquire and retain new perceptual and motor skills, even though he does not remember having practiced the tasks. The implication here is that the neural substrates for explicit and implicit memory are also distinct. Studies on amnesic patients suggest that different forms of memory are mediated by different brain structures.

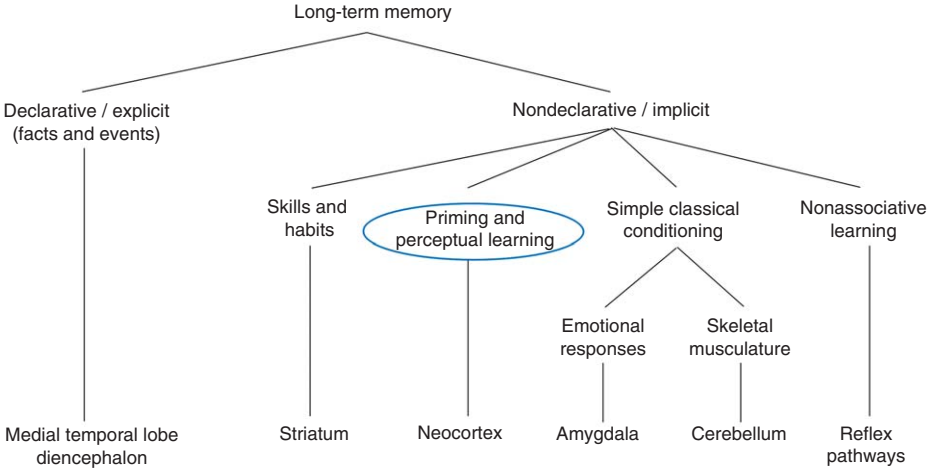

Figure 1 Classification of memory. Typical perceptual learning is a form of implicit memory whose encoding and retrieval do not reach conscious awareness. Reprinted from Neurobiol. Learn. Mem., 82, Squire, L. R., Memory systems of the brain: a brief history and current perspective, 171–177, Copyright 2004, with permission from Elsevier.

Perceptual learning is the unconscious acquisition of improved ability in simple discrimination and detection tasks with practice, and is an important form of implicit memory. It is a remarkable mechanism by which the brain adapts itself for better and more efficient processing of recurring stimuli. Some professionals, like artists, musicians, and gourmet chefs, rely on the extensive exercise of their sensory modalities to achieve extraordinary sensibility in vision, hearing, and taste. In a broad sense, perceptual learning is "any relatively permanent and consistent change in the perception of a stimulus array, following practice or experience with this array" (Gibson, E. J., 1963), or "any relatively long-lasting changes to an organism's perceptual system that improve its ability to respond to its environment and are caused by this environment" (Goldstone, R. L., 1998).

2.20.2 Psychophysical Studies on Perceptual Learning

In laboratory studies, perceptual learning is commonly seen as an improvement in performance after training on simple discrimination, detection, identification, and search tasks. This section will summarize some important findings from these psychophysical studies.

2.20.2.1 Time Course of Perceptual Learning

Perceptual learning causes a long-term change in perceptual skill. Subjects retain the learning effects derived from training on a perceptual task long after they stop practicing the task, for months or even years later (Ball, K. and Sekuler, R., 1982; Karni, A. and Sagi, D., 1993; Schoups, A. *et al.*, 1995; Crist, R. E. *et al.*, 1997). This enduring effect evolves with practice and time, showing different phases. A few tens of training trials suffice to improve a naïve subject's discrimination ability significantly in a vernier discrimination task (a visual task to discriminate the relative lateral offset of two end-to-end adjacent lines, Figure 2(c); Poggio, T. *et al.*, 1992; Fahle, M. *et al.*, 1995), indicating an early rapid phase in perceptual learning (see also Karni, A. and Sagi, D., 1993 for a fast learning phase in a texture detection task). The presence of a fast learning phase has also been demonstrated in an auditory frequency discrimination task after excluding the possible contribution of procedural learning (in which the subjects get used to the procedure of performing the task designed and instructed by the experimenters; Hawkey, D. J. C. *et al.*, 2004). Except for the quick learning phase within the initial test session, a subject's performance tends to stall within each daily training session

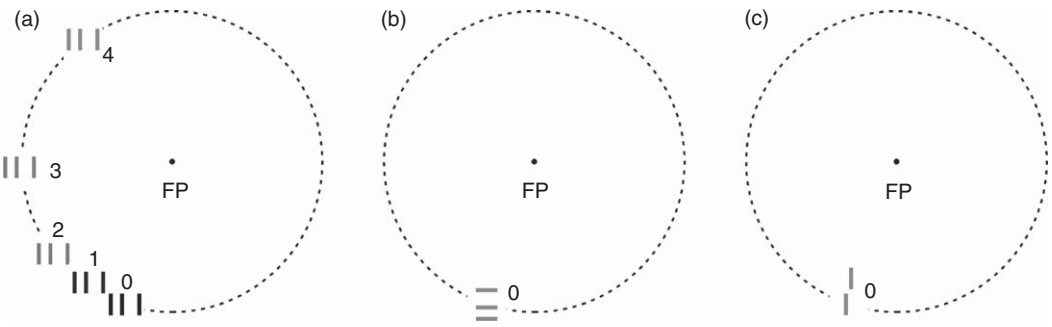

Figure 2 Specificity of perceptual learning in a three-line bisection discrimination task. The task stimulus used in this study consisted of three parallel lines. The two outer lines were fixed as a reference, while the central line was slightly displaced from the middle to either side. With fixation always at the fixation point (FP), the task was to determine whether the central line appeared closer to the left or to the right reference line. With a few weeks' training, the minimum displacement that was required for reliable discrimination of the positional offset of the middle line (i.e., the threshold for bisection discrimination) decreased by a factor of three on average. (a) The improved discrimination ability was restricted to the trained visual field location (labeled as position 0). When the same stimulus was moved away from the trained location (from 0 to 4) with the eccentricity kept constant, the training-resulted improvement gradually disappeared (denoted by a decrease in the darkness of lines). (b) Specificity of learning to stimulus orientation. At the trained location, a 90° rotation of the stimulus greatly diminished the learning effect. (c) Specificity of learning to stimulus context. Even if the task was to discriminate the lateral displacement of the same line at the same location, the learning effect did not transfer to a condition of new stimulus context, where a reference line was fixed at one end of the target line (this task is a form of the vernier task mentioned earlier). Adapted from Crist, R. E., Kapadia, M. K., Westheimer, G., and Gilbert, C. D. 1997. Perceptual learning of spatial localization: specificity for orientation, position, and context. J. Neurophysiol. 78, 2889–2894.

(Karni, A. and Sagi, D., 1993). Extensive training within the same day can even result in a decrease in performance, a phenomenon termed perceptual deterioration (Mednick, S. *et al.*, 2005). Nevertheless, relatively slow but steady improvement is evident across daily sessions (Karni, A. and Sagi, D., 1993; Schoups, A. *et al.*, 1995). This phase of gradual change lasts for many days before the subject's performance reaches an asymptote. Accumulated evidence shows that some rest (Karni, A. and Sagi, D., 1993) or sleep (Mednick, S. *et al.*, 2003; Atienza, M. *et al.*, 2004; Walker, M. P. *et al.*, 2005) after a training session is critical for the evolution and consolidation of improved discrimination ability. In fact, sleep may play an important role in memory formation and in cortical plasticity in general (for a recent review see Walker, M. P. and Stickgold, R., 2006). The requirement of a posttraining consolidation period is also supported by the finding that training on a new perceptual task immediately following a previous one without a sufficient delay interferences with the consolidation of the previously trained task (Seitzt, A. R. *et al.*, 2005).

2.20.2.2 Specificity of Perceptual Learning

Although perceptual learning occurs in virtually all kinds of perceptual tasks with repetitive exposure to the same stimulus and task conditions, the improved perceptual skill is usually highly specific to the conditions used for training. The specificity of perceptual learning is twofold. First, the improved perceptual skills obtained from training on different stimuli and tasks rarely interfere with each other (Ahissar, M. *et al.*, 1998; Seitzt, A. R. *et al.*, 2005). Second, there is little transfer of learning effect from a learned task and stimulus to a new task and stimulus. One has to undergo a new training process in order to improve under the changed conditions.

In visual perception, the commonly reported specificity of perceptual learning can be divided into four types. First, perceptual learning is restricted to the visual field location where the task stimulus is presented (Ball, K. and Sekuler, R., 1987; Berardi, N. and Fiorentini, A., 1987; Karni, A. and Sagi, D., 1991; Shiu, L. P. and Pashler, H., 1992; Fahle, M. *et al.*, 1995; Schoups, A. *et al.*, 1995; Ahissar, M. and Hochstein, S., 1996; Crist, R. E. *et al.*, 1997; Sigman, M. and Gilbert, C. D., 2000; Sowden, P. T. *et al.*, 2002). As the stimulus is moved away from the originally trained location, the observer's performance gradually regresses to the pretraining level (Crist, R. E. *et al.*, 1997; Figure 2(a)). Second, perceptual learning is specific to the stimulus used for training. Notably, a change in some simple attributes of the trained stimulus such as orientation (Ramachandran, V. S. and Braddick, O., 1973; Fiorentini, A. and Berardi, N., 1980; Schoups, A. *et al.*, 1995; Ahissar, M. and Hochstein, S., 1996; Crist, R. E. *et al.*, 1997; Sigman, M. and Gilbert, C. D., 2000; Figure 2(b)), moving direction (Ball, K. and Sekuler, R., 1982), spatial frequency (Fiorentini, A. and Berardi, N., 1980; Sowden, P. T. *et al.*, 2002; Yu, C. *et al.*, 2004), and size (Ahissar, M. and Hochstein, S., 1996), or even a change in stimulus context (Crist, R. E. *et al.*, 1997; Figure 2(c)), diminishes or abolishes the learning effect. Third, perceptual learning is specific to the particular perceptual task being practiced. Improved perceptual ability after training on one task does not usually generalize to other untrained tasks, even if the visual stimuli are very similar (Fahle, M. and Morgan, M., 1996; Fahle, M., 1997) or completely identical (Shiu, L. P. and Pashler, H., 1992; Ahissar, M. and Hochstein, S., 1993; Saffell, T. and Matthews, N., 2003). Since a perceptual task involves detecting or discriminating particular stimulus attributes, task-specificity is, in a sense, the specificity to the stimulus attributes that are relevant to the task. Learning to identify or discriminate one attribute has little effect on other tasks involving different attributes of the same stimulus. Finally, perceptual learning in some visual tasks is specific to the eye being trained. If only one eye is exposed to the task stimuli and the other eye is occluded, perceptual learning does not transfer to the untrained eye, as reported in a simple texture discrimination task (Karni, A. and Sagi, D., 1991), a luminance contrast detection task (Sowden, P. T. *et al.*, 2002), and a vernier discrimination task (Fahle, M., 2004).

While specificity is emphasized in most of the psychophysical studies, some have demonstrated partial or complete transfer of the learning effect under certain circumstances. It has been shown that the initial rapid learning phase is transferable between the two eyes, although some stimulus specificity remains (Karni, A. and Sagi, D., 1993; Fahle, M. *et al.*, 1995). Almost complete interocular transfer has been reported in an orientation discrimination task (Schoups, A. *et al.*, 1995), some acuity tasks (Beard, B. L. *et al.*, 1995), and pop-out detection tasks (Ahissar, M. and Hochstein, S., 1996; Schoups, A. A. and Orban, G. A., 1996). Some studies have shown that improvement in visual search tasks (involving the search for a unique target embedded in an array of similar distracters; Figure 3) transfers

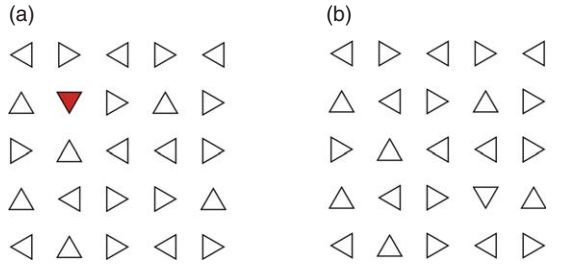

Figure 3 Learning effect on visual search. (a) An example of easy/parallel search. It is effortless to find a red target triangle pointing downward among an array of distracting triangles pointing to the other directions due to a salient difference between the target and distracters. (b) An example of difficult/serial search. To find the downward-pointing target triangle, a scrutiny of individual objects is required for naïve subjects. However, with a few days' practice, the serial/difficult search can be changed to parallel/easy search. Adapted from Sigman, M. and Gilbert, C. D. 2000. Learning to find a shape. Nat. Neurosci. 3, 264–269.

across different tasks, locations, and eyes, and is therefore less specific than the learning of simple discrimination tasks (Sireteanu, R. and Rettenbach, R., 1995; 2000; but see Ellison, A. and Walsh, V., 1998 and Sigman, M. and Gilbert, C. D., 2000 for some specificity in visual search tasks). Transfer of learning can also be manifested as an acceleration in learning speed when the stimulus parameters used for training are changed (Liu, Z. L. and Weinshall, D., 2000). In addition, learning an easy task can enable (Polat, U. and Sagi, D., 1994a) or facilitate (Liu, Z. L. and Weinshall, D., 2000) the learning of a difficult task. Perceptual learning can even transfer across sensory modalities: visual training on a shape discrimination task improves tactile discrimination ability of the same shapes (Hughes, B. *et al.*, 1990). It is still not clear under which circumstances the learned stimulus attributes or tasks are transferable. A recent study (Lu, Z. L. *et al.*, 2005) showed that the degree of interocular transfer increases with the amount of external noise added to the task stimuli, suggesting two distinct mechanisms in perceptual learning. In the presence of high external noise, a binocular mechanism of external noise exclusion, or perceptual template retuning, may be dominant, while in low external noise a monocular mechanism of stimulus enhancement may dominate. It has also been proposed that the degree of transfer depends on the task-relevant stimulus attributes and the difficulty of the perceptual task (Ahissar, M. and Hochstein, S., 1997; Liu, Z. L., 1999), and could reflect changes at different stages of information processing (Sireteanu, R. and Rettenbach, R., 1995; Ahissar, M. and Hochstein, S., 1997; Sireteanu, R. and Rettenbach, R., 2000; Ahissar, M. and Hochstein, S., 2004; for details see Section 2.20.4). But in any event, Thorndike's law of identical elements, which governs the generalization of learning, applies to perceptual learning as well (Thorndike, E. L. and Woodworth, R. S., 1901a).

2.20.2.3 Perceptual Learning and Contextual Interaction

Visual perception is usually affected by the global organization of the visual scene, namely, stimulus context. Early in the twentieth century Gestalt psychologists, typified by Max Wertheimer, proposed a set of laws governing perceptual organization. Rules like proximity, similarity and continuity determine how our visual system groups stimulus elements within a complex environment in order to properly identify individual objects (Wertheimer, M., 1923). Wertheimer also noticed that perceptual organization depends not only on the inner structure of stimulus context but also on past experience. The visual system tends to group those stimulus elements that have been previously associated with certain percepts (e.g., the well-known picture of hidden dalmatian dog created by R. C. James), suggesting an interaction between contextual influences and past experience.

That perceptual learning can modify contextual interactions is demonstrated by the observation that serial search can be changed into parallel search with training. Early studies of visual search suggested a dichotomy between parallel and serial search (Treisman, A. M. and Gelade, G., 1980; Julesz, B., 1981; Treisman, A. and Schmidt, H., 1982; Bergen, J. R. and Julesz, B., 1983). In parallel search, the target is distinct from its surrounding distracters in a certain conspicuous feature (e.g., color; Figure 3(a)). In this case, the target pops out by itself and little attention is required to locate the target. Therefore, the time needed to identify the unique target is independent of the number of distracters. In contrast, in serial search (such as the so-called conjunction search in which a combination of more than one feature is required to distinguish the target from the distracters), it is often necessary to serially direct one's attention to each object in the stimulus array. As a result, the search time is proportional to the number of distracters. Subsequent studies have revealed much more complex situations, suggesting that

parallel and serial search are simply two extremes of a continuum – an easy case and a difficult case – and that attentional state and training also affect the nature and speed of visual search. For example, some of the conjunction search tasks, which fall under the rubric of serial search by its original definition, can actually be performed in a parallel fashion (Nakayama, K. and Silverman, G. H., 1986). In contrast, for naive subjects, a parallel search task can be made serial if the subject's attention is taken away by a demanding task being performed simultaneously with the search task (Joseph, J. S. *et al.*, 1997). For experienced subjects, however, parallel search remains largely parallel regardless of the distracting task (Braun, J., 1998). A number of studies have also shown that a naïve observer's performance in some search tasks, being serial at the outset, becomes parallel with practice so that the hidden target pops out independently of the number of distracters (Figure 3(b); Sigman, M. and Gilbert, C. D., 2000; see also Wang, Q. *et al.*, 1994; Sireteanu, R. and Rettenbach, R., 1995; Ellison, A. and Walsh, V., 1998; Sireteanu, R. and Rettenbach, R., 2000; Yi, D. J. *et al.*, 2006). These studies suggest that perceptual learning can modify the interactions between contextual stimuli to facilitate the figure-ground segregation. This could be achieved by grouping a conjunction of features or a subset of visual elements into a single entity and by shifting the cortical representation of that entity from higher to lower areas (see Section 2.20.3.3.4).

Another example of the modification of contextual influences by perceptual learning is seen in collinear facilitation. Oriented stimulus elements, when arranged collinearly or smoothly along a continuous path, exhibit marked facilitatory interactions, as demonstrated in the phenomena of collinear brightness induction and contour saliency. In collinear brightness induction (Figure 4(a)), the contrast threshold for detecting the presence of a target drops significantly when the target is flanked by collinear stimuli (Dresp, B., 1993; Polat, U. and Sagi, D., 1993; 1994b; Kapadia, M. K. *et al.*, 1995; Polat, U. and Bonneh, Y., 2000). In contour saliency (Figure 4(b)), oriented stimulus elements that follow the Gestalt law of continuity are readily grouped together, forming a salient visual contour that pops out from its complex background (Field, D. J. *et al.*, 1993). This contour-linking process is known as contour integration. It has been shown that both collinear brightness induction and contour integration are significantly enhanced with training, with the enhancement

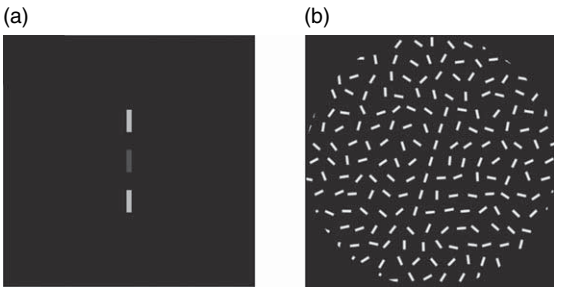

Figure 4 Collinear facilitation in visual perception is subject to perceptual learning. (a) Collinear brightness induction. The contrast threshold for detecting the presence of a target (the middle dim line) is significantly reduced in the presence of collinear flankers. (b) Contour integration. A stack of collinear lines embedded in a complex background are perceptually linked together, forming a salient contour. Perceptual learning strongly affects both collinear brightness induction and contour integration.

manifested both as an increase in the strength of collinear facilitation and as an increase in the effective spatial range within which the collinear interaction takes place (Polat, U. and Sagi, D., 1994a; Kovács, I. *et al.*, 1999; Li, W. and Gilbert, C. D., 2002;). In addition to pronounced learning effects in contour integration for both children and adults, contour integration ability improves with age in children, suggesting a late maturation of this perceptual ability (Kovács, I. *et al.*, 1999).

On the one hand, perceptual learning can modify contextual influences, but on the other hand, certain stimulus context could be helpful in learning to improve visual discrimination ability. It has been reported that contrast discrimination of an oriented target (a task to determine whether the target is brighter or dimmer than a reference) cannot be improved with training unless the training is conducted in the presence of collinear inducers (Adini, Y. *et al.*, 2002). This claim of context-enabled learning is currently under debate. Some recent studies have shown that contrast discrimination of an isolated target is learnable at different base (or reference) contrasts both in a blocked design (a single reference contrast is used within each block of trials; Yu, C. *et al.*, 2004) and in an interleaved design (different reference contrasts are mixed within the same block; Kuai, S. G. *et al.*, 2005). In the interleaved design, however, different reference contrasts must be presented in a fixed temporal order, as no learning effect takes place if they are randomly interleaved from trial to trial (Kuai, S. G. *et al.*, 2005). Here, a fixed

temporal pattern of stimulus presentation, namely temporal context, is critical in training on several mixed groups of stimuli, each of which has its own reference. These studies suggest that spatial and temporal contexts can be important for triggering the encoding mechanisms of perceptual learning.

2.20.2.4 Perceptual Learning and Top-Down Influences

Visual perception is generated by a combination of stimulus-driven bottom-up processes and behavior-driven top-down processes in the brain. A noticeable and extensively studied form of top-down influence is selective attention, which affords the attended objects or stimulus features more neuronal representation than the unattended ones.

Psychophysical studies reveal that attention is important not only for perception itself but also for perceptual learning. For the same visual stimulus, a subject's ability to discriminate a subtle change in a stimulus attribute can be improved only if the attribute is attended and used in the perceptual task (Shiu, L. P. and Pashler, H., 1992; Ahissar, M. and Hochstein, S., 1993; Saffell, T. and Matthews, N., 2003). The unattended attributes are unaffected in perception even though the subjects are repeatedly exposed to the same stimulus. For example, orientation and brightness are two different attributes of a straight line. When both attributes are altered from trial to trial, the discrimination ability of human subjects is improved only for the attended attribute (Shiu, L. P. and Pashler, H., 1992).

Despite the converging evidence that perceptual learning requires attention to the task-relevant stimulus attribute, some recent studies have shown that the discrimination of unattended and untrained stimuli is improvable under certain circumstances (Watanabe, T. *et al.*, 2001; 2002; Seitz, A. and Watanabe, T., 2003; Seitz, A. *et al.*, 2005). In these studies, the subjects' attentional resources were largely exhausted by performing a very demanding rapid-serial-visual-presentation (RSVP) task in the fovea, in which two white target letters had to be identified within a stream of rapidly displayed black distracter letters. Surrounding each letter was an array of dynamic random dots (DRDs) with subthreshold coherent motion (a small percentage of dots move in the same direction while the others move randomly). After extensive practice on the RSVP task while being passively exposed to the DRDs of subthreshold coherent motion, the subjects' ability to detect the coherent motion was significantly improved. Further investigation showed that the improvement only occurred for the coherent motion direction paired with the target letters, not for the other directions paired with the distracter letters (Seitz, A. R. and Watanabe, T., 2003; Seitz, A. *et al.*, 2005). That is, there is a strict temporal coupling between learning the unattended stimulus attribute (direction of coherent motion in DRDs) and the attended target. In this regard, attention is not completely dispensable in the subliminal learning. One possible explanation for the phenomenon is that attention is required for obtaining the reward signal that produces plasticity, but that this effect reinforces all stimuli that coincide with the attended stimulus (see Section 2.20.4). An enduring improvement in discrimination ability without training has been reported in somatosensory system. After extensive and passive stimulation of a small area on a finger tip, the subjects' spatial discrimination ability was improved for the stimulated skin area (Godde, B. *et al.*, 2000; Hodzic, A. *et al.*, 2004). In this case, the subjects had not been exposed to the task stimuli during the passive stimulation, so a possible role for top-down control was precluded. However, in this exceptional case, the enhancement in spatial discrimination ability was also accompanied by an impairment of temporal discrimination ability within the same skin area (Hodzic, A. *et al.*, 2004). As we will see later (see Section 2.20.3.3.1), prolonged passive stimulation incurs a reorganization of the somatosensory cortex, which is responsible for the change in tactile perception. This result pertains more to cortical plasticity than to typical modes of perceptual learning.

Another form of top-down influence on perceptual learning is the feedback that signals the observer's performance on the perceptual task. Although perceptual learning can take place without any external feedback signal (McKee, S. P. and Westheimer, G., 1978; Shiu, L. P. and Pashler, H., 1992; Fahle, M. *et al.*, 1995), strong effects of feedback have been reported. Correct feedback results in faster and more extensive improvement in performance than without it (Shiu, L. P. and Pashler, H., 1992; Herzog, M. H. and Fahle, M., 1997), whereas feedback uncorrelated with the subjects' responses prevents learning (Herzog, M. H. and Fahle, M., 1997). Moreover, there is no significant difference in the learning between the feedback given on a trial-by-trial basis or on a block-by-block basis (Shiu, L. P. and Pashler, H., 1992;

Herzog, M. H. and Fahle, M., 1997). These results indicate that nonattentional top-down influences also profoundly affect perceptual learning (Fahle, M., 2004).

While perceptual learning can be enabled or facilitated by top-down influences, the attentional mechanism itself is malleable and subject to learning. For example, perceptual learning results in a more effective attentional suppression of task-irrelevant stimuli, and this attentional learning is stimulus specific and long lasting (Vidnyanszk, Z. and Sohn, W., 2005). Moreover, perceptual learning ultimately leads to a release of the task from attentional control, resulting in automatization of the perceptual task (Shiffrin, R. M. and Schneider, W., 1977; Sigman, M. and Gilbert, C. D., 2000; see also Section 2.20.3.3.4).

2.20.2.5 Section Summary

The visual system can improve its performance on various perceptual tasks with training. For simple discrimination, detection and search tasks, the learned information is retained in the brain in the form of long-term implicit memory, which is usually specific to the trained task and the trained stimulus with little crosstalk. In addition to affecting the accuracy and speed of performing a task, perceptual learning, together with contextual modulation and top-down influences, strongly influences how we interpret visual stimuli. These modulatory factors also intimately interact with each other: perceptual learning can be affected by stimulus context and top-down control, and the mechanisms of contextual and attentional modulation themselves are subject to modification over the course of perceptual learning. These factors and their complex interactions necessarily determine the dynamic and creative nature of visual perception.

2.20.3 Cortical Mechanisms of Perceptual Learning

As mentioned in the introduction, the acquisition of explicit memory involves a rather unified memory system in the brain. This memory system is necessary neither for visual perception *per se* (for a recent study see Shrager, Y. *et al.*, 2006), nor for perceptual learning. For example, amnesic patients show learning effects that are comparable to normal observers in the vernier discrimination task (Fahle, M. and Daum, I., 2002). Several lines of evidence point to sensory cortices, including the primary sensory cortex, as the loci mediating perceptual learning.

2.20.3.1 Implications from Psychophysical Studies

Considered in conjunction with the functional organization of sensory systems, psychophysical findings offer insights into the cortical loci and mechanisms involved in perceptual learning. In the visual system, more than thirty cortical areas are associated with visual processing (Van Essen, D. C. *et al.*, 1992), and these areas are functionally specialized and hierarchically organized, forming partially segregated modules and pathways for processing different visual information (Van Essen, D. C. *et al.*, 1992; Zeki, S., 2001). The primary visual cortex (area V1) is the first stage of visual cortical processing, where neurons are selective for simple stimulus attributes like orientation and spatial frequency. In addition, the receptive fields (RFs) of V1 neurons are, on average, the smallest among all visual areas, and the visual inputs from the two eyes are still partially separate in V1. Ascending along the hierarchical pathway, response properties of neurons get more complex, the RFs get bigger, and the inputs from the two eyes become indistinguishable. Higher visual areas gain selectivity for more complex stimuli like faces, but loose spatial resolution and ocular identity. Therefore, given the specificity of perceptual learning to simple stimulus attributes, spatial location and the trained eye, the involvement of early visual areas in perceptual learning can be deduced from the functional organization of the visual system. For instance, the properties of V1 neurons – particularly their selectivity for simple stimulus parameters and their small RF sizes – make them suitable for learning tasks requiring high spatial resolution, like vernier and bisection discrimination. On the other hand, the dependence of perceptual learning on attention to specific stimulus attributes and tasks, together with the remarkable effects of feedback signals on learning, suggests the involvement of top-down control and an interaction between cortical areas. Moreover, the change from serial to parallel search with training and the release of perceptual task from attentional control – automatism of the task, in James' words (James, W., 1890) – suggest a shift of cortical

representation of the trained stimulus from higher to lower areas (Sigman, M. and Gilbert, C. D., 2000).

2.20.3.2 Implications from Lesion-Induced Cortical Plasticity

Another line of evidence suggesting the involvement of early sensory cortices in mediating perceptual learning comes from the accumulated findings that these cortical areas are highly plastic even in adults (fom reviews see Kaas, J. H. *et al.*, 1983; Weinberger, N. M., 1995; Edeline, J. M., 1999; Gilbert, C. D. *et al.*, 2001; see also Chapter Plasticity of Somatosensory Function during Learning, Disease and Injury).

In early postnatal development there are time windows, known as critical periods, during which the brain shows heightened plasticity and neural circuits are easily susceptible to modification by experience. The existence of critical periods was noticed by biologists nearly a century ago by studying the behavior of newborn animals. For example, Austrian ethologist Konrad Lorenz studied the phenomenon of imprinting, in which some birds (e.g., geese) have the tendency to treat the first moving object (e.g., Lorenz himself) they encounter after hatching as their parent and to attach themselves to this object. This imprinting behavior is restricted to a very short time period after hatching (Lorenz, K., 1935a; 1935b). Direct examination of cortical changes during the critical periods started from the 1960s. By suturing one eye of kittens for different periods of time after birth, Hubel D. H. and Wiesel T. N. observed a loss of responsiveness of V1 neurons to visual input from the sutured eye and determined the corresponding critical period for ocular dominance (Wiesel, T. N. and Hubel, D. H., 1963; Hubel, D. H. and Wiesel, T. N., 1970). They also anatomically demonstrated the changes that accompany monocular deprivation in the ocular dominance columns of juvenile monkeys (Hubel, D. H. *et al.*, 1977). So far a few clear critical periods in different sensory modalities and in different animal species have been well identified in terms of their timing, duration, and neural and molecular mechanisms (for a recent review see Hensch, T. K., 2004).

It was previously thought that the closure of the critical periods marks the maturation and stabilization of the brain, and that the neural connections and circuits should be fixed in adults. Nevertheless, since the late 1970s, pronounced reorganization of the central nervous system in adult animals has been observed after injury to the peripheral nervous system. For example, after severing the sciatic and saphenous nerves of adult cats, the spinal cord neurons on which the severed nerves used to terminate begin responding to adjacent intact nerves, thereby shifting their RFs (Devor, M. and Wall, P. D., 1978). A similar result has been observed in adult rats as well (Devor, M. and Wall, P. D., 1981). In the brain, striking reorganization of adult primary somatosensory cortex (area S1) has also been reported to follow deafferentation of the sensory input (Rasmusson, D. D., 1982; Merzenich, M. M. *et al.*, 1983a; 1983b; 1984; Calford, M. B. and Tweedale, R., 1988; Pons, T. P. *et al.*, 1991; Weiss, T. *et al.*, 2004). The cortical territory devoted to the representation of the deafferented body surface becomes responsive to adjacent body surfaces. Very similar plastic changes are also found in primary auditory cortex (area A1) of adult animals after restricted unilateral cochlear lesions (Robertson, D. and Irvine, D. R. F., 1989; Rajan, R. *et al.*, 1993), and in area V1 after retinal lesions (Gilbert, C. D. *et al.*, 1990; Kaas, J. H. *et al.*, 1990; Heinen, S. J. and Skavenski, A. A., 1991; Chino, Y. M. *et al.*, 1992; Gilbert, C. D. and Wiesel, T. N., 1992; Schmid, L. M. *et al.*, 1996; Eysel, U. T. *et al.*, 1999; Calford, M. B. *et al.*, 2000). A laser-induced retinal scotoma removes visual input to the corresponding retinotopic region in V1 and therefore silences neurons within that region, producing a cortical scotoma (Figure 5). However, several months following the retinal injury, the cortical scotoma shrinks: neurons within the cortical scotoma regain responsiveness by shifting their RFs outside the retinal scotoma. It has been shown that, rather than being derived from a rearrangement of thalamocortical afferents, the reorganization seen in V1 is cortically mediated, probably by the intrinsic horizontal connections in V1 (Darian-Smith, C. and Gilbert, C. D., 1995). The plasticity of early sensory cortices observed during recovery from injury has been suggested to serve as the neural basis of perceptual learning under normal physiological conditions.

2.20.3.3 Changes in Early Sensory Cortex Associated with Perceptual Learning

Since the 1990s, plastic changes associated with perceptual learning have also been demonstrated in early sensory cortices. In this section we will summarize these cortical changes into several categories, which to some extent depend on the nature of the perceptual tasks and could reflect different cortical

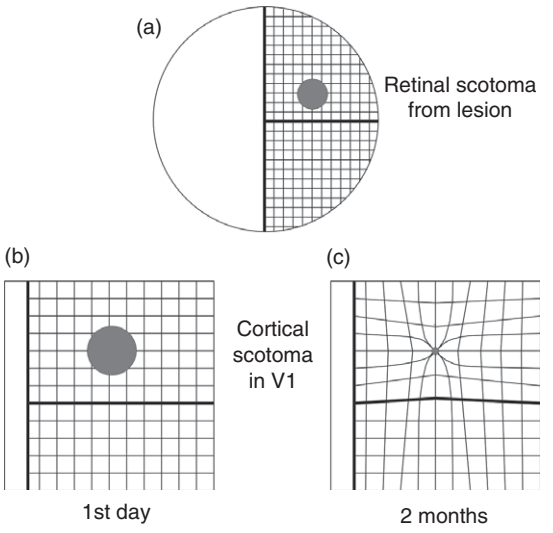

Figure 5 Reorganization of V1 after retinal lesion. A retinal scotoma caused by laser lesion (a, the small gray disc) creates a cortical scotoma in V1 (b). During recovery (c), neurons within the cortical scotoma regain responsiveness to visual input from the area surrounding the retinal scotoma. Adapted from Gilbert, C. D. 1992. Horizontal integration and cortical dynamics. Neuron 9, 1–13.

mechanisms of perceptual learning. We will describe in detail some cortical modifications that are well correlated with perceptual changes and can, therefore, account for perceptual learning.

2.20.3.3.1 Changes in cortical maps associated with discrimination training

The first piece of evidence that training on a discrimination task modifies early sensory cortex came from the observation of cortical recruitment, a process whereby the cortical area representing the trained sensory surface expands by recruiting the adjacent cortical areas previously representing the untrained surface. Intuitively, with the participation of a larger area of cortex and a proportionally greater number of neurons, better performance can be achieved in the discrimination task at the trained location due to probability summation: the probability of detecting a stimulus increases with the number of detectors/neurons, assuming that they are at least partially independent and that a subset is enough to signal the presence of the stimulus.

The primary sensory cortices are organized into orderly topographic maps to represent the sensory surfaces. These two-dimensional maps in S1, A1, and V1 are termed somatotopic, tonotopic and retinotopic maps, respectively. After training monkeys to perform a tactile frequency discrimination task using a small surface of one digit, remarkable reorganization of S1 has been observed, characterized by a significant increase in the size and complexity of the territory representing the trained skin area (Recanzone, G. H. *et al.*, 1992b; 1992c). Similarly, training on an acoustic frequency discrimination task results in up to a ninefold increase in cortical area representing the trained frequencies within A1 (Recanzone, G. H. *et al.*, 1993).

It is a matter of some debate whether the learning-associated cortical recruitment is actually responsible for the improved discrimination ability. There are several lines of evidence supporting the idea that it is, but some negative results have also been reported. Studies in monkey S1 (Recanzone, G. H. *et al.*, 1992c) and A1 (Recanzone, G. H. *et al.*, 1993) indicate that performing a tactile task while being passively stimulated by auditory stimuli mainly modifies S1 but not A1. Likewise, performing an auditory task while being passively stimulated by tactile stimuli mainly modifies A1 but not S1. Moreover, the reorganization is restricted to the cortical region representing the trained skin surface (S1) or the trained frequency range (A1). Therefore, cortical recruitment is specific to the sensory area where the task stimuli are processed. It has also been shown that increases in cortical representation are significantly correlated in A1 (Recanzone, G. H. *et al.*, 1993), and somewhat correlated in S1 (Recanzone, G. H. *et al.*, 1992c), with enhanced performance on the discrimination tasks. In a recent study (Polley, D. B. *et al.*, 2006), rats were trained to attend to either the frequency or the intensity attribute of an identical set of acoustic stimuli. Training on the frequency recognition task causes cortical recruitment in the frequency but not intensity domain of the topographic maps in A1 and higher auditory areas. In contrast, training on the intensity recognition task causes an increase in cortical sites that are sensitive to the target intensity but no change in the tonotopic maps. In both cases, cortical recruitment is correlated with improved performance. According to a study using the magnetic source imaging (MSI) technique (Braun, C. *et al.*, 2002), the topographic map in S1 is not only plastic, being modified by training on the discrimination task, but it is also rather dynamic, reorganizing according to different task requirements. Taken together, these findings suggest that the recruitment of specific cortical regions could be involved in solving specific discrimination tasks and

improving performance. While these studies emphasize the role of top-down influences in triggering the cortical recruitment, a recent human functional magnetic resonance imaging (fMRI) study has shown that prolonged passive tactile stimulation of a finger tip also significantly increases the cortical representation of the stimulated skin area in S1 and S2 (Hodzic, A. *et al.*, 2004). This augmentation is accompanied by a shift of the center of gravity of the reorganized cortical area, and the magnitude of the shift is strongly correlated with an improvement in spatial discrimination ability that is specific to the stimulated skin surface (Pleger, B. *et al.*, 2001; Hodzic, A. *et al.*, 2004).

Despite the evidence that cortical recruitment in S1 and A1 may account for perceptual learning, some issues remain unclear. In cat A1, a recent study (Brown, M. *et al.*, 2004) failed to show any cortical recruitment associated with training on an acoustic frequency discrimination task. Moreover, an expansion of cortical representation of a skin area in S1 or a frequency range in A1 occurs at the expense of the representation of adjacent skin areas or frequencies. If an increase in representation is responsible for the enhanced discrimination ability on the trained sensory surface, a decrease in representation would presumably result in impaired discrimination ability on the adjacent untrained sensory surface. Compelling evidence for such a phenomenon is still lacking, though it has been shown that training in a new skin area (Recanzone, G. H. *et al.*, 1992a) or in a new acoustic frequency range (Recanzone, G. H. *et al.*, 1993) degrades the learning effect for the previously trained skin area or frequency range. In addition, there is actually some evidence against a decrement in performance in untrained sensory surfaces (Brown, M. *et al.*, 2004). It is also worth pointing out that, in S1, the correlation between the area of cortical representation and the performance of the animal is not statistically significant (Recanzone, G. H. *et al.*, 1992c), but one would expect to see a close correlation if cortical recruitment mediates perceptual learning. Instead, a change in the temporal characteristics of S1 neuronal responses is suggested to be a more likely correlate with improvement in performance (Recanzone, G. H. *et al.*, 1992d; see Section 2.20.3.3.5). In the visual system, the lack of transfer between very similar tasks also argues against cortical recruitment. For example, in the bisection and vernier discrimination tasks mentioned earlier (Figure 2), the spatial offset of the same target line is discriminated in the same visual field location but in different stimulus contexts. If the improvement in one task is mediated by cortical recruitment, one would expect to see an improvement in the other task. Another argument against recruitment in visual learning is the absence of performance robbing from untrained visual field locations, which would be expected if the area of cortical representation correlates with performance. In fact, recent studies have shown that no change occurs in the retinotopic map in V1 after extensive training on bisection discrimination. However, changes do occur in V1 neuronal response properties that can account more for the context specificity of the learning and for the lack of transfer (Crist, R. E. *et al.*, 2001; Li, W. *et al.*, 2004b; see Section 2.20.3.3.2).

These mixed observations suggest that cortical recruitment is only one possible mechanism involved in perceptual learning. This mechanism could be specific to certain perceptual tasks in the somatosensory and auditory modalities, and it could be dependent on the stimulus and behavioral paradigms, or even on animal species (Brown, M. *et al.*, 2004). In addition to cortical recruitment, some changes in the basic properties of neurons within the reorganized cortical regions have been observed, such as an increase in the size and overlap of RFs (Recanzone, G. H. *et al.*, 1992c), a change in temporal response properties (Recanzone, G. H. *et al.*, 1992d), and a narrowing of tuning functions (Recanzone, G. H. *et al.*, 1993; Polley, D. B. *et al.*, 2006).

2.20.3.3.2 Changes in response properties of neurons associated with discrimination training

Response properties of visual neurons can be dynamically modified by a number of factors, notably stimulus context (for reviews see Allman, J. *et al.*, 1985; Gilbert, C. D., 1998; Albright, T. D. and Stoner, G. R., 2002; and Contextual Influences on Visual Processing: From Image-based to Scene-based Representations in this encyclopedia). The RFs of V1 neurons are usually mapped by moving a small bar of light in the visual field. The small responsive area determined in this way for a given cell is referred to as the cell's classical receptive field (CRF) or minimum responsive field. Within the last couple of decades, a large body of evidence has shown that V1 neuronal responses to a stimulus placed in the RF are profoundly modulated by contextual stimuli located outside the classically defined RF. Contextual modulation in V1 suggests that V1

neurons are involved in processing complex stimulus features in visual scenes, and in mediating many contextual interactions in visual perception (e.g., the collinear brightness induction and contour integration, Figure 4).

Recent studies have revealed that contextual influences in V1 can be strikingly altered by perceptual learning so as to fit the requirements of the perceptual task (Crist, R. E. *et al.*, 2001; Li, W. *et al.*, 2004b). V1 neuronal responses to a line positioned in the RF and orientated at the cell's preferred orientation are usually slightly inhibited by a second parallel line placed on either side of the RF (Kapadia, M. K. *et al.*, 2000). However, as shown by one study in which monkeys were trained on a three-line bisection discrimination task, this contextual influence in V1 can be greatly modified (Crist, R. E. *et al.*, 2001; Figure 6(a1) and 6(a2)). For a large proportion of cells, the contextual modulation of neuronal responses by the second line is profoundly increased during the performance of the bisection task. In a subset of these cells, weak contextual inhibition is even reversed to strong facilitation (Figure 6(a2)). The changes in magnitude and, in some cases, polarity, of contextual modulation are present only in the trained area, suggesting a task-specific modification of neuronal response properties. A more rigorous examination of task-specific contextual modulation was provided by a subsequent study (Li, W. *et al.*, 2004b). Monkeys were presented with an identical set of stimulus patterns on which they were trained to perform either a bisection or a vernier discrimination task (Figure 6(b1)). This study showed that V1 neuronal responses are strongly modulated by the stimulus attribute relevant to the immediate task, but that they are little affected by the other task-irrelevant attribute (Figure 6(b2)). Information theoretic analyses revealed that, compared with the task irrelevant condition, V1 neuronal responses carry significantly more information about the same stimulus attribute when it is used by the animal to solve the discrimination task. Taken together, these findings indicate that V1 neurons in the trained animals take on novel response properties related to the discrimination task, and that the exercise of these acquired response properties requires the same stimulus and behavior context as that during training. This cortical mechanism coincides with the specificity of perceptual learning. Interestingly, task-dependent modification of neuronal response properties has also been reported in auditory cortex. Neurons in ferret A1 respond differentially to identical tones used in tone detection versus frequency discrimination tasks (Fritz, J. B. *et al.*, 2005).

Not only can the complex responses properties of V1 neurons be modified by perceptual learning in a task-specific manner, but the basic tuning properties can also be changed by learning simple discrimination tasks. A study has reported an increase in orientation selectivity of V1 neurons after training monkeys in an orientation discrimination task (Schoups, A. *et al.*, 2001). Within the V1 region corresponding to the trained visual field location, a subgroup of neurons whose preferred orientations are between 12° and 20° away from the trained orientation show a significant increase in the slopes of their orientation tuning curves at the trained orientation (Figure 7). A steepening in the slope around the most sensitive orientations on the curves, which correspond to the trained orientation, would significantly enhance neuronal sensitivity to orientation differences at the trained orientation and thus improve orientation discrimination ability. This change in orientation tuning of V1 neurons is specific to the trained visual field location and trained orientation. A sharpening of the orientation tuning curve with training on orientation discrimination has also been reported in monkey V4 (a cortical area mainly involved in encoding visual information about color and form; Yang, T. M. and Maunsell, J. H. R., 2004).

Learning-associated cortical recruitment (see Section 2.20.3.3.1), as well as changes of neuronal tuning properties, requires attention to the stimulus attribute relevant to the task. This is consistent with the psychophysical finding that the encoding of the learned information is subject to top-down influences (see Section 2.20.2.4). Reorganized cortical maps in A1 and S1 are seen when the trained animals are anesthetized (Recanzone, G. H. *et al.*, 1992c; Recanzone, G. H. *et al.*, 1993; Polley, D. B. *et al.*, 2006), suggesting that these changes indeed take place in early sensory areas. However, in the visual system, neuronal response properties that emerge from learning the discrimination tasks are present only when the animal is executing the learned task. This suggests that top-down influences play a role in triggering recall of these acquired properties for the task at hand. One proposed neural mechanism is that (Li, W. *et al.*, 2004b), the information related to a given stimulus attribute is represented at the level of subsets of inputs to a cell, which are gated by the top-down signals via interactions between feedback connections from higher cortical areas and intrinsic connections within V1. This mechanism enables

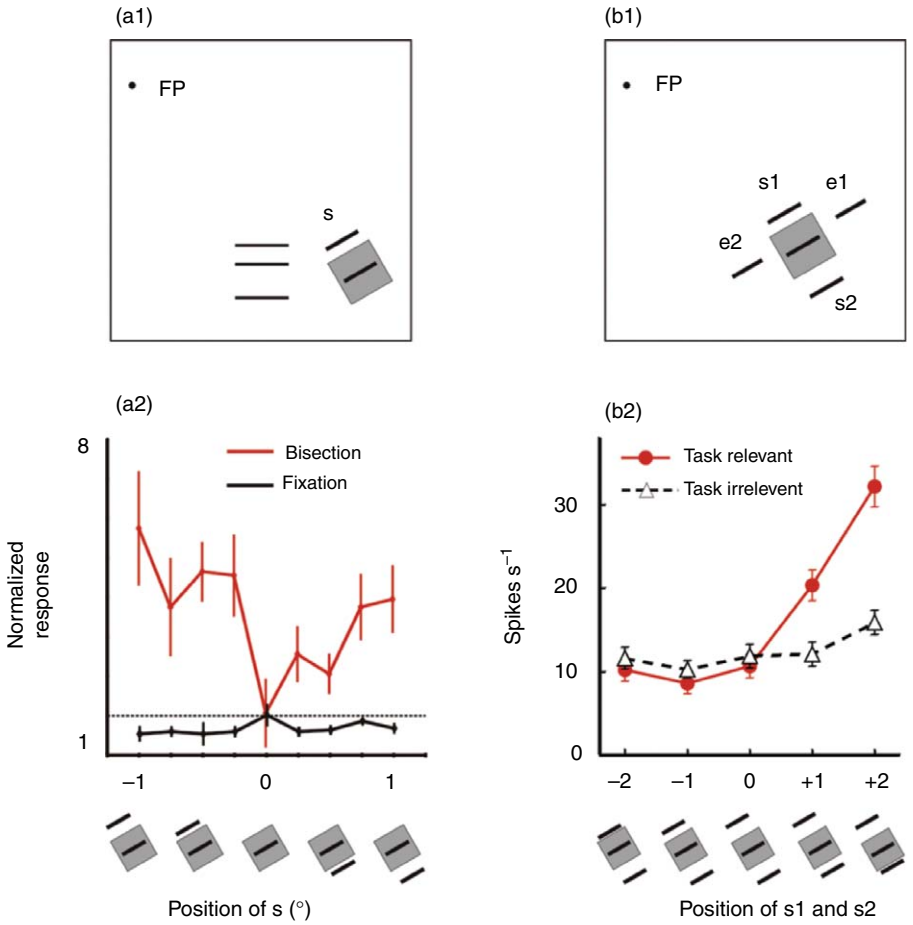

Figure 6 Perceptual learning modifies contextual interactions in V1 in a task-specific manner. (a1) Monkeys were trained to perform a three-line bisection discrimination task at a visual field location. The task stimuli consisted of three horizontal lines. Responses of single V1 neurons to another set of stimuli, the test stimuli, were recorded either when the animal did the trained bisection task or simply maintained its fixation at the fixation point (FP). The test stimuli consisted of two lines, an optimally oriented line fixed in the center of the RF (denoted by the small gray square), and a second parallel line (indicated by s) placed at different locations on either side of the RF (the cartoons at the bottom of (a2)). (a2) The normalized responses of a sample cell to the test stimuli are compared between the bisection and fixation task conditions. When the animal was performing the bisection discrimination task, the contextual modulation of neuronal responses by the second line was profoundly modified relative to the condition when the animal performed the fixation task. This change of contextual modulation was seen only in the trained area (for details see the text). (b1) Monkeys were trained to do two different discrimination tasks with identical stimulus patterns at the same visual field location. The stimuli consisted of five simultaneously presented lines: an optimally oriented line fixed in the RF center and flanked by four additional lines surrounding the RF. In different trials, the arrangement of the two side-flankers (s1, s2) was randomly assigned from a set of five different configurations (illustrated in the cartoons at the bottom of (b2) and labeled from -2 to $+2$). Each configuration differs from the others in the separation between the three side-by-side lines (in condition '0' the three lines were equidistant; in the other conditions either s1 or s2 was closer to the center line). In the same trials, the two end-flankers (e1, e2) were independently assigned a random configuration from a set of predefined arrangements, such that the end-flankers were collinear with each other but misaligned with the center line to either side. The animal was cued to perform either a bisection task based on the three side-by-side lines, or a vernier task based on the three end-to-end lines. (b2) One example of cells in response to the five-line stimuli under the two task conditions. Neuronal responses were examined as a function of the position of the two side-flankers s1 and s2 when the animal either performed the bisection task, in which s1 and s2 were task-relevant; or performed the vernier task, in which the same s1 and s2 were task-irrelevant. (a1,a2) Adapted from Crist, R. E., Li, W., and Gilbert, C. D. 2001. Learning to see: experience and attention in primary visual cortex. Nat. Neurosci. 4, 519–525. (b1,b2) From Li, W., Piech, V., and Gilbert, C. D. 2004b. Perceptual learning and top-down influences in primary visual cortex. Nat. Neurosci. 7, 651–657.

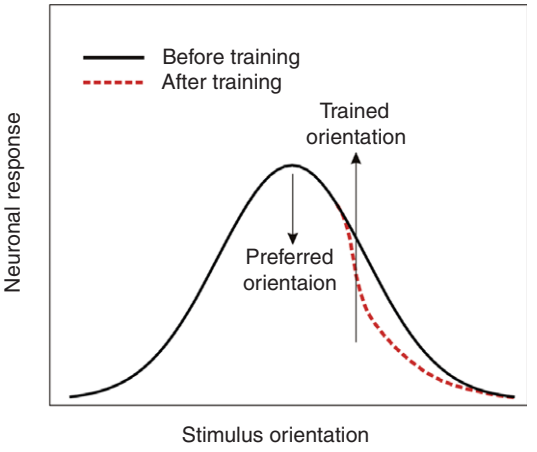

Figure 7 Increased orientation selectivity associated with training on an orientation discrimination task. The tuning curves shown here are only for schematic purpose. A significant change is observed for those neurons whose preferred orientations are at a certain distance from the trained orientation. The change is seen as an increase in the slope of orientation tuning curve on the flank that overlaps the trained orientation (Schoups, A. A. *et al.*, 2001; see also Teich, A. F. and Qian, N., 2003 for a model).

multiple learned attributes to be represented by the same cells without crosstalk, greatly expanding information processing capability in V1. Therefore, the top-down influences are critical in both encoding and retrieving the learned information.

2.20.3.3.3 Changes in neuronal responsiveness associated with discrimination and detection training

There is no reason *a priori* to expect that learning would always be associated with an increase in neural activity coming from a given cortical area. On the one hand, an increase in activity due to higher responses from individual neurons or from recruiting additional neurons could account for improvement because of an increase in the signal-to-noise ratio or probability summation. But on the other hand, a sharpening of tuning can also account for improvement in discrimination, yet this would mean that fewer cells would respond to the stimulus, leading to an overall decrease in neuronal responses.

Some discrimination tasks involve making a fine distinction between a target and a reference along a given stimulus dimension, like frequency, orientation or shape. It is not surprising, then, that training on such tasks would enhance neuronal selectivity for the task-related stimulus attributes (see Section 2.20.3.3.2). The changes in tuning properties are, in some cases, accompanied by changes in neuronal responsiveness. Some studies have reported increases in neuronal activity associated with discrimination learning. For example, over the course of learning a tone discrimination task in adult owl monkeys, an increase in sensitivity of A1 neurons to all frequencies is observed during the initial phase of improvement in performance. Subsequently, neuronal responses to the target stimuli are differentially intensified relative to the reference and nontarget stimuli (Blake, D. T. *et al.*, 2002). In monkey visual area V4, after training the animal on an orientation discrimination task, neurons with RFs overlapping the trained location show both narrower orientation tuning and stronger responses than neurons in the untrained hemisphere (Yang, T. M. and Maunsell, J. H. R., 2004). On the other hand, some studies have shown reversed results: a decrease of responsiveness in a subpopulation of neurons. A positron emission tomography (PET) study has shown decreased orientation-specific activity in early visual areas associated with orientation discrimination learning (Schiltz, C. *et al.*, 1999). Some studies have also shown both an increase and a decrease in neuronal responses in different subsets of V1 neurons, but both changes are associated with increased selectivity for the task stimuli (Crist, R. E. *et al.*, 2001; Li, W. *et al.*, 2004b). It is suggested that a change in neuronal responsiveness, with a corresponding change in the signal-to-noise ratio, is not directly related to the improvement in orientation discrimination, because a decreased signal-to-noise ratio in neuronal responses is observed at the trained orientation (Schoups, A. *et al.*, 2001). Therefore, the change of neuronal responsiveness in discrimination learning may be more closely related to the change in tuning properties, which better accounts for the improvement in discrimination ability (see Teich, A. F. and Qian, N., 2003 for a computational network simulation).

Unlike the discrimination tasks mentioned above, some perceptual tasks involve detection or identification of the presence or absence of a target, either in isolation near the detection threshold or within a noisy context. In this case, the intensity or signal-to-noise ratio of the target stimulus is more directly related to the task than any other stimulus attribute. Therefore, the responsiveness of neurons to the target is of key importance to solving the task. Depending on the nature of the target to be identified, activity in different visual areas is significantly

increased with training. It has been reported that an improvement in monkeys' performance on the detection of coherent motion of DRDs is predicted by an increase in neuronal activity in areas MT and MST (two cortical areas that are involved in processing motion signals; Zohary, E. *et al.*, 1994). Parallel results have been shown in visual area V4, which is at an intermediate stage along the hierarchical pathway for object recognition. Training monkeys to identify natural images degraded by noise specifically enhances V4 neuronal responses to those familiar and degraded pictures, and thus increases the amount of information that V4 neurons can extract from the stimuli (Rainer, G. *et al.*, 2004). In early visual areas, in particular in the most extensively studied area, V1, contextual modulation of neuronal responses is suitable for mediating center-surround interactions that are involved in many figure-ground detection tasks (for examples see Knierim, J. J. and Van Essen, D. C., 1992; Kapadia, M. K. *et al.*, 1995; Lamme, V. A., 1995; Rossi, A. F. *et al.*, 1996; Zipser, K. *et al.*, 1996; Nothdurft, H. C. *et al.*, 1999). Evidence from electrophysiological (Lee, T. S. *et al.*, 2002) and fMRI (Schwartz, S. *et al.*, 2002; Kourtzi, Z. *et al.*, 2005; Sigman, M. *et al.*, 2005) studies shows that training on detection of a target embedded in a background of noise or distracters significantly boosts activity in early visual areas. It has also been reported that the increased neuronal responses are correlated with the improvement in target detection (Lee, T. S. *et al.*, 2002). Training on target detection near the threshold and in the absence of any noise or distracter shows a similar effect (Furmanski, C. S. *et al.*, 2004). After training human subjects to detect a near-threshold grating patch, the fMRI signal in V1 for the trained orientation is significantly increased relative to the control orientation, and this change is correlated with the improvement in target detection.

In summary, the accumulated evidence indicates that an important mechanism of learning in target detection or identification near threshold or in the presence of external noise involves increasing the responsiveness of sensory neurons to the target and thus increasing the signal-to-noise ratio.

2.20.3.3.4 Shift of cortical representation of a learned stimulus with training on visual search

Visual search is a special kind of detection task in which the target is camouflaged in a background of similar distracters. In addition to engendering increased neuronal responsiveness in early cortical areas (see Section 2.20.3.3.3), learning to search for a particular shape results in a concomitant decrease in fMRI signals from higher visual areas involved in shape processing (Kourtzi, Z. *et al.*, 2005; Sigman, M. *et al.*, 2005) and from prefrontal and parietal areas involved in attentional control (Pollmann, S. and Maertens, M., 2005; Sigman, M. *et al.*, 2005; Figure 8). These studies suggest that another mechanism of perceptual learning involves a shift of cortical representation of the learned stimulus from higher to lower visual areas for more efficient and less effortful processing of the task stimulus. These findings also indicate that the attentional mechanism itself is pliable, being modified with training.

2.20.3.3.5 Changes in temporal properties of neuronal responses

The neural codes for sensory stimuli include not only the firing rates of neurons but also their temporal firing patterns, such as the synchrony of discharges across a population of neurons (for example see review Singer, W., 1999). It has been shown that temporal response properties of neurons can be modified by perceptual learning. For example, neuronal responses in monkey S1 become more coherent with training on tactile frequency discrimination. This change is highly predictive of the improved performance, and thus correlates better with learning than cortical recruitment does (Recanzone, G. H. *et al.*, 1992d). Similarly, after training rats to use the repetition rate of acoustic noise pulses to find food in a maze, with higher repetition rates indicating shorter distances between the animal and the food, A1 neuronal responses to high frequency noise pulses become stronger and more phase-locked to the stimuli (Bao, S. W. *et al.*, 2004). In the early visual areas (area 17, 18, and 21a) of the cat, gamma oscillations (an indication of response synchrony between neurons, see Singer, W., 1999) are increased for a behaviorally relevant stimulus on which the cats are trained, even if the animals are in a state of passive viewing and are not required to perform the associated task (Salazar, R. F. *et al.*, 2004). These studies suggest that the enhanced temporal response properties like increased synchrony and coherence of responses in a population of neurons can serve as another neural mechanism of perceptual learning.

2.20.3.4 Section Summary

In the search for the neural mechanisms of perceptual learning, it has been found that modifications in early

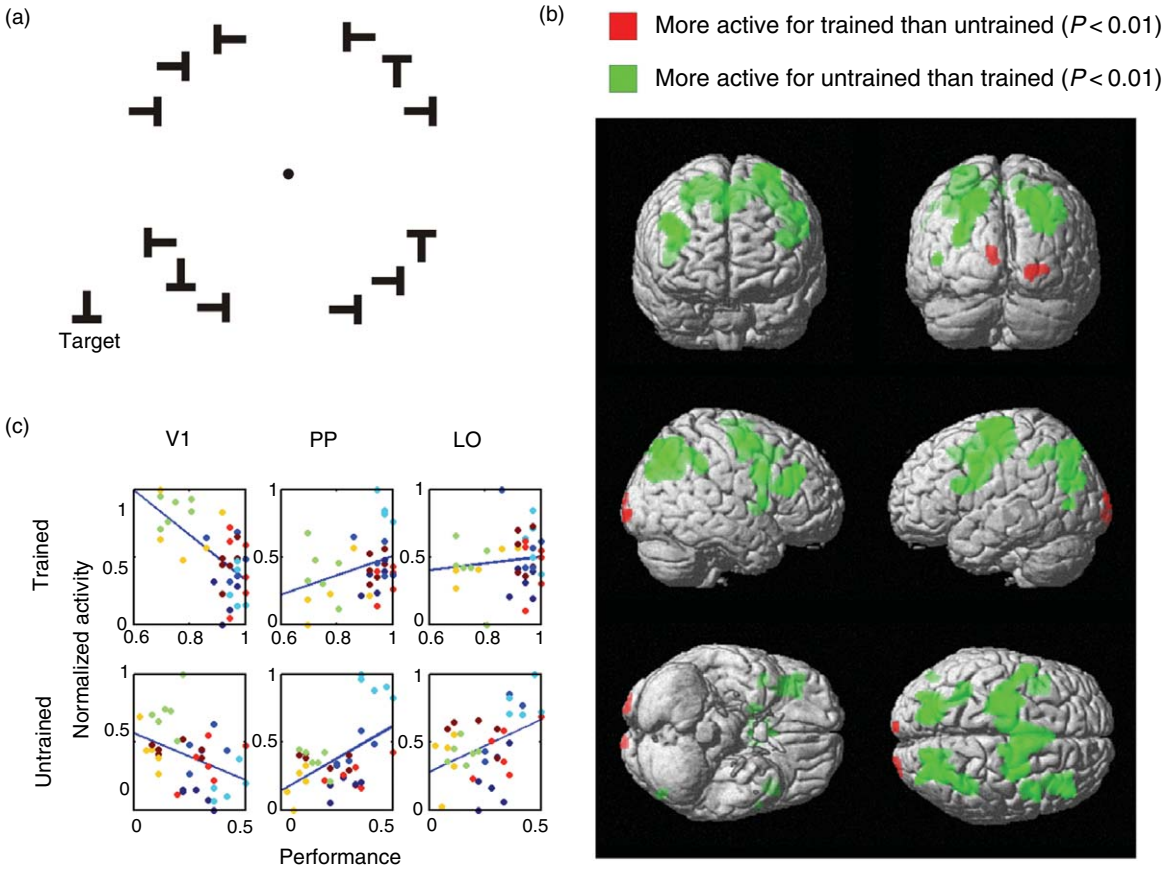

Figure 8 Shift of cortical representation of the learned shapes in training on visual search. (a) The task stimulus contained 12 Ts that were rotated by multiples of 90° and distributed in the four quadrants of the visual field. One rotated T was the target and the other Ts were distracters randomly pointing to the other three possible directions. The task was to report the quadrant within which the target T appeared. (b) Differential activation between the trained and untrained conditions. The first row shows the front and back views of the brain; the second row, the left and right hemispheres; the third row, the ventral and dorsal (bottom and top) views. The untrained condition was more active (shown in green) than the trained condition over an extended network that mainly involved the parietal and frontal cortices and lateral occipital cortices. The trained condition was more active (shown in red) than the untrained condition in the middle occipital cortex, corresponding to early visual areas in retinotopic cortex including V1. (c) Correlation between fMRI signals and behavioral performance for the three regions of interest – retinotopic cortex (RC), lateral occipital cortices (LO), and posterior parietal cortex (PP) – in the trained an untrained conditions. This analysis was based on the voxel that elicited the biggest difference between the trained and untrained conditions. At each voxel, the level of BOLD activity was calculated for each session and for each condition, and was correlated with the behavioral performance. For the trained condition, performance varied within the 60–100% range, and for the untrained condition, within the 0–50% range. RC activation is negatively correlated with behavioral performance, and the correlation becomes significantly stronger in the trained condition. LO and PP are positively correlated, and this correlation becomes substantially weaker in the trained condition. Reproduced from Sigman, M., Pan, H., Yang, Y. H., Stern, E., Silbersweig, D., and Gilbert, C. D. 2005. Top-down reorganization of activity in the visual pathway after learning a shape identification task. Neuron 46, 823–835.

sensory cortical areas are associated with training on various perceptual tasks. Some of these changes are well correlated with, and are therefore predictive of, the improvement in perception and the specificity of learning. These changes include an expansion of cortical representation; enhanced selectivity, responsiveness, and synchrony of neurons; and a shift of cortical representation of the learned stimuli. These plastic changes, which usually take place in a task-specific manner and are distributed across sensory cortices, are most likely involved in encoding the information about the learned stimuli, and thus

reflect the implicit memory formed during training. This is different from explicit memory, which involves a unified memory system located in the medial temporal lobe. Top-down influences specifically pertaining to the trained task may be required for both encoding and retrieving the learned information. This mechanism effectively prevents any potential interference between different perceptual tasks at the expense of the transfer of learning.

2.20.4 Theories and Models about Perceptual Learning

In addition to experimental studies, theoretical and computational approaches that endeavor to understand the possible neural circuitry can also provide insights into the mechanisms of perceptual learning. A few theories and models have been proposed, which emphasize different issues of perceptual learning, like different processes and stages of cortical processing.

Some of the computational models lay emphasis on plasticity at early stages of information processing. In a simple feedforward network model (Poggio, T. *et al.*, 1992), a task-specific module is synthesized based on simulated input from a few receptors on the retina that respond to vernier stimuli. This learning module improves its performance on vernier discrimination and reaches a hyperacuity level with only a few trials. Psychophysical observations are consistent with the simulated results in both the time course and orientation specificity. The algorithm can also be made to learn the hyperacuity task in the absence of feedback, with a corresponding decrease in learning speed, as is also observed with human subjects. A recurrent model has been proposed to explain V1 orientation selectivity (Benyishai, R. *et al.*, 1995; Douglas, R. J. *et al.*, 1995; Somers, D. C. *et al.*, 1995). Based on this model, a recent computational study has shown that the steepening of orientation tuning curves near the trained orientation (Figure 7) can be accounted for by slightly reducing the net excitatory connections to those cells tuned to the trained orientation (Teich, A. F. and Qian, N., 2003). This is consistent with some experimental observations (Schiltz, C. *et al.*, 1999; Schoups, A. *et al.*, 2001). In order to explain the context-enabled learning in contrast discrimination (see Section 2.20.2.3), a recurrent network model based on intrinsic inhibitory and excitatory interactions in V1 has been proposed (Adini, Y. *et al.*, 2002). Similarly, in another model (Hoshino, O., 2004), the strengths of lateral excitatory and inhibitory connections between neurons are modified according to a Hebbian learning rule (neuronal connections are strengthened if they fire together; for details see Section 2.20.5), and learning enhances the performance of the network by increasing the signal-to-noise ratio of neuronal activity. In a real situation of perceptual learning, due to small eye movements and fixation errors, there is a considerable amount of position variance in the visual signals, which presents a problem in solving hyperacuity tasks like bisection and vernier discrimination. However, as is shown by a modeling study (Zhaoping, L. *et al.*, 2003), a nonlinear recurrent network based on horizontal interactions can significantly outperform a feedforward network on the bisection task in the presence of positional uncertainty. The recurrent interactions in this network are highly specific to the stimulus parameters, and the recurrent connections in the model serve to modify the neural responses in a task-specific manner. Based on this model, the authors suggested that the fast phase in perceptual learning comes partly from learning the feedforward weights, and the slow learning phase results from learning the weights to implement the nonlinear transform.

By examining the training effect on visual discrimination tasks in the presence of different levels of external noise, a perceptual template model has been proposed (Dosher, B. A. and Lu, Z. L., 1998; 1999; Lu, Z. L. and Dosher, B. A., 2004; Lu, Z. L. *et al.*, 2005; Petrov, A. A. *et al.*, 2005). This model emphasizes two distinct mechanisms involved in perceptual learning – external noise exclusion (or perceptual template retuning) and stimulus enhancement. These studies also speculate that the improvement resulting from perceptual learning may simply reflect task-specific reweighting of the readout connections between early visual cortex and the decision stage, and thus perceptual learning does not necessarily involve modifications of early cortical areas. Similarly, by examining the effect of training on position discrimination at different noise levels, another study attributes the improvement to a retuning of the decision template (Li, R. W. *et al.*, 2004a). In the absence of external noise, some pooling models have made a similar claim that an improvement in performance does not need to change early sensory signals (Ghose, G. M. *et al.*, 2002). In contrast to the perceptual template model, by examining human performance

on identification of faces and textures embedded in noise, another study proposes the different view that perceptual learning entirely results from signal enhancement, not from noise reduction (Gold, J. *et al.*, 1999; for a debate see Lu, Z. L. and Dosher, B. A., 2004).

The central issue in the study of the neural basis of perceptual learning involves the loci in the brain where the plastic modifications occur. There is a considerable debate about whether the changes occur at early sensory cortices or higher cortical areas (for a review see Fahle, M., 2004). This discussion is also related to the specificity of perceptual learning and the role of top-down influences. A computational model (Herzog, M. H. and Fahle, M., 1998), which incorporates top-down mechanisms of internal evaluation of the performance and knowledge about the task, largely attributes the learning effect to a change in decision criteria. A reverse hierarchy theory (for a review see Ahissar, M. and Hochstein, S., 2004) suggests that learning-associated changes begin at higher levels in the visual pathway and progress backwards to lower levels. In particular, training on easy tasks modifies higher levels that are not sensitive to changes in simple stimulus parameters; therefore, the learning is transferable. In contrast, training on difficult tasks results in specific changes at lower levels, so the learning does not generalize.

A unified model has been proposed (Seitz, A. and Watanabe, T., 2005) in an attempt to reconcile task-irrelevant learning with task-relevant learning. According to this theoretical proposition, performing a task activates diffusive reinforcement signals, which interact not only with the task-relevant signals but also with those task-irrelevant signals that are temporally associated with the task stimulus. This theory compares task-irrelevant learning to classical conditioning in the sense that both phenomena rely on a temporal relationship between stimuli and reinforcers.

All the current models and theories have their own constraints, and can only address very limited aspects of perceptual learning (for a detailed comparison between different neural network models see review Tsodyks, M. and Gilbert, C., 2004). It will be important for a unified theory of perceptual learning to reconcile all the issues revealed by psychophysical and neurophysiological studies in the presence of complex behavioral and stimulus contexts.

2.20.5 Cellular and Molecular Basis

Significant strides have been made toward understanding the mechanisms of perceptual learning at the level of cortical plasticity. Another important direction of research has endeavored to relate perceptual learning to the changes seen at synaptic and molecular levels. This is particularly useful because at these levels all forms of cortical plasticity, including learning and memory, could share similar mechanisms, regardless of the different cortical structures or different experiences involved.

Cortical neurons are interconnected by synapses to construct intricate neural circuits, which are crucial determinants of brain functions like adaptive sensory processing. The synapses in the brain are formed at the cell bodies, dendritic shafts, dendritic spines, and the juxtaposition between specialized axonal swellings known as boutons. While synaptic stability is important for maintaining reliable neuronal functions like selectivity for primitive stimulus attributes, synapses must also be modifiable to endow neural circuits with adaptability to environmental changes. The dynamic and plastic nature of synaptic connections is seen as either an addition or elimination of synapses, or as a change in transmission at existing synapses.

More than a century ago, based on histological observations, Spanish histologist Santiago Ramón y Cajal proposed that changes in connections between neurons, which could be induced by cerebral gymnastics and which can take the forms of branching and strengthening, are responsible for our ability to learn (for a review see Jones, E. G., 1994). He also emphasized the integrative and plastic roles of pyramidal cells in neural circuitry because their axons provide long-range interarea and intra-area connections. Ramón y Cajal's propositions have been exemplified by modern experiments. It has been shown that lesion-induced cortical reorganization is associated with axonal sprouting in cat visual cortex (Darian-Smith, C. and Gilbert, C. D., 1994) and in monkey somatosensory cortex (Florence, S. L. *et al.*, 1998). Owing to the advances in two-photon microscopy, evidence from *in vivo* imaging on the same neurons at multiple time points indicates that, in the adult brain, the dendritic spines (Grutzendler, J. *et al.*, 2002; Trachtenberg, J. T. *et al.*, 2002; Holtmaat, A. J. G. D. *et al.*, 2005; Zuo, Y. *et al.*, 2005) and axonal boutons and branches (De Paola, V. *et al.*, 2006; Stettler, D. D. *et al.*, 2006) are rather dynamic, with

their elimination or formation occurring within days. These morphological changes have been shown to be associated with addition and subtraction of synapses (Trachtenberg, J. T. *et al.*, 2002; De Paola, V. *et al.*, 2006), and are most likely involved in mediating cortical plasticity. It has also been shown that a change in sensory experience increases the turnover rate of dendritic spines (Trachtenberg, J. T. *et al.*, 2002). In this study, a mouse's sensory experience was altered by trimming some of its whiskers. Reorganization of whisker representation in the barrel cortex is accompanied by an increase in transient spines and a concomitant decrease in stable spines – changes that are specific to the barrel cortex (Trachtenberg, J. T. *et al.*, 2002). Although similar changes have not yet been directly demonstrated over the course of perceptual learning, modern multiphoton microscopy may unveil the answer in the near future.

In addition to morphological changes, the transmission at existing synapses is also highly plastic, a phenomenon known as synaptic plasticity. In 1949, Canadian psychologist Hebb D. O. (1949) published his seminal theoretical postulate on the neural mechanism of learning, which states that "when an axon of cell A is near enough to excite a cell B and repeatedly or persistently takes part in firing it, some growth process or metabolic change takes place in one or both cells such that A's efficiency, as one of the cells firing B, is increased" (for a review on Hebb see Brown, R. E. and Milner, P. M., 2003). Since then, Hebb's idea has been contextualized in psychophysical, neurophysiological, and computational studies of learning, forming ideas like the Hebbian learning rule, the Hebbian neural network, the Hebbian synapse, and Hebbian synaptic plasticity. Synaptic plasticity is expressed in diverse forms and operates over a broad range of timescales (for a review see Abbott, L. F. and Regehr, W. G., 2004). The prevailing view is that long-term plastic changes of synaptic transmission are involved in learning and memory (for reviews see Martin, S. J. *et al.*, 2000; Morris, R. G. M., 2003; Lynch, M. A., 2004). Recent studies also emphasize the importance of pre- and postsynaptic spike timing in inducing synaptic plasticity (known as spike timing-dependent plasticity, see review Dan, Y. and Poo, M. M., 2004; Fox, K. and Wong, R. L., 2005). The contribution of short-term synaptic plasticity, however, is to enable complex dynamic information processing in neural circuits (for a review see Abbott, L. F. and Regehr, W. G., 2004).

One way to demonstrate a relationship between synaptic plasticity and perceptual learning is to show that the modulatory factors influencing synaptic plasticity also affect perceptual learning, as is done by a recent study (Dinse, H. R. *et al.*, 2003). This study employs the task-irrelevant learning paradigm (see Section 2.20.3.3.1) to show that inhibiting or facilitating synaptic plasticity has corresponding effects on perceptual learning. Recall that the passive stimulation of a finger tip improves spatial discrimination ability on the stimulated skin surface, and that this improvement is closely correlated with the cortical recruitment in S1. In human subjects, these changes can be completely eliminated by applying memantine, a drug that is known to block the *N*-methyl-D-aspartate (NMDA) receptors mediating Hebbian synaptic plasticity. In contrast, by applying a single dose of amphetamine (a central nervous system stimulant), the plastic effects are doubled.

Many studies have examined the neuromodulators that signal and control experience-dependent cortical plasticity. One of the neuromodulators noticeably involved in cortical reorganization and changes of RF properties is acetylcholine (ACh), which is released from the nucleus basalis (for reviews see Hasselmo, M. E., 1995; Weinberger, N. M., 1995; Edeline, J. M., 1999; Gu, Q., 2003; Weinberger, N. M., 2004; Wilson, D. A. *et al.*, 2004; Prakash, N. and Frostig, R. D., 2005; but see also Kamke, M. R. *et al.*, 2005). A large body of evidence has also shown that ACh is closely related to attentional mechanisms (for reviews see Everitt, B. J. and Robbins, T. W., 1997; Sarter, M. *et al.*, 2001; 2005). This coincidence may account for the close relationship between perceptual learning and top-down influences. One point of view is that the neuromodulators released while attentively performing a task serve as internal reinforcement (reward or feedback) signals; therefore, perceptual learning can take place even without any apparent reward or feedback, and can even occur for an unattended stimulus that coincides with the attended stimulus (Seitz, A. and Watanabe, T., 2005).

2.20.6 Concluding Remarks

This chapter outlines the current understanding of perceptual learning. It is evident that experience-dependent cortical plasticity is not restricted to early postnatal development or recovery from injury; it also serves as the neural basis of perceptual

learning throughout the life. Depending on the nature of the task stimuli, different cortical mechanisms are evoked to encode the learned information, which can be stored by modifying the functional properties and architecture of early sensory cortices. These changes usually take place in a task-specific fashion under top-down control. Similar top-down influences may also be required to retrieve the learned information relevant to a specific task. This provides an effective brain mechanism for avoiding interference across various perceptual tasks, as suggested by recent findings of task-specific plasticity in primary visual cortex (Crist, R. E. *et al.*, 2001; Li, W. *et al.*, 2004b).

It is worth noting that, for some complex visual tasks, in particular for those involving the recognition of complex objects and the association between different objects, learning is related to the formation of a more declarative form of memory (see Chapter High-level Visual Processing). In these cases, training on object discrimination results in modifications of neuronal response properties in monkey inferior temporal (IT) cortex (the last stage of the proposed object recognition pathway; Logothetis, N. K. *et al.*, 1995; Kobatake, E. *et al.*, 1998), and training on linking temporally associated objects creates neural codes in IT that represent long-term associative memory (Miyashita, Y., 1988; Sakai, K. and Miyashita, Y., 1991; Miyashita, Y., 1993; Miyashita, Y. and Hayashi, T., 2000; Messinger, A. *et al.*, 2005; Takeda, M. *et al.*, 2005). It has been suggested that both stimulus-driven bottom-up signals and behavior-driven top-down signals can trigger the retrieval of the associative information stored in IT (Miyashita, Y. and Hayashi, T., 2000).

It is also worth pointing out that, in spite of the diversity in the types of learning and the brain structures that are involved, different forms of learning and memory share some similar mechanisms. For example, the cortical mechanisms involved in perceptual learning are also found in motor learning (for reviews see Celnik, P. A. and Cohen, L. G., 2004; Paz, R. *et al.*, 2004). A recent study has shown that the encoding of implicit and explicit memory by exposure to the same stimuli shares the same processing factors, as the formation of both is intimately correlated (Turk-Browne, N. B. *et al.*, 2006). Given the similarities in neural mechanisms of different forms of learning and memory, understanding the neural basis of perceptual learning will have important implications for the study of learning and memory in general.

References

Abbott, L. F. and Regehr, W. G. 2004. Synaptic computation. Nature 431, 796–803.

Adini, Y., Sagi, D., and Tsodyks, M. 2002. Context-enabled learning in the human visual system. Nature 415, 790–793.

Ahissar, M. and Hochstein, S. 1993. Attentional control of early perceptual learning. Proc. Natl. Acad. Sci. U. S. A. 90, 5718–5722.

Ahissar, M. and Hochstein, S. 1996. Learning pop-out detection: specificities to stimulus characteristics. Vision Res. 36, 3487–3500.

Ahissar, M. and Hochstein, S. 1997. Task difficulty and the specificity of perceptual learning. Nature 387, 401–406.

Ahissar, M. and Hochstein, S. 2004. The reverse hierarchy theory of visual perceptual learning. Trends Cogn. Sci. 8, 457–464.

Ahissar, M., Laiwand, R., Kozminsky, G., and Hochstein, S. 1998. Learning pop-out detection: building representations for conflicting target-distractor relationships. Vision Res. 38, 3095–3107.

Albright, T. D. and Stoner, G. R. 2002. Contextual influences on visual processing. Annu. Rev. Neurosci. 25, 339–379.

Allman, J., Miezin, F., and McGuinness, E. 1985. Stimulus specific responses from beyond the classical receptive field: neurophysiological mechanisms for local-global comparisons in visual neurons. Annu. Rev. Neurosci. 8, 407–430.

Atienza, M., Cantero, J. L., and Stickgold, R. 2004. Posttraining sleep enhances automaticity in perceptual discrimination. J. Cogn. Neurosci. 16, 53–64.

Ball, K. and Sekuler, R. 1982. A specific and enduring improvement in visual motion discrimination. Science 218, 697–698.

Ball, K. and Sekuler, R. 1987. Direction-specific improvement in motion discrimination. Vision Res 27, 953–965.

Bao, S. W., Chang, E. F., Woods, J., and Merzenich, M. M. 2004. Temporal plasticity in the primary auditory cortex induced by operant perceptual learning. Nat. Neurosci. 7, 974–981.

Beard, B. L., Levi, D. M., and Reich, L. N. 1995. Perceptual learning in parafoveal vision. Vision Res. 35, 1679–1690.

Benyishai, R., Baror, R. L., and Sompolinsky, H. 1995. Theory of orientation tuning in visual cortex. Proc. Natl. Acad. Sci. U. S. A. 92, 3844–3848.

Berardi, N. and Fiorentini, A. 1987. Interhemispheric transfer of visual information in humans – spatial characteristics. J. Physiol. (Lond) 384, 633–647.

Bergen, J. R. and Julesz, B. 1983. Parallel versus serial processing in rapid pattern discrimination. Nature 303, 696–698.

Blake, D. T., Strata, F., Churchland, A. K., and Merzenich, M. M. 2002. Neural correlates of instrumental learning in primary auditory cortex. Proc. Natl. Acad. Sci. U. S. A. 99, 10114–10119.

Braun, C., Haug, M., Wiech, K., Birbaumer, N., Elbert, T., and Roberts, L. E. 2002. Functional organization of primary somatosensory cortex depends on the focus of attention. Neuroimage 17, 1451–1458.

Braun, J. 1998. Vision and attention: the role of training. Nature 393, 424–425.

Brown, M., Irvine, D. R. F., and Park, V. N. 2004. Perceptual learning on an auditory frequency discrimination task by cats: association with changes in primary auditory cortex. Cereb. Cortex 14, 952–965.

Brown, R. E. and Milner, P. M. 2003. Timeline – the legacy of Donald O. Hebb: more than the Hebb synapse. Nat. Rev. Neurosci. 4, 1013–1019.

Calford, M. B. and Tweedale, R. 1988. Immediate and chronic changes in responses of somatosensory cortex in adult flying fox after digit amputation. Nature 332, 446–448.
Calford, M. B., Wang, C., Taglianetti, V., Waleszczyk, W. J., Burke, W., and Dreher, B. 2000. Plasticity in adult cat visual cortex (area 17) following circumscribed monocular lesions of all retinal layers. J. Physiol. 524, 587–602.
Celnik, P. A. and Cohen, L. G. 2004. Modulation of motor function and cortical plasticity in health and disease. Restor. Neurol. Neurosci. 22, 261–268.
Chino, Y. M., Kaas, J. H., Smith, E. L., Langston, A. L., and Cheng, H. 1992. Rapid reorganization of cortical maps in adult cats following restricted deafferentation in retina. Vision Res. 32, 789–796.
Corkin, S. 2002. What's new with the amnesic patient HM? Nat. Rev. Neurosci. 3, 153–160.
Crist, R. E., Kapadia, M. K., Westheimer, G., and Gilbert, C. D. 1997. Perceptual learning of spatial localization: specificity for orientation, position, and context. J. Neurophysiol. 78, 2889–2894.
Crist, R. E., Li, W., and Gilbert, C. D. 2001. Learning to see: experience and attention in primary visual cortex. Nat. Neurosci. 4, 519–525.
Dan, Y. and Poo, M. M. 2004. Spike timing-dependent plasticity of neural circuits. Neuron 44, 23–30.
Darian-Smith, C. and Gilbert, C. D. 1994. Axonal sprouting accompanies functional reorganization in adult cat striate cortex. Nature 368, 737–740.
Darian-Smith, C. and Gilbert, C. D. 1995. Topographic reorganization in the striate cortex of the adult cat and monkey is cortically mediated. J. Neurosci. 15, 1631–1647.
De Paola, V., Holtmaat, A., Knott, G., Song, S., Wilbrecht, L., Caroni, P., and Svoboda, K. 2006. Cell type-specific structural plasticity of axonal branches and boutons in the adult neocortex. Neuron 49, 861–875.
Devor, M. and Wall, P. D. 1978. Reorganization of spinal cord sensory map after peripheral nerve injury. Nature 276, 75–76.
Devor, M. and Wall, P. D. 1981. Plasticity in the spinal cord sensory map following peripheral nerve injury in rats. J. Neurosci. 1, 679–684.
Dinse, H. R., Ragert, P., Pleger, B., Schwenkreis, P., and Tegenthoff, M. 2003. Pharmacological modulation of perceptual learning and associated cortical reorganization. Science 301, 91–94.
Dosher, B. A. and Lu, Z. L. 1998. Perceptual learning reflects external noise filtering and internal noise reduction through channel reweighting. Proc. Natl. Acad. Sci. U. S. A. 95, 13988–13993.
Dosher, B. A. and Lu, Z. L. 1999. Mechanisms of perceptual learning. Vision Res. 39, 3197–3221.
Douglas, R. J., Koch, C., Mahowald, M., Martin, K. A. C., and Suarez, H. H. 1995. Recurrent excitation in neocortical circuits. Science 269, 981–985.
Dresp, B. 1993. Bright lines and edges facilitate the detection of small light targets. Spat. Vis. 7, 213–225.
Edeline, J. M. 1999. Learning-induced physiological plasticity in the thalamo-cortical sensory systems: a critical evaluation of receptive field plasticity, map changes and their potential mechanisms. Prog. Neurobiol. 57, 165–224.
Ellison, A. and Walsh, V. 1998. Perceptual learning in visual search: some evidence of specificities. Vision Res. 38, 333–345.
Everitt, B. J. and Robbins, T. W. 1997. Central cholinergic systems and cognition. Annu. Rev. Psychol. 48, 649–684.
Eysel, U. T., Schweigart, G., Mittmann, T., Eyding, D., Qu, Y., Vandesande, F., Orban, G., and Arckens, L. 1999. Reorganization in the visual cortex after retinal and cortical damage. Restor. Neurol. Neurosci. 15, 153–164.
Fahle, M. 1997. Specificity of learning curvature, orientation, and vernier discriminations. Vision Res. 37, 1885–1895.
Fahle, M. 2004. Perceptual learning: a case for early selection. J. Vision 4, 879–890.
Fahle, M. and Daum, I. 2002. Perceptual learning in amnesia. Neuropsychologia. 40, 1167–1172.
Fahle, M. and Morgan, M. 1996. No transfer of perceptual learning between similar stimuli in the same retinal position. Curr. Biol. 6, 292–297.
Fahle, M., Edelman, S., and Poggio, T. 1995. Fast perceptual learning in hyperacuity. Vision Res. 35, 3003–3013.
Field, D. J., Hayes, A., and Hess, R. F. 1993. Contour integration by the human visual system: evidence for a local ''association field''. Vision Res. 33, 173–193.
Fiorentini, A. and Berardi, N. 1980. Perceptual learning specific for orientation and spatial frequency. Nature 287, 43–44.
Florence, S. L., Taub, H. B., and Kaas, J. H. 1998. Large-scale sprouting of cortical connections after peripheral injury in adult macaque monkeys. Science 282, 1117–1121.
Fox, K. and Wong, R. L. 2005. A comparison of experience-dependent plasticity in the visual and somatosensory systems. Neuron 48, 465–477.
Fritz, J. B., Elhilali, M., and Shamma, S. A. 2005. Differential dynamic plasticity of A1 receptive fields during multiple spectral tasks. J. Neurosci. 25, 7623–7635.
Furmanski, C. S., Schluppeck, D., and Engel, S. A. 2004. Learning strengthens the response of primary visual cortex to simple patterns. Curr. Biol. 14, 573–578.
Ghose, G. M., Yang, T. M., and Maunsell, J. H. R. 2002. Physiological correlates of perceptual learning in monkey V1 and V2. J. Neurophysiol. 87, 1867–1888.
Gibson, E. J. 1963. Perceptual learning. Annu. Rev. Psychol. 14, 29–56.
Gilbert, C. D. 1992. Horizontal integration and cortical dynamics. Neuron 9, 1–13.
Gilbert, C. D. 1998. Adult cortical dynamics. Physiol. Rev. 78, 467–485.
Gilbert, C. D. and Wiesel, T. N. 1992. Receptive field dynamics in adult primary visual cortex. Nature 356, 150–152.
Gilbert, C. D., Hirsch, J. A., and Wiesel, T. N. 1990. Lateral interactions in visual cortex. Cold Spring Harb. Symp. Quant. Biol. 55, 663–677.
Gilbert, C. D., Sigman, M., and Crist, R. E. 2001. The neural basis of perceptual learning. Neuron 31, 681–697.
Godde, B., Stauffenberg, B., Spengler, F., and Dinse, H. R. 2000. Tactile coactivation-induced changes in spatial discrimination performance. J. Neurosci. 20, 1597–1604.
Gold, J., Bennett, P. J., and Sekuler, A. B. 1999. Signal but not noise changes with perceptual learning. Nature 402, 176–178.
Goldstone, R. L. 1998. Perceptual learning. Annu. Rev. Psychol. 49, 585–612.
Grutzendler, J., Kasthuri, N., and Gan, W. B. 2002. Long-term dendritic spine stability in the adult cortex. Nature 420, 812–816.
Gu, Q. 2003. Contribution of acetylcholine to visual cortex plasticity. Neurobiol. Learn. Mem. 80, 291–301.
Hasselmo, M. E. 1995. Neuromodulation and cortical function – modeling the physiological basis of behavior. Behav. Brain Res. 67, 1–27.
Hawkey, D. J. C., Amitay, S., and Moore, D. R. 2004. Early and rapid perceptual learning. Nat. Neurosci. 7, 1055–1056.
Hebb, D. O. 1949. Organization of Behavior: a Neuropsychological Theory. Wiley.
Heinen, S. J. and Skavenski, A. A. 1991. Recovery of visual responses in foveal V1 neurons following bilateral foveal lesions in adult monkey. Exp. Brain Res. 83.
Helmholtz, H. 1866. Treatise on Physiological Optics. Dover Publications.

Hensch, T. K. 2004. Critical period regulation. Annu. Rev. Neurosci. 27, 549–579.
Herzog, M. H. and Fahle, M. 1997. The role of feedback in learning a vernier discrimination task. Vision Res. 37, 2133–2141.
Herzog, M. H. and Fahle, M. 1998. Modeling perceptual learning: difficulties and how they can be overcome. Biol. Cybern. 78, 107–117.
Hodzic, A., Veit, R., Karim, A. A., Erb, M., and Godde, B. 2004. Improvement and decline in tactile discrimination behavior after cortical plasticity induced by passive tactile coactivation. J. Neurosci. 24, 442–446.
Holtmaat, A. J. G. D., Trachtenberg, J. T., Wilbrecht, L., Shepherd, G. M., Zhang, X. Q., Knott, G. W., and Svoboda, K. 2005. Transient and persistent dendritic spines in the neocortex in vivo. Neuron 45, 279–291.
Hoshino, O. 2004. Neuronal bases of perceptual learning revealed by a synaptic balance scheme. Neural Comput. 16, 563–594.
Hubel, D. H. and Wiesel, T. N. 1970. Period of susceptibility to physiological effects of unilateral eye closure in kittens. J. Physiol. 206, 419–436.
Hubel, D. H., Wiesel, T. N., and Levay, S. 1977. Plasticity of ocular dominance columns in monkey striate cortex. Philos. Trans. R. Soc. Lond. B. Biol. Sci. 278, 377–409.
Hughes, B., Epstein, W., Schneider, S., and Dudock, A. 1990. An asymmetry in transmodal perceptual learning. Percept. Psychophys. 48, 143–150.
James, W. 1890. The Principles of Psychology. Dover Publications.
Jones, E. G. 1994. Santiago Ramón y Cajal and the Croonian-Lecture, March 1894. Trends Neurosci. 17, 190–192.
Joseph, J. S., Chun, M. M., and Nakayama, K. 1997. Attentional requirements in a 'preattentive' feature search task. Nature 387, 805–807.
Julesz, B. 1981. Textons, the elements of texture perception, and their interactions. Nature 290, 91–97.
Kaas, J. H., Krubitzer, L. A., Chino, Y. M., Langston, A. L., Polley, E. H., and Blair, N. 1990. Reorganization of retinotopic cortical maps in adult mammals after lesions of the retina. Science 248, 229–231.
Kaas, J. H., Merzenich, M. M., and Killackey, H. P. 1983. The reorganization of somatosensory cortex following peripheral nerve damage in adult and developing mammals. Annu. Rev. Neurosci. 6, 325–356.
Kamke, M. R., Brown, M., and Irvine, D. R. 2005. Basal forebrain cholinergic input is not essential for lesion-induced plasticity in mature auditory cortex. Neuron 48, 675–686.
Kapadia, M. K., Ito, M., Gilbert, C. D., and Westheimer, G. 1995. Improvement in visual sensitivity by changes in local context: parallel studies in human observers and in V1 of alert monkeys. Neuron 15, 843–856.
Kapadia, M. K., Westheimer, G., and Gilbert, C. D. 2000. Spatial distribution of contextual interactions in primary visual cortex and in visual perception. J. Neurophysiol. 84, 2048–2062.
Karni, A. and Sagi, D. 1991. Where practice makes perfect in texture discrimination: evidence for primary visual cortex plasticity. Proc. Natl. Acad. Sci. U. S. A. 88, 4966–4970.
Karni, A. and Sagi, D. 1993. The time course of learning a visual skill. Nature 365, 250–252.
Knierim, J. J. and Van Essen, D. C. 1992. Neuronal responses to static texture patterns in area V1 of the alert macaque monkey. J. Neurophysiol. 67, 961–980.
Kobatake, E., Wang, G., and Tanaka, K. 1998. Effects of shape-discrimination training on the selectivity of inferotemporal cells in adult monkeys. J. Neurophysiol. 80, 324–330.
Konorski, J. 1948. Conditioned Reflexes and Neuron Organization. Cambridge University Press.
Kourtzi, Z., Betts, L. R., Sarkheil, P., and Welchman, A. E. 2005. Distributed neural plasticity for shape learning in the human visual cortex. PLoS Biol. 3, 1317–1327.
Kovács, I., Kozma, P., Feher, A., and Benedek, G. 1999. Late maturation of visual spatial integration in humans. Proc. Natl. Acad. Sci. U. S. A. 96, 12204–12209.
Kuai, S. G., Zhang, J. Y., Klein, S. A., Levi, D. M., and Yu, C. 2005. The essential role of stimulus temporal patterning in enabling perceptual learning. Nat. Neurosci. 8, 1497–1499.
Lamme, V. A. 1995. The neurophysiology of figure-ground segregation in primary visual cortex. J. Neurosci. 15, 1605–1615.
Lee, T. S., Yang, C. F., Romero, R. D., and Mumford, D. 2002. Neural activity in early visual cortex reflects behavioral experience and higher-order perceptual saliency. Nat. Neurosci. 5, 589–597.
Li, R. W., Levi, D. M., and Klein, S. A. 2004a. Perceptual learning improves efficiency by re-tuning the decision 'template' for position discrimination. Nat. Neurosci. 7, 178–183.
Li, W. and Gilbert, C. D. 2002. Global contour saliency and local colinear interactions. J. Neurophysiol 88, 2846–2856.
Li, W., Piech, V., and Gilbert, C. D. 2004b. Perceptual learning and top-down influences in primary visual cortex. Nat. Neurosci. 7, 651–657.
Liu, Z. L. 1999. Perceptual learning in motion discrimination that generalizes across motion directions. Proc. Natl. Acad. Sci. U. S. A. 96, 14085–14087.
Liu, Z. L. and Weinshall, D. 2000. Mechanisms of generalization in perceptual learning. Vision Res. 40, 97–109.
Locke, J. 1689. An Essay Concerning Human Understanding, Prometheus Books.
Logothetis, N. K., Pauls, J., and Poggio, T. 1995. Shape representation in the inferior temporal cortex of monkeys. Curr. Biol. 5, 552–563.
Lorenz, K. 1935a. Der kumpan in der umwelt des vogels. J. Ornithol 83, 289–413.
Lorenz, K. 1935b. Der kumpan in der umwelt des vogels: der artgenosse als auslösendes moment sozialer verhaltungsweisen. J. Ornithol. 83, 137–213.
Lu, Z. L. and Dosher, B. A. 2004. Perceptual learning retunes the perceptual template in foveal orientation identification. J. Vision 4, 44–56.
Lu, Z. L., Chu, W., Dosher, B. A., and Lee, S. 2005. Independent perceptual learning in monocular and binocular motion systems. Proc. Natl. Acad. Sci. U. S. A. 102, 5624–5629.
Lynch, M. A. 2004. Long-term potentiation and memory. Physiol. Rev. 84, 87–136.
Martin, S. J., Grimwood, P. D., and Morris, R. G. M. 2000. Synaptic plasticity and memory: an evaluation of the hypothesis. Annu. Rev. Neurosci. 23, 649–711.
McKee, S. P. and Westheimer, G. 1978. Improvement in vernier acuity with practice. Percept. Psychophys. 24, 258–262.
Mednick, S., Nakayama, K., and Stickgold, R. 2003. Sleep-dependent learning: a nap is as good as a night. Nat. Neurosci. 6, 697–698.
Mednick, S. C., Arman, A. C., and Boynton, G. M. 2005. The time course and specificity of perceptual deterioration. Proc. Natl. Acad. Sci. U. S. A. 102, 3881–3885.
Merzenich, M. M., Kaas, J. H., Wall, J., Nelson, R. J., Sur, M., and Felleman, D. 1983a. Topographic reorganization of somatosensory cortical areas 3b and 1 in adult monkeys following restricted deafferentation. Neuroscience 8, 33–55.
Merzenich, M. M., Kaas, J. H., Wall, J. T., Sur, M., Nelson, R. J., and Felleman, D. J. 1983b. Progression of change following median nerve section in the cortical representation of the hand in areas 3b and 1 in adult owl and squirrel monkeys. Neuroscience 10, 639–665.
Merzenich, M. M., Nelson, R. J., Stryker, M. P., Cynader, M. S., Schoppmann, A., and Zook, J. M. 1984. Somatosensory

cortical map changes following digit amputation in adult monkeys. J. Comp. Neurol. 224, 591–605.
Messinger, A., Squire, L. R., Zola, S. M., and Albright, T. D. 2005. Neural correlates of knowledge: stable representation of stimulus associations across variations in behavioral performance. Neuron 48, 359–371.
Miyashita, Y. 1988. Neuronal correlate of visual associative long-term memory in the primate temporal cortex. Nature 335, 817–820.
Miyashita, Y. 1993. Inferior temporal cortex – Where visual perception meets memory. Annu. Rev. Neurosci. 16, 245–263.
Miyashita, Y. and Hayashi, T. 2000. Neural representation of visual objects: encoding and top-down activation. Curr. Opin. Neurobiol. 10, 187–194.
Morris, R. G. M. 2003. Long-term potentiation and memory. Philos. Trans. R. Soc. Lond. B 358, 643–647.
Nakayama, K. and Silverman, G. H. 1986. Serial and parallel processing of visual feature conjunctions. Nature 320, 264–265.
Nothdurft, H. C., Gallant, J. L., and Van Essen, D. C. 1999. Response modulation by texture surround in primate area V1: correlates of ''popout'' under anesthesia. Vis. Neurosci. 16, 15–34.
Pavlov, I. P. 1927. Conditioned Reflexes: an Investigation of the Physiological Activity of the Cerebral Cortex, Oxford University Press.
Paz, R., Wise, S. P., and Vaadia, E. 2004. Viewing and doing: similar cortical mechanisms for perceptual and motor learning. Trends Neurosci. 27, 496–503.
Petrov, A. A., Dosher, B. A., and Lu, Z. L. 2005. The dynamics of perceptual learning: an incremental reweighting model. Psychol. Rev 112, 715–743.
Pleger, B., Dinse, H. R., Ragert, P., Schwenkreis, P., Malin, J. P., and Tegenthoff, M. 2001. Shifts in cortical representations predict human discrimination improvement. Proc. Natl. Acad. Sci. U. S. A. 98, 12255–12260.
Poggio, T., Fahle, M., and Edelman, S. 1992. Fast perceptual learning in visual hyperacuity. Science 256, 1018–1021.
Polat, U. and Bonneh, Y. 2000. Collinear interactions and contour integration. Spat. Vis. 13, 393–401.
Polat, U. and Sagi, D. 1993. Lateral interactions between spatial channels: suppression and facilitation revealed by lateral masking experiments. Vision Res. 33, 993–999.
Polat, U. and Sagi, D. 1994a. Spatial interactions in human vision – from near to far via experience-dependent cascades of connections. Proc. Natl. Acad. Sci. U. S. A. 91, 1206–1209.
Polat, U. and Sagi, D. 1994b. The architecture of perceptual spatial interactions. Vision Res. 34, 73–78.
Polley, D. B., Steinberg, E. E., and Merzenich, M. M. 2006. Perceptual learning directs auditory cortical map reorganization through top-down influences. J. Neurosci. 26, 4970–4982.
Pollmann, S. and Maertens, M. 2005. Shift of activity from attention to motor-related brain areas during visual learning. Nat. Neurosci. 8, 1494–1496.
Pons, T. P., Garraghty, P. E., Ommaya, A. K., Kaas, J. H., Taub, E., and Mishkin, M. 1991. Massive cortical reorganization after sensory deafferentation in adult macaques. Science 252, 1857–1860.
Prakash, N. and Frostig, R. D. 2005. What has intrinsic signal optical imaging taught us about NGF-induced rapid plasticity in adult cortex and its relationship to the cholinergic system? Mol. Imaging Biol. 7, 14–21.
Rainer, G., Lee, H., and Logothetis, N. K. 2004. The effects of learning on the function of monkey extrastriate visual cortex. PLoS Biol. 2, 275–283.
Rajan, R., Irvine, D. R. F., Wise, L. Z., and Heil, P. 1993. Effect of unilateral partial cochlear lesions in adult cats on the representation of lesioned and unlesioned cochleas in primary auditory cortex. J. Comp. Neurol. 338, 17–49.
Ramachandran, V. S. and Braddick, O. 1973. Orientation-specific learning in stereopsis. Perception 2, 371–376.
Rasmusson, D. D. 1982. Reorganization of raccoon somatosensory cortex following removal of the 5th digit. J. Comp. Neurol. 205, 313–326.
Recanzone, G. H., Jenkins, W. M., Hradek, G. T., and Merzenich, M. M. 1992a. Progressive improvement in discriminative abilities in adult owl monkeys performing a tactile frequency discrimination task. J. Neurophysiol. 67, 1015–1030.
Recanzone, G. H., Merzenich, M. M., and Jenkins, W. M. 1992b. Frequency discrimination training engaging a restricted skin surface results in an emergence of a cutaneous response zone in cortical area 3A. J. Neurophysiol. 67, 1057–1070.
Recanzone, G. H., Merzenich, M. M., and Schreiner, C. E. 1992d. Changes in the distributed temporal response properties of S1 cortical neurons reflect improvements in performance on a temporally based tactile discrimination task. J. Neurophysiol. 67, 1071–1091.
Recanzone, G. H., Merzenich, M. M., Jenkins, W. M., Grajski, K. A., and Dinse, H. R. 1992c. Topographic reorganization of the hand representation in cortical area 3B of owl monkeys trained in a frequency-discrimination task. J. Neurophysiol. 67, 1031–1056.
Recanzone, G. H., Schreiner, C. E., and Merzenich, M. M. 1993. Plasticity in the frequency representation of primary auditory cortex following discrimination training in adult owl monkeys. J. Neurosci. 13, 87–103.
Robertson, D. and Irvine, D. R. F. 1989. Plasticity of frequency organization in auditory cortex of guinea pigs with partial unilateral deafness. J. Comp. Neurol. 282, 456–471.
Rossi, A. F., Rittenhouse, C. D., and Paradiso, M. A. 1996. The representation of brightness in primary visual cortex. Science 273, 1104–1107.
Saffell, T. and Matthews, N. 2003. Task-specific perceptual learning on speed and direction discrimination. Vision Res. 43, 1365–1374.
Sakai, K. and Miyashita, Y. 1991. Neural organization for the long-term memory of paired associates. Nature 354, 152–155.
Salazar, R. F., Kayser, C., and Konig, P. 2004. Effects of training on neuronal activity and interactions in primary and higher visual cortices in the alert cat. J. Neurosci. 24, 1627–1636.
Sarter, M., Givens, B., and Bruno, J. P. 2001. The cognitive neuroscience of sustained attention: where top-down meets bottom-up. Brain Res. Rev. 35, 146–160.
Sarter, M., Hasselmo, M. E., Bruno, J. P., and Givens, B. 2005. Unraveling the attentional functions of cortical cholinergic inputs: interactions between signal-driven and cognitive modulation of signal detection. Brain Res. Rev. 48, 98–111.
Schacter, D. L., Chiu, C. Y. P., and Ochsner, K. N. 1993. Implicit memory – a selective review. Annu. Rev. Neurosci. 16, 159–182.
Schiltz, C., Bodart, J. M., Dubois, S., Dejardin, S., Michel, C., Roucoux, A., Crommelinck, M., and Orban, G. A. 1999. Neuronal mechanisms of perceptual learning: changes in human brain activity with training in orientation discrimination. Neuroimage 9, 46–62.
Schmid, L. M., Rosa, M. G. P., Calford, M. B., and Ambler, J. S. 1996. Visuotopic reorganization in the primary visual cortex of adult cats following monocular and binocular retinal lesions. Cereb. Cortex 6, 388–405.
Schoups, A., Vogels, R., and Orban, G. A. 1995. Human perceptual learning in identifying the oblique orientation: retinotopy, orientation specificity and monocularity. J. Physiol. 483, 797–810.
Schoups, A., Vogels, R., Qian, N., and Orban, G. 2001. Practising orientation identification improves orientation coding in V1 neurons. Nature 412, 549–553.

Schoups, A. A. and Orban, G. A. 1996. Interocular transfer in perceptual learning of a pop-out discrimination task. Proc. Natl. Acad. Sci. U. S. A. 93, 7358–7362.
Schwartz, S., Maquet, P., and Frith, C. 2002. Neural correlates of perceptual learning: a functional MRI study of visual texture discrimination. Proc. Natl. Acad. Sci. U. S. A. 99, 17137–17142 [comment].
Scoville, W. B. and Milner, B. 1957. Loss of recent memory after bilateral hippocampal lesions. J. Neurol. Neurosurg. Psychiatry 20, 11–21.
Seitz, A. and Watanabe, T. 2005. A unified model for perceptual learning. Trends Cogn. Sci.. 9, 329–334.
Seitz, A., Lefebvre, C., Watanabe, T., and Jolicoeur, P. 2005. Requirement for high-level processing in subliminal learning. Curr. Biol. 15, R753–R755.
Seitz, A. R. and Watanabe, T. 2003. Is subliminal learning really passive? Nature 422, 36.
Seitzt, A. R., Yamagishi, N., Werner, B., Goda, N., Kawato, M., and Watanabe, T. 2005. Task-specific disruption of perceptual learning. Proc. Natl. Acad. Sci. U. S. A. 102, 14895–14900.
Shiffrin, R. M. and Schneider, W. 1977. Controlled and automatic human information processing. 2. Perceptual learning, automatic attending, and a general theory. Psychol. Rev. 84, 127–190.
Shiu, L. P. and Pashler, H. 1992. Improvement in line orientation discrimination is retinally local but dependent on cognitive set. Percept. Psychophys. 52, 582–588.
Shrager, Y., Gold, J. J., Hopkins, R. O., and Squire, L. R. 2006. Intact visual perception in memory-impaired patients with medial temporal lobe lesions. J. Neurosci. 26, 2235–2240.
Sigman, M. and Gilbert, C. D. 2000. Learning to find a shape. Nat. Neurosci. 3, 264–269.
Sigman, M., Pan, H., Yang, Y. H., Stern, E., Silbersweig, D., and Gilbert, C. D. 2005. Top-down reorganization of activity in the visual pathway after learning a shape identification task. Neuron 46, 823–835.
Singer, W. 1999. Neuronal synchrony: a versatile code for the definition of relations? Neuron 24, 49–65.
Sireteanu, R. and Rettenbach, R. 1995. Perceptual learning in visual search: fast, enduring, but non-specific. Vision Res. 35, 2037–2043.
Sireteanu, R. and Rettenbach, R. 2000. Perceptual learning in visual search generalizes over tasks, locations, and eyes. Vision Res. 40, 2925–2949.
Skinner, B. F. 1938. The Behavior of Organisms: an Experimental Analysis. D. Appleton-Century.
Somers, D. C., Nelson, S. B., and Sur, M. 1995. An emergent model of orientation selectivity in cat visual cortical simple cells. J. Neurosci. 15, 5448–5465.
Sowden, P. T., Rose, D., and Davies, I. R. L. 2002. Perceptual learning of luminance contrast detection: specific for spatial frequency and retinal location but not orientation. Vision Res. 42, 1249–1258.
Squire, L. R. 2004. Memory systems of the brain: a brief history and current perspective. Neurobiol. Learn. Mem. 82, 171–177.
Squire, L. R. and Zola, S. M. 1996. Structure and function of declarative and nondeclarative memory systems. Proc. Natl. Acad. Sci. U. S. A. 93, 13515–13522.
Squire, L. R., Knowlton, B., and Musen, G. 1993. The structure and organization of memory. Annu. Rev. Psychol. 44, 453–495.
Squire, L. R., Stark, C. E. L., and Clark, R. E. 2004. The medial temporal lobe. Annu. Rev. Neurosci. 27, 279–306.
Stettler, D. D., Yamahachi, H., Li, W., Denk, W., and Gilbert, C. D. 2006. Axons and synaptic boutons are highly dynamic in adult visual cortex. Neuron 49, 877–887.
Takeda, M., Naya, Y., Fujimichi, R., Takeuchi, D., and Miyashita, Y. 2005. Active maintenance of associative mnemonic signal in monkey inferior temporal cortex. Neuron 48, 839–848.
Teich, A. F. and Qian, N. 2003. Learning and adaptation in a recurrent model of V1 orientation selectivity. J. Neurophysiol. 89, 2086–2100.
Thorndike, E. L. 1911. Animal Intelligence. Macmillan.
Thorndike, E. L. and Woodworth, R. S. 1901a. The influence of improvement in one mental function upon the efficiency of other functions (I). Psychol. Rev. 8, 247–261.
Thorndike, E. L. and Woodworth, R. S. 1901b. The influence of improvement in one mental function upon the efficiency of other functions: (II) the estimation of magnitudes. Psychol. Rev 8, 384–395.
Thorndike, E. L. and Woodworth, R. S. 1901c. The influence of improvement in one mental function upon the efficiency of other functions: (III) functions involving attention, observation and discrimination. Psychol. Rev. 8, 553–564.
Trachtenberg, J. T., Chen, B. E., Knott, G. W., Feng, G. P., Sanes, J. R., Welker, E., and Svoboda, K. 2002. Long-term *in vivo* imaging of experience-dependent synaptic plasticity in adult cortex. Nature 420, 788–794.
Treisman, A. and Schmidt, H. 1982. Illusory conjunctions in the perception of objects. Cognit Psychol 14.
Treisman, A. M. and Gelade, G. 1980. A feature-integration theory of attention. Cognit. Psychol. 12, 97–136.
Tsodyks, M. and Gilbert, C. 2004. Neural networks and perceptual learning. Nature 431, 775–781.
Turk-Browne, N. B., Yi, D. J., and Chun, M. M. 2006. Linking implicit and explicit memory: common encoding factors and shared representations. Neuron 49, 917–927.
Van Essen, D. C., Anderson, C. H., and Felleman, D. J. 1992. Information processing in the primate visual system: an integrated systems perspective. Science 255, 419–423.
Vidnyanszk, Z. and Sohn, W. 2005. Learning to suppress task-irrelevant visual stimuli with attention. Vision Res. 45, 677–685.
Walker, M. P. and Stickgold, R. 2006. Sleep, memory, and plasticity. Annu. Rev. Psychol. 57, 139–166.
Walker, M. P., Stickgold, R., Jolesz, F. A., and Yoo, S. S. 2005. The functional anatomy of sleep-dependent visual skill learning. Cereb. Cortex 15, 1666–1675.
Wang, Q., Cavanagh, P., and Green, M. 1994. Familiarity and pop-out in visual search. Percept. Psychophys. 56, 495–500.
Watanabe, T., Nanez, J. E., and Sasaki, Y. 2001. Perceptual learning without perception. Nature 413, 844–848.
Watanabe, T., Nanez, J. E., Koyama, S., Mukai, I., Liederman, J., and Sasaki, Y. 2002. Greater plasticity in lower-level than higher-level visual motion processing in a passive perceptual learning task. Nat. Neurosci. 5, 1003–1009.
Weinberger, N. M. 1995. Dynamic regulation of receptive fields and maps in the adult sensory cortex. Annu. Rev. Neurosci. 18, 129–158.
Weinberger, N. M. 2004. Specific long-term memory traces in primary auditory cortex. Nat. Rev. Neurosci. 5, 279–290.
Weiss, T., Miltner, W. H. R., Liepert, J., Meissner, W., and Taub, E. 2004. Rapid functional plasticity in the primary somatomotor cortex and perceptual changes after nerve block. Eur. J. Neurosci. 20, 3413–3423.
Wertheimer, M. 1923. Untersuchungen zur lehre von der gestalt. Psychol. Forsch. 4, 301–350.
Wiesel, T. N. and Hubel, D. H. 1963. Single-cell responses in striate cortex of kittens deprived of vision in one eye. J. Neurophysiol. 26, 1003–1017.
Wilson, D. A., Fletcher, M. L., and Sullivan, R. M. 2004. Acetylcholine and olfactory perceptual learning. Learn. Mem. 11, 28–34.
Yang, T. M. and Maunsell, J. H. R. 2004. The effect of perceptual learning on neuronal responses in monkey visual area V4. J. Neurosci. 24, 1617–1626.

Yi, D. J., Olson, I. R., and Chun, M. M. 2006. Shape-specific perceptual learning in a figure-ground segregation task. Vision Res. 46, 914–924.

Yu, C., Klein, S. A., and Levi, D. M. 2004. Perceptual learning in contrast discrimination and the (minimal) role of context. J. Vision 4, 169–182.

Zeki, S. 2001. Localization and globalization in conscious vision. Annu. Rev. Neurosci. 24, 57–86.

Zhaoping, L., Herzog, M. H., and Dayan, P. 2003. Nonlinear ideal observation and recurrent preprocessing in perceptual learning. Network-Comp. Neural 14, 233–247.

Zielinski, K. 2006. Jerzy Konorski on brain associations. Acta Neurobiol. Exp. (Warsz.) 66, 75–84.

Zipser, K., Lamme, V. A., and Schiller, P. H. 1996. Contextual modulation in primary visual cortex. J. Neurosci. 16, 7376–7389.

Zohary, E., Celebrini, S., Britten, K. H., and Newsome, W. T. 1994. Neuronal plasticity that underlies improvement in perceptual performance. Science 263, 1289–1292.

Zuo, Y., Lin, A., Chang, P., and Gan, W. B. 2005. Development of long-term dendritic spine stability in diverse regions of cerebral cortex. Neuron 46, 181–189.

2.21 Face Recognition

B Duchaine, University College London, London, UK

G Yovel, Tel Aviv University, Tel Aviv, Israel

© 2008 Elsevier Inc. All rights reserved.

2.21.1	**Introduction**	330
2.21.2	**Cognitive Mechanisms**	330
2.21.2.1	Inversion Effects	331
2.21.2.2	Configural Processing	331
2.21.2.2.1	Holistic effects	332
2.21.2.2.2	Spacing effects	333
2.21.2.3	Are Faces Processed by Face-Specific or General-Purpose Configural Processing Mechanisms?	334
2.21.2.3.1	The face-house spacing-part task	334
2.21.2.3.2	Facelike processing of body stimuli	334
2.21.2.3.3	General expertise	335
2.21.2.4	The Other Race Effect	336
2.21.3	**Neural Basis of Face Recognition**	336
2.21.3.1	Single-Cell Recording	337
2.21.3.2	Event-Related Potentials	337
2.21.3.3	Magnetoencephalography Studies	338
2.21.3.4	Intracranial Recording of Neural Responses	338
2.21.3.5	Functional Magnetic Resonance Imaging Studies of Face Recognition	339
2.21.3.5.1	Face-selective functional magnetic resonance imaging regions	339
2.21.3.5.2	The nature of the face representation in face-selective regions	339
2.21.3.5.3	Two other face-selective regions: occipital face area and superior temporal sulcus	340
2.21.3.6	Combined Functional Magnetic Resonance Imaging and Electrophysiological Studies of Faces	341
2.21.4	**Neuropsychological Deficits of Face Recognition**	341
2.21.4.1	Acquired Prosopagnosia	342
2.21.4.1.1	Frequency of acquired prosopagnosia	343
2.21.4.1.2	Conditions associated with acquired prosopagnosia	343
2.21.4.1.3	Lesion location in acquired prosopagnosia	344
2.21.4.2	Developmental Prosopagnosia	345
2.21.4.2.1	Conditions associated with developmental prosopagnosia	346
2.21.4.2.2	Neural bases of developmental prosopagnosia	347
2.21.4.3	Face-Specificity in Prosopagnosia	347
2.21.5	**Development of Face Recognition**	348
2.21.5.1	Face Processing in Newborns	348
2.21.5.2	Infant Face Recognition	350
2.21.5.3	Critical Period in the Early Months of Life	350
2.21.5.4	Face Recognition in Childhood	351
2.21.6	**Conclusion**	351
References		352

Glossary

composite effect Behavioral effect seen when the top half of one face and the bottom half of another are combined. When these halves are aligned while upright, observers appear to fuse the two halves and so find it difficult to perceive the identity of either half. In contrast, performance with inverted composites shows little effect of alignment.

face inversion effects Perception and memory of faces is much more affected by stimulus inversion than other stimulus classes.

face-selective activation In functional magnetic resonance imaging studies, face-selective activations are areas that show a higher response to faces than other stimuli. They are usually defined by comparing the response to faces to the response to objects or places.

fusiform face area (FFA) A region in the fusiform gyrus defined by its greater response to faces than other visual stimuli. It is usually stronger in the right hemisphere than the left.

occipital face area (OFA) A region in the occipital cortex which shows face-selective activation.

other race effect The decrement in performance often seen when observers attempt to recognize faces from other races.

prosopagnosia A condition characterized by severe face recognition deficits. Acquired prosopagnosia occurs due to brain damage whereas developmental prosopagnosia is the result of a developmental failure.

superior temporal sulcus (STS) This sulcus in the temporal lobe contains areas which show face-selective activations.

2.21.1 Introduction

Face processing is one of the most important functions of the human visual system, and it is essential for normal social functioning. Gaze flits from face to face in social situations as we effortlessly assess identity, emotional state, attractiveness, and locus of attention. The use of faces in identification cards and police sketches attest to their primacy for identity recognition, and portraiture and busts are highly valued because viewers feel they gain insight into the personalities of the depicted individuals. Nonhuman animals also show great sensitivity to facial information (Sackett, G. P., 1966; Burghardt, G., 1990; Waitt, C. *et al.*, 2003), and natural selection has had eons to sculpt human face-processing abilities. When face processing is severely impaired due to brain damage or developmental problems, people experience great social difficulties (Duchaine, B. and Nakayama, K., 2006).

Consistent with its importance, face processing has been the focus of extensive research using a wide variety of methods. This work has led to the development of a number of models of face processing (Bruce, V. and Young, A. W., 1986; Burton, A. M. *et al.*, 1999; Haxby, J. V. *et al.*, 2000), with the Bruce and Young model (1986) providing the key cognitive framework for face-processing studies through the last 20 years (see Figure 1). In it, lower-level processes

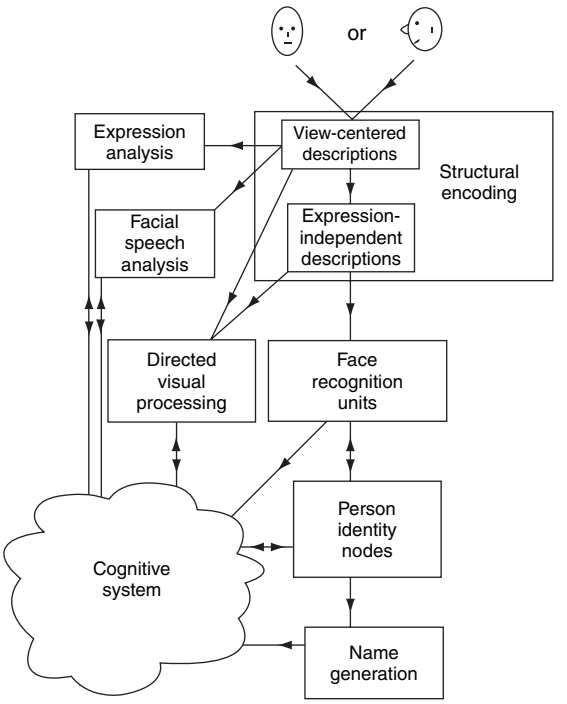

Figure 1 The Bruce and Young model of face processing. Reproduced with permission from the British Journal of Psychology © The British Psychological Society.

represent the facial image and later specialized modules carry out computations on different types of facial information such as identity, emotional expression, and mouth movements associated with speech. In this chapter, we review research investigating the processes involved in the recognition of facial identity, which is the best understood facet of face processing.

We first consider the nature of the perceptual/cognitive processes carrying out face recognition and discuss the special representation that is the basis of face recognition. Next, we review the neural basis of these computations, a research area which has seen an explosion of work in the last decade. We then discuss the neuropsychological impairments affecting these mechanisms and their implications for models of face recognition. We finish with a discussion of the development of face recognition mechanisms.

2.21.2 Cognitive Mechanisms

The idea that upright faces receive special processing has been supported by a number of cognitive experiments that reveal perceptual phenomena that are specific to faces. These studies suggest that faces are processed in a qualitatively different manner than objects or upside-down faces, and it is well accepted that they are represented holistically whereas nonfaces are processed in a more part-based manner. Although the term holistic has been defined differently in different papers (Maurer, D. *et al.*, 2002), it usually implies that faces are represented as one unit in which face parts are processed interactively rather than independently. Below we discuss several of the most robust cognitive effects indicative of holistic processing.

2.21.2.1 Inversion Effects

Aside from neuropsychological cases (see Section 2.21.4), cognitive studies provided the earliest and most convincing evidence that face processing engage specialized mechanisms. The first cognitive evidence came from a simple experimental procedure in which Yin R. (1969) asked subject to learn a set of faces and several sets of nonface objects (i.e., planes, houses, stick figures) to be recognize later. The stimuli were presented either upright or upside-down (inverted) during study and during test (see Figure 2). Although inversion of the stimuli resulted in lower recognition rates for all categories, the cost of inversion was much larger for faces. In fact, recognition rates for upright stimuli were best for faces whereas recognition rates for inverted stimuli were worst for faces. This robust phenomenon is typically referred to as the face inversion effect. It has been replicated numerous times since the original report and has been considered evidence that upright faces engage specialized mechanisms (e.g., Farah, M. J. *et al.*, 1998). Consequently, disproportionate inversion effects are sometimes used as a test to assess whether a given stimulus is processed by face-specific mechanisms or more general object mechanisms (Freire, A. *et al.*, 2000; Yovel, G. and Kanwisher, N., 2004; Duchaine, B. *et al.*, 2006).

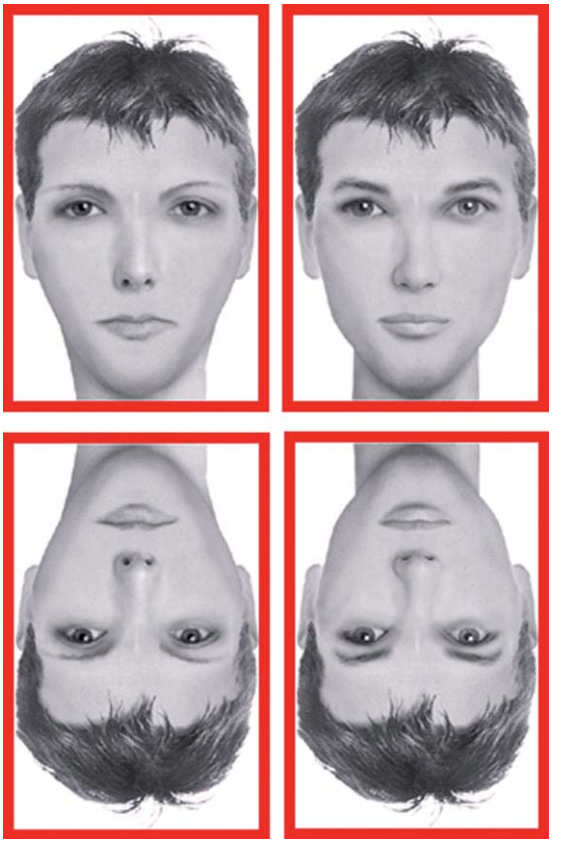

Figure 2 A pair of faces presented upright and inverted. Differences between the faces are much easier to perceive in the upright pair than the inverted pair.

2.21.2.2 Configural Processing

Later studies have tried to characterize the difference between upright and inverted face processing. Yin R. (1969) speculated that the difference involved a representation in which face configural information is better specified. Configural processing has referred

to two main phenomena: (1) holistic processing, that is, interactive processing of face parts and (2) sensitivity to spacing information (second-order relations; Maurer, D. *et al.*, 2002).

2.21.2.2.1 Holistic effects

Several paradigms demonstrate that face parts are processed interactively rather than independently.

2.21.2.2.1.(i) Composite effects In a seminal study that revealed holistic processing of upright faces, Young A. W. *et al.* (1987) presented subjects with composite faces created by combining the upper half of one famous face and the lower half of another famous face. The two halves were either aligned to create a coherent facial image or misaligned (see Figure 3). Subjects were asked to name either the upper or the lower half-face and ignore the other part. Response times were much longer for recognition of the one half of the face when it was aligned with the inconsistent half than when the halves were misaligned. Importantly, this effect was found for upright faces only. For inverted faces, subjects showed no difference in recognition time for aligned and misaligned faces. These findings suggest that halves are processed interactively when upright but independently when inverted. The composite face effect has also been demonstrated in perceptual matching tasks with unfamiliar faces in which subjects were asked to match the upper or lower halves of two sequentially presented faces (Hole, G., 1994; Le Grand, R. *et al.*, 2004). Thus, the two halves of the face are processed holistically at early perceptual stages and not only when they are stored for later recognition.

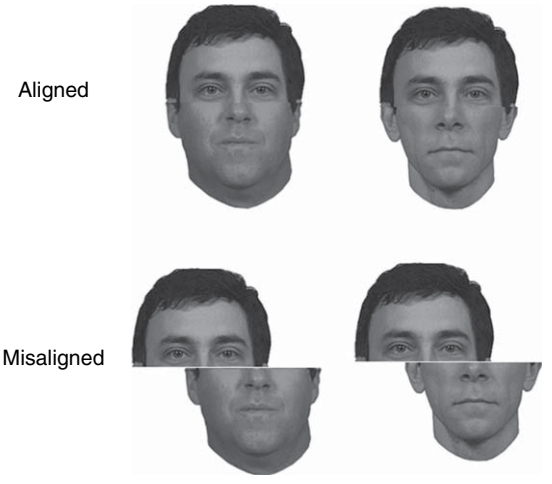

Figure 3 Composite faces created by combining the same top half with two different bottom halves. In tasks with composite faces, subjects find it much more difficult to determine whether the top halves are the same or different when they are aligned with the bottom halves than when they are misaligned. The difference between aligned and misaligned is much weaker or absent when the faces are inverted.

2.21.2.2.1.(ii) Part-whole effects Part-whole paradigms are another method that demonstrates that face parts are processed interactively for upright faces but not inverted faces. Tanaka J. W. and Farah M. J. (1993) presented subjects with a memory task in which subjects were asked to memorize a face and its name. During the test, a face part was presented to subjects either in isolation (part condition) or embedded in the original face (whole condition), and subjects decided whether the face part belonged to a given person (name). Performance was much better in the whole condition than the part condition (the part-whole effect). This effect was observed only for upright but not for inverted faces, upright houses, or inverted houses. In a follow-up study, Tanaka J. W. and Sengco J. A. (1997) showed that the precise location of the other face parts also interacts with recognition of individual parts. In particular, recognition of a face part was better when it was presented in the original face than in an original face in which the location of the other parts was altered. These findings suggest that face perception mechanisms encode both the shape of parts and their specific location (see also Section 2.21.2.2.2).

2.21.2.2.1.(iii) A whole face is more than the sum of its parts The composite face effect and the whole-part effect have examined recognition of face parts (e.g., a half-face, a face part) to determine how they are processed with relation to the rest of the face. Using a different paradigm, Yovel G. *et al.* (2005) estimated the extent to which face parts (i.e., right and left halves) are processed interactively or independently when subjects discriminate complete faces. In a face-matching task, facial stimuli were presented as either right half-faces, left half-faces, or complete faces. If the two halves are processed independently, the sum of accuracies for the right and left half-faces $[p(L) + p(R) - p(L)p(R)]$ will be comparable to the accuracy for complete faces. In contrast, if the two halves are processed interactively, performance with the complete faces will be better than the sum of the performance with the half-faces. Compared to this independence estimation, performance was higher for complete faces, which suggests interactive processing of the two half-faces. Like the composite and the

part-whole results, interactive processing of face parts was significantly reduced or absent for inverted faces.

2.21.2.2.2 Spacing effects

The experiments discussed above conceptualized configural processing as interactive processing of different parts or areas of the face. Configural processing has also been regarded as the sensitivity to the exact location of face parts or the spacing among the parts. Recent studies have tried to characterize what type of information is extracted by specialized face mechanisms. Studies of object recognition suggest that object processing is primarily part-based (Biederman, I., 1987; Braustein, M. L. *et al.*, 1989). In contrast, studies with faces have shown that we are very sensitive to minor dislocation of face parts (Haig, N. D., 1984) for upright but not inverted faces (Kemp, R., *et al* 1990). Thus, several studies have postulated that specialized face-processing mechanisms primarily extract information about the spacing among parts but not about the shape of the parts.

To assess this prediction directly, Freire A. *et al.* (2001) conducted a sequential same–different task with upright and inverted faces in which faces differed in one of two ways. On spacing pairs, faces differed only in the spacing among parts but the parts themselves were identical. Conversely, the part pairs consisted of faces in which the parts were different but the spacing of the parts remained the same (see Figure 4). The inversion effect was much larger for faces that differed only in spacing than for faces that differed only in parts. Based on the assumption that the size of the inversion effect reflects the extent to which information is extracted by specialized face-processing mechanisms, the authors concluded that these specialized mechanisms primarily extract information about the spacing but not the shape of parts (see also Leder, H. and Bruce, V., 2000; Le Grand, R. *et al.*, 2001; Mondloch, C. J. *et al.*, 2002).

However, the spacing and part tasks used by Freire A. *et al.* (2001) and Le Grand R. *et al.* (2001) were not matched for performance level (Yovel, G. and Kanwisher, N., 2004; Yovel, G., and Duchaine, B., 2006). In addition, the part manipulation was not limited to changes in the shape of parts, but these parts also differed in contrast and brightness. Thus, the absence of the inversion effect may reflect the operation of low-level visual mechanisms, which are

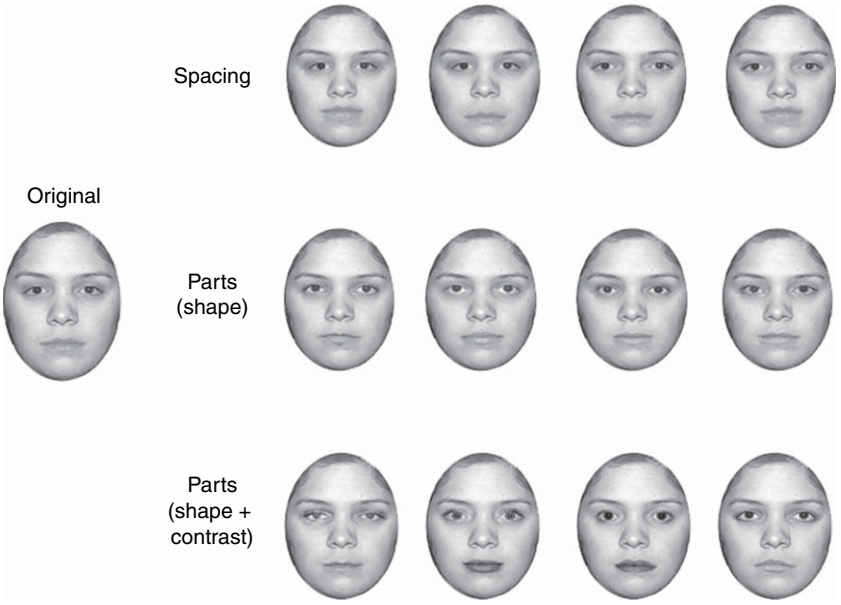

Figure 4 Faces from a same–different discrimination with three types of changes. The faces in the rows were created by modifying the original face on the left. In the spacing faces, the face parts are identical but the location of the eyes and mouth are varied. For the part (shape) faces, the locations of the features are identical but the face parts are different. The part (shape and contrast) faces also hold location constant but face parts differ in both shape and contrast. Rotate the figure to experience the inversion effect for the stimuli, differences are much more difficult to detect in the spacing and part (shape) variants than the part (shape and contrast) variants. Reproduced from Yovel, G., and Duchaine, B. 2006. Specialized face perception mechanisms extract both part and spacing information: evidence from developmental prosopagnosia. J. Cogn. Neurosci. 18, 580–593, with permission.

able to discriminate between the faces regardless of orientation based on color/contrast information. Indeed, several studies which matched performance for the spacing and part discriminations and which varied part shape but not contrast information found similar sized inversion effects for part and spacing discriminations (Riesenhuber, M. *et al.*, 2004; Yovel, G. and Kanwisher, N., 2004; Malcolm, G. *et al.*, 2005; Yovel, G. and Duchaine, B., 2006). Similar stimuli were presented in a fMRI study which examined the response of the face-selective fusiform regions during part and spacing discriminations with upright and inverted faces (Yovel, G. and Kanwisher, N., 2004). Face-selective regions showed a similar response to upright faces regardless of whether the discrimination involved parts or spacing and also showed a weaker response to inverted faces. Other evidence that face-specific mechanisms process parts and spacing comes from developmental prosopagnosia (Yovel, G., and Duchaine, B., 2006). These individuals have severe difficulties with both parts and spacing discriminations in faces despite normal performance on the same discriminations in houses. Furthermore, when face parts differ in contrast information, prosopagnosics were able to discriminate them as well as controls and control subjects showed no inversion effect for such face stimuli (Yovel, G. and Duchaine, B., 2006).

Finally, more direct evidence that spacing and parts are processed by shared rather than independent mechanisms was revealed in a study that employed an individual differences approach, in which the correlation across subjects between performance level for matching faces and house stimuli that differed in spacing or parts (Yovel, G. and Kanwisher, N., 2007). A significant positive correlation between performance for spacing and part discrimination was found only for upright faces. For inverted faces or houses, performance between the two tasks was not correlated. This suggests that face-processing mechanisms are special in that they represent information about spacing and parts, whereas general-object mechanisms processed the two types of information independently.

2.21.2.3 Are Faces Processed by Face-Specific or General-Purpose Configural Processing Mechanisms?

Whereas most researchers agree that faces are processed by holistic/configural mechanisms, the domain of these mechanisms is still debated. This mechanism could operate only on faces (Duchaine, B. *et al.*, 2006, Yovel, G. and Duchaine, B., 2006) or could process a wide variety of object classes (Levine, D. N. and Calvanio, R., 1989; Behrmann, M. *et al.*, 2005). Next we will review three nonface tasks that have been recently used to address this question.

2.21.2.3.1 The face-house spacing-part task

As mentioned above, several studies have shown that humans are very sensitive to the exact location of face parts and to the spacing among them (Freire A. *et al.*, 2000; Le Grand, R. *et al.*, 2001). These findings led researchers to suggest that face-processing mechanisms primarily extract spacing but not part based information. As we discussed above, recent studies have shown that both the spacing and the shape of parts are extracted by face-processing mechanisms, however, it is still not clear whether the ability to extract spacing information is limited to faces or is found also for nonface images. To answer this question Yovel G. and Kanwisher N. (2004) created house stimuli that, like the face stimuli, differed in the spacing among windows and doors or the shape of the windows and doors (part-task). These faces and houses were presented in a sequential matching task either upright or inverted. If configural-processing mechanisms are specific to faces, we should observe inversion effect for only faces but not houses. If, however, the mechanisms used with faces are also engaged in the processing of spacing information of non-faces, we should see an inversion effect in the house-spacing task. The results supported the face-specific hypothesis. Whereas faces yielded significant and equal sized inversion effects for both the spacing and the part task, there was no inversion effect for the house stimuli on either discrimination. These findings suggest that the specialized face-processing mechanism are specific to upright faces are not engaged by the processing of spacing information of non-faces.

2.21.2.3.2 Facelike processing of body stimuli

As mentioned above, the disproportionately large face inversion effect has been considered the hallmark of face-specific mechanisms. No other objects have produced a face-sized inversion effects until recently. Reed C. L. *et al.* (2003) have reported that human bodies yielded an inversion effect as large as they found with faces. In a perceptual matching task,

subjects were presented with upright or inverted pairs of faces and houses that differed in identity and whole bodies that differed in posture. Findings showed similar sized inversion effects for body posture and facial identity discriminations but no inversion effect for houses, though it is important to note that these effects (bodies = 5%; faces = 7%) were smaller than most face inversion effects (see Yovel, G. and Tambini, A., 2007 for a larger face than body inversion effect). In a more recent study, Reed C. L. *et al.* (2006) have examined whether the body inversion effect is specific for whole bodies or is also found for body parts. In one experiment, subjects matched whole bodies and houses or parts of bodies (leg, hand) and houses (window, door). Stimuli were presented either upright or inverted. Findings showed a larger inversion effect for whole bodies than whole houses and no inversion effect for body or house parts. In a second experiment, a comparison between whole bodies and faces to half bodies and half-faces revealed a similar significant inversion effect for all four conditions. These findings imply that, like upright faces, upright bodies are processed with special procedures.

Importantly, however, Reed's findings do not suggest that faces and bodies are mediated by the same configural mechanism. In fact, other studies suggest that they are mediated by distinct mechanisms. Yovel G. and Tambini A. (2007) found a larger inversion effect for faces and bodies and no correlation between performance on a face and body perception tasks (Yovel, G., and Tambini, A., 2007). Furthermore, recent functional magnetic resonance imaging (fMRI) findings revealed no overlap between face-selective and body-selective regions in the fusiform gyrus (Schwarzlose, R. F. *et al.*, 2005). Finally, developmental studies showed very early preference for the processing of upright than inverted faces (as early as the first day of life; Cassia, V. M., *et al.*, 2004), whereas the ability to discriminate between intact and jumbled body stimuli develops only during the second year of life (Slaughter, V. *et al.*, 2002). Thus, even if bodies are processed configurally, it appears likely that they are processed by configural mechanisms that are distinct from face configural mechanisms.

2.21.2.3.3 General expertise

A long-running debate in studies of face recognition concerns whether the putative face-specific effects are actually the hallmarks of expert processing (Diamond, R. and Carey, S., 1986; Tarr, M. J. and Gauthier, I., 2000; McKone, E., *et al.*, 2007). According to the expertise view, faces are processed in a qualitatively distinct manner but so are other object classes with which humans have substantial experience. Expert classes are claimed to be processed configurally, (Diamond, R. and Carey, S., 1986), and this predicts that experts will show the same effects that are seen for faces.

The seminal finding for the expertise view comes from Diamond and Carey's study of dog show judges (Diamond, R. and Carey, S., 1986). These dog experts, but not dog novices, showed face-sized inversion effects for the breed that they specialized in. To study the development of expertise in the laboratory, Gauthier and colleagues created the Greebles, a set of computer-generated objects designed to place similar demands on recognition mechanisms as faces. In training sessions, subjects learn individual Greeble names, their sex, or their family membership and are then tested on their recognition. A typical training regimen consists of eight sessions. Gauthier and colleagues have argued that Greeble training leads to behavioral results revealing configural/holistic effects (Gauthier, I. and Tarr, M. J., 1997; Gauthier, I. *et al.*, 1998; Gauthier, I. and Tarr, M. J., 2002) as well as neural effects similar to those seen in response to faces (Gauthier, I. *et al.*, 2000; Tarr, M. J. and Gauthier, I., 2000; Rossion, B. *et al.*, 2002).

New studies and close scrutiny of the evidence however reveals that the support for the expertise view of face recognition is weak (McKone, E. and Kanwisher, N., 2005; McKone, E., *et al.*, 2007). First, no findings with real world experts similar to the Diamond R. and Carey A. (1986) have been made in the intervening 20 years, and a recent study found that dog expertise did not show a larger inversion effect, part-whole effect, or composite effect than dog novices (Robbins, R. and McKone, E., 2007; for discussion, see McKone, E. and Robbins, R., 2007 and Gauthier, I. and Bukach, C., 2007). Despite many claims about Greeble effects, facelike effects do not emerge after Greeble training (Gauthier, I. and Tarr, M. J., 1997; Gauthier, I. *et al.*, 1998; Gauthier, I. and Tarr, M. J., 2002) and there has not even been a clear demonstration that Greeble training improves recognition of new Greebles (Gauthier, I. and Tarr, M. J., 1997). Recent fMRI work has found that expertise with objects increases responses in object-selective areas, not face-selective areas (Moore, C. D. *et al.*, 2006; Op de Beeck, H. *et al.*, 2006; Yue, X., *et al.*, 2006).

2.21.2.4 The Other Race Effect

The other race effect is a well-established, robust phenomenon in which individuals show better recognition for faces of their own race than faces of other races (e.g., Caucasian individuals recognize Caucasian faces better than Asian or black faces). As expected, it is not the race of the individual per se that determines the level of recognition of own and other race faces, but the type of faces that an individual has been exposed to throughout his life. For example, it has been shown that Caucasian individuals who frequently watch basketball games, which are dominated by black players, show good recognition of black faces (Li, J. C., *et al.*, unpublished). Interestingly, a study by MacLin O. H. and Malpass R. S. (2003) has shown that a racially ambiguous face will show another race effect when combined with other race hair but not when it is combined with own-race hair style. These findings suggest that when a face is categorized as another race face (based on non-facial features like hair), its facial features are not represented as well as when it is categorized as an own-race face. However, as discussed below, categorization is not the only factor that determines the way other race faces are represented.

Several studies have examined whether the poor recognition of other race faces may be associated with an absence of holistic processing for such faces. Earlier studies that examined the inversion effect for other-race relative to own-race faces have reported mixed results. Whereas some reported smaller inversion effect to other than own-race faces (Rhodes, G. *et al.*, 1989), other studies did not reveal similar findings (Valentine, T. and Bruce, V., 1986). One problem with studies that reported smaller inversion effect for other race faces is that they did not match performance level for the upright condition so the smaller inversion effect to other race faces may reflect scaling effect.

Studies that employed more direct measures of holistic processing, such as the abovementioned part-whole effect (Tanaka, J. W. *et al.*, 2004) or the composite face effect (Michel, C. *et al.*, 2006) revealed larger holistic effects for own than other race faces. Thus, the extensive exposure to own-race faces appears to be important for generating a holistic representation. It remains to be determined whether it is elevated holistic processing that allows better recognition of own-race faces or whether holistic representation and recognition abilities are two independent outcomes of extensive exposure.

The other race effect is typically attributed to perceptual mechanisms tuned to better represent same race faces than other race faces due to differential exposure. However, increased contact with other race faces has often failed to lessen the other race effect (reviewed in Levin, D., 2000). Levin D. (2000) suggests that other race effects are caused by selection of different facial features in same and other race faces. He proposes that individuating information is selected in same race faces whereas race specifying information is emphasized in representations of other race faces at the expense of individuating information. Consistent with this hypothesis and inconsistent with a simple perceptual tuning account, Levin D. (2000) found that subjects who showed the other race effect were better able to discriminate face race (e.g., which face is blacker?) than subjects who did not show the other race effect. Hence, for this task subjects with another race deficit better represented faces from other races than subjects who did not show an other face deficit. Levin argues that the differential selection is determined by higher-level cognitions such as whether an individual is concerned with the identity of a person or their race. This account is supported by recent findings showing that the other race deficit is eliminated by a positive mood induction (Johnson, K. J. and Fredrickson, B. L., 2005) and the effect of hair on faces with ambiguous race (MacLin, O. H. and Malpass, R. S., 2003).

2.21.3 Neural Basis of Face Recognition

Neurophysiological studies have reported ample evidence for specialized neural mechanism for faces. A robust face-selective response (a much higher response to faces than non-faces) has been reported with all relevant neurophysiological methods, including single-cell recordings, event-related potential (ERP), magnetencephalography (MEG), positron emission tomography (PET), and fMRI. Thus, the neural networks for face processing have been investigated with both high temporal resolution, which reveal face-selective neural response about 170–200 ms after stimulus onset, and with high-spatial resolution, which reveal face-selective regions in the occipitotemporal regions.

2.21.3.1 Single-Cell Recording

Single-cell recordings by Gross and colleagues and later in other laboratories during the 1970s and 1980s revealed cells in the superior temporal sulcus (STS) and inferior temporal cortex that showed highly specific responses to faces (Gross, C. G., *et al.*, 1972; for review see Gross, C. G., 2005). Examination of the response properties of these face cells has revealed a variety of response properties. The response of some cells was invariant to the size and position of the face image (Perrett, D. I. *et al.*, 1982). Others were view-selective with different cells responding to different views (e.g., Perrett, D. I. *et al.*, 1985; 1992), whereas others responded to all views (Desimone, R. *et al.*, 1984). Manipulations of the intactness of the face image, such as covering or scrambling face parts weakened the response of some of the cells, which responded vigorously only to intact faces (Perrett, D. I. *et al.*, 1982; Desimone, R. *et al.*, 1984). Head rotation and face inversion resulted in increased latencies of some of the cells (Perrett, D. I. *et al.*, 1998). Recent fMRI studies with monkeys, which will be discussed later, revealed activations that are consistent with this early single-cell recording work. Furthermore, studies with humans have also reported neural responses that are highly selective to faces as detailed below.

2.21.3.2 Event-Related Potentials

During the mid- and late 1990s, electrophysiological studies with humans revealed a robust and reliable selective response to faces. In particular, ERP studies measure a scalp electrical response that is time-locked to a given stimulus. ERP studies that presented subjects with various images such as faces, objects, or animals revealed a negative bilateral component that peaked 170 ms after stimulus onset (N170) at occipital-temporal electrodes that was much larger to faces than non-face images and larger over the right than the left temporal electrodes (Eimer, M., 1998; Bentin, S. *et al.*, 1996; see Figure 5). Further studies have shown that the N170 is influenced by variations in the intactness of the face image. Scrambling, contrast reversal, and orientation inversion elicit an N170 of slightly larger amplitude and a small but significant delay (George, N. *et al.*, 1996). Furthermore, the N170 shows a much larger response to presentation of eyes only (Bentin, S. *et al.*, 1996), which led some researchers to suggest that it is generated by the STS, which is sensitive to social aspects of facial information such as gaze (Hoffman, E. A. and Haxby, J. V., 2000; Hooker, C. I. *et al.*, 2003).

The question of whether the N170 encodes only the structure of the face image or also face identity information is still debated. Earlier studies found no difference between the response to familiar and unfamiliar faces and concluded that the N170 is not sensitive to face identity (Bentin, S. and Deouell, L. Y., 2000). However, studies that examined repetition effects (i.e., different response to second presentation of the same stimulus) to repeated presentation of unfamiliar faces reported mixed results. Whereas some studies found lower amplitude for repeated

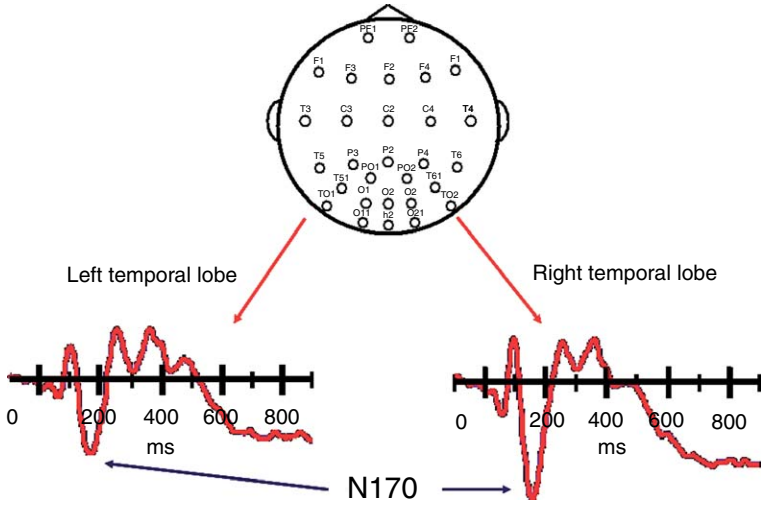

Figure 5 Schematic showing the sensors producing the largest N170 in event-related potential studies. The N170 to faces is much larger than that seen in response to other categories, and as in the figure, it is right lateralized.

presentation of the same individual face (Campanella, S. *et al.*, 2000; Itier, R. J., and Taylor, M. J., 2004a; Jacques, C., and Rossion, B., 2004), others reported no modulation by repetition (e.g., Yovel, G. *et al.*, 2003). The discrepancy between findings may be due to differences in the lag between repetitions and the number of repeated presentation. Thus, these studies suggest that, at least under some conditions (familiarization (Campanella, S. *et al.*, 2000), several repetitions (Itier, R. J., and Taylor, M. J., 2004a), or short delays (Jacques, C., and Rossion, B., 2004)), the N170 is sensitive to face identity information.

Another face-selective ERP component, the vertex positive potential (VPP), is observed at the same latency as the N170 but is maximal at a central electrode (Jeffreys, D. A., and Tukmachi, E. S., 1992). Like the N170, the VPP is delayed by face inversion or contrast inversion but it is not affected by familiarity and some studies have tried to assess the extent to which the VPP reflects the same neural source as the N170. In a recent systematic investigation, Joyce C. and Rossion B. (2005) have examined the effect of the location of the reference electrode and experimental manipulations on the VPP and N170 and found that the manipulated factors had similar effects on both components. Taking together with results of source localization, they concluded that the VPP and N170 are generated by the same source.

2.21.3.3 Magnetoencephalography Studies

MEG studies, which measure the magnetic fields produced by electrical activity in the brain, have revealed a similar face-selective negative component that also appears 170 ms after stimulus onset at lateral posterior electrodes. In addition, Liu J. *et al.* (2002) reported an earlier face-selective component that appeared 100 ms after stimulus onset (M100). Similar to the N170, the M100 and the M170 are delayed for orientation-inverted faces (Liu, J. *et al.*, 2000) and contrast-inverted faces (Itier, R. J. *et al.*, 2006); however, in contrast to the N170 these have no effect on amplitude. Another difference between the ERP and the MEG face-selective components is that the amplitude of the M170 is similar over the two hemispheres, whereas the N170 is larger over the right hemisphere (Bentin, S. *et al.*, 1996; Henson, R. N. *et al.*, 2002; Yovel, G. *et al.*, 2003).

In an elegant study, Liu J. *et al.* (2002) examined the role of the M100 and M170 in face categorization (discrimination between a face and a house) and face identification (discrimination between two faces). In a behavioral study, the authors determined the level of noise that allows categorization and the level that allows recognition for each subject. These at-threshold stimuli were presented to the subjects during MEG recordings and the evoked responses were classified based on subjects' success or failure in a face/house categorization and in their ability to recognize particular faces and houses. Results clearly showed that the M100 was sensitive to success in face categorization but not face identification. The M170 was sensitive to success in face categorization and identification. These components were not sensitive to performance for house stimuli or for stimuli for which subjects had expertise (Xu, Y. *et al.*, 2005). Finally, a recent study that examined category repetition effects for faces and houses (i.e., reduced amplitude for a second presentation of the same category) revealed that the M170 shows repetition effects (lower response for repetition of face–face than face–house) only when the delay between the first and second presentation is shorter than 400 ms (Harris, A. and Nakayama, K., 2007). These findings suggest that the M170 is generated by very early stages of face processing in which the facial image is not maintained for long durations.

In summary, although the N170 and M170 share some similar features in their response to faces, differences exist. It is unclear whether these reflect differences between electrical and magnetic responses from the same source or different sources (Itier, R. J. *et al.*, 2006).

2.21.3.4 Intracranial Recording of Neural Responses

Studies with epileptic patients enable intracranial recording of electrophysiological responses in humans. Such recording, which provides both high temporal and spatial resolution of the neural response, has been applied with face stimuli both with macroelectrodes which allow recording of evoked responses over the cortex and microelectrodes which allow recording of single cells. In an extensive investigation of intracranial ERPs of 98 epileptic patients, McCarthy G. *et al.* (1999) found a face-selective negative ERP component that appeared 200 ms after stimulus onset (N200). The face-selective component was maximal over certain patches in the ventral occipitotemporal cortex. Consistent with the N170 laterality, such patches were larger over the right than left hemisphere.

Investigation of the properties of this component showed invariance to size, color, and blurring. The response was largest for full faces and weaker for isolated face parts (eyes, nose, mouth), which evoked strong responses in other nearby locations. Similar to single-cell recordings, face rotation altered the amplitude of the N200, which was lowest for profile views (McCarthy, G. *et al.*, 1999). Like the N170, the N200 was not sensitive to face familiarity or to semantic priming and was therefore considered a neural correlates of initial structural encoding of face information prior to extraction of identity information (Puce, A. *et al.*, 1999).

In another study, single-cell recordings in epileptic patients conducted in the medial temporal lobe revealed neurons that responded selectively to images of faces, scenes, or objects (Kreiman, G. *et al.*, 2000). Further investigation of these cells (Quigora *et al.*, 2005) revealed that some of these cells respond selectively to certain individual familiar faces (e.g., Jennifer Aniston, Halle Barry) or familiar locations (Sydney Opera House). Furthermore, these cells are remarkably invariant to radical image variations (e.g., rotation, lighting, coloring) and in some cases were activated by letter strings of the name of the individual face/place. These findings suggest that some of these cells, which are anterior to the location of the N200 or the N170, are not purely visual but represent some abstract concept of individuals.

2.21.3.5 Functional Magnetic Resonance Imaging Studies of Face Recognition

2.21.3.5.1 Face-selective functional magnetic resonance imaging regions

Selective activation to faces in temporal occipital regions was first reported in PET studies. Sergent J. (1991) reported right lateralized fusiform activation to faces relative to scrambled faces. However, the first systematic investigations of brain regions that selectively respond to faces were fMRI studies by Kanwisher N. *et al.* (1997) and McCarthy G. *et al.* (1997). These studies revealed regions that elicited a much higher fMRI response to faces than non-face stimuli in the fusiform gyrus (see Figure 6). Kanwisher N. and colleagues (1997) referred to these face-selective regions as the fusiform face area (FFA). The FFA was larger over the right than the left hemisphere and showed a very selective response to any stimulus that contained facial information, including upright Mooney faces, animal faces, cartoon faces, and inverted faces (Tong, F. *et al.*, 2000),

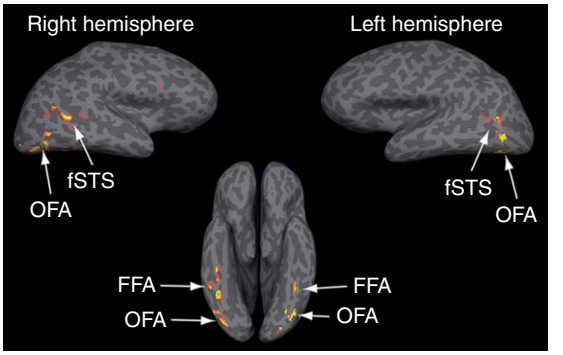

Figure 6 Inflated brain showing three face-selective areas: fusiform face area (FFA), occipital face area (OFA), and the face selective area in the posterior part of the superior temporal sulcus (fSTS).

but not to any objects or other body parts such as hands and feet (see also Schwarzlose, R. F. *et al.*, 2005). The FFA also showed selective response to imagery of faces (O'Craven and Kanwisher., 2000; Cox, D., *et al.*, 2004) and during periods when subjects perceive a face rather than a non-face when binocular rivalry is created by presenting different stimuli to each eye (Tong, F. *et al.*, 1998).

2.21.3.5.2 The nature of the face representation in face-selective regions

Several studies suggest that the FFA contributes to face identification. Grill-Spector K. *et al.* (2004) reported that the FFA response is modulated by successful recognition of familiar faces. Yovel G. and Kanwisher N. (2005) employed an event-related fMR-adaptation design in which the response to different stimuli is compared to the response of identical stimuli. A higher response to different than same pairs suggests that a given region is sensitive to the difference between the stimuli (for review see Grill-Spector, K. *et al.*, 2006). Findings show fMR-adaptation effect for unfamiliar upright faces in the FFA, but importantly non-face-selective regions, such as the object general lateral occipital complex (LOC), showed no fMR-adaptation for faces (see Figure 7).

As reviewed in Section 1, cognitive studies have demonstrated that faces are processed holistically. Do face-selective regions generate this holistic representation? Several early studies compared the response to upright and inverted faces in FFA and found a similar response to both. More recent studies however that measured fMR adaptation revealed that the

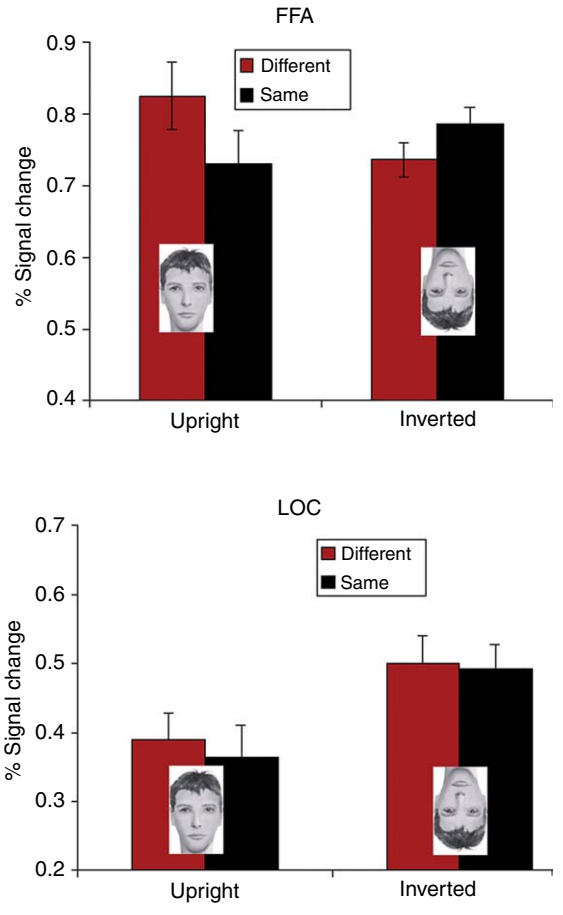

Figure 7 fMRI adaptation to same and different pairs of faces in the fusiform face area (FFA) and lateral occipital complex (LOC). FFA shows greater activation in response to different upright face pairs than same pairs. This adaptation is specific to upright faces in FFA in that LOC does not show adaptation to upright faces and neither FFA nor LOC show adaptation to inverted faces.

FFA showed a larger adaptation effect to upright than inverted faces (Yovel, G. and Kanwisher, N., 2005; Mazzard *et al.*, 2006; Schiltz, C. and Rossion, B., 2006), which is consistent with the behavioral phenomenon of better discrimination of upright than inverted faces. Interestingly, the general object region (LOC) showed an opposite effect of larger response to inverted than upright faces and no fMR adaptation to identity of upright or inverted faces (see Figure 7). These findings highlight the specialized representation for faces in face-selective mechanisms.

However, as mentioned above, the magnitude of the face inversion effect is not a direct measure of holistic processing. To directly assess the extent to which faces are represented holistically, paradigms such as the composite face task (Young, A. W. *et al.*, 1987) have been employed during fMRI experiments. Schiltz C. and Rossion B. (2006) found larger adaptation effect for aligned than misaligned faces, which is consistent with the behavioral composite effect in which identical half-faces are perceived as different faces when they are aligned to different faces than when they are misaligned.

2.21.3.5.3 Two other face-selective regions: occipital face area and superior temporal sulcus

In addition to the FFA, two other face-selective regions are commonly found in most fMRI studies: a region in the posterior STS and a lateral occipital region known as the occipital face area (OFA; see Figure 5). Several studies have shown clear dissociations between the role of the STS and FFA in face processing. The first study reporting such a dissociation revealed greater FFA activation when subjects attend to identity information than to gaze information and the opposite effect in the STS (Hoffman, E. A. and Haxby, J. V., 2000). These and other studies have led to the suggestion that the STS extracts dynamic aspects of face information such as emotion or gaze direction whereas the FFA represents nondynamic face information such as identity and sex (Haxby, J. V. *et al.*, 2000). Consistent with this finding, Grill-Spector K. *et al.* (2004) did not find modulation by successful face recognition in the STS, and Yovel G. and Kanwisher N. (2005) revealed similar response to same and different pairs of faces in the STS (no fMR adaptation). Furthermore, although both the FFA and the STS show lower response to inverted than upright faces, only the FFA inversion effect is correlated across subjects with the behavioral inversion effect as measured in a face identity discrimination task (Yovel, G. and Kanwisher, N., 2005).

The role of the OFA in face processing is less clear. For example, Rotshtein P., *et al.* (2005) presented subjects with pairs of different morphed famous faces that were either perceived as the same identity or were perceived as different identities. The FFA showed fMR adaptation for different morphs that were perceived as the same identity but not to different morphed faces that were perceived as different identities, which is consistent with its sensitivity to identity information. In contrast, the OFA appeared to be sensitive to physical differences, because it showed no adaptation to different morphed stimuli regardless of whether they

were perceived as the same identity or different identities. Yovel G. and Kanwisher N. (2005) also found dissociation between the OFA and FFA in a study that examined the role of face-selective regions in the behavioral face inversion effect. Whereas the FFA showed a higher response to upright than inverted faces and a correlation with the behavioral face inversion effect, the OFA showed a similar response to upright and inverted faces and no correlation with the behavioral inversion effect. These findings suggest that the OFA is primarily sensitive to physical information in the face image rather than its specific identity. In summary, the three face-selective regions seem to play different roles in the processing of the complex, rich information in the facial image.

2.21.3.6 Combined Functional Magnetic Resonance Imaging and Electrophysiological Studies of Faces

How face selective are regions showing a face-selective response in fMRI? This question has been impressively investigated by a recent study that combined fMRI and single-cell recording in monkeys (Tsao, D. Y. and Freiwald, W. A. 2006). Three face-selective patches are present in monkeys, and recordings from single cells were carried out in the middle face patch while the monkeys viewed face and various non-face stimuli. Of the nearly 200 visually responsive cells sampled, 97% showed a much higher response to faces than objects and the response to most objects was not significantly different from baseline. Of the non-face objects to which the cells responded, most had shapes similar to faces. These findings suggest that the face-selective response in face-selective areas human reflect the response of areas committed to face processing. The properties of the cells in the middle face patch were similar to the properties of face cells that were reported 20–30 years earlier without the guidance of fMRI (see Section 2.21.3.1 above). These unguided recordings usually found that about 20% of visually responsive cells were face selective, which suggested a seemingly sparse face-selective response. The new results demonstrate that face-selective cells are densely packed and reveal the great promise of studies combining fMRI with single-cell recording.

The relationship between the fMRI and electrophysiological responses to faces has also been assessed in humans in the few studies that collected data with both electroencephalography (EEG) and fMRI in different sessions under similar experimental procedures. Henson R. N. *et al.* (2002) examined the effect of familiarity and repetition with ERP and fMRI. The ERP and fMRI studies were conducted in different sessions on different groups of subjects. By examining the modulation of the N170 and fMRI measures to repetition and familiarity, the Henson R. N. and colleagues attempted to assess whether the N170 originates in the fusiform or the STS face regions. Because the N170 and the STS showed similar right hemisphere laterality and no effect of face familiarity and face repetition, the authors concluded that the N170 is associated with the face activity in the posterior STS. However, Horovitz S. G. *et al.* (2004) examined the effect of different levels of noise in a face on the pattern of response of the N170 and fMRI response to faces. Their results show a similar pattern of modulation of the stimulus on the N170 and the FFA. Recently, Iidaka T. *et al.* (2006) recorded ERP and fMRI using the same paradigm in separate sessions but revealed very weak correlations between the ERP and the fMRI response to faces. So far there have been no studies that recorded ERP and fMRI simultaneously. Hopefully such future studies will shed light on the relationship between temporal (ERP) and spatial (fMRI) aspects of the neural and response to faces.

2.21.4 Neuropsychological Deficits of Face Recognition

Deficits involving face recognition are some of the most dramatic conditions in neuropsychology and have provided powerful evidence that face recognition involves face-specific mechanisms. A variety of face recognition deficits have been documented, but we will focus our review on prosopagnosia, the most thoroughly researched and commonly reported deficit of face recognition.

Prosopagnosia is characterized by severe face recognition deficits which are not due to problems with lower-level visual problems or higher-level semantic problems. Prosopagnosics are usually able to perceive that they are viewing a face and the features that make them up, but they have great difficulties identifying individual faces (Blanc-Garin, J., 1984; Humphreys, G. W. and Riddoch, M. J., 1987; Ellis, H. D. and Florence, M., 1990). The

description of one of Bodamer's patients nicely illustrates the experience of many prosopagnosics:

> S is told to look at his own face in a mirror. At first he mistakes it for a picture but corrects himself. He stared for a long time as if a totally strange object is before him, then reports that he sees a face and describes its individual features. He knows it is his own face but does not recognize it as his own. It could be that of another person, even a woman. (Ellis, H. D. and Florence, M., 1990, p. 86).

This patient not only had deficits with facial identity recognition, but was also unable to discriminate gender from the face and other observations demonstrated that he was unable to recognize facial expressions of emotion (Ellis, H. D. and Florence, M., 1990). General deficits with face processing including expression, gender and identity are not uncommon in prosopagnosia (Bornstein, B., 1963; Ellis, H. D. and Florence, M., 1990; Duchaine, B. *et al.*, 2006), but dissociations between the processing of facial identity and other face-processing abilities have been reported (Duchaine, B. *et al.*, 2003) and suggest that different types of face processing involve separable components (Bruce, V. and Young, A. W., 1986; Haxby, J. V. *et al.*, 2000; Duchaine, B. *et al.*, 2006; but see Calder, A. J. and Young, A. W., 2005).

Prosopagnosia often leads to serious social difficulties. Prosopagnosics' failure to recognize acquaintances, friends, or family members can be perceived as an intentional snub and create offense when none is intended. Prosopagnosics who have contacted our laboratory have sadly described lost romantic opportunities, workplace disasters, and strained family relations due to failures of face recognition. Person recognition in neurologically typical individuals relies on a range of information including voice, gait, hair, body shape, and context, and prosopagnosics rely on these cues to identity (Bornstein, B., 1963; Duchaine, B. and Nakayama, K., 2006). They also often make use of distinctive facial features such as especially prominent features, moles, or scars (Ellis, H. D. and Florence, M., 1990; Duchaine, B., 2000). However, none of these means is as reliable or efficient as normal recognition of the face. Prosopagnosics not only fail to recognize people, but many also sometimes falsely recognize strangers as familiar (Duchaine, B. and Nakayama, K., 2006).

Until recently, the great majority of studies of prosopagnosia were restricted to patients who lost their face recognition ability due to brain damage. These acquired prosopagnosics were usually well aware of their face deficits, because they recalled how effortless face recognition was prior to their brain damage. In recent years, however, it has become clear that many individuals who have not experienced brain damage have severe deficit with face recognition (Kress, T. and Daum, I., 2003a; Behrmann, M. and Avidan, G., 2005; Duchaine, B. and Nakayama, K., 2006). These individuals are referred to as developmental or congenital prosopagnosics, and this condition appears to be much more common than acquired prosopagnosia.

2.21.4.1 Acquired Prosopagnosia

Given the difficulties that face recognition impairments present to patients, it is not surprising that prosopagnosia following brain damage was documented early on. In the first report in the neurological literature, Wigan A. L. (1844) described a man who could not recognize faces yet reported no other visual problems and could recognize people from their voices. There were a number of other reports of prosopagnosia in the late nineteenth century and early twentieth century (Charcot, J. M., 1883; Jackson, J. H., 1876; Quaglino, A. *et al.*, 2003; see Grusser, O. J. and Landis, T. 1991 for a review), but Hoff H. and Pöltz O. (1937) were the first to suggest that deficits with face recognition was a different disorder than object agnosia. Their patient was unable to identity familiar faces, including his own, but recovered his ability to read and retained some object recognition abilities.

A decade later, Bodamer in 1947 (Ellis, H. D. and Florence, M., 1990) described three patients who showed selective deficits of face perception or recognition subsequent to brain damage suffered in World War II. In his seminal paper, he extended the argument of Hoff H. and Pöltz O. (1937) and coined the term prosopagnosia by combining *prosopon*, the Greek word for face, with *agnosia*. One of Bodamer's patients was able to recognize faces normally but he experienced distortions restricted to faces. This metamorphopsia caused him to perceive faces as stretched or squished and features were sometimes displaced. In contrast, his perception of other objects was normal. The other two patients showed a number of characteristics typical of prosopagnosia. Both had suffered occipital lesions. They were impaired not only with face recognition, but had severe face perception deficits. Patient 1 described faces as "strangely flat, white with emphatic dark eyes, as if made from a flat surface, like white, oval plates, all

alike." Both patients also experienced deficits which sometimes co-occur with prosopagnosia such as object agnosia, cerebral achromatopsia, and difficulties with facial expression. Despite their severe difficulties with face recognition, their deficits were not readily apparent because both men compensated well by relying on non-facial information.

Since Bodamer's landmark paper, well over 100 cases of acquired prosopagnosia have been documented in the literature (see Farah, M. J., 1990; Grusser, O. J. and Landis, T., 1991 for reviews). These cases have contributed to debates about the neural areas involved in face recognition (Landis, T. *et al.*, 1986; Barton, J. J. *et al.*, 2002; Bouvier, S. E. and Engel, S. A., 2006), the nature of the mechanisms carrying out face recognition and face processing more generally (Damasio, A. *et al.*, 1982; Bruce, V. and Young, A. W., 1986; Farah, M. J., 1990; Farah, M. J. *et al.*, 1995), and even consciousness (Bauer, R. M., 1984; de Haan, E. *et al.*, 1987). However, despite the considerable research investigating acquired prosopagnosia, our understanding of this fascinating condition remains limited.

2.21.4.1.1 Frequency of acquired prosopagnosia

A number of studies have attempted to estimate the frequency of prosopagnosia in patients who have suffered brain damage. Such estimates are, of course, dependent on the criteria used for classification, the method by which patients are obtained, and the time since the event causing the brain damage. In the earliest studies addressing this issue, Hecaen H. and Angelergues R. (1962) found that only 6% of 382 patients who had suffered unilateral or bilateral posterior lesions experienced prosopagnosia. This low estimate was followed by a report from Gloning I. *et al.* (1967) that only one out of 241 patients with lesions to occipital or nearby areas experienced pure prosopagnosia. Similarly, Zihl J. and von Cramon D. (1986) reported that none of their 258 posterior lesioned patients had isolated prosopagnosia.

As we discuss below, prosopagnosia is often accompanied by a number of other deficits so strict criteria regarding purity are likely to make it appear extremely rare. Valentine T. *et al.* (2006) tested 91 brain-damaged subjects with a battery of cognitive and perceptual tests. These patients were a minimum of 6 months removed from their brain damage. Patients and their caregivers were asked to report on the patient's everyday face recognition abilities. Fifty per cent of patients and caregivers reported that patients would be able to recognize close acquaintances but would have difficulty recognizing people only seen a few times. Test results also indicated that many of the patients had trouble with face recognition, especially unfamiliar face recognition. On Warrington's Recognition Memory for Faces test, 77% scored more than two standard deviations below the mean. On less demanding tests of unfamiliar face memory, 20% were more than two standard deviations below. Many also had difficulties with famous face tests. Although the face recognition impairments many of these patients showed are likely to reflect higher level cognitive problems such as general memory deficits rather than problems with face-specific processes, the high proportion of impaired patients nonetheless indicate that problems with face recognition are more common than past studies suggested.

2.21.4.1.2 Conditions associated with acquired prosopagnosia

Acquired prosopagnosia often results from extensive bilateral lesions and is usually accompanied by a number of other visual impairments. Visual field defects are one of the most common co-occurring impairments. This was discussed by neurologists early on (Faust, C., 1955; Meadows, J. C., 1974), and a recent review found that only 12% of 69 prosopagnosic patients had no field defects (Bouvier, S. E. and Engel, S. A., 2006). Especially likely are defects in the left superior quadrant which result from lesions to the right inferior bank of the calcarine sulcus. This association fits nicely with neuroimaging (Sergent, J. *et al.*, 1992; Bentin, S. *et al.*, 1996; Kanwisher, N. *et al.*, 1997) and behavioral evidence (Levy, J. *et al.*, 1972; Gilbert, C. and Bakan, P., 1973; Christman, S. D. and Hackworth, M. D., 1993) indicating left visual field/right hemisphere dominance for face processing. Among the 41 patients in the review mentioned above who had visual field defects that could be assigned to a quadrant(s) or central vision (Bouvier, S. E. and Engel, S. A., 2006), 34 had defects in the upper left quadrant and 13 of these patients had defects restricted to this quadrant. In contrast, 22 had defects in the upper right field but only one patient had defects limited to it. Similarly, 15 had lower left defects and no patients had defects restricted to it.

Difficulties with face processing tasks other than identity computations are also common in acquired prosopagnosics. The quote about Bodamer's patient 1 revealed his problems with nonidentity face computations and similar difficulties have been repeatedly noted (Bornstein, B., 1963; Bowers, D. *et al.*, 1985;

Davidoff, J. B. and Landis, T., 1990; Ellis, H. D. and Florence, M., 1990; Humphreys, G. W., *et al.*, 1993; McNeil, J. and Warrington, E., 1993; de Renzi, E. and di Pellegrino, G., 1998; Humphreys, K. *et al.*, 2007). Some individuals with face recognition impairments have shown normal emotion recognition (Bruyer, R. *et al.*, 1983; Tranel, D. *et al.*, 1988), but Calder A. J. and Young A. W. (2005) have argued that limitations in these papers raise the question of whether identity and emotion can dissociate when tested under comparable conditions.

Object agnosia is also commonly associated with prosopagnosia. Below in our discussion about the specificity of prosopagnosia, we review cases that indicate that object and face recognition are dissociable, but the long-running debate revolving around this question (Damasio, A. *et al.*, 1982; Farah, M. J., 1990; McNeil, J. and Warrington, E., 1993; Moscovitch, M. *et al.*, 1997; Gauthier, I. *et al.*, 1999; Duchaine, B. and Nakayama, K., 2005) makes it clear that such dissociations are uncommon. Particularly rare are dissociations between recognition of individual objects (this car, this bird) and recognition of individual faces.

Meadows J. C. (1974) reviewed the many cases manifesting prosopagnosia and cerebral achromatopsia, and in their recent review, Bouvier S. E. and Engel S. A. (2006) found that the two conditions commonly co-occur. Of 73 cases of prosopagnosia they reviewed, 38 (52%) were also achromatopsic, and out of 38 achromatopics, 17 were prosopagnosic (Bouvier, S. E. and Engel, S. A., 2006).

Deficits impairing navigational abilities (topographagnosia) are also regularly seen. In some cases, representation of large-scale spatial information is impaired (Bornstein, B., 1963) while others are unable to recognize places (Bornstein, B., 1963). In the early analysis of Hecaen H. and Angelergues R. (1962) of the co-occurrence of prosopagnosia and topographagnosia in a large group of patients with unilateral lesions, they found that 38% of prosopagnosics also suffered from topographagnosia and that 77% of patients with topographagnosia were prosopagnosic. Landis T. *et al.* (1986a) examined their co-occurrence in 16 patients with topographic deficits and confirmed prosopagnosia in seven of these individuals.

2.21.4.1.3 Lesion location in acquired prosopagnosia

Neuroimaging and neurophysiology have demonstrated that occipitotemporal areas show a selective response to faces, particularly areas in the right hemisphere (Gross, C. G. *et al.*, 1972; Kanwisher, N. *et al.*, 1997; McCarthy, G. *et al.*, 1997). The consistent association of left field defects with prosopagnosia also argues for a right occipitotemporal locus for face recognition processing (Bouvier, S. E. and Engel, S. A., 2006), and studies of individuals born with cataracts demonstrate that the development of face recognition is more dependent on the right than the left hemisphere (Le Grand, R. *et al.*, 2003). In line with these findings, lesions in this region are crucial for acquired prosopagnosia. In fact, the debate about which areas were responsible for prosopagnosia centered not on whether right hemisphere lesions were necessary but whether they were sufficient (Hecaen, H. and Angelergues, R., 1962; Meadows, J. C., 1974; Landis, T. *et al.*, 1986b; de Renzi, E. *et al.*, 1994; Barton, J. J. *et al.*, 2002; Mayer, E. and Rossion, B., 2006). Most cases of prosopagnosia occur in individuals with bilateral lesions, so the decisive test cases were the few patients with unilateral lesions. With the advent of neuroimaging, this question has become much easier to address as it was no longer necessary to rely on autopsy findings. In recent years, structural imaging has demonstrated that lesions restricted to the right hemisphere are sufficient to cause prosopagnosia (Landis, T. *et al.*, 1988; Sergent, J. and Villemure, J. G., 1989; Sergent, J. and Signoret, J. L., 1992; Marotta, J. J. *et al.*, 2001; Barton, J. J. *et al.*, 2002; Uttner, L. *et al.*, 2002; Wada, Y. and Yamamoto, T., 2001). A few prosopagnosic cases have also been reported following lesions or atrophy not affecting posterior areas but more anterior temporal areas (Evans, J. J. *et al.*, 1995; Bukach, C. M. *et al.*, 2006).

Recent papers have attempted to more precisely assess lesion locations and their effects. Rossion and his colleagues carried out detailed structural and functional investigation of P.S., a prosopagnosic with especially face-selective deficits (Rossion, B. *et al.*, 2003; Schiltz, C., *et al.*, 2007; Sorger, B. *et al.*, 2007). These analyses showed that P.S. had lesions where the OFA is normally seen, activation in FFA though no adaptation, and an intact lateral occipital complex (an area selectively activated in object processing). A similar approach with other patients hold much promise. In the review of Bouvier S. E. and Engel S. A. (2006), lesion overlap in prosopagnosia was analyzed. Figure 8 shows the results of this, and as expected, high overlap was seen in right occipitotemporal areas with several peaks. Especially interesting to note is the lesion overlap results in comparison to face-selective activations seen in

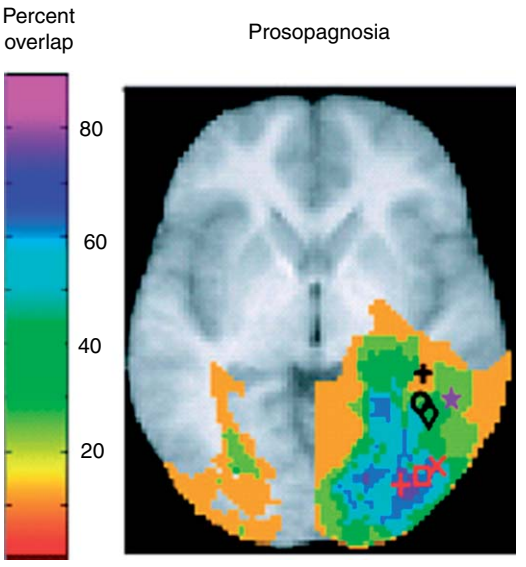

Figure 8 Lesion overlap results compared to face-selective activations in previous experiments with normal subjects. Three areas of peak overlap are shown in blue. Occipital face area activations are shown in red, fusiform face area in black, and superior temporal sulcus in purple. Bouvier, S. and Engel, S., Behavioral Deficits and Cortical Damage Loci in Cerebral Achromatopsia, Cerebral Cortex, 2006, 16, 2, 183–191, by permission of Oxford University Press.

fMRI experiments. The coordinates of OFA fall within the largest area of peak overlap whereas FFA and STS are anterior to this region and lateral to another peak. This suggests that lesions to OFA may be key to prosopagnosia, but given the apparent importance of FFA in face recognition (Grill-Spector, K. *et al*., 2004; Yovel, G. and Kanwisher, N., 2005), it is surprising that FFA did not overlap with a peak. Bouvier S. E. and Engel S. A. (2006) point out that sampling bias may have contributed to this finding as images with medial lesions are more likely to be included in papers because of the availability of landmarks. In discussing this finding, Mayer E. and Rossion B. (2006) also noted that isolated lesions to middle fusiform are rare because it receives blood from both posterior and middle cerebral arteries.

2.21.4.2 Developmental Prosopagnosia

Although Bornstein B. (1963) appears to have noted the existence of developmental prosopagnosia, McConachie H. (1976) provided the first case study of an individual with face recognition deficits in the absence of any identifiable brain damage. A.B. was a highly intelligent 12-year-old girl who reported that she had never been able to recognize faces, except for those with which she was very familiar. She had great difficulty recognizing her uniformed classmates at school. When tested with familiar faces, she hesitantly but correctly identified her friends, and she appeared to score normally on a test of unfamiliar face recognition. She showed normal visual fields, read well, and performed normally on tests of spatial ability and basic level object recognition. Lending support to a developmental etiology, her mother also reported problems with face recognition. Although this case hinted that developmental problems can give rise to prosopagnosia, A.B.'s deficits were not firmly established. In a follow-up study done 15 years later, de Haan E. H. and Campbell R. (1991) clearly demonstrated that A.B. did have face recognition problems as well as facial expression and object recognition problems. Intriguingly, her deficits with tasks other than identity recognition and anecdotal reports that she has navigational problems suggested that developmental prosopagnosia co-occurs with the same conditions as acquired prosopagnosia.

After A.B.'s case was reported, only one new case of developmental prosopagnosia (unaccompanied by autism spectrum disorder) was documented in the 1980s and early 1990s (Temple, C., 1992) so developmental prosopagnosia appeared to be extremely rare. Since that time though, more than 24 papers have reported on developmental prosopagnosics (for reviews, see Galaburda, A. M. and Duchaine, B., 2003; Kress, T. and Daum, I., 2003a; Behrmann, M. and Avidan, G., 2005; Duchaine, B. and Nakayama, K., 2006). The surge of papers is likely the result of the internet allowing researchers and developmental prosopagnosics to make contact and the increased attention to prosopagnosia in the media. Many of these individuals feel great relief upon learning about developmental prosopagnosia, because they finally have an explanation for the great difficulties they have with person recognition.

Like many acquired prosopagnosics (Grusser, O. J. and Landis, T., 1991), developmental prosopagnosics are sometimes able to recognize faces, but they experience severe, recurring problems and many fail to recognize family and close friends (McConachie, H., 1976; Duchaine, B. and Nakayama, K., 2006). Substantial variability in the severity of their face recognition deficit exists among developmental prosopagnosics. Some are able to recognize faces if seen often enough. One man told us that he could

recognize Bill Clinton after a few years of his presidency. Others recognize very few faces. One intelligent Englishman tested in our laboratory watches the news regularly yet failed to recognize Tony Blair, George Bush, Princess Diana, and Prince Charles. They tend to rely on nonfacial information to a much greater extent than people with normal face recognition. Movies and television programs are often difficult to follow because they cannot identify characters. Like acquired cases, many developmental prosopagnosics find ways to maneuver socially by faking recognition until verbal information clarifies identity and by preparing for or avoiding situations in which recognition will be challenging.

Although the prevalence of developmental prosopagnosia has not been firmly determined, it is clear that it is not as rare as once thought. From early 2002 until late 2006, approximately 1900 self-identified prosopagnosics contacted the website of the Harvard/UCL Prosopagnosia Research Center, and more than 1200 of these contacts came in 2006 due to media coverage. Of this sample, the great majority report no history of brain damage and years of difficulty with face recognition. When tested in the laboratory, we find that approximately 80% show severely impaired scores on our tests of face recognition. A German team recently estimated the prevalence of developmental prosopagnosia at 2% of the general population (Kennerknecht, I. *et al.*, 2006). While any estimate of prevalence is strongly dependent on the criteria used for diagnosis, this estimate suggests that there are millions of prosopagnosics in the world. Jane Goodall (Goodall, 1999) reports that she is prosopagnosic, and it appears that Robert Cecil, a late nineteenth century UK Prime Minister, was as well (Cecil, D., 1973). It is interesting to consider that individuals in modern societies are bombarded by faces whereas in ancestral environments the demands of face recognition were much less. In the small bands in which humans evolved (Foley, R. A., 1995), people with face recognition deficits may have been able to navigate the social world much more successfully than they can today.

It appears that a variety of causes can lead to developmental prosopagnosia. The first case study hinted at a genetic cause and other documented developmental prosopagnosics have mentioned that relatives share their difficulties (Duchaine, B., 2000; Behrmann, M. *et al.*, 2005; Duchaine, B. and Nakayama, K., 2005). de Haan E. (1999) found that three members of a family performed poorly on a famous face test. Approximately 30% of the developmental prosopagnosics who contact our website report genetic relatives with face recognition problems, and we have tested a number of families including one with ten affected members (Duchaine, B. *et al.*, 2007). A recent study using self-report data found that the inheritance patterns in seven families were consistent with dominant autosomal transmission (Kennerknecht, I. *et al.*, 2006). We also find that a substantial proportion (approximately 20%) of our contacts report severe early vision problems such as amblyopia, strabismus, and uncorrected myopia. This high proportion is consistent with developmental evidence indicating that visual input in the first months of life is crucial for the development of face processing (Le Grand, R. *et al.*, 2001; 2003). In many cases, there are no hints as to what may have led to prosopagnosia (Duchaine, B., *et al.*, 2003).

2.21.4.2.1 Conditions associated with developmental prosopagnosia

Like acquired prosopagnosia, developmental prosopagnosia shows considerable heterogeneity in the deficits commonly associated with it (Duchaine, B. and Nakayama, K., 2005; Harris, A., *et al.*, 2005; Le Grand, R. *et al.*, 2006). Many of the same deficits co-occur in both conditions, which suggests that developmental prosopagnosia sometimes results from a developmental failure which affects cortical areas near those areas involved with face recognition. Developmental cases sometimes have trouble recognizing facial expressions of emotion (Duchaine, B., 2000; Duchaine, B., *et al.*, 2006), classifying faces by sex (Duchaine, B. *et al.*, 2006), and judging facial attractiveness (Sadr, J. *et al.*, 2004). All documented developmental prosopagnosics perform normally with basic level object naming (car, dog), but many show deficits with tests of recognition of items from within a category (that car, that dog; Behrmann, M. *et al.*, 2005; Duchaine, B. and Nakayama, K., 2005). Also like acquired prosopagnosics, developmental prosopagnosics regularly report severe navigational problems. A.B.'s navigational difficulties were mentioned above, and among the prosopagnosics who have contacted the Prosopagnosia Research Center, approximately 15% report severe problems. In some especially severe cases, the navigations problems have a considerable impact. At present, almost no research has been carried out on developmental navigation deficits.

Although many associated conditions are seen in both forms of prosopagnosia, visual field defects and cerebral achromatopsia have not been reported in any developmental cases. Neuroimaging and neurophysiological work demonstrate that proximity explains their co-occurrence in acquired cases, so the absence in developmental cases is somewhat surprising. However, we expect that visual fields and color vision are often not assessed in developmental prosopagnosia. Lifelong defects such as these may be difficult to self-identify, especially defects limited to a small region of the visual field. Full-fledged achromatopsia would be apparent, but dyschromatopsia would be more difficult to detect.

2.21.4.2.2 Neural bases of developmental prosopagnosia

Given the cognitive heterogeneity in developmental prosopagnosia, it is likely that multiple neural abnormalities will be responsible for it. Studies that have investigated the neural bases in developmental cases have found some atypical neural responses but these atypicalities are not seen in all cases and no correspondence between response variability and cognitive variability has been identified.

Face-selective areas identified by fMRI were a natural first step in neural investigations of developmental prosopagnosia, but so far, few differences between controls and DPs have been found in these areas. Hassan U. *et al.* (2003) found that the magnitude of the FFA in Y.T. was normal, and normal FFA response was also found in a study involving four developmental prosopagnosics (Avidan, G. *et al.*, 2005). In addition, this study examined adaptation in FFA by comparing the response to 12 different faces to that of 12 repetitions of the same face. The developmental prosopagnosics showed adaptation comparable to the controls, which suggests that FFA is sensitive to identity information. However, adaptation in controls and the prosopagnosics was seen in a number of other visual areas, a finding consistent with an attentional account of the weakened response to repetition. Another recent single case study found weaker face activation in left FFA and bilaterally in the temporal poles (von Kriegstein, K. *et al.*, 2006).

The N170 and M170 have also been examined in developmental prosopagnosia. Bentin S. *et al.* (1999) found that the N170 in Y.T. was not as face-selective as controls, and Kress T. and Daum I. (2003b) found similar results in two other participants. In contrast, Harris A. *et al.* (2005) found mixed results when they examined the M170 in five developmental prosopagnosics. Two subjects showed a stronger response to faces than houses that was comparable to that for controls, while three failed to show a face-selective response. Analysis of the behavioral results for the two groups did not reveal any distinctions that mapped on to the M170 differences.

Behrmann M. *et al.* (in press) have reported structural abnormalities in developmental prosopagnosia. Morphometric and volumetric measurements were made in controls and six developmental prosopagnosics. Anterior fusiform gyrus was smaller in the developmental prosopagnosics than in controls, whereas middle temporal gyrus and posterior temporal gyrus were larger in the prosopagnosics than controls. Most impressively, the volume of the anterior fusiform gyrus was positively correlated with performance with famous faces in the developmental prosopagnosics.

2.21.4.3 Face-Specificity in Prosopagnosia

The cognitive and neural sections above described evidence indicating that faces are processed by face-specific mechanisms, and evidence from prosopagnosia has played a key role in the debate about specificity (Farah, M. J., 1990; Kanwisher, N., 2000; Tarr, M. J. and Gauthier, I., 2000). As mentioned above, many prosopagnosics experience both face and object recognition deficits. This association has led some researchers to argue that face recognition deficits are the most obvious manifestation of damage to more general purpose object recognition mechanisms (Damasio, A. *et al.*, 1982; Gauthier, I. *et al.*, 1999). Areas involved in face recognition, however, are adjacent to object recognition areas so an association is to be expected. The theoretically illuminating cases are those which show dissociations between face and object recognition, and such dissociations have been documented in both acquired and developmental prosopagnosia.

To demonstrate a dissociation between face and object recognition, it is crucial to test each at comparable levels of specificity. This has been done by comparing recognition of individual objects from within a category to recognition of individual faces (Davidoff, J., 1986; Moscovitch, M. *et al.*, 1997). A number of acquired cases have shown dissociations under such conditions. W.J. was a sheep farmer who experienced severe face-processing deficits following three vascular episodes (McNeil, J. and Warrington, E., 1993). In contrast, to his profound deficit with

faces, W.J. was able to recognize many of the sheep in his flock of 36 and performed better than all controls (including two sheep experienced controls) on two sheep face recognition memory tests and a paired associates learning test with sheep faces. Similarly, R.M., a car enthusiast who suffered a lesion that left him with profound prosopagnosia, was better able to name the make, model, and year of a large set of cars than any controls (Sergent, J. and Signoret, J. L., 1992). Reports with other acquired cases have found similar results with other non-face categories (Farah, M. J., 1996; Henke, K. *et al.*, 1998; Rossion, B. *et al.*, 2003).

Face-selective deficits have also been demonstrated in developmental prosopagnosia (Nunn, J. A. *et al.*, 2001; Duchaine, B. and Nakayama, K., 2005). The clearest demonstration involved testing the predictions of each proposed account of prosopagnosia in a man named Edward (Duchaine, B. *et al.*, 2004; 2006). His normal performance on a wide range of tests including inverted face matching, within-class object discrimination, non-face configural processing, and expert processing (Greebles and human bodies) showed that his prosopagnosia could not be explained by any of the accounts except the face-specific explanation (Duchaine, B. *et al.*, 2006).

If faces are processed by mechanisms specialized for face processing, cases with object agnosia and normal or relatively spared face recognition should exist. A number of these cases have been documented in brain damaged patients (Bruyer, R. *et al.*, 1983; Assal, G. *et al.*, 1984; Feinberg, T. E. *et al.*, 1986; McMullen, P. A. *et al.*, 2000), and multiple papers have explored the profile of Mr. C.K., an object agnosia with wholly spared face recognition (Moscovitch, M. *et al.*, 1997; Moscovitch, M. and Moscovitch, D. A., 2000). Normal recognition of faces has also been seen in combination with severe place recognition deficits (Carlesimo, G. A. *et al.*, 2001). At present, no developmental cases showing normal face recognition and impaired object recognition have been reported.

Evidence for face specificity has also come from metamorphopsia, a disorder involving perceptual distortions. In his classic paper, Bodamer reported a double dissociation (Ellis, H. D. and Florence, M., 1990): patient 3 reported perceptual distortions restricted to faces whereas patient 1 reported that the edges of all objects in a scene, but not faces, appeared to flicker at times. Davidoff J. B. and Landis T. (1986) reported a woman who perceived all faces to be distorted on the left-side, yet she perceived objects normally. Following a stroke, a prosopagnosic woman experienced several visual preservations including one amazing episode involving a poodle face (Landis, T. *et al.*, 1986b). While sitting on a bus, she observed a poodle sitting on the lap of a person across from her. Upon looking up from the poodle to the people in the bus, she now saw the poodle face instead of a human face on each person (see Figure 9). Her quick exit from the bus did not end this bizarre state, but fortunately after 30 min, the perseveration ended. Her perseveration revealed the specificity of face processing, because the poodle was only pasted on to other faces and not on to any other objects in the visual scene.

2.21.5 Development of Face Recognition

Like the cognitive, neural, and neuropsychological aspects of face recognition, the development of face recognition has received extensive attention. The majority of this work has addressed cognitive development, but neural issues are receiving increasing attention. Developmental studies have revealed much about face processing at different ages but little about the changes that lead to mature face recognition abilities.

2.21.5.1 Face Processing in Newborns

Infants are born with visual systems which, though limited in acuity and color perception, allow them to perceive and respond to coarse aspects of the visual world. Considerable research carried out over the last 30 years has demonstrated that newborns attend to faces more than many other comparable stimuli (Goren, C. *et al.*, 1975; Johnson, M. H. and Morton, J., 1991). This revealing ability was first demonstrated by Goren C. *et al.* (1975) in a study with newborns with a mean age of nine minutes. Each infant was presented with four stimuli which included a schematic face, two scrambled faces, and a blank face. The stimuli traversed 180° arcs in front of the child while the infants' head and eye movements were recorded. The infants looked significantly longer at the schematic face than the other three stimuli. Other experiments have replicated these findings (Johnson, M. H. *et al.*, 1991) and extended them to show that newborns prefer faces with open eyes (Batki, A., *et al.*, 2000) and direct eye gaze (Farroni, T. *et al.*, 2002; see Figure 10).

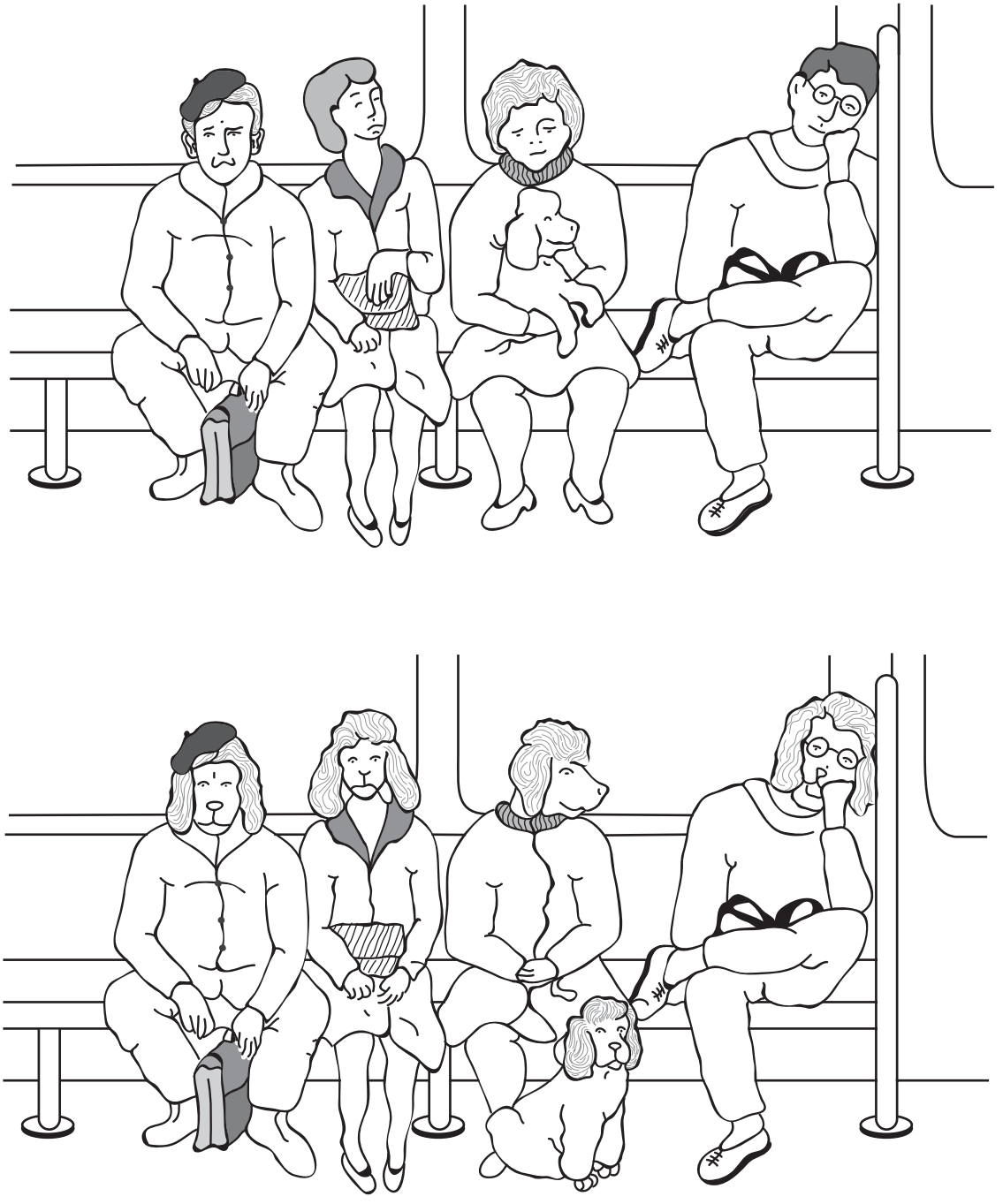

Figure 9 Drawing depicting the visual experiences of a woman experiencing metamorphopsia restricted to faces. Several weeks after suffering a stroke, she rode on a bus and viewed the scene in the top drawing. After looking at the face of the poodle, she looked back to the passengers. However, rather than seeing the faces of the passengers, she saw the poodle's face in place of all the other faces in the bus. This state lasted for approximately 30 min. Drawing by D. Starke.

Newborns also discriminate between different faces. Work examining newborn responsiveness to facial expressions and movements has demonstrated the existence of mechanisms sensitive to the face at birth. Field T. M. *et al.* (1982) found that neonates imitated facial expressions, and Meltzoff A. N. and Moore M. K. (1977) reported that neonates imitated facial gestures such as opening of the mouth and protrusion of the lips or tongue. Newborns also prefer attractive over unattractive faces (Slater, A., *et al.*,

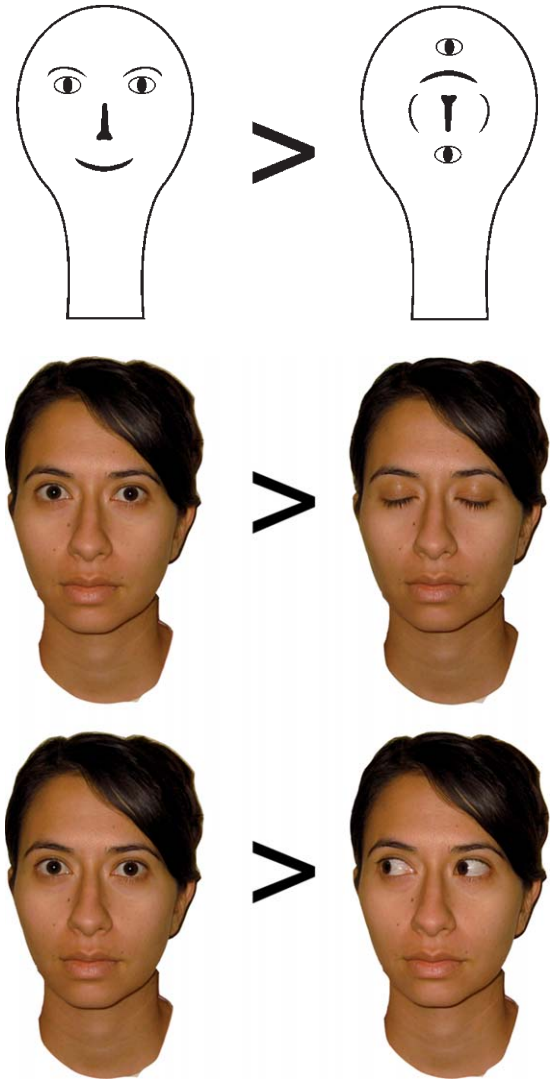

Figure 10 For each pair, newborns attend to the stimuli on the left longer than the stimuli on the right.

1998), and use the internal facial features to make this discrimination (Slater, A. *et al.*, 2000). While these experiments did not investigate face recognition, they clearly show that infants are born equipped to engage with faces.

2.21.5.2 Infant Face Recognition

In first days of life, infants look longer at their mother's face than a stranger's face (Field, T. M. *et al.*, 1984; Bushnell, I. W. *et al.*, 1989; Pascalis, O. *et al.*, 1995). It appears however that these discriminations are based on external features, particularly hair (Maurer, D. and Salapatek, P., 1976; Pascalis, O. *et al.*, 1995). Whether young infants are better able to recognize identity in upright faces than inverted faces is unknown.

The youngest evidence of the inversion effect is seen in infants at 4 or 5 months of age. Using a habituation paradigm, Turati C. *et al.* (2004) found that infants recognized facial identity better when faces were shown in different views in upright faces than inverted faces. Similarly, Bhatt R. S. *et al.* (2005) reported that 5-month-old infants were less sensitive to changes to the spacing of the eyes in inverted faces than upright faces. Neural measures have also demonstrated an early inversion effect. A differential ERP response to upright and inverted was seen in 6-month-old infants (de Haan, E. *et al.*, 2002), and near infrared spectroscopy, which noninvasively records hemodynamic changes, done with 5–8-month-old infants detected a stronger response to upright faces than inverted faces in right lateral areas (Otsuka, Y. *et al.*, 2007).

Recent work suggests that face recognition mechanisms in infants become tuned to the faces observed. Using preferential looking paradigms with infants and discrimination tests with adults, Pascalis O. *et al.* (2002) showed that 6-month-old infants, 9-month-old infants, and adults were able to discriminate between human faces but only 6-month-olds could discriminate between monkey faces. This phenomenon is similar to the loss of sensitivity to phonemes not used in the infant's native language (Werker, J. F. and Tees, R. C., 1984; Kuhl, P. K. *et al.*, 1992). As with phonemes, exposure to monkey faces during the period in which sensitivity is lost extends the period of sensitivity to monkey faces (Pascalis, O. *et al.*, 2005).

Differential processing of faces of different races follows a similar developmental course. Sangrigoli S. and de Schonen S. (2004) and Bar-Haim Y. *et al.* (2006) found that infants at 3 months discriminated between same race faces better than different race faces. This effect disappeared with pretest exposure to other race faces (Sangrigoli, S. and de Schonen, S., 2004). As expected, newborns show no preference for same race faces (Kelly, D. J. *et al.*, 2005).

2.21.5.3 Critical Period in the Early Months of Life

Some of the most revealing developmental studies have investigated face processing in individuals born with congenital cataracts (Le Grand, R. *et al.*, 2001; 2003). The lenses in these individuals were replaced

in the first few months of life, and they had relatively normal visual experience after surgery. Participants ranged in age between 9 and 21 years of age when their face discrimination was tested. Despite years of experience with faces, these individuals showed clear deficits with the face discriminations (Le Grand, R. *et al.*, 2001).

Further research done with participants born with unilateral cataracts, which again were repaired in the first months of life, found eye-specific effects. Cataracts in the right eye had no effect on face discriminations while left eye cataracts led to deficits comparable to those seen in participants with bilateral cataracts (Le Grand, R. *et al.*, 2003). The eye-specific effects are possible, because retinas in infancy are primarily responsive to the temporal visual field (Lewis, T. L. and Maurer, D., 1992) and the immaturity of the corpus callosum appears to make it unable to allow functional integration of visual information (Liegeois, F., *et al.*, 2000). Hence, visual information from each eye is primarily in the contralateral hemisphere. The effect of left eye cataracts indicates that the development of normal face discrimination requires early input to the right hemisphere. Lens replacements were carried out between 2 and 6 months of age, and length of deprivation had no effect on performance (Le Grand, R. *et al.*, 2001; 2003).

2.21.5.4 Face Recognition in Childhood

By 4 years of age, children can be tested using paradigms similar to those used with adults, and results using these paradigms show that children experience many of the same effects considered evidence of face-specific processing in adults. Pellicano E. and Rhodes G. (2003) showed that children as young as 4 years show a part-whole effect, with better recognition of parts within the context of face than in isolation (Tanaka, J. W. and Farah, M. J., 1993). de Heering *et al.* (2006) found additional evidence for holistic processing by demonstrating that 4–6-year-olds showed strong composite effects (Young, A. W. *et al.*, 1987). Similarly, McKone E. and Boyer B. L. (2006) showed that 4-year-olds and adults find that spacing and feature changes have similar effects on distinctiveness judgments.

Although these investigations suggest that face-specific processing procedures operate in early childhood, recognition of unfamiliar faces in children is far from adult levels (Diamond, R. and Carey, S., 1977). What leads to this improvement? Early work suggested that changes in face-processing mechanisms were responsible for much of the change as early studies suggested that the inversion effect was not evident until 10 years of age (Diamond R. and Carey, S., 1977). More sensitive measures however show inversion effects in infancy (Turati, C. *et al.*, 2004; Bhatt, R. S. *et al.*, 2005), and a recent elegant study indicates that the effect of both inversion and contrast reversal are constant from age 8 years through to adulthood (Itier, R. J., and Taylor, M. J., 2004b). Participants had to detect repetitions of upright, inverted, or contrast-reversed faces shown with no lag or a one trial lag. Older participants performed better than younger participants, but the effect of inversion and contrast-reversal had comparable effects on accuracy and response times at all ages. These comparable effects suggest that the improvement seen as children grow older is caused primarily by changes to higher-level processes such as working memory rather than face-specific processes.

2.21.6 Conclusion

Converging evidence from studies that employed cognitive, neural, neuropsychological, and developmental approaches suggest that faces engage specialized processing mechanisms that represent information about faces in a qualitatively different way than inverted faces and non-face objects. In particular, upright faces are represented in a more holistic manner, with the features and the spacing of the features coded more precisely and interactively than other types of objects are. Early studies that employed cognitive methods to examine the nature of the representation of faces in normal and brain damaged patients that suffer from face recognition deficits anticipated the existence of a specific neural substrate for face processing. Indeed, electrophysiological studies and the explosion of neuroimaging work in the last ten years have revealed neural responses that are highly face-specific and seem to play a special role in face recognition processes. A variety of neuropsychological deficits affect face processing. The best studied is prosopagnosia, and it can result from brain damage or a failure to develop face recognition mechanisms. Studies of the development of face recognition revealed that newborns attend to faces more than comparable stimuli and many of the holistic and configural effects emerge early in childhood. Most excitingly, growing connections between

these different levels of explanation are beginning to provide a more integrated theory of face recognition.

Although research into face recognition has led to an outline of what a detailed account of face recognition might look like, many fundamental questions remain unanswered. We still have little understanding of the stages of face processing, what sort of mix of face-specific and more general mechanisms contribute to face recognition, what operations different neural areas carry out, and how the system is modified by experience and maturation. Familial prosopagnosia reveals the existence of genes that are important for the development of face recognition, but little else is known about its genetic basis. Despite scores of neuropsychological studies, no effective treatments for face recognition deficits have been devised. However, the importance of face recognition in our daily life and the existence of specific neural, cognitive and possibly genetic mechanisms that are dedicated to face processing suggest that it will continue to be an area on the cutting edge that provides a model for research investigating other areas in cognitive neuroscience.

References

Assal, G., Favre, C., and Anderes, J. P. 1984. Nonrecognition of familiar animals by a farmer. Zooagnosia or prosopagnosia for animals? Rev. Neurol. (Paris) 140, 580–584.

Avidan, G., Hasson, U., Malach, R., and Behrmann, M. 2005. Detailed exploration of face-related processing in congenital prosopagnosia. 2. Functional neuroimaging findings. J. Cogn. Neurosci. 17, 1150–1167.

Bar-Haim, Y., Ziv, T., Lamy, D., and Hodes, R. M. 2006. Nature and nurture in own-race face processing. Psychol. Sci. 17, 159–163.

Barton, J. J., Press, D. Z., Keenan, J. P., and O'Connor, M. 2002. Lesions of the fusiform face area impair perception of facial configuration in prosopagnosia. Neurology 58, 71–78.

Batki, A., Baron-Cohen, S., Wheelwright, S., Connellan, J., and Ahluwalia, J. 2000. Is there an innate gaze module? Evidence from human neonates. Inf. Behav. Dev. 23, 223–229.

Bauer, R. M. 1984. Autonomic recognition of names and faces in prosopagnosia: a neuropsychological application of the Guilty Knowledge Test. Neuropsychologia 22, 457–469.

Behrmann, M. and Avidan, G. 2005. Congenital prosopagnosia: face-blind from birth. Trends Cogn. Sci. 9, 180–187.

Behrmann, M., Avidan, G., Gao, F., and Black, S. Structural imaging reveals anatomical alterations in inferotemporal cortex in congenital prosopagnosia. Cerebral Cortex. (in press).

Behrmann, M., Avidan, G., Marotta, J. J., and Kimchi, R. 2005. Detailed exploration of face-related processing in congenital prosopagnosia: 1. Behavioral findings. J. Cogn. Neurosci. 17, 1130–1149.

Bentin, S., Allison, T., Puce, A., Perez, E., and McCarthy, G. 1996. Electrophysiological studies of face perception in humans. J. Cogn. Neurosci. 8, 551–565.

Bentin, S. and Deouell, L. Y. 2000. Structural encoding and identification in face processing: ERP evidence for separate mechanisms. Cogn. Neuropsychol. 17, 35–54.

Bentin, S., Deouell, L. Y., and Soroker, N. 1999. Selective visual streaming in face recognition: evidence from developmental prosopagnosia. Neuroreport 10, 823–827.

Bhatt, R. S., Bertin, E., Hayden, A., and Reed, A. 2005. Face processing in infancy: developmental changes in the use of different kinds of relational information. Child Dev. 76, 169–181.

Biederman, I. 1987. Recognition-by-components: a theory of human image understanding. Psychol. Rev. 94, 115–147.

Blanc-Garin, J. 1986. Faces and Non-Faces in Prosopagnosic Patients. In: Aspects of Face Processing (*eds*. H. D. Ellis, M. A. Jeeves, F. Newcombe, and A. Young), pp. 273–278. Martinus Nijhoff.

Bornstein, B. 1963. Prosopagnosia. In: Problems in Dynamic Neurology (*ed*. L. Halpern). pp. 283–318. Hadassah Medical School.

Bouvier, S. E. and Engel, S. A. 2006. Behavioral deficits and cortical damage loci in cerebral achromatopsia. Cereb. Cortex 16, 183–191.

Bowers, D., Bauer, R. M., Coslett, H. B., and Heilman, K. M. 1985. Processing of faces by patients with unilateral hemisphere lesions. I. Dissociation between judgments of facial affect and facial identity. Brain Cogn. 4, 258–272.

Braunstein, M. L., Hoffman, D. D., and Saidpour, S. 1989. Parts of visual objects: an experimental test of the minima rule. Perception 18, 817–826.

Bruce, V. and Young, A. W. 1986. Understanding face recognition. Br. J. Psychol. 81, 305–327.

Bruyer, R., Laterre, C., Seron, X., Feyereisen, P., Strypstein, E., Pierrard, E., and Rectem, D. 1983. A case of prosopagnosia with some preserved covert remembrance of familiar faces. Brain Cogn. 2, 257–284.

Bukach, C. M., Bub, D. N., Gauthier, I., and Tarr, M. J. 2006. Perceptual expertise effects are not all or none: spatially limited perceptual expertise for faces in a case of prosopagnosia. J. Cogn. Neurosci. 18, 48–63.

Burghardt, G. 1990. Cognitive Ethology and Critical Anthropomorphism: A Snake with Two Heads and Hog-Nosed Snakes that Play Dead. In: Cognitive Ethology: The Minds of other Animals (*ed*. C. Ristau), pp. 53–90. Lawrence Erlbaum Associates.

Burton, A. M., Bruce, V., and Hancock, P. J. B. 1999. From pixels to people: a model of familiar face recognition. Cognit. Sci. 23, 1–31.

Bushnell, I. W., Sai, F., and Mullin, J. T. 1989. Neonatal recognition of the mother's face. Br. J. Dev. Psych. 7, 3–15.

Calder, A. J. and Young, A. W. 2005. Understanding the recognition of facial identity and facial expression. Nat. Rev. Neurosci. 6, 641–651.

Campanella, S., Hanoteau, C., Depy, D., Rossion, B., Bruyer, R., Crommelinck, M., and Guerit, J. M. 2000. Right N170 modulation in a face discrimination task: an account for categorical perception of familiar faces. Psychophysiology 37, 796–806.

Carlesimo, G. A., Fadda, L., Turriziani, P., Tomaiuolo, F., and Caltagirone, C. 2001. Selective sparing of face learning in a global amnesic patient. J. Neurol. Neurosurg. Psychiatry 71, 340–346.

Cassia, V. M., Turati, C., and Simion, F. 2004. Can a nonspecific bias toward top heavy patterns explain newborns' face preference? Psychol. Sci. 15, 379–383.

Cecil, D. 1973. The Cecils of Hatfield House, an English Ruling Family. Houghton Mifflin.

Charcot, J. M. 1883. Un cas de suppression brusque et isolé de la vision mentale des signes et des objets. Progr. Med. 11, 568–571.

Christman, S. D. and Hackworth, M. D. 1993. Equivalent perceptual asymmetries for free viewing of positive and negative emotional expressions in chimeric faces. Neuropsychologia 31, 621–624.
Cox, D., Meyers, E., and Sinha, P. 2004. Contextually evoked object-specific responses in human visual cortex. Science 303, 115–117.
Damasio, A., Damasio, H., and Van Hoesen, G. 1982. Prosopagnosia: anatomic basis and behavioral mechanisms. Neurology 32, 331–341.
Davidoff, J. 1986. The mental representation of faces: spatial and temporal factors. Percept. Psychphys. 40, 391–400.
Davidoff, J. B. and Landis, T. 1990. Recognition of unfamiliar faces in prosopagnosia. Neuropsychologia 28, 1143–1161.
de Haan, E. 1999. A Familial Factor in the Development of Face Recognition Deficits. J. Clin. Exp. Neuropsych. 21, 312–315.
de Haan, E., Young, A. W., and Newcombe, F. 1987. Faces interfere with name classification in a prosopagnosic patient. Cortex 23, 309–316.
de Haan, E. H. and Campbell, R. 1991. A fifteen year follow-up of a case of developmental prosopagnosia. Cortex 27, 489–509.
de Haan, M., Pascalis, O., and Johnson, M. H. 2002. Specialization of neural mechanisms underlying face recognition in human infants. J. Cogn. Neurosci. 14, 199–209.
de Renzi, E. and di Pellegrino, G. 1998. Prosopagnosia and alexia without object agnosia. Cortex 34, 403–415.
de Renzi, E., Perani, D., Carlesimo, G. A., Silveri, M. C., and Fazio, F. 1994. Prosopagnosia can be associated with damage confined to the right hemisphere – an MRI and PET study and a review of the literature. Neuropsychologia 32, 893–902.
Desimone, R., Albright, T. D., Gross, C. G., and Bruce, C. 1984. Stimulus-selective properties of inferior temporal neurons in the macaque. J. Neurosci. 4, 2051–2062.
Diamond, R. and Carey, S. 1977. Developmental changes in the representation of faces. J. Exp. Child. Psychol. 23, 1–22.
Diamond, R. and Carey, S. 1986. Why faces are and are not special: an effect of expertise. J. Exp. Psychol. Gen. 115, 107–117.
Duchaine, B. 2000. Developmental prosopagnosia and configural processing. Neuroreport 11, 79–83.
Duchaine, B. and Nakayama, K. 2005. Dissociations of face and object recognition indevelopmental prosopagnosia. J. Cogn. Neurosci. 17, 249–261.
Duchaine, B. and Nakayama, K. 2006. Developmental prosopagnosia: a window to content-specific processing. Curr. Opin. Neurobiol. 16, 166–173.
Duchaine, B., Dingle, K., Butterworth, E., and Nakayama, K. 2004. Normal greeble learning in a severe case of developmental prosopagnosia. Neuron 43, 469–473.
Duchaine, B., Germine, L., and Nakayama, K. 2007. Family resemblance: ten family members with prosopagnosia and within-class object agnosia. Cogn. Neuropsychol. 24, 419–430.
Duchaine, B., Nieminen-von Wendt, T., New, J., and Kulomaki, T. 2003. Dissociations of visual recognition in a developmental agnosic: evidence for separate developmental processes. Neurocase 9, 380–389.
Duchaine, B., Parker, H., and Nakayama, K. 2003. Normal recognition of emotion in a prosopagnosic. Perception 32, 827–838.
Duchaine, B., Yovel, G., Butterworth, E., and Nakayama, K. 2006. Prosopagnosia as an impairment to face-specific mechanisms: elimination of the alternative explanations in a developmental case. Cogn. Neuropsychol. 23, 714–747.
Eimer, M. 1998. Does the face-specific N170 component reflect the activity of a specialized eye processor? Neuroreport 9, 2945–2948.
Ellis, H. D. and Florence, M. 1990. Bodamer's (1947) paper on prosopagnosia. Cogn. Neuropsychol. 7, 81–105.
Evans, J. J., Heggs, A., Antoun, N., and Hodges, J. 1995. Progressive prosopagnosia with associated selective right temporal lobe atrophy: a new syndrome? Brain 118, 1–13.
Farah, M. J. 1990. Visual Agnosia. MIT Press.
Farah, M. J. 1996. Is face recognition 'special'? Evidence from neuropsychology. Behav. Brain Res. 76, 181–189.
Farah, M. J., Wilson, K. D., Drain, H. M., and Tanaka, J. 1995. The inverted face inversion effect in prosopagnosia: evidence for mandatory, face-specific perceptual mechanisms. Vision Res. 35, 2089–2093.
Farah, M. J., Wilson, K. D., Drain, M., and Tanaka, J. N. 1998. What is ''special'' about face perception? Psychol. Rev. 105, 482–498.
Farroni, T., Csibra, G., Simion, F., and Johhson, M. H. 2002. Eye contact detection in humans from birth. Proc. Nat. Acad. Sci. U. S. A. 99, 9602–9605.
Faust, C. 1955. Die zerebralen Herdstörungen nach Hinterhauptverletzungen und ihre Beurteilung. Thieme.
Feinberg, T. E., Gonzalez Rothi, L. J., and Heilman, K. M. 1986. Multimodal agnosia after unilateral left hemisphere lesion. Neurology 36, 864–867.
Field, T. M., Cohen, D., Garcia, R., and Greenberg, R. 1984. Mother–stranger face discrimination by the newborn. Inf. Behav. Dev. 7, 19–25.
Field, T. M., Woodson, R., Greenberg, R., and Cohen, D. 1982. Discrimination and imitation of facial expression by neonates. Science 218, 179–181.
Foley, R. A. 1995. Humans before Humanity: An Evolutionary Perspective, Blackwell.
Freire, A., Lee, K., and Symons, L. A. 2000. The face-inversion effect as a deficit in the encoding of configural information: direct evidence. Perception 29, 159–170.
Galaburda, A. M. and Duchaine, B. 2003. Developmental disorders of vision. Neurol. Clin. 21, 687–707.
Gauthier, I. and Bukach, C. 2007. Should we reject the expertise hypothesis? Cognition 103, 322–330.
Gauthier, I. and Tarr, M. J. 1997. Orientation priming of novel shapes in the context of viewpoint-dependent recognition. Perception 26, 51–73.
Gauthier, I. and Tarr, M. J. 2002. Unraveling mechanisms for expert object recognition: bridging brain activity and behavior. J. Exp. Psychol. Hum. Percept. Perform. 28, 431–446.
Gauthier, I., Behrmann, M., and Tarr, M. J. 1999. Can face recognition really be dissociated from object recognition? J. Cogn. Neurosci. 11, 349–370.
Gauthier, I., Skudlarski, P., Gore, J. C., and Anderson, A. W. 2000. Expertise for cars and birds recruits brain areas involved in face recognition. Nat. Neurosci. 3, 191–197.
Gauthier, I., Williams, P., Tarr, M. J., and Tanaka, J. 1998. Training 'greeble' experts: a framework for studying expert object recognition processes. Vision Res. 38, 2401–2428.
George, N., Evans, J., Fiori, N., Davidoff, J., and Renault, B. 1996. Brain events related to normal and moderately scrambled faces. Cogn. Brain Res. 4, 65–76.
Gilbert, C. and Bakan, P. 1973. Visual asymmetry in perception of faces. Neuropsychologia 11, 355–362.
Gloning, I., Gloning, K., and Hoff, H. 1967. On optic hallucinations. A study based on 241 patients with lesions of the occipital lobe and its surrounding regions verified by autopsy or surgery. Wien Z. Nervenheilkd. Grenzgeb. 25, 1–19.
Goodall, J. 1999. Reason for Hope, Warner.

Goren, C., Sarty, M., and Wu, P. Y. 1975. Abstract visual following and pattern discrimination of face-like stimuli by newborn infants. Pediatrics 56, 544–549.
Grill-Spector, K., Henson, R., and Martin, A. 2006. Repetition and the brain: neural models of stimulus-specific effects. Trends Cogn. Sci. 10, 14–23.
Grill-Spector, K., Knouf, N., and Kanwisher, N. 2004. The fusiform face area subserves face perception, not generic within-category identification. Nature Neurosci. 7, 555–562.
Gross, C. G. 2005. Processing the facial image: a brief history. Am. Psychol. 60, 755–763.
Gross, C. G., Rocha-Miranda, C. E., and Bender, D. B. 1972. Visual properties of neurons in intero-temporal cortex of the macaque. J. Neurophysiol. 35, 96–111.
Grusser, O. J. and Landis, T. 1991. Visual Agnosias and Other Disturbances of Visual Perception and Cognition. Macmillan.
Haig, N. D. 1984. The effect of feature displacement on face recognition. Perception 13, 5–12.
Harris, A. and Nakayama, K. 2007. Rapid face-selective adaptation of an early extrastriate component in MEG. Cereb. Cortex 17, 63–70.
Harris, A., Duchaine, B., and Nakayama, K. 2005. Normal and abnormal face selectivity of the M170 response in developmental prosopagnosics. Neuropsychologia 43, 2125–2136.
Hassan, U., Avidan, G., Deouell, L. Y., Bentin, S., and Malach, R. 2003. Face-selective activation in a congenital prosopagnosic subject. J. Cogn. Neurosci. 15, 419–431.
Haxby, J. V., Hoffman, E. A., and Gobbini, M. I. 2000. The distributed human neural system for face perception. Trends Cogn. Sci. 4, 223–233.
Hecaen, H. and Angelergues, R. 1962. Agnosia for faces (prosopagnosia). Arch. Neurol. 7, 92–100.
Henke, K., Schweinberger, S. R., Grigo, A., Klos, T., and Sommer, W. 1998. Cortex 34, 289–296.
Henson, R. N., Shallice, T., Gorno-Tempini, M. L., and Dolan, R. J. 2002. Face repetition effects in implicit and explicit memory tests as measured by fMRI. Cereb. Cortex 12, 178–186.
Hoff, H. and Pöltz, O. 1937. Über eine optisch-agnostische Störung des 'Physiognomie-Gedächtnisses'. Z. Ges. Neurol. Psychiat. 54, 55–88.
Hoffman, E. A. and Haxby, J. V. 2000. Distinct representations of eye gaze and identity in the distributed human neural system for face perception. Nat. Neurosci. 3, 80–84.
Hole, G. 1994. Configurational factors in the perception of unfamiliar faces. Perception 23, 65–74.
Hooker, C. I., Paller, K. A., Gitelman, D. R., Parrish, T. B., Mesulam, M. M., and Reber, P. J. 2003. Brain networks for analyzing eye gaze. Cogn. Brain Res. 17, 406–418.
Horovitz, S. G., Rossion, B., Skudlarski, P., and Gore, J. C. 2004. Parametric design and correlational analyses help integrating fMRI and electrophysiological data during face processing. Neuroimage 22, 1587–1595.
Humphreys, G. W. and Riddoch, M. J. 1987. To see but not to see: a case of visual agnosia, Lawrence Erlbaum.
Humphreys, G. W., Donnelly, N., and Riddoch, M. J. 1993. Expression is computed separately from facial identity, and it is computed separately for moving and static faces: neuropsychological evidence. Neuropsychologia 31, 173–181.
Humphreys, K., Minshew, N., Leonard, G. L., and Behrmann, M. 2007. A fine-grained analysis of facial expression processing in high-functioning adults with autism. Neuropsychologia 45, 685–695.
Iidaka, T., Matsumoto, A., Haneda, K., Okada, T., and Sadato, N. 2006. Hemodynamic and electrophysiological relationship involved in human face processing: evidence from a combined fMRI-ERP study. Brain Cogn. 60, 176–186.
Itier, R. J. and Taylor, M. J. 2004a. Effects of repetition learning on upright, inverted and contrast-reversed face processing using ERPs. Neuroimage 21, 1518–1532.
Itier, R. J. and Taylor, M. J. 2004b. Face inversion and contrast-reversal effects across development: in contrast to the expertise theory. Dev. Sci. 7, 246–260.
Itier, R. J., Herdman, A. T., George, N., Cheyne, D., and Taylor, M. J. 2006. Inversion and contrast-reversal effects on face processing assessed by MEG. Brain Res. 1115, 108–120.
Jackson, J. H. 1876. Case of large cerebral tumour without optic neuritis, and with left hemiplegia and imperception. Roy. Ophthalm. Hosp. Rep. 8, 434–444.
Jacques, C. and Rossion, B. 2004. Concurrent processing reveals competition between visual representations of faces. Neuroreport 15, 2417–2421.
Jeffreys, D. A. and Tukmachi, E. S. 1992. The vertex-positive scalp potential evoked by faces and by objects. Exp. Brain Res. 91, 340–350.
Johnson, K. J. and Fredrickson, B. L. 2005. ''We all look the same to me'': positive emotions eliminate the own-race effect in face recognition. Psychol. Sci. 16, 875–881.
Johnson, M. H. and Morton, J. 1991. Biology and Cognitive Development: The Case of Face Recognition, Blackwell.
Johnson, M. H., Dziurawiec, S., Ellis, H., and Morton, J. 1991. Newborns' preferential tracking of face-like stimuli and its subsequent decline. Cognition 40, 1–19.
Joyce, C. and Rossion, B. 2005. The face-sensitive N170 and VPP components manifest the same brain processes: the effect of reference electrode site. Clin. Neurophysiol. 116, 2613–2631.
Kanwisher, N. 2000. Domain specificity in face perception. Nat. Neurosci. 3, 759–763.
Kanwisher, N., McDermott, J., and Chun, M. 1997. The fusiform face area: a module in human extrastriate cortex specialized for face perception. J. Neurosci. 17, 4302–4311.
Kelly, D. J., Quinn, P. C., Slater, A., Lee, K., Gibson, A., Smith, M., Ge, L., and Pascalis, O. 2005. Three-month-olds, but not newborns, prefer own-race faces. Dev. Sci. 8, F31–F36.
Kemp, R., McManus, C., and Pigott, T. 1990. Sensitivity to the displacement of facial features in negative and inverted images. Perception 19, 531–543.
Kennerknecht, I., Grueter, T., Welling, B., Wentzek, S., Horst, J., Edwards, S., and Grueter, M. 2006. First report of prevalence of non-syndromic hereditary prosopagnosia (HPA). Am. J. Med. Genet. A 140, 1617–1622.
Kreiman, G., Koch, C., and Fried, I. 2000. Category-specific visual responses of single neurons in the human medial temporal lobe. Nat. Neurosci. 3, 946–953.
Kress, T. and Daum, I. 2003a. Developmental prosopagnosia: a review. Behav. Neurol. 14, 109–121.
Kress, T. and Daum, I. 2003b. Event-related potentials reflect impaired face recognition in patients with congenital prosopagnosia. Neurosci. Lett. 352, 133–136.
Kuhl, P. K., Williams, K., Lacerda, F., Stevens, K., and Lindblom, B. 1992. Linguistic experience alters phonetic perception in infants by 6 months of age. Science 255, 606–608.
Landis, T., Cummings, J. L., Benson, D., and Palmer, E. P. 1986a. Loss of topographic familiarity. An environmental agnosia. Arch. Neurol. 43, 132–136.
Landis, T., Cummings, J. L., Christen, L., Bogen, J. E., and Imhof, H. G. 1986b. Are unilateral right posterior cerebral lesions sufficient to cause prosopagnosia? Clinical and radiological findings in six additional patients. Cortex 22, 243–252.

Landis, T., Regard, M., Bliestle, A., and Kleihues, P. 1988. Prosopagnosia and agnosia for non-canonical views: an autopsied case. Brain 111, 1287–1297.
Le Grand, R., Cooper, P., Mondloch, C., Lewis, T., Sagiv, N., de Gelder, B., and Maurer, D. 2006. What aspects of face processing are impaired in developmental prosopagnosia? Brain Cogn. 61, 139–158.
Le Grand, R., Mondloch, C. J., Maurer, D., and Brent, H. P. 2001. Neuroperception. Early visual experience and face processing. Nature 410, 890.
Le Grand, R., Mondloch, C. J., Maurer, D., and Brent, H. P. 2003. Expert face processing requires visual input to the right hemisphere during infancy. Nat. Neurosci. 6, 1108–1112.
Le Grand, R., Mondloch, C. J., Maurer, D., and Brent, H. P. 2004. Impairment in holistic face processing following early visual deprivation. Psychol. Sci. 15, 762–768.
Leder, H. and Bruce, V. 2000. When inverted faces are recognized: the role of configural information in face recognition. Q. J. Exp. Psychol. A 53, 513–536.
Levin, D. 2000. Race as a visual feature: using visual search and perceptual discrimination tasks to understand face categories and the cross-race recognition deficit. J. Exp. Psychol. Gen. 129, 559–574.
Levine, D. N. and Calvanio, R. 1989. Prosopagnosia: a defect in visual configural processing. Brain Cogn. 10, 149–170.
Levy, J., Trevarthen, C., and Sperry, R. W. 1972. Reception of bilateral chimeric figures following hemispheric deconnexion. Brain 95, 61–78.
Lewis, T. L. and Maurer, D. 1992. The development of the temporal and nasal visual fields during infancy. Vision Res. 32, 903–911.
Liegeois, F., Bentejac, L., and de Schonen, S. 2000. When does inter-hemispheric integration of visual events emerge in infancy? A developmental study on 19- to 28-month-old infants. Neuropsychologia 38, 1382–1389.
Liu, J., Harris, A., and Kanwisher, N. 2002. Stages of processing in face perception: an MEG study. Nat. Neurosci. 5, 910–916.
Liu, J., Higuchi, M., Marantz, A., and Kanwisher, N. 2000. The selectivity of the occipitotemporal M170 for faces. Neuroreport 11, 337–341.
MacLin, O. H. and Malpass, R. S. 2003. The ambiguous-race face illusion. Perception 32, 249–252.
Malcolm, G., Leung, C., and Barton, J. J. S. 2005. Regional variations in the inversion effect for faces: differential effects for feature shape, spatial relations, and external contour. Perception 33, 1221–1231.
Marotta, J. J., Genovese, C. R., and Behrmann, M. 2001. A functional MRI study of face recognition in patients with prosopagnosia. Neuroreport 13, 1581–1587.
Maurer, D. and Salapatek, P. 1976. Developmental changes in the scanning of faces by young infants. Child Dev. 47, 523–527.
Maurer, D., Grand, R. L., and Mondloch, C. J. 2002. The many faces of configural processing. Trends Cogn. Sci. 6, 255–260.
Mayer, E. and Rossion, B. 2006. Prosopagnosia. In: The Behavioral and Cognitive Neurology of Stroke (*eds*. O. Godefroy and J. Bogousslavsky), pp. 316–334. Cambridge University Press.
McCarthy, G., Puce, A., Belger, A., and Allison, T. 1999. Electrophysiological studies of human face perception. II: Response properties of face-specific potentials generated in occipitotemporal cortex. Cereb. Cortex 9, 431–444.
McCarthy, G., Puce, A., Gore, J. C., and Allison, T. 1997. Face-specific processing in the human fusiform gyrus. J. Cogn. Neurosci. 9, 605–610.
McConachie, H. 1976. Developmental prosopagnosia. A single case report. Cortex 12, 76–82.
McKone, E. and Boyer, B. L. 2006. Sensitivity of 4-year-olds to featural and second-order relational changes in face distinctiveness. J. Exp. Child Psychol. 94, 134–162.
McKone, E. and Kanwisher, N. 2005. Does the Human Process Objects of Expertise Like Faces? A Review of the Evidence. In: From Monkey Brain to Human Brain (*eds*. S. Dehaene, J. R. Duhamel, M. Hauser, and G. Rizzolatti), pp. 339–356. MIT Press.
McKone, E. and Robbins, R. 2007. The evidence rejects the expertise hypothesis: a reply to Gauthier and Bukach. Cognition 103, 331–336.
McKone, E., Kanwisher, N., and Duchaine, B. 2007. Can generic expertise explain special processing for faces? Trends Cogn. Sci. 11, 8–15.
McMullen, P. A., Fisk, J. D., Phillips, S. J., and Maloney, W. 2000. Apperceptive agnosia and face recognition. Neurocase 6, 403–414.
McNeil, J. and Warrington, E. 1993. Prosopagnosia: a face-specific disorder. Q. J. Exp. Psychol. A 46, 1–10.
Meadows, J. C. 1974. The anatomical basis of prosopagnosia. J. Neurol. Neurosurg. Psychiat. 37, 489–501.
Meltzoff, A. N. and Moore, M. K. 1977. Imitation of facial and manual gestures by human neonates. Science 198, 74–78.
Michel, C., Rossion, B., Han, J., Chung, C. S., and Caldara, R. 2006. Holistic processing is finely tuned for faces of one's own race. Psychol. Sci. 17, 608–615.
Mondloch, C. J., Le Grand, R., and Maurer, D. 2002. Configural face processing develops more slowly than featural face processing. Perception 31, 553–566.
Moore, C. D., Cohen, M. X., and Ranganath, C. 2006. Neural mechanisms of expert skills in visual working memory. J. Neurosci. 26, 11187–11196.
Moscovitch, M. and Moscovitch, D. A. 2000. Super face-inversion effects for isolated internal or external features and for fractured faces. Cogn. Neuropsych. 18, 201–220.
Moscovitch, M., Winocur, G., and Behrmann, M. 1997. What is special about face recognition: nineteen experiments on a person with visual object agnosia and dyslexia but normal face recognition. J. Cogn. Neurosci. 9, 555–604.
Nunn, J. A., Postma, P., and Pearson, R. 2001. Developmental prosopagnosia: should it be taken at face value? Neurocase 7, 15–27.
Op de Beeck, H., Baker, C., DiCarlo, J., and Kanwisher, N. 2006. Discrimination training alters object representations in human extrastriate cortex. J. Neurosci. 26, 13025–13036.
Otsuka, Y., Nakato, E., Kanazawa, S., Yamaguchi, M. K., Watanabe, S., and Kakigi, R. 2007. Neural activation to upright and inverted faces in infants measured by near infrared spectroscopy. Neuroimage 34, 399–406.
Pascalis, O., de Haan, M., and Nelson, C. A. 2002. Abstract is face processing species-specific during the first year of life? Science 296, 1321–1333.
Pascalis, O., De Schonen, S., Morton, J., Deruelle, C., and Fabregrenet, M. 1995. Mothers face recognition by neonates – a replication and an extension. Inf. Behav. Dev. 18, 79–85.
Pascalis, O., Scott, L. S., Kelly, D. J., Shannon, R. W., Nicholson, E., Coleman, M., and Nelson, C. A. 2005. Plasticity of face processing in infancy. Proc. Natl. Acad. Sci. U. S. A. 102, 5297–5300.
Pellicano, E. and Rhodes, G. 2003. Holistic processing of faces in preschool children and adults. Psychol. Sci. 14, 618–622.
Perrett, D. I., Hietanen, J. K., Oram, M. W., and Benson, P. J. 1992. Organization and functions of cells responsive to faces in the temporal cortex. Phil. Trans. Royal Soc. Lond. B 335, 23–30.
Perrett, D. I., Oram, M. W., and Ashbridge, E. 1998. Evidence accumulation in cell populations responsive to faces: an account of generalisation of recognition without mental transformations. Cognition 67, 111–145.
Perrett, D. I., Rolls, E. T., and Caan, W. 1982. Visual neurones responsive to faces in the monkey temporal cortex. Exp. Brain Res. 47, 329–342.

Perrett, D. I., Smith, P. A., Potter, D. D., Mistlin, A. J., Head, A. S., Milner, A. D., and Jeeves, M. A. 1985. Visual cells in the temporal cortex sensitive to face view and gaze direction. Proc. Royal Soc. Lond. B 223, 293–317.

Puce, A., Allison, T., and McCarthy, G. 1999. Electrophysiological studies of human face perception. III: Effects of top-down processing on face-specific potentials. Cereb. Cortex 9, 445–458.

Quaglino, A., Borelli, G. B., Della Sala, S., and Young, A. W. 2003. Quaglino's 1867 case of prosopagnosia. Cortex 39, 533–540.

Quiroga, R. Q., Reddy, L., Kreiman, G., Koch, C., and Fried, I. 2005. Invariant visual representation by single neurons in the human brain. Nature 435, 1102–1107.

Reed, C. L., Stone, V. E., Bozova, S., and Tanaka, J. 2003. The body-inversion effect. Psychol. Sci. 14, 302–308.

Reed, C. L., Stone, V. E., Grubb, J. D., and McGoldrick, J. E. 2006. Turning configural processing upside down: part and whole body postures. J. Exp. Psychol. Hum. Percept. Perform. 32, 73–87.

Rhodes, G., Brake, S., Taylor, K., and Tan, S. 1989. Expertise and configural coding in face recognition. Br. J. Psychol. 80, 313–331.

Riesenhuber, M., Jarudi, I., Gilad, S., and Sinha, P. 2004. Face processing in humans is compatible with a simple shape-based model of vision. Biological letters.

Robbins, R. and McKone, E. 2007. No face-like processing for objects-of-expertise in three behavioural tasks. Cognition 103, 34–79.

Rossion, B., Caldara, R., Seghier, M., Schuller, A. M., Lazeyras, F., and Mayer, E. 2003. A network of occipito-temporal face-sensitive areas besides the right middle fusiform gyrus is necessary for normal face processing. Brain 126, 2381–2395.

Rossion, B., Curran, T., and Gauthier, I. 2002. A defense of the subordinate-level expertise account for the N170 component. Cognition 85, 189–196.

Rotshtein, P., Henson, R. N., Treves, A., Driver, J., and Dolan, R. J. 2005. Morphing Marilyn into Maggie dissociates physical and identity face representations in the brain. Nat. Neurosci. 8, 107–113.

Sackett, G. P. 1966. Monkeys reared in isolation with pictures as visual input: evidence for an innate releasing mechanism. Science 16, 1468–1473.

Sadr, J., Duchaine, B., and Nakayama, K. 2004. The perception of facial attractiveness in prosopagnosia. J. Vision 4, 249–250.

Sangrigoli, S. and De Schonen, S. 2004. Recognition of own-race and other-race faces by three-month-old infants. J. Child Psychol. Psychiatry 45, 1219–1227.

Schiltz, C. and Rossion, B. 2006. Faces are represented holistically in the human occipito-temporal cortex. Neuroimage 32, 1385–1394.

Schiltz, C., Goebel, R., Schiltz, C., and Rossion, B. 2007. Understanding the functional neuroanatomy of acquired prosopagnosia. Neuroimage 35, 836–852.

Schwarzlose, R. F., Baker, C. I., and Kanwisher, N. 2005. Separate face and body selectivity on the fusiform gyrus. J. Neurosci. 25, 11055–11059.

Sergent, J. 1991. Functional neuroanatomy of face recognition: a positron emission tomography study. Rev. Neuropsychol. 1, 119–156.

Sergent, J. and Signoret, J. L. 1992. Varieties of functional deficits in prosopagnosia. Cereb. Cortex 2, 375–388.

Sergent, J. and Villemure, J. G. 1989. Prosopagnosia in a right hemispherectomized patient. Brain 112, 975–995.

Sergent, J., Ohta, S., and MacDonald, B. 1992. Functional neuroanatomy of face and object processing. A positron emission tomography study. Brain 115, 15–36.

Slater, A., Bremner, J. G., Johnson, S. P., Sherwood, P., Hayes, R., and Brown, E. 2000. Newborn infants' preference for attractive faces: the role of internal and external facial features. Infancy 1, 265–274.

Slater, A., Von der Schulenburg, C., Brown, E., Badenoch, M., Butterworth, G., Parsons, S., and Samuels, C. 1998. Newborn infants prefer attractive faces. Inf. Behav. Dev. 21, 345–354.

Slaughter, V., Heron, M., and Sim, S. 2002. Development of preferences for the human body shape in infancy. Cognition 85, B71–B81.

Sorger, B., Goebl, R., Schiltz, C., and Rossion, B. 2007. Understanding the functional neuroanatomy of prosopagnosia. Neuroimage 35, 836–852.

Tanaka, J. W. and Farah, M. J. 1993. Parts and wholes in face recognition. Q. J. Exp. Psychol. A 46A, 225–245.

Tanaka, J. W. and Sengco, J. A. 1997. Features and their configuration in face recognition. Mem. Cognit. 25, 583–592.

Tanaka, J. W., Kiefer, M., and Bukach, C. M. 2004. A holistic account of the own-race effect in face recognition: evidence from a cross-cultural study. Cognition 93, B1–B9.

Tarr, M. J. and Gauthier, I. 2000. FFA: a flexible fusiform area for subordinate-level visual processing automatized by expertise. Nat. Neurosci. 3, 764–769.

Temple, C. 1992. Developmental Memory Impairment: Faces and Patterns. In: Mental Lives: Case Studies in Cognition (*ed*. R. Campbell), pp. 199–215. Blackwell.

Tong, F., Nakayama, K., Moscovitch, M., Weinrib, O., and Kanwisher, N. 2000. Response properties of the human fusiform face area. Cogn. Neuropsychol. 17, 257–279.

Tong, F., Nakayama, K., Vaughan, J. T., and Kanwisher, N. 1998. Binocular rivalry and visual awareness in human extrastriate cortex. Neuron 21, 753–759.

Tranel, D., Damasio, A. R., and Damasio, H. 1988. Intact recognition of facial expression, gender, and age in patients with impaired recognition of face identity. Neurology 38, 690–696.

Tsao, D. Y., Freiwald, W. A., Tootell, R. B., and Livingston, M. S. 2006. A cortical region consisting entirely of face-selective cells. *Science* 311, 670–674.

Tsao, D. Y. and Freiwald, W. A. 2006. What's so special about the average face? Trends Cogn. Sci. 10, 391–393.

Turati, C., Sangrigoli, S., Ruel, J., and de Schonen, S. 2004. Evidence of the face inversion effect in 4-month-old infants. Infancy 6, 275–297.

Uttner, L., Bliem, H., and Danek, A. 2002. Prosopagnosia after unilateral right cerebral infarction. J. Neurol. 249, 933–935.

Valentine, T. and Bruce, V. 1986. The effect of race, inversion and encoding activity upon face recognition. Acta Psychol. (Amst.) 61, 259–273.

Valentine, T., Powell, J., Davidoff, J., Letson, S., and Greenwood, R. 2006. Prevalence and correlates of face recognition impairments after acquired brain injury. Neuropsychol. Rehabil. 16, 272–297.

von Kriegstein, K., Kleinschmidt, A., and Giraud, A. L. 2006. Voice recognition and cross-modal responses to familiar speakers' voices in prosopagnosia. Cereb. Cortex 16, 1314–1322.

Wada, Y. and Yamamoto, T. 2001. Selective impairment of facial recognition due to a haematoma restricted to the right fusiform and lateral occipital gyrus. J. Neurol. Neurosurg. Psychiatry 71, 254–257.

Waitt, C., Little, A. C., Wolfensohn, S., Honess, P., Brown, A. P., Buchanon-Smith, H. M., and Perrett, D. I. 2003. Evidence from rhesus macaques suggests that male coloration plays a role in female primate mate choice. Proc. Biol. Sci. 270, S144–S146.

Werker, J. F. and Tees, R. C. 1984. Phonemic and phonetic factors in adult cross-language speech perception. J. Acoust. Soc. Am. 75, 1866–1878.
Wigan, A. L. 1844. The Duality of the Mind. Longman.
Xu, Y., Liu, J., and Kanwisher, N. 2005. The M170 is selective for faces, not for expertise. Neuropsychologia 43, 588–597.
Yin, R. 1969. Looking at upside down faces. J. Exp. Psychology 81, 141–145.
Young, A. W., Hellawell, D., and Hay, D. C. 1987. Configurational information in face perception. Perception 16, 747–759.
Yovel, G. and Duchaine, B. 2006. Specialized face perception mechanisms extract both part and spacing information: evidence from developmental prosopagnosia. J. Cogn. Neurosci. 18, 580–593.
Yovel, G. and Kanwisher, N. 2004. Face perception: domain specific, not process specific. Neuron 44, 1–20.
Yovel, G. and Kanwisher, N. 2005. The neural basis of the behavioral face-inversion effect. Curr. Biol. 15, 2256–2262.
Yovel, G. and Kanwisher, N. 2007. What makes upright faces special? Evidence from individual differences. Abstract presented in the Visual Sciences Society Meeting. Sarasota, USA.
Yovel, G. and Tambini, A. 2007. Are faces and bodies processed by separate mechanisms? Evidence from individual differences. Paper presented at the Cognitive Neuroscience Society Meeting, NY, USA.
Yovel, G., Levy, J., Graboweckey, M., and Paller, K. 2003. Neural correlates of the left-visual-field superiority in face perception appears at multiple stages of face perception. J. Cogn. Neurosci. 15, 462–467.
Yovel, G., Paller, K. A., and Levy, J. 2005. A whole face is more than the sum of its parts: Interactive processing in face perception. Vis. Cogn. 12, 337–352.
Yue, X., Tjan, B. S., and Biederman, I. 2006. What makes faces special? Vision Res. 46, 3802–3811.
Zihl, J. and von Cramon, D. 1986. Zerebrale Sehstörungen. Kohlhammer.

Further Reading

Allison, T., Puce, A., Spencer, D. D., and McCarthy, G. 1999. Electrophysiological studies of human face perception. I: Potentials generated in occipitotemporal cortex by face and non-face stimuli. Cereb. Cortex 9, 415–430.
Braunstein, M. L., Hoffman, D. D., and Saidpour, A. 1989. Parts of visual objects: an experimental test of the minima rule. Perception 18, 817–826.
Choisser, B. Faceblind! Available online at: http://www.choisser.com/faceblind, (accessed on 16 May 2007).
de Heering, A., Houthuys, S., and Rossion, B. 2007. Holistic face processing is mature at 4 years of age: Evidence from the composite face effect. J. Exp. Child Psychol. 96, 57–70.
Duchaine, B. and Nakayama, K. 2006. The Cambridge Face Memory Test: results for neurologically intact individuals and an investigation of its validity using inverted face stimuli and prosopagnosic participants. Neuropsychologia 44, 576–585.
Harris, A., Duchaine, B., and Nakayama, K. 2005. Normal and abnormal face selectivity of the M170 response in developmental prosopagnosics. Neuropsychologia 43, 2125–2136.
Hasson, U., Avidan, G., Deouell, L. Y., Bentin, S., and Malach, R. 2003. Face-selective activation in a congenital prosopagnosic subject. J. Cogn. Neurosci. 15, 419–431.
Henson, R. N., Goshen-Gottstein, Y., Ganel, T., Otten, L. J., Quayle, A., and Rugg, M. D. 2003. Electrophysiological and haemodynamic correlates of face perception, recognition and priming. Cereb. Cortex 13, 793–805.
Hooker, C. I., Paller, K. A., Gitelman, D. R., Parrish, T. B., Mesulam, M. M., and Reber, P. J. 2003. Brain networks for analyzing eye gaze. Brain Res. Cogn. Brain Res. 17, 406–418.
Jacques, C. and Rossion, B. 2004. Concurrent processing reveals competition between visual representations of faces. Neuroreport 15, 2417–2421.
Jeffreys, D. A. and Tukmachi, E. S. 1992. The vertex-positive scalp potential evoked by faces and by objects. Exp. Brain. Res. 91, 340–350.
Kelly, R. L. 1995. The Foraging Spectrum: Diversity in Hunter-Gatherer Lifeways. Smithsonian Institution Press.
Kemp, R., McManus, C., and Pigott, T. 1990. Sensitivity to the displacement of facial features in negative and inverted images. Perception 19, 531–543.
Kreiman, G., Koch, C., and Fried, I. 2001. Category-specific visual responses of single neurons in the human medial temporal lobe. Nat. Neurosci. 3, 946–953.
Liegeios, F., Bentejack, L., and de Schonen, S. 2000. When does inter-hemispheric integration of visual events emerge in infancy? A developmental study on 19- and 28-month old infants. Neuropsychologia 38, 1382–1389.
Malcolm, G., Leung, C., and Barton, J. J. S. 2005. Regional variations in the Inverson effect for Faces: Differential effects for feature shape, spatial relations, and external contour. Perception 33, 1221–1231.
Mazard, A., Schiltz, C., and Rossion, B. 2006. Recovery from adaptation to facial identity is larger for upright than inverted faces in the human occipito-temporal cortex. Neuropsychologia 44, 912–922.
Rotshtein, P., Henson, R. N., Treves, A., Driver, J., and Dolan, R. J. 2005. Morphing Marilyn into Maggie dissociates physical and identity face representations in the brain. Nat. Neurosci. 8, 107–113.
Schiltz, C., Sorger, B., Caldara, R., Ahmed, F., Mayer, E., Goebel, R., and Rossion, B. 2006. Impaired face discrimination in acquired prosopagnosia is associated with abnormal response to individual faces in the right middle fusiform gyrus. Cereb. Cortex 16, 574–586.
Slater, A. and Kirby, R. 1998. Innate and learned perceptual abilities in the newborn infant. Exp. Brain Res. 123, 90–94.
Tsao, D. Y. and Freiwald, W. A. 2006. What's so special about the average face? Trends Cogn. Sci. 10, 391–393.
Wada, Y. and Yamamoto, T. 2001. Selective impairment of facial recognition due to a haematoma to the right fusiform and lateral occipital region. J. Neurol. Neurosurg. Psychiatry 71, 254–257.
Yue, X., Tjan, B. S., and Biederman, I. 2006. What makes faces special? Vis. Res. 46, 3802–3811.

Relevant Website

http://www.faceblind.org – Harvard University/University College London Prosopagnosia Research Center. Faceblind

2.22 The VOR: A Model for Visual-Motor Plasticity

D E Angelaki, Washington University School of Medicine, St. Louis, MO, USA

© 2008 Elsevier Inc. All rights reserved.

2.22.1	Two Types of Vestibulo-Ocular Reflexes	360
2.22.1.1	Rotational Vestibulo-Ocular Reflex: Basic Properties and Frequency Dependence	360
2.22.1.2	Rotational Vestibulo-Ocular Reflex: Three-Neuron-Arc and Neural Integrator	362
2.22.1.3	Translational Vestibulo-Ocular Reflex: Basic Properties	363
2.22.1.4	Neural Circuits and Pathways	365
2.22.2	Functional Plasticity	365
2.22.2.1	Behavioral Observations	365
2.22.2.2	Neural Signatures of Plasticity: Identifying the Sites for Vestibulo-Ocular Reflex Learning?	367
References		368

Glossary

conjugate eye movements Eye movements of similar amplitude and direction for both eyes.

disjunctive eye movements Eye movements of different amplitude for the two eyes. Disjunctive components are typically quantified by measuring the vergence angle, defined as the difference between right and left eye position.

nystagmus A saw toothlike (zigzag) pattern where slow deviations in eye position are interleaved with oppositely directed quick phases (reflexive saccades) that keep eye position within the oculomotor range.

ocular following reflex Short-latency reflexive eye movements in response to the optic flow experienced during self-motion. These responses, which can be either conjugate or disjunctive, are typically studied during the first ~100 ms of brief presentations of visual motion (open-loop conditions).

optokinetic nystagmus (OKN) A reflexive visuo-ocular response to the en bloc motion of a large visual field that matches slow phase eye velocity to the velocity of the visual surround. Optokinetic after nystagmus (OKAN) refers to the decay of slow velocity to zero after surround rotation stops.

otolith organs Inertial sensors that are located in the inner ear and consist of receptor hair cells with different polarization vectors distributed over the utricular (approximately horizontal) and the saccular (approximately in the sagittal plane) maculae.

retinal image slip Difference between the velocity of the movement of a retinal image and the eye that is picked up by motion detectors in the visual system.

semicircular canal One of the two sets of vestibular end organs that measure angular acceleration of the head. In each ear, there are three semicircular canals: horizontal lateral, anterior, and posterior. Each canal senses angular motion in its respective plane.

vergence The angular difference between right and left eye position. Vergence angle is zero when looking at optical infinity and reaches higher values the closer the target is to the eyes.

vestibular end organs A set of balance receptors in the inner ear, consisting of the otolith organs (utricle and sacculus) that encode linear acceleration and the semicircular canals (horizontal lateral, anterior and posterior) that measure angular acceleration.

vestibulo-ocular reflex cancellation Head movement while fixating a head-fixed target that results in suppression of compensatory eye movements.

2.22.1 Two Types of Vestibulo-Ocular Reflexes

The vestibulo-ocular reflex (VOR) describes a group of eye movements whose goal is to rotate the eyeball in a particular direction and with a specific speed such that the world remains stable on the retina during head movement. The signals driving these eye movements arise from the vestibular labyrinths that house the sensory receptors of our sixth sense, enabling us to detect the movement of our head through space. The vestibular labyrinths contain two types of specialized sensory receptors (Figure 1(a)): (1) three semicircular canals (horizontal, anterior, and posterior) that transduce rotational head movements (angular acceleration); and (2) two otolith organs (utricle and saccule) that sense linear acceleration. Linear accelerations are typically experienced during translational movements and/or reorientations of the head relative to gravity (a form of linear acceleration). Collectively the five vestibular end organs contain sensory neuroepithelia that sense both angular and linear accelerations in three dimensions (3D).

Unlike the five senses described in this encyclopedia, there is limited conscious perception of this vestibular sense, largely because vestibular signals rarely occur in isolation in the central nervous system. Instead, neurons sensitive to vestibular stimulation are typically also responsive to visual, somatosensory, or motor-related signals. The VOR is unique in representing the sole behavior that is driven exclusively by labyrinthine signals. Because of this, as well as its relatively simple neuronal organization, the VOR has often been used to study vestibular function. Depending on whether the head movement consists of a rotation or a translation, these reflexive responses can be categorized into two types, the rotational VOR (RVOR; e.g., when the head rotates to the right, the eyes rotate to the left) and the translational VOR (TVOR; e.g., when the head translates to the right, the eyes rotate to the left). The RVOR represents a phylogenetically old reflex, shared by many invertebrates and all vertebrate species. In contrast, the TVOR is well developed in the primate brain where foveal visual acuity and stereovision are functionally important (Miles, F. A., 1993; 1998; Angelaki, D. E. and Hess, B. J., 2005). This chapter first outlines the unique properties of each VOR type and then describes their neuronal substrates and highly adaptive ability.

2.22.1.1 Rotational Vestibulo-Ocular Reflex: Basic Properties and Frequency Dependence

The RVOR is driven by semicircular canal signals that sense how fast our head rotates. It is studied

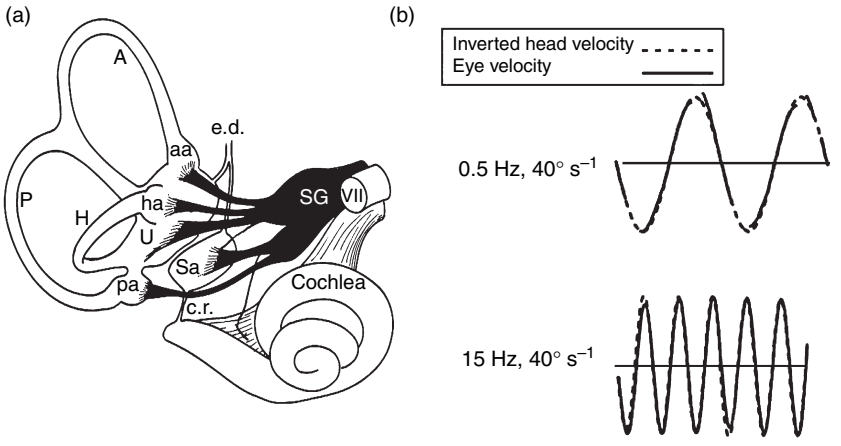

Figure 1 (a) The membranous vestibular labyrinth. Each semicircular canal encodes rotation in a particular plane and has a sensory organ located in an enlargement, the ampulla (aa, ha, and pa, ampullae of the anterior (A), horizontal (H) and posterior (P) canals, respectively). There are two otolith organs that sense linear accelerations, the utricle (U) and the saccule (Sa). The vestibular end organs are innervated by a separate branch of the VIII cranial nerve, whose cell bodies are in Scarpa's ganglion (SG). e.d., endolymphatic duct; c.r., canal reunions connecting the sacculus with the cochlea; VII, facial nerve. Redrawn with permission from Hardy, M. 1934. Observations on the innervation of the macula sacculi in man. Anat. Rec. 59, 403–418. (b) Typical rotational vestibulo-ocular reflex responses during sinusoidal rotation at 0.5 and 15 Hz. Redrawn from Sadeghi, S. G., Minor, L. B., and Cullen, K. E. 2006. Dynamics of the horizontal vestibuloocular reflex after unilateral labyrinthectomy: response to high frequency, high acceleration, and high velocity rotations. Exp. Brain Res. 175, 471–484, Springer.

using either sinusoidal oscillations (Figure 1(b)) or constant velocity rotations (Figure 2(a)). Its goal is to generate an eye movement with a velocity that is matched in amplitude but opposite in direction to head velocity (Figure 1(b)). For large head rotations, the RVOR is often manifested as nystagmus, a saw toothlike (zigzag) pattern where slow deviations in eye position are interleaved with oppositely directed quick phases (reflexive saccades) that keep eye position within the oculomotor range (Figure 2(a), top). The involuntary fast phase segments of the RVOR are generally ignored to facilitate analysis of the more salient slow phase compensatory response segments (Figure 2(a), bottom).

The effectiveness of the RVOR is characterized by its gain, defined as the ratio of eye velocity over head velocity. The exact value of RVOR gain varies from species to species, being largest in monkeys (where horizontal RVOR gain at frequencies above ~0.1 Hz in darkness is close to ideal; that is, ~0.9–1.0; Keller, E. L., 1978), but smaller in humans; that is, ~0.5–0.8; Benson, A. J., 1970; Tweed, D. *et al.*, 1994). High RVOR gains are also typical during rotation at high frequencies (Lasker, D. M. *et al.*, 1999; Huterer, M. and Cullen, K. E., 2002; Ramachandran, R. and Lisberger, S. G., 2005). Like the vestibular periphery that senses movement in 3D, the RVOR represents a 3D reflex (Robinson, D. A., 1982; Tweed, D. *et al.*, 1994; Angelaki, D. E. *et al.*, 1996): yaw (left–right) rotation elicits horizontal eye movements, pitch (up–down) rotation elicits vertical eye movements, and roll (right–left ear down) rotation elicits torsional eye movements.

For sinusoidal rotations, in addition to its gain, RVOR dynamics are also quantified by computing what is called the phase shift, defined as the timing difference between peak head and eye motion. The RVOR phase is typically perfectly compensatory, with phase near 0° (Figure 1(b); Tweed, D. *et al.*, 1994; Angelaki, D. E. and Hess, B. J., 1996; Lasker, D. M. *et al.*, 1999; Sadeghi, S. G. *et al.*, 2006). However, at frequencies lower than ~0.05–0.10 Hz gain declines and progressively larger phase leads are introduced. This occurs because of the properties of semicircular canal afferents, which accurately encode velocity only above ~0.05 Hz (Fernandez, C. and Goldberg, J. M., 1971). As a result, maintained constant velocity rotation results in an initial transient RVOR that decays out over several seconds (Figure 2(a)). Sudden cessation of rotation is encoded by the semicircular canals as a step in the opposite direction, eliciting a response typically referred to as postrotatory nystagmus (Raphan, T. and Cohen, B., 1985; Raphan, T. *et al.*, 1979; Figure 2(a)).

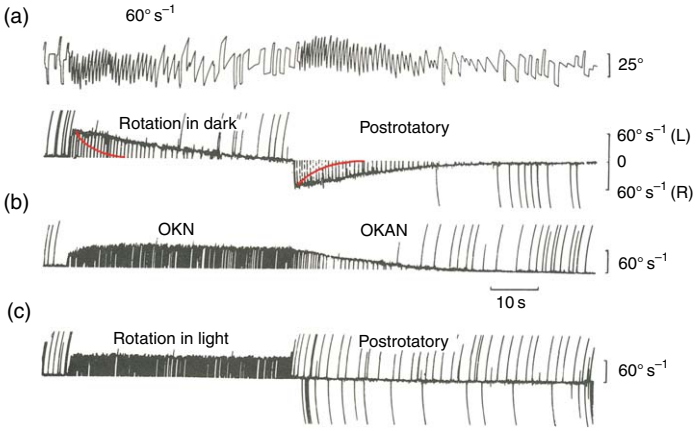

Figure 2 Interactions between the rotational vestibulo-ocular (RVOR) and optokinetic (OKN) reflexes. (a) Nystagmus in response to rotation at constant velocity (60° s^{-1}) in darkness. The top traces illustrate horizontal eye position, whereas the bottom traces plot slow-phase eye velocity (the large positive and negative spikes reflect the occurrence of fast phases). The solid red line in the lower trace illustrates the semicircular canal afferent time course, which is shorter than that of the RVOR. (b) Slow-phase eye velocity in response to a step in surround velocity, generating optokinetic nystagmus and optokinetic after nystagmus. (c) Slow-phase eye velocity in response to platform rotation in light. Note that during rotation in light the postrotatory RVOR and OKAN slow phase velocities are oppositely directed ((a) and (b)). Thus, the two after-responses cancel each other and postrotatory responses during rotation in light are small (c). Reprinted from Raphan, T. and Cohen, B. 1985. Velocity storage and the ocular response to multidimensional vestibular stimuli. Rev. Oculomot. Res. 1, 123–143, with permission from Elsevier.

How fast the RVOR decays is characterized by its time constant, defined as the time over which eye velocity decays to zero. In most species, including primates, the rate at which the RVOR response to a step in head velocity decays is slower than would be expected from semicircular canal afferents (Raphan, T. *et al.*, 1979). The difference represents a central prolongation or perseveration of the raw vestibular signal, referred to as the velocity storage integrator (for review, see Raphan, T. and Cohen, B., 1985). Although such low frequency or long duration stimuli are unnatural, particularly when delivered in darkness, they have been very useful experimentally to study multisensory interactions (for review, see Hess, B. J. and Angelaki, D. E., 1997).

An example of such velocity storage-mediated visual/vestibular interactions relates to optokinetic nystagmus (OKN), a reflexive visuo-ocular response elicited by a large patterned cylinder rotating around a stationary subject (Cohen, B. *et al.*, 1977; Collewijn, H., 1985). Following cessation of drum rotation, eye velocity declines to zero gradually (optokinetic after-nystagmus (OKAN); Cohen, B. *et al.*, 1977; Figure 2(b)). OKN provides a low-frequency complement to the RVOR during rotation in the light. Remember that during constant velocity rotation in darkness eye velocity decays to zero (Figure 2(a)). However, the same rotation in the presence of a visual surround elicits a steady-state nystagmus pattern that is sustained indefinitely, thus stabilizing the world on the retina (Figure 2(c)). This happens because the OKN increases at approximately the same rate as the RVOR decays. Similarly, when head rotation is suddenly halted, OKAN cancels out the postrotatory vestibular nystagmus, such that eye velocity drops quickly to zero. These visual/vestibular interactions are impaired after lesions that also impair velocity storage (Waespe, W. *et al.*, 1985; Schiff, D. *et al.*, 1990).

Activation of the otolith system during rotations that change head orientation relative to gravity also improves the low-frequency RVOR properties (Guedry, F. E., 1965; Baarsma, E. A. and Collewijn, H., 1975; Raphan, T. *et al.*, 1981; Cohen, B. *et al.*, 1983; Hess, B. J. and Dieringer, N., 1990; Angelaki, D. E. *et al.*, 1996). Similar to OKN, these otolith effects on the low-frequency RVOR are also mediated through the velocity storage mechanism (Cohen, B. *et al.*, 1983; Angelaki, D. E. and Hess, B. J., 1994; 1995; 1996).

2.22.1.2 Rotational Vestibulo-Ocular Reflex: Three-Neuron-Arc and Neural Integrator

One of the most important features of the RVOR is its very short latency (<10 ms; Minor, L. B. *et al.*, 1999; Huterer, M. and Cullen, K. E., 2002), which comes about because of a fast sensory vestibular transduction process and a direct, three-neuron-arc pathway (Lorente de No, R., 1935; Szentagothai, J., 1950; Figure 3). The RVOR is organized in a simple push–pull arrangement using signals from both labyrinths. For example, when the head rotates to the right, primary horizontal semicircular canal afferents on the right side increase their firing rates

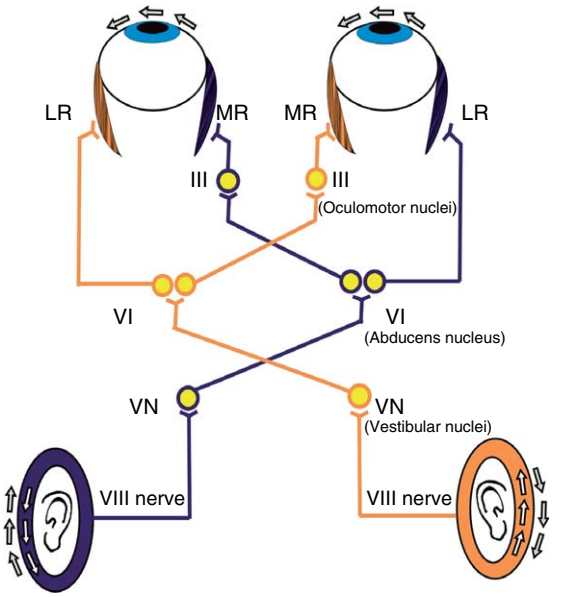

Figure 3 The push–pull organization of the horizontal (yaw) rotational vestibulo-ocular reflex. The direct path consists of a short tri-synaptic reflex consisting of vestibular afferents (VIII nerve), the vestibular nuclei (VN), motoneurons in the VI (abducens) and III (oculomotor) nuclei, and the lateral rectus (LR) and medial rectus (MR) muscles. When the head rotates to the right (arrows), the right horizontal semicircular canal afferents increase their firing rates, whereas the left afferents decrease their activities (orange versus blue colors, respectively). The excitation/inhibition is transmitted to the contralateral/ipsilateral abducens (VI) through neurons in the right/left VN, respectively. Internuclear neurons in the abducens nuclei cross the midline and terminate in the contralateral medial rectus motoneurons (III). Thus, motoneurons in the left VI and right III nuclei fire at a higher frequency, whereas those in the right VI and left III nuclei fire at a lower frequency. As a result, the left LR and right MR muscles contract, whereas the left MR and right LR muscles relax and both eyes rotate leftward.

(Figure 3, orange). This increase in activity is conveyed to the vestibular nuclei in the right side of the brain (Precht, W. and Shimazu, H., 1965) and subsequently through excitatory neuron projections to both motoneurons and internuclear neurons in the left (contralateral) abducens (IV) nucleus (Richter, A. and Precht, W., 1968; Precht, W. *et al.*, 1969). Whereas abducens motoneurons cause the left lateral rectus muscle to contract, internuclear neurons in the left abducens nucleus convey this activity onto medial rectus motoneurons in the right oculomotor nucleus (III; Highstein, S. M. and Baker, R., 1978). Activation of these pathways results in a simultaneous contraction of the lateral rectus muscle of the left eye and the medial rectus of the right eye (Figure 3, orange), causing them both to rotate to the left (open arrows). Importantly, these pathways are bilaterally symmetric, such that during rightward head rotation there is a simultaneous decrease in the firing rates of primary afferents from the left canal, which results in a parallel reduction in the tension of the antagonist muscles (i.e., the left medial rectus and the right lateral rectus; Figure 3, blue). This push–pull organization ensures appropriate yoking of the eyes, generating conjugate eye movements in the opposite direction to head movement.

Although appropriate to account for a fast and conjugate RVOR, the simple three-neuron-arc falls short of explaining other properties of the reflex. In particular, activity in semicircular canal afferents is proportional to rotational velocity, while the reflex generates a compensatory (i.e., of opposite direction) eye position change. Just like in math/calculus, converting velocity to position requires temporal integration. How this takes place in the RVOR has been well documented (Skavenski, A. A. and Robinson, D. A., 1973; Robinson, D. A., 1981). At high frequencies (>0.5 Hz), this transformation occurs automatically by the viscoelastic properties of the ocular plant (eyeball, muscles, and surrounding tissue). However, an additional neuronal circuitry is necessary at low frequencies. Because of this need, Robinson D. A. (1981) proposed a two parallel pathway solution, one of which is the direct three-neuron-arc and the second an indirect pathway that utilizes what has been known as the oculomotor neural integrator (Figure 4). This integrator circuitry involves several cerebellar and brainstem structures, including the prepositus hypoglossi for the horizontal system and the interstitial nucleus of Cajal for the vertical system), as documented by lesion studies (Cheron, G. *et al.*, 1986; Cannon, S. C. and Robinson, D. A., 1987; Fukushima, K., 1991).

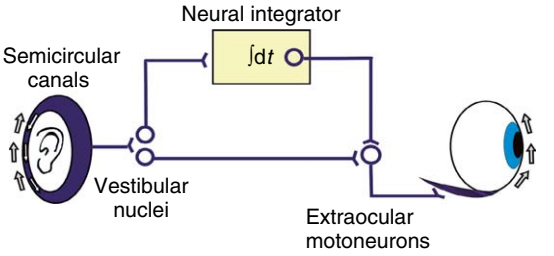

Figure 4 The now classical Robinson-style diagram for the rotational vestibulo-ocular reflex. Semicircular canal signals reach the extraocular motoneurons through two parallel pathways, a direct route through the vestibular nuclei (three-neuron arc; Figure 3) and an indirect pathway that functions like a neural integrator ($\int dt$).

2.22.1.3 Translational Vestibulo-Ocular Reflex: Basic Properties

The TVOR is elicited during translational displacements of the head and body (e.g., when we walk or drive in a car) and is driven by activation of otolith afferents. Unlike the RVOR where a head rotation is compensated by an eye rotation, the TVOR must convert translation into a compensatory eye rotation, a geometrical transformation that makes the magnitude of the evoked eye movement depend on target proximity (Figure 5(a)). Specifically, the same lateral displacement results in nearby objects moving on the retina more rapidly than distant ones. Several studies have indeed shown that the TVOR amplitude scales with vergence angle and the inverse of viewing distance: the eyes rotate by an amount that is larger as the target gets closer to the subject (Schwarz, U. *et al.*, 1989; Paige, G. D. and Tomko, D. L., 1991; Schwarz, U. and Miles, F. A., 1991; Figures 5(b)–5(d)). Like the RVOR, stimuli used to characterize the TVOR include either sinusoidal oscillations (Figure 5(b)) or transient displacements (Figure 5(c)).

A unique feature of the TVOR is that, unlike the RVOR, it often elicits disjunctive eye movements (each eye moves by a different amount). This occurs because the retinal flow experienced during translation can be complex and nonuniform. For example, when moving forward while looking straight ahead, we experience an expanding visual scene (Figure 6(a)) where (1) objects at the periphery of the visual field move faster than those in more central portions of the

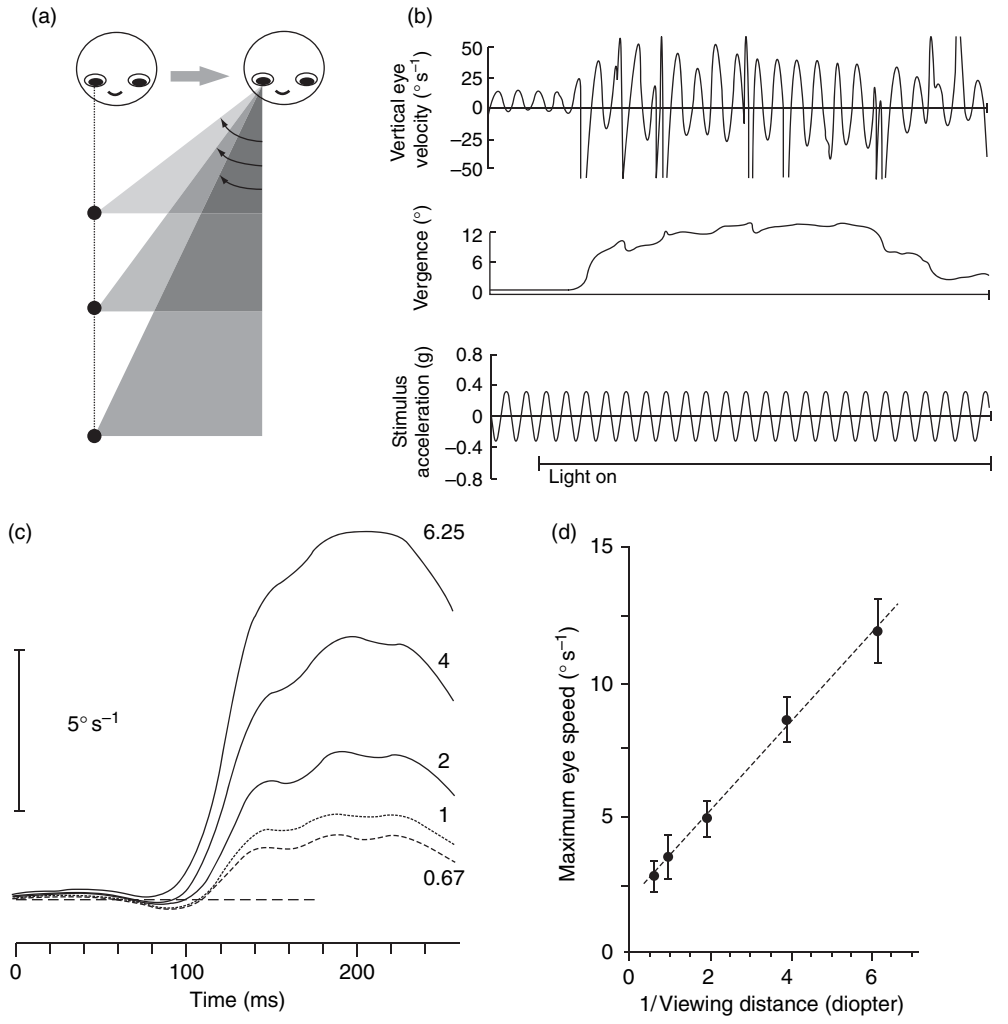

Figure 5 Dependence of the translational vestibulo-ocular reflex (TVOR) on viewing distance. (a) Schematic illustrating the geometry. (b) Eye velocity responses (top) and binocular vergence angle (middle) during 5 Hz oscillations. The monkey was initially in darkness and generated a small amplitude TVOR. After the light was turned on (bar), response amplitude increased as the monkey converged his eyes. Adapted from Paige, G. D. and Tomko, D. L. 1991. Eye movement responses to linear head motion in the squirrel monkey: II. Visualvestibular interactions and kinematic considerations. J. Neurophysiol. 65, 1183–1196, with permission from the American Physiological Society. (c) Mean eye velocity in response to leftward translation to a peak of 40 mm s^{-1} in darkness. The numbers next to each trace indicate viewing distance in diopters (reciprocal meters). (d) Maximum eye velocity (achieved within 250 ms of motion onset) plotted against the reciprocal of viewing distance (diopters). Dashed line is the linear regression. Adapted from Schwarz, U. *et al*., 1989. Ocular responses to linear motion are inversely proportional to viewing distance. Science 245, 1394–1396, with permission.

retina (similar to the star-field screen saver on a computer); (2) objects appear to move in different directions depending on their spatial location within the visual field; and (3) because forward motion is associated with distance changes, we must converge our eyes to keep images on corresponding locations on the two fovea. As a result, when moving forward while looking to the right, our eyes rotate further to the right (Figure 6(b), blue traces). In contrast, when looking to the left, the same translation elicits leftward eye velocity (Figure 6(b), red traces). The primate/human TVOR is typically undercompensatory for near viewing, with gains of ~0.5 (Paige, G. D. and Tomko, D. L., 1991; Telford, L. *et al*., 1997; Paige, G. D. *et al*., 1998; Angelaki, D. E. *et al*., 2000a; McHenry, M. Q. and Angelaki, D. E., 2000). The residual retinal image motion remaining after a less than ideal TVOR can be nulled by complementary visual stabilization mechanisms, known as the ocular following reflexes (for reviews, see Miles, F. A., 1993; 1998).

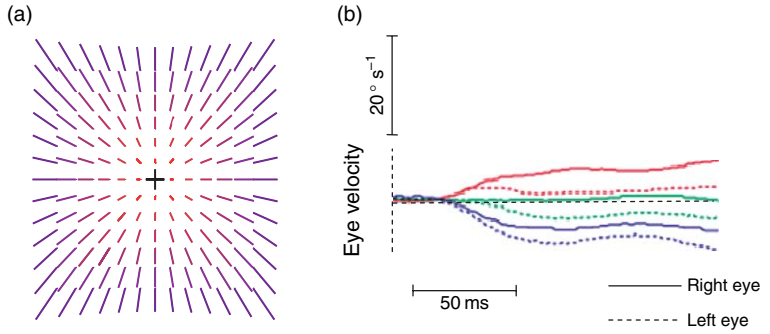

Figure 6 Complexities of the translational vestibulo-ocular reflex (TVOR). (a) Idealized optic flow pattern during forward motion while fixating straight-ahead. Shades from red to blue illustrate transition from the fovea to the retinal periphery. (b) Horizontal eye velocity (TVOR) amplitude during forward motion depends on target position and is disjunctive. Data plot eye velocity of the right and left eyes, while fixating one of three targets ~15° to the left (red), straight ahead (green), or 15° to the right (blue). Upward deflections illustrate leftward eye velocity. Adapted with permission from Macmillan Publishers Ltd: Angelaki, D. E. and Hess, B. J. 2005. Self-motion induced eye movements: effects on visual acuity and navigation. Nat. Rev. Neurosci. 6, 966–976. Panel (b) was redrawn from Hess, B. J. and Angelaki, D. E. 2003. Vestibular contributions to gaze stability during transient forward and backward motion. J. Neurophysiol. 90, 1996–2004, with permission from the American Physiological Society.

2.22.1.4 Neural Circuits and Pathways

The main brain areas that participate in the generation of the VORs include the vestibular nuclei (VN) and the vestibulocerebellum, which encompasses the cerebellar flocculus/ventral paraflocculus (FL/VPFL) and the posterior vermis (lobules X and XI). The FL/VPFL is critical for VOR plasticity (see Section 2.22.2.2). The posterior vermis is important for processing signals from the otolith organs and for controlling the RVOR at low frequencies (Solomon, D. and Cohen, B., 1994; Angelaki, D. E. and Hess, B. J., 1995; Angelaki, D. E., 2004). Purkinje cells in the vestibulocerebellum project to the vestibular nuclei, which house both the direct vestibulo-ocular connections (comprising the three-neuron-arc pathway; Figures 3 and 4), as well as some of the indirect projections involved in neural integration (Figure 4). Several VN cell types have been described, differing in their response properties to rotation and smooth pursuit eye movements. In particular, the position-vestibular-pause (PVP) cells are thought to represent the second-order neuron in the three-neuron-arc pathway (Figures 3 and 4; Scudder, C. A. and Fuchs, A. F., 1992). In contrast, eye-head cells, are thought to be involved in VOR adaptation (see Section 2.22.2.2), with many receiving inhibitory projections from FL/VPFL Purkinje cells (Lisberger, S. G. *et al.*, 1994a; 1994b).

2.22.2 Functional Plasticity

The VOR operates in what is called an open-loop fashion, where the signals activating the vestibular labyrinths are independent of the evoked eye movement. Thus, for this reflex to be functionally useful it is critical that the brain continuously monitors its performance by evaluating the clarity of vision during head movement. VOR recalibration is indeed a common experience in everyday life: whenever we try a newly prescribed pair of eyeglasses, we experience discomfort as we adjust to the changed optical magnification. With an increase in magnification, a movement of the head results in a faster movement of the image across the retina and requires an increase in VOR gain to maintain retinal stability. A magnification decrease will require a decrease in VOR gain.

2.22.2.1 Behavioral Observations

The first experimental demonstration of VOR plasticity was by Gonshor A. and Melvill Jones G. (1973; 1976a; 1976b), who studied the effects of wearing reversing prisms in both cats and humans going about their everyday activities. A few days after the prisms were put on, the RVOR (tested in darkness) was greatly reduced, and even reversed direction. Response reversal disappeared almost immediately after prism removal, but the return of gain took

several days. Less dramatic, but possibly more physiologically relevant gain increases and decreases were subsequently obtained with the use of spectacles that magnify or reduce the visual image (Gauthier, G. M. and Robinson, D. A., 1975; Miles, F. A. and Eighmy, B. B., 1980). Other studies used short-term adaptation by exposing the subject to a motion stimulus coupled with an abnormal visual stimulus (Lisberger, S. G. *et al.*, 1983; Raymond, J. L. and Lisberger, S. G., 1996). For example, head rotation paired with rotation of an optokinetic visual stimulus at the same speed but in the opposite direction results in an increase of RVOR gain (Figure 7, top). Similarly, rotating the subject and visual surround in tandem can be used to train the RVOR gain towards zero (Figure 7, bottom). Changes are typically frequency selective, with largest effects at the frequency used during training (Godaux, E. *et al.*, 1983; Lisberger, S. G. *et al.*, 1983; Powell, K. D. *et al.*, 1991; Raymond, J. L. and Lisberger, S. G., 1996). It is also possible to adapt RVOR gain in opposite directions at low versus high frequencies or during the two directions of motion (Hirata, Y. *et al.*, 2002).

RVOR plasticity is not only limited to gain changes. If the subject is rotated horizontally while the visual stimulus moves vertically, horizontal rotation in darkness will generate both horizontal and vertical eye movements (Schultheis, L. W. and Robinson, D. A., 1981; Baker, J. *et al.*, 1986; 1987; Angelaki, D. E. and Hess, B. J., 1998). Adaptive changes in RVOR phase are also possible (Kramer, P. D. *et al.*, 1995). Importantly, RVOR recalibration is context specific: static head position relative to gravity, the position of the eyes in the orbit, and the pattern of head movement have been used as contextual cues for gating different vestibular responses (Baker, J. *et al.*, 1987; Powell, K. D. *et al.*, 1991; Shelhamer, M. *et al.*, 1992; Kramer, P. D. *et al.*, 1998; Yakushin, S. B. *et al.*, 2003). The ability to store multiple calibrations is common in everyday life. For example, once accustomed to new spectacles, no adjustment is needed when the spectacles are removed. Similarly, persons wearing bifocals can instantly shift from one set of optics to the other.

Although less well characterized, the TVOR is also highly adaptable (Seidman, S. H. *et al.*, 1999; Wei, M. and Angelaki, D. E., 2001; Zhou, W. *et al.*, 2003). Notably, the VORs are modifiable not only in response to altered visual/vestibular interactions but also in response to a change in vestibular input brought on by disease or trauma (Paige, G. D., 1983; Fetter, M. and Zee, D. S., 1988; Curthoys, I. S. and Halmagyi, G. M., 1995; Angelaki, D. E. *et al.*, 2000b; Lasker, D. M. *et al.*, 2000; Sadeghi, S. G. *et al.*, 2006).

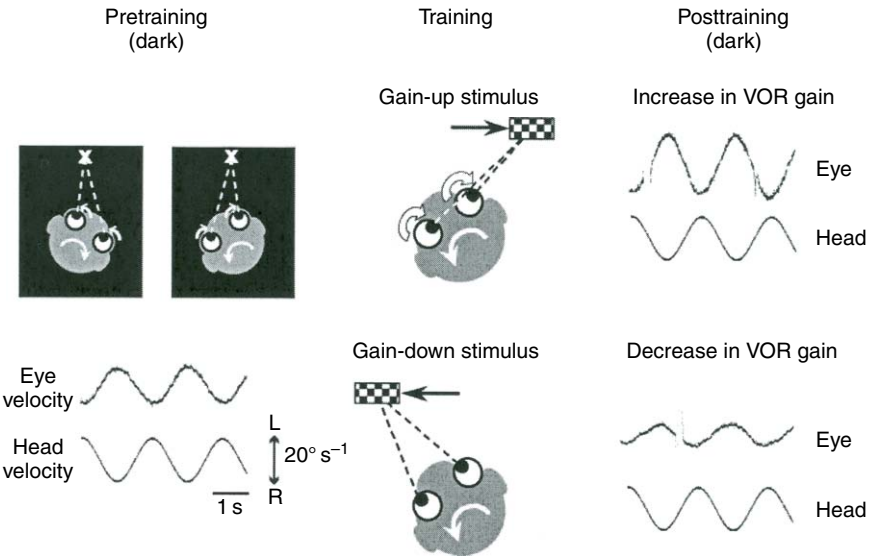

Figure 7 Example of rotational vestibulo-ocular reflex (RVOR) motor learning and adaptation. Prior to adaptation (pretraining dark) the eyes rotate with the same speed but in opposite direction from head rotation. The RVOR gain can be increased (top row) or decreased (bottom row) by simultaneously presenting image motion (OKN stimulus) in either the opposite or the same direction of head rotation, respectively (training). After each training session the RVOR is again measured during rotation in darkness (posttraining dark). Notice the difference in RVOR amplitude. Reprinted from Boyden, E. S., Katoh, A., and Raymond, J. L. 2004. Cerebellum-dependent learning: the role of multiple plasticity mechanisms. Annu. Rev. Neurosci. 27, 581–609, with permission.

2.22.2.2 Neural Signatures of Plasticity: Identifying the Sites for Vestibulo-Ocular Reflex Learning?

Following the theoretical works of Brindley G. S. (1964), Marr D. (1969), and Albus J. (1971) regarding a role for climbing fibers as the teacher signal for synapse modification, Ito M. (1972; 1982) pioneered the cerebellar hypothesis of motor learning, where the FL/VPFL provides a side path to the main brainstem three-neuron arc pathway that is used to adjust reflex performance (Figure 8). Ito proposed that the pairing of visual image motion and head motion causes coincident visually driven and vestibularly driven climbing fiber activity, resulting in long-term depression (LTD) of the corresponding parallel fibers. In this scheme, the instructive signal guiding learning is the retinal slip carried by climbing fibers. Early demonstrations that flocculectomy abolishes RVOR adaptation and LTD at the parallel fiber to Purkinje cell synapse supported this view (Ito, M. *et al.*, 1974; Robinson, D. A., 1976; Ito, M. *et al.*, 1982).

An alternative hypothesis proposed by Miles F. A. and Lisberger S. G. (1981) suggested that the modifiable synapses in the RVOR were located in the VN, while the FL/VPFL Purkinje cells provided the error signal to guide reflex recalibration. The Miles-Lisberger hypothesis was motivated by the observation that changes in Purkinje cell firing during VOR cancellation were often in the wrong direction to support reflex gain changes (Miles, F. A. *et al.*, 1980). However, PVP cells, the main interneurons in the three-neuron-arc pathway, did not exhibit sufficient and appropriate changes after learning (Lisberger, S. G. and Miles, F. A., 1980).

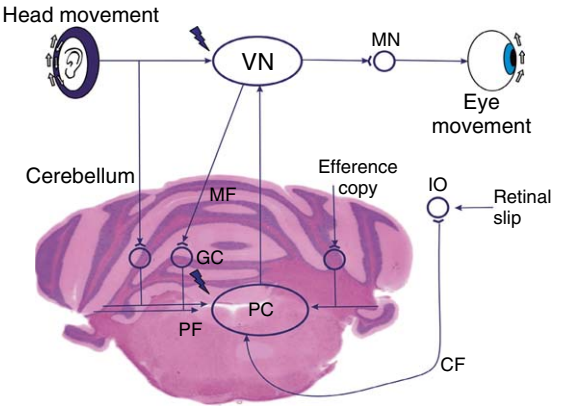

Figure 8 Proposed sites of plasticity for the rotational vestibulo-ocular reflex, one in the brainstem (vestibular nuclei, VN) and the other at the parallel fiber (PF) to Purkinje cell (PC) synapse (arrows). CF, climbing fiber; IO, inferior olive; GC, granule cell; MF, mossy fiber; MN, motoneurons. Adapted from Boyden, E. S., Katoh, A., and Raymond, J. L. 2004. Cerebellum-dependent learning: the role of multiple plasticity mechanisms. Annu. Rev. Neurosci. 27, 581–609.

Lisberger S. G. and colleagues have since described another VN cell type, flocculus-target neurons (FTNs), which receive direct inhibition from the FL/VPFL and monosynaptic inputs from the ipsilateral vestibular nerve (Lisberger, S. G. and Pavelko, T. A., 1988; Broussard, D. M. and Lisberger, S. G., 1992; Lisberger, S. G. *et al.*, 1994a). FTNs exhibited large changes following motor learning that were in the appropriate direction to support the adapted changes (Lisberger, S. G. and Pavelko, T. A., 1988; Lisberger, S. G. *et al.*, 1994b). Importantly, the latency at which these adaptive responses manifested was short, providing further support for FTNs being a site for plasticity (Lisberger, S. G. *et al.*, 1994b; for review, see du Lac, S. *et al.*, 1995). Similar sites for plasticity have also been described for the vertical RVOR (Partsalis, A. M. *et al.*, 1995a; 1995b; Highstein, S. M. *et al.*, 1997.

However, in some circumstances (e.g., during high frequency training), Purkinje cell firing fails to discriminate stimuli that increase and decrease RVOR gain, an observation that is incompatible with the Miles-Lisberger hypothesis (Raymond, J. L. and Lisberger, S. G., 1998). In contrast, several manipulations used to disrupt molecular pathways required for cerebellar LTD produced strong deficits in motor learning (for review, see Boyden, E. S. *et al.*, 2004). Thus, current opinion holds that there are multiple cites of plasticity (Figure 8; lightning bolts). Such a notion has been further supported by *in vitro* studies describing plasticity mechanisms (for review, see Hansel, C. *et al.*, 2001). Part of the argument for having multiple sites of plasticity stems from theoretical considerations showing that parallel changes in the strength of vestibular inputs to FTNs and Purkinje cells are required to maintain system stability (Lisberger, S. G. and Sejnowski, T. J., 1992; Lisberger, S. G., 1994). Notably, distinct differences between increasing and decreasing RVOR gain adaptation (Miles, F. A. and Eighmy, B. B., 1980) might arise because only the former depends on cerebellar LTD. The latter might utilize cerebellar long term potentiation (LTP) (for review, see Boyden, E. S. *et al.*, 2004).

In summary, there remains controversy regarding the sites for motor memory in the RVOR (with a complete lack of similar experiments in the TVOR). Reaching definite conclusions is often difficult and limited by incomplete knowledge of network structure and signal contents, as each can dramatically

influence interpretation of experimental results. Furthermore, sites for neural plasticity have typically been studied only during RVOR gain changes. It is unknown whether the same brainstem/cerebellar sites of plasticity might also apply to other types of VOR learning (e.g., cross-axis adaptation; Quinn, K. J. *et al.*, 1996). Further experimental investigations and the use of innovative analysis techniques that are less sensitive to assumptions regarding network structure are necessary to understand the sites of neural plasticity further. Yet, the richness of behavioral observations associated with different training paradigms points to the existence of multiple potential adaptation sites within the VOR pathways. Multiple plasticity mechanisms might be advantageous for storing motor memories over different timescales, enabling bidirectional amplitude changes, and refining the dynamics of the adapted movement.

References

Albus, J. 1971. A theory of cerebellar function. Math. Biosci. 10, 25–61.

Angelaki, D. E. 2004. Eyes on target: what neurons must do for the vestibuloocular reflex during linear motion. J. Neurophysiol. 92, 20–35.

Angelaki, D. E. and Hess, B. J. 1994. Inertial representation of angular motion in the vestibular system of rhesus monkeys. I. Vestibuloocular reflex. J. Neurophysiol. 71, 1222–1249.

Angelaki, D. E. and Hess, B. J. 1995. Lesion of the nodulus and ventral uvula abolish steady-state off-vertical axis otolith response. J. Neurophysiol. 73, 1716–1720.

Angelaki, D. E. and Hess, B. J. 1996. Three-dimensional organization of otolith-ocular reflexes in rhesus monkeys. II. Inertial detection of angular velocity, J. Neurophysiol. 75, 2425–2440.

Angelaki, D. E. and Hess, B. J. 1998. Visually induced adaptation in three-dimensional organization of primate vestibuloocular reflex. J. Neurophysiol. 79, 791–807.

Angelaki, D. E. and Hess, B. J. 2005. Self-motion induced eye movements: effects on visual acuity and navigation. Nat. Rev. Neurosci. 6, 966–976.

Angelaki, D. E., McHenry, M. Q., and Hess, B. J. 2000a. Primate translational vestibuloocular reflexes. I. High-frequency dynamics and the three-dimensional properties during lateral motion. J. Neurophysiol. 83, 1637–1647.

Angelaki, D. E., McHenry, M. Q., and Hess, B. J. 2000b. Primate translational vestibulo-ocular reflexes. III. Effect of bilateral labyrinthine electrical stimulation, J. Neurophysiol. 83, 1662–1676.

Baarsma, E. A. and Collewijn, H. 1975. Eye movements due to linear accelerations in the rabbit. J. Physiol. 245, 227–247.

Baker, J., Harrison, R. E. W., Isu, N., Wickland, C., and Peterson, B. 1986. Dynamics of adaptive change in vestibulo-ocular reflex direction: II. Sagittal plane rotations. Brain Res. 371, 166–170.

Baker, J., Wickland, C., and Peterson, B. 1987. Dependence of cat vestibulo-ocular reflex direction adaptation on animal orientation during adaptation and rotation in darkness. Brain Res. 408, 339–343.

Benson, A. J. 1970. Response of semicircular canal dependent units in vestibular nuclei to rotation of a linear acceleration vector without angular acceleration. J. Physiol. 210, 475–494.

Boyden, E. S., Katoh, A., and Raymond, J. L. 2004. Cerebellum-dependent learning: the role of multiple plasticity mechanisms. Annu. Rev. Neurosci. 27, 581–609.

Brindley, G. S. 1964. A new interaction of light and electricity in stimulating the human retina. J. Physiol. 171, 514–520.

Broussard, D. M. and Lisberger, S. G. 1992. Vestibular inputs to brain stem neurons that participate in motor learning in the primate vestibuloocular reflex. J. Neurophysiol. 68, 1906–1909.

Cannon, S. C. and Robinson, D. A. 1987. Loss of the neural integrator of the oculomotor system from brain stem lesions in monkey. J. Neurophysiol. 57, 1383–1409.

Cheron, G., Godaux, E., Laune, J. M., and Vanderkelen, B. 1986. Lesions in the cat prepositus complex: effects on the vestibulo-ocular reflex and saccades. J. Physiol. 372, 75–94.

Cohen, B., Matsuo, V., and Raphan, T. 1977. Quantitative analysis of the velocity characteristics of optokinetic nystagmus and optokinetic after-nystagmus. J. Physiol. 270, 321–344.

Cohen, B., Suzuki, J. I., and Raphan, T. 1983. Role of the otolith organs in generation of horizontal nystagmus: effects of selective labyrinthine lesions. Brain Res. 276, 159–164.

Collewijn, H. 1985. Integration of adaptive changes of the optokinetic reflex, pursuit and the vestibulo-ocular reflex. Rev. Oculomot. Res. 1, 51–69.

Curthoys, I. S. and Halmagyi, G. M. 1995. Vestibular compensation: a review of the oculomotor, neural, and clinical consequences of unilateral vestibular loss. J. Vestib. Res. 2, 67–107.

du Lac, S., Raymond, J. L., Sejnowski, T. J., and Lisberger, S. G. 1995. Learning and memory in the vestibulo-ocular reflex. Annu. Rev. Neurosci. 18, 409–441.

Fernandez, C. and Goldberg, J. M. 1971. Physiology of peripheral neurons innervating semicircular canals of the squirrel monkey. II. Response to sinusoidal stimulation and dynamics of peripheral vestibular system. J. Neurophysiol. 34, 661–675.

Fetter, M. and Zee, D. S. 1988. Recovery from unilateral labyrinthectomy in rhesus monkey. J. Neurophysiol. 59, 370–393.

Fukushima, K. 1991. The interstitial nucleus of cajal in the midbrain reticular formation and vertical eye movement. Neurosci. Res. 10, 159–187.

Gauthier, G. M. and Robinson, D. A. 1975. Adaptation of the human vestibuloocular reflex to magnifying lenses. Brain Res. 92, 331–335.

Godaux, E., Halleux, J., and Gobert, C. 1983. Adaptive change of the vestibulo-ocular reflex in the cat: the effects of a long-term frequency-selective procedure. Exp. Brain Res. 49, 28–34.

Gonshor, A. and Melvill Jones, G. 1973. Proceedings: Changes of human vestibulo-ocular response induced by vision-reversal during head rotation. J. Physiol. 234, 102–103.

Gonshor, A. and Melvill Jones, G. 1976a. Extreme vestibulo-ocular adaptation induced by prolonged optical reversal of vision. J. Physiol. 256, 381–414.

Gonshor, A. and Melvill Jones, G. 1976b. Short-term adaptive changes in the human vestibulo-ocular reflex arc. J. Physiol. 256, 361–379.

Guedry, F. E. 1965. Orientation of the rotation-axis relative to gravity: Its influence on nystagmus and the sensation of rotation. Acta Otolaryngol. 60, 30–48.

Hansel, C., Linden, D. J., and D'Angelo, E. 2001. Beyond parallel fiber LTD: the diversity of synaptic and non-synaptic plasticity in the cerebellum. Nat. Neurosci. 4, 467–475.

Hardy, M. 1934. Observations on the innervation of the macula sacculi in man. Anat. Rec. 59, 403–418.
Hess, B. J. and Angelaki, D. E. 1997. Kinematic principles of primate rotational vestibulo-ocular reflex. I. Spatial organization of fast phase velocity axes. J. Neurophysiol. 78, 2193–2202.
Hess, B. J. and Angelaki, D. E. 2003. Vestibular contributions to gaze stability during transient forward and backward motion. J. Neurophysiol. 90, 1996–2004.
Hess, B. J. and Dieringer, N. 1990. Spatial organization of the maculo-ocular reflex of the rat: responses during off-vertical axis rotation. Eur. J. Neurosci. 2, 909–919.
Highstein, S. M. and Baker, R. 1978. Excitatory termination of abducens internuclear neurons on medial rectus motoneurons: relationship to syndrome of internuclear ophthalmoplegia. J. Neurophysiol. 41, 1647–1661.
Highstein, S. M., Partsalis, A. M., and Arikan, R. 1997. Role of the y-group of the vestibular nuclei and flocculus of the cerebellum in motor learning of the vertical vestibulo-ocular reflex. Prog. Brain Res. 114, 383–397.
Hirata, Y., Lockard, J. M., and Highstein, S. M. 2002. Capacity of vertical VOR adaptation in squirrel monkey. J. Neurophysiol. 88, 3194–3207.
Huterer, M. and Cullen, K. E. 2002. Vestibuloocular reflex dynamics during high-frequency and high-acceleration rotations of the head on body in rhesus monkey. J. Neurophysiol. 88, 13–28.
Ito, M. 1972. Neural design of the cerebellar motor control system. Brain Res. 40, 81–84.
Ito, M. 1982. Cerebellar control of the vestibo-ocular reflex-around the floccululs hypothesis. Ann. Rev. Neurosci. 5, 275–296.
Ito, M., Shiida, T., Yagi, N., and Yamamoto, M. 1974. Visual influence on rabbit horizontal vestibo-ocular reflex presumably effected via the cerebellar flocculus. Brain Res. 65, 170–174.
Keller, E. L. 1978. Gain of the vestibulo-ocular reflex in monkey at high rotational frequencies. Vision Res. 18, 311–315.
Kramer, P. D., Shelhamer, M., and Zee, D. S. 1995. Short-term adaptation of the phase of the vestibulo-ocular reflex (VOR) in normal human subjects. Exp Brain Res. 106, 318–326.
Kramer, P. D., Shelhamer, M., and Zee, D. S. 1998. Short-term vestibulo-ocular adaptation: influence of context. Otolaryngol. Head Neck Surg. 119, 60–64.
Lasker, D. M., Backous, D. D., Lysakowski, A., Davis, G. L., and Minor, L. B. 1999. Horizontal vestibuloocular reflex evoked by high-acceleration rotations in the squirrel monkey. II. Responses after canal plugging. J. Neurophysiol. 82, 1271–1285.
Lasker, D. M., Hullar, T. E., and Minor, L. B. 2000. Horizontal vestibuloocular reflex evoked by high-acceleration rotations in the squirrel monkey. III. Responses after labyrinthectomy. J. Neurophysiol. 83, 2482–2496.
Lisberger, S. G. 1994. Neural basis for motor learning in the vestibuloocular reflex of primates. III. Computational and behavioral analysis of the sites of learning. J. Neurophysiol. 72, 974–998.
Lisberger, S. G. and Miles, F. A. 1980. Role of primate medial vestibular nucleus in long-term adaptive plasticity of vestibuloocular reflex. J. Neurophysiol. 43, 1725–1745.
Lisberger, S. G. and Pavelko, T. A. 1988. Brain stem neurons in modified pathways for motor learning in the primate vestibulo-ocular reflex. Science 242, 771–773.
Lisberger, S. G. and Sejnowski, T. J. 1992. Motor learning in a recurrent network model based on the vestibulo-ocular reflex. Nature 360, 159–161.
Lisberger, S. G., Miles, F. A., and Optican, L. M. 1983. Frequency-selective adaptation: evidence for channels in the vestibulo-ocular reflex? J. Neurosci. 3, 1234–1244.
Lisberger, S. G., Pavelko, T. A., and Broussard, D. M. 1994a. Responses during eye movements of brain stem neurons that receive monosynaptic inhibition from the flocculus and ventral paraflocculus in monkeys. J. Neurophysiol. 72, 909–927.
Lisberger, S. G., Pavelko, T. A., and Broussard, D. M. 1994b. Neural basis for motor learning in the vestibuloocular reflex of primates. I. Changes in the responses of brain stem neurons. J. Neurophysiol. 72, 928–953.
Lorente De No, R. 1935. Facilitation of motoneurones. Am. J. Physiol. 113, 505–523.
Marr, D. 1969. A theory of cerebellar cortex. J. Physiol. 202, 437–470.
McHenry, M. Q. and Angelaki, D. E. 2000. Primate translational vestibuloocular reflexes. II. Version and vergence responses to fore-aft motion. J. Neurophysiol. 83, 1648–1661.
Miles, F. A. 1993. The sensing of rotational and translational optic flow by the primate optokinetic system. Rev. Oculomot. Res. 5, 393–403.
Miles, F. A. 1998. The Neural processing of 3-D visual information: evidence from eye movements. Eur. J. Neurosci. 10, 811–22.
Miles, F. A. and Eighmy, B. B. 1980. Long-term adaptive changes in primate vestibuloocular reflex: behavioral observations. J. Neurophysiol. 43, 1406–1436.
Miles, F. A. and Lisberger, S. G. 1981. Plasticity in the vestibulo-ocular reflex: a new hypothesis. Ann. Rev. Neurosci. 4, 273–299.
Miles, F. A., Braitman, D. J., and Dow, B. M. 1980. Long-term adaptive changes in primate vestibuloocular reflex. IV. Electrophysiological observations in flocculus of adapted monkeys. J. Neurophysiol. 43, 1477–1493.
Minor, L. B., Lasker, D. M., Backous, D. D., and Hullar, T. E. 1999. Horizontal vestibuloocular reflex evoked by high-acceleration rotations in the squirrel monkey. I. Normal responses. J. Neurophysiol. 82, 1254–1270.
Paige, G. D. 1983. Vestibuloocular reflex and its interactions with visual following mechanisms in the squirrel monkey. I. Response characteristics in normal animals. J. Neurophysiol. 49, 134–151.
Paige, G. D. and Tomko, D. L. 1991. Eye movement responses to linear head motion in the squirrel monkey: II. Visual-vestibular interactions and kinematic considerations. J. Neurophysiol. 65, 1183–1196.
Paige, G. D., Telford, L., Seidman, S. H., and Barnes, G. R. 1998. Human vestibuloocular reflex and its interactions with vision and fixation distance during linear and angular head movement. J. Neurophysiol. 80, 2391–2404.
Partsalis, A. M., Zhang, Y., and Highstein, S. M. 1995a. Dorsal Y group in the squirrel monkey. II. Contribution of the cerebellar flocculus to neuronal responses in normal and adapted animals. J. Neurophysiol. 73, 632–650.
Partsalis, A. M., Zhang, Y., and Highstein, S. M. 1995b. Dorsal Y group in the squirrel monkey. I. Neuronal responses during rapid and long-term modifications of the vertical VOR. J. Neurophysiol. 73, 615–631.
Powell, K. D., Quinn, K. J., Rude, S. A., Peterson, B. W., Baker, J. F., and Powell, K. D. 1991. Frequency dependence of cat vestibulo-ocular reflex direction adaptation: single frequency and multifrequency rotations. Brain Res. 550, 137–141.
Precht, W., Richter, A., and Grippo, J. 1969. Responses of neurones in cat's abducens nuclei to horizontal angular acceleration. Pflugers Arch. 309, 285–309.
Precht, W. and Shimazu, H. 1965. Functional connections of tonic and kinetic vestibular neurons with primary vestibular afferents. J. Neurophysiol. 28, 1014–1028.
Quinn, K. J., Helminski, J. O., Didier, A. J., Baker, J. F., and Peterson, B. W. 1996. Changes in sensitivity of vestibular

nucleus neurons induced by cross-axis adaptation of the vestibulo-ocular reflex in the cat. Brain Res. 718, 176–180.
Ramachandran, R. and Lisberger, S. G. 2005. Normal performance and expression of learning in the vestibulo-ocular reflex (VOR) at high frequencies. J. Neurophysiol. 93, 2028–2038.
Raphan, T. and Cohen, B. 1985. Velocity storage and the ocular response to multidimensional vestibular stimuli. Rev. Oculomot. Res. 1, 123–143.
Raphan, T., Matsuo, V., and Cohen, B. 1979. Velocity storage in the vestibulo-ocular reflex arc (VOR). Exp. Brain Res. 35, 229–248.
Raphan, T., Cohen, B., and Henn, V. 1981. Effects of gravity on rotatory nystagmus in monkeys. Ann. N. Y. Acad. Sci. 374, 44–55.
Raymond, J. L. and Lisberger, S. G. 1996. Error signals in horizontal gaze velocity Purkinje cells under stimulus conditions that cause learning in the VOR. Ann. N. Y. Acad. Sci. 781, 686–689.
Raymond, J. L. and Lisberger, S. G. 1998. Neural learning rules for the vestibulo-ocular reflex. J. Neurosci. 18, 9112–9129.
Richter, A. and Precht, W. 1968. Inhibition of abducens motoneurones by vestibular nerve stimulation. Brain Res. 11, 701–705.
Robinson, D. A. 1976. Adaptive gain control of vestibuloocular reflex by the cerebellum. J. Neurophysiol. 39, 954–969.
Robinson, D. A. 1981. Control of Eye Movements. In: The Nervous System. Handbook of Physiology, Part 2. Vol. II. (*ed*. V. B. Brooks), pp. 1275–1320. Williams and Wilkins.
Robinson, D. A. 1982. The use of matrices in analyzing the three-dimensional behavior of the vestibulo-ocular reflex. Biol. Cybern. 46, 53–66.
Sadeghi, S. G., Minor, L. B., and Cullen, K. E. 2006. Dynamics of the horizontal vestibuloocular reflex after unilateral labyrinthectomy: response to high frequency, high acceleration, and high velocity rotations. Exp. Brain Res. 175, 471–484.
Schiff, D., Cohen, B., Buttner-Ennever, J., and Matsuo, V. 1990. Effects of lesions of the nucleus of the optic tract on optokinetic nystagmus and after-nystagmus in the monkey. Exp. Brain Res. 79, 225–239.
Schultheis, L. W. and Robinson, D. A. 1981. Directional plasticity of the vestibulo-ocular reflex in the cat. Ann. N. Y. Acad. Sci. 374, 504–512.
Schwarz, U. and Miles, F. A. 1991. Ocular responses to translation and their dependence on viewing distance. I. Motion of the observer. J. Neurophysiol. 66, 851–864.
Schwarz, U., Busettini, C., and Miles, F. A. 1989. Ocular responses to linear motion are inversely proportional to viewing distance. Science 245, 1394–1396.
Scudder, C. A. and Fuchs, A. F. 1992. Physiological and behavioral identification of vestibular nucleus neurons mediating the horizontal vestibuloocular reflex in trained rhesus monkeys. J. Neurophysiol. 68, 244–264.
Seidman, S. H., Paige, G. D., and Tomko, D. L. 1999. Adaptive plasticity in the naso-occipital linear vestibulo-ocular reflex. Exp. Brain Res. 125, 485–494.
Shelhamer, M., Robinson, D. A., and Tan, H. S. 1992. Context-specific adaptation of the gain of the vestibulo-ocular reflex in humans. J. Vestib. Res. 2, 89–96.
Skavenski, A. A. and Robinson, D. A. 1973. Role of abducens neurons in the vestibuloocular reflex. J. Neurophysiol. 36, 724–738.
Solomon, D. and Cohen, B. 1994. Stimulation of the nodulus and uvula discharges velocity storage in the vestibulo-ocular reflex. Exp. Brain Res. 102, 57–68.
Szentagothai, J. 1950. The elementary vestibulo-ocular reflex arc. J. Neurophysiol. 13, 395–407.
Telford, L., Seidman, S. H., and Paige, G. D. 1997. Dynamics of squirrel monkey linear vestibuloocular reflex and interactions with fixation distance. J. Neurophysiol. 78, 1775–1790.
Tweed, D., Sievering, D., Misslisch, H., Fetter, M., Zee, D., and Koenig, E. 1994. Rotational kinematics of the human vestibuloocular reflex. I. Gain matrices. J. Neurophysiol. 72, 2467–2479.
Waespe, W., Cohen, B., and Raphan, T. 1985. Dynamic modification of the vestibulo-ocular reflex by the nodulus and uvula. Science 228, 199–202.
Wei, M. and Angelaki, D. E. 2001. Cross-axis adaptation of the translational vestibulo-ocular reflex. Exp. Brain Res. 138, 304–312.
Yakushin, S. B., Raphan, T., and Cohen, B. 2003. Gravity-specific adaptation of the angular vestibuloocular reflex: dependence on head orientation with regard to gravity. J. Neurophysiol. 89, 571–586.
Zhou, W., Weldon, P., Tang, B., and King, W. M. 2003. Rapid motor learning in the translational vestibulo-ocular reflex. J. Neurosci. 23, 4288–4298.

3.01 Phylogeny and Evolution of Ciliated Mechanoreceptor Cells

G A Manley, Technische Universität München, Garching, Germany

R Ladher, RIKEN Centre for Developmental Biology, Kobe, Japan

© 2008 Elsevier Inc. All rights reserved.

3.01.1	**Introduction**	2
3.01.1.1	General Considerations	2
3.01.1.2	The Concepts of Morphological Homology and Molecular Homology	3
3.01.1.3	What Is a Ciliated Mechanoreceptor Cell?	4
3.01.2	**Phylogeny, Homology, and Homoplasy: The Historical Background of the Animal Groups**	5
3.01.3	**Ciliated Mechanosensory Cells of Vertebrates and Their Relatives**	6
3.01.3.1	Mechanoreceptors in Tunicate Sea Squirts and Lancelets	7
3.01.3.1.1	Mechanoreceptors in tunicate sea squirts	7
3.01.3.1.2	Mechanoreceptors in lancelets	8
3.01.3.2	Vertebrate Hair Cells	8
3.01.3.2.1	The typical vertebrate hair cell	8
3.01.3.2.2	Lateral-line hair cells of fish and Amphibia	10
3.01.3.3	The Origin and History of Vestibular Systems in Craniates	10
3.01.3.3.1	The structure and diversity of the vestibular organ	11
3.01.3.3.2	Auditory-vestibular sensory epithelia of fish	12
3.01.3.4	The Origin and Phylogeny of a Dedicated Auditory Epithelium	12
3.01.3.4.1	The hearing organs of amphibians (frogs and toads and their relatives)	13
3.01.3.4.2	The hearing organs of lepidosaurs (lizards and snakes)	14
3.01.3.4.3	The hearing organs of archosaur groups (dinosaurs, crocodilians, birds)	15
3.01.3.4.4	The hearing organs of mammals	16
3.01.3.5	A Synopsis of Hair Cell Phylogeny in Vertebrates	17
3.01.4	**Ciliated Mechanoreceptors of Nonchordate Animals**	17
3.01.4.1	Cnidarian Hair Cells	18
3.01.4.2	Mechanotransduction in *Caenorhabditis elegans*	19
3.01.4.3	Ciliated Mechanoreceptors in Insects	20
3.01.4.4	Mollusk Hair Cells	23
3.01.5	**Molecular Evolution of Mechanoreceptors**	25
3.01.5.1	Development of Ciliated Mechanoreceptors	26
3.01.5.1.1	Extrinsic factors regulating mechanoreceptor development	26
3.01.5.1.2	The role of transcription factors in mechanoreceptor development	27
3.01.5.2	Summary of Development	29
3.01.6	**Conclusion**	29
References		30

Glossary

amniote The largest group of land vertebrates, all originally egg-laying (lepidosaur and archosaur reptiles, birds, mammals).

apomorphy An evolutionarily new feature.

Bilateria Animals with three germ layers (endoderm, mesoderm, and ectoderm) and that show bilateral symmetry. All eumetazoans are Bilateria, except cnidarians and ctenophores.

cladistics The formal science of the study of evolutionary relationships.

deuterostomes Bilaterian animals in which during embryonic development the first opening, the

blastopore, becomes the anus. This includes the chordates as well as echinoderms and hemichordates.
ectopic Outside its normal location.
endothermy The ability to maintain body temperature independently of environmental sources of heat.
Eumetazoa Animals with true tissues – most of the multicellular animals.
homology The concept of sameness in evolution, where a structure can be traced back to a common origin.
homoplasy The concept of independent evolution of structures in different groups.
induction The effect of a tissue on the fate of another tissue, usually mediated by secreted signaling molecules.
innervation The establishment of functional contacts between nerve fibers and other cells.
neural/abneural The side of the auditory papilla where the nerve enters/the opposite side.
paleontology The science of the study of extinct organisms.
phylogeny The study of the evolutionary relationships of organisms.
plesiomorphy An evolutionarily old feature.
protostomes In these bilaterians, the blastopore becomes the mouth. Protostomes can be subdivided into ecdysozoans (molting animals such as arthropods and nematodes) and lophotrochozoans (such as mollusks and annelids). The split of the deuterostomes and protostomes represents one of the first major bifurcations in the phylogeny of eumetazoans.
signaling factor A secreted protein that binds to a cognate receptor to elicit a response. Its effect can be either cell autonomous (in which case signaling is autocrine) or nonautonomous (when signaling is paracrine) or both.
synapse The contact point between a nerve cell and another cell that permits fast signaling.
transcription factor A protein that binds DNA: it will bind to the promoter or enhancer of a particular gene to either activate or repress its transcription. This usually also requires binding of other transcription factors to different promoter or enhancer elements. Their function is cell autonomous.

The first vertebrate hair cells were probably located on the body surface. Such lateral-line organs specialized as a result of selection pressures to better analyze the stimuli from the environment. Hair cells in the inner ear organs of balance of fish also differentiated into different types and this became structurally obvious in the land vertebrates. Following the origin of a middle ear in lepidosaur, archosaur, and mammal ancestors, unique kinds of hair cell specializations arose that are recognizable along and across the respective epithelia. Structural features are accompanied by functional specializations that differ in the various groups, and in birds and mammals, there is a division of labor between two populations of highly specialized hair cells.

3.01.1 Introduction

3.01.1.1 General Considerations

This chapter is concerned with the history and relationships of a special type of sensory cell found in modern land vertebrates that subserves dual functions: detection of sound and of linear and rotational accelerations in the auditory and vestibular parts, respectively, of the inner ear. These sensory cells – the hair cells – are very similar to each other in both structure and function and they also strongly resemble the hair cells in the lateral-line system of fish and Amphibia. While there is little doubt that these sensory cells of vertebrates share the same phylogenetic origin, similar-looking sensory cells are found in quite different groups of organisms such as cnidarians, tunicates, and cephalopod mollusks (octopuses and relatives; reviews in Coffin, A. *et al.*, 2004; Holland, L. Z., 2005). Other sensory cells in organisms such as insects, which also respond to various kinds of mechanical stimuli, do not strongly resemble hair cells but may still have a common evolutionary history. In view of the presence of similar sensory cells in such a wide variety of species, extreme caution is necessary before making any statements concerning the phylogeny of these cells.

This chapter will have two main themes. Following an introduction to some of the important

concepts, it describes first the hair cell types in the various groups of vertebrates and their relatives, with a view to providing an overview of their evolutionary history and of their structural and molecular variation that is linked to sometimes subtle differences in function. Second, it examines some examples of mechanosensory cells from nonchordate animals and seeks to answer the question as to whether these sensory cells have independently evolved to perform similar functions to those of hair cells, that is, whether there is a basis for postulating that they are derived from the same kind of cells in an unbroken descent from a common ancestor (i.e., are they homologous and synplesiomorphic in the cladistic sense?) or whether they are homoplastic or analogous and only resemble each other due to convergence.

The criteria for determining common ancestry for morphological and molecular features are necessarily different and most conclusions must be preliminary in nature. The fossil history of soft-tissue structures such as sensory cells is virtually nonexistent, so any hypotheses based on the molecular constituents of sensory cells will probably never really be testable using comparisons of the morphological features of fossil organisms.

3.01.1.2 The Concepts of Morphological Homology and Molecular Homology

Homology is both a simple and an elusive concept. At its heart is the idea, rooted in comparative anatomy, of similarity due to common descent, and some have called it the central concept for all of biology (Wake, D. B., 1994). Classically, similarity was measured using a number of criteria: the relative position of a structure with respect to other structures, their continuity through intermediate forms, their connectivity to adjacent structures, their similarity in structural detail and histology, and the correspondence of their developmental origins (Remane, A., 1952; Brigandt, I., 2003). Other, more inclusive and tolerant concepts of homology, such as West-Eberhard's M. J. (2003) broad-sense homology, have not yet shown their usefulness in establishing ancestry and thus play no essential role in the discussion below. Homoplasy, that is, a similarity due to convergence, parallel evolution, and recurrence, needs to be identified; failure to recognize the characteristics of the homology concept can lead to fundamental misunderstandings of statements on evolutionary, historical commonality that are made from within different disciplines. These distinctions have become important since, in the last century, biology branched out into different experimental fields that use widely different techniques and seek different kinds of biologically relevant information (Brigandt, I., 2003). With regard to the discussion of mechanosensory cells, the usages of the homology concept in comparative biology show some very important differences.

Using the criteria defined above, comparative anatomists recognize structures in different species that are considered to correspond to each other and the inclusion of paleontological, comparative-anatomical evidence can provide powerful support for this notion. Homology in this context is a qualitative notion and structures or organs are either homologous or not. In molecular biology, however, the concept of homology is used in the context of the structure of genes and of the proteins they encode. The main criterion by which genes are considered to be homologous is the sequence of nucleic acids in the DNA or in their protein amino acid sequences. This concept is a quantitative one, in which it is said that two sequences are homologous to a certain degree (% sequence identity). At this level, the statement of homology permits comparisons between sequences with reference to their probable functions but only gives a statement of probability about the evolutionary origin of the sequences or about a potential common ancestor (Patterson, C., 1988; Brigandt, I., 2003).

Developmental biologists interested in evolutionary questions are faced with the problem of attempting to reconcile these two usages of homology, since at the level of organismic development, the question of the genetic control of ontogeny and the commonality of evolutionary history overlap. It would of course be expected that a homologous structure would be derived during ontogeny by the actions of the same set of genes, expressed in the same order at the same location in the body's bauplan. Since, however, genes can be involved in a wide variety of developmental processes and single genes may change their sequence during evolution and the gene may therefore change its function, the genetic background that leads to the building of homologous structures may in fact change over time. In addition, genes may become duplicated and diverge in their sequences. Orthologous genes are homologs that diverged as a result of a speciation event, whereas paralogous genes are homologs that diverged as a result of a gene duplication event (Hillis, D. M.,

1994). Here, the qualitative homology of comparative anatomy with its emphasis on common ancestry needs to be reconciled with the quantitative homology of molecular biology, a nontrivial problem indeed. For the purposes of the present chapter, concepts of evolutionary sameness need to be considered at different levels, especially those of the mechanosensory cells themselves, and also their integration into sensory organs in different animal groups. It is not sufficient to propose homology on the basis of the expression patterns of a few common genes (Adam, J. *et al.*, 1998).

A further distraction arises from the fact that frequently, homologous organs for hearing – or auditory organs – in terrestrial vertebrates are sought in invertebrate animals. As Budelmann B. U. (1992) pointed out, this is misguided, since all the invertebrate ancestors that come into question were aquatic and possessed sensory structures geared to respond to a variety of stimuli but not to classical auditory stimuli. To quote Budelmann B. U. (1992): "... any attempt to draw a direct evolutionary line of sound receptors or of hearing from any of the invertebrate groups, or via the hemi- and urochordates, to vertebrates must certainly fail. Also, we should not expect to find a direct *homolog* [his italics] precursor of the vertebrate hearing organ, or any other sense organ, in any of the invertebrate groups." Thus the search in the invertebrate phyla for homologs of vertebrate hair cells must be restricted to the search for possibly homologous sensory cells and their underlying genetic developmental background.

3.01.1.3 What Is a Ciliated Mechanoreceptor Cell?

Put briefly, the cells that are dealt with in this chapter are sensory elements that have a modified cilium (that arises from a basal body) that in some way is implicated in the cells' ability to respond to mechanical stresses of the cell membrane. Typically, such cells harbor certain ion-channel complexes in the cell membrane that are anchored both to the cell's cytoskeleton and outside the membrane to some nearby structure (Gillespie, P. G. and Walker, R. G., 2001). The channel can thus be mechanically stressed by changing the distance between the anchor points and this stress changes the open probability of the transduction (channel), increasing the flux of positive ions into the cell and thus depolarizing it.

As will become evident in this chapter, however, there is as yet no certainty that such mechanoreceptor cells of all animal species are derived from a common ancestral type, especially as mechanosensitive ionic channels are known even from bacteria and were thus most likely developed even before eukaryotic cells evolved. There are thus real problems in deciding evolutionary histories, especially when comparing on the one hand the ciliated mechanoreceptor cells of the chordates and their subgroup the vertebrates, which are specialized epithelial cells (hair cells, Figure 1) and thus belong to the group of secondary sensory cells, and on the other hand the ciliated mechanoreceptors of nonchordate groups that are, with few exceptions, specialized neurons with their own axon (Figure 1) and are thus primary sensory cells. In addition, these two kinds of cells show a fundamental difference in the involvement of the cilium in the sensory process. In the evolution of the vertebrate-type hair cell, the involvement of the cilium seems to have been steadily reduced until it may only be important in establishing the polarity of the cell's sensory outer segment (that consists of large microvilli or stereovilli) and, in some systems, is lost entirely during ontogeny. Not only in the primary ciliated mechanoreceptors, by contrast, but also in secondary ciliated mechanoreceptors of cephalopod mollusks, the cilium is an integral part of the sensory response apparatus and in many cases acts without the involvement of stereovilli.

In both kinds of receptor cells, the cilium is generally nonmotile, that is, the normal ability of the cilium to beat has been lost and is obviously not a requirement for the mechanosensory function. Instead, as in visual sensory cells of numerous animal groups (where the cilium has a vastly enlarged outer membrane segment based on a cilium), the cilium has been co-opted for another purpose. The original reason for the involvement of the cilium in chordate hair cells (and their predecessors, whatever they were) is unclear but may go as far back in evolution to ciliated single-celled organisms whose cilia are responsible for the sensitivity to touch. The cilium, the longest extension of the cell membrane, was perhaps used to anchor the mechanoreceptive channels. The cilium in the hair cell lineage (often called a kinocilium) later became supported by stereovilli, stiffened by an actin core, that form a symmetrical collar around the cilium. With the elongation of these stereovilli and their increase in numbers, the transduction channels

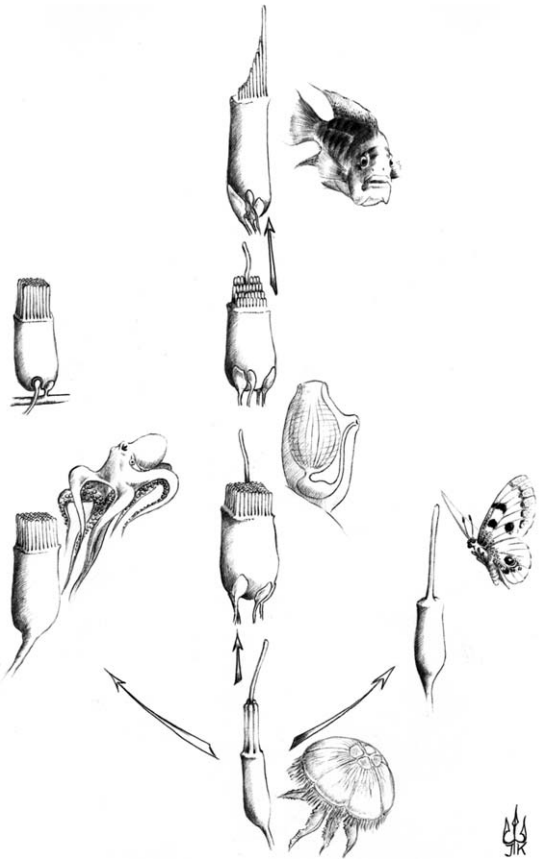

Figure 1 A schematic drawing of the evolution of hair cell like mechanosensitive cells. The figure should be read from bottom to top. Beginning with a mechanoreceptor of a cnidarian that possesses a normal cilium (kinocilium) surrounded by a small number of stereovilli, the evolution of these mechanoreceptors can be traced along three parallel paths in which the stereovilli and kinocilium have different fates. On the left is shown the lineage of the Lophotrochozoa, including annelids and mollusks. In this group, the best-studied case is that of *Octopus*, which possesses both primary (left, lower figure) and secondary (left, upper figure) receptor cells. In both cases, the receptor cells have no stereovilli but large numbers of kinocilia. On the right of the figure, the lineage to the ecdysozoans is shown using the example of insects, where the receptor cells are primary and there are no stereovilli but one enlarged kinocilium. The central lineage leads to the vertebrates (here represented by a fish) via primitive chordate groups, here represented by an ascidian tunicate. In this lineage, all receptor cells are secondary and both kinocilium and stereovilli are preserved. The bundle in vertebrates shows a stepped height of the stereovilli across the axis of sensitivity, with the tallest stereovilli next to the offset kinocilium. In mammals and birds, the kinocilium tends to degenerate during ontogeny. An original drawing by Johanna Kraus, all rights reserved.

apparently at least partly shifted to their membranes. In some lineages, this made the cilium somewhat redundant. In many vertebrate hair cells, one of the main functions of the remaining (kino-)cilium is as a contact area to overlying tectorial structures. In endothermic vertebrates, there is a strong tendency toward reduction or loss of the kinocilium during ontogeny, but the basal body remains in its position and likely plays an important role on the orientation of the bundle of stereovilli during ontogeny. In Ecdysozoa, such as arthropods and nematode worms, the supporting function of stereovilli was taken over by a connection of the cilium to the animal's cuticle. In these animals, therefore, all stereovilli have been lost and now only the modified cilium remains and carries the mechanotransductive channels (Thurm, U., 2001) (Figure 1).

3.01.2 Phylogeny, Homology, and Homoplasy: The Historical Background of the Animal Groups

It will be necessary to refer to a wide variety of animal groups in this chapter, since cilia-bearing mechanoreceptive cells have been described from the group considered to be the most primitive of the Eumetazoa (multicellular animals with true tissues), that is, the Cnidaria or jellyfish. In addition to their stinging cells that use a cilium as the sensor element, these organisms have small sensory organs, statocysts, able to encode to the brain the direction of gravitational force. It is believed that the eumetazoans are monophyletic, that is, have a single common origin. Therefore it may be expected that all following groups have inherited the ability to form such cells. However, abundant evidence from other sensory modalities and from considerations of the complement of cell-membrane channels that multicellular animals have inherited from their single-celled ancestors indicates that, although the genetic basis for mechanosensation exists in multiple cell types, it may only be expressed in a limited and varied subset. The question of homology at the level of cell types is thus not trivial.

The eumetazoans are extremely diverse and we will be concentrating on those groups that have been reasonably well studied. All other groups will not be mentioned or even shown in diagrams. A cladistic (phylogenetic) presentation of the groups to be

discussed is as follows (an indent step to the right indicates a subordinate group):

Common ancestor of eumetazoans
- Cnidaria (jellyfish)
- Common ancestor of bilaterally symmetrical eumetazoans
  - Ecdysozoa
    - Pseudocoelomata (e.g., nematode worms such as *Caenorhabditis*)
    - Arthropoda (e.g., insects such as the fruit fly *Drosophila*)
  - Lophotrochozoa
    - Molluska (e.g., the cephalopod *Octopus*)
  - Deuterostomia
    - Chordata
      - Tunicata (e.g., sea squirts)
      - Acrania (lancelets)
      - Craniata
        - Agnatha (Ostracodermi, hagfish, lampreys)
        - Vertebrata (animals with backbones)
          - Chondrichthyes (cartilaginous fish)
          - Osteichthyes (bony fish)
            - Teleostei (modern ray-finned fish)
            - Tetrapoda (land vertebrates)
              - Amphibia
              - Amniota
                - Lepidosauria (lizards and snakes)
                - Archosauria (birds and crocodilian)
                - Mammalia (mammals)

Evolutionary studies indicate clearly that the three major groups Ecdysozoa, Lophotrochozoa, and Deuterostomia diverged from one another very early and have long histories (more than 600 million years) of independent evolution behind them. In that time, their genomes have evolved completely without reference to each other (if we can exclude horizontal gene transfer via, e.g., common bacterial parasites). It might therefore be expected that their sensory substrates have diverged to a significant extent.

In the first section of this chapter, we will discuss the chordates and attempt to trace the history of their structure and function through the ancestral fish to modern aquatic and terrestrial groups. We will describe types of hair cell from the group of the sea squirts or Tunicata, chordate relatives of vertebrates, which may provide insights into possible ancestral states of the hair cells of vertebrates. Since vertebrate chordates are endowed with hard skeletal elements (cartilage or bone) that generally fossilize well, the fossil history of this group is extremely rich and as a result, the phylogenetic history is very well understood. In addition, the contours of some sensory structures are visible in some fossils. The history of hair cells in this group involves dealing initially with cells of the lateral-line system, then with vestibular, and finally with dedicated auditory sensory organs, whereby the functions of these organs may show considerable overlap.

The second part of the chapter will compare cilia-based mechanosensory cells from other major groups, such as the nematode worms and insects from the group of the Ecdysozoa and the cephalopod mollusks from the group Lophotrochozoa. Here, the question will be discussed as to the extent to which the molecular–genetic information concerning a possible homology to vertebrate hair cells is able to provide clear answers to questions of common ancestry.

3.01.3 Ciliated Mechanosensory Cells of Vertebrates and Their Relatives

A growing body of literature has demonstrated considerable heterogeneity in morphology and physiology of vertebrate hair cells in different taxa and even within different end organs of the same species. Electroreceptive sensory cells of vertebrates (which will not be discussed here) were also derived from hair cells (Jørgensen, J., 1989). Since they are no longer mechanoreceptive, their cilium has been lost and any stereovilli present are no longer stiffened.

Several lines of evidence support the presence of hair cells in the very earliest vertebrates, and in vertebrate ancestors, the early chordates. Such evidence includes the presence of hair cells in all craniates (Coffin, A. *et al.*, 2004) and in other chordates. Secondary sensory cells with one cilium and numerous stereovilli occur in tunicates (e.g., Bone, Q. and Ryan, K. P., 1978). Some of these hair cells in tunicates have symmetrical and some even have bilaterally symmetrical bundles (as in vertebrates), making it very likely that vertebrates inherited their basic hair cell pattern from their invertebrate ancestors (Shimeld, S. M. and Holland, P. W. H., 2000; Burighel, P. *et al.*, 2003). These animals, represented today by the tunicates and lancelets, may also have inherited their hair cells from even simpler ancestors going right back to the earliest eumetazoans, the cnidarians.

3.01.3.1 Mechanoreceptors in Tunicate Sea Squirts and Lancelets

Chordates are comprised of three groups: Tunicata (Urochordata, sea squirts, salps, and appendicularians), Acrania (Cephalochordata, lancelets), and Vertebrata (see, e.g., Hennig, W., 1983). There is no doubt concerning the close relationship of the three groups in the phylum Chordata and thus their relevance to questions concerning the phylogeny of vertebrate hair cells. However, the consistent association of vertebrate hair cells and their innervation with ectodermal placodes and neural crest cells, structures that do not occur in nonvertebrate chordates and for which no homologs have been firmly identified, makes considerations of sensory cell homologies difficult.

3.01.3.1.1 Mechanoreceptors in tunicate sea squirts

To illustrate the variety of mechanosensory cells in sea squirts, we will discuss recent data from ascidian tunicates (Burighel, P. *et al.*, 2003; Manni, L. *et al.*, 2004). These animals are filter feeders that are sessile as adults but have freely swimming larvae. As filter feeders, they use large areas of ciliated cells over the gill-slit supports to draw water through the filtering apparatus. Numerous mechanosensory cells are found, and many are presumably involved in monitoring such water currents.

Most of the superficial sensory cells of tunicates are of the primary receptor cell type, carrying their own axon. However, a recently described coronal organ in the oral siphon of ascidians contains secondary mechanoreceptive cells that bear strong resemblances to vertebrate hair cells (Burighel, P. *et al.*, 2003; Manni, L. *et al.*, 2004). This similarity is of great interest in view of the fact that the atrial chamber in these animals bears some ontogenetic and gene-expression similarities to the otic placodes of vertebrates with which hair cells are associated (Burighel, P. *et al.*, 2003). In the coronal organ of these tunicates, there are about 2000 mechanosensory cells which are secondary sensory cells that make contact to two different kinds of nerve fibers, both afferent and efferent. These hair cells are often arranged in rows of large numbers of cells. In addition, the stereovillar bundles (90–95 stereovilli) of the cells sometimes surround the cilium concentrically, but in other cases, the bundle is highly asymmetrical, with the cilium on one side (Figure 2; Burighel, P. *et al.*, 2003).

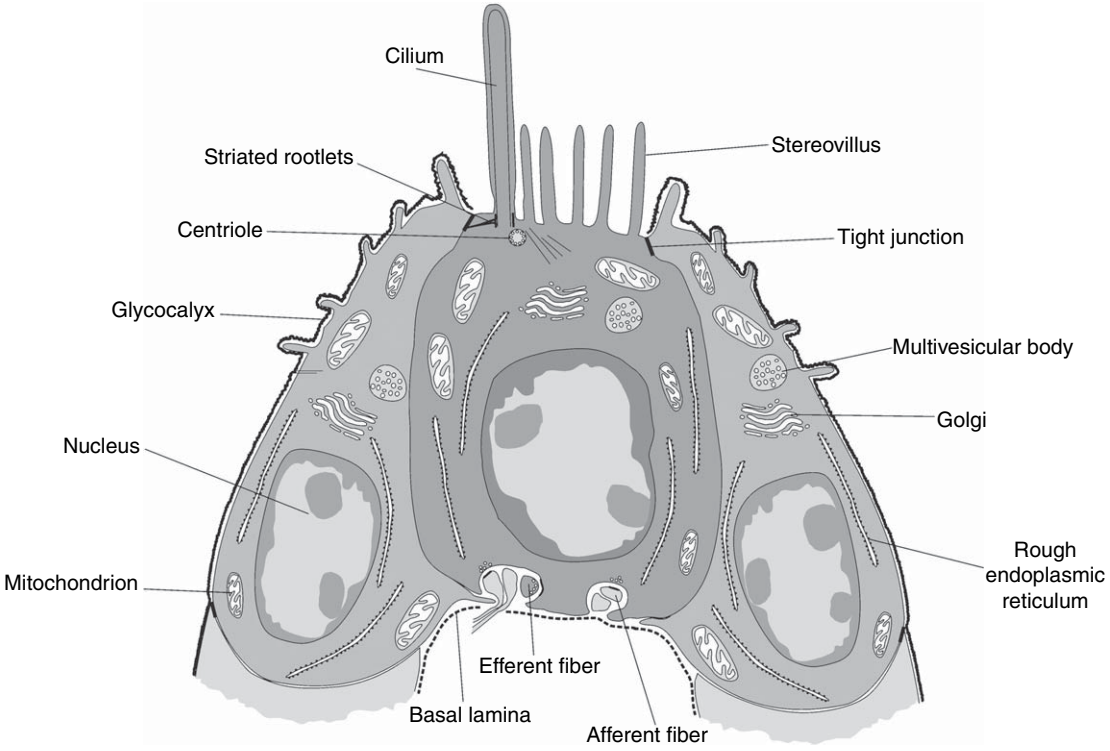

Figure 2 A schematic drawing of a hair cell accompanied by supporting cells in the coronal organ of the ascidian tunicate *Botryllus schlosseri*. Reproduced from Burighel, P., Lane, N. J., Fabio, G., Stefano, T., Zaniolo, G., Carnevali, M. D. C., and Manni, L. 2003. Novel, secondary sensory cell organ in ascidians: in search of the ancestor of the vertebrate latetal line. J. Comp. Neurol. 462, 236–249, with permission from John Wiley and Sons.

The stereovilli of these bundles are either of the same height or graded in height (Manni, L. *et al.*, 2004). In vertebrates, the stereovilli are always arranged such that there is a staircase of height up to the tallest and these are the closest to the cilium or basal body.

The suggestion that the above hair cells are homologous to vertebrate hair cells, even to the vertebrate lateral line (Burighel, P. *et al.*, 2003) has, however, been criticized, since none of the tunicate cells has all the characteristics of a vertebrate hair cell and there is a high degree of variation among ectodermal sensory cells within and between different species (review in Holland, L. Z., 2005). Thus, similarities between the ectodermal sensory cells of any one species of tunicate and craniate hair cells may possibly represent convergent evolution rather than homology. However, Shimeld S. M. and Holland P. W. H. (2000) concluded that since the atrium of ascidians develops from a pair of ectodermal invaginations that are topographically similar to the sensory placodes of vertebrates and since the atrial primordia also express members of the *Pax2/5/8* gene family as in placodes, these factors point to a possible homology between the atrial primordia of ascidia and the otic placodes of vertebrates. This strengthens the view that the hair cells in both the adult structures are also homologous (Manni, L. *et al.*, 2004). Obviously, further studies of the morphology and genetic control of ontogeny of these cells and their surrounding structures are necessary to enable firmer conclusions to be reached.

3.01.3.1.2 Mechanoreceptors in lancelets

The lancelets (often known as amphioxus and placed in a group known as cephalochordates, of which the best known are in the genus *Branchiostoma*) are small marine chordates that are most closely related to the vertebrates. Many primary, but also secondary sensory cells with cilia have been described in this group (review in Lacalli, T. C., 2004). Some are scattered in the rostral epithelium of the juvenile and classified as probable chemoreceptors. Others are in the spines of the mouth of the larvae. These cells bear a cilium, are grouped in clusters, and seem to be mechanoreceptors in synaptic contact with peripheral neurons. However, they do not possess a bundle of stereovilli. Lacalli T. C. (2004) concludes "There are a number of such [secondary receptor] cells in amphioxus, but none is an obvious precursor of any of the secondary sense cells of vertebrates, e.g., [hair cells of] neuromasts, taste buds, or solitary chemoreceptors". Thus with respect to sensory cells that are possible homologs of vertebrate hair cells, the lancelets show less promise than the sea squirts.

3.01.3.2 Vertebrate Hair Cells

3.01.3.2.1 The typical vertebrate hair cell

The hair cells of vertebrates have a typical structure that makes them immediately recognizable (Figure 3). This very strongly suggests that this kind of cell is plesiomorphic to vertebrates and that

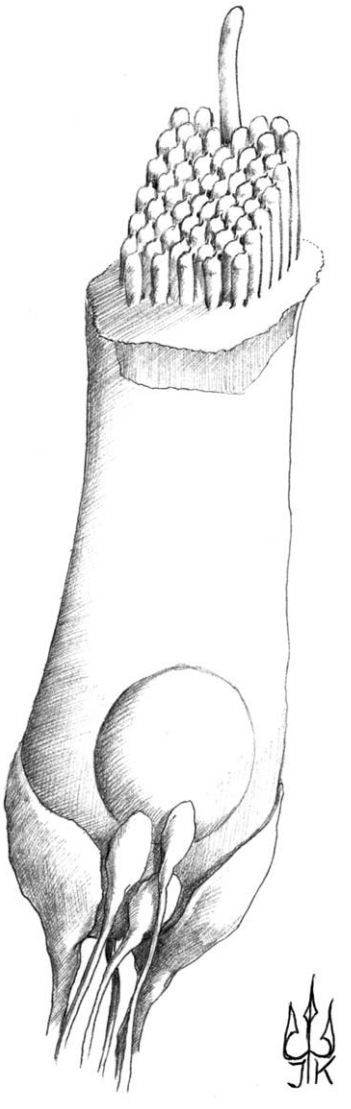

Figure 3 A schematic drawing of a typical vertebrate hair cell. This secondary receptor cell is innervated by both efferent (here drawn as larger synapses) and afferent nerve fibers. The cell bundle is polarized by the staircase structure of the rows of stereovilli that are joined by tip links. The bundle is also bilaterally symmetrical, based on the eccentric position of the kinocilium. An original drawing by Johanna Kraus, all rights reserved.

the first hair cells in vertebrate evolution would have resembled many modern ones. At their apical pole, each hair cell has a sensory hair bundle that is the sensory outer segment responsible for mechanoelectrical transduction (for reviews see Hudspeth, A. J., 1985; 1989). The bundle consists of a true cilium (in this context often referred to as a kinocilium and only lost during development in mammal and bird hearing organs and in electroreceptors) and a (generally shorter) bundle of large, stiff microvilli known as stereovilli (or, confusingly, stereocilia). The cilium is placed eccentrically on the cell surface, and the stereovilli show a gradient in their height, with the tallest next to the cilium. This gradient in height means that the bundle is bilaterally symmetrical and thus polarized in a particular direction.

Although we do not intend to review the detailed structure of such hair cells, we need to mention those features shown to have been the subject of natural selection during vertebrate evolution and thus differ between the hair cells seen in different groups, in different sensory organs, or even within one organ (reviewed in Lewis, E. R. *et al.*, 1985). The stereovillar component of the bundle consists of a number, between about 30 and 300, of rigid stereovilli that may have different thicknesses. The stereovilli are anchored not only in the cuticular plate (an actin matrix) of the hair cell's apex, but also to each other via various connections at different heights up the bundle. The connections between the stereovilli along their shafts help maintain their integrity, whereas the uppermost connections that form between the tip of the next lower stereovillus and the shaft of the taller neighbor (so-called tip links, Pickles, J. O. *et al.*, 1984) play a crucial role in sensory transduction (Hudspeth, A. J., 1989). A very small (a few nanometers) shift of the stereovilli toward the kinocilium puts tension on the mechanotransduction channels and increases their opening probability. This permits positive ions to flow into the cell, depolarizing it, and leading to an increased release of transmitter at the afferent synapse (Hudspeth, A. J., 1989).

The cell body of a hair cell can vary considerably in shape and size, from cylindrical cells with a height of over 70 µm, down to cup-shaped cells with a height of less than 4 µm. To a certain degree, the height of the cell body correlates – at least within the same auditory organ – with the bundle height, short bundles being found on shorter hair cells. The bundle height plays a role in determining the cell's frequency response (shorter bundles correlate with higher frequencies), and such higher frequencies are apparently better processed by smaller cell membranes. Under tectorial cupulae, bundle heights can exceed 130 µm (Lewis, E. R. *et al.*, 1985). The archaic state of vertebrate hair cells sees them connected synaptically to both afferent and efferent nerve fibers and this condition is maintained in almost all hair cell epithelia. The main exceptions are found in the cochleae of mammals and birds, where a clear specialization of the innervation is found, with a strong reduction or loss of the afferent innervation but increase in dominance of the efferent innervation of abneurally lying hair cells (Spoendlin, H., 1978; Fischer, F. P., 1994). In some areas of amniote auditory organs, efferent innervation is also completely lost (Manley, G. A., 2004; Vater, M. *et al.*, 2004).

Many features – visible and submicroscopic – of hair cells can change their stimulus–response properties. The response (depending on the sensory organ) will depend on whether the stereovillar bundle is connected to a gelatinous tectorial structure or not and whether this tectorium contains calcareous otoliths or not. It will also depend on the size, number, and thickness of the stereovilli, which together determine the bundle stiffness; stiffer bundles respond to higher stimulus frequencies. It will be noted below, using some examples, that hair cell micromechanics can be changed in a graduated fashion to produce frequency-response patterns that vary gradually over space (generally along a hearing organ, e.g., a phenomenon known as a tonotopic organization).

In many auditory organs (see below), the frequency response of the hair cells is largely determined by the stiffness of the bundle and the mass of the tectorial membrane. In lizards, the evolution of auditory organs was largely independent in different families and in some families, the tectorial mass over many of the hair cell bundles has been lost, but this loss of mass has been compensated for by an increase in bundle height and a reduction in stereovillar number of the bundles (see below and Manley, G. A., 2002; 2004). Of course, the type and number of transduction and other membrane channels in the outer and inner segments of the cell also play an important role in determining the cells' response characteristics. In some cases, as in turtle and bird auditory organs (see below), changes in the number, structure, and kinetics of membrane channels have been shown to strongly influence the gradient of the tonotopic organization (review in Köppl, C. *et al.*, 2000). Not surprisingly, variability in all of these features has produced a great variety of

morphological types and corresponding physiological responses. The following sections describe some of this diversity in different animal groups and different sensory epithelia.

3.01.3.2.2 Lateral-line hair cells of fish and Amphibia

Canals in dermal bone indicating the presence of an extensive lateral-line system have been described in the earliest of craniate fossils, in the jawless fish or ostracoderms (Carroll, R. L., 1987). Although there is no way to be sure what the sensory cells looked like, the structure of these canals, their distribution on the body (seven pairs in modern fish), and their innervation patterns indicate that they are homologous to the lateral lines of fish. Here, vertebrate-typical hair cells occur in groups that almost always have their stereovillar bundles embedded in sail-like tectorial masses called cupulae. Except in agnathans, both afferent and efferent fibers (the latter absent in agnathans, Görner, P., 1987) innervate typical hair cells.

There is evidence that the earliest hair cells occurred in groups associated with supporting cells in so-called neuromasts that were scattered in pits over the surface of the body, face, and mouth (Denison, R. H., 1966). This complexity was reduced very early by concentrating most or all of the neuromasts in a small number of canals with openings to the outside, most canals occurring on the animal's head. Such neuromast systems are found in all groups of modern fish and in the aquatic stages of amphibians, although in lampreys, slowly swimming, bottom-living fish and in amphibians, the neuromasts tend to lie in superficial pits rather than be sunken in canals (Young, J. Z., 1981). The lateral-line system is supposed to have given rise to electrosensory cells in at least two separate evolutionary events (Görner, P., 1987; Gibbs, M. A., 2004) and may also even be related to other secondary receptor cell systems such as taste cells (Smith, H. M., 1960). The origin of the lateral-line system as such must be sought in the earliest craniates, since only these have the dorsolateral placodal tissue from which this system (with few exceptions in amphibians) arises during ontogeny (Gibbs, M. A., 2004).

In a typical neuromast, the hair cells are arranged such that their bilaterally symmetrical stereovillar bundles show either of two orientations that are 180° opposed to each other. Thus these two groups of cells have their sensitive axes pointing in exactly opposite directions. Thus when one group of cells is stimulated, the other is not or even suppressed. Indeed, since these hair cells tend to be spontaneously active (indicating that at rest, their transduction channels have a significant opening probability), one population of hair cells would increase, the other decreasing its activity in response to the same stimulus. Neuromast hair cells respond with great sensitivity to displacement of the water over them and these responses provide information about the animal's own movements, the movements of other nearby organisms, and the presence of structures in the water (reviews in Flock, A., 1967; Russell, I. J., 1976; Sand, O., 1984; Bleckmann, H., 1986). There appears to be several stages in the evolution of lateral-line patterns and development in fish and amphibians (Pichon, F. and Ghysen, A., 2004).

Although hair cells in lateral-line neuromast systems tend to look similar to each other, there are few detailed studies of their fine structure and, given their different locations on the body, in canals, or on the surface, it would be surprising if specializations had not occurred. It is possible that the lateral-line mechanoreceptors of primitive hagfish resemble an early evolutionary stage of hair cell development, since they lack true stereovilli, their cilium being surrounded by microvilli and the cells lack polarization. It is, however, also possible that these cells in hagfish are degenerate. Lamprey lateral-line cells resemble typical hair cells but usually the neuromasts lack a cupula (review in Gibbs, M. A., 2004). In one study of the sensitivity of lateral-line hair cells to gentamicin that can destroy hair cells in hearing systems, hair cells in canal neuromasts were shown to be sensitive to gentamicin, whereas superficial hair cells were not (Song, J. *et al.*, 1995), indicating some kind of specialization. Since gentamicin acts through its ability to interact with the transduction channels, this suggests that the channels differ in some way between different groups of lateral-line hair cells, as has been noted in vestibular systems of vertebrates (Coffin, A. *et al.*, 2004). In addition, structurally differentiated types of hair cells that may correspond to different hair cell types found in vestibular organs have been demonstrated in a study of the lateral line of the ratfish (Ekström von Lubitz, D. K. J., 1981).

3.01.3.3 The Origin and History of Vestibular Systems in Craniates

A primitive vestibular organ was present in the earliest craniates, the ostracoderms (Carroll, R. L., 1987). Modern hagfish have one semicircular canal and lampreys have two (the anterior and posterior lateral

canals), as did the ostracoderms. It is possible that some ostracoderms had three or more, but the orientation of those canals did not allow for their preservation as fossils (Carroll, R. L., 1987). In addition to the sensory epithelia in these canals, agnathans only have a single additional area of sensory hair cells, the macula communis. The structural pattern typical for the vestibular organ of vertebrates, with three semicircular canals and two large spaces, the sacculus and utriculus, each with its own macula that can be supplemented by additional sensory organs in pouches (e.g., the lagenar macula) that arise from these spaces, obviously developed early in the evolution of the gnathostome fish (Figure 4; for details of the variety of organs and references, see Lewis, E. R. *et al.*, 1985). It appears that the sensory epithelium of the macula communis has been repeatedly and perhaps independently subdivided during the long evolutionary history of gnathostome vertebrates (Fritzsch, B. *et al.*, 2002).

3.01.3.3.1 The structure and diversity of the vestibular organ

In the semicircular canals, hair cells are restricted to so-called cristae in the terminal ampullae, where there is a cupula covering all hair cell bundles. In the sacculus and utriculus, there are – often large – sensory epithelia known as maculae and here, the hair cells are covered by an otolithic membrane. Other sensory epithelia (such as the macula neglecta and the macula lagenae) are generally small and carry otolithic membranes. All of these organs consist of sometimes very large hair cell epithelia that sit on a firm substrate (Lewis, E. R. *et al.*, 1985).

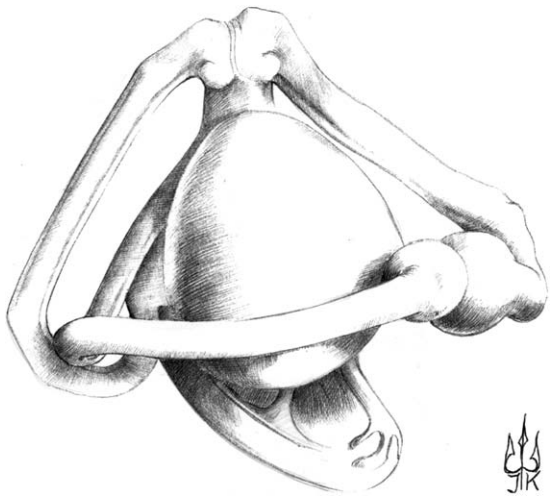

Figure 4 A schematic drawing of a typical vestibular organ of a vertebrate, here from the Australian bobtail skink *Tiliqua rugosa*. The vestibular system is seen from the animal's right side. Dorsal is up and the view is from lateral. The large globe in the center is the sacculus. The three semicircular canals can be seen, as can some of their ampullae. The lagena lies ventrally and is partially obscured by the sacculus. In the lagena, the finger processes of the nerve to the lagenar macula can be seen (right), as can the fan-shaped nerve to the basilar papilla. An original drawing by Johanna Kraus, all rights reserved.

The cristae are sensory epithelia that are stimulated by head rotation that causes a displacement of the cupula due to the inertia of the endolymphatic fluid in the semicircular canals. All hair cell stereovillar bundles in a crista are oriented in the same direction but those of different cristae may be oppositely oriented. In contrast to the relative uniformity of the cristae, great variety exists in the number, size, shape, and degree of specialization of the sensory maculae of the vestibular systems of different vertebrates (Lewis, E. R. *et al.*, 1985). The specializations are obviously not confined to macroscopic structural changes, since changes in the electrical properties of hair cells have also been found. Both structural and membrane properties of the hair cells will exert powerful influences on their sensory response properties.

Vestibular sensory epithelia in amniote vertebrates, both cristae and maculae with otoliths in their covering membranes, tend to show two types of hair cells that are differently distributed throughout the epithelia (see Lewis, E. R. *et al.*, 1985 for references). The more primitive kind of hair cell is the so-called type II. It is a mostly cylindrical hair cell that makes small synapses with afferent and, less frequently, efferent nerve fibers. Type I hair cells are more globular or flask-shaped, with a narrow neck and widened apex above it, and are a characteristic of amniote vestibular systems. There is some evidence that, ontogenetically, type I hair cells begin life as type II forms (Masetto, S. and Carreia, M. J., 1997). Most of the type I hair cell is surrounded by a large nerve terminal, the calyx, that may also enclose other hair cells. Efferent fibers synapse on this calyx and not on the hair cell. Especially in mammals, intermediate cell forms are known. Most physiological studies of these two hair cell types have been carried out in mammals, resulting in the tentative conclusion that type I hair cells respond to stimulation faster, with increased gain for small stimuli and an expanded dynamic range, whereas type II hair cells may be more sensitive. The huge synaptic calyx of type I hair cells apparently contains reciprocal

synapses with the hair cell that are responsible for a feedback process within the calyx that can produce large responses rapidly (Devau, G., 2000).

Different hair cell types are not distributed uniformly throughout vestibular epithelia, but their patterns are species-specific (Lewis, E. R. *et al.*, 1985). In general, type I hair cells tend to be concentrated along the center of the epithelium. Especially in otolith organs, a centrally lying strip of hair cells known as the striola tends to contain mainly type I, whereas type II hair cells are more numerous toward the periphery. Within these two types of hair cells and in nonamniotes, which show little evidence of such pronounced hair cell specializations, there is still a great variety in hair cell form due, for example, to the size, shape, and height of the bundles and the precise arrangement of stereovilli in the bundles.

3.01.3.3.2 Auditory-vestibular sensory epithelia of fish

In both cartilaginous and bony fish, hair cells of diverse vestibular maculae mediate the senses not only of rotational and linear acceleration, but also of hearing (for refs see Popper, A. N. and Fay, R. R., 1999; Ladich, F. and Popper, A. N., 2004). Hearing apparently coexists with vestibular responses from end organs that may or may not be covered by an otolithic membrane and, in fish as a whole, there is a great variety in size and structure of the various end organs between and even within systematic groups. The vestibular maculae display a variety of different hair cell orientation patterns, which are believed to contribute to the abilities of those fish to localize sounds (Fay, R. R. and Edds-Walton, P. L., 1997; Lu, Z. and Popper, A. N., 2001). In addition, in some fish groups, hearing sensitivity is improved by additional structures such as the Weberian ossicles to the swim bladder.

Although fish vestibular hair cells show no overt evidence of specialized cell types, such cells do have different arrangements of the kinocilium and stereovilli in their bundles (for references see Coffin, A. *et al.*, 2004). The columnar shape of the hair cells resembles the type earlier defined in amniotes as type II. However, biochemical studies using a calcium-binding protein and antibiotic agents revealed the presence of two types of hair cells with a differential distribution in the organs. Hair cells in different areas of fish maculae also show clear differences in their physiological response patterns. This suggests that during vertebrate evolution, hair cell specialization in terms of cell-membrane channels and other proteins, for example, began before obvious morphological specialization.

For agnathan fish, auditory function has not been localized to one of the various vestibular epithelia, and auditory function is poorly understood in cartilaginous fish (where the macula neglecta, lagena, and utricle may all play a role). However, it is well understood in bony fish (Ladich, F. and Popper, A. N., 2004). Whereas in these animals the utricular macula, with few exceptions, is relatively uniform, the saccular and (in fewer species) the lagenar macula vary greatly in size. There is evidence that this variety is linked to a function of these epithelia as both vestibular and auditory organs. The function of hearing is based on the sound in water moving the entire fish, whereby the denser otolithic material tends to lag in phase and therefore stimulate the underlying hair cells. In some groups, the frequency response goes up remarkably high, to several kilohertz, and the frequency responses may be spread systematically on the sensory epithelium. The latter implies a highly organized epithelium, with the properties of individual hair cells (presumably both structural and biochemical) varying systematically from place to place.

3.01.3.4 The Origin and Phylogeny of a Dedicated Auditory Epithelium

The dedicated auditory receptor of land vertebrates, the first epithelium in vertebrate evolution that responded exclusively to sound, is called the basilar papilla. It developed, like many vestibular epithelia, as an out-pocketing from the saccular macula. There is evidence that such an epithelium is present in the coelocanth *Latimeria* (Fritzsch, B., 1992) and thus by inference in the sister group of the ancestors of land vertebrates. It is, however, uncertain whether this was a unique event for all lobe-finned fish and their close relatives or whether *Latimeria* ancestors developed this epithelium independently of the true ancestors of land vertebrates. One of the difficulties with the assumption of an originating event in the common ancestor of lobe-finned fish and land vertebrates is the situation encountered in modern amphibians, where neither of the two auditory epithelia is conclusively considered to be homologous to the amniote basilar papilla. Thus either the ancestors of the Lissamphibia lost the basilar papilla and later developed their own two auditory organs or the *Latimeria* epithelium does not indicate that the basilar papilla of amniotes can be traced back to the

lobe-finned fish. Using the second possibility, this would mean that the amniote basilar papilla arose in the ancestors of the stem reptiles.

3.01.3.4.1 The hearing organs of amphibians (frogs and toads and their relatives)

In an extensive review of amphibian hearing mechanisms, Smotherman M. and Narins P., (2004) state that "Differences in the physiology of hearing can be seen within every branch of the amphibian phylogenetic tree, and range from such gross morphological differences as the absence of a middle ear down to subtle differences in hair cell stereovillar architecture." Considering this great diversity, we will ignore the middle ear and morphology of the endolymphatic system (that show important differences to the amniotes, Smotherman, M. and Narins, P., 2004), and restrict our discussion here to the specializations of the hair cells in the hearing organs of amphibians.

As noted above, modern amphibians, which are considered to be a monophyletic group, in addition to the retention of some acoustic sensitivity of the sacculus as in most fish, usually have two hearing epithelia, known as the basilar and the amphibian papillae. In contrast to the amphibian papilla, the basilar papilla is not found in all groups of Amphibia. The amphibian papilla is not considered to be homologous to the amniote basilar papilla, whereas there is considerable discussion as to whether the basilar papillae of amphibians and amniotes are homologous (for a review see Smotherman, M. and Narins, P., 2004). If the basilar papilla is a homolog, it has lost many of the structural (e.g., the freely moving basilar membrane) and functional characteristics of the amniote basilar papilla (i.e., the hair cell specialization and tonotopic organization).

The amphibian papilla probably originated as an outpocket near the duct joining the utriculus and the ventrally lying sacculus. It varies greatly in its structure throughout the amphibians. In some amphibian lineages, the amphibian papilla, with its tectorial membrane, is elongated and equipped with many more hair cells. At the distal end of the papilla there is a so-called contact membrane that permits pressure waves to leave the surrounding space, enabling sensitive responses to sound. The most primitive amphibian papilla is probably that seen in urodeles and the most primitive anurans and is a small patch of sensory hair cells located on the dorsomedial wall of the recess. More advanced anuran amphibians have a caudal extension to the sensory epithelium, the length of which correlates with an increase in the frequency-response range processed by this papilla (Smotherman, M. and Narins, P., 2004).

The basilar papilla of amphibians is found in all frogs, some salamanders, and a minority of caecilians. It contains a very small patch of 50 or so hair cells located beneath a thin tectorial membrane, the latter being stretched across the recess of the basilar papilla. Behind the sensory epithelium lies a contact membrane separating the recess from the periotic space. The basilar papilla is anatomically very uniform in all amphibian groups, but its exact location varies between the groups. In strong contrast to the hair cell array of the amphibian papilla (and indeed to hearing epithelia of amniotes), all the hair cells of the basilar papilla of the amphibians respond to a single, narrow frequency range that is species-specific. The basilar papilla thus appears to be a simple resonant structure (Meenderink, S. W. *et al.*, 2005) and it would not be expected that the hair cells would differ from one another in any pronounced way.

The amphibian papilla, by contrast, shows specializations in different amphibian groups in the presence or absence of electrically tuned hair cells, in the characteristics of the hair cell bundles and in the hair cell orientation patterns. Electrical tuning of hair cells, known from the fish and amphibian sacculus, probably arose fairly early in the evolution of hair cells and provides an important mechanism for frequency selectivity at least for frequencies below about 1 kHz (review in Fettiplace, R., 1987; Manley, G. A., 2000). It is found in about half of the hair cells of the amphibian papilla and in a small percentage of hair cells from the basilar papilla, although the latter only show this resonance in a different frequency range to that of their acoustic responses. In electrically tuned hair cells of the amphibian papilla in the anuran *Rana pipiens*, the hair cell response frequencies are organized into a tonotopic spatial array in which the best response frequency of any given hair cell is partly determined by the number and the kinetics of particular membrane channels that vary systematically along the epithelium (Smotherman, M. and Narins, P., 2004). The electrical properties of the saccular and amphibian papilla hair cells are fundamentally similar, but in the amphibian papilla, additional structural gradients in the hair cells influence the range of best frequencies along the epithelium.

Hair cell orientation patterns in the anuran amphibian papilla and basilar papilla are diverse. Most basilar papilla hair cells are polarized in the same direction, as are hair cells of the amphibian

papilla in the Caudata and Gymnophiona. In the more derived anuran amphibians, however, the amphibian papilla exhibits a much more complex array of hair cell orientation patterns, but no functional correlates have yet been reported (Smotherman, M. and Narins, P., 2004).

3.01.3.4.2 The hearing organs of lepidosaurs (lizards and snakes)

The phylogeny of the lepidosaur hearing epithelium has recently been extensively reviewed and will thus only be summarized here (Manley, G. A., 2000; 2002; 2004). The snake auditory papilla is very simple in its structure and resembles that of primitive lepidosaurs (tuataras) and the presumably primitive hearing organs of turtles. It consists of an elongated array of up to 1000 hair cells that are all oriented in the same direction (Miller, M. R., 1978; Wever, E. G., 1978) and whose response frequencies, which reach up to about 1 kHz, vary systematically from low frequencies apically to the highest frequencies basally. Although in the turtle papilla, the tonotopic arrangement of frequency responses is known to be due to both hair cell stereovillar bundle structure and electrical tuning (see Manley, G. A., 1990 for references), there are no recordings from hair cells or from the auditory nerve of snakes.

Considerably more information is available on specializations of hair cells in lizards (reviews in Wever, E. G., 1978; Miller, M. R., 1992; Manley, G. A., 2004). In these animals, the auditory epithelium is unique among amniotes in that it is always divided along its length into at least two hair cell arrays in which the hair cells belong to two different types which respond to different frequency ranges. In one of these areas, the hair cells (for which Miller, M. R., 1992 used the term UDT or unidirectional type to describe their unique morphology) are almost always oriented in one direction (abneurally), receive both afferent and efferent nerve fibers, are always covered by a tectorial membrane, and respond to frequencies below 1 kHz. Although in this respect they resemble the entire turtle papilla, there is no evidence for a pronounced electrical tuning of these lizard hair cells.

The other hair cell array consists of hair cells (Miller, M. R., 1992 referred to these as BDT or bidirectional type) which are generally in groups that have their bundles oppositely oriented (Figure 5) and have only an afferent innervation. Their response frequencies lie higher than 1 kHz and generally up to 5 kHz, in some cases higher. These hair cells may or may not be covered by a tectorial membrane, which

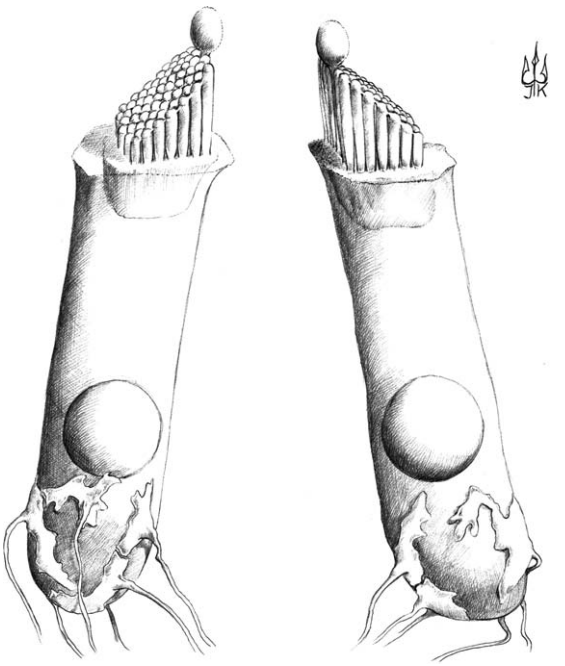

Figure 5 A schematic drawing of hair cell orientation pattern in lizards. In this figure, two hair cells are shown from the high-frequency area of a lizard papilla to illustrate the opposite orientation of the stereovillar bundles. In the species illustrated here (a lacertid lizard), the kinocilia are bulbed at their tips. Such high-frequency hair cells are micromechanically tuned and receive only an afferent innervation. An original drawing by Johanna Kraus, all rights reserved.

can take different forms. The response properties of these two hair cell populations differ not only in their frequency ranges but also in their intensity function patterns and their ability to phase lock to sinusoidal sound stimuli (Köppl, C. and Manley, G. A., 1990; Manley, G. A. *et al.*, 1990; Eatock, R. A. *et al.*, 1991; Manley, G. A., 2004).

It is likely that the plesiomorphic lizard basilar papilla contained three hair cell areas, one central area of UDT hair cells flanked at both ends by areas of BDT hair cells that were mirror images of each other (Manley, G. A., 2000; 2004). In some of the various families of lizards, one of these areas was lost (presumably because, being mirror images, one of them was redundant). In different lizard lineages, either the apical or the basal area was lost (Manley, G. A., 2002); in snakes, both areas were lost. Since the BDT areas respond to higher frequencies, primitive lizard papillae have a curious tonotopicity in which the cell response frequencies increase toward the two ends of the papilla. Where the apical high-frequency

area was lost, the tonotopicity resembles that of most other amniotes, increasing steadily toward the basal end of the papilla (Manley, G. A., 2000). Where the basal BDT area was lost, as in geckos, the tonotopicity is, as expected, reversed, a unique situation among amniotes (Manley, G. A. *et al.*, 1999).

It thus appears as if the specializations of hair cells in lizards vary between the plesiomorphic (for stem reptiles) UDT area, which in its properties continues in the long tradition established in the saccular macula. The BDT hair cells are almost unique among amniotes in their total loss of the efferent innervation (some specialized regions of some bat cochleae show this phenomenon). The BDT hair cell area(s) that are an apomorphy of lizards consist of hair cells that do not use electrical tuning, but instead perfected the mechanism of frequency selectivity known as micromechanical tuning. In such cells, the frequency selectivity results from the precise mechanical properties of the hair cell bundles (such as the bundle stiffness) and of the structures that surround them, such as the mass of the tectorial membrane (Figure 6). Precise and location-specific variations in these properties, often in groups of hair cells that are coupled, are the basis for the tonotopic organization. Knowledge of these gradients makes it possible to model the frequency-response limits and gradient (e.g., Manley, G. A. *et al.*, 1989). Since the basilar membrane in lizards is not tuned to different frequencies along its length (see Manley, G. A., 1990 for references), all of the frequency selectivity must originate in the hair cells and, if present, their local tectorial structure.

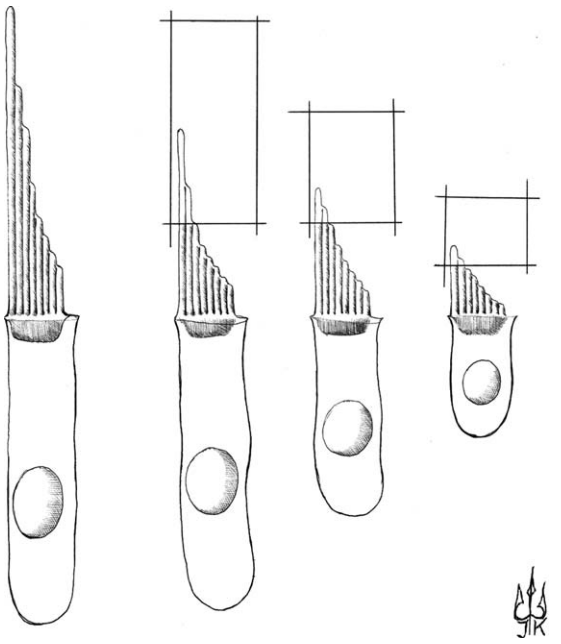

Figure 6 A schematic drawing of four hair cells to illustrate the principal structural changes underlying micromechanical tuning in the high-frequency hair cell areas of lizard auditory papillae. The hair cell on the left has no tectorial structure and this is associated with tall stereovillar bundles. The three cells to its right each carry a tectorial structure, which is shown highly schematically as if isolated, but could be part of a continuous tectorial membrane or of a local salletal unit. The mass of the tectorial structure and the bundle height vary systematically along the papilla and are responsible for the gradual change in the preferred response frequency of the hair cells. In this case, the frequency would rise from left to right hair cells. An original drawing by Johanna Kraus, all rights reserved.

3.01.3.4.3 The hearing organs of archosaur groups (dinosaurs, crocodilians, birds)

The evolution of the auditory epithelium of archosaurs has recently been reviewed (Gleich, O. *et al.*, 2004) and will therefore only be discussed here with reference to hair cell specializations. A comparison of the inner ears of the group of crocodilians with those of modern birds and an examination of recent fossil findings of casts of the inner ears of dinosaur groups have made it possible to speculate that the archosaur inner ear originated early in their lineage and is an apomorphy of the entire group. The hearing epithelium is elongated, up to 11 mm in length. It differs from that of lepidosaurs on the one hand and mammals on the other (both groups in which hair cells tend to be arranged in rows along the papilla) in that the hair cells and supporting cells form irregular mosaics. In addition, the width of the papilla can be large and there may be up to 50 hair cells in any transverse section of the wider, apical end of the epithelium. This contrasts with the 4–6 hair cells seen across the width of the papillae of lizards and mammals. Thus, although on average the avian and crocodilian papilla may be shorter than that of mammals, the number of hair cells can easily be as large or larger. In addition to the above, the archosaur epithelium is not all arrayed over the freely moving basilar membrane; instead, a substantial proportion of hair cells lies over the neural limbus, a firm and thick structure. It is thus apparent that the tectorial membrane, which is thick and covers all hair cells, surrounding their bundles in dome-like, individual concavities, plays a critical important role in hair cell stimulation (Manley, G. A., 1995).

The archosaur auditory papilla is also characterized by substantial gradients in different planes and in different structural and molecular features. It is presumed that together, these micromechanical and electrical features create the tonotopic organization of the papilla (Gleich, O. *et al.*, 2004). There are clear morphological gradients, such as in the mass of the tectorial membrane, the height and width of the hair cells, the height of their stereovillar bundles, and the number of stereovilli per bundle and the pattern of innervation (Figure 7). At the extremes, apical, neurally lying hair cells are very tall, their bundles have relatively few stereovilli that are tall and covered by a thick tectorial membrane. They receive both afferent and efferent innervation. At the other extreme, basal, abneural hair cells are much shorter, their bundles have 5–6 times as many stereovilli that are short and covered by a thinner tectorial membrane. These cells are only efferently innervated (Fischer, F. P., 1994; Gleich, O. *et al.*, 2004). In crocodilians, there tends to be a more sudden change from the one hair cell type to the other across the papilla.

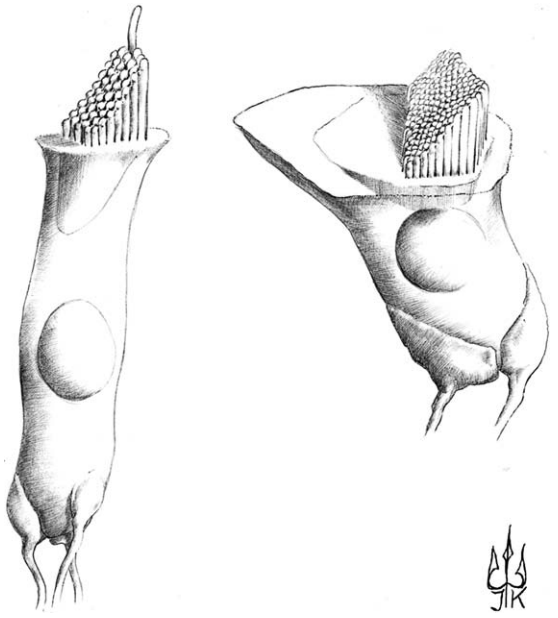

Figure 7 A schematic drawing of hair cell specializations in birds. These two hair cells illustrate the extremes of the structural differences shown by hair cells across and along the avian auditory papilla. On the left is a tall hair cell, which is both afferently and efferently innervated. The cuticular plate tends to go deeply into the cell. Such tall hair cells are typical for apical and neural hair cell areas. On the right is shown a short hair cell that is only efferently innervated. The apical surface of this cell is tilted somewhat toward the observer in order to more clearly show the broad, toothbrush-like, stereovillar bundle structure. Such short hair cells are typical of basal and abneural hair cell areas. An original drawing by Johanna Kraus, all rights reserved.

In addition and parallel to these morphological gradients, there are systematic changes in the molecular constituents of the cell membrane in various positions on the papilla, especially in those ion channels that are involved in electrical tuning (see, e.g., Rosenblatt, K. P. *et al.*, 1997; review in Köppl, C. *et al.*, 2000). The number and kinetics of K_{Ca} channels, which vary in their calcium and voltage sensitivities, are differentially distributed along the papilla, strongly suggesting that they also contribute to the tonotopic frequency arrangement. Alternative splicing can potentially generate thousands of ion-channel phenotypes that, combined with variations in calcium sensitivities, modulation by β subunits, and differing channel numbers per cell, would easily account for a large range of frequency responses. The avian auditory papilla provides one of the most interesting examples of genetic flexibility that creates a wide spectrum of functional variations within one type of cell.

The gradients described and the patterns of bundle orientation produce an exactly tonotopically organized auditory epithelium, with the lowest frequencies apically and the highest basally. There is also evidence that the tall hair cells lying over the neural limbus are more sensitive than hair cells lying further abneurally, with, in the starling, a change of 6 B per hair cell across the epithelium (see Gleich, O. *et al.*, 2004 for references). The expected change of hair cell sensitivity due to rotation of the bundle toward the middle of the papilla is compatible with these data, as is the fact that abneurally lying hair cells are not even afferently innervated. It is possible that abneural, short hair cells function as amplifiers in a similar way to the outer hair cells of mammals.

3.01.3.4.4 The hearing organs of mammals

With the exception of the egg-laying monotreme mammals, the auditory epithelium of mammals is coiled helically with the neural side on the inside of the helix. The hair cells are generally strictly arranged in rows, with a single row of inner hair cells and, except at the apex in some groups, three rows of outer hair cells (Figure 8). This specific arrangement, which is common to both placental and marsupial mammals, likely arose after their separation from the monotreme mammals that have

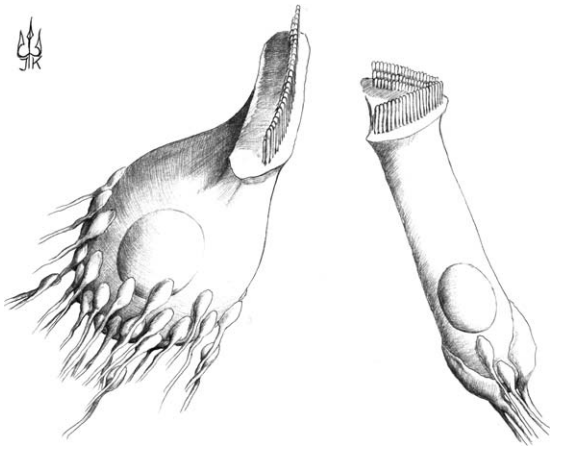

Figure 8 A schematic drawing of hair cell specializations in mammals. The two distinct hair cell populations of the mammalian cochlea are illustrated in this figure. On the left is a typically bulbous inner hair cell that is innervated by a large number of afferent fibers, which in turn receive synapses from a few efferent fibers. Its bundle is straight and made up of only a few rows of stereovilli. The outer hair cell on the right is typically cylindrical and mainly, but not exclusively, innervated by large efferent endings. Its bundle has a W shape, where the angle between the long arms of the W can vary with position along the cochlea. An original drawing by Johanna Kraus, all rights reserved.

more rows of both inner and outer hair cells (for references see Vater, M. *et al.*, 2004).

Inner hair cells are somewhat globular in shape, enclosed by supporting cells, and innervated by large numbers (15–30) of afferent nerve fibers that themselves (but seldom the hair cells) are efferently innervated. The hair bundle of inner hair cells contains only a few rows of stereovilli, and the bundle stands parallel to the long axis of the epithelium. Outer hair cells are more columnar in shape and their basal areas lie free in the fluid of Corti's organ. Their bundles contain more stereovilli and are in general arranged in a W-shape, with the open side of the W roughly pointing toward the inner hair cells. Outer hair cells, although numerically about 80% of all cochlear hair cells, are only innervated by 5–10% of the afferent nerve fibers, most of their basal synaptic area being contacted by large efferent endings (Spoendlin, H., 1978). There is much evidence that, in convergent evolution to the archosaur papilla, outer hair cells have a reduced afferent innervation because their main function is within the hearing organ, amplifying weak sounds. The resulting stimulus is then detected and transmitted to the brain via the inner hair cells.

This clear and profound specialization into two hair cell types that has been described in both birds and mammals is the clearest case of extreme differences between hair cell groups that has been observed in vertebrates. It exists at the same time as the general presence of gradients in both hair cell types along and across the papilla that determine, for example, their frequency responses and thus the pattern of the tonotopic organization.

3.01.3.5 A Synopsis of Hair Cell Phylogeny in Vertebrates

It is likely that the first vertebrate hair cell organs were lateral lines that contained a single type of hair cell. With differentiation of the lateral line into different types of organs, hair cell specialization set in as a result of selection pressures to better analyze the sensory information offered by the environment. Similarly, the analysis of stimuli by semicircular canal cristae and vestibular maculae depended not only on canal dimensions and the characteristics of the otolithic masses overlying the maculae, but also on hair cell differentiation. During the evolution of fish, the fundamental specialization of vestibular hair cells into two types began with minor structural and biochemical changes, but this became much more pronounced in the land vertebrates, where the two types are easily recognizable via overt structural features. Although it is likely that the hearing organs of land vertebrates began by utilizing only type II hair cells, unique kinds of hair cell specializations arose in lepidosaur, archosaur, and mammal ancestors that are recognizable along and across the respective epithelia. These generally show functional specializations at least as profound as their differing structural features to the extent that in birds and mammals at least, the functions of stimulus detection and stimulus amplification have been separated by a division of labor between two populations of highly specialized hair cells.

3.01.4 Ciliated Mechanoreceptors of Nonchordate Animals

Ciliated mechanoreceptors are found even in the earliest of Eumetazoa; however, the consideration of their homology with vertebrate auditory hair cells is not trivial. As we have already mentioned, considerations of homology can be made using comparative anatomy, which are qualitative (a structure

is either homologous or not), or can be made using molecular biology using sequence comparisons that are quantitative. As data exist on both anatomy and molecular biology, both aspects need to be considered. In this section we primarily focus on describing the anatomy of ciliated mechanoreceptors from a sampling of nonchordate groups, starting from the most primitive, the cnidarians, and progressing to ecdysozoans as exemplified by the nematode and dipteran insects and the lophotrochozoan cephalopod mollusks. We describe the structural characteristics of the ciliated mechanoreceptor found in these groups and discuss the molecular correlates that are known. While it is possible that an archetype for the ciliated mechanoreceptor is present (Vinnikov, Y. A., 1982), its significance must be placed within the context of the phylogeny (Adoutte, A. *et al.*, 2000).

In most cases the ciliated sensory neuron is of the primary type, that is, it can be thought of as a bipolar neuron, with its own axon. Secondary ciliated sensory neurons, seen in coelid cephalopod mollusks and in vertebrates, are modified epithelial cells and do not have axons.

3.01.4.1 Cnidarian Hair Cells

Cnidarians, the group containing hydra, jellyfish, and sea anemones, are basal eumetazoans positioned before the radiation of metazoans into deuterostomes and protostomes. This location highlights the importance of the cnidarians in any evolutionary discussion. Cnidarians do possess ciliated mechanoreceptors, responsible for both touch sensation and gravity sensation; they also show morphological variation depending not only on species but also on the function within an individual. In cnidarians, ciliated mechanoreceptors are found in specialized orientation organs, and also serve a combined chemosensory and mechanosensory role in the various types of stinging cell, the nematocysts.

The cnidocyte is a unique and defining feature of the phylum Cnidaria, playing a role in prey detection, capture, and defense (Ruppert, E. E. *et al.*, 2004; Figure 9). A cnidocyte itself houses a large fluid-filled sac, a cnidae which itself contains a large inverted tubule. Upon appropriate stimulation, the tubule is rapidly everted and penetrates the prey, in many cases concomitantly releasing toxin that causes stinging or paralysis. Three types of cnidocytes have been identified; two of them, spirocysts and pthychocysts, are only found in the class Anthozoa (corals, sea anemones, sea ferns, and sea pens); indeed

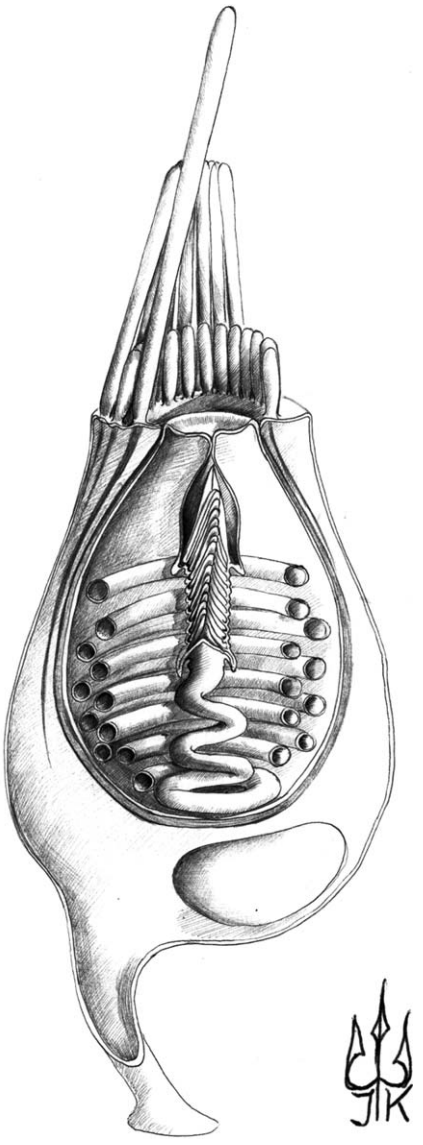

Figure 9 A schematic drawing of a nematocyte of the Cnidaria. These cells are connected synaptically at their base to nerve cells and/or epithelial muscle cells. Within the cell is the nematocyst, a capsule containing a thread that can be rapidly discharged into the prey. An original drawing by Johanna Kraus, all rights reserved.

pthychocysts are only found in the epidermis of the tube anemone. The third type of cnidocyte is the nematocyst, found throughout the cnidarian phylum and, for our purposes, the most interesting. These are associated with supporting cells.

The nematocyst itself is part of a type I sensory neuron and bears a sensory cilium. In anthozoans (sea anemones and corals), the cilium is motile (and called a ciliary cone) whereas in hydrozoans and

scyphozoans it is nonmotile (and called a cnidocil) (Peteya, D. J., 1975; Holstein, T. and Hausmann, K., 1988). The ciliary cone consists of a long cilium with a typical 9×2 (these are the peripheral doublets of A and B microtubules) +2 (a central pair of microtubules) configuration of microtubules, a common feature of sensory cilia (Vinnikov, Y. A., 1982). The cilium is surrounded by large diameter stereovilli of shorter length than the cnidocil itself, which are in turn surrounded by a palisade of shorter, smaller diameter stereovilli from the adjacent cells, the supporting cells (Peteya, D. J., 1975). The numbers of these larger and small stereovilli can vary; however, all seem to be stiffened by actin filaments (Wood, R. L. and Novak, P. L., 1982; Stidwill, R. P. *et al.*, 1988).

The resemblance of the sensory apparatus of the nematocyst to the hair cells of vertebrates suggests a mechanosensory function of these cilia, and indeed some data indicate that this is the case. Using a loose-patch, cell-associated recording method in slices of anemone tentacles, Mire and Watson measured the electrophysiological changes of the hair bundles of the nematocyst under mechanical stimulation (Mire, P. and Watson, G. M., 1997; Watson, G. M. and Mire, P., 1999). When the hair bundles were deflected using puffs of seawater, changes in membrane potential were recorded. Some cells were hyperpolarized in a graded manner, while others depolarized, depending on the direction of the deflection. By plotting the response amplitude as a function of the deflection magnitude, it became clear that the negative response is smaller and saturates relatively easily, whereas the positive response is larger and saturates more gradually, a characteristic of other mechanotransducers such as hair cells of the vertebrate inner ear (Hudspeth, A. J. and Corey, D. P., 1977). Indeed the presence of tip links in the nematocyst hair bundle may suggest that a process common to the vertebrate hair cell and involving a mechanically gated ion channel is responsible for mechanoreception (Watson, G. M. *et al.*, 1997).

Ciliated mechanoreceptors do not occur just in nematocysts; hydrozoan, scyphozoan, and cubozoan species also have a gravity-sensing organ known as the statocyst (Horridge, G. A., 1969). As shown by statocyst ablations in the hydrozoan *Aequorea*, this organ is responsible for the righting behavior of the animal (Singla, C. L., 1975). There is a huge variety of statocysts in the cnidarians, even within those of the same class; however, they all have a cell, the lithocyte, which contains a large concretion of some calcium salt (Horridge, G. A., 1969). The weighted lithocyte is deflected when the position or equilibrium of the animal is altered. Ciliated sensory cells that surround the concreted cell register this deflection. These ciliated cells are type I sensory cells, that is, cells that have a distal cilium and a proximal axon (Horridge, G. A., 1969). There are three types of ciliated sensory cells found in the cnidarian statocysts that have been examined. Leptomedusae typically have a single kinocilium and lack associated stereovilli. In Narcomedusae and Tracymedusae the sensory cells bear a kinocilium that is surrounded by a ring of stereovilli (Singla, C. L., 1983). The third type of ciliated sensory cell is found in a subset of statocysts in the basal cushion and sensory papilla. The kinocilia are extremely long and stiff with a well-developed rootlet system extending into the cytoplasm.

While the cytomechanics of nematocyst hair bundle function are beginning to be characterized, little work has been performed on the cytomechanical function of the cnidarian statocyst mechanoreceptor. Although it is likely that a mechanism consistent with the gated-channel model also functions in the statocyst hair cells of cnidarians, until the electrophysiology is investigated and until the molecular candidates are known, any proposed mechanism remains speculative.

3.01.4.2 Mechanotransduction in *Caenorhabditis elegans*

The nematode worm *C. elegans* has been used extensively as a model organism for developmental biology. The lineage of each individual cell has been traced and, when combined with the genetic tractability of the animal, has led to an understanding of the interactions that specify these lineages. *C. elegans* hermaphrodites are known to have 302 neurons, and a number of them are responsible for different mechanosensory behaviors: the gentle body touch, the harsh body touch, the nose touch, and a response to texture (Ernstrom, G. G. and Chalfie, M., 2002). As the neurons that mediate both the harsh and gentle body touch are not ciliated and detection appears to be mediated by varicosities, these will not be considered further (Chalfie, M. and Thomson, J. N., 1982; Chalfie, M. *et al.*, 1985).

There are some behaviors in *C. elegans* that are mediated by ciliated mechanosensory neurons. One is the nose touch avoidance, which causes the worm to move back if it bumps its anterior pole (Kaplan, J. M. and Horvitz, H. R., 1993). This behavior is mediated by

a number of sensory neurons, named ASH, FLP, and OLQ. The ASH neurons are mono-ciliated type I sensory neurons. Perkins, L. A. *et al.*, (1986) describe three segments to the cilium. The proximal zone, found at the base of the cilium, consists of 9×2 microtubules attached to the membrane by Y-shaped links arranged around a central cylinder. This cylinder contains a core of a variable number of singlet microtubules. Further distally, in the transition zone, there is no central cylinder, although the odd singlet microtubule can be seen. The peripheral microtubules spread apart, causing an apparent loss in the doublet structure and indeed the B subfibers are gradually lost toward the distal segment, the end of the microtubule. This, in effect, causes the cilium to flare, becoming thicker distally. The other neurons of this pathway, the FLP and OLQ neurons, rather resemble the CEP and ADE neurons which are described below.

The CEP and ADE neurons mediate a behavior related to texture sensation that indicates food (Sawin, E. R. *et al.*, 2000). When the worm encounters a bacterial lawn on an agar substrate, it slows down, presumably to dwell for longer so it can ingest more food. This behavior can be mimicked using sepharose beads and so it is likely that this slowing behavior is due to mechanoreception and not chemosensation. Indeed these cells express the worm homolog of the mechanotransduction channel found in *Drosophila* sensory bristles, *NompC* (Walker, R. G. *et al.*, 2000). The neurons themselves (i.e., the CEP, ADE, FLP, and OLQ) are mono-ciliated type I sensory neurons. The transition zone in their cilia resembles that of the ASH cilium, with 9×2 peripheral microtubules arranged around a central core (Perkins, L. A. *et al.*, 1986). However, some of these doublets terminate just distal to the transition zone. There is some variety in the characteristics of the distal segments of these neurons. For example, in the CEP cilia, the microtubules are interspersed with an electron-dense material and mold them into irregular rods. In OLQ neurons, the cores of the microtubules making up the doublets are filled. Both the CEP and OLQ neurons are anchored into the cuticle of the worm using a small nubbin, a varicosity on one side of the cilium, at the base of the transducing region.

An interesting property of the texture sensation behavior is its modulation depending on whether the animal is satiated or starved. This depends on serotonin and has provided some insights into the mechanisms by which neuromodulation can impact on mechanosensation (Sanyal, S. *et al.*, 2004). These kinds of studies highlight the strength of *C. elegans* for studies into neuromodulation. Synaptic contacts have been found on the CEP neurons from the neurons mediating the gentle touch (Chalfie, M. *et al.*, 1985). It is thought that encountering bacteria may register as a gentle touch (causing the animal to stop); by direct neurological input, the gentle touch response is abrogated when the animals encounter bacteria.

While *C. elegans* is a good model for the modulation of mechanosensation and the mechanisms by which other modalities can impact mechanoreception, there is still no clear mechanism as to how the mechanosensory transduction channels respond to vibrations, and indeed none that conforms to the gated-spring model proposed for hair cell stereovilli. One conjectured model could be similar to that proposed for *Drosophila* mechanotransduction (see below). Here NompC on the sensory neuron is attached to NompA anchored on a supporting cell. While NompC is found on mechanosensitive CEP neurons, a *C. elegans NompA* homolog has not yet been characterized.

3.01.4.3 Ciliated Mechanoreceptors in Insects

Insects have three basic types of ciliated mechanoreceptor: the bristle organ, the campaniform sensillum, and the chordotonal organ (Keil, T. A., 1997). All of them share common features, although they have become elaborated for their particular functions. The basic structure of what has been termed the organule is a central type I ciliated sensory neuron innervating a structure formed by three support cells (Lawrence, P. A., 1966). The cilium of the sensory neuron can be separated into two distinct domains. The cilium itself starts just above the distalmost centriole in the neuron and is initially of the $9 \times 2 + 0$ type. As the cilium extends distally, it may flare out, increasing in diameter and in the number of microtubules. At its most distal point the cilium contains a highly ordered cytoskeletal complex, the tubular body. This is made of a few to many thousands of short microtubules tightly packed into an electron-dense structure (Keil, T. A., 1997). This is attached to the membrane via various connectors, which is in turn attached to the dendritic cap, an extracellular matrix (ECM) structure secreted by the membrane of the sheath cell (also known as the theocogen) using fine connectors (Thurm, U. and Küppers, J., 1980).

As well as the sheath cell and the ciliated sensory neuron itself, two other cell types form the mechanosensory apparatus. The trichogen (shaft) cell forms the hair, which is most obvious in the bristle organ. The tormogen (socket) cell forms the joint membrane at the base of the hair. Both cells retract from the cuticle later in development to form the outer sensillum lymph cavity. This cavity is isolated from the rest of the subcuticular cavity by a seal formed by the periphery of the tormogen cell.

The sensillum lymph is high in K^+ and low in Na^+ ions (Thurm, U. and Küppers, J. 1980; Grünert, U. and Gnatzy, W., 1987). The supporting cells, actively transporting potassium ions from the hemolymph, maintain this ionic balance. By analogy with vertebrate hair cells, it is probable that the movement of the cilium causes an opening of cation channels allowing a rapid flood of K^+ into the neuron and leading to neuronal depolarization. As we have already discussed in relation to the cnidarian nematocyst, many mechanoreceptors show a directional sensitivity; movement of the cilium in the opposite direction inhibits receptor potential. Insect mechanoreceptors, at least those found on the bristle organ, also show the same profile (Corfas, G. and Dudai, Y., 1990). While many mechanoreceptors can be incredibly sensitive, the response decreases if deflection is sustained, that is, the cells show adaptation (Walker, R. G. *et al.*, 2000).

Models have been proposed that draw similarities to the gating-spring model proposed for vertebrate hair cell function (Gillespie, P. G. and Walker, R. G., 2001). This model requires that an ion channel be anchored under tension between the ciliary cytoskeleton and the dendritic cap. Deflection causes a certain number of channels to open; further deflection would cause more channels to open. Indeed adaptation is proposed to use a similar mechanism to the vertebrate hair cell, where the channel on the cilium would slide along the cytoskeletal tracks, in one direction passively and in the other direction using a molecular motor, thereby altering the tension on the channel.

The relevant structural features of insect mechanoreceptors can be clearly seen in the bristle mechanoreceptors. Here the dendritic cap links the cilium of the sensory neuron to the hair embedded in the cuticle of the insect. Another mechanoreceptor, the campaniform sensillum, is quite similar to the bristle organ and is responsive to deformation of the cuticle. Rather than connecting to a hair, the ciliated dendrite makes a connection with a button on the cuticle, the dome cuticle. The organization of this structure closely mirrors that of the bristle organ with perhaps some alteration in the function of the trichogen cell.

The structure of the chordotonal (also known as the scolopidial) cell is, at first sight, somewhat divergent; however, it still follows the organule plan of insect mechanoreceptors, even though the morphology and arrangement of the cells are somewhat different. The chordotonal organ is used as an internal pressure sensor; however, it is also the mechanoreceptor responsible for hearing in many insects. In contrast to the rather solitary bristles and sensilla, the chordotonal units (known as scolopidia) are organized into arrays in the various regions of the insect. The structure of a typical insect bristle mechanoreceptor is illustrated in Figure 10.

The main feature of the scolopidium is the scolapale space, a fluid-filled, spindle-shaped space (Todi, S. V. *et al.*, 2004; Yack, J. E., 2004). This space encloses the ciliated dendrite of the type I sensory neuron, the cilium of which is suspended between two surfaces where it responds to vertical deflections and deformation. The cilium itself is encased in the dendritic cap (more correctly called a dendritic sheath) made by the theocogen (sheath) cell. Just before entering the sheath, the cilia show a dilation containing an

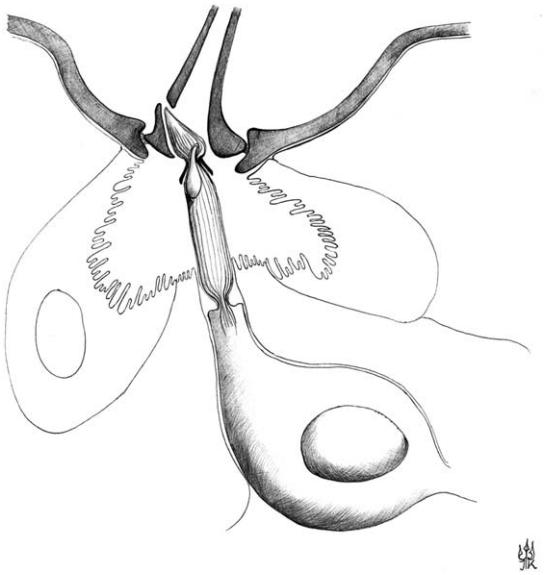

Figure 10 A schematic drawing of the structure of a typical superficial insect mechanoreceptor, in this case a bristle organ. The cytological plan of chordotonal organs is similar to that shown here. Mechanosensation is thought to depend on the relationship between the cilium and its dendritic cap. An original drawing by Johanna Kraus, all rights reserved.

electron-dense oval body. The cilium itself shows the same axoneme pattern, 9 peripheral doublets of microtubules without any central filaments ($9 \times 2 + 0$). Proximally there are extensive ciliary rootlets that run far into the cell body of the neuron, indeed some pass the nucleus. Scolopidia that are responsible for hearing are typically innervated by two or, sometimes, three type I ciliated sensory neurons (Hallberg, E. and Hansson, B. S., 1999). The significance of this is unclear. There is yet more variation at the distal end of the scolopidium; in one type of scolopidium, known as amphinematic, the cilium is attached to the distal cuticle through the elongated dendritic sheath connected to what can be considered to be a modified tubular body of the cilium. The other type of scolopidium is the mononematic. Here, the cilium is indirectly connected to the distal integument through a cuticular cap (provided by the dendritic sheath) that is in turn associated with one or two distally located attachment cells (Yack, J. E., 2004). In both types of scolopidium are massive bundles of actin cables, the scolopale rod, that give the scolopale cell (which can be considered to be a modified theocogen or sheath cell) its stiffness and afford some tension on the ciliated dendrite. These rods have also been used to suggest a mechanism of mechanotransduction based on a string on a bow model (Todi, S. V. *et al.*, 2004; 2005).

As mentioned earlier, the scolopidia are used in some insects as auditory mechanotransducers. The array of scolopidia that constitute the hearing organ is called, in flies, Johnston's organ (Boekhoff-Falk, G., 2005). In the fruit fly *Drosophila* and in the mosquito, this is found as a specialized region in the joints between basal segments of the antennae. However, this is not the case in all insects. In the bladder grasshopper, the main hearing organ is found in the first abdominal segment, with five smaller organs on abdominal segments A2–A6, and in the hawkmoth the hearing organ is found located just lateral to the tongue (van Staaden, M. J. and Römer, H., 1998; Göpfert, M. C. and Wasserthal, L. T., 1999). An interesting aside here, and one outside the scope of this chapter, is the further diversity of hearing organs within insects. In many insects, where sound plays a very important role in their lives (e.g., for mating, prey detection, and predator avoidance), as in some moths and true crickets, the animal uses a tympanal hearing organ (Stumpner, A. and von Helversen, D. 2001; Yack, J. E., 2004). This is characterized externally by a cuticular-derived tympanal membrane, which is deflected by sound. The tympanum is associated internally with an air sac derived from a trachea. The scolopidia are attached to the air sac or to the tympanal membrane.

Drosophila is used as the major insect model organism and the ability to identify molecules by directed genetic screens makes this preeminent in defining the components of the transduction system involved in mechanosensation. Two such screens have been carried out. Kernan M. *et al.* (1994) took extracellular recordings of bristle organs of mutagenized larvae, finding a number of genes through which mechanosensation was affected. Eberl D. F. *et al.* (1997) used a property of *Drosophila* courtship behavior for their screen. Male *Drosophila* will vigorously court when they hear a component of the mating sound (known as the pulse sound) produced when the wings are rubbed together (Bennet-Clark, H. C. and Ewing, A. W., 1970). In fact this sound is so effective that when presented with a recording of it, male *Drosophila* will court other males (von Schilcher, F., 1976). This provided a very simple behavioral screen.

In total, Eberl D. F. *et al.* (1997) identified 15 mutants in which auditory mechanosensation was perturbed. Many of these genes have now been identified. Possibly the most intriguing discovery, and one that indirectly led to the identification of a vertebrate mechanotransducing channel, is the identification of the *No mechanoreceptor potential C* gene or *NompC* (Walker, R. G. *et al.*, 2000). Flies that are mutant for *NompC* show a complete absence of mechanoreceptor potential in bristle organs. The product of the *NompC* gene is a part of the TRP (transient receptor potential) gene family. This provoked a great deal of interest, as the TRP family had been shown to mediate a large number of sensory processes such as vision, chemosensation, thermosensation, and osmosensation (Montell, C., 2005). Furthermore, this family was represented in numerous species from different phyla, ranging from nematodes (*C. elegans*) to vertebrates. The vertebrate homolog of NompC is in the TrpN subgroup and seems to form part of the mechanotransduction complex in fish (Sidi, S. *et al.*, 2003). However, the only vertebrates where a *TrpN*/*NompC* has been found are fish and frogs; *TrpN*/*NompC* has not been found in birds or mammals and indeed it appears to have been deleted in the mammalian and chicken genome (Boekhoff-Falk, G., 2005; Gillespie, P. G. *et al.*, 2005). *TrpN1* is expressed at the tip of the microtubule-based kinocilium of the frog hair cells (Shin, J. B. *et al.*, 2005), whereas TrpA1 is found at the tip of the actin-based stereovilli (Corey, D. P. *et al.*, 2004). As we

have already described, mammal and, to a significant extent, avian hair cells do not have a kinocilium, relying instead on just the stereovilli. Indeed it is possible to correlate the presence of TrpA1 and TrpN1/NompC with the presence of stereovilli and kinocilia in the ciliated mechanoreceptors. Unex-pectedly, the absence of an inner ear phenotype of *TrpA1* mutants (despite an absence of auditory response in other forms of ablation in the mouse) suggests that there may be another, as yet uncharacterized participant in the mechanoreceptor transduction channel of vertebrate hair cells (Kwan, K. Y. *et al.*, 2006).

A cautionary note: while *NompC* mutants show no mechanoreceptor potential in the bristle organs, auditory function is more or less normal. This indicates that other Trp channels operate in Johnston's organ, the auditory organs of the fly. Indeed two *TrpV* homologs can be detected, and both are localized to the proximal part of the ciliated dendrite (Kim, J. *et al.*, 2003; Gong, Z. *et al.*, 2004). Interestingly, the localization of TrpV channels is mediated by heterotetramerization with another unknown channel that is more localized. Mutants for either *Drosophila TrpV* channel show mislocalization of the other channel to the ciliated dendrite (Gong, Z. *et al.*, 2004). Thus far, *TrpV* homologs in vertebrates have not been characterized.

Other molecules that are important in vertebrate mechanoreception have also been shown to play a role in *Drosophila* mechanosensation. Mutations, in mammals, of the atypical myosin VIIa result in stereovilli that are incorrectly positioned and disarrayed, and indeed this is the cause of the human deafness syndrome Usher 1B (Hasson, T. *et al.*, 1995; Weil, D. *et al.*, 1995). In flies that are mutant for the myosin VIIa homolog *crinkled*, the scolopale cells are disorganized, perhaps due to a loss of the apical attachment of this cell (Todi, S. V. *et al.*, 2005).

Another molecule that appears in both mammalian and *Drosophila* hearing organs is prestin, a member of the solute carrier-26 (SLC26) family (Weber, T. *et al.*, 2003). The SLC26 family has diverse functions; in particular they are anion exchangers. In mammals, prestin is found in outer hair cells of the cochlea; however, it does not act as an anion transporter. Instead it acts as a motor driving cochlear amplification of sound signals (Zheng, J. *et al.*, 2000). Cochlear amplification via prestin (as contrasted with cochlear amplification by an active bundle mechanism; Manley, G. A., 2001) is a process that occurs exclusively in mammals (Géléoc, G. S. and Holt, J. R., 2003). Its presence in the auditory structure of the fly is therefore perhaps unexpected and until the function of *Drosophila* prestin is elucidated, statements about the relationship between the fly and vertebrate prestin homologs will be speculative.

This brings us to consider the larger issue of homology between the insect scolopidium and the vertebrate inner ear hair cell. Morphologically, the difference is simple; flies uses the deflection and deformation of a ciliated dendrite made of microtubules for mechanosensation, while vertebrates use actin-based stereovilli. Despite the presence of homologous molecules, mechanistically there must be differences between both modes of mechanosensation.

3.01.4.4 Mollusk Hair Cells

Thus far we have discussed nonchordate mechanoreceptors in cnidarians, a basal metazoan, and in nematodes and insects, both examples of Ecdysozoa (moulting animals). This leaves the lophotrochozoans. Ecdysozoa and Lophotrochozoa are protostomes; however, the two lineages diverged soon after the protostomes/deuterostomes split. Thus, an evolutionary perspective needs an example from the Lophotrochozoa. Mollusks are the largest group in this taxon and are also the most diverse. They range from chitons (Polyplacophora), snails and slugs (Gastropoda), bivalved animals such as oysters (Bivalvia) to octopuses, squids, and *Nautilus* (Cephalopoda). We will focus on the ciliated mechanoreceptors of cephalopods, which are perhaps the most advanced of invertebrate mechanoreceptors.

Cephalopods have a very well developed nervous system, and indeed remarkable sensory organs that are comparable in complexity to those found in vertebrates. It is the statocyst that attracts our attention. This organ helps maintain equilibrium, sensing linear (gravitational) and rotational acceleration (Budelmann, B. U. *et al.*, 1997). The statocyst is essentially a closed cavity that is lined with a complicated arrangement of specialized epithelia dotted with ciliated mechanoreceptors. Statocysts of simpler cephalopods (*Nautilus*) are completely lined with sensory epithelia and half-filled with a number of calciferous granular statoconia and with endolymph (Neumeister, H. and Budelmann, B. U., 1997). There are two types of mechanoreceptor in the *Nautilus* statocyst; type A is found in the ventral half, the hemisphere of the statocyst where the statoconia are found. type B mechanoreceptors are found in the dorsal hemisphere, in the region containing the endolymph.

The mechanoreceptors found in *Nautilus* are primary sensory neurons, that is, an axon leaves the basal part of the cell, joining with a complicated nerve plexus underneath the statocyst epithelium. A type A mechanoreceptor cell typically carries between 10 and 15 kinocilia, arranged in a single row, which is inclined toward the cell surface. The kinocilia are of the typical $9 \times 2 + 2$ configuration. The microtubules connect to the basal body, which in turn is part of an extensive basal root network. Running parallel to the kinociliary row and right beside each kinocilium is a row of shorter microvilli (Neumeister, H. and Budelmann, B. U., 1997). The rows of kinocilium and microvilli are not centered on the cells, but are polarized, displaced to the periphery on the cell. Not only the bundles but also the basal root network is polarized and points in the same direction as the kinocilium. Two interesting points are that the long axis of the kinociliary row is horizontal to the equator of the statocyst and that the polarization of each type A cell (that is to say the side of the cell to which the row is located) is the same for neighboring cells, suggesting a more global mechanism for polarizing type A mechanoreceptors in *Nautilus*. The association of these cells with the statoconia suggests a role in the sensation of gravity and other forms of linear acceleration.

A type B mechanoreceptor cell has 8–10 kinocilia, and as in the type A, these are placed on one side of the cell. Unlike the type A cells, however, the kinocilia are not arranged in a row but have an almost haphazard arrangement, although it is reported that some seem to have a circular configuration. There are again shorter microvilli on these cells, but they are more numerous than those found in the type A mechanoreceptors. These mechanoreceptors, and their association with the endolymph, are thought to be responsible for sensing angular acceleration (Neumeister, H. and Budelmann, B. U., 1997).

The statocysts of Coleoid cephalopods are more complicated than those of *Nautilus* (and in turn other mollusks). There are two main types, the Octopoda type and a Decapoda type which share some features. Contained in the statocyst is the gravity-sensing organs containing a macula/statolith system that is quite separate from the angular acceleration sensing organ that consists of a crista/cupula system. In the Octopoda type, the crista/cupula system is subdivided into nine segments, arranged so they can detect movements in the three spatial dimensions. The Decapoda type is irregularly shaped, as cartilaginous lobes protruding into the cyst direct the flow of the endolymph. It has three maculae, with a statolith attached to one and statoconia to the other two, arranged at right angles to each other. The crista/cupula system of the Decapoda is subdivided into four segments, arranged into three dimensions.

The mechanosensory cells found in these statocysts resemble the type A mechanoreceptors; however, while *Nautilus* has between 10 and 15 kinocilia per cell, the Octopoda- and Decapoda-type mechanoreceptors have between 50 and 150 kinocilia per cell (Figure 11). Cells similar to the type B mechanoreceptors in *Nautilus* are not found in these cephalopods (Budelmann, B. U. *et al.*, 1973). Again all

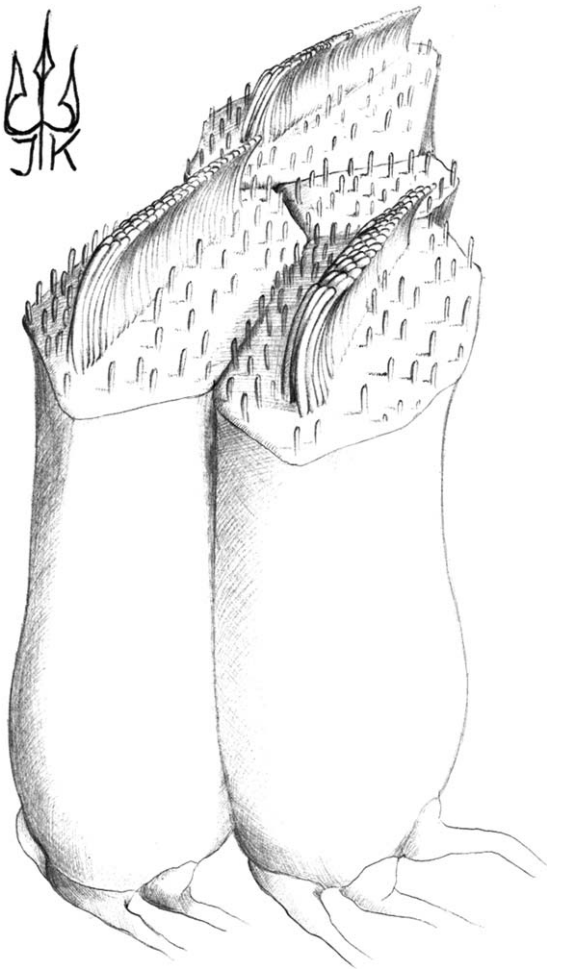

Figure 11 A schematic drawing of a cephalopod hair cell carrying a large number of kinocilia that are flanked by very much smaller microvilli. The ciliary bundles are displaced to one side of the cell, and the cilia themselves are angled toward the surface of the cell. An original drawing by Johanna Kraus, all rights reserved.

kinocilia are of the same length, arranged in a row along the long axis of the cell. All are inclined toward the surface of the cell, showing the same kind of polarization as found in *Nautilus*. The kinocilia are also associated with microvilli, found in parallel rows either side and next to the kinociliary row. These are not stereovilli as found in vertebrates, and there seem to be no tip links associating the microvilli to the kinocilia. Instead, each kinocilium is associated with the other by membrane junctions (Budelmann, B. U. *et al.*, 1973). The significance of this is still unclear.

At this point it is worth mentioning that other mollusks, that is, most gastropods and bivalves, have mechanoreceptors that are similar to the *Nautilus* type B mechanoreceptor (a random or circular arrangement of kinocilia); however, they are unpolarized. As such, the lack of polarization suggests that they are involved only in gravity sensation (McKee, A. E. and Wiederhold, M. L., 1974; Moir, A. J., 1977). Polarization of the basal feet with respect to the kinocilium is thought to correlate with the deflection of the kinocilia. Deflection in the direction of the basal feet causes maximum depolarization while deflection away from the basal foot causes hyperpolarization (Budelmann, B. U. and Williamson, R., 1994). This is important for detecting the directions of linear and angular acceleration.

One important difference between coelid cephalopods and other mollusks is that the mechanoreceptors found in the statocyst are predominantly secondary sensory cells (Stephens, P. R. and Young, J. Z., 1982; Budelmann, B. U. *et al.*, 1987). One exception is in the crista, which is a ridge of cells. In the middle of the ridge are 2 or 4 rows of larger hair cells and 2–4 less regularly arranged hair cells on either side. In the octopuses (the coelids that have been studied) the hair cells on one side of the ridge are primary, while on the other side, they are secondary. These secondary cells are large or small and are synaptically connected to two types of afferent neurons. No other animal has both primary and secondary sensory cells in the same epithelium.

The ionic character of the cephalopod hair cell is almost identical to that of vertebrates. This may indicate that a similar mechanoreceptor channel system acts, but as yet the molecular correlates for mechanosensation in mollusks are unknown. We would expect a Trp receptor to form a part of a presumptive spring-gated channel, similar to that found in vertebrates.

3.01.5 Molecular Evolution of Mechanoreceptors

In the preceding sections we described cellular relatedness between vertebrate and nonvertebrate ciliated mechanoreceptors and we find that these cells share certain characteristics that make them able to respond to mechanical stimuli. However, one important question remains: are ciliated mechanoreceptors in different species monophyletic or the result of convergent evolution? To fully answer this, the developmental program, or ontogeny, of mechanoreceptors from different species needs to be examined. In this section, the agents that transmit this information, the genes, are discussed. Only by understanding the molecular core of mechanoreceptor development can we be informed regarding a monophyletic or polyphyletic origin.

In a typical developmental/differentiation paradigm, an external signal – emitted, for example, by an adjacent group of cells – elicits a response in a target cell, a process known as induction. Induction usually results in the activation of a protein that acts on DNA. Such proteins, called transcription factors, bind stretches of DNA, known as *cis*-regulatory elements, and activate the genes controlled by these regions. These genes form a hierarchical organization of fate choices in the form of a transcription factor cascade. This becomes important when the consensus view of molecular evolution is taken into consideration. At the molecular level, developmental programs evolved as conserved genetic regulatory pathway are subtly modified, usually at the level of *cis*-regulatory elements and by equally subtle changes in the activity of a particular protein. Thus to extend the presumed cytological homology to the molecular level, an appreciation of the conservation of gene networks, in particular transcription factor cascades, is important. At this point we introduce an important caveat; developmental biology uses a limited number of model systems, comparative biology (by definition) needs far more. More specifically, much is known about the molecular networks that control the development of mechanoreceptors in vertebrates and in *Drosophila*; however, much less is known about the genetic cascades involved in the development of the other species considered. Therefore, any discussion about molecular comparisons makes large assumptions in the light of a somewhat limited data set. Notwithstanding, by identifying homologous genes from the phyla discussed, it is possible to be

informed on the validity of these assumptions, and indeed many genes involved in the development of vertebrate or fly mechanoreceptors can be found in cnidarians, nematodes, and cephalopods.

3.01.5.1 Development of Ciliated Mechanoreceptors

Ciliated mechanoreceptors are almost exclusively restricted to the ectodermal lineage of all animals. This highlights that the development of the mechanoreceptors is constrained by the molecular history of the cell. Indeed, mechanoreceptor cytodifferentiation can be thought of as the end product of a gradual restriction in cell fate, with each step being represented by a progression in the genetic transcription factor cascade.

In vertebrates, the ciliated mechanoreceptors form from a specialized, thickened region of epithelium, the sensory placode (Baker, C. V. and Bronner-Fraser, M., 2001). For the purpose of this review we discuss the vertebrate inner ear that forms from the otic placode. The otic placode is specified from ectoderm already committed to adopt a sensory fate. This pre-placodal domain is specified by surrounding tissues and refers to a territory of the vertebrate embryo that will give rise to not only the otic placode, but also other sense organs, peripheral neurons of the head and the lens. The pre-placodal domain is marked by families of transcription factors showing homology to a number of genes originally cloned in *Drosophila*: *distalless* (*dlx*) gene, the *sine oculis* (*six*) gene, and *eyeless* (*eya*) family (Schlosser, G., 2005). In flies these genes also play a role in epithelial patterning and outgrowth; however, it is not clear whether the role of these genes in the fly is to establish a field of competence or whether they participate more directly in the genetic cascade that leads directly to the formation of the mechanoreceptor.

3.01.5.1.1 Extrinsic factors regulating mechanoreceptor development

The early development of mechanoreceptors depends on the action of extrinsic factors. These act on competent ectoderm and are usually signaling molecules acting on cells to direct them to adopt a ciliated mechanoreceptor fate. The extrinsic mechanisms are not very well conserved between different phyla, and indeed there is considerable variability even within vertebrates. Thus their individual descriptions are not so pertinent to this discussion and will not be dealt with in depth. In vertebrates, a specific area of the pre-placodal region is acted upon by localized signaling interactions that direct the formation of the otic placode within this territory (Groves, A. K. and Bronner-Fraser, M., 2000; Ladher, R. K. *et al.*, 2000; Kil, S. H. *et al.*, 2005). This early phase of signaling is mediated, in vertebrates, by members of the fibroblast growth factor (FGF) family in combination with the wingless (WNT) family and induces pre-placodal ectoderm to adopt an otic fate (Schlosser, G., 2006). In *Drosophila*, the role of this early signaling in the development of the mechanoreceptors is not clear; Niwa N. *et al.* (2004) suggest the existence of a pre-proneural state that depends on the action of *decapentaplegic* (the fly homolog of *Bmp2/4*) and *wingless* (*wnt*).

The induced vertebrate inner ear invaginates to form an otocyst within the mesenchyme of the head. During this process extrinsic signals once again specify different territories within the inner ear. The otocyst is embedded in head mesoderm and flanked by the neural tube and endoderm, tissues that to varying extents exert some influence onto the otocyst (Wu, D. K. and Oh, S. H., 1996; Wu, D. K. *et al.*, 1998; Riccomagno, M. M. *et al.*, 2002; Bok, J. *et al.*, 2005; Riccomagno, M. M. *et al.*, 2005). In amniotes, where the studies have been performed, the hindbrain and the notochord provide the otocyst with dorsal and ventral identities, respectively. Recent reports described the antagonistic effect of Wnt3a, emanating from the hindbrain, and sonic hedgehog, from the notochord, directing development of the vestibular and auditory portions of the otocyst (Riccomagno, M. M. *et al.*, 2002; 2005). As has already been described, the morphology of hair cells is different in the two parts of the inner ear, leading to the speculation that the action of these extrinsic factors has a direct bearing on the differentiation of the hair cell subtypes. Finally, there is a role for extrinsic signals in the differentiation of the hair cells of the cochlea. Montcouquiol M. and Kelley M. W. (2004) showed that without mesenchyme, pattern and differentiation within the cochlea are perturbed.

Hair cells form from regions of the otocyst known as sensory patches. The sensory patches express a number of extrinsic factors that have been shown to play a role in mechanoreceptor development. In vertebrates, the sensory patches are specified by Notch and its ligands and by BMP molecules; however, both groups of molecules have additional functions later in development. As already mentioned, in flies, sensory

patches are though to be specified by the combined action of *decapentaplegic* and *wingless* (Niwa, N. *et al.*, 2004). Subsequent differentiation is triggered by the *Notch* ligand *Delta* (Schweisguth, F., 1995). It should be noted that in both vertebrates and insects, the mechanisms that specify exact mechanoreceptor identity do so in parallel to the differentiation of the sensory patches.

In vertebrates, *Bmp7* is expressed very early in the inner ear (Oh, S. H. *et al.*, 1996), with its close family member *Bmp4* appearing soon after. In chickens, *Bmp4* is expressed in all the sensory patches, and in mouse and zebrafish it is expressed in most (Oh, S. H. *et al.*, 1996; Morsli, H. *et al.*, 1998; Mowbray, C. *et al.*, 2001). While the overexpression of BMP7 has not been studied, BMP4 has been investigated. These data support a role for BMP4 as a permissive factor, allowing the differentiation of the inner ear hair cells; ectopic application of BMP4 increases the number of hair cells that are found, and application of a BMP4 antagonist decreases their number (Chang, W. *et al.*, 1999; Gerlach, L. M. *et al.*, 2000; Gerlach-Bank, L. M. *et al.*, 2004; Li, H. *et al.*, 2005). However in all cases, the experiments were performed too late to address any role in the formation of the sensory patches themselves. Furthermore, these experiments have only been performed in the chicken; and while BMP molecules are expressed in the inner ear, and more pertinently for us in the sensory patches, their function has not been addressed in other vertebrates.

The notch family of signaling molecules comprises the *Notch* receptors and its ligands, *Delta* and *Jagged/Serrate*. Signaling between these molecules occurs between neighboring cells and in the plane of the cell. More detail on the signaling pathway is provided in several excellent reviews (Fekete, D. M. and Wu, D. K., 2002). Notch–DSL (for Delta, Serrate, and Lag-2, the *C. elegans* homolog of Delta) signaling plays two roles in the development of ciliated mechanosensors; the first is in the specification of the sensory patches, imparting competence onto particular regions of the otocyst so that they can adopt a sensory fate. This property is mediated by the interaction of Notch with Jagged1 (also known as Serrate); Notch overexpression results in the production of supernumerary sensory patches, while knockouts of the *Jagged1* gene result in the loss of hair cells (Daudet, N. and Lewis, J., 2005; Brooker, R. *et al.*, 2006). The second role is within the sensory patch itself. It appears that Notch signaling is important in the fate choice between hair cells and the associated accessory cells, the supporting cells. The role of Notch in the binary fate choice between hair cells and supporting cells was demonstrated by work in fish, chicken, and mouse. Loss- and gain-of-function analysis using Notch, its ligands, or its downstream effectors has shown that sensory cells expressing one of the Notch ligands cause the activation of Notch in adjacent cells. Hair cell fate is inhibited in these adjacent cells which then become supporting cells. In contrast to sensory patch specification, this effect, termed lateral inhibition, is mediated by the interaction of Notch with Delta (Brooker, R. *et al.*, 2006).

Drosophila mechanoreceptors develop from patches of epidermis known as sensory organ precursors (SOPs). The development of the SOPs themselves is subject to patterning cues acting on the epidermis: *dpp* (the homolog of *Bmp/2/4*) and *wingless* act in concert to specify the SOP, together with ecdysone, the hormone that regulates the timing of metamorphosis of the *Drosophila* larva (Niwa, N. *et al.*, 2004). In addition, epidermal growth factor (EGF) signaling specifies some of this group of cells (Okabe, M. and Okano, H., 1997). This has parallels with the development of vertebrate hair cells: EGF is required for the survival and proliferation of mouse hair cells (Doetzlhofer, A. *et al.*, 2004). The concerted action of *dpp*, *wingless*, and EGF causes a group of cells within the *Drosophila* ectoderm to become specified as proneural. Lateral inhibition mediated by an interaction between Notch and Delta then specifies one of the proneural cells as the sensory precursor cell (Schweisguth, F., 1995).

3.01.5.1.2 The role of transcription factors in mechanoreceptor development

The action of extrinsic factors, that is, signaling molecules not acting cell-autonomously, has been described in the preceding section. These must provoke an intracellular response that affects the changes wrought on the cell by extracellular events. The intracellular response is invariably mediated by transcription factors that bind to specific DNA sequences, activating particular genes that lead to a particular developmental outcome. The transcription factor cascade involved in mechanoreceptor development is dynamic and the same transcription factors recur within different contexts and with slightly different functions as the mechanoreceptor becomes more and more differentiated.

Near the top of the hierarchy of transcription factors regulating mechanoreceptor development is the paired-box homeodomain-containing protein

Pax2. In vertebrates, *Pax2* is one of the first genes expressed in the inner ear primordia. In most phyla, the expression of *Pax2*, or its ancestral ortholog *Pax2/5/8*, prefigures the development of ciliated mechanoreceptors. The *Pax2/5/8* ancestor *PaxB* can be found in cnidarians (Sun, H. *et al*., 1997; Gröger, H. *et al*., 2000; Miller, D. J. *et al*., 2000). Expression analysis in hydrozoa localized *PaxB* to the developing sensory neurons of the tentacles (Gröger, H. *et al*., 2000) while in cubozoans, *PaxB* can be found in the statocyst (Kozmik, Z. *et al*., 2003). In *Drosophila*, the *Pax2* homolog is found in mechanoreceptors, and mutation results in a loss of the bristle organs; other mechanoreceptor subtypes were not investigated (Czerny, T. *et al*., 1997; Kavaler, J. *et al*., 1999). Mollusk *Pax2/5/8* has also been described and is expressed in both the chemosensory and mechanosensory cells (O'Brien, E. K., and Degnan, B. M., 2003). Finally, either *Pax2* itself or the *Pax2/5/8* gene can be found in deuterostome lineages, for example, in echinoderms (Czerny, T. *et al*., 1997), cephalochordates (Kozmik, Z. *et al*., 1999), and vertebrates (Krauss, S. *et al*., 1991; Rinkwitz-Brandt, S. *et al*., 1996; Torres, M. *et al*., 1996; Heller, N. and Brandli, A. W., 1997; Hutson, M. R. *et al*., 1999; Hidalgo-Sanchez, M. *et al*., 2000; McCauley, D. W. and Bronner-Fraser, M., 2002). It is tempting to suppose that the *Pax2* gene plays a fundamental role in establishing a mechanosensory propensity; however, as with all generalizations, caution must be applied.

In vertebrates, *Pax2* operates upstream of *Notch* to specify an area of ectoderm competent to become mechanosensory (Groves, A. K. and Bonner-Fraser, M., 2000). These cells then, through subsequent interactions, become definitively mechanosensory. In *Drosophila*, however, the role of *Pax2* is downstream of *Notch* and specifies the mechanosensory lineage (Kavaler, J. *et al*., 1999). However, this may reflect a difference between vertebrates and *Drosophila*; vertebrates use a placodal sense organ, arranging the ciliated mechanosensory receptors in specialized structures, whereas in *Drosophila* this is not the case. Analysis of *Pax2* mutants in the mouse and zebrafish indicate that the initial development of the inner ear is normal, due to a degree of redundancy with the *Pax8* gene, a close relative of *Pax2* (Hans, S. *et al*., 2004). In mice mutant for *Pax2*, however, the auditory portion of the inner ear fails to form (Favor, J. *et al*., 1996; Torres, M. *et al*., 1996). The formation of mechanoreceptors is apparently normal in the rest of the ear, as there are still cells positive for markers of early mechanoreceptors (Burton, Q. *et al*., 2004). Zebrafish have two *Pax2* genes, and mutations in one of them actually results in an increased number of hair cells by disrupting the expression of *Delta* (Riley, B. B. *et al*., 1999). Both sets of data do not emphatically rule out a role for *Pax2* in the direct specification of ciliated mechanoreceptors; the mouse study relied on molecular markers for assaying hair cells, without observing the final morphology of the hair cells. One cannot rule out the possibility that the hair cells had merely arrested at an earlier, *Pax2*-independent step of their development. In the zebrafish study, only one of the two *Pax2* genes was mutated. When both *Pax2a* and *Pax2b* are mutated, hair cell number is reduced (Whitfield, T. T. *et al*., 2002). These data are similar to those from *Drosophila*; when *Pax2* is lost, the external sensory organs of the fly are lost (Kavaler, J. *et al*., 1999).

Another transcription factor that plays an important role in the specification of the ciliated mechanoreceptors is the transcription factor *Atoh1*. *Atoh1* is one of the four vertebrate orthologs of the *Drosophila* gene *atonal*. Genetic ablation of *Atoh1* (formerly known as *Math1*) blocks the formation of the hair cells without any impact on other cell types (such as supporting cells) or on the overall morphology of the inner ear (Bermingham, N. A. *et al*., 1999). Mutation of the *Drosophila atonal* indicates its requirement for differentiation of the scolopidia in the fly; mutants of *atonal* completely lack these cells as well as some other sensory cell types. The functional similarity between the fly *atonal* and vertebrate *Atoh1* (*Atoh1* can rescue a fly *atonal* mutant and vice versa; Ben-Arie, N. *et al*., 2000; Wang, V. Y. *et al*., 2002) lends support to a homology between fly and vertebrate ciliated mechanoreceptors. However, closer inspection reveals important functional differences between *Drosophila* and vertebrates. These differences, reviewed by Hassan B. A. and Bellen H. J. (2000), highlight important mechanistic changes between the fly and vertebrates. In the fly, *atonal* functions in cell selection within the SOP and mediates the elaboration of chordotonal lineage identity, that is, proneural and lineage identities are coupled. In mouse, *Atoh1* functions in postmitotic cells, directing only terminal differentiation of the hair cell (Chen, P. *et al*., 2002). Indeed while *Atoh1* mutant mice do not have hair cells, the prosensory domain (the sensory patches) are unaffected. In vertebrates, the proneural and lineage identity function of *Atoh1* has become uncoupled. This is not because of a structural change in the molecule itself; *Atoh1* will rescue flies mutant for *atonal*, and *atonal* completely

rescues the *Atoh1* knockout mouse (Ben-Arie, N. *et al.*, 2000; Wang, V. Y. *et al.*, 2002). Furthermore, transfection of *Atoh1* into mammalian postnatal inner ears results in the formation of extra hair cells (Kawamoto, K. *et al.*, 2003; Woods, C. *et al.*, 2004). Seemingly *Atoh1* is both necessary and sufficient for the development of the vertebrate ciliate mechanoreceptor.

Atoh1 regulation is still unclear and thus is subject to some speculation. An ablation of the *Sox2* gene in the otocyst has been shown to also abolish the development of the hair cells (Kiernan, A. E. *et al.*, 2005). *Sox2* affects the development of the sensory patches rather than the differentiation of the hair cells themselves and epistatic studies have shown that *Sox2* functions upstream of *Atoh1* (Kiernan, A. E. *et al.*, 2005). *Atoh1* is also under negative regulation from the downstream effectors of notch–DSL signaling, the *HES* genes, genes that are the vertebrate orthologs of the *Drosophila enhancer of split* genes (Zine, A. *et al.*, 2001). Again this is not so surprising given the effect Notch has on the determination of the hair cells.

In *Drosophila*, *atonal* expression is regulated by a cascade of transcription factors. It is regulated by a zinc-finger protein called senseless and there are contributions from genes such as *pannier* and *u-shaped* as well as *distalless* and *homothorax* (Quan, X. J. *et al.*, 2004). While the vertebrate homolog of *senseless*, *Gfi1*, is involved in hair cell function, its relationship with *Atoh1* is not clear (Jafar-Nejad, H. and Bellen, H. J., 2004). *Gfi1* has itself been mutated in mice and these animals also show hair cell abnormalities (Wallis, D. *et al.*, 2003). In the inner ear, *Gfi1* has been identified as a downstream response of the transcription factor, *Pou4f3*, the causative mutation of the autosomal human hereditary deafness gene DFNA15. The relationship with *Atoh1* has not been elucidated, however, and it is still unclear whether *Atoh1* functions upstream, downstream, or in parallel with *Pou4f3*. Hertzano R. *et al.* (2004) showed that in mice mutant for *Pou4f3*, *Atoh1* expression was at 50% of its normal levels. *Gfi1* functions downstream of *Atoh1* in the development of secretory cells in the mouse intestine, suggesting that there may also be a similar relationship within the inner ear (Shroyer, N. F. *et al.*, 2005). Of the other genes suggested to play a role in the regulation of *Drosophila atonal*, homologs for *pannier* (*GATA*), *u-shaped* (*FOG*), *distalless* (*dlx*), and *homothorax* (*Meis*) can all be found in vertebrates and the expression can be detected in the inner ear. However, the detailed molecular relationships of these genes with each other and with *atonal*/*Atoh1*, either in the fly or in vertebrates, are still to be elucidated.

3.01.5.2 Summary of Development

Focusing on mechanoreceptor development in flies and in vertebrates allows important genes to be defined. Orthologs for these genes can also be found in all of the organisms we described. As discussed, *Pax2* orthologs can be found in every metazoan phylum including Porifera, the sponges (Hadrys, T. *et al.*, 2005). *Atonal*, involved in the development of mechanoreceptors in both vertebrates and insects, is also found in cnidarians, nematodes, and mollusks (Ladher, R., Tarui, H., and Agata, K. unpublished data). *Notch* and *Delta*, involved in fate choice within the sensory precursors in the fly and in the development of the sensory patches in vertebrates, can also be found in cnidarians, nematodes, and mollusks (Ladher, R., Tarui, H., and Agata, K. unpublished data). The list goes on, with genes involved in mechanoreceptor development in vertebrates being found as far back as cnidarians. This suggests a conservation of the molecular modules that could direct development of the ciliated mechanoreceptors. The could is important though, as in other organisms the involvement of these genes in mechanoreceptor development can only be postulated but has not yet been unequivocally shown. Indeed Fritzsch B. *et al.* (2006) have suggested that the presence of homologous genes suggests a deep homology describing a basic cellular property (such as the ability to rapidly proliferate), not really describing a derived structure, and that any attempt to describe further homologies is likely to fail. In fact many homologous genes are not exclusively mechanosensory but are found in other contexts during ontogeny.

Further resolution of the homology question will require more data, particularly from nonmodel species. At this stage, there is no doubt that ciliated mechanoreceptors share important molecular, structural, and cytological similarities. However, as well as these obvious similarities, ontogenetic differences become very important to characterize, enabling us to understand where and how the ciliated mechanoreceptor has arisen and how evolution has modified the ancestral prototype in the different lineages.

3.01.6 Conclusion

There is a considerable amount of information on the structure, function, and development of ciliated mechanosensory cells in vertebrates and invertebrate

animals. These provide tantalizing suggestions regarding their possible homology and make it possible to sketch the evolution of these cells through the major lines of multicellular animals. It is, however, still not possible to be sure whether all these cell types, in every organism, are derived from a common ancestor or whether the strong similarities they show are at least in some cases the result of developmental and physiological constraints. As so often in science, more data, especially from the less-studied invertebrates such as mollusks, will resolve this question.

Acknowledgments

Work in the authors' labs is supported by grants from the Deutsche Forschungsgemeinschaft (GAM) and from MEXT administered through RIKEN and the MEXT Leading Projects (RKL).

References

Adam, J., Myat, A., LeRoux, I., Eddison, M., Henrique, D., and Lewis, J. 1998. Cell fate choices and the expression of notch, delta and serrate homologs in the chick inner ear: parallel with *Drosophila* sense-organ development. Development 125, 4645–4654.

Adoutte, A., Balavoine, G., Lartillot, N., Lespinet, O., Prud'homme, B., and de Rosa, R. 2000. The new animal phylogeny: reliability and implications. Proc. Natl. Acad. Sci. U. S. A. 97, 4453–4456.

Baker, C. V. and Bronner-Fraser, M. 2001. Vertebrate cranial placodes. I. Embryonic induction. Dev. Biol. 232, 1–61.

Ben-Arie, N., Hassan, B. A., Bermingham, N. A., Malicki, D. M., Armstrong, D., Matzuk, M., Bellen, H. J., and Zoghbi, H. Y. 2000. Functional conservation of atonal and Math1 in the CNS and PNS. Development 127, 1039–1048.

Bennet-Clark, H. C. and Ewing, A. W. 1970. The love song of the fruit fly. Sci. Am. 223, 85–90.

Bermingham, N. A., Hassan, B. A., Price, S. D., Vollrath, M. A., Ben-Arie, N., Eatock, R. A., Bellen, H. J., Lysakowski, A., and Zoghbi, H. Y. 1999. Math1: an essential gene for the generation of inner ear hair cells. Science 284, 1837–1841.

Bleckmann, H. 1986. The Role of the Lateral Line in Fish Behaviour. In: The Behaviour of Teleost Fishes (*ed*. T. J. Pitcher), pp. 178–202. Sydney.

Boekhoff-Falk, G. 2005. Hearing in *Drosophila*: development of Johnston's organ and emerging parallels to vertebrate ear development. Dev. Dyn. 232, 550–558.

Bok, J., Bronner-Fraser, M., and Wu, D. K. 2005. Role of the hindbrain in dorsoventral but not anteroposterior axial specification of the inner ear. Development 132, 2115–24.

Bone, Q. and Ryan, K. P. 1978. Cupular sense organs in *Ciona* (Tunicata: Ascidiacea). J. Zool. (Lond.) 186, 417–429.

Brigandt, I. 2003. Homology in comparative, molecular, and evolutionary developmental biology: the radiation of a concept. J. Exp. Zool. B. Mol. Dev. Evol. 299, 9–17.

Brooker, R., Hozumi, K., and Lewis, J. 2006. Notch ligands with contrasting functions: Jagged1 and Delta1 in the mouse inner ear. Development. 133, 1277–86.

Budelmann, B. U. 1992. Hearing in Nonarthropod Invertebrates. In: The Evolutionary Biology of Hearing (*eds*. R. R. Fay, A. N. Popper, and D. B. Webster), pp. 141–155. Springer.

Budelmann, B. U. and Williamson, R. 1994. Directional sensitivity of hair cell afferents in the *Octopus* statocyst. J. Exp. Biol. 187, 245–259.

Budelmann, B. U., Barber, V. C., and West, S. 1973. Scanning electron microscopical studies of the arrangements and numbers of hair cells in the statocysts of *Octopus vulgaris*, *Sepia officinalis* and *Loligo vulgaris*. Brain Res. 56, 25–41.

Budelmann, B. U., Sachie, M., and Staudigl, M. 1987. The angular acceleration receptor system of the statocyst of *Octopus vulgaris*. Philos. Trans. R. Soc. Lond. B. 315, 305–343.

Budelmann, B. U., Schipp, R., and von Boletzky, S. 1997. Cephalopoda. In: Mollusca II (*eds*. F. W. Harrison and A. J. Kohn), pp. 119–414. Wiley-Liss.

Burighel, P., Lane, N. J., Fabio, G., Stefano, T., Zaniolo, G., Carnevali, M. D. C., and Manni, L. 2003. Novel, secondary sensory cell organ in ascidians: in search of the ancestor of the vertebrate lateral line. J. Comp. Neurol. 461, 236–249.

Burton, Q., Cole, L. K., Mulheisen, M., Chang, W., and Wu, D. K. 2004. The role of Pax2 in mouse inner ear development. Dev. Biol. 272, 161–75.

Carroll, R. L. 1987. Vertebrate Palaeontology and Evolution. Freeman.

Chalfie, M. and Thomson, J. N. 1982. Structural and functional diversity in the neuronal microtubules of *Caenorhabditis elegans*. J. Cell Biol. 93, 15–23.

Chalfie, M., Sulston, J. E., White, J. G., Southgate, E., Thomson, J. N., and Brenner, S. 1985. The neural circuit for touch sensitivity in *Caenorhabditis elegans*. J. Neurosci. 5, 956–964.

Chang, W., Nunes, F. D., De Jesus-Escobar, J. M., Harland, R., and Wu, D. K. 1999. Ectopic noggin blocks sensory and nonsensory organ morphogenesis in the chicken inner ear. Dev. Biol. 216, 369–381.

Chen, P., Johnson, J. E., Zoghbi, H. Y., and Segil, N. 2002. The role of Math1 in inner ear development: uncoupling the establishment of the sensory primordium from hair cell fate determination. Development 129, 2495–2505.

Coffin, A., Kelley, M., Manley, G. A., and Popper, A. N. 2004. Evolution of Sensory Hair Cells. In: Evolution of the Vertebrate Auditory System. (*eds*. G. A. Manley, A. Popper, and R. R. Fay), pp. 55–94. Springer.

Corey, D. P., Garcia-Añoveros, J., Holt, J. R., Kwan, K. Y., Lin, S.-Y., Vollrath, M. A., Amalfitano, A., Cheung, E. L.-M., Derfler, B. H., Duggan, A., Géléoc, G. S. G., Gray, P. A., Hoffman, M. P., Rehm, H. L., Tamasauskas, D., and Zhang, D.-S. 2004. TRPA1 is a candidate for the mechanosensitive transduction channel of vertebrate hair cells. Nature 432, 723–730.

Corfas, G. and Dudai, Y. 1990. Adaptation and fatigue of a mechanosensory neuron in wild-type *Drosophila* and in memory mutants. J. Neurosci. 10, 491–499.

Czerny, T., Bouchard, M., Kozmik, Z., and Busslinger, M. 1997. The characterization of novel Pax genes of the sea urchin and *Drosophila* reveal an ancient evolutionary origin of the Pax2/5/8 subfamily. Mech. Dev. 67, 179–92.

Daudet, N. and Lewis, J. 2005. Two contrasting roles for Notch activity in chick inner ear development: specification of prosensory patches and lateral inhibition of hair-cell differentiation. Development 132, 541–551.

Denison, R. H. 1966. The origin of the lateral-line sensory system. Am. Zool. 6, 369–370.

Devau, G. 2000. Glycine-induced calcium concentration changes in vestibular type I sensory cells. Hear. Res. 140, 126–136.

Doetzlhofer, A., White, P. M., Johnson, J. E., Segil, N., and Groves, A. K. 2004. *In vitro* growth and differentiation of mammalian sensory hair cell progenitors: a requirement for EGF and periotic mesenchyme. Dev. Biol. 272, 432–447.

Eatock, R. A., Weiss, T. F., and Otto, K. L. 1991. Dependence of discharge rate on sound pressure level in cochlear nerve fibers of the alligator lizard: implications for cochlear mechanisms. J. Neurophysiol. 65, 1580–97.

Eberl, D. F., Duyk, G. M., and Perrimon, N. 1997. A genetic screen for mutations that disrupt an auditory response in *Drosophila melanogaster*. Proc. Natl. Acad. Sci. U. S. A. 94, 14837–14842.

Ekström von Lubitz, D. K. J. 1981. Ultrastructure of the lateral-line sense organs of the ratfish, *Chimaera monstrosa*. Cell Tissue Res. 215, 651–665.

Ernstrom, G. G. and Chalfie, M. 2002. Genetics of sensory mechanotransduction. Annu. Rev. Genet. 36, 411–453.

Favor, J., Sandulache, R., Neuhauser-Klaus, A., Pretsch, W., Chatterjee, B., Senft, E., Wurst, W., Blanquet, V., Grimes, P., Sporle, R., and Schughart, K. 1996. The mouse Pax2$^{(1Neu)}$ mutation is identical to a human PAX2 mutation in a family with renal coloboma syndrome and results in developmental defects of the brain, ear, eye, and kidney. Proc. Natl. Acad. Sci. U. S. A. 93, 13870–13875.

Fay, R. R. and Edds-Walton, P. L. 1997. Directional response properties of saccular afferents of the toadfish, *Opsanus tau*. Hear. Res. 111, 1–21.

Fekete, D. M. and Wu, D. K. 2002. Revisiting cell fate specification in the inner ear. Curr. Opin. Neurobiol. 12, 35–42.

Fettiplace, R. 1987. Electrical tuning of hair cells in the inner ear. Trends Neurosci. 10, 421–425.

Fischer, F. P. 1994. General pattern and morphological specializations of the avian cochlea. Scanning Microsc. 8, 351–364.

Flock, A. 1967. Ultrastructure and Function in the Lateral Line Organs. In: Lateral Line Detectors, (*ed*. P. Cahn), pp. 163–197. Indiana University Press.

Fritzsch, B. 1992. The Water-to-Land Transition: Evolution of the Tetrapod Basilar Papilla, Middle Ear, and Auditory Nuclei. In: The Evolutionary Biology of Hearing. (*eds*. D. B. Webster, R. R. Fay, and A. N. Popper), pp. 351–375. Springer.

Fritzsch, B., Beisel, K. W., Jones, K., Farinas, I., Maklad, A., Lee, J., and Reichardt L. F. 2002. Development and evolution of inner ear sensory epithelia and their innervation. J. Neurobiol. 53, 143–56.

Fritzsch, B., Pauley, S., and Beisel, K. W. 2006. Cells, molecules and morphogenesis: the making of the vertebrate ear. Brain Res. Epub ahead of print, PMID: 16643865.

Géléoc, G. S. and Holt, J. R. 2003. Auditory amplification: outer hair cells pres the issue. Trends Neurosci. 26, 115–117.

Gerlach, L. M., Hutson, M. R., Germiller, J. A., Nguyen-Luu, D., Victor, J. C., and Barald, K. F. 2000. Addition of the BMP4 antagonist, noggin, disrupts avian inner ear development. Development 127, 45–54.

Gerlach-Bank, L. M., Cleveland, A. R., and Barald, K. F. 2004. DAN directs endolymphatic sac and duct outgrowth in the avian inner ear. Dev. Dyn. 229, 219–230.

Gibbs, M. A. 2004. Lateral line receptors: where do they come from developmentally and where is our research going? Brain Behav. Evol. 64, 163–181.

Gillespie, P. G. and Walker, R. G. 2001. Molecular basis of mechanosensory transduction. Nature 413, 194–202.

Gillespie, P. G., Dumont, R. A., and Kachar, B. 2005. Have we found the tip link, transduction channel, and gating spring of the hair cell? Curr. Opin. Neurobiol. 15, 389–396.

Gleich, O., Fischer, F. P., Köppl, C., and Manley, G. A. 2004. Hearing Organ Evolution and Specialization: Archosaurs. In: Evolution of the Vertebrate Auditory System, (*eds*. G. A. Manley, A. Popper, and R. R. Fay), pp. 224–255. Springer.

Gong, Z., Son, W., Chung, Y. D., Kim, J., Shin, D. W., McClung, C. A., Lee, Y., Lee, H. W., Chang, D. J., Kaang, B. K., Cho, H., Oh, U., Hirsh, J., Kernan, M. J., and Kim, C. 2004. Two interdependent TRPV channel subunits, inactive and Nanchung, mediate hearing in *Drosophila*. J. Neurosci. 24, 9059–9066.

Göpfert, M. C. and Wasserthal, L. T. 1999. Auditory sensory cells in hawkmoths: identification, physiology and structure. J. Exp. Biol. 202, 1579–1587.

Görner, P. 1987. Lateral Line System. In: Encyclopedia of Neuroscience, I (*ed*. G. Adelman), pp. 567–569. Birkhäuser.

Gröger, H., Callaerts, P., Gehring, W. J., and Schmid, V. 2000. Characterization and expression analysis of an ancestor-type Pax gene in the hydrozoan jellyfish *Podocoryne carnea*. Mech. Dev. 94, pp. 157–169.

Groves, A. K. and Bronner-Fraser, M. 2000. Competence, specification and commitment in otic placode induction. Development 127, 3489–3499.

Grünert, U. and Gnatzy, W. 1987. K^+ and Ca^{++} in the receptor lymph of arthropod cuticular mechanoreceptors. J. Comp. Physiol. A. 161, 329–333.

Hadrys, T., DeSalle, R., Sagasser, S., Fischer, N., and Schierwater, B. 2005. The Trichoplax PaxB gene: a putative Proto-PaxA/B/C gene predating the origin of nerve and sensory cells. Mol. Biol. Evol. 22, 1569–1578.

Hallberg, E. and Hansson, B. S. 1999. Arthropod sensilla: morphology and phylogenetic considerations. Microsc. Res. Tech. 47, 428–439.

Hans, S., Liu, D., and Westerfield, M. 2004. Pax8 and Pax2a function synergistically in otic specification, downstream of the Foxi1 and Dlx3b transcription factors. Development 131, 5091–102.

Hassan, B. A. and Bellen, H. J. 2000. Doing the MATH: is the mouse a good model for fly development? Genes Dev. 14, 1852–1865.

Hasson, T., Heintzelman, M. B., Santos-Sacchi, J., Corey, D. P., and Mooseker, M. S. 1995. Expression in cochlea and retina of myosin VIIa, the gene product defective in Usher syndrome type 1B. Proc. Natl. Acad. Sci. U. S. A. 92, 9815–9819.

Heller, N. and Brandli, A. W. 1997. Xenopus Pax-2 displays multiple splice forms during embryogenesis and pronephric kidney development. Mech. Dev. 69, 83–104.

Hennig, W. 1983. Stammesgeschichte der Chordaten. Verlag Paul Parey.

Hertzano, R., Montcouquiol, M., Rashi-Elkeles, S., Elkon, R., Yucel, R., Frankel, W. N., Rechavi, G., Moroy, T., Friedman, T. B., Kelley, M. W., and Avraham, K. B. 2004. Transcription profiling of inner ears from Pou4f3(ddl/ddl) identifies Gfi1 as a target of the Pou4f3 deafness gene. Hum. Mol. Genet. 13, 2143–2153.

Hidalgo-Sanchez, M., Alvarado-Mallart, R., and Alvarez, I. S. 2000. Pax2, Otx2, Gbx2 and Fgf8 expression in early otic vesicle development. Mech. Dev. 95, 225–229.

Hillis, D. M. 1994. Homology in Molecular Biology. In: Homology: The Hierarchical Basis of Comparative Biology (*ed*. B. K. Hall), pp. 339–368. Academic Press.

Holland, L. Z. 2005. Non-neural ectoderm is really neural: evolution of developmental patterning mechanisms in the non-neural ectoderm of chordates and the problem of sensory cell homologies. J. Exp. Zool. B. Mol. Dev. Evol. 304, 304–323.

Holstein, T. and Hausmann, K. 1988. The Cnidocil Apparatus of Hydrozoans: A Progenitor of Higher Metazoan Mechanoreceptors. In: The Biology of Nematocysts (*ed*. D. A. Hessinger and H. M. Lenhoff), pp. 53–73. Academic Press.

Horridge, G. A. 1969. Statocysts of medusae and evolution of stereocilia. Tissue Cell 1, 341–353.
Hudspeth, A. J. 1985. The cellular basis of hearing: the biophysics of hair cells. Science 230, 745–752.
Hudspeth, A. J. 1989. How the ear's works work. Nature 341, 397–404.
Hudspeth, A. J. and Corey, D. P. 1977. Sensitivity, polarity, and conductance change in the response of vertebrate hair cells to controlled mechanical stimuli. Proc. Natl. Acad. Sci. U. S. A. 74, 2407–2411.
Hutson, M. R, Lewis, J. E, Nguyen-Luu, D., Lindberg, K. H., and Barald, K. F. 1999. Expression of Pax2 and patterning of the chick inner ear. J. Neurocytol. 28, 795–807.
Jafar-Nejad, H. and Bellen, H. J. 2004. Gfi/Pag-3/senseless zinc finger proteins: a unifying theme? Mol. Cell Biol. 24: 8803–8812.
Jørgensen, J. 1989. Evolution of Octavolateralis Sensory Cells. In: The Mechanosensory Lateral Line: Neurobiology and Evolution (*eds*. S. Coombs, P. Görner, and H. Münz), pp. 115–145. Springer.
Kaplan, J. M. and Horvitz, H. R. 1993. A dual mechanosensory and chemosensory neuron in *Caenorhabditis elegans*. Proc. Natl. Acad. Sci. U. S. A. 90, 2227–2231.
Kavaler, J., Fu, W, Duan, H., Noll, M., and Posakony, J. W. 1999. An essential role for the *Drosophila* Pax2 homolog in the differentiation of adult sensory organs. Development. 126, 2261–72.
Kawamoto, K., Ishimoto, S., Minoda, R., Brough, D. E., and Raphael, Y. 2003. Math1 gene transfer generates new cochlear hair cells in mature guinea pigs *in vivo*. J. Neurosci. 23, 4395–4400.
Keil, T. A. 1997. Functional morphology of insect mechanoreceptors. Microsc. Res. Tech. 39, 506–531.
Kernan, M., Cowan, D., and Zuker, C. 1994. Genetic dissection of mechanosensory transduction: mechanoreception-defective mutations of *Drosophila*. Neuron 12, 1195–1206.
Kiernan, A. E., Pelling, A. L., Leung, K. K., Tang, A. S., Bell, D. M., Tease, C., Lovell-Badge, R., Steel, K. P., and Cheah, K. S. 2005. Sox2 is required for sensory organ development in the mammalian inner ear. Nature 434, 1031–1035.
Kil, S. H., Streit, A., Brown, S. T., Agrawal, N., Collazo, A., Zile, M. H., and Groves, A. K. 2005. Distinct roles for hindbrain and paraxial mesoderm in the induction and patterning of the inner ear revealed by a study of vitamin-A-deficient quail. Dev. Biol. 285, 252–271.
Kim, J., Chung, Y. D., Park, D. Y., Choi, S., Shin, D. W., Soh, H., Lee, H. W., Son, W., Yim, J., Park, C. S., Kernan, M. J., and Kim, C. 2003. A TRPV family ion channel required for hearing in *Drosophila.*. Nature 424, 81–84.
Köppl, C. and Manley, G. A. 1990. Peripheral auditory processing in the bobtail lizard *Tiliqua rugosa*. III. Patterns of spontaneous and tone-evoked nerve-fibre activity. J. Comp. Physiol. A. 167, 113–127.
Köppl, C., Manley, G. A., and Konishi, M. 2000. Auditory processing in birds. Curr. Opin. Neurobiol. 10, 474–481.
Kozmik, Z., Daube, M., Frei, E., Norman, B., Kos, L., Dishaw, L. J., Noll, M., and Piatigorsky, J. 2003. Role of Pax genes in eye evolution: a cnidarian PaxB gene uniting Pax2 and Pax6 functions. Dev. Cell 5, 773–85.
Kozmik, Z., Holland, N. D., Kalousova, A., Paces, J., Schubert, M., and Holland, L. Z. 1999. Charcterization of an amphioxus paired box gene, Amphi Pax 2/5/8: developmental expression patterns in optic support cells, nephridium, thyroid-like structures and pharyngeal gill slits, but not in the midbrain-hindbrain boundary region. Development 126, 1295–1304.
Krauss, S., Johansen, T., Korzh, V., and Fjose, A. 1991. Expression pattern of zebrafish pax genes suggests a role in early brain regionalization. Nature 353, 267–270.
Kwan, K. Y., Allchorne, A. J., Vollrath, M. A., Christensen, A. P., Zhang, D. S., Woolf, C. J., and Corey, D. P. 2006. TRPA1 contributes to cold, mechanical, and chemical nociception but is not essential for hair-cell transduction. Neuron. 50, 277–89.
Lacalli, T. C. 2004. Sensory systems in amphioxus: a window on the ancestral chordate condition. Brain Behav. Evol. 64, 148–162.
Ladher, R. K., Anakwe, K. U., Gurney, A. L., Schoenwolf, G. C., and Francis-West, P. H. 2000. Identification of synergistic signals initiating inner ear development. Science 290, 1965–1967.
Ladich, F. and Popper, A. N. 2004. Parallel Evolution in Fish Hearing Organs. In: Evolution of the Vertebrate Auditory System (*eds*. G. A. Manley, A. Popper, and R. R. Fay), pp. 95–127. Springer.
Lawrence, P. A. 1966. Development and determination of hairs and bristles in the milkweed bug, *Oncopeltus fasciatus* (Lygaeidae, Hemiptera). J. Cell Sci. 1, 475–498.
Lewis, E. R., Leverenz, E. L., and Bialek, W. S. 1985. The Vertebrate Inner Ear. CRC Press.
Li, H., Corrales, C. E., Wang, Z., Zhao, Y., Wang, Y., Liu, H., and Heller, S. 2005. BMP4 signaling is involved in the generation of inner ear sensory epithelia. BMC Dev. Biol. 5, 16.
Lu, Z. and Popper, A. N. 2001. Neural response directionality correlates of hair cell orientation in a teleost fish. J. Comp. Physiol. A. 187, 453–465.
Manley, G. A. 1990. Peripheral Hearing Mechanisms in Reptiles and Birds. Springer.
Manley, G. A. 1995. The Avian Hearing Organ: A Status Report. In: Advances in Hearing Research (*eds*. G. A. Manley, G. M. Klump, C. Köppl, H. Fastl, and H. Oeckinghaus), pp. 219–229. World Scientific Publishers.
Manley, G. A. 2000. The Hearing Organs of Lizards. In: Comparative Hearing: Birds and Reptiles (*eds*. R. Dooling, A. N. Popper, and R. R. Fay), pp. 139–196. Springer Handbook of Auditory Research.
Manley, G. A. 2001. Evidence for an active process and a cochlear amplifier in non-mammals. J. Neurophysiol. 86, 541–549.
Manley, G. A. 2002. Evolution of structure and function of the hearing organ of lizards. J. Neurobiol. 53, 202–211.
Manley, G. A. 2004. The Lizard Basilar Papilla and Its Evolution. In: Evolution of the Vertebrate Auditory System (*eds*. G. A. Manley, A. Popper, and R. R. Fay), pp. 200–223. Springer.
Manley, G. A., Köppl, C., and Sneary, M. 1999. Reversed tonotopic map of the basilar papilla in *Gekko gecko*. Hear. Res. 131, 107–116.
Manley, G. A., Köppl, C., and Yates, G. K. 1989. Micromechanical Basis of High-Frequency Tuning in the Bobtail Lizard. In: Mechanics of Hearing, (*eds*. J. P. Wilson and D. Kemp), pp. 143–150. Plenum.
Manley, G. A., Yates, G. K., Köppl, C., and Johnstone, B. M. 1990. Peripheral auditory processing in the bobtail lizard *Tiliqua rugosa*. IV. Phase locking of auditory-nerve fibres. J. Comp. Physiol. A. 167, 129–138.
Manni, L., Caicci, F., Gasparini, F., Zaniolo, G., and Burighel, P. 2004. Hair cells in ascidians and the evolution of lateral line placodes. Evol. Dev. 6, 379–381.
Masetto, S. and Carreia, M. J. 1997. Ionic currents in regenerating avian vestibular hair cells. Int. J. Dev. Neurosci. 15, 387–399.
McCauley, D. W. and Bronner-Fraser, M. 2002. Conservation of Pax gene expression in ectodermal placodes of the lamprey. Gene 287, 129–139.
McKee, A. E. and Wiederhold, M. L. 1974. *Aplysia* statocyst receptor cells: fine structure. Brain Res. 81, 310–313.
Meenderink, S. W., Narins, P. M., and van Dijk, P. 2005. Detailed f(1) f(2) area study of distortion product otoacoustic

emissions in the frog. J. Assoc. Res. Otolaryngol. 6, 3713–3726.
Miller, M. R. 1978. Scanning electron microscope studies of the papilla basilaris of some turtles and snakes. Am. J. Anat. 151, 409–435.
Miller, M. R. 1992. The Evolutionary Implications of the Structural Variations in the Auditory Papilla of Lizards. In: The Evolutionary Biology of Hearing (*eds*. R. R. Fay, A. N. Popper, and D. B. Webster), pp. 463–487. Springer.
Miller, D. J., Hayward, D. C., Reece-Hoyes, J. S., Scholten, I., Catmull, J., Gehring, W. J., Callaerts, P., Larsen, J. E., and Ball, E. E. 2000. Pax gene diversity in the basal cnidarian *Acropora millepora* (Cnidaria, Anthozoa): implications for the evolution of the Pax gene family. Proc. Natl. Acad. Sci. U. S. A. 97, 4475–4480.
Mire, P. and Watson, G. M. 1997. Mechanotransduction of hair bundles arising from multicellular complexes in anemones. Hear. Res. 113, 224–234.
Moir, A. J. 1977. Ultrastructural studies on the ciliated receptors of the long tentacles of the giant scallop, *Placopecten magellanicus* (gmelin). Cell. Tissue. Res. 184, 367–380.
Montcouquiol, M. and Kelley, M. W. 2004. Planar and vertical signals control cellular differentiation and patterning in the mammalian cochlea. J. Neurosci. 23, 9469–78.
Montell, C. 2005. The TRP superfamily of cation channels. Science STKE 2005, re3.
Morsli, H., Choo, D., Ryan, A., Johnson, R., and Wu, D. K. 1998. Development of the mouse inner ear and origin of its sensory organs. J. Neurosci. 18, 3327–3335.
Mowbray, C., Hammerschmidt, M., and Whitfield, T. T. 2001. Expression of BMP signalling pathway members in the developing zebrafish inner ear and lateral line. Mech. Dev. 108, 179–184.
Neumeister, H. and Budelmann, B. U. 1997. Structure and function of the *Nautilus* statocyst. Philos. Trans. R. Soc. Lond. B. Biol. Sci. 352, 1565–1588.
Niwa, N., Hiromi, Y., and Okabe, M. 2004. A conserved developmental program for sensory organ formation in *Drosophila* melanogaster. Nat. Genet. 36, 293–297.
O'Brien, E. K. and Degnan, B. M. 2003. Expression of Pax258 in the gastropod statocyst: insights into the antiquity of metazoan geosensory organs. Evol. Dev. 5, 572–578.
Oh, S. H., Johnson, R., and Wu, D. K. 1996. Differential expression of bone morphogenetic proteins in the developing vestibular and auditory sensory organs. J. Neurosci. 16, 6463–6475.
Okabe, M. and Okano, H. 1997. Two-step induction of chordotonal organ precursors in *Drosophila* embryogenesis. Development 124, 1045–1053.
Patterson, C. 1988. Homology in classical and molecular biology. Mol. Ecol. Evol. 5, 603–625.
Perkins, L. A., Hedgecock, E. M., Thomson, J. N., and Culotti, J. G. 1986. Mutant sensory cilia in the nematode *Caenorhabditis elegans*. Dev. Biol. 117, 456–487.
Peteya, D. J. 1975. The ciliary-cone sensory cell of anemones and cerianthids. Tissue Cell 7, 243–252.
Pichon, F. and Ghysen, A. 2004. Evolution of posterior latera line development in fish and amphibians. Evol. Dev. 6, 187–193.
Pickles, J. O., Comis, S. D., and Osborne, M. P. 1984. Cross-links between stereocilia in the guinea pig organ of Corti and their possible relation to sensory transduction. Hear. Res. 15, 103–112.
Popper, A. N. and Fay, R. R. 1999. The Auditory Periphery in Fishes. In: Comparative Hearing: Fish and Amphibians (*eds*. R. R. Fay and A. N. Popper), pp. 43–100. Springer.
Quan, X. J., Denayer, T., Yan, J., Jafar-Nejad, H., Philippi, A., Lichtarge, O., Vleminckx, K., and Hassan, B. A. 2004. Evolution of neural precursor selection: functional divergence of proneural proteins. Development 131, 1679–1689.
Remane, A. 1952. Die Grundlagen des natürlichen Systems, der vergleichenden Anatomie und der Phylogenetik. I. Theoretische Morphologie und Systematik. Geest und Portig.
Riccomagno, M. M., Martinu, L., Mulheisen, M., Wu, D. K., and Epstein, D. J. 2002. Specification of the mammalian cochlea is dependent on Sonic hedgehog. Genes Dev. 16, 2365–2378.
Riccomagno, M. M., Takada, S., and Epstein, D. J. 2005. Wnt-dependent regulation of inner ear morphogenesis is balanced by the opposing and supporting roles of Shh. Genes Dev. 19, 1612–1623.
Riley, B. B., Chiang, M., Farmer, L., and Heck, R. 1999. The deltaA gene of zebrafish mediates lateral inhibition of hair cells in the inner ear and is regulated by pax2.1. Development. 126, 5669–5678.
Rinkwitz-Brandt, S., Arnold, H. H., and Bober, E. 1996. Regionalized expression of Nkx5-1, Nkx5-2, Pax2 and sek genes during mouse inner ear development. Hear. Res. 99, 129–138.
Rosenblatt, K. P., Sun, Z.-P., Heller, S., and Hudspeth, A. J. 1997. Distribution of Ca^{2+}-activated K^{+} channel isoforms along the tonotopic gradient of the chicken's cochlea. Neuron, 19, 1061–1075.
Ruppert, E. E., Fox, R. S., and Barnes, R. D. 2004. Invertebrate zoology: a functional evolutionary approach. Belmont.
Russell, I. J. 1976. Amphibian Lateral Line Receptors. In: Frog Neurobiology (*eds*. R. Llinas and W. Precht), pp. 513–550. Springer.
Sand, O. 1984. Lateral Line Systems. In: Comparative Physiology of Sensory Systems, (*eds*. L. Bolish, R. Keynes, and S. H. P. Madrell), pp. 3–32. Cambridge University Press.
Sanyal, S., Wintle, R. F., Kindt, K. S., Nuttley, W. M., Arvan, R., Fitzmaurice, P., Bigras, E., Merz, D. C., Hebert, T. E., van der Kooy, D., Schafer, W. R., Culotti, J. G., and Van Tol, H. H. 2004. Dopamine modulates the plasticity of mechanosensory responses in *Caenorhabditis elegans*. EMBO J. 23, 473–482.
Sawin, E. R., Ranganathan, R., and Horvitz, H. R. 2000. *C. elegans* locomotory rate is modulated by the environment through a dopaminergic pathway and by experience through a serotonergic pathway. Neuron 26, 619–631.
Schlosser, G. 2005. Evolutionary origins of vertebrate placodes: insights from developmental studies and from comparisons with other deuterostomes. J. Exp. Zool. B. Mol. Dev. Evol. 304, 347–399.
Schlosser, G. 2006. Induction and specification of cranial placodes. Dev. Biol. (in press).
Schweisguth, F. 1995. Suppressor of hairless is required for signal reception during lateral inhibition in the *Drosophila* pupal notum. Development 121, 1875–1884.
Shimeld, S. M. and Holland, P. W. H. 2000. Vertebrate innovations. Proc. Nat. Acad. Sci. 97, 4449–4452.
Shin, J. B., Adams, D., Paukert, M., Siba, M., Sidi, S., Levin, M., Gillespie, P. G., and Grunder, S. 2005. *Xenopus* TRPN1 (NOMPC) localizes to microtubule-based cilia in epithelial cells, including inner-ear hair cells. Proc. Natl. Acad. Sci. U. S. A. 102, 12572–12577.
Shroyer, N. F., Wallis, D., Venken, K. J., Bellen, H. J., and Zoghbi, H. Y. 2005. Gfi1 functions downstream of Math1 to control intestinal secretory cell subtype allocation and differentiation. Genes Dev. 19, 2412–2417.
Sidi, S., Friedrich, R. W., and Nicolson, T. 2003. NompC TRP channel required for vertebrate sensory hair cell mechanotransduction. Science 301, 96–99.
Singla, C. L. 1975. Statocysts of hydromedusae. Cell Tissue Res. 158, 391–407.
Singla, C. L. 1983. Fine structure of the sensory receptors of *Aglantha digitale* (Hydromedusae: Trachylina). Cell Tissue Res. 231, 415–425.

Smith, H. M. 1960. Evolution of Chordate Structure. Reinhart and Winston.
Smotherman, M. and Narins, P. 2004. Evolution of the Amphibian Ear. In: Evolution of the Vertebrate Auditory System (*eds*. G. A. Manley, A. Popper, and R. R. Fay), pp. 164–199. Springer.
Song, J., Yan, H. Y., and Popper, A. N. 1995. Damage and recovery of hair cells in fish canal (but not superficial) neuromasts after gentamicin exposure. Hear. Res. 91, 63–71.
Spoendlin, H. 1978. The Afferent Innervation of the Cochlea. In: Evoked Electrical Activity in the Auditory Nervous System (*eds*. R. F. Naunton and C. Fernandez), pp. 3–19. Academic Press.
Stephens, P. R. and Young, J. Z. 1982. The statocyst of the squid, *Loligo*. J. Zool. 197, 241–266.
Stidwill, R. P., Honegger, T. G., and Tardent, P. 1988. Polymerized Actin in the Apical Region of Hydra Nematocytes. In: The Biology of Nematocysts (*eds*. D. A. Hessinger and H. M. Lenhoff), pp. 567–574. Academic Press.
Stumpner, A. and von Helversen, D. 2001. Evolution and function of auditory systems in insects. Naturwissenschaften 88, 159–170.
Sun, H., Rodin, A., Zhou, Y., Dickinson, D. P., Harper, D. E., Hewett-Emmett, D., and Li, W.-H. 1997. Evolution of paired domains: isolation and sequencing of jellyfish and hydra Pax genes related to Pax-5 and Pax-6. Proc. Natl. Acad. Sci. U. S. A. 94, 5156–5161.
Thurm, U. 2001. Mechanosensorik. In: Neurowissenschaften (*eds*. J. Dudel, R. Menzel, and R. F. Schmidt), pp. 333–353. Springer.
Thurm, U. and Küppers, J. 1980. Epithelial Physiology of Insect Sensilla. In: Insect Biology in the Future (*eds*. M. Locke and D. S. Smith), pp. 735–758. Academic Press.
Todi, S. V., Franke, J. D., Kiehart, D. P., and Eberl, D. F. 2005. Myosin VIIA defects, which underlie the Usher 1B syndrome in humans, lead to deafness in *Drosophila*. Curr. Biol. 15, 862–868.
Todi, S. V., Sharma, Y., and Eberl, D. F. 2004. Anatomical and molecular design of the *Drosophila* antenna as a flagellar auditory organ. Microsc. Res. Tech. 63, 388–399.
Torres, M., Gomez-Pardo, E., and Gruss, P. 1996. Pax2 contributes to inner ear patterning and optic nerve trajectory. Development. 122, 3381–91.
van Staaden, M. J. and Römer, H. 1998. Evolutionary transition from stretch to hearing organs in ancient grasshoppers. Nature 394, 773–776.
Vater, M., Meng, J., and Fox, R. C. 2004. Hearing Organ Evolution and Specialization: Early and Later Mammals. In: Evolution of the Vertebrate Auditory System (*eds*. G. A. Manley, A. Popper, and R. R. Fay), pp. 256–288. Springer.
Vinnikov, Y. A. 1982. Evolution of receptor cells. Cytological, membranous and molecular levels. Mol. Biol. Biochem. Biophys. 34, 1–141.
von Schilcher, F. 1976. The role of auditory stimuli in the courtship of *Drosophila melanogaster*. Anim. Behav. 24, 18–26.
Wake, D. B. 1994. Comparative terminology. Science 265, 268–269.
Walker, R. G., Willingham, A. T., and Zuker, C. S. 2000. A *Drosophila* mechanosensory transduction channel. Science 287, 2229–2234.
Wallis, D., Hamblen, M., Zhou, Y., Venken, K. J., Schumacher, A., Grimes, H. L., Zoghbi, H. Y., Orkin, S. H., and Bellen, H. J. 2003. The zinc finger transcription factor Gfi1, implicated in lymphomagenesis, is required for inner ear hair cell differentiation and survival. Development 130, 221–232.
Wang, V. Y., Hassan, B. A., Bellen, H. J., and Zoghbi, H. Y. 2002. *Drosophila* atonal fully rescues the phenotype of Math1 null mice: new functions evolve in new cellular contexts. Curr. Biol. 12, 1611–1616.
Watson, G. M. and Mire, P. 1999. A comparison of hair bundle mechanoreceptors in sea anemones and vertebrate systems. Curr. Top. Dev. Biol. 43, 51–84.
Watson, G. M., Mire, P., and Hudson, R. R. 1997. Hair bundles of sea anemones as a model system for vertebrate hair bundles. Hear. Res. 107, 53–66.
Weber, T., Gopfert, M. C., Winter, H., Zimmermann, U., Kohler, H., Meier, A., Hendrich, O., Rohbock, K., Robert, D., and Knipper, M. 2003. Expression of prestin-homologous solute carrier (SLC26) in auditory organs of nonmammalian vertebrates and insects. Proc. Natl. Acad. Sci. U. S. A. 100, 7690–7695.
Weil, D., Blanchard, S., Kaplan, J., Guilford, P., Gibson, F., Walsh, J., Mburu, P., Varela, A., Levilliers, J., and Weston, M. D. 1995. Defective myosin VIIA gene responsible for Usher syndrome type 1B. Nature 374, 60–61.
West-Eberhard, M. J. 2003. Developmental Plasticity and Evolution. Oxford University Press.
Wever, E. G. 1978. The Reptile Ear, Princeton Univ Press.
Whitfield, T. T., Riley, B. B., Chiang, M. Y., and Phillips, B. 2002. Development of the zebrafish inner ear. Dev. Dyn. 223, 427–58.
Wood, R. L. and Novak, P. L. 1982. The anchoring of nematocysts and nematocytes in the tentacles of *Hydra*. J. Ultrastruct. Res. 81, 104–116.
Woods, C., Montcouquiol, M., and Kelley, M. W. 2004. Math1 regulates development of the sensory epithelium in the mammalian cochlea. Nat. Neurosci. 7, 1310–1318.
Wu, D. K. and Oh, S. H. 1996. Sensory organ generation in the chick inner ear. J. Neurosci. 16, 6454–6462.
Wu, D. K., Nunes, F. D., and Choo, D. 1998. Axial specification for sensory organs versus non-sensory structures of the chicken inner ear. Development 125, 11–20.
Yack, J. E. 2004. The structure and function of auditory chordotonal organs in insects. Microsc. Res. Tech. 63, 315–337.
Young, J. Z. 1981. The Life of Vertebrates. Oxford.
Zheng, J., Shen, W., He, D. Z., Long, K. B., Madison, L. D., and Dallos, P. 2000. Prestin is the motor protein of cochlear outer hair cells. Nature 405, 149–155.
Zine, A., Aubert, A., Qiu, J., Therianos, S., Guillemot, F., Kageyama, R., and de Ribaupierre, F. 2001. Hes1 and Hes5 activities are required for the normal development of the hair cells in the mammalian inner ear. J. Neurosci. 21, 4712–4720.

Relevant Website

http://www.wzw.tu-muenchen.de – Wissenschaftszentrum Weihenstephan für Ernährung, Landnutzung und Umwelt.

3.02 Insect Ears

J E Yack and J W Dawson, Carleton University, Ottawa, ON, Canada

© 2008 Elsevier Inc. All rights reserved.

3.02.1	**Introduction**	36
3.02.2	**Tympanal Ears**	37
3.02.2.1	Evolutionary Origins of Tympanal Ears	39
3.02.2.2	Which Insects Have Tympanal Ears?	40
3.02.2.2.1	Lepidoptera	40
3.02.2.2.2	Orthoptera	42
3.02.2.2.3	Hemiptera (Homoptera + Heteroptera)	45
3.02.2.2.4	Diptera	46
3.02.2.2.5	Dictyoptera	47
3.02.2.2.6	Coleoptera	47
3.02.2.2.7	Neuroptera	47
3.02.3	**Nearfield Sound Receptors**	47
3.02.4	**Vibration-Sensitive Organs**	48
3.02.5	**Summary and Future Considerations**	48
References		51

Glossary

atympanate Refers to the condition of lacking a tympanal ear. Compare with tympanate.

campaniform sensillum A dome-shaped sensory organ normally occurring near joints. Campaniform sensillae are sensitive to distortion of the cuticle as typically occurs during joint movement. Each campaniform sensillum has a single mechanoreceptor cell associated with it.

chitin A major component of arthropod cuticle composed of amino-polysaccharide subunits of acetylglucosamine and glucosamine.

chordotonal organ A mechanosensory organ found in arthropods that functions primarily in detecting body movements and sound vibrations. A type of proprioceptive stretch receptor in arthropods consisting of thin, elastic strands of connective tissue stretched between adjacent body regions and comprised of individual mechanosensory units called scolopidia. Also called chordotonal sensillae.

cuticle The external layers of the integument of arthropods. It is secreted by the epidermis and is comprised of chitin and protein. Cuticle forms the arthropod exoskeleton.

exteroceptor A sense organ that responds to stimuli originating outside the body.

johnston's organ A sensory organ found within the antennal pedicel (second segment of the antennae) of many insects. It comprises several hundred chordotonal sensillae. The organ is stimulated by movements of the antennal flagellum typically in response to near-field sound or vibration.

mechanoreceptor A class of receptor whose adequate stimulus is a physical change in the position of a body part or surface. The mechanical deformation causes an electrical change within the receptor cell (i.e., the generator or receptor potential), and eventually an action potential in the nerve fibre(s) connected to the receptor organ.

proprioceptor A type of mechanoreceptor that provides information to an animal about the position and motion of the body and its appendages.

scolopidia (scolopidium) The individual mechanosensory receptor unit of an insect auditory organ that consists of a linear chain of four cell types: (1) one or more bipolar neurons, (2) a scolopale cell that forms a lumen around the cilium of the neuronal dendrite and whose cytoplasm contains electron-dense scolopale rods, (3) attachment cells that mechanically anchor and support the scolopale cell, and (4) accessory cells that envelop and provide nutritive and mechanical support to the neuronal soma.

spiracle An external opening of the trachea (insect respiratory system).

subgenual organ A chordotonal organ on the proximal tibia (fourth segment of the insect leg) that detects substrate vibration.
trachea (pl. tracheae) An internal component of the insect gas-exchange system; a tubular structure originating at the spiracles (specialized integumentary structures) and most typically branching extensively forming tracheoles within the insect body. Tracheae may be expanded to form air sacs in certain regions of the body.
trichoid sensilla A hair-like projection of the cuticle. Also called a hair, seta, or macrotrichium.
tympanal organ A type of mechanoreceptor used to detect acoustic signals. It is normally associated with a thinned region of cuticle – the tympanic membrane – whose motion directly corresponds to the pressure changes of an acoustic stimulus in the surrounding medium.
tympanate The condition of possessing a tympanal ear or organ. Compare with *atympanate*.

3.02.1 Introduction

An acoustic sense is well developed in many insects. Sounds and vibrations play key roles in detecting and evading predators, locating and choosing mates, establishing territories, forming and maintaining groups, coordinating social interactions, and locating hosts. Insects possess an impressive diversity of different hearing organs, which can be located on almost any part of the body. When discussing an acoustic sense in vertebrates, we typically refer to one type of hearing organ, ears, which are located on the head, and capable of detecting minute time-varying pressure changes transmitted through air or water. In insects however, an acoustic sense is not confined to the detection of sound-pressure waves, but also encompasses the detection of particle displacements, and in the broadest sense, solid-borne vibrations. Therefore, before discussing insect ears it is prudent to begin with a brief overview of the three kinds of acoustic stimuli important to insects: airborne sounds in the nearfield and farfield; and seismic, or solid-borne vibrations.

When a sound-producing source, like a speaker, vibrates back and forth, the molecules of the medium (air or water) in front of the source are displaced and transmit a disturbance to neighboring particles. In the acoustic nearfield, where the distance from the sound-producing source is less than the wavelength, there is a large particle velocity component which is out of phase with pressure. These particle displacements can be sufficient to move a lightweight structure, such as a hair or antenna. We call these nearfield sound receptors, movement receivers, or displacement receivers (Michelsen, A. and Nocke, H., 1974; Bennet-Clark, H. C., 1984; Römer, H. and Tautz, J., 1992). The speaker movement also causes fluctuations in air pressure that are propagated away from the speaker as a pressure wave. We call this the acoustic farfield, where the distance from the source is greater than the wavelength, and particle velocity is in phase with pressure. The pressure component of sound is detectable by farfield sound receptors, typically referred to as tympanal ears or tympanal organs, which can be either pressure-sensitive or pressure-gradient sensitive (Römer, H. and Tautz, J., 1992; Yager, D. D., 1999a; Yack, J. E., 2004). Finally, there is an increasing body of literature demonstrating that many adult and larval insects communicate using solid-borne (seismic) vibrations that are transmitted through sand, leaf litter, or living plant material. Although vibrational communication is often omitted from discussions of ears and hearing, in insects, inclusion of this topic is important since there are many similarities between structures that detect sound and vibrations. We felt that a review of insect hearing would be incomplete without a brief discussion of this sensory modality.

There are several comprehensive reviews on insect hearing organs (Michelsen, A. and Larsen, O. N., 1985; Römer, H. and Tautz, J., 1992; Hoy, R. R. and Robert, D., 1996; Field, L. H. and Matheson, T., 1998; Yager, D. D., 1999a; Mason, A. C. and Faure, P. A., 2004; Yack, J. E., 2004). The goal of this chapter is to present an overview of the structure and diversity of insect sound and vibration receptors, and to highlight some interesting examples among the various insect groups. Special emphasis will be placed on tympanal hearing, since this is where most research has been focused to date. Auditory processing at the level of the central nervous system is not covered here (reviews of this subject can be found in writings by Boyan, G. S., 1993; Pollack, G. S., 1998; 2000;

Stumpner, A. and von Helversen, D., 2001; Hennig, R. M. *et al*., 2004; and Wyttenbach, R. A. and Farris, H. E., 2004).

3.02.2 Tympanal Ears

Tympanal hearing is the best-described acoustic sense in insects, owing to the fact that the behaviors (e.g., singing crickets and cicadas), and receptor organs (tympanal membranes) associated with farfield sound communication are often conspicuous to humans. Tympanal ears are similar to vertebrate ears in that they employ a tympanal membrane (eardrum) to detect pressure changes transmitted through the air (or water). Unlike for vertebrates, however, insect tympanal ears can occur on almost any part of the body, and have evolved multiple times within and between various taxa (Figure 1). Many ears described to date are located at the thoracic-abdominal juncture

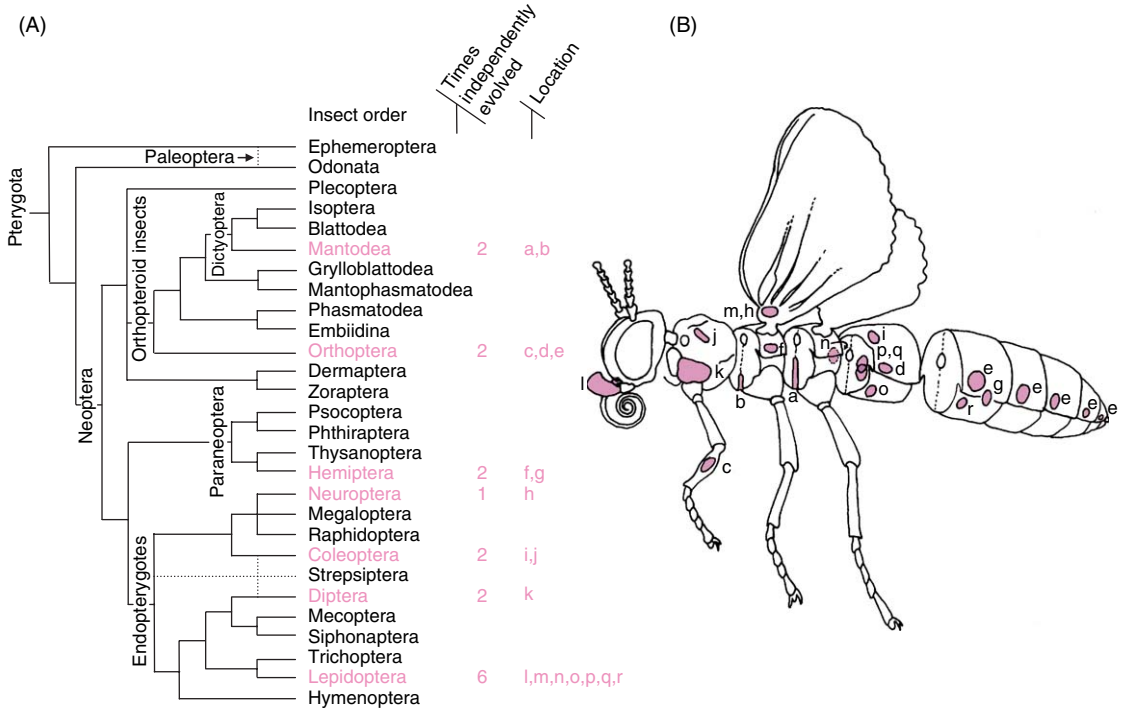

Figure 1 Distribution of tympanal hearing organs in insects. (A) A phylogeny of insects depicting the orders in which tympanal ears have evolved in at least some families. Numbers indicate how many times ears evolved independently within the order, and letters indicate where ears are located on the body, as shown in the drawing on the right. (B) A schematic drawing of a generalized insect showing where tympanal ears occur on insects. Please note that the sizes of the ears on figure are not to scale. Specific body locations according to each taxonomic division are as follows. *Mantodea*: (a) Within a deep groove on the ventral metathorax in many species; (b) In the same position on the mesothorax in Hymenopodidae. *Orthoptera*: (c) Ensifera, Gryllidae, Tettigoniidae. On the tibia of foreleg; (d) Acrididae. Within a tympanal cavity on the first abdominal segment; (d, e) Pneumoridae. On abdominal segment 1 (homologous to (d) in the Acrididae), and serial homologs on segments 2–6. *Hemiptera*: (f) Hydrocorisae. Lateral mesothorax, ventral to wing base; (g) Cicadidae. Within a cavity on the second abdominal segment. *Neuroptera*: (h) Chrysopidae. Base of ventral forewing. *Coleoptera*: (i) Cicindelidae. Dorsal surface of first abdominal segment, beneath the elytra; (j) Scarabidae. Dorsolateral region of prosternum. *Diptera*: (k) Sarcophagidae, Tachinidae. Ventral inflation of prosternum, between coxa (probably evolved independently in both groups). *Lepidoptera*: (l) Sphingidae (Choerocampini, Acherontini). Palp-pilifer region (probably evolved independently in both groups); (m) Papilionoidea, Hedyloidea. Ventral base of forewing (may have evolved independently in both groups); (n) Noctuoidea. Within a cavity on the posterior metathorax; (o) Pyraloidea. Within a cavity on ventral surface of first abdominal segment; (p) Geometridae. Within a cavity on anterior side of first abdominal segment; (q) Drepanidae. Internalized tympanal membrane located between two air-filled chambers on the first abdominal segment. (r) Uraniidae: within a cavity at the anterior (females) or posterior (males) end of the second abdominal segment. Phylogeny in (a) is from Gullan, P. J. and Cranston, P. S. 2005. The Insects: An Outline of Entomology, 3rd edn. Blackwell Publishing. (b) Redrawn from Yack, J. E. and Hoy, R. R. 2003. Hearing. In: Encyclopedia of Insects (*ed*. V. Resh and R. Cardé), pp. 498–505. Academic Press/Elsevier Science, with permission from Elsevier Science Publishers Ltd.

(the waist region of insects), but they also occur on more unusual body parts, including the neck area (some flies and beetles), the wings (some butterflies and lacewings), legs (crickets and katydids), and even the mouth-parts (some moths). Ears range in complexity, from those in notodontid and sphinx moths that possess a single auditory sensory cell (Surlykke, A., 1984; Göpfert, M. C. and Wasserthal, L. T., 1999), to those in some cicadas and bladder grasshoppers that can have up to 2000 sensory cells (Michel, K., 1975; Doolan, J. M. and Young, D., 1981; van Staaden, M. *et al.*, 2003). Tympanal ears in different insects are sensitive to a broad range of sound frequencies (~500 Hz to >100 kHz) at distances reaching up to 2 km. They have been reported in seven insect orders to date, and within most of these orders, ears have evolved more than once. Interestingly, some mantids and grasshoppers have multiple sets of ears on their bodies (discussed in Section 3.02.2.2). It is surprising that tympanal ears have not been reported for the large-bodied Odonates (dragon and damselflies), Hymenoptera (wasps, bees, ants), or Trichoptera (caddisflies), but it is expected that it is only a matter of time before hearing is described in at least some members of these groups.

Despite the wide diversity observed in their location and complexity, most tympanal ears follow a typical morphological plan, which includes three main components: (1) a tympanal membrane, (2) tracheal air sacs, and (3) a chordotonal organ (Figure 2). The tympanal membrane is a thinned region of cuticle, usually round or oval in shape, that is apposed to a tracheal air sac. When sound waves impinge upon the membrane, the auditory chordotonal organ, which is either directly or indirectly attached to the membrane, is stimulated by the vibration. The membrane thickness can vary from 0.4 μm in some noctuid moths (Ghiradella, H., 1971) to 100 μm in some wetas (Ball, E. E. and Field, L. H., 1981), and the diameter can range from ~500 μm (e.g., Hedylid butterflies; Yack J. E. and Fullard, J. H., 2000) to ~4 mm (e.g., some cicadas; Young, D. and Hill, K. G., 1977). In general, thinner membranes tend to be associated with sensitivity to higher frequencies. Finally, not all functional tympanal ears possess clearly differentiated tympanal membranes upon visual inspection of the insect (e.g., mantids, bladder grasshoppers, drepanid moths). A few of these examples will be discussed in this chapter.

The internal face of the tympanal membrane is directly adjacent to an air-filled chamber (tympanal

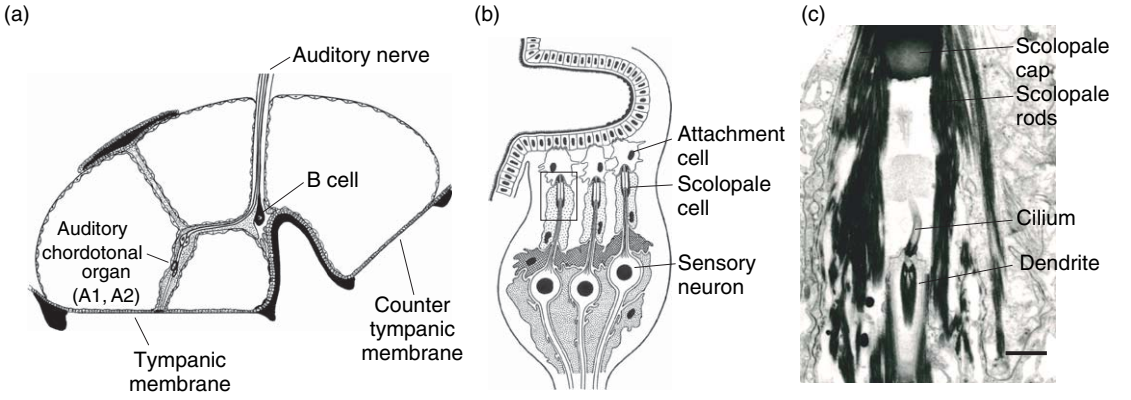

Figure 2 The principle features of a typical insect tympanal ear. (a) A cross section through the ear of a noctuid moth, illustrating the three main components of a tympanal hearing organ: the tympanic membrane, auditory chordotonal organ (which in this case has two scolopidia), and the tracheal air sac (white region). Another cell in the ear, the B cell, is a mutliterminal sensory neuron that does not respond to sound, and at present, the function is unknown. (b) A schematic of a chordotonal organ containing three monodynal, mononematic scolopidia. Each scolopidium comprises a single bipolar sensory neuron with a ciliated dendrite that inserts distally into a scolopale cap. A scolopale cell envelops the dendrite, and an attachment cell connects the entire structure to the integument. The boxed region is enlarged in (c). (c) Transmission electron micrograph of the distal dendritic region of a scolopidium. The ciliary segment passes through a lumen created by the surrounding scolopale cell, and inserts distally into the scolopale cap. Scolopale rod material, located inside the scolopale cell, surrounds the lumen. Scale bar = 0.5 μm. (a) Redrawn from Treat, A. E. and Roeder, K. D. 1959.A nervous element of unknown function in the tympanic organ of moths. J. Insect Physiol. 3, 262–270, with permission from Elsevier Science Publishers Ltd. (b) Reproduced from Gray, E. G. 1960. The fine structure of the insect ear. Phil. Trans. R. Soc. Lond. 243, 75–94. (c) Adapted from Yack, J. E. and Roots, B. I. 1992. The metathoracic wing-hinge chordotonal organ of an atympanate moth, *Actias luna* (Lepidoptera, Saturniidae): a light- and electron-microscopic study. Cell Tiss. Res., 267, 455–471.

chamber) formed by an enlargement of the trachea (part of the respiratory system of insects). The air chamber has an acoustic impedance matched to the external medium on the outside of the eardrum, allowing the membrane to vibrate (Figure 2(a)). In vertebrates, this impedance-matching is achieved by the air-filled middle ear. Although the tympanal chamber is almost always air-filled in insects, there is at least one exception in the green lacewing, *Chrysoperla carnea* (Chrysopidae) (Miller, L. A., 1970) where the ear is largely fluid-filled.

All insect tympanal ears described to date are innervated by a particular class of mechanoreceptors called chordotonal organs, which are unique to the Insecta and Crustacea (Howse, P. E., 1968; Moulins, M., 1976; Field, L. H. and Matheson, T., 1998). In insects, chordotonal organs are located throughout the body, and depending on their location and peripheral attachment sites, may function as proprioceptors (detecting self-induced movements of limbs and internal organs), or exteroreceptors (detecting gravitational forces, sounds, or vibrations). Chordotonal organs are structurally complex, and can be categorized into different morphological types. Briefly, each chordotonal organ comprises one or more units called scolopidia, and each scolopidium is made up of four cell types: (1) one to four bipolar sensory neurons, each with a distal dendrite that contains a modified stereocilium of the $9 \times 2 + 0$ type; (2) a scolopale cell that envelops the distal region of the sensory cell and dendrite and connects the attachment cell to the sensory cell; (3) one or more attachment cells that connect the scolopidium to the integument; and (4) one or more glial cells surrounding the sensory neuron cell bodies. Although little is known about how scolopidia transduce mechanical energy into electrical impulses of the sensory neuron, it is generally believed that longitudinal stretching of the dendritic cilium leads to permeability changes of the sensory cell at the base of the cilium. There is significant variation in the structure of chordotonal organs and their constituent scolopidia, and presumably these structural variations impart different functional characteristics to the sense organ.

Without exception, all chordotonal organs innervating insect tympanal ears (tympanal organs) that have been studied to date have certain ultrastructural features in common (Figures 2(b) and 2(c)). First, they are of the mononematic type, characterized by having an extracellular structure called a scolopale cap at the terminal end of the dendritic cilium. Second, they are of the monodynal type, meaning that there is only one dendrite associated with each scolopidium. Third, they possess type 1 scolopidia, which are distinguished by having a ciliary segment that has uniform diameter. At present, the functional importance of these ultrastructural features consistently found in tympanal organs is not understood. However, they are thought to be important for imparting a high degree of coupling between the vibrating membrane and the sensory cell, which would be a necessity for detecting small, rapid sound vibrations (Yack, J. E., 2004). While some structural features of tympanal organs are consistent, others, such as the number of scolopidia in the organ, or how the chordotonal organ is associated with the tympanal membrane, are variable. For further reading on the structure and function of chordotonal organs in general, the reader should consult Howse P. E. (1968), Moulins M. (1976), and Field L. H. and Matheson T. (1998). More specific reviews of chordotonal organs associated with insect hearing include the ones by Field L. H. and Matheson T. (1998), Eberl D. F. (1999), Yager D. D. (1999a), and Yack J. E. (2004).

3.02.2.1 Evolutionary Origins of Tympanal Ears

Why do insect tympanal ears occur in so many different body locations? One argument is that for insects, it is relatively easy to make an ear. There are now several lines of evidence demonstrating that tympanal ears evolved from chordotonal organs that previously served another function. As mentioned earlier, chordotonal organs occur throughout the insect body, where they commonly function as proprioceptors. It appears that through changes to peripheral structures associated with the chordotonal organ, a chordotonal organ that previously responded to proprioceptive or vibrational stimuli can be rendered sensitive to airborne vibrations, and thus converted to a hearing organ. Specific peripheral changes associated with the transition from proprioception to hearing might include the thinning of cuticle (i.e., development of a tympanum), enlargement of trachea, and other cuticular modifications that isolate the chordotonal organ from mechanical disturbances due to body movements. Support for the hypothesis that the evolutionary precursors of insect tympanal organs were vibration receptors or proprioceptors comes from comparative and developmental studies. For example, comparisons between primitively atympanate and tympanate moths show that the ultrasound sensitive thoracic ears of Noctuoid moths probably evolved from wing proprioceptors (Yack, J. E. and Fullard, J. H., 1990; Yack, J. E. *et al.*,

1999). Developmental studies on the abdominal ear of the locust demonstrate that the tympanal organ derives from an embryonic pleural chordotonal organ that monitors respiratory movements (Meier, T. and Reichert, H., 1990).

In discussing the transition from proprioception or vibration reception to hearing, many interesting questions arise. What are the genetic mechanisms governing the developmental processes leading to changes in peripheral structures, such as differences in the number of scolopidia, enlargement of tracheal air sacs, and the formation of a tympanal membrane? How is the wiring of the central nervous system modified for the animal to execute behaviors associated with hearing, such as positive phonotaxis, or evasive flight maneuvers? Why did ears evolve to be on any one particular body part in any given insect? Discussions of the developmental and evolutionary origins of insect tympanal ears are presented in research by Fullard J. H. and Yack J. E. (1993), Yack J. E. and Fullard J. H. (1993), Yager D. D. (1999a), Hasenfuss I. (2000), van Staaden M. *et al.* (2003), and Yack J. E. (2004).

3.02.2.2 Which Insects Have Tympanal Ears?

Tympanal ears are estimated to have evolved independently at least 17 times in insects (Figure 1), and this is not accounting for examples such as the multiple ears in bladder grasshoppers (van Staaden, M. *et al.*, 2003), or morphologically distinct tympanal membranes in some Lepidoptera that have not as yet been experimentally verified as functional hearing organs (Minet, J. and Surlykke, A., 2003). Even so, tympanal ears to date have only been described in seven of the 26 widely recognized extant neopteran insect orders. Why is it that some insect groups tend to be well equipped with ears, while others are deaf? A first answer is relatively clear to us, and this is that insect groups with members that are nocturnal and volant tend to have more members with ears. A great selection pressure for ear development arose about 60 million years ago, when bats began to use echolocation to detect their prey (Fullard, J. H., 1998), and this explains the origin of hearing in many insects, including moths, beetles, mantids, and lacewings. Lifestyle may explain why we do not see tympanal ears in some groups. For example, some insects that are nocturnally active may have alternative defense strategies. Mayflies, for example, are very short-lived as adults and synchronize their emergences to swamp their predators. Social Hymenoptera may lack tympanal hearing organs for communication purposes because of their communal lifestyle and the efficiency of near-field acoustic and substrate vibrations within a hive. Body size may also be an important factor in determining which insects have tympanal ears. Large insects may lack ears because their size offers some protection from bats (e.g., large silk- and hawk-moths, and dragonflies). In contrast, very small insects generally lack tympanal ears, and this could be for a couple of reasons. First, it is unlikely that a small-sized insect would use farfield sounds for communication because it would not have the mechanical power to generate sounds that will carry long distances (Bennet-Clark, H. C., 1998). Second, there is likely a size limit to how small an ear can be and still be functional. It could be that there is a minimum body size that can accommodate an ear, and that acoustic communication among small-bodied insects is restricted to the domain of solid-borne vibrations. The topic of ear size, with respect to the constraints imposed on miniature auditory systems and the selection pressures shaping ear size, is an interesting one (Surlykke, A. *et al.*, 1999; Robert, D., 2001). Following is a concise overview of tympanal ears described to date in the seven recognized tympanate insect orders.

3.02.2.2.1 Lepidoptera

Tympanal ears have evolved independently a minimum of six times in the Lepidoptera (moths and butterflies), where they are located on the thorax (Noctuoidea), abdomen (Pyraloidea, Geometroidea, Drepanoidea), mouth-parts (Bombycoidea), and wings (Hedyloidea, Papilionoidea). In addition, some members of the Tineoidea, Cossoidea, and Thyridoidea are likely to have ears, but confirmation of hearing in these groups awaits physiological and/or behavioral validation. All moth ears studied to date are sensitive to ultrasound (>20 kHz), and in most cases, function primarily as bat detectors (Miller, L. A. and Surlykke, A., 2001; Minet, J. and Surlykke, A., 2003). In species that also produce sounds, including some day-flying tiger moths (Arctiidae), hearing has secondarily assumed a role in social interactions (Spangler, H. G., 1988; Conner, W. E., 1999). Sonic hearing (<20 kHz) has only been demonstrated in a few species of Nymphalidae butterflies to date, and is believed to be used for conspecific communication and possibly the detection of bird predators (Ribaric, D. and Gogala, M., 1996; Yack J. E. *et al.*, 2000; Yack J. E., unpublished). The structure and function of moth ears has been studied extensively, and recently reviewed (Minet, J. and Surlykke, A., 2003). We restrict our

description of lepidopteran ears to two moth groups, the Noctuoidea, which have a very simple ear, and the Drepanoidea, which have a morphologically unconventional tympanal ear.

Noctuoidea ears are among the simplest of all insect ears studied to date, with only one (Notodontidae) or two (all other families) auditory cells (Figures 2(a) and 3). The ears are located on the posterior metathorax, nestled within a protective tympanal cavity (Figure 3(a)). The eardrum is an extremely thin (~0.4–1.0 μm) transparent membrane, bordered by a chitinous ring, and stretched across an enlarged tracheal air space, the tympanic chamber (Figure 3(b)). The tympanal organ attaches directly to the inner surface of the tympanal membrane. In those ears with two auditory cells (A1 and A2), both cells are broadly tuned to the same frequencies (25–50 kHz), but differ in their sensitivities by approximately 20 dB. The sensitivity range of moth ears overlaps with the same frequencies produced by the echolocation cries of

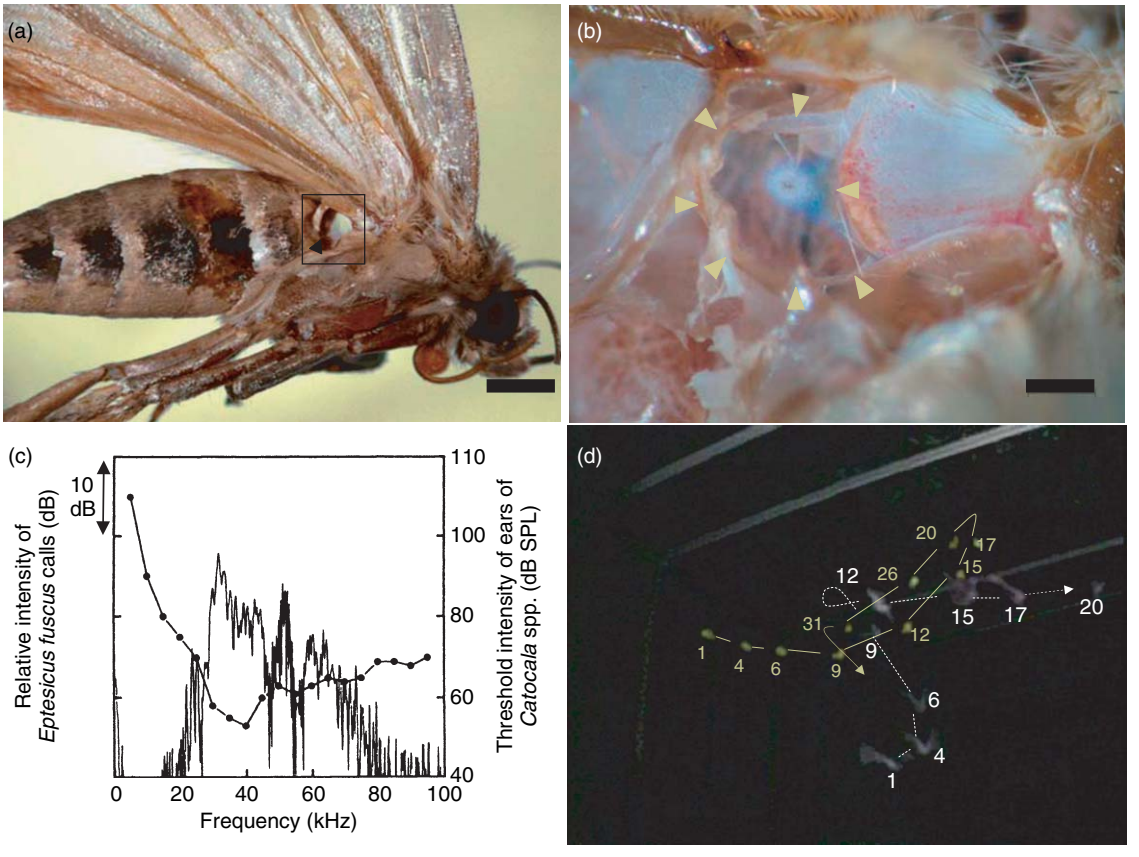

Figure 3 Hearing in noctuoid moths. (a) Photograph of the copper underwing moth, *Amphipyra pyramidoides,* indicating the location of the ear (boxed region) within a cleft at the junction of the thorax and abdomen (arrowhead). Scale bar = 3 mm. (b) Photograph showing the counter- tympanic membrane (indicated by arrowheads) and countertympanic membrane (translucent region to right of tympanic membrane). The attachment site of the auditory chordotonal organ appears as a small circular region of translucency and is partially visible through the courter-tympanic membrane. Scale bar = 500 μm. (c) Tuning curve of the A1 auditory receptor cell (filled circles) of an underwing moth (*Catocala* spp.) showing greatest sensitivity to sound pulses with 40 kHz carrier frequencies. The echolocation calls of the big brown bat, *Eptesicus fuscus*, a predator of underwing moths, have substantial energy in the 30–70 kHz band, the frequencies to which the ear of the moth is most sensitive. (d) A photo-montage created from a video capturing the interaction between a noctuid moth (dots and solid line highlighted in yellow) (unknown species) and a little brown bat, *Myotis lucifugus* (in gray with broken line). The moth is seen making changes in direction in response to the echolocation calls and flight path of the bat. Numbers indicate video frames compiled into the montage. (a, b) Photographs by J. Dawson. (c) Reproduced from Fullard, J. H. and Yack, J. E. 1993. The evolutionary biology of insect hearing. Trends Ecol. Evol. 8, 248–252, with permission from Elsevier Science Publishers Ltd. (d) Unpublished data by J. Dawson and A. Soutar.

insectivorous bats (Figure 3(c)). Flying moths stimulated with ultrasound respond by either turning away from the bat (negative phonotaxis), or engaging in an erratic evasive flight maneuver (Figure 3(d)) (reviewed by Roeder, K. D., 1967; Fullard, J. H., 1998; Miller, L. A. and Surlykke, A., 2001). This bi-modal response has in the past been attributed to the different thresholds of the two auditory cells. The lower threshold cell (A1) is thought to alert the moth to a far bat, and initiate negative phonotaxis, while the higher threshold cell (A2) warns of a close bat, to elicit evasive flight maneuvers. However, the jury is still out on how each of these cells contributes to evasive flight maneuvers (Fullard, J. H. *et al.*, 2003). Sound localization in moths can be achieved by comparing differences in sound intensities reaching each ear, since the wavelengths of the high-frequency sounds detected by moths are short enough to be diffracted by the moth's body.

The ears of hook-tip moths (Drepanoidea) are worth mentioning as a variation on the typical morphological plan of tympanal ears (Surlykke, A. *et al.*, 2003). In these moths, the eardrum is not directly exposed to the moth's exterior. Rather, the tympanal membrane occurs inside of the moth, stretched across an opening that joins two enlarged air-filled chambers (the dorsal chamber (dc) and ventral chamber (vc) in Figure 4). The scolopidia, instead of being attached to the tympanal membrane in a perpendicular orientation, as in the noctuid ear, are sandwiched between the tracheal air sac in the ventral chamber, and the tympanal membrane. It is believed that sound reaches this internal tympanum by two external membranes (anterior and posterior external membranes), and that the scolopidia are stretched lengthwise when sound impinges on the membrane. Like other moth ears, the drepanid ear is tuned to ultrasound, and represents another unique means by which insects have formed a high-frequency ear.

3.02.2.2.2 Orthoptera

Hearing has evolved independently in the suborders Caelifera (grasshoppers, locusts) and Ensifera (crickets, katydids, and wetas). In contrast to the Lepidoptera, the primary function for hearing in extant Orthoptera is conspecific communication, and secondarily, for predator detection.

In most grasshoppers and locusts, the ears are conspicuous, circular, translucent membranes located on the sides of the first abdominal segment (Figures 5(a) and 5(b)). The tympanal chordotonal organ (Müller's organ) attaches directly to the inner surface of the tympanum, and contains between 60 and 80 scolopidia, which are divided into groups (a, b, c, d) that attach to different parts of the membrane (Figure 5(d)) (Gray, E. G., 1960; Michel, K. and Petersen, M., 1982; Jacobs, K. *et al.*, 1999). The acridid ear is one of the few insect ears capable of pitch discrimination (Figure 5(c)). The mechanism has been explained by the place principle of frequency discrimination, whereby the tuning of the different cell groups is achieved by the unique resonance properties of the tympanal membrane to which they attach, and Müller's organ itself. This is similar to frequency discrimination in the mammalian cochlea where a traveling wave in the basilar membrane stimulates hair cells selectively.

Evidence for hearing in a primitively atympanate insect, the bladder grasshopper (*Bullacris membraciodes*) of South Africa, has made us reconsider our definition of tympanal hearing organs, since generally the term tympanal ear implies that the insect has an eardrum of some sort. These insects are highly acoustic, producing loud calls by which males and females 'duet' across distances up to 2 km. Bladder grasshoppers do not possess conspicuous tympanal membranes at all, but rather, have six pairs of abdominal chordotonal organs that are sufficiently sensitive to detect conspecific calls (van Staaden, M. J. and Römer, H., 1998; van Staaden, M. *et al.*, 2003) (Figures 5(e)–5(h)). Each ear of the most anterior pair of ears (on segment A1) comprises a large chordotonal organ with ~2000 scolopidia. The A1 chordotonal organ in bladder grasshoppers is homologous to Müller's organ in locusts, but in contrast to the latter, lacks an association with a tympanal membrane, and possesses far more scolopidia. In addition to the A1 ears, five simpler, serially homologous chordotonal organs with 11 scolopidia each, occur in the posterior segments A2–6. All of these chordotonal organs attach to thinned regions of cuticle on the body wall, and are sensitive to the sound frequencies and intensities of conspecific calls, despite the absence of a differentiated tympanal membrane. The bladder grasshopper is considered to represent a relatively ancient group of Acrididae, and it is argued that their hearing organs represent a living example of the evolutionary transition between proprioceptors and tympanal hearing.

Ears of crickets (Gryllidae) and katydids (Tettigoniidae) occur on the proximal tibia of the forelegs. There are two oval-shaped tympanal membranes on each leg – one on the front and one on the back. Each tympanum is apposed to a tracheal air sac, which

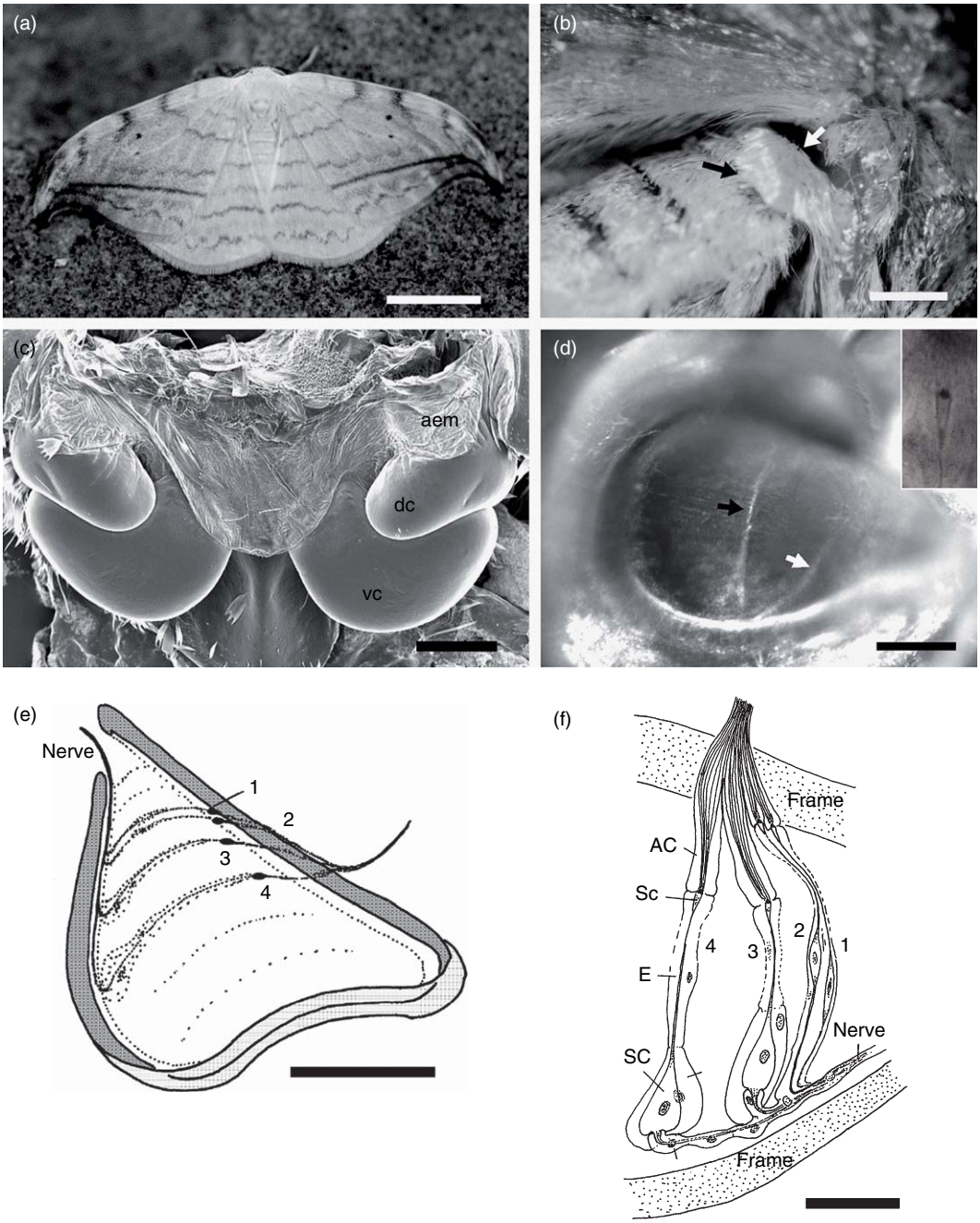

Figure 4 Tympanal ears in a hooktip moth (Drepanoidea). (a) A *Drepana arcuata* moth. Scale bar = 6 mm. (b) Right lateral view of the thorax and anterior abdomen, showing the general location of the abdominal ear. A white arrow points to the location of the anterior external membrane (aem in (c)), and a black arrow points to the location of the posterior external membrane. Scale bar = 0.75 mm. (c) Scanning electron micrograph of the anterior and ventral portion of the first abdominal segment. Each ear comprises a dorsal (dc) and ventral (vc) air chamber, between which the tympanal membrane is located. Sound is thought to enter the dorsal chamber by means of the anterior and posterior external membranes. Scale bar = 0.25 mm. (d) The internal tympanal membrane of the left ear as seen following removal of the dorsal chamber. Four scolopidia are suspended between the two tracheal sheets forming the tympanal membrane. The black and white arrows mark the location of scolopidia 4 and 3 respectively. Scale bar = 80 μm. The inset shows the distal tip of a scolopidium. (e) Drawing of the tympanic membrane with scolopidia 1–4 viewed from the dorsal chamber. Scale bar = 0.1 mm. (f) Further details of the tympanal scolopidia. SC, sensory cell; E, enveloping (scolopale) cell; Sc, scolopale region; AC, attachment cell. Scale bar = 0.05 mm. Reproduced from Surlykke, A., Yack, J. E., Spence, A. J., and Hasenfuss, I. 2003. Hearing in hooktip moths (Drepanidae, Lepidoptera). J. Exp. Biol. 206, 2653–2663.

in turn, is connected to other sound input sources, such as spiracles, and ears on the contralateral side of the body. In many insects, like the cricket, that use low-frequency sounds for communication, sound localization is a problem because the wavelength of the sound is greater than the width of the body (unlike for the noctuid moth, discussed earlier). Crickets solve this problem by having pressure-gradient ears, whereby the sound stimulates the tympanic membrane via both external and internal routes. In crickets, the tympanal membrane vibrates in response to sound reaching the ear from the external side of the

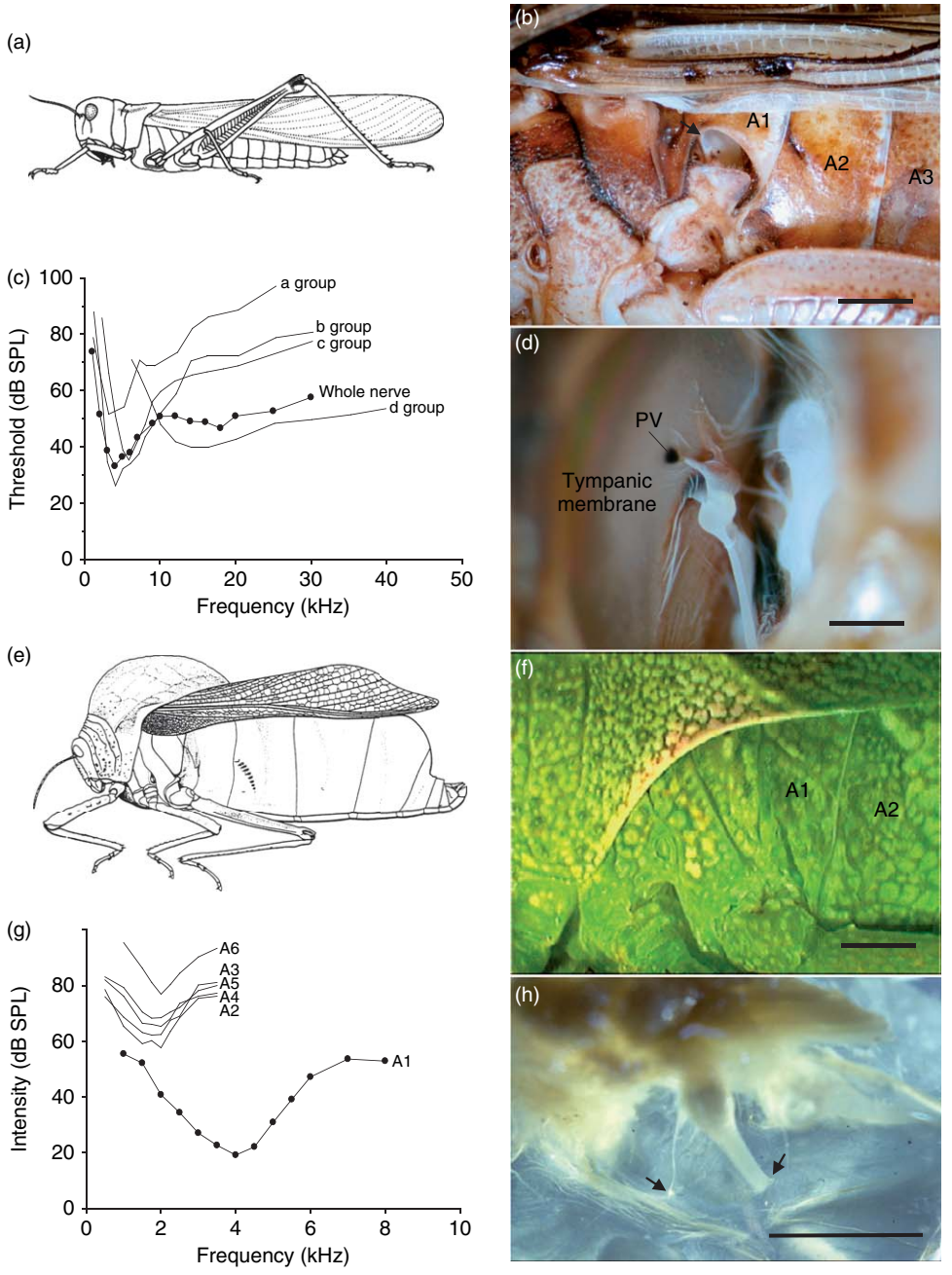

tympanum, but also from sounds that reach the inner side of the membrane by ipsilateral and contralateral spiracles. Because sound can reach the tympanal membranes from different routes, the relative lengths of the routes introduce phase delays between the ears, which provide directional cues for sound location.

In most Ensifera, the tympanal organ does not attach directly to the tympanal membranes, but rather, to the tracheal sac that lies adjacent to the anterior tympanal membrane. The scolopidia (60–70 in crickets, 20–50 in katydids) are arranged in a row down the leg, and are tonotopically organized, with the more distal units responding to higher frequencies (Stumpner, A., 1996). At present, the mechanism underlying the tuning properties of ensiferan ears is unknown, and there is experimental support that both intrinsic properties of the scolopidia themselves, and peripheral structures, such as trachea and membranes, play a role (see discussions by Field, L. H. and Matheson, T., 1998; Pollack, G. S. and Imaizumi, K., 1999). More extensive coverage of hearing in Orthoptera is provided by Michelsen A. and Larsen O. N. (1985), Ball E. E. *et al.* (1989), Bailey W. J. (1990), Field, L. H. and Matheson, T. (1998), and Yager D. D. (1999a).

3.02.2.2.3 Hemiptera (Homoptera + Heteroptera)

Cicadas (Homoptera, Cicadidae) are familiar to many of us because of the loud, high-pitched buzzing sounds they produce during hot weather. These sounds, usually produced by males calling to females, are generated by tymbal organs on the thorax, and often reach intensities close to 100 dB at close range, equivalent to what one might experience standing near a smoke alarm. Cicada ears comprise a pair of large oval tympanal membranes located inside a protective cavity on the ventral side of the second abdominal segment. The tympanal organ is contained within a sclerotized capsule and attaches to the lateral border of the eardrum. Cicada ears are among the largest of insect tympanal ears with respect to tympanal area (reaching 4 mm^2) and the number of scolopidia (up to 2000 scolopidia per ear). The large number of cells is thought to enhance frequency discrimination, thereby allowing females to exploit additional components of the calling song (Fonseca, P. J. *et al.*, 2000).

Many waterbugs (Heteroptera, subfamily Hydrocorisae) communicate acoustically (Aitken, R. B., 1985) but little is known about how they hear. Only one species, the water boatman, *Corixa punctata*, has been studied in detail. The round tympanal membrane occurs on the lateral mesothorax, between the forewing and the leg. A large club-shaped cuticular structure extends outward from the membrane, and the auditory organ, comprising only two scolopidia, attaches to the base of this club. Surprisingly, the acoustic cells in the left and right ears are asymmetrical in their tuning and thresholds, with the left ear being consistently more sensitive to higher frequencies than the right. These physiological differences have been attributed to differences in vibrational qualities of the tympanal membrane and

Figure 5 Homologous hearing organs in the tympanate African migratory locust, *Locusta migratoria* and the atympanate bladder grasshopper, *Bullacris membracioides*. (a) Line drawing of the gregarious phase *L. migratoria*. (b) Photograph of the thorax and first three abdominal segments (A1–3) of *L. migratoria*. The tympanic membrane is found on the first abdominal segment (arrow) within a recess protected by the tympanal hood. The metathoracic (jumping) leg has been lowered to reveal the ear. Scale bar = 4 mm. (c) Threshold tuning curves from *L. migratoria* recorded from the whole auditory nerve (closed circles) and from individual receptors (a, b, c, and d group) within the auditory nerve (solid lines). (d) The internal surface of the ear of *L. migratoria* showing Müller's organ. The tympanic membrane is composed of both thick and thin membranous areas. The black dot is the pyriform vesicle (PV); the site of attachment of the high-frequency (d group) auditory receptors. Scale bar = 200 μm. (f) Line drawing of *B. membracioides*. (f) The thorax and first two abdominal segments of *B. membracioides* showing the absence of an overt tympanum in the body wall of the first abdominal segment (A1) – compare with B above. Scale bar = 2 mm. (g) Threshold tuning curves recorded from the serially homologous abdominal chordotonal organs in *B. membracioides*. The curve recorded from the first abdominal segment, A1 (11 males and females combined) indicates this organ has lower thresholds than the organs located in abdominal segments 2–6 (A2–6; curves are from a single individual). (h) Internal view of the A1 abdominal segment showing the chordotonal organ with two attachment sites of the sensillae (arrows). This chordotonal organ is much larger with many more sensory cells than that found in Müller's organ in *L. migratoria* (compare with (d)). Scale bar = 1.2 mm. (a) Reproduced from Gullan, P. J. and Cranston, P. S. 2005. The Insects: An Outline of Entomology, 3rd edn. Blackwell Publishing. (b, d) Photographs by J. Dawson. (c) Adapted from Römer, H. 1976. Die Informationsverarbeitung tympanaler Rezeptorelemente von *Locusta migratoria* (Acrididae, Orthoptera). J. Comp. Physiol. 109, 101–122. (e, g) Reprinted from Van Staaden, M. J. and Römer, H. 1998. Evolutionary transition from stretch to hearing organs in ancient grasshoppers. Nature 394, 773–776. (f, h) Reproduced from Van Staaden, M., Rieser, M., Ott, S. R., Pabst, M. A., and Römer, H. 2003. Serial hearing organs in the atympanate grasshopper *Bullacris membracioides* (Orthoptera, Pneumoridae). J. Comp. Neurol. 465, 579–592.

the clubbed structure (Prager, J., 1976; Prager, J. and Larsen, O. N., 1981). The biological significance of this phenomenon is thought to be an accommodation for changes in the resonance properties of the tympanal membrane while the animal is diving (Prager, J. and Streng, R., 1982).

3.02.2.2.4 Diptera

Tympanal hearing in flies does not function for conspecific communication or predator detection, as it does for most insects, but rather, for eavesdropping on the communication signals of other insects. Certain species of parasitoid flies belonging to the families Tachnidae and Sarcophagidae have independently evolved tympanal ears on their prosternum, just behind the head in the neck region of the insect (Figures 6(a) and 6(b)). Hearing is best developed in females, whose ears are tuned to the calling song of their particular host (Figure 6(c)), such as crickets, katydids, and cicadas. Once located, the female fly lays endoparasitic larvae on the host, where the larvae feed until pupation. Female *Ormia ochracea* (Tachinidae, Ormiini) can localize the call of a male cricket in the dark with remarkable accuracy in the absence of visual or olfactory cues (Müller, P. and Robert, D., 2001) (Figure 6(d)). Directional hearing is attributable to a previously undescribed mechanism for sound localization, which involves a unique lever system that amplifies very small time and amplitude differences between the two eardrums. Fly hearing has been reviewed by Robert D. and Hoy R. R. (1998) and Yager D. D. (1999a).

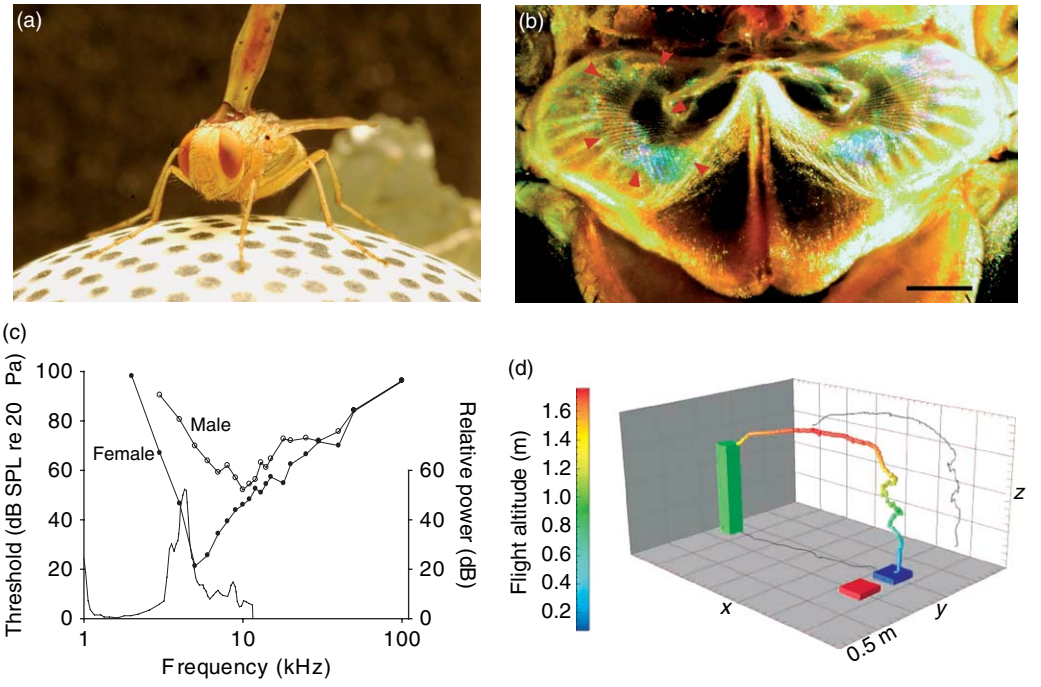

Figure 6 Hearing in the tachinid fly, *Ormia ochracea*. (a) Photograph of a tethered fly on a locomotion-tracking ball. (b) Photomicrograph of the ear. The head has been removed and the reader is looking at the neck region of the fly. The tympanic membrane is the region of thin cuticle outlined by arrowheads. A stiff cuticular rod connects the approximate centre of each tympanic membrane across the midline of the fly. This rod is used to facilitate extraction of directional information from the ear. Scale bar = 200 μm. (c) Threshold tuning curves of female (closed circles) and male (open circles) flies. The ears of females are more sensitive than the males and are frequency-matched to the calling song of their cricket host (solid line). (d) Three-dimensional reconstruction of the phonotactic flight path of a fly approaching a speaker broadcasting a synthesized cricket calling song. The fly takes off from the starting platform (green) and lands on the broadcasting speaker (blue); during the final stages of the approach, the fly exhibits a circling flight path. (a) Courtesy of Andrew Mason. (b) Reproduced from Yack, J. E. and Hoy, R. R. 2003. Hearing. In: Encyclopedia of Insects (eds. V. Resh and R. Cardé), pp. 498–505. Academic Press/Elsevier Science, with permission from Elsevier Science Publishers Ltd. (c) Redrawn from Robert, D., Amoroso, J., and Hoy, R. R. 1992. The evolutionary convergence of hearing in a parasitoid fly and its cricket host. Science 258, 1135–1137. (d) Reproduced from Müller, P. and Robert, D. 2001. A shot in the dark: the silent quest of a free-flying phonotactic fly. J. Exp. Biol. 204, 1039–1052.

3.02.2.2.5 Dictyoptera

Praying mantids (suborder Mantodea) were once thought to be deaf, but it is now estimated that hearing occurs in about 65% of all mantid species. The ear is located on the ventral midline of the metathorax, between the legs, inside a narrow groove. The teardrop-shaped eardrums, which are relatively thick (15–20 μm) and stiff compared to many other insect ears, are separated by a space of only 100–200 μm. As such, the mantid has been dubbed the auditory cyclops, and due to the close proximity of the ears to one another, lacks directional hearing. The ears are tuned to ultrasonic frequencies (25–50 kHz), and hearing triggers evasive flight maneuvers to escape bats. Ears are best developed in males, and the degree of sexual dimorphism seen in different species is positively correlated with wing length dimorphism. Interestingly, some species possess an additional set of ears on the mesothorax, which are serial homologs of the metathoracic ear. These are tuned to lower frequency sounds (2–4 kHz), and to date, their function remains a puzzle. Recent reviews of mantid hearing are provided by Yager D. D. (1999a; 1999b).

There is some evidence that *Periplaneta* cockroaches (suborder Blattidae) are capable of detecting farfield sounds below 5 kHz using the subgenual organs in their legs. There are no apparent tympanal membranes, and it is thought that sound arrives to the subgenual organ through the trachea (Shaw, S. R., 1994). There is no obvious function for detecting airborne sounds in *Periplaneta*, but other species, such as the hissing cockroach (*Gromphadorhina*), produce sounds in a social and defensive context, and it is possible that these insects use subgenual organs for communication (Nelson, M. C. and Fraser, J., 1980).

3.02.2.2.6 Coleoptera

Acoustic communication is widespread in beetles, which have a diversity of stridulatory structures that rivals no other insect order (Wessel, A., 2006). Surprisingly, little is known about their capabilities of detecting sounds or vibrations. To date, tympanal ears have been described in certain species belonging to two families. In tiger beetles (Cicindelidae), ears occur on the dorsum of the first abdominal segment in members of only one genus, the *Cicindela* (Yager, D. D. and Spangler, H. G., 1995; 1997; Yager, D. D. *et al.*, 2000). In some scarab beetles (Scarabidae, Dynastinae), ears are located on the anterior thorax, just behind the head (Forrest, T. G. *et al.*, 1995; 1997). In both tiger and scarab beetles, the ears are tuned to ultrasound, and thought to function in bat detection. It is somewhat surprising that hearing has not been discovered in more beetles, given their abundant numbers (350 000 described species) and that many species are nocturnal fliers, and communicate acoustically.

3.02.2.2.7 Neuroptera

Hearing in green lacewings (Chrysopidae) is tuned to ultrasound (30–60 kHz), and functions exclusively in bat detection. When approached by a bat at close range, a lacewing folds its wings and falls to the ground. The ears are located on the ventral forewing at the base of the radial vein, in a similar location described for some butterflies (Yack, J. E. and Fullard, J. H., 2000). The tympanal membrane is not at all conspicuous, but rather, comprises a thin region of cuticle on the ventral aspect of the wing that is associated with two chordotonal organs (Miller, L. A., 1970). Based on morphological evidence alone, one would not expect this organ to function as a hearing organ, yet its role as a bat detector has been indisputably supported through physiological and behavioral experiments. Lacewing ears are among the smallest of known insect ears, ~500–600 μm long, and are mostly fluid-filled. Perhaps the small size of the ear and the problem with impedance matching (due to being fluid-filled) explain its relatively high thresholds (60+ dB SPL at 50 kHz). However, since this functions as a last chance ear, when a bat has already detected and begun its attack upon the insect, such high thresholds are adaptive. Hearing in lacewings has been reviewed by Miller L. A. (1984) and Miller L. A. and Surlykke A. (2001).

3.02.3 Nearfield Sound Receptors

Typical sources of nearfield sounds relevant to insects include those produced by the beating wings of a flying predator or parasite, such as a wasp, or by a singing or flying conspecific. These sounds are typically restricted to lower frequencies (under 1 kHz) and do not travel distances of more than one wavelength from the sound source. For example, if the dominant frequency of the sound is 100 Hz, most of the nearfield component would have dissipated by 3.3 m, while the nearfield component of a 1 kHz sound would have dissipated within 33 mm. The antennae of some insects, including many Diptera (e.g., mosquitoes, fruit flies, and midges) are highly specialized to detect the nearfield sounds generated by the wing-beats of flying or singing mates. In the male mosquito, the long, plumous antennae fit loosely into sockets and resonate freely to frequencies produced by a flying female (Göpfert, M. C. *et al.*, 1999).

Antennal vibrations are transferred to an elaborate chordotonal organ, the Johnston's organ, comprising up to 15 000 sensory neurons (Boo, K. S. and Richards, A. G., 1975), that occurs in the pedicel at the antennal base. Recent studies suggest that nearfield hearing in mosquitoes and fruit flies may be enhanced through autonomous activity of the Johnston's organ, analogous to cochlear amplification in vertebrates (see Göpfert, M. C. and Robert, D., 2001; Göpfert, M. C. *et al.*, 2005). This is an interesting discovery, since hearing in insects has previously been considered to be a passive rather than an active process. There is evidence that nearfield sounds form an important component of the complex dance language of honeybees (*Apis mellifera*), and that these signals are detectable by the Johnston's organ (reviewed by Hrncir, M. *et al.*, 2006) (Figure 7). Some caterpillars use modified seta, called trichoid sensilla, to detect the nearfield sounds produced by flying predatory or parasitic wasps or flies. These elongate hairs insert into specialized sockets on the thorax. Each is innervated by a single bipolar sensory neuron, which is excited by deflection of the sensillum. Vibration of the hair in response to nearfield sounds of an approaching wasp initiates defensive reactions, including cessation of locomotion, squirming, and dropping to the ground. The best-studied example is the cabbage moth caterpillar, *Barathra brassicae* (Noctuidae) (Figure 8). Eight thoracic trichoid receptors project outward from the insect's body, and removal of these hairs abolishes the defensive responses (Markl, H. and Tautz, J., 1975). The trichoid sensillum's best frequency (resonance frequency) is ~150 Hz, the same frequency as the major sound component of the wing beat of *Dolichovespula media* (Hymenoptera: Vespidae), a tiny wasp that lays its eggs in the body of the larvae (Tautz, J. and Markl, H., 1978). The use of nearfield sounds is probably widespread in insects, and should be examined for its role in behavior more extensively. Reviews on the subject include the ones by McIver S. B. (1985), Römer H. and Tautz J. (1992), and Field L. H. and Matheson T. (1998).

3.02.4 Vibration-Sensitive Organs

Although vibrational, or seismic communication, in insects has been recognized for decades, it has often been overlooked, since generally these signals are undetectable by humans. A recent resurgence of literature on the subject is at least partly due to more scientists having access to sensitive vibration-recording methods, such as laser vibrometry. Indeed, seismic communication appears to be widespread among both adult and larval insects, and plays important roles in sexual communication, predator and prey localization, defense, and orientation (see Cocroft, R. B., 2001; Cokl, A. and Virant-Doberlet, M., 2003; Virant-Doberlet, M. and Cokl, A., 2004; Cocroft, R. B. and Rodriguez, R. L., 2005 for recent reviews).

Despite the ubiquitous presence of vibrational communication in insects, little has been reported on the receptor organs used for detecting seismic signals. Trichoid sensilla, campaniform sensilla, Johnston's organs, and scattered chordotonal organs have all been implicated as vibration receptors, but the most widely studied structure to date is the subgenual organ, located in the legs of most insects (reviewed by McIver, S. B., 1985; Field, L. H. and Matheson, T., 1998). These organs are best developed in species that are particularly sensitive to solid-borne vibrations, including some ants (Menzel, J. G. and Tautz, J., 1994), cockroaches (Moran, D. T. and Rowley, J. C. III, 1975), crickets (Friedman, M. H., 1972), wasps (Vilhelmsen, L. *et al.*, 2001), lacewings (Devetak, D. and Pabst M. A., 1994), and honeybees (Hrncir, M. *et al.*, 2006; Figure 7). The structure has probably been best studied in lacewings (*Chrysoperla*) that use vibrations for courtship. In *Chrysoperla carnea*, the attachment cells of the chordotonal organ form a septum that attaches to the walls and trachea of the leg. The scolopidia attach to the septum in a perpendicular orientation, and vibrations of the leg are thought to cause acceleration of the leg hemolymph, causing stimulation the scolopidia.

The subgenual organ has been implicated as the primary receptor in several insect groups that communicate seismically, but in most cases this has not been validated scientifically.

3.02.5 Summary and Future Considerations

Acoustic communication in insects is widespread and involves not only the detection of pressure waves, but also nearfield sounds and vibrational signals. A variety of different sound and vibration receptors have evolved in different insect groups, including tympanal ears, Johnston's organs, trichoid sensillae, and subgenual organs. Collectively, these acoustic sensory organs operate over a frequency range extending up to 150 kHz, and an intensity range of 100 dB. Sound and vibration receptors have evolved multiple times in different insect groups, and this enormous diversity of ear types is partially due to the fact that there are

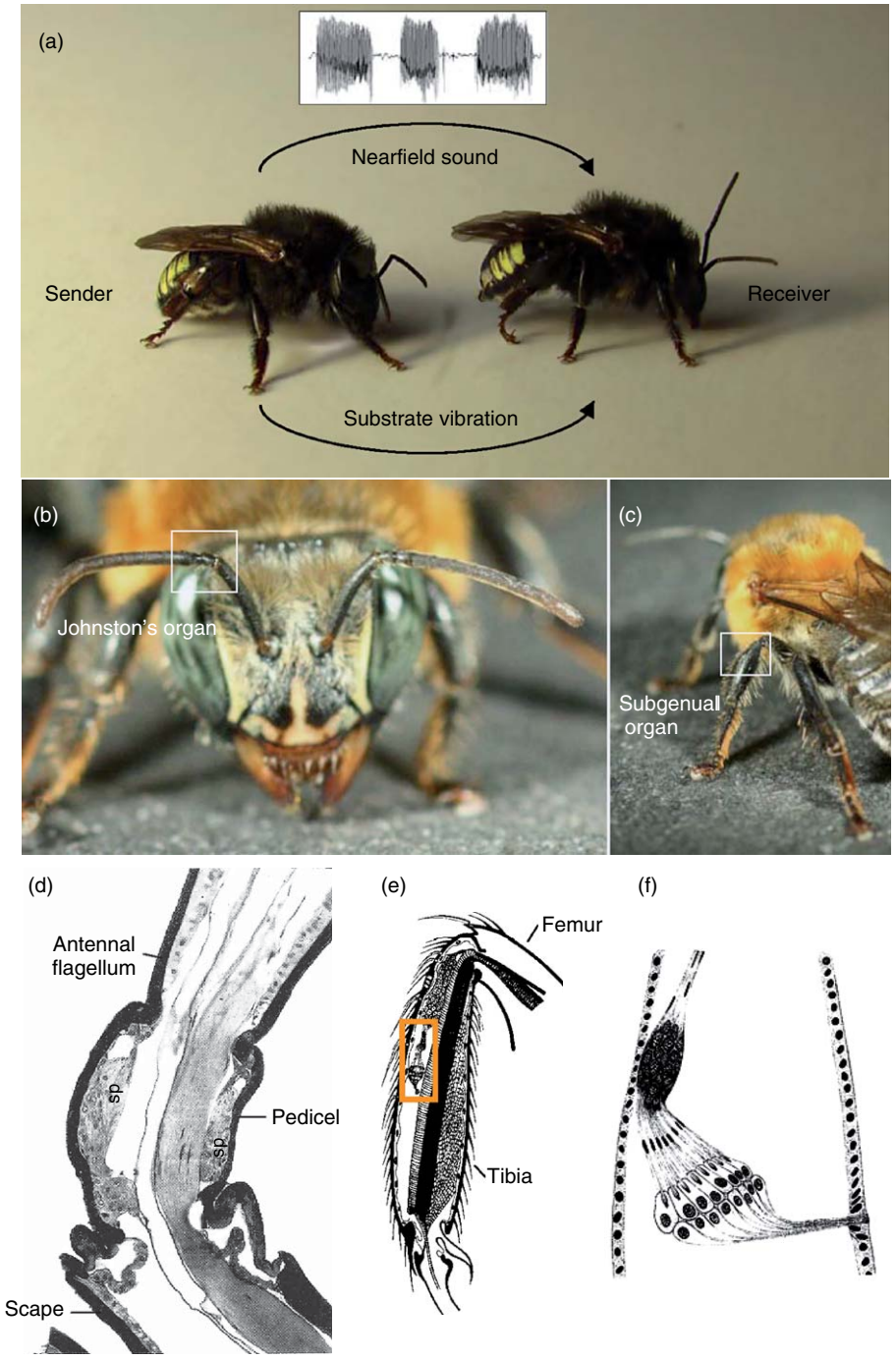

Figure 7 Acoustic communication in bees. (a) Schematic diagram depicting two possible communication channels between two honeybees: nearfield airborne sounds or substrate vibrations. (b) Airborne sounds induce vibrations of the antennal flagellum and stimulate sensory cells of the Johnston's organ. (c) The subgenual organ responds to axial vibrations of the tibia. The position of the leg (tibia) is important during signal reception. (d) Section of the antennal flagellum and pedicel of the honeybee antenna showing Johnston's organ. (e) Drawing of the subgenual organ of the leg of a honeybee. Boxed region is expanded in (f). (a–c) Photographs by M. Hrncir. (d) Reproduced from Dreller, C. and Kirchner, W. H. (1995) The sense of hearing in honey bees. Bee World 76(1), 6–17. (e, f) Reproduced from Schön, A. 1911. Bau und Entwicklung des tibialen Chordotonalorgans bei der Honigbiene und bei Ameisen. Zool. Jb. Anat. 31, 439–472, with permission from Elsevier Science Publishers Ltd.

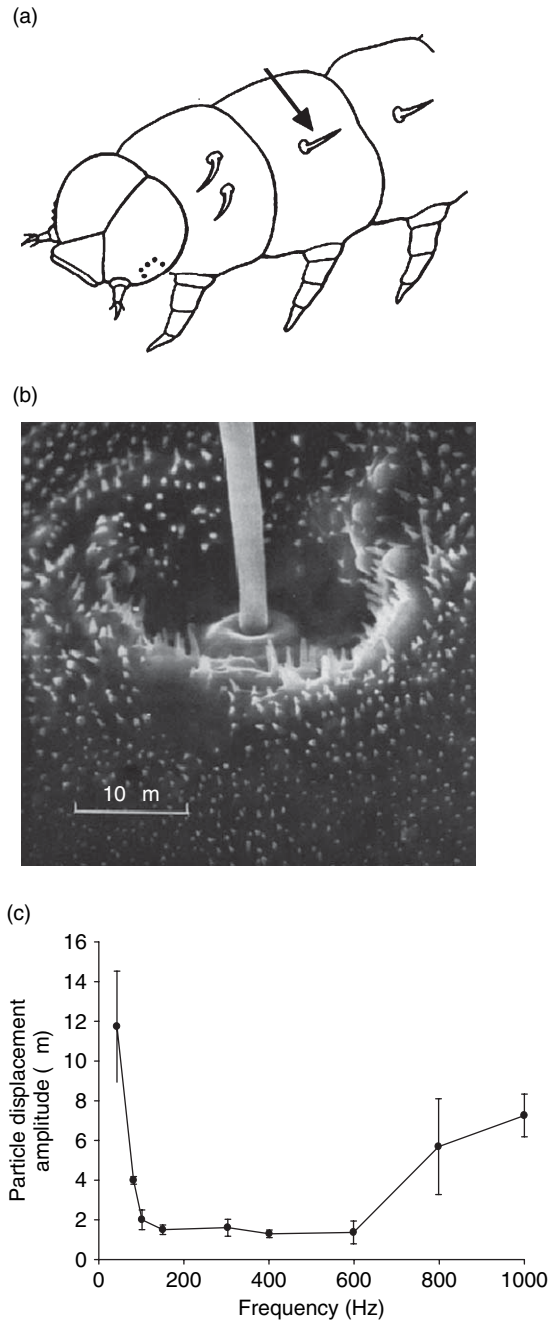

Figure 8 Nearfield sound receptors in a cabbage moth caterpillar *Barathra*. (a) The anterior end of the caterpillar, showing four thoracic trichoid sensilla. (b) A scanning electron micrograph of the base of a single trichoid sensillum. (c) Tuning curve of a single trichoid sensillum, which responds to the air particle displacements produced by the flight sounds of a parasitoid wasp, *Dolichovespula* sp. that lays eggs on the caterpillar. Adapted from Markl, H. and Tautz, J. 1975. The sensitivity of hair receptors in caterpillars of *Barathra brassicae* L. (Lepidoptera, Noctuidae) to particle movement in a sound field. J. Comp. Physiol. 99, 79–87.

few developmental steps to make a new ear from a preexisting proprioceptor. Some insects may rely on multiple tympanal ears, and a combination of sound and vibration receptors to form a perceptual construct of their environment. It is difficult for us to imagine a sensory world dominated by sounds and vibrations, which is probably the case for many insects.

Tympanal ears are structurally most similar to vertebrate ears in that they consist of an eardrum associated with sensory neurons that respond to far-field sounds (pressure waves). Unlike vertebrate ears, however, insect tympanal ears can occur on almost any part of the body (including the neck, wings, and mouth) and range in complexity from having a single auditory sense cell (in some moths) to over 2000 (in some grasshoppers and cicadas). Despite their small size, insect auditory systems are capable of performing complex tasks such as precise sound localization, frequency discrimination, pattern recognition, and categorical perception, similar to what we see in vertebrate auditory systems.

Much progress has been made in understanding insect auditory systems over the past few decades, thanks to developments in neural and vibrational recording techniques. Still, there are many puzzles, and exciting new avenues of research to explore in the field of insect sound and vibrational communication. First, we are still discovering new hearing organs. Recently it has been learnt that some insects possess highly sensitive hearing, but do not possess morphologically conspicuous hearing organs (i.e., they lack an obvious eardrum). It is very likely that hearing organs will be discovered in those insect groups that have been considered 'deaf', including the Hymenoptera (bees and wasps), and Odonates (dragonflies and damselflies). Second, despite our extensive knowledge of the structure of tympanal chordotonal organs, it's still not understood how these complex structures convert mechanical vibrations into nerve impulses. Developments in this area of study involving genetically manipulated auditory chordotonal organs, and insights into the molecular basis of mechanosensory channels, promise to shed light on this conundrum. Third, how acoustic signals are integrated at the level of the central nervous system to produce adaptive behaviors such as evasive flight, positive phonotaxis, or mate choice is an ongoing and exciting area of research. Finally, there is still much to learn about how insects detect and use solid-borne vibrations and nearfield sounds, and future explorations into these sensory modalities are sure to yield exciting new insights into the unique auditory sensory world of insects.

References

Aitken, R. B. 1985. Sound production by aquatic insects. J. Biol. Rev. 65, 163–211.

Bailey, W. J. 1990. The Anatomy of the Tettigoniid Hearing System. In: The Tettigoniidae: Biology, Systematics, and Evolution (*eds*. W. J. Bailey and D. C. F. Rentz), pp. 217–247. Springer.

Ball, E. E. and Field, L. H. 1981. Structure of the auditory system of the Weta (*Hemideina crassidens* (Blanchard, 1851) (Orthoptera, Ensifera, Gryllacridoidea, Stenopelmatidae). I. Morphology and histology. Cell Tiss. Res. 217, 321–343.

Ball, E. E., Oldfield, B. P., and Rudolf, K. M. 1989. Auditory Organ Structure, Development, and Function. In: Cricket Behavior and Neurobiology (*eds*. F. Huber and T. E. Moore), pp. 391–422. Cornell University Press.

Bennet-Clark, H. C. 1984. Insect Hearing: Acoustics and Transduction. In: Insect Communication (*ed*. T. Lewis), pp. 49–82. Academic Press.

Bennet-Clark, H. C. 1998. Size and scale effects as constraints in insect sound communication. Phil. Trans. R. Soc. Lond. B. 353, 407–419.

Boo, K. S. and Richards, A. G. 1975. Fine strucfture of the scolopidia in Johnston's organ of the male *Aedes aegypti* (L.) (Diptera: Culicidae). Int. J. Insect Morphol. Embryol. 4, 549–566.

Boyan, G. S. 1993. Another look at insect audition: the tympanic receptors as an evolutionary specialization of the chordotonal system. J. Insect Physiol. 39, 187–200.

Cocroft, R. B. 2001. Vibrational communication and the ecology of group-living, herbivorous insects. Amer. Zool. 41, 1215–1221.

Cocroft, R. B. and Rodriguez, R. L. 2005. The behavioral ecology of insect vibrational communication. Bioscience 55, 323–334.

Cokl, A. and Virant-Doberlet, M. 2003. Communication with substrate-borne signals in small plant-dwelling insects. Annu. Rev. Entomol. 48, 29–50.

Conner, W. E. 1999. ''Un chant d'appel amoureux'': acoustic communication in moths. J. Exp. Biol. 202, 1711–1723.

Devetak, D. and Pabst, M. A. 1994. Structure of the subgenual organ in the green lacewing, *Chrysoperla carnea*. Tiss. Cell. 26, 249–257.

Doolan, J. M. and Young, D. 1981. The organization of the auditory organ of the bladder cicada, *Cystosoma saundersii*. Phil. Trans. R. Soc. Lond. 291, 525–540.

Dreller, C. and Kirchner, W. H. 1995. The sense of hearing in honey bees. Bee World 76(1), 6–17.

Eberl, D. F. 1999. Feeling the vibes: chordotonal mechanisms in insect hearing. Curr. Opin. Neurobiol. 9, 389–393.

Field, L. H. and Matheson, T. 1998. Chordotonal organs of insects. Adv. Insect Physiol. 27, 1–228.

Fonseca, P. J., Münch, D., and Hennig, R. M. 2000. How cicadas interpret acoustic signals. Nature 405, 297–298.

Forrest, T. G., Farris, H. E., and Hoy, R. R. 1995. Ultrasound acoustic startle responses in scarab beetles. J. Exp. Biol. 198, 2593–2598.

Forrest, T. G., Read, M. P., Farris, H. E., and Hoy, R. R. 1997. A tympanal hearing organ in scarab beetles. J. Exp. Biol. 200, 601–606.

Friedman, M. H. 1972. An electron microscopic study of the tympanal organ and associated structures in the foreleg tibia of the cricket, *Gryllus assimilis*. J. Morphol. 138, 329–348.

Fullard, J. H. 1998. The Sensory Coevolution of Moths and Bats. In: Comparative Hearing: Insects (*eds*. R. R. Hoy, A. N. Popper, and R. R. Fay), pp. 279–326. Springer.

Fullard, J. H. and Yack, J. E. 1993. The evolutionary biology of insect hearing. Trends Ecol. Evol. 8, 248–252.

Fullard, J. H., Dawson, J. W., and Jacobs, D. S. 2003. Auditory encoding during the last moment of a moth's life. J. Exp. Biol. 206, 281–294.

Ghiradella, H. 1971. Fine structure of the noctuid moth ear. I. The transducer area and connections to the tympanic membrane in *Feltia subgothica* Hawthorn. J. Morphol. 134, 21–45.

Göpfert, M. C. and Robert, D. 2001. Active auditory mechanics in mosquitoes. Proc. R. Soc. Lond. B. 268, 333–339.

Göpfert, M. C. and Wasserthal, L. T. 1999. Auditory sensory cells in hawkmoths: Identification, physiology, and structure. J. Exp. Biol. 202, 1579–1587.

Göpfert, M. C., Briegel, H., and Robert, D. 1999. Mosquito hearing: sound-induced vibrations in male and female *Aedes aegypti*. J. Exp. Biol. 202, 2727–2738.

Göpfert, M. C., Humphris, A. D. L., Albert, J. T., Robert, D., and Hendrich, O. 2005. Power gain exhibited by motile mechanosensory neurons in *Drosophila* ears. Proc. Nat. Acad. Sci. USA 102, 325–330.

Gray, E. G. 1960. The fine structure of the insect ear. Phil. Trans. R. Soc. Lond. 243, 75–94.

Gullan, P. J. and Cranston, P. S. 2005. The Insects: An Outline of Entomology, 3rd edn. Blackwell Publishing.

Hasenfuss, I. 2000. Evolutionary pathways of truncal tympanal organs in Lepidoptera (Insecta: Holometabola). Zool. Anz. 239, 27–44.

Hennig, R. M., Franz, A., and Stumpner, A. 2004. Processing of auditory information in insects. Microsc. Res. Tech. 63, 351–374.

Howse, P. E. 1968. The fine structure and functional organization of chordotonal organs. Symp. Zool. Soc. (Lond.) 23, 167–198.

Hoy, R. R. and Robert, D. 1996. Tympanal hearing in insects. Ann. Rev. Ent. 41, 433–450.

Hrncir, M., Barth, F. G., and Tautz, J. 2006. Vibratory and Air-Borne Sound Signals in Bee Communication (Hymenoptera). In: Insect Sounds and Communication. Physiology, Behaviour, Ecology and Evolution (*eds*. S. Drosopoulos and M. F. Claridge), pp. 421–436. CRC, Taylor and Francis Group.

Jacobs, K., Otte, B., and Lakes-Harlan, R. 1999. Tympanal receptor cells of *Schistocerca gregaria:* correlation of soma positions and dendrite attachment sites, central projections and physiologies. J. Exp. Zool. 283, 270–285.

Markl, H. and Tautz, J. 1975. The sensitivity of hair receptors in caterpillars of *Barathra brassicae* L. (Lepidoptera, Noctuidae) to particle movement in a sound field. J. Comp. Physiol. 99, 79–87.

Mason, A. C. and Faure, P. A. 2004. The physiology of insect auditory afferents. J. Mic. Res. Tech. 63, 338–350.

McIver, S. B. 1985. Mechanoreception. In: Comprehensive Insect Physiology, Biochemistry and Pharmacology (*eds*. G. A. Kerkut and L. I. Gilbert), Vol. 6, pp. 71–132. Pergamon.

Meier, T. and Reichert, H. 1990. Embryonic development and evolutionary origin of the orthopteran auditory organs. J. Neurobiol. 21, 592–610.

Menzel, J. G. and Tautz, J. 1994. Functional morphology of the subgenual organ of the carpenter ant. Tiss. Cell. 26, 735–746.

Michel, K. 1975. Das tympanalorgan von *Cicada orni* L. (Cicadina, Homoptera). Zoomorphol. 82, 63–78.

Michel, K. and Petersen, M. 1982. Development of the tympanal organ of the migratory locust (*Locusta migratoria*). Cell Tiss. Res. 222, 667–676.

Michelsen, A. and Larsen, O. N. 1985. Hearing and Sound. In: Comprehensive Insect Physiology, Biochemistry, and Pharmacology (*eds*. G. A. Kerkut and L. I. Gilbert), pp. 495–556. Pergamon.

Michelsen, A. and Nocke, H. 1974. Biophysical aspects of sound communication in insects. Adv. Insect Physiol. 10, 247–296.

Miller, L. A. 1970. Structure of the green lacewing tympanal organ (*Chrysopa carnea,* Neuroptera). J. Morphol. 131, 359–382.

Miller, L. A. 1984. Hearing in Green Lacewings and Their Responses to the Cries of Bats. In: Biology of Chrysopidae (*eds*. M. Canard and Y. Séméria), pp. 134–149. W. Junk.

Miller, L. A. and Surlykke, A. 2001. How some insects detect and avoid being eaten by bats: tactics and countertactics of prey and predator. Bioscience 51, 571–582.

Minet, J. and Surlykke, A. 2003. Sound Producing and Auditory Organs. In: Handbook of Zoology/Handbuch der Zoologie: Lepidoptera, Moths and butterflies, Morphology and Physiology (*ed*. N. P. Kristensen), Vol. 2. IV, 35, pp. 289–323. Walter de Gruyter.

Moran, D. T. and Rowley, J. C. III. 1975. High voltage and scanning electron microscopy of the site of stimulus reception of an insect mechanoreceptor. J. Ultrastruct. Res. 50, 38–46.

Moulins, M. 1976. Ultrastructure of Chordotonal Organs. In: Structure and Function of Proprioceptors in the Invertebrates (*ed*. P. J. Mill), pp. 387–426. Chapman and Hall.

Müller, P. and Robert, D. 2001. A shot in the dark: the silent quest of a free-flying phonotactic fly. J. Exp. Biol. 204, 1039–1052.

Nelson, M. C. and Fraser, J. 1980. Sound production in the cockroach, *Gromphadorhina portentosa:* evidence for communication by hissing. Behav. Ecol. Sociobiol. 6, 305–314.

Pollack, G. S. 1998. Neural Processing of Acoustic Signals. In: Comparative Hearing: Insects (*eds*. R. R. Hoy, A. N. Popper, and R. R. Fay), pp. 139–196. Springer.

Pollack, G. S. 2000. Who, what, where? Recognition and localization of acoustic signals by insects. Curr. Opin. Neurobiol. 10, 763–767.

Pollack, G. S. and Imaizumi, K. 1999. Neural analysis of sound frequency in insects. Bioessays 21, 295–303.

Prager, J. 1976. Das mesothorakale Tympanalorgan von *Corixa punctata* Ill (Heteroptera, Corixidae). J. Comp. Physiol. 11, 33–50.

Prager, J. and Larsen, O. N. 1981. Asymmetrical hearing in the water bug *Corixa punctata* observed with laser vibrometry. Naturwissenschaften 68, 579–580.

Prager, J. and Streng, R. 1982. The resonance properties of the physical gill of *Corixa punctata* and their significance in sound reception. J. Comp. Physiol. A. 148, 323–335.

Ribaric, D. and Gogala, M. 1996. Acoustic behaviour of some butterfly species of the genus Erebia (Lepidoptera: Satyridae). Acta Entomol. Slov. 4, 5–12.

Robert, D. 2001. Innovative biomechanics for directional hearing in small flies. Biol. Bull. 200, 190–194.

Robert, D. and Hoy, R. R. 1998. The Evolutionary Innovation of Tympanal Hearing in Diptera. In: Comparative Hearing: Insects (*eds*. R. R. Hoy, A. N. Popper, and R. R. Fay), pp. 197–227. Springer.

Robert, D., Amoroso, J., and Hoy, R. R. 1992. The evolutionary convergence of hearing in a parasitoid fly and its cricket host. Science 258, 1135–1137.

Roeder, K. D. 1967. Nerve Cells and Insect Behavior. Harvard University Press.

Römer, H. 1976. Die Informationsverarbeitung tympanaler Rezeptorelemente von *Locusta migratoria* (Acrididae, Orthoptera). J. Comp. Physiol. 109, 101–122.

Römer, H. and Tautz, J. 1992. Invertebrate auditory receptors. Adv. Comp. Env. Phys. 10, 185–212.

Schön, A. 1911. Bau und Entwicklung des tibialen Chordotonalorgans bei der Honigbiene und bei Ameisen. Zool. Jb. Anat. 31, 439–472.

Shaw, S. R. 1994. Detection of airborne sound by a cockroach 'vibration detector': a possible missing link in insect auditory evolution. J. Exp. Biol. 193, 13–47.

Spangler, H. G. 1988. Moth hearing, defense, and communication. Ann. Rev. Entomol. 33, 59–81.

Stumpner, A. 1996. Tonotopic organization of the hearing organ in a bushcricket: physiological characterization and complete staining of auditory receptor cells. Naturwissenschaften 83, 81–84.

Stumpner, A. and von Helversen, D. 2001. Evolution and function of auditory systems in insects. Naturwissenschaften 88, 159–170.

Surlykke, A. 1984. Hearing in notodontid moths: a tympanic organ with a single auditory neurone. J. Exp. Biol. 113, 323–335.

Surlykke, A., Filskov, M., Fullard, J. H., and Forrest, E. 1999. Auditory relationships to size in noctuid moths: bigger is better. Naturwissenschaften 86, 238–241.

Surlykke, A., Yack, J. E., Spence, A. J., and Hasenfuss, I. 2003. Hearing in hooktip moths (Drepanidae, Lepidoptera). J. Exp. Biol. 206, 2653–2663.

Tautz, J. and Markl, H. 1978. Caterpillars detect flying wasps by hairs sensitive to airborne vibration. Behav. Ecol. Sociobiol. 4, 101–110.

Treat, A. E. and Roeder, K. D. 1959. A nervous element of unknown function in the tympanic organ of moths. J. Insect Physiol. 3, 262–270.

Van Staaden, M. J. and Römer, H. 1998. Evolutionary transition from stretch to hearing organs in ancient grasshoppers. Nature 394, 773–776.

Van Staaden, M., Rieser, M., Ott, S. R., Pabst, M. A., and Römer, H. 2003. Serial hearing organs in the atympanate grasshopper *Bullacris membracioides* (Orthoptera, Pneumoridae). J. Comp. Neurol. 465, 579–592.

Vilhelmsen, L., Isidoro, N., Romani, R., Basibuyuk, H. H., and Quicke, D. L. J. 2001. Host location and oviposition in a basal group of parasitic wasps: the subgenual organ, ovipositor apparatus and associatd structures in the Orussidae (Hymenoptera, Insecta). Zoomorphology 121, 63–84.

Virant-Doberlet, M. and Cokl, A. 2004. Vibrational communication in insects. Neotropical Entomology. 33, 121–134.

Wessel, A. 2006. Stridulation in the Coleoptera – An Overview. In: Insect Sounds and Communication. Physiology, Behaviour, Ecology and Evolution (*eds*. S. Drosopoulos and M. F. Claridge), pp. 397–403. CRC, Taylor and Francis.

Wyttenbach, R. A. and Farris, H. E. 2004. Psychophysics in insect hearing. Mic. Res. Tech. 63, 375–387.

Yack, J. E. 2004. The structure and function of auditory chordotonal organs in insects. J. Mic. Res. Tech. 63, 315–337.

Yack, J. E. and Fullard, J. H. 1990. The mechanoreceptive origin of insect tympanal organs: a comparative study of similar nerves in tympanate and atympanate moths. J. Comp. Neurol. 300, 523–534.

Yack, J. E. and Fullard, J. H. 1993. What is an insect ear? Ann. Ent. Soc. Am. 86, 677–682.

Yack, J. E. and Fullard, J. H. 2000. Ultrasonic hearing in nocturnal butterflies. Nature 403, 265–266.

Yack, J. E. and Hoy, R. R. 2003. Hearing. In: Encyclopedia of Insects (*eds*. V. Resh and R. Cardé), pp. 498–505. Academic Press/Elsevier Science.

Yack, J. E. and Roots, B. I. 1992. The metathoracic wing-hinge chordotonal organ of an atympanate moth, *Actias luna* (Lepidoptera, Saturniidae): a light- and electron-microscopic study. Cell Tiss. Res. 267, 455–471.

Yack, J. E., Otero, L. D., Dawson, J. W., Surlykke, A., and Fullard, J. H. 2000. Sound production and hearing in the blue cracker butterfly *Hamadryas feronia* (Lepidoptera, Nymphlidae) from Venezuela. J. Exp. Biol. 203, 3689–3702.

Yack, J. E., Scudder, G. G. E., and Fullard, J. H. 1999. Evolution of the metathoracic tympanal ear and its mesothoracic homologue in the Macrolepidoptera (Insecta). Zoomorphology 119, 93–103.

Yager, D. D. 1999a. Structure, development, and evolution of insect auditory systems. Micr. Res. Tech. 47, 380–400.

Yager, D. D. 1999b. Hearing. In: The Praying Mantids (*ed*. F. R. Prete), pp. 93–116. Johns Hopkins University Press.

Yager, D. D. and Spangler, H. G. 1995. Characterization of auditory afferents in the tiger beetle, *Cicindela marutha*. Dow J. Comp. Physiol. A. 176, 587–600.

Yager, D. D. and Spangler, H. G. 1997. Behavioral response to ultrasound by the tiger beetle *Cicindela marutha*. Dow J. Comp. Physiol. A. 176, 587–600.

Yager, D. D., Cook, A. P., Pearson, D. L., and Spangler, H. G. 2000. A comparative study of ultrasound-triggered behavior in tiger beetles (Cicindelidae). J. Zool. Lond. 251, 355–368.

Young, D. and Hill, K. G. 1977. Structure and function of the auditory system of the Cicada, *Cystosoma saundersii*. J. Comp. Physiol. A. 117, 23–45.

3.03 High-Frequency Hearing

H E Heffner and R S Heffner, University of Toledo, Toledo, OH, USA

© 2008 Elsevier Inc. All rights reserved.

3.03.1	Introduction	55
3.03.2	High-Frequency Hearing and Sound Localization	56
3.03.2.1	Binaural Spectral-Difference Cue	56
3.03.2.2	Pinna Localization Cues	57
3.03.2.3	Subterranean Mammals	58
3.03.2.4	Bats	58
3.03.2.5	Ultrasonic Communication	58
3.03.3	Conclusion	59
References		59

Glossary

azimuth Direction along the horizon relative to a listener.

functional head size The time it takes for sound to travel around the head from one ear to the other.

octave An interval between two frequencies that have a 2 to 1 ratio (0.25–0.5 kHz and 50–100 kHz are both intervals of one octave).

subterranean animals Animals that live their entire lives below ground.

Δt Difference in the time of arrival of a sound at the two ears.

Δfi Difference in the frequency–intensity spectra of a sound at the two ears.

3.03.1 Introduction

The first systematic study of high-frequency hearing was conducted by Francis Galton in the second half of the nineteenth century. Using a high-frequency whistle attached to his cane and operated by a rubber bulb, Galton observed the unconditioned responses of animals, including those of the London Zoological Gardens, to high-frequency sounds. His observations, which he briefly summarized in his book *Inquiries in Hhuman Faculty and Its Development* (1883), indicate that he found significant species differences in the ability to hear high frequencies or, as he referred to them, "shrill sounds." Of the animals he observed, he found cats to have the best high-frequency hearing, an ability he attributed to their need to hear the high-frequency sounds made by mice and the other small animals they catch. He also found small dogs to have good high-frequency hearing, although he believed that large dogs did not, as he was never able to get them to respond to his whistle. Thus, by the late nineteenth century, it was apparent that mammals vary in their ability to hear high-frequency sounds.

The purpose of this chapter is to explain both why mammals have good high-frequency hearing and why they differ in this ability. The explanation we offer does not address how mammals hear high frequencies, but why they do – mammals evolved high-frequency hearing for the purpose of localizing sound. Thus, the following is a description of the evolutionary pressures that have led to high-frequency hearing in mammals, rather than the mechanisms that underlie this ability.

Before beginning, some preliminary information will be useful. First, most nonmammalian vertebrates do not hear significantly above 10 kHz: birds have an upper limit of 8–12 kHz (Dooling, R. J. *et al.*, 2000) while reptiles, amphibians, and most fish do not hear above 5 kHz (Heffner, H. E. and Heffner, R. S., 1998; for an example of fish that hear high frequencies, see Mann, D.A. *et al.*, 2001). Thus, the almost universal ability of mammals to hear frequencies above 10 kHz

is a distinctly mammalian trait among vertebrates. Second, the term ultrasonic refers to frequencies above the nominal upper limit of humans, which is 20 kHz, and is therefore an anthropocentric term. A more appropriate perspective would be gained if we focus on the distinction between mammals and other vertebrates and consider any hearing above 10 kHz to be noteworthy. Finally, it should be noted that sound is perceived on a log scale, which in music is stated in octaves. Thus, although the difference between an upper limit of 50 and 100 kHz may seem greater than that between 5 and 10 kHz, both are differences of just one octave.

3.03.2 High-Frequency Hearing and Sound Localization

Although it was known that some mammals had better high-frequency hearing than others, it was not until 1967 that the discovery of systematic variation in mammalian high-frequency hearing was made by the late R. Bruce Masterton. In the course of determining the hearing abilities of several species of mammals, in preparation for a study of the auditory cortex, he noticed that smaller mammals had better high-frequency hearing than larger ones. Because he was studying sound localization at the time, he realized that this observation had implications for the use of the binaural locus cues: the difference in the time of arrival of a sound at the two ears (which he referred to as Δt), and the difference in the frequency–intensity spectra of the sound reaching the two ears (Δfi). Noting that the magnitude of the binaural time-difference cue depends on the size of an animal's head, he suggested that the smaller an animal's head, the more dependent it would be on the binaural spectral-difference cue (Masterton, B. *et al.*, 1969). However, to use the binaural spectral-difference cue, animals must hear frequencies high enough to be attenuated by their head and pinnae (thus generating intensity differences between the two ears) because small heads do not block low frequencies as effectively as they block higher ones. Therefore, the smaller an animal's functional head size (defined as the time it takes for sound to travel around the head from one ear to the other), the higher the frequencies it must hear to use the binaural spectral-difference cue for sound localization.

The relation between functional head size and high-frequency hearing has remained robust since its discovery ($r = -0.79$, $p < 0.0001$) and has been shown to hold for over 60 species ranging in size from mice and bats to humans and elephants (Figure 1). However, two points should be noted about this relationship. First, as can be seen in Figure 1, it does not apply to subterranean mammals; they are an exception that we shall later see proves the rule. Second, the relationship applies only to comparisons between species, not within species. For example, although dogs differ in head size by a factor of 2 (from Chihuahuas to St. Bernards), what little individual variation they show in high-frequency hearing is not related to their functional head size (Heffner, H. E., 1983). Thus, Galton, F. (1883) was wrong on one point – large dogs do have good high-frequency hearing. The failure of large dogs to respond to Galton's whistle demonstrates the weakness of using unconditioned responses for testing sensitivity and also suggests that large dogs may be unconcerned by objects that make only high-frequency sounds because such objects (usually other animals) are generally small.

3.03.2.1 Binaural Spectral-Difference Cue

The importance of high-frequency hearing for localizing sound in the horizontal (azimuthal) plane can be demonstrated by determining the ability of an animal to localize a broadband signal (i.e., noise) from which high frequencies are removed. Filtering out high frequencies has been shown to degrade azimuthal localization in monkeys, humans, chinchillas, and mice (Brown, C. H. *et al.*, 1982; Butler, R. A., 1986; Heffner, R. S. *et al.*, 1996; 2001a). Because the binaural time-difference cue is available in the low-frequency component of the signal, a decline in performance may be attributed to the absence of high frequencies necessary for using the binaural spectral-difference cue (assuming the use of pinna cues has been ruled out).

Although there is little doubt that the use of binaural spectral differences requires mammals to hear high frequencies, it is only part of the reason that mammals evolved high-frequency hearing. This point was dramatically demonstrated by the discovery that some mammals lack the ability to use the binaural spectral-difference cue but still hear high frequencies. Briefly, the ability to use the two binaural cues can be assessed by determining the ability of an animal to localize pure tones. Use of the binaural time-difference cue is indicated by the ability to localize low-frequency tones that pass around the head with little or no intensity difference between the ears. The ability to localize tones that are too high in frequency to permit the use of the

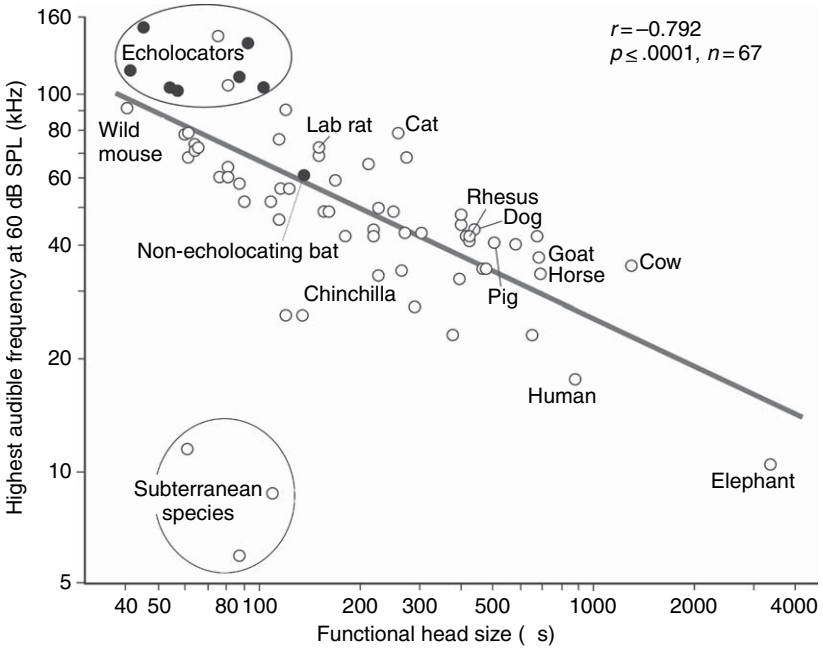

Figure 1 Relation between functional head size and high-frequency hearing (highest frequency audible at 60 dB sound pressure level) for mammals. This relationship is explained by the need of small mammals to hear higher frequencies than larger mammals in order to use the binaural spectral-difference cue and/or pinna cues to localize sound. Note that the subterranean species (naked mole-rat, blind mole-rat, and gopher), which do not localize sound, have lost the ability to hear high frequencies. Echolocating bats hear slightly higher than predicted based on their functional head size. Filled circles indicate bats, open circles indicate all other mammals. (The open circles among the echolocators are two species of cetacea.) For references to individual audiograms, see Koay G. *et al.* (1998a) and Heffner R. S. *et al.* (2003).

binaural time cue indicates that an animal can use the binaural spectral-difference cue (e.g., Heffner, R. S. *et al.*, 2001b; Heffner, H. E. and Heffner, R. S., 2003). The results of this test indicate that most mammals use both binaural cues (as, e.g., do humans, monkeys, and cats). Yet, some species do not use binaural time differences (such as hedgehogs, mice, laboratory rats, and some bats), and others are either partially or completely unable to use binaural spectral differences (Heffner, H. E. and Heffner, R. S., 2003). Specifically, Indian elephants and domestic goats are unable to localize pure tones in the upper end of their hearing range indicating that they do not use the spectral information in their highest audible frequencies to localize sound (Heffner, R. S. and Heffner, H. E., 1982; Heffner, H. E. and Heffner, R. S., 2003). Domestic pigs, horses, and cattle are more extreme in that they cannot localize high-frequency tones at all, leading to the conclusion that they have completely relinquished the ability to use the binaural spectral-difference cue (Heffner, R. S. and Heffner, H. E., 1986; 1989; Heffner, H. E. and Heffner, R. S., 2003). To explain the existence of good high-frequency hearing in animals that do not use the binaural spectral-difference cue, we turned to the third type of sound-localization cue which is produced by the external ear, namely the pinna cues.

3.03.2.2 Pinna Localization Cues

Although the role of the pinna in sound localization was demonstrated during the late nineteenth century, most twentieth century studies focused on the binaural locus cues (Butler, R. A., 1975). This resulted in the use of headphones for presenting stimuli thereby eliminating the pinnae, making it easy to lose sight of their importance. Over the years, the work of Robert Butler and others has demonstrated that the directionality of the pinna not only provides the primary cues for vertical localization and for preventing front–back confusions, but also provides effective cues for localizing sound in the horizontal plane (e.g., Butler, R. A., 1975; Musicant, A. D. and Butler, R. A., 1985). Indeed, as noted by Butler R. A. (1999), "We live in a world where many sounds emanating from the side are not sufficiently intense to stimulate the opposite ear," in which case a binaural comparison only indicates that

the sound source is somewhere within the hemifield of the ear receiving the sound and, in the absence of pinna cues, may result in the perception of the sound being located within the ear itself. Thus, there are situations in which the pinnae provide the only locus cues as to the horizontal and vertical location of a sound source within a hemifield. For pinna cues to be effective in humans, the sounds must contain frequencies above 4 kHz and even sounds as high as 15 kHz have been shown to be necessary for optimal localization performance. Thus, the upper two octaves of human hearing (from 4 to 16 kHz) appear to be used primarily, if not exclusively, for sound localization, as they are not necessary for the perception of speech.

Other mammals also require high frequencies for localizing in the vertical plane, as well as for preventing front–back confusions. For example, filtering out high frequencies from a broadband noise signal degrades sound-localization performance for front–back and vertical localization in chinchillas and for vertical localization in monkeys (Brown, C. H. *et al.*, 1982; Heffner, R. S. *et al.*, 1996). Horses, which lack the ability to use the binaural spectral-difference cue, still require high frequencies to use pinna cues for front–back localization (Heffner, H. E. and Heffner, R. S. 1983). Thus, although most mammals use their high-frequency hearing to obtain both binaural spectral differences and pinna cues, some, such as horses, pigs and cattle, use it only for pinna locus cues. In addition, it is likely that there are species that use their high-frequency hearing to obtain the binaural spectral-difference cue, but do not use pinna cues (such as cetacea and the pinnipeds that lack pinnae).

3.03.2.3 Subterranean Mammals

As previously noted, subterranean mammals do not have good high-frequency hearing and their upper limit of hearing does not fit the relation between functional head size and high-frequency hearing (Figure 1). However, the existence of these animals does not weaken the theory that mammals evolved good high-frequency hearing for sound localization, but, instead, strengthens it. This is because not only do the pocket gopher, naked mole-rat, and blind mole-rat lack good high-frequency hearing, they also lack the ability to localize sound (Heffner, R. S. and Heffner, H. E., 1990; 1992a; 1993). Thus, it appears that subterranean animals that are adapted to the one-dimensional world of an underground habitat have little use for sound localization and are therefore released from the selective pressure to hear high frequencies. In short, sound localization and high-frequency hearing go hand-in-hand in mammals. Mammals cannot optimally localize sound without high frequencies, and those that relinquish the ability to localize sound also give up their high frequency hearing.

3.03.2.4 Bats

Although bats require good high-frequency hearing for passive sound localization (Koay, G. *et al.*, 1998b), the question arises as to whether selective pressure for echolocation has caused bats to increase their high-frequency hearing beyond that required for passive sound localization. This possibility was recently examined by comparing the high-frequency hearing limits of bats with those of other mammals. The results of this comparison indicated that echolocating bats hear on average about 0.5 octaves higher than expected from their functional head size. Thus, although echolocating bats appear to owe 3.3 octaves of their high-frequency hearing to selective pressure for passive sound localization, they seem to have added an average of half an octave to their hearing ranges for use in echolocalization. In contrast, nonecholocating bats have not extended their high-frequency hearing beyond that expected for passive sound localization (Heffner, R. S. *et al.*, 2003).

3.03.2.5 Ultrasonic Communication

It is not unusual for small rodents to produce vocalizations that are above the range of human hearing, that is, ultrasonic (e.g., Nyby, J. and Whitney, G., 1978), and it has been suggested that high-frequency hearing evolved in order for animals to communicate via ultrasound (e.g., Sales, G. D. and Pye, J. D., 1974). Indeed, it would seem advantageous for small animals to use high-frequency communication signals because they are more directional and attenuate more rapidly over distance than low frequencies making them less likely to be detected by predators (Wilson, D. R. and Hare, F., 2004). However, whether such calls are inaudible to a predator depends on the predator's proximity as well as its auditory sensitivity.

Although the use of high-frequency communication signals by small mammals is well established, we have argued elsewhere that it appears to be a co-option of high-frequency hearing that originally evolved for sound localization (Heffner, H. E. and Heffner, R. S., 1985; Heffner, R. S., and Heffner, H. E.,

1985). One reason is that a species' upper limit of hearing often extends beyond that required for hearing its communication vocalizations, as in the case of cattle, dogs, and humans, which hear frequencies well above the dominant frequencies of their vocalizations. Another is that there is no clear sign that high-frequency communication has affected a species' auditory sensitivity. Although some species vocalize at frequencies corresponding to secondary peaks of sensitivity toward the midrange of their audiograms, these secondary peaks have been shown to result from the directionality of the pinnae and serve to enable animals to localize in the vertical plane (Koay, G. *et al*., 1998b). Finally, the fact that small animals produce high-frequency vocalizations is not surprising as it would require special adaptation for them to produce low-frequency calls as is the case for frogs and toads that use specialized vocal sacs to produce low-frequency call (e.g., Bradbury, J. W. and Vehrencamp, S. L., 1998).

3.03.3 Conclusion

The primary source of selective pressure for mammalian high-frequency hearing appears to be its role in localizing sound through use of the binaural spectral-difference cue, pinna cues, or both. Most mammals hear higher frequencies than humans because they have functionally smaller heads and therefore require higher frequencies to localize sound – when compared to the elephant, which only hears up to about 10 kHz, even humans have 'ultrasonic' hearing.

Finally, it may be noted that the understanding of high-frequency hearing is only one example of the insight that can be gained from a comparative analysis of hearing; other examples include low-frequency hearing (Heffner, R. S. and Heffner, H. E., 2001) and sound localization (Heffner, R. S., and Heffner, H. E., 1992b; Heffner, H. E. and Heffner, R. S., 2003). Indeed, the view that mammals evolved high-frequency hearing for sound localization suggests that nonmammals, such as birds, which lack high-frequency hearing, either do not localize sound as well as mammals (especially off to the side and in the vertical plane where pinna cues predominate) or else have evolved alternative mechanisms for sound localization, such as the facial ruff of the barn owl (Knudsen, E. I. and Konishi, M., 1979).

References

Bradbury, J. W. and Vehrencamp, S. L. 1998. Principles of Animal Communication. Sinauer.

Brown, C. H., Schessler, T., Moody, D., and Stebbins, W. 1982. Vertical and horizontal sound localization in primates. J. Acoust. Soc. Am. 72, 1804–1811.

Butler, R. A. 1975. The Influence of the External and Middle Ear on Auditory Discriminations. In: Handbook of Sensory Physiology: Auditory System (*eds*. W. D. Keidel and W. D. Neff), Vol. V/2, pp. 247–260. Springer.

Butler, R. A. 1986. The bandwidth effect on monaural and binaural localization. Hear. Res. 21, 67–73.

Butler, R. A. 1999. The unfolding of an auditory illusion. Perspect. Biol. Med. 42, 157–173.

Dooling, R. J., Lohr, B., and Dent, M. L. 2000. Hearing in Birds and Reptiles. In: Comparative Hearing: Birds and Reptiles (*eds*. R. J. Dooling, R. R. Fay, and A. N. Popper), pp. 308–359. Springer.

Galton, F. 1883. Inquiries in Human Faculty and Its Development. J. M. Dent and Sons.

Heffner, H. E. 1983. Hearing in large and small dogs: absolute thresholds and size of the tympanic membrane. Behav. Neurosci. 97, 310–318.

Heffner, H. E. and Heffner, R. S. 1983. Sound localization and high-frequency hearing in horses. J. Acous. Soc. Am. 73, S42.

Heffner, H. E. and Heffner, R. S. 1985. Hearing in two cricetid rodents: wood rat (*Neotoma floridana*) and grasshopper mouse (*Onychomys leucogaster*). J. Comp. Psychol. 99, 275–288.

Heffner, H. E. and Heffner, R. S. 1998. Hearing. In: Comparative Psychology, A Handbook (*eds*. G. Greenberg and M. M. Haraway), pp. 290–303. Garland.

Heffner, H. E. and Heffner, R. S. 2003. Audition. In: Handbook of Research Methods in Experimental Psychology (*ed*. S. F. Davis), pp. 413–440. Blackwell.

Heffner, R. S. and Heffner, H. E. 1982. Hearing in the elephant: absolute sensitivity, frequency discrimination, and sound localization. J. Comp. Physiol. Psychol. 96, 926–944.

Heffner, R. S. and Heffner, H. E. 1985. Hearing in mammals: the least weasel. J. Mammal. 66, 745–755.

Heffner, R. S. and Heffner, H. E. 1986. Localization of tones by horses: use of binaural cues and the superior olivary complex. Behav. Neurosci. 100, 93–103, 137.

Heffner, R. S. and Heffner, H. E. 1989. Sound localization, use of binaural cues and the superior olivary complex in pigs. Brain Behav. Evol. 33, 248–258.

Heffner, R. S. and Heffner, H. E. 1990. Vestigial hearing in a fossorial mammal, the pocket gopher (*Geomys bursarius*). Hear. Res. 46, 239–252.

Heffner, R. S. and Heffner, H. E. 1992a. Hearing and sound localization in blind mole rats. Hear. Res. 62, 206–216.

Heffner, R. S. and Heffner, H. E. 1992b. Visual factors in sound localization in mammals. J. Comp. Neurol. 317, 219–232.

Heffner, R. S. and Heffner, H. E. 1993. Degenerate hearing and sound localization in naked mole rats (*Heterocephalus glaber*), with an overview of central auditory structures. J. Comp. Neurol. 331, 418–433.

Heffner, R. S. and Heffner, H. E. 2001. Audiograms of five species of rodents: implications for the evolution of hearing and the perception of pitch. Hear. Res. 157, 138–152.

Heffner, R. S., Koay, G., and Heffner, H. E. 1996. Sound localization in chinchillas, III: effect of pinna removal. Hear. Res. 99, 13–21.

Heffner, R. S., Koay, G., and Heffner, H. E. 2001a. Sound-Localization Acuity Changes with Age in C57BL/6J Mice. In: Handbook of Mouse Auditory Research: From Behavior to Molecular Biology (*ed*. J. F. Willott) pp. 31–35. CRC Press.

Heffner, R. S., Koay, G., and Heffner, H. E. 2001b. Sound localization in a new-world bat, *Artibeus jamaicensis*: acuity, use of binaural cues, and its relationship to vision. J. Acoust. Soc. Am. 109, 412–421.
Heffner, R. S., Koay, G., and Heffner, H. E. 2003. Hearing in American leaf-nosed bats. III. *Artibeus jamaicensis.* Hear. Res. 184, 113–122.
Knudsen, E. I. and Konishi, M. 1979. Mechanisms of sound localization in the barn owl (*Tyto alba*). J. Comp. Physiol. A. 133, 13–21.
Koay, G., Heffner, R. S., and Heffner, H. E. 1998a. Hearing in a megachiropteran fruit bat (*Rousettus aegyptiacus*). J. Comp. Psychol. 112, 371–382.
Koay, G., Kearns, D., Heffner, H. E., and Heffner, R. S. 1998b. Passive sound-localization ability of the big brown bat (*Eptesicus fuscus*). Hear. Res. 119, 37–48.
Mann, D. A., Higgs, D. M., Tavolga, W. N., Souza, M. J., and Popper, A. N. 2001. Ultrasound detection by clupeiform fishes. J. Acoust. Soc. Am. 109, 3048–3054.
Masterton, B., Heffner, H., and Ravizza, R. 1969. The evolution of human hearing. J. Acoust. Soc. Am. 45, 966–985.
Musicant, A. D. and Butler, R. A. 1985. Influence of monaural spectral cues on binaural localization. J. Acoust. Soc. Am. 77, 202–208. Erratum in: J. Acoust. Soc. Am. 77, 2190.
Nyby, J. and Whitney, G. 1978. Ultrasonic communication of adult myomorph rodents. Neurosci. Biobehav. Rev. 2, 1014.
Sales, G. D. and Pye, J. D. 1974. Ultrasonic Communication by Animals. Wiley.
Wilson, D. R. and Hare, F. 2004. Ground squirrel uses ultrasonic alarms. Nature 430, 523.

Relevant Website

http://psychology.utoledo.edu/lch – The University of Toledo Department of Psychology Laboratory of Comparative Hearing

3.04 Sensory Ecology of Hearing

M Gridi-Papp and P M Narins, University of California, Los Angeles, CA, USA

© 2008 Elsevier Inc. All rights reserved.

3.04.1	**Introduction**	62
3.04.2	**Auditory Structure and Function in Vertebrates**	62
3.04.2.1	Otolith Organs	62
3.04.2.2	The Swim Bladder	63
3.04.2.3	Middle Ears	63
3.04.2.4	Sensory Epithelia	65
3.04.3	**Hearing Performance in the Vertebrate Classes**	65
3.04.4	**Relations Between Hearing Structure and the Medium**	67
3.04.5	**Allometry**	68
3.04.6	**Physiology**	69
3.04.7	**Localization**	69
3.04.8	**Management of the Acoustic Environment**	71
References		72

Glossary

audiogram A graphical representation of the sound amplitude threshold of hearing for a range of frequencies.

azimuth Angle in relation to the longitudinal axis of the body in the horizontal plane.

binaural Involving two ears.

clade A group of organisms that share a common ancestor. The group includes the ancestor and all its descendants.

cochlea The structure in the inner ear of reptiles, birds, and mammals that contains the sound sensitive sensory epithelium. In mammals only, the structure is coiled.

columella See stapes.

echolocation The use of acoustic reflections to infer the direction and distance of objects.

Eustachian tube A tube that links the middle ear to the pharynx and allows the passage of air, thus equalizing pressure across the tympanic membrane.

extracolumella See extrastapes.

extrastapes A cartilaginous element in the middle ear that connects the tympanic membrane to the stapes. Also known as the extracolumella.

fossorial Subterranean, living underground.

hair cells Auditory and vestibular transducers. Each possesses a stereovillar (hair) bundle protruding from its apical surface. The cell is sensitive to displacement of the hair bundle.

incus A bone in the mammalian middle ear that connects the malleus to the stapes. Also known as the anvil.

inferior colliculus The principal midbrain nucleus of the auditory pathway. It receives input from the peripheral auditory pathway, and from the auditory cortex.

interaural Between the two ears.

malleus A bone in the middle ear of mammals that connects the tympanic membrane to the incus. Also known as the hammer.

operculum Middle ear ossicle of amphibians that contacts the oval window and receives the insertion of muscles that attach to the scapula.

ostariophysan fishes Those belonging to the superorder *Ostariophysi* having four of the anterior vertebras modified for connecting the swim bladder to the inner ear (Weberian apparatus).

otolith A mineral concretion which makes contact with the hair bundles of several mechanoreceptive hair cells.
oval window A membrane-covered opening that separates the air-filled middle ear from the fluid-filled inner ear. It allows the middle ear ossicles to transmit vibrations from the tympanic membrane to the inner ear.
pinna The external ear.
spectral Relative to frequency.
stapes A bone in the middle ear that transmits vibrations to the oval window, and thus into the inner ear. Also known as the columella (in non-mammals) or stirrup.
swim bladder A gas-filled chamber with variable volume that allows fishes to control buoyancy. It can also have a role in hearing and sound production in some fishes.
tympanic membrane A thin membrane that senses airborne sound in the ears of vertebrates and separates the middle ear from the external environment. Also known as the eardrum.
ultrasound Sound with frequency above 20 kHz, which is about the nominal upper limit of human hearing.
weberian apparatus A set of bones that physically connect the swim bladder to the inner ears in order to enhance hearing.

3.04.1 Introduction

Most natural events involving physical movement produce some sound. The physical properties of the sound produced are correlated with properties of the body in motion and to properties of the movement. Vertebrates can detect many such sounds and may respond to them with adaptive behavior.

Hearing is unique among the senses in the combination of its functional attributes. It allows animals to respond to signals produced by remote sources. Sound is transmitted in the medium more quickly than odor and more slowly than light. Hearing is less affected than vision when an opaque object is present between the animal and the source of the stimulus. Hearing allows vertebrates to respond to vibrations in the air, underwater, and in the substrate (Fritzsch, B., 1992; Lewis, E. R. *et al.*, 2006). A close examination of vertebrate auditory systems frequently reveals specializations that match the acoustic environment that the animals inhabit or the structure of signals that are relevant to them (Numella, S. *et al.*, 2004; Pollak, G. D. and Casseday, J. H., 1989).

In this chapter, we focus on the ecological aspects of hearing in vertebrates. We review the structure and function of the auditory system in the main vertebrate clades and compare their performance. We also examine the current evidence on how habitat differences can affect vertebrate hearing. We intentionally omit a detailed discussion of auditory organization and processing in the central nervous system (for a review, see Carr, C. E., 1992; Grothe, B. *et al.*, 2004), but rather will focus on sound detection by the vertebrate peripheral auditory system.

More specifically, we compare threshold and frequency range across vertebrates. Next we examine auditory systems that transitioned between environments during evolution, as well as some of the effects of size and temperature on sound perception. We also review mechanisms of sound localization, an important capability for the detection of predators, prey, and potential mates. Finally, we present some examples illustrating the effects of noise derived from human activity on wildlife.

3.04.2 Auditory Structure and Function in Vertebrates

3.04.2.1 Otolith Organs

Vertebrates detect acoustic vibrations by sensing the relative motion between two parts of their body. A simple sensor has one element being moved by the sound and another element that remains stationary. In the underwater environment, this is complicated by the fact that most animal tissues are composed predominately of water and are transparent to sound. The problem is solved by adding a mineral concretion to the detector: the higher density of the mineral concretion results in a higher acoustic impedance than the surrounding tissues. When acoustic vibrations activate the sensor, the dense concretion lags behind the surrounding tissues, producing relative motion within the sensor.

The inner ears of fishes contain several otolith organs which can detect sound (Platt, C. and Popper, A. N., 1981; Popper, A. N. *et al.*, 2005; Figure 1). Each organ contains a mineral concretion called the otolith, which

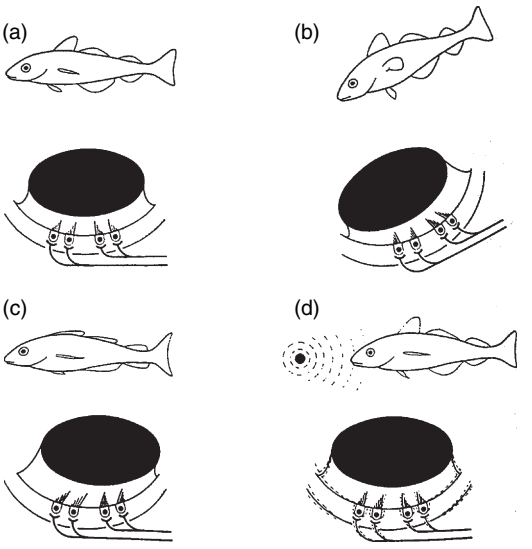

Figure 1 Schematic representation of an otolith organ showing the otolith in black and four hair cells under it. (a) The fish is static and horizontal; (b) The fish is static with the head down; (c) the fish is accelerating; (d) the fish is static, and detecting a sound that causes the otolith to vibrate over the hair cells. Reproduced from Behaviour of Telcost Fishes, 2nd, 1993, pp. 129–169, Underwater Sound and Fish Behaviour, Hawkins, A. D., figure 15.5, © Chapman and Hall, with kind permission of Springer Science and Business Media.

makes contact with a group of mechanoreceptive hair cells. The apical surface of each hair cell contains a hair (stereovillar) bundle, which is deflected when the otolith moves relative to the hair cell body. The patterns of neural output of the otolith organ depend on which hair cells are excited by the otolith and how the stereovillar bundle is deflected. Otolith organs respond to acceleration, which is produced in large part by gravity and by movements of the animal. Otolith organs allow fishes to sense the position of the head in relation to vertical and provide feedback to their movements. Position sensing is a general requirement in vertebrates and it was, most likely, the original function of the otolith organs (see articles in Manley, G. A. *et al.*, 2004).

Fishes do not have middle or external ears. As mentioned before, the flesh of the animal is composed mostly by water and it is transparent to sound. The inner ears can be very sensitive without being connected directly to the external world.

3.04.2.2 The Swim Bladder

Besides using the high density of the otolith to detect sound, many teleost fishes also take advantage of the very low density of the gas in their swim bladder (Ladich, F. and Bass, A. H., 2003). Sound pressure waves arriving at the animal produce larger volume changes in the swim bladder than in the flesh. It is thought that the swim bladder itself reradiates sound which is then detected by the ear. Experiments in which the gas was artificially removed from the swim bladder revealed a reduction in hearing sensitivity at high frequencies, whereas when a small air-filled balloon was placed under the head of the fish, hearing sensitivity increased (Sand, O. and Enger, P. S., 1973; Chapman, C. J. and Sand, O., 1974; Fay, R. R. and Popper, A. N., 1975). In the ostariophysan teleosts, the swim bladder is physically connected to the inner ears, via a series of four bones known as the Weberian apparatus: scaphium, claustrum, tripus, and intercalarium. This arrangement permits the direct transmission of swim bladder vibrations to the otolith organs, thus increasing the acoustic sensitivity of the fish (Hawkins, A. D., 1993). The Weberian apparatus is derived from vertebral elements that are not homologus to mammalian middle ear ossicles. This apparatus is analogous to the middle ear for transmitting sound pressure information to the inner ear.

3.04.2.3 Middle Ears

In the terrestrial environment, animals can detect acoustic vibrations arriving to them through the air or the substrate. The first terrestrial vertebrates lacked middle ears and probably preferentially perceived substrate vibrations over airborne vibrations (Clack, J. A., 1992; Clack, J. A. and Allin, E., 2004). Since air is much less dense and more elastic than water or flesh, a large acoustic impedance mismatch occurred between the skin of the animal and the air surrounding it. Most of the acoustic energy reaching the skin of the animal was reflected and did not reach the inner ear. Since soil is more similar in density and elasticity to animal tissues than is air, vibrations arriving from the soil could be coupled more efficiently to the tissues and would more likely be detected by the inner ear.

The evolution of the middle ear helped to resolve the acoustic impedance mismatch between animal tissues and air, greatly improving the airborne sound detection capabilities of terrestrial vertebrates. This occurred independently in the major clades (Clack, J. A. and Allin, E., 2004). Terrestrial animals evolved a tympanic membrane in contact with the external air (Figure 2). The thinness of the membrane and the presence of an air-filled cavity behind it reduces the impedance mismatch with the air and allows it to

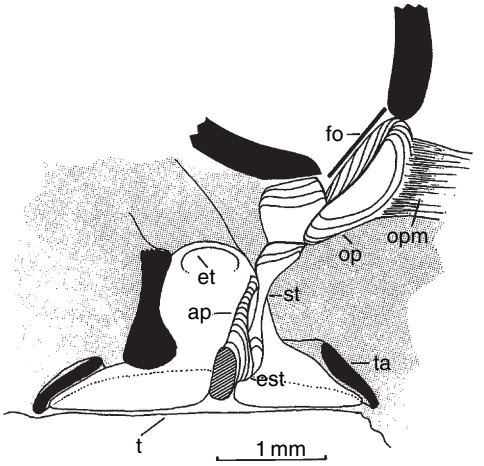

Figure 2 Dorsal view of an amphibian middle ear. t, tympanic membrane; et, Eustachian tube; est, extrastapes; ap, ascending process; st, stapes; op, operculum; fo, foramen ovalis; ta, tympanic annulus; opm, opercularis muscle. Reproduced from Jaslow A. P., Hetherington T. E., and Lombard R. E. 1988. Structure and Function of the Amphibian Middle Ear. In: The Evolution of the Amphibian Auditory System (*eds.* B. Fritzsch, M. J. Ryan, W. Wilczynski, T. E. Hetherington, and W. Walkowiak), pp. 69–91, with permission from John Wiley & Sons.

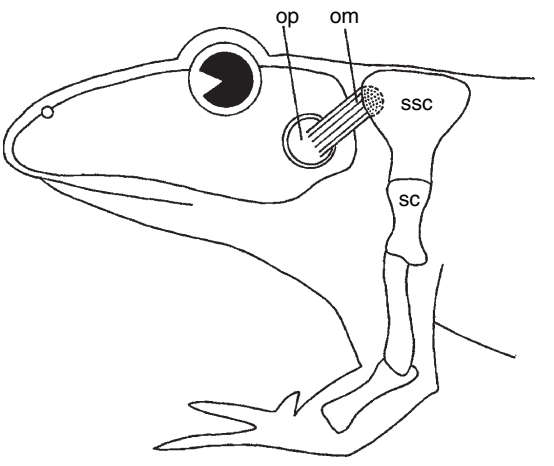

Figure 3 The opercularis muscle connects the shoulder of the frog to its middle ear and possibly plays a role in perception of substrate vibrations. op, operculum; om, opercularis muscle; sc, scapula; ssc, suprascapula. Reproduced from The Evolutionary Biology of Hearing, 1992, pp. 421–438, The Effects of Body Size on the Evolution of the Amphibian Middle Ear, Hetherington, T. E., figure 21.2, © Springer-Verlag, with kind permission of Springer Science and Business Media.

follow airborne pressure fluctuations within a range of frequencies. Vibrations of the tympanic membrane are conducted to the inner ear by a cartilaginous-bony ossicle called the columella or stapes. In amphibians, the stapes crosses the tissues of the back of the air-filled otic cavity to reach the inner ear (Smotherman, M. and Narins, P. M., 2004). In amniotes (reptiles, birds, and mammals), the otic cavity extends to the inner ear (Rosowski, J. J., 1994). The large area of the tympanic membrane relative to the stapes footplate, and the lever action performed at the connections of the stapes, allows the middle ear to approximately match the impedance of the air at the tympanic membrane to the impedance of the inner ear at the stapes footplate (Jorgensen, M. B. and Kanneworff, M., 1998; Mason, M. J. and Narins, P. M., 2002a).

In North American bullfrogs (*Rana catesbeiana*), the bony proximal portion of the stapes is rigid, but its distal segment forms a flexible articulation with a cartilaginous element called the plectrum (Capranica, R. R., 1976) or extrastapes (Mason, M. J. and Narins, P. M., 2002a). This flexible articulation confers on the amphibian middle ear a distinct mammal-like quality which in some species may be responsible for their extended high-frequency range (Mason, M. J. and Narins, P. M., 2002a). The tympanic membrane is also connected to the extrastapes. When the tympanic membrane vibrates, the extrastapes rocks over its flexible ascending process that attaches to the skull, and pushes or pulls the distal end of the stapes. If the ascending process is severed, transfer of vibrations from the extrastapes to the stapes is greatly reduced (Mason, M. J. and Narins, P. M., 2002a).

The stapes footplate contacts the inner ear at the oval window. In anuran amphibians, the oval window contains both the stapes footplate and a second bone called the operculum. The latter receives an insertion of the opercularis muscle, which connects it to the scapula, in the shoulder girdle (Figure 3). The opercularis system has been implicated both in the perception of vibrations from the substrate (Paton, J., 1971; Hetherington, T. E., 1985) and in the improvement of tympanic hearing by compensation for breathing (Mason, M. J. and Narins, P. M., 2002b).

In mammals, the evolution of a new jaw articulation point allowed the middle ear to incorporate two extra ossicles, the malleus and the incus (Rosowski, J. J., 1994; Clack, J. A. and Allin, E., 2004; Figure 4). Vibrations of the tympanic membrane are transmitted to the oval window by an articulated chain of three ossicles, as opposed to birds and reptiles, which transmit vibrations with a single ossicle, the stapes.

The extended high-frequency sensitivity of mammals relative to other vertebrates has been attributed to the incorporation of the tri-ossicular middle ear, consisting of an articulated structure composed of

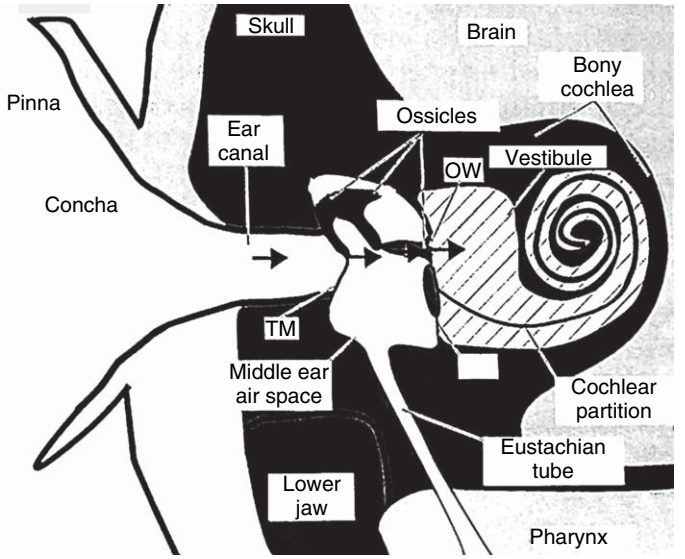

Figure 4 Schematic posterior view of the mammalian ear. OW, oval window; TM, tympanic membrane. Reproduced from Comparative Hearing: Mammals, 1994, pp. 172–248, Outer and Middle Ears, Rosowski, J. J., figure 6.2, © Springer-Verlag, with kind permission of Springer Science and Business Media.

three rigid elements. Moreover, in amphibians such as *Rana catesbeiana*, which rely on a single middle ear ossicle to transmit vibrations from the tympanic membrane to the inner ear, the articulation with the tympanum is cartilaginous and could potentially absorb high frequencies. In contrast, recent studies have recorded single-unit responses from the inferior colliculus (torus semicircularis) of the relatively small, arboreal frog *Amolops tormotus* at frequencies above 25 kHz (Feng, A. S. *et al.*, 2006). This species exploits a recessed tympanic membrane connected to low-mass ossicular elements, with a nonarticulated connection with the tympanum (personal observations). This calls into question the idea that a mono-ossicular middle ear is the main factor limiting the upper frequency range in nonmammalian vertebrates (see Mason, M. J. and Narins, P. M., 2002a).

3.04.2.4 Sensory Epithelia

The sensory organs in the inner ears of vertebrates vary in number, size, shape, and orientation of hair cell bundles (Lewis, E. R. *et al.*, 1985; Coffin, A. *et al.*, 2004). They also vary in number and types of hair cells that they contain and thus the homology among some vertebrate inner ear sensory organs is uncertain. The hearing organs of teleost fishes contain an otolith composed mainly of calcium carbonate and protein (Platt, C. and Popper, A. N., 1981; Hawkins, A. D., 1993; Popper, A. N. *et al.*, 2005). In elasmobranchs and other vertebrates, the otolithic structure is composed of a gelatinous mass containing calcium carbonate crystals, called otoconia.

Hair cells vary in their response to sound frequency (Fettiplace, R. and Fuchs, P. A., 1999; Smotherman, M. and Narins, P. M., 2000). In some inner ear organs such as the amphibian papilla of frogs and the cochlea in amniotes, hair cells are arranged by frequency sensitivity (tonotopic organization). These sensory organs tend to have an elongated structure (Miller, M. R., 1992; Figure 5), which reaches an extreme in birds and mammals (Manley, G. A. and Clack, J. A., 2004). In mammals other than monotremes, coiling of the cochlea not only allows for packing of an elongated epithelium in a small space but may also produce a low-frequency gain in sensitivity (Manoussaki, D. *et al.*, 2006). The epithelial length and the packing of the hair cells along the sensory epithelium are highly correlated both with the range of frequency sensitivity of the ear and its frequency resolution (Fay, R. R., 1992).

3.04.3 Hearing Performance in the Vertebrate Classes

Significant variation is found among and within behavioral audiograms of the five major classes of vertebrates (Fay, R. R., 1992; Figure 6). While most fishes cannot hear above 3 kHz, some species of the

Figure 5 Scanning electron microscope photograph of hair cell bundles on the elongated basilar papilla of the lizard *Agama agama*. ap, apical (direction); bhc, bidirectional region with hair cells oriented in opposite directions; uhc, unidirectional region with all hair cells oriented in the same direction. Reproduced from Further Scanning Electron Microscope Studies of Lizard Auditory Papillae, Miller, M. R.; Copyright © (1978 Wiley); reprinted with permission of Wiley-Liss, Inc., a subsidiary of John Wiley & Sons, Inc.

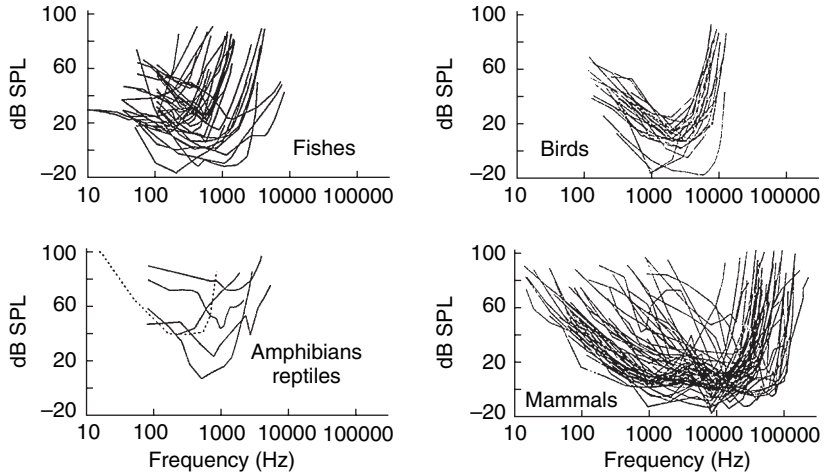

Figure 6 Behavioral audiograms of vertebrates. SPL, sound pressure level. Reproduced from The Evolutionary Biology of Hearing, 1992, pp. 229–264, Structure and Function in Sound Discrimination among Vertebrates, Fay, R. R., figure 14.1, © Springer-Verlag, with kind permission of Springer Science and Business Media.

order *Clupeiformes* have the capability of responding to ultrasound up to 180 kHz (Mann, D. A. *et al.*, 1997; Higgs, D. M., 2004). The mechanism and function of such capability is yet unknown, but its potential for use in avoidance of echolocating marine mammal predators is under investigation. Relatively few behavioral audiograms are available for amphibians and reptiles. Those that exist, together with neurophysiological recordings from anuran auditory nerve fibers, suggest a frequency range up to about 5 kHz (Feng, A. S. *et al.*, 1975; Wilczynski, W. and Capranica, R. R., 1984; Wilczynski, W. *et al.*, 1987; Narins, P. M. and Wagner, I., 1989; Wilczynski, W. *et al.*, 1992; 2001), with exceptions showing ultrasonic hearing (see below). Many birds can hear up to 8 kHz, this class being the most homogeneous among vertebrates. The extended hearing frequency range of birds has been ascribed to the elongation of the sensory epithelium in the cochlea (Manley, G. A. and Clack, J. A., 2004). Frequency range is further extended in mammals where it reaches above 100 kHz in cetaceans and bats. The lower limit of the frequency range in mammals is also variable; primates, elephants, and some rodents can perceive the lowest sound frequencies (Reuter, T. *et al.*, 1998; Webster, D. B. and Plassmann, W., 1992).

The lowest threshold of hearing is more variable within the classes than among the most sensitive or the average representatives of each class. The threshold of hearing is lowest in mammals, and lower in birds than in amphibians, reptiles, or fishes. Ostariophysan fishes have considerably lower hearing thresholds than nonostariophysans (see Section 3.04.2.2). Behavioral and neurophysiological recordings in amphibians have revealed lowest thresholds between 20 and 55 dB sound pressure level (SPL; Feng, A. S. *et al.*, 1975; Wilczynski, W. and Capranica, R. R., 1984, Wilczynski, W. *et al.*, 1987; Narins, P. M. and Wagner, I., 1989; Wilczynski, W. *et al.*, 1992; 2001). Eighth nerve recordings in geckos suggest lowest thresholds of about 20 dB SPL or lower (Manley, G. A., 1972; Dodd, F. and

Capranica, R. R., 1992; Werner, Y. L. and Wever, E. G., 1995) whereas lowest thresholds measured for snakes are about 40 dB SPL (Young, B., 2003).

The generalizations above should be taken with caution, as behavioral audiograms are only available for about 200 out of more than 50 000 species of vertebrates (Fay, R. R., 1992). Auditory specialists can often deviate significantly from the other members of their class, and can be instructive as a result. One example is the audiogram of the echolocating mustached bat (*Pteronotus parnellii*), with a very pronounced sensitivity peak at the dominant frequency of the echolocation calls (Figure 7). The sensitivity is not extreme, but the sharp peak in the audiogram clearly deviates from the common pattern for mammals, reflecting an adaptation to maximize reception of the echo (Pollak, G. D. and Casseday, J. H., 1989). Another apparent specialist is the concave-eared torrent frog, *Amolops tormotus*, which is a frog that lives in China near rushing streams that generate masking noise up to 20 kHz. It produces and detects calls at frequencies above those of the background noise (Narins, P. M. *et al.*, 2004; Feng, A. S. *et al.*, 2006). Ultrasonic communication might be an adaptation to the noisy environment, although other sympatric species such as the piebald odorous frog, *Odorrana schmackeri*, lack ultrasonic sensitivity (Yu, Z. L. *et al.*, 2006). Besides ultrasound, some frogs in similar noisy environments make use of visual signals for communication (Hödl, W. and Amézquita, A., 2001).

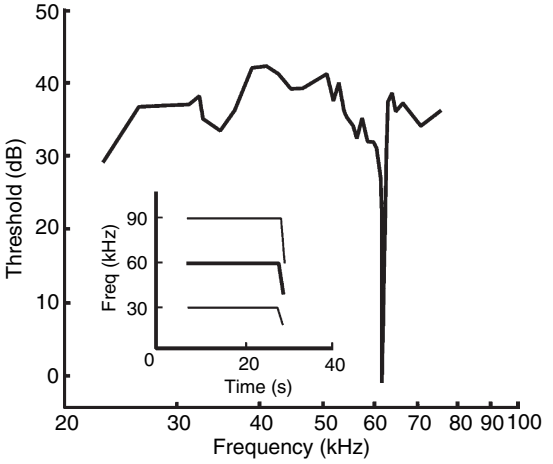

Figure 7 Cochlear microphonic audiogram of Parnell's mustached bat (*Pteronotus parnellii*). A schematic spectrogram of the echolocation call of the same species is inserted to show the close match between the dominant frequency of the call and the peak sensitivity of the ears. Reprinted with permission from Pollak G., Henson O. W., and Novick A. 1972. Cochlear microphonic audiograms in the "pure tone" bat *Chilonycteris parnellii parnellii*. Science 176, 66–68. Copyright 1972 AAAS.

3.04.4 Relations Between Hearing Structure and the Medium

Vertebrate ears frequently exhibit structural or mechanical adaptations to their acoustic environment. These are evident in diverse clades of animals with representatives living in contrasting environments.

Terrestrial rodent hearing is often characterized by high sensitivity and wide frequency range (Burda, H. *et al.*, 1992; Lange, S. *et al.*, 2004). Fossorial species usually show reduced high-frequency sensitivity and increased sensitivity at very low frequencies (Heffner, R. S. and Heffner, H. E., 1992b; 1993; Heffner, R. S. *et al.*, 1994). The reduced high-frequency sensitivity is likely related to the reduced availability of high-frequency sounds in the subterranean environment. Moreover, high-frequency sounds and sound filtering by the pinnae are important for sound localization by terrestrial animals. Fossorial species that lack pinnae spend much time in tunnels or burrows, where sound localization abilities are less essential. The low-frequency hearing of subterranean species, however, tends to be enhanced. Low frequencies are better transmitted by the soil and make up most of the acoustic input in the tunnels (Heth, G. *et al.*, 1986; Narins, P. M. *et al.*, 1992). Fossorial mammals in general exhibit middle ears with enlarged stapes footplates, reduced lever ratios and musculature, but similar tympanic membrane and ossicle sizes in relation to nonfossorial mammals (Burda, H. *et al.*, 1992; Mason, M. J., 2001). The reduced characters might relate to the loss of high-frequency sensitivity in fossorial mammals, but comparisons of the inner ears may reveal additional changes.

Snakes could, in principle, allow for an informative species comparison, having exemplars with auditory systems that operate in the terrestrial, aquatic, or fossorial environments (Young, B., 2003). The literature on snake hearing, however, is largely lacking, possibly because the species that have been studied revealed relatively limited frequency range and sensitivity (Wever, E. G. and Vernon, J. A., 1960; Wever, E. G., 1978).

The terrestrial–aquatic transition in cetaceans provides a fine example of adjustment of the hearing

apparatus to a change of medium. In terrestrial mammals, the impedance mismatch between air and tissues causes reflection of sound at the skin. Airborne sound, therefore, reaches the ear through the auditory meatus only (Figure 8).

When a terrestrial animal dives, the auditory meatus fills with water and reduces the efficacy of the tympanic membrane in transmitting sound. In addition, underwater sound can cross the head tissues and reach the ears from any direction, nullifying the effect of the head and external ears in sound localization. In odontocetes, the auditory meatus is nonfunctional and sound reaches the ears through a different path which is a large mandibular foramen that channels the sound through a fat pad that connects to the middle ear (Ketten, D. R., 2000). The ear is nearly acoustically isolated from the skull by a layer of air-filled sinuses. Such a system provides a novel path for sound to reach the inner ears and preserves directional cues. Intermediate stages in the specializations of the cetacean ear are observed in ontogeny (Kinkel, M. D. *et al.*, 2001) and in the fossil evidence, which documents gradual but rapid adaptation of the ears for effective hearing under water (Thewissen, J. G. M. and Hussain, S. T., 1993; Nummela, S. *et al.*, 2004).

3.04.5 Allometry

Allometric relations in vertebrate hearing have been best characterized at the macroscopic level. Studies of otolith size in fishes have found an association between the size of the fish, the size of the otolith, and frequency range (Cruz, A. and Lombarte, A., 2004; Popper, A. N. *et al.*, 2005). As the fish grows,

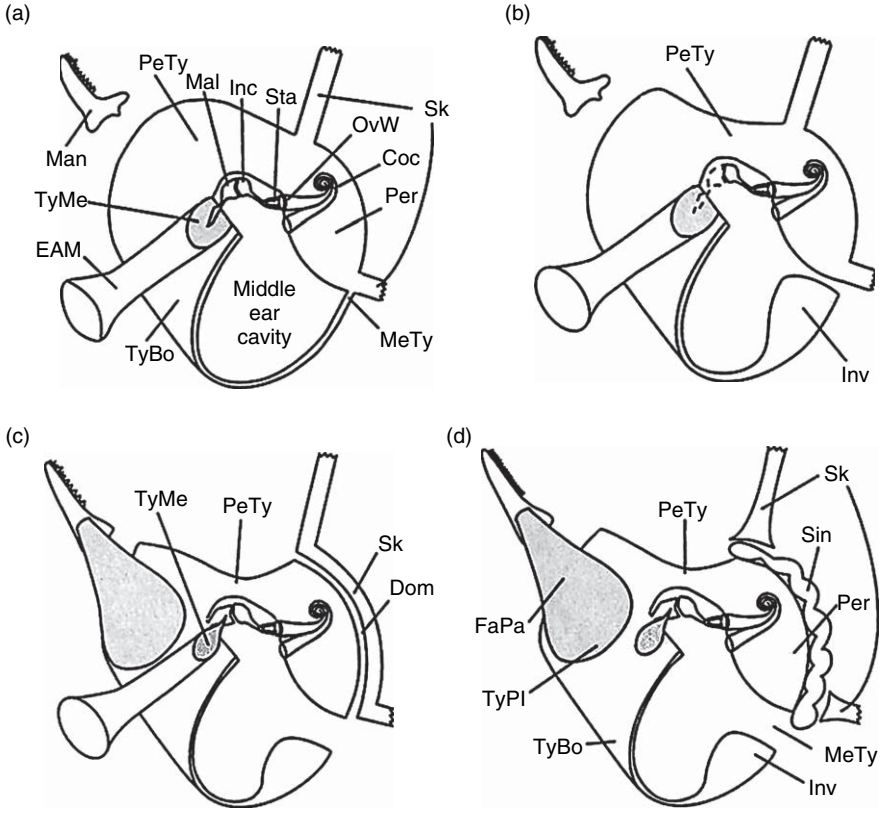

Figure 8 Sound transmission mechanisms in land mammals and whales. (a) Generalized land mammal; (b) a pakicetid, most primitive known whale; (c) an intermediate whale; (d) and a modern odontocete. Abbreviations: Coc, cochlea; Dom, dome-shaped depression for periotic; EAM, external auditory meatus; FaPa, fat pad; Inc, incus; Inv, involucrum; Mal, malleus; Man, mandible; MeTy, medial synostosis between periotic and tympanic bone; OvW, oval window; Per, periotic bone; PeTy, joint between periotic and tympanic; Sin, air-filled sinuses; Sk, skull, Sta, stapes; TyBo, tympanic bone; TM, tympanic membrane; TyPl, tympanic plate. Reproduced from Nummela S., Thewissen, J. G. M., Bajpal S., Hussain S. T., and Kumar K. 2004. Eocene evolution of whale hearing. Nature 430, 776–778.

more hair cells are added to the sensory epithelium, potentially expanding the frequency range of hearing, although direct confirmation of this association is still lacking (Popper, A. N. *et al.*, 2005).

In birds and mammals, the dimensions of the cochlea and packing of the hair cells provide close estimates of the frequency range and resolution of the auditory system. The tonotopic organization of the cochlea makes it possible to map sound frequency to a particular region of the cochlea, generating frequency-position maps (von Békésy, G., 1960). With the assumption that the frequency bands correspond to equal distances on the basilar membrane independent of frequency, a frequency-position map can be derived in which sound frequency is calculated based on position in the cochlea, a slope term, and the frequency range of the cochlear map (Greenwood, D. D., 1961).

Empirical data indicate that the slope term is constant among species if cochlear length is normalized and the frequency range term is a simple proportion of the highest frequency audible at 60 dB SPL (Greenwood, D. D., 1990; Fay, R. R., 1992). The cochlear map can therefore be derived based on the length of the basilar membrane and the maximum audible frequency, and produce exceptional fits with empirical measurements for birds and mammals. Such maps also generate precise predictions of frequency analysis capabilities in mammals and birds (Fay, R. R., 1992).

Poor fit of the model with empirical data was encountered in hearing specialists such as the greater horseshoe bat (*Rhinolophus ferrumequinum*) which performs detailed frequency analysis over a narrow range to compensate for Doppler shifts of its echolocation calls. The critical cochlear distance is however, rather constant for most other mammals, and for most studied birds, but it is about 3.3 larger in mammals than in birds. The reduced variation in critical cochlear distance found within mammals and birds results in species with long basilar membranes and poor high-frequency hearing having the best frequency acuity (Fay, R. R., 1992). Comparison of the audiograms of living birds with basilar papilla sizes in birds and fossils of their ancestors allowed for inference of the hearing capabilities of several dinosaurs, and indicated that they should have been mostly sensitive to very low frequencies (Gleich, O. *et al.*, 2005).

In general, large structures have increased mass and inertia, which tunes the hearing organ to low frequencies (Hetherington, T. E., 1992). High-frequency specialists such as the frog *Amolops tormotus* have a middle ear of reduced size, whereas low-frequency specialists tend to have large middle-ear ossicles (Feng, A. S. *et al.*, 2006). Golden moles (*Chrysochloridae*) are an extreme example, having highly hypertrophied mallei. Besides hearing airborne sounds that are detected by the tympanic membrane, golden moles can sense low-frequency seismic vibrations (Narins, P. M. *et al.*, 1997). The large mass of the malleus and the displacement of its center of mass from the rotation axis of the bone renders this ossicle a highly sensitive inertial motion detector (Mason, M. J. and Narins, P. M., 2002c; Willi, U. B. *et al.*, 2006).

3.04.6 Physiology

Several physiological factors can affect hearing in ectothermic vertebrates, especially temperature. For example, frogs carry out most of their sexual communication in conditions in which variations of 10 °C are frequently experienced throughout the course of one night, and variations of 20 °C are common over the breeding season. In addition, these animals can experience significant reductions of body temperature when they enter the water.

At low temperatures, hearing sensitivity is reduced and in some species the range and the frequency of best sensitivity also drops (Walkowiak, W., 1980; Stiebler, I. and Narins, P .M., 1990; van Dijk, P. *et al.*, 1990). In the gray treefrog, *Hyla versicolor*, temperature affects the preference of females for the rate of acoustic pulses in the advertisement calls emitted by males (Gerhardt, H. C., 1978). This is relevant because temperature also affects the acoustic pulse rate of male calls. *H. versicolor* frequently co-occurs with its sister species, *H. chrysoscelis*, and pulse rate is the main difference in their advertisement calls. The variation of female preference for pulse rate in response to temperature compensates for the variation in male call rate with temperature. This allows male trait and female preference to fluctuate with temperature in both species while matching males and females within each species and maintaining species isolation. The mechanism that couples female preference for call rate to temperature in either species is unknown.

3.04.7 Localization

Localizing a sound source involves estimating azimuth (angle in relation to the longitudinal axis of the body in the horizontal plane), elevation, and distance to the

source. Much is known about sound localization in humans and basic processes seem to be generalizable to some other mammals (Fay, R. R. and Popper, A. N., 2005). Other classes of vertebrates exhibit important differences in peripheral and central organization of the auditory system, and appear to have evolved independent mechanisms of sound source localization (for recent reviews, see Christensen-Dalsgaard, J., 2005; Chapter Interconnections Between the Ears in Nonmammalian Vertebrates).

Terrestrial vertebrates localize sound sources by cuing on interaural differences in the acoustic signal (binaural cues). Localization by binaural cues presents a greater challenge underwater. Sound transmission is about four times faster in water than in air, significantly reducing the time of arrival difference of off-axis sound to the ears (Ketten, D. R., 2000). The wavelength of sound is also about four times longer under water, resulting in a vanishingly small interaural phase difference for low frequencies. Nevertheless, several cetaceans have been shown to echolocate and to localize sound as well as humans, with an acuity of about 1° (Heffner, R. S. and Heffner, H. E., 1992a).

Binaural cues in terrestrial vertebrates are also formed by the sound reflected by the head, resulting in a sound shadow in which sound at the distal ear is attenuated relative to that at the proximal ear. This effect is especially salient for $\lambda \leq d/10$, where $\lambda =$ wavelength of sound, and $d =$ diameter of the head (Yost, W. A., 2000). This effect is strongly diminished under water, both because animal tissues are mostly composed of water and are transparent to underwater sound, and because the wavelength of sound is longer in water than in air, for any given frequency. Fish heads do not produce, therefore, a significant sound shadow.

Nevertheless, experimental evidence indicates that fishes can localize sound sources (Hawkins, A. D., 1993; Myrberg, A. A., Jr., 2001; Fay, R. R., 2005). They can be conditioned to approach sound sources that they would normally avoid, and they can perceive a change of source position of at least 20° of separation in azimuth or elevation, as well as changes in distance to the sound source. They show directional responses in the near and far sound fields. Fishes possess three otolith organs (utricle, sacculus, and lagena) that detect particle motion. Direction of movement in such organs can be encoded by the motion of the otolith, producing displacement of the bundles of specific hair cells (Fay, R. R., 1984). In addition, these organs are positioned at different orientations and their combined output facilitates orientation in three dimensions. If the outputs from the hair cells are analyzed independently in the central nervous system, fishes should be capable of detecting the direction of the sound source (Lu, Z. *et al.*, 1998; Lu, Z. and Popper, A. A., 2001).

While the otolith organs might inform the fish about the azimuth of sound propagation, it is not clear how the direction is determined, that is, how the 180° ambiguity problem is solved. For instance, if the azimuth is perpendicular to the longitudinal axis of the body, the sound source might be located to the left or to the right. Experiments with cod (*Gadus morhua*) suggest that these fishes cue on the phase delay between sound pressure and particle motion to solve the 180° ambiguity (Hawkins, A. D., 1993; Wubbels, R. J. and Schellart, N. A. M., 1997). Since the swim bladder can act as a sound pressure detector, coupling of its motion to that of the otolith organs might allow the fish to identify the direction of the source. Further studies should corroborate such a mechanism and explain how nonostariophysan fishes including those that lack swim bladders can determine the direction of the sound source.

In terrestrial vertebrates, external sound is transmitted to the inner ear by the middle ear, which evolved independently in the four clades (Clack, J. A. and Allin, E., 2004). Treefrogs have been shown to be capable of resolving azimuth separations down to about 16°, or 9° after head scanning, and elevations of about 30° (Feng, A. S. *et al.*, 1976; Gerhardt, H. C. and Rheinlaender, J., 1982; Michelsen, A. *et al.*, 1986). Data on reptiles are very scarce, in part because of the difficulty of training them to respond to changes in sound direction (Christensen-Dalsgaard, J., 2005). The best studied example of precise localization ability in birds is the barn owl (*Tyto alba*), with an azimuthal and elevational acuity of approximately 5°, but extensive variability is found in birds, and acuities up to 25° have been described (Knudsen, E. L. and Konishi, M., 1979; Bala, A. D. S. *et al.*, 2003; Christensen-Dalsgaard, J., 2005). Mammals range in both azimuthal and elevational acuities of about 1° to more than 20° and the extensive variability makes it difficult to establish causal links to features of anatomy or lifestyle (Heffner, R. S. and Heffner, H. E., 1992a).

Elevation in terrestrial vertebrates is mostly determined by analysis of the spectral attributes of the perceived sound. The head and the pinnae modify sounds of different frequencies by various amounts, and this varies with sound elevation due to the shape

of the head and pinnae (Brown, C. H. and May, B. J., 2005). Each elevation has, therefore, a signature of relative amplitudes of frequencies to which the animal may cue.

One important structural factor in sound localization in terrestrial vertebrates is the connection between the ears. In mammals, the Eustachian tubes are generally closed and comparisons between the inputs of the two ears are performed by the central nervous system. These acoustically isolated ears are called pressure detectors. In amphibians, the Eustachian tubes remain mostly open and in reptiles and many birds, the ears are often coupled via interaural canals (Lewis, B. and Coles, B., 1980; Klump, G. M., 2000; Christensen-Dalsgaard, J. and Manley, G. A., 2005). One consequence of the direct connection between the ears is that each ear contributes to the response of the other. In particular, the driving force on one tympanic membrane is the sound pressure difference or gradient across it at any moment, rather than simply the external sound pressure impinging upon it (Narins, P. M., 1995; Christensen-Dalsgaard, J., 2005).

Limitations and performance of the ears differ between connected and nonconnected middle ears. When the sound arrives from an angle which results in a phase difference of 180° across the eardrum of a pressure-gradient detector ear, the amplitude of the signal is doubled in relation to pressure difference detectors. At very low frequencies, the phase difference between the ears might be too small and not produce sufficient stimulation for localization by pressure gradient detectors. At very high frequencies, the sound might arrive to the two ears with phase differences of more than 360° and produce an input subject to ambiguous interpretation. Pressure gradient detectors (connected ears) offer the advantages of peripheral processing of binaural difference and increased sensitivity at intermediate frequencies, at the cost of being functionally restricted to the intermediate frequencies. Several birds, especially high-frequency hearing specialists such as owls, experience an intermediate situation. They have thin and long Eustachian tubes that add impedance to the connection between the ears, rendering them intermediates between pressure and pressure-gradient detectors.

The connection between the ears is relevant for altering the range and sensitivity of the ears but it can also have evolutionary implications as the output of connected ears likely requires very different neural processing for localization than the output of acoustically isolated ears.

3.04.8 Management of the Acoustic Environment

With advancement of technology, we have witnessed the inevitable increase in the diversity and abundance of human-made noisy devices present in the environment. Concern has been raised about the potentially negative effects on wildlife caused by human-made sound sources. This has inspired several research initiatives addressing various taxonomic groups, environments, and experimental setups.

The effect of noise in aquatic environments has received extensive reviews (Richardson, W. J. *et al.*, 1997; National Research Council U.S., 2005). In terrestrial environments, loud noise produced by airplanes, helicopters, and chainsaws was shown to have temporary deleterious effects on birds and mammals (Luick, B. R. *et al.*, 1996; Conomy, J. T. *et al.*, 1998; Delaney, D. K. *et al.*, 1999). Several studies have found behavioral adjustments by animals to anthropogenic noise. Nightingales call at higher intensities in territories where the background noise is intense (Brum, H., 2004), and great tits (*Parus major*) increase the pitch of their calls in noisy environments (Slabekoorn, M. and Peet, M., 2003). When exposed to playback of white noise, white-lipped frogs (*Leptodactylus albilabris*) switch their attention from the acoustic component of neighboring male calls to the seismic component, which is produced by thumping of the vocal sac against the substrate (Lewis, E. R. *et al.*, 2001). Marmoset monkeys (*Callithrix jacchus*) respond to noise playbacks by increasing the intensity and the duration of their calls (Brum, H. *et al.*, 2004). Studies on tree swallows (*Tachycineta bicolor*) showed that chicks increased begging call amplitude when exposed to white noise, both in the field and in captivity (Leonard, M. and Horn, A. G., 2005). The natural preference of parents to high begging-call rate disappeared under elevated noise, but it was reestablished when the intensity of the begging calls was increased to match the intensities produced by the chicks when exposed to noise.

Adjustments to the calling patterns in response to noise by males within a vocalizing assemblage may differ among species. Sun J. W. C. and Narins P. M. (2005) studied the responses of multiple species of frogs to playbacks of anthropogenic noise at a pond in central Thailand. Species varied widely on how their

call rates were affected by the noise. While most species silenced to various degrees following the stimuli, one species, the Taipei Frog (*Rana taipehensis*), increased its call rate. Anthropogenic noise might alter, therefore, the natural dynamics of frog choruses, and the degree of masking to which each species is exposed.

Besides behavior, studies have also found evidence of evolutionary adjustment of species to local environmental noise (Witte, K. *et al*., 2005). Cricket frogs (*Acris crepitans*) in Texas inhabit both open areas and pine forests. Male calls from forest areas degrade less than male calls from open areas when broadcast from either of the two environments. The auditory nerve fiber tuning curves of females from forest areas are also more sharply tuned than those of females from open areas, and therefore may more effectively filter out cricket frog calls from the local environmental noise in both environments. These results suggest that the environmental acoustics of the forest habitat has selected for adaptations of both male calls and female auditory systems of local cricket frogs to efficiently function in a noisy environment.

Considering the diversity of auditory systems and life history strategies found in nature, generalizations from these types of studies should be made with caution. Research must continue to access more species, environments, and noise sources as the impact caused by human-kind increases. As an added benefit, investigations of the responses of wildlife to anthropogenic noise produce new information about the hearing and behavior of those species in question. Such studies can also identify modifications to the noise-making devices that reduce their negative impact on wildlife without significantly compromising functionality.

Acknowledgments

Supported by NIH grant no. DC00222 to PMN.

References

Bala, A. D. S., Spitzer, M. W., and Takahashi, T. T. 2003. Prediction of auditory spatial acuity from neural images of the owl's auditory space map. Nature 424, 771–774.

Brown, C. H. and May, B. J. 2005. Comparative Mammalian Sound Localization. In: Sound Source Localization (*eds*. A. N. Popper and R. R. Fay), pp. 124–178. Springer.

Brum, H. 2004. The impact of environmental noise on song amplitude in a territorial bird. J. Anim. Ecol. 73, 434–440.

Brum, H., Voss, K., Köllmer, I., and Todt, D. 2004. Acoustic communication in noise: regulation of call characteristics in a new world monkey. J. Exp. Biol. 207, 443–448.

Burda, H., Bruns, V., and Hickman, G. C. 1992. The ear in subterranean Insectivora and Rodentia in comparison with ground-dwelling representatives. I. Sound conducting system of the middle ear. J. Morphol. 214, 49–61.

Capranica, R. R. 1976. Morphology and Physiology of the Auditory System. In: Frog Neurobiology, a Handbook (*eds*. R. Llinás and W. Precht), pp. 551–575. Springer.

Carr, C. E. 1992. Evolution of the Central Auditory System in Reptiles and Birds. In: The Evolutionary Biology of Hearing (*eds*. D. B. Webster, R. R. Fay, and A. N. Popper), pp. 511–544. Springer.

Chapman, C. J. and Sand, O. 1974. Field studies of hearing in two species of flatfish *Pleuronectes platessa* (L.) and *Limanda limanda* (L.). Comp. Biochem. Physiol. 47A, 371–385.

Christensen-Dalsgaard, J. 2005. Directional Hearing in Nonmammalian Tetrapods. In: Sound Source Localization (*eds*. A. N. Popper and R. R. Fay), pp. 67–123. Springer.

Christensen-Dalsgaard, J. and Manley, G. A. 2005. Directionality of the lizard ear. J. Exp. Biol. 208, 1209–1217.

Clack, J. A. 1992. The Stapes of Acanthostega-Gunnari and the Role of the Stapes in Early Tetrapods. In: The Evolutionary Biology of Hearing (*eds*. D. B. Webster, R. R. Fay, and A. N. Popper), pp. 405–420. Springer.

Clack, J. A. and Allin, E. 2004. The Evolution of Single- and Multiple-Ossicle Ears in Fishes and Tetrapods. In: Evolution of the Vertebrate Auditory System (*eds*. G. A. Manley, A. N. Popper, and R. R. Fay), pp. 128–163. Springer.

Coffin, A., Kelley, M., Manley, G. A., and Popper, A. N. 2004. Evolution of Sensory Hair Cells. In: Evolution of the Vertebrate Auditory System (*eds*. G. A. Manley, A. N. Popper, and R. R. Fay), pp. 55–94. Springer.

Conomy, J. T., Dubovsky, J. A., Collazo, J. A., and Fleming, W. J. 1998. Do black ducks and wood ducks habituate to aircraft disturbance? J. Wildl. Manage.62., 1135–1142.

Cruz, A. and Lombarte, A. 2004. Otolith size and its relationship with colour patterns and sound production. J. Fish Biol. 65, 1512–1525.

Delaney, D. K., Grubb, T. G., Beier, P., Pater, L. L., and Reiser, M. H. 1999. Effects of helicopter noise on Mexican spotted owls. J. Wildl. Manage. 63, 60–76.

Dodd, F. and Capranica, R. R. 1992. A comparison of anesthetic agents and their effects on the response properties of the peripheral auditory system. Hear. Res. 62, 173–180.

Fay, R. R. 1984. The goldfish ear codes the axis of acoustic particle motion in three dimensions. Science 225, 951–954.

Fay, R. R. 1992. Structure and Function in Sound Discrimination among Vertebrates. In: The Evolutionary Biology of Hearing (*eds*. D. B. Webster, R. R. Fay, and A. N. Popper), pp. 229–264. Springer.

Fay, R. R. 2005. Sound Source Localization by Fishes. In: Sound Source Localization (*eds*. A. N. Popper and R. R. Fay), pp. 36–66. Springer.

Fay, R. R. and Popper, A. N. 1975. Modes of stimulation of the teleost ear. J. Exp. Biol. 62, 379–387.

Fay, R. R. and Popper, A. N. 2005. Introduction to Sound Source Localization. In: Sound Source Localization (*eds*. A. N. Popper and R. R. Fay), pp. 1–5. Springer-Verlag.

Feng, A. S., Gerhardt, H. C., and Capranica, R. R. 1976. Sound localization behavior of the green treefrog (*Hyla cinerea*) and the barking treefrog (*H. gratiosa*). J. Comp. Physiol. 107, 241–252.

Feng, A. S., Narins, P. M., and Capranica, R. R. 1975. Three populations of primary auditory fibers in the bullfrog (*Rana catesbeiana*): their peripheral origins and frequency sensitivities. J. Comp. Physiol. A 100, 221–229.

Feng, A. S., Narins, P. M., Xu, C. H., Lin, W. Y., Yu, Z. L., Qiu, Q., Xu, Z. M., and Shen, J. X. 2006. Ultrasonic communication in frogs. Nature 440, 333–336.

Fettiplace, R. and Fuchs, P. A. 1999. Mechanisms of hair cell tuning. Ann. Rev. Physiol. 61, 809–834.

Fritzsch, B. 1992. The Water-to-Land Transition Evolution of the Tetrapod Basilar Papilla, Middle Ear and Auditory Nuclei. In: The Evolutionary Biology of Hearing (*eds*. D. B. Webster, R. R. Fay, and A. N. Popper), pp. 351–376. Springer.

Gerhardt, H. C. 1978. Temperature coupling in the vocal communication system of the gray tree frog, *Hyla versicolor*. Science 199, 992–994.

Gerhardt, H. C. and Rheinlaender, J. 1982. Localization of an elevated sound source by the green tree frog. Science 217, 663–664.

Gleich, O., Dooling, R. J., and Manley, G. A. 2005. Audiogram, body mass, and basilar papilla length: correlations in birds and predictions for extinct archosaurs. Naturwissenschaften 92, 595–598.

Greenwood, D. D. 1961. Critical bandwidth and the frequency coordinates of the basilar membrane. J. Acoust. Soc. Am. 33, 1344–1356.

Greenwood, D. D. 1990. A cochlear frequency-position function for several species – 29 years later. J. Acoust. Soc. Am. 87, 2592–2605.

Grothe, B., Carr, C. E., Casseday, J. H., Fritzsch, B., and Köppl, C. 2004. The Evolution of Central Pathways and their Neural Processing Patterns. In: Evolution of the Vertebrate Auditory System (*eds*. G. A. Manley, A. N. Popper, and R. R. Fay), pp. 289–359. Springer.

Hawkins, A. D. 1993. Underwater Sound and Fish Behaviour. In: Behaviour of Teleost Fishes ,2nd edn. (*ed*. T. J. Pitcher), pp. 129–169. Chapman and Hall.

Heffner, R. S. and Heffner, H. E. 1992a. Evolution of Sound Localization in Mammals. In: The Evolutionary Biology of Hearing (*eds*. D. B. Webster, R. R. Fay, and A. N. Popper), pp. 691–715. Springer.

Heffner, R. S. and Heffner, H. E. 1992b. Hearing and sound localization in blind mole rats. *Spalax ehrenbergi*. Hearing Res. 62, 206–216.

Heffner, R. S. and Heffner, H. E. 1993. Degenerate hearing and sound localization in naked mole rats (*Heterocephalus glaber*) with an overview of central auditory structures. J. Comp. Neurol. 331, 418–433.

Heffner, R. S., Heffner, H. E., Contos, C., and Kearns, D. 1994. Hearing in prairie dogs: transition between surface and subterranean rodents. Hear. Res. 73, 185–189.

Heth, G., Frankenberg, E., and Nevo, E. 1986. Adaptive optimal sound for vocal communication in tunnels of a subterranean mammal (*Spalax ehrenbergi*). Experientia 42, 1287–1289.

Hetherington, T. E. 1985. The role of the opercularis muscle in seismic sensitivity in the bullfrog *Rana catesbeiana*. J. Exp. Zool. 235, 27–34.

Hetherington, T. E. 1992. The Effects of Body Size on the Evolution of the Amphibian Middle Ear. In: The Evolutionary Biology of Hearing (*eds*. D. B. Webster, R. R. Fay, and A. N. Popper), pp. 421–438. Springer.

Higgs, D. M. 2004. Neuroethology and Sensory Ecology of Teleost Ultrasound Detection. In: The Senses of Fish: Adaptations for the Reception of Natural Stimuli (*eds*. G. von der Emde, J. Mogdans, and B. G. Kapoor), pp. 173–188. Kluwer Academic Publishers.

Hödl, W. and Amézquita, A. 2001. Visual Signaling in Anuran Amphibians. In: Anuran Communication (*ed*. M. J. Ryan), pp. 121–141. Smithsonian Institution Press.

Jaslow, A. P., Hetherington, T. E., and Lombard, R. E. 1988. Structure and Function of the Amphibian Middle Ear. In: The Evolution of the Amphibian Auditory System (*eds*. B. Fritzsch, M. J. Ryan, W. Wilczynski, T. E. Hetherington, and W. Walkowiak), pp. 69–91. John Wiley & Sons.

Jorgensen, M. B. and Kanneworff, M. 1998. Middle ear transmission in the grass frog, *Rana temporaria*. J. Comp. Physiol. 182, 59–64.

Ketten, D. R. 2000. Cetacean Ears. In: Hearing by Whales and Dolphins (*eds*. W. W. L. Au, A. N. Popper, and R. R. Fay), pp. 43–108. Springer.

Kinkel, M. D, Thewissen, J. G. M., and Oelschläger, H. A. 2001. Rotation of middle ear ossicles during cetacean development. J. Morphol. 249, 126–131.

Klump, G. M. 2000. Sound Localization in Birds. In: Comparative Hearing: Birds and Reptiles (*eds*. R. J. Dooling, R. R. Fay, and A. N. Popper), pp. 249–307. Springer.

Knudsen, E. L. and Konishi, M. 1979. Mechanisms of sound localization in the barn owl (*Tyto alba*). J. Comp. Physiol. 133, 13–21.

Ladich, F. and Bass, A. H. 2003. Underwater Sound Generation and Acoustic Reception in Fishes with Some Notes on Frogs. In: Sensory Processing in Aquatic Environments (*eds*. S. P. Collin and N. J. Marshall), pp. 173–193. Springer.

Lange, S., Stalleicken, J., and Burda, H. 2004. Functional morphology of the ear in fossorial rodents *Microtus arvalis* and *Arvicola terrestris*. J. Morphol. 262, 770–779.

Leonard, M. and Horn, A. G. 2005. Ambient noise and the design of begging signals. Proc. R. Soc. Lond. B 272, 651–656.

Lewis, B. and Coles, B. 1980. Sound localization in birds. Trends Neurosci. 3, 102–105.

Lewis, E. R., Leverenz, E. L., and Bialek, W. S. 1985. The Vertebrate Inner Ear. CRC Press.

Lewis, E. R., Narins, P. M., Cortopassi, K. A., Yamada, W. M., Poinar, E. H., Moore, S. W., and Yu, X. L. 2001. Do male white-lipped frogs use seismic signals for intraspecific communication? Amer. Zool. 41, 1185–1199.

Lewis, E. R., Narins, P. M., Jarvis, J. U. M., Bronner, G., and Mason, M. J. 2006. Preliminary evidence for the use of microseismic cues for navigation by the Namib golden mole. J. Acoust. Soc. Am. 119, 1260–1268.

Luick, B. R., Kitchens, J. A., White, R. G., and Murphy, S. M. 1996. Modeling energy and reproductive costs in caribou exposed to low flying military jet aircraft. Rangifer (Special Issue 9), 209–211.

Lu, Z. and Popper, A. A. 2001. Neural response directionality correlates of hair cell orientation in a teleost fish. J. Comp. Physiol. A 187, 453–465.

Lu, Z., Song, J., and Popper, A. A. 1998. Encoding of acoustic directional information by saccular afferents of the sleeper goby, *Dormitator latifrons*. J. Comp. Physiol. A 182, 805–815.

Manley, G. A. 1972. Frequency response of the ear of the tokay gecko. J. Exp. Zool. 181, 159–168.

Manley, G. A. and Clack, J. A. 2004. An Outline of the Evolution of Vertebrate Hearing Organs. In: Evolution of the Vertebrate Auditory System (*eds*. G. A. Manley, A. N. Popper, and R. R. Fay), pp. 1–26. Springer.

Manley, G. A., Popper, A. N., and Fay, R. R. 2004. Evolution of the Vertebrate Auditory System. Springer.

Mann, D. A., Lu, Z., and Popper, A. N. 1997. A clupeid fish can detect ultrasound. Nature 389, 341.

Manoussaki, D., Dimitriadis, E. K., and Chadwick, R. S. 2006. Cochlea's graded curvature effect on low frequency waves. Phys. Rev. Lett. 96, 088701.

Mason, M. J. 2001. Middle ear structure in fossorial mammals: a comparison with non-fossorial species. J. Zool. 255, 467–486.

Mason, M. J. and Narins, P. M. 2002a. Vibrometric studies of the middle ear of the bullfrog (*Rana catesbeiana*) I: the extrastapes. J. Exp. Biol. 205, 3153–3165.

Mason, M. J. and Narins, P. M. 2002b. Vibrometric studies of the middle ear of the bullfrog (*Rana catesbeiana*) II: the operculum. J. Exp. Biol. 205, 3167–3176.
Mason, M. J. and Narins, P. M. 2002c. Seismic sensitivity in the desert golden mole (*Eremitalpa granti*): a review. J. Comp. Psychol. 116, 158–163.
Michelsen, A., Jorgensen, M., Christensen-Dalsgaard, J., and Capranica, R. R. 1986. Directional hearing of awake, unrestrained treefrogs. Naturwissenschaften 73, 682–683.
Miller, M. R. 1978. Further scanning electron microscope studies of lizard auditory papillae. J. Morphol. 156, 381–418.
Miller, M. R. 1992. The Evolutionary Implications of the Structural Variations in the Auditory Papilla of Lizards. In: The Evolutionary Biology of Hearing (*eds*. D. B. Webster, R. R. Fay, and A. N. Popper), pp. 463–488. Springer.
Myrberg, A. A., Jr. 2001. The acoustical biology of elasmobranches. Environ. Biol. Fish 60, 31–45.
Narins, P. M. 1995. Frog communication. Sci. Am. 273, 78–83.
Narins, P. M. and Wagner, I. 1989. Noise susceptibility and immunity of phase locking in amphibian auditory-nerve fibers. J. Acoust. Soc. Am. 85, 1255–1265.
Narins, P. M., Feng, A. S., Schnitzler, H. U., Denzinger, A., Suthers, R. A., Lin, W., and Xu, C. H. 2004. Old World frog and bird vocalizations contain prominent ultrasonic harmonics. J. Acoust. Soc. Am. 115, 910–913.
Narins, P. M., Lewis, E. R., Jarvis, J. U. M., and O'Riain, J. 1997. The use of seismic signals by fossorial southern African mammals: a neuroethological gold mine. Brain Res. Bull. 44, 641–646.
Narins, P. M., Reichman, O. J., Jarvis, J. U. M., and Lewis, E. R. 1992. Seismic signal transmission between burrows of the Cape mole-rat, *Georychus capensis*. J. Comp. Physiol. A 170, 13–21.
National Research Council U.S. 2005. Marine Mammal Populations and Ocean Noise: Determining when Noise Causes Biologically Significant Effects. National Academies Press.
Nummela, S., Thewissen, J. G. M., Bajpal, S., Hussain, S. T., and Kumar, K. 2004. Eocene evolution of whale hearing. Nature 430, 776–778.
Paton, J. 1971. Microphonic Potentials in the Inner Ear of the Bullfrog. M.Sc. Thesis, Cornell University.
Platt, C. and Popper, A. N. 1981. Fine Structure and Function of the Ear. In: Hearing and Sound Communication in Fishes (*eds*. W. N. Tavolga, A. N. Popper, and R. R. Fay), pp. 3–38. Springer.
Pollak, G. D. and Casseday, J. H. 1989. The Neural Basis of Echolocation in Bats. Springer.
Popper, A. N., Ramcharitar, J., and Campana, S. E. 2005. Why otoliths? Insights from inner ear physiology and fisheries biology. Mar. Freshw. Res. 56, 497–504.
Reuter, T., Nummela, S., and Hemilä, S. 1998. Elephant hearing. J. Acoust. Soc. Am. 104, 1122–1123.
Richardson, W. J., Greene, C. R., Jr., Malme, C. I., and Thomson, D. H. 1997. Marine Mammals and Noise. Academic Press.
Rosowski, J. J. 1994. Outer and Middle Ears. In: Comparative Hearing: Mammals (*eds*. R. R. Fay and A. N. Popper), pp. 172–248. Springer.
Sand, O. and Enger, P. S. 1973. Evidence for an auditory function of the swimbladder in the cod. J. Exp. Biol. 59, 405–414.
Slabekoorn, H. and Peet, M. 2003. Birds sing at a higher pitch in urban noise. Nature 424, 267.
Smotherman, M. and Narins, P. M. 2000. Hair cells, hearing and hopping: a field guide to hair cell physiology in the frog. J. Exp. Biol. 203, 2237–2246.
Smotherman, M. and Narins, P. M. 2004. Evolution of the Amphibian Ear. In: Evolution of the Vertebrate Auditory System (*eds*. G. A. Manley, A. N. Popper, and R. R. Fay), pp. 164–199. Springer.
Stiebler, I. and Narins, P. M. 1990. Temperature dependence of auditory nerve response properties in the frog. Hear. Res. 46, 63–82.
Sun, J. W. C. and Narins, P. M. 2005. Anthropogenic sounds differentially affect amphibian call rate. Biol. Conserv. 121, 419–427.
Thewissen, J. G. M. and Hussain, S. T. 1993. Origin of underwater hearing in whales. Nature 361, 444–445.
van Dijk, P., Lewis, E. R., and Wit, H. P. 1990. Temperature effects on auditory nerve fiber response in the American bullfrog. Hear. Res. 44, 231–240.
von Békésy, G. 1960. Experiments in Hearing. McGraw-Hill.
Walkowiak, W. 1980. Sensitivity, range and temperature dependence of hearing in the grass frog and fire-bellied toad. Behav. Process. 5, 363–372.
Webster, D. B. and Plassmann, W. 1992. Parallel Evolution of Low-Frequency Sensitivity in Old World and New World Desert Rodents. In: The Evolutionary Biology of Hearing (*eds*. D. B. Webster, R. R. Fay, and A. N. Popper), pp. 633–653. Springer.
Werner, Y. L. and Wever, E. G. 1995. The function of the middle ear in lizards: *Gekko gecko* and *Eublepharis macularius* (Gekkonoidea). J. Exp. Zool. 179, 1–16.
Wever, E. G. 1978. The Reptile Ear: Its Structure and Function. Princeton University Press.
Wever, E. G. and Vernon, J. A. 1960. The problem of hearing in snakes. J. Aud. Res. 1, 77–83.
Wilczynski, W. and Capranica, R. R. 1984. The auditory system of anuran amphibians. Prog. Neurobiol. 22, 1–38.
Wilczynski, W., Keddy-Hector, A. C., and Ryan, M. J. 1992. Call patterns and basilar papilla tuning in cricket frogs. I. Differences among populations and between sexes. Brain Behav. Evol. 39, 229–237.
Wilczynski, W., Rand, A. S., and Ryan, M. J. 2001. Evolution of calls and auditory tuning in the *Physalaemus pustulosus* species group. Brain Behav. Evol. 58, 137–151.
Wilczynski, W., Resler, C., and Capranica, R. R. 1987. Tympanic and extratympanic sound transmission in the leopard frog. J. Comp. Physiol. A 161, 659–669.
Willi, U. B., Bronner, G. N., and Narins, P. M. 2006. Middle ear dynamics in response to seismic stimuli in the Cape golden mole (*Chrysochloris asiatica*). J. Exp. Biol. 209, 302–313.
Witte, K., Farris, H., Ryan, M. J., and Wilczynski, W. 2005. How cricket frog females deal with a noisy world: habitat-related differences in auditory tuning. Behav. Ecol. 16, 571–579.
Wubbels, R. J. and Schellart, N. A. M. 1997. Neuronal encoding of sound direction in the auditory midbrain of the rainbow trout. J. Neurophysiol. 77, 3060–3074.
Young, B. 2003. Snake bioacoustics: toward a richer understanding of the behavioral ecology of snakes. Q. Rev. Biol. 78, 303–325.
Yost, W. A. 2000. Fundamentals of Hearing. Academic Press.
Yu, Z. L., Qiu, Q., Xu, Z. M., and Shen, J. X. 2006. Auditory response characteristics of the piebald odorous frog and their implications. J. Comp. Physiol. 192, 801–806.

3.05 Genetics of Mechanoreceptor Evolution and Development

K W Beisel, D He, R Hallworth, and B Fritzsch, Creighton University, Omaha, NE, USA

© 2008 Elsevier Inc. All rights reserved.

3.05.1	**Introduction**	76
3.05.2	**The Origin of Mechanosensation Lies in Untethered, Membrane-Tension-Gated Channels**	76
3.05.2.1	Transient Receptor Potential and Degenerin/Epithelial Sodium Channels Genes of *Caenorhabditis elegans*, *Drosophila melanogaster*, *Ciona intestinalis*, *Danio rerio*, *Mus musculus*, and *Homo sapiens* Compared: Sequence Data Indicate Candidate Genes that Need to be Investigated	79
3.05.2.1.1	The transient receptor potential superfamily	79
3.05.2.1.2	The degenerin/epithelial sodium channels superfamily	89
3.05.2.2	Ancestry of Specialized Mechanosensory Cells	89
3.05.2.2.1	Known or suspected mechanosensory cells of multicellular animals	90
3.05.2.2.2	Mechanosensory cells in *Caenorhabditis elegans*: connecting degenerin/epithelial sodium channels channels to the cuticle?	92
3.05.2.2.3	Genetics of mechanotransduction in *Drosophila melanogaster*: tethering a kinocilium to the cuticle	93
3.05.3	**Mechanosensory Cells in Vertebrates**	94
3.05.3.1	The Zebrafish *NompC (TRPN-1)*: Is There a Divergent Base for Mechanosensory Transduction in the Apparently Structurally Conserved Vertebrate Hair Cells?	95
3.05.3.2	The Mammalian Cochlear Hair Cell: Adapting an Ancestral Cell to Very High Frequencies	96
3.05.3.3	Active Processes in Hair Cells	96
3.05.3.4	Development of Mechanoreceptor Cells: Molecular Transformation of an Epidermal Cell into a Mechanoreceptor	99
3.05.4	**Conclusions**	100
3.05.5	**Note Added in Proof**	101
References		101

Glossary

autosomal dominant An effect caused by mutations in a single allele of a gene in the autosomal chromosomes.

cochlear amplifier A mechanism to enhance the perception of stimuli of low intensity.

coelenterates Radial symmetric animals (jellyfish, corals).

DEG/ENAC Degenerin/epithelial sodium channels, a family of ion channels.

ecdysozoans Animals that shed the external layer of skin through the action of the hormone ecdyson.

eukaryotes Single and multicellular organisms that have all DNA (except for mtDNA) concentrated in one or more nuclei.

kinocilium A nonmotile flagellum like protrusion found in most mechanosensory cells.

mollusks Animals whose soft body is surrounded by a more or less developed shell (mussels, snails, octopus).

nociceptor A receptor that, if stimulated, causes the sensation of pain.

prokaryotes Single-celled organisms that lack the formation of a distinct nucleus.

stereocillia Modified microvilli that contain large amounts of actin filaments.

TRP Transient receptor potential, a superfamily of ion channel proteins.

3.05.1 Introduction

Any cell can be stimulated by almost any stimulus, provided the intensity is high enough. Defining the appropriate stimulus therefore requires finding the stimulus that is able to drive a receptor cell with the least amount of energy. This is important even at the molecular level, where solely mechanosensitive channels (Msc) (Goodman, M. B. *et al.*, 2004; O'Hagan, R. *et al.*, 2005) and channels that can respond to other stimuli have been identified (Syntichaki, P. and Tavernarakis, N., 2004; Kung, C., 2005; Zhou, X. L. *et al.*, 2005). Mutations have identified a number of candidate genes in several metazoan taxa that may be part of a mechanosensory transduction complex, but only in the nematode *Caenorhabditis elegans* are we approaching a molecular understanding of this complex (O'Hagan, R. *et al.*, 2005). Indeed, and in contrast to bacteria (Sukharev, S. and Corey, D. P., 2004; Anishkin, A. and Kung, C., 2005), without this genetic approach to mechanosensory function we would likely not even have those metazoan candidate genes identified. Problems in identifying mechanosensory channels seem to relate to their generally low abundance compared to those for phototransduction (Ernstrom, G. G. and Chalfie, M., 2002), making isolation of their mRNAs and proteins nearly impossible with current techniques. In addition, these channels have no known specific ligand to facilitate other approaches for protein purification, as used for ligand-gated channel discoveries.

The best-understood channels in terms of molecular modeling (Chiang, C. S. *et al.*, 2004) are the tension-gated mechanosensitive channels (large and small Msc: MscL and MscS, respectively) in bacteria that respond to tension of 5–10 $\mathrm{dyn\,cm^{-1}}$ (or 5–10 $\mathrm{mN\,m^{-1}}$) along the membrane with an iris-like opening in 10 ns (Anishkin, A. and Kung, C., 2005; Kung, C., 2005). Such gating times could accommodate even frequencies of over 100 kHz, which is as rapid as transduction in mammalian cochlear hair cells (Hudspeth, A. J., 2005). Comparison of absolute sensitivity of membrane tension to channels that are tethered to accessory structures is difficult (Sukharev, S. and Corey, D. P., 2004) and could best be accomplished by calculating the work done in opening an MscL channel (approximately 2×10^{-19} J) and an auditory transduction channel (approximately 2×10^{-21} J). Such calculations suggest that the tethered vertebrate channel may be up to two orders of magnitude more sensitive than the untethered bacterial channel. Specifying the molecular details of such sensitivity differences is beyond our current knowledge. Nevertheless, it appears appropriate to first explore what is known about the mechanosensory channels of bacteria followed by the molecularly less well-known channels in multicellular organisms.

3.05.2 The Origin of Mechanosensation Lies in Untethered, Membrane-Tension-Gated Channels

Mechanotransduction is likely as old as living cells (archaea, bacteria (prokaryotes), and eukaryotes) and is mediated by a number of transmembrane channels that have only a limited degree of conservation across and within phyla (Blount, P., 2003; Syntichaki, P. and Tavernarakis, N., 2004; Tobin, D. M. and Bargmann, C. I., 2004; Kung, C., 2005). In its simplest form, mechanoreception monitors cell turgor with a channel that responds to membrane tension (Figure 1). Such mechanotransduction serves single-cell homeostasis. Based on the finding of tethering threads in vertebrate mechanosensors, it has been proposed that the ability of hair cell to perceive displacements of a few nanometers with forces of <10 pN (Hudspeth, A. J., 2005) depends on such tethers. Likewise, attachments have been found in other highly sensitive mechanosensors of flies and nematodes (Ernstrom, G. G. and Chalfie, M., 2002; Emtage, L. *et al.*, 2004; Gong, Z. *et al.*, 2004). It is possible that, in the course of evolution, untethered channels were modified to respond even more effectively to stimuli across the membrane by tethering them to other structures such as other parts protruding from the same cell, extracellular matrix, or the internal cell skeleton (Figure 1). Alternatively, tethered and untethered channels may have evolved independently. The limited molecular data on tethered channels, combined with the great variety of molecular candidates for mechanically gated channels, make it difficult to exclude any of these possibilities at this moment. Indeed, it has been suggested that candidates for tethered channels in metazoans are as multimodal as those in bacteria (Kung, C., 2005) and direct evidence exists that shows that reconstituted TRPC1 or TRPY channels can be gated purely by membrane tension (Maroto, R. *et al.*, 2005; Zhou, X. L. *et al.*, 2005). These hypothesized and known similarities of certain tethered and untethered channels indicate that there may not be major structural

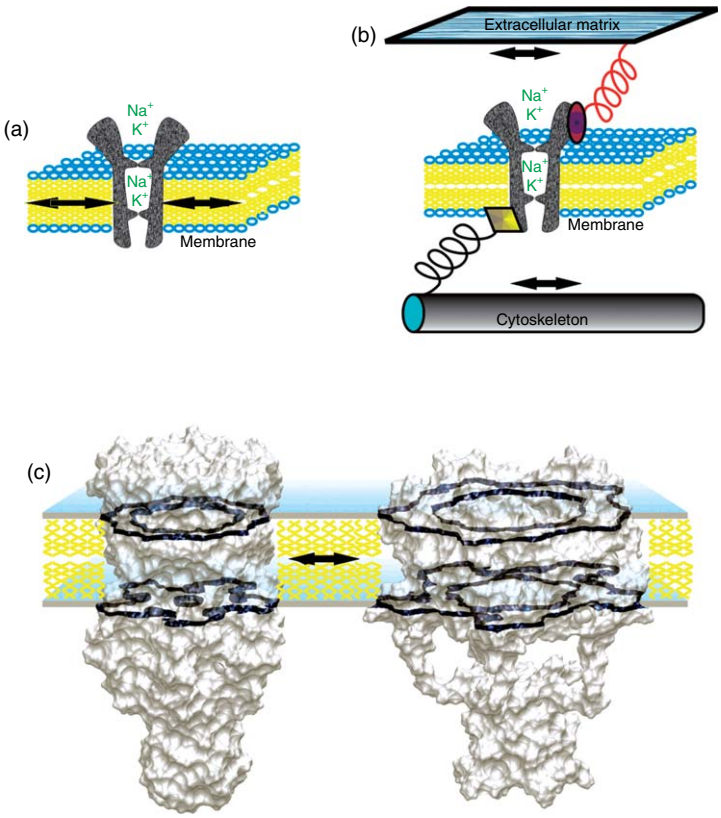

Figure 1 Various channels that respond to changes in turgor resulting in stretch of the membranes (double arrow in (a)) have been found in single-cell organisms. It is possible that such mechanosensitive channels (Msc) were modified in the unicellular ancestor of metazoans through extracellular or intracellular matrix attachments to provide increased sensitivity for shearing forces. Molecular evidence suggests that, across metazoans, only family members of degenerin/epithelial sodium channels (DEG/ENaC) and transient receptor potential (TRP) channel families are candidates for Msc. It thus remains possible that metazoan ancestors selected either or both families for specific properties that allow increased sensitivity to detect mechanical stimulations. What such properties could be remains unknown in the absence of any model of sensitive mechanosensory channel in any metazoan taxon. Detailed models of the pentameric large mechanosensitive channels (MscL) of bacteria suggest in iris-like opening upon tension acting in the plane of the membrane (c). Adopted from Chiang, C.S., Anishkin, A., and Sukharev, S. 2004. Gating of the large mechanosensitive channel *in situ*: estimation of the spatial scale of the transition from channel population responses. *Biophys. J. 86, 2846–2861,* with permission from S. Sukharev; and Syntichaki, P. and Tavernarakis, N. 2004. Genetic models of mechanotransduction: the nematode Caenorhabditis elegans. Physiol. Rev. 84, 1097–1153.

differences between those channels other than intra- and/or extracellular tethering.

Within recent years a number of candidates for untethered mechanotransduction channels have been molecularly defined in prokaryotes and eukaryotes (Blount, P., 2003; Syntichaki, P. and Tavernarakis, N., 2004). No sequence similarities exist between the Msc of prokaryotes and the likely Msc of eukaryotes, which belong to the degenerin/epithelial sodium channels (DEG/ENaC) and transient receptor potential (TRP) superfamily of genes (Goodman, M. B. *et al.*, 2004; Sukharev, S. and Corey, D. P., 2004; Tobin, D. M. and Bargmann, C. I., 2004; O'Hagan, R. *et al.*, 2005). In eukaryotes, TRP-like genes have also been found to form tension-sensitive TRP channels in yeast (Anishkin, A. and Kung, C., 2005; Kung, C., 2005; Zhou, X. L. *et al.*, 2005). Such tension-sensitive membrane channels therefore evolved before tethered mechanosensory channels, which appear to be restricted to fungi and multicellular animals. No DEG/ENaC channel has thus far been identified in fungi, suggesting that it evolved in metazoan ancestors (Figure 2). It is possible that different taxa of metazoa have recruited different channels or channel subunits to form specific Msc. Only the tethered mechanosensory channels are coupled with highly adaptable and not necessarily homologous connection(s) to accessory structures

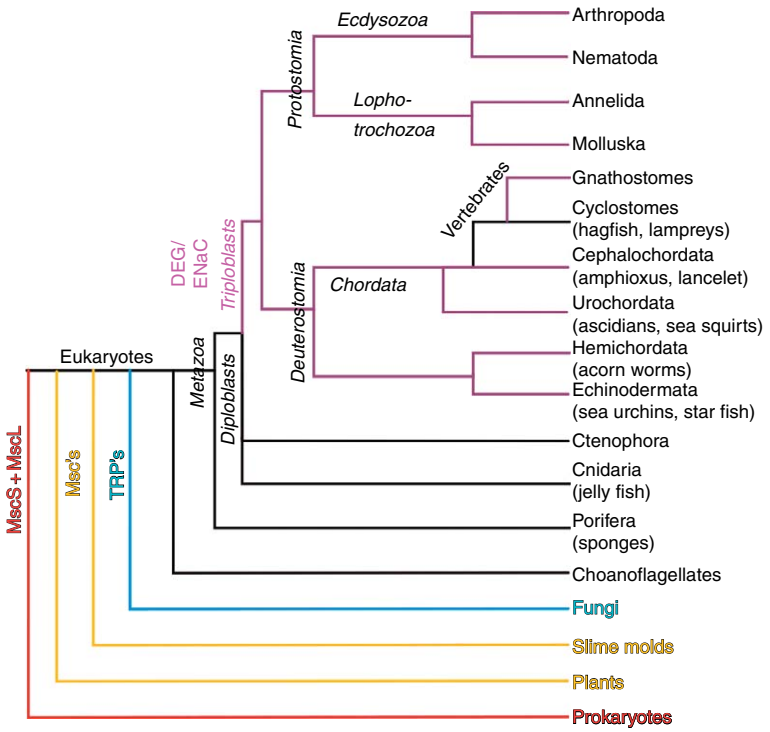

Figure 2 Distribution of the various known and putative mechanosensitive channels (Msc) is shown. All prokaryotes seem to share the large and small Msc (MscL and MscS, red). Plants and slime molds seem to have a variation of a modified form of this channel (Msc, yellow). There is no obvious sequence homology among these channels. Fungi and metazoans have transient receptor potential (TRP) channels, suggesting that the metazoan ancestors had at least this channel family (blue). Whether it functioned as a Msc remains unclear. At least triploblasts, but possibly all metazoa, have degenerin/epithelial sodium channels (DEG/ENaC) type of channels (lilac). As with TRP channels, it is unclear at which point they evolved into Msc. Adapted from Eichinger, L., Pachebat, J. A., Glockner, G., Rajandream, M. A., Sucgang, R., Berriman, M., Song, J., Olsen, R., Szafranski, K., Xu, Q., *et al*. 2005. The genome of the social amoeba *Dictyostelium discoideum*. Nature 435, 43–57; and Rokas A., Kruger, D., and Carroll, S. B. 2005. Animal evolution and the molecular signature of radiations compressed in time. Science 310, 1933–1938.

(Figure 1) that filter and amplify specific mechanical stimuli to enable a given mechanosensory cell to respond best to light touch, angular acceleration, gravity, or sound (Syntichaki, P. and Tavernarakis, N., 2004). This aspect is nowhere more obvious than in the various organs modified in vertebrates and invertebrates for sound energy detection (Sukharev, S. and Corey, D. P., 2004; Gillespie, P. G. *et al*., 2005; Hudspeth, A. J., 2005; Fritzsch, B. *et al*., 2006a).

Prokaryotic mechanosensitive multimeric channels share structural and functional similarities with the membrane-spanning domains (Figure 2). In contrast, eukaryotes have similarities only in the basic structural motifs (two membrane-spanning units) and membrane topology of these channels, in particular with the DEG/ENaC family of ion channels (Blount, P., 2003), as well as with the certain inward rectifying K^+ channels (Kung, C., 2005). Some of these similarities provide the basis for the multimodal sensitivity to heat, chemical stimuli, and osmolarity found in bacterial mechanosensors and TRP channels (Ernstrom, G. G. and Chalfie, M., 2002; Goodman, M. B. *et al*., 2004; Tobin, D. M. and Bargmann, C. I., 2004; O'Hagan, R. *et al*., 2005). In addition, it is noteworthy that the mammalian Shaker and other voltage-gated channels can also be modulated by membrane stretch, implying that, much like in the prokaryotic archaea and bacteria, both voltage changes and mechanical forces can activate the channel (Sukharev, S. and Corey, D. P., 2004; Kung, C., 2005).

The large conductance mechanosensitive channel (MscL) of bacteria has been shown to be a homopentamer with two iris-like openings at the extracellular and the intracellular sides. The size differences between the closed and the open states have been estimated to 23.3 nm^2 (Figure 1). Details of the movement are still debated, but it appears that most of the configuration change is a change in the position of

helices of domains near the lipid–water interface (Chiang, C. S. *et al.*, 2004; Tang, Y. *et al.*, 2006). It is possible that Msc can respond to either tension within the membrane or, if properly tethered, tension across the membrane. However, no reconstitution with a tether has been achieved in any channel to date, so the later assertion remains speculative.

In the following, we will explore the genetically identified candidates only for tethered channels and their variable, currently largely hypothetical, use in mechanotransduction. Specifically we will explore three main aspects of mechanosensory molecular and cellular evolution:

1. We will discuss the similarity and possible homology of presumed metazoan mechanosensory channels across the four main taxa where molecular data exist, the nematode *C. elegans* (Ce), the fly *Drosophila melanogaster* (Dm), the zebrafish *Danio rerio* (Dr), and the mouse *Mus musculus* (Mm).
2. We will put these molecular and structural data, including data on tethering molecules, into the context of our current understanding of mechanosensory cell and organ evolution and tethering to extracellular and intracellular structures.
3. We will discuss the molecular origin of hair cell transduction, with particular emphasis on mammals and what can be learned by comparison to other taxa.

3.05.2.1 Transient Receptor Potential and Degenerin/Epithelial Sodium Channels Genes of *Caenorhabditis elegans*, *Drosophila melanogaster*, *Ciona intestinalis*, *Danio rerio*, *Mus musculus*, and *Homo sapiens* Compared: Sequence Data Indicate Candidate Genes that Need to be Investigated

In the last 10 years, numerous putative mechanotransducer channels have been identified and their functions assessed. The emerging theme is that putative metazoan mechanosensory channels belong to the TRP or DEG/ENaC family of genes. With the completion of the genome of various vertebrates and invertebrates, it is now possible to establish sequence similarities and thereby assess whether a given gene is going through rapid sequence alteration even in closely related animals. Logically, given for example the ancient features of stereocilia in vertebrate hair cells that are responsible for mechanotransduction, one would like to find a putative channel that is at least conserved across vertebrates, if not shared with closely related deuterostome invertebrates such as *Ciona intestinalis* (Ci; Figure 2). Indeed, listing genes according to their conservation allows the identification of highly conserved as well as highly variable sequences (Table 1, Figure 3). Channel subunit homologies were determined based on current understanding of the known and predicted proteomes from these six species. It must be noted that the orthologs for both TRP and DEG/ENaC genes provided in Table 1 are not complete, since analyses of Dr and Ci genomes are still lagging behind in both the degree of completion of the genomic sequence and the subsequent annotation of the genes, transcripts, and predicted proteins (Okamura, Y. *et al.*, 2005).

The diversity among the members of the amiloride-sensitive cation sodium channels (ascNaC) superfamily is reflected primarily by the heterogeneity in the peptide sequences. However, the structural motif of these channels is highly conserved along with their generalized mechanoreception function. In comparison, the TRP superfamily is highly diversified, with a common channel motif being shared within each subfamily. This wide diversity is also highlighted by the extensive range of biophysiological and functional properties and use in rather diverse sensory stimulus acquisition. In order to emphasize this diversity, we will provide a summary of the members of each subfamily along with their associated channel properties and functional characteristics.

3.05.2.1.1 The transient receptor potential superfamily

The TRP superfamily of cation channels displays a wide range of gating versatility and associated functional properties. TRP channels play important roles in nonexcitable cells; however, an emerging theme is that many TRP-related proteins are expressed in the nervous system and function in sensory physiology. Most of the TRP channels are permeable for Ca^{2+} and in general provide Ca^{2+} influx pathways (Nilius, B. *et al.*, 2005). Members share a common structural motif that contains six putative transmembrane domains (TM1–TM6) with an intercalated pore (P) domain and the N- and C-terminal tails are located in the cytoplasm. Domains TM5, TM6, and P are thought to form the central cation-conducting pore, whereas TM1–TM4 and the cytoplasmic tails are proposed to contain the regulatory elements for channel formation and gating. The function of the

Table 1 Protein homology among the members of the TRP and DEG/ENaC superfamilies

Superfamily		*Ortholog*						
Family	***Gene***	***Ce***	***Dm***	***Ci***	***Dr***	***Mm***	***Hs***	***Function in mammals***
Trp								
TRPC	1	*trp-1* (55,92,11)[a] *spe-41(trp-3)* (42,81,7)	*trpl* (55,93,12) *trp* (53,92,11)	n/o	*LOC570841* (62,100,32)	*Trpc1* (95,100,4)	*TRPC1*	
	2	n/o	n/o	n/o	*trpc2* (75,94,3)	*Trpc2* (89,99,0)	*TRPC2*	*Trpc2* is required for male–male aggression, and initiation of sexual and courtship behaviors toward both males and females, and is caused by defective vomeronasal neurons.
	3	n/o	n/o	n/o	n/o	*Trpc3* (98,99,0)	*TRPC3*	
	4	n/o	n/o	n/o	*LOC555897* (89,70,2) *LOC566436* (81,60,4)	*Trpc4* (97,100,0)	*TRPC4*	*Trpc4* is an indispensable component of store-operated channels in native endothelial cells and these channels directly provide an Ca^{2+}-entry pathway essentially contributing to the regulation of blood vessel tone.
	5	n/o	n/o	ENSCINT013935 (53,61,6) ENSCINT017402 (50,81,13) ENSCINT004195 (48,71,12) ENSCINT007988 (46,71,12)	*LOC557533* (74,93,13) *LOC557456* (94,31,0)	*Trpc5* (98,100,0)	*TRPC5*	
	6	n/o	n/o	n/o	*bZ1P14.9* (80,95,8)	*Trpc6* (96,97,0)	*TRPC6*	The *FSGS2* form of focal segmental glomerulosclerosis is caused by mutations in the TRPC6 gene.
	7	n/o	n/o	n/o	n/o	*Trpc7* (99,100,0)	*TRPC7*	
TRPV		*ocr-1* (51,97,15) *ocr-2* (55,99,9) *ocr-3* (55,95,14) *ocr-4* (55,93,11)	*nan*[b]	ENSCINT004644 (54,85,9)	n/o	n/o	n/o	
	1	*osm-9* (46,66,12)	*CG4536 (iav)* (46,21,9)	n/o	n/o	*Trpv1* (82,100,0)	*TRPV1*	*Trpv1* is essential for inflammatory thermal hyperalgesia and is required for inflammatory sensitization to noxious thermal stimuli. Note that alternative mechanisms are sufficient for normal sensation of noxious heat.

	2	n/o	n/o	n/o	n/o	*Trpv2* (87,100,1)	*TRPV2*	
	3	n/o	n/o	n/o	n/o	*Trpv3* (96,100,0)	*TRPV3*	*Trpv3*-null mice have strong deficits in responses to innocuous and noxious heat in the skin.
	4	n/o	n/o	n/o	n/o	*Trpv4* (97,100,0)	*TRPV4*	*Trpv4* is necessary for the normal response to changes in osmotic pressure and functions as an osmotic sensor in the CNS.
	5	n/o	n/o	n/o	*Trpv6* (49.69,10)	*Trpv5* (89,99,0)	*TRPV5*	The key function of *Trpv5* in active Ca^{2+} resorption and plays an essential role in the Ca^{2+} homeostasis and bone remodeling by osteoclastic bone resorption.
	6	n/o	n/o	n/o	n/o	*Trpv6* (94,100,0)	*TRPV6*	
TRPM	1	n/o	n/o	n/o	*LOC569946* (78,68,6) *ENSDR66992* (73,99,9)	*Trpm1* (91,94,1)	*TRPM1*	
	2	n/o	n/o	n/o	*ENSDR53655* (64,96,7)	*Trpm2* (90,100,0)	*TRPM2*	
	3	*gon-2* (54,85,16) *gtl-1* (52,82,14) *gtl-2* (58,73,5)	*CG30078* (68,67,3)	n/o	*ENSDR51573* (86,99,1)	*Trpm3* (98,100,0)	*TRPM3*	
	4	n/o	n/o	n/o	*LOC557355* (59,98,9) *LOC556171* (54,49,13)	*Trpm4* (87,77,0)	*TRPM4*	
	5	n/o	n/o	n/o	*LOC557722* (74,93,3) *LOC563106* (62,54,9)	*Trpm5* (91,95,0)	*TRPM5*	Null *Trpm5* mice have an abolished sweet, amino acid, and bitter-taste reception, but sour or salty taste is normal.
	6	n/o	n/o	n/o	n/o	*Trpm6* (85,100,1)	*TRPM6*	
	7	n/o	n/o	n/o	*ENSDR36232* (72,100,5)	*Trpm7* (97,100,0)	*TRPM7*	
	8	n/o	n/o	n/o	*ENSDR66536* (50,81,11)	*Trpm8* (97,100,0)	*TRPM8*	
TRPML	1	*cup-5* (55,89,7)	*CG8743* (59,88,5)	*ENSCINT013096* (57,91,7)	*mcoln1* (77,43[a],4)	*Mcoln1* (94,100,0)	*MCOLN1*	Mutations in the human MCOLN1 gene leads to mucolipidosis type IV.
	2	n/o	n/o	n/o	*zgc:55310* (75,99,2)	*Mcoln2* (91,96,0)	*MCOLN2*	
	3	n/o	n/o	n/o	n/o	*Mcoln3* (96,100,0)	*MCOLN3*	Mutations are associated with deafness and pigmentation defects in varitint-waddler (Va) mice.

(*Continued*)

Table 1 (Continued)

Superfamily		*Ortholog*						
Family	***Gene***	***Ce***	***Dm***	***Ci***	***Dr***	***Mm***	***Hs***	***Function in mammals***
TRPP	1	*lov-1* (40,6,8)	n/o	n/o	n/o	*Pkd1* (85,99,0)	*PKD1*	Mutations in *PKD1* gene and lower *Pkd1* expression levels cause polycystic kidney disease.
	2	*pkd-2* (54,70,8)	*Pkd2* (49,40,1)	*ENSCINT008806* (74,67,5)	*pkd2*	*Pkd2* (92,100,0)	*PKD2*	*PKD2* mutations cause autosomal dominant polycystic kidney disease and *Pkd2* expression is both necessary and sufficient for renal cyst formation.
	3	n/o	n/o	n/o	n/o	*Pkd2l1* (92,94,0)	*PKD2L1*	
	4	n/o	n/o	n/o	n/o	*Pkd2l2* (92,98,0)	*PKD2L2*	
TRPA	1	*trpa-1* (43,94,12)	*TrpA1* (67,84,12)	*ENSCINT010301* (42,90,10) *ENSCINT022731* (43,94,11)	*trpa1a* (67,100,2) *trpa1b* (66,99,3)	*Trpa1* (98,100,0)	*TRPA1*	*Trpa1*-deficient mice exhibit pronounced deficits in bradykinin-evoked nociceptor excitation and pain hypersensitivity and *Trpa1* mediates the inflammatory actions of environmental irritants and proalgesic agents.
TRPN	1	*trp-4* (61,91,5)	*nompC*[b]	*ENSCINT015850* (58,92,6)	*trpn1* (62,97,7)			
DEG/ENac								
asc NaC	Group 1	*T28B8.5* *unc-105* *del-1* *asic-1* *mec-4* *mec-10* *deg-1* *unc-8* *asic-2* *F55G1.12*	n/o	n/o	n/o	n/o	n/o	
	Group 2	*F28A12.1* *C24G7.4* *T28F2.7* *C24G7.2* *flr-1* *tag-324*	n/o	n/o	n/o	n/o	n/o	

		n/o	*CG15555* *CG31105* *ppk19* *ppk21* *ppk20* *ppk23* *ppk16* *Nach* *CG32792* *CG33289* *ppk12* *ppk28* *ppk* *CG8546* *rpk*	n/o	n/o	n/o	n/o	
Scnn	αENaC	n/o	n/o	n/o	n/o	*Scnn1a* (91,93,0)	*SCNN1A*	*Scnn1a* null neonates develop respiratory distress and die within 40 h of birth from failure to clear their lungs of liquid. Autosomal recessive pseudohypoaldosteronism type I can be caused by *SCNN1A* mutations.
	βENaC	n/o	n/o	n/o	n/o	*Scnn1b* (90,100,0)	*SCNN1B*	Targeted *Scnn1b* mutant mice are hyperkalemic and exhibit neonatal death associated with a pseudohypoaldosteronism phenotype. Both autosomal recessive pseudohypoaldosteronism type I and Liddle syndrome can be caused by *SCNN1B* mutations.
	γENaC	n/o	n/o	n/o	n/o	*Scnn1g* (91,100,0)	*SCNN1G*	Both autosomal recessive pseudohypoaldosteronism type I and Liddle syndrome can be caused by *SCNN1G* mutations.
	δENaC	n/o	n/o	n/o	n/o	n/o	*SCNN1D*	

(*Continued*)

Table 1 (Continued)

Superfamily		*Ortholog*						
Family	***Gene***	***Ce***	***Dm***	***Ci***	***Dr***	***Mm***	***Hs***	***Function in mammals***
Accn	BNaC1	n/o	n/o	*ENSCINT005064* (44,72,4)	*accn1* (79,91,4)	*Accn1* (99,89,0)	*ACCN1*	Targeted *Accn1* null mutation have an increase in the rod electroretinogram α- and β-waves and thus show enhanced gain of visual transduction. These mice are also more sensitive to light-induced retinal degeneration
	BNaC2	n/o	n/o	n/o	*accn2a* (71,99,12) *accn2b* (74,94,9) *accn2c* (76,93,9)	*Accn2* (90,100,8)	*ACCN2*	*Accn2* null mice have reduced excitatory postsynaptic potentials and NMDA receptor activation during high-frequency stimulation. Consistent with these findings, null mice displayed defective spatial learning and eye blink conditioning
	Asic3	n/o	n/o	*ENSCINT013693* (59,91,7)	n/o	*Accn3* (91,42[a],0)	*ACCN3*	*Accn3* null mice show an increased sensitivity of mechanoreceptors detecting light touch, but reduced sensitivity of a mechanoreceptor responding to noxious pinch and decreased response to acid- and noxious heat-sensitive nociceptors
	Asic4	n/o	n/o	n/o	*accn4a* (72,84,6) *accn4b* (71,78,5)	*Accn4* (98,83,0)	*ACCN4*	
	Blinac	n/o	n/o	*ENSCINT025885* (55,77,4) *ENSCINT000995* (49,86,3) *ENSCINT027392* (50,39,8)	n/o	*Accn5* (89,98,0)	*ACCN5*	

[a]The scoring matrix for BLASTP alignment of human TRP and DEG/ENaC proteins in comparisons with the orthologs from mouse, zebrafish, sea squirt, fly, and worm. The three numbers represent the percent homology of positive amino acid, the percent length of homologous peptide fragment per total length of the human peptide sequence, and the percent of sequence gaps within the region of homology.

[b]Comparisons were done between the Dm nan and the nompC proteins and their respective orthologs.

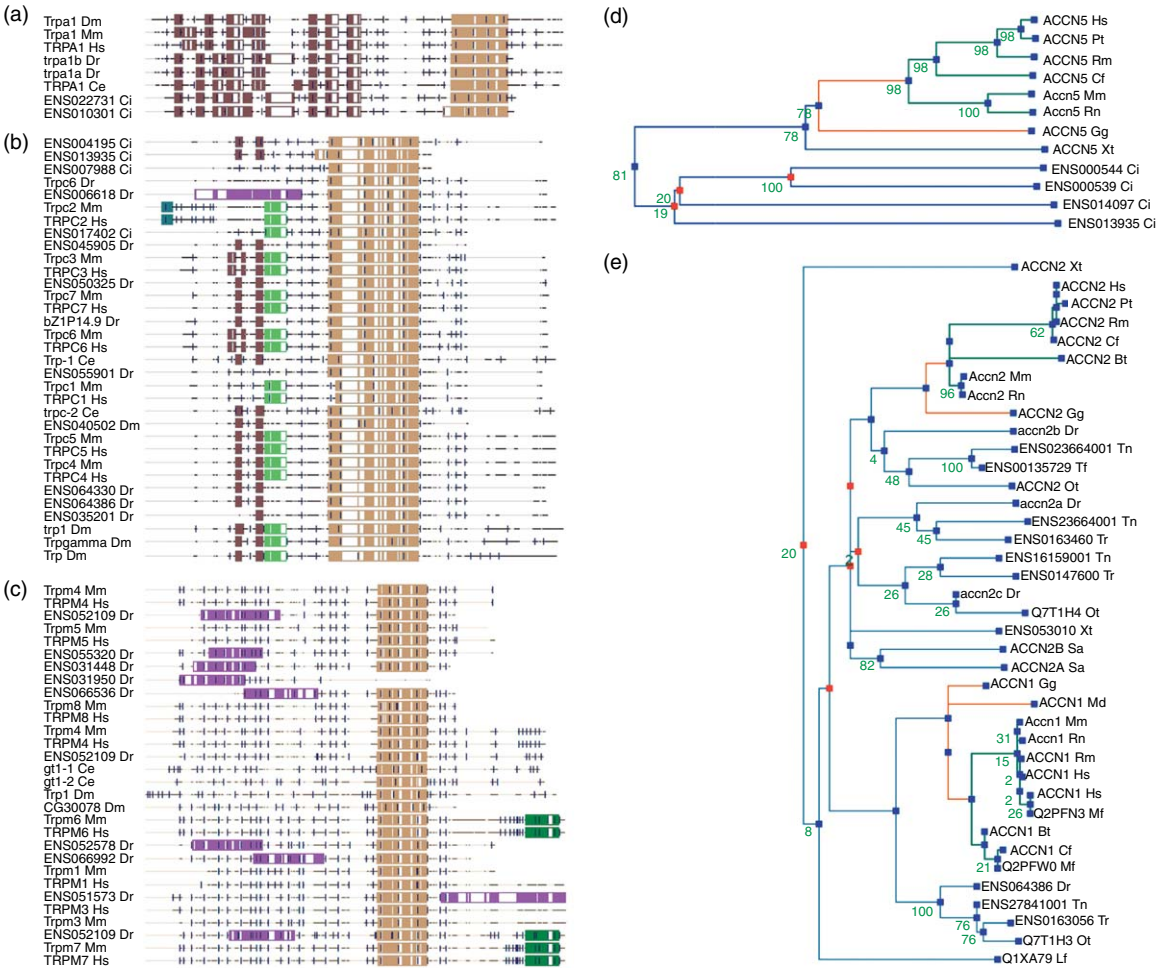

Figure 3 Similarities in channel proteins. The structural motifs of the orthologs and paralogs of the TRPA (a), TRPC (b), and TRPM (c) subfamilies are represented. Boxes correspond to protein family (Pfam) domains, while lines correspond to nondomain regions. Dark lines or boxes show matched parts, while light ones indicate homology gaps. Vertical dark-blue lines indicate splicing boundaries. The structural motifs represented are ion channel (■ – PF00520), transient receptor ion channel II (■ – PF08344), ankyrin repeat (■ – PF00023), IMP dehydrogenase/GMP reductase domain (■ – PF00478), α-kinase family domain (■ – PF02816), and XRCC1 N-terminal domain (■ – PF01834). A protein family tree is presented for the Accn5 (d) and Accn1/2 (e) orthologs where the full sequences were expanded from the seed through BLAST-HMMer pipeline and the full tree was reconstructed by constrained neighbor joining. The score in the TreeFam gene page is bootstrapping support rescaled around 100, where the higher the value the greater the homology. It measures how often the same ortholog (or within species paralog) pair can be inferred from a resampled tree.

N- and C-termini are still poorly understood. This general channel motif is similar to that associated with the family of voltage-gated potassium channels, except the S4 (TM4) membrane-spanning region does not contain positively charged amino acid R groups. Based on peptide sequence homologies and functional properties, these channels are grouped into seven subfamilies. The group 1 TRPs are the TRPC (canonical or classical), TRPV (vanilloid), TRPM (melastatin), TRPA (ankyrin), and TRPN (NOMP) channels and comprise closely related TRP subfamilies. Members of the group 2 TRP subfamilies, TRPML (mucolipin) and TRPP (polycystin), are distantly related to the group 1 TRPs. Each of these TRP subfamilies is represented by members in nematodes, flies and mice and provides the potential for using genetic approaches to characterize the normal functions and activation mechanisms of these channels.

In mammals the TRPC subfamily contains seven members that are all permeable for Ca^{2+} and are generally thought to mediate store-operated Ca^{2+}

entry (Montell, C., 2005). The selectivity P_{Ca}/P_{Na} ratio ranges from 1 for TRPC1 to 9 for the TRPC5 channels, and the conductance of the homomeric channels is 16 pS for TRPC1, 28–42 pS for TRPC2, TRPC4, and TRPC6, and ~65 pS for TRPC3 and TRPC5 (Nilius, B. *et al.*, 2005). It is suggested that these channels can also be activated by phospholipase C (PLC)-dependent pathways, but the precise mechanism of PLC stimulation still remains controversial. In addition, three channels, TRPC3, TRPC6, and TRPC7, appear to be activated by production of diacylglycerol in a manner that is independent of protein kinase C activity or regulated through an exocytotic mechanism (Trebak, M. *et al.*, 2003). These three subunits are homologous and do form heteromeric channels when expressed in human embryonic kidney (HEK) cells. Because of the functional redundancy of TRPC3/6/7, it may be necessary to generate double or triple nulls to examine their *in vivo* function. To date, only a *Trpc6*-null mouse line exists, and studies suggest that *Trpc3* expression increases as a compensatory mechanism (Dietrich, A. *et al.*, 2005). A nonredundant function for TRPC6 was identified in its role in controlling vascular smooth muscle tone. Missense mutations in the human *TRPC6* gene lead to a dominant form of focal segmental glomerulosclerosis (FSGS2) (Reiser, J. *et al.*, 2005; Winn, M. P. *et al.*, 2005) and cause a defective permeability barrier in the kidney, leading to renal failure. This pathology corresponds with TRPC6 being a component of the glomerular slit diaphragm associated with kidney podocytes.

Other functionally distinct heteromeric channels are formed by the closely related TRPC1, TRPC4, and TRPC5 subunits (Strubing, C. *et al.*, 2003). These genes are coexpressed in hippocampal neurons, but these paralogs are differentially expressed in most other tissues and cells (Freichel, M. *et al.*, 2004). *In vitro* expression studies have found that TRPC1 channels display an Msc-like membrane stretch activation, but whether or not the native TRPC1 channels exhibit this property still needs to be resolved. A TRPC1-null mutant mouse line that would permit testing this possibility has yet to be reported. Although TRPC1/4/5 subunits may compensate for each other, *Trpc4*-deficient mice exhibit loss of a store-operated Ca^{2+} current in vascular endothelial cells and an associated reduction in vasorelaxation capacity (Freichel, M. *et al.*, 2001; 2004). Unlike the other TRPC members, the TRPC2 has a highly restricted expression in neurons of the vomeronasal organ and in testis. Two independently derived knockout *Trpc2* mice found defective diacylglycerol-gated (DAG)-activated cation ion currents, a loss of sex discrimination among males and females, and male–male aggression (Leypold, B. G. *et al.*, 2002; Stowers, L. *et al.*, 2002).

The members of a second subfamily (TRPV) can be grouped into four highly related groups, which are TRPV1/2, TRPV3, TRPV4, and TRPV5/6. This TRP subfamily primarily functions in sensory physiology and responds to heat, changes in osmolarity, odorants, and mechanical stimuli. TRPV members 1–4 have a modest permeability for Ca^{2+} with a permeability P_{Ca}/P_{Na} ratio of ~1–10 whereas TRPV5 and TRPV6 are the only highly selective channels for Ca^{2+} ($P_{Ca}/P_{Na} > 100$) of all the TRP members (Clapham, D. E., 2003). The conductances of these homomeric channels are 35–90 pS for members 1, 4, –6, 190 pS for TRPV3, and TRPV2 has yet to be reported. Heat-activated TRP channels are primarily associated with TRPV1–4 and TRPM5 subunits and comprise one group of thermosensory channels (Nilius, B. *et al.*, 2005). The second group is the cold-activated TRP channels with TRPA1 and TRPM8. The range of temperatures (<10 to >50 °C) represented by these TRP channels corresponds with the physiological range of temperatures discriminated by humans. These channels are present not only in peripheral neurons and sensory fibers but also in the skin, with TRPV3 and TRPV4 primarily localizing to keratinocytes (Chung, M. K. *et al.*, 2003; Moqrich, A. *et al.*, 2005). Temperature sensitivity was verified in *Trpv1*-null mutants, where the mice are unable to respond to moderate heat (~43 °C), capsaicin, and lowering of pH (Caterina, M. J. *et al.*, 2000; Davis, J. B. *et al.*, 2000). TRPV1 also functions as a stretch receptor in bladder epithelial and urothelial cells with diminished responses to stretch and hyposmolal conditions in *Trpv1*-deficient mice (Birder, L. A. *et al.*, 2002). The TRPV2 and TRPV3 channels contrast with TRVP1 by their insensitivity to capsaicin and wider tissue distribution. TRPV3 is activated by temperatures ranging from 32 to 40 °C, which was confirmed in null mice (Moqrich, A. *et al.*, 2005). In comparison, TRPV2 channels respond to temperatures >52 °C and are associated predominantly with nociception. These data still need to be confirmed in *Trpv2* genetically altered mice. A rather surprising diversity of mechanosensory and nociceptive stimuli can activate TRPV4, which was confirmed in two independently produced null mutant lines (Liedtke, W. and Friedman, J. M., 2003; Suzuki, M. *et al.*, 2003). Interestingly, these mice also lose their hypotonicity responses and avoidance of

noxious odorants, which is similar to the worm mutants of osm-9 (Liedtke, W. *et al.*, 2003). Although there is functional homology between these two channels, a similar homology between their proteins is not apparent. Because of the high Ca^{2+} permeability of the TRPV5 and TRPV6 channels, these two paralogs are essential for Ca^{2+} homeostasis, with TRPV5 being essential for reabsorption in bone and TRVP6 found in the intestine. These two subunits can form heteromultimers. This has resulted in compensation by TRPV6 in *Trpv5*-deficient mice and has produced a milder bone phenotype with only a reduced bone thickness (Hoenderop, J. G. *et al.*, 2003). However, investigation of compensatory mechanisms between TRPV5 and TRPV6 still awaits the production of a *Trpv6*-null mouse line.

The TRPM subfamily members represent a functionally diverse set of channels. All the homomeric channels have a P_{Ca}/P_{Na} selectivity of 0.5–3 and conductances within the 40–130 pS range, except for TRPM4 and TRPM5, which have no cation selectivity and a conductance of 16–25 pS (Nilius, B. *et al.*, 2005). TRPM1 was the first channel identified and was initially named melastatin for its expression in highly metastatic melanoma cell lines. Further characterization of this channel is currently hindered by the difficulty of recording TRPM1 currents and the lack of identification of mutated forms of this gene in both humans and mice. The functional assessment of TRPM3 suggests that the channel current is nonselective, constitutively active and responsive to hypotonic stimuli with possible store-operated Ca^{2+} entry properties (Kraft, R. and Harteneck, C., 2005). TRPM3 is expressed in the kidney and nervous system. Like TRPM1, no mutant TRPM3 genes are presently known. The TRMP4 and TRMP5 channels are similar in being impermeable to Ca^{2+}, form ion channels permeable to monovalent cations, and are candidates for endogenous calcium-activated cation channels (Nilius, B. *et al.*, 2005). However, they are functionally very different. TRMP4 appears to be involved in negative-feedback regulation and release of interleukin 2 from T lymphocytes (Launay, P. *et al.*, 2004). In contrast, TRPM5 is highly expressed in taste receptors cells and, as demonstrated in *Trpm5*$^{-/-}$ mice, is essential for detection of sweet, bitter, and umami taste stimuli (Zhang, Y. *et al.*, 2003).

Besides TRPM5, the only TRPM member conveying sensory sensation is the TRPM8 channel, a thermosensory channel that is activated by temperatures <25 °C or cooling compounds such as menthol and icilin (Peier, A. M. *et al.*, 2002; Reid, G., 2005). Three TRPM proteins, TRPM2, TRPM6, and TRPM7, are classified as chanzymes, since these subunits contain a C-terminal α-kinase enzyme domain. TRPM2 is unique in possessing ADP-ribose hydrolase activity and appears to function as a sensor for cellular redox status by playing a role in responses to oxidative and nitrosative stresses (Perraud, A. L. *et al.*, 2005). Both TRPM6 and TRPM7 are similar, being involved in Mg^{2+} homeostasis, with TRPM7 playing an additional role in neuronal cell death (Levitan, I. B. and Cibulsky, S. M., 2001; Aarts, M. *et al.*, 2003). TRPM6 is predominantly expressed in the kidney and the gastrointestinal system, whereas TRPM7 is ubiquitously expressed. Null mutant mice are still needed to validate and extend functions of these three chanzymes.

The fourth and fifth subfamilies, TRPA and TRPN, include proteins with many ankyrin repeats. TRPN proteins function in mechanotransduction, whereas TRPA1 is also activated by noxious cold (Walker, R. G. *et al.*, 2000; Bautista, D. M. *et al.*, 2006; Kwan, K. Y. *et al.*, 2006; Li, W. *et al.*, 2006). The TRPA subfamily has only one member, *TRPA1*, and this gene is highly conserved and present in all species examined. The cytoplasmic N-termini of the TRPA1 orthologs contained 14–15 ankyrin domains. TRPA1 channels have a P_{Ca}/P_{Na} selectivity of 0.8–1.4 and a conductance of 40–105 pS and are expressed in sensory neurons and inner ear hair cells (Story, G. M. *et al.*, 2003; Corey, D. P. *et al.*, 2004; Nagata, K. *et al.*, 2005). Two independently derived null mutant mouse lines established that TRPA1 channels are activated by noxious cold and pungent substances, but the proposed role as the hair cell mechanically gated transduction channel was not validated (Bautista, D. M. *et al.*, 2006; Kwan, K. Y. *et al.*, 2006). The TRPN subfamily contains a single member that is unique from the other TRPs with the presence of 29 ankyrin motifs in the cytoplasmic amino tail (Walker, R. G. *et al.*, 2000). In mammals, the TRPN1 ortholog gene appears to be deleted from the genome. TRPN1 orthologs are present in the ciliated neurons of Ce and Dm, Dr, and in Xenopus hair cells (Walker, R. G. *et al.*, 2000; Sidi, S. *et al.*, 2003; Shin, J. B. *et al.*, 2005). In addition, frog TRPN1 channels were also localized to microtubule-based cilia in epithelial cells. Loss-of-function mutants resulted in the absence of mechanotransduction in the ciliated sensory neurons of worms and sensory bristles of flies (Walker, R. G. *et al.*, 2000). Morpholino-mediated removal of TRPN1 in

zebrafish eliminated transduction-dependent electrical responses in HCs (Sidi, S. *et al.*, 2003). Comparative genomics identify a single TRPN1-like gene in Ci.

The group 2 TRP subfamilies are responsible for human mucolipidosis type IV (MCOLN1) and polycystic kidney (PKD1 and PDK2) diseases. The three mammalian members, MCOLN1–3, of the TRPML subfamily have similar structural motifs, with a lipase domain between TM1 and TM2, a nuclear localization signal, and a putative late endosomal–lysosomal targeting signal. Functional assessment of these channels has been reported only for MCOLN1 channels, where the P_{Ca}/P_{Na} selectivity is ~1 and conductance is 46–83 pS. Mutations in the *MCOLN1* gene causing mucolipidosis type IV are primarily nonsense and deletions and result in premature termination of the protein. Missense mutations are also described and occur in the cation ion domain or prevent MCOLN1 channels to localize to late endosomes. Mouse mutants of *Mcoln1* and *Mcoln2* genes have yet to be reported. Interestingly, two spontaneous mutations in the varitint-waddler mouse *Mcoln3* gene cause deafness with pigmentation defects (Di Palma, F. *et al.*, 2002). MCOLN3 channels were found in the cytoplasmic compartments of hair cells and plasma membrane of stereocilia. Although correlation of pigmentation defects and deafness is observed in humans, the direct relationship between hearing and regulation of pigmentation is fully resolved in each case. Replication of the TRPML gene apparently occurred in vertebrates with only one ortholog found in the nonvertebrate species.

Four mammalian paralogs were identified in the TRPP subfamily with the homology among orthologs and paralogs appearing to reside primarily in polycistin domains (Delmas, P., 2005). Channel P_{Ca}/P_{Na} selectivity for the TRPP channels ranges from 1 to 5 and conductances of 44–300 pS. Although the polycystin domain is present in a number of genes, only the PKD1, PKD2, PKD2L1, and PKD2L2 orthologs have a cation ion channel domain. Null mutations in the mouse *Pkd1* and *Pdk2* genes have polycystic kidney disease and die *in utero* (Morsli, H. *et al.*, 1998; Boulter, C. *et al.*, 2001). Autosomal dominant polycystic kidney disease in man is caused by *PKD1* and *PKD2* mutations in genes, with majority of these mutations involving frame shift or nonsense mutations that lead to a premature termination of the proteins (Al-Bhalal, L. and Akhtar, M., 2005). Both these paralogs are ubiquitously expressed whereas the tissue distribution of PKD2L1 and PKD2L2 is more restricted, with PKD2L2 being highly expressed in the testis. PKD2L1 was found to form functional channels when expressed with PKD1 in a heterologous expression system. Interestingly, heteromeric channels composed of subunits of PKD2L1 and PKD1L3, which lacks the cationic ion channel domain, are candidates for sour taste receptors (Ishimaru, Y. *et al.*, 2006; LopezJimenez, N. D. *et al.*, 2006). Mutations in the *PDK2L1* and *PKD2L2* genes have yet to be identified to facilitate their characterization.

Representative members of each family are present in Mm and *H. sapiens* (Hs), with both sharing common orthologs with a high homology for all the members of the TRP superfamily. In comparison, Dr TRP subfamilies are similar to those of the mammal with the exception of a single member in the Dr TRPV subfamily and the presence of a TRPN gene, for which a suitable ortholog for mammals has yet to be identified. The superfamily representations in Ce, Dm, and Ci are very similar, although there are variations in both number of members and orthologs. It appears that expansion of the TRP superfamily occurred in vertebrates, accompanied by utilization in a wide variety of biological functions. Only two TRP members, TRPA1 and the TRPM MCOLN1, appear to be highly conserved across species.

Figures 3(a)–3(c) depicts the variation in structural motifs represented by members of the TRPA, TRPC, and TRPM subfamilies. Even within the conserved ion channel motif, there is significant variation among the members within a subfamily and between orthologs. This diversity is also reflected in the composition of additional structural motifs, such as the ankyrin repeat, transient receptor ion channel II, IMP dehydrogenase/GMP reductase, α-kinase, and XRCC1 N-terminal domains, within the TRPC, TRPA, and TRPN subfamily members. The number of ankryin repeat domains is increased in number from 3 to 4 in the TRPC genes, 14 to 15 in TRPA1, to ~29 for the TRPN orthologs. Use of the IMP dehyrogenase/GMP reductase domain appears to be a unique adaptation in the *Drosophila*, whereas the XRCC1 N-terminal domain is only present in the mammalian TRPC2 orthologs.

Further functional diversity can also be generated by formation of homo- and heterotetrameric channels, with homomeric channels usually being favored (reviewed in Schaefer, M., 2005). The configurational mechanisms, affinity among the subfamily members, and possible

heteromeric assembly between the subfamily members are currently being systematically studied.

3.05.2.1.2 The degenerin/epithelial sodium channels superfamily

In comparison to diversity observed in the TRP superfamily members, the members of DEG/ENaC family are more conserved in that they contain only an amiloride-sensitive cation (asc) channel motif (reviewed by Kellenberger, S. and Schild, L., 2002). This motif contains two TM regions with an intercalated pore domain. This domain is similar to that of the inward rectifier and twin-pore potassium ion channel subunits. However, this is where the conservation ends, since phylogenetic and sequence comparison demonstrate that the DEG/ENaC family has little to no sequence conservation among the nonmammalian species (see Tree families database). In Ce, there appear to be two conserved but distinct groups of ascNaC. Group 1 includes the original mechanosensitive sodium channel genes, *mec-4* and *mec-10* (Goodman, M. B. and Schwarz, E. M., 2003). In *Drosophila*, the ascNaC family is represented by an expansion of the pickpocket genes (Sukharev, S. and Corey, D. P., 2004). Orthologs of these genes are not found in the other species examined.

The ACCN subfamily of ascNaC genes is represented in Ce, Dr, Mm, and Hs. This family of channel subunits appears in the deuterostome invertebrates and five members exist in mammals. As depicted in Figure 3, the members of the ACCN5 subfamily are highly conserved across species, including the sea squirt, but surprisingly are absent in the zebrafish. Similar to the ascNaC in worms and flies, each of the ACCN subfamilies is distinct with little homology among the subfamilies. The ENaC or SCCN subfamily consists of three to four members. There is a high degree of similarity among both the orthologs and the paralogs of this subfamily. The prevailing model suggests that ascNaC are composed of four subunits, with both homo- and heterotetrameric configurations being formed. Mutational and biochemical data suggest that the ENaC SCNN1A, B, and G subunits form a functional channel as indicated by patients with pseudohypoaldosteronism type I and Liddle syndrome with mutations in any of these genes. Systematic efforts to examine heteromeric assembly between subfamily members of the TRP channels are under way (Sukharev, S. and Corey, D. P., 2004); similar studies of the DEG/ENaC superfamily interaction need to be pursued. The most extensive studies of DEG/ENaC channel interactions with other proteins are available for the *mec-4/10* ascNaC channel associated with touch sensation in the worm (Goodman, M. B. and Schwarz, E. M., 2003).

In summary, the current data on TRP and DEG/ENaC channels suggest that each superfamily shares some transmembrane motifs across taxa, evolved in fungi and possibly early metazoan ancestors, respectively, and plays roles in sensing of several stimuli through altering, in an as yet poorly known way, their pore properties. Sequence similarities suggest evolution of distinct units in several lines, with only closely associated taxa such as vertebrates showing high level of similarities. Only few units are conserved across metazoans, suggesting that involvement in mechanosensation does not massively constrain their sequences.

3.05.2.2 Ancestry of Specialized Mechanosensory Cells

Mechanosensation has been claimed to be the basis of gravity sensing in single-cell organisms to avoid sinking to the bottom (gravikinesis) (Syntichaki, P. and Tavernarakis, N., 2004) and likely precedes the evolution of multicellular organisms. Given the likely molecular ancestry of eukaryotic mechanosensory channels, it is not surprising that mechanosensation has been claimed for virtually all multicellular (metazoa) organisms. Despite this generally agreed-upon molecular ancestry, there are problems in establishing cellular identity because of anatomical differences between functionally comparable mechanosensory organs – such as acoustic organs – across phyla. Certainly, not all the various members of the two main families of mechanosensory channel candidate genes have been mutated to assess their function, and some mutations turned out to be early lethal, precluding thereby their functional evaluation. In addition, even when candidate molecules were identified through lack of function in mutants, direct test of function proved extremely difficult, as both the channel and the tether to extra- and intracellular structures (to provide the necessary gating tension and improved sensitivity) have to be molecularly defined and reconstituted in a heterologous system. Moreover, it is possible that a channel is composed of multiple units that may allow functional substitution of a single lost unit by others, thus rendering the past approach problematic at best and unsuccessful at worst. To date, not a single tethered mechanosensory channel candidate has passed this most stringent of all tests. All current

data on the putative function of tethered mechanosensory channel candidates rely on loss of function or correlative evidence, and must therefore be viewed as tentative. In this respect, the nematode mechanosensory channel is perhaps the best defined (O'Hagan, R. *et al.*, 2005). Recent success in identifying the TRPC1 stretch-activated channel through protein purification and characterization in a heterologous expression system indicates that possibly other Msc can be identified through such approaches (Maroto, R. *et al.*, 2005). Likewise, comparative mutagenic analysis of gating properties of DEG/ENaC channels demonstrated the power of a combined approach to specify functionally relevant parts for proton sensitivity of this channel (Coric, T. *et al.*, 2005).

Nevertheless, loss of function through mutational analysis was essential to identify several candidate genes in various animals, which are difficult to reconcile with each other in terms of conservation of structure and function (see TRP and DEG/ENaC genes of *C. elegans*, *D. melanogaster*, *C. intestinalis*, *Danio rerio*, *Mus musculus*, and *Homo sapiens* Compared: Sequence Data Indicate Candidate Genes that Need to be Investigated). With this caveat in mind, it appears as of this writing that, at a molecular level, different channels belonging to either the DEG/ENaC/BNaC or the TRP families have been incorporated into highly sensitive mechanoreceptors, indicating that the morphology of mechanosensory cells and organs may be intricately interwoven with molecularly and functionally distinct channels and tethers.

3.05.2.2.1 Known or suspected mechanosensory cells of multicellular animals

As with the mechanosensory channels, two ideas prevail for mechanosensory cell and organ evolution. The structural dissimilarities between them has been interpreted as either (1) an indication of independent evolution (Coffin, A. *et al.*, 2004; Holland, L. Z., 2005) at the cell and organ level or (2) a variation on a common theme at a cellular level accompanied by independent arrangement at the organ level (Jorgensen, J. M., 1989; Fritzsch, B. *et al.*, 2006a). For this review we will focus on known or suspected mechanosensory cells that show potential extracellular tethering with possibly molecularly dissimilar compounds. While such tethered channels may already play a role in single-cell organisms, we will not explore this possibility here.

Recent molecular evidence has clarified that choanoflagellates are the unicellular ancestor of all multicellular animals (King, N. and Carroll, S. B., 2001; Lavrov, D. V. *et al.*, 2005; Rokas, A. *et al.*, 2005; Steenkamp, E. T. *et al.*, 2006). These unicellular organisms have a single beating kinocilium with $9+2$ microtubules, surrounded by microvilli that are interconnected by filaments in several species. Choanoflagellates use the beating kinocilium to drive water through the mesh formed by the interconnected microvilli to catch microbes for consumption (King, N., 2005). In addition, choanoflagellates can secrete a mineralizing extracellular matrix in which the cell is embedded, much like a snail in its shell. It is conceivable that tethered channels exist either at the base of tethers between the extracellular matrix and the cell or at the base of the tethers that interconnect the microvilli. Also, intracellular tethers could exist in members of the myosin family, such as MyoVII. Indeed, these myosins have already been suggested to anchor mechanosensory channels to the cytoskeleton in slime molds (Eichinger, L. *et al.*, 2005) and clearly predate the evolution of multicellular organisms and specialized mechanosensory cells. Barring more detailed genomic analysis, mechanosensory channel proteins related to TRPs, as well as unrelated mechanosensory channels, exist in single-celled eukaryotic organisms such as yeast and slime molds (Eichinger, L. *et al.*, 2005; Kung, C., 2005). Thus TRP channels had to be present in the unicellular ancestors of metazoans (Figure 2). Some of the molecules also thought to play a role in tethering in mammals, such as cadherins (Gillespie, P. G. *et al.*, 2005; Senften, M. *et al.*, 2006), exist in those unicellular eukaryotes. It is possible that the entire channel/tether assembly is conserved across unicellular ancestors of metazoans. More molecular analysis of unicellular organisms is needed to fully understand the molecular basis of mechanosensation.

Various epidermal sensory cells exist in diploblastic and triploblastic metazoan organisms, and in some taxa they are grouped into organs suspected or known to be mechanosensory (Figure 4). For example, coelenterates (jellyfish and corals) have gravistatic sensors composed of more or less polarized microvilli bundles surrounding a single, immobile kinocilium (Arkett, S. A. *et al.*, 1988). Spiders have complex, lyriform slit organs with which they can detect minute vibrations elicited by prey captured in their webs (French, A. S. *et al.*, 2002; Hossl, B. *et al.*, 2006). The mechanotransducing elements are amiloride-sensitive (French, A. S. *et al.*,

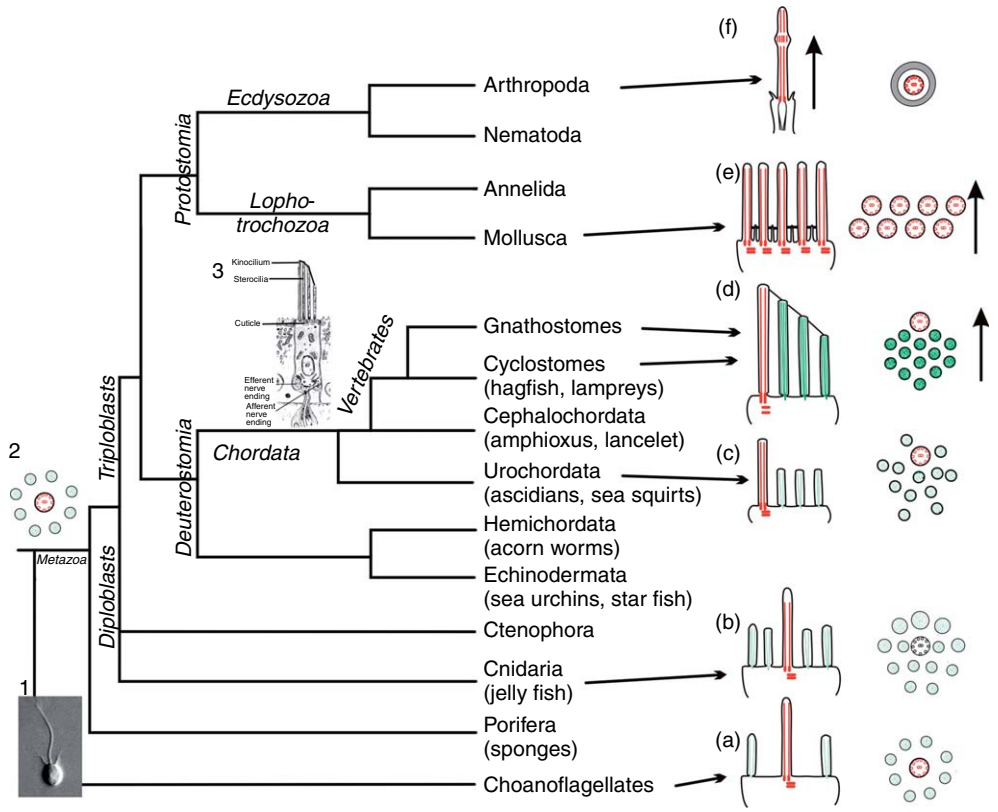

Figure 4 Kinocilia (red) and microvilli (light blue) of known or suspected mechanosensory cells in various eukaryotic unicellular and multicellular organisms are shown. Note that the single-celled ancestor of all multicellular animals, the choanoflagellates, has a single, actively beating kinocilium surrounded by microvilli that carry an actin core (a). In some diploblasts, the central kinocilium is surrounded by an asymmetric assembly of microvilli of various diameters, potentially providing directional sensitivity (b). Among deuterostomes, urochordates have various presumed mechanosensory cells that have a kinocilium with asymmetrically arranged microvilli (c). Vertebrates are unique in that a highly polarized, organ-pipe assembly of actin-rich stereocilia is attached via tip links with each other and the asymmetrically placed kinocilium (d). Among protostomes, mollusks may have numerous, interconnected kinocilia on mechanosensory cells (e). Ecdysozoans have either mechanosensory cells with cilia or a kinocilium that is stretched by the stimulus (f). Arrows indicate the direction of stimulation. Adapted from Fritzsch, B., Pauley, S., Feng, F., Matei, V., and Nichols, D. H. 2006b. The evolution of the vertebrate auditory system: transformations of vestibular mechanosensory cells for sound processing is combined with newly generated central processing neurons. Int. J. Comp. Psychol. 19, 1–24.

2002) and resemble in that respect mechanotransduction in many other taxa (Syntichaki, P. and Tavernarakis, N., 2004). Mollusks have statocysts, which have evolved into complex angular and linear perception detection organs that in cuttlefish rival the ears of vertebrates in their sensitivity (Budelmann, B. U., 1987). Cuttlefish also have hydrodynamic receptors that resemble the vertebrate lateral line (Budelmann, B. U. and Bleckmann, H., 1988; Budelmann, B. U. and Williamson, R., 1994). However, in contrast to vertebrates, the single sensory or neurosensory cells have apical specializations consisting of multiple kinocilia that are interconnected with each other near the base, possibly to activate tethered mechanosensory channels of unknown molecular composition. In multicellular organisms, there are many more examples of organizations that seem likely to provide an asymmetric mechanical input to tethered mechanosensory channels (Burighel, P. *et al.*, 2003; Mackie, G. O. and Singla, C. L., 2004; Fritzsch, B. *et al.*, 2006a).

Based on obvious cellular adaptations, it was proposed to distinguish between ciliated and nonciliated mechanosensory cells and some correlation between TRP and ciliated cells was noticed (Eberl, D. F. *et al.*, 2000; Goodman, M. B. *et al.*, 2004). Recent data suggest that mechanosensitive TRP channels exist in nematodes on ciliated and nonciliated cells (Li, W. *et al.*, 2006). Other variations of apical specializations can also be used to generate a different grouping. Most putative and known invertebrate mechanosensory

cells seem to be a variation of one basic organization, a kinocilium surrounded by microvilli (Jorgensen, J. M., 1989; Fritzsch, B. *et al.*, 2006b). Notable exceptions are the mollusks and the ecdysozoa (insects, nematodes, spiders, and crustaceans; Figure 4). In contrast to other multicellular organisms, ecdysozoans have an exoskeleton that leaves only limited openings for gas, water, and food exchange. It is possible that the evolution of this exoskeleton forced a radical reorganization of the mechanotransducer system: instead of variations on the theme of kinocilium and microvilli, these organisms have sensors with connections to the extracellular matrix that generate a force along a process rather than between different processes (Figure 4). Nevertheless, common features exist, such as the use of a kinocilium or special intracellular and extracellular tethering molecules, indicating that even these highly divergent forms may present derivations from the common theme of ancestral mechanosensory transduction (Figure 4). Tetrapod vertebrates, and in particular mammals, have also evolved mechanosensory transducers of various cellular compositions, such as Pacini and Meissner corpuscles, Merkel cells, and muscle spindles. In all these cases, the molecular basis for mechanosensation begins to emerge (Sukharev, S. and Corey, D. P., 2004), but a meaningful comparison with the evolutionarily ancestral mechanosensory cell, the vertebrate hair cell, is not possible in the absence of detailed information on the Msc in the latter cells. In summary, it appears that a distinction between ecdysozoans and nonecdysozoans can be made with respect to modifications of an ancestral kinocilum/microvilli specialization or with respect to a radical departure thereof.

Unfortunately, the genomes of only a few animals have been sequenced thus far, or the existing genome has not yet been fully annotated, and therefore the molecular composition of neither the mechanosensory channel nor the tethers can be assessed. Most of these organisms are unlikely to be used for genetic analyses comparable to those performed in the nematode (Ernstrom, G. G. and Chalfie, M., 2002; Goodman, M. B. and Schwarz, E. M., 2003), the fly (Kernan, M. *et al.*, 1994), the zebrafish (Sidi, S. *et al.*, 2003; Nicolson, T., 2005), or the mouse (Bryant, J. E. *et al.*, 2005; Gillespie, P. G. *et al.*, 2005). We will therefore limit our analysis to these four organisms (*C. elegans, D. melanogaster, D. reiro, M. musculus*) in which the putative mechanosensory elements have been molecularly identified and loss-of-function evidence exists for mechanosensory function.

3.05.2.2.2 Mechanosensory cells in Caenorhabditis elegans: connecting degenerin/epithelial sodium channels channels to the cuticle?

In *C. elegans*, numerous experiments have identified the cells, their structure, their development, and the mechanosensory channels that mediate fine touch such as elicited by a hair (Ernstrom, G. G. and Chalfie, M., 2002; Goodman, M. B. and Schwarz, E. M., 2003; Syntichaki, P. and Tavernarakis, N., 2004; Tobin, D. M. and Bargmann, C. I., 2004). Specifically, there are two pairs of anterior and posterior neurons and two ventral neurons that provide a total of six neurons that respond to light touch. In addition, these animals have two ciliated neurons that respond to light touch to the anterior pole, but these cells are polymodal nociceptors (Tobin, D. M. and Bargmann, C. I., 2004). If the six fine-touch mechanosensory neurons are ablated by lasers, the animals lose their ability to respond to mechanical stimuli along the body but are not otherwise negatively affected. The dendritic processes of all six cells run below and are interconnected to the extracellular matrix and the cuticle. Among neurons, these processes are uniquely characterized by unusual microtubules consisting of 15-protofilament microtubules (instead of the usual 13) that may provide a rigid internal core for mechanosensation. Eliminating only those 15-protofilament microtubules in *mec*-7 mutants, while maintaining other microtubules, leads to normal differentiation of sensory neurons but generates a 17-fold smaller mechanoreceptor current (O'Hagan, R. *et al.*, 2005). This indicates that the heavily crosslinked 15-protofilament microtubules play some role in increasing mechanosensation as previously suggested (Ernstrom, G. G. and Chalfie, M., 2002; Goodman, M. B. *et al.*, 2002). However, recent data (Emtage, L. *et al.*, 2004) suggest that extracellular tethering alone may suffice for mechanotransduction, with the 15-protofilament tubules adding increased sensitivity, possibly by providing added stiffness. Direct measurements of stiffness of the dendrite with or without these specialized microtubules are needed to resolve this question.

Mutational analysis has identified a total of 15 *mec* genes (mechanosensory abnormal) that can, if mutated, eliminate or significantly reduce fine-touch mechanosensation. Specifically, *mec-4* and *mec-10*, each coding for two closely related DEG/ENaC proteins, are expressed in the light-touch neurons, and the MEC-4 protein colocalizes with MEC-4 and MEC-6 proteins (Emtage, L. *et al.*, 2004). Most importantly, in the *mec-4* or *mec-10* mutants the mechanosensory neurons can still

respond to harsh touch, supporting the hypothesis that these genes code for essential units of the mechanosensory channel that specifically mediate light touch. Expression analysis in oocytes has shown that the channel is likely composed of two different DEG/ENaC units (MEC-2 and MEC-10) and two accessory proteins encoded by MEC-4 and MEC-6 (Goodman, M. B. *et al.*, 2002). Additional mutations that cause loss of fine-touch sensitivity are mutations in extracellular matrix components, in microtubules, and in genes necessary for the differentiation of mechanosensory cells (a bHLH gene, *lin-32*; a POU domain gene, *unc-86*; a LIM domain gene, *mec-3*). Such defects are caused by disrupted development and only indirectly relate to mechanosensory function, a general problem of mutational analysis. More targeted genes and conditional mutational approaches are needed to overcome this problem.

Single-cell recording (O'Hagan, R. *et al.*, 2005) has shown that the MEC-4/10 ion channel responds to force faster than the fastest known second messenger cascade and thus are likely recordings from a directly gated mechanosensory channel, a crucial verification of the basic assumption underlying the field (Ernstrom, G. G. and Chalfie, M., 2002; Goodman, M. B. and Schwarz, E. M., 2003). The mechanoreceptor currents are carried by Na^+ and can be blocked by amiloride, consistent with a mechanically gated DEG/ENaC channel type. It has been estimated that a single channel may exist at each focal point where the extracellular matrix and the neurite interact. The number of channels may be identical to the number of contact points of the dendrite with the cuticle. Despite all this progress, crucial molecular details of the channel (how many MEC-4 and MEC-10 units are assembled) and interaction with matrix (details of attachment to which unit of the channel) or attachment to the intracellular matrix (if attached at all) are unknown.

There are some similarities between the *C. elegans* mechanosensors and nonciliated mechanosensors in other taxa (such as the lyriform slit organs of spiders (French, A. S. *et al.*, 2002), the frog muscle spindles, and the Pacinian corpuscles of mammals) that may indicate that all these receptor cells use DEG/ENaC channels for mechanotransduction (Goodman, M. B. and Schwarz, E. M., 2003; O'Hagan, R. *et al.*, 2005). Several DEG/ENaC vertebrate genes have been mutated without any apparent effect, suggesting that either other mechanosensory systems such as the hair cells of the ear or the lateral line organs do not use DEG/ENaC channels for mechanosensation. Alternatively, and since not all these channels have been systematically mutated in any given vertebrate (and some mutations are neonatal lethal), it is possible that partially functional or normally functioning channels will form even if one unit is missing. Some DEG/ENaC channels are found in free nerve endings but also in endings at Meissner corpuscles, Merkel cells, hair follicles, and baroreceptors (Drummond, H. A. *et al.*, 1998; Price, M. P. *et al.*, 2000; Garcia-Anoveros, J. *et al.*, 2001; Sukharev, S. and Corey, D. P., 2004). Clearly, more work is needed before this circumstantial evidence is solid enough to warrant speculations about a uniform involvement of DEG/ENaC channels in mechanosensation across phyla.

3.05.2.2.3 *Genetics of mechanotransduction in Drosophila melanogaster*: tethering a kinocilium to the cuticle

Many fly mutants have defects in mechanosensory potentials and are grouped into the *nomp* (no mechanoreceptor potential) or *remp* (reduced mechanoreceptor potential) categories (Kernan, M. *et al.*, 1994). Cloning has identified several candidate genes involved in mechanosensory transduction, three of which belong to the TRP gene family. One of these is the TRPN channel, *nompC*, which has orthologs in nematodes, sea squirts, and zebrafish but not in mammals. *nompC*-null flies lose about half of their chordotonal organ sensitivity, and NOMPC may play an exclusive role in bristle mechanotransduction (Walker, R. G. *et al.*, 2000), but not in chordotonal organs such as the fly hearing organ (Eberl, D. F. *et al.*, 2000). Evidence suggests that NOMPC might form heteromultimers, but such channels have not yet been directly demonstrated. NOMPC has been proposed to connect via 29 ankyrin repeats to the cytoskeleton, thereby aiding in mechanotransduction of bristles and chordotonal organs (Walker, R. G. *et al.*, 2000). Another gene, *nompA*, eliminates, if mutated, all mechanosensation in bristles and chordotonal organs (Eberl, D. F. *et al.*, 2000). It was shown that this comes about by disrupting contacts between sensory neurons and cuticular structures, thus likely interfering with tethering of the dendrite (Chung, Y. D. *et al.*, 2001). Based on the differences between neuron and cuticular attachment, it was recently proposed that the different phenotypes of the *nompC* null in chordotonal organs and bristles relates to the attachment and thus indirectly to *nompA* (Gong, Z. *et al.*, 2004). *nompA* has sequence similarities to zona pelucida proteins and the N-terminal (N) domains of plasminogen/hepatocyte growth factor

proteins. Such domains fulfill diverse biological functions by mediating protein–protein or protein–carbohydrate interactions.

Two TRPV channels were recently shown to be essential for hearing in flies, *nanchung* (*nan*) and *inactive* (*iav*, the protein of the gene CG4536). Based on the loss of hearing in either *nan* or *iav* mutants, it has been suggested that both *nan* and *iav* contribute to the same complex. Green fluorescent protein (GFP)-labeled IAV is found in the proximal part of the cilium, whereas NOMPA is in the dendritic cap (secreted by the scolopale cell), requiring that the force transmission to NAN and IAV either pass through the cilium, possibly through the ciliary membrane, or be transmitted through the scolopidial space (Gong, Z. *et al.*, 2004). More work is needed to verify which of these modes of force transmission applies and whether NAN and IAV are indeed the channel(s) or yet another essential link in the force transmission chain (Gopfert, M. C. *et al.*, 2006).

More recently, it was found that mutation of the unconventional myosin VIIa fly ortholog, *crinkled* (*ck*), results in disorganization of the cilium and disruption of the scolopidia, and renders flies deaf (Todi, S. V. *et al.*, 2005). This work demonstrates that *ck*/myoVIIA functions to organize the auditory organ, that is, it is functionally required in neuronal and support cells, but that it is not required for TRPV channel localization or for scolopidial-cell-junction integrity. Conditional mutations of MyoVIIa are needed to establish adult function of MyoVIIa beyond that obvious developmental function. Only conditional adult null flies could show whether *ck* is also involved in intracellular tethering, comparable to functions suggested for mammals (Gillespie, P. G. *et al.*, 2005; Senften, M. *et al.*, 2006).

Flies also have multiple members of the DEG/ENaC family. One member of that gene family, pickpocket (*ppk*), has been implicated in mechanotransduction in larvae (Ainsley, J. A. *et al.*, 2003), and their presumptive role in adult cuticular mechanotransduction has not been tested (Lumpkin, E. A. and Bautista, D. M. 2005). Clearly, more DEG/ENaC genes have to be mutated alone, or in combination, before their involvement in mechanotransduction can be verified. For flies and nematodes it appears that both TRP and DEG/ENaC channels are involved in mechanosensation without clear correlation of either channel with specific receptor configurations (Goodman, M. B. *et al.*, 2002; Goodman, M. B. *et al.*, 2004; Hilliard, M. A. *et al.*, 2005; Li, W. *et al.*, 2006).

3.05.3 Mechanosensory Cells in Vertebrates

All vertebrates have placodally derived hair cells that mediate mechanotransduction in the lateral line (if present) and the inner ear (Lewis, E. R. *et al.*, 1985). Hair cells have been claimed to be "probably the most elegant solution for stimulus delivery" (Sukharev, S. and Corey, D. P., 2004). Mechanotransduction requires deflection of stiff actin-rich microvilli (called stereocilia), connected by tip links, and thus opening mechanotransducing channels located at the tips of stereocilia (Lewis, E. R. *et al.*, 1985; Hudspeth, A. J., 1989). With respect to overall organization, a hair cell with stereocilia and the eccentrically positioned kinocilium can be interpreted as a transformation of the ancestral mechanosensory cell (Figure 4) found in other deuterostomes, coelenterates, and even some single-celled organisms (Jorgensen, J. M., 1989; Fritzsch, B. *et al.*, 2006a). During development, hair cells start with microvilli surrounding a central kinocilium that eventually moves into an eccentric position under the influence of cell-polarizing signals (Barald, K. F. and Kelley, M. W., 2004). At the end of the differentiation process, an organ pipe distribution of the stereocilia is established with the kinocilium, being eccentric on one side of the cell or being lost in mammalian cochlear hair cells (Bryant, J. E. *et al.*, 2005). Below, we will highlight some genes found to play roles in the development and structural maturation of the hair cell apex.

Placodes produce not only the ear and the lateral line but also essential components of all head sensory systems (Schlosser, G., 2005). The so-called dorsolateral set of placodes produces not only the hair cells and the sensory neurons of the ear and the lateral line system of organs but also the electroreceptive hair cells and sensory neurons of ampullary electroreceptors (Northcutt, R. G. *et al.*, 1995). Given the polymodal nature of putative mechanosensory channels, it is possible that the still-unknown electrosensory channel or channels in electroreceptors of ampullary and tuberous organs (Bullock, T. H. and Heiligenberg, W., 1986) might have evolved from a mechanically gated channel that has lost its tethers.

As already introduced above, terrestrial vertebrates have numerous free and specialized nerve endings that respond to stretch or shearing forces, such as Pacinian corpuscles, Ruffini endings, Merkel cells, and muscle spindles. Since these structures are clearly derived features of terrestrial vertebrates they

cannot illustrate the early evolution of mechanosensory cells and the appropriate mechanosensory hair cell channel in vertebrate ancestors. We therefore do not consider most of those cells and concentrate on only one additional mechanosensory cell of vertebrates, the Merkel cell.

Like hair cells, which are the ancestral mechanosensory cell of vertebrates based on outgroup comparisons with invertebrates (Figure 4), Merkel cells have numerous microvilli extending, however, between the ectodermal cells that surround them rather then into the endolymph of the inner ear or into water (lateral line). Recent evidence suggests that the Merkel cell has the molecular machinery for synaptic transmission, thus likely representing a mechanosensory cell in its own right (Haeberle, H. *et al.*, 2004). However, Merkel cell afferent fibers also show the presence of DEG/ENaC proteins (Price, M. P. *et al.*, 2000). Most importantly, several genes relevant for hair cell differentiation are also expressed in developing Merkel cells (Bermingham, N. A. *et al.*, 1999; Leonard, J. H. *et al.*, 2002; Wallis, D. *et al.*, 2003). In contrast to hair cells, Merkel cells derive from the neural crest (Szeder, V. *et al.*, 2003) and Merkel cells are a source of stem cells that can turn carcinogenic, in particular in mutations of genes critical for differentiation of hair cells and Merkel cells (Leonard, J. H. *et al.*, 2002). Whether the mechanosensory channels of Merkel cells and hair cells are identical, as is possible based on detailed transcription factor identity, or are different based on the different embryonic origin, remains to be seen.

In summary, outgroup comparison indicates that the vertebrate hair cell represents many of the basic features also found in distantly related putative mechanosensory cells of nonecdysozoan invertebrates (Figure 4). The basic feature of the mechanotransduction apparatus of the vertebrate hair cell is the 20–300 stereocilia (modified microvilli with a dense actin core) organized in increasingly taller rows toward the kinocilium. Typically, a bundle of stereocilia with variable length is grouped adjacent to the single kinocilium. Stereocilia are interconnected with tip and other links, presumably providing directional sensitivity to stimuli and bundle integrity. Vestibular hair cells of vertebrates show a great many variations in the lengths of kinocilium and stereocilia and number of stereocilia (Lewis, E. R. *et al.*, 1985; Bryant, J. E. *et al.*, 2005). Similar features characterize the lateral line hair cell that derives from placodes adjacent to the ear placode.

3.05.3.1 The Zebrafish *NompC (TRPN-1)*: Is There a Divergent Base for Mechanosensory Transduction in the Apparently Structurally Conserved Vertebrate Hair Cells?

Mutagenetic studies of zebrafish have identified a number of animals that are defective in gravity, lateral line, and touch reception. The mutations underlying several of these defects have been cloned and their molecular basis has been identified (Ernstrom, G. G. and Chalfie, M., 2002; Syntichaki, P. and Tavernarakis, N., 2004; Nicolson, T., 2005). Most interesting is the finding that a zebrafish *nompC* ortholog apparently has defects in hair cell mechanotransduction (Sidi, S. *et al.*, 2003; Nicolson, T., 2005), suggesting that this TRPN molecule is a part of the channel complex. No data narrowing down the anatomical localization of the NOMPC protein exist in zebrafish. However, a frog TRPN-like gene with limited sequence similarity was recently cloned and antibodies were raised against the protein (Shin, J. B. *et al.*, 2005). The data suggest that the frog TRPN-like protein is associated with the kinocilium in hair cells and other epidermal cells. This essentially rules this gene out as a candidate for mechanosensory transduction in stereocilia (Hudspeth, A. J., 2005). What function TRPN plays in zebrafish hair cell mechanotransduction is at the moment unclear. Minimally, a conditional analysis needs to be performed to rule out that the apparent defects are not mediated by an as yet unknown crucial developmental function, analogous to the needed functional verification of MyoVIIa. In addition, screening of mouse and human genomes could not identify a TRPN gene ortholog (Goodman, M. B. *et al.*, 2004; Gillespie, P. G. *et al.*, 2005; Lin, S. Y. and Corey, D. P., 2005). Obviously, whatever function is performed by the TRPN in zebrafish is dispensable for mammalian hair cells and may be unique to zebrafish and other related teleosts. More needs to be known about the distribution of *nompC*-like genes in bony fish (teleosts?) before any detailed hypothesis about the significance of the zebrafish finding can be expanded to other bony fish.

These data highlight the strength but also the risk of a mutagenic approach: it can identify a candidate gene, but requires additional work to put the apparent functional defects into the context of known mechanotransduction data. In this context, several candidate genes of the TRPV and TRPA families have been identified in mammals. However, null mutants of each showed no effects, indicating that

those TRP genes, despite being expressed in hair cells, are not essential for mechanotransduction. Of note, the TRPA1 channel that was recently discussed as a potential candidate for the mammalian mechanosensory channel (Corey, D. P. *et al.*, 2004) has recently been knocked out and shown to mediate, as expected based on comparative data (Goodman, M. B. *et al.*, 2004; Tobin, D. M. and Bargmann, C. I., 2004), not mechanotransduction, but rather sensitivity to mechanical, chemical, and cold stimuli in nociceptors in various dorsal root ganglion neurons and hair cells (Bautista, D. M. *et al.*, 2006; Kwan, K. Y. *et al.*, 2006). The expression of *Trpa1* in ganglion neurons seems to be regulated by *Runx1* (Chen, C. L. *et al.*, 2006), a transcription factor that has not been identified in ear development.

3.05.3.2 The Mammalian Cochlear Hair Cell: Adapting an Ancestral Cell to Very High Frequencies

In contrast to the evolutionarily stable bundle configuration of vestibular hair cells, mammalian hair cell stereocilia show some derived features. First, mammalian auditory hair cells lose the kinocilium in neonates, signifying that this structure is functionally dispensable. In addition, the three rows of outer hair cells (OHCs) display a W-organization of stereocilia whereas the single row of inner hair cells displays a C-shaped bundle showing the greatest bundle differences in a single epithelium. Among vertebrate hair cells, mammalian outer and, to a lesser extent, inner hair cells are the most derived with respect to bundle organization. How these changes relate to the much expanded high-frequency hearing range of mammals, which can exceed 100 kHz, is unknown.

Much has been learned about the molecular organization of stereocilia. Obviously, the central role of shearing motion detection requires that stereocilia behave as stiff rods that slide along each other as the bundle is deflected in a specific direction. If deflection is in the direction of the kinocilium, the bundle sliding results in increased or reduced tension of the tip links, thereby opening still unknown cation channels that allow endolymphatic potassium to enter the hair cell and change its membrane potential. Many mutations have been identified in hair cell actin organization or in molecules suspected as functional components of the transduction apparatus (Table 2), and their molecular interactions, while not yet completely understood, have begun to emerge (Bryant, J. E. *et al.*, 2005; Ahmed, Z. M. *et al.*, 2006; Senften, M. *et al.*, 2006). Actin and several associated proteins that ensure the stability of the actin core are essential for the normal function of any hair cell by providing the stiff core of the stereocilia (Figure 5). Connecting and maintaining actin filaments is provided by various proteins such as *fimbrin*, *t-plastin*, and *espin*. Growth and anchoring of the actin filaments to the membrane is further ensured by additional proteins such as *whirlin* and several rare *myosins*, in particular MyoVI and MyoXV, to the cuticular plate and the tip of the stereocilia, respectively (Bryant, J. E. *et al.*, 2005). Ankle links near the base of stereocilia appear to be formed by *MyoVIIa*, *verzatin*, and an as yet uncharacterized ankle link antigen. *Protocadherin* 15 may participate in this complex or may participate in the tip link connections (Bryant, J. E. *et al.*, 2005; Gillespie, P. G. *et al.*, 2005; Ahmed, Z. M. *et al.*, 2006). The tip link complex is currently speculated to be composed of *Cadherin 23*, *Harmonin b*, *Protocadherin 15*, *Myo VIIa* (at least during development), and *Myo 1b* (Figure 5). Mutations of several of these genes affect either bundle formation or bundle cohesion, leaving them split open instead of tied together. No matter what aberration in bundle appearance is introduced by mutation, hearing is typically lost, demonstrating bundle integrity as a major component of mechanotransduction (Hertzano, R. and Avraham, K. B., 2005). These data show, even in the absence of molecular identification of the mechanotransducer channel, that both intracellular connections and stereocilia connections are essential for auditory sensitivity (Hudspeth, A. J., 2005). Insects have also evolved active mechanisms to amplify low-intensity auditory stimuli. Mosquito and fruit fly antennae (Johnston's organs) are excellent examples (Gopfert, M. C. and Robert, D., 2001).

3.05.3.3 Active Processes in Hair Cells

Unlike any other known sensory receptor, hair cells have found a way – perhaps more than one – to overcome the effect of viscous damping from the fluid in which they immerse. They have developed an active process, a motor for the mechanical amplification of low-intensity stimuli. By imparting mechanical energy to a hair bundle, this amplificatory process partly counters the loss of energy through viscous drag. This process evolved at least 380 million years ago, for it is employed by amphibians, reptiles, and birds, as well as by mammals. Fish

Table 2 Partial list of mutations in nematodes and mice that affect mechanosensation

C. elegans					*M. musculus*		
Gene	***Similarity***	***Function***	***Phenotype***	***Deafness***	***Gene***	***Function***	***Phenotype***
			Extracellular matrix and mantle connections				
mec-1	EGF/Kunitz	Mantle component	Touch insensitive				
mec-5	Collagen	Matrix component	Touch insensitive		DFNA13	Matrix component	Deaf
mec-9	EGF/Kunitz	Matrix component	Touch insensitive				
		Cupula, otoconia, tectorial membrane, and intercellular connections					
				DFNB12	Cdh23	Tip link connection	Deaf
				DFNB23	Pcdh15	Tip link connection	Deaf
					Tecta	Tectorial membrane	Reduced sensitivity
				DFNB22	Otoancorin	Tectorial membrane connection	Deaf
			Channel components				
mec-4	DEG/ENaC	Mechanosensitive channel	Touch insensitive				
mec-10	DEG/ENaC	Mechanosensitive channel	Touch insensitive				
mec-6	Arylesteras	Channel stability/activity	Touch insensitive				
mec-14	Shaker-type	Channel stability/activity	Touch insensitive				
mec-18	AMP-binding	Negative channel regulator	Touch insensitive				
			Intracellular matrix connections				
mec-2	Stomatin-like	Channel associated	Touch insensitive		Actin	Stereocilia skeleton	Unknown
mec-7	β-Tubulin	15-Filament tubule	Reduced touch sensitivity	DFNA11	MyoVIIa	Development and harmonin	Deaf
mec-12	α-Tubulin	15-Filament tubule	Reduced touch sensitivity	/DFNA22	MyoVI	Stereocilia disorganization	Deaf
mec-15	?	Tubule interaction?	Touch insensitive	DFNB30	MyoIIIa	?	Adult deaf
				DFNA17	Myh9	?	Deaf
				DFNB3	Myo15	Actin skeleton organization	born deaf
				?	Myo1c	Cdh23 connection	?
				DFNB16	Strc	Stereocilia protein	Deaf
				DFNB13	Whirlin	Actin skeleton organization	Deaf
				USH1	Harmonin	Interacts with MyoVIIa +Cdh23	Deaf
					MyoIc	Adaptor for channel?	?

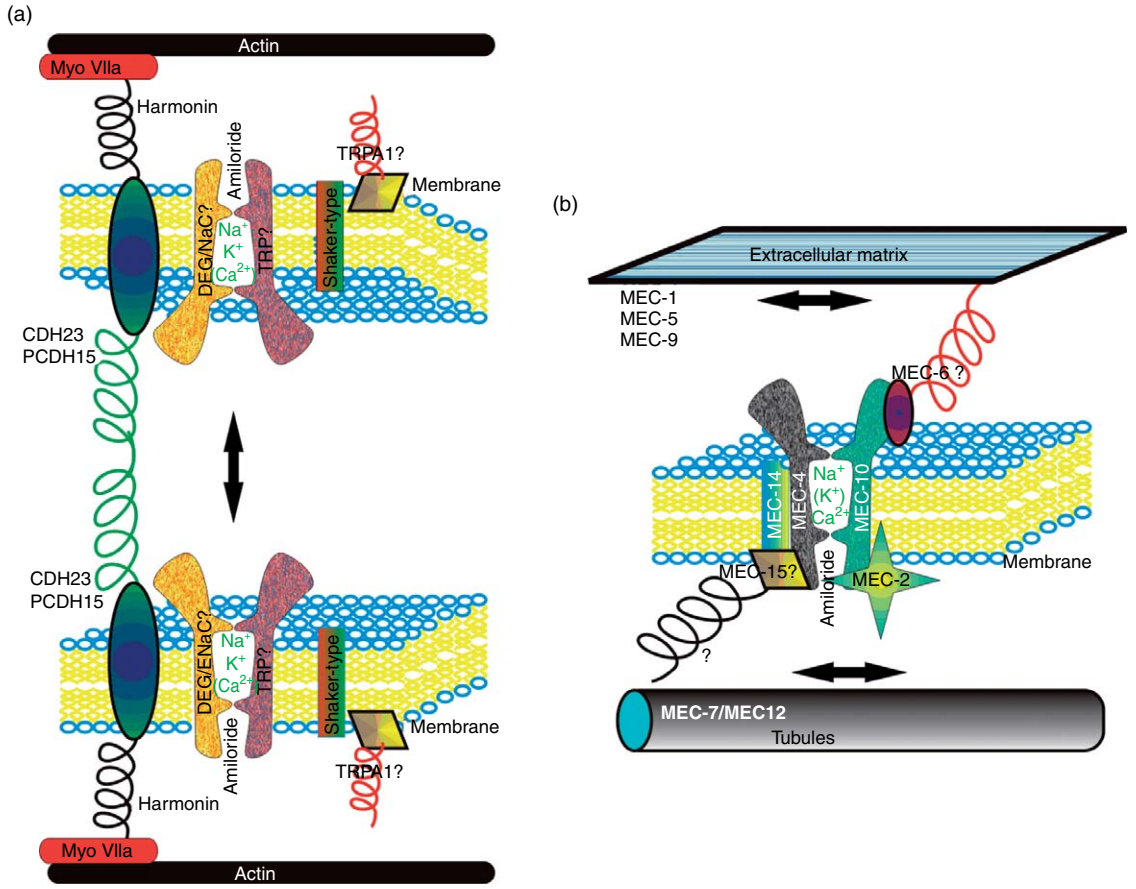

Figure 5 The basic organization of the mechanosensory channel of a vertebrate hair cell (a) and a nematode fine-touch sensor (b) are compared. Mutations analysis has identified several genes that are essential for the function in either taxon. In nematodes, fine touch is lost when either specific molecules of the extracellular matrix to which the channel is anchored are lost (Mec-1,5,9) or if specific components of the channel complex are lost (Mec-2,4,10,14). However, loss to the intracellular tubules (Mec-7, 12) may lead only to a reduced sensitivity, not a complete loss of sensation. In contrast, in vertebrates there is no extracellular matrix or cuticula connection. Instead, two stereocilia are interconnected presumably by Cdh23 that is hypothesized to be anchored to MyoVIIa via harmonin. Loss of any of these genes results in deafness indicating that in vertebrates mechanosensation requires relative movement against the actin core of the stereocilia. Additional connections exist between Cdh23 and Myo1c but no knockout data support the claimed function as an adaptor. It is speculated that MyoVIIa transports the still unknown amiloride-sensitive mechanosensory channel to the tip, but it is unclear whether this connection remains past development. In nematodes, at least two essential subunits of the DEG/ENaC channel are known whereas it is not clear whether the vertebrate channel is composed of DEG/ENaC or TRP channels. Certain candidates have been excluded as mutants in, for example, TRPA1 do hear excluding an essential role of this protein in mechanosensory transduction. Note that both nematode and vertebrate have a shaker-type channel associated with the mechanosensory channel, but details are unknown. Adapted from (Bryant, J.E., Forge, A., and Richardson, G.P. 2005. The Differentiation of Hair Cells. In: Development of the Inner Ear (*eds.* M.W. Kelley, D.K. Wu, A.N. Popper, R.R. Fay,), pp. 158–204. Springer. and O'Hagan, R., Chalfie, M., Goodman, M.B. 2005. The MEC-4 DEG/ENaC channel of *Caenorhabditis elegans* touch receptor neurons transduces mechanical signals. *Nat. Neurosci.* 8, 43–50.

ears too may well display mechanical amplification, which, like the structure of the hair cell, may prove to be a general feature of vertebrates.

Two mechanisms of active amplification have been proposed. In the mammalian cochlea, OHCs function as the key elements in a mechanical feedback loop in which the fast somatic motility of OHCs is thought to be the source of cochlear amplification. An alternative view is that amplification arises from active hair-bundle movements, similar to that seen in nonmammalian hair cells (Zheng, J. *et al.*, 2000; Hudspeth, A. J., 2005; Dallos, P. *et al.*, 2006). Although these mechanisms have been proposed, and evidence has been garnered in support of each,

there is no receptor organ in which the mechanism is unequivocally known. However, the strongest candidate to explain amplification in the mammalian cochlea is unlikely to operate in the receptor organs of amphibians, reptiles, or birds (He, D. Z. *et al.*, 2003).

The OHC of the mammalian cochlea functions not just as a receptor cell but, more importantly, as an effector. OHCs can convert voltage stimulation, the receptor potential, into somatic length change (Brownell, W. E. *et al.*, 1985; Kachar, B. *et al.*, 1986). Such electromechanical or reverse transduction can operate at high frequencies (Dallos, P. and Evans, B. N., 1995). The gene named *prestin* that codes the membrane-bound motor protein was identified (Zheng, J. *et al.*, 2000). Prestin belongs to a distinct anion transporter family called solute carrier protein 26 (SLC26) (Zheng, J. *et al.*, 2002). At present, 11 members of this family have been identified (Mount, D. B. and Romero, M. F., 2004). Several proteins in this family, including prestin, are involved in human diseases (Dawson, P. A. and Markovich, D., 2005). The human Prestin gene contains 21 exons crossing more than 90 kb in chromosome 7q22 (Liu, X. Z. *et al.*, 2003), a location near to those of other important SLC26 members, such as PDS (SLC26A4) (Everett, L. A. *et al.*, 1997) and DRA (SLC26A3) (Haila, S. *et al.*, 1998). The mouse Prestin gene has 20 exons spanning nearly 55 kb in chromosome 5 (Zheng, J. *et al.*, 2003). Eighteen of these exons code for prestin amino acids in both hPrestin and mPrestin. Among coding exons, 12 exons are exactly the same sizes as in other members of the SLC26 family, such as Pendrin, DRA, and CFEX (Zheng, J. *et al.*, 2003), indicating a high likelihood for homology among these genes. Several prestin isoforms have also been found in different stages of human cochlear development (Liu, X. Z. *et al.*, 2003).

Amphibian and reptilian ears are also sensitive and sharply tuned and produce otoacoustic emissions despite the fact that they lack OHCs (van Dijk, P. and Manley, G. A., 2001; Manley, G. A., 2001). This is consistent with a cochlear amplifier in which the stereocilia not only act as a receptor organelle, but also act as a force-generator (Hudspeth, A., 1997; Fettiplace, R. and Hackney, C. M., 2006). Indeed, active hair-bundle motion has been observed in hair cells of turtles and bullfrogs as reactions to hair-bundle displacement with compliant probes, and in response to changes in membrane potential. The active hair-bundle movements intimately related to the reclosure of the mechanotransducer channels and the myosin motors involved in adaptation can produce forces that amplify mechanical stimuli. The movements are sensitive to extracellular calcium concentration and can be altered by calcium influx through the mechanoelectrical transducer channels. However, the molecular basis of this active process is still unclear.

3.05.3.4 Development of Mechanoreceptor Cells: Molecular Transformation of an Epidermal Cell into a Mechanoreceptor

Numerous genes that appear to be essential for hair cell development in vertebrates and in Johnston's organs alike have been identified (Caldwell, J. C. and Eberl, D. F., 2002; Dong, P. D. *et al.*, 2003; Fritzsch, B. and Beisel, K. W. 2004; Boekhoff-Falk, 2005; Todi, S. V. *et al.*, 2005). Expanding this comparison to *C. elegans* allows a set of conclusions to be drawn about the stereotyped events that happen during mechanosensory organ development (Table 3). First, organ precursors have to be selected from ectoderm and turned into precursor cells able to respond to genes that initiate their differentiation. Such genes belong to

Table 3 Developmental genes compared

Human disease	*Mouse gene*	*Drosophila gene*	*C. elegans gene*	*Function*
Renal-coloboma syndrome	*Pax2*	*Dpax-2 (sparkling)*	?	Transcription factor
Branchio-oto-renal syndrome	*Eya1*	*Clift (eya)*	?	Transcription factor
Townes–Brocks syndrome	*Sall I*	*Spalt*	*sem-4*	Transcription factor
Di George syndrome	*Gata3*	*pannier*	?	Transcription factor
?	*Atoh1*	*atonal*	*lin-32*	Hair cell differentiation
DFNA15	*Pou4f3*	*Acj6*	*unc-86*	Transcription factor
Nonimmune chronic idiopathic neutropenia of adults	*Gfi1*	*senseless*	?	Hair cell survival
DFNA11	*MyoVIIA*	*crinkled*	?	Actin binding
DFNA17	*Myh9*	*zip*	?	Motor protein
DFNB3	*Myo15*	*CG2174*	?	Motor protein

the PAX domain factors (*Pax2*, *Dpax-2*) in vertebrates and in *D. melanogaster*. Other factors that have been specified in placodal induction belong to the *Wnt* and *Shh* genes, and these important diffusible morphogens likely also play a role in fly and nematode development. In vertebrates, several genes are necessary for the overall differentiation of the auditory organ or the ear, such as *Eya1*, *Gata3*, and *Sall/spalt*. Spalt-like transcription factors also contribute to touch cell fate in nematodes (Toker, A. S. *et al.*, 2003) and flies (Dong, P. D. *et al.*, 2003). Later expressed factors are essential for hair cell differentiation, such as the bHLH gene *Atoh1/atonal* of vertebrates and flies and the unrelated bHLH gene *lin-32* in nematodes. bHLH genes interact with POU domain and zinc finger genes to ensure proper differentiation of vertebrate hair cells and chordotonal organs alike. The latter genes are also found in diploblasts, suggesting that some developmental aspects of mechanosensory cell- and organ-specific transcription factors are conserved (Fritzsch, B. *et al.*, 2006a), even in the presence of the highly divergent morphology of such cells. In addition, the proper differentiation of hair cell and chordotonal transducer organs depends critically on several unconventional myosins, some of which are shared between flies and mice (Table 3) and are known already in the protist ancestors of multicellular organisms. It thus appears possible that development of mechanosensory cells may present a variation of a scheme already present in diploblasts and conserved in the molecular interactions, if not the molecules involved, across triploblast phyla. In simple terms, we can view these developmental transcription factors as conductors that orchestrate somehow the assembly of a molecular complex necessary for the mechanotransduction via a tethered mechanosensory channel to work. Unfortunately, how these transcription factors regulate the extra- and intracellular matrix development and the expression of mechanosensory channels and their tethering molecules is unknown at the moment.

3.05.4 Conclusions

Analyses of mutations in nematodes, flies, zebrafish, and mammals have identified a number of genes whose products play a role in mechanosensory function and development. However, only in nematodes do we have enough components of the transduction complex identified that we can begin to model the function of those proteins. The basic components are the channel, composed of at least two subunits, and an attachment to the cuticle. An intracellular attachment, previously deemed essential (Ernstrom, G. G. and Chalfie, M., 2002), is needed only for increased sensitivity of sensation (O'Hagan, R. *et al.*, 2005). Other animals such as zebrafish and mammals show sensitivity reduction or loss after mutations in over 100 genes, suggesting that the transduction complex requires more components for proper function, perhaps including a more sophisticated developmental regulation. Neither the detailed organization of the channel complex nor its connection to intra- and extracellular tethers is sufficiently known to explain the gating properties and its ability to follow repetitive stimuli to high frequencies.

Clearly, the past approach of unraveling the genetic basis of mechanosensory cell development and function by mutational analysis has been successful in identifying several genes necessary for proper development and/or function. The plethora of unsuccessful mutations in vertebrates that failed to demonstrate the mechanosensory function of a given gene because of limited viability, additional involvement in development, or absence of a phenotype perhaps related to redundancy suggest that it is may be time to alter our strategy. Single mutations assume that a given gene cannot be replaced by other genes (lack of functional redundancy). They further assume that the loss of function is associated only with adult mechanotransduction. Both of these assumptions may be untrue, and animals may not even mature in the absence of specific genes such as β-ENac (early lethal), or may not properly differentiate (MyoVIIa). In addition, while MEC-4 and -10 are different enough to be functionally distinct and cannot be substituted by each other, this may not be the case for all components of the possibly heteromultimeric vertebrate mechanotransducer channels.

Further progress requires the implementation of better strategies. Recently, mice were generated with hair cell-specific *Cre* expression (Matei, V. *et al.*, 2005; Tian, Y. *et al.*, 2006). Such mice could be crossed with mice in which all genes of a given family are floxed and can therefore be all eliminated at the same adult stage, simply by delayed activation of the hair cell-specific *Cre*. Once specific effects have been found, mice can be generated in which more and more of the putative channels are expressed. This way the relevant combination of genes necessary for proper function could be established. Ultimately, ear-specific conditional deletions of one or more of these genes, combined with the hair cell-targeted expression of

these genes, needs to be performed to verify that they are not only necessary but also sufficient. The way ahead therefore requires more work to generate floxed genes, clearly an effort that requires collaboration between multiple laboratories.

Analysis of mechanosensation has been a difficult road. What we learned thus far is that many channels can respond to mechanical force, albeit not with the high sensitivity of channels now considered to be dedicated to mechanosensation. In the absence of a clear-cut molecular definition of mechanosensory channels across phyla, we can only deal with an operational definition of a mechanosensitive cell to guide future research:

A mechanosensory channel responds maximally to low-intensity mechanical forces of a few micronewtons to piconewtons with a rapidly activating (pS), nondesensitizing, increased conductance. Such a channel will respond to membrane stretch (nontethered) or pull on extra- or intracellular attachments (tethered channels).

3.05.5 Note Added in Proof

Two recent papers have direct bearing for the review (Christensen, A. P. and Corey, D. P., 2007; Vollrath, M. A. *et al*., 2007). In addition, a recent paper established that coelenterates and deuterostomes show more genetic similarities with each other than either has with protostomes, essentially what we proposed based on the similarities in apical mechanosensory specializations (Putnam, N. H. *et al*., 2007).

Acknowledgments

This work was supported by NIH (DC005590) and a grant from Dr. Richard Bellucci. This investigation was conducted in a facility constructed with support from Research Facilities Improvement Program Grant Number 1 C06 RR17417-01 from the National Center for Research Resources, National Institutes of Health. We acknowledge the use of the confocal microscope facility of the NCCB, supported by EPSCoR EPS-0346476 (CFD 47.076). We would like to express our gratitude to Drs. Miriam B. Goodman and Dan Eberl for helpful insights and discussion that helped fine-tune this review. However, the perspective and views expressed are only those of the authors.

References

Aarts, M., Iihara, K., Wei, W. L., Xiong, Z. G., Arundine, M., Cerwinski, W., MacDonald, J. F., and Tymianski, M. 2003. A key role for TRPM7 channels in anoxic neuronal death. Cell 115, 863–877.

Ahmed, Z. M., Goodyear, R., Riazuddin, S., Lagziel, A., Legan, P. K., Behra, M., Burgess, S. M., Lilley, K. S., Wilcox, E. R., Riazuddin, S., *et al.* 2006. The tip-link antigen, a protein associated with the transduction complex of sensory hair cells, is protocadherin-15. J. Neurosci. 26, 7022–7034.

Ainsley, J. A., Pettus, J. M., Bosenko, D., Gerstein, C. E., Zinkevich, N., Anderson, M. G., Adams, C. M., Welsh, M. J., and Johnson, W. A. 2003. Enhanced locomotion caused by loss of the *Drosophila* DEG/ENaC protein Pickpocket1. Curr. Biol. 13, 1557–1563.

Al-Bhalal, L. and Akhtar, M. 2005. Molecular basis of autosomal dominant polycystic kidney disease. Adv. Anat. Pathol. 12, 126–133.

Anishkin, A. and Kung, C. 2005. Microbial mechanosensation. Curr. Opin. Neurobiol. 15, 397–405.

Arkett, S. A., Mackie, G. O., and Meech, R. W. 1988. Hair cell mechanoreception in a jellyfish *Aglantha digitale*. J. Exp. Biol. 135, 329–342.

Barald, K. F. and Kelley, M. W. 2004. From placode to polarization: new tunes in inner ear development. Development 131, 4119–4130.

Bautista, D. M., Jordt, S. E., Nikai, T., Tsuruda, P. R., Read, A. J., Poblete, J., Yamoah, E. N., Basbaum, A. I., and Julius, D. 2006. TRPA1 mediates the inflammatory actions of environmental irritants and proalgesic agents. Cell 124, 1269–1282.

Bermingham, N. A., Hassan, B. A., Price, S. D., Vollrath, M. A., Ben-Arie, N., Eatock, R. A., Bellen, H. J., Lysakowski, A., and Zoghbi, H. Y. 1999. Math1: an essential gene for the generation of inner ear hair cells. Science 284, 1837–1841.

Birder, L. A., Nakamura, Y., Kiss, S., Nealen, M. L., Barrick, S., Kanai, A. J., Wang, E., Ruiz, G., De Groat, W. C., Apodaca, G., *et al.* 2002. Altered urinary bladder function in mice lacking the vanilloid receptor TRPV1. Nat. Neurosci. 5, 856–860.

Blount, P. 2003. Molecular mechanisms of mechanosensation: big lessons from small cells. Neuron 37, 731–734.

Boekhoff-Falk, G. 2005. Hearing in *Drosophila*: development of Johnston's organ and emerging parallels to vertebrate ear development. Dev. Dyn. 232, 550–558.

Boulter, C., Mulroy, S., Webb, S., Fleming, S., Brindle, K., and Sandford, R. 2001. Cardiovascular, skeletal, and renal defects in mice with a targeted disruption of the Pkd1 gene. Proc. Natl. Acad. Sci. U. S. A. 98, 12174–12179.

Brownell, W. E., Bader, C. R., Bertrand, D., and de Ribaupierre, Y. 1985. Evoked mechanical responses of isolated cochlear outer hair cells. Science 227, 194–196.

Bryant, J. E., Forge, A., and Richardson, G. P. 2005. The Differentiation of Hair Cells. In: Development of the Inner Ear (*eds*. M. W. Kelley, D. K. Wu, A. N. Popper, and R. R. Fay), pp. 158–204. Springer.

Budelmann, B. U. 1987. Morphological Diversity of Equilibrium Receptor Systems in Aquatic Invertebrates. In: Sensory Biology of Aquatic Animals (*eds*. J. Atema, R. R. Fay, A. N. Popper, and W. N. Tavolga), pp. 757–782. Springer.

Budelmann, B. U. and Bleckmann, H. 1988. A lateral line analogue in cephalopods: water waves generate microphonic potentials in the epidermal head lines of *Sepia* and *Lolliguncula*. J. Comp. Physiol. A 164, 1–5.

Budelmann, B. U. and Williamson, R. 1994. Directional sensitivity of hair cell afferents in the octopus statocyst. J. Exp. Biol. 187, 245–259.

Bullock, T. H. and Heiligenberg, W. 1986. Electroreception. Wiley.

Burighel, P., Lane, N. J., Fabio, G., Stefano, T., Zaniolo, G., Carnevali, M. D., and Manni, L. 2003. Novel, secondary sensory cell organ in ascidians: in search of the ancestor of the vertebrate lateral line. J. Comp. Neurol. 461, 236–249.

Caldwell, J. C. and Eberl, D. F. 2002. Towards a molecular understanding of *Drosophila* hearing. J. Neurobiol. 53, 172–189.

Caterina, M. J., Leffler, A., Malmberg, A. B., Martin, W. J., Trafton, J., Petersen-Zeitz, K. R., Koltzenburg, M., Basbaum, A. I., and Julius, D. 2000. Impaired nociception and pain sensation in mice lacking the capsaicin receptor. Science 288, 306–313.

Chen, C. L., Broom, D. C., Liu, Y., de Nooij, J. C., Li, Z., Cen, C., Samad, O. A., Jessell, T. M., Woolf, C. J., and Ma, Q. 2006. Runx1 determines nociceptive sensory neuron phenotype and is required for thermal and neuropathic pain. Neuron 49, 365–377.

Chiang, C. S., Anishkin, A., and Sukharev, S. 2004. Gating of the large mechanosensitive channel *in situ*: estimation of the spatial scale of the transition from channel population responses. Biophys. J. 86, 2846–2861.

Christensen, A. P. and Corey, D. P. 2007. TRP channels in mechanosensation: direct or indirect activation? Nat. Rev. Neurosci. 8, 510–521.

Chung, M. K., Lee, H., and Caterina, M. J. 2003. Warm temperatures activate TRPV4 in mouse 308 keratinocytes. J. Biol. Chem. 278, 32037–32046.

Chung, Y. D., Zhu, J., Han, Y., and Kernan, M. J. 2001. nompA encodes a PNS-specific, ZP domain protein required to connect mechanosensory dendrites to sensory structures. Neuron 29, 415–428.

Clapham, D. E. 2003. TRP channels as cellular sensors. Nature 426, 517–524.

Coffin, A., Kelley, M. W., Manley, G. A., and Popper, A. N. 2004. Evolution of Sensory Hair Cells. In: Evolution of the Vertebrate Auditory System (*eds*. G. A. Manley, A. N. Popper, and R. R. Fay), pp. 55–94. Springer.

Corey, D. P., Garcia-Anoveros, J., Holt, J. R., Kwan, K. Y., Lin, S. Y., Vollrath, M. A., Amalfitano, A., Cheung, E. L., Derfler, B. H., Duggan, A., *et al.* 2004. TRPA1 is a candidate for the mechanosensitive transduction channel of vertebrate hair cells. Nature 432, 723–730.

Coric, T., Zheng, D., Gerstein, M., and Canessa, C. M. 2005. Proton sensitivity of ASIC1 appeared with the rise of fishes by changes of residues in the region that follows TM1 in the ectodomain of the channel. J. Physiol. 568, 725–735.

Dallos, P. and Evans, B. N. 1995. High-frequency motility of outer hair cells and the cochlear amplifier. Science 267, 2006–2009.

Dallos, P., Zheng, J., and Cheatham, M. A. 2006. Prestin and the cochlear amplifier. J. Physiol. 576, 37–42.

Davis, J. B., Gray, J., Gunthorpe, M. J., Hatcher, J. P., Davey, P. T., Overend, P., Harries, M. H., Latcham, J., Clapham, C., Atkinson, K., *et al.* 2000. Vanilloid receptor-1 is essential for inflammatory thermal hyperalgesia. Nature 405, 183–187.

Dawson, P. A. and Markovich, D. 2005. Pathogenetics of the human SLC26 transporters. Curr. Med. Chem. 12, 385–396.

Delmas, P. 2005. Polycystins: polymodal receptor/ion-channel cellular sensors. Pflugers Arch. 451, 264–276.

Di Palma, F., Belyantseva, I. A., Kim, H. J., Vogt, T. F., Kachar, B., and Noben-Trauth, K. 2002. Mutations in Mcoln3 associated with deafness and pigmentation defects in varitint-waddler (Va) mice. Proc. Natl. Acad. Sci. U. S. A. 99, 14994–14999.

Dietrich, A., Mederos, Y. S. M., Gollasch, M., Gross, V., Storch, U., Dubrovska, G., Obst, M., Yildirim, E., Salanova, B., Kalwa, H., *et al.* 2005. Increased vascular smooth muscle contractility in TRPC6−/− mice. Mol. Cell Biol. 25, 6980–6989.

Dong, P. D., Todi, S. V., Eberl, D. F., and Boekhoff-Falk, G. 2003. *Drosophila* spalt/spalt-related mutants exhibit Townes-Brocks' syndrome phenotypes. Proc. Natl. Acad. Sci. U. S. A. 100, 10293–10298.

Drummond, H. A., Price, M. P., Welsh, M. J., and Abboud, F. M. 1998. A molecular component of the arterial baroreceptor mechanotransducer. Neuron 21, 1435–1441.

Eberl, D. F., Hardy, R. W., and Kernan, M. J. 2000. Genetically similar transduction mechanisms for touch and hearing in *Drosophila*. J. Neurosci. 20, 5981–5988.

Eichinger, L., Pachebat, J. A., Glockner, G., Rajandream, M. A., Sucgang, R., Berriman, M., Song, J., Olsen, R., Szafranski, K., Xu, Q., *et al.* 2005. The genome of the social amoeba *Dictyostelium discoideum*. Nature 435, 43–57.

Emtage, L., Gu, G., Hartwieg, E., and Chalfie, M. 2004. Extracellular proteins organize the mechanosensory channel complex in *C. elegans* touch receptor neurons. Neuron 44, 795–807.

Ernstrom, G. G. and Chalfie, M. 2002. Genetics of sensory mechanotransduction. Annu. Rev. Genet. 36, 411–453.

Everett, L. A., Glaser, B., Beck, J. C., Idol, J. R., Buchs, A., Heyman, M., Adawi, F., Hazani, E., Nassir, E., Baxevanis, A. D., *et al.* 1997. Pendred syndrome is caused by mutations in a putative sulphate transporter gene (PDS). Nat. Genet. 17, 411–422.

Fettiplace, R. and Hackney, C. M. 2006. The sensory and motor roles of auditory hair cells. Nat. Rev. Neurosci. 7, 19–29.

Freichel, M., Philipp, S., Cavalie, A., and Flockerzi, V. 2004. TRPC4 and TRPC4-deficient mice. Novartis Found. Symp. 258, 189–199; discussion 199–203, 263–266.

Freichel, M., Suh, S. H., Pfeifer, A., Schweig, U., Trost, C., Weissgerber, P., Biel, M., Philipp, S., Freise, D., Droogmans, G., *et al.* 2001. Lack of an endothelial store-operated Ca^{2+} current impairs agonist-dependent vasorelaxation in TRP4−/− mice. Nat. Cell. Biol. 3, 121–127.

French, A. S., Torkkeli, P. H., and Seyfarth, E. A. 2002. From stress and strain to spikes: mechanotransduction in spider slit sensilla. J. Comp. Physiol. A Neuroethol. Sens. Neural Behav. Physiol. 188, 739–752.

Fritzsch, B. and Beisel, K. W. 2004. Keeping sensory cells and evolving neurons to connect them to the brain: molecular conservation and novelties in vertebrate ear development. Brain Behav. Evol. 64, 182–197.

Fritzsch, B., Pauley, S., and Beisel, K. W. 2006a. Cells, molecules and morphogenesis: the making of the vertebrate ear. Brain Res. 1091, 151–171.

Fritzsch, B., Pauley, S., Feng, F., Matei, V., and Nichols, D. H. 2006b. The evolution of the vertebrate auditory system: transformations of vestibular mechanosensory cells for sound processing is combined with newly generated central processing neurons. Int. J. Comp. Psychol. 19, 1–24.

Garcia-Anoveros, J., Samad, T. A., Zuvela-Jelaska, L., Woolf, C. J., and Corey, D. P. 2001. Transport and localization of the DEG/ENaC ion channel BNaC1alpha to peripheral mechanosensory terminals of dorsal root ganglia neurons. J. Neurosci. 21, 2678–2686.

Gillespie, P. G., Dumont, R. A., and Kachar, B. 2005. Have we found the tip link, transduction channel, and gating spring of the hair cell? Curr. Opin. Neurobiol. 15, 389–396.

Gong, Z., Son, W., Chung, Y. D., Kim, J., Shin, D. W., McClung, C. A., Lee, Y., Lee, H. W., Chang, D. J., Kaang, B. K., *et al.* 2004. Two interdependent TRPV channel subunits, inactive and Nanchung, mediate hearing in *Drosophila*. J. Neurosci. 24, 9059–9066.

Goodman, M. B., Ernstrom, G. G., Chelur, D. S., O'Hagan, R., Yao, C. A., and Chalfie, M. 2002. MEC-2 regulates *C. elegans* DEG/ENaC channels needed for mechanosensation. Nature 415, 1039–1042.

Goodman, M. B., Lumpkin, E. A., Ricci, A., Tracey, W. D., Kernan, M., and Nicolson, T. 2004. Molecules and mechanisms of mechanotransduction. J. Neurosci. 24, 9220–9222.

Goodman, M. B. and Schwarz, E. M. 2003. Transducing touch in *Caenorhabditis elegans*. Annu. Rev. Physiol. 65, 429–452.

Gopfert, M. C. and Robert, D. 2001. Active auditory mechanics in mosquitoes. Proc. Biol. Sci. 268, 333–339.

Gopfert, M. C., Albert, J. T., Nadrowski, B., and Kamikouchi, A. 2006. Specification of auditory sensitivity by *Drosophila* TRP channels. Nat. Neurosci. 9, 999–1000.

Haeberle, H., Fujiwara, M., Chuang, J., Medina, M. M., Panditrao, M. V., Bechstedt, S., Howard, J., and Lumpkin, E. A. 2004. Molecular profiling reveals synaptic release machinery in Merkel cells. Proc. Natl. Acad. Sci. U. S. A. 101, 14503–14508.

Haila, S., Hoglund, P., Scherer, S. W., Lee, J. R., Kristo, P., Coyle, B., Trembath, R., Holmberg, C., de la Chapelle, A., and Kere, J. 1998. Genomic structure of the human congenital chloride diarrhea (CLD) gene. Gene 214, 87–93.

He, D. Z., Beisel, K. W., Chen, L., Ding, D. L., Jia, S., Fritzsch, B., and Salvi, R. 2003. Chick hair cells do not exhibit voltage-dependent somatic motility. J. Physiol. 546, 511–520.

Hertzano, R. and Avraham, K. B. 2005. Developmental Genes Associated with Human Hearing Loss. In: Development of the Inner Ear (*eds*. M. W. Kelley, D. K. Wu, A. N. Popper, and R. R. Fay), pp. 204–233. Springer.

Hilliard, M. A., Apicella, A. J., Kerr, R., Suzuki, H., Bazzicalupo, P., and Schafer, W. R. 2005. *In vivo* imaging of *C. elegans* ASH neurons: cellular response and adaptation to chemical repellents. EMBO J. 24, 63–72.

Hoenderop, J. G., van Leeuwen, J. P., van der Eerden, B. C., Kersten, F. F., van der Kemp, A. W., Merillat, A. M., Waarsing, J. H., Rossier, B. C., Vallon, V., Hummler, E., *et al.* 2003. Renal Ca2+ wasting, hyperabsorption, and reduced bone thickness in mice lacking TRPV5. J. Clin. Invest. 112, 1906–1914.

Holland, L. Z. 2005. Non-neural ectoderm is really neural: evolution of developmental patterning mechanisms in the non-neural ectoderm of chordates and the problem of sensory cell homologies. J. Exp. Zool. B Mol. Dev. Evol. 304, 304–323.

Hossl, B., Bohm, H. J., Rammerstorfer, F. G., Mullan, R., and Barth, F. G. 2006. Studying the deformation of arachnid slit sensilla by a fracture mechanical approach. J. Biomech. 39, 1761–1768.

Hudspeth, A. J. 1989. How the ear's works work. Nature 341, 397–404.

Hudspeth, A. J. 1997. Mechanical amplification of stimuli by hair cells. Curr. Opin. Neurobiol. 7, 480–486.

Hudspeth, A. J. 2005. How the ear's works work: mechanoelectrical transduction and amplification by hair cells. C. R. Biol. 328, 155–162.

Ishimaru, Y., Inada, H., Kubota, M., Zhuang, H., Tominaga, M., and Matsunami, H. 2006. Transient receptor potential family members PKD1L3 and PKD2L1 form a candidate sour taste receptor. Proc. Natl. Acad. Sci. U. S. A. 103, 12569–12574.

Jorgensen, J. M. 1989. Evolution of Octavolateralis Sensory Cells. In: The Mechanosensory Lateral Line. Neurobiology and Evolution (*eds*. S. Coombs, P. Goerner, and H. Muenz), pp. 99–115. Springer.

Kachar, B., Brownell, W. E., Altschuler, R., and Fex, J. 1986. Electrokinetic shape changes of cochlear outer hair cells. Nature 322, 365–368.

Kellenberger, S. and Schild, L. 2002. Epithelial sodium channel/degenerin family of ion channels: a variety of functions for a shared structure. Physiol. Rev. 82, 735–767.

Kernan, M., Cowan, D., and Zuker, C. 1994. Genetic dissection of mechanosensory transduction: mechanoreception-defective mutations of *Drosophila*. Neuron 12, 1195–1206.

King, N. 2005. Choanoflagellates. Curr. Biol. 15, R113–R114.

King, N. and Carroll, S. B. 2001. A receptor tyrosine kinase from choanoflagellates: molecular insights into early animal evolution. Proc. Natl. Acad. Sci. U. S. A. 98, 15032–15237.

Kraft, R. and Harteneck, C. 2005. The mammalian melastatin-related transient receptor potential cation channels: an overview. Pflugers Arch. 451, 204–211.

Kung, C. 2005. A possible unifying principle for mechanosensation. Nature 436, 647–654.

Kwan, K. Y., Allchorne, A. J., Vollrath, M. A., Christensen, A. P., Zhang, D. S., Woolf, C. J., and Corey, D. P. 2006. TRPA1 contributes to cold, mechanical, and chemical nociception but is not essential for hair-cell transduction. Neuron 50, 277–289.

Launay, P., Cheng, H., Srivatsan, S., Penner, R., Fleig, A., and Kinet, J. P. 2004. TRPM4 regulates calcium oscillations after T cell activation. Science 306, 1374–1377.

Lavrov, D. V., Forget, L., Kelly, M., and Lang, B. F. 2005. Mitochondrial genomes of two demosponges provide insights into an early stage of animal evolution. Mol. Biol. Evol. 22, 1231–1239.

Leonard, J. H., Cook, A. L., Van Gele, M., Boyle, G. M., Inglis, K. J., Speleman, F., and Sturm, R. A. 2002. Proneural and proneuroendocrine transcription factor expression in cutaneous mechanoreceptor (Merkel) cells and Merkel cell carcinoma. Int. J. Cancer 101, 103–110.

Levitan, I. B. and Cibulsky, S. M. 2001. Biochemistry. TRP ion channels – two proteins in one. Science 293, 1270–1271.

Lewis, E. R., Leverenz, E. L., and Bialek, W. S. 1985. The Vertebrate Inner Ear. CRC Press.

Leypold, B. G., Yu, C. R., Leinders-Zufall, T., Kim, M. M., Zufall, F., and Axel, R. 2002. Altered sexual and social behaviors in trp2 mutant mice. Proc. Natl. Acad. Sci. U. S. A. 99, 6376–6381.

Li, W., Feng, Z., Sternberg, P. W., and Xu, X. Z. 2006. A *C. elegans* stretch receptor neuron revealed by a mechanosensitive TRP channel homologue. Nature 440, 684–687.

Liedtke, W. and Friedman, J. M. 2003. Abnormal osmotic regulation in trpv4−/− mice. Proc. Natl. Acad. Sci. U. S. A. 100, 13698–13703.

Liedtke, W., Tobin, D. M., Bargmann, C. I., and Friedman, J. M. 2003. Mammalian TRPV4 (VR-OAC) directs behavioral responses to osmotic and mechanical stimuli in *Caenorhabditis elegans*. Proc. Natl. Acad. Sci. U. S. A. 100(Suppl. 2), 14531–14536.

Lin, S. Y. and Corey, D. P. 2005. TRP channels in mechanosensation. Curr. Opin. Neurobiol. 15, 350–357.

Liu, X. Z., Ouyang, X. M., Xia, X. J., Zheng, J., Pandya, A., Li, F., Du, L. L., Welch, K. O., Petit, C., Smith, R. J., *et al.* 2003. Prestin, a cochlear motor protein, is defective in non-syndromic hearing loss. Hum. Mol. Genet. 12, 1155–1162.

LopezJimenez, N. D., Cavenagh, M. M., Sainz, E., Cruz-Ithier, M. A., Battey, J. F., and Sullivan, S. L. 2006. Two members of the TRPP family of ion channels, Pkd1l3 and Pkd2l1, are co-expressed in a subset of taste receptor cells. J. Neurochem. 98, 68–77.

Lumpkin, E. A. and Bautista, D. M. 2005. Feeling the pressure in mammalian somatosensation. Curr. Opin. Neurobiol. 15, 382–388.

Mackie, G. O. and Singla, C. L. 2004. Cupular organs in two species of Corella (Tunicata: Ascidiacea). Invert. Biol. 123, 269–281.

Manley, G. A. 2001. Evidence for an active process and a cochlear amplifier in nonmammals. J. Neurophysiol. 86, 541–549.

Maroto, R., Raso, A., Wood, T. G., Kurosky, A., Martinac, B., and Hamill, O. P. 2005. TRPC1 forms the stretch-activated cation channel in vertebrate cells. Nat. Cell. Biol. 7, 179–185.

Matei, V., Pauley, S., Kaing, S., Rowitch, D., Beisel, K. W., Morris, K., Feng, F., Jones, K., Lee, J., and Fritzsch, B. 2005. Smaller inner ear sensory epithelia in Neurog1 null mice are related to earlier hair cell cycle exit. Dev. Dyn. 234, 633–650.

Montell, C. 2005. The TRP superfamily of cation channels. Sci. STKE 2005 (272), re3 (1–24).

Moqrich, A., Hwang, S. W., Earley, T. J., Petrus, M. J., Murray, A. N., Spencer, K. S., Andahazy, M., Story, G. M., and Patapoutian, A. 2005. Impaired thermosensation in mice lacking TRPV3, a heat and camphor sensor in the skin. Science 307, 1468–1472.

Morsli, H., Choo, D., Ryan, A., Johnson, R., and Wu, D. K. 1998. Development of the mouse inner ear and origin of its sensory organs. J. Neurosci. 18, 3327–3335.

Mount, D. B. and Romero, M. F. 2004. The SLC26 gene family of multifunctional anion exchangers. Pflugers Arch. 447, 710–721.

Nagata, K., Duggan, A., Kumar, G., and Garcia-Anoveros, J. 2005. Nociceptor and hair cell transducer properties of TRPA1, a channel for pain and hearing. J. Neurosci. 25, 4052–4061.

Nicolson, T. 2005. Fishing for key players in mechanotransduction. Trends Neurosci. 28, 140–144.

Nilius, B., Talavera, K., Owsianik, G., Prenen, J., Droogmans, G., and Voets, T. 2005. Gating of TRP channels: a voltage connection? J. Physiol. 567, 35–44.

Northcutt, R. G., Brandle, K., and Fritzsch, B. 1995. Electroreceptors and mechanosensory lateral line organs arise from single placodes in axolotls. Dev. Biol. 168, 358–373.

O'Hagan, R., Chalfie, M., and Goodman, M. B. 2005. The MEC-4 DEG/ENaC channel of *Caenorhabditis elegans* touch receptor neurons transduces mechanical signals. Nat. Neurosci. 8, 43–50.

Okamura, Y., Nishino, A., Murata, Y., Nakajo, K., Iwasaki, H., Ohtsuka, Y., Tanaka-Kunishima, M., Takahashi, N., Hara, Y., Yoshida, T., *et al.* 2005. Comprehensive analysis of the ascidian genome reveals novel insights into the molecular evolution of ion channel genes. Physiol Genomics 22, 269–282.

Peier, A. M., Moqrich, A., Hergarden, A. C., Reeve, A. J., Andersson, D. A., Story, G. M., Earley, T. J., Dragoni, I., McIntyre, P., Bevan, S., *et al.* 2002. A TRP channel that senses cold stimuli and menthol. Cell 108, 705–715.

Perraud, A. L., Takanishi, C. L., Shen, B., Kang, S., Smith, M. K., Schmitz, C., Knowles, H. M., Ferraris, D., Li, W., Zhang, J., *et al.* 2005. Accumulation of free ADP-ribose from mitochondria mediates oxidative stress-induced gating of TRPM2 cation channels. J. Biol. Chem. 280, 6138–6148.

Price, M. P., Lewin, G. R., McIlwrath, S. L., Cheng, C., Xie, J., Heppenstall, P. A., Stucky, C. L., Mannsfeldt, A. G., Brennan, T. J., Drummond, H. A., *et al.* 2000. The mammalian sodium channel BNC1 is required for normal touch sensation. Nature 407, 1007–1011.

Putnam, N. H., Srivastava, M., Hellsten, U., Dirks, B., Chapman, J., Salamov, A., Terry, A., Shapiro, H., Lindquist, E., Kapitonov, V. V., Jurka, J., Genikhovich, G., Grigoriev, I. V., Lucas, S. M., Steele, R. E., Finnerty, J. R., Technau, U., Martindale, M. Q., and Rokhsar, D. S. 2007. Sea anemone genome reveals ancestral eumetazoan gene repertoire and genomic organization. Science 317, 86–94.

Reid, G. 2005. ThermoTRP channels and cold sensing: what are they really up to? Pflugers Arch. 451, 250–263.

Reiser, J., Polu, K. R., Moller, C. C., Kenlan, P., Altintas, M. M., Wei, C., Faul, C., Herbert, S., Villegas, I., Avila-Casado, C., *et al.* 2005. TRPC6 is a glomerular slit diaphragm-associated channel required for normal renal function. Nat. Genet. 37, 739–744.

Rokas, A., Kruger, D., and Carroll, S. B. 2005. Animal evolution and the molecular signature of radiations compressed in time. Science 310, 1933–1938.

Schaefer, M. 2005. Homo- and heteromeric assembly of TRP channel subunits. Pflugers Arch. 451, 35–42.

Schlosser, G. 2005. Evolutionary origins of vertebrate placodes: insights from developmental studies and from comparisons with other deuterostomes. J. Exp. Zool. B Mol. Dev. Evol. 304, 347–399.

Senften, M., Schwander, M., Kazmierczak, P., Lillo, C., Shin, J. B., Hasson, T., Geleoc, G. S., Gillespie, P. G., Williams, D., Holt, J. R., *et al.* 2006. Physical and functional interaction between protocadherin 15 and myosin VIIa in mechanosensory hair cells. J. Neurosci. 26, 2060–2071.

Shin, J. B., Adams, D., Paukert, M., Siba, M., Sidi, S., Levin, M., Gillespie, P. G., and Grunder, S. 2005. Xenopus TRPN1 (NOMPC) localizes to microtubule-based cilia in epithelial cells, including inner-ear hair cells. Proc. Natl. Acad. Sci. U. S. A. 102, 12572–12577.

Sidi, S., Friedrich, R. W., and Nicolson, T. 2003. NompC TRP channel required for vertebrate sensory hair cell mechanotransduction. Science 301, 96–99.

Steenkamp, E. T., Wright, J., and Baldauf, S. L. 2006. The protistan origins of animals and fungi. Mol. Biol. Evol. 23, 93–106.

Story, G. M., Peier, A. M., Reeve, A. J., Eid, S. R., Mosbacher, J., Hricik, T. R., Earley, T. J., Hergarden, A. C., Andersson, D. A., Hwang, S. W., *et al.* 2003. ANKTM1, a TRP-like channel expressed in nociceptive neurons, is activated by cold temperatures. Cell 112, 819–829.

Stowers, L., Holy, T. E., Meister, M., Dulac, C., and Koentges, G. 2002. Loss of sex discrimination and male-male aggression in mice deficient for TRP2. Science 295, 1493–1500.

Strubing, C., Krapivinsky, G., Krapivinsky, L., and Clapham, D. E. 2003. Formation of novel TRPC channels by complex subunit interactions in embryonic brain. J. Biol. Chem. 278, 39014–39019.

Sukharev, S. and Corey, D. P. 2004. Mechanosensitive channels: multiplicity of families and gating paradigms. Sci. STKE 219, 1–24.

Suzuki, M., Mizuno, A., Kodaira, K., and Imai, M. 2003. Impaired pressure sensation in mice lacking TRPV4. J. Biol. Chem. 278, 22664–22668.

Syntichaki, P. and Tavernarakis, N. 2004. Genetic models of mechanotransduction: the nematode *Caenorhabditis elegans*. Physiol. Rev. 84, 1097–1153.

Szeder, V., Grim, M., Halata, Z., and Sieber-Blum, M. 2003. Neural crest origin of mammalian Merkel cells. Dev. Biol. 253, 258–263.

Tang, Y., Cao, G., Chen, X., Yoo, J., Yethiraj, A., and Cui, Q. 2006. A finite element framework for studying the mechanical response of macromolecules: application to the gating of the mechanosensitive channel MscL. Biophys. J. 91, 1248–1263.

Tian, Y., James, S., Zuo, J., Fritzsch, B., and Beisel, K. W. 2006. Conditional and inducible gene recombineering in the mouse inner ear. Brain Res. 1091, 243–254.

Tobin, D. M. and Bargmann, C. I. 2004. Invertebrate nociception: behaviors, neurons and molecules. J. Neurobiol. 61, 161–174.

Todi, S. V., Franke, J. D., Kiehart, D. P., and Eberl, D. F. 2005. Myosin VIIA defects, which underlie the Usher 1B syndrome

in humans, lead to deafness in *Drosophila*. Curr. Biol. 15, 862–868.
Toker, A. S., Teng, Y., Ferreira, H. B., Emmons, S. W., and Chalfie, M. 2003. The *Caenorhabditis elegans* spalt-like gene sem-4 restricts touch cell fate by repressing the selector Hox gene egl-5 and the effector gene mec-3. Development 130, 3831–3840.
Trebak, M., Vazquez, G., Bird, G. S., and Putney, J. W., Jr. 2003. The TRPC3/6/7 subfamily of cation channels. Cell Calcium 33, 451–461.
van Dijk, P. and Manley, G. A. 2001. Distortion product otoacoustic emissions in the tree frog *Hyla cinerea*. Hear. Res. 153, 14–22.
Vollrath, M. A., Kwan, K. Y., and Corey, D. P. 2007. The micromachinery of mechanotransduction in hair cells. Annu. Rev. Neurosci. 30, 339–365.
Walker, R. G., Willingham, A. T., and Zuker, C. S. 2000. A *Drosophila* mechanosensory transduction channel. Science 287, 2229–2234.
Wallis, D., Hamblen, M., Zhou, Y., Venken, K. J., Schumacher, A., Grimes, H. L., Zoghbi, H. Y., Orkin, S. H., and Bellen, H. J. 2003. The zinc finger transcription factor Gfi1, implicated in lymphomagenesis, is required for inner ear hair cell differentiation and survival. Development 130, 221–232.
Winn, M. P., Conlon, P. J., Lynn, K. L., Farrington, M. K., Creazzo, T., Hawkins, A. F., Daskalakis, N., Kwan, S. Y., Ebersviller, S., Burchette, J. L., *et al.* 2005. A mutation in the TRPC6 cation channel causes familial focal segmental glomerulosclerosis. Science 308, 1801–1804.
Zhang, Y., Hoon, M. A., Chandrashekar, J., Mueller, K. L., Cook, B., Wu, D., Zuker, C. S., and Ryba, N. J. 2003. Coding of sweet, bitter, and umami tastes: different receptor cells sharing similar signaling pathways. Cell 112, 293–301.
Zheng, J., Long, K. B., Matsuda, K. B., Madison, L. D., Ryan, A. D., and Dallos, P. D. 2003. Genomic characterization and expression of mouse prestin, the motor protein of outer hair cells. Mamm. Genome 14, 87–96.
Zheng, J., Madison, L. D., Oliver, D., Fakler, B., and Dallos, P. 2002. Prestin, the motor protein of outer hair cells. Audiol. Neurootol. 7, 9–12.
Zheng, J., Shen, W., He, D. Z., Long, K. B., Madison, L. D., and Dallos, P. 2000. Prestin is the motor protein of cochlear outer hair cells. Nature 405, 149–155.
Zhou, X. L., Loukin, S. H., Coria, R., Kung, C., and Saimi, Y. 2005. Heterologously expressed fungal transient receptor potential channels retain mechanosensitivity *in vitro* and osmotic response *in vivo*. Eur. Biophys. J. 34, 413–422.

Relevant Website

http://www.treefam.org – Tree Familier Database, TF317359.

3.06 Molecular Anatomy of Receptor Cells and Organ of Corti

D N Furness, Keele University, Keele, UK

C M Hackney, University of Cambridge, Cambridge, UK

© 2008 Elsevier Inc. All rights reserved.

3.06.1	Introduction	108
3.06.1.1	Basic Anatomy of Auditory Epithelia and the Hair Cells	109
3.06.1.2	Composition of the Cells of Auditory Epithelia	112
3.06.1.2.1	Hair cells	112
3.06.1.3	The Mechanotransduction Apparatus	113
3.06.1.4	The Basolateral Membrane	121
3.06.1.5	The Outer Hair Cell Lateral Wall	125
3.06.1.6	The Cytoplasm	127
3.06.1.7	Supporting Cells	128
3.06.1.8	Concluding Remarks	131
References		131

Glossary

acousticolateralis system The system of organs associated with hearing, balance, and the lateral line (see sacculus).

BAPTA A specific calcium ion chelator (1,2-bis(*o*-aminophenoxy)ethane-*N*,*N*,*N*′,*N*′-tetraacetic acid) used to reduce or eliminate free calcium from a solution.

basilar membrane Tough fibrous membrane on which the organ of Corti sits and which forms the lower border of the cochlear duct.

cochlear amplifier Biophysical mechanism within the cochlea that enhances frequency selectivity and sensitivity.

cochlear duct Triangular chamber running longitudinally through the cochlear spiral and containing the organ of Corti.

cochleotopic Gradients that vary systematically along the cochlea.

cuticular plate An apical mat of cytoskeletal proteins in hair cells that supports the hair bundle (see cytoskeleton).

cytoskeleton Network of various kinds of filament and associated molecules that provide mechanical support, movement, and transport processes within cells.

electromotile Electrically induced cellular motility, usually used to describe outer hair cell somatic motility.

endocochlear potential Extracellular electrical potential in the cochlea generated by the lateral wall of the cochlear duct.

endolymph The fluid in the scala media, composed of a high concentration of potassium ions and low concentrations of other ions.

en passant Synapses formed in passing between two neural processes or nerve cells.

eukaryote Organism whose cells contain a membrane-bound, structurally discrete nucleus and other subcellular compartments.

freeze-fracture A technique of electron microscopy where tissue is broken open in a way that cleaves cell membranes along their central lipid bilayer to reveal the intrinsic membrane particles.

gap junctions Junctions between cells formed from arrays of proteins called connexons that cross a narrowed intercellular space and form pores that allow direct transfer of ions and small molecules between the cells.

immunocytochemical labeling (immunocytochemistry) A technique for specific labeling of proteins or particular regions of a protein molecule using antibodies.

ionotropic receptor A class of neurotransmitter receptor that is also an ion channel and exerts its effects via ionic currents into the stimulated cell (see metabotropic receptor).

isoform A subtype of a particular protein, displaying small differences in structure and properties.
junctional complex A region of junctions of several different types between cells.
kinocilium A subcellular protrusion, similar in external appearance to a stereocilium but based on an axoneme composed of microtubules, typical in structure to cilia from many other parts of the body (see stereocilium).
mechanoelectrical transduction Conversion of mechanical stimulus energy to electrical potentials.
membraneous cisternae Layers of membrane beneath the surfaces and in the cytoplasm of cells.
metabotropic receptor A class of neurotransmitter receptor molecule that exerts its effects via second messenger systems in the stimulated cell (see ionotropic receptor).
modiolus Central bony pillar of the cochlea.
orthologue A gene sequence of another species that shares a direct common ancestor with the species being considered.
paracrystalline A crystalline-like arrangement of filaments in an actin bundle.
perilymph The fluid in the scala vestibuli and scala tympani, containing principally sodium ions and with substantially lower concentrations of other ions.
permeant blocker An ion or small molecule that can pass through an ion channel but also blocks it and prevents other ions/molecules passing through.
prokaryote Cell or organism such as a bacterium that lacks a membrane-bound, structurally discrete nucleus and other subcellular compartments.
resting potential The membrane potential of an unstimulated sensory receptor.
reticular lamina Upper surface of the organ of Corti, consisting of the adjacent apices of hair cells and supporting cells.
sacculus One of the otolithic organs of the inner ear, associated with balance.
scala media Central compartment of the cochlear duct, containing endolymph.
scala tympani Longitudinal compartment running below the basilar membrane of the cochlear duct, containing perilymph.
scala vestibuli Longitudinal compartment running above Reissner's membrane of the cochlear duct, containing perilymph.
spiral ligament Structure containing fibrocytes and extracellular matrix which together with the stria vascularis forms the lateral wall of the cochlear duct.
stereocilia Hair-like subcellular protrusions similar in structure to microvilli but much larger, forming the characteristic cluster of hairs (the hair bundle) on the apex of the hair cell that contains the sensory apparatus (see kinocilium).
stria vascularis Vascular epithelium containing the blood vessel of the lateral wall of the cochlear duct.
tectorial membrane Fibrous flap of extracellular matrix overlying the organ of Corti, which is part of the structure that delivers the mechanical stimulus to the hair cells.
transgenic An animal that has been derived from genetically modified sperm or egg cells.

3.06.1 Introduction

The sensory cells of the auditory organs of vertebrates, the hair cells, are mechanosensory receptors that are adapted to detect minute mechanical stimuli. The receptor cell relies for this sensitivity on a cluster of organelles that project from its apex, the subcellular protrusions or hairs (stereocilia) which give the hair cell its name. Similar receptors are also found in vestibular organs where they are associated with the sense of balance and in the lateral line systems of fish and amphibians where they detect water movements. There are fundamental features shared by all hair cells that suggest that there is a common mechanism of mechanotransduction, the process by which they convert a mechanical stimulus into an electrical response that results in neurotransmission, the process by which their electrical response is sent to the brain. However, hair cells with varying morphologies and fine structure can be found, both within a single auditory or vestibular sensory epithelium and between sensory organs of

different vertebrate classes (see review by Furness, D. N. and Hackney, C. M., 2006). The hair cells are surrounded by supporting cells which also vary in morphology and organization, both in different epithelia and within an epithelium.

The cochlear hair cells and the supporting cells and other structures around them contain some molecules that are common to the equivalent cells in all auditory organs, and some that may be unique to a particular hair-cell or supporting-cell type or organ, either associated with distinct functional differences or performing an analogous role. The situation is further complicated by the fact that some molecules may have been described in certain tissues and hair-cell types but not in others, not necessarily because they are absent but because an appropriate method, molecular probe or genetic model, is not available or because the relevant investigation has not yet been done.

The purpose of this chapter is to review the molecular composition of hair cells and supporting cells determined from studies of a range of different hair-cell epithelia, including both vestibular and auditory organs, with the emphasis on the mammalian organ of Corti. These studies include genetic analysis of deafness genes (see Perspective a), molecular biological and immunohistochemical analysis of gene expression, electrophysiology and pharmacology, and correlated structural studies. Different molecules appear at different developmental stages, so account needs also to be taken of the age of the organisms studied. In general, this chapter will not consider developmental regulators or other factors that may play a transient role in the construction of the sensory epithelium but concentrate for the most part on molecules associated with its adult functional properties.

3.06.1.1 Basic Anatomy of Auditory Epithelia and the Hair Cells

The auditory organ of mammals is the cochlea, a snail-shell shaped part of the bony labyrinth of the inner ear lined by membranes and containing the membraneous cochlear duct. The sensory epithelium, the organ of Corti, is found within the cochlear duct (Figure 1). The epithelium is situated on the basilar membrane which forms the lower margin of the duct. This structure is composed of tough extracellular matrix molecules such as type IV collagen (Cosgrove, D. *et al.*, 1996a; 1996b), type II collagen, fibronectin, tenascin, 4S/6S chondroitin sulfate proteoglycans, decorin, αV and β1 integrins (Tsuprun, V. and Santi, P., 1999), emilin (Amma, L. L. *et al.*, 2003), and mainly laminin type 11 (Rodgers, K. D. *et al.*, 2001), the latter probably being located in the basement membrane which lies between the organ of Corti cells and the basilar membrane. Overlying the epithelium is a gelatinous flap, the tectorial membrane composed of collagen types II, V, and IX (Slepecky, N. B. *et al.*, 1992), with additional unique glycoproteins, α- and β-tectorin (Legan, P. K. *et al.*, 1997). The tectorial membrane is attached to the modiolar side of the cochlea (see below and Figure 1) where it arises from a ridge of tissue, the spiral limbus. The lateral wall of the cochlear duct stretches up from the outer edge of the basilar membrane inside the bony outer shell of the cochlea. It contains the stria vascularis, an epithelium composed of three layers of cells involved in homeostatic mechanisms that control the ionic balances of cochlear fluids, external to which is the spiral ligament that is composed mainly of extracellular material and fibrocytes (see, e.g., Spicer, S. S. and Schulte, B. A., 1991). A third membrane, Reissner's membrane that has two layers of cells, attaches the stria vascularis to the inner edge of the organ of Corti making the duct triangular in cross section (Figure 1). The central compartment of the duct, the scala media, is chemically and electrically isolated from the compartments above (the scala vestibuli) and below (scala tympani) by means of tight junctions connecting all of the cells that compose the inner lining. This allows a high potassium and low sodium content to be maintained in the fluid in the duct (endolymph) compared with fluid in the other scalae (perilymph), the latter being more typical of an extracellular solution as it is high in sodium (Konishi, T. and Salt, A. N., 1980). Various ion pumps and transport mechanisms situated in the lateral wall maintain the electrical potential of the scala media at around +80 mV compared with 0 mV in perilymph and negative potentials of the hair cells. The resultant endocochlear potential (EP) is vital for the maintenance of cochlear sensitivity as it provides a battery that powers both the mechanoelectrical and electromechanical properties crucial to normal hearing (see, e.g., Kirk, D. L. and Yates, G. K., 1998). Consequently, failure of the homeostatic mechanisms that generate and maintain the EP can result in impairment and loss of hearing (see Perspective b) and is potentially involved in Ménière's disease (see Perspective c).

The cochlear duct winds spirally around a central bony pillar, the modiolus (Figure 1), within which is the spiral ganglion of the auditory nerve. Peripheral processes of the spiral ganglion neurons emerge from the modiolus and innervate the hair cell via the

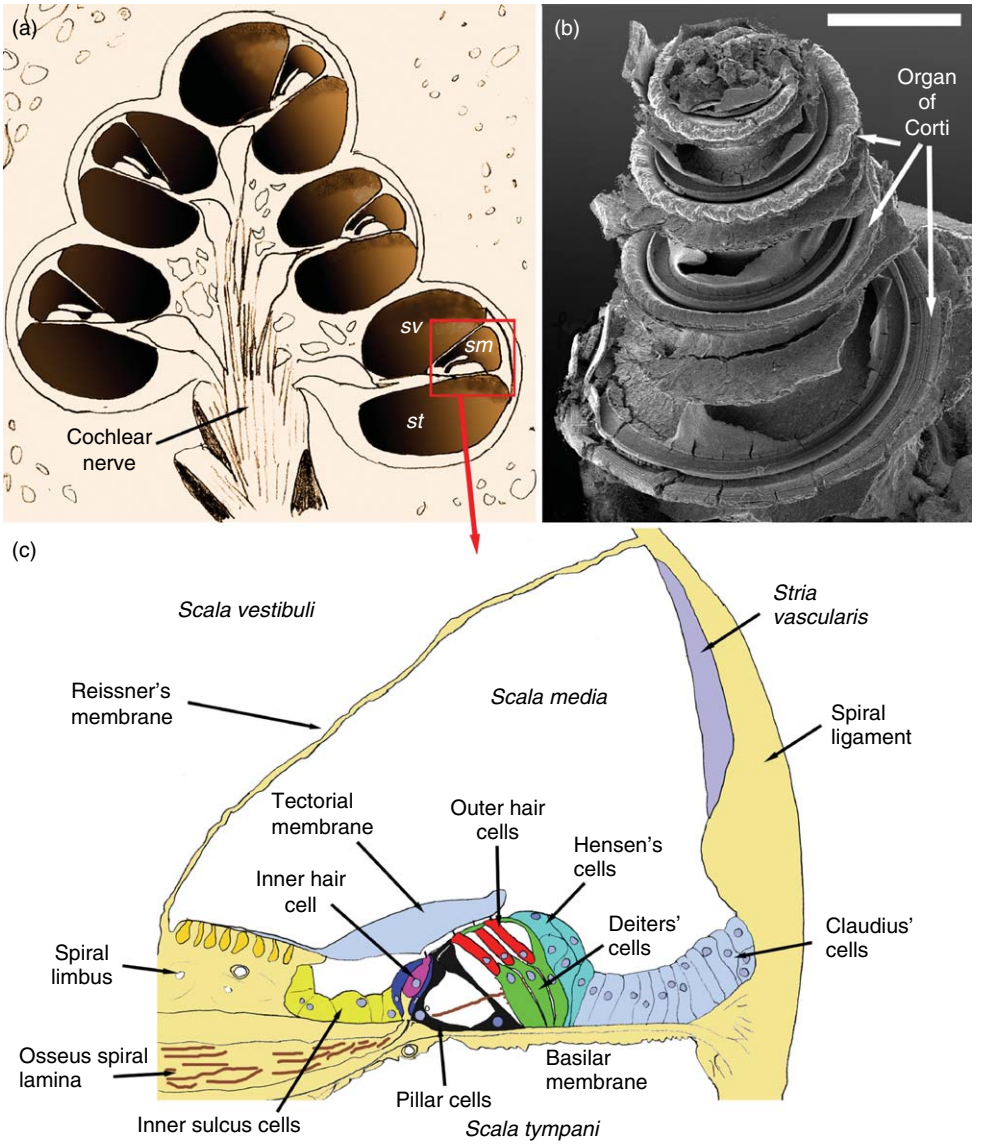

Figure 1 Gross anatomy of the cochlea and cytoarchitecture of the organ of Corti. (a) Diagrammatic cross section of a mammalian cochlea which consists of a canal that spirals around a central bony pillar, the modiolus, which contains the cochlear nerve. The canal is subdivided longitudinally by the central cochlear duct the scala media (*sm*), containing the organ of Corti, the scala vestibuli (*sv*) above and the scala tympani (*st*) below. (b) Scanning electron micrograph of a guinea pig cochlea dissected to reveal the organ of Corti. Scale bar = 0.5 mm. (c) Diagram of a cross section showing the scala media (the region enclosed by the red box in (a). The three boundaries are Reissner's membrane with scala vestibuli above, the lateral wall (composed of the stria vascularis and spiral ligament), and basilar membrane with scala tympani below. The organ of Corti sits on the basilar membrane and contains the inner and outer hair cells and supporting cells. The latter include the pillar cells and the Deiters' cells which support the outer hair cells and the Hensen's cells which are on the strial edge of the sensory epithelium. Other cells bordering the epithelium are, on the strial side, Claudius' cells and, on the modiolar side, the inner sulcal cells. The tectorial membrane is in contact with the tips of the hairs of the OHCs and is hinged along the spiral limbus. The innervation of the hair cells enters the organ of Corti via perforations in a bony shelf, the osseous spiral lamina.

osseous spiral lamina. Central processes of these neurons project to the cochlear nuclear complex. The cochlea is also innervated by efferent nerve fibers which predominantly originate in the superior olivary complex from neurones located both ipsilaterally in the lateral superior olivary nucleus (the lateral system) and contralaterally in the medial superior olivary nucleus (the crossed olivocochlear system).

The organ of Corti is composed of hair cells and supporting cells organized in a precise geometric array. Hair cells are of two types, inner hair cells (IHCs) forming one row along the cochlear spiral and consisting of flask-shaped cells with a more or less linear longitudinal (with respect to the direction of the spiral) array of stereocilia along their apices and three rows of outer hair cells (OHCs) with cylindrical cell bodies and an apical W-shaped bundle of stereocilia (Figure 2). In adults, the hair bundles are composed of around 50 stereocilia in IHCs and 90 in OHCs, although the precise number

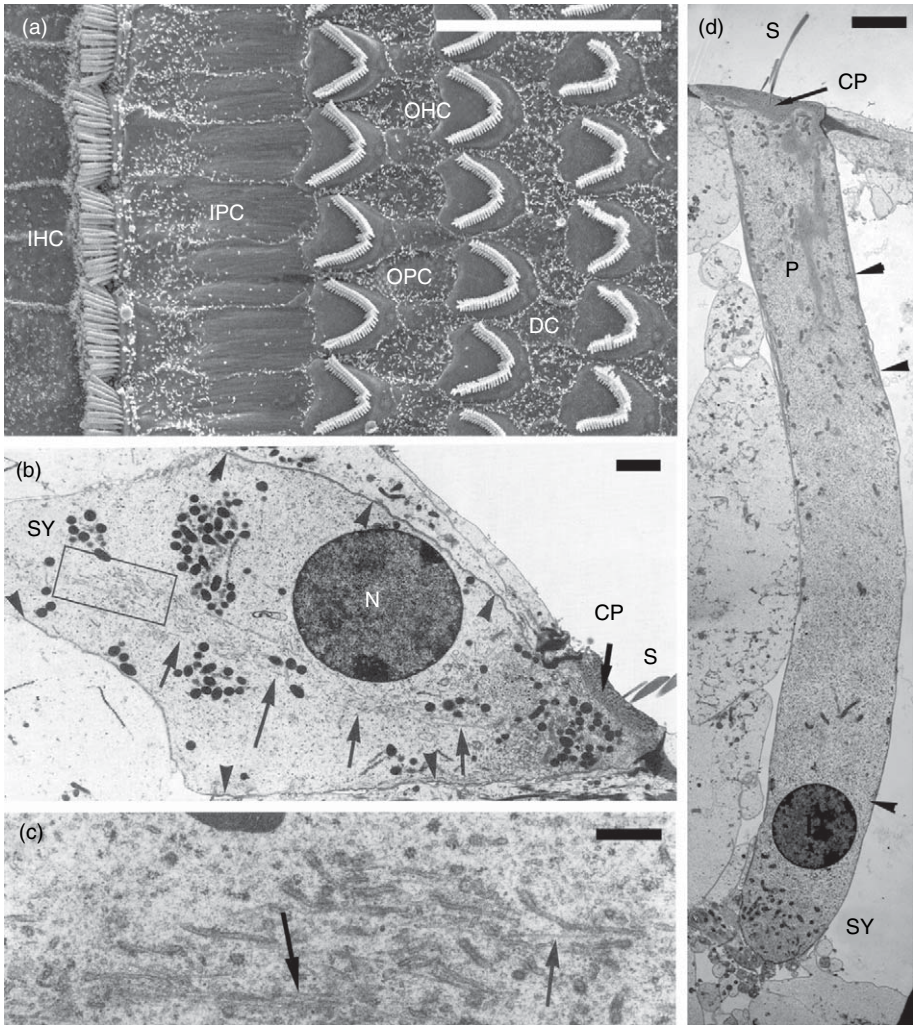

Figure 2 Organization of the sensory epithelium and the hair cells. (a) Scanning electron micrograph of the reticular lamina following removal of the tectorial membrane. The apices of the three rows of outer (OHC) and one row of inner (IHC) hair cells can be seen separated by supporting cells. The hair bundles of OHCs appear W-shaped, whilst those of IHCs appear more linear. Between the IHCs and the OHCs are the apices of inner pillar cells (IPC). The outer pillar cell (OPC) apices occur between OHCs of the first row, those of Deiters' cells (DC) between the remaining OHC rows. Scale bar = 20 μm. (b) Transmission electron micrograph of a guinea-pig IHC in longitudinal section showing stereocilia (S) projecting from the cuticular plate (CP). The cell body contains the nucleus (N) and a track of microtubules and vesicles (arrows) extending from the apex to the synaptic region (SY). The basolateral membrane has a subsurface cistern from the neck to just below the nucleus (arrowheads). The box is shown at higher enlargement in (c). Scale bar = 5 μm. (c) Membraneous tubules and vesicles are evident in association with longitudinally orientated microtubules (arrows). Scale bar = 500 nm. (d) Transmission electron micrograph of a guinea-pig OHC in longitudinal section. The apical stereocilia (S) and cuticular plate (CP), the lateral wall region, indicated by the arrowheads, and the synaptic region (SY) are illustrated. Note the central axial projection (P) of cuticular plate material. Scale bar = 5 μm. (b, c) Adapted from Furness, D. N., Hackney, C. M., and Steyger, P. S. 1990. Organization of microtubules in cochlear hair cells. J. Electron Microsc. Tech. 15, 261–279.

varies with species and position along the spiral, and there is a minimum of two rows of stereocilia always increasing in height stepwise across a bundle. The IHCs are supported by inner phalangeal cells and OHCs by Deiters' cells. Deiters' cells anchor the OHCs at their base in a cup and give rise to a strut which projects upward at an angle to terminate in the top of the organ of Corti (the reticular lamina) where it anchors adjacent OHC apices. Inner phalangeal cells almost completely enclose the IHCs. Between IHCs and OHCs are two rows of pillar cells which form a triangular arch in cross section, encompassing the longitudinally running tunnel of Corti (Figure 1).

The cochlear response to sound is related to the physical attributes of the array of hair cells and supporting cells, that is, the dimensions, angle, and shape of cells and projecting cellular processes, the basilar membrane, including changes in its width and thickness and the overlying tectorial membrane. These all vary systematically along the length of the spiral organ, and the result is a gradual change in mass and compliance that generates a cochleotopic gradient in resonant properties. Accordingly, sound input into cochlear fluids via the middle ear sets up traveling waves of displacement along the organ of Corti/basilar membrane complex such that low frequencies produce maximum displacement near the apex of the spiral and high frequencies near the base (see review by Robles, L. and Ruggero, M. A., 2001). The displacement is transferred to the hair bundles by means of the tectorial membrane, which contacts the OHC stereocilia and produces fluid movements that displace the IHC stereocilia. Movement of the hairs in the excitatory direction (i.e., toward the tallest row) depolarizes the hair cells whilst opposite deflections hyperpolarize them. The basilar membrane displacement also undergoes nonlinear amplification, via an electromechanical response attributed primarily to the OHCs, which enhances the separation of frequencies along the cochlea and the detection of low-intensity sound (see, e.g., review by Fettiplace, R. and Hackney, C. M., 2006a). In conjunction with physical changes, some aspects of the composition of the cells also vary systematically along the length of the spiral, with changes in the concentration of some proteins contributing to cochleotopic changes in the physiological properties of the organ of Corti.

Other auditory organs also contain hair cells and supporting cells of different types (see Chapter Phylogeny and Evolution of Ciliated Mechanoreceptor cells). The auditory epithelium of birds is a curved tapering ridge with two types of hair cell, short and tall. An overlying tectorial membrane similarly stimulates hair bundles. The cold-blooded vertebrates (amphibians and reptiles) also possess ridge-like auditory papillae with hair cells similar in overall organization to mammalian and avian hair cells (Figure 3) but of varying types often defined by differences in the geometric organization, size and morphology of the hair bundle (see, e.g., Manley, G. A., 1990; Hackney, C. M. *et al.*, 1993), and an overlying tectorial membrane, though not all hair bundles insert into it. In some amphibians, there are two auditory epithelia per inner ear whilst fish lack specific primary auditory epithelia but respond to auditory stimuli via other hair-cell epithelia in their inner ears (see, e.g., review by Popper, A. N., 2000).

3.06.1.2 Composition of the Cells of Auditory Epithelia

3.06.1.2.1 Hair cells

The hair cells are not only mechanically sensitive but also contribute to the general mechanical properties of auditory organs. These factors make their ultrastructure vital to the function of the hearing organs in a variety of ways; for example, in mammals, they must withstand and even contribute to the physical displacement of the basilar membrane in the organ of Corti whilst retaining a rapid, highly sensitive mechanotransduction mechanism. Thus, they are rich in cytoskeletal proteins, particularly actin, and the supporting cells are also structurally stiff because of large microtubule bundles and actin-rich anchoring structures. At the same time, the hair cells are innervated by nerve fibers of the cochlear nerve. IHCs are innervated by up to 20 afferent nerve fibers constituting around 90% of all afferent fibers, whilst several OHCs form synapses with branches from single nerve fibers that constitute the remaining 10% of afferents. The OHCs also receive direct input mainly from crossed olivocochlear efferents, whilst generally IHCs do not. Instead, the efferent innervation is received by their afferent fibers via *en passant* contacts from fibers of the lateral system, postsynaptic to the afferent terminal (see Chapter Genetic Hearing Loss).

The hair cells can accordingly be subdivided into an apical sensory pole containing the hair bundle which is the mechanotransduction apparatus that has evolved to detect mechanical stimuli and, at least in OHCs, is thought to contain a force-generating mechanism that may contribute to the cochlear amplifier (Chan, D. K. and Hudspeth, A. J., 2005;

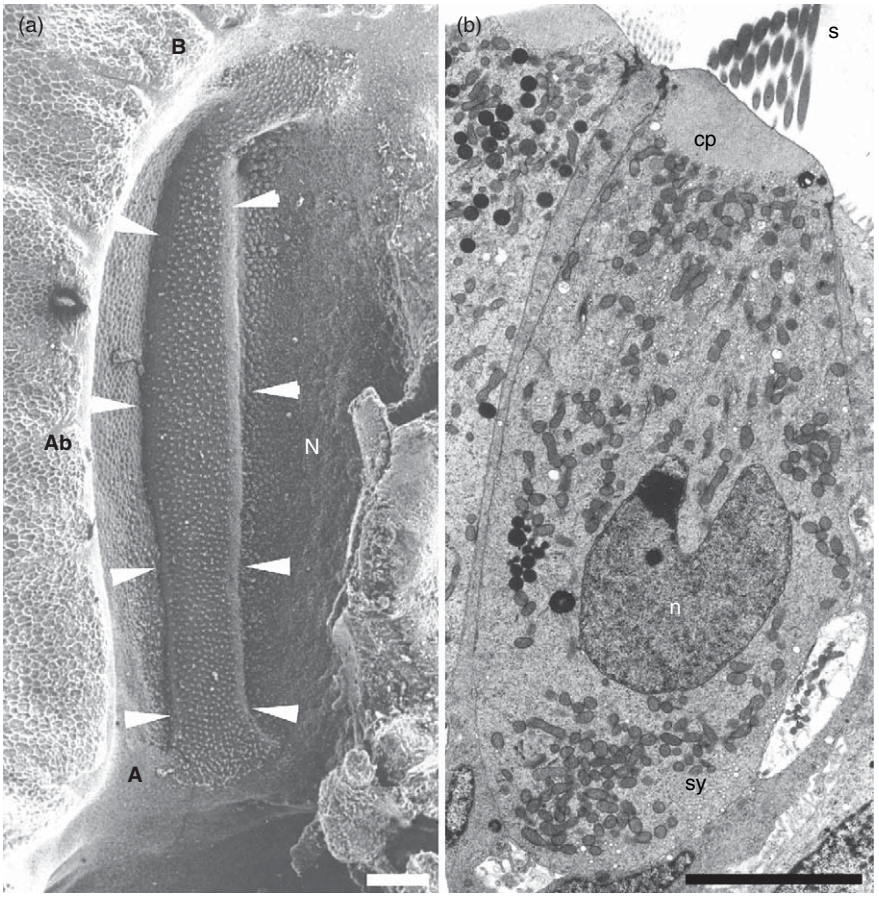

Figure 3 Auditory epithelium of a turtle. (a) Scanning electron micrograph showing the ridge-shaped epithelium (outlined by arrowheads), with the hair bundles appearing as light dots on the surface. High-frequency cells are located basally (**B**) and low-frequency cells apically (**A**). Auditory nerve fibers enter from the neural side (N) rather than the abneural (Ab) side. (b) Transmission electron micrograph of a hair cell from the turtle auditory epithelium. Like mammalian hair cells, these cells have an apical sensory region characterized by a stereociliary bundle (S) rooted into a cuticular plate (CP), and a basolateral region stretching down to the synaptic pole (SY). The nucleus (N) is central and here invaginated. The mitochondria are distributed throughout the cytoplasm but are more concentrated beneath the cuticular plate and nucleus, as is the case in mammalian cochlear hair cells.

Kennedy, H. J. *et al.*, 2005) and a basal synaptic pole which functions in both signaling to the central nervous system and receiving descending signals from the efferent auditory pathway (Figures 2 and 4). The extent of the synaptic region differs between cells; the OHCs can be relatively long cylinders, the length depending on species of origin and frequency location (Dannhof, B. J. *et al.*, 1991), with nuclei near their bases and synapses largely confined to a relatively small infranuclear region. The OHC lateral wall is a highly specialized region with a complex structure including layers of subsurface membraneous cisternae and a cytoskeletal cortical lattice. This region functions in the production of rapid cycle-by-cycle elongation/contractions involved in the biophysical amplification of basilar membrane motion (see, e.g., He, D. Z. *et al.*, 2003), which gives it properties distinct from either sensory or synaptic poles. In IHCs and other types of hair cells, this basolateral wall motility does not appear to be present.

The following descriptions will indicate the molecular organization of each of these regions in turn.

3.06.1.3 The Mechanotransduction Apparatus

The sensory pole of the hair cell is responsible for mechanotransduction (Corey, D. P. and Hudspeth, A. J., 1979a) and contains a complex apparatus that serves to deliver stimulus energy onto

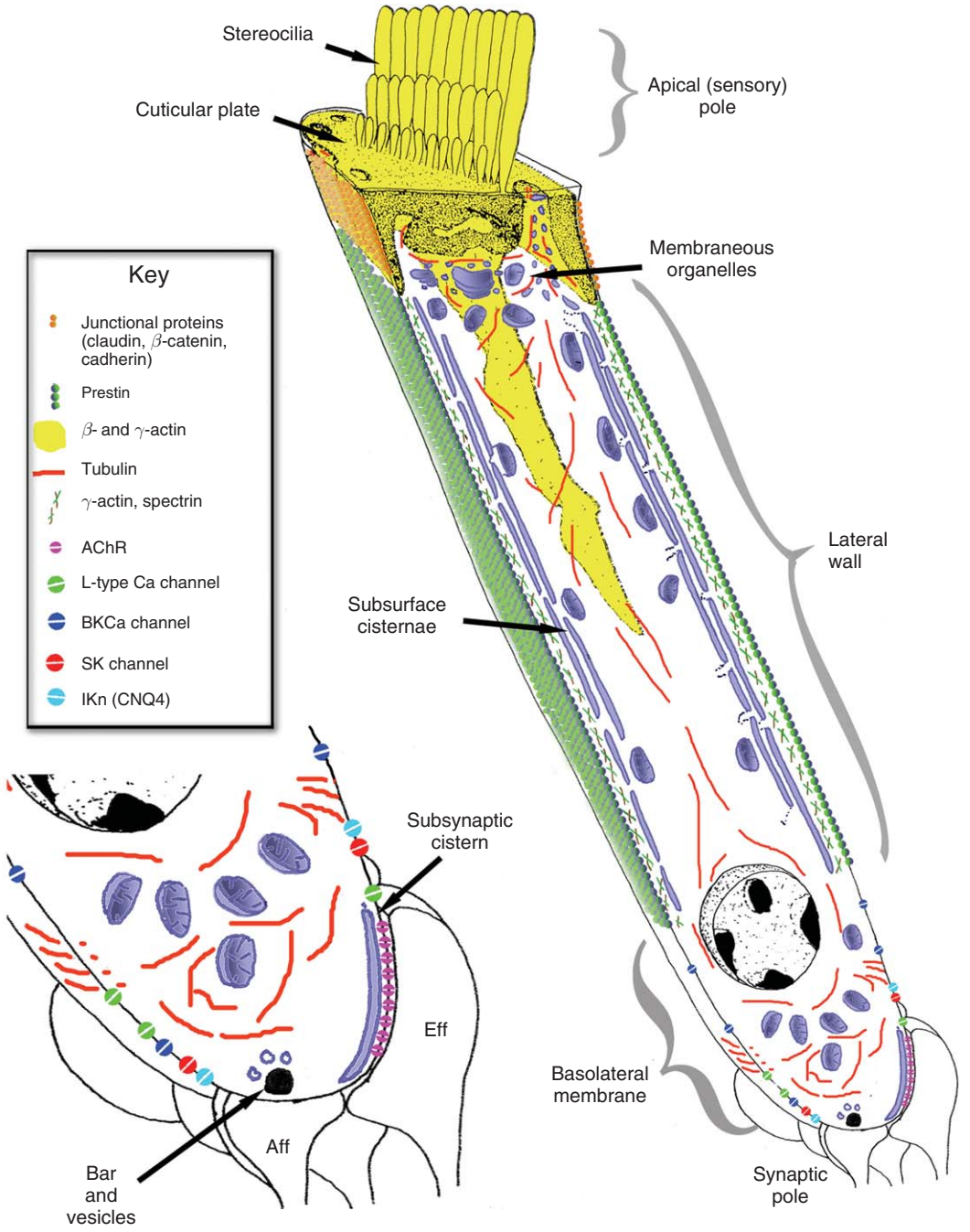

Figure 4 Diagram of an OHC showing the location of a number of important molecules as identified in the key. OHCs have a specialized lateral wall lined by cisternae and a cortical lattice. The plasma membrane contains a high density of prestin molecules. The stereocilia are rooted in the cuticular plate, both of which are rich in two nonmuscle isoforms of actin. (For clarity, other molecules important in the mechanotransduction apparatus have been omitted and are illustrated in a separate figure.) Around this region is the junctional complex composed of a number of molecules. The basolateral membrane and synaptic pole are illustrated at higher magnification on the lower left part of the plate. Note that the known ion channels associated with modulation of the receptor potential and neurotransmission are, for clarity, represented here although they are likely to be spread more apically among the prestin molecules. Membraneous organelles and cisternal membranes, including the subsynaptic cistern which apposes the efferent nerve endings, are depicted in blue. The synaptic bar and vesicles apposed to afferent nerve terminals are also shown, as is the microtubular cytoskeleton, composed of tubulin, depicted as red lines.

mechanoelectrical transduction (MET) channels in the hair-cell apex. This apparatus consists of the hair bundle (Figures 4 and 5) and an apical filamentous raft called the cuticular plate; the apical plasma membrane extends over the stereocilia and apical surface of the cuticular plate. Laterally there is a circumferential junctional complex around the plate that connects the cell with the apices of adjacent

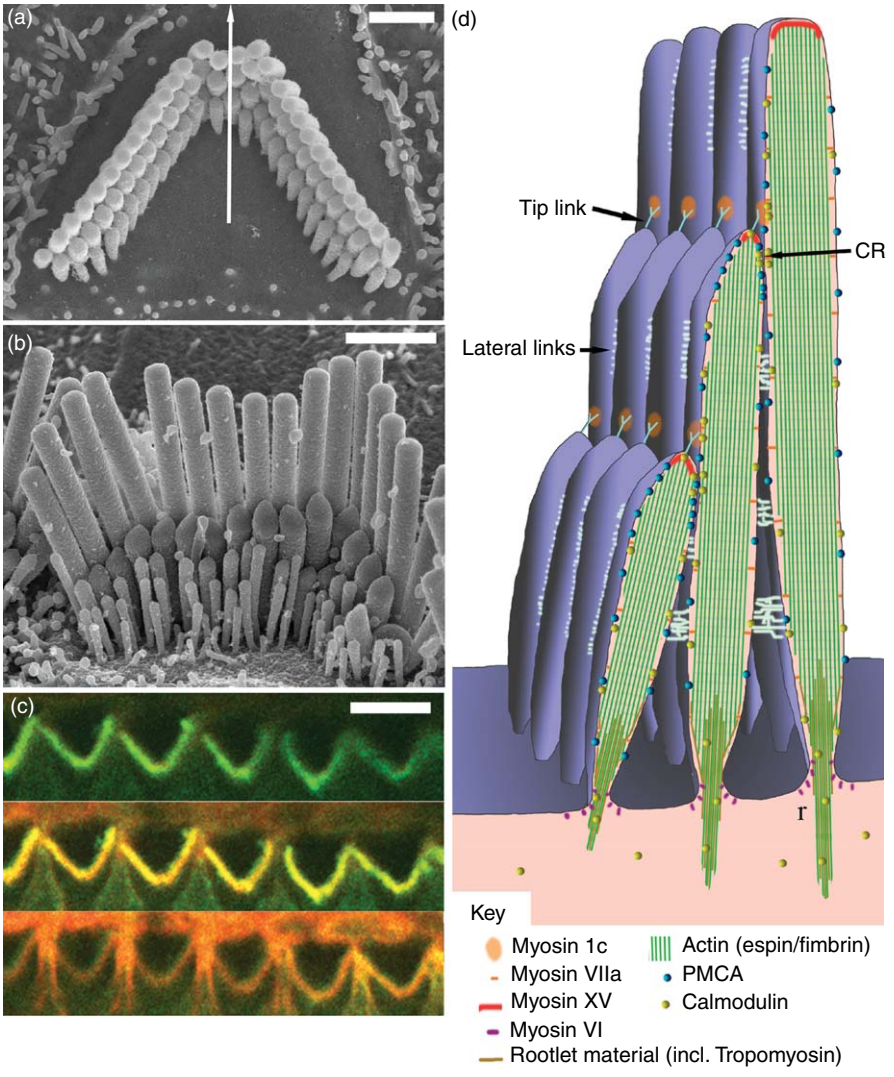

Figure 5 The stereociliary bundle and mechanotransducing apparatus. (a) Scanning electron micrograph of a rat OHC bundle. The direction of deflection of the bundle which leads to depolarization of the hair cell is shown. Scale bar = 1 μm. (b) Scanning electron micrograph of a rat IHC bundle. The bundle is more linear, and less precisely organized than the OHC, but shares most of the same anatomical features. Scale bar = 2 μm. (c) Confocal images of β (red) and γ (green) actin labeling in OHC bundles. The plane of section of the top image is near the stereociliary tips and moves lower through the middle and bottom panels. Colocalization, represented by a yellow color, is most apparent in the middle, whilst γ-actin labeling is stronger near the tips, and β-actin stronger near the ankles of the stereocilia. Scale bar = 10 μm. (d) Schematic diagram of a portion of a bundle showing the principle structures and molecules present, as indicated in the key. The stereocilia are linked by extracellular filaments, including the tip link which is forked. An actin paracrystal cross-linked by espin and fimbrin forms the core. Various myosin isoforms are enriched at different points as shown. Myosin XVa forms a cap over the actin core, myosin VIIa occurs along its periphery, myosin VI near the ankles, and myosin 1c, although found throughout the stereocilium, is enriched at the upper end of the tip link. Calcium ATPase (PMCA) and calmodulin are both associated with the plasma membrane but more concentrated in the tips of the stereocilia; calmodulin is known to be enriched at either ends of the tip link and in the contact region just below the tip link. At the lower end of the stereocilia, the shaft narrows to an ankle, and a small proportion of actin filaments appear to penetrate into the apex of the cell to form a rootlet (r) with dense material containing tropomyosin and calmodulin surrounding them. Putative localizations of the MET channels are depicted in Figure 6.

supporting cells, functionally separating the apical membrane from the basolateral membrane (Figure 4). This junctional complex contains β-catenin (Simonneau, L. *et al.*, 2003), cadherins (Mahendrasingam, S. *et al.*, 1997; Simonneau, L. *et al.*, 2003), and claudin 14 (Cldn 14 – Ben-Yosef, T. *et al.*, 2003). Null mutants for Cldn 14 have normal EPs but show rapid progressive loss of OHCs and slower IHC loss suggested to be due to altered ionic balances between endolymph and perilymph. Different isoforms of cadherin also show distinct distributions: N-cadherin is expressed in IHCs and E-cadherin in OHCs (Simonneau, L. *et al.*, 2003). Also around the pericuticular regions of IHCs, there is immunocytochemical evidence for the presence of a plasma membrane calcium ATPase isoform, PMCA3 (Dumont, R. A. *et al.*, 2001) presumably also assisting in ion control in that vicinity.

The hair bundle detects mechanical stimuli, directing the energy of the stimulus to the MET channels located in the stereocilia. The anatomical organization of the mechanotransduction apparatus of all hair cells, therefore, is quite precise; the stereocilia form well-defined rows, each row increasing in height stepwise in one direction across the bundle (Figure 5). Developmentally, there is a single kinocilium originating from an apical basal body, located initially in the center of the bundle at least in mammalian vestibular hair cells, which migrates to end up in the middle behind the tallest row (Forge, A. *et al.*, 1997). In the mature hair bundle, a line drawn from the kinocilium or basal body position to the middle of the shortest row of stereocilia represents an axis of symmetry whereby the structure on one side is an approximate mirror image of the other side and also lies along the excitatory–inhibitory axis of the bundle (Figure 5). The kinocilium is composed of a microtubular axoneme and is retained throughout life in all hair cells except for mammalian auditory hair cells where only the basal body remains in adults.

The stereocilia, and kinocilium when present, are covered by a surface coat of carbohydrate (Santi, P. A. and Anderson, C. B., 1987) and are linked together by a distinct array of extracellular strands called cross-links (Bagger-Sjoback, D. and Wersall, J., 1973; Pickles, J. O. *et al.*, 1984; Furness, D. N. and Hackney, C.M., 1985; Hackney, C. M. *et al.*, 1993). Typically, each shorter stereocilium is linked to a taller one in the adjacent row by an extracellular link emanating obliquely from the tip. The two attached stereocilia and the link ordinarily lie along a line that runs more or less parallel to the axis of symmetry of the bundle (Pickles, J. O. *et al.*, 1984; Furness, D. N. and Hackney, C. M., 1985). The tip link bifurcates part-way along its length, in examples from most vertebrate classes (see review by Furness, D. N. and Hackney, C. M., 2006), and at its upper end, the two strands attach to two points on the side of the taller stereocilium, coinciding with a circular plaque of electron dense material that is consistently present in all vertebrate classes (Figures 5 and 6). At its lower end, the tip link inserts into the shorter stereocilium near a dense cap of material over the actin core. Ultrastructural studies suggest that intracellular connections link the lower end of the tip link to this cap (Osborne, M. P. *et al.*, 1988; Kachar, B. *et al.*, 2000). Other cross-links include lateral links holding stereocilia together in all directions (Figure 6) and connectors below the tips, also joining short stereocilia to taller ones, in some cases in a region where the adjacent membranes are closely apposed, called the contact region (Hackney, C. M. *et al.*, 1992). Thus, in different hair-cell types, there are different constellations of links which can be distinguished to some extent by anatomical, immunological, and enzymatic means (see, e.g., Pickles, J. O. *et al.*, 1984; Furness, D. N. and Hackney, C. M., 1985; Osborne, M. P. and Comis, S. D., 1990; Goodyear, R. and Richardson, G. P. 1999; 2003), but all hair cells seem to possess tip links.

As noted above, during sound stimulation of the mammalian cochlea, displacement of the hair bundles occurs which, because of the sinusoidal nature of the traveling wave, will deflect the bundle cyclically along its axis of symmetry, alternately displacing the stereocilia in a direction toward and away from the tallest row. The likely outcome of displacement toward the tallest row of stereocilia is tension being placed on the tip links which could deliver energy and gate the MET channels at one or both ends of the link, resulting in a flow of potassium and calcium ions into the cell from the endolymph. Opposite displacement closes the channels restricting the current flow. Physiological evidence certainly accords with this hypothesis, since deflections toward the tallest stereocilia depolarize the cell and opposite displacements hyperpolarize it. When the MET channel opens, calcium entry initiates calcium-sensitive processes which include both rapid and slower force production that changes the operating point of the mechanotransduction apparatus (adaptation – see review by Fettiplace, R. and Hackney, C. M., 2006a).

Attempts are still being made to identify the different molecular composition of these components of

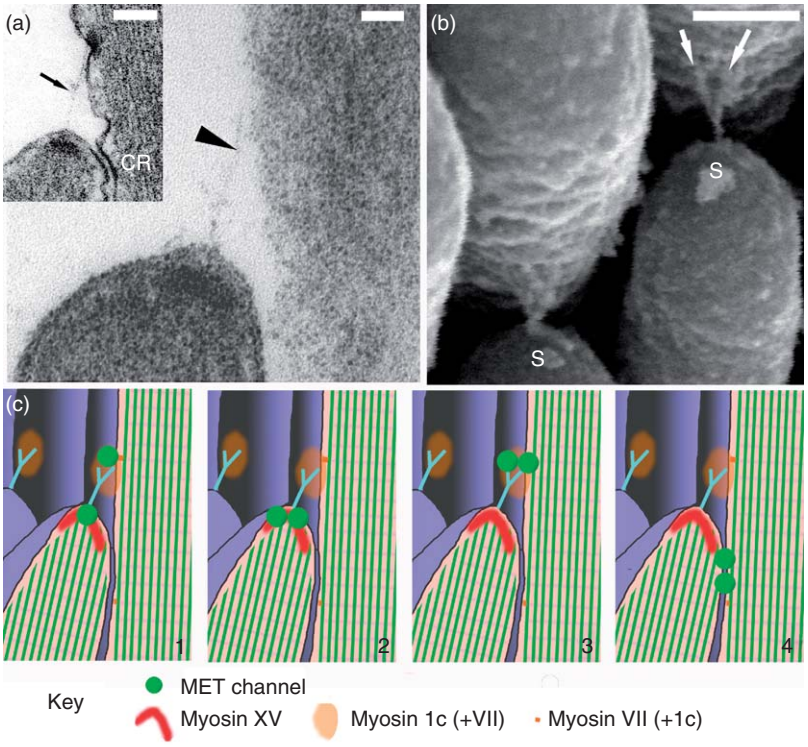

Figure 6 Possible models of the mechanotransduction apparatus. (a) (inset and main panel) Transmission electron micrographs of structures associated with gating of the MET channels. The tip link (arrow) runs between the tip of a shorter stereocilium and an adjacent taller stereocilium and appears to be forked between the two (arrowhead). The contact region (CR) is located just below the tip of the shorter stereocilium and is a point of close apposition with the taller stereocilium. Scale bars = 100 nm (inset) and 50 nm (main picture). (b) Scanning electron micrograph showing that each shorter stereocilium tip (S) is contacted by a tip link. The two forks are also illustrated (e.g., arrows). Scale bar = 100 nm. (c) Panels 1–4: different possible locations for the MET channels (green spheres). There is evidence for each of these models, but no one model currently satisfies all of the experimental data.

the mechanotransduction apparatus, in particular the identity of the MET channel itself and the composition of the tip links and associated adaptation mechanisms. The predominant apical material, the cytoskeletal protein actin, forms filaments with high-tensile strength that contribute to stiffness and motility in a variety of other cells throughout the body, including muscle cells. Between 30 and 3000 (depending on species, location, and hair-cell type), actin filaments fill the stereocilium, forming a paracrystalline bundle that constitutes the core (see review by Furness, D. N. and Hackney, C. M., 2006). The cuticular plate is composed of a network of actin filaments arranged in at least two domains in chick hair cells: a peripheral ring inside the junctional complex and a central matrix. Thus, the hair cell apices contain at least three different assemblies of actin, and these have their own constellation of associated proteins which help define and potentially modify their properties (Drenckhahn, D. *et al.*, 1991).

Actin is likely to determine the gross mechanical properties of the bundle and its anchor points. General actin stains, such as phalloidin or antibodies that are not isoform specific, label stereocilia and cuticular plate in all hair cells. However, where it has been examined (in chick and guinea pig), two specific isoforms of actin are present, cytoplasmic β- and γ-actins (Figure 5), which are distinct from the common muscle isoforms (Slepecky, N. B. and Savage, J. E., 1994; Hofer, D. *et al.*, 1997; Furness, D. N. *et al.*, 2005). Within the hair cells, these isoforms have varying ratios in different regions. Thus, the stereocilia and cuticular plate in mammals contain both, but there appears to be a peripheral enrichment of β-actin in the lower stereociliary shaft, with γ-actin more prominent toward the tip (Furness, D. N. *et al.*, 2005). In chick hair cells, β-actin may not be present in the cuticular plate (Hofer, D. *et al.*, 1997). It is not known how these isoform distributions are specified during development, nor has the relative

distribution been determined in hair cells from other vertebrates. The functional significance of the different isoform distributions is still being investigated.

The actin filaments in mammalian auditory stereocilia are cross-linked by espin which appears to be necessary for proper stereociliary elongation during development (Zheng, J. *et al.*, 2000) and, in adults, also by I-plastin (fimbrin – Pack, A. K. and Slepecky, N. B., 1995). During development, T-plastin is transiently expressed in the stereocilia (Daudet, N. and Lebart, M. C., 2002).

The stereocilia are thus stiffened by this core of actin and cross-linking proteins. Low levels of immunocytochemical labeling for the elastic molecule, spectrin, have also been detected along the shaft of the stereocilium, but this protein is more prominent in the cuticular plate and lateral wall (Mahendrasingam, S. *et al.*, 1998). The stereocilia also contain myosins (Figure 5), which commonly interact with actin to produce motility; myosin VIIa is located along the length of the actin core at its periphery (Hasson, T. *et al.*, 1997). Here, it may be associated with vezatin which can form links between catenin–cadherin complexes and myosin VIIa (Kussel-Andermann, P. *et al.*, 2000). Defects in the genes encoding myosin VIIa result in disturbance of hair bundle organization; the stereocilia can become splayed and, in scanning electron micrographs, some appear to have fallen onto the reticular lamina. These bundles require greater displacement to stimulate the hair cell than normal (Kros, C. J. *et al.*, 2002). Thus, myosin VIIa may be involved in maintaining the integrity of the bundle. Other proteins that may interact with myosin VIIa are harmonin, SANS, cadherin 23, and protocadherin 15, as defects in the genes for all of these proteins are associated with Ushers syndrome (Frolenkov, G. I. *et al.*, 2004 for a review) and PHR1, an integral membrane protein found in hair cells (Xu, S. *et al.*, 2004; Etournay, R. *et al.*, 2005).

A second myosin, myosin 1c, is distributed similarly to myosin VIIa but may be more concentrated near the stereociliary tips of shorter stereocilia and the upper end of the tip link in bullfrog where it is thought to be a component of the upper dense plaque (Garcia, J. A. *et al.*, 1998; Steyger, P. S. *et al.*, 1998). Genes for orthologs of myosin 1c have been identified in mouse (Crozet, F. *et al.*, 1997), and a transgenic model in which myosin 1c was manipulated suggest that it is involved in slow adaptation (Holt, J. R. *et al.*, 2002). Myosin 1c also interacts with PHR1 and calmodulin; all of these proteins may therefore be implicated in adaptation (Etournay, R. *et al.*, 2005).

Myosin XVa has been found to cap the actin core of mammalian stereocilia from the start of bundle development and in adulthood (Belyantseva, I. A. *et al.*, 2003; Rzadzinska, A. K. *et al.*, 2004) and is responsible for developmental delivery of whirlin to the tips of stereocilia, a process which is defective in whirler mice (Mburu, P. *et al.*, 2003). When either of the genes for myosin XVa and whirlin is defective, short stereocilia and deafness are the result; hence, both proteins are required for normal stereociliary growth (Belyantseva, I. A. *et al.*, 2005). Whirlin also associates with erythrocyte protein p55 and protein 4.1R, and it has been proposed that these form a complex involved in stereociliary development (Mburu, P. *et al.*, 2006). The expression of whirlin, p55 and protein 4.1R reduces at the end of development. During development, whirlin is also transiently present near the ankle regions, suggestive of an association with myosin VIIa as noted above.

Myosin VI has been localized to the hair-cell apex and cytoplasm, and in particular in developing hair bundles (Hasson, T. *et al.*, 1997). In zebrafish, it is localized to the ankle regions of stereocilia. A myo6 defective zebrafish mutant shows loss of mechanotransduction, and it is suggested that myosin VI is involved in tautening, then anchoring, the stereociliary membrane (Kappler, J. A. *et al.*, 2004). In mouse, defects in the *Myo,6* gene result in the Snell's Waltzer phenotype which has disorganized hair bundles (Avraham, K. B. *et al.*, 1997). Thus, myosin VI may also be involved in hair bundle development and maintenance.

The tip link is an extracellular filament and from immunocytochemical data and studies of mutant zebrafish, reported to be composed of cadherin 23 (Siemens, J. *et al.*, 2004; Sollner, C. *et al.*, 2004). However, in some studies, cadherin 23 has been detected developmentally but not in adults (Boeda, B. *et al.*, 2002). One reason for this discrepancy may be that there are multiple tip links in immature hair cells, and thus, cadherin may show a higher, more detectable, signal developmentally (see, Furness, D. N. *et al.*, 1989). Other studies suggest that protocadherin 15, which may be involved in the lateral links (see below), could be associated with the tip link (Ahmed, Z. M. *et al.*, 2006). Thus, it appears likely that some form of cadherin may be contained within the tip-link complex. If protocadherin 15 is part of the tip link, its interaction with myosin VIIa (Senften, M. *et al.*, 2006)

could form the basis of an adaptation motor in the MET apparatus.

Freeze-fracture studies show that the tip link is a braided macromolecule with an organization that suggests inelasticity (Kachar, B. *et al.*, 2000). This has led to the suggestion that the tip link is not itself the gating spring but connected to it, perhaps via ankyrin at the membrane that is then connected to the MET channel. Modeling has suggested that ankyrin has appropriate properties for a gating spring that could open the channel and is a component of transient receptor potential (TRP) channels, one candidate for the MET channel (Sotomayor, M. *et al.*, 2005).

Whilst the tip link seems to be anatomically, chemically, and structurally distinct from the lateral links, the latter also similarly seems to contain protocadherin 15 and myosin VIIa and possibly cadherin 23, especially those connecting to the kinocilium in hair cells that possess the latter. There are subsets of these links, which are differentially susceptible to agents such as BAPTA (Goodyear, R. and Richardson, G. P., 1999). Associated with all the links are keratan sulphate proteoglycans (Katori, Y. *et al.*, 1996).

The identity and location of the MET channels themselves remains controversial (see Figure 6 and Chapter Auditory Scene Analysis). Clues to the channel's identity may come from knowledge of its physiological properties. It has a large unitary conductance of between 50 and 160 pS (from chick, mouse, and turtle data *in vitro*). The conductance increases to as much as 300 pS when single channel measurements are made in the presence of low (50 μM) calcium which is a permeant blocker. The pore size is of the order of 1.26 nm (Farris, H. E. *et al.*, 2004). The channel can be blocked by other cations, such as magnesium, in millimolar concentrations, gadolinium (K_I 10 μM), and lanthanum (K_I 3.8 μM), by the diuretic amiloride (K_I 50 μM) and its derivative benzamil (K_I 6 μM), by aminoglycoside antibiotics such as dihydrostreptomycin (K_I 8–44 μM, varying with calcium concentration), and by several other agents (see review by Fettiplace, R. and Ricci, A. J., 2006b). None of the blockers yet found are irreversible, and so they are not effective as a means of isolating the channel protein biochemically. Estimates of the number of functional channels per stereocilium indicate that there may be one or (more likely) two, although this does not preclude the possibility that there could be nonfunctional channels or subunits *en route* through the hair cell or stereocilia (Hackney, C. M. *et al.*, 1992). Thus, the few channels per hair cell (about 100 or so in IHCs) coupled with the small number of hair cells in a cochlea or vestibular organ mean that the possibility of isolating channel proteins for characterization is limited.

There are a number of mechanosensory channels to consider as candidates for MET channels, in both prokaryotes and eukaryotes, and in the latter, in invertebrates and vertebrates, with a wide range of properties. These include the vertebrate MDEG – epithelial sodium channel superfamily. Like the hair-cell MET channels, these are blocked by amiloride but at lower concentrations, and they have a unitary conductance that is smaller than that of the MET channel. Another possible channel type is the cyclic nucleotide-gated channel. These are similar to the MET channel with respect to their amiloride sensitivity and calcium block but also have low unitary conductance (Farris, H. E. *et al.*, 2004). As a result of studies on invertebrate mutants with mechanosensory deficits, attention has also been drawn to the TRP channels. Studies of *Drosophila* revealed that NOMPC, a relative of the TRP channel OSM-9, was involved in mechanosensory bristles (Walker, R. G. *et al.*, 2000), and recent studies of zebrafish using antisense oligonucleotides to knock down channel function produced initial deafness and balance dysfunction (Sidi, S. *et al.*, 2003). NOMPC does not occur in mammalian hair cells, although another TRP channel TRPA1 has been suggested to be present. Antibodies to this channel label the stereocilia, and short interfering RNA for TRPA1 introduced into hair cells *in vitro* prevent mechanotransduction (Corey, D. P. *et al.*, 2004). However, knockout mice lacking TRPA1 appear to retain normal auditory function (Bautista, D. M. *et al.*, 2006; Kwan, K. Y. *et al.*, 2006), an observation that argues against this channel being the MET channel.

Another possible channel in the hair-cell apical membrane could be associated with purinergic receptors. There is evidence of ATP-gated channels in the stereocilia of hair cells, and labeling has been obtained in mammalian cochlear hair bundles for $P2X_2$ receptors. The precise location and function of these channels/receptors remain to be determined, but it has been suggested that they represent a possible way to modulate the transcellular driving force for mechanoelectrical and electromechanical transductions (Housley, G. D. *et al.*, 1999).

Recent immunocytochemical studies have also suggested the presence of two further types of channel in the hair-cell apex. The first is a chloride

channel, CLIC5, known to be associated with actin that has been detected in the region where radixin is found. A mouse mutant, jitterbug which lacks the CLIC5, has abnormal hair bundles and shows reduced labeling for radixin, suggesting that an interaction between the two is necessary for normal stereociliary formation (Gagnon, L. H. *et al.*, 2006). The second is an acid-sensing channel, ASIC1b (Ugawa, S. *et al.*, 2006). The ASICs are proton-gated sodium channels, also of the mammalian degenerin (MDEG) family, and have been localized especially near to the ankle region.

Despite all of these studies, the identity of the MET channel remains to be determined beyond doubt. It is possible that it is a channel common to other epithelia or neurones rather than one specific to the acousticolateralis system and is thus hard to distinguish from the other channels in this system.

The calcium sensitivity of mechanotransduction and its effects on adaptation mean that the MET apparatus also needs calcium-regulating and calcium-sensing proteins. In guinea-pig cochlear hair cells, calmodulin is enriched at the tips of the stereocilia, at either end of the tip link, and in the stereociliary contact region (Furness, D. N. *et al.*, 2002b; Figures 5 and 6). In these locations, calmodulin could be an integral component of the MET channel itself, since calcium appears to have a direct influence on channel gating. However, myosin molecules are likely to bind calmodulin, so some of the calmodulin in these regions may reflect an interaction with myosin 1c, myosin VIIa, representing the slow adaptation motor, or myosin XVa. In mammals, calmodulin also occurs along the lateral wall of the stereocilia where the myosin VIIa is found and so could also influence motile properties of the bundle from this location, more indirectly affecting the gating of the channels.

In the vicinity of the mechanotransduction apparatus, there is also thought to be a high density of plasma membrane calcium ATPases (pumps – PMCAs) that work together with endogenous diffusible calcium buffers, such as calbindin and parvalbumin, to exercise fine control over calcium concentration and thus regulate its effects on the MET channel (Figures 5 and 6). PMCAs have been immunolocalized in both adult frog sacculus and mammalian cochlear hair bundles, and a mouse mutant lacking PMCA (the deaf-waddler mouse) and PMCA2 knockouts become deaf and display vestibular dysfunction (Kozel, P. J. *et al.*, 1998; Street, V. A. *et al.*, 1998). The different isoforms of PMCA show distinct distributions; thus, the stereocilia contain predominantly or exclusively PMCA2 (Dumont, R. A. *et al.*, 2001), and there is evidence of rapid turnover of this protein in the stereociliary membrane (Grati, M. *et al.*, 2006).

Other proteins could also contribute to the control of calcium. A number of calcium buffers have been detected in hair cells. These include, parvalbumin-3 (Heller, S. *et al.*, 2002), a form of parvalbumin-β (oncomodulin), calbindin-D28K, and calretinin (Hackney, C. M. *et al.*, 2003; 2005), some of which may be involved in control of local calcium concentrations in the bundle associated with the modulation of mechanotransduction.

In the mouse, calretinin is present in hair cells developmentally but disappears, at least in OHCs, by P22 (Dechesne, C. J. *et al.*, 1994). The other calcium buffers are likely to play various roles in hair cells, and they are found in adults in the cytoplasm of the cell body (discussed further below). In rat cochlear hair cells, the concentration of these buffers appears to be lower in the stereocilia than in the hair-cell body (Hackney, C. M. *et al.*, 2005), a situation which differs from that seen in turtle cochlear hair cells where buffer concentrations appear to be similar in both compartments (Hackney, C. M. *et al.*, 2003). This implies an evolutionary change in calcium-handling mechanisms in the stereocilia perhaps related to changes in the sensitivity and frequency selectivity of the mammalian cochlea.

At their insertion into the apex of the hair cell, the stereocilia become narrower. In this vicinity and extending both up into the shaft and down into the cuticular plate is a rootlet of dense material which accompanies a smaller number of actin filaments that appear to continue into the plate. In mammals, this remains as a tightly packed bundle in the cuticular plate, surrounded by a clear zone relatively devoid of filaments (Itoh, M., 1982). In other vertebrates, the filaments may fan out in a conical array (Tilney, L. G. *et al.*, 1980; Hackney, C. M. *et al.*, 1993). The composition of the dense material in the mammalian rootlet remains obscure, although tropomyosin and calmodulin have been localized there in adult guinea pigs (Slepecky, N. and Chamberlain, S. C., 1985), and as noted before, myosin VI is present in the ankle region (Kappler, J. A. *et al.*, 2004).

Tropomyosin has a regulatory function modulating acto-myosin interactions in muscle. It is thus possible that the rootlet represents the site of an active mechanism that influences stereociliary stiffness or motion and perhaps is associated with force production. However, the relatively long distance

from the MET channels and the comparatively low speed of an enzymatically acting force-producing motor may limit how rapidly such a mechanism can work to modulate mechanotransduction at acoustic frequencies, which would be necessary for a process in this location to contribute significantly to the cochlear amplifier. On the other hand, a slower modulatory force might be used to tune the hair cells and optimize bundle properties better to the frequency location of the cells.

The ankle membrane of the stereocilia contains radixin (Pataky, F. *et al.*, 2004). Radixin interacts with myosin VIIa and myosin XVa, indicating possible formation of complexes between these proteins, binding actin to the membrane.

Other cytoskeletal and related proteins that have been detected in the cuticular plate include spectrin (Pack, A. K. and Slepecky, N. B., 1995; Mahendrasingam, S. *et al.*, 1998) profilin, I-plastin (fimbrin), α-actinin (Slepecky, N. B. and Ulfendahl, M., 1993), and calmodulin (Furness, D. N. *et al.*, 2005) as well as the aforementioned isoforms, myosin VI and myosin VIIa. The organization of the plate, at least by electron microscopy, is difficult to elucidate, but there are clearly arrays of cytoskeletal molecules within it or associated with it, examples being the striated Friedmann's body (Slepecky, N. B. *et al.*, 1981) and the infracuticular extension or network (Carlisle, L. *et al.*, 1988), the latter possibly unique to guinea pigs. This infracuticular protrusion is largest in apical long OHCs in guinea pig and decreases in size toward the base of the cochlea and from the third to the first row of OHCs. The cuticular plate of mammals also contains layers of discrete dense bodies, which may be enriched in α-actinin (Slepecky, N. and Chamberlain, S. C., 1985). In IHCs, the layers closer to the apical membrane contain larger-sized densities than those situated closer to nucleus; in addition, the cuticular plate may also be thicker in high-frequency regions (Furness, D. N. *et al.*, 1990). Thus, there are organizational features that suggest that the cuticular plate may influence hair bundle mechanics, but these properties require further biophysical investigation.

The apical membrane has some other structural and molecular features which indicate that active membrane cycling mechanisms may be occurring. The cuticular plate is interrupted by a wide channel of cytoplasm that reaches up to the apical membrane (Figures 4 and 7). In the membrane over this channel, there are frequently coated pits (Furness, D. N. *et al.*, 1990) and an apical subsurface cistern is also present in both IHCs and OHCs (Lim, D. J., 1986; Furness, D. N. *et al.*, 1990) of the mammalian cochlea. Endocytotic pits have been described in turtle cochlea (Hackney, C. M. *et al.*, 1993) and bullfrog sacculus (Kachar, B. *et al.*, 1997) at this location. Active membrane uptake has been confirmed in this region in both IHCs and OHCs by using the dye FM-1-43 (Gale, J. E. *et al.*, 2001; Meyer, J. *et al.*, 2001; Griesinger, C. B., *et al.*, 2002; 2004). In the IHCs, it has been estimated that approximately 0.5% of the surface area of the cell can be endocytosed each second. The membrane taken up seems to be transported to the base of IHCs by kinesin-dependent trafficking (Griesinger, C. B. *et al.*, 2002), probably along tracks of microtubules (Figures 2 and 7) that have been described running through the cell (Steyger, P. S. *et al.*, 1989; Furness, D. N. *et al.*, 1990; Kachar, B. *et al.*, 1997) where it appears to be accumulated near the synaptic pole perhaps associated with replenishment of synaptic membrane (Griesinger, C. B. *et al.*, 2002). Such a mechanism could also be indicative of an apical membrane recycling process, perhaps allowing turnover of the MET channels, although the source of new apical membrane has not been determined.

3.06.1.4 The Basolateral Membrane

The basolateral membrane region of hair cells, like other epithelial cells, is compositionally distinct from the apical membrane partly because of the periapical tight junctions, which are likely to restrict interchange of membrane components, and partly because of differences in cytoskeletal structures beneath the membranes. Whilst in the apical membrane, the ion channels presently thought to occur are the MET channels, ATP-gated channels, CLIC5 and ASIC1b, the basolateral membrane has a different complement of channels involved in shaping the receptor potential, calcium control and in neurotransmitter release (Figure 7).

The afferent synapses onto all hair cells are often called ribbon synapses as a consequence of their electron dense presynaptic bars or bodies, the shape of which varies between different hair-cell types. In mammalian IHCs, the synaptic bodies are usually tear-drop shaped, whereas in many nonmammalian vertebrates, they are round (Figure 7). They are surrounded by a halo of vesicles which are presumed to contain neurotransmitter. Other vesicles occur in the cytoplasm around these sites. The synaptic bar contains the marker ribeye in bullfrog saccular hair

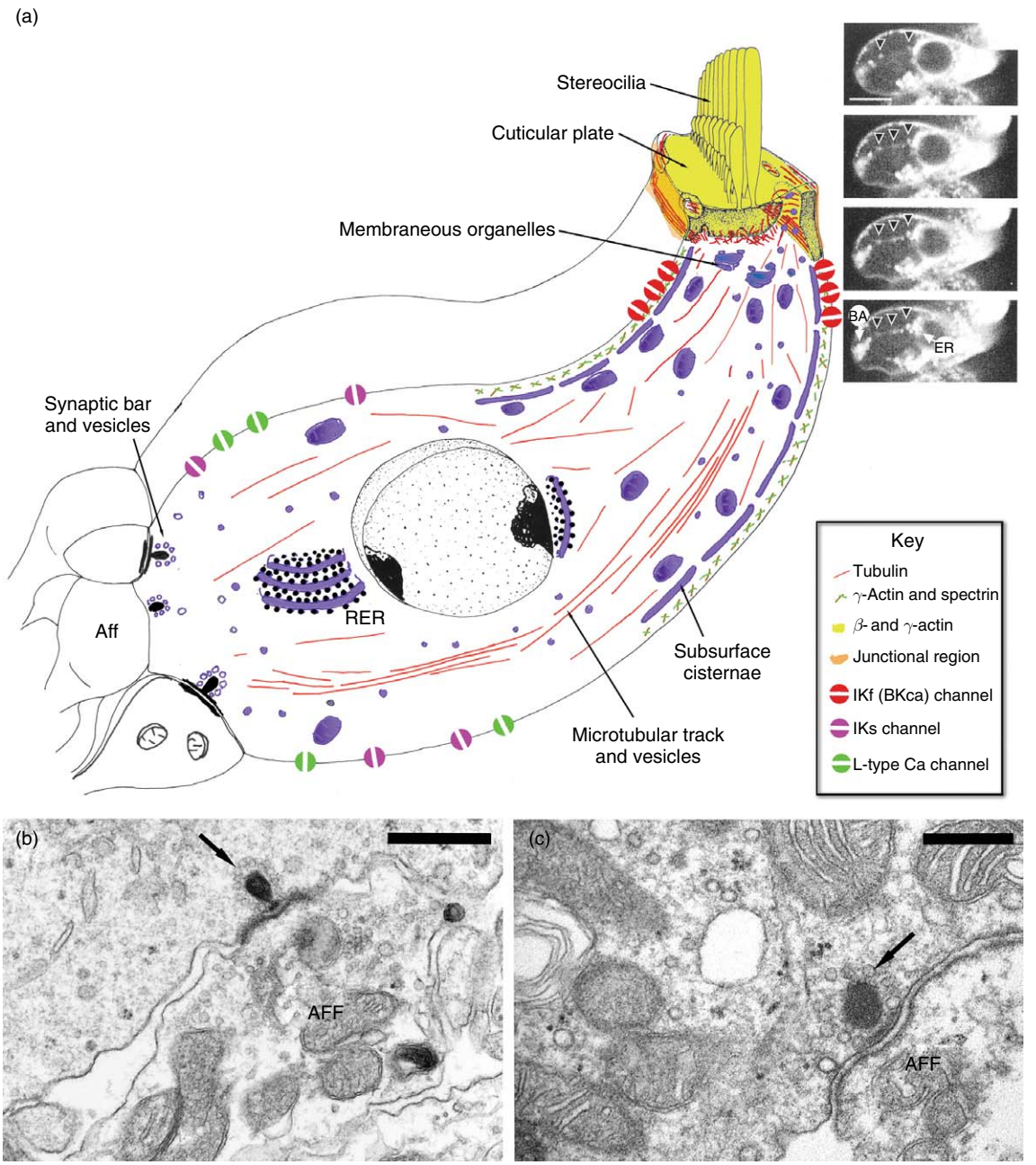

Figure 7 (a) Schematic diagram of an IHC showing several important molecules (see key for details). The IHC plasma membrane is lined by cisternae and a cortical lattice but lacks prestin. Ion channels of the basolateral membrane and synaptic region are mostly represented near the synapse, although in mammals BKCa channels may be mainly located in the neck region as indicated. Membraneous organelles, cisternal membranes, and vesicles are depicted in blue. The synaptic bars (ribbons) apposed to afferent nerve terminals are also shown. The extensive microtubular cytoskeleton, depicted as red lines, includes a specific track running through the cell (as illustrated microscopically in Figure 2). The inset shows time-lapse confocal images of a live IHC labeled with the dye FM 1-43, illustrating apico-basal movement of membrane along a track probably corresponding to the longitudinally running microtubules. Scale bar = 10 μm. (b) Structure of the IHC synapse viewed by transmission electron microscopy. Note the teardrop-shaped dense bar surrounded by a halo of vesicles (arrow) adjacent to pre- and postsynaptic densities at the synapse with afferent (AFF) nerve terminals. Scale bar = 500 nm. (c) Transmission electron micrograph showing the similar dense bar and vesicles (arrow) associated with AFF terminals onto a turtle hair cell. Scale bar = 500 nm. (Inset in a) reproduced from Griesinger, C. B., Richards, C. D., and Ashmore, J. F. 2002. FM1-43 reveals membrane recycling in adult inner hair cells of the mammalian cochlea. J. Neurosci. 22, 3939–3952, with permission, Copyright 2002 by the Society for Neuroscience.

cells (Zenisek, D. *et al.*, 2003) that is probably anchored to the membrane by the presynaptic scaffolding protein, Bassoon (Nemzou, N. R. M. *et al.*, 2006), since the anchoring of the bars is impaired in Bassoon-deficient mice (Khimich, D. *et al.*, 2005). Nemzou N. R. M. *et al.* (2006) found that the synaptic region of hair cells also contains Piccolo, which is part of the structural organization of the presynaptic specialization in neurones (see review by Schoch, S. and Gundelfinger, E. D., 2006), and cysteine string protein which is a component of synaptic (Mastrogiacomo, A. *et al.*, 1994) and other export vesicles, both noted for their functioning in exocytosis of neurotransmitter vesicles. Another molecule called otoferlin has been suggested from genetic and molecular studies to be part of the presynaptic complex (Roux, I. *et al.*, 2006) although it has also been implicated in vesicle trafficking from other regions of the hair cell (Schug, N. *et al.*, 2006). Although the molecular details are still being investigated, the synaptic bar is presumed to function in rapid release of the synaptic vesicles (see, e.g., Schnee, M. E. *et al.*, 2005) which is impaired when the bar is not anchored properly (Khimich, D. *et al.*, 2005). In OHCs, the synaptic structure is less clear-cut. The OHCs receive afferent innervation, but the synaptic bars and vesicles are less well defined (Furness, D. N. *et al.*, 2002a).

At their afferent presynaptic specializations the IHCs are contacted by the radial neurites of the type I spiral ganglion neurones. Whilst it is not our intention to discuss in detail the molecular composition of the neurones or the role of afferent neurotransmission, it is noteworthy that the postsynaptic membrane possesses glutamate receptors, in particular GluR2/3 and GluR4 (for review, see Parks, T. N., 2000). GluR4 may also be localized presynaptically in the IHC membrane (Furness, D. N. and Lawton, D. M., 2003). The hair cells may also express metabotropic glutamate receptors (Oestreicher, E. *et al.*, 2002), phosphate-activated glutaminase (Takumi, Y. *et al.*, 1999), and the vesicular glutamate transporter, VGLUT1 (Furness, D. N. and Lawton, D. M., 2003). These various proteins are associated with the handling of glutamate, the likely neurotransmitter, by the hair cells and their afferent endings.

The plasma membrane channels present in mammalian auditory hair cells give rise to a number of membrane currents detectable using intracellular recording techniques which are implicated in control of the membrane potential and transmitter release. The identification of these channels is primarily based on their physiological characteristics, but in some cases, molecular biological, genetic, and immunocytochemical data have also contributed. The three main categories are sodium, potassium, and calcium channels.

Sodium currents have been detected in hair cells, indicating the presence of sodium channels. These are tetrodotoxin-sensitive channels normally associated with spiking activity. These have been detected in the immature mammalian cochlea where IHCs transiently produce spontaneous calcium-based action potentials (Beutner, D. and Moser, T., 2001; Marcotti, W. *et al.*, 2003) prior to the onset of hearing. The role of this spiking may be to provide a signal for the maturation of synaptic function, and it is accompanied by membrane capacitance changes indicative of exocytosis. The exocytotic mechanism is likely to release glutamate from the hair cells, prior to the acquisition of functional auditory responses, which could help to drive the connection of afferent nerve synapses with the IHCs.

Most of the studies of potassium currents have been carried out on nonmammalian vertebrates, where their contribution to electrical tuning and other mechanisms associated with variations in the response to frequency has been well established (see, e.g., Art, J. J. and Fettiplace, R., 2006). However, similar potassium currents have also been found in mammalian hair cells. One of these is an inwardly rectifying current (K_{IR}) identified first in bullfrog vestibular hair cells (Corey, D. P. and Hudspeth, A. J. 1979b) but subsequently found in the cochlea of chick (Ohmori, H., 1984), turtle (Art, J. J. and Fettiplace, R., 1987), and mouse (Marcotti, W. *et al.*, 1999). In chick and turtle, these currents are inversely correlated with frequency.

Outward potassium currents have also been measured, although the role of these currents in the mammalian auditory system remains to be properly understood. Two main types of outward potassium channel seem to be present in mammalian cochlear hair cells, voltage-gated (K_V) underlying slow potassium current (IKs in IHCs), and calcium-activated potassium channels. In OHCs, the latter seem to be further subdivided into two types, the A (or SK) type and the B type. Whereas an SK-like channel is expressed only in immature IHCs (Marcotti, W. *et al.*, 2004), the BK_{Ca} channel is present in mature IHCs and probably gives rise to a rapid outward current (Kros, C. J. *et al.*, 1998); deletion of the BK_{Ca} channels leads to progressive hearing loss including loss of the OHCs (Ruttiger, L. *et al.*, 2004), and a

relatively high level of mRNA for the gene is expressed in IHCs (Langer, P. *et al.*, 2003). Immunocytochemistry suggests that the channels are clustered around the neck of the IHCs as well as occurring in the synaptic region of both types of hair cell and possibly on the basolateral membrane of the OHCs (Pyott, S. J. *et al.*, 2004; Hafidi, A. *et al.*, 2005).

Deafness is also associated with a mutation in KCNQ4, a slow K_V channel which leads to progressive OHC degeneration (Kubisch, C. *et al.*, 1999). KCNQ4 is expressed in OHCs and, like BK_{Ca} echannels, shows a tonotopic gradient, increasing in density toward the high-frequency region of the cochlea (Mammano, F. and Ashmore, J. F., 1996; Ruttiger, L. *et al.*, 2004). Knockout of the BK_{Ca} channel also leads to loss of the KCNQ4 channel. The slow potassium currents may be associated with setting the resting potential, acting as a shunt to reduce potassium accumulation through the MET channels. Their tonotopic gradient may also reflect a contribution to reducing the membrane time constant and thereby improving high-frequency signaling at the basal end of the mammalian cochlea.

Inward voltage-dependent calcium currents have been detected in mouse hair cells (Engel, J. *et al.*, 2002), and data from a range of species suggest they are based primarily on L-type Ca^{2+} channels (Fuchs, P. A. *et al.*, 1990; Schnee, M. E. and Ricci, A. J., 2003). L-type Ca^{2+} channels have a basic subunit structure of α, β, $\alpha 2\delta$, and sometimes γ (Hille, B., 2001), but there is a range defined by differences in the α subunit. Mammalian hair cells from a knockout mouse for the α1D (now known as Ca(V)1.3) subunit show substantially reduced Ca^{2+} current (Platzer, J. *et al.*, 2000) and failure of afferent synaptic transmission in IHCs despite having a structurally intact synapse up to 4 weeks of age (Nemzou, N. R. M. *et al.*, 2006). *In situ* hybridization reveals a strong signal for Ca(V)1.3 (α1D) compared with a weaker signal for α1C (Kollmar, R. *et al.*, 1997).

Use of calcium-sensitive dyes suggests that there are calcium hotspots (regions of significant calcium concentration changes) in the basal pole of some auditory hair cells. Thus, these channels may be clustered in the vicinity of the synaptic contacts, providing calcium influx required for neurotransmitter release (Roberts, W. M. *et al.*, 1990; Issa, N. P. and Hudspeth, A. J., 1994; Tucker, T. and Fettiplace, R., 1995). Calcium influx is also likely to affect other properties of the hair cell through intracellular calcium-induced calcium release, and in OHCs, there may be an interaction between the Ca^{2+} channels and acetylcholine (ACh) channels located around the basal pole (Figure 4). The lateral membrane also contains calcium pumps but a different isoform from that present in the stereocilia, PMCA1b (Dumont, R. A. *et al.*, 2001). It is likely that these pumps interact with calcium channels and the local intracellular calcium stores and buffers to control synaptic modulation by calcium. In IHCs, this will regulate synaptic transmission elicited by mechanotransduction-induced depolarization, but their roles in OHCs may be more associated with modulation of the cell's motile activity since afferent synaptic activity by OHCs and its role remain to be established definitively.

The calcium pumps of the lateral membrane and buffers in the cytoplasm also play a role in efferent modulation of hair-cell function. In OHCs, nonmammalian auditory hair cells, and vestibular hair cells, there is modulation by efferents at the synaptic pole. The OHC efferent fibers largely use ACh as their neurotransmitter, although a subset of GABAergic fibers is also present. Accordingly, isolated OHCs respond to application of ACh by activation of an early inward current and a later outward potassium current ($I_{K(ACh)}$), both blocked reversibly by α-bungarotoxin. The inward current is probably carried partially by calcium which then activates calcium-sensitive potassium channels (Evans, M. G., 1996), presumably the BK_{Ca} channels mentioned earlier. This idea is supported by observations of calcium concentrations rising initially at the basal pole in response to ACh application but then spreading apically (Evans, M. G. *et al.*, 2000).

The properties of hair-cell ACh receptors are mixed, in that they show some characteristics that are nicotinic-like and muscarinic-like according to studies of different hair cells. In vestibular hair cells, muscarinic (metabotropic) and nicotinic (ionotropic) receptor agonists evoke different responses (see review by Guth, P. S. and Norris, C. H., 1996). However, the most consistent features suggest a nicotinic-like receptor that allows an influx of calcium. Earlier studies (Elgoyhen, A. B. *et al.*, 1994) suggested that this receptor may be composed of a novel subunit (α9), but subsequently, a second subunit type was identified (α10). From recombinant studies, the likely composition of hair-cell ACh receptors is a pentamer with an (α9)2(α10)3 stoichiometry (Plazas, P. V. *et al.*, 2005).

ACh thus acts on the hair cells directly to alter the membrane potential through ionotropic mechanisms (see review by Fuchs, P. A. and Parsons, T. D., 2006), but responses can be prolonged and may thus involve second messenger systems. In this case, it is thought

that as well as relatively fast ion channel responses, there is a slower response involving internal mobilization of calcium through calcium-induced calcium release. This process is discussed further below in relation to efferent modulation of OHC motility.

In addition to the synaptic structures, the OHCs of the mammalian cochlea have a structurally and compositionally specialized lateral wall which shares only partial similarity with IHCs but not other hair cells. This consists of the cortical lattice of the OHC and the plasma membrane which uniquely displays a substantial concentration of protein particles probably involved in these cells unique electromotile response (see below).

3.06.1.5 The Outer Hair Cell Lateral Wall

The lateral wall of the OHCs has received a lot of attention since it was discovered that these cells are electromotile – that is, they respond to both field potentials and microelectrode-generated depolarization–hyperpolarization cycles by cyclical contraction–elongation movements – and that this motility could underlie the cochlear amplifier. Both IHCs (Furness, D. N. and Hackney, C. M., 1990) and OHCs (Bannister, L. H. *et al.*, 1988) have a submembrane network called the cortical lattice that is bounded on one side by one or more layers of subsurface cisternae and on the other side by the plasma membrane (Figure 8).

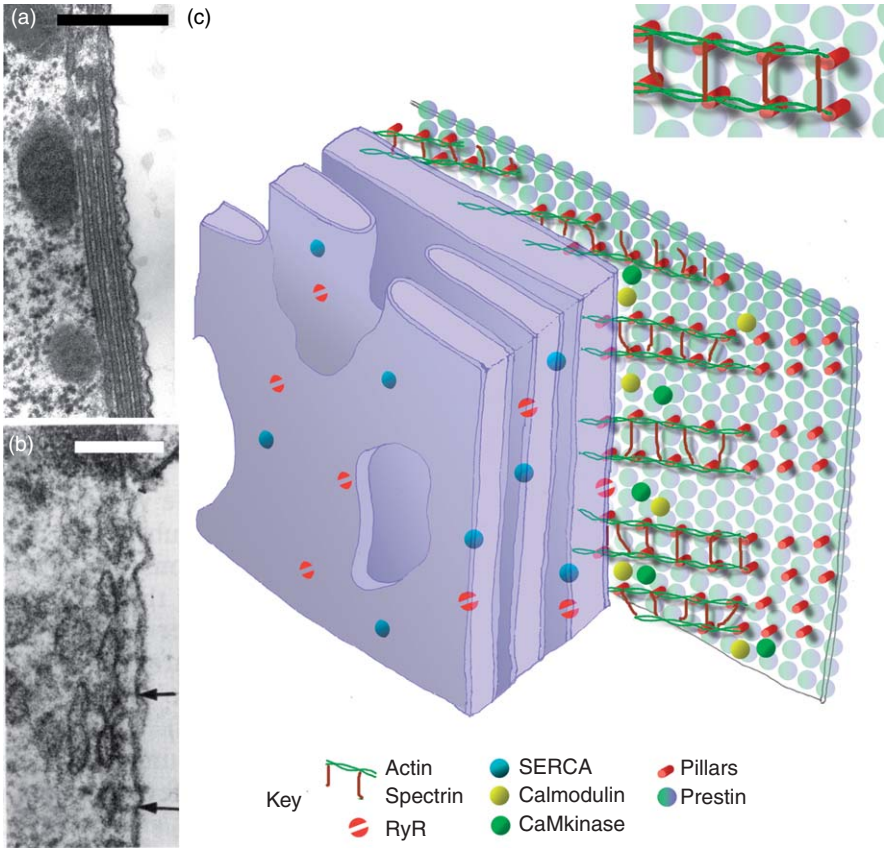

Figure 8 Lateral wall structures in an OHC. (a) Transmission electron micrograph showing the layers of membraneous cisternae and associated mitochondria. Scale bar = 500 nm. (b) Detail of the cortical lattice that lies between the plasma membrane and the first cisternal layer. Pillars connect the lattice with the membrane (arrows). Scale bar = 200 nm. (Adapted from Furness, D. N. and Hackney, C. M. 1985. Comparative ultrastructure of subsurface cisternae in inner and outer hair cells of the guinea pig cochlea. Eur. Arch. Otorhinolaryngol. 247, 12–15). (c) Schematic diagram of the cortical lattice and some associated molecules. The lattice is composed of actin filaments (primarily γ-actin) interconnected in tracks (as illustrated at higher magnification in the inset) by spectrin molecules. The lattice lies between the plasma membrane and the first cisternal layers and appears to be tied to the plasma membrane by pillars, the molecular composition of which has previously been suggested to be band 3 and protein 4.1R. Other molecules in the vicinity are calmodulin and CaM kinases which imply calcium-dependent process associated with the lattice. The cisternae contain other molecules involved in calcium-dependent processes such as ryanodine receptors and a calcium pump (SERCA).

Immunocytochemistry suggests that the lattice is composed predominantly of γ-actin filaments (Furness, D. N. *et al.*, 2005) and spectrin (Holley, M. C. and Ashmore, J. F., 1990; Mahendrasingam, S. *et al.*, 1998). The organization of this lattice has been studied by electron microscopy mainly in OHCs. Actin filaments in the lattice are preferentially circumferential in orientation and tend to occur in pairs (like railroad tracks) cross-linked by spectrin filaments (Holley, M. C. and Ashmore, J. F., 1990). Overlying the filament array and running along the tracks are pillar-like structures that extend up to the plasma membrane (Flock, A. *et al.*, 1986). Similar tracks and pillars have been observed in IHCs (Furness, D. N. and Hackney, C. M., 1990) and both actin and spectrin are localized there (Mahendrasingam, S. *et al.*, 1998; Furness, D. N. *et al.*, 2005).

The similarity of this lattice to that underlying the erythrocyte membrane has led to searches for similar proteins in OHCs. Thus, antibodies to band 3 and Protein 4.1 (now known as 4.1R and located also in stereocilia) have been used and labeling detected in the lateral wall of the hair cells, some of which could correspond to components of the lattice (Zine, A. and Schweitzer, L., 1997). Specific labeling of the pillars has yet to be clearly demonstrated so their composition remains uncertain. However, band 3 and protein 4.1R or related proteins could be associated with them. In erythrocytes, protein 4.1.R has multiple interactions with other lattice proteins, regulated by calcium and calmodulin, and is associated with stabilization of the membrane and cell shape (see review by Nunomura, W. and Takakuwa, Y., 2006); this could be a functionally relevant attribute in the OHCs.

In OHCs, freeze-fracture studies have shown that the plasma membrane adjacent to the lattice contains a high density of protein particles (Kalinec, F., *et al.*, 1992; Figures 4 and 8). These are thought to correspond to molecules of a protein called prestin, which is virtually unique to the OHC. Prestin, first reported by Zheng J. *et al.* (2000), is expressed throughout the basolateral membrane, though probably at a lower density in the synaptic region (Yu, N. *et al.*, 2006). It is believed to be a molecular motor that responds to voltage changes across the cell membrane by undergoing a conformational change. This in turn changes the area of the cell membrane and results in the elongation/contraction cycles that can be electrically evoked. Accordingly, the motility is reflected in nonlinear capacitance changes in the hair cells. There is also evidence of a higher density of the motor protein in freeze fractures of OHC membranes from high-frequency positions compared with low-frequency positions, which corresponds with gradients of motility-related charge along the cochlea (Santos-Sacchi, J. *et al.*, 1998).

Electromotility is absent in prestin-null mice, which also supports the notion that prestin is the motor that moves the OHC. However, the efficiency of this motor may be limited by the capacitance-filtering properties of the membrane which would reduce the effectiveness of the receptor potential in driving the prestin at the higher frequencies of mammalian hearing. Whilst this might be overcome by extracellular potential gradients driving the electromotility (Dallos, P. and Evans, B. N., 1995), another possibility is that an additional mechanism, perhaps related to bundle force generation (see above), may also be required; thus, there may be an interaction between hair bundle motility and somatic motility in cochlear amplification (Kennedy, H. J. *et al.*, 2006).

The subsurface cisternae (Figure 8) are membraneous compartments; only one layer is found in IHCs (Furness, D. N. and Hackney, C. M., 1990), but in OHCs, the number varies from 1 in hair cells near the basal end of the cochlea to between 10 and 20 apically in guinea pigs (Saito, K., 1983; Furness, D. N. and Hackney, C. M., 1990). In other species, such as bats, OHCs and IHCs also possess at least a single layer (Vater, M. *et al.*, 1992). It has been suggested that these cisternae are calcium stores and involved in calcium regulation of various cellular processes in OHCs. This could include motility of the lateral wall. Lim D. J. (1986) also suggests they have continuity with a single cisternal layer that lies adjacent to the membrane at the point of efferent contact, with the hair cell basal pole suggesting they may play a role in efferent modulation of the hair cell.

The relationship between the lattice, the prestin-based motor, and the cisternae and their role in calcium-dependent process is still being investigated. In rats, electromotility develops several days after prestin is first expressed at weak levels (Belyantseva, I. A. *et al.*, 2000) and simultaneously with the acquisition of calcium/calmodulin-sensitive motility dependent on the hair-cell cytoskeleton (Beurg, M. *et al.*, 2001). Specific localization of calmodulin (Nakazawa, K., 2001; Furness, Karkanavetos and Hackney, unpublished observations), CaMkinase (Koyama, M. *et al.*, 1999; Frolenkov, G. I. *et al.*, 2000), and protein phosphorylation cascade-IP(3) receptors (Frolenkov, G. I. *et al.*, 2000) along the lattice and adjacent subsurface cisternae suggests that it is a calcium-sensitive site with functions that could be

associated with second messenger-based modulation of the motility.

Belyantseva I. A. *et al.* (2000) argue that prestin expression and motility develop concurrently, but their data like those of Beurg M. *et al.* (2001) show an early dissociation in the time courses of the two that could reflect the deployment of components of the lattice. Thus, whilst the prestin may provide the motor, the lattice may be crucial for its efficient function within the cell.

The involvement of the cisternae in calcium-regulated processes is further supported by the presence of receptors for ryanodine (RyR – a molecule involved in calcium-induced calcium release) in them in both OHCs and IHCs. RyR are also found in a subset of rough endoplasmic reticulum located near the basal pole of the IHC (Grant, L. *et al.*, 2006). Ryanodine is involved in the response to ACh: the ryanodine receptor agonist caffeine initially facilitates the ACh response but then gradually suppresses it (Lioudyno, M. *et al.*, 2004). The latter authors suggest that the ryanodine receptors are localized to the subsynaptic cistern rather than the more distant subsurface cisternae. However, in rat cochleae, subsurface cisternae extend all the way round the basal pole of the hair cell up to the region of the efferent ending where they are briefly interrupted, so distances may not be so great (Furness, D. N., Mahendrasingam, S., and Hackney, C. M., unpublished observations) and continuity with the subsynaptic cistern could improve communication between these regions. Thus, it may well be that the subsurface cisternae and/or the subsynaptic cistern represent calcium stores and thus function in intracellular mobilization of calcium associated with efferent control.

The overall effect of efferent activation is to decrease cochlear sensitivity (see, e.g., Guinan, J. J. Jr. *et al*, 2005), but there are two different time courses, fast and slow. These presumably work by reducing the effective contribution of OHCs to the cochlear amplifier. The functional role of the efferent-based calcium mobilization is uncertain, as is the mechanism by which the amplifier is suppressed, because data obtained on OHC motility in response to ACh and calcium are somewhat contradictory. Ach-induced increased intracellular calcium can result in increased electromotility in a calmodulin-dependent manner, with a time constant of the order of 10 s (Dallos, P. *et al.*, 1997; Szonyi, M. *et al.*, 2001). Elevated intracellular calcium may also produce a long-term decrease in OHC axial stiffness (Frolenkov, G. I. *et al.*, 2003). Perhaps the decreased axial stiffness militates against the effectiveness of the increased motility and underlies the slow inhibition. These processes thus probably involve dynamic ACh-induced, calcium-dependent changes in the complex lattice and its linkage to the plasma membrane.

3.06.1.6 The Cytoplasm

In addition to the structural and functionally distinct regions already described, the remainder of the hair cell contains cytoplasmic components that include other molecules. Actin filaments and microtubules pervade the cytoplasm (Figures 2, 4, and 7). Microtubules are common in mammalian auditory hair cells (Furness, D. N. *et al.*, 1990; Steyger, P. S. *et al.*, 1991) and of the normal 13 protofilament variety, unlike the adjacent supporting cells (see below and Kikuchi, T. *et al.*, 1991). They are composed of βI and βII tubulin in IHCs and βI and βIV tubulin in OHCs (Jensen-Smith, H. C. *et al.*, 2003). In addition, the tubulin is tyrosinylated which makes the microtubules likely to be undergoing dynamic changes, again in contrast to those of the supporting cells (Slepecky, N. B. *et al.*, 1995; Bane, B. C., *et al.*, 2002). In both OHCs (Figure 4) and more prominently IHCs (Figure 7), the apical cuticular plate is surrounded by a basket of microtubules. These occur in a meshwork directly beneath the plate, in rings around the top and underside of the plate, and in the channel, presumably representing structural support for the apical MET apparatus. A basal body is found in all hair cells in the channel region or behind the rear of the cuticular plate, which in all except mammalian cochlear hair cells provides the base of the kinocilium. Microtubules extend down from the basal body region through the hair cell. In the IHCs, they form a prominent apico-basal track that probably constitutes a membrane trafficking path (Figures 2 and 7) between the apical endocytotic region described earlier and the basal synaptic pole (Steyger. P. S. *et al.*, 1989; Furness, D. N. *et al.*, 1990; Griesinger, C. B. *et al.*, 2002 – see Figures 2 and 7). They also enclose the projection of the cuticular plate found in long apical OHCs and encircle the circumference inside the membrane in the basal pole (Figure 4; Furness, D. N. *et al.*, 1990). Microtubules appear developmentally before the cuticular plate in some species (Heywood, P. *et al.*, 1975), indicating the possibility that they are involved in organizing some elements of the cytoskeleton.

Other vestibular and nonmammalian auditory hair cells probably contain similar microtubule patterns. There are apical concentrations and longitudinal tracks in rat vestibular hair cells (Jorgensen, J. M., 1982; Favre, D. and Sans, A., 1983), and longitudinally running microtubules have been described in chick (Cohen, G. M. and Fermin, C. D., 1978) and snake (Jorgensen, J. M., 1982) cochleae, ratfish lateral line (Ekstrom von Lubitz, D. K., 1981), and frog crista ampullaris (Flock, A. *et al.*, 1982).

Calcium-binding proteins including calbindin, calretinin, parvalbumin, and peptide 19 are found in hair cells (Imamura, S. and Adams, J. C., 1996; Hackney, C. M. *et al.*, 2003; 2005). Gradients of some of these proteins exist along the length of the mammalian cochlea, for example, calbindin appears to decrease toward the high-frequency region in mammals (Pack, A. K. and Slepecky, N. B., 1995) but increase in birds (Hiel, H. *et al.*, 2002). These discrepancies make determining the importance of buffers to the tonotopic variation in function difficult to evaluate. The role of intracellular calcium has already been discussed, and it is likely that these buffering proteins are associated with the precise control of calcium at different subcellular locations in the hair cell, for instance in modulating MET currents and adaptation, for modulation of the cytoskeleton involved in movements, both in the cytoplasm and the lateral wall of OHCs and in the synaptic region, where calcium regulates neurotransmitter release. There is a reduction in diffusible calcium buffers in mammalian IHCs during development in contrast to an increase to muscle-like levels in OHCs which suggests that calcium ions may play different roles in these two types of hair cells (Hackney, C. M. *et al.*, 2005).

3.06.1.7 Supporting Cells

The supporting cells of auditory epithelia surround the hair cells and in all except the mammalian organ of Corti completely enclose their basolateral regions. The base of each OHC is supported by a Deiters' cell cup and the apex by the process of a nearby Deiters' cell; each IHC is supported by inner phalangeal cells (Figure 9) and border cells. Between the IHC and first OHC rows, there are two rows of pillar cells, the inner and the outer. The supporting cells are characteristically shaped to support the hair cells mechanically within the epithelium, but they also assist in providing homeostatic support in a variety of ways for the various processes that occur in hair cells.

In the mammalian cochlea, the inner and outer pillar cells (IPC and OPC) both contain a rod-like process, filled with microtubules and actin filaments that extend up from a basal foot resting upon the basilar membrane to a head region (Figure 9). The foot and the head contain an anchoring mat of actin filaments composed of both β- and γ-actin and similar in appearance to the hair-cell cuticular plate. The head region has a second process extending across the organ of Corti radially, that of the IPC overlying the head of the OPC, whilst that of the OPC surfaces between the OHCs of the first row (Figure 2).

Compared with the cuticular plate of the hair cell, the actin-rich mats in the pillar cell apices contain approximately 10× (in IPC) to 20× (in OPC) the concentration of β-actin and about half the concentration of γ-actin. There is a greater overall concentration of actin which means that the actin filaments are probably more densely packed. Furthermore, the outer pillar cells have a higher proportion of β-actin in high-frequency regions compared with low-frequency regions, at least in guinea pig (Furness, D. N. *et al.*, 2005). The number of microtubules in the pillar cells also changes systematically, increasing toward the basal end of the cochlear spiral (Kikuchi, T. *et al.*, 1991). In addition, the pillar bundles contain tropomyosin, which could be associated with added stiffness (Slepecky, N. and Chamberlain, S. C., 1987). These high concentrations of significant cytoskeletal proteins indicate the importance of mechanical strengthening in the mammalian organ of Corti. There is little evidence of similar strut-like bundles in supporting cells of other auditory or vestibular epithelia.

Similar, but smaller, microtubule and actin bundles, also containing tropomyosin, occur in the other main supporting-cell type of the organ of Corti, the Deiters' cell (Slepecky, N. and Chamberlain, S. C., 1985; Slepecky, N. B. and Chamberlain, S. C., 1987; Steyger, P. S. *et al.*, 1989). Each Deiters' cell has a cylindrical body sitting with its base on the basilar membrane and reaching up to the bottom of the OHC above it. At this point, the Deiters' cell supports the synaptic pole and the incoming fibers of the OHC in a cup. The cup is rich in microtubules (Steyger, P. S. *et al.*, 1989; Furness, D. N. *et al.*, 1990), and actin filaments of both β- and γ-actin isoforms lie beneath the membrane directly opposed to the hair-cell base (Furness, D. N. *et al.*, 2005). Emanating from the strial side of the Deiters' cell body is a phalangeal process which also contains a microtubular and actin bundle (Figure 9). This process stretches up to the surface of

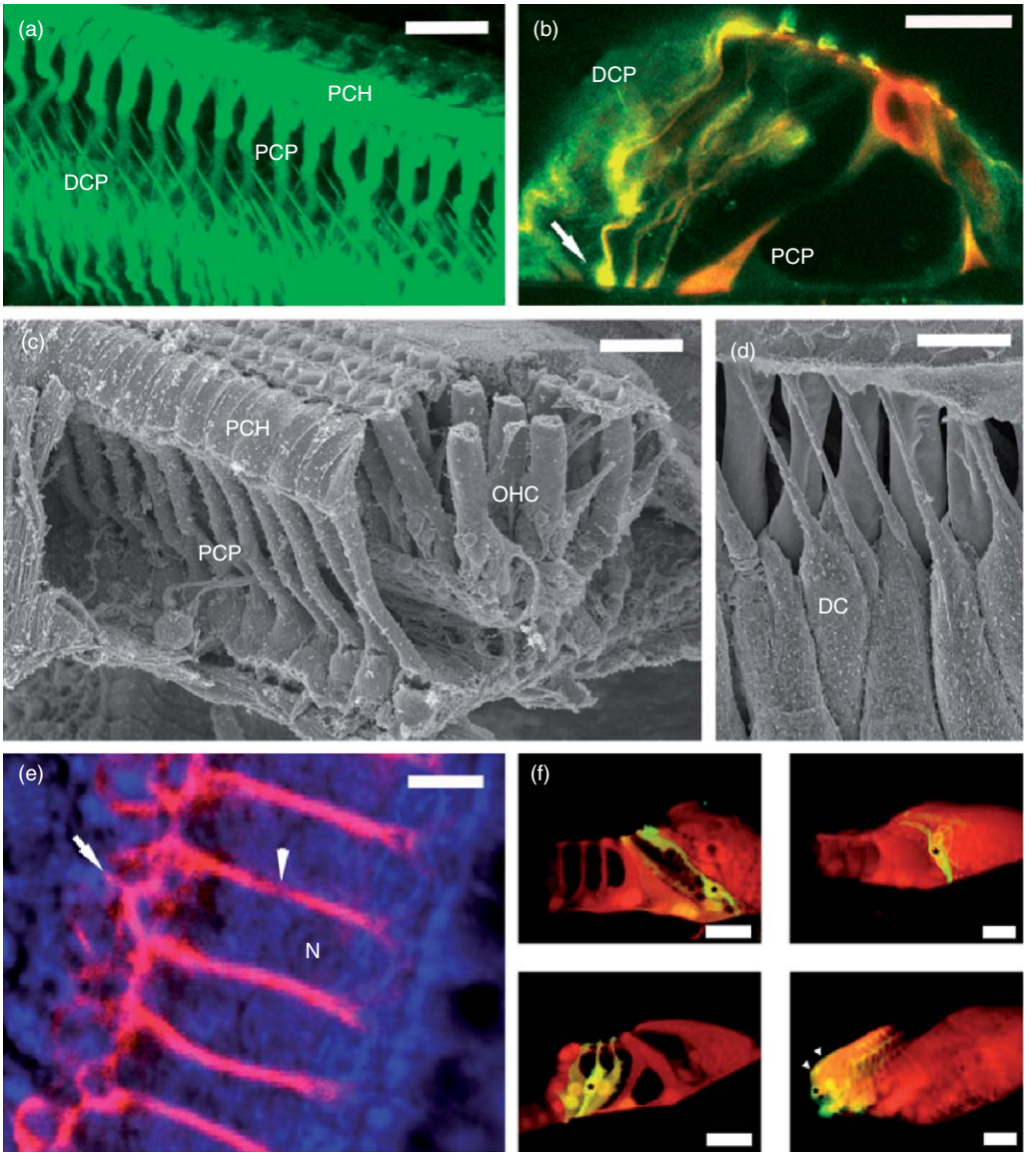

Figure 9 Structure and composition of supporting cells. (a) Deiters' cells and pillar cells labeled with tubulin antibodies and imaged using a confocal microscope. The microtubular bundles of the pillar cell processes (PCP) reach up to the pillar cell heads (PCH) and the thinner phalangeal processes of the Deiters' cells to their respective apical portions (DCP). Scale bar = 20 μm. (b) Cross section of the organ of Corti double labeled for β-actin (red) and γ-actin (green). Note colocalization (yellow-orange) in the Deiters' cell (DCP) and pillar cell (PCP) processes, especially in the former. The foot of both processes lies directly over the basilar membrane (indicated by an arrow for the DCP). The pillar cells have relatively more β-actin, as indicated by their redder coloration. Scale bar = 10 μm. (c) Scanning electron microscopy of a fracture of the organ of Corti showing the rod-like PCP culminating in the apical head (PCH). The OHCs are shown for orientation. Scale bar = 10 μm. (d) Scanning electron micrograph of Deiters' cells (DC) showing the cell bodies and thin phalangeal processes emanating obliquely from them. Scale bar = 10 μm. (e) Combined bright field (blue) and confocal fluorescent image (red) showing labeling for the glutamate transporter GLAST in mouse inner phalangeal cells around the IHCs which cup the IHC (identified by its central nucleus (N)) and send processes out to wrap incoming afferent nerves at the synaptic pole (arrow). Scale bar = 10 μm. (f) Demonstration of gap junctional coupling between supporting cells at postnatal day 8 (prior to the onset of hearing). Yellow represents Lucifer Yellow and red neurobiotin. Top panels show an inner phalangeal cell injected with both dyes but transfer only of neurobiotin to other supporting cells. Bottom panels illustrate Deiters' cells showing transfer of both dyes at this age. Scale bar = 20 μm. Reproduced, with permission, from Jagger, D. J. and Forge, A. 2006. Compartmentalized and signal-selective gap junctional coupling in the hearing cochlea. J. Neurosci. 26, 1260–1268, Copyright 2006 by the Society for Neuroscience.

the organ of Corti (called the reticular lamina) where it spreads to form a plate connected to the adjacent hair cells via junctional complexes. The microtubular-actin bundle approaches the complex but ends in a substantial mat of actin filaments prior to the junction. This mat contains intermediate amounts of β- and γ-actin between the cuticular plate of the hair cell and the head of the pillar cells (Furness, D. N. *et al.*, 2005).

As well as being rich in actin and tubulin, all mammalian cochlear supporting cells have a substantial cortical lattice containing spectrin and microfilaments (Mahendrasingam, S. *et al.*, 1998). This lattice does not appear to have the same systematic organization as found in the hair cells but presumably confers some elasticity on the periphery of the supporting cell, which is likely to prevent disruption of the cells in the mechanically active organ of Corti. They also express glial fibrillary acid protein (GFAP – Rio, C. *et al.*, 2002) which is characteristic of some glia, including astrocytes and nonmyelinating Schwann cells in the central nervous system, which implies functional similarity with glia.

The concentration of cytoskeletal proteins in these cells is consistent with the notion that one of their main functions is mechanical support. The extent to which this support is purely passive or actively modulated and able to change the mechanical properties of the organ of Corti is uncertain. As shall be seen below, some of the supporting cells possess ion channels and receptor molecules associated with possible homeostatic and modulatory functions and some may be innervated. The stalks of Deiters' cells can be induced to move by ATP (Bobbin, R. P., 2001), which suggests that they may have more than a passive role in cochlear mechanics.

The cells also express a number of proteins involved in homeostasis; inner phalangeal, border, and Deiters' cells express a major brain protein, the glutamate transporter, GLAST (Furness, D. N. and Lehre, K. P., 1997; Furness, D. N. *et al.*, 2002a). In astrocytes, GLAST functions in maintaining low extracellular levels of glutamate around glutamatergic synapses.

Deiters' cells contain a relatively low concentration of GLAST, and apical Deiters' cells express more GLAST than basal ones (Furness, D. N. *et al.*, 2002a; 2000b). This matches the pattern of afferent (presumptive glutamatergic) synapses to the OHCs and which suggests that they may release glutamate synaptically. The supporting cells around the IHCs, the inner phalangeal cells and border cells, in effect cup the IHC completely, except for its apical end. Both cell types express significant amounts of GLAST (Figure 9; Furness, D. N. and Lehre, K. P., 1997) with enrichment in finger-like processes around the nerve endings. These cells too show a cochleotopic gradient that matches the number of afferent endings on the IHCs which vary systematically along the cochlea (Furness, D. N. and Lawton, D. M., 2003). It is likely that GLAST here serves to take up glutamate from the synaptic clefts and surrounding extracellular space to help shape glutamate receptor activity in the afferent synapses and reduce the potential for excitotoxic damage to afferent terminals (Furness, D. N. and Lehre, K. P., 1997). GLAST knockout mice have no hearing defects but an enhanced susceptibility to trauma and elevated glutamate levels in cochlear fluids (Hakuba, N. *et al.*, 2000). The presence of GLAST thus seems likely to be a major player in glutamate homeostasis, especially associated with the primary receptor function of IHCs.

Supporting cells also express various calcium buffers although at lower levels than in hair cells. Thus, a low concentration of calretinin is present in Deiters' cells (Pack, A. K. and Slepecky, N. B., 1995; Hackney, C. M. *et al.*, 2005) and supporting cells of other vertebrates, such as turtles (Hackney, C. M. *et al.*, 2003). Another calcium-binding protein present in supporting cells is S-100 (Pack, A. K. and Slepecky, N. B., 1995). There is also expression of PMCA1b in the plasma membrane (Dumont, R. A. *et al.*, 2001).

Another common feature of the supporting cells seems to be the presence of gap junctions. These have been elegantly demonstrated in intracellular dye marking experiments with neurobiotin and Lucifer Yellow injected into individual supporting cells in cochlear slices from rats during development (Figure 9). Intracellular fluorescent neurobiotin (Jagger, D. J. and Forge, A., 2006) injected at postnatal day 12 (after the onset of hearing) spreads from one supporting cell to neighboring supporting cells in all directions (pillar cells, Deiters' cells, and inner phalangeal/border cells), indicating they have gap junctions containing connexin 30 only or connexin 30/26. However, dye injected into IPC does not transfer to outer pillar cells or vice versa. Injections of Lucifer Yellow (a marker for connexin 26-only gap junctions) are restricted in their spread at that age. Immunocytochemical data also suggested some colocalization of the two connexins, suggesting that gap junctions of either monomeric connexin 30 or heteromeric connexin 26/30 couple supporting cells together. The spread of Lucifer Yellow at postnatal

day 8 prior to the onset of hearing is wider (Figure 9), indicating a change in the gap junction distribution during maturation to the more restricted adult pattern, which it is suggested ultimately produces separate buffering compartments for IHCs and OHCs in the hearing cochlea (Jagger, D. J. and Forge, A., 2006). The significance of these findings relates to deafness genes which show that defects in both connexins result in hearing loss. The role of these junctions has been proposed to be in K^+ homeostasis, the supporting cells able to act as a passive sink for potassium.

A number of ion channels are expressed in supporting cells. $P2X_2$ (Housley, G. D. *et al.*, 1999) and P2y (Housley, G. D. *et al.*, 2006) receptors are found in the basolateral regions of Deiters' cells and pillar cells, as well as in other cells of the organ of Corti. The purinergic receptors presumably are involved in these cells' motile response to ATP (Bobbin, R. P., 2001). They also contain mRNA for voltage-insensitive potassium channels TASK-1 and TREK-1 (Kanjhan, R. *et al.*, 2004). Two possible types of voltage-sensitive outwardly rectifying potassium channels have been detected physiologically in Deiters' cells (Szucs, A. *et al.*, 2006). Finally, the water channel aquaporin 4 has been detected in Deiters' cells and inner phalangeal/border cells (Mhatre, A. N. *et al.*, 2002; Miyabe, Y. *et al.*, 2002).

Apart from their contribution to mechanics, the most likely role of supporting cells in the cochlea, therefore, is in homeostatic support for the hair cells. The presence of ion channels and gap junctions, the glutamate transporters, and water channels is likely to reflect control of the environment, particularly around the IHCs and OHCs.

Finally, mention should also be made of the innervation of supporting cells. There have been reports of synaptic structures onto some Hensen's and Deiters' cells (Burgess, B. J. *et al.*, 1997) and some evidence that they respond to ACh via an ACh receptor (Matsunobu, T. *et al.*, 2001). Whether this innervation has a functional role in cochlear mechanics or homeostasis remains to be determined.

3.06.1.8 Concluding Remarks

This review has attempted to draw together a large body of work to illustrate the complex molecular architectures of hair cells and supporting cells which together give the auditory epithelium its ability to perform mechanotransduction of acoustic signals, giving animals a highly sensitive and accurate auditory system. During evolution, the sensitivity, frequency selectivity, and dynamic range of auditory organs have been extended. To achieve this, a number of unique proteins and highly specialized molecular arrangements have also evolved – these include the mammalian motor protein, prestin, and the cortical lattice. Despite their specialization, mammalian hair cells share fundamental properties with all hair cells and the field still holds the potential for many interesting surprises – for example, mechanisms of amplification only recently being considered in mammalian hair bundles were first described more than 20 years ago in nonmammalian hair cells. The MET mechanism and the MET channel itself seem to be common to all hair cells, at least in its underlying principles, yet a proper understanding of the gating mechanism and the identity of the channel is still being sought.

Throughout this review, we have attempted to provide a description of the molecular composition of cells in the organ of Corti, but we have drawn on data from other species where relevant. However, there are many molecules that have not been discussed; apart from the basic molecules that are common to most or all eukaryotic cells, there are transient molecules, developmental regulators, and signaling molecules that shape the cells and the epithelium in which they lie, and there are most certainly interesting and potentially unique molecules as yet undiscovered. Some of the molecules we may have omitted or discussed only briefly may turn out to be crucial in terms of hearing and deafness, whilst others that are currently hot topics may turn out to be less important as their roles become better understood.

References

Ahmed, Z. M., Goodyear, R., Riazuddin, S., Lagziel, A., Legan, P. K., Behra, M., Burgess, S. M., Lilley, K. S., Wilcox, E. R., Riazuddin, S., Griffith, A. J., Frolenkov, G. I., Belyantseva, I. A., Richardson, G. P., and Friedman, T. B. 2006. The tip-link antigen, a protein associated with the mechanotransduction complex of sensory hair cells, is protocadherin-15. J. Neurosci. 26, 7022–7034.

Amma, L. L., Goodyear, R., Faris, J. S., Jones, I., Ng, L., Richardson, G., and Forrest, D. 2003. An emilin family extracellular matrix protein identified in the cochlear basilar membrane. Mol. Cell Neurosci. 23, 460–472.

Art, J. J. and Fettiplace, R. 1987. Variation of membrane properties in hair cells isolated from the turtle cochlea. J. Physiol. 385, 207–242.

Art, J. J. and Fettiplace, R. 2006. Contribution of Ionic Currents to Tuning in Auditory Hair Cells. In: Springer Handbook of Auditory Research: Vertebrate Hair Cells (*eds*. R. A. Eatock,

R. Fay, and A. N. Popper), pp. 204–288. Springer Science and Business Media.

Avraham, K. B., Hasson, T., Sobe, T., Balsara, B., Testa, J. R., Skvorak, A. B., Morton, C. C., Copeland, N. G., and Jenkins, N. A. 1997. Characterization of unconventional MYO6, the human homologue of the gene responsible for deafness in Snell's waltzer mice. Hum. Mol. Genet. 6, 1225–1231.

Bagger-Sjoback, D. and Wersall, J. 1973. The sensory hairs and tectorial membrane of the basilar papilla in the lizard Calotes versicolor. J. Neurocytol. 2, 329–350.

Bane, B. C., MacRae, T. H., Xiang, H., Bateman, J., and Slepecky, N. B. 2002. Microtubule cold stability in supporting cells of the gerbil auditory sensory epithelium: correlation with tubulin post-translational modifications. Cell Tissue Res. 307, 57–67.

Bannister, L. H., Dodson, H. C., Astbury, A. R., and Douek, E. E. 1988. The cortical lattice: a highly ordered system of subsurface filaments in guinea pig cochlear outer hair cells. Prog. Brain Res. 74, 213–219.

Bautista, D. M., Jordt, S. E., Nikai, T., Tsuruda, P. R., Read, A. J., Poblete, J., Yamoah, E. N., Basbaum, A. I., and Julius, D. 2006. TRPA1 mediates the inflammatory actions of environmental irritants and proalgesic agents. Cell 124, 1269–1282.

Belyantseva, I. A., Adler, H. J., Curi, R., Frolenkov, G. I., and Kachar, B. 2000. Expression and localization of prestin and the sugar transporter GLUT-5 during development of electromotility in cochlear outer hair cells. J. Neurosci. 20, RC116.

Belyantseva, I. A., Boger, E. T., and Friedman, T. B. 2003. Myosin XVa localizes to the tips of inner ear sensory cell stereocilia and is essential for staircase formation of the hair bundle. Proc. Natl. Acad. Sci. U. S. A. 100, 13958–13963.

Belyantseva, I. A., Boger, E. T., Naz, S., Frolenkov, G. I., Sellers, J. R., Ahmed, Z. M., Griffith, A. J., and Friedman, T. B. 2005. Myosin-XVa is required for tip localization of whirlin and differential elongation of hair-cell stereocilia. Nat. Cell Biol. 7, 148–156.

Ben-Yosef, T., Belyantseva, I. A., Saunders, T. L., Hughes, E. D., Kawamoto, K., Van Itallie, C. M., Beyer, L. A., Halsey, K., Gardner, D. J., Wilcox, E. R., Rasmussen, J., Anderson, J. M., Dolan, D. F., Forge, A., Raphael, Y., Camper, S. A., and Friedman, T. B. 2003. Claudin 14 knockout mice, a model for autosomal recessive deafness DFNB29, are deaf due to cochlear hair cell degeneration. Hum. Mol. Genet. 12, 2049–2061.

Beurg, M., Bouleau, Y., and Dulon, D. 2001. The voltage-sensitive motor protein and the Ca^{2+}-sensitive cytoskeleton in developing rat cochlear outer hair cells. Eur. J. Neurosci. 14, 1947–1952.

Beutner, D. and Moser, T. 2001. The presynaptic function of mouse cochlear inner hair cells during development of hearing. J. Neurosci. 21, 4593–4599.

Bobbin, R. P. 2001. ATP-induced movement of the stalks of isolated cochlear Deiters' cells. Neuroreport 12, 2923–2926.

Boeda, B., El-Amraoui, A., Bahloul, A., Goodyear, R., Daviet, L., Blanchard, S., Perfettini, I., Fath, K. R., Shorte, S., Reiners, J., Houdusse, A., Legrain, P., Wolfrum, U., Richardson, G., and Petit, C. 2002. Myosin VIIa, harmonin and cadherin 23, three Usher I gene products that cooperate to shape the sensory hair cell bundle. EMBO J. 21, 6689–6699.

Burgess, B. J., Adams, J. C., and Nadol, J. B., Jr. 1997. Morphologic evidence for innervation of Deiters' and Hensen's cells in the guinea pig. Hear. Res. 108, 74–82.

Carlisle, L., Zajic, G., Altschuler, R. A., Schacht, J., and Thorne, P. R. 1988. Species differences in the distribution of infracuticular F-actin in outer hair cells of the cochlea. Hear. Res. 33, 201–205.

Chan, D. K. and Hudspeth, A. J. 2005. Ca^{2+} current-driven nonlinear amplification by the mammalian cochlea *in vitro*. Nat. Neurosci. 8, 149–155.

Cohen, G. M. and Fermin, C. D. 1978. The development of hair cells in the embryonic chick's basilar papilla. Acta Otolaryngol. 86, 342–358.

Corey, D. P. and Hudspeth, A. J. 1979a. Ionic basis of the receptor potential in a vertebrate hair cell. Nature 281, 675–677.

Corey, D. P. and Hudspeth, A. J. 1979b. Response latency of vertebrate hair cells. Biophys. J. 26, 499–506.

Corey, D. P., Garcia-Anoveros, J., Holt, J. R., Kwan, K. Y., Lin, S. Y., Vollrath, M. A., Amalfitano, A., Cheung, E. L., Derfler, B. H., Duggan, A., Geleoc, G. S., Gray, P. A., Hoffman, M. P., Rehm, H. L., Tamasauskas, D., and Zhang, D. S. 2004. TRPA1 is a candidate for the mechanosensitive transduction channel of vertebrate hair cells. Nature 432, 723–730.

Cosgrove, D., Kornak, J. M., and Samuelson, G. 1996a. Expression of basement membrane type IV collagen chains during postnatal development in the murine cochlea. Hear. Res. 100, 21–32.

Cosgrove, D., Samuelson, G., and Pinnt, J. 1996b. Immunohistochemical localization of basement membrane collagens and associated proteins in the murine cochlea. Hear. Res. 97, 54–65.

Crozet, F., el Amraoui, A., Blanchard, S., Lenoir, M., Ripoll, C., Vago, P., Hamel, C., Fizames, C., Levi-Acobas, F., Depetris, D., Mattei, M. G., Weil, D., Pujol, R., and Petit, C. 1997. Cloning of the genes encoding two murine and human cochlear unconventional type I myosins. Genomics 40, 332–341.

Dallos, P. and Evans, B. N. 1995. High-frequency motility of outer hair cells and the cochlear amplifier. Science 267, 2006–2009.

Dallos, P., He, D. Z., Lin, X., Sziklai, I., Mehta, S., and Evans, B. N. 1997. Acetylcholine, outer hair cell electromotility, and the cochlear amplifier. J. Neurosci. 17, 2212–2226.

Dannhof, B. J., Roth, B., and Bruns, V. 1991. Length of hair cells as a measure of frequency representation in the mammalian inner ear. Naturwissenschaften 78, 570–573.

Daudet, N. and Lebart, M. C. 2002. Transient expression of the t-isoform of plastins/fimbrin in the stereocilia of developing auditory hair cells. Cell Motil. Cytoskeleton. 53, 326–336.

Dechesne, C. J., Rabejac, D., and Desmadryl, G. 1994. Development of calretinin immunoreactivity in the mouse inner ear. J. Comp. Neurol. 346, 517–529.

Drenckhahn, D., Engel, K., Hofer, D., Merte, C., Tilney, L., and Tilney, M. 1991. Three different actin filament assemblies occur in every hair cell: each contains a specific actin crosslinking protein. J. Cell Biol. 112, 641–651.

Dumont, R. A., Lins, U., Filoteo, A. G., Penniston, J. T., Kachar, B., and Gillespie, P. G. 2001. Plasma membrane Ca^{2+}-ATPase isoform 2a is the PMCA of hair bundles. J. Neurosci. 21, 5066–5078.

Ekstrom von Lubitz, D. K. 1981. Ultrastructure of the lateral-line sense organs of the ratfish, *Chimaera monstrosa*. Cell Tissue Res. 215, 651–665.

Elgoyhen, A. B., Johnson, D. S., Boulter, J., Vetter, D. E., and Heinemann, S. 1994. Alpha 9: an acetylcholine receptor with novel pharmacological properties expressed in rat cochlear hair cells. Cell 79, 705–715.

Engel, J., Michna, M., Platzer, J., and Striessnig, J. 2002. Calcium channels in mouse hair cells: function, properties and pharmacology. Adv. Otorhinolaryngol. 59, 35–41.

Etournay, R., El-Amraoui, A., Bahloul, A., Blanchard, S., Roux, I., Pezeron, G., Michalski, N., Daviet, L., Hardelin, J. P., Legrain, P., and Petit, C. 2005. PHR1, an integral membrane protein of the inner ear sensory cells, directly interacts with myosin 1c and myosin VIIa. J. Cell Sci. 118, 2891–2899.

Evans, M. G. 1996. Acetylcholine activates two currents in guinea-pig outer hair cells. J. Physiol. 491, 563–578.

Evans, M. G., Lagostena, L., Darbon, P., and Mammano, F. 2000. Cholinergic control of membrane conductance and intracellular free Ca^{2+} in outer hair cells of the guinea pig cochlea. Cell Calcium 28, 195–203.

Farris, H. E., LeBlanc, C. L., Goswami, J., and Ricci, A. J. 2004. Probing the pore of the auditory hair cell mechanotransducer channel in turtle. J. Physiol. 558, 769–792.

Favre, D. and Sans, A. 1983. Organization and density of microtubules in the vestibular sensory cells in the cat. Acta Otolaryngol. 96, 15–20.

Fettiplace, R. and Hackney, C. M. 2006. The sensory and motor roles of auditory hair cells. Nat. Rev. Neurosci. 7, 19–29.

Fettiplace, R. and Ricci, A. J. 2006. Mechanoelectrical transduction in Auditory Hair Cells. In: Springer Handbook of Auditory Research: Vertebrate Hair Cells (*eds*. R. A. Eatock, R. Fay, and A. N. Popper), pp. 154–203. Springer Science and Business Media.

Flock, A., Bretscher, A., and Weber, K. 1982. Immunohistochemical localization of several cytoskeletal proteins in inner ear sensory and supporting cells. Hear. Res. 7, 75–89.

Forge, A., Souter, M., and Denman-Johnson, K. 1997. Structural development of sensory cells in the ear. Semin. Cell Dev. Biol. Jun 8(3), 225–237.

Frolenkov, G. I., Belyantseva, I. A., Friedmann, T. B., and Griffith, A. J. 2004. Genetic insights into the morphogenesis of inner ear hair cells. Nature Rev. Gen. 5, 489–498.

Frolenkov, G. I., Mammano, F., Belyantseva, I. A., Coling, D., and Kachar, B. 2000. Two distinct $Ca^{(2+)}$-dependent signaling pathways regulate the motor output of cochlear outer hair cells. J. Neurosci. 20, 5940–5948.

Frolenkov, G. I., Mammano, F., and Kachar, B. 2003. Regulation of outer hair cell cytoskeletal stiffness by intracellular Ca^{2+}: underlying mechanism and implications for cochlear mechanics. Cell Calcium 33, 185–195.

Fuchs, P. A. and Parsons, T. D. 2006. The Synaptic Physiology of Hair Cells. In: Springer Handbook of Auditory Research: Vertebrate Hair Cells (*eds*. R. A. Eatock, R. Fay, and A. N. Popper), pp. 249–312. Springer Science and Business Media.

Fuchs, P. A., Evans, M. G., and Murrow, B. W. 1990. Calcium currents in hair cells isolated from the cochlea of the chick. J. Physiol. 429, 553–568.

Furness, D. N. and Hackney, C. M. 1985. Cross-links between stereocilia in the guinea pig cochlea. Hear. Res. 18, 177–188.

Furness, D. N. and Hackney, C. M. 1990. Comparative ultrastructure of subsurface cisternae in inner and outer hair cells of the guinea pig cochlea. Eur. Arch. Otorhinolaryngol. 247, 12–15.

Furness, D. N. and Hackney, C. M. 2006. The Structure and Composition of the Stereociliary Bundle of Vertebrate Hair Cells. In: Springer Handbook of Auditory Research: Vertebrate Hair Cells (*eds*. R. A. Eatock, R. Fay, and A. N. Popper), pp. 95–153. Springer Science and Business Media.

Furness, D. N. and Lawton, D. M. 2003. Comparative distribution of glutamate transporters and receptors in relation to afferent innervation density in the mammalian cochlea. J. Neurosci. 23, 11296–11304.

Furness, D. N. and Lehre, K. P. 1997. Immunocytochemical localization of a high-affinity glutamate-aspartate transporter, GLAST, in the rat and guinea-pig cochlea. Eur. J. Neurosci. 9, 1961–1969.

Furness, D. N., Hackney, C. M., and Steyger, P. S. 1990. Organization of microtubules in cochlear hair cells. J. Electron Microsc. Tech. 15, 261–279.

Furness, D. N., Hulme, J. A., Lawton, D. M., and Hackney, C. M. 2002a. Distribution of the glutamate/aspartate transporter GLAST in relation to the afferent synapses of outer hair cells in the guinea pig cochlea. J. Assoc. Res. Otolaryngol. 3, 234–247.

Furness, D. N., Karkanevatos, A., West, B., and Hackney, C. M. 2002b. An immunogold investigation of the distribution of calmodulin in the apex of cochlear hair cells. Hear. Res. 173, 10–20.

Furness, D. N., Katori, Y., Mahendrasingam, S., and Hackney, C. M. 2005. Differential distribution of beta- and gamma-actin in guinea-pig cochlear sensory and supporting cells. Hear. Res. 207, 22–34.

Furness, D. N., Richardson, G. P., and Russell, I. J. 1989. Stereociliary bundle morphology in organotypic cultures of the mouse cochlea. Hear. Res. 38, 95–109.

Gagnon, L. H., Longo-Guess, C. M., Berryman, M., Shin, J. B., Saylor, K. W., Yu, H., Gillespie, P. G., and Johnson, K. R. 2006. The chloride intracellular channel protein CLIC5 is expressed at high levels in hair cell stereocilia and is essential for normal inner ear function. J. Neurosci. 26, 10188–10198.

Gale, J. E., Marcotti, W., Kennedy, H. J., Kros, C. J., and Richardson, G. P. 2001. 2FM-143 dye behaves as a permanent blocker of the hair-cell-transducer channel. 21, 7013–7025.

Garcia, J. A., Yee, A. G., Gillespie, P. G., and Corey, D. P. 1998. Localization of myosin-Ibeta near both ends of tip links in frog saccular hair cells. J. Neurosci, 18, 8637–8647.

Goodyear, R. and Richardson, G. P. 1999. The ankle-link antigen: an epitope sensitive to calcium chelation associated with the hair-cell surface and the calycal processes of photoreceptors. J. Neurosci. 19, 3761–3772.

Goodyear, R. and Richardson, G. P. 2003. A novel antigen sensitive to calcium chelation that is associated with the tip links and kinocilial links of sensory hair bundles. J. Neurosci. 23, 4878–4887.

Grant, L., Slapnick, S., Kennedy, H., and Hackney, C. M. 2006. Ryanodine receptor localization in the mammalian cochlea: an ultrastructural study. Hear Res. 219, 101–209.

Grati, M., Schneider, M. E., Lipkow, K., Strehler, E. E., Wenthold, R. J., and Kachar, B. 2006. Rapid turnover of stereocilia membrane proteins: evidence from the trafficking and mobility of plasma membrane $Ca^{(2+)}$-ATPase 2. J. Neurosci. 26, 6386–6395.

Griesinger, C. B., Richards, C. D., and Ashmore, J. F. 2002. FM1-43 reveals membrane recycling in adult inner hair cells of the mammalian cochlea. J. Neurosci. 22, 3939–3952.

Griesinger, C. B., Richards, C. D., and Ashmore, J. F. 2004. Apical endocytosis in outer hair cells of the mammalian cochlea. Eur. J. Neurosci. 20, 41–50.

Guinan, J. J. Jr., Lin, T., and Cheng, H. 2005. Medial-olivocochlear-efferent inhibition of the first peak of auditory-nerve responses: evidence for a new motion within the cochlea. J. Acoust. Soc. Am. 118, 2421–2433.

Guth, P. S. and Norris, C. H. 1996. The hair cell acetylcholine receptors: a synthesis. Hear. Res. 98, 1–8.

Hackney, C. M., Fettiplace, R., and Furness, D. N. 1993. The functional morphology of stereociliary bundles on turtle cochlear hair cells. Hear. Res. 69, 163–175.

Hackney, C. M., Furness, D. N., Benos, D. J., Woodley, J. F., and Barratt, J. 1992. Putative immunolocalization of the mechanoelectrical transduction channels in mammalian cochlear hair cells. Proc. R. Soc. B. Biol. Sci. 248, 215–221.

Hackney, C. M., Mahendrasingam, S., Jones, E. M., and Fettiplace, R. 2003. The distribution of calcium buffering proteins in the turtle cochlea. J. Neurosci. 23, 4577–4589.

Hackney, C. M., Mahendrasingam, S., Penn, A., and Fettiplace, R. 2005. The concentrations of calcium buffering proteins in mammalian cochlear hair cells. J. Neurosci. 25, 7867–7875.

Hafidi, A., Beurg, M., and Dulon, D. 2005. Localization and developmental expression of BK channels in mammalian cochlear hair cells. Neuroscience 130, 475–484.

Hakuba, N., Koga, K., Gyo, K., Usami, S. I., and Tanaka, K. 2000. Exacerbation of noise-induced hearing loss in mice lacking the glutamate transporter GLAST. J. Neurosci. 20, 8750–8753.

Hasson, T., Gillespie, P. G., Garcia, J. A., MacDonald, R. B., Zhao, Y., Yee, A. G., Mooseker, M. S., and Corey, D. P. 1997. Unconventional myosins in inner-ear sensory epithelia. J. Cell Biol. 137, 1287–1307.

He, D. Z., Jia, S., and Dallos, P. 2003. Prestin and the dynamic stiffness of cochlear outer hair cells. J. Neurosci. 23, 9089–9096.

Heller, S., Bell, A. M., Denis, C. S., Choe, Y., and Hudspeth, A. J. 2002. Parvalbumin 3 is an abundant Ca^{2+} buffer in hair cells. J. Assoc. Res. Otolaryngol. 3, 488–498.

Heywood, P., Van de Water, T. R., Hilding, D. A., and Ruben, R. J. 1975. Distribution of microtubules and microfilaments in developing vestibular sensory epithelium of mouse otocysts grown *in vitro*. J. Cell Sci. 17, 171–189.

Hiel, H., Navaratnam, D. S., Oberholtzer, J. C., and Fuchs, P. A. 2002. Topological and developmental gradients of calbindin expression in the chick's inner ear. J. Assoc. Res. Otolaryngol. 3, 1–15.

Hille, B. 2001. Ion Channels of Excitable Membranes, 3rd edn. Sinauer Press.

Hofer, D., Ness, W., and Drenckhahn, D. 1997. Sorting of actin isoforms in chicken auditory hair cells. J. Cell Sci. 110, 765–770.

Holley, M. C. and Ashmore, J. F. 1990. Spectrin, actin and the structure of the cortical lattice in mammalian cochlear outer hair cells. J. Cell Sci. 96, 283–291.

Holt, J. R., Gillespie, S. K., Provance, D. W., Shah, K., Shokat, K. M., Corey, D. P., Mercer, J. A., and Gillespie, P. G. 2002. A chemical-genetic strategy implicates myosin-1c in adaptation by hair cells. Cell 108, 371–381.

Housley, G. D., Kanjhan, R., Raybould, N. P., Greenwood, D., Salih, S. G., Jarlebark, L., Burton, L. D., Setz, V. C., Cannell, M. B., Soeller, C., Christie, D. L., Usami, S., Matsubara, A., Yoshie, H., Ryan, A. F., and Thorne, P. R. 1999. Expression of the P2X(2) receptor subunit of the ATP-gated ion channel in the cochlea: implications for sound mechanotransduction and auditory neurotransmission. J. Neurosci. 19, 8377–8388.

Housley, G. D., Marcotti, W., Navaratnam, D., and Yamoah, E. N. 2006. Hair cells – beyond the MET. J. Membr. Biol. 209, 89–118.

Imamura, S. and Adams, J. C. 1996. Immunolocalization of peptide 19 and other calcium-binding proteins in the guinea pig cochlea. Anat. Embryol. (Berl.) 194, 407–418.

Issa, N. P. and Hudspeth, A. J. 1994. Clustering of Ca^{2+} channels and $Ca^{(2+)}$-activated K^+ channels at fluorescently labeled presynaptic active zones of hair cells. Proc. Natl. Acad. Sci. U. S. A. 91, 7578–7582.

Itoh, M. 1982. Preservation and visualization of actin-containing filaments in the apical zone of cochlear sensory cells. Hear. Res. 6, 277–289.

Jagger, D. J. and Forge, A. 2006. Compartmentalized and signal-selective gap junctional coupling in the hearing cochlea. J. Neurosci. 26, 1260–1268.

Jensen-Smith, H. C., Eley, J., Steyger, P. S., Luduena, R. F., and Hallworth, R. 2003. Cell type-specific reduction of beta tubulin isotypes synthesized in the developing gerbil organ of Corti. J. Neurocytol. 32, 85–97.

Jorgensen, J. M. 1982. Microtubules in inner ear hair cells of the snake. Neurosci. Lett. 31, 319–322.

Kachar, B., Battaglia, A., and Fex, J. 1997. Compartmentalized vesicular traffic around the hair cell cuticular plate. Hear. Res. 107, 102–112.

Kachar, B., Parakkal, M., Kurc, M., Zhao, Y., and Gillespie, P. G. 2000. High-resolution structure of hair-cell tip links. Proc. Natl. Acad. Sci. U. S. A. 97, 13336–13341.

Kalinec, F., Holley, M. C., Iwasa, K. H., Lim, D. J., and Kachar, B. 1992. A membrane-based force generation mechanism in auditory sensory cells. Proc. Natl. Acad. Sci. U. S. A. 89, 8671–8675.

Kanjhan, R., Balke, C. L., Housley, G. D., Bellingham, M. C., and Noakes, P. G. 2004. Developmental expression of two-pore domain K^+ channels, TASK-1 and TREK-1, in the rat cochlea. Neuroreport. 15, 437–441.

Kappler, J. A., Starr, C. J., Chan, D. K., Kollmar, R., and Hudspeth, A. J. 2004. A nonsense mutation in the gene encoding a zebrafish myosin VI isoform causes defects in hair-cell mechanotransduction. Proc. Natl. Acad. Sci. U. S. A. 101, 13056–13061.

Katori, Y., Hackney, C. M., and Furness, D. N. 1996. Immunoreactivity of sensory hair bundles of the guinea-pig cochlea to antibodies against elastin and keratan sulphate. Cell Tissue Res. 284, 473–479.

Kennedy, H. J., Crawford, A. C., and Fettiplace, R. 2005. Force generation by mammalian hair bundles supports a role in cochlear amplification. Nature 433, 880–883.

Kennedy, H. J., Evans, M. G., Crawford, A. C., and Fettiplace, R. 2006. Depolarization of cochlear outer hair cells evokes active hair bundle motion by two mechanisms. J. Neurosci. 26, 2757–2766.

Khimich, D., Nouvian, R., Pujol, R., Tom Dieck, S., Egner, A., Gundelfinger, E. D., and Moser, T. 2005. Hair cell synaptic ribbons are essential for synchronous auditory signalling. Nature 434, 889–894.

Kikuchi, T., Takasaka, T., Tonosaki, A., Katori, Y., and Shinkawa, H. 1991. Microtubules of guinea pig cochlear epithelial cells. Acta Otolaryngol. 111, 286–290.

Kirk, D. L. and Yates, G. K. 1998. 4-aminopyridine in scala media reversibly alters the cochlear potentials and suppresses electrically evoked oto-acoustic emissions. Audiol. Neurootol. 3, 21–39.

Kollmar, R., Montgomery, L. G., Fak, J., Henry, L. J., and Hudspeth, A. J. 1997. Predominance of the alpha1D subunit in L-type voltage-gated Ca^{2+} channels of hair cells in the chicken's cochlea. Proc. Natl. Acad. Sci. U. S. A. 94, 14883–14888.

Konishi, T. and Salt, A. N. 1980. Permeability to potassium of the endolymph–perilymph barrier and its possible relation to hair cell function. Exp. Brain Res. 40, 457–463.

Koyama, M., Spicer, S. S., and Schulte, B. A. 1999. Immunohistochemical localization of Ca^{2+}/calmodulin-dependent protein kinase IV in outer hair cells. J. Histochem. Cytochem. 47, 7–12.

Kozel, P. J., Friedman, R. A., Erway, L. C., Yamoah, E. N., Liu, L. H., Riddle, T., Duffy, J. J., Doetschman, T., Miller, M. L., Cardell, E. L., and Shull, G. E. 1998. Balance and hearing deficits in mice with a null mutation in the gene encoding plasma membrane Ca^{2+}-ATPase isoform 2. J. Biol. Chem. 273, 18693–18696.

Kros, C. J., Marcotti, W., van Netten, S. M., Self, T. J., Libby, R. T., Brown, S. D., Richardson, G. P., and Steel, K. P. 2002. Reduced climbing and increased slipping adaptation in cochlear hair cells of mice with Myo7a mutations. Nat. Neurosci. 5, 41–47.

Kros, C. J., Ruppersberg, J. P., and Rusch, A. 1998. Expression of a potassium current in inner hair cells during development of hearing in mice. Nature 394, 281–284.

Kubisch, C., Schroeder, B. C., Friedrich, T., Lutjohann, B., El-Amraoui, A., Marlin, S., Petit, C., and Jentsch, T. J. 1999. KCNQ4, a novel potassium channel expressed in sensory outer hair cells, is mutated in dominant deafness. Cell 96, 437–446.

Kussel-Andermann, P., El-Amraoui, A., Safieddine, S., Nouaille, S., Perfettini, I., Lecuit, M., Cossart, P., Wolfrum, U., and Petit, C. 2000. Vezatin, a novel transmembrane protein, bridges myosin VIIA to the cadherin-catenins complex. EMBO J. 19, 6020–6029.

Kwan, K. Y., Allchorne, A. J., Vollrath, M. A., Christensen, A. P., Zhang, D. S., Woolf, C. J., and Corey, D. P. 2006. TRPA1 contributes to cold, mechanical, and chemical nociception but is not essential for hair-cell mechanotransduction. Neuron 50, 277–289.

Langer, P., Grunder, S., and Rusch, A. 2003. Expression of Ca^{2+}-activated BK channel mRNA and its splice variants in the rat cochlea. J. Comp. Neurol. 455, 198–209.

Legan, P. K., Rau, A., Keen, J. N., and Richardson, G. P. 1997. The mouse tectorins. Modular matrix proteins of the inner ear homologous to components of the sperm–egg adhesion system. J. Biol. Chem. 272, 8791–8801.

Lim, D. J. 1986. Functional structure of the organ of Corti: a review. Hear. Res. 22, 117–146.

Lioudyno, M., Hiel, H., Kong, J. H., Katz, E., Waldman, E., Parameshwaran-Iyer, S., Glowatzki, E., and Fuchs, P. A. 2004. A 'synaptoplasmic cistern' mediates rapid inhibition of cochlear hair cells. J. Neurosci. 24, 11160–11164.

Mahendrasingam, S., Furness, D. N., and Hackney, C. M. 1998. Ultrastructural localisation of spectrin in sensory and supporting cells of guinea-pig organ of Corti. Hear. Res. 126, 151–160.

Mahendrasingam, S., Katori, Y., Furness, D. N., and Hackney, C. M. 1997. Ultrastructural localization of cadherin in the adult guinea-pig organ of Corti. Hear. Res. 111, 85–92.

Mammano, F. and Ashmore, J. F. 1996. Differential expression of outer hair cell potassium currents in the isolated cochlea of the guinea-pig. J. Physiol. 496, 639–646.

Manley, G. A. 1990. Peripheral Hearing Mechanisms in Reptiles and Birds. Springer.

Marcotti, W., Geleoc, G. S., Lennan, G. W., and Kros, C. J. 1999. Transient expression of an inwardly rectifying potassium conductance in developing inner and outer hair cells along the mouse cochlea. Pflugers Arch. 439, 113–122.

Marcotti, W., Johnson, S. L., and Kros, C. J. 2004. A transiently expressed SK current sustains and modulates action potential activity in immature mouse inner hair cells. J. Physiol. 560, 691–708.

Marcotti, W., Johnson, S. L., Rusch, A., and Kros, C. J. 2003. Sodium and calcium currents shape action potentials in immature mouse inner hair cells. J. Physiol. 552, 743–761.

Mastrogiacomo, A., Parsons, S. M., Zampighi, G. A., Jenden, D. J., Umbach, J. A., and Gundersen, C. B. 1994. Cysteine string proteins: a potential link between synaptic vesicles and presynaptic Ca^{2+} channels. Science 263, 981–982.

Matsunobu, T., Chung, J. W., and Schacht, J. 2001. Acetylcholine-evoked calcium increases in Deiters' cells of the guinea pig cochlea suggest alpha9-like receptors. J. Neurosci. Res. 63, 252–256.

Mburu, P., Kikkawa, Y., Townsend, S., Romero, R., Yonekawa, H., and Brown, S. D. 2006. Whirlin complexes with p55 at the stereocilia tip during hair cell development. Proc. Natl. Acad. Sci. U. S. A. 103, 10973–10978.

Mburu, P., Mustapha, M., Varela, A., Weil, D., El-Amraoui, A., Holme, R. H., Rump, A., Hardisty, R. E., Blanchard, S., Coimbra, R. S., Perfettini, I., Parkinson, N., Mallon, A. M., Glenister, P., Rogers, M. J., Paige, A. J., Moir, L., Clay, J., Rosenthal, A., Liu, X. Z., Blanco, G, Steel, K. P., Petit, C., and Brown, S. D. 2003. Defects in whirlin, a PDZ domain molecule involved in stereocilia elongation, cause deafness in the whirler mouse and families with DFNB31. Nature Genet. 34, 421–428.

Meyer, J., Mack, A. F., and Gummer, A. W. 2001. Pronounced infracuticular endocytosis in mammalian outer hair cells. Hear. Res. 161, 10–22.

Mhatre, A. N., Stern, R. E., Li, J., and Lalwani, A. K. 2002. Aquaporin 4 expression in the mammalian inner ear and its role in hearing. Biochem. Biophys. Res. Commun. 297, 987–996.

Miyabe, Y., Kikuchi, T., and Kobayashi, T. 2002. Comparative immunohistochemical localizations of aquaporin-1 and aquaporin-4 in the cochleae of three different species of rodents. Tohoku J. Exp. Med. 196, 247–257.

Nakazawa, K. 2001. Ultrastructural localization of calmodulin in gerbil cochlea by immunogold electron microscopy. Hear. Res. 151, 133–140.

Nemzou, N. R. M., Bulankina, A. V., Khimich, D., Giese, A., and Moser, T. 2006. Synaptic organization in cochlear inner hair cells deficient for the Ca(V)1.3 (alpha1D) subunit of L-type $GrCa^{(2+)}$ channels. Neuroscience. 141, 1849–1860.

Nunomura, W. and Takakuwa, Y. 2006. Regulation of protein 4.1R interactions with membrane proteins by Ca^{2+} and calmodulin. Front. Biosci. 11, 1522–1539.

Oestreicher, E., Wolfgang, A., and Felix, D. 2002. Neurotransmission of the cochlear inner hair cell synapse – implications for inner ear therapy. Adv. Otorhinolaryngol. 59, 131–139.

Ohmori, H. 1984. Studies of ionic currents in the isolated vestibular hair cell of the chick. J. Physiol. 350, 561–581.

Osborne, M. P. and Comis, S. D. 1990. Action of elastase, collagenase and other enzymes upon linkages between stereocilia in the guinea-pig cochlea. Acta Otolaryngol. 110, 37–45.

Osborne, M. P., Comis, S. D., and Pickles, J. O. 1988. Further observations on the fine structure of tip links between stereocilia of the guinea pig cochlea. Hear. Res. 35, 99–108.

Pack, A. K. and Slepecky, N. B. 1995. Cytoskeletal and calcium-binding proteins in the mammalian organ of Corti: cell type-specific proteins displaying longitudinal and radial gradients. Hear. Res. 91, 119–135.

Parks, T. N. 2000. The AMPA receptors of auditory neurons. Hear. Res. 147, 77–91.

Pataky, F., Pironkova, R., and Hudspeth, A. J. 2004. Radixin is a constituent of stereocilia in hair cells. Proc. Natl. Acad. Sci. U. S. A. 101, 2601–2606.

Pickles, J. O., Comis, S. D., and Osborne, M. P. 1984. Cross-links between stereocilia in the guinea pig organ of Corti, and their possible relation to sensory mechanotransduction. Hear. Res. 15, 103–112.

Platzer, J., Engel, J., Schrott-Fischer, A., Stephan, K., Bova, S., Chen, H., Zheng, H., and Striessnig, J. 2000. Congenital deafness and sinoatrial node dysfunction in mice lacking class D L-type Ca^{2+} channels. Cell 102, 89–97.

Plazas, P. V., Katz, E., Gomez-Casati, M. E., Bouzat, C., and Elgoyhen, A. B. 2005. Stoichiometry of the alpha9alpha10 nicotinic cholinergic receptor. J. Neurosci. 25, 10905–10912.

Popper, A. N. 2000. Hair cell heterogeneity and ultrasonic hearing: recent advances in understanding fish hearing. Philos. Trans. R. Soc. Lond., B, Biol. Sci. 355, 1277–1280.

Pyott, S. J., Glowatski, E., Trimmer, J. S., and Aldrich, R. W. 2004. Extrasyaptic localization of inactivating calcium-

activated potassium channels in mouse inner hair cells. J. Neurosci. 24, 9469–9474.
Rio, C., Dikkes, P., Liberman, M. C., and Corfas, G. 2002. Glial fibrillary acidic protein expression and promoter activity in the inner ear of developing and adult mice. J. Comp. Neurol. 442, 156–162.
Roberts, W. M., Jacobs, R. A., and Hudspeth, A. J. 1990. Colocalization of ion channels involved in frequency selectivity and synaptic transmission at presynaptic active zones of hair cells. J. Neurosci. 10, 3664–3684.
Robles, L. and Ruggero, M. A. 2001. Mechanics of the mammalian cochlea. Physiol. Rev. 81, 1305–1352.
Rodgers, K. D., Barritt, L., Miner, J. H., and Cosgrove, D. 2001. The laminins in the murine inner ear: developmental transitions and expression in cochlear basement membranes. Hear. Res. 158, 39–50.
Roux, I., Safieddine, S, Nouvian, R., Grati, M., Simmler, M. C., Bahloul, A., Perfettini, I., Le Gall, M., Rostaing, P., Hamard, G., Triller, A., Avan, P., Moser, T., and Petit, C. 2006. Otoferlin, defective in a human deafness form, is essential for exocytosis at the auditory ribbon synapse. Cell 127, 277–89.
Ruttiger, L., Sausbier, M., Zimmermann, U., Winter, H., Braig, C., Engel, J., Knirsch, M., Arntz, C., Langer, P., Hirt, B., Muller, M., Kopschall, I., Pfister, M., Munkner, S., Rohbock, K., Pfaff, I., Rusch, A., Ruth, P., and Knipper, M. 2004. Deletion of the Ca^{2+}-activated potassium (BK) alpha-subunit but not the BK beta1-subunit leads to progressive hearing loss. Proc. Natl. Acad. Sci. U. S. A. 101, 12922–12927.
Rzadzinska, A. K., Schneider, M. E., Davies, C., Riordan, G. P., and Kachar, B. 2004. An actin molecular treadmill and myosins maintain stereocilia functional architecture and self-renewal. J. Cell Biol. 164, 887–897.
Saito, K. 1983. Fine structure of the sensory epithelium of guinea-pig organ of Corti: subsurface cisternae and lamellar bodies in the outer hair cells. Cell Tissue Res. 229, 467–481.
Santi, P. A. and Anderson, C. B. 1987. A newly identified surface coat on cochlear hair cells. Hear. Res. 27, 47–65.
Santos-Sacchi, J., Kakehata, S., Kikuchi, T., Katori, Y., and Takasaka, T. 1998. Density of motility-related charge in the outer hair cell of the guinea pig is inversely related to best frequency. Neurosci. Lett. 256, 155–158.
Schnee, M. E. and Ricci, A. J. 2003. Biophysical and pharmacological characterization of voltage-gated calcium currents in turtle auditory hair cells. J. Physiol. 549, 697–717.
Schnee, M. E., Lawton, D. M., Furness, D. N., Benke, T. A., and Ricci, A. J. 2005. Auditory hair cell-afferent fiber synapses are specialized to operate at their best frequencies. Neuron 47, 243–254.
Schoch, S. and Gundelfinger, E. D. 2006. Molecular organization of the presynaptic active zone. Cell Tissue Res. 326, 379–391.
Schug, N., Braig, C., Zimmermann, U., Engel, J., Winter, H., Ruth, P., Blin, N., Pfister, M., Kalbacher, H., and Knipper, M. 2006. Differential expression of otoferlin in brain, vestibular system, immature and mature cochlea of the rat. Eur. J. Neurosci. 24, 3372–3380.
Senften, M., Schwander, M., Kazmierczak, P., Lillo, C., Shin, J. B., Hasson, T., Geleoc, G. S., Gillespie, P. G., Williams, D., Holt, J. R., and Muller, U. 2006. Physical and functional interaction between protocadherin 15 and myosin VIIa in mechanosensory hair cells. J. Neurosci. 26, 2060–2071.
Sidi, S., Friedrich, R. W., and Nicolson, T. 2003. NompC TRP channel required for vertebrate sensory hair cell mechanotransduction. Science 301, 96–99.
Siemens, J., Lillo, C., Dumont, R. A., Reynolds, A., Williams, D. S., Gillespie, P. G., and Muller, U. 2004. Cadherin 23 is a component of the tip link in hair-cell stereocilia. Nature 428, 950–955.
Simonneau, L., Gallego, M., and Pujol, R. 2003. Comparative expression patterns of T-, N-, E-cadherins, beta-catenin, and polysialic acid neural cell adhesion molecule in rat cochlea during development: implications for the nature of Kolliker's organ. J. Comp. Neurol. 459, 113–126.
Slepecky, N. and Chamberlain, S. C. 1985. Immunoelectron microscopic and immunofluorescent localization of cytoskeletal and muscle-like contractile proteins in inner ear sensory hair cells. Hear. Res. 20, 245–260.
Slepecky, N. B. and Chamberlain, S. C. 1987. Tropomyosin co-localizes with actin microfilaments and microtubules within supporting cells of the inner ear. Cell Tissue Res. 248, 63–66.
Slepecky, N. B. and Savage, J. E. 1994. Expression of actin isoforms in the guinea pig organ of Corti: muscle isoforms are not detected. Hear. Res. 73, 16–26.
Slepecky, N. B. and Ulfendahl, M. 1993. Evidence for calcium-binding proteins and calcium-dependent regulatory proteins in sensory cells of the organ of Corti. Hear. Res. 70, 73–84.
Slepecky, N. B., Hamernik, R., and Henderson, D. 1981. The consistent occurrence of a striated organelle (Friedmann body) in the inner hair cells of the normal chinchilla. Acta Otolaryngol. 91, 189–198.
Slepecky, N. B., Henderson, C. G., and Saha, S. 1995. Post-translational modifications of tubulin suggest that dynamic microtubules are present in sensory cells and stable microtubules are present in supporting cells of the mammalian cochlea. Hear. Res. 91, 136–147.
Slepecky, N. B., Savage, J. E., Cefaratti, L. K., and Yoo, T. J. 1992. Electron-microscopic localization of type II, IX, and V collagen in the organ of Corti of the gerbil. Cell Tissue Res. 267, 413–418.
Sollner, C., Rauch, G. J., Siemens, J., Geisler, R., Schuster, S. C., Muller, U., and Nicolson, T. 2004. Tubingen 2000 Screen consortium. Mutations in cadherin 23 affect tip links in zebrafish sensory hair cells. Nature 428, 955–959.
Sotomayor, M., Corey, D. P., and Schulten, K. 2005. In search of the hair-cell gating spring elastic properties of ankyrin and cadherin repeats. Structure 13, 669–682.
Spicer, S. S. and Schulte, B. A. 1991. Differentiation of inner ear fibrocytes according to their ion transport related activity. Hear. Res. 56, 53–64.
Steyger, P. S., Furness, D. N., Hackney, C. M., and Richardson, G. P. 1989. Tubulin and microtubules in cochlear hair cells: comparative immunocytochemistry and ultrastructure. Hear. Res. 42, 1–16.
Steyger, P. S., Gillespie, P. G., and Baird, R. A. 1998. Myosin Ibeta is located at tip link anchors in vestibular hair bundles. J. Neurosci. 18, 4603–4615.
Street, V. A., McKee-Johnson, J. W., Fonseca, R. C., Tempel, B. L., and Noben-Trauth, K. 1998. Mutations in a plasma membrane Ca^{2+}-ATPase gene cause deafness in deafwaddler mice. Nat. Genet. 19, 390–394.
Szonyi, M., He, D. Z., Ribari, O., Sziklai, I., and Dallos, P. 2001. Intracellular calcium and outer hair cell electromotility. Brain Res. 922, 65–70.
Szucs, A., Somodi, S., Batta, T. J., Toth, A., Szigeti, G. P., Csernoch, L., Panyi, G., and Sziklai, I. 2006. Differential expression of potassium currents in Deiters cells of the guinea pig cochlea. Pflugers Arch. 452, 332–341.
Takumi, Y., Matsubara, A., Laake, J. H., Ramirez-Leon, V., Roberg, B., Torgner, I., Kvamme, E., Usami, S., and Ottersen, O. P. 1999. Phosphate activated glutaminase is

concentrated in mitochondria of sensory hair cells in rat inner ear: a high resolution immunogold study. J. Neurocytol. 28, 223–237.

Tilney, L. G., Derosier, D. J., and Mulroy, M. J. 1980. The organization of actin filaments in the stereocilia of cochlear hair cells. J. Cell Biol. 86, 244–259.

Tsuprun, V. and Santi, P. 1999. Ultrastructure and immunohistochemical identification of the extracellular matrix of the chinchilla cochlea. Hear. Res. 129, 35–49.

Tucker, T. and Fettiplace, R. 1995. Confocal imaging of calcium microdomains and calcium extrusion in turtle hair cells. Neuron 15, 1323–1335.

Ugawa, S., Inagaki, A., Yamamura, H., Ueda, T., Ishida, Y., Kajita, K., Shimizu, H., and Shimada, S. 2006. Acid-sensing ion channel-1b in the stereocilia of mammalian cochlear hair cells. Neuroreport 17, 1235–1239.

Vater, M., Lenoir, M., and Pujol, R. 1992. Ultrastructure of the horseshoe bat's organ of Corti. II. Transmission electron microscopy. J. Comp. Neurol. 318, 380–391.

Walker, R. G., Willingham, A. T., and Zuker, C. S. 2000. A Drosophila mechanosensory transduction channel. Science 287, 2229–2234.

Xu, S., Wang, Y., Zhao, H., Zhang, L., Xiong, W., Yau, K. W., Hiel, H., Glowatzki, E., Ryugo, D. K., and Valle, D. 2004. PHR1, a PH domain-containing protein expressed in primary sensory neurons. Mol. Cell. Biol. 24, 9137–9151.

Yu, N., Zhu, M. L., and Zhao, H. B. 2006. Prestin is expressed on the whole outer hair cell basolateral surface. Brain Res. 1095, 51–58.

Zenisek, D., Davila, V., Wan, L., and Almers, W. 2003. Imaging calcium entry sites and ribbon structures in two presynaptic cells. J. Neurosci. 23, 2538–2548.

Zheng, J., Shen, W., He, D. Z., Long, K. B., Madison, L. D., and Dallos, P. 2000. Prestin is the motor protein of cochlear outer hair cells. Nature 405, 149–155.

Zine, A. and Schweitzer, L. 1997. Localization of proteins associated with the outer hair cell plasma membrane in the gerbil cochlea. Neuroscience 80, 1247–1254.

3.07 Genetic Hearing Loss

B J B Keats, Louisiana State University Health Sciences Center, New Orleans, LA, USA

© 2008 Elsevier Inc. All rights reserved.

3.07.1	**Introduction**	140
3.07.2	**USH1C**	141
3.07.2.1	Structure, Expression, and Function	142
3.07.2.2	Mutations	142
3.07.2.3	Mouse Models	143
3.07.3	**GJB2**	143
3.07.3.1	Structure, Expression, and Function	143
3.07.3.2	Mutations	143
3.07.3.3	Mouse Models	144
3.07.4	**OTOF**	144
3.07.4.1	Structure, Expression, and Function	144
3.07.4.2	Mutations	145
3.07.4.3	Mouse Models	145
3.07.5	**TECTA**	145
3.07.5.1	Structure, Expression, and Function	145
3.07.5.2	Mutations	146
3.07.5.3	Mouse Models	146
3.07.6	**Outlook for the Future**	146
References		147

Glossary

codon A set of three bases that specifies a single amino acid or signals the termination of the amino acid sequence.

compound heterozygote An individual with a recessive disorder who has a different mutation in the two copies of the gene (cf., homozygote).

cryptic splice site A DNA sequence that is similar to a consensus splice site sequence but is not usually used unless there is a mutation in the normal splice site, or a mutation in the cryptic splice site results in it being preferred over the normal splice site.

dominant negative The abnormal product of a mutant copy of a gene disrupts the function of the product of the normal copy of the gene.

exon Segment of a gene that is transcribed and present in mature mRNA.

founder effect A mutation that is present in a small ancestral population, which increases in frequency by chance due to the initial small population size.

frameshift mutation An insertion or deletion of a number of base pairs that is not a multiple of three, and therefore changes the codons that follow.

genome The complete DNA sequence. For example, the nuclear genome of a human germ cell (sperm or ovum) consists of 3 million kb of DNA.

genotype The two copies of the gene (one of each chromosome) that are present at a locus.

haploinsufficiency The product of the normal copy of a gene is not adequate to prevent the disease when the mutant copy of the gene does not have a functional product.

heterozygote An individual whose genotype consists of two different copies of the gene.

homozygote An individual whose genotype consists of two identical copies of the gene.

intron Segment of a gene that is not present in the mature mRNA.

isoform Alternate forms of a protein.

kilobase (kb) A unit of 1000 bases in a DNA sequence.

linkage A statistical method of analysis of family phenotype and genotype data that provides the probability that two or more loci are not assorting independently (i.e., they are linked).

locus The position of a gene on a chromosome.
messenger RNA (mRNA) An RNA transcribed from the DNA of a gene, which directs the sequence in which amino acids are added to the product encoded by that gene.
missense mutation A substitution of one base by another such that the amino acid specified by the codon is changed.
modifier gene A gene that alters the phenotype associated with mutations in another gene.
nonsense mutation A substitution of one base by another such that the resulting codon specifies termination of the amino acid sequence.
penetrance The probability that a given genotype will result in a particular phenotype.
phenocopy A phenotype that looks the same as one produced by a specific genotype, but has a different etiology.
phenotype The observed characteristics of an individual.
splice site The DNA sequence that specifies the boundary between an intron and an exon in a gene. The introns are removed in the generation of the mature mRNA.
stop codon One of three codons specifying the termination of the product encoded by a gene.
transcription The synthesis of a single-stranded mRNA molecule (transcript) from a DNA template.
translation The synthesis of a sequence of amino acids from the mature mRNA template.

3.07.1 Introduction

The human genome contains about 30 000 genes, and mutations in the DNA sequences of more than 100 of these genes are associated with hearing loss. The degree of genetic hearing loss may range from mild to profound and some frequencies may be affected more than others; for most individuals the loss is sensorineural, bilateral, and symmetric. Onset is often congenital (present at birth), but it can be later in childhood or in adulthood. Many different genetic forms of hearing loss may give similar pure tone air conduction audiograms. Thus, ideally, a battery of physiological measurements that include tympanometry, middle ear muscle reflexes, otoacoustic emissions (OAEs), speech audiometry, and auditory brainstem response/electrocochleography (ABR/EcochG) should be obtained for each patient in order to categorize the hearing loss accurately and determine the most effective management (Keats, B. J. B. and Berlin, C. I., 2002).

About 30% of genetic hearing loss is syndromic, meaning that there are associated abnormalities in other organs such as the eye (Usher syndrome), kidney (Alport syndrome), skin (Waardenburg syndrome), heart (Jervell and Lange-Nielsen syndrome), and thyroid (Pendred syndrome). For the remaining 70%, the hearing loss is nonsyndromic. Griffith A. and Friedman T. (2002) and Toriello H. V. *et al.* (2004) provide comprehensive descriptions of syndromic and nonsyndromic hearing loss.

The mode of inheritance of hearing loss in a family may be dominant or recessive, and the mutation may be in a gene on one of the autosomes (chromosomes 1–22) or on the X-chromosome; these chromosomes are in the nucleus of the cell. A pedigree showing who is affected and who is unaffected in the family helps to determine the inheritance pattern. Figure 1 shows an example of autosomal dominant inheritance in which individuals with one normal

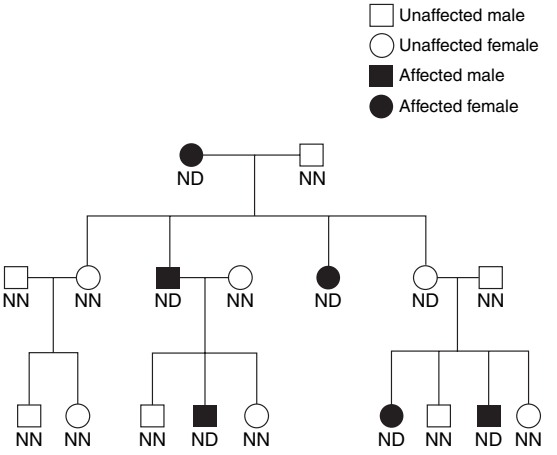

Figure 1 A pedigree showing an autosomal-dominant pattern of inheritance with incomplete penetrance. N is the normal form of the gene and D is the abnormal (mutant) form of the gene. Individuals with the NN genotype are unaffected and those with the ND genotype are expected to be affected. However, the sixth individual in the middle generation is unaffected but has an affected mother and two affected children. Thus, her genotype must be ND. This is an example of incomplete penetrance meaning that for individuals with the ND genotype, the probability of being affected is less than 1.

copy (N) and one abnormal copy (D) of the gene are usually affected; their genotype is ND and each of their offspring has a 50% chance of inheriting the D. However, the phenotype may be variable, and penetrance may be incomplete, meaning that some ND individuals may show no signs of being affected. The hearing loss is autosomal recessive if only individuals with the DD genotype are affected. Those with the ND genotype are unaffected and are referred to as carriers (or heterozygotes). Each offspring of two carrier parents has a 25% chance of inheriting the DD genotype and being affected. Family history is quite likely to be negative for a child with autosomal recessive hearing loss. Conversely, both parents may have autosomal recessive hearing loss but all their children may have normal hearing because mutations in different genes are responsible for the hearing loss in the parents. If all the affected individuals in a pedigree are male, and none of the affected males have affected sons, then the inheritance pattern is likely to be X-linked recessive. In this case, each son of a carrier mother has a 50% chance of being affected and all the daughters of an affected male will be carriers.

The symbols, DFNA*, DFNB*, and DFN*, are used to designate autosomal dominant, autosomal recessive, and X-linked hearing loss, respectively, where the asterisk represents a number. The symbol is assigned when the chromosomal location of the hearing loss gene is determined, usually through genetic linkage analysis. For example, DFNB21 means the twenty-first autosomal recessive locus mapped. When the abnormal gene at the locus is identified, a gene symbol is assigned. For human genes, the symbol is written in uppercase and italics. As a generalization, recessive hearing losses tend to be prelingual while dominant forms are postlingual and progressive, but there are exceptions. In some families the phenotype may vary from one affected child to another. Such findings may be examples of variable expression, but the possibility of phenocopies must be considered.

As well as the DNA in the nucleus, each of the several hundred mitochondria in a cell have multiple copies of their own DNA, and some forms of hearing loss are associated with mutations in this mitochondrial genome (mtDNA). Quite often the mutation is present in some copies of the mtDNA, but not others, a condition known as heteroplasmy. The number of base pairs of mtDNA is only about 16 000 compared with the three billion in the nuclear genome. Mitochondria are maternally inherited, so the pattern of inheritance is likely to be mitochondrial if all the offspring of an affected mother (but none of those of an affected father) are affected. However, because of heteroplasmy, the severity of the phenotype among the offspring may vary considerably. The majority of genetic hearing loss is autosomal recessive, but about 20% is autosomal dominant and 1–2% is X-linked or mitochondrial.

Throughout the body, the set of genes that are expressed varies among cell types, and from one stage of development to another. The characteristics of genetic forms of hearing loss are likely to differ depending on the cellular and subcellular localizations, and the functions of the proteins encoded by the associated genes. These proteins must be essential for normal hearing. They include cytoskeletal proteins, extracellular matrix proteins, transcription factors, and proteins required for ion homeostasis.

Because of the similarity between the mouse and human genomes, studies of mouse models are often quite informative in advancing understanding of genetic hearing loss. Many of the available mouse models are the result of spontaneous mutations, while others have been created using transgenic or gene knockout experimental approaches. The symbols for mouse genes are written in lowercase to differentiate them from human genes.

This perspective will focus on four genes (*USH1C*, *GJB2*, *OTOF*, and *TECTA*) that are associated with hearing loss and typify the range of phenotypes and modes of inheritance. They encode the proteins harmonin, connexin 26, otoferlin, and α-tectorin, which are expressed in four different cellular/subcellular locations in the inner ear and have diverse functions. Harmonin and otoferlin are cytoskeletal proteins, while connexin 26 is critical for maintaining ion homeostasis in the cochlear duct, and α-tectorin is an extracellular matrix protein that is an essential component of the tectorial membrane. Both dominant and recessive inheritance patterns have been found in families with mutations in *GJB2* and *TECTA*, while mutations in *GJB2* and *USH1C* are associated with both syndromic and nonsyndromic hearing loss, and mutations in *OTOF* have been found in children with auditory neuropathy/auditory dyssynchrony (AN/AD).

3.07.2 USH1C

Usher syndrome is clinically and genetically heterogeneous. Three clinical types have been described

based on the degree of hearing loss, vestibular function, and age of onset of retinal degeneration. Usher syndrome type I is the most severe, with profound hearing loss from birth, abnormal vestibular function, and retinal degeneration beginning with night blindness by the end of the first decade. As many as 6% of children born with profound hearing loss may have Usher syndrome type I. The pattern of inheritance is autosomal recessive, and mutations in at least six different genes are associated with Usher syndrome type I (Keats, B. J. B. and Savas, S., 2004). One of these genes is *USH1C*. It was mapped to the short arm of chromosome 11 in families of Acadian ancestry in south Louisiana. The original Acadians were French fishermen who left France in the early 1600s and settled in the Nova Scotia region (Acadia) of Canada. Their population size expanded dramatically until 1755 when they were forced to leave Canada. Over the next 40 years about 3000 Acadians moved to south Louisiana. Today more than 600 000 Louisiana residents consider themselves to be Acadians, and the frequency of Usher syndrome type IC is significantly higher than in any other population.

In 2000, the *USH1C* gene was identified and shown to encode a PDZ domain-containing cytoskeletal protein known as harmonin (Bitner-Glindzicz, M. *et al.*, 2000; Verpy, E. *et al.*, 2000). One mutation is specific to the Acadian population probably due to founder effect, but several others have been reported in different populations and some are associated with autosomal recessive nonsyndromic hearing loss (DFNB18) rather than Usher syndrome.

3.07.2.1 Structure, Expression, and Function

The *USH1C* gene contains 28 coding exons spanning approximately 50 kb of genomic DNA. As a result of alternative splicing of eight exons, multiple isoforms that are divided into three classes (a, b, c) are found. They vary in size from approximately 400 to 900 amino acids. Both a and b isoforms contain three PDZ domains while c isoforms have only two. The b isoforms are the longest and use exons that are not translated in either of the two shorter isoforms. The human and mouse proteins are 96% identical.

USH1C transcripts are present in many tissues, including colon, small intestine, kidney, brain, muscle, heart, and pancreas, in addition to the ear, eye, and vestibule. In the ear and eye, *USH1C* is expressed in the stereocilia of the hair cells and the photoreceptor cell synapses (Reiners, J. *et al.*, 2003). Isoforms a and c are widely expressed, but the longest isoforms (b) are found mostly in the stereocilia of the vestibular and cochlear hair cells. Developmental expression studies in mice detected harmonin b in the stereocilia from E15 until P30, suggesting that it is important for the development of the hair bundle (Boeda, B. *et al.*, 2002).

PDZ domain-containing proteins act as adapters for organizing protein complexes that usually involve transmembrane proteins. The protein products of other Usher type I genes (myosin VIIa, cadherin 23, protocadherin 15, and sans) cluster with harmonin via the first PDZ domain. This clustering, together with the localization of these proteins to the synaptic regions of the hair cells and photoreceptor cells, suggests this protein network may be involved in the organization or function of hair cell and photoreceptor cell synapses (Adato, A. *et al.*, 2005).

3.07.2.2 Mutations

Mutations in *USH1C* that are associated with Usher syndrome type IC include two frameshift mutations (insertions), four splice site mutations, and a nonsense mutation. All of these mutations are expected to result in a severely truncated transcript and no protein product. The causal mutation in Acadian Usher IC patients is a substitution (216G→A) that introduces a cryptic splice site in exon 3 and results in the deletion of 35 bases in the mature messenger RNA (mRNA; Lentz, J. *et al.*, 2005). The most common *USH1C* mutation, 238–239insC in exon 3, has been found in several different populations (Zwaenepoel, I. *et al.*, 2001).

The ability to diagnose Usher syndrome early enables appropriate management and provides time for the development of communication skills that do not rely on vision. In particular, an Acadian child with profound sensorineural hearing loss should be tested for the 216G→A mutation to determine if the correct diagnosis is actually Usher syndrome type IC.

Some mutations in *USH1C* are associated with hearing loss but not retinal degeneration. Because the b isoforms of harmonin are expressed at high levels only in the inner ear, and use some exons that are not translated in isoforms a and c, mutations in these exons would be predicted to cause nonsyndromic hearing loss. In fact, Ouyang X. *et al.* (2002) found four missense mutations in exons B and D, which are used only in isoform b, in patients with nonsyndromic hearing loss (DFNB18).

In contrast, Ahmed Z. M. *et al.* (2002) reported members of an Indian family with nonsyndromic hearing loss who were homozygous for a splice site mutation (IVS12+5G→C) in *USH1C*. *In vitro* studies showed that the presence of this mutation resulted in a mixture of both normal and aberrantly spliced mRNA. It is unlikely that the abnormal transcript forms a protein product; thus, the amount of harmonin that is produced must be adequate for normal retinal function, but not enough to preserve the cochlear hair cells.

3.07.2.3 Mouse Models

The deaf circler (*dfcr*) and deaf circler 2 Jackson (*dfcr 2J*) mice have spontaneous mutations in the *USH1C* gene and as with other mouse models for Usher syndrome type I, the stereocilia are disorganized (Johnson, K. R. *et al.*, 2003). However, the mouse models do not develop retinitis pigmentosa. The *dfcr* mutation is a large deletion that includes several exons, but does not change the reading frame, while the *dfcr 2J* mutation is a one base deletion in exon C. Only harmonin b is affected in *dfcr 2J*, but all isoforms are expected to be abnormal in *dfcr*.

ABR testing demonstrated that both *dfcr* and *dfcr 2J* mice were completely deaf (no response at 100 dB sound pressure level), and scanning electron microscopy revealed disorganized stereocilia by 3 weeks of age. A slight peripheral retinal degeneration was observed in three *dfcr* mice at 9 months of age, but electroretinograms (ERGs) were normal.

3.07.3 GJB2

Linkage analysis of two consanguineous families from Tunisia localized the DFNB1 locus to chromosome 13q12. The *GJB2* (Gap Junction Protein Beta 2) gene had been mapped to the same location, and Kelsell D. P. *et al.* (1997) identified mutations in this gene in children with nonsyndromic recessive deafness. The phenotype is usually severe-to-profound congenital hearing loss, but it may be mild-to-moderate and progressive. Although not common, syndromic (usually associated with skin abnormalities) and nonsyndromic (DFNA3) autosomal dominant families have been described with mutations in *GJB2*. In some populations, *GJB2* mutations explain as much as 50% of autosomal recessive hearing loss. Pandya A. *et al.* (2003) estimated that, on average, *GJB2* mutations account for about 22% of hearing loss in children, but pointed out that the percentages differ significantly among ethnic groups.

3.07.3.1 Structure, Expression, and Function

The *GJB2* gene consists of two exons, with exon 2 encoding the 208 amino acid protein. Exon 1 is not translated. The promoter region of the mouse and human genes is highly conserved, and includes GC boxes, GT boxes, and a TTAAAA box (Kiang, D. T. *et al.*, 1997). Because of the relatively short coding sequence, identification of mutations by sequencing is efficient and often provides a definitive diagnosis.

GJB2 is expressed in many tissues, including skin, liver, breast, bladder, and pancreas. In the inner ear, *GJB2* is expressed in both the epithelial and the connective cellular networks. These include the supporting cells of the hair cells, as well as the spiral limbus, spiral ligament, and stria vascularis.

The protein encoded by *GJB2* is usually called connexin 26. There are 20 different types of human connexins; two of these (connexin 26 and connexin 30) co-localize in the cochlea (Marziano, N. K. *et al.*, 2003). Each connexin consists of four transmembrane domains connected by one intracellular loop, two extracellular loops, and cytoplasmic N and C terminals. Connexons, which are comprised of six connexins, join with those in an adjacent cell to form homotypic, heterotypic, or heteromeric channels between the cells. The connexons are formed intracellularly and are trafficked to the plasma membrane. These gap junctions allow intercellular diffusion of small molecules and metabolites with a molecular mass up to about 1 kDa. The turnover time of connexins is very rapid, indicating that gap junction channels are replaced several times every day. They are thought to be important for maintaining high concentrations of K^+ in the endolymph via recycling from the perilymph. In turn, this recycling is necessary for the maintenance of the endocochlear potential, which is essential for normal auditory function. Normal forms of both connexin 26 and connexin 30 appear to be required for formation of functional gap junction channels in the support cells of the cochlea, indicating that they do not functionally compensate for one another (Ahmad, S. *et al.*, 2003).

3.07.3.2 Mutations

More than 90 different mutations have been reported in exon 2, the most common in the Caucasian

population (particularly those from southern Europe) being 35delG with a carrier frequency of about 2%. This deletion of a guanine in codon 12 means that codon 13 becomes a stop codon, and translation is terminated. Other mutations have been reported with increased frequencies in particular populations, such as 167delT and 235delC in the Ashkenazi Jewish and Asian populations, respectively.

Although most of the mutations in *GJB2* are associated with recessive hearing loss, some have been found in families with dominant hearing loss (DFNA3). All are missense mutations and for a few, the phenotype is syndromic with skin abnormalities in addition to the hearing loss.

Many variants that do not segregate with hearing loss have been reported. The M34T allele is controversial. Individuals with normal hearing based on pure-tone audiograms and 167delT/M34T and 35delG/M34T genotypes have been reported, but other studies suggest that M34T contributes to recessive mild-to-moderate- or high-frequency hearing loss.

Often, interpretation of diagnostic test results is not straight forward because only one mutation is found. Several explanations are possible: the second mutation may have been missed or the individual may be a carrier (by chance), with the hearing loss having nothing to do with the mutation. In some cases, it has been shown that the second mutation is a 309 kb deletion or a 232 kb deletion that encompasses all or part of the *GJB6* gene, which encodes connexin 30 (del Castillo, F. J. *et al.*, 2005). *GJB2* and *GJB6* are less than 50 kb apart, and share 77% identity in amino acid sequence, with connexin 30 having 37 more amino acids at its C-terminus than connexin 26.

The nonsyndromic recessive phenotype can vary from mild to profound hearing loss, even in individuals with the same *GJB2* mutations. This finding suggests that modifier genes may be involved, but a systematic study to find such genes has not yet been done.

3.07.3.3 Mouse Models

The knockout mouse is an embryonic lethal, but studies of conditional knockout mice suggest that interference with potassium recycling may explain the hearing loss that results when connexin 26 is missing in the inner ear (Cohen-Salmon, M. *et al.*, 2002). Mice do not hear until about 2 weeks after birth and the inner ears of the mutant mice were found to develop normally until P14 when apoptotic cell death began to occur. Supporting cells of the inner hair cells were the first to die, followed by outer hair cells and their supporting cells. However, the inner hair cells were generally preserved, although ultrastructural analysis revealed anomalies. The mice showed a significant hearing loss with an average of 30 dB at 8 kHz to 36 dB at 32 kHz relative to heterozygous and control mice. The endocochlear potential in adult mutants was significantly lower than in control mice as was the K^+ concentration in the endolymph. In contrast, the mutant mice did not show any vestibular dysfunction, suggesting that connexin 26 is not required for normal function of gap junctions in the vestibular system. Additionally, connexin 30 expression was not affected by the absence of connexin 26.

3.07.4 OTOF

The DFNB9 locus was mapped to chromosome 2p22–p23 in a large Lebanese family in which congenital profound sensorineural hearing loss followed an autosomal recessive pattern of inheritance. Yasunaga S. *et al.* (1999) showed that the affected individuals in this family were homozygous for a nonsense mutation in the *OTOF* gene. This gene encodes a cytoskeletal protein called otoferlin that may be involved in synaptic vesicle trafficking. Expression of otoferlin in the inner ear was found to be mostly in the inner hair cells. Because of this finding, Varga R. *et al.* (2003) searched for otoferlin mutations in children with recessive forms of AN/AD without peripheral neuropathy. These children had absent ABRs, but their OAEs were preserved, suggesting normal function of their outer hair cells. (For some of these children, OAEs disappeared with time.) In general, they did not benefit from hearing aids and their speech comprehension was poorer than expected based on their pure-tone audiograms, which ranged from moderate to profound. Several of these children received cochlear implants and found them helpful.

3.07.4.1 Structure, Expression, and Function

OTOF consists of 48 exons spanning about 90 kb of genomic DNA. Yasunaga S. *et al.* (2000) detected numerous alternate splice forms involving exons 6, 31, 47, and 48, and several translation initiation sites.

There are two classes of otoferlin isoforms: long ones with approximately 2000 amino acids and six C2-like domains, and short ones (encoded by exons 20–48) with about 1200 amino acids and only the last three C2-like domains. C2 domains bind Ca^{2+} and are often found in proteins involved in signal transduction, vesicle trafficking, and membrane fusion.

Numerous adult human and mouse tissues including the cochlea, vestibule, eye, brain, placenta, liver, heart, lungs, pancreas, skeletal muscle, and kidney, as well as total human fetus, showed *OTOF* expression, with the strongest expression being in the cochlea and brain. The short isoforms were not detected in mouse tissues, whereas the only human tissue in which the long isoforms were detected was the brain. Additionally, the 60 C-terminal amino acids in brain otoferlin are encoded by exon 47, whereas in the cochlea and other tissues, exon 47 is skipped and the 5′ part of exon 48 is used to encode the final 60 amino acids. The strongest expression of *OTOF* in the inner ear of the mouse is in the cochlear inner hair cells and vestibular type I sensory hair cells; it was detected at E19.5 and persisted until at least P20. *OTOF* expression was also detected in the cochlear outer hair cells and spiral ganglion cells of mouse embryos, but it was found only in inner hairs cells of mature cochleas (Yasunaga, S. *et al.*, 1999; 2000).

Otoferlin is related to the *C. elegans* FER-1 protein, as are two other proteins with C2 domains, dysferlin and myoferlin. They are all predicted to be C-terminal membrane-anchored cytosolic proteins, which interact with phospholipids and other proteins via their C2 domains. Otoferlin function is unknown, but the C2-like domains suggest that it may be involved in synaptic vesicle–plasma membrane fusion.

3.07.4.2 Mutations

In the original DFNB9 family, Yasunaga S. *et al.* (1999) showed that the affected individuals were homozygous for a nonsense mutation in exon 39. Of the17 frameshift, splice site, and missense mutations that have been reported so far, five are found in exons that are included only in the long isoforms, which are restricted to the brain. No mutations have been found in exon 47, but three are in exon 48, which is encoded in the cochlea but not in the brain. In the Spanish population, Migliosi V. *et al.* (2002) found that 4.4% of those without *GJB2* mutations have *OTOF* mutations (in particular, Q829X in exon 22), and Rodriguez-Ballesteros M. *et al.* (2003) reported that *OTOF* mutations account for at least 3.5% of prelingual hearing loss.

3.07.4.3 Mouse Models

A mouse model should provide some insight into clarifying the function of otoferlin. However, no spontaneous mutations have yet been reported, and a knockout mouse has not been created.

3.07.5 TECTA

Both dominant (DFNA8/12) and recessive (DFNB21) forms of hearing loss have been associated with mutations in the *TECTA* gene, which encodes α-tectorin, a noncollagenous extracellular matrix protein. The three loci were mapped to chromosome 11q22–q24 in three different families from Austria, Belgium, and Lebanon. *TECTA* was considered a likely candidate gene based on its location (Verhoeven, K. *et al.*, 1998). The dominant phenotype in the Belgian and Austrian families was nonsyndromic, prelingual, stable, moderate-to-severe hearing loss at all frequencies. This is in contrast to most dominant forms of hearing loss, which are progressive and have a postlingual onset. However, affected members of other DFNA8/12 families have the typical progressive loss starting in the high frequencies. The recessive phenotype in the family from Lebanon had a prelingual onset and was in the severe-to-profound range (Mustapha, M. *et al.*, 1999).

3.07.5.1 Structure, Expression, and Function

TECTA has 23 exons encoding a 2155 amino acid protein, α-tectorin. The human DNA sequence is predicted to have 95% identity with the mouse sequence. Splice variants may exist, but have not yet been systematically investigated. The protein has hydrophobic N-terminal signal sequences that are characteristic of secreted proteins. The C-terminal is also hydrophobic and is predicted to have a glycosyl-phosphatidylinositol (GPI) anchor, which is considered to be a signal for directing the protein to the apical surface of the inner ear sensory epithelia. It also has von Willebrand factor (vWF) type D repeats, which are similar to those found in the sperm membrane protein, zonadhesin, and are rich in cysteines, and a C-terminal ZP domain, which is found in proteins in the zona pellucida, the

extracellular matrix that surrounds the unfertilized egg. Zonadhesin is known to bind to the zona pellucida (Legan, P. K. *et al.*, 1997).

TECTA is expressed only in the inner ear, and, in particular, it is found in the tectorial membrane of the cochlea. Developmental studies in the mouse demonstrate that *tecta* mRNA is expressed in the basal cochlear duct by E12.5, throughout the cochlea by E14.5, and reaches its highest level at P3. After that, expression decreases with minimal detectable mRNA at P15 and none at P67 (Maeda, Y. *et al.*, 2001). These results indicate that *TECTA* is expressed at high levels only briefly during the development of the cochlea and suggest that α-tectorin is stable with a long half-life.

Tectorins are pepsin-sensitive glycoproteins that are resistant to digestion with bacterial collagenase. The tectorial membrane is a ribbonlike sheet of extracellular matrix that spirals along the length of the cochlea, and connects to the tips of the stereocilia of the outer hair cells. It is composed of collagens (types II, V, and IX) and a noncollagenous matrix, consisting mostly of α-tectorin and β-tectorin. These two proteins crosslink, and they appear to be critical for attachment of the tectorial membrane to the cochlear epithelium.

3.07.5.2 Mutations

Missense mutations have been found in affected individuals in DFNA8/12 families, and a dominant negative mechanism has been proposed, although haploinsufficiency is also considered possible (Verhoeven, K. *et al.*, 1998). The reasons for the differences in age of onset and phenotypes among affected individuals in DFNA8/12 families is not clear. However, three missense mutations that change cysteine residues at positions 1057, 1619, and 1837 are associated with progressive loss. So far, seven different missense mutations have been reported and to some extent it appears that mutations in the vWF regions cause high-frequency hearing loss, while those in the ZP domain cause mid-frequency loss (Naz, S. *et al.*, 2003).

In the Lebanese DFNB21 family, the affected individuals were homozygous for a splice site mutation. More recently, Naz S. *et al.* (2003) reported exon 5 and exon 20 frameshift mutations in two consanguineous DFNB21 families from Iran and Pakistan. In both families the hearing loss was prelingual and in the moderate-to-severe range.

3.07.5.3 Mouse Models

Homozygous knockout mice have moderate-to-severe hearing loss and abnormal and detached tectorial membranes with no known noncollagenous components. The tectorial membrane is synthesized, but within a few weeks after birth it is no longer attached at either end and the collagen fibers are disorganized. In contrast, the structure and orientation of the stereocilia of the cochlear hair cells are unaffected, although the cochlear microphonic is smaller and differs in phase and symmetry from the wild-type mice. The heterozygous mice appear to be normal (Legan, P. K. *et al.*, 2000). These findings demonstrate the importance of the tectorial membrane in amplifying auditory stimuli, presumably because it is essential for deflection of outer hair cell stereocilia.

3.07.6 Outlook for the Future

Progress in our understanding of genetic hearing loss has been enormous over the past decade. We have made great strides in determining many of the different molecular mechanisms that contribute to the genetic heterogeneity of hearing loss. However, more genes remain to be identified, and elucidating the function of the proteins encoded by these genes is challenging. The four genes discussed in this perspective provide examples of the phenotypic and genetic heterogeneity of hearing loss and the progress that has been made in understanding their function in the inner ear. It is clear that different mutations in the same gene can be associated with both nonsyndromic and syndromic forms of hearing loss, and in some cases a mutation in one copy of the gene (dominant) is sufficient while in others mutations in both copies (recessive) are required for hearing loss. These four genes show diverse expression patterns and the proteins they encode have quite different functions. But they are all critical for normal hearing.

Genetic diagnostic testing for mutations in the *GJB2* gene is becoming routine and other genes are likely to be added in the near future. In particular, testing for the Q829X mutation in the *OTOF* gene might be considered for those who do not have *GJB2* mutations. Ruling out a syndrome is important, especially for one such as Usher syndrome where the first signs of retinal degeneration may not appear for 10 or more years after the diagnosis of severe-to-profound

hearing loss. Because of the genetic heterogeneity of Usher syndrome, a genetic test for all mutations is not yet feasible, but Acadian children should be screened for the *USH1C* 216G→A mutation, and a mutation in the protocadherin 15 gene (R245X) should be considered in those with Ashkenazi Jewish ancestry who do not have mutations in the *GJB2* gene.

A genetic diagnosis is relevant not just to the affected individual but to all family members, some of whom may choose to be tested before making reproductive decisions. In many cases, knowing the genotype is not enough to give a precise phenotype and prognosis, but ongoing research is elucidating some of these relationships. The development of effective therapies based on knowledge of the underlying genetic abnormality is just beginning; however, the potential for molecular intervention strategies as a treatment for hearing loss is promising.

References

Adato, A., Michel, V., Kikkawa, Y., Reiners, J., Alagramam, K., Weil, D., Yonekawa, H., Wolfrum, U., El-Amraoui, A., and Petit, C. 2005. Interactions in the network of Usher syndrome type 1 proteins. Hum. Mol. Genet. 14, 347–356.

Ahmad, S., Chen, S., Sun, J., and Lin, X. 2003. Connexins 26 and 30 are co-assembled to form gap junctions in the cochlea of mice. Biochem. Biophys. Res. Comm. 307, 362–368.

Ahmed, Z. M., Smith, T. N., Riazuddin, S., Makishima, T., Ghosh, M., Bokhari, S., Menon, P. S. N., Deshmukh, D., Griffith, A. J., Riazuddin, S., Friedman, T. B., and Wilcox, E. R. 2002. Nonsyndromic recessive deafness DFNB18 and Usher syndrome type IC are allelic mutations of USHIC. Hum. Genet. 110, 527–531.

Bitner-Glindzicz, M., Lindley, K. J., Rutland, P., Blaydon, D., Smith, V., Milla, P., Hussain, K., Furth-Lavi, J., Cosgrove, J., Shepherd, R., Barnes, P., O'Brien, R., Farndon, P., Sowden, J., Liu, X. Z., Scanlan, M., Malcolm, S., Dunne, M., Aynsley-Green, A., and Glaser, B. 2000. A recessive contiguous gene deletion causing infantile hyperinsulinism, enteropathy and deafness identifies the Usher type 1C gene. Nat. Genet. 26, 56–60.

Boeda, B., El-Amraoui, A., Bahloul, A., Goodyear, R., Daviet, L., Blanchard, S., Perfettini, I., Fath, K. R., Shorte, S., Reiners, J., Houdusse, A., Legrain, P., Wolfrum, U., Richardson, G., and Petit, C. 2002. Myosin VIIa, harmonin and cadherin 23, three Usher I gene products that cooperate to shape the sensory hair cell bundle. EMBO J. 21, 6689–6699.

Cohen-Salmon, M., Ott, T., Michel, V., Hardelin, J., Perfettini, I., Eybalin, M., Wu, T., Marcus, D., Wangemann, P., Willecke, K., and Petit, C. 2002. Targeted ablation of connexin 26 in the inner ear epithelial gap junction network causes hearing impairment and cell death. Curr. Biol. 12, 1106–1111.

del Castillo, F. J., Rodriguez-Ballesteros, M., Alvarez, A., Hutchin, T., Leonardi, E., de Oliveira, C. A., Azaiez, H., Brownstein, Z., Avenarius, M. R., Marlin, S., Pandya, A., Shahin, H., Siemering, K. R., Weil, D., Wuyts, W., Aguirre, L. A., Martin, Y., Moreno-Pelayo, M. A., Villamar, M., Avraham, K. B., Dahl, H. M., Kanaan, M., Nance, W. E., Petit, C., Smith, R., Van Camp, G., Sartorato, E., Murgia, A., Moreno, F., and del Castillo, I. 2005. A novel deletion involving the connexin-30 gene, del(GJB6-d13s1854), found in trans with mutations in the GJB2 gene (connexin-26) in subjects with DFNB1 non-syndromic hearing impairment. J. Med. Genet. 42, 588–594.

Griffith, A. and Friedman, T. 2002. Autosomal and X-linked Auditory Disorders. In: Genetics and Auditory Disorders (*eds*. B. Keats, A. Popper, and R. Faye), pp. 121–227. Springer-Verlag.

Johnson, K. R., Gagnon, L. H., Webb, L. S., Peters, L. L., Hawes, N. L., Chang, B., and Zheng, Q. Y. 2003. Mouse models of USH1C and DFNB18: phenotypic and molecular analyses of two new spontaneous mutations of the *Ush1c* gene. Hum. Mol. Genet. 12, 3075–3086.

Keats, B. J. B. and Berlin, C. I. 2002. Introduction and Overview: Genetics in Auditory Science and Clinical Audiology. In: Genetics and Auditory Disorders (*eds*. B. Keats, A. Popper, and R. Faye), pp. 1–22. Springer.

Keats, B. J. B. and Savas, S. 2004. Genetic heterogeneity in Usher syndrome. Am. J. Med. Genet. 130A, 13–16.

Kelsell, D. P., Dunlop, J., Stevens, H. P., Lench, N. J., Liang, J. N., Parry, G., Mueller, R. F., and Leigh, I. M. 1997. Connexin 26 mutations in hereditary non-syndromic sensorineural deafness. Nature 387, 80–83.

Kiang, D. T., Jin, N., Tu, Z. J., and Lin, H. H. 1997. Upstream genomic sequence of the human connexin 26 gene. Gene 199, 165–171.

Legan, P. K., Lukashkina, V. A., Goodyear, R. J., Kossl, M., Russell, I. J., and Richardson, G. P. 2000. A targeted deletion in alpha-tectorin reveals that the tectorial membrane is required for the gain and timing of cochlear feedback. Neuron 28, 273–285.

Legan, P. K., Rau, A., Keen, J. N., and Richardson, G. P. 1997. The mouse tectorins: modular matrix proteins of the inner ear homologous to components of the sperm–egg adhesion system. J. Biol. Chem. 272, 8791–8801.

Lentz, J., Savas, S., Ng, S., Athas, G., Deininger, P., and Keats, B. 2005. The USH1C 216G>A splice site mutation results in a 35 base pair deletion. Hum. Genet. 116, 225–227.

Maeda, Y., Fukushima, K., Kasai, N., Maeta, M., and Nishizaki, K. 2001. Quantification of TECTA and DFNA5 expression in the developing mouse cochlea. Neuroreport 12, 3223–3226.

Marziano, N. K., Casalotti, S. O., Portelli, A. E., Becker, D. L., and Forge, A. 2003. Mutations in the gene for connexin 26 (GJB2) that cause hearing loss have a dominant negative effect on connexin 30. Hum. Mol. Genet. 12, 805–812.

Migliosi, V., Modamio-Hoybjor, S., Moreno-Pelayo, M. A., Rodriguez-Ballesteros, M., Villamar, M., Telleria, D., Menendez, I., Moreno, F., and del Castillo, I. 2002. Q829X, a novel mutation in the gene encoding otoferlin (OTOF), is frequently found in Spanish patients with prelingual non-syndromic hearing loss. J. Med. Genet. 39, 502–506.

Mustapha, M., Weil, D., Chardenoux, S., Elias, S., El-Zir, E., Beckmann, J. S., Loiselet, J., and Petit, C. 1999. An alpha-tectorin gene defect causes a newly identified autosomal recessive form of sensorineural pre-lingual non-syndromic deafness, DFNB21. Hum. Mol. Genet. 8, 409–412.

Naz, S., Alasti, F., Mowjoodi, A., Riazuddin, S., Sanati, M. H., Friedman, T. B., Griffith, A. J., Wilcox, E. R., and Riazuddin, S. 2003. Distinctive audiometric profile associated with DFNB21 alleles of TECTA. J. Med. Genet. 40, 360–363.

Ouyang, X. M., Xia, X. J., Verpy, E., Du, L. L., Pandya, A., Petit, C., Balkany, T., Nance, W. E., and Liu, X. Z. 2002. Mutations in the alternatively spliced exons of USH1C cause non-syndromic recessive deafness. Hum. Genet. 111, 26–30.

Pandya, A., Arnos, K. S., Xia, X. J., Welch, K. O., Blanton, S. H., Friedman, T. B., Sanchez, G. G., Jiu, X. Z., Morell, R., and Nance, W. E. 2003. Frequency and distribution of GJB2

(connexin 26) and GJB6 (connexin 30) mutations in a large North American repository of deaf probands. Genet. Med. 5, 295–303.

Reiners, J., Reidel, B., El-Amraoui, A., Boeda, B., Huber, I., Petit, C., and Wolfrum, U. 2003. Differential distribution of harmonin isoforms and their possible role in Usher-1 protein complexes in mammalian photoreceptor cells. Invest. Ophthalmol. Vis. Sci. 44, 5006–5015.

Rodriguez-Ballesteros, M., del Castillo, F. J., Martin, Y., Moreno-Pelayo, M. A., Morera, C., Prieto, F., Marco, J., Morant, A., Gallo-Teran, J., Morales-Angulo, C., Navas, C., Trinidad, G., Tapia, M. C., Moreno, F., and del Castillo, I. 2003. Auditory neuropathy in patients carrying mutations in the otoferlin gene (OTOF). Hum. Mutat. 22, 451–456.

Toriello, H. V., Reardon, W., and Gorlin, R. J. 2004. Hereditary Hearing Loss and its Syndromes, 2nd edn. Oxford University Press.

Varga, R., Kelley, P. M., Keats, B. J., Starr, A., Leal, S. M., Cohn, E., and Kimberling, W. J. 2003. Non-syndromic recessive auditory neuropathy is the result of mutations in the otoferlin (OTOF) gene. J. Med. Genet. 40, 45–50.

Verhoeven, K., Van Laer, L., Kirschhofer, K., Legan, P. K., Hughes, D. C., Schatteman, I., Verstreken, M., Van Hauwe, P., Coucke, P., Chen, A., Smith, R. J. H., Somers, T., Offeciers, F. E., Van de Heyning, P., Richardson, G. P., Wachtler, F., Kimberling, W. J., Willems, P. J., Govaerts, P. J., and Van Camp, G. 1998. Mutations in the human alpha-tectorin gene cause autosomal dominant non-syndromic hearing impairment. Nat. Genet. 19, 60–62.

Verpy, E., Leibovici, M., Zwaenepoel, I., Liu, X. Z., Gal, A., Salem, N., Mansour, A., Blanchard, S., Kobayashi, I., Keats, B., Slim, R., and Petit, C. 2000. A defect in harmonin, a PDZ domain-containing protein expressed in the inner ear sensory hair cells, underlies Usher syndrome type 1C. Nat. Genet. 26, 51–55.

Yasunaga, S., Grati, M., Chardenoux, S., Smith, T. N., Friedman, T. B., Lalwani, A. K., Wilcox, E. R., and Petit, C. 2000. OTOF encodes multiple long and short isoforms: genetic evidence that the long ones underlie recessive deafness DFNB9. Am. J. Hum. Genet. 67, 591–600.

Yasunaga, S., Grati, M., Cohen-Salmon, M., El-Amraoui, A., Mustapha, M., Salem, N., El-Zir, E., Loiselet, J., and Petit, C. 1999. A mutation in OTOF, encoding otoferlin, a FER-1-like protein, causes DFNB9, a nonsyndromic form of deafness. Nat. Genet. 21, 363–369.

Zwaenepoel, I., Verpy, E., Blanchard, S., Meins, M., Apfelstedt-Sylla, E., Gal, A., and Petit, C. 2001. Identification of three novel mutations in the USH1C gene and detection of thirty-one polymorphisms used for haplotype analysis. Hum. Mutat. 17, 34–41.

3.08 Homeostasis of the Inner Ear

B A Schulte, Medical University of South Carolina, Charleston, SC, USA

© 2008 Elsevier Inc. All rights reserved.

3.08.1	Introduction	149
3.08.2	Electrochemical Gradients and Cochlear Function	150
3.08.3	A Model of Cochlear K^+ Homeostasis	150
3.08.4	Genetic Evidence in Support of Cochlear K^+ Recycling	152
3.08.5	Fibrocyte Turnover and Replenishment	153
References		153

Glossary

Brn4 Brain 4 gene encoding Pou-domain transcription factor
Ca^{2+} Calcium
Cl^- Chloride
K^+ Potassium
KCNJ10 Inward rectifying K channel, subfamily J
Na^+ Sodium
Na^+, K^+-ATPase Sodium, potassium adenosine triphosphatase
NkCC1 Sodium, potassium, 2 chloride cotransporter, isoform 1

3.08.1 Introduction

Maintaining an appropriate ionic equilibrium between cells and extracellular fluids is essential to cell, organ, and organismal survival. Ion homeostasis is regulated mainly at the cell membrane by a wide variety of transport proteins specialized to selectively move different species of ions into or out of cells. Individual cells have taken advantage of these transport processes to develop their highly specialized functions such as nerve conduction and muscle contractility.

Epithelial cells form tight junctional connections to create barriers specialized to regulate the transcellular movement of ions and molecules between biological compartments. In other cases, groups of cells connected by gap junctions, which allow direct intercellular communication, form a functional syncytium such as in cardiac muscle. Disturbances in ion homeostasis in any of these systems, as occurs in numerous diseases, can lead to organ failure and death.

The inner ear and vestibular system are tiny yet complex organs that regulate the senses of hearing and balance. Both depend on highly organized and interdependent networks of specialized neural, epithelial, and connective tissue cells for normal physiological activity. Alterations in ion transport and fluid homeostasis in one or more of these inner ear cell types underlie the auditory dysfunction seen in metabolic disorders, ischemia, Meniere's disease (Juhn, S. K. *et al.*, 1987; Meyer zum Gottesberge, A. M., 1988; Doi, K. *et al.*, 1992; Salt, A. N. and DeMott, J., 1994; Nadol, J. B. *et al.*, 1995), some forms of presbyacusis (Schulte, B. A. and Schmiedt, R. A., 1992; Schmiedt, R. A., 1993), and in several genetic disorders (see below).

Comprehensive descriptions of structural and functional relationships (Slepecky, N. B., 1996) and homeostatic mechanisms (Wangemann, P. and Schacht, J., 1996; Juhn, S. K. *et al.*, 2001; Wangemann, P., 2002; Trune, D. R., 2006) in the inner ear are available. Much of the past work on hearing and balance disorders has focused on structural and functional changes in sensory HCs, neurons, and the stria vascularis. However, data accumulated over the past decade has established a role for highly specialized populations of fibrocytes in the lateral wall and limbus in maintaining cochlear electrochemical gradients. It is now known that pathological changes in subtypes of cochlear fibrocytes owing to mutation, noise trauma, and aging lead to profound hearing losses. This brief perspective will focus on the role of cochlear fibrocytes in the process, now referred to as potassium (K^+) recycling, and its importance to normal hearing.

3.08.2 Electrochemical Gradients and Cochlear Function

The high positive direct current (DC) resting potential or endocochlear potential (EP) and large K^+, sodium (Na^+), and calcium (Ca^{2+}) gradients between endolymph and perilymph are essential to normal hearing. The EP originates in the intrastrial space and its generation requires the active transport of K^+ into endolymph energized largely by Na^+, K^+-ATPase activity in strial marginal cells (Salt, A. N. *et al.*, 1987; Offner, F. F. *et al.*, 1987; Salt, A. N. and Thalmann, R., 1988; Takeuchi, S. *et al.*, 2000; Marcus, D. C. *et al.*, 2002; Wangemann, P., 2002). The majority of K^+ transported into endolymph is derived from perilymph rather than blood plasma (see Salt, A. N. and Thalmann, R., 1988). Davis H. (1965) first proposed that the EP and the negative diffusion potential of K^+ across the endolymph–perilymph barrier control acoustic transduction. He also postulated the existence of a standing current that exits the scala media through sensory HCs and flows radially across the scala tympani and back to the stria vascularis via the spiral ligament to form a local circuit. Indirect evidence for such a silent current was provided by subsequent physiological studies (Syka, J. *et al.*, 1981; Salt, A. N. and Konishi, T., 1982) and its existence was firmly established through direct measurements by Zidanic M. and Brownell W. E. (1990).

There is little doubt that K^+ is the primary cation carrying both this silent current (Zidanic, M. and Brownell, W. E., 1990; Dallos, P., 1995) and the much larger acoustically evoked transduction currents in auditory HCs (Corey, D. P. and Hudspeth, A. J., 1979; Ohmori, H., 1985; Kros, C. J., 1996). K^+ entering apical transduction channels is effluxed basolaterally through voltage- or Ca^{2+}-gated K^+ channels (Jiang, G. J. *et al.*, 1997; Dulon, D. *et al.*, 1998; Kharkovets, T. *et al.*, 2000; Wangemann, P., 2002). Low extracellular K^+ levels are critical for maintaining steep transmembrane voltage gradients in excitable cells (Giebisch, G. and Wang, W., 1998). Mammalian auditory HCs are bathed in perilymph which has a K^+ concentration ($[K^+]$) of around 3–4 mM. The accumulation of excess K^+ in fluid bathing HCs and neurons would promote depolarization adversely influencing their responses, and could be cytotoxic at too high a level. Thus, there is a need for a mechanism other than simple passive diffusion to maintain low K^+ levels in perilymph surrounding outer HCs as is discussed below.

3.08.3 A Model of Cochlear K^+ Homeostasis

The concept that K^+ leaked or effluxed from endolymph through HCs or supporting cells is actively recycled back to endolymph through a complex series of intercellular and intracellular pathways (Figure 1, Spicer, S. S. and Schulte, B. A., 1998) has rapidly gained acceptance (Steel, K., 1999; Wangemann, P., 2002). Physiological data supporting such a process have existed for years. Investigations showing that K^+ is cleared from the scala tympani to the scala vestibuli much more rapidly than vice versa indicate an active mechanism for K^+ recycling (Salt, A. N. and Ohyama, K., 1993). Evidence is also available documenting the noise-stimulated uptake of K^+ by supporting cells (Oesterle, E. and Dallos, P., 1985; Johnstone, B. M. *et al.*, 1989; Oesterle, E. and Dallos, P., 1990) and electrical connectivity between supporting cells in the organ of Corti (Santos-Sacchi, J. and Dallos, P., 1983; Santos-Sacchi, J., 1991). However, visualizing the nature and extent of the K^+ recycling pathways required new structural and biochemical information. Such data have been provided by studies showing unique morphological and ion transport specializations in inner ear epithelial cells and fibrocytes. At least five different subpopulations of fibrocytes have now been identified in the spiral ligament based on their location, ultrastructural characteristics, and differential expression of ion transport proteins (Schulte, B. A. and Adams, J. C., 1989; Spicer, S. S. and Schulte, B. A., 1991; Schulte, B. A., 1993; McGuirt, J. P. and Schulte, B. A., 1994; Schulte, B. A. and Steel, K. P., 1994; Crouch, J. J. *et al.*, 1997; Hibino, H. *et al.*, 2004). Three of these fibrocyte populations are rich in Na^+, K^+-ATPase and are strategically situated to resorb K^+ from perilymph in the scala tympani (type IV), the scala vestibuli (type V), and the region of the spiral ligament adjacent to the outer sulcus (type II). Each of these cell types is coupled to type I fibrocytes which serve as a final common pathway for moving the resorbed K^+ into the stria vascularis. In addition, electron microscopic studies have demonstrated significant differences in the fine structure of spiral ligament fibrocytes (SLFs) and outer sulcus, Claudius, Hensen, and Deiters cells along the place-frequency map (Spicer, S. S. and Schulte, B. A., 1994a; 1994b; 1996; Spicer, S. S. *et al.*, 2003) supporting their role in ion transport. These data, coupled with a new appreciation for the extent of direct cell-to-cell

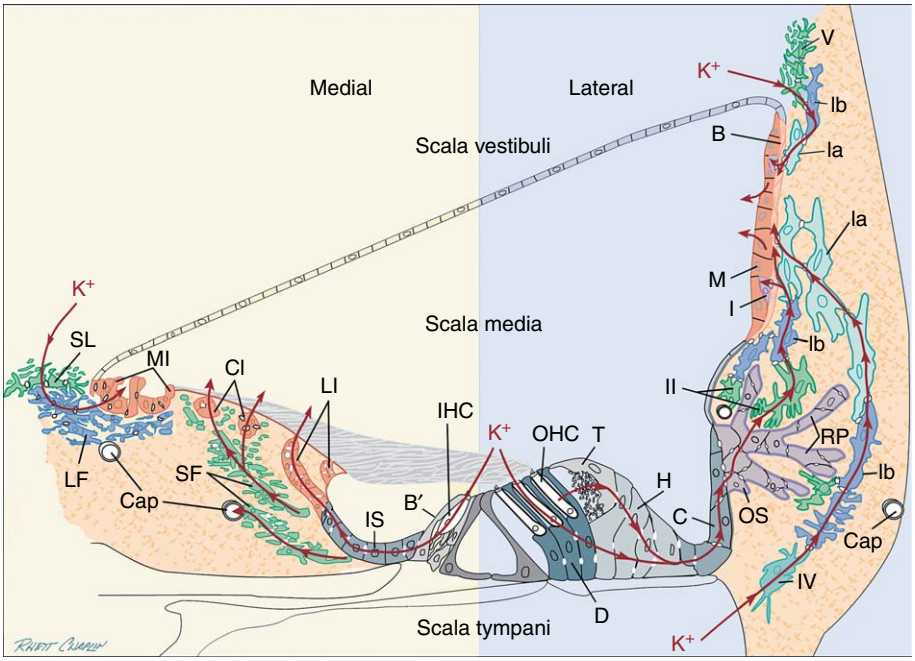

Figure 1 Proposed lateral and medial routes for K^+ homeostasis. In the lateral route, K^+ effluxing from outer hair cells (OHC) is resorbed by Deiters (D) and tectal (T) cells and flows via gap junctions through Hensen (H), Claudius (C), and outer sulcus (OS) cells and their root processes (RP) to efflux into stroma maintained at a low K^+ level by the Na^+,K^+-ATPase activity of type II fibrocytes. Other K^+ ions diffuse into scala tympani and are taken up by type IV fibrocytes. The resorbed K^+ subsequently diffuses via gap junctions through type I fibrocytes (Ia, Ib) and strial basal (B) and intermediate (I) cells into the intrastrial compartment kept low in K^+ by the pumping activity of strial marginal (M) cells. K^+ resorbed by type V fibrocytes from scala vestibuli diffuses downhill through Ib then Ia fibrocytes to the stria. In the medial circuit, ions released from inner hair cells (IHC) diffuse to endolymph through border (B′), inner sulcus (IS) and lateral interdental cells (LI) or pass from IS cells through stellate fibrocytes (SF) to capillaries (Cap) or to central interdental cells (CI) and into the scala media. K^+ pumped from scala vestibuli into supralimbal cells (SL) flows downgradient to light fibrocytes (LF) and medial interdental (MI) cells for return to scala media. Adapted from Spicer, S. S. and Schulte, B. A. 1998. Evidence for a medial K^+ recycling pathway from inner hair cells. Hear. Res., 118, 1–12, with permission from Elsevier.

communication in the inner ear via gap junctions gained by immunostaining for connexins 26, 30, 31, and 43 (Kikuchi, T. *et al.*, 1994; 1995; Lautermann, J. *et al.*, 1999; Kikuchi, T. *et al.*, 2000; Xia, A. P. *et al.*, 2000; Forge, A. *et al.*, 2002) have revealed at least three distinct networks of tightly coupled cells through which K^+ could be recycled (Figure 1). These networks include: (1) the supporting epithelial cells in the organ of Corti; (2) subpopulations of SLFs and basal and intermediate cells in the stria vascularis; and (3) subpopulations of fibrocytes in the spiral limbus.

Correlative electrophysiological and histochemical studies of the developing and aging gerbil inner ear have provided further evidence for the importance of SLFs in establishing and maintaining the EP and cochlear K^+ gradients. The expression of Na^+, K^+-ATPase and the Na–K–Cl cotransporter (NKCC1) in strial marginal cells reaches adult levels well before development of a measurable EP in neonatal gerbils (McGuirt, J. P. *et al.*, 1995; 1996; Sakaguchi, N. *et al.*, 1998). In contrast, expression of the $\alpha 2$ subunit of Na^+, K^+-ATPase and of NKCC1 in SLFs coincides precisely with the onset and rapid growth of the EP, as does the maturation of junctions between strial basal and intermediate cells (Souter, M. and Forge, A., 1998). Loss of Na^+, K^+-ATPase and NKCC1 expression in SLFs also correlates well with strial degeneration and EP declines in the aging cochlea (Schulte, B. A. and Schmiedt, R. A., 1992; Spicer, S. S. *et al.*, 1997; Sakaguchi, N. *et al.*, 1998).

The existence of a medial pathway for recycling K^+ effluxed by inner HCs and afferent nerves back to endolymph has also been postulated (Spicer, S. S. and Schulte, B. A., 1998). This medial route for K^+ homeostasis (Figure 1) is supported by patterns of expression of ion transport mediators in subpopulations of limbal fibrocytes (McGuirt, J. P. and Schulte, B. A., 1994; Schulte, B. A. and Steel, K. P.,

1994; Crouch, J. J. *et al.*, 1997) and similarities in the fine structure of inner phalangeal and Deiters cells, inner sulcus and Claudius cells, and interdental and outer sulcus cells (Spicer, S. S. and Schulte, B. A., 1998). As in the lateral transport system the developmental expression of Na^+, K^+-ATPase (McGuirt, J. P. *et al.*, 1996) and NKCC1 (Sakaguchi, N. *et al.*, 1998) in limbal fibrocytes coincides with the onset of auditory activity in the neonatal gerbil. Further evidence for this medical pathway was provided by the finding that the selective ablation of inner HCs by carboplatin alters cells in the medial flow route and disrupts the tectorial membrane (Spicer, S. S. *et al.*, 1999).

3.08.4 Genetic Evidence in Support of Cochlear K^+ Recycling

A large body of work now points to the importance of gap junctionally coupled syncytial networks to K^+ transport and normal auditory function. Mice lacking the K–Cl cotransporter, normally expressed exclusively in Deiters cells, suffer from deafness and renal tubular acidosis (Boettger, T. *et al.*, 2002). Several studies have revealed a direct link between mutations in connexins 26, 30, 31, and 43 and dominant and recessive forms of human nonsyndromic deafness (Kelsell, D. P. *et al.*, 1997; White, T. W. *et al.*, 1998; Grifa, A. *et al.*, 1999; Liu, X. Z. *et al.*, 2000; 2001). Targeted deletions of either connexin 26 or 30 disrupt the epithelial supporting cell network in the organ of Corti and result in a marked decline in the EP and the endolymphatic $[K^+]$ (Cohen-Salmon, M. *et al.*, 2002; Teubner, B. *et al.*, 2003).

More direct evidence of a role for SLFs in ion transport and normal auditory function derives from studies of mice with spontaneous or targeted mutations in the *Brn*4 gene, a model for DFN3 nonsyndromic deafness (Minowa, O. *et al.*, 1999; Phippard, D. *et al.*, 1999; Xia, A. P. *et al.*, 2002). These mutants have a profound hearing loss, a severely depressed EP, and develop hydrops with the major histopathologic change being chemical and histopathological alterations in SLFs. The sex-linked fidget mutation also results in abolished *Brn*4 gene expression making it an excellent mouse model for the most prevalent form of X-linked congenital deafness in humans (Phippard, D. *et al.*, 2000). Mice lacking a complete gene for pendrin, a model for human Pendred syndrome, fail to express the KCNJ10 protein on strial intermediate cells, lack a positive EP, and show a greatly reduced volume density of type I and II SLFs (Wangemann, P. *et al.*, 2004). Moreover, mice with a deletion of the *Otos* gene, encoding the protein otospiralin, which is normally produced by cochlear and vestibular fibrocytes, exhibit moderate deafness associated with degeneration of type II and IV fibrocytes as the primary pathology. It has been suggested that this dysfunction may predispose these mice to age-related hearing loss (Delprat, B. *et al.*, 2005).

Recent studies of age-related hearing loss further indicate the importance of SLFs to normal auditory function. Hequembourg S. and Liberman M. C. (2001) showed that degeneration of SLFs, in particular of type IV fibrocytes, is a primary cause of the age-related hearing loss, and ultimately sensory cell degeneration, in C57BL/6 mice. This strain carries the *ahl* gene (Johnson, K. R. *et al.*, 2000) as opposed to CBA/CaJ mice which lack this gene and show little age-related hearing loss and no fibrocyte pathology. Wu T. and Marcus D. C. (2003) found that CD-1 mice, which also carry the *ahl* gene, suffer from early onset age-related hearing loss associated with a reduced EP under anoxic conditions, a significant reduction in the endolymphatic $[K^+]$, and pathological changes in SLFs similar to those seen in aging C57BL/6 mice. Interestingly, damage to type II and IV SLFs is also reported to be a major pathology associated with noise-induced hearing loss in CBA/CaJ mice (Wang, Y. *et al.*, 2002).

Human hearing and balance disorders have also been associated with pathological changes in lateral wall fibrocytes which have a distribution and ion transport properties very similar to those found in rodents (Weber, P. C. *et al.*, 2001). An examination of temporal bones from 24 human subjects noted a significant correlation between the loss of type II and IV fibrocytes and age (Kusunoki, T. *et al.*, 2004). Another recent study concluded that the hydrops associated with Meniere's disease is likely the result of compromised cochlear ion homeostasis owing to pathological alterations in SLFs in human temporal bones (Merchant, S. N. *et al.*, 2005). The examination of human inner ears with cochlear otosclerosis, including spiral ligament hyalinization, revealed a loss or decrease of immunostaining for ion transport mediators in type I, II, and IV fibrocytes that was well correlated with degeneration of the stria vascularis and hearing loss (Doherty, J. K. and Linthicum, F. H., 2004). Evidence is thus accumulating that a wide range of inner ear disorders are associated with primary or secondary pathology of ion transport fibrocytes in both animal models and humans.

3.08.5 Fibrocyte Turnover and Replenishment

From a practical standpoint it is perhaps important that, unlike most inner ear cell types, at least some populations of fibrocytes maintain the capacity to divide in the normal and traumatized adult cochlea. Dividing cells have been reported in the spiral ligament and the stroma surrounding nerve fibers in 21-day-old gerbils (Roberson, D. W. and Rubel, E. W., 1994) and cell division has been documented in the spiral ligament of 4–5-week-old mice (Yamashita, H. *et al.*, 1999). Several cell types including fibrocytes in the spiral ligament, limbus, and the sacculus continue to divide in the mature gerbil cochlea, although there is a marked reduction in fibrocyte turnover in aged gerbils (Lang, H. *et al.*, 2003). The chronic administration of furosemide promoted a significant increase in the proliferation of SLFs which was associated with a marked recovery of EP values in 6-month-old gerbils (Lang, H. *et al.*, 2003). Increases in the number of (^{3}H)-thymidine labeled or 5-bromo-2-deoxyuridine (BrdU)-labeled nuclei have also been reported in the spiral ligament of gerbils and mice after acoustic trauma or streptomycin-induced injuries (Roberson, D. W. and Rubel, E. W., 1994; Yamashita, H. *et al.*, 1999). A recent study reported significant increases in the number of BrdU-positive cells in the spiral ligament and acoustic nerve of adult rats and guinea-pigs deafened with kanamycin and ethacrynic acid (Yamasoba, T. *et al.*, 2003). It is interesting to note that no labeling (cell division) was reported in the organ of Corti in the normal or injured ear in any of these investigations on adult animals.

The above data clearly demonstrate that fibrocytes in the spiral ligament and spiral limbus undergo continuous replacement in the adult cochlea and have the capacity to dramatically increase their proliferative index in response to chemical- or noise-induced injuries. This suggests the presence of a population of adult stem/progenitor cells capable of self renewal, although such cells have not yet been identified in the adult mammalian cochlea. It is generally accepted that fibrocytes, along with all other connective tissue elements in the inner ear including cartilage and bone, develop from periotic mesenchyme of mesodermal origin (Lang, H. and Fekete, D. M., 2001; Steel, K. P. *et al.*, 2002). The engraftment of cells derived from clonal expansion of single hematopoietic stem cells in regions corresponding to the location of fibrocytes and mesenchymal cells in the irradiated adult mouse inner ear has recently been documented (Lang, H. *et al.*, 2006). This finding suggests the alternative possibility that bone marrow stem/precursor cells continuously seeded to the inner ear throughout life may serve as a source of fibrocyte progenitors. It is also possible that this is not a normal occurrence but rather reflects the ability of stem/progenitor cells to home to the inner ear after injury, possibly induced by the ablative radiation treatment itself. It is also possible that both of these situations occur. In either event, these data raise the intriguing possibility of restoring or reversing disorders in inner ear ion homeostasis associated with injury to fibrocytes via the manipulation of endogenous or the introduction of exogenous stem/progenitor cells.

References

Boettger, T., Hubner, C. A., Maier, H., Rust, M. B., Beck, F. X., and Jentsch, T. J. 2002. Deafness and renal tubular acidosis in mice lacking the K–Cl co-transporter Kcc4. Nature 416, 874–878.

Cohen-Salmon, M., Ott, T., Michel, V., Hardelin, J. P., Perfettini, I., Eybalin, M., Wu, T., Marcus, D. C., Wangemann, P., Willecke, K., and Petit, C. 2002. Targeted ablation of connexin 26 in the inner ear epithelial gap junction network causes hearing impairment and cell death. Curr. Biol. 12, 1106–1111.

Corey, D. P. and Hudspeth, A. J. 1979. Ionic basis of the receptor potential in a vertebrate hair cell. Nature 281, 675–677.

Crouch, J. J., Sakaguchi, N., Lytle, C., and Schulte, B. A. 1997. Immunohistochemical localization of the Na–K–Cl co-transporter (NKCC1) in the gerbil inner ear. J. Histochem. Cytochem. 45, 773–778.

Dallos, P. 1995. The active cochlea. J. Neurosci. 12, 4575–4586.

Davis, H. 1965. A model for transducer action in the cochlea. Cold Spring Harb. Symp. Quant. Biol. 30, 181–190.

Delprat, B., Ruel, J., Guitton, M. J., Hamard, G., Lenoir, M., Pujol, R., Puel, J. L., Brabet, P., and Hamel, C. P. 2005. Deafness and cochlear fibrocyte alterations in mice deficient for the inner ear protein otospiralin. Molec. Cell Biol. 25, 847–853.

Doherty, J. K. and Linthicum, F. H. 2004. Spiral ligament and stria vascularis changes in cochlear otosclerosis: effect on hearing level. Otol. Neurotol. 25, 457–464.

Doi, K., Mori, N., and Matsunaga, T. 1992. Adenylate cyclase modulation of ion permeability in the guinea pig cochlea: a possible mechanism for the formation of endolymphatic hydrops. Acta Otolaryngol. 112, 667–673.

Dulon, D., Luo, L., Zhang, C., and Ryan, A. F. 1998. Expression of small-conductance calcium-activated potassium channels (SK) in outer hair cells of the rat cochlea. Eur. J. Neurosci. 10, 907–915.

Forge, A., Becker, D., Casalotti, S., Edward, J., Marziano, N., and Nickel, R. 2002. Connexins and gap junctions in the inner ear. Audiol. Neurootol. 7, 141–145.

Giebisch, G. and Wang, W. 1998. Potassium transport: from clearance to channels and pumps. Kidney Int. 49, 1624–1631.

Grifa, A., Wagner, C. A., D'Ambrosio, L., Melchionda, S., Bernardi, F., Lopez-Bigas, N., Rabionet, R., Arbones, M., Monica, M. D., and Estivill, X. 1999. Mutations in *GJB6* cause nonsyndromic autosomal dominant deafness at DFNA3 locus. Nat. Genet. 23, 16–18.

Hequembourg, S. and Liberman, M. C. 2001. Spiral ligament pathology: a major aspect of age-related cochlear degeneration in C57BL/6 mice. Assoc. Res. Otolaryngol. 2, 118–129.

Hibino, H., Higashi-Shingai, K., Fujita, A., Iwai, K., Ishii, M., and Kurachi, Y. 2004. Expression of an inwardly rectifying K^+ channel, *Kir*5.1, in specific types of fibrocytes in the cochlear lateral wall suggests its functional importance in the establishment of endocochlear potential. Eur. J. Neurosci. 19, 76–84.

Jiang, G. J., Zidanic, M., Michaels, R. L., Michael, T. H., Griguer, C., and Fuchs, P. A. 1997. CSIo encodes calcium-activated potassium channels in the chick's cochlea. Proc. Biol. Sci. 264, 731–737.

Johnson, K. R., Zheng, Q. Y., and Erway, L. C. 2000. A major gene affecting age-related hearing loss is common to at least ten inbred strains of mice. Genomics 70, 171–180.

Johnstone, B. M., Patuzzi, R., Syka, J., and Sykova, E. 1989. Stimulus-related potassium changes in the organ of Corti of guinea pig. J. Physiol. 408, 77–92.

Juhn, S. K., Hunter, B. A., and Odland, R. M. 2001. Blood–labyrinth barrier and fluid dynamics of the inner ear. Int. Tinnitus J. 7, 72–83.

Juhn, S. K., Papastavros, T., Jung, T. K., Rybak, L. P., Choquette, D., and Edlin, J. 1987. Biochemical Aspects of Endolymphatic Hydrops. In: Immunobiology, Histophysiology and Tumor Immunology in Otolaryngology. Proceedings of the Second International Academic Conference, 26–29 August, The Netherlands, pp. 83–93. Kugler Publications.

Kelsell, D. P., Dunlop, J., Stevens, H. P., Lench, N. J., Liang, J. N., Parry, G., Mueller, R. F., and Leigh, I. M. 1997. Connexin 26 mutations in hereditary non-syndromic sensorineural deafness. Nature 387, 80–83.

Kharkovets, T., Hardelin, J. P., Safieddine, S., Schweizer, M., El-Amraoui, A., Petit, C., and Jentsch, T. J. 2000. KCNQ4, a K^+ channel mutated in a form of dominant deafness, is expressed in the inner ear and the central auditory pathway. Proc. Natl. Acad. Sci. U. S. A. 98, 4333–4338.

Kikuchi, T., Adams, J. C., Miyabe, Y., So, E., and Kobayashi, T. 2000. Potassium ion recycling pathway via gap junction systems in the mammalian cochlea and its interruption in hereditary nonsyndromic deafness. Med. Electron Microsc. 33, 51–56.

Kikuchi, T., Adams, J. C., Paul, D. L., and Kimura, R. S. 1994. Gap junction systems in the rat vestibular labyrinth: immunohistochemical and ultrastructural analysis. Acta Otolaryngol. 114, 520–528.

Kikuchi, T., Kimura, R. S., Paul, D. L., and Adams, J. C. 1995. Gap junctions in the rat cochlea: immunohistochemical and ultrastructural analysis. Anat. Embryol. (Berl.) 191, 101–118.

Kros, C. J. 1996. Physiology of Mammalian Cochlear Hair Cells. In: The Cochlea. (*eds*. P. Dallos, A. N. Popper, and R. R. Fay), pp. 318–385. Springer.

Kusunoki, T., Cureoglu, S., Schachern, P. A., Baba, K., Kariya, S., and Paparella, M. M. 2004. Age-related histopathologic changes in the human cochlea: a temporal bone study. Otolaryngol. Head Neck Surg. 131, 897–903.

Lang, H. and Fekete, D. M. 2001. Lineage analysis in the chicken inner ear shows differences in clonal dispersion for epithelial, neuronal, and mesenchymal cells. Dev. Biol. 234, 120–137.

Lang, H., Schulte, B. A., and Schmiedt, R. A. 2003. Effects of chronic furosemide treatment and age on cell division in the adult gerbil inner ear. J. Assoc. Res. Otolaryngol. 4, 164–174.

Lang, H., Yasuhira, E., Schmiedt, R., Hitoshi, M., Zhou, D., Smythe, N., Liu, L., Ogawa, M., and Schulte, B. A. 2006. Contribution of bone marrow hematopoietic stem cells to adult mouse inner ear: mesenchymal cells and fibrocytes. J. Comp. Neurol. 496, 187–201.

Lautermann, J., Franck, H. G., Jahnke, K., Traub, O., and Winterhager, E. 1999. Developmental expression patterns of connexin-26 and -30 in the rat cochlea. Dev. Genet. 25, 306–311.

Liu, X. Z., Xia, X. J., Adams, J., Chen, Z. Y., Welch, K. O., Tekin, M., Ouyang, X. M., Kristiansen, A., Pandya, A., and Balkany, T. 2001. Mutations in GJA1 (connexin 43) are associated with non-syndromic autosomal recessive deafness. Hum. Mol. Genet. 10, 2945–2951.

Liu, X. Z., Xia, X. J., Xu, L. R., Pandya, A., Liang, C. Y., Blanton, S. H., Brown, S. D., Steel, K. P., and Nance, W. E. 2000. Mutations in connexin 31 underlie recessive as well as dominant non-syndromic hearing loss. Hum. Mol. Genet. 9, 63–67.

Marcus, D. C., Wu, T., Wangemann, P., and Kofuji, P. 2002. KCNJ10 (Kir4.1) potassium channel knockout abolishes the endocochlear potential. Am. J. Physiol. 282, 403–407.

McGuirt, J. P. and Schulte, B. A. 1994. Distribution of immunoreactive α and β subunit isoforms of Na, K-ATPase in the gerbil inner ear. J. Histochem. Cytochem. 42, 843–853.

McGuirt, J. P., Schmiedt, R. A., and Schulte, B. A. 1995. Development of cochlear potentials in the neonatal gerbil. Hear. Res. 84, 52–60.

McGuirt, J. P., Schmiedt, R. A., and Schulte, B. A. 1996. Na, K-ATPase and carbonic anhydrase expression in the developing gerbil cochlea. Aud. Neurosci. 2, 135–144.

Merchant, S. N., Adams, J. C., and Nadol, J. B. 2005. Meniere's syndrome: are symptoms caused by endolymphatic hydrops? Otol. Neurotol. 26, 74–81 .

Meyer Zum Gottesberge, A. M. 1988. Imbalanced calcium homeostasis and endolymphatic hydrops. Acta Otolaryngol. Suppl. 460, 18–27.

Minowa, O., Ikeda, K., Sugitani, Y., Oshima, T., Nakai, S., Katori, Y., Suzuki, M., Furukawa, M., Kawase, T., Zheng, Y., Ogura, M., Asada, Y., Watanabe, K., Yamanaka, H., Gotoh, S., Nishi-Takeshima, M., Sugimoto, T., Kikuchi, T., Takasaka, T., and Noda, T. 1999. Altered cochlear fibrocytes in a mouse model of DFN3 nonsyndromic deafness. Science 285, 1408–1411.

Nadol, J. B., Adams, J. C., and Kim, J. R. 1995. Degenerative changes in the organ of Corti and lateral cochlear wall in experimental endolymphatic hydrops and human Meniere's disease. Acta Otolaryngol. 519, 47–59.

Offner, F. F., Dallos, P., and Cheatham, M. A. 1987. Positive endocochlear potential: mechanism of production by marginal cells of stria vascularis. Hear. Res. 29, 117–124.

Ohmori, H. 1985. Mechano-electrical transduction currents in isolated vestibular hair cells of the chick. J. Physiol. 359, 189–217.

Oesterle, E. and Dallos, P. 1985. Intracellular recording from supporting cells in the organ of Corti. Hear. Res. 22, 229–232.

Oesterle, E. and Dallos, P. 1990. Intracellular recordings from supporting cells in the guinea pig cochlea: DC potentials. J. Neurophysiol. 64, 617–636.

Phippard, D., Boyd, Y., Reed, V., Fisher, G., Masson, W. K., Evans, E. P., Saunders, J. C., and Crenshaw, E. B. 2000. The sex-linked fidget mutation abolishes *Brn4*/*Pou3f4* gene expression in the embryonic inner ear. Hum. Mol. Genet. 9, 79–85.

Phippard, D., Lu, L., Lee, D., Saunders, J. C., and Crenshaw, E. B. 1999. Targeted mutagenesis of the POU-domain gene Brn4/Pou3f4 causes development defects in the inner ear. J. Neurosci. 19, 5980–5989.

Roberson, D. W. and Rubel, E. W. 1994. Cell division in the gerbil cochlea after acoustic trauma. Am. J. Otol. 15, 28–34.

Sakaguchi, N., Crouch, J. J., Lytle, C., and Schulte, B. A. 1998. Na–K–Cl cotransporter expression in the developing and senescent gerbil cochlea. Hear. Res. 118, 114–122.

Salt, A. N. and DeMott, J. 1994. Endolymph calcium increases with time after surgical induction of hydrops in guinea-pigs. Hear. Res. 74, 115–121.

Salt, A. N. and Konishi, T. 1982. Functional importance of sodium and potassium in the guinea pig cochlea studied with amiloride and tetraethylammonium. Jpn. J. Physiol. 32, 219–230.

Salt, A. N. and Ohyama, K. 1993. Accumulation of potassium in scala vestibuli perilymph of the mammalian cochlea. Ann. Otol. Rhinol. Laryngol. 102, 64–70.

Salt, A. N. and Thalmann, R. 1988. Cochlear Fluid Dynamics. In: Physiology of the Ear (*eds*. A. F. Juhn and J. Santos-Sacchi), pp. 341–357. Raven Press.

Salt, A. N., Melichar, I., and Thalmann, R. 1987. Mechanisms of endocochlear potential generation by stria vascularis. Laryngoscope 97, 984–991.

Santos-Sacchi, J. 1991. Isolated supporting cells from the organ of Corti: some whole cell electrical characteristics and estimates of gap junctional conductance. Hear. Res. 52, 89–98.

Santos-Sacchi, J. and Dallos, P. 1983. Intracellular communication in the supporting cells of the organ of Corti. Hear. Res. 9, 317–326.

Schmiedt, R. A. 1993. Cochlear Potentials in Quiet-Aged Gerbils: Does the Aging Cochlea Need a Jump Start? In: Sensory Research: Multimodal Perspectives (*ed*. R. T. Verrillo), pp. 91–104. Erlbaum and Associates.

Schulte, B. A. 1993. Immunohistochemical localization of intracellular Ca-ATPase in outer hair cells, neurons and fibrocytes in the adult and developing inner ear. Hear. Res. 65, 262–273.

Schulte, B. A. and Adams, J. C. 1989. Distribution of immunoreactive Na^+, K^+-ATPase in gerbil cochlea. J. Histochem. Cytochem. 37, 127–134.

Schulte, B. A. and Schmiedt, R. A. 1992. Lateral wall Na, K-ATPase and endocochlear potentials decline with age in quiet-reared gerbils. Hear. Res. 61, 35–46.

Schulte, B. A. and Steel, K. P. 1994. Expression of α and β subunit isoforms of Na, K-ATPase in the mouse inner ear and changes with mutations at the W^v or Sl^d loci. Hear. Res. 78, 65–76.

Slepecky, N. B. 1996. Structure of the Mammalian Cochlea. In: Springer Handbook of Auditory Research (*eds*. P. Dallos, A. N. Popper, and R. R. Fay), pp. 134–171. Springer.

Souter, M. and Forge, A. 1998. Intercellular junctional maturation in the stria vascularis: possible association with onset and rise of endocochlear potential. Hear. Res. 119, 81–95.

Spicer, S. S. and Schulte, B. A. 1991. Differentiation of inner ear fibrocytes according to their ion transport related activity. Hear. Res. 56, 53–64.

Spicer, S. S. and Schulte, B. A. 1994a. Ultrastructural differentiation of the first Hensen cell in the gerbil cochlea as a distinct cell type. Anat. Rec. 240, 149–156.

Spicer, S. S. and Schulte, B. A. 1994b. Differences along the place-frequency map in the structure of supporting cells in the gerbil cochlea. Hear. Res. 79, 161–177.

Spicer, S. S. and Schulte, B. A. 1996. The fine structure of spiral ligament cells relates to ion return to the stria and varies with place-frequency. Hear. Res. 100, 80–100.

Spicer, S. S. and Schulte, B. A. 1998. Evidence for a medial K^+ recycling pathway from inner hair cells. Hear. Res. 118, 1–12.

Spicer, S. S., Gratton, M. A., and Schulte, B. A. 1997. Expression patterns of ion transport enzymes in spiral ligament fibrocyte changes in relation to strial atrophy in the aged gerbil cochlea. Hear. Res. 111, 93–102.

Spicer, S. S., Salvi, R. J., and Schulte, B. A. 1999. Ablation of inner hair cells by carboplatin alters cells in the medial K^+ flow route and disrupts tectorial membrane. Hear. Res. 136, 139–150.

Spicer, S. S., Smythe, N., and Schulte, B. A. 2003. Ultrastructure indicative of ion transport in tectal, Deiters, and tunnel cells: differences between gerbil and chinchilla basal and apical cochlea. Anat. Rec. 271A, 342–359.

Steel, K. 1999. The benefits of recycling. Science 285, 1363–1364.

Steel, K. P., Erven, A., and Kierman, A. E. 2002. Mice as Models for Human Hereditary Deafness. In: Springer Handbook of Auditory Research (*eds*. B. J. Keats, A. N. Popper, and R. R. Fay), pp. 247–296. Springer.

Syka, J., Melichar, I., and Ulehlova, L. 1981. Longitudinal distribution of cochlear potentials and the K^+ concentration in the endolymph after acoustic trauma. Hear. Res. 4, 287–298.

Takeuchi, S., Ando, M., and Kakigi, A. 2000. Mechanism generating endocochlear potential: role played by intermediate cells in stria vascularis. Biophys. J. 79, 2572–2582.

Teubner, B., Michel, V., Pesch, J., Lautermann, J., Cohen-Salmon, M., Sohl, G., Jahnke, K., Winterhager, E., Herberhold, C., Hardelin, J. P., Petit, C., and Willecke, K. 2003. Connexin 30 (Gjb6)-deficiency causes severe hearing impairment and lack of endocochlear potential. Hum. Mol. Genet. 12, 13–21.

Wang, Y., Hirose, K., and Liberman, M. C. 2002. Dynamics of noise-induced cellular injury and repair in the mouse cochlea. J. Assoc. Res. Otolaryngol. 3, 248–268.

Wangemann, P. 2002. K^+ cycling and the endocochlear potential. Hear. Res. 165, 1–9.

Wangemann, P. and Schacht, J. 1996. Homeostatic Mechanisms in the Cochlea. In: Springer Handbook of Auditory Research (*eds*. P. Dallos, A. N. Popper, and R. R. Fay), pp. 130–185. Springer.

Wangemann, P., Itza, E. M., Albrecht, B., Wu, T., Jabba, S. V., Maganti, R. J., Lee, J. H., Everett, L. A., Wall, S. M., Royaux, I. E., Green, E. D., and Marcus, D. C. 2004. Loss of KCNJ10 protein expression abolishes endocochlear potential and causes deafness in Pendred syndrome mouse model. BMC Med. 2, 30.

Weber, P. C., Cunningham, C. D., and Schulte, B. A. 2001. Potassium recycling pathways in the human inner ear. Laryngoscope 111, 1156–1165.

White, T. W., Deans, M. R., Kelsell, D. P., and Paul, D. L. 1998. Connexin mutations in deafness. Nature 394, 630–631.

Wu, T. and Marcus, D. C. 2003. Age-related changes in cochlear endolymphatic potassium and potential in CD-1 and CBA/CaJ mice. J. Assoc. Res. Otolaryngol. 4, 353–362.

Xia, A. P., Ikeda, K., Katori, Y., Oshima, T., Kikuchi, T., and Takasaka, T. 2000. Expression of connexin 31 in the developing mouse cochlea. Neuroreport 11, 2449–2453.

Xia, A. P., Kikuchi, T., Minowa, O., Katori, Y., Oshima, T., Noda, T., and Ikeda, K. 2002. Late-onset hearing loss in a mouse model of DFN3 non-syndromic deafness: morphologic and immunohistochemical analyses. Hear. Res. 166, 150–158.

Yamashita, H., Shimogori, H., Sugahara, K., and Takahashi, M. 1999. Cell proliferation in spiral ligament of mouse cochlea damaged by dihydrostreptomycin sulfate. Acta Otolaryngol. 119, 322–325.

Yamasoba, T., Kondo, K., Miyajima, C., and Suzuki, M. 2003. Changes in cell proliferation in rat and guinea pig cochlea after aminoglycoside-induced damage. Neurosci. Lett. 347, 171–174.

Zidanic, M. and Brownell, W. E. 1990. Fine structure of the intracochlear potential field. I. The silent current. Biophys. J. 57, 1253–1268.

Further Reading

Trune, D. R. 2006. Ion Homeostasis and Inner Ear Disease. In: Medical Otology and Neurotology (*eds*. M. Hamid and A. Sismanis), pp. 21–32. Thieme Publishing.

3.09 Meniere's Disease

J P Harris, University of California, San Diego, CA, USA

A N Salt, Washington University School of Medicine, St. Louis, MO, USA

© 2008 Elsevier Inc. All rights reserved.

3.09.1	**Introduction**	157
3.09.2	**Pathophysiology**	157
3.09.3	**Epidemiology**	159
3.09.3.1	Sex Distribution	159
3.09.3.2	Age	159
3.09.3.3	Bilaterality	159
3.09.3.4	Hereditary Factors	159
3.09.3.5	Natural History	159
3.09.4	**Evaluation**	160
3.09.5	**Treatment**	160
3.09.5.1	Medical Therapy	161
3.09.5.2	Middle Ear Pressure Manipulations (the Meniett Device)	161
3.09.5.3	Intratympanic Therapies	161
3.09.5.3.1	Gentamicin	161
3.09.5.3.2	Steroids	161
3.09.5.4	Endolymphatic Sac Surgery	162
3.09.5.5	Vestibular Nerve Sectioning	162
3.09.5.6	Labyrinthectomy	162
References		162

Glossary

endolymphatic hydrops A swelling of the membrane-bound endolymphatic compartment of the inner ear.

intratympanic therapy Injection of drug through the tympanic membrane into the middle ear cavity, from where it diffuses into the inner ear through the round window membrane.

3.09.1 Introduction

Meniere's disease is a chronic illness that affects approximately 97 000 Americans annually, usually in adulthood, and with symptoms that subsequently wax and wane over time. Patients often experience a period of intense symptoms followed by years of remission, with relapses in later stages of the disease. Since it was first described by Prosper Meniere in 1861, this illness has defied scientific investigation into its etiology and cure.

The disorder is typically characterized by severe episodic vertigo, fluctuating hearing loss, roaring tinnitus, and a feeling of aural pressure. The characteristics are so unique that just the description of the attack by the patient can lead to a correct diagnosis of the condition. Selective tests can be performed to rule out other conditions in the short list of differential diagnoses.

3.09.2 Pathophysiology

Meniere's disease is characterized by the presence of endolymphatic hydrops, an enlargement of the endolymphatic compartment of the inner ear. Endolymphatic hydrops can be seen in histological sections of the temporal bone as a distension of the

membranous structures such as Reissner's membrane. However, the precise interdependence between endolymphatic hydrops and Meniere's disease remains unclear. Careful studies suggest that hydrops is present in the ears of all patients who exhibit Meniere's disease symptoms, but hydrops is also seen in the ears of substantial numbers of asymptomatic patients (Merchant, S. N. *et al.*, 2005). During the early phases of the disease, there are normal numbers of hair cells and neurons in the organ of Corti, but over time, damage occurs to many structures in the ear. In addition to derangements of the membranous labyrinth walls due to the swollen endolymphatic spaces, there are numerous other pathological changes. These include the loss of spiral ganglion cells, damage to the stereocilia of the hair cells, loss of inner and outer hair cells, and the degeneration of type I and type II fibrocytes of the lateral wall. These degenerative changes occur particularly in the apical turns of the cochlea.

There are a number of animal models of endolymphatic hydrops in which the physiological and anatomical changes have been compared to those in Meniere's disease patients. Endolymphatic hydrops can be induced by surgical ablation of the endolymphatic sac (Kimura, R. and Schuknecht, H. E., 1965), by partial ablation of the sac combined with aldosterone treatments (Dunnebier, E. A. *et al.*, 1997), or by treatments with vasopressin (antidiuretic hormone) (Takeda, T. *et al.*, 2000). Symptoms of Meniere's disease have been associated with hormonal changes during the menstrual cycle in females and may be related to elevated plasma vasopressin levels, but no systemic alterations of aldosterone levels are found in patients (Mateijsen, D. J. *et al.*, 2001).

In animals with surgically induced hydrops, similar anatomical changes are found to those in patients, including degeneration of fibrocytes in the lateral wall, loss of spiral ganglion cells, disruption of hair cell stereocilia, and eventual loss of hair cells (Nadol, J. B., Jr. *et al.*, 1995). In addition, physiological measures indicate that the endocochlear potential (the positive voltage in the endolymphatic space) is reduced, even though the major electrolytes of both endolymph and perilymph are unchanged (Sziklai, I. *et al.*, 1992). One chemical component of endolymph that is disturbed in the hydropic cochlea is the endolymph calcium concentration, which becomes elevated as hydrops develops, probably as a secondary consequence of the endocochlear potential decline (Salt, A. N. and DeMott, J., 1994). We can conclude that endolymphatic hydrops is far from the only pathological change occurring in the ear. It remains unknown how these different pathological processes interact and which are primary, secondary or tertiary. Although it is generally assumed that hydrops is the primary factor, and all other pathologies occur secondarily to hydrops, this remains to be proved. There is recent evidence that changes in fibrocytes in the lateral wall may precede the endolymph volume disturbance (Merchant, S. N. *et al.*, 2005). In this case, hydrops may occur as a secondary consequence of changes in ion transport in the lateral wall.

The observation of endolymphatic hydrops in asymptomatic human ears suggests that some types of hydrops may not be pathological and do not result in hearing loss or other inner ear dysfunction. In experimental animals, acute hydrops can be generated in the normal ear by exposure to loud, but not damaging, low-frequency tones (Salt, A. N., 2004). This type of hydrops does not impair function. On the contrary, the sensitivity of the ear is transiently increased after such tone exposures when hydrops is present. These combined observations demonstrate that endolymphatic hydrops may not be the primary cause of hearing loss in Meniere's disease. Alternative processes, such as the reduction of endocochlear potential and elevation of endolymph Ca^{2+}, may play a bigger role in hearing losses associated with chronic hydrops and Meniere's disease. Hearing acuity is known to be highly sensitive to reductions in endocochlear potential (Sewell, W. F., 1984), while increases in endolymph Ca^{2+} cause shrinkage of the tectorial membrane (Freeman, D. M. *et al.*, 2003) and alter transducer channel conductance and adaptation in hair cells (Hudspeth, A. J., 2005). The exact relationships between endolymphatic hydrops and electrochemical changes of the endolymph still remain uncertain.

When local volume regulation processes are disturbed in the cochlea, the mechanical properties of the endolymphatic system membranes result in volume flows toward or away from the saccule, which is the most compliant structure (Wit, H. P. *et al.*, 2000). Comparable to the weak spot on a balloon, the membranous walls of the saccule appear to be highly distensible. The interactions between the endolymphatic sac and the saccule are not well established, but it has been proposed that distension of the part of the saccule near the endolymphatic duct, called the endolymphatic sinus, may regulate endolymph movements into or out of the endolymphatic sac (Salt, A. N. and Rask-Andersen, H., 2004). The

endolymphatic sac appears to be capable of both resorption and secretion of substances, and is considered the likely ultimate locus for endolymph volume regulation (Rask-Andersen, H. *et al.*, 1999). It is also consistent with the observation of bone or detritus blocking the endolymphatic duct or sac in human temporal bones or vascular occlusions of the sac (Friberg, U. and Rask-Andersen, H., 2002), which may interfere with the sac's role in volume regulation. Another consequence of the distension of the saccular membrane in endolymphatic hydrops is the resulting contact the membrane makes with the undersurface of the stapes footplate. This is thought to lead to a positive Hennebert's sign (induction of dizziness or nystagmus when the stapes is displaced by pneumo-otoscopy) in approximately 30% of patients (Nadol, J. B., Jr., 1977).

3.09.3 Epidemiology

3.09.3.1 Sex Distribution

There is a slightly increased female preponderance among Meniere's patients, although there are some exceptions, such as in Sweden, where the incidence is 57% males to 43% females. In Japan in the 1970s, there was an equal male-to-female incidence that has changed over the last 30 years to a female predominance. The underlying reasons for this remain unknown.

3.09.3.2 Age

The patients who develop this condition are often in the prime of their working lives. The average age of onset has been reported to range between 38 and 50 years of age. The disease is rare in children.

3.09.3.3 Bilaterality

This is a very important consideration, since the illness can lead to severe hearing loss in the affected ear and can influence the treatment decision-making process, especially if destructive procedures are being considered. The incidence of bilaterality has been reported to range from as low as 2% to as high as 47%. Most practitioners will inform patients that the incidence is approximately 20–30%, with an increased incidence the longer they are followed. However, this depends on the criteria being used to determine when the second ear is affected. For instance, a second ear may show a hearing loss but no symptoms of dizziness; some physicians would consider this to be bilateral disease. In a recent study of Meniere's disease patients, 23% developed bilateral disease over an average of 7.6 years (House, J. W. *et al.*, 2006).

3.09.3.4 Hereditary Factors

There are some families that have a strong history of Meniere's disease. One recent study demonstrated that a COCH gene mutation was found in three families with Meniere's disease (Oliveira, C. A. and Braga, A. M., 1992), but in another study HLA class I and class II antigens were not found to increase the susceptibility of developing Meniere's disease (Koyama, S. *et al.*, 1993). Given the rapid identification of mutations that lead to derangements of gene products in the ear, it is reasonable to expect that mutations will be identified that have relevance to endolymph volume regulation.

3.09.3.5 Natural History

The presenting symptoms of Meniere's disease are variable. About 40% of the cases present with a sudden hearing loss, and approximately 50% report acute vertigo as their initial symptom. The incidence of these two symptoms occurring simultaneously ranges from 7% to 44%. When hearing loss is the presenting symptom, most of these patients begin to exhibit vertigo within 2 years. However, when vertigo is the initial symptom, fewer of these cases develop into Meniere's disease.

The audiograms of patients with Meniere's disease have a characteristic appearance. They often start with a low-frequency hearing loss averaging 35 dB, with fluctuations over time back to near-normal range. As the illness progresses, one begins to see associated high-frequency losses that result in a tent-like or peaked audiogram centered at 2000 Hz. Further along in the illness, the peak diminishes to a flat audiogram with further losses in the high frequencies and an associated loss in word identification scores.

Over time in humans, the hearing and vestibular losses plateau and the attacks abate. In this stage, hearing is reduced to the 50–60 dB range and the word identification scores are 50–60%. While these patients find the hearing loss disabling, hearing aids are usually not helpful, due to distortion and poor word discrimination. At this point there is still caloric function, but it, too, is reduced, on average by 50%. It is rare that the caloric function is not maintained to

some degree, but if it is lost 100%, the possibility of other retrocochlear pathology, such as an acoustic neuroma or even autoimmune inner ear disease, should be investigated.

Patients sometimes have a recrudescence of their illness after a period of relative calm. This may result in a frightening disorder characterized by a sudden drop attack known as the otolithic crisis of Tumarkin. During these spells, the patient falls to the ground, without losing consciousness or experiencing a change in hearing. If this occurs, the illness has moved to a dangerous phase, because these sudden drop attacks can cause serious injury. The patient should be treated aggressively at this point.

3.09.4 Evaluation

One of the essential issues in coming to a proper diagnosis of this disorder is to rely on the patient's history. If the patient presents with the classic symptoms of complex episodic vertigo, fluctuating hearing loss, roaring tinnitus, and aural pressure, the diagnosis is only a matter of confirmation and making sure no other condition that can mimic Meniere's disease exists. A thorough otoneurological examination is required and appropriate tests are ordered so that the possibility of retrocochlear pathology can be eliminated.

Electrocochleography can be performed, either with a noninvasive canal wick electrode or with a transtympanic electrode. The latter gives more accurate results, but may cause some injury to the tympanic membrane and, very rarely, to the inner ear. The value of the EcoG is controversial, because if a patient is asymptomatic, results may be normal. Its value for confirming the diagnosis, however, is only when it is positive, not negative. A form of stacked ABR, known as the CHAMP test, has recently been reported to be diagnostic of Meniere's disease although this has not yet been confirmed by other reports (Don, M. *et al.*, 2005).

Click-evoked otoacoustic emissions and $2f_1 - f_2$ distortion product otoacoustic emissions (DPOAE) are both suppressed in the ears of Meniere's patients, but the changes are related to the degree of hearing loss present, and are comparable to other types of hearing loss of similar magnitude. Conventional acoustic emissions are therefore of little additional value over conventional audiometry in the diagnosis of Meniere's disease. Although recent experimental results and theoretical models have shown that even-order distortions ($2f$, $f_2 - f_1$, $f_2 + f_1$) are much more sensitive to endolymph volume disturbances than are the conventional $2f_1 - f_2$ emissions (Sirjani, D. B. *et al.*, 2004), even-order distortions are difficult to record in humans.

Some patients with Meniere's disease have been found to have an autoimmune basis for their condition. If this is suspected, tests are ordered to look for this possibility, which include FTA-ABS, ANA, ESR, RF, CRP, C1q, and an Otoblot test (anti-68 kDa antibody). The Otoblot test (Otoimmune Diagnostics, Buffalo, NY) is especially important in cases of bilateral Meniere's disease. Studies of the basic immunity of the inner ear have shown that the inner ear is immunoresponsive and is quite capable of responding to an immunological challenge that, in itself, can damage inner ear function (Harris, J. P., 1983; Woolf, N. K. and Harris, J. P., 1986).

3.09.5 Treatment

Unfortunately, the common perception by patients, primary care physicians, and often general otolaryngologists is that there is no effective treatment for this disorder. The patient usually has no choice but to find a way to deal with the attacks until the disease burns itself out, which then coincides with the development of severe hearing and vestibular loss.

In a group of patients with Meniere's disease who performed quality-of-life evaluations between attacks and within days of an acute spell, the results were eye-opening. These patients, most of whom were middle-aged, were found to be severely impaired by their illness: their self-rated quality of well-being (QWB) was worse than that of adults with life-threatening illnesses (i.e., AIDS, cancer, renal and pulmonary disease). On days with acute symptoms, Meniere's patients were much more severely affected, scoring worse than noninstitutionalized Alzheimer's patients and elderly patients with severe obstructive pulmonary disease. Additionally, these patients were clinically depressed on the CES depression scale and were also one standard deviation below the mean for the general population on the SFA-12, a widely used measure of general health (Anderson, J. P. and Harris, J. P., 2001). Taken together, these findings underscore the importance of attempting to treat these patients aggressively, rather than letting the disease run its course.

3.09.5.1 Medical Therapy

The first step in managing patients with Meniere's disease is to explain their illness to them. The patients need to be engaged in their therapy to understand how they can take control of this condition. This often includes a change in lifestyle, reduction of stress, increased exercise, and reduced intake of salt and processed foods.

There are a number of studies that show that diuretics can significantly reduce the number of vertigo spells in Meniere's patients, but the hearing loss may continue (van Deelen, G. W. and Huizing, E. H., 1986).

Additionally, if the evaluation shows any form of autoimmunity or a positive Otoblot, high-dose prednisone (60 mg) will be administered for a 3- to 4-week taper. If a response is seen, the patient will either be given pulses of steroids or be referred to rheumatology for better-tolerated immunosuppressive agents such as Humira, Enbrel, or Rituxin.

3.09.5.2 Middle Ear Pressure Manipulations (the Meniett Device)

Experimental studies found that Meniere's patients responded well to treatment in a hypobaric pressure chamber. This effect was thought to be mediated by the positive pressure in the middle ear causing pressure to be applied to the labyrinth relative to the reduced body pressure. The Meniett is a device that, based on these observations, applies a controlled positive pressure to the middle ear space. Superimposed on the steady pressure are very low-frequency (infrasonic) pressure oscillations. The stimuli are transmitted to the middle ear through a pressure-equalizing tympanostomy tube in the tympanic membrane. The pressure manipulations are thought to influence inner ear pressures in a manner that reduces endolymphatic hydrops. This is supported by studies that have shown that low-frequency pressure pulses delivered to the ear of normal animals appear to drive endolymph from the saccule into the endolymphatic sac. In recent clinical trials, there has been a reduction in vestibular attacks after a period ranging from 6 weeks to 4 months (Odkvist, L. M. *et al.*, 2000; Gates, G. *et al.*, 2004; Thomsen, J. *et al.*, 2005). Patients still experience occasional attacks, but they are less frequent than before treatment. No change occurs in their hearing, tinnitus, or activities of daily living.

It should be noted that some patients who receive the pressure-equalizing tympanostomy tube in their tympanic membranes report that this, alone, is effective in controlling their Meniere's disease symptoms (Montandon, P. *et al.*, 1988). Animal studies also demonstrate that hydrops is less pronounced after surgical ablation of the sac, if the tympanic membrane is also perforated. Possible factors contributing to this effect include an increased oxygenation of the ear, a pH increase of inner ear fluids due to lowering of the middle ear CO_2 level, an attenuation of external low-frequency sounds entering the ear, or an increase in low-frequency displacements of the stapes produced by middle ear muscle contractions, such as those occurring during swallowing.

3.09.5.3 Intratympanic Therapies

3.09.5.3.1 Gentamicin

Vestibular ablation through chemical means has recently had resurgence in popularity. Once used only systemically for bilateral cases, it has now become a well-accepted and effective method to stop vestibular attacks in Meniere's disease (Carey, J., 2004; Chia, S. H. *et al.*, 2004). Low doses of gentamicin are injected into the middle ear, with gradual vestibular ablation occurring. The goal is not to destroy the vestibular end organ completely, but to titrate the dose until vestibular symptoms occur, and then watch for possible recurrence of episodic vertigo. By this low-dose titration method, the risk to hearing is reduced to approximately 6% and the overall effective vertigo control is 92%. Repeated doses can be administered as needed for new symptoms.

The only drawback to this method is the temporary instability patients develop as a consequence of vestibular injury incurred by the gentamicin.

3.09.5.3.2 Steroids

Recently, there has been a trend toward intratympanic (IT) injections of corticosteroids to control the symptoms of patients with steroid-responsive Meniere's disease (Barrs, D. M., 2004; Garduno-Anaya, M. A. *et al.*, 2005). This may permit a higher dose of drug to reach the ear than can be given by systemic therapy (Parnes, L. S. *et al.*, 1999), and carries less risk of hearing loss than does IT gentamicin therapy. The mechanism of action of direct application of steroids to the inner ear remains uncertain, and may be mediated indirectly through the immune system, or directly on fluid homeostasis mediated by

glucocorticoid receptors that are present on a variety of cell types in the inner ear, predominantly on the fibrocytes of the lateral wall of the cochlea.

3.09.5.4 Endolymphatic Sac Surgery

Patients who fail medical management may be considered for surgical therapy, although specialists dealing with this disorder differ markedly in their specific opinions. Many otologists recommend endolymphatic sac shunt surgery or endolymphatic sac decompression. This outpatient procedure involves a mastoidectomy to expose the endolymphatic sac; the site is then opened and a silastic drain is placed between the lumen of the sac and the mastoid. Alternatively, the sac is exposed without placing a shunt, a procedure known as decompression. These procedures have few risks to hearing or to other structures, and usually produce a reduction in vertigo in 65–80% of patients (Glasscock, M. E. *et al.*, 1984a; Ress, B. D. and Harris, J. P., 1999). Sac procedures do not statistically improve hearing or prevent tinnitus, but they have been reported to help people reach a stable point in their disease sooner than being left untreated (Quaranta, A. *et al.*, 1998). In controlled clinical studies, this procedure was found to be no more effective than sham surgery performed on the ears under general anesthesia. However, both groups of patients statistically improved over their baseline status, so the value of this surgery is controversial (Thomsen, J. *et al.*, 1981; Bretlau, P. *et al.*, 1984).

3.09.5.5 Vestibular Nerve Sectioning

Sectioning of the vestibular nerve was once a popular procedure, but it has been employed less over the last decade. In this surgery, the posterior fossa or the middle fossa approach exposes the vestibular nerve for its selective sectioning, sparing both the cochlear nerve and the facial nerve. This procedure has been recommended when symptoms are severe and hearing is still quite serviceable. It involves a craniotomy, and thus has the inherent risks of meningitis, CSF leak, and neurological injury (Glasscock, M. E., *et al.*, 1984b; Kemink, J. L. and Hoff, J. T., 1986; Silverstein, H. *et al.*, 1992).

3.09.5.6 Labyrinthectomy

When hearing is reduced by the illness to unserviceable levels (defined as at least 50 dB SRT or less than 50% word identification score), a labyrinthectomy can be recommended. This procedure is the gold standard for procedures in Meniere's disease treatment, against which other methods must be compared (Hammerschlag, P. E. and Schuknecht, H. F., 1981). In this operation, the five vestibular end organs are systematically removed under direct microscopic control, in an approach usually through the mastoid. After removal of these end organs, the inner ear can no longer generate vestibular attacks; but the residual hearing is destroyed as a consequence of the procedure. Patients will be unsteady for several weeks following the surgery, and must undergo central adaptation for the loss of vestibular function through vestibular exercises or physical therapy. This procedure is effective in approximately 95% of cases. One must be certain that there is adequate vestibular function on the contralateral side before the vestibular tissue is removed; otherwise, the patient may end up with a form of Dandy's syndrome where disabling oscillopsia and ataxia are experienced.

Financial disclosure. Dr. Harris holds the patent for the Otoblot test and has a financial interest in Otoimmune Diagnostics, Inc.

References

Anderson, J. P. and Harris, J. P. 2001. Impact of Ménière's disease on quality of life. Otol. Neurotol. 22(6), 888–894.

Barrs, D. M. 2004. Intratympanic corticosteroids for Ménière's disease and vertigo. Otolaryngol. Clin. North Am. 37, 955–972.

Bretlau, P., Thomsen, J., Tos, M., and Johnsen, N. J. 1984. Placebo effect in surgery for Ménière's disease: a three-year follow-up study of patients in a double blind placebo controlled study on endolymphatic sac shunt surgery. Am. J. Otol. 5(6), 558–561.

Carey, J. 2004. Intratympanic gentamicin for the treatment of Ménière's disease and other forms of peripheral vertigo. Otolaryngol. Clin. North Am. 37, 1075–1090.

Chia, S. H., Gamst, A. C., Anderson, J. P., and Harris, J. P. 2004. Intratympanic Gentamicin therapy for Ménière's disease: a meta-analysis. Otol. Neurotol. 25, 544–552.

Don, M., Kwong, B., and Tanaka, C. 2005. A diagnostic test for Ménière's disease and cochlear hydrops: impaired high-pass noise masking of auditory brainstem responses. Otol. Neurotol. 26(4), 711–722.

Dunnebier, E. A., Segenhout, J. M., Wit, H. P., and Albers, F. W. 1997. Two-phase endolymphatic hydrops: a new dynamic guinea pig model. Acta Otolaryngol. 117, 13–19.

Freeman, D. M., Masaki, K., McAllister, A. R., Wei, J. L., and Weiss, T. F. 2003. Static material properties of the tectorial membrane: a summary. Hear Res. 180, 11–27.

Friberg, U. and Rask-Andersen, H. 2002. Vascular occlusion in the endolymphatic sac in Ménière's disease. Ann. Otol. Rhinol. Laryngol. 111, 237–245.

Garduno-Anaya, M. A., Couthino De Toledo, H., Hinojosa-Gonzalez, R., Pane-Pianese, C., and Rios-Castaneda, L. C. 2005. Dexamethasone inner ear perfusion by intratympanic

injection in unilateral Ménière's disease: a two-year prospective, placebo-controlled, double-blind, randomized trial. Otolaryngol. Head Neck Surg. 133(2), 285–294.
Gates, G. A., Green, J. D., Jr., Tucci, D. L., and Telian, S. A. 2004. The effects of transtympanic micropressure treatment in people with unilateral Ménière's disease. Arch. Otolaryngol. Head Neck Surg. 130(6), 718–725.
Glasscock, M. E., Kveton, J. F., and Christiansen, S. G. 1984a. Current status of surgery for Ménière's disease. Otolaryngol. Head Neck Surg. 92, 67–72.
Glasscock, M. E., Kveton, J. F., and Christiansen, S. G. 1984b. Middle fossa vestibular neurectomy: an update. Otolaryngol. Head Neck Surg. 92(2), 216–220.
Hammerschlag, P. E. and Schuknecht, H. F. 1981. Transcanal labyrinthectomy for intractable vertigo. Arch. Otolaryngol. 107, 152–156.
Harris, J. P. 1983. Immunology of the inner ear: response of the inner ear to antigen challenge. Otolaryngol. Head Neck Surg. 91(1), 18–32.
House, J. W., Doherty, J. K., Fisher, L. M., Derebery, M. J., and Berliner, K. I. 2006. Ménière's disease: prevalence of contralateral ear involvement. Otol. Neurotol. 27(3), 355–361.
Hudspeth, A. J. 2005. How the ear's works work: mechanoelectrical transduction and amplification by hair cells. C. R. Biol. 328, 155–162.
Kemink, J. L. and Hoff, J. T. 1986. Retrolabyrinthine vestibular nerve section: analysis of results. Laryngoscope 96(1), 33–36.
Kimura, R. and Schuknecht, H. E. 1965. Membranous hydrops in the inner ear of the guinea pig after obliteration of the endolymphatic sac. Pract. Otorhinolaryngol. 27, 343–354.
Koyama, S., Mitsuishi, Y., Bibee, K., Watanabe, I., and Terasaki, P. I. 1993. HLA associations with Ménière's disease. Acta Otolaryngol. (Stockh.) 113, 575–578.
Mateijsen, D. J., Kingma, C. M., De Jong, P. E., Wit, H. P., and Albers, F. W. 2001. Aldosterone assessment in patients with Ménière's disease. ORL J. Otorhinolaryngol. Relat. Spec. 63, 280–286.
Merchant, S. N., Adams, J. C., and Nadol, J. B., Jr. 2005. Pathophysiology of Ménière's syndrome: are symptoms caused by endolymphatic hydrops? Otol. Neurotol. 26, 74–81.
Montandon, P., Guillemin, P., and Hausler, R. 1988. Prevention of vertigo in Ménière's syndrome by means of transtympanic ventilation tubes. ORL J. Otorhinolaryngol. Relat. Spec. 50(6), 377–381.
Nadol, J. B., Jr. 1977. Positive Hennebert's sign in Ménière's disease. Arch. Otolaryngol. 103(9), 524–530.
Nadol, J. B., Jr., Adams, J. C., and Kim, J. R. 1995. Degenerative changes in the organ of Corti and lateral cochlear wall in experimental endolymphatic hydrops and human Ménière's disease. Acta Otolaryngol. Suppl. 519, 47–59.
Odkvist, L. M., Arlinger, S., Billermark, E., Densert, B., Lindholm, S., and Wallqvist, J. 2000. Effects of middle ear pressure changes on clinical symptoms in patients with Ménière's disease – a clinical multicentre placebo-controlled study. Acta Otolaryngol. Suppl. 543, 99–101.
Oliveira, C. A. and Braga, A. M. 1992. Ménière's syndrome inherited as an autosomal dominant trait. Ann. Otol. Rhinol. Laryngol. 101, 590–594.
Parnes, L. S., Sun, A. H., and Freeman, D. J. 1999. Corticosteroid pharmacokinetics in the inner ear fluids: an animal study followed by clinical application. Laryngoscope 109(7 Pt. 2), 1–17.
Quaranta, A., Marini, F., and Sallustio, V. 1998. Long-term outcome of Ménière's disease: endolymphatic mastoid shunt versus natural history. Audiol. Neurootol. 3, 54–60.
Rask-Andersen, H., DeMott, J. E., Bagger-Sjoback, D., and Salt, A. N. 1999. Morphological changes of the endolymphatic sac induced by microinjection of artificial endolymph into the cochlea. Hear Res. 138, 81–90.
Ress, B. D. and Harris, J. P. 1999. Endolymphatic Sac Surgery. In: Ménière's Disease (*ed*. J. P. Harris), pp. 355–360. Kugler Publications.
Salt, A. N. 2004. Acute endolymphatic hydrops generated by exposure of the ear to nontraumatic low-frequency tones. J. Assoc. Res. Otolaryngol. 5, 203–214.
Salt, A. N. and DeMott, J. 1994. Endolymph calcium increases with time after surgical induction of hydrops in guinea-pigs. Hear Res. 74, 115–121.
Salt, A. N. and Rask-Andersen, H. 2004. Responses of the endolymphatic sac to perilymphatic injections and withdrawals: evidence for the presence of a one-way valve. Hear Res. 191(1–2), 90–100.
Sewell, W. F. 1984. The effects of furosemide on the endocochlear potential and auditory-nerve fiber tuning curves in cats. Hear Res. 14, 305–314.
Silverstein, H., Wanamaker, H., Flanzer, J., and Rosenberg, S. 1992. Vestibular neurectomy in the United States – 1990. Am. J. Otol. 13(1), 23–30.
Sirjani, D. B., Salt, A. N., Gill, R. M., and Hale, S. A. 2004. The influence of transducer operating point on distortion generation in the cochlea. J. Acoust. Soc. Am. 115, 1219–1229.
Sziklai, I., Ferrary, E., Horner, K. C., Sterkers, O., and Amiel, C. 1992. Time-related alteration of endolymph composition in an experimental model of endolymphatic hydrops. Laryngoscope 102, 431–438.
Takeda, T., Takeda, S., Kitano, H., Okada, T., and Kakigi, A. 2000. Endolymphatic hydrops induced by chronic administration of vasopressin. Hear Res. 140, 1–6.
Thomsen, J., Bretlau, P., Tos, M., and Johnsen, N. J. 1981. Placebo effect in surgery for Ménière's disease. A double-blind, placebo-controlled study on endolymphatic sac shunt surgery. Arch. Otolaryngol. 107(5), 271–277.
Thomsen, J., Sass, K., Odkvist, L., and Arlinger, S. 2005. Local overpressure treatment reduces vestibular symptoms in patients with Ménière's disease: a clinical, randomized, multicenter, double-blind, placebo-controlled study. Otol. Neurotol. 26(1), 68–73.
van Deelen, G. W. and Huizing, E. H. 1986. Use of a diuretic (Dyazide) in the treatment of Ménière's disease. A double-blind cross-over placebo-controlled study. ORL J. Otorhinolaryngol. Relat. Spec. 48(5), 287–292.
Wit, H. P., Warmerdam, T. J., and Albers, F. W. 2000. Measurement of the mechanical compliance of the endolymphatic compartments in the guinea pig. Hear Res. 145, 82–90.
Woolf, N. K. and Harris, J. P. 1986. Cochlear pathophysiology associated with inner ear immune responses. Acta Otolaryngol. 102, 353–364.

3.10 Mechano-Acoustical Transformations

S Puria and C R Steele, Stanford University, Stanford, CA, USA

© 2008 Elsevier Inc. All rights reserved.

3.10.1	**Introduction**	166
3.10.2	**Theories of Sound Transmission in the Ear**	167
3.10.2.1	Mechanical and Acoustic Levers	167
3.10.2.2	Newton's Second Law of Motion	167
3.10.2.3	Transmission Lines	168
3.10.2.4	Modes of Vibration	168
3.10.2.5	The Input and Output Variables	168
3.10.3	**External Ear**	169
3.10.3.1	Concha and Ear-Canal Resonance	169
3.10.3.2	Spatial Diffraction by the Pinna	170
3.10.3.3	Tympanic Membrane and Ear Canal Interface	170
3.10.4	**Middle Ear**	170
3.10.4.1	Tympanic Membrane Shape and Internal Structure	172
3.10.4.2	Tympanic Membrane Biomechanics	173
3.10.4.3	Middle-Ear Imaging	175
3.10.4.4	Malleus–Incus Complex	176
3.10.4.5	Lenticular Process	178
3.10.4.6	Stapes	178
3.10.4.7	Ossicular Reconstruction	179
3.10.4.8	Middle-Ear Muscles	179
3.10.4.9	Middle-Ear Cavity	180
3.10.4.10	Middle-Ear Acoustic Load	180
3.10.5	**Cochlear Hydrodynamics**	180
3.10.5.1	Vestibular Fluid Pressure	180
3.10.5.2	Partition Resonance	182
3.10.5.2.1	Plate	183
3.10.5.2.2	Fluid	183
3.10.5.2.3	Plate and fluid	184
3.10.5.3	Vestibular Fluid Pressure to Basilar Membrane Displacement	184
3.10.5.3.1	One-dimensional approximation	184
3.10.5.3.2	Two-dimensional approximation	185
3.10.5.3.3	Three-dimensional model and viscosity	186
3.10.5.3.4	Validation with physical modeling	186
3.10.5.4	Solution Methods	186
3.10.6	**Organ of Corti – Fluid Pressure to Neural Excitation**	188
3.10.6.1	Multiscale Organ of Corti Model	188
3.10.6.2	Outer Hair Cell Motility and the Push–Pull Motion of the Basiliar Membrane	189
3.10.6.3	Time Delay versus ''Feedforward''	192
3.10.6.4	Inner Hair Cell Excitation	193
3.10.7	**Summary of Some Issues**	195
3.10.7.1	Motion of the Tympanic Membrane for High Frequencies	195
3.10.7.2	Motion of the Ossicular Chain for High Frequencies	195
3.10.7.3	Bone Conduction	195
3.10.7.4	Traveling Waves	195
3.10.7.5	Cell Motility versus Stereociliary Forces	195
3.10.7.6	Outer Hair Cell Roll-Off	196

3.10.7.7	A Resonant Tectorial Membrane?	196
3.10.7.8	Multiple Traveling Wave Modes	196
3.10.7.9	Stiffness Change Along the Cochlea	196
3.10.8	**General Summary**	197
References		198

3.10.1 Introduction

The auditory periphery of mammals is one of the most remarkable examples of a biomechanical system. It is highly evolved, with tremendous mechanical complexity. What is the reason for such complexity? Why is it not the case for mammals to simply have hair cells tuned to various frequencies attached to their skin to detect motion due to sound? Clearly, the complexity serves the animal by providing greater functionality. This can be appreciated by looking at simpler auditory systems.

One of the simplest hearing organs is that of the fly (*Drosophila melanogaster*), which has tiny feather-like aristas that produce twisting forces in response to sound. This sound receiver mechanically oscillates to activate the Johnston's organ auditory receptors with a moderately damped resonance at about 430 Hz (Gopfert, M. C. and Robert, D., 2001). The sound pressure level (SPL) required to elicit a response, due to wing-generated auditory cues involved in courtship, is in the 70-100 dB range (Eberl, D. F. *et al.*, 1997). An example of a simple anatomy with more complex function than that of the fly is the Müller's organ of the locust. This invertebrate is capable of discriminating sounds at broadly tuned frequencies of approximately 3.5–5, 8, 12, and 19 kHz, corresponding to the four mechanotransduction receptors attached to the tympanic membrane (Michelsen, A., 1966). The best threshold for the receptor cells is about 40 dB SPL. The resonances of the tympanic membrane and attached organs provide the greater number of frequency channels than the fly (Windmill, J. F. *et al.*, 2005). Amphibians evolved to have a basilar papilla with at least a few hundred hair cell receptors in a fluid medium. Other amphibians, birds, and mammals have many thousands of hair cells. Other such examples, where structure that is more complex leads to greater hearing capability, are found in some of the other chapters in this volume.

The peripheral part of the auditory system, comprising the external ear, middle ear, and the inner ear, systematically transforms and transduces environmental sounds into neural impulses in the auditory nerve. The precise biophysical mechanisms relating the input variables to the output variables of some of the subsystems are still being debated. However, there is general agreement that these transformations lead to improved functionality. Five of the most important functional considerations are described below.

1. *Sensitivity.* The human ear is most sensitive to a range of sounds from the loudest at about 120 dB SPL to the softest at about −3 dB SPL. At its most sensitive frequency near 4 kHz, the displacement at the tympanic membrane at the threshold of hearing is less than one-tenth of the diameter of a hydrogen atom. At this threshold, the amount of work that is done at the eardrum is 3×10^{-18} J.[1] In comparison, the amount of work done for the perception of light at the retina is 4×10^{-18} J, which is close to the calculated value at the threshold of hearing.[2] This suggests that at its limits, the two sensory modalities have comparable thresholds.
2. *Dynamic range.* The dynamic range of psychophysical hearing in humans is about 120 dB SPL, corresponding to environmental sounds and vocalized sounds. However, the neurons of the auditory nerve have a dynamic range that is typically less than 60 dB SPL. The mechanics of the organ of Corti (OC) must compensate for this dynamic range mismatch problem.
3. *Frequency range.* Hearing in humans covers a frequency range of about 10 octaves, and in some other mammals this range can be as wide as 11.5 octaves (for ferrets). To handle this processing mechanically, the sensory receptors should have physical variations on a similar scale. However, the large range is achieved over an extraordinarily small space in comparison to the wavelengths of sound.
4. *Frequency resolution.* One of the most important functions of the cochlea is its tonotopic organization, which maps different input frequencies to characteristic places within the cochlea. Like a Fourier frequency analyzer, each characteristic place is most sensitive to a narrow band of

frequencies, which by limiting the bandwidth can reduce the input noise for the individual mechanoreceptor hair cells and thus the auditory nerve.

5. *Sound localization.* The physical characteristics of the pinna and head diffract sound in a spatially-dependent manner. The diffraction pattern provides important cues that allow the more central mechanisms to localize, segregate, and stream different sources of sound.

In this chapter, we follow the chain of acoustomechanical transformations of sound from the pinna to the modulation of tension in inner hair cell (IHC) tip links, which is the final mechanical output variable of the cochlea from our vantage point. The tension in the tip links opens ion channels in the stereocilia, which then starts a chain of biochemical events that leads to the firing of the auditory neurons. We term the physiologically-measurable output of each given subsystem a *proximate variable.* A chain of proximate variables can be thought to lead from the outer ear all the way to the tip-link tensions of the hair cells in the cochlea. Input variables, such as SPL, the morphometry of the anatomical structures, and the mechanical properties of those structures, combine with biomechanical processes to produce the values for these proximate variables.

3.10.2 Theories of Sound Transmission in the Ear

Starting with Helmholtz, mathematical models have played a key role in improving our understanding of the underlying biomechanical processes of the auditory periphery. In comparison to using natural languages to describe the observed phenomena, mathematical formulations have advantages and disadvantages. The advantages include providing a methodology by which it is possible to compactly describe correspondences with reality. The disadvantages are that the descriptions may be incomplete or difficult to validate. A mathematical model is also often a statement of a scientific theory that captures the essence of the current body of empirical observations. The power of a specific model is its ability to evolve as more facts become available, and to be able to predict facts not yet observed. Thus the interplay between theory and experiment allows one to test different hypotheses and generate new hypotheses. In this chapter we provide a foundation for physiological measurements in the form of mathematical models. We present below some common principles, applicable to many parts of the auditory periphery, that can help us understand the transformations of the input variables that lead to the ultimate output variable of hair cell tip-link tension. Several general concepts are presented, including how levers are formed, how Newton's laws apply to otobiomechanics, how sound transmission through different materials can be described by transmission line formulations, and how modes of vibration arise in structures of the ear. A combination of these principles is used to understand how the ear improves sensitivity, frequency range, frequency resolution, dynamic range, and sound localization within the constraints of biological materials and anatomic space.

3.10.2.1 Mechanical and Acoustic Levers

One of the simplest transformations of energy is achieved with a simple mechanical lever. There are numerous places in the auditory periphery where levers produce force and velocity transformations through anatomical changes in length and area. These transformations take place in the context of improving sound transmission at the interfaces of different anatomical structures where there is a change in the impedance. An example of a change in impedance is the low impedance of air to the high impedance of the fluid-filled cochlea. Examples of the lever action at work include an increase in sound pressure due to a decrease in area from the concha of the pinna to the ear canal, an increase in pressure due to the decrease in surface area from the tympanic membrane to the stapes footplate, an increase in force due to the lever ratio in the ossicular chain, an increase in velocity from the stapes footplate to the basilar membrane (BM) due to a decrease in surface area, and the transformation of the BM displacement to hair cell stereocillia tip-link tension due to relative shearing motion between the reticular lamina (RL) and tectorial membrane (TM).

3.10.2.2 Newton's Second Law of Motion

A key principle in describing the dynamic transformation of forces to accelerations in mechanical systems is the well-celebrated Newton's second law of motion, written as

$$F = ma, \qquad [1]$$

which states that when a force F acts upon a mass, it results in an acceleration a. Transformed to the frequency domain and extended to include the effects of resistance and stiffness, Newton's second law becomes,

$$F(\omega) = \left[M + \frac{R}{j\omega} + \frac{K}{(j\omega)^2}\right] a(\omega). \quad [2]$$

Here the sinusoidal force $F(w)$, with radian frequency ω, acts upon an object described by the variables in the square brackets. This object has now been generalized to include mass M, resistance R, and stiffness K. An alternative form of eqn [2] in terms of particle velocity $v(\omega)$ is,

$$F(\omega) = \left[j\omega M + R + \frac{K}{j\omega}\right] v(\omega), \quad [3]$$

where the term in the square bracket is the mechanical impedance Z_m. Sound pressure $P(\omega)$, measured with a microphone, is defined as the force per unit area A. Thus, eqn [3] can be rewritten for acoustics as

$$P(\omega) = \left[j\omega M_a + R_a + \frac{K_a}{j\omega}\right] V(\omega). \quad [4]$$

The term in the square bracket is now the acoustic impedance Z_a, which for uniform properties is the mechanical impedance Z_m divided by A^2, and $V(\omega) = v(\omega)A$ is the volume velocity. One thing to keep in mind is that impedance concepts are limited to linear steady-state analyses. Despite this limitation, eqns [3] and [4] play a prominent role in helping us understand the transformations of forces and pressures to velocities and volume velocities throughout the ear. It is clear from these equations that the velocity of any structure is proportional to the applied force, but inversely proportional to the impedance due to its mass (M), damping (R), and stiffness (K). At resonance the velocity reaches a maximum because the impeding effect of the mass is cancelled by the impeding effect of the stiffness. One of the challenges in efficient sound transmission to the hair cell detectors is in minimizing the impeding effects of fluid damping and stiffness and mass of structures.

3.10.2.3 Transmission Lines

Many problems in sound and vibration can be described by the wave equation that results in part from Newton's laws of motion. The one-dimensional (1D) version of the wave equation was formulated by d'Alembert in 1747 for a vibrating string. It did not take Euler very long (1759) to formulate the first derivation of the wave equation for sound transmission in 1D and later in three dimensions (3D). Solutions to the wave equation have stood the test of time, as is evident by their use in areas that include electromagnetic theory, transverse waves in stretched membranes, blood vessels, and electromagnetic transmission lines. Because it was used so extensively in telephone communication and power line transmission problems, the 1D wave equation is also known as the transmission line equation. In these equations the properties of the transmission system are assumed to be constant along the direction of propagation. A special form of the wave equation exists when a property along the propagation direction varies exponentially. As reviewed by Eisner E. (1967), these equations were originally formulated by Lord Rayleigh and are now known as Webster's horn equation.

Subsequent sections will show that the transmission line formulation can be used to describe ear canal acoustics, the coupling between the canal and tympanic membrane, wave propagation in the cochlea, and transverse motion on the BM. The series of transmission lines that are sequentially coupled may improve frequency bandwidth while maintaining sensitivity of the proximate variables.

3.10.2.4 Modes of Vibration

Anatomical structures and membranes have various modes of vibration with peak responses at modal frequencies due to resonance. These modes of vibrations are not very different from modes of vibrations in the strings of violins, guitars, and pianos, where both ends of the strings are fixed. The resonant frequency is directly proportional to the string tension and density, but inversely proportional to its length. More complicated modes of vibration are found in membranes and plates. In the ear, examples where resonances are a characteristic feature include the pinna and ear canal, tympanic membrane, ossicles, BM, OC, and hair cell stereocilia. Despite the presence of structural resonances in many of the proximate variables, the overall sensitivity of hearing varies smoothly with frequency and does not exhibit sudden changes.[3] Understanding this dichotomy has been challenging.

3.10.2.5 The Input and Output Variables

Which input variable at the ear canal entrance is representative of hearing sensitivity? Which output variable characterizes changes in tension of the inner-hair-cell stereocilia? Possible candidates for the input

variable are pressure as measured with a microphone, volume-velocity (acceleration and displacement), power, or transmittance and reflectance. Since these variables are interrelated, it is difficult to truly separate the effects of one variable from another. However, the use of pressure has some advantages.

Dallos P. (1973) showed that there is good agreement between hearing sensitivity measured behaviorally and the eardrum-to-cochlear pressure transfer function, also called the middle-ear pressure gain resulting from ossicular coupling. It appears that the combined properties of the middle ear and its cochlear load are the dominant determinants of the animal's measured behavioral sensitivity. This has been directly measured in cat (Nedzelnitsky, V., 1980), guinea-pig (Dancer, A. and Franke, R., 1979; 1980; Magnan, P. *et al.*, 1997), gerbil (Olson, E. S., 1998), and human (Puria, S. *et al.*, 1997; Aibara, R. *et al.*, 2001; Puria, S., 2003). In agreement with Dallos P. (1973), Puria S. *et al.* (1997) showed that there is good correlation between the human middle-ear-pressure gain and the behavioral threshold. This suggests that an important proximate variable, at least at the base of cochlea, is fluid pressure in the vestibule.[4]

In the OC it is well accepted that tension in the tip links is the ultimate mechanical variable for the mechanoelectric transduction (Corey, D. P. and Hudspeth, A. J., 1983; Howard, J. and Hudspeth, A. J., 1988). This tension opens ion channels and initiates the flow of ions through the stereocilia bundles, resulting in depolarization of the hair cell body, which results in firing of the auditory nerve.

In the sections that follow we generally follow the path taken by sound from the external ear, through the middle ear, into the fluid filled cochlea. We then analyze the mechanisms that cause the BM and the OC to vibrate, which then results in tension modulations of the hair cell stereocilia tip-links.

3.10.3 External Ear

The external ear consists of the highly visible cartilaginous pinna flange, the cavum concha, and the ear canal buried in the skull. It is generally accepted that sound source localization in a free field consists of two processes. The sound source azimuth is determined using interaural time differences or interaural intensity differences, whichever is the dominant, while sound source elevation is based on spectral cues from the pinna.

There is significant variability in both the size and the shape of the external ear amongst mammals, and the resulting pressure transformation from the free field to the tympanic membrane. Examples of anatomical variations include cone-shaped pinnae in cats to almost flat pinnae in ferrets, numerous invaginations and protuberances of the pinna flange and concha, and changes in ear canal cross-sectional area often accompanied by bends in the canal. The ear canal and concha boost the sound field in the middle frequency range. A key role of the pinna is to diffract the sound in a spatially-dependent manner, and thus augment the sound field's spectral cues. The torso also adds to elevation cues, particularly at low elevations and low frequencies, due to a shadowing effect (Algazi, V. R. *et al.*, 2002).

A common measure of the effects of the external ear is the free field pressure P_{ff} to tympanic membrane pressure P_{tm} transfer function, defined as P_{tm}/P_{ff}. When measured as a function of spatial angle, the magnitude of the ratio is often called the head-related transfer function (HRTF) Not surprisingly, the effects of the anatomical structures on the HRTF are likely to be unique for each species, and vary significantly in individuals of a given species.

The transformation of the free-field sound pressure to that measured at the tympanic membrane is determined by diffraction, scattering, and resonances due to the asymmetric structures along the way. The frequency region where different structures become important occurs when the wavelength of sound becomes smaller than the physical dimensions of a feature of the external ear.

3.10.3.1 Concha and Ear-Canal Resonance

Dimensionally, the largest feature of the human ear with some acoustic consequence is the ear canal, which is approximately 25 mm in length, and 7 mm in diameter, with a corresponding quarter-wavelength resonance near 2.5 kHz with an approximate pressure gain of about 10 dB (Békésy, G., 1960; Shaw, E. A. and Teranishi, R., 1968; Shaw, E. A., 1974). Significant developmental changes in the ear canal dimensions and wall properties take place even up to the age of 24 months (Keefe, D. H. *et al.*, 1993).

The next largest feature is the concha, with a typical height of 19 mm, a width of 16 mm, and a depth of about 10 mm. There is significant individual variation in these dimensions with very little correlation between them or with other pinna dimensions (Algazi, V. R. *et al.*, 2001). The depth mode resonance,

in the 4–5 kHz range, results in a pressure gain of about 10 dB. Both the canal and concha-depth resonances are complementary effects and are approximately independent of angle of the free-field sound and produce a pressure gain that starts at about 1.5 kHz reaching a maximum gain of up to 20 dB near 3–4 kHz and then decreasing again. At frequencies above 5 kHz, the width and depth modes of the concha become important and excitation of these modes is dependent on the angle of incident sound (Shaw, E. A. and Teranishi, R., 1968; Teranishi, R. and Shaw, E. A., 1968).

3.10.3.2 Spatial Diffraction by the Pinna

To a first-order approximation, the pinna flange and the surface of the head mechanically behave as rigid bodies to acoustic waves. In humans and in some animals like ferrets the pinna is immobile, while in other animals like mice and cats the pinna is mobile and able to move under muscular control independent of the skull. Many of the mobile pinnae have a horn-like structure, which improves their sound collecting ability. The larger cone may allow an effective interaural time delay that is greater than is possible for the head alone, while the mobility allows for the possibility to modulate the interaural time difference (Shaw, E. A. and Teranishi, R., 1968).

In humans, the pinna is relatively large (64 mm × 29 mm) but it does not seem to be strongly correlated with a resonant mode (Algazi, V. R. *et al.*, 2001). One role for the larger pinna is to increase directivity and thus reduce background noise. There are several unique geometric features of the pinna that contribute to resonant modes at frequencies above 6–7 kHz. These modes are dependent on the angle of the incident sound and are clearly important for determining the HRTFs measured in individual subjects.

The brain continually calibrates and interprets the HRTFs to infer the location of sound, indicating that there is plasticity in the perception of the spectral cues (Hofman, P. M. *et al.*, 1998). This was demonstrated by modifying the pinna of adult human subjects with a prosthesis so as to disrupt the spectral cues, resulting in poor spatial localization in the vertical plane. However, after a relearning period of about 30–45 days the subjects were able to localize accurately again. Furthermore, the subjects did just as well after removal of the prosthesis, suggesting that the new cues did not interfere with the ability to perceive previous cues.

3.10.3.3 Tympanic Membrane and Ear Canal Interface

The delicate tympanic membrane is located deep inside the skull at the end of the ear canal, likely for protection from mechanical damage. At frequencies above approximately 1 kHz the membrane response is very complex, while the cochlea provides a mainly resistive load (Onchi, Y., 1961; Møller, A. R., 1963; Zwislocki, J., 1963; Khanna, S. M. and Tonndorf, J., 1969; Lynch, T. J., 3rd, *et al.*, 1994; Puria, S. and Allen, J. B., 1998). This resistive load is the primary damping factor of the external ear resonances.

3.10.4 Middle Ear

The ear canal is filled with air that is continuous with the free field. In contrast, the cochlea is filled with cerebrospinal and other salty fluids. The mechanical properties of these media are shown in Table 1. What matters for effective wave propagation is the specific impedance, which is the product of the density and wave speed of the medium. Even though the fluid of the cochlea has mechanical properties close to those of saline, the flexibility of the cochlear partition greatly slows the wave speed, which causes a lower specific impedance and an air-to-cochlea specific impedance ratio of about 1/200.[5] Such a large impedance mismatch would normally cause most of the energy entering the ear canal to reflect and not enter the cochlea.

Table 1 Acoustical and mechanical properties of air, saline, and the input window to the cochlea

Medium	*Density* ρ *(kg m^{-3})*	*Speed of sound* c *(m s^{-1})*	*Specific impedance* $z = \rho c$ *(Pa-s m^{-1})*	*Impedance ratio* $\beta = z/z_{cochlea}$
Air	1.29	350	448	1/212 = 0.0047
Saline	1000	1500	1.5×10^6	15.7
Cochlear input	1000	95 (approx)[a]	9.5×10^4	1

[a]Actually the group velocity of the slow wave, discussed below.

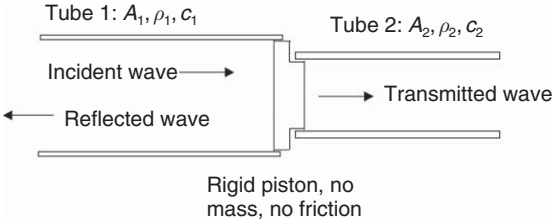

Figure 1 Greatly simplified model for the middle ear consisting of a piston connecting two acoustic tubes. Tube 1 represents the ear canal, containing an incident wave and a wave reflected from the piston. Tube 2 represents the fluid-filled inner ear, containing a transmitted wave.

The above shows that the slower speed of sound in the cochlear fluid reduces the air to fluid specific impedance mismatch by a factor of 15.7 (24 dB). A simple model in Figure 1 illustrates this concept. The model consists of two semi-infinite tubes of cross-sectional areas A_1 and A_2, with the ratio $\alpha = A_1/A_2$, filled with fluids with the densities ρ_1 and ρ_2 and speeds of sound c_1 and c_2. The specific acoustic impedances are $z_1 = \rho_1 c_1$ and $z_2 = \rho_2 c_2$, with the ratio $\beta = z_1/z_2$. The piston has one face in tube 1, and the other face in tube 2.

The hypothetical piston is free from constraint and is massless, so the forces on the two sides of the piston must be equal. An incoming acoustic wave in tube 1 (the ear canal) impinges upon the piston, causing the generation of a transmitted wave in tube 2 (the cochlea), as well as a reverse reflected wave in tube 1. The standard 1D transmission line analysis for acoustic waves yields the ratios of the amplitudes of transmitted and incident pressure (p_2 and $p_{1\text{in}}$ respectively) and energy (E_2 and $E_{1\text{in}}$ respectively),

$$\frac{p_2}{p_{1\text{in}}} = \frac{2\alpha}{1+\alpha\beta}\frac{E_2}{E_{1\text{in}}} = \frac{4\alpha\beta}{(1+\alpha\beta)^2}. \qquad [5]$$

The ratios of the areas of the tympanic membrane and the stapes footplate typical for human and cat give the results in Table 2. For conduction in air, the large ratio greatly improves the energy flowing into the cochlea. Since this is far from 100%, it is not impedance matching, but rather impedance mismatch alleviation. Perfect impedance matching $\alpha\beta = 1$ would provide for humans only a 15 dB improvement in the transmitted pressure, at the considerable cost of a tympanic membrane 10 times larger. It must be noted that larger areas enhance the signal-to-noise ratio at the hair cell level (Nummela, S., 1995).

So the large tympanic membrane is advantageous to humans and cats for hearing in air. It is interesting to consider a change to hearing under water. For this, the air in tube 1 is replaced by water, which yields the results in the bottom section of Table 2. The acoustic pressure transmitted to the cochlea is greatly reduced to a value insensitive to the area ratio. The difference in pressure in air and water of 49 dB is close to the behavioral threshold difference measured in divers (Brandt, J. F. and Hollien, H., 1967; DPA 2005). This supports the simple relation in eqn [5] as a fundamental consideration for the design of the middle ear.

In Table 3 the amplitude of the incident sound wave at threshold is given for hearing in air and water (Fay, R. R., 1988). The pinnipeds (marine mammals including sea lions, walruses, and true seals) spend time in both air and water and have hearing sensitivity worse than humans by a factor of 10 (20 dB) in air and better by a factor of 5 (14 dB) in water. However, the cetaceans (whales and dolphins) have better hearing sensitivity in water than humans by factor of 54 (36 dB) It is interesting that the intensity of the sound at threshold is about the same for humans in air and pinnipeds in water, and for humans in water and pinnipeds in air. Obviously, the middle ear of the pinniped is designed for the water environment. Quite a different middle-ear design provides the extraordinary sensitivity under water of cetaceans (Hemila, S. *et al.*, 1999).

Table 2 Effects of the middle-ear area ratio α and the specific impedance ratio β in transmitting sound pressure and energy into the cochlea, according to the basic model in Figure 1. Replacing the air in the ear canal (tube 1) with saline simulates underwater hearing, which has a great reduction in the transmitted pressure

Tube 1 (EC)	$\beta = z_1/z_2$	$\alpha = A_1/A_2$	p_2/p_1 *(lin)*	p_2/p_1 *(dB)*	E_2/E_1 *(lin)*
Air	0.0047	1	2	6	1.8%
		20 (human)	36	31	25
		40 (cat)	67	36	53
		212	212	46	100
Water	15.7	1	0.12	−18	22
		20 (human)	0.13	−18	1.7
		40 (cat)	0.13	−18	0.6

Table 3 Some approximate thresholds of hearing in air and water

	Air		*Water*	
	Pressure (μPa)	***Intensity ($W m^{-2}$)***	***Pressure (μPa)***	***Intensity ($W m^{-2}$)***
Human	20	8.9×10^{-13}	5400	2.0×10^{-11}
Pinnipeds	200	8.9×10^{-11}	1000	6.7×10^{-13}
Cetaceans	N/A	N/A	100	6.7×10^{-15}

As the simple estimate indicates, without an effective middle ear the sensitivity of the cochlea would be compromised and so would the overall bandwidth, as is evident by pathological conditions of the ear repaired by otologists. As discussed in a subsequent section, another important role of the middle ear is in exerting some degree of dynamic range control at high input levels via the three sets of muscles.

The simple model of Figure 1 is useful to a certain degree, but has significant limitations. In order to build an acoustic lever with an area change from the ear canal to the cochlea requires using biological materials consisting of bone and soft tissues. A rigid piston with a large area requires a large mass, which limits its ability to transduce sound, particularly at the higher frequencies. A membrane is lighter, but has a significant number of resonant modes, particularly at frequencies above 2–3 kHz. In a very thorough study, Nummela S. (1995) showed that malleus and incus masses scale with eardrum area, which further limits high-frequency hearing. These factors must be considered when formulating mathematical models of the middle ear.

More sophisticated models describing sound transmission in the middle ear have been around for some time. Early studies allocated various acoustic influences to the different middle-ear structures interconnected in five to six functional blocks. The blocks were then assigned more detailed elements, which consist of masses, springs, and dashpots. Some of the earliest models by Onchi Y. (1949; 1961), Zwislocki J. (1961), and Møller A. R. (1961) use dynamic analogies and represent the middle ear in the form of electrical circuit models. These phenomenological models have evolved and continue to be useful for understanding surgical interventions of the middle ear (Rosowski, J. J. and Merchant, S. N., 1995; Merchant, S. N. *et al.*, 1997; Rosowski, J. J. *et al.*, 2004). Nevertheless, they have limitations in that there is not a tight relationship between the underlying anatomical structure and function. To overcome these limitations requires models that explicitly incorporate morphometry of the middle ear into their formulation. The first and crucial component is the tympanic membrane, which converts sound pressures in the ear canal into vibrations of the ossicles.

3.10.4.1 Tympanic Membrane Shape and Internal Structure

There remain many unanswered questions regarding the biomechanics of the tympanic membrane. For example, why does the tympanic membrane have a conical shape? Why do the tympanic membrane sublayers have a highly-organized collagen fiber structure? What is the advantage of its angled placement in the ear canal? Why is there symmetrical malleus attachment to the eardrum in some animals while in others there is asymmetry? The functional significance of many of these gross anatomical features of the tympanic membrane is just beginning to be understood and the current status is discussed below.

Helmholtz H. L. F. (1868) discussed the need for impedance matching of the air in the environment and the fluid of the inner ear, and suggested that the tympanic membrane behaved as a piston. This assumption is widely used in lumped parameter (circuit) models of the middle ear, which build upon the free piston model (eqn [5]) by adding springs and the resonances of the malleus–incus complex and of the middle-ear cavity. However, instead of piston-like behavior, surface- displacement measurements on the tympanic membrane have revealed multiple modes of vibration for frequencies above a few kilohertz (Tonndorf, J. and Khanna, S. M., 1972). Since the to-and-fro motion of a resonance mode would reduce the effective area for the sound pressure, the presence of these modes has been difficult to explain. Pioneering work by Rabbitt R. D. and Holmes M. H. (1986) formulated a continuum analytic model with asymptotic approximations for the cat tympanic membrane. They included the membrane geometry and anisotropic ultrastructure in combination with curvilinear membrane equations, but did not analyze the effects of the eardrum angle and the conical shape of the eardrum, and neither have Eiber A. and Freitag H. G. (2002). Current finite-element models

represent the eardrum as an isotropic membrane (Wada, H. *et al.*, 1992; Koike, T. *et al.*, 2002; Gan, R. Z. *et al.*, 2004) and thus do not explain the need for the detailed fiber structure (Lim, D. J., 1995).

Two breakthroughs have increased our understanding of tympanic membrane mechanics. First was the observation that there is significant acoustic delay in eardrum transduction (Olson, E. S., 1998; Puria, S. and Allen, J. B., 1998). Second, the multiple modes of vibration seen on the surface of the eardrum are not transmitted to the cochlea. Rather, the pressure inside the cochlea as a function of frequency remains relatively smooth, even when measured at a high frequency resolution (Magnan, P. *et al.*, 1997; Puria, S. *et al.*, 1997; Olson, E. S., 1998; Aibara, R. *et al.*, 2001; Puria, S., 2003). Clearly these observations are tied to the complicated motions of the eardrum observed by Khanna S. M. and Tonndorf J. (1972), but need further explanation.

3.10.4.2 Tympanic Membrane Biomechanics

To understand the functional consequences of the tympanic membrane structure on its sound transducing capabilities, a biocomputational model has been formulated which leads to some insights on the posed questions (Fay, J. P., 2001; Fay, J. P. *et al.*, 2006). The model incorporates measurements of the geometry of the ear canal (Stinson, M. R. and Khanna, S. M., 1994), the 3D cone shape of the eardrum (Decraemer, W. F. *et al.*, 1991a), and details of the eardrum fiber structure (Lim, D. J., 1995).

The discrete model for the human eardrum is shown in Figure 2, in which a series of adjacent wedges approximate the eardrum. Near the center, the eardrum is attached to the malleus, while the outer edge is attached to the bony annulus (not shown). The 1D acoustic horn equation is used for a small cross-section of the ear canal. The change in area from the adjacent cross-section, the curvature of the centerline, and the flexibility of the portion of the eardrum that intersects with that section of the ear canal are all taken into account. Each strip of the eardrum is curved near the outer edge (locally a toroidal surface) and is straight in the central portion (locally conical) Because the main conical portion contains few circumferential fibers, the approximation is that the radial strips are weakly coupled in the circumferential direction.

The tympanic membrane is represented as a four-layer composite (Figure 2). The input parameters for the formulation are the thickness of each layer as a function of position and the Young's modulus of elasticity (a measure of resistance to deformation) for each layer. The outer-most epidermal layer and the inner-most submucosal layers are relatively flexible. Because the subepidermal and submucosal layers consists of connective tissue and are also relatively flexible, they are included within the epidermal and mucosal layers respectively (Figure 2). The inner two layers contain collagen fibers that are radially-oriented in one layer and circumferentially-oriented in the layer directly below. These two layers, unique to mammals, provide the majority of the scaffolding for the eardrum, and thus those layers mostly determine the stiffness compliance of the membrane. In contrast, the mass comes from the overall thickness of the membrane. Quantitative measurements for cat were used for the overall thickness (Kuypers, L. C. *et al.*, 2005). From these measurements and from sparse measurements of collagen sublayers, the thickness of each sublayer was estimated for human (Figure 2) and cat (Fay, J. P., *et al.*, 2005; 2006).

Direct measurements of the static elasticity of portions of the eardrum (Békésy, G., 1960; Decraemer, W. F. *et al.*, 1980) indicate an effective

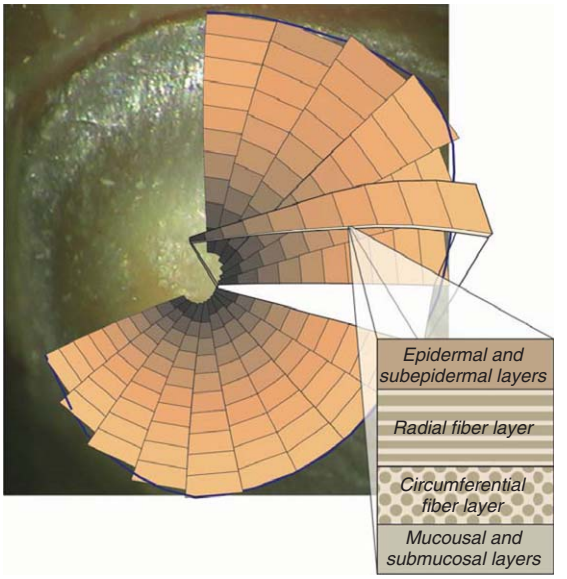

Figure 2 Human eardrum photograph with its biomechanical model representation composed of adjacent wedges. The zoomed box shows the four layer composite of each wedge. The inner radial and circumferential collagen fiber layers, unique to mammals, provide the scaffolding for the tympanic membrane. Dimension and material property differences of the wedges lead to mistuned resonances at high frequencies. The thickness of the eardrum layers increases from the umbo to the tympanic annulus.

modulus of elasticity of around 0.03 GPa. This was re-examined using three very different methods to determine the eardrum modulus of elasticity (Fay, J. P., *et al.*, 2005). First, constitutive models incorporating the Young's modulus of collagen and experimentally-observed fiber densities in cat and human were used. Second, experimental tension and bending measurements (Békésy, G., 1960; Decraemer, W. F. *et al.*, 1980) were reinterpreted using composite laminate theory. And third, dynamic measurements of the cat eardrum surface displacement patterns were combined with a composite shell model. All three methods lead to a similar modulus of elasticity value of 0.1–0.4 GPa for near the center of the eardrum. The corresponding values near the outer edge are approximately half of these values due to the linear taper in the elastic modulus. In previous models the eardrum was treated as a single layer having a uniform elastic modulus, resulting in a low value of elastic modulus (Funnell, W. R. *et al.*, 1987; Prendergast, P. J. *et al.*, 1999; Koike, T. *et al.*, 2002; Gan, R. Z. *et al.*, 2004). In the four-layer model, the collagen fiber sublayers are much thinner than the overall thickness, and hence the estimated elastic modulus is higher.

The modulus of elasticity was combined with the sublayer thickness to formulate a complete model of the cat tympanic membrane. The calculation for the dynamic response of each strip was performed with an algorithm for elastic shells (Steele, C. R. and Shad, K. R., 1995), which places no restriction on wavelength along the strip.

The full 1D interaction of the air in the ear canal and the eardrum is included. Behind the eardrum are the middle-ear cavities and the middle-ear bones connected to the cochlea, for which lumped-element approximations were used. Verification involved mesh refinement studies, comparisons with exact solutions for limiting cases, anatomical values of geometry, best estimate for elasticity, and comparisons with physiological measurements upto 20 kHz, all for the cat middle ear.

Different depths of the eardrum play an important role, as shown in Figure 3. With a shallow eardrum (no cone shape) there is a loss of more than 25 dB for frequencies above about 4 kHz (Figure 3(b), top panel). A deep eardrum shows a response similar to that seen in anatomic specimens, with little loss for low frequencies. Above 4 kHz, the phase for the normal and deep eardrum continues to decrease while for the shallow drum the phase tends to go in the opposite direction and increases. This suggests that there is more phase delay for the deep and normal shape than for shallow eardrums. In comparison to the normal eardrum, the deep drum requires more real estate in the skull, which competes for space with other organs.

The effects of the two collagen-fiber sublayers were also analyzed. This was done by examining the effects of isotropic eardrums that had the same stiffness in the radial and circumferential directions and orthotropic eardrums where there were radial fibers but no circumferential fibers (Fay, J. P., 2001; Fay, J. P. *et al.*, 2006). Results indicate that there is an advantage of the orthotropic microstructure with a dominance of radial fibers in the central region. In the normal drum when both are present, the radial fibers on the inner portion of the tympanic membrane result in an effectively orthotropic membrane while the outer circumferential fibers provide a low-impedance beam-like support. The orthotropic central portion allows maximal sound transmission at both low and high frequencies.

The model calculations indicate that sound transmission from the ear canal to the cochlea varies smoothly despite the fact that there are a significant number of resonances at different points on the eardrum. This suggests a design where drum sections are deliberately mistuned. Because these resonant points are added together at the malleus, no single mode ever dominates. Thus the ensemble of eardrum modes produces a relatively large and yet fairly smooth response at the malleus at the higher frequencies.

Understanding eardrum biomechanics is of critical importance to the development and improvement of myringoplasty, which is a surgical procedure for repairing damaged eardrums. The underlying disease process is often chronic inflammatory disease of the middle ear and mastoid, referred to as chronic otitis media (COM), which leads to a partial or total loss of the tympanic membrane or ossicles. Clinically, isotropic materials like temporalis fascia are used for myringoplasties. To improve hearing results at the higher frequencies, orthotropic material with collagen scaffolding preferentially oriented in the radial direction would be a better choice for improved high-frequency hearing outcomes. Improving postoperative high-frequency results may be important for the perception of sound localization cues present at high frequencies. Currently the standard practice is to measure clinically to 6 kHz. The above results suggest that clinical measurements at frequencies above 6 kHz might better show the effects of different materials.

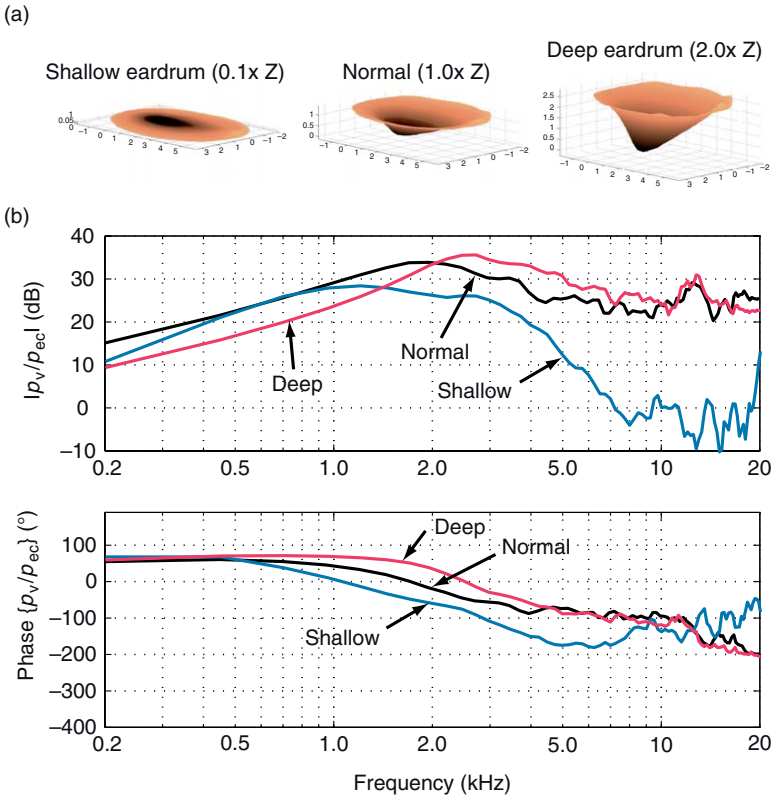

Figure 3 Effects of modifying the eardrum depth. (a) In the center is the anatomically normal eardrum. The *z*-coordinate of all the points is divided by a factor of 10 to obtain the shallow eardrum on the left, and multiplied by a factor of 2 to obtain the steep eardrum on the right. (b) Effects of eardrum depth on the middle-ear pressure transfer function, which is the ratio in decibels of the pressure delivered to the vestibule inside the cochlea (p_v) divided by the input pressure in the ear canal (p_{ec}). The deep eardrum calculation is nearly the same as the normal, but the shallow eardrum has more than a 20 dB loss at higher frequencies. For the normal and deep eardrums, the phase slope is steeper than it is for the shallow drum, indicating more acoustic delay. Reproduced from Fay, J. P., Puria, S., and Steele, C. R. 2006. The discordant eardrum. Proc. Natl. Acad. Sci. U. S. A. 103, 19743–19748, with permission.

Since the modulus of elasticity and the biocomputational approach using asymptotic methods has already been developed for the cat, the challenge will be to estimate eardrum morphometry for other species such as human (Figure 2 shows an approximate guess). Of particular interest is determining how the shape and thickness of the tympanic membrane varies from subject to subject. Such quantification will allow for the possibility of using the eardrum biocomputational model on individual subjects. Nondestructive high-resolution imaging methods are needed to obtain morphometry on individual subjects. A promising new imaging technology is described in the next section.

3.10.4.3 Middle-Ear Imaging

To obtain morphometry of the ear, histological methods have been the primary technique. However, this age-old technique is destructive and certainly not appropriate for *in vivo* imaging of individual subjects. One of the most recent advances for obtaining anatomical information is micro computed tomography (μCT) This has been used to obtain volume reconstructions of the temporal bone of living subjects at a resolution of less than 125 µm (Dalchow, C. V. *et al.*, 2006). *In vitro* resolution can be increased by an order of magnitude (Decraemer, W. F. *et al.*, 2003).

Figure 4 shows an image slice from an intact human cadaver temporal bone ear. The image resolution in the *x*, *y*, and *z* planes is 15 µm (isovolume) Most of the middle-ear structures, including the tympanic membrane cone shape and thickness, ossicles, and suspensory soft tissue, can be visualized because there is good density contrast between these structures and air in the ear canal and middle-ear cavity. Because they provide the best resolution,

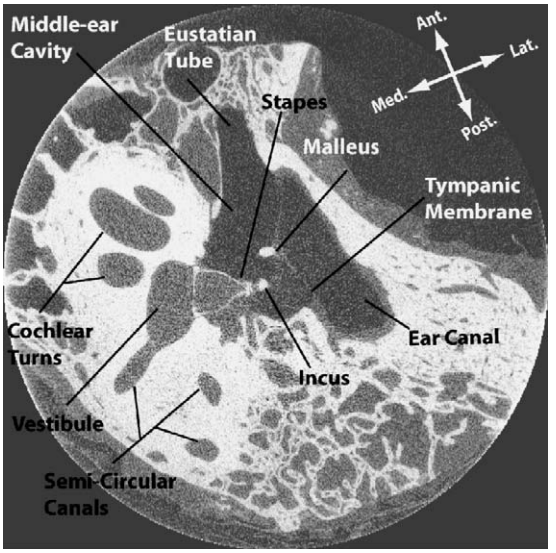

Figure 4 Micro computed tomography (μCT) image of an intact cadaver temporal bone. This is image #769, of 1897 images spanning a length of 28.455 mm. The image illustrates that most of the middle-ear structures can be visualized from an intact temporal bone ear scan. The resolution for both in-plane and out-of-plane (slice thickness) is 15 μm. The tympanic membrane although visible is faint, suggesting that the basic geometry and an approximate thickness can be obtained. The 30.72 mm scan diameter outline is clearly seen.

histological methods remain the standard. However, μCT imaging offers some distinct advantages (Decraemer, W. F. *et al.*, 2003; Puria, S. *et al.*, 2007; Sim, J. H. *et al.*, 2007; Sim and Puria, 2008). These include, (1) elimination of stretching distortions commonly found in histological preparations, (2) use of a nondestructive method, (3) shorter preparation time (hours rather than 12–16 months), and (4) results already in a digital format. This imaging technology is rapidly evolving and it is likely that similar resolutions will be possible for *in vivo* imaging in the near future.

3.10.4.4 Malleus–Incus Complex

The middle ear of most nonmammalian terrestrial animals consists of the tympanic membrane and a columella, while mammals have a tympanic membrane and a malleus–incus complex. Among vertebrates, a great majority of mammals are sensitive to ultrasonic sounds (above 20 kHz), while nonmammals are not.[6] This suggests that the mammalian hearing organ has evolved to be a superior organ for high-frequency hearing compared to those of non-mammals, and that the incorporation of the malleus–incus complex may have something to do with this capability (Fleischer, G., 1978; 1982). However, the biomechanics of this subsystem of the middle ear are not well understood.

Since the time of Helmholtz H. L. F. (1868) the handle of the malleus and the long process of the incus were described as the two arms of a lever with a fixed axis. Ossicle suspension also further supported the notion that the malleus and the incus rotate about a fixed axis while driving the stapes in a piston-like manner. However, detailed measurements of the ossicles have changed this view (Decraemer, W. F. *et al.*, 1991b; Decraemer, W. and Khanna, S., 1995). The malleus motion changes with frequency and all 3D components of translation and rotation are present at biologically relevant stimulation levels. These measurements suggest that a full 3D model of ossicle motion is required.

Between the malleus and incus is a saddle-shaped joint formed from an indentation in the head of the malleus, into which the surface of the body of the incus fits (Figure 5). The incus also has a depression into which a part of the malleus head fits, forming a cog-like mechanism as described by Helmholtz H. L. F. (1868). The significance of such a mechanism is thought to be a locking of the joint causing one part to move with the other during rotation in one direction, but leaving the parts free to rotate in the orthogonal direction (Wever, E. G. and Lawrence, M., 1954). However, measurements (e.g., Helmholtz, H. L. F., 1868; Békésy, G., 1960) have suggested that the incus and malleus are fused together, indicating that there is no slippage at the incudo-malleolar joint (IMJ). Making measurements in the cat ear, Guinan J. J., Jr. and Peake W. T. (1967) showed clear evidence

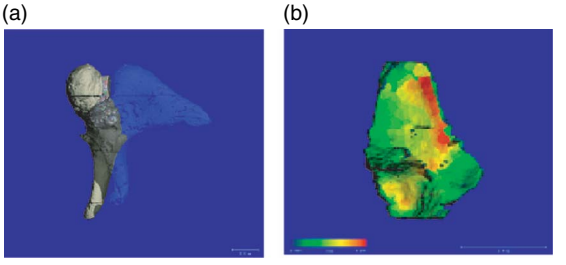

Figure 5 Volume reconstruction of the malleus and incus from μCT slices. (a) The incus is made transparent to allow better visualization of the incudomalleolar joint. (b) The incudomalleolar joint saddle shape and thickness map (0 is dark green while about 300 μm is red).

of slippage at the IMJ above about 8 kHz. Using time-averaged holography measurements Gundersen T. and Høgmoen K. (1976) concluded that the malleus and incus rotate like one stiff body for frequencies below about 2 kHz. Due to these measurements, mathematical models of the human middle ear generally treat the two ossicles as fused, and not allowing slippage (Goode, R. L. *et al.*, 1994; Koike, T. *et al.*, 2002). More recent measurements suggest slippage within the IMJ, and the apparent lack of slippage in previous measurements may have been due to methodological reasons such as the lack of a cochlear load and insensitive measurement techniques (Willi, U. B. *et al.*, 2002). In some animals, like guinea-pig and chinchilla, the IMJ is fused and thus there is no slippage (Puria, S. *et al.*, 2007). In contrast, there is no controversy regarding slippage at the joint between the incus and the stapes, and most mathematical models currently include it (e.g., Goode, R. L. *et al.*, 1994).

Natural mode shape calculations indicate that the ossicles can be treated as rigid bodies only for frequencies below about 3.5 kHz (e.g., Beer, H. J. *et al.*, 1999). Consequently, the ossicles have been modeled as finite elements, which require much more computation time. An alternative approach is to model the ossicles as elastic bodies incorporating just the first two or three modes in each body (Sim, J. H. *et al.*, 2003).

Not unlike the biological ligaments found in other parts of the body, the suspensory ligaments and tendons of the middle ear are a composite, consisting of collagen and elastin embedded in an amorphous intercellular material often called ground substance or matrix which is composed of proteoglycans, plasma constituents, metabolites, water, and ions. Almost two-thirds of the weight of ligaments is due to water, while about three-quarters of the remaining weight can be attributed to the fibrillar protein collagen (reviewed by Weiss, J. and Gardiner, J., 2001). Like the eardrum, the primary component resisting tensile stress in ligaments and tendons is collagen. The primary role of the ground substance is in maintenance of the collagen scaffolding. As such, the biomechanical behavior of a ligament is determined by its geometry, shape of the articulating joint surfaces, orientation and type of insertions to bone, *in situ* pretension, and material properties. What role do the suspensory ligaments play in the complicated 3D vibrations of the middle-ear bones? This question has yet to be addressed with any degree of satisfaction.

In the cat study discussed above, a simple ball and stick model for the malleus–incus complex was used (Fay, J. P. *et al.*, 2006). This was a gross simplification, but allowed concentration on the tympanic membrane biomechanics. A goal of several laboratories is to combine anatomical data with human cadaver temporal bone malleus–incus complex 3D motions into a computational model for individual ears, which should increase understanding of the functional consequences of the anatomy of the ossicles and suspensory ligaments and tendons.

The biomechanical characterization of the malleus–incus complex requires morphological and dynamical measurements from individual ears. The centers of mass, moments of inertia, and anatomical locations and orientations of the ligaments and tensor-tympani tendon are obtained from 3D volume reconstructions (Figure 6) based on μCT images of the isolated preparation.

The morphometry is used to construct a computational biomechanical model for the malleus–incus complex that includes ligament and tendon attachments to the bony walls and muscles, and slippage at the IMJ. Bending of the malleus and incus handles is also allowed. The viscoelastic parameters of each ligament, tensor tympani tendon, and the IMJ cannot be determined from the morphometry and thus 3D motion measurements are required.

As discussed in previous sections, the biomechanics of the tympanic membrane can be fairly complicated. This implies that the input to the malleus–incus complex is also relatively complicated, and thus it is difficult to deduce the dynamics of ossicles and soft tissue attachments with the sound-driven eardrum. To better understand ossicle dynamics an isolated malleus–incus complex preparation was developed where the tympanic membrane and the stapes were dissected. Without an eardrum or a cochlea, the middle-ear bones have to be driven directly. A tiny magnet and a coil around the tympanic annulus were used to drive the malleus–incus complex (Sim, J. H. *et al.*, 2003). The magnet on the tip of the malleus is oriented to drive it in the forward direction. The preparation is placed on a set of goniometers and malleus–incus motion measurements are made at several points at several different angles. The resulting three-dimensional x, y, and z vector components of velocity at each point are used within the biomechanical model to obtain the soft tissue viscoelastic parameters. The 3D volume reconstructions of the magnet and coil, combined with electromagnetic theory, allows

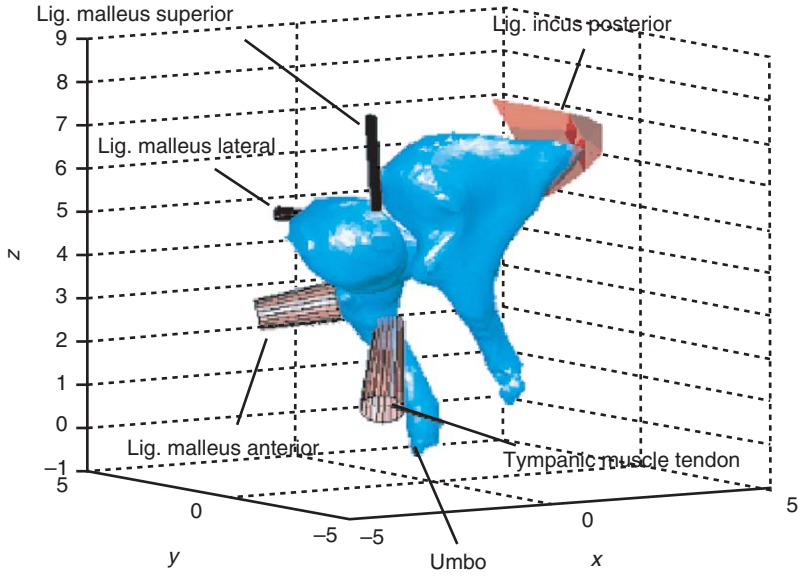

Figure 6 Three-dimensional volume reconstruction of the malleus (left bone), incus (right bone), suspensory ligaments, and the tensor tympani tendon. The soft tissue is represented as tapered cylinders or as a polyhedron. The origin is at the umbo. All dimensions are in millimeters.

accurate calculation of the 3D forces and moments exerted by the magnet onto the malleus. The combined imaging, physiology, and biomechanics approaches should help us better understand the structure and function relationships at audio frequencies in normal and pathological ears.

The above discussion concerns the dynamics of the malleus–incus complex. At high positive and negative static pressures such as during sneezing and coughing, the suspensory ligaments may also play a critical role (Huttenbrink, K. B., 1989). Incorporation of this mode of operation requires extension of the linear models to nonlinear models.

3.10.4.5 Lenticular Process

The inferior end of the long process of the incus terminates in a short perpendicular bend called the lenticular process, consisting of the pedicle and the lenticular plate surrounded by soft tissue. Between the lenticular plate and the stapes head is the incudostapedial joint. Motion from the incus is transmitted to the stapes via this process and thus its mechanical description is of significance.

Most previous modeling work has treated the lenticular process to be a rigid bone that transmits the incus motion directly to the stapes head, or with some slippage due to the incudo-stapedial joint (Beer, H. J. *et al.*, 1999; Koike, T. *et al.*, 2002). Recent anatomical measurements suggest that the platelike bony pedicle is perpendicular to the lenticular plate and is extremely thin and fragile. In cat the dimensions of the pedicle are 240 μm × 160 μm × 55 μm (Funnell, W. R. *et al.*, 2005). Model calculations of static displacements suggest that there is significant relative motion between the incus long process and stapes head (Funnell, W. R. *et al.*, 2005). Funnell W. R. and colleagues have hypothesized that one role for the thin pedicle and lenticular plate arrangement may be to convert the rotational modes of vibration of the incus into translational motion of the stapes. More work is needed to further test this hypothesis.

It has been observed that at high static pressures there is a large lateral displacement of the lenticular process, and that this serves to protect the cochlea from large motions (Huttenbrink, K. B., 1988). Clearly, bending of the pedicle may be involved in such cases.

3.10.4.6 Stapes

The interface between the malleus–incus complex and the vestibule of the fluid-filled cochlea is the stapes, which is held in place in the oval window (Fenestra vestibule) by the annular ligament. The mechanics of the stapes is quite independent of the

malleus–incus complex and of the cochlear fluid load. For this reason the stapes can be considered a semi-independent subsystem of the mammalian ear (Fleischer, G., 1978). This treatment of the stapes is widely accepted (Wada, H. and Kobayashi, T., 1990; Wada, H. *et al.*, 1992; Goode, R. L. *et al.*, 1994; Puria, S. and Allen, J. B., 1998; Beer, H. J. *et al.*, 1999; Koike, T. *et al.*, 2002).

3.10.4.7 Ossicular Reconstruction

While we are discussing the ossicles this is good place to discuss ossiculoplasty, which is the reconstruction of the middle-ear bones to improve hearing sensitivity. Two of the most common pathologies are a missing (or eroded) incus and an ossified stapes. Both result in significant hearing losses. Since the introduction of these surgical procedures more than 50 years ago, ossiculoplasty continues to pose significant challenges to otologists.

The interposition of passive prostheses between the malleus or tympanic membrane and the stapes head or footplate is used to reconstruct the transfer function of the middle ear in the missing or eroded incus condition. These are the incus replacement prostheses. Two types, used depending on the circumstances, are the partial ossicular reconstruction prosthesis (PORP), which is attached to the stapes head, and the total ossicular reconstruction prosthesis (TORP), which is attached to the stapes footplate. The PORP is typically used if there is an intact stapes superstructure. However, ear canal pressure to cochlear pressure transfer function and clinical measurements suggest that even if the stapes superstructure is present, there are acoustico-mechanical advantages to placing the foot of the prosthesis directly onto the footplate (Murugasu, E. *et al.*, 2005; Puria, S. *et al.*, 2005).

In a very different disease process called otosclerosis, the stapes becomes fixed to the surrounding oval window through ossification. The immobile stapes prevents sounds from entering the cochlea and results in significant hearing loss. The precise cause of otosclerosis is not well understood. However, it is becoming well established that otosclerosis is hereditary. Otolaryngologists repair the condition by a procedure called stapedotomy. A hole is made in the footplate, often with a surgical laser (Perkins, R. C., 1980), and then covered with soft tissue to prevent the inner-ear perilymph fluid from leaking out. Sound transmission is then restored with a piston-like prosthesis. One end of the prosthesis is crimped to the long process of the mobile incus, while the other end is inserted into the covered artificial hole in the footplate.

3.10.4.8 Middle-Ear Muscles

The malleus and stapes each have a tendon attached to a tiny muscle, the tensor tympani muscle and the stapedius muscle, respectively. The muscles contract when exposed to high-level sounds, and are part of the middle-ear reflex arc involving the spiral ganglion neurons, the auditory nerve, cochlear nucleus, the superior olive, the facial nerve nucleus, the facial nerve, and the two middle-ear muscles (Margolis, R. H., 1993). This reflex arc can reduce sound transmission through the middle ear at high levels, and may serve to control the dynamic range of the auditory system and to protect the cochlea at high sound levels. The reflex is slow, and thus does not provide protection to the cochlea against sudden impulsive sounds. The time for the stapedius reflex may be on the order of about 20 ms, while the tensor tympani arc is more than ten times slower (Teig, E., 1972).

Two additional functions are attributed to the middle-ear muscle reflex. Low-frequency sounds, particularly when they are high in level, normally tend to mask mid- and high-frequency sounds due to their upward excitation patterns on the BM. One role of the middle-ear muscles is to reduce the level of low-frequency inputs so they do not mask the higher frequency sounds on the BM (Pang, X. D. and Guinan, J. J., Jr., 1997). A second role of the middle-ear reflex is in the reduction of the audibility of self-generated sounds during speech, mastication, yawning, and sneezing (Simmons, F. B. and Beatty, D. L., 1962; Margolis, R. H. and Popelka, G. R., 1975). Because the reflex arc involves so many mechanisms, its measurement is used clinically to diagnose central and peripheral pathologies.

Recently it has been discovered that there are smooth muscle arrays within the peripheral edge of the tympanic membrane, the annulus fibrosus, in all four of the mammalian (bats, rodents, insectivores, and humans) species studied (Henson, O. W., Jr. and Henson, M. M., 2000; Henson, M. M. *et al.*, 2005). The role of this rim of contractile muscle cells in the par tensa region is not clear, but two suggested possibilities are to maintain tension of the tympanic membrane and to control blood flow to the membrane (Henson, M. M. *et al.*, 2005). Measurements indicate that these smooth muscles

can exert control over the input to the cochlea as measured by cochlear microphonics (Yang, X. and Henson, O. W., Jr., 2002).

3.10.4.9 Middle-Ear Cavity

One role of the middle-ear cavity is to act as a baffle for the tympanic membrane so that incident sound does not impinge on both sides of the eardrum. Without this, the sensitivity of the membrane, and thus hearing sensitivity, would be significantly reduced.[7] However, the presence of the cavity results in an increase in overall impedance, due to volume compliance at low frequencies and resonant modes at high frequencies. An increase in middle-ear impedance results in a decrease in hearing sensitivity (Wiener, F. M. *et al.*, 1966).

In humans the middle-ear cavity is relatively large, but is irregular in shape. The mastoid cavity portion has many air cells, or air pockets, that result in an increase in surface area. Each cell is lined by a mucous membrane of thin epithelial cells. It is thought that the irregular shape minimizes resonant modes, and that the air cells effectively dampen remaining resonances (Fleisher, G., 1978).

3.10.4.10 Middle-Ear Acoustic Load

The primary load to the middle ear is the acoustic input impedance of the cochlea Z_c. As defined by Zwislocki J. J. (1975), Z_c is the ratio of sound pressure in the scala vestibuli (SV) at the stapes footplate to the volume velocity of the footplate. Based on simplifications to the equations of motion at the base of the cochlea, Zwislocki J. J. (1948; 1965; 1975) predicted that the cochlear input impedance is primarily resistive. Direct measurements in the cat (Lynch, T. J., 3rd, *et al.*, 1982), guinea-pig (Dancer, A. and Franke, R., 1980), and human cadaver ears (Aibara, R. *et al.*, 2001) suggest that the prediction by Zwislocki was essentially correct for a broad range of frequencies.

Zwislocki's calculation had not included effects from the apical region of the cochlea. Calculations of the cochlear input impedance, using models that include the apical region and treat the cochlea as a box with constant scalae area, show that below approximately 1–2 kHz, the cochlear input impedance magnitude decreases and becomes more mass-like. This calculated result diverges from the measured data and from Zwislocki's prediction (Puria, S. and Allen, J. B., 1991; Shera, C. A. and Zweig, G., 1991). The decrease in the acoustic impedance and mass-like response is shown to be due to the use of a constant cross-sectional area for the scala vestibule and scala tympani (ST) in all standard box models. Using a more realistic scalae area that decreases from the base to the apex of the cochlea avoids the diverging catastrophe in the model calculations of cochlear input impedance at low frequencies.

The resistive nature of the cochlear input impedance, which is the primary damping component of sound transmission in the middle ear, has two consequences. Foremost is that a large fraction of the acoustic energy that enters the cochlea is absorbed by it rather than being reflected by it. Second, is that it smoothes out the peaks and valleys resulting from any resonances in the middle-ear structures.

3.10.5 Cochlear Hydrodynamics

In the preceding section, methods of imaging, physiology, and computational biomechanics were presented in the context of understanding the relationships between the various acousto-mechanical transformations performed by the middle ear. The end result is that the proximate output variable of the middle ear, which is the vestibule pressure at the base of cochlea, smoothly varies with frequency, and typically with pressure gain, for a wide bandwidth relevant to the species. In the following sections we analyze how sound energy at the base of the cochlea propagates within the cochlea. Much effort has been devoted to this topic, on which many survey papers have been written, as represented by Allen J. B. and Neely S. T. (1992), Nobili R. *et al.* (1998), and de Boer E. (1991; 2006), which provide a summary of current thought. Other chapters in this book address different aspects of cochlear function. Our focus is on what appear to be the key acousto-mechanical transformations that have a basis in the physiology.

3.10.5.1 Vestibular Fluid Pressure

A simple description of what happens to the pressure transmitted into the cochlea by the middle ear is shown in Figure 7 for a given frequency. This represents a standard tapered box model of the cochlea with two symmetric fluid ducts divided by a partition. The stapes provides the input pressure. The wall of the cochlea is bone, which is normally assumed to be rigid, so for air-conducted sound the stapes and round window have equal and opposite volume displacements, preserving the volume of

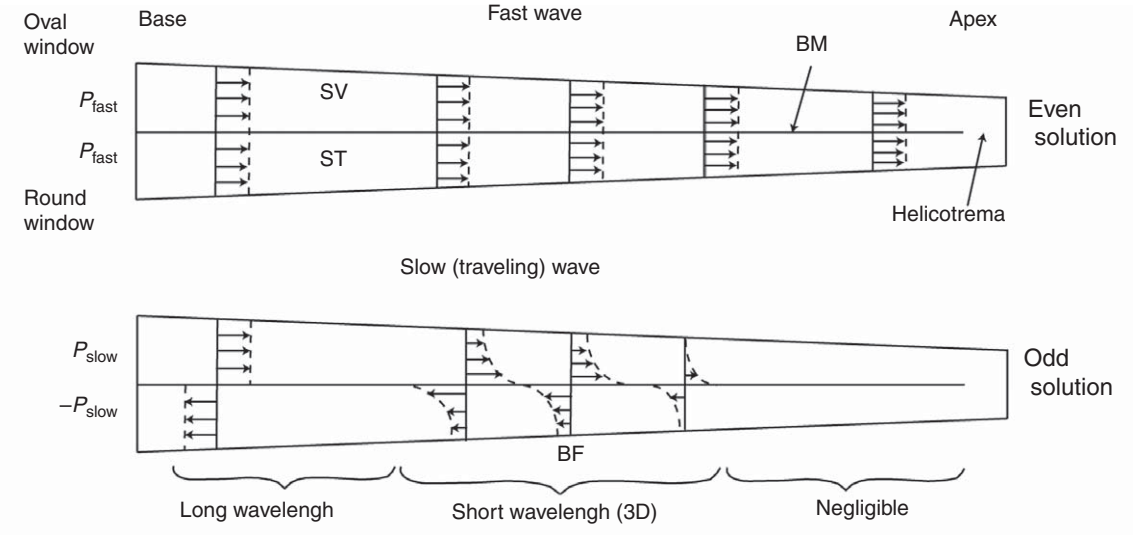

Figure 7 Simple tapered box model for the pressure in the cochlea. The fluid regions scala vestibuli (SV) and scala tympani (ST) with tapered areas are divided by the partition containing the elastic basilar membrane (BM). At the apex the partition has an opening, the helicotrema. The input sound pressure acts at the oval window (stapes) The response for a single frequency is divided into an even (symmetric) solution with equal pressure in SV and ST, and an odd (asymmetric) solution with the pressures in SV and ST of opposite sign. The symmetric solution causes a compression of the fluid, so the wave travels with the speed of sound in saline, which is the fast wave in the upper drawing. In contrast, the asymmetric solution has a net pressure on the partition, which causes a displacement of the BM that slows the wave considerably. This is the slow wave in the lower drawing. Because of the taper of the BM, the stiffness changes and the slow wave has a wavelength that is long near the input but becomes short near the region of maximum amplitude. The driving frequency is the best frequency (BF) for this place. In the region of short wavelength, the fluid motion is three-dimensional (3D), with a pressure that is maximum on the BM and decays exponentially with both the distance from the BM and the distance toward the apex. The round window is compliant, so the total fluid pressure at that location is nearly zero. Thus at the input end, the pressures from the slow and fast waves must cancel in the ST, and so are equal in magnitude.

fluid in the cochlea. However, a very compliant membrane covers the round window, so the fluid pressure at this point is nearly zero. Therefore the total pressure is divided into an even and an odd solution (Peterson, L. C. and Bogert, B. P., 1950), as indicated in Figure 7. The even distribution must cause a compression of the fluid. This corresponds to a wave that travels with the speed of sound in the fluid, which is relatively fast. The odd solution produces net pressure acting on the partition that causes an elastic deformation of the flexible portion of the partition, the BM. This interacts with the fluid motion, causing a wave that is relatively slow. This slow wave is the traveling wave first observed in the guinea-pig by Békésy G. (1952). Because the BM is narrow at the stapes and wide at the apex, there is a gradient in stiffness of the partition, which causes the traveling wave to have a long wavelength near the stapes, then build up to a maximum as the wavelength becomes short. In the very short wavelength region, the viscosity of the fluid causes this wave to die out exponentially. The traveling wave is so slow, relative to the fast wave, that the fast wave can often be approximated as instantaneous, that is, for incompressible fluid.

For simplicity, we consider the properties of the partition to be continuous. The actual tissue consists of discrete elements. As shown by Békésy G. (1960, p. 510) by models with coupled, discrete elements, behavior similar to that of a continuous system can be obtained. This holds, of course, for wavelengths of the response that are long in comparison with the spacing between elements. Many authors use discrete systems directly for advantage in computation and/or construction.

The description in Figure 7 of the spatial pressure distribution for a fixed frequency also holds for the waves seen at a fixed point as frequency varies. For frequencies less than the best frequency (BF), the slow wave has a long wavelength, and for frequencies greater than the BF, the slow wave decays to a negligible magnitude, leaving only the fast wave.

The first direct evidence for this behavior is provided by the measurement of pressure in the gerbil (Olson, E. S., 1998) at a distance 1.2 mm from the stapes. Some of the experimental values are shown in Figure 8,

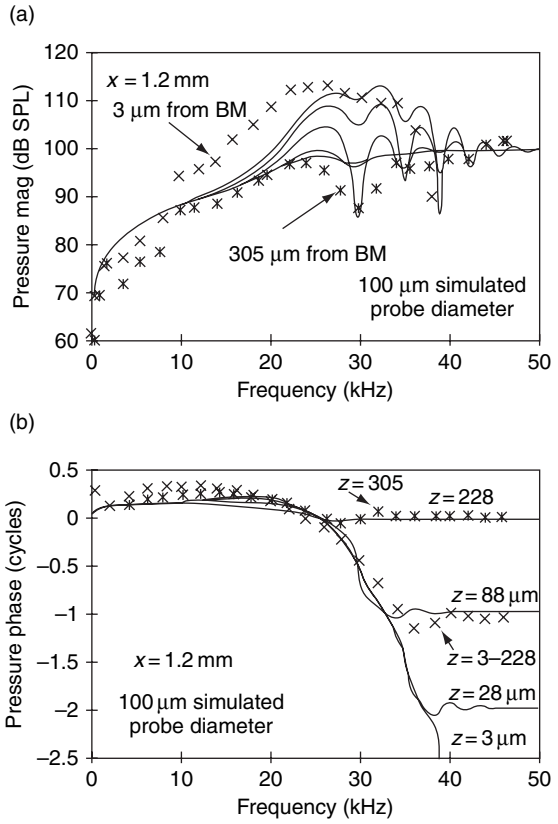

Figure 8 (a) Pressure magnitudes in the scala tympani (ST) region of the gerbil cochlea at a distance of 1.2 mm from the stapes, based on measurements (Olson, E. S., 1998) and calculations (Baker, G. J., 2000). For frequencies higher than best frequency (BF; >40 kHz), the slow wave is negligible and only the fast wave remains (Figure 7). For low frequencies, the fast and slow waves nearly cancel in the ST. Near BF (25 kHz), the fast wave dominates, with three-dimensional (3D) fluid motion that has much higher pressure near the basilar membrane (BM). The 'x' symbols represent measurement points at a distance of 3 μm from the BM, while the '*' symbols represent measurement points at a distance of 305 μm from the BM. Calculated values for some of the intermediate distances between 3 and 305 μm are shown as continuous curves. (b) Pressure phase relative to the simultaneously measured scala vestibule pressure at the base of the cochlea. For frequencies above the BF (>40 kHz), only the fast wave remains. The plateaus differ by one cycle, which shows that the fast wave is uniform with distance from the BM and exactly in phase with the eardrum pressure. For low frequencies, the phases at the different distances from the BM are also the same, corresponding to the fast wave and the long wavelength region of the slow wave. For frequencies approaching the BF (25 kHz), the slow wave dominates and shows the rapid decrease in phase signifying the traveling wave.

along with calculated values from a 3D cochlear model to be discussed later. Near the BF the pressure is strongly dependent on the distance from the BM, with much larger values near the BM (Figure 8(a)). This shows the 3D behavior of the fluid in the short-wavelength region. For low frequencies, the pressures at the different distances from the BM converge, showing the long wavelength region. The phase response shows the near cancellation of the waves for low frequencies (Figure 8(b)). For higher frequencies the slow wave dominates, and the rapid accumulation in phase is characteristic of a traveling wave. For even higher frequencies, the traveling wave disappears, so all that is left is the fast wave with constant phase, which at different distances from the BM differ by one cycle, so these are in fact the same. The phase measurements show that far from the BM (305 μm) the traveling wave quickly disappears, while the points closer (3–228 μm) all have the same phase. In contrast, the calculation shows differences at these points. This may be due to the large pressure probe interfering with the fluid motion, which is only simulated in the calculation by taking the average of the pressure at nine points in the 100 μm diameter of the probe. This is for 80 dB SPL input eardrum pressure. The measured pressure shows a constant value for high frequencies equal to 100 dB SPL. This corresponds to the 80 dB input to the eardrum, with a 26 dB gain through the middle ear, and a 6 dB drop because the fast wave has half the amplitude of the vestibular pressure at the stapes.

3.10.5.2 Partition Resonance

At one time or another almost every component of the cochlea has been suggested as a key tuned resonator that will cause a significant local response for a given frequency (the BF in Figure 7). The BM is the thin compliant portion of the partition that divides the two fluid ducts in Figure 7. The component for which the tuning can be best related to the physical dimensions is the pectinate zone (PZ) of the BM. Mathematical treatments of the BM include both bending stiffness and tension in addition to their interaction with the surrounding fluid. From the mathematical formulation, the frequency range and the place to frequency map of the cochlea can be predicted given the anatomical dimensions and material properties.

3.10.5.2.1 Plate

A cross-section of the BM is sketched in Figure 9. For many mammals, the BM PZ consists of a sandwich of collagen fibers in the radial (y) direction embedded in amorphous ground substance. For the same amount of material thickness, the sandwich provides increased bending stiffness. For simplicity, the details of the sandwich are omitted, and only the motion in the cross-section (y–z plane) is considered. For such a plate, the equation of motion in response to an applied pressure is,

$$D\frac{\partial^4 w}{\partial y^4} - T\frac{\partial^2 w}{\partial y^2} + \rho_P t_P \frac{\partial^2 w}{\partial t^2} = -2p_F, \qquad [6]$$

in which w is the displacement of the plate, T is the tension, ρ_P is the plate density, t_P is the plate thickness, p_F is the pressure in the fluid above the plate, which is doubled in eqn [6] for fluid above and below the plate, and the bending stiffness is $D = f\,Et_P^3/12$, where E is the Young's modulus of the fibers and f is the volume fraction of the fibers. For hinged edges at $y = 0$ and b, the solution is,

$$w = We^{j\omega t}\sin ny \quad n = \pi/b, \qquad [7]$$

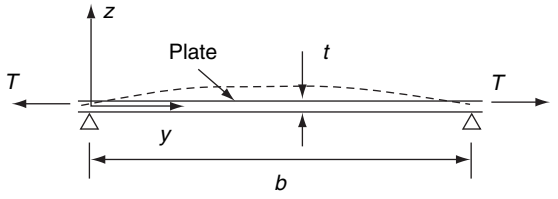

Figure 9 Cross section consisting of an elastic plate in vacuum with tension T. The plate thickness is t and the width between the support points is b. The resonant frequency is proportional to $(T/(tb^2))^{1/2}$. The dashed line shows the deformed position of the plate.

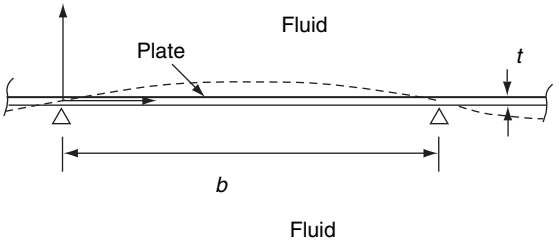

Figure 10 Cross section consisting of an elastic plate in infinite fluid. When the density of plate and fluid are the same, the plate density is negligible, and the resonant frequency is proportional to $(ft^3/b^5)^{1/2}$ where f is the volume fraction of basilar membrane fibers.

in which W is the amplitude and ω is the angular frequency. For static loading and for zero tension, the results for the volume stiffness and point load stiffness are,

$$K_{Vol} = \frac{2p_F}{b\bar{w}} = \frac{\pi}{8}Dn^5, \text{ and} \qquad k_{PtL} = \frac{P}{W} = \frac{48Dd}{b^3}, \qquad [8]$$

where $\bar{w}$ is the average displacement, and P is the magnitude of a load on a probe at the center with diameter d. With all terms retained, eqn [6] yields the impedance as the ratio of the pressure above and below the plate ($2p_F$) and the velocity (v), with $v = \bar{w}$

$$\frac{2p_F}{v} = -\frac{Dn^4 + Tn^2 - t_P\rho_P\omega^2}{j\omega}. \qquad [9]$$

3.10.5.2.2 Fluid

The BM is mainly covered with soft cells that are in contact with extracellular fluid. For the effect of the mass on the pressure distribution, there is little difference between fluid, soft cells, or a gel. As demonstrated by Békésy G. (1960, p. 445) in an experimental model, there is no change in localization when the fluid is replaced by gel. Consequently, for modeling, the soft cells are often replaced by fluid. Both have similar acoustical properties. The motion of an inviscid, incompressible fluid (or gel) is governed by the well-known Laplace's equation,

$$\frac{\partial^2\varphi}{\partial^2 y} + \frac{\partial^2\varphi}{\partial^2 z} = 0, \qquad [10]$$

in which φ is the displacement potential. The z-displacement and pressure are,

$$w = \frac{\partial\varphi}{\partial z}, \text{ and} \qquad p_F = -\rho_F\frac{\partial^2\varphi}{\partial t^2}. \qquad [11]$$

The solution giving the compatible displacement with the plate (eqn [7]) is,

$$\varphi = -\frac{W}{n}e^{j\omega t - nz}\sin ny, \qquad [12]$$

which gives the ratio of pressure to velocity,

$$\frac{p_F}{v} = -\frac{\rho_F\omega}{in} = j\rho_F\omega t_{effective}, \text{ and} \quad t_{effective} = \frac{1}{n} = \frac{b}{\pi}. \qquad [13]$$

Thus the inviscid, incompressible fluid has only the effect of a mass attached to the plate, with an effective thickness $t_{effective}$, over about a third of the plate width b. Soft cells or a gel, representing the OC, also satisfy the same equation, so eqn [13] holds for the fluid consisting of a thin or thick layer of soft cells and fluid. The difference between the fluid with and

without cells attached to the plate lies in the viscous correction, not the effective mass.

3.10.5.2.3 Plate and fluid

Equating the impedance of the plate (eqn [9]) to the impedance of the fluid (eqn [13]) gives the resonant frequency,

$$\omega^2 = \frac{Dn^4 + Tn^2}{\rho_P t_P + 2\rho_F / n}. \qquad [14]$$

Helmholtz H. L. F. (1868) proposed that the transverse fibers of the BM behaved as strings under tension in air, as in a harp. This corresponds to setting the bending stiffness D and the fluid inertia ρ_F to zero in eqn [14]. A sketch of this is in Figure 9 and the result for the first resonant frequency is,

$$\text{frequency}_{\text{Tension}} = \frac{1}{2}\left(\frac{T}{\rho_P t b^2}\right)^{1/2}. \qquad [15]$$

However, there is not much evidence for high tension in the BM and the density of the surrounding fluid is nearly the same as the BM. Consequently, the plate density term ρ_P in eqn [14] is negligible. Setting the tension T and the plate density to zero in eqn [14] gives the resonant frequency,

$$\text{frequency}_{\text{Bending}} = \frac{1}{2\pi}\left(\frac{Dn^5}{2\rho_F}\right)^{1/2} = \frac{1}{2\pi}\left(\frac{E\pi^5}{24\rho_F}\right)^{1/2}\left(\frac{ft^3}{b^5}\right)^{1/2}. \qquad [16]$$

With the BM dimensions and density of fibers (Cabezudo, L. M., 1978), eqn [16] provides a reasonable frequency range for several mammals (Steele, C. R. and Taber, L. A., 1983). The formula also works for recent measurements of the gerbil (Emadi, G. *et al.*, 2004). The wider frequency bandwidth capability for the bending case (eqn [16]) compared to the tension case (eqn [15]) is shown in Table 4. With a nominal Young's modulus of elasticity (E) for collagen, the frequencies computed from eqn [16] are close to the range for the guinea-pig. In contrast, a variation of tension by 10^4 would be required for the tension model to work, which is not justified by the modest change in the dimensions of the BM support. Shown in Table 4 is the width g of the spiral ligament. The tension is assumed to be proportional to g, and the tension frequency is set equal to the bending frequency at the apex for comparison. The conclusion is that it is bending stiffness that determines the frequency localization on the BM (Figure 10).

Table 4 Frequency range capability of the basilar membrane pectinate zone (for guinea-pig) for bending stiffness and tension stiffness

	Base	*Apex*	*Ratio*
Elastic modulus (E)	1 GPa	1 GPa	1
BM fiber vol fract (f)	0.08	0.01	8
BM width (b)	80 μm	180 μm	0.44
BM thickness (t)	7 μm	1 μm	7
Spiral ligament width (g)	200 μm	40 μm	5
Frequency tension	247 Hz	130 Hz	1.9
Frequency bending	52 000 Hz	130 Hz	400

3.10.5.3 Vestibular Fluid Pressure to Basilar Membrane Displacement

The equations for the slow wave (Figure 7), in the model with symmetric SV and ST without Reissner's membrane (e.g., Peterson, L. C. and Bogert, B. P., 1950; Zwislocki, J. J., 1953) can be written as,

$$\frac{\partial}{\partial x}(A\bar{p}) = -\rho_F \frac{\partial^2}{\partial t^2} Q, \text{ and} \qquad [17]$$

$$\frac{\partial}{\partial x} Q = -\Delta A = -\frac{1}{K_{Vol}} 2p_{BM}. \qquad [18]$$

The distance along the BM from the stapes is x, the average pressure in the SV is $\bar{p}$, the pressure acting on the BM is p_{BM}, the volume displacement of fluid in the SV is Q, the area of SV is $A(x)$, and the area displacement of the partition is $\Delta A = b\bar{w}$. Equation [17] follows directly Newton's second law of motion (eqn [1]) while eqn [18] is a statement about conservation of mass in a segment of scala. The equations above are valid for 1D, 2D, and 3D descriptions of the fluid flow by incorporating the dimensionality into the pressure p_{BM} acting on the BM.

3.10.5.3.1 One-dimensional approximation

For long wavelengths, the pressure is nearly constant on the cross section, so the approximation is $p_{BM} = \bar{p}$, and the system is a standard transmission line wave equation. For a single frequency, with all variables changing with $e^{j\omega t}$, this reduces to,

$$\frac{d^2}{dx^2}(A\bar{p}) + m^2(x,\omega)(A\bar{p}) = 0, \qquad [19]$$

where the coefficient m^2 is,

$$m^2(x,\omega) = \frac{2\rho\omega^2}{AK_{Vol}(x)}, \qquad [20]$$

which can be identified as the local wave number. The wavelength is proportional to the reciprocal of the wave number. For the cochlea, K_{Vol} decreases with distance from the stapes, so m increases with distance, meaning that the wavelength becomes short. Because of the simple interpretation, the 1D approximation continues to be the most widely used for cochlear modeling. Zwislocki J. J. (1953) and then later Dallos P. (1973) provide the history of the development. To improve the results, damping and mass are added to the stiffness, as in eqn [2]. However, these values have no physical basis, so this must be considered as a phenomenological model. Another approach is to ignore the physical basis completely and determine the complex wave number $m(x,\omega)$ from measurements of BM displacement phase and amplitude, and the neural response, so that eqn [19] will produce the measured response. This is often used in studies of the function of higher neural centers, for which a simple but reasonable input from the cochlea, described by eqn [19], is desired. Flanagan J. L. and Bird C. M. (1962) developed this approach using Békésy's postmortem measurements of the guinea-pig cochlear response. Of interest is their use of the Hilbert transform to show that the measurements are consistent for a causal and stable system. Zweig G. (1991) further developed the approach for the *in vivo* measurements of Rhode W. S. (1971) in squirrel monkey and obtained self-consistent effective BM impedance. Although the physical behavior is 3D, the traveling wave can indeed be described by an equation in the form of eqn [19]. So the choice is to fit the wave number from the measurements of the response or compute it from the actual stiffness and mass properties of the BM with the 3D fluid motion. Since measurements are difficult and restricted, there is interest in improving and verifying the capability for the direct calculation. de Boer E. (2006) provides a recent perspective on the issues.

3.10.5.3.2 Two-dimensional approximation

To place the cochlear model on a physical basis, more details of the fluid motion must be considered (Ranke, O., 1950; Berkley, D. A. and Lesser, M. B., 1973; Neely, S. T., 1981). When the wavelength is short for large m, the 1D approximation is not valid because the pressure on the BM is much larger than the average pressure, as indicated in the measurements (Figure 8). The 2D approximation (from Laplace's equation in the x–z plane) is,

$$\frac{p_{\mathrm{BM}}}{\bar{p}} = \frac{mH}{\mathrm{Tanh}(mH)} : \begin{cases} 1 & \text{for } mH < 1 \text{ long wavelength} \\ mH & \text{for } mH > 1 \text{ short wavelength} \end{cases}, \quad [21]$$

in which H is the height of the SV. With this, eqn [19] is the same, but the wave number is,

$$m^2 = \frac{2\rho\omega^2}{AK_{\mathrm{Vol}}(x)} \frac{mH}{\tanh(mH)}. \quad [22]$$

For the SV with a square cross-section (such that $A = H^2$) this can be rewritten as,

$$mH\tanh(mH) = \frac{2\rho\omega^2}{K_{\mathrm{Vol}}(x)}, \quad [23]$$

which has the approximation,

$$mH : \begin{cases} \left(\dfrac{2\rho_{\mathrm{F}}\omega^2}{K_{\mathrm{Vol}}(x)}\right)^{1/2} & \text{for } mH < 1 \text{ long wavelength} \\ \dfrac{2\rho_{\mathrm{F}}\omega^2}{K_{\mathrm{Vol}}(x)} & \text{for } mH > 1 \text{ short wavelength} \end{cases}. \quad [24]$$

Thus in the long wavelength region, the wave number is proportional to the frequency, which is the characteristic of nondispersive waves. For the short wavelength region, the wave number is quadratic with the frequency, which indicates dispersion. At the point of partition resonance defined by eqn [16], this has the value,

$$mH \approx \frac{8}{\pi} \quad \text{(partition resonance)}. \quad [25]$$

A dimensionless form of eqn [23] is,

$$\tilde{m} = \frac{8}{\pi} \frac{\bar{\omega}^2}{\tanh\bar{m}}, \quad [26]$$

in which,

$$\tilde{m} = mH, \quad \bar{\omega} = \omega/\omega_{\mathrm{ref}}, \quad \omega_{\mathrm{ref}} = \left(\frac{8}{\pi}\frac{K_{\mathrm{vol}}}{2\rho_{\mathrm{F}}}\right)^{1/2}, \quad \text{and} \quad \tilde{x} = xH.$$

The behavior indicated in the sketch of the slow wave in Figure 7 comes from eqn [23]. Near the stapes, where x is small, the stiffness is large, so the wave number is small, that is, the wavelength is long. As x increases, the wave number increases. The short wavelength region begins when $mH = 1$, after which the wave number increases more rapidly. A little past the beginning of the short wavelength region mH reaches the value shown in eqn [25]. So when the fluid–elastic behavior is considered, eqn [16] is seen

to be a transition point at which the wavelength becomes very short, rather than any local resonance similar to the strings of a harp. When the wavelength becomes rather short, the damping due to the fluid viscosity increases exponentially. It is therefore only a rough approximation to the actual BF. When the fluid viscosity increases, the BF shifts to the base, and when the cross-sectional area A of the scalae decreases, the BF shifts to the apex, with a less rapid decay of the amplitude (Lim, K. M., 2000).

3.10.5.3.3 Three-dimensional model and viscosity

The extension to the 3D analysis of the fluid, including the effects of viscosity, is straightforward but tedious. The pressure at the BM of the 3D fluid is included by making p_{BM} in eqn [21] a function of not just scalae height H, but also the scalae width W. Since the first development (Steele, C. R. and Taber, L. A., 1979), several authors have used various approaches. Advances include the proof that eqn [19] is valid for 3D without any assumption on the form of the solution; only the dispersion relation of eqn [23] is modified (Baker, G. J., 2000; Lim, K. M., 2000; Lim, K. M. and Steele, C. R., 2002). The viscosity of the fluid adds imaginary components to eqn [23], so the wave number m becomes complex. Incorporation of the 3D fluid becomes critical for capturing both the magnitude and phase behavior of the BM response with physical parameters. Several authors (de Boer, E. and Nuttall, A. L., 1999; Kolston, P. J., 2000) offer an alternate inverse approach, in which the 3D equations for the fluid are used to compute the impedance properties of the BM. The results show clearly that there is no significant mass attached to the BM and that near BF the damping becomes negative for low sound pressure, *in vivo*.

3.10.5.3.4 Validation with physical modeling

A comparison of the 1D, 2D, and 3D calculations is shown in Figure 11. For this calculation only the physical properties of fluid and partition measured by Helle R. (1974) are used. The gain in accuracy with 3D is well worth the slight extra effort of calculating the wave number m from the 3D generalization of eqn [23]. For the 1D model to have the correct BF, either the stiffness or mass must be modified from the physical value by a substantial amount.

In recent times, several laboratories have used micromachining to obtain life-sized box models of

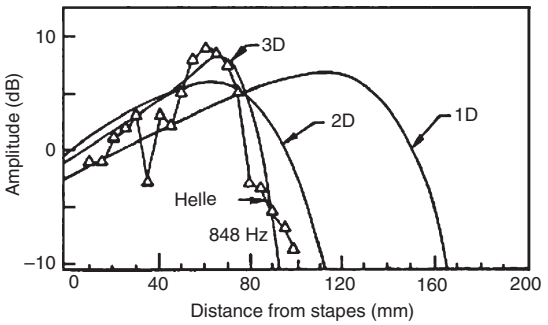

Figure 11 Motion of the basilar membrane (BM) relative to the input for a tone frequency of 848 Hz in an experimental model (Helle, R., 1974). This is a box model of the cochlea, six times human size, with an isotropic polymeric BM. The measured points are shown by Δ symbols. The computations from one-, two-, and three-dimensional approximations (labeled 1D, 2D, and 3D respectively) show that the three-dimensional approximation captures the behavior best (Steele, C. R. and Taber, L. A., 1979). Helle measured all properties, so there are no free parameters.

the cochlea. Traveling waves are found in models with fluid of the viscosity of saline for (1) fluid on one side and the partition stiffness dominated by tension (White, R. D. and Grosh, K., 2005) and (2) fluid on both sides and the stiffness dominated by bending, with 9000 ribs to simulate the orthotropic construction in the real cochlea (Wittbrodt, M. J. *et al.*, 2006). In the latter work, each of four different membrane thicknesses yields reasonable agreement between the calculation from the physical properties and the frequency localization from the 3D WKB calculation discussed in the next section. So finally there is solid evidence that the 3D fluid motion in the cochlea is captured properly by the transmission line eqn [19] with the 3D determination of wave number.

3.10.5.4 Solution Methods

With the advances in computing power, a direct finite difference computation for the full 3D cochlea is appealing. The problem is in the dimensions. With the typical cochlear length 30 times the width, and the BM only one-tenth of the width, and the fluid viscous boundary layer one-tenth of the width of the BM, a fixed mesh requires millions of degrees of freedom. Therefore, even full use of parallel processing (Givelberg, E. and Bunn, J., 2003) requires many hours of computing time, for limited results with a linear model in which the cochlea was coiled and the fluid was viscous. Kiefer J. *et al.* (2006) offer the model

closest to the actual geometry of the human cochlea with the full 3D coiling. However, they use inviscid fluid, which greatly reduces the computing challenge. In comparison, the 1D model eqn [19] can be solved by a variety of numerical methods. Most efficient is an asymptotic method often referred to as WKB. For this, the solution of eqn [19] is written as,

$$A\bar{p} \approx P(x,\omega)e^{j(\omega t-\phi(x,\omega))}, \qquad [27]$$

in which $P(x,\omega)$ is the amplitude function, and the exponential term provides the traveling wave, with the phase given by,

$$\phi(x,\omega) = \int_0^x m(x,\omega)\,\mathrm{d}x. \qquad [28]$$

The viscosity of the fluid contributes a negative imaginary part of the wave number m, which causes the exponential decrease in amplitude of the traveling wave in the short wavelength region. This approach was first used by Ranke O. (1950) on a 2D model for the cochlea. The viscous boundary layer of fluid adds an additional term to eqn [26],

$$\tilde{m} = \frac{8}{\pi}\frac{\tilde{\omega}^2}{\tanh\tilde{m} - \left(1 + j\tilde{\omega}\gamma/\tilde{m}^2\right)^{-1/2}}, \qquad [29]$$

in which the viscosity parameter is,

$$\gamma = \omega_{\mathrm{ref}} H^2 \rho_{\mathrm{F}}/\mu.$$

The viscosity of the fluid is μ. Generally, the term γ is large, so the expansion for the wave number is,

$$\tilde{m} \approx \frac{8\tilde{\omega}^2}{\pi}\left(1 + (1-j)\frac{8\tilde{\omega}^{3/2}}{\pi(2\gamma)^{1/2}} + \cdots\right), \qquad [30]$$

which shows that the fluid viscosity adds to the effective mass with the positive real part of the correction term, and provides the damping with the negative imaginary part. The damping is small for $\tilde{\omega} < 1$ but becomes significant for $\tilde{\omega} > 1$, causing the rapid high-frequency decay in amplitude.

A comparison of the 3D calculations and measurements in the chinchilla is shown in Figure 12. The BM displacement is divided by the stapes displacement, so a linear system would have this response independent of input amplitude. This is not the case for frequencies near the maximum. However, for amplitudes greater than 80 dB SPL, the responses converge, indicating a linear passive behavior, described well by eqn [19] with the 3D extension of eqn [22]. Particularly note the phase in Figure 12(b), which corresponds to eqn [24], linear in frequency for low frequencies and quadratic in frequency for frequencies approaching the BF and higher. This clearly shows the transition of wavelength from long to short near BF. The phase has some dependence on amplitude near BF, but is remarkably insensitive considering the huge change in the amplitude of the input sound.

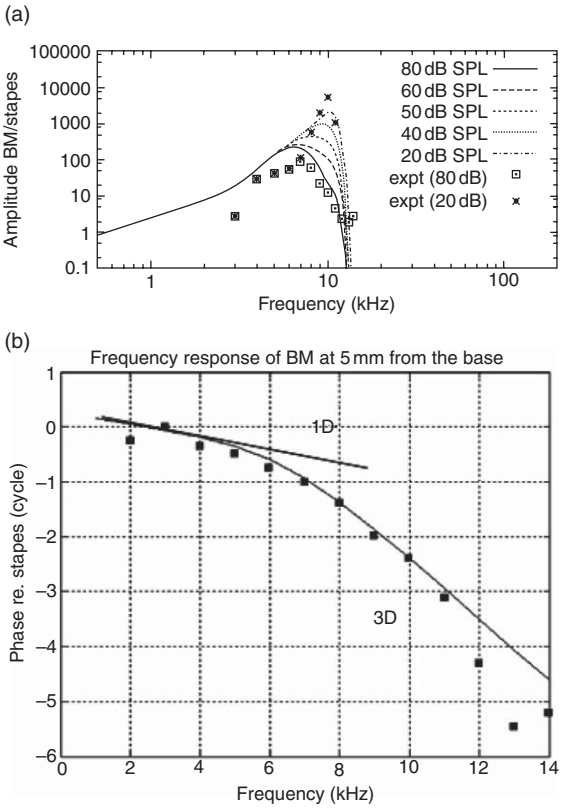

Figure 12 (a) Amplitude of basilar membrane (BM) displacement measured in chinchilla (Ruggero, M. A. *et al.*, 1997) and computed with a three-dimensional (3D) model with saturating feed forward (Lim, K. M. and Steele, C. R., 2002). The amplitude is normalized by the stapes displacement. Experimental points are shown for 20 and 80 dB sound pressure levels (SPL). The active process increases the relative amplitude for low input sound levels. (b) Phase relative to the stapes velocity of BM displacement measured (Ruggero, M. A. *et al.*, 1997) and computed (Lim, K. M. and Steele, C. R., 2002), corrected by Y. J. Yoon. The phase is generally insensitive to amplitude. For low frequencies, the phase is nearly linear with frequency (long wavelength one dimension) Approaching the BF for the given measurement location 5 mm from the base of the cochlea (10 kHz), the phase becomes quadratic, reflecting the dispersive 3D behavior.

A third region that appears in the BM measurements but not in the neural response is the plateau in amplitude and phase just beginning at 13 kHz in Figure 12(a). This has yet to receive an explanation,

but some consider this as evidence for the existence of additional waves. There may well be more than just the fast and slow waves shown in Figure 7.

The form of eqn [27] is also convenient for transients, since the energy for the wave of a given frequency arrives from the stapes at the point x in the time given by,

$$t_{\text{arr}}(x,\omega) = \frac{\partial}{\partial\omega}\phi(x,\omega) = \frac{\partial}{\partial\omega}\int_0^x m(x,\omega)\,\mathrm{d}x. \qquad [31]$$

This approximation can be used to estimate the neural delay (Anderson, D. J. *et al.*, 1971). Thus from Figure 12(b) the low frequencies have a constant low slope of phase, indicating a fast arrival independent of frequency. For higher frequencies, the slope increases in magnitude, indicating an increasingly longer time of arrival at this point and a dispersion of the signal. Note that the slopes depend on the location along the cochlea. We note that the passive cochlea is a causal and stable system. Equation [31] is the group delay of the transfer function relating the response at a point to the input at the stapes.

An important attribute of the auditory system is high-frequency resolution of auditory neurons (Kiang, N. Y. S. *et al.*, 1965). The source of the high resolution, measured as the bandwidth of the response from the peak, is in the BM response (Narayan, S. S. *et al.*, 1998). The sharp frequency discrimination resolution helps reject noise outside the bandwidth of interest for a specific neuron. Thus the sharp resolution is important for increasing the signal-to-noise ratio, particularly at low levels. It is well accepted that the bandwidth of the BM increases as the level increases (Rhode, W. S., 1971, see Figure 12) and this is now believed to be due to nonlinearity in the OC mechanics. Many consider this to be due to the active process that is significant at low levels. For high levels the BM response is linear and described well by the mechanics of the passive box model.

3.10.6 Organ of Corti – Fluid Pressure to Neural Excitation

The inner ear provides the neural excitation for acoustomechanical stimuli. Key to this are receptor cells (hair cells), which transduce mechanical force on cilia (hairs) on one end of the cell into increased firing of neurons via synapses near the other end. The hearing organs provide the sensation for the higher frequencies needed for sound localization and speech reception. Man has an upper frequency for hearing of 20 kHz, while the upper frequency for some bats and toothed whales extends over 150 kHz. As discussed in the previous section, the box model of the cochlea, consisting only of fluid and the BM, results in the localization of the BM displacement and fluid pressure to a certain region for a certain frequency. In the cochlea, the OC is attached to the BM and contains the receptor cells. This is the additional system needed to transform the BM displacements into forces delivered to the cilia. In addition, the OC provides an active input of energy into the traveling wave for low sound levels, which greatly increases the sensitivity and frequency resolution of the BM displacement and neural excitation.

In nonmammalian vertebrates, receptor cells achieve much of their frequency selectivity through the operation of electrical resonance. The ion channels in the basolateral membrane of each cell constitute a miniature electrical circuit that tunes the cell to a specific frequency of mechanical input. However, the mammalian OHC has the unique property of high-frequency electromotility, defined as a change in the cell length in response to a change in the electric potential difference across the cell membrane (Brownell, W. E. *et al.*, 1985). The potential difference across the cell membrane is the result of intracellular voltage depolarization due to ion flow in the stereocilia. Ion channels in the stereocilia are mechanically opened when there is displacement of the bundle in the excitatory direction. The mechanical opening of the ion channels in the inner ear is significantly faster than the cascade of chemical signals required for example in the retina. Therefore, while the sensory receptor hair cells are all mechanoreceptive in the three types of organs in the inner ear, the means for accomplishing their excitation for hearing are much more elaborate. Consequently, the cochlea remains more mysterious than the vestibular system on many levels. As a small example, the most striking geometric feature of coiling of the mammalian cochlea has yet to be adequately explained. Packaging is certainly a consideration. However, West C. D. (1985) finds correlation between hearing and coiling in land animals, while Cai H. *et al.* (2005) compute the low-frequency mechanical effects of coiling and in current work find remarkable correlation of coiling and hearing in sea mammals.

3.10.6.1 Multiscale Organ of Corti Model

The modeling of the OC with the inclusion of more complete anatomical details has received increasing attention in recent years. Kolston P. J. (1999) developed

the first detailed model, in which the components of the OC are simplified to a rectangular grid and the fluid viscosity neglected. He obtained the traveling waves in a significant length of the cochlea. The calculation is by the finite element method (FEM), which is now the prevalent method for structures and for fluid-structure interactions. Cai H. *et al.* (2004) and Andoh M. and Wada H. (2004) use this to consider more realistic geometry for the cross section, but use an approximation for the effect of the longitudinal motion, which is significant for higher frequencies. Another approach is to calculate the stiffness properties of the components of the OC first, and then incorporate the fluid motion in the various compartments of the OC. The components are shown in Figure 13 (Steele, C. R. and Puria, S., 2005).

It is safe to say that the complete solution for the transformation of the BM motion to hair cell excitation for the entire cochlea with a reasonable representation for the OC for all frequencies of excitation has yet to be attained. In the sections that follow, an approach to understanding the complex transduction that takes place in the OC is presented. The model is based on known anatomy and known material properties, with assumptions about how the outer hair cell (OHC) forces may be involved in active amplification using a "feedforward" mechanism. The Amplification and Feedback in Invertebrates chapter summarizes other methods of active amplication that have been proposed.

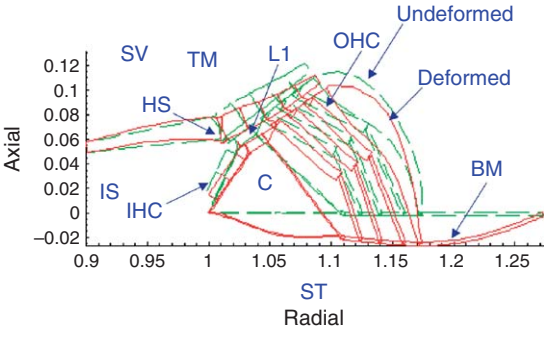

Figure 13 Shell model for guinea pig apex (*y*–*z* plane). The dashed lines show the undeformed configuration, while the solid lines show the deformed configuration due to static pressure loading toward ST, greatly amplified. The radial and axial distances are in mm. The labels are: SV scala vestibule, ST scala tympani, IS inner sulcus, C Cortilymph, TM tectorial membrane, IP inner pillar, OP outer pillar, BM basilar membrane, IHC inner hair cells, OHC outer hair cells, HS Hensen's stripe, and L1 sub-tectorial membrane fluid region.

3.10.6.2 Outer Hair Cell Motility and the Push–Pull Motion of the Basiliar Membrane

Many features of the geometry of the OC have been made clear from detailed measurements in the guinea pig and by a large physical model (Voldrich, L. and Ulehlova, L., 1987). The inclination of the OHC in the radial cross section is evident in Figures 13 and 14. The inclination in the longitudinal direction is shown in Figure 14. The synaptic end of the OHC is supported by Deiters' cell. Each cell has an intracellular axial column consisting of microtubules, referred to as Deiter's rod in Figure 14. One end of the rod cups the end of the OHC and the other end is attached to the BM. The Deiter's rod provides the dominant axial stiffness of the cell. The cup of Deiter's rod at the synaptic end of the OHC also has an attachment to the reticular lamina (RL) with a phalangeal process, shown in Figure 14. The process also consists of microtubules. Thus the triangular arrangement of OHC, RL, and Deiter's process provides a frame of significant elastic stiffness. The OHC is motile (see Chapter Amplification and Feedback in Invertebrates), so a shear of the cilia in the direction to cause hyperpolarization of the cell causes an expansion of the cell, which causes a push down on the BM through the rod. The interesting

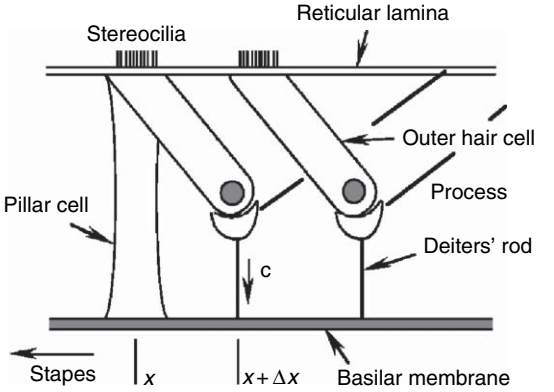

Figure 14 Side view of OHC showing the inclination (*x*–*z* plane). The end is supported by the cup of Deiter's cell, which has a rod providing mechanical attachment to the BM and a phalangeal process providing attachment to the RL. Inward shear of the stereocilia at the point x causes hyperpolarization of the OHC, which causes an elongation of the OHC, resulting in upward displacement of the RL and downward displacement of the BM. Because of the OHC inclination, this is a downward push on the Deiter's rod at the point $x + \Delta x$, "feed-forward". Because of the inclination of the phalangeal process, this rod will be pulled upward by an elongation of the OHC at the point $x + \Delta x_2$ which is a negative "feed-backward".

feature is that the shear on the cilia at the distance from the stapes given by x causes a push on the BM at the distance $x + \Delta x$.

Generally an active system with sensors and actuators that deliver energy to the system, which affects the input–output relation, is called feedback. For a system consisting of an input and output connected by a chain of processes, a sensor at one point that causes actuation at a preceding point in the chain, is called feedbackward, while a sensor that causes actuation at a subsequent point in the chain is called feedforward.

In birds and other nonmammals there is no motility and no stiff connection between the receptor cells and the BM. However, the hair bundle itself can have spontaneous oscillations and apparently is the source of a significant feedback of energy into the response. In this section we focus on the possible role of the OHC motility for mammals.

The structure of the OC shown in Figure 14 is elastic with the multiple attachments, so the elongation of a single OHC causes a ripple effect of loading of the BM in both directions. de Boer E. and Nuttall A. L. (2003) use a novel approach and take this into account with an array of impedances at different distances. The amplitudes of these feedforward and feedbackward elements are computed for a best fit with the experimental measurements of BM response, using the 3D calculation for the fluid. Here we offer a direct physical interpretation of a simpler version.

Another feature is that the fibers of the BM are in a sandwich in the PZ, then flatten to one layer in the arcuate zone (AZ) between the outer pillar (OP) and the inner pillar (IP). Since the bending stiffness D of a plate depends on the cube of the thickness, the BM AZ has roughly one-twenty-seventh of the stiffness of the PZ. Thus the OP offers significant support of the BM. Consequently, a simple model is the following sequence.

A downward pressure on the PZ, consisting of a positive fluid pressure p_F in the SV and an effective pressure from the Deiter's rods p_R causes a shear force on the OP foot of magnitude $(2p_F + p_R)b/2$ at the distance x from the stapes. The shear on the OP foot is roughly equal to the shear on the OHC cilia, if the details of the OC fluid-elastic motion are ignored. The shear is in the inhibitory direction and causes expansion of the OHC. The tendency of the OHC to expand causes a compressive force in the Deiter's rods, which is a downward force on the BM represented by the effective pressure p_R.

However, this occurs at the distance $x + \Delta x$. An equal and opposite force acts upward on the RL. Since this is more compliant, the displacement is more than for the BM, as shown in measurements in the cochlea and by calculations with the model in Figure 13. This upward displacement of the RL causes a tension in the phalangeal process, and an upward pull of the Deiter's rod. The equation for this is,

$$p_R(x+\Delta x,t) = \alpha[2p_F(x,t) + p_R(x,t)] - \alpha_2[2p_F(x+\Delta x_2,t) + p_R(x+\Delta x_2,t)]. \quad [32]$$

Thus the rod at the point $x + \Delta x$ is compressed by the OHC whose apex is at the point x by an amount proportional to the total pressure on the membrane, fluid plus rod, at x. So this is a positive feedforward with the amplitude α. The rod is also pulled by the phalangeal process by an amount proportional to the total pressure on the membrane at point $x + \Delta x_2$. So this is a negative feedbackward.

If the solution is used in the form eqn [27] with the assumption that Δx_2 and Δx are small, then eqn [32] becomes,

$$p_R e^{-jm\Delta x} = \alpha[2p_F + p_R] - \alpha_2[2p_F + p_R]e^{-jm\Delta x_2}, \quad [33]$$

with which the rod pressure p_R can be written in terms of the fluid pressure, so the total pressure becomes,

$$2p_F + p_R = \frac{2p_F}{1 - \alpha e^{jm\Delta x} + \alpha_2 e^{-jm(\Delta x_2 - \Delta x)}}. \quad [34]$$

Adding this feedforward and feedbackward to the previous eqn [29] for the dimensionless wave number yields,

$$\tilde{m} = \frac{8}{\pi} \times \frac{\tilde{\omega}^2}{\left[\tanh\tilde{m} - (1 + j\tilde{\omega}\gamma/\tilde{m}^2)^{-1/2}\right][1 - \alpha e^{j\tilde{m}\Delta\tilde{x}} + \alpha_2 e^{-j\tilde{m}(\Delta\tilde{x}_2 - \Delta\tilde{x})}]}. \quad [35]$$

Expanding this for small values as for eqn [30] gives the real and imaginary parts,

$$\mathrm{Re}(\tilde{m}) \approx \frac{8}{\pi}\tilde{\omega}^2\left[1 + \frac{1}{\sqrt{2\tilde{\omega}\gamma}}\frac{8}{\pi}\tilde{\omega}^2 + \alpha - \alpha_2\right], \text{ and} \quad [36]$$

$$\mathrm{Im}(\tilde{m}) \approx -\left(\frac{8}{\pi}\tilde{\omega}^2\right)^2\left[\frac{1}{\sqrt{2\tilde{\omega}\gamma}} - \alpha\Delta x - \alpha_2(\Delta x_2 - \Delta x)\right]. \quad [37]$$

Thus the feedforward and negative feedbackward tend to cancel in the real part. However, the positive feedforward and the negative feedbackward add to decrease the damping due to the fluid viscosity. In calculations it is far better to use the complete

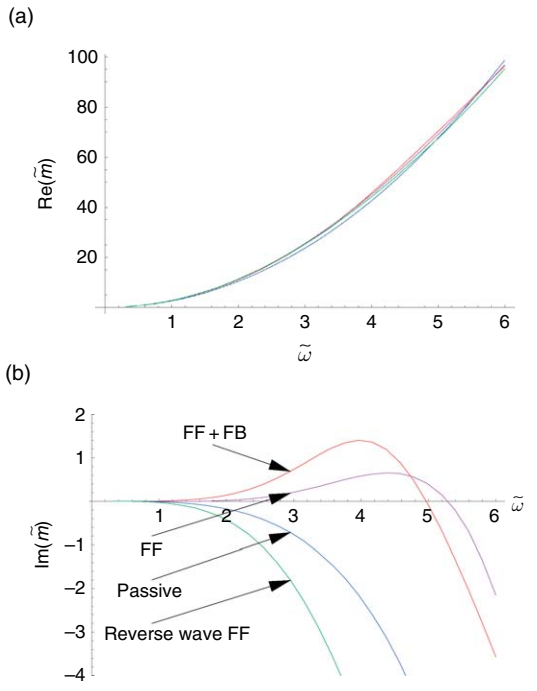

Figure 15 Wave number $\tilde{m}$ as a function of frequency $\tilde{\omega}$ from Equation xx. The curves "FF + FB" are for the feedforward due to the OHC inclination and the negative feedbackward due to the reverse inclination of the phalangeal processes, with parameters $\gamma = 10^5$, $\Delta\tilde{x} = 0.02$, $\Delta\tilde{x}_2 = 0.07\alpha = 0.08, \alpha_2 = 0.02$. The curves "FF" are with the effect of the feed-backward set to zero, $\alpha_2 = 0$. The curves "passive" are for both active effects turned off, $\alpha_2 = 0$ and $\alpha = 0$. Finally the curves "reverse FF" are for the traveling wave moving toward the stapes with $\Delta\tilde{x} = -0.02$ and $\alpha_2 = 0$. (a) The real part shows rapid accumulation for $\tilde{\omega} > 1$ and little sensitivity to feed-forward or feed-backward. (b) The imaginary part provides the effective damping of the wave, which is highly sensitive. The feed-forward push of the OHC causes a region of positive values, i.e., negative damping. The addition of the feed-backward "pull" of the phalangeal processes increases and sharpens the negative damping. For a wave in the reverse direction, the damping is increased by both effects. So the forward and backward waves are not the same.

relation (eqn [35]) and solve for the wave number iteratively. Results from this are shown in Figure 15. The real part of $\tilde{m}$, the spatial integral of which gives the phase, is not sensitive to the values for the parameters. However, the imaginary part of $\tilde{m}$ has dramatically different behavior. For the passive case, with both feedforward and feedbackward set to zero, the fluid viscosity provides the only damping. This is rather negligible for frequencies less than BF ($\tilde{\omega} < 1$), but increases rapidly for higher frequencies, and gives the rapid high-frequency decay in Figure 12(a). When feedforward is turned on with $\alpha = 0.08$, eqn [37] shows that the damping is decreased, but the full solution in Figure 15 shows that the imaginary part of $\tilde{m}$ actually is positive for a range of frequencies above BF. This can be interpreted as a negative damping due to the input of energy from the OHC motility. When the negative feedbackward is added, the positive range of the imaginary part of $\tilde{m}$ is decreased and sharpened.

With the approximation (eqn [32]), the details of the OC can be neglected and the transmission line model (eqn [19]) used. The effect is just a modification in the BM volume stiffness,

$$K_{\mathrm{Vol}}(x) \leftarrow K_{\mathrm{Vol}}(x)\left(1 - \alpha(x)e^{jm(x,\omega)\Delta x} + \alpha_2(x)e^{-jm(x,\omega)(\Delta x_2 - \Delta x)}\right). \quad [38]$$

Near the BF the changes in impedance is due to an apical shift in resonance for the low-level active case, but the phase change is small (Yoon, Y. J. *et al.*, 2006). This indicates that the zero crossings of the time domain response for the high-level passive case and the low-level active case will be nearly invariant. This suggests that force generation by OHCs in the feedforward formalism satisfies the near-invariance of fine time structure of the OC response predicted by Shera C. A. (2001).

The modification of BM stiffness is also valid in the 1D approximation (eqn [20]) and the 2D formulation (eqn. [23]) with the caveat that the stiffness may not be physical, as discussed above. Thus the feedforward causes a decrease in the effective partition stiffness and a negative damping. This is significant in the short wavelength region and corresponds to a significant input of energy into the traveling wave. For very short wavelengths, however, the fluid viscosity dominates.

The results for the 1D model for $\alpha_2 = 0$ (Geisler, C. D. and Sang, C., 1995) are excellent. The motility of the OHC saturates, which is represented by multiplying the factor α with a saturating function dependent on amplitude. The result for the dependence of the BM amplitude on input sound amplitude for the 3D model of the chinchilla cochlea is in Figure 12. The simulation results compare very well with other experimental measurements, capturing several nonlinear features observed in BM responses. These include compression of the response with stimulus level, two-tone suppressions, and generation of harmonic distortion and distortion products (Lim, K. M. and Steele, C. R., 2002). Transient click response has also been considered

(Lim, K. M. and Steele, C. R., 2003). The simulation results exhibit some of the characteristic nonlinear behavior of the BM commonly observed in experimental measurements, such as significant amplification and sustained ringing in the transient response at low stimulus levels. The simple feedforward mechanism is able to capture the properties of the active process in the cochlea without a second filter or resonance. All parameters are biologically based, with the feedforward needing only the inclination of the cells, assumed to be 30°, and the maximum value of α taken as 0.35 for the 3D calculation, which is modest.

The advantage of the distributed feedforward system should be appreciated. All the sensors and actuators are turned on, without the need for a "Maxwell's demon" to turn on the amplification where it is needed (Shera, C. A. and Guinan, J. J., Jr., 1999). For the long wavelength region, it has the effect of a small shift in the stiffness of the partition, but near BF, the negative damping is turned on with amplification of the signal of 40 dB or more. Then past BF there is little effect, and the high frequency fall-off is the same as for the passive case (Figure 12(a)). The assumption is that the OHC motility functions cycle by cycle without restriction on frequency, that is, α is independent of frequency. Whether the OHC actually performs this is a subject of current investigation in several laboratories.

3.10.6.3 Time Delay versus "Feedforward"

Similar to de Boer E. and Nuttall A. L. (2003) we ask for the time delay that would have the same effect as the spatial feedforward and feedbackward. With a time delay Δt in the pressure delivered to the BM from the OHC, eqn [32] is replaced by,

$$p_R(x, t + \Delta t) = \beta[2p_F(x, t) + p_R(x, t)]. \qquad [39]$$

The wave number-frequency relation eqn [35] is then,

$$\tilde{m} = \frac{8}{\pi} \frac{\tilde{\omega}^2}{\left[\tanh\tilde{m} - (1 + j\tilde{\omega}\gamma/\tilde{m}^2)^{-1/2}\right][1 - \beta e^{-j\tilde{\omega}\Delta\tilde{t}}]}, \qquad [40]$$

in which the dimensionless time delay is $\Delta\tilde{t} = \omega_{ref}\Delta t$. Expanding the wave number for small β and $\tilde{\omega} > 1$ as for eqn [35] gives the real and imaginary parts,

$$\mathrm{Re}(\tilde{m}) \approx \frac{8}{\pi}\tilde{\omega}^2\left[1 + \frac{1}{\sqrt{2\tilde{\omega}\gamma}}\frac{8}{\pi}\tilde{\omega}^2 + \beta\cos\tilde{\omega}\Delta\tilde{t}\right], \text{ and} \qquad [41]$$

$$\mathrm{Im}(\tilde{m}) \approx -\frac{8}{\pi}\tilde{\omega}^2\left[\frac{1}{\sqrt{2\tilde{\omega}\gamma}}\frac{8}{\pi}\tilde{\omega}^2 + \beta\sin\tilde{\omega}\Delta\tilde{t}\right]. \qquad [42]$$

Since β is positive, a small time delay *increases* the damping. The time delay must be tuned with $\Delta\tilde{t} > \pi$ for a decrease in the damping that corresponds to an energy input to the wave around the normalized BF $\tilde{\omega} \approx 1$. Another possibility is to make $\Delta\tilde{t} < 0$, to obtain negative damping for small time delays without tuning. However, this is a noncausal event, since what occurs at future time is having an effect at present time, as pointed out by de Boer E. and Nuttall A. L. (2003). with a different approach.

The stability can be examined by considering not a cochlea, but a simpler system consisting of a tube with constant properties over a finite length with a zero condition at the end $\tilde{x} = \tilde{L}$. The solution (eqn [27]), with forward and backward waves, provides the transfer function relating pressure at the general point x to the input pressure at $x = 0$,

$$\frac{\bar{p}(x)}{\bar{p}(0)} = \frac{e^{-j\tilde{m}\tilde{x}} - e^{j\tilde{m}_B(\tilde{x}-\tilde{L})-j\tilde{m}\tilde{L}}}{1 - e^{-j\tilde{m}_B\tilde{L}-j\tilde{m}\tilde{L}}}, \qquad [43]$$

where m_B is the wave-number for the backward traveling wave, defined by eqn [35] with the signs of Δx and Δx_2 changed. The poles are the zeros of the denominator at,

$$\tilde{m} + \tilde{m}_B = 2k\pi/\tilde{L}, \qquad [44]$$

in which k is an integer. For each k, this equation may be solved for the complex frequency. If the imaginary part of the frequency is negative, the solution is unstable in time. Remarkably, the feed-forward and feed-backward terms tend to cancel in the imaginary part, as can be seen by substituting the expanded eqns [36] and [37] into eqn [44]. Direct numerical calculations for the solution of eqn [44] support this, so it appears that the spatial delay expressed by the feedforward and feedbackward provides a stable system. Even when the imaginary part of the wave number is positive, as shown in Figure 15, the system remains stable. There is a limit to this, since for the gains $\alpha - \alpha_2 \to 1$, the stiffness becomes zero for small frequencies. A precise determination of the stability boundaries has not been carried out, but the gains used in Figure 15 can be increased by a factor of 3.9 until instability occurs. The zeros of the transfer function are the zeros of the numerator at,

$$\tilde{m} + \tilde{m}_B = 2k\pi/(\tilde{L} - \tilde{x}), \qquad [45]$$

which also have positive imaginary parts. So within certain limits, the feedforward system with a substantial gain in amplitude is stable and causal. This can be extended to the cochlea with variable properties. The condition (eqn [44]) becomes,

$$\int_0^{\bar{L}} (\tilde{m} + \tilde{m}_B) \mathrm{d}\tilde{x} = 2k\pi, \qquad [46]$$

which is more difficult to compute, but clearly with the same features.

In contrast, the forward and backward wave numbers are the same for the time delay system. Consequently, the solutions of eqn [39] show instability in time when the imaginary part (eqn [42]) is positive. Generally, feedback models incorporating time delay require additional components to prevent undesirable behavior. The measurements of Frank G. *et al.* (1999) show no time delay between the motile force and transmembrane potential. Therefore it appears most plausible that the frame structure in Figure 14 is for the purpose of the feedforward and negative feedbackward of energy into the traveling wave. Information on the exact inclination of the OHC and phalangeal process is lacking, but micrographs usually show a configuration similar to Figure 14. The one careful examination of this is from Karavitaki K. D. (2002), who finds in gerbil that the RL is nearly perpendicular to the OHC. Thus Δx is nearly zero. However, the Δx_2 is apparently equal to several OHC diameters, so the push–pull system works well.

3.10.6.4 Inner Hair Cell Excitation

In the preceding discussion an approximate relation (eqn [40]) is extracted from the physics of the OC, leaving only a modification of the BM model. Subsequently the details of the OC are avoided. However, the purpose of the OC is to provide the proper excitation of the IHC. The IHC cilia are not attached to the overlying tectorial membrane and are subject to the mechanical force of the fluid motion, which is dependent on the response of the entire structure of the OC. Consequently, the modeling of the OC is the subject of numerous recent studies. Böhnke F. and Arnold W. (1998) provide the most detailed FEM model, but without fluid. Kolston P. J. (1999) has inviscid fluid but with geometric simplification of the OC structure. Hubbard A. E. *et al.* (2003), Grosh K. *et al.* (2004), and Mountain D. C. and Hubbard A. E. (2006) use other geometric simplifications. Cai H. and Chadwick R. (2002), Andoh M. and Wada H. (2004), and Steele C. R. and Puria S. (2005) use detailed FEM models with realistic geometry and stiffness properties for the components.

As discussed by these authors, there is growing awareness that the flow of the fluid in the regions of the OC is important. Billone M. and Raynor S. (1973) provide perhaps the first careful analysis of the flow around the IHC cilia. One must keep in mind that in the hearing organ in lizards, there is considerable variety but always a group of receptor cells without a TM and with tall cilia free in the fluid. Freeman D. M. and Weiss T. F. (1990) have extensively investigated the mechanical behavior of these cilia through the relevant frequency range 1–3 kHz. It is of interest that the neural tuning and otoacoustic emissions from these receptor cells are similar to mammalian for the same frequency (Manley, G. A., 2006), without the TM, OHC motility, Deiter's cells, etc., that seem to be so important for mammals. For mammals, a feature recently established by Edge R. M. *et al.* (1998) is the proximity of the Hensen stripe, a protrusion of the tectorial membrane, to the tip of the IHC cilia, as indicated in Figure 15.

Nowotny M. and Gummer A. W. (2006) provide a breakthrough with measurements of the lower surface of the TM and the upper surface of the RL during electrical stimulation. They find that these surfaces do not remain parallel, as usually assumed. The calculation for the full elastic structure shows this as well. As can be seen in Figure 13, the region L1, near the IHC cilia between the TM and RL, opens with displacement of the BM toward ST. This tends to pull fluid in from the IS past the IHC cilia. Just how much depends on the relative stiffness of the TM and the proximity of the Hensen stripe (HS). Putting this together gives the effects on the phase of IHC excitation given in Table 5. The phase measured in neurons from the IHC in the middle and upper turns typically show for low frequencies something close to case 2, with a change toward case 1 as frequency increases (Cheatham, M. A. and Dallos, P., 1999). In the base with a relatively stiffer TM, Ruggero M. A. *et al.* (2000) report values similar to cases 3 and 4.

A strong mechanical nonlinearity comes from the restricted flow between the cilia, TM, and Hensen stripe (Steele, C. R. and Puria, S., 2005). A result of this is in Figure 17, which shows the tension in the tip link compared to the driving pressure, positive in the ST. Two peaks of the tension occur in each cycle of the pressure for a pressure level corresponding to

Table 5 Effects on phase of IHC tip-link tension for BM motion toward the ST, for which the pillar head and base of the cilium move radially outward. Cases 1 and 2 prevail for a soft TM, while cases 3 and 4 prevail for a stiff TM

Case	*Cause*	*Mechanism*	*Effect on IHC neurons*	*Phase*
1	Small gap with HS (or high frequency), cilium nearly sticks to HS	Tip lags the base, causing a decrease in tip-link tension in phase with the BM displacement.	Inhibition	0°
2	Large gap with HS and TM (or lower frequency), cilium is pulled through fluid	Tip lags the base, causing a decrease in tip-link tension in phase with the BM velocity.	Inhibition	90°
3	Small gap with HS, area of region L1 increases, cilium nearly sticks to HS, so L1 has negative pressure	Outward pressure on the cilium, causing an increase in tip-link tension in phase with the BM displacement.	Excitation	180°
4	Large gap with HS, area of region L1 increases, so fluid flows from IS into L1	Outward pressure on the cilium, causing an increase in tip-link tension in phase with the BM velocity.	Excitation	270°

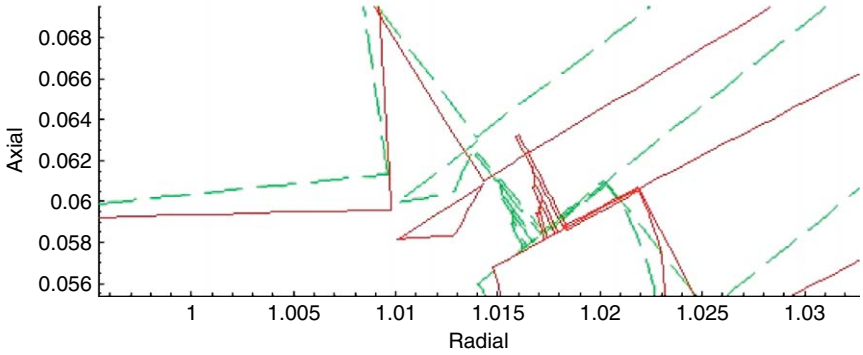

Figure 16 Close view of IHC cilia for guinea pig apex. The Hensen stripe (HS) is the triangle attached to the tectorial membrane above. The dashed lines show the undeformed configuration, with the tip of the IHC cilia near the HS. The solid lines show the deformed configuration due to static pressure loading toward ST, greatly amplified. The radial and axial distances are in mm.

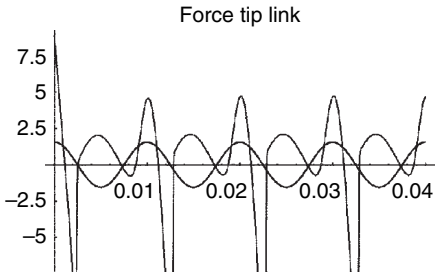

Figure 17 Nonlinear solution for the force in the tip link at the guinea pig base at 100 Hz. Around 90 dB SPL, two peaks of force (nonlinear curve) occur per cycle of ST pressure (cosine curve). This offers one possible explanation for the 180° change in phase and peak splitting sometimes observed in auditory nerve fibers (Kiang 1990).

around 90 dB SPL. For lower sound pressures, the peak that is out of phase with the pressure is the dominant one, and for higher sound pressures the only remaining peak is the one in phase with the pressure. This is remarkably close to the behavior of auditory neurons sometimes observed (Kiang, N. Y., 1990). A common expectation is that velocity of the BM toward the ST will cause the IHC cilia to be swept by the fluid in the inhibitory direction (to the left in Figure 13) (Figure 16). However, it seems that almost any phase of excitation is possible, depending on the specific geometry and relative stiffness properties. In the static response shown in Figure 13, the subtectorial fluid region L1 is seen to open with BM

displacement toward the ST. This will cause a fluid flow into L1 from the inner sulcus (IS) that will bend the cilia in the excitatory direction. BM motion toward the SV then is inhibitory. However, as the amplitude increases, the tall cilia are constrained by the Hensen stripe while the RL still moves to the left in Figure 13. This causes tension in the tip links seen as the in-phase peak in Figure 17.

3.10.7 Summary of Some Issues

Rapid development in measurement and computational techniques related to auditory biomechanics is ongoing. Perhaps the following issues soon will be completely resolved.

3.10.7.1 Motion of the Tympanic Membrane for High Frequencies

The simple model for the middle ear has the tympanic membrane acting as a rigid, massless piston. However, instead of piston-like behavior, surface displacement measurements have revealed multiple modes of vibration for frequencies above a few kilohertz (Tonndorf, J. and Khanna, S. M., 1972). This has provoked considerable discussion. A recent explanation offered in a preceding section is that the nonsymmetric material and geometric properties of the membrane provide mistuning without strong resonances. The consequence is a fairly uniform transmission of the pressure for the entire frequency range without the need for "woofer"-like or "tweeter"-like elements. Full validation for this notion is in progress.

3.10.7.2 Motion of the Ossicular Chain for High Frequencies

The nonmammalian vertebrates have a simple columella that transmits the tympanic membrane motion to the inner ear. In contrast, the mammals have a three-bone ossicular chain. In the simple model, this is represented by a simple lever with a fixed pivot point. However, measurements show that this is not the behavior for frequencies above a few kilohertz (Decraemer, W. F. *et al.*, 2003). The pivot point depends on frequency and the stapes wobbles, instead of directly providing a volume displacement of the cochlear fluid. The expectation is that this somehow permits the extension of the frequency range, but an explanation is totally lacking.

3.10.7.3 Bone Conduction

Hearing by bone conduction is of high clinical significance. There are many measurements showing that the volume displacements of the oval and round windows are exactly out of phase for air-conducted acoustic excitation, consistent with the two modes shown in Figure 7. All existing theory indicates that this is also the case for bone-conducted sound. However, measurements by Stenfeld S. *et al.* (2004) indicate that this is not the case for bone conduction. Indeed for some frequencies, the two windows are in phase. Thus there must be compliance in the cochlea not yet explained (often referred to as a third window) Dehiscence of the semi-circular canals has been clinically shown to produce a third window (Chien, W. *et al.*, 2007; Merchant, S. N. *et al.*, 2007; Minor, L. B. *et al.*, 2003). Sohmer H. and Freeman S. (2004) demonstrate that bone vibration generates acoustic pressure in the brain that can generate an auditory response. Estimates on the flow properties of the cochlear and vestibular aqueducts indicate that the compliance is too low to offer a reasonable acoustic pathway. Again, an explanation is totally lacking.

3.10.7.4 Traveling Waves

The traveling wave observed in the guinea-pig cochlea by Békésy G. (1960) was not anticipated by any theoretical consideration. There remain contrary opinions, for example Sohmer H. and Freeman S. (2004) consider their measurements as evidence against the existence of the traveling wave. The traveling wave does not occur in lizards and turtles, but most likely does occur in birds. For mammals, the evidence for the existence of the traveling wave seems overwhelming. We mention the direct *in vivo* observation of waves by Ren T. (2002), the close relation of BM displacement and neural excitation found in the same animal by Narayan S. S. *et al.* (1998), and the agreement in theory with the traveling wave, and experiment for the BM motion (Figure 12).

3.10.7.5 Cell Motility versus Stereociliary Forces

In nonmammalian hearing organs, there are no arches of Corti, Deiter's cells, or inner sulci as shown in Figure 13. Furthermore the cells similar to the OHCs cannot have somatic motility.

Nevertheless, in the responsive frequency range, the neural tuning is as sharp as in mammals, and evoked and spontaneous emissions occur very similarly to those in mammals (Manley, G. A., 2006). Crawford A. C. and Fettiplace R. (1985) discovered that the cilia on turtle hair cells have spontaneous activity, that is, they beat without external excitation. This mechanotransducer (MET) channel phenomenon is described as a Hopf bifurcation (Choe, Y. *et al.*, 1998). In all vertebrates, the cilia and transduction channels are similar. In mammals, is the energy of the active process generated by MET instability or somatic motility of the cell, or is it a combination? This is a subject of current investigation (e.g., Chan, D. K. and Hudspeth, A. J., 2005). Frank G. *et al.* (1999) discovered that the ratio of OHC motile force to transmembrane voltage remains constant to nearly 100 kHz without time delay, which supports the notion that motility is a unique feature of the OHC and must be important for mammalian hearing. Indeed the recent results on rat cochleas by Kennedy H. J. *et al.* (2006) offer evidence that both MET resonance and somatic motility are interacting.

3.10.7.6 Outer Hair Cell Roll-Off

The feedforward (and negative feedbackward) behavior discussed here depends on the force of motility of the OHC to be independent of frequency. However, the electrical properties of the OHC appear to be such that for a fixed amplitude of shear force on the cilia, there is a significant decrease in the intracellular potential at a frequency much less than the BF. Several laboratories propose more detailed analysis of intracellular or extracellular behavior that would maintain the effect of the motility for high frequencies. Without a more elaborate cell model, Baker G. J. (2000) and Grosh K. *et al.* (2004) use models with correct physical values for the electrical and mechanical properties of the OHC, but with a resonant TM, and find that the effects of the motility for high frequencies are preserved.

3.10.7.7 A Resonant Tectorial Membrane?

Many authors have used OC models with a strong resonance of the TM (e.g., Allen, J. B., 1980). Several laboratories have measured the properties of the TM, most recently Gueta R. *et al.* (2006) and Masaki K. *et al.* (2006). Details are different, but the general conclusion is that the TM is rather soft tissue, with an elastic Young's modulus in the 0.5–30 kPa range. Zwicker E. (1972) points out that squirrel monkeys and pigs have a huge difference in TM size. Such a difference for animals that have roughly the same frequency range of hearing makes a resonant TM seem unlikely. Nowotny M. and Gummer A. W. (2006) measure the TM response due to electrical stimulation and find no resonance for frequencies through the BF. So there are indications that the TM does not have a strong resonance.

3.10.7.8 Multiple Traveling Wave Modes

The common box model has the fast and slow waves indicated in Figure 7. However, each of the fluid spaces in the OC (Figure 13) can support an independent wave. Karavitaki K. D. (2002) offers measurements of motion of the OC that support the notion of multiple waves. As discussed by de Boer E. (2006) recent models, for example, Zhang L. *et al.* (1997) and Mountain D. C. and Hubbard A. E. (2006), have such a capability. The goal remains for a model of the OC with physically-realistic geometric and stiffness properties and with 3D viscous fluid, that can simulate the environment of the cilia for all frequencies. The expectation is that waves in the IS and tunnel space do play a significant role.

3.10.7.9 Stiffness Change Along the Cochlea

Almost every component of the cochlear cross-section has at one time or another been proposed as the fundamental resonance element. Most probably agree with Békésy G. (1960) that the BM has the strongest stiffness gradient and is the most likely candidate. The calculation in Table 4 shows that the modest variation in values of width, thickness, and fiber volume fraction of the PZ work together to explain the frequency range of the guinea-pig cochlea. The change in the volume compliance is five orders of magnitude. However, the direct measurement of the guinea pig cochlea by Békésy G. (1960) shows a change of three orders of magnitude, with a reasonable extrapolation to four orders of magnitude. Similarly, Zhang L. *et al.* (1997) find that the point load stiffness variation is inadequate to explain the frequency range in gerbil. With a different preparation, however, Emadi G. *et al.* (2004) find much more compliance in the apical region, which seems to fit the theoretical values from the geometry. The conclusion is that the soft cells covering the

BM make point load or volume compliance measurements difficult to interpret. As is often the case, a combination of theoretical and experimental approaches is needed.

3.10.8 General Summary

There are many acoustical and mechanical transformations performed by outer ear, middle ear, and cochlear structures. The components in the mammalian ear are more elaborate than those in nonmammalian vertebrates, with the advantage of a subsequently extended frequency range. The anatomic complexity of the mammalian ear ultimately results in greater functional capabilities. Some of quantifiable variables are sensitivity, frequency bandwidth, frequency resolution, dynamic range, and sound localization. The structures that lead to these capabilities do so given the available biological materials, space constraints within the skull, and limitations imposed by biophysics.

Several fundamental biophysical principles provide the means for obtaining the proper mechanical forcing of receptor cells in the inner ear. Each of the transformation steps can be described by a basic principle that can be readily understood using computational biomechanics. The objective of each transformation is to preserve the sound relevant to the species for the stated functionality. Each implementation is, however, much more complicated and involves biomechanical principles that are not all well characterized, are yet to be implemented in any man-made device, and are not free from controversy.

Less controversial is the spatially dependent transformation of sound by the pinna and the ear canal. The next step is the impedance alleviation between the air and fluid of the cochlea, which requires an area change provided by the eardrum and stapes footplate. It is not possible to have rigid, massless pistons for this purpose, so the tympanic membrane is an elaborate vibrating system with mistuning of the different radial sectors, each with significant resonances for frequencies over about 2 kHz. The ensemble, however, delivers a fairly smooth pressure to the ossicular chain. In the ossicular chain, the principle of a lever advantage is also readily grasped, but the chain does not behave as a simple lever for higher frequencies (>2 kHz) An adequate understanding of how the pressure is transmitted to the cochlea has yet to be attained.

In the cochlea, the local resonance at the BF is easily calculated for the BM immersed in fluid and soft cells. The reality of the transmission of the pressure to this point involves the fast and slow traveling waves, with their respective long and short wavelengths. The BF is not really a resonance in the sense of a set of tuned strings, but rather a point of transition to very short wavelengths. The actual BF location depends on fluid viscosity, width of the partition with respect to the BM, and sound level. The enhancement of the traveling wave by the active process for low levels of sound remains a subject of contention. The simplest model of feedforward provided by the geometry and the motility of the OHC appears to explain much. Such a distributed system of sensors and actuators is effective in enhancing the BM response near the BF. Finally, the transformation from BM motion to excitation of the IHC has the simple explanation of cilia being dragged through fluid. The details of the environment of the cilia and the proximity of the Hensen stripe make the actual cilia-fluid response much more complicated. Calculations for low frequencies have a resemblance to measurements in the IHC and in the neurons of the auditory nerve. However the full effect of the complex geometry for the full range of frequencies and amplitudes has yet to be examined. It is safe to predict that other mechanical design features are present in the OC to obtain the proper excitation of the IHC, which are not yet anticipated. The interplay between physiological measurements and bio-computational models helps to elucidate the knowns from the unknowns and thus provides a path toward greater understanding.

Acknowledgments

This work was supported in part by grant R01 DC 05960 from the National Institute of Deafness and other Communication Disorders of the National Institutes of Health and by grant RGP0051 from the Human Frontiers of Science Program.

Endnotes

[1] The work for the absolute threshold of hearing ($p^2/\rho c \times \text{area} \times \text{time}$) is easiest to estimate at the tympanic membrane, and it is about 6×10^{-18} J for humans, using a threshold of hearing of $p = 15\,\mu\text{Pa}$ (−3 dB SPL), pars tensa area $= 55\,\text{mm}^2$, $\rho = 1.18\,\text{kg m}^{-3}$, $c = 344\,\text{m s}^{-1}$, and time $= 0.2$ s. If we assume that there is a loss of a factor of two

between the middle ear and hair cell detectors, the threshold of hearing becomes about 3×10^{-18} J.

[2] A dark-adapted eye requires 90 photons within 0.1 s to perceive a flash. However, the estimate is that only 10% of the photons entering the eye actually reach the cones, so that gives about 10 photons necessary for the perception (Hecht, C. *et al.*, 1942). The energy of a single photon in the middle of the visible spectrum (hc/ν) is 4×10^{-19} J, using $h = 6.6 \times 10^{-34}$Js, $c = 3 \times 10^{8}\,\mathrm{m\,s^{-1}}$, and $\nu = 500 \times 10^{-9}$ m. Therefore, for 10 photons the energy is 4×10^{-18} J.

[3] It has been observed for some time that the threshold of hearing in subjects can have quasi-periodic peaks and valleys. However, the mechanism may be related to nonlinear properties of the cochlea at low levels and internal reflections leading to standing waves.

[4] Here it is assumed that the middle-ear cavity pressure at the round window is negligible, which is the case in normal ears. In pathological ears the pressure at the oval and round windows maybe more comparable, due to acoustic coupling, and thus the important determining variable there is the pressure difference between the two windows (Merchant, S. N. *et al.*, 1997).

[5] The specific impedance was calculated as the measured cochlear input impedance Zc times the footplate area. In humans the average magnitude of Zc is $2^{1/2} \times 21 \times 10^{9}\,\mathrm{kg\,s^{-1}\,m^{-4}}$ and the average footplate area is $3.21 \times 10^{-6}\,\mathrm{m^2}$ (Aibara, R. *et al.* 2001). The $2^{1/2}$ is to convert the peak velocity to rms velocity.

[6] The one exception to this is the recent finding that the concave-eared torrent frog species listens to mating calls that are present above 20 khz (Feng, A. S. *et al*., 2006).

[7] The reciprocal of this can be found in loudspeaker designs. If one takes an isolated loudspeaker (the output driver) it would operate as a dipole generating nearly equal and opposite signals from the two sides that would tend to cancel in the far field. To increase the acoustic output of a speaker driver, it is almost always placed in a cabinet that prevents cancellation from the opposite phase.

References

Aibara, R., Welsh, J. T., Puria, S., and Goode, R. L. 2001. Human middle-ear sound transfer function and cochlear input impedance. Hear. Res. 152, 100–109.

Algazi, V. R., Duda, R. O., Duralswami, R., Gumerov, N. A., and Tang, Z. 2002. Approximating the head-related transfer function using simple geometric models of the head and torso. J. Acoust. Soc. Am. 112, 2053–2064.

Algazi, V. R., Duda, R. O., Thompson, D. M., and Avendano, C. 2001. The CIPIC HRTF Database. Applications of Signal Processing to Audio and Acoustics, 2001 IEEE Workshop.

Allen, J. B. 1980. Cochlear micromechanics – a physical model of transduction. J. Acoust. Soc. Am. 68, 1660–1670.

Allen, J. B. and Neely, S. T. 1992. Micromechanical models of the cochlea. Phys. Today 45, 40–47.

Anderson, D. J., Rose, J. E., Hind, J. E., and Brugge, J. F. 1971. Temporal position of discharges in single auditory nerve fibers within the cycle of a sine-wave stimulus, frequency and intensity effects. J. Acoust. Soc. Am. 49, 1131.

Andoh, M. and Wada, H. 2004. Prediction of the characteristics of two types of pressure waves in the cochlea, theoretical considerations. J. Acoust. Soc. Am. 116, 417–425.

Baker, G. J. 2000. Pressure-feedforward and piezoelectric amplification models for the cochlea. PhD Thesis, Stanford University.

Beer, H. J., Bornitz, M., Hardtke, H. J., Schmidt, R., Hofmann, G., Vogel, U., Zahnert, T., and Huttenbrink, K. B. 1999. Modelling of components of the human middle ear and simulation of their dynamic behaviour. Audiol. Neurootol. 4, 156–162.

Berkley, D. A. and Lesser, M. B. 1973. Comparison of single- and double-chamber models of the cochlea. J. Acoust. Soc. Am. 53, 1037–1038.

Billone, M. and Raynor, S. 1973. Transmission of radial shear forces to cochlear hair cells. J. Acoust. Soc. Am. 54, 1143–1156.

Bö to mechanoelectrical-transduction channels Proc. Natl. Acad. Sci. U. S. A. 9515321–15326.

Crawford, A. C. and Fettiplace, R. 1985. The mechanical properties of ciliary bundles of turtle cochlear hair cells. J. Physiol. 364, 359–379.

Dalchow, C. V., Weber, A. L., Bien, S., Yanagihara, N., and Werner, J. A. 2006. Value of digital volume tomography in patients with conductive hearing loss. Eur. Arch. Otorhinolaryngol. 263, 92–99.

Dallos, P. 1973. The Auditory Periphery; Biophysics and Physiology. Academic Press.

Dancer, A. and Franke, R. 1979. Intracochlear acoustic pressure measurements in guinea-pigs. Scand. Audiol. Suppl. 9, 111–117.

Dancer, A. and Franke, R. 1980. Intracochlear sound pressure measurements in guinea-pigs. Hear. Res. 2, 191–205.

de Boer, E. 1991. Auditory physics. Physical principles in hearing theory. III. Physics Rep. 203, 125–231.

de Boer, E. and Nuttall, A. L. 1999. The 'inverse problem' solved for a three-dimensional model of the cochlea. III. Brushing-up the solution method. J. Acoust. Soc. Am. 105, 3410–3420.

de Boer, E. 2006. Cochlear Activity in Perspective. In: Auditory Mechanisms, Processes and Models (*eds*. A. L. Nuttall, T. Ren, P. Gillespie, K. Grosh, and E. deBoer), pp. 393–409. World Scientific.

de Boer, E. and Nuttall, A. L. 2003. Properties of Amplifying Elements in the Cochlea. In: Biophysics of the Cochlea (*ed*. A. W. Gummer), pp. 331–342. World Scientific.

Decraemer, W. and Khanna, S. 1995. Malleus vibration modelled as rigid body motion. Acta Otorhinolaryngol. Belg. 49, 139–145.

Decraemer, W. F., Dirckx, J. J., and Funnell, W. R. 1991a. Shape and derived geometrical parameters of the adult, human tympanic membrane measured with a phase-shift moire interferometer. Hear. Res. 51, 107–121.

Decraemer, W. F., Dirckx, J. J., and Funnell, W. R. 2003. Three-dimensional modelling of the middle-ear ossicular chain using a commercial high-resolution X-ray CT scanner. J. Assoc. Res. Otolaryngol. 4, 250–263.

Decraemer, W. F., Khanna, S. M., and Funnell, W. R. 1991b. Malleus vibration mode changes with frequency. Hear. Res. 54, 305–318.

Decraemer, W. F., Maes, M. A., and Vanhuyse, V. J. 1980. An elastic stress-strain relation for soft biological tissues based on a structural model. J. Biomech. 13, 463–468.

DPA 2005. Sound and Divers. http://www.mod.uk/dpa/projects/sonarenvir/impact.htm

Eberl, D. F., Duyk, G. M., and Perrimon, N. 1997. A genetic screen for mutations that disrupt an auditory response in Drosophila melanogaster. Proc. Natl. Acad. Sci. U. S. A. 94, 14837–14842.

Edge, R. M., Evans, B. N., Pearce, M., Richter, C. P., Hu, X., and Dallos, P. 1998. Morphology of the unfixed cochlea. Hear. Res. 124, 1–16.

Eiber, A. and Freitag, H. G. 2002. On Simulation models in otology. Multibody Syst. Dynam. 8, 197–217.

Eisner, E. 1967. Complete solutions of the Webster horn equations. J. Acoust. Soc. Am. 41, 1126–1146.

Emadi, G., Richter, C. P., and Dallos, P. 2004. Stiffness of the gerbil basilar membrane, radial and longitudinal variations. J. Neurophysiol. 91, 474–88.
Fay, J. P., Puria, S., Decraemer, W. F., and Steele, C. 2005. Three approaches for estimating the elastic modulus of the tympanic membrane. J. Biomech. 38, 1807–15.
Fay, J. P. 2001. Cat eardrum mechanics. PhD Thesis, Stanford University.
Fay, J. P., Puria, S., and Steele, C. R. 2006. The discordant eardrum. Proc. Natl. Acad. Sci. U. S. A. 103, 19743–19748.
Fay, R. R. 1988. Hearing in Vertebrates; a Psychophysics Databook. Hill-Fay Associates.
Flanagan, J. L. and Bird, C. M. 1962. Minimum phase response for the Basilar Membrane. J. Acoust. Soc. Am. 34, 114–118.
Fleischer, G. 1978. Evolutionary principles of the mammalian middle ear. Adv. Anat. Embryol. Cell Biol 55(5), 3–70.
Fleischer, G. 1982. [Hearing mechanisms in dolphins and baleen whales (author's transl)]. Hno 30, 123–30.
Frank, G., Hemmert, W., and Gummer, A. W. 1999. Limiting dynamics of high-frequency electromechanical transduction of outer hair cells. Proc. Natl. Acad. Sci. U. S. A. 96, 4420–4425.
Freeman, D. M. and Weiss, T. F. 1990. Hydrodynamic forces on hair bundles at high frequencies. Hear. Res. 48, 31–36.
Funnell, W. R., Decraemer, W. F., and Khanna, S. M. 1987. On the damped frequency response of a finite-element model of the cat eardrum. J. Acoust. Soc. Am. 81, 1851–1859.
Funnell, W. R., Shiah, H. T., McKee, M. D., Daniel, S. J., and Decraemer, W. F. 2005. On the coupling between the incus and the stapes in the cat. JARO 6, 9–18.
Gan, R. Z., Feng, B., and Sun, Q. 2004. Three-dimensional finite element modeling of human ear for sound transmission. Ann. Biomed. Eng. 32, 847–859.
Geisler, C. D. and Sang, C. 1995. A cochlear model using feed-forward outer-hair-cell forces. Hear. Res. 86, 132–146.
Givelberg, E. and Bunn, J. 2003. A comprehensive three-dimensional model of the cochlea. J. Comput. Physics 191, 377–391.
Goode, R. L., Killion, M., Nakamura, K., and Nishihara, S. 1994. New knowledge about the function of the human middle ear, development of an improved analog model. Am. J. Otol. 15, 145–154.
Gopfert, M. C. and Robert, D. 2001. Biomechanics. Turning the key on *Drosophila* audition. Nature 411, 908.
Grosh, K., Zheng, J., Zou, Y., de Boer, E., and Nuttall, A. L. 2004. High-frequency electromotile responses in the cochlea. J. Acoust. Soc. Am. 115, 2178–84.
Gueta, R., Barlam, D., Shneck, R. Z., and Rousso, I. 2006. Measurement of the mechanical properties of isolated tectorial membrane using atomic force microscopy. Proc. Natl. Acad. Sci. U. S. A. 103, 14790–14795.
Guinan, J. J., Jr. and Peake, W. T. 1967. Middle-ear characteristics of anesthetized cats. J. Acoust. Soc. Am. 41, 1237–1261.
Gundersen, T. and Høgmoen, K. 1976. Holographic vibration analysis of the ossicular chain. Acta Otolaryngol. 82, 16–25.
Hecht, C., Shlaer, S., and Pirenne, M. H. 1942. Energy, quanta, and vision. J Gen. Physiol. 25, 819–840.
Helle, R. 1974. Beobachtungen an hydromechanischen Modellen des Innenohres mit nachBuildung von Basilarmembran, Corti-Organ und Deckmembran. PhD Thesis, Technical University of Munich.
Helmholtz, H. L. F. 1868. Die Mechanik der Gehorknochelchen und des Trommelfells. M. Cohen und Sohn.
Hemila, S., Nummela, S., and Reuter, T. 1999. A model of the odontocete middle ear. Hear. Res. 133, 82–97.
Henson, M. M., Madden, V. J., Rask-Andersen, H., and Henson, O. W., Jr. 2005. Smooth muscle in the annulus fibrosus of the tympanic membrane in bats, rodents, insectivores, and humans. Hear. Res. 200, 29–37.
Henson, O. W., Jr. and Henson, M. M. 2000. The tympanic membrane, highly developed smooth muscle arrays in the annulus fibrosus of mustached bats. J. Assoc. Res. Otolaryngol. 1, 25–32.
Hofman, P. M., Van Riswick, J. G., and Van Opstal, A. J. 1998. Relearning sound localization with new ears. Nat. Neurosci. 1, 417–421.
Howard, J. and Hudspeth, A. J. 1988. Compliance of the hair bundle associated with gating of mechanoelectrical transduction channels in the bullfrog's saccular hair cell. Neuron 1, 189–99.
Hubbard, A. E., Mountain, D. C., and Chen, F. 2003. Time-Domain Responses for a Nonlinear Sandwich Model of the Cochlea. In: Biophysics of the Cochlea (*ed*. A. Gummer), pp. 315–330. World Scientific.
Huttenbrink, K. B. 1988. Mechanics of the ear ossicles in static pressures. II. Impaired joint function and surgical reconstruction of the ossicle chain. Laryngol. Rhinol. Otol. (Stuttg.) 67, 100–105.
Huttenbrink, K. B. 1989. The functional significance of the suspending ligaments of the ear ossicle chain. Laryngorhinootologie 68, 146–151.
Karavitaki, K. D. 2002. Measurements and models of electrically-evoked motion in the gerbil organ of Corti. PhD Thesis, Boston University.
Keefe, D. H., Bulen, J. C., Arehart, K. H., and Burns, E. M. 1993. Ear-canal impedance and reflection coefficient in human infants and adults. J. Acoust. Soc. Am. 94, 2617–2638.
Kennedy, H. J., Evans, M. G., Crawford, A. C., and Fettiplace, R. 2006. Depolarization of cochlear outer hair cells evokes active hair bundle motion by two mechanisms. J. Neurosci. 26, 2757–2766.
Khanna, S. M. and Tonndorf, J. 1969. Middle ear power transfer. Arch. Klin. Exp. Ohren. Nasen. Kehlkopfheilkd. 193, 78–88.
Khanna, S. M. and Tonndorf, J. 1972. Tympanic membrane vibrations in cats studied by time-averaged holography. J. Acoust. Soc. Am. 51, 1904–1920.
Kiang, N. Y. 1990. Curious oddments of auditory-nerve studies. Hear. Res. 49, 1–16.
Kiang, N. Y. S., Watanabe, T., Thomas, E. C., and Clark, L. F. 1965. Discharge Patterns of Single Fibers in the Cat's Auditory Nerve. MIT Press.
Kiefer, J., Bohnke, F., Adunka, O., and Arnold, W. 2006. Representation of acoustic signals in the human cochlea in presence of a cochlear implant electrode. Hear. Res. 221, 36–43.
Koike, T., Wada, H., and Kobayashi, T. 2002. Modeling of the human middle ear using the finite-element method. J. Acoust. Soc. Am. 111, 1306–1317.
Kolston, P. J. 1999. Comparing *in vitro*, *in situ*, and *in vivo* experimental data in a three-dimensional model of mammalian cochlear mechanics. Proc. Natl. Acad. Sci. U. S. A. 96, 3676–3681.
Kolston, P. J. 2000. The importance of phase data and model dimensionality to cochlear mechanics. Hear. Res. 145, 25–36.
Kuypers, L. C., Decraemer, W. F., Dirckx, J. J., and Timmermans, J. P. 2005. Thickness distribution of fresh eardrums of cat obtained with confocal microscopy. J. Assoc. Res. Otolaryngol. 3, 223–233.
Lim, D. J. 1995. Structure and function of the tympanic membrane, a review. Acta Otorhinolaryngol. Belg. 49, 101–115.
Lim, K. M. 2000. Physical and mathematical cochlear models. Ph.D. Thesis, Stanford University.

Lim, K. M. and Steele, C. R. 2002. A three-dimensional nonlinear active cochlear model analyzed by the WKB-numeric method. Hear. Res. 170, 190–205.
Lim, K. M. and Steele, C. R. 2003. Response suppression and transient behavior in a nonlinear active cochlear model with feed-forward. Int. J. Solids Struct. 40, 5097–5107.
Lynch, T. J., 3rd, Nedzelnitsky, V., and Peake, W. T. 1982. Input impedance of the cochlea in cat. J. Acoust. Soc. Am. 72, 108–130.
Lynch, T. J., 3rd, Peake, W. T., and Rosowski, J. J. 1994. Measurements of the acoustic input impedance of cat ears, 10 Hz to 20 kHz. J. Acoust. Soc. Am. 96, 2184–2209.
Magnan, P., Avan, P., Dancer, A., Smurzynski, J., and Probst, R. 1997. Reverse middle-ear transfer function in the guinea-pig measured with cubic difference tones. Hear. Res. 107, 41–45.
Manley, G. A. 2006. Spontaneous otoacoustic emissions from free-standing stereovillar bundles of ten species of lizard with small papillae. Hear. Res. 212, 33–47.
Margolis, R. H. 1993. Detection of hearing impairment with the acoustic stapedius reflex. Ear Hear. 14, 3–10.
Margolis, R. H. and Popelka, G. R. 1975. Loudness and the acoustic reflex. J. Acoust. Soc. Am. 58, 1330–1332.
Masaki, K., Weiss, T. F., and Freeman, D. M. 2006. Poroelastic bulk properties of the tectorial membrane measured with osmotic stress. Biophys. J. 91, 2356–2370.
Merchant, S. N., Ravicz, M. E., Puria, S., Voss, S. E., Whittemore, K. R., Jr., Peake, W. T., and Rosowski, J. J. 1997. Analysis of middle ear mechanics and application to diseased and reconstructed ears. Am. J. Otol. 18, 139–154.
Merchant, S. N., Rosowski, J. J., and McKenna, M. J. 2007. Superior semicircular canal dehiscence mimicking otosclerotic hearing loss. Adv. Otorhinolaryngol. 65, 137–145.
Michelsen, A. 1966. Pitch discrimination in the locust ear, observations on single sense cells. J. Insect. Physiol. 12, 1119–31.
Minor, L. B., Carey, J. P., Cremer, P. D., Lustig, L. R., Streubel, S. O., and Ruckenstein, M. J. 2003. Dehiscence of bone overlying the superior canal as a cause of apparent conductive hearing loss. Otol. Neurotol. 24, 270–278.
Mountain, D. C. and Hubbard, A. E. 2006. What Stimulates the Inner Hair Cell? In: Auditory Mechanisms, Processes and Models (*eds*. A. L. Nuttall, T. Ren, P. Gillespie, K. Grosh, and E. deBoer), pp. 466–473. World Scientific.
Murugasu, E., Puria, S., and Roberson, J. B., Jr. 2005. Malleus-to-footplate versus malleus-to-stapes-head ossicular reconstruction prostheses, temporal bone pressure gain measurements and clinical audiological data. Otol. Neurotol. 26, 572–582.
Møller, A. R. 1963. On transmission characteristic of middle ear. Acta Physiol. Scand. 59, 105–107.
Møller, A. R. 1961. Network model of middle ear. J. Acoust. Soc. Am. 33, 168–178.
Narayan, S. S., Temchin, A. N., Recio, A., and Ruggero, M. A. 1998. Frequency tuning of basilar membrane and auditory nerve fibers in the same cochleae. Science 282, 1882–1884.
Nedzelnitsky, V. 1980. Sound pressures in the basal turn of the cat cochlea. J. Acoust. Soc. Am. 68, 1676–1689.
Neely, S. T. 1981. Finite difference solution of a two-dimensional mathematical model of the cochlea. J. Acoust. Soc. Am. 69, 1386–1391.
Nobili, R., Mammano, F., and Ashmore, J. 1998. How well do we understand the cochlea? Trends Neurosci. 21, 159–167.
Nowotny, M. and Gummer, A. W. 2006. Nanomechanics of the subtectorial space caused by electromechanics of cochlear outer hair cells. Proc. Natl. Acad. Sci. U. S. A. 103, 2120–2125.
Nummela, S. 1995. Scaling of the mammalian middle ear. Hear. Res. 85, 18–30.
Olson, E. S. 1998. Observing middle and inner ear mechanics with novel intracochlear pressure sensors. J. Acoust. Soc. Am. 103, 3445–3463.
Onchi, Y. 1949. A study of the mechanism of the middle ear. J. Acoust. Soc. Am. 21, 404–410.
Onchi, Y. 1961. Mechanism of middle ear. J. Acoust. Soc. Am. 33, 794–805.
Pang, X. D. and Guinan, J. J., Jr. 1997. Effects of stapedius-muscle contractions on the masking of auditory-nerve responses. J. Acoust. Soc. Am. 102, 3576–3586.
Perkins, R. C. 1980. Laser stepedotomy for otosclerosis. Laryngoscope 90, 228–240.
Peterson, L. C. and Bogert, B. P. 1950. A dynamical theory of the cochlea. J. Acoust. Soc. Am. 22, 369–381.
Prendergast, P. J., Ferris, P., Rice, H. J., and Blayney, A. W. 1999. Vibro-acoustic modelling of the outer and middle ear using the finite-element method. Audiol. Neurootol. 4, 185–191.
Puria, S. 2003. Measurements of human middle ear forward and reverse acoustics, implications for otoacoustic emissions. J. Acoust. Soc. Am. 113, 2773–2789.
Puria, S. and Allen, J. B. 1991. A parametric study of cochlear input impedance. J. Acoust. Soc. Am. 89, 287–309.
Puria, S. and Allen, J. B. 1998. Measurements and model of the cat middle ear, evidence of tympanic membrane acoustic delay. J. Acoust. Soc. Am. 104, 3463–3481.
Puria, S., Kunda, L. D., Roberson, J. B., and Perkins, R. C. 2005. Malleus-to-footplate ossicular reconstruction prosthesis positioning, cochleovestibular pressure optimization. Otol. Neurotol. 26, 368–379.
Puria, S., Peake, W. T., and Rosowski, J. J. 1997. Sound-pressure measurements in the cochlear vestibule of human-cadaver ears. J. Acoust. Soc. Am. 101, 2754–2770.
Puria, S., Sim, J. H., Shin, M., Tuck-Lee, J., and Steele, C. R. 2007. Middle Ear Morphometry from Cadaveric Temporal Bone MicroCT Imaging. In: Middle Ear Mechanics in Research and Otology (*eds*. A. Eiber and A. Huber), World Scientific. pp. 260–269.
Rabbitt, R. D. and Holmes, M. H. 1986. A fibrous dynamic continuum model of the tympanic membrane. J. Acoust. Soc. Am. 80, 1716–1728.
Ranke, O. 1950. Theory of operation of the cochlea, a contribution to the hydrodynamics of the cochlea. J. Acoust. Soc. Am. 22, 772–777.
Ren, T. 2002. Longitudinal pattern of basilar membrane vibration in the sensitive cochlea. Proc. Natl. Acad. Sci. U. S. A. 99, 17101–6.
Rhode, W. S. 1971. Observations of the vibration of the basilar membrane in squirrel monkeys using the Mossbauer technique. J. Acoust. Soc. Am. 49, 1218.
Rosowski, J. J. and Merchant, S. N. 1995. Mechanical and acoustic analysis of middle-ear reconstruction. Am. J. Otol. 16, 486–497.
Rosowski, J. J., Songer, J. E., Nakajima, H. H., Brinsko, K. M., and Merchant, S. N. 2004. Clinical, experimental, and theoretical investigations of the effect of superior semicircular canal dehiscence on hearing mechanisms. Otol. Neurotol. 25, 323–332.
Ruggero, M. A., Narayan, S. S., Temchin, A. N., and Recio, A. 2000. Mechanical bases of frequency tuning and neural excitation at the base of the cochlea, comparison of basilar-membrane vibrations and auditory-nerve-fiber responses in chinchilla. Proc. Natl. Acad. Sci. U. S. A. 97, 11744–50.
Ruggero, M. A., Rich, N. C., Recio, A., Narayan, S. S., and Robles, L. 1997. Basilar-membrane responses to tones at the base of the chinchilla cochlea. J. Acoust. Soc. Am. 101, 2151–2163.

Shaw, E. A. 1974. Transformation of sound pressure level from the free field to the eardrum in the horizontal plane. J. Acoust. Soc. Am. 56(6), 1848–1861.
Shaw, E. A. and Teranishi, R. 1968. Sound pressure generated in an external-ear replica and real human ears by a nearby point source. J. Acoust. Soc. Am. 44, 240–249.
Shera, C. A. 2001. Intensity-invariance of fine time structure in basilar-membrane click responses, implications for cochlear mechanics. J. Acoust. Soc. Am. 110, 332–348.
Shera, C. A. and Guinan, J. J., Jr. 1999. Evoked otoacoustic emissions arise by two fundamentally different mechanisms, a taxonomy for mammalian OAEs. J. Acoust. Soc. Am. 105, 782–798.
Shera, C. A. and Zweig, G. 1991. Asymmetry suppresses the cochlear catastrophe. J. Acoust. Soc. Am. 89, 1276–1289.
Sim, J. H., Puria, S., and Steele, C. R. 2003. Three-Dimensional Measurements and Analysis of the Isolated Malleus–Incus Complex. In: Middle Ear Mechanics in Research and Otology (*eds*. K. Gyo, H. Wada, N. Hato, and T. Koike), pp. 61–67. World Scientific.
Simmons, F. B. and Beatty, D. L. 1962. A theory of middle ear muscle function at moderate sound levels. Science 138, 590–592.
Sohmer, H. and Freeman, S. 2004. Further evidence for a fluid pathway during bone conduction auditory stimulation. Hear. Res. 193, 105–110.
Steele, C. R. and Puria, S. 2005. Force on inner hair cell cilia. Int. J. Solids Struct. 42, 5887–5904.
Steele, C. R. and Shad, K. R. 1995. Asymptotic-numeric solution for shells of revolution. Appl. Mechan. Rev. 48, S44–S51.
Steele, C. R. and Taber, L. A. 1979. Comparison of WKB calculations and experimental results for three-dimensional cochlear models. J. Acoust. Soc. Am. 65, 1007–1018.
Stenfelt, S., Hato, N., and Goode, R. L. 2004. Fluid volume displacement at the oval and round windows with air and bone conduction stimulation. J. Acoust. Soc. Am. 115, 797–812.
Stinson, M. R. and Khanna, S. M. 1994. Spatial distribution of sound pressure and energy flow in the ear canals of cats. J. Acoust. Soc. Am. 96, 170–180.
Teig, E. 1972. Tension and contraction time of motor units of the middle ear muscles in the cat. Acta Physiol Scand, 84, 11–21.
Teranishi, R. and Shaw, E. A. 1968. External-ear acoustic models with simple geometry. J. Acoust. Soc. Am. 44, 257–263.
Tonndorf, J. and Khanna, S. M. 1972. Tympanic-membrane vibrations in human cadaver ears by time-averaged holography. J. Acoust. Soc. Am. 52, 1221–1233.
Voldrich, L. and Ulehlova, L. 1987. Cochlear micromechanics. Acta Otolaryngol. 103, 661–664.
Wada, H. and Kobayashi, T. 1990. Dynamical behaviour of middle ear, theoretical study corresponding to measurement results obtained by a newly developed measuring apparatus. J. Acoust. Soc. Am. 87, 237–245.
Wada, H., Metoki, T., and Kobayashi, T. 1992. Analysis of dynamic behaviour of human middle ear using a finite-element method. J. Acoust. Soc. Am. 92, 3157–3168.
Weiss, J. and Gardiner, J. 2001. Computational modeling of ligament mechanics. Crit. Rev. Biomed. Engin. 29, 1–70.
West, C. D. 1985. The relationship of the spiral turns of the cochlea and the length of the basilar membrane to the range of audible frequencies in ground dwelling mammals. J. Acoust. Soc. Am. 77, 1091–101.
Wever, E. G. and Lawrence, M. 1954. Physiological Acoustics. Princeton University Press.
White, R. D. and Grosh, K. 2005. Microengineered hydromechanical cochlear model. Proc. Natl. Acad. Sci. U. S. A. 102, 1296–1301.
Wiener, F. M., Pfeiffer, R. R., and Backus, A. S. 1966. On the sound pressure transformation by the head and auditory meatus of the cat. Acta Otolaryngol. 61, 255–269.
Willi, U. B., Ferrazzini, M. A., and Huber, A. M. 2002. The incudo-malleolar joint and sound transmission losses. Hear. Res. 174, 32–44.
Windmill, J. F., Gopfert, M. C., and Robert, D. 2005. Tympanal travelling waves in migratory locusts. J. Exp. Biol. 208, 157–68.
Wittbrodt, M. J., Steele, C. R., and Puria, S. 2006. Developing a physical model of the human cochlea using micro-fabrication methods. Audiol. Neurotol. 11, 104–112.
Yang, X. and Henson, O. W., Jr. 2002. Smooth muscle in the annulus fibrosus of the tympanic membrane, physiological effects on sound transmission in the gerbil. Hear. Res. 164, 105–114.
Yoon, Y. J., Puria, S., and Steele, C. R. 2006. Intracochlear pressure and organ of Corti impedance from a linear active three-dimensional model. ORL J. Otorhinolaryngol. Relat. Spec. 68, 365–372.
Zhang, L., Mountain, D. C., and Hubbard, A. E. 1997. Shape and stiffness changes of the organ of Corti from base to apex cannot predict characteristic frequency changes, are multiple modes the answer? In: Diversity in Auditory Mechanics (*eds*. E. R. Lewis, G. R. Long, P. M. Narins, C. R. Steele, and E. Hecht-Poinar), pp. 472–478. World Scientific.
Zweig, G. 1991. Finding the impedance of the organ of Corti. J. Acoust. Soc. Am. 89, 1229–1254.
Zwicker, E. 1972. Investigation of the inner ear of the domestic pig and the squirrel monkey with special regard to the hydrodynamics of the cochlear duct. Symp. Hear. Theory IPO, Eindhoven, Holland. 182–185.
Zwislocki, J. 1948. Theorie der Schneckenmechanik, qualitative und quantitative Analyse [Theory of cochlear mechanics.]. Acta Oto-Laryngol. 72, 1–76.
Zwislocki, J. 1961. Acoustic measurement of the middle ear function. Ann. Otol. Rhinol. Laryngol. 70, 599–606.
Zwislocki, J. 1963. An acoustic method for clinical examination of the ear. J. Speech Hear. Res. 13, 303–314.
Zwislocki, J. J. 1953. Review of recent mathematical theories of cochlear dynamics. J. Acoust. Soc. Am. 25, 743–751.
Zwislocki, J. 1965. Analysis of Some Auditory Characteristics. In: Handbook of Mathematical Physiology (*eds*. R. D. Luce, R. R. Bush, and E. Galanter), pp. 3–46. Wiley.
Zwislocki, J. 1975. The Role of the External and Middle Ear in Sound Transmission. In: The Nervous System. Vol. 3, Human Communication and its Disorders (*ed*. D. B. Tower), pp. 44–55. Raven Press.

3.11 Evolution of the Middle Ear and Inner Ear in Vertebrates

R R Fay, Loyola University Chicago, Chicago, IL, USA

© 2008 Elsevier Inc. All rights reserved.

References 208

Glossary

abneural A direction on the basilar papilla. Away from the side of the papilla containing the auditory nerve.

adenosine triphosphate (ATP) The source of energy in living cells.

columella A small, thin columnlike structure that transfers vibrations between the tympanic membrane and the fluid-filled basilar papilla.

farfield In acoustics, the region of a sound field, far from the source, in which sound propagates as a plane, progressive sound wave.

gnathostomes Jawed vertebrates.

homologous Characters in different species who were inherited from a common ancestor and thus share a similar ontogenetic pattern.

hyomandibular Pertaining both to the hyoidean arch and the mandible or lower jaw; as, the hyomandibular bone or cartilage, a segment of the hyoid arch which connects the lower jaw with the skull in fishes.

lagena The lower, posterior, and outer chamber of the inner ear projecting from the sacculus, probably responsible for hearing. Usually an otolith organ.

monotreme A primitive, egg-laying mammal.

nearfield In contrast to the farfield, a region close to a sound source where acoustic particle motion is largely due to hydrodynamic flow (fluid flow), rather than as part of a plane, progressive sound wave.

octaval Referring to the VIII cranial nerve, or auditory nerve.

otolith organ An organ of the ear characterized by a sensory epithelium overlain by an otolith, or substantially calcium carbonate ear stone operating as a restraint structure.

otophysans A sort of teleost fish having an efficient mechanical connection between the swimbladder and the ear known as Weberian ossicles.

sarcopterigians The three modern groups of lobe-finned bony fishes – the coelacanths, lungfishes, and tetrapods (amphibians). All have fleshy fins or limbs.

stereovilli The hairs of hair cells. The part of the hair cell, the deflection of which causes transduction, or the conversion of mechanical energy to electrochemical energy.

tectorial Pertaining to the structures of the ear that restrain the tips of the stereovilli so that they may be deflected by relative motion between the hair cell body and the tectorial structure.

telencephalic Pertaining to the most recently evolved portions of the brain (forebrain).

tetrapodomorphs Vertebrates having four legs and four feet.

thalamic Anatomical structure of the forebrain that connects brainstem structures with cerebral cortex.

tonotopic organization Organization of the ear or brain in which sound frequencies are spatially sorted and isomorphically projected.

vestibular Pertaining to the organs of the sense of balance.

Weberian ossicles In otophysan fishes, a series of bones connecting the ear and swimbladder, enhancing sound pressure sensitivity and upper hearing range.

This chapter summarizes what is currently thought about the evolution of the middle and inner ear of vertebrates. What is thought on this topic has varied over time, depending on the orientation of the author with respect to evolution in general, and auditory system evolution in particular. For example, the story of the evolution of the middle ear could be told by moving backward in time from the three-ossicle middle ear of humans (mammals) to the origins of this peculiar ossicular arrangement among early mammals, and then back through reptiles and early tetrapods, to the various fishes. The mammalian coiled cochlea could be treated similarly. This way of constructing a story emphasizes the unity of life (Dawkins, R., 2004). Another way to tell the story is through the history of all vertebrates, from fishes, to paleozoic tetrapods, to the great diversifications of species about 250 million years ago (mya) when there appeared crocodiles, dinosaurs, turtles, mammals, modern amphibians, and teleost fishes (Manley, G. and Clack, J., 2004). This is a more satisfying orientation to the evolutionary stories that extols the diversity of life (Dawkins, R., 2004). I choose this orientation in part because one particular extant form (e.g., the mammalian middle ear) is not portrayed as an inevitable evolutionary endpoint, and in part because it presents the various extant middle ears as alternative solutions to a problem and not as imperfect approximations of the mammalian (human) type.

What follows is one view of the evolution of middle and inner ears among vertebrate animals. This view arises primarily from the recently published volume, *Evolution of the Vertebrate Auditory System* (Manley, G. *et al.*, 2004), which represents the most recent and comprehensive treatment of this complex topic. The following depends heavily on this source, and is in some ways a selective summary of it.

The gnathostomes comprise the early fishes, splitting into three groups, lobe-finned fishes leading to Coelacanth (*Latimeria*) and the tetrapods; ray-finned fishes leading to most modern fishes; and sharks and rays. The first vertebrate inner ears appeared among fishes, and the same could be said of middle ears with a generous definition of middle ear. Of course, there is only speculation on the origin of the first vertebrate ear that responded to sound, but it is likely to have developed very early on from an ear that was initially adapted as a vestibular organ, with typically vestibular frequency response (fractions of a hertz to 10 Hz, or so). Organs with presumed vestibular functions have been identified in all three groups of gnathostomes, so were likely present in their common ancestor. It is not known whether the auditory organs observed in living representatives of these three groups are homologous or convergent (independently evolved). An auditory organ cannot be identified by appearance in fishes because the main distinction between a vestibular and auditory organ is in the frequency response and filtering properties (Cortopassi, K. A. and Lewis, E. R., 1988) of its filters, and its projections to the central nervous system (CNS). Any otolith organ such as the saccule can respond to sound (acoustic particle motion) by transducing relative motion between the otolith (density of about 3) and the sensory epithelium (de Vries, H. L., 1950). This relative motion can be caused by a nearfield or farfield wave passing through the animal and bringing the tissues into motion. Due to its high inertia, the otolithic mass will lag the motion of the tissues and a relative motion will result. When the frequency of this disturbance becomes sufficiently high (e.g., 100 Hz), we can say that it is sound. The animal can be said to hear if it could be expected to respond to the source as an external entity (Lewis, E. R. and Fay, R. R., 2004). This primitive or shared mode of hearing operates in all extant species and is the basis for their hearing which is apparently present in all species. Motional sensitivity of otolith organs is high; behavioral and physiological responses can be evoked by 100 Hz displacements as small as 0.1 nm (Chapman, C. J. and Sand, O., 1974; Fay, R. R. and Edds-Walton, P. L., 1997).

Among fishes, the presence of a sense of hearing is to be inferred, in many cases where behavioral data are lacking, by the organization of the CNS. All fishes examined so far have a central auditory system organization analogous to mammals and other tetrapods (see Chapters 3.30, 3.49). There are several first-order medullar nuclei that project to the auditory nucleus of the midbrain directly and via secondary octaval cell populations (in all fishes examined so far; McCormick, C., 2001). There is at least one thalamic auditory nucleus (Lu, Z. and Fay, R. R., 1996), and several telencephalic auditory nuclei, although these are not well known. This organization is the hallmark of an auditory system in other vertebrates, and is presumed to have the same function among fishes. It is certainly not a central vestibular system.

Many freshwater species have special adaptations that make them pressure sensitive as well as directly sensitive to acoustic particle motion (Braun, C. and Grande, T., in press). These species are generally referred to as hearing specialists, and all are

characterized by a gas bubble or gas bladder that is brought into close association with the ear by a short or efficient transmission pathway. These specialists are thought to be more sensitive to sound and to have a wider bandwidth of hearing than the generalists (by definition, all other fishes). As described by Boyles law, these gas bodies change volume in response to sound-pressure fluctuation, and this motion is transmitted to the organ(s) of the ear where they engage the otolith or hair cell sensory epithelium in motion. These ears therefore respond in proportion to sound pressure and would even be expected to respond to a pressure maximum of a standing wave where the wave impedance is nearly infinite (Fay, R. R. and Popper, A. N., 1975). In the Otophysans (goldfish, carp, minnows, suckers, knifefish, and catfish), this transmission pathway is the Weberian ossicles, a series of modified ribs and vertebral arches that directly connect the anterior swimbladder with the perilymphatic system of the ear, and ultimately to the endolymphatic fluids of the saccular organ. Another way that the swimbladder can be brought into proximity with the ear is by way of forward extensions of the swimbladder, or swimbladder horns. These can be found in species of the Holocentridae, Gadidae (cods), Cichlidae, Notopteridae, Elopomorphidae, and Percomorpha. Finally, there are the peculiar ears of clupeids (herrings) (Blaxter, J. H. S. *et al.*, 1981) in which an air-filled chamber directly apposes the utricular organ, and the Mormyridae (African electric fish; Crawford, J. D., 1997) in which the paired saccules have attached private gas bladders. In these species, the saccule (or utricle in herrings) can probably be identified as an exclusively auditory organ. Within teleosts, novel mechanisms for enhancing hearing may have evolved over 20 times (Braun, C. and Grande, T., in press). It has been speculated that these hearing enhancements probably required rather quiet environments in which to evolve (Amoser, S. and Ladich, F., 2005). Throughout the evolution of fishes, hearing has been subserved by otolith organs (commonly, the saccule) and there is little indication of the development a specifically auditory papilla in fishes as developed in tetrapods. However, Fritzsch B. (1987) described an unusual sensory papilla that he identified with the tetrapod basilar papilla in the ear of the Coelacanth (Latimeria), one of the only surviving species of sarcopterigians (lobe-finned fish) that are tetrapod ancestors. However, it is not known whether this organ is homologous with the basilar papilla of tetrapods.

These, and other morphological specializations for enhanced hearing, have evolved and are still evolving among teleosts. Teleosts appeared in the late Triassic (225 mya) roughly along with crocodiles, dinosaurs, turtles, modern amphibians, and mammals. The earliest known Weberian ossicles first appeared during the late Cretaceous period (40–50 mya; Clack, J. and Allin, E., 2004). Thus, there is a long time separating the earliest fishes (420 mya) from the diversification of species that included the teleosts and the presumed development of the hearing specialists (an interval of about 350 million years). Thus, the hearing enhancements among fishes appeared much later than the development of the tetrapod tympanic ear.

The first tetrapodomorphs appeared in the fossil record in the late Devonian about 350 mya, and they continued to evolve for 140 million years before the great diversification of species during the late Permian. For most of this period, these tetrapods were amphibious, and probably spent a significant portion of their life underwater. Their tetrapod limbs served locomotion underwater, and on land probably served getting the animal from one body of water to another. Presumably, the tetrapod basilar papilla first appeared among these Paleozoic tetrapods as a new organ in the lagenar resess, between the saccule and lagena, but there is no fossil evidence regarding the first appearance of the basilar papilla. Nor is there evidence that these amphibians developed arial hearing until the Triassic period (appearance of tympanic ears in various groups), so this new organ must have functioned primarily in bone conduction and underwater hearing (see Chapter 3.14). The basilar papilla of turtles and the Tuatara (*Sphenodon*) are probably the closest organs in living species to the original basilar papilla of tetrapods (Wever, E. G., 1978). Based on the ears of these species, the original papilla was probably of small size (less than 1 mm), contained between 100 and 1000 hair cells, had both afferent and efferent innervation, was covered by a tectorial membrane, and had hair cell orientations in only one, abneural direction (Manley, G. and Clack, J., 2004). It did not receive input from a tympanic ear, however.

The evolution of the stapes or columella (formerly in fishes, the hyomandibular bone) had begun among Paleozoic tetrapods (e.g., *Acanthostega* and *Ichthyostega*); its size, orientation, and relation to other skull structures give clues to its possible functions in hearing. Originally, apparently, it fit into the early equivalent of the oval window, but

its function is a matter of speculation. It was too massive to function as a stapes does, but could have functioned in bone conduction as an inertial mass (analogous to an otolith) in a mechanical circuit involving the basilar papilla. However, a pressure release window analogous to the round window did not evolve until later, and independently in mammals, crocodiles, birds, and dinosaurs (Clack, J. and Allin, E., 2004).

Throughout the Carboniferous period (350–290 mya) two groups of tetrapods developed; the line leading to amniotes (reptiles, crocodiles, birds, and mammals), and the line leading to modern amphibians (temnospondyls and lissamphibians). The temnospondyls were the first animals thought to have a terrestrially adapted ear, with a narrow-shafted stapes and a skull embayment presumed to be tympanic (e.g., *Balanerpeton* from the early Carboniferous; Clack, J. and Allin, E., 2004). These temnospondyls are thought to be the first species to make sounds. An alternative hypothesis places lissamphibians and amniotes closer to lepospondyls, small tetrapods that did not develop a tympanic ear until the late Triassic (210 mya). In any case, lissamphibians are the frogs and toads (Anura), salamanders and newts (Caudata), and caecilians (Gymnophonia). Modern forms are all thought to be highly derived (specialized) compared to their earliest ancestors, with the Caudata probably most closely resembling their early ancestors (Smotherman, M. and Narins, P., 2004). The ears of anurans consist of an amphibian papilla, a basilar papilla, a macula neglecta, a lagena, and a saccular organ, among others. The anuran basilar papilla may be homologous to the basilar papilla of reptiles and birds, but in spite of having the same name, this is not settled. The amphibian papilla has no counterpart among amniotes, yet it is tonotopically organized, unlike the anuran basilar papilla. Primary afferents are narrowly tuned and represent filters of high dynamic order (Lewis, E. R., 1992), so these characteristics evolved independently among amphibians and amniotes.

Remarkably, a tympanic middle ear developed independently among all amniotes during the Triassic (2220–250 mya), affording each group (Synapsids, Lepidosaurs, and Archroaurs) an enhanced sensitivity to airborne sound (Clack, J. and Allin, E., 2004; see Figure 1). This, in turn, apparently caused a rapid and simultaneous development and differentiation of the basilar papilla characteristic of these groups toward their modern forms (Manley, G. and Clack, J., 2004). Crocodiles, alligators, and birds are the descendants of the Archosaurs. The basilar papilla of these groups is wide and elongated, covered by a mosaic of hair cells and a thick tectorial membrane. In birds, there can be as many as 50 hair cells per cross-section,

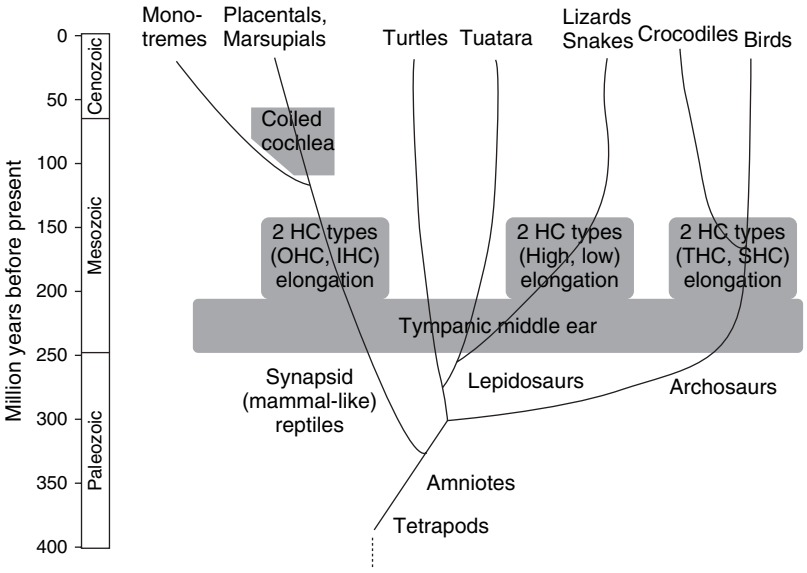

Figure 1 A family tree for amniote vertebrates emphasizing the independent evolution of the tympanic middle ear, and the independent development of two hair cell (HC) types. IHC, inner hair cell; OHC, outer hair cell; SHC, short hair cells; THC, tall hair cells. Reproduced from Manley, G. and Clack, J. 2004. An Outline of the Evolution of Vertebrate Hearing. In: Evolution of the Vertebrate Auditory System (*eds*. G. Manley, A. N. Popper, and R. R. Fay), pp. 1–26. Springer, with permission from Springer.

some so-called tall hair cells, and some short hair cells. Tall hair cells receive both afferent and efferent innervation, while short hair cells receive efferent but no afferent innervation. Apparently this dichotomy evolved independently and at the same time as inner and outer hair cells in mammals (late Triassic period).

Turtles represent their diapsid ancestors, and the Tuatara (lizard-like animal) is slightly later derived. The numerous species of lizards and snakes make up the most living descendents of diapsid lepisosaurs that developed during the Triassic. The basilar papillas of lizards is rather well described (Wever, E. G., 1978). It always has two types of hair cells; low-frequency and high-frequency. Low-frequency hair cells (<1 kHz) are primitive types derived from stem reptiles and snakes. High-frequency hair cells (up to 5 or 6 kHz) are more recently derived. These two types of hair cells arose independently of tall and short hair cells in birds, and inner and outer hair cells in mammals. The basilar papilla of iguanids is the most primitive. It consists of three areas; a central area of unidirectionally oriented, low-frequency hair cells (presumably representative of stem reptiles) flanked by areas of high-frequency hair cells on both sides, oriented in two, opposing directions. The central, unidirectional area is made up of hair cells that are electrically tuned to various best frequencies by virtue of particular membrane channels (Fettiplace, R. and Crawford, A. C., 1980). Extant lizards show remarkable diversity at the level of families, genus, and species (Manley, G., 2004). Surprisingly, this structural variation is not correlated with parallel functional variation; the peripheral anatomy is highly diverse among species, but the neurophysiology shows remarkable conservation of function and no comparable diversity (Manley, G., 2004).

Nonmammalian tetrapods all have a compound mandible consisting of many interrelated bones. The mammal mandible consists of the dentary bone alone, and the others of the complex jaw of mammal ancestors have been recruited into the new middle ear (angular, surangular, articular (malleus homolog), and preatricular) along with the quadrate (incus homolog), or are lost in mammals. This complex middle ear of mammals is probably responsible for the subsequent development of high-frequency hearing among mammals, but this capacity requires adaptations of the cochlea as well as of the middle ear.

The best-known early or stem mammal is *Morganucodon*, a small insectivorous animal of the late Triassic (200 mya). It is almost certain that this genus had a tympanic membrane; a malleus, incus, and stapes; and aerial hearing. Its cochlea has a finger-like shape, similar to that of birds. Rosowski J. J. (1992) has modeled the middle ear of *Morganucodon* as a mammalian microtype that was adapted to high-frequency hearing typical of some extant mammals. The elongated, coiled cochlea characteristic of modern placentals and marsupials (but not monotremes) appeared at least by the late Cretaceous (70 mya). So, it is thought that high-frequency hearing of modern mammals (well above 10 kHz) and echolocation capacities of some species, traits that set them apart from monotremes and all other tetrapods, appeared most definitely by this time (the late Cretaceous), and possibly earlier with *Morganucodon* during the late Triassic. High-frequency hearing predated a long, coiled cochlea.

Extant monotremes (platypus and echidnas) retain reptilian ear characteristics such as a short, uncoiled cochlea, the retention of a lagena at the distal end of the cochlea, and hearing probably no higher than 10 kHz. However, they have a three-ossicle middle ear that appears to have developed independently in monotremes and therian mammals (Rich, T. H. *et al.*, 2005), and the cochlea's internal structure is more similar to other mammals than to archosaurs (birds and reptiles) in having a clear distinction between inner and outer hair cells (Vater, M. *et al.*, 2004). The earliest known monotreme is from the early Cretaceous (140 mya), but the earliest known middle ear fossils are 115 million years old (from the Cretaceous period).

Recently, it has become clear that the mammalian cochlea is endowed with a unique mechanism for active amplification, motile outer hair cells that can feed back electrical-to-mechanical energy to basilar membrane motion. One mechanism identified in this process is prestin, a protein of the outer hair cell membrane that is capable of direct, rapid, electromechanical conversion without dependence on adenosine triphosphate (ATP; Zheng, J. *et al.*, 2000). It seems likely that prestin's functional role of active amplification appeared already in the first amniote ears (Manley, G. and Clack, J., 2004). Active amplification via the stereovillar bundle has been identified and analyzed in the saccular organ of bullfrogs (Hudspeth, A. J., 1997). While this organ has vestibular functions in amniotes, it functions as an organ of hearing in fishes and anurans (Lewis, E. R., 1992). Apparently, transduction channels on the stereovillar bundles cause a force on the bundle when they are

opened and closed. This general mechanism for fast stereocilliar motility has been observed in various hair cell systems, and appears to operate in the mammalian cochlea as well (Kennedy, H. J. *et al.*, 2003; Manley, G. and Clack, J., 2004). So, there seems to have been a parallel evolution of inner ear active amplification processes. The prestin mechanism is so far only identified with outer hair cells and the high-frequency hearing of mammals (well above 10 kHz).

In conclusion, one of the remarkable developments in our understanding of middle and inner ear evolution is the recent evidence for, and our willingness to accept, the ubiquity of parallel or independent evolution of many features of the auditory system. Not covered here is the story of the evolution of the CNS (Grothe, B. *et al.*, 2004), another example of parallel evolutionary trends among all vertebrates. In every vertebrate order the organization of the auditory CNS is analogous; it consists of multiple first-order medullar nuclei, several secondary nuclei, a lateral lemniscus, a midbrain auditory nucleus, thalamic nuclei, and telencephalic auditory areas. But all this analogy (including neurophysiological or functional analogy) has to be attributed to independent evolution because the evidence is against homology. Likewise, in the evolution of the middle and inner ears the recent evidence is inescapable that many features of vertebrate audition evolved independently. These features include the development of tympanic ears for aerial hearing; the development of two categories of hair cell; the three-boned middle ears of mammals; the inner ear organs themselves in fishes, amphibians, archosaurs, and mammals; mechanisms for frequency selectivity; and cochlear amplification. All this parallelism begs the question of what accounts for it. At least part of the answer must be that the requirements of auditory systems (the state demanded by the organism; Gans, C., 1992) are essentially similar for all species and for all time; the capacity to determine and perceptually segregate sources of sound, so that behavior may be appropriate with respect to them (Lewis, E. R. and Fay, R. R., 2004).

References

Amoser, S. and Ladich, F. 2005. Were hearing sensitivities of freshwater fishes selected by the ambient noise in their habitats. *Abstracts of the Midwinter Meeting of the Association for Research in Otolaryngology,* 19–24 February, New Orleans, LA.

Blaxter, J. H. S., Denton, E. J., and Gray, J. A. B. 1981. Acoustico-Lateralis Systems in Clupeid Fishes. In: Hearing and Sound Communication in Fishes (*eds*. W. N. Tavolga, A. N. Popper, and R. R. Fay), pp. 39–59. Springer.

Braun, C. and Grande, T. Evolution of Peripheral Mechanisms for the Enhancement of Sound Reception. In: Fish Bioacoustics (*eds*. J. Webb, R. R. Fay, and A. N. Popper). Springer (in press).

Chapman, C. J. and Sand, O. 1974. Field studies of hearing in two species of flatfish, *Pleuronectes platessa* (L.) and *Limanda limanda* (L.) (family Pleuronectidae). Comp. Biochem. Physiol. 47, 371–385.

Clack, J. and Allin, E. 2004. The Evolution of Single- and Multiple-Ossicle Ears in Fishes and Tetrapods. In: Evolution of the Vertebrate Auditory System (*eds*. G. Manley, A. N. Popper, and R. R. Fay), pp. 128–163. Springer.

Cortopassi, K. A. and Lewis, E. R. 1988. A comparison of the linear tuning properties of two classes of axons in the bullfrog lagena. Brain Behav. Evol. 51, 331–348.

Crawford, J. D. 1997. Feature-detecting auditory neurons in the brain of a sound-producing fish. J. Comp. Physiol. A 180, 439–450.

Dawkins, R. 2004. The Ancestor's Tale. Houghton-Mifflin.

de Vries, H. L. 1950. The mechanics of labyrinth otoliths. Acta Otolaryngol. 38, 262–273.

Fay, R. R. and Edds-Walton, P. L. 1997. Directional response properties of saccular afferents of the toadfish, *Opsanus tau*. Hear. Res. 111, 1–21.

Fay, R. R. and Popper, A. N. 1975. Modes of stimulation of the teleost ear. J. Exp. Biol. 62, 379–387.

Fettiplace, R. and Crawford, A. C. 1980. The origin of tuning in turtle cochlear hair cells. Hear. Res. 2, 447–454.

Fritzsch, B. 1987. The inner ear of the coelacanth fish *Latimeria* has tetrapod affinities. Nature 327, 153–154.

Gans, C. 1992. An Overview of the Evolutionary Biology of Hearing. In: The Evolutionary Biology of Hearing (*eds*. D. B. Webster, R. R. Fay, and A. N. Popper), pp. 3–14. Springer.

Grothe, B., Carr, C. E., Casseday, J. H., Fritzsch, B., and Koppl, C. 2004. The Evolution of Central Pathways and Their Neural Processing Patterns. In: Evolution of the Vertebrate Auditory System (*eds*. G. Manley, A. N. Popper, and R. R. Fay), pp. 289–359. Springer.

Hudspeth, A. J., Choe, Y., Mehta, A. D., and Martin, P. 1997. Putting ion channels to work: mechanoelectrical transduction, adaptation, and amplification by hair cells. Proc. Nat. Acad. Sci. 97, 11765–11772.

Kennedy, H. J., Evans, M. G., Crawford, A. C., and Fettiplace, R. 2003. Fast adaptation of mechanoelectrical transducer channels in mammalian cochlear hair cells. Nature Neurosci. 6, 790–791.

Lewis, E. R. 1992. Convergence of Design in Vertebrate Acoustic Sensors. In: The Evolutionary Biology of Hearing (*eds*. D. B. Webster, R. R. Fay, and A. N. Popper), pp. 163–184. Springer.

Lewis, E. R. and Fay, R. R. 2004. Environmental Variables and the Fundamental Nature of Hearing. In: Evolution of the Vertebrate Auditory System (*eds*. G. Manley, A. N. Popper, and R. R. Fay), pp. 27–54. Springer.

Lu, Z. and Fay, R. R. 1996. Two-tone interaction in auditory nerve fibers and midbrain neurons of the goldfish, *Carassius auratus*. Aud. Neurosci. 2, 257–273.

Manley, G. 2004. The Lizard Basilar Papilla and Its Evolution. In: Evolution of the Vertebrate Auditory System (*eds*. G. Manley, A. N. Popper, and R. R. Fay), pp. 200–223. Springer.

Manley, G. and Clack, J. 2004. An Outline of the Evolution of Vertebrate Hearing. In: Evolution of the Vertebrate Auditory System (*eds*. G. Manley, A. N. Popper, and R. R. Fay), pp. 1–26. Springer.

Manley, G., Popper, A. N., and Fay, R. R. (*eds*.) 2004. Evolution of the Vertebrate Auditory System. Springer.
McCormick, C. 2001. Brainstem acoustic areas in the marine catfish, *Arius felis*. Brain Behav. Evol. 57, 134–149.
Rich, T. H., Hopson, J. A., Musser, A. M., Flannery, T. F., and Vickers-Rich, P. 2005. Independent origins of middle ear bones in monotremes and therians. Science 307, 910–914.
Rosowski, J. J. 1992. Hearing in Transitional Mammals: Predictions from the Middle Ear Anatomy and Hearing Capabilities of Extant Mammals. In: The Evolutionary Biology of Hearing (*eds*. D. B. Webster, R. R. Fay, and A. N. Popper), pp. 615–632. Springer.
Smotherman, M. and Narins, P. 2004. Evolution of the Amphibian Ear. In: Evolution of the Vertebrate Auditory System (*eds*. G. Manley, A. N. Popper, and R. R. Fay), pp. 164–199. Springer.
Vater, M., Meng, J., and Fox, R. 2004. Hearing Organ Evolution and Specialization: Early and Later Mammals. In: Evolution of the Vertebrate Auditory System (*eds*. G. Manley, A. N. Popper, and R. R. Fay), pp. 256–288. Springer.
Wever, E. G. 1978. The Lizard Ear. Princeton University Press.
Zheng, J., Shen, W., He, D. Z., Madison, L. D., and Dallos, P. 2000. Prestin is the motor protein of cochlear outer hair cells. Nature 405, 149–155.

3.12 Biophysics of Chordotonal Organs

A S French, Dalhousie University, Halifax, NS, Canada

© 2008 Elsevier Inc. All rights reserved.

3.12.1	**Introduction**	211
3.12.2	**Structures of Chordotonal Organs**	212
3.12.3	**Locations and Functions of Chordotonal Organs**	212
3.12.3.1	Major Functions	212
3.12.3.2	Organs of Hearing	213
3.12.4	**Sensory Biophysics**	213
3.12.4.1	Mechanoreception in Arthropod Type I Mechanosensilla	213
3.12.4.2	Mechanical Coupling in Chordotonal Organs	214
3.12.4.3	Ciliary Functions in Type 1 Chordotonal Sensilla	214
3.12.4.4	Transduction and Action Potential Encoding in Chordotonal Sensilla	215
References		215

Glossary

arthropods Animals with segmented bodies and legs: insects, spiders, and crustaceans.

chordotonal organ Sensory organ found in insects and crustaceans. The name means long, thin structure, associated with hearing.

cilium, cilia Hairlike structures that form parts of many types of cells.

nematic Having molecules arranged in a linear, but not layered structure.

scolopale Twisted fence, a ring of electron-dense rods like the staves of a barrel.

tubular body Structure found in many arthropod mechanoreceptor neurons consisting of microtubules embedded in electron-dense material.

3.12.1 Introduction

Chordotonal organs are mechanosensory structures found in two of the three major classes of arthropods, insects, and crustacea (Graber, V., 1882; Howse, P. E., 1968; Moulins, M., 1976; Field, L. H. and Matheson, T., 1998). Arthropod mechanosensory neurons form two major groups, type I (cuticular) and type II (multipolar) (McIver, S. B., 1985; French, A. S., 1988). Type I neurons are bipolar, with cell bodies in the periphery between a single sensory dendrite and an axon that proceeds proximally to the central nervous system. They are closely associated with the exoskeleton, or cuticle, and innervate the hairs and bristles that cover many arthropods. In contrast, type II neurons have multiple sensory dendrites and are generally located in deeper structures such as muscles and internal organs.

Chordotonal organs contain type I sensory neurons. In insects, they are generally less directly connected to the exoskeleton than hairs or bristles. Instead, they are located below the cuticle, and detect relative movements of various body parts. In the case of joints in appendages, such as legs or antennae, this provides proprioception or gravity detection. In other cases the appendage is moved by currents in the air or water surrounding it, providing a sense of movements in the external environment. Chordotonal organs are often sensitive to rapid mechanical oscillations, making them vibration detectors and, for air-borne vibrations, organs of hearing. These include some elaborate hearing structures with comparable sensitivities and frequency ranges to vertebrate ears.

Less is known about crustacean chordotonal organs, although some have provided useful physiological models (Gamble, E. R. and DiCaprio, R. A., 2003). Crustacean chordotonal organs are more strongly associated with external mechanoreception, although nonchordotonal mechanosensory

innervation of sensory hairs in crustacea has also been reported (Crouau, Y., 1995).

3.12.2 Structures of Chordotonal Organs

General and specific structures of a variety of chordotonal organs have been described by light and electron microscopy (Howse, P. E., 1968; Moulins, M., 1976; Field, L. H. and Matheson, T., 1998; Yack, J. E., 2004). The central component is always a bipolar (type I) sensory neuron. The nomenclature is confusing because chordotonal sensory neurons are subdivided into type 1 and type 2, based on the form of the cilium (Figure 1; Field, L. H. and Matheson, T., 1998; Yack, J. E., 2004). Type 1 sensilla have long ciliary roots and a slender cilium with a dilation toward the distal end, whereas type 2 have reduced ciliary roots and the cilium expands distally with internal microtubules forming a tubular body.

The primary distinguishing feature of all chordotonal organs is the scolopale cell that surrounds the cilium, or several cilia, producing a dense set of intracellular scolopale rods, like barrel staves (Figure 1). Distally, the cilium is connected to an attachment cell and is embedded in an extracellular cuticular electron-dense structure forming a cap or tube. These forms are called mononematic or amphinematic, respectively (Graber, V., 1882; Moulins, M., 1976) reflecting the long, drawn-out form of the tube structure. Although type 1 and type 2 sensilla are generally associated with the cap and tube structures, respectively, chordotonal organs may contain more than one sensillum, of mixed types, embedded in the same distal structure. The terms monodynal and heterodynal refer to organs containing a single sensillum and multiple sensilla.

External to the cap or tube is an attachment cell, which connects the organ to the source of mechanical tension. However, tubes are often embedded in the external cuticle, which is presumed to provide the mechanical stimulation directly. Many fine ultrastructural details and significant variations exist within these broad patterns (Moulins, M., 1976; Field, L. H. and Matheson, T., 1998; Yack, J. E., 2004). Development, differentiation, and cell lineages of the various cells forming chordotonal organs have been reviewed by Field L. H. and Matheson T. (1998).

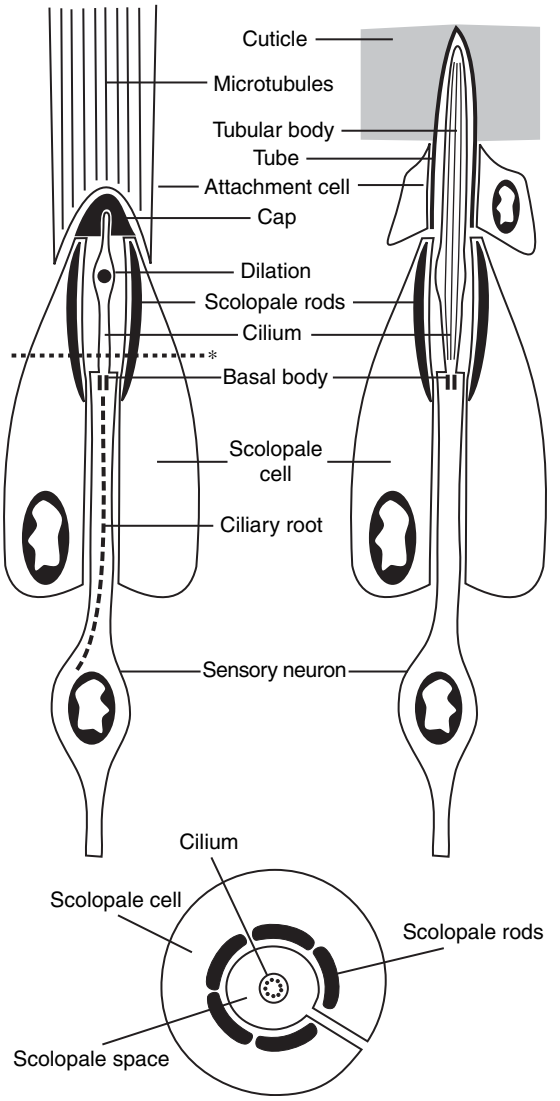

Figure 1 Chordotonal sensilla structures. Left: Type 1. Asterisk indicates the level of section shown in the lower figure. Right: Type 2. Note that other supporting cells are omitted for simplicity (based on material in Moulins, M. 1976; McIver, S. B., 1985; Field, L. H. and Matheson, T., 1998).

3.12.3 Locations and Functions of Chordotonal Organs

3.12.3.1 Major Functions

In insects, chordotonal organs are found in all major body regions (head, thorax, abdomen) and many appendages (antennae, mouthparts, legs, wings, ovipositors, cerci). Modalities include joint proprioception (connective chordotonal organs), substrate vibration (subgenual organs), sound (tympanal

organs) (Field, L. H. and Matheson, T., 1998), and infrared detection in the fire beetle (Mainz, T. *et al.*, 2004). Some organs are broadly homologous in many different species, such as the femoral chordotonal organ that detects femur–tibial movements and is involved in control of the leg musculature (Moran, D. T. *et al.*, 1975; Field, L. H. and Matheson, T., 1998; DiCaprio, R. A. *et al.*, 2002), and Johnston's organ in the pedicel (second segment) of insect antenna (McIver, S. B., 1985). Johnston's organs contains both type 1 and type 2 sensilla but they always terminate in one tube (amphinematic) ending. Johnston's organ is prominent in Diptera, with up to 20 000 sensory neurons in each male mosquito antenna, where they detect the sound produced by female mosquito wings (McIver, S. B., 1985).

3.12.3.2 Organs of Hearing

Sound sensitivity is known in many, but not all, insect groups. Organs of hearing occur in a wide variety of body locations in different species, including the mouthparts, thorax, abdomen, wings, and legs (Michelsen, A. and Larsen, O. N., 1985; Yack, J. E., 2004). Although some air movements are detected by long surface hairs, which are not chordotonal organs, most sounds are detected by structures based on chordotonal organs. The most elaborate of these use tympanal structures in the exoskeleton to collect and focus the sound vibrations onto sensilla. Tympanae are usually formed from the walls of trachea, which circulate gases within insect bodies (Michelsen, A. and Larsen, O. N., 1985; Yack, J. E., 2004).

Shaw S. R. (1994)suggested a model for the evolution of tympanal hearing organs in insects (Figure 2). In this model, chordotonal organs forming part of the vibration-detecting subgenual organ in the leg migrated to innervate the wall of an enlarged air sack in a leg trachea, increasing their sensitivity to vibration within the leg. This arrangement made the chordotonal organs sensitive to sound traveling through the tracheal system. Evolution to a true tympanal ear occurred by further enlargement of the air sack until it reached the exoskeleton, which thinned to form a tympanal membrane. Examples of these three stages exist in termites, cockroaches, and crickets (Shaw, S. R., 1994). Similar models could explain the occurrence of tympanae in other body regions.

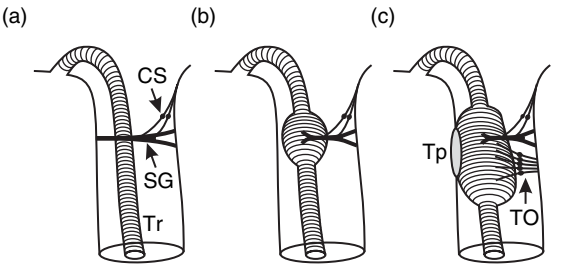

Figure 2 A model of the evolutionary development of tympanal hearing organs in insect legs. (a) Precursor state found in some termites. (b) Intermediate state found in cockroach. (c) Developed state found in some crickets. CS, chordotonal sensilla; SG, subgenual organ, Tr, trachea; TO, tympanal organ; Tp, tympanum. Based on material in Shaw, S. R. 1994. Detection of airborne sound by a cockroach 'vibration detector': a possible missing link in insect auditory evolution. J. Exp. Biol. 193, 13–47.

3.12.4 Sensory Biophysics

3.12.4.1 Mechanoreception in Arthropod Type I Mechanosensilla

Mechanoreception can be treated as a three-stage process (French, A. S., 1992): (1) coupling of the mechanical displacement to the membrane of a sensory cell; (2) transduction of mechanical stress in the membrane to ionic current through the membrane (receptor current) that changes the voltage across the membrane (receptor potential); and (3) encoding of the receptor potential into action potentials by voltage sensitive ion channels in the membrane. Encoding may be omitted where distances are short, or may occur in other cells that are synaptically activated by the primary receptor cell.

Chordotonal organs contain type I arthropod neurons, which are widely used as models of mechanosensation and provide a basis for understanding chordotonal biophysics. Most work has used insect or spider neurons with tubular bodies in the sensory dendrites, analogous to type 2 chordotonal sensilla. Coupling from external mechanical sources is not well understood in any type I system, although the consensus is that distortions of ~1–10 nm at the tip of the sensory dendrite lead to transduction (French, A. S., 1992). The tubular body may provide a rigid structure, against which external force can squeeze the dendrite membrane. However, destruction of the microtubules reduced but did not eliminate transduction (French, A. S., 1992; French, A. S. *et al.*, 2002).

The transduction step is believed to be due to mechanically activated ion channels in the dendrite

membrane. In some type I insect sensilla, the receptor current is driven by a potassium concentration and voltage gradient across the sensory dendrite that is maintained by metabolic pumping of potassium into an extracellular lymph space sealed by tight junctions (McIver, S. B., 1985; French, A. S., 1992), whereas some spider type I sensilla have a receptor current that is highly sodium selective (French, A. S. *et al.*, 2002). The identity of the mechanically activated ion channels is unknown in any receptor. Evidence that they are members of the TRP (transient receptor potential) channel family have been presented for *Drosophila* bristles (Walker, R. G. *et al.*, 2000), but there are also suggestions that members of the degenerin/acid sensitive ion channel families may be involved in spider mechanosensilla (French, A. S. *et al.*, 2002). Current models often include connections from the channels to both cytoskeleton and extracellular structures to provide mechanical stress (Walker, R. G. *et al.*, 2000; Gong, Z. *et al.*, 2004). Mechanically activated ion channels have been localized in spider sensilla, where direct extracellular recordings show that electrical activity is initiated at the distal dendrite tips (Gingl, E. *et al.*, 2004).

Type I neurons use sodium-dependent action potentials for axonal conduction (French, A. S., 1988). Several types of slowly and rapidly inactivating voltage-dependent potassium currents are found in insect and spider sensilla (Torkkeli, P. H. and French, A. S., 1995; French, A. S. *et al.*, 2002), but the dynamic properties of action potential encoding in spider sensilla can be explained by a model containing only voltage-activated sodium and delayed-rectifier potassium currents (French, A. S. *et al.*, 2002).

3.12.4.2 Mechanical Coupling in Chordotonal Organs

The complex morphology of chordotonal organs suggests mechanical functions for all or parts of the cilium, scolopale, cap, tube, and attachment cell. Field L. H. and Matheson T. (1998) discussed the mechanical properties of these structures, and the intercellular junctions and contacts that join them, to produce models of mechanical coupling. For mononematic sensilla, the attachment cell, cap, and scolopale are likely to be mechanically strong, and the primary stimulus is probably tension in the attachment cell. It is not clear if the scolopale acts as a rigid tube that transmits mechanical force from the cap to the basal body of the cilium, or if it forms a cage through which the cilium is pulled by the cap. Scolopale rigidity is not clearly established (Field, L. H. and Matheson, T., 1998). Some evidence suggests that lateral cap movement distorts the cilium sideways relative to the scolopale.

A major question is whether the mechanically activated ion channels are at the distal or proximal ends of the sensory dendrite. Type 2 chordotonal sensilla more closely resemble other type I arthropod sensilla, where the evidence favors distal transduction. Therefore, the primary stimulus in these sensilla is probably compression of the tube, causing stress of the dendrite membrane against the internal tubular body and opening mechanically activated ion channels in the membrane (Field, L. H. and Matheson, T., 1998). The issue is more complex for type 1 sensilla.

3.12.4.3 Ciliary Functions in Type 1 Chordotonal Sensilla

Type 1 sensilla have prominent ciliary structures with well-defined roots (Figure 1; Field, L. H. and Matheson, T., 1998; Yack, J. E., 2004). The axoneme contains nine doublet microtubules but lacks a central pair of singlet microtubules, except in some Lepidoptera. There is a dilation about two-thirds of the distance along the scolopale, where the microtubules are embedded in dense material and connected to the ciliary membrane. These structures probably play important roles in sensory transduction. Bending of the axoneme near the basal body (about the asterisk level in Figure 1) was seen, particularly during mechanical stimulation (Moran, D. T. *et al.*, 1975; Field, L. H. and Matheson, T., 1998; Yack, J. E., 2004). This was originally interpreted to mean that lateral movement of the distal dendrite produces active sliding of the axonemal microtubules, resembling a ciliary beat, distorting the neuronal membrane near the basal body, and opening mechanically activated channels located there (Moran, D. T. *et al.*, 1975).

Arguing against active axonemal beats are the lack of a central pair of microtubules, the fact that microtubules are not essential for transduction, and that transduction probably occurs at the tips of the dendrites in other type I sensilla (French, A. S., 1988). However, an active model has been revived by evidence that axonemes lacking the central pair of microtubules can be motile, that otoacoustic emissions can be recorded from some insect ears, and that mutations affecting the dynein arms of the axoneme prevent auditory transduction in *Drosophila* (Eberl, D. F., 1999; Eberl, D. F. *et al.*, 2000). These data support a model in which transduction occurs distally, but the sensitivity

of the sensillum is increased by positive feedback via axonemal movement. This could include direct connections between the microtubules and the transduction channels (Gong, Z. *et al*., 2004).

The importance of the ciliary dilation is shown by the strongly reduced receptor potentials in *Drosophila* mutants that specifically change the morphology of the dilation (Eberl, D. F. *et al*., 2000), but it is not clear if the primary role of the dilation is in transduction or in amplification. It is also possible that relatively slow, active movements of the scolopale or axoneme could adjust sensillum sensitivity to accommodate the stimulus level, providing adaptation similar to that in vertebrate ears.

3.12.4.4 Transduction and Action Potential Encoding in Chordotonal Sensilla

The scolopale lumen is assumed to provide the functional equivalent of the sensory lymph space in other type I sensilla. Morphological evidence of a sealed space supports this but no direct measurements of transepithelial potentials or concentration gradients exist (Yack, J. E., 2004).

Some of the evidence for mechanotransduction by TRP channels mentioned above was obtained in chordotonal sensilla. Several of these proteins are required for normal hearing function and are located in *Drosophila* chordotonal sensilla, but none has yet been shown to be part of the primary transduction channel (Gong, Z. *et al*., 2004).

The ionic basis of action potential encoding in chordotonal organs has not been directly demonstrated by voltage clamp experiments, but is assumed to resemble other type I sensilla. Action potential initiation probably occurs close to the mechanically activated ion channels in the distal dendrites. Evidence for this comes from extracellular recording and from observation of dendritic action potentials that sometimes fail to propagate through the soma (Hill, K. G., 1983). Firing rates in chordotonal organs show a range of adaptation behaviors (Field, L. H. and Matheson, T., 1998), which are probably controlled by voltage- and calcium-activated ion channels (DiCaprio, R. A. *et al*., 2002).

Acknowledgment

This work was supported by the Canadian Institutes of Health Research.

References

Crouau, Y. 1995. Association in a crustacean sensory organ of two usually mutually exclusive mechanosensory cells. Biol. Cell 85, 191–195.

DiCaprio, R. A., Wolf, H., and Buschges, A. 2002. Activity-dependent sensitivity of proprioceptive sensory neurons in the stick insect femoral chordotonal organ. J. Neurophysiol. 88, 2387–2398.

Eberl, D. F. 1999. Feeling the vibes: chordotonal mechanisms in insect hearing. Curr. Opin. Neurobiol. 9, 389–393.

Eberl, D. F., Hardy, R. W., and Kernan, M. J. 2000. Genetically similar transduction mechanisms for touch and hearing in *Drosophila*. J. Neurosci. 20, 5981–5988.

Field, L. H. and Matheson, T. 1998. Chordotonal organs of insects. Adv. Insect Physiol. 27, 1–228.

French, A. S. 1988. Transduction mechanisms of mechanosensilla. Ann. Rev. Entomol. 33, 39–58.

French, A. S. 1992. Mechanotransduction. Ann. Rev. Physiol. 54, 135–152.

French, A. S., Torkkeli, P. H., and Seyfarth, E. A. 2002. From stress and strain to spikes: mechanotransduction in spider slit sensilla. J. Comp. Physiol. A 188, 739–752.

Gamble, E. R. and DiCaprio, R. A. 2003. Nonspiking and spiking proprioceptors in the crab: white noise analysis of spiking CB-chordotonal organ afferents. J. Neurophysiol. 89, 1815–1825.

Gingl, E., French, A. S., Panek, I., Meisner, S., and Torkkeli, P. H. 2004. Dendritic excitability and localization of GABA-mediated inhibition in spider mechanoreceptor neurons. Eur. J. Neurosci. 20, 59–65.

Gong, Z., Son, W., Chung, Y. D., Kim, J., Shin, D. W., McClung, C. A., Lee, Y., Lee, H. W., Chang, D. J., Kaang, B. K., Cho, H., Oh, U., Hirsh, J., Kernan, M. J., and Kim, C. 2004. Two interdependent TRPV channel subunits, inactive and Nanchung, mediate hearing in *Drosophila*. J. Neurosci. 24, 9059–9066.

Graber, V. 1882. Die chordotonalen Sinnesorganes und das Gehör der Insekten. Arch. Mikro. Anat. Entwicklungsmech. 20, 506–640.

Hill, K. G. 1983. The physiology of locust auditory receptors II. Membrane potentials associated with the response of the receptor cell. J. Comp. Physiol. A 152, 483–493.

Howse, P. E. 1968. The fine structure and functional organization of chordotonal organs. Symp. Zool. Soc. Lond. 23, 167–198.

Mainz, T., Schmitz, A., and Schmitz, H. 2004. Variation in number and differentiation of the abdominal infrared receptors in the Australian 'fire-beetle' *Merimna atrata* Coleoptera, Buprestidae. Arth. Struct. Dev. 33, 419–430.

McIver, S. B. 1985. Mechanoreception. In: Comprehensive Insect Physiology Biochemistry and Pharmacology (*eds*. G. A. Kerkut and L. I. Gilbert), Vol. 6, pp. 71–132. Pergamon Press.

Michelsen, A. and Larsen, O. N. 1985. Hearing and Sound. In: Comprehensive Insect Physiology Biochemistry and Pharmacology (*eds*. G. A. Kerkut and L. I. Gilbert), Vol. 6, pp. 495–556. Pergamon Press.

Moran, D. T., Rowley, J. C., and Varela, F. G. 1975. Ultrastructure of the grasshopper proximal femoral chordotonal organ. Cell Tissue Res. 161, 445–457.

Moulins, M. 1976. Ultrastructure of Chordotonal Organs. In: Structure and Function of Proprioceptors in the Invertebrates (*ed*. P. J. Mill), pp. 387–426. Chapman and Hall.

Shaw, S. R. 1994. Detection of airborne sound by a cockroach 'vibration detector': a possible missing link in insect auditory evolution. J. Exp. Biol. 193, 13–47.

Torkkeli, P. H. and French, A. S. 1995. Slowly inactivating outward currents in a cuticular mechanoreceptor neuron of the cockroach (*Periplaneta americana*). J. Neurophysiol. 74, 1200–1211.

Walker, R. G., Willingham, A. T., and Zuker, C. S. 2000. A *Drosophila* mechanosensory transduction channel. Science 287, 2229–2234.

Yack, J. E. 2004. The structure and function of auditory chordotonal organs in insects. Microsc. Res. Tech. 63, 315–337.

3.13 Interconnections between the Ears in Nonmammalian Vertebrates

A S Feng, University of Illinois at Urbana-Champaign, Urbana, IL, USA

J Christensen-Dalsgaard, University of Southern Denmark, Odense, Denmark

© 2008 Elsevier Inc. All rights reserved.

3.13.1	**Introduction**	217
3.13.2	**Sound Localization in Nonmammalian Vertebrates**	218
3.13.3	**Interaural Acoustic Coupling**	218
3.13.3.1	Anurans and Lizards	219
3.13.3.1.1	Anurans	219
3.13.3.1.2	Lizards	221
3.13.3.2	Avians	221
3.13.4	**Concluding Remarks**	222
References		223

Glossary

columella The middle ear ossicle in frogs. It consists of three portions: pars externa (i.e., extracolumella), pars media, and pars interna.

diffraction Distortion of the sound field by an object, such as a head shadow.

directionality The directional sensitivity of a receiver.

directivity pattern The physical directional characteristics of a receiver.

dorsal medullary nucleus The first auditory nucleus in the frog brainstem, analogous to the cochlear nucleus in mammals.

extracolumella Pars externa of the columella. The part of the columella that attaches to the tympanic membrane.

extratympanic input Sound inputs to the ear other than that from the tympanic membrane.

interaural acoustic coupling The strength of acoustic coupling between the two ears in frogs, lizards, crocodiles, and some birds. The two ears are connected acoustically through Eustachian tubes and mouth cavity.

interaural level difference (ILD) Refers to the difference in sound pressure levels at the two ears (usually due to diffraction).

interaural time difference (ITD) Refers to the difference in time/phase at the two ears due to the disparity in the path lengths from an off-axis source.

pressure-difference receiver An acoustic receiver where tympanic membrane vibration is a product of interaction of sound arriving at both sides of the membrane.

Torus semicircularis Mid-brain auditory center, the homolog of the mammalian inferior colliculus.

3.13.1 Introduction

Most vertebrates can determine the location of a sound source by evaluating several interaural cues: interaural phase/time differences (ITD), interaural level differences (ILD), and interaural spectral differences. According to the duplex theory, localization of low- and high-frequency sounds largely depends on analysis of the ITD and ILD, respectively (Wightman, F. L. *et al.*, 1987). ITD processing is effective at low frequencies due to the facts that phase coding is prominent, and encoding of interaural phase differences is unambiguous. In contrast, ILD is most pronounced for high-frequency sounds. This is because when the head size is larger than one-quarter of the sound wavelength (as a general rule),

the head diffracts the sound and becomes an obstacle to sound propagation, thereby producing a head-shadowing effect.

For most nonmammalian vertebrates, the interaural distance is small. The sound energy of their communication signals is concentrated at low frequencies, and at the same time, hearing is generally restricted to low frequencies due to the limited high-frequency response of their middle ear bones (Manley, G. A., 1972; 1990; Mason, M. J., 2006). At low frequencies, vibration of the eardrum is transferred with little loss to the columellar footplate, but at higher frequencies energy is lost due to flexion in the extracolumella–columella link. A further limitation is that the tympanic membrane vibration tends to break up into higher vibration modes at higher frequencies (Anson, M. *et al.*, 1985; Purgue, A. P., 1997). In these modes, nodes can form at the extracolumellar attachment, effectively limiting the sound input to the inner ear to frequencies below 12 kHz in nonmammals. For most species, the auditory sensitivity drops around 5 kHz; here, the wavelength is 6.8 cm, so for the smallest animals (head size ~1 cm) the diffraction is only just measurable.

3.13.2 Sound Localization in Nonmammalian Vertebrates

Nonmammalian vertebrates can localize sound with varying degrees of accuracy. Frogs can locate a source of species' advertisement calls with an accuracy of ~20° (see reviews by Fay, R. R. and Feng, A. S., 1987; Christensen-Dalsgaard, J., 2005). Acuity of sound localization differs widely in birds, ranging from 3° to 5° in barn owls (Knudsen, E. I. *et al.*, 1979; Bala, A. D. S. *et al.*, 2003) and 2° to 8° in two hawk species (Rice, W. R., 1982), to ~25° in canaries (Klump, G. M., 2000; Christensen-Dalsgaard, J., 2005). In general, acuity of sound localization for small animals that hear low-frequency sounds is poorer than larger animals hearing higher-frequency sounds. Also, small animals must utilize special mechanical adaptations to achieve the localization acuity they possess (see Chapters 3.11, 3.35, 3.36, and 3.41).

3.13.3 Interaural Acoustic Coupling

In anurans (frogs and toads), lizards, crocodiles, and some bird species, the ears are connected acoustically through Eustachian tubes or interaural canal and mouth cavity. As a result, sound can travel relatively unobstructed from one ear to the other. Such acoustical coupling allows the direct component of sound at the external surface of the eardrum and the indirect component at the internal surface of the eardrum to interact, forming a pressure-gradient (or pressure-difference) receiver that enhances the directionality of the ear. In essence, for them, binaural interaction takes place on the tympanum itself. As to be described later, the interconnection between ears is most remarkable in the lizards, for which the eardrum directionality provides ILDs of up to 34 dB. In mammals, although the ears are also connected through the Eustachian tubes, the sound attenuation through the interaural pathways is so large that the ears act as independent pressure receivers. For them, directional information is extracted by the central nervous system by evaluating the interaural cues.

The pressure-difference receiver functions to amplify the amplitude and phase differences at the two eardrums, generating larger ITD and ILD than expected from the size of the animal. This amplification is strongly dependent on the acoustical coupling between the ears. The driving force for the eardrum vibrations is the instantaneous pressure difference between its sides, that is, $U = P_{\text{direct}} - P_{\text{indirect}}$. The indirect component is phase shifted and attenuated relative to the direct component when it reaches the internal side of the eardrum. For a sinusoidal sound, the expression becomes $U = \sin(\omega t) - B\sin(\omega t + \Delta\phi)$, where B is the amplitude ratio between direct and indirect sound, $\Delta\phi$ is thephase difference between direct and indirect sound, and ω is the frequency. It is useful to rewrite this expression as

$$U = \sqrt{1 + B^2 - 2B\cos\Delta\phi} \times \sin\left(\omega t + \arctan\left(\frac{-B\sin\Delta\phi}{1 - B\cos\Delta\phi}\right)\right) \quad [1]$$

The expression shows that the driving force strongly depends on the amplitude ratio B, that is, on the interaural attenuation, and on the phase shift between direct and indirect sound. The amplitude varies between $1 + B$ and $1 - B$, depending on the phase difference; for B with a value greater than zero the amplitude will be greater than the original signal at some phase differences. Note that for $B >> 1$ the phase shift of the difference signal approaches $\Delta\phi$, that is, the phase difference of the indirect sound. The operation thus results in larger interaural level and time differences compared to the cues generated by diffraction. Additionally, the greater ILD amplifies the ITD

further in light of the differential latency shifts of VIII nerve fibers on both sides (Feng, A. S., 1982).

The pressure-difference receiver ear is presumably the ancestral condition of the tetrapod tympanic ear, since the first eardrums were compliant, skin-covered fenestrations in the skull contacted by the middle ear ossicle and therefore coupled through the mouth cavity (Clack, J. A., 1997; Christensen-Dalsgaard, J., 2005). This configuration is similar to that found in present-day anurans and lizards, whereas the pressure-sensitive ear of mammals and some birds represent the derived condition of shielding the tympanum and ossicle in the middle ear cavity. The increasing isolation of the middle ear cavities may have evolved initially for isolating the ear from the respiratory and food-intake pathways (Christensen-Dalsgaard, J. and Manley, G. A., 2005a).

3.13.3.1 Anurans and Lizards

As shown above, pressure-difference receiver characteristics depend on the acoustical coupling between the ears. For frogs and lizards whose eardrums are acoustically coupled, the indirect component is non-negligible and frequency dependent. As such, frog and lizard ears behave like a combination pressure and pressure-difference receiver (Fay, R. R. and Feng, A. S., 1987). The directivity index V for such a receiver (consisting of a membrane, a cavity, and a second sound entry via the opposite membrane) is a function of the incident angle θ (Beranek, L. L., 1986) and can be modeled by

$$V = 20\log\frac{1 + B\cos\theta}{1 + B} \quad \text{where } B = \frac{\Delta L}{c\,C_A R_A}$$

B is a dimensionless constant with a value ranging from 0 to infinity, ΔL is the distance between the eardrums, c the speed of sound, C_A the acoustic compliance, and R_A the acoustic resistance of the cavity. If ears are uncoupled (i.e., thus having a large interaural resistance), B approaches zero; each ear then functions as a pure pressure receiver and is omnidirectional. Conversely, if the ears are tightly coupled (i.e., having a small interaural resistance or a very large B), the directivity will approach $V = 20\log\cos\theta$. This condition approximates a pure pressure-difference receiver and confers a figure 8 directionality with a prominent null for sound coming from the frontal and caudal directions. The acoustic receiver of frogs and lizards has moderate B values, showing frequency-dependent directional responses and giving rise to ILD that is greater than can be expected from the size of the animal.

More complicated models that also include the acoustical properties of the eardrums and of the Eustachian tubes can be made from electrical network analogs (Fletcher, N. and Thwaites, S., 1979; Fletcher, N. H., 1992). Briefly, any acoustical system where acoustical flow is one dimensional (e.g., propagation in tubes and through membranes) with all elements smaller than one half wavelength will have an analogous electrical circuit where cavities correspond to capacitors, tubes to inductances (at low frequencies; for high-frequency approximations, see Fletcher, N. H., 1992), and sound absorbers to resistances. See also Lewis E. R. (2004) for an introduction to modeling. Electrical network analogs have been used in modeling the acoustics of the frog and lizard ear (see below).

The external and middle ears of frogs and lizards share some similarities, even though their tympanic ears probably originated independently in the two groups (Clack, J. A., 1997). In both groups, the Eustachian tubes are wide and short with a considerable acoustical coupling between the two ears. Both frogs (see Lewis, E. R. and Narins, P. M., 1999 for general review of the auditory periphery) and lizards have a single middle ear ossicle connected to the eardrum via a cartilaginous extracolumella; flexion in the extracolumella–columella link limits the high-frequency sensitivity of the lizard ear (Manley, G. A., 1972; 1990) and probably also that of the anuran ear (Mason, M. J., 2006). However, there are notable differences between the directionality of frog and lizard ears (see Christensen-Dalsgaard, J., 2005). Frog ears generally show directional differences of up to 10 dB within a relatively narrow directional band (500 Hz), whereas lizards show directional differences of up to 34 dB and a wider directional bandwidth (>2 kHz; Christensen-Dalsgaard, J. and Manley, G. A., 2005a).

3.13.3.1.1 Anurans

Figure 1 shows the directionality of the eardrum of a treefrog *Eleutherodactylus coqui*, measured by laser vibrometry. The eardrum directionality is poor at low and high frequencies; maximum directionality is observed at ~1.7 kHz, having an ovoidal directional characteristic with the largest response from ipsilateral angles (Jørgensen, M. B., 1991; Jørgensen, M. B. *et al.*, 1991). The acoustics of the frog periphery are complicated, mainly due to its multiple acoustic

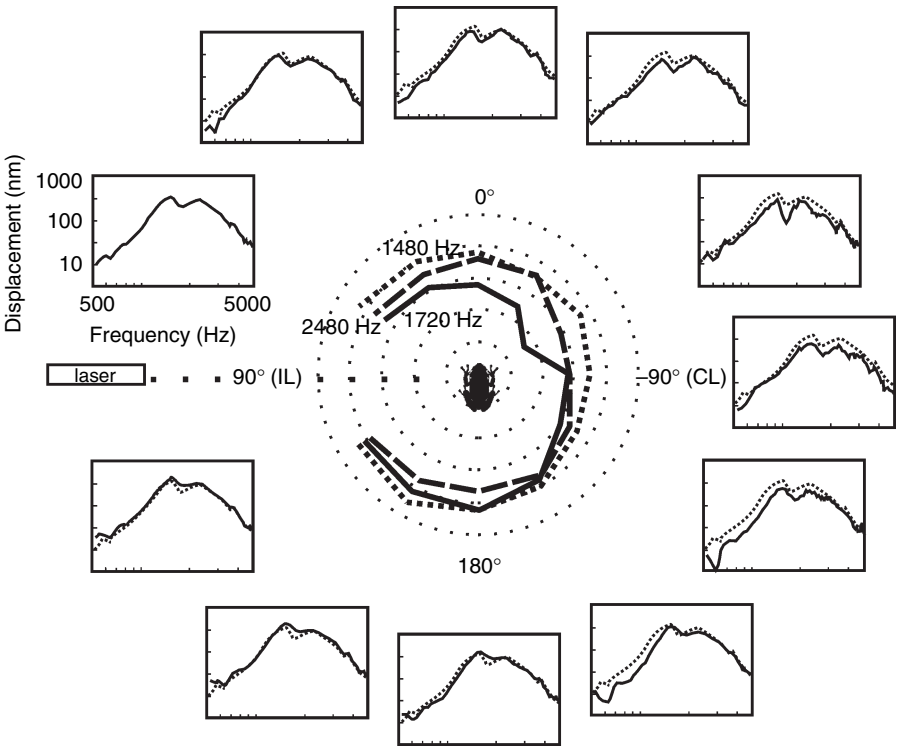

Figure 1 Directional response of the eardrum in *Eleutherodactylus coqui* measured by laser vibrometry. The figure shows polar plots at three frequencies, and the inset figures are vibration spectra taken at different directions. In each figure, the ipsilateral (IL) spectrum is shown as a reference (thin line). Reprinted from Jørgensen, M. B., Schmitz, B., and Christensen-Dalsgaard, J. 1991. Biophysics of directional hearing in the frog *Eleutherodactylus coqui*. J. Comp. Physiol. A 168, 223–232 and Christensen-Dalsgaard, J. 2005. Directional Hearing in Non-Mammalian Tetrapods. In: Sound Source Localization (*eds*. A. N. Popper and R. R. Fay), pp. 67–123. Springer, with kind permission of Springer-Verlag.

inputs. Sound is transmitted through not only the coupled eardrums, but the lungs are also efficient inputs for low-frequency sound (Narins, P. M. *et al.* 1988; Jørgensen, M. B. *et al.*, 1991). Also, the mouth cavity may be transparent to sound, and finally, there is an extratympanic low-frequency input (Feng, A. S. and Shofner, W. P., 1981; Wilczynski, W. *et al.* 1987; Wang, J. *et al.* 1996) that can be inferred from VIII nerve recordings. In response to low-frequency free-field sound (100–400 Hz), VIII nerve auditory fibers show a strong figure 8 directionality with a frontal null (Figure 2(a)), that is, decreased responses at frontal angles (Feng, A. S., 1980; Jørgensen, M. B., 1991; Jørgensen, M. B. and Christensen-Dalsgaard, J., 1997b), in spite of the fact that the tympanum is insensitive to sounds at such low frequencies and shows no directional characteristic. As shown in Figure 2(b), at higher frequencies, the directional characteristic of the auditory fibers is ovoidal and matches the directionality of the eardrum (Feng, A. S., 1980; Jørgensen, M. B. and Christensen-Dalsgaard, J., 1997a).

In *Rana pipiens* it was shown that the ear directionality as measured by the directional responses of primary auditory nerve fibers are altered when the interaural transmission is manipulated (Feng, A. F. and Shofner, W. P., 1981). Reducing the interaural transmission by filling the mouth cavity with moist cotton decreases the ear directionality at all frequencies; the ovoidal directivity pattern at high frequencies becomes omnidirectional and the figure 8 directivity pattern at low frequencies becomes ovoidal (second row of Figure 3). In contrast, coating the contralateral eardrum with rubber cement (which attenuates the sound through this ear) leaves the directionality and directivity pattern at low frequencies unchanged; the directionality of mid- and high-frequency fibers is reduced, and the directivity pattern becomes omnidirectional (third row of Figure 3), indicating that the tympanum is the source of the ear directionality at mid- and high frequencies. Finally, opening of the frog's mouth cavity that facilitates interaural transmission produces an increase in the

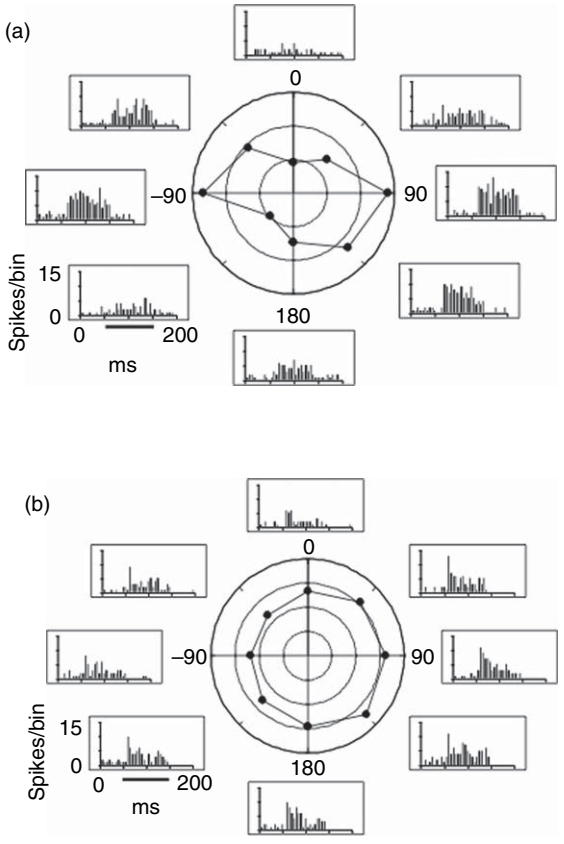

Figure 2 Directional responses of VIII nerve fibers in *Rana temporaria*. (a) Is the response of a low-frequency fiber stimulated at its best-frequency (BF) (300 Hz). Note the figure 8 response with low sensitivity at frontal directions. (b) Shows ovoidal response of a high-frequency fiber stimulated at its BF (1500 Hz). Reprinted from Jørgensen, M.B. and Christensen-Dalsgaard, J. 1997a. Directionality of auditory nerve fiber responses to pure tone stimuli in the grassfrog, *Rana temporaria*. I. Spike rate responses. J. Comp. Physiol. A 180, 493–502, with kind permission of Springer-Verlag.

ear directionality (suggesting that the mouth floor is not transparent to sound) and converts the directivity pattern at all frequencies into a figure 8 pattern (bottom row of Figure 3). These experiments are consistent with the results of mechanical measurements showing that the ear directionality at low frequencies is due mainly to the extratympanic route, whereas directionality at higher frequencies is produced by the acoustics of the coupled middle ear cavities and respiratory pathway, and that the frog's ear functions as a combination pressure–pressure difference receiver.

The source of the extratympanic input is unclear. Jørgensen M. B. and Christensen-Dalsgaard J. (1997b) suggested that sound-induced vibrations of the frog's skull likely produce movements of the inner-ear fluids that would have maximal amplitude in certain directions. However, since detympanation also affects the sensitivity and directionality at low frequencies (for which the source is extratympanic; Christensen-Dalsgaard, J. *et al.*, 1997), the tympanic and extratympanic pathways must be closely coupled, and the directionality is likely a product of interaction of these two pathways.

3.13.3.1.2 Lizards

In all lizards investigated, the middle ears are connected by large cavities in the upper palate. Thus, the lizard head is acoustically transparent, with an interaural attenuation of close to zero over a broad frequency range and thus large directionality of eardrum vibration (Figures 4(a) and 4(b), Christensen-Dalsgaard, J. and Manley, G. A., 2005b). The directional response is asymmetrical with a large gradient along the frontal directions (Christensen-Dalsgaard, J. and Manley, G. A., 2005a; 2005b). The directionality is abolished when one eardrum is occluded. A simple acoustical model having two tympanic inputs and a central cavity accurately describes the directionality of this ear (Figures 4(c) and 4(d)). By comparison, models of the directionality of the anuran ear do not fit the measured physiological responses, neither can they predict an increased directionality at low frequencies, a reduced directionality around the frequencies of maximal sensitivity (Aertsen, A. M. H. J. *et al.*, 1986), or a figure 8 response at low frequencies (Palmer, A. R. and Pinder, A. C., 1984). The discrepancy between model predictions and experimental data probably is due to the complicated acoustics of the frog periphery. For example, the lung input was not known at the time these models were made. Moreover, since the lung input covers most of the dorsum of the frog it is difficult to approximate by a single point input.

3.13.3.2 Avians

The ears of avians and crocodilians are similarly connected by an interaural canal. The functional significance of this connection varies among species and depends on the interaural attenuation (see reviews by Klump, G. M., 2000; Christensen-Dalsgaard, J., 2005). In the barn owl, for example, the interaural attenuation increases from 13 dB at 3.5 kHz to 63 dB at 7 kHz; at the behaviorally important high frequencies the ears are, therefore, functionally isolated (Moiseff, A. and Konishi, M.,

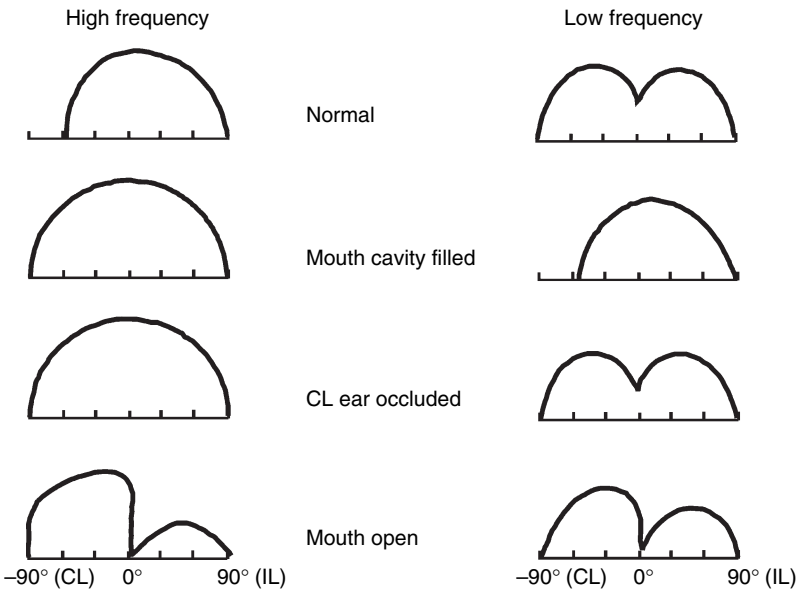

Figure 3 Directivity patterns of the frog's ear at low and high frequencies under several different experimental conditions. Top row shows directivity patterns from intact frogs. Second row shows directivity patterns from frogs whose mouth cavity was filled with moist cotton. Third row shows directivity patterns from frogs whose contralateral (CL) ear was occluded by coating with rubber cement. Fourth row shows directivity patterns from frogs whose mouth was artificially open during the recording session. IL, ipsilateral. Reprinted from Feng, A. S. and Shofner, W. P. 1981. Peripheral basis of sound localization in anurans. Acoustic properties of the frog's ear. Hear. Res. 5, 201–216, with kind permission of Elsevier B.V.

1981). In contrast, in quail (*Coturnix coturnix*), interaural attenuation is less than 5 dB at frequencies below 5 kHz; consequently the directivity patterns are cardioid at low frequencies and figure 8 at high frequencies with up to 10–20 dB directional differences (Hill, K. G. *et al.*, 1980). Similar directional characteristics have been reported for all other bird species that have prominent interaural canals.

Larsen O. N. *et al.* (1997) showed that the interaural coupling and normal operation of the tympanum of budgerigars is dependent on the intracranial air pressure, and that such pressure tends to decrease in anesthetized birds unless the middle ear cavity is vented. The result is that tympanic vibrations are impeded (with the tympanum sucked inwards), the interaural coupling is reduced by ~20 dB, and the tympanal directivity is at least 6 dB less in nonvented compared to vented birds.

Calford M. B. (1988) has modeled the bird's auditory receiver. The model calculates the pressure difference at the tympanum by adding the direct and indirect sound, delayed by travel time around the head and through the interaural canal. The model reveals the effects of interaural attenuation on the directional response and allows calculation of phase changes associated with the pressure-difference receiver. However, a drawback is that the attenuations and phase changes in the model are not frequency dependent.

3.13.4 Concluding Remarks

The interconnected ears are a primitive feature of the tetrapod tympanic ears and have been exploited for enhancing sound localization ability through fine-tuning of the acoustical elements. An inherent drawback of the pressure-difference receiver ear produced by the acoustical coupling is the strong frequency dependence of the directionality (notably in lizards and anurans) and the sensitivity to noise generated by respiration. Selection pressures associated with the need to localize high-frequency sounds probably have led to specialized, functionally isolated ears in some species of birds, most notably the barn owl. Because of the frequency dependence of directionality, central binaural processing may be different in animals having interconnected ears versus animals with isolated pressure receivers. As of to date, there is no clear evidence for separation of time and

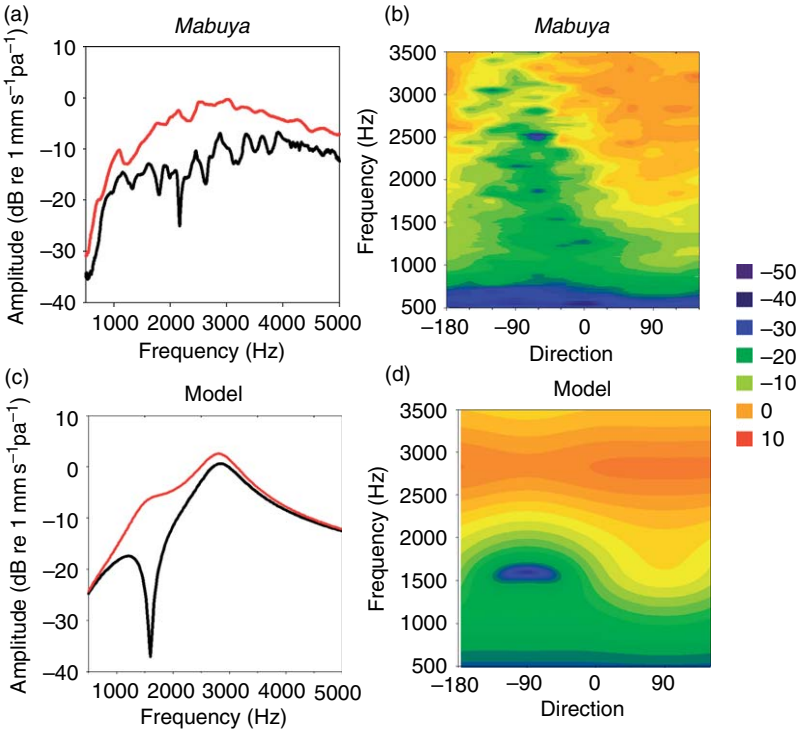

Figure 4 Eardrum vibrations in a lizard (*Mabuya macularia*) stimulated with directional sound (a, b). For comparison, data from a model based on physical parameters from Mabuya is shown in the lower row (c, d). In panels (a) and (c), ipsilateral and contralateral spectra are shown in red and black, respectively. Contour plots in (b) and (d) show the vibration amplitude (color scale, in dB re 1 mm s^{-1} pa^{-1}) as a function of direction (positive angles are ipsilateral sound directions) and frequency. Each horizontal line corresponds to a polar plot. Redrawn from Christensen-Dalsgaard, J. and Manley, G. A. 2005a. Directionality of the lizard ear. J. Exp. Biol. 208, 1209–1217, with kind permission of The Company of Biologists.

intensity processing pathways in frogs, as reported for the barn owl and mammals (Carr, C. and Code, R. A., 2000), and the existence of spatial maps also remains elusive. Instead, the available evidence suggests that central directional processing at the level of the dorsal medullary nucleus (Feng, A. S. and Capranica, R. R., 1976; Christensen-Dalsgaard, J. and Kanneworff, M., 2005) and torus semicircularis (Feng, A. S., 1981; Zhang, H. *et al.*, 1999) sharpens the peripheral directionality – this seems sufficient for providing the frog with ability to steer toward the direction of a sound source.

References

Aertsen, A. M. H. J., Vlaming, M. S. M. G., Eggermont, J. J., and Johannesma, P. I. M. 1986. Directional hearing in the grassfrog (*Rana temporaria* L.). II. Acoustics and modelling of the auditory periphery. Hear. Res. 21, 17–40.

Anson, M., Pinder, A. C., Keating, M. J., and Chung, S. H. 1985. Acoustic vibration of the amphibian eardrum studied by white noise analysis and holographic interferometry. J. Acoust. Soc. Am. 78, 916–923.

Bala, A. D. S., Spitzer, M. W., and Takahashi, T. T. 2003. Prediction of auditory spatial acuity from neural images on the owl's auditory space map. Nature 424, 771–774.

Beranek, L. L. 1986. Acoustics. American Institute of Physics.

Calford, M. B. 1988. Constraints on the coding of sound frequency imposed by the avian interaural canal. J. Comp. Physiol. A 162, 491–502.

Carr, C. and Code, R. A. 2000. The Central Auditory System of Reptiles and Birds. In: Comparative Hearing: Birds and Reptiles (*eds*. R. J. Dooling, R. R. Fay, and A. N. Popper), pp. 197–248. Springer.

Christensen-Dalsgaard, J. 2005. Directional Hearing in Non-Mammalian Tetrapods. In: Sound Source Localization (*eds*. A. N. Popper and R. R. Fay), pp. 67–123. Springer.

Christensen-Dalsgaard, J. and Kanneworff, M. 2005. Binaural interactions in the frog dorsal medullary nucleus. Brain Res. Bull. 66, 522–525.

Christensen-Dalsgaard, J., Kanneworff, M., and Jørgensen, M. B. 1997. Extratympanic Sound Sensitivity of Frog Auditory Fibers. In: Diversity in Auditory Mechanics (*eds*. E. R. Lewis, G. R. Long, R. F. Lyon, P. M. Narins, C. R. Steele, and E. Hecht-Poinar), pp. 64–68. World Scientific.

Christensen-Dalsgaard, J. and Manley, G. A. 2005a. Directionality of the lizard ear. J. Exp. Biol. 208, 1209–1217.

Christensen-Dalsgaard, J. and Manley, G. A. 2005b. Acoustical coupling of the lizard eardrums. Soc. Neurosci. Abs. 44.2.

Clack, J. A. 1997. The evolution of tetrapod ears and the fossil record. Brain Behav. Evol. 50, 198–212.
Fay, R. R. and Feng, A. S. 1987. Mechanisms for Directional Hearing Among Nonmammalian Vertebrates. In: Directional Hearing (*eds*. W. A. Yost and G. Gourevitch), pp. 179–213. Springer.
Feng, A. S. 1980. Directional characteristics of the acoustic receiver of the leopard frog (*Rana pipiens*): a study of the eighth nerve auditory responses. J. Acoust. Soc. Am. 68, 1107–1114.
Feng, A. S. 1981. Directional response characteristics of single neurons in the torus semicircularis of the leopard frog (*Rana pipiens*). J. Comp. Physiol. A 144, 419–428.
Feng, A. S. 1982. Quantitative analysis of intensity-rate and intensity-latency functions in peripheral auditory nerve fibers of the Northern leopard frogs (*Rana p. pipiens*). Hear. Res. 6, 241–246.
Feng, A. S. and Capranica, R. R. 1976. Sound localization in anurans. I. Evidence of binaural interaction in the dorsal medullary nucleus of the bullfrog (*Rana catesbeiana*). J. Neurophysiol. 39, 871–881.
Feng, A. S. and Shofner, W. P. 1981. Peripheral basis of sound localization in anurans. Acoustic properties of the frog's ear. Hear. Res. 5, 201–216.
Fletcher, N. H. 1992. Acoustic Systems in Biology. Oxford University Press.
Fletcher, N. and Thwaites, S. 1979. Physical models for the analysis of acoustical systems in biology. Q. Rev. Biophys. 12, 25–65.
Hill, K. G., Lewis, D. B., Hutchings, M. E., and Coles, R. B. 1980. Directional hearing in the Japanese quail (*Coturnix coturnix japonica*). I. Acoustical properties of the auditory system. J. Exp. Biol. 68, 135–151.
Jørgensen, M. B. 1991. Comparative studies of the biophysics of directional hearing in anurans. J. Comp. Physiol. A 169, 591–598.
Jørgensen, M. B. and Christensen-Dalsgaard, J. 1997a. Directionality of auditory nerve fiber responses to pure tone stimuli in the grassfrog, *Rana temporaria*. I. Spike rate responses. J. Comp. Physiol. A 180, 493–502.
Jørgensen, M. B. and Christensen-Dalsgaard, J. 1997b. Directionality of auditory nerve fiber responses to pure tone stimuli in the grassfrog, *Rana temporaria*. II. Spike timing. J. Comp. Physiol. A 180, 503–511.
Jørgensen, M. B., Schmitz, B., and Christensen-Dalsgaard, J. 1991. Biophysics of directional hearing in the frog *Eleutherodactylus coqui*. J. Comp. Physiol. A 168, 223–232.
Klump, G. M. 2000. Sound Localization in Birds. In: Comparative Hearing: Birds and Reptiles (*eds*. R. J. Dooling, R. R. Fay, and A. N. Popper), pp. 249–307. Springer.
Knudsen, E. I., Blasdel, G. G., and Konishi, M. 1979. Sound localization by the barn owl (*Tyto alba*) measured with the search coil technique. J. Comp. Physiol. A 133, 1–11.
Larsen, O. N., Dooling, R. J., and Ryals, B. M. 1997. Roles of Intracranial Air Pressure in Bird Audition. In: Diversity in Auditory Mechanics (*eds*. E. R. Lewis, G. R. Long, R. F. Lyon, P. M. Narins, C. R. Steele, and E. Hecht-Poinar), pp. 11–17. World Scientific.
Lewis, E. R. 2004. Appendix: Useful Concepts from Circuit Theory. In: Evolution of the Vertebrate Auditory System (*eds*. G. A. Manley, A. N. Popper, and R. R. Fay), pp. 369–400. Springer.
Lewis, E. R. and Narins, P. M. 1999. The Acoustic Periphery of Amphibians: Anatomy and Physiology. In: Comparative Hearing: Fish and Amphibians (*eds*. R. R. Fay and A. N. Popper), pp. 218–268. Springer.
Manley, G. A. 1972. The middle ear of the tokay gecko. J. Comp. Physiol. A 81, 239–250.
Manley, G. A. 1990. Peripheral Hearing Mechanisms in Reptiles and Birds. Springer.
Mason, M. J. 2006. Pathways for Sound Transmission to the Inner Ear of Amphibians. In: Hearing and Sound Communication in Amphibians (*eds*. P. M. Narins, A. S. Feng, R. R. Fay, and A. N. Popper), pp. 147–183. Springer.
Moiseff, A. and Konishi, M. 1981. Neuronal and behavioral sensitivity to binaural time differences in the owl. J. Neurosci. 1, 40–48.
Narins, P. M., Ehret, G., and Tautz, J. 1988. Accessory pathway for sound transfer in a neotropical frog. Proc. Natl. Acad. Sci. U. S. A. 85, 1255–1265.
Palmer, A. R. and Pinder, A. C. 1984. The directionality of the frog ear described by a mechanical model. J. Theor. Biol. 110, 205–215.
Purgue, A. P. 1997. Tympanic sound radiation in the bullfrog, *Rana catesbeiana*. J. Comp. Physiol. A 181, 438–445.
Rice, W. R. 1982. Acoustical location of prey by the marsh hawk: adaptation to concealed prey. Auk 99, 409–413.
Wang, J., Ludwig, T. A., and Narins, P. M. 1996. Spatial and spectral dependence of the auditory periphery in the northern leopard frog. J. Comp. Physiol. A 178, 159–172.
Wightman, F. L., Kistler, D. J., and Perkins, M. E. 1987. A New Approach to the Study of Human Sound Localization. In: Directional Hearing (*eds*. W. A. Yost and G. Gourevitch), pp. 26–48. Springer.
Wilczynski, W., Resler, C., and Capranica, R. R. 1987. Tympanic and extratympanic sound transmission in the leopard frog. J. Comp. Physiol. A 161, 659–669.
Zhang, H., Xu, J., and Feng, A. S. 1999. Effects of GABA-mediated inhibition on direction-dependent frequency tuning in the frog inferior colliculus. J. Comp. Physiol. A 184, 85–98.

Further Reading

Manley, G. A. 1981. A review of the auditory physiology of the reptiles. Prog. Sens. Physiol. 2, 49–134.

3.14 Underwater Hearing

A N Popper, University of Maryland, College Park, MD, USA

D R Ketten, Woods Hole Oceanographic Institution, Woods Hole, MA, USA

© 2008 Elsevier Inc. All rights reserved.

3.14.1	The Origins of Vertebrate Underwater Hearing	227
3.14.2	The Evolution of Vertebrate Hearing in Water	227
3.14.3	The Inner Ear of Fishes	228
3.14.4	Hearing Capabilities of Fishes	228
3.14.5	Marine Mammals	230
3.14.5.1	Marine Mammal Auditory Systems	230
3.14.5.2	Marine Mammal Audiometrics	232
References		235

Glossary

audiogram A graph of hearing ability conventionally displayed as frequency in hertz or kilohertz (abscissa) versus sensitivity expressed as sound pressure level or intensity measured in decibels (ordinate).

bony fishes All fishes with skeletons made of bone. This is the largest of all vertebrate groups and includes most of the species commonly thought of as fishes such as goldfish, tuna, etc.

cartilaginous fishes Sharks, skates, and rays. The skeleton in these species is made of very dense cartilage rather than bone.

Cetacea The name of the taxonomic order encompassing all whales, dolphins, and porpoises derived from the Latin word for whale, *cetus*. There are two suborders: Mysticeti (baleen whales) and Odontoceti (toothed whales) (see below).

cochlea The snail-shaped canals and sensory organs of the inner ear that provide hearing by transforming sound energy into neural impulses.

decibel (dB) A unit of measurement based upon the logarithm of the ratio of pressure versus an arbitrary reference pressure. For sound measurements, the decibel scale usually represents sound pressure level (SPL), but it may also be used as a measure of intensity (pressure squared). The reference pressures used are different for air (20 μPa) and underwater (1 μPa) sound measurements; therefore, the decibel level of a sound is properly stated in the form of *n* dB re *n* μPa. Two sounds that are perceived as equally loud may have different decibel values based on the reference pressures used in the measurements. Two sounds with equal intensity would have a 100 dB re 20 μPa in air but a decibel value in water of approximately 160 dB re 1 μPa.

echolocation The ability to image features of the environment including size, shape, and location of an object by analyzing echoes from a self-generated sound. Bats and toothed whales have the best known animal echolocation or biosonar.

end organ The sensory regions of the inner ear, particularly the otolithic receptors and the receptors of the semicircular canals.

hertz A unit of sound frequency equal to 1 cycle s^{-1} (see also kHz).

impedance A complex ratio of power versus flow properties, describing effectively the resistance or efficiency of transfer. Acoustic impedance can be thought of as the impact of the medium on sound transmission.

inner ear The combined organs of hearing and balance, the cochlea and vestibular system.

infrasonic Frequencies below 20 Hz, the lower extreme of human hearing.

kilohertz (kHz) Equals 1000 Hz (or 1000 cycles s^{-1}).

lagena One of the end organs of the ear in fishes. It is also present in all nonmammalian terrestrial vertebrates.

lamprey A group of primitive vertebrates that do not have a lower jaw. Lampreys represent the most primitive group of vertebrates.

mandible Lower jaw bone.

masking The impact of one sound on the ability to detect another sound.

middle ear The chamber and structures that amplify sound and connect the outer ear and inner ear. A form of middle ear is found in all terrestrial vertebrates.

Mysticetis The suborder of baleen-bearing or moustached whales comprising all great whales such as blue, finback, right, and humpback whales. Baleen is a series of horny overlapping plates with feathered edges that mysticetes use in lieu of teeth for straining food. Mysticetes have not been shown to echolocate.

octave An octave is broadly defined as a doubling of frequency. Thus, a one octave shift from 500 Hz is 1000 Hz; from 3000 Hz it is 6000 Hz. Adult humans have on typically an eight-octave functional hearing range of 32 Hz to 16 kHz.

octavolateralis system The term that refers to the combined ear and lateral line system of fishes.

Odontoceti The suborder of cetaceans comprising the toothed whales, such as sperm whales, dolphins, and porpoises. All odontocetes are believed to echolocate (to use sound for imaging the environment).

ossicles The bones that act as levers in the middle ear to amplify and transduce sound energy impinging on the tympanum or eardrum into mechanical forces driving the inner ear responses.

otoconia Calcium carbonate crystals found in the otolithic organs of terrestrial vertebrates, cartilaginous fishes, and primitive bony fishes. The crystals are embedded in a gelatinous matrix.

otolith Calcium carbonate structures found in the saccule, lagena, and utricle of most bony fishes. The otolith is several times denser than the rest of the fish body. Relative motion between the otolith and the sensory epithelium results in stimulation of the sensory hair cells. The saccular otolith has growth rings that can be visualized to determine fish age.

otolithic organs A general term for the saccule, lagena, and utricle of the inner ear. Each has a sensory epithelium and an overlying calcium carbonate mass (otoconia or otolith, depending on the species). Relative motion between the mass and the sensory epithelium causes excitation of the sensory hair cells.

Otophysi A group of fishes that includes goldfish, catfish, and carp. All members of this mostly freshwater group of fishes have a series of bones, the Weberian ossicles, which connect the swim bladder to the inner ear.

pinna The outer ear flap in most mammals, including humans. The pinnae assist with focusing sound and localization, the ability to detect the direction of a sound.

Pinnipedia The marine mammal order comprised of seals, sea lions, and walruses.

rorquals A type of baleen whale that feeds on small fish and zooplankton by lunge-feeding.

saccule One of the regions of the ear. In fishes the saccule is generally considered to be the major auditory end organ but it may also be used to determine head position relative to gravity. In terrestrial vertebrates and all mammals, the saccule, along with the utricle, provides information about head position relative to gravity and helps the animal maintain eye position as head position changes.

semicircular canals Fluid filled canals of the restibular system of the inner ear. Motion of these fluids excite cells that detect angular acceleration of the head. Feedback from the canals affects eye movements.

sensory hair cells The fundamental cell of the inner ear and lateral line of vertebrates. These cells detect mechanical motion and convert that motion to a signal that can stimulate the nerves that carry information to the brain.

sound localization Determination of the position of a sound source compared to the position of an animal based on differences in its intensity and arrival times between ears or receptors.

swim bladder An air chamber in the abdominal cavity of most bony fishes that is used to adjust buoyancy so that the animal can maintain its position in the water column without expenditure of energy. The swim bladder in some fishes is used in sound production and in sound detection.

ultrasonic Sounds above 20 kHz, which is the upper extreme of human hearing.

utricle One of the regions of the inner ear. In fishes the utricle is involved in both hearing and determination of head position relative to gravity. In terrestrial vertebrates and all mammals, the utricle is primarily a receptor for determination of head position relative to gravity and helps the animal maintain eye position as the head changes position.

vestibular system The part of the inner ear, that determines the position and acceleration of the head relative to gravity, commonly thought of as the balance system. The vestibular system includes the

sensory organs of the saccule and utricule plus the semicircular canals.

Weberian ossicles A series of bones between the swim bladder and inner ear of Otophysan fishes that appears to enhance hearing by serving as an acoustic coupling device between the pressure-receiving swim bladder and the saccule of the inner ear in a way that is functionally analogous to the middle ear of terrestrial vertebrates.

3.14.1 The Origins of Vertebrate Underwater Hearing

The vertebrate ear and hearing evolved in aquatic animals. Although there is no evidence as to when the first vertebrates were able to hear, it is likely this occurred several hundred million years ago.

Once vertebrates came onto land, they had to develop an array of new mechanisms to enable use of their fluid-filled and water-adapted inner ears for detection of airborne sounds. The problem that terrestrial vertebrates had to overcome was the difference in impedance between the fluids of the inner ear that had evolved to detect sound in water and the impedance of sound in air. Without special structures for capture, transduction, and amplification, the sound energy in air would not be efficiently transferred to the fluids of the inner ear. As a consequence, airborne sound would be largely undetectable. This need to accommodate the impedance mismatch of air and water led to the evolution of the middle ear present in virtually all terrestrial vertebrates.

Conversely, there was also a readaptation when air-adapted vertebrates once again entered the water. Air-adapted ears of land animals (including human divers) function poorly in water because they are not adapted to the higher pressures and faster sound speeds in water (approximately $1550\,m\,s^{-1}$ in water versus $330\,m\,s^{-1}$ in air) that are critical elements for discriminating between sounds and determining the position of a sound source in the space. Consequently, aquatic vertebrates have two levels of adaptation: the original water-derived ear of fishes and a range of partial to full remodifications of an air-to-water ear in animals that have returned to the marine environment.

3.14.2 The Evolution of Vertebrate Hearing in Water

The earliest vertebrates were jawless species resembling the modern-day lamprey. Lampreys, like their vertebrate ancestors, have a very recognizable ear with sensory cells and other structures similar to those of modern vertebrates. However, because the ear comprises both the vestibular and auditory senses, it is not clear whether the earliest ears were primarily for hearing or for detecting acceleration and head position.

Even if ears did not originally arise for hearing, they likely subsumed this role very early in the evolution of vertebrates because there were considerable selective pressures favoring sound detection (van Bergeijk, W. A., 1967; Wever, E. G., 1974; Fay, R. R. and Popper, A. N., 2000). In effect, hearing is likely to have arisen because other senses available to the earliest vertebrates, including vision, touch, and olfaction, function effectively only over short ranges. For example, vision can only function when there is sufficient light to excite photoreceptors in the eye (Fay, R. R. and Popper, A. N., 2000) and light does not penetrate very far into the ocean. In contrast to light, sound travels well in water, and the ocean is filled with sounds (Wenz, G. M., 1964) that can provide animals, through hearing, with a broader range of information about the environment at greater distances from the receiver than virtually any other sense.

Animals just detect presence of sound to use it effectively. Particularly for survival, the animal needs to be able to determine the direction and, ideally, the relative distance of sounds and to determine which are biologically relevant (e.g., predator, prey, mate, or competitor) in the presence of other sounds. Thus, it is possible to hypothesize that very early in the evolution of hearing, vertebrates developed mechanisms that would enabled them to localize sound sources, discriminate among signals, and detect signals in the presence of masking noise. This implies that in addition to evolving an ear, they also had to evolve the mechanisms for analyzing multiple features of sounds (e.g., Fay, R. R. and Popper, A. N., 2000).

It is likely also that use of sound for communication among animals of the same species, such as for mating, evolved later than hearing per se. Although data are limited, it is known that sharks and rays use sound to detect possible prey, but there is no evidence that any member of this very successful

vertebrate group uses sound for communication (Myrberg, A. A., 2001). Similarly, although goldfish have excellent hearing (Fay, R. R., 1988), no one has yet detected that goldfish producing sounds. Marine mammals by contrast employ complex signals not only for communication but, in some cases, for sophisticated acoustic imaging called echolocation or biosonar as discussed below.

3.14.3 The Inner Ear of Fishes

The ears of cartilaginous fishes (sharks and rays) and of bony fishes resemble those of terrestrial vertebrates (Figure 1). All vertebrate ears (other than jawless fishes) have three semicircular canals that are used for determination of angular acceleration. They also have several otolithic end organs, two of which, the saccule and utricle, are found in all vertebrates. The third end organ, the lagena, is found in all vertebrates except mammals but may have given rise to the cochlea (Wever, E. G., 1974). The function of the otolithic end organs in terrestrial animals is to determine head motion relative to gravity. For fishes, however, these organs provide vestibular functions as well as hearing (Platt, C., 1983; Popper, A. N. *et al.*, 2003).

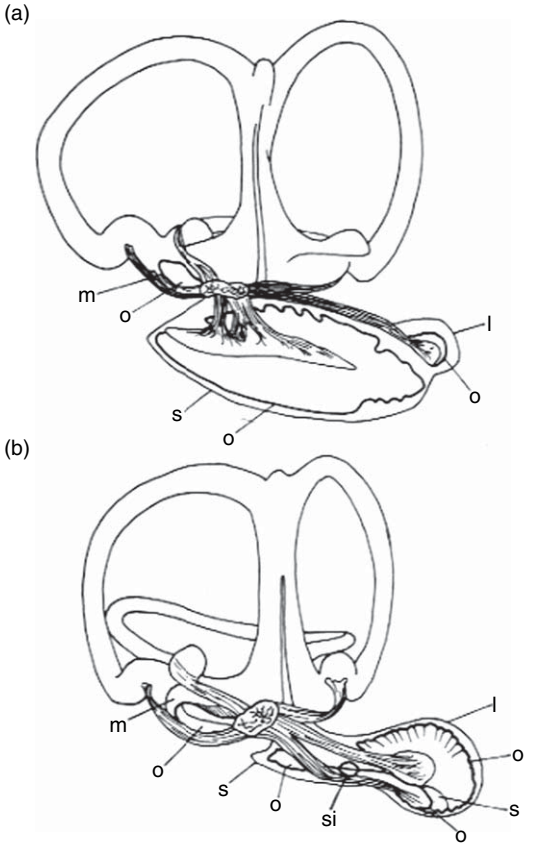

Figure 1 Illustrations of the right inner ears from the perch *Stizostedion lucioperca* (formerly *Lucioperca sandra*) (a) and goldfish *Carassius auratus* (b). Both from Retzius G. (1881). l, lagena; m, utricular macula; o, otolith; s, saccule; si, sinus impar (to connect left and right ears in goldfish). Anterior is to the left and dorsal to the top.

Fish hearing involves the use of sensory hair cells that are virtually the same as those found in terrestrial vertebrates (Coffin, A. *et al.*, 2004). In cartilaginous fishes (sharks and rays), terrestrial vertebrates, and more primitive bony fishes (e.g., sturgeon and lungfish), the sensory epithelium containing the sensory cells is overlain by a mass of calcium carbonate crystals (otoconia) embedded in a gelatinous matrix. In the majority of bony fishes, however, the calcium carbonate fuses into a single dense structure, the otolith. Hearing by fishes results when a sound field impinges on the body and moves tissues more readily than the denser otoliths. Because the ciliary bundles on the hair cells are mechanically coupled to the otoliths, the relative motion between the fish's body and the otolith results in bending of the ciliary bundles and stimulation of the hair cells, leading to detection of sound (or body motion in water).

The precise role of each of the end organs in fish hearing is not known, and it is likely that the specific roles vary among the more then 25 000 extant species of fish (Popper, A. N. *et al.*, 2003). For example, the saccule is thought to be the major auditory end organ in goldfish and related species (e.g., most catfish), whereas in a few species the utricle has a major role in hearing, as discussed below.

3.14.4 Hearing Capabilities of Fishes

Hearing has been measured in cartilaginous and bony fishes. These measures include both the range of frequencies detectable and the lowest sound levels that are detected at each frequency. While limited, these data show that cartilaginous fishes are able to detect sounds up to about 1000 Hz (Figure 2). Although there are hearing data on fewer than 100 of the 25 000 species of bony fish, it is clear that there is greater variation in the abilities of bony fish to detect in sound (Figure 2). Some fishes detect sounds only up to 500–1000 Hz, whereas others can detect sounds with better sensitivity and at frequencies up to 3000 or 4000 Hz. A few species are able to detect

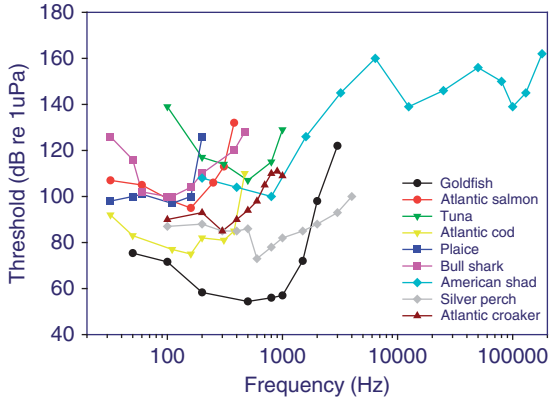

Figure 2 Auditory thresholds for a variety of different fish and shark species. Note that the audiograms were all determined using different methods. Moreover, while thresholds are most likely correctly represented using pressure values for hearing specialists such as goldfish and silver perch, it is not clear whether pressure or particle motion (not shown here) would be more suitable for the nonspecialists. All data from Fay, R. R. (1988) other than silver perch (Ramcharitar, J. U. *et al*., 2004) and Atlantic croaker (Ramcharitar, J. U. and Popper, A. N., 2004).

sounds well into the infrasonic and ultrasonic ranges (reviewed in Popper, A. N. *et al*., 2003; Ladich, F. and Popper, A. N., 2004).

Fishes that detect sounds above about 1500 Hz are often referred to as hearing specialists, whereas those that do not possess such capabilities are called nonspecialists (or generalists). It has been suggested that in the hearing specialists, one or more of the otolith organs may respond to sound pressure as well as to acoustic particle motion (e.g., Popper, A. N. *et al*., 2003). The response to sound pressure is thought to be mediated by mechanical coupling between the swim bladder (a gas-filled chamber in the abdominal cavity that enables a fish to maintain neutral buoyancy) or other gas bubbles and the inner ear. With this coupling, the expansion and contraction of the gas-filled structure in a pressure field is translated to the ear. In nonspecialists, however, the lack of a swim bladder or its lack of coupling to the ear probably results in any signal from the swim bladder attenuating before it gets to the ear. As a consequence, these fishes detect little or no pressure component of the sound (Popper, A. N. *et al*., 2003). Hearing generalists are most sensitive to sounds produced by relatively near sources.

While some hearing specialists, such as catfish, use sound for communication (as do some hearing generalists), others do not. Then here has been some question about why fishes that do not use sound for communication evolved the ability to detect higher frequencies. The most likely reason, at least for freshwater species, is that the fish evolved in shallow water where there is substantial and rapid attenuation of low frequencies (Rogers, P. H. and Cox, M., 1988). In order for these species to glean any information about their environment using sound, they would need adaptations to detect the higher frequencies that propagate over longer distances in such waters.

Specializations for enhancement of hearing generally involve mechanisms that acoustically couple an air bubble, such as the swim bladder, with the ear. It is likely that the swim bladder evolved to enable fishes to maintain neutral buoyancy, thus cutting down on energy used to maintain a particular depth in the water column. However, mechanisms have evolved that enable many fish species to use this organ for both sound production (Zelick, R. *et al*., 1999) and hearing (Ladich, F. and Popper, A. N., 2004).

The nature of the coupling between the swim bladder and inner ear varies among hearing specialists. The best-known coupling is found in the fishes of the superorder Otophysi, a group of primarily freshwater fishes that includes goldfish and catfish. These species have a series of bones, the Weberian ossicles, connecting the swim bladder directly to the inner ear. It has been hypothesized that motion of the walls of the swim bladder during sound stimulation results in motion of the Weberian ossicles that, in turn, moves the fluids of the inner ear (Alexander, R. McN., 1962) in a manner analogous to the function of the mammalian middle ear bones.

Beyond the Otophysi, there are diverse connections between the swim bladder or other air bubbles and the inner ear among taxonomically distinct species. These may include anterior projections of the swim bladder that terminate in contact with the ear and/or newly evolved air bubbles located near the ear.

One significant point about all of these structures is that multiple mechanisms evolved to enhance hearing that are spread throughout the fish taxa. Indeed, there are instances of closely related species with very different hearing capabilities and air bubble connections to the ear. For example, one species of the squirrel fish family (Holocentridae) only detects sounds to about 1000 Hz, whereas another species that lives in the same caves detects sounds to over 3000 Hz (Coombs, S. and Popper, A. N., 1979). The two species have substantial differences in ear structure and in the relationship between the swim bladder and ear.

Fishes of the commercially important family Sciaenidae (croakers and drums) also have great diversity in ear structure, in the relationship between the ear and swim bladder, and in hearing capabilities (Ramcharitar, J. U. *et al.*, 2001).

Although the saccule and lagena are most often implicated in fish hearing, there are a number of cases in which the utricle appears to have taken on a special role to enhance detection of low- or high-frequency sounds. There is evidence that some marine catfish use low-frequency echolocation to glean information about their environment (Tavolga, W. N., 1976), much as dolphins use high-frequency sounds for biosonar. Echolocating catfish have hypertrophied utricles that are hypothesized to function like a low-frequency accelerometer to detect echoes of their own sounds in order to navigate through the environment (Popper, A. N. and Tavolga, W. N., 1981).

At the other end of the frequency range, the clupeiform fishes (e.g., herring, anchovies, and sardines) have utricles unlike those found in any other vertebrate. Recent evidence has implicated this specialization for the detection of sounds up to 180 kHz in a number of clupeids including the American shad (Mann, D. A. *et al.*, 2001). The adaptive significance of this capability appears to be for the detection of sounds produced by the echolocating dolphins (Plachta, D. T. T. and Popper, A. N., 2003) that often prey upon schools of clupeids.

The bottom line is perhaps the exceptional diversity of structures that fishes have evolved that enable them to use sound to obtain environmental information. Although we are at the earliest stages of understanding this diversity, an example of the critical use of sound includes evidence that deep-sea fishes evolved specializations to enhance hearing at depths where there is little or no light (e.g., Buran, B. N. *et al.*, 2005). More recently, it has become apparent that some larval fishes use sounds produced by reefs to find places to settle (Simpson, S. D. *et al.*, 2005). Data is currently available on only a few extant species. It is likely that further study will continue to demonstrate that hearing not only evolved underwater but also that the broadest adaptations are in this environment as well.

3.14.5 Marine Mammals

Marine mammals, like fishes, encompass diverse groups of species, although it is arguable that they are less diverse than fishes. Marine mammals comprise five vertebrate groups. The two best known are the cetaceans (dolphins and whales) and the pinnipeds (seals, sea lions, and walruses). These will form the focus of this discussion because there are sufficient data on hearing in some of their component species to provide insights into how aquatic ears re-evolved from air-adapted ancestors. They also include species that range from totally aquatic to amphibious to primarily land (or ice), air-adapted ears.

Cetaceans are divided into two distinct groups. The Odontoceti (or toothed whales) are predatory high-frequency echolocators typified by the well-studied bottlenose dolphins. The Mysticeti (or baleen whales) include the largest species ever recorded, the blue whale, as well as some smaller rorqual whale species. All cetaceans live entirely in water and may spend as much as 80% of their time submerged. Pinnipeds, by contrast, are truly amphibious and all species spend some portion of their time and do key activities (e.g., breeding and rearing young) on land. The sirenians (manatees and dugongs) are, like cetaceans, obligate aquatics, but to date few manatees have been studied and there are no hearing data on dugongs. There are no hearing or ear data on any member of the two remaining and most recently evolved marine mammal groups, the sea otters and polar bears.

3.14.5.1 Marine Mammal Auditory Systems

Significant structural differences between marine and land mammal ears are primarily found in the outer and inner ears. All marine mammals have special adaptations of the external ear (valvular canal closure mechanisms, semioccluded canals, and wax plugs) and middle ear (heavily vascularized and innervated middle ear mucosa, diminished or absent mastoids, and broad-bore Eustachian tubes) consistent with deep, rapid diving and long-term submersion. However, recent data suggest that marine mammals retain air-filled middle ears and the same fundamental inner ear components and hearing mechanisms as terrestrial species.

Cetaceans have the most derived ear of any mammal, marine or otherwise. As cetaceans evolved into obligate aquatic mammals, their head tissues were pushed, inflated, and telescoped (Barnes, L. G. *et al.*, 1985) to form a novel cranium with elongated jaws (rostrum), scooped frontal bones, and nares transposed upward and rearward, dorsal to the eyes. Telescoping may have been driven head reshaping primarily to allow minimal head exposure at the surface, but the ear was effectively dragged along with other skull elements to new positions in the

head, and profound structural changes for sound transduction took place in virtually all parts of the peripheral auditory system.

In cetaceans, sound most likely arrives at the ear via specialized fatty tissues that are coupled to the middle ear and that act as both pinnae and external canals (Figure 3). Norris K. S. (1969) speculated that a fatty core in the posterior third of the mandible acts as a preferential path for underwater sound. Recent studies have determined that these perimandibular fats have complex shapes that effectively form internal pinnae (Ketten, D. R. *et al.*, 2004). They also are composed of very unusual lipids that have physical properties consistent with acting as a specialized channel matched to the acoustic impedance of underwater sound (Koopman, H. N. *et al.*, 2006).

Cetacean middle and inner ears in general were reshaped also to meet the demands of underwater physics of sound. They became encased in distinctive, shell-shaped bony capsules (tympanic and periotic bullae) that moved outside the brain case and, at least in most modern odontocetes, lost all firm bony connections to the skull. Instead, the tympanoperiotic bullae, and thus the middle and inner ears of dolphins, are suspended by ligaments or struts in a spacious, soft tissue-filled extracranial sinus. This accomplishes two critical things for underwater hearing. First, the ears have a three- to fivefold greater separation than if they retained the intracranial position common in land mammals, which means they are separated to match the increased speed of sound in water. Second, both the middle and inner ears are acoustically isolated from most head tissues that could conduct sound to the ear which improves sound localization which is critical for echolocation.

Odontocetes and mysticetes have middle ears adapted for radically different frequencies. Odontocetes follow the ultrasonic land mammal pattern but carry it to extremes with multiple stiffening agents for the middle ear ossicles that include both well-developed stapedial ligaments and incudal struts (Ketten, D. R., 2000). Further, the tympanic membrane is substantially reduced and relatively rigid in all odontocetes. Bottlenose dolphins (*Tursiops truncatus*) have recently been shown to have middle ear stiffnesses that are sixfold greater than those of land mammals (Miller, B. S. *et al.*, 2006). All of this is consistent with audiometric data for odontocetes (discussed below) that shows broad hearing ranges from about 150 Hz to well over 100 kHz, with peak hearing over 40 kHz for most dolphins species.

Mysticetes, by contrast, have low-frequency, mass-dominated middle ears. Unlike the small, stiff middle ear and eardrum of dolphins, the mysticetes

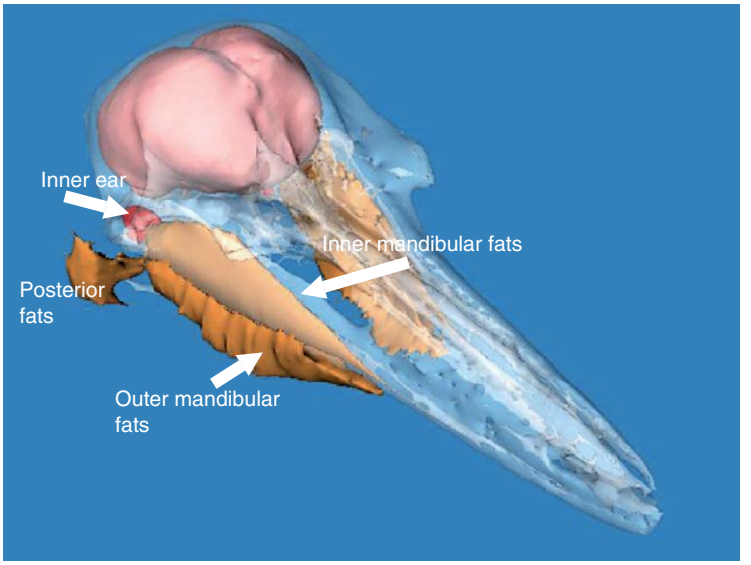

Figure 3 A three-dimensional reconstruction based on computerized tomography data of a bottlenose dolphin. The skull, including the upper and lower jaws or rostrum, are transparent to show the brain (pink) inside the skull and the ear bones (red). The ear bones, housing middle and inner ear structures, are outside the skull but inside the lower jaw (mandible) and are connected to the three fat bodies (orange) (Ketten, D. R. *et al.*, 2004, reprinted with permission, © Ketten, D. R., 2003). These fats form rabbit ears that are oriented anteriorly and slightly ventral and provide a low-impedance path to the middle ear compared to other head tissues. Reprinted by permission of Ketten, D. R.

have a thick, multilayered eardrum that is a unique elongated pouch called the glove finger (Reysenbach de Haan, F. W., 1956). This unusual structure not only reduces the probability of tympanic membrane perforation in diving but also increases middle ear volume and is coupled to a disproportionately large middle ear cavity, all of which are consistent with the expectation of good infrasonic to low-frequency hearing in most mysticetes (see Watkins, W. A. and Wartzok, D., 1985 for vocalizations and Ketten, D. R., 2000 for anatomical correlates). There is no evidence to date of echolocation by mysticetes, and whether they preceded, succeeded, or coevolved with odontocetes is not yet clear (Thewissen, J. G. M., 1998).

Thus, as a group, mysticete and odontocete middle ears span infra- to ultrasonic hearing with adaptations that clearly couple these ears so effectively to underwater sound that they may no longer be able to sense airborne sound at anything except very high levels.

There is no clear consensus on how whale and dolphin middle ears function underwater. Both conventional ossicular motion and translational bone conduction have been proposed for dolphins (see review in Ketten, D. R., 2000), and the role of the middle ear in cetaceans therefore remains an open question.

Cetacean inner ears have a well-developed spiral cochlea but substantially reduced vestibular systems. In some ways the cetacean cochlea is in fact hypertrophied in having more cells and more complex membrane structures than most land mammals. All whales and dolphins typically have more than 2000 ganglion cells mm^{-1} of basilar membrane, which is double to triple the ganglion cell densities of other mammals (Ketten, D. R., 2000). By contrast, the vestibular and optic nerves in cetaceans, in comparison to those of most land mammals, are depauperate. Cetacean vestibular systems have both far smaller canal radii than other mammals (the blue whale semicircular canals are comparable to those of mice) and very few nerve fibers. Vestibular fibers comprise less than 5% of the acousticovestibular nerve cetaceans in contrast to 40–50% in most terrestrial mammals.

In odontocetes, acute ultrasonic hearing is achieved by multiple stiffening elements in the inner ear, including doubled bony membrane suspensions and exceptional thickness-to-width basilar membrane ratios (1.0 : 0.01) that exceed even those of bats (Ketten, D. R. and Wartzok, D., 1990). Odontocete basilar membrane thicknesses typically range from 25 μm at the base to 5 μm at the apex or double those of most other species. Basilar membrane widths vary in the opposite direction; basal widths are 30–50 μm at the base and increase to 300–500 μm apically. Thus the odontocete basilar membrane is relatively thick and narrow. It therefore resembles a stiff beam throughout its length.

Mysticete membranes are thin rectangles throughout, with base-to-apex membrane ratios of 0.1 : 0.001 based on thicknesses from 7 μm at the base to 2 μm at the apex and widths ranging from 100 μm at the base (similar to the base in humans) to 2200 μm at the apex or threefold that of humans and 1.2-fold that of elephants (Ketten, D. R., 2000). These ratios are directly correlated with the resonant frequencies along the membrane, whereas the gradients reflect the octave range, which for all cetaceans implies hearing covering 10–12 octaves.

Pinniped ears are more conventional than those of cetaceans. External pinnae are reduced or absent in some species, but conventional external ear canals are present and functional at least for in-air hearing. One critical amphibious adaptation in seals and sea lions is a spiral cartilage–muscle sphincter that seals the meatus (Møhl, B., 1968), implying that the canal can be voluntarily closed. Whether the external canal remains air-filled, collapses, or floods when underwater remains unclear; neither is it known if the canal is a functional sound path to the ear in water.

The tympanic and periotic bones of pinnipeds resemble those of terrestrial mammals. The ear bones are not acoustically isolated as with those of cetaceans, and the middle ears only have a moderate layer of cavernous tissue with a wide range of ossicular chain configurations ranging from very massive (elephant seal) to moderately stiff (harbor seal; Møhl, B., 1968; Marsh, S. E. *et al.*, 2001), implying a wide variation in peak frequencies among species.

Most pinniped inner ears resemble those of terrestrial high-frequency generalists with evidence for some ultrasonic, but not well-developed, high ultrasonic hearing (Solntseva, G. N., 1990). At least one species, the elephant seal, has a membrane structure consistent with better low-frequency hearing than most other pinnipeds (Wartzok, D. and Ketten, D. R., 1999)

3.14.5.2 Marine Mammal Audiometrics

Audiograms are available for 11 of the nearly 80 cetacean species (Au, W. W. L., 2000), but the data are only from smaller odontocetes. Consistent with

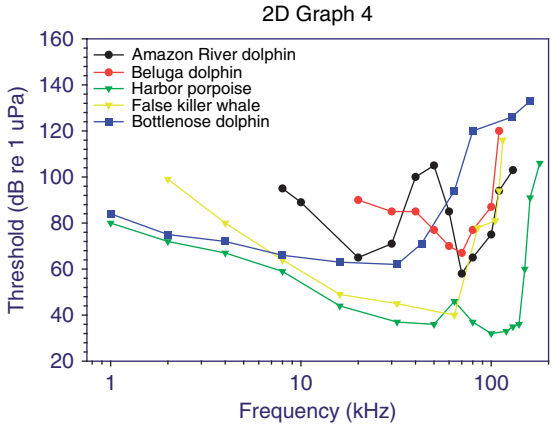

Figure 4 Hearing thresholds for a variety of odontocete cetaceans. Data for the Amazon River dolphin and the beluga dolphin (Popov, V. and Supin, A., 1990) were measured using auditory brainstem response methods. Data from the harbor porpoise (Kastelein, R. *et al*., 2002), false killer whale (Thomas, J. A. *et al*., 1988), and bottlenose dolphin (Johnson, C. S., 1967) were all obtained with behavioral measures.

the anatomically derived basilar membrane estimates, electrophysiological and behavioral measures show functional hearing ranges that span 10 octaves or more and excellent ultrasonic capacities for the species tested (Figure 4). Best thresholds measured to date typically range from 40 dB re 1 μPa to 60 dB re 1 μPa, with peak sensitivities ranging from 12 kHz in the killer whale (*Orcinus orca*) to well over 100 kHz in several species including the freshwater Amazonian boto (*Inia geoffrensis*) and the harbor porpoise (*Phocoena phocoena*; Nachtigall, P. E. *et al*., 2000; Kastelein, R. *et al*., 2002).

Ultrasonic echolocation signals produced by dolphins have been recorded from 21 species and are highly species specific, although active echolocation has been demonstrated unequivocally in only the 11 species tested to date (Nachtigall, P. E. *et al*., 2000). Virtually all parameters echolocation signals can be modified by the animal, including pulse repetition rate, interval, intensity, and spectra, given sufficient background interference (Au, W. W. L., 2000). However, the dominant normal click spectra for each species is relatively constant and ranges between 12 and 120 kHz, with source levels typically near 120–140 dB re 1 μPa but reportedly as high as 230 dB re 1 μPa (summary table in Wartzok, D. and Ketten, D. R., 1999). Species recorded to date produce species-stereotypic broadband echolocation clicks, with peak energy between 10 kHz and 200 kHz, burst-pulse click trains, and constant-frequency (CF) or frequency-modulated (FM) whistles with peak spectra from 4 to 16 kHz (Tyack, P., 1999) that appear to be used for intraspecific communication.

Functional significance for species variations in echolocation and communication signals has not been fully investigated, but habitat and peak spectra of echolocation signals are strongly correlated (Ketten, D. R. and Wartzok, D., 1990). Odontocetes that employ signals above 100 kHz tend to be inshore, estuarine, and freshwater dolphins that hunt in relatively shallow water environments such as harbors or rivers. These species locate small fish amidst tangled roots and stems in heavily silted waters. They have auditory systems adapted primarily to receive and analyze ultrahigh frequencies which have short wavelengths consistent with echolocating small, nearby objects.

Off-shore animals are generally larger, travel in highly social pods, and forage in deeper, clearer waters. These species have broader frequency-adapted ears consistent with processing ultrasonic but lower-frequency peak spectra and longer ranging echolocation signals as well as even lower mid-sonic frequency whistles for communication with podmates.

Bottlenose dolphins, the most commonly studied dolphin species, perform 6–8 dB better than an ideal receiver. Most species are capable of 1–4° azimuthal resolution, although as little as ~0.5° has been reported for harbor porpoises. Minimal intensity discrimination in bottlenose dolphins (1 dB) equals human values, and temporal discrimination (~8% of signal duration) is superior to that of humans. Frequency discrimination in dolphins is significantly better than in most mammals and is best, unsurprisingly, between 5 kHz and 60 kHz in the most common species which are mostly offshore (Popper, A. N., 1980). Intensity discrimination thresholds (ITD) for odontocetes equal those of any land mammal and decline with increasing sound level. Measured values range from 1–2 dB for bottlenose dolphins up to 3–5 dB for harbor porpoises and the Amazonian boto.

Detection of a source position, known as localization, is a third feature at which odontocetes excel. Two cues are critical for mammalian auditory system localization: differences in arrival time (interaural time) and sound level (interaural intensity). On land, the normal sound path is around the head, pinna to pinna, and thus the interaural time differences (ITDs) are calculated based on the distance

between receiver points in the head. In most mammals, this is the distance measured around the head from the center of each pinna divided by the speed of sound in air. In aquatic animals, however, sound could travel through the head via tissues with densities close to sea water.

As discussed above, anatomical evidence suggests that specialized jaw fats act as preferential, low-impedance channels that are able to carry sound to the middle ear in odontocetes. Behavioral experiments (Brill, R. L. *et al.*, 1988) found that echolocation by bottlenose dolphins is impaired if the jaws are blocked from receiving sounds by neoprene shields. These results suggest that interjaw distances are the appropriate measure for ITD values in odontocetes. The interjaw or interear distances of dolphins seem large but because of the speed of sound in water, they equate to the ear separations of larger bats, which is consistent with equally good angular resolution in both groups.

In addition to localization, detection of signals in noise is also critical for echolocation in natural environments. Critical bands and critical ratios are two measures of the ability of an ear to overcome masking, the phenomenon in which competing sounds eliminate or degrade perception of another (Yost, W. A., 1994). Odontocetes have more critical bands than most mammals and smaller critical ratios than humans or even many bats, making them better than most mammals at detecting signals in noise. The best critical ratios to date (8–40 dB) are for the false killer whale (*Pseudorca crassidens*) which is also the species that has performed best in echolocation discrimination tasks (Nachtigall, P. E. *et al.*, 2000; Supin, A. Y. *et al.*, 2003).

Recent studies using auditory evoked potentials (AEP) or auditory brainstem responses (ABR) employing amplitude-modulated stimuli (AMS) in bottlenose dolphins and false killer whales have demonstrated that odontocetes extract envelope features at higher modulation frequencies than other mammals, including humans where they are important for speech perception, particularly at low frequencies (Dolphin, W. F., 1995; Supin, A. Y. *et al.*, 2003). These data suggest that auditory central nervous system adaptations in toothed whales may include regions specialized for both low and high frequencies.

There are no direct behavioral or electrophysiologic hearing data for mysticetes, but deep ocean stationary arrays and deployable recording tags have substantially increased knowledge of mysticete sounds. In general, mysticete vocalizations are significantly lower in frequency than those of odontocetes, as hypothesized from anatomical evidence (Wartzok, D. and Ketten, D. R., 1999). Mysticete sounds are characterized as low-frequency moans (fundamental frequency below 200 Hz); simple calls (impulsive, narrowband signals below 1 kHz); complex calls (broadband pulsatile AM or FM signals); and complex, seasonally varied songs (Watkins, W. A. and Wartzok, D., 1985). Infrasonic signals, typically in the 10–16 Hz range, are well documented in at least two mysticetes, blue whales (*Balaenoptera musculus*) and fin whales (*Balaenoptera physalus*; Watkins, W. A., 1981). It has been speculated that mysticetes use infrasonic signals for long-distance communication or topographic scale echolocation, but there is not as yet any clear evidence or field tests that support the idea.

Pinnipeds are divided into three groups: Phocidae: true or non-eared seals; Otariidae: eared seals; and Odobenidae: walruses. Audiometric data show they vary from partially to fully adapted for underwater hearing (Figure 5). However, to date it is not certain how most species accomplish hearing in both media. One possibility is that pinnipeds have dual systems operating independently for aquatic and airborne stimuli and in different frequency ranges related to behaviors in each medium (e.g., feeding in water versus pup location on land). A second possibility is that pinnipeds are adapted primarily for one environment or the other or have one system for hearing in both media but not optimized for either. The current data suggest that among tested species both of these possible strategies have evolved.

The 11 pinniped species tested to date have peak sensitivities between 10 and 30 kHz, with a functional high-frequency limits up to 75 kHz (Richardson, W. J.

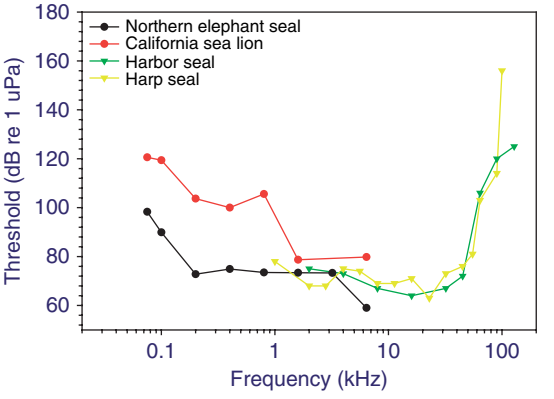

Figure 5 Underwater behavioral response auditory thresholds for four species of pinniped. Northern elephant seal and California sea lion from Kastak D. and Schusterman R. (1998); Harbor seal from Møhl B. (1964); Harp seal from Terhune J. M. and Ronald K. (1972).

et al., 1995, Kastelein, R. *et al.*, 2002; Southall, B. L. *et al.*, 2004). Low-frequency functional limits are not yet well established for most pinnipeds, but parallel studies of harbor seals (*Phoca vitulina*) versus elephant seals (*Mirounga angustirostris*) suggest that elephant seals have significantly better underwater low-frequency hearing sensitivity than other pinnipeds tested to date, with functional hearing down to 75 Hz (Kastak, D. and Schusterman, R., 1998).

In air pinniped audiograms have peak sensitivities at slightly lower frequencies than in water (3–10 kHz; Kastak, D. and Schusterman, R., 1998). Thresholds for airborne sounds are poorer, on average, in phocids, the seals, which have no overt pinna, but there is little difference in aerial versus underwater audiograms for otariids, the eared seals and sea lions. This implies that phocids may be better adapted for underwater hearing, whereas otariids evolved a single system that operates adequately but not optimally in air or water.

In frequency discrimination and localization tasks, pinnipeds perform more poorly than odontocetes. Angular resolution ranges from 1.5° to 9.0°, but most have 4.0° to 6.0° of resolution (Richardson, W. J. *et al.*, 1995). Minimal intensity discrimination (3 dB) in California sea lions is poorer than that of dolphins or humans, but frequency discrimination in phocids and sea lions is similar to that of bottlenose dolphins. Critical ratios for pinnipeds are generally equal to those of dolphins and humans. Like odontocetes, pinnipeds in water could have small-to-large functional inter-ear distances depending upon whether they use the external canal, specialized tissues, or the inner ear as the sound reception point underwater. However, to date, there are no clear data on the configuration of any pinniped underwater sound reception path.

Most pinniped sounds recorded to date are in the sonic range, and the repertoires are complex, varying by context, sex, and season (Watkins, W. A. and Wartzok, D., 1985; Richardson, W. J. *et al.*, 1995). Call descriptions run the gamut from grunts to rasps, rattles, and warbles in addition to whistles, clicks, and pulses ranging from 100 Hz to 15 kHz, with peak spectra below 5 kHz. Like cetaceans, source levels in water are commonly near 130 dB re 1 μPa although levels as high as 193 dB re 1 μPa have been reported (Richardson, W. J. *et al.*, 1995). Despite producing click-like sounds, there is no evidence that pinnipeds are able to echolocate. Infrasonic to seismic sounds are produced by northern elephant seals in air. Thus, both air and underwater vocalizations for these amphibious species, like those of cetaceans and other mammals, are consistent with conclusions from ear models and with the general characteristics of audiograms in tested species.

References

Alexander, R. McN. 1962. The structure of the Weberian apparatus in the *Cyprini*. Proc. Zool. Soc. Lond. 139, 451–473.

Au, W. W. L. 2000. Echolocation in Dolphins. In: Hearing by Whales and Dolphins (*eds*. W. W. L. Au, R. R. Fay, and A. N. Popper), pp. 364–408. Springer.

Barnes, L. G., Domning, D. P., and Ray, C. E. 1985. Status of studies on fossil marine mammals. Mar. Mamm. Sci. 1, 15–53.

Brill, R. L., Sevenich, M. L., Sullivan, T., Sustman, J. D., and Witt, R. E. 1988. Behavioral evidence for hearing through the lower jaw by an echolocating dolphin, *Tursiops truncatus*. Mar. Mamm. Sci. 4, 223–230.

Buran, B. N., Deng, X., and Popper, A. N. 2005. Structural variation in the inner ears of four deep-sea elopomorph fishes. J. Morphol. 265, 215–225.

Coffin, A., Kelley, M., Manley, G. A., and Popper, A. N. 2004. Evolution of Sensory Hair Cells. In: Evolution of the Vertebrate Auditory System (*eds*. G. A. Manley, A. N. Popper, and R. R. Fay), pp. 55–94. Springer.

Coombs, S. and Popper, A. N. 1979. Hearing differences among Hawaiian squirrelfishes (family Holocentridae) related to differences in the peripheral auditory system. J. Comp. Physiol. 132, 203–207.

Dolphin, W. F. 1995. Steady-State Auditory-Evoked Potentials in Three Cetacean Species Elicited Using Amplitude-Modulated Stimuli. In: Sensory Systems of Aquatic Mammals (*eds*. R. A. Kastelein, J. A. Thomas, and P. E. Nachtigall), pp. 25–47. DeSpil Publishers.

Fay, R. R. 1988. Hearing in Vertebrates, a Psychophysics Databook. Hill-Fay Associates.

Fay, R. R. and Popper, A. N. 2000. Evolution of hearing in vertebrates: the inner ears and processing. Hear. Res. 149, 1–10.

Johnson, C. S. 1967. Sound Detection Thresholds in Marine Mammals. In: Marine Bio-Acoustics (*ed*. W. N. Tavolga), pp. 247–260. Pergamon.

Kastak, D. and Schusterman, R. 1998. Low-frequency amphibious hearing in pinnipeds: methods, measurements, noise, and ecology. J. Acoust. Soc. Am. 103, 2216–2228.

Kastelein, R., Buskoek, P., Hageoom, M., Au, W., and de Haan, D. 2002. Audiogram of a harbor porpoise (*Phocoena phocoena*) measured with narrow-band frequency modulated signals. J. Acoust. Soc. Am. 112, 335–346.

Ketten, D. R. 2000. Cetacean Ears. In: Hearing by Whales and Dolphins (*eds*. W. Au, R. R. Fay, and A. N. Popper), pp. 43–108. Springer.

Ketten, D. R. and Wartzok, D. 1990. Three-Dimensional Reconstructions of the Dolphin Cochlea. In: Sensory Abilities of Cetaceans: Laboratory and Field Evidence (*eds*. J. A. Thomas and R. A. Kastelein), pp. 81–105. Plenum.

Ketten, D. R., Simmons, J., Hubbard, A. E., and Mountain, D. A. 2004. Dolphin and bat sonar: convergence, divergence, or parallelism. J. Acoust. Soc. Am. 115, 2517.

Koopman, H. N., Budge, S. M., Ketten, D. R., and Iverson, S. J. 2006. The topographical distribution of lipids inside the mandibular fat bodies of odontocetes: remarkable complexity and consistency. IEEE J. Ocean. Eng. 31, 95–106.

Ladich, F. and Popper, A. N. 2004. Parallel Evolution in Fish Hearing Organs. In: Evolution of the Vertebrate Auditory System (*eds*. G. A. Manley, A. N. Popper, and R. R. Fay), pp. 95–127. Springer.

Mann, D. A., Higgs, D. M., Tavolga, W. N., Souza, M. J., and Popper, A. N. 2001. Ultrasound detection by clupeiform fishes. J. Acoust. Soc. Am. 109, 3048–3054.

Marsh, S. E., Fischer, I., Arruda, J., and Ketten, D. R. 2001. Morphometric analyses of hearing in two families of pinnipeds. J. Acoust. Soc. Am. 110, 2749.

Miller, B. S., Zosuls, A. L., Ketten, D. R., and Mountain, D. A. 2006. Middle ear stiffness of the bottlenose dolphin (*Tursiops truncatus*). IEEE J. Ocean. Eng. 31, 87–94.

Møhl, B. 1964. Preliminary studies on hearing in seals. Videnskabelige Meddelelser Fra Dansk Naturhistorisk Forening I Kjobenhaven 127, 283–294.

Møhl, B. 1968. Hearing in Seals. In: The Behavior and Physiology of Pinnipeds (*eds*. R. Harrison, R. Hubbard, R. Peterson, C. Rice, and R. Schusterman), pp. 172–195. Appleton-Century.

Myrberg, A. A., Jr. 2001. The acoustic biology of elasmobranches. Environ. Biol. Fish 60, 31–45.

Nachtigall, P. E., Lemonds, D. W., and Roitblat, H. L. 2000. Psychoacoustic Studies of Dolphin and Whale Hearing. In: Hearing by Whales and Dolphins (*eds*. W. W. L. Au, R. R. Fay, and A. Popper), pp. 330–361. Springer.

Norris, K. S. 1969. The Echolocation of Marine Mammals. In: The Biology of Marine Mammals (*ed*. H. J. Andersen), pp. 391–423. Academic Press.

Plachta, D. T. T. and Popper, A. N. 2003. Evasive responses of American shad *(Alosa sapidissima)* to ultrasonic stimuli. Acoust. Res. Lett. Online 4, 25–30.

Platt, C. 1983. The Peripheral Vestibular System in Fishes. In: Fish Neurobiology (*eds*. R. G. Northcutt and R. E. Davis), pp. 89–124. University of Michigan Press.

Popov, V. and Supin, A. 1990. Electrophysiological Studies of Hearing in Some Cetaceans and a Manatee. In: Sensory Abilities of Cetaceans: Laboratory and Field Evidence (*eds*. J. A. Thomas and R. A. Kasterlein), pp. 405–415. Plenum.

Popper, A. N. 1980. Sound Emission and Detection by Delphinids. In: Cetacean Behavior: Mechanisms and Functions (*ed*. L. M. Herman), pp. 1–52. Wiley.

Popper, A. N. and Tavolga, W. N. 1981. Structure and function of the ear of the marine catfish, *Arius felis*. J. Comp. Physiol. 144, 27–34.

Popper, A. N., Fay, R. R., Platt, C., and Sand, O. 2003. Sound Detection Mechanisms and Capabilities of Teleost Fishes. In: Sensory Processing in Aquatic Environments (*eds*. S. P. Collin and N. J. Marshall), pp. 3–38. Springer.

Ramcharitar, J. U., Deng, X., Ketten, D., and Popper, A. N. 2004. Form and function in the unique inner ear of a teleost fish: the silver perch (*Bairdiella chrysoura*). J. Comp. Neurol. 475, 531–539.

Ramcharitar, J., Higgs, D. M., and Popper, A. N. 2001. Sciaenid inner ears: a study in diversity. Brain Behav. Evol. 58, 152–162.

Ramcharitar, J. U. and Popper, A. N. 2004. Masked auditory thresholds in sciaenid fishes: a comparative study. J. Acoust. Soc. Am. 116, 1687–1691.

Retzius, G. 1881. Das Gehörorgan der Wirbelthiere, Vol. I. Samson and Wallin.

Reysenbach de Haan, F. W. 1956. Hearing in whales. Acta Otolaryngol. Suppl. 134, 1–114.

Richardson, W. J., Greene, C. R., Jr., Malme, C. I., and Thomson, D. H. 1995. Marine Mammals and Noise. Academic Press.

Rogers, P. H. and Cox, M. 1988. Underwater Sound as a Biological Stimulus. In: Sensory Biology of Aquatic Animals (*eds*. J. Atema, R. R. Fay, A. N. Popper, and W. N. Tavolga), pp. 131–149. Springer.

Simpson, S. D., Meekan, M., Montgomery, J., McCauley, R., and Jeffs, A. 2005. Homeward sound. Science 308, 221.

Solntseva, G. N. 1990. Formation of an Adaptive Structure of the Peripheral Part of the Auditory Analyzer in Aquatic, Echo-Locating Mammals during Ontogenesis. In: Sensory Abilities of Cetaceans: Laboratory and Field Evidence (*eds*. J. A. Thomas and R. A. Kastelein), pp. 363–384. Plenum.

Southall, B. L., Schusterman, R. J., Kastak, D., and Kastak, C. R. 2004. Underwater hearing thresholds in pinnipeds measured over a 6-year period. J. Acoust. Soc. Am. 116, 2504.

Supin, A. Y., Nachtigall, P. E., Pawloski, J. L., and Au, W. W. L. 2003. Evoked potential recording during echolocation in a false killer whale *Pseudorca crassidens* (L). J. Acoust. Soc. Am. 113, 2408–2411.

Tavolga, W. N. 1976. Acoustic Obstacle Detection in the Sea Catfish (*Arius felis*). In: Sound Reception in Fish (*eds*. A. Schuijf and A. D. Hawkins), pp. 185–204. Elsevier.

Terhune, J. M. and Ronald, K. 1972. The harp seal (*Pagophilus groenlandicus* (Erxleben, 1777). III. The underwater audiogram Can. J. Zool. 50, 465–469.

Thewissen, J. G. M. 1998. The Emergence of Whales, Evolutionary Patterns in the Origin of Cetacea. Plenum.

Thomas, J. A., Chun, N., and Au, W. W. L. 1988. Underwater audiogram of a false killer whale (*Pseudorca crassidens*). J. Acoust. Soc. Am. 84, 936–940.

Tyack, P. 1999. Communication and Cognition. In: Biology of Marine Mammals (*eds*. J. Reynolds and S. Rommel), pp. 287–323. Smithsonian Institution Press.

van Bergeijk, W. A. 1967. The Evolution of Vertebrate Hearing. In: Contributions to Sensory Physiology (*ed*. W. D. Neff), pp. 1–49. Academic Press.

Wartzok, D. and Ketten, D. R. 1999. Marine Mammal Sensory Systems. In: Biology of Marine Mammals (*eds*. J. Reynolds and S. Rommel), pp. 117–175. Smithsonian Institution Press.

Watkins, W. A. 1981. The activities and underwater sounds of fin whales. Sci. Rep. Whales Res. Inst. 33, 83–117.

Watkins, W. A. and Wartzok, D. 1985. Sensory biophysics of marine mammals. Mar. Mamm. Sci. 1, 219–260.

Wenz, G. M. 1964. Curious Noises and the Sonic Environment in the Ocean. In: Marine Bio-Acoustics (*ed*. W. N. Tavolga), pp. 101–119. Pergamon.

Wever, E. G. 1974. The Evolution of Vertebrate Hearing. In: Handbook of Sensory Physiology. Vol. V/1 Auditory System. (*eds*. W. D. Keidel and W. D. Neff), pp. 423–454. Springer.

Yost, W. A. 1994. Fundamentals of Hearing: An Introduction, 3rd edn. Academic Press.

Zelick, R., Mann, D., and Popper, A. N. 1999. Acoustic Communication in Fishes and Frogs. In: Comparative Hearing: Fish and Amphibians (*eds*. R. R. Fay and A. N. Popper), pp. 363–411. Springer.

Further Reading

Popper, A. N., Ramcharitar, J., and Campana, S. E. 2005. Why otoliths? Insights from inner ear physiology and fisheries biology. Mar. Freshwater Res. 56, 497–504.

3.15 Otoacoustic Emissions

J Siegel, Northwestern University, Evanston, IL, USA

© 2008 Elsevier Inc. All rights reserved.

3.15.1	Introduction	237
3.15.2	A Brief History of Otoacoustic Emission	238
3.15.3	Otoacoustic Emission Phenomena	241
3.15.3.1	Spontaneous Acoustic Emission: A Response Without a Stimulus	241
3.15.3.2	Emissions Evoked by Low-Level Transients and Single-Frequency Tones	242
3.15.3.3	Emissions Evoked by Tone Pairs	243
3.15.3.4	Bidirectional Transduction Revealed by Acoustic Emissions Evoked by Electrical Stimuli	244
3.15.4	Models of Otoacoustic Emission	244
3.15.5	Interpreting Otoacoustic Emissions: Relation to Active Cochlear Mechanics and the Cochlear Amplifier	247
3.15.5.1	Emitted Sounds or a Change in the Cochlear Input Impedance?	247
3.15.5.2	Positive Feedback in the Mechanics of the Cochlea	248
3.15.5.3	Quasilinearity at Low Stimulus Levels	249
3.15.5.4	Nonlinear Behavior at Moderate Sound Levels	250
3.15.5.5	Nonlinear Emissions at Relatively High Stimulus Levels	253
3.15.6	Cellular Mechanisms of Otoacoustic Emission Generation	254
3.15.7	Conclusions and Future Directions	255
References		256

Glossary

cochlear microphonic An electrical field potential that originates in the summation of transduction currents of cochlear hair cells.

compressive nonlinearity A deviation from linear behavior of a system in which the amplitude of the response grows at a rate less than proportional to the amplitude of the input. This is also referred to as a saturating nonlinearity.

distortion products Frequencies generated by a nonlinear system that are not present in the input.

nonlinearity Deviation from linear behavior. Signs of nonlinearity include a compressive or expansive input-output relation and generation of distortion products.

quasilinearity A property of nonlinear systems with an input–output relation in which the slope does not change abruptly through the origin. The behavior of the system converges to linear for sufficiently small input amplitudes.

3.15.1 Introduction

Unlike other sensory receptor systems, the inner ear appears to generate signals of the same type as it is designed to receive. These sounds, called otoacoustic emissions (OAEs), have long been considered byproducts of the cochlear amplifier, the process that makes cochlear mechanics active by adding mechanical energy at the same frequency as a stimulus tone in a positive feedback process. This feature of the inner ear is one of the most important distinctions from other sensory receptors. In no other system is there such a profound collective reciprocal action of a population of sensory cells and supporting structures. In the eye, for example, the sensitivity of individual photoreceptors is essentially determined by the light absorption properties of the visual pigment, the rest of the eye serving passively to couple the light entering the pupil to the array of photoreceptors. The chemistry of the photopigments seems designed so that light absorption is virtually irreversible, so there is no apparent way for the eye to operate like the inner ear, where the receptor cells interact with accessory structures in a feedback loop to enhance sensitivity. One practical

implication is that photoreceptor mechanisms are much easier to study *in vitro* in single cells than are hair cell mechanisms, whose function is disrupted when they are removed from the intact hearing organ.

All normal cochleas appear to produce sounds in response to acoustic stimuli, for reasons that are the focus of intense discussion. OAEs are an epiphenomenon as they play no direct role in hearing. In principle, the ear could have a cochlear amplifier but not emit sounds. It is usually reasoned that, since the middle ear works efficiently in both directions and not all of the energy generated by the cochlear amplifier is dissipated within the cochlea, some of the added energy escapes through the middle ear and sets the eardrum in motion which in turn acts like a loudspeaker and radiates sounds out of the ear. But the story is much more complicated than that. There is ample evidence that OAEs are produced not only because cochleas amplify vibrations, but also because they exhibit nonlinearity. Nonlinearity is not only an essential characteristic of active cochlear mechanics, but also a hair cell phenomenon that may be manifest even when there is little or no mechanical amplification. Adding to the difficulty in understanding OAEs is the fact that they represent the collective action of a population of hair cells the size of which is not precisely known but is likely to depend on the levels of acoustic stimuli. The challenge in understanding emissions is that of adequately appreciating the entire signal chain, from the acoustics of the ear canal where evoking stimuli are presented, their propagation through the middle ear, the physics of wave motion in cochlear mechanics, the hair cell mechanism(s) that lie at the root of the phenomenon, and the summation and reverse propagation of the emission signals back out of the cochlea, through the middle ear, and into the ear canal.

Another conceptual problem in relating OAEs to active cochlear mechanics is the same as determining the cellular mechanism of the cochlear amplifier. Both are the product of a feedback loop that contains the transduction apparatus and both hair bundle and somatic motor mechanisms. So while both exhibit active gain and nonlinearity, these features may originate primarily in different components of the closed feedback loop. The loop can be opened to study the individual processes in isolated hair cells, but OAEs, active cochlear mechanics, and the cochlear amplifier itself are only features of the intact system.

There is no room for even an inadequate review of the OAE phenomenon. Individual published contributions now number in the thousands. The vast literature of OAEs can be accessed through several reviews (Probst, R. *et al.*, 1991; Shera, C. A. and Guinan, J. J., Jr., 1999; Kemp, D. T., 2007). But there are no current reviews with a focus of relating OAEs directly to active cochlear mechanics or to the cellular basis of the cochlear amplifier that are of greatest interest to those trying to understand the inner workings of the ear. I have therefore incorporated into this essay a mini review of a small part of the relevant literature that must be appreciated before this discussion can take place. My goal is to evaluate why OAEs are important, discuss how they are measured and interpreted, and examine the current limitations on both measurements and theories.

3.15.2 A Brief History of Otoacoustic Emission

One way to appreciate the importance of the OAE phenomenon is to review the state of understanding peripheral auditory mechanics at the time of the Kemp D. T. (1978) initial publication of his discovery. The picture of cochlear mechanics was still dominated by the pioneering studies of von Békésy G. (1960) in human cadavers (and those of other mammals), as well as in physical models. The basilar membrane was considered linear, passive, and broadly tuned. Many investigators were pursuing various schemes of an hypothesized second filter that could account for the frequency selectivity measured in auditory nerve fibers (Tasaki, I., 1954; Kiang, N. Y. S. *et al.*, 1965) versus Békésy's shallow mechanical tuning. The discovery of OAEs helped propel the study of cochlear mechanics into the modern era. Because so much had yet to be discovered of what is now known of the cochlear amplifier from direct studies of basilar membrane vibrations and motor mechanisms of cochlear hair cells, the acoustic emission phenomenon was interpreted largely using the time-honored black box engineering approach. The ear was probed by presenting acoustic stimuli and the characteristics of the emitted sounds were used to try to figure out what was inside the box that could produce this behavior. But now that we know much more about what is inside the box, it is important that theories and models of OAE be constrained by this new knowledge. In other words the outside-in black box approach should be paired with a comparable inside-out effort, and the theories and models that emerge must produce a satisfactory explanation of peripheral hearing mechanics, from hair cell motors to ear canal sounds. To some extent this is already being done, but there are many

examples of interpretations of OAEs that may not be consistent with well-established findings from more direct intracochlear studies. Examples abound in the OAE literature in which a theory or model that accounts for an emission phenomenon is described as though it was a proven fact, when direct demonstration of the predicted intracochlear phenomenon does not yet exist. I will attempt to examine the extent to which OAE phenomena have parallels in the cochlear amplifier and will address both the successes and failures of existing theories and models.

At the time when OAEs were discovered, a direct connection between basilar membrane nonlinearity, sensitivity, and frequency selectivity had not been established and so were initially considered separately. Evidence for mechanical nonlinearity accumulated in fragments. Insightful psychophysicists recognized that their studies of perceptual combination tones, at the frequencies of intermodulation distortion products generated by two-tone stimuli, gave strong evidence that mechanical nonlinearity was imposed on the basilar membrane by the healthy organ of Corti and that the resulting intermodulation distortion could be propagated as conventional traveling waves (Goldstein, J. L., 1967; Smoorenburg, G. F., 1972). Direct confirmation of basilar membrane nonlinearity came from the Rhode W. S. (1971; 1978) revolutionary studies in squirrel monkeys. This was also the first evidence that nonlinearity was accompanied with greater frequency selectivity and sensitivity at low levels, but there was still widespread skepticism about such heretical claims that vibrations so small could be nonlinear. Pfeiffer, Molnar, Kim, and colleagues had published evidence for mechanical nonlinearity, both in responses to combinations of click stimuli (Goblick, T. J., Jr. and Pfeiffer, R. R., 1969) and in populations of auditory nerve fibers (Pfeiffer, R. R. and Kim, D. O., 1975; Kim, D. O. *et al.*, 1979; Kim, D. O., 1980; Kim, D. O. *et al.*, 1980; Siegel, J. H. *et al.*, 1982). Dallos and colleagues provided the first evidence, albeit at high levels, that subharmonic distortion, measured in cochlear microphonic recordings, had an acoustic correlate in the ear canal (Dallos, P. J., 1966; Dallos, P. J. and Linnell, C. O., 1966). This was the first definitive demonstration that a distortion tone generated in the cochlea could be conducted through the middle ear and be radiated by the eardrum acting like a loudspeaker. In other words, Dallos should be credited with the discovery of OAE (see Kemp, D. T., 2007). While subharmonic distortion measured at 120 dB SPL may be generated by a mechanism different from emissions measured at lower levels, it is also possible that they are related. Dallos and colleagues also published the first clear evidence that outer hair cells were responsible for threshold sensitivity (Ryan, A. and Dallos, P., 1975; Dallos, P. and Harris, D., 1978), but it was not evident whether this facilitation was electrical or mechanical. Tuning curves of auditory nerve fibers sometimes appeared to show tip segments at elevated threshold with normal frequency selectivity (Dallos, P. and Harris, D., 1978). Frequency selectivity was envisioned as a feature of inner hair cells, with no direct link to sensitivity. The discovery of sharply tuned and sensitive inner hair cell receptor potentials (Russell, I. J. and Sellick, P. M., 1977) showed that these attributes were present in the mechanical input to the inner hair cells, restricting the possible mechanisms of interaction between the two hair cell populations. Despite the existence of the many pieces to the puzzle revealed in these studies, they were not sufficiently compelling to counter the dominant view, established by von Békésy, that the basilar membrane was linear, passive, and broadly tuned. Even as evidence accumulated for sharp, vulnerable basilar membrane tuning, it was not evident to some that this was the product of an active process. Passive second filter mechanisms were still invoked to account for selectivity.

Kemp's discovery helped tip the balance of opinion toward an active cochlea. OAEs, measured over the entire dynamic range of hearing, were undoubtedly mechanical. The evidence that they are generated by a frequency-selective and vulnerable mechanism originating in cochlear hair cells was clearly incompatible with von Békésy's passive and linear traveling wave. As studies emerged of basilar membrane vibrations in healthy cochleas using sensitive methods, attention among cochlear physiologists and theoreticians naturally shifted toward the intracochlear measurements of mechanics that would be the definitive experiments.

Adding to his direct contributions, Kemp also publicized the largely ignored proposal by the astronomer Gold T. (1948) that the ear possessed what became known as the cochlear amplifier. Gold's paper reviewed the phenomenon of objective tonal tinnitus, tones that are spontaneously emitted from some human ears that had appeared in the clinical literature. To Gold, these narrow-band signals indicated the presence of a highly tuned system that used positive feedback to counteract the damping of a passive mechanical resonance. If the gain is excessive, the circuit goes into self-sustained oscillation, predicting

the phenomenon now known as spontaneous otoacoustic emission (SOAE). If the feedback is carefully adjusted just shy of the point of oscillation, the amplifier has both very high gain and sharp frequency selectivity. Regenerative radio receivers based on this principle could detect faint transmitted radio signals, but were also susceptible to interference from strong signals from nearby transmitters, a sign that they could easily be driven into nonlinearity. A second filter would no longer be necessary, since the basilar membrane could exhibit high gain, sharp frequency selectivity, and nonlinearity, all three attributes of positive mechanical feedback in a real physical system. But rather than being the flash of light that spurred the study of peripheral auditory physiology into the modern era, the work of Gold was largely disregarded. So powerful was the impact of von Békésy that this strange-sounding notion of a regenerative receiver mechanism in the cochlea, proposed by an astronomer, sounded far-fetched. It was, except that Gold was right!

Inspired by Gold's ideas, Kemp discovered that acoustic stimuli could evoke acoustic emission from the ear (Kemp, D. T., 1978) and also confirmed with a physical measurement the clinical observations that the ear could spontaneously emit tones (Kemp, D. T., 1979a). One prominent characteristic of emissions evoked by transient sounds, commonly referred to as transient evoked otoacoustic emissions (TEOAE), was that they emerged with a delay that appeared to be too long to arise from the propagation delay of the traveling wave, as well as their prolonged duration. They also showed frequency dispersion, in that the highest frequencies in the spectrum of the emitted sound emerged from the cochlea with the shortest delay, followed by successively lower frequency components (Figure 1). A plausible interpretation of this finding was that the emission was generated by a bank of tuned mechanical resonators, each tuned to a slightly different frequency as Gold had predicted. The positive feedback mechanism within the cochlea would then add energy to the response to the evoking stimulus, some of which was coupled outward through the middle ear and radiated by the eardrum. Kemp's provocative discovery had virtually immediate impact and was rapidly confirmed and interpreted by several prominent scientists.

Looking back on that time, it is striking how many of the basic characteristics of OAEs and their significance were realized by the time the first international conference was held in London in the Fall of 1979 (published as *Hearing Research*, Vol. 2, nos. 3 and 4, 1980). For example, these earliest studies demonstrated that emissions exhibit relatively linear growth in amplitude with sound level below about 20 dB SPL, with

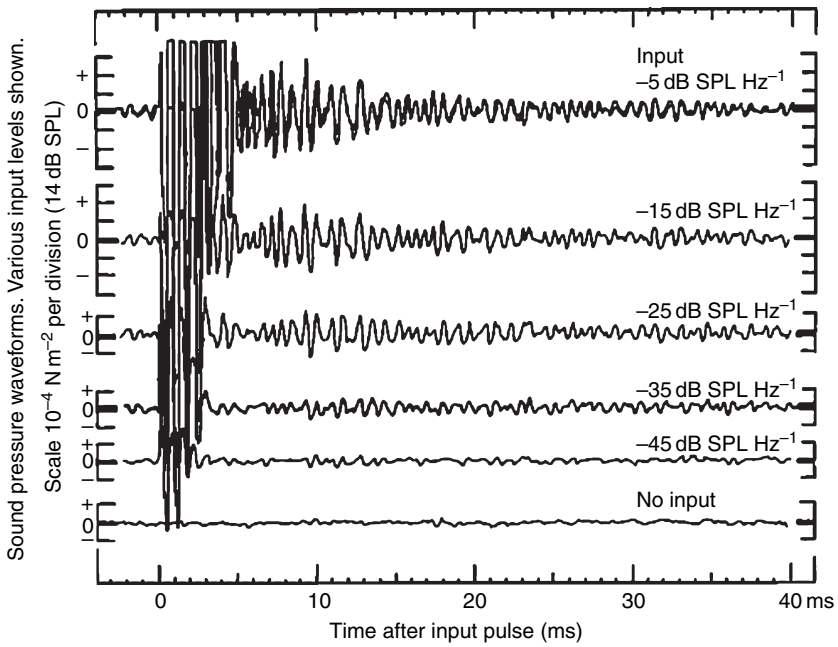

Figure 1 Otoacoustic emissions evoked by clicks from the Kemp D. T. (1978) first full report of his discovery. The delayed acoustic emission is clearly separated in time for the lowest levels of stimulation (bottom), but earlier components of the emission become evident with increasing level, but prolonged ringing of the acoustic click stimulus obscures the earliest part of the emission. Reused with permission from Kemp, D. T. The Journal of the Acoustical Society of America, 64, 1386 (1978). Copyright 1978, Acoustical Society of America.

strong saturating growth at higher levels (Kemp, D. T., 1978; Wit, H. P. and Ritsma, R. J., 1979; Anderson, S. D., 1980; Kemp, D. T. and Chum, R., 1980a), suppression by external stimuli (Kemp, D. T., 1979a; Wit, H. P. and Ritsma, R. J., 1979; Kemp, D. T. and Chum, R., 1980a; Wilson, J. P., 1980a; Kemp, D. T. and Chum, R., 1980b), and intermodulation distortion product generation with two-tone stimuli (Kemp, D. T., 1979a; Kim, D. O., 1980). The initial reports also revealed that emissions demonstrate evidence of sharp frequency selectivity (Kemp, D. T., 1978; Wit, H. P. and Ritsma, R. J., 1979; Kemp, D. T., 1979a; Wit, H. P. and Ritsma, R. J., 1980) and are vulnerable to acoustic overstimulation, hearing loss, and pharmacological agents known to impair hearing (Kemp, D. T., 1978; Anderson, S. D. and Kemp, D. T., 1979; Anderson, S. D., 1980; Rutten, W. L., 1980). Several attempts to model the new phenomenon had also appeared (de Boer, E., 1980; Kemp, D. T., 1980; Wilson, J. P., 1980b). In other words, OAEs were immediately shown to exhibit most of what are now understood to be the major characteristics of active cochlear mechanics in living ears. So direct was the presumed link that it has often been claimed that OAEs represent powerful ways to study active cochlear mechanics without having to open the cochlea. Perhaps, but the relation between the two is not as simple as usually implied. Kemp D. T. (2007) has summarized these complexities in some detail.

Although the cochlear amplifier is usually associated with the outer hair cells of the mammalian cochlea, OAEs are also present in nonmammals that lack outer hair cells and, in some cases, even a basilar membrane (reviewed by Manley, G. A., 2001). The nonmammalian emissions exhibit most of the characteristics of mammalian emissions, showing evidence for a tuned, nonlinear, and labile cochlear amplifier in nonmammals. These findings have added fuel to a lively discussion of the biophysical hair cell mechanisms that may underlie both OAEs and cochlear amplifier. For now I will focus on mammals, but will return later to a more general discussion of hair cell motor mechanisms.

3.15.3 Otoacoustic Emission Phenomena

A brief description of OAEs and how they are measured will serve as a prelude to discussing how they relate to the cochlear amplifier. Emissions are measured using the same type of device as invented by Kemp. A probe assembly containing a sensitive electret microphone is inserted into the ear canal and typically sealed into the canal using a foam ear tip to form a closed acoustic system. Sound sources are either incorporated into the probe assembly or are separate from it with the sounds coupled to the ear through small-diameter tubing. The specifics of how the emission signals are evoked, amplified, and quantified vary, but are most commonly performed using a computer-based acquisition system and standard digital signal processing procedures. It is practical to be able to distinguish emissions of –20 dB SPL or even smaller from the system's noise floor.

3.15.3.1 Spontaneous Acoustic Emission: A Response Without a Stimulus

Kemp D. T. (1979a) verified Gold's prediction of SOAEs. They have been reported for several mammals, including chinchillas, guinea pigs, dogs, monkeys, and humans. Spontaneous acoustic emission has been shown to have a correlate in spontaneous oscillation of the basilar membrane near the characteristic place of the emission frequency (Powers, N. L. *et al.*, 1995; Nuttall, A. L. *et al.*, 2004). They can be as large as 40–60 dB SPL (Ruggero, M. A. *et al.*, 1984), showing that the unstimulated ear is capable of emitting sounds with considerable acoustic power.

The spectra of the noise recorded in the ears of two humans are presented in Figure 2. The curves are slightly offset vertically (by 2 dB) to make both visible. One ear demonstrates no SOAEs, while the other emits ~11, with variable level and apparent

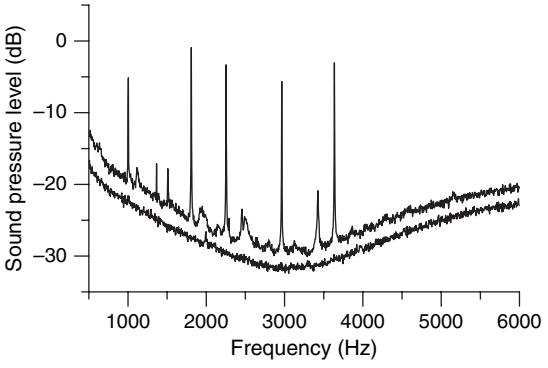

Figure 2 Spectrum of spontaneous otoacoustic emissions recorded from the ears of two humans with indistinguishable normal thresholds. One plot is displaced downward by 2 dB for illustrated. Only in one subject are spontaneous emissions present (upper plot).

bandwidth. Because these spectra are measured using long-term spectral averaging, an emission with relatively low amplitude and wide bandwidth could arise from a narrow-band oscillation that varies in frequency during averaging, but wider bandwidth for smaller emissions is predicted (reviewed by Shera, C. A., 2003). Behavioral thresholds for these two normal hearing subjects, measured using an accurate tracking method, are not significantly different over the entire frequency range of hearing and there is no indication that either individual has better hearing sensitivity in general. So while SOAEs may be absent in impaired ears, their presence is not required for normal hearing sensitivity.

3.15.3.2 Emissions Evoked by Low-Level Transients and Single-Frequency Tones

Early reports of approximately linear growth with level of OAEs evoked by low-level transient and tonal stimuli were of great interest and are even more so as reports have emerged that the basilar membrane response for characteristic frequency (CF) tones is also close to linear over the same range of stimulus level. It has become so common to associate active cochlear mechanics and OAE with nonlinearity that this low-level behavior has not been given the attention it deserves. Confusion arises because linearity at CF is also a property of cochleas in which the cochlear amplifier is not functional or at very high stimulus levels where the gain of the amplifier is small. However, nonlinearity at CF is apparent over most of the physiological range in normal living cochleas, so I will refer to the low-level behavior of both active mechanics and OAEs as quasilinear. This property characterizes many nonlinear physical systems that converge toward linearity for very small inputs. All that is required is that the slope of the function that defines the relation between the instantaneous input and the system's output should not change abruptly near the origin. That there have not been more studies of OAEs at very low levels is also partly due to technical limitations of the equipment and the procedures typically used to measure emissions.

A basic practical problem in studying OAEs is that the sound measured in the ear canal is composed of the sum of the acoustic stimulus pressure and the OAE pressure emitted by the cochlea. Click stimuli are often used so the stimulus can be separated from the emission on the basis of the time delay between the two. But emissions are often small compared to the evoking stimulus and even a well-engineered click can ring for several milliseconds, potentially overlapping the earliest part of the emission. This overlap increases as the level of the stimulus is raised, as is evident in Figure 1. Only emissions with long enough delays can be distinguished clearly from the stimulus. This fact has made it hard to study emissions originating in the basal turn that are expected to have the shortest delays, but short-latency emissions from more apical regions, should they exist, may also be obscured. This is why most studies of TEOAE do not use standard linear signal averaging. Kemp developed a clever technique to detect the presence of transient emissions that cancelled any part of the acoustic response that grows with increasing level, including most of the stimulus pressure (Kemp, D. T. *et al.*, 1986; Bray, P. and Kemp, D., 1987). A variant of this method, in which the method itself is compromised less by nonlinearity of the sound sources, has also been developed by Keefe D. H. (1998) and Keefe D. H. and Ling R. (1998). Either of these nonlinear extraction techniques removes the stimulus ringing, but unfortunately also any part of the emission that grows with level. So the technique does not measure the emission with any degree of fidelity, but only the degree to which it deviates from linear growth over a fairly narrow range of stimulus level. Because TEOAE are most commonly used in the clinic as a screening tool, only the presence or absence of an emission is at issue and the nonlinear technique works reliably for this intended purpose. But this measure of the nonlinearity of emissions is of questionable value for basic studies of emission mechanisms (Kalluri, R. and Shera, C. A., 2007).

Examining the type of experimental data used to study emissions at low levels is illuminating. To separate the stimulus and emission pressures, it is possible to estimate the stimulus pressure under conditions where the emission is negligible, using a method introduced by Kemp D. T. and Chum R. (1980b). At relatively high levels of stimulation, the pressure response in the ear canal appears to be dominated by the stimulus tone (Figure 3(a)). As the stimulus level is lowered, a periodic (with frequency) oscillation of the measured pressure around the intended value is observed, indicating the presence of a stimulus frequency otoacoustic emission (SFOAE) that goes in and out of phase with the stimulus. Plotted using the decibel scale, the fact that the pressure responses at low levels (<30–40 dB SPL) are vertically shifted versions of one another demonstrates that the amplitude of the emission

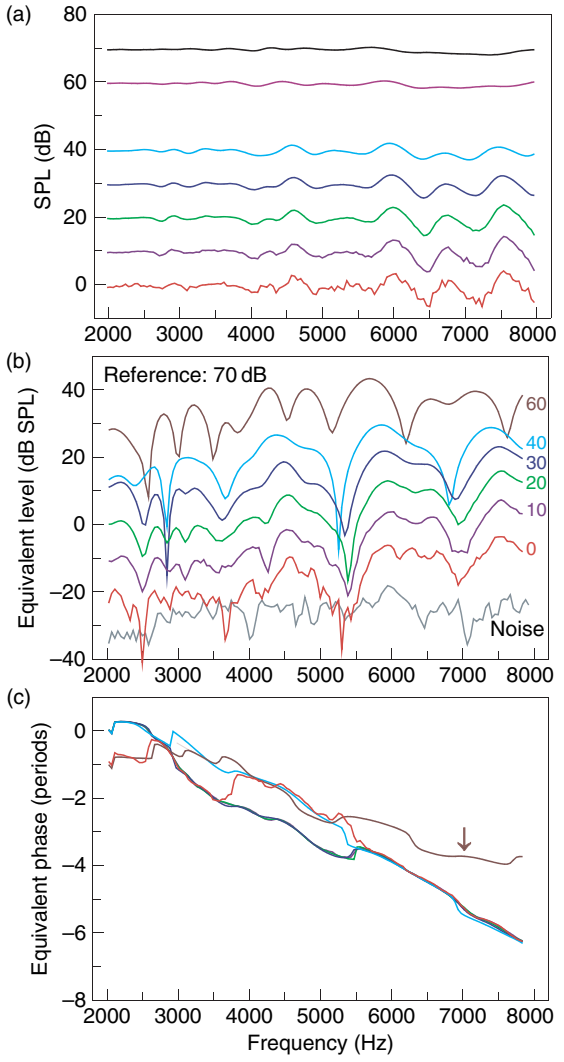

Figure 3 Stimulus frequency otoacoustic emissions measured in the ear canal of a chinchilla with normal compound neural thresholds. (a) The total pressure measured in the canal shows interaction between the stimulus tone and the emission, producing spectral fluctuations in level. The larger variations in the pressure seen with lower levels of stimulation indicate that the emission is relatively larger, compared with the stimulus, than at higher levels. Equivalent level (b) and phase (c) of the emission. The stimulus pressure is subtracted from the total pressure using the measurement at 70 dB SPL as the condition where the emission is relatively small. The level of the emission scales almost perfectly linearly with stimulus level below 30 dB SPL, but shows evidence of nonlinearity at higher levels. The phase of the emission is also relatively independent of level for stimuli below 30 dB SPL, and the overall slope is noticeably lower only at 60 dB SPL.

changes in quasilinear proportion to that of the stimulus. In these measurements from a chinchilla, there is evidence of a small contribution from the emission even at 70 dB SPL, the highest level used.

To measure the contribution of the emission at each level, the stimulus pressure is estimated by scaling down the amplitude of the pressure measured at 70 dB, then subtracting this from the pressure actually measured at each level. Since both the actually measured pressure and the stimulus estimate are vectors, the subtraction yields the vector that, when added to the stimulus pressure, yields the measured pressure. The result of this subtraction is the estimate of the emission, expressed as an equivalent SPL and phase in Figures 3(b) and 3(c). The emission magnitude exhibits regular peaks and nulls and the phase shows abrupt shifts of one half period at the frequencies of the magnitude nulls, superimposed on a general trend of increasing phase lag with frequency. The general trend in the slope of the phase in Figure 3 would be predicted if the SFOAE were delayed by around 1 ms relative to the stimulus, but the nulls and abrupt phase shifts likely represent an interference pattern between two or more signals that make up the SFOAE. As we will see later, these interactions have a behavioral correlate and likely have a mechanical correlate in the basilar membrane motion. Aside for near the frequencies of half-period shifts, the slope of the phase is remarkably independent of stimulus level, except above 5 kHz at a stimulus level of 60 dB where the slope is reduced (arrow). The magnitude grows in approximately linear proportion to the stimulus for levels of 30 dB or lower, but exhibits compressive growth at higher levels. The emission does not saturate completely.

Kemp D. T. and Chum R. (1980b) described an alternative method of separating the emission from the stimulus tone by using a second tone, near the frequency of a tone that evokes SFOAE but higher in level, to suppress the emission, leaving the stimulus pressure (see also Shera, C. A. and Guinan, J. J., Jr., 1999; Schairer, K. S. *et al.*, 2003; Siegel, J. H. *et al.*, 2005). Yet another method uses a time-domain windowing procedure that operates on the inverse fast fourier transform (FFT) or the response to the stimulus tone alone, measured across a range of frequencies (Kalluri, R. and Shera, C. A., 2001; Goodman, S. S. *et al.*, 2003). All methods yield essentially the same result, an important finding that I will return to later.

3.15.3.3 Emissions Evoked by Tone Pairs

Saturating growth of OAEs evoked by transients and tones provides evidence of cochlear mechanical nonlinearity, but the presence of two-tone distortion products and harmonics of the stimulus tones shows that the

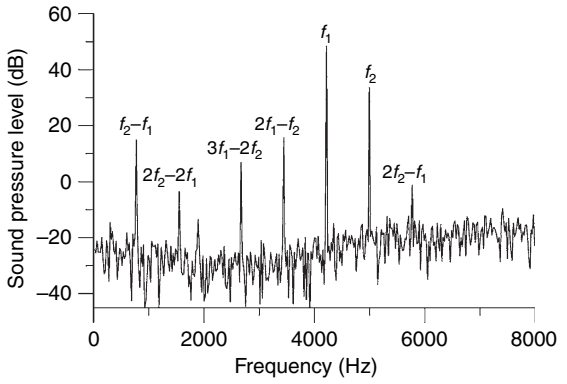

Figure 4 Distortion product otoacoustic emissions measured in the ear of a chinchilla in response to a two-tone stimulus. The frequencies of the distortion products are arithmetic combinations of the frequencies of the stimulus tones.

nonlinear mechanism(s) that generate them are fast compared to the duration of one period of the stimulus. One of the most widely used measures of OAE is to present a pair of tones (f_1 and $f_2, f_1 < f_2$) with a frequency ratio $f_2/f_1 < 1.4$. In addition to the stimulus tones the spectrum of the ear canal sound contains harmonic and intermodulation distortion products at frequencies that are simple arithmetical combinations of the two tones (Figure 4). The main practical advantage of measuring distortion products is that they are easily distinguished from the stimulus tones with narrow-band spectral analysis because they are at different frequencies from the stimuli. The most commonly measured distortion product otoacoustic emission (DPOAE) is at the frequency $2f_1 - f_2$. A problem with observing only one distortion product is the inherently incomplete information this measure provides. Not only is $2f_1 - f_2$ just one of the many distortion products that represent the emission, but each stimulus tone generates an SFOAE. Interpreting the relation between stimulus and response (i.e., all emission components together) would be difficult (reviewed by Kemp, D. T., 2007). In spite of this limitation, DPOAE has proven useful for detecting whether the cochlear amplifier and the outer hair cells that power it are normal, both in research labs and in clinical application (e.g., Martin, G. K. *et al.*, 1990; Gorga, M. P. *et al.*, 1999; Lapsley Miller, J. A. *et al.*, 2006).

3.15.3.4 Bidirectional Transduction Revealed by Acoustic Emissions Evoked by Electrical Stimuli

One of the most startling early discoveries was the demonstration that electrical currents delivered to the cochlea produce sounds in the ear canal that depend on intact hair cells (Hubbard, A. E. and Mountain, D. C., 1983; Mountain, D. C. and Hubbard, A. E., 1989; Xue, S. *et al.*, 1993; Nuttall, A. L. and Ren, T., 1995; Xue, S. *et al.*, 1995; Nuttall, A. L. *et al.*, 2001; Hu, N. *et al.*, 2005; Karavitaki, K. D. and Mountain, D. C., 2007). The extent of the region of the cochlea that contributes to electrically evoked emissions depends on how far the stimulating current spreads within the cochlea, but some place specificity results from focal current injection. It is not clear whether this phenomenon originates in somatic motility, a hair bundle motor, or some combination (e.g., Manley, G. A. *et al.*, 2001; Grosh, K. *et al.*, 2004; Chan, D. K. and Hudspeth, A. J., 2005a; 2005b). In spite of uncertainties of how to interpret electrically evoked emissions, these studies demonstrated directly that the hair cells are bidirectional transducers (Weiss, T. F., 1982) and do not simply respond passively to external stimuli.

3.15.4 Models of Otoacoustic Emission

Because of the complexity of the mechanics and cellular physiology of the inner ear, neither the cochlear amplifier nor OAEs will be understood without developing models of the ear that can account for the phenomena observed in experiments. On the other hand, models that are too abstract to formulate hypotheses that can be tested with experiments are of limited value. But a model that is designed to account for an OAE phenomenon may also have direct relevance to cellular mechanisms of the cochlear amplifier. A good example is the model developed by Shera C. A. (2003) to account for the characteristic minimum frequency spacing seen in mammalian spontaneous emissions. The model formalizes an explanation of how the passive mechanics of the cochlea and middle ear constrain the frequencies of SFOAE to particular values separated by regular intervals. Such behavior cannot arise from single hair cells in isolation, but can be modeled as a standing wave resonance produced by multiple internal reflections (see below). This strong dependence on accessory structures may distinguish active tuning mechanisms in mammals from those in nonmammals where frequency selectivity may arise from electrical or electromechanical resonance in individual cells (e.g., Crawford, A. C. and Fettiplace, R., 1985; Martin, P. *et al.*, 2001; 2003). Whatever the

mechanism of force production by hair cells, the constraints imposed by the strong coupling of individual hair cells to the passive mechanics by supporting structures, including the tectorial membrane in those hearing organs that have one, probably guarantee that the larger mechanical context must be considered. It has been proposed that mammalian outer hair cells have inherent tuning mechanisms (Fettiplace, R., 2006), but it is likely that the frequency selectivity of the active mammalian cochlea is the product of the passive mechanics of the cochlea with hair cells serving as relatively frequency-independent force generators. This is but one example of how models accounting for the behavior of OAEs, which must be understood as wave phenomena, can help evaluate models of active cochlear mechanics that incorporate force generation by hair cells.

Kemp developed a distinction between what he referred to as place-fixed and wave-fixed emissions (Kemp, D T., 1986, summarized by Kemp, D. T., 2007). He proposed that a linear, passive cochlea would dissipate essentially all of the energy of an incoming wave and no sound would be emitted in response. Even an ear with a cochlear amplifier would dissipate the added energy internally unless the forward-propagating traveling waves encountered an irregularity in the mechanical impedance of the basilar membrane. Reverse traveling waves arising from forces generated by hair cells would cancel in a smooth cochlea and only forward-propagating waves would exist. But the cancellation of reverse waves would be disrupted by impedance irregularities and reflected waves would become apparent. Spontaneous emissions and modulated SFOAE and TEOAE spectra would arise from standing waves caused by multiple internal reflections between fixed mechanical irregularities and the basal end of the cochlea (Kemp, D. T., 1979a; 1979b; see Kemp, D. T., 2007). The fraction of the energy in the forward wave that is reflected at the peak can be characterized as a reflectance. The same is true for the reflected wave when it encounters the impedance mismatch at the basal end of the cochlea. Thus, part of the energy is reflected to form a secondary forward traveling wave, while the rest enters the middle ear and is radiated into the ear canal. The secondary wave is amplified and reflected as before and so on. If the round-trip gain in energy due to the cochlear amplifier exceeds the total dissipated within the cochlea and escaping into and through the middle ear, sustained oscillation ensues. Another way of saying the same thing is that self-oscillation results when the product of the apical and basal reflectances exceeds unity. Since the reflectance at the basal end is passive and between 0 and 1, the apical reflectance can exceed 1 when the round-trip energy gain is near the point of instability. OAEs produced by this mechanism were described as place-fixed because the first reflection occurs at the place of each particular irregularity. In contrast, wave-fixed emissions were hypothesized to arise because of an impedance change created near the peak by mechanical nonlinearity. The origin of such waves would move with the envelope of the traveling wave as frequency is varied. They would be determined by the underlying wave pattern on the basilar membrane and are thus fixed to the wave. In a cochlea with a perfect logarithmic relation between frequency and place, the wave pattern simply shifts longitudinally with changing frequency, with no change in shape or even phase within the envelope. This property is termed shift symmetry. The phase of OAEs generated in this way would exhibit a shallow slope versus frequency (see also Shera, C. A. and Guinan, J. J., Jr., 1999). The underlying traveling wave delay would not be apparent in the emission. This applies to DPOAE originating in the region of overlap between the responses to the two stimulus tones if the ratio of the frequencies of the tones is fixed. Fixing the frequency of one of the two tones reveals the underlying wave propagation delays (Mahoney, C. F. and Kemp, D. T., 1995). Stimulus frequency emissions measured at levels high enough to become nonlinear would likewise be expected to exhibit shallow phase slopes versus frequency because of shift symmetry.

The most comprehensive and detailed model of OAE at present is the one described by Shera C. A. and Guinan J. J., Jr. (1999) (Figure 5). In a break with previous formulations, Shera and colleagues proposed that OAEs are the product of two fundamentally different mechanisms: linear coherent reflection and mechanical nonlinearity. Emissions are distinguished as reflection or distortion emissions corresponding to the mechanism of generation. To generate emissions with the long latencies observed for transient and stimulus frequency emissions and a delayed component of DPOAE requires a generation mechanism that is either fixed in location (Kemp, D. T., 1978) or that in some other way breaks shift symmetry. One proposed mechanism, termed the Theory of coherent linear reflection filtering (CRF) emerges as the result of small regular (Strube, H. W.,

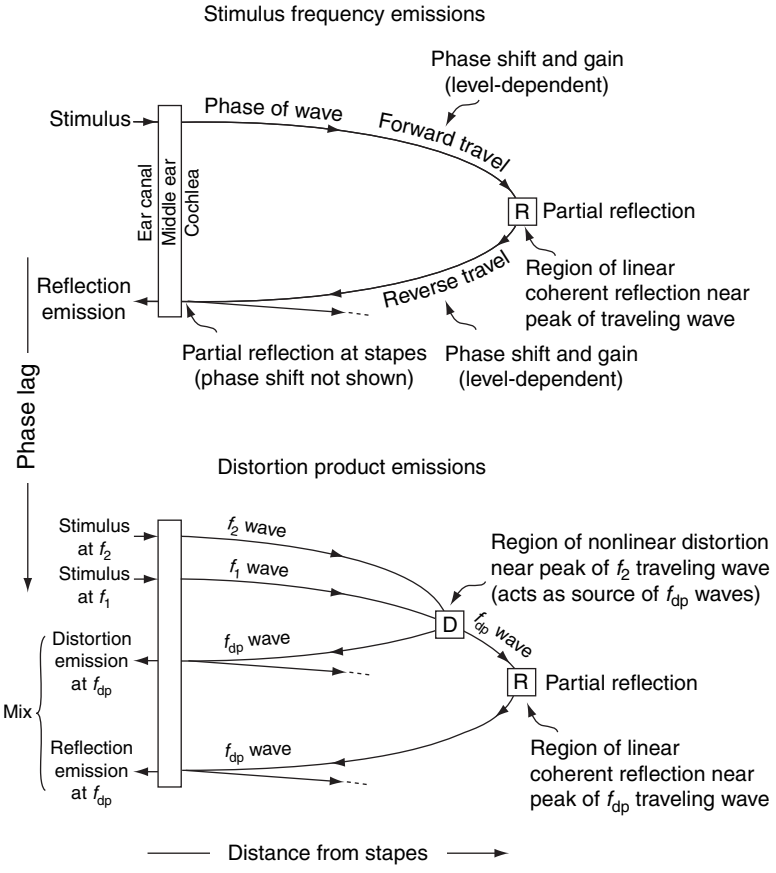

Figure 5 Classification scheme for otoacoustic emissions developed by Shera C. A. and Guinan J. J., Jr. (1999), based on their hypothesis that emissions can be distinguished based on fundamentally different mechanisms of generation. Reused with permission from Christopher A. Shera, The Journal of the Acoustical Society of America, 105, 782 (1999). Copyright 1999, Acoustical Society of America.

1989) or random (Zweig, G. and Shera, C. A., 1995) variations in basilar membrane impedance, which cause coherent reflections of forward-propagating traveling waves near the peak, but incoherent reflections from other regions that cancel one another. Coherent reflection from the peak region also depends on the fact that the peak is both tall and broad. Should the shape of the peak change, as with increasing stimulus level, suppression or other impairment of the cochlear amplifier, then the reflections should be reduced dramatically (Shera, C. A., 2004). Reflection emissions should then be especially well suited to detecting sensory cell hearing loss. Distortion emissions, measured at stimulus levels that drive cochlear mechanics into their nonlinear range, are predicted to exhibit not only different phase behavior, but different sensitivity to hair cell damage.

Both multiple internal reflection models envision the wave reflected from the apical location as a reverse version of von Békésy's traveling wave. If the reflected wave can approach and even exceed the amplitude of the incident wave, then reverse traveling waves should be readily observable, either directly in the motion of the basilar membrane or using indirect measures such as population responses of auditory nerve fibers. To date there have been no compelling experimental measurements of reverse traveling waves. The most clear-cut proof would be to observe them in longitudinal measurements of basilar membrane motion. This experiment, so far performed only in one laboratory, reported only forward-propagating waves (Ren, T., 2002; 2004; He, W. *et al.*, 2007), even in cochleas with normal sensitivity. Similarly, measurements of the basilar membrane response versus frequency at a single location should reveal the existence of standing waves for tones below CF, but this is not evident in any study of basilar membrane vibrations published till the time of

this writing. (A recent report of basilar membrane responses in chinchillas may contain the first evidence of this sort (Rhode, W. S., 2007). Quasiperiodic spectral fluctuations are noted for responses to tones at frequencies below CF at low stimulus levels, and disappear at levels above 30 dB SPL, similar to the behavior of SFOAEs in chinchillas (i.e., Figure 3).) The hypothesized reverse traveling waves should decrease in amplitude with increasing stimulus level, relative to the amplitude of the forward traveling wave, so there should be evidence of nonlinearity in I/O functions for single tones below CF, but significant deviations from linearity have not been observed in any set of data for frequencies an octave or more below CF. Conclusive data could be gathered by measuring both single tone responses in the basilar membrane and SFOAE in the same experimental animal. If reverse traveling waves exist, then wave interactions should be evident in both measures. If confirmed, this would be an example of an important cochlear mechanical wave phenomenon that was first detected in OAE measurements. Direct measurements of reverse traveling waves might then indicate that previous experiments that failed to demonstrate the phenomenon were compromised by the invasive techniques required to perform these extremely difficult experiments. But if such interactions are only present in SFOAE, then it would not be plausible to account for them with reverse traveling waves. Either basally directed basilar membrane traveling waves will eventually be demonstrated or it may be necessary to search for another mode of reverse propagation. However, until this question is resolved, it is wrong to speak of reverse-propagating conventional traveling waves and multiple internal reflections as though they are proven facts. Similar cautionary language is appropriate for describing emissions as wave- or place-fixed or in their origin using separate linear reflection or nonlinear distortion mechanisms until the physiological basis for these concepts is conclusively supported by experiments.

3.15.5 Interpreting Otoacoustic Emissions: Relation to Active Cochlear Mechanics and the Cochlear Amplifier

The background is now set to examine whether the measured behavior of OAEs directly corresponds to characteristics of the basilar membrane response attributed to the cochlear amplifier, implying a direct link. But I will first examine the question of whether what appears to be sound emitted by the ear is a cruel joke played on unsuspecting scientists by a cagy cochlea.

3.15.5.1 Emitted Sounds or a Change in the Cochlear Input Impedance?

Rather than sounds emitted by the ear, it has been proposed that OAEs can alternately be explained as the result of a passive, nonlinear modulation of the cochlear input impedance (Patuzzi, R., 1996) that is caused by intracochlear features such as nonlinear stereocilia stiffness or the action of prestin. The cochlear input impedance strongly influences the acoustic impedance of the eardrum (Zwislocki, J., 1962), so for typical high-impedance sound sources, a change in eardrum impedance will change the measured pressure. The change in measured sound pressure could equivalently be caused by the presence of a signal that is created in the cochlea. Recognizing this basic problem, Guinan J. J., Jr. (1990) suggested that SFOAE be expressed as an equivalent pressure and an equivalent phase. The change in the sound pressure for one tone induced by adding a second, more intense tone could also arise from a passive nonlinear interaction between the two tones. The concept of a nonlinear component of the eardrum reflectance, which may equivalently be considered the OAE, has been developed explicitly by Keefe D. H. (1998; Keefe, D. H. and Ling, R., 1998). But if emissions are measured at low enough levels that they become quasilinear, then they obviously cannot depend on nonlinearity. But this does not resolve the issue because a passive process that modulates the cochlear input impedance and is nonlinear may also converge to quasilinear behavior for small inputs.

The signal versus impedance explanation is not really the critical distinction. I like the way Chris Shera put it in a recent private communication: That OAE can be explained as a modulated cochlear input impedance is

> . . . right in a narrow technical sense: emissions measured in the ear canal do manifest themselves because they affect the cochlear input impedance. But saying that does not explain emissions, except in some superficial sense. Any satisfactory explanation would have to make clear how and why (i.e., through what cochlear process) the emission generation mechanisms modify the cochlear input impedance.

Regardless of whether the cochlear input impedance changes because the ear emits sounds or

because of a change in a passive and/or nonlinear component of the inner ear, if we make an impedance measurement we will measure an impedance! This is in fact the same problem as proving that the cochlear amplifier exists. If we measure the ratio of the differential pressure across the basilar membrane to the displacement caused by a tone at the characteristic frequency of the place of measurement, we can calculate the mechanical impedance at CF. If we reduce the gain of the cochlear amplifier by injecting furosemide into the blood supply to the cochlea, causing a drop in the endocochlear potential, then the same applied pressure causes much smaller displacements and the impedance is therefore much higher. Since we know that the change in impedance was caused by removing a source of power, then we also know exactly why the impedance changed. Similarly, if we inject into the fluid spaces of the organ of Corti of a living animal a substance like gelatin that increases the damping and/or stiffness of the cochlear partition, we will also measure reduced displacement for the same applied pressure and the mechanical impedance may increase by exactly the same factor as when we injected furosemide. But we know that the impedance changed in this case because we altered the passive mechanical properties of the cochlear partition. If we presented our impedance measurements to another scientist without telling how the cochlea was perturbed, then the scientist would have no way to interpret the results. In fact, consensus on the existence of a cochlear amplifier has depended not only on the discovery of motor mechanisms in hair cells or measurements of basilar membrane vibrations, but also on theories of cochlear mechanics and models that demonstrate that measured responses of the basilar membrane can only plausibly come from an active cochlea. The cochlear amplifier is a distributed phenomenon in which hair cells in a region extending basal from the peak supply the energy used to enhance the response at the peak. OAEs are likewise a distributed phenomenon that can likely be understood only through applicable theory-based models. There is as yet no direct demonstration that any hair cell motor function underlies the cochlear amplifier. So, while OAEs are one step removed from basilar membrane mechanics, the difficulties in interpreting them are fundamentally the same.

The view that emissions are signals that have correlates in basilar membrane vibrations is also supported by the demonstration that the low-level SFOAE is paired with a corresponding cochlear microphonic (Wilson, J. P., 1980b; Siegel, J. H., 2006), which is unambiguously a signal known to be generated by mechanical excitation of hair cell transduction (Dallos, P., 1973). Interpreting emission behavior at higher levels of stimulation where nonlinearity is evident is even more complex, because passive nonlinearities of the cochlea could originate in a mechanism separate from the cochlear amplifier. However, emissions that exhibit nonlinearity are usually measured under conditions where the basilar membrane is also known to demonstrate nonlinearity and disappear in situations where basilar membrane nonlinearity is abolished, so again the simplest interpretation is to assume a direct relationship. Resolving this question conclusively is beyond the scope of this contribution and will require definitive experimental data and a theory that can be proven correct.

3.15.5.2 Positive Feedback in the Mechanics of the Cochlea

Perhaps the most important insight gained from the existence of SOAE is that the ear has a positive feedback mechanism that is adjusted for maximum sensitivity, but does not allow large sustained self-oscillations that would interfere with hearing. Some mechanism appears to stabilize most SOAEs at very low levels. That SOAEs can sometimes be quite large is curious because the levels of SOAEs are typically below the threshold of hearing, even in humans where they are common. Compressive mechanical nonlinearity of the basilar membrane near CF, probably due to the saturating transduction apparatus, is likely to play a role (e.g., Talmadge, C. L. *et al.*, 2000). Whether this factor is sufficient to stabilize the amplitudes of very small SOAEs has not been established.

The amount of spontaneously emitted energy is typically so small that SOAE could represent random noise passed through a passive filter with very narrow bandwidth. Although the basis for such a sharp, passive filter was unclear, one way to approach the problem was to ask whether SOAEs represented net power production by the ear. This was accomplished definitively by showing that the power reflectance of the ear could become negative near the frequency of an SOAE, indicating that the acoustic energy emitted by the ear was greater than the power of the sounds used to measure reflectance (Burns, E. M. *et al.*, 1998; Tubis, A. and Talmadge, C. L., 1998). Strong evidence that SOAEs are noisy signals rather than filtered noise comes from statistical analyses of

SOAE amplitude distributions with time (Bialek, W. and Wit, H. P., 1984; Talmadge, C. L. *et al.*, 1991; van Dijk, P. *et al.*, 1996; Shera, C. A., 2003). These studies showed that SOAEs are incompatible with a passive filter model, but consistent with models of an amplitude-stabilized oscillator.

Multiple internal reflections were originally invoked to account for the long delays of stimulus-evoked emissions (Kemp, D. T., 1979a; 1980; reviewed by Shera, C. A. and Guinan, J. J., Jr. 1999). But it has since been shown that the delays measured for SFOAEs can be used to predict the characteristic minimum spacing between adjacent SOAEs, as well as the frequency dependence of their bandwidth and the influence of changes in the impedance of the middle ear (Shera, C. A., 2003). The power of being able to predict in such detail the behavior of SOAE from the behavior of SFOAE supports the CRF theory, but more importantly (in my view) strongly supports the notion that they originate in the same mechanism. Such a connection was proposed early on by Kemp, Wilson, and others (see Zwicker, E. and Schloth, E., 1984). Several of these studies documented that SOAE could be synchronized by external transient stimuli and that the SOAE could lock to the frequency of a nearby stimulus tone, a phenomenon described as capture (see Long, G. R. and Tubis, A., 1988). I have informally noted a strong association between SFOAE and SOAE in chinchillas. In an animal with an SOAE near 7.5 kHz, the magnitude of SFOAE evoked by tones <25 dB SPL slightly exceeded the stimulus pressure in the ear canal for frequencies near that of the SOAE. In many other cases where no SOAEs were detected, the level of SFOAEs was never larger than that of the stimulus (data not shown). The presence of strong SFOAE (or TEOAE) seems to indicate an ear that is close to being unstable.

3.15.5.3 Quasilinearity at Low Stimulus Levels

Both cochlear mechanics and OAEs exhibit quasilinear behavior at sound levels below 20–30 dB SPL. A common feature of many nonlinear physical systems is that they converge to linear behavior for very small inputs. Although nonlinear level dependence was emphasized as a hallmark of evoked acoustic emission in the Kemp D. T. (1978) first report, near-linear growth of OAEs at low levels was subsequently noted in several reports (Wit, H. P. and Ritsma, R. J., 1980; Wilson, J. P., 1980a; Kemp, D. T. and Chum, R., 1980b; Zwicker, E. and Schloth, E., 1984). Linearity is not only appealing for developing theories of both mechanics and emissions, but it may offer a situation to critically test proposed cellular mechanisms that underlie them. It was also evident to early investigators that emissions evoked by low-level tones and transients appeared to excite the same emission mechanism (Wilson, J. P., 1980a; Kemp, D. T. and Chum, R., 1980b). In a much more rigorous test, Kalluri R. and Shera C. A. (2007) have demonstrated that OAE evoked by transient stimuli and standard linear signal averaging can be predicted almost perfectly from measurements using single tones and vice versa. I believe this to be conclusive evidence that, at least for low-level stimuli, TEOAE, SFOAE (and SOAE) do in fact originate in the same mechanism.

It is also significant that widely differing methods of measuring SFOAE yield essentially the same result. One might argue that the suppression method yields a change in the response to the probe tone that appears as a signal but is instead the result of nonlinear interaction between the probe tone and the suppressor. But this explanation becomes implausible when an emission with almost exactly the same magnitude and phase is obtained using methods such as scaling and subtracting, changes in the response to the probe tone induced by the death of the animal or time-domain windowing, none of which require a simultaneous suppressor. So even for the suppression method, the change induced by the suppressor is most plausibly due to removing an SFOAE signal that is generated in the cochlea by the probe tone rather than an artifact induced by the suppressor. If SOAEs represent net power generated by the ear, in excess of that which is dissipated passively in the cochlea and middle ear, and if the levels of SFOAE can approach that of the evoking stimuli, then these linear low-level emissions are almost certainly the work of the cochlear amplifier.

As noted in Figure 3, the SFOAEs exhibit what appears to be an interference pattern of some kind. Although multiple internal reflections are one possibility, alternate mechanisms must be considered if reverse-propagating traveling waves do not exist in these conditions. At least for high-frequency regions of the cochlea, the group delay calculated from the SFOAE phase changes with frequency similar to the group delay at CF measured directly at one place along the spiral in the mechanical response or indirectly using responses of auditory nerve fibers (Siegel, J. H. *et al.*, 2005). How this similarity can come about despite the fact that emissions are a population

response is not understood. But at least in most cases, this finding demonstrates yet another strong correlation between cochlear mechanical wave propagation in living cochleas and emissions.

One of the fundamental predictions of the CRF theory is that the frequency-dependent slope of the phase of SFOAE, its group delay, should be twice the group delay measured at the characteristic place of the stimulus tone (Shera, C. A. and Guinan, J. J., Jr., 1999; 2003). This relation has been questioned based on a compilation of direct measures of mechanical group delay and comparable single unit measures (Siegel, J. H. *et al.*, 2005). In these sets of data the ratio of SFOAE and basilar membrane group delays appears closer to 1:1 than 2:1. Since then, Shera and colleagues have developed a more elaborate model that can generate both slow transverse waves and fast compression waves (Shera, C. A. *et al.*, 2005). Depending on the relative mix of transverse and compression waves, the ratio of SFOAE to BM group delays can range from practically zero to about 1.5:1. The revised group delay measures compare more favorably with model predictions but raise the question of whether the group delay prediction is robust enough to critically test the coherent reflection model, in light of both experimental and theoretical uncertainties.

Primates exhibit TEOAE and SFOAE with the longest delays of all mammals where emissions have been measured and CRF theory predicts that human frequency selectivity must be about three times sharper than small mammals (Shera, C. A. *et al.*, 2002; Shera, C. A., 2003). Using SFOAE measurements to predict frequency selectivity could be very useful. But Ruggero M. A. and Temchin A. N. (2007) have compared the best direct measures of group delay at CF for a wide range of vertebrates and do not find evidence that humans stand apart from other species. In particular, group delays calculated from direct measurements in human cadavers are remarkably similar to those measured in living chinchillas (which have much shorter cochleas than humans), despite 3–4 times longer SFOAE delays in humans. It is unfortunate that the relation between group delay at CF and SFOAE group delay may break down most clearly in a species where intracochlear measurements are impractical.

Low-level emission phenomena almost certainly have a direct correlate in basilar membrane mechanics because there are psychophysical observations that demonstrate corresponding phenomena that must be present in the outflow of neural signals via the inner hair cells. Fluctuations in behavioral threshold with frequency are clearly evident when thresholds are measured at closely spaced frequencies and this threshold microstructure is directly related to SFOAE and SOAE measured in the same ear (e.g., Kemp, D. T., 1979b; Wilson, J. P., 1980a; Long, G. R., 1984; Zwicker, E. and Schloth, E., 1984). This not only is a threshold phenomenon, but affects loudness perception at sound levels up to at least 40 dB SPL, where SFOAEs are partly saturated (Long, G. R., 1984; Mauermann, M. *et al.*, 2004). It seems very likely that the behavioral microstructure is caused by variations in the mechanical input to inner hair cells and should be observable in basilar membrane vibrations at low levels. Since the microstructure is variable even among humans with normal hearing thresholds, it may be labile and thus not easily preserved in invasive measurements of cochlear mechanics.

3.15.5.4 Nonlinear Behavior at Moderate Sound Levels

Evoked OAEs transition from quasilinear into compressive nonlinear growth over the same range of stimulus level as demonstrated in the basilar membrane at CF, hair cell, and single unit recordings. In other words, the energy in OAEs relative to the stimulus level declines in parallel with the decrease in gain of the cochlear amplifier at moderate stimulus levels ($< \sim$70–80 dB SPL). SFOAEs do not saturate fully at moderate stimulus levels, but continue to grow with increasing level in this range. This is also true of the basilar membrane for tones at CF, demonstrating that the cochlear amplifier provides some measurable gain at levels as high as 80–90 dB SPL. Intermodulation distortion products measured in basilar membrane vibrations show generally increasing level with stimulus level over this range as do DPOAE. These emissions demonstrate fast nonlinearity, but are not the product of a hard limiter, as distortion products are generally at least 20 dB below the levels of the stimulus tones. This is also the case for basilar membrane distortion products (reviewed by Robles, L. and Ruggero, M. A., 2001). Such behavior is expected if the compressive level dependence of the cochlear amplifier is caused by limited power in the feedback force generated by hair cells, rather than an overloading distortion mechanism, which would be expected to distribute stimulus energy into a much richer spectrum of distortion products than observed either in the basilar membrane or in OAEs. The frequency selectivity of the basilar

membrane also contributes by attenuating distortion products far from CF. Once again, the parallels between the cochlear amplifier and OAEs are striking.

The deviation from quasilinearity with increasing stimulus level shown in Figure 3 between 60 and 70 dB is interpreted as an SFOAE of roughly 40 dB SPL. Although the group delay derived from the slope of the phase curve in this case is somewhat smaller, on average, from that measured at lower levels, it is still far longer than predicted by nonlinear models (Talmadge, C. L. *et al.*, 2000).

The basilar membrane distortion product $2f_1 - f_2$ and others below f_1 have been shown to originate in two regions of the cochlea: the first being the region where the vibrations induced by the stimulus tones overlap, while the second is near the characteristic place of the distortion product frequency. Once generated in the stimulus interaction region, the distortion product propagated as a traveling wave as though it was present in the stimulus (Goldstein, J. L., 1967; Smoorenberg, G. F., 1972; Kim, D. O. *et al.*, 1980; Siegel, J. H. *et al.*, 1982; see Robles, L. and Ruggero, R. L., 2001). Kim D. O. (1980) was the first to propose that the DPOAE at $2f_1 - f_2$ also originated in these two regions. This was subsequently supported by several studies (Kemp, D. T. and Brown, A. M., 1983; Brown, A. M. *et al.*, 1996; Heitmann, J. *et al.*, 1998; Talmadge, C. L. *et al.*, 1999; Kalluri, R. and Shera, C. A., 2001; Dhar, S. *et al.*, 2002). When f_2/f_1 is held constant, the emission component originating in the interaction region of the stimulus tones appears to emerge with a relatively short delay, while the distortion product (DP) place component exhibits a delay similar to that of an SFOAE evoked by a stimulus tone at the frequency of the distortion product. Interaction between these two components at the same frequency but with different delays produces a microstructure similar to that seen for SFOAE. DPOAEs are thus envisioned as combinations of reflection and distortion emissions. This microstructure would only be apparent if the amplitudes of the two components are of the same order of magnitude. It is possible to separate the two components, either by selective suppression of the DP place component with an external tone or by spectral smoothing (e.g., Kalluri, R. and Shera, C. A., 2001). The DP place component is the more readily suppressed of the two (Kemp, D. T. and Brown, A. M., 1983).

Vulnerability to cochlear impairment has been used to classify DPOAE sources on the basis of stimulus level (e.g., Whitehead, M. L. *et al.*, 1992a), but it is likely that this distinction is based on the change in cochlear amplifier gain (Lukashkin, A. N. *et al.*, 2002) and the spatial spread of the stimulus tone interaction region with increased level. Both of these factors are likely to explain why DPOAE measured with high-level stimuli are relatively insensitive to mild impairment of hair cells. A basic but unresolved question is whether the distortion generation region for high-level stimuli extends beyond that required for the cochlear amplifier. Nonlinear interactions in transducer currents far basal to the peaks for the stimulus tones are evident in the cochlear microphonic (Dallos, P., 1973) and there is some evidence that two-tone interactions in SFOAE and cochlear microphonic (CM) appear coextensive (Siegel, J. H., 2006). Whether this basal region also contributes to the cochlear amplifier is unresolved.

It has been common to assume that the DPOAE is initially generated in a small region near the f_2 place, but this is based primarily on iso-suppression tuning curves, which are easily misinterpreted and are unsuited to evaluating relative contributions from different places (see Dreisbach, L. E. and Siegel, J. H., 2005). An extended generation region spreading basal from the f_2 place is supported by other studies (Martin, G. K. *et al.*, 1999; 2003; Fahey, P. F. *et al.*, 2006). Evidence that the DPOAE originates in the transduction process (Jaramillo, F. *et al.*, 1993; Carvalho, S. *et al.*, 2004; Liberman, M. C. *et al.*, 2004), combined with evidence from population studies of single auditory nerve fibers (e.g., Kim, D. O. *et al.*, 1980) further supports this view. Using the lowest stimulus levels that produce nonlinear interaction between the two tones restricts the size of the region of initial generation (Sutton, L. A. *et al.*, 1994). This strategy may be useful for trying to pinpoint regions of damage to the hair cells. At high stimulus levels, DPOAE can be measured even in the ears of recently dead animals (Whitehead, M. L. *et al.*, 1992b).

In sensitive cochleas, the basilar membrane I/O function becomes approximately linear at levels below about 20 dB SPL, where the displacement of hair bundles is about 10 nm (see Siegel, J. H., 2006). This is the range of transition between quasilinear behavior of the transducer for smaller displacements and nonlinearity at larger displacements (e.g., Kros, C. J. *et al.*, 1995; Lukashkin, A. N. and Russell, I. J., 1998; Martin, P. and Hudspeth, A. J., 2001). So the transducer function may underlie the compressive phase of basilar membrane level dependence, as

well as the appearance of intermodulation distortion in both intracochlear measures (Kim, D. O. *et al.*, 1980; Dallos, P. and Cheatham, M. A., 1989; Cheatham, M. A. and Dallos, P., 1990) and OAEs (e.g., Schairer, K. S. and Keefe, D. H., 2005; Siegel, J. H., 2006). The threshold for neural rate increase is also in this range of displacement, an inevitable consequence of the need for a depolarizing dc intracellular receptor potential, generated by transducer nonlinearity, to increase the average rate of neurotransmitter release by hair cells. It is probably not coincidental that the transition between linear and nonlinear SFOAE behavior is also at this inferred range of hair bundle displacement. To suppress an SFOAE evoked by a low-level tone, it is necessary that the amplitude of the displacement produced by the suppressor be large enough to drive the transducer into at least partial saturation (e.g., Lukashkin, A. N. and Russell, I. J., 1998; Siegel, J. H., 2006). Equal-level two-tone stimuli must also be presented at levels at least this high to generate measurable DPOAE (e.g., Schairer, K. S. and Keefe, D. H., 2005). In the transition into overtly nonlinear behavior, OAEs again mirror the cochlear amplifier and the hair cell transduction apparatus that may underlie all these forms of peripheral nonlinearity.

Stimuli that drive the basilar membrane into its nonlinear range should produce emissions via the nonlinear distortion mechanism. If distortion emissions arise from the cochlear amplifier, they should become evident for stimuli that exceed 30 dB SPL. Because distortion emissions generated in the interaction region of the stimulus tones are wave fixed, their phase should rotate slowly (Shera, C. A. and Guinan, J. J., Jr., 1999; Talmadge, C. L. *et al.*, 2000). But, as demonstrated in Figure 3, there is little evidence of contributions from a short-latency SFOAE except at considerably higher levels. Noting an essentially similar pattern in their measurements in guinea pigs, Goodman, S. S. *et al.* (2003) differentiated emission-level dependence presumably due to compressive growth of the basilar membrane response at CF from true nonlinear emissions which they detected only at much higher stimulus levels. It appears that basilar membrane compression was viewed as a slow-acting gain control, despite evidence for near instantaneous nonlinearity from basilar membrane intermodulation distortion measurements at relatively low levels. If distortion emissions (DPOAE) generated by two-tone stimuli are evident for stimulus levels exceeding 30 dB SPL and DPOAE microstructure indicates that they are of the same order as linear reflection emissions, then how is it possible that single tones do not generate short-latency emissions large enough to be detected unless stimuli are presented at 80 + dB SPL? How is it also possible that a slow-acting compressor generates significant intermodulation distortion, measured both in the basilar membrane and in ear canal DPOAE at comparably low stimulus levels? The answer may lie in yet another parallel between basilar membrane mechanics and emissions. The equivalency between emissions measured using clicks and tones noted by Kalluri R. and Shera C. A. (2007) was not limited to the quasilinear range at low levels as previously noted. They found that the equivalency extended to higher levels where the emissions exhibited compressive growth. As they noted, basilar membrane mechanics measured using clicks and tones of comparable levels are also surprisingly similar, despite pronounced compressive nonlinearity near CF (e.g., Recio, A. *et al.*, 1998; Robles, L. and Ruggero, M. A., 2001). As noted by the latter authors, this appears to parallel the observation that intermodulation distortion seldom exceeds −20 dB relative to the responses to two-tone stimuli, probably because nonlinearity is an inherent property of the active filter we call the cochlear amplifier, and the filter that reduces the levels of distortion products may also explain why responses to transient and tonal stimuli are so similar. While this parallel between basilar membrane mechanics and OAE is striking, it also suggests that in neither cochlear mechanics nor OAEs can linear versus nonlinear behavior be neatly distinguished by separate processes.

The CRF theory predicts that the condition for optimal reflection should depend critically on the shape of the peak of the traveling wave and reflection emissions should decline steeply as the gain of the cochlear amplifier is reduced, for example, as stimulus level is raised or when hair cells are damaged (Shera, C. A., 2004). This is another reason why short-latency nonlinear emissions should become dominant over reflection emissions over a relatively small range of stimulus level outside the linear range (Talmadge, C. L. *et al.*, 2000). In contrast, the phase behavior of the active basilar membrane does not change abruptly for CF stimulus tones at levels above 30 dB SPL. The phase of the response at the CF of the basilar membrane place barely budges over a 100 dB range of stimuli and the group delay at CF varies by less than a factor of 2. Comparable behavior is measured in SFOAE (Figure 3).

So to summarize the lessons learned from considering nonlinear behavior of emissions, the dual mechanism hypothesis attempts to separate the behavior of emissions into linear and nonlinear parts. On the other hand, we do not think of linear and nonlinear components of the cochlear amplifier, but of an amplifier that is compressive over most of the physiological range, but converges smoothly to linear behavior at levels less than 20–30 dB SPL. In light of what may be large deviations of basilar membrane and OAE phenomena from predictions drawn from the dual mechanism hypothesis, the apparent consistency of the level and phase behavior of the SFOAEs depicted in Figure 3 seems entirely consistent with the known response characteristics of active cochlear mechanics, but possibly not with the dual mechanism hypothesis. Relative to responses to single continuous tones, understanding intermodulation phenomena in the cochlea is considerably more complicated, particularly considering the uncertainties of defining the region of generation and how it may change with stimulus levels and the ratio of stimulus tone frequencies. This complexity can be readily appreciated by consulting attempts to model two-tone interactions (e.g., Kim, D. O. *et al.*, 1980; Shera, C. A. and Guinan, J. J., Jr., 2007; Shera, C. A. *et al.*, 2007). Single tones are rarely encountered in our natural environment, so studying the cochlea's response to complex stimuli is important. But I will confine most of my further comments to single tone phenomena because I believe that the basic issues of both OAE and the cochlear amplifier are best addressed, at least at present, using the simplest possible stimuli.

3.15.5.5 Nonlinear Emissions at Relatively High Stimulus Levels

The preceding parallels between OAEs and active cochlear mechanics may be compelling, but the biophysical mechanism of the cochlear amplifier itself is controversial and the region of generation of OAEs may extend beyond that of the active region that produces mechanical gain. One critically important fact that must be considered is that the region that participates in the amplifier in maintaining threshold sensitivity for a single tone is exceedingly small, no larger than about 0.5 mm (<200 outer hair cells) as demonstrated in a precisely controlled lesion study in guinea pigs (Cody, A. R., 1992). This is consistent with the common clinical finding of restricted and deep notches in audiograms and the steep slope of the audiogram commonly measured at the upper limit of hearing frequencies. This appears to rule out models of the cochlear amplifier that require the participation of large areas of the cochlea with hair cells contributing only a small gain (e.g., Lu, T. K. *et al.*, 2006). But the size of the population of hair cells contributing to the amplification (and nonlinear interactions) of above-threshold tones may expand beyond this estimate for threshold tones. Studies of two-tone suppression for above-threshold tones are relevant to this issue (reviewed by Robles, L. and Ruggero, M. A., 2001).

Contrasting with the restricted region of the cochlear amplifier near threshold in healthy living cochleas, it has been shown that DPOAE can be emitted at high stimulus levels, likely from a relatively large area, from ears in which the cochlear amplifier has been disabled, either following the death of the animal (Carvalho, S. *et al.*, 2004) or in mice with prestin knockouts (Liberman, M. C. *et al.*, 2004). These emissions, along with corresponding CM distortion products, have been reported to disappear rapidly following death (Liberman, M. C. *et al.*, 2004). If this is true, then the loss of both acoustic and microphonic distortion appears to be caused by dissipating the electrochemical driving force that powers the transduction current, rather than by disrupting a passive nonlinearity, perhaps inherent to the structure of the stereocilia bundles and/or gating transducer channels of hair cells. At relatively high levels (70–80 dB SPL), it appears that OAEs, even distortion products, can truly be signals actively generated by hair cells rather than exclusively the result of passive nonlinearity. It was this collection of facts that led Liberman and colleagues to conclude that hair bundles actively generate OAEs. They could not rule out the possibility that this was the dominant generator of DPOAEs even at lower stimulus levels in normal ears. The reduced emissions seen at lower stimulus levels might simply reflect the reduced mechanical drive to the hair cell transducers caused by the lower mechanical gain. But in a feedback loop such as the cochlear amplifier it is hard to differentiate cause and effect. These results demonstrate the potential for studies of OAEs to help solve the cochlear amplifier.

This scenario must, however, be tempered by studies in normal animals in which, at high (~75 dB SPL) stimulus levels, the postmortem decline in DPOAE is far more gradual (i.e., several hours; Whitehead, M. L. *et al.*, 1992b). At high enough levels truly passive distortion is observed, possibly

generated in the middle ear (Whitehead, M. L. *et al.*, 1992b). Further study is needed to determine whether the cochlear amplifier, both its gain and nonlinearity, are completely abolished by the above manipulations. Small OAEs measured in these animals may correspond to residual activity of the cochlear amplifier. The apparent discrepancy may be more a difference in culture and methodology between those who study OAEs and those who make intracochlear measurements. For example, the methods used to measure emissions are capable of detecting deviations from linearity as much as 100 dB below the stimulus levels, but clearly above the noise floor. On the other hand, observing a decline in cochlear amplifier gain of 95% (−26 dB) may lead one to conclude that active mechanisms have been abolished. Rigorous and applicable quantitative comparisons are required.

Because of the importance of the vulnerability of these high-level signals, it is especially important to verify that they are not artifacts that originate in the measuring system. While it is common practice to minimize distortion in the stimulus by using separate sound sources, nonlinearity in the microphone, its associated electronics, and data acquisition hardware and software can also generate artifacts. It is therefore essential to demonstrate that these passive emissions depend on the presence of intact hair cells. This is not trivial, since some manipulations such as perfusing the cochlea with fixative alter the passive mechanical properties of tissues and thus change the acoustic input impedance of the cochlea, which can influence the levels of artifact generated by the measuring system.

3.15.6 Cellular Mechanisms of Otoacoustic Emission Generation

The current debate over whether hair bundle or somatic motors produce the force required by the cochlear amplifier is equally relevant to the biophysical origin of OAEs. The cochlear amplifier ultimately derives its power source from the electrochemical gradient created by the stria vascularis. For the transduction current, this amounts to about 150 mV across the apical membrane. This driving force would be even higher, in excess of 200 mV, if the calcium component of the transducer current drives the amplifier (Chan, D. K. and Hudspeth, A. J., 2005a). A simple calculation verifies that either of the proposed motor mechanisms could generate forces large enough to account for OAEs, at least for low to moderate stimulus levels. For example, the force generated by active movements of hair bundles in the mammalian cochlea is reported to be about 500–1000 pN per outer hair cell (Kennedy, H. J. *et al.*, 2005). A recent estimate of the stiffness contributed by the hair bundle to the total stiffness of the cochlear partition indicates that the stiffness of the hair bundle and of the basilar membrane + organ of Corti are comparable (Chan, D. K. and Hudspeth, A. J., 2005b), so forces generated in the hair bundle could be delivered effectively to the basilar membrane. Nonmammalian hair bundles appear to generate an order of magnitude less force (e.g., Ricci, A. J. *et al.*, 2005). If the force generated by 200 outer hair cells was applied directly to the human eardrum, the resulting sound pressure level would be in the range of 50 dB SPL. Prestin motors generate around 0.1 nN mV^{-1} in a single OHC (Iwasa, K. H. and Adachi, M., 1997), so with a membrane voltage swing of 10 mV, this would produce a force comparable to that of the hair bundle motor. Of course the primary function of the cochlear amplifier (and the energy produced by it) is not to generate OAEs, but it speaks to the plausibility that either or both cellular motors may contribute to OAE. It is virtually certain that the mechanoelectrical transduction process controls the signal that drives prestin, but if the cochlea has evolved a solution to the high-frequency voltage attenuation problem (Santos-Sacchi, J., 1992), then contributions to OAEs could also originate in somatic electromotility (Brownell, W. E., 1990).

Close parallels between the cochlear microphonic potentials and evoked OAEs suggest a strong relation between the transducer currents of the population of contributing hair cells and acoustic emissions (Wilson, J. P., 1980b, Kemp, D. T. and Brown, A. M., 1984; Siegel, J. H., 2006). Like the cochlear microphonic, OAEs do not appear to be low-pass filtered, as would be expected for a current- rather than voltage-driven mechanism. This observation may indicate a fairly direct link between transduction currents and forces generated by the hair bundle motor, but this is far from being settled.

A critical question is which cellular mechanism can account for active mechanical action at threshold at high frequencies. Although the force generation capacity of proposed motors is an essential question, another is whether either one is ruled out by considering signal to noise ratio. There is strong evidence that the current model of hair cell transduction accounts for the threshold

performance of the system. The limit is determined by how strongly displacements of the hair bundle modulate the stochastic behavior of transduction channels (Martin, P. *et al.*, 2001). The animal can only detect the presence of a signal if there is strong enough modulation of transduction channel activity in the population of responding hair cells to be translated into a sufficient change in neural activity. The noisy transduction currents resulting from threshold stimulation in turn causes changes in the membrane potential of hair cells, but basolateral channel activity in quiescent hair cells adds another source of noise that is independent of transducer activity until synchronized transducer currents are large enough to create voltage changes in hair cells that are significant compared with the noise of the basolateral membrane caused by channel activity. Furthermore, the cochlear amplifier must produce its full gain for signal levels of 0 dB SPL and lower. The clear presence of microphonic and OAE signals below 0 dB SPL only confirms the obvious. If prestin is the cellular mechanism of the cochlear amplifier (and perhaps of OAE as well), then there must be an ac receptor potential that is sufficiently large compared with the voltage noise of the basolateral membrane to synchronize the activity of prestin motors. This must be true for frequencies as high as 100 kHz to account for hearing in bats and dolphins. Solving the low-pass filter problem for somatic electromotility requires not only a means of enhancing the ac voltage across the basolateral membrane, but also establishing a sufficiently favorable signal to noise ratio. An ac voltage of a few tens of microvolts (Fridberger, A. *et al.*, 2004) would be of little significance to hearing if the intracellular noise voltage were several orders of magnitude larger. The estimate that as few as 100 hair cells are required to account for cochlear threshold sensitivity to a tone places a bound on how much gain in signal to noise ratio can come from averaging the active mechanical contributions of a population of hair cells. Any scheme to counteract the capacitive reactance of the basolateral membrane with the electrical equivalent of an inductance transformed from the mechanical to the electrical domain through a bidirectional transducer must face the fact that the transformed impedance is subject to noise generated by the transducer. There would seem to be no benefit to increasing the ac receptor potential by raising the impedance of the basolateral membrane by canceling the capacitive reactance if the transformed inductance further degrades the signal to noise ratio.

The voltage attenuation problem is crying for the development of more biophysical-based models. But it is also not proven that a stereocilia motor can account for the cochlear amplifier or OAEs at 100 kHz. Just because the transducer is fast enough does not prove that active feedback from the hair bundle is comparably fast.

3.15.7 Conclusions and Future Directions

The numerous striking parallels between the behavior of OAEs and active cochlear mechanics suggest that emissions and the cochlear amplifier share a common origin. Understanding emissions is important not only because they can potentially tell us something about active cochlear mechanics, but also because they can be measured readily in humans and used as part of a diagnostic protocol to define the origin of hearing loss. In contrast to invasive direct studies of cochlear mechanics OAEs can be measured routinely without damaging the delicate workings of the inner ear. Studying either of these complex phenomena is hard partly because a wide range of disciplines must be focused on different aspects of the problem. Both involve wave phenomena that can only be adequately understood by applying principles of physics and engineering. At the other end are the cellular and molecular processes that require vastly different approaches. Each of us enters speaking the language we were trained to use and there is a great danger of constructing something of a Tower of Babel.

More clarity and precision are needed when describing emission data and theories to avoid circular reasoning. Those of us who live more in the experimental end of the spectrum need to have a firm enough understanding of the theories to know how to design experiments that can test them. Understanding either the cochlear amplifier or OAEs requires the use of theory and models. The system is far too complicated to solve through intuition. Experimental data are easy enough to describe, but seldom easy to interpret. We experimentalists have an obligation to acknowledge the practical limitations of our findings, particularly in the face of potential artifacts. For example, it is more useful to give a lower bound on the amplitudes of possible reverse traveling waves in the data we collect, due

to limits on our ability to detect them above the noise floor of our measuring system, than to claim that such waves do not exist. Those who live more in the theoretical domain have similar obligations. Until such major predictions of emission models such as reverse traveling waves, random impedance variations, and distinct linear and nonlinear mechanisms of emissions become firmly established in direct measurements of cochlear mechanics, it is important to make it clear that descriptions such as wave- versus placed-fixed or reflection versus distortion emissions are properties of the models developed to account for OAEs, but not necessarily of the actual cochlea. Future progress will depend not only on using better language, but also on focusing on the real question of whether OAEs arise in a fairly straightforward way from the cochlear amplifier. This does not mean that developing adequate theories and models will be easy, but neither is the problem of successfully modeling the cochlear amplifier. I suspect that OAEs will continue to prove their worth as ways to test cochlear models, but the burden is on those of us who study emissions to establish that they can be used this way and that trying to relate them to the cochlear amplifier is not a hopeless enterprise.

The dual mechanism model of Shera and Guinan is undoubtedly successful in reproducing a number of OAE phenomena, but is it a unique solution? Can a model that separates linear and nonlinear behaviors apply to active cochlear mechanics where the two properties appear to arise in a common mechanism? What may appear in the ear canal to suggest reverse-propagating conventional von Békésy traveling waves may be something else that cannot be easily distinguished from traveling waves. Whatever alternate theory might be proposed would have to do at least as well as existing theories and models. While existing models that assume shift invariance cannot account for emission phase behavior, it is not proven that the cochlea is such a system. Until it is proven that a single mechanism of OAE is positively ruled out, it is premature to conclude that two mechanisms are required. If our livelihood depends on acquiring a duck, then it behooves us to positively verify that an animal that looks, walks, and quacks like a duck really is a duck.

No active cochlear model yet exists that accurately replicates both cochlear partition mechanics and also incorporates detailed biophysical models of hair cells complete with prestin and hair bundle motors. Outside-in black box models of the OAE phenomenon have proven worthwhile, but a complimentary inside-out model intended to solve the cochlear amplifier from known properties of cochlear mechanics and hair cell force generation is critically important. To accomplish this would be a monumental achievement but is probably only a matter of time and effort. It is possible that such a model would also exhibit all the major OAE phenomena. If so, then it may well be possible to extract far more information about the workings of living cochleas from OAEs, both in the laboratory and in clinical practice, than is now possible.

References

Anderson, S. D. 1980. Some ECMR properties in relation to other signals from the auditory periphery. Hear. Res. 2, 273–296.

Anderson, S. D. and Kemp, D. T. 1979. The evoked cochlear mechanical response in laboratory primates. A preliminary report. Arch Otorhinolaryngol 224, 47–54.

Békésy, G. 1960. Experiments in Hearing. McGraw-Hill.

Bialek, W. and Wit, H. P. 1984. Quantum limits to oscillator stability: theory and experiments on acoustic emissions from the human ear. Phys. Lett. 104A, 173–178 (Abstract).

Bray, P. and Kemp, D. 1987. An advanced cochlear echo technique suitable for infant screening. Br. J. Audiol. 21, 191–204.

Brown, A. M., Harris, F. P., and Beveridge, H. A. 1996. Two sources of acoustic distortion products from the human cochlea. J. Acoust. Soc. Am. 100, 3260–3267.

Brownell, W. E. 1990. Outer hair cell electromotility and otoacoustic emissions. Ear Hear. 11, 82–92.

Burns, E. M., Keefe, D. H., and Ling, R. 1998. Energy reflectance in the ear canal can exceed unity near spontaneous otoacoustic emission frequencies. J. Acoust. Soc. Am. 103, 462–474.

Carvalho, S., Mom, T., Gilain, L., and Avan, P. 2004. Frequency specificity of distortion-product otoacoustic emissions produced by high-level tones despite inefficient cochlear electromechanical feedback. J. Acoust. Soc. Am. 116, 1639–1648.

Chan, D. K. and Hudspeth, A. J. 2005a. Ca^{2+} current-driven nonlinear amplification by the mammalian cochlea *in vitro*. Nat. Neurosci. 8, 149–155.

Chan, D. K. and Hudspeth, A. J. 2005b. Mechanical responses of the organ of Corti to acoustic and electrical stimulation *in vitro*. Biophys. J. 89, 4382–4395.

Cheatham, M. A. and Dallos, P. 1990. Two-tone interactions in inner hair cell receptor potentials: AC versus DC effects. Hear. Res. 43, 135–139.

Cody, A. R. 1992. Acoustic lesions in the mammalian cochlea: implications for the spatial distribution of the 'active process'. Hear. Res. 62, 166–172.

Crawford, A. C. and Fettiplace, R. 1985. The mechanical properties of ciliary bundles of turtle cochlear hair cells. J. Physiol. 364, 359–379.

Dallos, P. J. 1966. On the generation of odd-fractional subharmonics. J. Acoust. Soc. Am. 40, 1381–1391.

Dallos, P. 1973. The Auditory Periphery. Academic Press.

Dallos, P. and Cheatham, M. A. 1989. Nonlinearities in cochlear receptor potentials and their origins. J. Acoust. Soc. Am. 86, 1790–1796.

Dallos, P. and Harris, D. 1978. Properties of auditory nerve responses in absence of outer hair cells. J. Neurophysiol. 41, 365–383.

Dallos, P. J. and Linnell, C. O. 1966. Subharmonic components in cochlear-microphonic potentials. J. Acoust. Soc. Am. 40, 4–11.

de Boer, E. 1980. Nonlinear interactions and the 'Kemp echo'. Hear. Res. 2, 519–526.

Dhar, S., Talmadge, C. L., Long, G. R., and Tubis, A. 2002. Multiple internal reflections in the cochlea and their effect on DPOAE fine structure. J. Acoust. Soc. Am. 112, 2882–2897.

Dreisbach, L. E. and Siegel, J. H. 2005. Level dependence of distortion-product otoacoustic emissions measured at high frequencies in humans. J. Acoust. Soc. Am. 117, 2980–2988.

Fahey, P. F., Stagner, B. B., and Martin, G. K. 2006. Mechanism for bandpass frequency characteristic in distortion product otoacoustic emission generation. J. Acoust. Soc. Am. 119, 991–996.

Fettiplace, R. 2006. Active hair bundle movements in auditory hair cells. J. Physiol. 576, 29–36.

Fridberger, A., de Monvel, J. B., Zheng, J., Hu, N., Zou, Y., Ren, T., and Nuttall, A. 2004. Organ of Corti potentials and the motion of the basilar membrane. J. Neurosci. 24, 10057–10063.

Goblick, T. J., Jr. and Pfeiffer, R. R. 1969. Time-domain measurements of cochlear nonlinearities using combination click stimuli. J. Acoust. Soc. Am. 46, 924–938.

Gold, T. 1948. Hearing. II. The physical basis of the action of the cochlea. Proc. R. Soc. Lond., Ser. B, Biol. Sci. 135, 492–498 (Abstract).

Goldstein, J. L. 1967. Auditory nonlinearity. J. Acoust. Soc. Am. 41, 676–689.

Goodman, S. S., Withnell, R. H., and Shera, C. A. 2003. The origin of SFOAE microstructure in the guinea pig. Hear. Res. 183, 7–17.

Gorga, M. P., Neely, S. T., and Dorn, P. A. 1999. Distortion product otoacoustic emission test performance for a priori criteria and for multifrequency audiometric standards. Ear Hear. 20, 345–362.

Grosh, K., Zheng, J., Zou, Y., de Boer, E., and Nuttall, A. L. 2004. High-frequency electromotile responses in the cochlea. J. Acoust. Soc. Am. 115, 2178–2184.

Guinan, J. J., Jr. 1990. Changes in Stimulus Frequency Otoacoustic Emissions Produced by Two-Tone Suppression and Efferent Stimulation in Cats. In: Mechanics and Biophysics of Hearing (*eds*. P. Dallos, C. D. Geisler, J. W. Matthews, and C. R. Steele), pp. 170–177. Springer.

He, W., Nuttall, A. L., and Ren, T. 2007. Two-tone distortion at different longitudinal locations on the basilar membrane. Hear. Res. 228, 112–122.

Heitmann, J., Waldman, B., Schnitzler, H. U., Plinkert, P. K., and Zenner, H.-P. 1998. Suppression of distortion product otoacoustic emissions (DPOAE) near $2f_1 - f_2$ removes DP-gram fine structure – evidence for a secondary generator. J. Acoust. Soc. Am. 103, 1527–1531.

Hu, N., Nuttall, A. L., and Ren, T. 2005. Spatial distribution of electrically induced high frequency vibration on basilar membrane. Hear. Res. 202, 35–46.

Hubbard, A. E. and Mountain, D. C. 1983. Alternating current delivered into the scala media alters sound pressure at the eardrum. Science 222, 510–512.

Iwasa, K. H. and Adachi, M. 1997. Force generation in the outer hair cell of the cochlea. Biophys. J. 73, 546–555.

Jaramillo, F., Markin, V. S., and Hudspeth, A. J. 1993. Auditory illusions and the single hair cell. Nature 364, 527–529.

Kalluri, R. and Shera, C. A. 2001. Distortion-product source unmixing: a test of the two-mechanism model for DPOAE generation. J. Acoust. Soc. Am. 109, 622–637.

Kalluri, R. and Shera, C. A. 2007. Near equivalence of human click-evoked and stimulus-frequency otoacoustic emissions. J. Acoust. Soc. Am. 121, 2097–2110.

Karavitaki, K. D. and Mountain, D. C. 2007. Imaging electrically evoked micromechanical motion within the organ of Corti of the excised gerbil cochlea. Biophys. J. 92, 3294–3316.

Keefe, D. H. 1998. Double-evoked otoacoustic emissions. I. Measurement theory and nonlinear coherence. J. Acoust. Soc. Am. 103, 3489–3498.

Keefe, D. H. and Ling, R. 1998. Double-evoked otoacoustic emissions. II. Intermittent noise rejection, calibration and ear-canal measurements. J. Acoust. Soc. Am. 103, 3499–3508.

Kemp, D. T. 1978. Stimulated acoustic emissions from within the human auditory system. J. Acoust. Soc. Am. 64, 1386–1391.

Kemp, D. T. 1979a. Evidence of mechanical nonlinearity and frequency selective wave amplification in the cochlea. Arch. Otorhinolaryngol. 224, 37–45.

Kemp, D. T. 1979b. The evoked cochlear mechanical response and the auditory microstructure – evidence for a new element in cochlear mechanics. Scand. Audiol. Suppl. 35–47.

Kemp, D. T. 1980. Towards a model for the origin of cochlear echoes. Hear. Res. 2, 533–548.

Kemp, D. T. 1986. Otoacoustic emissions, travelling waves and cochlear mechanisms. Hear. Res. 22, 95–104.

Kemp, D. T. 2007. Exploring Cochlear Status with Otoacoustic Emissions: The Potential for New Clinical Applications. In: Otoacoustic Emissions: Clinical Applications, 3rd edn. (*eds*. M. S. Robinette and T. J. Glattke), pp. 7–42. Thieme Medical Publishers.

Kemp, D. T. and Brown, A. M. 1983. An Integrated View of Cochlear Mechanical Nonlinearities Observable from the Ear Canal. In: Mechanics of Hearing (*eds*. E. de Boer and M. A. Viergever), pp. 75–82. Delft University Press.

Kemp, D. T. and Brown, A. M. 1984. Ear canal acoustic and round window electrical correlates of 2f1–f2 distortion generated in the cochlea. Hear. Res. 13, 39–46.

Kemp, D. T. and Chum, R. 1980a. Observations on the Generator Mechanism of Stimulus Frequency Acoustic Emissions – Two Tone Suppression. In: Psychophysical Physiological and Behavioural Studies in Hearing (*eds*. G. V. D. Brink and F. A. Bilsen), pp. 34–42. Delft University Press.

Kemp, D. T. and Chum, R. 1980b. Properties of the generator of stimulated acoustic emissions. Hear. Res. 2, 213–232.

Kemp, D. T., Bray, P., Alexander, L., and Brown, A. M. 1986. Acoustic emission cochleography – practical aspects. Scand. Audiol. Suppl. 25, 71–95.

Kennedy, H. J., Crawford, A. C., and Fettiplace, R. 2005. Force generation by mammalian hair bundles supports a role in cochlear amplification. Nature 433, 880–883.

Kiang, N. Y. S., Watanabe, T., Thomas, E. C., and Clark, L. F. 1965. Discharge Patterns of Single Fibers in the Cat's Auditory Nerve. MIT Press.

Kim, D. O. 1980. Cochlear mechanics: implications of electrophysiological and acoustical observations. Hear. Res. 2, 297–317.

Kim, D. O., Molnar, C. E., and Matthews, J. W. 1980. Cochlear mechanics: nonlinear behavior in two-tone responses as reflected in cochlear-nerve-fiber responses and in ear-canal sound pressure. J. Acoust. Soc. Am. 67, 1704–1721.

Kim, D. O., Siegel, J. H., and Molnar, C. E. 1979. Cochlear nonlinear phenomena in two-tone responses. Scand. Audiol. Suppl. 9, 63–81.

Kros, C. J., Lennan, G. W. T., and Richardson, G. P. 1995. Voltage Dependence of Transducer Currents in Outer Hair Cells of Neonatal Mice. In: Active Hearing (*ed*. A. Flock), pp. 113–125. Elsevier Science.

Lapsley Miller, J. A., Marshall, L., Heller, L. M., and Hughes, L. M. 2006. Low-level otoacoustic emissions may predict susceptibility to noise-induced hearing loss. J. Acoust. Soc. Am. 120, 280–296.

Liberman, M. C., Zuo, J., and Guinan, J. J., Jr. 2004. Otoacoustic emissions without somatic motility: can stereocilia mechanics drive the mammalian cochlea? J. Acoust. Soc. Am. 116, 1649–1655.

Long, G. R. 1984. The microstructure of quiet and masked thresholds. Hear. Res. 15, 73–87.

Long, G. R. and Tubis, A. 1988. Investigations into the nature of the association between threshold microstructure and otoacoustic emissions. Hear. Res. 36, 125–138.

Lu, T. K., Zhak, S., Dallos, P., and Sarpeshkar, R. 2006. Fast cochlear amplification with slow outer hair cells. Hear. Res. 214, 45–67.

Lukashkin, A. N. and Russell, I. J. 1998. A descriptive model of the receptor potential nonlinearities generated by the hair cell mechanoelectrical transducer. J. Acoust. Soc. Am. 103, 973–980.

Lukashkin, A. N., Lukashkina, V. A., and Russell, I. J. 2002. One source for distortion product otoacoustic emissions generated by low- and high-level primaries. J. Acoust. Soc. Am. 111, 2740–2748.

Mahoney, C. F. and Kemp, D. T. 1995. Distortion product otoacoustic emission delay measurement in human ears. J. Acoust. Soc. Am. 97, 3721–3735.

Manley, G. A. 2001. Evidence for an active process and a cochlear amplifier in nonmammals. J. Neurophysiol. 86, 541–549.

Manley, G. A., Kirk, D. L., Koppl, C., and Yates, G. K. 2001. *In vivo* evidence for a cochlear amplifier in the hair-cell bundle of lizards. Proc. Natl. Acad. Sci. U. S. A. 98, 2826–2831.

Martin, P. and Hudspeth, A. J. 2001. Compressive nonlinearity in the hair bundle's active response to mechanical stimulation. Proc. Natl. Acad. Sci. U. S. A. 98, 14386–14391.

Martin, P., Hudspeth, A. J., and Julicher, F. 2001. Comparison of a hair bundle's spontaneous oscillations with its response to mechanical stimulation reveals the underlying active process. Proc. Natl. Acad. Sci. U. S. A. 98, 14380–14385.

Martin, G. K., Ohlms, L. A., Franklin, D. J., Harris, F. P., and Lonsbury-Martin, B. L. 1990. Distortion product emissions in humans. III. Influence of sensorineural hearing loss. Ann. Otol. Rhinol. Laryngol. Suppl. 147, 30–42.

Martin, G. K., Stagner, B. B., Jassir, D., Telischi, F. F., and Lonsbury-Martin, B. L. 1999. Suppression and enhancement of distortion-product otoacoustic emissions by interference tones above f(2). I. Basic findings in rabbits. Hear. Res. 136, 105–123.

Martin, G. K., Villasuso, E. I., Stagner, B. B., and Lonsbury-Martin, B. L. 2003. Suppression and enhancement of distortion-product otoacoustic emissions by interference tones above f(2). II. Findings in humans. Hear. Res. 177, 111–122.

Mauermann, M., Long, G. R., and Kollmeier, B. 2004. Fine structure of hearing threshold and loudness perception. J. Acoust. Soc. Am. 116, 1066–1080.

Mountain, D. C. and Hubbard, A. E. 1989. Rapid force production in the cochlea. Hear. Res. 42, 195–202.

Nuttall, A. L. and Ren, T. 1995. Electromotile hearing: evidence from basilar membrane motion and otoacoustic emissions. Hear. Res. 92, 170–177.

Nuttall, A. L., Grosh, K., Zheng, J., de Boer, E., Zou, Y., and Ren, T. 2004. Spontaneous basilar membrane oscillation and otoacoustic emission at 15 kHz in a guinea pig. J. Assoc. Res. Otolaryngol. 5, 337–348.

Nuttall, A. L., Zheng, J., Ren, T., and de Boer, E. 2001. Electrically evoked otoacoustic emissions from apical and basal perilymphatic electrode positions in the guinea pig cochlea. Hear. Res. 152, 77–89.

Patuzzi, R. 1996. Cochlear Micromechanics and Macromechanics. In: The Cochlea (*eds*., P. Dallos, A. N. Popper, and R. R. Fay), pp. 186–257. Springer.

Pfeiffer, R. R. and Kim, D. O. 1975. Cochlear nerve fiber responses: distribution along the cochlear partition. J. Acoust. Soc. Am. 58, 867–869.

Powers, N. L., Salvi, R. J., Wang, J., Spongr, V., and Qiu, C. X. 1995. Elevation of auditory thresholds by spontaneous cochlear oscillations. Nature 375, 585–587.

Probst, R., Lonsbury-Martin, B. L., and Martin, G. K. 1991. A review of otoacoustic emissions. J. Acoust. Soc. Am. 89, 2027–2067.

Recio, A., Rich, N. C., Narayan, S. S., and Ruggero, M. A. 1998. Basilar-membrane responses to clicks at the base of the chinchilla cochlea. J. Acoust. Soc. Am. 103, 1972–1989.

Ren, T. 2002. Longitudinal pattern of basilar membrane vibration in the sensitive cochlea. Proc. Natl. Acad. Sci. U. S. A. 99, 17101–17106.

Ren, T. 2004. Reverse propagation of sound in the gerbil cochlea. Nat. Neurosci. 7, 333–334.

Rhode, W. S. 1971. Observations of the vibration of the basilar membrane in squirrel monkeys using the Mossbauer technique. J. Acoust. Soc. Am. 49, 1218–1231.

Rhode, W. S. 1978. Some observations on cochlear mechanics. J. Acoust. Soc. Am. 64, 158–176.

Rhode, W. S. 2007. Basilar membrane mechanics in the 6–9 kHz region of sensitive chinchilla cochleae. J. Acoust. Soc. Am. 121, 2792–2804.

Ricci, A. J., Kennedy, H. J., Crawford, A. C., and Fettiplace, R. 2005. The transduction channel filter in auditory hair cells. J. Neurosci. 25, 7831–7839.

Robles, L. and Ruggero, M. A. 2001. Mechanics of the mammalian cochlea. Physiol. Rev. 81, 1305–1352.

Ruggero, M. A. and Temchin, A. N. 2007. Similarity of traveling-wave delays in the hearing organs of humans and other tetrapods. J. Assoc. Res. Otolaryngol. 8, 153–166.

Ruggero, M. A., Kramek, B., and Rich, N. C. 1984. Spontaneous otoacoustic emissions in a dog. Hear. Res. 13, 293–296.

Russell, I. J. and Sellick, P. M. 1977. Tuning properties of cochlear hair cells. Nature 267, 858–860.

Rutten, W. L. 1980. Evoked acoustic emissions from within normal and abnormal human ears: comparison with audiometric and electrocochleographic findings. Hear. Res. 2, 263–271.

Ryan, A. and Dallos, P. 1975. Effect of absence of cochlear outer hair cells on behavioural auditory threshold. Nature 253, 44–46.

Santos-Sacchi, J. 1992. On the frequency limit and phase of outer hair cell motility: effects of the membrane filter. J. Neurosci. 12, 1906–1916.

Schairer, K. S. and Keefe, D. H. 2005. Simultaneous recording of stimulus-frequency and distortion-product otoacoustic emission input–output functions in human ears. J. Acoust. Soc. Am. 117, 818–832.

Schairer, K. S., Fitzpatrick, D., and Keefe, D. H. 2003. Input–output functions for stimulus-frequency otoacoustic emissions in normal-hearing adult ears. J. Acoust. Soc. Am. 114, 944–966.

Shera, C. A. 2003. Mammalian spontaneous otoacoustic emissions are amplitude-stabilized cochlear standing waves. J. Acoust. Soc. Am. 114, 244–262.

Shera, C. A. 2004. Mechanisms of mammalian otoacoustic emission and their implications for the clinical utility of otoacoustic emissions. Ear Hear. 25, 86–97.

Shera, C. A. and Guinan, J. J., Jr. 1999. Evoked otoacoustic emissions arise by two fundamentally different mechanisms: a taxonomy for mammalian OAEs. J. Acoust. Soc. Am. 105, 782–798.

Shera, C. A. and Guinan, J. J., Jr. 2003. Stimulus-frequency-emission group delay: a test of coherent reflection filtering and a window on cochlear tuning. J. Acoust. Soc. Am. 113, 2762–2772.

Shera, C. A. and Guinan, J. J., Jr. 2007. Cochlear traveling-wave amplification, suppression, and beamforming probed using noninvasive calibration of intracochlear distortion sources. J. Acoust. Soc. Am. 121, 1003–1016.

Shera, C. A., Guinan, J. J., Jr., and Oxenham, A. J. 2002. Revised estimates of human cochlear tuning from otoacoustic and behavioral measurements. Proc. Natl. Acad. Sci. U. S. A. 99, 3318–3323.

Shera, C. A., Tubis, A., and Talmadge, C. L. 2005. Models of reflection- and distortion-source oaes with and without slow transverse retrograde waves. Assoc. Res. Otolaryngol. Abst. 28, 231. Available at: http://web.mit.edu/apg/shera-tubis-talmadge-ARO2005.pdf.

Shera, C. A., Tubis, A., Talmadge, C. L., de Boer, E., Fahe, P. F., and Guinan, J. J., Jr. 2007. Allen–Fahey and related experiments support the predominance of cochlear slow-wave otoacoustic emissions. J. Acoust. Soc. Am. 121, 1564–1575.

Siegel, J. H. 2006. The Biophysical Origin of Otoacoustic Emissions. In: Auditory Mechanisms: Processes and Models (*eds*. A. L. Nuttall, T. Ren, P. Gillespe, K. Grosh, and E. de Boer), pp. 361–368. World Scientific.

Siegel, J. H., Cerka, A. J., Recio-Spinoso, A., Temchin, A. N., van Dijk, P., and Ruggero, M. A. 2005. Delays of stimulus-frequency otoacoustic emissions and cochlear vibrations contradict the theory of coherent reflection filtering. J. Acoust. Soc. Am. 118, 2434–2443.

Siegel, J. H., Kim, D. O., and Molnar, C. E. 1982. Effects of altering the organ of Corti on cochlear distortion products f2–f1 and 2f1–f2. J. Neurophysiol. 47, 303–328.

Smoorenburg, G. F. 1972. Combination tones and their origin. J. Acoust. Soc. Am. 52, 615–632.

Strube, H. W. 1989. Evoked otoacoustic emissions as cochlear Bragg reflections. Hear. Res. 38, 35–45.

Sutton, L. A., Lonsbury-Martin, B. L., Martin, G. K., and Whitehead, M. L. 1994. Sensitivity of distortion-product otoacoustic emissions in humans to tonal over-exposure: time course of recovery and effects of lowering L2. Hear. Res. 75, 161–174.

Talmadge, C. L., Long, G. R., Tubis, A., and Dhar, S. 1999. Experimental confirmation of the two-source interference model for the fine structure of distortion product otoacoustic emissions. J. Acoust. Soc. Am. 105, 275–292.

Talmadge, C. L., Tubis, A., Long, G. R., and Tong, C. 2000. Modeling the combined effects of basilar membrane nonlinearity and roughness on stimulus frequency otoacoustic emission fine structure. J. Acoust. Soc. Am. 108, 2911–2932.

Talmadge, C. L., Tubis, A., Wit, H. P., and Long, G. R. 1991. Are spontaneous otoacoustic emissions generated by self-sustained cochlear oscillators? J. Acoust. Soc. Am. 89, 2391–2399.

Tasaki, I. 1954. Nerve impulses in individual auditory nerve fibers of guinea pig. J. Neurophysiol. 17, 97–122.

Tubis, A. and Talmadge, C. L. 1998. Ear canal reflectance in the presence of spontaneous otoacoustic emissions. I. Limit-cycle oscillator model. J. Acoust. Soc. Am. 103, 454–461.

van Dijk, P., Narins, P. M., and Wang, J. 1996. Spontaneous otoacoustic emissions in seven frog species. Hear. Res. 101, 102–112.

Weiss, T. F. 1982. Bidirectional transduction in vertebrate hair cells: a mechanism for coupling mechanical and electrical processes. Hear. Res. 7, 353–360.

Whitehead, M. L., Lonsbury-Martin, B. L., and Martin, G. K. 1992a. Evidence for two discrete sources of 2f1–f2 distortion-product otoacoustic emission in rabbit. II: Differential physiological vulnerability. J. Acoust. Soc. Am. 92, 2662–2682.

Whitehead, M. L., Lonsbury-Martin, B. L., and Martin, G. K. 1992b. Evidence for two discrete sources of 2f1–f2 distortion-product otoacoustic emission in rabbit: I. Differential dependence on stimulus parameters. J. Acoust. Soc. Am. 91, 1587–1607.

Wilson, J. P. 1980a. Evidence for a cochlear origin for acoustic re-emissions, threshold fine-structure and tonal tinnitus. Hear. Res. 2, 233–252.

Wilson, J. P. 1980b. Model for cochlear echoes and tinnitus based on an observed electrical correlate. Hear. Res. 2, 527–532.

Wit, H. P. and Ritsma, R. J. 1979. Stimulated acoustic emissions from the human ear. J. Acoust. Soc. Am. 66, 911–913.

Wit, H. P. and Ritsma, R. J. 1980. Evoked acoustical responses from the human ear: some experimental results. Hear. Res. 2, 253–261.

Xue, S., Mountain, D. C., and Hubbard, A. E. 1993. Acoustic enhancement of electrically-evoked otoacoustic emissions reflects basilar membrane tuning: experiment results. Hear. Res. 70, 121–126.

Xue, S., Mountain, D. C., and Hubbard, A. E. 1995. Electrically evoked basilar membrane motion. J. Acoust. Soc. Am. 97, 3030–3041.

Zweig, G. and Shera, C. A. 1995. The origin of periodicity in the spectrum of evoked otoacoustic emissions. J. Acoust. Soc. Am. 98, 2018–2047.

Zwicker, E. and Schloth, E. 1984. Interrelation of different oto-acoustic emissions. J. Acoust. Soc. Am. 75, 1148–1154.

Zwislocki, J. 1962. Analysis of the middle-ear function: Part I: Input impedance. J. Acoust. Soc. Am. 34, 1514–1523.

Further Reading

Abdala, C., Sininger, Y. S., Ekelid, M., and Zeng, F. G. 1996. Distortion product otoacoustic emission suppression tuning curves in human adults and neonates. Hear. Res. 98, 38–53.

Avan, P., Bonfils, P., Gilain, L., and Mom, T. 2003. Physiopathological significance of distortion-product otoacoustic emissions at 2f1–f2 produced by high- versus low-level stimuli. J. Acoust. Soc. Am. 113, 430–441.

Berlin, C. I., Hood, L. J., Wen, H., Szabo, P., Cecola, R. P., Rigby, P., and Jackson, D. F. 1993. Contralateral suppression of non-linear click-evoked otoacoustic emissions. Hear. Res. 71, 1–11.

Bozovic, D. and Hudspeth, A. J. 2003. Hair-bundle movements elicited by transepithelial electrical stimulation of hair cells in the sacculus of the bullfrog. Proc. Natl. Acad. Sci. U. S. A. 100, 958–963.

Brass, D. and Kemp, D. T. 1993a. Analyses of Mossbauer mechanical measurements indicate that the cochlea is mechanically active. J. Acoust. Soc. Am. 93, 1502–1515.

Brass, D. and Kemp, D. T. 1993b. Suppression of stimulus frequency otoacoustic emissions. J. Acoust. Soc. Am. 93, 920–939.

Brass, D. and Locke, A. 1997. The effect of the evanescent wave upon acoustic measurements in the human ear canal. J. Acoust. Soc. Am. 101, 2164–2175.

Brown, A. M. and Kemp, D. T. 1984. Suppressibility of the 2f1–f2 stimulated acoustic emissions in gerbil and man. Hear. Res. 13, 29–37.

Brown, A. M. and Kemp, D. T. 1985. Intermodulation distortion in the cochlea: could basal vibration be the major cause of round window CM distortion? Hear. Res. 19, 191–198.

Cheatham, M. A., Huynh, K. H., Gao, J., Zuo, J., and Dallos, P. 2004. Cochlear function in Prestin knockout mice. J. Physiol. 560, 821–830.

Cooper, N. P. and Guinan, J. J., Jr. 2006. Efferent-mediated control of basilar membrane motion. J. Physiol. 576, 49–54.

Dallos, P., Zheng, J., and Cheatham, M. A. 2006. Prestin and the cochlear amplifier. J. Physiol. 576, 37–42.

de Boer, E. and Nuttall, A. L. 2006. Spontaneous basilar-membrane oscillation (SBMO) and coherent reflection. J. Assoc. Res. Otolaryngol. 7, 26–37.

de Boer, E., Nuttall, A. L., and Shera, C. A. 2007. Wave propagation patterns in a ''classical'' three-dimensional model of the cochlea. J. Acoust. Soc. Am. 121, 352–362.

Fahey, P. F., Stagner, B. B., Lonsbury-Martin, B. L., and Martin, G. K. 2000. Nonlinear interactions that could explain distortion product interference response areas. J. Acoust. Soc. Am. 108, 1786–1802.

Gaskill, S. A. and Brown, A. M. 1990. The behavior of the acoustic distortion product, 2f1–f2, from the human ear and its relation to auditory sensitivity. J. Acoust. Soc. Am. 88, 821–839.

Gaskill, S. A. and Brown, A. M. 1996. Suppression of human acoustic distortion product: dual origin of 2f1–f2. J. Acoust. Soc. Am. 100, 3268–3274.

Guinan, J. J., Jr. 2006. Olivocochlear efferents: anatomy, physiology, function, and the measurement of efferent effects in humans. Ear Hear. 27, 589–607.

Harris, F. P., Probst, R., and Xu, L. 1992. Suppression of the 2f1–f2 otoacoustic emission in humans. Hear. Res. 64, 133–141.

He, N. and Schmiedt, R. A. 1997. Fine structure of the 2 f1–f2 acoustic distortion products: effects of primary level and frequency ratios. J. Acoust. Soc. Am. 101, 3554–3565.

Hofstetter, P., Ding, D., and Salvi, R. 2000. Induction of spontaneous otoacoustic emissions in chinchillas from carboplatin-induced inner hair cell loss. Hear. Res. 150, 132–136.

Hood, L. J. 1999. A review of objective methods of evaluating auditory neural pathways. Laryngoscope 109, 1745–1748.

Iwasa, K. H. 1997. Current noise spectrum and capacitance due to the membrane motor of the outer hair cell: theory. Biophys. J. 73, 2965–2971.

Kemp, D. T. 2002. Otoacoustic emissions, their origin in cochlear function, and use. Br. Med. Bull. 63, 223–241.

Kemp, D. T. and Brown, A. M. 1986. Wideband Analysis of Otoacoustic Intermodulation. In: Peripheral Auditory Mechanisms (*eds*. J. B. Allen, J. L. Hall, A. Hubbard, S. T. Neely, and A. Tubis), pp. 306–313. Springer.

Kemp, D. T., Ryan, S., and Bray, P. 1990. A guide to the effective use of otoacoustic emissions. Ear Hear. 11, 93–105.

Kennedy, H. J., Evans, M. G., Crawford, A. C., and Fettiplace, R. 2006. Depolarization of cochlear outer hair cells evokes active hair bundle motion by two mechanisms. J. Neurosci. 26, 2757–2766.

Knight, R. D. and Kemp, D. T. 2001. Wave and place fixed DPOAE maps of the human ear. J. Acoust. Soc. Am. 109, 1513–1525.

Kossl, M. and Vater, M. 1985. Evoked acoustic emissions and cochlear microphonics in the mustache bat, *Pteronotus parnellii*. Hear. Res. 19, 157–170.

Legan, P. K., Lukashkina, V. A., Goodyear, R. J., Lukashkin, A. N., Verhoeven, K., Van Camp, G., Russell, I. J., and Richardson, G. P. 2005. A deafness mutation isolates a second role for the tectorial membrane in hearing. Nat. Neurosci. 8, 1035–1042.

Lim, K. M. and Steele, C. R. 2002. A three-dimensional nonlinear active cochlear model analyzed by the WKB-numeric method. Hear. Res. 170, 190–205.

Long, G. R. and Tubis, A. 1988a. Investigations into the nature of the association between threshold microstructure and otoacoustic emissions. Hear. Res. 36, 125–138.

Long, G. R. and Tubis, A. 1988b. Modification of spontaneous and evoked otoacoustic emissions and associated psychoacoustic microstructure by aspirin consumption. J. Acoust. Soc. Am. 84, 1343–1353.

Long, G. R., Van Dijk, P., and Wit, H. P. 1996. Temperature dependence of spontaneous otoacoustic emissions in the edible frog (*Rana esculenta*). Hear. Res. 98, 22–28.

Lonsbury-Martin, B. L. and Martin, G. K. 1988. Incidence of spontaneous otoacoustic emissions in macaque monkeys: a replication. Hear. Res. 34, 313–317.

Lonsbury-Martin, B. L., Harris, F. P., Stagner, B. B., Hawkins, M. D., and Martin, G. K. 1990a. Distortion product emissions in humans. I. Basic properties in normally hearing subjects. Ann. Otol. Rhinol. Laryngol. Suppl. 147, 3–14.

Lonsbury-Martin, B. L., Harris, F. P., Stagner, B. B., Hawkins, M. D., and Martin, G. K. 1990b. Distortion product emissions in humans. II. Relations to acoustic immittance and stimulus frequency and spontaneous otoacoustic emissions in normally hearing subjects. Ann. Otol. Rhinol. Laryngol. Suppl. 147, 15–29.

Lukashkin, A. N. and Russell, I. J. 2001. Origin of the bell-like dependence of the DPOAE amplitude on primary frequency ratio. J. Acoust. Soc. Am. 110, 3097–3106.

Lukashkin, A. N. and Russell, I. J. 2002. Modifications of a single saturating non-linearity account for post-onset changes in 2f1–f2 distortion product otoacoustic emission. J. Acoust. Soc. Am. 112, 1561–1568.

Lukashkin, A. N. and Russell, I. J. 2003. A second, low-frequency mode of vibration in the intact mammalian cochlea. J. Acoust. Soc. Am. 113, 1544–1550.

Lukashkin, A. N. and Russell, I. J. 2005. Dependence of the DPOAE amplitude pattern on acoustical biasing of the cochlear partition. Hear. Res. 203, 45–53.

Lukashkin, A. N., Bashtanov, M. E., and Russell, I. J. 2005. A self-mixing laser-diode interferometer for measuring basilar membrane vibrations without opening the cochlea. J. Neurosci. Methods 148, 122–129.

Lukashkin, A. N., Lukashkina, V. A., Legan, P. K., Richardson, G. P., and Russell, I. J. 2004. Role of the tectorial membrane revealed by otoacoustic emissions recorded from wild-type and transgenic Tecta (deltaENT/deltaENT) mice. J. Neurophysiol. 91, 163–171.

Lukashkin, A. N., Smith, J. K., and Russell, I. J. 2007. Properties of distortion product otoacoustic emissions and neural suppression tuning curves attributable to the tectorial membrane resonance. J. Acoust. Soc. Am. 121, 337–343.

Manley, G. A. 2000. Cochlear mechanisms from a phylogenetic viewpoint. Proc. Natl. Acad. Sci. U. S. A. 97, 11736–11743.

Martin, P. and Hudspeth, A. J. 1999. Active hair-bundle movements can amplify a hair cell's response to oscillatory mechanical stimuli. Proc. Natl. Acad. Sci. U. S. A. 96, 14306–14311.

Martin, G. K., Lonsbury-Martin, B. L., Probst, R., and Coats, A. C. 1988. Spontaneous otoacoustic emissions in a nonhuman primate. I. Basic features and relations to other emissions. Hear. Res. 33, 49–68.

Martin, P., Bozovic, D., Choe, Y., and Hudspeth, A. J. 2003. Spontaneous oscillation by hair bundles of the bullfrog's sacculus. J. Neurosci. 23, 4533–4548.

Mom, T., Bonfils, P., Gilain, L., and Avan, P. 2001. Origin of cubic difference tones generated by high-intensity stimuli: effect of ischemia and auditory fatigue on the gerbil cochlea. J. Acoust. Soc. Am. 110, 1477–1488.

Mountain, D. C. 1980. Changes in endolymphatic potential and crossed olivocochlear bundle stimulation alter cochlear mechanics. Science 210, 71–72.

Nadrowski, B., Martin, P., and Julicher, F. 2004. Active hair-bundle motility harnesses noise to operate near an optimum of mechanosensitivity. Proc. Natl. Acad. Sci. U. S. A. 101, 12195–12200.

Norton, S. J. and Neely, S. T. 1987. Tone-burst-evoked otoacoustic emissions from normal-hearing subjects. J. Acoust. Soc. Am. 81, 1860–1872.

Ren, T. and Nuttall, A. L. 2006. Cochlear compression wave: an implication of the Allen–Fahey experiment. J. Acoust. Soc. Am. 119, 1940–1942.
Ren, T., He, W., Scott, M., and Nuttall, A. L. 2006. Group delay of acoustic emissions in the ear. J. Neurophysiol. 96, 2785–2791.
Rhode, W. S. and Cooper, N. P. 1993. Two-tone suppression and distortion production on the basilar membrane in the hook region of cat and guinea pig cochleae. Hear. Res. 66, 31–45.
Rhode, W. S. and Robles, L. 1974. Evidence from Mossbauer experiments for nonlinear vibration in the cochlea. J. Acoust. Soc. Am. 55, 588–596.
Ricci, A. 2003. Active hair bundle movements and the cochlear amplifier. J. Am. Acad. Audiol. 14, 325–338.
Ricci, A. J., Crawford, A. C., and Fettiplace, R. 2002. Mechanisms of active hair bundle motion in auditory hair cells. J. Neurosci. 22, 44–52.
Robles, L., Rhode, W. S., and Geisler, C. D. 1976. Transient response of the basilar membrane measured in squirrel monkeys using the Mossbauer effect. J. Acoust. Soc. Am. 59, 926–939.
Robles, L., Ruggero, M. A., and Rich, N. C. 1997. Two-tone distortion on the basilar membrane of the chinchilla cochlea. J. Neurophysiol. 77, 2385–2399.
Russell, I. J., Drexl, M., Foeller, E., Vater, M., and Kossl, M. 2003a. The development of a single frequency place in the mammalian cochlea: the cochlear resonance in the mustached bat *Pteronotus parnellii*. J. Neurosci. 23, 10971–10981.
Russell, I. J., Drexl, M., Foeller, E., Vater, M., and Kossl, M. 2003b. Synchronization of a nonlinear oscillator: processing the cf component of the echo-response signal in the cochlea of the mustached bat. J. Neurosci. 23, 9508–9518.
Russell, I. J., Legan, P. K., Lukashkina, V. A., Lukashkin, A. N., Goodyear, R. J., and Richardson, G. P. 2007. Sharpened cochlear tuning in a mouse with a genetically modified tectorial membrane. Nat. Neurosci. 10, 215–223.
Sellick, P. M., Patuzzi, R., and Johnstone, B. M. 1982. Measurement of basilar membrane motion in the guinea pig using the Mossbauer technique. J. Acoust. Soc. Am. 72, 131–141.
Shera, C. A. and Zweig, G. 1993. Noninvasive measurement of the cochlear traveling-wave ratio. J. Acoust. Soc. Am. 93, 3333–3352.
Shera, C. A., Tubis, A., and Talmadge, C. L. 2005. Coherent reflection in a two-dimensional cochlea: Short-wave versus long-wave scattering in the generation of reflection-source otoacoustic emissions. J. Acoust. Soc. Am. 118, 287–313.
Siegel, J. H. and Kim, D. O. 1982. Efferent neural control of cochlear mechanics? Olivocochlear bundle stimulation affects cochlear biomechanical nonlinearity. Hear. Res. 6, 171–182.
Sisto, R., Moleti, A., and Lucertini, M. 2001. Spontaneous otoacoustic emissions and relaxation dynamics of long decay time OAEs in audiometrically normal and impaired subjects. J. Acoust. Soc. Am. 109, 638–647.
Talmadge, C. L., Long, G. R., Murphy, W. J., and Tubis, A. 1993. New off-line method for detecting spontaneous otoacoustic emissions in human subjects. Hear. Res. 71, 170–182.
Trautwein, P., Hofstetter, P., Wang, J., Salvi, R., and Nostrant, A. 1996. Selective inner hair cell loss does not alter distortion product otoacoustic emissions. Hear. Res. 96, 71–82.
van Dijk, P., Narins, P. M., and Mason, M. J. 2003. Physiological vulnerability of distortion product otoacoustic emissions from the amphibian ear. J. Acoust. Soc. Am. 114, 2044–2048.
van Dijk, P., Wit, H. P., Tubis, A., Talmadge, C. L., and Long, G. R. 1994. Correlation between amplitude and frequency fluctuations of spontaneous otoacoustic emissions. J. Acoust. Soc. Am. 96, 163–169.
van Netten, S. M., Dinklo, T., Marcotti, W., and Kros, C. J. 2003. Channel gating forces govern accuracy of mechano-electrical transduction in hair cells. Proc. Natl. Acad. Sci. U. S. A. 100, 15510–15515.
Whitehead, M. L., Stagner, B. B., Martin, G. K., and Lonsbury-Martin, B. L. 1996. Visualization of the onset of distortion-product otoacoustic emissions, and measurement of their latency. J. Acoust. Soc. Am. 100, 1663–1679.
Wit, H. P. 1993. Amplitude fluctuations of spontaneous otoacoustic emissions caused by internal and externally applied noise sources. Prog. Brain Res. 97, 59–65.
Withnell, R. H. and Yates, G. K. 1998. Onset of basilar membrane non-linearity reflected in cubic distortion tone input–output functions. Hear. Res. 123, 87–96.
Zurek, P. M., Clark, W. W., and Kim, D. O. 1982. The behavior of acoustic distortion products in the ear canals of chinchillas with normal or damaged ears. J. Acoust. Soc. Am. 72, 774–780.
Zwicker, E. 1979. A model describing nonlinearities in hearing by active processes with saturation at 40 dB. Biol. Cybern. 35, 243–250.

3.16 Hair Cell Transduction and Adaptation: Physiology and Molecular Mechanisms

E A Stauffer, A Lelli, and J R Holt, University of Virginia School of Medicine, Charlottesville, VA, USA

© 2008 Elsevier Inc. All rights reserved.

3.16.1	**Introduction**	263
3.16.2	**Hair Bundle Anatomy**	264
3.16.3	**Biophysics of Hair Cell Transduction**	264
3.16.4	**The Gating-Spring Model**	267
3.16.5	**Tip Links**	267
3.16.6	**Adaptation**	269
3.16.6.1	The Mechanism of Slow Adaptation	270
3.16.6.2	The Mechanism of Fast Adaptation	273
3.16.7	**Active Hair Bundle Movements**	275
3.16.8	**Molecular Identification**	278
3.16.8.1	Slow Adaptation and Myosin-Ic	278
3.16.8.2	Myosin-Ic Binding Partners	280
3.16.8.3	Other Hair Bundle Myosins	280
3.16.8.4	Fast Adaptation	282
3.16.8.5	Tip Links	282
3.16.8.6	The Transduction Channel	285
3.16.8.7	The Gating Spring	288
3.16.9	**Conclusions**	288
References		289

3.16.1 Introduction

Each passing moment we are bombarded with information traveling in the form of light, sound, motion, and chemical signals. The rate at which the information arrives is so high and continuous that it would overwhelm the largest, fastest supercomputer ever built in short order. Yet, we expect our sensory systems to sort through the onslaught on a moment-by-moment basis and provide us with the small fraction of information that is most crucial to the task at hand. The fact that you are able to comprehend these words right now, whether transmitted in written or spoken form, attests to how remarkably well these systems work. The critical first step in this incredible process is sensory transduction, the conversion of physical information into electrical information, the language of the brain. Within the inner ear sensory transduction converts mechanical information carried by sound and head movements into electrical signals. The feat is accomplished by an array of exquisitely engineered mechanoreceptor cells, called hair cells. How hair cells transduce the enormous quantity of mechanical information that strikes the inner ear is the focus of this chapter.

Hair cells reside within patches of sensory epithelium distributed amongst the six end organs of the mammalian inner ear: one auditory organ and five vestibular, or balance, organs. Although the mechanical information transduced by each organ arrives in different forms (namely sound, rotational and linear head movements, and gravity), the fundamental mechanism by which hair cells convert mechanical energy into electrical energy is the same. Auditory and vestibular organs gain their sensitivity to the different modalities of inner ear stimuli through the anatomy and mechanics of accessory structures that serve to focus stimulus energy onto mechanosensitive hair cells. Although there are some interesting differences among hair cells of different organs and species, this chapter will focus primarily on the features of mechanotransduction common to all hair cells.

3.16.2 Hair Bundle Anatomy

The central player in the process is a mechanosensitive organelle, termed the hair bundle, which towers high above the apical surface of the cell body. The hair bundle, so named because it resembles the punkish coiffure proudly displayed atop the upper extremities of nonconformist youth (Figure 1(a)), actually consists of a staircase array of modified microvilli (Figures 1(b) and 1(c)) known as stereocilia. The stereocilia range in length from just over 1 μm up to ~40 μm, and the number of stereocilia per hair bundle ranges from 30 to 300. Each stereocilium contains a rigid bundle of actin filaments, cross-linked by fimbrin and espin, that taper at the base where it inserts into the apical surface, or cuticular plate of the hair cell (Figures 1(d) and 1(e)). In vestibular cells and immature auditory cells there is a single true cilium, called the kinocilium, that defines bundle orientation and serves to mechanically couple the hair bundle to overlying structures (Figure 1(c), arrows). Although the number, diameter, length and configuration of hair bundle stereocilia, and the presence of a kinocilium vary both within a single hair cell organ and between organs and species, they all have the same common function: to convert mechanical deflections into electrical signals.

3.16.3 Biophysics of Hair Cell Transduction

The unique cytoarchitecture of the sensory hair bundle allows the rigid stereocilia to pivot at their insertion points, causing the entire hair bundle to swing back and forth as a unit in response to mechanical forces applied at the tip of the bundle. Interestingly, the hair bundle is only sensitive to the vector component of forces applied along a bilateral axis of symmetry which runs parallel to the staircase array of stereocilia and bisects the kinocilium. By convention, hair bundle deflections toward the tallest stereocilia are defined as positive and tend to excite the cell, whereas deflections in the opposite direction are negative and tend to inhibit the cell. Hair bundle deflections 90° off the sensitive axis evoke no response (Figure 2(a)).

Positive deflections of different amplitudes evoke responses of different sizes (Figure 2(b), left panel). By

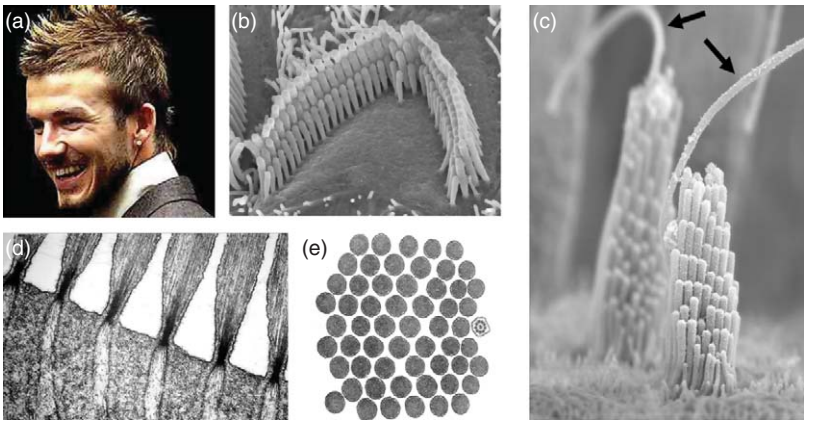

Figure 1 Hair bundle anatomy. (a) An example of a punk-style haircut which resembles the bundle arrangement of hair cells. (b) Scanning electron micrograph of an outer hair cell bundle of the guinea pig; the v arrangement of the three rows of stereocilia are evident. (c) Hair bundles from the mouse utricle; this scanning electron micrograph shows the staircase organization of the stereocilia and the presence of the kinocilium (arrows), the only true cilium in the bundle and a peculiarity of vestibular and immature cochlear hair cells. (d) Transmission electron micrograph of a hair bundle from the goldfish saccule. This longitudinal section shows the tapering of the stereocilia at the insertion into the cuticular plate. The stereocilia are filled with high density packed actin filaments that insert into the cuticular plate, forming rootlets. (e) When viewed in cross section, the hexagonal arrangement of stereocilia can be seen, as highlighted in this thin cross section of a bullfrog sacculus hair bundle; the kinocilium is located at the right with its 9 + 2 microtubule internal structure. (a) From http://hotdog.hu/_data/members3/923/76923/images/mohawk.jpg. (b) From Furness D. N and Hackney C. M. 2006. The Structure and Composition of the Stereociliary Bundle of Vertebrate Hair Cells. In: Vertebrate Hair Cells (*eds*. R. A. Eatock, R. R. Fay and A. N. Popper). Springer. (c) Reprinted from Holt, J. R., Gillespie, S. K., Provance, D. W., Shah, K., Shokat, K. M., Corey, D. P., Mercer, J. A., and Gillespie, P. G. 2002. A chemical-genetic strategy implicates myosin-1c in adaptation by hair cells. Cell 108, 371–381. (d) From Fawcett, D. W. 1981. The Cell, 2nd edn. W B Saunders. (e) From Hudspeth, A. J. 1983. The hair cells of the inner ear. They are exquisitely sensitive transducers that in human beings mediate the senses of hearing and balance. A tiny force applied to the top of the cell produces an electrical signal at the bottom. Sci. Am. 248, 54–64.

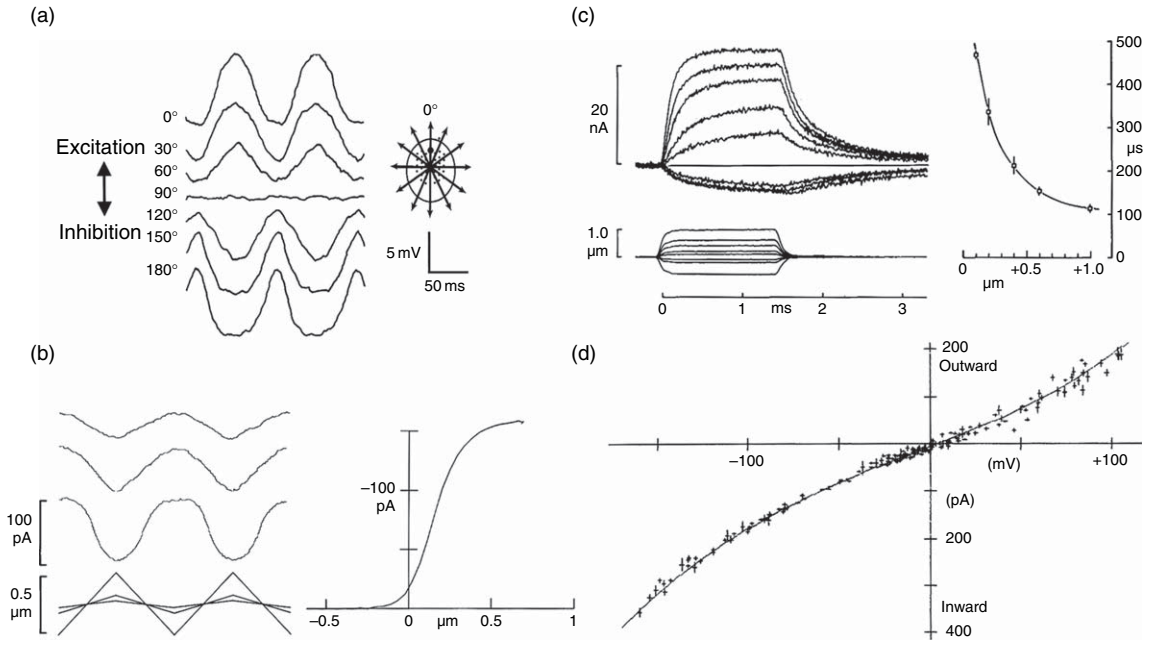

Figure 2 Biophysical properties of mechanotransduction in hair cells. (a) Directional sensitivity of mechanotransduction: receptor potentials recorded from a vestibular hair cell; the bundle was deflected along different axes as indicated. The maximal response was evoked for bundle deflections along the morphological axis of symmetry. (b) Amplitude sensitivity of mechanotransduction. Transduction currents recorded from a frog saccular hair cell, evoked by triangular mechanical stimuli of different amplitudes (left panel). Current-displacement relation from data in left panel is fitted with a second-order Boltzmann equation (right panel). (c) Fast activation of transduction current. The left panel shows fast activation kinetics of transduction currents from a vestibular hair cell stimulated with a fast probe. Time constants of single exponential fits to current activation are plotted versus stimulus amplitude (right panel). (d) The hair cell mechanotransduction channel is a nonselective, cation permeable channel. A plot of transduction currents measured at various membrane potentials shows that currents reverse around 0 mV. (a) From Shotwell, S. L., Jacobs, R., and Hudspeth, A. J. 1981. Directional sensitivity of individual vertebrate hair cells to controlled deflection of their hair bundles. Ann. N. Y. Acad. Sci. 374, 1–10. (b) From Hudspeth, A. J. and Corey, D. P. 1977. Sensitivity, polarity, and conductance change in the response of vertebrate hair cells to controlled mechanical stimuli. Proc. Natl. Acad. Sci. U. S. A. 74, 2407–2411. (c) From Corey, D. P. and Hudspeth, A. J. 1983. Kinetics of the receptor current in bullfrog saccular hair cells. J. Neurosci. 3, 962–976. (d) From Shotwell, S. L., Jacobs, R., and Hudspeth, A. J. 1981. Directional sensitivity of individual vertebrate hair cells to controlled deflection of their hair bundles. Ann. N. Y. Acad. Sci. 374, 1–10.

plotting the peak response as a function of stimulus amplitude, a stimulus–response relationship can be generated that reveals several noteworthy features (Figure 2(b), right panel). The relationship is sigmoidal and often best described by a second-order Boltzmann relation. The sensitivity of the cell is defined by the steepness of the curve at its midpoint, that is, the point at which 50% of the maximal response is evoked. Cells with a greater slope are more sensitive. The relationship also reveals the operating range of the cell, often measured as the deflection amplitude required to evoke between 10% and 90% of the response. Depending on the length, width and spacing of the stereocilia, the 10–90% operating range varies from ~100 nm in basal-turn cochlear hair cells (Russell, I. J. and Richardson, G. P. 1987; Kros, C. J. *et al.*, 1992) to a couple of microns in vestibular hair cells (Holt, J. R. *et al.*, 1997). However, differences in hair bundle geometry can be accounted for by using stereocilia length and width and interstereocilia distance to calculate the gamma factor (Jacobs, R. and Hudspeth, A. J., 1990). The product of gamma and the 10–90% operating range demonstrates that the sensitivity of the transduction apparatus at the tip of the hair bundle is remarkably similar even for diverse hair bundle geometries, species and organs (Holt, J. R. *et al.*, 1997). The stimulus–response relationship also reveals a nonzero open probability (P_o) at rest. In hair cells studied *in vitro* with perilymph-like solution (normal extracellular Na^+ and K^+, high Ca^{2+}) bathing the apical hair bundles, the open probability at rest is about 0.05–0.15, so that 5–15% of the transduction channels are

open in an undisturbed hair bundle (Holt, J. R. and Corey, D. P., 1999). In a frog saccule preparation with the hair cell's overlying accessory structure intact, the resting opening probability was found to be 0.15–0.20 (Corey, D. P. and Hudspeth, A. J., 1983). The open probability (P_o) may be even greater, up to 0.5, in outer hair cells from basal turns of the cochlea *in vivo* (Russell, I. J. and Kossl, M., 1992; Legan, P. K. *et al.*, 2000; Zou, Y. *et al.*, 2006). The resting P_o varies as a function of intracellular calcium concentration, which is largely determined by the extracellular calcium concentration (Corey, D. P. and Hudspeth, A. J., 1983; Hacohen, N. *et al.*, 1989; Crawford, A. C. *et al.*, 1991). Higher calcium concentrations favor a lower P_o. The significance of the nonzero P_o for sensory signaling in hair cells is threefold. It allows the hair cell to respond to bundle deflections in both directions. When the bundle swings from its rest position toward the shortest stereocilia, in the negative direction, the current that was on at rest declines. Conversely, when the bundle swings in the positive direction the response rises. The nonzero resting P_o also functions to position the hair bundle within a steeper region of the stimulus–response relationship. In other words, it allows the cell larger responses for smaller bundle deflections than if the resting P_o were closer to zero. Lastly, the pronounced asymmetry allows the cell to generate sustained depolarizing receptor potentials, which are particularly important at high frequencies because they promote neurotransmission at the afferent synapse.

Hair cell transduction currents have a reversal potential close to 0 mV (Figure 2(d)), which suggests the channels that carry the current are nonselective. Ion replacement experiments have revealed that the channels are permeable to monovalent and divalent cations. *In vivo*, the extracellular solution that bathes the hair bundle, known as endolymph, is high in potassium and low in sodium. Thus, transduction currents are carried mostly by potassium and calcium. At typical hair cell resting potentials, which range between −60 to −90 mV, the current is inward. *In vitro*, the maximal transduction current amplitudes range between ∼−200 pA in mouse vestibular cells and ∼−2 nA in gerbil auditory cells (Holt, J. R. *et al.*, 1997; 2002; He, D. Z. *et al.*, 2004). Inward transduction currents depolarize the cell with graded receptor potentials as large as 50–60 mV. Since mature hair cells do not express sodium channels, they do not fire action potentials and thus the sensory information is encoded within the receptor potential waveform. Under physiological conditions hair cells do not depolarize positive to the reversal potential of the transduction current.

Activation of hair cell transduction is extremely fast (Figure 2(c)). When chilled to 4 °C, the activation kinetics of frog saccular hair cells were found to be as fast as ∼100 μs, leading Corey D. P. and Hudspeth A. J. (1979) to hypothesize that hair cell transduction involves a direct gating mechanism of a mechanically sensitive ion channel. Although a provocative suggestion at the time, rapid submillisecond activation kinetics has proven to be a hallmark of nearly every mechanosensitive ion channel examined since. Furthermore, the rapid gating kinetics of hair cell mechanotransduction is in stark contrast to the sensory modalities of vision and olfaction, which make use of slower (100s of ms) second-messenger, G-protein-coupled cascades. The transduction process needs to be fast, as slow biochemical cascades would greatly restrict the frequency detection limit of the hair cell. Humans can hear sound frequencies up to approximately 20 kHz and some species of bats and marine mammals can detect frequencies up to 150 kHz (Hudspeth, A. J., 1989; Torre, V. *et al.*, 1995), which necessitates submicrosecond activation kinetics. Measurements from mammalian cochlear hair cells revealed response latencies of as fast as 10 μs, the limit of the recording device (Ricci, A. J. *et al.*, 2005).

Several experiments have revealed estimates of single-channel conductance for the hair cell transduction channel. Based on high quality whole-cell recordings from cells in which the transduction apparatus was disrupted to the extent that only a single transduction channel remained functional, Géléoc G. S. *et al.* (1997) measured single-channel conductances of ∼112 pS. Interestingly, other investigators have noted that single channel conductance varies tonotopically along the length of the turtle and rat auditory organs (Ricci, A. J. *et al.*, 2003; Beurg, M. *et al.*, 2006). In rat outer hair cells the single-channel conductance was found to be 95 pS at the low frequency end and increased to 139 pS toward the middle frequency range (Beurg, M. *et al.*, 2006). By comparison, the single-channel conductance in rat inner hair cells showed little variability and was ∼170 pS. The heterogeneity in the single-channel properties of hair cell transduction suggests that there may also be heterogeneity in the molecular composition of the transduction channel (see Section 3.16.8.6). In addition, the estimates of single-channel conductance have been compared to measures of whole cell conductance to determine the number of transduction channels per cell which range from 50 to 100, or 1–2 channels per stereocilium.

3.16.4 The Gating-Spring Model

Corey D. P. and Hudspeth A. J. (1983) considered various models to describe the transduction process based on the experimental response characteristics of hair cells from the bullfrog sacculus, a ground-borne vibration detector. The model that best fit their data involved a direct coupling between stereocilia displacement and transduction channel gating. In this model, stereocilia displacement directly regulates the energy difference between the open and closed states of a mechanosensitive transduction channel, in a probabilistic fashion. This is similar to the effect of membrane potential on charged amino acids of voltage-gated ion channels. Importantly, the rate of channel opening and closing is dependent on the magnitude of the displacement. The rate is also dependent on temperature. The stimulus–response relationship was found to be an asymmetric sigmoidal curve that was best fit by a three-state kinetic model, with two closed states and one open state (Corey, D. P. and Hudspeth, A. J., 1983).

The original model postulated the existence of an elastic element, termed a gating spring, that controls transduction channel gating (Corey, D. P. and Hudspeth, A. J., 1983; Howard, J. and Hudspeth, A. J., 1987). The gating-spring model is consistent with the response latency of the hair cell (requiring time to increase tension in the spring); the asymmetric sigmoidal relationship between steady-state transduction current and bundle displacement; and the dependence of the rate of gating on displacement stimulus size and on temperature. Corey, D. P. and Hudspeth, A. J. also noticed that, while channel opening becomes faster for larger positive displacements, negative displacements beyond a certain distance do not affect the amplitude or speed of the instantaneous receptor current. This implies that the gating spring is not a rigid element, but instead becomes slack during large negative displacements (Corey, D. P. and Hudspeth, A. J., 1983). The gating spring is therefore similar to an elastic string, in that a tensile force can be exerted, but not a compressive force (Figure 3(a)) In the three-state model, one of the closed states is thought to represent the transduction channel without tension on the gating spring, while the second closed state signifies a tensioned spring, but closed channel, and the third an open channel (Figure 3(b)). The biophysical data estimate that the gating spring has a stiffness of approximately 1 mN m^{-1}; should withstand forces of greater than 100 pN; and stretch to more than twice its resting length of ~150 nm (Shepherd, G. M. and Corey, D. P., 1994; Kachar, B. *et al.*, 2000). According to the model, the stiffness of the gating spring determines the steepness, or slope, of the $I(X)$ curve (Figure 2(b), right panel). The location of the curve along the displacement axis is determined by the tension of the spring at the resting bundle position.

3.16.5 Tip Links

Soon after the seminal publication of the gating-spring model, Pickles J. O. *et al.* (1984) noticed the presence of extracellular cross-links located at the tips of hair cell stereocilia (Figures 3(c) and 3(d)). These links, visible in both scanning and tunneling electron micrographs, were later termed tip links. Tip links connect the tip of the shorter stereocilium in one row to the side of the adjacent taller neighbor in the next row. The tip links are oriented along the hair bundle's axis of sensitivity and thus are ideally positioned to act as the biophysically defined gating spring. Deflecting the hair bundle towards the tallest row of stereocilia would stretch, or increase tension in the tip links and lead to channel opening. Deflecting the hair bundle in the negative direction, towards the row of shortest stereocilia, would relieve tension and allow the channels to close (Pickles, J. O. *et al.*, 1984). Off-axis displacements of the bundle would have little effect on tip link tension. Tip links are also sensitive to calcium chelators such as BAPTA, as well as lanthanum (Assad, J. A. *et al.*, 1991; Goodyear, R. and Richardson, G., 2003) and the protease elastase.

The tip link gating-spring model, then, fits both the biophysical and ultrastructural data. Consistent with the hypothesis that tip links were the biophysically defined gating springs, Assad J. A. *et al.* (1991) found that treating hair bundles with BAPTA eliminated tip links without otherwise adversely affecting hair bundle structure, as viewed in electron micrographs (Figure 3(c)). BAPTA solutions also abolished the mechanosensitivity of the hair bundle, causing a rapid loss in transduction currents (Assad, J. A. *et al.*, 1991). Perfusion of a low calcium solution (<1 μM) onto the hair bundle can similarly abolish mechanotransduction (Crawford, A. C. *et al.*, 1991). Secondly, a resting tension is exerted on the ends of the tip links by an adaptation motor (discussed in the next section) that tends to pull the hair bundle in the negative direction by approximately 130 nm. Indeed, applying BAPTA breaks tip links and allows the bundle to

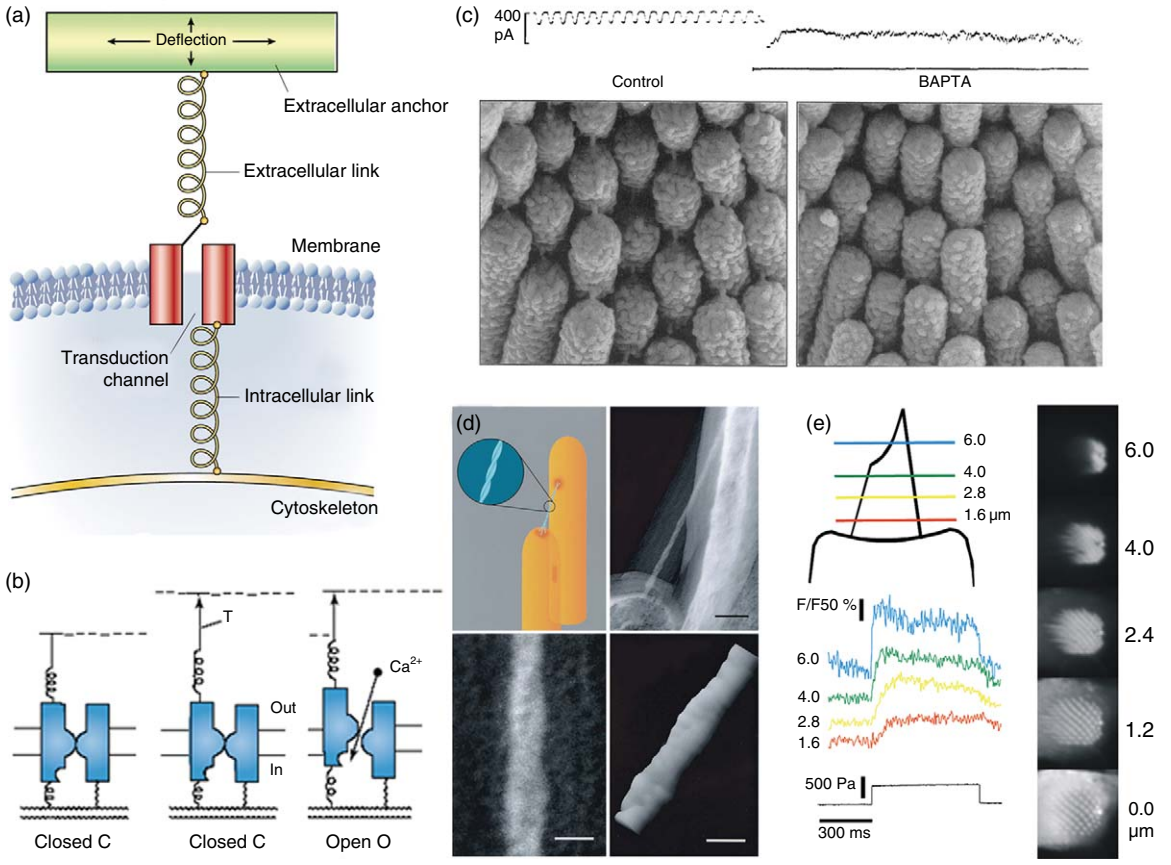

Figure 3 Tip link and gating spring. (a) Direct activation of mechanotransduction channels. A schematic diagram of a mechanosensitive channel that is gated by tension exerted perpendicular to the membrane. Deflection of a hair bundle increases tension across the membrane which directly opens the transduction channel. (b) According to the model for hair cell mechanotransduction, the channel can be found in three different states: closed with no tension on the gating spring (left), closed with the gating spring tensed (middle), and opened (right). (c) Sensitivity of mechanotransduction and tip links to calcium chelation. Transduction currents recorded from a frog saccular hair cell during sinusoidal mechanical stimulation of the bundle; when an extracellular solution containing the calcium chelator BAPTA was applied, the current was completely abolished (top panel). Scanning electron micrographs (lower panels) show frog saccular hair bundles before (left) and after (right) BAPTA treatment. Note the absence of tip links following BAPTA treatment. (d) High-resolution images of tip links from guinea pig cochlear hair cells. The top left panel shows a schematic diagram of tip link structure. Two helically intertwined protofilaments (Inset) are attached at two points to the taller stereocilium and contact three filaments emanating from the shorter stereocilium. The bottom left and top right panels are rapid-freeze deep-etched scanning electron micrographs showing a tip link visualized at different magnifications. The double coiled structure is apparent in the three dimensional reconstruction in the bottom right panel. Scale bars = 50 nm (top right), 10 nm (bottom left, right). (e) The transduction channel is located at the tips of stereocilia. A schematic diagram of a bullfrog saccular hair bundle (top left) indicates the focal plane of images shown at the right. The relative calcium concentration was monitored by the use of a fluorescent calcium indicator and two-photon scanning laser microscopy (lower left). When the bundle was stimulated by a fluid jet, the fluorescence intensity increased first at the tip of the bundle (bottom left) and then diffused to the rest of stereocilia. (a) From Gillespie, P. G. and Walker, R. G. 2001. Molecular basis of mechanosensory transduction. Nature 413, 194–202. (b) Adapted from Fettiplace, R. and Ricci, A. J. 2003. Adaptation in auditory hair cells. Curr. Opin. Neurobiol. 13, 446–451. (c) Reprinted from Assad, J. A., Shepherd, G. M., and Corey, D. P. 1991. Tip-link integrity and mechanical transduction in vertebrate hair cells. Neuron 7, 985–994. (d) Kachar, B., Parakkal, M., Kurc, M., Zhao, Y., and Gillespie, P. G. 2000. High-resolution structure of hair-cell tip links. Proc. Natl. Acad. Sci. U. S. A. 97, 13336–13341. (e) Reprinted from Denk, W., Holt, J. R., Shepherd, G. M., and Corey, D. P. 1995. Calcium imaging of single stereocilia in hair cells: localization of transduction channels at both ends of tip links. Neuron 15, 1311–1321.

relax forward (in the positive direction) by an average distance of 133 nm (Assad, J. A. *et al.*, 1991).

In a technical tour de force, Kachar B. *et al.* (2000) examined the hair cell tip link structure at high resolution by using rapid-freeze, deep-etch electron microscopy (Figure 3(d)). The authors determined that the tip link is a right-handed, periodic, coiled double filament that is 8–11 nm wide and 150–200 nm

long. The structure suggests that it is either a single wound polymer, or a pair of braided filamentous molecules, and is therefore likely to be relatively stiff and inextensible. These properties are inconsistent with the biophysical properties of the compliant transduction channel gating spring. The tip link branches at the upper end, attaching at two points to the insertional (side) plaque of the taller stereocilium. At the lower end, it seems to extend three filaments into the tip plaque. It is difficult to resolve the three filaments at the lower insertion point, but freeze–fracture images of stereociliary tips show three indentations likely left by the tip link insertions. Freeze–etch images and transmission electron micrographs of both stretched and compressed tip links were examined. A tenting phenomenon could be seen in the lower insertion of a tensioned tip link, as if the tip link is pulling the membrane away from the tip plaque, possibly straining some internal element below the membrane. A compressed tip link does not cause membrane tenting. The upper insertion point appears to remain rigid in both cases. Kachar B. *et al.* (2000) hypothesized that the tip link is not the gating spring, but that perhaps the gating spring is located elsewhere in series with the mechanotransduction apparatus. Elastic intracellular filaments at the lower end of the tip link could be components of the gating spring.

Although tip links were localized to the tips of stereocilia there was little direct evidence to suggest that this was also the site of transduction. Some investigators supported the idea that the channels were located along the latereral aspects of the stereocilia (Hackney, C. M. and Furness, D. N., 1995) or at the base of the hair bundle where the stereocilia insert into the cuticular plate (Ohmori, H. 1988).

Later studies, however, confirmed the hypothesis that the transduction channels are located at the tips of the stereocilia, imparting credence to the tip link's role in hair cell transduction. In one experiment, a transduction channel blocker was iontophoretically applied at various localized points along the hair bundle. The blocker was most effective when applied to the tips of the stereocilia, but had little or no effect when applied at the base of the bundle (Jaramillo, F., and Hudspeth, A. J., 1991). In a separate series of experiments, Denk W. *et al.* (1995) took advantage of the calcium permeability of the transduction channel and used two-photon laser-scanning microscopy, along with a fluorescent calcium indicator, to localize calcium entry in individual stereocilia. Upon positive bundle deflections, the calcium signal rose first at the tips of the stereocilia, and later in the bases, confirming that the transduction channels are located at the tips of the stereocilia (Figure 3(e)). Furthermore, calcium signals in individual stereocilia could be resolved in the two-photon imaging experiments, and the authors concluded that the transduction channels could be located at either end of the tips links (Denk, W. *et al.*, 1995). Interestingly, since transduction channels can be located at either end of the tip links, the asymmetric structure of the tip link suggests that the transduction channel is differently coupled to the tip link at each end (Kachar, B. *et al.*, 2000).

3.16.6 Adaptation

Sensory adaptation is defined as the decrease in a sensory response over time in the presence of a constant stimulus (Eatock, R. A. *et al.*, 1987) (Figure 4(a)). During and after adaptation, the full range of sensory response can still be evoked, a property that distinguishes adaptation from desensitization or inactivation. In hair cells, a large positive bundle displacement increases the open probability of the transduction channels to nearly 100%. If the bundle is held in that position, the transduction current decays over the subsequent 1–100 ms, as the transduction channels close (Figure 4(b)). However, even larger positive bundle displacements can reopen the channels that were closed by the adaptation process. Conversely, when the bundle is deflected in the negative direction, the 10% P_o at rest drops to near zero. In this case adaptation returns P_o back toward the resting level. This is particularly evident at the end of a negative step when the bundle is returned to the rest position. A rebound current is evoked before the cell adapts back the resting level. Hair cells exhibit two types of adaptation, termed slow and fast adaptation (Figure 4(c)). Slow and fast adaptation occur on different timescales, but both are regulated by calcium. Slow adaptation occurs over 10 to −100s of milliseconds and is thought to be mediated by a molecular motor, while fast adaptation occurs within a few milliseconds and is thought to result from either an inherent property of the transduction channel itself or from an associated accessory protein. Both types of adaptation shift the $I(X)$ curve in the direction of the applied stimulus (Figure 4(b), bottom panel). The shift may function to reset the operating range of the hair cell during either a positive or negative stimulus (Eatock, R. A., 2000). In vestibular hair cells, for example, the adaptation process allows the cells to remain responsive to stimuli in the presence of gravity, which exerts a relatively large tonic force on

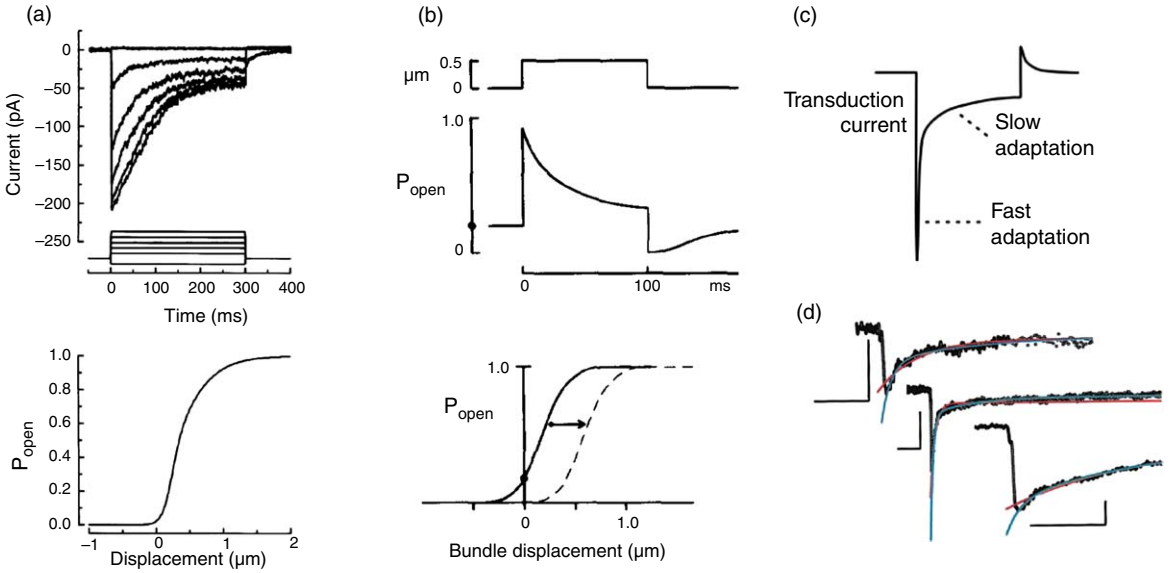

Figure 4 Hair cell adaptation. (a) A family of transduction currents from a mouse utricle hair cell evoked by the step displacements shown below. Note the decrease in current amplitude over time (due to adaptation) while the bundle is held in a fixed position. The peak current amplitude is plotted as a function of bundle displacement (bottom panel). (b) A bundle displacement increases gating-spring tension and channel open probability. Over the subsequent tens of milliseconds, adaptation proceeds and open probability declines (upper panels). Channel closure results from a shift of the sensitivity curve in the direction of the displacement (bottom panel), which suggests an adjustment of tension on channels. (c) A schematic diagram that highlights the different kinetics of fast and slow adaptation. Fast adaptation occurs within the first few milliseconds while slow adaptation follows over the subsequent tens to hundreds of milliseconds. (d) Separation of fast and slow adaptation. Mechanotransduction currents from frog sacculular hair cells fitted with single (red lines) and double (cyan) exponential curves. The data are best fit with a double exponential with time constant differing by an order of magnitude; scale bar 5 ms, 50 pA. Reprinted by permission, copyright 2003 by the American Physiological Society. (a) From Holt, J. R., Gillespie, S. K., Provance, D. W., Shah, K., Shokat, K. M., Corey, D. P., Mercer, J. A., and Gillespie, P. G. 2002. A chemical-genetic strategy implicates myosin-1c in adaptation by hair cells. Cell 108, 371–381. (b) Reprinted from Pickles, J. O. and Corey, D. P. 1992. Mechanoelectrical transduction by hair cells. Trends Neurosci. 15, 254–259. (c) LeMasurier, M. and Gillespie, P. G. 2005. Hair-cell mechanotransduction and cochlear amplification. Neuron 48, 403–415. (d) From Vollrath, M. A. and Eatock, R. A. 2003. Time course and extent of mechanotransducer adaptation in mouse utricular hair cells: comparison with frog saccular hair cells. J. Neurophysiol. 90, 2676–2689.

the hair bundles. Adaptation is not complete, as approximately 20–40% of the response remains after adaptation has reached steady state, which may serve to signal tonic stimulation.

Both types of adaptation may coexist to varying degrees among auditory and vestibular hair cells and amongst various species (Wu, Y. C. *et al.*, 1999; Eatock, R. O., 2000; Holt, J. R. and Corey, D. P., 2000). It is not entirely clear whether all hair cells possess both slow and fast adaptation. The type of stimulus used to deflect the hair bundle (stiff probe or fluid jet) and the speed, or rise time, of that stimulus can affect whether fast adaptation is observed or not (Vollrath, M. A. and Eatock, R. A., 2003). A stimulus that has a slow rise time can mask the appearance of fast adaptation. It is also sometimes difficult to separate the two processes (Figure 4(d)). In mouse utricular hair cells, slow adaptation is prominent, although fast adaptation has been observed (Holt, J. R. *et al.*, 2002; Vollrath, M. A. and Eatock, R. A., 2003; Stauffer, E. A. *et al.*, 2005). In frog saccular hair cells, fast adaptation is both faster and more prominent than in mouse vestibular hair cells (Vollrath, M. A. and Eatock, R. A., 2003). Although this chapter focuses on mechanotransduction and adaptation of the hair cell transduction process itself, it is important to note that additional factors may also contribute to adaptation in the inner ear, including voltage-dependent conductances in the hair cell, and the modulation of neurotransmitter release in the afferent neuron (Eatock, R. A., 2000).

3.16.6.1 The Mechanism of Slow Adaptation

Eatock R. A. *et al.* (1987) determined that adaptation involves a decrease in current entering through the transduction channel over time. Secondly, they found that adaptation involved a shift of the $I(X)$ relationship

along the displacement axis, in the direction of the applied stimulus. Slow adaptation allows hair cells to possess both high sensitivity and a broad operating range.

Eatock R. A. *et al.* (1987) revealed several important characteristics of hair cell adaptation. First, the $I(X)$ adaptive shift occurs in response to both negative and positive displacement stimuli. But, the rate of shift is nonlinear, as it occurs faster for positive displacements than for negative displacements. Second, the shift is dependent on the extracellular calcium concentration, and both the initial rate and the final extent of the adaptive shift increase upon increasing the calcium concentration. Third, the rate of shift is temperature dependent. Fourth, the extent of the adaptive shift to more negative displacements increases even after mechanotransduction has saturated. In other words, the amount of adaptation varies with displacement amplitude even if the amplitude of the current is constant (Eatock, R. A. *et al.*, 1987). All of these characteristics suggest that hair cell mechanotransducer adaptation is an active process.

Additional experiments suggested that hair cell adaptation involves a mechanical adjustment of the tension on the gating springs of the transduction channels. When Howard J. and Hudspeth A. J. (1987; 1988) displaced hair bundles in the positive direction with a flexible glass probe, a decrease in bundle stiffness occurred with a similar time course to the simultaneously measured adaptive decline in transduction current. The mechanical relaxation of the hair bundle in the positive direction was correlated with the polarity and direction of adaptation (Figure 5(a)). Furthermore, the mechanical adjustment during adaptation is thought to involve a movement of the gating spring. The $I(X)$ curve shifted along the displacement axis during adaptation, but the slope of the curve did not change substantially (Figure 5(b)). Howard J. and Hudspeth A. J. (1988) went on to show that the relationship between bundle stiffness and displacement also shifted along the displacement axis by the same amount (Figure 5(c)). The parallel shift in the two curves without changes in slope suggested that the attachment point of the gating spring actually moves during adaptation (Hacohen, N. *et al.*, 1989), perhaps slipping down the side of the taller stereocilia to relieve tip-link tension and allowing the channels to close (Figure 5(d)).

Calcium entering the stereocilia is additionally integral to the adaptation process. Lowering extracellular

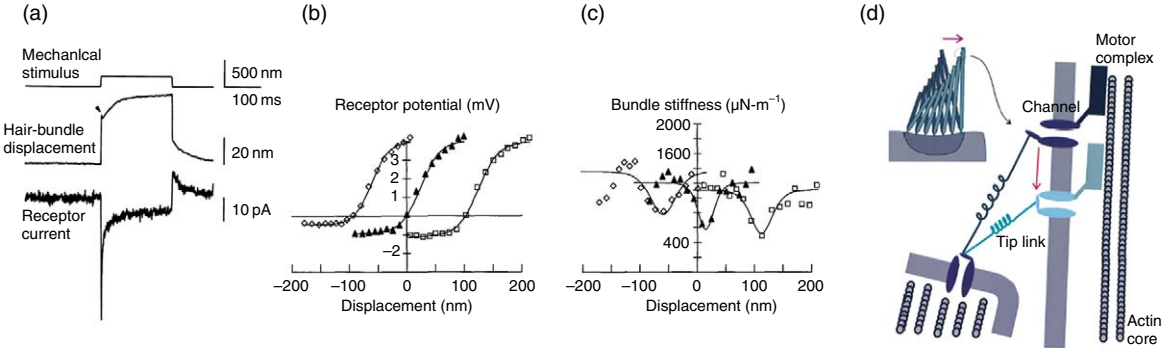

Figure 5 Bundle mechanics and slow adaptation. (a) Transduction current and bundle position were measured from a bullfrog vestibular hair cell stimulated by a force step (top panel). The force step was delivered by a flexible glass fiber of known stiffness. The bundle (middle trace) responded with an abrupt initial displacement, a twitch (arrowhead) and a slow relaxation. The current (bottom trace) revealed an initial, fast, inward transient followed by slow adaptation. The two components of adaptation in the receptor current had time courses similar to those of the mechanical relaxations. (b) As adaptation proceeds, the stimulus–response relationship shifts in the direction of the applied stimulus. (c) Hair bundle stiffness was estimated based on the amplitude of the probe displacement, the stiffness of the flexible stimulus probe, and the bundle displacement. The plot of bundle stiffness versus displacement shifted along the displacement axis parallel to the shift in the stimulus–response relationship (panel b). The dip in the stiffness-displacement curves corresponded to the midpoint of the respective stimulus–response relationships and presumably reflected a decrease in bundle stiffness due to transduction channel gating. (d) Model of slow adaptation: a motor complex in series with the channel and tip link is attach to an intracellular structure (probably the actin core): when tension is applied to the channel the motor complex releases and slips down the stereocilium which decreases gating-spring tension and allows the channel to close. (a) Howard, J. and Hudspeth, A. J. 1987. Mechanical relaxation of the hair bundle mediates adaptation in mechanoelectrical transduction by the bullfrog's saccular hair cell. Proc. Natl. Acad. Sci. U. S. A. 84, 3064–3068. (b, c) Reprinted from Howard, J. and Hudspeth, A. J. 1988. Compliance of the hair bundle associated with gating of mechanoelectrical transduction channels in the bullfrog's saccular hair cell. Neuron 1, 189–199. (d) Reprinted from Gillespie, P. G. and Corey, D. P. 1997. Myosin and adaptation by hair cells. Neuron 19, 955–958.

calcium (Eatock, R. A. *et al.*, 1987); including a high concentration of a calcium chelator in the intracellular recording solution; or depolarizing the hair cell to eliminate the entry of positively charged calcium ions during displacements (Crawford, A. C. *et al.*, 1989) all reduce the adaptation rate to positive stimuli. The rate of adaptation to negative stimuli is not dependent on extracellular calcium, however (Hacohen, N. *et al.*, 1989). These data, in sum, suggest that calcium entry into hair cell stereocilia, likely through the transduction channel itself, modulates the rate and extent of adaptation.

Finally, as alluded to earlier, slow adaptation is highly asymmetrical, with a faster rate for positive stimuli than for negative stimuli. In the positive direction, the initial rate of adaptation was found to increase linearly with the size of the displacement. The rate even increases for displacements beyond saturation, where the transduction current is at its maximum amplitude. On the other hand, the rate of adaptation for large negative displacements is nearly constant and does not depend on the size of the deflection. Large negative displacements, it is reasoned, would cause the gating spring to become slack, and allow an unloaded active adaptation element to re-tension the spring (Hacohen, N. *et al.*, 1989).

From these data, the active motor model of adaptation was developed as an extension of the gating-spring transduction model (Assad, J. A. and Corey, D. P., 1992). The active motor model involves an active force generator, or motor, which exerts a tension in the transduction channel's gating spring. During positive bundle displacements, the force generator passively slips at a rate that is dependent on displacement amplitude and calcium entry into the stereocilia (Figure 5(d)). Greater displacement amplitudes and higher concentrations of calcium increase the slipping rate. During saturating negative displacements, the unloaded motor actively tensions the gating spring by climbing, initially at a constant rate that is independent of displacement amplitude. This rate, calculated as the movement of the tip link along the stereocilium, was found to be 1–2 $\mu m\,s^{-1}$, similar to the rate of myosin moving along actin (Hacohen, N. *et al.*, 1989). After the motor senses the tension exerted by the gating spring, it slows and then stops when the channel open probability is about 10%. The open probability is determined by the opposing tensioning and slipping forces. At rest, the motor exerts a tension on the gating spring. In fact, the P_o at rest increases when extracellular calcium concentrations are decreased or the cell is depolarized to reduce calcium influx, just as decreasing extracellular calcium lowers the rate and extent of adaptation (Corey, D. P. and Hudspeth, A. J., 1983; Hacohen, N. *et al.*, 1989).

Thus, the active motor model postulates that the steady-state tension of the gating spring is set by a balance between slipping and climbing. In this model, the steady-state (i.e., at rest, or after adaptation has saturated) tension on the gating spring is adjusted by calcium, but is independent of the static position of the bundle. Also, according to this model, adaptation is complete so that the receptor current returns to the baseline value and the $I(X)$ curve shifts by an amount equal to the size of the displacement step. If the hair bundle was deflected in the positive direction by 1 μm, for example, then adaptation is predicted to cause the $I(X)$ curve to shift to the right, along the displacement axis, by 1 μm (Assad, J. A. and Corey, D. P., 1992).

However, this is not the case; adaptation is not complete. Rather, the extent of adaptation ranges between 60% and 80% of the displacement amplitude (Shepherd, G. M. and Corey, D. P., 1994; Holt, J. R. *et al.*, 1997). A 1 μm (nonsaturating) positive displacement will cause the $I(X)$ curve to shift by 0.6–0.8 μm in mouse utricular hair cells, for example, and 20–40% of the transduction current will remain at steady state, after adaptation is complete. According to the model, the movement of the upper tip link insertion point can also be calculated by multiplying the displacement of the bundle by a geometrical gain factor, gamma, that is approximately equal to the distance between the stereocilia divided by the height of the tallest stereocilium (Shepherd, G. M. and Corey, D. P., 1994). In mouse utricle hair cells, gamma is 0.047 (Holt, J. R. *et al.*, 1997), so that, at steady state, a 1 μm bundle displacement will cause the upper insertion point to slip down by about $1 \times 0.047 \times 80\% = 0.0376\,\mu m$. Shepherd G. M. and Corey D. P. (1994) added an adaptation extent spring into a revised motor model of adaptation to account for the incomplete extent of adaptation.

The original active motor model also treated the hair bundle as having no intrinsic set point, so that adaptation would occur regardless of bundle position. The hair bundle does, in reality, have a set point. In the positive direction, adaptation is essentially limitless. Larger positive stimuli increase the extent of the adaptive shift. Most hair cells are fairly resilient, but it is of course possible to damage the hair bundle with excessively large stimuli. In contrast, for large negative stimuli, the shift reaches a fixed limit. In bullfrog saccular hair cells, the fixed limit is 100–500 nm negative to the resting bundle position in 4 mM extracellular

calcium. Large negative displacements do not shift the $I(X)$ curve past this fixed limit. A negative stop was therefore added to the model to account for the negative limit (Shepherd, G. M. and Corey, D. P., 1994). The negative stop may be due to a fully extended extent spring (Yamoah, E. N. and Gillespie, P. G. 1996). Although the model for adaptation was developed for bullfrog saccular hair cells, the model applies equally well to mammalian vestibular hair cells, with minor adjustments allowed for differences in hair bundle geometry (Holt, J. R. *et al.*, 1997).

3.16.6.2 The Mechanism of Fast Adaptation

A second adaptation model, based on work with turtle auditory hair cells, posits that adaptation results as calcium enters the transduction channels and binds to an intracellular site which promotes channel closure (Crawford, A. C. *et al.*, 1991). Crawford A. C. *et al.* found that decreasing the concentration of calcium bathing turtle auditory hair cells led to a negative (leftward) shift and a decrease in the slope of the $I(X)$. The $I(X)$ shift and change in slope could be replicated by depolarizing a hair cell bathed in an extracellular solution high in calcium, suggesting that calcium is acting at an intracellular site (as depolarizing the cell toward the calcium equilibrium potential would reduce calcium influx). Note that the $I(X)$ curve actually broadens (decreases in slope), suggesting that the location of the gating spring is not climbing or slipping, as in the motor model. Rather, it was proposed that calcium, acting at an intracellular site, regulates the intrinsic open probability of the transduction channel by stabilizing one of its closed states (Crawford, A. C. *et al.*, 1991). Calcium influx therefore decreases the open probability of the transduction channel, leading to a fast decrease in transduction current amplitude during a sustained hair bundle displacement. This process was later named fast adaptation, to distinguish it from the slower active motor process. The intracellular fast adaptation sensor is unknown, but may be a calcium sensitive protein, such as calmodulin, associated with the transduction complex. Alternatively, a myosin motor may be involved in fast adaptation.

Although initially at odds, both the active motor model and the fast adaptation model seem to be valid. Each describes a physiologically distinct component of adaptation occurring on different timescales. Furthermore, they can coexist in the same hair cell, and both are calcium sensitive. Fast adaptation dominates in auditory hair cells of the turtle and rat, while slow adaptation is more prominent in vestibular hair cells of the bullfrog and mouse. The relative contribution of the two types of adaptation may depend on the frequency to which a particular type of hair cell is sensitive. In general, auditory hair cells encode higher frequencies than vestibular hair cells and thus are dominated by fast adaptation. The two components of adaptation are apparent in the adaptive decay in current amplitude in many hair cells and can be fit by a double exponential equation with fast and slow time constants. The fast time constant is usually below 5 ms, and the slower time constant is between 10 and 100 ms (Figure 4(c)) (Holt, J. R. *et al.*, 1997; 2002; Wu, Y. C. *et al.*, 1999). Rat outer hair cells exhibit fast adaptation time constants as fast as 100 μs (Kennedy, H. J. *et al.*, 2003).

Since fast adaptation can occur on a submillisecond timescale it is too fast for a system that requires the ATPase cycle of any known motor protein. While slow adaptation can be inhibited by dialyzing the hair cell with high concentrations of adenine nucleoside diphosphates and ATPase inhibitors, fast adaptation is not affected by ATPase inhibitors (Wu, Y. C. *et al.*, 1999; Holt, J. R. and Corey, D. P., 2000). Furthermore, unlike slow adaptation, the fast component of adaptation has a similar time constant for both positive and negative stimuli, suggesting that it is reversible (Wu, Y. C. *et al.*, 1999). Wu Y. C. *et al.* (1999) modeled adaptation by a scheme in which calcium ions enter through the transduction channels and act on two independent intracellular sites to modulate the activity of the fast and slow adaptation mechanisms. The initial model proposed for fast adaptation, now referred to as the channel re-closure model, suggested that calcium entry through open transduction channels alters the relationship between gating-spring tension and channel open probability such that greater tension is required to achieve the same open probability (Howard, J. and Hudspeth, A. J., 1988). In other words, with positive bundle deflections, channels open and allow calcium to enter; intracellular calcium in turn binds to a site on or near the channel. Although gating-spring tension remains, the fast adaptation mechanism causes rapid channel closure and thus a rapid decline in P_o and transduction current amplitude.

An alternate model, known as the release model, has recently been proposed (Bozovic, D. and Hudspeth, A. J., 2003; Martin, P. *et al.*, 2003; Stauffer, E. A. *et al.*, 2005; LeMasurier, M. and Gillespie, P. G., 2005). This model suggests that, following a bundle deflection, an element in series with the transduction apparatus releases tension which allows the transduction channels to

close. There are a couple of noteworthy differences between the two models. First, while the channel re-closure model suggests a fundamental change in the relationship between P_o and gating-spring tension, the release model suggests that this relationship remains constant. The re-closure model predicts that an unconstrained bundle deflected by a constant force will kick back in the negative direction (i.e., toward the shortest stereocilia) as fast adaptation proceeds (Figure 6(a), top panel). The amount of the negative movement depends on the extent of fast adaptation and the swing of the transduction channel gate. Conversely,

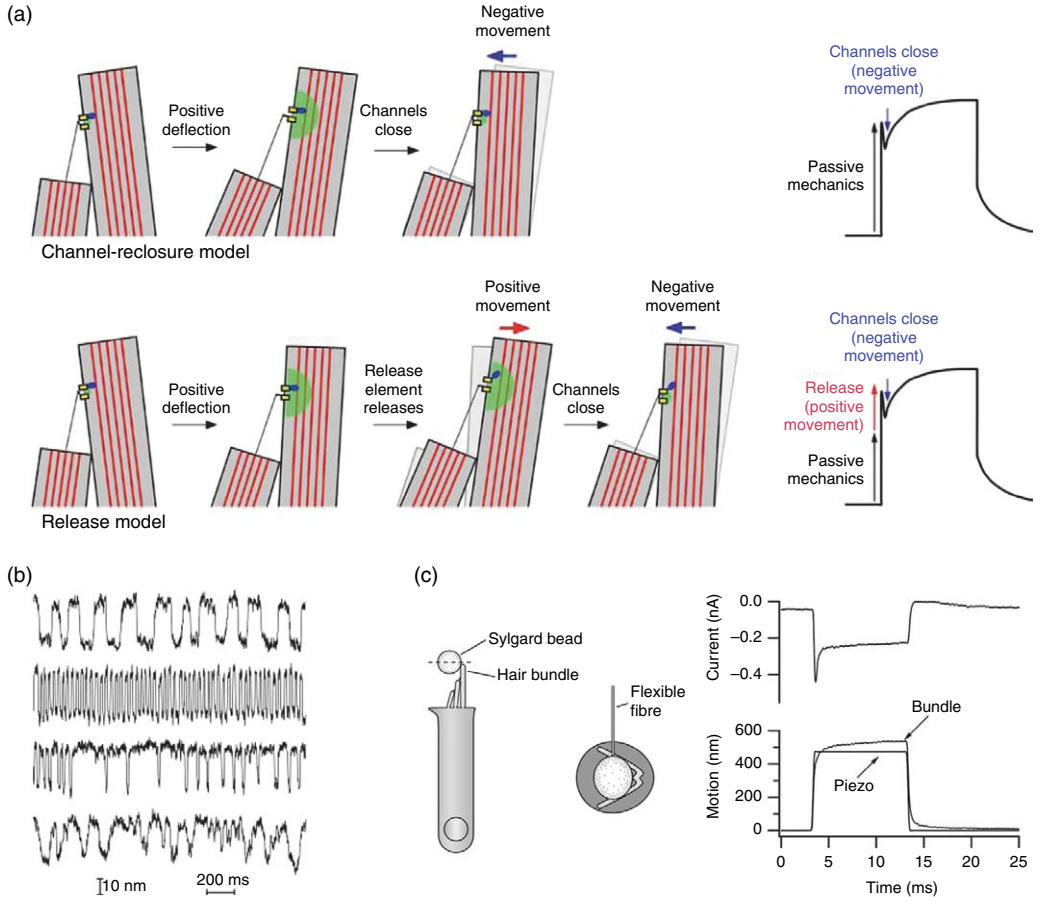

Figure 6 Fast adaptation and active hair bundle movements. (a) The cartoons present different scenarios for active hair bundle movements according to the channel reclosure model (top panel) and the release model (bottom panel). For both models, a positive deflection of the hair cell bundle causes transduction channels to open and allows Ca^{2+} to enter. In the channel reclosure model, Ca^{2+} binds to the transduction apparatus and forces the channel closed. Channel closure increases tension and moves the bundle back in the negative direction (top right). According to the release model, Ca^{2+} binding relieves tension within transduction apparatus by causing the release of an element in series. Thus, the bundle moves farther in the positive direction. The reduction in tension will subsequently allow the channel to close and rock the bundle back in the negative direction (bottom right). (b) Active bundle movements in a frog vestibular hair cell. The traces represent the spontaneous movement of saccular bundles, monitored by projecting the image of a flexible glass fiber attached to the bundle onto a pair of photodiodes. The tissue was bathed with an endolymph-like solution on the apical surface and a perilymph-like solution on the basolateral aspect. Spontaneous oscillations varied among cells from frequencies between 5 and 50 Hz with an average amplitude of 25 nm. (c) Active hair bundle movements in cochlear outer hair cells. The cartoon (left) shows the stimulus method for deflection of neonatal rat auditory hair bundles with a flexible fiber. The motion of the fiber and that of the bundle are shown at the bottom right. Interestingly, the bundle moved farther than the fiber, which indicates an active force generation. The transduction current recorded shows that the positive bundle movement paralleled fast adaptation (top right). (a) Reprinted from LeMasurier, M. and Gillespie, P. G. 2005. Hair-cell mechanotransduction and cochlear amplification. Neuron 48, 403–415. (b) Martin, P., Bozovic, D., Choe, Y., and Hudspeth, A. J. 2003. Spontaneous oscillation by hair bundles of the bullfrog's sacculus. J. Neurosci. 23, 4533–4548. (c) Kennedy, H. J., Crawford, A. C., and Fettiplace, R. 2005. Force generation by mammalian hair bundles supports a role in cochlear amplification. Nature 433, 880–883.

the release model suggests that an unconstrained bundle will swing further in the positive direction (Figure 6(a), bottom panel). As fast adaptation proceeds, the release of tension will allow a constant force to deflect the bundle even further. Second, the two models make different predictions for the effect of fast adaptation on slow adaptation. Since both fast and slow adaptations involve mechanical adjustments in series within the transduction apparatus they are intimately related. The channel re-closure model predicts that as fast adaptation proceeds, channel re-closure will increase tension within the transduction apparatus which will, in turn, increase the mechanical drive to slow adaptation. The release model, on the other hand, reduces tension as fast adaptation proceeds and thus is predicted to reduce the drive for slow adaptation. There is experimental evidence that supports both models for fast adaptation but the mechanism of fast adaptation remains unresolved.

In an elegant series of experiments, Cheung E. L. and Corey D. P. (2006) used a laser trap to deflect bullfrog vestibular hair bundles and measure the instantaneous forces applied to and produced by the hair bundle, which allowed them to resolve nanometer scale hair bundle movements. At the same time they developed a transduction model and simulated the effect of Ca^{2+} binding at different sites in the transduction complex. Their data were best fit with a fast adaptation model in which Ca^{2+} that entered the cell via the transduction channel reduced the P_o of the channel directly and caused an increase in gating-spring tension. A theoretical consequence of this effect is the movement of the bundle in the negative direction, which correlated with the bundle twitch documented by their data and by previous experiments (Benser, M. E. *et al.* 1996; Ricci, A. J. *et al.*, 2000).

Conversely, Stauffer E. A. *et al.* (2005) found evidence that supported the release theory for fast adaptation. They recorded transduction and adaptation from both frog and mouse vestibular hair cells and used the inferred shift method (Shepherd, G. M. and Corey, D. P., 1994) to translate the adaptive decay in the transduction current into the corresponding shift of the $I(X)$ relationship. By plotting the $I(X)$ shift as a function of time and fitting with a double-exponential equation, they were able to accurately distinguish the slow and fast components of adaptation evoked by different amplitude bundle deflections. They found that the drive for slow adaptation was greatly reduced over the narrow displacement range in which fast adaptation produced near-complete adaptation. Importantly they noted that the extent of slow adaptation was inversely proportional to that of fast adaptation. Both findings were consistent with the release model for fast adaptation but inconsistent with the channel re-closure model.

Although seemingly at odds, the Stauffer G. M. *et al.* (2005) and Cheung E. L. and Corey D. P. (2006) findings indicate that both the re-closure and release mechanisms may participate in fast adaptation in the same hair cell. Certainly it remains possible that the different techniques for hair bundle stimulation, displacement-clamp versus force-clamp, could highlight one fast adaptation mechanism more than the other.

3.16.7 Active Hair Bundle Movements

Both the slow and fast adaptation models predict that the adaptation mechanisms can exert active forces on the hair bundle, albeit on different timescales. These forces can evoke hair bundle movements which may provide feedback within the cochlea to amplify the motion of the basilar membrane. How the interplay between channel gating and the fast and slow adaptation mechanisms conspire to amplify bundle motion in the cochlea is an area of intensive and fruitful research. The observation that experimental depolarization can cause an unconstrained hair bundle to move in the negative direction was consistent with the motor model for slow adaptation (Assad, J. A. and Corey, D. P., 1992). The movement is thought to result from a reduction in the driving force on calcium during depolarization. A reduction in calcium entry at the adaptation motor in turn causes the $I(X)$ curve to shift in the negative direction. According to the active motor model, the leftward shift of the $I(X)$ results from an increase in the tension exerted on the transduction channel gating spring by a climbing motor. The model predicts that the increase in gating-spring tension will cause the hair bundle to pivot in the negative direction. Indeed, the hair bundle moves in the negative direction upon depolarization, and both the movement and $I(X)$ shift are abolished by reducing extracellular calcium or by application of transduction channel blockers (Assad, J. A. and Corey, D. P., 1992).

Fast adaptation has additionally been linked to the generation of active hair bundle forces, and with a speed that may allow it to contribute to amplification at the high frequencies to which cochlear hair cells are sensitive. During excitatory hair bundle displacements

with a flexible glass probe, turtle auditory hair cells were found to initially move in the positive direction, followed by rapid recoil in the negative direction. The positive movement is most likely due to the increase in gating compliance of the bundle as the transduction channels open. The recoil movement of the hair bundle, detected using a sensitive photodiode, followed the same time course of fast adaptation, had a similar calcium dependence as fast adaptation and was abolished by blocking the transduction channels. The negative bundle movement is therefore most likely caused by the fast adaptation process (Ricci, A. J. *et al*., 2000).

However, Benser M. E. *et al.* (1996) proposed an alternative mechanism to account for the initial positive bundle movement and subsequent recoil in the negative direction. The authors suggest that movements of the adaptation motors could provide a rapid decrease, followed by an increase, in gating-spring tension. In response to a positive stimulus (or to calcium), the adaptation motor could tilt, or rock backwards thereby causing a reduction in gating-spring tension. The reduced tension would allow the bundle to move in the positive direction. Subsequently, a single power stroke by the adaptation motors would increase the gating-spring tension, thereby pulling the bundle back in the negative direction. This model predicts that gating-spring tension should increase as the motors pull the bundle in the negative direction, thereby keeping the transduction channels open (Benser, M. E. *et al*., 1996).

The results of Kennedy H. J. *et al.* (2005) lend support to the model proposed by Benser M. E. *et al.* (1996). Using flexible glass fibers to displace bundles and measure the resulting forces, Kennedy H. J. *et al.* (2005) demonstrated that hair bundles of mammalian outer hair cells can produce force on a submillisecond timescale. The time course of force production was found to correlate with fast adaptation in these cells. Interestingly, force was generated in the positive direction during a positive displacement (Figure 6(c)). Therefore, the hair bundle actually moves further in the direction of the applied stimulus (Kennedy, F. J. *et al*., 2005). The authors suggest that an element in series with the transduction channel gate may rock in place during fast adaptation, thereby relieving tension and allowing the bundle to move further in the positive direction (Kennedy, F. J. *et al*., 2005). The identity of this putative element is currently unknown. Although the ATPase cycle of a myosin is too slow to account for this fast (<1 ms) force generation by outer hair cells, internal conformational changes within a myosin molecule to produce the rocking motion suggested by Benser M. E. *et al.* (1996) could presumably occur on a much faster timescale. As such, the model proposed by Benser M. E. *et al.* (1996) is still entirely feasible.

On the other hand, as previously mentioned, fast adaptation is associated with a bundle movement, or recoil, in a direction opposite that of the applied stimulus in turtle auditory hair cells. It is unclear why turtle hair cells exhibit fast adaptation-associated movements in a direction opposite to that of mammalian outer hair cells. The results of Ricci A. J. *et al.* (2000) suggest that the transduction channels actually close during the fast adaptation process in turtle hair cells, as the negative bundle movement appears to temporally coincide with the rapid closure of the transduction channels due to fast adaptation. The model proposed by Benser M. E. *et al.* (1996), however, suggests that the channels will remain open as the motor pulls the bundle in the negative direction, keeping tension on the gating spring. How can these results be reconciled? Turtle and mammalian auditory hair cells may simply utilize different fast adaptation mechanisms. Alternatively, both processes may occur simultaneously, or at different phases of a waveform stimulus.

The adaptation process can also cause the hair bundle to spontaneously oscillate in the absence of stimulation. Bullfrog saccular hair cells were placed in a chamber that separates the basolateral surfaces of the cells from the apical hair bundles, in order to replicate the *in vivo* ionic environment. When the hair bundles were perfused with an endolymph-like low calcium solution, and the basolateral cell bodies placed in a perilymph-like solution, the hair bundles were found to exhibit spontaneous oscillations at frequencies of 5–50 Hz (Figure 6(b)). Transduction channel blockers inhibited the oscillations and drugs that affect myosins altered their rate. Increasing calcium made the oscillations faster and smaller in amplitude, while decreasing calcium had the opposite effect. The oscillations, which still occur in a voltage-clamped cell, are therefore thought to result from the interaction of the transduction channel gating compliance with the calcium-dependent activity of the adaptation motor (Martin, P. *et al*., 2003). It is currently unknown whether mammalian vestibular or auditory hair bundles oscillate spontaneously *in vivo*.

The fast adaptation process could, in principle, cause an auditory hair cell's bundle to oscillate at

much higher frequencies than those found in bullfrog saccular hair cells. Turtle auditory hair cells can exhibit calcium-dependent oscillations at higher frequencies upon the sustained application of a bundle displacement (Ricci, A. J. *et al.*, 1998). Conceptually, one can imagine a sine-wave stimulus with a frequency that matches the innate resonant frequency of the cell impinging upon the hair bundle. When the hair bundle is deflected in the positive direction, during the positive phase of the stimulus, the increase in gating-spring compliance as the transduction channels open will act in a positive feedback manner to enhance hair bundle movement. Alternatively, according to the model proposed by Benser M. E. *et al.* (1996), the rocking of a myosin to reduce gating-spring tension will enhance bundle movement in the positive direction. Fast adaptation will ensue and lead to channel closure and reset the tension in the gating spring. If channel closure coincides with the negative-going phase of bundle displacement, the movement in the negative direction will also be enhanced. When the channels are closed, the calcium concentration at the intracellular fast adaptation sensor rapidly drops (due to calcium buffering, diffusion, and the operation of calcium ATPases), allowing the channel to open once again, and the process to be repeated. The mechanical forces exerted by the hair bundle, driven by fast adaptation, may therefore amplify the auditory stimulus, particularly at frequencies that match the characteristic frequency of the hair cell. Fast adaptation may therefore both amplify and tune the hair cell's response to a specific stimulus frequency.

Finally, the fast and slow adaptation processes may actually combine to produce oscillations at a frequency specific for the stimuli detected by the cell. The specific frequency and amplitude of the oscillations would be affected by the rates of slow and fast adaptation, hair bundle geometry, the number of functional transduction channels, the amount of calcium that enters the transduction channels, external calcium concentration, and intracellular calcium dynamics, among other things. As a side note, spontaneous otoacoustic emissions, the spontaneous production of sounds by the ear, are thought to result from active mechanical processes within the ear, possibly including hair bundle oscillations that result from the adaptation process (Jaramillo, F. *et al.*, 1993; Martin, P. *et al.*, 2003).

Slow and fast adaptation play important roles in hair cell mechanosensory transduction. First, slow adaptation allows hair cells to respond to phasic stimuli in the presence of tonic stimuli that would otherwise saturate the hair cell's response. Second, adaptation may function to tune and amplify the responses of auditory and vestibular hair cells. Third, adaptation serves to maximize the sensitivity of both auditory and vestibular hair cells by exerting a resting tension on the spring that gates the transduction channel. The tension exerted by the adaptation motor moves the resting position of the hair cell into the steep portion of the $I(X)$ curve, where it is most sensitive to hair bundle displacements. Fourth, a slipping adaptation motor may protect the integrity of the mechanotransduction apparatus. During large positive displacements, the motor slips to relieve tension in the gating spring. If the motor did not slip, excessive tension placed on the gating spring could conceivably break or irreversibly damage the transduction apparatus. Fifth, the adaptation motor may play a pivotal role in the assembly of the mechanotransduction apparatus by shuttling it along the actin filaments to the tips of the stereocilia (Zhao, Y. *et al.*, 1996; Géléoc, G. S. and Holt, J. R. 2003a; Gillespie, P. G. and Cyr, J. L. 2004).

To summarize, the biophysical model of mechanosensory transduction in hair cells postulates that an elastic gating spring directly opens mechanosensitive transduction channels located at stereociliary tips. Tip links are necessary for functional mechanotransduction, and their location and orientation suggest that they may function to gate the transduction channel. The motor model of adaptation, an extension of the gating-spring model, hypothesizes that a force generator, or molecular motor, exerts a resting tension on the gating spring. The motor can passively slip to relieve tension on the gating spring, and actively climb to increase tension in the gating spring. One fast adaptation theory proposes that calcium directly binds to an intracellular site and decreases the open probability of the transduction channel, while the other suggests that calcium promotes release of tension from an intracellular element which allows the channel to close. The biophysical model has provided a framework in which to examine the molecular components of the mechanotransduction and adaptation apparatus. The elements within the model, including the transduction channel, adaptation motor, elastic gating spring, adaptation extent spring, negative stop, the tip link, and the fast adaptation site are all amenable to molecular identification. Once identified, various tenets of the biophysical model can be further tested.

3.16.8 Molecular Identification

3.16.8.1 Slow Adaptation and Myosin-Ic

Slow adaptation is thought to be mediated by a molecular motor. Since hair cell stereocilia contain actin filaments, myosin molecules are ideal candidates for the slow adaptation motor. Furthermore, the actin cores of stereocilia support myosin motility. Myosin-2 coated beads were found to move at a rate of 1–2 $\mu m\,s^{-1}$ toward the tips of the actin cores of demembranated stereocilia, which matched the predicted direction and speed of a climbing adaptation motor (Shepherd, G. M. *et al.*, 1990). In addition, slow adaptation can be inhibited by dialyzing the hair cell with high concentrations of adenine nucleoside diphosphates, which inhibit ATPases, and by myosin ATPase inhibitors (Gillespie, P. G. and Hudspeth, A. J., 1993; Yamoah, E. N. and Gillespie, P. G., 1996). These preliminary findings launched a search for hair cell myosins that might participate in adaptation. The search focused on myosins that localized to the stereocilia and on myosins with biophysical properties consistent with the putative hair cell adaptation motor.

To identify the myosin isozymes expressed by hair cells, Solc C. K. *et al.* (1994) used an RT-PCR screen and found at least ten different myosin isozymes in the bullfrog saccule, including myosin-6, 7a, 1a, 1c, 5, 10, and four myosin-2 isozymes (Solc, C. K. *et al.*, 1994). A comprehensive antibody localization study found that myosin-1c (previously known as myosin-1*beta*), VI, and VIIa are all expressed in hair cell stereocilia, among other places (Hasson, T. *et al.*, 1997). More recently, myosins IIIa and XV have been localized to the hair bundle as well (Schneider, M. E. *et al.*, 2006; Belyantseva, I. A. *et al.*, 2003). Of these, myosin-1c was localized to the tips of stereocilia, the putative location of the adaptation motor. Myosin-7a colocalized with the more basal cross-links that connect adjacent stereocilia, and myosin-6 appeared to concentrate around the stereociliary rootlets at the cuticular plate (Hasson, T. *et al.*, 1997). Myosin-15a was also localized to the tips of stereocilia (Belyantseva, I. A. *et al.*, 2003) where it seems to play a role in stereocilia elongation and myosin-3a appears to cap stereocilia tips (Schneider, M. E. *et al.*, 2006).

High-resolution quantitative immunoelectron microscopy found the highest density of myosin-1c at both ends of the tip link. The labeling was greatest 100 nm above the side-plaque, an electron-dense region along the sides of the stereocilia at the upper tip-link insertion point, and at the tip plaques, the location of the lower tip-link insertion point at the tip of the stereocilium (Figure 7(a)) (Garcia, J. A. *et al.*, 1998). The presence of myosin-1c along the side plaque is in accord with the motor model of adaptation. In this position the motor may be either directly or indirectly attached to the tip link or the transduction channel and can slip or climb along the steroeciliary actin core in response to changes in gating-spring tension. The localization of myosin-1c at the tips of the steroecilia (i.e., the lower end of a tip link) is a bit more puzzling. It is possible that it is simply involved in anchoring the mechanotransduction apparatus. A second possibility is that an unloaded myosin-1c continues to climb to the end of the actin filament after the tip link or gating spring is broken.

Based on the immunolocalization data, myosin-1c therefore became a prime candidate for the adaptation motor. Myosin-1c, a (+)-directed motor, is a ~118 kDa single-headed myosin with three domains. The N-terminal globular head domain binds actin and hydrolyzes ATP. The neck region contains four calmodulin-binding IQ (isoleucine-glutamine) domains. The C-terminal basic tail domain binds anionic (negatively charged) phospholipids, including phosphatidylserine and phosphatidylinositol-4,5-bisphosphate (Gillespie, P. G. and Cyr, J. L., 2004).

To test the putative role of myosin-1c in adaptation, a myosin-1c targeted gene deletion, or knockout, mouse was created. Unfortunately, deleting myosin-1c was found to create embryonic lethality (Holt, J. R. and Corey, D. P., 2000). Therefore, a novel, chemical-genetic strategy was developed to test the role of myosin-1c in hair cell adaptation. Gillespie P. G. *et al.* (1999) designed a missense mutation in myosin-1c, replacing tyrosine-61 with a glycine (Y61G). This mutation has minimal effects on the normal ATP hydrolytic activity and motility of myosin-1c, but was found to confer a selective sensitivity to ADP analogs modified at the N^6 position with a bulky side group. The same modified nucleotides do not affect wild-type myosin-1c, due to unfavorable interactions between tyrosine-61 and the bulky N^6 substituent (Gillespie, P. G. *et al.*, 1999).

Multiple modified ADP analogs were screened for efficacy and selectivity, and N^6(2-methyl-butyl) ADP (termed NMB-ADP) was found to be the best. Indeed, NMB-ADP potently and selectively inhibited the ATPase activity of myosin-1c. The inhibition caused Y61G myosin-1c to remain tightly bound to actin in a rigor-like state. Furthermore, NMB-ADP and Y61G myosin-1c were dominant and inhibited mixtures with

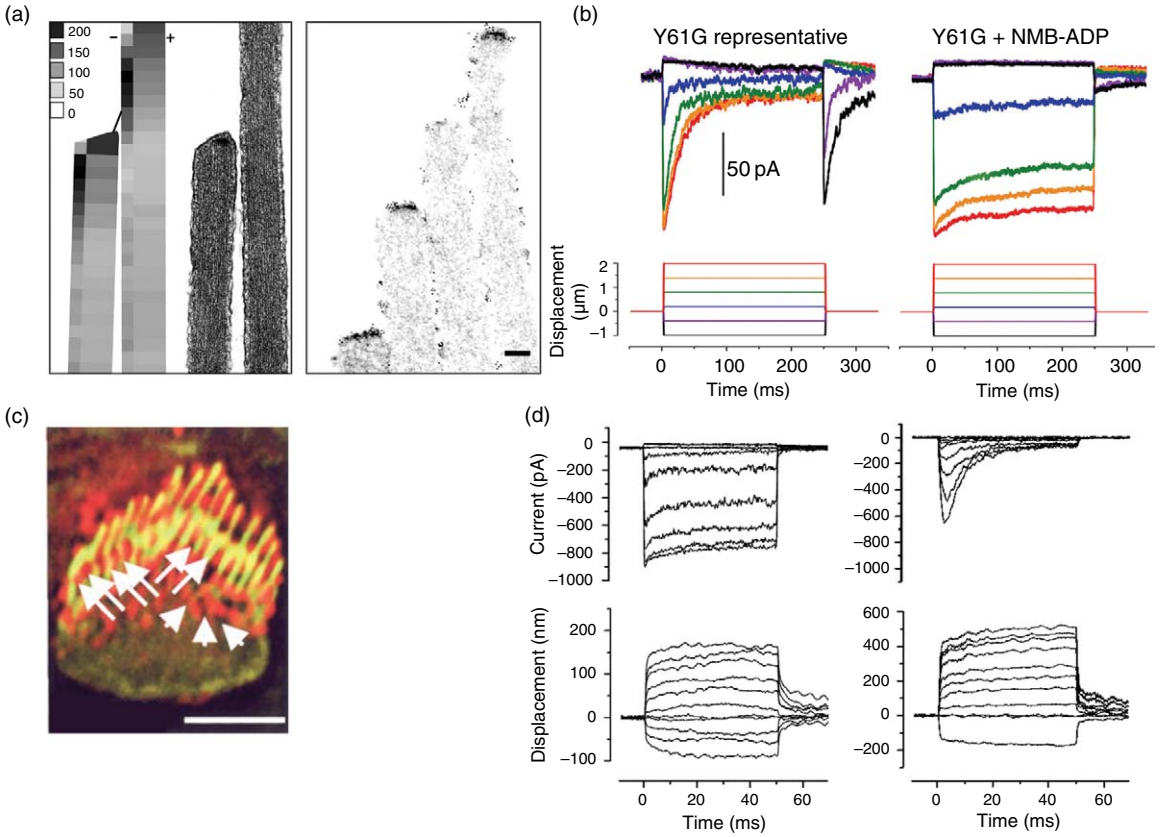

Figure 7 Myosins and adaptation. (a) Immuno-EM localizes myosin-1c to either end of the tip link in bullfrog saccular hair cells. A representative image is shown on the right. Quantification of data from multiple stereocilia is shown on the left. The intensity scale indicates immunogold particles per square micrometer; darker shading indicates an area with a higher density of particles and hence a presumably higher density of myosin-1c. (b) Myosin-1c participates in adaptation in mouse utricle hair cells. In the absence of the inhibitor, NMB-ADP, cells expressing Y61G myosin-1c exhibit normal adaptation (left). Notice the decline in current amplitude due to adaptation, as well as the rebound currents at the termination of steps in the negative direction. In contrast, inhibiting Y61G myosin-1c with NMB-ADP blocks adaptation (right). (c) Immunolocalization of myosin-7a (red) in an inner hair cell from a P5 mouse. F-actin bundles of the stereocilia are shown in green. Myosin-7a is localized toward the base of the longest stereocilia (arrows), at the cuticular plate (arrowheads), and toward tips of stereocilia. (d) A family of representative transduction currents, recorded at −84 mV, from a heterozygous myosin-7a control outer hair cell (top left) in response to a fluid-jet stimulus (bottom left). Bundle displacement at the tip of the hair bundle is indicated on the bottom left. Note that negative (inhibitory) bundle displacements turn off a small current on at rest. Homozygous myosin-7a mutant hair cells (top right) required larger bundle displacements (bottom right) to evoke transduction currents. Myosin-7a mutants also exhibited an open probability at rest of zero as well as slowed onset kinetics and a greater rate and extent of adaptation. (a) Reprinted from Garcia, J. A., Yee, A. G., Gillespie, P. G., and Corey, D. P. 1998. Localization of myosin-Ibeta near both ends of tip links in frog saccular hair cells. J. Neurosci. 18, 8637–8647. (b) Adapted from Stauffer, E. A., Scarborough, J. D., Hirono, M., Miller, E. D., Shah, K., Mercer, J. A., Holt, J. R., and Gillespie, P. G. 2005. Fast adaptation in vestibular hair cells requires Myosin-1c activity. Neuron 47, 541–553. (c) Adapted from Senften, M., Schwander, M., Kazmierczak, P., Lillo, C., Shin, J. B., Hasson, T., Géléoc, G. S., Gillespie, P. G., Williams, D., Holt, J. R., and Muller, U. 2006. Physical and functional interaction between protocadherin 15 and myosin VIIa in mechanosensory hair cells. J. Neurosci. 26, 2060–2071. (d) Adapted from Kros, C. J., Marcotti, W., van Netten, S. M., Self, T. J., Libby, R. T., Brown, S. D., Richardson, G. P., and Steel, K. P. 2002. Reduced climbing and increased slipping adaptation in cochlear hair cells of mice with Myo7a mutations. Nat. Neurosci. 5, 41–47.

wild-type myosin-1c that consisted of as little as 10% mutant myosin (Gillespie, P. G. *et al.*, 1999). With this tool in hand, Holt J. R. *et al.* (2002) created conventional transgenic mice that expressed Y61G myosin-1c as well as endogenous wild-type myosin-1c in order to examine the role of myosin-1c in vestibular hair cell adaptation.

Holt J. R. *et al.* (2002) used the whole-cell tight-seal recording technique to record transduction currents from transgenic mouse utricle hair cells while

deflecting the hair bundles with a stiff glass probe or a fluid jet. Adaptation was assayed by examining the decline in transduction current amplitude in the presence of constant bundle deflections, as well as by directly assessing the positive and negative shifts of the $I(X)$ that result from adaptation motor slipping and climbing, respectively. They found that Y61G myosin-1c expressing utricular hair cells have transduction and adaptation properties indistinguishable from wild-type in the absence of NMB-ADP. When cells were dialyzed with NMB-ADP, adaptation was normal early in the recording. However, later in the recording, after NMB-ADP was allowed to diffuse into the cell and, presumably, to the tips of the stereocilia, adaptation was blocked. NMB-ADP did not affect wild-type hair cells. The fact that NMB-ADP blocked adaptation to negative deflections, which requires an actively climbing adaptation motor, is perhaps the most convincing result. The authors concluded that myosin-1c participates in hair cell adaptation in the mouse utricle (Holt, J. R. *et al.*, 2002). These results were later confirmed using a knock-in mouse that expressed only the Y61G form of myosin-1c (Figure 7(b); Stauffer, E. A. *et al.*, 2005). Myosin-1c therefore became the first identified member of the mechanotransduction complex.

3.16.8.2 Myosin-Ic Binding Partners

These results begged the question: how and with what is myosin-1c interacting in the hair cell? Cyr J. L. *et al.* (2002) used various epitope-tagged recombinant myosin-1c fragments to identify myosin-1c binding sites within the hair cell, and to characterize the interactions of these sites with myosin-1c. Using immunohistochemistry, the authors found that myosin-1c seems to interact with unknown receptors (binding sites) at the tips of hair cell stereocilia using its calmodulin-binding IQ domains located in the neck region of the protein. Surprisingly, the tail domain is not required for these interactions to occur. It is not entirely clear which of the four IQ domains is important for binding *in vivo*. The first two IQ domains, IQ1 and IQ2, are sufficient for binding, but a calmodulin-occupied IQ3 site seems to enhance the interaction. Excess calmodulin blocks the interaction of myosin-1c with its hair cell binding partners, presumably by binding to previously unoccupied IQ domains. Finally, the fact that binding is affected by the calcium-sensitive protein calmodulin suggests that calcium may modulate interactions between the adaptation motor and other elements of the mechanotransduction apparatus (Cyr, J. L. *et al.*, 2002).

More recently, anionic membrane phospholipids, including phosphatidylinositol 4,5-bisphosphate (PIP2), were found to directly bind to the IQ domains of myosin-1c (Hirono, M. *et al.*, 2004) (although PIP2 does not seem to be the myosin-1c receptor discussed above). PIP2 localizes to the apical two-thirds of the stereocilia in some bullfrog saccular hair cells, appearing to be excluded from basal portions by the phosphatidylinositol lipid phosphatase, Ptprq. Interestingly, either blocking PIP2 synthesis or sequestering PIP2 using various drugs was found to reduce the rate of both slow and fast adaptation. Depletion of PIP2 also led to a decline in, and the eventual loss of, transduction current amplitude. PIP2 therefore seems to play an essential role in hair cell transduction and adaptation. Hirono M. *et al.* (2004) suggest that the lipid binding site within the IQ domains of myosin-1c might function to bring the calcium sensor for slow adaptation, presumed to be one of the IQ domains, closer to the stereociliary membrane, where calcium levels may be elevated. It is also possible that hair cells could vary PIP2 turnover dynamics in order to regulate transduction and adaptation (Hirono, M. *et al.*, 2004). Alternatively, PIP2 has been found to dynamically regulate the adhesive forces between actin-based cytoskeletal elements and the plasma membrane in fibroblasts (Raucher, D. *et al.*, 2000), and could function in a similar fashion at the location of the mechanotransduction complex.

3.16.8.3 Other Hair Bundle Myosins

Myosin-7a has emerged as an alternative candidate for the hair cell adaptation motor. Recessive mutations in the gene encoding myosin-7a have been linked to deafness in humans and in mice. Although myosin-7a is localized to hair cell stereocilia, it is not restricted to stereocilia tips (Figure 7(c)) (Hasson, T. *et al.*, 1997; Senften, M. *et al.*, 2006). Myosin-7a, a (+)-directed motor, contains an actin and ATP-binding head domain, and five IQ motifs in its neck domain. The tail contains two FERM (band 4.1 protein, ezrin, radixin, moesin) domains, which interact with certain cytoskeletal proteins (Inoue, A. and Ikebe, M. 2003).

Kros C. J. *et al.* (2002) examined transduction and adaptation in cochlear inner and outer hair cells of mice with myosin-7a mutations. One mutation is associated with reduced and presumably dysfunctional myosin-7a protein, while a second leads to a

very low expression level and a more severe phenotype, including disorganization of the hair bundle. The authors displaced hair bundles with a fluid jet stimulus, and recorded transduction currents (Figure 7(d)). Both myosin-7a homozygous mutants exhibited similar alterations in transduction and adaptation as compared to heterozygous controls. The resting open probability was zero in homozygotes, versus 4.8% in control. In addition, much larger than normal excitatory displacements were needed to elicit transduction currents in homozygotes. In response to a negative stimulus, the adaptation motor climbs up the stereocilium and increases tension on the gating spring. Therefore, an inward rebound current results upon returning to the resting bundle position at the termination of a negative stimulus. Controls exhibited this rebound, while homozygous mutants did not. The kinetics of transducer current activation were also slowed in the homozygous mutants. Taken together, these results suggest that the gating spring is abnormally slack in the homozygous myosin-7a mutants. Slipping adaptation evoked by positive steps was found to be faster in the homozygous mutants, and the extent of adaptation was greater as well. The authors therefore propose that myosin-7a participates in anchoring the stereociliary membrane to its actin core (possibly through its FERM domains), thereby tensioning membrane-bound elements of the transduction complex, including the channel and its gating spring, the tip link, and the adaptation extent spring (Kros, C. J. *et al.*, 2002).

Although the results of Holt J. R. *et al.* (2002) demonstrated that functional myosin-1c is crucial for adaptation, the data did not prove whether myosin-1c is the only myosin involved in the adaptation process. Locking Y61G myosin-1c onto actin in a rigor-like state apparently inhibited the motility of wild-type myosin-1c, and could similarly inhibit the motility of other myosins involved in adaptation, including myosin-7a. Also, the results of Kros C. J. *et al.* (2002) could be due to developmental effects of the myosin-7a mutation, and the immunolocalization data places myosin-7a along the entire stereocilium, not only at the ends of the tip links. Myosin-7a therefore may additionally participate in anchoring the lateral links along the sides of the stereocilia, further complicating interpretation of the data (Hasson, T. *et al.*, 1997; Kros, C. J. *et al.*, 2002). Or, myosin-7a may transport a component of the adaptation motor, but not participate in adaptation *per se*. The hair bundles of myosin-7a homozygous mutants are also structurally abnormal. Even though similar results were obtained with myosin-7a mutants that have differing severities of bundle disorganization, any disorganization at all confounds interpretation. Finally, Holt J. R. *et al.* (2002) only examined adaptation in vestibular hair cells, while Kros C. J. *et al.* (2002) only looked at auditory hair cells. It is possible that myosin-1c is the adaptation motor of vestibular hair cells, while myosin-7a serves a similar function in auditory hair cells.

Of course, it is also entirely possible that both myosins participate cooperatively as members of the mechanotransduction and adaptation apparatus. Myosin-7a may anchor the transduction complex at the opposite end of the gating spring as myosin-1c, so that myosin-7a and myosin-1c are in series. Therefore, the loss of one motor would make the other ineffective (Gillespie, P. G. 2002). Alternatively, myosin-1c and myosin-7a may interact with each other, possibly through intermediate binding partners, to affect the adaptation process. For example, PHR1, an integral membrane protein found in hair cells, has been found to interact, *in vitro*, with the tail regions of both myosin-1c and myosin-7a (Etournay, R. *et al.*, 2005). PHR1 contains a pleckstrin homology (PH) domain at its N-terminus and a transmembrane domain at its C-terminus (Xu, S. *et al.*, 2004). If PHR1 is present at the tips of stereocilia, it may participate in anchoring myosin-1c and/or myosin-7a to the cell membrane. PHR1 can apparently form homodimers, and so could conceivably interact with both myosin-1c and myosin-7a through the PH domain of each dimer (Etournay, R. *et al.*, 2005).

Myosin-7a also interacts with the cytoplasmic domain of protocadherin 15 (PCDH15), a member of the cadherin superfamily expressed in the hair cell bundle (Senften, M. *et al.*, 2006). Expression of PCDH15 is drastically reduced in stereocilia of myosin-7a deficient shaker-1 mice, whereas myosin-7a is strongly reduced in Ames waltzer^{av3j} mice, which lack PCDH15. This interaction is likely to play a role during bundle development as hair bundles of both Ames waltzer and shaker-1 mice show dramatic disorganization (Senften, M. *et al.*, 2006).

Myosin-15a is an additional hair cell myosin that could participate in adaptation (Belyantseva, I. A. *et al.*, 2003). Mutations in myosin-15a are associated with deafness in humans (DFNB3) and shaker (*Myo15*^{sh2}) mice. Myosin-15a localizes to stereocilia tips, overlapping with the barbed (+) ends of actin filaments and extending to the overlying apical plasma membrane. In deaf *Myo15*$^{sh2/sh2}$ mice, stereocilia appear to lack Myosin-15a, are abnormally short, and are nearly

equal in length (Belyantseva, I. A. *et al.*, 2003). During development, myosin-15a appears when the hair bundle begins to develop its staircase arrangement. Belyantseva I. A. *et al.* (2003) therefore proposed that myosin-15a is necessary for the staircase formation of the hair bundle. Additionally, in mature cells, the amount of myosin-15a at stereocilia tips is positively correlated with stereocilia length (Rzadzinska, A. K. *et al.*, 2004). Rzadzinksa A. K. *et al.* (2004) also suggested that myosin-15a may participate in the actin treadmilling process which serves to constantly renew and dynamically maintain stereocilia length. Due to its location near the tips of stereocilia (Rzadzinska, A. K. *et al.*, 2004), myosin-15a may also affect the tension applied to the tip links at the lower attachment points, and may therefore influence the adaptation process (Belyantseva, I. A. *et al.*, 2003). However, a recent report from Stepanyan R. *et al.* (2006) showed normal transduction and adaptation in myosin-15a deficient mice, suggesting that myosin-15a is not required for adaptation in mutant mice.

3.16.8.4 Fast Adaptation

The leading hypothesis for the mechanism of fast adaptation suggests that calcium binds directly to the transduction channel or a closely associated protein, and promotes channel reclosure. If this is indeed the case, identification of the molecular correlate of fast adaptation awaits molecular identification of the transduction channel itself (see Section 3.16.8.6).

However, there is a growing body of evidence that supports the release model for fast adaptation. In particular, a novel proposal suggests that, in addition to its role in slow adaptation, myosin-1c may be the release element that drives fast adaptation (Stauffer, E. A. *et al.*, 2005). Stauffer E. A. *et al.* (2005) used a chemical-genetic strategy similar to that used to identify the role of myosin-1c in slow adaptation (Holt, J. R. *et al.*, 2002). In this case, Stauffer E. A. *et al.* (2005) generated knock-in mice that expressed the Y61G mutation in myosin-1c instead of the wild-type form of the protein. Surprisingly, when they examined adaptation recorded from vestibular hair cells of Y61G knock-in mice with the selective inhibitor NMB-ADP in the recording pipette (Figure 7(b)), they found a significant reduction in the rates of both slow and fast adaptation. To separate the two components they used the inferred shift method (Shephred, G. M. and Corey, D. P., 1994) to analyze adaptation rates and found that NMB-ADP slowed the rate of fast adaptation by more than 80% relative to wild-type controls. This result held true for fast adaptation evoked both by positive and negative bundle deflections. The data suggested that in addition to its role in slow adaptation, which was also confirmed by these experiments, myosin-1c may also play a role in fast adaptation. Although the ATPase cycle of myosin-1c would be too slow to explain the rapid kinetics of fast adaptation, the authors hypothesized that an ATP-independent conformational change in the structure of myosin-1c may release tension within the transduction apparatus and allow transduction channels to close. The rapid release of tension would allow a constant force to deflect the hair bundle further in the positive direction. When the bundle is deflected back in the negative direction the hypothesis suggests that the decrease in tension will allow the myosin to rapidly flip back to its lower energy, resting conformation so that it is reprimed for the next cycle. Thus, myosin-1c may be a multifunctional molecule serving as the motor to drive slow adaptation, the release element to drive fast adaptation and, if the latter, perhaps a component of the cochlear amplifier as well, which serves to amplify and tune the auditory response to faint sounds. However, the role of myosin-1c in both slow and fast adaptation in cochlear hair cells has not yet been examined.

3.16.8.5 Tip Links

Nearly twenty years after the discovery of the tip link, two groups have identified cadherin-23 as a putative molecular component of the tip link (Siemens, J. *et al.*, 2004; Sollner, C. *et al.*, 2004). Cadherin-23 is a member of the large cadherin family of adhesive glycoproteins. Cadherin 23 contains an extracellular domain that consists of 27 cadherin repeats, a transmembrane domain, and a cytoplasmic domain that may be linked to the cell cytoskeleton. Cadherin repeats are independently folding motifs of around 110 amino acids that contain certain conserved sequences (Wheelock, M. J. and Johnson, K. R., 2003). Each cadherin repeat is approximately 3 nm wide and 5 nm long, and contains seven *Beta*-strands rigidly linked together by hydrogen bonds (Corey, D. P. and Sotomayor, M. 2004) (Figure 8(e)). The extracellular domains mediate the adhesive functions of cadherins in a calcium-dependent manner. Calcium binds to specific residues within the negatively charged cadherin repeat to ensure proper folding and impart rigidity to the extracellular domain (Wheelock, M. J. and Johnson, K. R., 2003). Calcium also promotes the interaction between adjacent cadherin repeats in

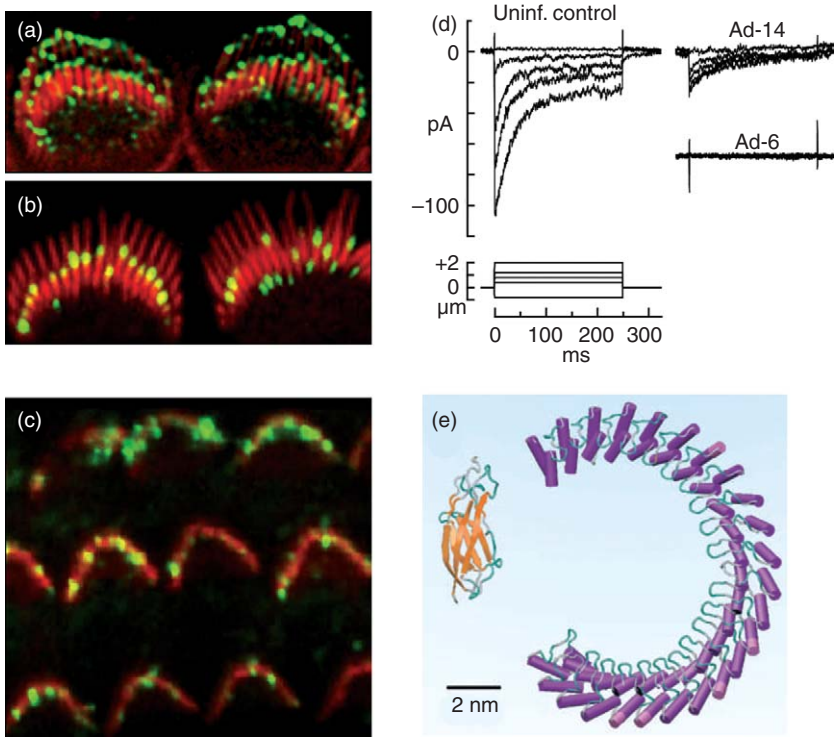

Figure 8 Localization and function of putative transduction molecules. (a) Immunolocalization of cadherin-23 (green) at the tips of stereocilia in inner hair cells from a P5 mouse cochlea. For (a–c), actin is shown in red. (b) Immunolocalization of protocadherin-15 (green) in stereocilia from inner hair cells of a P2 plus 1 day in vitro mouse cochlea. (c) Immunolocalization of TRPA1 (green) at the tips of stereocilia in outer hair cells from a P7 mouse cochlea. (d) Representative transduction currents from uninfected control mouse utricle cells (left) and cells infected with adenoviruses containing siRNAs directed against TRPA1 (right). Ad-6 and Ad-14 contain different siRNA constructs. (e) Models of a single cadherin domain (left) and 24 ankyrin repeats in series (right). Models suggest that a cadherin domain is relatively rigid and inelastic, while ankyrin domains assemble into an elastic spring-like superhelical structure. (a) Adapted from Senften, M., Schwander, M., Kazmierczak, P., Lillo, C., Shin, J. B., Hasson, T., Géléoc, G. S., Gillespie, P. G., Williams, D., Holt, J. R., and Muller, U. 2006. Physical and functional interaction between protocadherin 15 and myosin VIIa in mechanosensory hair cells. J. Neurosci. 26, 2060–2071. (b) Adapted from Ahmed, Z. M., Goodyear, R., Riazuddin, S., Lagziel, A., Legan, P. K., Behra, M., Burgess, S. M., Lilley, K. S., Wilcox, E. R., Griffith, A. J., Frolenkov, G. I., Belyantseva, I. A., Richardson, G. P., and Friedman, T. B. 2006. The tip-link antigen, a protein associated with the transduction complex of sensory hair cells, is protocadherin-15. J. Neurosci. 26, 7022–7034.(c,d) Adapted from Corey, D. P., Garcia-Anoveros, J., Holt, J. R., Kwan, K. Y., Lin, S. Y., Vollrath, M. A., Amalfitano, A., Cheung, E. L., Derfler, B. H., Duggan, A., Geleoc, G. S., Gray, P. A., Hoffman, M. P., Rehm, H. L., Tamasauskas, D., and Zhang, D. S. 2004. TRPA1 is a candidate for the mechanosensitive transduction channel of vertebrate hair cells. Nature 432, 723–730. (e) Corey D. P and Sotomayor M 2004. Hearing: tightrope act. Nature 428, 901–903.

both the *trans* and *cis* configurations (Goodyear, R and Richardson, G., 2003).

In young mice, cadherin-23 is found throughout the stereocilium, and is most abundant at the tips. In fact, cadherin-23, myosin-7a, and harmonin (a PDZ-containing actin-bundling protein) are all thought to interact during development to shape the cohesiveness of the hair bundle (Frolenkov, G. I. *et al.*, 2004). A defect in any one of these proteins leads to splayed hair bundles, and to Usher's syndrome, which is characterized by vision and hearing deficits. Some hypothesized that cadherin-23 plays a purely developmental role, as it was not initially found in mature stereocilia (Boeda, B. *et al.*, 2002).

However, Siemens J. *et al.* (2004) and Rzadzinska A. K. *et al.* (2005) localized cadherin-23 to the stereociliary tips of mature auditory and vestibular hair cells using a cadherin-23 antibody (Figure 8(a)). The labeling was absent in cadherin-23 deficient mutant mice. The authors went on to localize cadherin-23 intracellularly at tip-link insertion points with immunoelectron microscopy. In bullfrog vestibular cells, cadherin-23 also labeled the kinocilial links between the tallest stereocilia and the kinocilium.

Labeling was abolished in 75% of the hair cells treated with BAPTA, which destroys the tip link.

Cadherin-23 was found to mediate calcium-sensitive, homophilic interactions in a cell aggregation assay. Also, full-length cadherin-23, but not cadherin-23 lacking its cytoplasmic domain, was found to immunoprecipitate with myosin-1c, and to colocalize with myosin-1c when both were expressed in heterologous cells (Siemens, J. *et al.*, 2004). This result is somewhat puzzling, as, based on the mechanotransduction model, myosin-1c was not thought to bind directly to the tip link. The model may be incorrect - myosin-1c may bind to both the tip link and the channel at the lower end of the tip link, for example. In this case, the gating spring could be anchored to the intracellular cytoskeleton, so that the tip link, channel bound to myosin-1c, and gating spring are all in series. However, on the upper end of the tip link, it is difficult to imagine how such an arrangement would allow myosin-1c to exert tension on the channel by climbing. In this case, something other than the tip link would need to exert a force on the channel that opposes the force exerted by a climbing myosin. It remains possible that the assembly may be asymmetric with a different configuration at the upper end of the tip link or that the in vitro binding data do not represent the in vivo arrangement.

Sollner C. *et al.* (2004) separately identified cadherin-23 as a component of the tip link using a genetic approach in zebrafish. A random mutagenesis screen was employed to identify genes involved in vestibular and auditory function. Mutant zebrafish were found to have splayed hair bundles and defects in mechanotransduction. Multiple recessive alleles, all mapped to the cadherin-23 gene, were identified with varying phenotypic severities. Cadherin-23 was localized to the tips of stereocilia, and, importantly, was absent in fish with weak alleles of cadherin-23 that adversely affected mechanotransduction, but not bundle integrity. Transmission electron microscopy identified tip links in wild-type hair bundles, but not in bundles from cadherin-23 mutants.

Taken together, the results of Kachar B. *et al.* (2000), Siemens J. *et al.* (2004), and Sollner C. *et al.* (2004), as well as the similar biochemical and structural properties of cadherin-23 and the tip-link, all suggest that cadherin-23 is a component of the hair cell tip link. Furthermore, cadherin-23 and the tip link both share a number of similar features. Both mediate adhesive interactions between adjacent cell membranes in a calcium-sensitive manner. The tip link is sensitive to degredation by the protease elastase, but not to subtilisin (Goodyear, R. and Richardson, G., 1999a; 1999b). Likewise, cadherin-23 is degraded by elastase, but not by subtilisin (Siemens, J. *et al.*, 2004). Following enzymatic degradation, tip links regenerate within 24 hours. Likewise, cadherin-23 antibody labeling returns 24 hours after enzyme treatment (Siemens, J. *et al.*, 2004). The tip link appears to be a rigid, nonextensible structure consisting of repeating coiled filaments, and cadherin-23 can apparently form homomultimers (Siemens, J. *et al.*, 2004). Corey D. P. and Sotomayor M. (2004) predicted that a tip link could be formed from two parallel dimers of cadherin-23, as a dimer of dimers. Depending on the amount of interdigitation, this structure would be 8–12 nm wide and 140–280 nm long, consistent with the tip link electron microscopy data (Kachar, B. *et al.*, 2000; Corey, D. P. and Sotomayor, M., 2004).

Despite the substantial body of evidence, the conclusion that cadherin-23 is the tip link remains controversial. Other investigators have found that cadherin-23 plays a critical role during hair cell development, but is not present in the mature cell, which would suggest it cannot be a component of the tip link (Boeda, B. *et al.*, 2002; Lagziel, A. *et al.*, 2005; Michel, V. *et al.*, 2005). Michel V. *et al.* (2005) and Lagziel A. *et al.* (2005) both found cadherin-23 localized along the length of stereocilia early during development, was later restricted to the tips of stereocilia, but was no longer detected in the fully mature cell. Using immunogold labeling, cadherin-23 was localized to kinocilial links and to lateral links transiently present within and between stereociliary rows during development of the hair bundle (Michel, V. *et al.*, 2005). The immunolocalization data from these authors and the developmental phenotype of the *waltzer* mouse therefore suggest that cadherin-23 likely plays an essential role in maintaining the structure and cohesiveness of the developing hair bundle, but is not a constituent of the tip link. However, like other putative components of the mechanotransduction apparatus, including the transduction channel itself, the proteins of the tip link may easily elude detection due to exceedingly low expression levels. In addition, modifications to the tip-link proteins, such as glycosylation, may alter their immunoreactivity. The debate over whether cadherin-23 is a component of the tip link or a purely developmental hair cell element will surely continue.

Recently, another protein has emerged that may be a component of the mechano- transduction machinery and, perhaps, the tip link. Protocadherin-15, also a

member of the cadherin superfamily of Ca^{2+}-dependent adhesion glycoproteins, is important for normal hair bundle architecture and inner ear function in humans, mice, and zebrafish (Ahmed, Z. M. *et al.*, 2001; 2003; Alagramam, K. N. *et al.*, 2001a; 2001b; Ben-Yosef, T. *et al.*, 2003; Seiler, C. *et al.*, 2005). Mice carrying mutations in protocadherin-15 suffer from significant inner ear dysfunction and posses hair cells with disorganized bundles. Furthermore, mutant hair cells lack normal mechanotransduction currents (Alagramam, K. N. *et al.*, 2005; Senften, M. *et al.*, 2006). Recently, Ahmed Z. M. *et al.* (2006) identified protocadherin-15 as a component of the tip link antigen which was previously immunolocalized to the tip-link (Goodyear, R. and Richardson, G., 1999a; 1999b). Several splice variants of PCDH15 were identified, each with different localization and expression patterns in the inner ear (Ahmed, Z. M. *et al.*, 2006). While one of the isoforms was localized to the bottom half of stereocilia (Figure 8(b)), another was found just at the stereocilia tips (Ahmed, Z. M. *et al.*, 2006). Ahmed Z. M. *et al.* (2006) suggested that since protocadherin-15 is too short to span the ~150 nm between adjacent stereocilia, it may coassemble with a protein complex that includes cadherin-23, which together confers all the biophysical and structural properties of the filamentous tip link.

3.16.8.6 The Transduction Channel

Mechanosensation is ubiquitous; organisms as diverse as bacteria and blue whales utilize mechanosensation. The first mechanosensitive ion channel to be cloned was the MscL channel in *Escherichia coli*, which is gated by tension within the lipid bilayer and functions in osmoregulation. MscL can be mechanically gated when it is reconstituted in a lipid bilayer (Martinac, B., 2001). In contrast, most vertebrate and invertebrate mechanotransduction channels are thought to be gated by cytoskeletal and extracellular elements. Therefore, the mechanosensitivity of putative vertebrate channels often cannot be reconstituted in heterologous expression systems that lack these elements, making it much more difficult to directly demonstrate that individual proteins function as mechanotransducers.

Two families of ion channel proteins have been found to be necessary for mechanosensation in a variety of cell types: the degenerin/epithelial sodium channel (DEG/ENaC) family of ion channels and the transient receptor potential (TRP) family. In the worm *Caenorhabditis elegans*, a random mutagenesis screen was used to identify genes involved in mechanosensation, the *mec* genes. *MEC-4* and *MEC-10* are members of the DEG/ENac family of ion channels and are expressed in touch-sensitive neurons. They contain two transmembrane-domains, a large extracellular domain and a pore-forming loop. Certain gain-of function mutations in MEC-4 or MEC-10 cause the neurons to degenerate, hence the name degenerin (Huang, M. and Chalfie,M., 1994). MEC-2 and MEC-6 associate with MEC-4 and MEC-10, and can regulate channel activity (O'Hagan, R. *et al.*, 2005). In a heroic series of experiments, O'Hagan, R. *et al.* (2005) applied forces to the body wall of the worm using a flexible glass probe while simultaneously recording from the touch neurons *in vivo*. Null mutations in MEC-4, MEC-2, and MEC-6 did not affect voltage-gated currents in the neurons, but completely abolished mechanotransduction currents. The mechanotransduction currents are carried by Na^+ and can be blocked by amiloride, consistent with the properties of DEG/ENaC channels. Finally, more subtle mutations in specific glycine residues of both MEC-4 and MEC-10 reduced mechanotransduction current amplitudes and shifted the reversal potential of the current. O'Hagan R. *et al.* (2005) concluded that MEC-4 and MEC-10 must carry the mechanotransduction current. By directly demonstrating that the *C. elegans* DEG/ENaC complex composed of MEC-4, MEC-10, MEC-2, and MEC-6 forms a functional sensory mechanotransduction channel, O'Hagan R. *et al.* (2005) were the first to show that specific metazoan proteins are mechanotransducers. Based on similarities with *C. elegans* DEG/ENaC proteins, mammalian mechanosensitive BNaC channels were identified which are expressed in touch receptor cells (Garcia-Anoveros, J. *et al.*, 2001). Targeted gene deletion of BNaC1 caused a loss of touch sensitivity in mice (Price, M. P. *et al.*, 2000) but no deficits in auditory or vestibular function. Although the DEG/ENaC family of ion channels is of considerable interest to inner ear biologists, none of the members of the family have emerged as compelling candidates for the hair cell transduction channel.

Instead, attention has shifted to the TRP family of ion channels as several members were recently cloned from lower organisms, such as fruit flies and zebrafish, where they were found to be important for mechanotransduction (Walker, R. G. *et al.*, 2000; Kim, J. *et al.*, 2003; Sidi, S. *et al.*, 2003). TRP channels were first described in flies, where mutations in the *trp* gene expressed by photoreceptor cells cause transient

voltage responses to a continuous light stimulus (Clapham, D. E., 2003; Moran, M. M. *et al.*, 2004).

The TRP superfamily is extremely diverse, and channels are identified as belonging to the family based on homology, rather than on their selectivity or ligand sensitivity. In mammals, the TRP superfamily contains six subfamilies: the classical TRPs (TRPCs), vanilloid receptor TRPs (TRPVs), melastatin TRPs (TRPMs), the mucolipins (TRPMLs), the polycystins (TRPPs), and TRPA1 (also called ANKTM1, for ankyrin transmembrane protein 1) (Moran, M. M. *et al.*, 2004). The amino acid sequence identity among mammalian TRP channels is as low as 20%. TRP channels are involved in a diverse array of sensory processes, including hot and cold temperature sensation, the signaling of osmotic pressure, taste, alleged pheromone sensation, and mechanosensation (Clapham, D. E. 2003). TRP channels, with the exception of some TRPPs, are all predicted to form subunits consisting of six transmembrane (TM) domains with a pore-loop between TM5 and TM6, and may assemble into oligomers. They are generally nonselective, weakly voltage-sensitive, cation channels. Their properties are quite varied, and single TRP channels are often activated and modulated by multiple types of stimuli, second messengers, or other ligands (Clapham, D. E. 2003).

The fruitfly sensory bristle mechanotransduction channel, *nompC* or no mechanoreceptor potential C (later named TRPN1), was the first mechanosensitive TRP channel cloned (Walker, R. G. *et al.*, 2000). Fly sensory bristles consist of a hair shaft whose base is attached to the dendritic tip of a bipolar sensory neuron. Deflecting the hair shaft compresses the dendritic tip, and gates the mechanotransduction channel. The fly bristle mechanotransduction process is remarkably similar to the mammalian hair cell transduction process, in that it exhibits directional sensitivity, a submillisecond response latency, sensitivity to nanometer-scale deflections, a steep I(X) relationship, and similar adaptation. Flies carrying loss-of-function mutations in the *nompC* gene exhibit transduction currents that are ~10% of the wild-type response. Another *nompC* allele exhibits nearly normal transduction, but abnormally fast adaptation. The *nompC* gene was cloned, and found to encode a previously unidentified ion channel with 29 ankyrin (ANK) repeats on its NH_2-terminus, and six predicted transmembrane domains with a pore region between TM5 and TM6 (Walker, R. G. *et al.*, 2000).

The first putative vertebrate mechanotransduction channel to be cloned was the zebrafish ortholog of *nompC*. Zebrafish *nompC*, like fly *nompC*, belongs to the TRPN family within the TRP superfamily. It also contains 29 ANK repeats in its NH_2-terminus. Zebrafish injected with anti-sense morpholinos to disrupt *nompC* expression lacked an acoustic startle response. Hair cells within the ear of injected zebrafish did not take up the styryl dye FM-1-43, which permeates the transduction channel. Microphonic potentials, which are generated by current flowing through the transduction channels in a population of hair cells, were abolished in morpholino-injected zebrafish. The amount of dye uptake and the reduction in microphonic potential amplitudes were correlated with the severity of the acoustic startle phenotype. Finally, all three phenotypes were reversible; 24 hours after the morpholinos washed out nompC expression and all of the phenotypes returned to normal. Sidi S. *et al.* (2003) searched the mouse and human genomes but *nompC* homologs were not found.

The remarkable similarities between fruitfly mechanosensory bristle transduction, zebrafish hair cell transduction, and vertebrate hair cell mechanotransduction suggest that they may all use similar mechanotransduction channels. Yet, since *nompC* is not found in mammals, what is the mammalian transduction channel? The properties of the channel, namely its large single-channel conductance and permeability to cations, as well as the blocking effect of extracellular calcium, all suggest that it could be a member of the TRP family of ion channels.

In 2004 TRPA1 was presented as a mammalian hair cell transduction channel candidate (Corey, D. P. *et al.*, 2004, Nagata, K. *et al.*, 2005), but the suggestion remains controversial. TRPA1 was previously identified as a nonselective cation channel activated by noxious cold (~<17 °C) in a subset of nociceptive dorsal root ganglia neurons (Story, G. M. *et al.*, 2003; Bandell, M. *et al.*, 2004). TRPA1 is also activated by isothiocyanate compounds, such as mustard oil and wasabi, Delta(9)-tetrahydrocannabinol (THC) (Jordt, S. E. *et al.*, 2004), allicin, an unstable component of fresh garlic (Macpherson, L. J. *et al.*, 2005), and other pungent compounds such as in cinnamon oil (cinnamaldehyde), wintergreen oil (methyl salicylate), clove oil (eugenol), and ginger (gingerol) (Bandell, M. *et al.*, 2004).

Corey D. P. *et al.* (2004) presented TRPA1 as a candidate for the mammalian hair cell transduction channel based on several lines of indirect evidence. Corey D. P. *et al.* designed *in situ* hybridization probes for 33 TRP channels within the mouse genome, and looked for expression in the mouse ear. Only TRPA1

labeled hair cells above background levels. Hair cells of the mouse utricle first become sensitive to mechanical stimuli around embryonic day 17 (Géléoc, G. S. and Holt, J. R., 2003a). Quantitative RT-PCR was used to assess mRNA levels of various TRP channels during development of the mouse utricle, and TRPA1 levels were found to steadily increase to a prominent peak at E17. An antibody to the carboxy terminus of TRPA1 labeled the upper half of bullfrog stereocilia, along the length of the kinocilium, and the pericuticular zone around the cuticular plate. Light labeling was seen in the cell body. In mouse vestibular hair cells, light stereociliary labeling could be seen, along with stronger labeling within the kinocilium and pericuticular zone. In mouse auditory hair cells, labeling was the strongest in the stereocilia, but could be seen in the cell bodies (Figure 8(c)). Labeling at stereociliary tips could be seen in auditory hair cells from animals older than postnatal day 4. Interestingly, TRPA1 labeling in the stereocilia, like that of cadherin-23, was greatly diminished after treating cells with BAPTA or La^{3+} to break the tip links (Corey, D. P. *et al.*, 2004).

Corey D. P. *et al.* (2004) first inhibited TRPA1 expression in zebrafish hair cells. In zebrafish embryos injected with antisense morpholinos designed to inhibit TRPA1 protein expression, FM1-43 dye uptake by hair cells was significantly reduced, as compared to controls. Microphonic potentials, which result from current flow through transduction channels from multiple hair cells, were also reduced. TRPA1 morpholinos did not appear to simply delay hair cell development, as control and TRPA1 morpholino-injected fish had a similar number of hair cells. Finally, RT-PCR of TRPA1 message and immunoblots of extracted protein confirmed that TRPA1 levels were reduced in TRPA1 morpholino-injected animals as compared to control-injected animals. If TRPA1 and TPRN1 (*nompC*) are both required for hair cell transduction in zebrafish, it may be because they form heteromultimers together, or possibly because individual hair cells use one or the other (Corey, D. P. *et al.*, 2004).

Next, the functional consequences of inhibiting TRPA1 expression in mouse hair cells were investigated. Two hairpin small interfering RNAs (siRNAs) that targeted TRPA1 were packaged into adenoviral vectors along with the gene for green fluorescent protein. Mouse utricular hair cells were infected with the TRPA1 adenoviruses at embryonic day 16, before the onset of mechanotransduction. The authors recorded transduction currents at embryonic day 17–20 from siRNA treated cells, cells exposed to a control vector that expressed GFP alone and uninfected control cells. Both siRNA constructs yielded cells with reduced FM1-43 uptake and transduction current amplitudes relative to uninfected control cells (Figure 8(d)). From these data, the authors concluded that expression of siRNAs directed against TRPA1 resulted in a loss of hair cell mechanotransduction (Corey, D. P. *et al.*, 2004).

Based on the immunolocalization data, expression analysis, knock-down, and functional data, TRPA1 seemed a reasonable candidate for the hair cell transduction channel. However, recent data call that suggestion into question. Two groups generated mice that carried a targeted gene deletion of TRPA1, and both found that hearing and balance function in the knockout animals was identical to wild-type controls (Bautista, D. M. *et al.*, 2006; Kwan, K. Y. *et al.*, 2006). Furthermore, Kwan K. Y. *et al.* (2006) found normal FM1-43 uptake and mechanotranduction currents in $TRPA1^{-/-}$ animals. Several possibilities exist that may reconcile the observations of Corey D. P. *et al.* (2004) and Nagata K. *et al.* (2005) with those of Kwan K. Y. *et al.* (2006) and Bautista D. M. *et al.* (2006). First, TRPA1 could be an integral member of the transduction apparatus, coupling (either directly or indirectly) the actual transduction channel to the cytoskeleton using its ankyrin repeats (see Section 3.16.8.7). TRPA1 localizes along the kinocilium, and, like cadherin-23, at kinocilial links between the tallest stereocilia and the kinocilium. With its long ankyrin domain, TRPA1 could simply play a structural role in this location, as the kinocilium itself is not mechanosensitive. It is possible that TRPA1 is a nonessential structural component of the mechanotransduction apparatus. Secondly, it could be argued that TRPA1 plays a purely developmental role. Disruption of TRPA1 expression with siRNA- adenoviruses was performed between embryonic day 15 and 18 (Corey, D. P. *et al.*, 2004) whereas TRPA1-deficient mice were examined at later postnatal and adult stages (Kwan, K. Y. *et al.*, 2006). Third, the siRNAs designed to inhibit TRPA1 expression may have had unintended, nonspecific effects on the expression of other molecules required for transduction. Lastly, it remains a possibility that expression of some other transduction channel subunit compensated for the lack of TRPA1 expression in the knockout mice. Whatever the reason, two important questions remain. If TRPA1 is not the transduction channel, what is? And furthermore, what is the function of TRPA1 in hair cells?

Another TRP channel expressed in hair cells is TRPML3 (Di Palma, F. *et al.*, 2002). Mutations in TRPML3 are responsible for hair bundle disorganization, circling behavior, and hearing loss in the varitint-waddler mouse. TRPML3 localizes primarily to organelles within the cell body, suggesting that deafness results from abnormal organelle trafficking, rather than from defects in transduction. However, TRPML3 has not been ruled out as candidate for the hair cell transduction channel. A third candidate is TRPV4 (previously named VR-OAC), a mechanically sensitive channel that is activated by osmotic changes (cell swelling), fluid flow, and by heat. TRPV4 is expressed by multiple cells types within the inner ear, including the hair cells and the marginal cells within the stria vascularis. TRPV4 knockout mice have hearing deficits, but the deficits only appear in older mice and only shift hearing thresholds by about 20 dB. The mechanical activation of TRPV4 is also relatively slow, suggesting that a second messenger is involved, which is inconsistent with the rapid kinetics of the hair cell transduction channel (Corey, D. P., 2006). Although multiple candidates have been identified, the molecular identity (or identities) of the hair cell mechanotransduction channel is still unknown.

3.16.8.7 The Gating Spring

The tip link ultrastructural data and the finding that cadherin-23 (Figure 8(a)) and protocadherin-15 (Figure 8(b)) may be components of the tip link suggest that the tip link does not have the requisite elastic properties of the biophysically defined gating spring. Cadherin domains are predicted to be stiff and relatively inextensible. Furthermore, large forces would probably cause the complete unfolding of the cadherin repeat structure (Sotomayor, M. *et al.*, 2005), a characteristic poorly suited for the gating spring. Therefore, the search for the molecular correlate of the gating spring has recently shifted elsewhere. The gating spring may consist of the collective elasticity of multiple molecular elements in series with the transduction apparatus or it may be a single, as of yet, unidentified molecule. Several candidates have been proposed, including the 17 ankyrin repeats of TRPA1. TRPA1 is the only known mammalian TRP channel that, like *nompC*, contains a large number of ankyrin repeats in its NH_2-terminus. Ankyrin repeats have the ability to mediate protein-protein interactions by forming a scaffold that exposes certain interacting, or binding interfaces (Main, E. R. *et al.*, 2003). Ankyrin motifs consist of repeating units of 33 amino acids. Two anti-parallel alpha helices within the motif are linked by a beta hairpin/loop that is almost perpendicular to the alpha helices, thereby producing an L shape conformation. In the majority of ankyrin-mediated protein-protein interactions, the beta hairpin/loop region acts as the binding surface. Multiple ankyrin repeats stack together in parallel, and the stacking interactions cause a slight curvature and left-handed twist in the overall structure (Figure 8(e)) (Main, E. R. *et al.*, 2003).

Howard J. and Bechstedt S. (2004) suggested that a helix of ankyrin repeats within *nompC* may be the gating spring of zebrafish hair cells; might participate in gating the transduction channel of fruitfly mechanosensory bristles; and possibly act as the biophysically defined gating spring of mammalian hair cells as well. 29 ANK repeats are predicted to form almost exactly one helical turn with an expected stiffness of 1 mN m^{-1}. If *nompC* assembles into a tetramer, then four helices would have an upper limit stiffness of 4 mN m^{-1}. These values are similar to the stiffness of the gating spring of vertebrate hair cells (1 mN m^{-1}) and the fly hair bristle receptor (3 mN m^{-1}). Furthermore, molecular dynamic simulations suggested that the 17 ankyrin repeats found in TRPA1 would have a stiffness of a few mN m^{-1}, and that large forces can pull apart the packed alpha helices to extend the protein nearly tenfold, possibly acting as a safety release for extreme stimuli (Sotomayor, M. *et al.*, 2005). In addition, an ankyrin spring is predicted to have a relaxation time constant in the nanosecond range. As such, Corey D. P. *et al.* (2004) suggested that the ankyrin repeats of TRPA1 may act as the biophysically defined gating spring. But here again the lack of a hair cell transduction phenotype and hearing or vestibular deficits in the TRPA1-deficient mice call this attractive suggestion into question.

3.16.9 Conclusions

The biophysical properties of hair cell mechanotransduction and adaptation are fairly well understood. A flurry of recent activity has led to a number of suggestions regarding the molecular identity of components of the hair cell mechanotransduction complex (Figure 9). Cadherin-23 and protocadherin-15, myosin-1c and/or myosin-7a, TRPA1 and TRPML3, TRPV4 may play integral roles in hair cell mechanotransduction and adaptation, but many uncertainties remain. The identity of other molecular components, including the adaptation extent spring, the negative

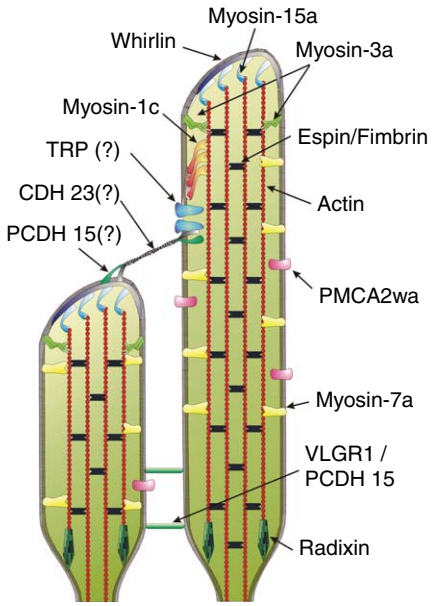

Figure 9 A schematic diagram showing known and hypothesized molecular components of the mechanosensory hair bundle.

limit and the fast adaptation mechanism, are still unknown. Other outstanding questions include: how are these components configured to render the fully functional mechanotransduction apparatus? By what molecular mechanism does conductance vary along the length of the cochlea? What role do second messengers or membrane phospholipids play in the transduction and adaptation processes? Does the transduction channel consist of heteromultimers of TRP or Deg/ENaC subunits? Do myosin-1c and myosin-7a, contribute to hair cell adaptation together or separately? Does the channel interact directly with myosin-1c or myosin-7a? Does the transduction apparatus contribute to active hair bundle movements that drive cochlear amplification?

Hair cell mechanotransduction and adaptation, like many biological processes, is probably more complex than first imagined. Even if the molecular components proposed thus far turn out not to be involved, the proposals themselves have accelerated the pace of research to either confirm or refute the hypotheses. Thus, the search continues for the channel and the rest of the components of this exquisite mechanosensitive system. As a final caveat, the transduction and adaptation model presented here will undoubtedly need to be modified as new discoveries clarify the true molecular and biophysical nature of hair cell transduction and adaptation. Stay tuned!

References

Ahmed, Z. M., Riazuddin, S., Bernstein, S. L., Ahmed, Z., Khan, S., Griffith, A. J., Morell, R. J., Friedman, T. B., and Wilcox, E. R. 2001. Mutations of the protocadherin gene PCDH15 cause Usher syndrome type 1F. Am. J. Hum. Genet. 69, 25–34.

Ahmed, Z. M., Riazuddin, S., Ahmad, J., Bernstein, S. L., Guo, Y., Sabar, M. F., Sieving, P., Griffith, A. J., Friedman, T. B., Belyantseva, I. A., and Wilcox, E. R. 2003. PCDH15 is expressed in the neurosensory epithelium of the eye and ear and mutant alleles are responsible for both USH1F and DFNB23. Hum. Mol. Genet. 12, 3215–3223.

Ahmed, Z. M., Goodyear, R., Riazuddin, S., Lagziel, A., Legan, P. K., Behra, M., Burgess, S. M., Lilley, K. S., Wilcox, E. R., Griffith, A. J., Frolenkov, G. I., Belyantseva, I. A., Richardson, G. P., and Friedman, T. B. 2006. The tip-link antigen, a protein associated with the transduction complex of sensory hair cells, is protocadherin-15. J. Neurosci. 26, 7022–7034.

Alagramam, K. N., Yuan, H., Kuehn, M. H., Murcia, C. L., Wayne, S., Srisailpathy, C. R., Lowry, R. B., Knaus, R., Van Laer, L., Bernier, F. P., Schwartz, S., Lee, C., Morton, C. C., Mullins, R. F., Ramesh, A., Van Camp, G., Hageman, G. S., Woychik, R. P., and Smith, R. J. 2001a. Mutations in the novel protocadherin PCDH15 cause Usher syndrome type 1F. Hum. Mol. Genet. 10, 1709–1718.

Alagramam, K. N., Yuan, H., Kuehn, M. H., Murcia, C. L., Wayne, S., Srisailpathy, C. R., Lowry, R. B., Knaus, R., Van Laer, L., Bernier, F. P., Schwartz, S., Lee, C., Morton, C. C., Mullins, R. F., Ramesh, A., Van Camp, G., Hageman, G. S., Woychik, R. P., and Smith, R. J. 2001b. Mutations in the novel protocadherin PCDH15 cause Usher syndrome type 1F. Hum. Mol. Genet. 10(22), 2603.

Alagramam, K. N., Stahl, J. S., Jones, S. M., Pawlowski, K. S., and Wright, C. G. 2005. Characterization of vestibular dysfunction in the mouse model for Usher syndrome 1F. J. Assoc. Res. Otolaryngol. 6(2): 106–118.

Assad, J. A. and Corey, D. P. 1992. An active motor model for adaptation by vertebrate hair cells. J. Neurosci. 12, 3291–3309.

Assad, J. A., Shepherd, G. M., and Corey, D. P. 1991. Tip-link integrity and mechanical transduction in vertebrate hair cells. Neuron 7, 985–994.

Bandell, M., Story, G. M., Hwang, S. W., Viswanath, V., Eid, S. R., Petrus, M. J., Earley, T. J., and Patapoutian, A. 2004. Noxious cold ion channel TRPA1 is activated by pungent compounds and bradykinin. Neuron 41, 849–857.

Bautista, D. M., Jordt, S. E., Nikai, T., Tsuruda, P. R., Read, A. J., Poblete, J., Yamoah, E. N., Basbaum, A. I., and Julius, D. 2006. TRPA1 mediates the inflammatory actions of environmental irritants and proalgesic agents.[see comment]. Cell 124, 1269–1282.

Belyantseva, I. A., Boger, E. T., and Friedman, T. B. 2003. Myosin XVa localizes to the tips of inner ear sensory cell stereocilia and is essential for staircase formation of the hair bundle. Proc. Natl. Acad. Sci. USA 100, 13958–13963.

Benser, M. E., Marquis, R. E., and Hudspeth, A. J. 1996. Rapid, active hair bundle movements in hair cells from the bullfrog's sacculus. J. Neurosci. 16, 5629–5643.

Ben-Yosef, T., Ness, S. L., Madeo, A. C., Bar-Lev, A., Wolfman, J. H., Ahmed, Z. M., Desnick, R. J., Willner, J. P., Avraham, K. B., Ostrer, H., Oddoux, C., Griffith, A. J., and Friedman, T. B. 2003. A mutation of PCDH15 among Ashkenazi Jews with the type 1 Usher syndrome. New England, J. Med. 348, 1664–1670.

Beurg, M., Evans, M. G., Hackney, C. M., and Fettiplace, R. 2006. A large-conductance calcium-selective

mechanotransducer channel in mammalian cochlear hair cells. J. Neurosci. 26, 10992–11000.
Boeda, B., El-Amraoui, A., Bahloul, A., Goodyear, R., Daviet, L., Blanchard, S., Perfettini, I., Fath, K. R., Shorte, S., Reiners, J., Houdusse, A., Legrain, P., Wolfrum, U., Richardson, G., and Petit, C. 2002. Myosin VIIa, harmonin and cadherin 23, three Usher I gene products that cooperate to shape the sensory hair cell bundle. EMBO J. 21, 6689–6699.
Bozovic, D. and Hudspeth, A. J. 2003. Hair-bundle movements elicited by transepithelial electrical stimulation of hair cells in the sacculus of the bullfrog. Proc. Natl. Acad. Sci. USA 100, 958–963.
Cheung, E. L. and Corey, D. P. 2006. Ca2+ changes the force sensitivity of the hair-cell transduction channel. Biophys., J. 90, 124–139.
Clapham, D. E. 2003. TRP channels as cellular sensors. Nature 426, 517–524.
Corey, D. P. 2006. What is the hair cell transduction channel? J. Physiol. 576, 23–28.
Corey, D. P. and Hudspeth, A. J. 1979. Response latency of vertebrate hair cells. Biophys. J. 26, 499–506.
Corey, D. P. and Hudspeth, A. J. 1983. Kinetics of the receptor current in bullfrog saccular hair cells. J. Neurosci. 3, 962–976.
Corey, D. P. and Sotomayor, M. 2004. Hearing: tightrope act [comment]. Nature 428, 901–903.
Corey, D. P., Garcia-Anoveros, J., Holt, J. R., Kwan, K. Y., Lin, S. Y., Vollrath, M. A., Amalfitano, A., Cheung, E. L., Derfler, B. H., Duggan, A., Geleoc, G. S., Gray, P. A., Hoffman, M. P., Rehm, H. L., Tamasauskas, D., and Zhang, D. S. 2004. TRPA1 is a candidate for the mechanosensitive transduction channel of vertebrate hair cells. Nature 432, 723–730.
Crawford, A. C., Evans, M. G., and Fettiplace, R. 1989. Activation and adaptation of transducer currents in turtle hair cells. J. Physiol. 419, 405–434.
Crawford, A. C., Evans, M. G., and Fettiplace, R. 1991. The actions of calcium on the mechano-electrical transducer current of turtle hair cells. J. Physiol. 434, 369–398.
Cyr, J. L., Dumont, R. A., and Gillespie, P. G. 2002. Myosin-1c interacts with hair-cell receptors through its calmodulin-binding IQ domains. J. Neurosci. 22, 2487–2495.
Denk, W., Holt, J. R., Shepherd, G. M., and Corey, D. P. 1995. Calcium imaging of single stereocilia in hair cells: localization of transduction channels at both ends of tip links. Neuron 15, 1311–1321.
Di Palma, F., Belyantseva, I. A., Kim, H. J., Vogt, T. F., Kachar, B., and Noben-Trauth, K. 2002. Mutations in Mcoln3 associated with deafness and pigmentation defects in varitint-waddler (Va) mice. Proc. Natl. Acad. Sci. U. S. A. 99, 14994–14999.
Eatock, R. A. 2000. Adaptation in hair cells. Ann. Rev. Neurosci. 23, 285–314.
Eatock, R. A., Corey, D. P., and Hudspeth, A. J. 1987. Adaptation of mechanoelectrical transduction in hair cells of the bullfrog's sacculus. J. Neurosci. 7, 2821–2836.
Etournay, R., El-Amraoui, A., Bahloul, A., Blanchard, S., Roux, I., Pezeron, G., Michalski, N., Daviet, L., Hardelin, J. P., Legrain, P., and Petit, C. 2005. PHR1, an integral membrane protein of the inner ear sensory cells, directly interacts with myosin 1c and myosin VIIa. J. Cell Sci. 118, 2891–2899.
Fawcett, D. W. 1981. The Cell, 2nd edn. W B Saunders.
Fettiplace, R. and Ricci, A. J. 2003. Adaptation in auditory hair cells. Current Opinion in Neurobiology 13, 446–451.
Frolenkov, G. I., Belyantseva, I. A., Friedman, T. B., and Griffith, A. J. 2004. Genetic insights into the morphogenesis of inner ear hair cells. Nat. Rev. Genet. 5, 489–498.
Furness, D. N. and Hackney, C. M. 2006. The Structure and Composition of the Stereociliary Bundle of Vertebrate Hair Cells. In: Vertebrate Hair Cells (*eds*. R. A. Eatock, R. R. Fay, and A. N. Popper), p. 105. Springer.
Garcia, J. A., Yee, A. G., Gillespie, P. G., and Corey, D. P. 1998. Localization of myosin-Ibeta near both ends of tip links in frog saccular hair cells. J. Neurosci. 18, 8637–8647.
Garcia-Anoveros, J., Samad, T. A., Zuvela-Jelaska, L., Woolf, C. J., and Corey, D. P. 2001. Transport and localization of the DEG/ENaC ion channel BNaC1alpha to peripheral mechanosensory terminals of dorsal root ganglia neurons. J. Neurosci. 21, 2678–2686.
Géléoc, G. S., Lennan, G. W., Richardson, G. P., and Kros, C. J. 1997. A quantitative comparison of mechanoelectrical transduction in vestibular and auditory hair cells of neonatal mice. Proc. R. Soc. Lond. B Biol. Sci. 264, 611–621.
Géléoc, G. S. and Holt, J. R. 2003a. Developmental acquisition of sensory transduction in hair cells of the mouse inner ear. Nat. Neurosci. 6, 1019–1020.
Gillespie, P. G. 2002. Myosin-VIIa and transduction channel tension [comment]. Nat. Neurosci. 5, 3–4.
Gillespie, P. G. and Cyr, J. L. 2004. Myosin-1c, the hair cell's adaptation motor. Annu. Rev. Physiol. 66, 521–545.
Gillespie, P. G. and Hudspeth, A. J. 1993. Adenine nucleoside diphosphates block adaptation of mechanoelectrical transduction in hair cells. Proc. Natl. Acad. Sci. USA 90, 2710–2714.
Gillespie, P. G. and Corey, D. P. 1997. Myosin and adaptation by hair cells. Neuron 19, 955–958.
Gillespie, P. G. and Walker, R. G. 2001. Molecular basis of mechanosensory transduction. Nature 413, 194–202.
Gillespie, P. G., Gillespie, S. K., Mercer, J. A., Shah, K., and Shokat, K. M. 1999. Engineering of the myosin-ibeta nucleotide-binding pocket to create selective sensitivity to N(6)-modified ADP analogs. J. Biol. Chem. 274, 31373–31381.
Goodyear, R. and Richardson, G. 1999a. The ankle-link antigen: an epitope sensitive to calcium chelation associated with the hair-cell surface and the calycal processes of photoreceptors. J. Neurosci. 19, 3761–3772.
Goodyear, R. and Richardson, G. 1999b. The ankle-link antigen: an epitope sensitive to calcium chelation associated with the hair-cell surface and the calycal processes of photoreceptors. J. Neurosci. 19(16), 7238–7239.
Goodyear, R. J. and Richardson, G. P. 2003. A novel antigen sensitive to calcium chelation that is associated with the tip links and kinocilial links of sensory hair bundles. J. Neurosci. 23, 4878–4887.
Hackney, C. M. and Furness, D. N. 1995. Mechanotransduction in vertebrate hair cells: structure and function of the stereociliary bundle. American J. Physiol. 268, C1–C13.
Hacohen, N., Assad, J. A., Smith, W. J., and Corey, D. P. 1989. Regulation of tension on hair-cell transduction channels: displacement and calcium dependence. J. Neurosci. 9, 3988–3997.
Hasson, T., Gillespie, P. G., Garcia, J. A., MacDonald, R. B., Zhao, Y., Yee, A. G., Mooseker, M. S., and Corey, D. P. 1997. Unconventional myosins in inner-ear sensory epithelia. J. Cell Biol. 137, 1287–1307.
He, D. Z., Jia, S., and Dallos, P. 2004. Mechanoelectrical transduction of adult outer hair cells studied in a gerbil hemicochlea. Nature 429, 766–770.
Hirono, M., Denis, C. S., Richardson, G. P., and Gillespie, P. G. 2004. Hair cells require phosphatidylinositol 4,5-bisphosphate for mechanical transduction and adaptation. Neuron 44, 309–320.
Holt, J. R. and Corey, D. P. 1999. Hair Cells: Sensory Transduction. In: Encyclopedia of Neuroscience, 2nd edn. (*eds*. G. Adelman and B. H. Smith), pp. 850–853. Elsevier.
Holt, J. R. and Corey, D. P. 2000. Two mechanisms for transducer adaptation in vertebrate hair cells. Proc. Natl. Acad. Sci. USA 97, 11730–11735.

Holt, J. R., Corey, D. P., and Eatock, R. A. 1997. Mechanoelectrical transduction and adaptation in hair cells of the mouse utricle, a low-frequency vestibular organ. J. Neurosci. 17, 8739–8748.

Holt, J. R., Gillespie, S. K., Provance, D. W., Shah, K., Shokat, K. M., Corey, D. P., Mercer, J. A., and Gillespie, P. G. 2002. A chemical-genetic strategy implicates myosin-1c in adaptation by hair cells. Cell 108, 371–381.

Howard, J. and Bechstedt, S. 2004. Hypothesis: a helix of ankyrin repeats of the NOMPC-TRP ion channel is the gating spring of mechanoreceptors. Curr. Biol. 14, R224–226.

Howard, J. and Hudspeth, A. J. 1987. Mechanical relaxation of the hair bundle mediates adaptation in mechanoelectrical transduction by the bullfrog's saccular hair cell. Proc. Natl. Acad. Sci. USA 84, 3064–3068.

Howard, J. and Hudspeth, A. J. 1988. Compliance of the hair bundle associated with gating of mechanoelectrical transduction channels in the bullfrog's saccular hair cell. Neuron 1, 189–199.

Huang, M. and Chalfie, M. 1994. Gene interactions affecting mechanosensory transduction in Caenorhabditis elegans.[see comment]. Nature 367, 467–470.

Hudspeth, A. J. 1983. The hair cells of the inner ear. They are exquisitely sensitive transducers that in human beings mediate the senses of hearing and balance. A tiny force applied to the top of the cell produces an electrical signal at the bottom. Sci. Am. 248, 54–64.

Hudspeth, A. J. 1989. How the ear's works work. Nature 341, 397–404.

Hudspeth, A. J. and Corey, D. P. 1977. Sensitivity, polarity, and conductance change in the response of vertebrate hair cells to controlled mechanical stimuli. Proc. Natl. Acad. Sci. USA 74, 2407–2411.

Inoue, A. and Ikebe, M. 2003. Characterization of the motor activity of mammalian myosin VIIA. J. Biol. Chem. 278, 5478–5487.

Jacobs, R. A. and Hudspeth, A. J. 1990. Ultrastructural correlates of mechanoelectrical transduction in hair cells of the bullfrog's internal ear. Cold. Spring Harb. Symp. Quant. Biol. 55, 547–561.

Jaramillo, F. and Hudspeth, A. J. 1991. Localization of the hair cell's transduction channels at the hair bundle's top by iontophoretic application of a channel blocker. Neuron 7, 409–420.

Jaramillo, F., Markin, V. S., and Hudspeth, A. J. 1993. Auditory illusions and the single hair cell. Nature 364, 527–529.

Jordt, S. E., Bautista, D. M., Chuang, H. H., McKemy, D. D., Zygmunt, P. M., Hogestatt, E. D., Meng, I. D., and Julius, D. 2004. Mustard oils and cannabinoids excite sensory nerve fibres through the TRP channel ANKTM1. Nature 427, 260–265.

Kachar, B., Parakkal, M., Kurc, M., Zhao, Y., and Gillespie, P. G. 2000. High-resolution structure of hair-cell tip links. Proc. Natl. Acad. Sci. USA 97, 13336–13341.

Kennedy, H. J., Crawford, A. C., and Fettiplace, R. 2005. Force generation by mammalian hair bundles supports a role in cochlear amplification.[see comment]. Nature 433, 880–883.

Kennedy, H. J., Evans, M. G., Crawford, A. C., and Fettiplace, R. 2003. Fast adaptation of mechanoelectrical transducer channels in mammalian cochlear hair cells. Nat. Neurosci. 6, 832–836.

Kim, J., Chung, Y. D., Park, D. Y., Choi, S., Shin, D. W., Soh, H., Lee, H. W., Son, W., Yim, J., Park, C. S., Kernan, M. J., and Kim, C. 2003. A TRPV family ion channel required for hearing in Drosophila.[see comment]. Nature 424, 81–84.

Kros, C. J., Marcotti, W., van Netten, S. M., Self, T. J., Libby, R. T., Brown, S. D., Richardson, G. P., and Steel, K. P. 2002. Reduced climbing and increased slipping adaptation in cochlear hair cells of mice with Myo7a mutations. Nat. Neurosci. 5, 41–47.

Kros, C. J., Rusch, A., and Richardson, G. P. 1992. Mechano-electrical transducer currents in hair cells of the cultured neonatal mouse cochlea. Proc. Biol. Sci. 249, 185–193.

Kwan, K. Y., Allchorne, A. J., Vollrath, M. A., Christensen, A. P., Zhang, D. S., Woolf, C. J., and Corey, D. P. 2006. TRPA1 contributes to cold, mechanical, and chemical nociception but is not essential for hair-cell transduction [see comment]. Neuron 50, 277–289.

Legan, P. K., Lukashkina, V. A., Goodyear, R. J., Kossi, M., Russell, I. J., and Richardson, G. P. 2000. A targeted deletion in alpha-tectorin reveals that the tectorial membrane is required for the gain and timing of cochlear feedback [see comment]. Neuron 28, 273–285.

Lagziel, A., Ahmed, Z. M., Schultz, J. M., Morell, R. J., Belyantseva, I. A., and Friedman, T. B. 2005. Spatiotemporal pattern and isoforms of cadherin 23 in wild type and waltzer mice during inner ear hair cell development. Dev. Biol. 280, 295–306.

LeMasurier, M. and Gillespie, P. G. 2005. Hair-cell mechanotransduction and cochlear amplification. Neuron 48, 403–415.

Macpherson, L. J., Geierstanger, B. H., Viswanath, V., Bandell, M., Eid, S. R., Hwang, S., and Patapoutian, A. 2005. The pungency of garlic: activation of TRPA1 and TRPV1 in response to allicin. Curr. Biol. 15, 929–934.

Main, E. R., Jackson, S. E., and Regan, L. 2003. The folding and design of repeat proteins: reaching a consensus. Curr. Opin. Struct. Biol. 13, 482–489.

Martin, P., Bozovic, D., Choe, Y., and Hudspeth, A. J. 2003. Spontaneous oscillation by hair bundles of the bullfrog's sacculus. J. Neurosci. 23, 4533–4548.

Martinac, B. 2001. Mechanosensitive channels in prokaryotes. Cell. Physiol. Biochem. 11, 61–76.

Michel, V., Goodyear, R. J., Weil, D., Marcotti, W., Perfettini, I., Wolfrum, U., Kros, C. J., Richardson, G. P., and Petit, C. 2005. Cadherin 23 is a component of the transient lateral links in the developing hair bundles of cochlear sensory cells. Dev. Biol. 280, 281–294.

Moran, M. M., Xu, H., and Clapham, D. E. 2004. TRP ion channels in the nervous system. Current Opin. Neurobiol. 14, 362–369.

Nagata, K., Duggan, A., Kumar, G., and Garcia-Anoveros, J. 2005. Nociceptor and hair cell transducer properties of TRPA1, a channel for pain and hearing. J. Neurosci. 25, 4052–4061.

O'Hagan, R., Chalfie, M., and Goodman, M. B. 2005. The MEC-4 DEG/ENaC channel of Caenorhabditis elegans touch receptor neurons transduces mechanical signals [see comment]. Nat. Neurosci. 8, 43–50.

Ohmori, H. 1988. Mechanical stimulation and Fura-2 fluorescence in the hair bundle of dissociated hair cells of the chick. J. Physiol. 399, 115–137.

Pickles, J. O. and Corey, D. P. 1992. Mechanoelectrical transduction by hair cells. Trends Neurosci. 15, 254–259.

Pickles, J. O., Comis, S. D., and Osborne, M. P. 1984. Cross-links between stereocilia in the guinea pig organ of Corti, and their possible relation to sensory transduction. Hear. Res. 15, 103–112.

Price, M. P., Lewin, G. R., McIlwrath, S. L., Cheng, C., Xie, J., Heppenstall, P. A., Stucky, C. L., Mannsfeldt, A. G., Brennan, T. J., Drummond, H. A., Qiao, J., Benson, C. J., Tarr, D. E., Hrstka, R. F., Yang, B., Williamson, R. A., and Welsh, M. J. 2000. The mammalian sodium channel BNC1 is required for normal touch sensation. Nature 407, 1007–1011.

Raucher, D., Stauffer, T., Chen, W., Shen, K., Guo, S., York, J. D., Sheetz, M. P., and Meyer, T. 2000. Phosphatidylinositol 4,5-bisphosphate functions as a second messenger that regulates cytoskeleton–plasma membrane adhesion. Cell 100, 221–228.

Ricci, A. J., Crawford, A. C., and Fettiplace, R. 2000. Active hair bundle motion linked to fast transducer adaptation in auditory hair cells. J. Neurosci. 20, 7131–7142.

Ricci, A. J., Crawford, A. C., and Fettiplace, R. 2003. Tonotopic variation in the conductance of the hair cell mechanotransducer channel. Neuron 40, 983–990.

Ricci, A. J., Wu, Y. C., and Fettiplace, R. 1998. The endogenous calcium buffer and the time course of transducer adaptation in auditory hair cells. J. Neurosci. 18, 8261–8277.

Ricci, A. J., Kennedy, H. J., Crawford, A. C., and Fettiplace, R. 2005. The transduction channel filter in auditory hair cells. J. Neurosci. 25, 7831–7839.

Russell, I. J. and Kossl, M. 1992. Sensory transduction and frequency selectivity in the basal turn of the guinea-pig cochlea. Philos. Trans. R. Soc. Lond. B Biol. Sci. 336, 317–324.

Russell, I. J. and Richardson, G. P. 1987. The morpology and physiology of hair cells in organotypic cultures of the mouse cochlea. Hear. Res. 31, 9–24.

Rzadzinska, A. K., Derr, A., Kachar, B., and Noben-Trauth, K. 2005. Sustained cadherin 23 expression in young and adult cochlea of normal and hearing-impaired mice. Hear. Res. 208, 114–121.

Rzadzinska, A. K., Schneider, M. E., Davies, C., Riordan, G. P., and Kachar, B. 2004. An actin molecular treadmill and myosins maintain stereocilia functional architecture and self-renewal. Journal of Cell Biol. 164, 887–897.

Schneider, M. E., Dose, A. C., Salles, F. T., Chang, W., Erickson, F. L., Burnside, B., and Kachar, B. 2006. A new compartment at stereocilia tips defined by spatial and temporal patterns of myosin IIIa expression. J. Neurosci. 26, 10243–10252.

Seiler, C., Finger-Baier, K. C., Rinner, O., Makhankov, Y. V., Schwarz, H., Neuhauss, S. C., and Nicolson, T. 2005. Duplicated genes with split functions: independent roles of protocadherin15 orthologues in zebrafish hearing and vision. Development 132, 615–623.

Senften, M., Schwander, M., Kazmierczak, P., Lillo, C., Shin, J. B., Hasson, T., Géléoc, G. S., Gillespie, P. G., Williams, D., Holt, J. R., and Muller, U. 2006. Physical and functional interaction between protocadherin 15 and myosin VIIa in mechanosensory hair cells. J. Neurosci. 26, 2060–2071.

Shepherd, G. M. and Corey, D. P. 1994. The extent of adaptation in bullfrog saccular hair cells. J. Neurosci. 14, 6217–6229.

Shepherd, G. M., Corey, D. P., and Block, S. M. 1990. Actin cores of hair-cell stereocilia support myosin motility. Proc. Natl. Acad. Sci. USA 87, 8627–8631.

Shotwell, S. L., Jacobs, R., and Hudspeth, A. J. 1981. Directional sensitivity of individual vertebrate hair cells to controlled deflection of their hair bundles. Ann. N. Y. Acad. Sci. 374, 1–10.

Sidi, S., Friedrich, R. W., and Nicolson, T. 2003. NompC TRP channel required for vertebrate sensory hair cell mechanotransduction. Science 301, 96–99.

Siemens, J., Lillo, C., Dumont, R. A., Reynolds, A., Williams, D. S., Gillespie, P. G., and Muller, U. 2004. Cadherin 23 is a component of the tip link in hair-cell stereocilia. Nature 428, 950–955.

Solc, C. K., Derfler, B. H., Duyk, G. M., and Corey, D. P. 1994. Molecular cloning of myosins from bullfrog saccular macula: a candidate for the hair cell adaptation motor. Aud. Neurosci. 1, 63–75.

Sollner, C., Rauch, G. J., Siemens, J., Geisler, R., Schuster, S. C., Muller, U., Nicolson, T., and Tubingen Screen, C. 2004. Mutations in cadherin 23 affect tip links in zebrafish sensory hair cells. Nature 428, 955–959.

Sotomayor, M., Corey, D. P., and Schulten, K. 2005. In search of the hair-cell gating spring elastic properties of ankyrin and cadherin repeats. Structure 13, 669–682.

Stauffer, E. A., Scarborough, J. D., Hirono, M., Miller, E. D., Shah, K., Mercer, J. A., Holt, J. R., and Gillespie, P. G. 2005. Fast adaptation in vestibular hair cells requires Myosin-1c activity. Neuron 47, 541–553.

Stepanyan, R., Belyantseva, I. A., Griffith, A. J., Friedman, T. B., and Frolenkov, G. I. 2006. Auditory mechanotransduction in the absence of functional myosin-XVa. J. Physiol. 576, 801–808.

Story, G. M., Peier, A. M., Reeve, A. J., Eid, S. R., Mosbacher, J., Hricik, T. R., Earley, T. J., Hergarden, A. C., Andersson, D. A., Hwang, S. W., McIntyre, P., Jegla, T., Bevan, S., and Patapoutian, A. 2003. ANKTM1, a TRP-like channel expressed in nociceptive neurons, is activated by cold temperatures. Cell 112, 819–829.

Torre, V., Ashmore, J. F., Lamb, T. D., and Menini, A. 1995. Transduction and adaptation in sensory receptor cells. J. Neurosci. 15, 7757–7768.

Vollrath, M. A. and Eatock, R. A. 2003. Time course and extent of mechanotransducer adaptation in mouse utricular hair cells: comparison with frog saccular hair cells. J. Neurophysiol. 90, 2676–2689.

Walker, R. G., Willingham, A. T., and Zuker, C. S. 2000. A Drosophila mechanosensory transduction channel. Science 287, 2229–2234.

Wheelock, M. J. and Johnson, K. R. 2003. Cadherins as modulators of cellular phenotype. Annual Review of Cell & Dev. Biol. 19, 207–235.

Wu, Y. C., Ricci, A. J., and Fettiplace, R. 1999. Two components of transducer adaptation in auditory hair cells. J. Neurophysiol. 82, 2171–2181.

Xu, S., Wang, Y., Zhao, H., Zhang, L., Xiong, W., Yau, K. W., Hiel, H., Glowatzki, E., Ryugo, D. K., and Valle, D. 2004. PHR1, a PH domain-containing protein expressed in primary sensory neurons. Mol. Cell. Biol. 24, 9137–9151.

Yamoah, E. N. and Gillespie, P. G. 1996. Phosphate analogs block adaptation in hair cells by inhibiting adaptation-motor force production. Neuron 17, 523–533.

Zhao, Y., Yamoah, E. N., and Gillespie, P. G. 1996. Regeneration of broken tip links and restoration of mechanical transduction in hair cells. Proc. Natl. Acad. Sci. USA 93, 15469–15474.

Zou, Y., Zheng, J., Ren, T., and Nuttall, A. 2006. Cochlear transducer operating point adaptation. J. Acoust. Soc. Am. 119, 2232–2241.

3.17 Amplification and Feedback in Invertebrates

M C Göpfert, University of Cologne, Cologne, Germany

© 2008 Elsevier Inc. All rights reserved.

3.17.1	Introduction	293
3.17.2	Evidence for Mechanical Feedback Amplification in Insect Auditory Systems	293
3.17.2.1	Essential Characteristics of Mechanical Feedback Amplification	293
3.17.2.2	Signatures of Mechanical Feedback Amplification in Insect Ears	294
3.17.3	Cellular and Molecular Basis of Mechanical Feedback Amplification in Invertebrates	295
3.17.3.1	Genetic Dissection of Mechanical Feedback Amplification	295
3.17.3.2	Candidate Sensors and Motors of the Feedback Loop	296
3.17.4	Parallel Evolution of Mechanical Feedback Amplification in Vertebrates and Invertebrates	297
3.17.5	Mechanical Feedback Amplification in Other Invertebrate Mechanosensory Systems?	298
References		298

3.17.1 Introduction

Sensitive hearing, as known from vertebrates, also occurs in certain invertebrates: many insects are endowed with exquisitely sensitive ears (see Chapter Insect Ears). The auditory systems of vertebrates and insects have evolved independently, display different anatomies, and house different types of mechanosensory cells: insect hearing relies on stretch-sensitive chordotonal sensory neurons that bear a true sensory cilium but lack the actin-based stereociliar hair bundle characteristic of vertebrate hair cells (see Chapter Biophysics of Chordotonal Organs). Notwithstanding this anatomical difference, it now appears that insect chordotonal neurons and vertebrate hair cells improve the sensitivity of hearing in equivalent ways: like hair cells, chordotonal neurons seem to generate forces to actively boost the mechanical sensitivity and frequency selectivity of the ear. This mechanical feedback amplification, its manifestations in the auditory mechanics, its cellular and molecular basis, and its evolution are the topic of this chapter, which reviews our current knowledge about the mechanical feedback processes in invertebrate ears.

3.17.2 Evidence for Mechanical Feedback Amplification in Insect Auditory Systems

3.17.2.1 Essential Characteristics of Mechanical Feedback Amplification

Feedback implies that the output signal, or some function thereof, is passed back to the input and modifies it. In hearing, the input signal is the mechanical vibration sound induces in the ear. This vibration, in turn, can trigger a mechanical output signal, which, in vertebrate auditory system, is an active, motile response of mechanosensory cells. Provided this motile response is constructively coupled back into the sound-induced vibration, it will amplify this vibration and, accordingly, augment the mechanical input of the ear. Mechanical feedback amplification introduces novel characteristics in the mechanics of the systems. In vertebrate auditory systems, these characteristics include (1) a compressive nonlinearity that condenses a wide range of sound intensities into a narrow range of responses by specifically boosting the mechanical sensitivity to low intensity sounds; (2) frequency-dependent amplification, whereby vibrations at certain frequencies are selectively enhanced; (3) power gain, reflecting the increase in the mechanical energy due to active energy contributions; and (4) self-sustained oscillations and their acoustic equivalent, spontaneous otoacoustic emissions, which may result from excessive feedback exerted by mechanosensory cells inside the ear (Dallos, P. *et al.*, 1996; Hudspeth, A. J., 1997; Manley, G. A., 2001; Robles, L. and Ruggero, M. A., 2001; Chan, D. K. and Hudspeth, A. J., 2005, see also Chapter Otoacoustic Emissions). Because all these characteristics are essentially linked to feedback amplification (Kruse, K. and Jülicher, F., 2005), they can be used to probe the existence of comparable feedback processes in other mechanosensory systems such as insect ears.

3.17.2.2 Signatures of Mechanical Feedback Amplification in Insect Ears

All the four essential characteristics of the amplificatory feedback that have been identified in vertebrate auditory systems have also been documented for insect ears. In the antennal hearing organ of the fruit fly *Drosophila melanogaster*, for example, nonlinear compression is observed when the vibrations of the sound receiver formed by the distal part of the antenna (Figure 1(a)) are measured in response to pure tones of different intensity. As long as the tone intensity is either very high or very low, the mechanical sensitivity of the receiver scales linearly with the loudness of the tone (Figure 1(b)). For intermediate intensities, however, a nonlinear relation is found: the sensitivity of the receiver increases as the stimulus intensity declines, leading to a *c.* tenfold gain in sensitivity for low-intensity sounds (Figure 1(b)). This compressive nonlinearity, which is reminiscent of that reported for actively oscillating hair bundles of frog hair cells (Martin, P. and Hudspeth, A. J., 2001), is only observed if the frequency of the tone approximates the best frequency of the receiver (*c.* 200 Hz, Figure 1(b)). If the stimulus frequency is much higher (600 Hz or more), the mechanical sensitivity of the receiver remains constantly low throughout the entire intensity range (Göpfert, M. C. *et al.*, 2006). Hence, nonlinear amplification in insects is frequency-specific, analogous to the frequency-dependent amplification in vertebrate hearing (Martin, P. and Hudspeth, A. J., 2001; Robles, L. and Ruggero, M. A., 2001).

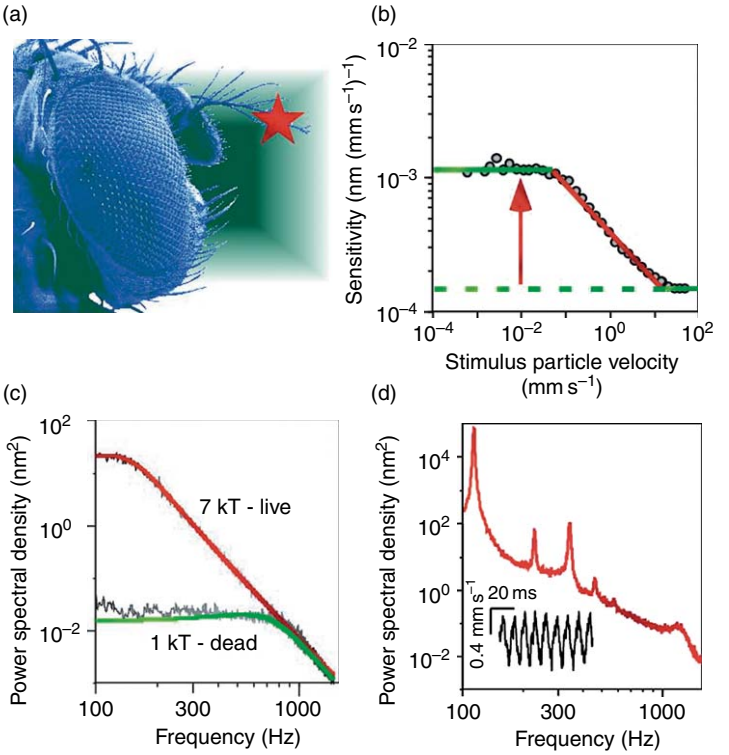

Figure 1 Signatures of feedback amplification in the mechanics of the *Drosophila* ear. (a) Lateral view of the *Drosophila* head depicting the measurement site (red star) on the antennal receiver from which the measurements in (b)–(d) were obtained. (b) Nonlinear amplification revealed by stimulating the receiver near its best frequency with pure tones of different intensities. Intensity is measured as particle velocity, and the mechanical sensitivity is expressed as the ratio between the phase-locked displacement of the receiver and the stimulus particle velocity. Green lines depict linear regimes, red lines nonlinear regimes, and the arrow indicates the gain in sensitivity due to nonlinear amplification. (c) Power gain. Power spectra of the mechanical fluctuations of a receiver (black traces) measured *in vivo* and postmortem and corresponding harmonic oscillator models (red and green lines). *In vivo*, the mean total energy of the fluctuations is lifted from 1 kT (thermal energy) to 7 kT, demonstrating that energy is injected into the system (for a detailed description, see Göpfert, M. C. *et al.*, 2005). (d) Self-sustained oscillations. Power spectrum and time trace (inset) of the displacement of a receiver oscillating spontaneously in the absence of external stimulation.

Nonlinear, frequency-specific amplification, as described here for the fly's auditory system, has also been documented for the antennal hearing organs of mosquitoes (Göpfert, M. C. and Robert, D., 2001) and seems also present in the tympanal ears of locusts (Kössl, M. and Boyan, G. S., 1998a; 1998b) and moths (Coro, F. and Kössl, M., 1998; 2001). In *Drosophila*, this amplification was shown to associate with power gain: mechanical measurements on live, dead, and mutant flies revealed that the receiver fluctuations in intact live flies exceed thermal noise (Göpfert, M. C. *et al.*, 2005); the mechanical energy of the fluctuations was found to amount to *c.* six times the thermal energy (Figure 1(c)), demonstrating that the fly expends biological energy to actively improve the mechanical sensitivity of its ear. Also the fourth characteristic of mechanical feedback amplification, self-sustained oscillations, has been documented for invertebrate ears: the antennal sound receivers of mosquitoes and *Drosophila* occasionally oscillate spontaneously with large amplitudes in the absence of acoustic stimulation (Göpfert, M. C. and Robert, D., 2001; 2003) (Figure 1(d)). These self-sustained oscillations, which cannot be explained by the activity of muscles, reliably occur when the physiological condition of the animal deteriorates, for example, after heat application to the thorax or after thoracic injection of ethanol of dimethylsulfoxide (DMSO). As described in the next section, self-sustained oscillations in the *Drosophila* auditory system can also result from genetic defects.

3.17.3 Cellular and Molecular Basis of Mechanical Feedback Amplification in Invertebrates

3.17.3.1 Genetic Dissection of Mechanical Feedback Amplification

The signatures of feedback amplification observed in the mechanics of insect auditory system suggest that insect chordotonal neurons, like vertebrate hair cells, are motile and exert feedback on the mechanics of the ear. Active movements of insect chordotonal neurons have hitherto not been directly observed, yet the motility of these cells has been inferred from the effects of genetic mutations on the mechanics of the ear (Göpfert, M. C. and Robert, D., 2003; Göpfert, M. C. *et al.*, 2005). In *Drosophila*, the signatures of feedback amplification observed in the mechanics of the antennal receiver are reportedly abolished by mutations in *no mechanoreceptor potential A* (*nompA*), *touch insensitive larva B* (*tilB*), and *beethoven* (*btv*) (Figure 2). All these mutations affect the chordotonal neurons in the antenna's base. *nompA*, for example, encodes a tectorin-related extracellular linker protein that connects the neurons to the antennal receiver (Chung, Y. D. *et al.*, 2001). Mutations in *nompA* disrupt this connection, separating the neurons from the receiver. Because this anatomical transection makes the receiver's mechanics linear and passive, it appears that the receiver is usually driven by the chordotonal neurons that connect to its base. Force generation by chordotonal neurons is supported by the elimination of the receiver's nonlinearity, self-sustained oscillations, and power gain by mutations in *tilB* and *btv*: these mutations specifically affect the structural and functional integrity of cilia, including the sensory cilia of the chordotonal neurons in the ear (Eberl, D. F. *et al.*, 2000). Also the transient receptor potential (TRP) channel (see Chapter Hair Cell Transduction and Adaptation: Physiology and Molecular Mechanisms) *NompC* (also known as *TRPN1*) is required for mechanical feedback amplification in the *Drosophila* ear: genetic disruption of this channel virtually abolishes

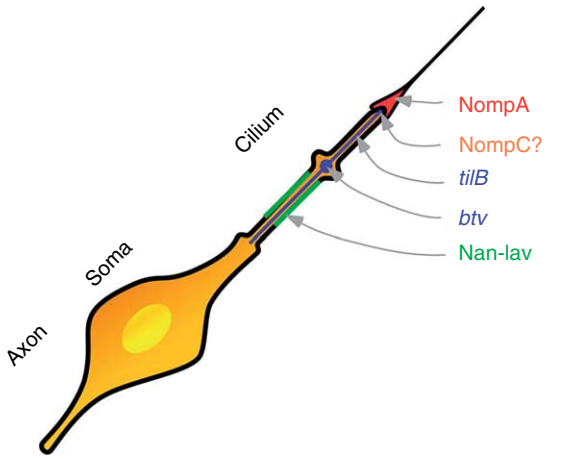

Figure 2 Molecular components involved in the mechanical feedback in the *Drosophila* ear. In the fly, feedback amplification is reportedly affected by mutations in *nompA*, *nompC*, *tilB*, *btv*, *nan*, and *iav*. *NompA* localizes to the extracellular cap that connects the auditory sensory neurons to the antennal receiver (Chung, Y. D. *et al.*, 2001). The NompC (=TRPN1) channel, though not definitely localized yet, may be a component of the ciliary tip. Mutations in *tilB* affect the structure of the ciliary axoneme, whereas mutations in *btv* cause structural defects of the ciliary dilation, a swelling in the distal region of the cilium (Eberl, D. F. *et al.*, 2000). In the region of the cilium proximal to the ciliary dilation, the Nan-Iav TRP channels are found (Kim, J. *et al.*, 2003; Gong, Z. *et al.*, 2004).

nonlinear amplification, and only some subtle nonlinearity seems to remain (Göpfert, M. C. and Robert, D., 2003; Göpfert, M. C. *et al.*, 2006). Interestingly, the opposite effect results from the disruption of another, presumably heteromultimeric TRP channel formed by the interdependent TRPV channel proteins Nanchung (Nan) and Inactive (Iav) (Kim, J. *et al.*, 2003; Gong, Z. *et al.*, 2004): mutations in the genes encoding for this channel facilitate amplification and induce self-sustained oscillations in the ear (Göpfert, M. C. *et al.*, 2006). Hence, while NompC is required for amplification, Nan-Iav seems required for adjusting the amplificatory gain. As shown by the examination of double mutants, this gain control requires NompC function, suggesting that NompC channel acts upstream of Nan-Iav. This functional placement accords with the presumptive anatomical placement of the two channels, for Nan-Iav localizes to the proximal region of the sensory cilia (Kim, J. *et al.*, 2003; Gong, Z. *et al.*, 2004), whereas – at least in frog hair cells – NompC localizes to ciliary tips (Shin, J. B. *et al.*, 2005) (Figure 2).

3.17.3.2 Candidate Sensors and Motors of the Feedback Loop

While the examination of *Drosophila* mutants has provided insights into the cellular basis of active amplification in invertebrate auditory systems (Figure 3), the identities of the sensor and motor elements that promote the feedback have remained unclear. Because all of the mutations mentioned above seem to affect both transduction and amplification, it seems plausible to assume that the sensor elements that sample the input signal in the course of the feedback are those ion channels that mediate

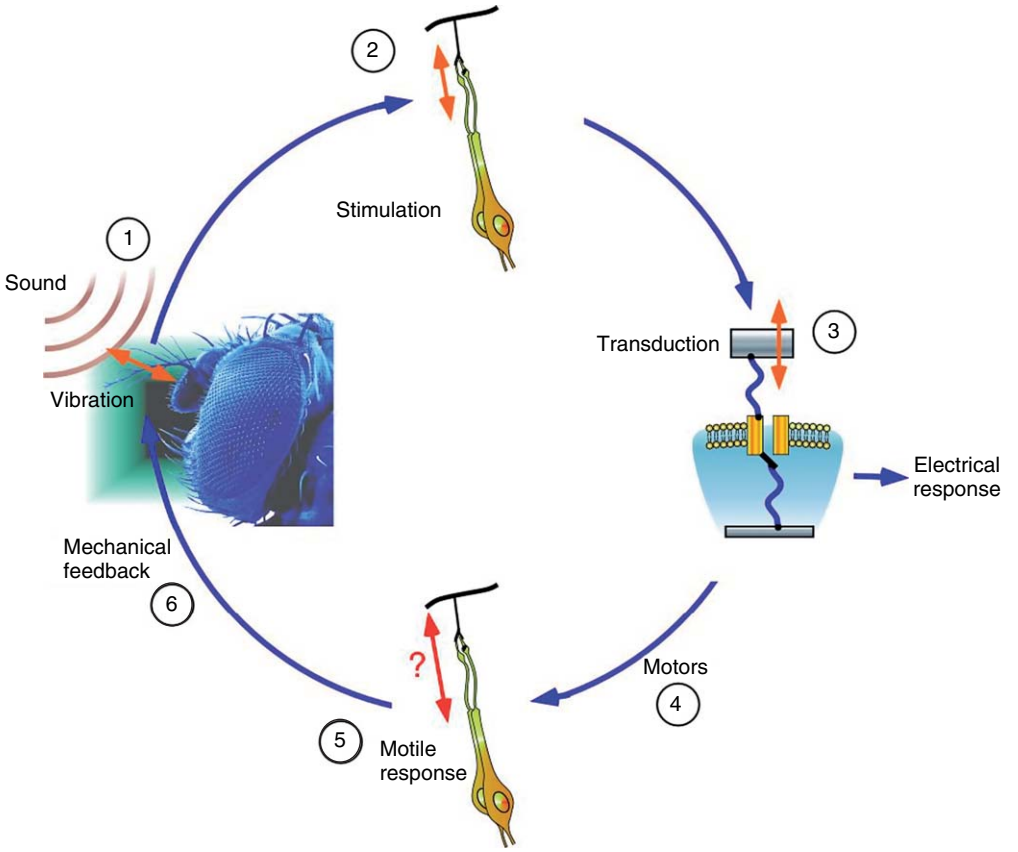

Figure 3 Simple scheme of the amplificatory feedback in *Drosophila* hearing. Sound-induced vibrations of the fly's antennal sound receiver (1) are directly coupled to the auditory neurons (2) and the mechanotransducer channels these neurons comprise (3). The resulting opening of channels leads to an electrical response and, in addition, triggers the activity of motors (4), leading to active mechanical responses of the cells. (5) This mechanical activity is coupled back into the receiver's vibrations (6), resulting in a mechanical feedback that amplifies the receiver's mechanical response to sound.

transduction in the *Drosophila* ear (Figure 3). Channels that have been proposed as candidate transducer in the fly's auditory system are the TRPs Nan-Iav and NompC (Eberl, D. F. *et al.*, 2000; Walker, R. G. *et al.*, 2000; Kim, J. *et al.*, 2003; Gong, Z. *et al.*, 2004). Of these two channels, NompC seems the better candidate, given its requirement for feedback amplification and its apparent functional and anatomical placement upstream of Nan-Iav. Disrupting the NompC channel, however, does not fully eliminate sound-induced electrical responses of the fly's auditory neurons (Eberl, D. F. *et al.*, 2000). Hence, NompC may participate in auditory transduction, but seems unlikely to be the only transducer in the *Drosophila* ear.

Also for the motor elements that exert the feedback in insect auditory systems (Figure 3), several candidates exist. Because chordotonal neurons are ciliated cells, it may well be that amplification involves active, kinesin- or dynein-driven movements of sensory cilia, in analogy to the cilium-based motility of sperm. This possibility is supported by the effects of mutations in *Drosophila tilB*, which abolish ciliary dynein arms, eliminate the amplificatory feedback, and lead to the immobility of sperm (Eberl, D. F. *et al.*, 2000; Göpfert, M. C. and Robert, D., 2003; Todi, S. V. *et al.*, 2004). Whether *tilB* codes for a dynein motor or an associated protein has not yet been determined. A second possibility is that force-generation by chordotonal neurons involves homologues of the mammalian outer hair cell motor protein prestin (see Chapter Prestin); prestin-related proteins are reportedly expressed in the antennal hearing organs of *Drosophila* and mosquitoes (Weber, T. *et al.*, 2003), yet whether these insect proteins serve as motors remains to be seen: a null allele of the *Drosophila* prestin gene has been generated, and its effects on the mechanical feedback amplification are currently being examined (Fritz, J. *et al.*, personal communication). Analogous to the hair bundle motility of hair cells, feedback amplification in invertebrate auditory systems may also rely on the interplay between the auditory transducer channels and associated adaptation motors (see Chapter Hair Cell Transduction and Adaptation: Physiology and Molecular Mechanisms). Adaptation characteristics as known from vertebrate hair cells have been documented for NompC-dependent currents in *Drosophila* sensory bristles, suggesting that insect mechanotransducer channels can associate with adaptation motors as well. Moreover, the fly's genome sequence comprises two close relatives of the hair cell adaptation motor myosin1c, which may contribute to active amplification. Whether dyneins, prestin homologs, or myosin1c relatives are the motors that promote active amplification in insect hearing cannot be answered yet. Given the list of candidates, however, it seems well possible that the motor mechanisms insects employ for amplification turn out to be similar to those found in vertebrate ears.

3.17.4 Parallel Evolution of Mechanical Feedback Amplification in Vertebrates and Invertebrates

The finding that mechanical feedback amplification, one of the presumably most elaborate aspects of vertebrate hearing, also occurs in certain invertebrates seems surprising as insects and vertebrates are only distantly related and independently evolved their ears (see Chapters Phylogeny and Evolution of Ciliated Mechano-Receptor Cells and Insect Ears). Accordingly, it seems most likely that the use of mechanical feedback has been independently invented within vertebrates and insects to improve the sensitivity of their ears. Such parallel evolution does not exclude the possibility that some of the molecular modules both groups employ for generating the feedback are evolutionarily conserved. Although the ears of insects and vertebrates have formed independently, evidence is accumulating that the mechanosensory cells that mediate hearing in these taxa have been derived from a common ancestral cell: insect chordotonal neurons and vertebrate hair cells are developmentally specified by homologous genes (Hassan, B. A. and Bellen, H. J., 2000) and share a variety of conserved molecular modules for mechanosensory cell formation and function (Fritzsch, B. and Beisel, K. W., 2004; Boekhoff-Falk, G., 2005, see Chapter Phylogeny and Evolution of Ciliated Mechano-Receptor Cells). Chordotonal neurons, for example, seem to express close relatives of motors implicated in amplification by hair cells and, conversely, hair cells express close relatives of channels chordotonal neurons need for amplification (see Chapter Hair Cell Transduction and Adaptation: Physiology and Molecular Mechanisms). Future research will show whether insects and vertebrates went back to the same conserved modules when independently implementing mechanical feedback into their ears.

3.17.5 Mechanical Feedback Amplification in Other Invertebrate Mechanosensory Systems?

One aspect that has hitherto not been addressed is whether the use of mechanical feedback amplification within invertebrates is unique to insect hearing, or whether other types of invertebrate mechanosensors employ the same trick. Invertebrates display an almost bewildering diversity of mechanosensory organs, including simple single-celled stretch receptors that, like chordotonal neurons and nonmammalian hair cells, express the NompC channel (Li, W. *et al*., 2006), and hair cell-based sensors such as the prey detectors of sea anemones and the balance organs of jellyfish, snails, mussels, and squids (Budelmann, B. U., 1988; Thurm, U. *et al*., 1997; Watson, G. M. *et al*., 1997). Testing for signatures of mechanical feedback amplification in these invertebrate systems may well hold some surprises, much as it still does in insect and vertebrate ears.

Acknowledgments

I would like to thank Jörg Albert and Björn Nadrowski for valuable comments and suggestions and the Volkswagen-Foundation for its support.

References

Boekhoff-Falk, G. 2005. Hearing in *Drosophila*: development of Johnston's organ and emerging parallels to vertebrate ear development. Dev. Dyn. 232, 550–558.

Budelmann, B. U. 1988. Morphological Diversity of Equilibrium Receptor Systems in Aquatic Invertebrates. In: Sensory Biology of Aquatic Animals (*eds*. J. Atema, R. R. Fay, A. N. Popper, and W. N. Tavolga), pp. 757–782. Springer.

Chan, D. K. and Hudspeth, A. J. 2005. Ca^{2+} current-driven nonlinear amplification *in vitro*. Nat. Neurosci. 8, 149–155.

Chung, Y. D., Zhu, J., Han, Y. G., and Kernan, M. J. 2001. *nompA* encodes a PNS-specific, ZP domain protein required to connect mechanosensory dendrites to sensory structures. Neuron 29, 415–428.

Coro, F. and Kössl, M. 1998. Distortion-product otoacoustic emissions from the tympanic organ in two noctuid moths. J. Comp. Physiol. A 183, 525–531.

Coro, F. and Kössl, M. 2001. Components of the 2f1-f2 distortion-product otoacoustic emission in a moth. Hear. Res. 162, 126–133.

Dallos, P., Popper, A. N., and Fay, R. R. 1996. The Cochlea. Springer Handbook of Auditory Research, Vol. 8. Springer.

Eberl, D. F., Hardy, R. W., and Kernan, M. J. 2000. Genetically similar transduction mechanisms for touch and hearing in *Drosophila*. J. Neurosci. 20, 5981–5988.

Fritzsch, B. and Beisel, K. W. 2004. Keeping sensory cells and evolving neurons to connect them to the brain: molecular conservation and novelties in vertebrate ear development. Brain Behav. Evol. 64, 182–197.

Gong, Z., Son, W., Chung, Y. D., Kim, J., Shin, D. W., McClung, C. A., Lee, Y., Lee, H., Chang, D. J., Kaang, B. K., Cho, H., Oh, U., Hirsh, J., Kernan, M. J., and Kim, C. 2004. Two interdependent TRPV channel subunits, Inactive and Nanchung, mediate hearing in *Drosophila*. J. Neurosci. 41, 9059–9066.

Göpfert, M. C. and Robert, D. 2001. Active auditory mechanics in mosquitoes. Proc. R. Soc. Lond. B 268, 333–339.

Göpfert, M. C. and Robert, D. 2003. Motion generation by *Drosophila* mechanosensory neurons. Proc. Natl. Acad. Sci. U. S. A. 100, 5514–5519.

Göpfert, M. C., Humphris, A. D. L., Albert, J. T., Robert, D., and Hendrich, O. 2005. Power gain exhibited by motile mechanosensory neurons in *Drosophila* ears. Proc. Natl. Acad. Sci. U. S. A. 102, 325–330.

Göpfert, M. C., Albert, J. T., Nadrowksi, B., and Kamikouchi, A. 2006. Specification of auditory sensitivity by *Drosophila* TRP channels. Nat. Neurosci. 9, 999–1000.

Hassan, B. A. and Bellen, H. J. 2000. Doing the MATH: is the mouse a good model for fly development? Genes Dev. 14, 1852–1865.

Hudspeth, A. J. 1997. Mechanical amplification by hair cells. Curr. Opin. Neurobiol. 7, 480–486.

Kim, J., Chung, Y. D., Park, D. Y., Choi, S., Shin, D. W., Soh, H., Lee, H. W., Son, W., Yim, J., Park, C. S., Kernan, M. J., and Kim, C. 2003. A TRPV family ion channel required for hearing in *Drosophila*. Nature 424, 81–84.

Kössl, M. and Boyan, G. S. 1998a. Acoustic distortion products from the ear of a grasshopper. J. Acoust. Soc. Am. 104, 326–335.

Kössl, M. and Boyan, G. S. 1998b. Otoacoustic emissions from a nonvertebrate ear. Naturwissenschaften 85, 124–127.

Kruse, K. and Jülicher, F. 2005. Oscillations in Cell Biology. Curr. Opin. Cell Biol. 17, 20–26.

Li, W., Feng, Z., Sternberg, P. W., and Xu, X. Z. 2006. A *C. elegans* stretch receptor neuron revealed by a mechanosensitive TRP channel homologue. Nature 440, 684–687.

Manley, G. A. 2001. Evidence for an active process and a cochlear amplifier in nonmammals. J. Neurophysiol. 86, 541–549.

Martin, P. and Hudspeth, A. J. 2001. Compressive nonlinearity in the hair bundle's active response to mechanical stimulation. Proc. Natl. Acad. Sci. U. S. A. 98, 14386–14391.

Robles, L. and Ruggero, M. A. 2001. Mechanics of the mammalian cochlea. Physiol. Rev. 81, 1305–1352.

Shin, J. B., Adams, D., Paukert, M., Siba, M., Sidi, S., Levin, M., Gillespie, P. G., and Grunder, S. 2005. *Xenopus* TRPN1 (NOMPC) localizes to microtubule-based cilia in epithelial cells, including inner-ear hair cells. Proc. Natl. Acad. Sci. U. S. A. 102, 12572–12577.

Thurm, U., Brinkmann, M., Golz, R., Lawonn, P., and Oliver, D. 1997. Studies of Mechanoelectric Transduction in Concentric Hair Bundles of Invertebrates. In: Diversity in Auditory Mechanics (*eds*. E. R. Lewis, G. R. Long, R. F. Lyon, P. M. Narins, C. R. Steele, and E. Hecht-Poinar), pp. 119–126. World Scientific.

Todi, S. V., Sharma, Y., and Eberl, D. F. 2004. Anatomical and molecular design of the Drosophila antenna as a flagellar auditory organ. Microsc. Res. Tech. 63, 388–399.

Walker, R. G., Willingham, A. T., and Zuker, C. S. 2000. A *Drosophila* mechanosensory transduction channel. Science 287, 2229–2234.

Watson, G. M., Mire, P., and Hudson, R. R. 1997. Hair bundles of sea anemones as a model system for vertebrate hair bundles. Hear. Res. 107, 53–66.

Weber, T., Gopfert, M. C., Winter, H., Zimmermann, U., Kohler, H., Meier, A., Hendrich, O., Rohbock, K., Robert, D., and Knipper, M. 2003. Expression of prestin-homologous solute carrier (SLC26) in auditory organs of nonmammalian vertebrates and insects. Proc. Natl. Acad. Sci. U. S. A. 100, 7690–7695.

Relevant Websites

http://scienceweek.com/2003/scc031107-1.htm ScienceWeek article on mechanosensory transduction

http://www.hearingcenteronline.com – Oregon Hearing Research Center Online on Drosophila hearing

http://www.polytec.com/usa/_files/LM_AN_INFO_0105_E_Hearing_Insects.pdf Polytec article about active feedback in the *Drosophila* ear

http://physicsweb.org/articles/world/15/5/8 PhysicsWeb article on the power of hearing by Tom Duke

http://www.uni-koeln.de/math-nat-fak/zoologie/tierphysiologie/goepfert/index.htm Group of Martin Gopfert at the University of Cologne

http://www.bio.bris.ac.uk/people/staff.cfm?key=726 Group of Daniel Robert at the University of Bristol

http://www.bio.uni-frankfurt.de/zoologie/nb/ Groups of Manfred Koessl and Ernst-August Seyfarth at the University of Frankfurt

http://www.biology.uiowa.edu/facultypage.php?ID=164 Group of Daniel Eberl at the University of Iowa

http://www.hsc.stonybrook.edu/som/neurobiology/kernan.cfm Group of Maurice Kernan at the State University of New York

http://www.ohsu.edu/ohrc/staff/walker/walker.html Group of Richard Walker at the Oregon Hearing Research Center

3.18 Tinnitus

J B Snow Jr., University of Pennsylvania, Philadelphia, PA, USA

© 2008 Elsevier Inc. All rights reserved.

3.18.1	**Definition of Tinnitus**	303
3.18.2	**Clinical Overview**	303
3.18.3	**Associated Decreased Sound Tolerance**	303
3.18.4	**Epidemiology of Tinnitus**	304
3.18.5	**Animal Models of Tinnitus**	305
3.18.6	**Neurophysiologic Model of Tinnitus**	305
3.18.7	**Theoretical Mechanisms of and Sites Associated with the Percept of Tinnitus**	305
3.18.7.1	Peripheral Processes Involved in Tinnitus	305
3.18.7.2	Otoacoustic Emissions	306
3.18.7.3	Neural Correlates of Tinnitus	306
3.18.7.4	Cortical Plasticity	306
3.18.7.5	Somatosensory Nuclei in Tinnitus	306
3.18.8	**Evaluation of the Individual with Tinnitus**	306
3.18.9	**Treatment of the Individual with Tinnitus**	307
References		307

Glossary

air conduction of sound Transmission of sound to the inner ear through the external auditory canal and middle ear.

anechoic chamber A room designed to absorb all sound to eliminate echo, used in auditory research.

audiometrically Performed with the use of an audiometer.

bone conduction of sound Transmission of sound to the inner ear through the bones of the skull.

characteristic frequency The frequency at which a neuron responds to the least intensity of sound.

cholinergic system The source of cholinergic agents (nucleus basilis) and the neurons that respond to them.

cochlear nucleus Brainstem center of the auditory pathway receiving input from the auditory nerve and providing the major output to the lateral lemniscus.

conditioned suppression Cessation or reduction of a learned response when the conditioned or warning stimulus is presented.

conductive hearing impairment or loss Hearing impairment or loss due to a lesion in the external auditory canal or middle ear.

decibel A unit of sound on a logarithmic scale used to measure hearing and sound; one-tenth of a bel, named after Scottish-American scientist, Alexander Graham Bell, 1847–1922.

dorsal cochlear nucleus The dorsal portion of the cochlear nucleus.

edge effect A contrast between two adjacent qualities.

effusion in the middle ear Fluid in the middle ear associated with otitis media.

external nucleus of the inferior colliculus Neuronal center located peripherally in the inferior colliculus.

frequency of sound Number of regular recurrences of vibrations of sound, measured in cycles per second; primary determinate of the pitch of a sound.

functional magnetic resonance imaging Use of magnetic resonance to measure the metabolic activity of a tissue or organ.

ginkgo biloba Extract of the leaves of the ginkgo tree, containing ginkgoheterosides and terpene lactones used medicinally in vascular insufficiency.

hertz A unit of frequency, one cycle per second, named after German physicist, Heinrich R. Hertz, 1857–1894.

hyperactivity Increased neuronal activity.

hyperacusis Physical discomfort from exposure to low or moderate sound intensity.
incidence Number of persons acquiring a new specific disease or disorder during a specific period of time in a specific population.
inferior colliculus Midbrain center of the auditory pathway receiving input from the lateral lemniscus and providing output to the medial geniculate body.
intense sound sound exceeding 85 dB sound pressure level, capable of causing a temporary threshold shift in hearing or permanent hearing impairment.
intensity of sound An objective measure of the amplitude of sound waves, expressed in decibels; primary determinant of the loudness of sound.
lemniscal pathway in the auditory system The pathway in the auditory system in the brain that is tonotopically organized and does not receive non-auditory input; it is characterized by the lateral lemniscus.
loudness The psychophysical attribute that depends on the intensity of sound.
maskability of tinnitus The intensity at which a specific spectrum of sound makes tinnitus imperceptible.
Meniere's disease A disease of the inner ear causing fluctuating and progressive hearing loss, episodic vertigo, low-pitched tinnitus and a feeling of aural fullness; its pathologic correlate is endolymphatic hydrops.
misophonia Strong dislike or hate of sound.
neuromodulatory systems Brain systems that produce and respond to specific neurotransmitters, as, for example, the cholinergic, serotonin, dopaminergic, and noradrenergic systems.
nonlemniscal pathway in the auditory system The pathway of the auditory system in the brain which is not tonotopically organized and receives multimodal (somatosensory and auditory) input.
objective tinnitus Tinnitus produced by body sound that can be heard or monitored by others.
octave The frequency interval between two tones that have a hertz ratio of 2:1.
otitis media Inflammation of the middle ear.
otoacoustic emissions Sound coming for the inner ear that can be measured in the external auditory canal, arising from the motion of the outer hair cells.
otosclerosis A disease affecting the bone encasing the inner ear and resulting in fixation of the footplate of the stapes and causing conductive and sensorineural hearing losses.
passive avoidance A procedure in which the adversive stimulus is delivered only if the subject fails to suppress a learned behavior when a conditioned stimulus is presented.
percept That which is perceived: a sensation or experience.
pitch The psychophysical attribute that depends on the frequency of the sound.
placebo effect The suggestive effect that occurs in response to an inert form of treatment.
positron emission tomography Images of metabolic activity in tissue with computer analysis of positrons emitted when radioactive substances are incorporated into the tissue.
prevalence Number of persons with a specific disease or disorder in a specific population at a specific time.
primary auditory cortex A major part of the auditory cortex; the other major parts are the secondary auditory cortex and the anterior auditory field.
psychoacoustic parameters of tinnitus They include pitch, loudness, timbre, and localization.
pulsatile tinnitus Objective tinnitus that is synchronous with the heartbeat.
selective serotonin reuptake inhibitors A group of relatively new antidepressive agents which act by inhibiting the re-uptake of serotonin in the vicinity of synapses.
sensorineural hearing impairment or loss Hearing impairment or loss due to a lesion in the inner ear or auditory nerve.
serotonin system The source of serotonin (raphe nuclei) and the neurons that respond to it.
somatic tinnitus Subjective tinnitus in which the onset can be attributed to some injury of the head or neck.
somatosound Body sound.
spontaneous activity Neuronal activity not preceded by a stimulus.
spontaneous otoacoustic emissions Otoacoustic emissions not preceded by an acoustic stimulus.
subjective tinnitus Tinnitus that can be heard only by the individual experiencing it.
synchrony Simultaneous increased neural activity from two or more sources.
temporary threshold shift Reversible hearing loss resulting from exposure to intense sound.
timbre The psychophysical quality of a sound that depends on the spectrum of the sound's frequencies.
trigeminal ganglion Sensory neuronal center of the trigeminal nerve located inside the base of the skull.
trigeminal nuclei Spinal and brainstem sensory neuronal centers of the trigeminal nerve.

3.18.1 Definition of Tinnitus

Tinnitus is the perception of a sound in the absence of an external acoustic stimulus. Tinnitus may be categorized as objective or subjective. Objective tinnitus is produced by an internal acoustic stimulus or somatosound (body sound) activating the inner ear by air conduction or bone conduction of the sound. Somatosounds include vibrations produced by muscular contractions (myoclonus) and vascular pulsations. Another form of objective tinnitus results from spontaneous otoacoustic emissions from the inner ear that can often be heard by the individual producing them. Objective tinnitus can be heard by another person with a stethescope or by electronic monitoring. Subjective tinnitus can be heard only by the individual experiencing it and has no acoustic source and, therefore, no activation of the inner ear. In current usage, the term tinnitus refers to subjective tinnitus, and somatosound refers to objective tinnitus. Pulsatile tinnitus is a variety of objective tinnitus that is synchronous with the heartbeat and due to vascular compression, malformations or tumors. Somatic tinnitus refers to subjective tinnitus in which the onset can be attributed to some somatic injury in the head and neck region and may or may not be associated with hearing impairment.

3.18.2 Clinical Overview

Nearly everyone occasionally experiences brief subjective tinnitus of a ringing quality lasting seconds or minutes. Indeed, many individuals experience tinnitus in a soundproof booth, and most experience tinnitus in near-perfect silence such as in an anechoic chamber (Heller, M. and Bergman, M., 1953). A more common experience is the transient ringing tinnitus that follows brief exposure to intense sound that is capable of producing a temporary threshold shift but not permanent hearing impairment. Likewise, ingestion of large amounts of salicylate or quinine may result in transient tinnitus.

Most clinical concern is with chronic tinnitus that may be frequently or continuously present. The vast majority of chronic tinnitus is caused by exposure to loud noise, but chronic tinnitus may be associated with any conductive or sensorineural hearing impairment. Among conductive hearing losses causing tinnitus are obstruction of the external auditory canal and middle-ear abnormalities including otitis media and effusion, tympanic membrane perforation, tympanosclerosis and ossicular discontinuity and fixation as in otosclerosis. In addition to noise exposure, tinnitus associated with sensorineural hearing impairment results from genetic mutations, ototoxic drugs, inner-ear infections, head injury, and aging.

Tinnitus is described as ringing, buzzing, hissing, and like the sounds of insects or, in Meniere's disease, as a low-pitched roaring. Tinnitus fluctuates in pitch, loudness and timbre in many individuals. Nevertheless, tinnitus can often be matched audiometrically for frequency and intensity. Most commonly, the pitch of tinnitus is matched to pure tones and the central frequency is found to be at 3 kHz or above. The results are often variable, and octave errors are common. The match frequency tends to correlate with the severity of the sensorineural hearing loss. Individuals with tinnitus below 1500 Hz tend to have more severe hearing losses, especially in the low frequencies, than do individuals with high-pitched tinnitus. Once the central frequency is determined, the intensity of the tinnitus can be matched and is usually about 10 dB above the threshold of hearing at that frequency. Tinnitus can often be modulated by somatic factors such as head and neck movements or clenching of the teeth.

Many people, perhaps 30 million in the United States, experience chronic tinnitus. Most of these individuals do not appear to be greatly bothered by their tinnitus. They seek professional care for diagnosis to determine if the tinnitus is a warning of an impending serious disease, such as a brain tumor, or impending deafness. Once the diagnostic evaluation is completed, most of them accept the reassurance and do not appear to be highly motivated to seek a cure for their tinnitus. Perhaps, only 10% of individuals experiencing tinnitus suffer from it in that it interferes with their occupational or social activities. They describe their tinnitus as annoying, irritating, intrusive, and distracting. It affects their sleep (getting to sleep and staying asleep), concentration, ability to understand conversation, and ability to relax and enjoy life. Many who suffer from tinnitus have anxiety and depression.

3.18.3 Associated Decreased Sound Tolerance

Individuals with tinnitus often have decreased sound tolerance in the form of hyperacusis and misophonia (Jastreboff, P. and Jastreboff, M., 2004a). Individuals with hyperacusis experience physical discomfort from exposure to low or moderate sound intensity.

They express a negative attitude toward sound and avoid sound. The discomfort depends on the spectrum and intensity of the sound. According to the theoretical concept of Jastreboff P. and Jastreboff M. (2004a) , hyperacusis is believed to result from an abnormally high level of neuronal activity in the auditory pathways due to excessive amplification of acoustically evoked neuronal signals. The limbic and autonomic nervous systems are activated due to the abnormal activity in the auditory pathways. Individuals with misophonia have a strong dislike or hate of sound and consequently avoid sound. The reaction depends on the individual's previous experience with a given sound, the context of the sound and the individual's psychological profile. According to the Jastreboff and Jastreboff hypothesis, misophonia is believed to be an abnormally strong reaction of the limbic and autonomic nervous systems to sound without abnormally high activation of the auditory system. Physiologic evidence for these appealing concepts has not so far been obtained. Frequently, hyperacusis and misophonia coexist.

3.18.4 Epidemiology of Tinnitus

The incidence of new cases of bothersome tinnitus in the age group 48–92 years is roughly 1.14% per year (Nondahl, D., Cruickshanks, K., Wiley T., *et al.*, 2002). The incidence appears to increase with age. Parenthetically, bothersome tinnitus is a term that has been used in interview surveys and should not be considered equivalent to suffering from tinnitus. The prevalence of tinnitus in individuals 20 years of age or greater is 10–15% in large national surveys. The age trend increases up to age 60–69 years, remains almost as high between 70 and 79 years and declines in the oldest age group, 80 years or greater (Hoffman, H. and Reed, G., 2004). Age-specific prevalence of tinnitus differs from the prevalence of hearing impairment's nearly exponential increase with age. Based on the 1990 Hearing Supplement to the National Health Interview Survey, Hoffman and Reed estimate that there were nearly 15 million adults with bothersome tinnitus in the United States (Hoffman, H. and Reed, G., 2004).

Among risk factors or associated characteristics for tinnitus are advancing age, male sex, less than a high school education, lower income, rural residence, occupational noise exposure, general health status reported as fair or poor, higher body mass index and hearing loss reported as of moderate or higher degree (Hoffman, H. and Reed, G., 2004). Men are 50% more likely than women to have chronic or bothersome tinnitus (Hoffman, H. and Reed, G., 2004). Although the age trends for tinnitus for men and women are similar in the 1994–95 United States National Health Interview Survey Disability Supplement, beginning at approximately age 30 years the prevalence of tinnitus in men rises more steeply and remains higher until age 85 years. There is a clear separation of men and women in prevalence from the age of 40–79 years probably due to men being more likely to be exposed to intense environmental noise from occupational or leisure (hunting) activities (Hoffman, H. and Reed, G., 2004). Strong associations between tinnitus and occupational noise exposure have previously been demonstrated.

With multivariate analysis, there is still a significantly greater risk of tinnitus for men aged 45–54 years; however, for men aged 75–84 years and 85+ years, there is a significant reduced risk of tinnitus (Hoffman, H. and Reed, G., 2004). Aging in men appears protective against tinnitus for reasons that are unclear.

There is a steady increase in risk of tinnitus with increasing hearing impairment. In addressing the issue of the role of aging once there is proper accounting for the hearing loss, Hoffman H. and Reed G. (2004) find that there is a lower prevalence of tinnitus as age cohort increases for any given level of hearing impairment.

Non-Hispanic whites are more likely than other races and ethnic groups to report chronic tinnitus although race and ethnicity do not appear to be strongly related to the risk of tinnitus in the United States (Hoffman, H. and Reed, G., 2004).

The odds ratio for chronic tinnitus is 50% greater in the West than in the Northeast of the United States (Hoffman, H. and Reed, G., 2004). The reason for this is uncertain but may be related to hunting and other forms of shooting.

Management or administrative and technical or sales occupational groups have a reduced risk of chronic tinnitus, and skilled or unskilled workers have a greater risk of chronic tinnitus. Prior military service carries a greater risk of chronic tinnitus (Hoffman, H. and Reed, G., 2004). Cigarette smoking increases the risk of bothersome tinnitus, whereas moderate drinking of alcohol of one drink per day or less reduces the risk.

There is a twofold increase in the risk of bothersome tinnitus for male and female siblings of individuals with

tinnitus, which suggests a familial association due to shared environmental factors or a genetic basis (Hoffman, H. and Reed, G., 2004).

3.18.5 Animal Models of Tinnitus

In 1988, Jastreboff and colleagues published their findings of conditioned suppression in rats that are trained to respond to silence and that fail to do so if tinnitus is present (Jastreboff, P. *et al.*, 1988). Tinnitus is induced with sodium salicylate, and the magnitude of the response is dose related. Extinction of the reflex occurs after several days. A rough estimate of intensity has been obtained. The results depend on group averages and do not yield information on individual subjects. Tinnitus in this model has also been induced with intense sound. It has been used to measure the therapeutic effectiveness of Ginkgo biloba in rats.

Jastreboff's animal model is a seminal contribution and has been followed by several others. Bauer and colleagues developed a passive avoidance procedure that allows determination of intense sound-induced tinnitus in rats over extended periods of time (Bauer, C. *et al.*, 1999). Bauer C. and Brozoski T. (2001) have used this procedure to measure the therapeutic effectiveness of gabapentin for tinnitus in rats. Heffner H. and Harrington I. (2002) used a somewhat similar procedure in hamsters. More recently, Heffner H. and Koay G. (2005) has, after training hamsters to respond to the direction from which sound is presented, induced unilateral tinnitus with intense sound and demonstrated that in the absence of acoustic stimulation the hamsters respond as if sound had been presented to the ear with tinnitus. This procedure allows gathering data from individual subjects without concern for the effect of hearing loss produced by the exposure to intense sound. However, the testing is limited because the testing is carried out to extinction.

3.18.6 Neurophysiologic Model of Tinnitus

The vast majority of tinnitus is associated with sensory hearing impairment. Although the initiation of tinnitus results from a lesion in the inner ear, once tinnitus is established it seems to take on a life of its own in the brain. In the individual who suffers from tinnitus, Jastreboff's neurophysiologic model of tinnitus offers the most plausible explanation of the responsible phenomena. Jastreboff P. and Jastreboff M. (2004b) contend that in individuals who suffer from tinnitus, the auditory system plays a minor role. They emphasize the role of the activation of the limbic and autonomic nervous systems, particularly the sympathetic part of the autonomic nervous system. When tinnitus-related neuronal activity is temporally associated with cognitively induced or high-stress-induced activation of the limbic and autonomic nervous systems, a conditioned reflex is established. Initially, this activation provides reinforcement for the reflex. Later the tinnitus signal activates the limbic and autonomic nervous systems without adverse cognition or stress. Physiologic and behavioral reactions caused by the activation of the limbic and autonomic nervous systems provide reinforcement of the reflex, and a vicious circle occurs. According to Jastreboff and Jastreboff, tinnitus is classified by the individual as important or not and with a positive or negative connotation. Reinforcement increases with greater importance, and the type of reaction is determined by the connotation. Continuous tinnitus-related neuronal activity and the reaction due to activation of the limbic and autonomic nervous systems preclude extinction of the reflex.

3.18.7 Theoretical Mechanisms of and Sites Associated with the Percept of Tinnitus

3.18.7.1 Peripheral Processes Involved in Tinnitus

Nuttall A. *et al.* (2004) recount a possible mechanism in the generation of tinnitus stemming from the edge effect of relatively normal hair cells on the low-frequency side and abnormal or absent hair cells on the high-frequency side of a lesion. They also note other possible peripheral mechanisms of generation of tinnitus including excessive release of neurotransmitter at the inner hair cell-type I afferent synapse, increased cochlear amplification resulting in mechanical noise from motion of the basilar membrane and reduced cochlear amplification decreasing the spontaneous rate in the neurons of the auditory nerve.

Based on correlations between psychoacoustic parameters of tinnitus, particularly pitch matching and localization, and the extent of inner ear damage, Meikle has pointed out that there is an ongoing

dynamic interaction between the inner ear and brain centers in tinnitus (Meikle, M., 1995).

3.18.7.2 Otoacoustic Emissions

Although there is usually no relationship between otoacoustic emissions and tinnitus, Lonsbury-Martin B. and Martin G. (2004). draw attention to a rare type of spontaneous otoacoustic emissions which is audible to the individual with it, much larger and at a higher frequency range than the usual spontaneous otoacoustic emissions and associated with a broad region of abnormal outer hair cells.

3.18.7.3 Neural Correlates of Tinnitus

Tinnitus induced with intense sound in animals is associated with increases in neuronal discharge rates in the dorsal cochlear nucleus; inferior colliculus, particularly in its external nucleus; and the primary auditory cortex. It is difficult to know if the hyperactivity is due to tinnitus or the associated hearing loss.

A recurring confounding problem in tinnitus research is that tinnitus is ordinarily associated with hearing impairment. Segregation of the correlates of tinnitus from the consequences of hearing impairment requires the inclusion of a second control group. Since some animals in which tinnitus induction has been attempted develop hearing impairment but no tinnitus, comparing healthy animals, animals with hearing impairment but no tinnitus and animals with hearing impairment and tinnitus improves the validity of the research. Clinical research on the mechanisms of or the sites associated with the percept of tinnitus is also confounded by this problem, and the solution is to include controls matched for hearing impairment who do not experience tinnitus.

Kaltenbach J. *et al.* (2004) suggest that hearing loss and tinnitus involve different mechanisms and a different time course in that the hyperactivity in the dorsal cochlear nucleus appears several days after the onset of the hearing loss following exposure to intense sound. They speculate that sound percepts of tinnitus are due to increased spontaneous activity and perhaps increased synchrony in the auditory cortex (Eggermont, J., 2004) and that the pitches of those percepts depend on characteristic frequencies that predominate in the expanded and reorganized region of the cortex as occurs in plasticity.

On the other hand, Eggermont points out that, in the tonotopically organized lemniscal pathway of the auditory system, a reduction in spontaneous activity is the rule in response to tinnitus-inducing agents (salicylate, quinine, and intense sound). Increased spontaneous activity has been found in the multimodal (auditory and somatosensory) dorsal cochlear nucleus and the nonlemniscal external nucleus of the inferior colliculus (Eggermont, J., 2004). Although it is generally assumed that the initiation, generation, and maintenance of tinnitus occurs as ascending phenomena in the auditory pathway, Eggermont calls attention to the temporal relationship of increased activity in the auditory cortex in hours and in the dorsal cochlear nucleus in days after exposure to intense sound and suggests that the initiation of increased spontaneous activity may occur in the auditory cortex first and secondarily in the dorsal cochlear nucleus.

3.18.7.4 Cortical Plasticity

Schreiner C. and Cheung S. (2004) point out that it is difficult to separate plastic changes due to hearing loss from those due to tinnitus. They suggest that acvtivity-dependent plasticity may be involved in the development of tinnitus. Stroke and trauma to the auditory cortex initiate injury-induced plasticity that may account for rare forms of tinnitus without peripheral injury.

3.18.7.5 Somatosensory Nuclei in Tinnitus

Somatic tinnitus apparently depends on the somatosensory innervation of the cochlear nucleus, superior olivary complex, and inferior colliculus. Stimulation of the trigeminal ganglion or nuclei causes excitation or inhibition of the neurons of the cochlear nucleus and inferior colliculus. Shore S. (2004) has demonstrated integration of acoustic and somatosensory stimuli causing an increased or decreased response in the cochlear nucleus or inferior colliculus that is greater or less than the sum of the parts. This integration could play a role in the generation of somatic tinnitus.

3.18.8 Evaluation of the Individual with Tinnitus

The neurotologic evaluation of the individual with tinnitus is similar to the evaluation of the individual with hearing impairment. The audiologic assessment includes matching of the pitch and loudness of the

tinnitus as well as estimation of the maskability of the tinnitus. Several tinnitus questionnaires have been developed and validated and serve as intake and outcome measures for the severity of the distress caused by tinnitus.

Brain imaging of tinnitus with functional magnetic resonance imaging and positron emission tomography is in the early stage of development. Already objective evidence of tinnitus has been demonstrated in the inferior colliculus and auditory cortex (Lockwood, A. *et al*., 1998; Melcher, J. *et al*., 2000). Brain imaging is likely to provide a level of objective evidence of tinnitus not previously attained.

3.18.9 Treatment of the Individual with Tinnitus

Antidepressive drugs are important therapy for individuals who suffer from tinnitus and have depression or insomnia and perhaps for those without depression. Hearing aids are an essential part of tinnitus management. Tinnitus retraining therapy and other psychological methods of treatment are effective for individuals who suffer from tinnitus (Jastreboff, P. and Jastreboff, M., 2003). Electrical suppression of tinnitus with high-rate ($5000\,s^{-1}$) pulse trains delivered to the inner ear has been demonstrated to occur without producing an auditory percept but continues to be experimental (Rubinstein, J. *et al*., 2003).

The neuromodulatory systems are sufficiently well understood to be directly or indirectly manipulated in the treatment for tinnitus with emotional associations of fear, depression, or decreased sound tolerance (Schreiner, C. and Cheung S., 2004). Since the cholinergic system is stimulus feature directed and the amygdala is critical in emotional processing, the cholinergic system may be helpful in therapy for emotionally laden tinnitus (Schreiner, C. and Cheung S., 2004). Drugs influencing the serotonin system, such as the selective serotonin reuptake inhibitors, may reduce the adverse aspects of tinnitus (Robinson, S. *et al*., 2005).

Because of the large placebo effect in individuals with tinnitus, randomized, placebo-controlled, double-masked clinical trials are required to evaluate therapy for tinnitus (Dobie, R., 1999). Furthermore, clinical trials should be limited to subjects who suffer from tinnitus as determined by a criterion score on validated tinnitus questionnaires.

Schreiner C. and Cheung S. (2004) propose that behavioral therapy enhanced with pharmacotherapy may be the most promising approach to tinnitus treatment.

References

Bauer, C. and Brozoski, T. 2001. Assessing tinnitus and prospective tinnitus therapeutics using a psychophysical animal model. J. Assoc. Res. Otolaryngol. 2, 54–64.

Bauer, C., Brozoski, T., Rojas, R., Boley, J., and Wyder, M. 1999. Behavioral model of chronic tinnitus in rats. Otolaryngol. Head Neck. Surg. 121, 457–462.

Dobie, R. 1999. A review of randomized clinical trials in tinnitus. Laryngoscope 109, 1202–1211.

Eggermont, J. 2004. The Auditory Cortex and Tinnitus. In: Tinnitus: Theory and Management (*ed*. J. Snow) pp. 171–188. BC Decker.

Heffner, H. and Harrington, I. 2002. Tinnitus in hamsters following exposure to intense sound. Hear Res. 170, 83–95.

Heller, M. and Bergman, M. 1953. Tinnitus aurium in normally hearing persons. Ann. Otol. Rhinol. Laryngol. 62, 73–83.

Heffner, H. E. and Koay, G. 2005. Tinnitus and hearing loss in hamsters (*Mesocricetus auratus*) exposed to loud sound. Behav. Neurosci. 119(3), 734–742.

Hoffman, H. and Reed, G. 2004. Epidemiology of Tinnitus. In: Tinnitus: Theory and Management (*ed*. J. Snow) pp. 16–41. BC Decker.

Jastreboff, P. and Jastreboff, M. 2003. Tinnitus retraining therapy for patients with tinnitus and decreased sound tolerance. Otolaryngol. Clin. North Am. 36, 321–336.

Jastreboff, P. and Jastreboff, M. 2004a. Decreased Sound Tolerance. In: Tinnitus: Theory and Management (*ed*. J. Snow) pp. 8–15. BC Decker.

Jastreboff, P. and Jastreboff, M. 2004b. The Neurophysiological Model of Tinnitus. In: Tinnitus: Theory and Management (*ed*. J. Snow) pp. 96–106. BC Decker.

Jastreboff, P., Brennan, J., Coleman, J., and Sasaki, C. 1988. Phantom auditory sensation in rats: an animal model for tinnitus. Behav. Neurosci. 102, 811–822.

Kaltenbach, J., Zhang, J., and Zacharek, M. 2004. Neural Correlates of Tinnitus. In: Tinnitus: Theory and Management (*ed*. J. Snow) pp. 141–161. BC Decker.

Lockwood, A., Salvi, R., Coad, M., Towsley, M. L., Wack, D. S., and Murphy, B. W. 1998. The functional neuroanatomy of tinnitus: evidence for limbic system links and neural plasticity. Neurology 50, 114–120.

Lonsbury-Martin, B. and Martin, G. 2004. Otoacoustic Emissions and Tinnitus. In: Tinnitus: Theory and Management (*ed*. J. Snow) pp. 69–78. BC Decker.

Meikle, M. 1995. The Interaction of Central and Peripheral Mechanisms in Tinnitus. In: Mechanisms of Tinnitus (*ed*. J. Vernon) pp. 181–206. Allyn and Bacon.

Melcher, J., Sigalovsky, I., Guinan, J., and Levine, R. 2000. Lateralized tinnitus studied with functional magnetic resonance imaging: abnormal inferior colliculus activation. J. Neurophysiol. 83, 1058–1072.

Nondahl, D., Cruickshanks, K., Wiley, T., Klein, R., Klein, B. E., and Tweed, T. S. 2002. Prevalence and 5-year incidence of tinnitus among older adults: the epidemiology of hearing loss study. J. Am. Acad. Audiol. 13, 323–331.

Nuttall, A., Meikle, M., and Trune, D. 2004. Peripheral Processes Involved in Tinnitus. In Tinnitus: Theory and Management (*ed*. J. Snow), pp. 52–68. BC Decker.

Robinson, S., Viirre, E., Bailey, K., Gerke, M. A., Harris, J. P., and Stein, M. B. 2005. Randomized placebo-controlled trial of a selective serotonin reuptake inhibitor in the treatment of nondepressed tinnitus subjects. Psychosom. Med. 67, 981–988. Erratum in: Psychosom. Med. 2006, 68 (1 p preceding 1. Stein, Murray B [added]).
Rubinstein, J., Tyler, R., Johnson, A, and Brown, C. 2003. Electrical suppression of tinnitus with high-rate pulse trains. Otol. Neurotol. 24, 478–485.
Schreiner, C. and Cheung, S. 2004. Cortical Plasticity and Tinnitus. In: Tinnitus: Theory and Management (*ed*. J. Snow), pp. 189–202. BC Decker.
Shore, S. 2004. Sensory Nuclei in Tinnitus. In: Tinnitus: Theory and Management (*ed*. J. Snow), pp. 125–137. BC Decker.

Further Reading

Henry, J., Schechter, M., Regelein, R., and Dennis, K. 2004. Veterans and Tinnitus. In: Tinnitus: Theory and Management (*ed*. J. Snow), pp. 125–137. BC Decker.
Jastreboff, P. and Hazell, J. 2004. Tinnitus Retraining Therapy Implementing the Neurophysiological Model. Cambridge University Press.
McFadden, D. 1982. Tinnitus Facts, Theories and Treatments. National Academy Press.
Snow, J. (*ed*.) 2004. Tinnitus: Theory and Management. BC Decker.
Tyler, R. (*ed*.) 2000. Tinnitus Handbook. Singular Publishing.

3.19 Prestin

D Oliver, Universität Freiburg, Freiburg, Germany

© 2008 Elsevier Inc. All rights reserved.

3.19.1	**Introduction: Outer Hair Cell Electromotility and Prestin**	309
3.19.2	**Molecular Structure of Prestin**	310
3.19.3	**Functional Properties of Prestin**	311
3.19.3.1	Electromechanical Activity	312
3.19.3.2	Charge Transfer	312
3.19.3.3	Voltage Dependence	312
3.19.3.4	Kinetics	313
3.19.3.5	Pharmacology	313
3.19.4	**The Generation of Force and Nonlinear Capacitance by Prestin: Molecular Mechanisms**	313
3.19.4.1	Biophysical Model	313
3.19.4.2	Molecular Mechanisms	314
3.19.5	**Future Directions**	315
References		316

Glossary

gating current A brief electrical current that precedes the opening and closing of voltage-gated ion channels. It results from the movement of a charged voltage sensor.

hydrophobicity analysis A method to identify possible/partial structural domains of proteins according to the hydrophobicity or hydrophilicity of the amino acids. A quantitative measure of the hydrophobicity of each amino acid is plotted against its order in the proteins sequence.

cystic fibrosis transmembrane conductance regulator (CFTR) A chloride channel, member of the superfamily of ATP-binding cassette (ABC) transporter proteins.

yeast-two-hybrid assay A molecular biological method to identify the direct interaction of two proteins, which is based on protein–protein association in living yeast cells.

nonlinear capacitance Voltage-dependent component of the membrane capacitance that results from the reversible translocation of an electrically charged particle through the membrane (also see 'gating current').

lock-in technique Phase-sensitive detection method that extracts a signal from a sinusoidal carrier wave at a certain phase angle.

3.19.1 Introduction: Outer Hair Cell Electromotility and Prestin

The cylindrical outer hair cells (OHCs) change their length in response to variation of the membrane potential; depolarization induces contraction of up to 4% and hyperpolarization leads to elongation. Unlike other cellular motile processes that depend on molecular motors acting on cytoskeletal elements, electromotility turns out to be an intrinsic membrane process residing in the lateral plasma membrane of the epithelial OHCs (reviewed by Holley, M. C., 1996). As such, it is not driven by adenosine triphosphate (ATP) hydrolysis, or triggered by ionic currents or rise in cytosolic Ca^{2+} but directly depends on the membrane potential. Analysis of the movements indicated that independent elementary motors distributed along the lateral membrane of the OHC generate electromotility (Dallos, P. *et al.*, 1991). Indeed, electromotility can be observed after removal of the entire cytoskeleton by proteolytic digestion and even in isolated patches of the OHC

membrane. This membrane motor mechanism is supported by an extremely high density of intramembrane particles in the lateral membrane of OHCs that can be visualized with electron-microscopic techniques. These particles are thought to be individual motor proteins. Central to the understanding of how distributed elementary motors in the membrane may generate movement is the observation that electromotility has an electrical signature: it is inextricably associated with the transfer of electrical charge across the membrane that can be measured as a gating current at the onset of a voltage jump (Dallos, P. and Fakler, B., 2002). Charge transfer and motility share the same voltage dependence, suggesting that the former results from the translocation of a charged particle (voltage sensor) within a membrane motor protein, which in turn directly triggers a force-producing conformational change.

In 2000, Dallos and colleagues used a subtractive cDNA library to isolate a cDNA encoding a protein present in OHCs but not in nonmotile inner hair cells and termed it prestin (Zheng, J. *et al.*, 2000). Prestin is selectively expressed in the inner ear (Zheng, J. *et al.*, 2000; Liu, X. Z. *et al.*, 2003), and specific antibodies directed against prestin label the lateral plasma membrane of OHCs exclusively and strongly (Belyantseva, I. A. *et al.*, 2000; Zheng, J. *et al.*, 2001). When expressed heterologously in culture cells prestin reproduces all the hallmarks of OHC electromotility. In particular, cells expressing prestin generate movement and force in response to electrical stimulation and produce charge movement, the electrical signature of electromotility (Zheng, J. *et al.*, 2000; Ludwig, J. *et al.*, 2001; Santos-Sacchi, J. *et al.*, 2001). Vice versa, OHCs from prestin knockout mice entirely lack electromotility (Liberman, M. C. *et al.*, 2002). Since it is both necessary and sufficient for electromotility, prestin is unquestionably the OHC membrane motor, or, at least, its core component.

3.19.2 Molecular Structure of Prestin

Prestin cDNAs from several rodents as well as from humans (Zheng, J. *et al.*, 2000; Ludwig, J. *et al.*, 2001; Liu, X. Z. *et al.*, 2003; Zheng, J. *et al.*, 2003) are now available, all coding for a protein of 744 amino acids (aa) with a predicted molecular weight of about 81 kDa. The aa sequence is highly conserved among mammalian species, showing sequence identity of 95% between mouse and human prestin with most exchanges occurring in the distal C- and N-termini. The prestin gene is localized on chromosomes 5 and 7 (location 7q22.1) in mice (Zheng, J. *et al.*, 2003) and humans (Liu, X. Z. *et al.*, 2003), respectively, and comprises 20 (mice) and 21 (humans) exons. Alternative shorter splice isoforms have been detected in the human fetal cochlea; however, their expression level is low and their functional role has not been examined (Liu, X. Z. *et al.*, 2003).

Prestin is the fifth mammalian member of the SLC26 family of anion transporters, and is therefore designated SLC26A5 (Zheng, J. *et al.*, 2000). Including prestin, the SLC26 family comprises 10 members in mammals and many homologs have been identified throughout eukaryotic and bacterial phyla (Mount, D. B. and Romero, M. F., 2004). The mammalian family members show aa sequence identities to prestin between 22% and 40% with SLC26A6 being the closest homolog.

Nonmammalian homologs of prestin have been identified in chicken, zebrafish, and drosophila (Weber, T. *et al.*, 2003; Schaechinger, T. J. and Oliver, D., 2007). The chicken and zebrafish molecules are clearly orthologs of mammalian prestin (with 58% and 52% aa sequence identity to rat prestin, respectively) while the insect homolog is more distantly related. Strikingly, these homologs are expressed in inner ear hair cells in zebrafish (Albert, J. T. *et al.*, 2007) and in mechanosensory organs of flies (Weber, T. *et al.*, 2003). However, they have no detectable electromotile properties (Albert, J. T. *et al.*, 2007), but are electrogenic anion transporters (Schaechinger, T. J. and Oliver, D., 2007). Thus, it seems possible that the molecular machinery of electromotility evolved from an ion transport mechanism present in the mechanosensory cells of nonmammalian ears.

Very similar to other SLC26 family members, hydrophobicity analysis of the aa sequence of prestin shows hydrophilic N- and C-termini and a hydrophobic core region with numerous hydrophobic stretches, indicative of transmembrane domains (Figure 1). The membrane topology of prestin is, as yet, incompletely resolved. Clearly, both N- and C-termini are located intracellularly since terminal epitopes are accessible to specific antibodies only in permeabilized cells (Ludwig, J. *et al.*, 2001; Zheng, J. *et al.*, 2001). This reduces the possible transmembrane topologies to those with an even number of complete membrane spans, possibly 10 or 12. Prestin contains two N-glycosylation consensus sites at positions 163 and 166 that are conserved among SLC26 family members. Interference with glycosylation shifted

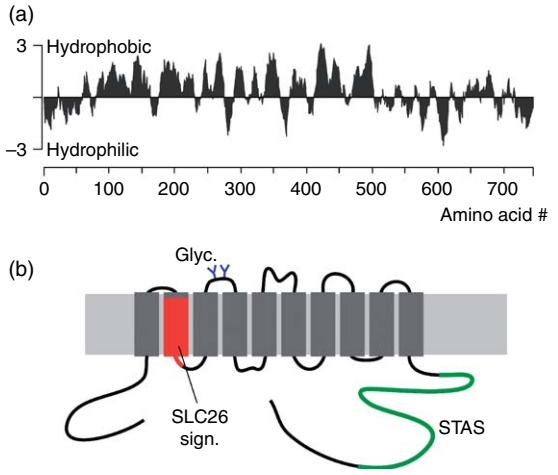

Figure 1 Molecular structure of prestin. a, Hydrophobicity plot of prestin, obtained with the Kyte-and-Doolittle algorithm. b, Hypothetic membrane topology of prestin. The full topology has not been determined experimentally and prediction algorithms yield divergent results (Zheng, J. *et al.*, 2001). Alternative models have been proposed (Oliver, D. *et al.*, 2001; Deak, L. *et al.*, 2005; Navaratnam, D. *et al.*, 2005). Structural motifs are outlined: STAS-domain (STAS, green); N-glycosylation sites (Oliver, D. *et al.*, 2001; Deak, L. *et al.*, 2005) (Glyc., blue); SLC26 transporter signature domain (SLC26 sign., red).

the apparent molecular weight of prestin and slightly affected its electrical properties (Matsuda, K. *et al.*, 2004), suggesting actual glycosylation at this site and extracellular localization of the short hydrophilic sequence stretch flanking this site, in agreement with preliminary epitope accessibility studies (Oliver, D. *et al.*, 2001). Unfortunately, more detailed topological information is currently not available for any other member of the SLC26 family. A preliminary suggestion for prestin's topology based on the above information and on hydrophobicity is shown in Figure 1. However, the actual membrane topology may be more complicated as it may contain partial membrane spans (Deak, L. *et al.*, 2005).

Prestin contains two highly conserved sequence stretches, one termed SLC26 transporters signature (Prosite entry PS01130), defined as a region highly conserved throughout family members, and a sulfate transporter and antisigma antagonists (STAS) domain (Prosite entry PS50801; Zheng, J. *et al.*, 2000; Mount, D. B. and Romero, M. F., 2004). The SLC26 signature motif approximately corresponds to the second putative transmembrane helix; its functional relevance is currently not known. The C-terminal STAS domain of the prestin relatives SLC26A3 and A6 is involved in the interaction between the SLC26 transporter and the cystic fibrosis transmembrane conductance regulator (CFTR) chloride channel. Here, the STAS domain appears to directly activate CFTR (Ko, S. B. *et al.*, 2004). A functional interaction of prestin with CFTR was also reported recently (Zheng, J. *et al.*, 2005).

Moreover, prestin harbors several potential protein phosphorylation sites, including consensus sites for protein kinase A (PKA), protein kinase G (PKG), protein kinase C (PKC), and protein kinase CK2. OHC electromotility is modulated by cGMP-dependent phosphorylation (Sziklai, I. *et al.*, 2001). Activation of PKG by cyclic guanosine monophosphate (cGMP) analogs indeed modified functional properties of recombinant prestin, suggesting phosphorylation at two PKG sites (Deak, L. *et al.*, 2005). In native OHCs, prestin's voltage dependence changes during postnatal development (Oliver, D. and Fakler, B., 1999) and is affected by agents that interfere with phosphorylation (Frolenkov, G. I. *et al.*, 2000), both consistent with a role for phosphorylation in the regulation of prestin's function.

Electron microscopy indicates that the OHC membrane may be mechanically linked to the underlying actin cytoskeleton (Holley, M. C., 1996), possibly in order to translate the force generated by the elementary motors into a macroscopic movement of the cell body. Such coupling suggests protein–protein interactions involving prestin. As yet, the promyelocytic leukemia zinc finger protein (PLZF) has been suggested as a direct interaction partner of prestin based on yeast-two-hybrid assays (Nagy, I. *et al.*, 2005). Moreover, given the size of particles in the OHC membrane (diameter $\approx$ 10 nm; Holley, M. C., 1996) it seems conceivable that each unitary motor is either an oligomer of prestin or may contain accessory proteins. Biochemical data (Zheng, J. *et al*, 2006) and fluorescence resonance energy transfer measurements (Navaratnam, D. *et al.*, 2005) are consistent with the oligomeric assembly of prestin.

3.19.3 Functional Properties of Prestin

As noted above, prestin can account for all mechanical and electrical hallmarks of OHC electromotility. When transfected into culture cells it generates voltage-dependent mechanical movement and electrical charge transfer (Zheng, J. *et al.*, 2000; Ludwig, J. *et al.*, 2001).

3.19.3.1 Electromechanical Activity

The electromechanical activity of prestin has been measured in cells transfected with gerbil and rat prestin using the microchamber method, where an isolated cell is partially drawn into a tightly fitting glass capillary (Holley, M. C., 1996; Zheng, J. *et al.*, 2000). Voltage commands applied across the cell depolarize and hyperpolarize the excluded and included segments of the cell's membrane in opposite polarity. The excluded segment of the cell was shown to move according to a sinusoidal voltage stimulus with amplitudes of up to 0.2 μm if prestin was present (Zheng, J. *et al.*, 2000). Using an atomic-force cantilever of known stiffness, Ludwig J. *et al.* (2001) showed that the excluded segment of prestin-expressing cells indeed generates force when stimulated electrically. The electromotile force resulted from the expression of prestin because it was inhibited by a known blocker of OHC electromotility, salicylate.

3.19.3.2 Charge Transfer

Electrical charge transfer mediated by prestin can be recorded as a gating current in response to a steplike displacement of the membrane voltage. On returning to the initial voltage, a current of the opposite sign but carrying the same amount of charge is observed. This reversibility of charge transfer and its high speed allow monitoring of it as a voltage-dependent capacitance (usually termed nonlinear capacitance, NLC; for details, see Dallos, P. and Fakler, B., 2002). Since membrane capacitance can be recorded with standard lock-in patch-clamp techniques, NLC is often used to characterize the properties of prestin. While control cells do not exhibit any appreciable NLC, expression of prestin is sufficient to produce NLC with properties equivalent to that seen in OHCs (Ludwig, J. *et al.*, 2001; Santos-Sacchi, J. *et al.*, 2001).

The specific voltage dependence and kinetics of both force generation and charge transfer have important implications for the physiological function of prestin in hearing and for understanding the underlying molecular mechanism. These properties have been studied extensively using the native protein in OHCs and have subsequently been confirmed with recombinant prestin.

3.19.3.3 Voltage Dependence

Both length changes and electrical charge transfer exhibit an identical sigmoidal dependence on membrane potential that saturates for very negative and positive voltages (Santos-Sacchi, J., 1991; Santos-Sacchi, J., 1992; Figure 2). Concerning motility, the OHC is short at depolarized and elongated at hyperpolarized potentials. Notably, the same polarity was observed in prestin-transfected cells (Ludwig, J. *et al.*, 2001). The sigmoidal voltage dependence can be accurately modeled by a first-order Boltzmann function, indicating that the underlying process is the voltage-dependent redistribution of molecules between two states (see Section 3.19.4.1). Accordingly, the derivative of charge transfer, NLC, is bell-shaped and corresponds to the derivative of a Boltzmann function (Santos-Sacchi, J., 1991; Figure 2). Fitting motility or charge movement with a Boltzmann function yields two main parameters that quantitatively characterize prestin's voltage dependence: (1) the slope (steepness) of the voltage dependence and (2) $V_{1/2}$, defined as the voltage at which half of the molecules reside in either conformation. The Boltzmann slope determined from recordings of electromotility or NLC of native or recombinant prestin is about 30 mV, which translates into the transport of about 0.8 elementary electrical

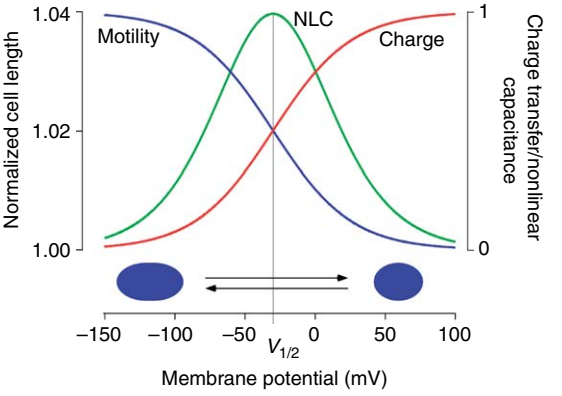

Figure 2 The characteristic mechanical and electrophysiological behavior of prestin. OHC length (blue) shortens with depolarization of the membrane potential in a saturating manner according to a first-order Boltzmann function. The underlying area change in the individual motor proteins is depicted schematically. Electromotility is coupled to electrical charge movement across the membrane (red). The amount of charge flowing for any given voltage change follows the same sigmoidal voltage dependence as motility. Charge movement can also be recorded as a voltage-dependent capacitance (nonlinear capacitance (NLC), green) that is the derivative of charge and thus has a bell-shaped voltage dependence.

charges through the whole transmembrane electrical field (see Section 3.19.4.1). $V_{1/2}$ is important because it characterizes the voltage of the highest electromechanical gain, that is, largest displacement of the cell for a given voltage change (Santos-Sacchi, J., 1992). $V_{1/2}$ also denotes the voltage at maximum NLC and in mature OHCs is typically around −30 mV (Santos-Sacchi, J., 1992; Kakehata, S. and Santos-Sacchi, J., 1995; Oliver, D. and Fakler, B., 1999). In contrast, heterologously expressed prestin yields a $V_{1/2}$ of ∼−70 mV, substantially hyperpolarized compared to the OHC (Ludwig, J. *et al.*, 2001; Santos-Sacchi, J. *et al.*, 2001). However, $V_{1/2}$ in OHCs can be shifted by various manipulations including agents that affect phosphorylation (Frolenkov, G. I. *et al.*, 2000) and is also more negative in immature OHCs (∼−90 mV; Oliver, D. and Fakler, B., 1999), suggesting that this difference in $V_{1/2}$ does not indicate a fundamental distinction between native and recombinant prestin but is more likely a regulatory issue.

3.19.3.4 Kinetics

The kinetics of electromotility and prestin-mediated charge movement are extremely rapid. Electromotility works at microsecond rates and has been measured up to 70 kHz from OHCs (Frank, G. *et al.*, 1999). Force generation by recombinant prestin shows no sign of attenuation up to at least 20 kHz (Ludwig, J. *et al.*, 2001). Electrophysiological measurements of the charge transfer are generally limited in time resolution because of low-pass filtering by the membrane capacitance in conjunction with a series resistance and the speed of the amplifier. However, using recordings from isolated membrane patches that yield high cut-off frequencies, microsecond rates for charge movements have been obtained (Gale, J. E. and Ashmore, J. F., 1997).

3.19.3.5 Pharmacology

Only few inhibitors of prestin-mediated electromotility are known, and none of them appears to act with high specificity. Salicylate reversibly inhibits electromotility at low millimolar concentrations (Kakehata, S. and Santos-Sacchi, J., 1996). This hydrophobic monovalent anion appears to affect prestin's function from the intracellular side by competing with the small inorganic anions that are crucial for mediating the voltage dependence of prestin (Oliver, D. *et al.*, 2001). Trivalent lanthanide ions like gadolinium (Gd^{3+}) that are known to block a variety of ion channels with little selectivity inhibit electromotility reversibly at millimolar concentrations (Kakehata, S. and Santos-Sacchi, J., 1996). The mechanism behind this action is unclear.

3.19.4 The Generation of Force and Nonlinear Capacitance by Prestin: Molecular Mechanisms

3.19.4.1 Biophysical Model

The tight coupling between charge movement and electromotility has led to the formulation of a biophysical model of force generation, the area motor model of electromotility (Dallos, P. *et al.*, 1993; Iwasa, K. H., 1994). In essence, the elementary motor, prestin, can adopt (at least) two conformational states, which occupy different areas in the plane of the membrane. The macroscopic movements that can be observed experimentally thus result from synchronous transitions of large numbers of prestin molecules from an extended to a compact conformation or vice versa. Occupancy of both states is voltage dependent. This voltage dependence requires an electrically charged particle, the voltage sensor that can move across the membrane electrical field to trigger the conformational area change in the protein, in doing so producing the charge transfer. Such a mechanism is analogous to the gating of voltage-dependent ion channels, where movement of the positively charged S4 helix triggers opening of the channel pore and can be observed as a gating current (Dallos, P. and Fakler, B., 2002). This simple two-state model is supported by the finding that charge and mechanics adhere to the same voltage dependence that can be accurately described by a two-state Boltzmann function. Though more complex reaction schemes are certainly possible, most experimental data are well described with this simplest model. Moreover, the tight coupling between conformational reorientation and charge transfer requires that electrical as well as mechanical energy terms should influence the occupation of either state. Such electromechanical reciprocity is indeed observed experimentally. Thus, altering the mechanical tension of the membrane shifts the voltage dependence of charge movement and electromotility along the voltage axis (Gale, J. E. and Ashmore, J. F., 1994; Kakehata, S. and Santos-

Sacchi, J., 1995). If tension is increased, $V_{1/2}$ is shifted to more positive potentials, meaning that more depolarization is necessary to push the prestin molecules into their compact conformation. This tension dependency is not only observed in OHCs, but has been confirmed with recombinant prestin (Ludwig, J. *et al.*, 2001; Santos-Sacchi, J. *et al.*, 2001), indicating that it is not due to the specific hair cell environment of prestin but is an intrinsic property of the molecule. Even more striking, changing membrane tension at a constant voltage should thrust molecules from one to the other conformational state, and consequently result in the reverse transfer of their voltage sensor across the membrane. This has been observed experimentally as an electrical current upon rapid stretching of the OHC membrane (Gale, J. E. and Ashmore, J. F., 1994). Estimates for the area change of a single motor molecule (Dong, X. X. and Iwasa, K. H., 2004) are 1–4 nm^2.

Measurements of OHC stiffness have shown that not only cell length but also axial stiffness is voltage dependent (He, D. Z. *et al.*, 2003). This may mean that prestin contributes significantly to the overall stiffness of the OHC and that the conformational states of prestin may differ in their intrinsic stiffness.

Alternative models for electromotility that involve generation of force by the membrane lipid bilayer have been put forward. In these models, prestin is assumed to provide voltage-dependent changes in dielectric properties of the membrane, which in turn may precipitate altered membrane tension (Zhang, P. C. *et al.*, 2001) or membrane bending (Raphael, R. M. *et al.*, 2000). While these models are based on established biophysical mechanisms, direct experimental evidence to support such an action of prestin is currently lacking.

3.19.4.2 Molecular Mechanisms

According to the biophysical model, the prestin molecule should comprise two principal functional domains, one that senses the membrane potential (voltage sensor) and one or more actuator domains that undergo the major conformational change. Since structural data for prestin or related transporters are currently not available, one basic approach to the underlying molecular mechanisms is to identify regions within the protein that are involved in either process.

So far, the issue of the voltage sensor has been addressed, exploiting the easy experimental accessibility of NLC. Using recombinant prestin or patches excised from the OHC membrane it was demonstrated that NLC depends on the presence of monovalent anions at the intracellular but not the extracellular side of the membrane (Oliver, D. *et al.*, 2001). Removal of the major anion chloride (Cl^-) from the cytoplasmic face of prestin reversibly abolished NLC in excised patches. The amount of NLC varied with the Cl^- concentration in a saturable manner, indicating the binding of Cl^- to prestin with millimolar affinity (dissociation constant (K_d) ~6 mM). Small monovalent anions like other halides, bicarbonate, and nitrate could substitute for Cl^-; in contrast, divalent anions like sulfate did not support NLC. While amplitude and $V_{1/2}$ of the NLC varied with the anion species, the steepness of voltage dependence was constant. However, if larger organic anions such as carboxylic acids were used, the steepness decreased with increasing molecule size, which in terms of the two-state voltage-sensor model translates into a reduced sensor charge or a smaller distance traversed by the sensor. These findings are consistent with the translocation of the anion itself through the electric field and suggest that the anion acts as an extrinsic voltage sensor of prestin (Figure 3(b)). In agreement with this idea, Cl^- removal also abolished electromotility, indicating that the force-producing steps are indeed triggered by the anion–prestin interaction (Oliver, D. *et al.*, 2001). Obviously, this model of anion-translocation nicely fits prestin's membership in an anion transporter family. In fact, it is tempting to hypothesize that the charge-translocation step functionally corresponds to a partial reaction in the anion transport cycle of other SLC26 transporters, which have been shown to mediate anion fluxes (Mount, D. B. and Romero, M. F., 2004).

One caveat to this simple model is that reducing the chloride concentration shifted the voltage dependence to more positive potentials (Oliver, D. and Fakler, B., 2002; Rybalchenko, V. and Santos-Sacchi, J., 2003). In other words, less negative intracellular potential is necessary to push an anion toward the extracellular side at a lower anion concentration – contrary to what is expected for a simple anion translocation. Thus, more complex reaction schemes may underlie the charge transfer and charged protein domains of prestin may contribute to it as well. An alternative model has been suggested in which anions bind to one or more distinct binding sites to allosterically regulate charge translocation

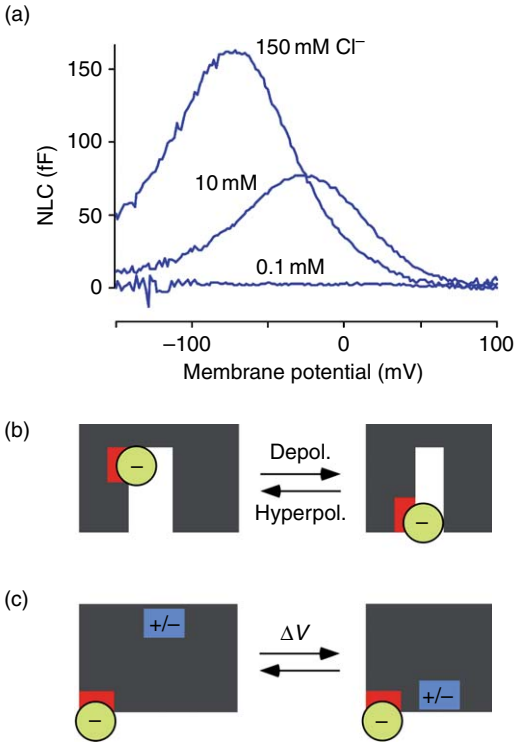

Figure 3 Anion dependence of prestin. a, nonlinear capacitance (NLC) generated by prestin is abolished when intracellular chloride is removed. NLC was measured in an inside–out membrane patch excised from an OHC with the indicated concentrations of Cl^- present at the cytoplasmic side (replacement of Cl^- by SO_4^{2-}). b, Model proposed to explain the anion dependence of prestin (Oliver, D. *et al.*, 2001). After binding to an anion-binding site (red), chloride (or other inorganic anions, yellow) can be translocated through the protein by changes of the membrane potential, and thereby trigger a conformational area change of prestin. The anion thus acts as an extrinsic voltage sensor. c, Alternative model (Rybalchenko, V. and Santos-Sacchi, J., 2003) in which binding of anions allosterically modifies the voltage dependence of prestin, which is mediated by charged residues acting as an intrinsic voltage sensor (blue).

and thus motility (Figure 3(c); Rybalchenko, V. and Santos-Sacchi, J., 2003). In this model, anion binding shifts the position of the NLC curve along the voltage axis. However, such a model predicts two populations of molecules either without or with Cl^- bound that differ in their voltage dependence, which is not observed experimentally (Oliver, D. *et al.*, 2001; Rybalchenko, V. and Santos-Sacchi, J., 2003).

In any case, the essential role of anions for prestin's function directly provokes the question about the molecular identity of the anion binding site. Recent structure–function studies have begun to address this issue. Mutational neutralization of charged aa residues present in prestin but not in the homologous protein SLC26A6 (which does not show charge movement) shifted NLC without abolishing it, suggesting rather an electrostatic effect of these residues on putative anion translocation than a direct involvement in anion binding (Oliver, D. *et al.*, 2001). Recently, mutations in a sequence stretch with similarity to anion coordination sites identified in a bacterial CLC chloride transporter were reported to abolish charge movement (Navaratnam, D. *et al.*, 2005), providing an exciting starting point for the identification of functional domains in prestin. However, due to the tight coupling of charge translocation and molecular motion any mutation that inhibits the conformational change may also arrest charge movement. Mutations that abolish NLC may therefore impair either anion binding, voltage sensor translocation, or the coupled conformational change.

3.19.5 Future Directions

Perhaps the most exciting questions for future research center around the molecular mechanisms of prestin's function. Does the NLC indeed result from physical translocation of anions through the electrical field; alternatively, how much of the sensor charge is supplied by movable residues of the protein? What is the anion-binding domain? And how does the sensor translocation subsequently trigger a gross conformational rearrangement that can even generate macroscopic cellular forces? Which are the domains of prestin that actually move upon changes in membrane voltage? Answers to these questions may arise from examining the mechanistic relationship between electromotility and the electrogenic anion exchange function of prestin's closest homologs (Schaechinger, T. J. and Oliver, D., 2007).

Thus, progress in understanding the molecular basis of electromotility may unexpectedly prove extremely helpful for understanding the currently completely unresolved mechanism of anion transport by other SLC26 transporters, whose essential roles in ion transport in many organs we are just beginning to appreciate (Mount, D. B. and Romero, M. F., 2004).

References

Albert, J. T., Winter, H., Schaechinger, T. J., Weber, T., Wang, X., He, D. Z. Z., Hendrich, O., Geisler, H. S., Zimmermann, U., Oelmann, K., Knipper, M., Gopfert, M. C., and Oliver, D. 2007. Voltage-sensitive prestin orthologue expressed in zebrafish hair cells. J. Physiol. 580, 451–461.

Belyantseva, I. A., Adler, H. J., Curi, R., Frolenkov, G. I., and Kachar, B. 2000. Expression and localization of prestin and the sugar transporter glut-5 during development of electromotility in cochlear outer hair cells. J. Neurosci. 20, RC116.

Dallos, P. and Fakler, B. 2002. Prestin, a new type of motor protein. Nat. Rev. Mol. Cell Biol. 3, 104–111.

Dallos, P., Evans, B. N., and Hallworth, R. 1991. Nature of the motor element in electrokinetic shape changes of cochlear outer hair cells. Nature 350, 155–157.

Dallos, P., Hallworth, R., and Evans, B. N. 1993. Theory of electrically driven shape changes of cochlear outer hair cells. J. Neurophysiol. 70, 299–323.

Deak, L., Zheng, J., Orem, A., Du, G. G., Aguinaga, S., Matsuda, K., and Dallos, P. 2005. Effects of cyclic nucleotides on the function of prestin. J. Physiol. 563, 483–496.

Dong, X. X. and Iwasa, K. H. 2004. Tension sensitivity of prestin: comparison with the membrane motor in outer hair cells. Biophys. J. 86, 1201–1208.

Frank, G., Hemmert, W., and Gummer, A. W. 1999. Limiting dynamics of high-frequency electromechanical transduction of outer hair cells. Proc. Natl. Acad. Sci. U. S. A. 96, 4420–4425.

Frolenkov, G. I., Mammano, F., Belyantseva, I. A., Coling, D., and Kachar, B. 2000. Two distinct Ca(2+)-dependent signaling pathways regulate the motor output of cochlear outer hair cells. J. Neurosci. 20, 5940–5948.

Gale, J. E. and Ashmore, J. F. 1994. Charge displacement induced by rapid stretch in the basolateral membrane of the guinea pig outer hair cell. Proc. Royal Soc. Lond. B 255, 243–249.

Gale, J. E. and Ashmore, J. F. 1997. An intrinsic frequency limit to the cochlear amplifier. Nature 389, 63–66.

He, D. Z., Jia, S., and Dallos, P. 2003. Prestin and the dynamic stiffness of cochlear outer hair cells. J. Neurosci. 23, 9089–9096.

Holley, M. C. 1996. Outer Hair Cell Motility. In: The Cochlea (*eds*. P. Dallos, A. N. Popper, and R. R. Fay), pp. 386–434. Springer.

Iwasa, K. H. 1994. A membrane motor model for the fast motility of the outer hair cell. J. Acoust. Soc. Am. 96, 2216–2224.

Kakehata, S. and Santos-Sacchi, J. 1995. Membrane tension directly shifts voltage dependence of outer hair cell motility and associated gating charge. Biophys. J. 68, 2190–2197.

Kakehata, S. and Santos-Sacchi, J. 1996. Effects of salicylate and lanthanides on outer hair cell motility and associated gating charge. J. Neurosci. 16, 4881–4889.

Ko, S. B., Zeng, W., Dorwart, M. R., Luo, X., Kim, K. H., Millen, L., Goto, H., Naruse, S., Soyombo, A., Thomas, P. J., and Muallem, S. 2004. Gating of CFTR by the STAS domain of SLC26 transporters. Nat. Cell Biol. 6, 343–350.

Liberman, M. C., Gao, J., He, D. Z., Wu, X., Jia, S., and Zuo, J. 2002. Prestin is required for electromotility of the outer hair cell and for the cochlear amplifier. Nature 419, 300–304.

Liu, X. Z., Ouyang, X. M., Xia, X. J., Zheng, J., Pandya, A., Li, F., Du, L. L., Welch, K. O., Petit, C., Smith, R. J., Webb, B. T., Yan, D., Arnos, K. S., Corey, D., Dallos, P., Nance, W. E., and Chen, Z. Y. 2003. Prestin, a cochlear motor protein, is defective in non-syndromic hearing loss. Hum. Mol. Genet. 12, 1155–1162.

Ludwig, J., Oliver, D., Frank, G., Klocker, N., Gummer, A. W., and Fakler, B. 2001. Reciprocal electromechanical properties of rat prestin: the motor molecule from rat outer hair cells. Proc. Natl. Acad. Sci. U. S. A. 98, 4178–4183.

Matsuda, K., Zheng, J., Du, G. G., Klocker, N., Madison, L. D., and Dallos, P. 2004. N-linked glycosylation sites of the motor protein prestin: effects on membrane targeting and electrophysiological function. J. Neurochem. 89, 928–938.

Mount, D. B. and Romero, M. F. 2004. The slc26 gene family of multifunctional anion exchangers. Pflugers Arch. 447, 710–721.

Nagy, I., Bodmer, M., Schmid, S., and Bodmer, D. 2005. Promyelocytic leukemia zinc finger protein localizes to the cochlear outer hair cells and interacts with prestin, the outer hair cell motor protein. Hear. Res. 204, 216–222.

Navaratnam, D., Bai, J. P., Samaranayake, H., and Santos-Sacchi, J. 2005. N-terminal-mediated homomultimerization of prestin, the outer hair cell motor protein. Biophys. J. 89, 3345–3352.

Oliver, D. and Fakler, B. 1999. Expression density and functional characteristics of the outer hair cell motor protein are regulated during postnatal development in rat. J. Physiol. 519, 791–800.

Oliver, D. and Fakler, B. 2002. Functional Properties of Prestin – How the Motormolecule Works Work. In: Biophysics of the Cochlea. From Molecules to Models (*ed*. A. W. Gummer), pp. 110–115. World Scientific.

Oliver, D., He, D. Z., Klocker, N., Ludwig, J., Schulte, U., Waldegger, S., Ruppersberg, J. P., Dallos, P., and Fakler, B. 2001. Intracellular anions as the voltage sensor of prestin, the outer hair cell motor protein. Science 292, 2340–2343.

Raphael, R. M., Popel, A. S., and Brownell, W. E. 2000. A membrane bending model of outer hair cell electromotility. Biophys. J. 78, 2844–2862.

Rybalchenko, V. and Santos-Sacchi, J. 2003. Cl^- flux through a non-selective, stretch-sensitive conductance influences the outer hair cell motor of the guinea-pig. J. Physiol. 547, 873–891.

Santos-Sacchi, J. 1991. Reversible inhibition of voltage-dependent outer hair cell motility and capacitance. J. Neurosci. 11, 3096–3311.

Santos-Sacchi, J. 1992. On the frequency limit and phase of outer hair cell motility: effects of the membrane filter. J. Neurosci. 12, 1906–1916.

Santos-Sacchi, J., Shen, W., Zheng, J., and Dallos, P. 2001. Effects of membrane potential and tension on prestin, the outer hair cell lateral membrane motor protein. J. Physiol. 531, 661–666.

Schaechinger, T. J. and Oliver, D. 2007. Nonmammalian orthologs of prestin (SLC26A5) are electrogenic divalent/chloride anion exchangers. Proc. Natl. Acad. Sci. U.S.A. 104, 7693–7698.

Sziklai, I., Szonyi, M., and Dallos, P. 2001. Phosphorylation mediates the influence of acetylcholine upon outer hair cell electromotility. Acta Otolaryngol. 121, 153–156.

Weber, T., Gopfert, M. C., Winter, H., Zimmermann, U., Kohler, H., Meier, A., Hendrich, O., Rohbock, K., Robert, D., and Knipper, M. 2003. Expression of prestin-homologous solute carrier (slc26) in auditory organs of nonmammalian vertebrates and insects. Proc. Natl. Acad. Sci. U. S. A. 100, 7690–7695.

Zhang, P. C., Keleshian, A. M., and Sachs, F. 2001. Voltage-induced membrane movement. Nature 413, 428–432.

Zheng, J., Aguiñaga, S., Anderson, C. T., Miller, K., and Dallos, P. 2005. Prestin's interaction with CFTR enhances its function. Assoc. Res. Otolaryngol. p.1045.

Zheng, J., Du, G. G., Anderson, C. T., Keller, J. P., Orem, A., Dallos, P., and Cheatham, M. A. 2006. Analysis of the

oligomeric structure of the motor protein prestin. J. Biol. Chem. 281, 19916–19924.
Zheng, J., Long, K. B., Matsuda, K. B., Madison, L. D., Ryan, A. D., and Dallos, P. D. 2003. Genomic characterization and expression of mouse prestin, the motor protein of outer hair cells. Mamm. Genome 14, 87–96.
Zheng, J., Long, K. B., Shen, W., Madison, L. D., and Dallos, P. 2001. Prestin topology: localization of protein epitopes in relation to the plasma membrane. Neuroreport 12, 1929–1935.
Zheng, J., Shen, W., He, D. Z., Long, K. B., Madison, L. D., and Dallos, P. 2000. Prestin is the motor protein of cochlear outer hair cells. Nature 405, 149–155.

Further Reading

Brownell, W. E., Bader, C. R., Bertrand, D., and de Ribaupierre, Y. 1985. Evoked mechanical responses in isolated cochlear outer hair cells. Science 227, 194–196.

3.20 Cochlear Receptor Potentials

I J Russell, University of Sussex, Brighton, UK

© 2008 Elsevier Inc. All rights reserved.

3.20.1	**Introduction**	320
3.20.2	**A History of Sensory Transduction**	321
3.20.3	**Compound Potentials Recorded from the Cochlea**	322
3.20.4	**Davis' Theory of Sensory Transduction**	323
3.20.5	**IHC Receptor Potentials**	324
3.20.5.1	Factors That Shape the Inner Hair Cell Receptor Potential	325
3.20.5.1.1	Intracellular calcium levels	326
3.20.5.1.2	Voltage-dependent basolateral conductances	326
3.20.5.1.3	Inner Hair Cell receptor potential transfer function and operating point depend on cochlear location	327
3.20.5.2	Transfer Functions of Afferent Synapses	329
3.20.5.3	Phase Relationships between Inner Hair Cell and Neural Excitation	332
3.20.5.4	Control of Transmitter Release from the Inner Hair Cell Afferent Synapse by the AC and DC Receptor Potentials	333
3.20.5.5	Inner Hair Cell Membrane Time Constant and Phase-Locking	333
3.20.5.5.1	Inner Hair Cell membrane time constant: significance for phase-locking	333
3.20.5.5.2	The problem of preserving high temporal resolution in synaptic transmission	335
3.20.5.5.3	The problem with owls	336
3.20.5.6	Dynamic Range	337
3.20.6	**Outer Hair Cell Receptor Potentials**	337
3.20.6.1	Phase and Magnitude of Outer Hair Cell and Inner Hair Cell Receptor Potentials as Indicators of Electromechanical Feedback	338
3.20.6.2	The Phase and Magnitude of Outer Hair Cell Receptor Potential and the Positive Feedback Model	339
3.20.6.3	Outer Hair Cell Excitation and the Parallel Resonance Model	340
3.20.6.4	The Phase of Outer Hair Cell Excitation: A Balance between the Tectorial Membranes Radial Stiffness and Rotational Stiffness of Outer Hair Cell Stereocilia	340
3.20.6.5	Hair Cell Isoresponse Tuning Curves: Comparison with Mechanical and Neural Tuning Curves	341
3.20.6.6	Factors Influencing Amplification along the Length of the Basilar Membrane	342
3.20.6.7	Operating Point of the Outer Hair Cell Receptor Potential	344
3.20.6.8	Control of the Outer Hair Cell Transducer-Operating Point	344
3.20.6.9	Displacement of the Outer Hair Cell Transducer-Operating Point and Gain Optimization	345
3.20.6.10	Temporary Threshold Shift in Cochlear Sensitivity and Changes in the Operating Point of the Outer Hair Cell Transducer	348
3.20.6.11	Control of the Outer Hair Cell Operating Point and Shaping of the Outer Hair Cell Receptor Potential Tuning Curve	350
3.20.7	**Exploiting Compound Potentials to Understand Cochlear Function and Dysfunction**	350
3.20.8	**The Nature of the Cochlear Amplifier**	351
References		352

Glossary

BM Basilar membrane
CAP Compound action potential
CF Characteristic frequency
CM Cochlear microphonic
EP Endocochlear potential
EPSPs Excitatory postsynaptic potentials
IHC Inner hair cell
MET Mechanoelectrical transducer channels
OHC Outer hair cell
TM Tectorial membrane
RL Reticular lamina
RW Round window
SP Summating potential

3.20.1 Introduction

Sensory processing in the cochlea is initiated when the hair cells respond to excitation by generating receptor potentials. Sensory transduction takes place in the organ of Corti, a strip of sensory epithelium consisting of a single row of inner hair cells (IHCs) and three rows of outer hair cells (OHCs) sandwiched between two extracellular matrices, the basilar membrane (BM), and tectorial membrane (TM) (Lim, D. J., 1986). Altogether, these structures comprise the cochlear partition. Hair cells are excited through sound-induced vibrations of the BM and the resultant reactions of their hair bundles with the overlying TM (ter Kuile, E., 1900; Davis, H., 1958; Allen, J. B., 1980; Zwislocki, J. J., 1980; Dallos, P., 2003; Legan, P. K. *et al.*, 2005; Chan, D. K. and Hudspeth, A. J., 2005; Nowotny, M. and Gummer, A. W., 2006; Fridberger, A. *et al.*, 2006) (Figure 1). IHCs, however, share a division of labor with the OHCs; OHCs are sensory-effector cells that both detect and influence mechanical interactions between the TM and the reticular lamina (RL) of the organ of Corti (Brownell, W. E. *et al.*, 1985; Mammano, F. and Ashmore, J. F., 1993; Dallos, P., 1992; Dallos, P. and Corey, M. E., 1991). They are most effective at exerting electromechanical feedback to the cochlear partition at frequencies close to the characteristic frequency (CF) of their location on the BM (Geisler, C. D., 1998). Their role is to amplify responses to low-level sounds and compress responses to high-level sounds (Geisler, C. D., 1998; Robles, L. and Ruggero, M. A., 2001). They are therefore instrumental in

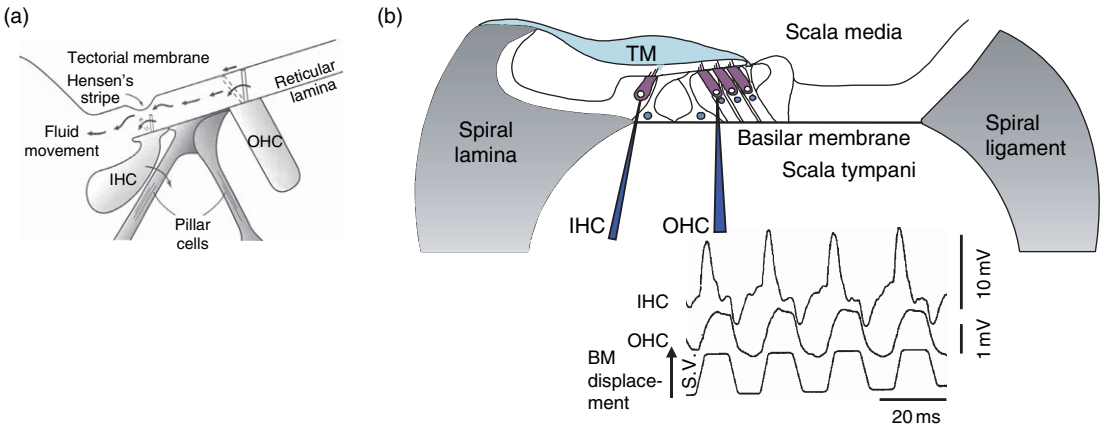

Figure 1 IHCs respond to the velocity and OHCs to the displacement of the BM. (a) OHC hair bundles are attached to the TM and thus OHCs are able to influence the BM movements. IHC hair bundles are coupled by viscous drag and respond passively to the cochlear partition's vibrations. (b) IHC receptor potentials (upper trace) recorded from the basal turn of a guinea-pig cochlea phase lead OHC responses (middle trace) recorded just outside the IHC in response to a 52 kHz, 89 dB SPL trapezoidal acoustic stimulus (lower trace). (a) Reproduced from figure 6.8 of Geisler, C. D. 1998. From Sound to Synapse. Oxford University Press. (b) From figure 1 of Sellick, P. M. and Russell, I. J. 1980. The responses of IHCs to basilar membrane velocity during low frequency auditory stimulation in the guinea pig cochlea. Hear. Res. 2, 439–446.

determining the exquisite sensitivity and frequency tuning of the cochlea and they define the enormous dynamic range of the auditory system. IHCs appear to be purely sensory, their hair bundles responding to the resultant interactions between the TM and RL (Dallos, P. *et al*., 1972; Russell, I. J. and Sellick, P. M., 1978), and their synapses transforming and transmitting the resulting receptor potentials to the afferent fibers, which conduct auditory responses in trains of nerve impulses to the hindbrain nuclei (Spoendlin, H., 1985). OHCs also, presumably, transmit their responses to the type II afferent fibers, although what these responses look like and their purpose remain mysteries (Robertson, D. and Gummer, M., 1985; Robertson, D. *et al*., 1999).

Their roles in cochlear sensory processing being different from each other, IHCs and OHCs thus have different design briefs. IHCs are designed to detect and relay interaction between the major extracellular matrices of the cochlear partition. OHCs are designed to optimize this interaction and hence the sensitivity and frequency selectivity of the cochlea. This chapter is concerned with our understanding of the workings of the cochlea largely from the measurement of receptor potentials from individual hair cells in the cochlea. This frustrating but fruitful line of research has been carried out in remarkably few laboratories over a relatively brief period of time. Only a few of us, including Mary Ann Cheatham, Peter Dallos, Fred Nuttall, Peter Sellick, Joe Zwislocki, and our hard put-upon colleagues decided that it might be easier to measure responses directly from hair cells rather than interpret extracellular potentials from the cochlea, except when the risk of confusion was relatively low. The major hazards with intracellular recording are limitations imposed by the frequency responses of the recording systems and their nonlinearity when strongly polarized. These limitations make it difficult to obtain quantitative measurements at high frequencies and high levels of electrical polarization. Other limitations are leak conductances caused by electrode penetration. These are often emphasized by patch clampers when attacking isolated cells with electrodes filled with nonphysiological solutions and obtaining findings that differ from those obtained with sharp electrodes *in vivo* measurements. These leak conductances can sometimes have real rather than imaginary consequences to the interpretation of the data. The findings from different laboratories using sharp electrodes to measure hair cell responses *in vivo* are remarkably consistent. Where they differ, the differences have usually been resolved. The origin and functional significance of cochlea potentials have been the subject of some outstanding reviews by Dallos P. (1992; 1996) .

3.20.2 A History of Sensory Transduction

This subject has been covered in a previous chapter, but it is worth reminding ourselves that our widely held understanding of hair cells as being excited by displacement of the hair bundle toward the tallest row or kinocilium, if one is present, is due to the combined electrophysiological measurements and electron microscopy of Löwenstein O. and Wersäll J. (1959) when working on the semicircular canals of the skate. The discovery that excitation was associated with hair cell depolarization is due to Flock A. (1965) measurements from lateral line organs of the freshwater cod *Lota*. He also revealed the exquisite asymmetry of the hair cell's electrical response and derived a hair cell-transfer function, which also offered an explanation for the double-frequency microphonic of the lateral line organ. Later, Hudspeth A. J. and Corey D. (1977) were the first to manipulate individual hair bundles and were able to relate the hair cell receptor potential to hair-bundle displacement in freestanding hair bundles, revealed by stripping away the otoconial membrane from the sensory epithelium of the isolated frog sacculus. The first measurements of receptor potentials from IHC (Russell, I. J. and Sellick, P. M., 1977) and OHC (Dallos, P. *et al*., 1982) depended very much on the earlier findings for their interpretation.

Sellick and Russell were also intrigued at this time by the nature of the hair cell receptor current. This came about as a consequence of Sellick's early research on the electrochemistry of the cochlea (Sellick, P. M. and Johnstone, B. M., 1975) and the present author's interest in the lateral line organs. As a consequence, we first worked on this problem in the lateral line organs of *Xenopus*, which swam in laboratory tap water, where the dominant cation was calcium. With help and encouragement from Keith Bosher, who had already made the definitive measurements of the ionic composition of endolymph (Bosher, S. K. and Warren, R. L., 1978), which bathes the hair bundles of cochlear hair cells, we discovered that the gelatinous cupula (equivalent to the TM) of lateral line organs can sustain a Donnan equilibrium and a micro, compartmentalized, environment of high levels of potassium and a positive endocupular

potential of several tens of millivolts (Russell, I. J. and Sellick, P. M., 1976). The environment bathing the apical surfaces of lateral line hair cells was, thus, remarkably similar to that bathing the apical surfaces of cochlear hair cells. From this we concluded, according to the Davis H. (1965) theory, that the dominant ion carrying the receptor current must be potassium. Olav Sand felt that we had missed a trick and insisted that we measure the free calcium concentration in the cupula. He was led to this suggestion by his frustration and finding that the tap water of Los Angeles was so contaminated with heavy metals, other than calcium, that salamander lateral line organs did not transduce if the salamanders were maintained in it (Sand, O., 1985). However, transduction was restored in the presence of calcium. He also pointed out that the calcium concentration of the endolymph measured by Bosher S. K. and Warren R. L. (1978) was very small (30 μM). Even so, 30 μM calcium is several orders larger than that which might be expected due to passive distribution of calcium in the endolymph, and therefore must be actively pumped and essential for sensory processing in the cochlea. We found similar calcium levels in the lateral line cupulae of *Xenopus*, although here we found no evidence of active pumping, but the high levels (10–30 μM) were due to diffusion from the surrounding tap water (McGlone, F. P. *et al.*, 1979). Thus Sand was the first to show that calcium was an essential element in hair cell mechanotransduction. These studies, and those of Krönester-Frei A. (1979) (see also Freeman, D. M. *et al.*, 2003a; 2003b) on the susceptibility of the TM to manipulations of the ionic composition of artificial endolymph, kept us aware that a drop in the endocochlear potential had many more implications for sensory transduction in the cochlea than a change in the driving voltage to the hair cell transducer. Our current understanding of endolymph and the production of the endocochlear potential has been the subject of several reviews in the early 2000s (e.g., Wangemann, P., 2002).

3.20.3 Compound Potentials Recorded from the Cochlea

Three important extracellular receptor potentials can be recorded, usually via an electrode placed on, or close to the round window (RW) membrane. These are the cochlear microphonic (CM), the summating potential (SP), and the compound action potential (CAP). They have been the subjects of seminal original papers and excellent reviews, including Dallos P. (1973). Experiments involving selective destruction of hair cells (Dallos, P. *et al.*, 1972) and later measurements from single hair cells (Russell, I. J. and Sellick, P. M., 1977; Dallos, P. *et al.*, 1982) provided the basis for a fuller understanding of the origin and nature of extracellular receptor potentials and their utility in studying the cellular mechanism of sensory transduction in the cochlea. Largely on the basis of these experiments, it was confirmed that the CM is a farfield potential produced almost exclusively from OHC cell-receptor currents (Dallos, P. *et al.*, 1972; 1982; Russell, I. J. and Sellick, P. M., 1983) and the CM recorded from the RW membrane is dominated by the responses of OHCs in the basal turn of the cochlea (Patuzzi, R. B. *et al* 1989; Zheng, X.-Y. *et al.*, 1997; Durrant, J. D. *et al.*, 1998; Legan, P. K. *et al.*, 2000). The SP is a DC component of the electrical response of the cochlea which, when recorded from the RW membrane, is dominated by the responses of basal turn hair cells. Experiments directed at the selective destruction of IHCs (Zheng, X.-Y. *et al.*, 1997; Durrant, J. D. *et al.*, 1998) appear to have resolved a long-standing issue on the origin of the SP concerning its generation, as least in the basal turn and for low-to-moderate stimulus levels, by attributing it largely to the IHCs when DC components of OHC responses are immeasurably small (Russell, I. J. and Sellick, P. M., 1978; Cody, A. R. and Russell, I. J., 1987; Russell, I. J. and Kössl, M., 1992a). It remains to be seen if this is the case in other turns of the cochlea. Controversy over the origin of the SP began when as a result of hair-cell lesion studies with streptomycin Davis H. *et al.* (1958a) concluded that the IHCs are the dominant source of the SP. By contrast Dallos P. (1973) proposed the OHCs as the primary source of the SP based on unpublished work with Bredberg in which they destroyed hair cells in the guinea-pig with kanamycin. Further support for an OHC origin for the SP was provided by Dallos P. and Cheatham M. A. (1976) who found SP recorded from the apical turn of the cochlea to be essentially unchanged with complete destruction of IHCs by kanamycin. In the light of later intracellular studies by Dallos P. and Cheatham M. A. (Dallos, P., 1986; Dallos, P. and Cheatham, M. A., 1991) which reveal that OHCs in the apical three turns of the guinea-pig cochlea can generate substantial DC potentials, the 3:1 outnumbering of IHCs by OHCs and that IHC receptor potentials are swamped by OHC responses when recording within the organ of Corti (Russell, I. J.

and Sellick, P. M., 1983; Cody, A. R. and Mountain, D. C., 1989), Dallos' conclusions that OHCs are the dominant source of SP, at least in the low-frequency turns of the cochlea, would appear to be justified.

The CAP is perhaps the easiest of the extracellular potentials to measure, through an electrode placed on the RW, and it is certainly the most useful. The RW electrode can record compound-action potentials from afferent fibers that innervate the entire extent of the cochlea. The same electrode will also record CM and SP, but these potentials are dominated by the responses of basal turn hair cells (Patuzzi, R. B. *et al.*, 1989). Accordingly the threshold responses of the CAP are an excellent indicator of sensitivity over the entire frequency range of the cochlea and can be used as a basis for comparison to determine the cochlear origin of sensory neural hearing loss (see Dallos, P., 1973). Simultaneous and forward-masking of the CAP can be used to produce tuning curves that are very similar in characteristics to those of single unit neural-tuning curves (Dallos, P. and Cheatham, M. A., 1976). Thus, through the relatively simple procedure of placing an electrode on the RW, one can measure the sensitivity and frequency response of the cochlea from the responses of the CAP.

3.20.4 Davis' Theory of Sensory Transduction

The significance of the remarkable ionic composition of endolymph, so similar to that of cytosol, and the associated positive endocochlear potential that usually exceeds +80 mV in most species, was first appreciated by Hallowell Davis in a model of cochlea function (Davis, H., 1965) (Figure 2(a)). According to this theory, the positive endocochlear potential in series with the hair cell resting-membrane potential provides the electromotive force for the flow of current through the gated transducer channels. At the

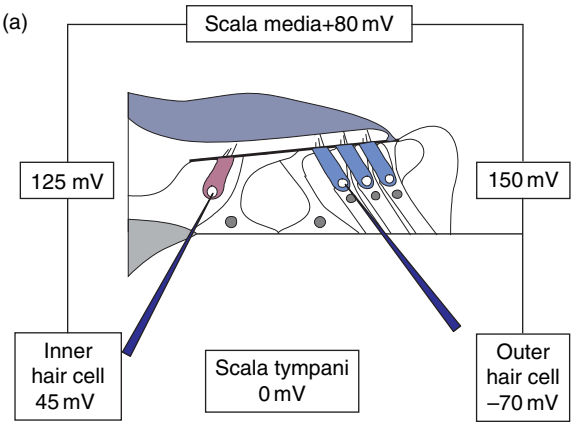

(b)

	K^+	Na^+	Ca^{2+}
Endolymph	150	1	0
Perilymph	5	140	2

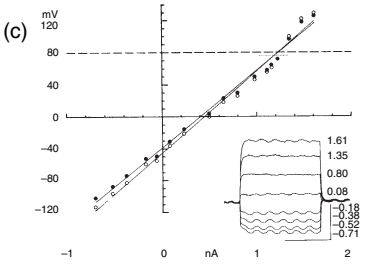

Figure 2 Davis' model of sensory transduction in the cochlea. (a) Current, largely carried by K^+ is driven by two batteries in series: the endocochlear potential (EP, +80 mV) and the cell-resting potential (−45 or −70 mV). K^+ is driven down the electrical gradient into the cell and down the chemical gradient out of the cell into the perilymph. Hair cells, therefore, expend little metabolic energy in restoring their ionic equilibrium or fatigue when transducing mechanical into electrical signals. (b) The ionic composition of the perilymph in the scala vestibuli and tympani and the endolymph of the scala media. (c) Evidence supporting Davis' theory: Reversal of the IHC receptor potential at close to the EP (+80 mV) by intracellular injection of positive current. From Russell, I. J. 1983. Origin of receptor potential in inner hair cells of the mammalian cochlea – evidence for Davis' theory. Nature 301, 334–336.

time when the model was conceived, the channels were visualized as variable resistors rather than elements with at least two states whose probability of opening was determined by hair bundle position (Kros, C. J., 1996). The current is carried by potassium, the dominant cation of the endolymph (Figure 2(b)), which is driven through the open transducer channel by the combined electromotive forces of the endocochlear potential and hair cell resting potential. The intracellular ionic composition is maintained within the hair cell by the diffusion of potassium down its concentration gradient through potassium conductances in the basolateral membrane into the surrounding perilymph.

Davis's theory was strongly supported by Sewell W. F. (1984) who found a direct association between the endocochlear potential and spontaneous discharge rates in auditory nerve fibers in that they both decreased synchronously following intravenous injections of the diuretic furosemide in anesthetized cats. He deduced that the injection of furosemide causes a decrease in the endocochlear potential, which produces a linearly related hyperpolarization of the IHC membrane potential by altering the standing current which flows through the transducer membrane. The logarithm of the rate of release of transmitter quanta decreases with the hyperpolarization of the IHC membrane potential, which decreases the rate of occurrence of action potentials at the postsynaptic terminal. The CM, SP, and CAP can all be altered through the polarization of the cochlea partition (e.g., Fernandez, C. *et al.*, 1950; Davis, H. *et al.*, 1958b). However, it was not until the experiments of Honrubia V. and Ward P. H. (1969) that polarization of the cochlear partition produced convincing evidence in support of Davis' theory. They discovered that the polarity of the CM and SP reversed at similar potentials and found a linear relationship between the magnitude and sign of these potentials and the magnitude and sign of the polarizing current in measurements from the cochleae of anoxic guinea-pigs. They were unable to reverse cochlear receptor potentials in the normal cochleae because they found it impossible to deliver sufficient current without polarizing the electrodes and short-circuiting the cochlear partition. Honrubia and Ward concluded that the results of their experiments supported Davis' theory, emphasized the role of the EP in the generation of the CM and SP, that the generation of SP and CM were related, and the major source of nonlinearity in the cochlea was the hair cell transducer. The same, but independently derived, conclusion was drawn by Santos-Sacchi J. (1993) more than two decades later. Further direct support for Davis' theory through a highly frustrating series of experiments was to inject positive current through an intracellular electrode inserted into a hair cell until the receptor potential reversed in sign (Russell, I. J., 1983; Russell, I. J. and Kössl, M., 1991). According to Davis' theory, the reversal potential should coincide with the EP. When current was injected into IHCs, the receptor potential reversed at the EP (Figure 2(c)). The frustration was caused by the electrodes, which usually had nonlinear electrical properties and had to be discarded, and the nonlinear electrical characteristics of the IHC membranes, which rectified and usually prevented depolarization to the EP. Thus support for Davis' theory came from IHCs where the transducer channels, but perhaps not the basolateral conductances, were functioning optimally.

3.20.5 IHC Receptor Potentials

IHCs are the true sensory receptors of the cochlea and respond to vibrations of the BM after they have been transformed through interactions between the OHCs, reticular laminar, TM, and the fluid of the subtectorial space. In contrast to the hair bundles of OHCs, which are firmly attached to the TM, the hair bundles of IHCs are freestanding (Lim, D. J., 1986) (Figure 1(a)). At low frequencies, IHC receptor potentials are proportional to the velocity of the BM and respond to the resultant interaction between the reticular laminar and the TM and fluid movement between them (Dallos, P. *et al.*, 1972; Sellick, P. M. and Russell, I. J., 1980; Patuzzi, R. and Yates, G., 1987; Cheatham, M. A. and Dallos, P., 1998) (Figure 1(b)). Thus IHC hair bundles are not sensitive to static displacements between the TM and reticular laminar, unless of course these static displacements influence the dynamic relationship between them. The precise way in which IHCs are excited is not understood. The mode of excitation has been inferred from the *in vivo* measurements described earlier and more recently from *in vivo* recordings from mice where the structure and relationship of the TM has been genetically modified. In these experiments it was deduced that the main drive to the fluid-coupled hair bundles of the IHCs in these mice was via radial motion of the RL at frequencies above and below the CF of the IHC and that radial

motion of the TM was required for driving the IHC hair bundles at the CF. IHC hair bundle can be directly observed in isolated preparations of the cochlea and organ of Corti (Dallos, P., 2003; Chan, D. K. and Hudspeth, A. J., 2005; Fridberger, A. *et al.*, 2006; Nowotny, M. and Gummer, A. W., 2006; Jia, S. *et al.*, 2007). This approach has the advantage of describing what can be seen, rather than inferring what is happening to the IHC hair bundles from electrical recordings and mechanical recordings from the cochlea. The disadvantage is that the slightest changes in the electrochemistry of the cochlea can have profound effects on the responses of IHCs and the properties of the TM, even at frequencies well below the CF (Russell, I. J. and Cowley, E. M., 1983; Russell, I. J. and Ashmore, J. F. 1983; Freeman, D. M., *et al.*, 2003a). Important factors in ensuring consistency between measurements made *in vivo* and *in vitro* are the calcium concentration of the ionic fluid bathing the hair bundles (see further) and the development stage of the preparation. In this respect the transducer conductance measured from mature IHCs in an isolated preparation (~30 nS, Jia, S. *et al.*, 2007) far exceeds that recorded from neonatal hair cells (~4 nS, Kros, C. J. *et al.*, 1992).

3.20.5.1 Factors That Shape the Inner Hair Cell Receptor Potential

IHCs respond to the acoustically evoked mechanical vibrations of the cochlear partition and relay these responses through synaptic transmission to the fibers of the cochlea nerve. They must perform this task over the entire frequency and dynamic ranges of the cochlea. The secret to coping with this task is encompassed within the nonlinear properties of IHC receptor potential and its operating point.

IH-receptor potentials are the products of the transducer function, which relates the hair bundle displacement to the open (or closed) probability of the mechanosensitive transducer channel (Kros, C. J. *et al.*, 1992) and the basolateral conductances and their voltage dependency (Kros, C. J., 1996; Housley, G. D. *et al.*, 2006) (Figure 3). The operating point of the hair cell transducer function is sensitive to extracellular calcium. The operating point of IHCs measured from cultures of neonatal mouse cochlea bathed in artificial perilymph with 1.4 mM Ca^{2+} is set so there is a probability of only 2–3% of the channels being open at rest. *In vivo* (Russell, I. J. and Sellick, P. M., 1978; 1983; Dallos, P., 1985), or *in vitro* (Jia, S. *et al.*, 2007) with 50 µm Ca^{2+}, the

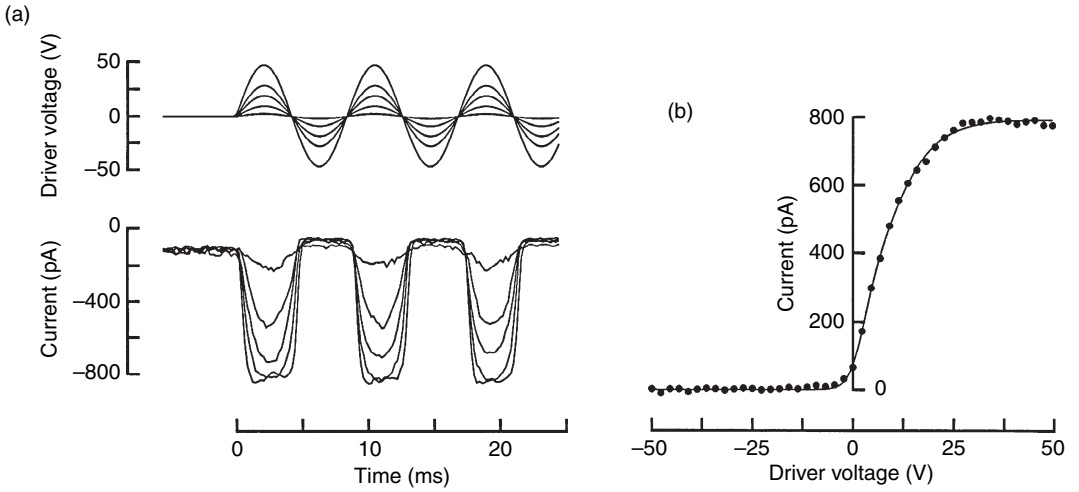

Figure 3 Transfer function of the transducer current. (a) Transducer currents of an OHC from the apical coil. Transducer currents (single traces) in response to five different driver voltages (records shown above). Responses to only the first three cycles of the sinusoid (119 Hz) are shown, to better appreciate the waveform of the responses. The currents can be seen to saturate for the largest driver voltages. The widening of the responses with increasing stimulus intensity indicates that the saturation occurs in the hair cell and not in the mechanical stimulus. Series resistance, 4.0 MΩ. (b) Transfer function of the cell of (a). Zero current is taken as the holding current when the force stimulus closes the transducer channels. Note that the currents have been inverted in this figure; inward current is plotted upwards. The maximum transducer current is 794 pA. When no force is exerted on the bundle, 66 pA of transducer current is flowing. From figure 3 of Kros, C. J., Rüsch, A., Richardson, G. P. 1992. Mechano-electrical transducer currents in hair cells of the cultured neonatal mouse cochlea. Proc. Roy. Soc. Lond. B 249, 185–193.

probability is 12–15% (Russell, I. J. and Sellick, P. M., 1978; 1983). The operating point is close to the point of maximum inflexion of the transducer function (Russell, I. J. and Kössl, M., 1992a), thereby causing the IHCs to generate a very asymmetrical receptor potential (Figures 4(a) and 4(b)).

3.20.5.1.1 Intracellular calcium levels

Intracellular calcium levels in the stereocilia in the vicinity of the mechanotransducer channel is one of the factors that determine the probability of these channels being open in their resting state (Ricci, A. J. and Fettiplace, R., 1997). These intracellular levels are also determined largely by the low extracellular levels of calcium rather than by calcium buffering in the hair bundle, which is believed to be weak. On the basis of calibrated immunogold labeling, four main calcium-buffering proteins (calbindin-D28k, calretinin, parvalbumin-α, and parvalbumin-β) are largely excluded from the hair bundles of mature rat cochlear hair cells (Hackney, C. M. *et al.*, 2005). The effect of high intracellular calcium levels is to cause adaptation by reducing the probability of the transducer channels being open at rest and to move the transducer function toward the right along the displacement axis (Kennedy, H. J. *et al.*, 2003; 2005). Thus the level of intracellular calcium determines the operating point of the transducer function. In turtle cochlear hair cells, the transducer function becomes almost symmetrical when the intracellular concentration of calcium in the hair bundles is very low, and thus the probability of mechanoelectrical channels being open in the resting state approaches 50% (Fettiplace, R. and Ricci, A. J., 2003; Fettiplace, R., 2006; Le Masurier, M. and Gillespie, P. G., 2005; Gillespie, P. G. and Cyr, J. L., 2004).

3.20.5.1.2 Voltage-dependent basolateral conductances

Another major influence that shapes the receptor potential-displacement function is the voltage-

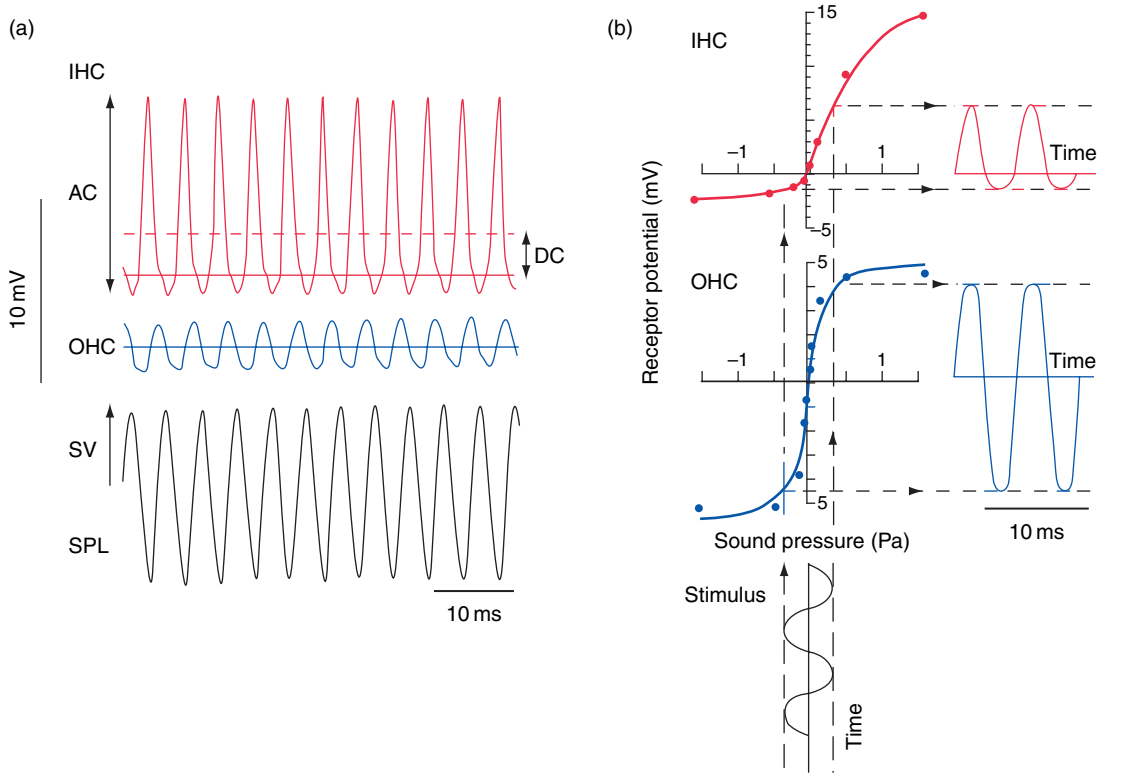

Figure 4 The operating characteristics of their transducer functions are related to the different roles of IHC and OHCs. (a, b) IHCs (red traces) operate about an asymmetrical point on their input–output curve. Thus they can generate DC voltage responses to high-frequency tones and hence signal their responses to the postsynaptic afferent fibers. OHCs (blue traces) operate about the steep, most sensitive region of their input–output curve. OHCs feed back energy to the cochlear partition, thereby boosting the swing of the BM to overcome viscous damping.

dependent basolateral conductances (Kros, C. J. and Crawford, A. C., 1990; Kros, C. J., 1996; Housley, G. D. *et al.*, 2006). These conductances are summarized in Figure 5. Recent models have taken into account the mechanotransducer channel as a mechanically driven potassium conductance and two time- and voltage-dependent basolateral potassium conductances: one with fast and one with slow kinetics (van Emst, M. G. *et al.*, 1997; Zeddies, D. G. and Siegel, J. H., 2004; Lopez-Poveda, E. A. and Eustaquio-Martín, A., 2006). The model developed by van Emst *et al.* was used to assess the contribution of basolateral potassium currents to the summating potential. Zeddies and Siegel used their model to investigate the homeostatic mechanisms responsible for the resting potential of the IHC, while Lopez-Poveda and Eustaquio-Martín developed a model to assess the contribution of basolateral potassium currents to the IHC nonlinear input/output transfer characteristics measured *in vitro* or *in vivo*. In the van Emst *et al.* model without the potassium conductances, the receptor potentials are determined by the properties of the transducer function and they are very asymmetrical with a correspondingly large DC component. The effect of switching on both the fast and slow potassium conductance as a consequence of the depolarization due to the activation of the transducer conductance is to decrease the overall amplitude of the receptor potential. This leads to a marked decrease in the DC component of the receptor potential as a consequence of a shift in the operating point to a more symmetrical location. Thus the nonlinearity of the receptor potential and its operating point, both so crucial for the generation of voltage responses to tones and their transmission to the afferent nerve fibers, are potentially vulnerable to voltage- and ion-dependent modification. Transient asphyxia causes profound modifications to the ionic and electrical environment of hair cells. It is possible, therefore, that the reduced nonlinearity and increased symmetry of their operating characteristics, and hence increased symmetry of the receptor potentials and decrease in the DC component recorded from asphyxic animals, are a consequence of changes in the electrochemistry of the cochlea (Russell, I. J. and Cowley, E. M., 1983; Russell, I. J. and Ashmore, J. F., 1983).

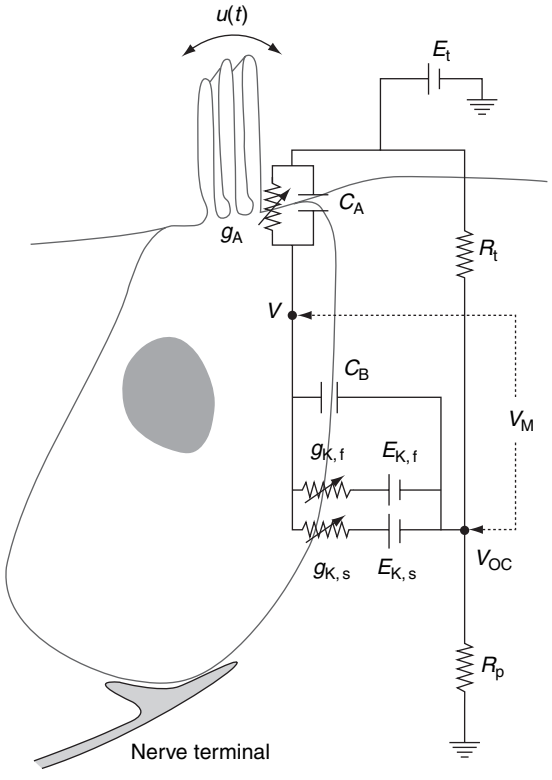

Figure 5 Model diagram: electrical equivalent circuit of the cell. E_t = endocochlear potential; R_t, R_p = epithelium resistances. C_A, C_B = capacitance of the apical and basal portions of the cell's membrane, respectively. g_A = conductance of the apical portion of the cell's membrane; it is assumed to be the sum of a mechanically sensitive K^+ conductance, $g_m(u)$, and a leakage conductance, g_l (not shown). $g_{K,f}$, and $g_{K,s}$ = fast and slow basolateral K^+ conductances. $E_{K,f}$ and $E_{K,s}$ = reversal potentials of the fast and slow basolateral K^+ conductances, u = stereocilia displacement, V = IHC intracellular potential. V_{OC} = extracellular potential. V_M = membrane potential, defined as $V - V_{OC}$. From figure 1 of Lopez-Poveda, E. A. and Eustaquio-Martin, A. 2006. A biophysical model of the inner hair cell: The contribution of potassium currents to peripheral auditory compression. J. Assoc. Res. Otolaryngol. 7, 218–235.

3.20.5.1.3 Inner Hair Cell receptor potential transfer function and operating point depend on cochlear location

IHC receptor potentials vary in shape and operating point depending on whether they are recorded from apical or basal turns of the cochlea. These differences are illustrated in Figure 6 and reveal that the receptor potentials of apical IHCs operate about a more symmetrical operating point and do not saturate so strongly in the negative direction compared to IHC receptor potentials from the basal region. Differences in operating point between apical and basal hair cells were not detected in whole cell measurements from IHCs in a hemicochlea preparation where the IHCs were excited through BM displacement and the apical surfaces were perfused with artificial endolymph

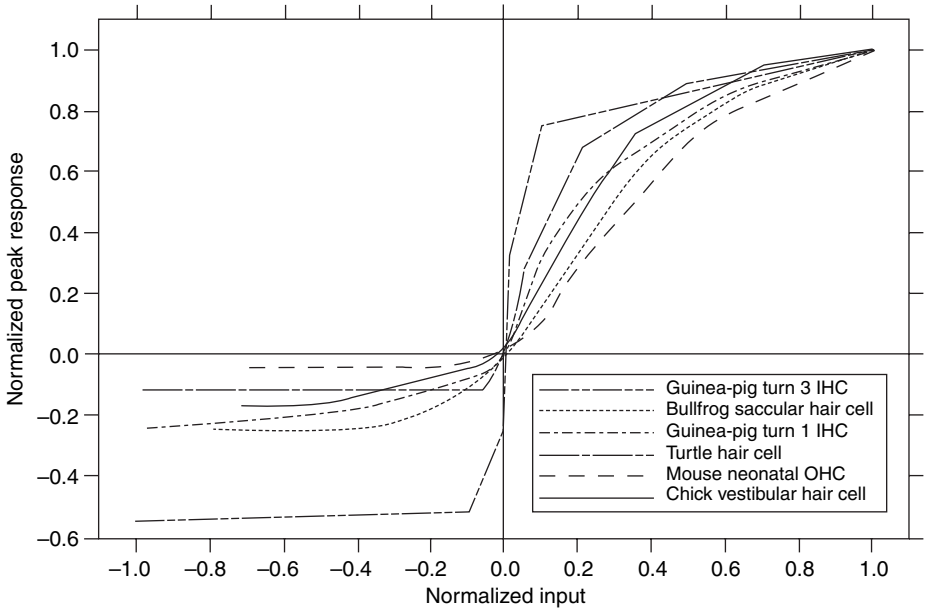

Figure 6 Sensory transducers in a variety of hair cell preparations. Transducer functions are plotted on normalized axes to facilitate comparisons *in vivo* from guinea-pig turn 3 (Cheatham, M. A. and Dallos, P. 1999) and turn 1 (Russell, I. J. and Sellick, P. M. 1983), and *in situ* from the turtle cochlea (Crawford, A. C. and Fettiplace, R. 1981). The *in vitro* data represent vestibular hair cells from bullfrog (Hudspeth, A. J. and Corey, D. P. 1977) and chick (Ohmori, H., 1987), as well as cochlear OHCs from a neonatal organ culture in the mouse (Kros, C. J. *et al.*, 1992). Only the chick and mouse results, however, provide true transducer functions. In all other preparations the receptor potential, rather than the receptor current, was measured. From figure 9 of Cheatham, M. A. and Dallos, P. 2000. The dynamic range of inner hair cell and organ of Corti responses. J. Acoust. Soc. Am. 107, 1508–1520.

(Jia, S. *et al.*, 2007). The slopes of the relationship between BM displacement and the mechanoelectrical transducer current were found, however, to be twice as steep for basal IHCs than for apical IHCs, although in contrast to OHCs (He, D. Z. Z. *et al.*, 2004), the total transducer conductances of apical and basal IHCs are similar. The finding that the BM displacement required in the apex to produce a given level of IHC (and OHC, He, D. Z. Z. *et al.*, 2004) excitation are about twice those needed to excite IHCs in the base of the cochlea, is due to a consequence of geometry. A given BM displacement in the base produces a larger hair bundle displacement (Dallos, P., 2003). It is hard to estimate IHC hair bundle displacement, however, because the stereocilia are not directly attached to the TM and their angular rotation due to TM displacement is frequency-dependent and difficult to deduce. The bases for regional differences in the shape of the IHC receptor potential recorded *in vivo* are not known. Possible candidates are regional differences in the intracellular levels of calcium in the vicinity of the transducer conductances and regional differences in the contributions of the voltage-dependent conductances. With respect to the latter possibility, the greatest density of voltage-dependent conductances is apparently found in hair cells in the base of the cochlea (Housley, G. D. and Ashmore, J. F., 1992; Mammano, F. *et al.*, 1995) and expression of KCNQ4 channels, which are represented by M-type conductances and are the linopiridine-sensitive $I_{K,n}$ present in IHCs and OHCs (Kros, C. J. *et al.*, 1998; Marcotti, W. and Kros, C. J., 1999; Marcotti, W. *et al.*, 2003; Oliver, D. *et al.*, 2003; Wong, W. H. *et al.*, 2004), are greatest in the IHCs and spiral ganglion neurones of the basal, high-frequency region of the cochlea (Beisel, K. W. *et al.*, 2000; 2005; Fritzsch, B. and Beisel, K. W., 2003). The functional significance of this distribution is, however, not fully appreciated at present, although mutations of the KCNQ4 channels known as *DFNA2* cause nonsyndromic, autosomal-dominant, progressive high-frequency hearing loss, whose cellular and molecular basis is unclear (Beisel, K. W. *et al.*, 2005).

Interestingly, the responses of IHCs to negative current injection depend on whether the IHCs are

from the apical or basal regions of the cochlea. One might anticipate that negative current injection, which hyperpolarizes the membrane, would tend to increase the driving voltage for calcium through the transducer conductance, thereby increasing the level of intracellular calcium in the hair bundle. Increased levels of intracellular calcium decrease the probability of the transducer conductance being open at rest (Crawford, A. C. *et al.*, 1991; Ricci, A. J. and Fettiplace, R., 1997). This change would shift the receptor potential displacement function toward the direction of reduced sensitivity, the operating point toward the point of maximum inflexion, and the DC component relative to the AC component would increase. Similar effects would also be produced as a consequence of inactivating the fast and slow potassium currents as a consequence of negative current injection, as predicted by van Emst M. G. *et al.* (1997). Indeed these predicted effects are observed when the apical turn IHCs are hyperpolarized (Cheatham, M. A. and Dallos, P., 2000) (Figure 7(a)). They are not seen, however, in the responses of basal turn IHCs, which become more symmetrical with a reduction in the saturation of the inhibitory phase of the receptor potential (Russell, I. J. and Kössl, M., 1991) (Figure 7(b)). The basis of this apical-basal difference in IHC response to current injection is unknown. Perhaps it is linked to an apex-to-base increase in the concentration of KCNQ4 channels (Beisel, K. W. *et al.*, 2005). Oliver D. *et al.* (2003) propose that KCNQ4 currents contribute substantially in establishing the resting membrane potential of IHCs and in so doing control low levels of intracellular $[Ca^{2+}]$. Moreover, several reports have suggested that intracellular Ca^{2+} may regulate KCNQ channels by reducing the magnitude of the current (Gamper, N. and Shapiro, M. S., 2003). The equilibrium conditions for the putative positive feedback between the conductance of KCNQ4 currents and intracellular $[Ca^{2+}]$ (Gamper, N. and Shapiro, M. S., 2003) may be finely balanced. Perhaps in basal IHCs, with a large concentration of KCN4 channels, hyperpolarization results in a stronger driving force for the influx of $[Ca^{2+}]$, but activation of the KCN4 channels results in lowering of intracellular $[Ca^{2+}]$ as a consequence of inactivating voltage-dependent conductance in the basolateral membranes (Hafidi, A. *et al.*, 2005). A reduction in intracellular calcium increases the probability of the transducer conductance being open at rest. The receptor potential displacement function will therefore shift to the left and increase the DC component of the receptor potential.

3.20.5.2 Transfer Functions of Afferent Synapses

IHCs are responsible for the translation of receptor potentials into neuronal signals with calcium playing an essential role in controlling the release of neurotransmitters at the IHC afferent synapse (Zhang, S. Y. *et al.*, 1999; Beutner, D. *et al.*, 2001). Sound-induced depolarizations of the IHC-membrane potential lead to the activation of $Ca_v1.3$ L-type voltage-gated channels located in the basolateral membrane (Dulon, D. *et al.*, 1995; Kros, C. J. *et al.*, 1998; Platzer, J. *et al.*, 2000; Brandt, A. *et al.*, 2003; Langer, P. *et al.*, 2003; Skinner, L. *et al.*, 2003; Hafidi, A. and Dulon, D., 2004; Marcotti, W. *et al.*, 2004). L-type calcium channels are believed to be primarily responsible for controlling both spontaneous and sound-evoked transmitter release from IHCs (Robertson, D. and Paki, B., 2002; Sueta, T *et al.*, 2004). Calcium entry leads to the fusion of vesicles and release of glutamate from the presynaptic membrane to bind with receptors on the afferent synaptic bouton (Glowatzki, E. and Fuchs, P. A., 2002).

The ribbon synapses of hair cells (Figure 8) release transmitter spontaneously and in a graded way in response to varying stimulus amplitudes over a wide frequency range (Raphael, Y. and Altschuler, R. A., 2003; Fuchs, P. A. *et al*, 2003; Fuchs, P. A., 2005). There are relatively few examples of *in vivo* intracellular recordings from the afferent terminals of hair cells. Furukawa and his colleagues (e.g., Furukawa, T. and Ishii, Y., 1967; Ishii, Y. *et al.*, 1971; Furukawa, T. and Matsuura, S., 1978; Furukawa, T. *et al*, 1978) made the first recordings from the giant afferent fibers of the goldfish sacculus, Flock A. and Russell I. J. (1973; 1976) recorded presynaptic and postsynaptic responses from hair cells and their afferent innervation from lateral line receptors in the freshwater cod *Lota*. Siegel J. H. and Dallos P. (1986) and Siegel J. H. (1992) recorded postsynaptic spikes and excitatory postsynaptic potentials (EPSPs) from afferent fibers close to IHCs (Figure 9(a)). Russell I. J. and Sellick P. M. (unpublished) and Palmer A. R. and Russell I. J. (1986) recorded IHC receptor potentials and postsynaptic potentials from an immediately adjacent afferent terminal, but did not record action potentials (Figure 9(b)). The vast majority of measurements have been from hair cell and isolated preparations of one form or another, with the advantages that

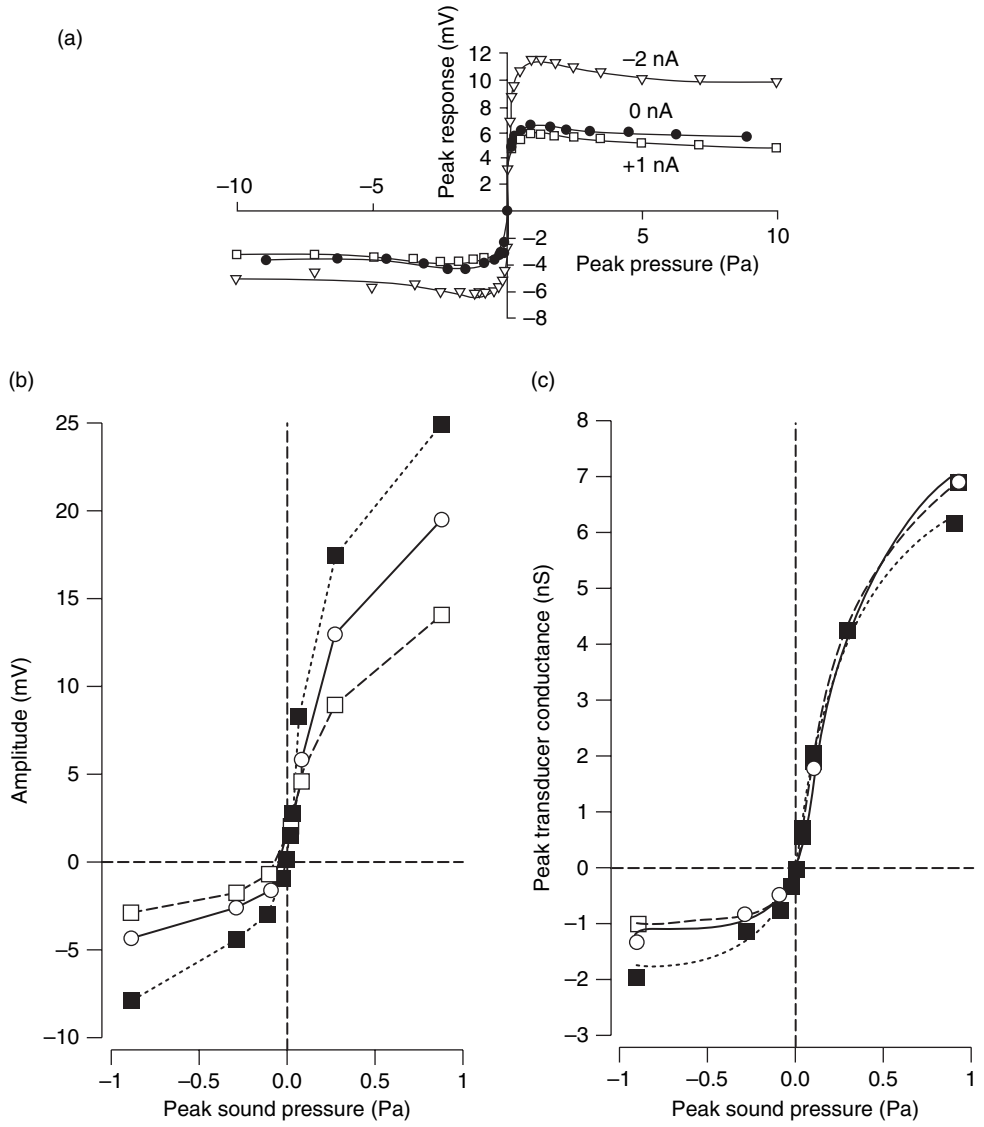

Figure 7 IHC transducer functions during current injection. (a) Input–output functions for the fundamental AC response recorded from a third-turn IHC plotted as linear response magnitude (depolarizing and hyperpolarizing peaks of the response) versus linear peak pressure from averaged waveforms. Data were obtained from Fourier transforms of the averaged responses to tone bursts. Stimulus frequency is 700 Hz. Data are shown for three current levels, 0, −2, and +1 nA passed into the cell through the recording electrode. Positive peaks are arbitrarily assigned to positive pressure. (b) Relationship between peak sound pressure and the peak negative and peak positive receptor potentials of an IHC. Zero current injection (○, continuous line); +1.2 nA (■, dashed line) current injection; −1.2 nA (□, dotted line) current injection. Stimulating frequency 300 Hz. (c) Peak transducer conductance estimates for the receptor potentials shown in (a) as functions of peak sound pressure and compensated for the IHC membrane time constant. The lines and symbols have the same meaning as in (a) and the curves are composed of two hyperbolic tangent functions. (a) From figure 3 of Dallos, P. and Cheatham, M. A. 1990. Effects of electrical polarization on inner hair cell receptor potentials. J. Acoust. Soc. Am. 87, 1636–1647. (b, c) From figure 4 of Russell, I. J.and Kössl M. 1991. The voltage responses of hair-cells in the basal turn of the guinea-pig cochlea. J. Physiol. Lond. 435, 493–511.

afferent transmission is more accessible for study but with various limitations imposed by the conditions of the experimental investigation. In the early 2000s, Glowatzky E. and Fuchs P. A. (2002) performed a major technological feat when they made whole-cell patch recordings from the postsynaptic terminals of single IHC afferent fibers in a cochlea slice preparation (Figure 10).

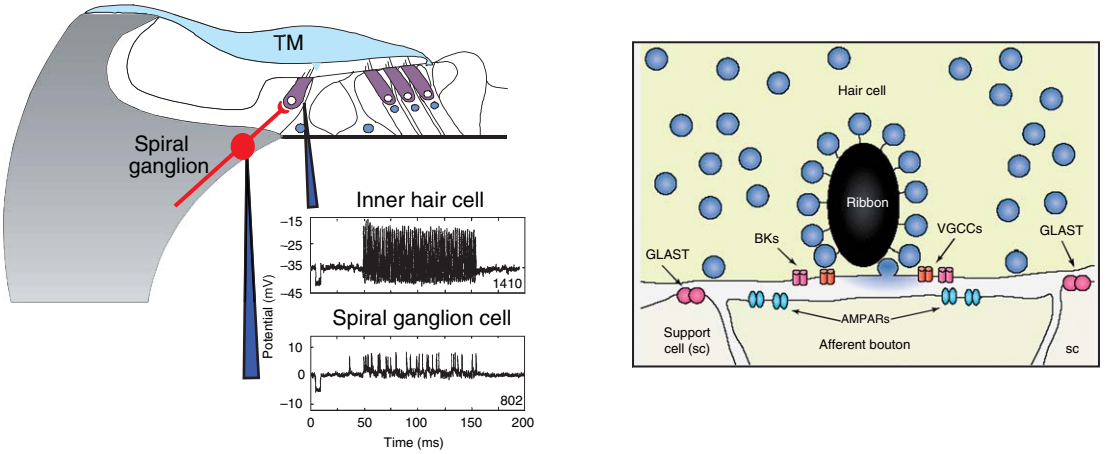

Figure 8 The hair cell's ribbon synapse. (a) Receptor potentials modulate transmitter release from the ribbon synapses at the basal membrane of the IHC and modulate the firing pattern of afferent neurons in the spiral ganglion. (b) The IHCs afferent synapse is demarcated by an electron-dense synaptic body, or ribbon, to which small, clear-core synaptic vesicles are tethered. In the mammalian cochlea the ribbon is around 0.2 μm in diameter, and the synaptic vesicles are 35–40 nm. Voltage-gated calcium channels (VGCCs) and BK-type (calcium-sensitive) voltage-gated potassium channels are clustered near the synaptic ribbons. AMPA receptors are found on the postsynaptic afferent bouton; glutamate transporters (GLAST) are expressed by supporting cells that surround the IHC and its afferent contacts. (a) From Zagaeski, M., Cody, A. R., Russell, I. J., and Mountain, D. C. 1994. Transfer characteristic of the inner hair cell synapse, steady state analysis. J. Acoust. Soc. Am. 95, 3430–3434. (b) From figure 1 of Fuchs, P. A., Glowatzki, E., and Moser, T. 2003. The afferent synapse of cochlear hair cells. Curr. Opin. Neurobiol. 13, 452–458.

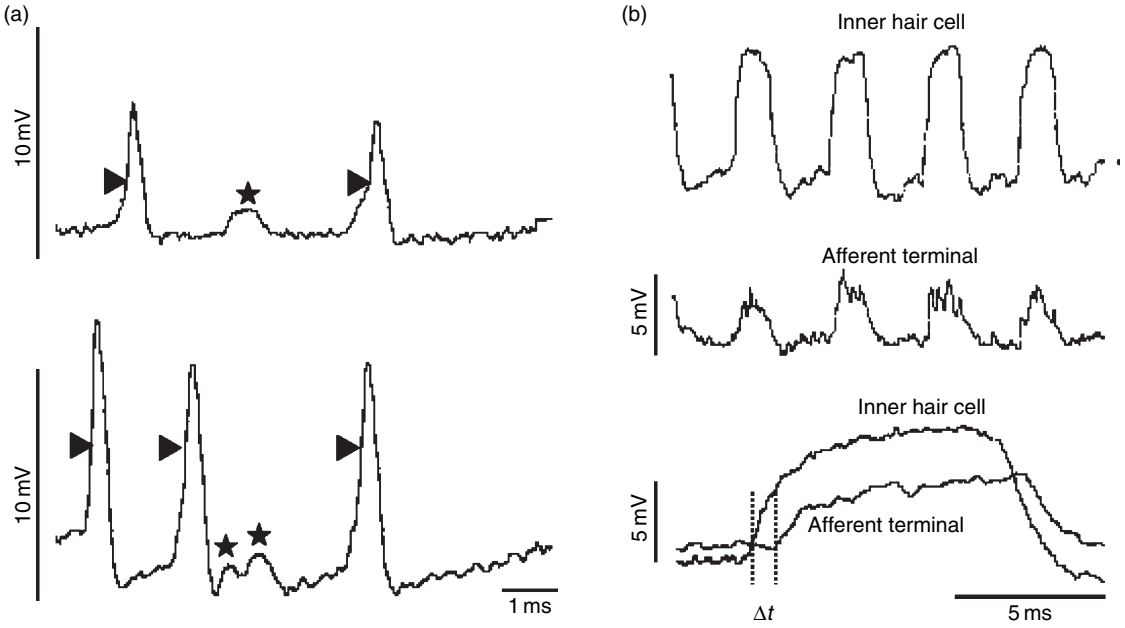

Figure 9 Excitatory postsynaptic potentials recorded from IHC afferent synapses *in vivo*. (a) AC-coupled intracellular recordings from two units showing prominent inflections on the rising edge of some spikes (arrowheads) and EPSPs which did not initiate spikes (asterisks). The resting membrane potentials in both (a) and (b) were approximately 10 mV. (b) Direct estimation of the 0.7–0.8 ms afferent synaptic delay (Δt) in the guinea-pig cochlea. (Top) Single receptor potential and postsynaptic potentials from immediately adjacent IHC and afferent terminal in response to 16 kHz tone bursts at 75 dB SPL. (Bottom) Averages of four successive responses from hair cell and afferent terminal shown on expanded timescale. The resting membrane potential of the IHC was −40 mV and of the afferent terminal was −52 mV. (a) From figure 12 of Palmer, A. R. and Russell, I. J. 1986. Phase-locking in the cochlear nerve of the guinea-pig and its relation to the receptor potential of inner hair-cells. Hear. Res. 24, 1–15. (b) From figure 3 of Siegel, J. H. and Dallos, P. 1986. Spike activity recorded from the organ of Corti. Hear. Res. 22, 245–248.

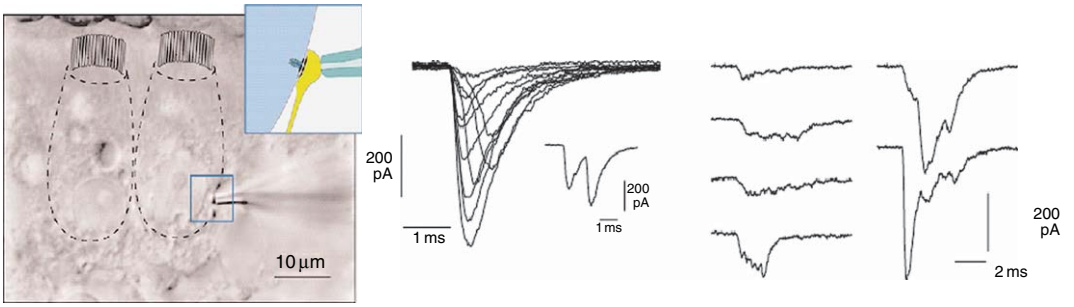

Figure 10 Excitatory postsynaptic currents (EPSCs) recorded from IHC afferent synapses *in vitro*. (a) Two afferent boutons visualized at the base of an IHC, one with attached pipette tip for whole-cell recording. (Right) EPSCs in afferent fibers of IHCs. Whole-cell recordings; holding potential (V_h) −94 mV. (b) Monophasic EPSCs with fast rise times and a slower exponential decay in 40 mM K^+, aligned at rise time. These represent about 70% of EPSCs in all recordings. Inset shows double EPSCs observed occasionally. (c) Multiphasic EPSCs with a wide range of waveforms, many consisting of a number of events dispersed in time. These represent about 30% of EPSCs in each recording From figure 2 of Glowatzki, E. and Fuchs, P. A., 2002. Transmitter release at the hair cell ribbon synapse. Nat. Neurosci. 5, 147–154.

3.20.5.3 Phase Relationships between Inner Hair Cell and Neural Excitation

On the basis of intracellular recordings from IHCs, the phase difference between the time when the hair cell depolarizes, thereby inducing transmitter release and neural excitation remains a contentious issue. At low frequencies, the relationship between hair cell depolarization and position of the BM is consistent in all frequency regions of the cochlea and IHC depolarization is generally observed near maximum BM velocity toward scala vestibuli, as might be expected if the hair bundles are freestanding (Dallos, P. *et al.*, 1972; Sellick, P. M. and Russell, I. J., 1980; Dallos, P. and Santos-Sacchi, J., 1983; Patuzzi, R. and Yates, G., 1987; Cody, A. R. and Mountain, D. C., 1989, Kössl, M. and Russell, I. J., 1992; Legan, P. K. *et al.*, 2000). In whole cell recordings from IHCs in the gerbil hemicochlea, Jia S. *et al.* (2007) pointed out that adaptation effects also contribute to the phase relationship between BM displacement and receptorpotential generation. The time constant of mechanoelectrical adaptation is level-dependent and at the lowest level behaves as a high-pass filter with a pole at 455 Hz. Thus IHC responses to frequencies above ~500 Hz should be minimally influenced by the effects of adaptation. It is likely, therefore, that adaptation is not the basis for the inconsistencies between timing between IHC and neural excitation that exist between the apex and base of the cochlea. IHC and neural excitation is associated with maximum velocity toward the scala vestibuli at the apex of the cochlea, but in the base of the cochlea, neural excitation is associated with BM velocity toward scala tympani (Ruggero, R. A. *et al.*, 1996), which is ~180° out of phase with IHC excitation measured in this region. Cheatham M. A. and Dallos P. (1998) suggest that the temporal disparity between IHC and neural data from the base of the cochlea may relate to several factors that influence transmembrane voltage in IHCs. Extracellular voltages (Sellick, P. M. *et al.*, 1982; Russell, I. J. and Sellick, P. M., 1983) can potentially affect low- and high-frequency regions differently because electrical interactions are more likely in the base of the cochlea than in the apex (Dallos, P., 1983, 1985). The velocity-dependence of IHCs in the apex appears to extend to higher frequencies than the velocity-dependence demonstrated for IHCs in the base of the cochlea. Sellick P. M. and Russell I. J. (1980) and Russell I. J. and Sellick P. M. (1983) observed that IHC excitation in the base of the cochlea switched from BM velocity to displacement toward scala vestibuli above ~200 Hz, compared with 340 Hz for apical OHCs (Cheatham, M. A. and Dallos, P., 1999). Cheatham and Dallos point out an anatomical correlation for this finding in that the tallest stereocilia at the base of the cochlea are found on inner rather than outer, hair cells (Lim, D. J., 1980; Wright, A., 1984). This is significant because it is the height of the stereocilia, in combination with the width of the subtectorial space, which determines input to the IHC (Freeman, D. M. and Weiss, T. F., 1990; Legan, P. K. *et al.*, 2005). The transition region where OHC stereocilia become shorter than IHC stereocilia occurs at a place along the cochlear partition (Eldredge, D. H. *et al.*, 1981) that is similar to the place where response phase changes in the single-unit recordings (Ruggero, M. A. *et al.*, 1996). It is, therefore, possible that the difference in response

phase, for low- versus high-BF nerve fibers, relates to the wider frequency range over which the velocity dependence of the IHC transducer contributes to apical IHC responses. Cheatham M. A. and Dallos P. (1999) also refer to the increased nonlinearity of the transducer conductance of basal turn IHCs compared to apical IHCs (see earlier in the chapter), and differences in basolateral voltage-dependent conductances with location along the length of the cochlea (also see earlier) as bases for the apparent phase difference between IHC and neural excitation in the base of the cochlea. They propose that a potentially confounding technical problem in attempting to resolve this issue is the possible short-circuiting of voltage-dependent conductances by leak conductances in the IHC membrane caused by the penetration of the micropipette used to make the intracellular recordings. In a schematic model, where they take into account these various considerations, they can, in theory, match the phase of IHC and neural excitation in the base of the cochlea (Figure 11).

3.20.5.4 Control of Transmitter Release from the Inner Hair Cell Afferent Synapse by the AC and DC Receptor Potentials

The asymmetry of the operating point of the receptor potential enables IHCs to generate DC receptor potentials to tones at all frequencies and levels within the range of the cochlea. At frequencies below the electrical cut-off of the IHC membrane time constant, IHCs generate both AC and DC components of the receptor potential and thus have the potential to signal both, the envelope of the acoustic stimulus and its phasic components. The AC component will depolarize the IHC during BM displacements toward the scala vestibuli and hyperpolarize it during BM displacements toward the scala tympani. IHC synapses release synaptic transmitter continuously, even in the absence of acoustic stimulation (Palmer, A. R. and Russell, I. J., 1986; Siegel, J. H. and Dallos, P., 1986; Siegel, J. H., 1992; Fuchs, P. A. *et al.*, 2003; Fuchs, P. A., 2005). Thus for frequencies below those set by the IHC's membrane time constant (<1 kHz), determined by the membrane capacitance (8–16 pF, Russell, I. J. and Sellick, P. M., 1978; 6–13 pF, Kros, C. J. and Crawford, A. C.1990) transmitter release can be both increased and decreased, during the depolarizing and hyperpolarizing phases of the IHC receptor potential, respectively (Palmer, A. R. and Russell, I. J., 1986). For frequencies above the membrane time constant, the IHC receptor potential is dominated by the depolarizing DC component and transmitter release can only be increased from the baseline spontaneous rate. The speed of vesicle fusion and transmitter release/diffusion contribute to low-pass filtering (Rose, C. and Weiss, T. F., 1988; Kidd, R. C. and Weiss, T. F., 1990), but the IHC membrane time constant is the most important factor in determining the range over which afferent fibers can code the phasic components of the receptor potential, otherwise known as phase-locking.

3.20.5.5 Inner Hair Cell Membrane Time Constant and Phase-Locking

In response to low-frequency sinusoidal stimuli the discharges in fibers of the auditory nerve do not occur randomly in time. Action potentials are elicited by unidirectional movements of the BM (Davis, H. *et al.*, 1950; Goldstein, M. H., 1968; Brugge, J. F. *et al.*, 1969) and thus discharges occur within a well-defined time window relative to a single cycle of the sinusoid. This preferred timing of action potentials has been termed phase-locking of the discharge (Rose, J. E. *et al.*, 1967) (Figures 12(a) and 12(b)). Phase-locking occurs in auditory neurons of all vertebrate classes (see Palmer, A. R. and Russell, I. J., 1986; Köppl, C., 1997; Figure 13). Phase-locking in response to low-frequencies can be observed in all auditory nerve fibers irrespective of their best frequency. However, the ability of the whole ensemble of auditory nerve fibers to phase-lock decreases with stimulus frequency. Interestingly there are large differences between species in the frequency range over which phase-locking is observed (Figure 13). Thus in cat, squirrel monkey, blackbird, and pigeon, phase-locking is constant up to about 2 kHz and then declines so that it is no longer detectable at 5–6 kHz (Rose, J. E. *et al.*, 1967; Kiang, N., 1965; Kim, D. O. and Molnar, C. E., 1979; Johnson, D. H., 1980; Sachs, M. B. *et al.*, 1974; 1980). In the guinea-pig phase-locking begins to decline at about 600 Hz and is no longer detectable above 3.5 kHz (Palmer, A. R. and Russell, I. J., 1986). The owl appears to be exceptional since good phase-locking is observed up to 9 kHz (Sullivan, W. E. and Konishi, M., 1984; Köppl, C., 1997).

3.20.5.5.1 Inner Hair Cell membrane time constant: significance for phase-locking

In a series of measurements from the guinea-pig cochlea Palmer A. R. and Russell I. J. (1986) found

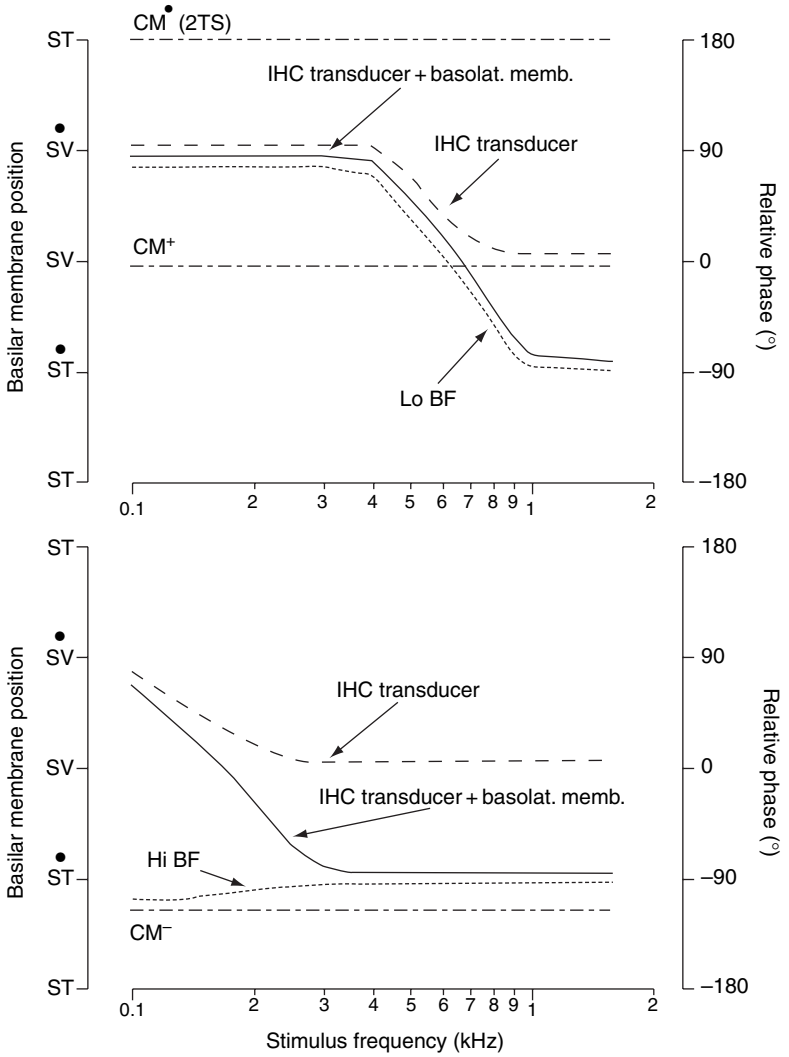

Figure 11 Resolving the phase ambiguity between IHC and neural excitation at the base of the cochlea. Summary representations of the response phase for hair cells and single-units in the apex (top panel) and base (bottom panel) of the cochlea, based on single-unit results in the chinchilla (Ruggero, M. A. *et al.*, 1996). The left ordinate represents BM position; the right, response phase plotted relative to SV displacement, with positive numbers indicating phase leads. The top panel indicates that the IHC transducer (dashed lines) responds to SV velocity at low frequencies. In other words, a 90° lead is expressed relative to the positive phase of the CM response (dot–dashed lines), which is associated with BM displacement to SV. As stimulus frequency increases, however, IHC excitation coincides with BM displacement to SV. In this case, the time of excitation is ~180° out of phase with the negative CM response. The phase of excitation for single units with low BFs (solid lines) indicates that they also respond to SV velocity at low frequencies. The IHC data reported here suggest that these neural responses should pass through SV displacement and finally settle at ST velocity as stimulus frequency increases. Above ~1000 Hz, the one fourth-cycle disparity between the single unit and the IHC transducer reflects the 90° phase lag associated with low-pass filtering by the IHC's basolateral membrane. For single units with high BFs, depicted at the bottom, a preference for ST velocity is demonstrated throughout the frequency range depicted here. The negative phase of the CM response is plotted near ST velocity to reflect nonlinearities associated with the high levels required to reach threshold for inputs well below BF. From figure 7 of Cheatham, M. A. and Dallos, P. 1999. Response phase: a view from the inner hair cell. J. Acoust. Soc. Am. 105, 799–810.

that the progressive decrease in the AC component compared to the DC component of the IHC receptor potential as the stimulus frequency was increased was closely associated with the decline in phase-locking of auditory nerve fibers (Figures 12(c) and 12(d)). Palmer and Russell concluded that the cut-off and slope of the decline in the AC component is consistent with the suggestion that this process is the limiting factor in

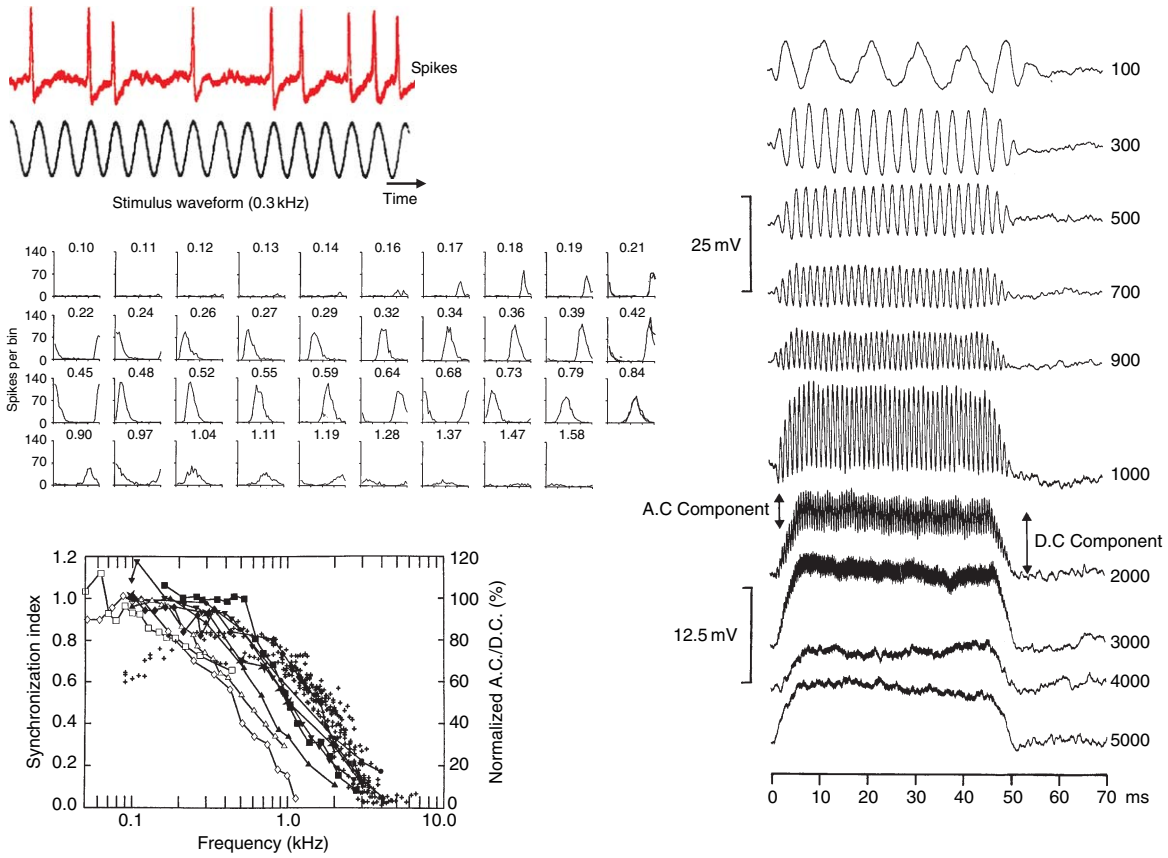

Figure 12 Comparison of the limits of phase-locking in the guinea-pig auditory nerve and the IHC membrane time constant. (a) Phase-locking of an auditory nerve spike discharge to a 300 Hz tone. (b) Period histograms of the response of a cochlear nerve fiber with a CF 0.6 kHz to sinusoidal stimulation. The numbers above the histograms indicate the stimulus frequency. The ordinate of each histogram is one cycle. (c) The membrane time constant attenuates the AC component of the IHC intracellular receptor potential recorded in the basal turn of the guinea-pig cochlea for frequencies above ~200 Hz. For frequencies below about 2 kHz, the AC component controls transmitter release, which is phase-locked to the stimulus. Above 2 kHz, the DC component predominates and controls the spike discharge rate. (d) Comparison of the limits of phase-locking in the guinea-pig auditory nerve and the ratio of the AC and DC components of the IHC receptor potential in 9 hair cells. The DC component was either calculated from the difference between the half-peak AC component and the resting potential or by the integral of the waveform. The hair cell data have been normalized by plotting as a percentage of the low frequency AC/DC ratio. (a) From Rose, J. E., Brugge, J. F., Anderson, D. J., and Hind, J. E. 1967. Phase locked response to low-frequency tones in single auditory nerve fibres of the squirrel monkey. J. Neurophysiol. 30. 769–793. (b–d) From figures 9 and 11 of Palmer, A. R. and Russell, I. J. 1986. Phase-locking in the cochlear nerve of the guinea-pig and its relation to the receptor potential of inner hair-cells. Hear. Res. 24, 1–15.

cochlear nerve fiber phase-locking. As pointed out subsequently by Rose C. and Weiss T. F. (1988), other mechanisms, probably due to time-limiting processes associated with synaptic transmission and afferent spike generation, also contribute to the high-frequency attenuation of phase-locking. For frequencies above ~3 kHz, phase-locking declines more rapidly than would be predicted from the membrane time constant of the IHC. The significance of synaptic mechanisms in providing a time-limited step in phase-locking is discussed ahead in relation to synaptic transmission.

3.20.5.5.2 The problem of preserving high temporal resolution in synaptic transmission

The superior temporal resolution of mammalian and avian auditory nerve fibers compared with those of amphibia and reptiles cannot be attributed to core temperature differences but to other differences, for example, in synaptic transmission and spike initiation in the afferent fibers (Palmer, A. R. and Russell, I. J., 1986; Rose, C. and Weiss, T. F., 1988; Köppl, C., 1997). The temporal resolution of

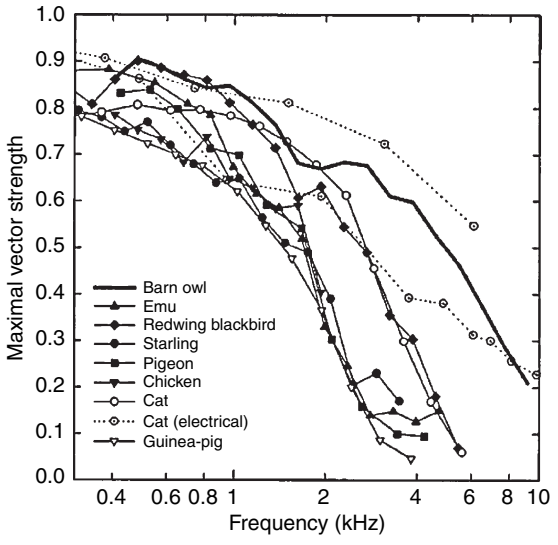

Figure 13 A comparison of maximal vector strength as a function of frequency in the auditory nerve of several avian and mammalian species. For the bird species, median values in mostly quarter octave bins are shown, taken or calculated from the following sources: barn owl, data from figure 4*A* in Köppl, C., 1997; emu, figure 9 in Manley G. A. *et al.* (1997); redwing blackbird, figure 11-9*B* in Sachs *et al.* (1980); starling, figure 4 in Gleich O. and Narins P. M. (1988); pigeon, graphic estimate of median values from figure 2 in Hill, K. G. *et al.* (1989); chicken, from figure 16 in Salvi R. J. *et al.* (1992). For the cat and guinea-pig, average values in 0.1 decade bins as determined by Weiss T. F. and Rose C. (1988, figure 3) from the original data (Johnson, D. H., 1980; Palmer, A. R. and Russell, I. J., 1986) are shown. The two different data sets for electrical stimulation in the cat (Hartmann, R. and Klinke, R. 1987; Dynes, S. B. C. and Delgutte, B., 1992) are mean values taken from figure 10 in Dynes S. B. C. and Delgutte B. (1992). From figure 11 of Köppl, C. 1997. Phase locking to high frequencies in the auditory nerve and cochlear nucleus magnocellularis of the barn owl, *Tyto alba*. J. Neurosci. 17: 3312–3321.

neural firing has also been assessed using Wiener–Kernel analysis of the responses to noise and tones by chinchilla auditory nerve fibers (Temchin, A. N. *et al.*, 2005; Recio-Spinosa, A. N. *et al.*, 2005). Temchin *et al.* and Recio-Spinosa *et al.* revealed that temporal responses are preserved in postsynaptic responses of chinchilla auditory nerves at least to 12 kHz. These events occur at frequencies beyond the limitations of the membrane time constant of the IHC. From *in vivo* recordings of afferent terminals the synaptic delay is 700–800 μs (Palmer, A. R. and Russell, I. J., 1986) (Figure 9(b)) and transmitter release is coordinated (Siegel, J. H. and Dallos, P., 1986; Siegel, J. H., 1992) (Figure 9(a)), which is in accord with more recent studies on isolated preparations (Glowatzki, E. and Fuchs, P. A., 2002; Edmonds, B. W. *et al.*, 2004; Singer, J. H. *et al.*, 2004; Khimich, D. *et al.*, 2005) that release from hair cell afferent fibers, including IHCs, and involves multivesicular release (Figure 10). Coordinated transmitter release provides a large safety factor and facilitates high temporal resolution. From studies on amphibian, chick, and mammalian auditory hair cells there is a large releasable pool of transmitter, its release is linearly proportional to the presynaptic calcium current, and the rate-limiting step seems to be release rather than refilling of the vesicles, with a critical role of vesicle-trafficking for the dense core bodies adjacent to the presynaptic membrane (Fuchs, P. A. *et al.*, 2003; Fuchs, P. A., 2005; Khimich, D. *et al.*, 2005). Ribbon synapses are specialized for fast synaptic transmission and their physiological properties that have so far been described will enable them to respond in the millisecond timescale (Parsons, T. D. and Sterling, P., 2003). The properties of the ribbon synapse would appear to optimize temporal resolution for transmitter release. At present we do not have a clear understanding of the factors that optimize temporal resolution and the brief interspike intervals in the postsynaptic afferent terminal. The major limitation to temporal resolution appears, however, to be largely presynaptic because electrically driven phase-locking in the cat auditory nerve, which bypasses the synapse, reveals that spike-generation is not the limiting factor (Dynes, S. B. C. and Delgutte, B., 1992) (Figure 13).

3.20.5.5.3 The problem with owls

If we accept that the limiting factor in phase-locking cut-off is a result of the hair-cell membrane time constant, then the time constants of the hair-cells at a particular frequency position in the cochlea would appear to be longer in rodents than those of cats, squirrel monkeys, pigeons, and blackbirds, which in turn are longer than those of owls. Given the two octave spread in phase-locking cut-off amongst these species the resistive or capacitive components in the hair cell membrane would have to change by about 4 times which would be an extremely large variation in the properties of the membrane. One further observation from phase-locking data from the guinea-pig cochlea is consistent with a variation in hair-cell properties. As a consequence of the increasing asymmetry of the IHC receptor potential with increasing frequency, phase-locking should

result in minimum instantaneous discharge rates below spontaneous rate for low frequency (below 1 kHz; Russell, I. J. and Sellick, P. M., 1983), but only down to spontaneous rate for high frequencies (above 1 kHz, see Figures 12 and 13). This phenomenon has been observed in guinea-pig data and it is clearly present in the cat data of Johnson D. H. (1980) . If the differing phase-locking cut-off frequencies are a result of the hair-cell membrane properties, we would expect the transition between minima below or above spontaneous rate to be species-dependent. For guinea-pigs, the transition is near 1.5 kHz whereas in a single fiber from cat (Johnson, D. H., 1980) it appears to be above 2 kHz, and from a single auditory nerve fiber in the owl (Köppl, C., 1997) it appears to be at least 7 kHz (Figure 13).

Phase-locking in cochlear nerve fibers responses is a consequence of two transfer functions (1) the mechanical to electrical transfer which results in the declining AC/DC ratio and (2) the transfer function of the hair-cell synapse. The sensitivity of the synaptic transfer function could be the key to phase-locking at high frequencies in the owl cochlea. If the sensitivity of the synaptic transfer function and the basal discharge rate of transmitter release were both higher in birds than in mammals, then a given magnitude of the AC receptor potential would modulate transmitter release to a greater depth from avian compared with mammalian hair cells. Correspondingly, avian afferent fibers would have higher phase-locking cut-off frequencies. While there are no apparent differences in the basal discharge rates of auditory nerve fibers in rodents and cats (3–25 spikes s^{-1} in guinea-pig, Palmer, A. R. and Russell, I. J. 1986), spontaneous discharge rate in the auditory fibers of owls is higher and up to 150 spikes s^{-1} (Köppl, C., 1997). Importantly, by comparison with mammalian auditory fibers, all auditory fibers in the bird cochlear nerves are spontaneously active. The basis for the high resting discharge rate in bird auditory fibers is not yet known. Appropriate experiments have yet to be conducted to ascertain if factors including hair-bundle biasing, increased resting calcium conductance, and postsynaptic mechanisms are responsible for the high resting discharge rates of avian auditory nerve fibers.

3.20.5.6 Dynamic Range

The combination of amplification of the BM vibrations at low levels and compression at high levels enables IHCs to signal responses over the entire dynamic range of the cochlea. The solution to coding this enormous dynamic range within the more limited scope of the spike-rate code of the auditory nerve fibers appears to be range fractionation. Extensive measurements of auditory nerve fibers in guinea-pigs led Winter I. M. *et al.* (1990) to divide the fibers into three categories. High spontaneous rate fibers display activity in the absence of any stimulus, have a low acoustic threshold, and a steep rate-intensity function at CF that almost completely saturates within 20–30 dB of the threshold. The rate-intensity functions at CF of medium spontaneous rate fibers are more sloping over their entire dynamic range. Low spontaneous rate fibers have almost no spontaneous activity, have high thresholds, and display a rate-intensity function at CF with a shallow slope. These different shapes are thought to reflect the linear and compressive regions of BM response (Yates, G. K. *et al.*, 1990). Accordingly, as demonstrated by Zagaesky M. *et al.* (1994) the synaptic transfer characteristics or hair cell receptor potential–spike rate functions must be quite different for each of the three different categories of fibers (Figure 14). A current goal is to understand the presynaptic and postsynaptic mechanisms that are the bases for these differences.

3.20.6 Outer Hair Cell Receptor Potentials

The tallest rows of stereocilia of the OHCs in the mammalian cochlea are attached by their tips to the TM and thus mechanically link the TM and BM (Figure 1). As a consequence of their strategic location in the cochlear partition, OHCs play an essential role in the frequency tuning and sensitivity of the cochlea. Following selective damage to the OHCs, the electrophysiological and mechanical responses of the cochlea to acoustic stimulation become insensitive, linear, and broadly tuned (Dallos, P., 1992; Robles, L. and Ruggero, M. A., 2001). OHCs have a bi-directional, interactive role in sensory transduction in the cochlea (Weiss, T. F., 1982; Davis, H., 1983) by both responding to vibrations of, and feeding forces back to, the cochlear partition that is the source of the cochlea's frequency tuning and sensitivity. It might be anticipated that the effectiveness of the proposed feedback depends on the mechanical properties of the BM, TM, and on the gain and phase of the feedback process.

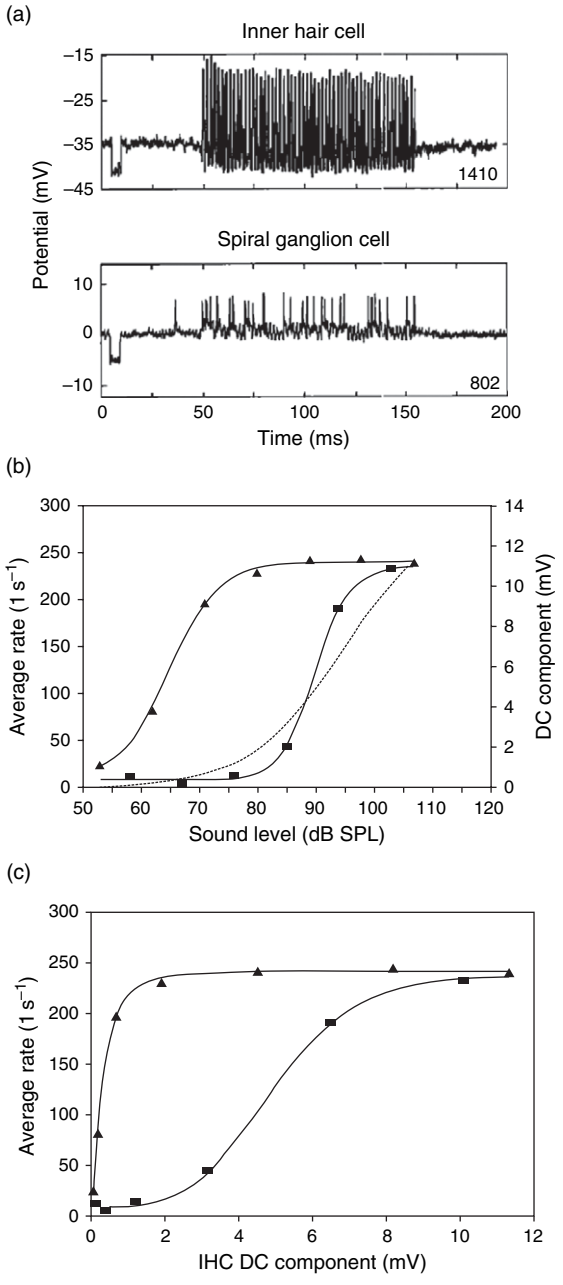

Figure 14 IHC–afferent fiber transfer function. (a) Waveforms of IHC and spiral ganglion cell responses to a 95 dB SPL 525 Hz tone. The negative deflection near the beginning of each panel is a 5 mV calibration pulse. (b) The average rate level data for two cells with CFs ~18 kHz to a stimulus frequency of 525 Hz. (c) The broken curve is the growth function of an IHC with a CF ~18 kHz IHC. (b) The neural data and associated functions from figure 4 plotted as a function of the DC receptor potential. From figures 1 and 4 of Zagaeski, M., Cody, A. R., Russell, I. J., and Mountain, D. C. 1994 Transfer characteristic of the inner hair cell synapse, steady state analysis. J. Acoust. Soc. Am. 95, 3430–3434.

3.20.6.1 Phase and Magnitude of Outer Hair Cell and Inner Hair Cell Receptor Potentials as Indicators of Electromechanical Feedback

If the OHCs operate in a true electromotor feedback loop, then they will contribute to their own responses and hence to the mechanical responses of the cochlear partition. The net mechanical response of the cochlear partition, that is, the radial shear displacement between the TM and BM, is detected by the IHCs (Davis, H., 1965) and reflected in the IHC receptor potentials (Russell, I. J. and Sellick, P. M., 1978) and in the firing pattern of the auditory nerve fibers (Kiang, N., 1965). OHCs might be expected to make a significant contribution to the mechanical properties of the cochlear partition at low and moderate levels of the acoustic stimulus that is within the most sensitive region of the OHC transducer function (Cody, A.R. and Russell, I. J., 1987; Russell, I. J. and Kössl, M., 1992a). For tone levels within this range, the magnitude of the AC response of the OHC receptor potential might provide a measure of the feedback contributed by the OHCs to the mechanics of the cochlear partition and the phase of the AC response relative to that of the passive mechanics of the BM indicates the sign of the feedback. For high levels of the acoustic stimulus, the OHC transducer is saturated and the mechanical responses of the BM and the voltage responses of the OHCs are governed by the passive mechanical properties of the BM (Patuzzi, R. B. *et al.*, 1989; Zwislocki, J. J., 1990).

The frequency and level dependence of the phase relationships of OHC and IHC AC receptor potentials (Dallos, P., 1986; Dallos, P. and Cheatham, M. A., 1989; Cheatham, M. A. and Dallos, P., 2001; Kössl, M. and Russell, I. J., 1992), BM vibrations (Robles, L. and Ruggero, M. A., 2001; Legan, P. K. *et al.*, 2000; 2005), and phase-locking of spike discharges in the auditory nerve (Anderson, D. J. *et al.*, 1971) are all similar for frequencies around the CF. Thus, as Anderson D. J. *et al.* (1971) were the first to show, for frequencies below the CF, the response phase increasingly lagged with increasing level and above the CF, the phase of the response increasingly led with increasing level. For levels below ~60 dB SPL, the phase at CF of OHC AC receptor potentials is level independent. In sensitive *in vivo* recordings from the basal turn of the cochlea, the appearance of compression (reduction in slope) in the OHC

AC and IHC DC level functions with increasing stimulus level, is associated with a phase lead of the OHC AC response, which asymptote at about 90° (Figure 15). A feedback model of amplification in the cochlea can provide a causal relationship between the magnitude and phase of the OHC responses at the CF.

3.20.6.2 The Phase and Magnitude of Outer Hair Cell Receptor Potential and the Positive Feedback Model

Mountain D. C. *et al.* (1983) proposed a model of cochlear amplification in which OHCs contribute negative feedback that reverses through a frequency-

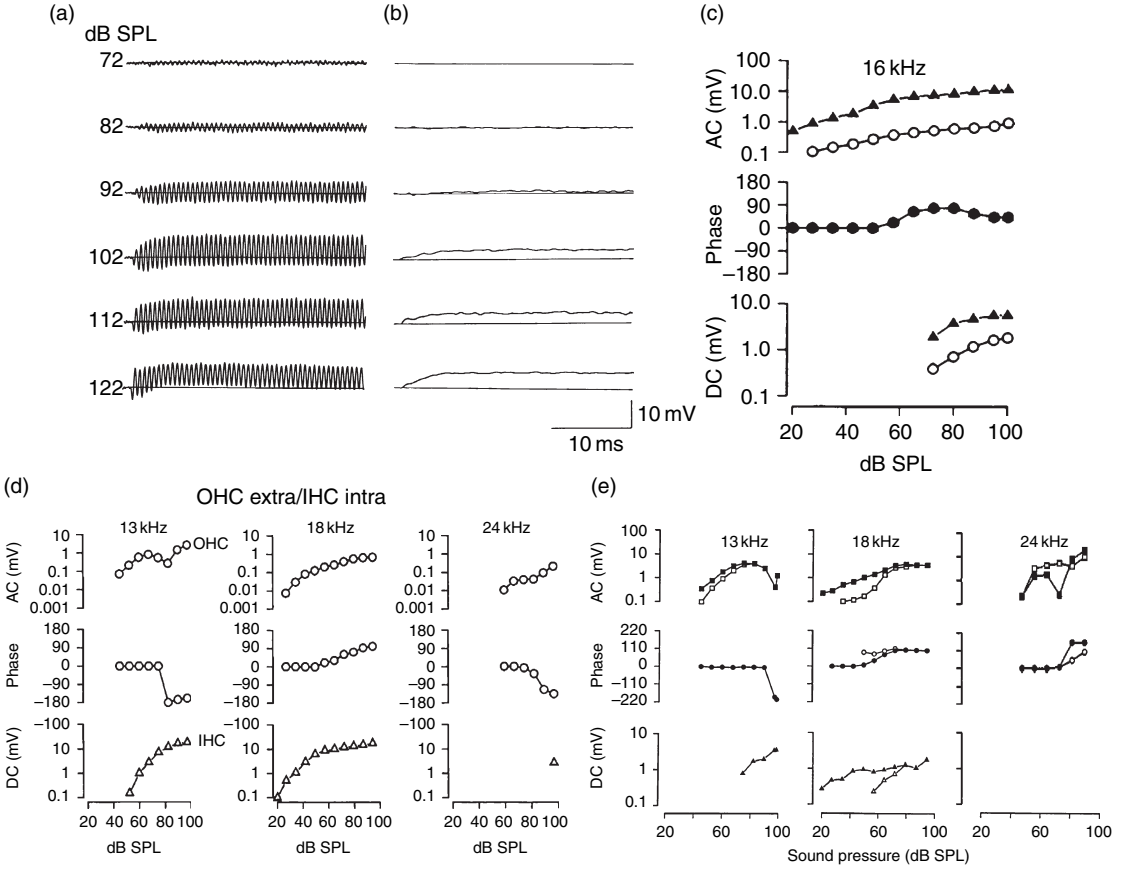

Figure 15 Receptor potential magnitudes and phase as functions of level and frequency. The OHC DC receptor potential appears when the AC potential begins to saturate, and the AC phase begins to change. (a) Receptor potentials recorded from a basal turn OHC CF ~18 kHz in response to a 3 kHz tone. (b) The same data but low-pass filtered at 1 kHz. (c) Tone-evoked voltage responses as functions of level (and at the frequencies shown) recorded intracellularly (solid triangles) and extracellularly (open circles) from an OHC. In each panel, the magnitude of the AC response (upper curves), the phase of the AC response (middle curves), and the amplitude of the DC receptor potential (lower curves) are plotted as a function of tone level. Resting potential of OHC, −70 mV, detection threshold at CF (16 kHz), 20 dB SPL. The magnitudes of the responses are root mean square (RMS) values, positive values of phase indicate leads, and the data have been compensated for recording system and membrane time constants of 3.5 and 1.1 kHz, respectively. (d) Magnitude and phase of AC responses recorded extracellularly from an OHC (open circles), and the amplitude of DC responses recorded intracellularly from an adjacent IHC (CF 18 kHz) (open triangles) as functions of level at the frequencies indicated. The magnitudes of the extracellular AC responses are corrected for the low-pass filtering of the recording electrode (corner frequency, 3 kHz). (e) Magnitude, phase, and DC response/level functions based on extracellular recordings close to an IHC at the frequencies indicated. The magnitude of the AC response is corrected by 6 dB/octave from 4 kHz to compensate for the low-pass filtering due to the recording system. (a, b) From figure 5 of Cody, A. R. and Russell, I. J. 1987. The responses of hair cells in the basal turn of the guinea-pig cochlea to tones. J. Physiol. Lond. 383, 551–569. (c, d) From figure 2 of Kössl, M. and Russell, I. J. 1992. The phase and magnitude of hair cell-receptor potentials and frequency tuning in the guinea-pig cochlea. J. Neurosci. 12, 1575–1586. (e) From figure 11 of Russell, I. J. and Kössl, M. 1992b. Modulation of hair cell voltage responses to tones by low-frequency biasing of the basilar membrane in the guinea pig cochlea. J. Neurosci. 12, 1587–l601.

dependent phase delay to positive feedback at the CF. That is, electromotor feedback from the OHCs opposes BM displacement at frequencies away from the CF, but augments BM velocity at the CF. This mechanism, through which fine-tuning of the phase of OHC feedback controls the gain of feedback, can also account for cochlear compression. If the magnitude of the OHC AC receptor potentials indicates the strength of the feedback, and their phase indicates the timing, then the phase of the feedback must be close to optimal at low stimulus levels. Presumably it is not optimal when the AC and DC level functions begin to compress, and in fact may be the cause of this compression as the vectorial strength of the feedback declines to a point where it begins to oppose rather than augment the swing of the BM. This model of compression of the electromechanical responses of the cochlea differs from the model of compression reviewed by Cooper N. P. (2003) where compression is defined by saturation of the OHC transducer function.

The proposal that OHC feedback can exert a frequency- and level-dependent negative gain on cochlea responses is supported by the findings of Kössl M. and Vater M (2000) findings that the resonance of the echo-response region of the moustached bat cochlea is enhanced following Amikacin ototoxicity. Amikacin selectively damaged the first row of the OHCs in the basal turn of the cochlea, leading Kössl and Vater to suggest that the resulting augmented resonance of the echolocation region of the cochlear partition that is largely attributable to the TM, and which is normally poised close to instability (Kössl, M. and Russell, I. J., 1995; Russell, I. J. and Kössl, M., 1999), is normally controlled through negative feedback. At the apical end of the cochlea, removal of the active attenuation/negative gain observed in BM responses above BF (Zinn, C. *et al*., 2000) could also result in hypersensitive tuning-curve tails when cochlear function is compromised.

3.20.6.3 Outer Hair Cell Excitation and the Parallel Resonance Model

Similar observations of hypersensitivity in the tuning-curve tails of neural, electrical, and mechanical responses of other cochlear regions may also be accounted for by this mechanism, although they have also been reproduced in a model by Zwislocki J. J. (1986). His model (reviewed in Zwislocki, J. J., 2002) is centered on the notion that elastically and hydromechanically coupled cochlear structures are likely to form a complex resonator. Consequently one can expect quite complex, frequency-dependent relative movements between these structures, particularly between the TM and the RL, which provides excitation of the cochlear hair cells. Some time ago Allen J. B. (1980) and Zwislocki J. J. (1980) postulated that this complex system possesses at least two resonant frequencies for each tonotopic place along the cochlea, one provided by the BM and the other by a parallel resonator formed by the TM mass and its elastic attachments to the spiral limbus and the OHC stereocilia. At the frequency of the parallel resonance, the TM moves in phase with the RL, thus resulting in a reduction in shear displacement between these structures and, as a consequence, a reduction in IHC and neural excitation. The reduction is greatest at the frequency of the parallel resonator. The same mechanism acts to reduce hair cell excitation throughout the frequency range of the low-frequency tails of cochlear response tuning curves According to this model, Zwislocki J. J. (1986) postulated that a reduction in the forces generated by the OHCs would reduce the radial motion of the TM, thereby sensitizing the low-frequency tail of tuning curves, as was first observed by Liberman M. C. and Dodds L. (1984) in neural tuning curves recorded from cochleae following acoustic trauma (Robertson, D. *et al*., 1980) and/or salicylate and ototoxicity (Murugasu, E. and Russell, I. J., 1995).

3.20.6.4 The Phase of Outer Hair Cell Excitation: A Balance between the Tectorial Membranes Radial Stiffness and Rotational Stiffness of Outer Hair Cell Stereocilia

At frequencies about one-half an octave below CF and again between one-third and one-half octave above CF, slight increases in the level of tones presented at moderate-to-high sound levels can cause the phase of the OHC AC response to jump by 180°. The phase transitions are associated with magnitude minima or notches in the fundamental AC response/level functions (Figures 15(c)–15(e)). It is suggested that these 180° phase jumps are not related to the feedback process associated with frequency tuning because they survive desensitization and loss of frequency tuning in the cochlea. These phase jumps are, furthermore, critically poised and close to instability so that biasing of the BM toward or away from the scala media can flip the phase from one state to the other (Figure 15(e) and see Russell, I. J. and Kössl, M., 1992b). These observations are in accordance with the results of similar measurements made on the gerbil cochlea by Zwislocki J. J. (1988; 1990). Phase jumps and notches have been

observed in the fundamental magnitude functions of IHCs but not OHCs in the apical turns of the guinea-pig cochlea (Dallos, P. and Cheatham, M. A., 1989; Cheatham, M. A. and Dallos, P., 2001), and magnitude minima and phase jumps have been observed in BM mechanics (Patuzzi, R. *et al.*, 1984). The 180° phase jumps may indicate that the direction of BM displacement associated with OHC excitation has become reversed. OHCs are excited by displacement of the hair bundle toward the tallest row (Russell, I. J. *et al.*, 1986a), and according to the Zwislocki J. J. (1986) mechanical model of the cochlear partition, this can be achieved by displacements of the BM toward either the scala vestibuli or the scala tympani, depending on the relative magnitude of the movements of the TM and RL. A change in the relationship, for example, between the rotational stiffness of OHC hair bundles and the radial stiffness of the TM, possibly as a consequence of a level-dependent change in the mechanical impedance of elements within the cochlear partition, could reverse the direction of excitation as proposed by Zwislocki J. J. (1986; 1988) and Mountain D. C. and Cody A. R. (1999). For example, the rotational stiffness of OHC hair bundles is reduced following intense mechanical stimulation (Saunders, D. C. and Flock, A., 1986).

3.20.6.5 Hair Cell Isoresponse Tuning Curves: Comparison with Mechanical and Neural Tuning Curves

In experiments where successive recordings were made from adjacent IHCs and OHCs tuned to the same frequency without a measurable change in cochlear sensitivity between and following the recordings, isoresponse tuning curves were found to share similar characteristics in the tip region (Dallos, P., 1985), and indeed with mechanical tuning curves measured from the same frequency region, but from another cochlea (Figure 16(a) and Russell, I. J. *et al.*, 1995). These findings were confirmed and extended when Narayan S. S. *et al.* (1998) compared BM and neural tuning curves measured from the same cochlea (Figure 16(b)). They also concluded that the tuning curves were almost

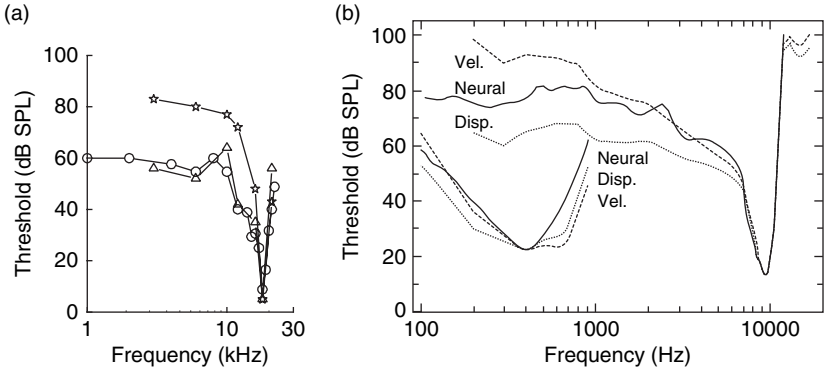

Figure 16 Hair cell, neural, and BM tuning curves compared. (a) Frequency tuning curves measured intracellularly from an IHC and OHC in the 18 kHz region of the same cochlea and isoresponse measurements of the displacement of the 18 kHz region of the BM of a different cochlea. The criteria for the isoresponse tuning curves were 0.5 mV (OHC, AC, △), 0.8 mV (IHC, DC, ○), 0.35 nm (BM, displacement ★). The resting potentials of the IHC and OHC were −45 and −65 mV respectively. The OHC AC responses are corrected for the low-pass filtering of the recording system (3.5 kHz) and OHC membrane filter (1 kHz). (b) Frequency tuning in cochlear vibrations and auditory nerve fibers in chinchilla. Curves at right: a frequency-threshold tuning curve for an auditory-nerve fiber (solid line) is compared with isoresponse curves for a BM site with identical CF (9.5 kHz) recorded in the same ear (244). At the fiber's CF threshold (13 dB SPL), BM vibrations had a peak displacement of 2.7 nm or, equivalently, 164 mm s^{-1}. These values were used to plot BM isodisplacement and isovelocity tuning curves (dotted and dashed lines, respectively). (A better mechanical/neural match was obtained by high-pass filtering the BM displacement curve at a rate of 3.8 dB/octave (not shown).) Curves at left: isodisplacement and isovelocity tuning curves (1 nm and 2.5 mm s^{-1}, respectively; dotted and dashed lines) for TM vibrations recorded at an apical cochlear site (299) are compared with a neural tuning curve (solid line), the average of recordings from many auditory-nerve fibers (Temchin, A. N., Rich, N. C., and Ruggero, M. A., unpublished observations). (a) From figure 3 of Russell, I. J., Kössl, M., and Murugasu, E. 1995. A Comparison between Tone-Evoked Voltage Responses of Hair Cells and Basilar Membrane Displacements Recorded in the Basal Turn of the Guinea Pig Cochlea. In: Advances in Hearing Research (*eds*. G. A. Manley,G.M. Klump, C. Köppl, H. Fastl, and H. Oeckinghaus), pp. 125–135. World Scientific. (b) From figure 18 of Robles, L. and Ruggero, M. A. 2001. Mechanics of the mammalian cochlea. Physiol. Rev. 81, 1305–1352.

identical in the tip region. When measured from the basal turn of the cochlea, the tuning curves of IHCs and nerve fibers are almost identical and differ from BM displacement (not velocity, Sellick, P. M. *et al.*, 1982; Narayan, S. S. *et al.*, 1998) and OHC tuning curves (which are also almost identical) in that the low-frequency tails of the tuning curves are 15–20 dB less sensitive. The similarity between neural and IHC tuning curves may indicate that synaptic transmission across the IHC afferent synapse is effectively frequency-independent, at least for frequencies above a few kilohertz. The 15–20 dB differences in the low-frequency tails of IHC and OHC tuning curves may be due to differences in the mechanical coupling between IHCs and OHCs with the TM (Dallos, P. *et al.*, 1972; Sellick, P. M. and Russell, I. J., 1980).

3.20.6.6 Factors Influencing Amplification along the Length of the Basilar Membrane

Amplification varies enormously along the length of the cochlea being about 1000-fold or more in the basal, high-frequency region of the cochlea, but little more than unity at the extreme low-frequency apex of the cochlea (Robles, L. and Ruggero, M. A., 2001; Sellick, P. M. *et al.*, 2006). What are the characteristics of the OHC's electrical responses to sound that vary down the length of the cochlea?

When recorded *in vivo* with sharp electrodes, the amplitudes of OHC receptor potentials do not appear to vary systematically down the length of the cochlea. OHC receptor potentials in response to low-frequency tones, at frequencies within the electrical time constants of the OHCs and recording systems, are similar and can exceed 30 mV in amplitude, irrespective of whether they are recorded in the apex or the base of the guinea-pig cochlea (Dallos, P., 1985; 1986; Russell, I. J. and Kössl, M., 1992b). The endocochlear potential does not vary substantially down the length of the guinea-pig cochlea being about +80 mV and neither does the resting-membrane potentials of the OHCs, being around −70 mV (Dallos, P. *et al.*, 1982; Dallos, P., 1986; Russell, I. J. and Sellick, P. M., 1983; Russell, I. J. *et al.*, 1986b). Intracellular *in vivo* recordings from hair cells are technically challenging and receptor potential magnitudes probably depend more on the quality and leakiness of the intracellular recording than on cochlear location. A systematic dependence of transducer currents and receptor potentials on cochlear location has, however, been shown from whole cell patch recordings made *in situ* in a gerbil hemicochlea preparation. He D. Z. Z. *et al.* (2004) , discovered that the transducer conductances of high-frequency basal OHCs were almost threefold greater in magnitude than those of the low-frequency apical OHCs, as indeed were the receptor currents when the OHCs were voltage-clamped at −70 mV (Figure 17). He D. Z. Z. *et al.* (2004) speculated that this variation could be a natural consequence of the increased number of stereocilia in the hair bundles of basal OHCs. They also proposed that the variation could be due to a gradation in the unitary conductance of the transducer channels, which for example in the turtle cochlea, ranges between 80 and 160 ps. Thus one basis for the vast difference in gain between the apical and basal region of the cochlea might be the differences in the size of the receptor current. Indeed, subsequent to the He D. Z. Z. *et al.* (2004) findings, Beurg, M. *et al.* (2006) found the single OHC channel conductance to vary with position along the length of the BM increasing from 145 ps in the apical coil to 210 ps in more basal locations.

An additional factor that might vary down the length of the cochlea is the sensitivity of the OHCs to BM displacement. In terms of linear displacement of the hair bundle, basal hair cells are more sensitive by a factor of six than apical hair cells. This is likely to be due to two factors, the larger transducer conductance of basal hair cells, mentioned earlier, and lever advantage between BM displacement and rotation of the hair bundle. From calculations based on the organ of Corti geometry and a kinematic study of the gerbil hemicochlea, Dallos P. (2003) proposed that the ratios of cilia angle and BM displacement for basal and apical OHCs are 20° and 10° μm^{-1}, respectively. The estimated angular sensitivity for basal and apical OHCs was 17.9 nS per degree and 2.9 nS per degree, which is ratio of about 6. He D. Z. Z. *et al.* (2004) estimated angular displacements and cilia ranges for OHCs between 10% and 90% activation of the transducer conductance from which they obtained 2.1° for the base and 1.9° for the apex. According these estimates by He D. Z. Z. *et al.* (2004) the physiological range of ciliary rotation remains constant throughout the cochlea, although it is unclear if these estimates take into account the huge differences in the magnitude of BM displacement at threshold between the apex and base of the cochlea (Robles, L. and Ruggero, M. A., 2001).

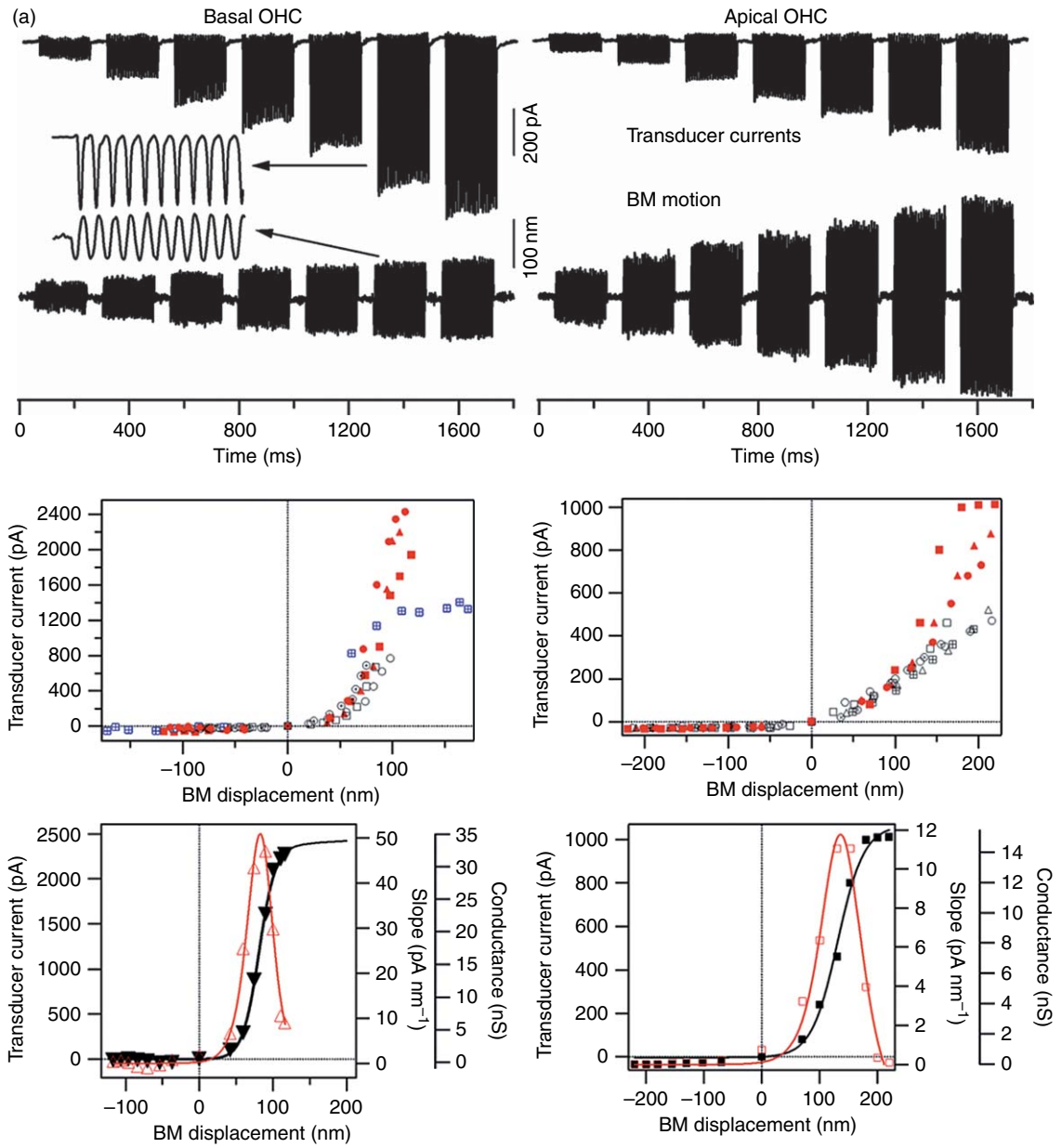

Figure 17 OHC transducer currents evoked by BM vibration. (a, b) Tight-seal recordings were made from two OHCs in the basal and apical turns at a holding potential of 270 mV. As shown on an expanded timescale in the insert, upward movement represents the BM moving toward the scala media, which evoked an increase in inward current (plotted downward in panels (a) and (b)). (c, d) Steady-state transducer current plotted as a function of BM displacement for eight basal (c) and eight apical (d) OHCs. Increase in inward current is plotted upward. Responses showing the most commonly observed behavior are plotted with black open symbols. Some of our best cells (filled red symbols) showed larger responses and intimate saturation. One fully saturated basal-turn cell, having small response and broad dynamic range, is also shown for comparison (blue symbols). (e, f) Transducer current, transducer conductance, and slope of the current function plotted for one good basal (e) and apical cell (f). The current plots are fitted with second-order Boltzmann functions, which are shown including the extrapolated saturation region (filled symbols). Slope functions (open symbols) are fitted with the derivatives of the second-order Boltzmann functions. From figure 2 of He, D. Z. Z., Jia, S., and Dallos, P. 2004. Mechanoelectrical transduction of adult outer hair cells studied in a gerbil hemicochlea. Nature 429, 766–770.

3.20.6.7 Operating Point of the Outer Hair Cell Receptor Potential

Receptor potentials and transducer currents have been recorded from isolated preparations of the neonatal mouse cochlea (Russell, I. J. *et al.*, 1986a; 1986b; Kros, C. J. *et al.*, 1992; Gèlèoc, G. S. G. *et al.*, 1997). In these preparations and in the gerbil hemicochlea, receptor potentials and transducer currents recorded from OHCs have a strong depolarizing asymmetry (Figure 3). The OHCs operate around the point of greatest inflexion such that at rest only about 6–10% of the transducer conductance is open and thus resemble the receptor potentials and currents recorded from hair cells in the frog sacculus, where the hair bundles are freestanding after the otolithic membrane is removed (Hudspeth, A. J. and Corey, D. P., 1977). The point of maximum sensitivity of the transducer conductance is not at this location on the OHC transfer function, but at the location of the maximum slope of the transfer function (Figures 18 and 19 and Russell, I. J. and Kössl, M., 1992a). From recordings made *in vivo*, OHCs in the basal turn of the guinea-pig cochlea operate close to this location (Russell, I. J. and Sellick, P. M., 1983; Russell, I. J. *et al.*, 1986b). There is however, a gradient of operating points down the length of the BM, such that OHCs in the upper coils of the cochlea produce largely depolarizing receptor potentials to tones of moderate levels (Dallos, P., 1985; 1986). The dependence of the operating point on the presence of the TM, as was demonstrated in measurements from mice where the TM is detached from the organ of Corti and the OHC receptor potentials, resemble those of other freestanding hair cells (Figure 20 and Legan, P. K. *et al.*, 2000).

3.20.6.8 Control of the Outer Hair Cell Transducer-Operating Point

The OHC transducer-operating point is not fixed but is a dynamic phenomenon and depends on the frequency, level, and duration of the tone and the frequency location of the OHC within the cochlea. Frequency and level-dependent changes in the symmetry of the receptor potential have been observed for middle and apical turn OHC in the guinea-pig cochlea (Dallos, P., 1985; 1986). In basal turn OHCs, the receptor potentials in response to tones several octaves in frequency below the CF, are symmetrical to tone-levels that generate responses close to the noise floor of the recording (~60 dB SPL). The receptor potentials become

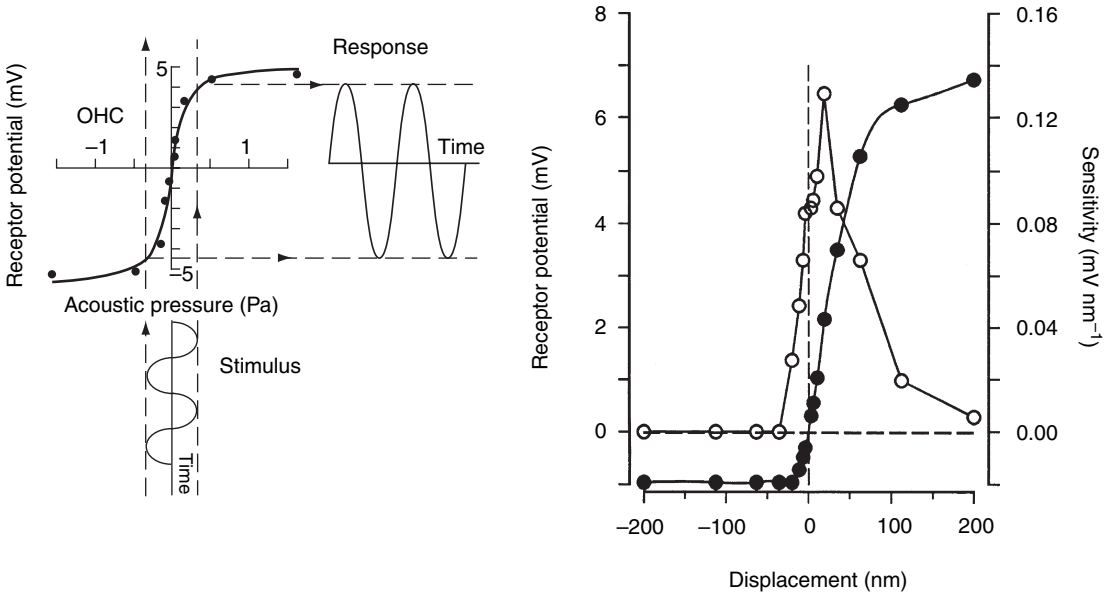

Figure 18 OHCs in the basal turn operate about the steep, most sensitive region of their input–output curve. (a) OHC transfer function based on *in vivo* data from Russell *et al.* 1986b. (b) OHC transfer function based on *in vivo* data (filled circles). The open circles plot the slope, and hence the sensitivity, of this relationship. (b) From Russell, I. J. and Kössl M. 1992a. Sensory transduction and frequency-selectivity in the basal turn of the guinea-pig cochlea. Philos. Trans. R. Soc. Lond. Ser. B. 336, 317–324.

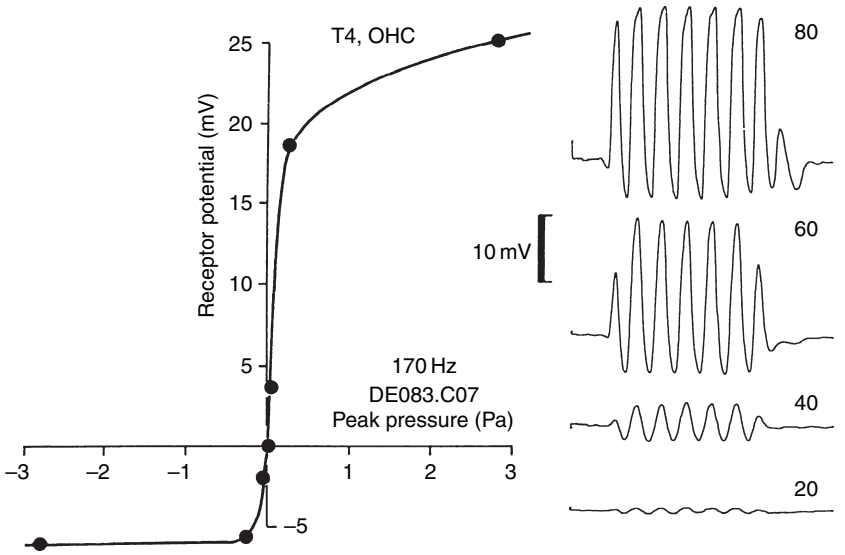

Figure 19 Peak AC response magnitude as a function of peak sound level for a fourth turn OHC. Stimulus frequency is near the BF of the cell. Corresponding waveforms are shown on the right side of the figure. From figure 9 of Dallos, P. 1986. Neurobiology of cochlear inner and outer hair cells, intracellular recordings. Hear. Res. 22, 185–198.

hyperpolarizing when the stimulus tone exceeds ~70 dB SPL, symmetrical at ~90 dB SPL, and depolarizing for levels above this. These level- and frequency-dependent changes in the OHC operating point are a natural consequence of the nonlinear properties of the OHC transducer function (Lukashkin, A. N. and Russell, I. J., 1998) and may also be due to interaction between the hair bundles and the TM rather than through interaction with the BM, at least for levels below 90 dB SPL. Level-dependent tonic displacements of the BM in the basal, high-frequency region of the cochlea have not been reported for levels below 90 dB SPL (Russell, I. J. *et al.*, 1986b).

3.20.6.9 Displacement of the Outer Hair Cell Transducer-Operating Point and Gain Optimization

From CM measurements to low-frequency tones following intense pure tone stimulation, Patuzzi R. *et al.* (1989) proposed that electromechanical feedback to the cochlea is directly related to the amplitude of the transducer current (Patuzzi, R. *et al.*, 1989). It has also been suggested that feedback is maximized when the DC component of the OHC receptor potential is minimized (Russell, I. J. *et al.*, 1986b; Russell, I. J. and Kössl, M., 1992a). In this feedback circuit, it was proposed that the error signal is the DC component of the OHC voltage response, which controls the OHC voltage-dependent motility and hence adjusts the length of the OHC to restore the radial displacement of the hair bundle and OHC transducer-operating point to optimum sensitivity. Changes in the membrane potential, length, and membrane tension of the OHCs alter voltage-dependent motility (Santos Sacchi, J., 2003) and hence should influence feedback gain. Thus, any displacement of the operating point of the OHC transducer away from the position of maximum sensitivity would reduce the gain of the transducer and hence the feedback.

There is evidence to support this proposal from *in vivo* intracellular current injection of OHCs in the basal turn of the cochlea that fast voltage-sensitive motility is responsible for automatic control of the OHC transducer-operating point. When single OHCs in the basal turn of the guinea-pig cochlea are injected *in vivo* through an intracellular electrode with current while the cochlea is stimulated with low-frequency tones, the OHC receptor potentials are decreased in amplitude and made more symmetrical with negative current (Figures 21(a) and 21(b)), which hyperpolarizes OHCs and presumably causes them to elongate. The OHCs receptor potentials are increased in amplitude and made positively asymmetrical with positive current, which depolarizes OHCs and presumably causes them to shorten (Russell, I. J. and Kössl, M., 1991). Current injection into IHCs does not

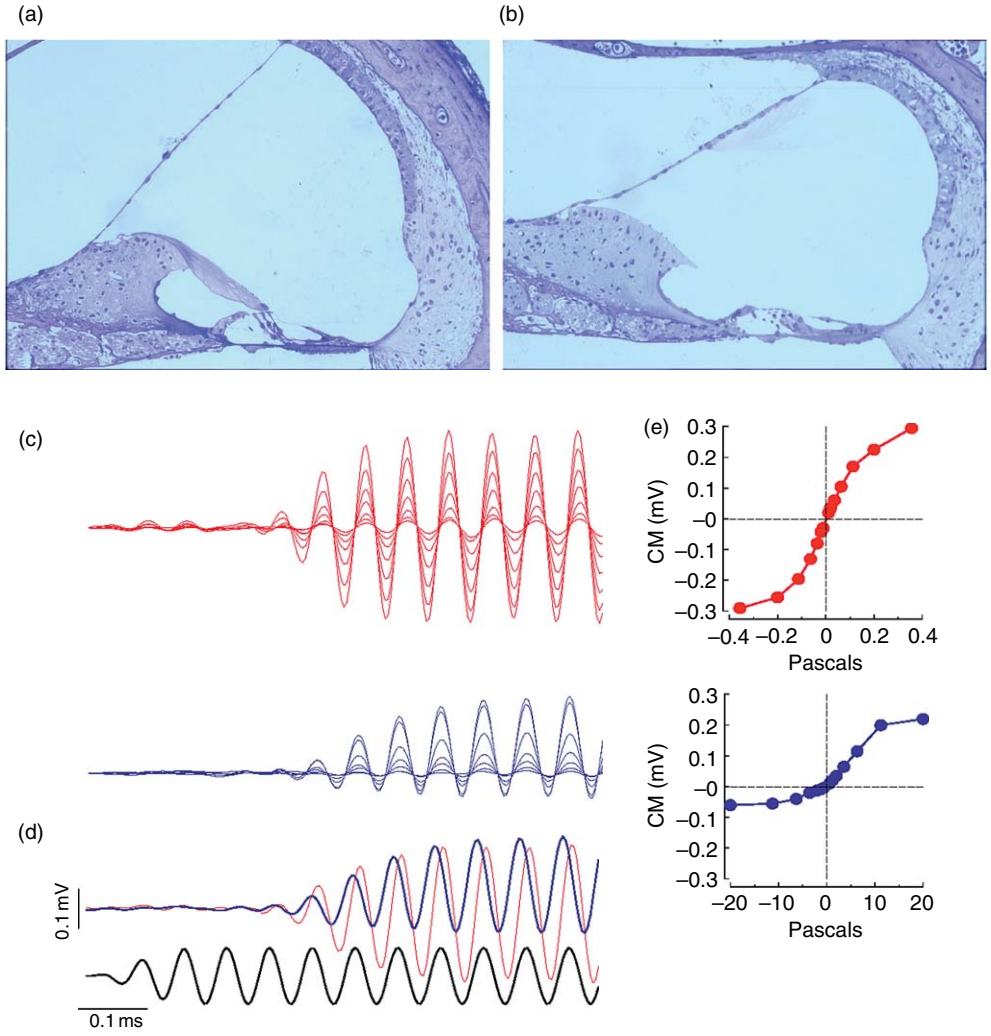

Figure 20 OHC operating point is controlled by the TM. Tolludin blue stained sections of the cochlea of (a) wild type mice and (b) *Tecta*Δ*ENT/DENT* mouse with detached TM. (c) CM measured in response to a 18 kHz tone. (Red) *Tecta*+/+ mouse at levels from 60–90 dB SPL in 5 dB SPL steps, (blue) *Tecta*Δ*ENT/DENT* mouse at levels from 95–125 dB SPL in 5 dB SPL steps. (d) Red line, *Tecta*+/+ mouse at 95 dB SPL, blue line, *Tecta* Δ*ENT/DENT* at 115 dB SPL. Black line control voltage to microphone driver. (e) Peak CM as function of r.m.s sound pressure at the tympanic membrane. (Red) *Tecta*+/+ mouse, (blue) *Tecta* Δ*ENT/DENT* mouse. From figure 7 of Legan, P. K., Lukashkina, V. A., Goodyear, R. J., Lukashkin, A. N., Verhoeven, K., Van Camp, G., Russell, I. J., and Richardson, G. P. 2000. A targeted deletion in α-tectorin reveals the tectorial membrane is required for the gain and timing of cochlear feedback. Neuron 28, 273–285.

strongly alter the waveforms of their low-frequency receptor potentials but they do alter the magnitudes in predictable ways (Figure 21(c)). This mechanism has also been proposed as a means for controlling the gain of OHCs following activation of the efferent medial olivocochlear system (Murugasu, E. and Russell, I. J., 1996).

Low-frequency biasing of the BM alters the gain of electromechanical feedback to the cochlear partition (Patuzzi, R. and Sellick, P. M. 1984; Russell, I. J. and Kössl, M. 1992b; Cheatham, M. A. and Dallos, P., 1994; 1997). The AC components of receptor potentials recorded from OHCs to tones close to their CF were suppressed when the BM was displaced away from its resting position toward either scala tympani or scala vestibuli by low-frequency (100 Hz) biasing tones (Russell, I. J. and Kössl, M., 1992b). Russell, I. J. and Kössl, M. suggested that this suppression was due to a reduction in feedback from the OHCs as a consequence of a reduction in the gain of mechanoelectrical transduction due to displacement of the OHC transducer operating. The AC responses were

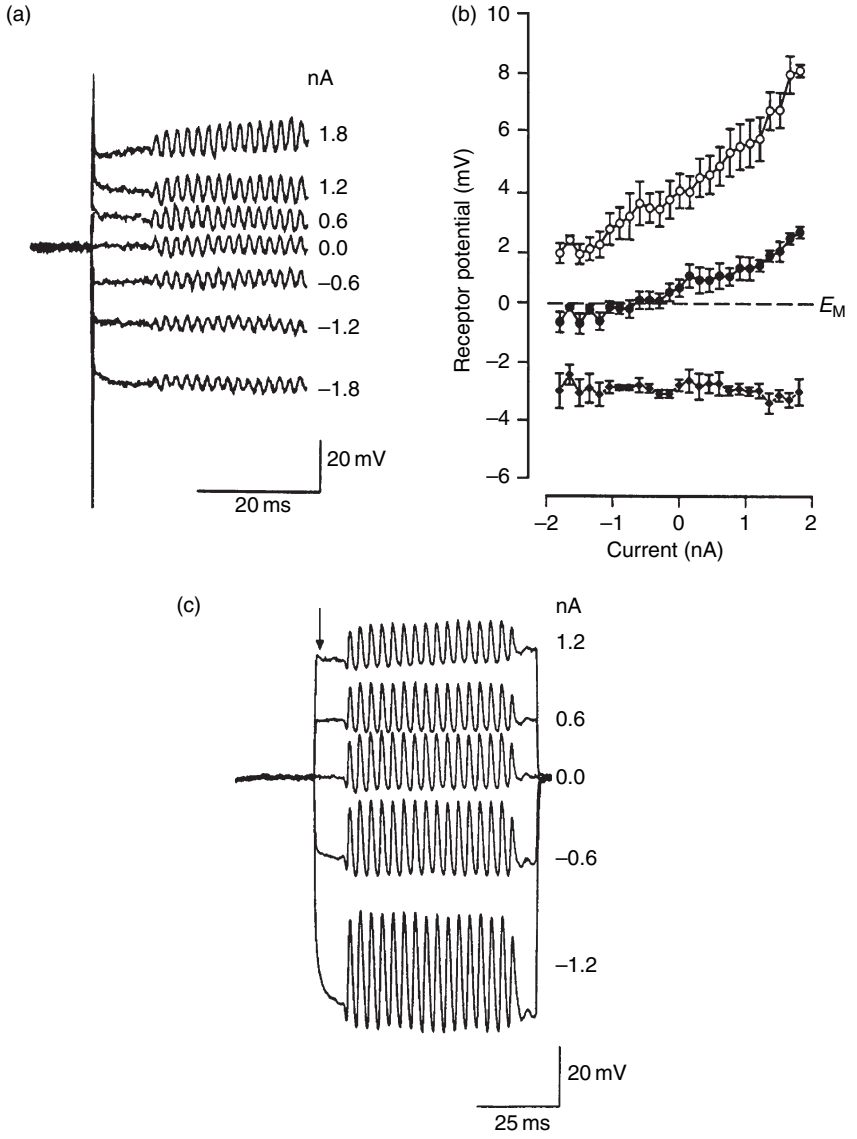

Figure 21 Intracellular current injection changes the symmetry of OHC but not IHC receptor potentials. (a) Receptor potentials recorded from an OHC when stimulated with 600 Hz tones at 80 dB SPL and during current injection. (b) Peak positive (○), peak negative (●) and DC (■) receptor potentials of the OHC and those of a further four OHCs in two other preparations as a function of injected current. EM (dashed line), indicates the membrane potential. Each point represents the mean and standard deviation of the pooled data. (b) Responses of an IHC to positive and negative current injection, voltage responses to 300 Hz tones at 90 dB SPL. From figures 1 and 6 of Russell, I. J. and Kössl M. 1991. The voltage responses of hair-cells in the basal turn of the guinea-pig cochlea. J. Physiol. Lond. 435, 493–511.

attenuated maximally at low levels of the near-CF tone when the combined levels of the biasing and CF tones are below the level of saturation of the transducer conductance (Patuzzi, R. *et al.*, 1989). Suppression was reduced when the high-frequency AC response became saturated and almost disappeared with the appearance of the OHC DC response to the HF tone.

Suppression of IHC responses to tones at frequencies around CF by low-frequency biasing of the cochlear partition (Patuzzi, R. and Sellick, P. M., 1984; Russell, I. J. and Kössl, M., 1992b) is due, therefore, primarily to changes in the mechanical input to the OHCs that are brought about as a consequence of the suppression of the OHC AC responses by the biasing tone. Displacement of the OHC operating

point can have profound effects on the gain of cochlear amplification as revealed in the responses of the IHCs. Indeed, in insensitive preparations, biasing of the cochlear partition can enhance IHC responses, presumably through shifting the operating point of the OHC transducer to a more sensitive position (Figure 22).

Zou Y. *et al.* (2006) re-examined these earlier proposals and findings and plotted the operating point movement of OHC stereociliary bundles derived from an analysis of the second and third harmonics of the CM waveform (Frank, G. and Kössl, M., 1997; Kirk, D. L. and Patuzzi, R., 1997; Bian, L. *et al.*, 2002; Lukashkin, A. N. and Russell, I. J., 2005). On the basis of this analysis, Zou Y. *et al.* (2006) inferred that the operating point was shifted by sound or by applied force to the otic capsule. Through the application of perfusion hydraulic pressure, force, and loud sound Zou Y. *et al.* (2006) , revealed that maintenance of the operating point was a dynamic process. They argued that fast prestin-based motility could be the basis for restoring the operating point, but the long-time constants of recovery they observed might be a consequence of slower potential mechanisms such as depolarization of the OHCs from potassium accumulation in the spaces of Nuel (Johnstone, B. M. *et al.*, 1989), calcium and ATP-dependent motility (Zenner, H. P., 1986), and mechanical processes such as cell turgor or stiffness (Santos-Sacchi, J., 2003).

3.20.6.10 Temporary Threshold Shift in Cochlear Sensitivity and Changes in the Operating Point of the Outer Hair Cell Transducer

Experiments based on direct measurements of IHC and OHC responses to intense tones challenge the view that cochlear desensitization is associated with saturation of the transducer conductance and may also provide insight into the way in which OHC responses can shape the frequency responses and dynamic ranges of IHCs at frequencies at and away from the CF. In experiments where responses to intense tones were measured from adjacent IHCs and OHCs in the basal high-frequency region of the same cochlea, Cody A. R. and Russell I. J. (1995) showed that although the hair bundles of IHCs are freestanding, IHC transducer functions can be controlled by the OHCs, even at frequencies several octaves below the CF. When the mammalian cochlea is exposed to brief (<200 ms) loud tones (~110 dB SPL), both IHCs and OHCs develop rapid and sustained AC voltage

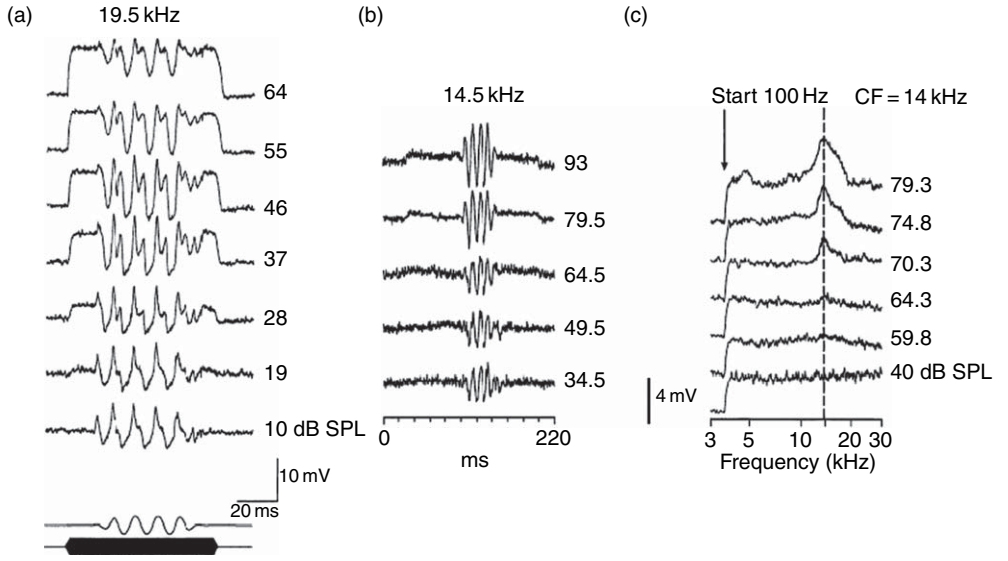

Figure 22 Intracellular voltage responses of an IHC to a combination of 80 dB SPL, 100 Hz tones and a tone at 19.5 kHz (CF) at the levels shown to the right. The waveform of the 100 Hz tone and the envelope of the HF tone are shown at the bottom. Resting membrane potential, −40 mV. The voltage responses are low-pass filtered at 3 kHz. Intracellular responses of an insensitive IHC to combined 100 Hz, 80 dB SPL tones and HF tones. (a) Voltage responses of the IHC to 100 Hz and 14 kHz tones at the levels shown to the right. (b) Magnitude of the 100 Hz response measured with the lock-in amplifiers as a function of the frequency and level of the HF tone when it is swept from 3 to 30 kHz. Resting membrane potential, −40 mV. From Russell, I. J. and Kössl, M. 1992b. Modulation of hair cell voltage responses to tones by low-frequency biasing of the basilar membrane in the guinea pig cochlea. J. Neurosci. 12, 1587–l601.

responses. The DC component of the IHC receptor potential is developed concurrently with the AC potential and it is sustained, with little variation, for the duration of the acoustic stimulus. In contrast, the DC component of the OHC receptor potential develops at a significantly slower rate and continues to grow as long as the acoustic stimulus is present. At tone-offset, the membrane potential returns over periods of 10s of ms to the resting-membrane potential (Figure 23). For longer stimuli (up to 8 s) at frequencies about half an octave below the CF, the OHC response is simply an extension of the response to the short tone burst. That is, the AC component of the voltage response remains constant and the DC component continues to grow with time. The magnitude of the IHC AC component also remains constant throughout the tone burst, but the DC component declines by more than 50% for an 8 s exposure. During long-term exposures, the complex time constants for the growth of the OHC DC and the decay of the IHC DC are very similar, although opposite in sign, indicating a common origin. Presentations of a low-frequency tone, either during the intense tone or immediately afterwards, reveals a basis for the decline in the IHC DC response; the receptor potentials become more symmetrical. Consequently the DC component declines relative to the magnitude of the AC component, which remains constant for the duration of the intense tone, although the harmonic distortion of the waveform decreases, which might be expected if the IHCs are operating in a more linear region of the transfer function. What, therefore, cause the depolarization and shift in symmetry of the OHC receptor potentials and how might this influence the waveforms of the IHC responses?

Depolarzsation of OHCs and other cellular elements of the organ of Corti during intense tones is believed to be due to the accumulation of potassium ions in the extracellular fluid-filled spaces of Nuel that surround the basolateral membranes of the OHCs (Cody, A. R. and Russell, I. J., 1985; 1987; Johnstone, B. M. *et al.*, 1989; Oesterle, E. C. and Dallos, P., 1986; 1990). The subsequent depolarization of the OHCs would cause the OHCs to shorten, thereby altering the way IHCs are stimulated so that their hair bundles become biased to a more linear region of the transducer transfer function. Other possible factors, such as intracellular accumulation of calcium in the stereocilia and change in stiffness of the OHC hair bundles (and indeed in the IHC

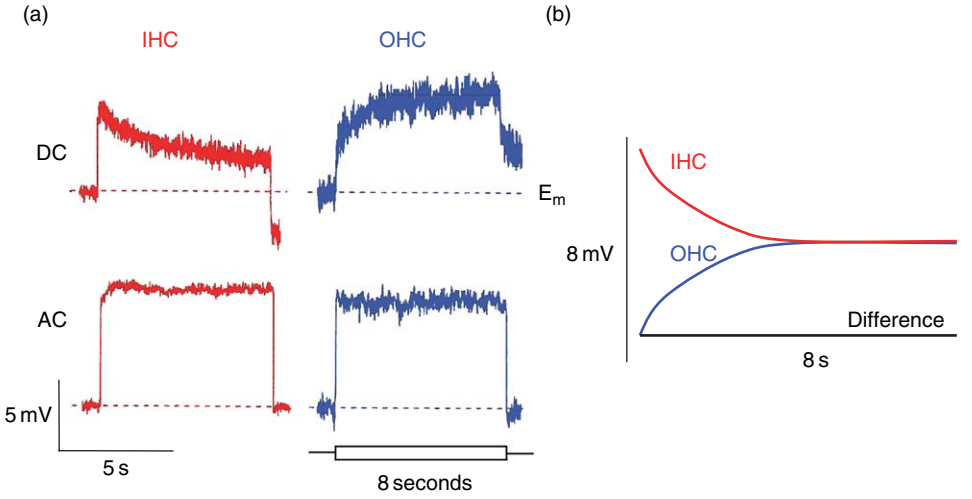

Figure 23 DC receptor potentials recorded from IHCs and OHCs in response to intense tones are mirror opposites of each other. (a) Intracellular receptor potentials generated by an IHC and an OHC) in response to a 12.5 kHz continuous tone at a level of 105 dB sound pressure level. The upper half of the figure represents the DC component of the receptor potential and the lower half represents the magnitude of the AC or phasic component measured using a lock-in amplifier (time constant 10 ms). In this case the fundamental component (12.5 kHz) is shown. Em. is the intracellular resting membrane potential (IHC, −32 mV; OHC, −78 mV). The period of the 8-second tone is indicated at the bottom of the figure. (b) An expanded and averaged plot of the data shown in the left hand figure. IHC (red trace) DC voltage response to a tone delivered for 8 seconds (12.5 kHz, 105 dB SPL). OHC (blue trace) DC voltage response to an 8-second continuous tone (12.5 kHz, 105 dB SPL). Difference (black trace) in membrane potential change for the IHC and OHC (OHC-IHC) depicted in (a). Redrawn and recalculated from original data used in Cody and Russell, 1995.

bundles), could also contribute to the forces exerted on the TM that might reduce the subtectorial space and hence bias the freestanding bundles of the IHCs.

3.20.6.11 Control of the Outer Hair Cell Operating Point and Shaping of the Outer Hair Cell Receptor Potential Tuning Curve

The level- and frequency-dependent behavior of the operating point of the OHC transducer function could also potentially contribute to shaping the high- and low-frequency shoulders of the tuning curve, although experiments directed at this question remain to be performed. There are hints from hair cell responses to low-frequency biasing tones that the OHC operating point does have a role in shaping the tuning curve from earlier experiments. For example, IHC DC/level functions and OHC AC/level functions share similar characteristics for frequencies around CF (Figures 15(c) and 15(d)). OHC and IHC AC and IHC DC receptor potentials are also similarly suppressed by BM displacements both toward and away from scala tympani (Figure 15(e)). At frequencies more than about 3 kHz below CF, however, the OHC AC/level functions are more sensitive than the IHC DC level functions (Figures 15(d) and 15(e)). At these frequencies, the OHC AC responses are suppressed by biasing tones at levels below those that elicit IHC DC responses (Figure 15(e)). At threshold levels for the IHC DC responses (~70 dB SPL), the suppressive influence of the 100 Hz tone on the OHC AC response (and hence on the IHC DC response) is no longer apparent. Thus control of the operating point of the OHC transducer can control the gain of cochlear amplification at frequencies away from the CF, and thereby shape the tip of the tuning curve.

3.20.7 Exploiting Compound Potentials to Understand Cochlear Function and Dysfunction

There is renewed interest in the measurement of extracellular receptor potentials from the cochlea and the extent to which they can reveal information about the transducer current and the way this is shaped by the basolateral conductances of hair cells. This approach is important because the technique is technically less demanding and far less invasive than the making of electrophysiological measurements from hair cells or sections of the organ of Corti isolated from the cochlea, where there have to be serious concerns about the extent to which these measurements reflect normal, *in vivo* function in the cochlea. The ability to probe the molecular basis of sensory transduction and amplification in the mammalian cochlea using techniques that are relatively noninvasive and easy to conduct is of great potential value in experiments using transgenic mice where proteins associated with the transduction apparatus and the dominant extracellular matrices have been modified. There have been several interesting attempts to explore the possibility of using the CM and SP to derive cochlear transducer functions largely from Patuzzi's laboratory in Perth (Patuzzi, R. and Moleirinho, A., 1998; Patuzzi, R. and O'Beirne, G. A., 1999) using custom-built electronics and software. Patuzzi and his colleagues estimated the transfer curve relating instantaneous sound pressure in the ear canal to instantaneous receptor current through the OHCs in the basal turn of the guinea-pig cochlea using the CM in response to 200 Hz tones. The transfer curve was approximated by a first-order Boltzmann activation curve which they analyzed automatically to continuously and swiftly derive the three parameters defining the curve. Their techniques offer a convenient method of monitoring changes in OHC mechanoelectrical transduction in the basal turn of the cochlea (Patuzzi, R. *et al.*, 1989) due to cochlear disturbances.

More recently Choi C.-H. *et al.* (2004) have constructed a cochlear transducer function from the SP recorded from the RWs of gerbils using a low-frequency bias tone. They assumed that the SP generated in the basal turn of the cochlea is due largely to the IHCs (Durrant, J. D. *et al.*, 1998). The transducer function could be fitted with a second-order Boltzmann function in line with the treatment of transducer functions constructed from electrical recordings of vestibular and cochlear hair cells (Hudspeth, A. J., 1982; Kros, C. J. *et al.*, 1992). Choi C.-H. *et al.* (2004) were conservative and did not attribute the derived transfer function specifically to IHCs. This is in part because at the 70–90 dB SPL levels of the 6 kHz and 12 kHz probe tones and a 25 Hz bias tone at 130 dB SPL they employed, OHCs in the basal turn might be expected to generate DC components in their receptor potentials, as has been shown for OHCs in the basal turn of the guinea-pig cochlea (Cody, A. R. and Russell, I. J., 1987).

The CAP is the synchronous sound-evoked activity of cochlear neurons that can be monitored by

placing an electrode on the RW. This compound neural potential has been used extensively throughout the history of cochlear electrophysiology to assess the sensitivity of the cochlea and as a criterion for determining if cochlear function has been impaired (see Dallos, P., 1973). The ability to derive masking frequency tuning curves from the CAP that closely resemble single unit threshold tuning curves (Dallos, P. and Cheatham, M. A., 1976) has been used more recently to examine frequency tuning in the cochleae of mice with deletions and mutations of the motor protein prestin (Cheatham, M. A. *et al*, 2004; 2005) and the tectorins of the TM (Legan, P. K. *et al*., 2005; Russell, I. J. *et al*., 2007).

The discoveries that the spontaneous neural activity of the cochlear nerve could be monitored as an electrical noise, with an electrode on the cochlear nerve trunk (Weinberger, N. M. *et al*., 1970; Snyder, R. L. and Schreiner, C. E., 1984; Schreiner, C. E. *et al*., 1986) and by Dolan D. F. *et al*. (1990) that electrical noise recorded from the RW was associated with the generation of spontaneous activity in the auditory nerve enabled others to exploit this finding to examine its apparent synchronicity (Cazals, Y. and Huang, Z. W., 1996). Later studies, however by McMahon C. M. and Patuzzi R. B. (2002) confirmed an original suggestion by Dolan D. F. *et al*. that the apparent synchronicity of 900 Hz is determined by the principal frequency component of the waveform of the action potentials in the type I neurons of the cochlear nerve, which is also shared by the CAP. McMahon C. M. and Patuzzi R. B. reassessed the basis of the neural noise recorded at the round window and concluded that changes in this neural noise, which Cazals Y. *et al*. (1998) had proposed as an indicator of peripheral tinnitus, was a rather ambiguous indicator because according to the findings by McMahon C. M. and Patuzzi R. B. it "can indicate changes in either the neural firing rate, as determined by stochastic quantal transmitter release or efficiency of spike initiation from excitatory post-synaptic potentials, or alternatively in the resonant properties of the primary afferent dendrites." More recently, Patuzzi and his colleagues discovered that the CAP waveform and its spectrum could be modulated either by direct current injection into scala media of the basal turn or through the RW (Brown, D. J. *et al*., 2004), or by changes to the auditory brainstem (McMahon, C. M. and Patuzzi, R. B., 2002; Sellick, P. M. *et al*., 2003). They proposed that these changes are due to the modulation of the membrane potential of the type I afferent neurons, caused by changing the extracellular potential in the case of the current injection, or via the lateral olivocochlear system of efferent neurons in the case of the brainstem manipulations (McMahon, C. M. *et al*., 2004). The measurements of neural noise at the RW membrane appear to hold considerable promise for understanding the cellular and molecular mechanisms of synaptic transmission, tinnitus, and efferent modulation of synaptic transmission by the lateral olivocochlear efferent system. Indeed measurement of neural noise at the RW has been very useful in determining the role of L-type calcium channels in mediating the release of transmitter from IHC afferent synapses (Sueta, T. *et al*., 2004). For the moment, however, the origin and properties of the noise remain to be fully understood (Patuzzi, R. B. *et al*., 2004).

3.20.8 The Nature of the Cochlear Amplifier

One of the most important challenges in understanding the workings of the cochlea concerns the identity of the amplification process itself. Shortly after Davis H. (1983) coined the phrase "cochlear amplifier," fast somatic electromotility was discovered in OHCs (Brownell, W. E. *et al*., 1985; Ashmore, J. F., 1987; Dallos, P., 1992) and the Dallos-lab (Zheng, J. *et al*., 2000) famously identified prestin, the motor molecule associated with this process in the lateral membranes of OHCs. A targeted deletion of prestin in mice (Liberman, M. C. *et al*., 2002) resulted in loss of OHC electromotility *in vitro* and a 35–60 dB loss of cochlear sensitivity *in vivo* (Cheatham, M. A. *et al*., 2004), while mechanoelectrical transduction was preserved in OHCs (Cheatham, M. A. *et al*., 2004; Jia, S. and He, D. Z., 2005). Liberman *et al*. suggested that prestin was "indeed the motor protein," and "that there is a simple and direct coupling between electromotility and cochlear amplification and that there is no need to invoke additional active processes to explain cochlear sensitivity in the mammalian ear." Detractors to the prestin theory of amplification point to fact that the hearing organs of nonmammalian vertebrates, which are without prestin, also amplify sounds and their frequency tuning is at least as good, if not better, than that of the mammalian cochlea at the same, low, frequencies (Manley, G. A. *et al*., 2001). Moreover, nonmammalian hearing organs display many of the characteristics of the mammalian cochlea and generate spontaneous emissions and distortion product otoacoustic emissions. Amplification in these organs harnesses forces provided

by the hair bundle linked to gating of the mechano-electrical transducer (MET) channels (Crawford, A. C. and Fettiplace, R., 1985; Howard, J. and Hudspeth, A. J., 1987; Martin, P. and Hudspeth, A. J., 1999). Active hair bundle movements have been detected first in non-mammalian hair cells. Here they have been correlated with two phases of MET channel adaptation (Fettiplace, R. and Ricci, A. J., 2003). Myosin-mediated slow adaptation occurs over tens of milliseconds (Gillespie, P. G. and Cyr, J. L., 2004), whereas fast adaptation occurs in tens of microseconds as the MET channel re-closes following its opening by positive deflection on the bundle. This twitch of the hair bundle is the result of a transient increase of intracellular Ca^{2+} following gating of the MET channel (Fettiplace, R. and Hackney, C. M., 2006). Fast adaptation has also been demonstrated in mammalian OHCs (Kros, C. J. *et al.*, 1992; Kennedy, H. J. *et al.*, 2003), and is associated with force generation by hair bundles (Kennedy, H. J. *et al.*, 2005). Thus both mechanisms can potentially fulfill the role of the cochlear amplifier. In nonmammalian hearing organs there is apparently no contest, and hair bundle motility is currently the only available candidate. In the cochlea there is strong, but currently not unequivocal, evidence that prestin provides amplification in the cochlea. However, does prestin act on its own (Jia, S. and He, D. Z., 2005). Does it supplement hair bundle motility (Kennedy, H. J. *et al.*, 2005)? Perhaps it mediates and modulates hair bundle motility (Chan, D. K. and Hudspeth, A. J., 2004)?

In an attempt to resolve the relative roles of hair bundle motility and somatic motility in cochlear amplification, Santos-Sacchi J. *et al.* (2006) investigated the nature of the cochlear amplifier based on the hypothesis that chloride ions interact with the intracellular domain of prestin to confer voltage sensitivity (Oliver, D. *et al.*, 2001) and that that chloride movements via the OHC lateral membrane conductance *G*metL, could serve to underlie cochlear amplification (Rybalchenko, V. and Santos-Sacchi, J., 2003). Santos-Sacchi J. *et al.* (2006) used salicylate, which competes with the putative anion binding or interaction site of prestin, to determine the resting level of chloride in OHCs. They found this to be near or below 10 mM, whereas perilymphatic levels are known to be ~120 mM. Using this observation, they explored the effects of perilymphatic chloride levels on BM amplification in the guinea-pig cochlea. Reductions in perilymphatic chloride resulted in reversible reductions in OHC electromechanical activity and cochlear amplification. They argued that changes in the extracellular chloride levels will not influence the cation-selective hair bundle MET channels process and associated fast adaptation, and that their findings lend further support to the proposal that prestin activity is dominant in underpinning the cochlear amplifier.

Chan D. K. and Hudspeth A. J. (2004; 2005) have measured hair bundle motility from IHCs in cochlear explants and mechanical responses of the organ of Corti of the explants to electrical and acoustic stimuli. Their measurements of the stiffness of the TM, BM, and hair bundles and modeling studies support the notion that "active forces generated by hair bundles can amplify movements of the basilar membrane."

From their studies and earlier measurements, they attribute the hair bundles' stiffness largely to the tip links, which are ideally located as bi-directional mechanoelectrical, electromechanical, transducers of energy between the TM and hair bundle. "An active process based on the transduction channels themselves, or on the myosin motors that anchor the channels to the stereociliary actin cores, would therefore be able to drive movement of the cochlear partition and contribute to active amplification." Thus Hudspeth and Chan seem to concur with Kennedy H. J. *et al.* (2005) that prestin and hair bundle motility share the role of cochlea amplifier. This is all well and good if both mechanisms work in synergy. Perhaps they do not. Perhaps one acts to amplify, and the other to compress, the cochlea's responses to the enormous dynamic range of stimuli it can cope with. At this moment, there is also no unequivocal evidence from measurements made *in vivo* that isolate a role for hair bundle motility in cochlear amplification in the mammalian cochlea. Otoacoustic emissions, that are distortion products and can signature cochlea amplification, have been recorded from mice with a targeted deletion of prestin where they have been tentatively attributed to hair bundle motility (Liberman, M. C. *et al.*, 2004), although otherwise these mice are profoundly insensitive (Liberman, M. C. *et al.*, 2002; Cheatham, M. A. *et al.*, 2004).

References

Allen, J. B. 1980. Cochlear micromechanics – a physical model of transduction. J. Acoust. Soc. Am. 68, 1660–1670.

Anderson, D. J., Rose, J. E., Hind, J. E., and Brugge, J. F. 1971. Temporal position of discharges in single auditory nerve fibres within the cycle of a sine-wave stimulus, frequency and intensity effects. J Acoust. Soc. Am. Suppl. 2, 1131.

Ashmore, J. F. 1987. A fast motile response in guinea-pig outer hair cells, the cellular basis of the cochlear amplifier. J. Physiol. Lond. 388, 323–347.

Beutner, D., Voets, T., Neher, E., and Moser, T. 2001. Calcium dependence of exocytosis and endocytosis at the cochlear inner hair cell afferent synapse. Neuron 29, 681–690.

Beisel, K. W., Nelson, N. C., Delimont, D. C., and Fritzsch, B. 2000. Longitudinal gradients of KCNQ4 expression in spiral ganglion and cochlear hair cells correlate with progressive hearing loss in DFNA2. Brain Res. Mol. Brain. Res. 82, 137–149.

Beisel, K. W, Wang-Lundberg, Y., Maklad, A., and Fritzsch, B. 2005. Development and evolution of the vestibular sensory apparatus of the mammalian ear. J. Vestib. Res. 15(5–6), 225–241.

Beurg, M., Evans, M. G., Hackney, C. M., and Fettiplace, R. 2006. A large-conductance calcium-selective mechanotransducer channel in mammalian cochlear hair cells. J. Neurosci. 26, 10992–11000.

Bian, L., Chertoff, M. E., and Miller, E. 2002. Deriving a cochlear transducer function from low-frequency modulation of distortion product otoacoustic emissions. J. Acoust. Soc. Am. 112, 198–210.

Bosher, S. K. and Warren, R. L. 1978. Very low calcium content of cochlear endolymph, an extracellular fluid. Nature 273, 377–378.

Brandt, A., Striessnig, J., and Moser, T. 2003. CaV1.3 channels are essential for development and presynaptic activity of cochlear inner hair cells. J. Neurosci. 23, 10832–10840.

Brown, D. J, McMahon, C. M, and Patuzzi, R. B. 2004. $K^{(+)}$ currents produce P(1) in the RW CAP: evidence from DC current bias, $K^{(+)}$ channel blockade and recordings from cochlea and brainstem. Hear Res. 190, 60–74.

Brownell, W. E., Bader, C. R., Bertrand, D., and de Ribaupierre, Y. 1985. Evoked mechanical responses of isolated cochlear outer hair-cells. Science 227, 194–196.

Brugge, J. F., Anderson, D. J., Hind, J. E., and Rose, J. E. 1969. Time structure of discharges in single auditory nerve fibers in the squirrel monkey in response to complex periodic sounds. J. Neurophysiol. 32, 386–401.

Cazals, Y. and Huang, Z. W. 1996. Average spectrum of cochlear activity: a possible synchronized firing, its olivo-cochlear feedback and alterations under anesthesia. Hear Res. 101, 81–92.

Cazals, Y., Horner, K. C., and Huang, Z. W. 1998. Alterations in average spectrum of cochleoneural activity by long-term salicylate treatment in the guinea pig: a plausible index of tinnitus. J. Neurophysiol. 80, 2113–2120.

Chan, D. K. and Hudspeth, A. J. 2004. Ca^{2+} current-driven nonlinear amplification by the mammalian cochlea *in vitro*. Nat. Neurosci. 8, 149–155.

Chan, D. K. and Hudspeth, A. J. 2005. Mechanical responses of the organ of Corti to acoustic and electrical stimulation *in vitro*. Biophys. J. 89, 4382–4395.

Cheatham, M. A. and Dallos, P. 1994. Stimulus biasing: a comparison between cochlear hair cell and organ of Corti response patterns. Hear. Res. 75, 103–113.

Cheatham, M. A. and Dallos, P. 1997. Low-frequency modulation of inner hair cell and organ of Corti responses in the guinea pig cochlea. Hear. Res. 108, 191–212.

Cheatham, M. A. and Dallos, P. 1998. The level dependence of response phase: Observations from cochlear hair cells. J. Acoust. Soc. Am. 104, 356–369.

Cheatham, M. A. and Dallos, P. 1999. Response phase: a view from the inner hair cell. J. Acoust. Soc. Am. 105, 799–810.

Cheatham, M. A. and Dallos, P. 2000. The dynamic range of inner hair cell and organ of Corti responses. J. Acoust. Soc. Am. 107, 1508–1520.

Cheatham, M. A. and Dallos, P. 2001. Inner hair cell response patterns, implications for low-frequency hearing. J. Acoust. Soc. Am. 1104, 2034–2044.

Cheatham, M. A., Huynh, K. H., Gao, J., Zuo, J., and Dallos, P. 2004. Cochlear function in Prestin knockout mice. J. Physiol. 560, 821–830.

Cheatham, M. A, Zheng, J., Huynh, K. H., Du, G. G., Gao, J., Zuo, J., Navarrete, E., and Dallos, P. 2005. Cochlear function in mice with only one copy of the prestin gene. J. Physiol. 569, 229–241.

Choi, C.-H., Chertoff, M. E., Bian, L., and Lerner, D. 2004. Constructing a cochlear transducer function from the summating potential using a low-frequency bias tone. J. Acoust. Soc. Am. 1116, 2996–3007.

Cody, A. R. and Mountain, D. C. 1989. Low-frequency responses of inner hair cells. Evidence for a mechanical origin of peak splitting. Hear. Res. 41, 89–100.

Cody, A. R. and Russell, I. J. 1985. Outer hair cells in the mammalian cochlea and noise-induced hearing loss. Nature 315, 662–665.

Cody, A. R and Russell, I. J. 1987. The responses of hair cells in the basal turn of the guinea-pig cochlea to tones. J. Physiol. Lond. 383, 551–569.

Cody, A. R. and Russell, I. J. 1995. Time-varying voltage responses of mammalian hair cells to isoamplitude acoustic stimulation. Aud. Neurosci. 1, 351–361.

Cooper, N. P. 2003. Compression in the Peripheral Auditory System. In: Compression: From Cochlea to Cochlear Implants (*eds*. S. P. Bacon, R. R. Fay, and A. N. Popper), pp. 18–61. Springer.

Crawford, A. C. and Fettiplace, R. 1981. Non-linearities in the responses of turtle hair cells. J. physiol. 315, 317–338.

Crawford, A. C. and Fettiplace, R. 1985. The mechanical properties of ciliary bundlesof turtle cochlear hair cells. J. Physiol. Lond. 364, 359–379.

Crawford, A. C., Evans, M. G., and Fettiplace, R. 1991. The actions of calcium on the mechano-electrical transducer current of turtle hair cells. J. Physiol. 434, 369–398.

Dallos, P. 1973. Whole-Nerve Action Potential. In: The Auditory Periphery (*ed*. P. Dallos), pp. 329–353. Academic Press.

Dallos, P. 1983. Some electrical circuit properties of the organ of Corti. I. Analysis without reactive elements. Hear. Res. 12, 89–119.

Dallos, P. 1985. Response characteristics of mammalian cochlear hair cells. J. Neurosci. 5, 1591–1608.

Dallos, P. 1986. Neurobiology of cochlear inner and outer hair cells, intracellular recordings. Hear. Res. 22, 185–198.

Dallos, P. 1992. The active cochlea. J. Neurosci. 12, 4575–4585.

Dallos, P. 1996. Overview, Cochlear Neurobiology. In: The Cochlea (*eds*. P. Dallos, A. N. Popper, and R. R. Fay), pp. 1–43. Springer.

Dallos, P. 2003. Organ of Corti kinematics. J. Assoc. Res. Otolaryngol. 4, 416–421.

Dallos, P. and Cheatham, M. A. 1976. Production of cochlear potentials by inner and outer hair cells. J. Acoust. Soc. Am. 60, 510–512.

Dallos, P. and Cheatham, M. A. 1989. Nonlinearities in cochlear receptor potentials in their origins. J. Acoust. Soc. Am. 86, 1790–1796.

Dallos, P. and Cheatham, M. A. 1990. Effects of electrical polarization on inner hair cell receptor potentials. J. Acoust. Soc. Am. 87, 1636–1647.

Dallos, P. and Cheatham, M. A. 1991. Cochlear Hair Cell Function Reflected in Intracellular Recordings *In Vivo*. In: Sensory Transduction (*eds*. D. P. Corey and S. D. Roper), pp. 371–393. The Rockefeller University Press.

Dallos, P. and Corey, M. E. 1991. The role of outer hair cell motility in cochlear tuning. Curr. Opin. Neurobiol. 1, 215–220.

Dallos, P. and Santos-Sacchi, J. 1983. AC receptor Potentials from Hair Cells in the Low-Frequency Region of the Guinea Pig Cochlea. In: Mechanisms of Hearing

(*eds*. W. R. Webster and L. M. Aitkin), pp. 11–16. Monash University Press.
Dallos, P., Billone, M. C., Durrant, J. D., Wang, C., and Raynor, S. 1972. Cochlear inner and outer hair cells, functional differences. Science 177, 356–358.
Dallos, P. J., Santos-Sacchi, J., and Flock, A. 1982. Cochlear outer hair cells, Intracellular recordings. Science 218, 582–584.
Davis, H. 1958. Transmission and transduction in the cochlea. Laryngoscope 68, 359–382.
Davis, H. 1965. A model for transducer action in the cochlea. Cold Spring Harbor Symp. Quant. Biol. 30, 181–190.
Davis, H. 1983. An active process in cochlear mechanics. Hear. Res. 9, 79–90.
Davis, H., Deatherage, B. H., Eldredge, D. H., and Smith, C. A. 1958a. Summating potentials of the cochlea. Am. J. Physiol. 195, 251–261.
Davis, H., Eldredge, D. H., and Gannon, R. P. 1958b. Some effects of electrical polarization of the organ of Corti. Physiologist 1, 15.
Davis, H., Fernandez, C., and McAuliffe, D. R. 1950. The excitatory process in the cochlea. Proc. Natl. Acad. Sci. U. S. A. 30, 580–587.
Dolan, D. F., Nuttall, A. L., and Avinash, G. 1990. Asynchronous neural activity recorded from the round window. J. Acoust. Soc. Am. 87, 2621–2627.
Dulon, D., Sugasawa, M., Blanchet, C., and Erostegui, C. 1995. Direct measurement of Ca^{2-+} activated K^{+} currents in inner hair cells of the guinea-pig cochlea using photolabile Ca^{2+} chelators. Pflügers. Arch 430, 365–373.
Durrant, J. D., Wang, J., Ding, D. L., and Salvi, R. J. 1998. Are inner or outer hair cells the source of summating potentials recorded from the round window? J. Acoust. Soc. Am. 104, 370–377.
Dynes, S. B. C. and Delgutte, B. 1992. Phase-locking of auditory-nerve discharges to sinusoidal electric stimulation of the cochlea. Hear. Res. 58, 79–90.
Edmonds, B. W., Gregory, F. D., and Schweizer, F. E. 2004. Evidence that fast exocytosis can be predominantly mediated by vesicles not docked at active zones in frog saccular hair cells. J. Physiol. 560, 439–450.
Eldredge, D. H., Miller, J. D., and Bohne, B. A. 1981. A frequency-position map for the chinchilla cochlea. J. Acoust. Soc. Am. 69, 1091–1095.
Fernandez, C., Gernand, B. E., Davis, H., and McAuliffe, D. R. 1950. Electrical injury of the cochlea of the guinea pig. Proc. Soc. Exp. Biol. Med. 75, 452–455.
Fettiplace, R. 2006. Active hair bundle movements in auditory hair cells. J. Physiol. 576, 29–36.
Fettiplace, R. and Hackney, C. M. 2006. The sensory and motor roles of auditory hair cells. Nature Neuro. Rev. 7, 19–29.
Fettiplace, R. and Ricci, A. J. 2003. Adaptation in auditory hair cells. Curr. Opin. Neurobiol. 13, 446–51.
Flock, Å. 1965. Transducing mechanisms in the lateral line canal organ receptors. Cold Spring Harb. Symp. Quant. Biol. 30, 133–145.
Flock, Å and Russell, I. J. 1973. Efferent nerve fibers – postsynaptic action on hair cells. Nature-New Biol. 243, 89–91.
Flock, Å and Russell, I. J. 1976. Inhibition by efferent nerve-fibers - action on hair cells and afferent synaptic transmission in lateral line canal organ of burbot Lota lota. J. Physiol. Lond. 257, 45–62.
Frank, G. and Kössl, M. 1996. The acoustic two-tone distortions 2f1-f2 and f2-f1 and their possible relation to changes in the gain and the operating point of the cochlear amplifier. Hear. Res. 98, 104–115.
Frank, G. and Kössl, M. 1997. Acoustical and electrical biasing of the cochlear partition. Effects on the acoustic two tone distortions f_2-f_1 and $2f_1$-f_2. Hear. Res. 113, 57–68.
Freeman, D. M. and Weiss, T. F. 1990. Hydrodynamic forces on hair bundles at high frequencies. Hear. Res. 48, 31–36.
Freeman, D. M., Abnet, C. C., Hemmert, W., Tsai, B. S., and Weiss, T. F. 2003a. Dynamic material properties of the tectorial membrane: a summary. Hear. Res. 180, 1–10.
Freeman, D. M., Masaki, K., McAllister, A. R., Wei, J. L., and Weiss, T. F. 2003b. Static material properties of the tectorial membrane: a summary. Hear. Res. 180, 11–27.
Fridberger, A., Tomo, I., Ulfendahl, M., and Boutet de Monvel, J. 2006. Imaging hair cell transduction at the speed of sound, dynamic behavior of mammalian stereocilia. Proc. Natl. Acad. Sci. U. S. A. 103, 1918–23.
Fritzsch, B. and Beisel, K. W. 2003. Molecular conservation and novelties in vertebrate ear development. Curr. Top. Dev. Biol. 57, 1–44.
Fuchs, P. A. 2005. Time and intensity coding at the hair cell's ribbon synapse. J. Physiol. 566, 7–12.
Fuchs, P. A., Glowatzki, E., and Moser, T. 2003. The afferent synapse of cochlear hair cells. Curr. Opin. Neurobiol. 13, 452–458.
Furukawa, T. and Ishii, Y. 1967. Neurophysiological studies of hearing in the goldfish. J. Neurophysiol. 30, 1377–1403.
Furukawa, T. and Matsuura, S. 1978. Adaptive run down of excitatory post synaptic potentials at synapses between hair cells and eighth nerve fibres in goldfish. J. Physiol. 276, 193–209.
Furukawa, T., Hayashida, Y., and Matsuura, S. 1978. Quantal analysis of the size of excitatory post-synaptic potentials at synapses between hair cells and afferent nerve fibres in goldfish. J. Physiol. 276, 211–226.
Gamper, N. and Shapiro, M. S. 2003. Calmodulin mediates Ca^{2+}-dependent modulation of M-type K^{+} channels. J. Gen. Physiol. 122, 17–31.
Geisler, C. D. 1998. From Sound to Synapse. Oxford University Press.
Géléoc, G. S. G., Lennan, G. W. T., Richardson, G. P., and Kros, C. J. 1997. A quantitative comparison of mechano-electrical transduction in vestibular and auditory hair cells of neonatal mice. Proc. Roy. Soc. Lond. B. 264, 611–621.
Gillespie, P. G. and Cyr, J. L. 2004. Myosin-1c, the hair cell's adaptation motor. Annu. Rev. Physiol. 66, 521–545.
Gleich, O. and Narins, P. M. 1988. The phase response of primary auditory afferents in a songbird (Sturnus vulgaris L.). Hear. Res. 32, 81–91.
Glowatzki, E. and Fuchs, P. A. 2002. Transmitter release at the hair cell ribbon synapse. Nat. Neurosci. 5, 147–154.
Goldstein, M. H. 1968. The Auditory Periphery. In: Medical Physiology (*ed*. V. B. Mountcastle), Vol. 2, pp. 1165–1198. Mosby.
Hackney, C. M., Mahendrasingam, S., Penn, A., and Fettiplace, A. 2005. The concentrations of calcium buffering proteins in mammalian cochlear hair cells. J. Neurosci. 25, 7867–7886.
Hafidi, A. and Dulon, D. 2004. Developmental expression of calcium channels in mouse inner ear. Exp. Brain. Res. 150, 167–175.
Hafidi, A., Beurg, M., and Dulon, D. 2005. Localization and developmental expression of BK channels in mammalian cochlear hair cells. Neuroscience 130, 475–484.
Hartmann, R. and Klinke, R. 1987. Impulse pattern in auditory-nerve fibres to extra- and intra-cochlear electrical stimulation. In: Cochlear implants: current situation (*ed*. P. Banfai), pp. 73–86. International Cochlear Implant Symposium.
He, D. Z. Z., Jia, S., and Dallos, P. 2004. Mechanoelectrical transduction of adult outer hair cells studied in a gerbil hemicochlea. Nature 429, 766–770.

Hill, K. G., Stange, G., and Mo, J. 1989. Temporal synchronization in the primary auditory response in the pigeon. Hear. Res. 39, 63–74.
Honrubia, V. and Ward, P. H. 1969. Dependence of the cochlear microphonics and the summating potential on the endocochlear potential. J Acoust. Soc Am. 46, 388–392.
Housley, G. D. and Ashmore, J. F. 1992. Ionic currents of outer hair cells isolated from the guinea-pig cochlea. J. Physiol. 448, 73–98.
Housley, G. D., Marcotti, W., Navaratnam, D., and Yamoah, E. N. 2006. Hair cells – beyond the transducer. J. Membr. Biol. 209, 89–118.
Howard, J. and Hudspeth, A. J. 1987. Compliance of the hair bundle associated with gating of mechanoelectrical transduction channels in the bullfrog's saccular hair cell. Neuron 1, 189–199.
Hudspeth, A. J. 1982. Extracellular current flow and the site of transduction by vertebrate hair cells. J. Neurosci. 2, 1–10.
Hudspeth, A. J. and Corey, D. P 1977. Sensitivity, polarity and conductance change in the response of vertebrate hair cells to controlled mechanical stimuli. Proc. Natl. Acad. Sci. U. S. A. 74, 2407–2411.
Ishii, Y., Matsuura, S., and Furukawa, T. 1971. An input–output relation at the synapse between hair cells and eighth nerve fibers in goldfish. Jpn. J. Physiol. 21, 91–98.
Jia, S. and He, D. Z. 2005. Motility-associated hair-bundle motion in mammalian outer hair cells. Nat. Neurosci. 8, 1028–1034.
Jia, S., Dallos, P., and He, D. Z. Z. 2007. Mechanoelectric transduction of adult inner hair cells. J. Neurosci. 27, 1006–1014.
Johnson, D. H. 1980. The relationship between spike rate and synchrony in responses of auditory-nerve fibers to single tones. J. Acoust. Soc. Am. 68, 1115–1122.
Johnstone, B. M., Patuzzi, R., Syka, J., and Sykova, E. 1989. Stimulus related potassium changes in the organ of Corti of guinea-pig. J. Physiol. London 408, 77–92.
Kennedy, H. J., Crawford, A. C., and Fettiplace, R. 2005. Force generation by mammalian hair bundles supports a role in cochlear amplification. Nature 433, 880–883.
Kennedy, H. J., Evans, M. G., Crawford, A. C., and Fettiplace, R. 2003. Fast adaptation of mechanoelectrical transducer channels in mammalian cochlear hair cells. Nat. Neurosci. 6, 832–836.
Kiang, N. 1965. Discharge Patterns of Single Fibers in the Cat's Auditory Nerve, MIT Press.
Kidd, R. C. and Weiss, T. F. 1990. Mechanisms that degrade timing information in the cochlea. Hear. Res. 49, 181–207.
Kim, D. O. and Molnar, C. E. 1979. A population study of cochlear nerve fibers, comparison of spatial distributions of average rate and phase-locking of responses to single tones. J. Neurophysiol. 42, 16–30.
Kirk, D. L. and Patuzzi, R. 1997. Transient changes in cochlear potentials and DPOAEs after low-frequency tones, the 'two-minute bounce' revisited. Hear. Res. 112, 49–68.
Khimich, D., Nouvian, R., Pujol, R., tom Dieck, S, Egner, A., Gundelfinger, E. D., and Moser, T. 2005. Hair cell synaptic ribbons are essential for synchronous auditory signalling. Nature 434, 889–894.
Köppl, C. 1997. Phase locking to high frequencies in the auditory nerve and cochlear nucleus magnocellularis of the barn owl, *Tyto alba*. J. Neurosci. 17, 3312–3321.
Kössl, M. and Russell, I. J. 1992. The phase and magnitude of hair cell-receptor potentials and frequency tuning in the guinea-pig cochlea. J. Neurosci. 12, 1575–1586.
Kössl, M. and Russell, I. J. 1995. Basilar membrane resonance in the cochlea of the mustached bat. Proc. Natl. Acad. Sci. U. S. A. 921, 276–279.
Kössl, M. and Vater, M. 2000. Consequences of outer hair cell damage for otoacoustic emissions and audio-vocal feedback in the mustached bat. J. Assoc. Res. Otolaryngol. 14, 300–314.
Krönester-Frei, A. 1979. The e!ect of changes in endolymphatic ion concentrations on the tectorial membrane. Hear. Res. 1, 81–94.
Kros, C. J. 1996. Physiology of Mammalian Cochlear Hair Cells. In: The Cochlea (*eds*. P. Dallos, A. N. Popper, and R. R. Fay), pp. 318–385. Springer.
Kros, C. J. and Crawford, A. C. 1990. Potassium currents in inner hair cell isolated from the guinea-pig cochlea. J. Physiol. 421, 263–291.
Kros, C. J., Ruppersberg, J. P., and Rüsch, A. 1998. Expression of a potassium current in inner hair cells during development of hearing in mice. Nature 394, 281–284.
Kros, C. J., Rüsch, A., and Richardson, G. P. 1992. Mechano-electrical transducer currents in hair cells of the cultured neonatal mouse cochlea. Proc. Roy. Soc. Lond. B 249, 185–193.
Langer, P, Grunder, S., and Rusch, A. 2003. Expression of Ca^{2+}-activated BK channel mRNA and its splice variants in the rat cochlea. J. Comp. Neurol. 455, 198–209.
Legan, P. K., Lukashkina, V. A, Goodyear, R. J., Lukashkin, A. N., Verhoeven, K., Van Camp, G., Russell, I. J., and Richardson, G. P. 2000. A targeted deletion in α-tectorin reveals the tectorial membrane is required for the gain and timing of cochlear feedback. Neuron 28, 273–285.
Legan, P. K., Lukashkina, V. A., Goodyear, R. J., Verhoeven, K., Van Camp, G., Russell, I. J., and Richardson, G. P. 2005. A deafness mutation demonstrates a second role for the tectorial membrane in hearing. Nat. Neurosci. 8, 1035–1042.
LeMasurier, M. and Gillespie, P. G. 2005. Hair-cell mechanotransduction and cochlear amplification. Neuron. 48, 403–415.
Liberman, M. C. and Dodds, L. W. 1984. Single-neuron labeling and chronic cochlear pathology. III. Stereocilia damage and alterations of threshold tuning curves. Hear. Res. 16, 55–74.
Liberman, M. C., Gao, J., He, D. Z., Wu, X., Jia, S., and Zuo, J. 2002. Prestin is required for electromotility of the outer hair cell and for the cochlear amplifier. Nature 419, 300–304.
Liberman, M. C., Zuo, J., and Guinan, J. J., Jr. 2004. Otoacoustic emissions without somatic motility: can stereocilia mechanics drive the mammalian cochlea? J. Acoust. Soc. Am. 116, 1649–1655.
Lim, D. J. 1980. Cochlear anatomy related to cochlear mechanics. A Review. J. Acoust. Soc. Am. 67, 1686–1695.
Lim, D. J. 1986. Functional structure of the organ of Corti – a review. Hear. Res. 22, 117–146.
Lopez-Poveda, E. A. and Eustaquio-Martin, A. 2006. A biophysical model of the inner hair cell: The contribution of potassium currents to peripheral auditory compression. J. Assoc. Res. Otolaryngol. 17, 218–235.
Löwenstein, O. and Wersäll, J. 1959. A functional interpretation of the elctronmicroscopic structure of the sensory hairs in the cristae of the elasmobranch *Raja clavata* in terms of directional sensitivity. Nature 184, 1807–1808.
Lukashkin, A. N. and Russell, I. J. 1998. A descriptive model of the receptor potential nonlinearities generated by the hair cell mechanoelectrical transducer. J. Acoust. Soc. Am. 103, 973–980.
Lukashkin, A. N. and Russell, I. J. 2005. Dependence of the DPOAE amplitude pattern on acoustical biasing of the cochlear partition. Hear. Res. 203, 45–53.
McMahon, C. M. and Patuzzi, R. B. 2002. The origin of the 900 Hz spectral peak in spontaneous and sound-evoked round-window electrical activity. Hear. Res. 173, 134–152.
McMahon, C. M., Brown, D. J., and Patuzzi, R. B. 2004. Transient focal cooling at the round window and cochlear

nucleus shows round window CAP originates from cochlear neurones alone. Hear. Res. 190, 75–86.
Mammano, F. and Ashmore, J. F. 1993. Reverse transduction measured in the isolated cochlea by laser Michelson interferometry. Nature 365, 838–841.
Mammano, F., Kros, C. K., and Ashmore, J. F. 1995. Patch clamped responses from outer hair cells in the intact adult organ of Corti. Pflügers Arch. 430, 745–750.
Manley, G. A. 2001. Evidence for an active process and a cochlear amplifier in nonmammals. J. Neurophysiol. 862, 541–549.
Manley, G. A., Köppl, C., and Yates, G. K. 1997. Activity of primary auditory neurons in the cochlear ganglion of the emu Dromaius novaehollandiae: spontaneous discharge, frequency tuning, and phase locking. J. Acoust. Soc. Am. 101, 1560–1573.
Manley, G. A., Kirk, D. L., Köppl, C., and Yates, G. K. 2001. *In vivo* evidence for a cochlear amplifier in the hair-cell bundle of lizards. Proc. Natl. Acad. Sci. U. S. A. 98, 2826–2831.
Marcotti, W. and Kros, C. J. 1999. Developmental expression of the potassium current I K,n contributes to maturation of mouse outer hair cells. J. Physiol. 520, 653–660.
Marcotti, W., Johnson, S. L., and Kros, C. J. 2003. Sodium and calcium currents shape action potentials in immature mouse inner hair cells. J. Physiol. Lond. 552, 743–761.
Marcotti, W., Johnson, S. L., and Kros, C. J. 2004. A transiently expressed SK current sustains and modulates action potential activity in immature mouse inner hair cells. J. Physiol. Lond. 560, 691–708.
Martin, P. and Hudspeth, A. J. 1999. Active hair-bundle movements can amplify a hair cell's response to oscillatory mechanical stimuli. Proc. Natl. Acad. Sci. USA 96, 14306–14311.
McGlone, F. P., Russell, I. J., and Sand, O. 1979. Measurement of calcium ion concentration in the lateral line system of *Xenopus laevis*. J. Exp. Biol. 83, 123–130.
Mountain, D. C. and Cody, A. R. 1999. Multiple modes of inner hair cell stimulation. Hear. Res. 132, 1–14.
Mountain, D. C., Hubbard, A. E, and Mcmullen, T. A. 1983. Electromechanical Processes in the Cochlea. In: Mechanics of Hearing (*eds*. E. de Boer and M. A. Viergever), pp. 119–126. Delft University Press.
Murugasu, E. and Russell, I. J. 1995. Salicylate ototoxicity, the effects on basilar membrane displacement, cochlear microphonics, and neural responses in the basal turn of the guinea pig cochlea. Auditory Neurosci. 1, 139–150.
Murugasu, E. and Russell, I. J. 1996. The effect of efferent stimulation on basilar membrane displacement in the basal turn of the guinea pig cochlea. J. Neurosci. 16, 325–332.
Narayan, S. S., Temchin, A. N., Recio, A., and Ruggero, M. A. 1998. Frequency tuning of basilar membrane and auditory nerve fibers in the same cochleae. Science 282, 1882–1884.
Nowotny, M. and Gummer, A. W. 2006. Nanomechanics of the subtectorial space caused by electromechanics of cochlear outer hair cells. Proc. Natl. Acad. Sci. U. S. A. 103, 2120–2125.
Oesterle, E. C. and Dallos, P. 1986. Intracellular recordings from supporting cells in the organ of Corti. Hear. Res. 22, 229–232.
Oesterle, E. C. and Dallos, P. 1990. Intracellular recordings from supporting cells in the guinea pig cochlea: DC potentials. J. Neurophysiol. 64, 617–636.
Ohmori, H. 1987. Gating properties of the mechano-electrical transducer channel in the dissociated vestibular hair cell of the chick. J. Physiol. 87, 589–609.
Oliver, D., He, D. Z., Klocker, N., Ludwig, J., Schulte, U., Waldegger, S., Ruppersberg, J. P., Dallos, P., and Fakler, B 2001. Intracellular anions as the voltage sensor of prestin, the outer hair cell motor protein. Science 292, 2340–2343.
Oliver, D., Knipper, M., Derst, C., and Fakler, B. 2003. Resting potential and submembrance calcium concentration of inner hair cells in the isolated mouse cochlea are set by KCNQ-type potassium channels. J. Neurosci. 23, 2141–2149.
Palmer, A. R. and Russell, I. J. 1986. Phase-locking in the cochlear nerve of the guinea-pig and its relation to the receptor potential of inner hair-cells. Hear. Res. 24, 1–15.
Parsons, T. D. and Sterling, P. 2003. Synaptic ribbon: conveyor belt or safety belt? Neuron 37, 379–382.
Patuzzi, R. and Moleirinho, A. 1998. Automatic monitoring of mechanoelectrical transduction in the guinea pig cochlea. Hear. Res. 125, 1–16.
Patuzzi, R. and O'Beirne, G. A. 1998. Boltzmann analysis of CM waveforms using virtual instrument software. Hear. Res. 133, 155–159.
Patuzzi, R. and Sellick, P. M. 1984. The modulation of the sensitivity of the mammalian cochlea by low frequency tones. II. Inner hair cell receptor potentials. Hear. Res. 13, 9–18.
Patuzzi, R. and Yates, G. 1987. The low-frequency response of inner hair cells in the guinea pig cochlea. Implications for fluid coupling and resonance of the stereocilia. Hear. Res. 30, 83–98.
Patuzzi, R., Sellick, P. M., and Johnstone, B. M. 1984. The modulation of the sensitivity of the mammalian cochlea by low frequency tones. III. Basilar membrane motion. Hear. Res. 13, 19–27.
Patuzzi, R. B., Yates, G. K., and Johnstone, B. M. 1989. Outer hair cell receptor current and sensorineural hearing loss. Hear. Res. 42, 47–72.
Patuzzi, R. B., Brown, D. J., McMahon, C. M., and Halliday, A. F. 2004. Determinants of the spectrum of the neural electrical activity at the round window: transmitter release and neural depolarisation. Hear. Res. 190, 87–108.
Platzer, J., Engel, J., Schrott-Fischer, A., Stephan, K., Bova, S., Chen, H., Zheng, H., and Striessnig, J 2000. Congenital deafness and sinoatrial node dysfunction in mice lacking class D L-type Ca^{2+} channels. Cell 102, 89–97.
Raphael, Y. and Altschuler, R. A. 2003. Structure and innervation of the cochlea. Brain Res. Bull. 60, 397–422.
Recio-Spinoso, A., Temchin, A. N., van Dijk, P., Fan, Y-H., and Ruggero, M. A. 2005. Wiener–Kernel analysis of responses to noise of Chinchilla auditory-nerve fibers. J. Physiol. 93, 3615–3634.
Ricci, A. J. and Fettiplace, R. 1997. The effects of calcium buffering and cyclic AMP on mechano-electrical transduction in turtle auditory hair cells. J. Physiol. 501, 111–124.
Ricci, A. J., Wu, Y. C., and Fettiplace, R. 1998. The endogenous calcium buffer and the time course of transducer adaptation in auditory hair cells. J. Neurosci. 18, 8261–8277.
Robertson, D. and Gummer, M. 1985. Physiological and morphological characterization of efferent neurones in the guinea pig cochlea. Hear. Res. 201, 63–77.
Robertson, D. and Paki, B, 2002. Role of L-type Ca^{2+} channels in transmitter release from mammalian inner hair cells. II. Single-neuron activity. J. Neurophysiol. 87, 2734–2740.
Robertson, D., Johnstone, B. M., and McGill, T. J. 1980. Effects of loud tones on the inner ear, a combined electrophysiological and ultrastructural study. Hear. Res. 21, 39–43.
Robertson, D., Sellick, P. M., and Patuzzi, R. 1999. The continuing search for outer hair cell afferents in the guinea pig spiral ganglion. Hear. Res. 136, 151–158.
Robles, L. and Ruggero, M. A. 2001. Mechanics of the mammalian cochlea. Physiol. Rev. 81, 1305–1352.
Rose, C. and Weiss, T. F. 1988. Frequency dependence of synchronization of cochlear nerve fibers in the alligator lizard: evidence for a cochlear origin of timing and non-timing neural pathways. Hear. Res. 33, 151–165.

Rose, J. E., Brugge, J. F., Anderson, D. J., and Hind, J. E. 1967. Phase locked response to low-frequency tones in single auditory nerve fibres of the squirrel monkey. J. Neurophysiol. 30, 769–793.

Ruggero, M. A., Rich, N. C., Shivapuja, B. G., and Temchin, A. N. 1996. Auditory-nerve responses to low-frequency tones: intensity dependence. Aud. Neurosci. 2, 159–185.

Russell, I. J. 1983. Origin of receptor potential in inner hair cells of the mammalian cochlea – evidence for Davis' theory. Nature 301, 334–336.

Russell, I. J. and Ashmore, J. F. 1983. Inner Hair Cell Receptor Potentials Investigated During Transient Asphyxia: A Model For Hair Cell Coupling. In: Hearing – Physiological Basis and Psychophysics (*eds*. R. Klinke and R. Hartman), pp. 10–16. Academic Press.

Russell, I. J. and Cowley, E. M. 1983. The influence of transient asphyxia on receptor potentials in inner hair cells of the guinea pig cochlea. Hear. Res. 11, 373–384.

Russell, I. J. and Kössl, M. 1991. The voltage responses of hair-cells in the basal turn of the guinea-pig cochlea. J. Physiol. Lond. 435, 493–511.

Russell, I. J. Kössl, M. 1992a. Sensory transduction and frequency-selectivity in the basal turn of the guinea-pig cochlea. Philos. Trans. R. Soc. Lond. Ser. B. 336, 317–324.

Russell, I. J. and Kössl, M. 1992b. Modulation of hair cell voltage responses to tones by low-frequency biasing of the basilar membrane in the guinea pig cochlea. J. Neurosci. 12, 1587–1601.

Russell, I. J. and Kössl, M. 1999. Micromechanical responses to tones in the auditory fovea of the greater mustached bat's cochlea. J. Neurophysiol. 22, 676–686.

Russell, I. J. and Sellick, P. M. 1976. Measurement of potassium and chloride ion concentrations in the cupulae of the lateral line of *Xenopus laevis*. J. Physiol. 257, 245–255.

Russell, I. J. and Sellick, P. M. 1977. The tuning properties of cochlear hair cells. Nature, 267, 858–860.

Russell, I. J. and Sellick, P. M. 1978. Intracellular studies of cochlear hair cells. J. Physiol. Lond. 84, 261–290.

Russell, I. J and Sellick, P. M. 1983. Low-frequency characteristics of intracellularly recorded receptor potentials in guinea-pig cochlear hair cells. J. Physiol. Lond. 338, 179–206.

Russell, I. J., Kössl, M., and Murugasu, E. 1995. A Comparison between Tone-Evoked Voltage Responses of Hair Cells and Basilar Membrane Displacements Recorded in the Basal Turn of the Guinea Pig Cochlea. In: Advances in Hearing Research (*eds*. G. A. Manley, G. M. Klump, C. Köppl, H. Fastl, and H. Oeckinghaus), pp. 125–135. World Scientific.

Russell, I. J., Richardson, G. P., and Cody, A. R. 1986a. The mechanosensitivity of mammalian auditory hair cells *in vitro*. Nature, 321, 517–519.

Russell, I. J, Cody, A. R, and Richardson, G. P 1986b. The responses of inner and outer hair-cells in the basal turn of the guinea-pig cochlea and in the mouse cochlea grown *in vitro*. Hear Res 22, 199–216.

Russell, I. J, Legan, P. K, Lukashkina, V. A., Lukashkin, A. N., Goodyear, R. J., and Richardson, G. P. 2007. Sharpened cochlear tuning in a mouse with a genetically modified tectorial membrane. Nature Neurosci. 10, 215–223.

Rybalchenko, V. and Santos-Sacchi, J. 2003. Cl flux through a non-selective, stretch-sensitive conductance influences the outer hair cell motor of the guinea-pig. J. Physiol. (Lond.) 547, 873–891.

Sachs, M. B., Woolf, N. K., and Sinnott, J. M. 1980. Response Properties of Neurons in the Avian Auditory System: Comparisons with Mammalian Homologues and Consideration of the Neural Encoding of Complex Stimuli. In: Comparative Studies of Hearing in Vertebrates (*eds*. A. N. Popper and R. R. Fay), pp. 323–353. Springer.

Salvi, R. J., Saunders, S. S., Powers, N. L., and Boettcher, F. A. 1992. Discharge patterns of cochlear ganglion neurons in the chicken. J. Comp. Physiol. A 170, 227–241.

Sachs, M. B., Young, E. D., and Lewis, R. H. 1974. Discharge patterns of single fibers in the pigeon auditory nerve. Brain Res. 70, 431–447.

Sand, O. 1985. Effects of different ionic environments on the mechano-sensitivity of lateral line organs I the mudpuppy. J. Comp. Physiol. Ser. A 102, 27–42.

Santos-Sacchi, J. 1993. Harmonics of hair cell motility. Biophys. J. 65, 2217–2227.

Santos-Sacchi, J. 2003. New tunes from Corti's organ: the outer hair cell boogie rules. Curr. Opin. Neurobiol. 13, 459–468.

Santos-Sacchi, J., Song, L., Zheng, J., and Nuttall, A. L. 2006. Control of mammalian cochlear amplification by chloride anions. J. Neurosci. 26, 3992–3998.

Saunders, J. C. and Flock, Å. 1986. Recovery of threshold shift in hair-cell stereocilia following exposure to intense stimulation. Hear Res 23, 233–244.

Schreiner, C. E., Snyder, R. L., and Johnstone, B. M. 1986. Effects of extracochlear direct current stimulation on the ensemble auditory nerve activity of cats. Hear. Res. 21, 213–226.

Sellick, P. M. and Johnstone, B. M. 1975. Production and role of inner ear fluid. Prog. Neurobiol. 54, 337–362.

Sellick, P. M. and Russell, I. J. 1980. The responses of inner hair cells to basilar membrane velocity during low frequency auditory stimulation in the guinea pig cochlea. Hear. Res. 2, 439–446.

Sellick, P. M., Patuzzi, R., and Johnstone, B. M. 1982. Modulation of responses of spiral ganglion cells in the guinea pig cochlea by low frequency sound. Hear. Res. 7, 199–222.

Sellick, P. M., Patuzzi, R, and Robertson, D. 2003. Primary afferent and cochlear nucleus contributions to extracellular potentials during tone-bursts. Hear Res. 176, 42–58.

Sellick, P. M., Robertson, D., and Patuzzi, R. 2006. The effect of BAPTA and 4AP in scala media on transduction and cochlear gain. Hear. Res. 111, 7–15.

Sewell, W. F. 1984. The relation between the endocochlear potential and spontaneous activity in auditory nerve fibres of the cat. J. Physiol. 347, 685–696.

Siegel, J. H. 1992. Spontaneous synaptic potentials from afferent terminals in the guinea pig cochlea. Hear. Res. 59, 85–92.

Siegel, J. H. and Dallos, P. 1986. Spike activity recorded from the organ of Corti. Hear. Res., 22, 245–248.

Singer, J. H., Lassova, L., Vardi, N., and Diamond, J. S. 2004. Coordinated multivesicular release at a mammalian ribbon synapse. Nat. Neurosci. 7, 826–833.

Skinner, L., Enée, V., Beurg, M., Hak Hyun, J., Ryan, A. F., Hafidi, A., Aran, J. M., and Dulon, D. 2003. Contribution of BK Ca^{2+}-activated K^{+} channels to auditory neurotransmission in the guinea pig cochlea. J. Neurophysiol. 90, 320–332.

Snyder, R. L. and Schreiner, C. E. 1984. The auditory neurophonic: basic properties. Hear Res. 15, 261–280.

Spoendlin, H. 1985. Anatomy of cochlear innervation. Am. J. Otolaryngol. 6, 453–467.

Sueta, T., Zhang, S. Y., Sellick, P. M., Patuzzi, R., and Robertson, D. 2004. Effects of a calcium channel blocker on spontaneous neural noise and gross action potential waveforms in the guinea pig cochlea. Hear. Res. 188, 117–125.

Sullivan, W. E. and Konishi, M. 1984. Segregation of stimulus phase and intensity coding in the cochlear nucleus of the barn owl. J. Neurosci. 4, 1781–1786.

Temchin, A. N., Recio-Spinoso, A., van Dijk, P., and Ruggero, M. A. 2005. Wiener Kernels of Chinchilla auditory-nerve fibers, verification using responses to tones, clicks,

and noise and comparison with basilar-membrane vibrations. J. Physiol. 93, 3635–3648.
ter Kuile, E. 1900. Die übertragung der energie von der grundmembran auf die haarzellen. Pflügers Arch. 79, 146–157.
van Emst, M. G., Giguère, C., and Smoorenburg, G. F. 1997. The generation of DC potentials in a computational model of the organ of Corti, effects of voltage-dependent K^+ channels in the basolateral membrane of the inner hair cell. Hear. Res. 115, 184–196.
Wangermann, P. 2002. K^+ cycling and the endocochlear potential. Hear. Res. 165, 1–9.
Weinberger, N. M., Kitzes, L. M., and Goodman, D. A. 1970. Some characteristics of the 'auditory neurophonic'. Experientia. 26, 46–48.
Weiss, T. F. 1982. Bidirectional transduction in vertebrate hair cells. A mechanism for coupling mechanical and electrical processes. Hear. Res. 7, 353–360.
Weiss, T. F. and Rose, C. 1988. A comparison of synchronization filters in different auditory receptor organs. Hear. Res. 33, 175–180.
Winter, I. M., Robertson, D., and Yates, G. K. 1990. Diversity of characteristic frequency rate-intensity functions in guinea pig auditory nerve fibre. Hear. Res. 45, 191–202.
Wong, W. H., Hurley, K. M., and Eatock, R. A. 2004. Differences between the negatively activating potassium conductances of mammalian cochlear and vestibular hair cells. J. Assoc. Res. Otolaryngol. 5, 270–284.
Wright, A. 1984. Dimensions of the cochlear stereocilia in man and theguinea pig. Hear. Res. 13, 89–98.
Yates, G. K., Winter, I. M., and Robertson, D 1990. Basilar membrane nonlinearity determines auditory nerve rate-intensity functions and cochlear dynamic range. Hear. Res. 203–220.
Zagaeski, M., Cody, A. R., Russell, I. J., and Mountain, D. C. 1994. Transfer characteristic of the inner hair cell synapse, steady state analysis. J. Acoust. Soc. Am. 95, 3430–3434.
Zeddies, D. G. and Siegel, J. H. 2004. A biophysical model of an inner hair cell. J. Acoust. Soc. Am. 116, 426–441.
Zenner, H. P. 1986. Motile responses in outer hair cells. Hear. Res. 22, 83–90.
Zhang, S. Y., Robertson, D., Yates, G., and Everett, A. 1999. Role of 1-type Ca^{2+} channels in transmitter release from mammalian inner hair cells I, gross sound-evoked potentials. J. Neurophysiol., 82, 3307–3315.
Zheng, X-Y., Ding, D-L., McFadden, S. L., and Henderson, D. 1997. Evidence that inner hair cells are the major source of cochlear summating potentials. Hear. Res. 113, 76–88.
Zheng, J., Shen, W., He, D. Z., Long, K. B., Madison, L. D., and Dallos, P. 2000. Prestin is the motor protein of cochlear outer hair cells. Nature. 783, 149–55.
Zinn, C., Maier, H., Zenner, H. P., and Gummer, A. W. 2000. Evidence for active,nonlinear, negative feedback in the vibration response of the apical region of the *in vivo* guinea-pig cochlea. Hear. Res. 142, 159–183.
Zou, Y., Zheng, J., Ren, T., and Nuttall, A. 2006. Cochlear transducer operating point adaptation. J. Acoust. Soc. Am. 94, 2232–41.
Zwislocki, J. J. 1980. Two Possible Mechanisms for the Second Cochlear Filter. In: Psychophysical, Physiological and Behavioural Studies in Hearing (*eds*. G. van den Brink and F. A. Bilsen), Delft University Press.
Zwislocki, J. J. 1986. Analysis of cochlear mechanics. Hear. Res. 22, 155–169.
Zwislocki, J. J. 1988. Phase Reversal of OHC Response at High Sound Intensities. In: Cochlear Mechanisms, Structure Function and Models (*eds*. J. P. Wilson and D. T. Kemp), pp. 163–168. Plenum.
Zwislocki, J. J. 1990. Active Cochlear Feedback, Required Structure and Response Phase. In: Mechanics and Biophysics of Hearing (*eds*. P. Dallos, C. D. Geisler, J. W. Mathews, M. Ruggero, and C. R. Steele), pp. 114–120. Springer.
Zwislocki, J. J. 2002. Auditory sound transmission: An Autobiographical perspective, Erlbaum.

Further Reading

Evans, E. F. 1972. The frequency response and other properties of single fibres in the guinea-pig cochlear nerve. J. Physiol. 226, 263–287.
He, D. Z. Z., Jia, S., and Dallos, P. 2003. Prestin and the dynamic stiffness of cochlear outer hair cells. J. Neurosci. 23, 9089–9096.
Oliver, D., Klocker, N., Schuck, J., Baukrowitz, T., Ruppersberg, J. P., and Fakler, B. 2000. Gating of Ca^{2+}-activated K^+ channels controls fast inhibitory synaptic transmission at auditory outer hair cells. Neuron 26, 595–601.
Woolf, N. K., Ryan, A. F., and Bone, R. C. 1981. Neural phase-locking properties in the absence of cochlear outer hair cells. Hear. Res. 4, 346–355.

3.21 Manifestations of Cochlear Events in the Auditory Brain-stem Response and Its Clinical Applications

J D Durrant, University of Pittsburgh, Pittsburgh, PA, USA

© 2008 Elsevier Inc. All rights reserved.

References 364

Glossary

acoustic click Sound stimulus – a brief transient – that is composed of most audible frequencies, produced by exciting an earphone with a brief direct-current pulse (e.g., 100 μs duration for a bandwidth of nearly 10 kHz).

auditory brainstem response (ABR) Electrical potential derived via computer averaging to extract a sensory (auditory) signal evoked by the applied (sound) stimulus, generated by the auditory nerve and brainstem auditory pathways (namely, pontine level).

cochlear mechanics Sum of hydromechanical events of the cochlea (auditory portion of the inner ear) involved in the transduction of sound.

frequency-following response (FFR) Variation of the auditory brainstem response elicited by tone bursts and whose waveform follows the waveform of the stimulus.

frequency-specific Characteristic of sound stimuli whose energy is largely concentrated around a particular frequency.

latency Time delay between the onset of a stimulus and the onset of a given wave of a stimulus-evoked potential.

masking A stimulus used to obscure/eliminate a sensory response evoked by another (probe or target) stimulus.

place encoding mechanism Effect of cochlear mechanics such that the displacement maxima occur at a place specific to the stimulus frequency and wherein high-frequency maxima tend to occur toward the base, and low-frequency maxima toward the apex.

threshold In sensory physiology and psychology, the concept that there is a stimulus magnitude that is just adequate to reliably excite a response (e.g., action potential, sensory-evoked potentials like the auditory brainstem response, behavioral response such as pushing a button, etc.).

tone burst Sinusoidal pulse, formed by abruptly turning on and off a sine wave.

traveling wave The wavelike motion peculiar to the cochlea by which sound energy is efficiently coupled to the basilar membrane and travels along this structure from the cochlear base toward the apex, reaching a maximum at a place according to the sound's frequency.

vertex (Cz) Location on the scalp at the top of the head, frequently used as a recording site for sensory-evoked potentials like the auditory brainstem response.

whole-nerve action potential (AP) Compound action potential of the auditory (VIII cranial) nerve in response to sound stimulation, thereby a population response of first-order auditory neurons.

The auditory brainstem response (ABR) is a compound neural potential recorded from the scalp. Obtaining the ABR requires computer signal averaging to extract this $0.5 = \mu V$ signal from background electrical noise. The ABR comprises a series of waves falling within the first approximately 10 ms of bioelectrically generated response to the onset of sound (Figure 1(a)), representing in turn the initial stages of activation of the auditory nervous system. This signal has found extensive clinical use via four major applications (see reviews by Hall, III, J. W., 1991; Durrant, J. D. and Ferraro, J. A., 1999; Goldstein, R. and Aldrich, W. M., 1999). The first is neurodiagnostic testing wherein the waveform and/or timing of the

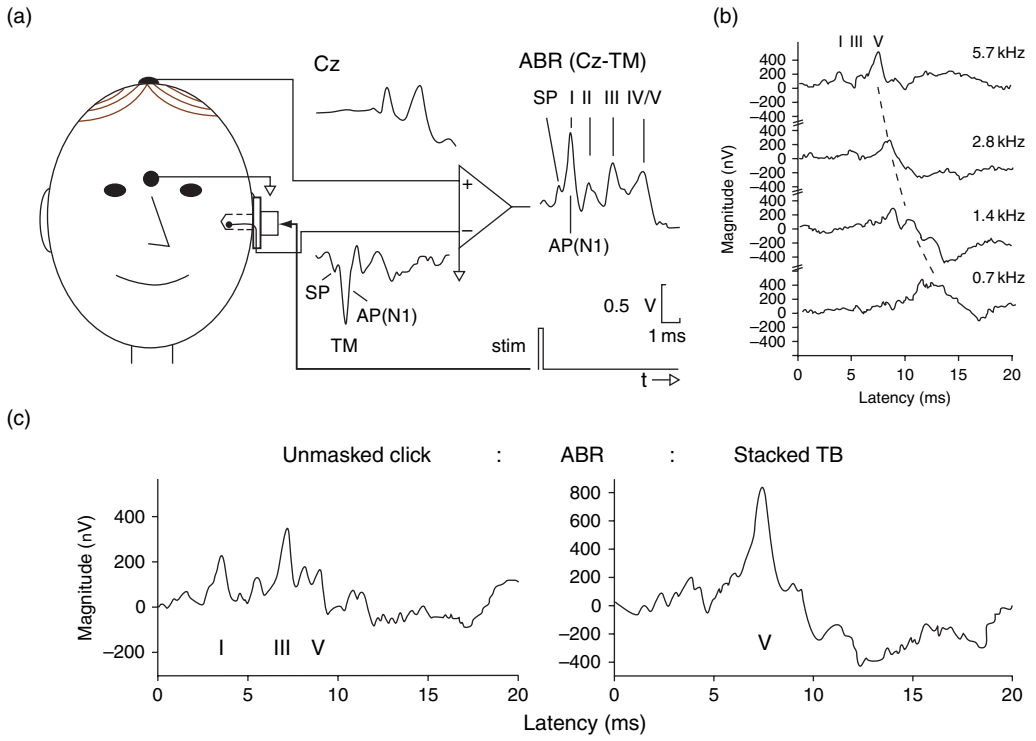

Figure 1 (a) The auditory brainstem response (ABR) is recorded between electrodes placed on or near the vertex (Cz) of the head and the ear (earlobe, mastoid, ear canal, or deeper). Enhancement of the diminutive wave I recorded at the scalp's surface can be accomplished by combining ABR recording with electrocochleography (ECochG), using an electrode deep in the ear canal or on the tympanic membrane (TM). Here, even the cochlear summating potential is detected, along with a more prominent N1 component of the whole-nerve action potential (AP). A third electrode, at nasion, completes the electrode montage for electrical grounding and safety of the subject. The stimulus (stim) derives from exciting the earphone with a brief direct-current pulse, delivering energy essentially at all frequencies shaped by the transducer's frequency response. The ABR component waves are labeled by Roman numerals (according to Jewett, D. L. and Williston, J. S., 1971). (b) A strictly surface recording method (vertex to mastoid) was used to record ABRs in response to sinusoidal pulses of various frequencies, as indicated. The dashed line traces the latency shift associated with effectively shifting the place of stimulation from near the cochlear base (high frequencies) to near the apex (low frequencies). (c) Tone-burst responses were aligned according to wave-V latency and summated to produce the stacked ABR (panel: stacked TB (tone burst)), reducing the untoward effects of traveling-wave dispersion (panel b) and dramatically improving ABR magnitude compared to that elicited by the broadband, unfiltered click (panel: unmarked click).

ABR waves are evaluated to detect neural blockage from space-occupying lesions, demyelinating diseases, etc. The second is newborn hearing screening which takes advantage of the strong correlation between ABR detection levels and behavioral hearing thresholds, plus the ability to record ABRs in sleeping/sedated patients, even premature infants. The third application is hearing threshold estimation which combines the advantages of ABR testing for newborn screening with the use of frequency-specific stimuli to estimate the audiogram (the pattern of hearing loss across frequency) in young pediatric, mentally handicapped, and other difficult-to-test subjects. The last application, intraoperative monitoring, capitalizes on most of the features above to provide a test keenly sensitive to conditions adverse to neural conduction in peripheral nerve and pontine-brainstem structures; monitoring the status of the ABR can help to minimize damage from neurosurgical procedures.

It may be asked, "What is such a topic as the ABR doing as follow-up to a chapter on cochlear function?" The short answer is that the ABR is actually a misnomer; the first two waves of the ABR derive from responses of the VIII nerve. Generally recorded between metal electrodes placed near the top of the head (vertex) and the stimulated ear (Figure 1(a)), the first barrage of electrical activity registered is nothing more than the N1 component of the whole-nerve action potential (AP). Indeed, using an

electrode deep in the ear canal or on the tympanic membrane enhances the AP (Figure 1(a)) and may reveal stimulus-related cochlear potentials, such as the summating potential (SP) – a method known as electrocochleography (ECochG). ECochG can also be performed using a needle electrode to penetrate the tympanic membrane, resting on the promontory (lateral wall of the cochlea, near the niche of the round window). The other potential that can be recorded is the cochlear microphonic. The SP and AP have been found useful for the differential diagnosis of Meniere's disease, characterized by a condition known as cochlear hydrops. In hydrops cases, the SP tends to be exaggerated in absolute magnitude or relative to the AP, perhaps reflecting asymmetrical mechanical biasing of the cochlear partition and/or biochemical effects due to this condition. Figure 1(a) illustrates another application of ECochG, combined with ABR recording (Durrant, J. D., 1986), to enhance wave I of the ABR, as this wave may be easily obscured by peripheral hearing loss. After the VIII nerve traverses the highly dense and electrically insulating temporal bone (specifically, the petrous pyramid), a second electrical wave develops as the nerve exits in the cerebellopontine angle, en route to the brainstem (Moller, A. R., 1994; Martin, W. H. *et al.*, 1995). This too is a manifestation of activity of the VIII nerve, that is the first-order neurons of the auditory pathway. Consequently, not until the third wave is the ABR truly a brainstem response; this and later waves are registered more prominently by the vertex (Cz) electrode (Figure 1(a)).

The longer and less obvious answer, regarding relevance of the ABR here, is that its nuances are strongly determined in the auditory periphery, despite the fact that waves III–V (Figure 1(a)) are generated in the pons between the dorsal–ventral cochlear nucleus complex and the inferior colliculus (Scherg, M. and von Cramon, D., 1985; Moore, J. K., 1987; Durrant, J. D. *et al.*, 1994). The representation of stimulus onset in the discharge patterns of auditory neurons is quite robust regardless of neuron type (Kiang, N. Y. S., 1975). Thus, the onset of the stimulus excites a high spike-discharge rate such that this feature of the primary-neural discharge pattern is prevalent throughout the auditory pathways. The several waves of the ABR are readily attributable to the sequential connectivity of the nerve and brainstem pathways which provide a combination of axonal (propagation) and synaptic delays at each major nucleus (Scherg, M. and von Cramon, D., 1985; Moore, J. K., 1987). Consequently, the activity at each level of the pathway will be passed on to the next, as in a relay race. The result is a multiphasic compound neural response of several milliseconds duration.

As conventionally tested, a simple wideband stimulus, called the acoustic click, is used to elicit the ABR. As such, the ABR may be considered as the impulse response of the combined VIII-nerve and brainstem systems. The input sound approximates an ideal impulse (a very brief transient). The click is created by exciting the earphone transducer with a brief direct-current pulse, typically 100 μs in duration (Figure 1(a)), providing equal power at all frequencies up to nearly 10 000 Hz (see Durrant, J. D. and Lovrinic, J. H., 1995 for review of underlying principles). Consequently, the output signal (waves of the ABR) is expected to reflect activity representing a broad frequency range, if, in fact, the frequency content of the input stimulus was well encoded by the hearing organ. The preceding chapter has established that, indeed, it should have been, but through the rather special transform effected by traveling-wave mechanics. The brainstem thus sees the outside world through the VIII nerve, which, in turn, sees the world through an array of variably tuned narrow-band filters produced by the place-encoding mechanism of the basilar membrane and the outer hair cells. Recall that, by this mechanism, the basilar membrane is not excited all at once, rather the traveling-wave motion is propagated with finite speed from the base toward the apex. The result is that the different best-frequency regions are excited sequentially, progressing from high- (basal) to low-frequency (apical) places.

Due to cochlear mechanics, the AP reflects activity at most audible frequencies in response to the simple (unfiltered) click, yet not instantaneously. Consequently, the click waveform (or its frequency content) is not obvious in the recorded signal. In other words, the AP (ABR wave I) does not mimic the input signal. True, it still is brief, roughly 1 ms in duration and thus is itself a transient. In contrast, it would take several milliseconds of activity to represent the entire cochlear response, again due to traveling-wave propagation. In VIII-nerve activity alone this would outlast the entire click-evoked ABR! So where did the rest of the activity go? Well, this same encoding mechanism, by virtue of the cochlear propagation delay, as well as filtering properties of the cochlear hydromechanics, causes phase dispersion. Activity from the base, where the traveling-wave velocity is high and the propagation delay

(and thus phase dispersion) is minimum, dominates the recorded response, yielding the robust but temporally compact wave observed. In contrast, activity from more apical regions tends to cancel out. Still, an appropriate masking technique (use of interfering noise of different cut-off frequencies) or frequency-specific stimuli (use of sinusoidal pulses (tone bursts)) can be used to isolate more apical places of excitation.

The same approach can be taken with the entire ABR (which suffers the same fate as the AP, accounting for its own compactness), as shown in Figure 1(b). Note the shifting latency (delay from the start of the stimulus), namely increasing latency as frequency of the stimulus decreases. Recombining the frequency- or place-specific responses, while compensating for the traveling-wave delays (stacked TB ABR in Figure 1(c)), produces a substantially greater magnitude of response (Philibert, B. *et al.*, 2003). Interestingly, stimulus intensity also has a dramatic and related effect (Figure 2(a)). As stimulus intensity decreases, not only does the response magnitude decrease (as expected), but the peaks of the earlier/smaller waves disappear, and the waves occur at progressively longer latencies. This results from a combination of effects, including a basic neural effect – the characteristic increase of latency with decreasing stimulus intensity (Kiang, N. Y. S., 1965), and a cochlear mechanical effect – progressively fewer neurons excited on the tails of their turning curves (Ozdamar, O. and Dallos, P., 1976). The latency-intensity tradeoff is the hallmark of auditory-evoked responses. Given such pervasive influence of cochlear mechanics on the ABR, it seems likely that traveling-wave velocity could be estimated using ABR latency measures, as indeed is the case (e.g., see Donaldson, G. S. and Ruth, R. A., 1993). This entirely noninvasive clinical tool thus permits the examination of cochlear function in intact humans and other animals.

With all this attention to place-frequency encoding, what about time synchrony? In fact, a high degree of synchrony of neural discharge is essential

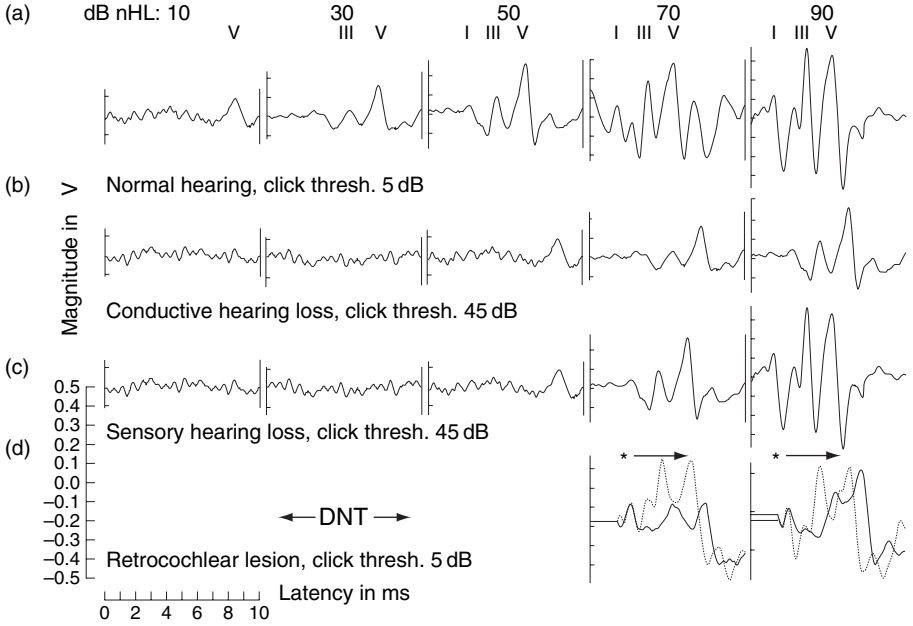

Figure 2 Illustration of typical effects of level of the acoustic-click stimulus (a), peripheral auditory pathology (b, c), and retrocochlear lesion on the auditory brainstem response (ABR). a, Normal ABR recorded at click hearing levels indicated: just at/above hearing threshold of the acoustic click stimulus, and several levels above, yielding at 70 and 90 dB hearing level full complements of waves. b, Simulated flat conductive loss, typical of middle-ear disease, leading merely to simple attenuation of the stimulus, i.e., the 90 dB response corresponds to the 70 dB, and the detection level of the response is elevated. c, Simulated high-frequency sensory loss, yielding similar effects to the conductive loss at low levels but by 90 dB, in this case, an essentially normal amount of activity is recruited due, in part, to basalward spread of excitation. d, Actual responses from a case of acoustic tumor which, in this case, had virtually no adverse effects on the usual tests of hearing, yet causing a clear delay in neural conduction in the VIII nerve (indicated by prolongation of the I–III∗ interpeak interval). DNT, did not test; nHL, normal hearing level.

for a good ABR. Stimuli with relatively long rise times yield poor responses (Hecox, K. *et al.*, 1976). The click is highly effective, not only because of its broad bandwidth, but also its abruptness. Subtle timing cues, in fact, are readily evident in the ABR, for example, the slight time difference between condensation (C) and rarefaction (R) polarity stimuli – stimuli initiated with a push versus a pull on the eardrum. The result in the average subject is that there is a subtle, yet measurable, difference in waveform and latency between the C- and R-evoked ABRs (see Durrant, J. D. and Ferraro, J. A., 1999). This follows from the fact that the excitatory phase of stimulation in the cochlea is basilar membrane movement (displacement and velocity) going from scala tympani to the scala vestibuli (Dallos, P. and Durrant, J. D., 1972); this motion corresponds to R.

Still more compelling is the extent to which phase synchrony can be expressed in the ABR under appropriate recording conditions. Returning to Figure 1, inspection of the ABR reveals a pseudosinusoidal waveform. It may not be too surprising, then, that short sinusoidal pulses can be used to drive this feature to produce a frequency-following response (FFR) that more-or-less mimics the stimulus waveform (e.g., see Ananthanarayan, A. K. and Durrant, J. D., 1992). The FFR responses are most robust in the mid-frequency range of hearing, roughly 500–2000 Hz, the upper range being consistent with the upper limit of the most efficient phase locking of single auditory neurons (the lower limit perhaps reflects the general deterioration of the ABR at low frequencies, as low-frequency stimuli have inherently slower onsets. In general, the ABR is not quite as robust/distinctive when elicited below 1000 Hz; e.g., see Kiang, N. Y. S., 1965; Joris, P. X. *et al.*, 1994a; 1994b). This temporal synchrony is robust enough that the FFR can be used to study encoding of complex stimuli, most notably vowels of speech (Krishnan, A., 2002). So complete is this reflection of cochlear events, that yet another manifestation of cochlear function, that is, nonlinearity (e.g., intermodulation distortion products), is also expressed in FFR activity (Pandya, P. K. and Krishnan, A., 2004).

To outline this of clinical correlation, a few examples of applications and related concepts will be worthwhile. The most basic manifestation of cochlear function is hearing sensitivity. While it certainly takes the rest of the auditory pathways to provide the sense of hearing and related conscious/voluntary responses, as sampled via conventional (behavioral) audiometry, it is well established that the limits of hearing sensitivity are determined by the peripheral auditory system. It was noted earlier that a common application of the ABR is found in newborn hearing screening and hearing threshold estimation in young children and others incapable of participating in the standard (behavioral) clinical test. This application enjoys broad utility, providing reliable screening for hearing impairment and threshold estimation often to within an accuracy of 10 dB, as illustrated in Figure 2(a). Such results, in practice, are usually obtained while the subject is asleep naturally or under sedation or general anesthesia. This is possible because the generators of the ABR are below the inferior colliculus and strongly driven by the peripheral nerve, as revealed above. In many pediatric patients, a common problem of hearing is fluid in the middle ear which attenuates sound delivered to the inner ear and causes changes in the ABR (see Figure 2(b)). Hearing loss in the population at large, however, is most often caused by loss of hair-cell function, frequently limited to the higher frequencies. This also causes deterioration in the ABR. However, moderate or less severe losses may be overcome with increasing stimulus intensity due to basalward spread of excitation from the traveling wave, which may finally overcome the impaired thresholds of more basal or high-frequency neurons (Figure 2(c)). Consequently, the ABR may be used to explore/define such losses and the nuances of their effects. The latency-intensity relationship, specifically, can help predict hearing loss type (conductive versus sensory) and degree. At the same time, such peripheral effects must be fully appreciated before retrocochlear neural influences can be confidently deduced.

This brings the discussion to another major application of ABR testing, that of differential diagnosis (see Durrant, J. D. and Ferraro, J. A., 1999, for review). The effects of a common space-occupying retrocochlear lesion (the acoustic tumor) also is illustrated in Figure 2. In this case, the compression of the VIII nerve by the tumor appears not to significantly affect hearing sensitivity, at least not as clinically tested, yet the lesion has clear impact on the ABR. The delay between waves I and III is consistent with the site of lesion, i.e., blockage of VIII-nerve conduction. Over the past decade, the clinical importance of the ABR for detection of such tumors has diminished with advancements in imaging. However, Don M. *et al.* (1997) have shown that, by using an approach similar to that represented in Figures 1(b) and 1(c) (i.e., stacked ABR analysis),

the ABR can be enhanced, providing a more thorough test of VIII-nerve function, that is, not merely the higher-frequency response elicited via the unfiltered click (Don, M. *et al*., 1997; Philibert, B. *et al*., 2003). Interestingly, the basic stimulus-analysis paradigm of the stacked-ABR test was developed over four decades ago for the purpose of breaking down the click-evoked AP into its (equivalent) component frequency bands (Teas, D. C. *et al*., 1962). The method represents the results of the much more tedious and invasive analysis of single-unit-response measurement along the nerve trunk well (Kiang, N. Y. S., 1975), again reflecting propagation events along the cochlear partition. Lastly, the acoustic-tumor example also demonstrates the basis for use of the ABR in intraoperative monitoring, in this case the possible compression of the VIII-nerve or more central fiber tracts during neurosurgery.

In summary, cochlear events are strongly manifested in, and determine many characteristics of, the ABR. While a powerful and sensitive clinical tool for investigating or ruling out retrocochlear pathology and objective hearing screening, ABR recording is an equally valuable investigative tool in the evaluation of peripheral auditory sensorineural events.

References

Ananthanarayan, A. K. and Durrant, J. D. 1992. The frequency following response and the onset response: evaluation of frequency specificity using a forward masking paradigm. Ear Hear. 13, 228–232.

Dallos, P. and Durrant, J. D. 1972. On the derivative relationship between stapes displacement and cochlear microphonics. J. Acoust. Soc. Am. 52, 1263–1265.

Don, M., Masuda, A., Nelson, R., and Brackmann, D. 1997. Successful detection of small acoustic tumors using the stacked derived-band auditory brain stem response amplitude. Am. J. Otol. 18, 608–621.

Donaldson, G. S. and Ruth, R. A. 1993. Derived band auditory brain-stem response estimates of traveling wave velocity in humans. I. Normal-hearing subjects. J. Acoust. Soc. Am. 93, 940–951.

Durrant, J. D. 1986. Combined ECochG-ABR versus conventional ABR recordings. Semin. Hear. 7, 289–305.

Durrant, J. D. and Ferraro, J. A. 1999. Short-Latency Evoked Potentials: Electrocochleography and Auditory Brainstem Response. In: Contemporary Perspectives in Hearing Assessment (*eds*. F. Musiek and W. Rintlemann), pp. 197–242. Allyn-Bacon.

Durrant, J. D. and Lovrinic, J. H. 1995. Bases of Hearing Science, 3rd edn. Williams & Wilkins.

Durrant, J. D., Martin, W. H., Hirsch, B., and Schwegler, J. 1994. 3CLT ABR analyses in a human subject with unilateral extirpation of the inferior colliculus. Hear. Res. 72, 99–107.

Goldstein, R. and Aldrich, W. M. 1999. Evoked Potential Audiometry. Allyn and Bacon.

Hall, J. W. III, 1991. Handbook of Auditory Evoked Responses. Allyn and Bacon.

Hecox, K., Squires, N., and Galambos, R. 1976. Brainstem auditory evoked responses in man. I. Effect of stimulus rise–fall time and duration. J. Acoust. Soc. Am. 60, 1187–1192.

Jewett, D. L. and Williston, J. S. 1971. Auditory-evoked far fields averaged from the scalp of humans. Brain 94, 681–696.

Joris, P. X., Carney, L. H., Smith, P. H., and Yin, T. C. 1994a. Enhancement of neural synchronization in the anteroventral cochlear nucleus. I. Responses to tones at the characteristic frequency. J. Neurophysiol. 71, 1022–1036.

Joris, P. X., Smith, P. H., and Yin, T. C. 1994b. Enhancement of neural synchronization in the anteroventral cochlear nucleus. II. Responses in the tuning curve tail. J. Neurophysiol. 71, 1037–1051.

Kiang, N. Y. S. 1965. Discharge Patterns of Single Fibers in the Cat's Auditory Nerve. MIT Press.

Kiang, N. Y. S. 1975. Stimulus Representation in the Discharge Patterns of Auditory Neurons. In: The Nervous System – Vol. 3: Human Communication and Its Disorders (*ed*. E. L. Eagles), pp. 81–96. Raven Press.

Krishnan, A. 2002. Human frequency-following responses: representation of steady-state synthetic vowels. Hear. Res. 166, 192–201.

Martin, W. H., Pratt, H., and Schwegler, J. W. 1995. The origin of the human auditory brain-stem response wave II. Electroencephalogr. Clin. Neurophysiol. 96, 357–370.

Moller, A. R. 1994. Neural Generators of Auditory Evoked Potentials. In: Principles and Applications in Auditory Evoked Potentials (*ed*. J. T. Jacobson), pp. 23–46. Allyn and Bacon.

Moore, J. K. 1987. The human auditory brain stem as a generator of auditory evoked potentials. Hear. Res. 29, 33–43.

Ozdamar, O. and Dallos, P. 1976. Input–output functions of cochlear whole-nerve action potentials: interpretation in terms of one population of neurons. J. Acoust. Soc. Am. 59, 143–147.

Pandya, P. K. and Krishnan, A. 2004. Human frequency-following response correlates of the distortion product at 2F1-F2. J. Am. Acad. Audiol. 15, 184–197.

Philibert, B., Durrant, J. D., Ferber-Viart, C., Duclaux, R., Veuillet, E., and Collet, L. 2003. Stacked tone-burst-evoked auditory brainstem response (ABR): preliminary findings. Int. J. Audiol. 42, 71–81.

Scherg, M. and von Cramon, D. 1985. A new interpretation of the generators of BAEP waves I–V: results of a spatio-temporal dipole model. Electroencephalogr. Clin. Neurophysiol. 62, 290–299.

Teas, D. C., Eldrege, D. H., and Davis, H. 1962. Cochlear responses to acoustic transients: an interpretation of whole nerve action potentials. J. Acoust. Soc. Am. 34, 1438–1459.

Further Reading

Burkard, R. F., Don, M., and Eggerment, J.J (eds.) 2007. Auditory Evoked Potentials: Basic Principles and clinical Application Lippincott Williams & Wilkins.

3.22 Afferent Synaptic Mechanisms

M A Rutherford and W M Roberts, University of Oregon, Eugene, OR, USA

© 2008 Elsevier Inc. All rights reserved.

3.22.1	**Introduction**	366
3.22.2	**Afferent Neurons of Acousticolateralis Sensory Systems**	366
3.22.2.1	Spiral Ganglion Neurons	367
3.22.2.2	Auditory Nerve Fibers	368
3.22.2.3	Innervation Patterns and the Function of Auditory Organs	371
3.22.3	**Hair Cells**	372
3.22.3.1	Hair Cell Shape in Relation to Synaptic Signaling	372
3.22.3.2	The Synaptic Body and Synaptic Vesicle Pools	372
3.22.3.3	Calcium Buffering in Hair Cells	375
3.22.4	**Ribbon Synapses – A Small but Diverse Class**	377
3.22.4.1	The Synaptic Body (Ribbon) and Its Vesicles	377
3.22.4.2	Molecular Specializations of Ribbon Synapses	378
3.22.4.3	Anatomy of the Synaptic Body: Heterogeneity of Structure	380
3.22.5	**The Synaptic Vesicle Cycle in Hair Cells**	381
3.22.5.1	Endocytosis	381
3.22.5.2	Vesicle Mobility	381
3.22.5.3	Docking and Priming	382
3.22.5.4	Transmitter Release and Clearance	382
3.22.5.5	Relating Anatomical and Functional Vesicle Pools	383
3.22.6	**Physiology of the Hair Cell Afferent Synapse**	384
3.22.6.1	Encoding of Phase	385
3.22.6.2	Encoding of Frequency	386
3.22.6.3	Baseline and Evoked Synaptic Activity	386
3.22.6.4	Tuning Mechanisms in Hair Cells	388
3.22.6.4.1	Frequency-selective augmentation of membrane potential oscillation	388
3.22.6.4.2	Synaptic frequency selectivity	388
3.22.7	**Auditory Nerve Fiber Firing Patterns Mirror Presynaptic Vesicle Pool Dynamics**	389
3.22.7.1	Adaptation of the Auditory Nerve Response	389
3.22.7.2	The Role of the Synaptic Body in Auditory Nerve Fiber Spike Timing	390
3.22.8	**Synapse to Psychophysics**	391
References		391

Glossary

active zone (AZ) The area where synaptic vesicles fuse with the presynaptic membrane. The AZ is juxtaposed to the postsynaptic terminal across the synaptic cleft.

afferent The flow of signals from the periphery toward the central nervous system (CNS).

auditory nerve fiber (ANF) The axon of an auditory afferent neuron that projects to the brainstem in the vestibulocochlear (eighth cranial) nerve. In mammals, ANFs have cell bodies in the spiral ganglion.

characteristic frequency (CF) The frequency of maximum sensitivity to sound.

cytomatrix at the active zone (CAZ) The cytoskeletal meshwork comprised of multidomain proteins that aggregate through specific protein–protein and protein–lipid interactions. The CAZ creates a scaffold upon which the presynaptic machinery is assembled.

hair cells The sensory receptors of the auditory system and related sense organs of the ear and lateral line of vertebrate animals.

inner hair cell (IHC) One of the highly innervated hair cells in the mammalian ear that are primarily responsible for the perception of sound. They are located in a single row near the modiolar (inner) edge of the organ of Corti.

root mean square (RMS) A type of average computed by first squaring a set of values, then computing the mean of the squared values, then taking the square root of the mean. The RMS average deviation of N samples from their mean is $\sqrt{(N-1)}$ times the standard error of the mean.

sound pressure level (SPL) The RMS pressure change during a sound, expressed on the logarithmic decibel (dB) scale, measured in the vicinity of the listener during a specified time period.

spiral ganglion The cell bodies of the afferent neurons that innervate the organ of Corti; housed in the bony spiral lamina of the mammalian cochlea.

spontaneous rate (SR) Frequency of spikes in an auditory nerve fiber in the absence of an applied sound stimulus.

synaptic body or ribbon (SB) The most obvious presynaptic structure at hair cell afferent synapses, and the subject of many carefully designed experiments to reveal its function(s). There is general agreement that the SB serves an important purpose, which is not presently known. It harbors synaptic vesicles attached to it via fine filaments that are thought to either facilitate or impede the movement of vesicles along its surface.

synaptic vesicle (SV) Spherical lipid bilayer that contains neurotransmitter.

synaptic vesicle cycle The recurrent processes by which SVs are continuously created, used and recreated. Exocytosis of the neurotransmitter is triggered by calcium and involves fusion of the SV membrane with the plasmalemma and/or the formation of a transient aqueous connection between the SV and the extracellular space. After exocytosis, SVs are reformed, refilled, and reenter the exocytic pathway.

threshold The SPL needed to produce a criterion response. Defined in this way, threshold is a measure of sensitivity to sound: low threshold means high sensitivity. Sensitivity is usually expressed in units of response/stimulus, but in auditory physiology threshold is traditionally defined in units of stimulus only, omitting explicit reference to the response criterion used in a particular experiment.

3.22.1 Introduction

We will begin with an overview of the hair cell afferent synapse and related structures, with a focus on mammalian inner hair cells (IHCs) and spiral ganglion neurons. Our review will then turn to electrophysiological studies and discussions of the specializations that may endow these first auditory synapses with their ability to maintain fast and reliable, information-rich signaling to the brain. Readers unfamiliar with the basics of cellular neuroscience will better appreciate the unique properties of auditory afferent synapses after reviewing the properties of conventional chemical synapses described in the many excellent neuroscience textbooks (e.g., Delcomyn, F., 1998; Kandel, E. R. *et al.*, 2000; Hille, B., 2001; Nicholls, J. G. *et al.*, 2001). Additional information specific to hair cell afferent synapses can be found in recent literature reviews (Nouvian, R. *et al.*, 2006; Moser, T. *et al.*, 2006a; 2006b).

3.22.2 Afferent Neurons of Acousticolateralis Sensory Systems

The primary afferent neurons in the auditory and vestibular organs of all vertebrate species, and in related mechanosensory and electrosensory organs of the lateral line system of aquatic vertebrates are bipolar neurons that have cell bodies located in or near the ear. They extend one process peripherally to the sensory epithelium, the other centrally to the brainstem. The peripheral processes have often been called dendrites, but most are myelinated and can properly be called axons. This distinction is likely to be important for the assembly and maintenance of afferent synapses because axons and dendrites use different protein-targeting signals (Burack, M. A. *et al.*, 2000). The afferent neurons in auditory and vestibular organs have cell bodies located close to the corresponding sensory epithelium, and therefore have short peripheral axons.

Lateral line afferent neurons have long peripheral axons that extend from cell bodies in the lateral line ganglia near the ear to sensory neuromasts on the head and trunk (Dambly-Chaudiere, C. *et al.*, 2003).

3.22.2.1 Spiral Ganglion Neurons

In mammals, the cell bodies of auditory afferent neurons reside in the spiral ganglion, which parallels the inner (modiolar) edge of the organ of Corti (Figure 1(a)). Type I spiral ganglion neurons are responsive to acoustic stimulation and constitute 90–95% of cochlear nerve afferents (Spoendlin, H., 1969; Liberman, M. C., 1982). Intracellular labeling with horseradish peroxidase and subsequent histological processing revealed that they contact only the IHCs (Robertson, D., 1984). Both the peripheral and the central axons of a type I afferent neuron are myelinated and have a cluster of voltage-gated Na^+ channels (Na_v 1.6) at each node of Ranvier. Na^+ channels are also found in the unmyelinated axon segment between the postsynaptic terminal and the most distal peripheral node, suggesting that spikes may be initiated at or near the site of synaptic input (Hossain, W. A. *et al.*, 2005), as occurs in vertebrate skeletal muscle (Kandel, E. R. *et al.*, 2000). Minimizing the distance from the synapse to the spike initiation site is expected to minimize attenuation and low-pass filtering of excitatory postsynaptic potentials (EPSPs). The cell bodies of type I spiral ganglion neurons are also wrapped in a loose myelin-like sheath that may speed conduction, reduce temporal jitter, or decrease the probability of conduction failure across the cell body during high-frequency firing (Hossain, W. A. *et al.*, 2005).

In mammals, the peripheral axons of type I afferents (also known as radial fibers) remain unbranched and contact only a single IHC. Unlike most neurons, which receive synaptic inputs from hundreds or thousands of separate sites of synaptic contact (active zones; AZs), each type I afferent neuron typically receives sensory input from a single hair cell AZ (Spoendlin, H., 1969; Liberman, M. C., 1980; Spoendlin, H., 1985; Hashimoto, S. *et al.*, 1990). In other vertebrates, most auditory afferent neurons make multiple postsynaptic contacts on one or more hair cells (Lewis, E. R. *et al.*, 1982).

Each mammalian IHC provides the sole input to 5–30 type I afferent axons, which vary in number by species and hair cell position on the cochlear tonotopic axis (Kiang, N. Y. S. *et al.*, 1982; Liberman, M. C., 1982; Fuchs, P. A. *et al.*, 2003). The mammalian cochlea thus represents a case of synaptic divergence in which each IHC controls many private communication channels to the brain. The function of this unusual arrangement is only partially understood, but it is easy to speculate that the dynamic membrane potential of the hair cell contains more information than can be transmitted across one synapse and encoded in a single spike train.

Information is degraded by events that alter a signal in an unpredictable way (noise). The synaptic noise introduced by the stochastic nature of exocytosis can be reduced by having synaptic currents from many AZs converge on the spike initiation zone of one afferent axon, as occurs at the calyx synapses of vestibular hair cells (Goldberg, J. M., 1996); but the mammalian auditory system uses a different strategy in which the maximum possible separation of information channels to the brain is maintained by having each synaptic AZ control action potential generation in a separate afferent axon. If separate information channels later converge onto a single higher-order neuron in the brain stem (e.g., a globular bushy cell in the cochlear nucleus that detects coincident input), this arrangement can reduce the effects of variability in the spike conduction time from the ear to the central nervous system (CNS) and other noise sources that are downstream of the afferent synapse.

A small population of afferent axons in the mammalian cochlea (type II; Figure 1(a)) are unmyelinated (Liberman, M. C. *et al.*, 1990). Like the type I afferents, they are labeled by antibodies against Na_v 1.6 and may initiate action potentials near their distal tips (Hossain, W. A. *et al.*, 2005). These outer hair cell (OHC) afferents are thought to monitor the state of the organ of Corti, but not to contribute directly to the perception of sound, the role ascribed to the IHCs. Very little is known about the physiology of type II afferents, and they will not be considered further in this chapter.

Although the peripheral neural network in the ear is less elaborate than that of the retina and contains far fewer cell types, electron micrographs of the organ of Corti do show several additional types of synapses that could provide important functional interactions, including local feedback (Raphael, Y. and Altschuler, R. A., 2003; Sobkowicz, H. M. *et al.*, 2003). These include connections between IHCs and OHCs via afferent and efferent fibers that contact both hair cell types (Sobkowicz, H. M. *et al.*, 2004). Nothing is known about the function of these synapses in auditory signal processing. Efferent synapses are typically seen on the postsynaptic

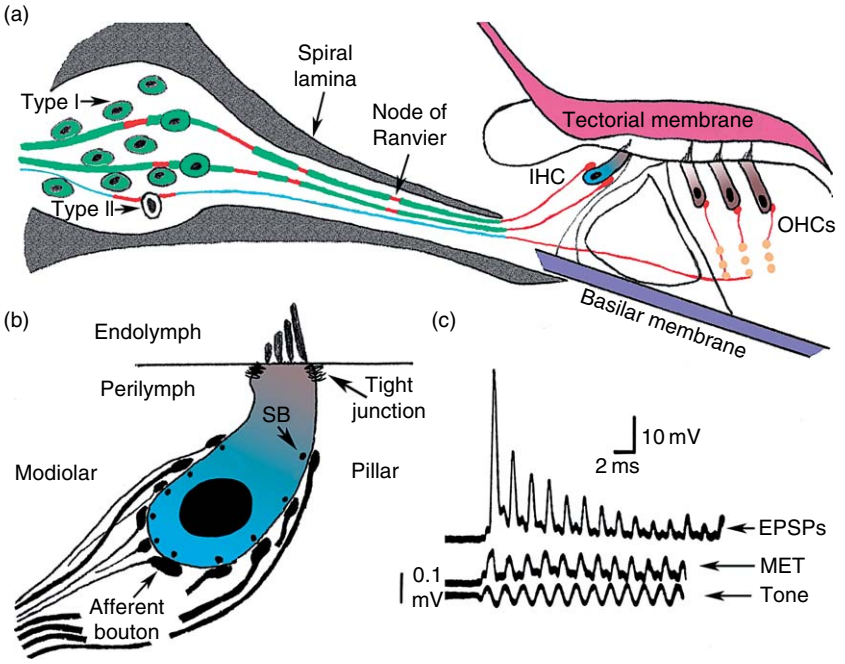

Figure 1 Auditory afferent synapses. (a) Schematic cross section through the mammalian organ of Corti, showing the bipolar cell bodies of afferent neurons (left), which each send one axon peripherally toward the hair cells and another axon centrally to the brainstem. In mammals, most afferent axons (type I) are myelinated (green), unbranched, and contact a single inner hair cell (IHC). A smaller population (type II) are unmyelinated and branch to contact several outer hair cells. A high density of voltage-gated sodium channels (Na_v 1.6, red) are located at nodes of Ranvier, on the unmyelinated distal axon segments of all afferent neurons, and at both axon hillocks of type II neurons. (b) Each IHC supplies the only input to tens of type I afferent neurons at active zones. Large-diameter afferent axons usually contact the pillar face of the IHC, whereas smaller-diameter axons contact the modiolar side. (c) Electrophysiological recording of afferent synaptic activity *in vivo*. A 200 Hz sinusoidal sound delivered to the goldfish sacculus (bottom trace) evoked an extracellular field potential (middle trace), analogous to a cochlear microphonic potential (see Chapter Hair Cell Transduction and Adaptation: Physiology and Molecular Mechanisms), that is primarily a measure of mechanoelectrical transduction (MET). The top trace is an intracellular recording from an afferent axon, in which spikes had been blocked to reveal the EPSPs, which are synchronized to the sound waveform and show strong synaptic depression. (c) Adapted from Furukawa, T. and Matsuura, S. 1978. Adaptive rundown of excitatory postsynaptic potentials at synapses between hair cells and eighth nerve fibres in the goldfish. J. Physiol. 276, 193–209, with permission from Blackwell Publishing.

terminals of mammalian type I afferents, where they may modulate synaptic transmission from the hair cell to the afferent axon. Efferent axons also make inhibitory cholinergic synapses directly onto hair cells in most vertebrate auditory and vestibular organs, including mammalian IHCs and OHCs (see Chapter Efferent System).

3.22.2.2 Auditory Nerve Fibers

The central axons of spiral ganglion neurons project to the brainstem in the eighth cranial nerve, where they are called auditory nerve fibers (ANFs). Nearly all recordings of action potentials in mammalian ANFs are presumed to be from axons of type I spiral ganglion neurons because they are larger and much more numerous than the axons of type II neurons (Liberman, M. C., 1982).

In vivo recordings from single ANFs show that nearly all fire action potentials spontaneously (i.e., in a quiet laboratory environment with no experimentally imposed stimulus). The baseline or spontaneous firing rate (SR) in some ANFs exceeds 100 spikes s^{-1}, while others fire fewer than 5 spikes s^{-1}, with no apparent correlation between a fiber's characteristic frequency (CF) and SR (Kiang, N. Y. S. *et al.*, 1965; Tsuji, J. and Liberman, M. C., 1997). CF varies with position along the tonotopic axis whereas SR has been correlated with both axon diameter and subcellular synaptic structure in the guinea-pig and cat (Liberman, M. C., 1980; Merchan-Perez, A. and Liberman, M. C., 1996; Tsuji, J. and Liberman, M. C., 1997). In these studies of afferent structure/function,

intracellular recording and labeling of individual ANFs followed by serial-section electron microscopy (EM) showed that ANFs of high SR belong to spiral ganglion neurons that have large diameter peripheral axons and contact IHCs predominantly on the pillar face (Figure 1(b)); however, this segregation of axonal diameters around the hair cell circumference was not observed in one study of the gerbil (Slepecky, N. B. *et al*., 2000). Low- and intermediate-SR fibers of the cat and guinea-pig contact the modiolar face and have synapses with larger presynaptic dense bodies (called synaptic bodies, SBs, or ribbons) and more vesicles than synapses with high-SR fibers. Because the 5–30 afferent synapses on each IHC display this range of ultrastructural characteristics and modiolar/pillar position, and because ANFs of the same CF differ in SR, it is inferred that each IHC synapses onto both high-SR fibers and intermediate-/low-SR fibers.

To quantify the strength of a sound, most experimenters report the sound pressure level (SPL), expressed on the logarithmic decibel scale (dB). Each 20 dB increase in SPL corresponds to a tenfold multiplication of root mean square (RMS) sound pressure. The zero point (0 dB) is often defined as 20 μPa, which is approximately the amplitude of a barely perceptible sound at frequencies where human hearing is most sensitive (2–5 kHz). Compared to the standard atmospheric pressure of ~100 kPa, 20 μPa amounts to a change of only about 1 part in 5 billion.

An ANF's sensitivity to sound (Figure 2) is typically measured as the SPL needed to increase its firing rate by a criterion number of spikes per second above the SR, or alternatively, to produce a criterion increase in ANF discharge synchrony with the sound stimulus (Rose, J. E. *et al*., 1967; 1971; Johnson, D. H., 1980). This measure, which is often called the fiber's threshold, depends on the response criterion, stimulus duration, and other factors that are specific to the experimental protocol (Heil, P. and Neubauer, H., 2003). The term threshold is typically used in biology to mean a stimulus level below which there is no response (e.g., the threshold for generating an action potential), and therefore implies the existence of a strong nonlinearity in the stimulus–response relation (a cut-off below which there is no response). The use of the term threshold in auditory physiology is quite different. It carries no implication of a threshold nonlinearity, only that the response has fallen below some criterion level. In fact, the initial stages of auditory processing are constructed to avoid threshold nonlinearities.

A threshold nonlinearity in the peripheral auditory system would be detrimental to subsequent neural processing because it would eliminate information that could otherwise be recovered by temporal averaging (integration) or filtering, which can in principle pull an arbitrarily small periodic signal out of aperiodic background noise. This ability is crucial for systems designed to detect small noisy signals. For example, a sinusoidal signal that is superimposed on additive white noise can be passed through a narrow-band linear filter that leaves the signal unchanged while reducing the noise in proportion to the bandwidth of the filter. Narrowing the filter's bandwidth can thus increase the signal-to-noise ratio as much needed to detect an arbitrarily small periodic signal, albeit at the expense of temporal resolution (Bracewell, R. N., 1999). The auditory system's use of temporal integration to improve signal-to-noise ratio is seen experimentally as an inverse relation between threshold and sound duration (Jeffress, L. A., 1968; Heil, P. and Neubauer, H., 2001; 2003). The observation that sounds too soft to be audible can nevertheless influence the audibility of subsequent sounds (Plack, C. J. *et al*., 2006) supports the idea that subthreshold sounds still produce some response.

The peripheral auditory system eliminates any threshold cut-off in the afferent response to faint sounds by eliminating all slack from the system, ensuring that arbitrarily weak sounds evoke a change in ANF firing rate that is proportional to the sound amplitude, at least for low-frequency tones. This begins with mechanosensory transduction, which uses feedback to maintain partial activation of the transduction channels even in complete silence. The resulting resting transduction current places the hair cell's resting membrane potential in a range where the presynaptic calcium channels are also partially activated (Koschak, A. *et al*., 2001; Xu, W. and Lipscombe, D., 2001; Johnson, S. L. *et al*., 2005). This steady-state activation of the calcium current (i.e., the random, thermally driven, independent gating of individual calcium channels that occurs at constant membrane potential) may be sufficient to catalyze baseline transmitter release (Brandt, A. *et al*., 2005) that drives the so-called spontaneous spiking in ANFs (Liberman, M. C. and Kiang, N. Y. S., 1978; Sewell, W. F., 1984; Glowatzki, E. and Fuchs, P. A., 2002; Keen, E. C. and Hudspeth, A. J., 2006). Thus, each stage of processing is maintained in a partially active state even in complete silence, thereby avoiding a threshold nonlinearity and the resulting loss of

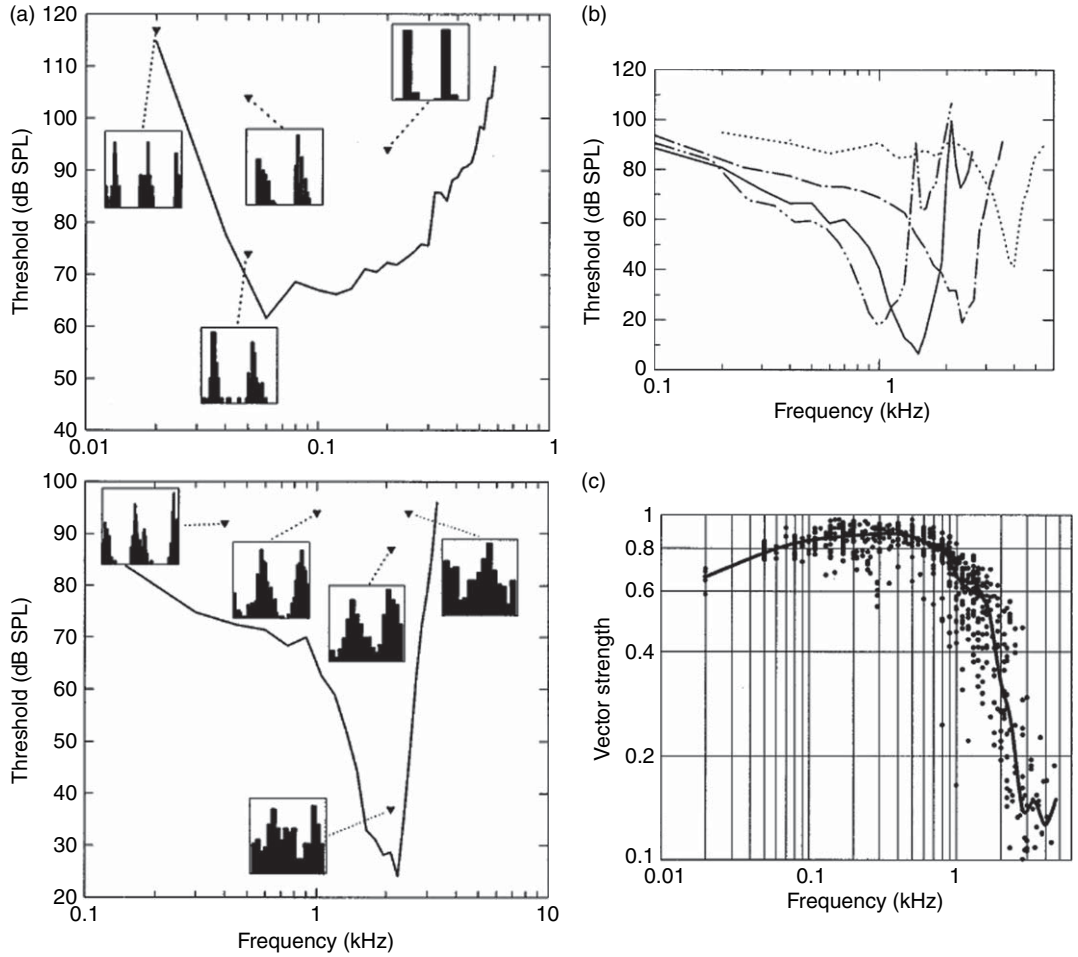

Figure 2 Tuning curves and phase locking in avian (emu) auditory nerve fibers (ANFs). (a) The sound pressure level (SPL) required to evoke a criterion response, in this case, a 20 Hz increase in ANF firing rate above the spontaneous rate (SR), plotted as a function of the frequency of the tonal stimulus. This type of measurement is often called the fiber's threshold, although it does not mean that the fiber fails to respond to less intense sounds, only that the response falls below the experimenter's criterion. Data from two ANFs are shown. Each panel shows one fiber's tuning curve as a continuous line and phase histograms (insets) from the same fiber, each spanning a time frame of two cycles on the *x*-axis and displaying the probability of a spike in particular time bins within the cycle. The stimulus for the insets was at the frequency-level combinations indicated by the associated filled, inverted triangles. The phase relationship of spike occurrence to the period of the tonal stimulus changes as a function of frequency, but at the characteristic frequency (the low point on the curve) the phase relationship does not vary with changes in sound intensity (dB SPL). (b) Tuning curves for four ANFs of different characteristic frequency. (c) When vector strength (a measure of the degree of phase locking, on a scale of 0 to 1, derived from phase histograms like those shown in (a)) is plotted as a function of stimulus frequency around characteristic frequency for 73 different afferent fibers, it is apparent that cochlear ANFs in the emu exhibit a sharp decline in phase-locked firing at frequencies above 1 kHz. Reprinted with permission from Manley, G. A., Köppl, C., and Yates, G. K., J. Acoust. Soc. Am., Vol. 101, pages 1560-1573, 1997. Copyright 1997, American Institute of Physics.

information about small signals. Because several steps in auditory reception involve discrete all-or-none events (e.g., the opening of individual ion channels, the fusion of individual synaptic vesicles (SVs) with the plasmalemma, and the generation of individual action potentials in ANFs), the presence of thermally driven noise in the system is crucial to maintaining high sensitivity to small sounds (Indresano, A. A. *et al.*, 2004). This phenomenon has been studied in many physical systems under the odd name of stochastic resonance.

At frequencies above a few kilohertz, where sound perception relies on nonlinear transduction at the foot of the stimulus–response curve to produce the

DC component of the receptor potential (see Section 3.22.6), a nonlinear response to small sounds may be unavoidable.

Fibers that are the most sensitive to sound also have the highest SR. The equivalent statement in terms of threshold is that SR varies inversely with threshold. In cats, ANFs have been divided into three classes based on SR: low-SR fibers (<0.5 Hz) have the highest threshold (20–60 dB higher than high-SR fibers), high-SR fibers (≥18 Hz) have the lowest thresholds, and medium-SR fibers have an intermediate sensitivity (Merchan-Perez, A. and Liberman, M. C., 1996). Because ANFs with the same CF can have high-, intermediate-, or low-SR, it seems likely that a single IHC forms synapses with representatives of all three functional groups.

Unlike many types of neurons that fire either with a fairly constant interspike interval or in bursts, the exponential distribution of interspike intervals for baseline activity in mammalian ANFs suggests that their activity in the absence of sound is driven by independent random events (i.e., it is a Poisson process), except during a neural refractory period following each spike (Johnson, D. H. and Kiang, N. Y. S., 1976) rather than by an oscillation in the pre- or postsynaptic membrane potential or by any of the other well-known mechanisms that underlie bursting or rhythmic firing in neurons. The independent events may be the brief openings of individual presynaptic calcium channels, in which case the afferent synapses onto ANFs with higher SRs could have more calcium channels or a higher probability of transmitter release in response to the opening of a single calcium channel. Another possibility to explain the correlation between an ANF's sensitivity and its SR is that the voltage dependence of the calcium channels at high-SR synapses is shifted such that the channel's resting open probability is increased, which would also move the resting potential to a steeper place on the channel's sigmoidal activation curve. In all of these cases, high SR would be associated with greater sensitivity to sound. Since a single hair cell can make synapses onto several ANFs that have widely varying SRs, these differences must be specific to individual synapses.

If the Poisson events that trigger exocytosis are the openings of individual calcium channels, then a simple calculation shows that the probability of exocytosis associated with each channel opening is likely to be very small. Calcium channels in hair cells have mean open times of <1 ms and a steady-state open probability of ∼10% at the resting potential, implying a mean closed time of <10 ms. If calcium channels in IHCs have properties similar to these, then each channel is expected to generate >100 openings per second at the resting potential, and the ensemble of ∼100 calcium channels at a typical AZ are expected to generate $>10^4$ openings per second. Given that the highest SRs in ANFs are $\sim 100\,s^{-1}$, fewer than 1% of calcium channel openings are predicted to trigger exocytosis.

3.22.2.3 Innervation Patterns and the Function of Auditory Organs

The pattern of afferent innervation onto hair cells contributes greatly to the response properties observed in afferent fiber recordings. To illustrate this, we will consider two very different auditory organs of the inner ear: the mammalian cochlea and the frog sacculus.

As mentioned above, sensory information from a single IHC in the mammalian cochlea diverges onto multiple ANFs, which can be regarded as a set of parallel channels that relay information from a single IHC to the brain. Because each IHC has a slightly different CF, and a slightly different phase relationship to the sound, restricting each ANF's input to a single IHC preserves these two important features of the cochlear tonotopy. Having multiple outputs from each IHC with different sensitivities (range fractionation) may be important for maintaining a high signal-to-noise ratio for faint sounds in some ANFs while avoiding saturation by loud sounds in other ANFs. Even if some of the ANFs have identical response properties, maintaining redundant information channels can be important for increasing the signal-to-noise ratio. Two important sources of noise are uncertainty in when (or whether) a spike will be generated in a given ANF and variation in the conduction time of ANF spikes to the brain. This noise can, in principle, be reduced by combining information transmitted over separate channels that have independent noise sources. Each ANF postsynaptic to a given IHC shares a common input signal (the hair cell's membrane potential), but the subsequent steps of synaptic transmission, spike generation and conduction to the brain are carried out independently in each AFN, and therefore are subject to independent noise. The innervation pattern of the mammalian cochlea thus appears to be optimized to provide the spectral and temporal information needed for complex computations involved in speech recognition and generating a map of auditory space.

The frog sacculus has a very different structure and pattern of innervation (reviewed in Smotherman, M. S. and Narins, P. M., 2000). It is (in addition to its function as a vestibular organ) exquisitely sensitive to both airborne sound and substrateborne vibration (Koyama, H. *et al.*, 1982). The frog saccular hair cells reside in a roughly circular patch of sensory epithelium beneath the otolithic membrane, and all are attached to it through their kinocilia. There is no evidence of tonotopic organization. Instead, the hair cells fall into only a few anatomical classes, suggesting that many may be functionally equivalent to each other (Edmonds, B. *et al.*, 2000). Unlike the mammalian cochlea, each saccular afferent neuron branches to contact many hair cells (Lewis, E. R. *et al.*, 1982). Summation of synaptic inputs from multiple hair cells is expected to increase the sensitivity and, perhaps more important, the signal-to-noise ratio of ANFs from the frog sacculus, which is expected to contribute to the organ's extreme sensitivity to sound and vibration.

3.22.3 Hair Cells

Hair cells are part of the tight epithelium that separates endolymph from perilymph. Each hair cell is sealed to its neighbors by tight junctions that form an extracellular diffusion barrier across the epithelium and divides the cell membrane into an apical domain that is primarily involved in mechanosensory transduction and a basolateral domain where the synapses reside (Figure 1(b)). Hair cells are both pre- and postsynaptic, and have other neuronal properties, including voltage- and calcium-gated ion channels that, in concert with the transduction current and the membrane's electrical capacitance, determine how the membrane potential changes with time. The hair cell's compact shape has important consequences for both the electrical signal and the ensuing calcium signal that controls transmitter release at afferent synapses.

3.22.3.1 Hair Cell Shape in Relation to Synaptic Signaling

The hair cell body has a diameter-to-length ratio that is too large to allow significant spatial variation in the membrane potential, except in OHCs of the mammalian cochlea, where extensive internal membranes lining the plasmalemma might impede intracellular current flow (Nakagawa, T. *et al.*, 2006). Other types of hair cells, including IHCs of the mammalian cochlea, are expected to be nearly isopotential even to the tips of the stereocilia (Roberts, W. M. *et al.*, 1990). This means that the electrical signal for synaptic transmission is the same at each of the afferent synaptic sites, and implies that the different properties of the afferent synapses on a single hair cell must arise downstream of the electrical signal. Similarly, the membrane capacitance is expected to attenuate high-frequency voltage oscillations to the same degree at all AZs in a given hair cell, leaving only a steady depolarization in response to high-frequency sounds (Section 3.22.6).

The hair cell's large radius of membrane curvature compared to the diameter of a single synaptic AZ (several micrometers vs. hundreds of nanometers) simplifies the understanding and modeling of afferent synaptic transmission because for some purposes the membrane can be regarded as a planar boundary separating two infinite spaces (Neher, E. and Augustine, G. J., 1992; Roberts, W. M., 1994). Clearly, the hair cell's ~1 pl volume is less than infinite and cannot serve as an infinite sink for calcium entering at synapses, but as long as calcium extrusion can keep pace with calcium entry, the details of how and where calcium is pumped back into the extracellular space are expected to be less important than in the confined space of a typical presynaptic bouton.

3.22.3.2 The Synaptic Body and Synaptic Vesicle Pools

Afferent synapses on all hair cells and related electroreceptors are distinguished by a prominent presynaptic structure, the synaptic body (SB). One or more SBs are found at each site of synaptic contact, in close association with the presynaptic plasma membrane (Figures 3 and 4). Numerous functions have been proposed for the SB (Sjostrand, F. S., 1958; Bunt, A. H., 1971; Gray, E. G. and Pease, H. L., 1971; Osborne, M. P. and Thornhill, R. A., 1972; Wagner, H.-J., 1978; King, T. S. and Dougherty, W. J., 1982; Schmitz, F. *et al.*, 2000; Lenzi, D. and von Gersdorff, H., 2001; Parsons, T. D. and Sterling, P., 2003), but none proved.

The hair cell contains a large population of ~40 nm, clear-core vesicles that are presumed to contain the neurotransmitter, glutamate. These SVs have been partitioned into several conceptual pools, defined either structurally with EM or functionally

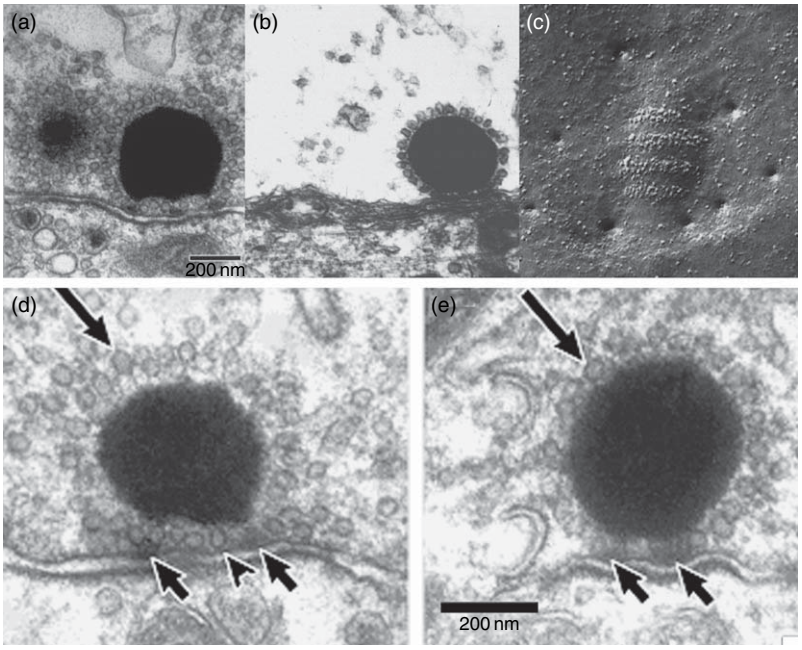

Figure 3 Afferent synapse ultrastructure. All panels are electron micrographs of afferent synapses in frog saccular hair cells. (a) Each site of synaptic contact between a hair cell (top) and afferent nerve ending (bottom) typically contains one synaptic body, which is darkly stained and surrounded by ~40 nm-diameter vesicles. A second synaptic body (SB) is faintly visible to the left. The region of close apposition between pre- and postsynaptic membranes is marked by a fuzzy appearance that extends 100–400 nm beyond the edge of the synaptic body, but the presumed region where synaptic vesicles release their contents (the active zone) is restricted to the area beneath the SB and perhaps ~100 nm beyond. The presynaptic membrane at the active zone contains several densities that anchor the SB. (b) The SB and its attached vesicles remain anchored to the presynaptic active zone after the cell is broken open in extracellular saline (contains 1.8 mM calcium) and the cytoplasm washed away prior to fixation. (c) A freeze-fracture electron micrograph shows rows of particles in the presynaptic membrane that may align with the presynaptic densities and correspond to ion channels. The membrane dimples around the periphery of the active zone are most likely the openings of membrane tubules rather than sites of vesicle fusion, which are expected to occur closer to the ion channels at the active zone. (d, e) Filamentous links tether the SB to the cytomatrix at the active zone (short arrows) and synaptic vesicles to the SB (long arrows). Synapses that had been inhibited before and during fixation (d) had a high density of docked vesicles in the space between the SB and the plasmalemma (arrowhead points to one). Synapses that had been stimulated before and during fixation (e) had few docked vesicles and numerous cisternal structures in the cytoplasm. (c) Reproduced with permission from Roberts W. M. 1994. Localization of calcium signals by a mobile calcium buffer in frog saccular hair cells. J. Neurosci. 14, 3246–3262. Copyright by the Society for Neuroscience. (d,e) Reprinted from Lenzi, D., Crum, J., Ellisman, M .H., and Roberts, W. M. 2002. Depolarization redistributes synaptic membrane and creates a gradient of vesicles on the synaptic body at a ribbon synapse. Neuron 36, 649–659, Copyright (2002) with permission from Elsevier.

with electrophysiological assays of SV fusion and neurotransmitter release.

Experiments on a wide variety of chemical synapses in many animals have shown that SVs can generally be assigned to one of three groupings: the readily releasable pool (RRP), the recycling pool, and the reserve pool (reviewed in Rizzoli, S. O. and Betz, W. J., 2005). Parallel definitions of these pools at hair cell afferent synapses are useful to facilitate comparisons with more conventional chemical synapses, although this is hampered somewhat by their different anatomical and functional characteristics. At both types, maximal activation of the presynaptic calcium current exhausts a small SV pool, defined as the RRP, within a few milliseconds. At conventional synapses, the RRP comprises 1–2% of the total vesicle population, but considering the hair cell cytoplasm as an unrestricted volume for SV movement containing hundreds of thousands of SVs (Lenzi, D. *et al.*, 1999; Holt, M. *et al.*, 2004), the RRP in hair cells comprises a miniscule fraction of the total (Moser, T. and Beutner, D., 2000; Schnee M. E. *et al.*, 2005; Rutherford, M. A. and Roberts, W. M., 2006).

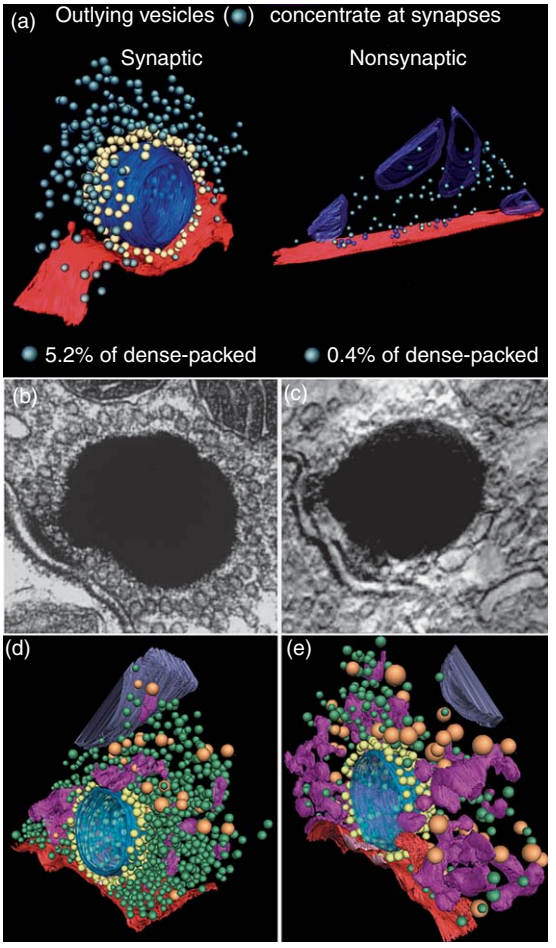

Figure 4 Tomographic reconstructions of afferent synapses in frog saccular hair cells. (a) Tethered vesicles (yellow) surround the SB (blue), which lies close to the plasmalemma (red) at the Active zone (AZ). Other (outlying) synaptic vesicles (green) are also highly concentrated within a few hundred nanometers of the SB, and populate the rest of the cytoplasm at much lower density. (b) An inhibited synapse shows mostly spherical vesicles around the SB. (c) A stimulated synapses has numerous irregular membrane structures near the SB that could be the result of compound vesicle fusion and/or membrane retrieval. (d, e) Tomographic reconstructions give a clear view of the more extensive cisternal structures (magenta) at stimulated synapses (e) compared to inhibited synapses (d). Coated vesicles (orange) and mitochondria (dark blue) are also shown. Other colors are the same as in (a). (a) Reproduced with permission from Lenzi, D., Runyeon, J. W., Crum, J., Ellisman, M. H., and Roberts, W. M. 1999. Synaptic vesicle populations in saccular hair cells reconstructed by electron tomography J. Neurosci. 19, 119–132; Copyright by the Society for Neuroscience. (d,e) Reprinted from Lenzi, D., Crum, J., Ellisman, M. H., and Roberts, W. M. 2002 Depolarization redistributes synaptic membrane and creates a gradient of vesicles on the synaptic body at a ribbon synapse. Neuron 36, 649–659; Copyright (2002) with permission from Elsevier.

At conventional synapses, the RRP is generally thought to correspond to the docked vesicles, those seen in EM to be in contact with the plasmalemma at the AZ. The corresponding pool of morphologically docked vesicles at ribbon synapses consists mostly of vesicles that occupy the space between the SB and the plasmalemma at each AZ (Figures 3 and 4). Differences in the precise criteria used for anatomical classification of vesicles can cause estimates of the size of the docked vesicle pool to differ by a factor of two, even in careful quantitative studies.

There is ambiguity about how to classify vesicles that are tethered to the SB but do not contact the plasma membrane. Direct evidence that these vesicles even participate in transmitter release under normal conditions is scant (Siegel, J. H. and Brownell, W. E., 1986), but assuming that they do, are they part of the RRP, the recycling pool, or some other pool? One reason to think that even though they reside far from the plasmalemma they might still be in the RRP is that they may be able to fuse with each other, forming a chain that connects to the cell surface (reviewed in Parsons, T. D. and Sterling, P., 2003; Edmonds, B. W. *et al.*, 2004). Figure 4(c) shows what may be a chain of fused vesicles. If the morphological criterion that has been used to determine whether a vesicle is docked to the plasmalemma is applied to vesicles on the SB, then many of these vesicles are morphologically docked to each other, and thus could conceivably be ready to fuse together, although the calcium signal is expected to be highly attenuated more than a few vesicle diameters from the calcium channels on the cell surface (Roberts, W. M., 1994). Alternatively, the type of structures shown in Figure 4(c), which were observed after extended depolarization in high potassium (Lenzi, D. *et al.*, 2002), could reflect membrane retrieval.

The available physiological evidence indicates that the RRP in the frog sacculus and mouse cochlea is much smaller than the total pool of SB-associated vesicles, and is close to the number of vesicles docked at the plasmalemma (Khimich, D. *et al.*, 2005; Rutherford, M. A. and Roberts, W. M., 2006), which supports the more conventional hypothesis that only vesicles docked at the plasmalemma are part of the RRP, and that other SB-associated vesicles are part of the recycling vesicle pool that replenishes the RRP. Physiological correlates of these anatomical definitions are discussed in more detail in the following sections of this chapter.

Tens of thousands of clear-core vesicles are found in the hair cell cytoplasm within several hundred

nanometers of the cell surface, and hundreds of thousands more reside in the vast cell interior. They occur at a low average density in frog saccular hair cells (0.4% of dense packed = ~100 vesicles per μm^3), but are much more concentrated within 700 nm of each synapse (5–10% of dense packed = ~1200–2400 vesicles per μm^3; Lenzi, D. *et al.*, 1999; 2002). The contribution of these vesicles to synaptic transmission under normal physiological conditions is unclear. At conventional synapses, there is a physiologically distinct (but sometimes not anatomically distinct; Rizzoli, S. O. and Betz, W. J., 2005) recycling pool of SVs that are reused preferentially by local endocytosis (Pyle, J. L. *et al.*, 2000; Stevens, C. F. and Williams, J. H., 2000), whereas vesicles in the reserve pool enter the exocytic pathway only under strong stimulus conditions that also cause bulk endocytosis and vesicle reconstitution through an endosomal compartment. It remains unknown whether hair cell afferent synapses have distinct recycling and reserve SV pools.

The AZ at most brain synapses contains only a few docked vesicles, and a single presynaptic action potential seldom evokes exocytosis of neurotransmitter from more than one of them, with frequent failures (Dobrunz, L. E. and Stevens, C. F., 1997; for a review see Sudhof, T. C., 2000). In contrast, the docked vesicle pool is considerably larger at AZs in hair cells of the turtle papilla (mean of 30; Schnee, M. E. *et al.*, 2005), mouse cochlea (16–30, IHC; Khimich, D. *et al.*, 2005), and the frog sacculus (mean of 43; Lenzi, D. *et al.*, 2002). Furthermore, both pre- and postsynaptic assays of SV exocytosis (see Sections 3.22.5–3.22.7) have indicated that more than one SV can fuse in response to a single, brief presynaptic stimulus (reviewed in Fuchs, P. A., 2005). The stimulus to open voltage-gated calcium channels (VGCCs) in hair cells is not an all-or-none action potential that lasts on the order of 1 ms, rather, they respond to depolarizations of varying duration and intensity with graded release of neurotransmitter. Thus, while some generalizations can be made across all synapse types, there may be important differences between SV pools at conventional synapses and hair cell afferent synapses.

3.22.3.3 Calcium Buffering in Hair Cells

Exogenous calcium buffer can be introduced into a hair cell through a micropipette recording electrode, and has been shown to influence synaptic transmission. Interestingly, a high concentration of calcium buffer with fast binding kinetics is required to interfere with exocytosis from the RRP, whereas refilling of the RRP can be inhibited by low concentrations of slower buffer (Moser, T. and Beutner, D., 2000). It is concluded that although both processes are regulated by calcium, refilling of the RRP involves signaling over a longer distance, and is therefore more susceptible to disruption by calcium buffers. To understand the interaction between calcium ions and calcium buffers that can diffuse in cytoplasm one must think about the rates of binding and diffusion, not just equilibrium binding of calcium to the buffer. A brief introduction to the essential concepts needed to understand the nonequilibrium interaction between a mobile calcium buffer and the calcium ions that enter through a calcium channel and diffuse into a large cytoplasmic volume is given below.

High concentrations of calcium-binding proteins can limit the spread of calcium signals within a cell (Roberts, W. M., 1994). This may be particularly important in hair cells, because they use calcium signals for several distinct cellular processes, including feedback inhibition of the transduction current, which involves calcium entry and action at the stereociliary tips (see Chapter Hair Cell Transduction and Adaptation: Physiology and Molecular Mechanisms), and efferent synaptic transmission see Chapter Efferent System at postsynaptic sites, which intermingle with afferent presynaptic sites on the hair cell's basolateral surface. In addition to localized transmembrane calcium signals, hair cells also exhibit localized calcium-induced calcium release from intracellular stores near sites of efferent contact (Lioudyno, M. *et al.*, 2004).

The equilibrium interaction between calcium and a molecule that has a single calcium-binding site is characterized by a single number, the dissociation constant, K_D (units: molar, M), or its reciprocal, K_A (M^{-1}):

$$K_D = \frac{[Ca][B]}{[CaB]}$$

where [Ca] and [B] are the concentrations (M) of free Ca and free buffer, and [CaB] is the concentration of calcium bound to the buffer. Free means that they are able to interact with each other (i.e., not already bound to something else, hidden inside an organelle, etc.); whether or not they are free to diffuse in the cytoplasm is a separate issue that is also important. Time does not appear in the units of these variables. It is assumed that enough time has elapsed for equilibrium to be attained.

The equilibrium equation does not apply near an open calcium channel because equilibrium is never

reached while the calcium current persists (which requires an extrusion mechanism to keep the cell from filling up with calcium). The existence of a calcium current is *prima facie* evidence of disequilibrium, at least locally around the mouth of the channel. We will not specifically consider the calcium pump here, except to note that the maximum flux of calcium ions through a single pump ($\sim 10^3\,s^{-1}$) is roughly one ten thousandth the flux through an open calcium channel ($\sim 10^7\,s^{-1}$), so that the local calcium gradient around a single pump is miniscule compared to the gradient near the mouth of a single calcium channel. Therefore, it makes sense to consider the calcium extrusion process to be distributed over a large region of cell surface, and ignore its effect on the localized region of extremely high free calcium near an open calcium channel.

Two parameters, k_{on} ($M^{-1}\,s^{-1}$) and k_{off} (s^{-1}), are needed to describe the kinetics of calcium binding to a single-site buffer. $k_{on}[B]$ and k_{off} are, respectively, the rate constants for calcium binding to and unbinding from the buffer. The three parameters, k_{on}, k_{off}, and K_D are related by $K_D = (k_{off}/k_{on})$, so any two specify the third.

A calcium ion is initially free as it enters the cell through a calcium channel. The mean time required to encounter and bind to a buffer molecule is $1/(k_{on}[B])$, which for the buffering conditions encountered in many hair cells ($[B] >> K_D$) is close to the equilibration time constant (τ) in response to a step change in free calcium:

$$\tau = \frac{1}{k_{on}([B] + K_D)}$$

During this time, a free calcium ion diffuses a characteristic distance of

$$\lambda = \sqrt{\tau D_{Ca}}$$

where D_{Ca} is the diffusion coefficient for free calcium in cytoplasm (Neher, E. and Augustine, J. G, 1992; Roberts, W. M., 1993). The parameters τ and λ are, respectively, the time and space constants for calcium binding to the buffer in the vicinity of an open calcium channel.

If the distance between the presynaptic calcium channels and the calcium sensors that trigger exocytosis is substantially less than λ then the buffer has little effect. If the distance is substantially greater than λ then the buffer has time to come into equilibrium with global free calcium and binding kinetics are not important. If the distance is similar to λ then the binding kinetics are important and the buffer's effects can be complex. The diffusion coefficient for the buffer in cytoplasm is also important because slow diffusion reduces the rate at which calcium-free buffer is replenished near the open channel, which reduces the local [B], and in turn locally increases both τ and λ. At hair cell afferent synapses, exocytosis of RRP vesicles falls into the first category, where cytoplasmic buffers are irrelevant, but some other important calcium-dependent steps in the SV cycle appear to fall into the complex category, where buffer concentration, binding kinetics, and diffusion coefficient all come into play.

To assign approximate values to τ and λ one needs to know the concentration and k_{on} for the predominant diffusionally mobile calcium buffer(s) in the cell. Many types of hair cells are intensely labeled by fluorescent antibodies against one or more of the diffusible calcium-binding proteins calbindin-D28k, calretinin, parvalbumin-α, and parvalbumin-β (also known as oncomodulin or PV-3). For example, some hair cells in the frog sacculus contain calretinin at a concentration above 1 mM, which provides more than 5 mM calcium-binding sites (Edmonds, B. *et al.*, 2000). Other frog saccular hair cells contain predominantly parvalbumin β, at the extraordinary concentration of 4 mM (Heller, S. *et al.*, 2002), which amounts to 8 mM calcium-binding sites. OHCs in the mammalian cochlea contain different calcium-binding proteins than are found in the IHCs, and appear to express them at a tenfold higher concentration (calbindin-D28k and parvalbumin-β equivalent to 5 mM calcium-binding sites; Hackney, C. M. *et al.*, 2005). These extreme concentrations of calcium buffer are certain to have important consequences for many calcium signals in the cell. It is also worth remembering that some calcium-binding proteins may serve both as buffers and as calcium sensors that influence exocytosis or participate in other steps in the SV cycle.

For typical values of $K_D = 1\,\mu M$ and $k_{on} = 10^7\,M^{-1}\,s^{-1}$, the buffer space constant and time constant in a cell that has a moderate calcium buffer concentration of $[B] = 100\,\mu M$ are $\lambda = 450\,nm$ and $\tau = 1\,ms$. Increasing the buffer concentration 100-fold to 10 mM decreases λ to 44 nm and τ to 10 µs. From this calculation, one can see that an extremely high concentration of a calcium buffer can reduce the buffering space constant from approximately the diameter of the entire AZ (Figure 3(c)) to approximately the diameter of a single SV, thereby minimizing the overlap of calcium

domains around each open calcium channel, particularly at barely perceptible sound intensities where only a few calcium channels are open at each afferent synapse. The close association between calcium channels and AZs (Lewis, R. S. and Hudspeth, A. J., 1983; Art, J. J. and Fettiplace, R., 1987; Roberts, W. M. *et al.*, 1990; Issa, N. P. and Hudspeth, A. J., 1994; Martinez-Dunst, C. *et al.*, 1997; Rodriguez-Contreras, A. and Yamoah, E. N., 2001; Zenisek, D. *et al.*, 2003; Brandt, A. *et al.*, 2005) means that steep spatial calcium gradients and the nonequilibrium calcium binding to buffer are important at afferent synapses.

At distances on the order of λ from an open channel, the buffer serves as a calcium sink, and can greatly reduce the free calcium concentration (Roberts, W. M., 1994). At larger distances, where free calcium falls below the buffer's K_D, the buffer becomes a calcium source as it dumps its bound calcium, although the large volume available to receive this calcium means that the calcium rise associated with unbinding from the buffer is orders of magnitude smaller than the calcium concentration near the source. Because the buffer molecules are large compared to a calcium ion, bound calcium diffuses more slowly than free calcium. The net result is that the buffer can greatly increase total calcium near an open calcium channel, and can slightly increase free calcium at certain distances from the channel, but its main effect is to greatly reduce the extremely high concentration of free calcium that accumulates near the channel (i.e., at distances on the order of λ).

More detailed discussions of these and other properties of mobile calcium buffers are in the literature (e.g., Stern, M. D., 1992; Roberts, W. M., 1993; 1994; Dargan, S. L. and Parker, I., 2003). One interesting result is that the average distance that a calcium ion travels while remaining bound to the buffer is >1 μm, which is large compared to the AZ diameter. Thus, the mobile buffer gives a calcium ion only one brief chance to exert its effect. Either it binds to its target, such as the calcium sensor that triggers exocytosis, or it is captured by the mobile buffer and is carried away. If the buffer has reasonably fast binding kinetics ($k_{on} = 10^7\,M^{-1}\,s^{-1}$) and provides 5–10 mM of mobile binding sites for Ca (Edmonds, B. *et al.*, 2000; Heller, S. *et al.*, 2002), then the average time available for a calcium ion to encounter and bind to its target (i.e., the binding time constant, τ) is only 10–20 μs.

3.22.4 Ribbon Synapses – A Small but Diverse Class

The SBs of hair cells are homologous to the presynaptic ribbons found in rods, cones, and bipolar cells in the retina, and pinealocytes in the pineal body. Like hair cells, these cells usually do not make action potentials. Because of their anatomical, physiological, and molecular similarities, we include the afferent synapses of hair cells in the class of ribbon synapses, but one should also keep in mind the differences, including, for example, the slow-time scale of the visual system compared to the auditory system.

Ribbon synapses are understood to be specialized for sustained transmitter release. For example, vertebrate photoreceptors release neurotransmitter continuously in the dark (Rea, R. *et al.*, 2004) and the hair cell afferent synapse is active in the absence of an applied stimulus (Siegel, J. H., 1992). However, the hair cell is also capable of releasing transmitter phasically (e.g., EPSPs that are correlated with the periodicity of the stimulus for afferent fibers at frequencies up to a few kilohertz; Figures 1(c) and 2(c), see also Section 3.22.6). The details of synaptic physiology that vary among ribbon synapses from different tissues and cell types are likely to be essential for their function (for a review, see Sterling, P. and Matthews, G., 2005). Nevertheless, the first synapse in the pathways for vision, hearing, balance, and lateral line senses in all vertebrate animals is a ribbon synapse.

3.22.4.1 The Synaptic Body (Ribbon) and Its Vesicles

The term ribbon originates from the flat, almost 2D morphology of the presynaptic structures observed in transmission EMs of retinal photoreceptors and bipolar cells. Serial reconstructions of gluteraldehyde-fixed hair cells from many preparations, including mammalian cochlea, have shown that the SB in hair cells has a more spherical or ellipsoid shape. IHCs rely exclusively on ribbon synapses for afferent transmission. The role of SBs in OHCs is more uncertain as they (the SBs) are far fewer and often seen only during development (Smith, C. A. and Sjostrand, F. S., 1961; Siegel J. H. and Brownell W. E., 1981; Sobkowicz, H. M. *et al.*, 1986).

Although SBs are heavily stained by osmium, which typically labels lipid membranes, they are thought to be composed primarily of protein

(Krstic, R., 1976). The osmiophilic nature of the SB is well-known because OsO_4 is a common EM fixative and is electron-dense. Perhaps more relevant to function, the ribbon has been reported to bind both calcium and phosphate (Schmitz, F. and Drenckhahn, D., 1991), although there is no evidence that it binds or releases these ions in the process of synaptic transmission.

SBs at AZs are always found in association with ~40 nm-diameter clear-cored vesicles, which are attached to it by thin filaments (Usukura, J. and Yamada, E., 1987) and often cover its surface nearly completely (Figures 3 and 4; Lenzi, D. *et al.*, 2002). SBs can sometimes be found in the cell interior, either singly or in clusters, where they are also covered in vesicles (Miller, M. R. and Beck, J., 1987). The molecular identity of the filaments is not known, except that they are thought not to contain synapsins I or II, which form filaments linking SVs to cytoskeleton at other synapses (Hirokawa, N. *et al.*, 1989), but are absent from ribbon synapses (von Kriegstein, K. *et al.*, 1999). Based on antibody labeling, the filaments could contain the KIF3A subunit of the kinesin 2 motor complex (Muresan, V. *et al.*, 1999), which forms 50 nm-long rods *in vitro* (Yamazaki, H. *et al.*, 1995), or possibly one or more of the many other KIF3 isoforms that may cross react with the antibody.

SBs and ribbons can be regarded as elaborations of the cytomatrix at the active zone (CAZ) seen at all synapses (Zhai, R. G. and Bellen, H. J., 2004), but in EM the SB appears as a separate structure, connected to the CAZ by filamentous links (Usukura, J. and Yamada, E., 1987; Lenzi, D. *et al.*, 2002). The tight association between the SVs and the SB, and between the SB and the presynaptic plasma membrane is evident in cells that were broken open prior to fixation (Figure 3(b)). If the binding were weak or disrupted by exposure to the high-calcium concentration of extracellular saline, these structures would not have remained behind while the rest of the cytoplasm was washed away.

3.22.4.2 Molecular Specializations of Ribbon Synapses

Understanding of the molecular composition of hair cell afferent synapses has begun (Figure 5), but is far from complete (Wagner, H.-J., 1997). A protein, Ribeye

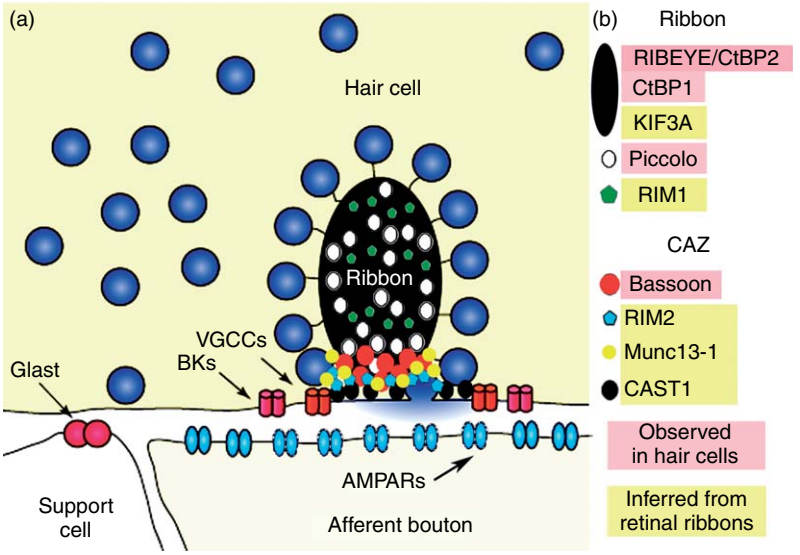

Figure 5 Molecular specializations of the hair cell ribbon synapse. (a) Localization of proteins associated with the synaptic ribbon and plasma membrane density of the cytomatrix at the active zone (CAZ), labeled in (b). Voltage-gated calcium channels (VGCCs) are clustered underneath the ribbon and juxtaposed to postsynaptic α-amino-3-hydroxy-5-methylisoxazole-4-propionic acid (AMPA)-type glutamate receptors. In some hair cells, presynaptic calcium-sensitive voltage-gated (BK) potassium channels intermingle with the VGCCs. Glutamate transporters in supporting cells clear neurotransmitter from the cleft. Bassoon anchors the ribbon to the Cytomatrix at the active zone (CAZ) plasma membrane density via its interaction with the RIBEYE. Bassoon, RIBEYE/CtBP2, CtBP1, and Piccolo have been observed at hair cell afferent synapses. The existence of the other proteins at the hair cell's ribbon synapse is by inference from observations at retinal ribbon synapses (tom Dieck, S. *et al.*, 2005). Reproduced from The Journal of Cell Biology, 2005, 168, 825–836 by Copyright permission of The Rockefeller University Press; and Reprinted from Curr. Opin. Neurobiol. Vol. 13, Fuchs, P. A., Glowatzki, E., and Moser, T., The afferent synapse and cochlear hair cells, 452–458, Copyright 2003, with permission from Elsevier.

(Schmitz, F. *et al.*, 2000), has been identified that appears to be a component of all synaptic ribbons, and is expressed nowhere else. This finding justifies exclusion of T-bar synapses of arthropods (e.g., *Drosophila*) from the class of ribbon synapses because the *Drosophila* genome contains no DNA sequences that code for a homolog of the unique exon 1 of the Ribeye protein (Bradford, Y. and Roberts, W. M., unpublished observations). Ribeye is one of two known protein products of the CtBP2 gene. The other product, CtBP2, is a transcription regulator (reviewed in Chinnadurai, G., 2002). A recent report suggests that the CtBP1 protein, which is the product of a closely related gene and also a known transcription regulator, is a presynaptic component of both hair cell (Moser, T., personal communication) and retinal (tom Dieck, S. *et al.*, 2005) ribbon synapses, as well as conventional synapses, raising the possibility that the ancestral CtBP protein had a presynaptic function in addition to being a transcriptional corepressor, and conceivably could link synaptic activity to gene expression. The CAZ-associated protein Bassoon was recently shown to anchor the ribbon at the photoreceptor synapse via a physical interaction with Ribeye (tom Dieck, S. *et al.*, 2005). Bassoon and the related protein Piccolo, are also present at hair cell afferent synapses (Khimich, D. *et al.*, 2005). Bassoon appears to interact with both Ribeye and CtBP1, which are both localized to ribbons even in the absence of functional Bassoon protein.

Drosophila has a single CtBP gene that produces a transcription regulator essential for embryonic development (Nibu, Y. *et al.*, 1998; Poortinga, G. *et al.*, 1998), but it is not known whether CtBP is present at synapses in *Drosophila*. Similarly, the *Ciona* genome (a urochordate) has a single CtBP gene that lacks the coding sequence for Ribeye (Bradford, Y. and Roberts, W. M., unpublished observations). The simplest evolutionary scenario consistent with the data is that a gene duplication event early in the vertebrate lineage, but after the divergence of urochordates from vertebrates, gave rise to paralogous genes, CtBP1 and CtBP2. The CtBP2 gene then acquired an alternate first exon, which became involved in aggregation of CAZ components (Schmitz, F. *et al.*, 2000) into large structures (ribbons), with important, but largely unknown consequences for afferent synaptic transmission in the eye and ear. Ribeye expression became limited to the small class of ribbon synapses, while CtBP1 continues to be expressed at other synapses. An additional gene duplication gave rise to two CtBP2/ribeye genes in teleost fishes (Wan, L. *et al.*, 2005).

Besides Ribeye, only one other protein, the B16 antigen, has been proposed to be a unique component of all ribbon synapses. This protein is known only as an antigenic epitope (amino sequence: DTYQHPPKDS; Balkema, G. W., 1991; Nguyen, T. H. and Balkema, G. W., 1999). A search of the human genome and expressed sequence tag (EST) databases shows that only one gene, aconitase, contains a nucleotide sequence that codes for this exact amino acid sequence. Aconitase is a transcription regulator and a regulator of iron metabolism, but reportedly is not present in synaptic ribbons (Nguyen, T. H. and Balkema, G. W., 1999). Human CtBP2 and Ribeye contain a sequence (TYxxPP) near the C-terminus that is part of the B16 antigen and thus might bind the B16 antibody, but synaptic ribbons in fish reportedly also bind the B16 antibody (Balkema, G. W., 1991) even though this sequence is entirely absent from their CtBP2 and Ribeye proteins. Thus, the component of the ribbon that binds antibodies raised against the DTYQHPPKDS peptide remains unknown.

There are other proteins that may be unique to ribbon synapses but are not expressed at all ribbon synapses. The α_{1D} calcium channel is found only in hair cells and is essential for normal hair cell Ca^{2+} current, neurotransmitter release, and for hearing (reviewed in Moser, T. *et al.*, 2006a). Most synapses express N, P/Q, or R-type calcium channels, but hair cells express L-type calcium channels (Cav 1.3) formed by this unique splice variant. This channel opens at unusually hyperpolarized voltages (Koschak, A. *et al.*, 2001; Brandt, A. *et al.*, 2003; Rodriguez-Contreras, A. and Yamoah, E. N., 2003; Schnee, M. E. and Ricci, A. J., 2003), which may cause the transmitter release responsible for the baseline action potential rate (i.e., SR) in afferent neurons. Retinal rods express a different L-type calcium channel at ribbon synapses, Cav 1.4 (α_{1F}; Morgans, C. W., 2001).

Another protein that may be unique to ribbon synapses is complexin IV (Pabst, S. *et al.*, 2000; Reim, K. *et al.*, 2006). Based on similarity of complexin I and II, and the ability to rescue synaptic transmission in complexin I/II knockout mice, both complexin III and complexin IV are potential calcium-dependent regulators of synaptic transmission. Complexins I and II are known to bind to the soluble NSF (*N*-ethylmaleimide-sensitive factor) attachment receptor (SNARE) complex that forms the core of the vesicle fusion machinery at many synapses (McMahon, H. T. *et al.*, 1995; Reim, K. *et al.*, 2001; Chen, X. *et al.*, 2002; for a review, see Sudhof, T. C., 2004). Complexins III and IV have both been

described at ribbon synapses in the retina, but only complexin IV was found to be unique to retinal ribbon synapses. It was not reported whether complexins III or IV are present in the ear.

Otoferlin is another protein that may be involved in synaptic transmission by hair cells. This protein was discovered by genetic mapping of familial deafness (Yasunaga, S. *et al*., 1999), and is essential for hearing. The otoferlin gene is large and complex, having 48 exons and many splice variants (Yasunaga, S. *et al*., 2000). It is similar to the FER-1 protein of *Caenorhabditis elegans*, which has been implicated in vesicle membrane fusion (Achanzar, W. E. and Ward, S., 1997). Otoferlin is a candidate to substitute for synaptotagmin as the calcium sensor for transmitter release (Yasunaga, S. *et al*., 2000).

Several other presynaptic proteins, including synapsins and synaptotagmins, are notable by their absence from ribbon synapses (Safieddine S. and Wenthold R. J., 1999; von Kriegstein, K. *et al*., 1999). Syntaxin 1, a component of the core SNARE complex is also missing, replaced by syntaxin 3 (Morgans, C. W. *et al*., 1996).

3.22.4.3 Anatomy of the Synaptic Body: Heterogeneity of Structure

SBs come in a bewildering variety of shapes and sizes. Most synapses have one SB at the synaptic complex, others have two or three (Liberman, M. C. *et al*., 1990). In addition to the typically spherical or ellipsoidal shapes of SBs in hair cells from mice, turtles, frogs, and chicks (Sneary, M. G., 1988; Martinez-Dunst, C. *et al*., 1997; Lenzi, D. *et al*., 1999; Khimich, D. *et al*., 2005), SBs of different geometries and densities have been observed in EM (Giannessi, F. and Ruffoli, R., 1996). In many types of hair cells, the SB appears as a uniformly dense blob, with no internal structure but it also can have a laminar appearance, as in some cochlear IHCs. In old world monkeys the SBs of IHCs nearly always appear ring shaped (Bodian, D., 1980). It is unclear how much of this variability is an artifact of fixation and staining. For example, in the frog retina, synaptic ribbons of a lamellar nature were observed with conventional transmission electron microscope (TEM) thin sections, but were not so apparent when freeze-etching and freeze-substitution methods were employed for tissue preparation (Usukura, J. and Yamada, E., 1987).

SBs vary in size and number among organs, within and between species, as well as among cells within a particular organ. Furthermore, SBs vary in size and shape within individual cells. The dimensions of the SB are typically submicron, ranging from ~200 nm for the shortest principle axis of the ellipsoid SBs in mouse IHCs (Khimich, D. *et al*., 2005) to ~400 nm in hair cells of frog and goldfish sacculus (Gleisner, L. *et al*., 1973; Hama, K. and Saito, K., 1977; Jacobs, R. A. and Hudspeth, A. J., 1990; Lenzi, D. *et al*., 1999). Estimates of the number of ribbon-containing synapses per cell ranged from 10 in mouse cochlear IHCs (Khimich, D. *et al*., 2005) to 85 in the high-frequency hair cells of the turtle papilla (Sneary, M. G., 1988).

Several studies have provided clues regarding the function of SBs in hair cells by demonstrating that the size and number of synaptic ribbons, as well as the numbers of associated calcium channels and SVs, is correlated with the position of the hair cell on the tonotopic axis of the organ. In the turtle papilla, high-frequency cells have three times more SBs, higher vesicle densities near SBs, more calcium channels, and larger calcium currents than do lower-frequency cells (Sneary, M. G., 1988; Art, J. J. *et al*., 1995; Schnee, M. E. *et al*., 2005). Upon depolarization, the high-frequency cells released more vesicles and with faster kinetics. A model of SV trafficking that incorporated all of these data predicted that these differences result in transmission being optimized to the CF of the hair cell (Schnee, M. E. *et al*., 2005). In the papilla of the chick, the diameter of the SB ranged from 120 to 210 nm with increasing CF from apical to more basal positions along the tonotopic axis (Martinez-Dunst, C. *et al*., 1997). These two studies used different experimental approaches to reach a similar conclusion; that the morphology of the SB has influence over the numbers of SVs that are maintained at well-defined positions with respect to the source of calcium influx. SVs close to the center of the AZ may be more responsive to calcium influx if the channels are clustered there (Furukawa, T. and Matsuura, S., 1978; Furukawa, T. *et al*., 1982; reviewed for the case of CNS synapses in Schneggenburger, R. and Neher, E., 2005).

A study in the mammalian cochlea has reported presynaptic morphological correlates of ANF SR and threshold (Merchan-Perez, A. and Liberman, M. C., 1996). Analysis of ultrastructure at the EM level showed that the size and complexity of SBs tended to increase as SR decreased, accompanied by an increase in the total number of SVs clustered at the AZ. These data suggest that the size of the SB has something to do with the regulation of vesicle release that determines the baseline afferent discharge rate

and sensitivity to faint sounds, but the relationship is opposite what is expected based on the prevailing view that the ribbon collects vesicles and conveys them to the release sites. Instead, these data seem to suggest that a larger SB may somehow inhibit SV fusion for weak sounds. Clearly, more work needs to be done to understand the relationship between SB morphology and postsynaptic properties.

3.22.5 The Synaptic Vesicle Cycle in Hair Cells

The basic features of the SV cycle are similar at conventional chemical synapses and ribbon synapses. Both baseline and evoked EPSCs at ribbon synapses require presynaptic calcium influx through channels (Robertson, D. and Paki, B., 2002; Keen, E. C. and Hudspeth, A. J., 2006) and are completely and reversibly blocked by antagonists of the α-amino-3-hydroxy-5-methylisoxazole-4-propionic acid (AMPA)-type glutamate receptor (Glowatzki, E. and Fuchs, P. A., 2002; Keen, E. C. and Hudspeth, A. J., 2006; Holt, J. C. *et al.*, 2006). The calcium-controlled release of glutamate into the synaptic cleft is quantal, involving exocytosis from SVs that fuse with the plasmalemma and are later retrieved for reuse.

3.22.5.1 Endocytosis

Various routes for vesicle recycling at chemical synapses have been proposed, including two controversial types of fast, local reuse in which the neurotransmitter leaves the SV through a fusion pore without full collapse of the SV membrane into the plasmalemma. In one of these hypothetical fast recycling routes, named kiss-and-stay, the vesicle remains docked to the AZ where it is presumably refilled with glutamate after discharging its contents. In the other, named kiss-and-run, the vesicle undocks and enters a local recycling pool. Slower recycling pathways involve full fusion of the SV with the plasmalemma, followed by clathrin-dependent endocytosis of vesicles or bulk membrane retrieval and reprocessing of SVs either directly or via an endosomal route (reviewed in Sudhof, T. C., 2004). The extent to which each of these processes contributes to the SV cycle under natural physiological conditions remains unclear.

Recent work in the cochlea showed that IHCs may be able to draw upon the vast supply of preformed vesicles present throughout the cytoplasm, and thus may not have to rely on endocytic routes for replenishment of releasable SVs for even the longest stimuli used in many experiments (Griesinger, C. B. *et al.*, 2005). For example, a hair cell that contains 1 million vesicles could, in principle, sustain the exocytosis of 10 vesicles per millisecond for 100 s, although is hard to imagine how the hair cell could accommodate the resultant threefold increase in surface area. Clearly, in the long run endocytosis still must keep pace with exocytosis.

3.22.5.2 Vesicle Mobility

The movement of vesicular membrane through the cytoplasm is an essential step in the SV cycle, except for the case of kiss-and-stay. At conventional synapses, the vesicle-associated phosphoproteins, called synapsins, play essential roles in regulating the movement and clustering of SVs (Rosahl, T. *et al.*, 1995). Studies on hippocampal synapses in synapsin knockout mice have shown that synapsins contribute to the SV cycle by maintaining the reserve pool and the RRP at glutamatergic and GABAergic terminals, respectively (Gitler, D. *et al.*, 2004). The synapsins tether SVs to actin filaments in a phosphorylation-dependent manner (for a review, see Hilfiker, S. *et al.*, 1999).

Synapsins are absent at ribbon synapses, supporting the idea that vesicle clustering and mobilization are different in these cells (von Kriegstein, K. *et al.*, 1999). Recent work in retinal bipolar cells utilized EM, confocal microscopy, and total internal reflection microscopy to demonstrate that cytoplasmic vesicle movement is rapid, random, and not altered by calcium influx or cytoskeletal interactions (Holt, M. *et al.*, 2004, reviewed in Sterling, P. and Matthews, G., 2005). The authors concluded that SVs 2 are highly mobile in bipolar cells ($D = 1.5 \times 10^{-2}\ \mu m\ s^{-1}$), and that random vesicle movement (i.e., diffusion) is sufficient to account for the translocation of vesicles from the large cytoplasmic pool to release sites.

If baseline spike rates in ANFs are due to fusion of SVs, then the diffusion coefficient reported for SVs in bipolar terminals is far too low to support continuous resupply of release sites at mammalian hair cell synapses that sustain SRs of >100 Hz unless some additional mechanism exists to concentrate vesicles in the vicinity of the synapse. Even assuming that diffusion is used only to transport vesicles to the SB, whereupon they are instantly transported to release sites by some other means, and ignoring the

plasmalemma and other barriers that restrict diffusional access to the SB, the maximum steady-state rate at which vesicles can reach the SB by diffusion is

$$F = 4\pi DRC$$

where C is the global concentration of vesicles in the volume. Substituting $D = 1.5 \times 10^{-2}\,\mu m^2\,s^{-1}$, $F = 100\,s^{-1}$, and $R = 100\,nm$, and solving for C yields $C = 5000$ vesicles μm^3, which is more than 50 times the density reported in the nonsynaptic regions of hair cells. This calculation shows that the average concentration of SVs throughout the cytoplasm is too low to continuously supply the SB with vesicles by diffusion unless some additional process operates to maintain the locally high concentration of SVs within a few hundred nanometers of the SB (Lenzi, D. *et al.*, 1999; 2002).

Experiments like these, combined with the observed presence of synaptic ribbons in cell types that support continuous exocytosis have led to the view that the structural and molecular specializations of ribbon synapses assist high rates of sustained vesicle supply to AZs, but crucial questions remain unanswered. For example, data for the refilling of the RRP by vesicles on the SB are indirect; it is still unknown whether or not vesicles actually move on the ribbon.

3.22.5.3 Docking and Priming

In addition to translocation to the AZ, other things must occur before a vesicle is ready for exocytosis. Two important but relatively poorly understood steps are called docking and priming, each of which likely embodies a series of associated events. Docking refers to the placement of a SV in contact with the inner leaflet of the plasma membrane whereas priming refers to the molecular reactions, some ATP-dependent, required to make a vesicle immediately ready for fusion upon calcium influx. It is unclear whether a vesicle must first be docked in order to be primed.

For clues to the relationship between fast exocytosis and docking/priming at ribbon synapses, we look to experimental evidence from retinal bipolar cells. Here the ribbon is plate-like and the anatomical picture of rows of vesicles tethered to both sides of the ribbon led to the model in which the vesicles move along the ribbon to docking sites. One hypothesis is that during a 100 ms strong depolarization all vesicles on the ribbon are depleted via exocytosis. Assuming that this exocytosis requires movement of vesicles along the ribbon to the plasmalemma, several lines of evidence argue against the involvement of ATP-dependent, kinesin-mediated translocation of vesicles to the plasmalemma (Heidelberger, R. *et al.*, 2002). This observation led to the alternative hypothesis that SVs on the ribbon can fuse with each other (reviewed in Parsons, T. D. and Sterling, P., 2003), creating chains that extend to the plasmalemma. This mechanism can account for the large EPSCs recorded postsynaptically at hair cell synapses (see Section 3.22.6.3), and implies that vesicles on the ribbon can be primed and fuse with each other. However the protein Munc13-1, thought to be necessary for priming (Rosenmund, C. *et al.*, 2003), was found to cluster with calcium channels at the plasma membrane and not on the ribbon (tom Dieck, S. *et al.*, 2005), implying that the final priming steps must take place near the membrane.

3.22.5.4 Transmitter Release and Clearance

Glutamate released into the synaptic cleft binds to postsynaptic AMPA receptors (Ruel, J. *et al.*, 2000; Glowatzki, E. and Fuchs, P. A., 2002; Keen, E. C. and Hudspeth, A. J., 2006), causing a depolarization of the postsynaptic membrane and, if the depolarization is sufficient, one or more action potentials. *N*-Methyl-D-aspartate (NMDA) receptor antagonist had no effect on ANF activity, suggesting that they are functionally absent. The pattern of spikes depends on the temporal pattern of neurotransmitter release, the kinetics of AMPA receptor activation, stochastic spike generation, and neuronal refractoriness. Most *in vivo* studies have focused on the firing properties of ANFs in response to pure tones of varying intensities.

If quantal release of neurotransmitter is to accurately reflect the temporal pattern of the sound stimulus, then the chemical signal in the synaptic cleft must rapidly be terminated, which involves uptake of glutamate from the synaptic cleft by excitatory amino acid transporters (e.g., GLAST) in surrounding supporting cells and afferents (Furness, D. N. and Lehre, K. P., 1997; Furness, D. N. and Lawton, D. M., 2003). Voltage-clamp recordings from inner phalangeal cells in the cochlea of normal rats and GLAST knockout mice showed the presence and absence, respectively, of currents produced by these transporters (Hakuba, N. *et al.*, 2000). Normal glutamate reuptake from the synaptic cleft is also thought to be important for the prevention of noise-induced damage to afferent terminals, which can be mimicked by GLAST blockers (Hakuba, N. *et al.*, 2000; Rebillard, G. *et al.*, 2003) and prevented by AMPA receptor blockers.

3.22.5.5 Relating Anatomical and Functional Vesicle Pools

The hair cell's compact shape has proved fortuitous for experimental measurements of synaptic exocytosis by observing the increase in electrical capacitance associated with the increased cell surface that occurs when SVs fuse with the plasmalemma (Figures 6(a)–6(d); Lindau, M. and Neher, E., 1988; reviewed in Nouvian, R. *et al.*, 2006). Because the surface area of a single SV can be estimated, capacitance changes can be translated into numbers of SVs exocytosed, although given the uncertainties in SV diameter and specific membrane capacitance, such calculations are probably only accurate to within a factor of two. These functionally derived SV counts can be compared to numbers obtained with anatomical studies at the EM level in order to test hypotheses about the relationships between the structure and the function of SV pools. The reliability of this technique in accurately monitoring the release of neurotransmitter has been verified by combining capacitance

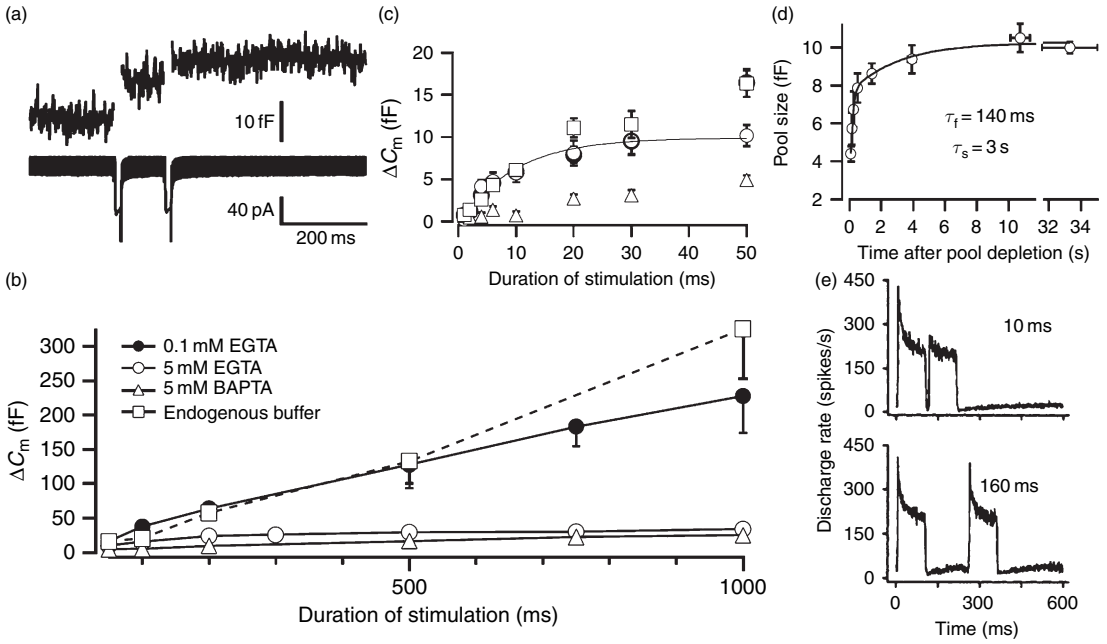

Figure 6 Exocytosis from inner hair cells, recovery from synaptic vesicle pool depletion, and adaptation/disadaptation of auditory nerve fiber responses. (a) Plasma membrane capacitance changes (upper) caused by depolarization-induced synaptic vesicle exocytosis that depends on calcium influx (lower). Two 15 ms depolarizations to the peak of the IV curve for calcium (−15 mV) were separated by 100 ms. Although the calcium currents evoked by the paired pulses were the same, the exocytic response to the first pulse was greater than the response to the second pulse (secretory depression). (b, c) The amplitude of stimulus-evoked capacitance changes is plotted as a function of the duration of the depolarization for different intracellular calcium-buffering conditions. (c) The first 50 ms of (b) at higher temporal resolution. With the cell's endogenous buffer present, the readily releasable pool (RRP) is depleted within the first 10 ms, after which exocytosis continues at a slower rate that is sustained for at least 1 s. The slow calcium buffer (EGTA) of 5 mM abolishes the sustained release while leaving exocytosis of the RRP intact. The fast calcium buffer (BAPTA) of 5 mM inhibits both fast exocytosis of the RRP and the slower component of exocytosis. (d) Strong depolarizations sufficient to deplete the RRP were followed by a second identical stimulus with varying interstimulus intervals as indicated on the *x*-axis. Recovery of the RRP as a function of time after pool depletion has both rapid and slow components. (e) Auditory nerve fiber spike rate *in vivo* as a function of time after sound onset. The sound is interrupted by 10 ms (upper) or 160 ms (lower). During a sound presentation, the spike rate is initially very high followed by two phases of fast reduction in firing rate called rapid and short-term adaptation, with time courses of about 10 and 100 ms, respectively. The 10 ms interruption (upper) is not enough for recovery from rapid adaptation of the spike rate whereas the 160 ms interruption (lower) is sufficient for nearly complete recovery of the initial spike rate. Note the depression of baseline rate and its recovery after sound offset. Panels (a)–(d) are for the mouse: Reproduced with permission from, Copyright (2000) National Academy of Sciences, U. S. A., Moser, T. and Beutner, D., Kinetics of exocytosis and endocytosis at the cochlear inner hair cell afferent synapsis of the mouse. Proc. Natl. Acad. Sci. U S A 97, 883–888. Panel (e) is from the chick: JARO, Vol. 5, 2004, Evidence that rapid vesicle replenishment of the synaptic ribbon mediates recovery from short-term adaptation at the hair cell afferent synapse, Spassova, M. A., Avissar, M., Furman, A. C., Crumling M. A., Saunders, J. C., and Parsons, T. D., Copyright Springer, with kind permission of Springer Science and Buisness Media.

measurements with simultaneous detection of glutamate release in bipolar cells of the vertebrate retina (von Gersdorff, H. *et al.*, 1998).

To estimate the size of the RRP in hair cells, synaptic transmission is first inhibited by hyperpolarization (to fill vesicle pools), then a depolarizing voltage stimulus that maximally stimulates exocytosis is delivered, and the ensuing capacitance increase is observed (Figures 6(b) and 6(c); reviewed in Fuchs, P. A. *et al.*, 2003). Pairs of brief strong depolarizations that evoke maximal calcium currents typically cause paired-pulse depression (Figures 6(a) and 6(d)), implying that the first stimulus partially or totally depletes the RRP, which is refilled more slowly. The size of the RRP can also be measured by applying strong continuous depolarizations of various durations, which evoke continuous calcium currents from the L-type calcium channels at ribbon synapses. Exocytosis of the RRP is seen as an initial rapid increase in capacitance that lasts only a few milliseconds before giving way to a sustained secretory component (SSC) that lasts for seconds (Figure 6(b); Moser, T. and Beutner, D., 2000; Spassova, M. A. *et al.*, 2004; Rutherford, M. A. and Roberts, W. M., 2006). Generally, the size of the RRP measured by change in capacitance is in good agreement with the size of the docked SV pool, as measured by EM, and is smaller than the pool of vesicles on the SB. The presence of a SB and the size of the RRP are both important for normal ANF responses (Khimich, D. *et al.*, 2005; see also Section 3.22.7.2).

The density of vesicles on the SB and in the cytoplasm surrounding the AZ is sensitive to the physiological state of the hair cell before and during fixation (Lenzi, D. *et al.*, 2002). In frog saccular hair cells, prolonged depolarization by high extracellular potassium reduces the density of vesicles on the SB from 79% to 42% of 3D dense-packed, with the greatest reduction occurring in the number of docked SVs in the narrow space between the SB and the plasmalemma. Fixation under resting conditions yielded intermediate values (Lenzi, D. *et al.*, 2002). Whole-cell measurements of SV exocytosis support the notion that all of the docked, SB-associated vesicles can fuse with the plasmalemma within 10 ms (Rutherford, M. A. and Roberts, W. M., 2006). Vesicles in the cytoplasm that are not attached to the SB are also massively depleted by prolonged depolarization (from 10% to 2% of 3D dense-packed in reconstructed volumes within 800 nm perpendicular to the plasmalemma; Figure 4).

Exocytosis of the SSC is slow compared to the RRP (but still a fast resupply rate of hundreds of vesicles per second per AZ), and may indicate the rate at which the RRP is replenished from a recycling pool in the presence of a continuing calcium influx. Dialyzing the cell with the calcium buffer EGTA to inhibit the spread of free calcium away from the AZ (Figures 6(b) and 6(c)) blocked the SSC but not the initial exocytic burst from the RRP (Spassova, M. A. *et al.*, 2004; Moser, T. and Beutner, D., 2000), which suggests that refilling of the RRP is stimulated by long-distance calcium signaling that can be blocked by a slow calcium buffer. Exocytosis of the RRP was inhibited only with the fast calcium buffer BAPTA, as is expected for the case of tight spatial coupling between the release-ready vesicles and the calcium channels (i.e., the RRP docked at the AZ). At present, it is unknown whether the SSC involves vesicles on the SB, other cytoplasmic vesicles that move to the AZ, or possibly even vesicles that are not located at AZs. Experiments that combine capacitance measurements with other techniques to monitor the flow of membrane through the SV cycle will be required to answer such questions.

3.22.6 Physiology of the Hair Cell Afferent Synapse

Precise encoding at the first synapse in the auditory system is absolutely critical for the complete range of behavioral interactions with the acoustic world. To produce a neural representation of the acoustic environment in the CNS, the mammalian cochlea first decomposes complex stimuli into separate frequency components, each of which has an amplitude and a phase. The simplest statement that can be made about sensory encoding in the mammalian cochlea is that the amplitude of the sound at a given frequency is encoded by the spike rate in the ANFs of corresponding CF, while phase and other temporal patterns (e.g., amplitude modulations) are specified by the timing of ANF spikes. Decades of work have produced a wealth of detail about sensory encoding in the auditory system, but much remains to be discovered. The following will barely scratch the surface of what is known. For additional information, the mechanisms underlying the temporal precision of sound coding at the IHC ribbon synapse have been recently reviewed (Moser, T. *et al.*, 2006b).

3.22.6.1 Encoding of Phase

For low-frequency sinusoidal (tonal) stimuli, action potentials in ANFs occur within a narrow time window relative to each cycle of the sinusoid (Anderson, D. J. *et al*., 1970). The discharge of the ANF is said to be phase-locked to the stimulus (Rose, J. E. *et al*., 1967). Phase locking has been observed experimentally in the auditory pathways of mammals, birds, reptiles, amphibians, and fish, and is thought to be an important mechanism for the temporal encoding of low-frequency sound. For example, phase differences between the two ears provide important binaural cues for localizing sounds horizontally (Knudsen, E. I. and Konishi, M., 1978; see Chapter Encoding of Interaural Timing for Binaural Hearing).

Phase locking declines as frequency increases until action potentials in the auditory nerve become nearly random with respect to the stimulus period. The frequency where this transition occurs in the cochlear nerve is generally between 1 and 4 kHz, but it varies among species and even within an individual cochlea. In part, the decline of phase locking with increasing frequency can be attributed to the low-pass filtering of the AC component of the receptor potential by the hair cell membrane (Figure 7). When intracellular receptor potentials were recorded *in vivo* from a guinea-pig cochlear IHC, the receptor potential was quasisinusoidal with the periodicity of the stimulus for low-frequency tones (Palmer, A. R. and Russell, I. J., 1986; Cheatham, M. A. and Dallos, P., 1993). The AC (periodic) component of the receptor potential began to decline at 600 Hz and was not detectable above 3.5 kHz, leaving only a DC (steady) depolarization (Figures 7(a) and 7(b)). The diminution of the presynaptic AC component was mirrored by a decline in postsynaptic phase locking (Figure 7(c)).

Recordings of spike trains in the saccular branch of the eighth nerve in frogs have shown that vibrations at frequencies $\leq$50 Hz evoke a single, phase-locked spike for each cycle of the stimulus (Koyama, H. *et al*., 1982; Christensen-Dalsgaard, J. and Narins P. M., 1993). When expressed as spikes per second, the response thus decreases in proportion to frequency below 50 Hz. Because for low frequencies the depolarizing phase of the hair cell receptor potential may be

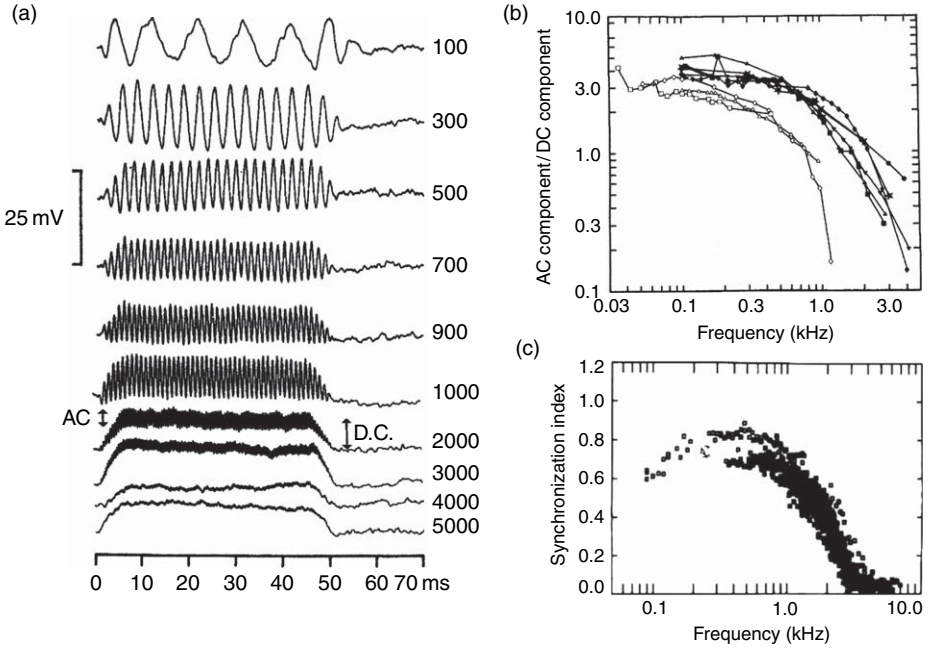

Figure 7 The relationship between receptor potentials in inner hair cells (IHCs) and phase locking in auditory nerve fibers. (a) Intracellular recordings of receptor potentials in one IHC of the guinea-pig cochlea in response to loud (80 dB sound pressure level) tones at the frequency (Hz) indicated by the right side of each trace. The receptor potential has an oscillatory (AC) component and a steady-state (DC) component. The AC component dominates at low frequencies but is almost absent above 3000 Hz. (b) The ratio of AC to DC component across frequency for the receptor potentials from nine different IHCs. (c) The synchronization index (a measure of phase locking to the tonal stimulus) plotted as a function of tone frequency. (Reprinted from Palmer, A. R. and Russell, I. J. 1986. Phase-locking in the cochlear nerve of the guinea-pig and its relation to the receptor potential of inner hair-cells. Hear Res. 24, 1–15, with permission from Elsevier.)

relatively long (e.g., 5 ms for 100 Hz) compared to the duration required for fusion of a single vesicle, the synapse could generate a single spike per cycle if synaptic exocytosis occurred primarily within a narrow time window in response to the onset of each depolarizing phase of a periodic stimulus, and was subsequently suppressed until the next depolarization. This possibility was tested using capacitance measurements as the assay of SV exocytosis (Rutherford, M. A. and Roberts, W. M., 2006). A 30 ms depolarization to −55 mV was interrupted with a return to −80 mV, thus creating a pair of 10 ms depolarizations separated by 10 ms. If the synapse responds primarily to stimulus onset, then the response to the interrupted depolarization is expected be twice the response to a maintained 30 ms depolarization, even though the interposed hyperpolarization reduces the total calcium influx. The total capacitance change in response to the interrupted stimulus was nearly twice as large as the response to the sustained depolarization. The result may reflect the mechanism by which hair cell limits the ANF discharge to a single phase-locked spike per stimulus cycle at low frequencies.

3.22.6.2 Encoding of Frequency

In general, all ANFs phase lock to low frequencies, regardless of their CF. Therefore, the timing of ANF spikes can provide information about the frequency of a low-frequency sound independent of the fiber's CF (Figure 2). For frequencies above 3–4 kHz, the alternative to temporal coding is place-rate coding (Javel, E. and Mott, J. B., 1988), which does not rely upon the temporal (fine timing) pattern of spikes to communicate frequency. In the case of the mammalian cochlea, which performs exquisite mechanical tuning, frequency can be determined from peaks in action potential rates in ANFs that innervate specific CF regions (labeled lines) in the organ of Corti. Therefore, an increase in the mean firing rate of an ANF that originates from a particular place in the organ of Corti is a mechanism for specifying frequency to the brain. Auditory nuclei in the brain stem may use different decoding algorithms for different frequency ranges in order to interpret firing patterns of the auditory nerve.

3.22.6.3 Baseline and Evoked Synaptic Activity

Whole-cell recordings from postsynaptic afferent terminals demonstrated EPSCs (Figure 8) resulting from baseline and evoked SV exocytosis from rat IHCs (Glowatzki, E. and Fuchs, P. A., 2002) and from hair cells of the frog amphibian papilla (Keen, E. C. and Hudspeth, A. J., 2006). In both cases, EPSCs were fast (1–2 ms for the rat, 2–3 ms for the frog) with very rapid onset and exponential decay. Sensitivity to AMPA receptor antagonists provided a functional confirmation of previous *in vivo* and EM studies (Matsubara, A. *et al.*, 1996), showing that the glutamatergic receptor subunits GluR2/3 and 4 are present.

The amplitude distribution of EPSCs recorded under baseline conditions (i.e., extracellular saline with normal concentration of potassium) showed ∼20-fold variation in the rat and ∼10-fold variation in the frog with mean sizes of 190 and 100 pA, respectively (Figure 8). This is remarkable considering that spontaneous glutamatergic EPSCs recorded elsewhere in the CNS are distributed normally with much smaller variation around a quantal size of 20–40 pA.

Presynaptic depolarization via paired whole-cell recordings in the frog, and by perfusion with high-potassium saline in the rat, greatly increased the EPSC rate (Figure 8(a)) while the amplitude distribution remained relatively unchanged (Figures 8(d) and 8(e)). In both preparations, individual small events (miniature EPSCs) were observed, but the amplitude distributions were skewed to larger events for both baseline and evoked EPSCs. For example, in the rat the peak in the amplitude distribution changed from about 18 pA in 5.8 mM potassium (baseline, Figure 8(d), left) to about 36 pA in 40 mM potassium (evoked, Figure 8(e), left), as the mean rate changed from about 1.5 to 27 events per second. Interestingly, the mean EPSC size was slightly less for evoked EPSCs, perhaps due to SV depletion with the sharp increase in EPSC frequency. Combined with the positive shift in the peak of the amplitude distribution, this results in a tightening of the EPSC amplitude distribution (e.g., smaller interquartile range), although the total range remains unchanged (cf. Figures 8(d) and 8(e), left). In both frog and rat hair cells, the larger EPSCs were sometimes multiphasic, but the durations of the larger monophasic events were not appreciably longer than the smaller monophasic events (Figure 8(b), frog; Figures 8(c)–8(e), rat), which suggests that if the large EPSCs are due to the fusion of several SVs, then these fusion events are highly synchronized (reviewed in Parsons, T. D. and Sterling, P., 2003; Singer, J. H. *et al.*, 2004). Two possible mechanisms might explain such multiquantal events. One possibility is that the opening of

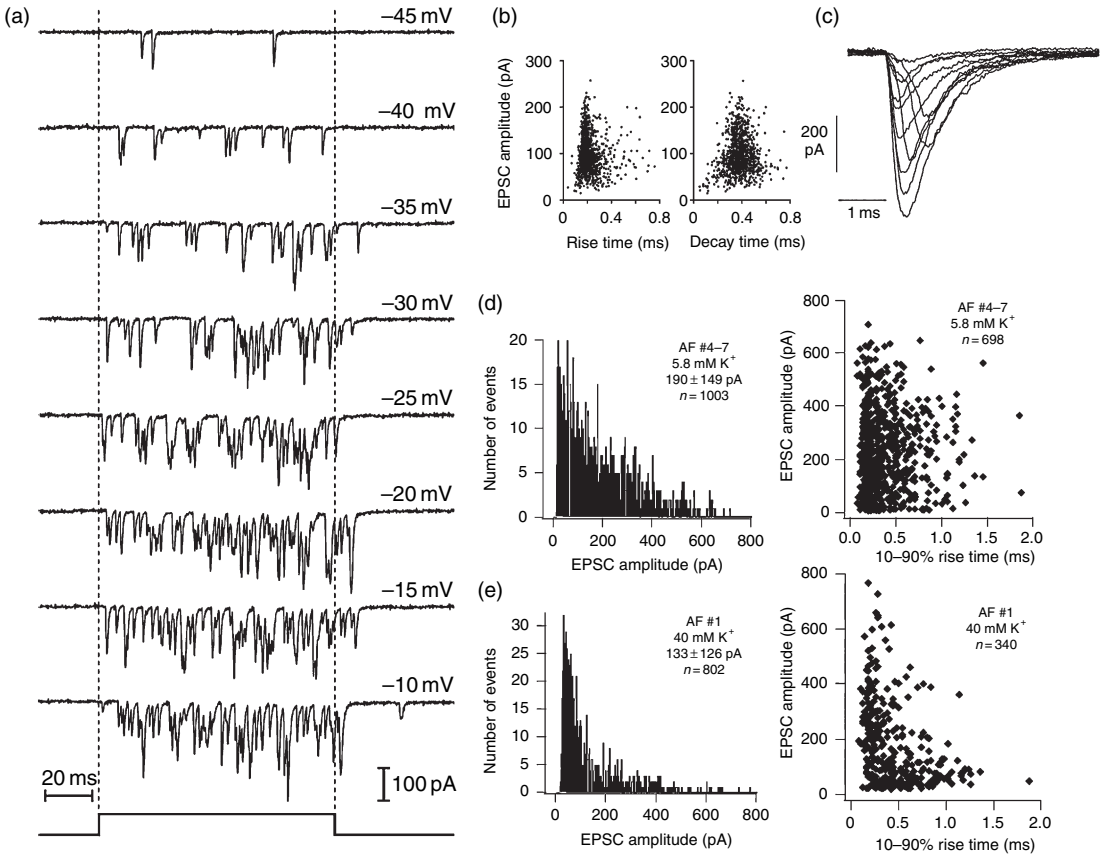

Figure 8 Excitatory postsynaptic currents (EPSCs) in afferent fibers indicate the size and frequency of glutamate release from hair cells. (a) EPSCs recorded in afferent fibers of the frog amphibian papilla while the presynaptic hair cell was depolarized to the voltages indicated at the right of each trace. The predominant effect of depolarization was an increase in EPSC frequency, with little change in EPSC amplitudes. (b) The rise and decay times for baseline EPSCs (frog) are tightly distributed despite a wide range of amplitudes. (c) EPSCs evoked from rat cochlear afferent fibers in response to inner hair cell depolarization by 40 mM extracellular potassium, aligned in time, exhibit a large range in the amplitude of monophasic events. (d, e) Left: EPSC amplitude distributions from rat afferent fibers show the number of events observed in each amplitude bin along the *x*-axis. Baseline EPSC amplitudes from four afferents are shown in (d), evoked EPSC amplitudes from one afferent in (e). The distributions are positively skewed, suggestive of multivesicular release events from individual hair cell active zones. The range of baseline EPSC amplitudes observed in a normal concentration of extracellular potassium (5.8 mM) spans the entire range of EPSC amplitudes evoked by depolarization in high potassium (see text). Mean amplitudes were 190 pA (baseline) and 133 pA (evoked). Right: The relationship between EPSC amplitude and 10–90% rise time is very similar for baseline (d) and evoked (e) events. (a, b) Reproduced from Keen, E. C. and Hudspeth, A. J. 2006. Transfer characteristics of the hair cell's afferent synapse. Proc. Natl. Acad. Sci. U. S. A. 103, 5537–5542; Copyright (2006) National Academy of Sciences, U. S. A. (c–e) Glowatzki, E. and Fuchs, P. A., 2002. Transmitter release at the hair cell ribbon synapse. Nat. Neurosci. 5, 147–154; Copyright (2002) Nature Publishing Group.

a single presynaptic calcium channel, or a few channels that happen to be close together, triggers the synchronized fusion of several nearby vesicles. Another is that several vesicles undergo nonsynchronous fusion with each other, but their contents are not released until one of them fuses with the plasmalemma.

When spikes are present in intracellular recordings from ANFs, the peak EPSP amplitude is obliterated by the action potential that it triggers, but the slope of the initial rise can be used instead to measure the EPSP size. *In vivo* recordings from afferent units in the guinea-pig cochlea demonstrated a range of EPSP slopes (Siegel, J. H., 1992). Similar to the EPSCs recorded *in vitro* and discussed above, the distribution of EPSP slopes was positively skewed, suggesting the existence of synchronous multiquantal release events. Interestingly, nearly all EPSPs that did not occur during neural refractory periods triggered action potentials.

What then is the consequence of multivesicular release to synaptic function? One possibility is that large EPSCs trigger action potentials with less temporal jitter (Anderson, D. J. *et al.*, 1970; reviewed in Fuchs, P. A., 2005), but this leaves open the question of whether there is some value in having a large variance in EPSP amplitude rather than all being equally large. An intriguing possibility has to do with the role of efferent innervation on the input resistance of afferent terminals. The terminal bouton of a type I afferent is typically postsynaptic to both an IHC and an efferent axon (see Chapter Efferent System). Spikes in the efferent axon release transmitter that opens postsynaptic channels, thereby reducing the input resistance of the afferent terminal. The effect of efferent activity may therefore be to reduce the size of the EPSP produced by a given EPSC. Since efferent activity increases in loud environments, the effect may be to render small EPSCs from the hair cell unable to trigger ANF spikes in loud environments. In this case, the wide distribution of EPSC amplitudes associated with multiquantal events may be important for efferent control of ANF firing rate. Similarly, efferent innervation directly onto hair cells is proposed to evoke inhibitory conductances in hair cells during strong stimuli. The expected effect would be a decrease in hair cell depolarization and calcium influx. Since efferent modulation of synaptic activity is expected to be largely absent from *in vitro* preparations, the effects of such inhibition on the EPSC amplitude and frequency in response to varying presynaptic stimulus levels are unknown.

If large EPSCs are due to the fusion of vesicles with each other on the SB before one of them fuses with the plasmalemma, this could be a mechanism to integrate sound amplitude over many cycles while preserving phase locking of glutamate release to the sound waveform. For this to work, the fusion of SVs with each other on the SB would have to be triggered by the relatively small changes in free calcium that are predicted to occur at distances of tens to hundreds of nanometers from the plasmalemma, whereas the fusion of the resulting multivesicular structure with the cell surface membrane would be phase locked to the large, rapid calcium changes that occur close to the presynaptic calcium channels. In favor of this hypothesis, large irregularly shaped structures that appear to be attached to the SB are seen much more frequently at stimulated synapses than inhibited or resting synapses (Lenzi, D. *et al.*, 1999; 2002, Figure 4). Opposed to this hypothesis, the mean EPSC amplitude did not increase following stimulation (Glowatzki, E. and Fuchs, P. A., 2002; Keen, E. C. and Hudspeth, A. J., 2006).

3.22.6.4 Tuning Mechanisms in Hair Cells

Auditory organs of fish, amphibians, reptiles, and birds all show frequency selectivity resulting from the properties of individual hair cells. These mechanisms are different from the frequency tuning seen in the mammalian cochlea, which is the result of the gradient in stiffness of the basilar membrane (acellular) and active mechanical feedback from hair bundle motion and OHC motility (cellular). Our focus will be on tuning in the other four classes of vertebrate animals.

3.22.6.4.1 Frequency-selective augmentation of membrane potential oscillation

In the turtle auditory papilla, there is no apparent frequency tuning extrinsic to the hair cell (i.e., transduction currents are equal over a broad frequency range). Instead, each cell is intrinsically tuned to a different frequency band by a process that has been called electrical resonance. The resonant frequency is determined primarily by the number and kinetics of the cell's calcium-activated potassium channels, voltage-activated potassium and calcium channels, and electrical capacitance (Ricci, A. J. *et al.*, 2000; and reviewed in Fettiplace, R. and Fuchs, P. A., 1999). Each hair cell preferentially amplifies the receptor potential in a frequency band, with peak amplification near the resonant frequency. The tonotopic axis in this organ is generated by the systematic variation of the hair cells' preferred frequencies along the length of the sensory epithelium. Low-frequency cells have low channel density and slower potassium channel kinetics than high-frequency cells. These variations in channel kinetics are caused by differential expression of potassium channel genes and differential splicing of the mRNAs (Jones, E. M. C. *et al.*, 1999). The result is a continuum of resonant frequencies along the papilla. Similar electrical tuning has been studied in the frog sacculus (Armstrong, C. E. and Roberts, W. M., 1998; 2001) and chick cochlea (Correia, M. J., 1992), but there is no evidence of electrical tuning in the mammalian cochlea.

3.22.6.4.2 Synaptic frequency selectivity

Experiments employing capacitance measurements in hair cells typically use very strong depolarizations

that evoke maximal calcium currents in order to measure vesicle pool sizes by depletion. This approach has been very fruitful for understanding vesicle pools, but the stimuli used for these experiments are much larger than *in vivo* receptor potentials, drawing into question the physiological relevance of the evoked exocytosis. A recent study of frog saccular hair cells (Rutherford, M. A. and Roberts, W. M., 2006) used smaller, sinusoidal fluctuations in membrane potential as the voltage-clamp stimulus to mimic the size and frequency of *in vivo* receptor potentials and looked for frequency selectivity downstream of the known mechanical and electrical tuning mechanisms in these cells. Changes in membrane capacitance were measured in response to small sinusoidal voltage changes (±5 mV centered at −60 mV) delivered at 5, 50, and 200 Hz to test the hypothesis that exocytosis would be largest at 50 Hz, the frequency where the sacculus is most sensitive to airborne and groundborne vibrations. Consistent with this hypothesis, exocytosis was twice as large at 50 Hz than at 5 or 200 Hz, even though the total calcium influx was the same at the three frequencies. This preference for 50 Hz disappeared when stronger sinusoidal stimuli (±10 mV centered at −55 mV) were applied, which is reminiscent of other tuning mechanisms that are saturated by large stimuli (e.g., de Boer, E. and Nuttall, A. L., 2000). It is important to note that the ±5 mV sinusoidal stimulus, while small compared to the stimuli used in most voltage-clamp studies, is well above the amplitude of oscillations that occur at sensory threshold (Dallos, P., 1985). The exocytosis in response to the small stimulus at 50 Hz corresponded to the net fusion of 1.7 SV per AZ per stimulus cycle. This amounts to twice the number of vesicles in the docked pool fusing during the 1 s stimulus, and suggests that new vesicles can dock and be primed for release during the stimulus. This synaptic tuning, operating in series with mechanical and electrical tuning, is expected to contribute to the overall tuning of the sacculus, which has been measured by action potential firing rates and sensitivity in afferent axons of the eighth cranial nerve (Koyama, H. *et al.*, 1982; Lewis, E. R. and Narins, P. M., 1985; Yu, X. *et al.*, 1991; Christensen-Dalsgaard, J. and Narins, P. M., 1993). Similar synaptic tuning could contribute to frequency selectivity at other ribbon synapses, particularly in auditory and vestibular organs where synaptic transmission results in phased-locked action potentials in the postsynaptic neuron.

3.22.7 Auditory Nerve Fiber Firing Patterns Mirror Presynaptic Vesicle Pool Dynamics

Until recently, physiological studies of cochlear output have focused on *in vivo* recordings of spike trains in ANFs in response to sound stimuli (e.g., pure tones of varying SPL). Advances in patch-clamp techniques *in vitro*, such as capacitance measurements as a presynaptic assay of SV exocytosis, have allowed more direct comparisons between presynaptic activity and postsynaptic spike trains.

3.22.7.1 Adaptation of the Auditory Nerve Response

Adaptation of ANF responses is thought to be necessary for the peripheral processing of speech (Delgutte, B., 1980). Two types of fast adaptation have been described to explain the reduction in ANF discharge rate following the onset of a sustained acoustic stimulation (Figure 6(e)). These have been called rapid adaptation and short-term adaptation, with durations of approximately 10 and 20–90 ms, respectively. Although the precise time courses can vary by species, SR of the fiber, and sound intensity; both processes are thought to arise from mechanisms downstream of IHC receptor potential *in vivo*, which is not reduced in amplitude during a sustained stimulus (Russell, I. J. and Sellick, P. M., 1978; Holton, T. and Weiss, T. F., 1983). Fast adaptation is thought to involve presynaptic depression (as described below), but not via inactivation of the presynaptic calcium current which shows no significant decline over this time course under voltage clamp (Parsons, T. D. *et al.*, 1994; Moser, T and Beutner, D., 2000; Schnee, M. E. and Ricci, A. J., 2003; Eisen, M. D. *et al.*, 2004).

Fast adaptation of ANF firing and its subsequent recovery seem to be predominantly due to depletion and refilling of the RRP. Recovery from adaptation takes hundreds of milliseconds (Smith, R. L., 1977; Harris, D. M. and Dallos, P., 1979; Chimento, T. C. and Schreiner, C. E., 1991), and this time course is thought to reflect refilling of the RRP. In the chick, using a combination of *in vivo* single unit recordings of ANF activity and *in vitro* patch-clamp recordings of SV fusion, it was found that sound-evoked ANF activity adapted and recovered with similar time courses as RRP depletion and recovery (Figure 6; Spassova, M. A. *et al.*, 2004). After RRP exhaustion,

its recovery was 95% complete after a 200 ms rest period, similar to the time course of recovery from adaptation. In comparison, analogous recovery in retinal bipolar neurons takes about 100 times longer (20 s; von Gersdorff, H. and Matthews, G., 1997). In the mouse IHC, RRP refilling is biphasic, possibly reflecting the refilling of two functionally distinct types of AZs (Moser, T. and Beutner, D., 2000). Differences among AZs in a single IHC could provide the basis for the variable properties of ANFs (Merchan-Perez, A. and Liberman, M. C., 1996). Indeed high- and low-SR fibers exhibit different times needed for recovery from prior stimuli (Relkin, E. M. and Doucet, J. R., 1991) that are a close match to the biphasic refilling of the RRP (Figure 6(d)).

3.22.7.2 The Role of the Synaptic Body in Auditory Nerve Fiber Spike Timing

Computational attempts at predicting psychophysical performance on auditory tasks based on the activity of ANFs have generally concluded that the probabilistic nature of action potentials (the variability of spike timing during repeated presentations of the same stimulus) limits the precision of acoustic information sent to the brain (Mountain, D. C. and Hubbard, A. E., 1996). Upon repeated presentation of a pure tone, an ANF will fire a first spike with variable latency. The variance of first spike latency in mice with a targeted deletion of the gene for the cytomatrix AZ protein Bassoon was increased by a factor of 12 compared to controls (Buran, B. N. *et al.*, 2006). Bassoon is thought to anchor SBs at AZs by interacting with Ribeye (Khimich, D. *et al.*, 2005; tom Dieck, S. *et al.*, 2005); ultrastructural inspection demonstrated a 90% reduction in the number of SBs anchored at AZs. This work suggests that the presence of SBs at release sites helps to reduce the temporal jitter of ANF discharge, and hence improve phase locking.

In the absence of an applied stimulus, the temporal firing pattern of ANFs *in vivo* is often represented as a poison process, but on a short timescale it is more accurately described as a renewal process that is a function of neurotransmitter concentration in the cleft (presynaptic effect) and neural refractoriness (postsynaptic effect), the combination of which causes the firing probability to be depressed for more than 20 ms following a spike (Gaumond, R. P. *et al.*, 1983). Furukawa and co-workers recorded synaptic potentials from afferent units in the saccular branch of the eighth nerve of the goldfish and observed a 20 ms delay in firing upon a decrement in the intensity of tone. They attributed this delay to the time required for SVs to refill the depleted low-threshold release sites between the SB and the calcium channels at the plasmalemma. Furthermore, quantal analysis of the size of EPSPs showed a negative correlation between the amplitude of two consecutive events (i.e., large EPSPs tend to be followed by smaller ones and vice versa). These data support the idea that adaptive rundown of EPSPs is the result of SV depletion (Furukawa, T. and Matsuura, S., 1978; Furukawa, T. *et al.*, 1978).

Additional evidence for the involvement of the SB in maintenance of the functional RRP comes from the Bassoon mutant mice, in which the first phase of exocytosis and the calcium current are both reduced (Khimich, D. *et al.*, 2005). The large reduction of SB-associated docked SVs at AZs in the mutant provides additional support for the contribution of these docked vesicles to the functional RRP measured in capacitance experiments. The reduced calcium current supports previous evidence that calcium channel expression is coregulated with and restricted spatially to SV release sites adjacent to SBs (Martinez-Dunst, C. *et al.*, 1997; Zenisek, D. *et al.*, 2003). Intriguingly, the sustained component of the capacitance rise was relatively intact in the mutant mice compared to the 50% reduction in ANF discharge rate after short-term adaptation to tonal stimuli (Buran, B. N. *et al.*, 2006). One interpretation is that the sustained component in the mutant mice is relatively asynchronous or not properly localized to postsynaptic fibers. In contrast, the sustained exocytosis in wild-type mice is likely to reflect synaptic release as indicated by the massive sustained release measure by EPSCs in high potassium and higher levels of sustained ANF discharge rate *in vivo*. The sound-evoked onset firing rate (before adaptation) and steady-state firing rate (after fast adaptation) were decreased and threshold was increased, in accordance with the reduction of the functional RRP measured presynaptically. In spite of this, the shapes of rate-level functions were normal in the mutants. Indeed a recent modeling study showed that the effect of increasing the maximum number of transmitter quanta held in the immediate store (analogous to the concept of increasing the size of the RRP) is to scale the release rate linearly across the entire dynamic range (Sumner, C. J. *et al.*, 2002).

Work with the Bassoon mutant mouse has shown that the localization of synaptic ribbons to hair cell

AZs is required for transmitter release to be precisely synchronized to the onset of sound at each AZ, which is required for synchronous auditory signaling carried to the brain stem (Khimich, D. *et al*., 2005; Buran, B. N. *et al*., 2006). If simultaneously activated fibers provide input to a single neuron in the cochlear nucleus, then converging synaptic inputs arriving closely in time could be the physiological basis for a coincidence detector to differentiate between baseline activity and stimulus-evoked (synchronous) hair cell afferent synaptic activity. It seems probable that the precise configurations of SBs and their associated cytomatrices at AZs are important for establishing both the sensitivity and the phase relationship of ANF spikes to the sound.

3.22.8 Synapse to Psychophysics

One of the goals of auditory research is to provide an explanation of the behavior of the auditory system based upon the functions of its cellular components and the circuits they make. For example, numerous experiments have examined the ability of the auditory system to detect weak sounds. These experiments have been carried at the level of ANFs, cortical neurons, and behavior, in a variety of mammals, including humans. Recently it has been proposed that the inverse relationship between the duration and the SPL needed to attain a threshold criterion for detection seen at all levels of auditory processing can be explained by the properties of hair cell afferent synapses. One interpretation of these results is that the statistics of individual events, which may correspond to the exocytosis of individual SVs at the afferent synapse, underlies the trade-off between strength and duration for barely detectable sounds (Heil, P. and Neubauer, H., 2003) that is measured in psychophysical experiments of sound perception.

References

Achanzar, W. E. and Ward, S. 1997. A nematode gene required for sperm vesicle fusion. J. Cell Sci. 110, 1073–1081.

Anderson, D. J., Rose, J. E., Hind, J. E., and Brugge, J. F. 1970. Temporal position of discharges in single auditory nerve fibers within the cycle of a sine-wave stimulus: frequency and intensity effects. J. Acoust. Soc. Am. 49, 1131–1139.

Armstrong, C. E. and Roberts, W. M. 1998. Electrical properties of frog saccular hair cells: distortion by enzymatic dissociation. J. Neurosci. 18, 2962–2973.

Armstrong, C. E. and Roberts, W. M. 2001. Rapidly inactivating and non-inactivating calcium-activated potassium currents in frog saccular hair cells. J. Physiol. 536, 49–65.

Art, J. J. and Fettiplace, R. 1987. Variation of membrane properties in hair cells isolated from the turtle cochlea. J. Physiol. 385, 207–242.

Art, J. J., Wu, Y. C., and Fettiplace, R. 1995. The calcium-activated potassium channels of turtle hair cells. J. Gen. Physiol. 105, 49–72.

Balkema, G. W. 1991. A synaptic antigen (B16) is localized in retinal synaptic ribbons. J. Comp. Neurol. 312, 573–583.

Bodian, D. 1980. Presynaptic bodies of auditory hair cells in old world monkeys. Anat. Rec. 197, 379–386.

Bracewell, R. N. 1999. The Fourier Transform and Its Applications. McGraw-Hill Co.

Brandt, A., Khimich, D., and Moser, T. 2005. Few Cav1.3 channels regulate the exocytosis of a synaptic vesicle at the hair cell ribbon synapse. J. Neurosci. 25, 11577–11585.

Brandt, A., Striessng, J., and Moser, T. 2003. CaV1.3 channels are essential for development and presynaptic activity of cochlear inner hair cells. J. Neurosci. 23, 10832–10840.

Bunt, A. H. 1971. Enzymatic digestion of synaptic ribbons in amphibian retinal photoreceptors. Brain Res. 25, 571–577.

Burack, M. A., Silverman, M. A., and Banker, G. 2000. The role of selective transport in neuronal protein sorting. Neuron 26, 465–474.

Buran, B. N., Moser, T., Gundelfinger, E. D., and Liberman, M. C. 2006. Role of synaptic ribbons in auditory nerve responses in mice lacking the synaptic scaffolding protein Bassoon. Assoc. Res. Otolaryngol (ARO) Poster, 2006, Baltimore.

Cheatham, M. A. and Dallos, P. 1993. Longitudinal comparisons of IHC ac and dc receptor potentials recorded from the guinea pig cochlea. Hear Res. 68, 107–114.

Chen, X., Tomchick, D. R., Kovrigin, E., Arac, D., Machius, M., Sudhof, T. C., and Rizo, J. 2002. Three-dimensional structure of the complexin/SNARE complex. Neuron 33, 397–409.

Chimento, T. C. and Schreiner, C. E. 1991. Adaptation and recovery from adaptation in single fiber responses of the cat auditory nerve. J. Acoust. Soc. Am. 90, 263–273.

Chinnadurai, G. 2002. CtBP family proteins: more than transcriptional corepressors. Bioessays 25, 9–12.

Christensen-Dalsgaard, J. and Narins, P. M. 1993. Sound and vibration sensitivity of VIIIth nerve fibers in the frogs *Leptodactylus albilabris* and *Rana pipiens pipiens*. J. Comp. Physiol. A 172, 653–662.

Correia, M. J. 1992. Filtering properties of hair cells. Ann. N. Y. Acad. Sci. 656, 49–57.

Dallos, P. 1985. Response characteristics of mammalian cochlear hair cells. J. Neurosci. 5, 1591–1608.

Dambly-Chaudiere, C., Sapede, D., Soubiran, F., Decorde, K., Gompel, N., and Ghysen, A. 2003. The lateral line of zebrafish: a model system for the analysis of morphogenesis and neural development in vertebrates. Biol. Cell 95, 579–587.

Dargan, S. L. and Parker, I. 2003. Buffer kinetics shape the spatiotemporal patterns of IP3 evoked Ca^{2+} signals. J. Physiol. 553, 775–788.

de Boer, E. and Nuttall, A. L. 2000. The mechanical waveform of the basilar membrane. III. Intensity effects. J. Acoust. Soc. Am. 107, 1497–1507.

Delcomyn, F. 1998. Foundations of Neurobiology. W. H. Freeman.

Delgutte, B. 1980. Representation of speech-like sounds in the discharge patterns of auditory-verve fibers. J. Acoust. Soc. Am. 68, 843–857.

tom Dieck, S., Altrock, W. D., Kessels, M. M., Qualmann, B., Regus, H., Brauner, D., Fejtova, A., Bracko, O.,

Gundelfinger, E. D., and Brandstatter, J. H. 2005. Molecular dissection of the photoreceptor ribbon synapse: physical interaction of Bassoon and Ribeye is essential for the assembly of the ribbon complex. J. Cell Biol. 168, 825–836.

Dobrunz, L. E. and Stevens, C. F. 1997. Heterogeneity of release probability, facilitation, and depletion at central synapses. Neuron 18, 995–1008.

Edmonds, B. W., Gregory, F. D., and Schweizer, F. E. 2004. Evidence that fast exocytosis can be predominantly mediated by vesicles not docked at active zones in frog saccular hair cells. J. Physiol. 560, 439–450.

Edmonds, B., Reyes, R., Schwaller, B., and Roberts, W. M. 2000. Calretinin modifies presynaptic calcium signaling in frog saccular hair cells. Nat. Neurosci. 3, 786–790.

Eisen, M. D., Spassova, M., and Parsons, T. D. 2004. Large releasable pool of synaptic vesicles in chick cochlear hair cells. J. Neurophysiol. 91, 2422–2428.

Fettiplace, R. and Fuchs, P. A. 1999. Mechanisms of hair cell tuning. Annu. Rev. Physiol. 61, 809–834.

Fuchs, P. A. 2005. Time and intensity coding at the hair cell's ribbon synapse. J. Physiol. 566, 7–12.

Fuchs, P. A., Glowatzki, E., and Moser, T. 2003. The afferent synapse of cochlear hair cells. Curr. Opin. Neurobiol. 13, 452–458.

Furness, D. N. and Lawton, D. M. 2003. Comparative distribution of glutamate transporters and receptors in relation to afferent innervation density in the mammalian cochlea. J. Neurosci. 23, 11296–11304.

Furness, D. N. and Lehre, K. P. 1997. Immunocytochemical localization of a high-affinity glutamate-aspartate transporter, GLAST, in the rat and guinea-pig cochlea. Eur. J. Neurosci. 9, 1961–1969.

Furukawa, T. and Matsuura, S. 1978. Adaptive rundown of excitatory post-synaptic potentials at synapses between hair cells and eighth nerve fibers in the goldfish. J. Physiol. 276, 193–209.

Furukawa, T., Hayashida, Y., and Matsuura, S. 1978. Quantal analysis of the size of excitatory post-synaptic potentials at synapses between hair cells and afferent nerve fibers in the goldfish. J. Physiol. 276, 211–226.

Furukawa, T., Kuno, M., and Matsuura, S. 1982. Quantal analysis of a decremental response at hair cell-afferent fibre synapses in the goldfish sacculus. J. Physiol. 322, 181–195.

Gaumond, R. P., Kim, D. O., and Molnar, C. E. 1983. Response of cochlear nerve fibers to brief acoustic stimuli: role of discharge-history effects. J. Acoust. Soc. Am. 74, 1392–1398.

von Gersdorff, H. and Matthews, G. 1997. Depletion and replenishment of vesicle pools at a ribbon-type synaptic terminal. J. Neurosci. 17, 1919–1927.

von Gersdorff, H., Sakaba, T., Berglund, K., and Tachibana, M. 1998. Submillisecond kinetics of glutamate release from a sensory synapse. Neuron 21, 1177–1188.

Giannessi, F. and Ruffoli, R. 1996. Fine structure of the afferent synapses in the paratympanic organ of the chicken, with special reference to the synaptic bodies. Ann. Anat. 178, 127–131.

Gitler, D., Takagishi, Y., Feng, J., Ren, Y., Rodriguiz, R. M., Wetsel, W. C., Greengard, P., and Augustine, G. J. 2004. Different presynaptic roles of synapsins at excitatory and inhibitory synapses. J. Neurosci. 24, 11368–11380.

Gleisner, L., Flock, A., and Wersall, J. 1973. The ultrastructure of the afferent synapse on hair cells in the frog labyrinth. Acta Otolaryngol. 76, 199–207.

Glowatzki, E. and Fuchs, P. A. 2002. Transmitter release at the hair cell ribbon synapse. Nat. Neurosci. 5, 147–154.

Goldberg, J. M. 1996. Theoretical analysis of intercellular communication between the vestibular type I hair cell and its calyx ending. J. Neurophysiol. 76, 1942–1957.

Gray, E. G. and Pease, H. L. 1971. On understanding the origins of the retinal receptor synapses. Brain Res. 35, 1–15.

Griesinger, C. B., Richards, C. D., and Ashmore, J. F. 2005. Fast vesicle replenishment allows indefatigable signaling at the first auditory synapse. Nature 435, 212–215.

Hackney, C. M., Mahendrasingam, S., Penn, A., and Fettiplace, R. 2005. The concentrations of calcium buffering proteins in mammalian cochlear hair cells. J. Neurosci. 25, 7867–7886.

Hakuba, N., Koga, K., Gyo, K., Usami, S., and Tanaka, K. 2000. Exacerbation of noise-induced hearing loss in mice lacking the glutamate transporter GLAST. J. Neurosci. 20, 8750–8753.

Hama, K. and Saito, K. 1977. Fine structure of the afferent synapse of the hair cells in the saccular macula of the goldfish, with special reference to the anastomosing tubules. J. Neurocytol. 6, 361–373.

Harris, D. M. and Dallos, P. 1979. Forward masking of auditory nerve fiber responses. J. Neurophysiol. 42, 1083–1107.

Hashimoto, S., Kimura, R. S., and Takasaka, T. 1990. Computer-aided 3-dimensional reconstruction of the inner hair-cells and their nerve-endings in the guinea-pig. Acta Otolaryngol. 109, 228–234.

Heidelberger, R., Sterling, P., and Matthews, G. 2002. Roles of ATP in depletion and replenishment of the releasable pool of synaptic vesicles. J. Neurophysiol. 88, 98–106.

Heil, P. and Neubauer, H. 2001. Temporal integration of sound pressure determines thresholds of auditory nerve fibers. J. Neurosci. 21, 7404–7415.

Heil, P. and Neubauer, H. 2003. A unifying basis of auditory thresholds based on temporal summation. Proc. Natl. Acad. Sci. U. S. A. 100, 6151–6156.

Heller, S., Bell, A. M., Charlotte, S. D., Choe, Y., and Hudspeth, A. J. 2002. Parvalbumin 3 is an abundant Ca^{2+} buffer in hair cells. JARO 3, 488–498.

Hilfiker, S., Pieribone, V. A., Czernik, A. J., Kao, H. T., Augustine, G. J., and Greengard, P. 1999. Synapsins as regulators of neurotransmitter release. Phil. Trans. R Soc. Lond. B 354, 269–279.

Hille, B. 2001. Ionic Channels of Excitable Membranes. Sinauer Associates.

Hirokawa, N., Sobue, K., Kanda, K., Harada, A., and Yorifuji, H. 1989. The cytoskeletal architecture of the presynaptic terminal and molecular structure of synapsin 1. J. Cell Biol. 108, 111–126.

Holt, M., Cooke, A., Neef, A., and Lagnado, L. 2004. High mobility of vesicles supports continuous exocytosis at a ribbon synapse. Curr. Biol. 14, 173–183.

Holt, J. C., Xue, J. T., Brichta, A. M., and Goldberg, J. M. 2006. Transmission between type II hair cells and bouton afferents in the turtle posterior crista. J. Neurophysiol. 95, 428–452.

Holton, T. and Weiss, T. F. 1983. Receptor potentials of lizard cochlear hair cells with free-standing stereocilia in response to tones. J. Physiol. 345, 205–240.

Hossain, W. A., Antic, S. D., Yang, Y., Rasband, M. N., and Morest, D. K. 2005. Where is the spike generator of the cochlear nerve? J. Neurosci. 25, 6857–6868.

Indresano, A. A., Frank, J. E., Middleton, P., and Jaramillo, F. 2004. Mechanical noise enhances signal transmission in the bullfrog sacculus. JARO 4, 363–370.

Issa, N. P. and Hudspeth, A. J. 1994. Clustering of Ca^{2+} channels and Ca^{2+}-activated K^{+} channels at fluorescently labeled presynaptic active zones of hair cells. Proc. Natl. Acad. Sci. U. S. A. 91, 7578–7582.

Jacobs, R. A. and Hudspeth, A. J. 1990. Ultrastructural correlates of mechanoelectrical transduction in hair-cells of the bullfrogs internal ear. Cold Spring Harb. Symp. Quant. Biol. 55, 547–561.

Javel, E. and Mott, J. B. 1988. Physiological and psychophysical correlates of temporal processes in hearing. Hear Res. 34, 275–294.

Jeffress, L. A. 1968. Mathematical and electrical models of auditory detection. J. Acoust. Soc. Am. 44, 187–203.

Johnson, D. H. 1980. The relationship between spike rate and synchrony in responses of auditory-nerve fibers to single tones. J. Acoust. Soc. Am. 68, 1115–1122.

Johnson, D. H. and Kiang, N. Y. S. 1976. Analysis of discharges recorded simultaneously from pairs of auditory nerve fibers. Biophys. J. 16, 719–734.

Johnson, S. L., Marcotti, W., and Kros, C. J. 2005. Increase in efficiency and reduction in Ca^{2+} dependence of exocytosis during development of mouse inner hair cells. J. Physiol. 563, 177–191.

Jones, E. M. C., Gray-Keller, M., and Fettiplace, R. 1999. The role of Ca^{2+}-activated K^+ channel spliced variants in the tonotopic organization of the turtle cochlea. J. Physiol. 518, 653–665.

Kandel, E. R., Schwartz, J. H., and Jessell, T. M. 2000. Principles of Neural Science. McGraw-Hill.

Keen, E. C. and Hudspeth, A. J. 2006. Transfer characteristics of the hair cell's afferent synapse. Proc. Natl. Acad. Sci. U. S. A. 103, 5537–5542.

Khimich, D., Nouvian, R., Pujol, R., tom Dieck, S., Egner, A., Gundelfinger, E. D., and Moser, T. 2005. Hair cell synaptic ribbons are essential for synchronous auditory signalling. Nature 434, 889–894.

Kiang, N. Y. S., Rho, J. M., Northrop, C. C., Liberman, M. C., and Ryugo, D. K. 1982. Hair-cell innervation by spiral ganglion cells in adult cats. Science 217, 175–177.

Kiang, N. Y. S., Watanabe, T., Thomas, E. C., and Clark, L. F. 1965. Discharge Pattern of Single Fibers in the Cat's Auditory Nerve. MIT Press.

King, T. S. and Dougherty, W. J. 1982. Effect of denervation on ''synaptic'' ribbon population in the rat pineal gland. J. Neurocytol. 11, 19–28.

Knudsen, E. I. and Konishi, M. 1978. A neural map of auditory space in the owl. Science 200, 795–797.

Koschak, A., Reimer, D., Huber, I., Grabner, M., Glossmann, H., Engel, J., and Striessnig, J. 2001. α1D (Cav1.3) subunits can form L-type Ca^{2+} channels activating at negative voltages. J. Biol. Chem. 276, 22100–22106.

Koyama, H., Lewis, E. R., Leverenz, E. L., and Baird, R. A. 1982. Acute seismic sensitivity in the bullfrog ear. Brain Res. 250, 168–172.

von Kriegstein, K., Schmitz, F., Link, E., and Sudhof, T. C. 1999. Distribution of synaptic vesicle proteins in the mammalian retina identifies obligatory and facultative components of ribbon synapses. Eur. J. Neurosci. 11, 1335–1348.

Krstic, R. 1976. Ultracytochemistry of the synaptic ribbons in the rat pineal organ. Cell Tissue Res. 166, 135–143.

Lenzi, D. and von Gersdorff, H. 2001. Structure suggests function: the case for synaptic ribbons as exocytotic nanomachines. Bioessays 23, 831–840.

Lenzi, D., Crum, J., Ellisman, M. H., and Roberts, W. M. 2002. Depolarization redistributes synaptic membrane and creates a gradient of vesicles on the synaptic body at a ribbon synapse. Neuron 36, 649–659.

Lenzi, D., Runyeon, J. W., Crum, J., Ellisman, M. H., and Roberts, W. M. 1999. Synaptic vesicle populations in saccular hair cells reconstructed by electron tomography. J. Neurosci. 19, 119–132.

Lewis, E. R. and Narins, P. M. 1985. Do frogs communicate with seismic signals? Science 227, 187–189.

Lewis, R. S. and Hudspeth, A. J. 1983. Voltage- and ion-dependent conductances in solitary vertebrate hair cells. Nature 304, 538–541.

Lewis, E. R., Baird, R. A., Leverenz, E. L., and Koyama, H. 1982. Inner ear: dye injection reveals peripheral origins of specific sensitivities. Science 215, 1641–1643.

Liberman, M. C. 1980. Morphological differences among radial afferent fibers in the cat cochlea: an electron-microscopic study of serial sections. Hear Res. 3, 45–63.

Liberman, M. C. 1982. Single-neuron labeling of the cat auditory nerve. Science 216, 1239–1241.

Liberman, M. C. and Kiang, N. Y. S. 1978. Acoustic trauma in cats. Cochlear pathology and auditory-nerve activity. Acta Otolaryngol. Suppl. 358, 1–63.

Liberman, M. C., Dodds, L. W., and Pierce, S. 1990. Afferent and efferent innervation of the cat cochlea: quantitative analysis with light and electron microscopy. J. Comp. Neurol. 301, 443–460.

Lindau, M. and Neher, E. 1988. Patch-clamp techniques for time-resolved capacitance measurements in single cells. Pflugers Arch. 411, 137–146.

Lioudyno, M., Hiel, H., Kong, J. H., Katz, E., Waldman, E., Parameshwaran-Iyer, S., Glowatzki, E., and Fuchs, P. A. 2004. A ''synaptoplasmic cistern'' mediates rapid inhibition of cochlear hair cells. J. Neurosci. 24, 11160–11164.

Manley, G. A., Köppl, C., and Yates, G. K. 1997. Activity of primary auditory neurons in the cochlear ganglion of the emu *Dromaius novaehollandiae*: spontaneous discharge, frequency tuning, and phase locking. J. Acoust. Soc. Am. 101, 1560–1573.

Martinez-Dunst, C., Michaels, R. L., and Fuchs, P. A. 1997. Release sites and calcium channels in hair cells of the chick's cochlea. J. Neurosci. 17, 9133–9144.

Matsubara, A., Laake, J. H., Davanger, S., Usami, S., and Ottersen, O. P. 1996. Organization of AMPA receptor subunits at a glutamate synapse: a quantitative immunogold analysis of hair cell synapses in the rat organ of Corti. J. Neurosci. 16, 4457–4467.

McMahon, H. T., Missler, M., Li, C., and Sudhof, T. C. 1995. Complexins: cytosolic proteins that regulate SNAP receptor function. Cell 83, 111–119.

Merchan-Perez, A. and Liberman, M. C. 1996. Ultrastructural differences among afferent synapses on cochlear hair cells: correlations with spontaneous discharge rate. J. Comp. Neurol. 371, 208–221.

Miller, M. R. and Beck, J. 1987. Heterotopic synaptic bodies in the auditory hair cells of adult lizards. Anat. Rec. 218, 338–344.

Morgans, C. W. 2001. Localization of the α1F calcium channel subunit in the rat retina. Invest. Ophthalmol. Vis. Sci. 42, 2414–2418.

Morgans, C. W., Brandstatter, J. H., Kellerman, J., Betz, H., and Wassle, H. 1996. SNARE complex containing syntaxin 3 is present in ribbon synapses of the retina. J. Neurosci. 16, 6713–6721.

Moser, T. and Beutner, D. 2000. Kinetics of exocytosis and endocytosis at the cochlear inner hair cell afferent synapse of the mouse. Proc. Natl. Acad. Sci. U. S. A. 97, 883–888.

Moser, T., Brandt, A., and Lysakowski, A. 2006. Hair cell ribbon synapses. Cell Tissue Res. 326, 347–359.

Moser, T., Neef, A., and Khimich, D. 2006. Mechanisms underlying the temporal precision of sound coding at the inner hair cell ribbon synapse. J. Physiol. 576, 55–62.

Mountain, D. C. and Hubbard, A. E. 1996. Computational Analysis of Hair Cell and Auditory Nerve Processes. In: Auditory Computation (*eds*. H. L. Hawkins, T. A. McMullen, A. N. Popper, and R. R. Fay), p. 121. Springer.

Muresan, V., Lyass, A., and Schnapp, B. J. 1999. The kinesin motor KIF3A is a component of the presynaptic ribbon in vertebrate photoreceptors. J. Neurosci. 19, 1027–1037.

Nakagawa, T., Oghalai, J. S., Saggau, P., Rabbitt, R. D., and Brownell, W. E. 2006. Photometric recording of

transmembrane potential in outer hair cells. J. Neural. Eng. 3, 79–86.
Neher, E. and Augustine, G. J. 1992. Calcium gradients and uffers in bovine chromaffin cells. J. Physiol. 450, 273–301.
Nguyen, T. H. and Balkema, G. W. 1999. Antigenic epitopes of the photoreceptor synaptic ribbon. J. Comp. Neurol. 413, 209–218.
Nibu, Y., Zhang, H., Bajor, E., Barolo, S., Small, S., and Levine, M. 1998. dCtBP mediates transcriptional repression by Knirps, Krueppel and Snail in the *Drosophila* embryo. EMBO J. 17, 7009–7020.
Nicholls, J. G., Martin, A. R., Wallace, B. G., and Fuchs, P. A. 2001. From Neuron to Brain. Sinauer Associates.
Nouvian, R., Beutner, D., Parsons, T. D., and Moser, T. 2006. Structure and function of the hair cell ribbon synapse. J. Memb. Biol. 209, 1–13.
Osborne, M. P. and Thornhill, R. A. 1972. The effect of monoamine depleting drugs upon the synaptic bars in the inner ear of the bullfrog. Z. Zellforsch. Mikrosk. Anat. 127, 347–355.
Pabst, S., Hazzard, J. W., Antonin, W., Sudhof, T. C., Jahn, R., Rizo, J., and Fasshauer, D. 2000. Selective interaction of complexin with the neuronal SNARE complex. J. Biol. Chem. 275, 19808–19818.
Palmer, A. R. and Russell, I. J. 1986. Phase-locking in the cochlear nerve of the guinea-pig and its relation to the receptor potential of inner hair-cells. Hear Res. 24, 1–15.
Parsons, T. D. and Sterling, P. 2003. Synaptic ribbon: conveyor belt or safety belt? Neuron 37, 379–82.
Parsons, T. D., Lenzi, D., Almers, W., and Roberts, W. M. 1994. Calcium-triggered exocytosis and endocytosis in an isolated presynaptic cell: capacitance measurements in saccular hair cells. Neuron 13, 875–883.
Plack, C. J., Oxenham, A. J., and Drga, V. 2006. Masking by inaudible sounds and the linearity of temporal summation. J. Neurosci. 26, 8767–8773.
Poortinga, G., Watanabe, M., and Parkhurst, S. M. 1998. *Drosophila* CtBP: a hairy-interacting protein required for embryonic segmentation and hairy-mediated transcriptional repression. EMBO J. 17, 2067–2078.
Pyle, J. L., Kavalali, E. T., Piedras-Renteria, E. S., and Tsien, R. W. 2000. Rapid reuse of readily releasable pool vesicles at hippocampal synapses. Neuron 28, 221–231.
Raphael, Y. and Altschuler, R. A. 2003. Structure and innervation of the cochlea. Brain Res. Bull. 60, 397–422.
Raymond, J., Puel, J. L., and Devau, G. 2003. Glutamate transporters in the guinea-pig cochlea: partial mRNA sequences, cellular expression and functional implications. Eur. J. Neurosci. 17, 83–92.
Rea, R., Li, J., Dharia, A., Levitan, E. S., Sterling, P., and Kramer, R. H. 2004. Streamlined synaptic vesicle cycle in cone photoreceptor terminals. Neuron 41, 755–766.
Rebillard, G., Ruel, J., Nouvian, R., Saleh, H., Pujol, R., Dehnes, Y., Raymond, J., Puel, J. L., and Devau, G. 2003. Glutamate transporters in the guinea-pig cochlea: partial mRNA sequences, cellular expression and functional implications. Eur J. Neurosci. 17, 83–92.
Reim, K., Mansour, M., Varoqueaux, F., McMahon, H. T., Sudhof, T. C., Brose, N., and Rosenmund, C. 2001. Complexins regulate a late step in Ca^{2+}-dependent neurotransmitter release. Cell 104, 71–81.
Reim, K., Wegmeyer, H., Brandstatter, J. H., Xue, M., Rosenmund, C., Dresbach, T., Hofmann, K., and Brose, N. 2006. Structurally and functionally unique complexins at retinal ribbon synapses. J. Cell Biol. 169, 669–680.
Relkin, E. M. and Doucet, J. R. 1991. Recovery from prior stimulation. I. Relationship to spontaneous firing rates of primary auditory neurons. Hear Res. 55, 215–222.
Ricci, A. J., Gray-Keller, M., and Fettiplace, R. 2000. Tonotopic variations of calcium signalling in turtle auditory hair cells. J. Physiol. 524, 423–436.
Rizzoli, S. O. and Betz, W. J. 2005. Synaptic vesicle pools. Nat. Rev. Neurosci. 6, 57–69.
Roberts, W. M. 1993. Spatial calcium buffering in saccular hair cells. Nature 363, 74–76.
Roberts, W. M. 1994. Localization of calcium signals by a mobile calcium buffer in frog saccular hair cells. J. Neurosci. 14, 3246–3262.
Roberts, W. M., Jacobs, R. A., and Hudspeth, A. J. 1990. Colocalization of ion channels involved in frequency selectivity and synaptic transmission at presynaptic active zone of hair cells. J. Neurosci. 10, 3664–3684.
Robertson, D. 1984. Horseradish peroxidase injection of physiologically characterized afferent and efferent neurons in the guinea pig spiral ganglion. Hear Res. 15, 113–121.
Robertson, D. and Paki, B. 2002. A role for purinergic receptors at the inner hair cell-afferent synapse? Audiol. Neurootol. 7, 62–67.
Rodriguez-Contreras, A. and Yamoah, E. N. 2001. Direct measurement of single-channel Ca^{2+} currents in bullfrog hair cells reveals two distinct channel subtypes. J. Physiol. 534, 669–689.
Rodriguez-Contreras, A. and Yamoah, E. N. 2003. Effects of permeant ion concentrations on the gating of L-type Ca^{2+} channels in hair cells. Biophys. J. 84, 3457–3469.
Rosahl, T., Spillane, D., Missler, M., Herz, J., Selig, D., Wolff, J. R., Hammer, R. E., Malenka, R. C., and Sudhof, T. C. 1995. Essential functions of synapsins I and II in synaptic vesicle regulation. Nature 375, 488–493.
Rose, J. E., Brugge, J. F., Anderson, D. J., and Hind, J. E. 1967. Phase-locked response to low-frequency tones in single auditory nerve fibers of the squirrel monkey. J. Neurophysiol. 30, 769–793.
Rose, J. E., Hind, J. E., Anderson, D. J., and Brugge, J. F. 1971. Some effects of stimulus intensity on response of auditory-nerve fibers in the squirrel monkey. J. Neurophysiol. 34, 685–699.
Rosenmund, C., Rettig, J., and Brose, N. 2003. Molecular mechanisms of active zone function. Curr. Opin. Neurobiol. 13, 509–519.
Ruel, J., Bobbin, R. P., Vidal, D., Pujol, R., and Puel, J. L. 2000. The selective AMPA receptor antagonist GYKI 53784 blocks action potential generation and excitotoxicity in the guinea pig cochlea. Neuropharmacology 39, 1959–1973.
Russell, I. J. and Sellick, P. M. 1978. Intracellular studies of hair cells in the mammalian cochlea. J. Physiol. 284, 261–290.
Rutherford, M. A. and Roberts, W. M. 2006. Frequency selectivity of exocytosis in frog saccular hair cells. Proc. Natl. Acad. Sci. U. S. A. 103, 2898–2903.
Safieddine, S. and Wenthold, R. J. 1999. SNARE complex at the ribbon synapses of cochlear hair cells: analysis of synaptic vesicle- and synaptic membrane-associated proteins. Eur. J. Neurosci. 11, 803–812.
Schmitz, F. and Drenckhahn, D. 1991. Influence of Ca^{2+} on synaptic morphology of fish cone photoreceptors. Brain Res. 546, 341–344.
Schmitz, F., Konigstorfer, A., and Sudhof, T. C. 2000. RIBEYE, a component of synaptic ribbons: a protein's journey through evolution provides insight into synaptic ribbon function. Neuron 28, 857–872.
Schnee, M. E. and Ricci, A. J. 2003. Biophysical and pharmacological characterization of voltage-gated calcium currents in turtle auditory hair cells. J. Physiol. 549, 697–717.
Schnee, M. E., Lawton, D. M., Furness, D. N., Benke, T. A., and Ricci, A. J. 2005. Auditory hair cell-afferent fiber synapses are specialized to operate at their best frequencies. Neuron 47, 243–254.

Schneggenburger, R. and Neher, E. 2005. Presynaptic calcium and control of vesicle fusion. Curr. Opin. Neurobiol. 15, 266–274.
Sewell, W. F. 1984. The relation between the endocochlear potential and spontaneous activity in auditory nerve fibres of the cat. J. Physiol. 347, 685–696.
Siegel, J. H. 1992. Spontaneous synaptic potentials from afferent terminals in the guinea pig cochlea. Hear Res. 59, 85–92.
Siegel, J. H. and Brownell, W. E. 1981. Synaptic bodies in outer hair cells of the chinchilla organ of Corti. Brain Res. 220, 188–193.
Siegel, J. H. and Brownell, W. E. 1986. Synaptic and golgi membrane recycling in cochlear hair cells. J. Neurocytol. 15, 311–328.
Singer, J. H., Lassova, L., Vardi, N., and Diamond, J. S. 2004. Coordinated multivesicular release at a mammalian ribbon synapse. Nat. Neurosci. 7, 826–833.
Sjöstrand, F. S. 1958. Ultrastructure of retinal rod synapses of the guinea pig eye as revealed by three-dimensional reconstructions from serial sections. J. Ultrastruct. Res. 5, 13–17.
Slepecky, N. B., Galsky, M. D., Swartzentruber-Martin, H., and Savage, J. 2000. Study of afferent nerve terminals and fibers in the gerbil cochlea: distribution by size. Hear Res. 144, 124–134.
Smith, R. L. 1977. Short-term adaptation in single auditory nerve fibers: some poststimulatory effects. J. Neurophysiol. 40, 1098–1111.
Smith, C. A. and Sjostrand, F. S. 1961. Structure of the nerve endings on the external hair cells of the guinea pig cochlea as studied by serial sections. J. Ultrastruct. Res. 5, 523556.
Smotherman, M. S. and Narins, P. M. 2000. Hair cells, hearing and hopping: a field guide to hair cell physiology in the frog. J. Exp. Biol. 203, 2237–2246.
Sneary, M. G. 1988. Auditory receptor of the red-eared turtle: II. Afferent and efferent synapses and innervation patterns. J. Comp. Neurol. 276, 588–606.
Sobkowicz, H. M., August, B. K., and Slapnick, S. M. 2004. Synaptic arrangements between inner hair cells and tunnel fibers in the mouse cochlea. Synapse 52, 299–315.
Sobkowicz, H. M., Rose, J. E., Scott, G. L., and Levenick, C. V. 1986. Distribution of synaptic ribbons in the developing organ of Corti. J. Neurocytol. 15, 693–714.
Sobkowicz, H. M., Slapnick, S. M., and August, B. K. 2003. Reciprocal synapses between inner hair cell spines and afferent dendrites in the organ of corti of the mouse. Synapse 50, 53–66.
Spassova, M. A., Avissar, M., Furman, A. C., Crumling, M. A., Saunders, J. C., and Parsons, T. D. 2004. Evidence that rapid vesicle replenishment of the synaptic ribbon mediates recovery from short-term adaptation at the hair cell afferent synapse. JARO 5, 376390.
Spoendlin, H. 1969. Innervation patterns in the organ of Corti of the cat. Acta Otolaryngol. 67, 239–254.
Spoendlin, H. 1985. Anatomy of cochlear innervation. Am. J. Otolaryngol. 6, 453–467.
Sterling, P. and Matthews, G. 2005. Structure and function of ribbon synapses. Trends Neurosci. 28, 20–29.
Stern, M. D. 1992. Buffering of calcium in the vicinity of a channel pore. Cell Calcium 13, 183–192.
Stevens, C. F. and Williams, J. H. 2000. ''Kiss and run'' exocytosis at hippocampal synapses. Proc. Natl. Acad. Sci. U. S. A. 97, 12828–12833.
Sudhof, T. C. 2000. The synaptic vesicle cycle revisited. Neuron 28, 317–320.
Sudhof, T. C. 2004. The synaptic vesicle cycle. Annu. Rev. Neurosci. 27, 509–547.
Sumner, C. J., Lopez-Poveda, E. A., O'Mard, L. P., and Meddis, R. 2002. A revised model of the inner-hair cell and auditory nerve complex. J. Acoust. Soc. Am. 111, 2178–2188.
Tsuji, J. and Liberman, M. C. 1997. Intracellular labeling of auditory nerve fibers in the guinea pig: central and peripheral projections. J. Comp. Neurol. 381, 188–202.
Usukura, J. and Yamada, E. 1987. Ultrastructure of the synaptic ribbons in photoreceptor cells of *Rana catesbeiana* revealed by freeze-etching and freeze-substitution. Cell Tissue Res. 247, 483–488.
Wagner, H.-J. 1978. Cell types and connectivity patterns in mosaic retinas. Adv. Anat. Embryol. Cell Biol. 55, 1–81.
Wagner, H.-J. 1997. Presynaptic bodies (''ribbons''): from ultrastructural observations to molecular perspectives. Cell Tissue Res. 287, 435–446.
Wan, L., Almers, W., and Chen, W. 2005. Two ribeye genes in teleosts: the role of Ribeye in ribbon formation and bipolar cell development. J. Neurosci. 25, 941–994.
Xu, W. and Lipscombe, D. 2001. Neuronal Cav1.3α1 L-type channels activate at relatively hyperpolarized membrane potentials and are incompletely inhibited by dihydropyridines. J. Neurosci. 21, 5944–5951.
Yamazaki, H., Nakata, T., Okada, Y., and Hirokawa, N. 1995. KIF3A/B: a heterodimeric kinesin superfamily protein that works as a microtubule plus end-directed motor for membrane organelle transport. J. Cell Biol. 130, 1387–1399.
Yasunaga, S., Grati, M., Chardenoux, S., Smith, T. N., Friedman, T. B., Lalwani, A. K., Wilcox, E. R., and Petit, C. 2000. OTOF encodes multiple long and short isoforms: genetic evidence that the long ones underlie recessive deafness DFNB9. Am. J. Hum. Genet. 67, 591–600.
Yasunaga, S., Grati, M., Cohen-Salmon, M., El-Amraoui, A., Mustapha, M., Salem, N., El-Zir, E., Loiselet, J., and Petit, C. 1999. A mutation in OTOF, encoding Otoferlin, a FER-1-like protein, causes DFNB9, a nonsyndromic form of deafness. Nat. Gen. 21, 363–369.
Yu, X., Lewis, E. R., and Feld, D. 1991. Seismic and auditory tuning curves from bullfrog saccular and amphibian papillar axons. J. Comp. Physiol. A 169, 241–248.
Zenisek, D., Davila, V., Wan, L., and Almers, W. 2003. Imaging calcium entry sites and ribbon structures in two presynaptic cells. J. Neurosci. 23, 2538–2548.
Zhai, R. G. and Bellen, H. J. 2004. The architecture of the active zone in the presynaptic nerve terminal. Physiology 19, 262–270.

Further Reading

Rizzoli, S. O. and Betz, W. J. 2004. The structural organization of the readily releasable pool of synaptic vesicles. Science 303, 2037–2039.

3.23 Perspectives on Auditory Neuropathy: Disorders of Inner Hair Cell, Auditory Nerve, and Their Synapse

A Starr, F G Zeng, and H J Michalewski, University of California, Irvine, CA, USA

T Moser, University of Goettingen, Goettingen, Germany

© 2008 Elsevier Inc. All rights reserved.

3.23.1	Introduction	397
3.23.2	Testing for Auditory Neuropathy	397
3.23.3	Clinical Features of Auditory Neuropathy	398
3.23.4	Exceptions to the Criteria for Defining Auditory Neuropathy	400
3.23.5	Pathophysiology of Auditory Neuropathy	401
3.23.6	Psychoacoustic Deficits of Auditory Neuropathy	402
3.23.7	Molecular Mechanisms of Auditory Neuropathy	406
3.23.7.1	Inner Hair Cell Channelopathy-Knockout of the Inner Hair Cell $Ca_V1.3$	406
3.23.7.2	Impaired Inner Hair Cell Transmitter Release	408
3.23.7.3	Auditory Nerve Ion Channel Displacement	408
3.23.7.4	Auditory Nerve Fiber Myelin Disorder	408
3.23.7.5	Loss of Spiral Ganglion Neurons	411
3.23.8	Conclusions	411
References		411

3.23.1 Introduction

The term auditory neuropathy (Starr, A. *et al.*, 1996) was first used to describe a hearing disorder due to altered function of the auditory nerve in the presence of preserved functions of cochlear outer hair cells (OHCs; Starr, A. *et al.*, 1991). The hearing loss has specific features reflecting impairment of auditory temporal processes that are typically unaffected with sensory outer hair disturbances (Zeng, F. G. *et al.*, 1999). The disorder has also been referred to as type I afferent neuron dysfunction (Berlin, C. I. *et al.*, 1993), auditory neuropathy/auditory dys-synchrony (Berlin, C. I. *et al.*, 2003), and neural hearing loss (Rapin, I. and Gravel, J., 2003). We now know that dysfunction of the auditory nerve, having quite similar clinical features, accompanies a variety of disorders acting on the nerve, the inner hair cell, and/or their synapse. We will refer to the disorder as auditory neuropathy and emphasize whenever possible the site(s) of involvement in the auditory periphery. We will review how the varieties of auditory neuropathy are identified, the special psychoacoustic features of the hearing loss, candidate pathophysiological mechanisms, and cochlear and auditory nerve pathologies. We will introduce recent advances in knowledge of molecular organization of cochlear inner hair cell synapses and auditory nerve that suggest some mechanisms likely to be involved in auditory nerve dysfunction.

3.23.2 Testing for Auditory Neuropathy

Auditory brainstem responses (ABRs) are the far-field reflection of potentials arising in the cochlea, auditory nerve, and auditory brainstem pathways during the first 10–15 ms after a transient acoustic signal. These potentials are of small amplitude in humans (<0.5 μV) and their resolution requires averaging brain activity to several thousand acoustic stimuli. Those potentials that are time-locked to the stimuli appear in the averaged ABR whereas potentials that are not sufficiently time-locked to the acoustic signals are attenuated. The averaged ABR is therefore especially sensitive to the temporal pattern of neural discharge in auditory nerve and brainstem auditory pathways.

The ABR has five major components, labeled in sequence by Roman numerals I through V, which are generated by distinct regions of the auditory pathway. The absolute latencies of the components change with signal intensity but the time difference between each of the components remains relatively

constant independent of stimulus intensity (Starr, A. and Achor, J., 1975). Wave I is generated in the distal portions of auditory nerve in the region of the ganglion cells; wave II is generated in the proximal portions of the auditory nerve in the region of its entry into the brainstem; wave III is generated in the region of the ipsilateral cochlear nucleus; waves IV and V are generated bilaterally in the region of the midbrain tegmentum (Starr, A. and Achor, J., 1975; Starr, A. and Hamilton, A. E., 1976; Martin, W. H. *et al.*, 1995; Melcher, J. R. *et al.*, 1996). Thus the ABR components provide a longitudinal view of sequential activities arising from both the auditory nerve and brainstem portions of the auditory pathway.

Cochlear microphonics (CMs) are receptor potentials generated by both inner and OHCs. Since the dominant type of hair cell is outer, one would expect that the amplitude of cochlear microphonics derives predominantly from outer rather than inner hair cells. that can also be identified in the ABR by separately averaging potentials to condensation and rarefaction stimuli to define phase reversed components in the two averages (Starr, A. *et al.*, 1991; Berlin, C. I. *et al.*, 1998). If the condensation and rarefaction stimuli are presented in an alternating fashion, the CMs to each polarity stimulus cancel and do not appear in the ABR average.

Otoacoustic emissions (OAEs) are faint sounds produced by OHCs (Kemp, D. T., 1978; Brownell, W. E., 1984) that can be recorded by a small microphone in the ear canal and provide a measure of mechanical activity (electromotility) of cochlear OHCs.

By combining measures of ABRs, CMs, and OAEs, the site(s) of altered functions can be identified as affecting one or several of the components comprising the auditory periphery including OHCs, auditory nerve, and auditory brainstem structures. At present, there are no physiological measures available for clinical applications that are specific for identifying disorders of inner hair cells (IHCs) or their pre- and postsynaptic functions with auditory nerve.

3.23.3 Clinical Features of Auditory Neuropathy

The ABR was introduced in the 1970s as a screening method to identify auditory impairments in neonates and children (Hecox, K. and Galambos, R., 1974). There were occasional observations that ABRs could be absent even though the subject was subsequently shown to have preserved hearing by behavioral measures (Davis, H. and Hirsh, S. K., 1979; Kaga, K. *et al.*, 1979; Worthington, D. W. and Peters, J. F., 1980; Lenhardt, M. L., 1981). These authors recognized the paradox these findings posed and suggested explanations ranging from technical limitations of the ABR as a test of hearing to the possibility that the abnormal ABRs might reflect a particular kind of peripheral auditory disorder (Kraus, N. *et al.*, 1984).

Special patients can occasionally provide a solution to clinical paradoxes. We examined such a subject (Starr, A. *et al.*, 1991) identified by her teachers as possibly having a hearing problem. Audiological measures showed absent ABRs inconsistent with the mild low-frequency threshold loss. Speech comprehension was impaired and acoustic middle ear muscle reflexes were absent. When ABRs were tested separately to condensation or rarefaction clicks, short latency components appeared that were phased reversed when the two averages were superimposed consistent with their being CMs rather than neural components. OAEs were also present. Figure 1 contains the test results (audiograms, ABRs, CMs, OAEs, and cortical-evoked potentials) for another patient with the same disorder showing a mild threshold elevation (in this example affecting high frequencies), impaired speech comprehension out-of-proportion to the pure tone threshold elevation, a low amplitude and delayed wave V, and preserved hair cell measures of both CMs and OAEs. The test results for a subject with normal hearing are shown for comparison in Figure 1. The results obtained from the patient were consistent with preserved functions of cochlear OHC functions (normal CMs and OAEs) but impaired function of auditory nerve and brainstem. The failure to obtain an averaged ABR was attributed to altered synchrony of neural activity of auditory nerve rather than to a loss of auditory nerve activity because hearing thresholds were only modestly impaired. Auditory cortical-evoked potentials were present suggesting that neural synchrony was still sufficiently preserved to allow an averaged cortical response to be detected. Finally, psychoacoustic studies in this patient (Starr, A. *et al.*, 1991) and subsequently in others (Zeng, F. G. *et al.*, 1999; 2005) summarized below in this chapter revealed that the hearing disorder is indeed relatively specific for auditory percepts dependent on temporal cues (e.g., speech comprehension, gap detection, masking level differences, and low-frequency difference limens) whereas percepts dependent on intensity cues were normal. The disorder appeared

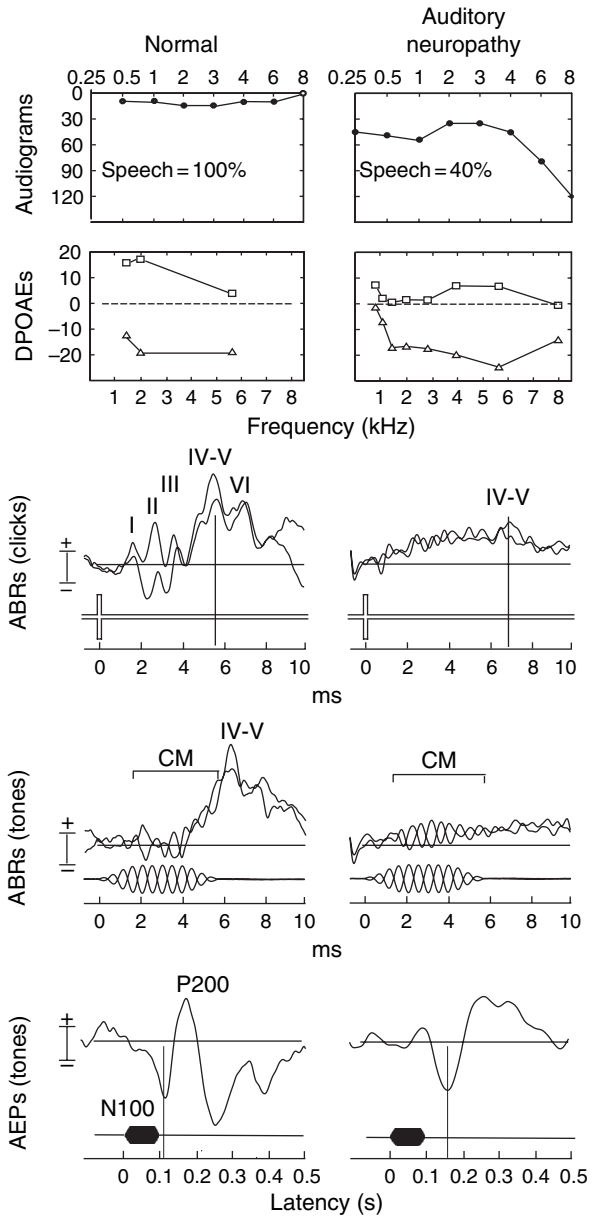

Figure 1 The audiogram (with speech comprehension), distortion product otoacoustic emissions (DPOAEs), auditory brainstem responses (ABRs) to clicks of opposite polarity, ABRs to brief tones (1 kHz) of opposite polarity and auditory cortical-evoked potentials (AEPs) to a 100 ms 1 kHz tone burst are shown for a normal-hearing and auditory neuropathy subjects. The analog stimuli used for the electrophysiological procedures are depicted below the averaged responses. The patient displays a moderate low-frequency threshold elevation that becomes less affected in mid-frequencies, and severe at high frequency (8 kHz). DPOAEs and cochlear microphonics (CMs) are present whereas only a low amplitude delayed wave V can be seen in the click-evoked ABR. The auditory cortical N100 component is present in the patient of delayed latency (160 ms) compared to the N100 in normal hearing subject (N100). Amplitude calibration is 0.25 μV for ABRs and 5 μV for AEPs.

to involve the auditory nerve and/or its synapses with inner hair cells while sparing cochlear OHCs.

Soon, additional subjects with absent ABRs and preserved OAEs and/or CMs were identified. Neurological studies of 11 adolescent and adult subjects with absent ABRs and preserved OHC activity revealed the presence of a peripheral neuropathy in eight, consistent with the presence of a concomitant neuropathy of the auditory nerve (Starr, A. *et al.*, 1996). Subsequently, the temporal bone of a subject with

neural hearing loss and peripheral neuropathy due to a mutation of the *MPZ* gene was examined and revealed marked depletion of auditory neurons with preservation of both inner and OHCs (Starr, A. *et al.*, 2003). The pathological changes in the peripheral sensory nerves and the auditory nerve were similar and consisted of nerve fiber loss (deafferentation) as well as demyelination and incomplete remyelination of the remaining fibers. These results indicate that a hearing loss characterized by a temporal processing disorder, absent ABRs, preserved OAEs and CMs can be a consequence of a neuropathy of the auditory nerve. Both Hallpike C. S. *et al.* (1980) and Spoendlin H. (1974) reported similar temporal bone findings 30 years earlier, in individuals with deafness and hereditary peripheral neuropathies. Satya-Murti S. *et al.* (1980) showed ABRs were absent or severely abnormal in subjects with hereditary neuropathy due to Fredreichs' ataxia and interpreted their findings as reflecting a disorder of the VIII nerve. Thus both a loss of fibers (deafferentation) and/or altered synchrony of nerve impulses in the remaining fibers due to demyelination and incomplete remyelination are likely factors contributing to the temporal processing defects in auditory neuropathy.

Disorders of inner hair cells and their synapses with auditory nerve fibers can also lead to a hearing disorder that is essentially indistinguishable clinically from that accompanying a neuropathy of the auditory nerve. An example of such an inner hair cell disorder occurs with mutations of genes encoding otoferlin (*OTOF*), a putative synaptic protein identified in inner hair cells (Yasunaga, S. *et al.*, 1999; Rodriguez-Ballesteros, M. *et al.*, 2003; Varga, R. *et al.*, 2003). These patients have absent ABRs and in some, preserved OAEs. The hearing loss is severe-to-profound and speech comprehension is a major impairment. Otoferlin belongs to the family of the FER-1 like proteins which are involved in membrane trafficking. Thus the some clinical findings are present with disorders of the nerve and in Otoferlin disorder of inner hair cells. It is likely that a synaptic disorder underlies the hearing loss in these patients, who do not have any evidence of peripheral or other cranial neuropathies.

The findings of auditory neuropathy and Otoferlin inner hair cell disorder (absence of ABRs with preserved OHC functions) are also recognized at high incidence in newborns tested as part of universal infant hearing screening evaluation (Kraus, N. *et al.*, 1984; Doyle, K. J. *et al.*, 1998). It is likely that many of these infants have disorders of both inner hair cells affecting synaptic function and auditory nerves due to metabolic disorders such as hypoxia, hyperbilirubinemia, infections, and prematurity. The infants are typically without clinical evidence of a peripheral neuropathy. In a study of temporal bones of premature infants dying with abnormal ABRs (OAEs were not tested) there were several who showed isolated loss of inner hair cells with preservation of both auditory ganglion cells and OHCs (Amatuzzi, M. G. *et al.*, 2001).

Thus, auditory neuropathy with quite similar physiological and audiological findings can occur as a consequence of pathology of inner hair cell, their synapses, and/or the auditory nerve due to a host of etiologies (Starr, A. *et al.*, 2001a). The common denominators are absence or profound abnormalities of ABRs, absence or profound abnormalities of acoustic reflexes of middle ear muscles and olivocochlear bundle (OCB; Berlin, C. I. *et al.*, 1993), and impaired perceptions dependent on temporal cues. Both the physiological expressions and the types of hearing impairment are remarkably similar whether the disorder is at the inner hair cell, its synapses, or the auditory nerve.

3.23.4 Exceptions to the Criteria for Defining Auditory Neuropathy

The criteria for defining auditory neuropathy have exceptions. First, ABRs are not always absent and a delayed wave V can be defined in approximately 40% of subjects. However, the changes of wave V are beyond those expected for the degree of hearing loss. Second, while it is typical to find absent acoustic middle ear muscle and efferent OCB reflexes, there are some subjects who show the reflexes to be present at elevated thresholds. Third, the impairment of speech comprehension may only be manifest in the presence of noise. Fourth, while OAEs and/or CMs are typically preserved, almost one-third of subjects show OAEs to be absent on retesting. And fifth, while hearing aid amplification is typically without benefit for understanding speech in most subjects, occasionally there are exceptions that do benefit.

The disorder can occur across the age spectrum (Hood, L. J. and Berlin, C. I., 2001; Sininger, Y. and Oba, S., 2001) reflecting a host of etiologies (e.g., hereditary, infectious, and metabolic) and risk factors (hypoxia and hyperbilirubinemia). Almost half of patients cannot be assigned an etiology. The high incidence in neonates and in children at entry to school likely reflects the use of universal auditory screening in neonates (OAEs and/or ABRs) and universal behavioral auditory testing (audiograms) in schools.

The clinical and physiological findings originally used for identifying auditory neuropathy can change over time. Audiograms and speech comprehension decline or remain stationary (Sininger, Y. and Oba, S., 2001). There are documented instances of improvement of ABRs in newborn infants after discharge from the neonatal intensive care unit and even recovery in adults affected with immune disorders acting on nerve fiber (e.g., Guillain-Barré syndrome; Ropper, A. H. and Chiappa, K. H., 1986). OAEs that are present initially may not be obtainable in approximately 30% of subjects (Starr, A. *et al.*, 2001b). CMs appear to persist longer but they too can become attenuated and difficult to detect when patients are over the age of 50 years (Starr, A., *et al.*, 2001b). These findings are consistent with the idea that some forms of auditory neuropathy may be progressive and in others also involve OHC functions.

3.23.5 Pathophysiology of Auditory Neuropathy

The remarkable similarity of electrophysiological findings in subjects with different forms of auditory neuropathy suggests a common pathophysiology independent of site of affliction. Each IHC forms separate synaptic contacts with several afferent fibers. Each of these synapses consists of the presynaptic ribbon-containing active zone and a small (~1 μm) dendritic swelling. Each active zone contains up to 80 $Ca_V1.3$ Ca^{2+} channels and approximately 60 readily releasable glutamate-containing synaptic vesicles, several of which can be released in parallel within milliseconds or less (Khimich, D. *et al.*, 2005). The individual release sites appear to be controlled by few active $Ca_V1.3$ Ca^{2+} channels in nanometer proximity, which activate rapidly upon depolarization and drive vesicle fusion at near saturating speed (Ca^{2+} nanodomain control). The released glutamate rapidly opens postsynaptic alpha-amino-3-hydroxy-5-methylisoxazole-4-propionic acid (AMPA)-type glutamate receptors (Glowatzki, E. and Fuchs, P. A., 2002), which are clustered at the postsynaptic density. Excitatory postsynaptic currents (EPSCs) measured in the nerve terminals display both rapid rise (<0.50 ms) and rapid decay (<2 ms) enhancing nerve spike generation at short latency and the ability to discharge again at short intervals. Synchronous transmission of nerve impulses is optimized by their relatively uniform fiber diameter and corresponding similar conduction velocity. When the nerve impulses reach the first node of Ranvier, conduction is speeded by becoming saltatory.

Mechanisms enhancing temporal precision of auditory information coding and transmission include precise receptor potential generation, rapid Ca^{2+}-channel gating, the nanodomain control of exocytosis, parallel release of multiple vesicles at one active zone, rapid glutamate receptor signaling, and small size of postsynaptic terminal. This precise timing enables synchronization of spiking in fibers driven by one hair cell (same receptor potential). However, there are a host of opportunities for degrading neural synchrony including changes in hair cell mechanics; hair cell metabolic functions; transmitter release and reuptake; receptor sensitivity; nerve terminal nerve spike initiation; and transmission, axonal, and myelin disorders.

If there were a disorder of inner hair cells affecting transmitter release, a synaptic disorder affecting the number or sensitivity of receptor sites, or a disorder of nerve fibers affecting speed of conduction, both the synchrony of discharge and the number of fibers that were active would likely be compromised. We have modeled the general effects of such disorders in Figure 2 (gray spikes) and compared with the normal condition (black spikes). Normally the fibers all discharge at short latency with little variability. However, with a disorder of inner hair cells, the synapse, and/or the nerve fibers, the affected population's response would likely show both altered temporal patterns of discharge and overall amplitude changes. These changes are modeled in Figure 2 by reducing the number of fibers activated by 30%, and introducing in the remaining fibers a variable delay in their latency of discharge. The effects of these alterations impair both temporal synchrony and overall amplitude of response of the population of fibers and are plausible pathophysiological mechanisms accounting for the electrophysiological and psychoacoustic changes.

Figure 3 depicts how neural desynchrony could affect the appearance of the ABR (see details in Starr, A. *et al.*, 1991). The top tracing is of an ABR in which the averaging process always begins 3 ms after each click stimulus. There are five positive peaks present labeled as P1 through P5. Neural desynchrony is simulated in the lower trace by delaying the stimulus in a variable manner from between 3 and 4 ms after the start of the averaging process. Note that components P1 through P5 are markedly attenuated whereas the slow potential shift or pedestal on which the peaks arise is maintained. The attenuation of ABR peaks occurred because the neural events were made to vary in latency to cancel one another

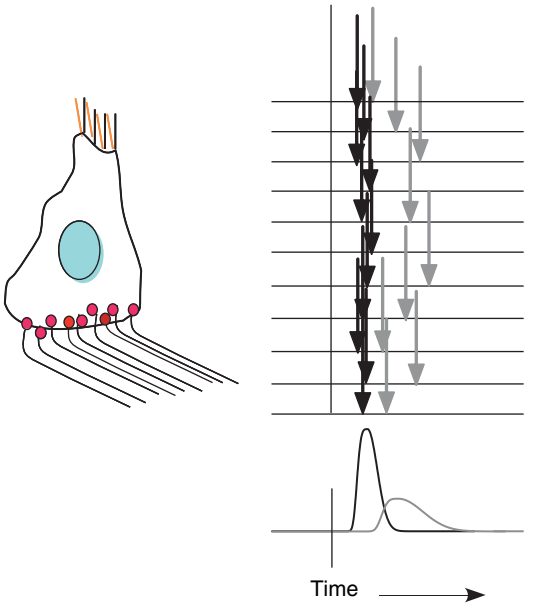

Figure 2 A representation of the patterns of activity of afferent auditory nerve fibers with synaptic connections to an inner hair cell. The onset of a transient stimulus is indicated by the vertical line below. The occurrence of fiber activity in a normally functioning system is represented by black arrows while fiber activity in an abnormal system is represented by gray arrows. The patterns of activity in the two conditions are shown below. The abnormalities of fiber activity that are represented include (a) variable delay in the latency of discharge and (b) absence of a response in 30% of the fibers. Note the short latency and synchrony of the population's response when the system is normal and the delayed latency, temporal dispersion, and reduced amplitude of the population's response when the system is abnormal. We suggest that the pattern of abnormality of activity would be similar whether the disorder were at inner hair cell, the synapse including neurotransmitter release, reuptake and binding to receptor sites, or in the nerve fibers. However, the extent of latency delay and variability as well as in the proportion of fibers that are activated would vary according to the type and extent of the pathological processes.

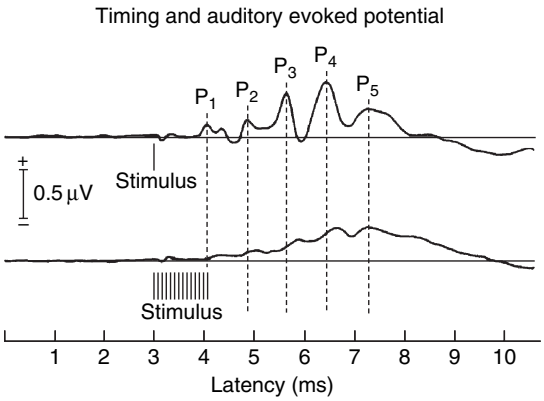

Figure 3 The effect of desynchrony on the ABR. The recordings were obtained from a cat when the stimuli were applied at precisely 3 ms after the onset of the averaging process. There are five peaks identified by the polarity (P for positive) and approximate latency in milliseconds. Another ABR was constituted when the stimulus was applied in a random manner between 3 and 4 ms after the onset of the averaging process. Note the marked attenuation of the five peaks that now appear as small variations in a sustained positive shift.

in the averaging process. The slow pedestal is not affected by the introduction of such a small variation in synchrony. We expect that such an attenuation of ABR components would accompany disorders of inner hair cells, auditory nerve fibers and/or their synapses affecting desynchrony of discharge, and/or a reduction of the number of neural elements activated making the population's response difficult to distinguish from background activity.

We suggest distinguishing the clinical disorder is known as auditory neuropathy by the presumed site of disorder. If the auditory nerve were involved with sparing of the inner hair cells and their synapses, the classification as auditory nerve disorder is appropriate. The finding of concomitant peripheral or cranial neuropathies appears to be the best evidence we have now for inferring the presence of auditory nerve disease. If the inner hair cells and/or the synapses with the auditory nerve were affected with sparing of the auditory nerve, the classification as auditory synaptic disorder is appropriate. The lack of a concomitant neuropathy of peripheral and/or cranial nerves and a positive response to electrical stimulation of the auditory nerve cell bodies is the best evidence we now have to suggest the disorder is distal in the auditory periphery in the region of the inner hair cell and its synapse with auditory nerve terminals. Synaptic disorders could involve alterations in the timing and magnitude of transmitter release and/or the availability of receptor sites on the afferent nerve terminals. There are likely many instances when both auditory nerve and inner hair cells would be affected and the classification of auditory nerve disorder, unspecified may be appropriate.

3.23.6 Psychoacoustic Deficits of Auditory Neuropathy

Auditory psychoacoustics have identified the major perceptual consequences of dysfunction of the auditory nerve (Figure 4). The mean measures of

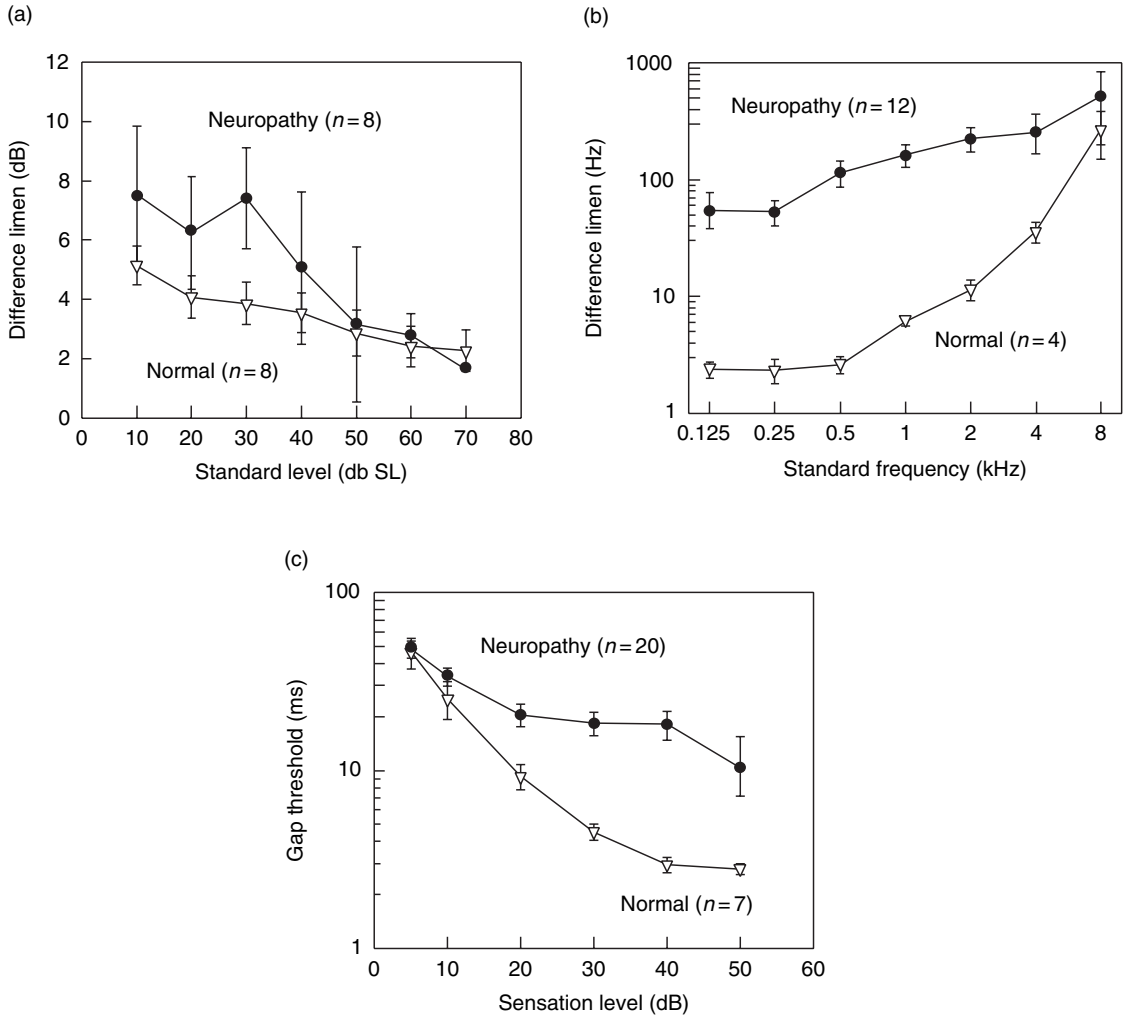

Figure 4 The means and standard errors (vertical lines) of psychoacoustic measures in patients with auditory neuropathy (filled circles) and in normal hearing subjects (unfilled, inverted triangles). The numbers of subjects tested are indicated each panel: (a) intensity discrimination; (b) frequency discrimination, and (c) gap detection. The magnitude of detection limens (DLs) for intensity discrimination was not significantly different between the two groups. In contrast, the difference limens for low frequencies up to 4 kHz were significantly higher in the auditory neuropathy group than the control group. DLs for high frequency (8 kHz) did not differ. Gap thresholds were elevated in auditory neuropathy subjects for intensities that were suprathreshold (>20 dB).

intensity discrimination (Figure 4(a)), frequency discrimination (Figure 4(b)), and temporal gap detection (Figure 4(c)) are plotted for the patients (filled circles) along with normal-hearing controls (unfilled, inverted triangles).

Although the hearing-impaired subjects tended to have greater than normal difference limen in intensity discrimination at low sensation levels, there was no overall significant difference between the affected and normal subjects. In contrast, the auditory neuropathy subjects showed significantly impaired frequency discrimination at low frequencies (125 Hz to 4 kHz) but normal difference limens at the high frequency (8 kHz). Similarly, the hearing-impaired subjects showed significantly impaired gap detection at high sensation levels (20–50 dB) but normal results at low sensation levels (5–10 dB).

Detailed description of other psychoacoustic measures has been obtained to reveal a unique pattern for persons with auditory neuropathy, in which auditory percepts dependent on temporal cues are particularly impaired whereas percepts dependent on intensity cues are preserved (Zeng, F. G. *et al.*, 2005).

Examples of impaired percepts related to temporal cues included pitch discrimination at low frequencies, temporal integration, gap detection, temporal modulation detection, backward and forward masking, signal detection in noise, binaural beats, and sound localization using interaural time differences. Examples of preserved percepts related to intensity cues included loudness discrimination, pitch discrimination at high frequencies, and sound localization using interaural level differences. These results are unique because cochlear or sensory hearing typically affects intensity related percepts (e.g., loudness recruitment) but not temporally related percepts as long as the intensity impairment is taken into account.

Objective measures of gap thresholds can also be defined using cortical potentials evoked by the interruption of a continuous noise with a silent period of different duration. (Michalewski, H. J. *et al.*, 2005). This is particularly relevant for defining temporal functions in children or adult patients who might not be able perform the normal behavioral measures of gap threshold. Figure 5 contains cortical responses to gaps from subjects with normal hearing and two individuals with auditory neuropathy and an elevated gap threshold. Note that an N100 component is clearly present in subjects with normal hearing in response to gaps as short as 5 ms whereas in the patients, N100 appears only with prolonged gap durations that approximate their psychoacoustic detection thresholds.

There were no significant differences between temporal psychoacoustic measures in subjects with a concomitant peripheral neuropathy presumed to also have a disease of the auditory nerve and those without a peripheral neuropathy presumed to have a disease affecting inner hair cells, the nerve terminals, and/or the synapse. Moreover, significant impairment in detecting tonal signals in noise has been observed in neuropathy subjects (Zeng, F. G. *et al.*, 2005). This large excess of masking, along with impaired temporal processing, contributes to the difficulty of understanding speech in noise so frequently observed in neuropathy subjects. We shall note that similar impairment in detecting tonal signals in noise has also been reported in persons who have inner hair cell loss or the so-called dead regions in cochlea (Moore, B. C., 2004). At present, we do not have a means to differentiate between the inner hair cell loss and the nerve loss.

Figure 6 presents possible mechanisms of auditory nerve responses to gaps of short duration when there are normal numbers of nerve fibers responding in a synchronous manner (Figure 6(a)) and the consequences of both impaired synchrony (Figure 6(b)) and reduced numbers of nerve fibers activated (Figure 6(c)). The normal neural response shows a clear spike pattern corresponding to the temporal gap in the stimuli. However, both the reduced neural synchrony and input will diminish this temporal

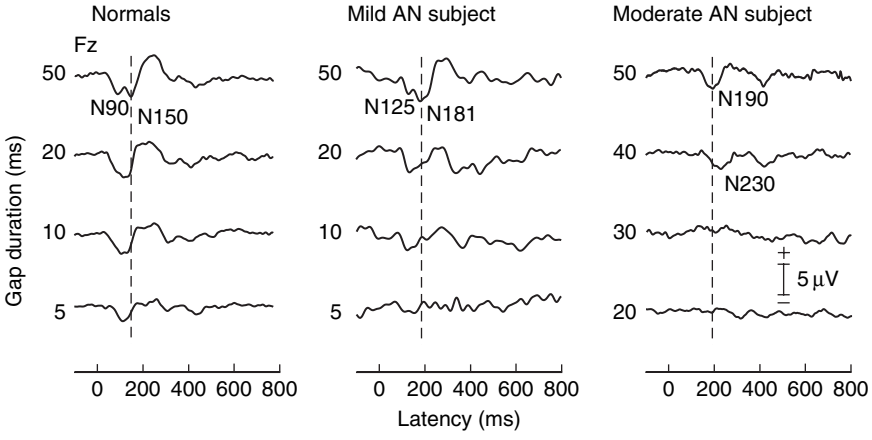

Figure 5 Cortical potentials as objective measure of gap threshold. Scalp-recorded brain potentials to gaps at 50 ms (top traces) and decreasing in duration in subsequent traces indicated on the left of each panel. In normal subjects (psychoacoustic gap threshold was 3 ms) clear N100 components indicated by dashed vertical line can be identified down to 5-ms gaps. In a subject with mild auditory neuropathy (psychoacoustic gap threshold was 8 ms), N100 can be identified at 50, 20, and 10 ms but not at 5 ms. In a subject with a moderate auditory neuropathy (AN; psychoacoustic gap threshold was 30 ms), N100 was delayed and identified at 50 and 40 ms, but not at 30 or 20 ms.

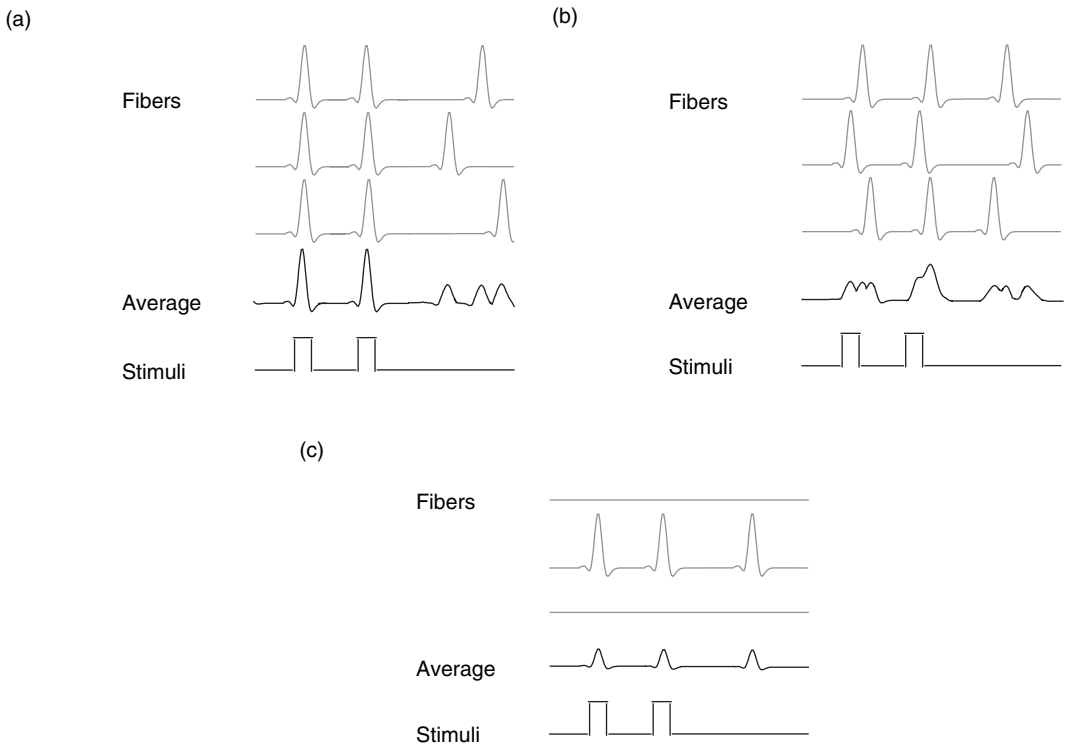

Figure 6 Population of auditory nerve fiber responses of to transient signals separated by a brief temporal gap when there is (a) normal synchrony; (b) desynchronized; and (c) deafferentation but preserved synchrony. Note that the neural representation of the two stimuli and their intervening gap are degraded when there is desynchrony or deafferentation. The condition when both desynchrony and deafferentation coexist would result in further loss of correlation with the acoustic stimuli.

gap at the neural level, making it difficult to discriminate from spontaneous background activity.

At present, we are lacking effective means to differentiate between these two models, as they all tend to show similar audiological, electrophysiological, and behavioral symptoms. Future studies using electric stimulation of the auditory nerve via a cochlear implant (CI) might be able to differentiate these two models, as selective loss of inner hair cells or dysfunctional synapses should not present a significant problem in electric stimulation, which bypasses these structures and activates the neuron's cell body or axon directly.

Clinical management of auditory neuropathy is difficult and not yet standardized. Because of the lack of success with conventional hearing aids, CIs have become the choice of treatment for many clinicians (Shallop, J. K. *et al.*, 2001). The psychoacoustic results suggest that novel features may need to be introduced in hearing aids in order for them to have any chance to help persons with neural hearing loss. One new feature would be to perform modulation expansion as opposed to compression in a typical hearing aid to compensate for the impaired temporal processing abilities. Another feature would be to perform upward frequency shift as opposed to downward frequency shift to take advantage of relatively normal pitch processing at high frequencies in persons with auditory neuropathy.

Individuals with disorders of the inner hair cells or their synapses appear especially likely to benefit from CIs. For instance, auditory neuropathy accompanying mutations of the otoferlin gene (*OTOF*; Rodriquez-Ballesteros, M. *et al.*, 2003; Varga, R. *et al.*, 2003) respond well to cochlear implantation. It is likely that in this disorder there are sufficient numbers of auditory nerve fibers and ganglion cells present capable of responding to electrical stimulation.

Cochlear implantation has also benefited subjects with a dominantly inherited deafness without peripheral nerve involvement (Starr, A. *et al.*, 2004). These subjects initially have absent ABRs and preserved OAEs and CMs. The latter two measures become lost within a few years of onset reflecting an

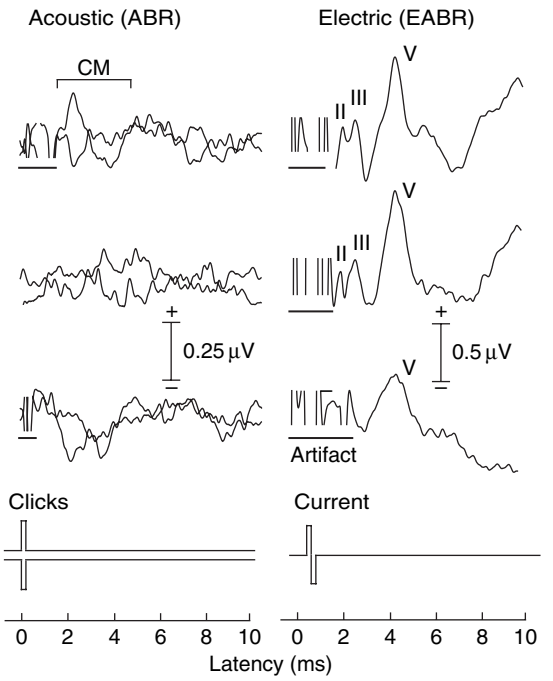

Figure 7 ABRs in three family members with a dominantly inherited disorder producing auditory nerve dysfunction (Starr, A. *et al.*, 2004). Prior to cochlear implantation, ABRs in response to acoustic stimulation do not show neural responses but cochlear microphonics (CM) were identified in one. After implantation electrical stimulation applied through the implant evoked large-amplitude neural components in all three. The artifacts of stimulation are indicated by the horizontal line for both the acoustic and electrical stimulation. Gap detection and speech comprehension improved remarkably following implantation.

involvement of OHCs only later in the course of the disorder. It is likely that the disorder affects inner hair cells/nerve terminals allowing the CI to provide striking benefits. Figure 7 contains ABRs and electrically evoked ABRs (EABRs) from three affected family members before and after implantation. The absence of acoustic ABRs prior to implantation contrasts with the well-developed EABRs after implantation. The subjects' abnormalities of gap thresholds and speech comprehension were also benefited after implantation.

3.23.7 Molecular Mechanisms of Auditory Neuropathy

We will present examples of mice (see Table 1) with genetically engineered defects affecting inner hair cells, synapses, or auditory nerve functions that provide an opportunity to define how specific genes alter auditory functions. Audiological tests of these mutants can identify similarities and differences to auditory neuropathies in humans. There is a particular need to develop both behavioral and objective measures of specific features of the accompanying auditory deficits such as cortical potential measures in response to gaps (Michalewski, H. J. *et al.*, 2005). We expect that characterizing the disorder at the cellular and molecular levels in these mutants may facilitate the development of tests and therapies in human disorders of hearing. The auditory findings on selective examples of gene mutants with various forms of auditory nerve dysfunction are presented below.

3.23.7.1 Inner Hair Cell Channelopathy-Knockout of the Inner Hair Cell $Ca_V1.3$

The molecular identity of the mammalian hair cell Ca^{2+} channel was proven to be $Ca_V1.3$ by a knockout experiment by Platzer J. *et al.* (2000) and Dou H. *et al.* (2004). The Ca^{2+} current of $Ca_V1.3^{-/-}$ inner hair cells is reduced by ~90% in inner hair cells causing a major defect of inner hair cell exocytosis (Figure 8(b); Brandt, A. *et al.*, 2003). $Ca_V1.3^{-/-}$ mice have absent ABRs (Figure 8(c)). Inner hair cells maintain their morphology for at least 2 months after birth but progressively loose their afferent synapses (Nemzou *et al.*, 2006). OHCs at the basilar turn of the cochlear are morphologically preserved for several weeks and produce high-frequency distortion product OAEs. In contrast, OHCs at the apical coil lose their stereovilli and tend to degenerate. There also appears to be an associated reduction of the numbers of surviving spiral ganglion neurons (Glueckert, R. *et al.*, 2003; Dou, H. *et al.*, 2004). A massive exocytosis of transmitter can still be elicited in inner hair cells by artificially increasing the cytosolic Ca^{2+} concentration (Brandt, A. *et al.*, 2003). Together, the results indicate that the lack of inner hair cell $Ca_V1.3$ channels disrupts the coupling of receptor potential and transmitter release. Thus a profound dysfunction of auditory nerve occurs in animals in the neonatal period with a gene defect disabling Ca^{2+} influx into inner hair cell with consequences of disrupting synaptic transmitter release. The disorder is progressive and can also affect the survival of both OHCs and auditory nerve.

Table 1 Animal examples of the variety of auditory nerve dysfunctions

	Primary mechanism	*Animal model (examples)*	*Human disease*	*OAE/CM*	*ABR*	*Morphology*	*Cellular phenotype/ molecular defect*
Disorders of inner hair cells and their synapses	IHC channelopathy	$Ca_V1.3$ KO [a,b,c]		+	Absent	Stereociliar defect of apical OHCs, age-dependent loss of apical OHCs, reduction of SGN	~90% reduction of Ca^{2+} current. Near complete block of IHC transmitter release
Auditory synaptopathy	Defect of presynaptic active zone	Bassoon KO [d]		+	Abnormal	No obvious morphological changes	Defect of synaptic ribbon anchorage at the active zone. Selective defect of synchronous transmitter release
	Inner hair cell vesicle fusion IHC transmitter release	To be generated Otoferlin KO (Roux *et al.*, Cell 2006)	Otoferlin inner hair cell disorders	+	Absent	Normal synaptogenesis, rapid loss of synapses	Major reduction of IHC transmitter release, defect of late step of exocytosis
	Defect of postsynaptic zone	Tubby mouse[e]	Profound prelingual deafness DFNB9				
Disorders of auditory nerve	Mislocalization of ion channels at axon initial segments and nodes of Ranvier	β-4-Spectrin-mutants[f,g]		+	Abnormal	Ultrastructural changes of nerve fibers	Impaired scaffolding of channels and cytoskeletal anchorage
Auditory neuropathy							Impaired nerve conduction
	Demyelination	PMP22-mutants MPZ-mutants[h,i]	Hereditary neuropathies		Abnormal	Demyelination, loss of dendrites, SGN reduction	Impaired nerve conduction due to short internodes, demyelinated axon segments, loss of SGN
	Axon/SGN loss	Dominant-negative erbB4-mutant[j]		+	Abnormal	SGN loss	Loss of axons and SGN

+, present; ABR, auditory brainstem response; CMs, cochlear microphonics; IHC, inner hair cell; KO, knockout; OAEs, otoacoustic emissions; OHC, outer hair cell; SGN, spiral ganglion neurons;
[a]Platzer J. *et al*. (2000).
[b]Brandt A. *et al*. (2003).
[c]Dou H. *et al*. (2004).
[d]Khimich D. *et al*. (2005).
[e]Noben-Trauth K. *et al*. (1996).
[f]Parkinson N. J. *et al*. (2001).
[g]Lacas-Gervais S. *et al*. (2004).
[h]Zhou R. *et al*. (1995).
[i]Zhou *et al*. (1995).
[j]Stankovic K. *et al*. (2004).

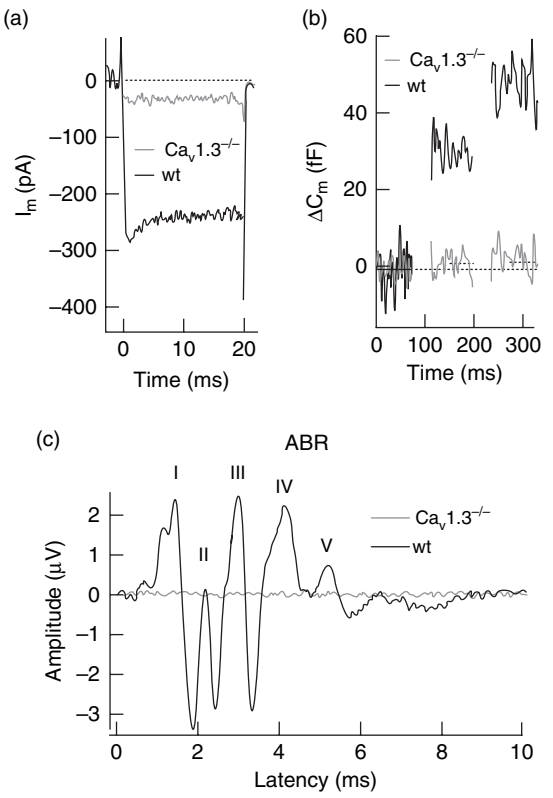

Figure 8 Auditory synaptic nerve dysfunction in a mutant mouse ($Ca_V1.3$-deficient) accompanying profound impairment of hair cell transmitter release due to loss of Ca^{2+} influx. (a) Voltage-gated Ca^{2+}currents in normal (Im: membrane current) (black) and a $Ca_V1.3$-deficient (gray) inner hair cells. There is a major reduction of Ca^{2+} influx in the mutant (~90%). (b) The absence of exocytic capacitance changes (ΔC_m) to paired depolarizations in a $Ca_V1.3$-deficient inner hair cell compared to the normal response. c, ABRs from a 3-week-old wild-type (WT) mouse (black trace) showing normal neural components and the absence neural components in a $Ca_V1.3$-deficient mouse (gray trace).

3.23.7.2 Impaired Inner Hair Cell Transmitter Release

Bassoon is a large matrix protein, which helps to anchor ribbons to the hair cell active synaptic zones. Quantitative assessment of the number of synapse-anchored ribbons of mature mutant mice (stained as green in Figures 9(a) and 9(b)) showed that inner hair cells on average contained one anchored ribbon compared to 10 ribbons in wild-type (WT) animals (Khimich, D. *et al.*, 2005). This reduction in synaptic function is accompanied by abnormal ABRs (Figure 9(c)) showing a marked attenuation and delay of wave I whereas subsequent components were affected only slightly. The thresholds for evoking the ABR were elevated up to 30 dB (Figure 9(d)). OHC activity reflected by CMs and distortion product OAEs were normal. Patch-clamp analysis of inner hair cell presynaptic function revealed a reduced readily releasable pool of synaptic vesicles and a slight reduction of the Ca^{2+} current in ribbon-deficient inner hair cells (Figures 9(e) and 9(f)). Thus, a reduction of ribbon-anchored synapses results in auditory nerve dysfunction reflected by impaired spiral ganglion activation (wave I) without changes in OAEs. The relative preservation of activity arising in brainstem portions of the auditory pathway may indicate that the change of synchrony in the auditory periphery is mild and can be compensated by central auditory mechanisms.

3.23.7.3 Auditory Nerve Ion Channel Displacement

The location of voltage-gated sodium channels in clusters at the nodes of Ranvier in auditory nerves is essential for normal saltatory propagation of action potentials along axons. Beta-4 spectrins are cytoskeletal proteins, which are involved in the positioning and linkage of voltage-gated sodium and potassium channels at the nodes of Ranvier (Bennett, V. and Baines, A. J., 2001). Beta-4 spectrin mutants are also known as Quivering mice because of their abnormal motor behaviors. The alterations in the locations of the voltage-gated channels are shown in Figures 10(d)–10(f). These animals can also have hearing impairments that vary with the mutation. Spontaneous mouse mutants with truncated beta-4 spectrin showed an intriguing correlation of the length of the remaining spectrin protein with the transmission along the auditory pathway (Parkinson, N. J. *et al.*, 2001). In the animals most severely affected only a wave I was present. Auditory studies in less affected mutant animals (Lacas-Gervais, S. *et al.*, 2004) showed auditory thresholds were unaffected (Figure 10(c)) whereas there was progressive delay of ABR peaks consistent with involvement of conduction along the brainstem auditory pathway (Figures 10(a) and 10(b)).

The delay in latency increased at higher stimulation rates and could be consistent with conduction deficits and/or conduction block in the affected fibers.

3.23.7.4 Auditory Nerve Fiber Myelin Disorder

Defects of genes coding for myelin proteins result in hereditary neuropathy (review in Suter, U. and

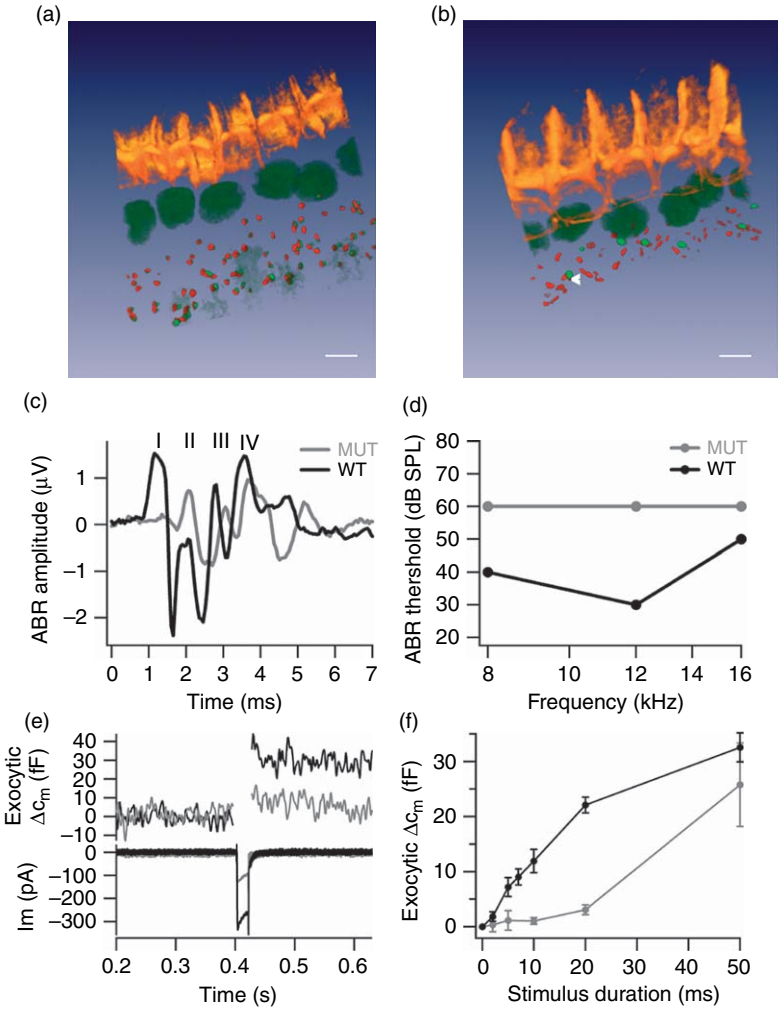

Figure 9 Auditory nerve dysfunction accompanying reduction in the numbers of synaptic ribbons in inner hair cells, the Bassoon mutant. a and b, immunostaining for RIBEYE/CtBP-2 (green): labeling ribbons and nuclei, postsynaptic glutamate receptors (red) adjacent to inner hair cell ribbons. Inner hair cells in mutants (MUT) (a) show fewer ribbon-postsynapstic pairs (arrow) than in wild-type (WT) animals (b). Actin filaments in. . . were labeled with Phalloidin and rendered gold. The apical part of inner hair cell and the adjacent pillar cells are labeled gold. Scale bar: 5 μm. (c) ABR of a representative pair of MUT (gray) and WT (black) mice in response to suprathreshold clicks (80 dB peSPL). Note that wave I was delayed and profoundly attenuated in the MUTs whereas the subsequent waves were only slightly attenuated but delayed in latency. (d) ABR threshold as function of frequency. The MUTs have normal otoacoustic emissions (not shown). (e) Representative Ca^{2+} currents and C_m changes recorded from WT and MUT inner hair cells (20 ms step depolarization). (f) Kinetics of exocytosis constructed from ΔC_m of the same inner hair cells in response to depolarization of varying durations showing depressed response in the MUT. SPL, sound pressure level; Im, membrane current; ΔC_m, exocytic membrane capacitance change.

Scherer, 2003). For example, mutations of the PMP22 gene cause hypomyelination, impaired nerve conduction and consequently neural hearing loss (Verhagen, W. I. *et al.*, 2005) in human Charcot–Marie–Tooth disease (Suter, U. and Scherer, S. S., 2003). Animal models with *PMP22* gene mutations have been described with altered auditory functions. The mutant known as Trembler because of their motor abnormalities shows reduced amplitudes and latency delay of ABR components. There are alterations of myelination of auditory nerve accompanied by a delayed spiral ganglion loss (Zhou, R. *et al.*, 1995a; 1995b). OHC functions have not been defined. These mutant animals have auditory nerve dysfunction due to a nerve disorder affecting myelin.

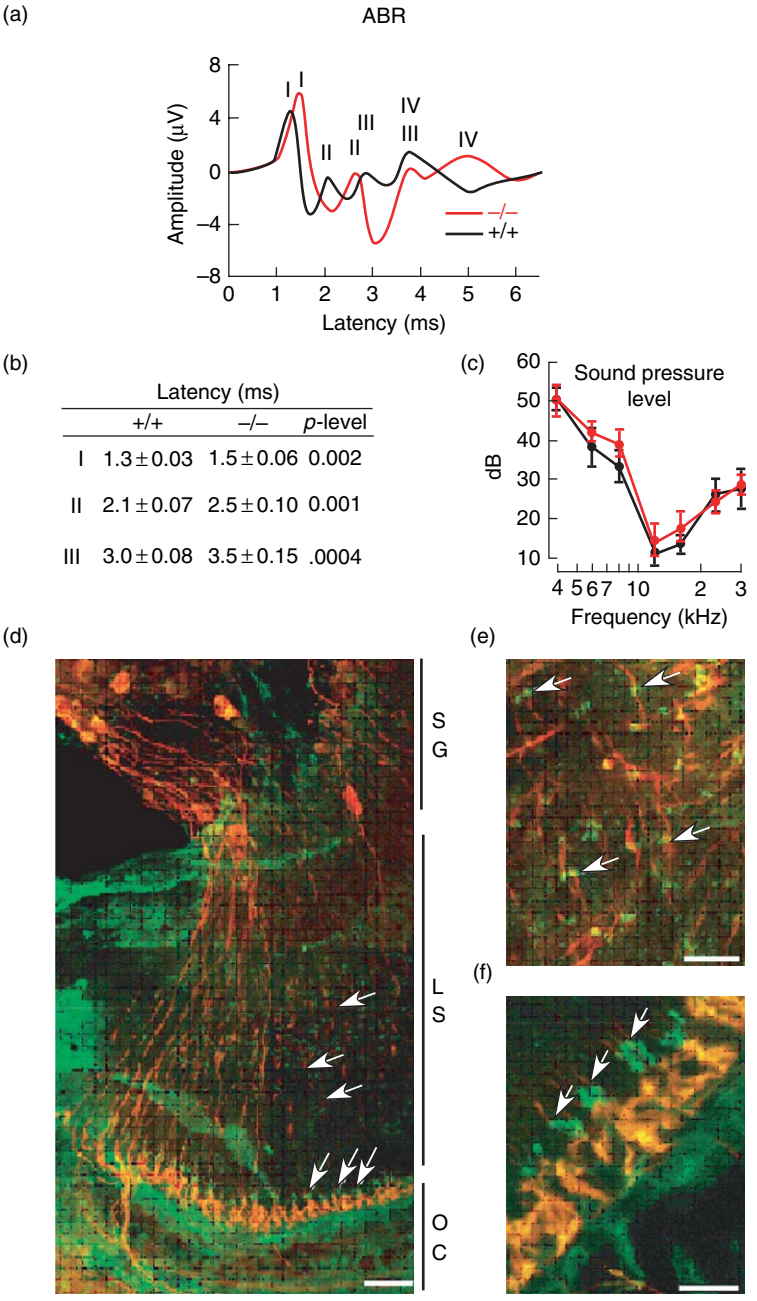

Figure 10 Auditory nerve dysfunction accompanying reduction in the numbers of synaptic ribbons in inner hair cells, the Bassoon mutant. (a) and (b) immunostaining for RIBEYE/CtBP-2 (green): labeling ribbons and nuclei, glutamate receptors (red) adjacent to IHC ribbons. Inner hair cells in mutants (a) show fewer ribbon-postsynapstic pairs (arrow) than in wild type animals (b). The apical part of inner hair cell and the adjacent pillar cells are labeled gold. Scale bar: 5 μm. (c) ABR of a representative pair of mutant (grey) and wild type (WT) (black) mice in response to suprathreshold clicks (80 dB peSPL). Note that Wave I was delayed and profoundly attenuated in the mutant whereas the subsequent waves were only slightly attenuated but delayed in latency. (d) ABR threshold as function of frequency. The mutants have normal otoacoustic emissions. (e) Representative Ca^{2+} currents and C_m changes recorded from WT and mutant IHCs (20 ms step depolarization). (f) Kinetics of exocytosis constructed from ΔC_m of the same IHCs in response to depolarization of varying durations showing depressed response in the wild type.

3.23.7.5 Loss of Spiral Ganglion Neurons

Spiral ganglion neurons may be affected as both a primary and a secondary effect of gene mutations. Recent data demonstrated that the survival of spiral ganglion neurons depends on a complex regulation involving the neuregulin-erbB system and neurotrophin signaling (Stankovic, K. *et al.*, 2004). Their study showed a primary expression of erbB in the supporting cells of the organ of Corti. Disabling the erbB receptor function results in a rapid and ~80% loss of spiral ganglion neurons. Immediately prior to the neuronal loss, downregulation of cochlear neurotrophin-3 expression occurred, which appears to be important for ganglion cell maintenance. The audiological findings are consistent with auditory neuropathy showing absent or profoundly abnormal ABRs and preserved OAEs. Both IHCs and OHCs appear to be little affected. This gene mutation results in auditory nerve dysfunction consistent with loss of spiral ganglion cells without other peripheral or cranial neuropathies.

3.23.8 Conclusions

There has been considerable advance in identifying and characterizing auditory nerve dysfunction in humans. We have highlighted physiological criteria for defining the disorder and identified the diversity of affected structures in the auditory periphery that, when affected, can be accompanied by auditory neuropathy. Psychoacoustic results show that the deficits of auditory nerve dysfunctions primarily affect those percepts dependent on temporal cues. The development of experimental animal models with auditory nerve dysfunction has begun to provide insights into basic molecular mechanisms of the disorders and will hopefully lead to the development of treatment therapies.

Acknowledgments

This research was supported in part by grants DC-02618 (Starr) and DC-02267 (Zeng) from the National Institutes of Health, and the MPG (Tandemproject) and DFG (CMPB) to T Moser.

References

Amatuzzi, M. G., Northrop, C., Liberman, M. C., Thornton, A., Halpin, C., Herrmann, B., Pinto, L. E., Saenz, A., Carranza, A., and Eavey, R. D. 2001. Selective inner hair cell loss in premature infants and cochlear pathological patterns from neonatal intensive care unit autopsies. Arch. Otolaryngol. Head Neck Surg. 127, 629–636.

Bennett, V. and Baines, A. J. 2001. Spectrin and ankyrin-based pathways: metazoan inventions for integrating cells into tissues. Physiol. Rev. 81, 1353–1392.

Berlin, C. I., Bordelon, J., St John, P., Wilensky, D., Hurley, A., Kluka, E., and Hood, L. J. 1998. Reversing click polarity may uncover auditory neuropathy in infants. Ear Hear. 19, 37–47.

Berlin, C. I., Hood, L. J., Cecola, R. P., Jackson, D. F., and Szabo, P. 1993. Does type I afferent neuron dysfunction reveal itself through lack of efferent suppression? Hear. Res. 65, 40–50.

Berlin, C. I., Hood, L. J., Morlet, T., Rose, K., and Brashears, S. 2003. Auditory neuropathy/dys-synchrony: diagnosis and management. Ment. Retard. Dev. Disabil. Res. Rev. 9, 225–231.

Brandt, A., Striessnig, J., and Moser, T. 2003. $Ca_V1.3$ channels are essential for development and presynaptic activity of cochlear inner hair cells. J. Neurosci. 23, 10832–10840.

Brownell, W. E. 1984. Microscopic observation of cochlear hair cell motility. Scan. Electron Microsc. Pt 3, 1401–1406.

Davis, H. and Hirsh, S. K. 1979. A slow brain stem response for low-frequency audiometry. Audiology 18, 445–461.

Dou, H., Vazquez, A. E., Namkung, Y., Chu, H., Cardell, E. L., Nie, L., Parson, S., Shin, H. S., and Yamoah, E. N. 2004. Null mutation of alpha1D Ca^{2+} channel gene results in deafness but no vestibular defect in mice. J. Assoc. Res. Otolaryngol. 5, 215–226.

Doyle, K. J., Sininger, Y., and Starr, A. 1998. Auditory neuropathy in childhood. Laryngoscope 108, 1374–1377.

Glowatzki, E. and Fuchs, P. A. 2002. Transmitter release at the hair cell ribbon synapse. Nat. Neurosci. 5, 147–154.

Glueckert, R., Wietzorrek, G., Kammen-Jolly, K., Scholtz, A., Stephan, K., Striessnig, J., and Schrott-Fischer, A. 2003. Role of class D L-type Ca^{2+} channels for cochlear morphology. Hear. Res. 178, 95–105.

Hallpike, C. S., Harriman, D. G., and Wells, C. E. 1980. A case of afferent neuropathy and deafness. J. Laryngol. Otol. 94, 945–964.

Hecox, K. and Galambos, R. 1974. Brain stem auditory evoked responses in human infants and adults. Arch. Otolaryngol. 99, 30–33.

Hood, L. J. and Berlin, C. I. 2001. Auditory Neuropathy (Auditory Dys-synchrony) Disables Efferent Suppression of Otoacoustic Emissions. In: Auditory Neuropathy: A New Perspective on Hearing Disorders (*eds*. Y. Sininger and A. Starr), pp. 183–202. Singular.

Kaga, K., Kitazumi, E., and Kodama, K. 1979. Auditory brain stem responses of kernicterus infants. Int. J. Pediatr. Otorhinolaryngol. 1, 255–264.

Kemp, D. T. 1978. Stimulated acoustic emissions from within the human auditory system. J. Acoust. Soc. Am. 64, 1386–1391.

Khimich, D., Nouvian, R., Pujol, R., Tom Dieck, S., Egner, A., Gundelfinger, E. D., and Moser, T. 2005. Hair cell synaptic ribbons are essential for synchronous auditory signaling. Nature 434, 889–894.

Kraus, N., Ozdamar, O., Stein, L., and Reed, N. 1984. Absent auditory brain stem response: peripheral hearing loss or brain stem dysfunction? Laryngoscope 94, 400–406.

Lacas-Gervais, S., Guo, J., Strenzke, N., Scarfone, E., Kolpe, M., Jahkel, M., De Camilli, P., Moser, T.,

Rasband, M. N., and Solimena, M. 2004. BetaIVSigma1 spectrin stabilizes the nodes of Ranvier and axon initial segments. J. Cell Biol. 166, 983–990.

Lenhardt, M. L. 1981. Childhood central auditory processing disorder with brainstem evoked response verification. Arch. Otolaryngol. 107, 623–625.

Martin, W. H., Pratt, H., and Schwegler, J. W. 1995. The origin of the human auditory brain-stem response wave II. Electroencephalogr. Clin. Neurophysiol. 96, 357–370.

Melcher, J. R., Knudson, I. M., Fullerton, B. C., Guinan, J. J., Jr., Norris, B. E., and Kiang, N. Y. 1996. Generators of the brainstem auditory evoked potential in cat. I. An experimental approach to their identification. Hear. Res. 93, 1–27.

Michalewski, H. J., Starr, A., Nguyen, T. T., Kong, Y. Y., and Zeng, F. G. 2005. Auditory temporal processes in normal-hearing individuals and in patients with auditory neuropathy. Clin. Neurophysiol. 116, 669–680.

Moore, B. C. 2004. Dead regions in the cochlea: conceptual foundations, diagnosis, and clinical applications. Ear Hear. 25, 98–116.

Noben-Trauth, K., Naggert, J. K., North, M. A., and Nishina, P. M. 1996. A candidate gene for the mouse mutation tubby. Nature 380, 534–538.

Parkinson, N. J., Olsson, C. L., Hallows, J. L., McKee-Johnson, J., Keogh, B. P., Noben-Trauth, K., Kujawa, S. G., and Tempel, B. L. 2001. Mutant beta-spectrin 4 causes auditory and motor neuropathies in quivering mice. Nat. Genet. 29, 61–65.

Platzer, J., Engel, J., Schrott-Fischer, A., Stephan, K., Bova, S., Chen, H., Zheng, H., and Striessnig, J. 2000. Congenital deafness and sinoatrial node dysfunction in mice lacking class D L-type Ca^{2+} channels. Cell 102, 89–97.

Rapin, I. and Gravel, J. 2003. ''Auditory neuropathy'': physiologic and pathologic evidence calls for more diagnostic specificity. Int. J. Pediatr. Otorhinolaryngol. 67, 707–728.

Rodriguez-Ballesteros, M., del Castillo, F. J., Martin, Y., Moreno-Pelayo, M. A., Morera, C., Prieto, F., Marco, J., Morant, A., Gallo-Teran, J., Morales-Angulo, C., Navas, C., Trinidad, G., Tapia, M. C., Moreno, F., and del Castillo, I. 2003. Auditory neuropathy in patients carrying mutations in the otoferlin gene (OTOF). Hum. Mutat. 22, 451–456.

Ropper, A. H. and Chiappa, K. H. 1986. Evoked potentials in Guillain-Barré syndrome. Neurology 36, 587–590.

Satya-Murti, S., Cacace, A., and Hanson, P. 1980. Auditory dysfunction in Friedreich ataxia: result of spiral ganglion degeneration. Neurology 30, 1047–1053.

Shallop, J. K., Peterson, A., Facer, G. W., Fabry, L. B., and Driscoll, C. L. 2001. Cochlear implants in five cases of auditory neuropathy: postoperative findings and progress. Laryngoscope 111, 555–562.

Sininger, Y. and Oba, S. 2001. Patients With Auditory Neuropathy: Who Are They and What Can They Hear? In: Auditory Neuropathy: A New Perspective on Hearing Disorders (*eds*. Y. Sininger and A. Starr), pp. 15–35. Singular.

Spoendlin, H. 1974. Optic cochleovestibular degenerations in hereditary ataxias. II. Temporal bone pathology in two cases of Friedreich's ataxia with vestibule-cochlear disorders. Brain 97, 41–48.

Stankovic, K., Rio, C., Xia, A., Sugawara, M., Adams, J. C., Liberman, M. C., and Corfas, G. 2004. Survival of adult spiral ganglion neurons requires erbB receptor signaling in the inner ear. J. Neurosci. 24, 8651–8661.

Starr, A. 2001. The Neurology of Auditory Neuropathy. In: Auditory Neuropathy: A New Perspective on Hearing Disorders (*eds*. Y. Sininger and A. Starr), pp. 37–49. Singular.

Starr, A. and Achor, J. 1975. Auditory brain stem responses in neurological disease. Arch. Neurol. 32, 761–768.

Starr, A. and Hamilton, A. E. 1976. Correlation between confirmed sites of neurological lesions and abnormalities of far-field auditory brainstem responses. Electroencephalogr. Clin. Neurophysiol. 41, 595–608.

Starr, A., Isaacson, B., Michalewski, H. J., Zeng, F. G., Kong, Y. Y., Beale, P., Paulson, G. W., Keats, B. J., and Lesperance, M. M. 2004. A dominantly inherited progressive deafness affecting distal auditory nerve and hair cells. J. Assoc. Res. Otolaryngol. 5, 411–426.

Starr, A., McPherson, D., Patterson, J., Don, M., Luxford, W., Shannon, R., Sininger, Y., Tonakawa, L., and Waring, M. 1991. Absence of both auditory evoked potentials and auditory percepts dependent on timing cues. Brain 114, 1157–1180.

Starr, A., Michalewski, H. J., Zeng, F. G., Fujikawa-Brooks, S., Linthicum, F., Kim, C. S., Winnier, D., and Keats, B. 2003. Pathology and physiology of auditory neuropathy with a novel mutation in the MPZ gene (Tyr145->Ser). Brain 126, 1604–1619.

Starr, A., Picton, T. W., and Kim, R. 2001a. Pathophysiology of Auditory Neuropathy. In: Auditory Neuropathy: A New Perspective on Hearing Disorders (*eds*. Y. Sininger and A. Starr), pp. 67–82. Singular.

Starr, A., Picton, T. W., Sininger, Y., Hood, L. J., and Berlin, C. I. 1996. Auditory neuropathy. Brain 119, 741–753.

Starr, A., Sininger, Y., Nguyen, T., Michalewski, H. J., Oba, S., and Abdala, C. 2001b. Cochlear receptor (microphonic and summating potentials, otoacoustic emissions) and auditory pathway (auditory brain stem potentials) activity in auditory neuropathy. Ear Hear. 22, 91–99.

Suter, U. and Scherer, S. S. 2003. Disease mechanisms in inherited neuropathies. Nat. Rev. Neurosci. 4, 714–726.

Varga, R., Kelley, P. M., Keats, B. J., Starr, A., Leal, S. M., Cohn, E., and Kimberling, W. J. 2003. Non-syndromic recessive auditory neuropathy is the result of mutations in the otoferlin (OTOF) gene. J. Med. Genet. 40, 45–50.

Verhagen, W. I., Huygen, P. L., Gabreels-Festen, A. A., Engelhart, M., van Mierlo, P. J., and van Engelen, B. G. 2005. Sensorineural hearing impairments in pateints with Pmp22 duplication, deletion, and frame shift mutations. Otol. Neurotol. 26, 405–414.

Worthington, D. W. and Peters, J. F. 1980. Quantifiable hearing and no ABR: paradox or error? Ear Hear. 1, 281–285.

Yasunaga, S., Grati, M., Cohen-Salmon, M., El-Amraoui, A., Mustapha, M., Salem, N., El-Zir, E., Loiselet, J., and Petit, C. 1999. A mutation in OTOF, encoding otoferlin, a FER-1-like protein, causes DFNB9, a nonsyndromic form of deafness. Nat. Genet. 21, 363–369.

Zeng, F. G., Kong, Y. Y., Michalewski, H. J., and Starr, A. 2005. Perceptual consequences of disrupted auditory nerve activity. J. Neurophysiol. 93, 3050–3063.

Zeng, F. G., Oba, S., Garde, S., Sininger, Y., and Starr, A. 1999. Temporal and speech processing deficits in auditory neuropathy. Neuroreport 10, 3429–3435.

Zhou, R., Abbas, P. J., and Assouline, J. G. 1995a. Electrically evoked auditory brainstem response in peripherally myelin-deficient mice. Hear. Res. 88, 98–106.

Zhou, R., Assouline, J. G., Abbas, P. J., Messing, A., and Gantz, B. J. 1995b. Anatomical and physiological measures of auditory system in mice with peripheral myelin deficiency. Hear. Res. 88, 87–97.

3.24 Efferent System

L Robles and P H Delano, Universidad de Chile, Santiago, Chile

© 2008 Elsevier Inc. All rights reserved.

3.24.1	**Introduction**	414
3.24.2	**Anatomy of the Efferent System**	414
3.24.2.1	Olivocochlear Anatomy	414
3.24.2.1.1	Medial olivocochlear anatomy	415
3.24.2.1.2	Lateral olivocochlear anatomy	416
3.24.2.1.3	Medial olivocochlear neurotransmitters	417
3.24.2.1.4	Lateral olivocochlear neurotransmitters	417
3.24.2.2	Cortico-Cochlear Pathways	419
3.24.3	**Physiology of the Efferent System**	421
3.24.3.1	Electrical Stimulation of the Efferent System	421
3.24.3.1.1	Effects on cochlear electrical responses and otoacoustic emissions	421
3.24.3.1.2	Medial olivocochlear effects on cochlear mechanics	424
3.24.3.1.3	Efferent modulation by electrical activation of the inferior colliculus	425
3.24.3.1.4	Efferent modulation by electrical activation of the auditory cortex	425
3.24.3.2	Acoustic Activation of the Efferent System	426
3.24.3.2.1	Acoustic efferent effects in experimental animals	426
3.24.3.2.2	Acoustic efferent effects measured in humans	428
3.24.3.3	Lesion Studies of the Efferent System	428
3.24.3.3.1	Section of olivocochlear efferents in animals	428
3.24.3.3.2	Vestibular-nerve section in humans	429
3.24.3.3.3	Ablation of the auditory cortex	430
3.24.3.4	Manipulating Efferent Neurotransmission	430
3.24.3.4.1	Knockout Mice (α9-nicotinic acetylcholine, αCGRP, $GABA_A$)	430
3.24.3.4.2	Drugs that alter the auditory-efferent function	431
3.24.3.4.3	Neurochemical and lesion studies of lateral olivocochlear transmission	432
3.24.4	**Proposed Functions of the Auditory Efferent System**	433
3.24.4.1	Antimasking of Auditory Stimuli in Noise	433
3.24.4.1.1	Antimasking in experimental animals	434
3.24.4.1.2	Antimasking of tones and speech in humans	434
3.24.4.2	Protection to Loud Sounds	435
3.24.4.2.1	Medial olivocochlear protection to loud sounds	435
3.24.4.2.2	Lateral olivocochlear protection to loud sounds	436
3.24.4.3	Modulation of Sensory Input During Sleep	436
3.24.4.4	Modulation of Cochlear Sensitivity by Selective Attention	437
3.24.4.4.1	Cross-modal attenuation of auditory stimuli	437
3.24.4.4.2	Intra-modal frequency filter	437
3.24.4.5	Balance of Interaural Sensitivity	437
3.24.5	**Some Clinical Findings**	437
3.24.6	**Conclusions**	439
References		439

Glossary

round-window electrode A metal electrode is positioned near the round window of the cochlea to record cochlear potentials from the auditory nerve and cochlear hair cells, as: auditory-nerve compound action potential (CAP), cochlear microphonic potential (CM), and VIII nerve ensemble background activity.

auditory-nerve compound action potential (CAP) This neural response reflects the summed and synchronous responses of auditory-nerve fibers elicited by clicks or by tone bursts. The amplitude of the N1 wave of the CAP and its latency are the most commonly used measures.

cochlear microphonic potential (CM) It is an alternating potential that resembles the time course of the acoustic stimulus. This potential originates from the outer hair cells of the cochlea.

eighth-nerve ensemble background activity Also known as round-window noise, it is the spontaneous neural activity of auditory-nerve fibers, recorded without auditory stimulation. It is characterized by a frequency peak between 0.5 and 1.5 kHz.

otoacoustic emissions They are low-level sounds emitted by the cochlea, which are believed to originate in outer hair cells. They are classified in spontaneous and evoked otoacoustic emissions. Evoked emissions include transiently evoked and distortion products otoacoustic emissions.

3.24.1 Introduction

The cochlea has highly specialized receptor cells that transform the mechanical energy from acoustic stimuli into changes of cell-membrane electrical potentials. These electrical responses give origin to action potentials that conduct the information through afferent neural pathways to the central nervous system, where auditory perception takes place. Until recently auditory research was mainly focused on the study of transduction mechanisms, afferent neural responses, and psychoacoustics. However, in addition to afferent pathways, the auditory system has conspicuous efferent pathways that project from the central nervous structures to the periphery, as far as to the receptor hair cells from the inner ear, and that can modify the incoming sensory information. This chapter provides a general and comprehensive summary of the current knowledge about the auditory efferent system in mammals, discussing research data obtained in animals as well as in humans. It reviews the main findings on the anatomy, neurotransmission, and physiology of the auditory efferent system and it discusses some of the functions that have been proposed for the efferent system and possible clinical implications.

3.24.2 Anatomy of the Efferent System

The auditory efferent system in mammals originates in the auditory cortex, comprises the inferior colliculus (IC) and the superior olivary complex, and reaches the cochlea through the olivocochlear (OC) fibers. Following the chronological order of anatomical findings in the auditory efferent system, this section first reviews the extensively studied OC efferent system and then the more recently discovered cortico-cochlear connections.

3.24.2.1 Olivocochlear Anatomy

Inner-ear efferent fibers are part of a centrifugal pathway, known in vertebrates as the octavolateralis efferent system, which originates in a group of neurons located in the brainstem and terminates in the hair cells or the eight-nerve ganglion cells of auditory and vestibular organs in mammals and birds, and in the hair cells of the lateral line in fish. In mammals, the brainstem neurons giving origin to auditory and vestibular efferent fibers are completely separated (Simmons, D. D., 2002).

Rasmussen G. L. (1946) was the first to identify in the cat a group of efferent fibers that originate in the ventral brainstem, at the medial region of the superior olivary complex. These fibers that constitute the crossed olivococlear bundle cross at the floor of the fourth ventricle and reach the contralateral cochlea. In a later work (Rasmussen, G. L., 1960), he described a second group of thin fibers that originate in the same region and project to the ipsilateral cochlea, known as the uncrossed OC bundle.

Afterward, using neuronal retrograde tracers Warr W. B. (1975) elucidated the central origin and

the distribution of the crossed and uncrossed OC bundles in the cat. From this and other studies using anterograde tracers (Warr,W. B. and Guinan, J. J., 1979) emerged a new classification of the OC fibers, in which according to their central origin in the brainstem they were separated into: medial OC (MOC) fibers and lateral OC (LOC) fibers. The MOC fibers correspond to large diameter, myelinated axons from neurons located in the medial region of the superior olivary complex, whereas the LOC fibers are thin, unmyelinated axons from small neurons located in the lateral region of the superior olivary complex (Figure 1).

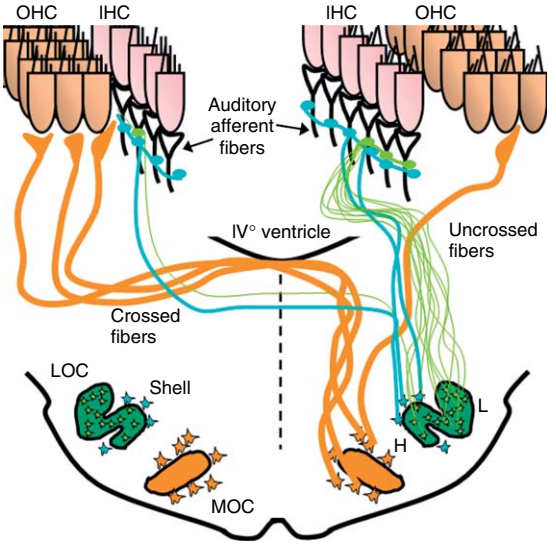

Figure 1 Illustration of the olivocochlear (OC) anatomy. Three different groups of efferent neurons have been identified in the superior olivary complex: (1) intrinsic lateral olivocochlear (LOC) neurons (green), (2) shell neurons from the lateral superior olive (light blue), and (3) medial olivocochlear (MOC) neurons from the medial superior olive (orange). MOC neurons have thick and myelinated axons that mainly project to the contralateral cochlea and make synapses with OHCs. LOC neurons and shell neurons project mainly to the ipsilateral cochlea and make synapses with afferent auditory-nerve fibers. Shell neurons originate in the periphery of the LOC nuclei, and their projections bifurcate to the base and apex of the cochlea. LOC intrinsic neurons are the largest component of the OC system and emerge from the LOC nuclei themselves. LOC axons project unidirectionally to the apex or base of the cochlea. Neurons located in the LOC medial limb project to the base of the cochlea (H: high frequencies), whereas those located in the lateral limb project to the apex (L: low frequencies). Differences in the distribution of OC neurons among mammals can be found in Table 1 (OHC: outer hair cell; IHC: inner hair cell).

These two bundles of OC efferents, besides their different origin, project to different targets in the cochlea. The MOC fibers project mostly contralaterally, making synaptic contact with the three rows of outer hair cells (OHCs), while LOC fibers project mostly ipsilaterally, making synaptic contact with radial afferent auditory-nerve fibers beneath inner hair cells (IHCs; Guinan, J. J., Jr., 1996).

In the following sections the anatomy and neurotransmitters of the medial and lateral OC systems are reviewed separately. For further information in the anatomy and physiology of these systems see Guinan J. J., Jr. (1996) or in cochlear neurotransmitters see Eybalin M. (1993).

3.24.2.1.1 Medial olivocochlear anatomy

MOC fibers emerge from the ventral nucleus of the trapezoid body, and in some species (cats and guinea-pigs) also from the superior periolivary nucleus. In the mature mammalian cochlea, MOC fibers make direct synaptic contact only with OHCs; however, during development, immature IHCs also receive transient innervation from MOC efferents that disappears in later developmental stages (Simmons, D. D., 2002). Although there are differences in the distribution of efferent fibers among species, in all of those studied, most of the MOC fibers cross to the contralateral cochlea through the floor of the fourth ventricle (Table 1). In cats, crossed MOC fibers project mainly to the more basal turns of the cochlea, while uncrossed MOC projections are largest in the center of the cochlea (Guinan, J. J., Jr., 1996). In contrast, the largest MOC projections in mice are directed toward the middle of the cochlea, a location that in this species corresponds to characteristic frequencies around 10 kHz (Maison, S. F. *et al.*, 2003a). Another species-specific difference in efferent innervation is that the MOC synaptic terminal area in cats is four times larger for the first row than that for the third row of OHCs (Liberman, M. C. *et al.*, 1990), whereas in mice there is no gradient of MOC innervation across OHC rows (Maison, S. F. *et al.*, 2003a). In addition to their well-studied cochlear projections, MOC neurons in various species also send axon collaterals to the ventral cochlear nucleus and the vestibular nuclei (Brown, M. C. *et al.*, 1991; Brown, M. C., 1993; Horvath, M. *et al.*, 2000).

An analysis of the anatomy of single MOC neurons performed in selectively labeled axons in rats demonstrated great morphological diversity of MOC neurons, which was evident at the organ of Corti in the number of tunnel-crossing fibers (1–15) and of

Table 1 Species differences in the distribution of olivocochlear efferent fibers

	Medial olivocochlear system (MOC)		*Lateral olivocochlear system (LOC)*			
			Intrinsic LOC		*Shell LOC*	
Species	*Number of neurons*	*Percentage of contralateral fibers*	*Number of neurons*	*Percentage of ipsilateral fibers*	*Number of neurons*	*Percentage of ipsiateral fibers*
Chinchilla (Azeredo, W. J., *et al.*, 1999)	280	80% contralateral	787	99% ipsilateral	101	70% ipsilateral
Rat (Vetter, D. E. and Mugnaini, E., 1992)	316	60% contralateral	619	100% ipsilateral	111	95% ipsilateral
Cat (Warr, W. B., *et al.*, 2002)	549	75% contralateral	769	87% ipsilateral	251	75% ipsilateral
Hamster (Sanchez-Gonzalez, M. A., *et al.*, 2003)	80	75% contralateral	164	97% ipsilateral	65	80% ipsilateral
Guinea-pig (Robertson, D., *et al*., 1987)	543	69% contralateral	690 LOC fibers (99% ipsilateral)			
Mouse (Campbell, J. P. and Henson, M. M., 1988)	164	75% contralateral	311 LOC fibers (99% ipsilateral) (around 30 shell neurons, suggested by Darrow, K. N. *et al*., 2006a)			
Human (Arnesen, A. R., 1984)	360 myelinated fibers (MOC)		1005 unmyelinated fibers (LOC)			

synaptic boutons contacting OHCs (Warr,W. B. and Boche, J. E., 2003). According to their pattern of axonal branching within the cochlea, MOC neurons were sorted into two subtypes: a more common sparsely branched and a quite rare highly branched. In the limited sample of MOC axons analyzed in that study all highly branched fibers projected ipsilaterally and innervated short spans of the cochlea.

3.24.2.1.2 Lateral olivocochlear anatomy

The unmyelinated axons of the lateral OC system originate from two subgroups of efferent brainstem neurons: intrinsic and shell LOC neurons (Figure 1; Vetter, D. E. and Mugnaini, E., 1992). The intrinsic LOC neurons are small neurons located within the lateral superior olivary nucleus that project almost exclusively to the ipsilateral cochlea and have dendrites restricted to the nucleus. Intrinsic neurons have a coarse tonotopic distribution in the lateral superior olive (LSO); as neurons located in the lateral limb project to the cochlear apex and those located in the medial limb project to the base (Robertson, D. *et al*., 1987). In contrast with the intrinsic neurons, shell LOC neurons are a small group of large neurons that surround the LSO and project mainly to the ipsilateral cochlea (Vetter, D. E. and Mugnaini, E., 1992). Shell neurons have extensive dendrites that reach into the lateral superior olivary nucleus and probably make contact with other brainstem nuclei. In the rat, shell neurons, like MOC neurons, send axon collaterals that innervate the ventral cochlear nucleus, whereas intrinsic LOC neurons do not project into the ventral cochlear nucleus (Horvath, M. *et al*., 2000).

Based upon the patterns of cochlear innervation in the guinea-pig, LOC axons have been classified into two groups (Brown, M. C., 1987). The largest group of LOC fibers runs unidirectionally (either apically or basally), usually less than 1 mm, in a spiral path within the cochlea and make discrete terminations with synaptic contacts beneath IHCs, while the smallest group of fibers runs bidirectionally in the cochlea, forming axonal swellings throughout a more extended spiral course. A later study also found two types of LOC axons in the rat and showed that axons with focal terminal patterns beneath IHCs

corresponded to intrinsic neurons, whereas those with diffuse terminal patterns corresponded to shell neurons (Warr, W. B. *et al.*, 1997; Warr, W. B. and Boche, J. E., 2003). Although, it is known that lateral OC fibers make synaptic contacts with the dendrites of afferent auditory neurons, just beneath their synapses with the IHCs, it is not clear yet whether these efferent synapses correspond to either one or the other or to both types of LOC axons. Lateral efferents have also been reported to make sporadically synapses directly onto the IHCs (Liberman, M. C., 1980; Liberman, M. C. *et al.*, 1990).

3.24.2.1.3 Medial olivocochlear neurotransmitters

It is well established that the main neurotransmitter of the MOC efferent system, that makes synaptic contact onto OHCs, is acetylcholine (ACh; Eybalin, M. 1993). In some species, there is also evidence that a subset of MOC neurons release gamma-aminobutyric acid (GABA) and calcitonin gene related peptide (CGRP) (Raphael, Y. and Altschuler, R. A., 2003).

Acetylcholine activates a nicotinic receptor located in the basolateral membrane of the OHCs, which has only recently been identified. Elgoyhen A. B. *et al.*, 1994 and collaborators isolated and characterized $\alpha 9$, a new member of the nicotinic ACh receptor subunit gene family, which injected in Xenopus oocytes expressed a homomeric receptor-channel complex. This ion channel, as the other members of the family, is permeable to Na^+ and Ca^{2+} and is activated by acetylcholine. The $\alpha 9$ nicotinic receptor displays unusual pharmacological properties, as it is blocked by nicotinic as well as muscarinic antagonists. *In situ* hybridization studies in the rat show that the $\alpha 9$ nicotinic receptor is expressed in only a few regions of the brain and in the hair cells of the cochlea, both in IHCs and OHCs. Based on this information, the $\alpha 9$ nicotinic receptor was postulated as a candidate for efferent transmission in the cochlea. However, there were still some differences between the biophysical properties of the heterologous expressed homomeric $\alpha 9$ nicotinic receptor and those of the native cholinergic receptor from isolated OHCs. In a later study, Elgoyhen A. B. *et al.* (2001) found another α nicotinic subunit, the $\alpha 10$, which in the adult rat is only expressed in OHCs. Their data show that a heteromeric $\alpha 9/\alpha 10$ nicotinic ACh receptor presents pharmacological and biophysical properties indistinguishable from those of the native cochlear hair-cell receptor. Recent studies in a heterologous expression of $\alpha 9$ and $\alpha 10$ subunits with different mutations in Xenopus oocytes (Plazas, P. V. *et al.*, 2005) suggest that the native $\alpha 9/\alpha 10$ nicotinic receptor is constituted by a pentamer with a $(\alpha 9)_2(\alpha 10)_3$ stoichiometry (Figure 2). For a review in nicotinic acetylcholine receptors in the auditory efferent system, see Lustig L. R. (2006).

There is evidence in mice and guinea-pigs that a subset of MOC fibers releases GABA (Fex, J. *et al.*, 1986; Maison, S. F. *et al.*, 2003a) and CGRP (Safieddine, S. and Eybalin, M., 1992). The presence of GABA and glutamic acid decarboxylase in efferent endings has been shown by inmunocytochemistry, and $GABA_A$ receptors have also been detected in the basolateral domain of OHCs by monoclonal antibodies against α and β subunits of the $GABA_A$ receptor (Plinkert, P. K. *et al.*, 1989; 1993; see also Eybalin, M., 1993). These results, obtained in the guinea-pig cochlea, show a tonotopical distribution of gabaergic fibers and $GABA_A$ receptors, with a predominant presence in the upper cochlear turns. This tonotopical arrangement of gabaergic efferent fibers seems to be opposite to that of cholinergic fibers which are primarily located in the more basal regions of the cochlea (Plinkert, P. K. *et al.*, 1993). In contrast, in mice OHC efferent innervation presents a density peak, similar for acetylcholine, GABA, and CGRP markers, in the central cochlear region (near 10 kHz) and lower values of density in the apical and basal regions (Maison, S. F. *et al.*, 2003a). Furthermore, in mice near 100% co-localization between the three neurotransmitters has been found (Maison, S. F. *et al.*, 2003a), whereas in guinea-pigs only a subset of MOC cholinergic fibers co-localizes for ACh and CGRP (Safieddine, S. and Eybalin, M., 1992) and another subset co-localizes for ACh and GABA (Fex, J. *et al.*, 1986).

3.24.2.1.4 Lateral olivocochlear neurotransmitters

Several neurotransmitters and neuromodulators are known to be released by the LOC system: Acethylcholine, GABA, dopamine, dynorphines, enkephalin, and CGRP (Eybalin, M., 1993), and some of them have been shown to co-localize in LOC neurons. An early work demonstrated in cats that most LOC neurons stained with retrograde tracers (injected into the cochlea), also co-stained with acetylcholinesterase (AChE) (Warr, W. B., 1975). Another work using inmunohistochemistry, in cats and guinea-pigs, found that lateral efferent fibers beneath IHCs exhibited enkephaline-like

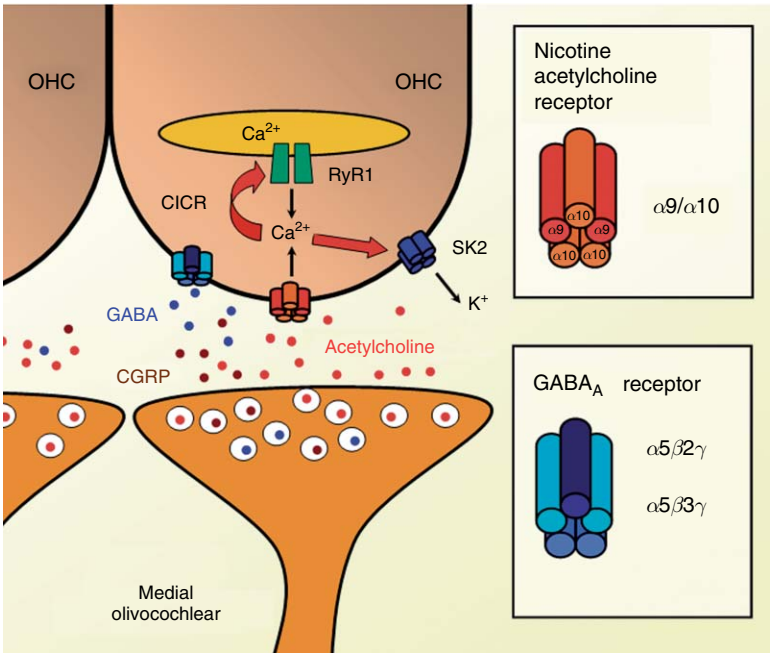

Figure 2 Medial olivocochlear (MOC) synapses with OHCs. The main neurotransmitter released by MOC fibers is acetylcholine that in mice co-localizes with GABA and CGRP (Maison, S. F. *et al.*, 2003a). The opening of $\alpha 9/\alpha 10$ acetylcholine receptors generates an inward Ca^{2+} current in OHCs. An outward current through small-conductance Ca^{2+}-activated K^+ channels (SK2) hyperpolarizes OHCs. It is also postulated that the opening of acetylcholine receptors produces a Ca^{2+}-induced Ca^{2+} release (CICR) from an intracellular cistern through ryanodine receptors (RyR 1). Inset panels on the right show the putative conformations of the pentameric $\alpha 9/\alpha 10$ acetylcholine receptor, and of the GABA receptor at the mouse cochlea (Plazas, P. V. *et al.*, 2005; Maison, S. F. *et al.*, 2006). OHC, outer hair cell.

reactivity (Fex, J. and Altschuler, R. A., 1981). Later, by means of double and triple inmunofluorescence co-localization techniques it was demonstrated, in guinea-pigs and rats, the presence of extensive co-localization of ACh, dynorphines and enkephalines (Abou-Madi, L. *et al.*, 1987) and of ACh, GABA, dopamine, CGRP and enkephaline in most lateral efferent neurons (Safieddine, S. *et al.*, 1997). In contrast, Darrow K. N. *et al.* (2006a) using inmunostaining for tyrosine hydroxylase (dopamine marker) and vesicular acetylcholine transporter in mouse cochleae showed little co-localization of both neurotransmitters in axon terminals beneath IHCs. Consistently, they found that in the brainstem most dopaminergic neurons are distinct from cholinergic neurons (Figure 3). Their results also suggested that in mice the bulk of the lateral efferent fibers reaching the cochlea are cholinergic and only 10–20% of them are dopaminergic (tyrosine-hydroxylase positive).

Acetylcholine released by OC lateral efferents probably activates cholinergic receptors composed by $\alpha 6$, $\alpha 7$, and $\beta 2$ subunits (Morley, B. J. *et al.*, 1998) that depolarize afferent auditory-nerve fibers and enhance glutamatergic transmission from IHCs (Felix, D. and Ehrenberger, K., 1992). Recent studies using inmunocytochemistry in guinea-pig cochlea have established the presence of dopamine transporters in the lateral efferent fibers below IHCs and in the inner spiral bundle (Ruel, J. *et al.*, 2006) and also the presence of D1 receptors in the spiral ganglion neurons and in the afferent nerve endings beneath IHC synapses (Niu, X. and Canlon B., 2006).

In the brainstem, dopaminergic neurons are mainly located surrounding the LSO and they probably correspond to the shell neurons (Vetter, D. E. and Mugnaini, E., 1992), while AChE stained neurons are located within the LSO nucleus, corresponding to LOC intrinsic neurons (Darrow, K. N. *et al.*, 2006a). In a recent study combining intracochlear injections of a fluorescent retrograde tracer and inmunofluorescent staining of tyrosine hydroxylase in the guinea-pig, Mulders W. H. and Robertson D. (2004) succeeded in demonstrating that dopaminergic neurons from the LSO project to the

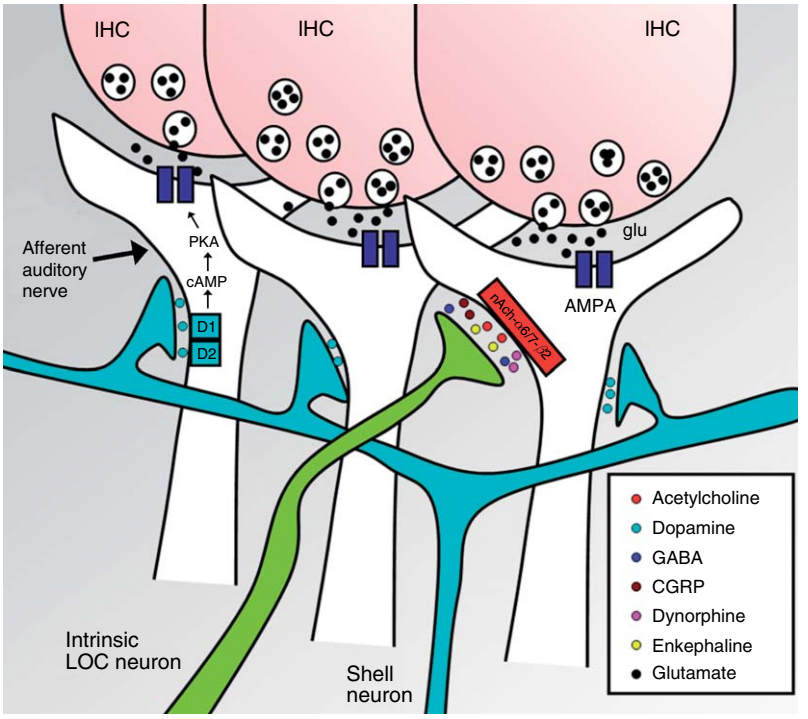

Figure 3 Lateral olivocochlear synapses with auditory-nerve fibers. Neurotransmitters released by lateral olivocochlear (LOC) fibers include: acetylcholine, dopamine, GABA, CGRP, dynorphines, and enkephalines. The main neurotransmitter between IHCs and auditory-nerve fibers is glutamate. In mice, LOC dopaminergic fibers originate from shell neurons (light blue) and are a separate group from LOC intrinsic fibers (green) that release acetylcholine and other neurotransmitters (Darrow, K. N. *et al.*, 2006a). The dopamine receptors in the auditory-nerve afferent fiber (D1/D2) through a G-protein regulate the intracellular concentration of cAMP and thus the activity of the protein kinase A (PKA), which phosphorilates AMPA glutamate-receptors (Niu, X. and Canlon, B. 2006). Acetylcholine released by LOC fibers is thought to activate receptors conformed by α6, α7, and β2 subunits (Morley, B. J. *et al.*, 1998). IHC, inner hair cell.

cochlea through the lateral efferent fibers. In agreement with previous observations (Safieddine, S. *et al.*, 1997), they also found that dopaminergic neurons are not equally distributed over the LSO. Most of them originate from the medial limb, the region of the LSO that receives high-frequency input. Consistently, they found dense tyrosine-hydroxylase labeling in the first and second cochlear turns and sparse or no labeling in the apical cochlear regions. These results are in contrast with evidence that shows no differences in the distribution of D1 receptors beneath IHCs along the guinea-pig cochlea (Niu, X. and Canlon, B., 2006) and a uniform dopaminergic innervation from base to apex in the mouse cochlea (Darrow, K. N. *et al.*, 2006a). It has been suggested that dopaminergic innervation may be important for high frequencies in the mammalian cochlea. This fact would explain the presence of dopaminergic fibers only in the basal turns of the cochlea in guinea-pig and through the whole cochlea in the mouse, which is a high-frequency mammal.

3.24.2.2 Cortico-Cochlear Pathways

Anatomic studies performed in a variety of animals have shown the existence of corticofugal pathways that originate in the auditory cortex and, after making synaptic contacts in various nuclei of the brainstem, reach the cochlea through the OC efferent fibers. This section presents a summary of the main findings on these cortico-cochlear pathways; for a more thorough review on the subject see Huffman R. F. and Henson O. W., Jr. (1990) and Winer J. A. (2005). A schematic view of the basic anatomy of the cortico-cochlear pathways is presented in Figure 4.

The largest descending pathway from the auditory cortex projects to the medial geniculate body, that is, the auditory thalamus. Each of the three main subdivisions of the medial geniculate body and the thalamic reticular nucleus receive projections from various auditory cortices (Winer, J. A. *et al.*, 2001). Tonotopic cortical areas project mainly to the tonotopic medial geniculate body and nontonotopic cortical areas

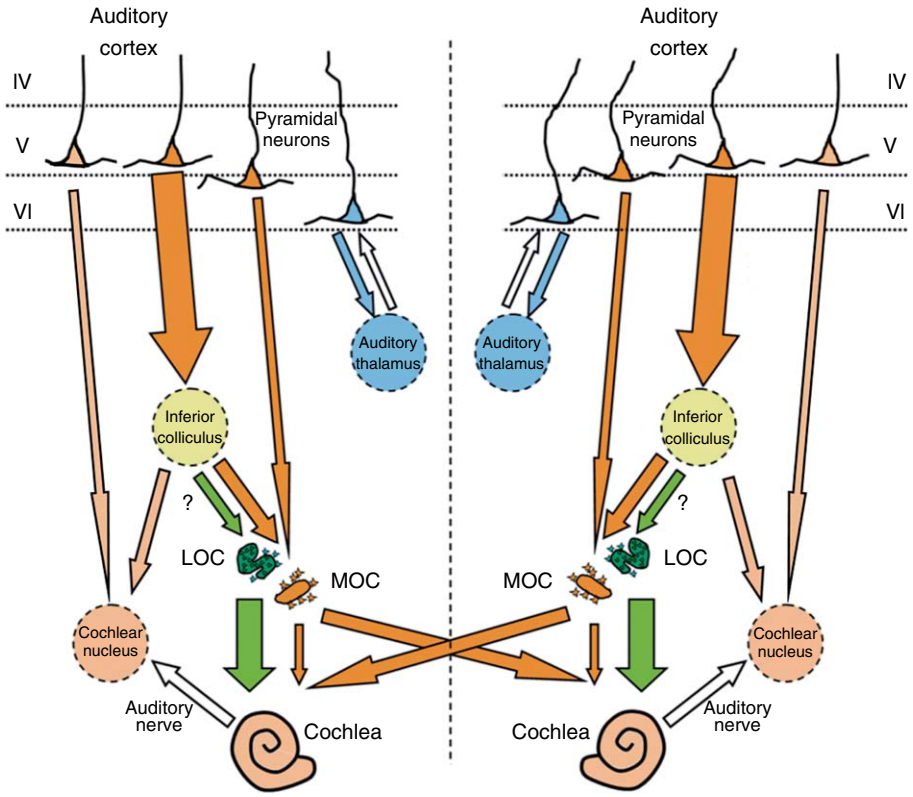

Figure 4 Diagram of cortico-cochlear pathways. Descending projections to the auditory thalamus emerge from pyramidal neurons located in layer VI of the auditory cortex (light blue arrows and cortical neurons). Corticofugal projections to the ipsilateral IC, superior olivary complex (orange arrows and cortical neurons), and to the cochlear nucleus (beige arrows and cortical neurons) emerge from different populations of pyramidal neurons located in layer V of the auditory cortex. There are also contralateral projections from the auditory cortex to the IC, superior olivary complex and cochlear nucleus (not shown in this schematic figure). Through the OC fibers (MOC and LOC fibers) the cortical pathways reach the contralateral and ipsilateral cochleae. Possible IC to LOC projection (green arrow with?; Groff, J. A. and Liberman, M. C. 2003).

project largely to nontonotopic thalamic regions. These projections emerge from pyramidal neurons located in the deepest part of layer V, and throughout layer VI of the auditory cortex (Winer, J. A. and Prieto, J. J., 2001). There is, however, no evidence of thalamic projections that reach the cochlea, and it seems that the projections from the auditory cortex to the medial geniculate body and to the reticular nucleus form a feedback loop with the ascending fibers to the auditory cortex.

For a long time the IC was seen as an obligatory synaptic station in the descending auditory pathways that reach the cochlear nucleus and the cochlea (Huffman, R. F. and Henson, O. W., Jr., 1990). The cortical fibers innervating the IC have their origin in pyramidal neurons located in layer V of the auditory cortex and project mainly to the dorsal and external cortices of the ipsilateral IC (Andersen, R. A. *et al.*, 1980; Faye-Lund, H., 1985; Herbert, H. *et al.*, 1991), although they also innervate other regions of the IC, including the central nucleus (Saldaña, E. *et al.*, 1996). There are multiple studies showing the presence of descending fibers that originate in the IC central nucleus and terminate in the dorsal cochlear nucleus and the superior olivary complex (Malmierca, M. S. *et al.*, 1996; Coomes, D. L. and Schofield, B. R., 2004a). Studies using double labeling have shown that descending collicular axons that innervate primarily the ipsilateral superior olivary complex make synaptic contacts mainly with MOC neurons (Thompson, A. M and Thompson, G. C., 1993; Vetter, D. E. *et al.*, 1993). Also, studies using multilabeling techniques in guinea-pigs have demonstrated the existence of cortico-colliculo-cochlear nucleus projections (Schofield, J. R. and Coomes, D. L., 2006).

In 1995, Feliciano and collaborators demonstrated in rats the presence of auditory-cortex projections that, bypassing the IC, reach directly the brainstem nuclei,

like lateral lemniscus, superior olivary complex, and cochlear nucleus (Feliciano, M. *et al.*, 1995). The existence of a direct cortico-cochlear nucleus pathway has also been confirmed in the guinea-pig (Schofield, J. R. and Coomes, D. L., 2006). Injections of a retrograde tracer in the cochlear nucleus and an anterograde tracer in the auditory cortex of the rat made it possible to show that the cochlear-nucleus cortical projections originate from large pyramidal neurons in layer V of the ipsilateral primary auditory cortex (Weedman, D. L. and Ryugo, D. K., 1996a) and that the pyramidal neurons make synapses exclusively with neurons located in the granule cell layer of the cochlear nucleus (Weedman, D. L. and Ryugo, D. K., 1996b).

Mulders W. H. and Robertson D. (2000a) combined auditory-cortex anterograde and cochlear retrograde tracing techniques to demonstrate in the rat that projections from pyramidal neurons located in layer V of the primary auditory cortex make synaptic contacts with MOC neurons that project to the cochlea. Afterward, using anterograde tracers, the presence of direct projections from the auditory cortex to the superior olivary complex was also demonstrated in the guinea-pig (Coomes, D. L. and Schofield, B. R., 2004b). The majority of the cortical axons terminate in the ipsilateral side where they innervate most of the superior olivary complex nuclei, with the largest number of fibers reaching the ventral nucleus of the trapezoid body and few fibers reaching the LSO. It has been established that the pyramidal neurons that project to the cochlear nucleus and to the superior olivary complex belong to different populations of neurons (Doucet, J. R. *et al.*, 2002). These anatomical results show that cortical neurons may exert a direct action on the activity of MOC neurons and consequently could modulate cochlear sensitivity (Mulders, W. H. and Robertson, D., 2000a).

3.24.3 Physiology of the Efferent System

From the early classical works on the physiology of the efferent system it is known that efferent OC neurons respond to sound at regular firing rates with frequency tuned responses (Brown, M. C., 1989) and that their activation produces an inhibitory effect in cochlear responses (Galambos, R., 1956; Fex, J., 1959; 1962).

Two main methods have been used to study the function of auditory efferents, activation and blocking of the efferent pathways. Activation has been performed by electrical stimulation at different levels of the efferent path and by contra- and ipsilateral acoustical stimulation. Blocking of the efferent function has been achieved by: surgical lesions, pharmacological neurotransmitter antagonists, and molecular deletion of relevant genes.

3.24.3.1 Electrical Stimulation of the Efferent System

To activate the efferent system, electrical stimulation with high-frequency current pulses has been applied at different levels of the efferent pathway: (1) at the midline of the floor of the fourth ventricle; (2) at the medial superior olive region; (3) at the round window; (4) at the IC; and (5) at the auditory cortex.

3.24.3.1.1 Effects on cochlear electrical responses and otoacoustic emissions

Most of the early information on the physiology of the efferent system was obtained by electrical activation of the MOC fibers with current pulses delivered at the point of fiber crossing in the midline of the floor of the fourth ventricle. The electrical stimulation of efferent fibers produced a reduction in the amplitude of the compound action potential (CAP) (Galambos, R., 1956), that is, the summated activity of the auditory nerve, and an increase in the amplitude of cochlear microphonics (CM) (Fex, J., 1959; 1962), that reflect a voltage drop produced by some weighted sum of currents generated in multiple hair cells. These CAP reductions and CM increases elicited by efferent stimulation disappeared after systemic injection of strychnine, a known blocker of efferent function (Figure 5; Desmedt, J. E. and Monaco, P., 1961). Efferent electrical stimulation was also shown to suppress the responses to tones recorded from single auditory-nerve fibers and intracellularly from IHCs, particularly at the characteristic frequency of the fiber or IHC (Guinan, J. J., Jr., 1996).

Soon after the discovery of otoacoustic emissions (OAEs) (Kemp, D. T., 1978), Mountain D. C. (1980) showed that electrical stimulation of MOC fibers reduces the amplitude of distortion product OAEs (DPOAEs) recorded in the ear canal. The fact that electrical activation of the MOC efferents can modify OAEs and IHC receptor potentials demonstrates that the efferent system through the activity of OHCs can regulate the tuning and sensitivity of cochlear mechanics and IHC responses (Dallos, P., 1992; Robles, L. and Ruggero, M. A., 2001).

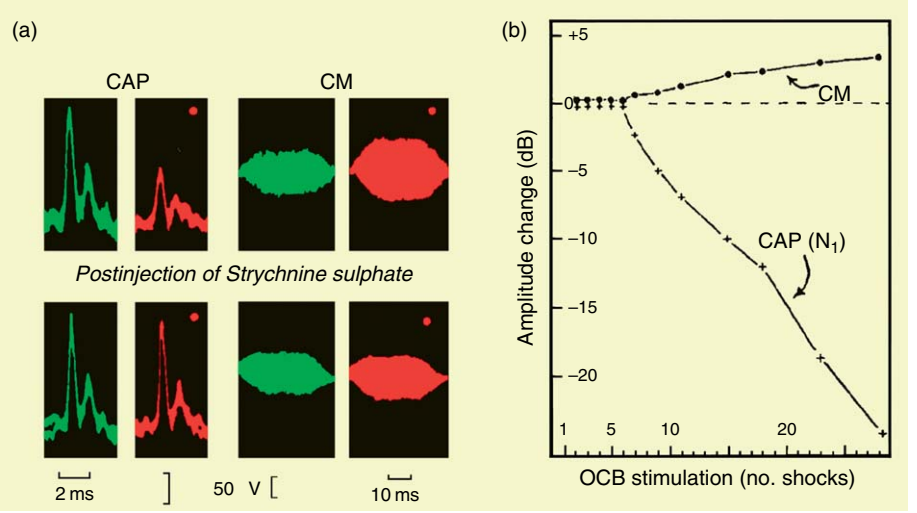

Figure 5 Effect of the electrical activation of MOC fibers on cochlear potentials. (a) Green traces show cochlear CAP and CM potentials in response to sound without efferent electrical stimulation. Red traces show same cochlear responses preceded by electrical activation of MOC fibers at the midline of the floor of the fourth ventricle. In the upper row a clear CAP reduction and CM increase is evident during electrical activation of MOC fibers. In the lower row this effect is blocked after an injection of strychnine. (b). Change of CAP and CM amplitudes as a function of the number of shocks at the fourth ventricle (OCB: olivocochlear bundle). Adapted from Desmedt, J. E. and Monaco, P. 1961. Mode of action of the efferent olivo-cochlear bundle on the inner ear. Nature 192, 1263–1265.

It has been shown in guinea-pigs that electrical stimulation at the round window produces similar reductions in CAP amplitude that the activation of efferent fibers at the floor of the fourth ventricle, and consequently this less invasive technique has been proposed as an alternative method of activation of efferent fibers innervating the cochlea (Rajan, R. and Johnstone, B. M., 1983).

A comparison of the effects of selective electrical stimulation of MOC efferents by an electrode placed near MOC cell bodies and of stimulation of efferent fibers at the floor of the fourth ventricle was performed by Gifford M. L. and Guinan J. J., Jr. (1987) to differentiate the effects produced by medial and lateral OC efferent fibers. The results showed qualitatively similar reductions in CAP and increases in CM amplitudes produced by electrical activation of the MOC neurons and the fourth-ventricle fibers. However, a quantitative analysis showed that the reduction in CAP amplitude produced by fourth-ventricle stimulation amounted to about the sum of the CAP amplitude reductions produced by selective electrical stimulation of one-side MOC neurons in the contra and ipsilateral ears. Consequently, the authors postulated that in their experiments, as well as in previous ones, the efferent effects elicited with fourth-ventricle OC stimulation, due to the proximity of the uncrossed fibers to the stimulation place, most probably corresponded to the joint effect of crossed and uncrossed medial OC fibers. Some studies have reported that the electrical stimulation of MOC fibers, concomitant to the changes in CAP amplitude, produces increases in CAP (N1) latency (Dayal, V. S., 1968; Gifford, M. L. and Guinan, J. J., Jr., 1987), but other studies have failed to observe them (Desmedt, J. E. *et al.*, 1971; Rajan, R. and Johnstone, B. M., 1983).

In auditory-nerve fibers, electrical stimulation of MOC neurons (and at the fourth ventricle) produces a decrease in spontaneous rate, which is stronger for the lower spontaneous rate fibers, and shifts the fiber firing rate–sound level functions to higher sound levels, decreasing their spike rate at the plateau. MOC activation also raises the thresholds for tones at the characteristic frequency and decreases the sharpness of the nerve-fiber tuning curves. High-spontaneous-rate fibers have smaller increases in threshold, and low-spontaneous-rate fibers larger increases (Guinan, J. J., Jr. and Gifford, M. L., 1988; Guinan, J. J., Jr.,1996). Figure 6 illustrates some of the efferent effects on auditory-nerve responses discussed in this section.

3.24.3.1.1.(i) Mechanisms of inhibition of OHC activity Electrical stimulation of efferent fibers in the turtle isolated cochlea was shown to produce slow hyperpolarizing postsynaptic potentials in hair cells (Art, J. J. *et al.*, 1982). Later experiments in guinea-pig

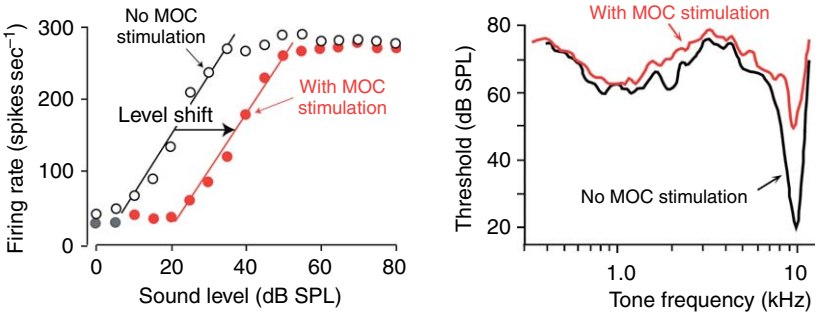

Figure 6 Examples of MOC effects on the activity of auditory nerve fibers. Left panel shows auditory-nerve firing rate versus sound-pressure level with and without MOC stimulation. Data are from a high-spontaneous fiber recorded from a cat. MOC activity produces a shift of the nerve-fiber firing-rate curve to higher sound-pressure levels. Right panel: Tuning curves with and without MOC stimulation. MOC stimulation increases the response thresholds at frequencies around the characteristic frequency of the auditory-nerve fiber. Adapted from Guinan, J. J., Jr. 2006. Olivocochlear efferents: Anatomy, physiology, function, and the measurement of efferent effects in humans. Ear Hear. 27: 589–607.

isolated OHCs demonstrated that ACh applied to their basal pole binds to the ACh nicotinic receptor inducing a Ca^{2+} influx current. The increase in intracellular Ca^{2+} activates Ca^{2+}-dependent K^+ channels producing an increase in cell input conductance and an outward K^+ current that hyperpolarizes the OHC (Housley, G. D. and Ashmore, J. F., 1991; Erostegui, C. *et al.*, 1994; Evans, M. G., 1996) (Figure 2). This unusual fast inhibitory synapse, which through nicotinic ACh receptors activates low-conductance Ca^{2+}-dependent SK2 channels, has short rise and decay time constants of 6 and 30 ms, respectively, mainly determined by the Ca^{2+} gating of the K^+ currents (Oliver, D. *et al.*, 2000). A Ca^{2+}-dependent potassium channel has been reconstituted within a heterologous system by co-expressing a low-conductance potassium channel cloned from the mouse cochlea with the $\alpha 9/\alpha 10$-nicotinic acetylcholine receptor, showing that these two elements are sufficient to reconstitute the efferent synaptic response (Nie, L. *et al.*, 2004).

It has been shown that OHCs have a membrane potential-dependent motor capability by which they elongate and contract under hyperpolarization and depolarization, respectively (Brownell, W. E. *et al.*, 1985; Ashmore, J. F., 1987). This electromotile effect, driven by voltage-dependent conformational changes of a transmembrane protein, prestin (Zheng, X. Y. *et al.*, 2000), performs as a cochlear amplifier by boosting cochlear vibrations at each cochlear location for stimuli at frequencies close to its characteristic frequency. Both of the effects of ACh on OHCs, described above, which induce changes in their electrical responses affect cochlear amplification, since hyperpolarization of OHCs would elongate them and the increase in input conductance would reduce sound-induced receptor potentials modifying the OHC electromotile response. However, ACh has been found to also produce increases in OHC axial compliance and electromotile response that occur with a significantly greater latency than the effects on OHC electrical responses and that are simultaneous with Ca^{2+} release from intracellular stores (Dallos, P. *et al.*, 1997). The ACh-induced increase in OHC electromotile response is probably accounted by the increase in axial compliance and may be related to slow effects produced by OC activation (see following section). Surprisingly, this increase in electromotility induced by ACh in isolated OHCs is opposite to the *in vivo* effects of efferent-system activation and cochlear ACh perfusion that reduce cochlear amplification; it is not clear how these different results can be reconciled.

3.24.3.1.1.(ii) Fast and slow effects of olivocochlear activation Sridhar T. S. *et al.* (1995) described new slow effects on cochlear responses produced by electrical activation of OC fibers, which occur with time constants of 25–50 s, three orders of magnitude slower than the previously reported efferent cochlear effects. These slow effects are similar to the fast effects in that they include a reduction in eight-nerve CAP concomitant to an increase of CM during electrical activation of the MOC bundle (Figure 7). The new slow effects are also similar to the classical fast effects in that they are blocked by similar concentrations of various cholinergic antagonists, suggesting that both effects are mediated by the same cellular receptor. However, one important

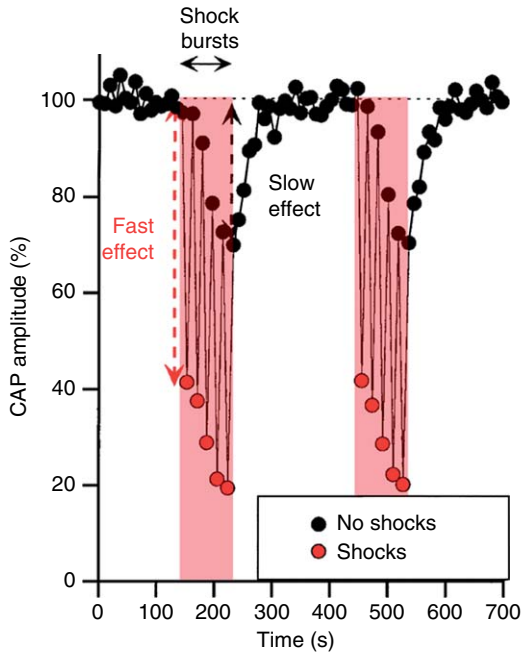

Figure 7 Fast and slow OC effects on CAP amplitude. The fast effect (red arrow) is a reduction in magnitude of CAP responses to tones with shocks (red circles) compared with the CAP magnitudes without shocks (black circles). The slow effect is measured as the cumulative decrease in the amplitude of CAP with repeated shock bursts (black arrow). Adapted from Sridhar, T. S., Brown, M. C., and Sewell, W. F. 1997. Unique postsynaptic signaling at the hair cell efferent synapse permits calcium to evoke changes on two time scales. J. Neurosci. 17, 428–437.

difference between the fast and slow effects in guinea-pig, besides their time courses, is that the former has a peak effect for frequencies between 6 and 10 kHz and the latter for frequencies between 12 and 16 kHz.

Perfusion of the cochlea with ryanodine, an agonist of calcium-induced calcium release from endoplasmic reticulum, enhanced the fast and slow effects on CAP and CM, probably by increasing calcium concentration at the cell membrane and thus increasing the conductance of OHCs. On the other hand, cochlear perfusion with an antagonist of reticulum calcium ATPase (SERCA) enhanced selectively the slow effects, suggesting that these effects are dependent on calcium stored in a compartment other than the OHC synaptic region (Sridhar, T. S. *et al.*, 1997). Expression of type-I ryanodine receptors has been demonstrated in OHCs of the apical turn of the rat cochlea and consistently, whole-cell voltage-clamp recordings made in OHCs from that location have shown that ryanodine modulates the potassium current evoked by acethylcholine (Lioudyno, M. I. *et al.*, 2004). These results suggest that, as in muscle sarcoplasmic reticulum, the cistern (synaptoplasmic cistern) in OHCs could act to assure a fast activation of the Ca^{2+}-dependent K^{+} current that turns the nicotinic receptor excitation into synaptic inhibition.

3.24.3.1.2 Medial olivocochlear effects on cochlear mechanics

Mountain D. C. (1980), and later Siegel J. H. and Kim D. O. (1982), showed that the electrical activation of OC fibers at the fourth ventricle can modulate the amplitude of distortion-product OAEs, an effect that reflects changes in cochlear mechanics. Afterward, direct mechanical measurements demonstrated that electrical activation of MOC fibers produces a characteristic-frequency-specific loss of sensitivity in basilar membrane vibrations (Murugasu, E. and Russell, I. J., 1996a; Dolan, D. F. *et al.*, 1997). For tones near the characteristic frequency, efferent stimulation linearizes the compressive basilar membrane displacement–intensity functions and shifts the steep segment of the curves to higher intensities, by up to 30 dB. All of these efferent effects were blocked by strychnine, a known blocker of efferent function. Consistent with the electrically produced efferent effects, cochlear perfusion with acetylcholine produced transient losses of sensitivity and linearization of the compressive displacement–intensity functions of tone-evoked basilar membrane responses (Murugasu, E. and Russell, I. J., 1996b). In addition, electrical efferent stimulation has been reported to enhance basilar membrane responses at frequencies well above the characteristic frequency and at high intensities (Dolan, D. F. *et al.*, 1997); however, a comparable effect has not been observed previously in auditory nerve responses.

Sound-evoked cochlear vibrations were also shown to be modulated over two different time scales by electrical activation of MOC fibers (Cooper, N. P. and Guinan, J. J., Jr., 2003). As previously demonstrated in cochlear potentials (see Section 3.24.3.1.1.(ii)), both fast (10–100 ms) and slow (10–100 s) efferent effects decreased cochlear mechanical responses for low and moderate intensity tones at frequencies close to the characteristic frequency. The fast inhibition of basilar membrane motion was accompanied by phase leads, while the slow inhibition was accompanied by phase lags, suggesting that two different mechanical processes underlie these two effects. (For further information, see Cooper, N. P. and Guinan, J. J., Jr., 2006.)

3.24.3.1.3 Efferent modulation by electrical activation of the inferior colliculus

Electrical stimulation of the central nucleus and external cortex of the IC produced large reductions in DPOAE magnitudes (up to 25 dB), while stimulation of the dorsal cortex produced little or no change in DPOAEs (Scates, K. W. *et al.*, 1999). However, since much smaller DPOAE reductions were observed in paralyzed animals (Mulders, W. H. and Robertson, D., 2000b) than those previously obtained in unparalyzed animals, it is likely that the observed large effects could partly be due to middle-ear muscle contractions. The stronger effects obtained with the stimulating electrodes positioned in the central nucleus and external cortex, compared with those obtained with the electrodes in the dorsal cortex, are consistent with previous anatomical evidence showing that the former regions have numerous and the latter region only sparse projections to the ipsilateral superior olivary complex (see Section 3.24.2.2).

Electrical activation of the central nucleus and external cortex of the IC also produces reductions in CAP amplitude and increases in CM potentials that are similar, although smaller than those obtained by direct electrical stimulation of MOC fibers at the fourth ventricle (Mulders, W. H. and Robertson, D., 2000b). Using the same microelectrodes to electrically stimulate and to record from neurons from different IC sites it was shown that, in the central nucleus, the characteristic frequency of the sharply tuned recorded units closely matches the stimulus frequency at which the maximum CAP reduction was observed. In contrast, neurons from the external cortex presented broad tuning and their stimulation had a weak and broadly tuned effect in CAP amplitudes. The stimulation of the IC dorsal cortex had no effect on cochlear responses (Ota, Y. *et al.*, 2004).

Surprisingly, in addition to these efferent effects, electrical stimulation at other IC sites elicited bilaterally CAP amplitude enhancements or reductions that could last for periods of 3–20 min after shock termination. These novel long-lasting efferent effects were attributed to activation of LOC fibers that enhance or reduce auditory-nerve activity (CAP and eighth-nerve ensemble background activity; see Section 3.24.3.4.2.(i)) without affecting measures of OHC function (cochlear microphonics and DPOAEs). They differed from the efferent effects elicited by MOC activation, in that their magnitudes were independent of the frequency and intensity of acoustic stimuli (Groff, J. A and Liberman, M. C., 2003).

Consistent with the previous observations, it has been shown that the IC can produce diverse effects on the activity of auditory-nerve single fibers. In a recent study, electrical activation of the IC produced inhibitory effects, with a loss in response sensitivity to tones in 53% of the recorded fibers and excitatory effects, with an increase in response sensitivity in 5% of the fibers (Mulders, W. H. and Robertson, D., 2005). The activation of the LOC system, in addition to the MOC system, could explain the diversity of effects produced by the IC at the level of single auditory nerve fibers.

3.24.3.1.4 Efferent modulation by electrical activation of the auditory cortex

There are several lines of physiological evidence indicating that corticofugal projections from the auditory cortex modulate the responses of subcortical nuclei. Moreover, a few studies show that the auditory cortex can modulate auditory responses even at a cochlear level.

Electrical activation of the ipsilateral and contralateral auditory cortices modulates the spontaneous and sound-evoked activity of units recorded in the central nucleus of the IC in guinea-pigs. The contralateral cortex is more effective in eliciting inhibitory effects in IC units, while the ipsilateral cortex is more effective in producing excitatory effects on spontaneous activity of the units (Torterolo, P. *et al.*, 1998). Electrical stimulation of the auditory cortex also modulates the response properties of units recorded intracellularly from the medial geniculate body, producing excitatory as well as inhibitory modulations (Xiong, Y. *et al.*, 2004).

It has been shown in the mustached bat that focal electrical stimulation (or pharmacological inactivation) of the constant-frequency Doppler-shift area of the auditory cortex can modulate in a highly specific way the amplitude and tuning of cochlear microphonics. This effect, although bilaterally present, is stronger at the contralateral auditory cortex (Xiao, Z. and Suga, N., 2002a; 2002b).

Corticofugal modulations of cochlear responses have also been studied in humans, in a group of patients with refractory epilepsy during their presurgical chronic intracerebral electroencephalography. In these patients, during this protocol, in which the auditory cortex and other nonauditory cortices are electrically stimulated to delimit epileptogenic areas in the brain, evoked OAEs were simultaneously recorded, as a measure of cochlear function. Electrical stimulation of the contralateral auditory cortex

produced a significant reduction of evoked OAEs in all the patients, while there was no change under stimulation of nonauditory cortical areas (Perrot, X. *et al.*, 2006). These results imply that, in humans, as in bats, the anatomical pathways from the auditory cortex to the cochlea are functional, providing a top-down control on incoming auditory information.

3.24.3.2 Acoustic Activation of the Efferent System

Since it was known that acoustical stimulation activates the medial OC neurons (Fex, J., 1962) and that these neurons can modify cochlear responses (Galambos, R., 1956), it was natural to look for acoustically evoked efferent effects in cochlear responses. Acoustic stimulation is certainly a more physiological method to activate the OC system than electric stimulation, and since it is noninvasive, it has been used to asses the auditory efferent function in awake animals and in humans. Figure 8 displays a schematic diagram explaining the experimental setting for the acoustic activation experiments.

3.24.3.2.1 Acoustic efferent effects in experimental animals

Buño W. (1978) showed in anesthetized animals that contralateral acoustic stimulation at low intensities modifies the tone-evoked responses of single auditory-nerve fibers in the ipsilateral ear. The suppression effect is maximal for low- and medium-spontaneous-rate fibers with characteristic frequencies below 3 kHz and is highly dependent on the intensity and frequency of the tones, being strongest for ipsi- and contralateral

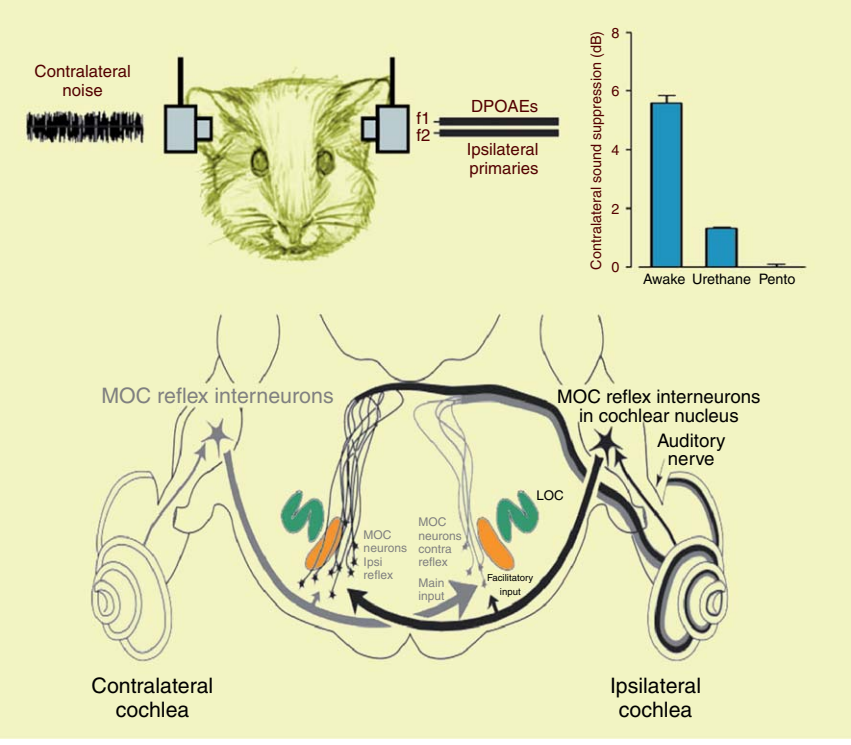

Figure 8 Acoustic activation of the efferent system. Top: Illustration of the method used to measure the acoustic efferent effect. The amplitude of ipsilateral DPOAEs is measured in the presence of contralateral noise. Bottom: Anatomy of the acoustic efferent effect. The anatomic pathway of the ipsilateral acoustic efferent reflex has double crossing fibers: (1) from the ipsilateral cochlea, through the cochlear nucleus, to the contralateral MOC neurons and (2) from contralateral MOC neurons to the ipsilateral cochlea. In contrast the contralateral reflex has only one crossing (light gray arrow pathway in the illustration) of afferent fibers from the contralateral cochlear nucleus to the subset of MOC uncrossed neurons that project to the ipsilateral cochlea (see de De Venecia, R. K. *et al.*, 2005). Top right: Effective attenuation of the efferent effect measured in awake and urethane- and pentobarbitone-anesthetized guinea-pigs. Adapted from De Venecia, R. K., Liberman, M. C., Guinan, J. J. Jr., Brown, M. C. 2005. Medial olivocochlear reflex interneurons are located in the posteroventral cochlear nucleus: a kainic acid lesion study in guinea-pigs. J. Comp. Neurol. 487, 345–360 and Guitton, M. J., Avan, P., Puel, J. L., and Bonfils, P. 2004. Medial olivocochlear efferent activity in awake guinea-pigs. Neuroreport. 15, 1379–1382.

tones with frequencies close to the nerve-fiber characteristic frequency. This contralateral-sound suppression has a much slower time course than two-tone suppression, with onset and offset times of more than 100 ms. The fact that the suppressive effect is eliminated by a complete section of the OC bundle within the internal auditory meatus, but remains after section of the crossed OC fibers at the floor of the fourth ventricle implies that it is mediated by uncrossed MOC fibers (Warren, E. H., 3rd and Liberman, M. C., 1989). There is evidence showing that ipsilateral noise also suppresses ipsilateral tone-evoked responses through MOC efferents.

Two MOC reflex circuits have been described for each cochlea, one that is activated by contralateral and another by ipsilateral acoustic stimulation (Figure 8). The ipsilateral MOC reflex circuit crosses twice the midline of the brainstem, comprising: afferent auditory-nerve fibers that reach the ipsilateral posteroventral cochlear nucleus (PVCN), interneurons from the PVCN whose axons cross the midline to make synaptic contact at the opposite side with efferent MOC neurons, that project back across the midline to the OHCs of the ipsilateral cochlea. In contrast, the contralateral MOC reflex has only one midline crossing, the contralateral afferent auditory-nerve fibers make synaptic contact with interneurons from the contralateral PVCN, which cross the midline to contact ipsilateral MOC neurons that project through uncrossed fibers to the OHCs of the ipsilateral cochlea (De Venecia, R. K. *et al.*, 2005). This means that contralateral noise efferent suppression is mediated by uncrossed MOC fibers, while ipsilateral efferent suppression is mediated by crossed MOC fibers.

In awake guinea-pigs, noise in the contralateral ear reduces the power of eighth-nerve ensemble background activity recorded from the ipsilateral round window, revealing a decrease in auditory-nerve spontaneous activity (Lima da Costa, D. *et al.*, 1997a; Dolan, D. F. *et al.*, 1990). Contralateral tones or noise also decrease(s) the amplitude of the ipsilateral auditory-nerve CAP, with a frequency and level dependency similar to that of tone-evoked responses from auditory-nerve fibers. In spite of the constancy of auditory-nerve-fiber thresholds between animals, the magnitudes of efferent CAP reductions display significant interanimal variability, attributed mainly to variability in the level of activity of OC efferent neurons. Consequently, the measurement of CAP suppression by contralateral sound has been proposed as a rapid assessment of the strength of the OC reflex, which depends on the activity level of efferent MOC neurons (Liberman, M. C., 1989).

The magnitude of the DPOAEs recorded in the ipsilateral ear is also reduced by the presence of a simultaneous noise in the contralateral ear. This suppression is completely abolished by a midline sagittal section of the brainstem, demonstrating that it is an effect mediated by the MOC fibers (Puel, J. L. and Rebillard, G., 1990). It is, however, difficult to compare the strengths of the efferent effect assessed by measuring the changes in magnitude of auditory-nerve CAP and those of DPOAEs. The former measure reflects the summed activity of the whole auditory nerve, which could also be affected by LOC effects, while the latter reflects a mechanical nonlinear response whose magnitude is not clearly related to the amplitude of the traveling wave at the primary sites. A direct comparison in anesthetized cats of the magnitudes of contralateral-noise suppression obtained with the two measures showed that the effective suppression measured with CAP is generally larger than that measured with DPOAEs, with differences reaching as much as 10 dB (Puria, S. *et al.*, 1996).

Interestingly, measuring DPOAEs it has been found that the activation of the efferent system can not only produce reductions in the amplitude of OAEs, but also enhancements. The first to report this kind of enhancements were Siegel J. H. and Kim D. O. (1982), who used electrical activation of the OC fibers at the floor of the fourth ventricle in chinchilla. More recently, it has been reported that efferent activation can elicit decreases and also enhancements in DPOAEs, and that the change from one effect to the other is level dependent. A change in just 1 dB in sound-pressure level in one of the stimulus primary tones can produce a transition in the effect, from decrease to enhancement of the DPOAEs (Maison, S. F. and Liberman, M. C., 2000). This phenomenon, named the bipolar effect, has also been observed in DPOAEs measured in humans during contralateral acoustic stimulation (Muller, J. *et al.*, 2005).

A pharmacological study of the acoustic efferent effect found that cochlear perfusions of nanomolar concentrations of bungarotoxin (a nicotine antagonist) and of strychnine (a glycine antagonist that also blocks nicotinic receptors) blocked the suppression of DPOAEs produced by contralateral-noise activation of MOC neurons, indicating that the suppression was mediated by a nicotinic receptor (Kujawa, S. G. *et al.*, 1994). Enhancements of neural potentials and DPOAEs have recently been reported during recovery from acoustic activation of auditory efferents (Maison, S. F. *et al.*, 2007a). In contrast to the classical suppressive efferent effect, the enhancement effect is not blocked by strychnine and is present in mice with deletion of

the $\alpha 9$ cholinergic receptor (see Section 3.24.3.3.2), implying that this enhancement effect is not dependent on cholinergic neurotransmission.

Most of the effects of MOC fibers in cochlear responses had been previously studied in anesthetized animals, and since there was evidence showing that the activity of medial OC neurons was dependent on the level of anesthesia it became important to make the measurements in awake animals. A comparison of contralateral-sound suppression in awake and anesthetized guinea-pigs found that the efferent suppression is much weaker in the urethane-anesthetized than in the awake animal, and that it is even weaker in the pentobarbitone-anesthetized animal (Figure 8; Guitton, M. J. *et al.*, 2004; Boyev, K. P. *et al.*, 2002). These results suggested that suppression measurements performed in anesthetized animals probably underestimate the magnitude of the physiological efferent effects.

3.24.3.2.2 Acoustic efferent effects measured in humans

As stated by Puria S. *et al.* (1996), it is difficult to compare the strength of the OC reflex reported in humans, usually assessed by measuring OAE magnitude changes, with that reported in experimental animals, appraised by the changes in auditory-nerve CAP magnitude. Most of the studies on acoustic stimulation of the efferent pathway performed in humans have measured the effect on OAEs, because it involves a relatively easy and noninvasive measurement. Only exceptionally the acoustic efferent effect has been assessed by measuring auditory-nerve CAPs, recorded at the external ear canal or at the eighth nerve in patients undergoing surgery.

Folsom R. C. and Owsley R. M. (1987) recording click-evoked CAPs from the external ear canals of normal subjects found a reduction in the amplitude of N1 during the presentation of contralateral tones, with no change in N1 latency. Later studies found that contralateral acoustic stimulation, at sound levels below the stapedial-reflex threshold, could modulate different types of OAEs recorded in the ipsilateral ear of human subjects. Contralateral tones at frequencies within an octave of the frequency of an ipsilateral spontaneous OAE changed the frequency and amplitude of the emission (Mott, J. B. *et al.*, 1989). Also, broadband noise stimulation of the contralateral ear in humans produced a reduction in the amplitude of transiently evoked OAEs (TEOAEs) (Collet, L. *et al.*, 1990) and also in DPOAEs (Moulin, A. *et al.*, 1993). The facts that, in both of these studies, suppressions were not found in unilateral deaf subjects discarded that the observed effects could be produced by acoustic bone transmission.

The effect of contralateral noise on CAP responses was subsequently studied by recording directly from the auditory nerve during retrosigmoid surgery in humans (Chabert, R. *et al.*, 2002). Using this method, which produces more stable results than the recordings from the ear canal, the effective attenuation of contralateral noise on CAP amplitudes reached up to 10 dB. The study concluded that, as in the case of experimental animals, contralateral-sound suppression measured at the neural level is considerably higher than that measured with OAEs (about 10 dB vs. 1–4 dB).

Interestingly, the medial OC system strength, measured as equivalent attenuation of the click-evoked OAEs during contralateral-noise stimulation is stronger in the right than left ear in right-handers (Khalfa, S and Collet, L., 1996), while being symmetrical in left-handers (Khalfa, S. *et al.*, 1998). It is known that TEOAEs are larger in the right than in the left ear (Khalfa, S. *et al.*, 1997; Sininger, Y. S. and Conne-Wesson, B., 2004), but this cochlear asymmetry is independent of the greater attenuation effect in the right than left ear, which is mediated by MOC efferents (Khalfa, S. *et al.*, 1998). Also, contralateral acoustic suppression is stronger in professional musicians than in nonmusicians, with a similar left/right asymmetry in both groups (Perrot, X. *et al.*, 1999).

3.24.3.3 Lesion Studies of the Efferent System

Lesion studies to evaluate the efferent function in most cases have disrupted the efferent pathway at one of three locations: (1) the midline of the floor of the fourth ventricle, severing the crossed OC fibers; (2) the vestibular nerve or at the vestibulo-cochlear anastomosis, disrupting all efferent fibers that innervate one cochlea; or (3) at the level of the auditory cortex, eliminating the central control to the periphery (the first is performed in animals and the last two in animals and humans).

3.24.3.3.1 Section of olivocochlear efferents in animals

Acute sections of the OC fibers at the midline of the fourth-ventricle floor have often been used to eliminate the electrical or acoustic efferent effects measured in cochlear responses, to confirm the efferent involvement in the observed effects. In this section only the

physiological and behavioral consequences of chronic cochlear de-efferentation are presented.

3.24.3.3.1.(i) Physiological consequences of olivocochlear sections Several studies have shown evidence, although not always consistent, of the presence of tonic activity in the efferent system. A section of the OC bundle at the midline of the fourth ventricle in the guinea-pig produced a reduction of about 5% in CM amplitude, whereas a complete section of the OC fibers to the cochlea produced a reduction near 14% (Rossi, G. *et al.*, 1964). Later studies in the same species also found reductions in CM amplitude for lateral sectioning of the brainstem (which probably sections both the crossed and uncrossed medial fibers), but not for midline sections at the fourth ventricle, which sections only the crossed fibers (Bonfils, P. *et al.*, 1987). Sectioning of both, the medial and lateral OC fibers in chinchillas produced increases in DPOAEs of 5–20 dB, at high intensity levels and frequencies between 1 and 2 kHz, but no changes at frequencies of 4 and 8 kHz. In contrast, de-efferented chinchillas presented reductions in CM amplitude at all frequencies tested (1–8 kHz) and at all intensities (Zheng, X. Y. *et al.*, 2000).

Chronic de-efferentation in adult cats did not change thresholds, tuning curves and firing rate–level functions of single auditory-nerve fibers, but produced significant decreases in spontaneous rates (Liberman, M. C., 1990). However, chronic de-efferentation in neonatal cats after a year produced threshold increases and decreases in sharpness of tuning of auditory-nerve fiber responses, suggesting that OC efferent innervation may be critical for the proper development of the active mechanical processes (Walsh, E. J. *et al.*, 1998). Chronic de-efferentation in chinchillas produced a significant decrease in the spontaneous discharge rate of auditory nerve fibers (Zheng, X. Y. *et al,* 1999), consistent with previous observations in cats. However, de-efferentation in chinchillas also produced changes in neural responses not observed previously in cats, as decreases in the dynamic range of discharge rate–level functions and hypersensitive tails in the tuning curves of auditory-nerve fibers with characteristic frequencies between 2 and 8 kHz.

3.24.3.3.1.(ii) Behavioral consequences of olivocochlear sections The behavioral consequences of chronic sections of the OC fibers in quiet conditions are controversial. On the other hand, most studies that have assessed the effects of chronic sections in background noise have found some impairment after severing the efferent pathway.

In cats, the section of the crossed efferent fibers at the midline of the fourth-ventricle floor did not affect pure tone detection thresholds in quiet between 250 Hz and 14 kHz (Trahiotis, C. and Elliott, D. N., 1970; Igarashi, M. *et al.*, 1972), neither did it affect frequency discrimination thresholds for stimuli at 8 kHz or intensity discrimination thresholds at 10 kHz (Igarashi, M. *et al,* 1979a; 1979b). However, in monkeys it was found that transection of the crossed OC fibers produced increases in frequency discrimination thresholds, for tones at 1 and 4 kHz presented in quiet conditions (Capps, M. J. and Ades, H. W., 1968).

May B. J. and McQuone S. J. (1995) trained cats in an intensity discrimination task in quiet and in the presence of noise, and performed bilateral lesions of the OC efferent fibers at the fourth-ventricle floor. Olivocochlear lesions were confirmed by AChE staining of efferent projections to the cochlea and by measuring the contralateral-noise CAP suppression. They found that intensity discrimination of tones at 8 kHz was affected by the lesions only when tested in the presence of noise, but not in quiet. Similarly, in cats trained in a sound localization task, bilateral lesions of OC efferents at the brainstem produced a significant deficit in localization only when tested in noise, but not in quiet (May, B. J. *et al.*, 2004). However, this initial deficit in sound localization observed in the presence of noise disappeared after five to six sessions of testing, suggesting that compensatory behaviors minimize the functional deficits along weeks, and that probably in humans these compensatory behaviors are also present.

In monkeys trained to discriminate human speech sounds in noise, a lesion in the midline of the fourth ventricle significantly impaired their performance in the behavioral task (Dewson, J. H., 3rd, 1968). Likewise, bilateral lesions of the OC system in cats produced significant impairment in the discrimination of vowel formants in the presence of noise, especially for high-intensity-noise backgrounds (Hienz, R. D. *et al.*, 1998).

3.24.3.3.2 Vestibular-nerve section in humans

Since OC fibers reach the cochlea through the vestibular nerve, patients whose vestibular nerve has been severed due to pharmacological untreatable vertigo constitute a human model of auditory de-efferentation. Several psychoacoustic tasks indicate that sound

detection, intensity discrimination, frequency selectivity, and loudness adaptation are not affected after vestibular neurotomy (Scharf, B. *et al.*, 1994; 1997). The only clear difference in these patients is that most of them detect unexpected frequencies in noise better than before surgery, suggesting that the efferent system is involved in the filtering of frequencies during attention (see Section 3.24.4.4.2).

In a study performed in a group of patients who had undergone vestibular neurotomy, the suppression produced by contralateral broad band noise on click-evoked OAEs was greatly reduced in comparison with normal subjects. In another group of patients with facial nerve paralyses (Bell's palsy), that abolishes the stapedial reflex, no difference was found in the magnitude of contralateral suppression by noise with that measured in control ears (Giraud, A. L. *et al.*, 1995). Although these results are evidence that the MOC efferent system is involved in the suppression by contralateral acoustic stimulation, the existence of residual contralateral-sound suppression in supposedly de-efferented patients suggests that maybe in humans not all efferent fibers travel along the vestibular nerve (Labrousse, M. *et al.*, 2005).

Amplitude suppression produced by contralateral sound in click-evoked OAEs is accompanied in normal subjects by a phase advance, which was reduced in de-efferented (vestibulotomized) patients (Giraud, A. L. *et al.*, 1996). Similarly, contralateral sound reduces DPOAE latencies for low-frequency primary tones at levels below 60 dB SPL, except in vestibular neurotomized patients who, in identical experimental conditions, showed increased latencies, suggesting the involvement of two different mechanisms in the modulation of DPOAEs latencies (Giraud, A. L. *et al.*, 1997a).

3.24.3.3.3 Ablation of the auditory cortex

Bilateral removal of the insular–temporal cortex in cats, changes the temporal properties of evoked potentials to paired clicks at the cochlear nucleus, suggesting a corticofugal regulation of afferent responses in the first synapses of the auditory pathway (Dewson, J. H. *et al.*, 1966). Khalfa S. D. *et al.* (2001a) studied humans in whom the temporal superior gyrus (auditory cortex location) was surgically removed due to epilepsy refractory to pharmacological treatment. After the cortical resection the patients showed a reduction in MOC function, assessed by TEOAEs and contralateral broadband noise, in both cochleae, but especially in that contralateral to the cortical ablation. These results imply that the auditory-cortex activity modulates the MOC efferent reflex in humans.

3.24.3.4 Manipulating Efferent Neurotransmission

This section presents experimental results obtained by different means of modifying efferent neurotransmission. It first describes the consequences of molecular deletion of target genes (*α9-nicotinic acetylcholine, αCGRP, $GABA_A$*) relevant for the efferent function in mice. Then, it reviews evidences showing that some drugs commonly used in clinical practice alter the efferent function (gentamicin, benzodiazepines, opiates, and quinoline derivates). Finally, it discusses the dopaminergic neurotransmission in LOC efferent fibers that has been reported to modulate the efferent function.

3.24.3.4.1 Knockout Mice (α9-nicotinic acetylcholine, αCGRP, $GABA_A$)

3.24.3.4.1.(i) α9-Nicotinic acetylcholine receptor knockout mice In 1999 Vetter and collaborators developed an α9-nicotinic acetylcholine receptor knockout mouse. Based on external examination, the α9-knockout mice had no evident phenotype; it presented a clear startle reflex and no difficulties with balance or movement. At a microscopic level, cochlear hair cells, supporting cells, and primary auditory neurons were not affected by the mutation and OC fibers, marked with choline-acetyltransferase inmunostaining, were seen at their normal crossing on the floor of the fourth ventricle. Efferent innervation was evaluated with specific antibodies against vesicular acetylcholine transporter or synaptophysin, an integral protein of the synaptic vesicle membrane. In knockout mice OHCs were innervated by one large efferent terminal instead of multiple smaller terminals as in wild-type mice; however, cholinergic innervation was present from base to apex in the cochlea.

Physiological tests in the α9-knockout mouse showed normal CAP thresholds across most of the hearing range and normal growth for CAP and DPOAE magnitudes with increasing intensity. However, these tests failed to show the best-known effect of OC activation, a reduction in cochlear sensitivity. Electrical stimulation of the crossed OC fibers at their crossing in the fourth ventricle did not elicit a decrease in CAP and DPOAE magnitudes in the α9-knockout, as in the wild-type mouse (Vetter, D. E. *et al.*, 1999). Several attempts have

been made to identify functional deficits in the α9-knockout, which could provide clues about the efferent-system functions. However, no significant differences were found between α9-knockout and control mice in behavioral thresholds for pure-tone detection and intensity discrimination under quiet conditions and in presence of noise (Prosen, C. A. *et al.*, 2000; May, B. J. *et al.*, 2002).

3.24.3.4.1.(ii) αCGRP knockout mice In an effort to learn about the role of the CGRP neuropeptide in the auditory function, Maison S. F. *et al.* (2003b) assessed auditory thresholds, input/output functions and MOC functions in mice in which the αCGRP receptor gene was deleted. No differences were found between wild type and αCGRP-null mice in auditory thresholds measured with auditory brainstem responses and DPOAEs. Also, the electrical activation of the MOC fibers at the fourth ventricle and the resistance to acoustic injury were similar in control and mutant mice. The αCGRP deletion did not affect the input/output functions for DPOAEs; however, it consistently reduced the amplitude of auditory-brainstem responses at suprathresholds sound levels. The authors concluded that the observed decrease in sound-evoked neural responses in the αCGRP knockout is most probably caused by the LOC system. The mechanism of action of CGRP in mammalian auditory efferents is unknown, but the activation of αCGRP receptors in myocites from the heart in rats increases the levels of cyclic adenosine monophosphate (cAMP), suggesting the presence of a G-protein-coupled receptor (Poyner, D. R. *et al.*, 1992).

3.24.3.4.1.(iii) $GABA_A$ receptor knockout mice Despite the clear evidence of the presence of GABA in both medial and lateral OC efferents, its functional role in the cochlea is still unknown. To elucidate the physiological function of this neurotransmitter, Maison S. F. *et al.* (2006) studied the cochlear phenotypes of seven lines of mice with targeted deletion of different $GABA_A$ receptor subunit genes. Four of the lines (α1, α2, α6, and δ) were found to be normal, without any sign of afferent or efferent cochlear histopathology or dysfunction. In contrast, mice with deletion on α5, β2, and β3 GABA subunits showed threshold elevations, decrease in efferent function or decreased density of efferent or afferent innervation. The authors concluded that the GABAergic component of OC innervation contributes to the long-term maintenance of cochlear hair cells and neurons.

3.24.3.4.2 Drugs that alter the auditory-efferent function

3.24.3.4.2.(i) Gentamicin Gentamicin is an aminoglycoside antibiotic that has well-known side effects as ototoxicity, nephrotoxicity and neuromuscular blockage. Brown R. D. (1972) (see also Brown, R. D. and Daigneault, E. A. 1973) showed that the suppressive effect of the electrical activation of OC fibers was reduced after a chronic systemic treatment with aminoglycosides, but he also observed some damage and loss of hair cells. Afterward, in a seminal work, Smith, D. W. *et al.* (1994) showed that a single dose of gentamicin (150 mg kg^{-1}) in awake guinea-pigs can block the reduction in CAP amplitude produced by activation of OC fibers by nonsimultaneous contralateral noise. This pharmacological effect, which did not affect CAP thresholds, was completely reversed after 72 h of the antibiotic treatment. Similarly, a single injection of gentamicin (150 mg kg^{-1}) abolished the suppression of DPOAE produced by contralateral white noise in awake guinea-pigs (Avan, P. *et al.*, 1996; Guitton, M. J. *et al.*, 2004). Gentamicin is believed to have pre- as well as postsynaptic effects in OHC efferent synapses. Aminoglycosides at a presynaptic level inhibit maxi-K^+ channels in isolated efferent auditory-nerve fibers (Takeuchi, S. and Wangemann, P., 1993) and at a postsynaptic level inhibit Ca^{2+} influx through voltage dependent calcium channels (Dulon, D. *et al.*, 1989) or via the α9/α10 nicotinic receptor, thus reducing the Ca^{2+}-activated K^+ currents in OHC (Blanchet, C. *et al.*, 2000; Rothlin, C. V. *et al.*, 2000).

Recordings of the unstimulated eighth-nerve ensemble background activity in awake guinea-pigs (Lima da Costa, D. *et al.*, 1997a; 1997b) showed different effects of gentamicin in the fast and slow suppression produced by contralateral acoustic activation of OC efferents (see Section 3.24.3.1.1.(ii)). The rapid OC effect was reversibly blocked by a single injection of gentamicin at a dose of 150 mg kg^{-1}, whereas higher doses were required to completely (although reversibly) block the slow effect, implying that these two effects may involve different cellular mechanisms. However, no dose dependency of the effect of gentamicin was found on the fast and slow effects of electrically evoked OC efferent activation in anesthetized guinea-pigs (Yoshida, N. *et al.*, 1999a). It is not clear whether the differences in the results of these two studies are due to the difference in OC efferent activation, contralateral sound versus electrical pulses at the fourth ventricle, or to the conditions of the animals, awake versus the deeply anesthetized.

Gentamicin has also been shown to block the efferent effects produced by electrical activation of the IC in anesthetized guinea-pigs (Popelar, J. *et al.*, 2002; Mulders, W. H. and Robertson, D., 2006). A single injection of gentamicin (210–250 mg kg^{-1}) abolished the efferent suppression of DPOAE produced by contralateral broadband noise and by electrical activation of the IC (Popelar, J. *et al.*, 2002). The administration of gentamicin, whether in a single injection (200 mg kg^{-1}) or by intracochlear perfusion, blocked the inhibitory and the excitatory effects produced by electrical activation of the IC (Mulders, W. H. and Robertson, D., 2006; Groff, J. A. and Liberman, M. C., 2003). These last results have been interpreted as suggesting that both the inhibitory as well as excitatory effects of the electrical stimulation of the IC are mediated by the MOC (Mulders, W. H. and Robertson, D., 2006).

3.24.3.4.2.(ii) Benzodiazepines Benzodiazepines are well-known drugs that potentiate the inhibitory chloride currents of GABA receptors in the nervous system. As discussed above, a group of GABAergic fibers that project to the OHCs has been identified in the MOC system. Velluti R. and Pedemonte M. (1986) showed in guinea-pig that systemic (i.p.) administration of benzodiazepines (chlordiazepoxide or midazolam) increases CAP amplitudes and reduces CM in a dose-dependent manner. These effects on cochlear potentials are opposite to those of electrical activation of the OC bundle, suggesting the presence of a tonic gabaergic activity on the cochlea. However, a later work in humans showed that oral intake of oxazepam (20 mg) does not affect the evoked OAEs (EOAEs) baseline amplitude, but produces a slight reduction in contralateral broadband noise suppression of EOAEs (Morand, N. *et al.*, 1998), indicating that benzodiazepines in humans can partially block the acoustic activation of the MOC system.

3.24.3.4.2.(iii) Opiod peptides It has been observed *in vitro* that morphine inhibits $\alpha 9$-nicotinic acetylcholine receptors and that the endogenous opioid peptides endomorphine-1 (μ-agonist) and dynorphine-B (κ-agonist) directly inhibit $\alpha 9/\alpha 10$ nicotinic acetylcholine receptors, by a mechanism not involving opioid receptors (Lioudyno, M. I. *et al.*, 2000; 2002). Intravenous administration of κ-agonist, μ-agonist (-)pentazocine in chinchillas produced a marked increase in CAP amplitude and no effect on CM (Sahley, T. L. *et al*, 1991, Sahley, T. L. and Nodar, R. H. 1994). Since this effect was blocked by the opiod antagonist naloxene, it must be mediated by opiod receptors located in LOC efferents (Sahley, T. L. *et al.*, 1996).

3.24.3.4.2.(iv) Quinoline derivates Quinine and chloroquine are medications commonly used in treatment of malaria. Their auditory side effects include sensorineural hearing loss and tinnitus (Jung, T. T. *et al.*, 1993). It has been shown *in vitro* that chloroquine and quinine block ACh-evoked currents in the $\alpha 9/\alpha 10$ nicotinic acetylcholine receptor through a competitive mechanism the former, and a mixed competitive and noncompetitive manner the latter (Ballestero, J. A. *et al.*, 2005).

3.24.3.4.3 Neurochemical and lesion studies of lateral olivocochlear transmission

Although the physiology of lateral efferents has remained elusive for many years, neurochemical and lesion studies have provided some clues about their physiological role, especially about the cochlear efferent function of dopamine.

3.24.3.4.3.(i) Neurochemistry of lateral olivocochlear dopaminergic transmission Intracochlear perfusion of dopamine in guinea-pigs reduced auditory-nerve CAP amplitudes, increased thresholds and decreased spontaneous and evoked auditory-nerve fiber activity, with no significant effect in CM amplitudes. It is known that dopamine acts on two types of receptors, D1- and D2-like receptors that activate and inhibit adenilate cyclase, respectively. Although antagonists to the two types of receptors had different effects in auditory-nerve units with different spontaneous rates, for low-spontaneous-rate fibers they increased spontaneous activity, improved threshold sensitivity and decreased maximum evoked firing rates, suggesting that dopamine in lateral efferents could exert a tonic inhibition on auditory-nerve activity (Ruel, J. *et al.*, 2001).

Inmunocytochemical evidence obtained in guinea-pigs strongly suggests the presence of dopamine in efferent varicosities that make synaptic contacts with afferent auditory dendrites postsynaptic to IHCs (D'Aldin, C. *et al.*, 1995). In the same study the intracochlear administration of piribedil, a D2-dopamine agonist, produced a dose-dependent decrease in auditory-nerve CAP amplitude that was more evident at high stimulus intensities. The fact that the D2 agonist produced no changes on CM potentials implied that the effect of dopamine does not involve OHCs.

Moreover, intracochlear perfusion of selective inhibitors of dopamine transporters, increased the cochlear dopamine level and diminished spontaneous and evoked neural activity, but had no effect on CM and DPOAE amplitudes (Ruel, J. *et al.*, 2006).

Electrical stimulation of cochlear tissue *in vitro* produced release of dopamine, which could be blocked by tetrodotoxin and cadmium, which inhibit axonal activity and Ca^{2+} influx respectively, indicating its neuronal origin. The dopamine release, probably from lateral efferents, could be modulated by D1, but not by D2, receptors (Gaborjan, A. *et al.*, 1999).

Niu X. and Canlon B. (2006) found by inmunohistochemistry that the D1 receptor is located at the auditory afferent dendrites and thus, that it is a postsynaptic target for dopamine released from lateral efferents. No differences were found in the distribution of D1 positively stained dendrites along the base, middle or apex of the cochlea. They showed that cochlear perfusion with a D1 agonist produced an increase in CAP amplitude, whereas perfusion with a D1 antagonist produced CAP reductions and increased CAP thresholds. Furthermore, they demonstrated that D1 effects on afferent fibers are mediated by a mechanism involving phosphorylation of glutamate receptors via protein kinase A/cAMP. They proposed a dual effect of dopamine; at high-level sounds D2 receptors would dominate and inhibit auditory nerve responses providing protection to acoustic injury (see Section 3.24.4.2.2), while at normal low-level sounds D1 receptors would dominate enhancing neural responses.

3.24.3.4.3.(ii) Selective lesions of lateral olivocochlear efferents In an attempt to selectively damage lateral efferents the cholinotoxin etylcholine aziridinium ion (AF64A) was injected into the cochlea in chinchillas. Cochlear infusion of 1 μM AF64A produced damage of lateral efferents, but not of MOC fibers or OHC, as evaluated 7 days after the injection by light and electron microscopy. Cochlear injection of 10 μM AF64A produced a significant disruption of LOC and MOC fibers, but also of cochlear supporting cells (Smith, D. W. *et al.*, 1989; Morley, B. J. *et al.*, 1991; Smith, D. W. and Mount, R. J., 1993). However, because cholinotoxin damages cholinergic neurons, it is difficult to rule out damage to MOC neurons.

Melittin, a cytotoxic chemical, has been used to selectively lesion the LOC nucleus in the guinea-pig brainstem finding a reduction in CAP amplitude, without changes in N1 latency (Le Prell, C. G. *et al.*, 2003). Adaptation of the DPOAEs, which is thought to be mediated by MOC efferents, was present in the severed animals, suggesting a selective lesion of lateral efferents. Although these results confirmed the notion that LOC efferents modulate eigth-nerve activity, it is not clear whether the ascending auditory pathway that passes through the lateral superior olive may also have been damaged.

Le Prell C. G. *et al.* (2005) used intracochlear administration of MPTP, a known dopaminergic toxin, to selectively disrupt the dopaminergic subset of LOC fibers in guinea-pigs. As in their study with LSO lesions (Le Prell, C. G. *et al.*, 2003), after disruption of LOC efferents they found CAP decreases at all tested frequencies (2–18 kHz) and CAP-threshold elevations at 16 and 18 kHz. The toxin applied to the cochlea affected neither amplitude nor adaptation of DPOAEs, leading to the conclusion that it did not affect OHC function, but selectively disrupted dopaminergic function of lateral efferents.

3.24.4 Proposed Functions of the Auditory Efferent System

The role of the auditory efferent system in hearing is still unknown. However, based on the available experimental evidence, various possible roles have been proposed for it. It has been suggested that the efferent system: (1) is involved in antimasking of auditory stimuli in noisy backgrounds, like in speech perception in noise; (2) has a protective role in preventing hearing loss caused by exposure to high-intensity sounds; (3) modulates cochlear sensitivity to filter unattended tones in auditory tasks or in tasks that require selective attention to stimuli of other sensory modalities; (4) modulates auditory afferent responses during sleep or awake states; and (5) could balance interaural sensitivity.

3.24.4.1 Antimasking of Auditory Stimuli in Noise

It has been suggested that the efferent system can enhance neural responses to acoustic stimuli in the presence of masking noise. Physiological and behavioral studies performed in animals and humans support this antimasking role of the efferent system, which, in humans, becomes quite important for the detection and discrimination of speech in noisy environments.

3.24.4.1.1 Antimasking in experimental animals

As described above (Section 3.24.3.3.1.(ii)), a chronic section of the OC bundle at the midline of the fourth-ventricle floor impairs, in the presence of background noise, intensity discrimination (May, B. J. and McQuone, S. J., 1995), sound localization (May, B. J. *et al.*, 2004), and human-speech sounds discrimination (Dewson, J. H., 3rd, 1968; Hienz, R. D. *et al.*,1998).

In acute physiological studies in guinea-pigs, it has been demonstrated that electrical stimulation of OC fibers at the midline of the fourth ventricle produces an antimasking effect, increasing neural responses to loud clicks recorded in the presence of masking noise (Nieder, P. and Nieder, I., 1970; Dolan, D. F. and Nuttall, A. L., 1988). Afterward, recording responses of auditory-nerve afferent fibers to tones in background noise, it was shown in cats that electrical stimulation of MOC fibers reduces the low-level noise-driven discharge rate and increases the saturation discharge rate (Winslow, R. L. and Sachs, M. B., 1987). Consequently, the effect of MOC electrical stimulation was to counteract the compression produced by broadband noise on auditory-nerve fiber discharge rate–level functions, improving the discriminability of the signal in the presence of background noise.

More recently, it has been shown in cats that the acoustic activation of efferent fibers also has an antimasking effect for sounds presented in the presence of noise (Kawase, T. and Liberman, M. C., 1993). The amplitude of the CAP elicited by a click presented together with an ipsilateral masker is larger in the presence of a simultaneous contralateral noise, which activates the OC efferents, than when the ipsilateral stimuli are presented alone (Figure 9). In these experiments, in some of the animals there was an enhancement of CAP responses during contralateral-noise stimulation even in the absence of an ipsilateral masker. This phenomenon was interpreted as a release from masking caused by internally generated sounds.

3.24.4.1.2 Antimasking of tones and speech in humans

The role of auditory efferents in the reduction of masking of sounds in noise has also been studied in human subjets. The OC efferent function can be assessed in humans by the magnitude of the suppression produced by contralateral noise in EOAEs (Collet, L. *et al.*, 1990; Moulin, A. *et al.*, 1993; see Section 3.24.3.2.2). In behavioral studies of

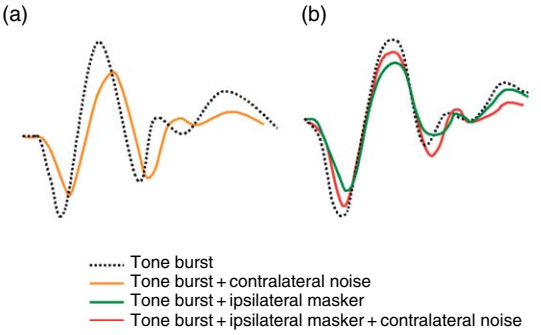

Figure 9 (a) Suppression of CAP by contralateral noise in quiet conditions (orange trace). (b) Antimasking effect of contralateral noise stimulation. An ipsilateral masker produces a CAP reduction (green trace). In this condition, the contralateral noise produces a CAP enhancement (red trace). In both panels, the segmented black traces indicate CAPs evoked with tone bursts alone. Adapted from Kawase, T. and Liberman, M. C. 1993. Antimasking effects of the olivocochlear reflex. I. Enhancement of compound action potentials to masked tones. J. Neurophysiol. 70, 2519–2532.

performance in detection and intensity discrimination of tones in noise, significant correlations have been reported between the magnitude of contralateral-noise suppression of EOAEs and the detection thresholds for a 2 kHz tone in noise, and the performance in intensity discriminations in noise (Micheyl, C. and Collet, L., 1996; Micheyl, C. *et al.*, 1997).

In other psychoacoustic tests, it has been shown that contralateral acoustic suppression also enhances speech perception in the presence of ipsilateral noise, and that the magnitude of the enhacement is correlated with the strength of the contralateral suppression of EOAEs, mediated by the efferent system (Giraud, A. L. *et al.*, 1997b; Kumar, U. A. and Vanaja, C. S., 2004). Furthermore, the same tests in patients in whom the efferent pathway had been sectioned (through vestibular neurotomy; see Section 3.24.3.3.1) showed almost no enhancement in word recognition in the de-efferented ear, but a greater enhancement in the healthy ear than that of normal subjects (Giraud, A. L. *et al.*, 1997b). In another study performed in vestibular neurotomized patients, little effect of the de-efferentation was found in pure-tone detection and frequency discrimination in quiet; however, several deficits of auditory perception in noise were found in most of the patients, such as worse intensity discrimination and speech recognition in noise (Zeng, F. G. *et al.*, 2000).

3.24.4.2 Protection to Loud Sounds

One of the proposed roles of the efferent system that has received more attention is its putative protection to acoustic injury from loud sounds. After the influential work by Cody A. R. and Johnstone B. M. (1982), showing that the losses in hearing sensitivity produced by an intense pure tone could be reduced by a tone of the same frequency simultaneously delivered to the contralateral ear, several other evidences have implicated the MOC system in protection to temporary hearing loss (Rajan, R. and Johnstone, B. M., 1988; Reiter, E. R. and Liberman, M. C., 1995) and to permanent hearing loss induced by loud sounds (Kujawa, S. G. and Liberman, M. C., 1997; Yamasoba, T. and Dolan, D. F., 1997). Recently, the LOC system has also been implicated in protection to temporary hearing loss (Darrow, K. N. *et al.*, 2007).

3.24.4.2.1 Medial olivocochlear protection to loud sounds

Electrical stimulation of the crossed OC fibers has been shown to reduce temporary thresholds shifts (TTSs) after brief exposures to high-intensity tones in anesthetized guinea-pigs. Crossed OC stimulation at any fixed rate produces the greatest reductions in TTSs for the exposures that would have caused the largest amounts of TTSs. On the other hand, OC electrical stimulation is always most effective when presented at a high rate and simultaneous with the exposure, and has a tonic effect that can last up to several minutes (Rajan, R., 1988a; 1988b). Electrical activation of the IC in guinea-pigs also produces a reduction of TTSs caused by loud sounds. Furthermore, chronic section or strychnine inactivation of the OC fibers increases the noise-induced permanent threshold shift in guinea-pigs and chinchillas (Kujawa, S. G. and Liberman, M. C., 1997; Zheng, X. Y. *et al.*, 1997a; 1997b; Yamasoba, T. and Dolan, D. F., 1997).

There is a high degree of intersubject variability in susceptibility to permanent hearing loss due to exposure to loud sounds, and it is known that some subjects have tough ears, whereas others have tender ears (Cody, A. R. and Robertson, D., 1983). Maison S. F. and Liberman M. C. (2000) found, in awake guinea-pigs, that the strength of sound-evoked efferent activity is inversely correlated with the degree of permanent hearing loss produced after an acoustic trauma. Moreover, a correlation has been found between cochlear expression of the $\alpha 9$ subunit of the cholinergic receptor and strength of the efferent function, thus implying that intersubject variability in vulnerability to noise damage may be partly caused by intersubject variability in $\alpha 9$ subunit cochlear expression (Luebke, A. E. and Foster, P. K., 2002). However, a previous study in guinea-pigs did not find any correlation between magnitude of the acoustic efferent reflex and susceptibility to TTSs (Zennaro, O. *et al.*, 1998).

There is also evidence in human subjects recovering from impulse noise trauma (young military subjects), suggesting that higher activity of the efferent system improves the short-term recovery of auditory thresholds (Veuillet, E. *et al.*, 2001a). In contrast, another study in human subjects participating in shooting exercises did not find any correlation between acoustic contralateral suppression of DPOAEs and susceptibility to TTSs (Wagner, W. *et al.*, 2005).

In a study aimed to determine whether the putative OC protective effect to acoustic trauma was mediated by the $\alpha 9$ nicotinic receptor, hearing was assessed after noise exposure in $\alpha 9$-knockout mice (129/SvEv strain). No differences in permanent threshold shift were found between homozygotes, heterozygotes, and wild-type mice a week after exposure to high-intensity broadband noise (Yoshida, N. *et al.*, 1999b). However, the 129/SvEv mice strain used to generate the $\alpha 9$-knockout mice (Vetter, D. E. *et al.*, 1999) tested for vulnerability to acoustic injury was later shown to be exceptionally resistant to noise-induced hearing loss (Yoshida, N. *et al.*, 2000). The special characteristic of high resistance to acoustic injury observed on this mice strain must reflect mechanisms other than those involving the $\alpha 9$-nicotinic receptor. More recent evidence supports the idea that OC protection to acoustic trauma is mediated by the $\alpha 9$ nicotinic receptor. Overexpression of the $\alpha 9$ nicotinic receptor has been shown to increase MOC suppression effects in the cochlea and to enhance ear protection to temporary and permanent acoustic trauma in mice, without changes in auditory thresholds (Maison,S. F. *et al.*, 2002).

The time course of the protective effect from acoustic trauma, and the exposure frequencies at which it is more effective (10 kHz) suggest that the slow rather than fast effect of OC activation is responsible for this protective effect (Reiter, E. R. and Liberman, M. C., 1995). Recently, Maison S. F. *et al* (2007b) studied mice overexpressing the SK2 channel (Ca^{2+}-activated K^+ channel; see Section

3.24.2.1.3; Figure 2) in OHCs, finding that cochlear morphology, auditory thresholds, and OAEs were normal, but electrically evoked fast efferent suppression was enhanced, similarly as in $\alpha 9$ nicotinic-receptor overexpresser mice (Maison, S. F. *et al.*, 2002). These mice, however, did not show enhanced resistance to acoustic trauma, suggesting that the efferent protective effects from acoustic overexposure are not dependent on the function of the SK2 channel and probably depend on other cellular mechanisms activated by Ca^{2+} entry into OHCs.

3.24.4.2.2 Lateral olivocochlear protection to loud sounds

It has been proposed that the release of dopamine by the lateral efferents could have a functional role in the postsynaptic regulation of the glutamatergic activity of IHCs and in mediating a protection of auditory nerve dendrites against loud sounds that induce massive releases of glutamate from IHCs and produce swelling of auditory nerve fibers (D'Aldin, C. *et al.*, 1995; Oestreicher, E. *et al.*, 1997; Niu, X. and Canlon, B., 2002; Niu, X. *et al.*, 2004).

Niu X. and Canlon B. (2002) found an up-regulation of tyrosine-hydroxylase-positive efferent terminals on the guinea-pig cochlea during sound preconditioning (the protective effect of exposure to low-level sounds against a subsequent exposure to loud sounds), and that the protective effects of preconditioning can be blocked by 6-hydroxidydopamine, which disrupts tyrosine hidroxylase in the lateral efferent terminals. These results suggest a role of lateral efferents in protection to acoustic trauma by sound conditioning.

Selective, unilateral destruction of the LSO by stereotaxically injected melittin in mice increased the ipsilateral frequency- and level-independent suprathreshold auditory-nerve component (wave 1) of brainstem responses, with no evident simultaneous changes in DPOAE amplitudes (Darrow, K. N. *et al*, 2007). In these mice, exposure to an acoustic trauma produced greater TTSs in neural responses from the cochlea ipsilateral than contralateral to the LSO lesion.

Consequently, both, the medial and lateral, components of the efferent system seem to be involved in protection to acoustic injury by loud sounds. However, it is unlikely that the auditory efferent system may have evolved primarily as a protective mechanism from acoustic trauma, because it has been present in vertebrates for millions of years of evolution, while high-intensity sounds are rarely found in nature, and they only appeared in the last 200 years of human history, after the industrial revolution (Kirk, E. C. and Smith, D. W., 2003).

3.24.4.3 Modulation of Sensory Input During Sleep

Significant increases in CM and auditory-nerve CAPs have been found in guinea-pigs during slow wave sleep, as compared to in the awake state and in paradoxical sleep (Velluti, R. *et al.*, 1989). In these experiments the changes in both cochlear potentials could not be attributed to middle-ear muscle reflex, because the middle-ear ossicles and muscles were removed and auditory stimuli were directly delivered to the animal's bulla. These results imply that during sleep the central nervous system modulates auditory input through OC efferents. A single systemic injection of gentamicin ($150\,mg\,kg^{-1}$) that blocks MOC efferent effects in unanesthetized guinea-pigs (see Section 3.24.3.4.2.(i)) did not affect the central modulations of cochlear responses produced through OC efferents by sleep/awake state changes (Pedemonte, M. *et al.*, 2004). However, it is possible that the gentamicin dose used in these experiments was too low to block the efferent effect, and a higher dose may be required. This was the case for the slow suppression produced by contralateral-sound activation of OC efferents that was not blocked by a single dose of $150\,mg\,kg^{-1}$ gentamicin, but was completely blocked by a $250\,mg\,kg^{-1}$ dose (Lima da Costa, D. *et al.*, 1997a).

In relation to humans, Campbell K. B. and Bartoli E. A. (1986) did not find any reliable differences in the amplitude or latency of brainstem auditory evoked potentials recorded during wakefulness and various stages of sleep. A later study, recording TEOAE during sleep in adults found a progressive increase in TEOAE amplitudes through the night that could reach up to 4 dB at the end of the night, but that was not related to the sleep stages (Froehlich, P. *et al.*, 1993). The work also evaluated the effect of contralateral noise on the amplitude of TEOAE and found a decrease in the reduction of TEOAEs by contralateral noise during the night. Although this study suggests a role of auditory efferents during sleep, another factor that could also modify the magnitude of TEOAEs, as middle-ear muscle activity, was not excluded.

3.24.4.4 Modulation of Cochlear Sensitivity by Selective Attention

Hernandez-Peón *et al.* (1956) showed a reduction in click-evoked potentials recorded from the cochlear nucleus in cats while receiving stimuli of other sensory modalities. They postulated the existence of peripheral filters that would selectively inhibit unattended inputs at early stages of the sensory pathways. This proposition became controversial as other groups fail to replicate their findings (Dunlop, C. W. *et al.*, 1965; Wickelgren, W. O., 1968). However, later experiments confirmed the hypothesis that cross-modal attention to visual stimuli could attenuate peripheral auditory responses, as reductions in CAP amplitude were found in cats attending to visual stimuli (Oatman, L. C., 1971).

3.24.4.4.1 Cross-modal attenuation of auditory stimuli

Reductions in the amplitude of CAP responses during periods of visual attention have been demonstrated in cats and chinchillas performing visual discrimination tasks (Oatman, L. C., 1971; Delano, P. H. *et al.*, 2007). Similarly, in humans, the auditory-nerve component of tone-pip evoked brainstem potentials were significantly reduced in subjects when instructed to count letters flashed on a screen (Lukas, J. H., 1980). In another study in humans, attention to a visual task produced a small but significant amplitude decrease of click-evoked OAEs, indicating changes in cochlear mechanics (Puel, J. L. *et al.*, 1988).

Recently, it has been shown, in chinchillas performing a visual discrimination task, that reductions of CAP amplitude during periods of visual attention are also accompanied by increases in CM amplitude (Figure 10; Delano, P. H. *et al.*, 2007). Two facts are worth mentioning in these results: (1) The reduction of cochlear sensitivity is transient (a few seconds), during the period of high expectancy; and (2) the reduction of cochlear sensitivity is larger for higher attentional loads of the task (shorter target stimuli). These facts could probably explain why some works have failed to find a reduction of cochlear sensitivity during visual attention. An easy task or an inadequate temporal resolution of the method to assess cochlear responses can lead to negative results.

Auditory efferents are most probably involved in this cochlear cross-modal attentional effect. Sectioning the tendons of the middle-ear muscles did not abolish this effect (Oatman, L. C., 1971) and increases in CM amplitudes simultaneous with CAP reductions are incompatible with a middle-ear muscle effect (Delano, P. H. *et al.*, 2007). Also, the CAP amplitude reductions concomitant to CM increases observed in the cross-modal attentional effect are reminiscent of the efferent effects produced by electrically evoked activation of MOC fibers (Gifford, M. L. and Guinan, J. J., Jr., 1987).

3.24.4.4.2 Intra-modal frequency filter

There is experimental evidence in anesthetized animals of a frequency-dependent loss of sensitivity in basilar membrane vibrations during efferent stimulation (Murugasu, E. and Russell, I. J., 1996a; Dolan, D. F. *et al.*, 1997) that could account for similar neural effects (Robles, L and Ruggero, M. A., 2001). Likewise, psychophysical measurements in humans show frequency-specific effects of attention in detection of target tones of unexpected frequencies in noise (Greenberg, G. Z. and Larkin, W. D., 1968). Furthermore, humans in whom the auditory efferent pathway has been sectioned present higher detection levels of unexpected target frequencies in noise than before surgery (Scharf, B. *et al.*, 1994; 1997), suggesting that the efferent system is required to maintain an attentional band-pass filter.

3.24.4.5 Balance of Interaural Sensitivity

Recently, Darrow K. N. *et al.* (2006b) suggested a new role for the LOC efferents. Using the protocol mentioned above (see Section 3.24.3.4.3.(ii)), in which an injection of melittin selectively destroys LSO cells, they reported that in mice in which LSO cells were effectively destroyed there was an amplitude increase of wave 1 of the auditory brainstem responses, without changes in DPOAE amplitudes. Surprisingly, they also found an amplitude reduction in the contralateral wave 1 of the auditory brainstem response. As it is known that LSO neurons are involved in processing interaural intensity differences for sound localization, they proposed that the LOC system may provide a binaural sensitivity balance required for accurate sound localization.

3.24.5 Some Clinical Findings

Little is known about the involvement of the auditory efferent system in clinical pathologies. Only a few findings have been reported about its

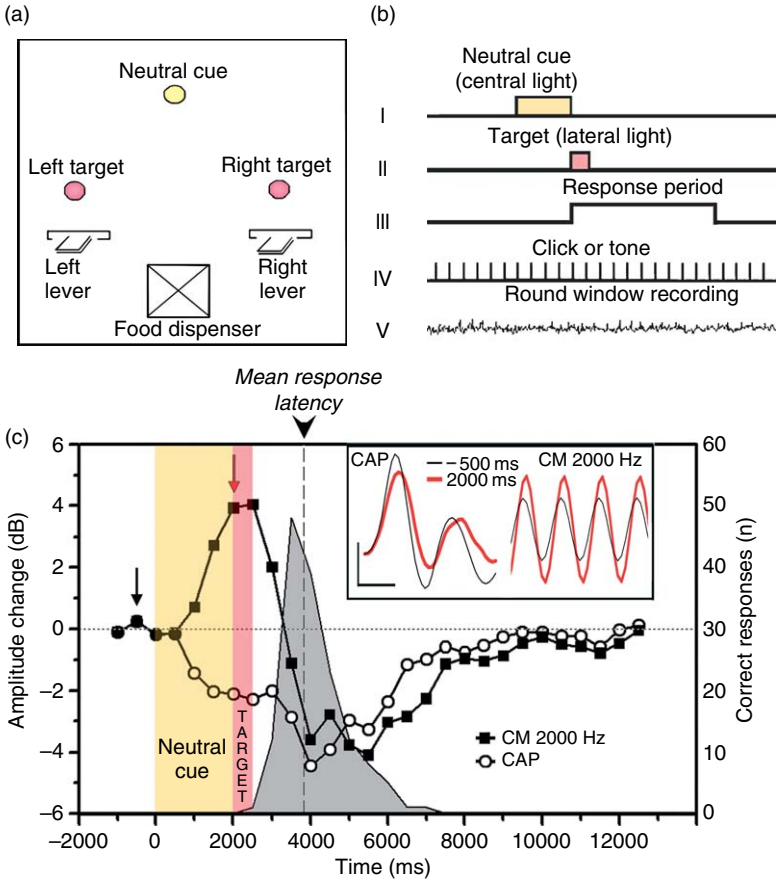

Figure 10 Reduction of cochlear sensitivity during visual attention. (a) Schematic diagram of the frontal panel of the operant cage used in the visual discrimination task. (b) Time sequence of this task. I–III: A neutral cue (central light) was turned on before one of two lateral lights (targets); the chinchilla had 5 s to respond by pressing a lever under the target light. IV: Simultaneously an irrelevant click and/or tone train was presented at 2 Hz rate. V: The round-window electrical signal was acquired during the task. (c) Example of CM augmentation (solid squares) concomitant to CAP reductions (open circles) during the period of visual attention. Symbols on each trace represent CAP and CM amplitude changes measured in dB, referenced to the average amplitude of the respective cochlear potential measured before the onset of the neutral cue. The figure also shows a histogram for the latencies of correct responses to the target (dark gray shaded area; scale in right *y*-axis). The upper-right inset shows examples of averaged CAP and CM traces from −500 ms (thin trace) and 2000 ms (thick trace) (see vertical arrows in panel (c); scale bar: *x*-axis: 0.5 ms; *y*-axis: 40 μV for CAP, 80 μV for CM). The mean correct-response latency measured from the target-light onset was 1833 ms (vertical segmented line). Adapted from Delano, P. H., Elgueda, D., Hamame, C. M., and Robles, L. 2007. Selective attention to visual stimuli reduces cochlear sensitivity in chinchillas. J. Neurosci. 27, 4146–4153.

possible role in some auditory and psychiatric disorders and in myasthenia gravis disease.

A dysfunction of auditory efferents has been postulated in the physiopathology of acute tinnitus, although diverse results have been obtained by different groups (Chery-Croze, S. *et al.*, 1993; Riga, M. *et al.*, 2007). Significantly lower efferent suppression of EOAEs was reported in children with impaired learning than in normal children (Veuillet, E. *et al.*, 1999); however, no difference was found in efferent activity between children with specific language impairments and controls (Clarke, E. M. *et al.*, 2006).

Auditory efferent dysfunctions have been found in relation to some behavioral disorders. A decrease in acoustically evoked efferent activity and differences in the right–left asymmetry of efferent suppression have been reported in subjects with autism and in schizophrenic patients (Collet, L. *et al.*, 1993; Khalfa, S. *et al.*, 2001b; Veuillet, E. *et al.*, 2001b). A reduction in auditory efferent activity has also been found in some children with selective mutism, a

psychiatric disorder in which patients are reluctant or not able to speak in specific situations (Bar-Haim, Y. *et al.*, 2004).

The possible involvement of cochlear-efferent nicotinic-ACh receptors in patients affected by myasthenia gravis has been reported by several authors. Myasthenia gravis is an autoimmune neuromuscular disease characterized by the presence of circulating antibodies against nicotinic acetylcholine receptors, in which patients have muscle weakness and fatigability. Myasthenic patients present significantly reduced levels of DPOAEs, TEOAEs, and efferent activity before pharmacological treatment, which after administration of acetylcholinesterase inhibitors recover almost control levels (Toth, L. *et al.*, 1998; Paludetti, G. *et al.*, 2001; Di Girolamo, W. *et al.*, 2001); however, chronic myasthenic patients develop a permanent cochlear efferent damage (Hamed, S. A. *et al.*, 2006). Based on these findings, it has been suggested that recordings of OAE may be useful in early diagnosis and in the evaluation of treatments in some forms of myasthenia gravis.

3.24.6 Conclusions

The evidence reviewed in this chapter shows a significant presence of efferent auditory pathways that originate in the auditory cortex, project to various levels of the afferent auditory path, and reach as far as the cochlea. An important number of efferent nerve fibers make direct synaptic contact with cochlear hair cells and dendrites of auditory nerve cells. This significant efferent innervation makes possible a tight top-down control on incoming auditory information. However, despite the clear evidence showing that activation of the efferent fibers produces mainly suppressive effects on cochlear responses, the function of the efferent system in audition is still uncertain. Probably, the difficulty found in the assessment of the auditory deficits produced by lesions of the efferent system in experimental animals and in humans, made more difficult to resolve the role of the efferent system in audition. Among the various functions that have been proposed for the auditory efferent system, three of them have concentrated most of the research efforts: cochlear protection to acoustic trauma, antimasking of sound in noise, and modulation of cochlear sensitivity by selective attention. In the first of these, acoustical activation of a reflex circuit comprising the brainstem prevents hearing losses caused by exposure to loud sounds. In the latter two functions, which are closely related, top-down neural pathways originating in the auditory cortex modulate cochlear sensitivity at particular times or for specific frequencies, making it possible to unmask sounds in noisy environments or to attend to specific stimuli.

References

Abou-Madi, L., Pontarotti, P., Tramu, G., Cupo, A., and Eybalin, M. 1987. Coexistence of putative neuroactive substances in lateral olivocochlear neurons of rat and guinea pig. Hear. Res. 30, 135–146.

Andersen, R. A., Knight, P. L., and Merzenich, M. M. 1980. The thalamocortical and corticothalamic connections of AI, AII, and the anterior auditory field (AAF) in the cat: evidence for two largely segregated systems of connections. J. Comp. Neurol. 194, 663–701.

Arnesen, A. R. 1984. Fibre population of the vestibulocochlear anastomosis in humans. Acta Otolaryngol. 98, 501–18.

Art, J. J., Crawford, A. C., Fettiplace, R., and Fuchs, P. A. 1982. Efferent regulation of hair cells in the turtle cochlea. Proc. R. Soc. Lond. B 216, 377–384.

Ashmore, J. F. 1987. A fast motile response in guinea pig outer hair cells: the cellular basis of the cochlear amplifier. J. Physiol. (Lond). 388, 323–347.

Avan, P., Erre, J. P., da Costa, D. L., Aran, J. M., and Popelar, J. 1996. The efferent-mediated suppression of otoacoustic emissions in awake guinea pigs and its reversible blockage by gentamicin. Exp. Brain Res. 109, 9–16.

Azeredo, W. J., Kliment, M. L., Morley, B. J., Relkin, E., Slepecky, N. B., Sterns, A., Warr, W. B., Weekly, J. M., and Woods, C. I. 1999. Olivocochlear neurons in the chinchilla: a retrograde fluorescent labelling study. Hear. Res. 134, 57–70.

Ballestero, J. A., Plazas, P. V., Kracun, S., Gomez-Casati, M. E., Taranda, J., Rothlin, C. V., Katz, E., Millar, N. S., and Elgoyhen, A. B. 2005. Effects of quinine, quinidine, and chloroquine on alpha9alpha10 nicotinic cholinergic receptors. Mol. Pharmacol. 68, 822–829.

Bar-Haim, Y., Henkin, Y., Ari-Even-Roth, D., Tetin-Schneider, S., Hildesheimer, M., and Muchnik, C. 2004. Reduced auditory efferent activity in childhood selective mutism. Biol Psychiatry. 55, 1061–1068.

Blanchet, C., Erostegui, C., Sugasawa, M., and Dulon, D. 2000. Gentamicin blocks ACh-evoked K^+ current in guinea-pig outer hair cells by impairing Ca^{2+} entry at the cholinergic receptor. J. Physiol. 525, 641–54.

Bonfils, P., Remond, M. C., and Pujol, R. 1987. Variations of cochlear microphonic potential after sectioning efferent fibers to the cochlea. Hear. Res. 30, 267–271.

Boyev, K. P., Liberman, M. C., and Brown, M. C. 2002. Effects of anesthesia on efferent-mediated adaptation of the DPOAE. J. Assoc. Res. Otolaryngol. 3, 362–373.

Brown, M. C. 1987. Morphology of labeled efferent fibers in the guinea pig cochlea. J. Comp. Neurol. 260, 605–18.

Brown, M. C. 1989. Morphology and response properties of single olivocochlear fibers in the guinea pig. Hear. Res. 40, 93–109.

Brown, M. C. 1993. Fiber pathways and branching patterns of biocytin-labeled olivocochlear neurons in the mouse brainstem. J. Comp. Neurol. 337, 600–13.

Brown, M. C., Pierce, S., and Berglund, A. M. 1991. Cochlear-nucleus branches of thick (medial) olivocochlear fibers in the mouse: a cochleotopic projection. J. Comp. Neurol. 303, 300–315.

Brown, R. D. 1972. Influence of chronic treatment with neomycin and kanamycin on N 1 suppression produced by contralateral olivo-cochlear bundle stimulation in cats. Acta Otolaryngol. 73, 335–40.

Brown, R. D. and Daigneault, E. A. 1973. Neomycin: ototoxicity and the cochlear efferents. Acta Otolaryngol. 76, 128–35.

Brownell, W. E., Bader, C. R., Bertrand, D., and de Ribaupierre, Y. 1985. Evoked mechanical responses of isolated cochlear hair cells. Science. 227, 194–196.

Buño, W. 1978. Auditory-nerve fiber activity influenced by contralateral ear sound stimulation. Exp. Neurol. 59, 62–74.

Campbell, K. B. and Bartoli, E. A. 1986. Human auditory evoked potentials during natural sleep: the early components. Electroencephalogr. Clin. Neurophysiol. 65, 142–149.

Campbell, J. P. and Henson, M. M. 1988. Olivocochlear neurons in the brainstem of the mouse. Hear. Res. 35, 271–274.

Capps, M. J. and Ades, H. W. 1968. Auditory frequency discriminaion after transection of the olivocochlear bundle in squirrel monkeys. Exp. Neurol. 21, 147–158.

Chabert, R., Magnan, J., Lallemant, J. G., Uziel, A., and Puel, J. L. 2002. Contralateral sound stimulation suppresses the compound action potential from the auditory nerve in humans. Otol. Neurotol. 23, 784–788.

Chery-Croze, S., Collet, L., and Morgon, A. 1993. Medial olivo-cochlear system and tinnitus. Acta Otolaryngol. 113, 285–90.

Clarke, E. M., Ahmmed, A., Parker, D., and Adams, C. 2006. Contralateral suppression of otoacoustic emissions in children with specific language impairment. Ear Hear. 27, 153–160.

Cody, A. R. and Johnstone, B. M. 1982. Temporary threshold shift modified by binaural acoustic stimulation. Hear. Res. 6, 199–205.

Cody, A. R. and Robertson, D. 1983. Variability of noise-induced damage in the guinea pig cochlea: electrophysiological and morphological correlates after strictly controlled exposures. Hear. Res. 9, 55–70.

Collet, L., Kemp, D. T., Veuillet, E., Duclaux, R., Moulin, A., and Morgon, A. 1990. Effect of contralateral auditory stimuli on active cochlear micro-mechanical properties in human subjects. Hear. Res. 43, 251–61.

Collet, L., Roge, B., Descouens, D., Moron, P., Duverdy, F., and Urgell, H. 1993. Objective auditory dysfunction in infantile autism. Lancet. 342, 923–924.

Coomes, D. L. and Schofield, B. R. 2004a. Separate projections from the inferior colliculus to the cochlear nucleus and thalamus in guinea pigs. Hear. Res. 191, 67–78.

Coomes, D. L. and Schofield, B. R. 2004b. Projections from the auditory cortex to the superior olivary complex in guinea pigs. Eur. J. Neurosci. 19, 2188–2200.

Cooper, N. P. and Guinan, J. J. Jr. 2003. Separate mechanical processes underlie fast and slow effects of medial olivocochlear efferent activity. J. Physiol. 548, 307–312.

Cooper, N. P. and Guinan, J. J., Jr. 2006. Efferent-mediated control of basilar membrane motion. J Physiol. 576, 49–54.

D'Aldin, C., Eybalin, M., Puel, J. L., Charachon, G., Ladrech, S., Renard, N., and Pujol, R. 1995. Synaptic connections and putative functions of the dopaminergic innervation of the guinea pig cochlea. Eur. Arch. Otorhinolaryngol. 252, 270–274.

Dallos, P. 1992. The active cochlea. J. Neurosci. 12, 4575–4585.

Dallos, P., He, D. Z. Z., Lin, X., Sziklai, I., Mehta, S., and Evans, B. N. 1997. Acetylcholine, outer hair cell electromotility, and the cochlear amplifier. J. Neurosci. 17, 2212–2226.

Darrow, K. N., Maison, S. F., and Liberman, M. C. 2006b. Cochlear efferent feedback balances interaural sensitivity. Nat. Neurosci. 9, 1474–1476.

Darrow, K. N., Maison, S. F., and Liberman, M. C. 2007. Selective removal of lateral olivocochlear efferents increases vulnerability to acute acoustic injury. J. Neurophysiol. 97, 1775–1785.

Darrow, K. N., Simons, E. J., Dodds, L., and Liberman, M. C. 2006a. Dopaminergic innervation of the mouse inner ear: evidence for a separate cytochemical group of cochlear efferent fibers. J. Comp. Neurol. 498, 403–14.

Dayal, V. S. 1968. The effects of olivocochlear bundle stimulation on latency of action potential. Laryngoscope. 78, 1590–1596.

Delano, P. H., Elgueda, D., Hamame, C. M., and Robles, L. 2007. Selective attention to visual stimuli reduces cochlear sensitivity in chinchillas. J. Neurosci. 27, 4146–4153.

Desmedt, J. E. and Monaco, P. 1961. Mode of action of the efferent olivo-cochlear bundle on the inner ear. Nature. 192, 1263–1265.

Desmedt, J. E., La Grutta, V., and La Grutta, G. 1971. Contrasting effects of centrifugal olivo-cochlear inhibition and of middle ear muscle contraction on the response characteristics of the cat's auditory nerve. Brain Res. 1971. 30, 375–384.

Dewson, J. H., 3rd. 1968. Efferent olivocochlear bundle: some relationships to stimulus discrimination in noise. J. Neurophysiol. 31, 122–130.

Dewson, J. H., 3rd., Nobel, K. W., and Pribram, K. H. 1966. Corticofugal influence at cochlear nucleus of the cat: some effects of ablation of insular-temporal cortex. Brain Res. 2, 151–159.

De Venecia, R. K., Liberman, M. C., Guinan, J. J., Jr., and Brown, M. C. 2005. Medial olivocochlear reflex interneurons are located in the posteroventral cochlear nucleus: a kainic acid lesion study in guinea pigs. J. Comp. Neurol. 487, 345–360.

Di Girolamo, S., d'Ecclesia, A., Quaranta, N., Garozzo, A., Evoli, A., and Paludetti, G. 2001. Effects of contralateral white noise stimulation on distortion product otoacoustic emissions in myasthenic patients. Hear. Res. 162, 80–84.

Dolan, D. F., Guo, M. H., and Nuttall, A. L. 1997. Frequency-dependent enhancement of basilar membrane velocity during olivocochlear bundle stimulation. J. Acoust. Soc. Am. 102, 3587–3596.

Dolan, D. F. and Nuttall, A. L. 1988. Masked cochlear whole-nerve response intensity functions altered by electrical stimulation of the crossed olivocochlear bundle. J. Acoust. Soc. Am. 83, 1081–1086.

Dolan, D. F., Nuttall, A. L., and Avinash, G. 1990. Asynchronous neural activity recorded from the round window. J. Acoust. Soc. Am. 87, 2621–2627.

Doucet, J. R., Rose, L., and Ryugo, D. K. 2002. The cellular origin of corticofugal projections to the superior olivary complex in the rat. Brain Res. 925, 28–41.

Dulon, D., Zajic, G., Aran, J. M., and Schacht, J. 1989. Aminoglycoside antibiotics impair calcium entry but not viability and motility in isolated cochlear outer hair cells. J. Neurosci. Res. 24, 338–346.

Dunlop, C. W., Webster, W. R., and Simons, L. A. 1965. Effect of attention on evoked responses in the classical auditory pathway. Nature. 206, 1048–50.

Elgoyhen, A. B., Johnson, D. S., Boulter, J, Vetter, D. E., and Heinemann, S. 1994. Alpha-9: an acetylcholine receptor with novel pharmacological properties expressed in rat cochlear hair cells. Cell 79, 705–715.

Elgoyhen, A. B., Vetter, D. E., Katz, E., Rothlin, C. V., Heinemann, S. F., and Boulter, J. 2001. alpha10: a determinant of nicotinic cholinergic receptor function in mammalian vestibular and cochlear mechanosensory hair cells. Proc. Natl. Acad. Sci. 98, 35013506.

Erostegui, C., Norris, C. H., and Bobbin, R. P. 1994. *In vitro* pharmacologic characterization of a cholinergic receptor on outer hair cells. Hear. Res. 74, 135–147.

Evans, M. G. 1996. Acetylcholine activates two currents in guinea-pig outer hair cells. J. Physiol. (Lond). 491, 563–578.

Eybalin, M. 1993. Neurotransmitters and Neuromodulators of the Mammalian Cochlea. Physiol. Rev. 73, 309–373.

Faye-Lund, H. 1985. The neocortical projection to the inferior colliculus in the albino rat. Anat Embryol. 173, 53–70.

Feliciano, M., Saldaña, E., and Mugnaini, E. 1995. Direct projections from the rat primary auditory neocortex to nucleus sagulum, paralemniscal regions, superior olivary complex and cochlear nuclei. Audit. Neurosci. 1, 287–308.

Felix, D. and Ehrenberger, K. 1992. The efferent modulation of mammalian inner hair cell afferents. Hear. Res. 64, 1–5.

Fex, J. 1959. Augmentation of cochlear microphonic by stimulation of efferent fibres to the cochlea; preliminary report. Acta Otolaryngol. 50, 540–541.

Fex, J. 1962. Auditory activity in centrifugal and centripetal cochlear fibres in cat. A study of a feedback system. Acta Physiol. Scand. Suppl. 1962; 189, 1–68.

Fex, J. and Altschuler, R. A. 1981. Enkephalin-like immunoreactivity of olivocochlear nerve fibers in cochlea of guinea pig and cat. Proc. Natl. Acad. Sci. 78: 1255–1259.

Fex, J., Altschuler, R. A., Kachar, B., Wenthold, R. J., and Zempel, J. M. 1986. GABA visualized by immunocytochemistry in the guinea pig cochlea in axons and endings of efferent neurons. Brain Res. 366, 106–17.

Folsom, R. C. and Owsley, R. M. 1987. N1 action potentials in humans. Influence of simultaneous contralateral stimulation. Acta Otolaryngol. 103, 262–265.

Froehlich, P., Collet, L., Valatx, J. L., and Morgon, A. 1993. Sleep and active cochlear micromechanical properties in human subjects. Hear. Res. 66, 1–7.

Gaborjan, A., Lendvai, B., and Vizi, E. S. 1999. Neurochemical evidence of dopamine release by lateral olivocochlear efferents and its presynaptic modulation in guinea-pig cochlea. Neuroscience. 90, 131–138.

Galambos, R. 1956. Suppression of auditory nerve activity by stimulation of efferent fibers to cochlea. J. Neurophysiol. 19, 424–437.

Gifford, M. L. and Guinan, J. J., Jr. 1987. Effects of electrical stimulation of medial olivocochlear neurons on ipsilateral and contralateral cochlear responses. Hear. Res 29, 179–194.

Giraud, A. L., Collet, L., Chery-Croze, S., Magnan, J., and Chays, A. 1995. Evidence of a medial olivocochlear involvement in contralateral suppression of otoacoustic emissions in humans. Brain Res. 705, 15–23.

Giraud, A. L., Garnier, S., Micheyl, C., Lina, G., Chays, A., and Chery-Croze, S. 1997b. Auditory efferents involved in speech-in-noise intelligibility. Neuroreport. 8, 1779–1783.

Giraud, A. L., Perrin, E., Chery-Croze, S., Chays, A., and Collet, L. 1996. Contralateral acoustic stimulation induces a phase advance in evoked otoacoustic emissions in humans. Hear. Res. 94, 54–62.

Giraud, A. L., Wable, J., Chays, A., Collet, L., and Chery-Croze, S. 1997a. Influence of contralateral noise on distortion product latency in humans: is the medial olivocochlear efferent system involved? J. Acoust. Soc. Am. 102, 2219–2227.

Greenberg, G. Z. and Larkin, W. D. 1968. Frequency-response characteristic of auditory observers detecting signals of a single frequency in noise: the probe-signal method. J. Acoust. Soc. Am. 44, 1513–1523.

Groff, J. A. and Liberman, M. C. 2003. Modulation of cochlear afferent response by the lateral olivocochlear system: activation via electrical stimulation of the inferior colliculus. J. Neurophysiol. 90, 3178–3200.

Guinan, J. J., Jr. 1996. Physiology of Olivocochlear Efferents. In: The Cochlea (*eds*. P. Dallos, A. Popper, and R. Fay), pp. 435–502. Springer.

Guinan, J. J., Jr. and Gifford, M. L. 1988. Effects of electrical stimulation of efferent olivocochlear neurons on cat auditory-nerve fibers. II. Spontaneous rate. Hear. Res. 33, 115–128.

Guitton, M. J., Avan, P., Puel, J. L., and Bonfils, P. 2004. Medial olivocochlear efferent activity in awake guinea pigs. Neuroreport. 15, 1379–1382.

Hamed, S. A., Elattar, A. M., and Hamed, E. A. 2006. Irreversible cochlear damage in myasthenia gravis – otoacoustic emission analysis. Acta Neurol. Scand. 113, 46–54.

Herbert, H., Aschoff, A., and Ostwald, J. 1991. Topography of projections from the auditory cortex to the inferior colliculus in the rat. J. Comp. Neurol. 304, 103–22.

Hernandez-Peón, R., Scherrer, H., and Jouvet, M. 1956. Modification of electric activity in cochlear nucleus during attention in unanesthetized cats. Science 123, 331–332.

Hienz, R. D., Stiles, P., and May, B. J. 1998. Effects of bilateral olivocochlear lesions on vowel formant discrimination in cats. Hear. Res. 116, 10–20.

Horvath, M., Kraus, K. S., and Illing, R. B. 2000. Olivocochlear neurons sending axon collaterals into the ventral cochlear nucleus of the rat. J. Comp. Neurol. 422, 95–105.

Housley, G. D. and Ashmore, J. F. 1991. Direct measurement of the action of acetylcholine on isolated outer hair cells of the guinea pig cochlea. Proc. R. Soc. Lond. B. 244, 161–167.

Huffman, R. F. and Henson, O. W., Jr. 1990. The descending auditory pathway and acousticomotor systems: connections with the inferior colliculus. Brain Res. Rev. 15, 295–323.

Igarashi, M., Alford, B. R., Nakai, Y., and Gordon, W. P. 1972. Behavioral auditory function after transection of crossed olivo-cochlear bundle in the cat. I. Pure-tone threshold and perceptual signal-to-noise ratio. Acta Otolaryngol. 73, 455–466.

Igarashi, M., Cranford, J. L., Allen, E. A., and Alford, B. R. 1979b. Behavioral auditory function after transection of crossed olivo-cochlear bundle in the cat. V. Pure-tone intensity discrimination. Acta Otolaryngol. 87, 429–433.

Igarashi, M., Cranford, J. L., Nakai, Y., and Alford, B. R. 1979a. Behavioral auditory function after transection of crossed olivo-cochlear bundle in the cat. IV. Study on pure-tone frequency discrimination. Acta Otolaryngol. 87, 79–83.

Jung, T. T., Rhee, C. K., Lee, C. S., Park, Y. S., and Choi, D. C. 1993. Ototoxicity of salicylate, nonsteroidal antiinflammatory drugs and quinine. Otolaryngol. Clin. North Am. 26, 791–810.

Kawase, T. and Liberman, M. C. 1993. Antimasking effects of the olivocochlear reflex. I. Enhancement of compound action potentials to masked tones. J. Neurophysiol. 70, 2519–2532.

Kemp, D. T. 1978. Stimulated acoustic emissions from within the human auditory system. J. Acoust. Soc. Am. 64, 1386–1391.

Khalfa, S. and Collet, L. 1996. Functional asymmetry of medial olivocochlear system in humans. Towards a peripheral auditory lateralization. Neuroreport. 7, 993–996.

Khalfa, S., Bougeard, R., Morand, N., Veuillet, E., Isnard, J., Guenot, M., Ryvlin, P., Fischer, C., and Collet, L. 2001a. Evidence of peripheral auditory activity modulation by the auditory cortex in humans. Neuroscience. 104, 347–358.

Khalfa, S., Bruneau, N., Roge, B., Georgieff, N., Veuillet, E., Adrien, J. L., Barthelemy, C., and Collet, L. 2001b. Peripheral auditory asymmetry in infantile autism. Eur. J. Neurosci. 13, 628–632.

Khalfa, S., Morlet, T., Micheyl, C., Morgon, A., and Collet, L. 1997. Evidence of peripheral hearing asymmetry in humans: clinical implications. Acta Otolaryngol. 17, 192–196.

Khalfa, S., Veuillet, E., and Collet, L. 1998. Influence of handedness on peripheral auditory asymmetry. Eur. J. Neurosci. 10, 2731–2737.

Kirk, E. C. and Smith, D. W. 2003. Protection from acoustic trauma is not a primary function of the medial olivocochlear efferent system. J. Assoc. Res. Otolaryngol. 4, 445–465.

Kujawa, S. G. and Liberman, M. C. 1997. Conditioning-related protection from acoustic injury: effects of chronic deefferentation and sham surgery. J. Neurophysiol. 78, 3095–3106.

Kujawa, S. G., Glattke, T. J., Fallon, M., and Bobbin, R. P. 1994. A nicotinic-like receptor mediates suppression of distortion product otoacoustic emissions by contralateral sound. Hear. Res. 74, 122–34.

Kumar, U. A. and Vanaja, C. S. 2004. Functioning of olivocochlear bundle and speech perception in noise. Ear Hear. 25, 142–146.

Labrousse, M., Leveque, M., Ouedraogo, T., Avisse, C., Chays, A., and Delattre, J. F. 2005. An anatomical study of the vestibulocochlear anastomosis (anastomosis of Oort) in humans: preliminary results. Surg. Radiol. Anat. 27, 238–242.

Le Prell, C. G., Halsey, K., Hughes, L. F., Dolan, D. F., and Bledsoe, S. C., Jr. 2005. Disruption of lateral olivocochlear neurons via a dopaminergic neurotoxin depresses sound-evoked auditory nerve activity. J. Assoc. Res. Otolaryngol. 6, 48–62.

Le Prell, C. G., Shore, S. E., Hughes, L. F., and Bledsoe, S. C., Jr. 2003. Disruption of lateral efferent pathways: functional changes in auditory evoked responses. J. Assoc. Res. Otolaryngol. 4, 276–290.

Liberman, M. C. 1980. Efferent synapses in the inner hair cell area of the cat cochlea: an electron microscopic study of serial sections. Hear. Res. 3, 189–204.

Liberman, M. C. 1989. Rapid assessment of sound-evoked olivocochlear feedback: suppression of compound action potentials by contralateral sound. Hear. Res. 38, 47–56.

Liberman, M. C. 1990. Effects of chronic cochlear de-efferentation on auditory-nerve response. Hear. Res. 49, 209–23.

Liberman, M. C., Dodds, L. W., and Pierce, S. 1990. Afferent and efferent innervation of the cat cochlea: quantitative analysis with light and electron microscopy. J. Comp. Neurol. 301, 443–460.

Lima da Costa, D., Erre, J. P., Charlet de Sauvage, R., Popelar, J., and Aran, J. M. 1997a. Bioelectrical cochlear noise and its contralateral suppression: relation to background activity of the eighth nerve and effects of sedation and anesthesia. Exp. Brain Res. 116, 259–269.

Lima da Costa, D., Chibois, A., Erre, J. P., Blanchet, C., de Sauvage, R. C., and Aran, J. M. 1997b. Fast, slow, and steady-state effects of contralateral acoustic activation of the medial olivocochlear efferent system in awake guinea pigs: action of gentamicin. J. Neurophysiol. 78, 1826–1836.

Lioudyno, M., Hiel, H., Kong, J. H., Katz, E., Waldman, E., Parameshwaran-Iyer, S., Glowatzki, E., and Fuchs, P. A. 2004. A ''synaptoplasmic cistern'' mediates rapid inhibition of cochlear hair cells. J. Neurosci. 24, 11160–11164.

Lioudyno, M. I., Verbitsky, M., Glowatzki, E., Holt, J. C., Boulter, J., Zadina, J. E., Elgoyhen, A. B., and Guth, P. S. 2002. The alpha9/alpha10-containing nicotinic ACh receptor is directly modulated by opioid peptides, endomorphin-1, and dynorphin B, proposed efferent cotransmitters in the inner ear. Mol. Cell. Neurosci. 20, 695–711.

Lioudyno, M. I., Verbitsky, M., Holt, J. C., Elgoyhen, A. B., and Guth, P. S. 2000. Morphine inhibits an alpha9-acetylcholine nicotinic receptor-mediated response by a mechanism which does not involve opioid receptors. Hear. Res. 149, 167–177.

Luebke, A. E. and Foster, P. K. 2002. Variation in inter-animal susceptibility to noise damage is associated with alpha 9 acetylcholine receptor subunit expression level. J. Neurosci. 22, 4241–4247.

Lukas, J. H. 1980. Human auditory attention: the olivocochlear bundle may function as a peripheral filter. Psychophysiology 17, 444–452.

Lustig, L. R. 2006. Nicotinic acetylcholine receptor structure and function in the efferent auditory system. Anat. Rec. A Discov. Mol. Cell. Evol. Biol. A 288, 424–434.

Maison, S. F. and Liberman, M. C. 2000. Predicting vulnerability to acoustic injury with a noninvasive assay of olivocochlear reflex strength. J. Neurosci 20, 4701–4707.

Maison, S. F., Adams, J. C., and Liberman, M. C. 2003a. Olivocochlear innervation in the mouse: immunocytochemical maps, crossed versus uncrossed contributions, and transmitter colocalization. J. Comp. Neurol. 455, 406–416.

Maison, S. F., Emeson, R. B., Adams, J. C., Luebke, A. E., and Liberman, M. C. 2003b. Loss of alpha CGRP reduces sound-evoked activity in the cochlear nerve. J. Neurophysiol. 90, 2941–2949.

Maison, S. F., Luebke, A. E., Liberman, M. C., and Zuo, J. 2002. Efferent protection from acoustic injury is mediated via alpha9 nicotinic acetylcholine receptors on outer hair cells. J. Neurosci. 22, 10838–10846.

Maison, S. F., Parker, L. L., Young, L., Adelman, J. P., Zuo, J., and Liberman, M. C. 2007b. Overexpression of SK2 channels enhances efferent suppression of cochlear responses without enhancing noise resistance. J. Neurophysiol. 97, 2930–2936.

Maison, S. F., Rosahl, T. W., Homanics, G. E., and Liberman, M. C. 2006. Functional role of GABAergic innervation of the cochlea: phenotypic analysis of mice lacking GABA(A) receptor subunits alpha 1, alpha 2, alpha 5, alpha 6, beta 2, beta 3, or delta. J. Neurosci. 26, 10315–26.

Maison, S. F., Vetter, D. E., and Liberman, M. C. 2007a. A novel effect of cochlear efferents: *in vivo* response enhancement does not require {alpha} 9 cholinergic receptors. J. Neurophysiol. 97, 3269–3278.

Malmierca, M. S., Le Beau, F. E., and Rees, A. 1996. The topographical organization of descending projections from the central nucleus of the inferior colliculus in guinea pig. Hear. Res. 93, 167–80.

May, B. J. and McQuone, S. J. 1995. Effects of bilateral olivocochlear lesions on pure-tone intensity discrimination in cats. Audit. Neurosci. 1, 385–400.

May, B. J., Budelis, J., and Niparko, J. K. 2004. Behavioral studies of the olivocochlear efferent system: learning to listen in noise. Arch. Otolaryngol. Head Neck Surg. 130, 660–664.

May, B. J., Prosen, C. A., Weiss, D., and Vetter, D. 2002. Behavioral investigation of some possible effects of the central olivocochlear pathways in transgenic mice. Hear. Res. 171, 142–157.

Micheyl, C. and Collet, L. 1996. Involvement of the olivocochlear bundle in the detection of tones in noise. J. Acoust. Soc. Am. 99, 1604–1610.

Micheyl, C., Perrot, X., and Collet, L. 1997. Relationship between auditory intensity discrimination in noise and olivocochlear efferent system activity in humans. Behav. Neurosci. 111, 801–807.

Morand, N., Veuillet, E., Gagnieu, M. C., Lemoine, P., and Collet, L. 1998. Benzodiazepines alter cochleo-cochlear loop in humans. Hear. Res. 121, 71–76.

Morley, B. J., Li, H. S., Hiel, H., Drescher, D. G., and Elgoyhen, A. B. 1998. Identification of the subunits of the nicotinic cholinergic receptors in the rat cochlea using RT-PCR and *in situ* hybridization. Brain Res. Mol. Brain Res. 53, 78–87.

Morley, B. J., Spangler, K. M., Schneider, B. L., and Javel, E. 1991. Selective degeneration of a putative cholinergic pathway in the chinchilla cochlea following infusion with ethylcholine aziridinium ion. Brain Res. 544, 94–100.

Mott, J. B., Norton, S. J., Neely, S. T., and Warr, W. B. 1989. Changes in spontaneous otoacoustic emissions produced by acoustic stimulation of the contralateral ear. Hear. Res. 38, 229–242.

Moulin, A., Collet, L., and Duclaux, R. 1993. Contralateral auditory stimulation alters acoustic distortion products in humans. Hear. Res. 65, 193–210.

Mountain, D. C. 1980. Changes in endolymphatic potentials and crossed olivocochlear bundle stimulation alter cochlear mechanics. Science 210, 71–72.

Mulders, W. H. and Robertson, D. 2000a. Evidence for direct cortical innervation of medial olivocochlear neurones in rats. Hear. Res. 144, 65–72.

Mulders, W. H. and Robertson, D. 2000b. Effects on cochlear responses of activation of descending pathways from the inferior colliculus. Hear. Res. 149, 11–23.

Mulders, W. H. and Robertson, D. 2004. Dopaminergic olivocochlear neurons originate in the high frequency region of the lateral superior olive of guinea pigs. Hear. Res. 187, 122–30.

Mulders, W. H. and Robertson, D. 2005. Diverse responses of single auditory afferent fibres to electrical stimulation of the inferior colliculus in guinea-pig. Exp. Brain Res. 160, 235–244.

Mulders, W. H. and Robertson, D. 2006. Gentamicin abolishes all cochlear effects of electrical stimulation of the inferior colliculus. Exp. Brain Res. 174, 35–44.

Muller, J., Janssen, T., Heppelmann, G., and Wagner, W. 2005. Evidence for a bipolar change in distortion product otoacoustic emissions during contralateral acoustic stimulation in humans. J. Acoust. Soc. Am. 118, 3747–3756.

Murugasu, E. and Russell, I. J. 1996a. The effect of efferent stimulation on basilar membrane displacement in the basal turn of the guinea pig cochlea. J. Neurosci. 16, 325–332.

Murugasu, E. and Russell, I. J. 1996b. The role of calcium on the effects of intracochlear acetylcholine perfusion on basilar membrane displacement in the basal turn of the guinea pig cochlea. Audit. Neurosci. 2, 363–376.

Nie, L., Song, H., Chen, M. F., Chiamvimonvat, N., Beisel, K. W., Yamoah, E. N., and Vazquez, A. E. 2004. Cloning and expression of a small-conductance Ca(2+)-activated K+ channel from the mouse cochlea: coexpression with alpha9/alpha10 acetylcholine receptors. J. Neurophysiol. 91, 1536–44.

Nieder, P. and Nieder, I. 1970. Stimulation of efferent olivocochlear bundle causes release from low level masking. Nature. 227, 184–185.

Niu, X. and Canlon, B. 2002. Activation of tyrosine hydroxylase in the lateral efferent terminals by sound conditioning. Hear. Res. 174, 124–132.

Niu, X. and Canlon, B. 2006. The signal transduction pathway for the dopamine D1 receptor in the guinea-pig cochlea. Neuroscience. 137, 981–990.

Niu, X., Bogdanovic, N., and Canlon, B. 2004. The distribution and the modulation of tyrosine hydroxylase immunoreactivity in the lateral olivocochlear system of the guinea-pig. Neuroscience 125, 725–733.

Oatman, L. C. 1971. Role of visual attention on auditory evoked potentials in unanesthetized cats. Exp. Neurol. 32, 341–356.

Oestreicher, E., Arnold, W., Ehrenberger, K., and Felix, D. 1997. Dopamine regulates the glutamatergic inner hair cell activity in guinea pigs. Hear. Res. 107, 46–52.

Oliver, D., Klocker, N., Schuck, J., Baukrowitz, T., Ruppersberg, J. P., and Fakler, B. 2000. Gating of Ca^{2+}-activated K^{+} channels controls fast inhibitory synaptic transmission at auditory outer hair cells. Neuron. 26, 595–601.

Ota, Y., Oliver, D. L., and Dolan, D. F. 2004. Frequency-specific effects on cochlear responses during activation of the inferior colliculus in the guinea pig. J. Neurophysiol. 91, 2185–2193.

Paludetti, G., Di Nardo, W., D'Ecclesia, A., Evoli, A., Scarano, E., and Di Girolamo, S. 2001. The role of cholinergic transmission in outer hair cell functioning evaluated by distortion product otoacoustic emissions in myasthenic patients. Acta Otolaryngol. 121, 119–121.

Pedemonte, M., Drexler, D. G., and Velluti, R. A. 2004. Cochlear microphonic changes after noise exposure and gentamicin administration during sleep and waking. Hear. Res. 194, 25–30.

Perrot, X., Micheyl, C., Khalfa, S., and Collet, L. 1999. Stronger bilateral efferent influences on cochlear biomechanical activity in musicians than in non-musicians. Neurosci. Lett. 262, 167–170.

Perrot, X., Ryvlin, P., Isnard, J., Guenot, M., Catenoix, H., Fischer, C., Mauguiere, F., and Collet, L. 2006. Evidence for corticofugal modulation of peripheral auditory activity in humans. Cereb. Cortex. 16, 941–948.

Plazas, P. V., Katz, E., Gomez-Casati, M. E., Bouzat, C., and Elgoyhen, A. B. 2005. Stoichiometry of the alpha9alpha10 nicotinic cholinergic receptor. J. Neurosci. 25, 10905–10912.

Plinkert, P. K., Gitter, A. H., Mohler, H., and Zenner, H. P. 1993. Structure, pharmacology and function of GABA-A receptors in cochlear outer hair cells. Eur. Arch Otorhinolaryngol. 250, 351–357.

Plinkert, P. K., Mohler, H., and Zenner, H. P. 1989. A subpopulation of outer hair cells possessing GABA receptors with tonotopic organization. Arch Otorhinolaryngol. 246, 417–422.

Popelar, J., Mazelova, J., and Syka, J. 2002. Effects of electrical stimulation of the inferior colliculus on 2f1-f2 distortion product otoacoustic emissions in anesthetized guinea pigs. Hear. Res 170, 116–126.

Poyner, D. R., Andrew, D. P., Brown, D., Bose, C., and Hanley, M. R. 1992. Pharmacological characterization of a receptor for calcitonin gene-related peptide on rat, L6 myocytes. Br. J. Pharmacol. 105, 441–447.

Prosen, C. A., Bath, K. G., Vetter, D. E., and May, B. J. 2000. Behavioral assessments of auditory sensitivity in transgenic mice. J. Neurosci. Methods. 97, 59–67.

Puel, J. L. and Rebillard, G. 1990. Effect of contralateral sound stimulation on the distortion product 2F1-F2: evidence that the medial efferent system is involved. J. Acoust. Soc. Am. 87, 1630–1635.

Puel, J. L., Bonfils, P., and Pujol, R. 1988. Selective attention modifies the active micromechanical properties of the cochlea. Brain Res. 447, 380–1383.

Puria, S., Guinan, J. J., Jr., and Liberman, M. C. 1996. Olivocochlear reflex assays: effects of contralateral sound on compound action potentials versus ear-canal distortion products. J. Acoust. Soc. Am. 99, 500–507.

Rajan, R. 1988a. Effect of electrical stimulation of the crossed olivocochlear bundle on temporary threshold shifts in auditory sensitivity. I. Dependence on electrical stimulation parameters. J. Neurophysiol. 60, 549–568.

Rajan, R. 1988b. Effect of electrical stimulation of the crossed olivocochlear bundle on temporary threshold shifts in auditory sensitivity. II. Dependence on the level of temporary threshold shifts. J. Neurophysiol. 60, 569–579.

Rajan, R. and Johnstone, B. M. 1983. Efferent effects elicited by electrical stimulation at the round window of the guinea pig. Hear. Res. 12, 405–417.

Rajan, R. and Johnstone, B. M. 1988. Binaural acoustic stimulation exercises protective effects at the cochlea that mimic the effects of electrical stimulation of an auditory efferent pathway. Brain Res. 459, 241–255.

Raphael, Y. and Altschuler, R. A. 2003. Structure and innervation of the cochlea. Brain Res. Bull. 60, 397–422.

Rasmussen, G. L. 1946. The olivary peduncle and other fiber projections of the superior olivary complex. J. Comp. Neurol. 84, 141–219.

Rasmussen, G. L. 1960. Efferent Fibers of the Cochlear Nerve and Cochlear Nucleus. In: Neural Mechanisms of the Auditory and Vestibular Systems (*eds*. G. L. Rasmussen and W. F. Windle), pp. 105–115. C. C. Thomas.

Reiter, E. R. and Liberman, M. C. 1995. Efferent-mediated protection from acoustic overexposure: relation to slow effects of olivocochlear stimulation. J. Neurophysiol. 73, 506–514.

Riga, M., Papadas, T., Werner, J. A., and Dalchow, C. V. 2007. A clinical study of the efferent auditory system in patients with normal hearing who have acute tinnitus. Otol. Neurotol. 28, 185–190.

Robertson, D., Anderson, C. J., and Cole, K. S. 1987. Segregation of efferent projections to different turns of the guinea pig cochlea. Hear. Res. 25, 69–76.

Robles, L. and Ruggero, M. A. 2001. Mechanics of the mammalian cochlea. Physiol. Rev. 81, 1305–1352.

Rossi, G., Voena, G., Cortesina, G., and Buongiovanni, S. 1964. Changes in the cochlear-microphonic potential due to resection of the efferent cochlear fibers. J. Acoust. Soc. Am. 36, 1845–1849.

Rothlin, C. V., Katz, E., Verbitsky, M., Vetter, D. E., Heinemann, S. F., and Elgoyhen, A. B. 2000. Block of the alpha9 nicotinic receptor by ototoxic aminoglycosides. Neuropharmacology. 39, 2525–2532.

Ruel, J., Nouvain, R., D'Aldin, C. G., Pujol, R., Eybalin, M., and Puel, J. L. 2001. Dopamine inhibition of auditory nerve activity in the adult mammalian cochlea. Eur. J. Neurosci. 14, 977–986.

Ruel, J., Wang, J., Dememes, D., Gobaille, S., Puel, J. L., and Rebillard, G. 2006. Dopamine transporter is essential for the maintenance of spontaneous activity of auditory nerve neurones and their responsiveness to sound stimulation. J. Neurochem. 97, 190–200.

Safieddine, S. and Eybalin, M. 1992. Triple immunofluorescence evidence for the coexistence of acetylcholine, enkephalins and calcitonin gene-related peptide within efferent (olivocochlear) neurons of rats and guinea-pigs. Eur. J. Neurosci. 4, 981–992.

Safieddine, S., Prior, A. M., and Eybalin, M. 1997. Choline acetyltransferase, glutamate decarboxylase, tyrosine hydroxylase, calcitonin gene-related peptide and opioid peptides coexist in lateral efferent neurons of rat and guinea-pig. Eur. J. Neurosci. 9, 356–367.

Sahley, T. L. and Nodar, R. H. 1994. Improvement in auditory function following pentazocine suggests a role for dynorphins in auditory sensitivity. Ear Hear. 15, 422–431.

Sahley, T. L., Kalish, R. B., Musiek, F. E., and Hoffman, D. W. 1991. Effects of opioid be drugs on auditory evoked potentials suggest a role of lateral olivocochlear dynorphins in auditory function. Hear. Res. 55, 133–142.

Sahley, T. L., Musiek, F. E., and Nodar, R. H. 1996. Naloxone blockade of (-) pentazocine-induced changes in auditory function. Ear Hear. 17, 341–353.

Saldaña, E., Feliciano, M., and Mugnaini, E. 1996. Distribution of descending projections from primary auditory neocortex to inferior colliculus mimics the topography of intracollicular projections. J. Comp. Neurol. 371, 15–40.

Sanchez-Gonzalez, M. A., Warr, W. B., and Lopez, D. E. 2003. Anatomy of olivocochlear neurons in the hamster studied with FluoroGold. Hear. Res. 185, 65–76.

Scates, K. W., Woods, C. I., and Azeredo, W. J. 1999. Inferior colliculus stimulation and changes in 2f1-f2 distortion product otoacoustic emissions in the rat. Hear. Res. 1999 128, 51–60.

Scharf, B., Magnan, J., and Chays, A. 1997. On the role of the olivocochlear bundle in hearing: 16 case studies. Hear. Res 103, 101–122.

Scharf, B., Magnan, J., Collet, L., Ulmer, E., and Chays, A. 1994. On the role of the olivocochlear bundle in hearing: a case study. Hear. Res. 75, 11–26.

Schofield, B. R. and Coomes, D. L. 2006. Pathways from auditory cortex to the cochlear nucleus in guinea pigs. Hear. Res. 216–217, 81–89.

Siegel, J. H. and Kim, D. O. 1982. Efferent neural control of cochlear mechanics? Olivocochlear bundle stimulation affects cochlear biomechanical nonlinearity. Hear. Res. 6, 171–182.

Simmons, D. D. 2002. Development of the inner ear efferent system across vertebrate species. J. Neurobiol. 53, 228–250.

Sininger, Y. S. and Cone-Wesson, B. 2004. Asymmetric cochlear processing mimics hemispheric specialization. Science. 305, 1581.

Smith, D. W. and Mount, R. J. 1993. Damage to cochlear efferents following AF64A intoxication. Acta Otolaryngol. 113, 512–518.

Smith, D. W., Erre, J. P., and Aran, J. M. 1994. Rapid, reversible elimination of medial olivocochlear efferent function following single injections of gentamicin in the guinea pig. Brain Res. 652, 243–248.

Smith, D. W., Mount, R. J., and Callahan, J. W. 1989. Selective damage to cochlear efferents by the choline neurotoxin ethylcholine mustard aziridinium ion (AF64A) in the chinchilla. Hear. Res. 42, 113–117.

Sridhar, T. S., Brown, M. C., and Sewell, W. F. 1997. Unique postsynaptic signaling at the hair cell efferent synapse permits calcium to evoke changes on two time scales. J. Neurosci. 17, 428–437.

Sridhar, T. S., Liberman, M. C., Brown, M. C., and Sewell, W. F. 1995. A novel cholinergic ''slow effect'' of efferent stimulation on cochlear potentials in the guinea pig. J. Neurosci. 15, 3667–3678.

Takeuchi, S. and Wangemann, P. 1993. Aminoglycoside antibiotics inhibit maxi-K^+ channel in single isolated cochlear efferent nerve terminals. Hear. Res. 67, 13–9.

Thompson, A. M. and Thompson, G. C. 1993. Relationship of descending inferior colliculus projections to olivocochlear neurons. J. Comp. Neurol. 335, 402–412.

Torterolo, P., Zurita, P., Pedemonte, M., and Velluti, R. A. 1998. Auditory cortical efferent actions upon inferior colliculus unitary activity in the guinea pig. Neurosci. Lett. 249, 172–176.

Toth, L., Racz, T., Dioszeghy, P., Repassy, G., and Lampe, I. 1998. Otoacoustic emission in myasthenia gravis patients and the role of efferent activation. Hear. Res. 126, 123–125.

Trahiotis, C. and Elliott, D. N. 1970. Behavioral investigation of some possible effects of sectioning the crossed olivocochlear bundle. J. Acoust. Soc. Am. 47, 592–596.

Velluti, R. and Pedemonte, M. 1986. Differential effects of benzodiazepines on cochlear and auditory nerve responses. Electroencephalogr. Clin. Neurophysiol. 64, 556–562.

Velluti, R., Pedemonte, M., and Garcia-Austt, E. 1989. Correlative changes of auditory nerve and microphonic potentials throughout sleep. Hear. Res 39, 203–208.

Vetter, D. E. and Mugnaini, E. 1992. Distribution and dendritic features of three groups of rat olivocochlear neurons. A study with two retrograde cholera toxin tracers. Anat. Embryol. 185, 1–16.

Vetter, D. E., Liberman, M. C., Mann, J., Barhanin, J., Boulter, J., Brown, M. C., Saffiote-Kolman, J., Heinemann, S. F., and Elgoyhen, A. B. 1999. Role of α9 nicotinic ACh receptor subunits in the development and function of cochlear efferent innervation. Neuron. 23, 93–103.

Vetter, D. E., Saldana, E., and Mugnaini, E. 1993. Input from the inferior colliculus to medial olivocochlear neurons in the rat: a double label study with PHA-L and cholera toxin. Hear. Res. 70, 173–186.

Veuillet, E., Bazin, F., and Collet, L. 1999. Objective evidence of peripheral auditory disorders in learning-impaired children. J. Audio. Med. 8, 18–29.
Veuillet, E., Georgieff, N., Philibert, B., Dalery, J., Marie-Cardine, M., and Collet, L. 2001b. Abnormal peripheral auditory asymmetry in schizophrenia. J. Neurol. Neurosurg. Psychiatry. 70, 88–94.
Veuillet, E., Martin, V., Suc, B., Vesson, J. F., Morgon, A., and Collet, L. 2001a. Otoacoustic emissions and medial olivocochlear suppression during auditory recovery from acoustic trauma in humans. Acta Otolaryngol. 121, 278–283.
Wagner, W., Heppelmann, G., Kuehn, M., Tisch, M., Vonthein, R., and Zenner, H. P. 2005. Olivocochlear activity and temporary threshold shift-susceptibility in humans. Laryngoscope. 115, 2021–2028.
Walsh, E. J., McGee, J., McFadden, S. L., and Liberman, M. C. 1998. Long-term effects of sectioning the olivocochlear bundle in neonatal cats. J. Neurosci. 18, 3859–3869.
Warr, W. B. 1975. Olivocochlear and vestibular efferent neurons of feline brain-stem - their location, morphology and number determined by retrograde axonal-transport and acetylcholinesterase histochemistry. J. Comp. Neurol. 161, 159–181.
Warr, W. B. and Boche, J. E. 2003. Diversity of axonal ramifications belonging to single lateral and medial olivocochlear neurons. Exp. Brain Res. 153, 499–513.
Warr, W. B. and Guinan, J. J. 1979. Efferent Innervation of the Organ of Corti – 2 Separate Systems. Brain. Res. 173, 152–155.
Warr, W. B., Beck Boche, J. E., Ye, Y., and Kim, D. O. 2002. Organization of olivocochlear neurons in the cat studied with the retrograde tracer cholera toxin-B. J Assoc Res Otolaryngol. 3, 457–478.
Warr, W. B., Boche, J. B., and Neely, S. T. 1997. Efferent innervation of the inner hair cell region: origins and terminations of two lateral olivocochlear systems. Hear. Res. 108, 89–111.
Warren, E. H., 3rd. and Liberman, M. C. 1989. Effects of contralateral sound on auditory-nerve responses. I. Contributions of cochlear efferents. Hear. Res. 37, 89–104.
Weedman, D. L. and Ryugo, D. K. 1996a. Pyramidal cells in primary auditory cortex project to cochlear nucleus in rat. Brain Res. 706, 97–102.
Weedman, D. L. and Ryugo, D. K. 1996b. Projections from auditory cortex to the cochlear nucleus in rats: synapses on granule cell dendrites. J. Comp. Neurol. 371, 311–324.
Wickelgren, W. O. 1968. Effects of walking and flash stimulation on click-evoked responses in cats. J. Neurophysiol. 31, 769–776.
Winer, J. A. 2005. Decoding the auditory corticofugal systems. Hear. Res. 207, 1–9.
Winer, J. A. and Prieto, J. J. 2001. Layer V in cat primary auditory cortex (AI): cellular architecture and identification of projection neurons. J. Comp. Neurol. 434, 379–412.
Winer, J. A., Diehl, J. J., and Larue, D. T. 2001. Projections of auditory cortex to the medial geniculate body of the cat. J. Comp. Neurol. 430, 27–55.
Winslow, R. L. and Sachs, M. B. 1987. Effect of electrical stimulation of the crossed olivocochlear bundle on auditory nerve response to tones in noise. J. Neurophysiol. 57, 1002–1021.
Xiao, Z. and Suga, N. 2002a. Modulation of cochlear hair cells by the auditory cortex in the mustached bat. Nat. Neurosci. 5, 57–63.
Xiao, Z. and Suga, N. 2002b. Reorganization of the cochleotopic map in the bat's auditory system by inhibition. Proc. Natl. Acad. Sci. 99, 15743–15748.
Xiong, Y., Yu, Y. Q., Chan, Y. S., and He, J. 2004. Effects of cortical stimulation on auditory-responsive thalamic neurones in anaesthetized guinea pigs. J. Physiol. 560, 207–217.
Yamasoba, T. and Dolan, D. F. 1997. Chronic strychnine administration into the cochlea potentiates permanent threshold shift following noise exposure. Hear. Res. 112, 13–20.
Yoshida, N., Hequembourg, S. J., Atencio, C. A., Rosowski, J. J., and Liberman, M. C. 2000. Acoustic injury in mice: 129/SvEv is exceptionally resistant to noise-induced hearing loss. Hear. Res. 141, 97–106.
Yoshida, N., Liberman, M. C., Brown, M. C., and Sewell, W. F. 1999a. Gentamicin blocks both fast and slow effects of olivocochlear activation in anesthetized guinea pigs. J. Neurophysiol. 82, 3168–3174.
Yoshida, N., Vetter, D., Heinemann, S., and Liberman, M. C. 1999b. Mice lacking alpha 9 acethylcholine receptors have normal vulnerability to acoustic injury. Abs. Soc. Neuroscience. 25, 133.
Zennaro, O., Erre, J. P., Aran, J. M., and Dauman, R. 1998. Short-term effectiveness of medial efferents does not predict susceptibility to temporary threshold shift in the guinea pig. Acta Otolaryngol. 118, 681–684.
Zeng, F. G., Martino, K. M., Linthicum, F. H., and Soli, S. D. 2000. Auditory perception in vestibular neurectomy subjects. Hear. Res 142, 102–112.
Zheng, J., Shen, W., He, D. Z., Long, K. B., Madison, L. D., and Dallos, P. 2000. Prestin is the motor protein of cochlear outer hair cells. Nature 405, 149–155.
Zheng, X. Y., Henderson, D., Hu, B. H., Ding, D. L., and McFadden, S. L. 1997b. The influence of the cochlear efferent system on chronic acoustic trauma. Hear. Res. 1997 107, 147–59.
Zheng, X. Y., Henderson, D., McFadden, S. L., Ding, D. L., and Salvi, R. J. 1999. Auditory nerve fiber responses following chronic cochlear de-efferentation. J. Comp. Neurol. 406, 72–86.
Zheng, X. Y., Henderson, D., McFadden, S. L., and Hu, B. H. 1997a. The role of the cochlear efferent system in acquired resistance to noise-induced hearing loss. Hear. Res. 104, 191–203.
Zheng, X. Y., McFadden, S. L., Henderson, D., Ding, D. L., and Burkard, R. 2000. Cochlear microphonics and otoacoustic emissions in chronically de-efferented chinchilla. Hear. Res. 143, 14–22.

Further Reading

Engström, H. 1958. Structure and innervation of the inner ear sensory epithelia. Int. Rev. Cytol. 7, 535–585.
Liberman, M. C. and Guinan, J. J., Jr. 1998. Feedback control of the auditory periphery: antimasking effects of middle ear muscles vs. olivocochlear efferents. J. Commun. Disord. 31, 471–482.

3.25 Overview of Treatment of Hearing Loss

H Staecker, P Gochee, and J Ferraro, University of Kansas Medical Center, Kansas City, KS, USA

R Storms, Veterans Administration Medical Center, Kansas City, MO, USA

© 2008 Elsevier Inc. All rights reserved.

3.25.1	**Introduction**	448
3.25.2	**Medical/Surgical Treatments**	450
3.25.2.1	Conductive Hearing Loss	450
3.25.2.1.1	Debridement of the ear canal	450
3.25.2.1.2	Myringotomy and pressure equalization tube placement	450
3.25.2.1.3	Tympanoplasty	450
3.25.2.1.4	Pharmacological treatments	451
3.25.2.1.5	Eustachian tube dysfunction	451
3.25.2.1.6	Otitis media	451
3.25.2.1.7	Perforation of the tympanic membrane	451
3.25.2.1.8	Stapedectomy	452
3.25.2.1.9	Ossicular chain reconstruction	452
3.25.2.1.10	Otosclerosis	452
3.25.2.1.11	Cholesteatoma	452
3.25.2.1.12	Bone-anchored hearing aid	452
3.25.2.2	Sensorineural Hearing Loss	453
3.25.2.2.1	Pharmacological treatments	453
3.25.3	**Surgical Treatments**	456
3.25.3.1	Cochlear Implants	456
3.25.3.2	Endolymphatic Sac Decompression	457
3.25.3.3	Treatment for Acoustic Neuromas	457
3.25.4	**Nonmedical/Nonsurgical Treatments**	458
3.25.4.1	Hearing Aid Types	458
3.25.4.2	Hearing Aid Styles	458
3.25.4.2.1	Completely-in-the-canal	458
3.25.4.2.2	In-the-canal and in-the-ear	459
3.25.4.2.3	Behind-the-ear	459
3.25.4.2.4	Mini-behind-the-ear	459
3.25.4.3	Binaural versus Monaural Amplification	460
3.25.4.4	Recent Technological Advancements in Hearing Aids	460
3.25.4.4.1	Microphone technology	460
3.25.4.4.2	Directional microphone hearing aid technology	461
3.25.4.4.3	Digital signal processing	462
3.25.4.5	Hearing Aid Fitting Verification	463
3.25.4.6	Assistive Listening Devices	463
3.25.4.7	Aural Rehabilitation	464
3.25.5	**Summary**	464
References		464

Glossary

air–bone gap The difference between air- and bone-conduction hearing thresholds at specific frequencies.

assistive listening device (ALD) Any device, such as a hearing aid, designed to be worn or used to improve hearing.

aural rehabilitation Nonmedical/surgical approaches designed to overcome/help minimize the effects of hearing loss on communication and quality-of-life.

autoimmune Pertaining to disorders of the body's immune system.

bone-anchored hearing aid (BAHA) A hearing aid implanted behind the ear designed to bypass the conductive portion of the auditory system and deliver sound to the inner ear via bone conduction.

cochlear implant An electronic device implanted into the inner ear designed to provide electrical stimulation to the auditory nerve in response to sound.

conductive hearing loss Hearing loss that prevents the transmission of sound to the inner ear.

mixed hearing loss Hearing loss that includes both conductive and sensorineural components.

myringotomy A tiny surgical incision made in the tympanic membrane under microscopy that permits drainage of the middle ear and/or placement of a pressure equalization tube.

ossiculoplasty Surgical reconstruction of the ossicular chain.

ototoxic/ototoxicity Pertaining to pharmaceutical agents or other chemicals that are toxic to hearing.

pharmacological Pertaining to the use of pharmaceutical agents in the treatment of hearing loss.

sensorineural hearing loss Hearing loss that involves the inner ear (cochlea) and/or auditory nerve.

stapedectomy A surgical procedure for the treatment of otosclerosis that involves removing the stapes and replacing it with a prosthetic device.

tympanoplasty A surgical procedure to heal chronic perforations of the tympanic membrane.

3.25.1 Introduction

Disorders of the auditory system have become prevalent in modern society due to the combined effects of noise, aging, disease, and heredity. Approximately 28 million Americans have hearing loss, with this number expected to rapidly climb and nearly double by 2030 (National Institute on Deafness and Other Communication Disorders, 1996). A primary reason for this prediction is that the incidence of hearing loss increases with age, and older Americans constitute the fastest growing segment of the population. For adults over the age of 65 years, hearing disorders represent the third most prevalent chronic condition, ranking behind only arthritis and hypertension as primary health concerns (Brechtelsbauer, D. A., 1990).

The most common causes of hearing loss in adults are presbyacusis (hearing loss related to aging) and noise exposure. The most significant consequences of decreased hearing are increased difficulty understanding speech, and the effects of this condition on communication. If left untreated, adults experience social/emotional difficulties, such as increased stress, anger, guilt, depression, anxiety, and withdrawal (Chartrand, M. S., 1990). This situation is cause for considerable concern since only approximately 20% of the total adult hearing-impaired population owns hearing aids, and many of these individuals may not be using their aids correctly, or at all (Kochkin, S., 2002).

Genetic/hereditary factors and middle ear pathology constitute the most common causes of hearing loss in children. It is well recognized that normal auditory function is essential for normal speech and language development, communication, and learning. Therefore, early identification of hearing loss in children is critical. If left unidentified and untreated, hearing loss causes delay in development of receptive and expressive communication, reduced academic achievement, and can lead to social isolation and poor self-concept. These disabilities can be minimized by early intervention.

Traditionally, hearing loss has been classified into three categories or types: conductive, sensorineural, and mixed. Conductive disorders are conditions that prevent sound waves from reaching the inner ear. Sensorineural disorders involve the cochlea and/or auditory nerve, while mixed hearing losses include both conductive and sensorineural components.

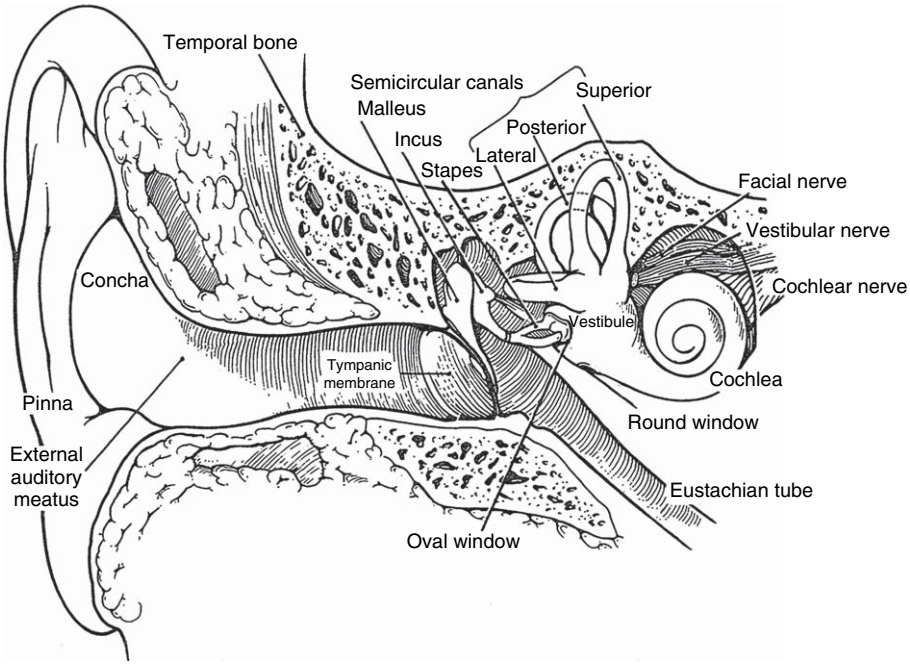

Figure 1 Schematic of the human peripheral auditory system. From Bess, F. H. and Humes, L. E. 2003. Audiology: the Fundamentals, 3rd edn. Lippincott Williams & Wilkins.

Conductive losses traditionally have been considered as treatable through medical and/or surgical approaches. Examples include the treatment of otitis media with antibiotics and the reconstruction of the tympanic membrane for perforations. Sensorineural hearing losses such as those caused by noise exposure or presbyacusis have largely been managed by amplification. This paradigm is slowly changing with the appreciation that a number of complex inner ear diseases that include sensorineural hearing loss as a manifestation are actually treatable through pharmacologic intervention. In addition to progress in the pharmacologic treatment of inner ear disease, significant advances in the surgical treatment of hearing loss have been made in the area of cochlear implantation. Cochlear implants now offer the clinician the ability to rehabilitate profoundly hearing-impaired patients. Development of bilateral implantation and the utilization of hybrid devices in which patients use a cochlear implant in conjunction with residual hearing are further improving outcomes.

Figure 1 displays a drawing of the auditory periphery. This figure can be used as a reference for the anatomical sites/structures that may be involved in the various types of hearing loss described in this chapter as well as the areas where treatments are focused.

Degree of hearing loss refers to the severity of the loss. Table 1 identifies the five broad categories that are typically used to classify the degree of loss. The numbers displayed represent hearing thresholds (i.e., the lowest intensity of sound that is perceived at least 50% of the time). A key indicator of posttreatment outcome is the level to which the degree of loss has improved.

The treatment of hearing loss varies considerably according to the cause (if known), type, and degree of impairment. Generally, these approaches can be categorized as either medical/surgical or nonmedical/nonsurgical. This chapter will provide an overview of current treatments under these two broad categories.

Table 1 Classification of hearing loss according to degree

Hearing threshold in dB HL	*Degree of loss classification*
0–15	Normal
16–25	Slight
26–40	Mild
41–55	Moderate
56–70	Moderately severe
71–90	Severe
>90	Profound

Adapted from Martin, F. N. and Clark, J. G. 2000. Introduction to Audiology. 7th Edn. Needham Heights.

3.25.2 Medical/Surgical Treatments

3.25.2.1 Conductive Hearing Loss

As indicated above, conductive hearing loss is the impairment or loss of transmission of sound to the inner ear. Normally, the coordinated action of the external auditory canal (EAC), tympanic membrane, and ossicular chain amplify sound entering the EAC by as much as 30 dB as it is delivered to the inner ear. This phenomenon occurs through a combination of factors, including resonance of the EAC, the ratio of the surface areas of the tympanic membrane to oval window opening, and the mechanical lever action of the ossicular chain. Pure tone audiometry, assessing both air conduction and bone conduction, can measure the degree of conductive hearing loss by determining the difference between air conduction and bone conduction hearing thresholds at specific frequencies. This difference is termed the air–bone gap. A key indicator of posttreatment outcome for conductive losses is the degree to which the air–bone gap has been closed. Although lacking in precision, various tuning fork tests also can be applied to gain quick insight as to whether or not hearing loss is conductive in nature. Tympanometry is another tooluseful in the identification of conductive hearing loss.

As overviewed in Table 2, multiple etiologies of conductive hearing loss exist. The following section will include a description of treatment options for managing, and often curing the more common causes of such disorders.

Table 2 Common etiologies for conductive hearing loss

External ear
- Cerumen impaction
- Congenital aural atresia
- Exostoses
- Foreign body
- Otitis externa
- Tumor of the external auditory canal

Middle ear
- Acute otitis media
- Cholesteatoma
- Glomus tumor
- Mastoiditis
- Osteogenesis imperfects
- Otosclerosis
- Paget's disease
- Serous otitis media
- Temporal bone trauma
- Tympanic membrane perforation

3.25.2.1.1 Debridement of the ear canal

Perhaps the most common form of acquired conductive hearing loss in adults is cerumen impaction. Although the EAC is normally self-cleaning, abnormal narrowing of the canal, whether congenital or acquired from a variety of factors, including multiple bouts of otitis externa, can retard the ear's natural ability to eliminate cerumen buildup. This situation can lead to deposition and, eventually, complete occlusion of the EAC. In addition, use of cotton-tipped applicators can push cerumen deep into the canal leading to compaction, analogous to packing the barrel of a cannon. Fortunately, removal of the cerumen by a physician or audiologist via debridement (irrigation/suction or curettage under microscopic examination) of the ear canal readily reverses the associated conductive hearing loss.

3.25.2.1.2 Myringotomy and pressure equalization tube placement

A myringotomy is a tiny surgical incision made in the tympanic membrane under microscopy that permits placement of a pressure equalization tube. Pressure equalization tubes allow the middle ear space to ventilate via the EAC and significantly reduce complications from Eustachian tube dysfunction and resolve any associated conductive hearing loss. Indications for this procedure include chronic Eustachian tube dysfunction, multiple episodes of acute otitis media (AOM), and chronic serous otitis media (described below).

3.25.2.1.3 Tympanoplasty

A tympanoplasty is a surgical procedure to heal chronic tympanic membrane perforations. An incision is made behind the ear or through the EAC skin and the remaining tympanic membrane is elevated. A graft, most commonly postauricular fascia, is then placed lateral to the head of the malleus and either medial or lateral to the native tympanic membrane. The graft is secured in place by packing the EAC with small gelatin sponges. If the etiology of the tympanic membrane perforation is infectious causes, tympanoplasty often is performed in combination with a mastoidectomy, a procedure that removes diseased tissue from the mastoid air cells and helps improve aeration of the middle ear space. Approximately 90–95% of patients who

undergo a tympanoplasty will obtain complete closure of the perforation with an accompanying reduction of the air–bone gap. Should the first operation fail to heal the perforation completely, additional attempts using the same procedure can be made.

3.25.2.1.4 Pharmacological treatments

AOM (described below) can cause a conductive hearing loss secondary to fluid present behind the tympanic membrane. In 2000, there were 16 million physician office visits in the USA for AOM (Cherry, D. K. and Woodwell, D. A., 2002). Prescriptions for antibiotics were given in approximately 80% of these visits. Common pathogens cultured from infected ears in AOM include *Streptococcus pneumonia* (25–50%), nontypeable *Haemophilus influenzae* (15–30%), and *Moraxella catarrhalis* (3–20%; Klein, J. O., 1994). A current recommendation for initial antibiotic treatment is amoxicillin, a penicillin analog, with or without clavulanate (American Academy of Pediatrics Subcommittee on Management of Acute Otitis Media, 2004). In patients who are penicillin allergic, other options include cephalosporins, clindamycin, or macrolide antibiotics. In general, treatment is given for 7–10 days to eradicate the pathogen completely and resolve the middle ear effusion.

Myringotomy, pressure-equalization tubes, tympanoplasty, and antibiotics are used to treat a variety of middle ear disorders. Some of the more common ones are described below.

3.25.2.1.5 Eustachian tube dysfunction

The Eustachian tube is a bony and fibrocartilaginous structure that connects the middle ear space with the nasopharnyx and functions to regulate the middle ear pressure to maintain equilibrium between −50 mm H_2O and +150 mm H_2O. Under normal conditions, the middle ear mucosa absorbs gases contained within the middle ear space creating negative air pressure (Bluestone, C. D. *et al.*, 2005). To maintain equilibrium, the Eustachian tube opens in the nasopharnyx and permits movement of air into the middle ear space to compensate for air-pressure changes. If the Eustachian tube fails to open, continued negative middle ear pressure impairs tympanic membrane mobility and reduces mechanical transmission of sound through the ossicular chain. This phenomenon is commonly observed when ascending or descending in an airplane, creating a temporary conductive hearing loss which resolves once the Eustachian tubes open. Several factors can impair the ability of the Eustachian tube to open, including rapid weight loss causing a patulous Eustachian tube (Tideholm, B. *et al.*, 1999), congenital disorders such as cleft palate, and obstruction of the opening of the Eustachian tube observed with adenoidal hypertrophy in children. Chronic decreased middle ear pressure as a result of Eustachian tube dysfunction lead to retraction of the tympanic membrane, which in severe cases is adherent to the middle ear mucosa.

3.25.2.1.6 Otitis media

Otitis media is the collection of fluid behind the tympanic membrane. The pathophysiology is often related to Eustachian tube dysfunction that leads to serous fluid accumulation from the surrounding middle ear mucosa (Bluestone, C. D. *et al.*, 2005). This fluid results in impaired vibration of the ossicles. In AOM, the fluid can become infected from nasopharyngeal flora leading to acute suppurative otitis media, which is common in children. This condition is exacerbated by the relatively short length of the pediatric Eustachian tube in combination with retrograde reflux of nasopharyngeal contents through the Eustachian tube into the middle ear space (Tasker, A. *et al.*, 2002; Bluestone, C. D. *et al.*, 2005). Chronic serous otitis media is a condition in which the fluid is benign and persists for greater than 1 month. If this fluid becomes infected, the term chronic suppurative otitis media is applied. As children grow, the Eustachian tube develops a more anterior and inferior course which prohibits Eustachian tube reflux as well as allows better opening of the nasopharyngeal opening of the Eustachian tube to permit gas exchange with the middle ear space (Daly, K. A. *et al.*, 2005). Diagnosis is made clinically by inspection of the tympanic membrane and can be augmented with audiometric tympanometry, with characteristic findings of a flattened tympanogram.

3.25.2.1.7 Perforation of the tympanic membrane

Trauma, acute or chronic otitis media, Eustachian tube dysfunction, and a variety of other conditions can cause a tear in the tympanic membrane which is usually preceded by severe pain (Boedts, D., 1995). Diagnosis is made by inspection of the tympanic membrane during

otoscopy. Depending on its size and location, a perforation can lead to a conductive hearing impairment. Fortunately, the majority of tympanic membrane perforations heal spontaneously. For perforations refractory to conservative management, tympanoplasty can be performed to correct the defect and help restore hearing.

3.25.2.1.8 Stapedectomy

Stapedectomy is a short outpatient surgical procedure, usually lasting 60–90 min, for the treatment of otosclerosis (described below). During this procedure, the tympanic membrane is reflected anteriorly through a postauricular or EAC surgical approach. After confirming fixation of the stapes at the oval window, the incudostapedial joint is separated and the stapes is fractured at the footplate using a laser. A small hole is made in the center of the stapes with the laser and prosthesis is placed over the oval window and secured to the incus. After confirming complete mobility of the ossicular chain, a small soft tissue graft is placed around the prosthesis and the tympanic membrane returned to its anatomical position and the EAC packed with small gelatin sponges. Approximately 90% of individuals with otosclerosis will achieve reduction of the air–bone gap to <10 dB.

3.25.2.1.9 Ossicular chain reconstruction

Ossicular erosion, discontinuity, or fixation is most commonly caused by cholesteatoma (described below) or chronic suppurative otitis media. With complete disruption of the ossicular chain, conductive hearing losses as high as 60 dB are observed, but ossicular chain discontinuity should be suspected in any individual with an air–bone gap greater than 30 dB. Ossicular chain reconstruction, termed ossiculoplasty, is a surgical procedure performed to improve the conductive portion of hearing loss. After removal of diseased tissue, including affected portions of the ossicular chain, grafts are placed to replicate the eroded ossicles. The type of graft used is determined by the extent and location of disease as well as the preference of the surgeon. Common grafts include autogenous cartilage and hydroxyapatite incorporated materials. Successful reconstruction can achieve air–bone gap closure to within 5–10 dB.

Stapedectomy and ossicular chain reconstruction generally are used to treat otosclerosis and cholesteatomas, which are described below. Both of these conditions cause conductive hearing loss.

3.25.2.1.10 Otosclerosis

The most common form of congenital conductive hearing disorder is otosclerosis. The hallmark of this disease is abnormal bone growth in portions of the ossicular chain. The most common location of bone deposition is around the stapes footplate, which can progress to eventual fixation of the footplate. Once the stapes footplate is fixated, mechanical sound transmission through the oval window is prohibited. Approximately 10% of Caucasians have histological evidence of otosclerosis at autopsy, but only 10% of these individuals have clinical evidence of disease (Cole, R. A. and McKenna, M., 2001). African Americans are affected less, with only 1% having histological evidence at autopsy. Women are affected more frequently than men with a 2:1 ratio. A characteristic finding in patients with otosclerosis is the Carhart notch. This finding is denoted by an apparent sensorineural hearing loss of 20–30 dB at 2000 Hz by audiometry. Interestingly, this finding disappears after surgical correction of otosclerosis, and does not represent a true sensorineural hearing loss in affected individuals. Patients with a reversed tuning fork test by Rinne examination, showing bone conduction better than air conduction when using the 512-Hz and 1024-Hz tuning forks, are best candidates for surgery. Surgical options include stapedectomy or stapedotomy plus placement of prosthesis.

3.25.2.1.11 Cholesteatoma

Cholesteatomas are congenital or acquired destructive lesions of the temporal bone. These lesions consist of squamous epithelium trapped within the skull base that slowly grows and erodes into surrounding structures (Kazahaya, K. and Potsic, W. P., 2004). Drainage from the ear, termed otorrhea, often is observed in the affected ear. In advanced disease, the erosion of the incus and malleus leads to a conductive hearing loss often greater than 30 dB. Surgery is performed to remove the cholesteatoma with reconstruction of the ossicular chain to restore hearing and reduce the air–bone gap.

Many of the conditions described above affect the appearance of the tympanic membrane. Figure 2 shows otoscopic photographs of a normal tympanic membrane along with tympanic membranes affected by different conductive disorders.

3.25.2.1.12 Bone-anchored hearing aid

A bone-anchored hearing aid (BAHA) is an implantable hearing aid that consists of three parts: (1) an

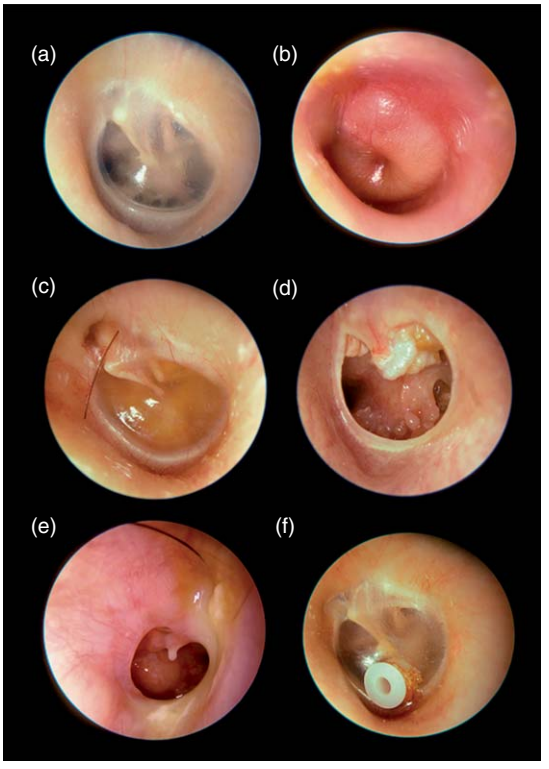

Figure 2 Otoscopic view of (a) normal tympanic membrane, (b) acute otitis media, (c) chronic serous otitis media, (d) cholesteatoma, (e) tympanic membrane perforation, and (f) myringotomy with pressure equalization tube placement. Reproduced from http://me.hawkelibrary.com, with permission.

implanted titanium screw placed behind the ear, (2) an abutment attached to the screw and visible on the surface of the skin, and (3) an external sound processor (Snik, A. F. *et al.*, 2005). The BAHA has been approved by the US Food and Drug Administration (FDA) for conductive and mixed hearing loss and more recently for unilateral sensorineural hearing loss. The device acts by translating sound into bone vibration at the site of the implant. Vibration is then conducted through bone to stimulate the cochlea directly, completely bypassing the middle ear. Since the BAHA is attached to an abutment behind the ear with no portion contained within the EAC, a variety of individuals can benefit from this device, including patients with congenital EAC atresia, chronic otitis externa or otitis media, or individuals unable to tolerate conventional hearing aids. Moreover, when the BAHA is implanted behind the affected ear in patients with unilateral profound sensorineural hearing loss, the vibration of bone from the BAHA is transmitted to the cochlea of the opposite ear

Figure 3 Bone-anchored hearing aid (BAHA) abutment implanted behind patient's right ear. The signal-processing device is connected to the abutment and translates sound into bone conduction for patients with conductive hearing loss or unilateral sensorineural hearing loss. Reprinted from http://www.headandneck.ucalgary.ca/postop_baha.htm, with permission.

allowing the perceived sensation of sound from the side of the head with the dead ear.

Figure 3 is a photograph of a patient implanted with a BAHA. The signal-processing device is connected to the abutment and translates sound into bone conduction.

3.25.2.2 Sensorineural Hearing Loss

As indicated earlier, sensorineural hearing losses involve the cochlea and/or auditory nerve (cochlear branch of VIII cranial nerve). Medical treatments for such losses include the administration of pharmacologic agents generally applied to stabilize hearing and, in some cases, reverse the progression of loss. Surgical treatments include cochlear implants, removal of space-occupying lesions, and surgeries designed to reduce fluid pressure within the endolymphatic system. The following section will describe the use of such treatments related to more common disorders of the inner ear/auditory nerve that cause/lead to sensorineural hearing loss.

3.25.2.2.1 Pharmacological treatments

A number of diseases have been identified in which pharmacological intervention potentially controls the progression of, or even reverses, sensorineural hearing loss. Some of the more common ones are described below.

3.25.2.2.1.(i) Menière's syndrome Menière's syndrome is the model disease when considering the treatment of inner ear disorders. First described by Prospère Menière in 1868, the disease consists of a triad of symptoms including attacks of vertigo, tinnitus, and fluctuating sensorineural hearing loss. The observation that sensorineural hearing loss can fluctuate is one of the earliest examples demonstrating that this type of loss can be reversible. Treatment of Menière's syndrome is mostly aimed at stabilizing the patient's balance. Two types of medications have emerged for the management of this often disabling disease. Diuretics are widely used based on the hypothesis that Menière's syndrome involves a disorder of inner ear fluid homeostasis and the observation that increased dietary salt is associated with more severe manifestation of the disease. Most clinicians would agree that dietary salt restriction and diuretics improve patients' symptoms and in many cases result in hearing returning to normal. Definitive clinical evidence has remained elusive, mainly due to the fluctuating nature of Menière's disease (Thirlwall, A. and Kundu, S., 2006). Beyond these measures a variety of other nonsurgical interventions have been used to help patients with Menière's syndrome, including positive pressure via hyperbaric treatment, or a hand-held pressure pump (termed the Meniett device) applied to the ear canal (Gates, G. A. and Green, J. D., 2002). Many of these approaches, although promising, have yet to demonstrate long-term effectiveness in the treatment of Menière's syndrome. Surgical interventions for the intractable form of the disease include endolymphatic sac decompression and intratympanic gentamicin treatment (Gates, G. A., 2005; Wittner, S., 2006). Menière's syndrome, despite being well described for over 150 years and estimated to affect about 50/100 000–75/100 000 adults (Pfaltz, C. R. and Matéfi, L., 1981), is emblematic of the problems encountered in the treatment of inner ear disease: (1) the pathophysiology of the disorder is not completely understood, (2) no absolutely reliable diagnostic modality exists, and (3) funding has not been committed to the execution of well-designed clinical trials.

3.25.2.2.1.(ii) Sudden sensorineural hearing loss Idiopathic sudden sensorineural hearing loss (ISSHL) occurs over a maximum of a 3-day period and can be associated with mild vertigo and tinnitus. The cause and pathogenesis of ISSHL remain unknown. Proposed theories of the pathogenesis of include viral cochleitis, vascular occlusion, and Reissner's membrane breaks (Mattox, D. E. and Simmons, F. B., 1977; Hughes, G. B. *et al.*, 1996). Several reports have described the postmortem pathologic findings in the temporal bones of cases of sudden deafness (Schuknecht, H. F. and Donovan, E. D., 1986). The majority of these cochleae showed atrophy of hair cells and supporting cells of the organ of Corti, with additional losses of the tectorial membrane, stria vascularis, and cochlear neuronal cells in varying combinations and severity. Recently, the hypothesis that ISSHL may be the result of pathologic activation of cellular stress pathways within the cochlea also was proposed (Merchant, S. N. *et al.*, 2005). The incidence of this disease in the US is estimated to range from 5/100 000 to 10/100 000.

Numerous drugs have been tested in an attempt to improve the outcome in patients presenting sudden sensory hearing loss. Among them, glucocorticoids are thought to influence the course of sensorineural hearing loss by decreasing inflammation resulting from viral infection or from altering immune response in the ear. Recent studies have demonstrated glucocorticoid receptors in the inner ear (Rarey, K. E. and Luttge, W. G., 1989), and glucocorticoids have been shown to influence the level of a variety of transcription factors that control inflammatory mediators. A study conducted by Wilson W. R. *et al.* (1980), who treated patients with ISSHL with steroids in a double-blind controlled trial, showed a significant improvement in hearing in steroid-treated individuals. Since then, steroid treatment for moderate-to-profound ISSHL has been the intervention of choice. Unfortunately, steroids can have significant side effects including gastric ulcers, mood changes, insomnia, and, in rare cases, avascular necrosis of joints. Intratympanic therapy for ISSHL also has been attempted (Chandrasekhar, S. S. *et al.*, 2000; Chandrasekhar, S. S., 2001; Kopke, R. D. *et al.*, 2001). Parnes L. S. *et al.* (1999) demonstrated a 54% improvement in ISSHL patients treated either with intratympanic methylprednisolone or dexamethasone. Other studies report some success with transtympanic steroid therapy for treatment of hearing loss in patients with various inner ear problems (Silverstein, H. *et al.*, 1996). Delivery of steroids to the middle ear and to the inner ear via the round window may achieve higher inner ear steroid concentrations while minimizing systemic side effects.

The partial or complete response rate to systemic steroid treatment for ISSHL is reported to range from 49 to 89% (Mattox, D. E. and Simmons, F. B.,

1977; Wilson, W. R. *et al.*, 1980; Hughes *et al.*, 1996). Several studies have demonstrated a much higher penetration of corticosteroids into inner ear fluids following topical application as compared with systemic administration presenting an opportunity to improve the treatment of this disease (Parnes, L. S. *et al.*, 1999; Chandrasekhar, S. S. *et al.*, 2000).

3.25.2.2.1.(iii) Autoimmune inner ear disease

There is considerable evidence to suggest that hearing and vestibular function can be influenced by autoimmune processes. In 1979, McCabe B. F. reported 18 cases of patients with progressive bilateral hearing loss responding to corticosteroids and/or cyclophosphamide. An autoimmune mechanism was suggested and he called this entity autoimmune sensorineural hearing loss (McCabe, B. F., 1979). A number of systemic autoimmune disorders include hearing loss and vertigo as part of their constellation of symptoms. Although classic evidence for a specific autoimmune etiology mediated by immune response directed solely at the inner ear is elusive, it appears that autoimmune damage can also exist as an entity confined to the labyrinth. Antigenic targets of autoimmunity within the labyrinth seem to be diverse. Partly because of this characteristic, the condition is difficult to diagnose (Ryan, A. F. *et al.*, 2001). Various tests can be used to detect several specific antibodies directed against antigens such as 58 kDa protein (Boulassel, M. R. *et al.*, 2001), 68 kDa protein (Ryan, A. F. *et al.*, 2001), or P0 protein (Cao, M. Y. *et al.*, 1996). Reactivity of patient sera against tissue sections of the inner ear has produced convincing labeling of sensorineural structures in some cases, but remains primarily a research tool (Soliman, A. M. and Zanetti, F., 1988). Diagnosis of autoimmune inner ear disease (AIED) is, therefore, based on the clinical findings and on the responsiveness to steroid therapy. Immune-mediated inner ear disease includes clinical conditions associated with unilateral or bilateral rapidly progressive sensorineural hearing loss. A systemic autoimmune disorder can be present in one-third of the cases (Welling, D. B., 1996). AIED has been reported in association with autoimmune diseases such as rheumatoid arthritis, systemic lupus erythematosus, Sjögren's syndrome, polyarthritis nodosa, relapsing polychondritis, Cogan's disease (Froelich, F. *et al.*, 1994), and Crohn's disease (Staecker, H. and Lefebvre, P. P., 2002; ten Cate, W. J. and Bachor, E., 2005).

Immunosuppressive drugs have been used to halt the progression of the hearing loss and in some cases were found to improve hearing. Early institution of high-dose oral prednisone daily for about 1 month is now widely used. Prednisone is then tapered slowly if a positive response to therapy is obtained (McCabe, B. F., 1979). Corticosteroids may have serious effects such as cataracts, gastrointestinal disturbances, and aseptic necrosis of the femoral head. Some patients develop a dependency on steroids with disease progression directly linked to the decrease of the steroid dosage. Recent progress in the development of novel treatments for autoimmune disease will hopefully lead to better treatments for AIED.

3.25.2.2.1.(iv) Ototoxicity and sound trauma

A wide variety of common medications have been found to be toxic to the auditory system. The most commonly seen in practice are aspirin, which reversibly inhibits outer hair cell motility; loop diuretics (Koegel, L., 1985), and aminoglycoside antibiotics, which are toxic to hair cells; and cisplatin, carboplatin, or any platinum-containing therapeutic, which are toxic to hair cells and auditory neurons (Moroso, M. J. and Blair, R. L., 1983; Tucci, D. L. and Rubel, E. W., 1990; Tsuji, K. *et al.*, 2000; Rauch, S. D., 2001; Shine, N. P. and Coates, H., 2005). Less commonly seen in clinical practice is ototoxicity due to vancomycin, quinine compounds, and industrial solvents such as styrene (Shine, N. P. and Coates, H., 2005; Lawton, B. W. *et al.*, 2006). Most efforts to treat ototoxicity have focused on dose limitation, careful monitoring, and avoiding combining ototoxins such as diuretics and aminoglycosides in clinical settings (Catlin, F. I., 1985; Stavroulaki, P. *et al.*, 2001; Shine, N. P. and Coates, H., 2005). Recently a better understanding of the molecular pathways that are induced in ototoxicity have led to a variety of strategies that may become useful for preventing ototoxicity (Chiodo, A. A. and Alberti, P. W., 1994; Lopez, I. *et al.*, 1999; Rybak, L. P. *et al.*, 1999; Schacht, J., 1999; Yagi, M. *et al.*, 1999). A recent human clinical trial has also demonstrated the ability to prevent aminoglycoside ototoxicity using pretreatment with aspirin (Sha, S. H. *et al.*, 2006). This finding is somewhat surprising in that aspirin, as described above, also can cause sensorineural hearing loss (although, aspirin-induced loss usually is reversible upon cessation of the drug). Postulations on why aspirin may have a protective effect on hearing include its role in reducing oxidative stress and/or increasing vascular flow to the cochlea.

Sound trauma (noise-induced hearing loss) is another very common cause of sensorineural hearing

loss that is largely preventable through the use of hearing protection and monitoring of individuals routinely exposed to high sound levels, be it through the workplace or recreational/leisure activities (van der Laan, F. L., 2001; Davis, R. R. *et al.*, 2003; Le Prell, C. G. *et al.*, 2003; Miller, K., 2004). Application of molecular strategies to prevent sound trauma to the inner ear are being actively explored (Sohmer, H., 1997; Henderson, D. *et al.*, 1999; Waters, C., 1999; Kopke, R. *et al.*, 2005; Henderson, D. *et al.*, 2006).

3.25.3 Surgical Treatments

3.25.3.1 Cochlear Implants

Despite the progress made in understanding and treating sensorineural hearing loss, rehabilitation of hearing with amplification is the primary treatment for most patients with this general condition. The effectiveness of amplification is dependant on the patient having a functional sound transduction mechanism. Without hair cells, an endocochlear potential, and a reasonable complement of auditory neurons, amplification using hearing aids is not possible. Cochlear implantation has enabled patients who do not have the capacity of sound transduction to hear by bypassing the function of hair cells and directly stimulating surviving auditory neurons. This process is accomplished by combining an implanted electrode array that is driven by an external speech processor (Merzenich, M. M. *et al.*, 1980; Clark, G. M. and Tong, Y. C., 1981; Harrison, R. V., 1987; Schloss, M. D., 1987; Nadol, J. B. and Eddington, D. K., 1988). Figure 4 illustrates the components of an adult cochlear implant. Figure 5 is a photograph of an actual device.

Candidates for cochlear implantation range from patients with poor speech discrimination and relatively normal hearing thresholds to patients with profound sensorineural hearing loss. Evaluation of patients is divided into adult and pediatric populations (Merzenich, M. M. *et al.*, 1980; Gantz, B. J., 1989; Kveton, J. and Balkany, T. J., 1991; Tyler, R. S. and Lowder, M. W., 1992; Souliere, C. R. *et al.*, 1994). For adult patients key criteria include prior presence of hearing and development of speech. Patients who never possessed hearing tend to have poor outcomes and results in noncompliance with the device. Outcomes in adults vary from sound awareness to open set speech recognition with duration of deafness being a predictor of successful implantation. Implantation in infants is a rapidly evolving field. Evidence is mounting that, for children who are born profoundly deaf, earlier implantation results in better speech/language development. Age of implantation is becoming younger as hearing screening and genetic testing combine to give a definitive diagnosis of hearing loss (Merzenich, M. M. *et al.*, 1980; Cullen, R. D.

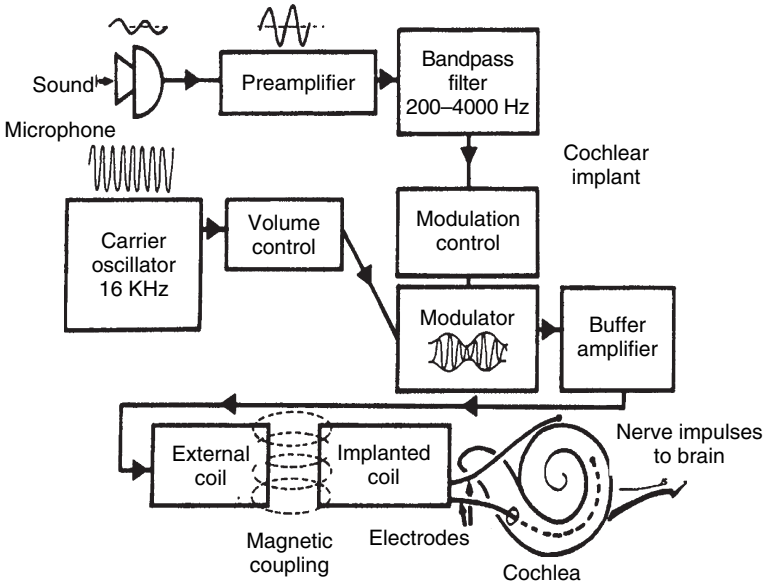

Figure 4 Basic components of an adult cochlear implant. From Waltzman, S. B. and Shapiro, W. H. Cochlear implants in adults. In: M. Valente, H. Hossford-Dunn, and R. Roesser (*eds.*) Audiology: Treatment. Thieme Medical Publishing; 2000: 537–546. Reprinted by permission.

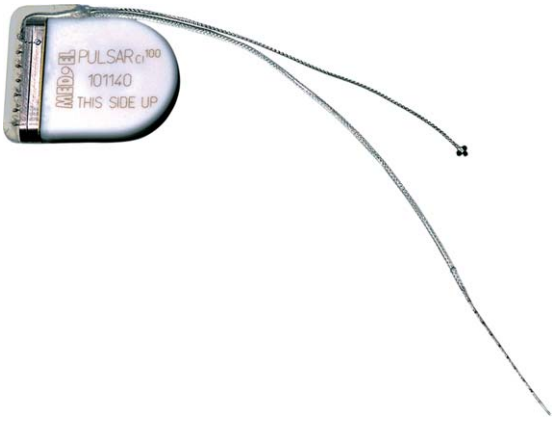

Figure 5 Adult cochlear implant device.

et al., 2004; Horn, D. L. *et al.*, 2005; Fitzpatrick, E. *et al.*, 2006; Wiley, S. *et al.*, 2006).

Evolution of cochlear implant technology is occurring on several fronts. The devices are becoming smaller with a larger number of electrodes and are capable of progressively higher stimulation rates. In parallel, new software is being developed that takes advantage of improved hardware and features reduced channel interference and the ability to use advanced speech processing. Bilateral implantation studies have been performed in both adults and children and have demonstrated improved sound localization and hearing in background noise (Das, S. and Buchman, C. A., 2005).

For patients who have agenesis of the cochlear nerve, trauma with bilateral transection of the cochlear nerve, or neurofibromatosis type 2, implantation with standard cochlear implants is not possible. For these patients auditory brainstem implants can provide some hearing rehabilitation (Cervera-Paz, F. J. and Manrique, M. J., 2005; Ramsden, R. *et al.*, 2005).

3.25.3.2 Endolymphatic Sac Decompression

The endolymphatic sac is a blind pouch, connected to the saccule and utricle of the membranous labyrinth of the vestibular system via the endolymphatic duct. In patients with sensorineural hearing loss related to Menière's disease, elevated pressure within the endolymphatic system has been postulated to contribute to both vestibular symptoms of this disease and hearing loss (Ghossaini, S. N. and Wazen, J. J., 2006). In select patients refractory to medical management, surgical decompression of the endolymphatic sac or placement of a shunt to divert fluid can reduce endolymphatic pressures and help stabilize sensorineural hearing loss (Shah, D. K. and Kartush, J. M., 1997). Since its initial description in the 1920s, an active debate within the literature continues regarding the effectiveness (or lack thereof) of endolymphatic sac surgery for the treatment of Menière's disease.

3.25.3.3 Treatment for Acoustic Neuromas

Acoustic neuromas are benign tumors of the auditory nerve, with the majority affecting vestibular function. Figure 6 displays the radiographic image of a patient with a left, cerebellopontine angle acoustic neuroma.

Data suggest that the annual incidence of acoustic neuromas in the general population is 1/100 000 (Tos, M. and Thomsem, J., 1984), although autopsy studies indicate that asymptomatic tumors have a much higher prevalence (Leonard, J. R. and Talbot, M. L., 1970). As these tumors grow, clinical manifestations occur due to compression of surrounding structures due to the limited space of the cerebellopontine angle where the auditory nerve traverses.

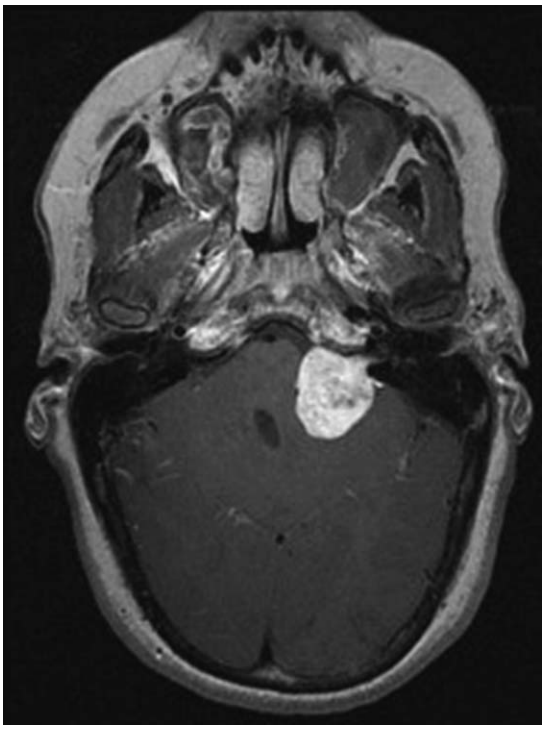

Figure 6 Acoustic neuroma of the left cerebellopontine angle. Notice the tail of the tumor entering the internal auditory canal. This patient had surgical removal of the tumor with a behind the ear approach.

The majority of acoustic neuromas occur as spontaneous mutations, but 5% are associated with neurofibromatosis type 2. In these individuals, acoustic neuromas develop at an earlier age, are more aggressive, and are bilateral. Unilateral hearing loss is observed in more than 85% of affected individuals (Selesnick, S. H. and Jackler, R. K., 1993). Tinnitus is the second most common symptom, affecting over 50% of afflicted individuals, and usually is described as hissing, ringing, or buzzing.

The gold standard for diagnosis of acoustic neuromas is magnetic resonance imaging (MRI) with gadolinium contrast. The auditory brainstem response also can also be used for diagnosis, often as a precursor to MRI. Treatment options are necessarily limited for acoustic neuromas and include surgical removal or stereotactic gamma irradiation. If the tumor is small, slow growing, and accompanied by minimal symptoms, surgery/irradiation may be withheld in favor of careful monitoring over time via imaging and electrophysiological tests, and patient feedback.

3.25.4 Nonmedical/Nonsurgical Treatments

Approximately 95% of adult hearing loss cases cannot be treated medically/surgically. In cases when medical management cannot reduce the hearing loss, hearing aids are the primary treatment. Most people become a candidate for hearing aid use when communication is negatively affected by their hearing loss. By pursuing amplification the patient hopes to gain improved speech understanding, a comfortable physical fit, and good sound quality. It is important to determine patient expectations and provide counseling on benefits and limitations of hearing aids. Hearing-impaired individuals have unique self-perceived communication needs that must be identified prior to hearing aid selection. Several self-assessment instruments such as The Abbreviated Profile of Hearing Aid Benefit (APHAB; Cox, R. and Alexander, G., 1995) and the Client Oriented Scale of Improvement (COSI; Dillon, H. *et al.*, 1997) are available to help the audiologist determine these communication needs. Although hearing aid use is beginning to increase, Kochkin S. (1994) reported that only 20% of those who needed hearing aids actually purchased them. Numerous factors contribute to this poor market penetration, including denial of communication difficulties and stigma related to hearing aid use. In general, however, hearing aid use has been shown to improve social, emotional, and communication function, as well as improve the user's self-concept and cognitive function, and decrease depression (Harless, E. and McConnnell, F., 1982; Mulrow, C. D. *et al.*, 1990; Cox, R. *et al.*, 1991; Mulrow, C. D. *et al.*, 1992).

3.25.4.1 Hearing Aid Types

There are two fundamental types of hearing aids, analog and digital. The basic components of an analog hearing aid comprise a microphone, amplifier, and receiver. The microphone picks up the acoustic signal from the environment and converts it to an electrical signal. The electrical signal is then passed through an analog amplifier before being sent to the receiver for reconversion to an acoustic signal. A volume control allows the user to adjust the loudness of the hearing aid and a telecoil option enhances telephone communication. Since 2000, there has been a dramatic increase in the availability of digital hearing aids, which employ digital technology to manipulate the input signal. The current generation of digital hearing aids provides variable gain at selective frequencies, compression of high-level signals, and attenuation of background noise through adaptive filtering, directional microphones (DMs), and multiple programs.

3.25.4.2 Hearing Aid Styles

Hearing aid components can be packaged into a variety of hearing aid styles as illustrated in Figure 7. A brief description of these styles is presented below.

3.25.4.2.1 Completely-in-the-canal

The completely-in-the-canal (CIC) is the smallest style of hearing aid made and is cosmetically appealing since it is almost invisible in the ear. All the components are housed in a small case that fits deep into the ear canal. This deep insertion allows use of the ear's natural sound-modifying resonance, and offers easy telephone usage. Less gain is needed, particularly for the higher frequencies, because the decrease in ear canal volume allows for a higher sound pressure at the tympanic membrane. Users typically report less wind noise with CICs because the microphone is protected by the ear canal and tragus. Also, users report less occlusion effect (quality of the user's voice; Killion, M. *et al.*, 1988). However,

Figure 7 Various hearing aid styles. CIC, completely-in-the-canal; ITC, in-the-canal; ITE, in-the-ear; BTE, behind-the-ear.

advanced digital circuits often cannot be incorporated into a CIC due to its small size and there is a slightly higher repair rate due to cerumen build up. CICs are custom made for each ear and are restricted to persons with ear canals large enough to accommodate the insertion depth. Also, the CIC style uses a very small battery that requires good manual dexterity for insertion. This type of hearing aid is suitable for persons with mild-to-moderate hearing loss.

3.25.4.2.2 In-the-canal and in-the-ear

These two custom-made hearing aids (in-the-canal (ITC) and in-the-ear (ITE)) fit completely in the external canal and protrude into the concha of the external ear. The ITC is smaller and fills about half of the concha. Because of their larger size in comparison to CIC aids, ITCs can accommodate recent technological advancements such as DM and telephone options, if the patient's ear canal is large enough to permit housing of these features. ITCs can also incorporate a volume control for the user and are more cosmetically appealing than hearing aids worn more external to the EAC. ITCs are appropriate for mild-to-moderately severe losses. ITE aids are larger and fill the entire concha area. Since the 1980s, ITC/ITE hearing aids have been the most popular styles of hearing aids in the USA, being chosen by approximately 90% of new users (Mueller, H. G. and Budinger, A. C., 1990). ITE aids are less popular in Europe where they account for approximately 40% of new hearing aids issued (Vonlanthen, A., 2000). ITE aids are easier to handle because of their larger size and typically have better battery life than smaller hearing aids and are capable of housing all the advanced circuits of hearing aid technology. ITEs are appropriate for mild-to-severe hearing loss.

3.25.4.2.3 Behind-the-ear

With behind-the-ear (BTE) hearing aids, the components are housed in a case that fits behind the ear. This type of hearing aid is connected to a custom-made earmold that directs the sound into the EAC. Because of its larger size and physical separation of the microphone and receiver, higher gain and output can be achieved without acoustic feedback. BTE hearing aids are the most flexible and durable style of hearing aid, which makes them especially appropriate for young children. BTE hearing aids can provide more amplification than smaller devices due to the powerful amplifier and the larger battery. One of the biggest advantages, however, is the ability to couple the BTE hearing aid to assistive technology, which will be discussed later in this chapter. This hearing aid style is the most powerful of the ear level hearing aids and is appropriate for mild-to-profound hearing losses. BTEs are gaining popularity in the USA as miniaturization has made them smaller and more cosmetically appealing to consumers. In fact, recent market trends indicate approximately 40% of new users are now selecting BTE aids.

3.25.4.2.4 Mini-behind-the-ear

The newest hearing aid style on the market is the mini-BTE. It is not as strong as a traditional BTE hearing aid and is fitted with an open noncustomized ear piece. These hearing aids are optimum for mild-to-severe high-frequency hearing loss and are cosmetically appealing because they are nearly invisible. Since the ear piece is noncustom these hearing aids can be fitted on the same day as the hearing evaluation. They are easy to insert and also reduce the occlusion effect for persons with normal low-frequency hearing. Mini-BTEs are not compatible with assistive technology. However, they can incorporate other modern technologies, but rarely have a volume control.

Hearing aid industry studies have documented that approximately 80% of people who need hearing aids do not purchase them. While there are numerous factors that contribute to the stigma of wearing a hearing aid, cosmetics issues appear to be a primary reason (Kochkin, S., 1994). Cosmetic aspects of hearing aid use include not only the concern

about wearing a device that calls attention to a sensory deficit, but that this deficit often is associated with growing older. Recently, Johnson C. E. *et al.* (2005) found that observers rated the CIC as having the least visibility and the mini-BTE and mini-ITC the next most invisible. Abrams H. *et al.* (2004) found that new hearing aid users are willing to pay more for CICs than other styles. These findings are important as hearing aid dispensers counsel potential reluctant hearing aid wearers. However, the dispenser must balance the cosmetic concerns with the needs of the hearing-impaired individual.

3.25.4.3 Binaural versus Monaural Amplification

In most cases, binaural amplification has significant advantages over monaural amplification. Two primary advantages are improvement in localization of sound and speech understanding in noise (Ricketts, T. A., 2005). Another advantage is loudness summation, which can provide a 3 dB improvement in thresholds. Binaural amplification helps eliminate the head shadow effect by allowing sound to be received on both sides of the head. With only one hearing aid, sounds from the unaided side, particularly high frequencies, can be attenuated by as much as 15 dB. In addition, binaural amplification provides a signal-to-noise improvement of approximately 3 dB, which can result in a 30–40% improvement in speech understanding (Mueller, H. G. and Hawkins, D. B., 1990). There is sufficient evidence to conclude that individuals with bilateral hearing loss should be fitted with two hearing aids (Valente, M., 1982a; 1982b).

3.25.4.4 Recent Technological Advancements in Hearing Aids

Miniaturizations with enhanced signal processing and improved microphone technology have been at the forefront of recent hearing aid advancements. Hearing aids now have multiple memories, microphones and channels, expansion and noise reduction circuits, feedback cancellation, and digital signal processing (DSP). Most modern hearing aids have computerized programming capabilities, which allow the audiologist to adjust frequency, gain, and output characteristics. The biggest challenges facing hearing aid users today is the ability to understand speech in the presence of background noise. A great deal of research and development has focused on resolving this problem. Primarily, two technologies have been used to enhance speech understanding in noise: DMs, and DSP.

3.25.4.4.1 Microphone technology

Until the mid-1990s most hearing aids incorporated omni-DMs, which consist of a single microphone that transduces sound uniformly from all directions. Directionality with regard to hearing aids means the hearing aid treats sounds differently depending on the location of the sound source. Conventionally directional hearing aids used a single microphone with two ports and acoustic delay. Newer directional hearing aids use two microphones (two omni-directional or a directional plus omni-directional) with electronic delay and subtraction. Understanding the benefits of current hearing aid DM technology requires familiarity with microphone polar plots, since newer hearing aids support multiple directional responses. Varying by microphone design and frequency, polar plots simply provide a graphical display of microphone output for different incident sound directions. Figure 8 displays polar plots for the types of microphones described below.

Omni-directional. The omni-DM treats all directions as equals. There is no differential attenuation of sound from any direction. However, even the use of omni-DMs can yield some directional characteristics such as a decrease in ipsilateral and contralateral sounds because of the shadow of the head, and pinna effects (Dillion, H., 2001).

Cardioid. Cardioid microphones are sometimes described as heart-shaped, which is the type of directionality pattern this microphone possesses. Sound is picked up mostly from the front and to a lesser extent from the sides. As shown in Figure 8, maximum rejection (null) is at the rear of the microphone. The maximum difference in sound reception is between the front and the back of the microphones. This response pattern is ideal if speech originates from the front and noise from the back. However, this situation rarely happens in the real world as noise is typically diffuse and rarely comes from one direction.

Supercardioid. Supercardioid microphones have a response pattern similar to cardioid microphones, but do allow some reception of sound from the rear. Note from Figure 8 that there are two nulls (one on each side) of maximum sound rejection. This response pattern has a higher directivity index (DI) than the cardioid pattern.

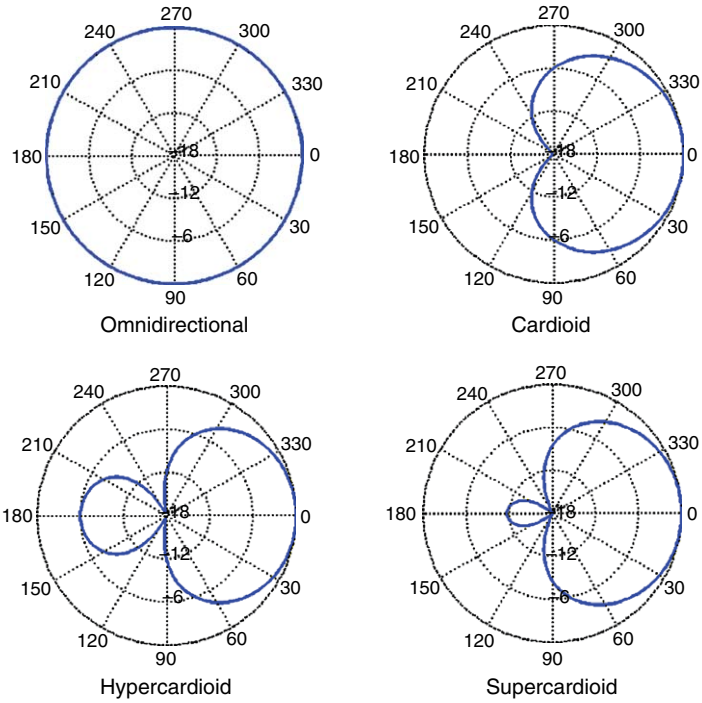

Figure 8 Polar plots for different types of hearing aid microphones. The contours provide a graphical display of microphone output from different directions.

Hypercardioid. Hypercardioid microphones have a similar response pattern to supercardioid microphones but are more responsive to sounds arriving at 180°. As shown in Figure 8, there are two nulls, with maximal attenuation at 130° and 230°. The hypercardioid pattern has a higher DI than cardioid and supercardioid patterns and theoretically provides more directional benefit.

3.25.4.4.2 Directional microphone hearing aid technology

DM hearing aid technology is an exciting advancement in modern hearing aids due to its potential for improving speech understanding in noise. It is well documented that use of DMs is able to increase the signal-to-noise ratio (SNR), therefore improving speech understanding in noise (Valente, M. *et al.*, 1995; Ricketts, T. A. and Mueller, H. G., 2000; Ricketts, T. A. and Dittberner, A. B., 2002). The improvement of the SNR varies, depending on environmental reverberation, the noise source, and distance from the listener (Hawkins, D. B. and Yacullo, W. S., 1984; Novick, M. *et al.*, 2001). The amount of microphone directionality is quantified by measuring the DI, which compares the reception of sounds originating from the front of the hearing aid to sounds originating from all other locations. The DI is expressed in decibel (dB) levels and the higher the DI the more directional the response of the hearing aid. An omni-DM would be expected to have a DI of 0 dB, while a cardioid or hypercardioid microphone might have a DI of 5–6 dB. Theoretically, speech understanding in noise increases as DI increases.

Directionality can be fixed at a certain point in space or made adaptive, so that the response pattern changes depending on the location of the sound source. No directionality benefit has been demonstrated between fixed and adaptive DMs in a diffuse noise environment (Bentler, R. A. *et al.*, 2004). However, speech understanding in noise was significantly worse for the omni-DM condition, when compared to all the DM conditions. Directionality can be manually controlled by the hearing aid wearer with a push button on the hearing aid, or automatically with the hearing aid deciding when to switch from omni- to directional mode. Automatic features are widely used in current hearing aid technology. However, Walden B. E. *et al.* (2004) and Palmer C. *et al.* (2006) have indicated that automatic directionality may not always be preferred by the hearing aid users. One disadvantage of

automatic features is the tendency to switch to directional when the overall intensity of the input level reaches a certain value, even if speech is not present. Also, automatic options sometimes switch into directional mode even when speech is coming from the back, which puts the listener at a significant disadvantage for understanding speech.

In general, DMs are used in modern hearing aids with impressive benefits and few limitations. However, if the noise source is in front of the listener, the DM will be of no benefit. Some DM users have reported higher levels of internal noise that may be audible in quiet environments, and more sensitivity to wind noise. However, these problems can usually be eliminated by using the expansion feature of the aid or switching the aid to omni-directional mode. The limitations of microphone directionality primarily relate to the environmental listening conditions, and the number of microphone ports, which is limited by the size of the hearing aid. Although there are some isolated limitations of DMs, this technology is the only one that is proven to provide improved speech understanding in noise.

3.25.4.4.3 Digital signal processing

With DSP hearing aids the acoustic analog signal is converted into discrete positive and negative electrical signals (i.e., into a digital form). Various signal-processing algorithms are incorporated into the microprocessor, and multiple algorithms can be incorporated into a single hearing aid. One algorithm might control the frequency response, one might enhance speech in noise, and yet another might control the loudness output of the hearing aid. Sophisticated DSP algorithms provide increased alternatives and enhanced options for hearing aid users.

The advantages of hearing aid DSP technology lie in its expanded capacity for processing the signal. DSP technology allows the hearing aid to adapt to the individual listening needs of the hearing aid user. For example, adaptive directional systems can change the response pattern of the microphone to improve the SNR and maximize speech understanding in noise. Also, DSP algorithms allow automatic switching between omni- and DM modes, and multiband directionality. Adaptive feedback management can analyze the feedback path to minimize or eliminate feedback without decreasing gain or output.

DSP technology also has limitations. Despite advancements in hearing aid DSP, laboratory studies have yet to demonstrate improved speech understanding in noise as compared to analog hearing aids (Walden, B. E. *et al.*, 2004; Alcantara, J. *et al.*, 2003). In addition, DSP technology is expensive and cost-prohibitive for many potential hearing aid candidates. No technology, including DSP, can restore the exquisite processing of a normal auditory system. This basic truth is an important consideration when counseling patients regarding the benefits and limitations of DSP hearing (and hearing aids in general for that matter). Without the ability to change the pathophysiology or neurology of the impaired cochlea or auditory nerve there always will be limits to hearing aid benefit. If a hearing-impaired individual has poor speech understanding abilities, they will receive limited benefit from even the most sophisticated DSP or analog hearing aid, as these devices cannot improve the distortion of speech secondary to ear pathologies.

In the early stages of digital hearing aid use consumers had high expectations. Kochkin S. (2002) reported that 95% of hearing aid users would like improved speech intelligibility in background noise; 88% wanted better sound quality; 83% wanted to be able to hear soft sounds better; and 81% wanted greater comfort for loud sounds. More recently, Kochkin S. (2005) has reported significant improvement in hearing aid customer satisfaction, with mostly digital hearing aids. For hearing instruments 0–5 years old, customer satisfaction was 71% while satisfaction with 1-year-old instruments was 78%. According to Kochkin S. this satisfaction rating placed hearing aids in the top third of all products and services measured in the USA. Eighty five per cent of users were satisfied with the ability of their hearing aids to improve their hearing, which is interpreted to mean they were receiving tremendous benefit. Hearing aid users received the most benefit (90%) for one-on-one conversations and the least benefit for cell phone use (59%). Six out of 10 hearing aid wearers surveyed were satisfied with their instrument in 80% of the listening situations measured. Hearing aid benefit was lower when the user had severe-to-profound hearing loss. In general, digital hearing aids provided significantly higher overall satisfaction, benefit, sound quality, feedback reduction, and improved performance in noisy environments. There have been significant enhancements in quality-of-life issues with DSP hearing aids. Ninety-three per cent of the hearing aid wearers reported more effective communication and enhanced social life. In addition, seven out of 10 hearing aid wearers reported improved mental/cognitive abilities and physical health. Improved customer

satisfaction and hearing aid benefit has resulted in an increase in the utilization of DSP, with 90% of hearing aids dispensed in 2005 being digital. In 1999, when only 5% of the hearing aids dispensed were digital, customer satisfaction was only 59% (Kochkin, S., 1994). Although these surveys are based primarily on perception, they do indicate an obvious preference for digital technology by hearing users; however, comparative studies between analog and digital hearing aid performance fail to demonstrate superiority of digital instruments. In addition, the specific features that tend to make digital technology more preferred by hearing aid users have not been well defined and tend to be very subjective.

3.25.4.5 Hearing Aid Fitting Verification

As hearing aid technology becomes more complicated, appropriate fitting and programming of the aids also has become more complex. Much of the success of the hearing aid user depends on the professional expertise of the audiologist or hearing aid dispenser. It has become increasingly important to verify that the hearing aid is actually performing according to the manufacturer's specifications and is meeting the needs and expectations of the patient. When a custom hearing aid is ordered, the manufacturer will pre-program the hearing aid based on the users hearing loss, an average ear canal resonance, and one of several commercially available fitting algorithms. Some audiologists question the need for verifying the manufacturer's pre-programming with digital instruments, assuming the manufacturer's estimate will accurately predict the appropriate output and gain needs of individual hearing aid users. However, several studies have noted dramatic differences between manufacturer's estimates and the actual gain measured in the patient's ear canal with real-ear measurements (Hawkins, D. B. and Cook, J. A., 2003; Aarts, N. L. and Caffee, C. S., 2005). In fact, Aarts N. and Caffee C. S. (2005) reported that the values predicted by the manufacturer were inaccurate for almost all the subjects studied. Because of these discrepancies it is incumbent on the audiologist to validate hearing aid function routinely. This task can be accomplished by several measures.

The most effective (gold standard) measurement technique for validating hearing aid function is real ear probe microphone measurement, which requires no response from the patient. A small silicone tube is placed in the patient's ear canal, and a signal is presented to a monitoring microphone located near the ear. Sound pressure level (SPL) ear canal measurements are made with and without the hearing aid in place. These SPLs can then be used in a hearing aid fitting program that provides target output for different input levels. In addition, real ear measures can be used to measure effectiveness of DMs and the smoothness of the frequency response of the hearing aid. Other verification measures for hearing aid performance include functional gain measurements and assessment of aided and unaided speech understanding in quiet and in the presence of background noise.

In addition to verification of hearing aid performance, self-reported outcome measures are helpful to ensure that the hearing aid is meeting the needs and expectations of the patient. Outcomes are simply defined as measurable differences resulting from treatment (Frattali, C. M., 1998). Outcome measures fall into two general categories: self-report from the patient such as the previously mentioned APHAB, and objective measurement of performance such as tests of speech in noise and real ear measurements. Self-reported outcomes provide a complement to real ear measures because they reflect how the user performs with the hearing aid and its perceived benefit. These measures allow the audiologist to determine the effectiveness of hearing aid intervention. In addition, they help the consumer determine efficacy of treatment, provide objective evidence for third party payment, and assess quality-of-life issues (Saunders, G. H. and Jutai, J. W., 2004). The audiological evaluation determines the type and degree of hearing impairment, but the disability (activity limitation) or handicap (participation restriction) of the hearing loss on the individual can only be assessed with self-reported measures (World Health Organization, 2001). A combination of real ear measures and self-reported outcome measures help assure that individual amplification goals are met.

3.25.4.6 Assistive Listening Devices

Even with the best hearing aid technology, some hard of hearing individuals have continued communication or safety needs because of the nature of their hearing loss and/or daily communication demands. Assistive listening devices (ALDs) help to meet these needs. Compton C. L. (2000) suggests hearing-impaired individuals have four basic communication needs that ALDs should address: face-to-face communication, enjoyment of broadcast or other media, telephone communication, and alerting devices.

Frequency-modulated (FM) systems are a type of ALD used to enhance face-to-face communication, which incorporate a microphone transmitter and a receiver worn by the hard of hearing individual. The primary advantage of this system is improved SNR. FM systems can be coupled to a BTE hearing aid or used independently. Because the microphone of the transmitter is located in close proximity to the speaker's mouth, the FM system minimizes the effects of room reverberation, distance, and noise on speech understanding (Crandell, C. *et al.*, 1995).

Other ALD devices such as infrared and induction loop systems can be used to enhance reception of television, movie, and other media. Numerous ALDs are available to assist with telephone communication. Examples include amplified telephones with volume controls and text telephones which allow the user to read the incoming conversation on an LCD screen and respond by typing or speaking. Various alerting devices help hard of hearing individuals hear environmental sounds necessary for safety and daily living such as smoke alarms, telephones, and alarm clocks. These devices also require a microphone transmitter to send a message to a receiver. The receiver can be attached to loud auditory signals, visual stimuli such as a bright flashing light, or vibrotactile stimuli such as a bed shaker.

3.25.4.7 Aural Rehabilitation

Aural rehabilitation (AR) emerged as a result of World War II for the purpose of minimizing or lessening the negative effects of hearing loss on communication, and continues to be an important supplement to hearing aid and cochlear implant use. Initially AR emphasis was on use of visual cues and auditory training. However, AR has advanced to new levels, with individualized training programs. An adult AR program might include speech reading, lip-reading, assertiveness training, communication strategies training, and counseling regarding psychosocial and emotional aspects of hearing loss. For children, an AR program might additionally include auditory training, speech-language therapy, and academic assessment. Recently computerized AR programs have been developed, which allow the hearing-impaired individual and their families to implement the program at home.

3.25.5 Summary

Although significant progress has been made in the treatment and management of hearing loss, many hurdles still remain in the quest to improve the hearing of individuals who suffer from this condition. This chapter described more common causes for hearing loss and their current treatments. As can be seen from this material, most conductive losses respond well to medical and/or surgical treatment. Unfortunately, it remains the case that there are few if any real cures for the majority of sensorineural disorders. As we have described, medical and surgical treatments can sometimes halt and even reverse the progression of sensorineural losses. In addition, coping with hearing loss has been made considerably easier by great strides in technology, such as cochlear implants, hearing aids, and other ALDs as well as behavioral modification strategies. Despite these advances, the secrets to revitalizing human cochlear hair cells or auditory nerve fibers that have been destroyed by genetic aberrations, disease, trauma, ototoxic chemicals, or aging continue to elude us. On the plus side, cochlear hair cell regeneration represents one of the hottest areas of current research in the hearing sciences. The emerging technology of stem-cell therapy is yet another tool that may have a role in future the treatment of hearing loss. The notion of inserting stem cells into the inner ear that eventually develop into functional sensory hair cells is attracting considerable scientific interest throughout the world.

References

Aarts, N. L. and Caffee, C. S. 2005. The accuracy and clinical usefulness of manufacturer-predicted REAR values in adult hearing aid fittings. Hear. Rev. 12, 16–22.

Abrams, H., Hnath-Chisolm, T., and Block, M. 2004. The effects of signal processing and style on perceived value of hearing aids. Hear. Rev. 11, 16–21.

Alcantara, J., Moore, B., Kuhnel, V., and Launer, S. 2003. Evaluation of the noise reduction system in a commercial digital hearing aid. Int. J. Audiol. 32, 34–42.

American Academy of Pediatrics Subcommittee on Management of Acute Otitis Media. 2004. Diagnosis and Management of Acute Otitis Media. Pediatrics 113, 1451–1465.

Bentler, R. A., Egge, J. L. M., Tubbs, J. L., Dittberner, A. B., and Flamme, G. A. 2004. Quantification of directional benefit across different polar response patterns. J. Am. Acad. Audiol. 15, 649–659.

Bess, F. H. and Humes, L. E. 2003. Audiology: the Fundamentals 3rd edn. Lippincott Williams & Wilkins.

Bluestone, C. D., Hebda, P. A., and Alper, C. M. 2005. Recent advances in otitis media: Eustachian tube, middle ear, and mastoid anatomy; physiology, pathophysiology, and pathogenesis. Ann. Otol. Rhinol. Laryngol. Suppl. 194, 16–30.

Boedts, D. 1995. Tympanic membrane perforation. Acta Otorhinolaryngol. Belg. 49, 149–158.

Boulassel, M. R., Deggouj, N., Tomasi, J. P., and Gersdorff, M. 2001. Inner ear autoantibodies and their targets in patients with autoimmune inner ear diseases. Acta Otolaryngol. 121, 28–34.

Brechtelsbauer, D. A. 1990. Adult hearing loss. J. Prim. Care 17, 249–266.

Cao, M. Y., Dupriez, V. J., Rider, M. H., Deggouj, N., Gersdorff, M. C., Rousseau, G. G., and Tomasi, P. 1996. Myelin protein Po as a potential autoantigen in autoimmune inner ear disease. FASEB J. 10, 1635–1640.

Catlin, F. I. 1985. Prevention of hearing impairment from infection and ototoxic drugs. Arch. Otolaryngol. 111, 377–384.

Cervera-Paz, F. J. and Manrique, M. J. 2005. Traditional and emerging indications in cochlear and auditory brainstem implants. Rev. Laryngol. Otol. Rhinol. (Bord.) 126, 287–292.

Chandrasekhar, S. S. 2001. Intratympanic dexamethasone for sudden sensorineural hearing loss: clinical and laboratory evaluation. Otol. Neurotol. 22, 18–23.

Chandrasekhar, S. S., Rubinstein, R. Y., Kwartler, J. A., Gatz, M., Connelly, P. E., Huang, E., and Baredes, S. 2000. Dexamethasone pharmacokinetics in the inner ear: comparison of route of administration and use of facilitating agents. Otolaryngol. Head Neck Surg. 22, 521–528.

Chartrand, M. S. 1990. Working with the psychology of the hearing impaired. Hear. Instr. 3, 38–66.

Cherry, D. K. and Woodwell, D. A. 2002. National ambulatory medical care survey: 2000 summary. Adv. Data 328, 1–32.

Chiodo, A. A. and Alberti, P. W. 1994. Experimental, clinical and preventive aspects of ototoxicity. Eur. Arch. Otorhinolaryngol. 251, 375–392.

Clark, G. M. and Tong, Y. C. 1981. Multiple-electrode cochlear implant for profound or total hearing loss: a review. Med. J. Aust. 1, 428–429.

Cole, R. A. and McKenna, M. 2001. Pathophysiology of otosclerosis. Otol. Neurotol. 22, 249–257.

Compton, C. L. 2000. Assistive Technology for the Enhancement of Receptive Communication. In: Rehabilitative Audiology: Children and Adults 3rd Edn. (*eds*. J. G. Alpiner and P. A. McCarthy), pp. 503–505. Lippincott Williams & Wilkins.

Cox, R. and Alexander, G. 1995. The Abbreviated Profile of Hearing Aid Benefit. Ear Hear. 16, 176–183.

Cox, R., Alexander, G., and Gilmore, C. 1991. Objective and Self-Report Measures of Hearing Aid Benefit. In: The Vanderbilt Hearing Aid Report II (*eds*. G. Studebaker, F. Bess, and L. Beck), pp. 201–213. York Press.

Crandell, C., Smaldino, J., and Flexer, C. 1995. Sound-Field Amplification. Theory and Practical Applications. Singular Press.

Cullen, R. D., Buchman, C. A., Brown, C. J., Copeland, B. J., Zdanski, C., Pillsbury, H. C., III, and Shores, C. G. 2004. Cochlear implantation for children with GJB2-related deafness. Laryngoscope 114, 1415–1419.

Daly, K. A., Rovers, M. M., and Hoffman, H. J. 2005. Recent advances in otitis media: epidemiology, natural history, and risk factors. Ann. Otol. Rhinol. Laryngol. Suppl. 194, 8–15.

Das, S. and Buchman, C. A. 2005. Bilateral cochlear implantation: current concepts. Curr. Opin. Otolaryngol. Head Neck Surg. 13, 290–293.

Davis, R. R., Kozel, P., and Erway, L. C. 2003. Genetic influences in individual susceptibility to noise: a review. Noise Health 5, 19–28.

Dillion, H. 2001. Hearing Aids: a Comprehensive Text. Thieme Medical Publishers.

Dillion, H., James, A., and Ginis, J. 1997. Client Oriented Scale of Improvement (COSI) and its relationship to several other measures of benefit and satisfaction provided by hearing aids. J. Am. Acad. Audiol. 8, 27–43.

Fitzpatrick, E., McCrae, R., and Schramm, D. 2006. A retrospective study of cochlear implant outcomes in children with residual hearing. BMC Ear Nose Throat Disord. 6, 7.

Frattali, C. M. 1998. Outcome Measurement: Definitions, Dimensions and Perspectives. In: Measuring Outcomes in Speech-Language Pathology (*ed*. C. Fratalli), p. 161. Thieme Medical Publishers.

Froehlich, F., Fried, M., Gonvers, J. J., Saraga, E., Thorens, J., and Pecoud, A. 1994. Association of Crohn's disease and Cogan's syndrome. Dig. Dis. Sci. 39, 1134–1137.

Gantz, B. J. 1989. Issues of candidate selection for a cochlear implant. Otolaryngol. Clin. North Am. 22, 239–247.

Gates, G. A. 2005. Treatment of Meniere's disease with the low-pressure pulse generator (Meniett device). Expert. Rev. Med. Devices 2(5), 533–537 (Review).

Gates, G. A. and Green, J. D. 2002. Intermittent pressure therapy of intractable Menière's disease using the Meniett® device: a preliminary report. Laryngoscope 112, 1489–1493.

Ghossaini, S. N. and Wazen, J. J. 2006. An update on the surgical treatment of Menière's diseases. Am. J. Audiol. 17, 38–44.

Harless, E. and McConnell, F. 1982. Effects of hearing aid use on self-concept in older persons. J. Speech Hear. Disord. 47, 305–309.

Harrison, R. V. 1987. Cochlear implants: a review of the principles and important physiological factors. J. Otolaryngol. 16, 268–275.

Hawkins, D. B. and Cook, J. A. 2003. Hearing aid software and predictive gain values: how accurate are they? Hear. J. 56, 26–34.

Hawkins, D. B. and Yacullo, W. S. 1984. Signal-to-noise ratio advantage of binaural hearing aids and directional microphones under different levels of reverberation. J. Speech Hear. Disord. 49, 277–279.

Henderson, D., Bielefeld, E. C., Harris, K. C., and Hu, B. H. 2006. The role of oxidative stress in noise-induced hearing loss. Ear Hear. 27, 1–19.

Henderson, D., Hu, B., McFadden, S., and Zheng, X. 1999. Evidence of a common pathway in noise-induced hearing loss and carboplatin ototoxicity. Noise Health 2, 53–70.

Horn, D. L., Pisoni, D. B., Sanders, M., and Miyamoto, R. T. 2005. Behavioral assessment of prelingually deaf children before cochlear implantation. Laryngoscope 115, 1603–1611.

Hughes, G. B., Freedman, M. A., Haberkamp, T. J., and Guay, M. E. 1996. Sudden sensorineural hearing loss. Otolaryngol. Clin. North Am. 29, 393–405.

Johnson, C. E., Danhauer, J. L., Gavin, R. B., Karns, S. R., Reith, A. C., and Lopez, I. P. 2005. Am. J. Audiol. 14, 169–175.

Kazahaya, K. and Potsic, W. P. 2004. Congenital cholesteatoma. Curr. Opin. Otolaryngol. Head Neck Surg. 12, 398–403.

Killion, M., Wilbur, L., and Gundmundsen, G. 1988. Zwislocki was right . . .. a potential solution to the ''hollow voice'' problem. Hear. Instrum. 39, 32–37.

Klein, J. O. 1994. Otitis media. Clin. Infect. Dis. 19, 823–833.

Kochkin, S. 1994. MarkeTrak IV: impact of purchase intent on cosmetics, stigma, and style of hearing instrument. Hear. J. 47, 29–36.

Kochkin, S. 2002. MarkeTrak VI: consumers rate improvements sought in hearing instruments. Hear. Rev. 9, 18–22.
Kochkin, S. 2005. MarkeTrak VII: customer satisfaction with hearing instruments in the digital age. Hear. J. 58, 30–43.
Koegel, L., Jr. 1985. Ototoxicity: a contemporary review of aminoglycosides, loop diuretics, acetylsalicylic acid, quinine, erythromycin, and cisplatinum. Am. J. Otol. 6, 190–199.
Kopke, R., Bielefeld, E., Liu, J., Zheng, J., Jackson, R., Henderson, D., and Coleman, J. K. 2005. Prevention of impulse noise-induced hearing loss with antioxidants. Acta Otolaryngol. 125, 235–243.
Kopke, R. D., Hoffer, M. E., Wester, D., O'Leary, M. J., and Jackson, R. L. 2001. Targeted topical steroid therapy in sudden sensorineural hearing loss. Otol. Neurotol. 22, 475–479.
Kveton, J. and Balkany, T. J. 1991. Status of cochlear implantation in children. American Academy of Otolaryngology-Head and Neck Surgery Subcommittee on Cochlear implants. J. Pediatr. 118, 1–7.
Lawton, B. W., Hoffmann, J., and Triebig, G. 2006. The ototoxicity of styrene: a review of occupational investigations. Int. Arch. Occup. Environ. Health 79, 93–102.
Leonard, J. R. and Talbot, M. L. 1970. Asymptomatic acoustic neurolimoma. Arch. Otolaryngol. 91, 117–124.
Le Prell, C. G., Dolan, D. F., Schacht, J., Miller, J. M., Lomax, M. I., and Altschuler, R. A. 2003. Pathways for protection from noise induced hearing loss. Noise Health 5, 1–17.
Lopez, I., Honrubia, V., Lee, S. C., Chung, W. H., Li, G., Beykirch, K., and Micevych, P. 1999. The protective effect of brain-derived neurotrophic factor after gentamicin ototoxicity. Am. J. Otol. 20, 317–324.
Martin, F. N. and Clark, J. G. 2000. Introduction to Audiology. 7th Edn. Needham Heights.
Mattox, D. E. and Simmons, F. B. 1977. Natural history of sudden sensorineural hearing loss. Ann. Otol. Rhinol. Laryngol. 86, 463–480.
McCabe, B. F. 1979. Autoimmune sensorineural hearing loss. Ann. Otol. Rhinol. Laryngol. 113, 526–530.
Merchant, S. N., Adams, J. C., and Nadol, J. B., Jr. 2005. Pathology and pathophysiology of idiopathic sudden sensorineural hearing loss. Otol. Neurotol. 26, 151–160.
Merzenich, M. M., Byers, C. L., White, M., and Vivion, M. C. 1980. Cochlear implant prostheses: strategies and progress. Ann. Biomed. Eng. 8, 361–368.
Miller, K. 2004. Occupational health injuries: a brief review of three disorders. Nurs. Clin. North Am. 39, 395–402.
Moroso, M. J. and Blair, R. L. 1983. A review of cis-platinum ototoxicity. J. Otolaryngol. 12, 365–369.
Mueller, H. G. and Budinger, A. C. 1990. Selection of hearing aid style. Rep. Hear. Instrum. Technol. 2, 5–10.
Mueller, H. G. and Hawkins, D. B. 1990. Considerations in Hearing Aid Selection. In: Handbook of Hearing Aid Amplification, II: Clinical Considerations and Fitting Practices (ed (*ed*. R. Sandlin), pp. 31–60. College Hill Press.
Mulrow, C., Michael, T., and Aguilar, C. 1992. Correlates of successful hearing aid use in older adults. Ear Hear. 13, 108–113.
Mulrow, C. D., Aguilar, C., Endicott, J. E., Velex, R., Tuley, M. R., Charlip, W. S., and Hill, J. A. 1990. Association between hearing impairment and the quality of life of elderly individuals. J. Am. Geriatr. Soc. 38, 45–50.
Nadol, J. B., Jr. and Eddington, D. K. 1988. Treatment of sensorineural hearing loss by cochlear implantation. Annu. Rev. Med. 39, 491–502.
National Institute on Deafness and Other Communication Disorders. 1996. National Strategic Research Plan: Hearing and Hearing Impairment. Department of Health and Human Services, National Institutes of Health.
Novick, M., Benter, R., Dittberner, A., and Flamme, G. 2001. The effects of release time and directionality on unilateral and bilateral hearing aid fittings in complex sound fields. J. Am. Acad. Audiol. 12, 493–504.
Palmer, C., Benter, R., and Mueller, H. G. 2006. Evaluation of a second-order directional microphone hearing aid: II self-report outcomes. J. Am. Acad. Audiol. 27, 190–201.
Parnes, L. S., Sun, A. H., and Freeman, D. J. 1999. Corticosteroid pharmacokinetics in the inner ear fluids: an animal study followed by clinical application. Laryngoscope 109, 1–17.
Pfaltz, C. R. and Matéfi, L. 1981. Menière's disease or syndrome? A critical review of diagnosis criteria. In: Menière's Disease: Pathogenesis. Diagnosis and Treatment (*eds*. K. H. Vosteen, H. Schuknecht, C. R. Pfaltz, J. Wersäll, R. S. Kimura, C. Morgenstern, and K. Juhn), pp. 1–10. Thieme Medical Publishing.
Ramsden, R., Khwaja, S., Green, K., O'Driscoll, M., and Mawman, D. 2005. Vestibular schwannoma in the only hearing ear: cochlear implant or auditory brainstem implant? Otol. Neurotol. 26, 261–264.
Rarey, K. E. and Luttge, W. G. 1989. Presence of type I and type II/IB receptors for adrenocorticosteroid hormones in the inner ear. Hear. Res. 41, 217–221.
Rauch, S. D. Vestibular histopathology of the human temporal bone. 2001. What can we learn? Ann. N. Y. Acad. Sci. 942, 25–33.
Ricketts, T. A. 2005. Directional hearing aids: then and now. J. Rehabil. Res. Dev. 42, 133–144.
Ricketts, T. A. and Dittberner, A. B. 2002. Directional Amplification for Improved Signal-to-Noise Ratio: Strategies, Measurement and Limitations. In: Hearing Aids: Standards, Options and Limitations, 2nd edn. (*ed*. M. Valente), pp. 274–346. Thieme Medical Publishers.
Ricketts, T. A. and Mueller, H. G. 2000. Predicting directional hearing aid benefit for individual listeners. J. Am. Acad. Audiol. 11, 561–569.
Ryan, A. F., Keithley, E. M., and Harris, J. P. 2001. Autoimmune inner ear disorders. Curr. Opin. Neurol. 14, 35–40.
Rybak, L. P., Whitworth, C., and Somani, S. 1999. Application of antioxidants and other agents to prevent cisplatin ototoxicity. Laryngoscope 109, 1740–1744.
Saunders, G. H. and Jutai, J. W. 2004. Hearing specific and generic measures of the psychosocial impact of hearing aids. J. Am. Acad. Audiol. 15, 238–248.
Schacht, J. 1999. Antioxidant therapy attenuates aminoglycoside-induced hearing loss. Ann. N. Y. Acad. Sci. 884, 125–130.
Schloss, M. D. 1987. Cochlear implants in children. J. Otolaryngol. 16, 307–310.
Schuknecht, H. F. and Donovan, E. D. 1986. The pathology of idiopathic sudden sensorineural hearing loss. Arch. Otorhinolaryngol. 243, 1–15.
Selesnick, S. H. and Jackler, R. K. 1993. Atypical hearing loss in acoustic neuroma patients. Laryngoscope 103(4 pt 1), 437–441.
Sha, S. H., Qiu, J. H., and Schacht, J. 2006. Aspirin to prevent gentamicin-induced hearing loss. N. Engl. J. Med. 354, 1856–1857.
Shah, D. K. and Kartush, J. M. 1997. Endolymphatic sac surgery in Menière's disease. Otolaryngol. Clin. North Am. 30, 1061–1074.
Shine, N. P. and Coates, H. 2005. Systemic ototoxicity: a review. East Afr. Med. J. 82, 536–539.
Silverstein, H., Choo, D., Rosenberg, S. I., Kuhn, J., Seidman, M., and Stein, I. 1996. Intratympanic steroid

treatment of inner ear disease and tinnitus (preliminary report). Ear Nose Throat J. 75, 468–471, 474, 476.
Snik, A. F., Mylanus, J. A., and Proops, D. W. 2005. Consensus statements on the BAHA system: where do we stand at present? Ann. Otol. Rhinol. Laryngol. Suppl. 195, 2–12.
Sohmer, H. 1997. Pathophysiological mechanisms of hearing loss. J. Basic Clin. Physiol. Pharmacol. 8, 113–125.
Soliman, A. M. and Zanetti, F. 1988. Improvements of a method for testing autoantibodies in sensorineural hearing loss. Adv. Otorhinolaryngol. 39, 13–17.
Souliere, C. R., Jr., Quigley, S. M., and Langman, A. W. 1994. Cochlear implants in children. Otolaryngol. Clin. North Am. 27, 533–556.
Staecker, H. and Lefebvre, P. P. 2002. Autoimmune sensorineural hearing loss improved by tumor necrosis factor-alpha blockade: a case report. Acta Otolaryngol. 122, 684–687.
Stavroulaki, P., Apostolopoulos, N., Segas, J., Tsakanikos, M., and Adamopoulos, G. 2001. Evoked otoacoustic emissions – an approach for monitoring cisplatin induced ototoxicity in children. Int. J. Pediatr. Otorhinolaryngol. 59, 47–57.
Tasker, A., Detmar, P. W., Panetti, M., Koufman, J. A., Birchall, J. P., and Pearson, J. P. 2002. Reflux of gastric juice and glue ear in children. Lancet 359, 493.
ten Cate, W. J. and Bachor, E. 2005. Autoimmune-mediated sympathetic hearing loss: a case report. Otol. Neurotol. 26, 161–165.
Thirlwall, A. and Kundu, S. 2006. Diuretics for Menière's disease or syndrome. Cochrane Database Syst. Rev. 3: CD003599.
Tideholm, B., Carlborg, B., and Brattmo, M. 1999. Continuous long-term measurements of middle ear pressure in subjects with symptoms of patulous Eustachian tube. Acta Otolaryngol. 119, 809–815.
Tos, M. and Thomsen, J. 1984. Epidemiology of acoustic neuromas. J. Laryngol. Otol. 98, 685–692.
Tsuji, K., Velazquez-Villasenor, L., Rauch, S. D., Glynn, R. J., Wall, C., III, and Merchant, S. N. 2000. Temporal bone studies of the human peripheral vestibular system. Aminoglycoside ototoxicity. Ann. Otol. Rhinol. Laryngol. Suppl. 181, 20–25.
Tucci, D. L. and Rubel, E. W. 1990. Physiologic status of regenerated hair cells in the avian inner ear following aminoglycoside ototoxicity. Otolaryngol. Head Neck Surg. 103, 443–450.
Tyler, R. S. and Lowder, M. W. 1992. Audiological management and performance of adult cochlear-implant patients. Ear Nose Throat J. 71, 117–118.
Valente, M. 1982a. Binaural amplification: part I. Audiology. J. Contin. Educ. 7, 7–9.
Valente, M. 1982b. Binaural amplification: part II. Audiology. J. Contin. Educ. 7, 9–11.
Valente, M., Fabry, D. A., and Potts, L. G. 1995. Recognition of speech in noise with hearing aids using dual microphones. J. Am. Acad. Audiol. 6, 440–450.
van der Laan, F. L. 2001. Noise exposure and its effect on the labyrinth, part II. Int. Tinnitus J. 7, 101–104.
Vonlanthen, A. 2000. Hearing Instrument Technology for the Hearing Healthcare Professional, 2nd Edn. Delmar Learning.
Walden, B. E., Surr, R. K., Cord, M. T., and Dyrlund, O. 2004. Predicting hearing aid microphone preference in everyday listening. J. Am. Acad. Audiol. 15, 365–396.
Waltzman, S. B. and Shapiro, W. H. 2000. Cochlear implants in adults. In: Audiology: Treatment (*eds*. M. Valente, H. Hossford-Dunn, and R. Roesser), pp. 537–546. Thieme Medical Publishing.
Waters, C. 1999. Molecular mechanisms of cell death in the ear. Ann. N. Y. Acad. Sci. 884, 41–51.
Welling, D. B. 1996. Clinical evaluation and treatment of immune-mediated inner ear disease. Ear Nose Throat J. 75, 301–305.
Wiley, S., Choo, D., Meinzen-Derr, J., Hilbert, L., and Greinwald, J. 2006. GJB2 mutations and additional disabilities in a pediatric cochlear implant population. Int. J. Pediatr. Otorhinolaryngol. 70, 493–500.
Wilson, W. R., Byl, F. M., and Laird, N. 1980. The efficacy of steroids in the treatment of idiopathic sudden hearing loss. A double-blind clinical study. Arch. Otolaryngol. 106, 772–776.
Wittner, S. 2006. Diagnosis and treatment Menière's disease. JAAPA 19, 34–39.
World Health Organization. 2001. International Classification of Functioning, Disability and Health (ICF). Geneva.
Yagi, M., Magal, E., Sheng, Z., Ang, K. A., and Raphael, Y. 1999. Hair cell protection from aminoglycoside ototoxicity by adenovirus-mediated overexpression of glial cell line-derived neurotrophic factor. Hum. Gene Ther. 10, 813–823.

Further Reading

Cruz, R. M., Lambert, P. R., and Rubel, E. W. 1987. Light microscopic evidence of hair cell regeneration after gentamicin toxicity in chick cochlea. Arch. Otolaryngol. Head Neck Surg. 113, 1058–1062.
Dulon, D., Aran, J. M., Zajic, G., and Schacht, J. 1986. Comparative uptake of gentamicin, netilmicin, and amikacin in the guinea pig cochlea and vestibule. Antimicrob. Agents Chemother. 30, 96–100.
Gates, G. A. 2006. Menière's disease review 2005. J. Am. Acad. Audiol. 17, 16–26.
Kessel, R. G. and Kardon, R. H. 1979. Tissues and Organs: a Text-Atlas of Scanning Electron Microscopy. W. H. Freeman.
Kochkin, S. 2000. MarkeTrak V: ''baby boomers'' spur growth in potential market but penetration rate declines. Hear. J. 52, 33–48.
National Council on the Aging. Senior Research Group. 1999. The consequences of untreated hearing loss in older persons. Available online at: http://www.ncoa.org/attachments/UntreatedHearingLossReport.pdf (last accessed 18 January 2007).
Ricketts, T. and Hornsby, G. 2005. Sound quality measures for speech in noise through a commercial hearing aid implementing ''digital noise reduction''. J. Am. Acad. Audiol. 16, 270–277.
Selesnick, S. H. and Jackler, R. K. 1992. Clinical manifestations and audiological diagnosis of acoustic neuromas. Otolaryngol. Clin. North Am. 25, 521–551.

Relevant Websites

http://me.hawkelibrary.com – Me.
http://www.headandneck.ucalgary.ca/postop_baha.htm – Otolaryngology – Head & Neck Surgery at the University of Calgary Medical Clinic.

3.26 Cochlear Implants

R V Shannon, House Ear Institute, Los Angeles, CA, USA

© 2008 Elsevier Inc. All rights reserved.

3.26.1	Introduction	469
3.26.2	Cochlear Implants	469
3.26.3	Cochlear Implant Psychophysics	470
3.26.3.1	Amplitude Coding	470
3.26.3.2	Temporal Coding	470
3.26.3.3	Spectral (Tonotopic) Coding	471
3.26.4	Speech Recognition	471
3.26.5	Bilateral Cochlear Implants	472
3.26.6	Combined Acoustic and Electric Hearing	472
3.26.7	Cochlear Implants as a Tool for Neuroscience	472
References		473

3.26.1 Introduction

When the concept of cochlear implants was initially proposed it was dismissed as absurd – it was thought that an artificial device replacing the complex function of the inner ear was impossible. Replacing the functionality of 30 000 nerve fibers with a small number of electrodes did not seem like a viable prosthesis. Auditory researchers were so focused on the cochlea and its complexity, that they overlooked a highly important part of hearing – the brain. Now it is clear that to understand hearing fully and to design the next generation of prosthetic devices we must have better understanding of the ear–brain system. Some aspects of hearing do not require the intricate complexities of cochlear physiological responses, while other auditory tasks rely critically on specialized details of cochlear processing. In this chapter we will review basic design and signal processing of cochlear implants, basic perceptual capabilities, and implications for future research.

3.26.2 Cochlear Implants

Most types of deafness are caused by loss or malfunction of the sensory hair cells in the inner ear. The inner row of hair cells normally converts the vibrational energy of sound into neurotransmitter release, which activates auditory neurons. When the inner hair cells are damaged, sound-induced vibration in the cochlea is not converted to nerve impulses. Cochlear implants are prosthetic devices that are intended to bypass the damaged inner hair cells and stimulate the auditory neurons directly with small electrical pulses. Multiple electrodes are placed through the round window of the cochlea and into the scala tympani. Present cochlear implants have 12–22 electrodes placed along the tonotopic dimension of the cochlea. Insertion depth of the electrodes varies across the device designs, and also depends on the anatomical pathology of the individual patient, but typically extend 20–30 mm inside the round window. Figure 1 shows a typical cochlear implant. The electrode array is inserted through a cochleostomy and sealed at the round window. The wires exit through the surgical opening and connect to the internal electronics package, which is fixed to the skull near the mastoid. The implanted electronics package contains an antenna-receiver that receives the radio signal transmitted across the skin and hermetically sealed circuitry that decodes the signal and routes the appropriate electrical stimulating pulse to the appropriate electrodes. Stimulating pulses are typically biphasic current pulses. Some devices contain multiple current sources and so can stimulate multiple electrodes simultaneously while others contain a single current source that is rapidly switched across electrodes. Modern devices have microprocessor circuitry that can contain simple programs to implement complex stimulation algorithms, and most have reverse telemetry capabilities – sending electrical potentials from the electrodes out across the skin to external devices. These components allow recording of evoked potentials and electrical fields from electrodes inside the cochlea.

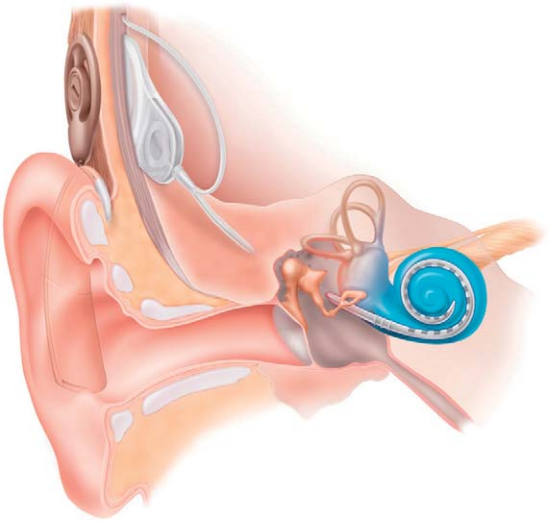

Figure 1 A diagram of a cochlear implant, which is composed of external and internal portions. The external portion contains a microphone and signal processor (shown behind the ear) and a transmission coil (located above the ear) that sends the coded signal across the skin to the implanted portion. The implanted portion of the implant contains a pick-up antenna coil, a receiver-stimulator which decodes the signal received from the external transmitter, and the intracochlear electrode, which is inserted into the cochlea. Reproduced with kind permission of Cochlear Ltd.

The external portion of a cochlear implant is worn on a belt or behind the ear, much like a hearing aid. The external portion contains a microphone, a signal processor, and a transmitter coil that sends the coded signals to the implanted portion of the implant.

3.26.3 Cochlear Implant Psychophysics

Cochlear implants produce auditory sensation by electrically activating neurons near the stimulating electrodes in the scala tympani. The patterns of activation of those nerves are quite different to those produced by acoustic stimulation of a normal cochlea. In electrical stimulation, the activated region is essentially symmetrical around the stimulating electrode, complicated by the spiral geometry of the cochlea, and the pattern spreads equally to the apex and base as the current level is increased (van den Honert, C. and Stypulkowski, P. H., 1984; 1987a). In contrast, acoustic stimulation produces a localized pattern of activation at low stimulus levels and the pattern spreads asymmetrically as level is increased. Electrical activation spreads linearly with stimulating current while acoustic activation is strongly compressed. In addition, the normal cochlea produces a high rate of spontaneous activity in the auditory nerve, and the response becomes strongly (but stochastically) phase locked to periodic stimuli as the sound level is increased. Electrical stimulation produces highly abnormal phase-locking even at levels just above threshold (van den Honert, C. and Stypulkowski, P. H., 1987b). At stimulation rates below 300 Hz, the phase-locking produced by electrical stimulation is much stronger in both time and place than for acoustic stimulation; neurons fire on every stimulus cycle. Neurons fire in a more stochastic temporal pattern when electrical pulses are presented at rates of 4 kHz or higher, due to the probabilistic nature of recovery from refractoriness (Wilson, B. S. *et al.*, 1997).

3.26.3.1 Amplitude Coding

As electrical stimulation current is raised above threshold the loudness increases. The dynamic range of electrical hearing, defined as the range between threshold and the loudness level that is tolerably but not uncomfortably loud, is typically 10–20 dB. Since the acoustic dynamic range is 120 dB there is a need for compression mapping from acoustic to electric amplitude in a cochlear implant. This is not surprising because electrical stimulation bypasses the normally compressive mechanical function of the cochlea, which is principally produced by outer hair cells. Studies of loudness in cochlear implants and auditory brainstem implants indicate that loudness for an electric stimulus increases as an exponential function of the stimulating current (Zeng, F. G. and Shannon, R. V., 1994; Zeng, F. G. *et al.*, 1998; Zeng, F. G. and Shannon, R. V., 1999). Within the electrically produced dynamic range, people with cochlear implants can only differentiate 20–40 steps of intensity, compared to more than 200 discriminable intensity steps for acoustic hearing (Nelson, D. A. *et al.*, 1996). Studies have shown that only eight steps in amplitude are adequate for speech recognition (Loizou, P. C. *et al.*, 2000), but more resolution may help in difficult listening situations.

3.26.3.2 Temporal Coding

Although electrical stimulation produces an abnormal temporal response in the auditory nerve,

temporal perceptual responses are relatively similar to those of acoustic hearing. Psychophysical measures of gap detection, forward masking, modulation detection, temporal integration, and pulse rate discrimination show similar performance in implants and acoustic hearing. Implant patients can typically detect silent gaps of 1–3 ms (Shannon, R. V., 1989), show a time constant of about 100 ms for recovery form forward masking (Shannon, R. V., 1990) and temporal integration, and can detect changes in modulation rate or pulse rate up to about 300 Hz (Shannon, R. V., 1983a; Tong, Y. C. *et al.*, 1983; Shannon, R. V., 1992). All of these capabilities are similar to those of normal acoustic hearing, suggesting that these temporal perceptual capabilities are not limited by peripheral synaptic processes. It appears that electrical stimulation, in spite of the considerable differences in the physiological temporal response, produces similar temporal perceptual abilities to acoustic hearing. One study has shown a strong correlation between individual differences in patients' ability to detect modulation and speech recognition (Fu, Q. J., 2002).

3.26.3.3 Spectral (Tonotopic) Coding

One of the places where electrical stimulation is vastly inferior to acoustic hearing is in spatial (tonotopic) resolution. The normal cochlea has more than 5000 inner hair cells that each transmit independent information to auditory neurons. Although longitudinal coupling along the basilar membrane produces some correlation across adjacent hair cells, the biological responses are stochastically independent in time and across location (Johnson, D. H. and Kiang, N. Y., 1976). In contrast, electrical stimulation activates all neurons synchronously within the electrical field of the stimulated electrode (van den Honert, C. and Stypulkowski, P. H., 1987b). Within that region all neurons are activated in a highly deterministic manner, at least for relatively low stimulating pulse rates (below 1000 pulses s^{-1}). Nerve fibers that are adjacent along the tonotopic dimension of the cochlea are all fired in tight neural synchrony by each electrical pulse.

The spatial selectivity of electrical activation is at least partially determined by the configuration of the electrodes. Monopolar stimulation, in which an intracochlear electrode is stimulated relative to a remote ground electrode, produces a broad pattern of activation (Shannon, R. V., 1983b; van den Honert, C. and Stypulkowski, P. H., 1987a). Bipolar stimulation, in which the current source and sink are both intracochlear electrodes that are close to each other, produces activation in a more restricted region. Bipolar electrodes that are more widely spaced produce intermediate activation patterns. Tripolar (also called quadrapolar) electrode configurations, in which a center electrode is activated and the return electrodes flank the active electrode, produces the most restrictive pattern of activation (Spelman, F. A. *et al.*, 1995).

Psychophysically, spatial selectivity can be evaluated with many methods that produce different results depending of the task. Some tasks are quite sensitive to differences in the overlap of the excitation produced by two electrodes while other tasks are not. For example, to discriminate two electrodes may only require that any aspect of the excitation produced by the two electrodes be different. In contrast, loudness may be a relatively insensitive measure of the degree of overlap of the excitation produced by two electrodes: it may require considerable separation of the two excitation patterns to produce a change in loudness (Shannon, R. V. *et al.*, 2004). Recent studies have shown modest differences in perceptual interference for monopolar, bipolar, and tripolar stimulation, broadly consistent with the physiological results (Bierer, J. A. and Middlebrooks, J. C., 2004). However, the perceptual measures appear to be more similar across electrode configurations than the physiological results. One possible explanation for this pattern of results is that the differences in electrode configuration would be expected to diminish if the electrodes are located distant from the nerve to be stimulated. In the physiological experiments the electrodes could be positioned close to the nerves, while in the behavioral experiments the electrodes are likely to be further from the nerves. Overall, there appears to be a modest correlation between psychophysical measures of electrode selectivity and speech recognition (Donaldson, G. S. and Nelson, D. A., 2000).

3.26.4 Speech Recognition

Early single-channel cochlear implants did not produce significant levels of open set speech recognition, but patients still found the sound from the implants to be quite useful and patient acceptance and satisfaction were high. Even single channel implants could provide significant improvements in speech recognition when the sensation produced by the

implant was combined with lip-reading. In addition, the sensation produced by the implant, even when the source of the sound was not identifiable, provided a sense of connection with the world of sound, relieving the isolation of deafness. Many people report that deafness makes them feel isolated and cut off from the world around them. Even minimal hearing provided by a single-channel cochlear implant removed that barrier of silence and made them feel connected again, even if they could not understand speech or identify the sounds.

Multichannel cochlear implants use multiple electrodes to stimulate different tonotopic locations along the scala tympani. Information from the low-frequency region of speech is coded and presented to the most apical electrode location. It is clear that speech recognition improves as the number of spectral channels increases (Fu, Q. J. *et al.*, 1998; Dorman, M. F. *et al.*, 1997), but implant listeners do not appear to be able to utilize all the channels of information presented fully. Although modern cochlear implants have 16–22 electrodes, implant listeners appear to only use a smaller number of effective channels. A study by Fishman K. *et al.* (1997) measured speech recognition in cochlear implant listeners as the number of electrodes was changed. Speech recognition performance increased as the number of electrodes increased only up to four to seven electrodes. From seven to 22 electrodes there was no significant improvement in speech recognition. Even patients who had excellent stimulation selectivity showed no increase in performance as the number of electrodes was increased above seven. A follow-up study (Friesen, L. *et al.*, 2001) showed the same result for speech recognition in quiet and for speech recognition in noise.

One of the most important factors in the tonotopic representation is to preserve the absolute and relative distribution of frequency information in the cochlea, at least as far as is possible with electrical stimulation. Once the brain is highly trained to understand patterns of excitation produced by sound in the normal tonotopic positions in a normal acoustic cochlea, then electrical activation must match that distribution for the patterns to be recognized. If the pattern of nerve activity produced by electrical stimulation is shifted or distorted relative to the normal acoustic tonotopic pattern then speech is not recognized (Shannon, R. V. *et al.*, 1998; Fu, Q. J. and Shannon, R. V., 1999; Baskent, D. and Shannon, R. V., 2003; 2004; 2005). In some cases, speech recognition can be learned even if the sensory pattern is shifted in the cochlea or distorted from the normal acoustic pattern (Fu, Q. J. and Nogaki, G., 2005; Fu, Q. J. *et al.*, 2005a; 2005b). However, congenitally deaf individuals who receive the cochlear implant as adults do not recognize speech with the device even after years of use.

3.26.5 Bilateral Cochlear Implants

Recently hearing-impaired patients have received cochlear implants in both ears in an attempt to restore directional hearing. These trials have demonstrated mixed success, with some implant listeners able to localize sounds in space and others unable to localize. Research is ongoing to determine the factors that lead to binaural fusion and localization with two cochlear implants (van Hoesel, R. J., 2004; Litovsky, R. Y. *et al.*, 2004).

3.26.6 Combined Acoustic and Electric Hearing

The average level of speech understanding with modern cochlear implants is so good that implants are now being applied to patients with relatively good acoustic hearing at low frequencies, but poor to no hearing at mid- and high frequencies. The implant is intended to activate nerves in mid- and high-frequency regions to combine with the acoustic hearing in low frequencies. Preliminary clinical trials are showing mixed success of this approach with some patients showing clear synergy combining acoustic and electric hearing (Gantz, B. J. *et al.*, 2005; Kiefer, J. *et al.*, 2005). Success of an implant in such cases will clearly depend on the survival of neurons in the deafened high-frequency region of the cochlea.

3.26.7 Cochlear Implants as a Tool for Neuroscience

One of the most interesting outcomes of the cochlear implant is in its implications for auditory neuroscience. Although much is known about the function of the cochlea, relatively little is known about central perceptual processing mechanisms in hearing. Cochlear implants have already advanced our knowledge about the interaction between peripheral and central processing in hearing. In people who become deaf as adults, the implant provides

an abnormal and distorted peripheral signal to a well-trained auditory brain. Experiments have demonstrated that a coarse peripheral signal can still produce good speech understanding and poor music understanding. Sound quality and musical pitch require relatively fine information from the periphery whereas pattern recognition of speech requires only relatively coarse peripheral information. Measurements of long-term learning show the plasticity of central processing in adapting to an abnormal peripheral signal (Fu, Q. J. and Nogaki, G., 2005; Fu, Q. J. *et al*., 2005a; 2005b). Children who receive cochlear implants before 2 years of age are showing not only normal speech and language development, but there are also reports of musical abilities that are beyond those available to adult implant patients (Svirsky, M. A. *et al*., 2000). In contrast, congenitally deaf individually who receive the implant as adults derive limited benefit from the implant even after many years of daily use. Central plasticity, critical periods for complex pattern recognition, and the plasticity of early development are all areas in which cochlear implants can provide a tool for research as well as a successful prosthesis.

References

Baskent, D. and Shannon, R. V. 2003. Speech recognition under conditions of frequency-place compression and expansion. J. Acoust. Soc. Am. 113, 2064–2076.

Baskent, D. E. and Shannon, R. V. 2004. Frequency-place compression and expansion in cochlear implant patients. J. Acoust. Soc. Amer. 116, 3130–3140.

Baskent, D. E. and Shannon, R. V. 2005. Interactions between cochlear implant electrode insertion depth and frequency-place mapping. J. Acoust. Soc. Am. 117, 1405–1416.

Bierer, J. A. and Middlebrooks, J. C. 2004. Cortical responses to cochlear implant stimulation: channel interactions. JARO 5, 32–48.

Donaldson, G. S. and Nelson, D. A. 2000. Place-pitch sensitivity and its relation to consonant recognition by cochlear implant listeners using the MPEAK and SPEAK speech processing strategies. J. Acoust. Soc. Am. 107, 1645–1658.

Dorman, M. F., Loizou, P. C., and Rainey, D. 1997. Speech intelligibility as a function of the number of channels of stimulation for signal processors using sine-wave and noise-band outputs. J. Acoust. Soc. Am. 102, 2403–2411.

Fishman, K., Shannon, R. V., and Slattery, W. H. 1997. Speech recognition as a function of the number of electrodes used in the SPEAK cochlear implant speech processor. J. Speech Hear. Res. 40, 1201–1215.

Friesen, L., Shannon, R. V., Baskent, D., and Wang, X. 2001. Speech recognition in noise as a function of the number of spectral channels: comparison of acoustic hearing and cochlear implants. J. Acoust. Soc. Am. 110, 1150–1163.

Fu, Q. J. 2002. Temporal processing and speech recognition in cochlear implant users. Neuroreport 13, 1635–1639.

Fu, Q. J. and Nogaki, G. 2005. Noise susceptibility of cochlear implant users: the role of spectral resolution and smearing. J. Assoc. Res. Otolaryngol. 6, 19–27.

Fu, Q. J. and Shannon, R. V. 1999. Recognition of spectrally degraded and frequency-shifted vowels in acoustic and electric hearing. J. Acoust. Soc. Am. 105, 1889–1900.

Fu, Q. J., Galvin, J. J., III, Wang, X., and Nogaki, G. 2005b. Moderate auditory training can improve speech performance of adult cochlear implant users. Acoust. Res. Lett. Online 6, 106–111.

Fu, Q. J., Nogaki, G., and Galvin, J. J., III. 2005a. Auditory training with spectrally shifted speech: an implication for cochlear implant users' auditory rehabilitation. J. Assoc. Res. Otolaryngol. 6, 180–189.

Fu, Q. J., Shannon, R. V., and Wang, X. 1998. Effects of noise and spectral resolution on vowel and consonant recognition: acoustic and electric hearing. J. Acoust. Soc. Am. 104, 3586–3596.

Gantz, B. J., Turner, C., Gfeller, K. E., and Lowder, M. W. 2005. Preservation of hearing in cochlear implant surgery: advantages of combined electrical and acoustical speech processing. Laryngoscope 115, 796–802.

Johnson, D. H. and Kiang, N. Y. 1976. Analysis of discharges recorded simultaneously from pairs of auditory nerve fibers. Biophysics J. 16, 719–734.

Kiefer, J., Pok, M., Adunka, O., Sturzebecher, E., Baumgartner, W., Schmidt, M., Tillein, J., Ye, Q., and Gstoettner, W. 2005. Combined electric and acoustic stimulation of the auditory system: results of a clinical study. Audiol. Neurootol. 10, 134–144.

Litovsky, R. Y., Parkinson, A., Arcaroli, J., Peters, R., Lake, J., Johnstone, P., and Yu, G. 2004. Bilateral cochlear implants in adults and children. Arch. Otolaryngol. Head Neck Surg. 130, 648–655.

Loizou, P. C., Dorman, M., Poroy, O., and Spahr, T. 2000. Speech recognition by normal-hearing and cochlear implant listeners as a function of intensity resolution. J. Acoust. Soc. Am. 108, 2377–2387.

Nelson, D. A., Schmitz, J. L., Donaldson, G. S., Viemeister, N. F., and Javel, E. 1996. Intensity discrimination as a function of stimulus level with electric stimulation. J. Acoust. Soc. Am. 100, 2393–2414.

Shannon, R. V. 1983a. Multichannel electrical stimulation of the auditory nerve in man. I. Basic psychophysics. Hear. Res. 11, 157–189.

Shannon, R. V. 1983b. Multichannel electrical stimulation of the auditory nerve in man. II. Channel interaction. Hear. Res. 12, 1–16.

Shannon, R. V. 1989. Detection of gaps in sinusoids and pulse trains by patients with cochlear implants. J. Acoust. Soc. Am. 85, 2587–2592.

Shannon, R. V. 1990. Forward masking in patients with cochlear implants. J. Acoust. Soc. Am. 88, 741–744.

Shannon, R. V. 1992. Temporal modulation transfer functions in patients with cochlear implants. J. Acoust. Soc. Am. 91, 1974–1982.

Shannon, R. V., Fu, Q. J., Galvin, J. J., III, and Friesen, L. 2004. Speech Perception with Cochlear Implants. In: Auditory Prostheses (*eds*. F. G. Zeng, A. N. Popper, and R. R. Fay), Vol. X, pp. 334–376., Springer Handbook of Auditory Research, Springer.

Shannon, R. V., Zeng, F. G., and Wygonski, J. 1998. Speech recognition with altered spectral distribution of envelope cues. J. Acoust. Soc. Am. 104, 2467–2476.

Spelman, F. A., Pfingst, B. E., Clopton, B. M., Jolly, C. N., and Rodenheiser, K. L. 1995. Effects of electrical current configuration on potential fields in the electrically stimulated cochlea: field models and measurements. Ann. Otol. Rhinol. Laryngol. 166, 131–136.

Svirsky, M. A., Robbins, A. M., Kirk, K. I., Pisoni, D. B., and Miyamoto, R. T. 2000. Language development in profoundly deaf children with cochlear implants. Psychol. Sci. 11, 153–158.

Tong, Y. C., Blamey, P. J., Dowell, R. C., and Clark, G. M. 1983. Psychophysical studies evaluating the feasibility of a speech processing strategy for a multiple-channel cochlear implant. J. Acoust. Soc. Am. 74, 73–80.

van den Honert, C. and Stypulkowski, P. H. 1984. Physiological properties of the electrically stimulated auditory nerve. II. Single fiber recordings. Hear. Res. 14, 225–243.

van den Honert, C. and Stypulkowski, P. H. 1987a. Single fiber mapping of spatial excitation patterns in the electrically stimulated auditory nerve. Hear. Res. 29, 195–206.

van den Honert, C. and Stypulkowski, P. H. 1987b. Temporal response patterns of single auditory nerve fibers elicited by periodic electrical stimuli. Hear. Res. 29, 207–222.

van Hoesel, R. J. 2004. Exploring the benefits of bilateral cochlear implants. Audiol. Neurootol. 9, 234–246.

Wilson, B. S., Finley, C. C., Lawson, D., and Zerbi, M. 1997. Temporal representations with cochlear implants. Am. J. Otol. 18, S30–S34.

Zeng, F. G. and Shannon, R. V. 1994. Loudness coding mechanisms inferred from electric stimulation of the human auditory system. Science 264, 564–566.

Zeng, F. G. and Shannon, R. V. 1999. Psychophysical laws revealed by electric hearing. Neuroreport 10, 1–5.

Zeng, F. G., Galvin, J., and Zhang, C. Y. 1998. Encoding loudness by electric stimulation of the auditory nerve. Neuroreport 9, 1845–1848.

Further Reading

Eddington, D. K., Dobelle, W. H., Brackmann, D. E., Mladevosky, M. G., and Parkin, J. L. 1978. Auditory prosthesis research with multiple channel intracochlear stimulation in man. Ann. Otol. Rhinol. Laryngol. 87, 1–39.

3.27 Hearing Loss and Hearing Aids: A Perspective

M C Killion, Etymotic Research Ltd., Elk Grove Village, IL, USA

© 2008 Elsevier Inc. All rights reserved.

3.27.1	**Background**	475
3.27.2	**Hearing Loss and Signal-to-Noise Ratio Loss**	476
3.27.2.1	Hearing Loss	476
3.27.2.2	Signal-to-Noise Ratio Loss	476
3.27.3	**Hearing Aids**	477
3.27.3.1	Early Hearing Aids	477
3.27.3.2	Modern Digital Hearing Aids – Limitations	478
3.27.3.3	Modern Digital Hearing Aids – Improvements	479
3.27.4	**Satisfaction and Technology**	480
3.27.5	**Over-the-Counter Hearing Aids**	481
3.27.6	**The Future**	482
References		482

Glossary

automatic gain control (AGC) Nonlinear hearing aid compression circuitry designed to automatically change gain as signal level changes or limit output when signal level reaches a specified criterion.

conductive loss Reduction in hearing sensitivity, despite normal cochlear function, due to impaired sound transmission through the external auditory meatus, tympanic membrane, and ossicular chain.

feedback Sound produced when an amplification system goes into oscillation, produced by amplified sound from the receiver reaching the microphone and being re-amplified.

minimum audible pressure (MAP) Denotes the sound pressure level (SPL) at the eardrm required by a listener to detect a tone.

over-the-counter (OTC) Hearing aids hearing enhancement devices that provide amplification of sounds, available without the assistance of a hearing professional.

sensorineural loss Hearing loss resulting from damage to the sensory end organs and/or their associated nerve fibers.

signal-to-noise ratio (SNR) Relative difference in decibels between a sound of interest and a background of noise.

SNR loss Increase in SNR, relative to normal-hearing performance, required to understand speech in noise.

sound pressure level (SPL) Magnitude of sound expressed in decibels above the reference level of 20 μpa.

wide-dynamic-range compression (WDRC) A form of automatic gain control that provides greater gain for quiet sounds than for loud sounds, with a smooth change in gain spread out between the two conditions.

3.27.1 Background

There are two difficulties that accompany hearing loss: loss of ability to hear quiet sounds (usually accompanied by a much smaller loss of ability to hear stronger sounds), and loss of ability to understand speech, especially speech in noise. The two losses often but not always go together: either loss can occur without the other. Someone who cannot even detect quiet speech may be able to understand almost as well as someone with normal hearing at an extremely noisy party, while another person who can still detect quiet speech may be unable to understand speech in the presence of noise at any presentation level.

The common term sensorineural loss includes both types of loss whenever they arise from inner-ear or neural pathology. A conductive loss from middle-ear pathology causes a sensitivity loss only. Fortunately, the majority of conductive losses can be treated medically or surgically, and will not be discussed further here.

Hearing aids can do an excellent job of restoring the ability to hear quiet sounds. As discussed below, the task of improving one's ability to hear in noise is much more difficult to solve. Other problems facing hearing aid wearers – feedback (sometimes that only others can hear), a hollow sound in the wearer's own voice called occlusion effect, disappointing sound quality, size, cost, and an unwillingness to see a professional presumably account for the fact that only 20% of those who say they need a hearing aid get one. These issues will be discussed below.

3.27.2 Hearing Loss and Signal-to-Noise Ratio Loss

3.27.2.1 Hearing Loss

The term minimum audible pressure (MAP) denotes the sound pressure level (SPL) at the eardrum required by a listener to detect a tone. As shown in Figure 1, the average MAP for a normal-hearing person is about 12 dB SPL between 500 and 8000 Hz. (The standards specify that MAP be generated by an earphone. Different numbers come from the use of different sound sources and their calibrating methods, but all produce the same eardrum pressure at threshold.)

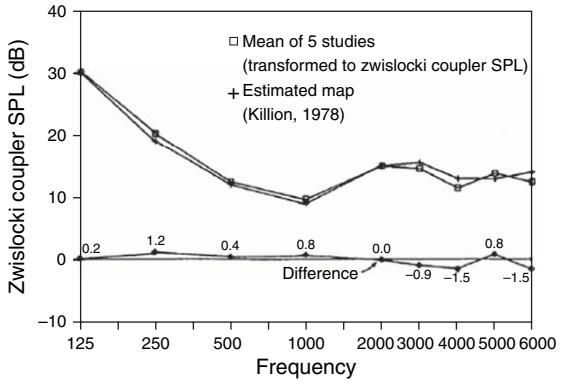

Figure 1 Minimum audible pressure (MAP) at the eardrum estimated from data obtained over a 40-year period (Killion, 1978), plus, five subsequent studies using insert earphones. From Wilber, L. A., Kruger, B., and Killion, M. C. 1988. Reference thresholds for the ER-3A insert earphone. J. Accoust. Soc. Am. 83, 669–676, used with permission.

What is commonly called hearing loss is more precisely called pure tone hearing loss. This is defined as the number of decibels increase in SPL, over normal-hearing response, that is required for a pure tone to elicit a response 50% of the time. It is thus a loss of ability to hear quiet tones; that is, a sensitivity loss. Normal-hearing performance for SPLs at the eardrum that can be detected 50% of the time is shown in Figure 1.

3.27.2.2 Signal-to-Noise Ratio Loss

The second type of hearing loss has recently been dubbed signal-to-noise ratio (SNR) loss, a term derived from the decreased tolerance to noise when the listener is trying to understand speech. Speech is highly redundant. If it was necessary to hear 100% of the available speech cues to carry on a conversation, none of us could enjoy noisy social situations where much of the desired talker's speech is masked by the voices of other talkers. Fortunately, only about 26% of the speech cues must be heard by normal-hearing persons in order for them to understand 90% of sentences correctly. In laboratory experiments, it has been found that it is possible to carry on a conversation with all sounds above 800 Hz filtered out, or all sounds below 2200 Hz filtered out, or even all sounds between 600 and 3500 Hz filtered out, each of which corresponds approximately to removing 75% of the speech cues.

Someone who requires more than 26% of speech cues in order to understand speech is said to have an SNR loss. Rather than express SNR loss in the number of speech cues required, we normally express it as the number of decibels improvement in SNR required to reach normal performance. Normal performance is about 50% words in sentences correct at a roughly 0 dB SNR (signal and noise at equal levels). Three popular tests, the Hearing In Noise Test (HINT), the Quick Speech in Noise (QuickSIN), and the BKB-SIN test each start with a sentence in virtual quiet and progressively increase the noise until the patient can repeat only 50% of the words in sentences correctly. It turns out that if a person requires twice the number of speech cues (i.e., requires 52% instead of 26%) of the cues, he or she will require an 8 dB increase in SNR in order to repeat 50% of the words in sentences correctly.

As shown in Figure 2, patients with similar hearing loss can have dramatically different abilities to

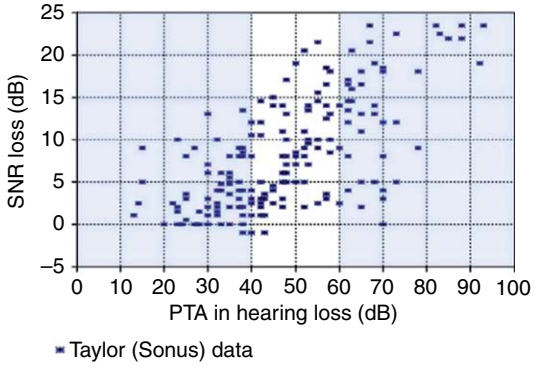

Figure 2 Relationship between signal-to-noise ratio (SNR) loss and pure tone average (PTA) hearing loss for 100 hearing aid wearers. Shaded region of moderate hearing loss shows range of SNR loss from normal (0 dB) to severe loss (23 dB).

understand speech in noise. A loss in sensitivity may or may not be accompanied by a significant loss of ability to hear in noise. For example, an SNR loss ranging from normal (SNR loss = 0 dB) to severely impaired (SNR loss = 24 dB) is found in persons all of whom have a moderate hearing loss.

The distribution in SNR loss among hearing aid wearers has been reported by several groups. Approximately 50% of subjects have a 5 dB SNR loss or greater, 20% have a 10 dB or greater loss, and 5% have a 15 dB or greater loss. A person with a 15–20 dB loss of ability to hear in noise finds it impossible to enjoy a dinner out with family and friends because the restaurant noise makes everyone's normal speech unintelligible to that person.

3.27.3 Hearing Aids

3.27.3.1 Early Hearing Aids

Pre-electric ear trumpets provided acoustic amplification in the 1800s and earlier. In the 1930s, hearing aids consisted of table models, thus the brand name Radio Ear, or relatively large body aids. They used carbon microphones (similar to those used in telephones but generally larger and often used in pairs to obtain 6 dB greater gain), a rheostat as volume control, and an earphone sealed to the ear. The complete electric circuit was battery–microphone–rheostat–earphone–battery. When additional gain was needed, an amplifier consisting of a miniature earphone mechanism connected to a miniature carbon element was added. The carbon element of the earphone was used as an amplifier. Such hearing aids had peak real-ear gains of 50 dB, along with, unfortunately, high distortion and a very peaky frequency response.

By 1952, hearing aids containing miniature vacuum tubes could provide an amount of gain limited only by the quality of the seal (to prevent feedback whistling) between the earmold and the ear. By 1962, continuing miniaturization of the components had made all-in-the-ear hearing aids possible. Figure 3 illustrates the three types which make up the vast majority of hearing aid fittings today. The smallest completely-in-the-canal hearing aids can lie deeply enough in the ear canal to be invisible for all practical purposes.

By the early 1980s, integrated circuits had made improved automatic signal processing possible, the best-known of which was perhaps the Manhatten circuit, which dramatically reduced the distortion for high-level signals by automatically reducing the gain and low-frequency response of the hearing aid as the input sound level increased.

By 1990, zinc–air batteries and high-efficiency class D amplifiers made it practical to provide hearing aids with fidelity equal to the best home stereo systems: 16 kHz bandwidth, low distortion, and an improved signal-processing scheme called wide-dynamic-range compression (WDRC). WDRC is now used in all analog and digital hearing aids. A WDRC amplifier mainly amplifies the quieter sounds, especially the high-frequency sounds rendered inaudible by a typical high-frequency hearing loss, leaving loud sounds with much less amplification. While this approach seems obvious now, it met with great resistance when it was introduced.

Recent data have added further support for providing high fidelity in hearing aids. One surprising – almost astonishing – finding is that the ability of hearing-aid wearers to understand speech in noise can be predicted almost exactly by the fidelity rating given those same aids by normal-hearing subjects, as illustrated in Figure 4. This is counter to common myths, which state that hearing-aid wearers need only digital signal processing and noise reduction, and that limited frequency response is not important.

We find experimentally that hearing-aid wearers assign fidelity ratings nearly identical to those assigned by subjects with normal hearing, further evidence that intelligibility and fidelity are interlinked. More details can be found in Killion M. (2004).

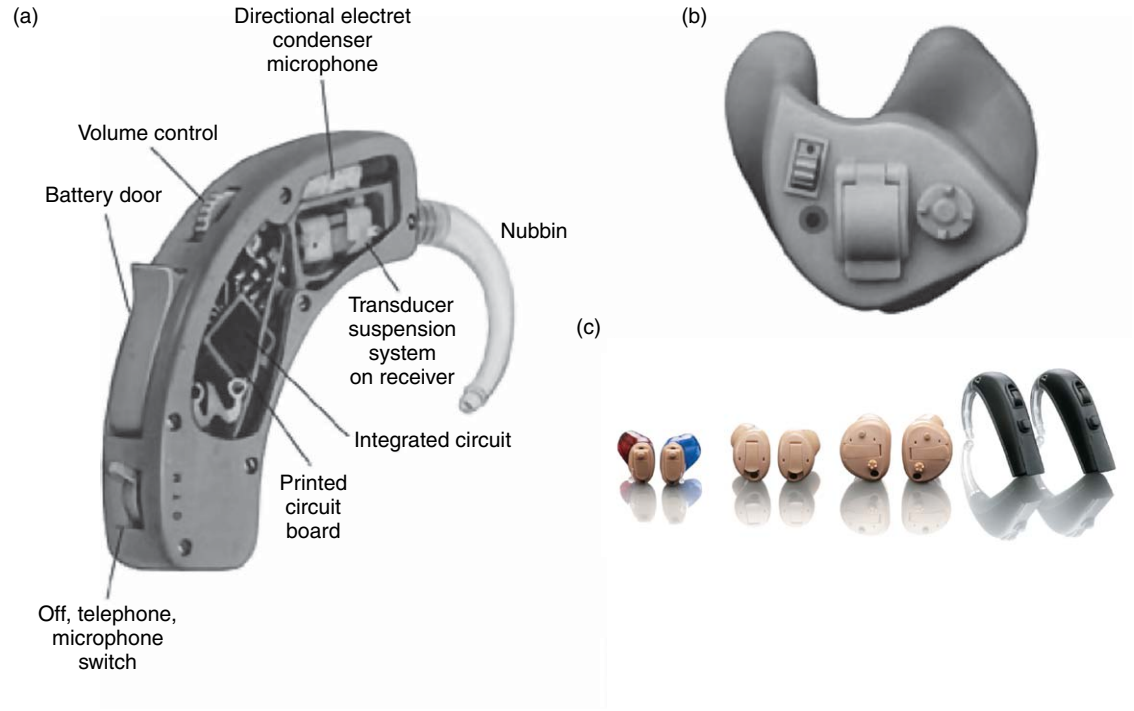

Figure 3 (a) Behind-the-ear (BTE), (b) in-the-ear (ITE), and (c) completely-in-the-canal (CIC) hearing aids. Courtesy of Beltone Corporation.

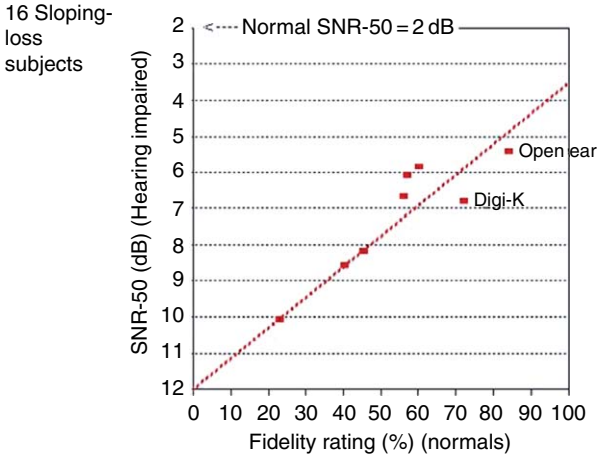

Figure 4 Intelligibility versus fidelity rating for different hearing aid types. SNR, signal-to-noise ratio.

3.27.3.2 Modern Digital Hearing Aids – Limitations

The most recent of the digital hearing aids is probably the cellphone, with its Dick Tracy ability to let us carry on a conversation from almost anywhere in the world. Ironically enough, the emphasis on special features, such as sending pictures, has come at the expense of further improvements in intelligibility. The severe distortion from data compression in today's cellphones results in degradation of 5–6 dB in SNR, measured with QuickSIN tests at a volume control setting of loud but OK, which generally produces maximum intelligibility. Indeed, part of the reason cellphone users speak so loudly that people around them can overhear their conversation is the frequent "what?"

response from listeners who cannot understand. (To be fair, a larger part results from the fact that the candy bar cellphones and Bluetooth cellphones have moved the microphone so far from the mouth that the transmitted SNR is degraded by 20 dB or more compared to the old Western Electric telephone handsets that picked up sound directly in front of the mouth.)

A similar problem in sound quality exists today with some digital hearing aids, whose advertised CD quality contrasts with the reality of distortion (from feedback cancellation, noise reduction, internal time-delay-induced ringing, etc.), ragged frequency response, poor overload characteristics, and improper automatic-gain-control (AGC) time delays. In one example, the AGC action was so fast that the sound of a drummer playing rhythmic shh-shh-shh-shh cymbals sounded more like a nearly continuous shhhhhhhhhhhh.

As of 2002, the typical digital hearing-aid bandwidth was restricted to only 5.8 kHz, which causes a theoretical 0.9 dB (and measured 1 dB) loss in effective SNR for actual hearing aid wearers. In one experiment, the average SNR loss from all causes for seven modern digital hearing aids was 1.7 dB compared to the results with a near-perfect-fidelity amplification system (Killion, M., 2004) using the same subjects. The subjects were 11 hearing aid wearers with flat hearing loss and 16 subjects with sloping loss (greater high-frequency loss).

A 1.7 dB SNR is equivalent to a 17% reduction in the intelligibility of words in sentences, using a test such as the QuickSIN test (Killion, M. *et al.*, 2004). For conversational speech, it represents a 27% decrease in intelligibility in marginal conditions. Fortunately, the best directional-microphone hearing aids provide 5 dB improvement in SNR by rejecting sounds from the back and sides in favor of sounds from directly in front. Interestingly enough, the hearing aids with the best signal processing often contain the best directional microphones, and the manufacturers indicate the performance as Articulation Index–Directivity Index (AI-DI) on the data sheet. (AI-DI is a method used to predict the effect of the directivity on speech recognition performance.) The average directional aids, unfortunately, use directional microphones with only about 3 dB SNR improvement, and usually do not list AI-DI on their data sheets.

Since it has only recently become common practice of audiologists to measure SNR loss, the purchaser of a hearing aid is not always warned in advance that his loss is mostly a loss of ability to hear in noise, so making the sound louder will not help much except in very quiet situations. The patient's high expectations are not always tempered by realistic advice, whether the hearing aids are analog or digital.

3.27.3.3 Modern Digital Hearing Aids – Improvements

Three improvements brought about by the use of digital signal processing are: (1) significant reduction in feedback without reducing the average high-frequency response, (2) the automatic sensing of listening conditions in order to change the circuit configuration, (3) the smoothing of the frequency response and tailoring the response to the desired real-ear response for near-perfect fidelity (used in only a few hearing aids).

What is the practical significance of these improvements? While some feedback reduction schemes accomplish the result by filtering out high-frequency sounds (and thus muffling the incoming speech), the better ones provide increased gain without feedback when the seal of the eartip in the earcanal is lost by chewing, yawning, or even smiling. Thus the better designs represent a real advance for the user with moderate–severe hearing loss. In addition, the improved feedback-rejection methods permit open-ear fittings, where only a thin tube goes into the ear from a behind-the-ear hearing aid. It is now practical to obtain enough gain without feedback for open-ear fittings to be useful for many patients with mild–moderate high-frequency hearing loss. This type of fitting has become increasingly common in recent years, approaching 25% of fittings today.

The automatic sensing of listening conditions has been a boon for many listeners who cannot easily decide (or remember) when to switch between omni- and directional-microphone operation, giving them the optimum omni operation in quiet conditions and directional operation for noisy conditions.

Although digital noise reduction schemes sound attractive in advertisements, to date none has shown any ability to improve intelligibility in noise (except where the hearing aid had been misfit and a side effect of the processing was to improve the fitting). And it is unlikely that any will provide intelligibility improvement in the future, until the hearing-aid circuit can recognize and differentiate between speakers. To explain: most of us have had the experience at a party of hearing the person in front of us drone on tediously, and finding ourselves listening to the left and right for a more interesting conversation (while nodding politely to the person in front at appropriate times). Without

recognition of the speaker by the hearing aid, there is no way for the hearing aid circuit to decide which voice is the desired speech and which voices are part of the interfering babble to be suppressed. The best noise-reduction schemes we have tested do little harm, but no good. The worst cause serious degradation of intelligibility in noise (recall Figure 4).

3.27.4 Satisfaction and Technology

Available surveys show a nearly constant 60% of hearing-aid wearers are satisfied overall (Figure 5). This percentage goes back to as early as 1968, when many people wore body or eyeglass hearing aids, although differences in survey methods prevent direct comparison among the surveys except for the last four conducted by Kochkin K. (2002). Kochkin's surveys cover the period of the transition from analog aids to digital aids, and suggest that the introduction of digital hearing aids did not increase overall satisfaction.

The explanation for these disappointing results appears to lie in the wearer's hearing aid expectations as much as in the hearing aids. Back in 1944, when it was considered a miracle that a simple body-worn hearing aid could provide so much benefit, Hughson W. and Thompson E. (1944) reported a 90% satisfaction rate among those who had purchased their hearing aids from a hospital clinic.

The above history is pertinent today, because for some time hearing aids have solved the audibility part of the hearing loss, but exacerbated the problem of hearing in noise because of their narrow bandwidth. Many hearing-aid input circuits (analog or analog-to-digital converters) are designed to be distortion-free only up to 85–90 dB SPL. At a noisy party where overall levels of 90 dB SPL are not uncommon and resulting speech-peaks reach 100–105 dB, this design choice appears to explain the report of some hearing aid wearers that under those conditions they hear better without their hearing aids. The author has estimated that a deficit equivalent to 6–10 dB in SNR was introduced by the frequency response and distortion of early hearing aids. They were a boon in quiet to those with pure conductive loss (e.g., otosclerosis) and the early carbon-mic aids could handle inputs of 115 dB SPL, but those aids would have been nearly worthless in noise to someone with a 10 dB SNR loss. Indeed, early authors strongly cautioned against fitting someone with nerve deafness, the term used at the time for what we now call sensorineural loss, because of the high failure rate of such fittings. Virtually all hearing aids at the time of Hughson's report were fitted to those with conductive loss; virtually none to those with nerve deafness.

Today, the opposite is true. Because of medical alleviation of most conductive losses, virtually all hearing aids are fitted to those with sensorineural hearing loss, 50% of whom have a 5 dB SNR loss or greater. For those with 0–5 dB SNR loss, their primary problem will be difficulty in hearing quiet sounds and they may be well satisfied with nearly any reasonable hearing aid circuit if properly fitted, especially if the aids contain good directional microphones.

But 40% of hearing aid wearers are dissatisfied with their hearing aids. This includes an estimated 12–16% of US owners who put away their aids in dresser drawers (Kochkin, K., 2000), and an estimated

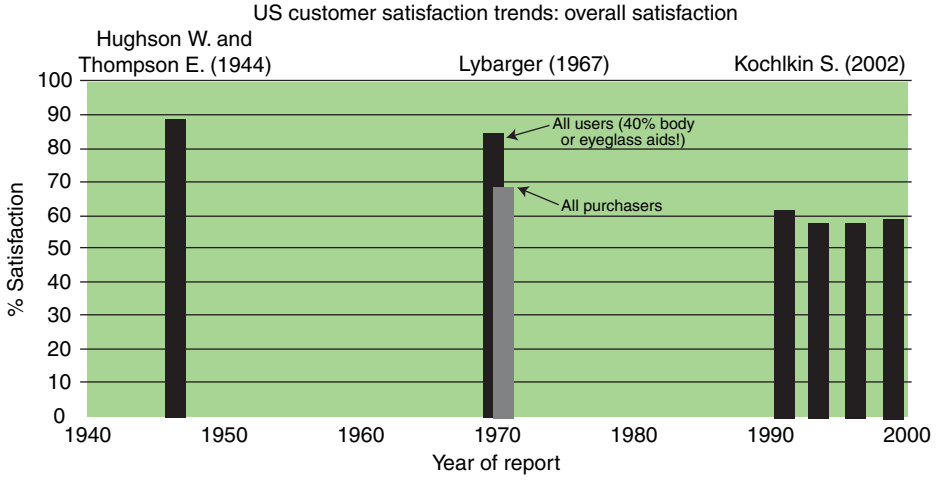

Figure 5 Percentage overall satisfaction with user's hearing aids: data over the years.

25% of owners in England who do the same thing (Davis, A., 2006). Those nonusers presumably include persons whose hearing aids were not properly fitted (or were inappropriate to the loss); those whose earmold fit does not prevent feedback or does not prevent a hollow voice sound; and a small percentage who will not be satisfied with having to wear a hearing aid under any circumstances.

The most important reason for dissatisfaction by those with SNR loss in the 10–15 dB range is their resultant inability to understand speech in the presence of noise at restaurants, parties, etc. Some report that they take off their hearing aids in loud social situations where audibility is not a problem but their inability to separate speech from noise (typically interfering with speech) is. For such persons, the better analog aids and the best digital aids fail equally under those high-noise circumstances: the hearing aids may be solving a problem they do not have in high-level noise (audibility), while failing to solve the problem they do have (SNR loss).

Not surprisingly, user surveys show no difference in overall satisfaction between low-priced analog and high-priced digital hearing aids (Figure 6). One finding is that both types of hearing aids containing directional microphones (Ana Dir and Dig Dir) produce the highest overall satisfaction. Many of the claims that digital circuits are better than analog circuits appear unfounded, based on intelligibility in noise testing, listening tests, and satisfaction ratings.

However, the better digital aids today provide sophisticated feedback reduction that does not simultaneously reduce audibility or intelligibility, and many persons appreciate the convenience of having a digital circuit analyze the sound environment and adjust the hearing aid to the processing the manufacturer has chosen for that environment (directional microphones versus omni microphones), rather than having to readjust the controls. Indeed studies show that many owners of directional hearing aids need this self-adjustment, because they simply leave the hearing aid in the omni setting all the time, even under circumstances when the directional setting would presumably improve their sentence intelligibility by 50–80% (Killion, M. C., *et al.*, 1998).

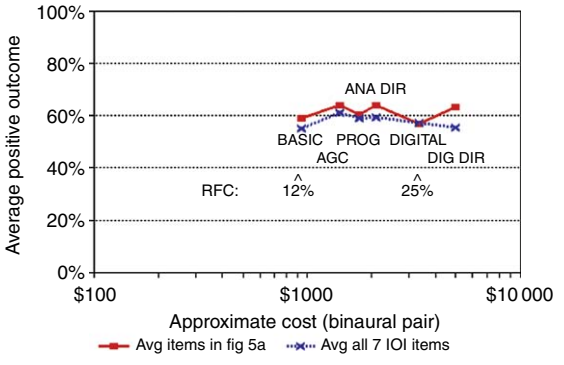

Figure 6 Percentage overall satisfaction as a function of hearing aid cost and technology. No increase with cost or technology is apparent From Van Vliet, D. 2002. User satisfaction as a function of hearing aid technology. Paper presented at: American Auditory Society Scientific/Technology Meeting, 14–16, March, 2002, Scottsdale, AZ.

3.27.5 Over-the-Counter Hearing Aids

Nearly everyone who needs reading glasses in the US gets them, often from the local pharmacy. This option was debated years ago, but no-one now suggests that purchasing over-the-counter (OTC) reading glasses has caused medical damage to the buyers, that they must see a professional to obtain properly fitted reading glasses, that they will be discouraged from buying another pair out of disappointment with the first pair they try, or that OTC reading glasses will destroy the professions of optometry and ophthalmology. Yet analogous arguments have been used to argue the alleged dangers of OTC hearing aids.

Only about 20% of those who need hearing aids in the US choose to purchase them. Several explanations have been offered: the high cost of professionally dispensed hearing aids, a reluctance to see any medical professional, and the failure of friends to be satisfied with their own hearing aids are among them.

With regard to the possible effect of cost, in the US 4.1 persons per 1000 are fitted with one or two hearing aids. Twice that percentage (8.6 per 1000) are fitted with aids in England and three times that percentage (12.4 per 1000) are fitted in Denmark. In both countries hearing aids are free; in the US they cost an average of nearly $3000 a pair (Arlinger, S., 2006). The fact that it takes up to 6 months to get an appointment for a hearing aid fitting in England may influence the lower rate in England.

The percentage of persons who need hearing aids that actually obtain hearing aids can be estimated if the average lifetime of the hearing aids is known. Such an estimate is shown in Table 1, assuming an average life of either 4 years or 7 years for the hearing aids. It appears that 16–29% of those who need hearing aids obtain them in the US, 34–60% in England, and 50–87% in Denmark.

Table 1 Estimate of percentage of those needing hearing aids who get them, assuming the average life of hearing aids is 4 years and 7 years

Country	*# Persons fitted per 1000 inhabitants*	*Percentage ot those needing hearing aids who obtain them if life=*	
		4 years	*7 years*
Sweden	6.3	25%	44%
Denmark	12.4	50%	87%
Norway	7.5	30%	53%
Finland	2.7	11%	19%
Poland	1.3	5%	9%
Netherlands	5.2	21%	36%
Belgium	2.6	10%	18%
Germany	5.5	22%	38%
England	8.6	34%	60%
France			
Australia	8.6	34%	60%
Ontario, Canada	3.9	15%	27%
USA	4.1	16%	29%

Data from Arlinger, S. 2006. A survey of public health policy on bilateral fittings and comparison with market trends: the evidence-base required to frame policy. Int. J. Audiol. 45, S45–S48.

With regard to the possibility that reluctance to see professionals causes the low usage rate in the US, national Medicare statistics indicate that some 60% of those with significant hearing loss have already seen an otolaryngologist, audiologist, or hearing aid specialist, suggesting that most persons who need hearing aids have already received a recommendation to obtain them but chose not to (Freeman, B., 2006, personal communication).

With regard to the argument that only a professional can properly decide if a hearing aid is appropriately fitted, the fact that some 25% of high-end digital hearing aid purchasers return their aids for credit suggests that consumers can and do decide for themselves when a product provides satisfactory service. Similarly, the McLaughlin W. (1995) survey of mail-order hearing aid customers found a satisfaction level of 78%; significantly higher than the 60% reported satisfaction for professionally dispensed hearing aids. One might speculate that obtaining a reasonably adequate hearing aid at one-tenth the price is more satisfactory than obtaining a presumably better fitted digital hearing aid from a professional for $3000.

3.27.6 The Future

Hearing aids at all prices already provide a solution to hearing the quiet sounds that are otherwise missing: grandchildren, quiet speech, and even the songs of distant birds. The better directional-microphone hearing aids can provide significant help for those whose hearing problems include great difficulty understanding speech in noise. In the near future, the technology of assistive listening devices with a microphone for each of three or more talkers will make it possible for virtually everyone having difficulty hearing in noise to enjoy going out to noisy restaurants again.

References

Arlinger, S. 2006. A survey of public health policy on bilateral fittings and comparison with market trends: the evidence-base required to frame policy. Int. J. Audiol. 45, S45–S48.

Davis, A. 2006. Modernizing hearing health care: epidemiological and public health consideration. Hearing Care for Adults: An International Conference, Chicago, IL, November 13–15.

Hughson, W. and Thompson, E. 1944. Hearing aids. Arch. Otolaryngol. 39, 245–249.

Killion, M. 2004. Myths that discourage improvements in hearing aid design. Hear. Rev. 11, 32–40.

Killion, M., Niquette, P., Gudmundsen, G., Revitt, L., and Banerjee, S. 2004. Development of a quick speech-in-noise test for measuring signal-to-noise ratio loss normal-hearing and hearing-impaired listeners. J. Acoust. Soc. Am. 116, 2395–2405.

Killion, M. C., Schulein, R., Christensen, L. A., Fabry, D., Revit, L., Niquette, P., and Chung, K. 1998. Real-world performance of an ITE directional microphone. Hear. J. 51, 24–38.

Kochkin, K. 2000. MarkeTrak V: why my hearing aids are in the drawer: the consumers' perspective. Hear. J. 53, 34–42.

Kochkin, S. 2002. 10-Year customer satisfaction trends in the U.S. hearing instrument market. Hear. Rev. 9, 14–25.

McLauchlan, W. 1995. Customer satisfaction and benefit with direct-by-mail hearing instruments. Survey conducted by McLauchlan & Assoc., Cincinnati, OH.

Van Vliet, D. 2002. User satisfaction as a function of hearing aid technology. Paper presented at: American Auditory Society Scientific/Technology Meeting, 14–16, March 2002, Scottsdale, AZ.

Wilber, L. A., Kruger, B., and Killion, M. C. 1998. Reference thresholds for the ER-3A insert earphone. J. Accoust. Soc. Am. 83, 669–676.

3.28 Sensory Regeneration in the Vertebrate Ear

M E Warchol, Washington University School of Medicine, St. Louis, MO, USA

© 2008 Elsevier Inc. All rights reserved.

3.28.1	Ongoing Hair Cell Production in the Ears of Cold-Blooded Vertebrates	485
3.28.2	Regeneration in the Avian Ear	485
3.28.3	Regulation of Supporting Cell Proliferation	486
3.28.4	Recovery of Hair Cells and Sensory Function	487
3.28.5	Regeneration in the Absence of Cell Proliferation	487
3.28.6	Summary	488
References		488

3.28.1 Ongoing Hair Cell Production in the Ears of Cold-Blooded Vertebrates

The production and replacement of hair cells in the mature ear was first demonstrated in cold-blooded vertebrates. Fishes and amphibians continue to grow throughout life and, as a consequence, new cells are continuously added to most tissues and organ systems. Postembryonic production of hair cells has been observed in the ear of fishes (e.g., sharks, Corwin, J. T., 1981; rays, Corwin, J. T., 1983; teleost fish, Popper, A. N. and Hoxter, B., 1984), frogs (Lewis, E. R. and Li, C. W., 1973), and toads (Corwin, J. T., 1985). The majority of newly produced hair cells arise from division of precursor cells near the edges of the sensory epithelia (e.g., Popper, A. N. and Hoxter, B., 1984; Corwin, J. T., 1985). Given this potential for postembryonic hair cell generation, it is not surprising that these sensory organs can also regenerate lost hair cells (Baird, R. A. *et al.*, 2000; Taylor, R. R. and Forge, A., 2005). All of these studies clearly demonstrate that hair cell production is not necessarily confined to embryonic development, but their direct relevance to warm-blooded vertebrates is unclear. The addition and regeneration of hair cells in mature fishes and amphibians might simply be a consequence of their ongoing growth.

3.28.2 Regeneration in the Avian Ear

Interest in the potential for sensory regeneration in the ear was heightened by the demonstration that the cochlea and vestibular organs of birds can replace hair cells after acoustic overstimulation or treatment with ototoxic antibiotics. Like their counterparts in mammals, the sensory organs of the avian ear do not exhibit continued growth during mature life; hair cell production is mainly confined to a fixed period of embryonic development. Unlike mammals, however, the mature avian ear can quickly generate new hair cells after injury (Cotanche, D. A., 1987; Cruz *et al.*, 1987; Corwin, J. T. and Cotanche, D. A., 1988; Ryals, B. M. and Rubel, E. W., 1988; Weisleder, P. and Rubel, E. W., 1993). Regeneration in the both avian cochlea and vestibular organs has been extensively studied and appears to involve very similar mechanisms. Loss of hair cells leads to an increase in the proliferation of nearby epithelial supporting cells (Figure 1). This response occurs very quickly; supporting cells can enter the S-phase of the cell cycle as early as 12–16 h after hair cell death (Warchol, M. E. and Corwin, J. T., 1996). Also, the number of proliferating cells is related to the extent of the hair cell lesion. Studies of utricles maintained in organ culture have demonstrated that about 1000 supporting cells are in the S-phase of the cell cycle at 48 h after a high-dose streptomycin treatment (Matsui, J. I. *et al.*, 2000). Present evidence suggests that these proliferating supporting cells serve as progenitors for replacement hair cells. They may undergo several rounds of cell division, but ultimately some of the newly divided cells go on to differentiate as hair cells. Once the original hair cell population has been restored, the proliferation of these progenitors ceases. Notably, similar ototoxic injury to the mammalian vestibular organs also leads to the proliferation of supporting cells, but the overall level of cell division is much lower than that observed in the avian ear (e.g., Warchol, M. E. *et al.*, 1993). Finally, there is no evidence for injury-evoked proliferation of supporting cells within the mammalian cochlea (Roberson, D. W. and Rubel, E. W., 1994).

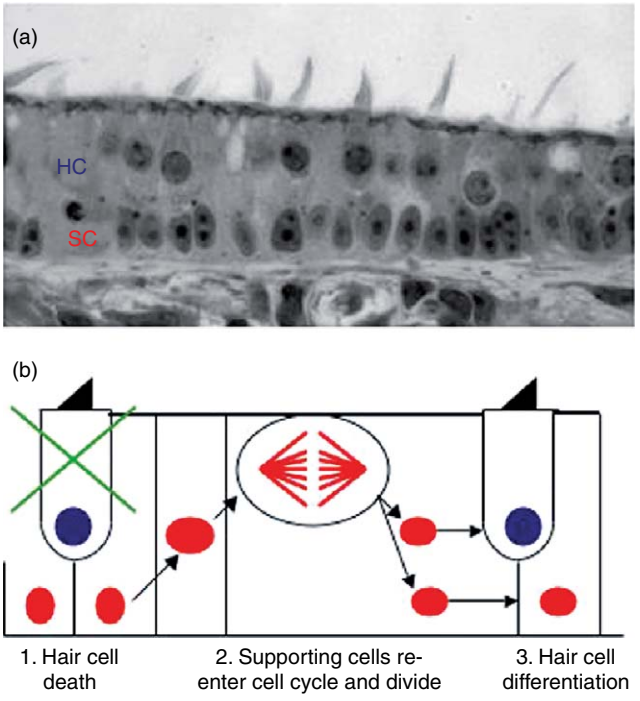

Figure 1 (a) Cross-section of the vertebrate utricle. Hair cell (HC) nuclei reside in the upper stratum of the sensory epithelium, while supporting cell (SC) nuclei are mainly confined to the lower stratum. (b) After hair cell injury, supporting cell nuclei begin to synthesize new DNA and ascend toward the lumenal surface. Cell division takes place near the lumen. The progeny then begin to descend and differentiate as replacement hair cells and supporting cells.

3.28.3 Regulation of Supporting Cell Proliferation

Since proliferation of supporting cells can lead to the production of new hair cells, it is of great interest to understand how cell cycle entry is regulated within the supporting cell phenotype. Much attention has focused on possible signaling near the sites of cell–cell junctions. In the avian ear, all hair cells are linked to their neighboring supporting cells via cell adhesion molecules of the cadherin family (e.g., Raphael, Y. *et al.*, 1988; Warchol, M. E., 2002). Once they die, hair cells are either extruded from the epithelium or are engulfed by nearby supporting cells. In either case, the cadherin-mediated junctions between hair cells and adjoining supporting cells will be disrupted and this may be the initial injury signal. Consistent with this notion, studies of supporting cells in primary culture have indicated that maintenance of N-cadherin-mediated contact is a negative regulator of supporting cell proliferation (Warchol, M. E., 2002). Tyrosine phosphorylation, another common early signaling event in cell cycle entry, is also observed at cell–cell junctions in cultures of proliferating sensory epithelia (Warchol, M. E., 2002). Finally, the proliferation of cultured supporting cells is inversely proportional to the local cell density, suggesting that the ability of a cell to expand its cytoplasm and cytoskeleton can regulate proliferation (Warchol, M. E., 2002). This observation is notable because the apical surfaces of avian supporting cells also contain a novel receptor tyrosine phosphatase, which might deactivate tyrosine kinases (and suppress proliferation) when cells are packed together at high densities (Kruger, R. P. *et al.*, 1999).

The proliferation of nontransformed cells is normally regulated by peptide mitogens, and cultures of such cells typically stop proliferating unless exogenous mitogens are added to the culture medium. In contrast, studies of cultured utricles and their isolated sensory epithelia have suggested that supporting cells produce their own mitogens, which then act in an autocrine or paracrine fashion (Warchol, M. E. and Corwin, J. T., 1993; Warchol, M. E., 1995). The identity of the mitogens(s) that regulate proliferation in the avian ear remains uncertain. Proliferation of cultured supporting cells can be moderately increased by treatment with insulin, insulin-like

growth factor-1 (IGF-1), transforming growth factor-α (TGF-α), and tumor necrosis factor-α (TNF-α; Oesterle, E. C. *et al.*, 1997; Warchol, 1999), and decreased by treatment with fibroblast growth factor-2 (FGF2) and transforming growth factor-β1 (TGF-β1; Warchol, M. E., 1999; Oesterle, E. C. *et al.*, 2000). Unfortunately, there is little direct evidence to date for the involvement of any of these factors in the regenerative process *in vivo*.

More recent studies have focused on identification of downstream signaling pathways that are activated in response to injury. Signaling via a cyclic-adenosine monophosphate (AMP)-dependent pathway can induce proliferation in the avian cochlea and the mammalian vestibular organs (Navaratnam *et al.*, 1996; Montcouquiol, M. and Corwin, J. T., 2001a). Activation of the phosphatidylinosital-3-kinase (PI3-K) is also required for supporting cell proliferation (Montcouquiol, M. and Corwin, J. T., 2001b; Witte, M. C. *et al.*, 2001). In addition, several transcription factors have been implicated in regenerative proliferation. The homeoboxlike factor cPROX1 is expressed in hair cell progenitors during both embryonic development and regeneration (Stone, J. S. *et al.*, 2004). The paired box factor PAX2 is associated with regions of cell proliferation in the developing inner ear (Li, H. *et al.*, 2004), and expression of this factor is maintained in the vestibular organs of mature birds (Warchol, M. E., 2007). At present, several groups are using microarray methodology to examine large-scale changes in gene expression during regeneration (e.g., Hawkins, R. D. *et al.*, 2003). Such studies have the potential to identify the specific regulatory pathways that promote regeneration in the avian ear.

3.28.4 Recovery of Hair Cells and Sensory Function

Supporting cells continue to proliferate for several days after hair cell injury. Beginning about 48–72 h after injury, a subset of the progeny start to differentiate as replacement hair cells. In the chick cochlea, new hair cells are observed as early as 3 days after acoustic injury and reasonably complete repair of the sensory epithelium is apparent after about 10–14 days (Cotanche, D. A., 1987; Corwin, J. T. and Cotanche, D. A., 1988). Because they require systemic treatment with ototoxic drugs, studies of regeneration in the avian vestibular organs typically involve longer time courses. Treatment for 5–7 days with a moderate dose of streptomycin results in the death of nearly all hair cells in the striolar region of the utricle (e.g., Weisleder, P. and Rubel, E. W., 1993; Matsui, J. I. *et al.*, 2003). Hair cells in this region begin to reappear after about 2 weeks, but recovery is still incomplete after 8 weeks (Warchol, M. E. and Speck, J. D., 2007). Specification of hair cell phenotype in the regenerating ear is accomplished via a Notch–Delta interaction, whereby a differentiating hair cell actively inhibits its neighboring cells from taking on a hair cell phenotype (Stone, J. S. and Rubel, E. W., 1999). A very similar mechanism specifies hair cell fate during embryonic development (Adam, J. *et al.*, 1998). Finally, numerous studies have demonstrated nearly complete return of auditory and vestibular function after regeneration (reviewed in Bermingham-McDonogh, O. and Rubel, E. W., 2003).

3.28.5 Regeneration in the Absence of Cell Proliferation

Most studies of regeneration in the hair cell epithelia of fishes, amphibians, and birds have pointed to a key role for supporting cell proliferation in the regenerative process. Thus, it is somewhat surprising that a significant amount of hair cell recovery can be observed in these organs even when cell proliferation has been blocked by treatment with antimitotic drugs (e.g., Adler, H. J. *et al.*, 1997; Steyger, P. S. *et al.*, 1997; Baird, R. A. *et al.*, 2000). Also, during ordinary regeneration, a small number of new hair cells can be produced by means other than proliferation (Roberson, D. W. *et al.*, 2004; Taylor, R. R. and Forge, A., 2005). In both of these cases, regenerated hair cells appear to arise by (at least) two distinct mechanisms. First, aminoglycoside treatment does not always lead to the complete death of target hair cells. Instead, a subset of injured hair cells appear to lose their stereociliary bundles and cuticular plates, but remain alive within the sensory epithelia. These surviving hair cells can then grow new stereocilia bundles (Zheng, J. L. *et al.*, 1999; Gale, J. E. *et al.*, 2002). Also, some supporting cells appear to be capable of changing directly into new hair cells, without first undergoing proliferation (e.g., Adler, H. J. *et al.*, 1997; Li, L. and Forge, A., 1997; Roberson, D. W. *et al.*, 2004). The cellular basis of phenotypic conversion has been particularly difficult to study, since there is no unambiguous method of labeling and identifying cells that have undergone a phenotypic change.

3.28.6 Summary

Although much has been learned about the basic biology of hair cell regeneration, most of the fundamental questions remain unanswered. Taken together, the results summarized above suggest that regenerative ability is critically linked to the capacity for cellular proliferation within the mature ear, even when replacement hair cells are not produced via cell division. One key unanswered question is: how is cell cycle entry differentially regulated within the supporting cells of mammals and nonmammals? In order to resolve this issue, it will first be necessary to identify the signaling pathways and transcriptional regulators that maintain the differentiated state and/or permit proliferation in nonmammalian supporting cells. Finally, it is notable that mammals are the only vertebrates that lack the capacity for hair cell regeneration. This suggests that regenerative ability is the default condition of vertebrate ear, and it will be of great interest to understand why regenerative ability has been lost from the mammalian ear and which genetic modifications are responsible for its absence.

Acknowledgments

Work in the author's laboratory was supported by grants from the NIH/NIDCD, NASA, and the National Organization for Hearing Research.

References

Adam, J., Myat, A., Le Roux, I., Eddison, M., Henrique, D., Ish-Horowicz, D., and Lewis, J. 1998. Cell fate choices and the expression of Notch, Delta and Serrate homologues in the chick inner ear: parallels with Drosophila sense-organ development. Development 125, 4645–4654.

Adler, H. J., Komeda, M., and Raphale, Y. 1997. Further evidence for supporting cell conversion in the damaged avian basilar papilla. Int. J. Dev. Neurosci. 15, 375–385.

Baird, R. A., Burton, M. D., Fashena, D. S., and Naeger, R. A. 2000. Hair cell recovery in mitotically-blocked cultures of the bullfrog saccule. Proc. Natl. Acad. Sci. U. S. A. 97, 11722–11729.

Bermingham-McDonogh, O. and Rubel, E. W. 2003. Hair cell regeneration: winging our way towards a sound future. Curr. Opin. Neurobiol. 13, 119–126.

Corwin, J. T. 1981. Postembryonic production and aging in inner ear hair cells in sharks. J. Comp. Neurol. 201, 541–553.

Corwin, J. T. 1983. Postembryonic growth of the macula neglecta auditory detector in the ray, *Raja clavata*: continual increases in hair cell number, neural convergence, and physiological sensitivity. J. Comp. Neurol. 217, 345–356.

Corwin, J. T. 1985. Perpetual production of hair cells and maturational changes in hair cell ultrastructure accompany postembryonic growth in an amphibian inner ear. Proc. Natl. Acad. Sci. U. S. A. 82, 3911–3915.

Corwin, J. T. and Cotanche, D. A. 1988. Regeneration of sensory hair cells after acoustic trauma. Science 240, 1772–1774.

Cotanche, D. A. 1987. Regeneration of hair cell stereociliay bundles in the chick cochlea following severe acoustic trauma. Hear. Res. 30, 181–195.

Cruz, R. M., Lambert, P. R., and Rubel, E. W. 1987. Light microscopic evidence of hair cell regeneration after gentamicin toxicity in chick cochlea. Arch. Otolaryngol. Head Neck Surg. 113, 1058–1062.

Gale, J. E., Meyers, J. R., Periasamy, A., and Corwin, J. T. 2002. Survival of bundleless hair cells and subsequent bundle replacement in the bullfrog's saccule. J. Neurobiol. 50, 81–92.

Hawkins, R. D., Bashiardes, S., Helms, C. A., Hu, L., Saccone, N. L., Warchol, M. E., and Lovett, M. 2003. Gene expression differences in quiescent versus regenerating hair cells of avian sensory epithelia: implications for human hearing and balance disorders. Hum. Mol. Genet. 12, 1261–1272.

Kruger, R. P., Goodyear, R. J., Legan, P. K., Warchol, M. E., Raphael, Y., Cotanche, D. A., and Richardson, G. P. 1999. The supporting cell antigen: a receptor-like protein phosphatase expressed in the sensory epithelia of the avian inner ear. J. Neurosci. 19, 4815–4827.

Lewis, E. R. and Li, C. W. 1973. Evidence concerning the morphogenesis of saccular receptors in the bullfrog (*Rana catesbeiana*). J. Morphol. 139, 351–361.

Li, L. and Forge, A. 1997. Morphological evidence for supporting cell to hair cell conversion in mammalian utricular maculae. Int. J. Dev. Neurosci. 15, 433–446.

Li, H., Liu, H., Corrales, C. E., Matai, H., and Heller, S. 2004. Correlation of Pax-2 expression with cell proliferation in the developing chicken inner ear. J. Neurobiol. 60, 61–70.

Matsui, J. I., Haque, A., Huss, D., Messana, E. P., Alosi, J. A., Roberson, D. W., Cotanche, D. A., Dickman, J. D., and Warchol, M. E. 2003. Caspase inhibitors promote vestibular hair cell function and survival following aminoglycoside treatment *in vivo*. J. Neurosci. 23, 6111–6122.

Matsui, J. I., Oesterle, E. C., Stone, J. S., and Rubel, E. W. 2000. Characterization of damage and regeneration in cultured avian utricles. J. Assoc. Res. Otolaryngol. 1, 46–63.

Montcouquiol, M. and Corwin, J. T. 2001a. Brief treatments with forskolin enhance S-phase entry in balance epithelial form the ears of rats. J. Neurosci. 21, 974–982.

Montcouquiol, M. and Corwin, J. T. 2001b. Intracellular signals that control cell proliferation in mammalian balance epithelia: key roles for phosphatidylinositol-3 kinase, mammalian target of rapamycin, and S6 kinases in preference to calcium, protein kinase C, and mitogen-activated protein kinase. J. Neurosci. 21, 570–580.

Navaratnam, D. S., Su, H. S., Scott, S. P., and Oberhottzer, J. C. 1996. Proliferation in the auditory receptor epithelium mediated by a cyclic AMP-dependent signaling pathway. Nat. Med. 2, 1136–1139.

Oesterle, E. C., Bhave, S. A., and Coltrera, M. D. 2000. Basic fibroblast growth factor inhibits cell proliferation in cultured avian inner ear sensory epithelia. J. Comp. Neurol. 424, 307–326.

Oesterle, E. C., Tsue, T. T., and Rubel, E. W. 1997. Induction of cell proliferation in avian inner ear sensory epithelia by insulin-like growth factor-I and insulin. J. Comp. Neurol. 380, 262–274.

Popper, A. N. and Hoxter, B. 1984. Growth of a fish ear. 1. Quantitative analysis of hair cell and ganglion cell proliferation. Hear. Res. 15, 133–142.
Raphael, Y., Volk, T., Crossin, K. L., Edelman, G. M., and Geiger, B. 1988. The modulation of cell adhesion molecule expression and intercellular junction formation in the developing avian inner ear. Dev. Biol. 128, 222–235.
Roberson, D. W. and Rubel, E. W. 1994. Cell division in the gerbil cochlea after acoustic trauma. Am. J. Otolaryngol. 15, 28–34.
Roberson, D. W., Alosi, J. A., and Cotanche, D. A. 2004. Direct transdifferentiation gives rise to the earliest new hair cells in regenerating avian auditory epithelium. J. Neurosci. Res. 78, 461–471.
Ryals, B. M. and Rubel, E. W. 1988. Hair cell regeneration after acoustic trauma in adult Coturnix quail. Science 240, 1774–1776.
Steyger, P. S., Burton, M., Hawkins, J. R., Schuff, N. R., and Baird, R. A. 1997. Calbindin and parvalbumin are early markers of non-mitotically regenerating hair cells in the bullfrog vestibular otolith organs. Int. J. Dev. Neurosci. 15, 417–432.
Stone, J. S. and Rubel, E. W. 1999. Delta1 expression during avian hair cell regeneration. Development 126, 961–973.
Stone, J. S., Shang, J. L., and Tomarev, S. 2004. cProx1 immunoreactivity distinguishes progenitor cells and predicts hair cell fate during avian hair cell regeneration. Dev. Dynam. 230, 597–614.
Taylor, R. R. and Forge, A. 2005. Hair cell regeneration in sensory epithelia from the inner ear of a urodele amphibian. J. Comp. Neurol. 484, 105–120.
Warchol, M. E. 1995. Supporting cells in isolated sensory epithelia of avian utricles proliferate in serum-free culture. Neuroreport 6, 981–984.
Warchol, M. E. 1999. Immune cytokines and dexamethasone influence sensory regeneration in the avian vestibular periphery. J. Neurocytol. 28, 889–900.
Warchol, M. E. 2002. Cell density and N-cadherin interactions regulate cell proliferation in the sensory epithelia of the inner ear. J. Neurosci. 22, 2607–2616.
Warchol, M. E. 2007. Characterization of supporting cell phenotype in the avian inner ear: implications for memory regeneration. Hear. Res. 227, 11–18.
Warchol, M. E. and Corwin, J. T. 1993. Supporting cells in avian vestibular organs proliferate in serum-free culture. Hear. Res. 71, 28–36.
Warchol, M. E. and Corwin, J. T. 1996. Regenerative proliferation in organ cultures of the avian cochlea: identification of the initial progenitors and determination of the latency of the proliferative response. J. Neurosci. 16, 5466–5477.
Warchol, M. E. and Speck, J. D. 2007. Expression of GATA3 and tenascin in the avian vestibular maculae: normative patterns and changes during sensory regeneration. J. Comp. Neurol. 500, 646–657.
Warchol, M. E., Lambert, P. R., Goldstein, B. J., Forge, A., and Corwin, J. T. 1993. Regenerative proliferation in inner ear sensory epithelia from adult guinea pigs and humans. Science 259, 1619–1622.
Weisleder, P. and Rubel, E. W. 1993. Hair cell regeneration after streptomycin toxicity in the avian vestibular system. J. Comp. Neurol. 331, 97–110.
Witte, M. C., Montcouquiol, M., and Corwin, J. T. 2001. Regeneration in avian hair cell epithelia: identification of intracellular signals required for S-phase entry. Eur. J. Neurosci. 14, 829–838.
Zheng, J. L., Keller, G., and Gao, W. Q. 1999. Immunocytochemical and morphological evidence for intracellular self-repair as an important contributor to mammalian hair cell recovery. J. Neurosci. 19, 2161–2170.

Further Reading

Forge, A., Li, L., Corwin, J. T., and Nevill, G. 1993. Ultrastructural evidence for hair cell regeneration in the mammalian inner ear. Science 259, 1616–1619.
Oesterle, E. C., Cunningham, D. E., Westrum, L. E., and Rubel, E. W. 2003. Ultrastructural analysis of [3H]thymidine-labeled cells in the rat utricular macula. J. Comp. Neurol. 463, 177–195.
Stone, J. S. and Rubel, E. W. 2000. Cellular studies auditory hair cell regeneration in birds. Proc. Natl. Acad. Sci. U. S. A. 97, 11714–11721.

3.29 Treatment of Hearing Loss: Viral Transfection

D M Zeitler and A K Lalwani, New York University School of Medicine, New York, NY, USA

© 2008 Dr A. Lalwani. Published by Elsevier Inc.

3.29.1	Introduction	491
3.29.2	Viral Vectors: An Overview	492
3.29.3	Gene Therapy and Hearing Impairment: Cochlear Gene Transfer	493
3.29.4	Intracochlear Viral Gene Delivery	493
3.29.5	Cochlear Gene Therapy: Safety Considerations	495
3.29.6	Viral Gene Therapy: Preclinical Applications	496
3.29.7	Future Implications	496
References		497

Glossary

gene therapy Treatment by replacing, supplementing, or manipulating the expression of genes with the introduction of genetic material or genes.

liposomes Artificial, single or multilaminar vesicles made from lipids that can be used for the delivery of a genes to cells.

round window membrane A trilaminar membrane that separates the basal turn of the cochlea from the middle ear space.

viral vector A gene transfer vehicle composed of viral DNA and usually containing a therapeutic or experimental gene of interest.

3.29.1 Introduction

Congenital and acquired sensorineural hearing loss is the most prevalent inherited sensory disorder associated with significant morbidity and deterioration in quality of life. Despite its prevalence, therapeutic intervention is limited to assistive electrical devices such as frequency modulation (FM) systems, hearing aids, and cochlear implants that partially restore audition. While these technologies objectively and subjectively improve hearing, as well as the patient's quality of life, significant shortcomings of electrical rehabilitation remain including poor sound localization, inadequate clarity of hearing especially in background noise, and inability to appreciate complex auditory signals such as music. These technologies fail because they do not regenerate or recreate the physiologic mechanism of hearing. Gene therapy holds the promise of restoring natural, high-fidelity hearing by re-establishing normal physiology.

The potential to introduce normal genes to replace defective ones to restore normal function was suggested nearly 30 years ago by Friedmann T. and Roblin R. (1972). Over the past three decades, several lines of research elucidating normal biology and physiology of hearing have raised the expectation that gene therapy may play a role in the treatment of hearing disorders. These include the demonstration of avian inner hair cell regeneration in the late 1980s (Corwin, J. T. and Cotanche, D. A., 1988; Ryals, B. M. and Rubel, E. W., 1988) with the recent identification of handful of genes important in inner ear and hair cell development and regeneration (e.g., math1, retinoblastoma protein) (Bermingham, N. A. *et al.*, 1999; Cotanche, D. A., 1999; Kawamoto, K. *et al.*, 2003; Sage, C. *et al.*, 2006). In the 1990s, a variety of growth factors were shown to mitigate inner ear damage following ototoxic insult; however, their effect was temporally limited and waned with physiologic breakdown of the protein. Methods for increasing availability of the growth factor over time, possibly with gene therapy, were needed. Over the last decade, rapid discovery of nearly 75 genes responsible for nonsyndromic deafness has led to the elucidation of the molecular basis for hearing and hearing loss. The identification of molecular targets to arrest, prevent, or restore hearing loss has spurred the development of cellular and molecular therapies and it has come to occupy a significant portion of current otologic research.

Gene therapy is the introduction of genetic material for therapeutic benefit by the process of gene transfection. Both viral and nonviral vectors have

been used for gene transfection and each is associated with its advantages and disadvantages. The objective of this review is to examine viral gene transfection.

3.29.2 Viral Vectors: An Overview

Since Smithies O. *et al.* (1985) reported the first chromosomal gene targeting in mammalian cells in 1985, both viral and nonviral vectors have been used for the transfection of eukaryotic cells. However, viral vectors have several advantages over nonviral vectors given their innate ability to infect human cells including a specific mechanism for cell binding and entry, an efficient targeting mechanism of the transgene to the nucleus of the cell, and avoidance of intracellular degradation. Additionally, virions are able to use the host cell's machinery to express the viral genome. In order to prevent host cell lysis via immune-mediated processes, the viral agents are usually altered so that they can no longer replicate within the transduced cell. Viral gene delivery has been performed using a number of different viruses including both DNA (e.g., adeno-, adeno-associated-, and herpes) and RNA (e.g., retro- and influenza) viruses. Each is characterized by both desirable and undesirable characteristics that make them more or less suitable for gene therapy and none is ideal for all applications.

The first viral vector used for mammalian gene targeting and the prototype for viral-mediated gene transfer is the retrovirus murine leukemia virus (Ellis, J. and Berstein, A., 1989; Berkener, K. L., 1992; Merrouche, Y. and Favrot, M. C., 1992). Retroviruses are RNA viruses that are reverse transcribed into DNA and are able to integrate into the host chromosome of dividing cells. Thus, in rapidly proliferating cells such as cancer cells, they are ideal for stable long-term transgene expression and have been extensively used in both *in vivo* and *in vitro* cancer models. However, retroviral DNA expression in eukaryotic host cells has been shown to activate a cascade of sophisticated defense mechanisms designed to reject the retrovirus as foreign thereby leading to its inactivation (Bestor, T. H. and Tycko, B., 1996; Bestor, T. H., 2000). Additionally, the neurosensory epithelial cells of the cochlea are postmitotic, making retroviral vectors unsuitable for cochlear gene therapy.

Unlike other retroviral vectors, the lentiviral vector, based on the human immunodeficiency virus (HIV), can integrate into both dividing cells as well as nondividing cells leading to stable long-term expression of the transgene (Naldini, L. *et al.*, 1996). This would make the lentivirus an ideal candidate for gene transfection of the postmitotic cochlear neuroepithelia and spiral ganglions. *In vivo* infusion of the lentivirus vector via a cochleostomy into a guinea-pig cochlea revealed a highly restricted fluorescence pattern limited to the periphery of the perilymphatic space and spiral ligament suggesting limited distribution of the large virus within the cochlea or inability to transfect the other inner ear cell types (Han, J. J. *et al.*, 1999). *In vitro*, lentivirus was able to transduce auditory neurons thus suggesting that it is limited physical distribution that is responsible for the restricted transfection pattern seen. While robust in transfection efficiency and facilitates long-term transgene expression, concerns remain about the use of a HIV-based vector in human trials.

Like the retroviruses, the adenovirus is a well characterized and extensively studied viral vector for gene therapy applications; it has also been shown to be an effective vector for intracochlear gene transfer (Raphael, Y. *et al.*, 1996; Staecker, H. *et al.*, 2001). This vector is highly effective for transient gene transfer due to its capacity for introducing large foreign genes, the ability to transduce both dividing and nondividing cells with high efficiency, and the relative ease with which it can be produced in high titers (Friedmann, T., 1997). However, the transgene expression is temporally limited as adenovirus does not integrate into the host cell genome and the recombinant gene is expressed as an extrachromosomal element for a period of only several weeks. The native adenovirus also provokes a strong immune response that can cause significant tissue damage *in vivo*, thereby limiting its usefulness. Newer generations of attenuated adenovirus vectors have deleted viral sequences making them less immunogenic; however, their efficacy in the cochlear microenvironment still awaits validation.

Adeno-associated viruses (AAVs) are able to overcome some of the shortcomings of the adenovirus. AAV is a single-stranded DNA parvovirus endogenous to diverse mammalian species and is not known to cause any disease in humans. Its ability to infect and integrate into both dividing and nondividing cells with high frequency makes it an ideal candidate for work on quiescent cells of the inner ear. AAV can persist as an integrated provirus without lyses of the host cell; if the host cell is superinfected with a helper virus (adenovirus or herpes virus), the integrated AAV genome is able to carry out lytic growth. AAV

has previously been used for the long-term correction of hemophilia B in a dog model (Herzog, R. *et al.*, 1999; Mount, J. D. *et al.*, 2002; Arruda, V. R. *et al.*, 2005) and has been shown in phase I trials to result in successful, dose-dependent gene transfer of the cystic fibrosis transmembrane conductance regulator (CFTR) gene into the maxillary sinus of patients with cystic fibrosis and sinusitis (Wagner, J. A. *et al.*, 1999). A major disadvantage of AAV is its small packaging limit, restricting the size of potential transgenes to 4.5 kb of DNA.

Herpes simplex virus (HSV) is a double-stranded DNA virus with demonstrated tropism for mammalian neural tissues. HSV is a relatively large virus with several characteristics, which make it an attractive vector for gene therapy: broad host cell range with vectors that are highly infectious; the ability to infect nondividing cells with efficient transduction; a large proportion of nonessential viral genes allowing accommodation of multiple or large transgenes (Krisky, D. M. *et al.*, 1998); and the latent behavior of the virus allowing stable long-term expression of the transgene (Lachmann, R. H. and Efstathiou, S., 1997). HSV-1 has been used as a vector for inner ear gene transfer in mammals (Derby, M. L. *et al.*, 1999); however, its use is limited. These vectors are difficult to produce, have low infection efficiency, and many people have been previously infected by this virus, with subsequent immunity to various components of HSV.

3.29.3 Gene Therapy and Hearing Impairment: Cochlear Gene Transfer

The feasibility of gene therapy as a therapeutic strategy for hearing loss rests on the elucidation of the cellular and molecular targets of hearing. While much progress has been made in the last decade, and genes for both syndromic and nonsyndromic hearing loss have been discovered and proposed as potential therapeutic targets, gene therapy for hearing disorders is still not ready for clinical application. Current focus of inner ear gene therapy is largely on the manipulation of genes responsible for hair cell regeneration and the introduction of neurotrophic factors to promote neuronal survival. Nonetheless, substantial progress has been made in the exploration of the potential of gene therapy for inner ear disorders.

Lalwani A. K. *et al.* (1996) and Raphael Y. *et al.* (1996) independently reported on the feasibility of intracochlear transfection using AAV and adenovirus vectors, respectively, in the guinea-pig. Using β-galactosidase as a reporter gene, the AAV vector was found to transduce nearly all tissue types in the cochlea, including spiral limbus, spiral ligament, spiral ganglion, and the organ of Corti; however, the stria vascularis did not show transgene expression (Figure 1). The marker gene expression was shown to be present for up to 24 weeks following osmotic minipump-mediated infusion of the AAV-β-galactoside vector. Adenovirus-mediated gene transfer was characterized by expression of the reporter gene in nearly all cell types including stria vascularis; however, the expression was temporally limited and an immune response was noted. Subsequently, a variety of vectors have been successfully used to mediate gene transfer to the inner ear including AAVs (Lalwani, A. K. *et al.*, 1998a; 1998b), lentiviruses (Han, J. J. *et al.*, 1999), HSV type 1 (Geschwind, M. D. *et al.*, 1996; Jin, B. K. *et al.*, 1996; Staecker, H. *et al.*, 1998; Van de Water, T. R. *et al.*, 1999), retroviruses (Zheng, J. L. *et al.* 1998), and adenoviruses (Raphael, Y. *et al.*, 1996; Weiss, M. A. *et al.*, 1997; Yagi, M. *et al.*, 1999) and the features of viral-mediated gene transfer has been further characterized. Table 1 summarizes the characteristics of cochlear transgene expression with different viral vectors, with differences likely reflecting the unique properties of the vectors such as size of the viral particle, presence or absence of viral receptors, promoters used, or differences in host cell susceptibility to infection.

While the seminal work on auditory gene transfection was performed using guinea-pigs, subsequent studies have shifted their focus to using the mouse as the animal model. The mouse genome is better characterized than that of the guinea-pig. There are a number of available mutant mice strains with inherited hearing loss, with the genetic basis of their hearing loss identified (Avraham, K. B., 2003). Additionally, transgenic mice have been generated in order to study the knockout effect of mutant alleles on nonsyndromic and syndromic hearing loss (Anagnostopoulos, A. V., 2003).

3.29.4 Intracochlear Viral Gene Delivery

Delivery of viral vector to the cochlea can be accomplished via systemic administration of the virus, intratympanic injection, or direct intracochlear administration (Figure 2). The potential for systemic delivery of viral vector for inner ear therapy is

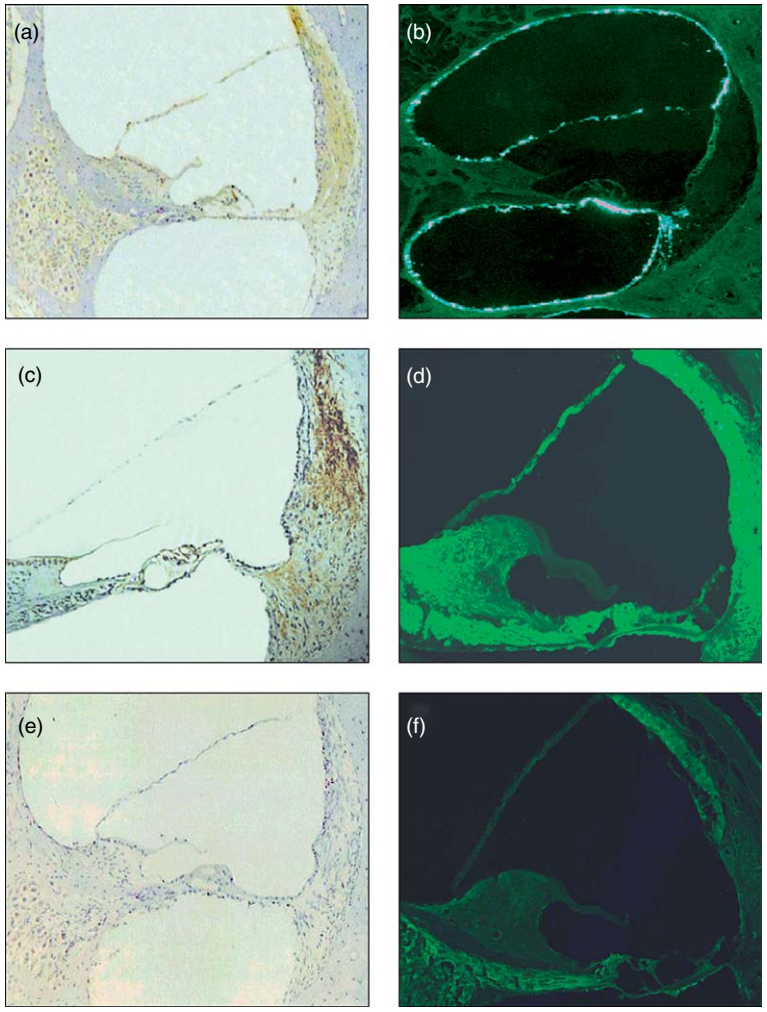

Figure 1 Intracochlear transgene expression. (a) Liposome- and (c) adeno-associated virus (AAV)-mediated beta-galactosidase (β-gal) transgene expression within guinea-pig cochleae. (b) Lentivirus- and (d) liposome-mediated humanized green fluorescent protein (GFP) transgene expression within (b) guinea-pig and (d) mouse cochleae. Transgene expression of β-gal or GFP following infusion (a–c) and direct instillation through the intact round window membrane (d) is seen ipsilaterally in the cochleae, but not in the control cochleae (e, f). Reprinted with permission from Anil K. Lalwani, MD, New York University School of Medicine.

Table 1 Transfection of cochlear cells and tissues by viral vectors

Vector	*Hair cells*	*Supporting cells*	*Auditory neurons*	*Stria vascularis*	*Reissner's membrane*	*Spiral ligament*	*Immune response*
AAV	+	+	+	−	+	+	−
Adenovirus	+	+	+	+	+	+	+
Herpes virus	−	+	+	−	+	+	+
Vaccinia	+	+	−	−	+	+	+
Lentivirus	−	−	+	−	+	+	−
Liposomes	+	+	+	−	+	+	−

AAV, adeno-associated virus.

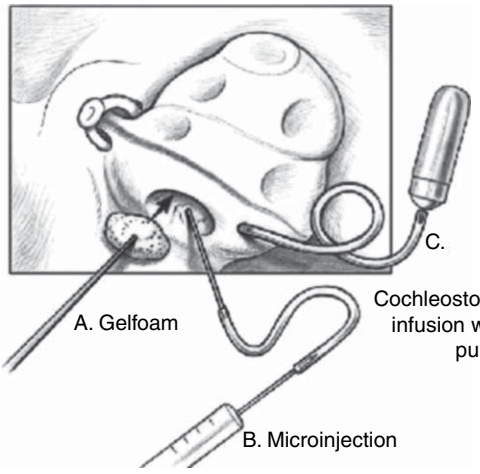

Figure 2 Routes of delivery for cochlear gene therapy. The delivery of a therapeutic agent to the cochlea can be performed by: direct instillation of the agent through an intact round window membrane with a gelatin sponge (A); direct injection through the round window membrane (B); and, infusion with osmotic minipump through cochleostomy (C). Reprinted with permission from Anil K. Lalwani, MD, New York University School of Medicine.

hampered by the blood–cochlear barrier preventing efficient delivery, the relatively limited cochlear blood flow compared to the remainder of circulation, and potential for unwanted systemic toxicity (Wareing, M. J. and Lalwani, A. K., 1999). Intratympanic delivery with subsequent diffusion of the vector across the round window membrane (RWM) is attractive as it avoids systemic toxicity. This route has the additional advantage of significant prior clinical experience as various pharmacotherapeutic agents (e.g., aminoglycosides, steroids) are routinely administered in this manner (Jero, J. *et al.*, 2001a). However, the permeability of RWM is quite variable depending on the conditions of the middle ear, the anatomy of the area, the presence or absence of mucosal adhesions obstructing the round window, and the nature of the administered agent including its charge and size. Direct gene transfer to the inner ear via injection or perfusion through a cochleostomy is conceptually preferable as the virus is delivered directly to the organ of interest with restricted distribution; the dose of the virus can also be controlled. However, direct intracochlear introduction can be associated with hearing loss.

To date, several methods of *in vivo* gene delivery to the inner ear have been tested. Most studies have used either a cochleostomy through the basal turn of the scala tympani (Lalwani, A. K. *et al.*, 1996; Carvalho, G. J. and Lalwani, A. K., 1999; Han, J. J. *et al.*, 1999) or via the RWM in order to deliver the vector to the perilymphatic space (Raphael, Y. *et al.*, 1996; Derby, M. L. *et al.*, 1999; Yagi, M. *et al.*, 1999). Other methods such as endolymphatic sac injection (Yamasoba T. *et al.*, 1999), posterior semicircular canalostomy (Kawamoto, K. *et al.*, 2001), and scala media injection via cochleostomy (Ishimoto, S. *et al.*, 2002) have also been attempted with varying success. Due to the small volume of perilymphatic fluid within the scala tympani of mice and guinea-pigs (~5 and 12 µl respectively) (Thorne, M. *et al.*, 1999), infusion methods such as osmotic minipumps (Davies, E. *et al.*, 1994) and microinjections are used with RWM or scala tympani exposure in order to protect against disturbance of the delicate fluid homeostasis. Despite these precautions, introduction of viral vectors with a miniosmotic pump through a cochleostomy has been shown to incite an inflammatory response and connective tissue deposition adjacent to the site (Davies, E. *et al.*, 1994) as well as causing a mild to marked rise in ABR thresholds at mid- and high frequencies, respectively (Carvalho, G. J. and Lalwani, L. K., 1999). Recently, noninvasive infusion of the gene vector via gelfoam soaked with a therapeutic agent against the round window has been demonstrated with minimal elevation of postoperative ABR thresholds. This technique is minimally invasive, avoids direct manipulation of the cochlear apparatus and iatrogenic hearing loss, as well as reduces dissemination outside the target cochlea, making it a clinically viable option for human gene therapy in the future (Jero, J. *et al.*, 2001a; 2001b).

3.29.5 Cochlear Gene Therapy: Safety Considerations

Lalwani A. K. *et al.* (1996) initially reported the potential of transgene expression at a distant site following cochlear infusion of viral vector. Utilizing AAV as the gene therapy vector, they observed transgene expression within the contralateral cochlea of the AAV-perfused animal, albeit much weaker than within the directly perfused cochlea (Lalwani, A. K. *et al.*, 1996). Expression of the transgene within the contralateral cochlea raises concern about the risks associated with dissemination of the virus from the target tissue. The appearance of the virus, distant from the site of infection, may be due to its hematogenous dissemination to near and distant tissues. However, this is unlikely as the viral vector was not

detected in near and distant tissues. Other possible explanations include migration of AAV via the bone marrow space of the temporal bone or via the cerebrospinal fluid (CSF) space to the contralateral ear (Kho, S. T. *et al.*, 2000). The perilymphatic space into which the virus was perfused is directly connected to the CSF via the cochlea aqueduct; transgene expression within the contralateral cochlea aqueduct has been demonstrated following introduction of the viral vector in the ipsilateral cochlea. Collectively, these results suggest potential routes for AAV dissemination from the infused cochlea via the cochlea aqueduct or by extension through the temporal bone marrow spaces. The potential for leakage from the infused cochlea can be diminished or eliminated by avoiding continuous infusion; when a smaller volume of injection was used in the cochlea, contralateral transgene expression was not seen.

3.29.6 Viral Gene Therapy: Preclinical Applications

Although viral gene therapy for hearing loss has not yet been attempted in human subjects, it has shown to be efficacious in animal models. First, several transgenic products expressed in the cochlea have been shown to protect the sensory hair cells and primary auditory neurons against atrophy and degeneration following ototoxic exposure. Using virally transduced brain-derived growth factor (BDGF) in the inner ear, Staecker H. *et al.* (1998) were able to show a survival effect on spiral ganglion neurons exposed to toxic levels of aminoglycoside. Similarly, Lalwani A. K. *et al.* (2002) demonstrated the protective effect of AAV-mediated BDNF expression on spiral ganglion neurons exposed to aminoglycoside both *in vitro* and *in vivo* with region specificity – the protection occurred predominantly at the basal turn of the cochlea with relative sparing of the middle and apical regions. Other investigators have shown protective effects of neurotrophin-3 (NT-3) (Chen X. *et al.*, 2001; Bowers, W. J. *et al.*, 2002) and glial-derived nerve growth factor (GDNF) on the spiral ganglion cells and hair cells (Yagi, M. *et al.*, 1999; 2000).

A second application of viral gene therapy has been in the introduction of antioxidant gene expression to counteract reactive oxygen species in the inner ear. Oxygen radicals are thought to play a role in many of the mechanisms of acquired hearing loss, and free radical scavengers such as superoxide dismutase (SOD) have demonstrated protective effects on hearing damage secondary to noise exposure (Seidman, M. D. and Shivapuja, B. G., 1993), aging (McFadden, S. L. *et al.*, 1999), and aminoglycoside treatment (Kawamoto, K. *et al.*, 2004). Although these trials have only been performed in animal models, the preservation of hair cells and auditory thresholds in the treated animal population offers the hope for future treatment potential in humans.

Finally, and perhaps most exciting, is the use of gene transfer technology to induce the differentiation of organ of Corti cells toward hair cell fates – a preliminary step toward hair cell regeneration. The auditory sensory epithelia within the organ of Corti are terminally differentiated cells that lack basal stem cells. For this reason, it was long assumed that regeneration of damaged or lost hair cells could not occur. However, as was shown in the avian inner ear, supporting cells can be induced to change their phenotype and become new hair cells (Corwin, J. T. and Cotanche, D. A., 1988; Ryals, B. M. and Rubel, E. W., 1988). Recently *math1* or *atoh1*, a basic transcription factor, already known to induce hair cell differentiation during development of the cochlea (Bermingham, N. A. *et al.*, 1999), was shown to have similar effects in the adult (Kawamoto, K. *et al.*, 2004) mammalian cochlea. Using viral transfection and subsequent overexpression of the *math1* gene in the inner ear, Kawamoto K. *et al.* (2004) showed the induction of rudimentary hair cell growth in ectopic locations near the organ of Corti with some auditory function.

3.29.7 Future Implications

The past 10 years of research in cochlear gene therapy has shown that viral transfection for hearing disorders holds significant promise. There is great deal of excitement of its potential to improve rehabilitative outcomes in patients with cochlear implants with concomitant gene therapy (with neurotrophic factors allowing for outgrowth of auditory neuronal processes toward the implant electrode). Perhaps fetal genetic screening will someday include tests for known genetic mutations causing both syndromic and nonsyndromic hearing loss, and *in utero* gene therapy using viral vectors could ameliorate congenital deafness. As our understanding of gene therapy using viral vectors for the inner ear improves, and translational research shifts from the laboratory bench to the bedside, several concerns will need to be addressed. Safety issues regarding gene therapy using viral vectors have been raised in the wake of

three children, all having received gene therapy for severe combined immunodeficiency in France, developing leukemia-like lymphoproliferative malignancies (Hacein-Bey-Abina, S. *et al.*, 2003). Regulation of gene expression, specifically regional and distant dissemination of the therapeutic agent, will need to be optimized. Finally, surgical procedures that minimize both damage to the inner ear microarchitecture and hearing loss will need to be perfected. Gene therapy using viral transduction has shown significant advances in the last decade. These advances will serve as the foundation for the introduction of novel gene therapeutics for the inner ear in the future.

References

Anagnostopoulos, A. V. 2003. A compendium of mouse knockouts with inner ear defects. Trends Genet. 18(10), S21–S38.

Arruda, V. R., Stedman, H. H., Nichols, T. C., *et al.* 2005. Regional intravascular delivery of AAV-2-F.IX to skeletal muscle achieves long-term correction of hemophilia B in a large animal model. Blood 105(9), 3458–3464.

Avraham, K. B. 2003. Mouse models for deafness: lessons for the human inner ear and hearing loss. Ear Hear. 24(4), 332–341.

Berkener, K. L. 1992. Expression of heterologous sequences in adenoviral vectors. Curr. Top. Microbiol. 158, 39–66.

Bermingham, N. A., Hassan, B. A., Price, S. D., *et al.* 1999. Math 1: an essential gene for the generation of inner ear hair cells. Science 284(5421), 1837–1841.

Bestor, T. H. 2000. Gene silencing as a threat to the success of gene therapy. J. Clin. Invest. 105(4), 409–411.

Bestor, T. H. and Tycko, B. 1996. Creation of genomic methylation patterns. Nat. Genet. 12, 363–367.

Bowers, W. J., Chen, X., Guo, H., *et al.* 2002. Neurotrophin-3 transduction attenuates cisplatin spiral ganglion neuron ototoxicity in the cochlea. Mol. Ther. 6(1), 12–18.

Carvalho, G. J. and Lalwani, A. K. 1999. Effect of cochleostomy and intracochlear infusion on auditory brainstem response thresholds in the guinea pig. Am. J. Otolaryngol. 20, 87–90.

Chen, X., Frisina, R. D., Bowers, W. J., Frisina, D. R., and Federoff, H. J. 2001. HSV amplicon-mediated neurotrophin-3 expression protects murine spiral ganglion neurons from cisplatin-induced damage. Mol. Ther. 3(6), 958–963.

Corwin, J. T. and Cotanche, D. A. 1988. Regeneration of sensory hair cells after acoustic trauma. Science 240(4860), 1772–1774.

Cotanche, D. A. 1999. Structural recovery from sound and aminoglycoside damage in the avian cochlea. Audiol. Neurootol. 4(6), 271–285.

Davies, E., Gladstone, H. B., Williams, H., *et al.* 1994. A model for long-term intracochlear administration of pharmacologic agents. Am. J. Otolaryngol. 15, 757–761.

Derby, M. L., Sena-Esteves, M., Breakefield, X. O., and Corey, D. P. 1999. Gene transfer into the mammalian inner ear using HSV-1 and vaccine virus vectors. Hearing Res. 134, 1–8.

Ellis, J. and Bernstein, A. 1989. Gene targeting with retroviral vectors: recombination by gene conversion into regions of nonhomology. Mol. Cell. Biol. 9, 1621–1627.

Friedmann, T. 1997. Overcoming the obstacles to gene therapy. Sci. Am. 276, 96–101.

Friedmann, T. and Roblin, R. 1972. Gene therapy for human genetic disease? Science 175, 949–955.

Geschwind, M. D., Hartnick, C. J., Liu, W., *et al.* 1996. Defective HSV-1 vector expressing BDNF in auditory ganglia elicits neurite outgrowth: model for treatment of neuron loss following cochlear degeneration. Hum. Gene Ther. 7, 173–182.

Hacein-Bey-Abina, S., Von Kalle, C., Schmidt, M., *et al.* 2003. LMO2-associated clonal T cell proliferation in two patients after gene therapy for SCID-X1. Science 302, 415–419.

Han, J. J., Mhatre, A. N., Wareing, M., *et al.* 1999. Transgene expression of the guinea-pig cochlea mediated by a lentivirus-derived gene transfer vector. Hum. Gene Ther. 10(11), 1867–1873.

Herzog, R., Yang, E., Couto, L., *et al.* 1999. Long-term correction of canine hemophilia B by gene transfer of blood coagulation factor IX mediated by adeno-associated viral vector. Nat. Med. 5, 56–63.

Ishimoto, S., Kawamoto, K., Kanzaki, K., and Raphael, Y. 2002. Gene transfer into supporting cells of the organ of Corti. Hear. Res. 173(1–2), 187–197.

Jero, J., Mhatre, A. N., Tseng, C. J., *et al.* 2001a. Cochlear gene delivery through an intact round window membrane in mouse. Hum. Gene Ther. 12, 539–548.

Jero, J., Tseng, C. J., Mhatre, A. N., and Lalwani, A. K. 2001b. A surgical approach appropriate for targeted cochlear gene therapy in the mouse. Hear. Res. 151, 106–114.

Jin, B. K., Belloni, M., Conti, B., *et al.* 1996. Prolonged *in vivo* gene expression drive by a tyrosine hydroxylase promoter in a defective herpes simplex virus amplicon vector. Hum. Gene Ther. 7, 2015–2024.

Kawamoto, K., Ishimoto, S., Minoda, R., Brough, D. E., and Raphael, Y. 2003. Math1 gene transfer generates new cochlear hair cells in mature guinea pigs *in vivo*. J. Neurosci. 23(11), 4395–4400.

Kawamoto, K., Oh, S. H., Kanzaki, S., Brown, N., and Raphael, Y. 2001. The functional and structural outcome of inner ear gene transfer via the vestibular and cochlear fluids in mice. Mol. Ther. 4(6), 575–585.

Kawamoto, K., Sha, S. H., Minoda, R., *et al.* 2004. Antioxidant gene therapy can protect hearing and hair cells from ototoxicity. Mol. Ther. 9(2), 173–181.

Kho, S. T., Pettis, R. M., Mhatre, A. N., and Lalwani, A. K. 2000. Safety of adeno-associated virus as cochlear gene transfer vector: analysis of distant spread beyond injected cochleae. Mol. Ther. 2(4), 368–373.

Krisky, D. M., Marconi, P. C., Oligino, T., *et al.* 1998. Development of herpes simplex virus replication-defective multigene vectors for combination gene therapy applications. Gene Ther. 5, 1517–1530.

Lachmann, R. H. and Efstathiou, S. 1997. Utilization of the herpes simplex virus type 1 latency-associated regulatory region to drive stable reporter gene expression in the nervous system. J. Virol. 71, 3197–3207.

Lalwani, A. K., Han, J. J., Castelein, C. M., Carvalho, G. J., and Mhatre, A. N. 2002. *In vitro* and *in vivo* assessment of the ability of adeno-associated virus brain-derived neurotrophic factor to enhance spiral ganglion cell survival following ototoxic insult. Laryngoscope 112(8 Part 1), 1325–1334.

Lalwani, A. K., Walsh, B. J., Carvalho, G. J., *et al.* 1998a. Expression of adeno-associated virus integrated transgene within the mammalian vestibular organs. Am. J. Otolaryngol. 19, 390–395.

Lalwani, A. K., Walsh, B. J., Reilly, P. G., *et al.* 1998b. Long-term *in vivo* cochlear transgene expression mediated by recombinant adeno-associated virus. Gene Ther. 5, 277–281.

Lalwani, A. K., Walsh, B. J., Reilly, P. G., *et al.* 1996. Development of *in vivo* gene therapy for hearing disorders: introduction of adeno-associated virus into the cochlea of the guinea pig. Gene Ther. 3(7), 588–592.

McFadden, S. L., Ding, D., Reaume, A. G., Flood, D. G., and Salvi, R. J. 1999. Age-related cochlear hair cell loss is enhanced in mice lacking copper/zinc superoxide dismutase. Neurobiol. Aging 20, 1–8.

Merrouche, Y. and Favrot, M. C. 1992. Retroviral gene therapy and its application in oncohematology. Hum. Gene Ther. 3, 285–291.

Mount, J. D., Herzog, R. W., Tillson, D. M., *et al.* 2002. Sustained phenotypic correction of hemophilia B dogs with a factor IX null mutation by liver-directed gene therapy. Blood 99(8), 2670–2676.

Naldini, L., Blomer, U., Gallay, P., Ory, D., Mulligan, R., *et al.* 1996. *In vivo* gene delivery and stable transduction of non-dividing cells by a lentiviral vector. Science 272, 263–267.

Raphael, Y., Frisancho, J. C., and Roessler, B. J. 1996. Adenoviral-mediated gene transfer into guinea pig cochlear cells *in vivo*. Neurosci. Lett. 207, 137–141.

Ryals, B. M. and Rubel, E. W. 1988. Hair cell regeneration after acoustic trauma in adult Coturnix quail. Science 240(4860), 1774–1776.

Sage, C., Huang, M., Vollrath, M. A., *et al.* 2006. Essential role of retinoblastoma protein in mammalian hair cell development and hearing. Proc. Natl. Acad. Sci. U. S. A. 103(19), 7345–7350.

Seidman, M. D. and Shivapuja, B. G. 1993. The protective effects of allopurinol and superoxide dismutase on noise-induced cochlear damage. Otolaryngol. Head Neck Surg. 109, 1052–1056.

Smithies, O., Gregg, R. G., Boggs, S. S., *et al.* 1985. Insertion of DNA sequences into the human chromosomal beta-globin locus by homologous recombination. Nature 317, 230–234.

Staecker, H., Gabaizadeh, R., Federoff, H., *et al.* 1998. Brain-derived neurotrophic factor gene therapy prevents spiral ganglion degeneration after hair cell loss. Otolaryngol. Head Neck Surg. 119, 7–13.

Staecker, H., Li, D., O'Malley, B. W., Jr., *et al.* 2001. Gene expression in the mammalian cochlea: a study of multiple vector systems. Acta Otolaryngol. 121(2), 157–163.

Thorne, M., Salt, A. N., DeMott, J. E., *et al.* 1999. Cochlear fluid space dimensions for six species derived from reconstructions of three-dimensional magnetic resonance images. Laryngoscope 109(10), 1661–1668.

Van de Water, T. R., Staecker, H., Halterman, M. W., and Federoff, H. J. 1999. Gene therapy in the inner ear: mechanisms and clinical implications. Ann. N. Y. Acad. Sci. 884, 345–360.

Wagner, J. A., Messner, A. H., Moran, M. L., *et al.* 1999. Safety and biological efficacy of an adeno-associated virus vector–cystic fibrosis transmembrane regulator (AAV–CFTR) in the cystic fibrosis maxillary sinus. Laryngoscope 109(2 Pt 1), 266–274.

Wareing, M. J. and Lalwani, A. K. 1999. Cochlear gene therapy: current perspectives. Int. J. Pediatr. Otorhinolaryngol. 49(Suppl 1), S27–S30.

Weiss, M. A., Frisancho, J. C., Roessler, B. J., and Raphael, Y. 1997. Viral-mediated gene transfer in the cochlea. Int. J. Dev. Neurosci. 15, 577–583.

Yagi, M., Kanzaki, S., Kawamoto, K., *et al.* 2000. Spiral ganglion neurons are protected from degeneration by GDNF gene therapy. J. Assoc. Res. Otolaryngol. 1(4), 315–325.

Yagi, M., Magal, E., Sheng, Z., Ang, K. A., and Raphael, Y. 1999. Hair cell protection from aminoglycoside ototoxicity by adenovirus-mediated overexpression of glial cell line-derived neurotrophic factor. Hum. Gene Ther. 10, 813–823.

Yamasoba, T., Jagi, M., Roessler, B. J., *et al.* 1999. Inner ear transgene expression after adenoviral vector inoculation in the endolymphatic sac. Hum. Gene Ther. 10(5), 769–774.

Zheng, J. L., Lewis, A. K., and Gao, W. Q. 1998. Establishment of conditionally immortalized rat utricular epithelial cell lines using a retrovirus-mediated gene transfer technique. Hear. Res. 117, 13–23.

3.30 Vertebrate Auditory Pathways

C E Carr, University of Maryland, College Park, MD, USA

P L Edds-Walton, Parmly Hearing Institute, Chicago, IL, USA

Published by Elsevier Inc.

3.30.1	**Introduction**	500
3.30.1.1	Sensory Receptors	500
3.30.1.2	Overview of General Auditory Pathway for All Vertebrates	501
3.30.2	**Functional Organization in Fishes**	502
3.30.2.1	The Auditory Periphery of Fishes	503
3.30.2.2	The Auditory Medulla in Fishes	505
3.30.2.3	The Auditory Midbrain of Fishes	506
3.30.2.4	The Auditory Forebrain of Fishes	508
3.30.3	**Functional Organization in Lissamphibians**	508
3.30.3.1	The Auditory Periphery of Lissamphibians	509
3.30.3.2	The Auditory Medulla of Amphibians	510
3.30.3.3	The Auditory Midbrain of Anurans	511
3.30.3.4	The Auditory Forebrain of Anurans	511
3.30.4	**Functional Organization in Reptilia**	512
3.30.4.1	The Auditory Periphery of Reptilia	512
3.30.4.2	The Auditory Medulla of Reptilia	513
3.30.4.3	The Auditory Midbrain of Reptilia	514
3.30.4.4	The Auditory Forebrain of Reptilia	514
3.30.5	**Functional Organization in Mammals**	515
3.30.5.1	The Auditory Receptors of Mammals	516
3.30.5.2	The Auditory Medulla of Mammals	516
3.30.5.3	The Auditory Midbrain of Mammals	518
3.30.5.4	The Auditory Forebrain of Mammals	518
3.30.6	**Summary**	519
References		519

Glossary

chopper cells A physiological term to describe neurons with regular chopping discharge patterns characterized by narrow initial peaks in poststimulus time histograms.

clade A taxonomic group of organisms consisting of a single common ancestor and all the descendants of that ancestor.

interaural level difference (ILD) The difference between sound levels at the left versus the right ear; used by the central nervous system to compute sound source location.

interaural time difference (ITD) The difference between the timing of the sound stimulus to the left versus the right ear; used by the central nervous system to compute sound source location, in particular, azimuth.

monophyletic A group consisting of an inferred common ancestor and all its descendants.

nucleus As used in anatomy to describe a grouping of cells that form a functional unit; often, but not always, there is a dominant cell type (e.g., fusiform or multipolar cells).

onset cells A physiological term to describe neurons that fire at the beginning of the stimulus and are often silent thereafter.

phase-locking A physiological term based on a cell's ability to encode the phase of a sinusoidal stimulus. Phase-locking is quantified using the

coefficient of synchronization (R) to calculate the probability that the cell will fire at the specified phase.

phasic A physiological term based on a cell's response to a specific stimulus; the cell generally responds at the onset of stimulation, but not throughout (cf. tonic).

polyphyletic A group is polyphyletic if the trait its members have in common evolved separately in different places in the phylogenetic tree. Equivalently, a polyphyletic taxon does not contain the most recent common ancestor of all its members.

tonic A physiological term based on a cell's response to a specific stimulus; the cell fires continuously as long as the stimulus is presented at an appropriate level (cf. phasic).

3.30.1 Introduction

Members of all vertebrate groups have sensory receptors to detect sound energy, though there is much diversity in their capabilities. Within each vertebrate group, there are species for which hearing is critical for normal behavior. In this chapter we will concentrate on how the nervous system encodes particular characteristics of sound along the auditory pathway from the ear to the highest levels of the brain. Our approach to the neuroanatomy will therefore have a functional slant. Emphasis will be placed on how sound becomes categorized by the brain, as needed to sort out the biologically relevant components from the auditory scene. For a detailed discussion of the concept of auditory scene, the reader is referred to Chapter Auditory Scene Analysis.

Sound is a longitudinal wave of alternating pressure increases (compressions of the molecules in the medium) and decreases (rarefactions of the molecules in the medium). Hearing is something quite different. An old question is pertinent here: if a tree falls in the forest, does it make a sound if no one is there to hear it? There can be no doubt that the impact of the tree on the forest floor will make vibrations that could be detected as sound in the air and in the surrounding ground, but it is not heard unless there is an animal with a specialized receptor present in the air or ground. Hearing requires the transformation of the energy in a sound wave to a code that the nervous system can use. There are two components to sound that can be detected by the auditory systems in animals: pressure changes and/or particle motion. In this chapter, we will discuss the process by which sound in the environment is perceived by vertebrates and encoded in a way that is useful to the nervous system.

3.30.1.1 Sensory Receptors

The sensory receptor for the transduction of sound to electrical signals in all vertebrates is a mechanoreceptor that responds to deformation of its surface structures. This mechanoreceptor has been called a hair cell due to the shaggy appearance of the surface structures in the earliest laboratory examinations of the ear. The hair cell varies somewhat in its form among vertebrate groups and the response properties of the cells vary as well (see Chapter Phylogeny and Evolution of Ciliated Mechano-Receptor Cells). In general, there are rows of stereovillae in a very orderly, stair-step array on the surface of the cell. The relative movement of the stereovillae is influenced by an overlying or associated structure, such as a gelatinous cupula, a suspension of small calcareous otoconia, a dense calcified otolith connected to the stereovillae via a gelatinous matrix, or a tectorial membrane. For further details about the structural variations and the distribution of hair cell types among vertebrates, see Chapter Phylogeny and Evolution of Ciliated Mechano-Receptor Cells. For this chapter, we will briefly describe the qualities of the hair cell that are related to response properties of unique importance to each vertebrate group.

Auditory hair cells are always found in groups on an epithelium (or macula) that also contains supporting cells (Figure 1). The base of the cell is within the epithelium, and the stereovillae extend from the apical surface of the cell into a fluid (endolymph). The stereovillae vary in length and stiffness, both of which affect the frequency responsiveness of the individual cell. For example, hair cells with long stereovillae respond best (produce the greatest output to an afferent neuron) to lower frequencies than do hair cells with short, stiff stereovillae. In addition, the stair-step array of stereovillae imposes directionality to the responsiveness of the hair cell.

Bending of the hair cell stereovillae along the cell's best axis results in maximum excitation of the hair cell and maximum neurotransmitter release to the postsynaptic afferent neuron. Bending of the stereovillae in the opposite direction (180° difference in the axis of stimulation) causes the cell to hyperpolarize to its maximum extent, meaning that the hair cell does not

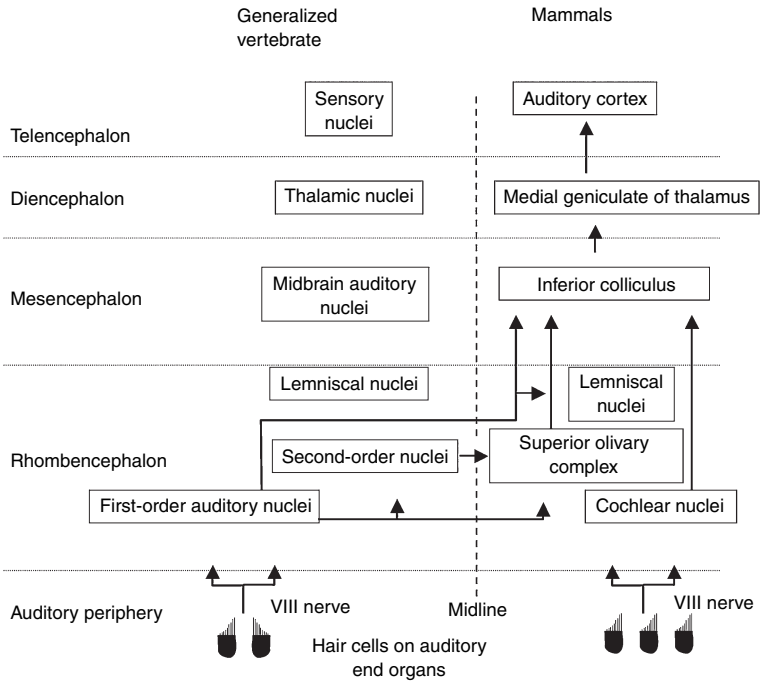

Figure 1 Simplified ascending auditory pathway in vertebrates. A generalized pathway common to all vertebrates is shown on the left, with the mammalian pathway compared on the right. Note that not all components are shown (see text).

relay excitatory information to the afferent neuron. Stimulation at angles in between these two results in a graded response that reflects how close the stimulus axis is to the best axis. Therefore, the surface structures of the hair cell can impart both frequency sensitivity and directional sensitivity to the ear, both of which can be used to encode specific attributes of a sound source to the central nervous system.

The auditory system takes many forms among the vertebrates. Some vertebrates have outer ears, but many do not. The outer ear may consist of paired pinnae (mammals), membrane-covered openings, or simply an opening on both sides of the skull that leads to a middle ear (some amphibians and Sphenodon). Fishes lack an outer ear and do not have a true middle ear. Hair cells are found in the inner ear, which is also quite variable when viewed across the vertebrates. There are two components within the ear of all vertebrates that serve different purposes. Vestibular structures encode tilt and angular motion, providing information about orientation and movement with respect to gravity. Auditory structures encode the particle motion associated with sound. The task of encoding sound may be done by multiple end organs, which usually have parceled out sound detection by frequency or sensitivity. In other words, two end organs may have hair cells that respond to similar frequencies, but the sounds may be encoded differently in the afferent neurons that send the information to the brain (e.g., with broader frequency responses or only at higher sound levels). Thus, in fishes, there can be three or four end organs that encode sound, and in mammals there are at most two, with the second playing a very limited role in auditory processing, and which may be a remnant of the ancestral inner ear.

3.30.1.2 Overview of General Auditory Pathway for All Vertebrates

The organization of the central auditory system is similar among all vertebrates with functional ears (Figure 1). Despite the similarities, it is not clear whether the components of the central auditory system are homologous, or whether the evolution of the central auditory system merely follows the organizational pattern common to the octaval system (Grothe, B. *et al.*, 2004). Evolutionary changes in the peripheral auditory end organs, combined with a lack of detailed embryological studies on the origins of the central auditory cells, are the basis for the present uncertainty in determining homologies in the central auditory system.

The auditory nerve projects to a column of first-order auditory nuclei, also termed cochlear nuclei in birds and mammals (Table 1). These projections are tonotopically organized, when tonotopic organization

Table 1 Comparison of hindbrain components along the auditory pathway in vertebrates

Level	*Bony fish*	*Anuran amphibians*	*Reptilia*	*Mammals*
Periphery				
Origin of primary afferents (species dependent)	Saccule Lagena (Utricle)	Saccule[a] (Lagena) Amphibian papilla Basilar papilla	Basilar membrane Saccule[a]	Cochlea Saccule[a]
Medulla				
First order auditory nuclei with ascending projections	Descending octaval[b] (anterior octaval)	Ventral zone Dorsal medullary nucleus[b,c]	Angularis Magnocellularis[d]	Cochlear nuclei: DCN, AVCN, PVCN
Second order nuclei (SON)	Secondary octaval populations (SOP) (dorsal/intermed/ventral)	Superior olive (SO)	Laminaris[e] Superior olive (SO)	Superior olivary complex: LSO, MSO, periolivary MNTB

[a]Auditory sensitivity demonstrated in amphibians, reptiles, birds, and mammals reviewed by Todd N. P. and Merker B. (2004).
[b]There is evidence for commissural pathways linking the first order nucleus in bony fishes and anurans.
[c]The dorsal medullary nucleus has also been called the dorsolateral or the dorsal nucleus in anurans.
[d]Magnocellularis only projects to laminaris.
[e]Laminaris is not found in all snakes and lizards.
AVCN, anteroventral cochlear nucleus; DCN, dorsal cochlear nucleus; LSO, lateral superior olive; MNTB, medial nucleus of the trapezoid body; MSO, medial superior olive; PVCN, posteroventral cochlear nucleus.

is found in the periphery. The projections to different first-order nuclei mediate the emergence of coding for different aspects of the auditory stimulus, such as sound timing and level. Furthermore, the first-order nucleus projections contribute to two ascending streams, one binaural, combining information from the two ears, and the other monaural. The binaural stream is formed when projections from the ipsilateral and contralateral nuclei converge on second-order hindbrain nuclei that project in parallel with the monaural nuclei to the midbrain. The auditory brainstem shows substantial anatomical diversity between the major vertebrate taxa (reviews in Cant, N. B., 1992; McCormick, C. A., 1998; Carr, C. E. and Code, R. A., 2000; Grothe, B. *et al*., 2004). The auditory midbrain receives ascending inputs from both monaural and binaural hindbrain nuclei, and physiological recordings have revealed the emergence of complex response properties there. The midbrain projects to the thalamus, which in turn projects to auditory stations in the telencephalon. The organization of the telencephalon is structurally and functionally diverse. In all vertebrate clades (monophyletic groups of organisms), the telencephalon exhibits large changes associated with the increased use of sound for communication. Finally, in addition to these ascending pathways, the central auditory system is characterized by multiple descending projections.

3.30.2 Functional Organization in Fishes

In this chapter, we will use the term fishes to include only the jawed fishes, that is, the Chondrichthyes and Osteichthyes. We will not include the jawless Agnatha (lampreys and hagfish) in this review since there is nothing known about auditory processing in those fishes. (However, it is important to note that they have hair cells on end organs that may function in audition.) The Chondrichthyes include the sharks, skates, and rays. The Osteichthyes (bony fishes) include primitive fishes and modern fishes commonly called teleosts.

Sound may reach the inner ear of bony fishes in two ways. The most common pathway is directly through the fish's body to the auditory end organs. The compressions and rarefactions of the water medium cause particle motion that is easily transmitted through the fish's soft tissues due to the similarity in the density of water and tissue. The second pathway, called the indirect pathway, utilizes the presence of an air-filled structure (gas bladder or special otic sac) that is mechanically coupled in some way to the fluids surrounding the auditory end organs. The pressure component of sound causes the air-filled structure to expand and contract, thus producing particle motion

that is transmitted to the ear via the mechanical connection. The indirect pathway is found in a group of fishes called the otophysines (most of which are freshwater species), weakly electric fishes (mormyrids), and herrings. The presence of this second pathway is correlated with greater sensitivity to higher frequencies (>1 kHz) than is found among fish species that have only the direct pathway and hear best below about 500 Hz. There is controversy at present as to whether the indirect pathway can function in fishes that have a gas bladder but lack a mechanical link to the inner ear, since the tissues between the gas bladder and the ear may conduct particle motion (see discussion by Popper, A. N. *et al.*, 2003 and Chapter Underwater Hearing). This indirect pathway does not exist in cartilaginous fishes because they do not have gas bladders.

The majority of the data on the sense of hearing in fishes has been collected from teleosts (Fay, R. R. and Simmons, A. M., 1999; Popper, A. N. *et al.*, 2003), and we will focus on their ascending auditory pathway, with less attention to the cartilaginous and primitive fishes. In addition, there are reciprocal connections between auditory nuclei and descending projections to auditory and nonauditory nuclei at different levels of the pathway, which are not well documented in many fish species, and for simplicity, will not be discussed here. The reader interested in more detailed information about the auditory pathways in cartilaginous and primitive fishes is encouraged to refer to McCormick C. A. (1999) for a comparison of central auditory pathways among all fishes.

3.30.2.1 The Auditory Periphery of Fishes

The auditory periphery refers to the components of the auditory system that are not part of the central nervous system. The periphery of the auditory system of all vertebrates includes the auditory end organs with their sensory hair cells (Figure 2(a)) and the afferents in the acoustic cranial nerve (VIII) that innervate the hair cells and project to auditory processing areas in the medulla. In fishes more than any other vertebrate, the variation in the morphology and orientations of sensory hair cells in the ear have the capability of encoding the axis of stimulation. For that reason, we will provide some background information about hair cells that is pertinent for the discussion of fish auditory circuitry that follows.

The sensory hair cells in the ears of fishes have the stair-step array of stereovillae that is present on the hair cells of all vertebrates (see Chapter Phylogeny and Evolution of Ciliated Mechano-Receptor Cells). In addition, each hair cell has a single kinocilium. The most excitatory direction for a hair cell is along the axis that points from the shortest row of stereovillae to the kinocilium (Figure 2(a)). In all vertebrates, the hair cells are organized on auditory epithelia in specific ways that are predictable within a given species. There is much variety in hair cell orientation among the auditory end organs of different teleosts (Popper, A. N. and Coombs, S., 1982). Their most important feature is that the variety in hair cell orientations on the auditory end organs of fishes provides the ear with the ability to respond to sounds originating from different directions and also provides the potential for relaying that directional information to the brain.

There are four potential auditory end organs in the ears of fishes: the macula neglecta, saccule, lagena, and utricle. The macula neglecta (sometimes called the papilla neglecta) differs in two major ways from the other three end organs. First, the hair cells of the macula neglecta are in contact with a gelatinous cupula; the hair cells of the saccule, lagena, and utricle are associated with an otolith. Second, the hair cells of the macula neglecta are oriented in various directions, with best directions often organized radially from the center of the epithelium. The hair cells on the saccule, lagena, and utricle are oriented in various directions as well, but in nearly all cases, each hair cell has a 180° counterpart.

The detection of hair cell motion in the ear depends on both the frequency and amplitude (level or loudness) of the stimulus. The effective stimulus can be very low frequency (e.g., $<1\,\mathrm{Hz\,s^{-1}}$), as in linear acceleration or tilt of the head, or may consist of higher frequencies, such as environmental sounds. Hair cells with very different frequency sensitivities may be mixed on the same epithelium in the ear (e.g., vestibular vs. auditory). Therefore, the sensory role for any end organ in the ear of fishes cannot be assumed – physiological investigations are needed to confirm the range of response characteristics, although the organization of sensory afferent projections to the brain provides useful clues. In this section, we will base our descriptions of auditory pathways in fishes on comparative anatomy as well as physiological investigations.

The macula neglecta appears to be the primary auditory end organ among sharks (Corwin, J. T., 1989). The size of this end organ varies among shark species and its role in hearing may vary as well. In an adult Carcharhinid shark, the macula is composed of two patches, containing about 200 000 hair cells that project to about 4700 myelinated nerve

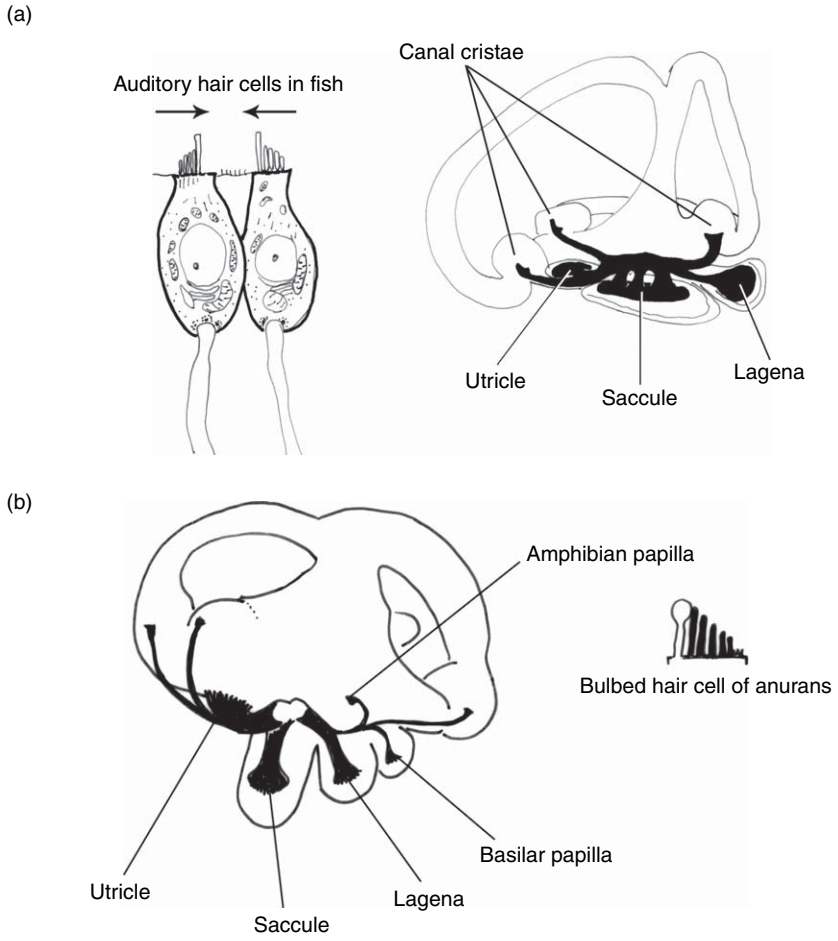

Figure 2 Illustrations of anamniote inner ears, medial view. The sensory end organs and the branches of VIII are shown in black. (a) Generalized teleost fish. Note that the hair cells on each of the sensory epithelia occur in opposing orientations (arrows indicate best directions for the two hair cells shown; they are separated by a support cell). Hair cells of fishes have both a kinocilium (white) and stair-step arrays of stereovillae (black). The semicircular canal cristae are included for completeness, but are not auditory structures. (b) Generalized anuran ear. The hair cells are oriented in various patterns, as in fishes, but a unique hair cell, with a bulbed kinocilium occurs in anurans. Note the relative sizes and locations of the amphibian papilla and basilar papilla. Adapted from Lewis, E. R., Leverenz, E. L., and Bialek, W. S. 1985. The Vertebrate Inner Ear. CRC Press, figures 4 and 8; and Will, U. and Fritzsch, B. 1988. The Eighth Nerve of Amphibians: Peripheral and Central Distribution. In: The Evolution of the Amphibian Auditory System (*eds*. B. Fritzsch, M. J. Ryan, W. Wilczynski, T. E. Hetherington, and W. Walkowiak), pp. 159–183. Wiley, figure 1.

fibers (Corwin, J. T., 1977). Some teleost fishes have a macula neglecta, but in general, the end organ is very small, and its function has not been determined physiologically in any teleost.

The paired saccules are the most common otolithic end organ associated with hearing in fishes. The hair cells have a variety of apical bundle morphologies, including differences in the relative height of the kinocilium versus the stereovillae (Platt, C. and Popper, A. N., 1981; 1984), that no doubt influence the response characteristics (Chapter Mechano-Acoustical Transformations). Most of the work on auditory responses of the saccule have been conducted in teleost fishes (Fay, R. R. and Simmons, A. M., 1999), but an auditory function for the saccule was demonstrated in the lemon shark, *Negaprion brevirostris*, by Corwin J. T. (1981). Lowenstein O. and Roberts T. D. M. (1951) estimated that two-thirds of the saccule in some sharks, skates, and rays respond to sound vibrations. The remaining portion of the saccule responds to tilt.

The lagena is intriguing due to the apparent flexibility in both the structure and function of this end organ. In sharks, skates, and rays, the lagena, in addition to a portion of the saccule, may be sensitive to

tilt. In bony fishes, the lagena may respond to vibration for auditory processing (e.g., goldfish, Fay, R. R., 1984; and freshwater goby, Lu, Z. *et al.*, 2003) and/or respond to tilt for vestibular processing (e.g., toadfish, Locke, R. *et al.*, 1999). Lu Z. *et al.* (2003) have suggested that the lagena may be important for extending the dynamic range of the auditory system in teleost fishes, since it is less sensitive to auditory frequencies than the saccule in the sleeper goby. There are no data indicating the presence (or absence) of a frequency map on the lagena in species for which auditory responses have been documented, although Platt C. (1977) documented considerable variation in apical bundle morphology on the goldfish lagena.

In most fishes, the utricle is very similar in appearance to the utricle of other vertebrates. The utricle is assumed to play a major role in encoding linear acceleration in the horizontal plane. However, Lowenstein O. and Roberts T. D. M. (1951) found that although most of the utricle of a skate (*Raja clavata*) responds to tilt, a small portion responds to vibration. There is evidence that the utricle could respond to higher frequencies and contribute to directional hearing (Fay, R. R., 1984; Lu, Z. *et al.*, 2004). Tomchik S. M. and Lu Z. (2005) presented strong anatomical evidence for a mixture of vestibular and auditory functions in the utricle based on the interdigitation of utricular afferents with those of the other two otolith organs in the dorsal medulla and with the semicircular canal cristae projections in the ventral medulla of the sleeper goby. In addition, Wallace A. C. and McCormick C. A. (2005) showed utricular and saccular afferents terminating on the same cells in the descending octaval nucleus (see below). In some teleost fishes, the utricle has a very different morphology with distinct subdivisions of the macula. In at least one herring species, one of the utricular subdivisions clearly functions in auditory processing (Denton, E. J. *et al.*, 1979; Mann, D. A. *et al.*, 2001).

The diversity of response characteristics for the end organs in the ear of fishes makes generalizations about the auditory periphery among fishes difficult. The best data are from species for which both auditory physiology and neuroanatomical analyses have been conducted. In the next section, we will discuss the organization of auditory inputs from the ear to the medulla, based on anatomical data from species for which the peripheral auditory end organs have been identified.

3.30.2.2 The Auditory Medulla in Fishes

Primary afferents innervating the end organs with auditory responses may send their axons to one or more nuclei in the medulla. Four nuclei are arranged rostrocaudally in the octaval column in the medulla of cartilaginous and primitive bony fishes: anterior, descending, magnocellular, and posterior. In teleost fishes, the octaval column has an additional nucleus, the tangential nucleus. Of these nuclei in the octaval column, only the anterior (AON) and/or descending (DON) octaval nuclei have ascending projections to the auditory midbrain. Although the magnocellular and tangential octaval nuclei may also be involved in directional responses to sound, in that they have been implicated in coordinating reflex responses to sound via the spinal cord (Highstein, S. M. *et al.*, 1992; Puzdrowski, R. L. and Leonard, R. B., 1993; Suwa, H. *et al.*, 1999), there is no evidence that either nucleus is a component of the ascending auditory circuit.

All of the octaval nuclei appear to receive a mixture of inputs from multiple end organs. Auditory inputs tend to be more dorsal and extend more medially than vestibular inputs in the anterior and descending nuclei in both cartilaginous and bony fish species for which inner ear projections have been examined in detail (McCormick, C. A., 1992; 1999). Similarly, the subset of cells in these first-order nuclei that project to higher-order auditory nuclei are located in the more medial zones of the anterior and descending nuclei (Figure 1, Table 1).

One study has characterized the auditory responses of single primary saccular afferents in the toadfish and revealed their central projections with intracellular injections of neurobiotin (Edds-Walton, P. L. *et al.*, 1999). Some, though not all, saccular afferents bifurcated upon entering the medulla. The rostral branch of the axon projected to the AON, and the caudal branch projected to the dorsal zones of the DON. Each branch tended to have multiple termination sites in each nucleus, although cells in the DON received the greatest proportion of inputs from the bifurcating saccular fibers. The distribution of the auditory inputs to those nuclei was distinctively different, however. Projections into the AON were radially organized. Projections into the DON tended to extend rostrocaudally with multiple synaptic sites at intervals down the length of this elongate nucleus. The functional significance of that organization is not yet known. Given that most saccular afferents are broadly tuned with overlapping response areas, as is the case in all fishes for which such data are available

(Fay, R. R. and Simmons, A. M., 1999), a tonotopic organization is unlikely.

No studies have documented the range of response properties of first-order auditory nuclei in cartilaginous fishes or primitive fishes, and only a few studies have been done in teleost fishes. Some of these studies have been carried out on teleosts that vocalize, including toadfish, midshipmen, and mormyrid fishes. Phase-locking is characteristic of the majority of auditory cells in the medulla of fishes (see discussion in Feng, A. S. and Schellart, N. A. M., 1999). In the weakly electric mormyrid fishes, *Pollimyrus* sp. evidence was presented for both frequency and timing computations in the medulla that might contribute to conspecific call recognition (Kozloski, J. and Crawford, J. D., 1998). In the toadfish, recordings from identified sites in the DON revealed more specific frequency and directional responses than found in the nerve (Edds-Walton, P. L. and Fay, R. R., 2005b).

The requirements of directional hearing might be reflected in the organization of the DON. Binaural interactions can occur at this level of the auditory circuit of fishes in two ways. First, in some fishes, a subset of afferents from the auditory end organ(s) projects to a dorsomedial zone of both the ipsilateral and contralateral DONs (McCormick, C. A., 1992; 1999). Second, in some teleosts, cells in the DON have reciprocal connections with cells in the contralateral DON (Nieuwenhuys, R. and Pouwels, E., 1983; Edds-Walton, P. L., 1998; Tomchik, S. M. and Lu, Z., 2005). The reciprocal connections provide the potential for left–right comparisons for directional computations. Alternatively, the binaural interactions may be part of a common mode rejection circuit to eliminate self-generated noise (Duman, C. H. and Bodznick, D., 1996; 1997). At present no physiological studies have documented the response properties of binaurally driven cells in the DON. However, binaurally driven cells have been found in undocumented sites in the medulla of the cod (Horner, K. *et al.*, 1980).

Another potential site for binaural interactions in the medulla is among cells in the secondary octaval population (SOP). There are a minimum of two divisions of secondary octaval cells usually located in the rostral medulla, near the entrance of eighth nerve. The two divisions are (1) a dorsal grouping of cells lying near the ventricle and (2) a ventral grouping located more medially and often near the internal arcuate tract. A third division, consisting of spherical cells that lie intermediate to the dorsal and ventral divisions, has been described for the goldfish (McCormick, C. A. and Hernandez, D. V., 1996), but the intermediate division may not be present in all teleosts (McCormick, C. A., 1999). In addition, a primitive fish, the bowfin (*Amia calva*) has only the ventral division (McCormick, C. A. and Braford, M. R., Jr., 1988), suggesting that a single ventral nucleus may be the primitive vertebrate condition.

The sources of inputs to the SOP are not known with any certainty. The cells of the dorsal division have a ventral process that extends into the more dorsal and medial regions of the DON (where saccular input is also found) and a dorsal process that traverses the lateral line nucleus medialis and enters the cerebellar crest (McCormick, C. A., 1999). Therefore, the dorsal division could be integrating primary saccular input, DON cell input, and medialis input, with modulation from the cerebellum. McCormick C. A. (1999) suggests that the ventral and intermediate divisions of the SOP may be components of a descending acoustic pathway since those divisions receive input from the auditory midbrain in goldfish. At present there is no evidence to suggest that any division of the SOP is homologous to the superior olivary nuclei of tetrapods.

The pathway from the medulla to the auditory midbrain is the same in fishes as in other vertebrates. Projections from the first- and second-order auditory nuclei ascend via the lateral lemniscus. There is also some evidence for an intermediate nucleus (e.g., paralemniscal nucleus or nucleus of the lateral lemniscus) that may act as a relay for some of the projections to the auditory midbrain (McCormick, C. A., 1999; Edds-Walton, P. L. and Fay, R. R., 2005a).

3.30.2.3 The Auditory Midbrain of Fishes

The midbrain is a major site of convergence for the many sensory systems found among fishes: vision, audition, lateral line, and the electric sense. The lateral mesencephalic complex (LMC) in the midbrain of cartilaginous fishes can be subdivided into as many as four nuclei in some species (e.g., skates and rays), but the identification of a discrete auditory nucleus has proved elusive, particularly in sharks, likely due to a substantial amount of sensory integration. The strongest evidence indicates that the medioventral nucleus of the LMC can be an auditory center (e.g., Barry, M. A., 1987). In bony fishes, a physiologically and anatomically distinctive auditory region (nucleus centralis) is usually dorsal to, and sometimes medial to, the lateral line nucleus (nucleus

ventrolateralis or n. ventralis) in the torus semicircularis (torus) of the midbrain (see figure 17.11 in McCormick, C. A., 1992). In electroreceptive fishes, the auditory nucleus may be sandwiched between the electrosensory nucleus and the lateral line nucleus, but in another variation, the lateral line and auditory inputs may converge (in the mediodorsal nucleus), as demonstrated in a weakly electric fish (Crawford, J. D., 1993).

Spontaneous activity and phase-locking are reduced in the midbrain compared to primary afferents (summarized by Feng, A. S. and Schellart, N. A. M., 1999). Two studies have been conducted similarly and provide comparable data. In the goldfish torus, Lu Z. and Fay R. R. (1993) found cells with either no spontaneous activity or activity below 20 spikes s^{-1}. Cells in the toadfish torus also had a similar range of activity, with most below 5 spikes s^{-1} (Edds-Walton, P. L. and Fay, R. R., 2003). Phase-locking is present among a subset of cells in the auditory torus, though there are no data to indicate that they are located in a particular functional subunit of the torus.

Auditory recordings in the torus provide evidence for additional computations along the auditory pathway or within the torus that produce cells with unique frequency response areas (compared to saccular inputs) and cells with sharpened directional responses (Lu, Z. and Fay, R. R., 1993; Ma, W. L. and Fay, R. R., 2002; Edds-Walton, P. L. and Fay, R. R., 2003; Edds-Walton, P. L. and Fay, R. R., 2005b). Edds-Walton P. L. and Fay R. R. (2003) compared frequency tuning with directional sharpening and found that the computations are independent. In other words, a directionally sharpened cell in the torus is not necessarily highly tuned.

Bimodal sites have been documented in the midbrain of fishes by several investigators, however, no functional neuroanatomy has been conducted in the midbrain of fishes using all potential stimuli to sort out multimodal sites. As McCormick C. A. (1999) notes, the presence of a nucleus that receives input predominantly from one sensory pathway does not preclude the presence of multimodal cells or areas. Bimodal auditory and visual (AV) cells were found in the tegmentum, deep to the torus of goldfish (Page, C. H. and Sutterlin, A. M., 1970) and the trout (Schellart, N. A. M., 1983; Schellart, N. A. M. and Kroese, A. B. A., 1989). Schellart N. A. M. *et al.* (1987) also found a vertical gradation in relative responsiveness to auditory versus visual stimulation, with unimodal cells tending to lie at the extremes (auditory most dorsal, visual most ventral).

Bimodal auditory and lateral line cells were found throughout the torus of the toadfish (Edds-Walton, P. L. and Fay, R. R., 2003). Neurobiotin injections at sites with auditory and lateral line bimodality revealed multipolar cells with processes that extended throughout both subdivisions of the torus. In addition, retrogradely filled input cells indicated that bimodality was the result of convergence of inputs from medullary auditory and lateral line cells rather than interconnections between lateral line responsive cells in nucleus ventrolateralis and auditory cells in nucleus centralis (Edds-Walton, P. L. and Fay, R. R., 2005a). Finally, Edds-Walton P. L. and Fay R. R. (2003) presented physiological data that indicated a dorsal–ventral gradation in relative responsiveness to auditory versus lateral line stimulation. As was found with auditory and vestibular cells in trout, auditory and lateral line-responsive cells in toadfish tended to be more common at intermediate depths, and auditory-only cells tended to be located most dorsally in the torus.

The data on unimodal versus bimodal cells in the torus reflect sensory mapping across sensory modalities; however, maps within a sensory modality, such as audition, have not been well demonstrated in fishes. Tonotopy may be present in a relatively gross way, but there are no data to indicate a strict tonotopic organization in the auditory torus. In several physiological surveys of the torus, more cells with high best frequencies were found in the rostral torus than in the caudal torus (carp, *Cyprinus carpio*, Echteler, S. M., 1985; rainbow trout, *Oncorhynchus mykiss*, Schellart, N. A. M. *et al.*, 1987; toadfish, *Opsanus tau*, Edds-Walton, P. L. and Fay, R. R., 2003).

Only one study has provided evidence for a spatial auditory map in a trout, based on directional stimuli in the horizontal plane (Wubbels, R. J. *et al.*, 1995). Furthermore, these authors suggested a columnar organization in the torus based on similar response characteristics among consecutive recording sites along vertical tracts. Another study in toadfish, using horizontal and vertical plane directional stimuli, did not reveal a simple spatial auditory map in the toadfish nucleus centralis (Edds-Walton, P. L. and Fay, R. R., 2003).

In summary, the midbrain of cartilaginous and bony fishes is not easily separated into functional neuroanatomical units. In teleosts, there is mounting evidence that multimodal cells are not strictly segregated from unimodal cells in the midbrain, and there is considerable variety in midbrain organization. The amount of overlap among sensory systems in the

midbrain may be species dependent and may reflect species-typical requirements for emphasizing particular aspects of the sensory experience (Feng, A. S. and Schellart, N. A. M., 1999).

3.30.2.4 The Auditory Forebrain of Fishes

The forebrain includes the diencephalon and telencephalon; both will be discussed in this section. Auditory components have been identified from tract-tracing studies, but much remains to be learned about auditory processing in the forebrain. We will focus on what is known about the ascending projections to the diencephalon and telencephalon. More detailed discussions are available in Braford M. R., Jr. (1995), Striedter G. F. (1997), and Northcutt R .G. (2006).

The auditory torus projects to the central posterior nucleus of the dorsal thalamus in all fishes examined to date and the ventromedial nucleus of the ventral thalamus in some species (see McCormick, C. A., 1999). Lu Z. and Fay R. R. (1995) confirmed the presence of auditory responses in the central posterior nucleus in goldfish, though their data indicated less auditory specificity (broader frequency tuning and less phase-locking) than previously recorded in the goldfish midbrain. Projections from the midbrain have also been noted in the anterior tuberal nucleus of the hypothalamus, with reciprocal connections noted in some species (reviewed in McCormick, C. A., 1999; Northcutt, R. G., 2006).

The lateral preglomerular complex of the diencephalon is a recipient of midbrain projections that are likely to have auditory components (McCormick, C. A., 1999). Auditory inputs have been revealed in goldfish: the auditory torus projects to the caudal subnucleus of the lateral preglomerular complex, while the rostral subnucleus of the lateral preglomerular nucleus receives input from the medial pretoral nucleus (Northcutt, R. G., 2006). The medial pretoral nucleus is found in the midbrain of otophysines (no other teleost groups to date) and receives inputs from the auditory torus. Therefore, in otophysines, there may be an additional auditory pathway from the midbrain to the diencephalon. This is of special interest due to the potential for parallel processing of pressure versus particle motion components of sound that may be used for directional hearing (Fay, R. R., 2005).

The auditory pathway culminates in the dorsal region of the telencephalon. Within the dorsal telencephalon, two pallial divisions, medial (Dm) and lateral (Dl), receive auditory input either from ascending pathways or intrinsic connections. The relative contributions of ascending auditory input from dorsal thalamus versus the preglomerular complex may vary among fish species (see discussion in Northcutt, R. G., 2006); however, what constitutes the thalamus in teleosts remains an issue. Projections to the pallium are believed to originate in the central posterior nucleus and/or the anterior nucleus of the dorsal thalamus. The rostral subnucleus of the lateral preglomerular nucleus projects to both Dm and Dl; the caudal subnucleus of the lateral preglomerular complex and the anterior preglomerular nucleus project only to Dm. Braford M. R., Jr. (1995) and Northcutt R. G. (2006) have argued that much of the dorsal telencephalon in goldfish and other teleosts may be more limbic than isocortical in organization.

Physiological studies have revealed both unimodal and multimodal sites in the telencephalon. An investigation using four different sensory stimuli (auditory, visual, electrosensory, and lateral line) and electrode arrays found that most sites in the Dm of a weakly electric fish were unimodal (Prechtl, J. C. *et al.*, 1998). The comparatively rare bimodal or multimodal sites were clustered at the borders of unimodal sites in Dm. Included among the bimodal loci were auditory-lateral line and auditory-electrosensory sites. Clearly, more data are needed before we can begin to understand sensory processing in the telencephalon. Physiological studies of diencephalic/telencephalic sites in representatives of the major groups of fishes could provide much needed insights into the functional organization of the auditory pathway.

3.30.3 Functional Organization in Lissamphibians

There are three major radiations of lissamphibians (extant amphibians): the frogs and toads (Anura), the salamanders and aquatic newts (Urodeles or Caudata), and the limbless caecilians (Gymnophiona). There is considerable diversity in the structures involved in transducing sound from the environment to the inner ear (e.g., presence or absence of a tympanum) and in the role of hearing in the behavioral ecology of lissamphibia, which we cannot cover here. Several recent publications provide excellent reviews of the diversity of auditory systems and hearing among the amphibians (e.g., Fritzsch, B. *et al.*, 1988; Fay, R. R. and Simmons, A. M., 1999; Lewis, E. R. and Narins, P. M., 1998; Smotherman, M. and Narins, P. M., 2004; Rose, G. J.

and Gooler, D. M., 2007). There are also interesting variations in the ways that sound reaches the fluid-filled inner ear among the lissamphibia that cannot be described here. For a detailed discussion about the columellar subsystem (for underwater and airborne sound) and the opercular subsystem (for substrate vibrations) of anurans, see Lewis E. R. and Narins P. M. (1998) and Mason M. J. (2007).

Frogs have garnered most of the attention of research scientists interested in amphibian hearing. Most anurans are vocal, providing the experimenter with an obvious starting point in determining the types of sounds most likely to be encoded by the auditory system. Far less is known about auditory processing in salamanders, newts, and caecilians, and they will not be described here.

3.30.3.1 The Auditory Periphery of Lissamphibians

Diversity in the range of auditory end organs is arguably the greatest among the lissamphibians. Lissamphibian auditory end organs include some of those present in fishes, plus two end organs not found in any teleost fish, though there may be an homologous structure in an ancient fish (see Fritzsch, B., 1992). In addition, the hair cells of most anurans have a unique kinocilium with a bulbed tip (Figure 2(b)).

The auditory end organs that amphibians have in common with fishes are the lagena and saccule. Hair cells are oriented in specific patterns on those end organs as in fishes. Unlike those end organs in teleost fishes, there is not a single dense otolith, but rather an otoconia (a suspension of calcareous particles) associated with a gelatinous matrix that contacts the apical structures of the hair cells. The lagena appears to be a mixed auditory/vestibular end organ in at least some of the anurans, with sensitivity to low-frequency vibration and sensitivity to linear acceleration (posture) in different regions of the lagena (Cortopassi, K. A. and Lewis, E. R., 1995; 1996). There is no evidence for mixed vestibular and auditory function in the amphibian saccule. The saccule and the lagena encode the lowest frequencies, including substrate vibrations from predators or prey. In some burrowing anurans, the saccule may also be part of the auditory circuit that encodes calls transmitted through the substrate. The utricle, which has auditory sensitivity in some teleost fishes, is believed to be sensitive only to head movements and not to vibration in lissamphibians.

The two additional auditory epithelia found among the lissamphibians are the low-frequency sensitive amphibian papilla and the higher-frequency sensitive basilar papilla. The amphibian papilla is found in all lissamphibians; the basilar papilla is present in most of the lissamphibians. The sensory hair cells are oriented in characteristic patterns along these papilla, with systematic variations in surface morphology (e.g., relative height of kinocilium vs. stereovillae). Associated with the surface of the hair cells on the amphibian and basilar papillae is a gelatinous structure called a tectorium or tectorial membrane. The tectorium of the amphibian papilla varies in relative thickness, which, in addition to variations in hair cell morphologies, has been correlated with the tonotopic map common along that end organ (Shofner, W. P., 1988). The tectorium of the basilar papilla varies among amphibian groups, having greatest complexity in the anurans (Lewis, E. R. and Narins, P. M., 1998). Both the amphibian and basilar papilla vary in relative size among amphibians. The amphibian papilla is usually the largest end organ, and its size is associated with the frequency response. The larger the amphibian papilla, the broader the frequency response for that end organ, with the range extended to higher frequencies rather than lower. Hair cells with shorter ciliary bundles and higher-frequency responses are found most caudally. Although there are systematic variations in hair cell morphologies, there is no evidence for tonotopy on the basilar papilla.

Lewis E. R. and Narins P. M. (1999) note that frequency sensitivity seems to be distributed among the different end organs in a systematic way: the saccule encodes the lowest frequencies (<100 Hz), the amphibian papilla encodes intermediate frequencies (around 80–1000 Hz), and the basilar papilla encodes the highest frequencies (around 1–4 kHz). They also state that in all species studied thus far, the basilar papilla encodes some component in the species' vocalizations. The amphibian papilla may also respond to lower-frequency components of a conspecific call.

In general, auditory afferents have low spontaneous activity (0–80 spikes s^{-1}), have fairly distinct best frequencies, and phase-lock well up to about 1 kHz (Christensen-Dalsgaard, J. *et al.*, 1998; Lewis, E. R. and Narins, P. M., 1998). However, the higher-frequency fibers from the basilar papilla do not exhibit good phase-locking and are more broadly tuned than the fibers from the amphibian papilla. Zakon H. H. and Wilczynski W. (1988) suggested that the combined output of the two end organs may be critical for recognition of communication signals

that sweep through a wide range of frequencies (frequency-modulated or FM signals).

3.30.3.2 The Auditory Medulla of Amphibians

The majority of the work on amphibian auditory physiology and anatomy has been conducted on frogs or salamanders. Comparisons of the ascending auditory systems can be found in Will U. and Fritzsch B. (1988) and McCormick C. A. (1999). Here we present a general summary with highlights of some of the differences between anuran and nonanuran amphibians.

Input from the peripheral auditory end organs enters the medulla via the anterior and posterior rami of VIII. The fibers from the amphibian and basilar papillae travel in the posterior ramus with lagenar fibers (Figure 2(b)). Saccular fibers may travel in either the anterior or posterior ramus. All auditory fibers bifurcate as they enter the medulla, resulting in ascending tracts to the primary auditory nuclei and cerebellum and descending octaval tracts to the region of the obex (Will, U. and Fritzsch, B., 1988). The organization of the medulla varies depending on the presence of a lateral line system. When a lateral line region is present in larval amphibians and the aquatic urodeles, inputs to the auditory medulla are located more laterally and ventrally (see figure 3 in Will, U. and Fritzsch, B., 1988). Among octaval inputs, the auditory processing regions tend to be more dorsal than the vestibular sites.

The acoustic region in the medulla among urodeles and caecilians is more diffuse than in anurans (McCormick, C. A., 1999) and there is much overlap in the projections of the auditory end organs. The region of the medulla that receives octaval inputs in nonanurans is designated as the ventral zone. The anurans have a similarly organized ventral zone, but also have a well-defined auditory nucleus that lies dorsal to the ventral zone, the dorsal medullary nucleus (DMN, Feng, A. S. and Capranica, R. R., 1976; Feng, A. S., 1986; also called the dorsal lateral nucleus or the dorsal nucleus; see Table 1).

Afferents from the lagena and the saccule project to the ventral zone in both nonanurans and anurans. We have noted earlier that a region of the lagena and the entire saccule respond to low-frequency, vibrational stimuli. In addition, both lagenar and saccular inputs overlap with inputs from the canal cristae and the utricle in other octaval projection sites in the medulla. This region has not been well characterized physiologically, but the distribution of input is consistent with the fact that the majority of the hair cells in the lagena are vestibular. The functional significance of the saccular overlap is less clear, since there is no evidence for vestibular responses among saccular afferents. Cells of the ventral zone project down the spinal cord in the vestibulospinal tract (Will, U., 1988), and thus, the saccular input could be involved in a reflex orientation circuit that coordinates responses to seismic stimuli (e.g., predator movements). In addition, saccular afferents also project to the nucleus saccularis of Matesz (see McCormick, C. A., 1999), which does not receive inputs from the amphibian and basilar papillae. The distribution of saccular inputs among octaval sites in the medulla is intriguing and may be a function of the behavioral significance of low-frequency, seismic stimuli to the species under consideration.

Inputs from the amphibian papilla and the basilar papilla are organized tonotopically in the ventral zone in both anurans and nonanurans and in the DMN in anurans. Saccular afferent inputs are generally most ventral in the ventral zone in nonanurans and are not intermingled with amphibian and basilar papilla inputs in the DMN of anurans. Response characteristics of DMN cells are similar to those of primary auditory afferents in about half the cells, but new firing patterns also emerge, for example, onset-only and phasic bursting cells (discussed in more detail in Feng, A. S. and Schellart, N. A. M., 1999). Phase-locking to tones is poor among those cells, and their frequency responses are relatively low. Feng A. S. and Schellart N. A. M. (1999) suggest that these DMN cells are most important for encoding temporal patterns.

A commissural tract exists between the two DMN, making this the first site along the auditory pathway in which binaural interactions occur (Feng, A. S. and Capranica, R. R., 1976; Christensen-Dalsgaard, J. and Kanneworff, M., 2005). Feng A. S. and Capranica R. R. (1976) presented anatomical and physiological evidence that the commissural connections are homotopic, and that a proportion of the binaural cells are sensitive to interaural time differences (ITDs). Other interconnections exist among primary octaval regions of the medulla and the cerebellum that we will not discuss as their role in auditory processing is unknown. None of those areas project to the auditory midbrain.

Among amphibians, only anurans have a secondary acoustic nucleus in the ventral medulla, called the superior olivary (SO) nucleus. The SO of anurans is a single nucleus (not a complex as found in teleosts or

mammals) that receives bilateral input from the DMN and from a portion of the ventral zone that has inputs from all four auditory end organs. Contralateral inputs tend to predominate. The inputs are organized both tonotopically and by laterality: the ipsilateral DMN inputs terminate more ventrally than the contralateral DMN inputs (Will, U., 1988). Sensitivity to temporal characteristics of stimuli is retained among cells in the SO (Walkowiak, W., 1988), and the range of firing patterns recorded in the DMN are also present in the SO (Condon, C. J. *et al.*, 1995). However, additional frequency, amplitude modulation, and temporal encoding are evident as more specific combinations of these features are required by some cells (described in detail by Feng, A. S. and Schellart, N. A. M., 1999).

Auditory projections ascend to the midbrain in the lateral lemniscus in amphibians, as in all vertebrates. Wilczynski W. (1988) and McCormick C. A. (1999) have suggested that a nucleus found in close proximity to the lateral lemniscus may have a role similar to the nucleus of the lateral lemniscus in other tetrapods, which is also supported by some physiological work (Rose, G. J. and Wilczynski, W., 1984). Since the relationship of this nucleus to the lemniscal nuclei of other tetrapods is unclear, it is referred to as the superficial reticular nucleus by McCormick C. A. (1999), as a portion of the nucleus lies just lateral to the reticular formation. The superficial reticular nucleus receives input from the ipsilateral superior olive and also direct input from the contralateral DMN.

3.30.3.3 The Auditory Midbrain of Anurans

The auditory midbrain of amphibians, the torus semicircularis (torus), is considered to be homologous to the auditory midbrains of tetrapods. Our examination of the auditory pathway through the midbrain will be restricted to that of anurans due to a paucity of information on urodeles and caecilians.

The torus is described by Wilczynski W. (1988) as the largest site for auditory processing in the anuran brain. The auditory torus has a central core surrounded by concentric shells. The most dorsal shell, the laminar nucleus, and the underlying, more caudal principal nucleus are both laminar structures with a subset of cells whose dendrites extend dorsoventrally into other layers. The ventral toral zone lies just above the tegmentum and is partially enclosed by the laminar and principal nuclei. The ventral toral zone consists of medium and large multipolar cells whose distributions vary within the ventral toral zone of different anurans. In some species, the large multipolar cells predominate in the ventral torus and are designated as the toral magnocellular nucleus.

The torus receives bilateral projections from the DMN, SO (ipsilateral predominance), and superficial reticular nucleus (or the nucleus of the lateral lemniscus). The ventral toral zone appears to be the major auditory integration site in the torus (Wilczynski, W., 1988). Some studies indicate there may be a loosely organized tonotopic organization with more high-frequency cells caudally and more low-frequency cells rostrally. Other studies have suggested a frequency map with concentric circles, resulting in lower-frequency cells surrounded by higher-frequency cells during vertical physiological excursions through the torus (discussed in Fuzessery, Z. M., 1988; Feng, A. S. and Schellart, N. A. M., 1999). Detection of a map is confounded by differences in tuning curves (broad vs. narrow) for torus cells and the convergence of other sensory systems in the torus that result in multimodal cells in all three subdivisions.

Physiological studies in the torus of anurans have revealed complex frequency responses, including cells that respond best to two or three simultaneous tones, cells with discontinuous tuning curves (e.g., intermediate frequencies are inhibitory), and cells that require very specific stimulus durations (Gooler, D. M. and Feng, A. S., 1992). Overall, the anuran torus has cells that exhibit complex acoustic feature detection, but there are still a few cells that retain primarylike responses. Feng A. S. and Schellart N. A. M. (1999) provide a more detailed discussion of the auditory response properties documented in the torus of anurans.

3.30.3.4 The Auditory Forebrain of Anurans

Cells in the auditory torus project to the central and posterior nuclei of the thalamus, though the projections are not distributed equally (McCormick, C. A., 1999). The central thalamic nucleus has reciprocal connections with the magnocellular and principal nuclei of the torus and also receives direct input from the SO. The posterior thalamic nucleus receives input primarily from the laminar nucleus of the torus. Hall J. C. and Feng A. S. (1987) suggested that the central and posterior thalamic nuclei conduct parallel processing for temporal and spectral aspects of sound, respectively. However, Neary T. J. (1988) suggested that the posterior nucleus integrates sensory information and is best thought

of as multimodal rather than acoustic based on extensive visual and somatosensory inputs. Although a third subdivision of the thalamus, the anterior nucleus, responds to acoustic stimuli, this area also receives substantial visual and somatosensory inputs (Neary, T. J., 1988).

Feng A. S. and Schellart N. A. M. (1999) suggest that signal discrimination in frogs such as conspecific, nonpredator, or predator may lie in the coincident activity of groups of cells in the thalamus, forming a population code whose activity reflects the convergence of various acoustic characteristics encoded at lower levels of the auditory pathway. This population code idea is an attractive one, since a similar organization has been suggested for other sensory systems in vertebrates.

The central thalamic nucleus projects to the hypothalamus and the preoptic area in the diencephalon, and to the striatum of the telencephalon. The anterior thalamic nucleus also sends light projections to the hypothalamus and the pallium of the telencephalon (primarily medial). Neither the preoptic area nor the hypothalamus are involved in auditory processing, but both are components of the circuitry that regulates seasonal, reproductive sound production. The role of the telencephalon may primarily be descending feedback pathways to coordinate behavioral responses to the relevant aspects of the auditory scene.

3.30.4 Functional Organization in Reptilia

The reptilia or sauropsida are a clade that includes turtles (Testudines), snakes and lizards (Lepidosauria), crocodiles and their relatives (Crocodilia), and birds (Aves), as well as a number of extinct groups. The birds and crocodiles (Archosaurs) are more closely related to each other than they are to lepidosaurs, while the position of turtles is controversial (Hedges, S. B. and Poling, L. L., 1999). Because birds arise from within the group traditionally considered to be reptiles, systematists now consider birds to be a subgroup within Reptilia. Most archosaurs are vocal, and birds have provided a major model for studies of complex sound processing and vocal communication.

3.30.4.1 The Auditory Periphery of Reptilia

Reptilia usually have an external ear and tympanum, with the only exception being Sphenodon, the surviving member of the order Rhynchocephalia, and the only living genus that shows an unmodified diapsid skull. Reptilia have one middle ear bone, the columella, which connects the tympanum and the oval window. The hearing organ of turtles, lizards, and archosaurs develops as an out-pocket from the saccule (Morsli, H. *et al.*, 1998). This ear has a new feature, the elongate basilar membrane (Wever, E. G., 1978). The evolution of the stereotypical basilar papilla of modern amniotes appears to have begun with the stem reptiles (Miller, M. R., 1980; Manley, G. A., 2000), and its key features are seen in turtles. The turtle basilar papilla is a flat strip of membrane populated by approximately 1000 tonotopically organized hair cells (see Chapter Phylogeny and Evolution of Ciliated Mechano-Receptor Cells). Salient features in papilla evolution include lengthening and curvature of the sensory epithelia, features thought to both enhance sensitivity and extend the audible frequency range (Manley, G. A. and Gleich, O., 2000).

The major tetrapod lineages are thought to have diverged from the stem reptiles quite early, and the ears of these groups are believed to have evolved in parallel. Tonotopic organization and the elongation of the papilla is seen in all groups. In addition, lizards display a unique population of free-standing hair cells that are not associated with a tectorial membrane. Free-standing hair cells are thought to be an adaptation that enables lizards to respond to higher frequencies (Manley, G. A. and Gleich, O., 2000). Tectorial hair cells in lizards resemble those found in birds and mammals. Usually lizard auditory nerve fibers encode low-center frequencies (100–800 Hz) and have sharp asymmetric tuning curves. Fibers from free-standing hair cells have high center frequencies (900–4000 Hz), high spontaneous rates, and broad symmetric tuning curves.

The basilar membrane of birds contains rows of hair cells that vary in height across the membrane. The number varies with species, with about 16 000 hair cells in the barn owl, 17 000 in the emu, and 6000 in the starling (Köppl, C., 2001). The avian basilar membrane does not contain the two types of hair cells found in mammals, but there are differences in innervation. Tall hair cells closest to the neural edge of the papilla provide the most afferent input to the auditory nerve dendrites, while short hair cells furthest from the neural edge receive purely efferent innervation. In general, the height of the hair cell stereocilia varies smoothly from one end of the papilla to the other, with long stereocilia at the apical low-frequency end of the papilla, and short stereocilia at the basal

high-frequency end. Birds hear higher frequencies than turtles, snakes, and lizards (Dooling, R. J., 2000; Klump, G., 2000). Most birds hear up to 5–6 kHz, while the barn owl has exceptional high-frequency hearing, with characteristic frequencies of 9–10 kHz in the auditory nerve (Konishi, M., 1973).

Additional auditory sensitivity to lower frequencies may be contributed by the saccule. In reptilia and mammals, the saccule had been assumed to be purely vestibular. Auditory sensitivity has been shown in reptiles (Lewis, E. R. and Narins, P. M., 1998), birds (Wit, H. *et al.*, 1984), and mammals (Young, E. D. *et al.*, 1977), however, and an accumulating body of evidence suggests that the saccule has retained some acoustic sensitivity (see Todd, N. P. and Merker, B., 2004 for review).

3.30.4.2 The Auditory Medulla of Reptilia

Tonotopic organization appears to be a key feature of the central auditory system of birds and crocodilians. Each point on the basilar membrane projects to an isofrequency plane across the extent of the first-order auditory nuclei. Thus the cochlear place representation is expanded into a second dimension in the brain, unlike the visual and somatosensory systems, which are point to point. These tonotopic sheets are preserved all the way to the forebrain, although it is not clear what features are processed in these isofrequency slabs. Divergent and convergent connections within isofrequency planes may be observed at all levels.

The reptilian central auditory system is organized in a common plan (Carr, C. E. and Code, R. A., 2000; Figure 1, Table 1). The auditory nerve enters the brain and divides into two, with the ascending branch terminating in the nucleus angularis and the descending branch in the nucleus magnocellularis. Except in some lizards, the nucleus magnocellularis projects to the nucleus laminaris, which in turn projects to the superior olive, to the lemniscal nuclei, and to the central nucleus of the auditory midbrain. The nucleus angularis projects to the superior olive, to the lemniscal nuclei, and to the central nucleus of the auditory midbrain. The parallel ascending projections of angularis and laminaris may or may not overlap with one another. Hindbrain auditory connections are generally bilateral, although contralateral projections predominate.

The evolutionary relationships among the elements of the central auditory systems of reptiles and mammals are beginning to be assessed using developmental comparisons. The early development of the avian hindbrain has been described in terms of rhombomere(r)-derived domains (Marin, F. and Puelles, L., 1995; Cramer, K. S. *et al.*, 2000). The nuclei of the lateral lemniscus originate between r1 and r3; nucleus angularis from r3 to r6; nucleus laminaris mostly from r5 with a small contribution from r6; nucleus magnocellularis from r5, r6, and r7; and the superior olivary nucleus from r5. The vestibular and sensory trigeminal columns both extend from r1 caudal throughout the hindbrain. A new study of the origins of the mouse cochlear nuclei has revealed distinct and not entirely overlapping origins from those observed in the chicken. The neurons of the cochlear nuclei arise largely from r2–r5, although a contribution arising from more caudal territories cannot be ruled out (Farago, A. F. *et al.*, 2006).

The first-order auditory nuclei encode parallel ascending auditory information streams (compare with other vertebrate nuclei in Table 1). In the owl, the nucleus magnocellularis is the origin of a neural pathway that encodes timing information, while a parallel pathway for encoding sound level originates with nucleus angularis (Takahashi, T. *et al.*, 1984). Auditory responses in the nucleus angularis include primarylike, onset, chopper, and complex-type-IV responses (Köppl, C. and Carr, C. E., 2003). Recordings in the chicken cochlear nuclei have found a similar but less clear segregation of function (Warchol, M. E. and Dallos, P., 1990). The similarities between the owl and the chicken suggest that the functional separation of time and level coding is a common feature of the avian auditory system. Although the anatomical divisions into angular and magnocellular nuclei characterize turtles, lizards, and archosaurs, there are no similar physiological data from turtles and lizards.

The auditory system uses phase-locked spikes to encode the timing of the stimulus. Phase-locking underlies accurate detection of temporal information, including detection of ITDs and gap detection (see Chapters Biophysical Specializations of Neurons that Encode Timing and Encoding of Interaural Timing for Binaural Hearing). Neural substrates for phase locking include the specialized endbulb terminal in the nucleus magnocellularis, termed an endbulb of Held. This large synapse has been documented in mammals, birds, and crocodilians, and conveys the phase-locked discharge of the auditory nerve fibers to its postsynaptic targets in the nucleus magnocellularis (see Chapter Central Synapses that Preserve Auditory Timing). Alpha-amino-3-hydroxy-5-methyl-4-isoxazole propionic acid (AMPA)-type glutamate receptors

contribute to the rapid response of the postsynaptic cell by virtue of their rapid desensitization kinetics (Parks, T. N., 2000). In birds, the nucleus magnocellularis projects to the nucleus laminaris, where sensitivity to ITDs emerges (see Chapter Encoding of Interaural Timing for Binaural Hearing). In the barn owl and chicken, nucleus laminaris neurons generate ITD selectivity by coincidence detection between binaural excitatory inputs and encode ITD in a place map according to the Jeffress model (Chapter Encoding of Interaural Timing for Binaural Hearing).

The lemniscal nuclei are located caudal and ventral to the auditory midbrain. There are two identified lemniscal nuclei in lizards and turtles (dorsal and ventral) and three in birds (dorsal, intermediate, and ventral). They receive input from the first-order auditory nuclei and from the nucleus laminaris, and they project to midbrain, thalamic, and forebrain targets. The dorsal lemniscal nucleus mediates detection of interaural level differences (ILDs) in the barn owl, which are important for the determination of elevation of sound sources (Konishi, M., 2003). The ILD pathway begins with the nucleus angularis, which responds to changing sound levels over about a 30 dB range (Köppl, C. and Carr, C. E., 2003). Each nucleus angularis projects to the contralateral dorsal nucleus of the lateral lemniscus, where sensitivity to ILDs emerges. Since dorsal lemniscal neurons do not encode elevation unambiguously, they are described as sensitive to ILD, but not selective because they are not immune to changes in sound level. The encoding of elevation improves in the auditory midbrain.

3.30.4.3 The Auditory Midbrain of Reptilia

The auditory midbrain in reptilia is termed the torus semicircularis or inferior colliculus. It receives ascending input and projects to the thalamus. It is surrounded rostrally and laterally by an intercollicular area that receives descending input from the forebrain archistriatum (Puelles, L. *et al.*, 1994). The auditory midbrain mediates auditory processing, while the intercollicular area appears to mediate vocalization and other auditory-motor behaviors.

In birds, the auditory midbrain is divided into an external nucleus and a central nucleus. The nucleus angularis, lemniscal nuclei, and nucleus laminaris project to regions of the central nucleus (Conlee, J. W. and Parks, T. N., 1986; Takahashi, T. T. and Konishi, M., 1988). Studies of the owl auditory midbrain have shown that most neurons are binaural, excited by inputs from the contralateral ear and inhibited by the ipsilateral ear, although bilateral excitation and contralateral excitation are also present. The tonotopic organization is consistent with the tonotopy observed in lizards and crocodiles, with low best frequencies dorsal.

Physiological recordings from the midbrain in barn owls and songbirds show the emergence of biologically relevant responses (Konishi, M., 2003; Woolley, S. M. *et al.*, 2005). Behavioral studies have identified the relevant stimulus features for barn owl sound localization (Takahashi, T. T. *et al.*, 2003). These nocturnal predators have excellent sound localization ability, and their midbrain responses are dominated by binaural computations underlying localization. Most barn owl inferior colliculus neurons are binaural, and many are sensitive to changes in ILD and ITD. Physiological properties are subdivision specific and reflect the inputs to each subdivision. The central nucleus projects both to the auditory thalamus and external nucleus. Space-specific responses emerge in the external nucleus (Konishi, M., 2003; Takahashi, T. T. *et al.*, 2003). The external nucleus projects topographically to the optic tectum, which contains aligned maps of visual and auditory space. Activity in the tectum directs the rapid head movements made by the owl in response to auditory and visual stimuli (Knudsen, E. I. *et al.*, 2000).

3.30.4.4 The Auditory Forebrain of Reptilia

In reptilia, the central nucleus of the auditory midbrain projects bilaterally to a dorsal thalamus region made up of a central nucleus surrounded by a shell (Grothe, B. *et al.*, 2004). The core and shell receive ascending input from the central nucleus and from the lemniscal nuclei, respectively. In both birds and crocodilians, the core and shell thalamic regions project to separate, nonoverlapping regions of forebrain, suggesting a basic division of auditory input to the forebrain into two separate streams (Grothe, B. *et al.*, 2004). Although the connections and dorsal thalamic locations are consistent throughout amniote phylogeny, suggesting these structures are homologous, the anatomical terminology differs. The dorsal thalamus is called nucleus reuniens in turtles, nucleus medialis in lizards and crocodilians, and nucleus ovoidalis in birds. The avian nucleus ovoidalis is tonotopically organized, with high best frequencies located dorsally, and low best frequencies ventrally. There is not a great deal known about the physiological properties of the auditory dorsal thalamus. In

the barn owl, all divisions of the central nucleus project to the nucleus ovoidalis, and the physiological responses in ovoidalis reflect this diverse array of inputs. Most neurons respond to ITD and/or ILD, at stimulus frequencies similar to those found in the midbrain. In contrast to the mapping found in the owl midbrain, however, nucleus ovoidalis contains no systematic representation of sound localization cues. Nevertheless, space-specific responses are found in the forebrain, and sound localization and gaze control are mediated in parallel in the midbrain and forebrain of the barn owl (Konishi, M., 2003).

In birds, the nucleus ovoidalis projects to field L (Karten, H. J., 1968; Wild, J. M. *et al.*, 1993). Field L is the primary auditory area of the avian telencephalon, and is divided into three parallel layers; L1, L2, and L3, with L2 further divided into L2a and L2b. Auditory units in L2 generally have narrow tuning curves with inhibitory sidebands, which might be expected from their direct input from the dorsal thalamus, while the cells of L1 and L3 exhibit more complex responses (Karten, H. J., 1968; Scheich, H. *et al.*, 1979). The general avian pattern is that Field L projects to the adjacent nidopallium and to other nuclei of the caudal nidopallium. These nidopallial nuclei project to the auditory areas of the arcopallium (ventromedial nucleus of the intermediate arcopallium (AIVM), robust nucleus of the arcopallium (RA)), which project back down to the auditory thalamus and midbrain (Carr, C. E. and Code, R. A., 2000). Karten H. J. (1968) has hypothesized that the organization of the ovoidalis to field L circuit in birds resembles the pathway in mammals from the ventral medial geniculate nucleus to primary auditory cortex (see Reiner, A. *et al.*, 2005 for review).

The auditory forebrain exhibits large changes associated with the increased use of sound for communication in archosaurs and mammals. In the archosaurs, the clearest examples are the specialized communication systems that have evolved in parallel in songbirds, parrots, and humming birds. Birds that learn their vocal motor behavior have a strong dependence on hearing. Their telencephalic song system is composed of an anterior and posterior pathway. The posterior pathway is composed of a circuit from the higher vocal center (HVC) to the RA and then down to the motor nuclei that control the syrinx and respiration (Nottebohm, F., 1980; Brainard, M. S. and Doupe, A. J., 2000). The posterior pathway is required throughout life for song production. The anterior forebrain pathway is a basal ganglia–forebrain circuit critical for song learning and for adult modification of vocal output. The anterior pathway projects to the posterior pathway, and is thus well positioned to provide a guiding influence on the developing vocal motor program.

The anterior pathway is homologous to basal ganglia circuits in mammals (Bottjer, S. W. and Johnson, F., 1997). A modern revision of the avian anatomical nomenclature has provided a common language for studying the function of the cortical–basal ganglia–cortical loop, enabling neuroscientists to take advantage of the specialization of basal ganglia areas in various birds (Doupe, A. J. *et al.*, 2005; Jarvis, E. D. *et al.*, 2005). In both birds and mammals, the basal ganglia contain similar cell types, which project to the midbrain substantia nigra and globus pallidus, and receive a major glutaminergic input from the overlying pallium, dopaminergic input from the midbrain, and a lesser glutamatergic input from the thalamus. The two types of striatal projection neuron, a substantia nigra and a globus pallidus are present in all jawed vertebrates, supporting the idea that the basal ganglia performs a fundamental role in telencephalic function (Doupe, A. J. *et al.*, 2005). Studies of the role of the anterior pathway in auditory learning are illuminating the interaction between sensory, motor, and reward signals in the basal ganglia, and the function of these signals in task learning and execution.

3.30.5 Functional Organization in Mammals

Mammals are a monophyletic group composed of the placental mammals (or eutheria) and two sister taxa, the monotremes and marsupials (Janke, A. *et al.*, 1997). One of the defining mammalian characters is the presence of three middle ear bones. Mammals also differ from other vertebrates in often having moveable external ears and sensitivity to high-frequency sound. The mammalian central auditory system is further characterized by the addition of type II auditory nerve fibers and by additional nuclei including the dorsal cochlear nucleus (DCN), the nuclei of the trapezoid body, and multiple olivary nuclei. The mammalian auditory system has been the subject of numerous books and articles, and will only be briefly reviewed here.

3.30.5.1 The Auditory Receptors of Mammals

Mammals usually have external ears that collect sound and act as directional filters. Three middle ear bones work together as a lever system to amplify the force of sound vibrations (see Chapter Mechano-Acoustical Transformations). In mammals, auditory hair cells in the cochlea (Figure 3(b)) are organized on the basilar membrane into rows of inner and outer hair cells. Inner hair cells innervate type I primary afferents and are innervated by a very few efferents. Outer hair cells sparsely innervate by type II primary afferents and receive more efferent terminals.

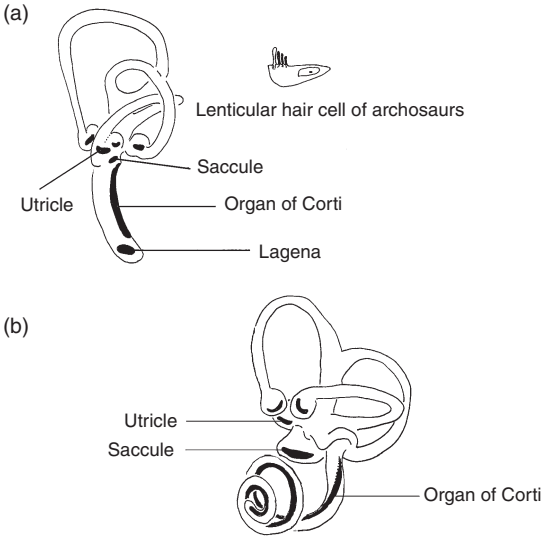

Figure 3 Comparison of archosaurian and mammalian inner ears. The branching of nerve VIII has not been included. The semicircular canal cristae of the vestibular system are shown but not labeled (compare to Figure 2). (a) Generalized archosaur ear (crocodilian/avian). Note the relationship between the lagena and the elongate basilar papilla (also called the basilar membrane and organ of Corti). The archosaurs have a unique lenticular hair cell, which varies in shape and frequency response with location along the basilar membrane (see figures 3.1 and 3.5 in Gleich, O., and Manley, G. A., 2000). (b) Generalized mammalian ear (guinea-pig). Note the loss of the lagena and the impressive increase in the length of the organ of Corti (cochlea), associated with a greater range of frequency sensitivity than found in archosaurs. Mammalian hair cells lack a kinocilium and are oriented identically all along the cochlea, with systematic changes in surface morphology correlated to their frequency response. Note that micromechanical factors also influence frequency sensitivity along the cochlea. Adapted from Lewis, E. R., Leverenz, E. L., and Bialek, W. S. 1985. The Vertebrate Inner Ear. CRC Press.

Mammals hear relatively high frequencies compared to other vertebrates. Most mammals hear up to 20 kHz, while microchiropteran bats and some toothed whales have evolved high-frequency hearing for use in sonar, with characteristic frequencies of 50–120 kHz. Some mammals (e.g., elephants and baleen whales) are sensitive to infrasound, which they use for communication (Payne, K. *et al.*, 1986; Edds-Walton, P. L., 1997). Auditory sensitivity has been documented in saccular afferents of guinea-pigs, cats, and squirrel monkeys (see Todd, N. P. and Merker, B., 2004 for review). Saccular responses are like those associated with type I hair cells, with a best stimulus frequency between about 200 and 1000 Hz, and a rate threshold of about 90 dB sound pressure level (SPL).

3.30.5.2 The Auditory Medulla of Mammals

The auditory nerve enters the brain and divides into two, with the ascending branch projecting to the anterior region of the ventral cochlear nucleus (VCN) and the descending branch to the posterior region of the VCN and to the new DCN. The cochlear nucleus complex develops modularly from progenitor populations arrayed as rostrocaudal microdomains both within and outside the lower rhombic lip region of rhombomeres 3–5 (Farago, A. F. *et al.*, 2006). VCN subdivisions arise from more rostral lower rhombic lip than the DCN, which arises from the region of rhombomere 5, both caudal and noncontiguous to the cerebellar primordium. Thus, although the DCN has a laminar, cerebellum-like organization that includes a granule cell system (Oertel, D. and Young, E. D., 2004), its embryonic origins suggest that it is evolutionarily separate from the cerebellar primordium in rhombomere 1. The VCN contains both large cells and a granule cell cap. These two populations are also embryonically separable, since VCN neurons arise from lower rhombic lip and coaxial nonlip progenitors while the granule cells derive principally from the lower rhombic lip (Farago, A. F. *et al.*, 2006).

The auditory nerve contains both type I and type II afferents. Type I are the most numerous, receive sharply tuned inputs from inner hair cells, and send thick myelinated axons into the brain. Type II afferents are assumed to be unique to mammals, are innervated by outer hair cells, and have thin, unmyelinated axons. They project to granule cell regions of VCN and DCN, and also are involved in the efferent feedback circuit to the cochlea (Ryugo, D. K. and May, S. K.,

1993). Tonotopy is preserved in the projections of the auditory nerve. In mammals, the ventral part of each cochlear nucleus receives low-frequency (apical) input and dorsal areas receive high-frequency input. The auditory nerve forms different types of terminals onto different cell types in the cochlear nucleus (Ryugo, D. K. and May, S. K., 1993). Endbulb of Held terminals are formed on bushy cells (see below), while more varicose or boutonlike terminals are formed on other cell types in the cochlear nuclei. The auditory nerve appears to use glutamate as a transmitter, often with the postsynaptic cell expressing fast AMPA-type glutamate receptors that can mediate precise temporal coding (Parks, T. N., 2000; see Chapter Central Synapses that Preserve Auditory Timing).

There are nine distinguishable projection neurons in the cochlear nucleus – seven in the VCN and two in the DCN (Rouiller, E. M. and Ryugo, D. K., 1984; Rhode, W. S., 1991; Young, E. D., 1998; Cant, N. B. and Benson, C. G., 2003). In the VCN, bushy cells receive endbulb inputs from the auditory nerve and exhibit accurate temporal coding (see Chapter Biophysical Specializations of Neurons that Encode Timing). Spherical bushy cells dominate the anterior VCN, respond to lower best frequencies, and project to the medial superior olive (MSO), which is sensitive to ITDs. Globular bushy cells respond to higher frequencies and project to the lateral superior olive (LSO) and the medial nucleus of the trapezoid body (MNTB). These projections may mediate detection of ILDs (see Chapter Encoding of Interaural Level Differences for Sound Localization). Octopus cells in the posterior VCN are multipolar, with thick dendrites that extend across the nerve root (Oertel, D. *et al.*, 2000). This morphology enables them to integrate auditory nerve inputs across a range of frequencies. Octopus cells encode the time structure of stimuli with great precision and exhibit onset responses to tonal stimuli (Oertel, D. *et al.*, 2000). Onsets play an important role in theories of speech perception, and segregation and grouping of sound sources (Bregman, A. S., 1990).

The DCN appears for the first time in mammals, and is assumed to have evolved with the development of high-frequency hearing and motile external ears. It is composed of a cerebellar-like circuit in the superficial layers, with projection cells below that receive auditory nerve inputs (Oertel, D. and Young, E. D., 2004). The granule cells in the superficial layers receive ascending somatosensory input that may convey information about head and ear position. The deep portion of the DCN contains fusiform and stellate cell types. Fusiform cells exhibit complex (type IV) frequency tuning curves, with small areas of excitation at best frequency and at sides. This response is well suited to detecting the notches in sound level created by the external pinna, which provide cues for locating sound in elevation (Brown, C. and May, B. J., 2005).

The olivary nuclei regulate the binaural convergence of acoustic information and mediate spatial hearing. Neural computations for sound localization begin at this first site of binaural convergence. The LSO encodes ILD (see Chapter Encoding of Interaural Level Differences for Sound Localization), while the MSO encodes time differences (see Chapter Encoding of Interaural Timing for Binaural Hearing). Information conveyed by temporal and rate codes appears to be transformed in the olivary nuclei into codes for location. The LSO principal cells receive excitatory inputs from ipsilateral globular bushy cells, and inhibitory glycinergic inputs onto their cell bodies and proximal dendrites, relayed from the contralateral ear via the MNTB. The MNTB input acts to reverse the sign of bushy cell input from excitatory to inhibitory to make an EI response and create sensitivity to ILDs (see Chapter Encoding of Interaural Level Differences for Sound Localization). In general, as the strength of the contralateral input increases with increasing loudness in the contralateral ear, the maximum rate decreases. Thus, LSO firing rate signals a range of ILDs (for review, see Kuwada, S. *et al.*, 1997).

Sensitivity to ITDs originates in the MSO (see Chapter Encoding of Interaural Timing for Binaural Hearing). Neurons of the MSO act as coincidence detectors, as do the neurons of the reptilian nucleus laminaris. Nevertheless, there may be differences in how birds and mammals encode ITDs. Recent evidence from guinea-pigs and gerbils indicates that in mammals, ITDs are not represented by maximal discharges of a small subpopulation of neurons within one frequency contour, but rather by the relative activity of the frequency contours of both MSOs. This activity is regulated by inhibition, not delay-lines (see reviews in Grothe, B., 2003; McAlpine, D. and Grothe, B., 2003). It is possible that neuronal representation of auditory space differs in reptiles and mammals indicating again a parallel, independent evolution of spatial hearing (Grothe, B. *et al.*, 2004).

There are three mammalian lemniscal nuclei: ventral, intermediate, and dorsal. They receive projections from the cochlear nuclei and olivary complex (Cant, N. B. and Benson, C. G., 2003). The ventral lemniscal

nucleus contains a columnar region characterized by broad-frequency tuning and temporally precise inputs that encode stimulus onset time. The dorsal lemniscal nucleus is largely binaural, and receives ITD information from the superior olivary complex. The dorsal lemniscal nucleus provides a strong GABAergic inhibitory input to the inferior colliculus, and may serve to transform the coding of ITDs there (Winer, J. A. *et al.*, 1995; Kuwada, S. *et al.*, 2006).

3.30.5.3 The Auditory Midbrain of Mammals

The inferior colliculus is the midbrain target of ascending auditory information. It has three major divisions, the central nucleus, the lateral nucleus, and dorsal cortex (see Winer, J. A. and Schreiner, C. E., 2005). In the central nucleus, the inputs from brainstem auditory nuclei are either distributed across or superimposed upon maps to form what are believed to be locally segregated functional zones for processing different aspects of the auditory stimulus (Oliver, D. L. and Morest, D. K., 1984; Ehret, G., 1997; Covey, E. and Carr, C. E., 2005; Winer, J. A. and Schreiner, C., 2005). The central nucleus receives both direct monaural input and indirect binaural input (Winer, J. A. and Schreiner, C., 2005). Physiological studies show both binaural and monaural responses (Ehret, G., 1997), and the emergence of coding for biologically important parameters. Input sources include the cochlear nucleus, olivary complex (Glendenning, K. K. *et al.*, 1992), lemniscal nuclei, and descending inputs from auditory cortical areas (Winer, J. A. *et al.*, 1998). There are also commissural and intrinsic projections. The inferior colliculus projects back to almost all auditory brainstem nuclei, and projects bilaterally to the auditory thalamus.

The central nucleus is exclusively auditory and is essential for normal hearing, the lateral nucleus is multisensory, and the dorsal cortex receives most of its projections from the cerebral cortex. Physiological properties that arise in the auditory midbrain distinguish it from medullary auditory nuclei, and Casseday J. H. and Covey E. (1996) have proposed that tuning processes in the inferior colliculus are related to the biological importance of sounds. They propose that the changes in timing properties at the inferior colliculus, from rapid input to output timing related to the timing of specific behaviors.

3.30.5.4 The Auditory Forebrain of Mammals

In mammals, the ascending auditory projections share many features with other vertebrates, although the origins and homologies of mammalian cortex are not yet well understood (Aboitiz, F. *et al.*, 2003). The isocortex is a distinctive feature of mammalian brains, and has no clear counterpart in the cerebral hemispheres of other amniotes. Current studies suggest that the isocortex may have originated from the dorsal pallium (Northcutt, R. G. and Kaas, J. H., 1995). As in birds and frogs, the auditory regions of the mammalian forebrain exhibit large changes in size and number of auditory areas, possibly associated with the increased use of sound for communication.

Mammalian auditory cortex receives ascending input from the medial geniculate complex. Primary auditory cortex (A1) generally contains three primary-like areas that are tonotopically organized and highly responsive to pure tones (see Chapter The Functional Neuroanatomy of the Auditory Cortex). Auditory information is then distributed from these core areas to surrounding belt regions that are less precisely cochleotopic and generally more responsive to complex stimuli. Belt and parabelt regions may be concerned with integrative and associative functions involved in pattern perception and object recognition. At least one tonotopic representation has been found in all species studied. Primitive mammals like tenrecs have few auditory areas (Krubitzer, L. *et al.*, 1997), there are at least seven tonotopic maps in the cat and mustached bat (Winer, J. A., 1992), and eight in the macaque monkey (Petkov, C. I. *et al.*, 2006).

Functional analyses demonstrate independent processing streams for sound localization and identification, analogous to the what and where streams in visual cortex (Rauschecker, J. P. and Tian, B., 2000). The nature of both these streams is still elusive. Spatial representation (where) in the mammalian auditory cortex has proven to be a difficult issue. Unlike the superior colliculus, there is no topographic organization of binaural cues or spatial sensitivity (see Chapter Sound Localization and the Auditory Cortex). Detection of salient sounds (what) is also only incompletely understood. Recordings from marmoset auditory cortex reveal very similar preferences for species-specific vocalizations to those found in songbirds.

Mechanisms underlying the emergence of responses to complex sounds also have been addressed in the most vocal mammals, bats, which use sound for both echolocation and communication. Bats determine

target distance from the time delay between their sonar vocalizations and the returning echoes and use the three-dimensional information about target location to guide the features of their sonar vocalizations. In the mustached bat (*Pteronotus parnellii*), numerous auditory cortical areas are related to identification of echolocated prey. A1 systematically represents frequency with an enlarged representation of the Doppler shift compensation region, mapping not just frequency, but amplitude. There are several maps of echo delay, for delays that represent near, mid-range, and far targets. There are also maps of the contralateral azimuth and a second Doppler shift region. Suga N. (1988) has used these data to construct a parallel-hierarchical scheme for signal processing. Two major principles have emerged from studies of bat auditory processing. First, since different components of echolocation calls differ in frequency, they are processed in parallel channels in the auditory system by virtue of their tonotopy. In the cortex, however, combination sensitive neurons may be created by comparing across frequency channels (Suga, N., 1988). Second, this work has shown that the auditory system has the potential for reorganization as a function of experience. In particular, corticofugal projections can affect the properties of subcortical neurons in response to sound (Suga, N. and Ma, X., 2003).

3.30.6 Summary

There are exceptions that limit our ability to make generalizations about auditory processing that apply to all members of any vertebrate group. While all vertebrates hear, there is great variation in their auditory periphery and in the frequencies detected. Nevertheless, phase-locking, frequency tuning, temporal sensitivity, and binaural processing are present in all vertebrates.

Fishes lack an outer ear but have auditory end organs that function similarly to those of terrestrial vertebrates. The auditory epithelia are stimulated by particle motion, with best frequencies below 500 Hz being most common. Physiologically polarized hair cells are oriented in various directions within and among the auditory end organs of fishes, and form an anatomical basis for sound source localization. Pressure sensitivity is a specialization found primarily in freshwater fishes, usually accompanied by an extended sensitivity to higher frequencies.

Evolutionarily, the amphibians developed an external tympanum and a middle ear, plus a unique auditory inner ear end organ, the amphibian papilla, not found among other vertebrates. The tympanum/middle ear transduces air- or water-borne pressure waves into particle motion in the fluids surrounding the auditory end organs. Some also detect substrate vibrations via bone conduction. Sound source localization and discrimination of species-specific calls critical to reproduction appear to be the major driving forces in the organization of both the periphery and the central nervous system in anurans. Primary afferent responses are similar to those of fishes, but feature detection is well-developed at the midbrain level in anurans and the forebrain may primarily coordinate appropriate responses to input from auditory and other sensory systems.

Among the Reptilia, evolutionarily new specializations of the auditory periphery emerge, with an elongate basilar membrane, systematic variations in hair cell morphology and tonotopic organization. There is great variability in the auditory periphery of the lizards. Birds are the most intensively studied Reptilia, and provide a model for studies of complex sound processing and vocal communication. Parallel pathways for encoding interaural time and level differences mediate sound source localization.

Mammals have a further elongated and coiled cochlea in the inner ear with specialized inner and outer hair cells and great diversity in hearing capabilities, from infrasound to ultrasound. Localization was improved by the development of moveable external ears. The forebrain auditory processing areas are characterized by complex responses to auditory stimuli, including those related to sound source localization and communication.

Despite similarities in the organization of the central auditory systems of vertebrates, it is not clear whether the components are homologous, or whether the evolution of the central auditory system merely follows the organizational pattern common to the octaval system. The auditory processing observed in modern vertebrates shows many examples of parallel solutions to similar problems.

References

Aboitiz, F., Morales, D., and Montiel, J. 2003. The evolutionary origin of the mammalian isocortex: towards an integrated developmental and functional approach. Behav. Brain Sci. 26, 535–552.

Barry, M. A. 1987. Afferent and efferent connections of the primary octaval nuclei in the clearnose skate, *Raja eglanteria*. J. Comp. Neurol. 266, 457–477.

Bottjer, S. W. and Johnson, F. 1997. Circuits, hormones, and learning: vocal behavior in songbirds. J. Neurobiol. 33, 602–618.

Braford, M. R., Jr. 1995. Comparative aspects of forebrain organization in the ray-finned fishes: touchstones or not? Brain Behav. Evol. 46, 259–274.

Brainard, M. S. and Doupe, A. J. 2000. Auditory feedback in learning and maintenance of vocal behaviour. Nat. Rev. Neurosci. 1, 31–40.

Bregman, A. S. 1990. Auditory Scene Analysis. MIT Press.

Brown, C. and May, B. J. 2005. Comparative Mammalian Sound Localization. In: Sound Source Localization (*eds*. A. N. Popper and R. R. Fay), pp. 124–178. Springer.

Cant, N. B. 1992. The Cochlear Nucleus: Neuronal Types and their Synaptic Organization. In: The Mammalian Auditory Pathway: Neuroanatomy (*eds*. D. B. Webster, A. N. Popper, and R. R. Fay), pp. 66–116. Springer.

Cant, N. B. and Benson, C. G. 2003. Parallel auditory pathways: projection patterns of the different neuronal populations in the dorsal and ventral cochlear nuclei. Brain Res. Bull. 60, 457–474.

Carr, C. E. and Code, R. A. 2000. The Central Auditory System of Reptiles and Birds. In: Comparative Hearing: Birds and Reptiles (*eds*. R. J. Dooling, R. R. Fay, and A. N. Popper), pp. 197–248. Springer.

Casseday, J. H. and Covey, E. 1996. A neuroethological theory of the operation of the inferior colliculus. Brain Behav. Evol. 47, 311–336.

Christensen-Dalsgaard, J. and Kanneworff, M. 2005. Binaural interaction in the frog dorsal medullary nucleus. Brain Res. Bull. 66, 522–525.

Christensen-Dalsgaard, J., Jorgensen, M. B., and Kanneworff, M. 1998. Basic response characteristics of auditory nerve fibers in the grassfrog (*Rana temporaria*). Hear. Res. 119, 155–163.

Condon, C. J., Chang, S. H., and Feng, A. S. 1995. Classification of the temporal discharge patterns of single auditory neurons in the frog superior olivary nucleus. Hear. Res. 83, 190–202.

Conlee, J. W. and Parks, T. N. 1986. Origin of ascending auditory projections to the nucleus mesencephalicus lateralis pars dorsalis in the chicken. Brain Res. 367, 96–113.

Cortopassi, K. A. and Lewis, E. R. 1995. Tuning Properties of Acoustic and Equilibrium Axons: A Comparison of Frequency Response Curves in the Bullfrog Lagena. In: Nervous Systems and Behaviour (*eds*. M. Burrows, T. Matheson, P. L. Newland, and H. Shuppe), p. 344. Georg Thieme Verlag.

Cortopassi, K. A. and Lewis, E. R. 1996. High-frequency tuning properties of bullfrog lagenar vestibular afferent fibers. J. Vestib. Res. 6, 105–119.

Corwin, J. T. 1977. Morphology of the macula neglecta in sharks of the genus Carcharhinus. J. Morphol. 152, 341–362.

Corwin, J. T. 1981. Peripheral auditory physiology in the lemon shark: evidence of parallel otolithic and non-otolithic sound detection. J. Comp. Physiol. A 142, 370–390.

Corwin, J. T. 1989. Functional anatomy of the auditory system in sharks and rays. J. Exper. Biol. (Zool. Suppl.) 2, 62–74.

Covey, E. and Carr, C. E. 2005. The Auditory Midbrain in Bats and Birds. In: The Inferior Colliculus (*eds*. J. A. Winer and C. Schreiner), pp. 493–536. Springer.

Cramer, K. S., Fraser, S. E., and Rubel, E. W. 2000. Embryonic origins of auditory brain-stem nuclei in the chick hindbrain. Dev. Biol. 224, 138–151.

Crawford, J. D. 1993. Central auditory neurophysiology of a sound producing mormyrid fish: the mesencephalon of *Pollimyrus isidori*. J. Comp. Physiol. A 172, 1–14.

Denton, E. J., Gray, J. A. B., and Blaxter, J. H. S. 1979. The mechanics of the clupeid acousticolateralis system: frequency responses. J. Mar. Biol. Assoc. UK 59, 27–47.

Dooling, R. J. 2000. Hearing in Birds and Reptiles. In: Comparative Hearing: Birds and Reptiles (*eds*. R. Dooling, A. N. Popper, and R. R. Fay), pp. 308–359. Springer.

Doupe, A. J., Perkel, D. J., Reiner, A., and Stern, E. A. 2005. Birdbrains could teach basal ganglia research a new song. Trends Neurosci. 28, 353–363.

Duman, C. H. and Bodznick, D. 1996. A role for GABAergic inhibition in electrosensory processing and common mode rejection in the dorsal nucleus of the little skate, *Raja erinacea*. J. Comp. Physiol. A 179, 797–807.

Duman, C. H. and Bodznick, D. 1997. Distinct but overlapping populations of commissural and GABAergic neurons in the dorsal nucleus, *Raja erinacea*. Brain Behav. Evol. 49, 99–109.

Echteler, S. M. 1985. Organization of the auditory midbrain in a teleost fish, *Cyprinus carpio*. J. Comp. Physiol. A 156, 267–280.

Edds-Walton, P. L. 1997. Acoustic communication signals of mysticete whales. Bioacoustics 8, 47–60.

Edds-Walton, P. L. 1998. Anatomical evidence for binaural processing in the descending octaval nucleus of the toadfish (*Opsanus tau*). Hear. Res. 123, 41–54.

Edds-Walton, P. L. and Fay, R. R. 2003. Directional selectivity and frequency tuning of midbrain cells in the oyster toadfish, *Opsanus tau*. J. Comp. Physiol. A 189, 527–543.

Edds-Walton, P. L. and Fay, R. R. 2005a. Medullary projections to bimodal sites in the torus semicircularis of the toadfish, *Opsanus tau*. Brain Behav. Evol. 66, 73–87.

Edds-Walton, P. L. and Fay, R. R. 2005b. Sharpening of directional responses along the auditory pathway of the oyster toadfish, *Opsanus tau*. J. Comp. Physiol. A 191, 1079–1086.

Edds-Walton, P. L., Fay, R. R., and Highstein, S. M. 1999. Dendritic arbors and central projections of physiologically characterized auditory fibers from the saccule of the toadfish, *Opsanus tau*. J. Comp. Neurol. 411, 212–238.

Ehret, G. 1997. The auditory cortex. J. Comp. Physiol. A 181, 547–557.

Farago, A. F., Awatramani, R. B., and Dymecki, S. M. 2006. Assembly of the brainstem cochlear nuclear complex is revealed by intersectional and subtractive genetic fate maps. Neuron 50, 205–218.

Fay, R. R. 1984. The goldfish ear codes the axis of acoustic particle motion in three dimensions. Science 225, 951–954.

Fay, R. R. 2005. Sound Source Localization by Fishes. In: Sound Source Localization, Springer Handbook of Auditory Research (*eds*. R. R. Fay and A. N. Popper), Vol. 25, pp. 71–96. Springer.

Fay, R. R. and Simmons, A. M. 1999. The Sense of Hearing in Fishes and Amphibians. In: Comparative Hearing: Fish and Amphibians (*eds*. R. R. Fay and A. N. Popper), pp. 269–318. Springer.

Feng, A. S. 1986. Afferent and efferent innervation patterns of the cochlear nucleus (dorsal medullary nucleus) of the leopard frog. Brain Res. 367, 183–191.

Feng, A. S. and Capranica, R. R. 1976. Sound localization in anurans. II. Binaural interaction in dorsal medullary nucleus of bullfrogs (*Rana catesbeiana*). J. Neurophysiol. 39, 871–881.

Feng, A. S. and Schellart, N. A. M. 1999. Central Auditory Processing in Fish and Amphibians. In: Comparative Hearing: Fish and Amphibians (*eds*. R. R. Fay and A. N. Popper), pp. 218–268. Springer.

Fritzsch, B. 1992. The Water to Land Transition: Evolution of the Tetrapod Basilar Papilla, Middle Ear, and Auditory Nuclei. In: The Evolutionary Biology of Hearing (*eds*. D. B. Webster, R. R. Fay, and A. N. Popper), pp. 351–375. Springer.

Fritzsch, B., Ryan, M. J., Wilczynski, W., Hetherington, T. E., and Walkowiak, W. 1988. The Evolution of the Amphibian Auditory System. Wiley.

Fuzessery, Z. M. 1988. Frequency Tuning in the Anuran Central Auditory System. In: The Evolution of the Amphibian Auditory System (*eds*. B. Fritzsch, M. J. Ryan, W. Wilczynski, T. E. Hetherington, and W. Walkowiak), pp. 253–273. Wiley.

Gleich, O. and Manley, G. A. 2000. The Hearing Organ of Birds and Their Relatives. In: Comparative Hearing: Birds and Reptiles, Springer Handbook of Auditory Research (*eds*. R. Dooling, A. N. Popper, and R. R. Fay), pp. 70–138. Springer.

Glendenning, K. K., Baker, B. N., Hutson, K. A., and Masterton, R. B. 1992. Acoustic chiasm V: inhibition and excitation in the ipsilateral and contralateral projections of lso. J. Comp. Neurol. 319, 100–122.

Gooler, D. M. and Feng, A. S. 1992. Temporal coding in the frog auditory midbrain: the influence of duration and rise-fall time on the processing of complex amplitude-modulated stimuli. J. Neurophysiol. 67, 1–22.

Grothe, B. 2003. New roles for synaptic inhibition in sound localization. Nat. Rev. Neurosci. 4, 540–550.

Grothe, B., Carr, C. E., Casseday, J. H., Fritzsch, B., and Köppl, C. 2004. The Evolution of Central Pathways and their Neural Processing Patterns. In: Evolution of the Vertebrate Auditory System (*eds*. G. A. Manley, A. N. Popper, and R. R. Fay), pp. 289–359. Springer.

Hall, J. C. and Feng, A. S. 1987. Evidence for parallel processing in the frog's auditory thalamus. J. Comp. Neurol. 258, 407–419.

Hedges, S. B. and Poling, L. L. 1999. A molecular phylogeny of reptiles. Science 283, 998–1001.

Highstein, S. M., Kitch, R., Carey, J., and Baker, R. 1992. Anatomical organization of the brainstem octavolateralis area of the oyster toadfish, *Opsanus tau*. J. Comp. Neurol. 319, 501–518.

Horner, K., Sand, O., and Enger, P. S. 1980. Binaural interactions in the cod. J. Exp. Biol. 85, 323–331.

Janke, A., Xu, X., and Arnason, U. 1997. The complete mitochondrial genome of the wallaroo (*Macropus robustus*) and the phylogenetic relationship among monotremata, marsupialia, and eutheria. Proc. Natl. Acad. Sci. U. S. A. 94, 1276–1281.

Jarvis, E. D., Gunturkun, O., Bruce, L., Csillag, A., Karten, H., Kuenzel, W., Medina, L., Paxinos, G., Perkel, D. J., Shimizu, T., Striedter, G., Wild, J. M., Ball, G. F., Dugas-Ford, J., Durand, S. E., Hough, G. E., Husband, S., Kubikova, L., Lee, D. W., Mello, C. V., Powers, A., Siang, C., Smulders, T. V., Wada, K., White, S. A., Yamamoto, K., Yu, J., Reiner, A., and Butler, A. B. 2005. Avian brains and a new understanding of vertebrate brain evolution. Nat. Rev. Neurosci. 6, 151–159.

Karten, H. J. 1968. The ascending auditory pathway in the pigeon (*Columba livia*). II. Telencephalic projections of the nucleus ovoidalis thalami. Brain Res. 11, 134–153.

Klump, G. 2000. Sound Localization in Birds. In: Comparative Hearing: Birds and Reptiles (*eds*. R. J. Dooling, R. R. Fay, and A. N. Popper), pp. 249–307. Springer.

Knudsen, E. I., Zheng, W., and DeBello, W. M. 2000. Traces of learning in the auditory localization pathway. Proc. Natl. Acad. Sci. U. S. A. 97, 11815–11820.

Konishi, M. 1973. Locatable and nonlocatable acoustic signals for barn owls. Am. Naturalist 107, 775–785.

Konishi, M. 2003. Coding of auditory space. Annu. Rev. Neurosci. 26, 31–55.

Köppl, C. 2001. Efferent axons in the avian auditory nerve. Eur. J. Neurosci. 13, 1889–1901.

Köppl, C. and Carr, C. E. 2003. Computational diversity in the cochlear nucleus angularis of the barn owl. J. Neurophysiol. 89, 2313–2329.

Kozloski, J. and Crawford, J. D. 1998. Functional neuroanatomy of auditory pathways in the sound-producing fish *Pollimyrus*. J. Comp. Neurol. 401, 227–252.

Krubitzer, L., Kunzle, H., and Kaas, J. 1997. Organization of sensory cortex in a madagascan insectivore, the tenrec (*Echinops telfairi*). J. Comp. Neurol. 379, 399–414.

Kuwada, S., Batra, R., and Fitzpatrick, D. C. 1997. Neural Processing of Binaural Temporal Cues. In: Binaural and Spatial Hearing in Real and Virtual Environments (*eds*. R. H. Gilkey and T. R. Anderson), pp. 399–426. Erlbaum.

Kuwada, S., Fitzpatrick, D. C., Batra, R., and Ostapoff, E. M. 2006. Sensitivity to interaural time differences in the dorsal nucleus of the lateral lemniscus of the unanesthetized rabbit: comparison with other structures. J. Neurophysiol. 95, 1309–1322.

Lewis, E. R. and Narins, P. M. 1999. The Acoustic Periphery of Amphibians: Anatomy and Physiology. In: Comparative Hearing: Fish and Amphibians (*eds*. R. R. Fay and A. N. Popper), pp. 101–154. Springer.

Lewis, E. R., Leverenz, E. L., and Bialek, W. S. 1985. The Vertebrate Inner Ear. CRC Press.

Locke, R., Vautrin, J., and Highstein, S. 1999. Miniature EPSPs and sensory encoding in the primary afferents of the vestibular lagena of the toadfish, *Opsanus tau*. Ann. N. Y. Acad. Sci. 871, 35–50.

Lowenstein, O. and Roberts, T. D. M. 1951. The localization and analysis of the responses to vibration from the isolated elasmobranch labyrinth. A contribution to the problem of the evolution of hearing in vertebrates. J. Physiol. 114, 471–489.

Lu, Z. and Fay, R. R. 1993. Acoustic response properties of single units in the torus semicircularis of the goldfish, *Carassius auratus*. J. Comp. Physiol. A 173, 33–48.

Lu, Z. and Fay, R. R. 1995. Acoustic response properties of single units in the central posterior nucleus of the thalamus of the goldfish, *Carassius auratus*. J. Comp. Physiol. A 176, 747–760.

Lu, Z., Xu, Z., and Buchser, W. J. 2003. Acoustic response properties of lagenar nerve fibers in the sleeper goby, *Dormitator latifrons*. J. Comp. Physiol. A 189, 889–905.

Lu, Z., Xu, Z., and Buchser, W. J. 2004. Acoustic response properties of utricular nerve fibers in the sleeper goby, *Dormitator latifrons*. J. Comp. Physiol. A 190, 923–938.

Ma, W. L. and Fay, R. R. 2002. Neural representations of the axis of acoustic particle motion in the auditory midbrain of the goldfish, *Carassius auratus*. J. Comp. Physiol. A 188, 301–313.

Manley, G. A. 2000. Cochlear mechanisms from a phylogenetic viewpoint. Proc. Natl. Acad. Sci. 97, 11736–11743.

Manley, G. A. and Gleich, O. 2000. The Peripheral Auditory System of Birds and their Relatives. In: Comparative Hearing: Birds and Reptiles (*eds*. R. J. Dooling, A. N. Popper, and R. R. Fay), pp. 70–138. Springer.

Mann, D. A., Higgs, D. M., Tavolga, W. N., Souza, M. J., and Popper, A. N. 2001. Ultrasound detection by clupeiform fishes. J. Acoust. Soc. Am. 109, 3048–3054.

Marin, F. and Puelles, L. 1995. Morphological fate of rhomboneres in quail/chick chimeras: a segmental analysis of hindbrain nuclei. Eur. J. Neurosci. 7, 1714–1738.

Mason, M. J. 2007. Pathways for Sound Transmission to the Inner Ear in Amphibians. In: Hearing and Sound Communication in Amphibians (*eds*. P. M. Narins, A. S. Feng, R. R. Fay, and A. N. Popper), pp. 147–183. Springer.

McAlpine, D. and Grothe, B. 2003. Sound localization and delay lines – do mammals fit the model? Trends Neurosci. 26, 347–350.

McCormick, C. A. 1992. Evolution of Central Auditory Pathways in Anamniotes. In: The Evolutionary Biology of Hearing (*eds*. D. B. Webster, R. R. Fay, and A. N. Popper), pp. 323–350. Springer.

McCormick, C. A. 1998. Anatomy of the Central Auditory Pathways of Fish and Amphibians. In: Comparative Hearing: Fish and Amphibians (*eds*. R. R. Fay and A. N. Popper), pp. 155–217. Springer.

McCormick, C. A. 1999. Anatomy of the Central Auditory Pathways of Fish and Amphibians. In: Comparative Hearing: Fish and Amphibians (*eds*. A. N. Popper and R. R. Fay), pp. 155–121. Springer.

McCormick, C. A. and Braford, M. R., Jr. 1988. Central Connections of the Octavolateralis System. In: Sensory Biology of Aquatic Animals (*eds*. J. Atema, R. R. Fay, A. N. Popper, and W. N. Tavolga), pp. 733–756. Springer.

McCormick, C. A. and Hernandez, D. V. 1996. Connections of the octaval and lateral line nuclei in the medulla of the goldfish, including cytoarchitecture of the secondary octaval population in goldfish and catfish. Brain Behav. Evol. 47, 113–137.

Miller, M. R. 1980. The Reptilian Cochlear Duct. In: Comparative Studies of Hearing in Vertebrates (*eds*. A. N. Popper and R. R. Fay), pp. 169–204. Springer.

Morsli, H., Choo, D., Ryan, A., Johnson, R., and Wu, D. K. 1998. Development of the mouse inner ear and origin of its sensory organs. J. Neurosci. 18, 3327–3335.

Neary, T. J. 1988. Forebrain Auditory Pathways in Ranid Frogs. In: The Evolution of the Amphibian Auditory System (*eds*. B. Fritzsch, M. J. Ryan, W. Wilczynski, T. E. Hetherington, and W. Walkowiak), pp. 233–252. Wiley.

Nieuwenhuys, R. and Pouwels, E. 1983. The Brain Stem of Actinopterygian Fishes. In: Fish Neurobiology, Vol. I, Brainstem and Sensory Organs (*eds*. R. G. Northcutt and R. E. Davis), pp. 25–87. University of Michigan Press.

Northcutt, R. G. 2006. Connections of the lateral and medial divisions of the goldfish telencephalic pallium. J. Comp. Neurol. 494, 903–943.

Northcutt, R. G. and Kaas, J. H. 1995. The emergence and evolution of mammalian neocortex. Trends Neurosci. 18, 373–379.

Nottebohm, F. 1980. Brain pathways for vocal learning in birds: a review of the first 10 years. Prog. Psychobiol. Physiol. Psychol. 9, 85–124.

Oertel, D. and Young, E. D. 2004. What's a cerebellar circuit doing in the auditory system? Trends Neurosci. 27, 104–110.

Oertel, D., Bal, R., Gardner, S. M., Smith, P. H., and Joris, P. X. 2000. Detection of synchrony in the activity of auditory nerve fibers by octopus cells of the mammalian cochlear nucleus. Proc. Natl. Acad. Sci. U. S. A. 97, 11773–11779.

Oliver, D. L. and Morest, D. K. 1984. The central nucleus of the inferior colliculus in the cat. J. Comp. Neurol. 222, 237–264.

Page, C. H. and Sutterlin, A. M. 1970. Visual and auditory responses in the goldfish tegmentum. J. Neurophysiol. 33, 129–136.

Parks, T. N. 2000. The AMPA receptors of auditory neurons. Hear. Res. 147, 77–91.

Payne, K., Langbauer, W. R., Jr., and Thomas, E. M. 1986. Infrasonic calls of the Asian elephant (*Elephas maximus*). Behav. Ecol. Sociobiol. 18, 297–301.

Platt, C. 1977. Hair cell distribution and orientation in goldfish otolith organs. J. Comp. Neurol. 172, 283–297.

Platt, C. and Popper, A. N. 1981. Structure and Function in the Ear. In: Hearing and Sound Communication in Fishes (*eds*. W. N. Tavolga, A. N. Popper, and R. R. Fay), pp. 3–38. Springer.

Platt, C. and Popper, A. N. 1984. Variation in lengths of ciliary bundles on hair cells along the macula of the sacculus in two species of teleost fishes. Scan. Electron. Microsc. Pt. 4, 1915–1924.

Petkov, C. I., Kayser, C., Augath, M., and Logothetis, N. K. 2006. Functional imaging reveals numerous fields in the monkey auditory cortex. PLoS Biol. 4, e215.

Popper, A. N. and Coombs, S. 1982. The morphology and evolution of the ear in Actinopterygian fishes. Am. Zool. 22, 311–328.

Popper, A. N., Fay, R. R., Platt, C., and Sand, O. 2003. Sound Detection Mechanisms and Capabilities of Teleost Fishes. In: Sensory Processing in Aquatic Environments (*eds*. S. P. Colin and N. J. Marshall), pp. 3–38. Springer.

Prechtl, J. C., vonder Emde, G., Wolfart, J., Karamaursel, S., Akoev, G. N., Andrianov, Y. N., and Bullock, T. N. 1998. Sensory processing in the pallium of a mormyrid fish. J. Neurosci. 18, 7381–7393.

Puelles, L., Robles, C., and Martinez-de-la-Torre, M. 1994. New subdivision schema for the avian torus semicircularis: neurochemical maps in the chick. J. Comp. Neurol. 340, 98–125.

Puzdrowski, R. L. and Leonard, R. B. 1993. The octavolateral systems in the stingray, *Dasyatis sabina*. I. Primary projections of the octaval and lateral line nerves. J. Comp. Neurol. 332, 21–37.

Rauschecker, J. P. and Tian, B. 2000. Mechanisms and streams for processing of ''what'' and ''where'' in auditory cortex. Proc. Natl. Acad. Sci. U. S. A. 97, 11800–11806.

Reiner, A., Yamamoto, K., and Karten, H. J. 2005. Organization and evolution of the avian forebrain. Anat. Rec. A Discov. Mol. Cell Evol. Biol. 287, 1080–1102.

Rhode, W. S. 1991. Physiological–Morphological Properties of the Cochlear Nucleus. In: Neurobiology of Hearing: the Central Auditory System (*eds*. R. A. Altschuler, R. P. Bobbin, B. M. Clopton, and D. W. Hoffman), pp. 47–77. Raven Press.

Rose, G. J. and Gooler, D. M. 2007. Function of the Amphibian Central Auditory System. In: Hearing and Sound Communication in Amphibians (*eds*. P. M. Narins, A. S. Feng, R. R. Fay, and A. N. Popper), pp. 250–290. Springer.

Rose, G. J. and Wilczynski, W. 1984. The anuran superficial reticular nucleus: evidence for homology with nuclei of the lateral lemniscus. Brain Res. 304, 170–172.

Rouiller, E. M. and Ryugo, D. K. 1984. Intracellular marking of physiologically characterized cells in the ventral cochlear nucleus of the cat. J. Comp. Neurol. 225, 167–186.

Ryugo, D. K. and May, S. K. 1993. The projections of intracellularly labeled auditory nerve fibers to the dorsal cochlear nucleus of cats. J. Comp. Neurol. 329, 20–35.

Scheich, H., Langner, G., and Bonke, D. 1979. Responsiveness of units in the auditory neostriatum of the guinea fowl (*Numida meleagris*) to species-specific calls and synthetic stimuli. J. Comp. Physiol. A 132, 257–276.

Schellart, N. A. M. 1983. Acoustical and visual processing and their interaction in the torus semicircularis of the trout, *Salmo gairdneri*. Neurosci. Lett. 42, 39–44.

Schellart, N. A. M. and Kroese, A. B. A. 1989. Interrelationship of Acousticolateral and Visual Systems in the Teleost Midbrain. In: The Mechanosensory Lateral Line: Neurobiology and Evolution (*eds*. S. Coombs, P. Gorner, and H. Munz), pp. 421–443. Springer.

Schellart, N. A. M., Kamermans, M., and Nederstigt, L. J. A. 1987. An electrophysiological study of the topographical organization of the multisensory torus semicircularis of the rainbow trout. Comp. Biochem. Physiol. 88A, 461–469.

Shofner, W. P. 1988. Postmetamorphic Changes in the Auditory System. In: The Evolution of the Amphibian Auditory System (*eds*. B. Fritzsch, M. J. Ryan, W. Wilczynski, T. E. Hetherington, and W. Walkowiak), pp. 377–392. Wiley.

Smotherman, M. and Narins, P. M. 2004. Evolution of the Amphibian Ear. In: Evolution of the Vertebrate Auditory

System (*eds*. G. A. Manley, A. N. Popper, and R. R. Fay), pp. 164–199. Springer.
Striedter, G. F. 1997. The telencephalon of tetrapods in evolution. Brain Behav. Evol. 49, 179–213.
Suga, N. 1988. Auditory Neuroethology and Speech Processing: Complex-Sound Processing by Combination-Sensitive Neurons. In: Auditory Function (*eds*. G. Edelman, W. Gall, and W. Cowan), pp. 679–720. Wiley.
Suga, N. and Ma, X. 2003. Multiparametric corticofugal modulation and plasticity in the auditory system. Nat. Rev. Neurosci. 4, 783–794.
Suwa, H., Gilland, E., and Baker, R. 1999. Otolith ocular reflex function of the tangential nucleus in a teleost fish. Ann. N. Y. Acad. Sci. 871, 1–14.
Takahashi, T. T. and Konishi, M. 1988. Projections of nucleus angularis and nucleus laminaris to the lateral lemniscal nuclear complex of the barn owl. J. Comp. Neurol. 274, 212–238.
Takahashi, T. T., Bala, A. D., Spitzer, M. W., Euston, D. R., Spezio, M. L., and Keller, C. H. 2003. The synthesis and use of the owl's auditory space map. Biol. Cybern. 89, 378–387.
Takahashi, T., Moiseff, A., and Konishi, M. 1984. Time and intensity cues are processed independently in the auditory system of the owl. J. Neurosci. 4, 1781–1786.
Todd, N. P. and Merker, B. 2004. Siamang gibbons exceed the saccular threshold: intensity of the song of hylobates syndactylus. J. Acoust. Soc. Am. 115, 3077–3080.
Tomchik, S. M. and Lu, Z. 2005. Octavolateral projections and organization in the medulla of a teleost fish, the sleeper goby (*Dormitator latifrons*). J. Comp. Neurol. 481, 96–117.
Walkolwiak, W. 1988. Central Temporal Coding. In: The Evolution of the Amphibian Auditory System (*eds*. B. Fritzsch, M. J. Ryan, W. Wilczynski, T. E. Hetherington, and W. Walkowiak), pp. 275–294. Wiley.
Wallace, A. C. and McCormick, C. A. 2005. Otolith endorgan input to auditory projection neurons in the goldfish: a confocal microscopic analysis. Soc. Neurosci. Program No. 182.2, Abstract/Itinerary Planner, Washington, DC (online).
Warchol, M. E. and Dallos, P. 1990. Neural coding in the chick cochlear nucleus. J. Comp. Physiol. A 166, 721–734.
Wever, E. G. 1978. The Reptile Ear. Princeton University Press.
Wilczynski, W. 1988. Brainstem Auditory Pathways. In: The Evolution of the Amphibian Auditory System (*eds*. B. Fritzsch, M. J. Ryan, W. Wilczynski, T. E. Hetherington, and W. Walkowiak), pp. 209–231. Wiley.
Wild, J. M., Karten, H. J., and Frost, B. J. 1993. Connections of the auditory forebrain in the pigeon (*Columba livia*). J. Comp. Neurol. 337, 32–62.
Will, U. 1988. Organization and Projections of the Area Octavolateralis in Amphibians. In: The Evolution of the Amphibian Auditory System (*eds*. B. Fritzsch, M. J. Ryan, W. Wilczynski, T. E. Hetherington, and W. Walkowiak), pp. 185–208. Wiley.
Will, U. and Fritzsch, B. 1988. The Eighth Nerve of Amphibians: Peripheral and Central Distribution. In: The Evolution of the Amphibian Auditory System (*eds*. B. Fritzsch, M. J. Ryan, W. Wilczynski, T. E. Hetherington, and W. Walkowiak), pp. 159–183. Wiley.
Winer, J. A. 1992. The Functional Architecture of the Medial Geniculate Body and the Primary Auditory Cortex. In: The Mammalian Auditory Pathway: Neuroanatomy (*eds*. A. N. popper, R. R. Fay, and D. B. Webster), Vol. 1, pp. 222–409. Springer.
Winer, J. A. and Schreiner, C. E. (*eds*.) (2005) The Inferior Colliculus, pp. 1–705. Springer.
Winer, J. A., Larue, D. T., and Pollak, G. D. 1995. Gaba and glycine in the central auditory system of the mustache bat: structural substrates for inhibitory neuronal organization. J. Comp. Neurol. 355, 317–353.
Winer, J. A., Larue, D. T., Diehl, J. J., and Hefti, B. J. 1998. Auditory cortical projections to the cat inferior colliculus. J. Comp. Neurol. 400, 147–174.
Wit, H., Bleeker, J., and Mulder, H. 1984. Response of pigeon vestibular nerve fibres to sound and vibration with audio frequencies. J. Acoust. Soc. Am. 75, 202–208.
Woolley, S. M., Fremouw, T. E., Hsu, A., and Theunissen, F. E. 2005. Tuning for spectro-temporal modulations as a mechanism for auditory discrimination of natural sounds. Nat. Neurosci. 8, 1371–1379.
Wubbels, R. J., Schellart, N. A. M., and Goossens, J. H. L. M. 1995. Mapping of sound direction in the trout lower midbrain. Neurosci. Lett. 199, 179–182.
Young, E. D. 1998. Cochlear Nucleus. In: The Synaptic Organization of the Brain (*ed*. G. M. Shepherd), pp. 121–158. Oxford University Press.
Young, E. D., Fernandez, C., and Goldberg, J. M. 1977. Responses of squirrel monkey vestibular neurons to audio-frequency sound and head vibration. Acta Otolaryngol. 84, 352–360.
Zakon, H. H. and Wilczynski, W. 1988. The Physiology of the Anuran Eighth Nerve. In: The Evolution of the Amphibian Auditory System (*eds*. B. Fritzsch, M. J. Ryan, W. Wilczynski, T. E. Hetherington, and W. Walkowiak), pp. 125–155. Wiley.

Further Reading

Cant, N. B. and Benson, C. G. 2003. Parallel auditory pathways: projection patterns of the different neuronal populations in the dorsal and ventral cochlear nuclei. Brain Res. Bull. 60, 457–474.
Narins, P. M. and Lewis, E. R. 1984. The vertebrate ear as an exquisite seismic sensor. J. Acoust. Soc. Am. 76, 1384–1387.
Narins, P. M., Feng, A. S., Fay, R. R., and Popper, A. N. (*eds*) 2007. Hearing and Sound Communication in Amphibians, Springer Handbook of Auditory Research, Vol. 28. Springer.
Popratiloff, A. and Peusner, K. D. 2007. Otolith fibers and terminals in chick vestibular nuclei. J. Comp. Neurol. 502, 19–37.
Striedter, G. F. 1991. Auditory, electrosensory, and mechanosensory pathways through the diencephalon and telencephalon of channel catfishes. J. Comp. Neurol. 312, 311–331.
Wilczynski, W. and Endepols, H. 2007. Central Auditory Pathways in Anuran Amphibians: The Anatomical Basis of Hearing and Sound Communication. In: Hearing and Sound Communication in Amphibians (*eds*. P. M. Narins, A. S. Feng, R. R. Fay, and A. N. Popper), pp. 221–249. Springer.

3.31 Invertebrate Auditory Pathways

B Hedwig, University of Cambridge, Cambridge, UK

G S Pollack, McGill University, Montreal, QC, Canada

© 2008 Elsevier Inc. All rights reserved.

3.31.1 General Introduction 526
3.31.1.1 Distribution and Design of Ears 527
3.31.2 Peripheral Processing 528
3.31.2.1 Central Projections of Auditory Receptors 528
3.31.2.1.1 Common features of receptor projections 528
3.31.2.1.2 Functional organization of central afferent projections 529
3.31.2.2 Processing and Physiology 533
3.31.2.3 Coding of Stimulus Amplitude 533
3.31.2.4 Temporal Coding 533
3.31.2.5 Frequency Sensitivity 534
3.31.2.5.1 Lepidoptera 534
3.31.2.5.2 Acridids 535
3.31.2.5.3 Tettigoniids 535
3.31.2.5.4 Gryllids 535
3.31.2.5.5 Mantises 536
3.31.2.5.6 Cicadas 536
3.31.3 Central Pathways 536
3.31.3.1 Overview 536
3.31.3.2 Noctuid Moths 536
3.31.3.3 Acridids 537
3.31.3.4 Ensiferans (Tettigoniids and Gryllids) 537
3.31.3.5 Sound Frequency 537
3.31.3.6 Noctuid Moths 537
3.31.3.7 Mantises 538
3.31.3.8 Acridids 539
3.31.3.9 Tettigoniids 539
3.31.3.10 Gryllids 541
3.31.3.11 Temporal Processing and Pattern Recognition 545
3.31.3.12 Pattern Recognition in Grasshoppers 545
3.31.3.12.1 Gap detection 546
3.31.3.13 Gryllids 546
3.31.3.14 Tettigoniids 548
3.31.3.15 Selective Attention: Detecting the Loudest Singer 549
3.31.3.16 Flies 549
3.31.3.17 Directional Processing 550
3.31.3.18 What Is the Neural Code for Sound Direction? 550
3.31.3.19 Enhancement of Interaural Differences Through Bilateral Interactions 551
3.31.3.20 Contralateral Inhibition in Gryllids 551
3.31.3.21 Contralateral Inhibition in Acridids 553
3.31.3.22 Integration of Pattern Recognition and Sound Localization 554
3.31.3.22.1 Gryllids 554
3.31.3.22.2 Acridids 554
3.31.4 Integrating Hearing with Other Activities 554
3.31.4.1 Ventilation and Flight 554
3.31.4.2 Sound Production 555

3.31.4.2.1	Cicadas	555
3.31.4.2.2	Grasshoppers	555
3.31.4.2.3	Crickets	555
References		557

Glossary

auditory neuropil Projection area in the central nervous system of primary auditory afferents.
chordotonal organ A highly sensitive mechanoreceptive organ that comprises several scolopidial sensilla. Chordotonal organs insert on different parts in the body and have a proprioceptive function.
crista acoustica Hearing organ in the ear of Ensiferans, in which the auditory afferents are arranged tonotopically.
phonotaxis Orientation behavior toward or away from a sound source.
precedence effect Behavioral preference of animals for the earlier of two identical sound signals.
scolopidium An internal mechanoreceptive sensillum consisting of 1–3 bipolar sensory neurons with ciliated dendrites, a scolopale cell that forms a scolopale around the cilia and an attachment cell that links the sensillum to the cuticle.
template matching A mechanism proposed for auditory pattern recognition based on an internal template that is compared with any perceived acoustic signals.
tonotopy Mapping between sound frequency and the spatial distribution of cell bodies or axonal arborizations pattern of auditory afferents.
tympanic membrane Eardrum in the hearing organ of insects.

3.31.1 General Introduction

In comparison to olfaction or vision, hearing in invertebrates probably appeared only recently during evolution, as an adaptation to permit detection of sounds made by predators, especially by bats, or by acoustically active hosts, and to mediate intraspecific communication. Although many groups of invertebrates possess sensory organs capable of responding to sound (particularly in water), insects are the only group in which hearing is used widely. Indeed, the use of airborne acoustic signals in behavior by invertebrates is known, outside the insects, only for some crustaceans (Budelmann, B. U., 1992). Moreover, only scant information is available on the neurobiology of hearing in noninsect groups. Therefore, this chapter focuses exclusively on hearing in insects.

Two functionally different types of sound sensors evolved in insects, which exploit different physical principles and work in completely different frequency ranges. Tympanic membranes attached to some cuticular framework respond to acoustically mediated changes in the air pressure. Fragile elongated hair- or feather-like structures act as velocity receptors and respond to the coherent movements of air that occur close to a sound source. Velocity receptors are sensitive to sounds with frequencies well below 1 kHz, whereas sensitivity of pressure receivers is best for frequencies in the range of about 3–50 kHz and is poor for low frequencies due to constraints of body size. Auditory systems allow the insects to deal with several fundamental tasks:

1. The detection of predator signals to prepare for an evasive response.
2. The recognition and localization of species-specific acoustic communication signals, for example, for territorial spacing, mate attraction and/or the transfer of information on food resources.
3. The localization, by parasitoid insects, of acoustically conspicuous hosts.

But to do so auditory systems have to cope with self-generated sounds and with signal degradation due to the impact of motor activity on the auditory organs, and due to degradation of sound as it travels through the environment.

The acoustically induced oscillations of velocity or pressure receivers are picked up by auditory afferent neurons. In all insects the afferents of pressure receivers are components of scolopidia, which are

highly sensitive mechanosensory sensilla. The number of sensilla per ear may vary from a single one in some moths to more than a thousand in cicadas or mosquitoes. It is still a matter of debate to what degree absolute sensitivity and frequency tuning are determined by the biomechanical frequency analysis of the ears and/or by inherent active properties of the auditory sensilla. Spike activity of afferents is precisely timed to the onset of sound pulses and forwarded from the auditory afferents to first order interneurons in the thoracic ganglia.

The central auditory pathways are located in the thoracic ganglia and the brain. The principal tasks for processing may be summarized as follows:

1. Behaviorally relevant information, including the frequency, direction, and temporal pattern of acoustic signals, must be extracted from the spike trains of afferents.
2. This information must be distributed to decision-making centers, generally believed to reside in the brain, where features such as species identity, gender, and perhaps genetic quality of the signaler can be assessed.
3. Finally, information must be forwarded to the motor centers that generate behavioral responses to the acoustic signals.

Structural and functional specializations that support the various tasks of auditory processing appear to occur very early in the auditory pathway and allow parallel processing of specific auditory features within the central nervous system (CNS). Since thoracic auditory neuropils and even identified interneurons appear to be homologous in different groups of related insects, species-specific adaptations can be revealed.

We would like to note in passing that the terminology for auditory interneurons is not uniform. The same names are given to what may be nonhomologous neurons in different groups of insects; for example, a neuron named AN1 in crickets, a prothoracic neuron, is certainly nonhomologous with a metathoracic neuron of the same name in acridids. However, AN1s of crickets and tettigoniids are structurally and functionally similar, and thus may be homologs.

3.31.1.1 Distribution and Design of Ears

Hearing organs for the detection of sound pressure are generally composed of three components (Yager, D. D., 1999): a thin tympanic membrane that vibrates in response to acoustic stimulation; a cuticular frame that anchors the membrane; and an air-filled tracheal chamber that is apposed against the inner surface of the tympanal membrane to match the acoustic impedance of the surrounding air. From one (in some moths) to more than a thousand (in some cicadas) mechanosensitive scolopidial sensilla form the auditory organ and transduce the mechanical oscillations of the tympanum into series of action potentials in auditory receptor neurons. With the exception of some sensory hairs (sensilla trichodia) that can respond to particle velocity, scolopidial sensilla are the auditory sensors for all insect ears, reflecting the evolution of ears from chordotonal organs, which are also comprised of scolopidia (Boyan, G. S., 1993). The basic building blocks for acoustic pressure receivers (cuticle, membrane, and scolopidia) are present in almost all insects. This may explain partly the frequency with which pressure receivers have evolved independently (at least 12 times in eight orders of insects (Yager, D. D. and Spangler, H. G., 1995)), in at least ten different locations on the body (Yack, J. E. and Fullard, J. H., 1993). However, outside the group of insects, specialized hearing organs have not been described among invertebrates.

Long-distance acoustic signaling and hearing is used by the ancient bladder grasshopper *Bullacris membracioides* (van Staaden, M. J. and Römer, H., 1997; 1998; van Staaden, M. J. *et al.*, 2003). Auditory organs in males and females may represent an early evolutionary stage. They lack a tympanum but consist of chordotonal organs directly attached to the pleural cuticle of the abdominal segments A1–A6, the first containing about 2000 bipolar sensory neurons. In Lepidoptera, where pressure receivers have evolved several times, tympanal ears occur on the mouth (Roeder, K. D., 1972; Göpfert, M. C. and Wasserthal, L. T., 1999a; 1999b), the first abdominal segment (von Kennel, J. and Eggers, F., 1933; Roeder, K. D. and Treat, A. E., 1957), the thorax (Eggers, F., 1911; 1919; Richards, A. G., 1933) and the wings (Vogel, R. 1912; Yack, J. E. and Fullard, J. H. 1999; Yack, J. E. *et al.*, 2000). Ears situated on the wings also occur in lacewings (Miller, L. A. 1970; 1971).

In beetles, pressure receivers evolved in at least two groups independently. In scarab beetles (*Dynastinae*), ears are located in the cervical membrane behind the head with 3–8 scolopidia directly attached to the tympanic membrane (Forrest, T. G. *et al.*, 1997). In tiger beetles (*Cicindelidae*), hearing organs are positioned laterally on the first abdominal tergum (Spangler, H. G., 1988; Yager, D. D. and

Spangler, H. G., 1995). In the praying mantis (*Mantis religiosa*), pressure receivers are located in a groove stretching caudally along the midline of the metathoracic segment. The left and right tympana are formed by stiff nonmembranous cuticular ovals in the walls of the groove with large tracheal sacs adhering to the tympana from the inside. The tympanal organ contains about 32 scolopidial sensilla, which are attached to the anterior end of a tympanum by a ligament (Yager, D. D. and Hoy, R. R., 1986; 1987).

In the Hemiptera, tympanal hearing evolved at least twice, in cicadas (*Homoptera/Cicadidae*) and in water bugs (*Heteroptera/Corixidae*), both of which use sound for intraspecific signaling. In *Corixidae*, sounds are picked up by mesothoracic tympanal hearing organs containing two auditory afferents. The tympanic membranes are covered by an air-filled space that is enclosed by the basal parts of the wings and maintained when the animals dive (Wotzel, F., 1933; Schaller, F., 1951; Arntz, B., 1975; Prager, J., 1976). In *Cicadidae*, the auditory capsule containing the structures of the ear is located ventro-laterally between the first and second abdominal segments (Vogel, R., 1923; Michel, K., 1975; Young, D. and Hill, K. G. 1977). Each auditory organ contains about 1300–2200 auditory afferents (Michel, K. 1975; Doolan, J. M. and Young, D. 1981; Huber, F. *et al.*, 1990).

Pressure receivers have no inherent directional sensitivity but some directionality may be present due to sound diffraction at the animal's body, which is especially effective for short-wavelength ultrasound signals.

Pressure difference receivers are more complex and allow for access of the sound waves to both sides of the tympanic membrane. The oscillations of the tympanum depend on the amplitude and phase of the forces acting on the inside and outside respectively. Since these vary with the direction of sound incidence pressure difference receivers are therefore inherently directionally sensitive. Pressure difference receivers occur in the first abdominal segments of grasshoppers and in the tibiae of the front legs in crickets and katydids (Yager, D. D., 1999). In acridid grasshoppers, tympana are present in the pleura of the first abdominal segment (Schwabe, J., 1906). Both ears are acoustically coupled due to large air sacs within the abdomen that allow sound in the range of 3–5 kHz to pass through the body and act on the inside of the contralateral tympanum (Michelsen, A. and Rohrseitz, K., 1995; Schul, J. *et al.*, 1999). In bushcrickets and crickets, an air-filled acoustic trachea with a spiracular opening at the first thoracic segment acts like a hearing tube which guides sound into the tibia of the front leg where it can act upon the inner surface of the tympanum. In addition, in crickets branches of the left and right trachea meet at the midline and are functionally coupled by a median septum, permitting acoustical interaction between the two ears. Depending on the group and species about 20–70 auditory afferents are arranged along the length of the leg trachea, forming the hearing organ. The afferents are divided into anatomically distinct groups: a proximal group with about 10–20 sensilla (referred to as the *intermediate organ* in bushcrickets); a main group with up to 40 sensilla (the *crista acoustica*) and, in crickets, a distal group with about 10–20 sensilla (Ball, E. E. *et al.*, 1989).

In two groups of parasitic flies (*Tachinidae and Sarcophagidae*), evolution has driven the development of a different type of a highly directional hearing organ that is used by the females for locating and approaching singing crickets, bushcrickets or cicadas (Lakes-Harlan, R and Heller, K.-G. 1992; Robert, D. *et al.*, 1992). These ears are located at the midline of the ventral prosternum and comprise two tympanal membranes backed by an air-filled chamber in the sternum. Although the design varies in different species (Robert, D. *et al.*, 1994; Robert, D. *et al.*, 1999; Lakes-Harlan, R. *et al.*, 1999) as a functional principle both membranes are mechanically coupled. The hearing organs (*bulba acoustica*) are located within the air sac behind the tympanal membranes and comprise about 90–100 (*Ormia ochracea*) or 200 (*Therobia leonideii*) auditory afferents, which are attached to each tympanum (Stumpner, A. and Lakes-Harlan, R., 1996; Oshinsky, M. L. and Hoy, R. R., 2002).

3.31.2 Peripheral Processing

3.31.2.1 Central Projections of Auditory Receptors

The anatomical substrate for the first level of central processing, that is, that of first-order interneurons, is established by the projections to the CNS of auditory receptors. We will first discuss some general issues regarding central projections before considering in detail the functional organization of the afferent projections in the few insects in which this has been analyzed.

3.31.2.1.1 Common features of receptor projections

In all systems studied to date, receptor neurons of one side (i.e., left or right) project to the same side of

the CNS (moths: Surlykke, A. and Miller, L. A., 1982; mantises: Yager, D. D. and Hoy, R. R., 1987; flies: Lakes-Harlan, R. *et al.*, 1999; cicadas: Wohlers, D. W. *et al.*, 1979; Doolan, J. M. and Young, D., 1981; see below for references for crickets, locusts, and tettigoniids). Only in mantises and cicadas have a few fibers been described as crossing the midline. Presumably, keeping input from the two ears separate facilitates binaural comparison at the interneuron level, which forms the basis for sound localization (see below).

A second common finding is that axonal projections are generally plurisegmental (references as above); single afferents form terminal arbors in several adjacent ganglia (or neuromeres of fused ganglia) within the CNS. For example, afferents of the locust may have axonal branches in all three thoracic ganglia and also in one or more abdominal neuromeres that form part of the metathoracic ganglion complex (Jacobs, K. *et al.*, 1999). The A1 afferent of noctuid moths has an even more extensive reach. The axon proceeds to the head ganglia, probably to the brain (although the final arborizations in the brain have not yet been demonstrated (Surlykke, A and Miller, L. A. 1982, Boyan, G. S. *et al.*, 1990). Plurisegmental projections of auditory afferents also occur in cicadas (Wohlers, D. W. *et al.*, 1979; Doolan, J. M. and Young, D., 1981), mantises (Yager, D. D. and Hoy, R. R., 1987 and flies (Lakes-Harlan, R. and Heller, K-G., 1992). A different scheme is found in the ensiferans (crickets and tettigoniids), where the axonal arborizations of auditory afferents are restricted to the prothoracic ganglion.

Despite the enormous variation in the locations and structures of insect ears, the central neuropils in which the axonal branches of auditory afferents terminate are similar across many insects. The internal organization of insect ganglia is highly structured, and specific axon tracts, commissures, and neuropil regions can be recognized across taxa. In each segmental ganglion, a region, variously known as the anterior ring tract, the medial ventral association center (mVAC), or the anterior intermediate sensory neuropil (iASN), is the target of auditory afferents of insects as diverse as moths, flies, crickets, grasshoppers, katydids, and wetas (Wohlers, D. W. and Huber, F., 1985; Römer, H. *et al.*, 1988; Boyan, G. S. *et al.*, 1990; Lakes-Harlan, R. and Heller, K.-G., 1992; Jacobs, K. *et al.*, 1999; Nishino, H. and Field, L. H., 2003; Imaizumi, K. and Pollack, G. S., 2005). This region is also the target of many nonacoustic chordotonal organs (Pflüger, J. *et al.*, 1988), suggesting that the conservation of auditory projections reflects the origin of auditory receptors from nonauditory chordotonal organs (Meier, T. and Reichert, H., 1990; Boyan, G. S., 1993).

3.31.2.1.2 Functional organization of central afferent projections

The organization of afferent projections has been studied at fine scale by injecting dye into single physiologically characterized receptor neurons, permitting a detailed histological analysis of axonal projection patterns. Such studies have been performed for only four groups (moths, acridids, tettigoniids, and gryllids) and reveal a functional organization of central projections.

Moths. Three sensory neurons are associated with the ear of noctuid moths. Two of these, designated A1 and A2, are sound sensitive, and the third, the B cell, may serve proprioceptive functions. Retrograde staining of the auditory nerve reveals three axons entering the metathoracic neuromere (Paul, D. H., 1973; Surlykke, A. and Miller, L. A., 1982). Two of these, provisionally identified as A1 and B, have highly similar branching patterns. They bifurcate soon after entering the CNS, projecting axonal branches both anteriorly and posteriorly. The posterior branch arborizes in the metathoracic neuromere as well as in the anterior abdominal neuromeres. Several auditory interneurons have dendritic branches in the same region of the metathoracic ganglion as the branches of A1, providing an anatomical substrate for monosynaptic connections between A1 and the interneurons. The anteriorly directed axons of A1 (and B) also have terminal branches in the mesothoracic neuromere, before coursing further anteriorly through the prothoracic neuromere, where there are no branches, and into the cervical connectives. The central branches of the neuron provisionally identified as A2 are restricted to the mesothoracic and anterior abdominal neuromeres. These branches overlap in some regions with those of A1 and B, but A2 also projects to distinct regions of neuropil.

Only A1 has been identified unambiguously through intracellular staining of the physiologically identified neuron. The identification of A2 was based on comparisons of the anatomy of the neurons, as revealed by retrograde labeling, with the sites in the CNS at which action potentials from A2 can be recorded extracellularly (Surlykke, A. and Miller, L. A., 1982). More recently, it has been suggested that A2 and B may have been misidentified; that is, the neuron with anatomy identical to that of A1 may be A2, rather than B (Lewis, F. P. and Fullard, J. H., 1996).

Acridids. Receptor axons, traveling within the tympanal nerve, enter the metathoracic ganglion complex. Here, some of these form two distinct terminal arbors, one caudal, in the first abdominal neuromere, and one rostral in the anterior metathoracic neuromere. Many receptors axons then continue further anteriorly, arborizing in the mesothoracic and prothoracic ganglia. The sites of these anterior arborizations are segmentally homologous with the rostral termination site in the metathoracic ganglion (Jacobs, K. *et al*., 1999).

Three groups of receptors have been distinguished based on their attachment sites at the tympanic membrane (Figure 1(a)). The groups differ in the probability and extent of arborizations in the central termination sites (Jacobs, K. *et al*., 1999). For example, within the metathoracic ganglion, group I receptors have abundant terminals in the caudal site and relatively sparse terminals in the rostral site. The converse is true for group II, and the majority of group III receptors have no terminals in the caudal site. All group II cells ascend to more anterior ganglia whereas only 60% of group I and 46% of group III receptors have ascending axons.

Histological analysis reveals that, within the rostral neuropil of the metathoracic ganglion, terminals of the three receptor types are anatomically segregated, with group I cells terminating most anteriorly, group II cells most posteriorly, and group III cells sandwiched between these. Because of the differences in frequency tuning between these groups, this arrangement is tonotopic, with low sound frequencies represented anteriorly, and high frequencies posteriorly (Römer, H. *et al*., 1988; (Figure 1(b)).

Tettigoniids. Like the peripheral positions of the cell bodies in the *crista acoustica*, the central projections are tonotopic (Oldfield, B. P., 1983; Römer, H., 1983; Stölting, H. and Stumpner, A., 1998). The gradual shift in frequency tuning from receptor to receptor in the periphery is paralleled by a shift in the positions of their terminal branches in the sensory neuropil within the prothoracic ganglion. The axis of tonotopy is from anterior for low-frequency-tuned receptors to posterior for high-frequency-tuned receptors, with the highest sound frequencies represented dorsally along the posterior edge of the auditory neuropil (Figure 2). In addition, receptors

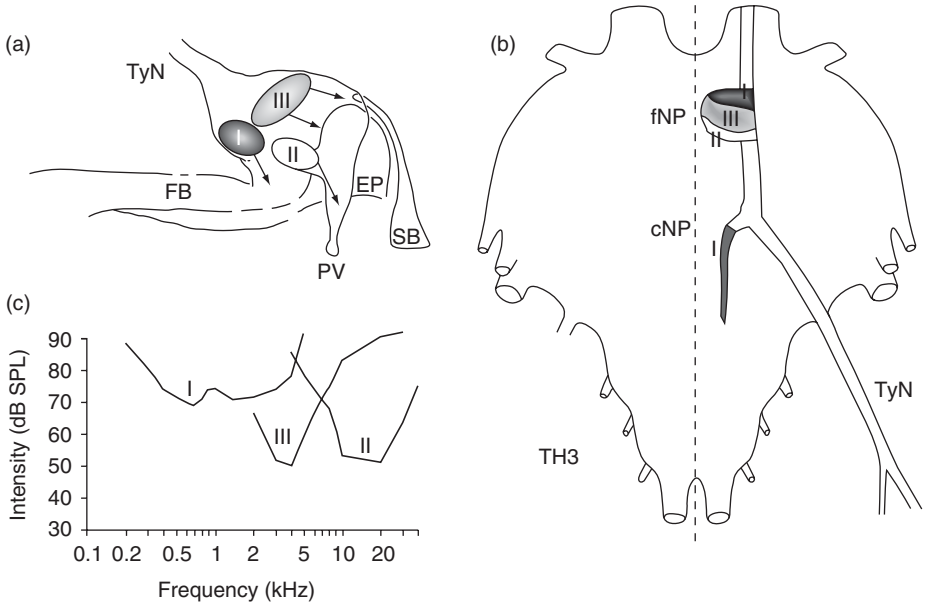

Figure 1 Organization of three groups of afferents in the auditory organ and in the metathoracic ganglion of the locust *Schistocerca gregaria.* (a) Soma positions of group I–III afferents and dendrite attachment sites (indicated by arrows) in Müllers organ. Tympanal nerve (TyN), folded body (FB), pyriform vesicle (PV), elevated process (EP), styliform body (SB). (b) Metathoracic ganglion with frontal (fNP) and caudal (cNP) and frontal/rostral (fNP) auditory neuropil. Axons of group I–III auditory afferents arborise somatotopically and, thus, tonotopically in the anterior neuropil. (c) Schematic representation of group I–III auditory threshold curves. From Jacobs K., Otte, B., and Lakes-Harlan, R. 1999. Tympanal receptor cells of *Schistocerca gregaria*: correlation of soma positions and dendrite attachment sites, central projections and physiologies. J. Exp. Zool. 283, 270–285.

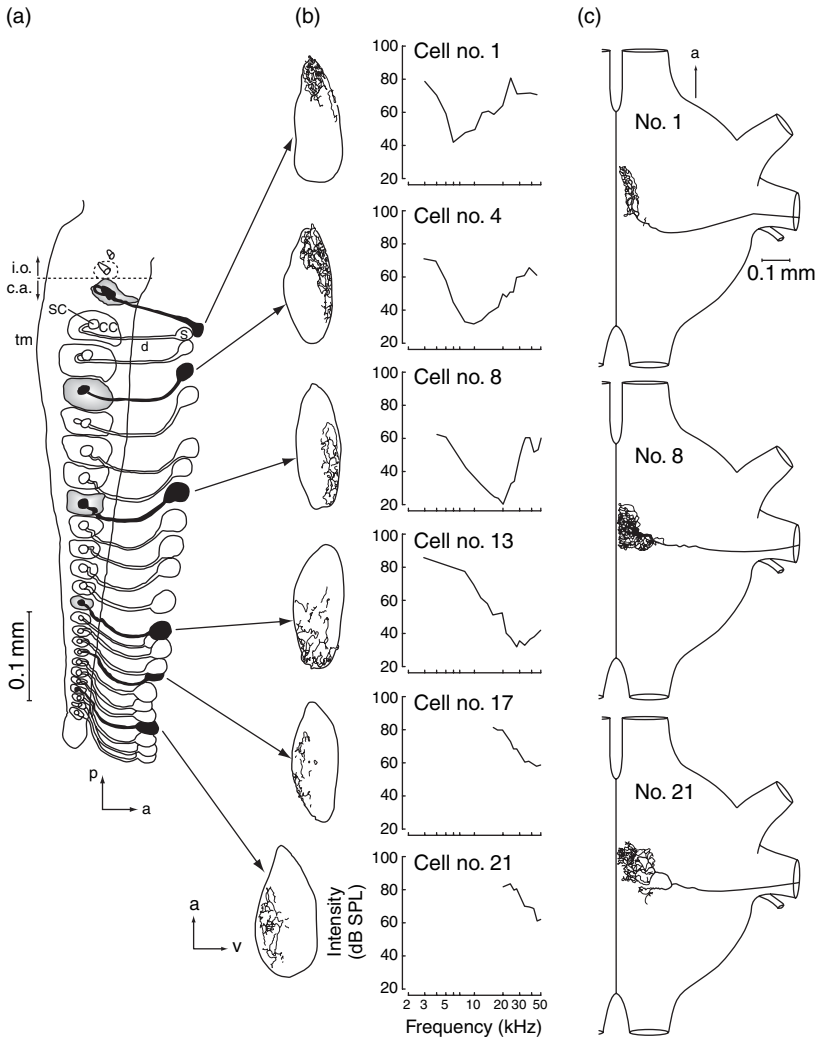

Figure 2 Tuning and organization of auditory afferents in the ear and in the prothoracic auditory neuropil in the bushcricket *Pholidoptera griseoaptera.* (a) Linear arrangement of the 24 auditory afferents in the *crista acoustica*. Soma (s) and dendrites (d) of identified afferents are drawn in black, Cap cell (cc), intermediate organ (i.o.), *crista acoustica* (c.a.), tectorial membrane (tm), proximal (p) anterior (a). (b) Axonal arborizations patterns in the prothoracic neuropil, viewed in parasagittal sections, and corresponding tuning curves of identified afferents, anterior (a), ventral (v, c) Branching pattern of three afferents within the prothoracic ganglion, viewed in the horizontal plane. From Stölting, H. and Stumpner, A. 1998. Tonotopic organization of auditory receptors of the bushcricket *Pholidoptera griseoaptera* (Tettigoniidae, Decticinae). Cell Tissue Res. 294, 377–386.

that are tuned to the dominant frequencies of communication signals may have particularly abundant terminal arbors (Oldfield, B. P., 1983), suggesting that the weighting of synaptic inputs to central neurons is uneven across the audible range.

Crickets. Based on the anatomy of their central arborizations, receptor neurons occur as two distinct types. One of these, designated medially terminating (MT), ends with a dense cluster of branches close to the midline. The other, denoted bifurcating (BC), has a characteristic bifurcating terminal arbor which is more lateral and posterior than the terminations of MT-types (Imaizumi, K. and Pollack, G. S., 2005) (Figure 3). Ultrasound-tuned, mid-frequency-tuned, and about half of the receptor neurons tuned to the carrier frequency of the calling song are MT-type; the remaining receptors tuned to the calling song (but none of the mid-frequency or ultrasound-tuned receptors) are BC-type. All of the MT-type receptors project to the same region of the auditory neuropil, where their terminal arbors overlap extensively. The terminal processes of the MT-type afferents overlap

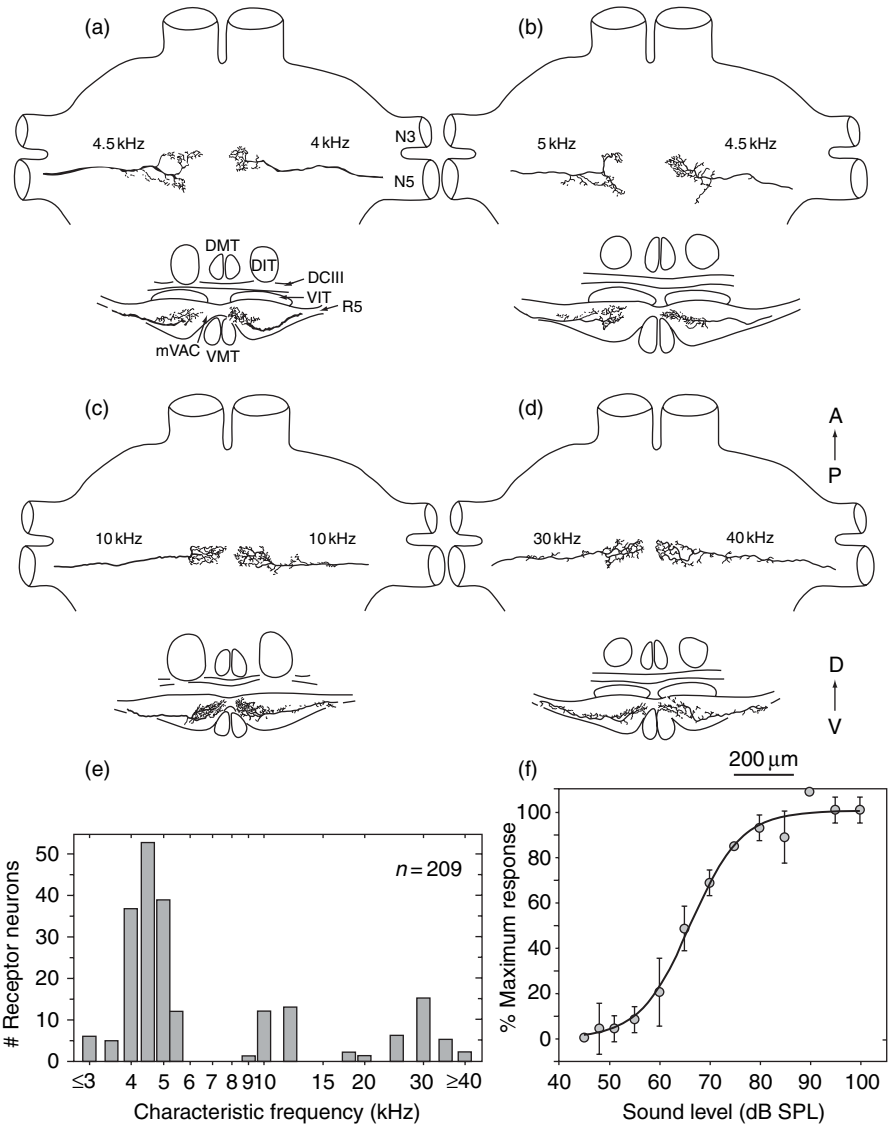

Figure 3 Anatomy and physiology of auditory receptor neurons of crickets. (a, b) Central projections of two anatomical types of low-frequency-tuned receptors; BC (left side of each drawing) and MT (right sides). Top drawings show projections in horizontal view; bottom drawings show transverse view of central neuropil. (c, d) projections mid-frequency-tuned (c) and ultrasound-tuned (d) receptors. DMT: dorsal median tract; DIT: dorsal intermediate tract: DCIII: dorsal commisure III: VIT: ventral intermediate tract; R5: root of nerve 5; mVAC: median ventral association center; VMT: ventral median tract, A-P: anterior–posterior, D-V: dorsal–ventral. (e) Histogram showing distribution of characteristic frequencies (frequency at which threshold is lowest). (f) Intensity–response curve of a typical receptor neuron, showing how spike count (normalized with respect to the maximum) varies as a function of stimulus amplitude. (a – d) From Imaizumi, K., Pollack, G. S. 2005. Central projections of auditory receptor neurons of crickets. J. Comp. Neurol. 493, 439–447. (e, f) From Imaizumi, K., and Pollack, G. S. 2001. Neural representation of sound amplitude by functionally different auditory receptors in crickets. J. Acoust. Soc. Am. 109, 1247–1260.

with the dendrites of interneurons that carry acoustic information to the brain (AN1 and AN2 – see further ahead), as well as to a local interneuron (ON1) that modifies ascending information through contralateral inhibition; thus MT-type receptors can provide direct input to these neurons. By contrast, the terminals of BC-type receptors are situated too far posteriorly and laterally to interact substantially with these interneurons. BC terminals do, however, overlap with the dendritic processes of another interneuron, DN1 that relays auditory information to more posterior ganglia, possibly to influence the

thoracic motor output. It thus seems possible that information about calling song stimuli is parsed into separate pathways as early as the level of receptor neurons.

3.31.2.2 Processing and Physiology

By comparison with vertebrates, insect ears are relatively insensitive, with minimum thresholds of receptor neurons sometimes as low as 20 dB SPL, but more typically in the range 30–60 dB SPL. The range of audible frequencies varies widely across species, but seldom extends below 2–3 kHz, and often reaches as high as 100 kHz.

The first step in the neural coding of behaviorally relevant features of acoustic signals, including intensity, pattern of amplitude modulation, and spectral composition, is accomplished by auditory receptor neurons. The transduction machinery (see Chapter 3; Perspectives 7b, 10c) in the scolopidium translates this information into sequences of action potentials in the receptor neurons. Here, we summarize the nature of receptor neuron responses.

3.31.2.3 Coding of Stimulus Amplitude

Auditory receptor neurons respond to sound-induced mechanical oscillations at their attachment site in the ear and transmit series of actions potentials toward the CNS. For comparatively long (>50 ms) acoustic stimuli responses of most receptor neuron are phasi-tonic, that is, spike rate is high at stimulus onset, and after a few tens of milliseconds adapts to a lower level, with spiking continuing for the duration of a long-lasting stimulus. As in most other sensory neurons, increasing stimulus amplitude leads to shorter response latency and higher firing rate. For brief stimuli, firing rate generally increases approximately linearly with increasing sound level (but see Imaizumi, K. and Pollack, G. S., 2001 for exceptions) until saturating, generally at quite high firing rate, for example, 300–500 Hz (Imaizumi, K. and Pollack, G. S., 2001; Benda, J. *et al.*, 2001; Benda, J. and Herz. A. V., 2003; Figure 3(f)). For stimuli lasting longer than 100 ms or so, however, including many communication signals, responses are affected strongly by adaptation, resulting in a flattening of the steady-state intensity–response function as well as an increase in response latency. Moreover, the degree of adaptation depends on the temporal structure of the stimulus (Sippel, M. and Breckow, J., 1984; Givois, V. and Pollack G. S., 2000; Benda, J. *et al.*, 2001). For some stimuli adaptation is sufficiently severe that the time-averaged firing rate loses all value as an indicator of stimulus amplitude.

Another potential code for stimulus intensity stems from the fact that most insect ears contain several sensory neurons that differ in sensitivity. Consequently, the number and identities of receptor neurons for which threshold has been reached changes with increasing stimulus amplitude (Roeder, K. D., 1974; van Staaden, M. J. and Römer, H., 1998; Oshinsky, M. L. and Hoy, R. R., 2002), a coding scheme known as range fractionation. One of the clearest and simplest examples of range fractionation occurs in noctuid moths, which have two auditory receptor neurons per ear, denoted A1 and A2. A1 is the most sensitive of these, with threshold typically in the range 35–55 dB SPL (Fullard, J. H. *et al.*, 2003), but in some species as low as 20–30 dB (Fullard, J. H., 1984b). A2 is about 20 dB less sensitive, reaching threshold at approximately the same stimulus level at which firing rate of A1 begins to saturate (Roeder, K.D. and Treat, A. E., 1957; Madsen, B. M. and Miller, L. A., 1987; Waters, D. A. and Jones, G., 1996).

3.31.2.4 Temporal Coding

Behaviorally relevant stimuli, including communication sounds and sounds produced by predators, are modulated in amplitude through time, establishing the signal's temporal structure, or rhythm. Behavioral tests have shown for a number of insects that temporal pattern is a crucial cue for signal recognition. Stimulus temporal structure must, then, be represented by the responses of receptor neurons. One important temporal feature, the timing of sound-pulse onsets, is accentuated by the receptor population (Nabatiyan, A. *et al.*, 2003), both because of adaptation (see above) and because of synchronized spiking across the receptor population at stimulus onset (Adam, L.-J., 1977; Ronacher, B. and Römer, H., 1985; Pollack, G. S. and Faulkes, Z., 1998).

A recent approach to characterizing the temporal coding properties of receptors utilizes information theory, which allows one to express quantitatively the extent to which the temporal structure of the stimulus amplitude envelope can be recovered from the timing of spikes within a neuron's response (Rieke, F. *et al.*, 1997). Experiments on receptors of grasshoppers (Machens, C. K. *et al.*, 2001, Edin, F. *et al.*, 2004) and crickets (Marsat, G. S. and Pollack, G. P. 2004), show that receptors are broadly tuned

with respect to rates of amplitude modulation, varying only slightly in the accuracy with which they encode modulation rates from *c.* 10 to 100 Hz.

In auditory afferents of grasshoppers, spike rates of 200 Hz appear to be optimal to transmit information about the amplitude modulation of the communication signals to the CNS. Information transfer improves when input from several afferents is combined, saturating at 5–8 afferents (Machens, C. K. *et al.*, 2001). Nevertheless, the spike patterns of single afferents relay sufficient information to allow a reliable discrimination between different song patterns (Machens, C. K. *et al.*, 2003). A particularly salient feature of grasshopper songs, the rapid increase in sound level at the onset of each syllable, is detected by receptor neurons with remarkable temporal precision, with spike-time jitter of as little as 0.15 ms (Rokem, A. *et al.*, 2006). This high precision may play a role in downstream analysis of the syllable-pause structure of the song, which is the key to its recognition by conspecifics (Balakrishnan, R., *et al.*, 2001).

A subset of auditory receptors of the parasitoid fly, *Ormia ochracea*, exhibit properties adapted to the processing of sound pulses produced by their cricket hosts (Oshinsky, M.L. and Hoy, R. R., 2002). These neurons have highly phasic response properties, producing only a single spike at the beginning of a sound pulse. They then require a silent period of at least 4.3 ms before they can spike again. This response property supports synchronous afferent activity at the onset of sound pulses and, moreover, may provide a low-pass filter for pulse repetition rates.

3.31.2.5 Frequency Sensitivity

Early students of insect hearing believed that insects were tone deaf (Pumphrey, R. J., 1940). This view changed in 1960 with the discovery, in a locust (Horridge, G. A., 1960) and in a tettigoniid (Katsuki, Y. and Suga, N., 1960), that different auditory neurons in the same specimen could be most sensitive to different sound frequencies. There are two aspects of frequency sensitivity: (1) frequency *tuning*, that is, variation in sensitivity as a function of frequency and (2) frequency *discrimination*, the ability to respond in different ways to different frequencies independent of stimulus intensity. All auditory systems show tuning to at least some degree, but the capacity for frequency discrimination is more limited.

Sound frequency plays several roles in behavior. First, if an auditory system is sensitive to a restricted range of frequencies that matches the bandwidth of important signals, then extraneous sounds outside this frequency range will not be perceived, thus increasing the signal-to-noise ratio of signal detection. Second, sound frequency can serve as a code for the signal's meaning. For example, crickets are attracted to the low frequency (3–6 kHz) calling song of conspecific males, but they are repelled by ultrasonic (15–80 kHz) bat-like sounds (Moiseff, A. *et al.*, 1978). Indeed, ultrasound elicits avoidance or startle responses in many night-flying insects (Hoy, R. R., 1992). Third, some grasshoppers and tettigoniids determine the sex of a signaling partner in part by the signal's spectrum (von Helversen, D. and von Helversen, O., 1997; Dobler, S. *et al.*, 1994). And a fourth possible role of frequency discrimination is distance estimation. Natural environments act as low-pass filters of sound frequency, with the result that the spectrum of a signal changes as it travels from sender to receiver. Tettigoniids may use this change in spectrum to estimate the distance of a singing conspecific (Römer, H., 1987).

In the following paragraphs we describe the response to and processing of sound frequency by auditory receptors for those insect groups in which this has been studied most thoroughly.

3.31.2.5.1 *Lepidoptera*

In most moths, receptor neurons are tuned rather broadly to ultrasonic frequencies and follow the tuning of the tympanic membrane. Although ears may contain up to four receptor neurons, there is no evidence that these are differently tuned (Roeder, K. D., 1966a; Surlykke, A. and Filskov, M., 1997).

Like moths, nocturnal butterflies have evolved ultrasound-sensitive ears. The presumed sensory organ in this case is Vogel's organ, which is located at the base of the forewing (Yack, J. E. and Fullard, J. H., 1999; Rydell, J. *et al.*, 2003). This consists of three groups of chordotonal organs that are attached directly to the tympanal membrane. In contrast to the usual lepidopteran ear, which contains only a few scolopidia, Vogel's organ may contain 100–200 scolopidia (Yack, J. E. *et al.*, 2000). Vogel's organ has been shown to mediate hearing in some diurnal butterflies as well, in which males produce sounds in interactions with conspecifics (Yack, J. E. *et al.*, 2000). The sounds have peak energy between 8 and 18 kHz.

Neurophysiological recordings have so far been made from only one of the three chordotonal organs,

and peak sensitivity, rather than being in the same range as conspecific signals, is at 1.75 kHz. It remains to be determined whether one of the other chordotonal organs is tuned to the higher-frequency range of conspecific signals. If so, then this would provide the first evidence for frequency discrimination in *Lepidoptera*.

3.31.2.5.2 Acridids

Four groups of receptor neurons were originally identified in the ear of acridids based on the locations of their somata, the attachment sites of their dendrites to the tympanic membrane, response threshold and frequency sensitivity (Gray, E. G., 1960; Michelsen, A., 1971; Römer, H., 1976; Halex, H. *et al.*, 1988). More recent work, in which the physiology, peripheral anatomy, and central projection sites of individual receptor neurons were studied, proposes three functional groups (Jacobs, K. *et al.*, 1999; Figure 1). Group I cells, which number *c.* 20 neurons in *Schistocerca gregaria,* have relatively high thresholds (*c.* 60 dB SPL at the most sensitive frequency), and have two rather broadly tuned regions of best sensitivity: one in the range 400–700 Hz, and the second in the range 1–4 kHz. Cells in group II ($n = 12$–14) are broadly tuned to higher frequencies, ranging from 4–7 kHz to >40 kHz. Sensitivity is greatest in the range 12–25 kHz, with thresholds between 40 and 60 dB SPL. The most populous group, group III with about 40 afferents, is physiologically heterogeneous. Best sensitivity is to frequencies in the range 3–4 kHz, but absolute sensitivity (minimum threshold: 40–60 dB SPL), and breadth of tuning vary widely.

3.31.2.5.3 Tettigoniids

Peripheral discrimination of sound frequency is perhaps best developed in the *crista acoustica* of tettigoniids. Receptor neurons are aligned linearly along the proximo-distal axis of the tibia, reminiscent of the basal-to-apical organization of hair cells within the organ of Corti of vertebrates (see Chapter 6). As in the latter, this organization is tonotopic, with low frequencies represented proximally and high frequencies distally (Oldfield, B. P., 1982; 1984; 1985); Stölting, H. and Stumpner, A., 1998; Figure 2). The auditory organ is attached to the acoustic trachea and has no direct contact to the tympanum. Mapping a frequency range of about 4–50 kHz with wavelength ranging from 82.5 to 6 mm on a less than 1 mm long receptor array probably does not result from pure biomechanics of the auditory trachea but may be due to intrinsic tuning of the receptor cells (Oldfield, B. P., 1985) or to the specific mechanical properties of the accessory structures (dorsal wall, cap cells, tectorial membrane) adjacent to the receptor cells within the *crista acoustica* (Kalmring, K. *et al.*, 1996). The ability of this receptor array to analyze the spectrum of acoustic signals is determined by the number of receptor neurons that are tuned to specific frequencies, the sharpness of their tuning, their absolute sensitivity, and the spacing between their best frequencies. These parameters are often tailored to the spectral composition of behaviorally relevant signals. For example, among three related species, each of which has 25–30 receptor neurons in its *crista acoustica*, the proportions of receptor neurons tuned to low or to high frequencies differ in accordance with the differences in spectral composition of the songs of the species (Kalmring, K. *et al.*, 1993). Adjacent to the *crista acoustica* in bushcrickets (Lin, Y. *et al.*, 1993; Kalmring, K. *et al.*, 1996) lies the bimodal auditory–vibratory intermediate organ which contains about 15 afferents and appears to have a lower auditory sensitivity (Rössler, W. *et al.*, 1994; Stölting, H. and Stumpner, A., 1998).

3.31.2.5.4 Gryllids

As in tettigoniids, auditory afferents of crickets are organized tonotopically within the *crista acoustica* in the tibia (Oldfield, B. P. *et al.*, 1986). Based on structural evidence the *crista acoustica* is divided into three anatomical groups: the proximal group with about ten sensilla, a main group with about 40 sensilla and a distal group with about 10–20 sensilla (Ball, E. E. *et al.*, 1989).

At the single-cell level, the physiology of cricket receptor neurons has been studied most thoroughly in *Teleogryllus oceanicus* (Imaizumi, K. and Pollack, G. S., 1999; 2001). Rather than preferred sound frequency shifting gradually from receptor to receptor, as occurs in the tettigoniids, cricket receptors fall into one of three distinct groups that are most sensitive, respectively, to sound frequencies similar to the dominant frequency of the species' calling song (4–5.5 kHz), to ultrasonic frequencies similar to those used by echolocating bats (>18 kHz), or to an intermediate range of frequencies (9–12 kHz) (Imaizumi, K. and Pollack, G. S., 1999; 2001). The three frequency groups are unequal in size: of the 65–70 receptor neurons in the ear, approximately three quarters fall into the low-frequency group, and one eighth into each of the other two groups (Figure 3(e)).

These three categories are based on responses to sound levels near threshold. When suprathreshold responses are considered, the situation becomes considerably more complicated. Most receptor neurons not only have a particular best frequency, they also have enhanced sensitivity to one or more additional frequencies. Because of these additional sensitivity peaks, the dominant frequency of a stimulus cannot be coded simply by the identities of the activated receptor neurons. Instead, this must be determined by integrating the response magnitudes across the entire receptor population.

3.31.2.5.5 Mantises

A remarkable example of frequency discrimination at the peripheral level occurs in mantises. Many mantises possess an ultrasound-sensitive ear on the midline of the metathorax, which responds best to bat-like sounds (35 kHz) (Yager, D. D. and Hoy, R. R., 1986; Yager, D. D. and May, M. L., 1990). Members of the genus *Creobroter*, however, have an additional, serially homologous ear on the mesothorax (Yager, D. D., 1996). In contrast to the metathoracic ear, the mesothoracic organ is tuned to frequencies in the range 2–4 kHz. Sound production by mantises has not been reported, and as yet the function of low-frequency hearing is unknown.

3.31.2.5.6 Cicadas

The ears of cicadas contain up to 2500 scolopidia. Frequency tuning has not been studied at the level of individual receptor neurons. At the interneuron level, however, different individual cells may be most sensitive to different frequencies, implying that this must be true as well at the receptor-neuron level (Fonseca, P. J. *et al.*, 2000).

3.31.3 Central Pathways

3.31.3.1 Overview

In the central auditory pathway behaviorally relevant information (e.g., sound direction, temporal pattern, or frequency components), is extracted from the afferent spike trains. The first level of central processing occurs within the thoracic auditory neuropil(s). Intersegmental interneurons then forward information to the brain, where adaptive behavioral sequences may be elicited and coordinated via the activation of descending pre-motor interneurons. The properties of the interneurons that accomplish these tasks are shaped by their patterns of connectivity with receptor neurons and with each other, as well as by their intrinsic properties.

As noted above, aspects of early auditory processing, such as the cell biology of receptors and the overall organization of their central projections, are in many ways similar across insect groups. At the interneuron level, however, taxon-specific features become increasingly evident. Here we summarize the general organization of central pathways for those insects in which sufficient information is available. More detailed examinations of specific neural circuits and properties are presented later.

3.31.3.2 Noctuid Moths

Auditory afferents enter the metathoracic neuromere of the fused pterothoracic ganglion and project anteriorly, probably as far as the brain and posteriorly, to abdominal neuromeres, by ascending and descending axonal branches (Surlykke, A. and Miller, L. A., 1982; Lewis, F. P. and Fullard, J. H., 1996). A total of 14 local and ascending interneurons have been characterized in the meta- and mesothoracic neuromeres (Boyan, G.S. and Fullard, J. H., 1986; 1988; Boyan, G.S. and Miller, L. A., 1991; Boyan, G.S. *et al.*, 1990). In each neuromere, some of these receive direct synaptic input from receptors and others are excited polysynaptically. Most interneurons, like the afferents, have local, ascending and descending axonal branches that may interact with motor circuits that drive behavioral responses to acoustic stimulation. The responses of some thoracic neurons resemble those of receptor neurons (these were called repeater neurons by Roeder, K. D., 1966b), but others extract stimulus features such as pulse onset (Roeder's pulse-marker) and repetition rate (Boyan, G.S. and Fullard, J. H., 1986; Boyan, G. S. and Miller, L.A., 1991).

Although auditory interneurons have been recorded in the brain (Roeder, K. D., 1973), cerebral circuits have not been identified. Thoracic processing alone is sufficient to implement some aspects of acoustic behavior. Arctiid moths respond to bat-like stimuli by producing ultrasonic clicks, which appear to interfere with the bat's ability to locate the moth using echolocation (Fullard, J. H. *et al.*, 1994; Ratcliffe, J. M. and Fullard, J. H., 2005). Click generation in response to ultrasound pulses can occur even in moths that have been decapitated. Descending input from the brain does, however, affect the probability and duration of responses (Fullard, J. H., 1982, Dawson J. W. and Fullard J. H., 1995), in agreement with Roeder's (1970; 1973)

speculation that the brain could modulate local auditory reflexes operating in the thoracic ganglia.

3.31.3.3 Acridids

Within the rostral metathoracic and mesothoracic auditory neuropil auditory information is forwarded to local and intersegmental ascending and T-shaped interneurons. Interneurons may project from the metathoracic ganglion to the mesothoracic neuropil or up to the lateral protocerebrum in the brain. Most of the interneurons leaving the meta- or mesothoracic auditory neuropil receive auditory input indirectly, via local and/or bisegmental neurons (Römer, H. and Marquart, V., 1984; Marquart, V., 1985). Descending axons of T-fibers project to motor areas in the metathoracic ganglion.

Surgical manipulations (Ronacher, B. *et al.*, 1986) as well as neurophysiological recordings (Römer, H. *et al.*, 1981; Römer, H. and Marquart, V., 1984; Stumpner, A. and Ronacher, B., 1991; Stumpner, A. *et al.*, 1991) point to the metathoracic auditory neuropil as a site at which important steps in auditory processing take place. This is the site of origin of at least six pairs of local interneurons and 17 pairs of ascending neurons, many of which extract specific features of acoustic signals. For example, some neurons are highly directional but poor at representing stimulus temporal pattern, whereas others have poor directionality but extract particular aspects of temporal pattern, such as the onsets of syllables, their durations, and their continuity. These various snippets of information are presumably integrated in the brain, where the recognition of species-specific song patterns occurs (Bauer, M. and von Helversen, O., 1987). Descending commands from the brain then mediate behavioral responses to acoustic signals, such as song production (Hedwig, B. and Heinrich, R., 1997 and phonotaxis (Ronacher, B. *et al.*, 1986).

3.31.3.4 Ensiferans (Tettigoniids and Gryllids)

Tettigoniids and gryllids are treated together here because the overall organization of early processing appears to be similar in these groups. About 30 (tettigoniids) to 70 (gryllids) afferents enter, and are restricted to, the prothoracic ganglion, where they synapse with local, ascending, and descending neurons. Selectivity of interneurons for sound frequency is established by specific connectivity with receptor neurons as well as by local inhibitory circuits. Local inhibition also plays a role in enhancing the directionality of interneuron responses (Selverston, A., *et al.*, 1985; Horseman, G. and Huber, F., 1994a; Faulkes, Z. and Pollack, G. S., 2000; Marsat, G. and Pollack, G. S., 2005).

A hallmark of this group is that information is carried to the brain by relatively few ascending neurons. In crickets, ascending neurons may number as few as four: two on each side of the midline, with best sensitivity, respectively, to the carrier frequency of the calling song (3–6 kHz) or to higher frequencies such as occur in courtship song of some species (12–16 kHz) and in the echolocation calls of hunting bats (>20 kHz). However, in at least one species of tettigoniid, at least five ascending neurons occur on each side. Unlike the situation in acridids, in ensiferans most ascending neurons are both highly directional and also represent accurately the temporal structures of behaviorally relevant signals (Wohlers, D.W. and Huber, F., 1982; Hennig, R. M., 1988; Marsat, G. and Pollack, G. S. 2004; 2005; Stumpner, A. and Molina, J. 2006).

The ascending neurons provide input to separate networks within the brain for processing of low- and high-frequency signals. Descending neurons carry the results of brain processing back to the thoracic ganglia, where they contribute to the generation of motor responses (Brodfuehrer, P. D. and Hoy, R.R. 1989; Staudacher, E. M., 2001).

3.31.3.5 Sound Frequency

In the following sections we examine how information about sound frequency is processed in the CNS. We focus first on two insect groups, moths and mantises, in which the main role of hearing is to detect the ultrasonic probes of echolocating bats. We then turn to the Orthoptera, where the CNS must deal both with sounds produced by predators, and with intraspecific communication signals.

3.31.3.6 Noctuid Moths

Although some moths use ultrasound signals for intraspecific communication (Conner, W. E., 1999; Sanderford, M. V.. *et al.*, 1998), the earliest function of hearing in this group was probably to detect the ultrasound pulses of echolocating bats, which elicit evasive flight responses (Roeder, K. D., 1962). Hunting bats progress through a series of ultrasound pulse patterns: a search phase, with pulses emitted at relatively low rate, followed by an approach phase,

when pulse rate increases and pulse duration decreases, to the terminal attack phase, when pulse rate may exceed 100 Hz. With natural sequences of bat calls (Fullard, J. H. *et al.*, 2003), escape behavior and defensive sound production (Blest, A. D. *et al.*, 1963; Dunning, D.C. and Roeder, K. D., 1965; Fullard, J. H. *et al.*, 1994) are triggered at the transition between the bat's approach phase and terminal attack phase.

The A1 auditory afferent connects monosynaptically to local and ascending thoracic auditory interneurons (Boyan, G.S. and Fullard, J. H., 1986; 1988). A noise filter at the synapse between the afferent and interneuron 501 appears to prevent escape responses to spontaneous A1 activity and arbitrary sounds. A1 elicits short, rapidly decaying EPSPs in interneuron 501, so that postsynaptic summation reaches threshold only when the spike rate of A1 approaches 250–300 Hz. It has been proposed that this mechanism ensures responses only to bat cries (Boyan, G. S. and Fullard, J.H., 1988).

Evasive behavioral responses are best elicited by ultrasound pulse rates of 25–45 Hz (Roeder, K. D., 1964; Fullard, J. H., 1984a). The neural basis of temporal tuning underlying the avoidance behavior is not completely established. Crucial elements for auditory processing could be pulse marker neurons, which – independent of sound intensity and duration – respond to the onset of sound pulses only (Roeder, K. D., 1966b). Their spike activity will be at maximum at the transition from search to attack calls. Differences across interneurons in the decay times of EPSPs allow differences in sensitivity to pulse repetition rates (Boyan, G. S. and Miller, L. A., 1991). In some interneurons (e.g., 501 and 502) the extended duration of EPSPs leads to temporal summation at approximately 40 sound pulses s^{-1}, whereas in 504, with faster decaying EPSPs, higher repetition rates are necessary (Boyan, G.S. and Fullard, J. H., 1986, Boyan, G. S. and Miller, L. A., 1991). Thus time constants of EPSPs in first-order auditory interneurons may be crucial for the temporal tuning of moth evasive behavior (Figure 4).

3.31.3.7 Mantises

In mantises a prominent interneuron (MR-501-T3) in the metathoracic ganglion appears to mediate ultrasound triggered evasive flight maneuvers, which occur in response to approaching bats (Yager, D. D. *et al.*, 1990; Yager, D. D. and Hoy, R. R., 1989; Triblehorn, J. D. and Yager, D. D., 2005). The neuron

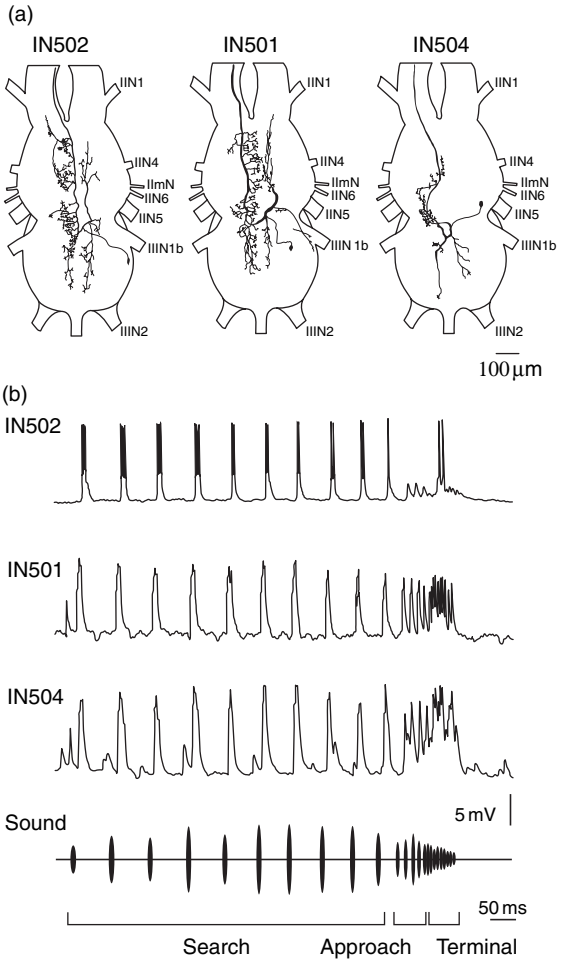

Figure 4 (a) First-order auditory interneurons IN502, IN501, and IN504 in the pterothoracic ganglion of *Heliothis virescens*. Neurons have dendritic branches ipsilateral to the cell body. Axons project within the contralateral connective at least to the prothoracic ganglion and axonal arborisations branch off contralateral to the soma. (b) Intracellular recorded response of the interneurons in *Noctua pronuba* to sound pulses in the call of an echolocating bat, *M. siligorensis* (bottom trace). The call shows a complete sequence containing search (S), approach (A), and the terminal (T) phase. Peak sound level for the pulses with maximum amplitude in the search phase was 80 dB SPL. During the terminal phase the response of IN501 merges to a tonic response whereas IN504 reflects the pattern of the sound due to its faster EPSP decay time. Scale: vertical 5 mV, horizontal 100 µm or 50 ms. (a) From Boyan, G.S. and Fullard, J.H. 1986. Interneurones responding to sound in the tobacco budworm moth *Heliothis virescens* (Noctuidae): morphological and physiological characteristics. J. Comp. Physiol. A 158, 391–404. (b) From Boyan, G. S. and Miller, L. A. 1991. Parallel processing of afferent input by identified interneurons in the auditory pathway of the noctuid moth *Noctua pronuba* (L.). J. Comp. Physiol. A 168, 727–738.

has a large (17 μm) axon that projects anteriorly (Yager, D. D. and Hoy, R. R. 1989) and its structure strongly resembles that of identified, sound-sensitive neurons (the G and B cells) of locusts (Rehbein, H., 1976). Responsiveness to high-frequency sounds (25–60 kHz), fast conduction of spikes (4 m s^{-1}) and reliable high firing rate spike responses to sound pulses repeated even at 60 Hz match the requirements for bat-avoidance behavior (Yager, D. D. and Hoy, R. R., 1989). During live bat attacks, the neuron responds to each sonar pulse of the approaching bat with a high-frequency burst of spikes. The neuron stops responding about 270 ms before contact at the beginning of the terminal phase when the bat homes in on the prey with a series of short sound pulses emitted at more than 100 pulses s^{-1} (Triblehorn, J. D. and Yager, D. D., 2002). Flight evasive responses of the mantis start when pulse repetition rates of the bat reach 20–40 pulses s^{-1}. MR-503-T3 is thus a good candidate for triggering the evasive responses, but a robust electrophysiological test demonstrating the sufficiency of the neuron's activity is not yet available.

3.31.3.8 Acridids

Sound frequency plays several roles in behavioral responses of acridids. Flying locusts exhibit avoidance responses to 30 kHz sound stimuli. Stimuli with frequency of 5 kHz are not effective, and in fact suppress responses to simultaneously delivered ultrasound (Robert, D., 1989). Acridids also use complex sound signals for intraspecific communication. Their songs are generally quite broadband (2–40 kHz), but species-specific and sex-specific spectral differences exist that could contribute to recognition (Meyer, J. and Elsner, N., 1997). A clear role for sound spectrum in communication has been demonstrated in the grasshopper *Chorthippus biguttulus*. Courtship in this species is mediated by an acoustic duet: males emit calling songs, which may evoke a female's response song. If the male recognizes this, he responds with a phonotactic turn and walks toward the female. Both male and female songs have peaks at 5 and *c.* 30 kHz, but high frequencies are more prominent in the songs of males. Tests with female song models show that males respond best with phonotaxis to the low-frequency song components only, and in fact their response is suppressed when high frequencies are added to the model songs, presumably preventing inappropriate approaches to other males (although males will respond with rivalry song to songs of other males). By contrast, females respond best to male song models containing both low- and high-frequency components (von Helversen, D. and von Helversen, O., 1997). Finally, because acridid songs are broadband, and because high frequencies are more strongly attenuated as sound travels through the environment (Römer, H., 1987), the spectrum of the signal at the position of its recipient can, in principle, carry information about the distance to its source.

Auditory receptors of acridids are tuned to either low (<6 kHz) or high (>12 kHz) sound frequencies (see above), and auditory interneurons of the metathoracic ganglion receive direct and/or indirect input from these groups of afferents, with one group (most often the high-frequency afferents) providing mainly excitation and the other providing polysynaptic inhibition. As a result of this mixed input, the responses of the interneurons are quite complex, and often depend strongly on stimulus intensity. For stimuli with broad bandwidth, such as natural songs, the interaction of excitation and inhibition causes many neurons to become intensity tuned, that is, they respond maximally to a particular intensity range (Römer, H. and Marquart, V., 1984; Römer, H. and Seikowski, V., 1985). Thus intensity coding through frequency-specific inhibition may be an additional function of frequency discrimination in acridids.

The mixture of excitatory and inhibitory input to most interneurons also shapes the temporal structure of their responses. For example, low-frequency-induced inhibition precedes excitation in the neuron AN2, increasing its response latency. In AN1, by contrast, inhibition is delayed, causing the neuron's response to be phasic.

The sources of low-frequency-tuned inhibition include the identified interneuron, SN1 (Marquart, V., 1985) and, probably, another identified neuron, TN1 (Sokoliuk, T. *et al.*, 1989). A population of GABA-immunoreactive neurons, with somata at the dorsal midline and processes in the auditory neuropil, comprises another set of candidates (Thompson, K.J., and Siegler, M. V. S., 1991). Although these neurons are sound sensitive, their auditory characteristics (e.g., thresholds, best frequencies) have not been described.

3.31.3.9 Tettigoniids

Sound frequency is important in a number of behavioral contexts, distinguishing the songs of different species (Keuper, A. *et al.*, 1988), of different genders (Dobler, S. *et al.*, 1994), and even of different

individuals (Latimer, W. and Sippel, M., 1987). Tettigoniids, like acridids (and gryllids, see below) also respond to bat-like ultrasound signals by negative phonotaxis, interruption of flight, and cessation of singing (Libersat, F. and Hoy, R. R., 1991; Faure, P. A. and Hoy, R. R., 2000a; Schultz, W. and Schul, J., 2001). The sophisticated frequency-discrimination capabilities of the array of receptors in the tettigoniid ear (see above), together with their tonotopic projections to the CNS, provide the basis for central frequency processing.

The initial stage of frequency processing in the CNS is established by the patterns of connectivity between receptor neurons and interneurons. This in turn is determined by the positions, within the tonotopic receptor projection, of the interneurons' dendrites. The Omega neuron of *Tettigonia viridissima* has dendritic processes that are coextensive with the entire projection area of receptors, except for a small anterior region, which is the target area of low-frequency-tuned receptors. Accordingly, frequency sensitivity of the Omega neuron matches that of the entire auditory nerve except for low frequencies, where Omega is comparatively less sensitive. Similarly, a descending neuron in *Mygalopsis marki,* with dendrites that are restricted to the anterior, low-frequency, portion of the receptor projection, responds only to low frequencies (Figure 5).

Although specific connectivity does impart a degree of frequency selectivity, many interneurons clearly receive convergent input from a large number of differently tuned receptor neurons, with the result that the relatively fine-scaled frequency tuning available at the periphery is lost. Tuning of auditory interneurons may, however, be recovered through frequency-specific inhibition. In a group of related species in the subfamily *Phaneropterinae*, an ascending neuron, AN1, has frequency tuning that matches the spectrum of communication signals. AN1's tuning is species-specific, in contrast to the Omega neuron, the tuning of which is indistinguishable between the species (Stumpner, A., 1997; 2002). AN1's dendrites, like those of the Omega neuron, are widespread throughout the auditory neuropil, suggesting that specific connectivity cannot account for the difference in tuning of these two neurons. Intracellular recordings show that AN1 receives frequency-specific inhibitory inputs. When these are blocked pharmacologically, the species-specific differences in tuning disappear. Thus inhibition, rather than excitation, accounts for the species-specific difference in tuning of this neuron.

Another function of frequency-tuned neurons may be to facilitate distance estimation. The spectrum of tettigoniid songs typically extends from a few kHz into the ultrasonic range. However, as the sound

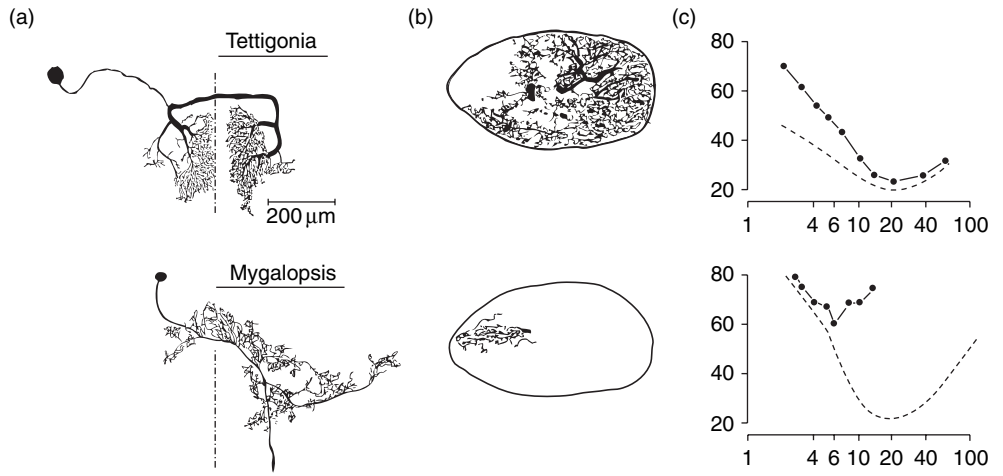

Figure 5 (a) Structure of the Omega neuron in *Tettigonia viridissima* and of a descending auditory neuron in *Mygalopsis marki*. (b) Dendritic branching pattern in the prothoracic auditory neuropil. Level of histological sections of the neurons indicated by the stippled line in the whole-mount drawings. (c) Correlation between the dendritic branching pattern and broad or narrow frequency tuning of the interneurons. Tuning of the interneurons (dots, solid line) is compared with the tuning of the ears as measured by recordings of the whole auditory nerve (dashed line). Ordinate: threshold sound level (dB SPL); abscissa: sound frequency (kHz). From Römer, H., Marquardt, V., and Hardt, M. 1988. Organisation of a sensory neuropile in the auditory pathway of two groups of Orthoptera. J. Comp. Neurol. 275, 201–215.

signal travels through the biotope its spectrum changes, with high-frequency components being attenuated more severely than low-frequency components. As a consequence, the identities of the receptors that are activated, and their degree of activation, could provide information on the distance of the signaler. Depending on the signal spectrum as emitted by the sender, different groups of receptors will be able to track the signal over different ranges of distance. For example, one group might just be reaching threshold at distances where another group begins to saturate. Thus, frequency tuning of the afferents implements a form of range fractionation for signal distance. In *Mygalopsis marki*, receptors that are tuned to low (4–6 kHz) or high (>28 kHz) frequencies respond best over close ranges, the former because the signal emitted by the male contains relatively little power at low frequencies, and the latter because of the severe attenuation of high-frequency components. Receptors tuned to intermediate frequencies (10–20 kHz) operate over longer distances (Römer, H., 1987; Figure 6(a)–(e)). Moreover, the tonotopic organization of receptors translates this relationship between receptor tuning and distance into an odotopic map; the locus of activity within the auditory neuropil shifts systematically with the distance from the sound source (Figure 6(f)). As discussed above, different interneurons sample different regions of this neuropil, and thus differences in operating range occur at the interneuron level as well. For at least one class of interneuron (possibly homologous with AN1, described above), range selectivity is enhanced by frequency-specific inhibition. This results in range-tuned neurons, for which response is maximal for signals arising from a particular distance.

A large, T-shaped interneuron (Suga, N. and Katsuki, Y., 1961; Kalmring, K. *et al*., 1979; Oldfield, B. P. and Hill, K. G., 1983) has been most closely associated with ultrasound-elicited evasive responses. In *Neoconocephalus ensiger* the lowest threshold (30–40 dB SPL) occurs at 20–25 kHz with sensitivity extending to 100 kHz (Faure, P. A. and Hoy, R. R., 2000b). The tuning curve closely matches the tuning of the evasive behavior (Faure, P. A. and Hoy, R. R., 2000a), however, the threshold of the T-fiber is 15–20 dB lower. The neuron responds more strongly to bat-like high-frequency pulses (30 kHz) than to sound pulses with the dominant frequency (15 kHz) of the *N. ensiger* song (Libersat, F. and Hoy, R. R., 1991). Temporal coding of repetitive sound signals is reliable up to 30 pulses s^{-1} for short (10 ms) constant frequency (40 kHz) or frequency modulated (80→30 kHz) bat-like signals. In contrast responses to patterns mimicking the conspecific calling song (12–15 kHz, 30 ms) fail at 5–10 Hz repetition rate (Faure, P. A. and Hoy, R. R., 2000b; 2000c). Also the response latency is shorter (13 ms) for bat-like sounds than for calling song signals (18 ms). This evidence indicates a functional role for the T-fiber in ultrasound mediated startle responses. However, the same neuron has also been proposed to play a role in intraspecific communication in the genus *Tettigonia* (Schul, J., 1997).

3.31.3.10 Gryllids

Male crickets produce calling songs to attract females, and aggression songs in interactions with males. The songs are relatively sharply tuned, with most power at the fundamental frequency, which for field crickets is typically in the range 3–6 kHz. A third signal, courtship song, is emitted when male and female come into contact and elicits a mounting response in females, a prerequisite for mating. In many species courtship song contains sound pulses of two spectral types: a low-amplitude pulse dominated by the fundamental frequency, and an intense pulse dominated by its third harmonic, whereas in other taxa (e.g., *Teleogryllus*) courtship song is spectrally similar to calling song. The importance of song spectrum for behavioral function has been demonstrated in a number of behavioral studies. For example, attraction of females is tuned to the fundamental frequency component of the calling song (Hennig, R. M. and Weber, T., 1997), although the addition of higher harmonics improves both attractiveness and accuracy of localization (Latimer, W. and Lewis, D. B., 1986). Mounting responses during courtship are also best elicited by the dominant frequency of the courtship song (Balakrishnan, R. and Pollack, G. S., 1996; Libersat, F. *et al*., 1994). In addition, crickets are sensitive to ultrasonic frequencies (20–40 kHz) similar to those produced by echolocating bats. Stimulation with ultrasound elicits avoidance responses (Moiseff, A. *et al*., 1978; Pollack, G. S. *et al*., 1984; Nolen, T. G. and Hoy, R. R., 1986a).

Although three frequency ranges are represented peripherally (see above), in the CNS neurons are generally tuned either to a low-frequency range, centered on the dominant frequency of calling song, and/or to a broad, high-frequency range that includes the frequencies that occur in courtship song (for some species) and bat calls. Most attention has focused on neurons that carry auditory information from the prothoracic ganglion to the brain and on local,

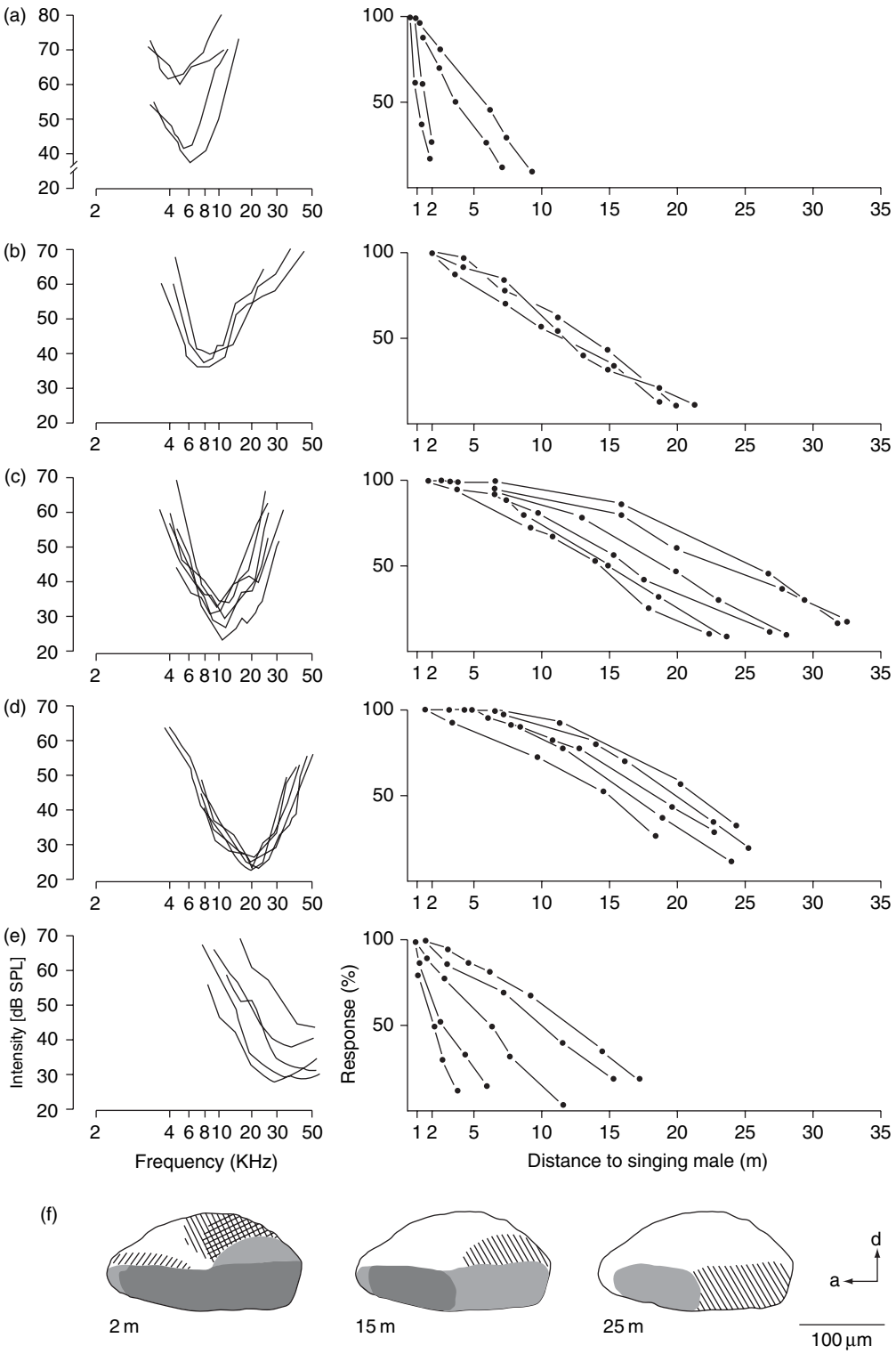

Figure 6 Representation of distance by auditory afferents in *Mygalopsis marki*. (a – e) Tuning curves (left) and distance response characteristics (right) of 26 auditory afferents with optimum frequencies of 4 and 6 kHz (a), 8 kHz (b), 10–12 kHz (c), 20 kHz (d), and above 28 kHz (e). The response magnitude is given as a percentage of the maximum number of spikes/song. Note that whereas all of the receptors are active for nearby sources, activity of the different groups drops off with distance at different rates. (f) Schematic representation of the spatial distribution of receptor fiber activity within the neuropil at three different distances (2, 15, and 25 m) to a calling male. Dark area indicates the relative amount of afferent activity. At intermediate distances dorsal areas also start to be activated. anterior (a), dorsal (d). From Römer, H. 1987. Representation of auditory distance within a central neuropile of the bushcricket *Mygalopsis marki*. J. Comp. Physiol. A 161, 33–42.

prothoracic neurons that shape this information. As described below, manipulation of neural activity in behaving animals has revealed the functional roles of some of these interneurons. Other interneurons, with axons descending from the prothorax to posterior ganglia, and with both ascending and descending axons, have also been described but their roles in behavior are less clear.

There is some disagreement about the number of ascending neurons. Some workers report two on each side (left or right) of the prothoracic ganglion, one, denoted AN1, that is sharply tuned to the calling-song fundamental, and another, AN2, with broad tuning to high frequencies (Wohlers, D. W. and Huber, F., 1982; Hennig, R. M., 1988). Others report a third ascending neuron, but without agreement on its physiological properties (Atkins, S. *et al.*, 1989; Boyd, P. *et al.*, 1984).

The roles of AN1 and AN2 in frequency-specific behaviors have been demonstrated by manipulating their activity in behaving animals (Schildberger, K., 1994; Nolen, T. G. and Hoy, R. R., 1984). When one of the AN1s of *Gryllus bimaculatus* is hyperpolarized (and thus silenced) while a cricket tracks a calling song model by walking on a spherical treadmill, the cricket turns toward the other side, no matter from which side the song is played (Schildberger, K. and Hörner, M., 1988; Figure 7). Similarly, destruction of L1, the presumed homolog to AN1 in *Acheta domesticus,* results in deviation and circling toward the intact side, and phonotaxis stops when this ear is blocked (Atkins, G. *et al.*, 1992). Thus, information about low-frequency stimuli carried to the brain by AN1 and L1 is clearly behaviorally relevant.

AN2 is most sensitive to high sound frequencies and participates in bat-avoidance responses of flying crickets. When AN2 is hyperpolarized while a cricket performs tethered flight, avoidance responses to ultrasound stimuli played from the same side are abolished. When AN2 is caused to fire at high frequency by release from hyperpolarization, an avoidance response occurs, even though no sound is played. These links between AN2 and behavior are operational only when the cricket is flying. High-firing-rate activity of AN2, whether elicited by release from hyperpolarization or by sound, is not accompanied by a behavioral response in quiescent animals. Thus, AN2's activity is both necessary and sufficient for the response, so long as the cricket is actively flying (Figure 8). Crickets also perform negative phonotaxis while walking (Pollack, G. S. *et al.*, 1984). It is not yet known whether AN2 plays any role in this behavior.

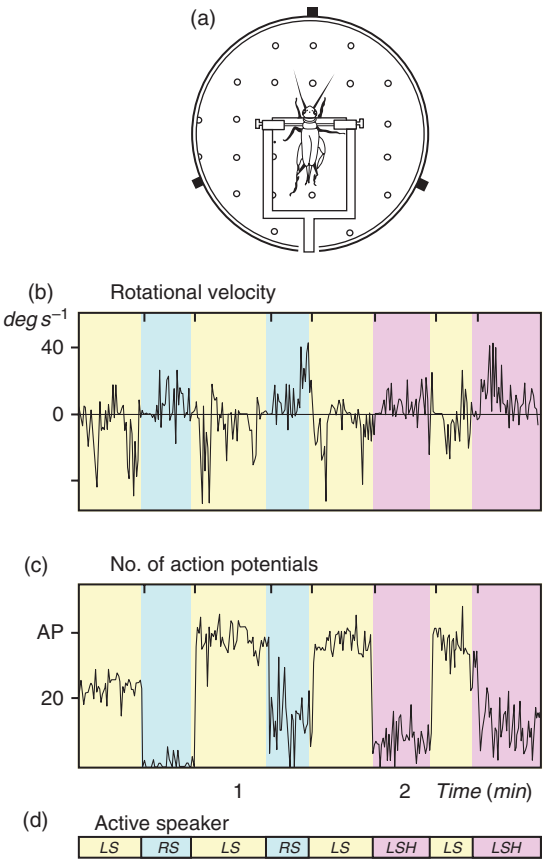

Figure 7 Role of an identified interneuron, AN1, in phonotaxis. (a) The cricket was tethered to a holder in a manner that permitted it to walk on the surface of an air-supported sphere, while AN1 was impaled with a microelectrode to record and manipulate its activity. Walking direction was monitored by tracking the movements of the sphere. (b) Rotational velocity of the sphere; positive rotational velocity indicates turns to the right, and negative velocity indicates left turns. (c) Spike rate of the left AN1. (d) Indicator of experimental conditions. During the time periods indicated by yellow shading, a calling-song model was played from the left side, resulting in firing of AN1 and turns to the left. During the periods indicated with cyan shading, the sound was played from the right; spike rate in left AN1 was low, and the cricket turned right. The crucial periods are indicated with magenta shading; sound was played from the left, but the left AN1 was hyperpolarized, decreasing its spike rate; the cricket turned right. Adapted from Schildberger, K. and Hörner, M. 1988. The function of auditory neurons in cricket phonotaxis I. Influence of hyperpolarization of identified neurons on sound localisation. J. Comp. Physiol. A 163, 621–631.

AN2 elicits behavioral responses only if it fires at high rate (Nolen, T.G. and Hoy, R. R., 1984). For continuous dynamic stimulation with ultrasound, as

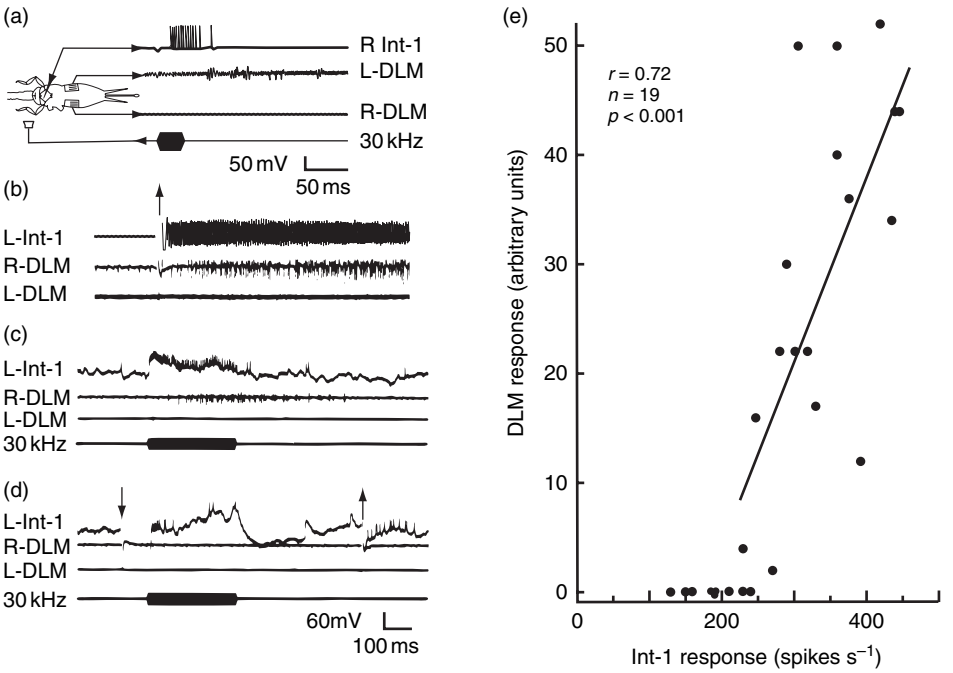

Figure 8 Effect of Int-1 (=AN2) on flight steering in *Teleogryllus oceanicus.* (a) Preparation for simultaneous recordings of Int-1, abdominal dorsal-longitudinal flight-steering muscle activity (DLM), and acoustic stimulation with 30 kHz, 85 dB SPL, 30 ms at 90° to the animal's length axis. A sound pulse elicits a burst of spikes in the left Int-1 and a burst of activity in the right DLM, indicating an attempt to steer to the right. (b) Release of the left Int-1 from hyperpolarizing current injection with −8 nA elicits a spike rate of 400 Hz and causes a steering response in the right DLM. (c) A sound stimulus (30 kHz, 300 ms, 82 dB SPL) presented to the left ear elicits a steering response. (d) When Int-1 is hyperpolarized with −15 nA, its spike activity during acoustic stimulation is reduced to less than 170 Hz and the steering response is suppressed. Duration of current injection is indicated by arrows. (e) Relation between Int-1 spike activity and activity of the steering muscle. Muscle activity correlates with Int-1 spike rates above 230 Hz. Reprinted with permission from Nolen, T. G. and Hoy, R. R. 1984. Initiation of behavior by a single neurons: the role of behavioural context. Science 226, 992–994. Copyright (1984) AAAS.

might occur under natural conditions, AN2 produces brief bursts of high-frequency firing following sharp increases in sound amplitude. The bursts follow these important stimulus features reliably and, moreover, they reliably encode the sound-source direction through binaural differences in bursting. By contrast, isolated spikes of AN2, which also occur in the responses, perform poorly at both tasks. And, as expected from the work of Nolen and Hoy, bursts, but not isolated spikes, elicit avoidance responses (Marsat, G. and Pollack, G. S., 2006).

Both AN1 and AN2 terminate in the brain. Auditory processing here involves local neurons with arborizations restricted to the brain as well as intersegmental neurons with axons that descend to the thoracic ganglia, where they may mediate motor responses to sound. Within both types, there are neurons that are tuned to the calling-song frequency, and others that are most sensitive to high-frequency sounds (Boyan, G. S., 1980; 1981; Schildberger, K., 1984; Brodfuehrer, P. D. and Hoy, R. R., 1990).

The separation of low- and high-frequency processing has its origins in the properties of receptor neurons, but is enhanced through central inhibition. High-frequency-tuned interneurons, both in the prothorax and in the brain, are inhibited by simultaneous low-frequency stimuli (Moiseff, A. and Hoy, R. R., 1983; Nolen, T. G. and Hoy, R. R. 1986a; Boyd, P. *et al.*, 1984; Boyan, G. S. 1980;1981). In those species in which the courtship song includes higher harmonics, inhibition of the high-frequency pathway by low-frequency stimuli would prevent inappropriate activation of putative courtship-song-detecting circuits by the higher harmonics of calling song (Boyan, G. S., 1981). In species that exhibit negative phonotaxis to ultrasound, low-on-high inhibition would prevent inappropriate avoidance of a calling male (Nolen, T.G. and Hoy, R. R., 1986b). Another possible function of this inhibition is to restrict the responses of high-frequency-tuned interneurons to the middle of their dynamic range, thus preventing response

saturation. This would allow the neurons to track the stimulus temporal pattern over a wide range of intensities (Hutchings, M. and Lewis, B., 1984).

3.31.3.11 Temporal Processing and Pattern Recognition

Acoustic signaling for mate attraction requires the identification of the species-specific song pattern by the receiver. In behavioral experiments pattern recognition can only be analyzed through an observable reaction in the receiving animal (Alexander, R. D., 1967; Weber, T. and Thorson, J., 1989). Generally, the singing response or phonotactic orientation of the receiver is used as an indicator to explore the tuning of the recognition process and to elucidate underlying neural mechanisms. Additional complexity may be added by the interaction of recognition and localization, since the underlying neural mechanisms need to be separated in space and/or time. Pattern recognition may benefit from summing the afferent responses of both ears, whereas localization and steering depend on the difference between both signals, which requires their comparison, either prior to the generation of steering commands (von Helversen, D., 1984; von Helversen, D. and von Helversen, O., 1990), or at the level of the motor output (Stabel, J. *et al.*, 1989). Crucial information about pattern recognition has been obtained from behavioral and neurophysiological evidence. Peripheral specializations allow frequency filtering of the species-specific signals, but the final task of identifying the species-specific signal is accomplished in the CNS and in particular the brain (Bauer, M. and von Helversen, O., 1987). Neural mechanisms underlying pattern recognition are best analyzed in crickets and acridid grasshoppers. Only little information is available on cicada, katydids, moths, and other groups.

3.31.3.12 Pattern Recognition in Grasshoppers

Acridid grasshoppers (*Gomphocerinae*) produce broad-frequency (2–40 kHz) sound signals (Meyer, J. and Elsner, N., 1996) by rubbing the hind legs against the wings. Signal amplitude is initially low and may increase to a maximum of 60–66 dB SPL in males (at 10 cm distance, von Helversen, O. and von Helversen , D., 1994). Songs last for several seconds and are characterized by a species-specific pattern of amplitude modulation, that is, sequences of sound pulses and pauses, which are grouped into subunits (syllables). Signals are different in males and females (von Helversen, D. and von Helversen, O., 1997) and are crucial for intraspecific communication and mate attraction. Studies of pattern recognition and orientation have especially focused on the group of *Chorthippus* species (von Helversen, D., 1997).

The general organization of pattern recognition is well characterized (von Helversen, D., 1997) but specific details are not yet understood. From the ears about 60 auditory afferents (Pauls, S. *et al.*, 2001) forward auditory information to the metathoracic ganglion. But the afferent activity does not provide a filter for species-specific signal features (Römer, H., 1976). A crucial step occurs at the first level of auditory processing. In the recognition pathway, which is separate from the processing of sound direction (see below), the afferent information of both ears is merged. Split-song sound patterns (i.e., different song components presented to each ear) that are not effective when presented by their own to one ear, release a behavioral response when the complete pattern is reconstructed by presenting some components to one ear and the remainder simultaneously to the other ear (von Helversen, D., 1984; 1997); thus, input from both ears can be combined prior to pattern recognition. Micro lesions of the thoracic connectives point to the metathoracic ganglion as the location of auditory summation (Ronacher, B. *et al.*, 1986). In the metathoracic ganglion at least six types of local interneurons and at least 17 different ascending interneurons receive afferent information and forward their spike trains to the brain (Stumpner, A. and Ronacher, B., 1991) where they terminate in the lateral protocerebrum (Rehbein, H., 1976; Hedwig, B., 1986). Most of these ascending neurons exhibit poor directionality and show different degrees of phasic, tonic, excitatory, and inhibitory responses. The interneurons differ in details of their activity patterns and seem to forward different features of the sound signal to the brain; however, none appears to be particularly tuned to the species-specific song pattern (Stumpner, A. *et al.*, 1991). More specific functions may be assigned to the interneuron AN4, which is involved in gap detection (see below) and to AN12, which phasically responds only to the onset of syllables (Stumpner, A. *et al.*, 1991). Pattern recognition is located in the brain (Bauer, M. and von Helversen, O., 1987). A central question is whether the animals use the repetitive song structure to integrate auditory information over time or whether they rely on real time processing based on parallel auditory information provided by the ascending interneurons. Songs of *Ch.*

biguttulus females last for 1–1.5 s and are composed of 12 subunits. However, under ideal auditory conditions – with subunits presented at maximum natural amplitude – pattern recognition by males is achieved within just 250 ms by processing only three subunits (Ronacher, B. and Krahe, R., 1998). Thus pattern recognition does not require a long-term sampling strategy but rather is a real-time analysis (Ronacher, B. *et al.*, 2004). Obviously the cross fiber pattern of the numerous ascending neurons provides the information for a rapid identification of the species-specific signal. A model for feature extraction from the species-specific pattern of amplitude-modulated sound has been proposed (Balakrishnan, R. *et al.*, 2001). The model is based on a syllable onset detector, a filter for the syllable periods and a syllable pause detector. So far only some general physiological responses of brain neurons have been characterized in the locust (Römer, H. and Seikowski, U., 1985). The large number of ascending auditory neurons and the unknown recognition network in the brain may allow for subtle changes in cellular and network properties corresponding to receiver variability and species-specific pattern recognition, which has to match intraspecific signal variation and the diversity of *Gomphocerine* songs.

3.31.3.12.1 Gap detection

Songs of acridid grasshoppers are generated by the movements of the hind legs, each scratching a row of cuticular pegs against the front wings. Calling songs of *Ch. biguttulus* males are composed of sequences of amplitude modulated broadband noise of 2–3 s duration. The legs move slightly out of phase, so that the brief silent intervals of 2–3 ms duration (gaps) that occur at the transitions between upward and downward movements of a single leg are filled in by sound produced by the other leg. The loss of one hind leg reveals these gaps within the syllables of a song (von Helversen, D., 1972; von Helversen, O., 1979). When *Ch. biguttulus* females are exposed to male songs with gaps ranging from 0 to 4 ms their response is gradually abolished (von Helversen, D., 1972; Ronacher, B. and Stumpner, A., 1988). Mating success of males having only one hind leg is reduced by 87.2% (Kriegbaum, H., 1989), demonstrating a strong preference of females for the calling song of intact males. Although the spike pattern of individual auditory afferents cannot resolve the gaps, spike synchronization over the population of 60–80 afferents is sufficient to forward the occurrence of silent intervals to the CNS (Ronacher, B. and Römer, H., 1985). Gaps have no effect on the responses of most ascending auditory interneurons, but they drastically affect that of interneuron AN4. This neuron receives pronounced IPSPs at the onset of a sound pulse followed by synaptic excitation during the tonic sound component. In response to a continuous sound (i.e., gap-free pulses) AN4 therefore spikes after an initial transient inhibition; but its spike response is completely suppressed when short silent gaps consecutively re-trigger the inhibition. The decay of AN4's spike response closely matches the decay of the female behavior for increasing gap duration (Ronacher, B. and Stumpner, A., 1988). In *Ch. biguttulus* this property of AN4 appears to be involved in efficient selection against males that have lost one hind leg. Since female responses are suppressed when AN4 is not spiking, activity of this neuron may be essential to activate the calling-song recognition network in the brain (Figure 9).

3.31.3.13 Gryllids

Cricket calling songs are characterized by high-intensity sound pulses ranging from 6 to 50 ms duration which are arranged in long lasting sequences of pulses, or grouped in chirps and intermittent silent intervals, or organized in alternations of chirps and trills with different pulse rates (Alexander, R. D., 1961). Since the carrier frequency of the signal shows little modulation, far-field recognition of the male's calling song depends on the temporal structure of the pulse pattern. Behavioral experiments point to the pulse rate as the most important character for pattern recognition (Zaretsky, M. D., 1972; Thorson, J. *et al.*, 1982). Phonotaxis is maximum at the species-specific pulse rate and decreases at higher and lower rates. Other song features, such as pulse duration, pulse duty cycle, and the organization of pulses into higher-order structures such as chirps and trills, can also influence the phonotactic response (Doherty, J. A., 1985; Stout, J. F. and McGhee, R., 1988; Pollack, G. S. and Hoy, R. R., 1979; Hennig, R. M. and Weber, T., 1997; Hennig, R. M., 2003).

Phonotaxis during flight (Pollack, G. S. and Hoy, R. R., 1981) and during walking on a sensitive trackball system (Hedwig, B. and Poulet, J. F. A., 2004; 2005) demonstrated fast reflex-like steering movements toward individual sound pulses that underlie the orientation behavior. The females also steer toward nonattractive pulses if these are inserted into a sequence of the calling song. The amplitude of steering responses gradually increases at the start

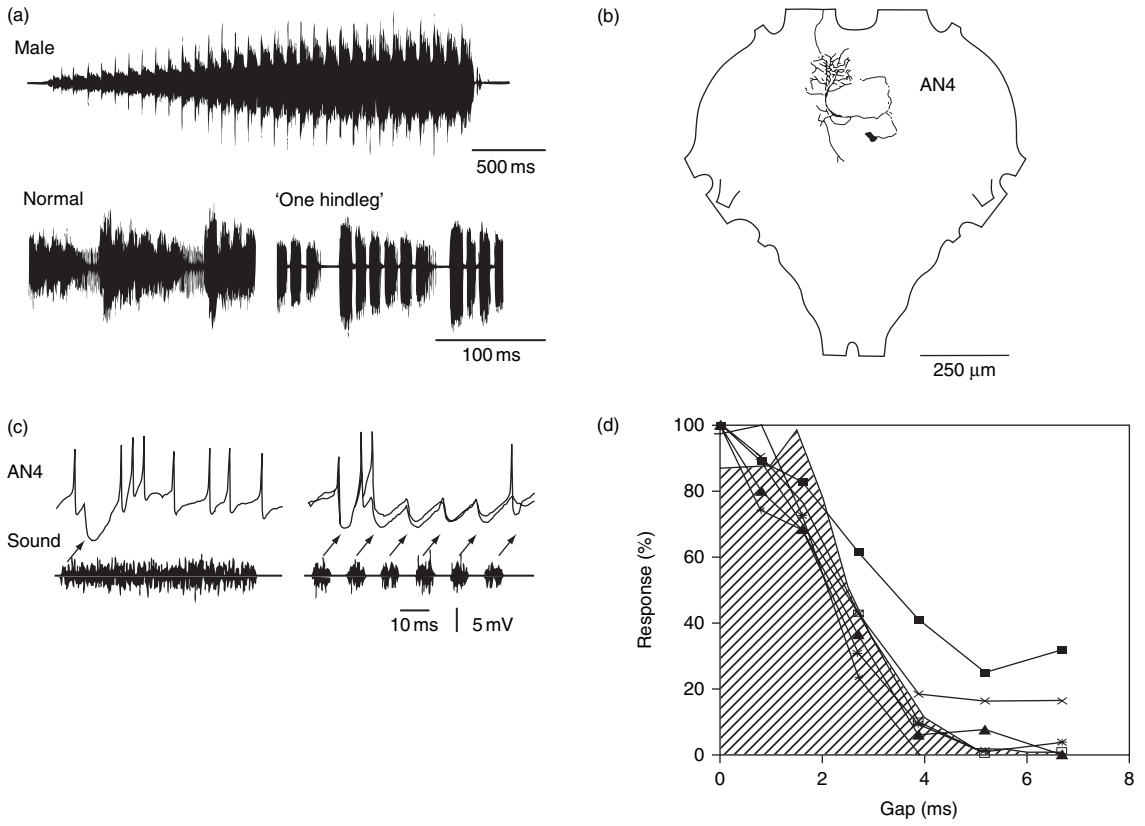

Figure 9 Detection of silent gaps in the song of a grasshopper. (a) Normal song of a male grasshopper *Chorthippus biguttulus* (top). Section of a normal song at higher temporal resolution (lower left) and of a song produced with one hind leg only (lower right). (b) Structure of the ascending auditory interneuron AN4 in the metathoracic ganglion. Main dendritic branches are located in the rostral auditory neuropil, the axon projects to the brain. (c) Intracellularly recorded response to acoustic stimulation with a normal conspecific syllable (left) and with a syllable interrupted by silent gaps (right). Two recordings are superimposed on the right. Each sound onset triggers a pronounced IPSP. (d) Relative response of four AN4 interneurons to syllables with different gap durations at intensities between 66 and 78 dB SPL. The relative behavioral response toward the sound stimuli with increasing gaps is based on three females and indicated by the shaded area. From Stumpner, A. and Ronacher, B. 1994. Neurophysiological aspects of song pattern recognition and sound localization in grasshoppers. Amer. Zool. 34, 696–705.

of phonotaxis and the response to nonoptimal test pulses decreases over several seconds after a sequence of phonotaxis (Poulet, J. F. A. and Hedwig, B., 2005; Hedwig, B. 2006). These results indicate that the pattern recognition process modulates the gain of auditory steering and that pattern recognition itself is not directly involved in the fast steering responses. This modulation appears to be mediated by the brain, since phonotactic steering fails after the brain has been disconnected from the CNS (Pollack, G. S. and Hoy, R. R., 1981).

Various possible mechanisms for pattern recognition have been discussed, including template matching (Hoy, R. R., 1978; Pollack, G. S. and Hoy, R. R., 1979), cross- and autocorrelation (Weber, T. and Thorson, J., 1989; Hennig, R. M., 2003), band-pass filtering (Schildberger, K., 1984), and instantaneous discharge rate coding (Nabatiyan, A. *et al.*, 2003), and some neurobiological evidence relates to the filtering of the syllable rate. Afferents respond with phasi-tonic spike patterns to acoustic stimuli. At the population level the synchronous activity of the afferents leads to a strong onset response highlighting the onsets of sound pulses (Nabatiyan, A. *et al.*, 2003), possibly facilitating downstream measurement of pulse rate. The time constant of mutual inhibition between the local thoracic ON1 neurons has been proposed to constitute a temporal filter matched to the species-specific syllable rate (Wiese, K. and Eilts-Grimm, K., 1985), but Marsat G. and Pollack G. S. (2004) found no change in ON1's temporal coding properties when the contralateral neuron was deafferented. The ascending

thoracic interneurons of crickets, AN1 and AN2, are not selective for temporal patterns if only their spike numbers are considered. They respond to different types of pulse patterns with the same mean spike rate and appear to copy and forward a wide range of patterns to the brain (Wohlers, D.W. and Huber, F., 1982; Huber, F., 1983). However, when the coding properties of the neurons are analyzed using an information-theoretic approach, ON1 and AN1 in *Teleogryllus oceanicus* code best for amplitude modulations in the range 5–30 Hz, corresponding to the range of modulation rates which occur in the species' songs (Marsat, G. and Pollack, G. S., 2004; 2005). If the instantaneous spike rates are analyzed in response to different syllable rates, ON1 generates a maximum number of high-frequency discharges (200–300 Hz) at the species-specific syllable period. This indicates thoracic filtering of the species-specific pulse rate. The activity of any postsynaptic neuron that is driven by such a spike pattern will exhibit band-pass characteristics, like the tuning of phonotactic behavior (Nabatiyan, A. *et al.*, 2003). Boyan, G. S. (1984) provides evidence for local brain neurons clearly responding to the pattern of the calling song. The activity of other local brain neurons, some with rather weak auditory responses, has been interpreted to support a concept that pattern recognition is based on a series of low-pass and high-pass filters which in combination lead to a band-pass filter for the syllable rate (Schildberger, K., 1984). The arborization patterns of all local auditory brain neurons are restricted to one side of the brain only (Boyan, G. S., 1980; Schildberger, K., 1984). Since the ascending auditory information is also strictly side-specific, two separate recognition systems may exist, one located in each half of the brain (Pollack, G. S., 1986). The functional properties of these recognition networks still have to be elucidated.

3.31.3.14 Tettigoniids

Phonotaxis behavior and its neural correlates have also been analyzed in a group of closely related Tettigoniids (Schul, J., 1997; Schul, J. *et al.*, 1998;, Schul, J., 1998) where males attract females by series of sound pulses comprising low (8–12 kHz) and high carrier frequency (25–45 kHz) components. In one species (*T. cantans*) pattern recognition is based on a pulse-rate mechanism, whereas *T. caudata* uses the detection of a minimum duty cycle. The species *T. viridissima* has a more complex recognition system based on pulse duration and the interval between double-pulses. Interestingly in two species (*T. caudata* and *T. viridissima*) the pulse structure of the songs are more elaborate than the requirements of the pattern recognition system (Schul, J., 1998).

The central auditory pathway in tettigoniids shares common features and homologous neurons with crickets. Ascending auditory neurons (AN1, AN2) and T-shaped interneurons copy the pulse structure of the song and forward this information to the brain. The T-fiber has been implicated in pattern recognition (Schul, J., 1997); however, it responds best to high sound frequencies and rather may be involved in predator avoidance (see above). Pattern recognition and directional information appear to be processed in a serial manner in the brain (Schul, J. *et al.*, 1998; Section 3.31.3.22). Behavioral experiments provide evidence for resonant neural networks underlying pulse-rate recognition in *T. cantans* (Bush, S. L. and Schul, J., 2006). Female phonotaxis is activated by the pulse rate of the species-specific song and by subharmonics of it. This type of response selectivity is expected if acoustically driven activity interacts with a neural network that oscillates at the species-typical rate (see also Hennig, R.M. *et al.*, 2004).

A fundamentally different method of pattern recognition underlies acoustic communication in duetting phaneropterine tettigoniids. Males and females communicate with sequences of short high-frequency sound pulses (Spooner, J. D., 1968; Hartley, J. C. and Robinson, D. J., 1976; Robinson, D. J. *et al.*, 1986; Heller, K.-G. and von Helversen, O., 1986; von Helversen, O. *et al.*, 2001; Stumpner, A. and Meyer, S., 2001). Males generate a chirp, that is, a series of sound pulses, which in some species are terminated with a final trigger pulse. When listening to the first series of sound pulses of a singing male the stationary females open their wings, in preparation for producing a response. The response occurs after the male's (trigger) pulses. By closing their wings females generate one to three high-frequency clicks less than 1 ms in duration. The time delay of the response is fixed and species-specific. In *Leptophyes* the response latency is just 28 ms (Zimmermann, U. *et al.*, 1989) and seems to constitute a thoracic acoustic motor reflex (Robinson, D. J. *et al.*, 1986), which is armed once the females have recognized the species-specific sequence of male sound pulses. Female sound pulses are extremely similar in different species (Stumpner, A. and Meyer, S., 2001) but males approach a conspecific female only if they perceive its response within a certain sensitive time window after their own song (Heller, K.-G. and

von Helversen, D., 1986; Dobler, S. *et al.*, 1994). At the neural level, males must have a temporarily sensitized network that expects the female response and initiates phonotactic steering. Interneurons of tettigoniids have been described with respect to frequency processing (Stumpner, A., 1997; 1999; 2002), however the neural basis of this temporal filter is not known.

Some species of tettigoniids sing in choruses, with calls of individuals generated either in synchrony or alteration (Sismondo, E., 1990; Greenfield, M. D. and Roizen, I., 1993). The synchrony of signaling is not perfect and one male will lead its neighbors. When females are exposed to identical calls presented in close succession they prefer the leading signals (Greenfield, M. D. and Roizen, I., 1993; Snedden, W. A. and Greenfield, M. D., 1998). This is not due to physical masking of the following signal but rather to a neuronal precedence effect (Wallach, H. *et al.*, 1949; Wyttenbach, R. A. and Hoy, R. R., 1993) in which the first of two temporally and spatially separated signals reaching the CNS inhibits the response to the second signal. When two identical chirps separated in space (180°) and time (e.g., 120 ms) are presented to the tettigoniid *Mecopoda elongata,* simultaneous recordings from both thoracic local ON1 neurons demonstrate that the leading signal inhibits the response to the follower signal in the contralateral neuron. This inhibition is due to the reciprocal inhibition between ON1 neurons, an arrangement that functions to enhance the bilateral auditory contrast in directional processing, but in this system also contributes to the female preference for the calls of leading animals (Römer, H. *et al.*, 2002).

3.31.3.15 Selective Attention: Detecting the Loudest Singer

Complex acoustic situations are generated when several animals sing at the same time. Phonotaxis of a receiver then may be dominated by sound intensity (Greenfield, M.D. and Shelly, T. E., 1990) since intensity indicates the loudest/fittest singer or a nearby male that can be approached with the lowest risk of predation. Of course a loud signal will activate auditory afferents more strongly than simultaneously perceived softer signals. However, in crickets (Pollack, G. S., 1988; Poulet, J. F. A. and Hedwig, B., 2003b) and tettigoniids (Römer, H., 1993; Römer, H. and Krusch, M., 2000) additionally a cellular mechanism decreases and even suppresses the response to the quieter sound in central neurons. In local (ON1, cricket and tettigoniid) and in ascending thoracic auditory interneurons (AN1 cricket, AN2, tettigoniids) repetitive acoustic stimulation with the species-specific song elicits an excitatory response to each sound pulse. At the same time excitation leads to a slow hyperpolarization, caused by a fast increase in cytosolic Ca^{2+} that probably triggers a Ca^{2+}-activated K^{+} current (Sobel, E.C. and Tank, D. W., 1994. Baden, T. and Hedwig, B., 2007). Ca^{2+}-activated potassium currents depend on the level of cytosolic calcium and thereby indirectly on stimulus intensity. This has a significant consequence for the activity of the auditory neurons. When loud and soft sound pulses are presented simultaneously to a cricket (80/60 dB) or tettigoniid (60/45 dB), only the loud pulses that cause a strong depolarization overcome the inhibition and consequently govern the spike activity of the auditory neuron. The excitatory response to the softer sound pulses is shunted and these are not represented in the spike pattern (Pollack, G. S., 1988; Sobel, E. C. and Tank, D. W., 1994; Römer, H. and Krusch, M., 2000). This cellular mechanism, based on the coupling of inhibitory membrane conductances to excitation, acts like an automatic gain control. It adjusts the output of these auditory neurons depending on the input and drastically decreases the response to background noise. In tettigoniids it is effective at intensity differences of only 2–5 dB (Römer, H. and Krusch, M. 2000). Humans can switch their process of recognition to either ear at will (thereby solving the cocktail party problem (Cherry, E. C., 1953)). The mechanism described here for insects does not entail a volitional shift in attention, but combined with the directional sensitivity of the ears it allows the loudest signal to dominate perception at each side. Consequently side-specific different temporal patterns ascend to the brain for pattern recognition (Pollack, G. S., 1986; Figure 10).

3.31.3.16 Flies

Some members of two groups of parasitic flies (*Sarcophagidae/Emblemasoma* and *Tachinidae/Ormiini*) use acoustic cues to approach singing crickets and tettigoniids. Female flies locate the singing males of host species and deposit their larvae on them (Cade, W. H., 1975; Walker, T. J., 1993; Allen, G. R., 1995). Frequency sensitivity of the flies' ears is adapted to the host's communication signals. This allows peripheral filtering of an essential feature for host recognition (Robert, D. *et al.*, 1992; Lakes-Harlan, R. and Heller, K.-G., 1992). Convergent song preferences are shared between female crickets, *G. lineaticeps* (38 pulses s^{-1} 0.8–4.6 chirps s^{-1}) and the fly *O. ochracea* in Californian populations. Both crickets and flies prefer male calling songs with

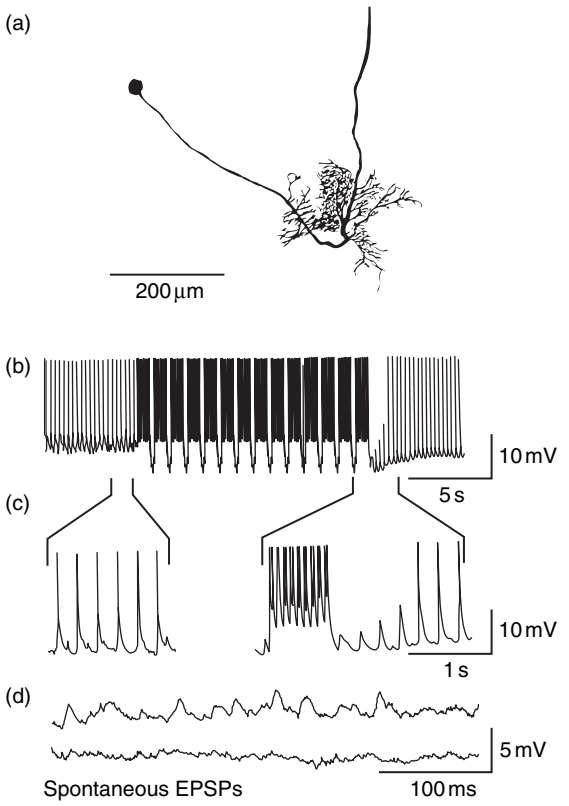

Figure 10 Suppression of background noise in tettigoniids. (a) Branching pattern of the ascending interneuron AN2 in the prothoracic ganglion of *Tettigonia viridissima*. Dendritic arborisations are located in the auditory neuropil, the axon ascends to the brain, and the soma is positioned to the left. (b) Intracellular recording of AN2. The neuron is stimulated via two ipsilateral speakers with a continuous sequence of pure tone bursts at a rate of 5 Hz (20 kHz, 50 dB SPL) and additionally with a conspecific song at 55 dB SPL. Note the hyperpolarization and the reduction in the EPSP amplitude at the end of the stimulation with the song pattern. Same data given in (c) with higher temporal resolution. (d) shows the amplitude of spontaneous EPSPs before and immediately after prolonged stimulation with the conspecific signal. (a) From Römer, H., Marquardt, V., and Hardt, M. 1988. Organisation of a sensory neuropile in the auditory pathway of two groups of Orthoptera. J. Comp. Neurol. 275, 201–215. (b–d) From Römer, H. and Krusch, M. 2000. A gain-control mechanism for processing of chorus sounds in the afferent auditory pathway of the bushcricket *Tettigonia viridissima* (Orthoptera; Tettigoniidae). J. Comp. Physiol. A 186, 181–191.

relatively high chirp rates and long chirp durations (Wagner, W. E., 1995). In *Therobia leonidei*, which parasitize tettigoniids, three auditory interneurons with tonic and phasic response properties have been characterized. They ascend from the sensory neuropil in the thoracic ganglion complex and terminate in the brain (Stumpner, A. and Lakes-Harlan, R., 1996).

3.31.3.17 Directional Processing

The physical cues for sound localization are generated by the properties of sound. For a source that is not in the median plane, the distance sound travels to each ear differs in a direction-dependent manner, generating an interaural time difference. Diffraction, reflection, and absorption of sound by body parts interposed between the ears will generate an interaural intensity difference. Because insects are small, both sorts of difference are minute. However, as described in Section 3.31.1.1 and elsewhere in this volume (see Monaural Sound Localization Using Spectral Cues) insects have evolved a number of mechanical specializations that exploit these small differences (Michelsen, A. and Löhe, G., 1995), bringing them into the working range of neural circuitry. In this section we consider how localization cues are represented and processed further within the CNS.

Time-of-arrival differences, even after mechanical preprocessing, are only on the order of a few tens of microseconds. Although such small differences can be resolved by brain circuits of higher vertebrates, there is no evidence that the nervous systems of insects are capable of such fine temporal processing. However, the relationship between stimulus amplitude and response latency of receptor neurons (see above) may generate millisecond-level interaural latency differences (Mörchen, A. *et al.*, 1978). Thus there are several ways in which interaural difference in stimulus amplitude (after mechanical preprocessing) may be represented: as differences in response latency of receptor neurons, in firing rates, and in the numbers of receptors for which threshold has been reached. These differences provide the raw material with which central circuits can work.

3.31.3.18 What Is the Neural Code for Sound Direction?

Translation of the physical cues for sound direction into behavior by flies is discussed by Hoy, R.R. and Robert, D. (Chapter 21, Perspective). Here we examine the processing of directional information in Orthoptera, the other group in which this issue has received considerable attention.

As noted above, a binaural difference in stimulus amplitude will lead to bilateral differences in both response latency and response strength. For natural stimuli, these two measures co-vary with stimulus direction, and tests of their relative contributions to

sound localization require that they be uncoupled. Independent stimulation of the two ears is difficult to achieve in freely behaving insects. However, quasi-dichotic stimulation of grasshoppers (*Ch. biguttulus*) was achieved by presenting stimuli from separate free-field loudspeakers on the insect's left and right (von Helversen, D. and Rheinlaender, J., 1988). Male grasshoppers turned toward the leading side with 75% accuracy for a time difference as small as 0.4 ms; performance was nearly perfect for a difference of 1.5 ms. These values are well within the range of bilateral latency differences of receptor neurons (Mörchen, A. *et al.*, 1978). The possible role of interaural intensity difference was investigated by playing just suprathreshold stimuli simultaneously from the two sides and varying their relative intensities. Reliable turning toward the more intense signal occurred for differences as small as 1–2 dB, values within the range that would be produced by the acoustic mechanisms for directionality. Similar sensitivity to binaural intensity difference has been shown in a tettigoniid (Rheinlaender, J. *et. al.*, 2006).

The effectiveness of binaural intensity difference was also demonstrated in crickets, which performed open-loop phonotaxis while walking on a spherical treadmill (Hedwig, B. and Poulet, J. F. A., 2005). Again, a bilateral difference of 1–2 dB was sufficient to elicit reliable steering toward the more intense stimulus. Time difference is apparently less important for crickets, with a modest tendency to turn toward the earlier signal appearing only for differences of 4 ms or more.

Bilateral differences in response timing and strength have also been decoupled by exploiting the adaptation characteristics of receptor neurons. Adaptation to rapidly repeated stimulation is expressed both as a decrease in spike rate and as an increase in latency. The effect on spike rate is greater for higher intensities (and thus for receptors serving the ear ipsilateral to the sound source), but the effect on latency is intensity independent (Sippel, M. and Breckow, J., 1984; Givois, V. and Pollack, G. S., 2000). Thus, adaptation causes a decrease, and sometimes even a reversal in sign, of the bilateral difference in response strength, but little or no change in the bilateral latency difference.

When crickets were exposed to a stimulus that produced strong adaptation but that was not behaviorally attractive, and were subsequently stimulated with an attractive pulse train, interaural differences in response strength and in latency could be uncoupled, at least transiently; for the first several sound pulses of the attractive stimulus, response strength could be greater on one side (the side opposite the adapting signal), yet latency could be shorter on the other side. Thus, the two potential cues for sound location disagreed. Under these conditions, crickets (assayed while performing tethered flight) turned most frequently toward the side where response strength was greatest (Pollack, G. S., 2003). Thus, as also shown by Hedwig B. and Poulet J. F. A . (2005), in crickets the bilateral difference in response strength, rather than in latency, is the dominant cue for localization.

3.31.3.19 Enhancement of Interaural Differences Through Bilateral Interactions

Bilateral differences in activity at the level of receptor neurons are amplified centrally through contralateral inhibition. The best-studied example of contralateral inhibition is that provided by the Omega neurons of crickets and tettigoniids.

3.31.3.20 Contralateral Inhibition in Gryllids

Two omega-shaped neurons occur on each side of the prothoracic ganglion of crickets. Omega neuron 1 (ON1) is a large, local interneuron in the prothoracic ganglion of crickets (Casaday, G. B. and Hoy, R. R., 1977; Popov, A. V. *et al.*, 1978; Wohlers, D. W. and Huber, F., 1978). It is most sensitive to the fundamental frequency of calling song, but also responds robustly to higher (including ultrasonic) frequencies (Wohlers, D. W. and Huber, F., 1982; Atkins, G. and Pollack, G. S., 1986). It has extensive processes in the auditory neuropil on both sides of the ganglion. The branches on the soma-ipsilateral side are dendritic and mainly postsynaptic, whereas the soma-contralateral branches show axonal terminals and are mainly presynaptic (Watson, A. H. D. and Hardt, M., 1996). The neuron receives input from receptors of the soma-ipsilateral ear, and inhibits several neurons receiving input from the other ear, including the ascending neurons AN1 and AN2, and its contralateral homolog (Selverston, A. *et al.*, 1985; Horseman, G. and Huber, F., 1994a; Faulkes, Z. and Pollack, G. S., 2000, Figure 11). This contralateral inhibition enhances binaural contrast (Kleindienst, H.-U. *et al.*, 1981; Horseman, G. and Huber, F., 1994b; Marsat, G. and Pollack, G. S., 2005), presumably facilitating sound localization. ON2 is similar in morphology, except that it has a dendritic process that crosses the midline. Ultrastructural studies suggest that, as

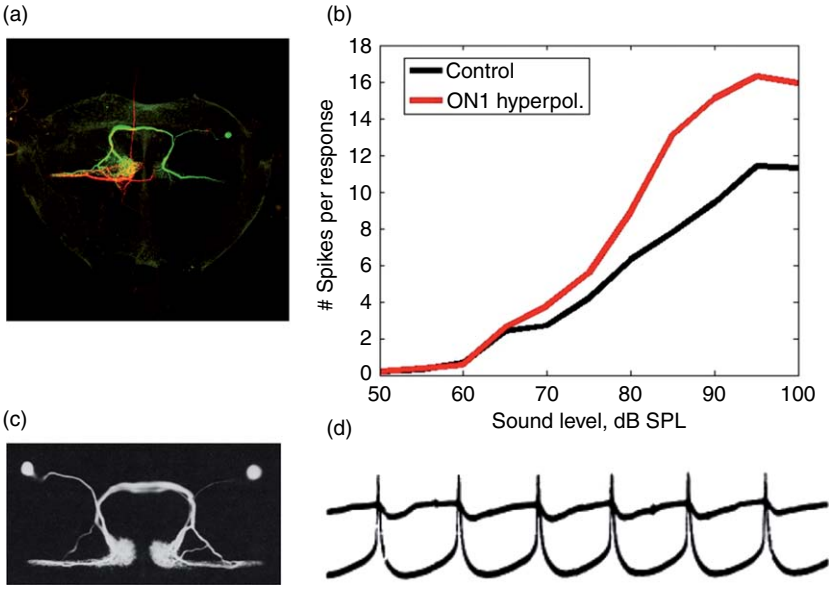

Figure 11 Contralateral inhibition in crickets. (a) The identified interneurons ON1 (green) and AN2 (red). Each neuron exists as a mirror–image pair. The AN2 shown receives auditory input from receptor neurons from the ear (not shown) to the left in this image; ON1 receives input from the ear to the right, and provides inhibitory input to AN2 (as well as to another identified neuron, AN1 – not shown – and to its contralateral homolog – see (c) and (d)). (b) Demonstration of contralateral inhibition. The curves show spike counts of AN2 responses to 30 kHz sound pulses, at various amplitudes, both without (black) and with (red) hyperpolarization of the contralateral ON1. When ON1 is hyperpolarized and its spikes suppressed, spike count of AN2 increases. (c) and (d) Mutual inhibition between the left and right ON1s. (c) Shows the anatomical relationships of the two neurons, both of which were stained here with intracellular dye injection. (d) Action potentials in one of the ON1s (bottom trace) are followed with short, constant latency, by IPSPs in the other ON1. (a) Pollack, G. S. (unpublished). (b) From Marsat, G. and Pollack, G. S., 2007. Efficient inhibition of bursts by bursts in the auditory system of crickets. J. Comp. Physiol. A 193, 625–633. (c, d) From Selverston, A. I, Kleindienst, H.-U., and Huber, F. 1985. Synaptic connectivity between cricket auditory interneurons as studied by selective photoinactivation. J. Neurosci. 5, 1283–1292.

for ON1, the soma-ipsilateral and soma-contralateral branches are mainly post- and presynaptic, respectively. However, unlike ON1, ON2 responds nearly equally well to stimuli from both sides (Wohlers, D. W. and Huber, F., 1982).

As noted above (see the section 'Frequency Analysis'), activity of the ascending neurons AN1 and AN2 influence the direction of phonotaxis; hyperpolarizing either of these neurons in crickets performing phonotaxis while walking results in directional errors away from the side of the silenced neuron. Horseman G. and Huber F. (1994b) the effect of contralateral inhibition in the network comprised of the left and right AN1s, AN2s, and ON1s. Contralateral inhibition received by ON1 and AN1 is relatively strong, whereas that of AN2 is weaker. Modeling the auditory pathway showed that contralateral inhibition strongly affects the bilateral difference in AN1s response, and more weakly affects that of AN2, in accordance with the relatively strong and weak effects of silencing these neurons on phonotaxis. The structure of this prothoracic network predicts that silencing ON1 should also affect phonotaxis accuracy. Hyperpolarization of ON1 in behaving animals resulted in a decrease in the tendency to turn toward the sound source, but only in three of eight animals tested (Schildberger, K. and Hörner, M., 1988). Killing ON1 (in another species) caused a tendency to circle toward the intact side. However, in this case the effects were seen only for stimuli with marginally acceptable temporal patterns; for an optimal stimulus pattern, killing ON1 had little effect on accuracy (Atkins, G. *et al.*, 1984).

A neuron probably homologous to ON1 of crickets also occurs in tettigoniids (Römer, H., 1987). As in crickets, ON1 of tettigoniids inhibits its contralateral partner. However, ablation experiments show that unlike ON1 of crickets, which accounts for all measurable contralateral inhibition (Faulkes, Z. and Pollack, G. S., 2000), this neuron is not the only source of contralateral inhibition in tettigoniids

(Molina, J. and Stumpner, A., 2005). Since there appears to be no ON2 in tettigoniids the additional source of contralateral inhibition is not yet known.

3.31.3.21 Contralateral Inhibition in Acridids

At least one local interneuron (BSN1) and two ascending neurons (AN1, AN2) of acridids are highly directional (Stumpner, A. and Ronacher, B., 1991); although micro-lesions in the connectives leading from the thorax to the brain point toward AN2 as the key neuron forwarding directional information to the brain and question the importance of AN1 (Ronacherl, B. *et al.*, 1993). The directionality of thoracic neurons is caused in part by contralateral inhibition (Suga, N., 1963). Direction-dependent inhibitory inputs are apparent as IPSPs in intracellular recordings of thoracic interneurons (Römer, H. *et al.*, 1981; Römer, H. and Dronse, R., 1982; Figure 12(a)),

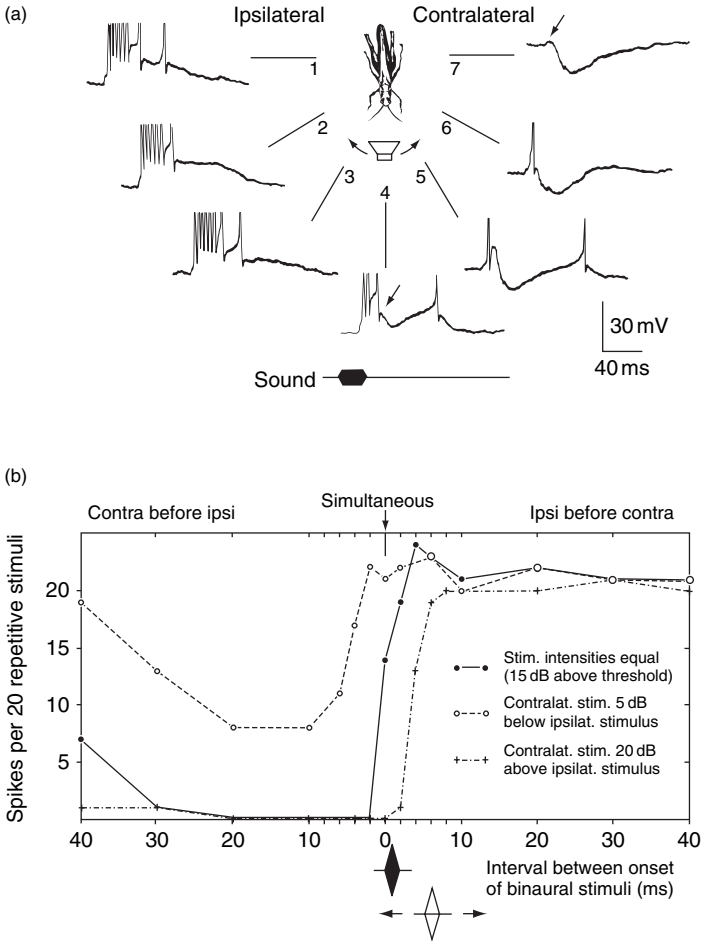

Figure 12 Directional processing in the locust auditory pathway. (a) Intracellular response of a directional sensitive interneuron in the metathoracic ganglion of the locust *Locusta migratoria*. Sound direction changed in steps of 30°. Excitatory responses are elicited upon ipsilateral stimulation (position 1) and pronounced IPSPs follow an initial excitation (arrow) when the stimulus is presented from contralateral (position 7). IPSPs occur at the transition of the speaker from ipsilateral to contralateral (arrow, position 4). Sound stimulus 20 ms, 20 kHz, 20 dB above ipsilateral threshold. (b) Effect of interaural time and intensity differences on the response of an auditory interneuron in the locust *Locusta migratoria*. Tympanic membranes were stimulated with contact-mechanical stimuli (69 kHz, 2 ms duration, repeated at 1 Hz). Excitation of the interneuron by ipsilateral stimulation (◆) and inhibition by contralateral stimulation (◇). The interval between binaural stimuli is systematically varied. The slope of the curves shifts by changing the difference in interaural stimulation intensities. (a) From Römer, H., Rheinlaender, J., and Dronse, R. 1981. Intracellular studies on auditory processing in the metathoracic ganglion of the locust. J. Comp. Physiol. A 144, 305–312. (b) From Rheinlaender, J. and Mörchen, A. 1979. 'Time-intensity trading' in locust auditory interneurons. Nature 281, 672–674.

but their source has not yet been identified. As for behavior (see above), responses of interneurons may be exquisitely sensitive to small difference in binaural timing and intensity (Rheinlaender, J. and Mörchen, A., 1979; Figure 12(b)).

3.31.3.22 Integration of Pattern Recognition and Sound Localization

3.31.3.22.1 Gryllids

Since crickets are selective for the more attractive pattern – when patterns are presented from different directions – it was proposed that inhibitory interaction between the two recognition systems might allow for discrimination of the better pattern (Pollack, G. S., 1986). Crickets steer to the side where the auditory pattern is represented best in the activity of ascending neurons. This led to the conclusion that pattern recognition and localization are organized serially, with the bilateral comparison that is the basis of localization being performed only after auditory information has passed through a recognition filter (Stabel, J. *et al.*, 1989, von Helversen, D. and von Helversen, O., 1995). However, rapid steering responses occur toward individual sound pulses in flying (Pollack, G. S. and Hoy, R. R., 1981) and walking (Hedwig, B. and Poulet, J. F. A., 2004; 2005) crickets. Rapid reflex-like steering is even elicited by the first pulses of chirps, when the animals had no chance to analyze the pulse rate of the perceived song. This demonstrates that orientation is not based on comparing the activity in both recognition systems. Moreover, orientation during phonotactic walking emerges from consecutive reactive steering responses to individual sound pulses. Even when an optimal pattern is presented from one side, the animals still respond toward nonattractive sound patterns presented on the other side (Hedwig, B. and Poulet, J. F. A., 2004). The reflex-like steering responses are under control of the brain and fail once the brain is disconnected from the CNS (Pollack, G. S. and Hoy, R. R., 1981).

3.31.3.22.2 Acridids

Directional information is functionally separated from pattern recognition at the metathoracic level, and ascends in a side-specific manner to the brain (Ronacher, B. *et al.*, 1986; von Helversen, D., 1997). The decision on turning direction appears to be made in the brain by a system comparing the directional information from both sides of the nerve cord (von Helversen, D. and von Helversen, O., 1990; 1995). When an efficient sound pattern is presented to one ear of a grasshopper and a nonefficient pattern with better directional cues to the other, the animals will turn not toward the attractive sound pattern, but rather toward the pattern with the better directional information. This indicates that the turning decision is independent of pattern recognition, however pattern recognition finally gates the turning response (von Helversen, D. and von Helversen, O., 1990; 1995).

3.31.4 Integrating Hearing with Other Activities

Insect hearing organs are adapted to respond to sounds of predators and conspecifics. Because of their design and sensitivity, however, they may also be affected by the animal's own motor activity. Furthermore, during sound production the ears are exposed to the animal's self-generated sound. Here we look at the impact of motor activity on sound processing and demonstrate that different insects adopted different strategies ranging from behavioral adaptations to neural attenuation of the auditory pathway to deal with this problem.

3.31.4.1 Ventilation and Flight

In grasshoppers and crickets the ears are closely related to the ventilatory system and they are not mechanically decoupled from the animal's body. Consequently, ventilation and other motor activities have a strong impact on hearing. Changes in the air pressure of the tracheal system cause inward and outward movements of the tympanic membrane in grasshoppers (Schwabe, J., 1906; Meyer, J. and Hedwig, B., 1995; Meyer, J. and Elsner, N., 1995) reaching 90–120 µm in *Locusta migratoria*. These slow movements of the tympanic membrane change its auditory response properties and modulate the afferent activity. Tympanic membrane oscillations are generally attenuated in the range of 2–10 kHz and enhanced above 10 kHz, leading to corresponding changes in auditory afferent responses (Meyer, J. and Elsner, N., 1995). Ventilation thus distorts the perception of conspecific communication signals. In the grasshopper *Ch. biguttulus*, which uses frequency components for sex

recognition (von Helversen, D. and von Helversen, O., 1997), the males stop breathing for some seconds after generating a calling song. This is the time during which a female response would be most likely to occur (Meyer, J. *et al.*, 1993).

In grasshoppers and locusts ventilatory movements and flight motor activity also activate the primary auditory afferents so that they discharge in the rhythm of the motor pattern (Hedwig, B., 1988; 1989). In crickets the activity of auditory interneurons may be coupled to ventilation (Stout, J. F. and Huber, F., 1972) and during walking auditory afferents are activated by the front leg movements (Schildberger, K. *et al.*, 1988). Thus during motor activity auditory afferents and interneurons convey auditory responses and nonauditory noise and furthermore auditory activity may be transiently suppressed. This decreases the reliability of auditory information that is available for pattern recognition and orientation within the CNS.

3.31.4.2 Sound Production

A particular challenge for auditory processing occurs during acoustic communication since the auditory system of the singing animal is also exposed to any self-generated sounds. This may desensitize the sender's auditory pathway and self-generated and external sound may be mixed and muddled. Different strategies are used to deal with this problem.

3.31.4.2.1 Cicadas

In male cicadas the tympanal membranes of the ears and the sound producing tymbals are both backed by a large abdominal air chamber (Pringle, J. W. S., 1954; Hennig, R. M. *et al.*, 1994). Since the animals generate high-intensity sound patterns in the vicinity of their hearing organs (Young, D., 1990) the auditory organ is prone to overloading by self-generated sound. During singing, however, the detensor tympani and ventral longitudinal muscles contract and act on the tympanal rim so that the tympana relax and fold (Pringle, J. W. S., 1954; Hennig, R. M. *et al.*, 1994). Folding of the tympana reduces their tension and the sensitivity of the ears by 20 dB; however, it does not completely disable sound perception.

3.31.4.2.2 Grasshoppers

During singing acridid grasshoppers use the hind legs to scratch a row of cuticular pegs against the wings and produce broad frequency songs of 60–70 dB SPL. The tympanic membranes, which are positioned just beneath the wings, oscillate in phase with the self-generated sound and also move in phase with the stridulatory hind leg movements (Hedwig, B. and Meyer, J., 1994). Even in silently singing males – with wings removed – the contractions of the thoracic singing muscles cause tympanic membrane vibrations. The self-generated sounds and the mechanical vibrations of the thorax activate auditory afferents leading to depolarization and spiking of auditory interneurons during singing (Hedwig, B., 1986; 1990). Due to the limited dynamic range of the afferents their response to external sound stimuli is strongly masked and reduced. When sound stimuli occur in phase with self-generated sounds extracellular recordings give the impression that auditory interneurons may be switched off (Wolf, H. and von Helversen, O., 1986). Intracellular recordings however demonstrate that the neurons are depolarized and that there is no indication of central inhibition acting on the auditory pathway (Hedwig, B., 1990). Short silent intervals, which occur in most songs, allow the animals to perceive external stimuli (Hedwig, B. and Meyer, J., 1994). The impact of self-generated sounds on auditory processing may be one reason for some species of grasshoppers to use alternating singing activity during intraspecific communication.

3.31.4.2.3 Crickets

Male crickets produce songs of over 100 dB SPL. At least some species are enduring singers and constantly expose their auditory system to the self-generated sounds. No attenuation occurs within the peripheral auditory system and the ears and afferents fully respond to the self-generated sound pulses (Poulet, J. F. A. and Hedwig, B., 2001). Processing of self-generated sounds is modulated within the first stage of auditory processing. A corollary discharge interneuron (Poulet, J. F. A. and Hedwig, B., 2002; 2006) is driven by the singing central pattern generator and spikes in phase with sound production. The interneuron projects into the prothoracic auditory neuropil and presynaptically inhibits the auditory afferent terminals and at the same time postsynaptically inhibits the local and ascending auditory interneurons ON1, AN1, and AN2 (Poulet, J. F. A. and Hedwig, B., 2003a; 2003b). Inhibiting sound processing in phase with the self-generated sounds prevents the auditory pathway from desensitization and maintains the animal's sensitivity to respond to external sounds (Poulet, J. F. A. and Hedwig, B., 2002; 2003a; Figure 13).

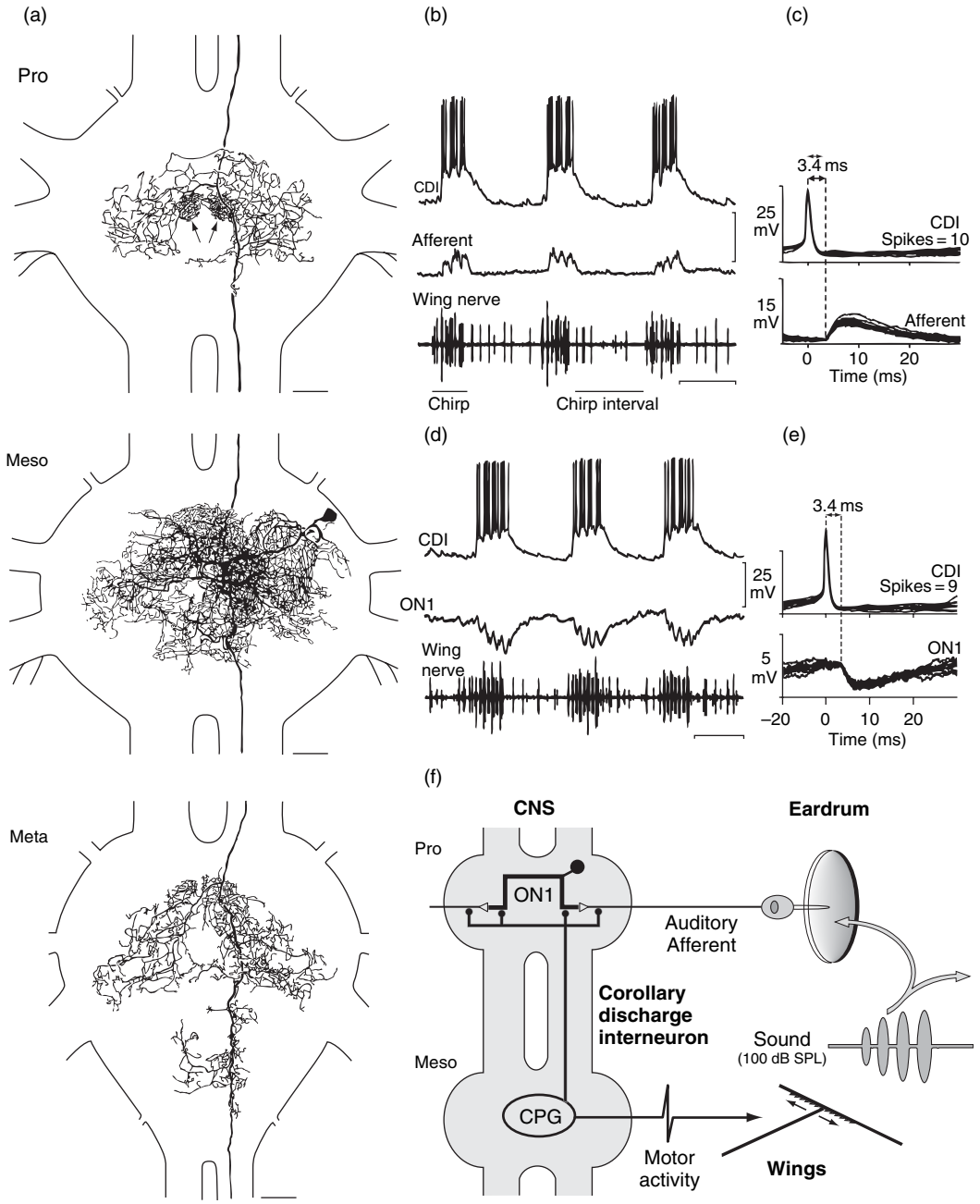

Figure 13 Corollary discharge interneuron controlling auditory processing in singing crickets. (a) Structure of the corollary discharge interneuron (CDI) in the CNS of a cricket that inhibits auditory neurons during stridulation. Extensive dendritic branches occur in the dorsal area of the mesothoracic ganglion and axonal branches in the prothoracic, the ventral area of the mesothoracic, and in the metathoracic ganglion. Axonal terminals are particular densely packed in the prothoracic auditory neuropil. The axons of the neuron extend to the brain and the terminal ganglion. The interneuron causes presynaptic inhibition of primary auditory afferents (b). Each spike in the neuron elicits a primary afferent depolarization in fictively singing crickets (c). The interneuron makes monosynaptic inhibitory connections to the ON1 neuron. Pronounced inhibition of ON1 occurs during the spike activity of CDI during singing (d). Each spike in CDI elicits an IPSP in the ON1 neuron (e). (f) During singing the ears of crickets are exposed to the self-generated sound. The CDI interneuron appears to be driven by the CPG for singing and pre- and postsynaptically inhibits the auditory pathway at afferent and interneuron level. (a–e) From Poulet, J. F. A. and Hedwig, B. 2006. The cellular basis of a corollary discharge. Science 311, 518–522. (f) From Hedwig, B. 2006. Pulses, patterns, paths: neurobiology of auditory behaviour in crickets. J. Comp. Physiol. A 192, 677–689.

References

Adam, L.-J. 1977. The oscillating summed action potential of an insect's auditory nerve (*Locusta migratoria*, Acrididae). II. Underlying spike pattern and causes of spike synchronisation. Biol. Cybern. 28, 109–119.

Alexander, R. D. 1961. Aggressiveness, territoriality and sexual behavior in field crickets. Behaviour 17, 130–223.

Alexander, R. D. 1967. Acoustical communication in arthropods. Ann. Rev. Entomol. 12, 495–526.

Allen, G. R. 1995. The biology of the phonotactic parasitoid, *Homotrixa sp*. (Diptera: Tachinidae), and its impact on the survival of the male *Sciarasaga quadrata* (Orthoptera: Tettigoniidae) in the field. Ecol. Entomol. 20, 103–110.

Arntz, B. 1975. Das Hörvermögen von *Nepa cinera* L. J. Comp. Physiol. A 96, 53–72.

Atkins, G. and Pollack, G. S. 1986. Age dependent occurrence of an ascending axon on the omega neuron of the cricket, *Teleogryllus oceanicus.*. J. Comp. Neurol. 243, 527–534.

Atkins, G., Henley, J., Handysides, R., and Stout, J. F. 1992. Evaluation of the behavioral roles of ascending auditory interneurons in calling song phonotaxis by the female cricket (*Acheta domesticus*). J. Comp. Physiol. A 170, 363–372.

Atkins, G., Ligmann, S., Burghardt, F., and Stout, J. F. 1984. Changes in phonotaxis by the female cricket *Acheta domesticus* L. after killing identified acoustic interneurons. J. Comp. Physiol. A 154, 795–804.

Atkins, S., Atkins, G., Rhodes, M., and Stout, J. F. 1989. Influence of syllable period on song encoding properties of an ascending auditory interneuron in the cricket *Acheta domesticus*. J. Comp. Physiol. A 165, 827–836.

Baden, T. and Hedwig, B. 2007. Neurite specific Ca2+ dynamics underlying sound processing in an auditory interneurone. J. Neurobiol. 67, 68–80.

Balakrishnan, R. and Pollack, G. S. 1996. Recognition of courtship song in the field cricket, *Teleogryllus oceanicus*. Anim. Behav. 51, 353–366.

Balakrishnan, R, Helversen, von D., and Helversen, von O. 2001. Song pattern recognition in the grasshopper *Chorthippus biguttulus*: the mechanism of syllable onset and offset detection. J. Comp. Physiol. A 187, 255–264.

Ball, E. E., Oldfield, B. P., and Michel, R. K. 1989. Auditory Organ Structure, Development, and Function. In: Cricket Behaviour and Neurobiology (*eds*. F. Huber, T. E. Moore, and W. Loher), pp. 391–422. Cornell University Press.

Bauer, M. and Helversen, von O. 1987. Separate localisation of sound recognition and sound producing neural mechanisms in a grasshopper. J. Comp. Physiol. A 161, 95–101.

Benda, J. and Herz, A. V. 2003. A universal model for spike-frequency adaptation. Neural Comput. 15, 2523–2564.

Benda, J., Bethge, M., Hennig, R. M., Pawelzik, K., and Herz, A. V. M. 2001. Spike frequency adaptation: phenomenological model and experimental tests. Neurocomput. 38–40, 105–110.

Blest, A. D., Collett, J. D., and Pye, J. D. 1963. The generation of ultrasonic signals by a New World arctiid moth. Proc. Roy. Soc. Lond. B 158, 196–207.

Boyan, G. S. 1980. Auditory neurones in the brain of the cricket *Gryllus bimaculatus* (De Geer). J. Comp. Physiol. A 140, 81–93.

Boyan, G. S. 1981. Two-tone suppression of an identified auditory neurone in the brain of the cricket *Gryllus bimaculatus* (De Geer). J. Comp. Physiol. A 144, 117–125.

Boyan, G. S. 1984. Neural mechanisms of auditory information processing by identified interneurons in orthoptera. J. Insect Physiol. 30, 27–41.

Boyan, G. S. 1993. Another look at insect audition: the tympanic receptors as an evolutionary specialization of the chordotonal system. J. Insect Physiol. 39, 187–200.

Boyan, G. S. and Fullard, J. H. 1986. Interneurones responding to sound in the tobacco budworm moth *Heliothis virescens* (Noctuidae): morphological and physiological characteristics. J. Comp. Physiol. A 158, 391–404.

Boyan, G. S. and Fullard, J. H. 1988. Information processing at a central synapse suggests a noise filter in the auditory pathway of the noctuid moth. J. Comp. Physiol. A 164, 251–258.

Boyan, G. S. and Miller, L. A. 1991. Parallel processing of afferent input by identified interneurones in the auditory pathway of the noctuid moth *Noctua pronuba* (L.). J. Comp. Physiol. A 168, 727–738.

Boyan, G. S., Williams, J. L. D., and Fullard, J. H. 1990. Organisation of the auditory pathway in the thoracic ganglia of noctuid moths. J. Comp. Neurol. 295, 248–267.

Boyd, P., Kühne, R., Silver, S., and Lewis, B. 1984. Two-tone suppression and song coding by ascending neurones in the cricket *Gryllus campestris* L. J. Comp. Physiol. A 154, 423–430.

Brodfuehrer, P. D. and Hoy, R. R. 1989. Integration of ultrasound and flight inputs on descending neurons in the cricket brain. J. Exp. Biol. 145, 157–171.

Brodfuehrer, P. D. and Hoy, R. R. 1990. Ultrasound sensitive neurons in the cricket brain. J. Comp. Physiol. A 166, 651–662.

Bush, S. L. and Schul, J. 2006. Pulse-rate recognition in an insect: evidence of a role for oscillatory neurons. J. Comp. Physiol. A 192, 113–121.

Cade, W. H. 1975. Acoustically orienting parasitoids: fly phonotaxis to cricket song. Science 190, 1312–1313.

Casaday, G. B. and Hoy, R. R. 1977. Auditory interneurons in the cricket *Teleogryllus oceanicus*: physiological and anatomical properties. J. Comp. Physiol. A 121, 1–13.

Cherry, E. C. 1953. Some experiments on the recognition of speech with one and with two ears. J Acoust. Soc. Am. 25, 975–979.

Conner, W. E. 1999. 'Un chant d'appel amoureux': acoustic communication in moths. J. Exp. Biol. 202, 1711–1723.

Dawson, J. W. and Fullard, J. H. 1995. The neuroethology of sound production in tiger moths (Lepidoptera, Arctiidae). II. Location of the tymbal central pattern generator in *Cycnia tenera* Hübner. J. Comp. Physiol. A 176, 541–549.

Dobler, S., Heller, K.-G., and Helversen, von O. 1994. Song pattern recognition and an auditory time window in the female bushcricket *Ancistura nigrovittata* (Orthoptera: Phaneropteridae). J. Comp. Physiol. A 175, 67–74.

Doherty, J. A. 1985. Trade-off phenomena in calling song recognition and phonotaxis in the cricket, *Gryllus bimaculatus* (Orthoptera, Gryllidae). J. Comp. Physiol. A 156, 787–801.

Doolan, J. M. and Young, D. 1981. The organization of the auditory organ of the bladder cicada, *Cystosoma saundersii*. J. Exp. Biol. 291, 525–540.

Dunning, D. C. and Roeder, K. D. 1965. Moth sounds and the insect-catching behaviour of bats. Science 147, 173–174.

Edin, F., Machens, C. K., Schütze, H., and Herz, A. V. M. 2004. Searching for optimal sensory signals: interative stimulus reconstruction in closed-loop experiments. J. Comp. Neurosci. 17, 47–56.

Eggers, F. 1911. Über das thorakale Tympanalorgan der Noctuiden. Sitzungsberichte der Naturforscher-Gesellschaft bei der Universität Tartu (Dorpat) 20, 139–146.

Eggers, F. 1919. Das thorakale bitympanale Organ einer Gruppe der Lepidoptera Heterocera. Zool. Jb. Anat. 41, 273–376.

Faulkes, Z. and Pollack, G. S. 2000. Effects of inhibitory timing on contrast enhancement in auditory circuits in crickets (*Teleogryllus oceanicus*). J. Neurophysiol. 84, 1247–1255.

Faure, P. A. and Hoy, R. R. 2000a. The sounds of silence: cessation of singing and sound pausing are ultrasound-induced acoustic startle behaviours in the katydid *Neoconocephalus ensiger* (Orthoptera; Tettigoniidae). J. Comp. Physiol. A 186, 129–142.

Faure, P. A. and Hoy, R. R. 2000b. Neuroethology of the katydid T-cell. I. Tuning and responses to pure tones. J. Exp. Biol. 203, 3225–3242.

Faure, P. A. and Hoy, R. R. 2000c. Neuroethology of the katydid T-cell. II. response to acoustic playback of conspecific and predatory signals. J. Exp. Biol. 203, 3243–3254.

Fonseca, P. J., Münch, D., and Hennig, R. M. 2000. Auditory perception: how cicadas interpret acoustic signals. Nature 405, 297–298.

Forrest, T. G., Read, M. P., Farris, H. E., and Hoy, R. R. 1997. A tympanal hearing organ in scarab beetles. J. Exp. Biol. 200, 601–606.

Fullard, J. H. 1982. Cephalic influences on a defensive behaviour in the dogbane tiger moth, *Cycnia tenera*. Physiol. Entomol. 7, 157–162.

Fullard, J. H. 1984a. Listening for bats: pulse repetition rate as a cue for a defensive behaviour in *Cycnia tenera* (Lepidoptera:Arctiidae). J. Comp. Physiol. A 154, 249–252.

Fullard, J. H. 1984b. Acoustic relationships between tympanate moths and the Hawaiian hoary bat (*Lasiurus cinereus semotus*). J. Comp. Physiol. A 155.

Fullard, J. H., Dawson, J. W., and Jacobs, D. S. 2003. Auditory encoding during the last moment of a moth's life. J. Exp. Biol. 206, 281–294.

Fullard, J. H., Simmons, S. J., and Saillant, P. A. 1994. Jamming bat echolocation: the dogbane tiger moth *Cycnia tenera* times its clicks to the terminal attack calls of the big brown bat *Eptesicus fuscus*. J. Exp. Biol. 194, 285–298.

Givois, V. and Pollack, G. S. 2000. Sensory habituation of auditory receptor neurons: implications for sound localization. J. Exp. Biol. 201, 2529–2537.

Gray, E. G. 1960. The fine structure of the insect ear. Phil. Trans. R. Soc. Lond B 243, 75–94.

Greenfield, M. D. and Roizen, I. 1993. Katydid synchronous chorusing is an evolutionary stable outcome of female choice. Nature 364, 618–620.

Greenfield, M. D. and Shelly, T. E. 1990. Territory-Based Mating Systems in Desert Grasshoppers: Effects of Host Plant Distribution and Variation. In: Biology of Grasshoppers (*eds*. Chapman R. F. and Joern A), pp. 315–335. Wiley.

Halex, H., Kaiser, W., and Kalmring, K. 1988. Projection areas and branching patterns of the tympanal receptor cells in migratory locusts, *Locusta migratoria* and *Schistocerca gregaria*. Cell Tissue Res. 253, 517–528.

Hartley, J. C. and Robinson, D. J. 1976. Acoustic behaviour of both sexes of the speckled bush cricket *Leptophyes punctatissima*. Physiol. Entomol. 1, 21–25.

Hedwig, B. 1986. On the role in stridulation of plurisegmental interneurons of the acridid grasshopper *Omocestus viridulus* L. II. Anatomy and physiology of ascending and T-shaped interneurons. J. Comp. Physiol. A 158, 429–444.

Hedwig, B. 1988. Activation and modulation of auditory receptors in *Locusta migratoria* by respiratory movements. J. Comp. Physiol. A 162, 237–246.

Hedwig, B. 1989. Modulation of auditory information processing in tethered flying locusts. J. Comp. Physiol. A 164, 409–422.

Hedwig, B. 1990. Modulation of auditory responsiveness in stridulating grasshoppers. J. Comp. Physiol. A 167, 847–856.

Hedwig, B. 2006. Pulses, patterns, paths: neurobiology of auditory behaviour in crickets. J. Comp. Physiol. A 192, 677–689.

Hedwig, B. and Heinrich, R. 1997. Identified descending brain neurons control different stridulatory motor patterns in an acridid grasshopper. J. Comp. Physiol. A 180, 285–295.

Hedwig, B. and Meyer, J. 1994. Auditory information processing in stridulating grasshoppers: tympanic membrane vibrations and neurophysiology. J. Comp. Physiol. A 174, 121–131.

Hedwig, B. and Poulet, J. F. A. 2004. Complex auditory behaviour emerges from simple reactive steering. Nature 430, 781–785.

Hedwig, B. and Poulet, J. F. A. 2005. Mechanisms underlying phonotactic steering in the cricket *Gryllus bimaculatus* (de Geer) revealed with a fast trackball system. J. Exp. Biol. 208, 915–927.

Heller, K-G. and Helversen, von D. 1986. Acoustic communication in phaneropterid bushcrickets: species-specific delay of female stridulatory response and matching male sensory time window. Behav. Ecol. Sociobiol. 18, 189–198.

Helversen, von D. 1972. Gesang des Männchens und Lautschema des Weibchens bei der Feldheuschrecke *Chorthippus biguttulus* (Orthoptera, Acrididae). Z. vergl. Physiol. 81, 381–422.

Helversen, von D. 1984. Parallel processing in auditory pattern recognition and directional analysis by the grasshopper *Chorthippus biguttulus* L. (Acrididae). J. Comp. Physiol. A 154, 837–846.

Helversen, von D. 1997. Acoustic Communication and Orientation in Grasshoppers. In: Orientation and Communication in Arthropods (*ed*. M. Lehrer), pp. 301–341. Birkhäuser.

Helversen, von D. and Helversen, von O. 1990. Pattern Recognition and Directional Analysis: Routes and Stations of Information Flow in the CNS of a Grasshopper. In: Sensory Systems and Communication in Arthropods. (*eds*. F. Gribakin, K. Wiese, and A. V. Popov), pp. 209–216. Birkhäuser.

Helversen, von D. and Helversen, von O. 1995. Acoustic pattern recognition and orientation in orthopteran insects: parallel or serial processing? J. Comp. Physiol. A 177, 767–774.

Helversen, von D. and Helversen, von O. 1997. Recognition of sex in the acoustic communication of the grasshopper *Chorthippus biguttulus* (Orthoptera, Acrididae). J. Comp. Physiol. A 180, 373–386.

Helversen, von D. and Rheinlaender, J. 1988. Interaural intensity and time discrimination in an unrestrained grasshopper: a tentative approach. J. Comp. Physiol. A 162, 333–340.

Helversen, von O. 1979. Angeborenes Erkennen akustischer Schlüsselreize. Verh. Dtsch. Zool. Ges. 1979, 42–59.

Helversen, von O. and Helversen, von D. 1994. Forces Driving the Coevolution of Song and Song Recognition in Grasshoppers. In: Progress in Zoology (*eds*. K. Schildberger and N. Elsner), pp. 253–284. Fischer Verlag Stuttgart.

Helversen, von O., Schul, J., and Kleindienst, H-U. 2001. Male recognition mechanism for female responses implies a dilemma for their localisation in a phaneropterine bushcricket. J. Comp. Physiol. A 186, 1153–1158.

Hennig, R. M. 1988. Ascending auditory interneurons in the cricket *Teleogryllus commodus* (Walker): comparative physiology and direct connections with afferents. J. Comp. Physiol. A 163, 135–143.

Hennig, R. M. 2003. Acoustic feature extraction by cross-correlation in crickets? J. Comp. Physiol. A 189, 589–598.

Hennig, R. M. and Weber, T. 1997. Filtering of temporal parameters of the calling song by cricket females of two closely related species: a behavioural analysis. J. Comp. Physiol. A 180, 621–630.

Hennig, R. M., Franz, A., and Stumpner, A. 2004. Processing of auditory information in insects. Microsc. Res. Tech. 63, 351–374.

Hennig, R. M., Weber, T., Huber, F., Kleindienst, H.-U., Moore, T. E., and Popov, A. V. 1994. Auditory threshold change in singing cicadas. J. Exp. Biol. 187, 45–55.

Horridge, G. A. 1960. Pitch discrimination in Orthoptera (Insecta) demonstrated by responses of central auditory neurones. Nature 165, 623–624.

Horseman, G. and Huber, F. 1994a. Sound localisation in crickets I. Contralateral inhibition of an ascending interneuron (AN1) in the cricket *Gryllus bimaculatus*. J. Comp. Physiol. A 175, 389–398.

Horseman, G. and Huber, F. 1994b. Sound localisation in crickets II. Modelling the role of a simple network in the prothoracic ganglion. J. Comp. Physiol. A 175, 399–413.

Hoy, R. R. 1978. Acoustic communication in crickets: a model system of feature detection. Fed. Proc. 37, 2316–2323.

Hoy, R. R. 1992. The Evolution of Hearing in Insects as an Adaptation to Predation from Bats. In: The Evolutionary Biology of Hearing (*eds*. D. B. Webster, R. R. Fay, and A. N. Popper), pp. 115–129, Springer.

Huber, F. 1983. Neural Correlates of Orthopteran and Cicada Phonotaxis. In: Neuroethology and Behavioural Physiology (*eds*. F. Huber and H. Markl II.), pp. 108–135. Springer, Berlin.

Huber, F., Kleindienst, H.-U., Moore, T. E., Schildberger, K., and Weber, T. 1990. Acoustic Communication in Periodical Cicadas: Neuronal Responses to Songs of Sympatric Species. In: Sensory Systems and Communication in Arthropods. (*eds*. F. Gribakin, K. Wiese, and A. V. Popov), pp. 217–228. Birkhäuser.

Hutchings, M. and Lewis, B. 1984. The role of two-tone suppression in song coding by ventral cord neurones in the cricket *Teleogryllus oceanicus* (Le Guillou). J. Comp. Physiol. A 154, 103–112.

Imaizumi, K. and Pollack, G. S. 1999. Neural coding of sound frequency by cricket auditory receptors. J. Neuroscience 19, 1508–1516.

Imaizumi, K. and Pollack, G. S. 2001. Neural representation of sound amplitude by functionally different auditory receptors in crickets. J. Acoust. Soc. Am. 109, 1247–1260.

Imaizumi, K. and Pollack, G. S. 2005. Central projections of auditory receptor neurons of crickets. J. Comp. Neurol. 493, 439–447.

Jacobs, K., Otte, B., and Lakes-Harlan, R. 1999. Tympanal receptor cells of *Schistocerca gregaria*: correlation of soma positions and dendrite attachment sites, central projections and physiologies. J. Exp. Zool. 283, 270–285.

Kalmring, K., Hoffmann, E., Jatho, M., Sickmann, T., and Grossbach, M. 1996. The auditory-vibratory sensory system of the bushcricket *Polysarcus denticauda* (Phaneropterinae, Tettigoniidae) II. Physiology of receptor cells. J. Exp. Zool. 276, 315–329.

Kalmring, K., Rehbein, H., and Kühne, R. 1979. An auditory giant neuron in the ventral cord of *Decticus verrucivorus* (Tettigoniidae). J. Comp. Physiol. A 132, 225–234.

Kalmring, K., Rössler, W., Ebendt, R., Ahi, J., and Lakes, R. 1993. The auditory receptor organs in the forelegs of bushcrickets: physiology, receptor cell arrangement, and morphology of the tympanal and intermediate organs of three closely related species. Zool Jb Physiol. 97, 75–94.

Katsuki, Y. and Suga, N. 1960. Neural mechanism of hearing in insects. J. Exp. Biol. 37, 279–290.

Kennel, von J. and Eggers, F. 1933. Die abdominalen Tympanalorgane der Lepidopteren. Zoologische Jahrbücher Abteilung für Anatomie und Ontogenie der Tiere 57, 1–105.

Keuper, A., Weidemann, S., Kalmring, K., and Kaminski, D. 1988. Sound production and sound emission in seven species of European tettigoniids. The different parameters of the song: their relation to the morphology of the bushcricket. Bioacoustics 1, 31–48.

Kleindienst, H.-U., Koch, U. T., and Wohlers, D. W. 1981. Analysis of the cricket auditory system by acoustic stimulation using a closed sound field. J. Comp. Physiol. A 141, 282–296.

Kriegbaum, H. 1989. Female choice in the grasshopper *Chorthippus biguttulus*. Naturwissenschaften 76, 81–82.

Lakes-Harlan, R. and Heller, K-G. 1992. Ultrasound-sensitive ears in a parasitoid fly. Naturwissenschaften 79, 224–226.

Lakes-Harlan, R., Stölting, H., and Stumpner, A. 1999. Convergent evolution of insect hearing organs from a preadaptive structure. Proc. Roy. Soc. Lond. B 266, 1161–1167.

Latimer, W. and Lewis, D. B. 1986. Song harmonic content as a parameter determining acoustic orientation behaviour in the cricket *Teleogryllus oceanicus* (Le Guillou). J. Comp. Physiol. A 158, 538–591.

Latimer, W. and Sippel, M. 1987. Acoustic cues for female choice and male competition in *Tettigonia cantans*. Anim. Behav. 35, 887–900.

Lewis, F. P. and Fullard, J. H. 1996. Neurometamorphosis of the ear in the gypsy moth, *Lymantria dispar*, and its homologue in the earless forest tent caterpillar moth, *Malacosomosa disstria*. J. Neurobiol. 31, 245–262.

Libersat, F. and Hoy, R. R. 1991. Ultrasonic startle behaviour in bushcrickets (Orthoptera; Tettigoniidae). J. Comp. Physiol. A 169, 507–514.

Libersat, F., Murray, J. A., and Hoy, R. R. 1994. Frequency as a releaser in the courtship song of two crickets, *Gryllus bimaculatus* (de Geer) and *Teleogryllus oceanicus*: a neuroethological analysis. J. Comp. Physiol. A 174, 485–494.

Lin, Y., Kalmring, K., Jatho, M., Sickmann, T., and Rössler, W. 1993. Auditory receptor organs in the foreleg of *Gamsocleiis gratiosa* (Tettigoniidae): morphology and function of the organs in comparison to the frequency parameters of the conspecific song. J. Exp. Zool. 267, 377–388.

Machens, C. K., Schütze, H., Franz, A., Kolesnikova, O., Stemmler, M. B., Ronacher, B., and Herz, A. V. M. 2003. Single auditory neurons rapidly discriminate conspecific communication signals. Nat. Neurosci. 6, 341–342.

Machens, C. K., Stemmler, M. B, Prinz, P., Krahe, R., and Ronacher, B. 2001. Representation of acoustic communication signals by insect auditory receptor neurons. J. Neurosci. 21, 3215–3227.

Madsen, B. M. and Miller, L. A. 1987. Auditory input to motor neurones of the dorsal longitudinal flight muscle of the noctuid moth (*Barathra brassicae* L.). J. Comp. Physiol. A 160, 23–31.

Marquart, V. 1985. Local interneurons mediating excitation and inhibition onto ascending neurons in the auditory pathway of grasshoppers. Naturwissenschaften 72, 42–44.

Marsat, G. and Pollack, G. S. 2004. Differential temporal coding of rhythmically diverse acoustic signals by a single interneuron. J. Neurophysiol. 92, 939–948.

Marsat, G. and Pollack, G. S. 2005. Effect of the temporal pattern of contralateral inhibition on sound localization cues. J. Neurosci. 25, 6137–6144.

Marsat, G. and Pollack, G. S. 2006. A behavioral role for feature detection by sensory bursts. J. Neurosci. 26, 10542–10547.

Marsat, G. and Polllaus, G. S. 2007. Efficient inhibition of bursts by bursts in the auditory system of crickets. J. Comp. Physiol. A 193, 625–633.

Meier, T. and Reichert, H. 1990. Embryonic development and evolutionary origin of the orthopteran auditory system. J. Neurobiol. 21, 592–610.

Meyer, J. and Elsner, N. 1995. How respiration affects auditory sensitivity in the grasshopper *Chorthippus biguttulus* (L.). J. Comp. Physiol. A 176, 563–573.
Meyer, J. and Elsner, N. 1996. How well are frequency sensitivities of grassshopper ears tuned to species-specific song spectra. J. Exp. Biol. 199, 1631–1642.
Meyer, J. and Elsner, N. 1997. Can spectral cues contribute to species separation in closely related grasshoppers? J. Comp. Physiol. A 180, 171–180.
Meyer, J. and Hedwig, B. 1995. The influence of tracheal pressure changes on the responses of the tympanal membrane and auditory receptors in the locust *Locusta migratoria* L. Laservibrometric, laserinterferometric and neurophysiological studies. J. Exp. Biol. 198, 1327–1339.
Meyer, J., Hedwig, B., and Elsner, N. 1993. Auditory Information Processing and Pattern Recognition in Ventilating Grasshoppers. In: Gene-Brain-Behaviour: Proceedings of the 21st Göttingen Neurobiology Conference. (*eds*. N. Elsner and M. Heisenberg), p. 81. Thieme.
Michel, K. 1975. Das Tympanalorgan von *Cicada orni* L. (Cicadina, Homoptera). Zoomorphologie 82, 63–78.
Michelsen, A. 1971. The physiology of the locust ear. J. Comp. Physiol. A 71, 49–128.
Michelsen, A. and Löhe, G. 1995. Tuned directionality in cricket ears. Nature 375, 639.
Michelsen, A. and Rohrseitz, K. 1995. Directional sound processing and interaural sound transmission in a small and a large grasshopper. J. Exp. Biol. 1817–1827.
Miller, L. A. 1970. Structure of the green lacewing tympanal organ (*Chrysopa carnea,* Neuroptera). J. Morphol. 131, 359–382.
Miller, L. A. 1971. Physiological responses of green lacewings (Chrysopa, Neuroptera) to ultrasound. J. Insect Physiol. 17, 491–506.
Moiseff, A. and Hoy, R. R. 1983. Sensitivity to ultrasound in an identified auditory interneuron in the cricket: a possible link to phonotactic behaviour. J. Comp. Physiol. A 152, 155–167.
Moiseff, A., Pollack, G. S., and Hoy, R. R. 1978. Steering responses of flying crickets to sound and ultrasound: mate attraction and predator avoidance. Proc. Natl. Acad. Sci. 75, 4052–4056.
Molina, J. and Stumpner, A. 2005. Effects of pharmacological treatment and photoinactivation on the directional responses of an insect neuron. J. Exp. Zool. 303A, 1085–1103.
Mörchen, A, Rheinlaender, J., and Schwartzkopff, J. 1978. Latnecy shift in insect auditory nerve fibers. Naturwiss 65, 656–657.
Nabatiyan, A., Poulet, J. F. A., de Polavieja, G. G., and Hedwig, B. 2003. Temporal pattern recognition based on instantaneous spike rate coding in a simple auditory system. J. Neurophysiol. 90, 2484–2493.
Nishino, H. and Field, L. H. 2003. Somatotopic mapping of chordotonal organ neurons in a primitive Ensiferan, the New Zealand tree weta *Hemideina femorata*: II. Complex tibial organ. J. Comp. Neurol. 464, 327–342.
Nolen, T. G. and Hoy, R. R. 1984. Initiation of behavior by a single neuron: the role of behavioral context. Science 226, 992–994.
Nolen, T. G. and Hoy, R. R. 1986a. Phonotaxis in flying crickets. I. Attraction to the calling song and avoidance of bat-like ultrasound are discrete behaviors. J. Comp. Physiol. A 159, 423–439.
Nolen, T. G. and Hoy, R. R. 1986b. Phonotaxis in flying crickets. II. Physiological mechanisms of two-tone suppression of the high frequency avoidance steering behavior by the calling song. J. Comp. Physiol. A 159, 441–456.
Oldfield, B. P. 1982. Tonotopic organization of auditory receptors in Tettigoniidae (Orthoptera: Ensifera). J. Comp. Physiol. A 147, 461–469.
Oldfield, B. P. 1983. Central projections of primary auditory fibers in Tettigoniidae (Orthoptera: Ensifera). J. Comp. Physiol. A 151, 389–395.
Oldfield, B. P. 1984. Physiology of auditory receptors in two species of Tettigoniidae (Orthoptera: Ensifera): alternative tonotopic organisations of the auditory organ. J. Comp. Physiol. A 155, 689–696.
Oldfield, B. P. 1985. The Role of the Tympanal Membrane and the Receptor Array in the Tuning of Auditory Receptors in Bushcrickets. In: Acoustic and Vibrational Communication in Insects (*eds*. K. Kalmring and N. Elsner), pp. 17–24. Parey.
Oldfield, B. P. and Hill, K. G. 1983. The physiology of ascending auditory interneurons in the tettigoniid *Caedica simplex* (Orthoptera: Ensifera): response properties and a model of integration in the afferent auditory pathway. J. Comp. Physiol. A 152, 495–508.
Oldfield, B. P, Kleindienst, H.-U., and Huber, F. 1986. Physiology and tonotopic organization of auditory recptors in the cricket *Gryllus bimaculatus* DeGeer. J. Comp. Physiol. A 15, 457–464.
Oshinsky, M. L. and Hoy, R. R. 2002. Physiology of the auditory afferents in an acoustic parasitoid fly. J. Neurosci. 15, 7254–7263.
Paul, D. H. 1973. Central projections of the tympanic fibres in noctuid moths. J. Insect Physiol. 19, 1785–1792.
Pauls, S., Pauls, M., Elsner, N., and Lakes-Harlan, R. 2001. Composition of the Tympanal Nerves of Different Grasshopper Species. In: Göttingen Neurobiology Report (*eds*. N. Elsner and G. W. Kreutzberg), p. 372. Thieme.
Pflüger, H.-J, Bräunig, P., and Hustert, R. 1988. The organization of mechanosensory neuropiles in locust thoracic ganglia. Phil. Trans. R. Soc. Lond. B 321, 1–26.
Pollack, G. S. 1986. Discrimination of calling song models by the cricket, *Teleogryllus oceanicus:* the influence of sound direction on neural encoding of the stimulus temporal pattern and on phonotactic behavior. J. Comp. Physiol. A 158, 549–561.
Pollack, G. S. 1988. Selective attention in an insect auditory neuron. J. Neurosci. 8(7), 2635–2639.
Pollack, G. S. 2003. Sensory cues for sound localization in the cricket *Teleogryllus oceanicus:* interaural difference in response strength versus interaural latency difference. J. Comp. Physiol. A 189, 143–151.
Pollack, G. S. and Faulkes, Z. 1998. Representation of behaviourally relevant sound frequencies by auditory receptors in the cricket *Teleogryllus oceanicus*. J. Exp. Biol. 201, 155–163.
Pollack, G. S. and Hoy, R. R. 1979. Temporal pattern as a cue for species-specific calling song recognition in crickets. Science (204) 429–432.
Pollack, G. S. and Hoy, R. R. 1981. Phonotaxis in flying crickets: neural correlates. J. Insect Physiol. 27, 41–45.
Pollack, G. S, Huber, F., and Weber, T. 1984. Frequency and temporal pattern dependent phonotaxis of crickets (*Teleogryllus oceanicus*) during tethered flight and compensated walking. J. Comp. Physiol. 154, 13–26.
Popov, A. V., Markovich, A. M., and Andjan, A. S. 1978. Auditory interneurons in the prothoracic ganglion of the cricket, *Gryllus bimaculatus* deGeer. I. The large segmental auditory neuron (LSAN). J. Comp. Physiol. A 126, 183–192.
Poulet, J. F. A. and Hedwig, B. 2001. Tympanic membrane oscillations and auditory receptor activity in the singing cricket *Gryllus bimaculatus*. J. Exp. Biol. 204, 1281–1293.
Poulet, J. F. A. and Hedwig, B. 2002. A corollary discharge maintains auditory sensitivity during sound production. Nature 418, 872–876.
Poulet, J. F. A. and Hedwig, B. 2003a. A corollary discharge modulates central auditory processing in singing crickets. J. Neurophysiol. 89, 1528–1540.

Poulet, J. F. A. and Hedwig, B. 2003b. Corollary discharge inhibition of ascending auditory neurons in the stridulating cricket. J. Neurosci. 23, 4717–4725.
Poulet, J. F. A. and Hedwig, B. 2005. Auditory orientation in crickets: pattern recognition controls reactive steering. PNAS 102, 15665–15669.
Poulet, J. F. A. and Hedwig, B. 2006. The cellular basis of a corollary discharge. Science 311, 518–522.
Prager, J. 1976. Das mesothorakale Tympanalorgan von *Corixa punctata* Ill. (Heteroptera, Corixidae). J. Comp. Physiol. A 110, 33–50.
Pringle, J. W. S. 1954. A physiological analysis of cicada song. J. Exp. Biol. 31, 525–560.
Pumphrey, R. J. 1940. Hearing in insects. Biol. Rev. 15, 107–132.
Ratcliffe, J. M. and Fullard, J. H. 2005. The adaptive function of tiger moth clicks against echolocating bats: an experimental and synthetic approach. J. Exp. Biol. 208, 4689–4698.
Rehbein, H. 1976. Auditory neurons in the ventral cord of the locust: morphological and functional properties. J. Comp. Physiol. A 110, 233–250.
Rheinlaender, J. and Mörchen, A. 1979. 'Time-intensity trading' in locust auditory interneurones. Nature 281, 672–674.
Rheinlaender, J., Shen, J.-X., and Römer, H. 2006. Auditory lateralization in bushcrickets: a new dichotic paradigm. J. Comp. Physiol. A 192, 389–397.
Richards, A. G. 1933. Comparative skeletal morphology of the noctuid tympanum. Entomologica Americana 13, 1–43.
Rieke, F., Warland, D., Ruyter van Steveninck, R., and Bialek, W. 1997. Spikes Exploring the Neural Code, 395 pp. MIT Press.
Robert, D. 1989. The auditory behaviour of flying locusts. J. Exp. Biol. 147, 279–301.
Robert, D., Amoroso, J., and Hoy, R. R. 1992. The evolutionary convergence of hearing in a parasitoid fly and its cricket host. Science 258, 1135–1137.
Robert, D., Miles, R. N., and Hoy, R. R. 1999. Tympanal hearing in the sarcophagid parasitoid fly *Emblemasoma sp*.: the biomechanics of directional hearing. J. Exp. Biol. 1865–1876.
Robert, D., Read, M. P., and Hoy, R. R. 1994. The tympanal hearing organ of the parasitoid fly *Ormia ochracea* (Diptera, Tachinidae, Ormiini). Cell Tissue Res. 275, 63–78.
Robinson, D. J., Rheinlaender, J., and Hartley, J. C. 1986. Temporal parameters of male-female sound communication in *Leptophyes punctatissima*. Physiol. Entom. 11, 317–323.
Roeder, K. D. 1962. The behaviour of free flying moths in the presence of artificial ultrasonic pulses. Anim. Behav. 10, 300–304.
Roeder, K. D. 1964. Aspects of the noctuid tympanic nerve response having significance in the avoidance of bats. J. Insect Physiol. 10, 529–546.
Roeder, K. D. 1966a. Auditory system of noctuid moths. Science 154, 1515–1521.
Roeder, K. D. 1966b. Interneurons of the thoracic nerve cord activated by tympanic nerve fibres in noctuid moths. J. Insect Physiol. 12, 1227–1244.
Roeder, K. D. 1970. Episodes in insect brains. Am. Sci. 58, 378–389.
Roeder, K. D. 1972. Acoustic and mechanical sensitivity of the distal lobe of the pilifer in choerocampine hawkmoths. J. Insect Physiol. 18, 1249–1264.
Roeder, K. D. 1973. Brain interneurons in noctuoid moths: binaural excitation and slow potentials. J. Insect Physiol. 19, 1591–1601.
Roeder, K. D. 1974. Responses of the less sensitive acoustic sense cells in the tympanic organs of some noctuid and geometrid moths. J. Insect Physiol. 20, 55–66.
Roeder, K. D. and Treat, A. E. 1957. Ultrasonic reception by the tympanic organ of noctuid moths. J. Exp. Zool. 134, 127–157.
Rokem, A., Watzl, S., Gollish, T., Stemmler, M., Herz, A. V. M., and Samengo, I. 2006. Spike-timing precision underlies the coding efficiency of auditory receptor neurons. J. Neurophysiol. 95, 2541–2552.
Römer, H. 1976. Die Informationsverarbeitung tympanaler Rezeptorelemente von *Locusta migratoria* (Acrididae, Orthoptera). J. Comp. Physiol. A 109, 101–122.
Römer, H. 1983. Tonotopic organisation of the auditory neuropil in the bushcricket *Tettigonia viridissima*. Nature 306, 60–62.
Römer, H. 1987. Representation of auditory distance within a central neuropile of the bushcricket *Mygalopsis marki*. J. Comp. Physiol. A 161, 33–42.
Römer, H. 1993. Environmental and biological constraints for the evolution of long-range signalling and hearing in acoustic insects. Phil. Trans. R. Soc. Lond. B 340, 179–185.
Römer, H. and Dronse, R. 1982. Synaptic mechanisms of monaural and binaural processing in the locust. J. Insect Physiol. 28, 365–370.
Römer, H. and Krusch, M. 2000. A gain-control mechanism for processing of chorus sounds in the afferent auditory pathway of the bushcricket *Tettigonia viridissima* (Orthoptera; Tettigoniidae). J. Comp. Physiol. A 186, 181–191.
Römer, H. and Marquart, V. 1984. Morphology and physiology of auditory interneurons in the metathoracic ganglion of the locust. J. Comp. Physiol. A 155, 249–262.
Römer, H. and Seikowski, U. 1985. Response to model songs of auditory neurons in the thoracic ganglia and brain of the locust. J. Comp. Physiol. A 156, 845–860.
Römer, H, Hedwig, B., and Ott, S. R. 2002. Contralateral inhibition as a sensory bias: the neural basis for a female preference in a synchronously calling bushcricket, *Mecopoda elongata*. Eur. J. Neurosci. 15, 1655–1662.
Römer, H., Marquardt, V., and Hardt, M. 1988. Organisation of a sensory neuropile in the auditory pathway of two groups of Orthoptera. J. Comp. Neurol. 275, 201–215.
Römer, H., Rheinlaender, J., and Dronse, R. 1981. Intracellular studies on auditory processing in the metathoracic ganglion of the locust. J. Comp. Physiol. A 144, 305–312.
Ronacher, B. and Krahe, R. 1998. Song recognition in the grasshopper *Chorthippus biguttulus* is not impaired by shortening song signals: implications for neural encoding. J. Comp. Physiol. A 183, 729–735.
Ronacher, B. and Römer, H. 1985. Spike synchronisation of tympanic receptor fibres in a grasshopper (*Chorthippus biguttulus* L., Acrididae). J. Comp. Physiol. A 157, 631–642.
Ronacher, B. and Stumpner, A. 1988. Filtering of behavioural relevant temporal parameters of a grasshopper's song by an auditory interneurone. J. Comp. Physiol. A 163, 517–523.
Ronacher, B., Franz, A., Wohlgemuth, S., and Hennig, R. M. 2004. Variability of spike trains and the processing of temporal patterns of acoustic signals – problems, constraints, and solutions. J. Comp. Physiol. A 190, 257–277.
Ronacher, B., Helversen, von D., and Helversen, von O. 1986. Routes and stations in the processing of auditory directional information in the CNS of a grasshopper, as revealed by surgical experiments. J. Comp. Physiol. A 158, 363–374.
Ronacher, B., Stumpner, A., Sokoliuk, T., and Herrmann, B. 1993. Acoustic communication of grasshopper males after lesions in the thoracic connectives: correlation with the ascending projections of identified auditory neurons. Zoo. Jb. Physiol. 97, 199–214.
Rössler, W., Hübschen, A., Schul, J., and Kalmring, K. 1994. Functional morphology of bushcricket ears: comparison

between two species belonging to the Phaneropterineae und Decticinae (Insecta, Ensifera). Zoomorphology 114, 39–46.
Rydell, J., Kaerma, S., Hedelin, H., and Skals, N. 2003. Evasive response to ultrasound by the crepuscular butterfly *Mataria maculata*. Naturwissenschaften 90, 80–83.
Sanderford, M. V., Coro, F., and Conner, W. E. 1998. Courtship behaviour in *Empyreunma affinis* Roths. (Lepidoptera, Arctiidae, Ctenuchinae): acoustic signals and tympanic response. Naturwissenschaften 85, 82–87.
Schaller, F. 1951. Lauterzeugung und Hörvermögen von *Corixa (Callicorixa) striata* L. Z. vergl Physiol 33, 476–486.
Schildberger, K. 1984. Temporal selectivity of identified auditory neurons in the cricket brain. J. Comp. Physiol. A 155, 171–185.
Schildberger, K. 1994. The auditory pathway of crickets: adaptations for intraspecific acoustic communication. In: Neural basis of behavioural adaptations. (*eds*. Schildberger K., Elsner N.), pp. 209–226. Gustav Fischer Verlag Stuttgart.
Schildberger, K. and Hörner, M. 1988. The function of auditory neurons in cricket phonotaxis I. Influence of hyperpolarization of identified neurons on sound localisation. J. Comp. Physiol. A 163, 621–631.
Schildberger, K., Milde, J. J., and Hörner, M. 1988. The function of auditory neurons in cricket phonotaxis II. Modulation of auditory responses during locomotion. J. Comp. Physiol. A 163, 633–640.
Schul, J. 1997. Neuronal basis of phonotactic behaviour in *Tettigonia viridissima*: processing of behaviourally relevant signals by auditory afferents and thoracic interneurons. J. Comp. Physiol. A 180, 573–583.
Schul, J. 1998. Song recognition by temporal cues in a group of closely related buschcrickets (genus Tettigonia). J. Comp. Physiol. A 183, 401–410.
Schul, J., Helversen, von O., and Weber, T. 1998. Selective phonotaxis in *Tettigonia cantans* and *T. viridissima* in song recognition and discrimination. J. Comp. Physiol. A 182, 687–694.
Schul, J., Holderied, M., Helversen, von D., and Helversen, von O. 1999. Directional hearing in a grasshopper: neurophysiological testing of a bioacoustical model. J. Exp. Biol. 202, 121–133.
Schultz, W. and Schul, J. 2001. Ultrasound avoidance behaviour in the bushcricket *Tettigonia viridissima* (Orthoptera: Tettigoniidae). J. Exp. Biol. 204, 733–740.
Schwabe, J. 1906. Beiträge zur Morphologie und Histologie der tympanalen Sinnesapparate der Orthopteren. Zoologica 50, 1–154.
Selverston, A. I, Kleindienst, H.-U., and Huber, F. 1985. Synaptic connectivity between cricket auditory interneurons as studied by selective photoinactivation. J. Neurosci. 5, 1283–1292.
Sippel, M. and Breckow, J. 1984. Non-monotonic response-intensity characteristics of auditory receptor cells in *Locusta migratoria*. J. Comp. Physiol. A 155, 633–638.
Sismondo, E. 1990. Synchronous. alternating, and phase-locked stridulation by a tropical katydid. Science 249, 55–58.
Snedden, W. A. and Greenfield, M. D. 1998. Females prefer leading males: relative call timing and sexual selection in katydid choruses. Anim. Behav. 56, 1091–1098.
Sobel, E. C. and Tank, D. W. 1994. In vivo Ca^{2+} dynamics in a cricket auditory neuron: an example of chemical computation. Science 263, 823–826.
Sokoliuk, T., Stumpner, A., and Ronacher, B. 1989. GABA-like immunoreactivity suggests an inhibitory function of the thoracic low-frequency neuron (TN1) in acridid grasshoppers. Naturwissenschaften 76, 223–225.
Spangler, H. G. 1988. Hearing in tiger beetles (Cicindelidae). Physiol. Entomol. 13, 447–452.
Spooner, J. D. 1968. Pair-forming acoustic systems of phaneropterine katydids (Orthoptera, Tettigoniidae). Anim. Behav. 16, 197–212.
Staaden, van M. J, Rieser, M., Ott, S. R., Pabst, M. A., and Römer, H. 2003. Serial hearing organs in the atympanate grasshopper *Bullacris membracioides* (Orthoptera, Pneumoridae). J. Comp. Neurol. 465, 579–592.
Stabel, J., Wendler, G., and Scharstein, H. 1989. Cricket phonotaxis: localisation depends on recognition of the calling song patern. J. Comp. Physiol. A 165, 165–177.
Staudacher, E. M. 2001. Sensory responses of descending brain neurons in the walking cricket, *Gryllus bimaculatus*. J. Comp. Physiol. A 187, 1–17.
Stölting, H. and Stumpner, A. 1998. Tonotopic organization of auditory receptors of the bushcricket *Pholidoptera griseoaptera* (Tettigoniidae, Decticinae). Cell Tissue Res. 294, 377–386.
Stout, J. F. and Huber, F. 1972. Response of central auditory neurons of female crickets (*Gryllus campestris* L.) to the calling song of the male. J. Comp. Physiol. A 76, 302–313.
Stout, J. F. and McGhee, R. 1988. Attractiveness of the male *Acheta domestica* calling song to females II. The relative importance of syllable period, intensity, and chirp rate. J. Comp. Physiol. A 164, 277–287.
Stumpner, A. 1997. An auditory interneurone tuned to the male song frequency in the bushcricket *Ancistura nigrovittata* (Orthoptera, Phaneropteridae). J. Exp. Biol. 200, 1089–1101.
Stumpner, A. 1999. An interneurone of unusual morphology is tuned to the female song frequency in the bushcricket *Ancistura nigrovittata* (Orthoptera, Phaneropteridae). J. Exp. Biol. 202, 2071–2081.
Stumpner, A. 2002. A species-specific frequency filter through specific inhibition, not specific excitation. J. Comp. Physiol. A 188, 239–248.
Stumpner, A. and Lakes-Harlan, R. 1996. Auditory interneurons in a hearing fly (*Therobia leonidei*, Ormiini, Tachinidae, Diptera). J. Comp. Physiol. A 178, 227–233.
Stumpner, A. and Meyer, S. 2001. Songs and the function of song elements in four duetting bushcricket species (Ensifera, Phaneropteridae, Barbitistes). J. Ins. Physiol. 14, 511–534.
Stumpner, A. and Molina, J. 2006. Diversity of Intersegmental auditory neurons in a bush cricket. J. Comp. Physiol. A. 192, 1359–1376.
Stumpner, A. and Ronacher, B. 1991. Auditory interneurones in the metathoracic ganglion of the grasshopper *Chorthippus biguttulus*. I. Morphological and physiological characterization. J. Exp. Biol. 158, 391–410.
Stumpner, A. and Ronacher, B. 1994. Neurophysiological aspects of song pattern recognition and sound localization in grasshoppers. Amer. Zool. 34, 696–705.
Stumpner, A., Ronacher, B., and Helversen, von O. 1991. Auditory interneurones in the metathoracic ganglion of the grasshopper *Chorthippus biguttulus*. II. Processing of temporal patterns of the song of the male. J. Exp. Biol. 158, 411–430.
Suga, N. 1963. Central mechanism of hearing and sound localization in insects. J. Insect Physiol. 9, 867–873.
Suga, N. and Katsuki, Y. 1961. Central mechanism of hearing in insects. J. Exp. Biol. 38, 545–558.
Surlykke, A. and Filskov, M. 1997. Hearing in Geometrid moths. Naturwissenschaften 84, 356–359.
Surlykke, A. and Miller, L. A. 1982. Central branchings of three axons from a moth ear (*Agrotis segetum*, Noctuidae). J. Insect Physiol. 28, 357–364.
Thomson, K. J. and Siegler, M. V. S. 1991. Anatomy and physiology of spiking local and intersegmental interneurons in the median neuroblast lineage of the grasshopper. J. Comp. Neurol. 305, 659–675.

Thorson, J., Weber, T., and Huber, F. 1982. Auditory behaviour of the cricket. II. Simplicity of calling-song recognition in Gryllus, and anomalous phonotaxis at abnormal carrier frequencies. J Comp. Physiol, A 146, 361–378.
Triblehorn, J. D. and Yager, D. D. 2002. Implanted electrode reecordings from a praying mantis auditory interneuron during flying bat attacks. J. Exp. Biol. 205, 307–320.
Triblehorn, J. D. and Yager, D. D. 2005. Timing of praying mantis evasive responses during simulated bat attack sequences. J. Exp. Biol. 208, 1867–1876.
van Staaden, M. J. and Römer, H. 1997. Sexual signalling in bladder grasshoppers: tactical design for maximising calling range. J. Exp. Biol. 200, 2597–2608.
van Staaden, M. J. and Römer, H. 1998. Evolutionary transition from stretch to hearing organs in ancient grasshoppers. Nature 394, 773–776.
van Staaden, M. J., Rieser, M., Ott, S. R., Pabst, M. A., and Römer, H. 2003. Serial hearing organs in the atympanate grasshopper *Bullacris membraciodes* (Orthoptera, Pneumoridae). J Comp Neurol 465, 579–592.
Vogel, R. 1912. Über die Chordotonalorgane in der Wurzel der Schmetterlingsflügel. Z wiss Zool 100, 210–244.
Vogel, R. 1923. Über ein tympanales Sinnesorgan, das mutmaßliche Hörorgan der Singzikaden. Zeitschrift für Anatomie und Entwicklungsgeschichte der Tiere 67, 190–231.
Wagner, W. E. 1995. Convergent song preferences between female crickets and acoustically orienting parasitoid flies. Behav. Ecol. 7, 279–285.
Walker, T. J. 1993. Phonotaxis in female *Ormia ochracea* (Diptera: Tachinidae), a parasitoid of field crickets. J. Insect Behav. 6, 389–410.
Wallach, H., Newman, E. B., and Rosenzweig, M. R. 1949. The precedence effect in sound localization. Am. J. Psychol. 62, 315–336.
Waters, D. A. and Jones, G. 1996. The peripheral auditory characteristics of noctuid moths: responses to the search-phase echolocation calls of bats. J. Exp. Biol. 199, 847–856.
Watson, A. H. D. and Hardt, M. 1996. Distribution of synapses on two local auditory interneurons, ON1 and ON2 in the prothoracic ganglion of the cricket: relationships with GABA-immunoreactive neurons. Cell Tissue Res. 283, 231–246.
Weber, T. and Thorson, J. 1989. Phonotactic Behaviour of Walking Crickets. In: Cricket Behaviour and Neurobiology (*eds*. F. Huber, T. E. Moore, and W. Loher), pp. 310–339. Cornell University Press.
Wiese, K. and Eilts-Grimm, K. 1985. Functional Potential of Recurrent Lateral Inhibition in Cricket Audition. In: Acoustic and Vibrational Communication in Insects. (*eds*. K. Kalmring and N. Elsner), pp. 3–40. Parey.
Wohlers, D. W. and Huber, F. 1978. Intracellular recording and staining of cricket auditory interneurons (*Gryllus campestris* L.., *Gryllus bimaculatus* DeGeer). J. Comp. Physiol. A 127, 11–28.
Wohlers, D. W. and Huber, F. 1982. Processing of sound signals by six types of neurons in the prothoracic ganglion of the cricket, *Gryllus campestris* L. J. Comp. Physiol. A 146, 161–173.
Wohlers, D. W. and Huber, F. 1985. Topographical organization of the auditory pathway within the prothoracic ganglion of the cricket *Gryllus campestris* L. Cell Tissue Res. 239, 555–565.
Wohlers, D. W., Williams, J. L. D., Huber, F., and Moore, T. E. 1979. Central projections of fibres in the auditory and tensor nerves of cicadas (Homoptera: Cicadidae). Cell Tissue Res. 203, 35–51.
Wolf, H. and von Helversen, O. 1986. ''Switching off'' of an auditory interneuron during stridulation in the acridid grasshopper *Chorthippus biguttulus* L. J. Comp. Physiol. A 158, 861–871.
Wotzel, F. 1933. Zur Kenntnis der Tympanalorgane der Hydrocores. Z wiss Zool 143, 241–262.
Wyttenbach, R. A. and Hoy, R. R. 1993. Demonstration of the precedence effect in an insect. J. Acoust. Soc. Am. 94, 777–784.
Yack, J. E. and Fullard, J. H. 1993. What is an insect ear? Ann. Entomol. Soc. Am. 86, 677–682.
Yack, J. E. and Fullard, J. H. 1999. Ultrasonic hearing in nocturnal butterflies. Nature 403, 265–266.
Yack, J. E., Otero, L. D, Dawson, J. W, Surlykke, A., and Fullard, J. H. 2000. Sound production and hearing in the blue cracker butterfly *Hamadryas feronia* (Lepidoptera, Nymphalidae) from Venezuela. J. Exp. Biol. 203, 3689–3702.
Yager, D. D. 1996. Serially homologeous ears perform frequency range fractionation in the praying mantis, *Creobroter* (Mantodea, Hymenopodidae). J. Comp. Physiol. A 178, 463–475.
Yager, D. D. 1999. Structure, development, and evolution of insect auditory systems. Microsc. Res. Tech. 47, 380–400.
Yager, D. D. and Hoy, R. R. 1986. The cyclopean ear: a new sense for the praying mantis. Science 231, 727–729.
Yager, D. D. and Hoy, R. R. 1987. The midline metathoracic ear of the praying mantis, *Mantis religiosa*. Cell. Tissue Res. 250, 531–541.
Yager, D. D. and Hoy, R. R. 1989. Audition in the praying mantis, *Mantis religiosa* L.: identification of an interneuron mediating ultrasonic hearing. J. Comp. Physiol. A 165, 471–493.
Yager, D. D. and May, M. L. 1990. Ultrasound-triggered, flight-gated evasive maneuvers in the praying mantis *Parasphendale agrionina*. II. Tethered flight. J. Exp. Biol. 152, 41–58.
Yager, D. D. and Spangler, H. G. 1995. Characterization of auditory afferents in the tiger beetle, *Cicindela marutha* Dow. J. Comp. Physiol. A 176, 587–599.
Yager, D. D, May, M. L., and Fenton, M. B. 1990. Ultrasound-triggered, flight-gated evasive maneuvers in the praying mantis *Parasphendale agrionina*. I. Free flight. J. Exp. Biol. 152, 17–39.
Young, D. 1990. Do cicadas radiate sound through their ear drums? J. Exp. Biol. 151, 41–56.
Young, D. and Hill, K. G. 1977. Structure and function of the auditory system of the cicada, *Cystosoma saundersii*. J. Comp. Physiol. A 117, 23–45.
Zaretsky, M. D. 1972. Specificity of the calling song and short term changes in the phonotactic response by female crickets *Scapsipedus marginatus* (Gryllidae). J. Comp. Physiol. A 79, 153–172.
Zimmermann, U., Rheinlaender, J., and Robinson, D. 1989. Cues for male phonotaxis in the duetting bushcricket *Leptophyes punctatissima*. J. Comp. Physiol. A 164, 621–628.

Further Reading

Boyan, G. S. 1984. Neural mechanisms of auditory information processing by identified interneurons in Orthoptera. J. Insect Physiol. 30, 27–41.
Boyan, G. S. 1993. Another look at insect audition: The tympanic receptors as an evolutionary specialization of the chordotonal system. J. Insect Physiol. 39, 187–200.
Budelmann, B. U. 1992. Hearing in Crustacea. In: The Evolutionary Biology of Hearing (*eds*. D. B. Webster, R. R. Fay, and A. N. Popper), pp. 131–139. Springer.
Coro, F. and Perez, M. 1993. Threshold and suprathreshold responses of the arctiid moth. Experientia 49, 285–290.

Ewing, A. W. 1978. The antenna of Drosophila as a ''love song'' receptor. Physiol. Entomol. 3, 33–36.
Finke, C. 1968. Lautäußerungen und Verhalten von *Sigara striata* und *Callicorixa praeusta* (Corixidae Leach., Hydrocorisae Latr.). J. Comp. Physiol. A 58, 398–422.
Fullard, J. H. 1998. The Sensory Coevolution of Moths and Bats. In: Comparative Hearing: Insects (*eds*. R. R. Hoy, A. N. Popper, and R. R. Fay), pp. 279–327. Springer.
Gerhardt, H. C. and Huber, F. 2002. Acoustic Communication in Insects and Anurans: Common Problems and Diverse Solutions. University of Chicago Press.
Göpfert, M. C. and Wasserthal, L. T. 1999a. Hearing with the mouthparts: behavioural responses and the structural basisi of ultrasound perception in acherontiine hawkmoths. J. Exp. Biol. 202, 909–918.
Göpfert, M. C. and Wasserthal, L. T. 1999b. Auditory sensory cells in hawkmoths: identification, physiology and structure. J. Exp. Biol. 202, 1579–1587.
Hedwig, B. 2006. Pulses, patterns and paths: neurobiology of acoustic behaviour in crickets. J Comp. Physiol. A 192, 677–689.
Helversen von, D. 1997. Acoustic Communication and Orientation in Grasshoppers. In: Orientation and Communication in Arthropods (*ed*. M. Lehrer), pp. 301–341. Birkhäuser.
Helversen, von D. and Helversen, von O. 1983. Species Recognition and Acoustic Localization in Arcridid Grasshoppers: A Behavioural Approach. In: Neuroethology and Behavioural Physiology (*eds*. F. Huber and H. Markl), pp. 95–107. Heidelberg.
Hennig, R. M., Franz, A., and Stumpner, A. 2004. Processing of auditory information in insects. Microsc. Res. Tech. 63, 351–374.
Hoy, R. R., Popper, A. N., and Fay, R. R. 1988. Springer Handbook of Auditory Research. Comparative Hearing: Insects. Springer.
Pollack, G. S. 2000. Who, what, where? Recognition and localization of acoustic signals by insects. Curr. Opin. Neurobiol. 10, 763–767.
Pollack, G. S. and Imaizumi, K. 1999. Neural analysis of sound frequency in insects. BioEssays 21, 295–303.
Römer, H. and Tautz, J. 1992. Invertebrate auditory receptors. Adv. Comp. Environ. Physiol. 10, 185–212.
Robinson, D. J. 1980. Acoustic communication between sexes of the bush cricket*, Leptophyes punctatissima.* Physiol. Entomol. 5, 183–189.
Römer, H. and Tautz, J. 1992. Invertebrate auditory receptors. Adv. Comp. Envir. Physiol. 10, 185–212.
Ronacher, B., Franz, A., Wohlgemuth, S., and Hennig, R. M. 2004. Variability of spike trains and the processing of temporal patterns of acoustic signals-problems, constraints, and solutions. J. Comp. Physiol. A 190, 257–277.
Stumpner, A. and Helversen von, D. 2001. Evolution and function of auditory systems in insects. Naturwissenschaften 88, 159–170.
Surlykke, A. 1984. Hearing in notodontid moths: a tympanic organ with a single auditory neurone. J. Exp. Biol. 113, 323–335.
Tautz, J. 1979. Reception of particle oscillation in a medium - an unorthodox sensory capacity. Naturwissenschaften 66, 452–461.
Yack, J. E. 2004. The structure and function of auditory chordotonal organs in insects. Microsc. Res. Tech. 63, 315–337.
Yager, D. D. 1999. Structure, development, and evolution of insect auditory systems. Microsc. Res. Tech. 47, 380–400.

3.32 Biophysical Specializations of Neurons that Encode Timing

P B Manis, The University of North Carolina at Chapel Hill, Chapel Hill, NC, USA

© 2008 Elsevier Inc. All rights reserved.

3.32.1	**Introduction**	566
3.32.2	**Firing Patterns**	567
3.32.3	**Voltage-Gated Potassium Channels**	569
3.32.3.1	The Kv Family	569
3.32.3.1.1	The Kv1 family	570
3.32.3.1.2	The Kv2 family	570
3.32.3.1.3	The Kv3 family	570
3.32.3.1.4	The Kv4 family	571
3.32.3.1.5	Kv5–Kv9	571
3.32.4	**Channel Specialization and Biophysical Characterization of the Channels in the Vertebrate Auditory Cental Nervous System**	571
3.32.4.1	Spiral Ganglion Cells	572
3.32.4.2	Ventral Cochear Nucleus Bushy Cells	572
3.32.4.2.1	The low voltage-activated potassium conductance	572
3.32.4.2.2	The high voltage-activated potassium conductance	573
3.32.4.2.3	The transient potassium conductances	574
3.32.4.2.4	The hyperpolarization-activated conductances	574
3.32.4.3	Ventral Cochlear Nucleus Stellate/Multipolar Cells	574
3.32.4.4	Octopus Cells	574
3.32.4.5	Dorsal Cochlear Nuclear Pyramidal Cells	575
3.32.4.6	Superior Olivary Complex	576
3.32.4.6.1	Medial nucleus of trapezoid body	576
3.32.4.7	Medial Superior Olive	576
3.32.4.8	Other Auditory Structures	577
3.32.4.8.1	Superior olive	577
3.32.4.8.2	Nuclei of the lateral lemniscus	577
3.32.4.8.3	Inferior colliculus	577
3.32.5	**Summary of Channel Expression**	578
3.32.6	**The Role of Low-Voltage-Activated K^+ Channels in Temporal Integration**	578
3.32.6.1	Tonotopic Channel Expression Patterns, and Relationship to Integrative Roles	580
3.32.7	**Conclusion**	581
References		581

Glossary

action potential The action potential is a stereotyped electrical signal, consisting of a rapid, millisecond long, decrease in membrane potential, with a rapid return to the resting potential. Action potentials are typically 50–100 mV in amplitude. Action potentials serve to encode information as it is transmitted from one neuron to the next, and drive transmitter release from synapses.

anomalous rectifier Anomalous rectifier channels are those that are opened by hyperpolarization of the cell membrane as opposed to depolarization. They are anomalous because most channels are opened by depolarization.

brain slice The brain slice is a reduced preparation of the nervous system, in which a thin section of live brain tissue is obtained and maintained in an

artificial oxygenated balanced salt solution. Brain slices are typically between 0.25 and 0.5 mm thick. The slices have the advantages of mechanical stability and optical access, allowing careful biophysical analyses of individual cells and local neuronal circuits.

cation-selective channels Membrane proteins that are permeable to K, Na, and/or Ca are cation selective. Often this term is used for channels that do not have high selectivity, and so are permeable to more than one cation.

delayed rectifier Delayed rectifier is a term used to refer to the set of potassium conductances that repolarize the action potential. The term arises from the time-delayed activation of the membrane conductance, and because the membrane current–voltage relationship is nonlinear (nonohmic) when this conductance is active. Delayed rectifiers typically do not show significant inactivation.

depolarization Depolarization refers to movement of the membrane potential from its resting value, typically near −60 mV, toward more positive potentials, such as 0 mV. Depolarization of the neuronal membrane is often excitatory, in the sense that it increases the probability of triggering action potentials, or increasing the frequency of action potentials.

EPSC (excitatory postsynaptic current) EPSC refers to the current flow created when excitatory ligand-gated ion channels (such as glutamate and some acetylcholine receptors) are activated. The change in conductance, associated with a cation-selective channel, depolarizes the neuron and increases the probability of firing.

hyperpolarization Hyperpolarization refers to movement of the membrane potential from its resting value, typically near −60 mV, toward more negative potentials, such as −80 mV. Hyperpolarization of the neuronal membrane is often inhibitory, in the sense that it decreases the probability of triggering action potentials, or decreases the frequency of action potentials.

intrinsic firing pattern Intrinsic firing pattern refers to the temporal pattern of action potentials elicited by an extrinsic depolarization of the neuron membrane, in the absence of synaptic inputs. Typically, the pattern is defined with respect to simple rectangular current pulses injected into the cell.

node of Ranvier The node of Ranvier is a specialized region of the axon, where ion channels (sodium and potassium channels) are clustered. The nodes are located between the long stretches of the myelin sheath created by different myelinating glial cells (Schwann cells and oligodendrocytes).

pore loop The pore loop is the region of an ion channel protein that helps determine the selectivity of the channel, and plays a role in regulating the channel open or closed states. The pore loop often consists of a hairpin length of the protein inserted into the membrane, that begins and ends on the same side of the membrane.

tetrameric Tetrameric proteins have four subunits, often arising from the assembly of four distinct proteins encoded by different genes.

transient potassium current (or A current) The transient potassium currents are those that show inactivation, or an intrinsic closing, of the channels during a sustained change in membrane potential. This inactivation distinguishes these channels from delayed rectifiers. The time course of inactivation of transient potassium currents varies from about 10 ms to seconds, depending on the potassium channel subunits that make up the channel.

transmembrane domain Transmembrane domains are regions of a protein that are hydrophobic, so that they prefer to be inserted into the cell membrane such that the parts of the protein on either side of the domain are on opposite sides of the membrane.

3.32.1 Introduction

The auditory system faces unique challenges in processing the temporal and spectral features of sound, because sound contains biologically relevant information in timescales that are much faster than the capabilities of most common neuronal mechanisms. Most forebrain neurons have synaptic potentials that last tens of milliseconds and action potentials that are 2–5 ms wide. In comparison, the task of localizing sound in the azimuthal plane requires that the central auditory system compare spike trains with microsecond precision. Specializations of the standard neural processing mechanisms are thus necessary in the neurons and synapses of the auditory brainstem to meet these challenges (Oertel, D., 1999). Over the

past 15 years, these mechanisms have been identified and characterized in some detail. In particular, neurons in the auditory brainstem have phenotypes that result from the expression of specific patterns of ion channels and neurotransmitter receptors that produce temporal processing performance appropriate to the tasks of sound localization, sound identification, and sound perception for communication. In this chapter, the roles of voltage-gated potassium channels, which are highly expressed in auditory brainstem nuclei, and the role of cation-selective hyperpolarization-activated currents will be discussed. Equally important to the task of neural computation based on fine timing information are the synapses and their receptors; these too are specialized in the brainstem auditory system and are reviewed in 3.33.

We will begin by discussing the four primary firing pattern motifs that are found in brainstem auditory neurons. Next, we will briefly review the biophysics and structure of potassium channels, as these are the critical elements that endow auditory neurons with their ability to encode timing information. We will then review the expression of these channels along the auditory pathway in specific cell types. In the last section, we will discuss specific roles for these channels from the perspective of synaptic integration.

3.32.2 Firing Patterns

There are four fundamental motifs of electrical excitability that predominate in the brainstem auditory system (Figure 1). The first intrinsic pattern is a simple regular spiking pattern that is common to many neurons in the nervous system. In this case, a step depolarization of the cell membrane leads to a train of evenly spaced action potentials that can be sustained indefinitely (Figure 1(a)). The interval between the action potentials decreases as the injected current increases, and the rate does not change over time (in other words, there is no adaptation or slowing of firing as seen in many other neurons). The action potentials are narrow, and even in the best recordings reach only to about +10 mV (as compared to +40 mV for cortical neurons). The firing pattern is not sensitive to the membrane potential of the cell before depolarization (this will be important later). The cells in the ventral cochlear nucleus (VCN) that have this pattern are multipolar (or stellate) neurons (Wu, S. H. and Oertel, D., 1984) that receive many small bouton synapses from the auditory nerve fibers (ANFs). In response to sound *in vivo*, multipolar neurons fire trains of evenly spaced action potentials, similar to what is seen in brain slices with current injection. Cells with this firing pattern do not convey fine timing information necessary for speech perception or some types of sound localization, but may encode information about sound intensity or slower modulation of sound amplitude with their firing rate (Sullivan, W. E. and Konishi, M., 1984; Rhode, W. S. and Smith, P. H., 1986; Frisina, R. D. *et al.*, 1990; Kim, D. O. *et al.*, 1990).

The second intrinsic pattern is characterized by the presence of only one or two action potentials (Figure 1(b)) at the beginning of a depolarizing current step (Oertel, D., 1983). After these initial action potentials, the membrane potential stays close to the resting potential, and the membrane conductance is high. The action potentials may be wider than those in multipolar cells, and are often quite short. *In vivo*, neurons with these electrical properties may respond with patterns of action potentials that are similar to their inputs, or may respond only at the onset of a sound, depending on the strength and convergence of the inputs. Some neurons with these intrinsic properties can actually improve the temporal precision of firing relative to their inputs (Joris, P. X. *et al.*, 1994; Paolini, A. G. *et al.*, 2001; Louage, D. H. *et al.*, 2005). Neurons with this intrinsic pattern are commonly found in cells that process fine timing information, and the mechanisms underlying this processing will be discussed in more detail below.

The third intrinsic pattern is uniquely characterized by sensitivity of the cell's firing pattern to the membrane potential prior to a depolarization. Cells with this firing motif can fire a regular train of action potentials when the membrane potential has been at rest before current is injected (Figure 1(c), trace 1), but the timing of the first few spikes changes when the membrane potential is negative (hyperpolarized) to the resting potential before depolarization (Manis, P. B., 1990). Two different, related discharge patterns can occur. The first pattern has a first spike latency that is tens of milliseconds (Figure 1(c), trace 2), and the second pattern has a short first spike latency (Figure 1(c), trace 3), but long first interspike interval. The firing of subsequent spikes in these cells in response to depolarization is regular, and does not show adaptation, similar to the regular firing cells discussed above. A surprising feature is that these patterns closely resemble the patterns reported for

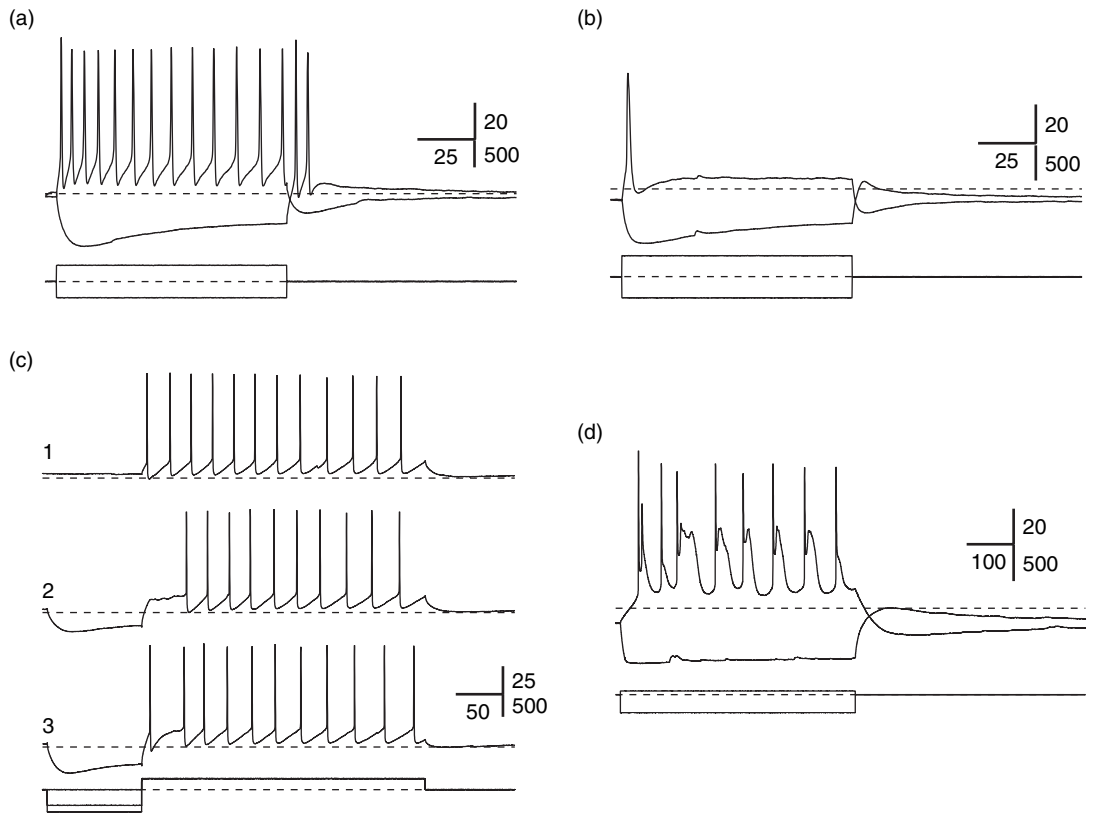

Figure 1 Example recording from cells in the cochlear nucleus with different intrinsic firing patterns. (a) Regular firing pattern (type I) found in stellate–multiploar cells of the ventral cochlear nucleus. Note occasional anodal break spikes following a hyperpolarizing current injection. Data from P23 mouse (DBA) ventral cochlear nucleus. (b) Phasic firing pattern (type II) found in bushy cells (including spherical and globular bushy cells); a slightly modified version of this pattern is found in octopus cells. Data from P35 mouse (DBA) ventral cochlear nucleus. (c) Three different voltage-dependent discharge patterns of dorsal cochlear nucleus (DCN) pyramidal cells. Trace 1 shows the regular firing elicited when the membrane potential is at rest. Trace 2 shows the delay to the first spike following a hyperpolarization. Trace 3 shows the slightly longer first interspike interval that is seen with larger hyperpolarizations, or with different hyperpolarization–depolarization sequences. Data from P13 rat DCN pyramidal cell. (d) Complex spiking pattern seen in cartwheel cells of the DCN. Note the related complex bursts and broad after depolarization when only single spikes are generated. Data from P12 rat DCN cartwheel cell. Calibrations: horizontal bars indicate time in milliseconds. Upward vertical bars are voltage in millivolts. Downward vertical bars indicate current, in picoamperes. For voltage traces the dashed lines are at −60 mV, except in (d), where they are at −75 mV. For current traces, the dashed lines are at 0 pA. Recordings in (a) and (b) from Wang Y. and Manis P. B. (unpublished data). Recording in (c) from Manis P. B. (unpublished data) Recording in (d) from Mancilla J. and Manis P. B. (unpublished data)

the responses to tone bursts for these cells *in vivo*. While these cells are not normally thought of as being involved in precise timing circuits, their intrinsic mechanisms are capable of encoding timing information (Manis, P. B. *et al.*, 2003; Kanold, P. O. and Manis, P. B., 2005) and so they are briefly discussed below.

The fourth motif is a bursting or complex spiking pattern, in which groups of action potentials occur closely together in time, with much longer intervals between the bursts (Figure 1(d)). This pattern is seen in cartwheel cells of the dorsal cochlear nucleus (DCN) (Zhang, S. and Oertel, D., 1993; Manis, P. B. *et al.*, 1994). Because these cells do not seem to be involved in timing circuits *per se*, and little is known about their channels, they will not be discussed further.

Each of these patterns is generated by neurons that express different complements, densities and possibly distributions of ion channels in their membrane. While the discharge patterns result from the interplay between the membrane voltage and all of the time and voltage dependences of the ion conductances, the potassium conductances vary most between the cells with different patterns. Therefore, we will focus on the potassium channels in this chapter.

3.32.3 Voltage-Gated Potassium Channels

Phylogenetically, the voltage-gated potassium channels are ancient, and homologous channels can be found in plants (Cherel, I., 2004). Even the ionotropic glutamate receptors have a pore domain that closely resembles an inverted pore from the voltage-gated potassium channels (Wo, Z. G. and Oswald, R. E., 1995; McFeeters, R. L. and Oswald, R. E., 2004). In mammals, voltage-gated potassium channels arise from several gene families with different properties (reviewed in Coetzee, W. A. *et al.*, 1999). The major known families include the Kv series, which are principally gated by membrane voltage, the KCNQ family (Robbins, J., 2001), some of which form the G-protein-gated channels associated with muscarinic receptors, the ether-a-go-go (ERG) channels that play a role in cardiac action potential repolarization (Schwarz, J. R. and Bauer, C. K., 2004), two calcium-dependent families (Sah, P. and Faber, E. S., 2002; Stocker, M., 2004), and a host of smaller two pore channels (O'Connell, A. D. *et al.*, 2002). In addition, cellular excitability is regulated by hyperpolarization-activated currents (HCN) (Robinson, R. B. and Siegelbaum, S. A., 2003). Each of these sets of channels performs different functions in regulating the excitability of neurons, and each exhibits a selective pattern of cellular expression in the nervous system. This review will focus on the Kv family; however, the HCN currents will also be discussed. Indeed, the principal regulation of electrical excitability in the brain seems to depend on the Kv, HCN, and K(Ca) currents, which together form the major voltage-dependent K^+ conductances in the cell membrane. The next best-studied group of channels, the calcium-activated potassium channels, are also important in some auditory neurons for regulating spike frequency and firing rate accommodation.

For the other classes of channels, much less is known about their distribution in the central auditory system or their contribution to electrical excitability. In particular, KCNQ4 channels have a very interesting pattern of expression in brainstem auditory nuclei, being prominent in the anterior ventral cochlear nucleus (AVCN), and ventral nucleus of the lateral lemniscus (Kharkovets, T. *et al.*, 2000). The pattern of expression is limited to just a few brainstem nuclei (not all of which are auditory). So far, no currents attributable to these channels have been identified. Two other sets of channels are also known to be expressed at high levels in some neurons of the auditory brainstem. Two-pore potassium channels are found throughout the nervous system, and some show high levels of expression in specific auditory brainstem nuclei (Karschin, C. *et al.*, 2001; Pal, B. *et al.*, 2005; Chen, W. C. and Davis, R. L., 2006; Holt, A. G. *et al.*, 2006). The TASK-5 channel is specifically highly expressed in cochlear nucleus and some nuclei of the superior olivary complex, but is notably not expressed in the medial nucleus of trapezoid body (MNTB) (Karschin, C. *et al.*, 2001). Potassium-dependent sodium channels, Slick and Slack (Bhattacharjee, A. and Kaczmarek, L. K., 2005) are also found widely, but have a particular pattern of expression in the auditory system. Slack has been localized to the calyces of Held in the MNTB (Bhattacharjee, A. *et al.*, 2002), while Slick is found in the VCN, lateral superior olive (LSO), and MNTB (Bhattacharjee, A. *et al.*, 2005). It is likely that these channels play an important role in regulating repetitive firing. While these and other channels are likely very important for some aspects of neural processing, and in setting the membrane potential, they are in need of further experimental analysis. This requires pharmacological and genetic tools that allow specific analysis of their contribution to the physiological functions of neurons.

3.32.3.1 The Kv Family

Voltage-gated potassium channels consist of tetrameric assemblies of proteins with six transmembrane domains, with a pore loop located between the fifth and sixth transmembrane spans. The specific assembly of the channel subunits is thought to be governed by C-terminal protein interactions such that all of the subunits of a given channel must belong to a single family. Thus, while there are specific rules regarding assembly, the number of different combinations of channel assemblies that can be produced is potentially quite large.

Several Kv genes are known to have splice variants (Kv1.5, Kv3.1, Kv3.2, Kv3.3, Kv3.4, and Kv4.3). However, there is no evidence for posttranslational editing of these channels in mammals. At least for Kv1, glycosylation can alter channel function (Thornhill, W. *et al.*, 1996). In addition, the biophysical behavior of the channels can vary considerably, even within a family, giving a wide range of potential channel function according to the rules of assembly. The details of channel assembly are not well understood, but are known to depend on both targeting motifs in the

protein that regulate channel trafficking to the membrane, and specific interactions among subunits at the level of the endoplasmic reticulum (Heusser, K. and Schwappach, B., 2005). In addition, auxiliary subunits (β subunits) have been shown to act as chaperones, and influence the targeting and assembly of the channels, as well as gating in assembled channels.

Ultimately, the pore-conducting portion of the Kv channels (referred to as the α subunits) are associated with β subunits in a 1:1 α–β stoichiometry. The β subunits play an important modulatory role in channel function, sometimes in conjunction with channel interacting proteins. Furthermore, the localization of Kv channels can be regulated by motifs that can target the channels to postsynaptic densities. Channel localization in the membrane is not random, but is, at least for some channels, quite focal. For example, Kv4.2 has been found to be targeted to postsynaptic densities in preoptic neurons (Alonso, G. and Widmer, H., 1997). This allows the channels to interact with other proteins, and may also facilitate local modulation by short-range messengers.

Because specific families of Kv channels have particular properties, it is useful to briefly review the families and the properties of the channels as expressed as homomers in heterologous systems. Such a description is useful in considering the potential functional contribution of the channels in auditory neurons.

3.32.3.1.1 The Kv1 family

The Kv1 family of channels is homologous to the Drosophila *shaker* family. There are currently seven genes that are known to be associated with this family, and their functional conductance and kinetics in heterologous expression systems is somewhat diverse. All of these have been detected in at least some regions of the brain, although Kv1.7 is not highly expressed (Kalman, K. *et al.*, 1998). Kv1.1 and Kv1.2 channels are found principally in axons, terminals (such as cerebellar basket cells) and cell somata, although Kv1.2 can also be found in dendrites (Sheng, M. *et al.*, 1994). In the axon, they are localized in a juxtaparanodal position (Rasband, M. N. and Trimmer, J. S., 2001; Rasband, M. N., 2004). These channels play the role of a delayed rectifier, where they repolarize the axonal action potential. Kv1.1 and Kv1.2 are also highly expressed in the auditory brainstem, as will be discussed in detail below. Kv1.4 channels are also found principally in axons and axon terminals (Sheng, M. *et al.*, 1992), and form an inactivating current that is sensitive to tetraethylammonium (TEA) and 4-aminopyridine (4-AP) (however, a unique localization has been reported in the auditory system, as discussed below). Kv1.4 gating is strongly accelerated by β subunit association (Castellino, R. C. *et al.*, 1995). While Kv1.4 contributes to some A currents (inactivating or transient potassium currents) in brain, other channels, such as Kv3.4, Kv4.2, and Kv4.3 can also be responsible for these currents (see below). Simply taking into account the seven members of the Kv1 α family and their tetrameric assembly, and ignoring issues related to β subunits or other proteins, or assembly order (adjacency), it is obvious that there exists the potential for a large number of different subunit combinations. In practice, however, any given cell seems to express only a subset of the family, and so the potential heteromultimeric composition of membrane channels is far more limited. In brain, immunoprecipitation experiments have shown that heteromeric combinations of Kv1.1–Kv1.2, Kv1.1–Kv1.4, Kv1.1–Kv1.2–Kv1.6, and homomeric Kv1.2 predominate (Wang, H. *et al.*, 1999).

3.32.3.1.2 The Kv2 family

The Kv2 family of channels is homologous to the Drosophila *shab* family. There are two known members of this family, and both are widely expressed in brain. Kv2 channels are high-voltage-activated, TEA- and 4-AP-sensitive delayed rectifiers (Shi, G. *et al.*, 1994). Kv2 channels have not been extensively studied in the auditory system, although they are reported to be expressed in the cochlear nucleus (Fitzakerley, J. L. and Quale, M., 2005) and inferior colliculus (Hwang, P. M. *et al.*, 1993; Richardson, F. C. and Kaczmarek, L. K., 2000).

3.32.3.1.3 The Kv3 family

The Kv3 family of channels is homologous to the Drosophila *shaw* family. There are four known members of the family, and one member, Kv3.1 can exist as one of two splice variants, known as Kv3.1*a* and and Kv3.1*b* (Luneau, C. J. *et al.*, 1991). While Kv3.1 is especially found in the forebrain in gamma-aminobutyric acid (GABA)ergic interneurons, it is highly expressed in auditory brainstem neurons that are both glutamergic and glycinergic (Perney, T. M. *et al.*, 1992; Perney, T. M. and Kaczmarek, L. K., 1997), and thus is of significant interest in auditory processing. Kv3.1 channels form high-threshold delayed rectifiers, with activation near −10 mV and incomplete slow inactivation. Kv3.2 channels are also delayed rectifiers, and are expressed in many cells, including in the auditory brainstem (Weiser, M. *et al.*,

1994). Kv3.3 and Kv3.4, in contrast, show a relatively deep, slow inactivation.

3.32.3.1.4 The Kv4 family

The Kv4 family of channels is homologous to the Drosophila *shal* family. There are three known members of the family, and one member, Kv4.3 can exist in multiple splice variants (Ohya, S. *et al.*, 1997). Kv4.1 is not expressed in the brain, but Kv4.2 and Kv4.3 are expressed in throughout the neural axis, but in specific populations of neurons (Serodio, P. and Rudy, B., 1998). Due to a particular targeting motif (Rivera, J. F. *et al.*, 2003), these channels are largely found in dendrites, and not in axons or synaptic terminals (Sheng, M. *et al.*, 1992). The channels are all rapidly and nearly completely inactivating, and their gating is subject to modulation by a number of factors, including arachidonic acid (Villarroel, A. and Schwartz, T. L., 1996) and phosphorylation by various kinases (Yuan, L. L. *et al.*, 2002; Varga, A. W. *et al.*, 2004). A particularly important set of regulatory proteins that interact with the Kv4 family of channels are the the KChip proteins (An, W. F. *et al.*, 2000). These proteins confer a calcium sensitivity, as well as modulate activation and inactivation voltage dependence and gating kinetics. A surprisingly linear relationship between Kv4 family mRNA (including Kv4.2, Kv4.3, and *shal*) and the rapidly inactivating transient potassium current has been demonstrated in several cell types (Baro, D. J. *et al.*, 1997; Tkatch, T. *et al.*, 2000; Liss, B. *et al.*, 2001).

3.32.3.1.5 Kv5–Kv9

These are all accessory proteins that do not, on their own, form ion channels, but which can associate with other Kv channels (Coetzee, W. A. *et al.*, 1999). Their roles are less well defined, and their presence in auditory neurons has not been extensively explored. Kv9.1, which is present in the inferior colliculus, has been shown to modify Kv2.1 gating, so that cells may be able to fire more rapidly or entrain better (Richardson, F. C. and Kaczmarek, L. K., 2000).

3.32.4 Channel Specialization and Biophysical Characterization of the Channels in the Vertebrate Auditory Cental Nervous System

Since the initial work of Oertel D. (1983) it has been evident that neurons in the auditory brainstem could be differentiated by their intrinsic firing responses to rectangular current pulses. For many cell types, the intrinsic firing responses can be shown to be related or to underlie the acoustically evoked spike patterns, although this is not always a trivial relationship. The intrinsic firing patterns are regulated by three principal features of cells. First, and often most important, is the cell-specific selection of specific ion channels complexes; for example, which sets of Kv α and β subunits, in conjunction with any auxillary proteins such as the KChips, are expressed. Second, the firing patterns depend on the location and density of the channel proteins, which is a function of channel targeting. Finally, and to a lesser extent, the shape of the dendritic tree affects the patterns of current flow through the cell (Mainen, Z. F. and Sejnowski, T. J., 1996), so dendritic structure also influences the cell voltage at the spike initiation site, which is usually in the initial segment (Colbert, C. M. and Johnston, D., 1996; Stuart, G. *et al.*, 1997; Colbert, C. M. and Pan, E., 2002).

In this section, we will review the patterns of ion channel expression in a number of nuclei and cell types of the auditory brainstem. There are a number of caveats on the interpretation of data in the literature that should be recognized before we delve into this section. The first is that expression of channels in a single cell population can show differences among species; a prime example of this is in heart, where atrial I_{to} (the transient outward current) is mediated by Kv4.2 channels in rat (Bou-Abboud, E. and Nerbonne, J. M., 1999), but is mediated by heteromultimers of Kv4.2 and Kv4.3 channels in mice (Guo, W. *et al.*, 2002). While the intrinsic physiology of most auditory neurons seems comparable across species, the underlying channel composition may vary. Second, channel expression is regulated during development, sometimes in a nonmonotonic manner, and is not complete (in rodents) until late adolescence (e.g., ~30 days of age in rats and mice). Thus, the ages of animals used for physiological analyses is an important variable. Third, the technical limitations of message and protein localization studies should always be carefully considered. The presence of a particular mRNA in a cell does reveal the cellular localization of the presumptive protein(s); in most cases the level of mRNA is also not necessarily correlated with the level of functional protein in the membrane (an exception is for Kv4.2, as discussed above). Proteins can be localized by immunocytochemistry, but the limits on the specificity of the available antibodies suggest some caution is warranted in interpreting these results, and localization of proteins in relevant membrane compartments can be difficult to demonstrate, particularly in the auditory brainstem where the nuclei often have

a complex neuropil, multiple fiber systems, and nonlaminar organization. Physiological studies directly demonstrate the existence of different kinds of channels in specific cell types, but require the use of pharmacological or genetic manipulations to identify specific types of channels, and frequently cannot assay protein function in dendritic or axonal processes.

3.32.4.1 Spiral Ganglion Cells

A recent discovery was the identification of a diversity of discharge characteristics in spiral ganglion cells (SGCs). SGCs are endowed with rapidly inactivating sodium channels, a low-voltage-activating potassium current, a transient potassium current, hyperpolarization-activated currents, and calcium channels (Yamaguchi, K. and Ohmori, H., 1990; Sheppard, D. N. *et al.*, 1992; Valverde, M. A. *et al.*, 1992; Santos-Sacchi, J., 1993; Garcia-Diaz, J. F., 1999; Adamson, C. L. *et al.*, 2002b; Mo, Z. L. *et al.*, 2002). Studies using cultured neurons showed that the transient current and the low-voltage-activating current could vary along the length of the modiolus (Adamson, C. L. *et al.*, 2002a; 2002b). In response to current pulses, high-frequency (cochlear base) cells showed shorter latency action potentials and phasic firing, and in older cultures, narrower action potentials, whereas low-frequency (cochlear apex) cells more frequently showed repetitive firing and longer latency action potentials to current pulses. These physiological features correlated with a higher expression (as assayed by a semiquantitive immunocytochemical method) of Kv1.1 and Kv3.1 in the base, whereas Kv4.2 was slightly more highly expressed in the apex. These results suggest that there may be differential processing of temporal information along the length of the cochlea. Given that the representation of the temporal structure of sound in SGCs varies with cochlear location (e.g., see Louage, D. H. *et al.*, 2004), perhaps this is not surprising. Nonetheless, the role of these channel configurations in temporal coding in the spiral ganglion cell (SGC) is still not well understood, although some clues may be derived from work in the central auditory system, as discussed next.

3.32.4.2 Ventral Cochear Nucleus Bushy Cells

3.32.4.2.1 The low voltage-activated potassium conductance

Since the pioneering studies of Oertel (Oertel, D., 1983; Wu, S. H. and Oertel, D., 1984) in mouse cochlear nucleus brain slices, it has been evident that bushy neurons have specialized electrical excitability. The principal signature of these cells when recorded in current clamp is a strong outward rectification that opposes depolarizing currents, and limits the cell membrane potential to not move too far above the resting potential (Figure 1(b)). This rectification was associated with a significant increase in membrane conductance. Initial voltage clamp studies from acutely isolated guinea-pig VCN neurons showed that the rectification could be explained by the presence of a strong, low-voltage-activated (often called low-threshold, or I_{LTK}) potassium conductance (Manis, P. and Marx, S., 1991) that was partially blocked by 4-AP, but was not blocked by TEA. The cardinal characteristics of this conductance are that it is partially activated at rest, it shows modest, voltage-dependent inactivation, and that activation from potentials near rest (−60 mV) has a monoexponential time course. Subsequently, depolarization from more negative potentials revealed a sigmoidal activation time course (Rothman, J. S. and Manis, P. B., 2003a), consistent with cooperative gating of four subunits during channel opening. Estimates of the maximal conductance in isolated cells revealed a mean value of about 200 nS for a 12 pF cell, but the conductance varied over a wide range. In addition, the voltage at which the conductance yielded a current of 0.1 nA also showed wide variability (Rothman, J. S. and Manis, P.B., 2003c), suggesting that the voltage dependence of activation, and therefore the availability of the conductance to participate in synaptic integration, is not constant among VCN cells.

In both rat and guinea-pig, I_{LTK} has been shown to be sensitive to the mamba snake toxin, dendrotoxin (DTX)-I (Dodson, P. D. *et al.*, 2003; Rothman, J. S. and Manis, P.B., 2003a; 2003c; Pal, B. *et al.*, 2004), which blocks Kv1.1- and Kv1.2-containing channels (Hopkins, W. F., 1998). The low-voltage-activated conductance has been reported to be blocked in a subset of bushy cells by tityustoxin-Kα, which blocks only Kv1.2-containing channels (Dodson, P. D. *et al.*, 2003), suggesting that either bushy cells are heterogeneous in their channel expression, or that not all cells express Kv1.2-containing channels within the spatial reach of the voltage clamp, for example, on or near the soma. A very similar conductance is present in neurons of the chicken nucleus magnocellularis that are homologous to the mammalian bushy cells (Reyes, A. D. *et al.*, 1994; Zhang, S. and Trussell, L. O., 1994; Rathouz, M. and Trussell, L., 1998;

Fukui, I. and Ohmori, H., 2003; 2004; Lu, Y. *et al.*, 2004). The similarities of the conductance extend to the voltage dependence, apparent density (as estimated from currents recorded in somatic voltage clamp), sensitivity to 4-AP and DTXs, and the presence of partial inactivation with prolonged steps.

The pharmacological profile of block by 4-AP and DTXs suggests that the low-voltage-activated conductance in bushy neurons is mediated by channel complexes containing both Kv1.1 and Kv1.2. Three additional lines of evidence support this conclusion. First, the mRNA for both channel subunits is widely expressed in mouse VCN (Grigg, J. J. *et al.*, 2000), although colocalization of multiple messages has not been attempted. In addition, while it is clear that the major populations of bushy and octopus neurons have the message (see below), it is less clear whether the multipolar cell classes express the message. Neither immunocytochemical nor *in situ* hybridization studies have attempted to positively identify cell types using classical criteria. Second, preliminary single-cell PCR studies (Sonnenburg, R. *et al.*, 2002) have shown coexpression of Kv1.1 and Kv1.2 message in individual bushy neurons in the rat VCN, but surprisingly, these channels were also found in a subset of regular firing (stellate) neurons, suggesting that their expression is not limited to cells expressing a low-voltage-activated conductance. Third, positive immunostaining for Kv1.1 and Kv1.2 is widely apparent in the VCN, including in the bushy cell populations (Dodson, P. D. *et al.*, 2003; Caminos, E. *et al.*, 2005; Pal, B. *et al.*, 2005; Bortone, D. S. *et al.*, 2006), as might be expected from their expression of DTX-sensitive low-voltage-activated K^+ currents. However, it remains unclear as to whether the channels are coexpressed in individual cells, and if they are, whether the functional channels are actually coassembled in the membrane. In addition, a recent report of immunostaining for Kv1.3 and Kv1.6 in the rat VCN (Pal, B. *et al.*, 2005) raises additional questions about the composition of channel complexes. Thus, while Kv1.1 and Kv1.2 seem likely to be key components of the conductance, the pharmacological data, together with immunocytochemical observations and the variations in the activation threshold of the potassium conductance (Rothman, J. S. and Manis, P. B., 2003c), also support the idea that there is heterogeneity across cells in the function and molecular composition of the low-voltage-activated current in the VCN.

Hallows J. L. and Tempel B. L. (1998) examined the developmental profile of Kv1.1 message in whole brain. The mRNA for Kv1.1 showed a spike during embryonic development, and did not increase again until between P12 and P15, with levels remaining stable after P15. Using real-time PCR, message in cochlear nucleus increases from P3 until P28 (Manis, P. *et al.*, 2002; Bortone, D. S. *et al.*, 2006). The reason for the later maturation compared to whole brain is not clear; however, the results suggest regional differences in the development of potassium channels. Mechanisms related to the control of expression of these channels are not well understood. Transcriptional control of Kv1 channels has only partially been elucidated (Wymore, R. S. *et al.*, 1996; Jang, G. M. *et al.*, 2004).

3.32.4.2.2 The high voltage-activated potassium conductance

In the initial studies of guinea-pig VCN neurons (Manis, P. and Marx, S., 1991), a second potassium conductance was characterized. This conductance activated at more positive voltages, and was blocked both by TEA and 4-AP. It also showed slower activation kinetics, and only a small amount of inactivation. A similar conductance, which is also insensitive to DTXs, but which can be blocked by low concentrations of 4-AP, has been seen in all subsequent studies in both mammals and avians (Reyes, A. D. *et al.*, 1994; Rathouz, M. and Trussell, L., 1998; Rothman, J. S. and Manis, P. B., 2003a; 2003c; Pal, B. *et al.*, 2004). This high-threshold conductance (I_{HT}) is not as strong as the low-voltage-activated conductance, activates slightly more slowly, and appears to have two kinetically distinct activation components (Rothman, J. S. and Manis, P.B., 2003a). There is also evidence for heterogeneity in deactivation time constants (Manis, P. *et al.*, 1996) suggesting that there may be multiple channels contributing to the conductance. This conductance is thought to be mediated by channels containing Kv3.1, as this subunit is highly expressed in the auditory brainstem, and particularly in bushy neurons of the cochlear nucleus (Perney, T. M. *et al.*, 1992; Perney, T. M. and Kaczmarek, L. K., 1997; Grigg, J. J. *et al.*, 2000). The properties and pharmacology of the conductance are generally consistent with those of heterologously expressed channels.

In whole brain (Perney, T. M. *et al.*, 1992), in the cochlear nucleus (Bortone, D. S. *et al.*, 2006), and in the inferior colliculus (Liu, S. J. and Kaczmarek, L. K., 1998a; Liu, S. Q and Kaczmarek, L. K., 1998b), Kv3.1 mRNA increases through development. Kv3.1 transcription is regulated by a cAMP response element (Gan, L. *et al.*, 1996), and indirectly by electrical

activity (Liu, S. J. and Kaczmarek, L. K., 1998a; Liu, S. Q and Kaczmarek, L. K., 1998b; von Hehn, C. A. *et al.*, 2004). In DBA2/J mice, which undergo an age-related high-frequency hearing loss (Zheng, Q. Y. *et al.*, 1999), the expression pattern of Kv3.1 is disrupted in high-frequency regions of the VCN, suggesting an activity-dependent regulation (von Hehn, C. A. *et al.*, 2004).

3.32.4.2.3 The transient potassium conductances

While rapidly inactivating potassium currents (I_A) are not a feature of bushy neurons in adult guinea-pig, even when conditions were optimized for their detection (Manis, P. and Marx, S., 1991; Rothman, J. S. and Manis, P. B., 2003a), they have been reported in embryonic chickens (Rathouz, M. and Trussell, L., 1998), and early postnatal rats and gerbils (Schwarz, D. W. and Puil, E., 1997; Pal, B. *et al.*, 2004). Consistent with their possible presence in bushy cells in rats and mice, Kv4.2 (but not Kv4.1 or Kv4.3) has been detected immunocytochemically in the VCN of P4-10 rats (Pal, B. *et al.*, 2005), and by *in situ* hybridization in the juvenile mouse cochlear nucleus (Fitzakerley, J. L. *et al.*, 2000). There are several possible explanations for the different expression patterns, including age or species differences.

3.32.4.2.4 The hyperpolarization-activated conductances

VCN bushy neurons have a strong hyperpolarization-activated conductance (I_H), which has been partially characterized (Rusznak, Z. *et al.*, 1996). This conductance is effectively blocked by cesium, but not barium, shows half-activation at −95 mV, and reverses at −33 mV. It is not prominent in isolated cells, presumably because the enzymatic treatment inactivates the channels. HCN1 and HCN2 are both strongly expressed by VCN bushy neurons (Koch, U. *et al.*, 2004). The specific roles of HCN channels in the VCN are not known, although it is likely that they contribute to setting the membrane potential and thereby regulating the level of activation of I_{LTK}. As such, they may be served as a transducer of modulatory influences, as suggested in the MNTB (Banks, M. I. and Smith, P. H., 1992).

3.32.4.3 Ventral Cochlear Nucleus Stellate/Multipolar Cells

Stellate neurons are not normally associated with the processing of high-frequency auditory events. They are characterized by having longer time constants as measured with small hyperpolarizing current pulses from rest, typically between 3 and 10 ms (White, J. A. *et al.*, 1994; Francis, H. W. and Manis, P. B., 2000), and regular firing (Figure 1(a)) upon depolarization (Oertel, D., 1983; Wu, S. H. and Oertel, D., 1984). Estimates of electrotonic structure suggest that these cells will significantly filter excitatory postsynaptic potentials (EPSPs) impinging on their dendrites (White, J. A. *et al.*, 1994). Voltage clamp studies show that stellate cells lack the low-voltage-activated conductance of bushy cells. However, they express a high-threshold K^+ current that is kinetically and pharmacologically indistinguishable from that in bushy neurons (Manis, P. and Marx, S., 1991; Rothman, J. S. and Manis, P.B., 2003a; 2003c).

Stellate cells can be distinguished along two different dimensions with respect to ion channel expression. The first is that the I_H currents show slower activation kinetics in T-stellate cells than in D-stellate cells (Fujino, K. and Oertel, D., 2001; Rodrigues, A. R. and Oertel, D., 2006). The second is that some cells (not classified as T- or D-stellate cells) exhibit a 4-AP-sensitive transient potassium current, whereas others do not (Manis, P. *et al.*, 1996; Rothman, J. S. and Manis, P. B., 2003c). The significance of these differences is not known.

3.32.4.4 Octopus Cells

Octopus cells are arguably one of the most interesting and perhaps extreme neurons in the cochlear nucleus. These cells have long dendrites that extend across the fascicles of ANFs in the posterior VCN, and so receive input from a broad region of the cochlea. In spite of this massive input, the cells fire only a single action potential at the beginning of tone bursts, with excellent precision (standard deviation 20–50 μs). They have also been reported to entrain, cycle by cycle, to tonal stimuli up to 1 kHz (Rhode, W. S. and Smith, P. H., 1986; Rhode, W. S. and Kettner, R. E., 1987). As such, they may also be among the most rapidly firing neurons in the brain.

Recordings from octopus cells show that they have very strong rectification around the resting potential, small action potentials at the soma (typically 10–20 mV), a low-input resistance of about 2.5 MΩ, and a short membrane time constant of 0.21 ms (Golding, N. L. *et al.*, 1999), which is close to the limit that can be measured with whole-cell recordings. These general properties arise from high levels of expression of both the low-voltage-activated

potassium current and I_H. I_{LTK} is similar to the current in bushy neurons. It is active at the resting potential, shows some inactivation over time in voltage clamp, and is variably blocked by DTX-I, DTX-K, α-DTX, δ-DTX, and tityustoxin (Bal, R. and Oertel, D., 2001). The selectivity of these toxins indicates that I_{LTK} in octopus cells includes Kv1.1, Kv1.2, and possibly Kv1.4 channels. The variability of block among cells by different toxins suggests that the pattern of channel expression varies among cells. The estimate of the total conductance in octopus cells is on the order of 500 nS, or roughly 2.5 times the conductance in bushy cells. While the low-voltage-activated current is so large that it is difficult to analyze across a wide voltage range under voltage clamp with patch pipettes, these estimates were obtained by partially blocking the current with α-DTX. However, it is quite possible that the conductance is even larger than this.

Octopus cells have DTX-resistant, TEA-sensitive current that activates at more positive voltages than the DTX-sensitive current (Bal, R. and Oertel, D., 2001). This I_{HT} is weak relative to the low-voltage-activated current, but is still substantial, with an estimated maximal conductance of about 115 nS (Bal, R. and Oertel, D., 2001). While there is a low level of Kv3.1 immunoreactivity in the octopus cell area (Perney, T. M. and Kaczmarek, L. K., 1997), Kv3.3 mRNA is clearly present in the octopus cells (Li, W. *et al.*, 2001) and could be the substrate for the I_{HT} current.

The I_H current in octopus cells has been more extensively characterized than in bushy cells (Bal, R. and Oertel, D., 2000), and it appears that I_H is much larger in these cells than any other cells in the brain. Similar to the current in bushy cells, it is blocked by extracellular cesium and ZD7288, but not by barium. The conductance is half-activated at −66 mV, and has a mixed cation (sodium and potassium) selectivity with a reversal potential of −38 mV. Perhaps most remarkable, the conductance is estimated to be 41% activated at rest, contributing about 62 nS of conductance to the cell membrane. Kinetics of activation showed two components at 44 and 180 ms, at −77 mV. This suggests a rapidly activating I_H. In terms of subunit composition, HCN1 is particularly clearly expressed in immunocytochemistry in octopus cells, whereas HCN2 is less clearly expressed in these cells, although it is found elsewhere (Koch, U. *et al.*, 2004). This conductance approximately balances the currents through the low-voltage-activated K channel at rest (Bal, R. and Oertel, D., 2001), so that subtle variations in voltage dependence or modulation by second messengers will affect the activation of the low-voltage-activated current (Cai, Y. *et al.*, 1997).

3.32.4.5 Dorsal Cochlear Nuclear Pyramidal Cells

DCN pyramidal cells can exhibit multiple discharge patterns in response to tones (Godfrey, D. A. *et al.*, 1975; Rhode, W. S. *et al.*, 1983) and in response to intracellular current steps (Manis, P. B., 1990). These discharge patterns (Figure 1(c)) are regulated by an interaction between transient potassium currents with different rates of inactivation (Kanold, P. O. and Manis, P. B., 1999) and subthreshold sodium conductances (Manis, P. B. *et al.*, 2003). One of the transient K^+ currents inactivates with a time constant between 11 and 20 ms, and shows a variable half-inactivation voltage. The other transient current inactivates with a time constant of about 200 ms, and activates at a more positive voltage. Following a hyperpolarization, depolarization activates the rapidly inactivating conductance, which can keep the membrane potential from reaching spike threshold. However, as this conductance inactivates, the membrane depolarizes. The depolarization is slowed by the slowly inactivating conductance, which continues to activate during the slow depolarization. The insensitivity of the rapidly inactivating current to 4-AP and TEA suggests that it is mediated by Kv4 family channels, of which Kv4.2 is most highly expressed in the DCN (Serodio, P. and Rudy, B., 1998; Fitzakerley, J. L. *et al.*, 2000). The slowly inactivating channel is sensitive to 4-AP and TEA, and may be mediated by a Kv3 or Kv1 family channel. A persistent (or slowly activating, relatively noninactivating) sodium current also provides the depolarizing drive necessary to produce long latency spikes in these cells. While pyramidal cells do not encode temporal information by phase locking, except at low frequencies, they may be able to encode a different kind of temporal information. Modeling based on the experimental measurements and range of kinetic parameters suggests that the relative timing of inhibitory and excitatory inputs can be reported by a small population of cells in which the half-inactivation (or magnitude) of the rapidly inactivating current varies (Kanold, P. O. and Manis, P. B., 2005). Thus, the cells may help analyze information about the relative timing of auditory and nonauditory events.

3.32.4.6 Superior Olivary Complex

3.32.4.6.1 Medial nucleus of trapezoid body

Neurons of the MNTB are often compared to VCN bushy cells, because they share several features, including a strong, multisite, afferent synapse (the calyx of Held), and they have firing properties and voltage-dependent conductances that resemble those of bushy cells (Banks, M. I. and Smith, P. H., 1992; Forsythe, I. D. and Barnes-Davies,M., 1993; Brew, H. M. and Forsythe, I. D., 1995). However, there are notable differences also. For example, MNTB neurons rarely fire more than one action potential when depolarized (Banks, M. I. and Smith, P. H., 1992; Forsythe, I. D. and Barnes-Davies, M., 1993), whereas VCN bushy neurons usually fire one, but up to three action potentials to a depolarizing current step. However, in mice at 22–25 °C, multiple action potentials have been reported (Brew, H. M. *et al.*, 2003). Second, the action potential height, as measured in brain slices at 33–34 °C, is slightly larger in MNTB neurons (~50 mV; Banks, M. I. and Smith, P. H., 1992) than in bushy neurons, where it averages 30–40 mV (Oertel, D., 1983; Francis, H. W. and Manis, P.B., 2000).

As with the VCN bushy cells, MNTB principal neurons possess a low-voltage-activated, potassium current and a high-threshold delayed rectifier. The low-voltage-activated current is reduced by 4-AP, and is blocked by DTX-I (Banks, M. I. and Smith, P. H., 1992; Forsythe, I. D. and Barnes-Davies, M., 1993; Brew, H. M. and Forsythe, I. D., 1995; Dodson, P. D. *et al.*, 2002). A detailed pharmacological dissection of the currents in rats (Dodson, P. D. *et al.*, 2002) showed that block by DTX-I is relatively complete, implicating Kv1 channels in the generation of the conductance. The current is also largely blocked by DTX-K, which is selective for Kv1.1-containing channels. Tityustoxin-Kα blocks about half of the low-voltage-activated current, suggesting that only a subpopulation of the channels contain Kv1.2. Noxiustoxin, which also blocks Kv1.2, as well as Kv1.3- and Kv 1.7-containing channels, also blocked about half of the current. Taken together, these data suggest that the low-voltage-activated current in MNTB neurons may be composed of a roughly equal mixture of channels containing Kv1.1 and Kv1.2, or Kv1.1 without Kv1.2, but possibly Kv1.6 (Dodson, P. D. *et al.*, 2002). The presence of other channels is not clear, although a compound that blocks Kv1.3 channels did not affect the current. Consistent with these data, immunostaining revealed Kv1.1, Kv1.2, Kv1.6, but not Kv1.4 or Kv1.5, in the MNTB (Dodson, P. D. *et al.*, 2002), and the high levels of Kv1.1 and Kv1.2 mRNA present in the MNTB by *in situ* hybridization (Grigg, J. J. *et al.*, 2000).

Further evidence regarding the contribution of Kv1.1 to the low-voltage-activated currents in the MNTB was obtained in a study of Kv1.1 knockout mice by Brew H. M. *et al.* (2003). In these mice, the low-voltage-activated current, as measured near threshold, was reduced in the knockouts, but not eliminated. DTX-I blocked about half of the current in both normal and knockout mice; the remaining current activated with a different time course and was not identified (although as it was not blocked by DTX-I, it appears to not be generated by Kv1 family channels). Nonetheless, in the knockouts, there was a substantial increase in the number of action potentials evoked during a rectangular current pulse. These results support not only Kv1.1 in MNTB neurons, but also show that in the absence of Kv1.1, Kv1.2, and/or Kv1.6 remain and generate a low-voltage-activated current. In this study, a small transient, rapidly inactivating current was also identified, although it appeared to be largely inactivated at rest.

The most detailed studies of the high-threshold current have been done on MNTB neurons. Both Kv3.1 and Kv3.3 are present in these cells by immunocytochemistry (Perney, T. M. *et al.*, 1992; Li, W. *et al.*, 2001) and by *in situ* hybridization (Wang, L. Y. *et al.*, 1998). A comparison of I_{HT} in MNTB neurons and Kv3.1 homomultimers in CHO cells (Wang, L. Y. *et al.*, 1998) shows that the currents are very similar. The similarity extends to the voltage dependence of the activation kinetics, and the magnitude of sensitivity to block by TEA. In these cells, the Kv3.1-like current contributes to action potential repolarization, and allows the cells to fire rapidly in response to trains of depolarizing current pulses (Wang, L. Y. *et al.*, 1998).

3.32.4.7 Medial Superior Olive

In terms of temporal precision, the neurons of the medial superior olive (MSO) have one of the most daunting tasks. These cells are responsible for comparing information from the two ears and generating a representation that the rest of the nervous system can use to make judgments about differences in sound arrival times that are on the order of 10 µs. The ion channels of MSO neurons are central to analyzing synaptic events with this level of temporal precision. It is not surprising then, that their discharge patterns

under current clamp is similar to that of bushy or MNTB neurons (Smith, P. H., 1995) (also, similar excitability is seen in the avian homolog, n. laminaris; Reyes, A. D. *et al.*, 1996). The conductance underlying this behavior was found first to be blocked by 4-AP (Smith, P. H., 1995), and subsequently by DTX-I and DTX-K (Svirskis, G., 2002; Scott, L. L. *et al.*, 2005), again implicating Kv1.1 and/or Kv1.2 channels in its generation. Similar observations have been made in n. laminaris (Kuba, H. *et al.*, 2002; 2005). While the general features of the conductances have been examined, so far no detailed kinetic analyses of the currents in these cells have been reported. Immunocytochemical analyses in both the MSO and n. laminaris support the presence of Kv1.1 and Kv1.2 channels. These cells also possess a high-threshold conductance that is revealed in the presence of DTX or 4-AP. Immunocytochemical analyses and *in situ* studies suggest that Kv3.3, rather than Kv3.1, may be responsible for this conductance in mammalian MSO (Li, W. *et al.*, 2001), although Kv3.1 is present in n. laminaris (Parameshwaran, S. *et al.*, 2001).

The operation of MSO and n. laminaris neurons as coincidence detectors in the traditional model (Jeffress, L. A., 1948) requires that the cells have a narrow temporal integration window. The presence of the low-voltage-activated conductance allows these cells to function as coincidence detectors of subthreshold inputs (Reyes, A. D. *et al.*, 1996; Kuba, H. *et al.*, 2005).

3.32.4.8 Other Auditory Structures

The conductances present in the principal nuclei involved in the processing of rapid timing information are recapitulated in other auditory brainstem nuclei, although in general less is known from a functional standpoint. Because, in general, these have not been investigated as extensively as the regions just discussed, they will be discussed as a group.

3.32.4.8.1 Superior olive

Nuclei that show high expression of Kv1.1 include scattered neurons in the ventral and lateral periolivary nuclei (Grigg, J. J. *et al.*, 2000; Rosenberger, M. H. *et al.*, 2003) and a few neurons in the LSO (Barnes-Davies, M. *et al.*, 2004); however, in general, the superior olive shows low levels of Kv1.2 (Grigg, J. J. *et al.*, 2000). HCN1 is highly visible in all nuclei of the SOC except the MNTB, whereas HCN2 is principally seen in the MNTB and the LSO (Koch, U. *et al.*, 2004). Kv3.1 is not highly expressed except in some cells of the superior paraolivary nucleus, whereas Kv3.3 appears to be widely expressed in all the principal nuclei and in surrounding periolivary cells (but see Grigg, J. J. *et al.*, 2000; Li, W. *et al.*, 2001). Most neurons of the superior olivary complex fire in a regular discharge pattern (Wu, S. H. and Kelly, J. B., 1991; Fujino, K. *et al.*, 1997; Adam, T. J. *et al.*, 1999; 2001; Barnes-Davies, M. *et al.*, 2004), although some neurons in the LSO (Barnes-Davies, M. *et al.*, 2004) and the lateral nucleus of the trapezoid body (Spirou, G. A. *et al.*, 1995) exhibit phasic responses and rectification.

3.32.4.8.2 Nuclei of the lateral lemniscus

Some, but not all, neurons of the ventral nucleus of the lateral lemniscus have phasic responses to current pulses (Wu, S. H., 1999) that are similar to those of VCN bushy neurons. Kv1.1 immunoreactivity is evident in this nucleus (Rosenberger, M. H. *et al.*, 2003), as is message for Kv3.1 and Kv3.3, and light immunostaining for Kv3.1 (Li, W. *et al.*, 2001). HCN1 and HCN2 are both found in the ventral nucleus also (Koch, U. *et al.*, 2004). Neurons in this nucleus can exhibit accurate onset timing in bats (Covey, E. and Casseday, J. H., 1991). The GABAergic neurons of the dorsal nucleus of the lateral lemniscus, in contrast, fire regular trains of action potentials (Wu, S. H. and Kelly, J. B., 1995). Kv3.1 and Kv3.3 are highly expressed as assayed by *in situ* hybridization (Li, W. *et al.*, 2001), and in bat in some neurons are lightly immunoreactive for Kv1.1 (Rosenberger, M. H. *et al.*, 2003).

3.32.4.8.3 Inferior colliculus

Neurons of the inferior colliculus can show a variety of sustained firing patterns to depolarization (Peruzzi, D. *et al.*, 2000; Sivaramakrishnan, S. and Oliver, D., 2001). However, a subset of cells show an onset response to current steps and an associated outward rectification (Wagner, T., 1994; Peruzzi, D. *et al.*, 2000) that is generated by a 4-AP-sensitive current (Sivaramakrishnan, S. and Oliver, D., 2001), and which allows the cells to follow higher rates of stimulation than other collicular neurons (Peruzzi, D. *et al.*, 2000). IC neurons express Kv3.1 and Kv3.3 at fairly high levels (Perney, T. M. *et al.*, 1992; Grigg, J. J. *et al.*, 2000; Li, W. *et al.*, 2001). Kv1.1 and Kv1.2 are also present (Grigg, J. J. *et al.*, 2000; Rosenberger, M. H. *et al.*, 2003), although some regional variation in expression patterns are evident. HCN1 and HCN2 are also both present (Koch, U. *et al.*, 2004).

There are hints that upper levels of the auditory system may have some specializations to improve temporal processing relative to neurons in nonauditory pathways. For example, action potentials of

thalamocortical recipient neurons in cat auditory cortex are narrower than those in similar neurons of the visual cortex (Smith, P. H. and Populin, L. C., 2001). In addition, GABAergic IPSPs have a faster time course in layer V neurons (Hefti, B. J. and Smith, P. H., 2003). Finally, at least during postnatal development, some auditory cortical neurons may have rectifying current–voltage relationships and phasic firing similar to the auditory brainstem neurons that convey timing information (Metherate, R. and Aramakis, V., 1999). Kv3.1 is highly expressed in auditory cortical interneuorns, apparently at higher levels than in surrounding regions (Li, W. *et al.*, 2001). The significance of these specializations is not known.

3.32.5 Summary of Channel Expression

As can be seen from the above review, there are several themes in the patterns of ion channel expression and discharge patterns in the auditory brainstem. Cells expressing low-voltage-activated potassium channels are present in circuits involved in processing timing information. These cells tend to fire a single action potential (or sometimes just a few action potentials) with step depolarization. Cells lacking this conductance are present in those auditory brainstem circuits that are not involved in processing precise timing information, and these cells tend to fire regular trains of action potentials. It is not clear to what extent these two motifs truly exist as canonical forms. Some evidence is consistent with the hypothesis that the expression of channels is in fact a continuum, with a graded variation of total conductance, and this may vary along to tonotopic axis, or even across tonotopic sheets of cells. The idea that there is a tonotopic distribution of conductances is supported by several lines of recent evidence, and is discussed later.

Because of the bifurcation of the cell voltage trajectory that results from the nonlinear interactions of the sodium and potassium channels over time, cells with similar qualitative but quantitatively different channel expression can show different firing patterns. For example, expression of the low-voltage-activated K^+ currents is not sufficient to make a cell fire phasically at all current levels. If a cell has relatively weak low-voltage-activated potassium conductance, it might fire phasically only for weak current injections that are just suprathreshold for an AP, but larger current injections could be sufficient to counter the outward current and push the cell into a repetitive firing mode (Rothman, J. S. and Manis, P. B., 2003b). Current clamp recordings in the VCN and MNTB have consistently shown (in mice, rats, and guinea-pigs, e.g., see Oertel, D., 1983; Francis, H. W. and Manis, P. B., 2000) that some cells fire with a type II phasic pattern of a single action potential for weak currents can generate a short, although not sustained, train of repetitive spikes for larger currents. Thus, the simple expression of channel transcripts is not sufficient for the elaboration of a particular discharge pattern; both the density and distribution of the channels in the membrane play a critical role. These two factors are difficult to measure accurately.

3.32.6 The Role of Low-Voltage-Activated K^+ Channels in Temporal Integration

The low-voltage-activated K^+ channels play several roles in the temporal integration of synaptic inputs in auditory neurons (Trussell, L. O., 1999). Each of these roles serves to enhance the ability of the cells to fire precisely timed action potentials in response to afferent activity. The first role is as a conductance shunt. Because it is generally found that the low-voltage-activated channels are partially conducting at rest, they participate in both setting the resting potential and in setting the membrane conductance (and therefore, time constant). Estimates of the fraction of channels open at rest in cochlear nucleus neurons vary from 10% to 15%, based on calculations using Boltzman fits to the voltage dependence of the conductance in mammals (Manis, P. and Marx, S., 1991; Bal, R. and Oertel, D., 2001; Rothman, J. S and Manis, P. B., 2003a), to about 30% in avian n. magnocellularis (Rathouz, M. and Trussell, L., 1998). The conductance contributed by the low-voltage-activated channels at rest then corresponds to 20–60 nS, which can be nearly as large as the resting conductance of the cell. This conductance may also be balanced by the conductance of I_H channels, which are of similar magnitude at rest in octopus cells (Bal, R. and Oertel, D., 2000). This is also on the same order of magnitude as the conductance contributed by single endbulb of held synapses in mouse VCN (a typical single auditory nerve fibre (ANF) input generating a 5 nA excitatory postsynaptic currents (EPSCs) at −60 mV in mouse VCN bushy cells (Wang, Y. and Manis, P. B., 2005) would correspond to 83 nS). Because the membrane time constant is short, the synaptic conductance can charge and discharge the

cell membrane very rapidly; thus the excitatory postsynaptic potential (EPSP) is not much longer than the duration of the synaptic conductance, and the conductances themselves are very brief (Trussell, L. O., 1999). In addition, this shunting effect limits the window for temporal summation of subthreshold EPSPs, so that close temporal coincidence of subthreshold events is necessary to reach threshold; this can enhance temporal precision by averaging inputs to the cell and may be responsible for the ability of some cells to show greater phase locking than their inputs (Rothman, J. and Young, E., 1996).

Second, the low-voltage-activated channel limits extra action potentials that might be produced by strong excitatory inputs (Brew, H. M. and Forsythe, I. D., 1995; Gittelman, J. X. and Tempel, B. L., 2006). This occurs because the conductance activates during action potentials, and so contributes to action potential repolarization (Rothman, J. S. and Manis, P. B., 2003b; Klug, A. and Trussell, L. O., 2006). Limiting extraneous action potentials in response to a cyclical input (click train or tones) would improve temporal signaling, especially when this signaling is compared to that of other neurons responding to the same temporal pattern of input, and is analyzed by higher-order neurons receiving convergent input. Suppression of multiple action potentials would also maximize the opportunity for action potentials to be phase locked to subsequent cycles of a tonal stimulus, and would reduce the refractory period by providing additional hyperpolarization between cycles. A similar role for these channels in the presynaptic terminal has been shown (Dodson, P. D. *et al.*, 2003). In this context, the high- and low-voltage-activated currents are likely to interact during periods of high synaptic drive to promote sustained and temporally precise high rate firing (Fernandez, F. R. *et al.*, 2005; Klug, A. and Trussell, L. O., 2006).

Third, the low-voltage-activated channels makes the cells more sensitive to rapidly changing events than to slowly changing events; in other words, they become sensitive to the slope of the EPSP, such that rapidly rising EPSPs have a much higher probability of bringing the cell to threshold than slowly rising events (Ferragamo, M. J. and Oertel, D., 2002; McGinley, M. J. and Oertel, D., 2006). The slope sensitivity arises in part because activating the low-voltage-activated conductance can raise spike threshold (Brew, H. M. *et al.*, 2003; see also Fukui, I. and Ohmori, H., 2004), and in part because slowly rising EPSPs will allow the low-voltage-activated conductance to turn on before the peak of the EPSP, which reduces the amplitude of the EPSP. In contrast, rapidly rising events bring the cell to threshold before the low-voltage-activated currents become fully activated. In the case of octopus cells, this allows the cells to respond to synchronous synaptic inputs with precisely timed action potentials, but will tend to suppress responses to desynchronized inputs (Ferragamo, M. J. and Oertel, D., 2002; McGinley, M. J. and Oertel, D., 2006). The slope sensitivity varies among cells in the VCN that express different amounts of low-voltage-activated conductances (McGinley, M. J. and Oertel, D., 2006). The way in which these channels impart slope sensitivity will depend on their rates of activation. Although the low-voltage-activated channel activates with fourth-order kinetics, at a resting potential of −60 mV the energetics are such that the channels need only move through a single gating transition to achieve the open state (Rothman, J. S. and Manis, P. B., 2003a). Thus, at rest, they will open with first-order kinetics with no delay (Manis, P. and Marx, S., 1991; Rathouz, M. and Trussell, L., 1998; Rothman, J. S. and Manis, P. B., 2003a), so that they will be engaged at the first sign of depolarization. A covariance analysis of the membrane potential preceding spikes in n. magnocellularis was undertaken to examine the temporal nonlinearities present in these cells (Slee, S. J. *et al.*, 2005). Spike generation depended on two features of the input: a short-term (2 ms wide) smoothing function and a short-term (<5 ms wide) derivative-like function. Sensitivity to the derivative-like function was largely abolished with the low-voltage-activated conductance was blocked with α-DTX, whereas the short-term smoothing component remained. This analysis thus supports the contention that the low-voltage-activated conductance confers sensitivity to rapidly fluctuating voltage changes, rather than the time-averaged membrane potential.

Fourth, activation of the low-voltage-activated channels can improve the signal-to-noise ratio for detection of weak excitatory events against a background of uncorrelated activity (Svirskis, G., 2002; Svirskis, G. *et al.*, 2004). These authors used dynamic clamp to simulate synaptic conductances onto MSO neurons. The contribution of the low-voltage-activated channels to signal detection was found to be twofold. First, reducing the low-voltage-activated current with DTX reduced the synchrony of the response to specific, slightly larger, inputs, largely because decreasing the conductance permitted weaker, uncorrelated, inputs to generate extraneous spikes. Second, using reverse correlation (spike-triggered averaging), it was found that the average

synaptic current that brought the cell to threshold was rapidly rising (see also Slee, S. J. *et al.*, 2005), and that in the presence of DTX, more slowly rising events could also be effective. These properties are consistent with results described above for MNTB principal neurons, n. magnocellularis neurons, and cochlear nucleus octopus cells.

Together, these features suggest that low-voltage-activated potassium conductances optimize detection of rapidly changing synchronous synaptic input (whether from a few or many synapses), while simultaneously suppressing the contributions of asynchronous and slow inputs, and suppressing asynchronous postsynaptic spikes. Which contribution is most important for processing for a given cell type seems to depend on the pattern of afferent convergence, and perhaps the relative size of the low-voltage-activated conductance.

3.32.6.1 Tonotopic Channel Expression Patterns, and Relationship to Integrative Roles

The fundamental organizing principle of the auditory system is the representation of sound frequency as position (tonotopic organization). In many species, there are clear and well-established gradients of cellular mechanisms along the tonotopic axis in the auditory end organs (cochlea and basilar papilla) that support the temporal requirements for sensory processing of different frequency sounds (Fettiplace, R. and Fuchs, P. A., 1999). Such gradients make sense for peripheral processing. Perhaps not surprisingly, similar gradients have been described in central nuclei, even though their existence might not be predicted to be necessary. Because sound is converted into a train of action potentials at the level of the auditory nerve, the sound frequency itself is no longer represented in terms of a continuously variable signal. Instead, frequency is represented as the place of activity, and other attributes such as intensity or stimulus phase are encoded in action potential intervals in single fibers or as temporally correlated firing across fibers. The information represented by these action potentials is, in some senses, independent of acoustic stimulus frequency. However, both the tonotopic variation in ion channel expression in the SGCs (discussed above), and the variation in the precision of temporal structure in ANF responses to broadband noise suggests that ANFs represent other kinds of temporal information that do change with tonotopic position. For example, the temporal dispersion of spike times sufficient to attain a vector strength of 0.9 at 500 Hz is much greater than the dispersion necessary to attain a lower vector strength at 2 kHz (Koppl, C., 1997; Paolini, A. G. *et al.*, 2001); hence, the temporal requirements for detection of correlated afferent activity are more stringent for high-frequency cells. Finally, phase locking in the low-frequency tail of cat high characteristic frequency (CF) ANF response areas is better than the phase locking seen at the same frequencies, near CF, for low-frequency ANFs (Joris, P. X. *et al.*, 1994), which suggests that timing information in high CF fibers is more precise than in low CF fibers. This is also reflected in the temporal correlations in response to broadband noise. The interstimulus correlations of responses to noise in cat ANFs show a central peak whose width varies from about 1 ms for 4 kHz fibers to 400 μs for 12 kHz fibers (Louage, D. H. *et al.*, 2004). Translating this into the response of many fibers of a given CF to the same stimulus, it suggests that certain features of the stimulus generate correlations in synaptic input whose relative timing is in the 1–0.4 ms range, depending on CF. Postsynaptic cells that receive subthreshold inputs (globular bushy cells and octopus cells) could detect these coincident synaptic events and forward this information to higher-order nuclei.

Tonotopic gradients in cellular mechanisms of information processing are present in some central auditory nuclei. High levels of Kv3.1 immunostaining are seen in the high-frequency regions of the avian n. magnocellularis and n. laminaris (Parameshwaran, S. *et al.*, 2001). A similar gradient of Kv3.1 expression is present along the tonotopic axis of the rat and mouse MNTB (Li, W. *et al.*, 2001; von Hehn, C. A. *et al.*, 2004) and possibly VCN (von Hehn, C. A. *et al.*, 2004). Because Kv3.1 is a high-threshold delayed rectifier channel, it is largely involved in action potential repolarization (Rothman, J. S. and Manis, P. B., 2003b; Klug, A. and Trussell, L. O., 2006). Thus, the gradient suggests that the high-frequency cells might recover from a spike more rapidly and could have greater firing precision for high afferent rates. However it is unclear why the low-frequency cells do not have a similar expression level; it is possible that they utilize another channel. Physiological measurements in the MNTB are consistent with this, revealing a gradient in the low- and high-voltage-activated K^+ conductances (largest conductance in the high-frequency regions), whereas an unidentified K^+ conductance showed an opposing gradient (Brew, H. M. and Forsythe, I. D., 2005). In n. magnocellularis, there is higher Kv1.1 expression in the high-frequency regions, which correlates well with the intrinsic physiology of the cells

(Fukui, I. and Ohmori, H., 2004). The higher expression of Kv1.1 endows the high-frequency cells with shorter time constants, and a shorter window for coincidence detection. This kind of gradient is also consistent with the smaller timing dispersion for afferent synapses from high-frequency regions of the basilar papilla (Koppl, C., 1997). In n. laminaris, which expresses Kv1.1 at a lower level than Kv1.2, Kv1.2 is found to be maximal in the middle region, and lower at higher and lower frequencies (Kuba, H. *et al.*, 2005). This is also consistent with cells in the mid-frequency region having shorter time constants, lower input resistances, and more rapidly decaying EPSPs (however, cf. Reyes, A. D. *et al.*, 1996). In rat LSO, Kv1.1 protein and low-voltage-activated conductance expression are higher in the low-frequency regions (Barnes-Davies, M. *et al.*, 2004). With the exceptions of the LSO and n. laminaris, the central K^+ channel gradients follow a general pattern similar to that reported for the SGC: Kv1.1 (or Kv1.2) and Kv3.1 are more highly expressed in the higher-frequency neurons. Thus, it appears that the biophysical mechanisms that support fine temporal processing are optimized to match the tonotopic variation in the precision of afferent spikes.

3.32.7 Conclusion

Many neurons of the auditory system are specialized for rapid temporal processing. Although the specific mechanisms that participate in the analysis of timing information are most evident in the brainstem, there is also evidence that some specialization in terms of receptors and channels may be present even in primary auditory cortex. The key elements appear to be combinations of voltage-gated potassium and hyperpolarizatation-activated conductances that appear as repeated motifs in the cells involved in temporal processing. These include low-voltage-activated potassium channels that operate in a subthreshold voltage regime to determine the rules of synaptic integration as well as participate in dynamically regulating spike threshold, hyperpolarization-activated cation channels that presumably control the level of activation of the subthreshold potassium conductances and perhaps the availability of sodium conductances, and high-voltage-activated potassium channels that rapidly repolarize action potentials and support the ability of the cells to fire precisely timed spikes at high rates. These combinations are seen both in avians and mammals, attesting to their fundamental importance in auditory temporal processing. Many of the neurons with these channel combinations were once thought to operate as relays that forwarded temporal information with little modification. However, this is clearly not an accurate depiction of their operation, as the cells do not fire in response to all afferent spikes (Li, R.Y.-S. and Guinan, J. J., 1966; Kopp-Scheinpflug, C. *et al.*, 2002; 2003). Temporal processing in these cells is influenced by many additional processes, such as synaptic depression (Brenowitz, S. and Trussell, L., 1998; Cook, D. L. *et al.*, 2003), contributions from dendritic and electrotonic structure (Agmon-Snir, H. *et al.*, 1998; Zhou, Y. *et al.*, 2005), regulation by neuromodulators (Kossl, M. and Vater, M., 1989; Banks, M. I. *et al.*, 1993), and of course, inhibition (Caspary, D. M., *et al.*, 1994; Grothe, B. and Sanes, D. H., 1994; Brand, A. *et al.*, 2002; Kopp-Scheinpflug, C. *et al.*, 2002). It is the dynamic interaction between all of these influences and the different sets of ion channels that ultimately determines the exquisite temporal acuity of the auditory system.

Acknowledgment

This work was supported by NIDCD grant R01 DC004551 to PBM.

References

Adam, T. J., Finlayson, P., and Schwarz, D. W. 2001. Membrane properties of principal neurons of the lateral superior olive. J. Neurophysiol. 86, 922–934.

Adam, T. J, Schwarz, D. W., and Finlayson, P. 1999. Firing properties of chopper and delay neurons in the lateral superior olive of the rat. Exp. Brain Res. 124, 489–502.

Adamson, C. L., Reid, M. A., and Davis, R. L. 2002a. Opposite actions of brain-derived neurotrophic factor and neurotrophin-3 on firing features and ion channel composition of murine spiral ganglion neurons. J. Neurosci. 22, 1385–1396.

Adamson, C. L., Reid, M. A., Mo, Z. L., Bowne-English. J., and Davis, R. L. 2002b. Firing features and potassium channel content of murine spiral ganglion neurons vary with cochlear location. J. Comp. Neurol. 447, 331–350.

Agmon-Snir, H., Carr, C. E., and Rinzel, J. 1998. The role of dendrites in auditory coincidence detection. Nature 393, 268–272.

Alonso, G. and Widmer, H. 1997. Clustering of Kv4.2 potassium channels in postsynaptic membrane of rat supraoptic neurons: an ultrastructural study. Neuroscience 77, 617–621.

An, W. F., Bowlby, M. R., Betty, M., Cao, J., Ling, H. P., Mendoza, G., Hinson, J. W., Strassle, B. W., Trimmer, J. S., and Rhodes, K. J. 2000. Modulation of A-type potassium channels by a family of calcium sensors. Nature 403, 553–556.

Bal, R. and Oertel, D. 2000. Hyperpolarization-activated, mixed-cation current (I_h) in octopus cells of the mammalian cochlear nucleus. J. Neurophysiol. 84, 806–817.

Bal, R. and Oertel, D. 2001. Potassium currents in octopus cells of the mammalian cochlear nucleus. J. Neurophysiol. 86, 2299–2311.

Banks, M. I. and Smith, P. H. 1992. Intracellular recordings from neurobiotin-labeled cells in brain slices of the rat medial nucleus of the trapezoid body. J. Neurosci. 12, 2819–2837.

Banks, M. I., Pearce, R. A. and Smith, P. H. 1993. Hyperpolarization-activated cation current (I_h) in neurons of the medial nucleus of the trapezoid body: voltage-clamp analysis and enhancement by norepinephrine and cAMP suggest a modulatory mechanism in auditory brain stem. J. Neurophysiol. 70, 1420–1432.

Barnes-Davies, M., Barker, M. C., Osmani, F., and Forsythe, I. D. 2004. Kv1 currents mediate a gradient of principal neuron excitability across the tonotopic axis in the rat lateral superior olive. Eur. J. Neurosci. 19, 325–333.

Baro, D. J., Levini, R. M., Kim, M. T., Willms, A. R., Lanning, C. C., Rodriguez, H. E., and Harris-Warrick, R. M. 1997. Quantitative single-cell-reverse transcription-PCR demonstrates that A-current magnitude varies as a linear function of shal gene expression in identified stomatogastric neurons. J. Neurosci. 17, 6597–6610.

Bhattacharjee, A. and Kaczmarek, L. K. 2005. For K^+ channels, Na^+ is the new Ca^{2+}. Trends Neurosci. 28, 422–428.

Bhattacharjee, A., Gan, L., and Kaczmarek, L. K. 2002. Localization of the Slack potassium channel in the rat central nervous system. J. Comp. Neurol. 454, 241–254.

Bhattacharjee, A., von Hehn, C. A., Mei, X., and Kaczmarek, L. K. 2005. Localization of the Na^+-activated K^+ channel Slick in the rat central nervous system. J. Comp. Neurol. 484, 80–92.

Bortone, D. S., Mitchell, K., and Manis, P. B. 2006. Developmental time course of potassium channel expression in the rat cochlear nucleus. Hear. Res. 211, 114–125.

Bou-Abboud, E. and Nerbonne, J. M. 1999. Molecular correlates of the calcium-independent, depolarization-activated K^+ currents in rat atrial myocytes. J. Physiol. (Lond.) 517, 407–420.

Brand, A., Behrend, O., Marquardt, T., McAlpine, D., and Grothe, B. 2002. Precise inhibition is essential for microsecond interaural time difference coding. Nature 417, 543–547.

Brenowitz, S. and Trussell, L. 1998. Enhancement of synaptic efficacy by presynaptic $GABA_B$ receptors. Neuron 20, 135–141.

Brew, H. M. and Forsythe, I. D. 1995. Two voltage-dependent K^+ conductances with complementary functions in postsynaptic integration at a central auditory synapse. J. Neurosci. 15, 8011–8022.

Brew, H. M. and Forsythe, I. D. 2005. Systematic variation of potassium current amplitudes across the tonotopic axis of the rat medial nucleus of the trapezoid body. Hear. Res. 206, 116–132.

Brew, H. M., Hallows, J. L., and Tempel, B. L. 2003. Hyperexcitability and reduced low threshold potassium currents in auditory neurons of mice lacking the channel subunit Kv1.1. J. Physiol. 548, 1–20.

Cai, Y., Walsh, E. J., and McGee, J. 1997. Mechanisms of onset responses in octopus cells of the cochlear nucleus: implications of a model. J. Neurophysiol. 78, 872–883.

Caminos, E., Vale, C., Lujan, R., Martinez-Galan, J. R., and Juiz, J. M. 2005. Developmental regulation and adult maintenance of potassium channel proteins (Kv 1.1 and Kv 1.2) in the cochlear nucleus of the rat. Brain Res. 1056, 118–131.

Caspary, D. M., Backoff, P. M., Finlayson, P. G., and Palombi, P. S. 1994. Inhibitory inputs modulate discharge rate within frequency receptive fields of anteroventral cochlear nucleus neurons. J. Neurophysiol. 72, 2124–2133.

Castellino, R. C., Morales, M. J., Strauss, H. C., and Rasmusson, R. L. 1995. Time- and voltage-dependent modulation of a Kv1.4 channel by a beta-subunit (KvBeta3) cloned from ferret ventricle. Am. J. Physiol. 269, H385–H391.

Chen, W. C. and Davis, R. L. 2006. Voltage-gated and two-pore-domain potassium channels in murine spiral ganglion neurons. Hear. Res. 222, 89–99.

Cherel, I. 2004. Regulation of K^+ channel activities in plants. from physiological to molecular aspects. J. Exp. Bot. 55, 337–351.

Coetzee, W. A., Amarillo, Y., Chiu, J., Chow, A., Lau, D., McCormack, T., Moreno, H., Nadal, M. S., Ozaita, A., Pountney, D., Saganich, M., Vega-Saenz de Miera, E., and Rudy, B. 1999. Molecular diversity of K^+ channels. Ann. N. Y. Acad. Sci. 868, 233–285.

Colbert, C. M. and Johnston, D. 1996. Axonal action-potential initiation and Na^+ channel densities in the soma and axon initial segment of subicular pyramidal neurons. J. Neurosci. 16, 6676–6686.

Colbert, C. M. and Pan, E. 2002. Ion channel properties underlying axonal action potential initiation in pyramidal neurons. Nat. Neurosci. 5, 533–538.

Cook, D. L., Schwindt, P. C., Grande, L. A. and Spain, W. J. 2003. Synaptic depression in the localization of sound. Nature 421, 66–70.

Covey, E. and Casseday, J. H. 1991. The monaural nuclei of the lateral lemniscus in an echolocating bat: parallel pathways for analyzing temporal features of sound. J. Neurosci. 11, 3456–3470.

Dodson, P. D., Barker, M. C., and Forsythe, I. D. 2002. Two heteromeric Kv1 potassium channels differentially regulate action potential firing. J. Neurosci. 22, 6953–6961.

Dodson, P. D., Billups, B., Rusznak, Z., Szucs, G., Barker, M. C., and Forsythe, I. D. 2003. Presynaptic rat Kv1.2 channels suppress synaptic terminal hyperexcitability following action potential invasion. J. Physiol. 550, 27–33.

Fernandez, F. R., Mehaffey, W. H., Molineux, M. L., and Turner, R. W. 2005. High-threshold K^+ current increases gain by offsetting a frequency-dependent increase in low-threshold K^+ current. J. Neurosci. 25, 363–371.

Ferragamo, M. J. and Oertel, D. 2002. Octopus cells of the mammalian ventral cochlear nucleus sense the rate of depolarization. J. Neurophysiol. 87, 2262–2270.

Fettiplace, R. and Fuchs, P. A. 1999. Mechanisms of hair cell tuning. Annu. Rev. Physiol. 61, 809–834.

Fitzakerley, J. L. and Quale, M. 2005. Differential expression of potassium channel Kv2.1 in the adult mouse cochlear nucleus. Association for Research in Otolaryngology, Midwinter Meeting, New Orleans, LA.

Fitzakerley, J. L., Star, K. V., Rinn, J. L., and Elmquist, B. J. 2000. Expression of Shal potassium channel subunits in the adult and developing cochlear nucleus of the mouse. Hear. Res. 147, 31–45.

Forsythe, I. D. and Barnes-Davies, M. 1993. The binaural auditory pathway: membrane currents limiting multiple action potential generation in the rat medial nucleus of the trapezoid body. Proc. Biol. Sci. 251, 143–150.

Francis, H. W. and Manis, P. B. 2000. Effects of deafferentation on the electrophysiology of ventral cochlear nucleus neurons. Hear. Res. 149, 91–105.

Frisina, R. D., Smith, R. L., and Chamberlain, S. C. 1990. Encoding of amplitude modulation in the gerbil cochlear nucleus. I. A hierarchy of enhancement. Hear.Res. 44, 99–122.

Fujino, K. and Oertel, D. 2001. Cholinergic modulation of stellate cells in the mammalian ventral cochlear nucleus. J. Neurosci. 21, 7372–7383.

Fujino, K., Koyano, K., and Ohmori, H. 1997. Lateral and medial olivocochlear neurons have distinct electrophysiological properties in the rat brain slice. J. Neurophysiol. 77, 2788–2804.

Fukui, I. and Ohmori, H. 2003. Developmental changes in membrane excitability and morphology of neurons in the nucleus angularis of the chicken. J. Physiol. 548, 219–232.

Fukui, I. and Ohmori, H. 2004. Tonotopic gradients of membrane and synaptic properties for neurons of the chicken nucleus magnocellularis. J. Neurosci. 24, 7514–7523.

Gan, L., Perney, T. M., and Kaczmarek, L. K. 1996. Cloning and characterization of the promoter for a potassium channel expressed in high frequency firing neurons. J. Biol. Chem. 271, 5859–5865.

Garcia-Diaz, J. F. 1999. Development of a fast transient potassium current in chick cochlear ganglion neurons. Hear. Res. 135, 124.

Gittelman, J. X. and Tempel, B. L. 2006. Kv1.1-containing channels are critical for temporal precision during spike initiation. J. Neurophysiol. 96, 1203–1214.

Godfrey, D. A., Kiang, N. Y., and Norris, B. E. 1975. Single unit activity in the dorsal cochlear nucleus of the cat. J. Comp. Neurol. 162, 269–284.

Golding, N. L., Ferragamo, M. J., and Oertel, D. 1999. Role of intrinsic conductances underlying responses to transients in octopus cells of the cochlear nucleus. J. Neurosci. 19, 2897–2905.

Grigg, J. J., Brew, H. M., and Tempel, B. L. 2000. Differential expression of voltage-gated potassium channel genes in auditory nuclei of the mouse brainstem. Hear. Res. 140, 77–90.

Grothe, B. and Sanes, D. H. 1994. Synaptic inhibition influences the temporal coding properties of medial superior olivary neurons: an *in vitro* study. J. Neurosci. 14, 1701–1709.

Guo, W., Li, H., Aimond, F., Johns, D. C., Rhodes, K. J., Trimmer, J. S., and Nerbonne, J. M. 2002. Role of heteromultimers in the generation of myocardial transient outward K+ currents. Circ. Res. 90, 586–593.

Hallows, J. L. and Tempel, B. L. 1998. Expression of Kv1.1, a Shaker-like potassium channel, is temporally regulated in embryonic neurons and glia. J. Neurosci. 18, 5682–5691.

Hefti, B. J. and Smith, P. H. 2003. Distribution and kinetic properties of GABAergic inputs to layer V pyramidal cells in rat auditory cortex. J. Assoc. Res. Otolaryngol. 4, 106–121.

von Hehn, C. A., Bhattacharjee, A., and Kaczmarek, L. K. 2004. Loss of Kv3.1 tonotopicity and alterations in cAMP response element-binding protein signaling in central auditory neurons of hearing impaired mice. J. Neurosci. 24, 1936–1940.

Heusser, K. and Schwappach, B. 2005. Trafficking of potassium channels. Curr. Opin. Neurobiol. 15, 364–369.

Holt, A. G., Asako, M., Keith Duncan, R., Lomax, C. A., Juiz, J. M., and Altschuler, R. A. 2006. Deafness associated changes in expression of two-pore domain potassium channels in the rat cochlear nucleus. Hear. Res. 216–217, 146–153.

Hopkins, W. F. 1998. Toxin and subunit specificity of blocking affinity of three peptide toxins for heteromultimeric, voltage-gated potassium channels expressed in Xenopus oocytes. J. Pharmacol. Exp. Ther. 285, 1051–1060.

Hwang, P. M., Fotuhi, M., Bredt, D. S., Cunningham, A. M., and Snyder, S. H. 1993. Contrasting immunohistochemical localizations in rat brain of two novel K^+ channels of the Shab subfamily. J. Neurosci. 13, 1569–1576.

Jang, G. M., Leong, L. E., Hoang, L. T., Wang, P. H., Gutman, G. A., and Semler, B. L. 2004. Structurally distinct elements mediate internal ribosome entry within the 5′-noncoding region of a voltage-gated potassium channel mRNA. J. Biol. Chem. 279, 47419–47430.

Jeffress, L. A. 1948. A place theory of sound localization. J. Comp. Physiol. Pyschol. 41, 35–39.

Joris, P. X., Carney, L. H., Smith, P. H., and Yin, T. C. 1994. Enhancement of neural synchronization in the anteroventral cochlear nucleus. I. Responses to tones at the characteristic frequency. J. Neurophysiol. 71, 1022–1036.

Kalman, K., Nguyen, A., Tseng-Crank, J., Dukes, I. D., Chandy, G., Hustad, C. M., Copeland, N. G., Jenkins, N. A., Mohrenweiser, H., Brandriff, B., Cahalan, M., Gutman, G. A., and Chandy, K. G. 1998. Genomic organization, chromosomal localization, tissue distribution, and biophysical characterization of a novel mammalian shaker-related voltage-gated potassium channel, Kv1.7. J. Biol. Chem. 273, 5851–5857.

Kanold, P. O. and Manis, P. B. 1999. Transient potassium currents regulate the discharge patterns of dorsal cochlear nucleus pyramidal cells. J. Neurosci. 19, 2195–2208.

Kanold, P. O. and Manis, P. B. 2005. Encoding the timing of inhibition. J. Neurophysiol. 93, 2887–2897.

Karschin, C., Wischmeyer, E., Preisig-Muller, R., Rajan, S., Derst, C., Grzeschik, K. H., Daut, J., and Karschin, A. 2001. Expression pattern in brain of TASK-1, TASK-3, and a tandem pore domain K(+) channel subunit, TASK-5, associated with the central auditory nervous system. Mol. Cell. Neurosci. 18, 632–648.

Kharkovets, T., Hardelin, J. P., Safieddine, S., Schweizer, M., El-Amraoul, A., Petit, C., and Jentsch, T. J. 2000. KCNQ4, a K^+ channel mutated in a form of dominant deafness, is expressed in the inner ear and the central auditory pathway. Proc. Natl. Acad. Sci. U. S. A. 97, 4333–4338.

Kim, D. O., Sirianni, J. G., and Chang, S. O. 1990. Responses of DCN–PVCN neurons and auditory nerve fibers in unanesthetized decerebrate cats to AM and pures tones: analysis with autocorrelation/power-spectrum. Hear. Res. 45, 95–113.

Klug, A. and Trussell, L. O. 2006. Activation and deactivation of voltage-dependent K^+ channels during synaptically driven action potentials in the MNTB. J. Neurophysiol. 96, 1547–1555.

Koch, U., Braun, M., Kapfer, C., and Grothe, B. 2004. Distribution of HCN1 and HCN2 in rat auditory brainstem nuclei. Eur. J. Neurosci. 20, 79–91.

Koppl, C. 1997. Phase locking to high frequencies in the auditory nerve and cochlear nucleus magnocellularis of the barn owl, *Tyto alba*. J. Neurosci. 17, 3312–3321.

Kopp-Scheinpflug, C., Dehmel, S., Dorrscheidt, G. J., and Rubsamen, R. 2002. Interaction of excitation and inhibition in anteroventral cochlear nucleus neurons that receive large endbulb synaptic endings. J. Neurosci. 22, 11004–11018.

Kopp-Scheinpflug, C., Lippe, W. R., Dorrscheidt, G. J., and Rubsamen, R. 2003. The medial nucleus of the trapezoid body in the gerbil is more than a relay: comparison of pre- and postsynaptic activity. J. Assoc. Res. Otolaryngol. 4, 1–23.

Kossl, M. and Vater, M. 1989. Noradrenaline enhances temporal auditory contrast and neuronal timing precision in the cochlear nucleus of the mustache bat. J. Neurosci. 9, 4169–4179.

Kuba, H., Koyano, K., and Ohmori, H. 2002. Development of membrane conductance improves coincidence detection in the nucleus laminaris of the chicken. J. Physiol. 540, 529–542.

Kuba, H., Yamada, R., Fukui, I., and Ohmori, H. 2005. Tonotopic specialization of auditory coincidence detection in nucleus laminaris of the chick. J. Neurosci. 25, 1924–1934.

Li, R. Y.-S. and Guinan, J. J. 1966. Antidromic and orthodromic stimulation of neurons receiving calyces of Held. MIT Q. Progr. Rep. No 100, 227–234.

Li, W., Kaczmarek, L. K., and Perney, T. M. 2001. Localization of two high-threshold potassium channel subunits in the rat central auditory system. J. Comp. Neurol. 437, 196–218.

Liss, B., Franz, O., Sewing, S., Bruns, R., Neuhoff, H., and Roeper, J. 2001. Tuning pacemaker frequency of individual dopaminergic neurons by Kv4.3L and KChip3.1 transcription. EMBO J. 20, 5715–5724.

Liu, S. J. and Kaczmarek, L. K. 1998a. The expression of two splice variants of the Kv3.1 potassium channel gene is regulated by different signaling pathways. J. Neurosci. 18, 2881–2890.

Liu, S. Q. and Kaczmarek, L. K. 1998b. Depolarization selectively increases the expression of the Kv3.1 potassium channel in developing inferior colliculus neurons. J. Neurosci. 18, 8758–8769.

Louage, D. H., van der Heijden, M., and Joris, P. X. 2004. Temporal properties of responses to broadband noise in the auditory nerve. J. Neurophysiol. 91, 2051–2065.

Louage, D. H., van der Heijden, M., and Joris, P. X. 2005. Enhanced temporal response properties of anteroventral cochlear nucleus neurons to broadband noise. J. Neurosci. 25, 1560–1570.

Lu, Y., Monsivais, P., Tempel, B. L., and Rubel, E. W. 2004. Activity-dependent regulation of the potassium channel subunits Kv1.1 and Kv3.1. J. Comp. Neurol. 470, 93–106.

Luneau, C. J., Williams, J. B., Marshall, J., Levitan, E. S., Oliva, C., Smith, J. S., Antanavage, J., Folander, K., Stein, R. B., Swanson, R., Kaczmarek, L. K., and Buhrow, S. A. 1991. Alternative splicing contributes to K^+ channel diversity in the mammalian central nervous system. Proc. Natl. Acad. Sci. U. S. A. 88, 3932–3936.

Mainen, Z. F. and Sejnowski, T. J. 1996. Influence of dendritic structure on firing pattern in model neocortical neurons. Nature 382, 363–366.

Manis, P. B. 1990. Membrane properties and discharge characteristics of guinea pig dorsal cochlear nucleus neurons studied *in vitro*. J. Neurosci. 10, 2338–2351.

Manis, P. and Marx, S. 1991. Outward currents in isolated ventral cochlear nucleus neurons. J. Neurosci. 11, 2865–2880.

Manis, P., Marx, S., and White, J. 1996. Integrative Mechanisms of Ventral Cochlear Nucleus Stellate Cells: Membrane Conductances and Electrotonic Structure. In: Cochlear Nucleus: Structure and Function in Relation to Modeling (*eds*. W. A. Ainsworth, E. F. Evans, and C. M. Hackney), Vol. 3, pp. 213–229. JAI Press.

Manis, P., Mitchell, K., and Bortone, D. 2002. Developmental pattern of potassium channel expression in rat cochlear nucleus. *Association for Research in Otolaryngology, Midwinter Meeting,* St. Petersburg, FL.

Manis, P. B., Molitor, S. C., and Wu, H. 2003. Subthreshold oscillations generated by TTX-sensitive sodium currents in dorsal cochlear nucleus pyramidal cells. *Exp. Brain Res.* 153, 443–451.

Manis, P. B., Spirou, G. A., Wright, D. D., Paydar, S., and Ryugo, D. K. 1994. Physiology and morphology of complex spiking neurons in the guinea pig dorsal cochlear nucleus. J. Comp. Neurol. 348, 261–276.

McFeeters, R. L. and Oswald, R. E. 2004. Emerging structural explanations of ionotropic glutamate receptor function. FASEB J. 18, 428–438.

McGinley, M. J. and Oertel, D. 2006. Rate thresholds determine the precision of temporal integration in principal cells of the ventral cochlear nucleus. Hear. Res. 216–217, 52–63.

Metherate, R. and Aramakis, V. 1999. Intrinsic electrophysiology of neurons in thalamarecipient layers of developing rat auditory cortex. Brain Res. Dev. Brain Res. 115, 131–144.

Mo, Z. L., Adamson, C. L., and Davis, R. L. 2002. Dendrotoxin-sensitive K(+) currents contribute to accommodation in murine spiral ganglion neurons. J. Physiol. 542, 763–778.

O'Connell, A. D., Morton, M. J., and Hunter, M. 2002. Two-pore domain K^+ channels-molecular sensors. Biochim. Biophys. Acta 1566, 152–161.

Oertel, D. 1983. Synaptic responses and electrical properties of cells in brain slices of the mouse anteroventral cochlear nucleus. J. Neurosci. 3, 2043–2053.

Oertel, D. 1999. The role of timing in the brain stem auditory nuclei of vertebrates. Annu. Rev. Physiol. 61, 497–519.

Ohya, S., Tanaka, M., Oku, T., Asai, Y., Watanabe, M., Giles, W. R., and Imaizumi, Y. 1997. Molecular cloning and tissue distribution of an alternatively spliced variant of an A-type K^+ channel alpha-subunit, Kv4.3 in the rat. FEBS Lett. 420, 47–53.

Pal, B., Por, A., Pocsai, K., Szucs, G., and Rusznak, Z. 2005. Voltage-gated and background K^+ channel subunits expressed by the bushy cells of the rat cochlear nucleus. Hear. Res. 199, 57–70.

Pal, B., Rusznak, Z., Harasztosi, C., and Szucs, G. 2004. Depolarization-activated K^+ currents of the bushy neurones of the rat cochlear nucleus in a thin brain slice preparation. Acta. Physiol. Hung. 91, 83–98.

Paolini, A. G., FitzGerald, J. V., Burkitt, A. N., and Clark, G. M. 2001. Temporal processing from the auditory nerve to the medial nucleus of the trapezoid body in the rat. Hear. Res. 159, 101–116.

Parameshwaran, S., Carr, C. E., and Perney, T. M. 2001. Expression of the Kv3.1 potassium channel in the avian auditory brainstem. J. Neurosci. 21, 485–494.

Perney, T. M. and Kaczmarek, L. K. 1997. Localization of a high threshold potassium channel in the rat cochlear nucleus. J. Comp. Neurol. 386, 178–202.

Perney, T. M., Marshall, J., Martin, K. A., Hockfield, S., and Kaczmarek, L. K. 1992. Expression of the mRNAs for the Kv3.1 potassium channel gene in the adult and developing rat brain. J. Neurophysiol. 68, 756–766.

Peruzzi, D., Sivaramakrishnan, S., and Oliver, D. 2000. Identification of cell types in brain slices of the inferior colliculus. Neuroscience 101, 403–416.

Rasband, M. N. 2004. It's ''juxta'' potassium channel! J. Neurosci. Res. 76, 749–757.

Rasband, M. N. and Trimmer, J. S. 2001. Developmental clustering of ion channels at and near the node of Ranvier. Dev. Biol. 236, 5–16.

Rathouz, M. and Trussell, L. 1998. Characterization of outward currents in neurons of the avian nucleus magnocellularis. J. Neurophysiol. 80, 2824–2835.

Reyes, A. D., Rubel, E. W., and Spain, W. J. 1994. Membrane properties underlying the firing of neurons in the avian cochlear nucleus. J. Neurosci. 14, 5352–5364.

Reyes, A. D., Rubel, E. W., and Spain, W. J. 1996. *In vitro* analysis of optimal stimuli for phase-locking and time-delayed modulation of firing in avian nucleus laminaris neurons. J. Neurosci. 16, 993–1007.

Rhode, W. S. and Kettner, R. E. 1987. Physiological study of neurons in the dorsal and posteroventral cochlear nucleus of the unanesthetized cat. J. Neurophysiol. 57, 414–442.

Rhode, W. S. and Smith, P. H. 1986. Encoding timing and intensity in the ventral cochlear nucleus of the cat. J. Neurophysiol. 56, 261–286.

Rhode, W. S., Smith, P. H., and Oertel, D. 1983. Physiological response properties of cells labeled intracellularly with horseradish peroxidase in cat dorsal cochlear nucleus. J. Comp. Neurol. 213, 426–447.

Richardson, F. C. and Kaczmarek, L. K. 2000. Modification of delayed rectifier potassium currents by the Kv9.1 potassium channel subunit. Hear. Res. 147, 21.

Rivera, J. F., Ahmad, S., Quick, M. W., Liman, E. R., and Arnold, D. B. 2003. An evolutionarily conserved dileucine motif in Shal K^+ channels mediates dendritic targeting. Nat. Neurosci. 6, 243–250.

Robbins, J. 2001. KCNQ potassium channels: physiology, pathophysiology, and pharmacology. Pharmacol. Ther. 90, 1–19.

Robinson, R. B. and Siegelbaum, S. A. 2003. Hyperpolarization-activated cation currents: from molecules to physiological function. Annu. Rev. Physiol. 65, 453–480.

Rodrigues, A. R. and Oertel, D. 2006. Hyperpolarization-activated currents regulate excitability in stellate cells of the mammalian ventral cochlear nucleus. J. Neurophysiol. 95, 76–87.

Rosenberger, M. H., Fremouw, T., Casseday, J. H., and Covey, E. 2003. Expression of the Kv1.1 ion channel subunit in the auditory brainstem of the big brown bat, *Eptesicus fuscus*. J. Comp. Neurol. 462, 101–120.

Rothman, J. S. and Manis, P. B. 2003a. Kinetic analyses of three distinct potassium conductances in ventral cochlear nucleus neurons. J. Neurophysiol. 89, 3083–3096.

Rothman, J. S. and Manis, P. B. 2003b. The roles potassium currents play in regulating the electrical activity of ventral cochlear nucleus neurons. J. Neurophysiol. 89, 3097–3113.

Rothman, J. S. and Manis, P. B. 2003c. Differential expression of three distinct potassium currents in the ventral cochlear nucleus. J. Neurophysiol. 89, 3070–3082.

Rothman, J. and Young, E. 1996. Enhancement of neural synchronization in computational models of ventral cochlear nucleus bushy cells. Aud. Neurosci. 2, 47–62.

Rusznak, Z., Forsythe, I. D., and Stanfield, P. R. 1996. Characterization of the hyperpolarization activated nonspecific cation current (Ih) of bushy neurones from the rat anteroventral cochlear nucleus studied in a thin brain slice preparation. Neurobiology (Bp) 4, 275–276.

Sah, P. and Faber, E. S. 2002. Channels underlying neuronal calcium-activated potassium currents. Prog. Neurobiol. 66, 345–353.

Santos-Sacchi, J. 1993. Voltage-dependent ionic conductances of type I spiral ganglion cells from the guinea pig inner ear. J. Neurosci. 13, 3599–3611.

Schwarz, D. W. and Puil, E. 1997. Firing properties of spherical bushy cells in the anteroventral cochlear nucleus of the gerbil. Hear. Res. 114, 127–138.

Schwarz, J. R. and Bauer, C. K. 2004. Functions of erg K^+ channels in excitable cells. J. Cell. Mol. Med. 8, 22–30.

Scott, L. L., Mathews, P. J., and Golding, N. L. 2005. Posthearing developmental refinement of temporal processing in principal neurons of the medial superior olive. J. Neurosci. 25, 7887–7895.

Serodio, P. and Rudy, B. 1998. Differential expression of Kv4 K^+ channel subunits mediating subthreshold transient K+ (A-type) currents in rat brain. J. Neurophysiol. 79, 1081–1091.

Sheng, M., Tsaur, M. L., Jan, Y. N., and Jan, L. Y. 1992. Subcellular segregation of two A-type K^+ channel proteins in rat central neurons. Neuron 9, 271–284.

Sheng, M., Tsaur, M. L., Jan, Y. N., and Jan, L. Y. 1994. Contrasting subcellular localization of the Kv1.2 K^+ channel subunit in different neurons of rat brain. J. Neurosci. 14, 2408–2417.

Sheppard, D. N., Valverde, M. A., Represa, J., and Giraldez, F. 1992. Transient outward currents in cochlear ganglion neurons of the chick embryo. Neuroscience 51, 631–639.

Shi, G., Kleinklaus, A. K., Marrion, N. V., and Trimmer, J. S. 1994. Properties of Kv2.1 K^+ channels expressed in transfected mammalian cells. J. Biol. Chem. 269, 23204–23211.

Sivaramakrishnan, S. and Oliver, D. 2001. Distinct K currents result in physiologically distinct cell types in the inferior colliculus of the rat. J. Neurosci. 21, 2861–2877.

Slee, S. J., Higgs, M. H., Fairhall, A. L., and Spain, W. J. 2005. Two-dimensional time coding in the auditory brainstem. J. Neurosci. 25, 9978–9988.

Smith, P. H. 1995. Structural and functional differences distinguish principal from nonprincipal cells in the guinea pig MSO slice. J. Neurophysiol. 73, 1653–1667.

Smith, P. H. and Populin, L. C. 2001. Fundamental differences between the thalamocortical recipient layers of the cat auditory and visual cortices. J. Comp. Neurol. 436, 508–519.

Sonnenburg, R., Bortone, D., and Manis, P. 2002. Differential potassium channel gene expression in ventral cochlear nucleus neurons. American Academy of Otolaryngology-Head and Neck Surgery Annual Meeting, San Diego, CA.

Spirou, G. A., Smith, P. H., and Manis, P. B. 1995. Intracellular recording and labeling of neurons in the lateral nucleus of the trapezoid body. Soc. Neurosci. Abstr. 21, 400.

Stocker, M. 2004. Ca(2+)-activated K^+ channels: molecular determinants and function of the SK family. Nat. Rev. Neurosci. 5, 758–770.

Stuart, G., Schiller, J., and Sakmann, B. 1997. Action potential initiation and propagation in rat neocortical pyramidal neurons. J. Physiol. 505(Pt 3), 617–632.

Sullivan, W. E. and Konishi, M. 1984. Segregation of stimulus phase and intensity coding in the cochlear nucleus of the barn owl. J. Neurosci. 4, 1787–1799.

Svirskis, G. 2002. Enhancement of signal-to-noise ratio and phase locking for small inputs by a low-threshold outward current in auditory neurons. J. Neurosci. 22, 11019–11025.

Svirskis, G., Kotak, V., Sanes, D. H., and Rinzel, J. 2004. Sodium along with low-threshold potassium currents enhance coincidence detection of subthreshold noisy signals in MSO neurons. J. Neurophysiol. 91, 2465–2473.

Thornhill, W., Wu, M. B., Jiang, X., Wu, X., Morgan, P. T., and Margiotta, J. F. 1996. Expression of Kv1.1 delayed rectifier potassium channels in Lec mutant Chinese hamster ovary cell lines reveals a role for sialidation in channel function. J. Biol. Chem. 271, 19093–19098.

Tkatch, T., Baranauskas, G., and Surmeier, D. J. 2000. Kv4.2 mRNA abundance and A-type K(+) current amplitude are linearly related in basal ganglia and basal forebrain neurons. J. Neurosci. 20, 579–588.

Trussell, L. O. 1999. Synaptic mechanisms for coding timing in auditory neurons. Annu. Rev. Physiol. 61, 477–496.

Valverde, M. A., Sheppard, D. N., Represa, J., and Giraldez, F. 1992. Development of Na(+)- and K(+)-currents in the cochlear ganglion of the chick embryo. Neuroscience 51, 621–630.

Varga, A. W., Yuan, L. L., Anderson, A. E., Schrader, L. A., Wu, G. Y., Gatchel, J. R., Johnston, D., and Sweatt, J. D. 2004. Calcium-calmodulin-dependent kinase II modulates Kv4.2 channel expression and upregulates neuronal A-type potassium currents. J. Neurosci. 24, 3643–3654.

Villarroel, A. and Schwartz, T. L. 1996. Inhibition of the Kv4 (Shal) family of transient K^+ currrents by arachidonic acid. J. Neurosci. 16, 2522–2532.

Wagner, T. 1994. Intrinsic properties of identified neurones in the central nucleus of mouse inferior colliculus. NeuroReport 6, 89–93.

Wang, L. Y., Gan, L., Forsythe, I. D., and Kaczmarek, L. K. 1998. Contribution of the Kv3.1 potassium channel to high-frequency firing in mouse auditory neurones. J. Physiol. 509(Pt 1), 183–194.

Wang, H., Parcej, D. N., and Dolly, J. O. 1999. Alpha subunit compositions of Kv1.1-containing K^+ channel subtypes fractioned from rat brain using dendrotoxins. Eur. J. BioChem. 263, 230–237.

Wang, Y. and Manis, P. B. 2005. Synaptic transmission at the cochlear nucleus endbulb synapse during age-related hearing loss in mice. J Neurophysiol. 94, 1814–1824.

Weiser, M., Vega-Saenz de Miera, E., Kentros, C., Moreno, H., Franzen, L., Hillman, D., Baker, H., and Rudy, B. 1994. Differential expression of Shaw-related K+ channels in the rat central nervous system. J. Neurosci. 14, 949–972.

White, J. A., Young, E. D., and Manis, P. B. 1994. The electrotonic structure of regular-spiking neurons in the

ventral cochlear nucleus may determine their response properties. J. Neurophysiol. 71, 1774–1786.
Wo, Z. G. and Oswald, R. E. 1995. Unraveling the modular design of glutamate-gated ion channels. Trends Neurosci. 18, 161–168.
Wu, S. H. 1999. Physiological properties of neurons in the ventral nucleus of the lateral lemniscus of the rat: intrinsic membrane properties and synaptic response. J. Neurophysiol. 81, 2862–2874.
Wu, S. H. and Kelly, J. B. 1991. Physiological properties of neurons in the mouse superior olive: membrane characteristics and postsynaptic responses studied *in vitro*. J. Neurophysiol. 65, 230–246.
Wu, S. H. and Kelly, J. B. 1995. *In vitro* brain slice studies of the rat's dorsal nucleus of the lateral lemniscus. I. Membrane and synaptic response properties. J. Neurophysiol. 73, 780–793.
Wu, S. H. and Oertel, D. 1984. Intracellular injection with horseradish peroxidase of physiologically characterized stellate and bushy cells in slices of mouse anteroventral cochlear nucleus. J. Neurosci. 4, 1577–1588.
Wymore, R. S., Negulescu, D., Kinoshita, K., Kalman, K., Aiyar, J., Gutman, G. A., and Chandy, K. G. 1996. Characterization of the transcription unit of mouse Kv1.4, a voltage-gated potassium channel gene. J. Biol. Chem. 271, 15629–15634.
Yamaguchi, K. and Ohmori, H. 1990. Voltage-gated and chemically gated ionic channels in the cultured cochlear ganglion neurone of the chick. J. Physiol. 420, 185–206.
Yuan, L. L., Adams, J. P., Swank, M., Sweatt, J. D., and Johnston, D. 2002. Protein kinase modulation of dendritic K^+ channels in hippocampus involves a mitogen-activated protein kinase pathway. J. Neurosci. 22, 4860–4868.
Zhang, S. and Oertel, D. 1993. Cartwheel and superficial stellate cells of the dorsal cochlear nucleus of mice: intracellular recordings in slices. J. Neurophysiol. 69, 1384–1397.
Zhang, S. and Trussell, L. O. 1994. A characterization of excitatory postsynaptic potentials in the avian nucleus magnocellularis. J. Neurophysiol. 72, 705–718.
Zheng, Q. Y., Johnson, K. R., and Erway, L. C. 1999. Assessment of hearing in 80 inbred strains of mice by ABR threshold analyses. Hear. Res. 130, 94–107.
Zhou, Y., Carney, L. H., and Colburn, H. S. 2005. A model for interaural time difference sensitivity in the medial superior olive: interaction of excitatory and inhibitory synaptic inputs, channel dynamics, and cellular morphology. J. Neurosci. 25, 3046–3058.

3.33 Central Synapses that Preserve Auditory Timing

L O Trussell, Oregon Health and Science University, Portland, OR, USA

© 2008 Elsevier Inc. All rights reserved.

3.33.1	Introduction	588
3.33.2	Synaptic Transmission	588
3.33.3	Overview of the Types and Morphology of Synapses in Auditory Pathways	589
3.33.3.1	Bushy Cells and the Endbulbs of Held	590
3.33.4	Medial Nucleus of the Trapezoid Body	591
3.33.5	Dendritic Coincidence Detectors	592
3.33.6	Transmission at Giant Synapses	592
3.33.7	Synaptic Strength at Auditory Relays	593
3.33.8	Reliability of Timing	594
3.33.9	Synaptic Depression	594
3.33.10	Alpha-Amino-3-Hydroxy-5-Methyl-4-Isoxazolepropionic Acid Receptors and K^+ Channels	595
3.33.11	Determination of Synaptic Information Transfer	596
3.33.12	Endbulbs versus Calyces versus Hair Cells	596
3.33.13	Comparison to Other Fast Synapses	597
3.33.14	Control of Fast Auditory Signaling	597
3.33.14.1	Inhibition	597
3.33.14.2	Presynaptic Modulation	598
References		599

Glossary

action potential or spike Unit electrical signal in the functioning nervous system.

AMPA receptor Glutamate receptors which selectively bind the drug alpha-amino-3-hydroxy-5-methyl-4-isoxazolepropionic acid (AMPA). These are the major excitatory postsynaptic receptors in the vertebrate central nervous system.

calyx synapse Very large terminals of globular bushy cell axons onto principle cells of the medial nucleus of the trapezoid body (MNTB).

endbulb synapse Large terminals of auditory nerve fibers onto spherical bushy cells in the cochlear nucleus.

EPSC Excitatory postsynaptic current, the excitatory current flow through transmitter receptor/channels such as AMPA or NMDA receptors.

EPSP Excitatory postsynaptic potential, the potential generated as the EPSC discharges the postsynaptic membrane.

exocytosis Secretion of neurotransmitter by fusion of transmitter-filled vesicles with the presynaptic plasma membrane.

GABA receptor Receptor for the inhibitory transmitter gamma-aminobutyric acid (GABA).

glycine receptor Receptor for the inhibitory transmitter glycine.

intrinsic response properties A neuron's stereotyped response to a given stimulus as a consequence of its geometrical arrangement and the complement of voltage-gated ion channels it expresses.

IPSP Inhibitory postsynaptic potential, the potential change due to anionic current flow through GABA or glycine receptor channels.

NMDA receptor Glutamate receptors which selectively bind the drug *N*-methyl-D-aspartic acid (NMDA).

release site Equivalent to active zone, the region of the presynaptic membrane from which transmitter is exocytosed.

3.33.1 Introduction

The central nervous system (CNS) must preserve and detect the timing of action potentials, or spikes, in the auditory nerve in order to localize sounds and to understand complex spectral information encoded in vocalizations. For example, spike timing in different fibers must at some point translate to a neural map for sound location relative to head position. The timing must be preserved along the pathway until the point at which the map is laid out. In localization of sound in the horizontal plane, phase shifts of tens of microseconds between sounds at the two ears changes significantly the perceived location of the sound source (Carr, C. E., 1986). Thus, acoustically driven spikes conducted along sequential neural stations must have minimal trial-to-trial error in their timing. Moreover, conduction through synaptic relays must be very fast, to enable precise convergence of signals from different nerve fibers, and so that a rapid succession of information can be processed. This dual requirement for precision and speed places special demands upon synapses in the auditory system. While the speed of conduction in nerve fibers is a problem solved by myelinated axons throughout the nervous system, precise and rapid synaptic transmission has required special refinements of physiology and morphology. This chapter will explore these refinements in some of the major cell types associated with acoustic timing pathways.

3.33.2 Synaptic Transmission

First, it may be helpful to review some of the basic elements of synaptic function, in order to appreciate better the unique adaptations in auditory synapses. Readers unfamiliar with this topic are also encouraged to consult well-known textbooks for a more complete account (e.g., Nicholls, J. G. *et al.*, 2001). Those trained in cellular neuroscience may skip ahead.

Classical central synapses formed between two neurons usually consist of just a few synapses or boutons, each one a site for exocytosis of the chemical transmitter from synaptic vesicles (Figure 1). For most vertebrate excitatory synapses, that transmitter is the amino acid glutamate, and the postsynaptic receptors that detect the glutamate are of two types, the alpha-amino-3-hydroxy-5-methyl-4-isoxazolepropionic acid (AMPA) receptor and the *N*-methyl-D-aspartic acid (NMDA) receptor. These subtypes are distinguished by their pharmacological sensitivities, their timecourse or kinetics of activation, and the change in ion permeability they induce in the postsynaptic cell (Dingledine, R. *et al.*, 1999). There are other types of glutamate receptors, but these will not be discussed here. Arrival of an action potential at the nerve terminals leads to a rapid elevation of presynaptic intracellular Ca^{2+}, which then triggers exocytosis of the transmitter. Figure 2 details the steps involved in transmission. At most synapses, the delay between the presynaptic spike and the onset of the postsynaptic response to the transmitter is 0.5 ms or less. Each synaptic site typically liberates one or fewer synaptic vesicles per presynaptic spike, which is to say that the probability of release at each site is between zero and one. Thus, the effectiveness of transmission can be increased by having more synaptic sites (i.e., more boutons), higher release probability at each site, or by increasing the number of receptors available to respond to the transmitter. A

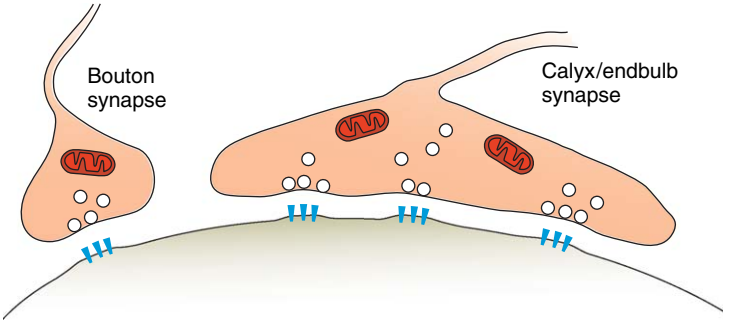

Figure 1 Two types of excitatory synapses that preserve spike timing that are found in auditory pathways. Bouton terminals have only one or two sites of transmitter release, each with a few docked vesicles. Calyceal and endbulb terminals feature a large number of transmitter release sites. In all cases, the transmitter is glutamate, which mediates its effect by binding postsynaptic alpha-amino-3-hydroxy-5-methyl-4-isoxazolepropionic acid (AMPA) receptors.

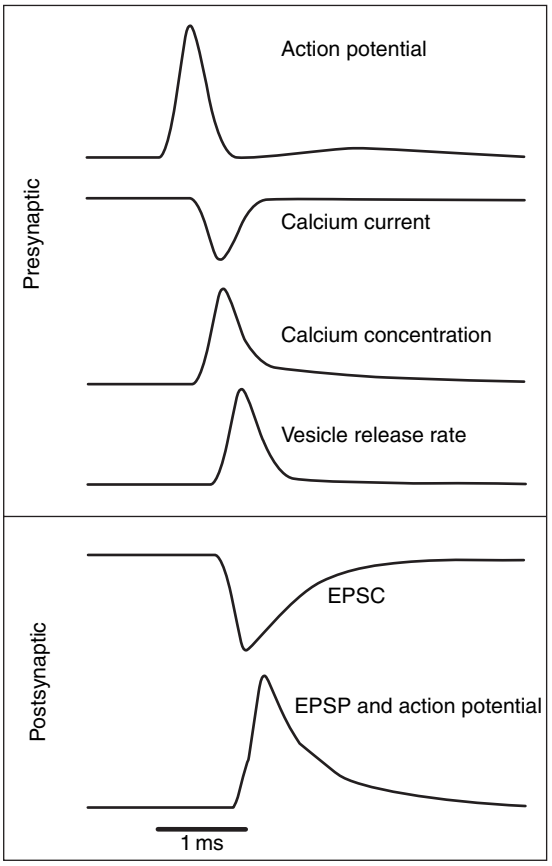

Figure 2 The steps involved in chemical synaptic transmission. Arrival of an action potential in the axon terminal triggers an inward calcium current and a rise in intraterminal calcium levels. This rise in calcium triggers a sharp increase in the rate of exocytosis, releasing the contents of synaptic vesicles into the synaptic cleft. The transmitter binds and activates postsynaptic receptors, generating an inward, excitatory current, the EPSC. The resulting depolarization is the EPSP, which drives the membrane potential past threshold for triggering an action potential. The time between the peak of the pre- and postsynaptic spikes can be less than 1 ms.

similar scenario holds for the major inhibitory transmitters gamma-aminobutyric acid (GABA) and glycine. Generally, a single vesicle's worth of glutamate has little depolarizing power to trigger a postsynaptic spike, but when many synapses are simultaneously active, summation of the depolarizing response occurs, and brings the postsynaptic membrane potential across spike threshold. Often, activation of many presynaptic neurons (each making several synaptic boutons) is required to trigger a postsynaptic spike, although there are well known cases where activation of a single presynaptic axon is sufficient, as described below.

Following the activation of the glutamate receptors, positive ionic current flows into the postsynaptic cell (EPSC), leading to membrane depolarization (EPSP). However, the consequence of this depolarization, in terms of the timing and pattern of spikes, varies dramatically in different types of neurons. This topic is explored in the chapter on Biophysical Specializations of Neurons that Encode Timing, by Paul B. Manis, and so only a brief overview will be made. Synaptic depolarization is limited in size and shape by the intrinsic electrical resistance and capacitance of the cell membrane. This resistive property, generated by an assortment of membrane ion channels, is highly nonlinear, with strong voltage and time dependencies. The morphology of the cell also plays a significant role; when synapses are made onto dendrites, the electrical filtering that is produced by dendrites typically leads to distortion of synaptic responses as the signals pass to the cell body and the axonal spike-trigger regions (Stuart, G. *et al.*, 1999). Because of these factors, a cell's shape, location of synapses, and the exact complement and distribution of ion channels are key determinants of the response to activation of the postsynaptic receptors.

3.33.3 Overview of the Types and Morphology of Synapses in Auditory Pathways

In this overview, we will focus primarily on a subset of auditory brainstem synapses within the sound localization pathways. Later we will consider the properties of these synapses in more detail and also in relation to that of the hair cell synapse, the site at which timing information is first encoded as neuronal action potentials. Readers should also consult the chapter on Afferent Synaptic Mechanisms by William Roberts.

Action potentials arrive at nerve terminals in the cochlear nucleus via the highly branched auditory nerve fibers. This branching accomplishes a division of information into multiple parallel pathways for computation (Cant, N. B. and Benson, C. G., 2003). For example, in the mammalian ventral cochlear nucleus (VCN), auditory nerve terminals onto the large spherical bushy cells initiate a pathway involved in localization of sounds along the azimuth using interaural timing cues. In birds, spherical bushy cells are the principal cells of the nucleus magnocellularis (NM). Terminals on the small spherical and globular bushy cells of mammals initiate azimuthal

localization by interaural intensity cues (Oertel, D., 1999; Cant, N. B. and Benson, C. G. 2003). In the mammalian dorsal cochlear nucleus (DCN), auditory nerve terminals onto fusiform neurons are believed to play a role in sound localization-based monaural spectral cues (Oertel, D. and Young, E. D., 2004). As discussed below, the different synapses made by the auditory nerve are diverse in both morphology and physiological mechanisms, in keeping with their different roles in information transfer. Figure 3 diagrams the major regions and cell types discussed in this chapter.

3.33.3.1 Bushy Cells and the Endbulbs of Held

Auditory nerve terminals onto large spherical bushy cells are called endbulbs of Held. Unlike classical boutons, each endbulb is a collection of hundreds to thousands of synaptic release sites distributed among thick fingers and fine branchlets of a terminal that enshrouds the postsynaptic cell body (Cant, N. B. and Morest, D. K., 1979; Ryugo, D. K. *et al.*, 1996; Nicol, M. J. and Walmsley, B., 2002; Figure 4). Each large spherical bushy cell typically receives one to three such terminals, and activation of each endbulb can

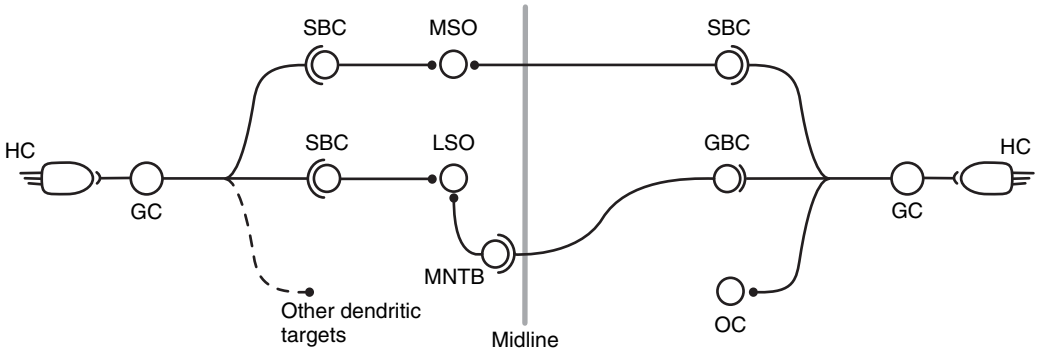

Figure 3 Diagram of the primary mammalian cell types, brain regions, and interconnections discussed in this review. GBC, globular bushy cell; GC, ganglion cell; HC, hair cell; LSO, lateral superior olive; MNTB, medial nucleus of the trapezoid body; MSO, medial superior olive; OC, octopus cell; SBC, spherical bushy cell.

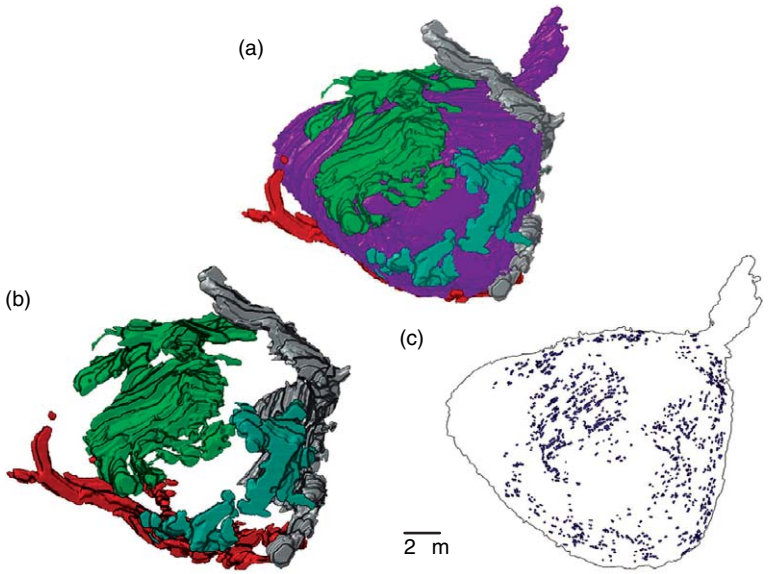

Figure 4 Electron microscopic reconstruction of four endbulbs terminating on a single bushy cell from the rat. (a) Each endbulb is in a different color; the postsynaptic neuron is shaded purple; (b) the postsynaptic cell is removed to show how the endbulbs enshroud the cell surface; (c) the postsynaptic cell is outlined and the location of synaptic release sites is indicated by the spots. Figure adapted from the study of Nicol M. J. and Walmsley B. (2002). with permission.

reliably trigger postsynaptic spikes. Accordingly, spherical bushy cells show a response pattern to tonal inputs similar to that of auditory nerve fibers (Rhode, W. S. *et al.*, 1983). This is characterized in a peristimulus time histogram (PSTH), which plots the frequency of spiking during a stimulus. Such plots for spherical bushy cells or auditory nerve show, for low-frequency sounds stimuli, peaks in activity associated with the phase of the sound. This concentration of the response within the phase of the sound wave cycle is called phase locking. For higher-frequency stimuli, beyond about 2 kHz, phase locking is lost both pre- and postsynaptically; after an initial well-timed spike, subsequent activity occurs randomly with respect to sound, but at an average rate reflecting the intensity of the sound energy (Joris, P. X. *et al.*, 1994). Because of this matching of pre- and postsynaptic spike behavior (Pfeiffer, R. R., 1966), large endbulb synapses are often characterized as synaptic relays.

The gross morphology of endbulbs has been shown to vary with the activity level of the presynaptic fiber. Endbulbs of genetically deaf cats and mice, for example, are characterized by an increase in the complexity of the synapse's branchlets as compared to conspecifics with normal hearing (Ryugo, D. K. *et al.*, 1997; Lee, D. J. *et al.*, 2003). Some studies indicate that this morphological pattern is paralleled by physiological changes in the strength of transmission, although this effect seems to vary with the genetic model (Oleskevich, S. *et al.*, 2004; Wang, Y. and Manis, P. B., 2005). Differences in morphology are also associated with the average activity level of the auditory nerve fiber, such that axons that have higher spontaneous (background) activity levels make synapses of simpler morphology (Sento, S. and Ryugo, D. K., 1989). In avian bushy cells, neurons in the regions receiving signals from higher-frequency sound information (i.e., high characteristic frequency) have larger, simpler terminals and fewer endbulbs per cell body (Koppl, C., 1994; Fukui, I. and Ohmori, H., 2004). Thus, these data suggest the possibility that the endbulb may dynamically adjust for changing average levels of acoustic stimulation.

In contrast to the spherical cells that host the large endbulbs, globular bushy cells are believed to be contacted by up to 30 auditory nerve terminals (Smith, P. H. and Rhode, W. S., 1987; Liberman, M. C., 1991). While the so-called modified endbulbs are, like the large endbulbs, confined mainly to the cell body, their smaller size means that each terminal has less influence, by itself, on postsynaptic cell firing. As a result, globular bushy cells probably fire only when multiple presynaptic fibers are synchronously active (Rothman, J. S. *et al.*, 1993; Joris, P. X. *et al.*, 1994). Such a mechanism has the ability to reduce the jitter in the firing of signals relative to the phase of the sound source. Indeed, the firing of globular bushy cells, measured by recordings made from their axons in the trapezoid body, show significant improvements in spike timing relative to that of auditory nerve fibers (Joris, P. X. *et al.*, 1994). For these cells, the peristimulus time histogram of the response to low-frequency sound is characterized by very narrow peaks around the phase of the sound cycle. With higher sound frequencies, an extremely well-timed initial spike is followed by a pause in firing, perhaps due to the spike refractory period of the fibers, and then a much lower level of randomized firing (Smith, P. H. and Rhode, W. S., 1987).

3.33.4 Medial Nucleus of the Trapezoid Body

The very large axons of globular bushy cells terminate on the principal cells of the medial nucleus of the trapezoid body (MNTB) as calyces of Held, among the largest synaptic terminals in the mammalian brain. Each principal cell receives only one such calyx, which occupies nearly half of the cell body surface (Smith, P. H. *et al.*, 1998; Satzler, K. *et al.*, 2002). Calyces, like endbulbs, are riddled with synaptic release sites; in the rat, each terminal contains over 600 active zones (Meyer, A. C. *et al.*, 2001; Satzler, K. *et al.*, 2002; Taschenberger, H. *et al.*, 2002), more than enough to drive the postsynaptic cell quickly to spike threshold (Taschenberger, H. and von Gersdorff, H. 2000). Calyces are therefore the ultimate synaptic relay, and accordingly the firing of principal cells generally follows closely that of calyces (Guinan, J. J., Jr. and Li, R. Y., 1990). As these synapses must quickly ferry signals from the contralateral bushy cells to the ipsilateral lateral superior olive (LSO), all aspects of the axons and synapse are suited to minimizing delays. Indeed, the time delay for signals to travel through this pathway, as compared for signals between ipsilateral cochlear nucleus and LSO, is less than 0.2 ms in cats (Joris, P. X. and Yin, T. C., 1998). In the later sections we will examine more carefully the functional differences between calyces and endbulbs, and possible modifications to their relay function.

3.33.5 Dendritic Coincidence Detectors

Many cell types in the cochlear nucleus and superior olive receive synaptic inputs on dendrites, rather than on (or in addition to) their cell bodies; for some of these cells, their spike output is highest when their inputs fire in precise synchrony. Such coincidence detectors include the octopus cells of the posteroventral cochlear nucleus and the principal cells of the medial superior olive (or its avian homolog, the nucleus laminaris (NL)). Octopus cells receive auditory nerve inputs representing a broad range of frequencies, an exception to the rule of highly frequency-specific, tonotopic innervation of other auditory brainstem neurons (Golding, N. L. *et al.*, 1995). Octopus cells will fire only in response to synchronous activation of groups of synaptic inputs, a feature well suited for the detection of acoustic elements of speech (Oertel, D. *et al.*, 2000). However, because so many axons contact these cells, and not all need fire to drive the cell to threshold, the firing of octopus cells can entrain to higher-frequency sounds, firing on a one-to-one basis with the sound cycle up to nearly 1 kHz (Rhode, W. S. and Smith, P. H., 1986; Oertel, D. *et al.*, 2000). In terms of both precision and entrainment, they are among the most specialized cells in the mammalian nervous system.

Bipolar or bitufted neurons of the mammalian medial superior olive/avian NL receive frequency-specific inputs segregated onto their two dendritic fields, physically segregating the inputs from ipsi- and contralateral spherical bushy cells. According to classical models of sound localization, the precise convergence of ipsi- and contralateral excitatory inputs forms the basis for encoding interaural time delays ((Joris, P. X. *et al.*, 1998) see chapter by E. Rubel). More recent models suggest an important role for precise convergence of inhibitory inputs as well as excitatory inputs, at least in mammals (Brand A. *et al.*, 2002). In any case, it is thought that the ability of these cells to fire only when their synaptic inputs are well timed (with submillisecond accuracy) is an essential feature of their role in sound localization.

With these examples we have a paradox. Why is it that endbulbs and calyces of Held require large somatic synapses for their role in timing circuits, yet octopus and medial superior olive (MSO)/laminaris cells are able to function with small synapses on dendrites? Several aspects of this question are worth investigating. The role of large synapses is very different from that of coincidence detectors, namely to permit one or a few axons to exert complete control over the firing of the postsynaptic cell and to relay signals quickly. Large somatic synapses enable presynaptic axons to drive the postsynaptic cell to threshold reliably and without much delay. By contrast, coincidence detectors function through precise integration of well-timed signals. Some physiological features are common to all of these synapses, for example the types of synaptic receptors and ion channels that are employed. Still, it is not clear how fast, reliable timing information can be encoded in cells with dendrites. Some clues may be found in the fact that the dendrites are not particularly long, and can be rather stout, conditions that certainly minimize distortions of signals by electrical cable effects. One extreme example is in medial regions of the avian NL, in which cells have dozens of remarkably short dendrites, resembling the roots of a green onion (Smith, D. J. and Rubel, E. W., 1979; Carr, C. E. and Konishi, M., 1990). Dispersing synaptic inputs onto different dendrites has been proposed to favor the integration of synaptic signals between dendrites rather than within a dendrite (Agmon-Snir, H. *et al.*, 1998). This is because when adjacent synapses are active, the local depolarization they generate will tend to reduce the electrical driving force for synaptic current flow; synapses far away from one another will therefore tend to contribute to more effectively to depolarization of the soma and nearby spike generating regions. Other factors need to be investigated, however, such as unusual distributions of ion channels, which might shape the electrical profile of dendritic responses. Critically timed inhibition may also play an important role in this process (Brand, A. *et al.*, 2002; Zhou, Y. *et al.*, 2005).

3.33.6 Transmission at Giant Synapses

In this section we will focus on the properties of giant synapses, in part because they represent the quintessential spike timing relay, but also because their large size has made them particularly amenable to biophysical and molecular analyses. Many of their detailed, physiological, features are probably common to all of the synapses described above. Most of the attention to presynaptic function has taken advantage of the calyx of Held, and therefore this will be described most extensively below. However, where appropriate, information derived from studies of endbulb synapses will also be included.

3.33.7 Synaptic Strength at Auditory Relays

The hallmark of endbulb and calyceal synapses is their size. As noted above, electron microscopic reconstructions indicate that each terminal probably contains at least 600 synaptic active zones. At each active zone, two to seven vesicles are touching the plasma membrane; these are termed docked vesicles and it is assumed that any of these is available for exocytosis (Satzler, K. *et al.*, 2002; Taschenberger, H. *et al.*, 2002). Thus, one may conclude that the pool of releasable vesicles numbers in the thousands. This estimate roughly coincides with several physiological estimates of the readily releasable pool, although the definition of this pool remains highly method-dependent (Sun, J. Y. and Wu, X. S., 2001).

For low-frequency calyceal stimuli, the quantal content (evoked EPSC/miniature EPSC (mEPSC)) of each EPSC is about 200–400, indicating that only a fraction (presumably a random fraction) of release sites and vesicles are used in each response (Zhang, S. and Trussell, L. O., 1994b; Iwasaki, S. and Takahashi, T., 2001). Still higher estimates of spike-evoked release come from measurements of presynaptic capacitance during exocytosis (Taschenberger, H. *et al.*, 2002; Sun, J. Y. *et al.*, 2004). To view the vesicle pool size and quantal content with respect to what the synapse needs for effective transmission, we should consider the depolarizing power of a vesicle's worth of glutamate. The response to the release of one vesicle of glutamate results in 30–50 pA of current at a membrane potential of −70 mV (Sahara, Y. and Takahashi, T., 2001); this in turn may depolarize the membrane by roughly 1 mV. With spike threshold of only about 20 mV positive to the resting potential (Awatramani, G. B. *et al.*, 2004), the number of released vesicles needed to trigger a spike is relatively small. Even though nonlinearities in summation of synaptic currents and in membrane conductance will increase the quantal number needed to reach threshold, these data indicate that the calyx releases many more vesicles than are needed to reach spike threshold. This surplus is evident in experiments on endbulbs which showed that release could be blocked by over 80% and reliable transmission is still maintained (Brenowitz, S. *et al.*, 1998). Such a high safety factor is not only an insurance policy for suprathreshold transmission. Large synaptic currents drive the postsynaptic cell to threshold sooner than small currents; thus, a high safety factor ensures that spike latencies and jitter is small (see the section Reliablity of Timing).

The rapid termination of the transmitter release process is essential to high-frequency transmission. Experiments in which voltage clamp stimuli of variable duration were delivered to the nerve terminals demonstrated that the release process could be critically shaped by the waveform of the presynaptic spike (Borst, J. G. and Sakmann, B., 1999; Fedchyshyn, M. J. and Wang, L. Y., 2005). Spike width is tightly regulated during brain development. Between postnatal ages 7 and 14, the duration of the EPSC becomes significantly shorter, and parallels an age-dependent narrowing of the presynaptic spike (Taschenberger, H. and von Gersdorff, H., 2000). Presumably, enhanced expression in mature animals of presynaptic K^+ currents that repolarize the spike is key to the fast performance of this synapse (Dodson, P. D. *et al.*, 2003; Ishikawa, S. *et al.*, 2003).

Additional presynaptic features necessary for fast synapses is the precise location of Ca^{2+} channels relative to the synaptic release machinery and Ca^{2+} buffers and extrusion mechanisms. As noted above, the duration of the transmitter release process is critically dependent on the spike width. The spike width determines the duration of Ca^{2+} entry, and recent studies show that the Ca^{2+} near the release apparatus decays in less than 1 ms (Bollmann, J. H. and Sakmann, B., 2005). The major wave of Ca^{2+} entry is thought to be controlled by diffusible Ca^{2+} buffers, and indeed during postnatal weeks 2–4 in rats, there is a sharp increase in expression of the buffers calretinin and parvalbumin in the calyces of Held (Felmy, F. and Schneggenburger, R., 2004). Interestingly, the narrower spike-evoked Ca^{2+} profile observed in more mature calyces is insufficient to drive release from younger calyces. By correlating the amount of release with the amount of Ca^{2+} entry, Fedchyshyn M. J. and Wang L. Y. (2005) argued that the degree of cooperativity in Ca^{2+} action at the release site is lower in mature animals. They explain this by saying that Ca^{2+} channels are closer to the releasable vesicles and so that fewer channels are needed to trigger exocytosis. Thus, with maturation the nerve terminal is modified to release a large number of vesicles over a very narrow time period. Synaptic relays are therefore optimized presynaptically for both power and precision.

3.33.8 Reliability of Timing

Reliability can be viewed not only as the likelihood of driving the postsynaptic cell to spike threshold but in terms of temporal precision. When an action potential reaches the presynaptic terminal there is a small delay before the postsynaptic response ensues. This latency, termed the synaptic delay, lasts about 0.3 ms in mature synapses (Guinan, J. J., Jr. and Li, R. Y., 1990; Taschenberger, H. and von Gersdorff, H., 2000) and is extremely reproducible, that is to say it exhibits little trial to trial jitter (Borst, J. G. and Sakmann, B., 1996; Sahara, Y. and Takahashi, T., 2001). Indeed, at mature endbulbs, the standard deviation of jitter in transmission, including the triggering of the action potential, is only 20 μs (Brenowitz, S. and Trussell, L. O., 2001). Thus, even though action potentials themselves may be several hundred microseconds in duration (Brenowitz, S and Trussell, L. O., 2001; Taschenberger, H. and von Gersdorff, H., 2000), the giant synapses have the ability to transmit with much greater precision.

3.33.9 Synaptic Depression

When endbulb or calyceal synapses are activated at high frequencies (>20 Hz), the peak amplitudes of the resulting synaptic currents decline to a steady level over 5–10 stimuli, a process termed synaptic depression. Synaptic depression has been intensively studied in giant synapses because their large size affords the opportunity to work out the pre- and postsynaptic mechanisms of this ubiquitous synaptic feature.

Depression has two sources. In prehearing rodents or embryonic chicks, the transmitter glutamate is not effectively cleared from the synapses and AMPA receptors desensitize (Trussell, L. O. *et al.*, 1993; Otis, T. *et al.*, 1996; Scheuss, V. *et al.*, 2002; Wong, A. Y. *et al.*, 2003). This poor clearance is probably a result of both the immature, sheet-like structure of the synapses and the high probability of exocytosis at neighboring release sites (Kandler, K. and Friauf, E., 1993; Taschenberger, H. *et al.*, 2002). Because glutamate uptake sites reside generally on glial cells (e.g., Turecek, R. and Trussell, L. O., 2000), these factors together lead to pooling and delayed clearance of glutamate. However, in older animals, transmitter release probability declines, the synapses become more fenestrated, and desensitization is minimized (Kandler, K. and Friauf, E., 1993; Brenowitz, S. and Trussell, L. O., 2001; Taschenberger, H. *et al.*, 2002).

The second, and more common, source of depression is a use-dependent reduction in transmitter release. Two views exist as to the basis of presynaptic depression. Depletion of vesicles that are immediately available for exocytosis is reported to account for the majority of depression, even outweighing postsynaptic factors (Schneggenburger, R. *et al.*, 1999; Scheuss, V. *et al.*, 2002). By voltage clamping the presynaptic terminals, one can deliver strong voltage pulses that result in depletion of the readily releasable pool of vesicles. This pool can also be depleted by repetitive presynaptic action potentials. These studies showed that synaptic depression is associated with a significant depletion of the readily releasable pool of vesicles. Moreover, it was apparent that not all vesicles are the same in terms of their likelihood of depletion or their ability to build up again (Sakaba, T. and Neher, E., 2001). One population released quickly but recovered slowly while another had the opposite characteristics. These populations may consists of vesicles with either different distances to Ca^{2+} channels (Wadel, K. *et al.*, 2007) or different sensitivities to Ca^{2+} (Wolfel, M. *et al.*, 2007).

Another view of presynaptic depression at giant auditory synapses is that the probability of release is reduced for docked vesicles, rather than (or in addition to) vesicle depletion. Wu L. G. and Borst J. G. (1999) showed in the calyx of Held that the fraction of the total releasable pool of vesicles that are released by a spike-like stimulus is reduced after a strong, depressing presynaptic voltage step. In endbulbs of Held, where such presynaptic recordings are rare, there is also some evidence for a nondepletion mechanism at work. Bellingham M. C. and Walmsley B. (1999) demonstrated a phase of depression that was Ca^{2+} dependent but apparently not due to depletion, and suggested that Ca^{2+} triggers an event inhibitory to exocytosis. Finally, one component of depression, restricted to lower-frequency responses, is produced by the inactivation of Ca^{2+} currents (Xu, J. and Wu, L. G., 2005). Although this inactivation is rather small for a brief spike-evoked Ca^{2+} current (~10% change), the high degree of cooperativity for Ca^{2+} needed for release means that small changes in the current has a large effect of transmitter output.

As noted above, postsynaptic depression declines with synaptic maturation. While presynaptic depression remains prominent, it also declines in magnitude in the first 2–3 weeks after birth in rodents, but

apparently does not disappear. One reason for this decline is that during the period that the synapse grows, and the number of synaptic release sites increases, the probability of release for each vesicle declines (Brenowitz, S. and Trussell, L. O., 2001; Iwasaki, S. and Takahashi, I., 2001; Taschenberger, H. *et al.*, 2002). In this way, effective transmission is maintained while the likelihood of vesicle depletion diminishes. Thus, several developmental processes converge to improve the ability of giant synapses to sustain release at high frequencies. Despite the continued presence of depression, sufficient numbers of vesicles are released with each impulse that EPSPs are well above spike threshold. Interestingly, depression has been shown to have a physiological role in improvement of coincidence detection in the chick NL. There, frequency-dependent depression of EPSPs ensures that a critical number of coincident events are required for summation, regardless of the frequency of inputs (Kuba, H. *et al.*, 2002; Cook, D. L. *et al.*, 2003).

3.33.10 Alpha-Amino-3-Hydroxy-5-Methyl-4-Isoxazolepropionic Acid Receptors and K^+ Channels

Postsynaptically, the auditory synapse has several physiological properties that allow it to respond to the released glutamate reliably, with negligible delay, and to recover from the response quickly. These include specializations in glutamate receptors and potassium channels (Trussell, L. O., 1999b). As noted above, glutamate activates two main subtypes of ionotropic receptors, the AMPA and NMDA receptors. NMDA receptors, although essential for transmission in many other brain regions, play a minor role in auditory relays. Indeed these receptors show a striking developmental downregulation, so that by the onset of hearing they contribute little to postsynaptic depolarization (Bellingham, M. C. *et al.*, 1998; Taschenberger, H. and von Gersdorff, H., 2000; Iwasaki, S. and Takahashi,T., 2001; Lu, T. and Trussell, L., 2007). AMPA receptors, therefore, mediate almost all excitation at these synapses. EPSCs in auditory relays have a remarkably faster time course than at other CNS synapses. For example, spike-evoked EPSCs in the chick NM rise and decay with a timecourse of around 200 μs (Zhang, S. and Trussell, L. O., 1994b; Brenowitz, S. and Trussell, L. O., 2001). By contrast, EPSCs mediated by AMPA receptors in cortical pyramidal neurons decay in at least 2 ms (Hausser, M. and Roth, A., 1997). The basis for these differences lies in the fact that the AMPA receptors are structurally and functionally different in these two regions. This was initially explored by excising membrane patches from bushy cells and rapidly applying glutamate, which resulted in ionic currents with time courses several fold faster in than glutamate responses in nonauditory neurons (Raman, I. M. *et al.*, 1994). Currents like these were also observed in experiments in which AMPA receptor complimentary DNA (cDNA) was expressed in a heterologous expression system. Specifically, the flop alternative splice variants of the GluR3 or 4 subunits produced currents almost indistinguishable from those of chick or mouse bushy cells (Mosbacher, J. *et al.*, 1994). Similar currents were also obtained from several other auditory cell types, and all of these were shown to express this molecular subtype of AMPA receptor (Gardner, S. M. *et al.*, 2001; Koike-Tani, M. *et al.*, 2005). These results have led to the idea that cells contacted by the auditory nerve, as well as some cell types downstream of the cochlear nucleus, have a particular pattern of gene expression leading to production of a fast auditory AMPA receptor.

The presence of GluR3/4 flop subunits in the AMPA receptors heteromeric complex gives these receptors their characteristic speed. The absence of other subunits also has some meaning for auditory function. The GluR1 subunit is associated with synapses exhibiting use-dependent, long-term potentiation of the EPSP, and the absence of these subunits suggests that many auditory synapses are not plastic (Wang, Y. X. *et al.*, 1998b; Petralia, R. S. *et al.*, 2000). The GluR2 subunit is associated with a reduced Ca^{2+} permeability and enhanced receptor channel conductance (Dingledine, R. *et al.*, 1999), and is poorly expressed in neurons of the cochlear nucleus (Otis, T. S. *et al.*, 1995; Wang, L. Y. *et al.*, 1998b; Gardner, S. M. *et al.*, 1999; Petralia, R. S. *et al.*, 2000; Gardner, S. M. *et al.*, 2001). Accordingly, many cells of the cochlear nucleus express AMPA receptors which allow Ca^{2+} entry with each synaptic response (Otis, T. S. *et al.*, 1995; Gardner, S. M. *et al.*, 1999; Gardner, S. M. *et al.*, 2001); it should not be surprising then that these neurons also express high levels of Ca^{2+} binding proteins (Lohmann, C. and Friauf, E. 1996; Hack, N. J. *et al.*, 2000). The physiological function of this Ca^{2+} is not known. However, the elevated channel conductance may serve a specific role in some cases, to ensure a large synaptic response. mEPSCs are the response to single vesicles of glutamate, and synapses with larger mEPSCs will

produce a larger spike-evoked EPSPs. Comparison of mEPSC among different CNS neurons indicates that bushy cells, contacted by endbulbs of Held, have some of the largest in the brain (Trussell, L. O., 1999a). Interestingly, MNTB neurons have rather normal sized mEPSCs. Perhaps the larger size of the calyx, as compared to the endbulb, obviates the need to enhance mEPSC amplitude.

The second factor promoting rapid relay of synaptic signals is the intrinsic properties of the postsynaptic cell, generally determined by the complement of K^+ channels. This aspect of the physiology is covered by Paul Manis in this series, and so will only be addressed briefly. Neurons of avian NM and NL cells, as well as mammalian bushy, octopus and MSO cells, express several major voltage-gated currents. Two of these are most notable here, a low-voltage-activated K^+ current (LVA), blockable with dendrotoxin, and a high-voltage-activated current (HVA) blocked by tetraethylammonium (TEA) (Trussell, L. O., 1999b). The latter is the major outward current repolarizing the action potential. The former plays a very different role: once the cell becomes slightly depolarized above rest, this current activates and effectively raises spike threshold. Because of this, the cell can only spike if it can reach threshold before the current activates. After the spike, the cell must return back to rest to be able to spike again; thus synaptic currents must be brief to allow rapid firing. Blockade of the HVA in bushy or MNTB cells broadens the spike (Zhang, S. and Trussell, L. O., 1994a; Wang, L. Y. *et al.*, 1998a), while block of LVA promotes repetitive firing (Brew, H. M. and Forsythe, I. D., 1995; Rathouz, M. and Trussell, L., 1998; Wang, L. Y. *et al.*, 1998a). Thus, the LVA helps maintain a single postsynaptic spike for a single presynaptic spike (Brew, H. M. and Forsythe, I. D., 1995). The effect of the LVA on spike threshold is probably essential to the detection of coincidence of synaptic inputs. Because the LVA turns on quickly, subthreshold EPSPs produced by convergent inputs must all occur within a narrow time window to allow summation to threshold (Ferragamo, M. J. and Oertel, D., 2002).

3.33.11 Determination of Synaptic Information Transfer

Auditory nerve fibers innervate diverse cell types each with very specific processing roles. What are the common physiological elements at these synapses? We have seen that synapses of the auditory nerve use glutamate receptors with rapid kinetics; however, this is not always the case. Synapses and AMPA receptors on basal dendrites of fusiform cells of the DCN exhibit much slower kinetics than synapses in the VCN or synapses onto interneurons in the DCN (Gardner, S. M. *et al.*, 1999; Gardner, S. M. *et al.*, 2001). Fusiform cells also receive glutamatergic contacts of granule cells on their apical dendrites, and these synapses also have slow kinetics. Thus, it may be that the fast synaptic phenotype is restricted to cells whose primary excitatory input is the auditory nerve. Interestingly, although synapses on both apical and basal dendrites are slower than VCN synapses, they employ different receptor subunits, which are differentially targeted to the two dendrites (Rubio, M. E. and Wenthold, R. J., 1999), suggesting very local control of synaptic properties.

Even among these auditory nerve-dominant neurons, synaptic function may vary. In birds, auditory nerve fibers terminate in two cochlear nuclei, the NM and the nucleus angularis, the latter being involved in sound localization using intensity cues (Takahashi, T. *et al.*, 1984). Fast AMPA receptors appear to mediate transmission in both nuclei (Raman, I. M. *et al.*, 1994; MacLeod, K. M. and Carr, C. E., 2005b), despite their neurons having very different membrane firing properties (Soares, D. *et al.*, 2002; Fukui, I. and Ohmori, H., 2003; Zhang, S. and Trussell, L. O, 1994a). Moreover, EPSPs in nucleus angularis are slower than in NM, due to their different postsynaptic membrane properties, and do not exhibit the acute presynaptic synaptic depression seen in calyceal synapses (MacLeod, K. M. and Carr, C. E., 2005a; 2005b). These features are ideal for promoting integration of EPSPs generated by multiple auditory nerve fibers in nucleus angularis. Thus, both pre- and postsynaptic physiology may vary in a cell-type-specific manner despite a common presynaptic source of input. This is reminiscent of the varying synaptic properties among different neocortical excitatory synapses (Markram, H. *et al.*, 1998), and suggests that synaptic properties are determined not just by the identity of the pre- or postsynaptic cell but in a synapse-specific manner.

3.33.12 Endbulbs versus Calyces versus Hair Cells

Up to this point we have treated endbulbs and calyces of Held as being equivalent in their physiological properties, on the assumption that relays are

relays. However, the differences between these synapses may give insight into their respective roles. Endbulbs are smaller synapses, which concentrate as much transmission power as a calyx into a smaller space. Because each bushy cells received several axonal inputs, some synaptic integration is possible. Indeed, Xu-Friedman M. and Regehr W. (2005) have shown that even though these inputs are suprathreshold, the degree of jitter in firing of presynaptic inputs can be reduced in the output of the bushy cell. Say that three input fibers fire with some jitter around the phase of the sound stimulus. The first EPSP will trigger a spike and therefore the average timing of the output spikes will be concentrated and shifted slightly earlier in phase. Each calyx, by contrast, is the sole excitatory drive for the MNTB principle cell. These synaptic features, as well as the very large size of the presynaptic axon, suggest that the synaptic adaptations of the calyx are geared for reliability and minimizing transmission delays, rather than preservation or improvement in phase locking.

Because all precise auditory signaling arises from the hair cell synapse, it is of interest to compare the functioning of this synapse to that of its downstream partners in the CNS.

As described in the chapter by William Roberts, hair cells utilize a very different synaptic structure; accordingly, they encode neural information through a different cellular algorithm. Each auditory nerve fiber is driven by a single synaptic release site, called a ribbon synapse, which is suited for graded, rather than spike-triggered, transmission (Fuchs, P. A., 2005). Because the postsynaptic fiber is excited following exocytosis from a single release site, involving one or a few vesicles (Crawford, A. C. and Fettiplace, R., 1980; Siegel, J. H., 1992), the number of vesicles released per cycle of sound contains little information. Rather, what seems to matter at this synapse is the phase-locked rise in probability of release at each cycle for low-frequency sounds (<2 kHz) or the average number of randomized releases for higher-frequency sound. Unlike CNS synapses, in which higher-frequency presynaptic firing reflects higher intensity sounds, sound intensity in the hair cell is encoded by the amplitude of membrane depolarization (Palmer, A. R. and Russell, I. J., 1986). At the level of the hair cell synapse, this higher depolarization should increase the frequency of exocytic events and thus the frequency of spikes in the nerve fiber.

At the other end of the auditory nerve fiber, single release sites contribute only slightly to raising the postsynaptic cell to threshold, and so find strength in numbers; postsynaptic excitation requires either endbulb synapses or many convergent fibers. These nerve terminals are only excited by all-or-nothing spikes. Although such transmission is not graded, release is very sensitive to variation in spike width (Borst, J. G. and Sakmann, B., 1999; Bollmann, J. H. and Sakmann, B., 2005); this variation eventually may be shown to be an essential means for regulation of transmission in auditory synapses.

3.33.13 Comparison to Other Fast Synapses

How special are auditory timing synapses compared to others in the CNS? Certainly the jitter in postsynaptic spike timing is greater in cortical and hippocampal neurons, even for those that are considered to provide well-timed signaling. We have already seen that AMPA receptor kinetics are several times slower in most nonauditory brain regions. On the other hand, some of the specializations we have described are found in a few brain regions that are not associated with such precise temporal fidelity. For example, the fast-gating AMPA receptors that are characteristic of auditory nerve targets mediate transmission in retinal horizontal cells, even though glutamate is released onto them much more asynchronously than in fast, phasic synapses (Eliasof, S. and Jahr, C. E., 1997). EPSCs almost as fast as auditory EPSCs are also found in cerebellar stellate cells (Carter, A. G. and Regehr, W. G., 2002). Cerebellar granule cells feature EPSCs whose timing of multi-vesicular glutamate release from mossy fibers is extremely precise, with a temporal dispersion in release of less than 100 μs (Sargent, P. B. *et al.*, 2005). However, unlike auditory relays, these synapses also show considerable trial-to-trial fluctuation in strength. Thus, precisely timed or fast EPSCs has been selected for in several other brain regions, but it remains unclear what function it serves there.

3.33.14 Control of Fast Auditory Signaling

3.33.14.1 Inhibition

Auditory relay neurons and coincidence detectors all receive substantial inhibitory input from interneurons or from cells in nearby nuclei. Glyinergic inputs

on mammalian bushy cells of the VCN, which probably originate from subtypes of stellate cell within the VCN and from tuberculoventral cells of the DCN, may regulate multiple aspects of acoustic responses (Wickesberg, R. E. and Oertel, D., 1990; Backoff, P. M. *et al.*, 1997; Ferragamo, M. J. *et al.*, 1998; Kopp-Scheinpflug, C. *et al.*, 2002). MNTB receives very powerful glycinergic inputs (Banks, M. I. and Smith, P. H., 1992; Awatramani, G. B. *et al.*, 2004), possibly originating from MNTB collaterals or from neighboring olivary nuclei (Kuwabara, N. *et al.*, 1991). Avian cochlear nuclei and NL receive GABAergic input from the superior olivary nucleus (Burger, R. M. *et al.*, 2005). MNTB provides fast inhibition to LSO and probably also to MSO (Kuwabara, N. and Zook, J. M., 1991; Banks, M. I. and Smith, P. H., 1992; Kuwabara, N. and Zook, J. M., 1992; Wu, S. H. and Kelly, J. B., 1992; Kim, G. and Kandler, K., 2003). Birds and mammals employ strikingly different mechanisms for mediating inhibition of synaptic relays. Here we will focus on the rat MNTB and the chick NM to contrast these very different inhibitory systems.

Glycine serves as the major inhibitory transmitter of the lower auditory pathways, and elicits fast, hyperpolarizing synaptic potentials. In the MNTB, these inhibitory postsynaptic potentials (IPSPs) are driven by very large conductance and fast kinetic synaptic responses, which are blocked by the glycine receptor antagonists strychnine (Banks, M. I. and Smith, P. H., 1992; Awatramani, G. B. *et al.*, 2004; 2005b). In mature rats, the size of the synaptic conductance is almost as great as that of the calyceal EPSC (Awatramani, G. B. *et al.*, 2004). Moreover, the currents are quite brief, with decay times of evoked responses less than 2 ms, and quantal currents of less than 1 ms at physiological temperature (Awatramani, G. B. *et al.*, 2004). The IPSCs are in fact the fastest glycine synaptic events that have been observed, suggesting the possibility that, like the AMPA receptor, the auditory system has employed a receptor modification to gain fast signaling properties. The size and speed of the IPSCs are well suited for abbreviating a train of calyceal-evoked EPSPs, and could therefore play a role in rapidly sculpting the response to a complex acoustic stimulus. Indeed, one recent study observed two-tone suppression in the MNTB that appeared to arise by a postsynaptic mechanism, as one might expect of inhibition triggered in response to frequencies near an MNTB neuron's characteristic frequency (Kopp-Scheinpflug, C. *et al.*, 2003). It will be essential to determine the source of this inhibition and how it is activated *in vivo* in order to develop more testable hypotheses about the role of inhibition.

By contrast, inhibition in avian auditory brainstem is mediated by GABA (Yang, L. *et al.*, 1999; Monsivais, P. *et al.*, 2000). Both the kinetics and ionic driving force of the GABAergic synaptic responses are geared for tonic inhibition through prolonged depolarization of the postsynaptic cell, rather than abrupt well-timed hyperpolarization as in mammals (Lu, T. and Trussell, L. O., 2000; Lu, T. and Trussell, L. O., 2001). GABAergic synaptic currents have a decay time over 10 times slower than the glycinergic currents. Moreover, when stimulated in high-frequency trains, the GABA release becomes desynchronized from the timing of the presynaptic spikes, thus generating a tonic GABAergic current (Lu, T. and Trussell, L. O., 2000). Remarkably, the reversal potential for GABA is far above spike threshold, between −36 and −25 mV in neurons of NM, due to an elevated intracellular Cl^- concentration (Lu, T. and Trussell, L. O., 2001; Monsivais, P. and Rubel, E. W., 2001). Although some IPSPs can trigger spikes at their onset, their tonic activation keeps the neuron depolarized; by activating K^+ currents and inactivating Na^+ currents, spike threshold is raised and excitation quickly ceases. Given the physiology and circuitry of inhibition, it has been proposed that GABAergic transmission serves to offset the effects of interaural level differences in auditory timing pathways (Burger, R. M. *et al.*, 2005). Thus, in mammals and birds, decidedly different modes of inhibition are employed, despite the remarkable similar mechanisms for fast excitation using calyces, fast glutamate receptors, and a complement of high- and low-threshold K^+ channels.

3.33.14.2 Presynaptic Modulation

Endbulbs and calyces are endowed with a variety of presynaptic mechanisms for modulation of transmitter release, besides the use-dependent synaptic depression described above (Trussell, L. O., 2002). Most work has focused on the calyx of Held, because its large size enables direct evaluation of the presynaptic effects of modulatory agents. These agents act on presynaptic receptors for norepinephrine, GABA (two receptor types), glycine, adenosine, glutamate (two types), and endocannabinoids (Takahashi, T. *et al.*, 1996; Brenowitz, S. *et al.*, 1998; Takahashi, T. *et al.*, 1998; Turecek, R. and Trussell, L. O., 2001;

Leao, R. M. and von Gersdorff. H., 2002; Turecek, R. and Trussell, L. O., 2002; Kimura, M. *et al.*, 2003; Sakaba, T. and Neher, E., 2003; Kushmerick, C. *et al.*, 2004; Takago, H. *et al.*, 2005). Two major schemes have been described for how these receptors work. Activation of presynaptic G-protein-coupled receptors inhibit Ca^{2+} channels and thus reduce the Ca^{2+} signal needed to trigger exocytosis (Takahashi, T. *et al.*, 1998; Kajikawa, Y. *et al.*, 2001). On the other hand, activation of ionotropic receptors depolarize the terminal, weakly activate Ca^{2+} channels, and induce a facilitation of glutamate release (Turecek, R. and Trussell, L. O., 2001; Awatramani, G. B. *et al.*, 2005a). In addition to effects on baseline synaptic strength, these receptors can also alter how quickly the synapse can recover from a period of synaptic depression. GABA, acting via a G-protein-coupled receptor, reduces cAMP levels in the synapse and slows the replenishment of vesicle pools after synaptic depression (Sakaba, T. and Neher, E., 2003). By contrast, glutamate, acting on group III metabotropic receptors, accelerates recovery from depression (Billups, B. *et al.*, 2005). Thus, calyces are endowed with a multitude of presynaptic receptor subtypes, which regulate glutamate release through many signaling pathways.

What are the physiological roles of these presynaptic receptors? Remarkably, only two studies have shown activation of such receptors by synaptically released transmitter. Synaptically released glutamate reaches presynaptic group III receptors (von Gersdorff, H. *et al.*, 1997; Billups, B. *et al.*, 2005), while activation of glycinergic inputs to MNTB principle cells releases sufficient glycine to modulate calyceal function (Turecek, R. and Trussell, L. O., 2001). For the other modulators, a physiological role is obscure, in part because the sources of endogenous transmitters is not known. It is of interest that some of these receptors, such as noradrenergic and metabotropic receptors, are downregulated during development. It may be that young synapses simply express many types of receptor, and these are pared down according to the needs of the mature functioning system. Alternatively, such mechanisms may act *in vivo*, but under conditions that have not yet been replicated in the brain slice studies. An important area for future research will be to identify how these various receptors are activated by endogenous transmitters and how such activation modifies the relay function of giant auditory synapses.

References

Agmon-Snir, H., Carr, C. E., and Rinzel, J. 1998. The role of dendrites in auditory coincidence detection. Nature 393, 268–272.

Awatramani, G. B., Price, G., and Trussell, L. O. 2005a. Modulation of transmitter release by presynaptic resting potential and background calcium levels. Neuron 48, 109–121.

Awatramani, G. B., Turecek, R., and Trussell, L. O. 2004. Inhibitory control at a synaptic relay. J. Neurosci. 24, 2643–2647.

Awatramani, G. B., Turecek, R., and Trussell, L. O. 2005b. Staggered development of GABAergic and glycinergic transmission in the MNTB. J. Neurophysiol. 93, 819–828.

Backoff, P. M., Palombi, P. S., and Caspary, D. M. 1997. Glycinergic and GABAergic inputs affect short-term suppression in the cochlear nucleus. Hear. Res. 110, 155–163.

Banks, M. I. and Smith, P. H. 1992. Intracellular recordings from neurobiotin-labeled cells in brain slices of the rat medial nucleus of the trapezoid body. J. Neurosci. 12, 2819–2837.

Bellingham, M. C. and Walmsley, B. 1999. A novel presynaptic inhibitory mechanism underlies paired pulse depression at a fast central synapse. Neuron 23, 159–170.

Bellingham, M. C., Lim, R., and Walmsley, B. 1998. Developmental changes in EPSC quantal size and quantal content at a central glutamatergic synapse in rat. J. Physiol. 511, 861–869.

Billups, B., Graham, B. P., Wong, A. Y., and Forsythe, I. D. 2005. Unmasking group III metabotropic glutamate autoreceptor function at excitatory synapses in the rat CNS. J. Physiol. 565, 885–896.

Bollmann, J. H. and Sakmann, B. 2005. Control of synaptic strength and timing by the release-site Ca^{2+} signal. Nat. Neurosci. 8, 426–434.

Borst, J. G. and Sakmann, B. 1996. Calcium influx and transmitter release in a fast CNS synapse. Nature 383, 431–434.

Borst, J. G. and Sakmann, B. 1999. Effect of changes in action potential shape on calcium currents and transmitter release in a calyx-type synapse of the rat auditory brainstem. Philos. Trans. R. Soc. Lond. B Biol. Sci. 354, 347–355.

Brand, A., Behrend, O., Marquardt, T., McAlpine, D., and Grothe, B. 2002. Precise inhibition is essential for microsecond interaural time difference coding. Nature 417, 543–547.

Brenowitz, S. and Trussell, L. O. 2001. Maturation of synaptic transmission at end-bulb synapses of the cochlear nucleus. J. Neurosci. 21, 9487–9498.

Brenowitz, S., David, J., and Trussell, L. 1998. Enhancement of synaptic efficacy by presynaptic GABA(B) receptors. Neuron 20, 135–141.

Brew, H. M. and Forsythe, I. D. 1995. Two voltage-dependent K^+ conductances with complementary functions in postsynaptic integration at a central auditory synapse. J. Neurosci. 15, 8011–8022.

Burger, R. M., Cramer, K. S., Pfeiffer, J. D., and Rubel, E. W. 2005. Avian superior olivary nucleus provides divergent inhibitory input to parallel auditory pathways. J. Comp. Neurol. 481, 6–18.

Cant, N. B. and Benson, C. G. 2003. Parallel auditory pathways: projection patterns of the different neuronal populations in the dorsal and ventral cochlear nuclei. Brain. Res. Bull. 60, 457–474.

Cant, N. B. and Morest, D. K. 1979. The bushy cells in the anteroventral cochlear nucleus of the cat. A study with the electron microscope. Neuroscience 4, 1925–1945.

Carr, C. E. 1986. Time coding in electric fish and barn owls. Brain Behav. Evol. 28, 122–133.
Carr, C. E. and Konishi, M. 1990. A circuit for detection of interaural time differences in the brain stem of the barn owl. J. Neurosci. 10, 3227–3246.
Carter, A. G. and Regehr, W. G. 2002. Quantal events shape cerebellar interneuron firing. Nat. Neurosci. 5, 1309–1318.
Cook, D. L., Schwindt, P. C., Grande, L. A., and Spain, W. J. 2003. Synaptic depression in the localization of sound. Nature 421, 66–70.
Crawford, A. C. and Fettiplace, R. 1980. The frequency selectivity of auditory nerve fibres and hair cells in the cochlea of the turtle. J. Physiol. 306, 79–125.
Dingledine, R., Borges, K., Bowie, D., and Traynelis, S. F. 1999. The glutamate receptor ion channels. Pharmacol. Rev. 51, 7–61.
Dodson, P. D., Billups, B., Rusznak, Z., Szucs, G., Barker, M. C., and Forsythe, I. D. 2003. Presynaptic rat Kv1.2 channels suppress synaptic terminal hyperexcitability following action potential invasion. J. Physiol. 550, 27–33.
Eliasof, S. and Jahr, C. E. 1997. Rapid AMPA receptor desensitization in catfish cone horizontal cells. Vis. Neurosci. 14, 13–18.
Fedchyshyn, M. J. and Wang, L. Y. 2005. Developmental transformation of the release modality at the calyx of held synapse. J. Neurosci. 25, 4131–4140.
Felmy, F. and Schneggenburger, R. 2004. Developmental expression of the Ca^{2+}-binding proteins calretinin and parvalbumin at the calyx of held of rats and mice. Eur. J. Neurosci. 20, 1473–1482.
Ferragamo, M. J. and Oertel, D. 2002. Octopus cells of the mammalian ventral cochlear nucleus sense the rate of depolarization. J. Neurophysiol. 87, 2262–2270.
Ferragamo, M. J., Golding, N. L., and Oertel, D. 1998. Synaptic inputs to stellate cells in the ventral cochlear nucleus. J. Neurophysiol. 79, 51–63.
Fuchs, P. A. 2005. Time and intensity coding at the hair cell's ribbon synapse. J. Physiol. 566, 7–12.
Fukui, I. and Ohmori, H. 2003. Developmental changes in membrane excitability and morphology of neurons in the nucleus angularis of the chicken. J. Physiol. 548, 219–232.
Fukui, I. and Ohmori, H. 2004. Tonotopic gradients of membrane and synaptic properties for neurons of the chicken nucleus magnocellularis. J. Neurosci. 24, 7514–7523.
Gardner, S. M., Trussell, L. O., and Oertel, D. 1999. Time course and permeation of synaptic AMPA receptors in cochlear nuclear neurons correlate with input. J. Neurosci. 19, 8721–8729.
Gardner, S. M., Trussell, L. O., and Oertel, D. 2001. Correlation of AMPA receptor subunit composition with synaptic input in the mammalian cochlear nuclei. J. Neurosci. 21, 7428–7437.
von Gersdorff, H., Schneggenburger, R., Weis, S., and Neher, E. 1997. Presynaptic depression at a calyx synapse: the small contribution of metabotropic glutamate receptors. J. Neurosci. 17(21), 8137–8146.
Golding, N. L., Robertson, D., and Oertel, D. 1995. Recordings from slices indicate that octopus cells of the cochlear nucleus detect coincident firing of auditory nerve fibers with temporal precision. J. Neurosci. 15, 3138–3153.
Guinan, J. J., Jr. and Li, R. Y. 1990. Signal processing in brainstem auditory neurons which receive giant endings (calyces of Held) in the medial nucleus of the trapezoid body of the cat. Hear. Res. 49, 321–334.
Hack, N. J., Wride, M. C., Charters, K. M., Kater, S. B., and Parks, T. N. 2000. Developmental changes in the subcellular localization of calretinin. J. Neurosci. 20, RC67.
Hausser, M. and Roth, A. 1997. Estimating the time course of the excitatory synaptic conductance in neocortical pyramidal cells using a novel voltage jump method. J. Neurosci. 17, 7606–7625.
Ishikawa, T., Nakamura, Y., Saitoh, N., Li, W. B., Iwasaki, S., and Takahashi, T. 2003. Distinct roles of Kv1 and Kv3 potassium channels at the calyx of Held presynaptic terminal. J. Neurosci. 23, 10445–10453.
Iwasaki, S. and Takahashi, T. 2001. Developmental regulation of transmitter release at the calyx of Held in rat auditory brainstem. J. Physiol. 534, 861–871.
Joris, P. X. and Yin, T. C. 1998. Envelope coding in the lateral superior olive. III. Comparison with afferent pathways. J. Neurophysiol. 79, 253–269.
Joris, P. X., Carney, L. H., Smith, P. H., and Yin, T. C. 1994. Enhancement of neural synchronization in the anteroventral cochlear nucleus. I. Responses to tones at the characteristic frequency. J. Neurophysiol. 71, 1022–1036.
Joris, P. X., Smith, P. H., and Yin, T. C. 1998. Coincidence detection in the auditory system: 50 years after Jeffress. Neuron 21, 1235–1238.
Kajikawa, Y., Saitoh, N., and Takahashi, T. 2001. GTP-binding protein beta gamma subunits mediate presynaptic calcium current inhibition by GABA(B) receptor. Proc. Natl. Acad. Sci. U. S. A. 98, 8054–8058.
Kandler, K. and Friauf, E. 1993. Pre- and postnatal development of efferent connections of the cochlear nucleus in the rat. J. Comp. Neurol. 328, 161–184.
Kim, G. and Kandler, K. 2003. Elimination and strengthening of glycinergic/GABAergic connections during tonotopic map formation. Nat. Neurosci. 6, 282–290.
Kimura, M., Saitoh, N., and Takahashi, T. 2003. Adenosine A(1) receptor-mediated presynaptic inhibition at the calyx of Held of immature rats. J. Physiol. 553, 415–426.
Koike-Tani, M., Saitoh, N., and Takahashi, T. 2005. Mechanisms underlying developmental speeding in AMPA–EPSC decay time at the calyx of Held. J. Neurosci. 25, 199–207.
Kopp-Scheinpflug, C., Dehmel, S., Dorrscheidt, G. J., and Rubsamen, R. 2002. Interaction of excitation and inhibition in anteroventral cochlear nucleus neurons that receive large endbulb synaptic endings. J. Neurosci. 22, 11004–11018.
Kopp-Scheinpflug, C., Lippe, W. R., Dorrscheidt, G. J., and Rubsamen, R. 2003. The medial nucleus of the trapezoid body in the gerbil is more than a relay: comparison of pre- and postsynaptic activity. J. Assoc. Res. Otolaryngol. 4(1), 1–23.
Koppl, C. 1994. Auditory nerve terminals in the cochlear nucleus magnocellularis: differences between low and high frequencies. J. Comp. Neurol. 339(3), 438–446.
Kuba, H., Koyano, K., and Ohmori, H. 2002. Synaptic depression improves coincidence detection in the nucleus laminaris in brainstem slices of the chick embryo. Eur. J. Neurosci. 15(6), 984–990.
Kushmerick, C., Price, G. D., Taschenberger, H., Puente, N., Renden, R., Wadiche, J. I., Duvoisin, R. M., Grandes, P., and von Gersdorff, H. 2004. Retroinhibition of presynaptic Ca^{2+} currents by endocannabinoids released via postsynaptic mGluR activation at a calyx synapse. J. Neurosci. 24(26), 5955–5965.
Kuwabara, N. and Zook, J. M. 1991. Classification of the principal cells of the medial nucleus of the trapezoid body. J. Comp. Neurol. 314(4), 707–720.
Kuwabara, N. and Zook, J. M. 1992. Projections to the medial superior olive from the medial and lateral nuclei of the trapezoid body in rodents and bats. J. Comp. Neurol. 324(4), 522–538.
Kuwabara, N., DiCaprio, R. A., and Zook, J. M. 1991. Afferents to the medial nucleus of the trapezoid body and their collateral projections. J. Comp. Neurol. 314(4), 684–706.

Leao, R. M. and Von Gersdorff, H. 2002. Noradrenaline increases high-frequency firing at the calyx of held synapse during development by inhibiting glutamate release. J. Neurophysiol. 87(5), 2297–2306.

Lee, D. J., Cahill, H. B., and Ryugo, D. K. 2003. Effects of congenital deafness in the cochlear nuclei of Shaker-2 mice: an ultrastructural analysis of synapse morphology in the endbulbs of Held. J. Neurocytol. 32(3), 229–243.

Liberman, M. C. 1991. Central projections of auditory-nerve fibers of differing spontaneous rate. I. Anteroventral cochlear nucleus. J. Comp. Neurol. 313(2), 240–258.

Lohmann, C. and Friauf, E. 1996. Distribution of the calcium-binding proteins parvalbumin and calretinin in the auditory brainstem of adult and developing rats. J. Comp. Neurol. 367(1), 90–109.

Lu, T. and Trussell, L. O. 2000. Inhibitory transmission mediated by asynchronous transmitter release. Neuron 26(3), 683–694.

Lu, T. and Trussell, L. O. 2001. Mixed excitatory and inhibitory GABA-mediated transmission in chick cochlear nucleus. J. Physiol. 535(Pt 1), 125–131.

Lu, T. and Trussell, L. O. 2007. Development and elimination of end bulb synapses in the click cochlear nucleus. J. Neurosci. 27(4), 808–817.

MacLeod, K. M. and Carr, C. E. 2005a. Synaptic Dynamics and Intensity Coding in the Cochlear Nucleus. In: Auditory Signal Processing: Physiology, Psychoacoustics, and Models (*eds*. D. Pressnitzer, A. deCheveigné, S. McAdams, and L. Collet), pp. 501–509. Springer.

MacLeod, K. M. and Carr, C. E. 2005b. Synaptic physiology in the cochlear nucleus angularis of the chick. J. Neurophysiol. 93(5), 2520–2529.

Markram, H., Wang, Y., and Tsodyks, M. 1998. Differential signaling via the same axon of neocortical pyramidal neurons. Proc. Natl. Acad. Sci. U. S. A. 95(9), 5323–5328.

Meyer, A. C., Neher, E., and Schneggenburger, R. 2001. Estimation of quantal size and number of functional active zones at the calyx of held synapse by nonstationary EPSC variance analysis. J. Neurosci. 21(20), 7889–7900.

Monsivais, P. and Rubel, E. W. 2001. Accommodation enhances depolarizing inhibition in central neurons. J. Neurosci. 21(19), 7823–7830.

Monsivais, P., Yang, L., and Rubel, E. W. 2000. GABAergic inhibition in nucleus magnocellularis: implications for phase locking in the avian auditory brainstem. J. Neurosci. 20(8), 2954–2963.

Mosbacher, J., Schoepfer, R., Monyer, H., Burnashev, N., Seeburg, P. H., and Ruppersberg, J. P. 1994. A molecular determinant for submillisecond desensitization in glutamate receptors. Science 266(5187), 1059–1062.

Nicholls, J. G., Martin, A. R., Wallace, B. G., and Fuchs, P. A. 2001. From Neuron to Brain. Sinauer Associates.

Nicol, M. J. and Walmsley, B. 2002. Ultrastructural basis of synaptic transmission between endbulbs of Held and bushy cells in the rat cochlear nucleus. J. Physiol. 539(Pt 3), 713–723.

Oertel, D. 1999. The role of timing in the brain stem auditory nuclei of vertebrates. Annu. Rev. Physiol. 61, 497–519.

Oertel, D. and Young, E. D. 2004. What's a cerebellar circuit doing in the auditory system? Trends Neurosci. 27(2), 104–110.

Oertel, D., Bal, R., Gardner, S. M., Smith, P. H., and Joris, P. X. 2000. Detection of synchrony in the activity of auditory nerve fibers by octopus cells of the mammalian cochlear nucleus. Proc. Natl. Acad. Sci. U. S. A. 97(22), 11773–11779.

Oleskevich, S., Youssoufian, M., and Walmsley, B. 2004. Presynaptic plasticity at two giant auditory synapses in normal and deaf mice. J. Physiol. 560(Pt 3), 709–719.

Otis, T. S., Raman, I. M., and Trussell, L. O. 1995. AMPA receptors with high Ca^{2+} permeability mediate synaptic transmission in the avian auditory pathway. J. Physiol. 482(Pt 2), 309–315.

Otis, T., Zhang, S., and Trussell, L. O. 1996. Direct measurement of AMPA receptor desensitization induced by glutamatergic synaptic transmission. J. Neurosci. 16(23), 7496–7504.

Palmer, A. R. and Russell, I. J. 1986. Phase-locking in the cochlear nerve of the guinea-pig and its relation to the receptor potential of inner hair-cells. Hear. Res. 24(1), 1–15.

Petralia, R. S., Rubio, M. E., Wang, Y. X., and Wenthold, R. J. 2000. Differential distribution of glutamate receptors in the cochlear nuclei. Hear. Res. 147(1–2), 59–69.

Pfeiffer, R. R. 1966. Classification of response patterns of spike discharges for units in the cochlear nucleus: tone-burst stimulation. Exp. Brain Res. 1(3), 220–235.

Raman, I. M., Zhang, S., and Trussell, L. O. 1994. Pathway-specific variants of AMPA receptors and their contribution to neuronal signaling. J. Neurosci. 14(8), 4998–5010.

Rathouz, M. and Trussell, L. 1998. Characterization of outward currents in neurons of the avian nucleus magnocellularis. J. Neurophysiol. 80(6), 2824–2835.

Rhode, W. S. and Smith, P. H. 1986. Encoding timing and intensity in the ventral cochlear nucleus of the cat. J. Neurophysiol. 56(2), 261–286.

Rhode, W. S., Oertel, D., and Smith, P. H. 1983. Physiological response properties of cells labeled intracellularly with horseradish peroxidase in cat ventral cochlear nucleus. J. Comp. Neurol. 213(4), 448–463.

Rothman, J. S., Young, E. D., and Manis, P. B. 1993. Convergence of auditory nerve fibers onto bushy cells in the ventral cochlear nucleus: implications of a computational model. J. Neurophysiol. 70(6), 2562–2583.

Rubio, M. E. and Wenthold, R. J. 1999. Differential distribution of intracellular glutamate receptors in dendrites. J. Neurosci. 19(13), 5549–5562.

Ryugo, D. K., Pongstaporn, T., Huchton, D. M., and Niparko, J. K. 1997. Ultrastructural analysis of primary endings in deaf white cats: morphologic alterations in endbulbs of Held. J. Comp. Neurol. 385(2), 230–244.

Ryugo, D. K., Wu, M. M., and Pongstaporn, T. 1996. Activity-related features of synapse morphology: a study of endbulbs of held. J. Comp. Neurol. 365(1), 141–158.

Sahara, Y. and Takahashi, T. 2001. Quantal components of the excitatory postsynaptic currents at a rat central auditory synapse. J. Physiol. 536(Pt 1), 189–197.

Sakaba, T. and Neher, E. 2001. Quantitative relationship between transmitter release and calcium current at the calyx of held synapse. J. Neurosci. 21(2), 462–476.

Sakaba, T. and Neher, E. 2003. Direct modulation of synaptic vesicle priming by GABA(B) receptor activation at a glutamatergic synapse. Nature 424(6950), 775–778.

Sargent, P. B., Saviane, C., Nielsen, T. A., DiGregorio, D. A., and Silver, R. A. 2005. Rapid vesicular release, quantal variability and spillover contribute to the precision and reliability of transmission at a glomerular synapse. J. Neurosci. 25(36), 8173–87.

Satzler, K., Sohl, L. F., Bollmann, J. H., Borst, J. G., Frotscher, M., Sakmann, B., and Lubke, J. H. 2002. Three-dimensional reconstruction of a calyx of Held and its postsynaptic principal neuron in the medial nucleus of the trapezoid body. J. Neurosci. 22(24), 10567–10579.

Scheuss, V., Schneggenburger, R., and Neher, E. 2002. Separation of presynaptic and postsynaptic contributions to depression by covariance analysis of successive EPSCs at the calyx of held synapse. J. Neurosci. 22(3), 728–739.

Schneggenburger, R., Meyer, A. C., and Neher, E. 1999. Released fraction and total size of a pool of immediately available transmitter quanta at a calyx synapse. Neuron 23(2), 399–409.

Sento, S. and Ryugo, D. K. 1989. Endbulbs of held and spherical bushy cells in cats: morphological correlates with physiological properties. J. Comp. Neurol. 280(4), 553–562.

Siegel, J. H. 1992. Spontaneous synaptic potentials from afferent terminals in the guinea pig cochlea. Hear. Res. 59(1), 85–92.

Smith, D. J. and Rubel, E. W. 1979. Organization and development of brain stem auditory nuclei of the chicken: dendritic gradients in nucleus laminaris. J. Comp. Neurol. 186(2), 213–239.

Smith, P. H and Rhode, W. S. 1987. Characterization of HRP-labeled globular bushy cells in the cat anteroventral cochlear nucleus. J. Comp. Neurol. 266(3), 360–375.

Smith, P. H., Joris, P. X., and Yin, T. C. 1998. Anatomy and physiology of principal cells of the medial nucleus of the trapezoid body (MNTB) of the cat. J. Neurophysiol. 79(6), 3127–3142.

Soares, D., Chitwood, R. A., Hyson, R. L., and Carr, C. E. 2002. Intrinsic neuronal properties of the chick nucleus angularis. J. Neurophysiol. 88(1), 152–162.

Stuart, G., Spruston, N., and Hausser, M. 1999. Dendrites. Oxford University Press.

Sun, J. Y. and Wu, L. G. 2001. Fast kinetics of exocytosis revealed by simultaneous measurements of presynaptic capacitance and postsynaptic currents at a central synapse. Neuron 30(1), 171–182.

Sun, J. Y., Wu, X. S., Wu, W., Jin, S. X., Dondzillo, A., and Wu, L. G. 2004. Capacitance measurements at the calyx of Held in the medial nucleus of the trapezoid body. J. Neurosci. Methods 134(2), 121–131.

Takago, H., Nakamura, Y., and Takahashi, T. 2005. G protein-dependent presynaptic inhibition mediated by AMPA receptors at the calyx of Held. Proc. Natl. Acad. Sci. U. S. A. 102(20), 7368–7373.

Takahashi, T., Forsythe, I. D., Tsujimoto, T., Barnes-Davies, M., and Onodera, K. 1996. Presynaptic calcium current modulation by a metabotropic glutamate receptor. Science 274(5287), 594–597.

Takahashi, T., Kajikawa, Y., and Tsujimoto, T. 1998. G-Protein-coupled modulation of presynaptic calcium currents and transmitter release by a GABAB receptor. J. Neurosci. 18(9), 3138–3146.

Takahashi, T., Moiseff, A., and Konishi, M. 1984. Time and intensity cues are processed independently in the auditory system of the owl. J. Neurosci. 4(7), 1781–1786.

Taschenberger, H. and von Gersdorff, H. 2000. Fine-tuning an auditory synapse for speed and fidelity: developmental changes in presynaptic waveform, EPSC kinetics, and synaptic plasticity. J. Neurosci. 20(24), 9162–9173.

Taschenberger, H., Leao, R. M., Rowland, K. C., Spirou, G. A., and von Gersdorff, H. 2002. Optimizing synaptic architecture and efficiency for high-frequency transmission. Neuron 36(6), 1127–1143.

Trussell, L. O. 1999a. Physiology of Glutamatergic Transmission at Calyceal And Endbulb Synapses of Central Auditory Pathway. In: Handbook of Experimental Pharmacology (*eds*. P. Jonas and H. Monyer). Springer-Verlag.

Trussell, L. O. 1999b. Synaptic mechanisms for coding timing in auditory neurons. Annu. Rev. Physiol. 61, 477–496.

Trussell, L. O. 2002. Modulation of transmitter release at giant synapses of the auditory system. Curr. Opin. Neurobiol. 12(4), 400–404.

Trussell, L. O., Zhang, S., and Raman, I. M. 1993. Desensitization of AMPA receptors upon multiquantal neurotransmitter release. Neuron 10(6), 1185–1196.

Turecek, R. and Trussell, L. O. 2000. Control of synaptic depression by glutamate transporters. J. Neurosci. 20(5), 2054–2063.

Turecek, R. and Trussell, L. O. 2001. Presynaptic glycine receptors enhance transmitter release at a mammalian central synapse. Nature 411(6837), 587–590.

Turecek, R. and Trussell, L. O. 2002. Reciprocal developmental regulation of presynaptic ionotropic receptors. Proc. Natl. Acad. Sci. U. S. A. 99(21), 13884–13889.

Wadel, K., Neher, E., and Sakaba, T. 2007. The coupling between synaptic vesicles and Ca^{2+} channels determines fast neurotransmitter release. Neuron. 53(4), 563–575.

Wang, L. Y., Gan, L., Forsythe, I. D., and Kaczmarek, L. K. 1998a. Contribution of the Kv3.1 potassium channel to high-frequency firing in mouse auditory neurones. J. Physiol. 509(Pt 1), 183–194.

Wang, Y. and Manis, P. B. 2005. Synaptic transmission at the cochlear nucleus endbulb synapse during age-related hearing loss in mice. J. Neurophysiol. 99, 1814–1824.

Wang, Y. X., Wenthold, R. J., Ottersen, O. P., and Petralia, R. S. 1998b. Endbulb synapses in the anteroventral cochlear nucleus express a specific subset of AMPA-type glutamate receptor subunits. J. Neurosci. 18(3), 1148–1160.

Wickesberg, R. E. and Oertel, D. 1990. Delayed, frequency-specific inhibition in the cochlear nuclei of mice: a mechanism for monaural echo suppression. J. Neurosci. 10(6), 1762–1768.

Wolfel, M., Lou, X., and Schneggenburger, R. 2007. A mechanism intrinsic to the vesicle fusion machinery determines fast and slow transmitter release at a large CNS synapse. J. Neurosci. 27(12), 3198–3210.

Wong, A. Y., Graham, B. P., Billups, B., and Forsythe, I. D. 2003. Distinguishing between presynaptic and postsynaptic mechanisms of short-term depression during action potential trains. J. Neurosci. 23(12), 4868–4877.

Wu, L. G. and Borst, J. G. 1999. The reduced release probability of releasable vesicles during recovery from short-term synaptic depression. Neuron 23(4), 821–832.

Wu, S. H. and Kelly, J. B. 1992. Binaural interaction in the lateral superior olive: time difference sensitivity studied in mouse brain slice. J. Neurophysiol. 68(4), 1151–1159.

Xu-Friedman, M. and Regehr, W. 2005. Dynamic clamp analysis of the effects of convergence on spike timing II: Few synaptic inputs. J. Neurophysiol. 94(4), 2526–34.

Xu, J. and Wu, L. G. 2005. The decrease in the presynaptic calcium current is a major cause of short-term depression at a calyx-type synapse. Neuron 46(4), 633–645.

Yang, L., Monsivais, P., and Rubel, E. W. 1999. The superior olivary nucleus and its influence on nucleus laminaris: a source of inhibitory feedback for coincidence detection in the avian auditory brainstem. J. Neurosci. 19(6), 2313–2325.

Zhang, S. and Trussell, L. O. 1994a. A characterization of excitatory postsynaptic potentials in the avian nucleus magnocellularis. J. Neurophysiol. 72(2), 705–718.

Zhang, S. and Trussell, L. O. 1994b. Voltage clamp analysis of excitatory synaptic transmission in the avian nucleus magnocellularis. J. Physiol. 480(Pt 1), 123–136.

Zhou, Y., Carney, L. H., and Colburn, H. S. 2005. A model for interaural time difference sensitivity in the medial superior olive: interaction of excitatory and inhibitory synaptic inputs, channel dynamics, and cellular morphology. J. Neurosci. 25(12), 3046–3058.

3.34 Acoustic Startle in Mice and Rats

J F Willott, University of South Florida, Tampa, FL, USA

© 2008 Elsevier Inc. All rights reserved.

3.34.1	**Introduction**	603
3.34.2	**The Acoustic Startle Response as a Research Tool**	604
3.34.3	**Properties of the Acoustic Startle Response**	604
3.34.3.1	Description and Measurement of the Behavior	604
3.34.3.1.1	Suprathreshold performance is not related to threshold in a simple manner	604
3.34.3.2	Modulation of the Acoustic Startle Response by History, Environment, Genes, and Other Variables	604
3.34.3.2.1	Prepulse inhibition	604
3.34.3.2.2	Fear-potentiated startle	605
3.34.3.2.3	Sensitization	605
3.34.3.2.4	Habituation	605
3.34.3.2.5	Ambient noise	605
3.34.3.2.6	Circadian rhythms	606
3.34.3.2.7	Genetics	606
3.34.3.2.8	Neurotransmitter systems	606
3.34.3.2.9	Psychological states or pathology	606
3.34.3.2.10	Relationship between hearing loss and central plasticity	606
3.34.4	**Anatomical Pathways**	607
3.34.4.1	The Acoustic Startle Response Pathway	607
3.34.4.2	The Prepulse Inhibition Pathway	607
3.34.4.3	Other Modulating Pathways	607
3.34.5	**Auditory Neurophysiology**	607
3.34.6	**Function and Adaptive Significance**	608
References		609

Glossary

inbred strain Mice of an inbred strain are genetically identical to one another and homozygous at all genetic loci.

sound pressure level (SPL) Decibels re: 20 μPa

3.34.1 Introduction

The acoustic startle response (ASR) provides an important behavioral tool for assessing properties of the auditory system, as discussed below. More importantly, however, the ASR is a phenomenon having relevance for a wide variety of issues important in the study of sensory systems. Whereas the ASR is by definition a behavior, it is more importantly a sensorimotor reflex and as such cannot be divorced from the auditory processes that trigger it. We can conceptualize the ASR as a sensorimotor system for which the behavioral component is linked to certain aspects of the acoustic stimuli that evoke the response and to events that surround it in space and time. The adequate stimuli for activating the system are intense sounds with an abrupt onset that are unexpected and/or not monotonous (Fleshler, M., 1965; Willott, J. F. *et al.*, 1979; Ison, J. R., 2001). Arguably, the sensory, central modulatory, and motor circuits that comprise the ASR system can be viewed as a sensory filter or detector of these features. The ASR may be influenced by location, spectral

content, and other qualities, but these properties are not critical for activation of the system. Importantly, activation of this sensorimotor system is strongly modified by emotional states, temporally proximal events, and ambient stimulus conditions, as discussed below.

3.34.2 The Acoustic Startle Response as a Research Tool

The ASR has enjoyed wide use as a tool in auditory and other research, and there are good reasons for its popularity. The ASR:

- is a fundamental auditory behavior, occurring widely in mammals, including humans (Landis, C. and Hunt, W., 1939; Davis, M., 1984; Ison, J. R., 2001) and has been well studied in the latter species (Dawson, M. E. *et al.*, 1999);
- is simple enough to be accurately isolated and measured;
- is an interesting and important auditory behavior in its own right;
- can be used as a measure of behavioral responsiveness to intense or unexpected sounds;
- serves as a behavioral probe to evaluate responses to environmental conditions, emotional situations, neurobehavioral disorders, strain differences, or drugs (e.g., Hoffman, H. S. and Ison, J. R., 1980; Braff, D. *et al.*, 1992; Glowa, J. R. and Hansen, C. T., 1994; Falls, W. A. *et al.*, 1997a; 1997b; Geyer, M. A., 1998; Kline, L. *et al.*, 1998; Zhang, J. *et al.*, 2000; Ison, J. R., 2001);
- can be used as a measure of auditory processing in neurobehaviorally normal populations (Reiter, L. A. and Ison, J. R., 1979; Young, J. S. and Fechter, L. D., 1983; Carlson, S. and Willott, J. F., 1996; Jeskey, J. E. and Willott, J. F., 2000; Willott, J. F. and Turner, J. G., 2000);
- is an auditory behavior for which the neurophysiological and neurochemical mechanisms, neural pathways, and physiology are reasonably well understood;
- is an auditory behavior for which quantitative measurement is relatively simple, fast, and reliable; and
- varies substantially among different genetic strains of mice and/or mutants in order for inheritance mapping and other genetic techniques to be applied.

3.34.3 Properties of the Acoustic Startle Response

3.34.3.1 Description and Measurement of the Behavior

In rats and mice, the ASR is manifested as a transient, crouchlike movement of the body and flinching of the head and pinnae. To measure the response, the animal is typically placed in a movement-sensitive device that produces a voltage that can be recorded. A startle evokes a transient voltage spike within relatively short latency (5–30 ms, depending on the inertia and sensitivity of the device). ASR parameters that are easily measured include the amplitude (e.g., peak voltage of the response) and latency (time elapsed between onset of stimulus and onset of response). Amplitude-intensity functions and startle thresholds can be measured by varying the level of the startle stimuli.

3.34.3.1.1 Suprathreshold performance is not related to threshold in a simple manner

ASRs are elicited by stimulus levels well above the sensory threshold (Willott, J. F. *et al.*, 1979; 1984) and startle amplitude has little if any relationship to threshold unless hearing loss is quite severe (Parham, K. and Willott, J. F., 1988; Carlson, S. and Willott, J. F., 1996). Indeed, some hearing-impaired mice have very large startle responses. For example, mice of the BUB/BnJ inbred strain have very large ASRs (see Figure 1), yet they exhibit substantial threshold elevations (Willott, J. F. *et al.*, 2003).

3.34.3.2 Modulation of the Acoustic Startle Response by History, Environment, Genes, and Other Variables

An extraordinary aspect of the ASR system is the ease by which it is modified by precedent sensory stimuli (prepulse inhibition; PPI), fear (fear-potentiated startle; FPS), monotonous repetition (habituation), continuous background noise, and other variables. Whereas the ASR is sensitive to certain stimulus features mentioned earlier, behavioral manifestation of the ASR system is affected by many variables.

3.34.3.2.1 Prepulse inhibition

PPI reflects the perceptual impact or salience of sensory stimuli and their regulation by the central nervous system. PPI is manifested as follows: an

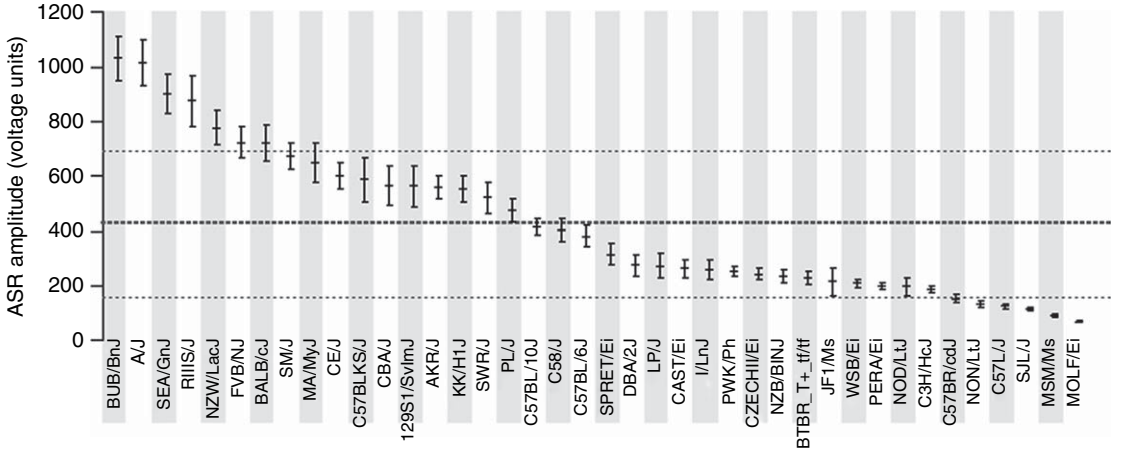

Figure 1 Mean startle amplitudes of 40 inbred strains, males and females combined (in most cases 10 of each per strain), evoked by 100 dB sound pressure level (SPL) noise bursts. Error bars represent standard error of mean for each strain. Bold dashed line, grand mean for all strains. Light dashed lines, ±1 standard deviation of grand mean. Reprinted from Willott, J. F., Tanner, L., O'Steen, J., Johnson, K. R., Bogue, M. A., and Gagnon, L. 2003. Startle and prepulse inhibition in forty inbred strains of mice. Behav. Neurosci. 117, 716-727. Copyright © 2003 by the American Psychological Association, with permission.

audible prepulse stimulus (S1) is presented about 100 ms before an intense startle-eliciting stimulus (S2). Whether the prepulse is a tone burst, a gap in the background noise, or other sensory change, activation of the PPI circuit inhibits the startle pathway for a period lasting several hundred milliseconds, resulting in an inhibited ASR with a reduced amplitude during this interval. PPI can be expressed by the simple ratio of ASR amplitude evoked by S2 when S1 has been presented, to ASR amplitude when S2 has been presented without S1.

3.34.3.2.2 Fear-potentiated startle

FPS is widely used to investigate the neurobiological basis of fear or anxiety. In FPS a subject learns to fear an auditory or visual cue that was paired with footshock; later, when startled in the presence of the cue, startle amplitude is increased as a function of the learned fear. Because FPS utilizes Pavlovian conditioning procedures, it is also used to investigate the neurobiological basis of learning and memory (Davis, M. and Astrachan, D. I., 1978; Miserendino, M. J. D. *et al.*, 1990; Campeau, S. and Davis, M., 1992; Falls, W. A. *et al.*, 1992; Campeau, S. and Davis, M., 1995a; Falls, W. A. *et al.*, 1997b; Gewirtz, J. C. and Davis, M., 1997).

3.34.3.2.3 Sensitization

Sensitization is the phenomenon whereby responsiveness is generally enhanced in a nonspecific (nonassociative) manner, usually by an intense or highly arousing event. The nonassociative aspect differentiates it from FPS, although in both cases ASR amplitude is increased. The ASR can be used as a model to study sensitization involving sensory stimuli (Koch, M., 1999; Plappert, C. F. and Pilz, P. K., 2001).

3.34.3.2.4 Habituation

The ASR exhibits rapid habituation and can be used as a model to study the phenomenon (Thompson, R. F. and Spencer, W. A., 1966; Groves, P. M., *et al.*, 1974; Davis, M., 1984; Koch, M., 1999). Habituation occurs when repeated, monotonous presentation of a startle stimulus results in diminution or cessation of the response, despite the fact that the stimuli are still being processed by the auditory system (i.e., threshold shifts, adaptation, or fatigue have not taken place). A good understanding of, and access to, the startle pathway allows habituation to be studied at many levels. For example, Weber M. *et al.* (2002) explored distinct synapses of the neuronal startle pathway in rat brain slices by patch-clamp recordings neurons in the startle pathway and found that response parameters associated with synaptic depression *in vitro* matched those of ASR habituation *in vivo*.

3.34.3.2.5 Ambient noise

The presence of continuous background noise modulates the ASR system. In general, a relatively low

level of continuous background noise tends to potentiate the ASR whereas high levels tend to suppress the ASR (see Carlson, S. and Willott, J. F., 2001 for a review). It is common for researchers to use a constant background noise during ASR testing, and this runs the risk of unintentionally modulating the ASR up or down.

3.34.3.2.6 Circadian rhythms

The ASR system exhibits circadian modulation, with amplitudes greater at night in nocturnal rats and mice. The changes in ASR amplitude do not appear to be correlated with general motor activity (Horlington, M., 1970) or auditory sensitivity (Chabot, C. C. and Taylor, D. H., 1992). At least one site of circadian modulation appears to occur at the level below the brainstem (Frankland, P. W. and Ralph, M. R., 1995), so it is not clear if the modulation is occurring in the brain.

3.34.3.2.7 Genetics

Because the ASR and PPI have been well studied in mice, a number of studies have used the behaviors as a behavior-genetics tool (e.g., Bullock, A. E. *et al.*, 1997; Logue, S. F. *et al.*, 1997; Paylor, R. and Crawley, J. N., 1997; Hitzemann, R. *et al.*, 2001; Plappert, C. F. and Pilz, P. K., 2001; Ralph, R. J. *et al.*, 2001; Willott, J. F. *et al.*, 2003). Whereas, aspects of these studies are not necessarily aimed at the genetics of hearing or auditory behavior *per se*, they often provide insights. Figure 1 summarizes ASR amplitudes from 40 inbred strains of mice all having similar age and rearing conditions. It is evident that the size of startle varies greatly among strains – presumably as a function of genetic differences. Some of the strains with very large or very small ASRs have similar, normal hearing suggesting that genetic effects on central auditory processes and/or gating is responsible for the differences, rather than cochlear sensitivity.

3.34.3.2.8 Neurotransmitter systems

The ASR system is readily amenable to experiments on neurotransmitter systems and drug effects. For example, drugs affecting central dopamine (DA) systems (especially the mesolimbic system) have been well studied and shown to play an important role in startle (Meloni, E. G. and Davis, M., 2000) and PPI and related paradigms. A number of studies in humans and rodents have shown that overactivity of DA induced by DA agonists or other means results in reduced PPI and reduced gating of evoked potentials (Koch, M. and Hauber, W., 1998; Swerdlow, N. R. *et al.*, 1990; Zhang, J. *et al.*, 2000).

Another example is the role of acetylcholine. Fendt M. and Koch M. (1999) showed that the nucleus reticularis pontis caudalis (PnC) receives an inhibitory cholinergic projection that might be important for PPI.

3.34.3.2.9 Psychological states or pathology

The startle reflex is highly sensitive to various factors that are of interest in the studies of emotional disorders and has promoted new areas of investigations in psychiatry. Alteration of the startle response (by PPI in particular) has been widely used in models of psychiatric conditions (Koch, M., 1999; Grillon, C. and Baas, J., 2003) including schizophrenia (Braff, D. L. and Geyer, M. A., 1990; Geyer, M. A. *et al.*, 1990; Cadenhead, K. S. *et al.*, 1993; Braff, D. L. *et al.*, 1995; Swerdlow, N. R. and Geyer, M. A., 1998), Huntington's disease (Swerdlow, N. R. *et al.*, 1995), posttraumatic stress disorder (Pitman, R. K. *et al.*, 1999), fear and anxiety, affective disturbances, sensitization, and motivational states (Dawson, M. E. *et al.*, 1999). Most notably, schizophrenic patients exhibit deficits in both the PPI of startle and the habituation of startle, and evidence supports involvement of mesolimbic dopaminergic systems in the modulation of PPI or sensorimotor gating and the importance of central serotonergic systems in the habituation of startle (Geyer, M. A. *et al.*, 1990). Whereas these studies have tended to focus on gating mechanisms, alterations in central auditory processing may also be involved, and this topic deserves additional attention (Willott, J. F. *et al.*, 2003).

3.34.3.2.10 Relationship between hearing loss and central plasticity

High-frequency hearing loss results in plasticity of the central auditory system, whereby audible lower frequencies become more strongly represented in the inferior colliculus (IC) and elsewhere (Willott, J. F., 1996). This plasticity is accompanied by parallel changes in the strength of PPI (Willott, J. F. *et al.*, 1994; Carlson, S. and Willott, J. F., 1996; Willott, J. F. and Turner, J. G., 2000). As high-frequency S1s become ineffective, lower-frequency S1s become more salient, producing stronger PPI.

3.34.4 Anatomical Pathways

3.34.4.1 The Acoustic Startle Response Pathway

The primary neural pathway for the ASR resides in the lower brainstem, with auditory neurons in the cochlear nucleus and/or cochlear nerve root projecting to startle-triggering neurons of the reticular formation. The most basic acoustic startle pathway is supported by only a few synaptic relays: auditory nerve ⇒ ventral cochlear nucleus (VCN) ⇒ giant neurons of the PnC ⇒ spinal cord and motor neurons ⇒ muscles (Davis, M. *et al.*, 1982; Huffman, R. F. and Henson, O. W., 1990; Kandler, K. and Herbert, H., 1991; Lingenhöhl, K. and Friauf, E., 1994; Lee, Y. *et al.*, 1996; Yeomans, J. S. and Frankland, P. W., 1996; Koch, M., 1999; Scott, B. W. *et al.*, 1999; Swerdlow, N. R. and Geyer, M. A., 1999; Weber, M. *et al.*, 2002). The PnC, whose axons descend the spinal cord is especially important. Koch M. and Schnitzler H. U. (1997) noted the PnC is also the target of input from various brain nuclei which are involved in modulation of the ASR (e.g., PPI, FPS, sensitization, habituation). Hence, the PnC can be described as a sensorimotor interface, where the transition of sensory input into the motor output can be directly influenced by excitatory or inhibitory afferents.

3.34.4.2 The Prepulse Inhibition Pathway

PPI results from modulation of the startle pathway by circuit(s) that include prepulse-activated auditory nuclei, with efferents from the IC playing an especially important role (Parham, K. and Willott, J. F., 1990; Carlson, S. and Willott, J. F., 1996; Li, L. *et al.*, 1998a; 1998b). Neural output from the central auditory system activates other postauditory components of the PPI neural circuitry, including pathways that ultimately descend to the PnC and inhibit the giant neurons that trigger the startle reflex (e.g., Hoffman, H. S. and Ison, J. R., 1980; Davis, M., 1984; Willott, J. F. *et al.*, 1994; Carlson, S. and Willott, J. F., 1998; Li, L. *et al.*, 1998b; Koch, M., 1999; Ison, J. R., 2001).

3.34.4.3 Other Modulating Pathways

A number of brain structures appear capable of modulating the ASR and/or PPI neural circuitry. Anatomical and lesion-behavior studies have indicated that auditory cortex, IC, and substantia nigra pars reticulata project to the startle circuitry and may provide tonic inhibition and/or modulation of the ASR (Parham, K. and Willott, J. F., 1990; Hunter, K. P. and Willott, J. F., 1993; Koch, M. *et al.*, 2000; Leaton, R. N. and Brucato, F. H., 2001). In various neurobehavioral conditions associated with impaired PPI or startle (see Section 3.34.3.2.9), brain regions such as the limbic cortex, ventral striatum, pallidum, and pedunculopontine nucleus have been implicated (Koch, M., 1999; Swerdlow, N. R. and Geyer, M. A., 1999). Finally, a key structure of the FPS pathway is the amygdala, which receives information from the auditory system via the auditory thalamus and cortex and projects to the startle circuit (e.g., Rosen, J. B. *et al.*, 1991; Romanski, L. M. and LeDoux, J. E., 1992; Campeau, S. and Davis, M., 1995a; 1995b; Falls, W. A. *et al.*, 1997a; Leaton, R. N., 2003).

3.34.5 Auditory Neurophysiology

Carlson S. and Willott J. F. (1998) studied single-unit responses of PnC neurons that presumably trigger the ASR in mice. They performed the study in the fashion of a typical auditory single-unit study: stimuli were presented and the extracellular responses elicited were recorded and described. Responses of PnC neurons generally paralleled those of the ASR (see also Wu, M. F. *et al.*, 1988; Lingenhöhl, K. and Friauf, E., 1992; 1994). In order to evoke auditory responses in these neurons, stimuli had to be intense (e.g., about 100 dB sound pressure level (SPL)), have an abrupt onset, and be repeated at a relatively slow rate. The responses of most PnC neurons were transient – one or a few responses occurred shortly after the onset of the sound. The latency of these onset responses were short enough (as short as 4 ms) to trigger the ASR behavior. PnC neurons exhibited little or no spontaneous activity. PnC neurons responded to a startle stimulus when it was repeated at a slow rate of one every 10 s, as shown in Figure 2 ($0.1\,s^{-1}$; filled circles). By contrast, when the stimulus was presented at a rate of $1\,s^{-1}$ (unfilled circles) the evoked discharges quickly waned, as does the ASR. Stimuli with moderate intensities (e.g., 70 dB SPL) – well above the absolute threshold of hearing but ineffective startle stimuli – excited PnC neurons weakly, if at all. However, when a 70 dB tone was presented 100 ms before an effective (100 dB) startle stimulus the responses to the startle stimulus was inhibited – that is, PPI was exhibited a the neuronal level. Figure 3 presents examples of such responses; when the startle

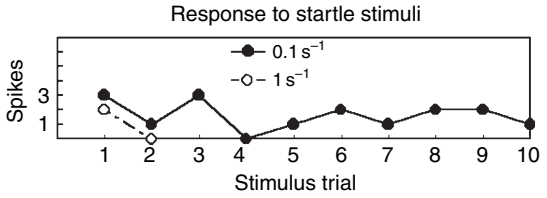

Figure 2 Effects of stimulus presentation rate on responses of a nucleus reticularis pontis caudalis neuron to a series of 10 startle stimuli (100 dB sound pressure level noise bursts). At a rate of 1 s^{-1} (unfilled circles, dashed lines), two action potentials were evoked by the first stimulus, but thereafter, subsequent stimuli no longer elicited responses. By contrast, presentation of the startle stimulus at a slower rate of 0.1 s^{-1} (filled circles, unbroken line) continued to elicit action potentials for most stimuli. Reproduced from Carlson, S. and Willott, J. F. 1998. Caudal pontine reticular formation of C57BL/6J mice: responses to startle stimuli, inhibition by tones, plasticity. J. Neurophysiol. 79, 2603–2614, use with permission from the American Physiological Society.

stimulus (S2) was preceded by a prepulse (S1), few spikes were evoked (filled squares) compared to those evoked by S2 alone (unfilled squares).

3.34.6 Function and Adaptive Significance

Sensory systems evolved to trigger, guide, direct, or modulate behaviors. The fundamental nature of the startle – retraction/withdrawal of head and body – suggests a protective role from sudden, potentially injurious events. Yeomans J. S. *et al.* (2002) noted that intense tactile, acoustic, or vestibular stimuli activate their respective cranial nerves and primary sensory nuclei which all project to PnC giant neurons critical for the startle reflex. Cross-modal summation of this input to the PnC is strong, suggesting convergence of modalities in startle. This summation declines sharply if the cross-modal stimuli are not synchronous. Head impact stimuli activate trigeminal, acoustic, and vestibular systems together, suggesting that the startle response protects the body from impact stimuli.

There are, however, issues that do not fit nicely with the notion that the ASR has adaptive value. For example, an ASR might be evoked by predator movement, giving away prey position, a seemingly maladaptive response. Moreover, some species (e.g., rabbits and chinchillas) do not readily exhibit ASRs suggesting that prey species can be successful

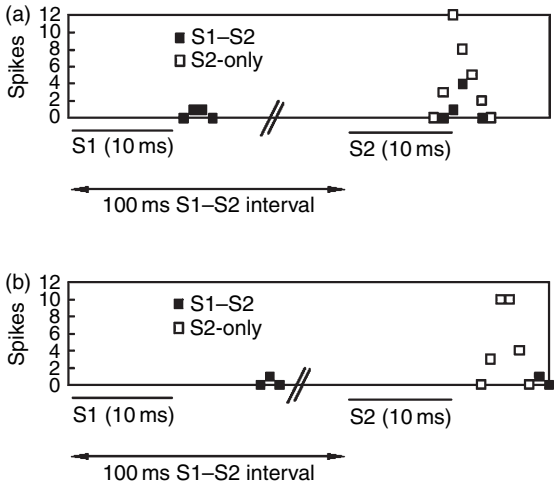

Figure 3 Action potentials in nucleus reticularis pontis caudalis neurons evoked by S1–S2 pairs and by S2 alone. Poststimulus time histograms show extracellularly recorded action potentials in response to a 100 dB sound pressure level (SPL) startle stimuli (S2, horizontal line under right portion of the panel) and to a 70 dB SPL 10 ms tone (horizontal line under left portion of panel) paired with S2. The number of action potentials when S2 was presented alone is indicated by unfilled squares; the number of action potentials evoked by both S1 and S2 (when S2 was preceded by S1) is indicated by filled squares. In each case, 10 stimuli or stimulus pairs were presented at a rate of one per 10 s and the total number of action potentials at each 1 ms time bin was summed. In example (a), S2, when not preceded by S1, evoked almost 30 action potentials for 10 stimulus presentations. When a 4 kHz tone S1 preceded S2, the number of action potentials evoked by S2 was reduced (a few responses were also evoked by S1). In (b), S1 did not evoke any action potentials (left portion of panel) but caused a substantial reduction in action potentials evoked by S2 (right portion of panel). Reproduced from Carlson, S., and Willott, J. F. 1998. Caudal pontine reticular formation of C57BL/6J mice: responses to startle stimuli, inhibition by tones, plasticity. J. Neurophysiol. 79, 2603–2614, used with permission from the American Physiological Society.

without startle. Perhaps the ASR has minimal survival value but is an epiphenomenon – an escape response that is initiated by a sudden event, then aborted by inhibition as the nervous system determines that escape is unwarranted or detrimental; by this time, however a burst of movement has already occurred.

Acknowledgment

Preparation of this chapter was supported by NIH grant R01 AG07554.

References

Braff, D. L. and Geyer, M. A. 1990. Sensorimotor gating and schizophrenia. Human and animal studies. Arch. Genet. Psychiatry 47, 181–188.

Braff, D., Grillon, C., and Geyer, M. A. 1992. Gating and habituation of the startle reflex in schizophrenic patients. Arch. Genet. Psychiatry 49, 206–215.

Braff, D. L., Swerdlow, N. R., and Geyer, M. A. 1995. Gating and habituation deficits in the schizophrenia disorders. Clin. Neurosci. 3, 131–139.

Bullock, A. E., Slobe, B. S., Vazquez, V., and Collins, A. C. 1997. Inbred mouse strains differ in the regulation of startle and prepulse inhibition of the startle response. Behav. Neurosci. 111, 1353–1360.

Cadenhead, K. S., Geyer, M. A., and Braff, D. L. 1993. Impaired startle prepulse inhibition and habituation in patients with schizotypal personality disorder. Am. J. Psychiatry 150, 1862–1867.

Campeau, S. and Davis, M. 1992. Fear-potentiation of the acoustic startle reflex in rats using noises of various spectral frequencies. Anim. Learn. Behav. 20, 177–186.

Campeau, S. and Davis, M. 1995a. Involvement of subcortical and cortical afferents to the lateral nucleus of the amygdala in fear conditioning measured with fear-potentiated startle in rats trained concurrently with auditory and visual conditioned stimuli. J. Neurosci. 15, 2312–2327.

Campeau, S. and Davis, M. 1995b. Involvement of the central nucleus and basolateral complex of the amygdala in fear conditioning measured with fear-potentiated startle in rats trained concurrently with auditory and visual conditioned stimuli. J. Neurosci. 15, 2301–2312.

Carlson, S. and Willott, J. F. 1996. The behavioral salience of tones as indicated by prepulse inhibition of the startle response: relationship to hearing loss and central neural plasticity in C57BL/6J mice. Hear. Res., 99, 168–175.

Carlson, S. and Willott, J. F. 1998. Caudal pontine reticular formation of C57BL/6J mice: Responses to startle stimuli, inhibition by tones, plasticity. J. Neurophysiol. 79, 2603–2614.

Carlson, S. and Willott, J. F. 2001. Modulation of the Acoustic Startle Response by Background Sound in C57BL/6J Mice. In: Handbook of Mouse Auditory Research: from Behavior to Molecular Biology (*ed*. J. F. Willott), pp. 83–90. CRC Press.

Chabot, C. C. and Taylor, D. H. 1992. Circadian modulation of the rat acoustic startle response. Behav. Neurosci. 106, 846–852.

Davis, M. 1984. The Mammalian Startle Response. In: Neural Mechanisms of Startle Behavior (*ed*. R. C. Eaton), pp. 287–351. Plenum.

Davis, M. and Astrachan, D. I. 1978. Conditioned fear and startle magnitude: effects of different footshock or backshock intensities used in training. J. Exp. Psychol. Anim. Behav. Proc. 4, 95–103.

Davis, M., Gendelman, D. S., Tischler, M. D., and Gendelman, P. M. 1982. A primary acoustic circuit: lesion and stimulation studies. J. Neurosci. 2, 791–805.

Dawson, M. E., Schell, A. M., and Böhmelt, A. H. 1999. Startle Modification. Cambridge University Press.

Falls, W. A., Bakken, K., and Heldt, S. 1997a. Lesions of the perirhinal cortex block conditioned excitation but not conditioned inhibition of fear. Behav. Neurosci. 111, 476–486.

Falls, W. A., Carlson, S., Turner, J., and Willott, J. F. 1997b. Fear-potentiated startle in two strains of inbred mice. Behav. Neurosci. 111, 855–861.

Falls, W. A., Miserendino, M. J. D., and Davis, M. 1992. Extinction of fear-potentiated startle: blockade by infusion of an excitatory amino acid antagonist into the amygdala. J. Neurosci. 12, 854–863.

Fendt, M. and Koch, M. 1999. Cholinergic modulation of the acoustic startle response in the caudal pontine reticular nucleus of the rat. Eur. J. Pharmacol. 370, 101–107.

Fleshler, M. 1965. Adequate acoustic stimulus for startle reaction in the rat. J. Comp. Physiol. Psychol. 60, 200–207.

Frankland, P. W. and Ralph, M. R. 1995. Circadian modulation in the rat acoustic startle circuit. Behav. Neurosci. 109, 43–48.

Gewirtz, J. C. and Davis, M. 1997. Second-order fear conditioning prevented by blocking NMDA receptors in amygdala. Nature 388, 471–474.

Geyer, M. A. 1998. Behavioral studies of hallucinogenic drugs in animals: implications for schizophrenia research. Pharmacopsychiatry 31, 73–79.

Geyer, M. A., Swerdlow, N. R., Mansbach, R. S., and Braff, D. L. 1990. Startle response models of sensorimotor gating and habituation deficits in schizophrenia. Brain Res. Bull. 25, 485–498.

Glowa, J. R. and Hansen, C. T. 1994. Differences in response to an acoustic startle stimulus among forty-six rat strains. Behav. Genet. 24, 79–84.

Grillon, C. and Baas, J. 2003. A review of the modulation of the startle reflex by affective states and its application in psychiatry. Clin. Neurophysiol. 114, 1557–1579.

Groves, P. M., Wilson, C. J., and Boyle, R. D. 1974. Brain stem pathways, cortical modulation, and habituation of the acoustic startle response. Behav. Biol. 10, 391–418.

Hitzemann, R., Bell, J., Rasmussen, E., and McCaughran, J. 2001. Mapping the Genes for the Acoustic Startle Response (ASR) and Prepulse Inhibition of the ASR in the BXD Recombinant Inbred Series: Effect of High-Frequency Hearing Loss and Cochlear Pathology. In: Handbook of Mouse Auditory Research: From Behavior to Molecular Biology (*ed*. J. F. Willott), pp. 441–455. CRC Press.

Hoffman, H. S. and Ison, J. R. 1980. Reflex modification in the domain of startle. I. Some empirical findings and their implications for how the nervous system processes sensory input. Psychol. Bull. 87, 175–189.

Horlington, M. 1970. Startle response circadian rhythm in rats: lack of correlation with motor activity. Physiol. Behav. 5, 49–53.

Huffman, R. F. and Henson, O. W. 1990. The descending auditory pathway and acousticomotor systems: connections with the inferior colliculus. Brain Res. Rev. 15, 295–323.

Hunter, K. P. and Willott, J. F. 1993. Effects of bilateral lesions of auditory cortex in mice on the acoustic startle response. Physiol. Behav. 54, 1133–1139.

Ison, J. R. 2001. The Acoustic Startle Response: Reflex Elicitation and Reflex Modification by Preliminary Stimuli. In: Handbook of Mouse Auditory Research: From Behavior to Molecular Biology (*ed*. J. F. Willott), pp. 59–82. CRC Press.

Jeskey, J. E. and Willott, J. F. 2000. Modulation of prepulse inhibition in the DBA/2J mice by an augmented acoustic environment. Behav. Neurosci. 114, 991–997.

Kandler, K. and Herbert, H. 1991. Auditory projections from the cochlear nucleus to pontine and mesencephalic reticular nuclei in the rat. Brain Res. 562, 230–242.

Kline, L., Decena, E., Hitzemann, R., and McCaughran, J. 1998. Acoustic startle, prepulse inhibition, locomotion, and latent inhibition in the neuroleptic-responsive (NR) and neuroleptic-nonresponsive (NNR) lines of mice. Psychopharmacology 139, 322–331.

Koch, M. 1999. The neurobiology of startle. Prog. Neurobiol. 59, 107–128.

Koch, M., Fendt, M., and Kretschmer, B. D. 2000. Role of the substantia nigra pars reticulata in sensorimotor gating, measured by prepulse inhibition of startle in rats. Behav. Brain Res. 117, 153–162.

Koch, M. and Hauber, W. 1998. Regulation of sensorimotor gating by interactions of dopamine and adenosine in the rat. Behav. Pharmacol. 9, 23–29.

Koch, M. and Schnitzler, H. U. 1997. The acoustic startle response in rats – circuits mediating evocation, inhibition and potentiation. Behav. Brain Res. 89, 35–49.

Landis, C. and Hunt, W. 1939. The Startle Pattern: Ferrar and Rinehart.

Leaton, R. N. 2003. Electrolytic, but not neurotoxic, lesions to the lateral tegmental tract increase acoustic startle amplitude and reduce startle stimulus-induced freezing. Neurobiol. Learn. Memory 79, 89–98.

Leaton, R. N. and Brucato, F. H. 2001. Startle amplitude and fear in an acoustic startle paradigm: lesions to the brachium of the inferior colliculus or the lateral tegmental tract. Behav. Neurosci. 115, 477–492.

Lee, Y., Lopez, D. E., Meloni, E. G., and Davis, M. 1996. A primary acoustic startle pathway: obligatory role of cochlear root neurons and the nucleus reticularis pontis caudalis. J. Neurosci. 16, 3775–3789.

Li, L., Korngut, L. M., Frost, B. J., and Beninger, R. J. 1998a. Prepulse inhibition following lesions of the inferior colliculus: prepulse intensity functions. Physiol. Behav. 65, 133–139.

Li, L., Priebe, R. P., and Yeomans, J. S. 1998b. Prepulse inhibition of acoustic or trigeminal startle of rats by unilateral electrical stimulation of the inferior colliculus. Behav. Neurosci. 112, 1187–1198.

Lingenhöhl, K. and Friauf, E. 1992. Giant neurons in the caudal pontine reticular formation receive short latency acoustic input: an intracellular recording and HRP-study in the rat. J. Comp. Neurol. 325, 473–492.

Lingenhöhl, K. and Friauf, E. 1994. Giant neurons in the rat reticular formation: a sensorimotor interface in the elementary acoustic startle circuit? J. Neurosci. 14, 1176–1194.

Logue, S. F., Owen, E. H., Rasmussen, D. L., and Wehner, J. M. 1997. Assessment of locomotor activity, acoustic and tactile startle, and prepulse inhibition of startle in inbred mouse strains and F1 hybrids: implications of genetic background for single gene and quantitative trait loci analyses. Neuroscience 80, 1075–1086.

Meloni, E. G. and Davis, M. 2000. Enhancement of the acoustic startle response by dopamine agonists after 6-hydroxydopamine lesions of the substantia nigra pars compacta: corresponding changes in c-Fos expression in the caudate-putamen. Brain Res. 879, 93–104.

Miserendino, M. J. D., Sananes, C. B., Melia, K. R., and Davis, M. 1990. Blocking of acquisition but not expression of conditioned fear-potentiated startle by NMDA antagonists in the amygdala. Nature 345, 716–718.

Parham, K. and Willott, J. F. 1988. The acoustic startle response in young and aging C57BL/6J and CBA/J mice. Behav. Neurosci. 102, 881–886.

Parham, K. and Willott, J. F. 1990. The effects of inferior colliculus lesions on the acoustic startle response. Neurosci. Behav. 104, 831–840.

Paylor, R. and Crawley, J. N. 1997. Inbred strain differences in prepulse inhibition of the mouse startle response. Psychopharmacology 132, 169–180.

Pitman, R. K., Orr, S. P., Shalev, A. Y., Metzger, L. J., and Mellman, T. A. 1999. Psychophysiological alterations in post-traumatic stress disorder. Semin. Clin. Neuropsychiatry 4, 234–241.

Plappert, C. F. and Pilz, P. K. 2001. The acoustic startle response as an effective model for elucidating the effect of genes on the neural mechanism of behavior in mice. Behav. Brain Res. 125, 183–188.

Ralph, R. J., Paulus, M. P., Fumagalli, F., Caron, M. G., and Geyer, M. A. 2001. Prepulse inhibition deficits and perseverative motor patterns in dopamine transporter knock-out mice: differential effects of D1 and D2 receptor antagonists. J. Neurosci. 21, 305–313.

Reiter, L. A. and Ison, J. R. 1979. Reflex modulation and loudness recruitment. J. Audit. Res. 19, 201–207.

Romanski, L. M. and LeDoux, J. E. 1992. Equipotentiality of thalamo-amygdala and thalamo-cortico-amygdala circuits in auditory fear conditioning. J. Neurosci. 12, 4501–4509.

Rosen, J. B., Hitchcock, J. M., Miserendino, M. J. D., Falls, W. A., Campeau, S., and Davis, M. 1991. Lesions of the perirhinal cortex, but not of the frontal, medial pre-frontal, visual or insular cortex block fear-potentiated startle using a visual conditioned stimulus. J. Neurosci. 12, 4624–4633.

Scott, B. W., Frankland, P. W., Li, L., and Yeomans, J. S. 1999. Cochlear and trigeminal systems contributing to the startle reflex in rats. Neuroscience 91, 1565–1574.

Swerdlow, N. R. and Geyer, M. A. 1998. Using an animal model of deficient sensorimotor gating to study the pathophysiology and new treatment of schizophrenia. Schizophr. Bull. 24, 285–301.

Swerdlow, N. R., Mansbach, R. S., Geyer, M. A., Pulvirenti, L., Koob, G. F., and Braff, D. L. 1990. Amphetamine disruption of prepulse inhibition of acoustic startle is reversed by depletion of mesolimbic dopamine. Psychopharmacology 100, 413–416.

Swerdow, N. R., Paulsen, J., Braff, D. L., and Butters, N. 1995. Impaired prepulse inhibition of acoustic and tactile startle response in patients with Huntington's disease. J. Neurol. Neurosurg. Psychiatry 58, 192–200.

Thompson, R. F. and Spencer, W. A. 1966. Habituation: a model phenomenon for the study of neuronal substrates of behavior. Psychol. Rev. 73, 16–43.

Weber, M., Schnitzler, H. U., and Schmid, S. 2002. Synaptic plasticity in the acoustic startle pathway: the neuronal basis for short-term habituation? Eur. J. Neurosci. 16, 1325–1332.

Willott, J. F. 1996. Auditory System Plasticity in the Adult C57BL/6J Mouse. In: Auditory Plasticity and Regeneration (*eds*. R. J. Salvi, D. H. Henderson, V. Colletti, and F. Fiorino), pp. 297–316. Thieme Medical Publishers.

Willott, J. F., Carlson, S., and Chen, H. 1994. Prepulse inhibition of the startle response in mice: relationship to hearing loss and auditory system plasticity. Behav. Neurosci. 108, 703–713.

Willott, J. F., Kulig, J, and Satterfield, T. 1984. The acoustic startle response in DBA/2 and C57BL/6 mice: relationship to auditory neuronal response properties and hearing impairment. Hear. Res. 16, 161–167.

Willott, J. F., Shnerson, A., and Urban, G. P. 1979. Sensitivity of the acoustic startle response and neurons in subnuclei of the mouse inferior colliculus to stimulus parameters. Exp. Neurol. 65, 625–644.

Willott, J. F., Tanner, L., O'Steen, J., Johnson, K. R., Bogue, M. A., and Gagnon, L. 2003. Startle and prepulse inhibition in forty inbred strains of mice. Behav. Neurosci. 117, 716–727.

Willott, J. F. and Turner, J. G. 2000. Neural plasticity in the mouse inferior colliculus: relationship to hearing loss, augmented acoustic stimulation, and prepulse inhibition. Hear. Res. 147, 275–281.

Wu, M. F., Suzuki, S. S., and Siegel, J. M. 1988. Anatomical distribution and response patterns of reticular neurons active in relation to acoustic startle. Brain Res. 457, 399–406.

Yeomans, J. S. and Frankland, P. W. 1996. The acoustic startle reflex: neurons and connections. Brain Res. Rev. 21, 301–314.

Yeomans, J. S., Li, L., Scott, B. W., and Frankland, P. W. 2002. Tactile, acoustic and vestibular systems sum to elicit the startle reflex. Neurosci. Biobehav. Rev. 26, 1–11.

Young, J. S. and Fechter, L. D. 1983. Reflex inhibition procedures for animal audiometry: a technique for assessing ototoxicity. J. Acoust. Soc. Am. 73, 1686–1693.

Zhang, J., Forkstam, C., Engel, J. A., and Svensson, L. 2000. Role of dopamine in prepulse inhibition of acoustic startle. Psychopharmacology 149, 181–188.

Further Reading

Swerdlow, N. R., Geyer, M. A., Hartman, P. L., Sprock, J., Auerbach, P. P., Cadenhead, K., Perry, W., and Braff, D. L. 1999. Sex differences in sensorimotor gating of the human startle reflex: all smoke? Psychopharmacology (Berl.) 146, 228–232.

Willott, J. F. and Carlson, S. 1995. Modification of the acoustic startle response in hearing-impaired C57BL/6J mice: prepulse augmentation and prolongation of prepulse inhibition. Behav. Neurosci. 109, 396–403.

3.35 Encoding of Interaural Timing for Binaural Hearing

R M Burger, Lehigh University, Bethlehem, PA, USA

E W Rubel, University of Washington, Seattle, WA, USA

© 2008 Elsevier Inc. All rights reserved.

3.35.1	**Overview and Background**	613
3.35.1.1	Interaural Time Disparity: The Cue for Low-Frequency Sound Localization	614
3.35.1.2	Processing Interaural Time Disparities: The Jeffress Model	615
3.35.1.3	Processing Interaural Time Disparities: Physiology	615
3.35.2	**Interaural Time Disparity Processing in Birds**	616
3.35.2.1	Inputs to Nucleus Laminaris	616
3.35.2.2	Encoding of Interaural Time Disparities in Nucleus Laminaris	618
3.35.2.3	Intrinsic Properties of Nucleus Laminaris Neurons Specialized for Interaural Time Disparity Computation	619
3.35.2.4	The Role of Inhibition in Nucleus Luminaris Function	621
3.35.3	**Interaural Time Disparity Processing in the Medial Superior Olive**	623
3.35.3.1	Mammalian Interaural Time Disparity-Encoding Circuitry	623
3.35.3.2	Response Properties of Medial Superior Olive Neurons	624
3.35.3.3	Intrinsic Properties of Medial Superior Olive Neurons	625
3.35.3.4	The Role of Inhibition in the Medial Superior Olive	625
3.35.3.5	The Neural Code for Interaural Time Disparity in Mammals	626
3.35.4	**Summary and Conclusion**	627
References		627

Glossary

avian Of or pertaining to birds.

azimuth The angular distance or position in the horizontal plane.

delay line A component of either a model or physical circuit that introduces time delays into a processing unit where time delay is proportional to the length of the component.

dichotic The binaural presentation of stimuli that differ in one or more aspects (i.e., frequency, intensity, etc.).

diotic The binaural presentation of identical stimuli to the two ears.

interaural phase disparity The difference in stimulus phase at the two ears, which varies with interaural time disparity for freefield stimuli.

interaural intensity disparity The difference in stimulus intensity measured at the two ears, the magnitude of which depends on physical features of the listener, such as head size, and stimulus frequency.

interaural time disparity The difference in arrival time for a particular sound stimulus at the two ears, the magnitude of which depends primarily on head size and the speed of sound in the medium.

K^+_{HT} High-threshold potassium conductance through a membrane, usually associated with Kv3 family potassium channels.

K^+_{LVA} Low-threshold potassium conductance through a membrane, usually associated with Kv1 family potassium channels.

3.35.1 Overview and Background

Binaural hearing provides important perceptual information for localizing acoustic information in space and for enhancing signal-to-noise characteristics, especially in noisy environments. Interaural time disparities (ITDs) are the principal cue animals use to localize low-frequency sounds in the azimuthal plane (horizon). In reptiles, birds, and mammals specialized regions in the auditory brainstem are devoted to

processing this cue (Carr, C. E. and Code, R. A., 2000; Carr, C. E. and Soares, D., 2002). These regions express specializations for temporal processing at the network, synaptic, and cellular levels, providing striking examples of neural architecture and molecular properties that are clearly related to the function of the circuit and the behavior for which it is utilized. Some of the features of the specialized synaptic physiology in these pathways have been discussed in previous chapters. This chapter will focus primarily on the input pathways and intrinsic properties of neurons in nucleus laminaris (NL) and the medial superior olive (MSO), binaural brainstem nuclei in birds and mammals that first process ITDs. These regions provide some of the clearest examples in neurobiology of how neuronal circuits perform computations.

Our discussion will first explore the nature of ITD cues highlighting some early historical contributions in the field, and we will review the current state of knowledge regarding the anatomy and physiology of both NL and MSO circuitry. We will focus on inhibitory components of both systems, because while inhibition has long been recognized as an important component of ITD processing circuitry, recent work has generated renewed interest in resolving its contribution to ITD processing.

3.35.1.1 Interaural Time Disparity: The Cue for Low-Frequency Sound Localization

The difference in the arrival time of sound to each ear varies systematically with a sound source's position in space along the azimuth (Figure 1(a)). A particular ITD value depends on: (1) the acoustic distance between the ears (interaural distance), (2) the speed of sound in air (or water), and (3) the angle of incidence of the sound to the listener. For example, a sound source emanating from a position in space on the midline with respect to the listener arrives at both ears simultaneously yielding an ITD of 0 μs. This value will systematically increase as the sound is shifted laterally such that a sound source at roughly 90° to the midline will lead in the ipsilateral ear by the maximal ITD, a value that is generally determined by the distance between the two ears. For humans the maximal ITD is ~700 μs (Wightman, F. L. and Kistler, D. J., 1993), while for small mammals such as the gerbil it is ~130 μs (Maki, K. and Furukawa, S., 2005).

These ITDs result in stable interaural phase differences (IPDs) for ongoing periodic sounds such as

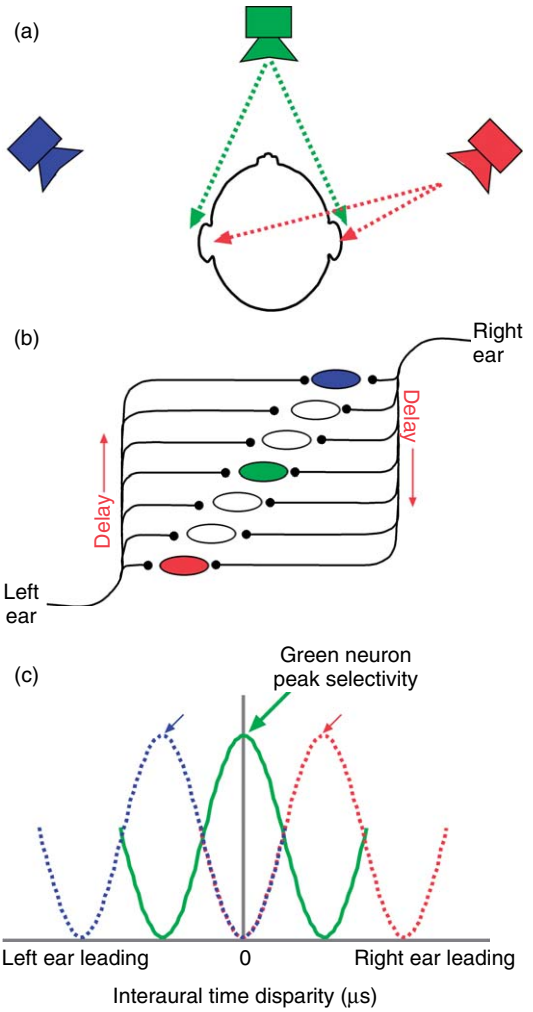

Figure 1 Illustration of the fundamental principles of ITD processing. (a) ITD varies systematically with sound source position. Three sound sources are represented by the three colored speakers. The sound path from the green speaker positioned on the midline is equidistant to each ear, resulting in an ITD of 0 μs. The blue and red speakers will lead in the left and right ears respectively and thus generate large ITDs. The maximum ITD for a human listener is about 700 μs. (b) The Jeffress model for processing ITDs. The ovals represent an array of coincidence detecting neurons and the black lines indicate the input axons to the coincidence detectors. The crucial feature is the increase in axon length (delay lines) from each ear across the array of coincidence detectors. The axon length gradient ensures that each cell in the array is maximally activated at a particular ITD with a value that is determined by the intrinsic delay of the input circuitry. The green neuron, with equal length input axons is selective for an ITD value of 0 μs, while the blue and red neurons prefer ITDs that favor the left and right ear (blue and red sound source positions), respectively. (c) The neural response functions are schematically shown for each of the three colored neurons from panel (b).

tone stimuli. The ongoing phase differences resulting from ITDs provide the principal cue animals use to localize low-frequency sounds in space. The phase difference generated at a given ITD will depend on the frequency of the stimulus. Low-frequency (long wavelength) stimuli generate relatively small IPDs. As frequency increases, the wavelength of the stimulus decreases, thus a greater change in phase (or IPD) will occur per unit time (ITD). Figure 2 illustrates this principle. For simplicity, we will refer to the auditory cue as ITD unless specifically discussing phase. The salience of ITD as a cue for sound location was demonstrated in the early 1900s by Rayleigh L. S. (1907).

Rayleigh's observations defined what is now referred to as the duplex theory of sound localization (Rayleigh, L. S., 1907; Colburn, H. S. and Durlach, N. I., 1978). The duplex theory states that sounds are lateralized on the basis of differences in both arrival time and intensity at the two ears. Arrival time cues are useful at low frequencies where wavelengths are broad and sound intensity is not significantly attenuated by the head. At higher frequencies, when wavelengths are smaller than the interaural distance (roughly 1500 Hz for humans), sound is attenuated by its interaction with the head generating substantial interaural spectral differences (intensity differences, IIDs) between the two ears. ITDs and IIDs are processed in separate parallel pathways that appear to interact through the inhibitory circuitry in both mammals and birds. The circuitry for processing IIDs is beyond the scope of this chapter, but is discussed in Chapter 3.36 (Pollak, G. D. *et al.*, 2002; Pollak, G. D. *et al.*, 2003; Tollin, D. J., 2003).

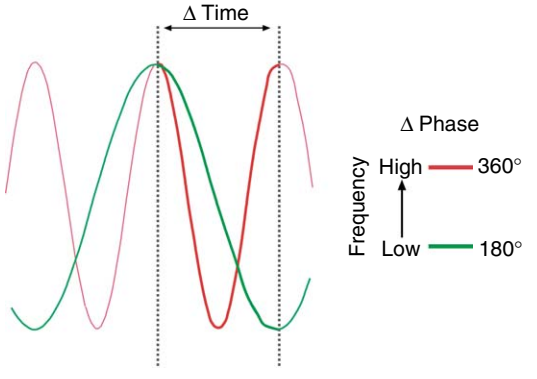

Figure 2 Illustration of the relationship between ITD and IPD. A given ITD defined by the gray dashed lines yields IPDs bold lines that depend on stimulus frequency. In this simple example, the high-frequency stimulus red waveform has a change in phase of 360° for this ITD while the low-frequency green waveform (half the frequency of the red stimulus) has a change in phase of only 180° with the same ITD.

3.35.1.2 Processing Interaural Time Disparities: The Jeffress Model

With the acoustic cues necessary for localizing sounds in azimuth well established, a second major contribution to the field was made by Lloyd Jeffress (1948). He conceived a simple model for the computation of ITDs that has been perhaps the most enduring and influential model in auditory neuroscience. The Jeffress model comprises two major components (Figures 1(b) and 1(c)). The first is an array of coincidence detecting binaural neurons. These neurons require simultaneous or near-simultaneous input from each ear to evoke a maximal response. The second component of his model is a particular arrangement of input axons to the coincidence detectors. The inputs are arranged such that input from a given ear innervates each successive coincidence detector in the array with increasing axon lengths, thus establishing an orderly series of delay lines. A complimentary delay line array is provided by circuitry from the contralateral ear. The model's opposing sets of delay lines compensate for interaural delays such that each consecutive coincidence detecting neuron is optimally responsive to a particular interaural delay and thus systematically shifting locations in space.

3.35.1.3 Processing Interaural Time Disparities: Physiology

These early works by both Raleigh and Jeffress set the stage for decades of behavioral and physiological auditory research. Several studies in the 1960s began to explore auditory brainstem regions that exhibited binaural interactions suggestive of sensitivity to ITD (Hall, J. L., 2nd, 1965; Moushegian, G. *et al.*, 1967; Goldberg, J. M. and Brown, P. B., 1969). Among the most significant of these early pioneering studies was that of Goldberg J. M. and Brown P. B. (1969). Their work represents the first comprehensive physiological study of the MSO. MSO neurons responded primarily to low-frequency stimuli and were remarkably sensitive to ITDs. The authors showed that MSO neurons had spike rates that varied several fold over just a few hundred microseconds shifts in ITD, revealing some of the most temporally sensitive neurons ever observed in the nervous system.

Furthermore, Goldberg and Brown showed that the ITD to which the neurons were most sensitive, referred to as the neuron's "best ITD," was predictable on the basis of the latency of excitatory input from each ear. In other words, the MSO neurons were optimally driven when the time between the ears was adjusted so that the intrinsic delays from the inputs from each ear arrived simultaneously at the MSO neuron. This finding solidified support for the delay line concept proposed by Jeffress and demonstrated that neurons in the mammalian brain are selective for particular ITDs, the localization cue established by Raleigh.

Further investigation of this system in mammals as diverse as cats, kangaroo rats, gerbils, and rabbits has supported and expanded on the major findings of Goldberg and Brown (Hall, J. L., 2nd, 1965; Moushegian, G. *et al.*, 1967; Moushegian, G. *et al.*, 1975; Yin, T. C. and Chan, J. C., 1990; Spitzer, M. W. and Semple, M. N., 1995; Batra, R. and Fitzpatrick, D. C., 1997; Batra, R. *et al.*, 1997b; 1997a). Indeed, the processing of ITDs of airborne sounds appears to be a general feature of auditory systems including insects, reptiles, birds, and mammals (Hoy, R. R. and Robert, D., 1996; Robert, D. *et al.*, 1996; Carr, C. E. *et al.*, 2001). The most comprehensive literature on ITD processing has arisen from studies in birds where behavioral, anatomical, and physiological studies offer a relatively complete picture of sound localization circuitry in the auditory system.

3.35.2 Interaural Time Disparity Processing in Birds

The components of the avian auditory pathway devoted to processing interaural time cues compose what is arguably one of the most elegant and well-understood circuits in the vertebrate nervous system. The elegance of this circuit derives from the remarkable correspondence between its functional role and its anatomical and physiological characteristics. NL is the first nucleus in the avian brainstem to receive information from the two ears and appears to be the initial region where sound location is computed. In addition, it appears that both ITDs and sound frequency are mapped along orthogonal directions in NL.

Current understanding of this circuit relies primarily on studies of two species, the chicken and barn owl. Fortuitously, the data acquired from studies of each species are largely complimentary because the attributes of each preparation are optimal for different but overlapping methods of investigation. For example, studies of the chicken have yielded exceptionally detailed developmental, cell physiological, and anatomical data, whereas the barn owl's remarkable sound localization related behavior has contributed much in relating anatomical and *in vivo* physiological observations to psychophysical and behavioral studies. The general features common to both species will be discussed, but a few of the differences will be highlighted.

3.35.2.1 Inputs to Nucleus Laminaris

In birds, sound is transduced by hair cells of the basilar papilla and relayed to the central nervous system by the auditory nerve (nVIII). nVIII fibers enter the brainstem and bifurcate to innervate two cochlear nuclei (Figure 3). The first, nucleus angularis (NA) is not directly involved in temporal coding, but does interact with this circuit through its connections with inhibitory inputs (see below). The second is nucleus magnocellularis (NM) where large endbulb of Held synaptic complexes from 2 to 4 nVIII fibers make direct contact with the somata of NM cells. This unusually secure synaptic connection preserves the spike timing information encoded in the nVIII and represents one of the early specializations in the ITD coding pathway in birds. There is

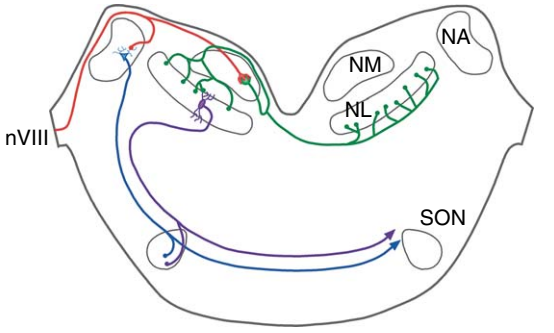

Figure 3 Excitatory pathways in the avian brainstem ITD-processing pathway. Information from the ear is conveyed over the nVIII red line to two cochlear nuclei, nucleus angularis (NA), and nucleus magnocellularis (NM). In NM the nVIII makes large endbulb of Held synapses onto the NM neurons. NM cells in turn project bilaterally to NL green projection. The NM projections to NL are the source of internal delays for ITD processing in birds. Both NA and NL blue and purple lines project to higher-order auditory centers including a fourth brainstem nucleus, the SON. The SON is the primary source of inhibition to all of the brainstem auditory nuclei.

now a vast literature on the nature of this synapse, although much of it is beyond the scope of this chapter. Excellent reviews are presented in Chapter 3.33 and in the writings of Oertel D. (1997) and Trussell L. O. (1997; 1999).

NM cell axons project bilaterally to a third nucleus, NL, the first center to receive binaural input. As with NM, NL is tonotopically organized such that neurons receiving low-frequency NM input are located at the caudolateral pole while high-frequency cells are located rostromedially (Rubel, E. W. and Parks, T. N., 1975). In the chicken, throughout most of its extent, NL is composed of a monolayer of neurons, the exception being the low-frequency caudolateral region which is a few cells thick.

The pattern of NM inputs to NL is a critical feature for the ITD-processing function of NL. Each NM cell axon branches upon exiting the nucleus medially. The ipsilateral branch arcs dorsally, passes back through the nucleus, and then courses rostrally before dipping ventrally to ramify along the dorsal dendrites and on the cell bodies of an isofrequency sheet of NL neurons. Physiological and anatomical studies have shown that the axon length to the ipsilateral NL neurons is equivalent along the isofrequency dimension (Young, S. R. and Rubel, E. W., 1983; Overholt, E. M. *et al.*, 1992). The contralateral collateral from the same NM neuron extends across the midline and branches several times to create an orderly, serial set of axonal branches extending along an analogous isofrequency band of NL neurons. These contralateral collaterals innervate the ventral dendrites and cell bodies of NL neurons within an isofrequency band (Young, S. R. and Rubel, E. W., 1983). This arrangement of innervation, predominantly along the medial to lateral dimension, results in medial laminaris cells receiving contralateral input with the shortest input axons and lateral NL cells the longest. The systematic increase of axon lengths across the nucleus effectively establishes a series of delay lines that compensate for interaural time delays. This corresponds remarkably well to the Jeffress model. One notable exception is that in the chicken NL, the delay line arises solely from the contralateral ear input, rather than bilaterally. Thus, neurons in the lateral NL will respond most vigorously to sounds with ITDs that lead in the contralateral ear (sounds that emanate from contralateral sound fields) and medial laminaris neurons that have receptive fields near the midline. Thus, each NL topographically maps a sound field composed primarily of the contralateral sound field.

The orderly arrangement of input axons across the roughly medial to lateral dimension defines a topography of contralateral delay within NL. Orthogonal to this axis is the tonotopic axis that runs caudolaterally to rostromedially at about 30° to the sagittal plane. Precisely along this tonotopic axis, chicken NL neurons express a gradient of dendrite length (Figure 4) (Smith, D. J. and Rubel, E. W., 1979). In mature animals, dendrite length varies 11-fold from the low- to high-frequency poles of NL (Smith, D. J. and Rubel, E. W., 1979). Low-frequency cells have one or two long primary dendrites that branch profusely, while high-frequency cells have a few short ones. The possible role of this intriguing feature of NL will be discussed in Section 3.35.2.4.

The NL of the barn owl is similar to that described in the chicken, with a few important differences. First, in the high-frequency portion of NL, dendrites of mature barn owl NL neurons are short and are not restricted to the dorsal and ventral poles of the neurons (Carr, C. E. and Boudreau, R. E., 1996; Kubke, M. F. *et al.*, 2002). This may be related to the unusual ability of the barn owl to process ITD information for much higher-frequency signals than other birds and most other mammals (see below). ITDs remain a useful cue up to about 9 kHz and the owl's greatest ITD selectivity is in the range of 4–8 kHz (Knudsen, E. I. and Konishi, M., 1979). A second major difference between the barn owl and chicken is that the barn owl NL is several hundred μm thick and composed of layers of neurons throughout its extent. The input axons to these neurons enter the nucleus at the dorsal or ventral surface and course perpendicularly to the mediolateral trajectory of input axons from the contralateral NM (Carr, C. E. and Konishi, M., 1990). This arrangement of input axons through several layers of NL neurons will be discussed in Section 3.35.2.2, but it represents an expansion of the sound-localization circuitry in this predator, presumably specialized for acoustically localizing prey in the dark.

In addition to the orderly pattern of excitatory inputs to NL, GABAergic inhibitory inputs are abundant (Carr, C. E. *et al.*, 1989; Code, R. A. *et al.*, 1989; Lachica, E. A. *et al.*, 1994; Burger, R. M. *et al.*, 2005). These arise from two sources, a small population of multipolar neurons residing in the neuropil between NM and NL and a prominent projection from the ipsilateral superior olivary nucleus (SON) (von Bartheld, C. S. *et al.*, 1989; Lachica, E. A. *et al.*, 1994;

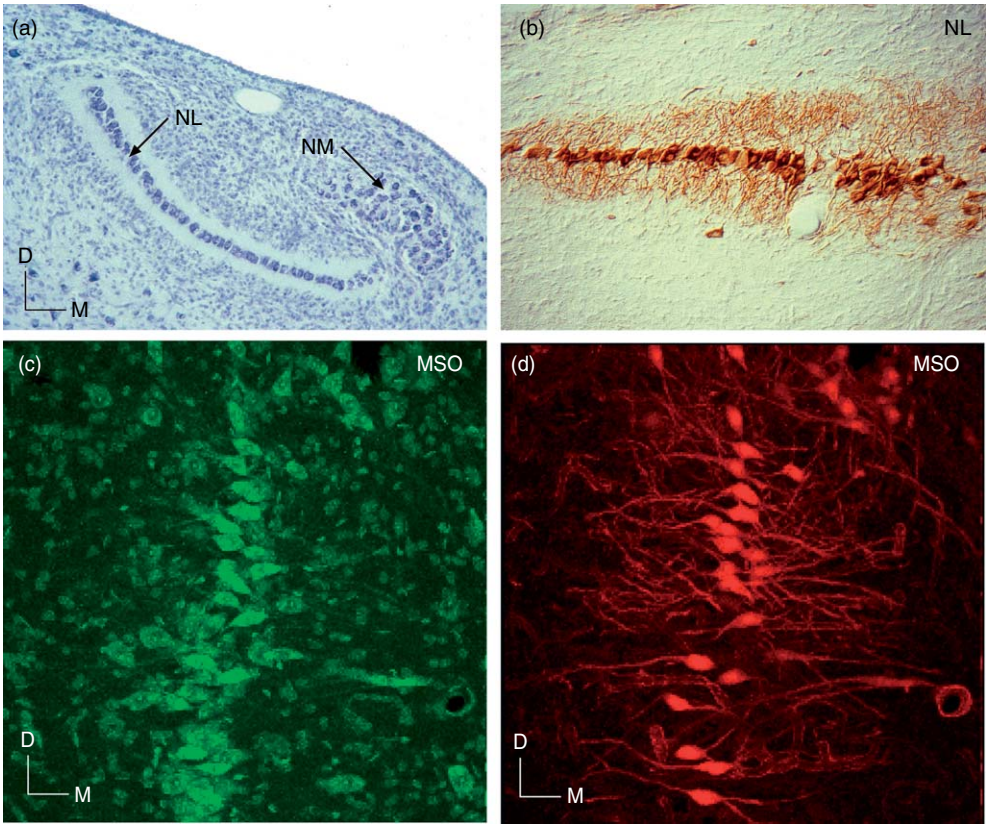

Figure 4 Comparison of NL and MSO neurons. (a) A Nissl-stained section through the auditory brainstem of the chicken showing the laminar structure of NL and the neighboring ipsilateral NM. (b) The dendrite length gradient in NL can be clearly observed in the section through NL stained for MAP2 antigen. Higher best frequency neurons are to the left, lower BF NL cells are to the right. Additionally, one can appreciate the dorsoventrally oriented bipolar dendrites. (c) Neurons of the Gerbil MSO can be seen clustered along a dorsoventral running axis in this fluorescent Nissl-stained section. (d) The bipolar mediolaterally oriented dendrites of rhodamine conjugated dextran-labeled MSO neurons in the same section as that shown in (c).

Westerberg, B. D. and Schwarz, D. W., 1995; Yang, L. *et al.*, 1999; Burger, R. M. *et al.*, 2005). The functional impact of this inhibitory input has been the focus of intense study and current understanding of inhibition's role in the computation of ITDs will be discussed in some detail further in this chapter.

3.35.2.2 Encoding of Interaural Time Disparities in Nucleus Laminaris

NL's primary function appears to be the computation and topographic representation of ITDs across the nucleus. The most compelling data available on a topographic ITD representation has derived from studies of the barn owl nucleus laminaris and *in vitro* data from the chicken (Parks, T. N. and Rubel, E. W., 1975; Sullivan, W. E. and Konishi, M., 1986; Carr, C. E. and Konishi, M., 1990; Overholt, E. M. *et al.*, 1992; Joseph, A. W. and Hyson, R. L., 1993). The suggestion that innervation pattern of NL from the contralateral NM may represent a Jeffress-type delay line was first suggested for the chicken by Parks T. N. and Rubel E. W. (1975) where the topography of these connections was initially described. Later physiological and anatomical work in both the barn owl and chicken has confirmed the hypothesis of Parks T. N. and Rubel E. W. (1975).

While the anatomical substrate of the delay line that generates the topographic representation was identified and described in the chick by Young S. R. and Rubel E. W. (1983) (Figure 5), the contribution of delay lines to the resultant topographic representation of ITD was demonstrated physiologically *in vivo* by a sequence of papers from the Konishi lab (Sullivan, W. E. and Konishi, M., 1986; Carr, C. E. and Konishi, M., 1990). In the first paper, roughly dorsal to ventral electrode penetrations were made through NL transecting the contralateral NM axon

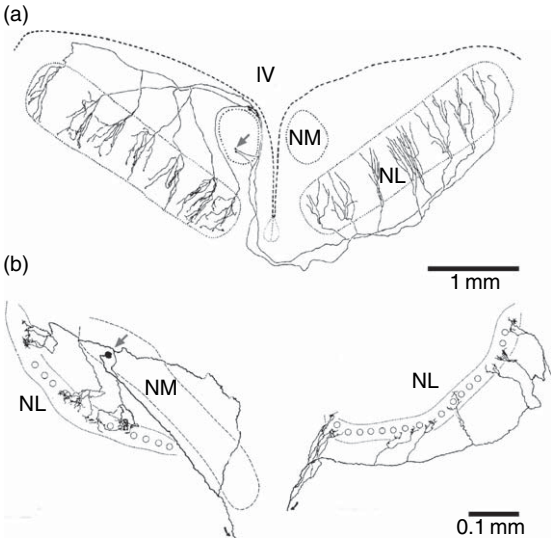

Figure 5 A comparison of the inputs from NM to NL in the barn owl and chicken reveals the exquisite architecture of the avian ITD-coding system. (a) Reconstruction of projections from two barn owl NM neurons to their targets in NL and in (b) reconstruction of an NM neuron projection in the chicken. In both barn owl and chicken, the contralateral projections innervate medial NL neurons with the shortest axon segments while the lateral NL cells receive the longest NM axon length inputs. In the barn owl, the orderly and opposing innervation from the dorsal and ventral borders of NL by NM axons may lead to additional sources of delay. NM neuron somas are labeled by gray arrows in both panels. (a) From Carr, C. E. and Konishi, M. 1990. A circuit for detection of interaural time differences in the brain stem of the barn owl. J. Neurosci. 10, 3227–3246. (b) From Young, S. R. and Rubel, E. W. 1983. Frequency-specific projections of individual neurons in chick brainstem auditory nuclei. J. Neurosci. 3, 1373–1378.

length gradient obliquely. Sullivan W. E. and Konishi M. (1986) demonstrated that as the electrode advanced ventrally (and roughly across the gradient of medial to lateral input axon lengths) the ITD for eliciting a maximum field potential shifted systematically toward the contralateral ear.

A later study by Carr C. E. and Konishi M. (1990) in which recordings were made from NM axons in addition to NL cells, demonstrated that when electrode penetrations were made perpendicular to the mediolateral running plexus of NM input axons in the ventral NL, delays increased or decreased with depth, depending on whether the axon was from ipsilateral or contralateral NM, respectively. In addition, a given interaural phase delay was often represented more than once in a single penetration. These authors have suggested that in the barn owl, the topographic representation of the entire range of ITDs is represented along the dorsal–ventral axis of NL, and this representation is repeated many times along the predominantly mediolateral dimension that is orthogonal to the tonotopic dimension. In other words, the layered expansion of NL in barn owls could generate an additional source of delay lines not present in other bird species.

The presence of delay lines in the bird auditory pathway was directly demonstrated by *in vitro* chick brainstem slice studies in the Rubel lab (Overholt, E. M. *et al.*, 1992; Joseph, A. W. and Hyson, R. L., 1993). Hyson and colleagues recorded postsynaptic field potentials from NL neurons while systematically shifting the timing of stimulated inputs from the ipsilateral and contralateral NM. In these studies, a dramatic difference was observed when stimulating the ipsilateral versus contralateral input to NL neurons. Increasing delays were observed as the electrode was moved along an isofrequency line of NL neurons; that is, rostrolaterally parallel to the main axis of input axons thus confirming the source of input delays. Consistent with predictions from the anatomical observations of Young S. R. and Rubel E. W. (1983), latencies of the postsynaptic responses to ipsilateral stimulation did not vary as the electrode is moved from medial to lateral. On the other hand, the latencies of postsynaptic responses to contralateral stimulation systematically increased along the delay line dimension. Furthermore, these studies showed that NL cells were most optimally driven by binaural inputs timed to compensate for the mismatch in delay from each NM.

3.35.2.3 Intrinsic Properties of Nucleus Laminaris Neurons Specialized for Interaural Time Disparity Computation

The studies reviewed above provided the anatomical and physiological groundwork for a next generation of studies that have explored the unique specializations of intrinsic physiological properties in NM and NL that contribute to ITD calculations. Perhaps the most ubiquitous attribute of neurons involved in processing temporal aspects of auditory stimuli is the prevalence of potassium conductances that are suited to enhance temporal encoding. These include both a low-threshold potassium conductance (K^+_{LVA}) associated with Kv1 family channel subunits and a high-threshold (K^+_{HT}) conductance associated with Kv3 family channel subunits.

The K^+_{LVA} conductances have been investigated in a large number of auditory neurons (Oertel, D., 1983; Manis, P. B. and Marx, S. O., 1991; Banks, M. I. and Smith, P. H., 1992; Reyes, A. D. *et al.*, 1994; Zhang, S. and Trussell, L. O., 1994; Brew, H. M. and Forsythe, I. D., 1995; Smith, P. H., 1995; Reyes, A. D. *et al.*, 1996; Rathouz, M. and Trussell, L., 1998; Bal, R. and Oertel, D., 2001; Adamson, C. L. *et al.*, 2002; Svirskis, G. *et al.*, 2002; Svirskis, G. *et al.*, 2003; Kuba, H. *et al.*, 2005; Scott, L. L. *et al.*, 2005). The channels underlying this conductance are activated at voltages at or just above rest and have several influences on information processing. First, the strong outward conductance causes a reduced membrane input resistance thus shortening the time constant of the membrane. This has the dual effect of reducing the time course of voltage changes from a given input and correspondingly reducing the time window during which inputs can summate. Second, these neurons typically respond to sustained depolarizing currents with a single action potential, allowing the membrane to recover quickly from an excitatory input. This property has been observed in many auditory neurons involved in temporal processing. A classic example of responses in a mammalian medial nucleus of the trapezoid body (MNTB) neuron from a study by Brew H. M. and Forsythe I. D. (1995) is shown in Figure 6. A third effect of this conductance is to raise the neuron's threshold. Together, these effects may increase the requirement for inputs to be coincident in order to evoke a postsynaptic action potential, a property which provides improved temporal processing ability advantageous for the encoding of ITDs (Carney, L. H., 1992; Rothman, J. S. *et al.*, 1993).

The channels underlying the K^+_{HT} conductances activate at high voltages in the range of −20 mV and thus may only be activated by action potentials (Gan, L. and Kaczmarek, L. K., 1998; Rudy, B. and McBain, C. J., 2001). These channels' protein subunits or their mRNAs have been shown to be highly expressed in both NL and NM (Parameshwaran, S. *et al.*, 2001; Parameshwaran-Iyer, S. *et al.*, 2003; Lu, Y. *et al.*, 2004), as well as in mammalian time-coding neurons (Perney, T. M. *et al.*, 1992; Perney, T. M. and Kaczmarek, L. K., 1997; Grigg, J. J. *et al.*, 2000). The K^+_{HT} conductances confer upon neurons the ability to rapidly repolarize following an action potential and thus the primary role of K^+_{HT} currents appears to be the preservation of high-frequency firing (Brew, H. M. and Forsythe, I. D., 1995; Gan, L. and Kaczmarek, L. K., 1998; Wang, L. Y. *et al.*, 1998). Several studies have shown that in the presence of low concentrations of tetraethylammonium chloride (TEA) which blocks K^+_{HT}, cells fail to sustain the high-firing frequencies typically achieved by temporal coding neurons (Brew, H. M. and Forsythe, I. D., 1995; Wang, L. Y. *et al.*, 1998). Figure 6 shows that a TEA-sensitive conductance in MNTB cells contributes to the brevity of action potentials. Furthermore, recent studies suggest that K^+_{HT} conductances can be modulated through phosphorylation in an activity-dependent manner (Macica, C. M. *et al.*, 2003; Song, P. *et al.*, 2005). This finding suggests the possibility that this conductance may be tuned to optimally preserve temporal fidelity over a large range of firing frequencies (Song, P. *et al.*, 2005).

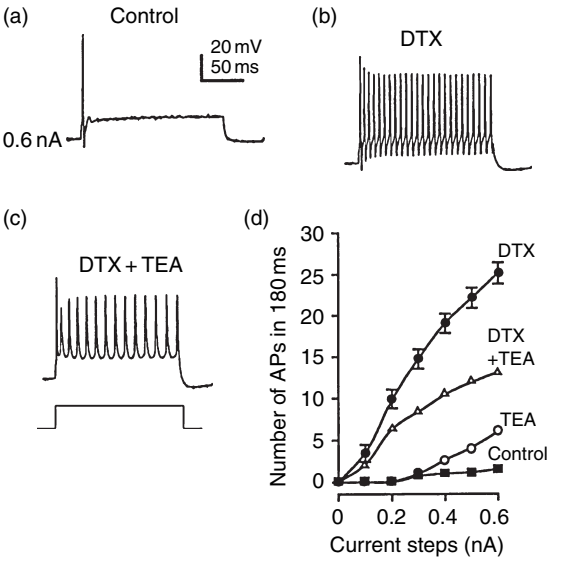

Figure 6 Potassium currents enhance signal processing in time-coding neurons. Shown are responses of MNTB neurons to current injections. (a) In the control condition, cells typically respond to depolarizing current steps with a single rapid action potential followed by a steady-state depolarization. The steady-state response is normally highly outward rectified (not shown). (b) When DTX, a Kv1 subunit specific blocker, is applied to the neuron, multiple spiking is evoked by the same current pulse. (c) Shows that by TEA application, high-threshold K^+ channels play an additional role in controlling membrane voltage. (d) Shows the firing rates across the population for the conditions in (a) through (c) and the TEA alone condition for two additional cells. Adapted from Brew, H. M. and Forsythe, I. D. 1995. Two voltage-dependent K^+ conductances with complementary functions in postsynaptic integration at a central auditory synapse. J. Neurosci. 15, 8011–8022. Change to the current values from original was made at the request of H. Brew.

The impact of K^+_{LVA} conductances on phase-locking and modulation of firing frequency in NL was investigated by Reyes A. D. *et al.* (1996). Reyes and colleagues recorded evoked excitatory postsynaptic conductances (EPSCs) in NL, and then, based on these recordings, computed model input trains and injected the summed current into the cells through a patch pipette. This strategy allowed the experimenters to model variations in the size, number, and temporal properties of the inputs. They were able to show that as stimulus frequency increased, a reduction of the number and an increase in size of the inputs was necessary to maintain high firing rates and phase-locked discharges in NL cells. They demonstrated that NL neurons characteristically possess a large low-threshold potassium conductance and that this conductance was crucial for temporal coding. NL neurons in which this current was pharmacologically blocked or other brainstem neurons that did not possess this conductance, were unable to phase-lock to high input frequencies.

Work by Ohmori and colleagues investigated the tonotopic distribution of Kv1.1 type potassium channel subunits, which are often incorporated into voltage gated K^+ channels that underlie K^+_{LVA} conductances. Using both physiological and immunohistochemical methods, they show that Kv1.1 subunits are not distributed evenly across the tonotopy of NL. NL cells in the mid- and high-frequency range appear to express Kv1.1 subunits and the associated conductance at higher levels than low-frequency neurons. Correlated with this effect is the observation that the middle-frequency NL neurons, the subset that physiologically had the strongest K^+_{LVA} conductances, appear to have the smallest coincidence window. The authors suggested that these findings may explain behavioral data showing that sound localization is most precise in the middle-frequency range for many birds (Kuba, H. *et al.*, 2005).

An additional important observation from this series of studies was the demonstration that the input properties vary across the tonotopy such that low-frequency cells produce Excitatory post synaptic potentials (EPSPs) with a longer time course than their mid- and high-frequency counterparts. The long EPSP duration was attributable to dendritic filtering of low-frequency NL cells that results from the large surface area of dendrites (Rall, W., 1969; Koch, C. and Segev, I., 2000; Kuba, H. *et al.*, 2005). A possible consequence of this filtering property is that it may enhance the electrical isolation of dorsal and ventral dendrites and, thus, the inputs from either ear from each other. This finding is significant because it is the first direct data to support the notion that the dendrite length gradient in NL is an adaptation for ITD processing of particular stimulus frequencies.

A fascinating assessment of the possible contribution of NL dendrites to ITD computation was made in an influential modeling study (Agmon-Snir, H. *et al.*, 1998). These authors proposed that the segregation of the ipsilateral and contralateral inputs to the dorsal and ventral dendrites, respectively, of NL neurons provides semi-isolated electrical compartments in which a series of inputs arriving near-simultaneously will add sublinearly within one electrical compartment. On the other hand, inputs arriving on separate dendrites will sum linearly in the soma. This mechanism could greatly enhance coincidence detection. Put simply, two inputs that arrive on separate dendrites and provide just enough current necessary to reach threshold would add sublinearly in a single dendrite and thus not generate a postsynaptic action potential. This mechanism would function to enhance a cell's responsiveness to binaural inputs, while suppressing the signaling of responses from coincident monaural input. The model also provided a rationale for the reduction of dendrite length with increasing frequency. Due to the amount of temporal error in phase-locking (or jitter), long dendrites, with longer duration membrane time constants, may expand their inputs in time and cause excess monaural summation at high frequencies where the stimulus period is brief, relative to the temporal jitter.

3.35.2.4 The Role of Inhibition in Nucleus Luminaris Function

The release of GABA in both NM and NL has unusual and important properties. GABA-receptor activation evokes a depolarizing response in these neurons. This property, first discovered by Hyson R. L. *et al.* (1995) in NL, is due to an unusually high internal Cl^- concentration. The reversal potential for the Cl^- conductance through $GABA_A$ receptors has been reported to be -25 and -37 mV by two separate studies using gramicidin perforated patch-clamp recording of NM cells (Lu, T. and Trussell, L. O., 2001; Monsivais, P. and Rubel, E. W., 2001). Depolarizing responses to GABA are not unusual at early stages of development in the auditory system or in other central neurons (Ben-Ari, Y. *et al.*, 1990; Cherubini, E. *et al.*, 1990; Kandler, K. and Friauf, E., 1995; Ehrlich, I. *et al.*, 1999; Kakazu, Y. *et al.*, 1999), but

are normally rapidly converted to hyperpolarizing responses. In mammalian auditory systems this generally occurs around the time of onset of hearing (Kandler, K. and Friauf, E., 1995; Smith, A. J. *et al.*, 2000; Magnusson, A. K. *et al.*, 2005). The precise mechanism underlying this shift is unknown, but is likely due to a change in Cl^- transporter expression (Kakazu, Y. *et al.*, 1999). In the chicken, depolarizing responses to GABA have been recorded well beyond hearing onset and appear to persist into maturity (Hackett, J. T. *et al.*, 1982; Jackson, H. *et al.*, 1982; Hyson, R. L. *et al.*, 1995; Yang, L. *et al.*, 1999; Monsivais, P. *et al.*, 2000; Lu, T. and Trussell, L. O., 2001).

What functional benefit is gained by this unusual property? In a series of studies from our laboratory, Monsivais and colleagues (Yang, L. *et al.*, 1999; Monsivais, P. *et al.*, 2000; Monsivais, P. and Rubel, E. W., 2001) showed that despite the depolarizing response to GABA, this input is generally inhibitory although occasional spiking from GABAergic input has been observed *in vitro* (Lu, T. and Trussell, L. O., 2001; Lu, Y. *et al.*, 2005). Indeed, Monsivais P. and Rubel E. W. (2001) showed that GABAergic depolarization into a superthreshold voltage range maintains its inhibitory function, and even exceeds the inhibitory potency that would derive from equal strength hyperpolarizing inputs. This depolarizing and potent inhibitory response is mediated through three cooperative mechanisms.

First, GABA release at NM or NL activates $GABA_A$ channels generating a Cl^- conductance. High stimulation rates of inhibitory inputs to NM cause Ca^{2+} accumulation in GABAergic terminals resulting in a long-lasting postsynaptic plateau inhibition characterized by asynchronous release of GABA (Lu, T. and Trussell, L. O., 2000). The outward flux of Cl^- ions depolarizes the cell membrane activating strong K^+_{LVA} conductances that dramatically lower the input resistance and thus provide a shunting inhibition for subsequent excitatory inputs. Finally, the slow and sustained GABA-induced depolarization causes inactivation of voltage gated Na^+ channels and, as a consequence, threshold shifts to depolarized values (Monsivais, P. and Rubel, E. W., 2001). Our recent study suggested that excessive GABA-evoked depolarization might be limited by $GABA_B$ receptor activation on the GABAergic terminals. $GABA_B$ receptor activation at these sites reduces the release of transmitter and subsequently generates less postsynaptic depolarization (Lu, Y. *et al.*, 2005).

Funabiki K. *et al.* (1998), in the Ohmori lab, tested the hypothesis that GABAergic input to NL improves coincidence detection as well. In an elegant series of experiments, they simulated binaural inputs by current injection or direct stimulation of NM axons and varied the interval between inputs to simulate a range of ITDs. They showed that during GABA application, the range of binaural intervals that evoked responses in the NL neurons (or response window) was reduced by 70%. This study clearly demonstrated GABA's potentially advantageous effect on the computational properties of NL.

To date, there have been no *in vivo* studies in birds to directly address the role of endogenous GABAergic input to the temporal coding nuclei. However, several studies have been done that underscore the potentially critical influence inhibition may have on ITD coding. Among the most important of these, Peña and colleagues in the Konishi lab published a pair of studies using loose-patch recording of NM and NL neurons providing superior isolation of responses. The NL recordings explored the stability of ITD tuning when neurons were challenged with a range of intensity changes to the two ears such that levels were shifted simultaneously in both ears (diotically) or differentially in each ear (dichotically) (Pena, J. L. *et al.*, 1996; Viete, S. *et al.*, 1997). Figure 7 shows that NL neurons possess a remarkable ability to maintain their best ITD (the ITD evoking the strongest response) and large firing-rate modulations with ITD over a large dynamic range of diotically presented intensity changes (Pena, J. L. *et al.*, 1996). Additionally, in the second paper, Viete S. *et al.* (1997) showed that for broadband stimuli, a neuron's best ITD remained fairly stable when the input intensity to either ear was unequal, suggesting that the system may include a mechanism to correct for differences in input strengths. These authors suggested that inhibition might provide the input necessary to preserve the stability of the ITD selective response under a broad range of conditions, although in their hands, evidence for such a mechanism was not forthcoming.

Our recent studies on the detailed anatomy of the GABAergic input to these nuclei from the SON led to predictions about a specific inhibitory mechanism for the observations noted earlier and further suggest that the inhibitory components of the ITD processing circuitry may have a fundamental role in ITD processing (Burger, R. M. *et al.*, 2005). In the chicken, most of the inhibitory input to the cochlear nuclei and NL is provided by the ipsilateral SON (Lachica,

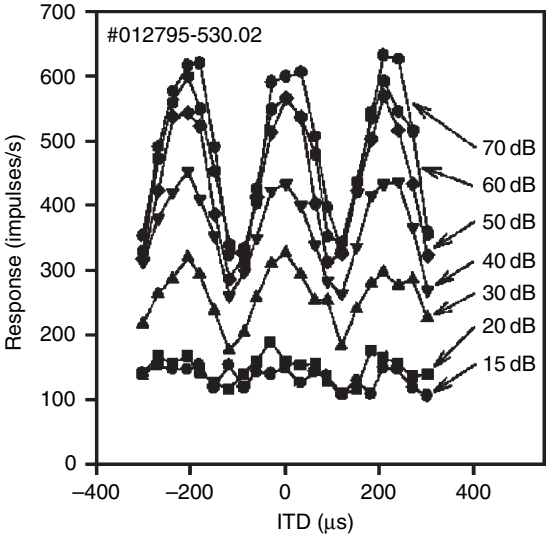

Figure 7 NL neurons possess a remarkable ability to maintain ITD selectivity over a broad dynamic range. In this figure, Pena and colleagues showed that NL neurons preserve their best ITD and a fairly large dynamic response over a large range of binaurally presented intensity changes. These data suggest that some mechanism, perhaps inhibition, may adjust the gain of the NL neuron's responses, allowing it to be selective at low intensities and preventing saturation at high intensities. Reproduced from Pena, J. L., Viete, S., Albeck, Y., and Konishi, M. 1996. Tolerance to sound intensity of binaural coincidence detection in the nucleus laminaris of the owl. J. Neurosci. 16, 7046–7054.

E. A. *et al.*, 1994; Westerberg, B. D. and Schwarz, D. W., 1995; Yang, L. *et al.*, 1999; Burger, R. M. *et al.*, 2005). The SON, in turn, receives its input from three sources, NA, NL, and the contralateral SON (Yang, L. *et al.*, 1999). The NA and NL input is glutamatergic and excitatory, and the contralateral SON input is likely to be inhibitory. Thus, the inhibitory circuitry of the avian auditory system is composed of a negative feedback loop on each side of the brainstem. In addition, these two feedback circuits appear to be negatively coupled to one another (Figure 8).

This anatomical arrangement provides clues as to how the system may work. We developed a conceptual model that suggested that this arrangement would provide a mechanism to preserve ITD encoding by equalizing the input strength to NL (Burger, R. M. *et al.*, 2005). A computational model went further in testing this hypothesis in a model avian auditory brainstem network using realistic biological parameters (Dasika, V. K. *et al.*, 2005).

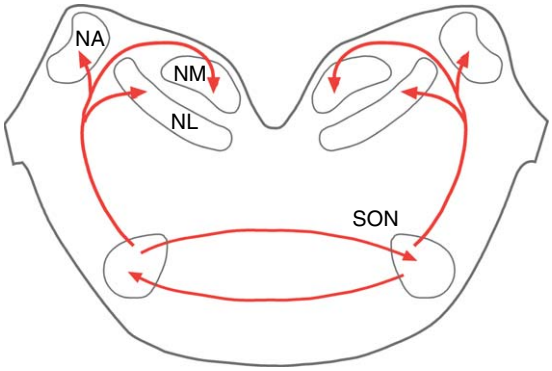

Figure 8 The inhibitory circuitry of the avian auditory brainstem. The majority of inhibitory input to the time-coding system emanates from the predominantly GABAergic SON. The SON which receives excitatory input from both NA and NL provides inhibition back to all ipsilateral brainstem nuclei forming an inhibitory feedback loop. These parallel feedback loops are coupled by the crossed reciprocal and putatively inhibitory connection between the SONs. These negatively coupled feedback circuits may be involved in offsetting bilateral differences in input strength to NL.

3.35.3 Interaural Time Disparity Processing in the Medial Superior Olive

The MSO in mammals receives a similar complement of inputs to that of NL in avians. However, important differences exist which raise interesting comparative questions as to the nature of ITD processing in MSO. In this section, we will first discuss the known anatomy and physiology of the MSO leading to some current issues in the field of ITD processing in the final section.

3.35.3.1 Mammalian Interaural Time Disparity-Encoding Circuitry

The MSO receives four principal inputs, one excitatory and one inhibitory, driven from each ear (Figure 9). The excitatory inputs derive bilaterally from the spherical bushy cells of the anteroventral cochlear nucleus (AVCN) where neurons specialized to faithfully transmit temporal aspects of the acoustic signal project to the MSO (Stotler, W. A., 1953; Glendenning, K. K. *et al.*, 1985; Cant, N. B. and Hyson, R. L., 1992; Smith, P. H. *et al.*, 1993). For a thorough review of superior olive anatomy see Thompson A. M. and Schofield B. R. (2000). MSO neurons, like their avian NL counterparts, have bipolar dendrites oriented roughly in the mediolateral plane, with each dendrite receiving input from

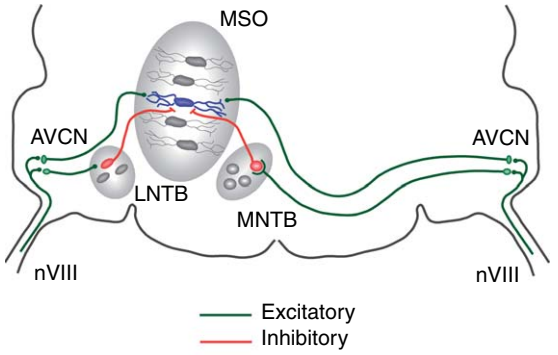

Figure 9 Input pathways to the MSO. The MSO receives excitatory input green pathways from both ears via bushy cells of the AVCN where nVIII inputs convey phase-locked discharges with large endbulb of Held synapses. Inhibition from both ears is also derived from input circuitry that is specialized to preserve temporal information. Input from the contralateral ear is conveyed via the glycinergic MNTB where bushy cell axons make large Caylx of Held synapses onto MNTB neuron somas. The ipsilateral inhibitory input is derived from the LNTB where enlarged synaptic endings from AVCN neurons appear to be specialized for temporal encoding.

its proximal ear (Figure 4) (Stotler, W. A., 1953; Smith, P. H. *et al.*, 1993).

The inhibitory input from the contralateral ear is derived from the medial nucleus of the trapezoid body (MNTB) (Kuwabara, N. and Zook, J. M., 1992; Smith, P. H. *et al.*, 1998). The glycinergic MNTB receives input from the anteroventral cochlear nucleus (AVCN) through large caliciform synapses that convert the precisely timed excitatory input into a precisely timed inhibitory output. The ipsilateral inhibition to the MSO is derived from the lateral nucleus of the trapezoid body (LNTB) where similar large synapses from AVCN bushy cells drive its glycinergic inhibitory output (Cant, N. B. and Hyson, R. L., 1992; Kuwabara, N. and Zook, J. M., 1992; Spirou, G. A. *et al.*, 1998).

A fundamental component of ITD-encoding circuitry according to the Jeffress hypothesis is an orderly series of input delay lines. In birds, NM input to the contralateral NL exhibits a clear anatomical axon length gradient that corresponds to the orderly representation of interaural phase delays. The evidence for delay lines in mammals is controversial. In the cat MSO, some compelling data suggests that the input axons from the contralateral ear may be arranged to generate delay lines, such that the rostral MSO cells receive the shortest length input collateral and the caudal cells receive the longest (Smith, P. H. *et al.*, 1993; Beckius, G. E. *et al.*, 1999). This anatomical arrangement agrees fairly well with the physiologically observed rough topography of ITD representation reported in the cat (Yin, T. C. and Chan, J. C., 1990). However, data from both anatomical studies shows that many input axons innervate only small segments of the MSO and not the entire extent of the nucleus as they do in NL. In addition, there have not been similar systematic physiological studies of the inputs to MSO at the level of those in NL (Sullivan, W. E. and Konishi, M., 1986; Carr, C. E. and Konishi, M., 1990; Overholt, E. M. *et al.*, 1992; Joseph, A. W. and Hyson, R. L., 1993) to confirm the presence of functional delay lines as a general feature in mammals.

3.35.3.2 Response Properties of Medial Superior Olive Neurons

The classic work of Goldberg J. M. and Brown P. B. (1969) was the first thorough study of the MSO role in ITD processing. Goldberg and Brown showed that MSO neurons in the dog were: (1) excited by input to both ears, (2) phase-locked to the stimulus waveform, and (3) optimally driven by binaural input with a particular delay that could be predicted based on the ITD required for the coincidence of monaural delays from each ear. They also observed several features of MSO neural responses that they attributed to inhibition, such as frequency selectivity, nonmonotonic input/output functions when driven by sound to one or both ears, and binaural firing rates that fell below the firing rate to either ear alone at the worst ITD (the ITD evoking the lowest firing rate).

The presence of brainstem neurons that process ITDs in a similar fashion to those observed in the dog have been documented in the cat, rabbit, gerbil, and kangaroo rat (Moushegian, G. *et al.*, 1967; Moushegian, G. *et al.*, 1975; Yin, T. C. and Chan, J. C., 1990; Spitzer, M. W. and Semple, M. N., 1995; Batra, R. and Fitzpatrick, D. C., 1997; Batra, R. *et al.*, 1997a; 1997b). In most of these studies the dominant class of MSO neurons exhibited evidence of phase-locked excitatory input from each ear and responded selectively to ITD selectivity to varying binaural stimuli. This suggests that most MSO neurons derive their response properties by cross-correlation of the phase-locked excitation from each ear.

A series of studies from Batra and colleagues (Batra, R. and Fitzpatrick, D. C., 1997; Batra, R. *et al.*, 1997a; 1997b) investigated ITD processing in the superior olivary complex. An important finding

of these studies was that coincidence of excitation from one ear and inhibition from the opposite ear also can impart ITD sensitivity on a neuron. Such neurons were referred to as troughers, following the nomenclature of Kuwada S. and Yin T. C. (1983) and Yin T. C. and Kuwada S. (1983a; 1983b), and were also observed in earlier studies of the LSO (Finlayson, P. G. and Caspary, D. M., 1991; Joris, P. X. and Yin, T. C., 1995). Spiking in trougher neurons is suppressed at a particular ITD regardless of stimulus frequency. Thus, these neurons are inactivated by coincidence of their inputs. However, it remains inconclusive whether or not this class of neurons resides within the MSO proper, but rather, may be the predominant ITD selective cell type in the neighboring lateral superior olive.

3.35.3.3 Intrinsic Properties of Medial Superior Olive Neurons

MSO neurons share several morphological and physiological properties with NL cells. Similar to other neurons that are specialized for processing temporal information (as cited earlier), injection of depolarizing current into principal MSO cells typically results in a single action potential followed by a sustained depolarization (Smith, P. H., 1995). The sustained portion of the response shows strong outward rectification. Application of 4-AP increases the number of action potentials and reduces the degree of rectification. This suggests that the large K^+_{LVA} type currents dominate the intrinsic membrane voltage responses in MSO neurons (Smith, P. H., 1995).

A study utilizing both physiological and modeling methods tested the role of K^+_{LVA} in signal detection in the presence of noisy inputs. Using a similar approach to that used by Reyes A. D. *et al.* (1996) in NL, Svirskis G. *et al.* (2002) injected subthreshold simulated excitatory postsynaptic conductances (EPSGs) as signals in a background of noisy subthreshold currents into normal and dendrotoxin (DTX)-treated MSO cells. DTX is a specific blocker of Kv1 family subunit containing channels (Robertson, B. *et al.*, 1996). They used a spike-triggered reverse correlation paradigm to determine the optimal current waveform to evoke spiking and found that control cells required very rapid inward currents, indicating a brief integration window. In DTX-treated cells the integration window was broader and the phase-locking to simulated EPSGs was poor. Thus, NL and MSO possess similar intrinsic mechanisms to enhance ITD selectivity.

In a later paper Svirskis G. *et al.* (2004) showed that at rest, many voltage-gated Na^+ channels are inactivated in MSO cells. Spike-triggered reverse correlations showed that MSO neurons fired optimally following a brief hyperpolarizing current. Manipulations of the Na^+ current showed that brief hyperpolarizing inputs have a role in releasing Na^+ channels from inactivation, thereby increasing the spike probability for a subsequent depolarizing input. Thus, the Na^+ channel properties in MSO cells may interact with inhibitory inputs to shape the coincidence window.

3.35.3.4 The Role of Inhibition in the Medial Superior Olive

Speculation on the contribution of inhibition in MSO responses has persisted in the literature since Goldberg J. M. and Brown P. B. (1969) noted that the firing rate to binaural stimuli that were at the worst ITD were below the rates evoked by stimulation of either ear alone. Similar observations have been noted in subsequent studies (Yin, T. C. and Chan, J. C., 1990; Spitzer, M. W. and Semple, M. N., 1995; 1998). Abundant anatomical evidence shows direct innervation of the MSO by both the glycinergic MNTB and the LNTB (Cant, N. B. and Hyson, R. L., 1992; Kuwabara, N. and Zook, J. M., 1992; Smith, P. H. *et al.*, 1998).

Investigation of these inputs has been made in slice preparations of both gerbil and rat (Grothe, B. and Sanes, D. H., 1993; 1994; Smith, A. J. *et al.*, 2000; Magnusson, A. K. *et al.*, 2005). Grothe B. and Sanes D. H. (1994) showed that glycinergic input suppressed firing of MSO cells *in vitro* at particular stimulus intervals between shocks to ipsilateral and contralateral inputs. Studies by Smith A. J. *et al.* (2000) in the rat and Magnusson A. K. *et al.* (2005) in the gerbil investigated the development of inhibitory input to the MSO and showed that between the early postnatal period and the week following the onset of hearing, inhibitory inputs to MSO switch from slow depolarizing and predominantly GABAergic to relatively fast, hyperpolarizing, and predominantly glycinergic inputs. A similar developmental pattern has been described in the neighboring lateral superior olive (LSO), which receives collateral MNTB input (Kandler, K. and Friauf, E., 1995; Kotak, V. C. *et al.*, 1998; Nabekura, J. *et al.*, 2004; Magnusson, A. K. *et al.*, 2005). In the LSO the developmental conversion of inhibitory inputs represents a gradual switch from GABA to glycine transmitter expression within individual inhibitory terminals rather than a replacement

of GABAergic input axons by glycinergic ones (Nabekura, J. *et al.*, 2004).

The first study to test the role of inhibition in MSO coding *in vivo* by manipulating the glycinergic receptor activation yielded striking results. These results suggest a critical difference between avian and mammalian strategies for computation of ITDs. Brand A. *et al.* (2002) recorded from the gerbil MSO using multibarrel microelectrodes that allowed them to block the glycinergic input to MSO neurons with strychnine during recordings. Their data revealed that in the presence of strychnine, all MSO neurons had maximal responses at ITD values near 0 μs (Figure 10). In control recordings, on the other hand, most neurons had a best ITD favoring sounds leading in the contralateral ear and outside the physiological range (the maximum range of ITD experienced by the animal under normal conditions). These data suggest that ITD processing in the gerbil may not rely on delays imposed on MSO by input axons but rather, the inhibitory inputs provided by the MNTB and/or the LNTB shape the selectivity.

Brand A. *et al.* (2002) supported their conclusions with computational modeling that showed that interaction between very rapid glycinergic inputs and the glutamatergic AVCN inputs is sufficient to generate the normal ITD responses. Since inhibitory inputs possessing such rapid kinetics have not been observed in intracellular studies of MSO neurons (Smith, A. J. *et al.*, 2000; Magnusson, A. K. *et al.*, 2005), further studies will be required to resolve exactly how inhibition imparts its apparently critical contribution to MSO response properties.

3.35.3.5 The Neural Code for Interaural Time Disparity in Mammals

A second important finding of the Brand A. *et al.* (2002) study is that the peaks of the ITD functions in the control condition almost always occurred outside of the physiological range of ITDs. Similar results have been observed in the gerbil DNLL and the guinea pig inferior colliculus (McAlpine, D. *et al.*, 2001; Seidl, A. H. and Grothe, B., 2005). These organisms share the characteristics of having both, low-frequency hearing and small heads. As a consequence, the role of inhibition identified in the gerbil raises considerable doubt regarding the notion that ITD processing is simply a function of coincidence of binaural excitatory delays.

The recent progress discussed earlier has compelled researchers in the field to re-evaluate the nature of ITD representation in the mammalian nervous system. This topic has been thoroughly and clearly discussed elsewhere (Grothe, B., 2003; McAlpine, D. and Grothe, B., 2003) and the arguments will not be recounted here, but the discussion rests on two possible, and not mutually exclusive, strategies of ITD representation in the nervous system.

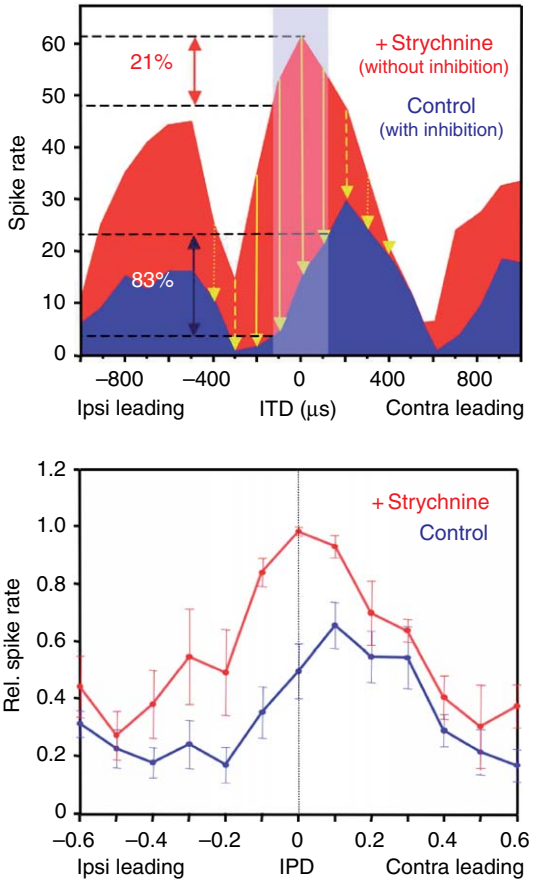

Figure 10 Inhibition shapes ITD functions in MSO. The top panel shows the ITD response functions of an MSO neuron before blue function and after red function application of strychnine, a glycine-receptor antagonist. The control condition data indicate that the peak response falls outside the range of naturally occurring ITDs shaded area but that the steepest slope of the function falls across zero ITD. When strychnine was applied, the neuron shifted its best ITD to near-zero, and had a rather small dynamic response within the physiological range. In the lower panel, the population data suggests that a primary consequence of inhibition in the MSO is to shift the location of the peak (or the slope) of ITD functions toward ITDs that lead in the contralateral ear. Reproduced from Macmillan Publishers LTD: Nature, from the study by Brand, A., Behrend, O., Marquardt, T., McAlpine, D., and Grothe, B. 2002. Precise inhibition is essential for microsecond interaural time difference coding. Nature 417, 543–547.

The first possible coding strategy can be likened to a labeled line paradigm and is derived from the Jeffress model. In this scheme a neuron will have a peak response at a particular ITD within the physiological range of ITDs. Across the population of coding neurons (i.e., MSO, NL) all spatial positions (ITDs) will be represented by different subsets of neurons according to where their peak sensitivity lies within auditory space. The second strategy depends on comparing population responses, between two broadly tuned spatial channels (McAlpine, D. *et al*., 2001; Palmer, A. R., 2004). In this scheme, information on the sound source location would depend not on the firing rate of particular neurons sensitive to small regions of space, but on a comparison of activity between the two MSOs. Each MSO neuron would respond to many positions in space, but in a graded way such that sound sources in the ipsilateral hemifield will evoke little activity while sound sources in the contralateral hemifield will evoke strong responses. Under this scheme sound source position is resolved only after a higher-order comparison of activity from the two MSOs.

The relative utility of these two coding schemes depends on the physical relationships between the stimulus frequency (wavelength) and the animal's head size. At the extremes, a low-frequency sound for an animal with a small head, the range of available IPDs is relatively small; thus broad population coding may be optimal. For higher frequencies and for animals with wide heads, there is an ample range of IPDs for which neurons could be constructed to be differentially sensitive. A recent modeling study took into account the relationships between stimulus frequency, interaural phase, and head size for four animals with different hearing ranges and head sizes (Harper, N. S. and McAlpine, D., 2004). The authors showed that across the tonotopic range for each animal, one or a combination of both coding strategies may be optimal depending on the stimulus frequency.

3.35.4 Summary and Conclusion

In both birds and mammals elegant circuitry has evolved to compute sound source location. The circuits devoted to low-frequency processing involving NL and MSO share many features designed to preserve or enhance extraction of temporal information from nVIII inputs. These include both morphological and intrinsic membrane specializations throughout the circuitry that are remarkably similar across these vertebrate classes. That being said, two systems appear to differ in several ways that are still under investigation. These include the presence or absence of delay lines, the nature of the ITD code, as well as the role of inhibitory components of each system.

A suite of studies spanning the last two decades in both birds and mammals has elucidated the importance of inhibitory circuitry for ITD processing. The mammalian studies have demonstrated that MSO neurons receive a rapid and glycinergic hyperpolarizing inhibition from auditory pathways specialized to process temporal information from each ear. In contrast, avian ITD-processing neurons in NL receive a depolarizing slow GABAergic input that is derived from an auditory center that appears not to preserve phase-locked timing information with both monaural and binaural responses. In mammals, the limited data available suggest that a temporally constrained inhibitory input is a crucial factor in setting ITD selectivity in the MSO, but at this time a well-supported model for how the inhibition imparts selectivity on these cells is lacking. In birds, the slow inhibitory input seems to be involved in both enhancing the intrinsic membrane properties of time-coding neurons and perhaps binaurally controlling the system gain. The contrasting nature of inhibition in these systems represents one of the most fundamental differences between avian and mammalian circuits for processing ITDs. A clear understanding of inhibitory function in both NL and MSO will be critical to resolving the nature of ITD encoding at these primary sites of binaural computation.

Acknowledgments

We thank Mark Konishi, Helen Brew, Benedikt Grothe, the Society for Neuroscience, and Nature Publishing Group for permission to present their figures in our review. Finally, we thank Staci Sorensen, Olga Alexandrova, and Michael Pecka for contributions of images used in this chapter.

References

Adamson, C. L., Reid, M. A., Mo, Z. L., Bowne-English, J., and Davis, R. L. 2002. Firing features and potassium channel content of murine spiral ganglion neurons vary with cochlear location. J. Comp. Neurol. 447, 331–350.

Agmon-Snir, H., Carr, C. E., and Rinzel, J. 1998. The role of dendrites in auditory coincidence detection. Nature 393, 268–272.

Bal, R. and Oertel, D. 2001. Potassium currents in octopus cells of the mammalian cochlear nucleus. J. Neurophysiol. 86, 2299–2311.

Banks, M. I. and Smith, P. H. 1992. Intracellular recordings from neurobiotin-labeled cells in brain slices of the rat medial nucleus of the trapezoid body. J. Neurosci. 12, 2819–2837.

Batra, R. and Fitzpatrick, D. C. 1997. Neurons sensitive to interaural temporal disparities in the medial part of the ventral nucleus of the lateral lemniscus. J. Neurophysiol. 78, 511–515.

Batra, R., Kuwada, S., and Fitzpatrick, D. C. 1997a. Sensitivity to interaural temporal disparities of low- and high-frequency neurons in the superior olivary complex. II. Coincidence detection. J. Neurophysiol. 78, 1237–1247.

Batra, R., Kuwada, S., and Fitzpatrick, D. C. 1997b. Sensitivity to interaural temporal disparities of low- and high-frequency neurons in the superior olivary complex. I. Heterogeneity of responses. J. Neurophysiol. 78, 1222–1236.

Beckius, G. E., Batra, R., and Oliver, D. L. 1999. Axons from anteroventral cochlear nucleus that terminate in medial superior olive of cat: observations related to delay lines. J. Neurosci. 19, 3146–3161.

Ben-Ari, Y., Rovira, C., Gaiarsa, J. L., Corradetti, R., Robain, O., and Cherubini, E. 1990. GABAergic mechanisms in the CA3 hippocampal region during early postnatal life. Prog. Brain Res. 83, 313–321.

Brand, A., Behrend, O., Marquardt, T., McAlpine, D., and Grothe, B. 2002. Precise inhibition is essential for microsecond interaural time difference coding. Nature 417, 543–547.

Brew, H. M. and Forsythe, I. D. 1995. Two voltage-dependent K^+ conductances with complementary functions in postsynaptic integration at a central auditory synapse. J. Neurosci. 15, 8011–8022.

Burger, R. M., Cramer, K. S., Pfeiffer, J. D., and Rubel, E. W. 2005. Avian superior olivary nucleus provides divergent inhibitory input to parallel auditory pathways. J. Comp. Neurol. 481, 6–18.

Cant, N. B. and Hyson, R. L. 1992. Projections from the lateral nucleus of the trapezoid body to the medial superior olivary nucleus in the gerbil. Hear. Res. 58, 26–34.

Carney, L. H. 1992. Modelling the sensitivity of cells in the anteroventral cochlear nucleus to spatiotemporal discharge patterns. Philos. Trans. R. Soc. Lond. B. Biol. Sci. 336, 403–406.

Carr, C. E. and Boudreau, R. E. 1996. Development of the time coding pathways in the auditory brainstem of the barn owl. J. Comp. Neurol. 373, 467–483.

Carr, C. E. and Code, R. A. 2000. Anatomy and Physiology of the Central Auditory System of Birds and Reptiles. In: Comparative Hearing: Birds and Reptiles (*eds*. A. N. Popper, R. R. Fay, and R. J. Dooling), pp. 197–248. Springer.

Carr, C. E. and Konishi, M. 1990. A circuit for detection of interaural time differences in the brain stem of the barn owl. J. Neurosci. 10, 3227–3246.

Carr, C. E. and Soares, D. 2002. Evolutionary convergence and shared computational principles in the auditory system. Brain. Behav. Evol. 59, 294–311.

Carr, C. E., Fujita, I., and Konishi, M. 1989. Distribution of GABAergic neurons and terminals in the auditory system of the barn owl. J. Comp. Neurol. 286, 190–207.

Carr, C. E., Soares, D., Parameshwaran, S., and Perney, T. 2001. Evolution and development of time coding systems. Curr. Opin. Neurobiol. 11, 727–733.

Cherubini, E., Rovira, C., Gaiarsa, J. L., Corradetti, R., and Ben Ari, Y. 1990. GABA mediated excitation in immature rat CA3 hippocampal neurons. Int. J. Dev. Neurosci. 8, 481–490.

Code, R. A., Burd, G. D., and Rubel, E. W. 1989. Development of GABA immunoreactivity in brainstem auditory nuclei of the chick: ontogeny of gradients in terminal staining. J. Comp. Neurol. 284, 504–518.

Colburn, H. S. and Durlach, N. I. 1978. Models of Binaural Interaction. In: Handbook of Perception (*eds*. E. C. Carterette, and M. Friedman), pp. 467–518. Academic Press.

Dasika, V. K., White, J. A., Carney, L. H., and Colburn, H. S. 2005. Effects of inhibitory feedback in a network model of avian brain stem. J. Neurophysiol. 94, 400–414.

Ehrlich, I., Lohrke, S., and Friauf, E. 1999. Shift from depolarizing to hyperpolarizing glycine action in rat auditory neurones is due to age-dependent Cl^- regulation. J. Physiol. 520(Pt 1), 121–137.

Finlayson, P. G. and Caspary, D. M. 1991. Low-frequency neurons in the lateral superior olive exhibit phase-sensitive binaural inhibition. J. Neurophysiol. 65, 598–605.

Funabiki, K., Koyano, K., and Ohmori, H. 1998. The role of GABAergic inputs for coincidence detection in the neurones of nucleus laminaris of the chick. J. Physiol. 508(Pt 3), 851–869.

Gan, L. and Kaczmarek, L. K. 1998. When, where, and how much? Expression of the Kv3.1 potassium channel in high-frequency firing neurons. J. Neurobiol. 37, 69–79.

Glendenning, K. K., Hutson, K. A., Nudo, R. J., and Masterton, R. B. 1985. Acoustic chiasm II: anatomical basis of binaurality in lateral superior olive of cat. J. Comp. Neurol. 232, 261–285.

Goldberg, J. M. and Brown, P. B. 1969. Response of binaural neurons of dog superior olivary complex to dichotic tonal stimuli: some physiological mechanisms of sound localization. J. Neurophysiol. 32, 613–636.

Grigg, J. J., Brew, H. M., and Tempel, B. L. 2000. Differential expression of voltage-gated potassium channel genes in auditory nuclei of the mouse brainstem. Hear. Res. 140, 77–90.

Grothe, B. 2003. New roles for synaptic inhibition in sound localization. Nat. Rev. Neurosci. 4, 540–550.

Grothe, B. and Sanes, D. H. 1993. Bilateral inhibition by glycinergic afferents in the medial superior olive. J. Neurophysiol. 69, 1192–1196.

Grothe, B. and Sanes, D. H. 1994. Synaptic inhibition influences the temporal coding properties of medial superior olivary neurons: an *in vitro* study. J. Neurosci. 14, 1701–1709.

Hackett, J. T., Jackson, H., and Rubel, E. W. 1982. Synaptic excitation of the second and third order auditory neurons in the avian brain stem. Neuroscience 7, 1455–1469.

Hall, J. L., 2nd 1965. Binaural interaction in the accessory superior-olivary nucleus of the cat. J. Acoust. Soc. Am. 37, 814–823.

Harper, N. S. and McAlpine, D. 2004. Optimal neural population coding of an auditory spatial cue. Nature 430, 682–686.

Hoy, R. R. and Robert, D. 1996. Tympanal hearing in insects. Annu. Rev. Entomol. 41, 433–450.

Hyson, R. L., Reyes, A. D., and Rubel, E. W. 1995. A depolarizing inhibitory response to GABA in brainstem auditory neurons of the chick. Brain Res. 677, 117–126.

Jackson, H., Hackett, J. T., and Rubel, E. W. 1982. Organization and development of brain stem auditory nuclei in the chick: ontogeny of postsynaptic responses. J. Comp. Neurol. 210, 80–86.

Jeffress, L. A. 1948. A place theory of sound localization. J. Comp. Physiol. Psychol. 41, 35–39.

Joris, P. X. and Yin, T. C. 1995. Envelope coding in the lateral superior olive. I. Sensitivity to interaural time differences. J. Neurophysiol. 73, 1043–1062.

Joseph, A. W. and Hyson, R. L. 1993. Coincidence detection by binaural neurons in the chick brain stem. J. Neurophysiol. 69, 1197–1211.

Kakazu, Y., Akaike, N., Komiyama, S., and Nabekura, J. 1999. Regulation of intracellular chloride by cotransporters in

developing lateral superior olive neurons. J. Neurosci. 19, 2843–2851.
Kandler, K. and Friauf, E. 1995. Development of glycinergic and glutamatergic synaptic transmission in the auditory brainstem of perinatal rats. J. Neurosci. 15, 6890–6904.
Knudsen, E. I. and Konishi, M. 1979. Mechanisms of sound localization in the barn owl (Tyto alba). J. Comp. Physiol. A Neuroethol. Sens. Neural. Behav. Physiol. 133, 13–21.
Koch, C. and Segev, I. 2000. The role of single neurons in information processing. Nat. Neurosci. 3(Suppl), 1171–1177.
Kotak, V. C., Korada, S., Schwartz, I. R., and Sanes, D. H. 1998. A developmental shift from GABAergic to glycinergic transmission in the central auditory system. J. Neurosci. 18, 4646–4655.
Kuba, H., Yamada, R., Fukui, I., and Ohmori, H. 2005. Tonotopic specialization of auditory coincidence detection in nucleus laminaris of the chick. J. Neurosci. 25, 1924–1934.
Kubke, M. F., Massoglia, D. P., and Carr, C. E. 2002. Developmental changes underlying the formation of the specialized time coding circuits in barn owls (Tyto alba). J. Neurosci. 22, 7671–7679.
Kuwabara, N. and Zook, J. M. 1992. Projections to the medial superior olive from the medial and lateral nuclei of the trapezoid body in rodents and bats. J. Comp. Neurol. 324, 522–538.
Kuwada, S. and Yin, T. C. 1983. Binaural interaction in low-frequency neurons in inferior colliculus of the cat. I. Effects of long interaural delays, intensity, and repetition rate on interaural delay function. J. Neurophysiol. 50, 981–999.
Lachica, E. A., Rubsamen, R., and Rubel, E. W. 1994. GABAergic terminals in nucleus magnocellularis and laminaris originate from the superior olivary nucleus. J. Comp. Neurol. 348, 403–418.
Lu, T. and Trussell, L. O. 2000. Inhibitory transmission mediated by asynchronous transmitter release. Neuron 26, 683–694.
Lu, T. and Trussell, L. O. 2001. Mixed excitatory and inhibitory GABA-mediated transmission in chick cochlear nucleus. J. Physiol. 535, 125–131.
Lu, Y., Burger, R. M., and Rubel, E. W. 2005. GABA(B) receptor activation modulates GABA(A) receptor-mediated inhibition in chicken nucleus magnocellularis neurons. J. Neurophysiol. 93, 1429–1438.
Lu, Y., Monsivais, P., Tempel, B. L., and Rubel, E. W. 2004. Activity-dependent regulation of the potassium channel subunits Kv1.1 and Kv3.1. J. Comp. Neurol. 470, 93–106.
Macica, C. M., von Hehn, C. A., and Wang, L. Y., *et al.* 2003. Modulation of the kv3.1b potassium channel isoform adjusts the fidelity of the firing pattern of auditory neurons. J. Neurosci. 23, 1133–1141.
Magnusson, A. K., Kapfer, C., Grothe, B., and Koch, U. 2005. Maturation of Glycinergic Inhibition in the Gerbil Medial Superior Olive after Hearing Onset. J. Physiol. 568, 497–512.
Maki, K. and Furukawa, S. 2005. Acoustical cues for sound localization by the Mongolian gerbil, Meriones unguiculatus. J. Acoust. Soc. Am. 118, 872–886.
Manis, P. B. and Marx, S. O. 1991. Outward currents in isolated ventral cochlear nucleus neurons. J Neurosci 11, 2865–2880.
McAlpine, D. and Grothe, B. 2003. Sound localization and delay lines – do mammals fit the model? Trends Neurosci 26, 347–350.
McAlpine, D., Jiang, D., and Palmer, A. R. 2001. A neural code for low-frequency sound localization in mammals. Nat. Neurosci. 4, 396–401.
Monsivais, P. and Rubel, E. W. 2001. Accommodation enhances depolarizing inhibition in central neurons. J. Neurosci. 21, 7823–7830.
Monsivais, P., Yang, L., and Rubel, E. W. 2000. GABAergic inhibition in nucleus magnocellularis: implications for phase locking in the avian auditory brainstem. J. Neurosci. 20, 2954–2963.
Moushegian, G., Rupert, A. L., and Langford, T. L. 1967. Stimulus coding by medial superior olivary neurons. J. Neurophysiol. 30, 1239–1261.
Moushegian, G., Rupert, A. L., and Gidda, J. S. 1975. Functional characteristics of superior olivary neurons to binaural stimuli. J. Neurophysiol. 38, 1037–1048.
Nabekura, J., Katsurabayashi, S., Kakazu, Y., *et al.* 2004. Developmental switch from GABA to glycine release in single central synaptic terminals. Nat. Neurosci. 7, 17–23.
Oertel, D. 1983. Synaptic responses and electrical properties of cells in brain slices of the mouse anteroventral cochlear nucleus. J. Neurosci. 3, 2043–2053.
Oertel, D. 1997. Encoding of timing in the brain stem auditory nuclei of vertebrates. Neuron 19, 959–962.
Overholt, E. M., Rubel, E. W., and Hyson, R. L. 1992. A circuit for coding interaural time differences in the chick brainstem. J. Neurosci. 12, 1698–1708.
Palmer, A. R. 2004. Reassessing mechanisms of low-frequency sound localisation. Curr. Opin. Neurobiol. 14, 457–460.
Parameshwaran, S., Carr, C. E., and Perney, T. M. 2001. Expression of the Kv3.1 potassium channel in the avian auditory brainstem. J. Neurosci. 21, 485–494.
Parameshwaran-Iyer, S., Carr, C. E., and Perney, T. M. 2003. Localization of KCNC1 (Kv3.1) potassium channel subunits in the avian auditory nucleus magnocellularis and nucleus laminaris during development. J. Neurobiol. 55, 165–178.
Parks, T. N. and Rubel, E. W. 1975. Organization and development of brain stem auditory nuclei of the chicken: organization of projections from n. magnocellularis to n. laminaris. J. Comp. Neurol. 164, 435–448.
Pena, J. L., Viete, S., Albeck, Y., and Konishi, M. 1996. Tolerance to sound intensity of binaural coincidence detection in the nucleus laminaris of the owl. J. Neurosci. 16, 7046–7054.
Perney, T. M. and Kaczmarek, L. K. 1997. Localization of a high threshold potassium channel in the rat cochlear nucleus. J. Comp. Neurol. 386, 178–202.
Perney, T. M., Marshall, J., Martin, K. A., Hockfield, S., and Kaczmarek, L. K. 1992. Expression of the mRNAs for the Kv3.1 potassium channel gene in the adult and developing rat brain. J. Neurophysiol. 68, 756–766.
Pollak, G. D., Burger, R. M., and Klug, A. 2003. Dissecting the circuitry of the auditory system. Trends Neurosci. 26, 33–39.
Pollak, G. D., Burger, R. M., Park, T. J., Klug, A., and Bauer, E. E. 2002. Roles of inhibition for transforming binaural properties in the brainstem auditory system. Hear. Res. 168, 60–78.
Rall, W. 1969. Time constants and electrotonic length of membrane cylinders and neurons. Biophys. J. 9, 1483–1508.
Rathouz, M. and Trussell, L. 1998. Characterization of outward currents in neurons of the avian nucleus magnocellularis. J. Neurophysiol. 80, 2824–2835.
Rayleigh, L. S. 1907. On our perception of sound direction. Philos. Mag. 13, 214–232.
Reyes, A. D., Rubel, E. W., and Spain, W. J. 1994. Membrane properties underlying the firing of neurons in the avian cochlear nucleus. J. Neurosci. 14, 5352–5364.
Reyes, A. D., Rubel, E. W., and Spain, W. J. 1996. *In vitro* analysis of optimal stimuli for phase-locking and time-delayed modulation of firing in avian nucleus laminaris neurons. J. Neurosci. 16, 993–1007.
Robert, D., Miles, R. N., and Hoy, R. R. 1996. Directional hearing by mechanical coupling in the parasitoid fly Ormia ochracea. J. Comp. Physiol. A 179, 29–44.
Robertson, B., Owen, D., Stow, J., Butler, C., and Newland, C. 1996. Novel effects of dendrotoxin homologues on subtypes

of mammalian Kv1 potassium channels expressed in Xenopus oocytes. FEBS Lett. 383, 26–30.
Rothman, J. S., Young, E. D., and Manis, P. B. 1993. Convergence of auditory nerve fibers onto bushy cells in the ventral cochlear nucleus: implications of a computational model. J. Neurophysiol. 70, 2562–2583.
Rubel, E. W. and Parks, T. N. 1975. Organization and development of brain stem auditory nuclei of the chicken: tonotopic organization of n. magnocellularis and n. laminaris. J. Comp. Neurol. 164, 411–433.
Rudy, B. and McBain, C. J. 2001. Kv3 channels: voltage-gated K^+ channels designed for high-frequency repetitive firing. Trends Neurosci. 24, 517–526.
Scott, L. L., Mathews, P. J., and Golding, N. L. 2005. Posthearing developmental refinement of temporal processing in principal neurons of the medial superior olive. J. Neurosci. 25, 7887–7895.
Seidl, A. H. and Grothe, B. 2005. Development of sound localization mechanisms in the Mongolian Gerbil is shaped by early acoustic experience. J. Neurophysiol. 94, 1028–1036.
Smith, A. J., Owens, S., and Forsythe, I. D. 2000. Characterisation of inhibitory and excitatory postsynaptic currents of the rat medial superior olive. J. Physiol. 529(Pt 3), 681–698.
Smith, D. J. and Rubel, E. W. 1979. Organization and development of brain stem auditory nuclei of the chicken: dendritic gradients in nucleus laminaris. J. Comp. Neurol. 186, 213–239.
Smith, P. H. 1995. Structural and functional differences distinguish principal from nonprincipal cells in the guinea pig MSO slice. J. Neurophysiol. 73, 1653–1667.
Smith, P. H., Joris, P. X., and Yin, T. C. 1993. Projections of physiologically characterized spherical bushy cell axons from the cochlear nucleus of the cat: evidence for delay lines to the medial superior olive. J. Comp. Neurol. 331, 245–260.
Smith, P. H., Joris, P. X., and Yin, T. C. 1998. Anatomy and physiology of principal cells of the medial nucleus of the trapezoid body (MNTB) of the cat. J. Neurophysiol. 79, 3127–3142.
Song, P., Yang, Y., Barnes-Davies, M., *et al.* 2005. Acoustic environment determines phosphorylation state of the Kv3.1 potassium channel in auditory neurons. Nat. Neurosci. 8, 1335–1342.
Spirou, G. A., Rowland, K. C., and Berrebi, A. S. 1998. Ultrastructure of neurons and large synaptic terminals in the lateral nucleus of the trapezoid body of the cat. J. Comp. Neurol. 398, 257–272.
Spitzer, M. W. and Semple, M. N. 1995. Neurons sensitive to interaural phase disparity in gerbil superior olive: diverse monaural and temporal response properties. J. Neurophysiol. 73, 1668–1690.
Spitzer, M. W. and Semple, M. N. 1998. Transformation of binaural response properties in the ascending auditory pathway: influence of time-varying interaural phase disparity. J. Neurophysiol. 80, 3062–3076.
Stotler, W. A. 1953. An experimental study of the cells and connections of the superior olivary complex of the cat. J. Comp. Neurol. 98, 401–431.
Sullivan, W. E. and Konishi, M. 1986. Neural map of interaural phase difference in the owl's brainstem. Proc. Natl. Acad. Sci. USA 83, 8400–8404.
Svirskis, G., Dodla, R., and Rinzel, J. 2003. Subthreshold outward currents enhance temporal integration in auditory neurons. Biol. Cybern. 89, 333–340.
Svirskis, G., Kotak, V., Sanes, D. H., and Rinzel, J. 2002. Enhancement of signal-to-noise ratio and phase locking for small inputs by a low-threshold outward current in auditory neurons. J. Neurosci. 22, 11019–11025.
Svirskis, G., Kotak, V., Sanes, D. H., and Rinzel, J. 2004. Sodium along with low-threshold potassium currents enhance coincidence detection of subthreshold noisy signals in MSO neurons. J. Neurophysiol. 91, 2465–2473.
Thompson, A. M. and Schofield, B. R. 2000. Afferent projections of the superior olivary complex. Microsc. Res. Tech. 51, 330–354.
Tollin, D. J. 2003. The lateral superior olive: a functional role in sound source localization. Neuroscientist 9, 127–143.
Trussell, L. O. 1997. Cellular mechanisms for preservation of timing in central auditory pathways. Curr. Opin. Neurobiol. 7, 487–492.
Trussell, L. O. 1999. Synaptic mechanisms for coding timing in auditory neurons. Annu. Rev. Physiol. 61, 477–496.
Viete, S., Pena, J. L., and Konishi, M. 1997. Effects of interaural intensity difference on the processing of interaural time difference in the owl's nucleus laminaris. J. Neurosci. 17, 1815–1824.
von Bartheld, C. S., Code, R. A., and Rubel, E. W. 1989. GABAergic neurons in brainstem auditory nuclei of the chick: distribution, morphology, and connectivity. J. Comp. Neurol. 287, 470–483.
Wang, L. Y., Gan, L., Forsythe, I. D., and Kaczmarek, L. K. 1998. Contribution of the Kv3.1 potassium channel to high-frequency firing in mouse auditory neurones. J. Physiol. 509(Pt 1), 183–194.
Westerberg, B. D. and Schwarz, D. W. 1995. Connections of the superior olive in the chicken. J. Otolaryngol. 24, 20–30.
Wightman, F. L. and Kistler, D. J. 1993. Sound Localization. In: Human Psychophysics (*eds*. W. A. Yost, A. N. Popper, and R. R. Fay), pp. 155–192. Springer.
Yang, L., Monsivais, P., and Rubel, E. W. 1999. The superior olivary nucleus and its influence on nucleus laminaris: a source of inhibitory feedback for coincidence detection in the avian auditory brainstem. J. Neurosci. 19, 2313–2325.
Yin, T. C. and Kuwada, S. 1983a. Binaural interaction in low-frequency neurons in inferior colliculus of the cat. III. Effects of changing frequency. J. Neurophysiol. 50, 1020–1042.
Yin, T. C. and Kuwada, S. 1983b. Binaural interaction in low-frequency neurons in inferior colliculus of the cat. II. Effects of changing rate and direction of interaural phase. J. Neurophysiol. 50, 1000–1019.
Yin, T. C. and Chan, J. C. 1990. Interaural time sensitivity in medial superior olive of cat. J. Neurophysiol. 64, 465–488.
Young, S. R. and Rubel, E. W. 1983. Frequency-specific projections of individual neurons in chick brainstem auditory nuclei. J. Neurosci. 3, 1373–1378.
Zhang, S. and Trussell, L. O. 1994. Voltage clamp analysis of excitatory synaptic transmission in the avian nucleus magnocellularis. J. Physiol. 480(Pt 1), 123–136.

3.36 Encoding of Interaural Level Differences for Sound Localization

D J Tollin, University of Colorado Health Sciences Center, Aurora, CO, USA

© 2008 Elsevier Inc. All rights reserved.

3.36.1	**Introduction**	631
3.36.1.1	The Duplex Theory of Sound Localization	632
3.36.1.2	The Superior Olivary Complex	632
3.36.2	**The Three Main Acoustical Cues to Sound Source Location**	633
3.36.2.1	Interaural Time Differences	635
3.36.2.2	Interaural Level Differences	635
3.36.2.3	Monaural Spectral Shape Cues	636
3.36.3	**Interaural Level Differences Are Initially Processed in the Lateral Superior Olive**	636
3.36.3.1	Lateral Superior Olive Neurons Receive Excitatory Inputs from One Ear and Inhibitory Inputs from the Other Ear	636
3.36.3.2	Inputs Encode the Spectral and Temporal Characteristics of the Sounds at Each Ear	637
3.36.3.2.1	Spectral representation by lateral superior olive afferents	637
3.36.3.2.2	Temporal representation by lateral superior olive afferents	638
3.36.3.3	The Inputs from Each Ear to Individual Neurons Have Similar Frequency Tuning	638
3.36.3.4	Inputs from the Two Ears Reach Lateral Superior Olive Neurons in Approximate Temporal Register	640
3.36.3.5	Lateral Superior Olive Neurons Have Short Integration Times	643
3.36.3.6	Lateral Superior Olive Neurons Encode the Interaural Level Difference Present in the Sounds at the Two Ears	643
3.36.3.6.1	Sensitivity to interaural level differences in pure-tone stimuli	643
3.36.3.6.2	Sensitivity to interaural level differences in virtual space (VS) stimuli that mimic free-field sounds	645
3.36.4	**Comparative Studies Implicate the LSO as Necessary for ILD Processing**	649
3.36.5	**Conclusion**	650
References		650

Glossary

ANF Auditory nerve fiber.
AVCN Anteroventral cochlear nucleus.
CF Characteristic frequency.
CN Cochlear nucleus.
EPSP Excitatory postsynaptic potential.
GBC Globular bushy cell.
HRTF Head-related transfer function.
IC Inferior colliculus.
ILD Interaural level difference.
IPSP Inhibitory postsynaptic potential.
ITD Interaural time difference.
LSO Lateral superior olive.
MNTB Medial nucleus of the trapezoid body.
MSO Medial superior olive.
PSTH Poststimulus time histogram.
SBC Spherical bushy cell.
SOC Superior olivary complex.
VS Virtual space.

3.36.1 Introduction

A primary function of the auditory system is to determine the location of objects in the environment. Although this function is also shared by the visual and somatosensory systems, the peripheral receptors comprising these systems can encode the locations of visual and tactile objects directly via the topographic organization of the rods and cones of the retina and the mechanoreceptors of the skin, respectively. In

contrast, the hair cells of the cochlea have no mechanism to sense sound location directly, but rather encode sound frequency and intensity owing to their position along the basilar membrane and the frequency- and intensity-dependent mechanical properties of the basilar membrane itself. Thus, sound location must be computed at more central levels of the auditory system based on the neural representations of the spectral and temporal characteristics of the acoustic stimuli arriving at the two ears.

The quick and accurate determination of sound location has considerable functional significance in directing the behavior of most mammals. Some species, like bats and cats, rely heavily on localization to capture prey, while others rely on it to avoid capture. Localization also confers additional perceptual benefits, like facilitating auditory scene analysis, binaural unmasking, and increasing comprehension of speech in noisy and reverberant environments. The importance of localization was recognized early in the history of experimental psychology and physiology, and sound localization has been investigated for over 200 years. A main goal of these studies has been to determine how the direction-dependent physical parameters of sounds, or cues, arriving at the ears are used for localization. There are three primary cues to location, each of which is created by direction-dependent interactions of the incident sound waves with the head and outer ears, or pinnae:

1. interaural time differences (ITDs),
2. ILDs, and
3. monaural spectral shape cues.

Accurate localization and the associated perceptual benefits that location confers require that the cues be extracted and encoded by neurons accurately. This chapter focuses on the neural and anatomical mechanisms by which one of the cues, ILDs, is initially encoded in the auditory system. Although much of the behavioral work in sound localization has been done in human observers, we use here the cat as the model system because it is one of the only animals for which the anatomy, physiology, and psychophysics of the localization system have been well-studied and for which there is a good understanding of the acoustical cues to sound location available to them.

3.36.1.1 The Duplex Theory of Sound Localization

Psychophysical studies in humans have endeavored to discover how the ITD, ILD, and spectral cues are used for the perception of location. At present, the consensus on what the cues are and how they are used is strongest for the case of sources varying in azimuth along the horizontal plane. Psychophysical experiments in this area have consistently revealed that low- and high-frequency tones can be accurately localized by both humans and cats, but that midfrequency tones (1.5–3.0 kHz in humans, slightly higher frequencies in cats) cannot. The presence of such discontinuities in the function relating localization accuracy to tone frequency is suggestive of separate physiological mechanisms that mediate, in this case, the localization of high- and low-frequency sources, respectively. The poor performance for the midfrequency tones presumably reflects the transition from using one cue and/or mechanism to another, the cues being ITDs and ILDs. Based on the behavioral and acoustic evidence, a dual mechanism for localization, the so-called duplex theory, was proposed whereby low-frequency sounds are localized based on the ITD cues while higher-frequency sounds are localized based on the ILD cue (Rayleigh, L. J. S., 1907; Stevens, S. and Newman, E., 1936; Mills, A. W., 1958; Casseday, J. H. and Neff, W. D., 1973).

3.36.1.2 The Superior Olivary Complex

While the duplex theory has served as the principal model of localization in azimuth for over a century, the exact mechanisms by which each of the localization cues are first encoded and then ultimately integrated in the responses of auditory neurons are not known in detail. Early anatomical studies revealed that the first places in the auditory pathway to receive large-scale and systematic converging inputs from both ears were two of the primary nuclei comprising the superior olivary complex (SOC, Figure 1), the medial superior olive (MSO, not shown in Figure 1) and the LSO.

Later, physiological studies found that the neurons in the MSO and LSO were, in general, separately sensitive to ITDs and ILDs, respectively. And lesion studies showed that sectioning the afferent inputs to the SOC (Masterton, B. *et al.*, 1967) or lesioning the SOC (Kavanagh, G. L. and Kelly, J. B., 1992) dramatically decreases the ability of experimental animals to localize sounds in the horizontal plane suggesting that the SOC nuclei are necessary for localization. The anatomical, physiological, and psychophysical evidence suggests that at this very early stage, the MSO and the LSO provide the anatomical and physiological bases for the duplex theory.

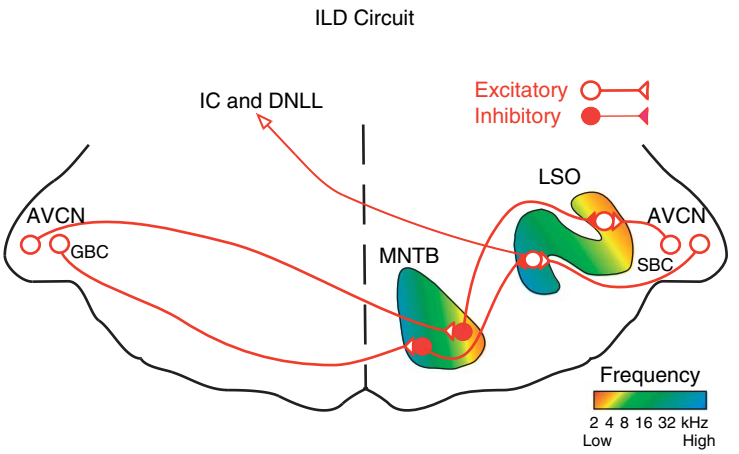

Figure 1 Illustration of a frontal section through the cat brainstem showing the ascending pathways through the lateral superior olive (LSO), which is believed to be responsible for encoding interaural level differences (ILDs). LSO neurons receive bilateral inputs from both ears. The input from the ipsilateral ear via the spherical bushy cells (SBCs) is excitatory (open symbols) but the input from the contralateral ear via the globular bushy cells (GBCs) of the contralateral anteroventral cochlear nucleus (AVCN) is inhibitory (filled symbols) due to the additional synapse in the ipsilateral medial nucleus of the trapezoid body (MNTB). The ipsilateral excitation and contralateral inhibition allows LSO neurons to encode ILDs. LSO neurons send excitatory projections to the contralateral inferior colliculus (IC) and dorsal nucleus of the lateral lemniscus (DNLL) and inhibitory projections (not shown) to the ipsilateral IC and DNLL. The color bar and shading indicates the tonotopic organization and shows that the neurons comprising the MNTB and LSO are sensitive to predominantly high-frequency sounds. The SBCs and GBCs receive excitatory input from the auditory nerve (not shown).

The hypothesis that ILDs are first encoded in the LSO is examined here. (Review of the mechanisms for ITD and spectral cue coding can be found elsewhere in this volume.) The LSO ILD-coding hypothesis was founded upon two classical observations. First, the LSO is one of the most peripheral nuclei receiving massive convergence of inputs from the two ears. Second, the LSO neurons respond systematically to ILDs of stimuli presented to the two ears. Since these initial observations, strong support for this hypothesis has come from disparate scientific fields, which we cover here. First, the ILD as an acoustical cue to location will be considered. Second, we will examine the anatomical, biophysical and physiological characteristics of the neurons comprising the LSO circuit (Figure 1) that are responsible for ILD coding. Finally, we consider comparative studies that have examined the functional roles of the SOC nuclei through combined anatomical, physiological, and psychophysical observations.

3.36.2 The Three Main Acoustical Cues to Sound Source Location

The task of localizing a sound's source differs from localization by the other spatial senses because the physical cues for location are different. The cues for sound localization are generated by the interaction of the sound waves with the anatomical structures supporting the receptors of the ear, namely the head and pinnae, and not by the topographic organization of the receptors themselves. Therefore, in order to understand the neural mechanisms for localization based on ILDs, the acoustical basis for the ILD cue and how the cue varies with sound location must be considered.

The three primary cues to location are illustrated in Figure 2 for an adult cat (acoustical recordings from Tollin, D. J., 2004). The cues are measured by placing small probe tube microphones deep inside the ear canal near the tympanic membranes of both ears. A sound with known spectral and temporal characteristics is delivered from a loudspeaker (Figure 2(a)) and the acoustical responses that result are recorded by the microphones. This process is repeated as the loudspeaker is systematically placed at various locations around the subject.

Consider the cues available to a cat for a broadband transient sound (i.e., a click) delivered from just one location (−40°, 0°, Figure 2(a)). Figure 2(b) shows the averaged acoustical responses recorded at the left and right ears to multiple clicks presented from this location. For each location (i.e., our example location), the acoustic transfer function is

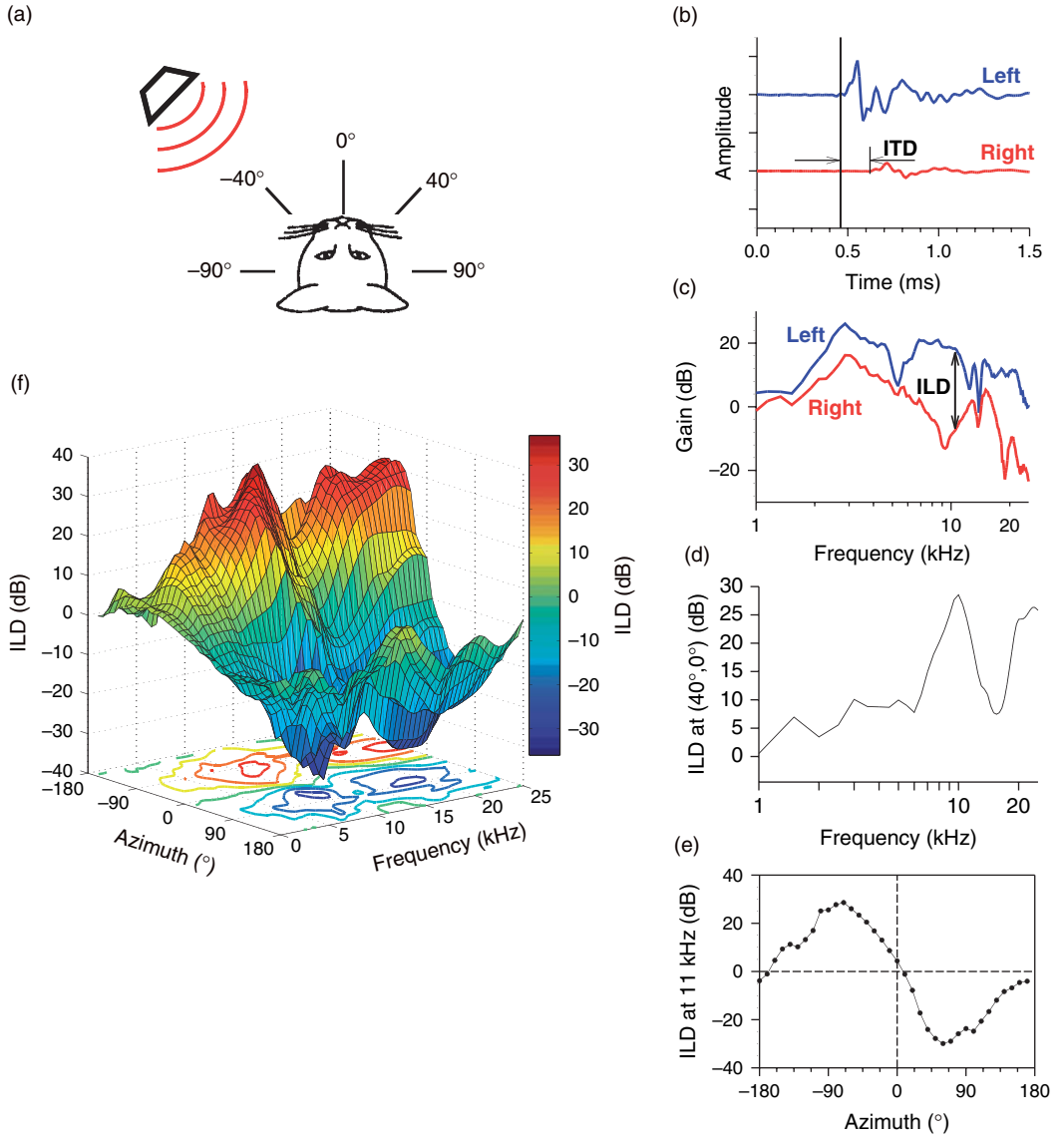

Figure 2 The acoustical cues to sound location in the cat. (a) Broadband clicks are presented repeatedly from a loudspeaker at −40°, 0°. (b) Averaged acoustical responses recorded by microphones near the eardrums in the left and right ears to the clicks presented from −40°, 0°. The interaural time difference (ITD) cue is represented by the relative differences in the onset times of the impulse responses at each ear. (c) The head-related transfer functions (HRTFs) plot the spectrum of the acoustical responses in (b) in terms of the acoustical gain introduced by the presence of the head and pinnae relative to the sound level in response to the click recorded in the absence of the cat. The monaural spectral cues are captured by the changes in the shapes of the spectra as a function of source location. (d) The interaural level difference (ILD) cue is indicated by the relative differences in the gains of the HRTFs as a function of frequency as shown in (c) for a source at −40°, 0°. The ILDs were computed by taking the difference of the left and right ear HRTFs after filtering them though a bank of 1/6-octave Gaussian filters with different center frequencies. (e) At any one frequency, ILDs vary systematically with source azimuth. Frequency is 11 kHz in the example. (f) The joint spatial and frequency dependence of ILDs. ILDs are a complicated function of azimuth and frequency for high stimulus frequencies. For illustrative purposes, sources were restricted to the horizontal plane and only in the frontal hemisphere for frequencies between 1 and 30 kHz. The HRTFs and ILDs were derived directly from the acoustical measurements of Tollin D. J. (2004).

computed by removing from the left and right ear recordings the response recorded at the microphones but in the absence of the cat. This correction procedure effectively removes the stimulus, loudspeaker, and microphone frequency responses leaving only the response due to the torso, head, and pinnae. Figure 2(b) shows the corrected responses, commonly called the impulse responses. Figure 2(c)

shows the Fourier transform of the impulse responses, called head-related transfer functions (HRTFs), for the (−40°, 0°) location; the HRTFs are plotted in terms of the acoustical gain resulting from the head and pinnae relative to the sound level in response to the click in the absence of the cat. A left and right ear pair of HRTFs for any given location captures the frequency- and direction-dependent changes to the acoustic stimulus from that location due to interactions of the incident sound waves with the head, pinnae, and torso.

3.36.2.1 Interaural Time Differences

The ITD and ILD cues are readily apparent in the differences between the impulse responses (Figure 2(b)) and the spectra (Figure 2(c)) of the HRTFs. These binaural cues result because the ears are physically separated in space by the head, which is also acoustically opaque. Direction-dependent differences in path lengths that sound must travel to reach each ear give rise to the ITD cue. In the cat, ITDs increase monotonically with azimuth along the horizontal plane up to a maximum of 300–400 μs (Roth, G. L. *et al*, 1980). The range of ITDs is directly proportional to head diameter so species with larger heads exhibit a larger range of ITDs (Masterton, B. and Diamond, I. T., 1973). For example, the maximum ITD in humans can exceed ∼700 μs. Yet some species of bats and rodents, which have head diameters <1 cm, can have maximum ITDs as small as 40 μs. While such small ITDs are likely to be of little use for localization, substantial ILD cues that can be used for localization will be available at high frequencies.

3.36.2.2 Interaural Level Differences

The ILD cue results from frequency-dependent modifications of the incident sound pressure waves made by the head and pinnae and is defined as the difference in sound pressure level of the signals arriving at the two ears as a function of sound frequency (e.g., Figure 2(c)). ILDs result in part from an acoustic shadow effect that occurs for sounds whose wavelengths are shorter than the diameter of the head so that they are reflected off the head. As a result, relative to the sound level at the ear ipsilateral (same side) to the source, the head effectively attenuates the sound arriving at the contralateral (opposite side) ear. Two main factors contribute to ILDs, both of which can be seen in the sound spectra at the ears (Figure 2(c)). First, there is a general boosting of sound level by the ipsilateral pinna, as evidenced by gains >0 dB. (The gains at ∼3 kHz are due to the ear canal resonance.) Second, the shadowing effect attenuates sounds at the contralateral ear resulting in smaller gains at every frequency than the gains at the ipsilateral ear (Figure 2(c)). Measurements in adult cats confirm the observations made in Figure 2 (Wiener, F. M. *et al*., 1966; Phillips, D. P. *et al*., 1982; Calford, M. B. and Pettigrew, J. D. 1984; Irvine, D. R., 1987). Although the amplification provided by the ipsilateral pinna can approach 20–25 dB sound pressure level (SPL) at some frequencies (Phillips, D. P. *et al*., 1982; Musicant, A. D. *et al*., 1990), for most frequencies, the acoustic head shadow accounts for much of the magnitude of the ILD (Irvine, D. R., 1987).

The ILD cue varies systematically with location in cats (Wiener, F. M. *et al*., 1966; Moore, D. R. and Irvine, D. R., 1979; Phillips, D. P. *et al*., 1982; Calford, M. B. and Pettigrew, J. D., 1984; Irvine, D. R., 1987; Martin, R. L. and Webster, W. R., 1989; Musicant, A. D. *et al*., 1990; Rice, J. J. *et al*., 1992; Tollin, D. J., 2004). However, at any one location, the ILD also varies with frequency. The example in Figure 2 illustrates the dual nature of this complexity. First, the frequency-dependent ILD for the source at (−40°, 0°) is given by the difference in the gains at the two ears (Figure 2(c)), which is plotted in Figure 2(d) as a function of frequency. Second, Figure 2(e) shows how the ILD at one frequency (11 kHz) varies with azimuth. Finally, to illustrate the joint direction- and frequency-dependent patterns of ILD, Figure 2(f) shows ILDs as a function of azimuth and frequency for sources along the horizontal plane. Three main points are apparent. First, at each azimuth, the ILD–frequency functions (e.g., Figure 2(d)) are nonmonotonic and exhibit complex shapes. As expected from physical acoustics, ILDs are small for low frequencies and systematically increase in magnitude for frequencies approaching ∼10 kHz. Frequencies >∼10 kHz have wavelengths that are on the order of the dimensions of the pinnae, so the pinnae begin to contribute in complex ways to ILDs at these higher frequencies. Second, for frequencies <∼10 kHz, the ILD–azimuth functions are nearly sinusoidal (Figure 2(e); and sigmoidally shaped for sources between ±90°), and the rate of change of ILD with azimuth near the midline increases with frequency. Third, for frequencies >10 kHz, the ILD–azimuth functions are highly nonmonotonic and exhibit peaks and dips. In general, the nonmonotonicity of the ILD–azimuth functions (a pattern also

present in measurements of human ILDs) creates problems for the use of this cue in any single frequency band to represent azimuthal location unambiguously (see Martin, R. L. and Webster, W. R., 1989). However, the *pattern* of ILD across frequency for any one location (e.g., Figure 2(d) for the source at (−40°, 0°)) might be used to resolve the ambiguity.

3.36.2.3 Monaural Spectral Shape Cues

Monaural spectral shape cues arise from direction- and frequency-dependent reflection and diffraction of the pressure waveforms of sounds by the head, torso, and pinna that result in broadband spectral patterns, or shapes, that change with location. Prominent direction-dependent features in the spectra, such as the deep notches that occur at some locations (e.g., 5.5 and 9.5 kHz for the left and right ear, respectively, in Figure 2(c)), are thought to be critical both for localization in elevation, where the binaural cues change little with variations in elevation, as well as facilitating the distinction between sources in front of an observer from sources behind. These spectral features are believed to be initially extracted by the principal neurons of the dorsal cochlear nucleus (CN).

3.36.3 Interaural Level Differences Are Initially Processed in the Lateral Superior Olive

For ILDs to be useful for localization there must be neural mechanisms to encode them. It is easy to imagine a group of neurons where the neural representation of sound level at one ear is simply subtracted from the representation of sound level at the other ear. Insofar as the inputs to this hypothetical mechanism represent the sound levels accurately, this neural differencer could produce a neural correlate of the acoustical ILD cue.

Research has suggested that a correlate of ILD is encoded by the discharge rates of LSO neurons. ILD sensitivity results because LSO neurons are inhibited by sounds presented to the contralateral ear and excited by sounds presented to the ipsilateral ear (Boudreau, J. C. and Tsuchitani, C., 1968). The inhibition can be thought of as the neural equivalent of subtraction. Many neurons in higher auditory nuclei, including the dorsal nucleus of the lateral lemniscus (DNLL), inferior colliculus (IC), medial geniculate body, and auditory cortical areas, are sensitive to changes in sound location, usually for sounds in the contralateral hemifield (Irvine, D. R. F., 1986). These neurons likely derive that sensitivity in large part from the initial processing in LSO neurons, which, as indicated in Figure 1, project excitatory afferents to the contralateral DNLL and IC and inhibitory afferents (not shown) to the ipsilateral IC and DNLL (Glendenning, K. K. and Masterton, R. B., 1983; Glendenning, K. K. *et al.*, 1992; Loftus, W. C. *et al.*, 2004). The initial processing of ILDs by the LSO may place limitations on the spatial selectivity exhibited in higher-order nuclei and, thus, might ultimately limit behavioral sound localization performance. For this reason, we restrict our review of ILD processing to the LSO.

It has been long hypothesized that the functional role of the LSO is to extract and represent the ILD cue as a function of frequency (Tollin, D. J., 2003). But what does ILD processing entail? We review here the anatomical, biophysical, and physiological specializations of the LSO and its afferents (Figure 1) that are necessary for the accurate encoding of ILD.

3.36.3.1 Lateral Superior Olive Neurons Receive Excitatory Inputs from One Ear and Inhibitory Inputs from the Other Ear

Figure 1 summarizes the major afferent inputs from the two ears to the LSO. The principal neurons of the LSO receive excitatory inputs from the ipsilateral ear through the spherical bushy cells (SBCs) of the ipsilateral anteroventral cochlear nucleus (AVCN) (Stotler, W. A., 1953; Warr, W. B., 1966; Osen, K. K., 1969; Warr, W. B., 1972; Tolbert, L. P. *et al.*, 1982; Glendenning, K. K. *et al.*, 1985; Shneiderman, A. and Henkel, C. K., 1985; Cant, N. B. and Casseday, J. H., 1986; Saint Marie, R. L. *et al.*, 1989; Smith, P. H. *et al.*, 1993). LSO neurons receive inhibitory afferents from the contralateral ear via neurons in the ipsilateral medial nucleus of the trapezoid body (MNTB) (Harrison, J. M. and Warr, W. B., 1962; 1972; Elverland, H. H., 1978; Tolbert, L. P. *et al.*, 1982; Glendenning, K. K. *et al.*, 1985; Spangle, K. M. *et al.*, 1985; Friauf, E. and Ostwald, J., 1988; Bledsoe, S. C. *et al.*, 1990; Smith, P. H. *et al.*, 1991; Banks, M. I. and Smith, P. H., 1992; Smith, P. H. *et al.*, 1998) which in turn receive excitatory input from the globular bushy cells (GBCs) of the contralateral AVCN (Harrison, J. M. and Warr, W. B., 1962; Warr, W. B., 1972; Tolber, L. P. *et al.*, 1982; Glendenning, K. K. *et al.*, 1985; Smith, P. H. *et al.*, 1991). The SBCs and GBCs receive a

direct excitatory input from the auditory nerve (not shown in Figure 1).

The hypothesis that the LSO detects differences in the strengths of synaptic inputs received from each ear was first inferred from the patterns of neural discharges elicited when presented with acoustic stimuli containing ILDs (Boudreau, J. C. and Tsuchitani, C., 1968). The early studies found that ipsilateral sound-evoked discharges could be systematically reduced by increasing the level of the stimuli presented to the contralateral ear. Although this hypothesis was attractive, a change in discharge rate with ILD does not by itself directly implicate the LSO as the actual site where ILD is computed. The actual computation could have occurred more peripherally.

Moore M. J. and Caspary D. M. (1983) provided the first conclusive evidence that ILD sensitivity results directly from the nature of the synaptic inputs on LSO neurons. These experiments showed that the input from the ipsilateral MNTB was glycinergic and inhibitory. Inhibition that was evoked by an acoustic stimulus at the contralateral ear was blocked by iontophoretic application of the glycine receptor antagonist, strychnine. Moreover, an inhibitory effect comparable to that evoked by acoustic stimulation could also be elicited by iontophoretic application of glycine. Immunocytochemical studies have since confirmed that the principal neurons of the MNTB are glycinergic (Wenthold, R. J. *et al.*, 1987; Glendenning, K. K. and Baker, B. N., 1988; Helfert, R. H. *et al.*, 1989; Saint Marie, R. L. *et al.*, 1989; Adams, J. C. and Mugnaini, E., 1990; Bledsoe, S. C. *et al.*, 1990; Henkel, C. K. and Brunso-Bechtold, J. K., 1995) and that glycine receptors are abundantly expressed on the principal neurons of the LSO (Sanes, D. H. *et al.*, 1987; Glendenning, K. K. *et al.*, 1991; Korada, S. and Schwartz, I. R., 1999).

Intracellular recordings *in vivo* from single LSO neurons show that acoustic stimulation of the ipsilateral and contralateral ears generates excitatory (EPSPs) and inhibitory (IPSPs) postsynaptic potentials, respectively (Finlayson, P. G. and Caspary, D. M., 1989). Moreover, *in vitro* recordings, which allow the afferent pathways to LSO from each ear to be electrically stimulated directly and independently, also showed that ipsilateral inputs generated glutamatergic EPSPs while contralateral inputs generated glycinergic IPSPs, although there were exceptions (Caspary, D. M. and Faingold, C. L., 1989; Sanes, D. H., 1990; Wu, S. H. and Kelly, J. B., 1991; 1992). For example, some LSO neurons could be inhibited by ipsilateral electrical stimulation from glycinergic inputs directly to LSO neurons themselves, although the source of this input is not clear (Wu, S. H. and Kelly, J. B., 1991; 1994). Such inputs were also inferred from *in vivo* studies, where some LSO neurons could be inhibited by ipsilateral presentation of tones with frequencies away from the characteristic frequency (CF) consistent with side-band inhibition (Brownell, W. E. *et al.*, 1979; Caird, D. and Klinke, R., 1983). Sideband inhibition could play a role in sharpening the frequency tuning of the ipsilateral input.

3.36.3.2 Inputs Encode the Spectral and Temporal Characteristics of the Sounds at Each Ear

3.36.3.2.1 Spectral representation by lateral superior olive afferents

A hypothesized role of the LSO is to compute a correlate of the ILD across frequency for any one location (e.g., Figure 2(d)). For this to take place, the afferent inputs to the LSO must accurately encode the broadband spectral characteristics of the sounds at each ear (e.g., Figure 2(c)). Clearly, the population of auditory nerve fibers (ANFs) must initially encode sound spectra sufficiently for the computation of ILDs. This representation must be preserved in the pathways to the LSO through the bushy cells and the MNTB neurons. At the periphery, ANFs display narrow frequency selectivities, evidenced by sharp frequency tuning curves (Kiang, N. Y. S. *et al.*, 1965). Therefore, the broadband spectrum of high-frequency stimuli is likely represented via the pattern of discharge rates across the population of ANFs, with the spectral level at each frequency being proportionally represented by the discharge rate of ANFs with that CF (Pfeiffer, R. R. and Kim, D. O., 1975). ANFs project to the CN, which is tonotopically organized (Rose, J. E. *et al.*, 1959), so the representation of the spectrum by the ANF array will be available to the CN, including the bushy cells of the AVCN.

Several studies have examined the ability of the ANF population to represent the spectral shapes of HRTFs themselves (e.g., Figure 2(c)). These studies recorded the responses from populations of cat ANFs, spanning a broad range of CFs, to broadband noise stimuli that had been filtered by HRTFs measured from adult cats. An early study suggested that single ANFs could encode the spatial location-dependent spectral features of HRTFs via their discharge rates (Poon, P. W. and Brugge, J. F., 1993).

However, another concluded that the most salient spectral characteristics, such as the deep spectral notches, could not be accurately encoded (Rice, J. J. *et al.*, 1995). Rice J. J. *et al.* (1995) used a limited set of HRTF measurements, so it is not clear from that study whether the ANF population could encode the more global spectral characteristics necessary for the computation of ILD independent of the sharp notches. This possibility was reexamined with a computational model (May, B. J. and Huang, A. Y., 1997). By simulating the responses of a larger population of ANFs, May B. J. and Huang A. Y. revealed that the discharge rates represented across the ANF population contained information that was sufficient to account for the behavioral measurements of sound localization acuity by cats for the high-frequency sounds where ILD cues predominate (Martin, R. L. and Webster, W. R., 1989).

Less is known about the spectral-encoding capabilities of bushy cells and MNTB neurons, which provide the inputs to LSO, since studies similar to those described above have not yet been performed. However, SBCs (Rhode, W. S. and Smith, P. H., 1986; Spirou, G. A. *et al.*, 1990; Smith, P. H. *et al.*, 1993) and MNTB neurons (Guinan, J. J., Jr. *et al.*, 1972a; Tsuchitani, C., 1997; Smith, P. H. *et al.*, 1998; Kopp-Scheinpflug, C. *et al.*, 2003) have physiological response characteristics that are nearly identical to their ANF or GBC inputs, respectively: narrow frequency tuning, primary-like or primary-like with notch responses to tone pips at CF; similar dynamic ranges, etc. Based on this similarity, it is possible that the ANF rate representation of the spectrum is preserved through the SBCs and GBCs as well as the MNTB.

3.36.3.2.2 Temporal representation by lateral superior olive afferents

Many natural sounds, like speech and animal vocalizations, are modulated over time in both frequency and amplitude. Other sounds are brief and transient, like rustling leaves and snapping twigs. To compute the ILD present in these signals at the LSO requires special care because the inputs from the two ears must encode the temporal variations in the spectra with high fidelity. Surprisingly, the neurons comprising the ascending pathway through the LSO (Figure 1) contain remarkable anatomical and biophysiological specializations that appear suited to accurate encoding of temporal information. This is particularly interesting because it is contrary to the hypothesis that the ILD pathway is concerned only with the encoding of sound spectra.

The ANF synapses onto the bushy cells of the CN (Brawer, J. R. and Morest, D. K., 1975; Cant, N. B. and Morest, D. K., 1979; Smith, P. H. and Rhode, W. S., 1987) along with the intrinsic biophysical properties of the bushy cells themselves (Trussel, L. O., 2002) are specialized to permit the accurate preservation of temporal information. Consistent with these biophysical specializations, the encoding of temporal variations in the fine structure of low-frequency sounds is enhanced over that of their ANF input (Joris, P. X. *et al.*, 1994). Yet at high frequencies where ILDs are useful, ANFs do not encode temporal fine structure (Johnson, D. H., 1980), but they can encode the amplitude (AM) (Figure 4) (Joris, P. X. and Yin, T. C. T., 1992) and frequency (FM) modulations of the stimuli (Britt, R. and Starr, A., 1976). The representations of AM and FM stimuli are preserved in the bushy cells and MNTB neurons (e.g., Figure 4) (Moller, A. R., 1974; Rhode, W. S. and Smith, P. H., 1986; Rhode, W. S. and Greenberg, S., 1994; Joris, P. X. and Yin, T. C. T., 1998). MNTB neurons have similar membrane properties as bushy cells, with short membrane time constants and nonlinear current–voltage relationships (Wu, S. H. and Kelly, J. B., 1991; Banks, M. I. and Smith, P. H., 1992), also making them well suited to preserve temporal information. Indeed, low-CF MNTB neurons exhibit phase locking that is enhanced over similar CF ANFs (Tollin, D. J. and Yin, T. C.T., 2005). Together, these specializations ensure that rapidly time-varying changes in the amplitude and frequency content of stimuli at each ear are accurately represented through the pathway to the LSO neurons.

3.36.3.3 The Inputs from Each Ear to Individual Neurons Have Similar Frequency Tuning

In order for the LSO to compute a faithful correlate of the ILD, the afferents to individual LSO neurons must encode corresponding frequency regions of the spectrum. Like the CN, the LSO exhibits a tonotopic organization with neurons responding to high frequencies located in the ventromedial limb and neurons responding to lower frequencies represented in the dorsolateral limb (see shading in Figure 1). The representation of frequency is skewed such that most LSO neurons respond to frequencies $>\sim$2 kHz (Tsuchitani, C. and Boudreau, J. C., 1966; Guinan, J. J., Jr. *et al.*, 1972b; Tsuchitani, C., 1977). A similar

and parallel disproportionate representation of high frequencies exists in the MNTB (e.g., Figure 1; Guinan, J. J., Jr. *et al.*, 1972b). There is evidence that the frequency selectivity of GBCs is also skewed towards high frequencies (Smith, P. H. *et al.*, 1991). The parallel overrepresentation of high-frequency-selective neurons in GBCs, the MNTB, and the LSO correlates well with the acoustical measurements in cats showing that the ILD cue becomes prominent only for frequencies above ~2–3 kHz (e.g., Figure 2(f)).

There is strong anatomical and physiological support for matched-frequency inputs to LSO. First, anatomically, the tonotopic organization of LSO determined from physiological studies matches the topography of the afferent projections to the LSO from the ipsilateral CN (Warr, W. B., 1966) and from the ipsilateral MNTB (Elverland, H. H., 1978; Glendenning, K. K. *et al.*, 1985; Spangler, K. M. *et al.*, 1985; Smith, P. H. *et al.*, 1998). Second, frequency tuning curves for the contralateral inhibitory ear have been measured by determining the sound level of tones presented to the contralateral ear, at different frequencies, that just inhibited a set percentage of the discharges evoked by a fixed-level CF tone presented to the ipsilateral ear (Figure 3(a)).

The inhibitory frequency tuning curves that result (black lines, Figure 3(b)) were similar in shape and yielded nearly identical estimates of the CF as the ipsilateral excitatory tuning curves (red dashed line, Figure 3(b) (Boudreau, J. C. and Tsuchitani, C., 1968; Caird, D. and Klinke, R., 1983; Tsuchitani, C., 1997). That is, the lowest intensity of contralateral stimulation that can evoke inhibition occurs when the frequencies of the tones presented to the two ears are matched at the CF (11 kHz in the example). However, as is apparent in Figure 3(b) there was a tendency for the bandwidths of the frequency tuning estimated from the inhibitory input to be wider than those of the ipsilateral excitatory tuning curves. Because the tuning curves of MNTB neurons of similar CFs have been found to be narrower than the inhibitory tuning curves of LSO neurons, there is likely a convergence of inhibitory MNTB

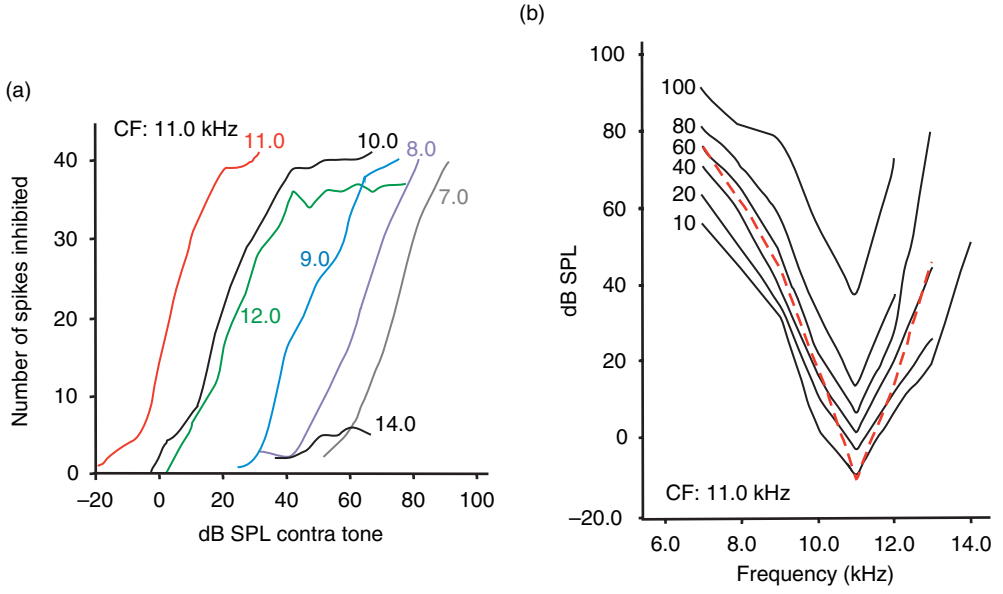

Figure 3 Frequency selectivity of the contralateral inhibitory and ipsilateral excitatory input to lateral superior olive (LSO) neurons is matched. (a) The number of spikes by which the response to a tone presented at the neuron's characteristic frequency (CF, 11.0 kHz) to the ipsilateral ear was reduced or inhibited by the simultaneous presentation to the contralateral ear of tones with different frequencies (indicated by colored lines and associated numbers) and at different sound levels (abscissa). Spikes are inhibited at the lowest sound levels when the tones presented to the two ears were matched at the CF (red line). (b) Inhibitory threshold tuning curves calculated from the functions plotted in (a). The shape of the frequency threshold curve for the excitatory ear (dashed red line) is well matched by the inhibitory tuning curves (black lines). Each inhibitory tuning curve represents the sound levels and frequencies at which equal inhibitory effects were found in (a). Inhibitory effects are expressed as the percentage of inhibition relative to the ipsi-only stimulus (values next to each curve). Reprinted with permission from Boudreau, J. C. and Tsuchitani, C. 1968. Binaural interaction in the cat superior olive S segment. J. Neurophysiol. 31, 442–454.

inputs with slightly different CFs onto LSO neurons (Boudreau, J. C. and Tsuchitani, C., 1968; Sanes, D. H. and Rubel, E. W., 1988; Tsuchitani, C., 1997).

3.36.3.4 Inputs from the Two Ears Reach Lateral Superior Olive Neurons in Approximate Temporal Register

If the peripheral representations of sounds that are brief or have rapid AM and/or FM do not arrive at the LSO in approximate temporal register, then the computation of the ILD in those stimuli will be compromised. This ILD-timing problem has been illustrated nicely by Joris P. X. and Yin T. C. T. (1995), which is reprinted in Figure 4.

The illustration shows hypothetical responses to an AM tone by the constituent neurons in the ILD pathway (Figure 1). In Figure 4(a), three periods of the AM waveform are shown as arriving at the ears with zero time delay, or zero interaural phase difference in the envelopes, which approximates a sound source at the midline. The temporal fluctuations in the amplitude of the stimulus are conveyed in the timing of the discharges of the ANFs, bushy cells, and the MNTB neuron. In this example, for the LSO to compute the correct acoustic ILD, which is 0 dB because the source is at the midline, the inputs from the ipsilateral SBC and the ipsilateral MNTB neuron must arrive at the LSO neuron simultaneously. For the ideal case in Figure 4(a) where the inputs have been forced to arrive in register, the LSO neuron's response is minimal when the ILD of the stimulus is 0 dB.

If at any point along the pathway from the sound source to the synaptic inputs to the LSO there are additional time delays, then the inputs will not arrive in register. And because the magnitude of the responses of the inputs fluctuates in time, there will be a corresponding change in the relative levels of excitation and inhibition at the LSO neuron. The functional consequences of temporal delays on ILD coding are illustrated in Figure 4(b) in which the neural input from the contralateral ear is delayed and arrives at the LSO later than the ipsilateral input. The ILD of the stimuli remains 0 dB. In this hypothetical case, the delay is imposed on the acoustical stimuli themselves, but in principle a comparable delay could result at any point in the LSO circuit (Figure 1). Due to the delay, the excitatory and inhibitory representations of the AM waveforms at the inputs to LSO are not in register. Consequently, relative to the zero-delay condition (Figure 4(a)) there is a release from inhibition leading to a large increase in the discharge rate of the LSO neuron. Clearly the encoding of the ILDs in such stimuli via the discharge rate of LSO neurons can be confounded by delays at any point in the circuit.

There are at least three ways in which the contralateral input is delayed relative to the ipsilateral. First, the neural path to the LSO is ~5.5–7.0 mm (in the cat; Tsuchitani, C. and Johnson, D. H., 1991) longer from the contralateral ear than the ipsilateral ear. Assuming that the axons of all neurons had equal diameters (and thus, equal conduction velocities), the contralateral input to LSO would arrive ~0.26–0.33 ms after the ipsilateral input (Tsuchitani, C. and Johnson, H., 1991). Second, the additional synapse through the MNTB adds an additional delay of ~0.5 ms (Smith, P. H. *et al.*, 1998). Finally, the sound source may not be equidistant from the two ears generating a delay due to the ITD of maximally ~0.4 ms (Roth, G. L. *et al.*, 1980). Even without the ITD, the neural circuitry could theoretically impose a delay on the contralateral input to LSO of nearly 1.0 ms. As illustrated in Figure 4, the consequences of such delays on ILD processing can be great.

Fortunately, there are at least three anatomical specializations along the contralateral pathway that work in concert to compensate for the delay brought about by the added path length and extra synapse in the contralateral ear input. First, the axonal diameters of the GBCs, which provide the input to the contralateral MNTB, are about three times larger and MNTB axons two times larger than the axons from the SBCs that provide the excitatory input from the ipsilateral CN (Brownell, W. E., 1975; Spangler, K. M. *et al.*, 1985). Thus, conduction times through axons are relatively shorter in the contralateral than in the ipsilateral circuit. Second, although the MNTB has traditionally been thought of as just a relay nucleus whose sole purpose is to invert the sign of the synaptic input to the LSO from the contralateral CN from excitatory to inhibitory, the GBC/MNTB synapse may have further functions (e.g., Kopp-Scheinpflug, C. *et al.*, 2003). The input from contralateral GBCs onto MNTB neurons forms one of the largest and most secure synapses in the whole CNS, referred to as the calyx of Held (Morest, D. K., 1973). Each MNTB principal neuron receives only a single calyx from a GBC, which envelops about half of the available surface of the soma, and large presynaptic terminals that produce large postsynaptic currents (Banks, M. I. and Smith, P. H., 1992; Smith, P. H. *et al.*, 1998). MNTB neurons have short time constants, receptors with fast kinetics, and specialized ion channels that together

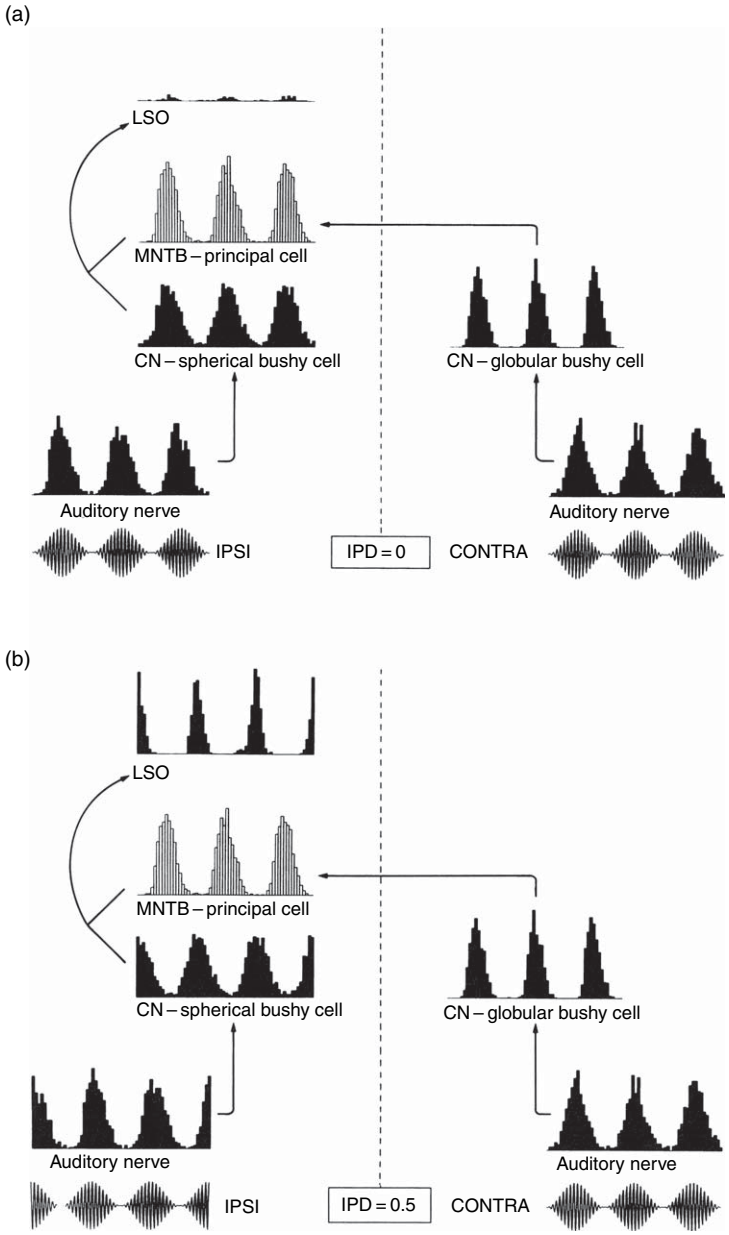

Figure 4 Illustration of the effect on interaural level difference (ILD) coding of delayed contralateral inhibition. (a) Hypothetical responses of a lateral superior olive (LSO) neuron and its afferents (e.g., Figure 1) to an amplitude-modulated (AM) stimuli presented in phase (0 time delay) to the two ears with an ILD of 0 dB plotted as poststimulus time histograms. The afferents encode the ongoing amplitude modulations of the stimuli. In the example, the excitatory and inhibitory representations arrive at the LSO neuron in temporal register resulting in a small discharge rate for this stimulus with an ILD of 0 dB. (b) Hypothetical responses of the same LSO neuron and its afferents to the AM stimuli that still has an ILD of 0 dB but contralateral stimulus has been delays in time (equivalent to an IPD in the envelopes of 0.5). The time delay is preserved by the responses of the contralateral afferents. Consequently, the excitation and inhibition do not arrive in temporal register and there is an effective release from inhibition resulting in an increased discharge rate of the LSO neuron relative to that in (a). Even though the ILDs of the stimuli in (a) and (b) were identical, the LSO response was not the same due to the relative delay between the excitation and inhibition. The delay in the example was imposed on the acoustic stimuli themselves, but a similar effect could occur by imposing a delay at any point along the contralateral pathway to the LSO (Figure 1). Reprinted with permission from Joris, P. X. and Yin, T. C. T. 1995. Envelope coding in the lateral superior olive. I. Sensitivity to interaural time differences. J. Neurophysiol. 73, 1043–1062.

with specializations in the calyx result in large, rapid EPSPs that excite MNTB neurons with nearly invariant synaptic delays (Trussell, L. O., 2002). Collectively, these synaptic specializations allow the physiological response properties of MNTB to be virtually identical to their GBC inputs not only in their representation of the stimulus spectrum but also in their representation of the time structure of the stimulus (Guinan, J. J. *et al.*, 1972a; Tsuchitani, C., 1997; Smith, P. H. *et al.*, 1998; Kopp-Scheinpflug, C. *et al.*, 2003; Tollin, D. J. and Yin, T. C. T., 2005). Finally, further reducing the functional delays in the contralateral pathway, MNTB inputs synapse right on or near the soma of LSO neurons while the excitatory inputs from the ipsilateral CN synapse on the distal dendrites (Cant, N. B., 1984; Helfert, R. H. *et al.*, 1992; Smith, P. H. *et al.*, 1998).

The functional implication of rapid transmission to the LSO of the contralateral inhibition is that for transient sounds or sounds with ongoing rapid AM (e.g., Figure 4) or FM, the inhibition of the discharge rate of the LSO should be nearly maximal when these stimuli are presented to the two ears with no delay between their onsets (i.e., a source at the midline). Physiological experiments have indeed shown that inhibition of LSO responses can often be maximal when the delay between the onsets of transients (Figure 5), low-frequency tones, or

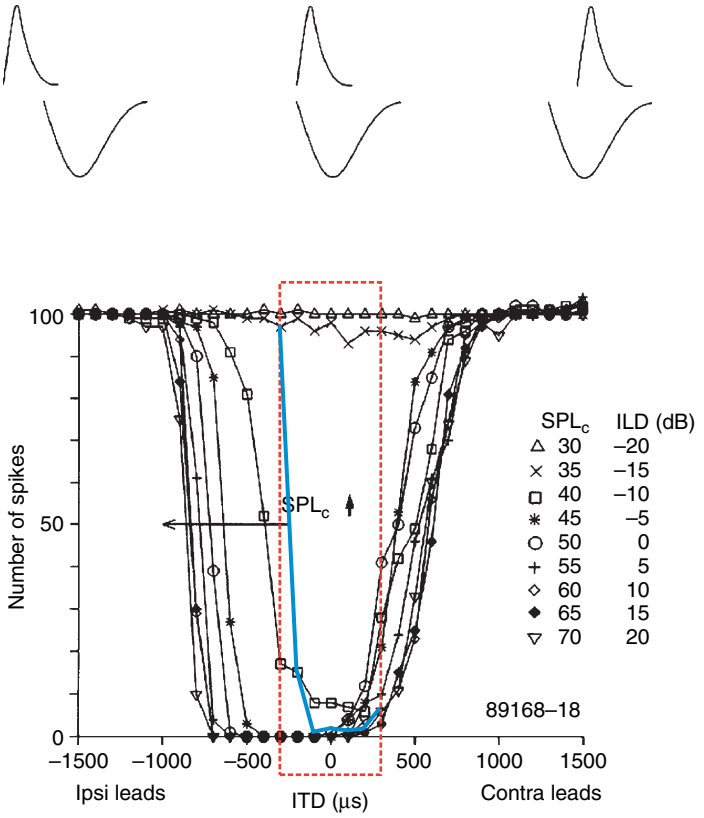

Figure 5 Lateral superior olive (LSO) neurons compare excitation and inhibition over short time intervals. Tracings at the top illustrate the relative durations of EPSPs (top, positive-going traces) and IPSPs (bottom, negative-going traces) in LSO neurons and their potential interactions as a function of the time delay between them (abscissa, bottom graph). The graph shows the number of spikes elicited from an LSO neuron as a function of both interaural time difference (ITD) (abscissa) and interaural level difference (ILD) (different symbols) in clicks presented to the two ears. For most ILDs, the response as a function of ITD has a characteristic U shape with substantial inhibition occurring primarily for ITDs between ~±500 μs. Therefore, the functional binaural integration time over which there is effective inhibition is ~1 ms. The physiological range of ITDs in cats (~±300 μs) is indicated by the box (red). The blue function plots the change in response that would likely result from the joint changes in ILD and ITD that would be expected by varying an actual sound source in azimuth. A functional consequence of the short integration time is that the ILD in transient stimuli like the clicks used in this example can still be represented by LSO neurons without the confounding effects on responses that time delays produce. Reprinted with permission from Joris, P. X. and Yin, T. C. T. 1995. Envelope coding in the lateral superior olive. I. Sensitivity to interaural time differences. J. Neurophysiol. 73, 1043–1062.

amplitude-modulated stimuli of equal level are presented to the two ears simultaneously (Caird, D. and Klinke, R., 1983; Finlayson, P. G. and Caspary, D. M., 1991; Joris, P. X. and Yin, T. C. T., 1995; Park, T. J. *et al.*, 1996; Batra, R. *et al.*, 1997; Irvine, D. R. *et al.*, 2001). Joris P. X. and Yin T. C. T. (1998) showed using two independent methods that, on average, the contralateral inhibitory input reaches the LSO within ~200 μs of the ipsilateral excitatory input. These data confirm earlier reports that the initial onset discharges to simultaneous and equal amplitude sounds could be inhibited in some LSO neurons (Boudreau, J. C. and Tsuchitani, C., 1968) and are also consistent with *in vitro* intracellular recordings of synaptic potentials that demonstrate that the relative time of arrival of evoked EPSPs and IPSPs can have a dramatic effect on the discharge probability of LSO neurons (Wu, S. H. and Kelly, J. B., 1991). The unique and remarkable anatomical and biophysical specializations observed in the long contralateral pathway to the LSO likely serve to minimize both the relative timing delays and the jitter in the synaptic delays incurred along the ILD pathway so that ILDs in the stimulus, particularly for brief, transient stimuli, can be accurately represented.

3.36.3.5 Lateral Superior Olive Neurons Have Short Integration Times

The highly accurate encoding of rapid temporal variations in stimuli by LSO afferents and the comparison of those inputs in temporal register by LSO neurons would not be necessary unless those inputs were also compared over short time intervals. For this to happen, the integration time of the comparison should be short so that a correlate of ILD is only computed over brief, temporally corresponding portions of the stimuli at each ear. Indeed, it has been shown that contralateral stimulus-evoked IPSPs recorded intracellularly in LSO neurons tend to have relatively long durations (3.2–8.1 ms) that are nearly twice the duration of ipsilaterally evoked EPSPs (1.5–4.2 ms) (Sanes, D. H., 1990). Functionally, however, the contralateral inhibition is effective in suppressing ipsilaterally evoked discharges of LSO neurons for only about ~1.0–2.0 ms (Sanes, D. H., 1990; Wu, S. H. and Kelly, J. B., 1992; Joris, P. X. and Yin, T. C. T., 1995; Park, T. J. *et al.*, 1996; Irvine, D. R. *et al.*, 2001).

To illustrate the functional integration time, Figure 5 shows an example of the responses of an LSO neuron to presentations of click stimuli to the two ears that contain combinations of ITDs and ILDs (Joris, P. X. and Yin, T. C. T., 1995). The drawings above the graph illustrate the relative durations of and the delays between the click-evoked EPSPs and IPSPs, respectively, as the ITD is varied. For a given ILD, as the ITD varied, responses were suppressed for delays ranging from ~±500 μs; in other words, IPSPs and EPSPs interacted functionally for ~1 ms. Integration times of 1–2 ms would presumably allow ongoing ILD computation for stimulus fluctuations up to ~1 kHz before synaptic inputs would be temporally integrated. Supporting this, some LSO neurons track ILDs in binaural AM stimuli at rates up to 800 Hz (Joris, P. X., 1996).

A potentially important consequence of the short integration time is that the output of the LSO neuron is still modulated monotonically as a function of ILD (Figure 5(b), blue line) despite the changes in ITD over the physiological range of ITDs in cats (±300 μs, red box; Roth, G. L. *et al.*, 1980). The neuron's response that would likely result under the natural situation where both ILD and ITD vary with source azimuth (blue line) changes in an orderly way as the source is moved from the ipsilateral (negative delays and ILDs) to the contralateral (positive delays and ILDs) side. Short integration times, then, presumably allow LSO neurons to accurately encode the ILDs of transient sounds via discharge rate without the confounding influence of time delays induced by the ITD.

3.36.3.6 Lateral Superior Olive Neurons Encode the Interaural Level Difference Present in the Sounds at the Two Ears

3.36.3.6.1 Sensitivity to interaural level differences in pure-tone stimuli

The responses of single LSO neurons are correlated with ILDs (Boudreau, J. C. and Tsuchitani, C., 1968; Guinan, J. J., Jr. *et al.*, 1972a; Caird, D. and Klinke, R., 1983; Sanes, D. H. and Rubel, E. W., 1988; Joris, P. X. and Yin, T. C. T., 1995; Park, T. J. *et al.*, 1997; Irvine, D. R. *et al.*, 2001; Tollin, D. J. and Yin, T. C. T., 2002a; Park, T. J. *et al.*, 2004).

For example, Figure 6 shows the responses of an LSO neuron to changes in the ILD of CF tones. ILD was manipulated by presenting a constant-level tone to the ipsilateral excitatory ear while varying the sound level of a simultaneously presented tone to the contralateral ear. Figures 6(a)–6(d) shows the responses at four different ILDs displayed as dot rasters and associated poststimulus time histograms

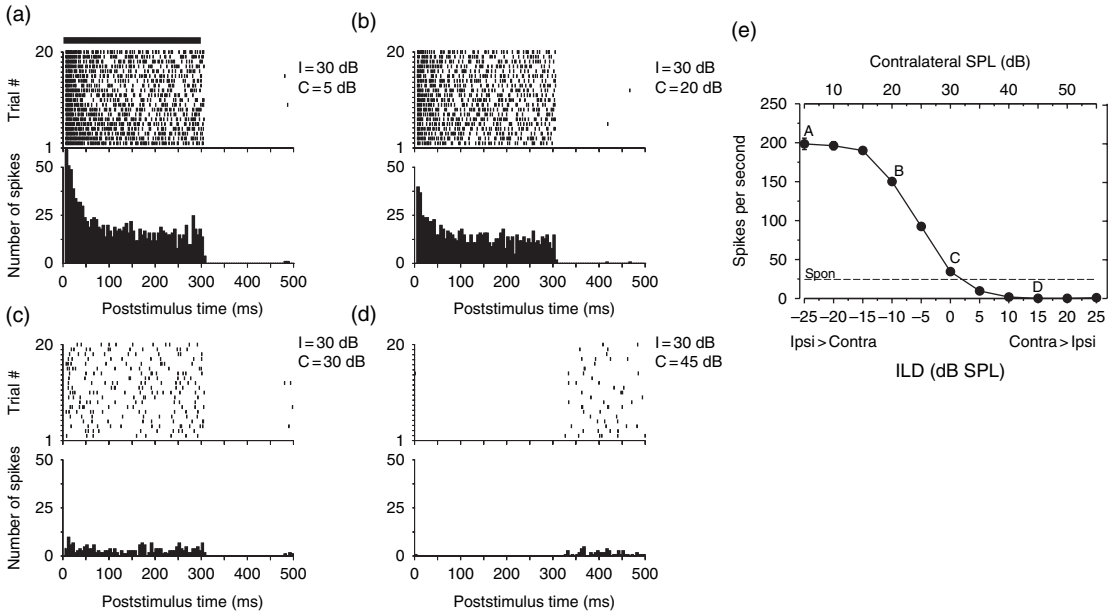

Figure 6 Lateral superior olive (LSO) neurons are sensitive to interaural level differences (ILDs) in pure tone stimuli. (a)–(d) Responses of one LSO neuron (CF (characteristic frequency) = 16 kHz) displayed as dot rasters and PSTHs to CF-tone bursts presented 20 times for each ILD (top right-hand corner). Stimulus duration was 300 ms (bar at top of (a)). The level of the tone at the ipsilateral ear was fixed at 30 dB SPL (~20 dB re: threshold) while the level of the same CF tone presented to the contralateral ear was increased. (e) Mean discharge rate ±1 SEM of the neuron computed over the duration of the stimuli and across the 20 repetitions as the level of the stimulus to the contralateral ear was increased (top abscissa), which changes the ILD (bottom abscissa). ILD is defined as the difference between the sound level at the contralateral ear and that at the ipsilateral ear so negative ILDs indicate greater sound levels at the excitatory ear. The dashed horizontal line indicates spontaneous firing rate. Reprinted with permission from Tollin, D. J. and Yin, T. C. T. 2002. The coding of spatial location by single units in the lateral superior olive of the cat. I. Spatial receptive fields in azimuth. J. Neurosci. 22, 1454–1467.

(PSTHs). The data points marked A–D in Figure 6(e) show the mean discharge rates evoked at these four ILD values. With the ipsilateral level held constant, the firing rate decreased systematically as the level of the contralateral tone was increased. For positive ILDs that favor the contralateral ear, the response was completely inhibited, with the discharge rate falling even below the spontaneous rate (horizontal dashed line), as shown for an ILD of 15 dB (Figure 6(d)). This neuron preferentially responded to stimuli with ILDs favoring the ipsilateral excitatory ear. In fact, studies have shown that most neurons in the LSO respond preferentially to ipsilateral ILDs (Boudreau, J. C. and Tsuchitani, C., 1968; Caird, D. and Klinke, R., 1983; Sanes, D. H. and Rubel, E. W., 1988; Joris, P. X. and Yin, T. C. T., 1995; Park, T. J. *et al.*, 1997; Tollin, D. J. and Yin, T. C. T., 2002a; Park, T. J. *et al.*, 2004). Extrapolating from the ILD cues actually available to cats (e.g., Figure 2), the neurons comprising each LSO, then, would likely encode information primarily about ipsilateral sound sources as most neurons would be inhibited for contralateral sources. That is, the left and right LSOs encode sources in the left and right hemispheres, respectively.

Neurons in the LSO can collectively, across the population, respond to ILDs over a range sufficient to encode the range of physical ILDs that are expected from acoustical measurements (see Figure 2(b)). Moreover, individual neurons are sensitive to different absolute ranges of ILDs and can also signal the ILD for different types of acoustical signals provided the stimuli fall within the frequency selectivity of the neuron (Boudreau, J. C. and Tsuchitani, C., 1968; Caird, D. and Klinke, R., 1983; Sanes, D. H. and Rubel, E. W., 1988; Joris, P. X. and Yin, T. C. T., 1995; Batra, R. *et al.*, 1997; Park, T. J. *et al.*, 1997; Tollin, D. J. and Yin, T. C. T., 2002a; Park, T. J. *et al.*, 2004). However, there are complications to the notion that LSO neurons faithfully represent ILDs. First, responses generally are not invariant to changes in the more global aspects of the stimuli. For example, the responses of most LSO neurons change dramatically as the overall level of the stimuli is changed despite a constant ILD (Tsuchitani, C. and

Boudreau, J. C., 1969; Tollin, D. J. and Yin, T. C. T., 2002a; Park, T. J. *et al.*, 2004). Second, as reviewed in earlier sections, for some stimuli large delays in the contralateral input to the LSO can change the discharge rate irrespective of any ILD changes (e.g., Figure 4). Consequently, a given physical ILD in a stimulus does not always correspond to a fixed discharge rate. It is likely that populations of LSO neurons and/or the differential responses of comparable LSO neurons comprising the left and the right LSOs compute a more accurate correlate of the ILD (e.g., Park, T. J. *et al.*, 2004).

3.36.3.6.2 Sensitivity to interaural level differences in virtual space (VS) stimuli that mimic free-field sounds

Most physiological studies of ILD coding have used stimuli presented over headphones to the two ears. But what about the ability of LSO to encode ILDs present in more natural stimuli, in which the ILDs (and ITDs and spectral shape cues) are created by the interactions of the sound waveforms with the head and pinnae (e.g., Figure 2)? Can LSO neurons encode the ILDs present in broadband stimuli that contain all the acoustical cues to location in their native combinations, such as would be the case for sounds presented in the free field? Complicating any discussion of ILD coding of free-field sources is the fact that LSO neurons are sensitive not only to ILD, but also to each of the other cues to azimuth when they are presented in isolation; that is, certain types of ITDs (Caird, D. and Klinke, R., 1983; Finlayson, P. G. and Caspary, D. M., 1991; Joris, P. X. and Yin, T. C. T., 1995; Park, T. J. *et al.*, 1996; Batra, R. *et al.*, 1997; Irvine, D. R. *et al.*, 2001; Tollin, D. J. and Yin, T. C. T., 2005) and overall sound level, which is important for the spectral cues (Tsuchitani, C. and Boudreau, J. C., 1966; Tsuchitani, C., 1997; Tollin, D. J. and Yin, T. C. T., 2002a). Moreover, free-field studies of spatial sensitivity are further complicated by the fact that the cues covary with changes in source azimuth. So without acoustical measurements, it is difficult to determine which cues or combinations of cues were responsible for the neural responses.

This issue of which cues contribute to the spatial selectivity of LSO neurons was recently addressed in experiments where broadband noises were first filtered by left- and right-ear HRTFs from a desired location and then presented over earphones (Tollin, D. J. and Yin, T. C. T., 2002a; 2002b). HRTFs contain the complete spatial- and frequency-dependent transformation a sound undergoes as it travels from source to eardrum (see Figure 2(a)), so HRTF-filtered sounds presented to the two ears from the earphones are comparable to those that would have arisen had the cat been stimulated by the sound stimuli delivered from that chosen location in space. This is the basis of the so-called VS technique. The obvious advantage of the VS technique is that the stimuli contain all the cues to location and the cues can be computed by the experimenter, which facilitates the correlation of a neuron's response with the values of the cues.

Figure 7 shows the responses of the same LSO neuron as in Figure 6 but to broadband noise from five different VS azimuths along the horizontal plane under two different stimulus conditions. When the stimuli were presented to both ears so that all the acoustical cues to location were presented in their natural combinations (Figure 7(a), normal condition), there were vigorous responses for ipsilateral sources, diminishing responses at the midline, and inhibited responses for sources in the contralateral field. This pattern of responses is partly expected because this neuron was sensitive to ILDs (e.g., Figure 6) and for ipsilateral sources, the sound level to the excitatory ear, as processed through the frequency selectivity of the neuron, exceeded the sound level at the inhibitory ear and *vice versa* for sources in the contralateral field. The experiment was repeated with stimuli presented only to the ipsilateral ear, the contralateral earphone having been turned off (Figure 7(b), ipsi-only condition). The contribution of contralateral inhibition to spatial sensitivity was clear, as evidenced by the increased responsiveness for sounds at all locations, particularly at the midline and for contralateral locations where the inhibition seen in the binaural condition (Figure 7(a)) was no longer apparent. The binaural sensitivity of this neuron is further illustrated by plotting the responses as continuous dot rasters for 21 different azimuths in the frontal hemisphere for the normal binaural (Figure 7(a), right) and monaural ipsi-ear only (Figure 7(b), right) conditions. By comparing the rasters as a function of azimuth for the two conditions, the effect of the contralateral inhibition is evident. Figure 9(a) plots the mean discharge rate as a function of azimuth for this neuron, which we call the spatial receptive fields (SRFs) in azimuth.

Different LSO neurons were shown to be sensitive to variations in the azimuth of sounds consistent with their ipsi-excitatory and contra-inhibitory binaural interaction as assessed from the pure tone stimuli (Tollin, D. J. and Yin, T. C. T., 2002a; 2002b).

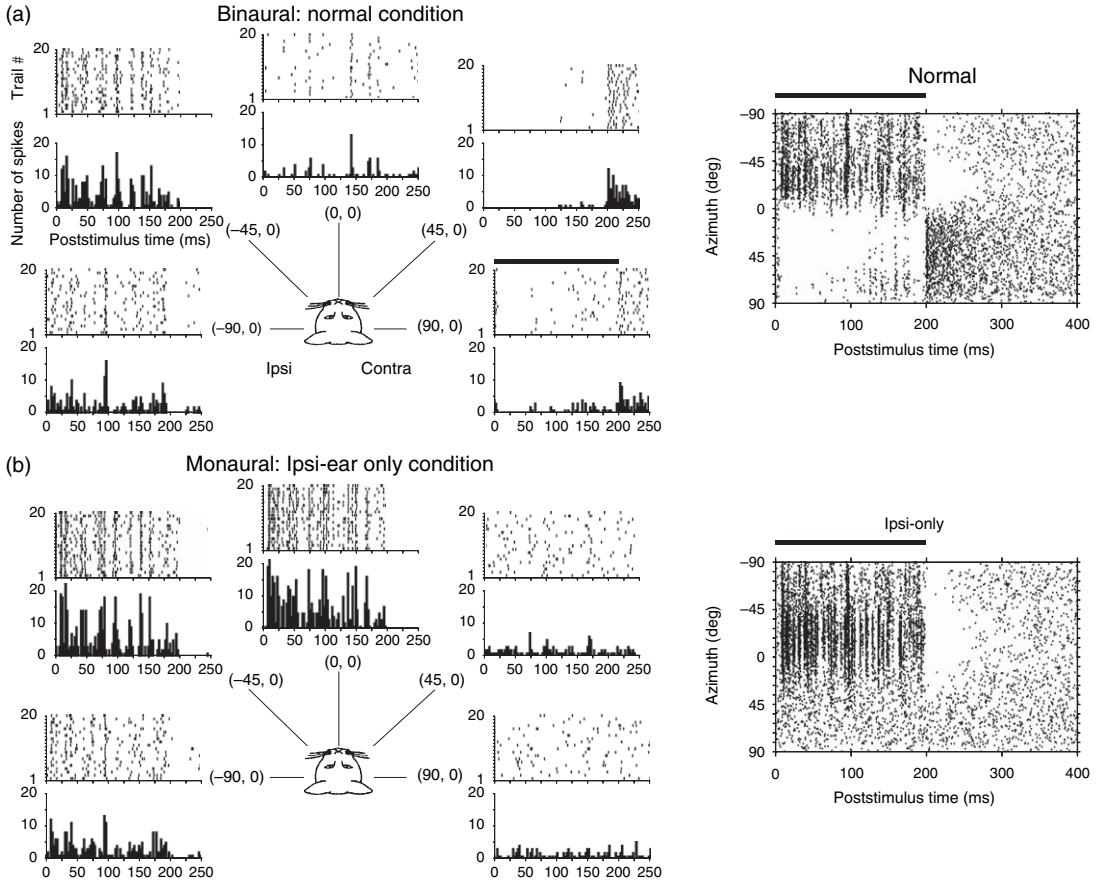

Figure 7 Lateral superior olive (LSO) neurons are sensitive to the azimuthal location of virtual-space stimuli. Responses of the same LSO neuron in Figure 6 shown as dot rasters and associated PSTHs to variations in the virtual-space azimuth of 200-ms broadband noise (black bar) stimuli. Source azimuth was manipulated by filtering noise with a left- and right-ear head-related transfer function (HRTF) appropriate for each position and presenting the stimuli over earphones. The stimuli were presented 20 times each at 21 different azimuths (right column), the responses to five of which are shown in detail (left column), and under two conditions, binaural (a) and monaural (b). (a) Responses for the normal binaural condition for which all the acoustical cues to location were presented to the two ears in their natural combination at each azimuth. The strong responses for ipsilateral azimuths and the apparent inhibition for contralateral azimuths were expected because ipsilateral sources result in higher sound levels at the excitatory ear relative to those at the contralateral ear, whereas contralateral sources result in higher sound levels at the inhibitory ear than at the excitatory ear. The raster to the right plots the responses of the neuron for all 21 azimuths. Note the strong suppression of responses during stimulus presentation for contralateral (positive) azimuths. (b) Responses in the monaural ipsi-ear only condition. The stimulus was presented only to the excitatory ear as a function of azimuth; the contralateral earphone was simply shut off. At all azimuths, responses are greater than was the case for binaural stimulation revealing the effect of the contralateral inhibition observed in the example shown in (a). The raster to the right shows the responses for all 21 azimuths. Inhibition that was apparent in the binaural condition (a) is no longer present. Reprinted with permission from Tollin, D. J. and Yin, T. C. T. 2002. The coding of spatial location by single units in the lateral superior olive of the cat. I. Spatial receptive fields in azimuth. J. Neurosci. 22, 1454–1467.

Consistent with that found with tone stimuli, all neurons appeared to encode information about sound location only for stimuli in the ipsilateral field as most were inhibited for sources contralateral to the midline (Figure 8; normalized SRFs).

Strong correlations were documented between the shapes of the SRFs as a function of the CF of the neuron being studied and the azimuth-dependent patterns of ILD actually present in a narrow band of frequencies around the CF of the neurons (see Figure 2(b)). For example, neurons with CFs <10 kHz had sigmoidally shaped SRFs with shallow rate-azimuth slopes at the midline (Figure 8, black) while neurons with CFs >10 kHz (Figure 8, red) had more complex-shaped SRFs and steeper rate–azimuth slopes at the midline. The sensitivity to

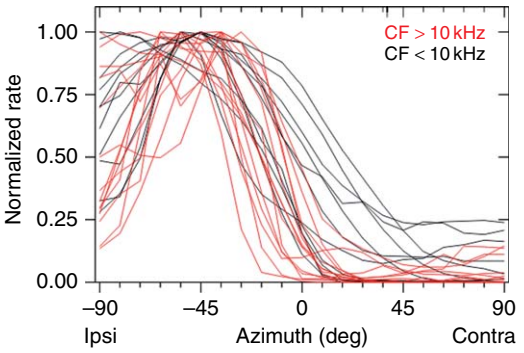

Figure 8 Spatial receptive fields (SRFs) in azimuth of lateral superior olive (LSO) neurons. LSO neurons encode azimuth for sources in the ipsilateral hemisphere as the responses of most neurons for contralateral sources are suppressed. SRF shape also depends upon the characteristic frequency (CF) of each neuron. Neurons with CFs <10 kHz (black) have sigmodally shaped SRFs and the slope of the rate-azimuth function near the midline is shallow. Neurons with CFs >10 kHz (red) have complex SRFs that exhibit peaks and dips and the slope of the rate–azimuth function near the midline is steep. In many ways, the CF dependence on SRF shape mirrors the CF dependence that the interaural level difference (ILD) cue itself displays as a function of azimuth (e.g., Figure 2(f)). This reinforces the hypothesis that LSO neurons are encoding the ILD computed through their frequency selectivity. Reprinted with permission from Tollin, D. J. and Yin, T. C. T. 2002. The coding of spatial location by single units in the lateral superior olive of the cat. I. Spatial receptive fields in azimuth. J. Neurosci. 22, 1454–1467.

azimuth in LSO neurons was also found to be maintained over a wider range of overall sound levels under binaural than monaural ipsi-only stimulation where the neural responses saturated at higher levels (Tollin, D. J. and Yin, T. C. T., 2002a).

But what about the documented sensitivity of LSO neurons to the other cues and what do those cues contribute, if any, to the SRFs? To test this, the VS stimuli were digitally manipulated in such a way as to hold constant (or vary) with changes in stimulus azimuth each of the localization cues in turn while varying (or holding constant) the remaining cues (Tollin, D. J. and Yin, T. C. T., 2002b). Figure 9 shows the normal binaural and ipsi-only SRFs (Figure 9(a)) for the same neuron as in Figures 6 and 7 and the SRFs that result from manipulating the ILD cues (Figure 9(b)), the ITD cues (Figure 9(c)), and the monaural spectral cues (Figure 9(d)). In each of these three panels, the normal SRF is shown for reference (filled circles) and the two additional plots show the effect on the SRF of manipulating one of the cues by holding it at a constant value for all azimuths while letting the remaining cues vary naturally (open squares) or allowing only that cue to vary with azimuth while holding the remaining two cues constant (red squares). When a cue or cues were held constant, they were set to values consistent with the cues provided by a stimulus delivered from the midline (i.e., 0 dB ILD, 0 μs ITD, and the spectral shape for this position). When the ILD cue was manipulated it was done so by appropriately increasing or decreasing the amplitude of the stimuli presented to each ear until the desired ILD, as computed through a 1/3-octave Gaussian filter centered on the CF of the unit being studied, was obtained.

Through the selective manipulation of the cues, it was determined directly that the ILDs present in a small band of frequencies around the CF of each neuron were the primary determinants of the VS fields that were measured under the normal binaural conditions for which all the cues varied naturally (Tollin, D. J. and Yin, T. C. T., 2002b). For example, when the ILD cue varied naturally with azimuth but the ITD and the monaural spectral shape cues held constant (Figure 9(b), Δ-ILD), the SRF was similar to that measured when all three of these cues varied naturally with azimuth. The ITD and spectral cues were held fixed for all azimuths in the Δ-ILD condition, so the close correspondence between the resulting SRF and the normal SRF strongly implicate the ILD in the narrowband of frequencies around the CF of the stimuli as the primary determinant of the normal SRF for this neuron. Supporting this notion, for those manipulation conditions where the ILD cue in the same narrowband was held constant at 0 dB for all azimuths (red squares in Figure 9(c), Δ-ITD condition and in Figure 9(d), Δ-ISD condition), there was no modulation of the response with azimuth. Although ILD was held constant at 0 dB in those latter two conditions, the ITD and spectral cues were changed naturally, but the response was not modulated. Hence, ILDs and not ITDs or the monaural spectral shape determined the SRF for this LSO neuron. Similar results were obtained across a population of LSO neurons with different CFs (Tollin, D. J. and Yin, T. C. T., 2002b). The finding that ITDs and the spectral cues contributed little to the spatial selectivity is consistent with earlier reports of ILD dominance in LSO responses to complex sounds with limited combinations of physiologically plausible ITDs and ILDs (Caird, D. and Klinke, R., 1983; Joris, P. X. and Yin, T. C. T., 1995). However, for stimuli of transient nature, ITDs

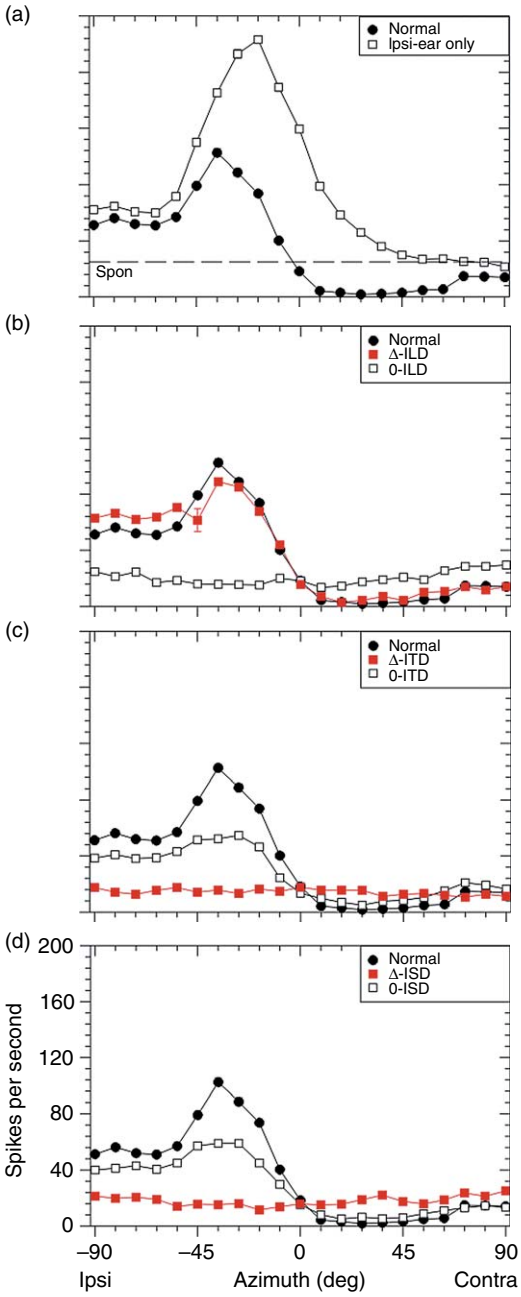

Figure 9 The primary determinant of the spatial selectivity of lateral superior olive (LSO) neurons is the interaural level difference (ILD) cue. (a) The spatial receptive field (SRF) in azimuth of the same LSO neuron shown in Figures 6 and 7 plotted as the mean discharge rate ± 1 SEM for both the normal binaural condition (filled circles) and the monaural ipsi-ear only condition (open squares). The inhibition resulting from contralateral sound sources (e.g., Figure 7(a)) is visible in the SRFs. The contribution of the contralateral inhibition to the SRF can be seen by comparing the normal SRF to the ipsi-ear only SRF. The dashed line indicates the spontaneous discharge rate. (b)–(d) Effects on the SRF in azimuth of manipulating the three cues to location. Each cue was either held constant while the remaining two cues were allowed to vary naturally with changes in the azimuth of the sound sources (open squares) or changed naturally with azimuth while the remaining cues were held at fixed values (red squares). Cues held constant took values consistent with those for the midline location; that is, zero ITD and ILD and monaural spectral shape cues identical for a stimulus at the midline. For comparison, the normal binaural SRF is shown in each panel (filled circles). (b) Effects of manipulating the ILD cues. (c) Effects of manipulating the ITD cues. (d) Effects of manipulating the monaural spectral cues. Only for those conditions were the ILD cues were changed with azimuth (Δ-ILD in (b), 0-ITD in (c), and 0-ISD in (d)) were the responses similar to the response under the normal binaural condition where all the cues varied with azimuth. As shown in (c) and (d), there was little response modulation as either ITD (Δ-ITD) or the spectral cues (Δ-ISD) were varied in isolation with azimuth.

can have a larger effect through the mechanisms described in Figure 4; however, the ranges of ITDs used in those experiments were often well outside the physiological range (Caird, D. and Klinke, R., 1983; Park, T. J. *et al.*, 1996; Irvine, D. R. *et al.*, 2001).

3.36.4 Comparative Studies Implicate the LSO as Necessary for ILD Processing

There are marked differences in the relative sizes of the major nuclei comprising the SOC across mammalian species (Harrison, J. M. and Irving, R., 1966; Irving, R. and Harrison, J. M., 1967; Glendenning, K. K. and Masterton, R. B., 1998; Moore, J. K., 2000). The correlation between the sizes of the SOC nuclei and the availability and use of the localization cues provides important clues to the different functions of these nuclei. On the one hand, mice, hedgehogs, and echolocating bats have extremely large and well-developed LSO and MNTB but small and sparse MSO. On the other hand, in primates, including humans, the LSO and MNTB tend to be small but the MSO large and well developed. In the middle are mammals, like cats, dogs, chinchillas, and guinea-pigs, for which all three nuclei are well developed. Despite differences in overall size, there is a consistent parallel development of MNTB and LSO in virtually all species examined such that mammals with large LSOs typically also have large MNTBs and *vice versa*. This finding supports the hypothesis that the LSO and the ipsilateral MNTB form a functional circuit. Interestingly, in a study of 53 mammalian species, while all mammals possessed a LSO and MNTB, the MSO was the only nucleus out of 10 examined that was found to be entirely absent in some mammals (Glendenning, K. K. and Masterton, R. B., 1998).

If both the LSO and the MSO contribute to sound localization, why are there large variations in the relative sizes of the MSO and LSO in different species? One possibility is that the types and magnitudes of the localization cues available to these species differ because of variations in the diameter of the head (see Section 3.36.2). For example, ITDs are not useful for animals with very small heads because the magnitude of the maximum ITDs is small. Yet in these same mammals large ILDs are available, but only for high-frequency sounds with wavelengths smaller than the diameter of the head. Based on this logic, it has been hypothesized that the main selective pressure for the evolution of high-frequency hearing in mammals has been the need to use ILDs for accurate localization, rather than for communication (Masterton, B. *et al.*, 1969). Supporting this hypothesis, there is a large significant correlation between high-frequency hearing and interaural diameter so that mammals with smaller heads have higher-frequency hearing limits than those with larger heads (Masterton, B. and Diamond, I. T., 1967). Moreover, anatomically, the ratios of the sizes of the major nuclei of the SOC are also closely related to the frequency range of hearing in the species (Masterton, B. and Diamond, I. T., 1973) so that, in general, the higher the frequency the animals can detect, the larger and more developed the MNTB/LSO circuit, whereas the lower the frequencies that animals can detect, the larger and more well-developed the MSO.

Given the comparative anatomical findings and the useable localization cues available to different species, Masterton B. and Diamond I. T. (1967) suggested that the MSO encodes ITDs and the LSO encodes ILDs. Psychophysical data supports this hypothesis. For example, the hedgehog lacks an MSO and cannot use ITDs to localize low-frequency sounds, but can use ILDs for high frequencies (Masterton, B. *et al.*, 1975). Horses and cattle have diffuse and disorganized LSOs and cannot use ILDs to localize high-frequency sounds (Heffner, R. S. and Heffner, H. E., 1986). In general, those species that localize low-frequency sounds poorly or that rely exclusively on high-frequency sound have well-developed LSO and MNTB and poorly developed MSO (Irving, R. and Harrison, J. M., 1967; Masterton, B. *et al.*, 1969; Masterton, B. and Diamond, I. T., 1973; Masterton, B. *et al.*, 1975; Heffner, R. S. and Heffner, H. E., 1986). Conversely, animals that localize high-frequency sounds poorly or that typically use low-frequency sounds for communication, like humans, tend to have a prominent MSO but a smaller LSO and MNTB (Harrison, J. M. and Feldmam, 1970; Moore, J. K., 2000). Finally, in species that are sensitive to low and high frequencies, like the cat, both the MSO and the LSO/MNTB are prominent and they are able to locate accurately sounds of both low and high frequencies.

Naturally, there are exceptions. For example, many hoofed mammals including pigs, cattle, horses, and goats possess a LSO and MNTB, but seem unable to use ILDs in high-frequency sounds for localization (Heffner, R. S. and Heffner, H. E., 1986; 1989). And due to increased head diameter and good low-frequency hearing humans have a predictably smaller

LSO; however, the MNTB is either very small (Richter, E. A. *et al.*, 1983) or nonexistent (Moore, J. K., 2000; Bazwinsky, I. *et al.*, 2003) despite our extraordinary behavioral sensitivity to ILDs over virtually the entire range of hearing (Mills, A. W., 1960). Given these important exceptions, in addition to head diameter and the differential availability of the ITD and ILD cues, there must have been additional evolutionary pressures for the divergent development of the SOC nuclei across mammals. Interestingly, head diameter alone accounts for only a fraction of the variance of sound localization abilities in a large number of mammals tested (Heffner, R. S., 1997). The one factor (among many tested) that can account for much of this variability is the width of the best field of vision (Heffner, R. S., 1997), supporting earlier hypotheses that the primary function of the binaural auditory system is to direct the eyes to the source of the sound to permit further visual inspection (Harrison, J. M. and Irving, R., 1966). Taken as a whole, these comparative studies strongly implicate the LSO as necessary for ILD processing consistent with our review of the anatomical and physiological data above.

3.36.5 Conclusion

The duplex theory posits that the localization of low- and high-frequency sounds is based on ITDs and ILDs, respectively. Early in the ascending auditory pathway, anatomical and physiological specializations in the nuclei of the SOC form a neural basis for the duplex theory where the MSO is thought to encode ITD cues while the LSO, along with the inhibitory input from the MNTB, is thought to encode ILDs. Acoustically, ILDs are available predominately for high frequencies with wavelengths smaller than the diameter of the head and depend jointly on sound source azimuth and frequency. The processing of ILD was shown to be dependent upon several remarkable specializations in the anatomy, biophysical characteristics, and the physiological response properties of the LSO neurons and their afferents. The specializations in the LSO afferents permit the faithful representation of the spectral and temporal attributes of the sound arriving at the two ears. And the specializations at the LSO allow ILD to be encoded based on these representations on nearly a frequency-by-frequency and time-by-time basis. From a functional perspective, comparative studies of the SOC nuclei, the available localization cues, and the localization abilities of a large number of mammals have substantiated these findings. In summary, the literature reviewed here collectively supports the hypothesis that the LSO is the initial ILD processor in the mammalian ascending auditory pathway.

Acknowledgment

This work was supported by NIH grant DC006865.

References

Adams, J. C. and Mugnaini, E. 1990. Immunocytochemical evidence for inhibitory and disinhibitory circuits in the superior olive. Hear. Res. 49, 281–298.

Banks, M. I. and Smith, P. H. 1992. Intracellular recordings from neurobiotin-labeled cells in brain slices of the rat medial nucleus of the trapezoid body. J. Neurosci. 12, 2819–2837.

Batra, R., Kuwada, S., and Fitzpatrick, D. C. 1997. Sensitivity to interaural temporal disparities of low- and high- frequency neurons in the superior olivary complex. I. Heterogeneity of responses. J. Neurophysiol. 78, 1222–1236.

Bazwinsky, I., Hilbig, H., Bidmon, H. J., and Rubsamen, R. 2003. Characterization of the human superior olivary complex by calcium binding proteins and neurofilament H (SMI-32). J. Comp. Neurol. 456, 292–303.

Bledsoe, S. C., Jr., Snead, C. R., Helfert, R. H., Prasad, V., Wenthold, R. J., and Altschuler, R. A. 1990. Immunocytochemical and lesion studies support the hypothesis that the projection from the medial nucleus of the trapezoid body to the lateral superior olive is glycinergic. Brain Res. 517, 189–194.

Boudreau, J. C. and Tsuchitani, C. 1968. Binaural interaction in the cat superior olive S segment. J. Neurophysiol. 31, 442–454.

Brawer, J. R. and Morest, D. K. 1975. Relations between auditory nerve endings and cell types in the cat's anteroventral cochlear nucleus seen with the Golgi method and Normarski optics. J. Comp. Neurol. 160, 491–506.

Britt, R. and Starr, A. 1976. Synaptic events and discharge patterns of cochlear nucleus cells. II. Frequency-modulated tones. J. Neurophysiol. 39, 179–194.

Brownell, W. E. 1975. Organization of the cat trapezoid body and the discharge characteristics of its fibers. Brain Res. 94, 413–433.

Brownell, W. E., Manis, P. B., and Ritz, L. A. 1979. Ipsilateral inhibitory responses in the cat lateral superior olive. Brain Res. 177, 189–193.

Caird, D. and Klinke, R. 1983. Processing of binaural stimuli by cat superior olivary complex neurons. Exp. Brain Res. 52, 385–399.

Calford, M. B. and Pettigrew, J. D. 1984. Frequency dependence of directional amplification at the cat's pinna. Hear. Res. 14, 13–19.

Cant, N. B. 1984. The fine structure of the lateral superior olivary nucleus of the cat. J. Comp. Neurol. 227, 63–77.

Cant, N. B. and Casseday, J. H. 1986. Projections from the anteroventral cochlear nucleus to the lateral and medial superior olivary nuclei. J. Comp. Neurol. 247, 457–476.

Cant, N. B. and Morest, D. K. 1979. Organization of the neurons in the anterior division of the anteroventral cochlear nucleus of the cat. Light-microscopic observations. Neuroscience 4, 1909–1923.

Caspary, D. M. and Faingold, C. L. 1989. Non-*N*-methyl-D-aspartate receptors may mediate ipsilateral excitation at lateral superior olivary synapses. Brain Res. 503, 83–90.

Casseday, J. H. and Neff, W. D. 1973. Localization of pure tones. J. Acoust. Soc. Am. 54, 365–372.

Elverland, H. H. 1978. Ascending and intrinsic projections of the superior olivary complex in the cat. Exp. Brain Res. 32, 117–134.

Finlayson, P. G. and Caspary, D. M. 1989. Synaptic potentials of chinchilla lateral superior olivary neurons. Hear. Res. 38, 221–228.

Finlayson, P. G. and Caspary, D. M. 1991. Low-frequency neurons in the lateral superior olive exhibit phase-sensitive binaural inhibition. J. Neurophysiol. 65, 598–605.

Friauf, E. and Ostwald, J. 1988. Divergent projections of physiologically characterized rat ventral cochlear nucleus neurons as shown by intra-axonal injection of horseradish peroxidase. Exp. Brain Res. 73, 263–284.

Glendenning, K. K. and Baker, B. N. 1988. Neuroanatomical distribution of receptors for three potential inhibitory neurotransmitters in the brainstem auditory nuclei of the cat. J. Comp. Neurol. 275, 288–308.

Glendenning, K. K. and Masterton, R. B. 1983. Acoustic chiasm: efferent projections of the lateral superior olive. J. Neurosci. 3, 1521–1537.

Glendenning, K. K. and Masterton, R. B. 1998. Comparative morphometry of mammalian central auditory systems: variation in nuclei and form of the ascending system. Brain Behav. Evol. 51, 59–89.

Glendenning, K. K., Baker, B. N., Hutson, K. A., and Masterton, R. B. 1992. Acoustic chiasm V: inhibition and excitation in the ipsilateral and contralateral projections of LSO. J. Comp. Neurol. 319, 100–122.

Glendenning, K. K., Hutson, K. A., Nudo, R. J., and Masterton, R. B. 1985. Acoustic chiasm. II: Anatomical basis of binaurality in lateral superior olive of cat. J. Comp. Neurol. 232, 261–285.

Glendenning, K. K., Masterton, R. B., Baker, B. N., and Wenthold, R. J. 1991. Acoustic chiasm. III: Nature, distribution, and sources of afferents to the lateral superior olive in the cat. J. Comp. Neurol. 310, 377–400.

Guinan, J. J., Jr., Guinan, S. S., and Norris, B. E. 1972a. Single auditory units in the superior olivary complex. I: Responses to sounds and classifications based on physiological properties. Int. J. Neurosci. 4, 101–120.

Guinan, J. J., Jr., Norris, B. E., and Guinan, S. S. 1972b. Single auditory units in the superior olivary complex. II: Location of unit categories and tonotopic organization. Int. J. Neurosci. 4, 147–166.

Harrison, J. M. and Feldman, M. L. 1970. Anatomical aspects of thecochlear nucleus and superior olivary complex. Contrib. Sens. Physiol. 4, 95–142.

Harrison, J. M. and Irving, R. 1966. Visual and nonvisual auditory systems in mammals. Anatomical evidence indicates two kinds of auditory pathways and suggests two kinds of hearing in mammals. Science 154, 738–743.

Harrison, J. M. and Warr, W. B. 1962. A study of the cochlear nuclei and ascending auditory pathways of the medulla. J. Comp. Neurol. 119, 341–380.

Heffner, R. S. 1997. Comparative study of sound localization and its anatomical correlates in mammals. Acta Otolaryngol. Suppl. 532, 46–53.

Heffner, R. S. and Heffner, H. E. 1986. Localization of tones by horses: use of binaural cues and the role of the superior olivary complex. Behav. Neurosci. 100, 93–103.

Heffner, R. S. and Heffner, H. E. 1989. Sound localization, use of binaural cues and the superior olivary complex in pigs. Brain Behav. Evol. 33, 248–258.

Helfert, R. H., Bonneau, J. M., Wenthold, R. J., and Altschuler, R. A. 1989. GABA and glycine immunoreactivity in the guinea pig superior olivary complex [published erratum appears in Brain Res. 1990 Feb 12; 509(1): 180]. Brain Res. 501, 269–286.

Helfert, R. H., Juiz, J. M., Bledsoe, S. C., Jr., Bonneau, J. M., Wenthold, R. J., and Altschuler, R. A. 1992. Patterns of glutamate, glycine, and GABA immunolabeling in four synaptic terminal classes in the lateral superior olive of the guinea pig. J. Comp. Neurol. 323, 305–325.

Henkel, C. K. and Brunso-Bechtold, J. K. 1995. Development of glycinergic cells and puncta in nuclei of the superior olivary complex of the postnatal ferret. J. Comp. Neurol. 354, 470–480.

Irvine, D. R. F. 1986. The Auditory Brainstem: Processing of Spectral and Spatial Information, pp. 1–277. Springer-Verlag.

Irvine, D. R. 1987. Interaural intensity differences in the cat: changes in sound pressure level at the two ears associated with azimuthal displacements in the frontal horizontal plane. Hear. Res. 26, 267–286.

Irvine, D. R., Park, V. N., and McCormick, L. 2001. Mechanisms underlying the sensitivity of neurons in the lateral superior olive to interaural intensity differences. J. Neurophysiol. 86, 2647–2666.

Irving, R. and Harrison, J. M. 1967. The superior olivary complex and audition: a comparative study. J. Comp. Neurol. 130, 77–86.

Johnson, D. H. 1980. The relationship between spike rate and synchrony in responses of auditory-nerve fibers to single tones. J. Acoust. Soc. Am. 68, 1115–1122.

Joris, P. X. 1996. Envelope coding in the lateral superior olive. II. Characteristic delays and comparison with responses in the medial superior olive. J. Neurophysiol. 76, 2137–2156.

Joris, P. X. and Yin, T. C. T. 1992. Responses to amplitude-modulated tones in the auditory nerve of the cat. J. Acoust. Soc. Am. 91, 215–232.

Joris, P. X. and Yin, T. C. T. 1995. Envelope coding in the lateral superior olive. I. Sensitivity to interaural time differences. J. Neurophysiol. 73, 1043–1062.

Joris, P. X. and Yin, T. C. T. 1998. Envelope coding in the lateral superior olive. III. Comparison with afferent pathways. J. Neurophysiol. 79, 253–269.

Joris, P. X., Carney, L. H., Smith, P. H., and Yin, T. C. T. 1994. Enhancement of neural synchronization in the anteroventral cochlear nucleus. I. Responses to tones at the characteristic frequency. J. Neurophysiol. 71, 1022–1036.

Kavanagh, G. L. and Kelly, J. B. 1992. Midline and lateral field sound localization in the ferret (*Mustela putorius*): contribution of the superior olivary complex. J. Neurophysiol. 67, 1643–1658.

Kiang, N. Y. S., Watanabe, T., Thomas, E. C., and Clark, L. F. 1965. Discharge patterns of sinlge fibers in the cat's auditory nerve. MIT Press.

Kopp-Scheinpflug, C., Lippe, W. R., Dorrscheidt, G. J., and Rubsamen, R. 2003. The medial nucleus of the trapezoid body in the gerbil is more than a relay: comparison of pre- and postsynaptic activity. J. Assoc. Res. Otolaryngol. 4, 1–23.

Korada, S. and Schwartz, I. R. 1999. Development of GABA, glycine, and their receptors in the auditory brainstem of gerbil: a light and electron microscopic study. J. Comp. Neurol. 409, 664–681.

Loftus, W. C., Bishop, D. C., Saint Marie, R. L., and Oliver, D. L. 2004. Organization of binaural excitatory and inhibitory inputs to the inferior colliculus from the superior olive. J. Comp. Neurol. 472, 330–344.

Martin, R. L. and Webster, W. R. 1989. Interaural sound pressure level differences associated with sound-source locations in the frontal hemifield of the domestic cat. Hear. Res. 38, 289–302.

Masterson, B. and Diamond, I. T. 1967. Medial superior olive and sound localization. Science 155, 1696–1697.
Masterton, B. and Diamond, I. T. 1973. Hearing: Central Neural Mechanisms. In: Handbook of Perception: Biology of Perceptual Systems (*eds*. E. C. Carterett and M. P. Friedman), pp. 408–448. Academic.
Masterton, B., Heffner, H., and Ravizza, R. 1969. The evolution of human hearing. J. Acoust. Soc. Am. 45, 966–985.
Masterton, B., Jane, J. A., and Diamond, I. T. 1967. Role of brainstem auditory structures in sound localization. I. Trapezoid body, superior olive, and lateral lemniscus. J. Neurophysiol. 30, 341–359.
Masterton, B., Thompson, G. C., Bechtold, J. K., and RoBards, M. J. 1975. Neuroanatomical basis of binaural phase-difference analysis for sound localization: a comparative study. J. Comp. Physiol. Psychol. 89, 379–386.
May, B. J. and Huang, A. Y. 1997. Spectral cues for sound localization in cats: a model for discharge rate representations in the auditory nerve. J. Acoust. Soc. Am. 101, 2705–2719.
Mills, A. W. 1958. On the minimum audible angle. J. Acoust. Soc. Am. 30, 237–246.
Mills, A. W. 1960. Lateralization of high frequency tones. J. Acoust. Soc. Am. 32, 132–134.
Moller, A. R. 1974. Responses of units in the cochlear nucleus to sinusoidally amplitude-modulated tones. Exp. Neurol. 45, 105–117.
Moore, D. R. and Irvine, D. R. 1979. A developmental study of the sound pressure transformation by the head of the cat. Acta Otolaryngol. 87, 434–440.
Moore, J. K. 2000. Organization of the human superior olivary complex. Microsc. Res. Tech. 51, 403–412.
Moore, M. J. and Caspary, D. M. 1983. Strychnine blocks binaural inhibition in lateral superior olivary neurons. J. Neurosci. 3, 237–242.
Morest, D. K. 1973. Auditory neurons of the brain stem. Adv. Otorhinolaryngol. 20, 337–356.
Musicant, A. D., Chan, J. C., and Hind, J. E. 1990. Direction-dependent spectral properties of cat external ear: new data and cross-species comparisons. J. Acoust. Soc. Am. 87, 757–781.
Osen, K. K. 1969. The intrinsic organization of the cochlear nuclei in the cat. Acta Otolaryngol. 67, 352–359.
Park, T. J., Grothe, B., Pollak, G. D., Schuller, G., and Koch, U. 1996. Neural delays shape selectivity to interaural intensity differences in the lateral superior olive. J. Neurosci. 16, 6554–6566.
Park, T. J., Klug, A., Holinstat, M., and Grothe, B. 2004. Interaural level difference processing in the lateral superior olive and the inferior colliculus. J. Neurophysiol. 92, 289–301.
Park, T. J., Monsivais, P., and Pollak, G. D. 1997. Processing of interaural intensity differences in the LSO: role of interaural threshold differences. J. Neurophysiol. 77, 2863–2878.
Pfeiffer, R. R. and Kim, D. O. 1975. Cochlear nerve fiber responses: distribution along the cochlear partition. J. Acoust. Soc. Am. 58, 867–869.
Phillips, D. P., Calford, M. B., Pettigrew, J. D., Aitkin, L. M., and Semple, M. N. 1982. Directionality of sound pressure transformation at the cat's pinna. Hear. Res. 8, 13–28.
Poon, P. W. and Brugge, J. F. 1993. Virtual-space receptive fields of single auditory nerve fibers. J. Neurophysiol. 70, 667–676.
Rayleigh, L. J. S. 1907. On our perception of sound direction. Philos. Mag. Ser. 6, 214–232.
Rhode, W. S. and Greenberg, S. 1994. Encoding of amplitude modulation in the cochlear nucleus of the cat. J. Neurophysiol. 71, 1797–1825.
Rhode, W. S. and Smith, P. H. 1986. Encoding timing and intensity in the ventral cochlear nucleus of the cat. J. Neurophysiol. 56, 261–286.
Rice, J. J., May, B. J., Spirou, G. A., and Young, E. D. 1992. Pinna-based spectral cues for sound localization in cat. Hear. Res. 58, 132–152.
Rice, J. J., Young, E. D., and Spirou, G. A. 1995. Auditory-nerve encoding of pinna-based spectral cues: rate representation of high-frequency stimuli. J. Acoust. Soc. Am. 97, 1764–1776.
Richter, E. A., Norris, B. E., Fullerton, B. C., Levine, R. A., and Kiang, N. Y. S. 1983. Is there a medial nucleus of the trapezoid body in humans? Am. J. Anat. 68, 157–166.
Rose, J. E., Galambos, R., and Hughes, J. R. 1959. Microelectrode studies of the cochlear nuclei of the cat. Bull. Johns Hopkins Hosp. 104, 211–251.
Roth, G. L., Kochhar, R. K., and Hind, J. E. 1980. Interaural time differences: implications regarding the neurophysiology of sound localization. J. Acoust. Soc. Am. 68, 1643–1651.
Saint Marie, R. L., Ostapoff, E.-M., Morest, D. K., and Wenthold, R. J. 1989. Glycine immunoreactive projection of the cat lateral superior olive: possible role in midbrain ear dominance. J. Comp. Neurol. 279, 382–396.
Sanes, D. H. 1990. An *in vitro* analysis of sound localization mechanisms in the gerbil lateral superior olive. J. Neurosci. 10, 3494–3506.
Sanes, D. H. and Rubel, E. W. 1988. The ontogeny of inhibition and excitation in the gerbil lateral superior olive. J. Neurosci. 8, 682–700.
Sanes, D. H., Geary, W. A., Wooten, G. F., and Rubel, E. W. 1987. Quantitative distribution of the glycine receptor in the auditory brainstem of the gerbil. J. Neurosci. 7, 3793–3802.
Shneiderman, A. and Henkel, C. K. 1985. Evidence of collateral axonal projections to the superior olivary complex. Hear. Res. 19, 199–205.
Smith, P. H. and Rhode, W. S. 1987. Characterization of HRP-labeled globular bushy cells in the cat anteroventral cochlear nucleus. J. Comp. Neurol. 266, 360–375.
Smith, P. H., Joris, P. X., Carney, L. H., and Yin, T. C. T. 1991. Projections of physiologically characterized globular bushy cell axons from the cochlear nucleus of the cat. J. Comp. Neurol. 304, 387–407.
Smith, P. H., Joris, P. X., and Yin, T. C. T. 1993. Projections of physiologically characterized spherical bushy cell axons from the cochlear nucleus of the cat: evidence for delay lines to the medial superior olive. J. Comp. Neurol. 331, 245–260.
Smith, P. H., Joris, P. X., and Yin, T. C. T. 1998. Anatomy and physiology of principal cells of the medial nucleus of the trapezoid body (MNTB) of the cat. J. Neurophysiol. 79, 3127–3142.
Spangler, K. M., Warr, W. B., and Henkel, C. K. 1985. The projections of principal cells of the medial nucleus of the trapezoid body in the cat. J. Comp. Neurol. 238, 249–262.
Spirou, G. A., Brownell, W. E., and Zidanic, M. 1990. Recordings from cat trapezoid body and HRP labeling of globular bushy cell axons. J. Neurophysiol. 63, 1169–1190.
Stevens, S. and Newman, E. 1936. The localization of actual sources of sound. Am. J. Psychol. 48, 297–306.
Stotler, W. A. 1953. An experimental study of the cells and connections of the superior olivary complex of the cat. J. Comp. Neurol. 98, 401–432.
Tolbert, L. P., Morest, D. K., and Yurgelun-Todd, D. A. 1982. The neuronal architecture of the anteroventral cochlear nucleus of the cat in the region of the cochlear nerve root: horseradish peroxidase labelling of identified cell types. Neuroscience 7, 3031–3052.
Tollin, D. J. 2003. The lateral superior olive: a functional role in sound source localization. Neuroscientist 9, 127–143.

Tollin, D. J. 2004. The development of the acoustical cues to sound location in cats. J. Assoc. Res. Otolaryngol. 27–56.
Tollin, D. J. and Yin, T. C. T. 2002a. The coding of spatial location by single units in the lateral superior olive of the cat. I. Spatial receptive fields in azimuth. J. Neurosci. 22, 1454–1467.
Tollin, D. J. and Yin, T. C. T. 2002b. The coding of spatial location by single units in the lateral superior olive of the cat. II. The determinants of spatial receptive fields in azimuth. J. Neurosci. 22, 1468–1479.
Tollin, D. J. and Yin, T. C. T. 2005. Interaural phase and level difference sensitivity in low-frequency neurons in the lateral superior olive. J. Neurosci. 25, 10648–10657.
Trussell, L. O. 2002. Cellular Mechanisms for Information Coding in Auditory Brainstem Nuclei. In: Integrative Functions in the Mammalian Auditory Pathway (*eds*. D. Oertel, A. N. Popper, and R. R. Fay), pp. 72–98. Springer-Verlag.
Tsuchitani, C. 1977. Functional organization of lateral cell groups of cat superior olivary complex. J. Neurophysiol. 40, 296–318.
Tsuchitani, C. 1997. Input from the medial nucleus of trapezoid body to an interaural level detector. Hear. Res. 105, 211–224.
Tsuchitani, C. and Boudreau, J. C. 1966. Single unit analysis of cat superior olive S segment with tonal stimuli. J. Neurophysiol. 29, 684–697.
Tsuchitani, C. and Boudreau, J. C. 1969. Stimulus level of dichotically presented tones and cat superior olive S-segment cell discharge. J. Acoust. Soc. Am. 46, 979–988.
Tsuchitani, C. and Johnson, D. H. 1991. Binaural Cues and Signal Processing in the Superior Olivary Complex. In: Neurobiology of Hearing: The Central Auditory System (*eds*. R. A. Altschuler, R. P. Bobbin, B. M. Clopton, and D. W. Hoffman), pp. 163–193. Raven.
Warr, W. B. 1966. Fiber degeneration following lesions in the anterior ventral cochlear nucleus of the cat. Exp. Neurol. 14, 453–474.
Warr, W. B. 1972. Fiber degeneration following lesions in the multipolar and globular cell areas in the ventral cochlear nucleus of the cat. Brain Res. 40, 247–270.
Wenthold, R. J., Huis, D., Altschuler, R. A., and Reeks, K. A. 1987. Glycine immunoreactivity localized in the cochlear nucleus and superior olivary complex. Neuroscience 22, 897–912.
Wiener, F. M., Pfeiffer, R. R., and Backus, A. S. N. 1966. On the sound pressure transformation by the head and auditory meatus of the cat. Acta Otolaryngol. 61, 255–269.
Wu, S. H. and Kelly, J. B. 1991. Physiological properties of neurons in the mouse superior olive: membrane characteristics and postsynaptic responses studied *in vitro*. J. Neurophysiol. 65, 230–246.
Wu, S. H. and Kelly, J. B. 1992. Synaptic pharmacology of the superior olivary complex studied in mouse brain slice. J. Neurosci. 12, 3084–3097.
Wu, S. H. and Kelly, J. B. 1994. Physiological evidence for ipsilateral inhibition in the lateral superior olive: synaptic responses in mouse brain slice. Hear. Res. 73, 57–64.

Further Reading

Tollin, D. J., Populin, L. C., Moore, J., Ruhland, J. L., and Yin, T. C. T. 2005. Sound localization performance in the cat: the effect of restraining the head. J. Neurophysiol. 93, 1223–1234.

3.37 Monaural Sound Localization Using Spectral Cues

B J May, The Johns Hopkins University School of Medicine, Baltimore, MD, USA

© 2008 Elsevier Inc. All rights reserved.

3.37.1	Overview	656
3.37.2	The Acoustic Basis of Monaural Sound Localization	657
3.37.3	Early Studies of Human Head-Related Transfer Functions	657
3.37.4	Modern Studies of Human Head-Related Transfer Functions	659
3.37.5	Directional Transfer Functions	662
3.37.5.1	Peripheral Coding of Monaural Localization Cues	663
3.37.5.2	Representation by the Rate Profiles of Auditory-Nerve Fibers	663
3.37.5.3	Modeling the Auditory-Nerve Representation of Monaural Spectral Cues	663
3.37.5.4	Distinguishing Sound Localization and Directional Acuity	666
3.37.6	Pathways of the Dorsal Cochlear Nucleus and Inferior Colliculus	668
3.37.6.1	Dorsal Cochlear Nucleus	668
3.37.6.2	Inferior Colliculus	670
3.37.7	Acoustic Manipulations of the Spectral Processing Pathway	674
3.37.7.1	Altering the Ear's Input to the Brain	674
3.37.7.2	Spectral Manipulations	675
3.37.8	Lesions of the Spectral Processing Pathway	679
3.37.8.1	Cochlear Deficits	679
3.37.8.2	Experimental Lesions of the Dorsal Cochlear Nucleus	680
3.37.8.3	Experimental Lesions of the Inferior Colliculus and Its Projections	682
3.37.9	Species Comparisons of the Spectral Processing Pathway	685
References		689

Glossary

binaural sound localization Directional hearing that requires two ears. These processes are important for localization based on the interaural time and level differences that are associated with sources in the horizontal plane. See interaural time difference, interaural level difference.

directional transfer function Acoustic measure of the outer ear's responses to free-field sounds. Unlike the head-related transfer function, this measure is based on filtering effects at a single source location versus common effects at all locations. The directional transfer function reveals which acoustic properties are idiosyncratic for the location and therefore of greatest directional significance. See head-related transfer function.

dorsal acoustic stria The output pathway of the dorsal cochlear nucleus. The projections convey spectral representations that are created in the brainstem to the inferior colliculus (ICC). See dorsal cochlear nucleus.

dorsal cochlear nucleus The dorsal subdivision of the cochlear nucleus receives inputs from the auditory nerve and projects to the inferior colliculus by way of the dorsal acoustic stria. The structure is implicated in the initial processing of spectral cues for sound localization. See spectral cues for sound localization.

head-related transfer function (HRTF) Acoustic measure of the outer ear. The transfer function is obtained by placing a probe microphone in the ear canal and measuring responses to free-field auditory stimuli. Unlike the directional transfer function, this is an absolute measure of the acoustic properties of the ear. See directional transfer function.

head shadow Attenuation created when the ear obstructs the path of a free-field sound en route to the ear. These effects are determined by the wavelength of the sound and the physical dimensions of the head. The attenuation is largest for sounds with short wavelengths and establishes the interaural level differences that dictate high-

frequency localization in the horizontal plane. See interaural level differences, lateral superior olive.

horizontal plane Imaginary plane that intersects the head at the interaural axis. A rotation in the plane proceeds front, right, back, left, and front. Tests in this plane emphasize the importance of binaural localization cues. See binaural sound localization.

inferior colliculus The auditory midbrain integrates inputs from all of the major auditory nuclei and a number of nonauditory sources. Ascending pathways with important localization roles include the essentially monaural dorsal cochlear nucleus, and the binaural lateral and medial superior olives. See dorsal cochlear nucleus, lateral superior olive, medial superior olive.

interaural level difference Difference in the level of a free-field stimulus at the two ears. The stimulus is attenuated at the ear remote to the source by the sound shadowing effect of the head. See head shadow.

interaural time difference Difference in the time of arrival of a free-field auditory stimulus at the two ears. The stimulus is delayed at the ear remote to the source by the increased distance the sound wave must travel. See medial superior olive.

lateral superior olive Binaural nucleus that receives a direct excitatory input from the ipsilateral ventral cochlear nucleus and an indirect inhibitory input from the contralateral ventral cochlear nucleus via the trapezoid body. The excitatory–inhibitory interaction endows lateral superior olive neurons with a sensitivity to interaural level differences. These binaural cues dictate high-frequency localization in the horizontal plane. See interaural level difference, horizontal plane.

lesion Surgical destruction of a neuroanatomical pathway. Resulting behavioral deficits confirm the functional significance of the damaged structure.

medial superior olive Auditory brainstem nucleus that receives bilateral excitatory inputs from the ventral cochlear nuclei. The binaural excitatory interactions are the primary site for the processing of interaural time differences. These binaural cues dominate low-frequency sound localization in the horizontal plane. See interaural time difference, horizontal plane.

median plane Imaginary plane that intersects the head at the vertical axis. A rotation in the plane proceeds front, above, back, below, and front. Tests in this plane reveal the importance of monaural localization cues. See monaural sound localization.

monaural sound localization Directional hearing in the absence of binaural localization cues. The process is demonstrated by testing impaired listeners with monaural deafness, impeded listeners with one ear plugged or partially occluded, and normal listeners attending to the median plane where binaural cues are minimized. See binaural sound localization.

spectral cues for sound localization Directional information arising from the acoustic transfer function of the outer ear. Reflections and diffractions of sound energy shape the high-frequency spectrum of complex sounds with directionally dependent notches and peaks. These cues play a dominant role in monaural sound localization. See head-related transfer function, directional transfer function, monaural sound localization.

trapezoid body Binaural pathway linking the cochlear nuclei to the superior olives. Lesions of the pathway produce profound localization deficits in the horizontal plane because they disrupt the processing of interaural time and level differences. See interaural time differences, interaural level differences, binaural sound localization.

virtual sound field Sounds that are delivered through headphones but impart the perception of externalized spatial coordinates because they convey synthetic sound localization cues. The sounds may represent the cues in isolation, in combination, or in competition to determine the acoustic basis of directional responses.

3.37.1 Overview

Monaural sound localization is traditionally defined in three experimental contexts: impaired listeners with monaural deafness, impeded listeners with one ear plugged or partially occluded, and normal listeners attending to the median plane where binaural cues are minimized. Under these conditions, source location is derived from spectral features that are added to complex sounds by the transfer function of

the head and external ear. These acoustic cues and their initial representation in the auditory system are essentially monaural. Nevertheless, there is good evidence that spectral information takes on binaural properties at higher processing levels and exerts a pervasive influence on the localization of both elevation and azimuth. This chapter uses the term monaural to distinguish these processes from the binaural comparisons of interaural time and levels differences (ITDs and ILDs, respectively) that are described elsewhere in this publication.

We begin by summarizing the acoustic basis of monaural sound localization. Classical studies continue to provide informative descriptions of the human head-related transfer functions (HRTFs) at low-frequency. Modern techniques push these measures to higher frequencies with richer spectral detail. Differences between absolute HRTF measures and directional transfer functions (DTFs) are explained. This latter measure emphasizes acoustic information that can only be revealed by identifying the uncommon features of individual HRTFs.

Virtual space stimuli derived from HRTF acoustics provide a solid foundation for neurophysiological characterizations of the mechanisms that shape directional hearing. These representations are followed from a generalized peripheral coding of monaural localization cues to specialized pathways of the dorsal cochlear nucleus and inferior colliculus (ICC). This extensive literature is organized by the concept of a discrete spectral processing pathway that functions in parallel with binaural localization processes.

A section on acoustic manipulations of the spectral processing pathway reviews a century of research with monaural listeners, ear plugging procedures, and spectral manipulations. Subsequent psychoacoustic studies with more sophisticated signal processing techniques have elaborated on these early accounts but not contradicted their basic findings. A striking aspect of this classic work is its ability to provide timeless insights into constantly evolving physiological characterizations.

A section on lesions of the spectral processing pathway explores the neuroanatomical basis of monaural sound localization. Although the definitive behavior/ablation studies of Masterton R. B. and Neff W. D. were designed to explicate the central processes that govern horizontal localization, the universal importance of monaural spatial hearing is highlighted by the patterns of recovery that follow destruction of the binaural system.

The descriptions of monaural sound localization here rely heavily on anatomical, physiological, and behavioral data from domestic cats. Another section on species comparisons of the spectral processing pathway addresses the potential specificity of specialized localization processes by relating directional acuity to the brainstem physiology of common mammalian species. Although behavioral tests are lacking in this area of comparative hearing, interesting links exist between the keen localization sense of predatory species and physiological specializations for monaural spectral coding.

3.37.2 The Acoustic Basis of Monaural Sound Localization

When sound propagates to the eardrum, it is shaped by the directional filtering properties of the HRTF. The HRTF describes the linear distortion of the sound's amplitude and phase spectrum by the reflective, dispersive, and diffractive properties of the torso, head, and pinna (Kuhn, G. F., 1987). The resulting patterns of interference combine to increase and decrease sound energy entering the ear canal. The constructive or destructive nature of interference is determined by the wavelength of the sound and the angle of incidence upon which it impinges on the ear. Consequently, HRTF-based spectral peaks and nulls (notches) change with the direction of a sound source providing robust localization cues.

3.37.3 Early Studies of Human Head-Related Transfer Functions

Early studies of the acoustic basis of human sound localization were strongly influenced by Lord Rayleigh's duplex theory (Rayleigh, L., 1907). The theory postulates the existence of two frequency-dependent processes. Low-frequency sounds are localized on the basis of ITDs and high-frequency sounds by ILDs.

Contemporary psychoacoustic assessments of human sound localization offered behavioral proof of the dual processing mode (Hartley, R. V. L. and Fry, T. C., 1921; Stevens, S. S. and Newman, E. B., 1936). Systematic errors were noted when pure tone localization was measured in the horizontal plane. The largest deficits occurred at intermediate frequencies, revealing the transition between reliable ITD and ILD cues. To a first approximation, these localization patterns could be explained by simple

geometric models that considered the physical dimensions of the head, the wavelength of the stimulus, and the direction of the sound source (Teranishi, R and Shaw, E. A. G., 1968; Woodworth, R. S., 1938).

Early characterizations of the human HRTF offered empirical support for geometric interpretations of horizontal localization. Wiener F. M. and Ross D. A. (1946) obtained these data by inserting a small, flexible probe microphone deeply into the ear canal of human subjects. The combined directional filtering effects of the torso, head, and ear were measured by recording the transformation of sound pressure near the eardrum relative to free field. An example of these measures is shown in Figure 1, which plots the average gain of 6–12 adult men at three locations in the horizontal plane. Additional measures in women were not published but apparently did not differ significantly from men.

Several features of the transfer functions are noteworthy. First, virtually all of the gains are greater than zero. The outer ear acts as an acoustic amplifier that is most efficient at frequencies between 2 and 5 kHz, where signal levels can increase by more than 20 dB relative to free field. The boost in signal energy is created by the quarter-wave resonances of the ear canal and surrounding concha (Shaw, E. A., 1974a). This property of the outer ear enhances signal detection but is not inherently directional. A similar gain profile is observed at the three locations.

Two sources of potential directional information are visible in Figure 1. As the sound location moves from in front of the observer (0° azimuth) to the ear with the probe microphone (90° azimuth), the HRTF translates to a higher gain. The shift is produced by a lessening of the head's sound shadow; that is, the attenuation of the sound by head reflections. A microphone in the contralateral ear would show a concomitant decrease in gain for the same movement because the head would more effectively block the stimulus. The resulting ILD is an essential cue for horizontal localization.

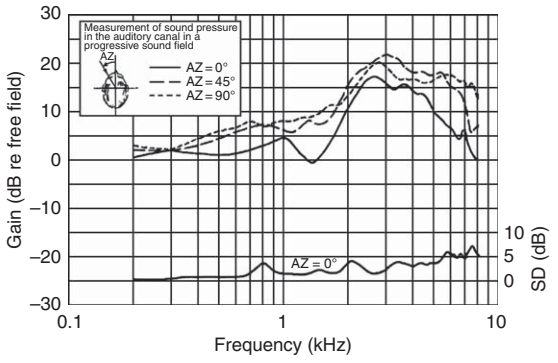

Figure 1 Gain of the head-related transfer function (HRTF) at three azimuths (AZs) in the horizontal plane. Each function represents the average of 6–12 adult men. Variation between subjects is indicated by the SD of frequency measures at 0° azimuth (bottom). Reused with permission from Wiener, F. M. and Ross, D. A. The Journal of the Acoustical Society of America, 18, 401 (1946). Copyright 1946, Acoustical Society of America.

The magnitude of the head shadow depends on the wavelength of the sound in relation to the observer's head size. The functions converge at long wavelengths below 400 Hz and diverge by as much as 15 dB at short wavelengths above 4 kHz. As a result, the ILD increases in magnitude and exerts a more direct influence on localization behavior at higher frequencies. The binaural disparity may be conveyed by broadband sounds or simple tones.

Further inspection of high-frequency filtering effects reveals that the acoustic axis of the outer ear is pointed slightly forward. Sounds reaching the ear canal from 45° are less attenuated than the more forward or eccentric locations. By analogy to retinal acuity, this preferred path has been designated the *acoustic fovea* (Middlebrooks, J. C., and Green, D. M., 1991).

A second directional cue is communicated by changes in the spectral shape of the HRTFs. Each function reflects movements of sound source azimuth with a unique maximum gain. The frequency of the prominent null seen in the 0° HRTF is similarly affected by movements in elevation that are not shown here. These spectral peaks and notches are only fully represented in broadband sounds. As a result, sound localization in the horizontal plane is sensitive to manipulations of stimulus bandwidth (Butler, R. A. and Flannery, R., 1980; Flannery, R. and Butler, R. A., 1981) and accurate localization in the median plane is virtually impossible for narrowband stimuli (Blauert, J., 1969/1970; Middlebrooks, J. C., 1992). These perceptual effects will be described later.

The stability of the HRTF measures is indicated by standard deviations (SDs) at the bottom of Figure 1. The statistical analysis was applied across subjects to each frequency in the HRTF at 0° azimuth. Although variation was quite low at low frequencies, the SD progressively increased at higher frequencies. This variability arises from the inconsistency of high-frequency acoustic measures (Wightman, F. L. and Kistler, D. J., 1989a), as well as actual individual differences (Middlebrooks, J. C., 1999a).

3.37.4 Modern Studies of Human Head-Related Transfer Functions

Early studies of the human HRTF provide only partial descriptions of the spectral features that are critical for monaural sound localization. Technical limitations of the era made it impossible to record inside the ear canal at frequencies approaching the upper bounds of human hearing. When recordings were possible, measurements were often made at discrete frequency steps and the transfer function estimated by interpolation. This lack of sampling content and resolution obscured the potential perceptual significance of directional changes in the sharp spectral features that populate high frequencies of the HRTF. Modern acoustic studies have focused on expanding the accurate characterization of these directional filtering effects.

This new approach to human sound localization may be viewed as a three stage process (for a review, see Wightman, F. L. *et al.*, 1987). The acoustic properties of the HRTF are measured at free-field locations. The properties are imposed upon synthetic stimuli to create a virtual sound field (VSF) that simulates the directional properties of the HRTF in closed field. The fidelity of the synthesis is verified by asking subjects to identify the apparent free-field location of VSF stimuli that are presented with headphones. Psychoacoustic validation is a defining characteristic of modern studies of the human HRTF (Wightman, F. L. and Kistler, D. J., 1989b).

The ability to measure and validate the HRTF in the same subject places a premium on efficient recording procedures. Most modern studies use a variant of the approach introduced by Mehrgardt S. and Mellert V. (1977), which replaces sinusoidal stimuli with pseudorandom noise. The spectrum of the noise is crafted using inverse Fourier transforms to have a broad bandwidth, random phase, and an amplitude spectrum that complements the output characteristics of the free-field speaker. The duration of the stimulus is made as short as possible to allow repetitive presentations from the free-field source while sound energy is recorded in the ear canal with a probe microphone. Averaging the microphone response across hundreds of presentations increases signal-to-noise ratios by lowering the noise floor of the recording. Consequently, deep spectral notches may be observed at low stimulus levels without eliciting middle ear reflexes that change the resonant properties of the ear canal. The Fourier transform of the averaged microphone response is divided by the Fourier transform of the noise burst to estimate the transfer function of the ear.

Figure 2 compares a modern description of the human HRTF (Wightman, F. L. and Kistler, D. J., 1989a), with representative results from three earlier studies (Mehrgardt, S. and Mellert, V., 1977; Shaw, E. A. G., 1974b; Wiener, F. M. and Ross, D. A., 1946). The measures were recorded at a source location of 0° azimuth, 0° elevation. Data from Figure 1 have been replotted to illustrate the remarkable consistency of independent measures by early investigators. Although all of the functions show good agreement at lower frequencies, early measures deviate considerably from the modern HRTF at frequencies above 2.5 kHz. These discrepancies are due in part to the presence of a deep spectral notch at frequencies between 7 and 10 kHz that was not revealed by early recording procedures. Wightman F. L. and Kistler D. J. (1989a) noted similar differences in the high-frequency HRTF throughout the horizontal and median planes.

The individual HRTFs of three subjects are presented in Figure 3. These results were obtained at locations in the horizontal plane that ranged from in front of the observer (0° azimuth) to behind the observer (180° azimuth). Each panel compares the function of the right ear (solid line) and left ear (dashed line). The right ear is the near ear for the two lateral locations (45° and 135° azimuth). The functions have been partitioned at 2.5 kHz, which is

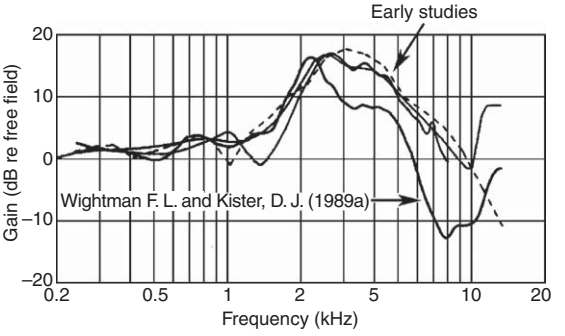

Figure 2 Comparison of early versus modern measures of the head-related transfer function at 0° azimuth, 0° elevation. The results of modern recording techniques are represented by Wightman F. L. and Kistler D. J. (1989a). Early measures are taken from Wiener and Ross (1946, solid bold line), Shaw (1974, light bold line), and Mehgardt and Mellert (1977, dashed line). Reused with permission from Wightman, F. L. and Kistler, D. J. The Journal of the Acoustical Society of America, 85, 858 (1989). Copyright 1989, Acoustical Society of America.

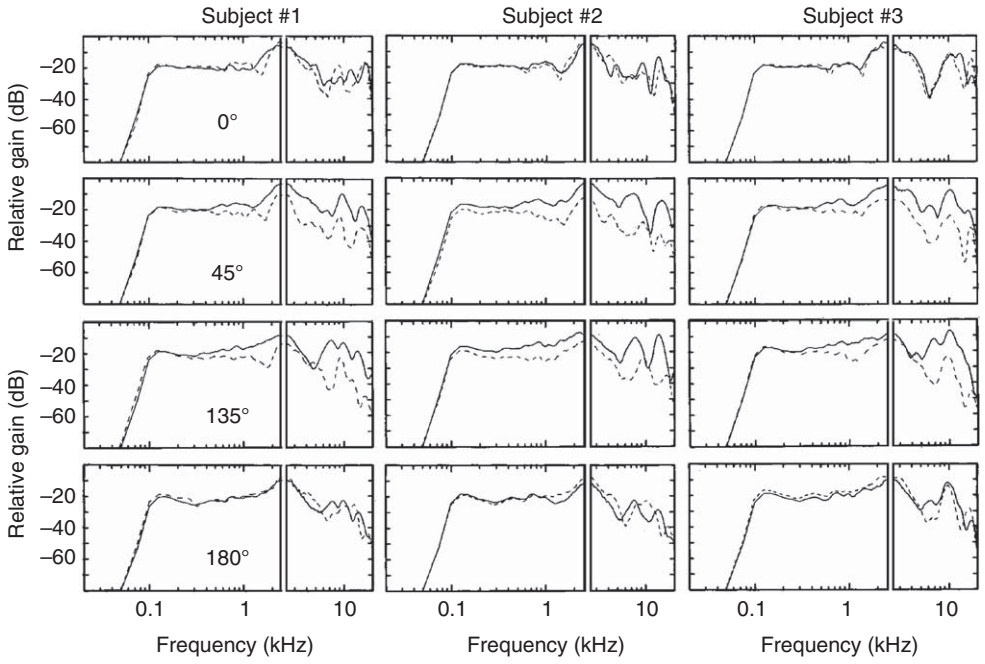

Figure 3 Comparison of individual head-related transfer functions (HRTFs) for three subjects at four locations in the horizontal plane. The solid curves indicate responses from right ears (near the speaker). The dashed curves are responses from left ears. Numerical labels indicate the azimuth of the sound source. The functions are separated at 5 kHz to emphasize intersubject differences in high-frequency spectral features. Adapted from Wightman, F. L., Kistler, D. J., and Perkins, M. E. 1987. A New Approach to the Study of Human Sound Localization. In: Directional Hearing (*eds.* W. A. Yost and G. Gourevitch). Springer: With kind permission of Springer Science and Business Media.

the frequency where the high-frequency measures of Wightman F. L. and Kistler D. J. (1989a) began to deviate from earlier recordings (Figure 2).

An examination of the low-frequency transfer functions verifies basic observations that were made more than 40 years earlier by Wiener F. M. and Ross D. A. (1946). The gain profile of each function rises to a maximum near 2.5 kHz, is higher in the near ear for lateral locations in the horizontal plane, and shows little variation between subjects.

The high-frequency transfer functions in Figure 3 reveal a very different pattern of localization cues. Here, the functions are marked by sharp spectral peaks and deep notches. On average, head-shadowing effects become more pronounced and yield larger ILD cues. At some frequencies, contradictory ILD cues are created by the presence of a spectral notch in the near ear or a spectral peak in the far ear. Individuals show clear differences in the frequency, shape, and magnitude of the spectral features.

Wightman F. L. and Kistler D. J. (1989b) obtained psychophysical validation of their acoustic measures by asking subjects to localize noise bursts that were presented under free-field conditions and with headphones. The latter stimuli were shaped by the HRTF of the free-field locations. Veridical simulations and actual locations are expected to elicit identical percepts. Figure 4 presents results from two subjects, with best and worst performances.

The scatterplots in Figure 4 contrast the target position of the stimulus with the judged position of the observer. Free-field responses are shown in Figure 4(a) and simulations in Figure 4(b). In the case of headphone stimuli, target position refers to the source location for the HRTF that was used in the simulation. A perfect correlation between stimulus and response ($r = 1$) is indicated by the unity line. Responses at six elevations are combined at each azimuth. Twenty-four azimuths are combined at each elevation.

Localization accuracy was excellent in the azimuth dimension of free-field responses. Statistical tests indicated a strong correlation between the judged positions and target positions of both subjects ($r > 0.98$). The errors generated by headphone stimuli only slightly exceeded those for natural sounds ($r > 0.97$). These results depict a best-case scenario

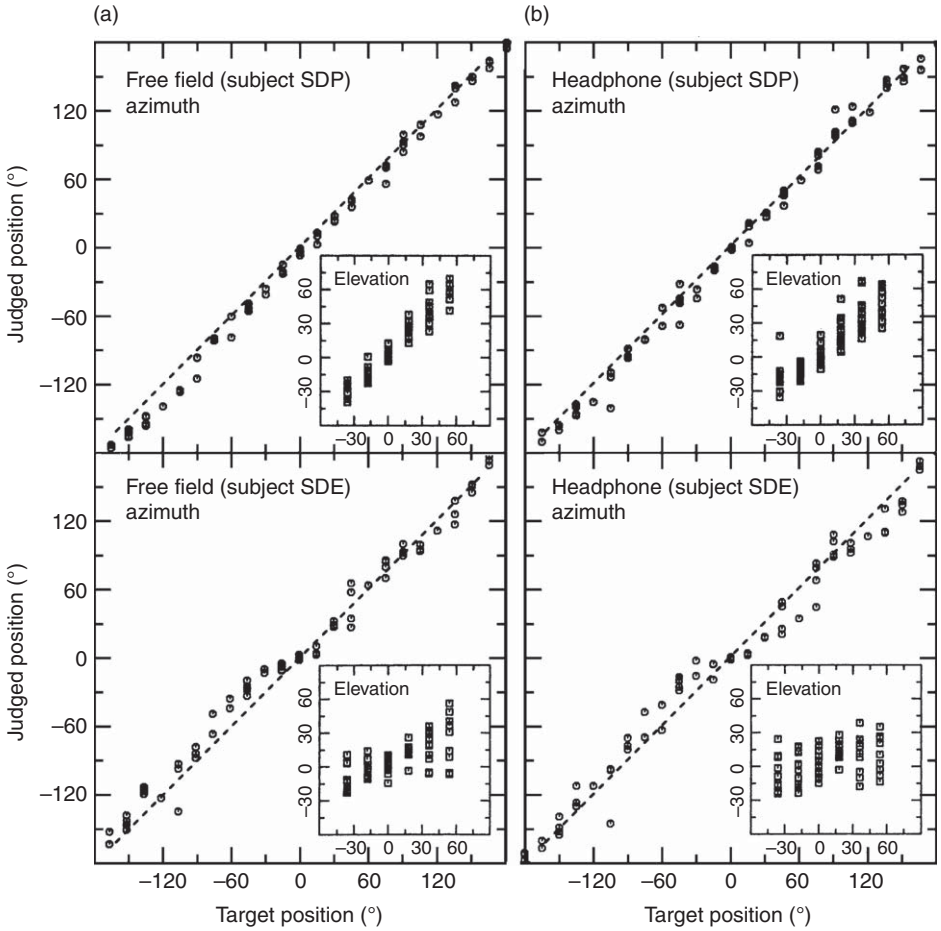

Figure 4 Comparison of free-field (a) and headphone (b) localization for two subjects. Judged positions are related to the azimuth of target positions in the main panels. Correct responses fall along the dashed line. The target positions of headphone stimuli indicate source locations during HRTF recordings. Inset: Responses to the elevation of target positions. Reused with permission from Wightman, F. L. and Kistler, D. J. The Journal of the Acoustical Society of America, 85, 858 (1989). Copyright 1989, Acoustical Society of America, 1989b.

where source location is derived from redundant ILD, ITD, and spectral cues. When these cues are placed in conflict, the azimuth directionality of a VSF stimulus is dominated by low-frequency ITDs (Wightman, F. L. and Kistler, D. J., 1992).

A missing detail in Figure 4 is the occurrence of front–back confusions; that is, the attribution of a front-hemisphere location to the back-hemisphere, or the less common opposite impression. To facilitate the comparison of free-field versus headphone performance, these potentially large errors have been removed by reflecting the data around the vertical axis to the correct hemisphere. Both subjects exhibited a greater tendency to make front–back confusions under closed-field conditions. The errors of subject SDP increased from three in free field to six with headphones. Subject SDE made substantially more of these errors in free field than SDP (12 confusions), and also displayed a loss of performance when tested with headphones (20 confusions).

Bandwidth manipulations of free-field stimuli suggest that front–back confusions are resolved by monaural spectral cues (Blauert, J., 1969/1970; Oldfield, S. R. and Parker, S. P., 1986). Because these cues are essential for localization in the median plane, the prevalence of confusion errors in the azimuth data of subject SDE predicts poor performance in the elevation dimension of localization responses. These results are presented in the inset panels of Figure 4.

Both subjects displayed elevation responses that were less accurate and more variable than their azimuth responses. The stimulus–response correlation

of subject SDP decreased slightly in free field (0.96), but showed a more precipitous drop under closed-field conditions (0.88). As predicted, subject SDE was especially challenged by this dimension of the task. Responses were poorly correlated in free field (0.68) and with headphones (0.43).

The increase of elevation errors for synthetic HRTFs suggests that the simulations failed to capture the full complement of spectral features that contribute to vertical sound localization. Notwithstanding the limitations of modern synthesis techniques, it is apparent that the high-frequency HRTF is highly individualized. Human subjects may display informative (SDP) or impoverished (SDE) localization cues under normal listening conditions (Middlebrooks, J. C., 1999a; Wenzel, E. M. *et al*., 1993).

3.37.5 Directional Transfer Functions

HRTFs provide a detailed description of outer ear acoustics. They do not reveal what acoustic features are influenced by changes in sound source direction and therefore provide veridical localization cues. The DTF is the spectral shape that remains after common nondirectional components of the HRTF are removed by statistical methods (Middlebrooks, J. C. and Green, D. M., 1990). This analysis provides a useful link between the quality of directional information and the accuracy of perceptual behavior (Middlebrooks, J. C.,1992).

Middlebrooks J. C. and Green D. M. (1990) recorded ear canal responses at hundreds of loudspeaker locations evenly distributed around the observer. Their methods for averaging microphone responses to noise bursts and converting the time domain signal into the frequency domain were essentially the same as those used by (Mehrgardt, S. and Mellert, V., 1977). Figure 5(a) presents two unprocessed magnitude spectra for recordings at 0° azimuth, 0° elevation. The responses were simultaneously recorded from the same ear with two probe microphones.

Dividing the spectral shapes in Figure 5(a) by the spectrum of the noise burst is expected to yield HRTFs that are equivalent to results from Wightman F. L. and Kistler D. J. (1989a) in Figure 2(a). Middlebrooks J. C. and Green D. M. (1990) argued that the HRTF is the product of the desired DTF and an unknown common transfer function that can be estimated by averaging the microphone response across all sampled locations. Thus, the DTF can be calculated by dividing the microphone responses in Figure 5(a) by the stimulus spectrum and the common transfer function.

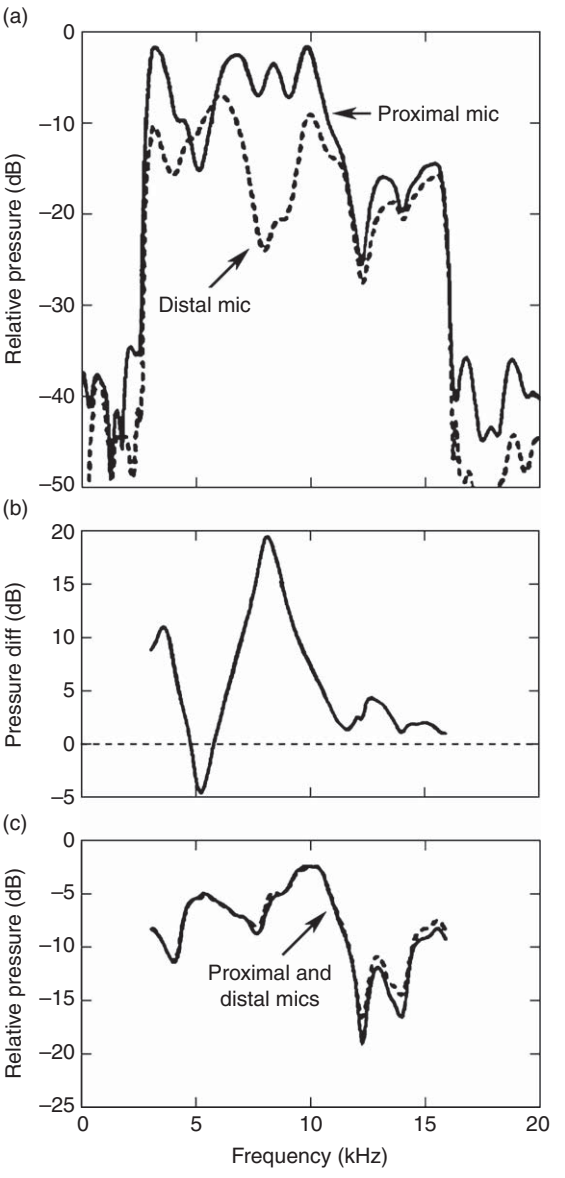

Figure 5 Directional transfer functions measured at proximal and distal locations in the ear canal. (a) Unprocessed magnitude spectra of responses to noise bursts. The responses were measured simultaneously with a 9 mm microphone separation. The sound source was located at 0° azimuth, 0° elevation. (b) Sound pressure differences between the two recordings. (c) Directional transfer functions derived by dividing the microphone responses by the stimulus spectrum and the common transfer function. Reused with permission from Middlebrooks, J. C. and Green, D. M. The Journal of the Acoustical Society of America, 87, 2149 (1990). Copyright 1990, Acoustical Society of America.

Figure 5(b) illustrates how placement can alter acoustic measures. Approximately 9 mm separate the proximal and distal microphones. The unprocessed magnitude spectra differ by as much as 24 dB between the recording sites. These pressure differences are produced by standing waves in the ear canal that may cancel or amplify select wavelengths according to insertion depth. These artifacts persist when microphone responses are converted to HRTFs.

Figure 5(c) compares the results of DTF calculations for the two recordings. Despite the large pressure differences in the raw magnitude spectra, the transfer functions are virtually identical. The ear canal resonances that give rise to standing waves are sensitive to microphone placement, but they are not affected by changes in source location. Consequently, this nondirectional component of the microphone signal is removed as part of the common transfer function.

Unlike the deep spectral notch in the HRTF of Wightman F. L. and Kistler D. J. (Figure 2), the DTF reveals a prominent spectral peak at frequencies between 7 and 10 kHz. The differences suggest that most transfer functions have the spectral notch, but it is less pronounced at frontal locations (0° azimuth, 0° elevation). As described later, these so-called covert peaks can exert profound effects on sound localization (Musicant, A. D. and Butler, R. A., 1984b).

3.37.5.1 Peripheral Coding of Monaural Localization Cues

The mechanical properties of the peripheral auditory system decompose the HRTF shape into its constituent frequency components (for general reviews of the auditory coding of complex sounds, see Evans, E. F., 1992; Lopez-Proveda, E. A., 2005). These elements are arrayed along the cochlear partition in a frequency dependent manner that establishes the first principle of auditory coding, the frequency to place transformation known as tonotopy (Narayan, S. S. *et al.*, 1998; Ruggero, M. A. *et al.*, 2000). Auditory-nerve fibers make spatially restricted synaptic contact with the tonotopic axis, and therefore respond selectively to a limited frequency range of the HRTF spectrum (Kim, D. O. and Molnar, C. E., 1979). Consequently, spectral cues for sound localization must be encoded by multiple fibers with complementary tuning properties. Fibers that are tuned to high-energy spectral peaks show high discharge rates and fibers that are tuned to spectral notches show low rates (Sachs, M. B. and Young, E. D., 1979).

3.37.5.2 Representation by the Rate Profiles of Auditory-Nerve Fibers

The representation of HRTF-based spectral shapes has been measured by recording the discharge rates of populations of auditory-nerve fibers in domestic cats (Poon, P. W. and Brugge, J. F., 1993; Rice, J. J. *et al.*, 1995). The localization behaviors of this predatory species is strongly influenced by directional properties of notches that are observed at mid frequencies of the HRTF (Musicant, A. D. *et al.*, 1990; Phillips, D. P. *et al.*, 1982; Rice, J. J. *et al.*, 1992). Examples of two HRTFs are shown in Figure 6(a). The locations that produced the HRTFs differed slightly in elevation. As the sound source changed in elevation, the spectral notch changed in frequency. Similar patterns have been observed for the outer ear acoustics of humans (Bloom, P. J., 1977; Butler, R. A. and Belendiuk, K., 1977).

The directional dependence of the mid-frequency notch causes the amplitude spectra of the two stimuli to diverge at frequencies between 10 and 20 kHz. These localization cues are illustrated in Figure 6(b) by plotting the level difference between the two HRTFs. Auditory-nerve fibers respond to these level differences with increases and decreases of discharge rate.

3.37.5.3 Modeling the Auditory-Nerve Representation of Monaural Spectral Cues

Quantitative descriptions of the peripheral representation of HRTF-based spectral shapes are facilitated by the largely homogeneous discharge properties of the auditory nerve. Figure 6(c) plots the rate differences that were observed when a population of auditory-nerve fibers was tested with the two HRTFs. The frequency location of each data point indicates the fiber's best frequency (BF: the most sensitive frequency). The magnitude of the level difference between the two stimuli is superimposed on the rate difference profile to emphasize the straightforward relationship between rate and level.

The effect of spectrum level on the auditory nerve is strikingly linear (May, B. J. and Huang, A. Y., 1997). This relationship is revealed in Figure 7 by plotting discharge rates in terms of the magnitude of the

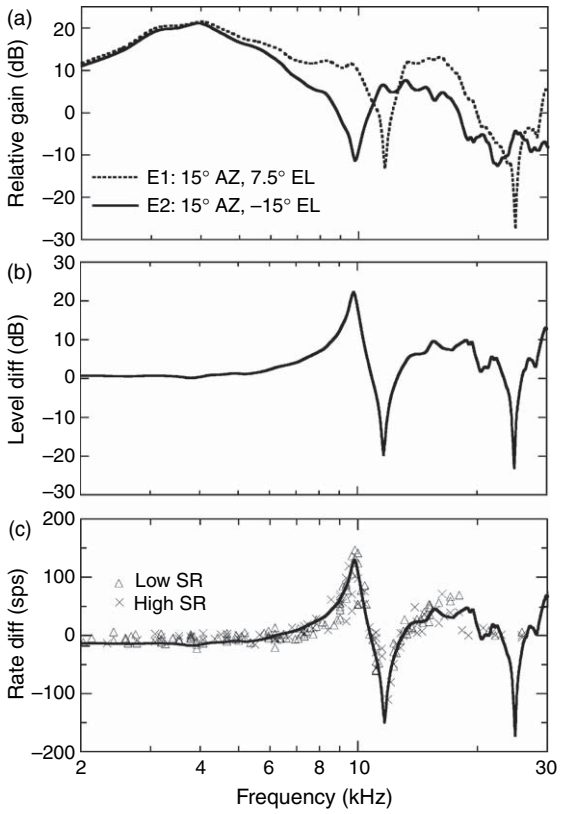

Figure 6 The auditory-nerve representation of the head-related transfer function (HRTF). (a). The relative gain of the cat's HRTF at two elevations. As the source moves from a negative elevation (E2) to a positive elevation (E1), the prominent mid-frequency notch moves to a higher frequency. (b). The level difference contour created by subtracting E2 from E1. Major directional effects are related to changes in the frequencies of spectral notches. (c). The rate differences of auditory responses to the two HRTFs. Each symbol is the E1–E2 rate difference for a single fiber, which is plotted at the fiber's BF. Different symbols distinguish fibers with high versus low spontaneous rates (SRs). The E1–E2 level contour is superimposed on the population response to emphasize the close correspondence between stimulus features and discharge rates. Reused with permission from May, B. J. and Huang, A. Y. The Journal of the Acoustical Society of America, 101, 2705 (1997). Copyright 1997, Acoustical Society of America.

amplitude difference at each fiber's BF. Fibers with high spontaneous rates produce a steeply sloped function, which indicates the neuron's robust representation of spectral peaks and notches (Figure 7(a)). Fibers with low spontaneous rates exhibit smaller differences because they are less sensitive to moderate sound levels (Figure 7(b)). The fibers play a critical role in the coding of spectral information at high sound levels and in the presence of background noise (Le Prell, G. S. *et al.*, 1996).

The quality of a neural code depends not only on response magnitude but also the variability of responses under identical stimulus conditions. Conveniently, the average SD of auditory-nerve discharge rates is proportional to the magnitude of sound-driven activity and is well fit by the power function in Figure 7(c).

Implicit in the linear rate–level relationship is the potential to model the auditory-nerve representation under conditions that simulate localization behavior (May, B. J. *et al.*, 1996; May, B. J. and Huang, A. Y., 1997). Because the relationship is linear, HRTF gain can be translated to a predicted discharge rate by a simple respecification of the amplitude axis. The simulated rates in Figure 8(a) are based on the rate–level relationship of high SR fibers (Figure 7(a)).

The two HRTFs used in the simulation re-create a change in lateral location. The sound source begins at a reference location directly in front of the subject and shifts to a positive (rightward) azimuth of 45°. Because the response of the right ear is being modeled, the sound takes a more direct route to the ear when it originates from the positive azimuth and the movement is associated with a frequency dependent gain (Calford, M. B. and Pettigrew, J. D., 1984). Level differences between the reference and comparison locations are reflected by positive discharge rates at the BF of most model fibers. The exception is a sharp rate decrease where the comparison HRTF displays its mid-frequency notch.

The rate profile may be expressed in terms of d' statistics to evaluate the information content of the simulated population response (Delgutte, B., 1989; Green, D. M. and Swets, J. A., 1974). This signal detection analysis specifies rate differences in units of SD. The d' statistics in Figure 8(b) were derived by dividing the simulated rates in Figure 8(a) by the SD values in Figure 7(c). By convention, the detection of an acoustic event is assumed when d' scores are greater than 1 or less than -1 (i.e., ± 1 SD). These frequency regions have been highlighted with shading to emphasize the potential physiological salience of the change in location.

The acuity of directional hearing is defined by the minimum audible angle (MAA) (Mills, A. W., 1958). This psychophysical threshold represents the just-detectable change in location relative to a reference that is usually directly in front of the observer (0° azimuth, 0° elevation). The comparison source locations are arranged in the horizontal plane to

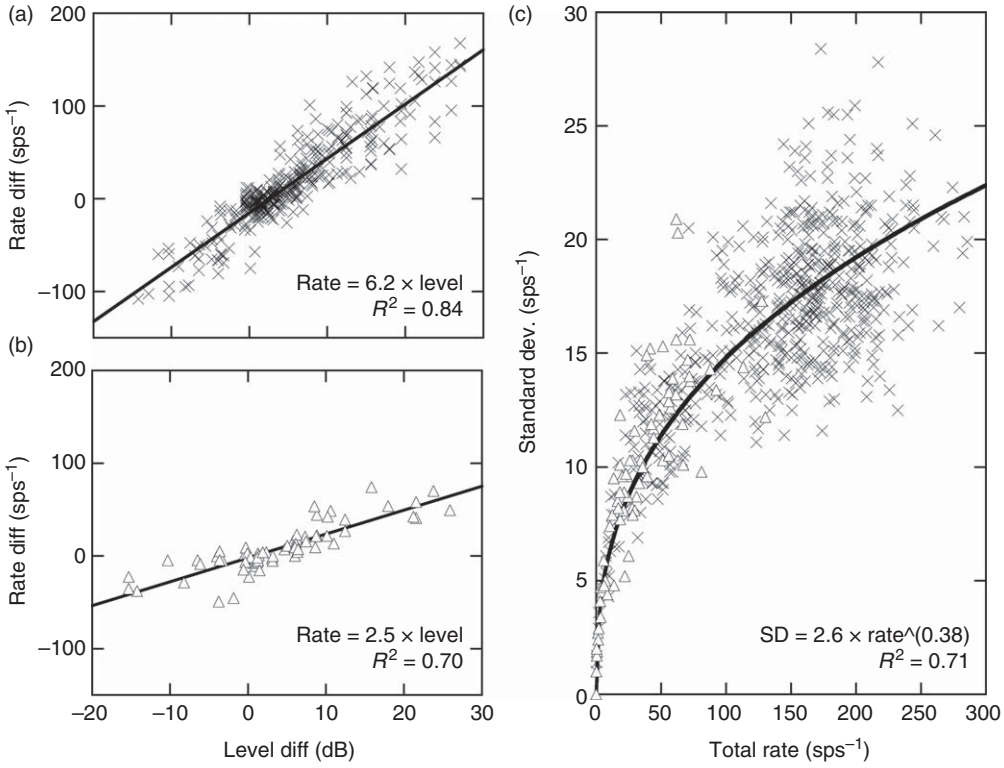

Figure 7 Statistical descriptions of the auditory-nerve representation of the head-related transfer function (HRTF). (a). The rate differences of high spontaneous rate (SR) auditory-nerve fibers for pairwise combinations of HRTF stimuli. Discharge rates are linearly related to the magnitude of the level difference at the fiber's BF. (b) Same relationship for low SR fibers. (c) The SD of discharge rates in the auditory nerve. SD was calculated from multiple presentations of the same stimulus. It increased with rate magnitude and was well fit by a power function. Reused with permission from May, B. J. and Huang, A. Y. The Journal of the Acoustical Society of America, 101, 2705 (1997). Copyright 1997, Acoustical Society of America.

determine the smallest detectable change in azimuth, or in the median vertical plane to determine the threshold for elevation.

The simulated d' values in Figure 9 compare the quality of localization cues at ten locations in the horizontal plane (15° increments) and at 16 locations in the median plane (7.5° increments). To incorporate the design of a minimum audible angle task, the d' statistic represents the magnitude of the rate differences between the set of comparison HRTFs and the fixed reference HRTF (0° azimuth, 0° elevation). In Figure 9(a), the most noticeable source of azimuth information is a systematic increase in the magnitude of d' as the comparison HRTF becomes more lateralized. Sounds originating at negative (leftward) azimuths are attenuated by the sound shadow of head, while sounds at positive (rightward) azimuth are amplified by the *acoustic fovea*. Acoustic differences between symmetrical positive and negative azimuths are equivalent to the binaural ILD cues reaching the two ears from a single lateralized location.

The head's sound shadow is less obvious in the median plane. Nevertheless, as shown in Figure 9(b), changes in elevation also produce systematic rate differences when the sound source moves from the reference location to positive (high) or negative (low) elevations. Unlike changes in azimuth, these localization cues tend to be less uniform, smaller in magnitude, and restricted to high frequencies (>6 kHz).

The broadly distributed rate increases that extend across positive azimuths and elevations are marked by a sharp negativity at frequencies between 10 and 20 kHz. The paradoxical rate decrease is created by the mid-frequency notch in the cat's HRTF. Although most frequencies are amplified by the HRTF, this select frequency range is attenuated to levels below the reference HRTF. The frequency of the notch displays a continuous increase as the sound

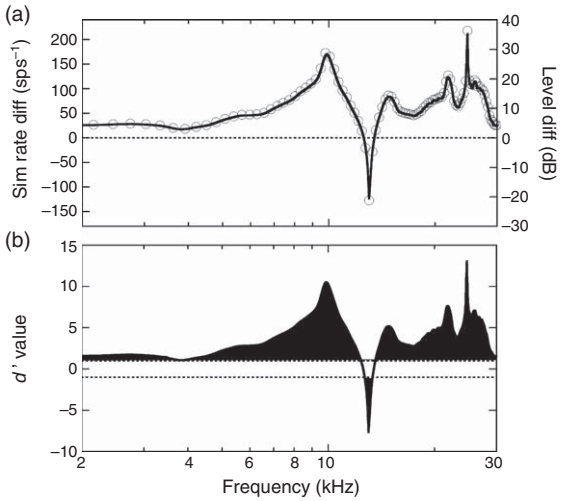

Figure 8 Simulated auditory-nerve responses to two HRTFs in the horizontal plane. (a). The level difference contour (line, right ordinate) was created by subtracting a reference HRTF (0° azimuth, 0° elevation) from a more lateralized comparison HRTF (45° azimuth, 0° elevation). The higher gain of the comparison HRTF is reflected in positive level differences. Simulated high SR discharge rates (symbols, left ordinate) were derived by applying the statistics in Figure 7(a) to rate differences. Because the rate–level relationship is linear, the simulated rate profile is identical to the level profile. (b) The simulated auditory-nerve response has been further transformed into the d' index of sensitivity by standardizing the magnitude of the rate difference. The SDs used in this calculation are taken from Figure 7(c). The information content of simulated discharge rates is indicated by shading regions where d' values are greater than 1 (black) or less than –1 (gray). Reused with permission from May, B. J. and Huang, A. Y. The Journal of the Acoustical Society of America, 101, 2705 (1997). Copyright 1997, Acoustical Society of America.

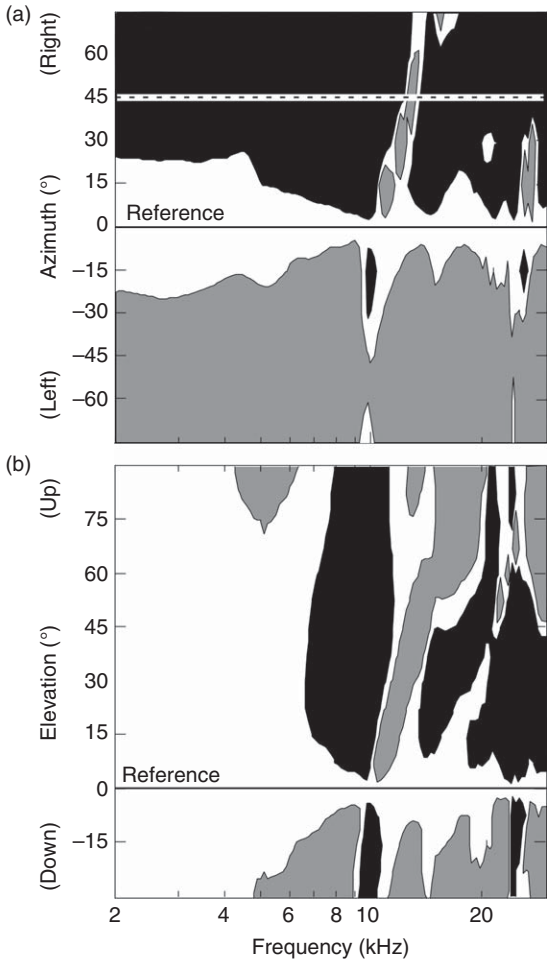

Figure 9 Simulated auditory-nerve responses in a minimum audible angle task. (a). Rate differences were calculated by applying the linear model to level differences between the reference HRTF (0° azimuth, 0° elevation) and 10 comparison HRTFs that were arrayed at 15° intervals along the horizontal plane. Regions where d' values are greater than 1 or less than −1 are indicated with black and gray shading, respectively. The d' contour in Figure 8(b) is indicated by the dashed line. (b). The same analysis for 16 elevations in the median plane. Reused with permission from May, B. J. and Huang, A. Y. The Journal of the Acoustical Society of America, 101, 2705 (1997). Copyright 1997, Acoustical Society of America.

source moves from the reference location to more lateralized azimuths in the right hemifield or higher elevations in the median plane. The unambiguous association between frequency and location suggests that accurate sound localization may be achieved by combining rate information at the same frequency across ears (i.e., binaural processing of ILDs) or across frequencies at the same ear (i.e., monaural processing of spectral cues).

The magnitude of d' in the MAA simulation suggests that strong localization cues are communicated by high frequencies of the HRTF. This prediction has been verified by training cats to release a lever when a sound source changed from a reference location in front of the subject to a comparison location at a positive azimuth or elevation (Huang, A. Y. and May, B. J., 1996b). Best performance was observed with bursts of broadband noise or high-pass noise (>20 kHz).

3.37.5.4 Distinguishing Sound Localization and Directional Acuity

Distinctions between sound localization and spatial discrimination (e.g., the MAA task) have been noted

since the earliest psychophysical assessments of human directional hearing (Mills, A. W., 1958; Starch, D., 1908). A subject is only required to respond to acoustic differences that are correlated with directional changes. The subject may perceive change without absolute knowledge of the locations that contribute to the effect. In the context of directional acuity, a mid-frequency notch exerts less impact on the auditory-nerve population response because it is more localized in frequency and smaller in magnitude than the complex spectral variations found at high frequencies of the HRTF. The singularity of the notch does not lessen its importance in situations where the absolute location of the sound source must be determined (Hebrank, J. and Wright, D., 1974; Butler, R. A. and Belenduik, K., 1977; Bloom, P. J., 1977).

The ability to localize a discrete acoustic event implies that the auditory system can derive the absolute directionality of a sound source from physical characteristics of the HRTF. This process requires some unique directional property that distinguishes each HRTF from all other HRTFs. In Figure 10(a), the acoustic basis of absolute sound localization is explored by comparing an individual HRTF (0° azimuth, 0° elevation) to the statistical distribution of HRTF gains at over a 150 locations in the frontal sound field. Absolute localization cues are defined as spectral features that fall beyond the average HRTF shape by at least one SD. This statistical analysis emphasizes the unique directionality of spectral features in the same way as DTFs (Middlebrooks, J. C. and Green, D. M., 1991; Musicant, A. D. and Butler, R. A., 1984b). In this context, high-frequency cues are rendered less salient by a frequency-dependent increase in variability between HRTFs. The mid-frequency notch is the only feature that consistently extends beyond the ±1 SD criterion.

Figures 10(b) and 10(c) simulate the auditory-nerve representation of absolute sound localization cues. This analysis involves identifying frequencies where individual HRTFs deviate from the average HRTF by at least one SD, calculating the magnitude of the level difference relative to the SD boundary, and transforming the level difference into discharge rate with the linear model. The resulting d' statistics suggest a critical role for mid-frequency spectral notches. They are the only cue available for central locations in the horizontal and median planes, where cats show their most accurate sound localization behaviors (Populin, L. C. and Yin, T. C., 1998a; 1998b).

Predictions of the absolute localization model have been tested by measuring the cat's ability to

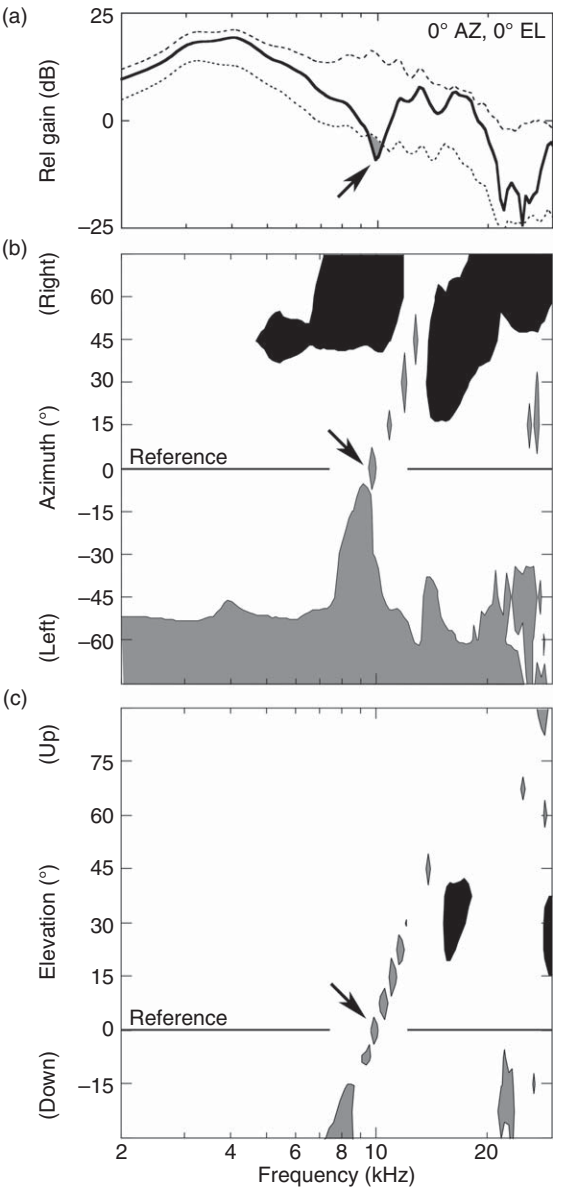

Figure 10 Simulated auditory-nerve responses in an absolute localization task. (a) Comparison of an individual HRTF (0° azimuth, 0° elevation) to the statistical distribution of HRTF gains at 179 locations in the frontal sound field. Dashed lines indicate ±1 SD relative to the mean of the distribution. The mid-frequency spectral notch where the HRTF falls below −1 SD is indicated by gray shading (arrow). (b) Simulated d' values based on the magnitude of individual HRTFs relative to SD contours. Rate responses to the HRTF at 0° azimuth, 0° elevation is indicated by the line. The arrow points to the statistically significant rate decrease at the mid-frequency spectral notch. Additional plotting conventions are described in Figure 9. (c) Same analysis for 16 elevations in the median plane. Reused with permission from May, B. J. and Huang, A. Y. The Journal of the Acoustical Society of America, 101, 2705 (1997). Copyright 1997, Acoustical Society of America.

orient to discrete sound presentations (May, B. J. and Huang, A. Y., 1996). Cats make this natural reflexive behavior with very little training (Sutherland, D. P. *et al.*, 1998b). If the bandwidth of the orientation stimulus is modified in a manner that conserves mid-frequency spectral information, accurate behavior is maintained. Limiting the sound spectrum to high frequencies elicits poorly directed head movements (Huang, A. Y. and May, B. J., 1996a).

3.37.6 Pathways of the Dorsal Cochlear Nucleus and Inferior Colliculus

The central nervous system is known for its remarkable diversity of anatomical and physiological adaptations for encoding binaural directional information. Monaural localization cues also play an important role in the biological world of most mammalian species and there is good evidence that the auditory system has developed similar specializations to ensure efficient spectral processing. When the auditory-nerve representation of spectral cues for sound localization enters the brain, the dorsal cochlear nucleus (DCN) integrates this ascending input to create a neuron that is sensitive to the sharp spectral features of HRTF-shaped sounds (Oertel, D. and Young, E. D., 2004). Ascending projections from the DCN bypass the binaural brainstem and climb directly to the central nucleus of the ICC where monaural spectral representations are further transformed to enhance spatial selectivity.

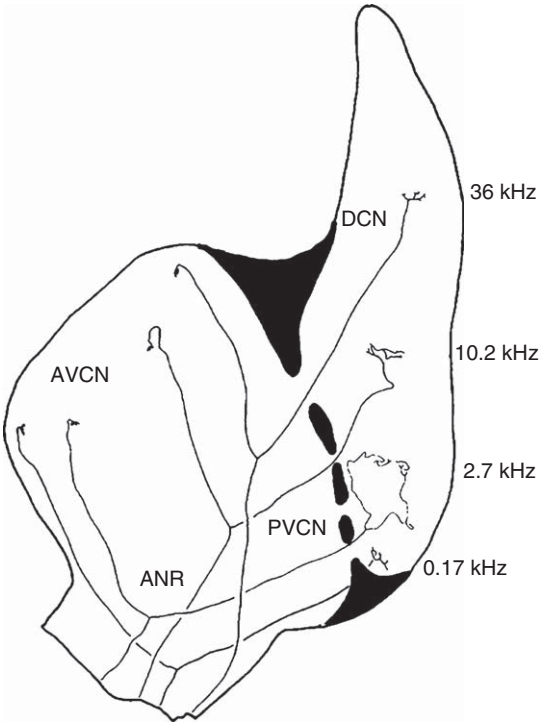

Figure 11 Drawing tube reconstruction of the central processes of four auditory-nerve fibers. Frequency tuning characteristics were measured electrophysiologically before intracellular labeling with horseradish peroxidase. Numerical labels indicate BF. Descending projections pass through the posteroventral cochlear nucleus to terminate in a tonotopically organized manner in the dorsal cochlear nucleus. ANR, auditory-nerve root; AVCN, anteroventral cochlear nucleus; DCN, dorsal cochlear nucleus; PVCN, posteroventral cochlear nucleus. Reproduced from Ryugo, D. K. and Parks, T. N. Primary innervation of the avian and mammalian cochlear nucleus. Brain Res. Bull. 60, 435–456. Copyright (2003), with permission from Elsevier.

3.37.6.1 Dorsal Cochlear Nucleus

The central projections of the auditory nerve bifurcate upon entering the cochlear nucleus to send an ascending branch to the anteroventral subdivision and a descending branch to the posteroventral and dorsal subdivisions (Lorente De Nó, R., 1933; Ryugo, D. K. and Parks, T. N., 2003). The highly structured topography of these projects is shown in Figure 11. Fibers from the low-frequency apex of the cochlea terminate in the ventral DCN, while fibers from the high-frequency base terminate dorsally. As a result, the tonotopic organization of the cochlea is transferred to the brainstem (Spirou, G. A. *et al.*, 1993). It is common for central auditory nuclei to exaggerate the tonotopic representation of functionally relevant frequencies. For example, the medial superior olive is primarily involved with low-frequency binaural temporal processing (Tsuchitani, C., 1977). The cat's DCN shows a similar bias for the mid-frequency sounds that convey important HRTF directional features (Spirou, G. A. *et al.*, 1993).

Auditory-nerve inputs to the DCN are modified by a complex intrinsic circuitry (for recent reviews, see Oertel, D. and Young, E. D., 2004; Young, E. D. and Davis, K. A., 2002). These largely inhibitory influences activate selectively under different conditions of stimulation. The hypothesized circuit is summarized by the simple model in Figure 12(b). The anatomical counterparts of the model are shown in Figure 12(a).

Before the excitatory inputs of the auditory nerve are relayed to the ICC by type-IV projection neurons (pyramidal cells), they are shaped by two sources of

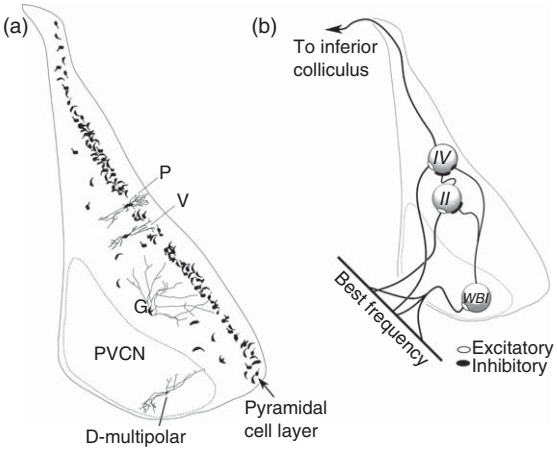

Figure 12 Summary of the functional anatomy of the DCN. (a) Principal anatomical cell types. Ascending projections originate from pyramidal (P) and giant cells (G). These responses are shaped by excitatory inputs from the auditory nerve (not shown) and inhibitory inputs from vertical cells (V) and D-multipolar cells. (b) Neural circuit model. The type-IV response pattern is assumed to arise from pyramidal or giant cells. Vertical neurons are a likely source of type-II inhibition. WBI is associated with inputs from D-multipolar cells. The excitatory tuning of the response types is indicated by the distribution of inputs along the BF axis. PVCN, posteroventral cochlear nucleus. Adapted from Young, E. D. and Davis, K. A., 2002. Circuitry and function of the dorsal cochlear nucleus. In: Integrative Functions in the Mammalian Auditory Pathway (*eds.* D. Oertel, R. R. Fay and Popper, A. N.), pp. 160–206. Springer, Copyright (2002), with kind permission of Springer Science and Business Media.

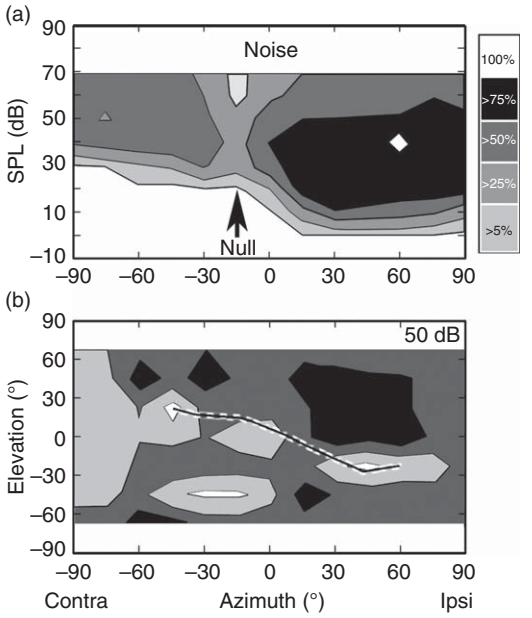

Figure 13 Responses of two DCN pauser neurons to free-field noise bursts. (a) Discharge rates evoked from one neuron (BF = 10 kHz) by sound sources in the horizontal plane. The magnitude of the response is expressed as a percentage of maximum (gray scale on right). The decrease in noise-driven rate at the −15° azimuth is explained by a mid-frequency null at the neuron's BF (arrow). (b) Responses of a second neuron (BF = 11 kHz) to sound sources at different azimuths and elevations in the frontal sound field. The predicted trajectory of an 11 kHz null (line) coincides with rate decreases. Reproduced from Imig, T. J., Bibikov, N. G., Poirier, P., and Samson, F. K., 2000. Directionality derived from pinna-cue spectral notches in cat dorsal cochlear nucleus. J Neurophysiol, 83, 907–925. Copyright (2000), used with permission from The American Physiological Society.

inhibition (Nelken, I. and Young, E. D., 1994). The frequency tuning of these inhibitory neurons is indicated by the distribution of connections on the BF axis of the model. The type-II inhibitory input to the type-IV unit is sharply tuned in frequency and tends to have a BF that is slightly lower than the type-IV neuron (Hancock, K. E. *et al.*, 1997). These responses have been attributed to vertical cells in the deep layers of the DCN (Spirou, G. A. *et al.*, 1999; Young, E. D. and Voigt, H. F., 1982). A second inhibitory input is weaker and more broadly tuned (Hancock, K. E. and Voigt, H. F., 1999; Nelken, I. and Young, E. D., 1994). Wide-band inhibition (WBI) is assumed to arise from multipolar cells in the posteroventral cochlear nucleus (Arnott, R. H. *et al.*, 2004; Doucet, J. R. *et al.*, 1999; Hancock, K. E. and Voigt, H. F., 1999; Nelken, I. and Young, E. D., 1996; Oertel, D. *et al.*, 1990).

The model predicts the output of the DCN under a variety of stimulus conditions. Type-IV units are weakly driven by broadband noise with a uniform amplitude spectrum because they are simultaneously excited by auditory-nerve inputs and inhibited by a combination of type-II and WBI inputs. Adding a directional notch to the noise spectrum may either potentiate or reduce the response. If energy is removed from frequencies that excite the type-II unit, the type-IV unit will be less inhibited. If energy is removed from frequencies that excite the type-IV unit, it will show stronger inhibitory responses. A spectral peak evokes the opposite pattern of responses.

The predicted notch sensitivity of type-IV units has been confirmed by the responses of DCN neurons to free-field stimuli (Imig, T. J. *et al.*, 2000). Figure 13(a) plots the responses of a pauser unit that was recorded in an anesthetized cat. This

temporal pattern is associated with type-IV activity in unanesthetized preparations (Pfeiffer, R. R., 1966). As the stimulus moves in the horizontal plane, the neuron's discharge rates capture the essential properties of the auditory-nerve population response (Figures 9(a) and 10(b)). Higher discharge rates are observed at positive (ipsilateral) azimuths, and lower discharge rates at negative (contralateral) azimuths. Minimum rates signal locations where spectral notches coincide with BF.

A more complete picture of the directional properties of the DCN is obtained by plotting discharge rates as a function of both azimuth and elevation. The responses of a second pauser neuron (BF = 11 kHz) are shown in Figure 13(b). A distinguishing feature of the neuron's spatial response map is the consistent rate decrease that follows the trajectory of an 11 kHz spectral notch (line). Because this notch frequency exists at multiple locations, rate decreases define a spatial contour and not a point in space (Rice, J. J. *et al.*, 1992). The representation of a specific location along the isonotch contour requires additional spectral processing. This more selective coding has been observed in the ICC (Davis, K. A., 2005).

3.37.6.2 Inferior Colliculus

It may be argued that the central nucleus of the ICC is an obligatory relay for the ascending projections of the auditory brainstem (Aitkin, L. M. and Phillips, S. C., 1984). Although these pathways converge within the midbrain (Adams, J. C., 1979; Malmierca, M. S. *et al.*, 2005; Oliver, D. L. *et al.*, 1997), ICC neurons exhibit physiological properties that appear to be dominated by discrete sources of input under certain conditions of stimulation (Davis, K. A. *et al.*, 1999; Ramachandran, R. *et al.*, 1999). The directional sensitivity of the resulting physiological response types may be influenced by binaural processes that are performed in the superior olive or by monaural spectral cues that encoded by the DCN (Davis, K. A., 2002; Ramachandran, R. and May, B. J., 2002).

A number of studies have characterized the spatial tuning of ICC neurons with free-field stimuli (Aitkin, L. M. *et al.*, 1984; Bock, G. R. and Webster, W. R., 1974; Leiman, A. L. and Hafter, E. R., 1972; Moore, D. R. *et al.*, 1984; Semple, M. N. *et al.*, 1983). Much of this work has focused on responses to pure tones in the horizontal plane. Under these restricted testing conditions, spatial selectivity is strongly influenced by the binaural processing of interaural time and level differences (Aitkin, L. M. and Martin, R. L., 1987; Aitkin, L. M. *et al.*, 1985). Nevertheless, an enhanced directional selectivity is observed when neurons are tested with broadband sounds containing HRTF-based spectral cues (Poirier, P. *et al.*, 2003).

The specific contributions of spectral cues for sound localization are potentially isolated by measuring the responses of ICC neurons to changes in the elevation of free-field sounds. As in studies of horizontal acuity, these experiments typically involve sound sources that are restricted to a single plane. In this case, it is the median vertical plane.

The cat's HRTF does not show sharp spectral filtering at low frequencies, so it is not surprising that elevation sensitivity is limited to neurons with BFs above 6 kHz (Aitkin, L. M. and Martin, R. L., 1990). An unexpected observation is that the spatial tuning is similar for azimuth and elevation and can be induced with both broadband and tonal stimuli. Examples of these measures are shown in Figure 14.

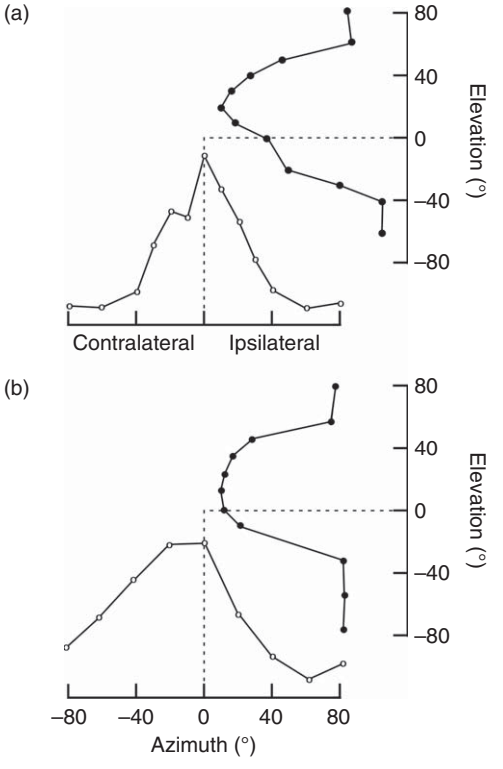

Figure 14 Responses of two ICC neurons to free-field sounds. (a) Unit showing spatial tuning for both azimuth and elevation when tested with noise bursts. (b) Unit showing similar tuning when tested with BF tones. The speaker array was fixed at an elevation of 40° for testing in azimuth and an azimuth of 0° for testing in elevation. Reproduced from Aitkin, L. and Martin, R., 1990. Neurons in the ICC of cats sensitive to sound-source elevation. Hear Res, 50, 97–105. Copyright (1990), with permission from Elsevier.

These results have led to the conclusion that elevation sensitivity may be partly mediated by the same binaural comparisons that dictate azimuthal sensitivity. It should be pointed out, however, that this method for defining the directionality of a neural response has the same shortcomings as the spatial discrimination procedure in Figure 9. Any acoustic change between sound sources has the capacity to modulate neural discharge rates. Consequently, spatially selective responses may reflect veridical localization cues or simple changes in sound pressure level that are given directional significance by the restricted spatial context in which they are examined. Well-established psychoacoustic effects argue against the accurate vertical localization of pure tones (Butler, R. A. and Planert, N., 1976).

The independent contributions of binaural and monaural localization processes have been studied in isolation with VSFs (Chase, S. M. and Young, E. D., 2006; Davis, K. A., 2005; Delgutte, B. *et al.*, 1999). This paradigm simulates a free-field environment under closed-field conditions by shaping broadband sounds with the directional properties of the HRTF. Individual localization cues may be modified, removed, or placed in competition with the remaining directional properties of the simulated sound source.

The VSF selectivity of ICC neurons recapitulates their responses to free-field stimuli (Delgutte, B. *et al.*, 1999). Examples of typical responses are shown in Figure 15. When ITD cues are removed from VSF stimuli and electrophysiological recording is restricted to neurons with best frequencies above 4 kHz, most neurons respond preferentially to contralateral azimuths, reflecting the strong excitatory input from the opposite ear. This tuning may encompass the contralateral field (Figure 15(a)) or rise to a peak at a best azimuth (Figure 15(b)). For the majority of azimuth sensitive neurons, directional tuning is sharpened by the binaural inhibitory interactions of the opposite ear and degrades under monaural testing conditions.

Binaural sensitivity is not an absolute prerequisite of azimuth sensitivity (Delgutte, B. *et al.*, 1999). The discharge rates of monaural neurons are also modulated by changes in the azimuth of VSF stimuli. As discussed before, this azimuth sensitivity may arise from the monaural processing of spectral cues or simple changes in the gain of the HRTF in the contralateral ear.

Approximately half of ICC neurons respond selectively to VSF elevations in the median plane

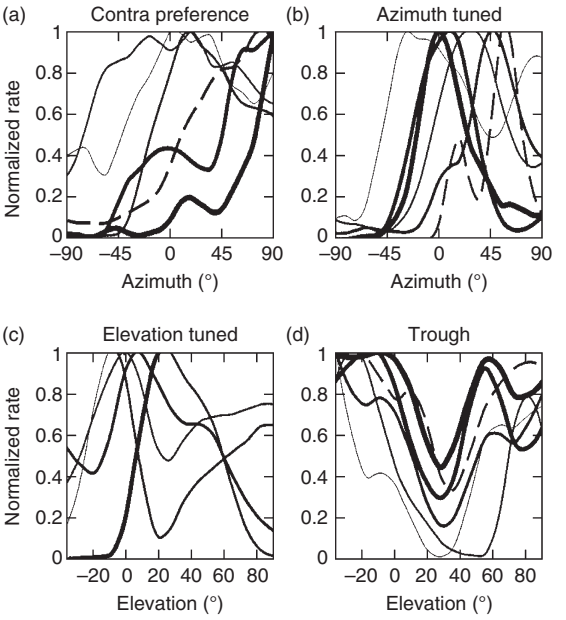

Figure 15 Responses of ICC neurons to VSF stimuli. (a, b) Examples of common azimuth tuning properties. (c, d) Common elevation tuning properties. Reproduced from Delgutte, B., Joris, P. X., Litovsky, R. Y., and Yin, T. C. 1999. Receptive fields and binaural interactions for virtual-space stimuli in the cat ICC. J. Neurophysiol. 81, 2833–2851., Copyright (1999), used with permission from The American Physiological Society.

(Delgutte, B. *et al.*, 1999). Unlike the results of earlier free-field experiments, many neurons with azimuth sensitivity fail to respond to changes in elevation. The neurons that do respond to these changes tend to display sharply tuned rate peaks (Figure 15(c) or troughs (Figure 15(d)). These strongly modulated responses imply a sensitivity to HRTF-based spectral peaks or notches, or combinations of both features in patterns that maximize excitatory inputs.

The dichotomy between azimuth and elevation sensitivity implies two modes of directional processing. A binaural mode imparts azimuth sensitivity through the interaction of contralateral excitatory and ipsilateral inhibitory inputs. A monaural mode modulates responses to changes in elevation or azimuth depending on the relationship between the tuning properties of the neuron and the directional properties of the HRTF. Neurons showing monaural sensitivity tend to have BFs that fall within the mid-frequency notch region of the HRTF.

ICC neurons can be linked to their brainstem inputs by shared response patterns (Davis, K. A.

et al., 1999; Ramachandran, R. *et al.*, 1999). Type-I neurons are distinguished by a frequency response map (FRM) with lateral inhibition (Figure 16(a)). As a result, excitatory tuning is restricted to an I-shaped region above the best-frequency threshold. The neurons are strongly inhibited when the frequency of a spectral notch coincides with BF and thus removes energy from the narrowly tuned excitatory field (Figure 16(b)). Similar inhibitory properties are displayed by the projection neurons of the lateral superior olive (LSO) implying that ascending projections from the binaural brainstem may preferentially target type-I units (Ramachandran, R. *et al.*, 2000).

Additional inferences regarding the ascending innervation of type-I units may be drawn from their binaural sensitivity and spatial selectivity (Davis, K. A. *et al.*, 1999; Ramachandran, R. *et al.*, 1999; Ramachandran, R. and May, B. J., 2002). Like LSO neurons, type-I units are excited when sounds are presented to the contralateral ear (E) and inhibited when sounds are presented to the ipsilateral ear (I). This so-called EI interaction is modulated by the timing of binaural stimulation. As demonstrated with closed-field stimuli in Figure 16(c), maximum ipsilateral inhibition is observed at a characteristic delay (CD) (Kuwada, S. *et al.*, 1987). The delay compensates for asymmetries of the binaural auditory system to deliver coincident inhibitory and excitatory inputs to the LSO (Batra, R. *et al.*, 1997). The requisite ITD is conferred under free-field conditions by the azimuth of the sound source.

The spatial tuning of type-I units is illustrated with a VSF procedure in Figure 16(d). As predicted by the EI binaural interaction, there is a sharp transition from excitatory to inhibitory responses as the simulated sound source moves from contralateral to ipsilateral locations. Although the responses of this unit were sampled across a broad range of azimuths

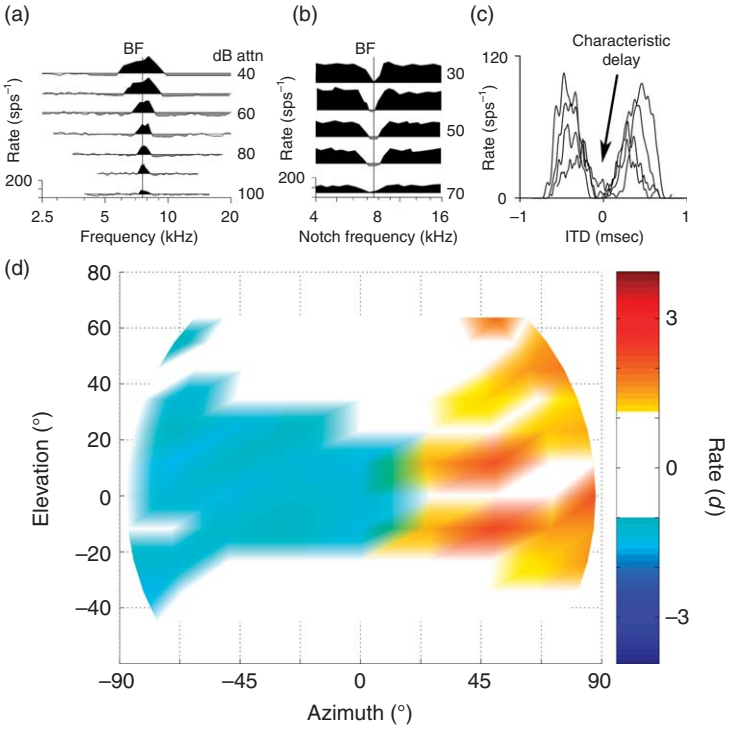

Figure 16 Physiological characteristics of ICC type-I units. (a) The narrow I-shaped excitatory tuning of the frequency response map (black) is dictated by lateral inhibition (gray). These inhibitory effects are potentiated when a spectral notch falls at BF (b) or binaural stimuli reach the two ears with a characteristic time delay (c). These response patterns are associated with the projection neurons of the lateral superior olive. (d) The binaural inhibitory properties of type-I units create contralateral preferences when the units are tested with VSF stimuli. Most units are excited by contralateral (positive) azimuths and inhibited by ipsilateral (negative) azimuths. Sound-driven rates are specified in units of SD relative to spontaneous activity (d'). Regions in red or blue represent statistically significant responses. Reproduced from Ramachandran, R. and May, B. J. 2002. Functional segregation of ITD sensitivity in the inferior colliculus of decerebrate cats. J. Neurophysiol. 88, 2251–2261. Copyright (2002), used with permission from The American Physiological Society.

and elevations, a subset of the stimulus conditions were arranged along the interaural horizontal axis (0° elevation) and therefore is equivalent to those shown in Figures 15(a) and 15(b). Under matching conditions, type-I units display the same directional properties as contra-preferring neurons. This spatial tuning is dictated by ILDs that are relatively unaffected by changes in elevation.

Type-O responses in the ICC are established by ascending projections from the DCN (Davis, K. A., 2002; 2005). As shown by the FRM in Figure 17(a), this response type takes its name from the O-shaped island of excitation that is consistently observed near the BF threshold (Ramachandran, R. *et al.*, 1999). In addition to sharing the strong on-BF inhibitory effects of DCN projection neurons, most type-O units show monaural responses when tested with ITD procedures (Figure 17(c)). They are silenced by surgical or pharmacological manipulations that disrupt the output pathways of the DCN (Davis, K. A., 2002).

Type-O units further transform the spectral integration properties of their DCN counterparts to optimize the processing of monaural localization cues (Davis, K. A. *et al.*, 2003). In Figure 17(b), the frequency of a spectral notch is swept across the receptive field of a type-O unit. Unlike the inhibitory responses that are observed for DCN type-IV units (Figure 8) or ICC type-I units (Figure 16(b)), type-O units exhibit strong excitatory responses at their characteristic notch frequency. This selectivity arises because a sharply tuned inhibitory input is turned off by the removal of spectral energy at frequencies near BF. When local GABAergic inhibition is blocked by administration of bicuculine, type-O units display the more generalized response patterns of type-IV and type-I units (Davis, K. A., 2002).

From a sound localization perspective, spectral selectivity is synonymous with spatial tuning. As shown in Figure 17(d), type-O units respond to the narrow range of azimuths and elevations where the HRTFs of VSF stimuli display the characteristic

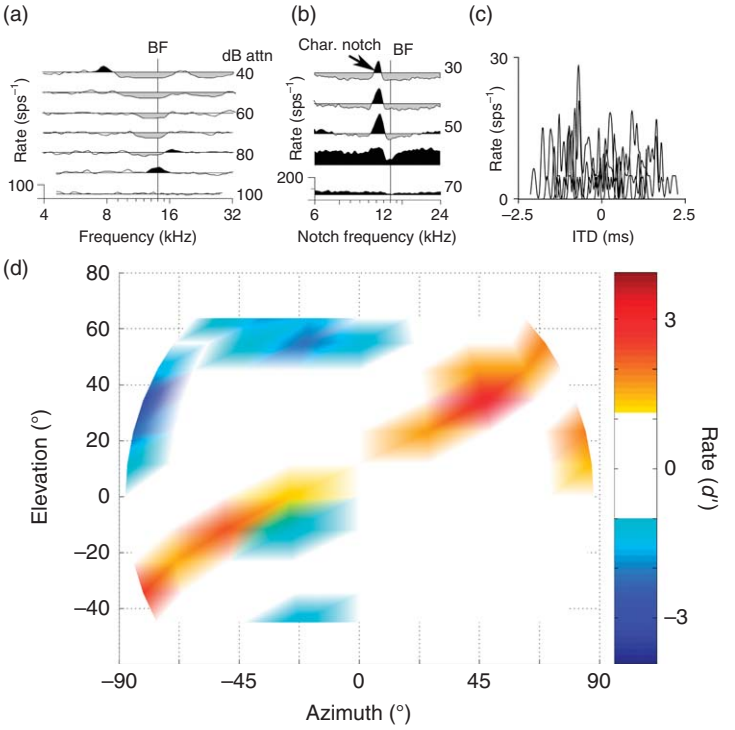

Figure 17 Physiological characteristics of ICC type-O units. (a) The frequency response map is largely inhibitory with the exception of an O-shaped island of excitation at the best-frequency threshold. The discharge rates of type-O units are strongly modulated when a spectral notch sweeps over BF (b) but most are insensitive to binaural cues (c). (d) Despite their lack of binaural sensitivity, the notch selectivity of type-O units tunes their excitatory responses to the azimuth and elevation of VSF stimuli. Plotting conventions are described in Figure 16. Reproduced from Ramachandran, R. and May, B. J., 2002. Functional segregation of ITD sensitivity in the inferior colliculus of decerebrate cats. J. Neurophysiol. 88, 2251–2261. Copyright (2003), used with permission from The American Physiological Society.

notch frequency. When responses are limited to a single horizontal or vertical plane, directional properties compare favorably with the tuned azimuth and elevation responses in Figures 15(b) and 15(c). Although these results were obtained with binaural stimuli, the weakly binaural type-O units are not significantly affected by the removal of ipsilateral stimulation.

Despite the discrete nature of ICC unit types, most neurons are sensitive to multiple sound localization cues (Chase, S. M. and Young, E. D., 2005). Chase S. M. and Young E. D. applied an information theory approach to discharge rates that were evoked by parametric manipulations of ITD, ILD, and spectral notches. The feature of interest was presented under closed field conditions and adjusted to conform to the frequency tuning characteristics and threshold of individual neurons. For example, in one series of experiments, the playback rate of HRTF stimuli was varied to sweep the mid-frequency spectral notch across BF. Under these conditions, type-I units provided the most information regarding changes in notch frequency and ILD.

An important distinction to be made with these findings is the unique role of auditory neurons that are generalists versus specialists. In the context of spectral cues for sound localization, these characteristics are synonymous with narrowband versus wideband integration. The lateral inhibitory properties of type-I units sharpen frequency tuning and endow the neurons with the ability to encode spectral peaks and notches (Ramachandran, R. *et al.*, 2000). These narrowband responses are sensitive to variations in the magnitude of local HRTF features but ignore the broader context in which they occur. As a result, the neurons show strongly modulated responses to notch frequency sweeps (Figure 16(b)) but little directional selectivity (Figure 16(c)). By contrast, the wideband integration properties of type-O units diminish their generalized spectral sensitivity, but maximize the selectivity of their spatial coding (Figure 17(c)).

3.37.7 Acoustic Manipulations of the Spectral Processing Pathway

In good agreement with physiological descriptions of the sound localization pathways, an extensive psychophysical literature suggests that binaural and monaural processes merge to support the accurate localization of sound source azimuth and elevation (for a general review of human psychophysical literature, see Middlebrooks, J. C. and Green, D. M., 1991). The relative importance of binaural and monaural pathways has been addressed by acoustic manipulations that alter the ear's input to the brain or the spectral content of the stimulus that impinges on the ear.

3.37.7.1 Altering the Ear's Input to the Brain

Complete unilateral deafness may be considered the most profound manipulation of the ear's input (Gatehouse, R. W., 1976). In parallel with Lord Rayleigh's (1907) classic treatise on the duplex theory of binaural sound localization, Angell and Fite (Angell, J. R. and Fite, W., 1901a; 1901b) introduced the concept of spectral based directional cues by describing the localization abilities of an individual who was profoundly deaf in one ear. Although localization was extremely uncertain in the region opposite the affected ear, the individual was able to make accurate responses to sound sources on the side of the intact ear. Sounds with increased spectral complexity were associated with faster and more accurate localization, which led these investigators to propose that directional quality is imparted by the frequency-dependent damping and reinforcement of sound energy by pinna acoustics. These observations have been confirmed in subsequent studies of unilateral deafness (Slattery, W. H., 3rd and Middlebrooks, J. C., 1994; Starch, D., 1908; Viehweg, R. and Campbell, R. A., 1960).

Prior to detailed descriptions of the human HRTF and the digital signal processing techniques that are required to synthesize these acoustic effects, Gardner M. B. and Gardner R. S. (1973) linked the directional properties of the pinna to sound localization by progressively occluding the ear cavities of human listeners. These simple, yet elegant experiments systematically related perceptual errors to the extent of occlusion, the location of the sound source, and the high-frequency content of the auditory stimulus. Their basic findings on the importance of pinna-based spectral cues in vertical localization have not been challenged by decades of ensuing research and more sophisticated testing procedures.

Other investigators have attempted to simulate monaural localization effects by completely plugging one ear of normal listeners (Oldfield, S. R. and Parker, S. P., 1986). These procedures are somewhat controversial because even low levels of sound in the occluded ear provide access to interaural localization

cues (Wightman, F. L. and Kistler, D. J., 1997). Noteworthy among these studies are experiments by Slattery W. H., 3rd and Middlebrooks J. C. (1994) that have explored the limitations of plugging procedures with direct comparisons of acute versus chronic unilateral deficits. Although there is considerable variation in the performance of individuals with congenital deafness in one ear, most subjects show the remarkably normal abilities that were observed by Angell J. R. and Fite W. (1901a; 1901b). By contrast, plugging one ear of normal listeners leads to the highly inaccurate perception of a sound source that is translated toward the unobstructed ear. The temporary distortion of binaural input has less effect on vertical localization. Two alternative conclusions may be drawn from the powerful immediate deficits of monaural plugging procedures. Spectral cues may play only a supportive role in horizontal localization (Batteau, D. W., 1967; Musicant, A. D. and Butler, R. A., 1984a), or their spatial attributes may be enhanced by the binaural processing of interaural spectral differences (Searle, C. L. *et al.*, 1975).

The clear differences in acute versus chronic manipulations suggest that ear plugs do not adequately unmask the full utility of monaural spectral cues (Jin, C. *et al.*, 2004). With sufficient experience, listeners can learn to rely exclusively on the directional properties of the pinna for the localization of both azimuth and elevation (Musicant, A. D. and Butler, R. A., 1980; Van Wanrooij, M. M. and Van Opstal, A. J., 2004). This compensation has also been observed when individuals are given sufficient time to adapt to the sound altering effects of ear cavity occlusion (Hofman, P. M. *et al.*, 1998; McPartland, J. L. *et al.*, 1997; Van Wanrooij, M. M. and Van Opstal, A. J., 2005) or supernormal localization cues (Shinn-Cunningham, B. G. *et al.*, 1998). From a clinical perspective, the effects of conductive hearing loss on sound localization show similar patterns of compensation in patients with chronic versus acute otitis media (Kawase, T. *et al.*, 1999).

3.37.7.2 Spectral Manipulations

An alternate strategy for characterizing the perceptual impact of monaural spectral cues is to manipulate the frequency content of the stimulus. In their simplest incarnation, these experiments can be traced to Pratt C. C. (1930), who noted that the frequency of a pure tone altered the spatial character of sound source elevation. Similar perceptual effects have been described for narrow bands of noise (Blauert, J., 1969/1970, 1997). For example, as the frequency content of a noise band changes from 1 to 5 kHz, the spatial attributes of the sound source shifts from behind to in front of the listener regardless of its actual angle of incidence. Acoustic measures indicate that these location judgments are correlated with a directional boost of the energy band. That is, the DTF exerts a high gain when frequencies near 4–5 kHz reaches the ear from a frontal location (Figure 5(c)). A rearward enhancement is noted at frequencies near 1–2 kHz.

A subtle property of Blauert's directional bands is that they are derived localization cues. That is, they are based on the relative acoustic differences that distinguish individual transfer functions from the average spectral shape of all transfer functions. Because they are not an absolute property of the transfer function, Musicant A. D. and Butler R. A. (1984b) have described these features as covert peaks.

Frequency also exerts strong effects on monaural localization in the horizontal plane. When Butler R. A. and Flannery R. (1980) disrupted normal binaural processing with a unilateral ear plug, the frequency content of a noise band altered the perceived laterality of the sound source. As illustrated in Figure 18, increasing the noise frequency from 4 to 8 kHz moved the apparent azimuth of the stimulus from opposite the unobstructed ear (negative 90°) to a frontal location (negative 15°). The pattern repeated at frequencies above 8 kHz, suggesting the existence of multiple spatial referent maps. Accurate localization was observed when the bandwidth of the stimulus was sufficient to overlap adjacent maps.

Implicit in studies of narrow band sound localization is a processing scheme that establishes sound source location by matching the proximal spectrum of the stimulus to the directional properties of outer ear acoustics. This relationship was directly tested by Middlebrooks J. C. (1992). Figure 19 plots the stimulus locations and ensuing responses of one subject for noise bands with a center frequency of 12 kHz. The columnar organization of the data in Figure 19(a) suggest that the azimuth of the sound source was localized with reasonable accuracy, presumably by attending to ILDs. Regardless of actual vertical and front–back coordinates, the subject most often identified a sound source near the horizontal plane (Figure 19(a)) and in the frontal field (Figure 19(b)). Two properties of these errors are noteworthy: they are systematic and they are confined to the dimensions of localization that are most closely linked to monaural spectral processing.

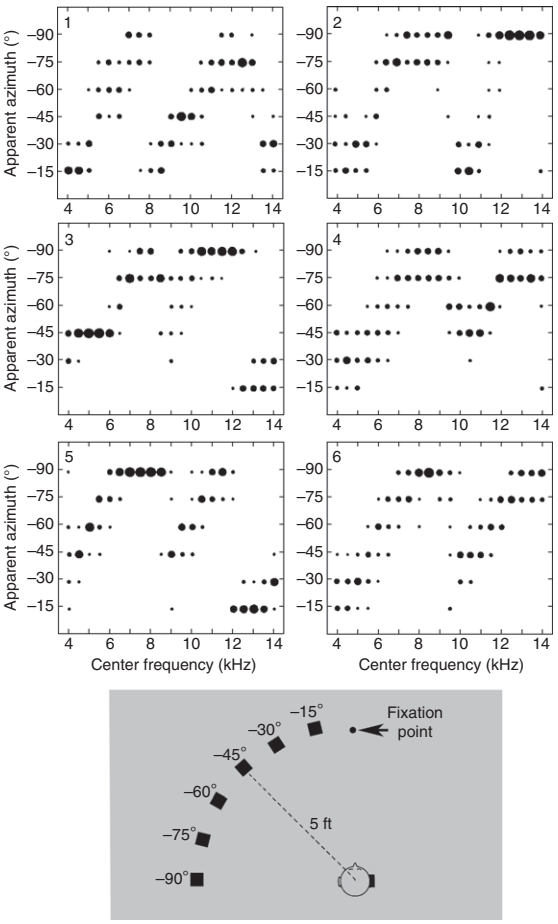

Figure 18 Apparent azimuth of 1 kHz wide noise bands with center frequencies of 4–14 kHz. Number of judgments is indicated by the size of the circle. Individual results are shown for six subjects. The arrangement of the speaker array is shown below. Adapted from Butler, R. A. and Flannery, R. 1980. The spatial attributes of stimulus frequency and their role in monaural localization of sound in the horizontal plane. Percept. Psychophys. 28, 449–457. with permission.

The spectral cues that potentially influence the localization behaviors of the listener are shown in Figure 19(c). These four DTFs have been selected because they correspond to response locations that occurred with the greatest frequency for 6, 8, 10, and 12 kHz noise bursts. Each function displays a tuned bandpass effect near the frequency that generated the matching spatial attribute. The filter shapes are reminiscent of the directional bands of Blauert J. and covert peaks of Musicant A. D. and Butler R. A.

Experiments with narrow bands of noise emphasize the importance of energy peaks in monaural localization. Other psychoacoustic procedures have focused on the directional properties of spectral notches. Hebrank, J. and Wright D., (1974) evaluated localization in the median plane using a number of high-pass, low-pass, band-pass, and band-stop filter conditions. Accurate localization required a sound spectrum with frequencies between 4 and 16 kHz. The noise band imparted a frontal directionality if it contained a spectral notch at frequencies between 4 and 10 kHz and increased energy at frequencies above 13 kHz. Increases in the lower cutoff of the notch raised the apparent elevation of the sound source.

A similar notch–frequency relationship was found by Butler R. A. and Belendiuk K. (1977). These investigators recorded the ear canal responses for noise sources in the median plane. Subjects could localize closed-field presentations of the recordings almost as well as their free-field counterparts. A spectral analysis of the recordings revealed a deep notch at frequencies between 5 and 9 kHz. The frequency of the notch changed with sound source elevation. The DTF in Figure 5(c) shows the notch for an elevation of 0°.

Bloom P. J. (1977) extended the findings of Butler R. A. and Belendiuk K. using a novel psychophysical approach. He assumed that tone detection thresholds would manifest pinna filtering effects if they were obtained under monaural conditions and if head movements were eliminated. After measuring thresholds at frequencies between 4 and 16 kHz using sound sources in the median plane, he derived the psychoacoustic eqivalent of DTFs by subtracting the average sensitivity curve from curves at individual locations. As previously noted in other psychoacoustic studies (Hebrank, J. and Wright, D. 1974; Butler, R. A. and Belendiuk, K. 1977), this behavioral method revealed a spectral notch that changed systematically in frequency with sound source elevation.

Bloom hypothesized that the spatial attributes of sounds in the median plane could be modified by adding spectral notches to the source spectrum. Subjects first listened to an unmodified reference stimulus from target elevations that ranged from ±45° and then created a matching vertical percept by adjusting the synthetic notch of a comparison stimulus from an eccentric location with a relatively featureless transfer function. He noted a strong correlation between natural occurring notches and the synthetic notches of illusionary source locations.

The subjects of animal behavioral studies are also sensitive to perturbations of the natural spectral cues that govern vertical sound localization. Cats make

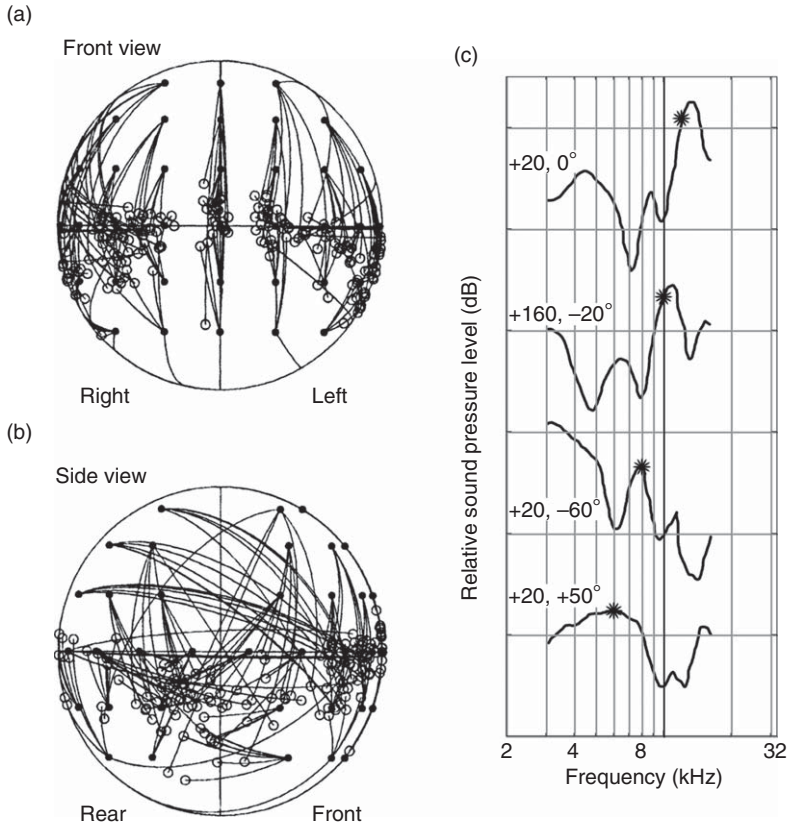

Figure 19 Localization responses of a human subject for narrow bands of noise. (a, b) The spatial distribution of responses to noise with a center frequency of 12 kHz. Stimulus locations (filled circles) and response locations (open circles) are joined by lines. (c) Directional transfer functions for the same subject. Numerical labels indicate the azimuth and elevation associated with each function. Stars mark the center frequency of noise bands that generated responses near the four locations. Reproduced from Middlebrooks, J. C. 1992. Narrow-band sound localization related to external ear acoustics. J. Acoust. Soc. Am., 92, 2607–2624. Copyright (1992), used with permission from American Institute of Physics.

accurate head orientation responses to brief bursts of broadband noise (May, B. J. and Huang, A. Y., 1996). If the noise spectrum is truncated in a manner that preserves mid-frequency spectral notches (Figure 10), performance is spared (Huang, A. Y. and May, B. J., 1996a). Broadband sounds lacking notch frequencies and pure tones elicit large elevation errors. These deficits are not observed in spatial acuity tasks that do not require absolute localization of the sound source (Huang, A. Y. and May, B. J., 1996b).

An unexpectedly robust demonstration of the directionality of spectral notches was observed in the context of summing localization by Tollin D. J. and Yin T. C. (2003). Like humans, cats may confuse two sound sources as a single spatial image. The fused location is determined by the relative timing of stimulus onsets. Short interstimulus delays sum to create the illusion of an intermediate location that is biased toward the leading speaker. When Tollin, D. J. and Yin, T. C. applied this principle, they noticed that sound sources in the horizontal plane evoked orientation responses that were also shifted toward higher elevations.

An explanation for the ventriloquial quality of the summed stimulus is presented in Figure 20. As previously noted by May B. J. and Huang A. Y. (1996) , systematic changes in notch frequency are correlated with accurate orientation responses to single sound sources in the median plane (Figure 20(a)). Notch frequencies of 12–13 kHz are associated with elevations of 9–18°. When broadband energy from symmetrical locations in the horizontal plane is summed, binaural difference cues are minimized and monaural spectral cues mimic the HRTF of an elevated source (Figure 20(b)).

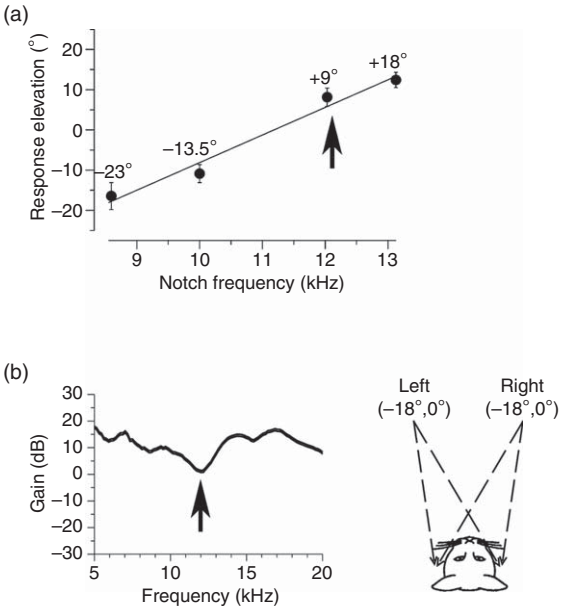

Figure 20 Role of spectral notches in the illusion of vertical location. (a) Response elevation as a function of notch frequencies in the cat's head-related transfer functions. Numerical labels indicate the actual locations associated with the spectral features. (b) Illusory transfer function created by the summation of paired speakers in the horizontal plane. The inset describes the physical arrangement of the speakers and subject. Arrows relate the pseudonotch to actual directional cues in the median plane. Reproduced from Tollin, D. J. and Yin, T. C. 2003. Spectral cues explain illusory elevation effects with stereo sounds in cats. J. Neurophysiol. 90, 525–530. Copyright (2003), used with permission from The American Physiological Society.

The spectral manipulations that alter the spatial hearing of humans and animals suggest that members of the same species rely on a common set of localization cues. A principal component analysis by Kistler D. J. and Wightman F. L. (1992) has confirmed that 90% of the individual variance of human HRTFs can be explained by the linear summation of five basis functions. Middlebrooks J. C. and Green D. M. (1992) reached the same conclusion using different analysis techniques. Similarities between the independently derived basis functions are remarkable.

Although the gross acoustic properties of the external ear are conserved across individuals, best immediate virtual localization is achieved when sounds are shaped by the listener's own HRTFs (Butler, R. A. and Belendiuk, K., 1977; Morimoto, M. and Ando, Y., 1982; Wenzel, E. M. *et al.*, 1993). Nonindividualized transfer functions evoke poor elevation accuracy and front–back confusion. The binaural processes that support horizontal localization are more robust, presumably because their directional properties are less individualized (Wightman, F. L. and Kistler, D. J., 1998).

Intersubject differences in localization cues are highly correlated with the physical dimensions of the listener (i.e., interaural delays, size of the external ear, and head width) (Middlebrooks, J. C., 1999a; Xu, L. and Middlebrooks, J. C., 2000). Acoustic measurements have shown that the disparities are reduced by compressing or expanding the frequency axis of DTFs. This relationship suggests that virtual sound localization may be enhanced by scaling procedures that align synthetic spectral shapes with the listener's natural cues. These findings have important implications for the design of generic sound fields with realistic directional qualities.

Frequency scaling has been used successfully to improve performance in virtual localization tasks (Middlebrooks, J. C., 1999b). The resulting benefits are particularly evident when elevation judgments are based on other-ear transfer functions. The magnitude of response errors is halved in most listeners.

A limitation for the practical application of frequency scaling is that detailed acoustic measurements are needed to optimize the match between synthetic and natural localization cues. In the absence of these measures, the most veridical scale factor must be estimated from an individual's physical dimensions or by confirming its reliability with psychophysical procedures (Middlebrooks, J. C. *et al.*, 2000).

The spatial illusions created by spectral peaks and notches imply that the auditory system is making assumptions regarding the transformation of the source spectrum by the directional filtering properties of the outer ear. The dilemma is: how does the auditory system distinguish a spectral feature that is introduced by the ear from a feature that exists at the sound source? It remains a matter of debate whether this information is available for familiar sounds or must be recovered by the auditory system.

Rakerd B. *et al.* (1999) addressed the question of stimulus familiarity by training listeners to identify band–band noise tokens with different spectral peaks and notches. After a brief training period, identification errors were uncommon when the stimuli were presented from a fixed location in the median plane but increased when the source location changed randomly across presentations. The magnitude of the deficit in the roving speaker condition was related to the center frequency of the noise. Frequencies less

than 3 kHz yielded near normal identification rates, while frequencies above 8 kHz approached chance performance. This dependency suggests that listeners could not dissociate the source spectrum from pinna-based features that are introduced at frequencies above 3 kHz. Knowledge of the sound's location did not influence these results. Listeners did not show better identification for spectral shapes that were accurately localized.

In contrast to the narrow bands of noise or spectral notches that evoke spatial illusions, most naturally occurring sounds have locally constant slopes (Zakarauskas, P. and Cynader, M., 1993). Consequently, very sharp pinna-filtering effects create spectral discontinuities that can support accurate monaural localization. In addition, each ear exerts a unique filtering effect when sounds outside the median plane contact the head with different incident angles. Subtle disparities in the transfer functions of the two pinnae yield similar differences when sounds occur within the median plane (Searle, C. L. *et al.*, 1975). Binaural spectral comparisons may allow the listener to isolate these local filtering effects. Regardless of the mechanism, the auditory system resolves these ambiguities under all but the most extreme stimulus conditions. Such spatial illusions are rare for natural sounds.

3.37.8 Lesions of the Spectral Processing Pathway

Lesions of the spectral processing pathway reveal the contributions of the ear and brain to sound localization behavior. Critical central auditory nuclei can be silenced by design in experimental animals with controlled surgical lesions. No less profound are the unplanned processing deficits that afflict humans when the cochlea is damaged by disease, acoustic overexposure, or aging.

3.37.8.1 Cochlear Deficits

A complete loss of auditory function in one ear does not preclude accurate sound localization if normal hearing is maintained in the opposite ear (Slattery, W. H., 3rd and Middlebrooks, J. C., 1994). A more common form of peripheral deafness is the progressive bilateral loss of high-frequency hearing that affects virtually all adult humans. This condition is known as presbycusis (Gates, G. A. and Mills, J. H., 2005). Assessments of directional hearing in presbycusis patients suggest that sound localization is resistant to high-frequency hearing loss (Colburn, H. S., 1982; Rosenhall, U., 1985). Existing audiological measures have focused on sound localization in the horizontal plane. Under these conditions, sound source laterality may be derived from ITD cues, if low frequencies are present and the listener possesses residual low-frequency hearing (Wightman, F. L. and Kistler, D. J., 1992).

Rakert B. *et al.* (1998) extended the psychophysical assessments of presbycusis patients to locations that were more closely linked to high-frequency spectral processing. These subjects showed normal localization in the horizontal plane but rarely scored above chance for sources in the median or sagittal planes. Hearing aid amplification of the high-frequency spectral cues significantly improved performance.

The deficits in spatial processing that accompany hearing loss are not exclusively directional. A listener's ability to segregate simultaneous streams of competing sounds or separate auditory signals from background noise is intricately bound to localization processes (Cherry, E. C., 1953; Hirsh, I. J., 1950). For these reasons, presbycusis often leads to perceptual abnormalities in masking, speech intelligibility, and loudness recruitment before overt hearing loss. As the far ranging consequences of spatial hearing are recognized, strategies for deafness rehabilitation are placing greater emphasis on the preservation of binaural hearing and pinna acoustics (Lin, L. M. *et al.*, 2006).

Outer hair cells are a primary site for the early stages of cochlear deafness (Rokay, E. and Penzes, L., 1988; Soucek, S. *et al.*, 1987). These sensory neurons are innervated by descending olivocochlear efferent fibers (Kimura, R. and Wersall, J., 1962). The cholinergic effects of the olivocochlear projections modulate cochlear sensitivity and frequency tuning by altering the voltage-sensitive electromotile properties of outer hair cells (Fuchs, P., 2002). Electrical stimulation of the olivocochlear bundle can expand the dynamic range properties of auditory-nerve fibers, particularly when transient signals are embedded in continuous background noise (Guinan, J. J., Jr. and Gifford, M. L., 1988; Wiederhold, M. L., 1970; Winslow, R. L. and Sachs, M. B., 1987).

An intriguing aspect of olivocochlear anatomy is the prolific innervation of the middle turns of the cat's cochlea (Liberman, M. C. *et al.*, 1990). This projection pattern augments efferent feedback at frequencies between 5 and 20 kHz (Wiederhold, M. L., 1970), and therefore may enhance the coding of

mid-frequency spectral notches that are critical for accurate localization behaviors (Huang, A. Y. and May, B. J., 1996a). May B. J. *et al.* (2004) investigated the role of efferent feedback in sound localization by lesioning the olivocochlear bundle of domestic cats. The specificity of the resulting deficits was striking. Lesioned cats maintained normal directional hearing when sound sources changed location in the horizontal plane. Spatial acuity decreased moderately in the median plane under quiet conditions and was severely disrupted in the presence of background noise. With sufficient training, a number of cats recovered normal function. These findings suggest that the peripheral representation of spectral cues was altered but not eliminated by the disruption of efferent feedback.

3.37.8.2 Experimental Lesions of the Dorsal Cochlear Nucleus

The behavioral significance of spectral processing in the DCN has been explored by evaluating the auditory deficits of cats with surgical lesions of the dorsal acoustic stria (May, B. J., 2000). These fibers are the ascending axons of the type-IV principal cells that link the DCN to ICC. In previous studies, the surgical procedure did not change hearing sensitivity or the detection of signals in noise (Masterton, R. B. and Granger, E. M., 1988; Masterton, R. B. *et al.*, 1994). It did diminish the accuracy of reflexive head orientations to bursts of noise in the median plane (Sutherland, D. P. *et al.*, 1998b). The surgical procedure had no effect on the discrimination of sound source elevation (Sutherland, D. P. *et al.*, 1998a), leading Sutherland and Masterton to hypothesize that the loss of function involved the formulation of the orientation response. One explanation for the specificity of the deficit is that absolute localization competency is required to make accurate head orientations but not to discriminate spatial differences.

The orientation plots in Figure 21(a) illustrate the head pointing behaviors of one cat before lesions of the dorsal acoustic stria (May, B. J., 2000). These tests were conducted with band-pass noise to restrict the domain of HRTF-based spectral information to the mid-frequency notches that exist at 5–20 kHz. As predicted by the results of previous spectral manipulations (Huang, A. Y. and May, B. J., 1996a), the cat exhibited well-directed orientation responses prior to the lesion. The cat slightly underestimated locations when the noise bursts were presented from high elevations. Mid-frequency spectral notches are not a

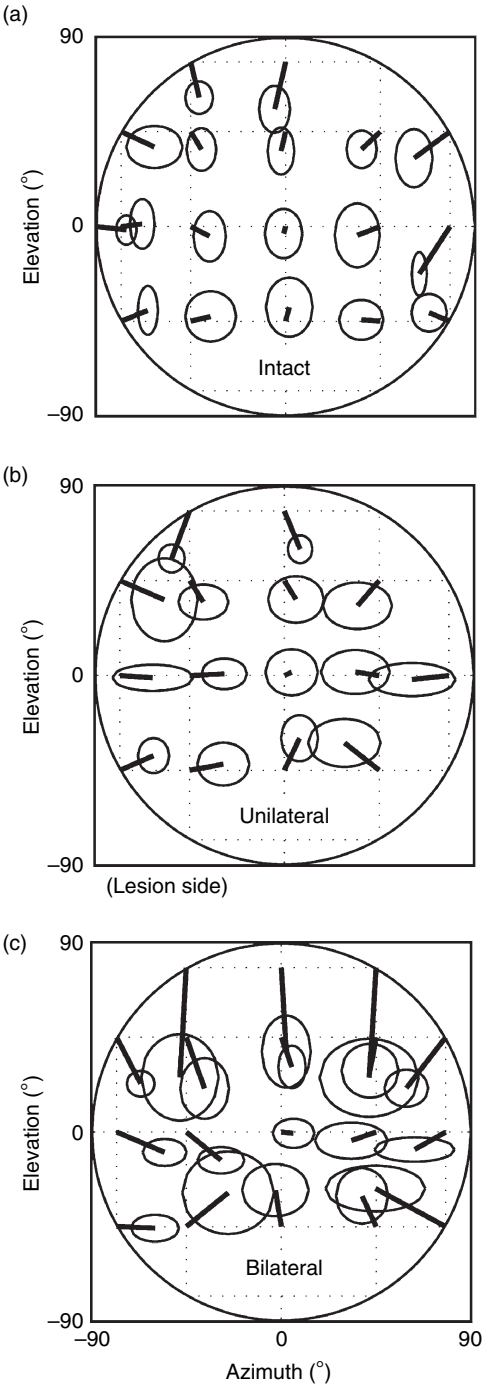

Figure 21 Effects of strial lesions on sound-evoked orientation behavior. Results are shown for one cat before the lesions (a), and after unilateral (b) and bilateral lesions of the dorsal acoustic striae (c). Each ellipse represents the SD of azimuth and elevation for orientation responses to the speaker location indicated by the adjoining line segment. Reproduced from May, B. J. 2000. Role of the dorsal cochlear nucleus in the sound localization behavior of cats. Hear. Res. 148, 74-87. Copyright (2000), with permission from Elsevier.

prominent feature of the HRTF at these eccentric angles of incidence (Rice, J. J. *et al.*, 1992).

Orientation behaviors were only slightly degraded if the dorsal acoustic stria was left intact on one side of the brain (Figure 21(b)). The cat distinguished the elevation and azimuth of most test locations, although the variability of responses increased slightly. Errors at eccentric locations grew in magnitude but remained localized to those spatial regions that proved most difficult to intact subjects. These results suggest that monaural spectral cues can support relatively accurate localization over a wide range of source locations. Similar response patterns have been noted in psychophysical studies of monaural humans (Angell, J. R. and Fite, W., 1901b; Slattery, W. H., 3rd and Middlebrooks, J. C., 1994).

Large localization errors were noted after a second lesion disrupted spectral processing pathways on both sides of the brain (Figure 21(c)). These localization deficits were statistically significant only in terms of response elevation. Regardless of the actual location of the sound source, the subject's orientation responses were seldom directed toward elevations that deviated more than 20° from the interaural horizontal plane. The systematic underestimations could exceed 60° for extreme source locations.

It is likely that cats with bilateral DCN lesions maintained accurate lateral localization by relying on the ILD and ITD cues that are processed in the intact binaural pathways (Batteau, D. W., 1967; Musicant, A. D. and Butler, R. A., 1984a). This interpretation was investigated by acutely disrupting binaural processing in lesioned cats with unilateral ear plugs. The manipulation is predicted to have less impact on intact cats that can learn to rely on monaural spectral cues (Hofman, P. M. *et al.*, 1998; Van Wanrooij, M. M. and Van Opstal, A. J., 2005).

The effects of a unilateral ear plug before and after DCN lesions are contrasted in Figure 22. Orientation responses of an intact cat conform well to target localizations except at extreme lateral positions opposite the plugged ear (Figure 22(a)). These results were collected after the cat had habituated to the plug. Acute ear plug effects were more severe, as has been noted in humans (Slattery, W. H., 3rd and Middlebrooks, J. C., 1994).

When monaural spectral processing was surgically eliminated and binaural inputs acoustically altered (Figure 22(b)), the lesioned cat made robust errors at all target locations. A direct comparison of the orientation behaviors of the lesioned cat with normal binaural processing (Figure 21(c)) and the lesioned

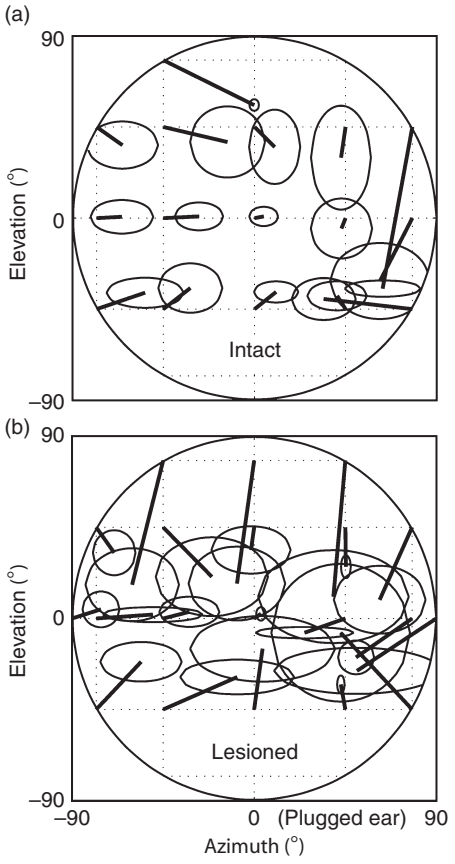

Figure 22 Effects of an acute ear plug (right ear) on orientation behavior. Responses of one cat are compared before (a) and after bilateral lesions of the dorsal acoustic striae (b). Plotting conventions are described in Figure 21. Reproduced from May, B. J. 2000. Role of the dorsal cochlear nucleus in the sound localization behavior of cats. Hear. Res. 148, 74–87. Copyright (2000), with permission from Elsevier.

cat with an ear plug (Figure 22(b)) suggests that horizontal accuracy is the critical difference in their localization abilities.

Spatial discrimination procedures have been conducted in cats with bilateral DCN lesions to verify the specificity of deficits first reported by Sutherland and Masterton (May, B. J., 2000). These experiments are summarized by the psychometric functions in Figure 23. Each function represents the postlesion performance of one cat for directional changes in the horizontal (Figure 23(a)) and median planes (Figure 23(b)). The test stimuli were mid-frequency noise bursts.

All of the cats exhibited orientation deficits. None of the subjects showed signs of impaired spatial

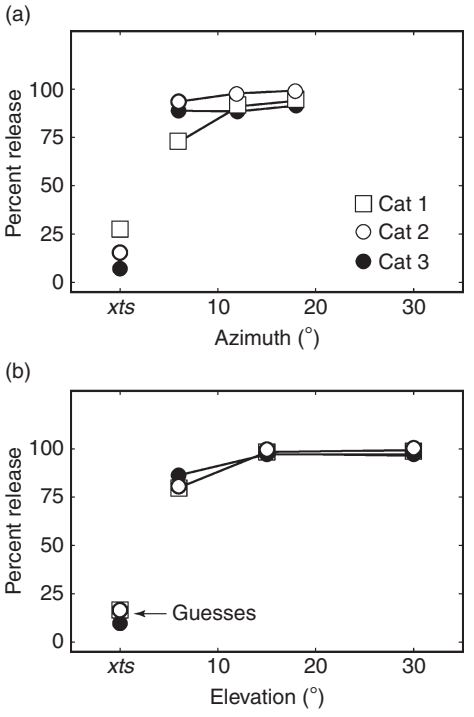

Figure 23 Effects of strial lesions on the discrimination of sound sources in the horizontal (a) and median planes (b). Results are shown for one cat after bilateral lesions of the dorsal acoustic striae. Psychometric functions plot the percentage of correct responses in relation to the magnitude of changes in location. False-positive responses (guesses) are estimated by catch trials that did not include changes in location (xts). Reprinted from May, B. J. 2000. Role of the dorsal cochlear nucleus in the sound localization behavior of cats. Hear. Res. 148, 74–87. Copyright (2000), with permission from Elsevier.

discrimination. These results confirm that DCN lesions do not lead to generalized hearing deficits and further support the notion that spatial acuity and directional identification are based on different auditory cues and processing pathways.

A loss of cochlear inputs to the DCN has been associated with the perception of phantom sound, or tinnitus (Moller, A. R., 2003). Although the etiologies and physiological consequences of this pervasive hearing disorder are varied, elevated activity in the absence of sound stimulation is a common outcome when animal models are subjected to experimental manipulations that are known to induce tinnitus in humans.

Tinnitus-related hyperactivity has been observed in the DCN (Brozoski, T. J. and Bauer, C. A., 2005; Imig, T. J. and Durham, D., 2005; Kaltenbach, J. A. *et al.*, 2005) and ICC (Chen, G. D. and Jastreboff, P. J., 1995; Jastreboff, P. J. and Sasaki, C. T., 1986; Ma, W. L. *et al.*, 2006). A unifying property of these structures is that their normal sound-driven responses are sculpted by both auditory and nonauditory inputs. For example, the granule cell layer of the DCN receives somatosensory and vestibular inputs that are thought to integrate the auditory processing of sound localization cues with head and pinna movements (Davis, K. A. *et al.*, 1996; Kanold, P. O. and Young, E. D., 2001). Interestingly, many patients can modify the strength of their tinnitus percepts by maneuvers of the jaw, head, and neck (Levine, R. A. *et al.*, 2003). Tinnitus may arise when these somatosensory–auditory interactions are no longer regulated by the intrinsic inhibitory circuitry of the DCN (Ma, W. L. and Young, E. D., 2006). This is an area of intense physiological research.

3.37.8.3 Experimental Lesions of the Inferior Colliculus and Its Projections

The neuroanatomical basis of sound localization has also been investigated by evaluating the effects of surgical lesions beyond the cochlear nucleus (Aitkin, L. M., 1986). None of these paradigms have looked exclusively at monaural spectral processing but they are nevertheless relevant because they often involve bilateral lesions that are completed in a two-stage process. Functional assessments that precede the second surgical procedure offer insights into monaural performance.

A consensus among lesioning studies is that damage to the lower commissural pathways exerts a pervasive effect on sound localization (Casseday, J. H. and Neff, W. D., 1975; Jenkins, W. M. and Masterton, R. B., 1982; Masterton, R. B. *et al.*, 1967; Moore, C. N. *et al.*, 1974). Masterton and colleagues demonstrated these deficits with shock-avoidance procedures. Cats were conditioned to avoid the shock by jumping a barrier to the safe side of a double grill box. A warning sound indicated the shock was about to be delivered. The procedure was adapted to sound localization by training the cats to wear a helmet that was equipped with binaural hearing aids. The closed-field sound system allowed the investigators to precisely control the directional properties of the auditory stimuli. Pinna-based localization cues and ILDs were eliminated, but ITD cues gave the stimuli a spatial lateralization within the head (Plenge, G., 1974).

The complexity of the stimulus conditions that warned of the impending shock were manipulated to

determine the specificity of lateralization deficits. In two tasks, the warning stimulus was a train of clicks in the right ear and the safe stimulus was either silence (discrimination #1) or a train of clicks in the left ear (discrimination #2). These tests did not assess binaural hearing. They were used as a procedural control to ensure that lesioned subjects maintained the ability to hear auditory stimuli.

Discrimination #3 was more directly linked to binaural processing. A right to left pattern of click pairs (RL) signaled the warning state and a left to right pattern (LR) indicated the safe condition. The binaural click pairs were separated by 50 μs. For cats with normal ITD processing, this short interaural delay creates a fused lateralized percept making the task equivalent to R versus L discrimination (discrimination #2). Lesions that impair ITD processing produce a specific loss of discrimination #3. The magnitude of the deficit was quantified by varying the time delay between clicks (Δt).

Cats with a complete unilateral lesion of the trapezoid body continued to perform the L versus R tasks but exhibited a severe disruption of LR versus RL binaural discrimination (Masterton, R. B. *et al.*, 1967). The deficit was related to a large shift in Δt sensitivity. Although normal cats discriminated time delays of less than 50 μs, lesioned cats required delays greater than 500 μs. Time disparities of this magnitude cannot be realized under natural free-field conditions (Roth, G. L. *et al.*, 1980).

Complete unilateral lesions of the trapezoid body also involved the dorsal and intermediate acoustic striae and the superior olive. Given this extensive damage, it is not clear how the central auditory pathways retained any capacity for binaural processing. Observations in cats with partial lesions of the trapezoid body or lateral lemniscus suggest that ITD processing is robust to surgical manipulation (Masterton, R. B. *et al.*, 1967). Near normal LR versus RL discrimination was possible if surgical procedures spared only a fraction of the projections in either pathway. It is likely that broadband clicks enhanced the usefulness of any surviving fibers by conveying Δt cues across the widest possible frequency range.

The effects of ICC lesions also may be dissociated by comparing the functional consequences of complete versus partial lesions (Masterton, R. B. *et al.*, 1968). A deep bilateral lesion of the nucleus, or its ascending pathways (brachium), impaired not only LR versus RL discrimination but also the discrimination of L versus R clicks. In the latter case, monaural discrimination could be improved by additional ILD cues. Superficial lesions that were restricted to the apical ICC did not disrupt lateralization behaviors. Consequently, ITD discrimination was possible if binaural information could enter the basal nucleus via the lateral lemniscus and then ascend to the forebrain via the brachium.

Masterton and his colleagues isolated ITD processing deficits by forcing subjects to attend to a single directional cue under closed-field conditions. Although these lateralization paradigms provide classic examples of functional organization, they do not predict how sounds are localized under circumstances that afford the full complement of ITD, ILD, and spectral cues. For example, cats with unilateral cochlear ablations fail to lateralize LR versus RL stimuli because they lack the requisite binaural processes (Masterton, R. B. *et al.*, 1967), but unilaterally deaf humans show surprisingly good directional hearing because they have learnt to replace compromised binaural processes with monaural spectral information (Angell, J. R. and Fite, W., 1901b; Slattery, W. H., 3rd and Middlebrooks, J. C., 1994). The localization deficits of lesioned cats change dramatically when performance is measured in free field.

Neff and colleagues revisited the effects of central auditory lesions on sound localization in cats (for a complete contemporary review, see Neff, W. D. *et al.*, 1975). Their lesioning procedures were similar to those used in earlier studies by the Masterton group, but behavioral deficits were characterized in a free-field testing arena (Figure 24). In their two-alternative forced-choice paradigm, an active speaker signaled the availability of a food reward that could be taken from a proximal receptacle. The goal box on the alternative speaker could not be opened. Directional thresholds were determined by changing the physical separation between speakers.

An advantage of the goal-box paradigm is that it is a true localization task that requires the subject to identify and approach a sound source (the testing environment is darkened to minimize visual cues). A disadvantage, at least for the analysis of spectral processing pathways, is that the speaker/goal box combinations are arranged along the floor of the testing arena and therefore measure localization only in the horizontal plane.

Moore C. N. *et al.* (1974) used the goal-box paradigm to investigate the effects of commissural lesions on sound localization. As a baseline measure, one cochlea was destroyed in two cats. The lesion elevated average prelesion directional thresholds of less than 5° to postlesion thresholds of over 15°. The

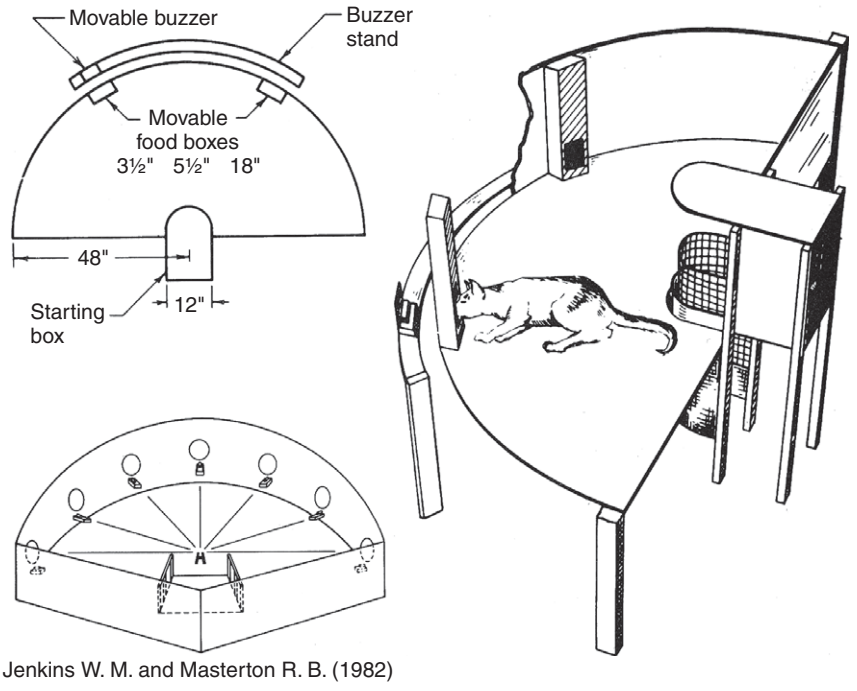

Figure 24 Goal-box apparatus for measuring horizontal localization. The subject is released from the starting box and approaches the active sound source to obtain a food reward. Initial experiments were conducted with two speaker choices. Jenkins W. M. and Masterton R. B. (1982) increased the speaker number to seven. Adapted from Irvine, D. R. F. 1986. The Auditory Brainstem, Springer. Copyright (1986), with kind permission of Springer Science and Business Media.

subjects' performance was not greater than chance during initial postoperative sessions but showed a gradual improvement with extensive retraining. The auditory stimulus for these experiments was a broadband buzzer making it likely that the recovery of function reflects an increased attention to monaural spectral cues.

The remaining seven cats were subjected to lesions of the trapezoid body, commissure of the ICC, and corpus callosum. Although the extent of the lesions varied between subjects and multiple lesions were performed on some cats, the results suggest a striking lack of effect for lesions at higher processing levels. Destruction of the commissures of the ICC or cerebral cortex changed average prelesion thresholds by less than 0.5°. The cats did not require postoperative retraining.

Lesions of the trapezoid body produced more variable results. At the extreme, one cat (459) showed a complete loss of directional acuity that gradually recovered to a 25° threshold increase over more than 500 training trials. Another cat (559) was virtually unaffected by the lesion. In part, these differences may be explained by the extent of damage. The lesion in cat 459 effectively isolated the left cochlear nucleus by destroying all ascending fibers (dorsal and intermediate acoustic striae and lateral lemniscus) as well as crossing fibers in the trapezoid body. The lesion in cat 559 destroyed the left superior olive and transected the trapezoid body, but spared the dorsal and intermediate acoustic striae.

From the perspective of sound localization pathways, the lesion of cat 459 must compromise not only the binaural interactions that are established by the crossing projections of the ventral cochlear nuclei but also the monaural ascending projections of the DCN. By contrast, the lesion of cat 559 suggests extensive damage to the binaural system but less involvement of the spectral processing pathway. Given recent functional measures (May, B. J., 2000), it is possible that binaural deficits in cat 559 were masked by the availability of spectral cues in both ears.

Like Masterton and his colleagues, Casseday J. H. and Neff W. D. (1975) lesioned the trapezoid body, lateral lemniscus, and brachium of the ICC. Consequential localization deficits were only noted for trapezoid body lesions, and as noted in their previous study (Moore, C. N. *et al.*, 1974), these

effects were complete and permanent in only a subset of subjects. An interesting distinction between these and previous trapezoid body lesions is that they were performed near the midline of the brainstem and therefore did not directly involve the cochlear nuclei. Here, the magnitude of the impairment was related to the depth of the lesion. Cats with the deepest lesions made localization errors that exceeded those observed after unilateral cochlear ablation. Histological results suggest that the deep medullary incisions included a bilateral transection of the intermediate and dorsal acoustic striae as they crossed the brainstem en route to the ICC. Presumably, one spectral pathway is spared by unilateral cochlear ablation. These results provide further evidence that severe localization impairments require the combined disabling of binaural and spectral processing.

Subsequent results by Jenkins W. M. and Masterton R. B. (1982) raise important questions regarding the use of the goal-box paradigm. The issue is not the task itself, but the potential to apply other decision criteria to the two-alternative forced choice. For example, when two sound sources are located to the left and right of the listener, a normal subject may perform the task by discriminating left versus right. On the other hand, a subject with a rightward directional impairment may maximize correct responses by discriminating left versus not-left, or even loud versus quiet if there is an accompanying hearing loss. These ambiguities were corrected by increasing the number of sound sources in the semi-circular arena. With the seven speaker array, the cat was required to select the active speaker from multiple locations in the left or right hemifield (Figure 24). The correct choice offered brief access to a water reward.

The effects of trapezoid body lesions on performance in the more complex localization task were similar to those previously noted with the two-choice paradigm (Casseday, J. H. and Neff, W. D., 1975; Moore, C. N. *et al.*, 1974). Results for lesions of higher auditory structures were quite different. Unlike the transient effects observed by Casseday and Neff, unilateral damage of the lateral lemniscus, ICC and brachium yielded profound and permanent impairments. In most instances, the deficits were confined to locations that were contralateral to the lesion site.

Representative lesioning results are summarized in Figure 25. This cat (case 907) received a complete lesion of the left lateral lemniscus (Figure 25(a)). When tested with the multispeaker array, the cat showed a high percentage of correct localization responses for speakers in the ipsilateral (left) field (Figure 25(b)). Correct responses declined precipitously as source locations moved toward contralateral (right) azimuths. The cat rarely responded to locations in the contralateral field.

A more detailed description of the pattern of localization errors is provided in Figure 25(c). The stimulus–response matrix plots the azimuth of the speaker on the horizontal axis and the azimuth of the response on the vertical axis. Numerical values indicate the number of incorrect responses for each speaker–response combination out of 30 postoperative trials. For example, the 90° speaker in the ipsilateral field produced only eight errors out of 30 trials, while the 90° speaker in the contralateral field was never correctly localized. Most incorrect responses in the ipsilateral field occurred when the subject responded to the adjacent speaker. Errors in the contralateral field spanned the entire 180° speaker range.

To explain the discrepancies between these responses and previous results with the two-speaker paradigm, Jenkins W. M. and Masterton R. B. (1982) conducted additional tests using single speakers at left and right azimuths of 30°. Responses of cat 907 in the simplified testing environment are indicated by the star symbols in Figure 25(b). As noted by Casseday J. H. and Neff W. D. (1975), the subject was able to attain near-perfect discrimination of left versus right locations.

Results with the seven-speaker array led Masterton and his colleagues to propose the existence of an acoustic chiasm (Glendenning, K. K. and Masterton, R. B., 1983; Masterton, R. B., 1997), that creates a contralateral representation of auditory space at processing levels above the decussation of the trapezoid body. Physiological support for this interpretation can be seen in the contralateral preference of spatial tuning in the ICC (Figure 15). A significant proportion of these directional effects are observed under monaural conditions (Delgutte, B. *et al.*, 1999).

3.37.9 Species Comparisons of the Spectral Processing Pathway

Ablation paradigms evaluate the functional importance of neuroanatomical structures by comparing the behavioral performance of subjects with normal and surgically altered systems. A persistent problem

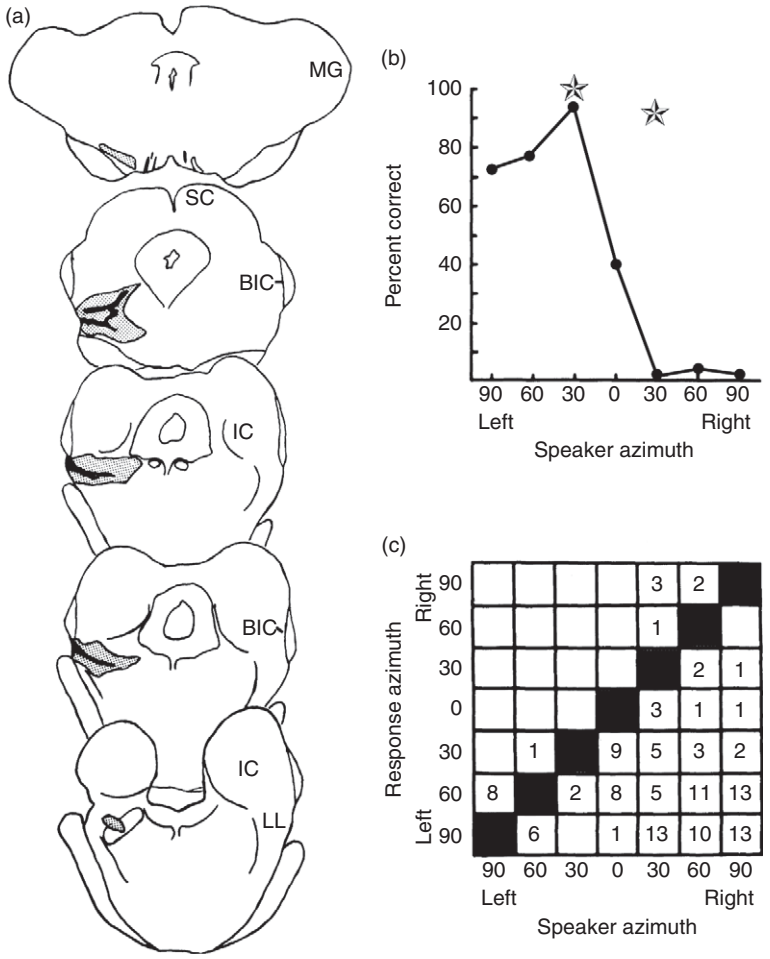

Figure 25 Effects of a unilateral inferior colliculus lesion on sound localization. (a) Histological reconstruction of the unilateral lateral lemniscus lesion in case 907. (b) Psychometric function plotting the percentage of correct localization responses in relation to the azimuth of seven speakers. Results obtained with two speakers are indicated by star symbols. (c) Stimulus–response matrix for the localization errors of case 907. Each column of numbers indicates the total errors out of 30 trials for the speaker location indicated on the horizontal axis. The spatial distribution of the errors is indicated on the vertical axis. Abbreviations: BIC, brachium of the inferior colliculus; IC, inferior colliculus; LL, lateral lemniscus; MG, medial geniculate nucleus; SC, superior colliculus. Reproduced from Jenkins, W. M. and Masterton, R. B. 1982. Sound localization: effects of unilateral lesions in central auditory system. J. Neurophysiol. 47, 987–1016. Copyright (1982), used with permission from The American Physiological Society.

with the lesioning approach is its inherent variability. When the lesion is too small, destruction is incomplete. When the lesion is too large or misplaced, surrounding structures are compromised. Either outcome leads to ambiguous structure/function relationships. Masterton followed his lesioning studies of the auditory brainstem with a novel alternative to surgical ablations (Masterton, B. *et al.*, 1975). These natural ablation studies compared the sound localization behaviors of domestic cats to a menagerie of unusual mammalian species representing the evolutionary development of the medial superior olive (MSO). As shown in Figure 26(a), hedgehogs have no MSO. Rats, tree shrews, and cats form a continuum of increasing MSO size and cell number (additional species are described in Heffner, R. S. and Masterton, R. B., 1990). Thus, naturally occurring variations in the anatomy of the ITD pathway could be systematically related to directional acuity without surgical intervention.

Sound localization accuracy was measured with the two-speaker paradigm that was developed by the Neff group (Figure 24). The left/right speaker separation was 60°, which is an easily detectable

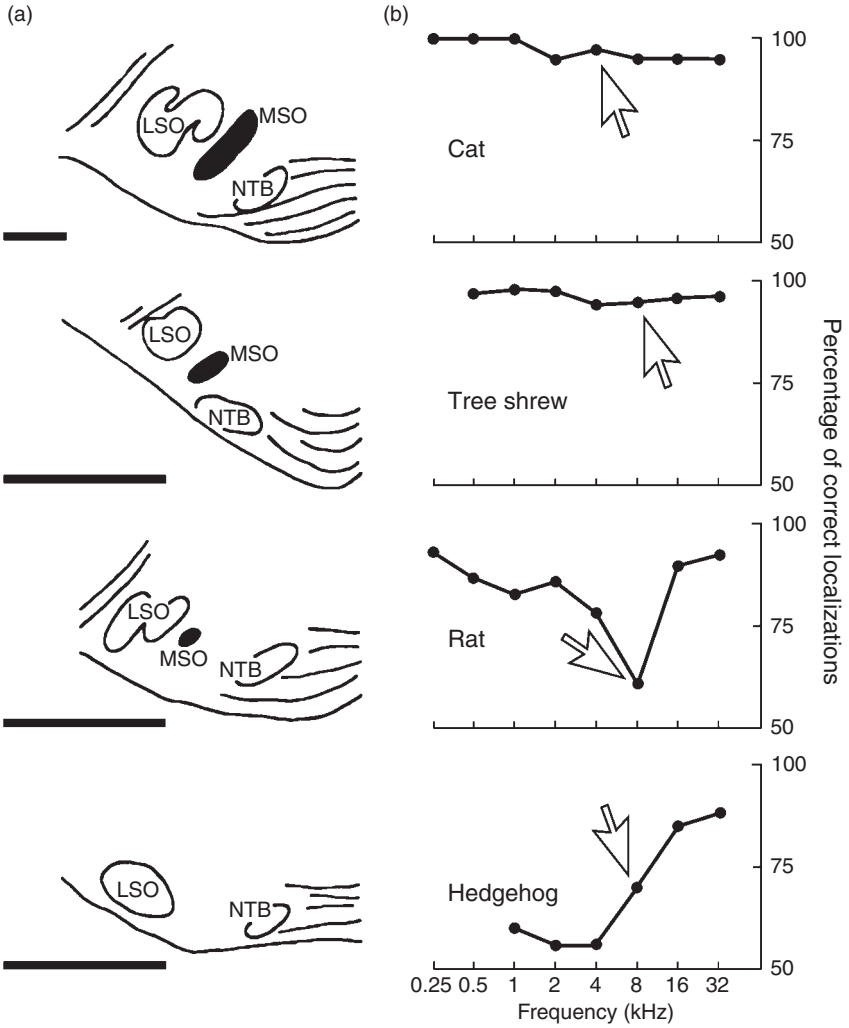

Figure 26 Comparative analysis of ITD processing. (a) Brainstem anatomy showing species variations of the medial superior olive (black fill). The structure is missing in the hedgehog. (b) Effects of frequency on the correct localization of a 60° speaker change. Arrows indicate the low-frequency cutoff of ILD cues based on the physical dimensions of the subject's head. Hedgehogs failed to localize pure tones below 16 kHz and were not tested at the lowest frequencies. Abbreviations: LSO, lateral superior olive; MSO, medial superior olive; NTB, nucleus of the trapezoid body. Scale bar indicates 1 mm. Reprinted from Masterton, R. B., Thompson, G. C., Bechtold, J. K., and RoBards, M. J. 1975. Neuroanatomical basis of binaural phase-difference analysis for sound localization: a comparative study. J. Comp. Physiol. Psychol. 89, 379–386 (1975) ©, with permission from American Physiological Association.

change in source location for most mammalian species (Fay, R. R., 1988). Instead of the usual noise burst, the auditory stimulus was a tone pip that ranged in frequency from 250 to 32 kHz. This important modification of the testing procedure allowed the investigators to compare each species' performance at low versus high frequencies. Accurate responses across the entire frequency range reflect the subject's ability to make use of both ITD and ILD cues (Casseday, J. H. and Neff, W. D., 1973; Mills, A. W., 1958).

The effects of frequency varied across species (Figure 26(b)). All subjects showed near-perfect discrimination at high frequencies where the physical dimensions of the head are expected to create large ILD effects. These binaural cues were presumably processed in the lateral superior olive. The three species with an anatomically distinct MSO also performed well at low frequencies, although the performance of the rat declined at intermediate frequencies where there is a transition between ILD and ITD cues. Humans show comparable deficits at lower

frequencies because of their larger head size (Stevens, S. S. and Newman, E. B., 1936). Of particular interest is the complete breakdown of the hedgehog's behavior at frequencies below 16 kHz. The frequency dependency of the deficit suggests an inability to process ITD information.

Application of the natural ablation method to the spectral processing pathway is problematic. All mammalian species possess a DCN and ICC. Nevertheless, the essence of the approach may be achieved by supplanting anatomical classifications with criteria that are based on unique physiological characteristics. It may even be argued that physiological dichotomies are more closely linked to species-specific perceptual behaviors.

Figure 27 contrasts the spectral integration properties of ICC neurons in the cat and mouse. Both species show the same types of frequency response maps (Figure 27(a)), but there are clear differences in the prevalence of the major unit types (Figure 27(b)).

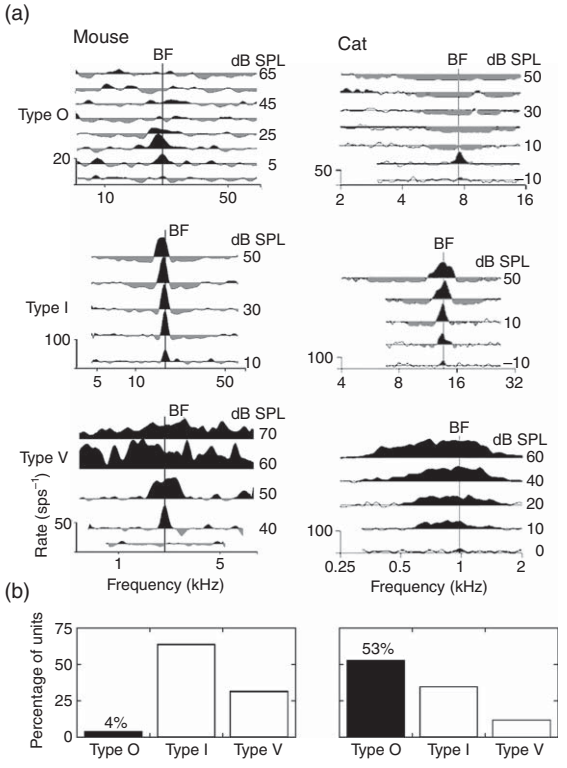

Figure 27 Comparative analysis of spectral processing. (a) Frequency response maps in the inferior colliculus of mice (left column) and cats (right column). Both species show the same physiological response types. (b) The distribution of response types. Type-O responses (black fill) are rare in mice but common in cats. Plotting conventions of frequency response maps are described in Figure 16.

Notch-selective type-O responses are common in cats (Ramachandran, R. *et al.*, 1999), but rarely encountered in mice (Egorova, M. *et al.*, 2001; Ehret, G. *et al.*, 2003; Ma, W. L. *et al.*, 2006). Additional physiological results from the mouse ICC (Vartanyan, I. A. and Malinina, E. S., 2004) confirm the more generalized notch frequency sensitivity of type-I units (Figure 16), and not the spatially selective responses of type-O units (Figure 17). A similar under-representation of spectral processing specializations has been observed in guinea pigs (LeBeau, F. E. *et al.*, 2001), rats (Malmierca, M. S. *et al.*, 2003), and gerbils (Gdowski, G. T. and Voigt, H. F., 1997).

The lack of a dedicated spectral processing pathway in the prey species predicts poor monaural sound localization. As previously noted, well-established physiological and psychophysical procedures are capable of validating this conclusion. Unfortunately, not one of these critical functional assessments has been performed in the requisite species. Without these cross-species comparisons, function interpretations must be extracted from a psychophysical literature that is highly skewed toward the horizontal localization of spectrally rich stimuli (for a convenient source of animal psychophysical data, see Fay, R. R., 1988).

Figure 28 presents a sample of the animal psychophysical tests that have used broadband noise to determine localization thresholds in the horizontal plane (Heffner, R.S. and Masterton, R. B., 1990). Results from eight different species are organized according to predator (Figure 28(a)) versus prey lifestyles (Figure 28(b)). Included in the comparison are domestic cats and three of the four prey species where physiological results suggest an impoverished spectral processing pathway (mice, rats, and gerbils). A functional void appears to exist between the subject groups. The most acute sense of direction is limited to predatory species, where there is an evolutionary premium on accurate localization.

The least weasel is a carnivore that feeds on mice and voles (Figure 28(c)). Because it is comparable in size to a mouse or gerbil, head-shadowing effects are expected to produce equivalent ITD and ILD cues. Despite this similarity in binaural acoustics, the small predator's directional hearing is approximately twice as accurate as the localization behaviors of size-matched prey (Heffner, R. S. and Heffner, H. E., 1987). The neuroanatomical source of this advantage has not been explored with electrophysiological or more detailed psychophysical methods. It is intriguing to speculate that the refinements for

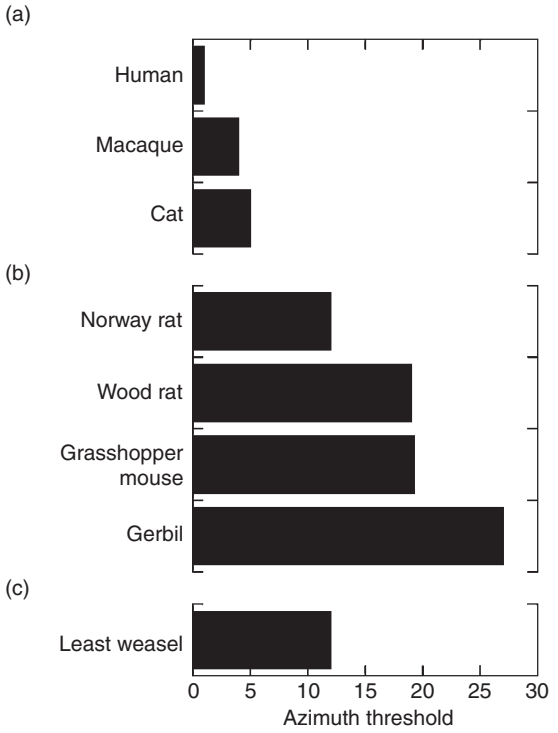

Figure 28 Representative azimuth thresholds for primates and predatory species (a), prey species (b), and a small predator (c). Best thresholds are observed among predatory species. Although the least weasel's head size is equivalent to the mouse and gerbil, the small predator exhibits more accurate localization behaviors. Thresholds were obtained with a variety of psychophysical procedures using noise bursts. The data were compiled by Heffner R. S. and Masterton R. B. (1990).

spectral processing found in the cat contribute to a general enhancement of localization abilities among other predatory species.

This chapter uses the concept of the spectral processing pathway as an organizing principle for the extensive literature on monaural sound localization. Unlike the overt structural underpinnings of the binaural auditory system, the spectral pathway is implied by unusual physiological patterns in the central auditory system of the cat. Many details of these processes remain to be discovered and are likely to change with further elaboration in additional animal models. The lasting value of this construct may be its ability to serve as a theoretical foundation for future studies of the stimulus properties, neural responses, anatomical structures, and species differences that shape directional hearing. For several decades, models of binaural processing have exerted a profound influence on auditory physiology and psychoacoustics (Colburn, H. S., 1973; Jeffress, L. A., 1948). Similar hypothesis-driven research into the role of spectral cues for sound localization is just beginning.

Acknowledgment

These projects were made possible by the continued support of NIDCD grant DC000954.

References

Adams, J. C. 1979. Ascending projections to the inferior colliculus. J. Comp. Neurol. 183, 519–538.

Aitkin, L. 1986. The Auditory Midbrain: Structure and Function in the Central Auditory Pathway. Humana Press.

Aitkin, L. and Martin, R. 1990. Neurons in the inferior colliculus of cats sensitive to sound-source elevation. Hear Res. 50, 97–105.

Aitkin, L. M. and Martin, R. L. 1987. The representation of stimulus azimuth by high best-frequency azimuth-selective neurons in the central nucleus of the inferior colliculus of the cat. J. Neurophysiol. 57, 1185–1200.

Aitkin, L. M. and Phillips, S. C. 1984. Is the inferior colliculus an obligatory relay in the cat auditory system? Neurosci. Lett. 44, 259–264.

Aitkin, L. M., Gates, G. R., and Phillips, S. C. 1984. Responses of neurons in inferior colliculus to variations in sound-source azimuth. J. Neurophysiol. 52, 1–17.

Aitkin, L. M., Pettigrew, J. D., Calford, M. B., Phillips, S. C., and Wise, L. Z. 1985. Representation of stimulus azimuth by low-frequency neurons in inferior colliculus of the cat. J. Neurophysiol. 53, 43–59.

Angell, J. R. and Fite, W. 1901a. Further observations on the monaural localization of sound. Psychol. Rev. 8, 449–458.

Angell, J. R. and Fite, W. 1901b. The monaural localization of sound. Psychol. Rev. 8, 225–246.

Arnott, R. H., Wallace, M. N., Shackleton, T. M., and Palmer, A. R. 2004. Onset neurones in the anteroventral cochlear nucleus project to the dorsal cochlear nucleus. J. Assoc. Res. Otolaryngol. 5, 153–170.

Batra, R., Kuwada, S., and Fitzpatrick, D. C. 1997. Sensitivity to interaural temporal disparities of low – and high-frequency neurons in the superior olivary complex. II. Coincidence detection. J. Neurophysiol. 78, 1237–1247.

Batteau, D. W. 1967. The role of the pinna in human localization. Proc. R. Soc. Lond. B Biol. Sci. 168, 158–180.

Blauert, J. 1969/1970. Sound localization in the median plane. Acustica 22, 205–213.

Blauert, J. 1997. Spatial Hearing: The Psychophysics of Human Sound Localization. MIT Press.

Bloom, P. J. 1977. Creating source elevation illusions by spectral manipulation. J. Audio Eng. Soc. 25, 560–565.

Bock, G. R. and Webster, W. R. 1974. Coding of spatial location by single units in the inferior colliculus of the alert cat. Exp. Brain Res. 21, 387–398.

Brozoski, T. J. and Bauer, C. A. 2005. The effect of dorsal cochlear nucleus ablation on tinnitus in rats. Hear Res. 206, 227–236.

Butler, R. A. and Belendiuk, K. 1977. Spectral cues utilized in the localization of sound in the median sagittal plane. J. Acoust. Soc. Am. 61, 1264–1269.

Butler, R. A. and Flannery, R. 1980. The spatial attributes of stimulus frequency and their role in monaural localization of sound in the horizontal plane. Percept. Psychophys. 28, 449–457.

Butler, R. A. and Planert, N. 1976. The influence of stimulus bandwidth on localization of sound in space. Percept. Psychophys. 19, 103–108.

Calford, M. B. and Pettigrew, J. D. 1984. Frequency dependence of directional amplification at the cat's pinna. Hear Res. 14, 13–19.

Casseday, J. H. and Neff, W. D. 1973. Localization of pure tones. J. Acoust. Soc. Am. 54, 365–372.

Casseday, J. H. and Neff, W. D. 1975. Auditory localization: role of auditory pathways in brain stem of the cat. J. Neurophysiol. 38, 842–858.

Chase, S. M. and Young, E. D. 2005. Limited segregation of different types of sound localization information among classes of units in the inferior colliculus. J. Neurosci. 25, 7575–7585.

Chase, S. M. and Young, E. D. 2006. Spike-timing codes enhance the representation of multiple simultaneous sound-localization cues in the inferior colliculus. J. Neurosci. 26, 3889–3898.

Chen, G. D. and Jastreboff, P. J. 1995. Salicylate-induced abnormal activity in the inferior colliculus of rats. Hear Res. 82, 158–178.

Cherry, E. C. 1953. Some experiments on the recognition of speech, with one and with two ears. J. Acoust. Soc. Am. 25, 975–979.

Colburn, H. S. 1973. Theory of binaural interaction based on auditory-nerve data. I. General strategy and preliminary results on interaural discrimination. J. Acoust. Soc. Am. 54, 1458–1470.

Colburn, H. S. 1982. Binaural interaction and localization with various hearing impairments. Scand. Audiol. Suppl. 15, 27–45.

Davis, K. A. 2002. Evidence of a functionally segregated pathway from dorsal cochlear nucleus to inferior colliculus. J. Neurophysiol. 87, 1824–1835.

Davis, K. A. 2005. Spectral processing in the inferior colliculus. Int. Rev. Neurobiol. 70, 169–205.

Davis, K. A., Miller, R. L., and Young, E. D. 1996. Effects of somatosensory and parallel-fiber stimulation on neurons in dorsal cochlear nucleus. J. Neurophysiol. 76, 3012–3024.

Davis, K. A., Ramachandran, R., and May, B. J. 1999. Single-unit responses in the inferior colliculus of decerebrate cats. II. Sensitivity to interaural level differences. J. Neurophysiol. 82, 164–175.

Davis, K. A., Ramachandran, R., and May, B. J. 2003. Auditory processing of spectral cues for sound localization in the inferior colliculus. J. Assoc. Res. Otolaryngol. 4, 148–163.

Delgutte, B. 1989. Physiological Mechanisms of Masking and Intensity Discrimination. In: Interactions between Neurophysiology and Psychoacoustics (*ed*. C. W. Turner), pp. 81–101. Acoustical Society of America.

Delgutte, B., Joris, P. X., Litovsky, R. Y., and Yin, T. C. 1999. Receptive fields and binaural interactions for virtual-space stimuli in the cat inferior colliculus. J. Neurophysiol. 81, 2833–2851.

Doucet, J. R., Ross, A. T., Gillespie, M. B., and Ryugo, D. K. 1999. Glycine immunoreactivity of multipolar neurons in the ventral cochlear nucleus which project to the dorsal cochlear nucleus. J. Comp. Neurol. 408, 515–531.

Egorova, M., Ehret, G., Vartanian, I., and Esser, K. H. 2001. Frequency response areas of neurons in the mouse inferior colliculus. I. Threshold and tuning characteristics. Exp. Brain Res. 140, 145–161.

Ehret, G., Egorova, M., Hage, S. R., and Muller, B. A. 2003. Spatial map of frequency tuning-curve shapes in the mouse inferior colliculus. Neuroreport 14, 1365–1369.

Evans, E. F. 1992. Auditory processing of complex sounds: an overview. Philos. Trans. R. Soc. Lond. B Biol. Sci. 336, 295–306.

Fay, R. R. 1988. Comparative psychoacoustics. Hear Res 34, 295–305.

Flannery, R. and Butler, R. A. 1981. Spectral cues provided by the pinna for monaural localization in the horizontal plane. Percept. Psychophys. 29, 438–444.

Fuchs, P. 2002. The synaptic physiology of cochlear hair cells. Audiol Neurootol 7, 40–44.

Gardner, M. B. and Gardner, R. S. 1973. Problem of localization in the median plane: effect of pinnae cavity occlusion. J. Acoust. Soc. Am. 53, 400–408.

Gatehouse, R. W. 1976. Further research in localization of sound by completely monaural subjects. J. Aud. Res. 16, 263–273.

Gates, G. A. and Mills, J. H. 2005. Presbycusis. Lancet 366, 1111–1120.

Gdowski, G. T. and Voigt, H. F. 1997. Response map properties of units in the dorsal cochlear nucleus of barbiturate-anesthetized gerbil (Meriones unguiculatus). Hear Res. 105, 85–104.

Glendenning, K. K. and Masterton, R. B. 1983. Acoustic chiasm: efferent projections of the lateral superior olive. J. Neurosci. 3, 1521–1537.

Green, D. M. and Swets, J. A. 1974. Signal Detection Theory and Psychophysics. Robert E. Krieger.

Guinan, J. J., Jr. and Gifford, M. L. 1988. Effects of electrical stimulation of efferent olivocochlear neurons on cat auditory-nerve fibers. III. Tuning curves and thresholds at CF. Hear Res. 37, 29–45.

Hancock, K. E. and Voigt, H. F. 1999. Wideband inhibition of dorsal cochlear nucleus type IV units in cat: a computational model. Ann. Biomed. Eng. 27, 73–87.

Hancock, K. E., Davis, K. A., and Voigt, H. F. 1997. Modeling inhibition of type II units in the dorsal cochlear nucleus. Biol. Cybern. 76, 419–428.

Hebrank, J. and Wright, D. 1974. Spectral cues used in the localization of sound sources in the median plane. J. Acoust. Soc. Am. 56, 1829–1834.

Hartley, R. V. L. and Fry, T. C. 1921. The binaural localization of pure tones. Phys. Rev. 18, 431–442.

Heffner, R. S. and Heffner, H. E. 1987. Localization of noise, use of binaural cues, and a description of the superior olivary complex in the smallest carnivore, the least weasel (Mustela nivalis). Behav. Neurosci. 101, 701–708, 744–705.

Heffner, R. S. and Masterton, R. B. 1990. Sound Localization in Mammals: Brain-Stem Mechanisms. In: Comparative Perception (*eds*. M. A. Berkley and W. C. Stebbins). Wiley.

Hirsh, I. J. 1950. The relation between localization and intelligibility. J. Acoust. Soc. Am. 22, 196–200.

Hofman, P. M., Van Riswick, J. G., and Van Opstal, A. J. 1998. Relearning sound localization with new ears. Nat. Neurosci. 1, 417–421.

Huang, A. Y. and May, B. J. 1996a. Sound orientation behavior in cats. II. Mid-frequency spectral cues for sound localization. J. Acoust. Soc. Am. 100, 1070–1080.

Huang, A. Y. and May, B. J. 1996b. Spectral cues for sound localization in cats: effects of frequency domain on minimum audible angles in the median and horizontal planes. J. Acoust. Soc. Am. 100, 2341–2348.

Imig, T. J. and Durham, D. 2005. Effect of unilateral noise exposure on the tonotopic distribution of spontaneous activity in the cochlear nucleus and inferior colliculus in the cortically intact and decorticate rat. J. Comp. Neurol. 490, 391–413.

Imig, T. J., Bibikov, N. G., Poirier, P., and Samson, F. K. 2000. Directionality derived from pinna-cue spectral notches in cat dorsal cochlear nucleus. J. Neurophysiol. 83, 907–925.

Irvine, D. R. F. 1986. The Auditory Brainstem. Springer.

Jastreboff, P. J. and Sasaki, C. T. 1986. Salicylate-induced changes in spontaneous activity of single units in the inferior colliculus of the guinea pig. J. Acoust. Soc. Am. 80, 1384–1391.

Jeffress, L. A. 1948. A place theory of sound localization. J. Comp. Psychol. 41, 35–39.

Jenkins, W. M. and Masterton, R. B. 1982. Sound localization: effects of unilateral lesions in central auditory system. J. Neurophysiol. 47, 987–1016.

Jin, C., Corderoy, A., Carlile, S., and van Schaik, A. 2004. Contrasting monaural and interaural spectral cues for human sound localization. J. Acoust. Soc. Am. 115, 3124–3141.

Kaltenbach, J. A., Zhang, J., and Finlayson, P. 2005. Tinnitus as a plastic phenomenon and its possible neural underpinnings in the dorsal cochlear nucleus. Hear. Res. 206, 200–226.

Kanold, P. O. and Young, E. D. 2001. Proprioceptive information from the pinna provides somatosensory input to cat dorsal cochlear nucleus. J. Neurosci. 21, 7848–7858.

Kawase, T., Koiwa, T., Yuasa, R., Yuasa, Y., Hidaka, H., Takasaka, T., Ozawa, K., Suzuki, Y., and Sone, T. 1999. Sound localization for a virtual sound source in cases of chronic otitis media. Audiology 38, 83–90.

Kim, D. O. and Molnar, C. E. 1979. A population study of cochlear nerve fibers: comparison of spatial distributions of average-rate and phase-locking measures of responses to single tones. J. Neurophysiol. 42, 16–30.

Kimura, R. and Wersall, J. 1962. Termination of the olivo-cochlear bundle in relation to the outer hair cells of the organ of Corti in guinea pig. Acta Otolaryngol. 55, 11–32.

Kistler, D. J. and Wightman, F. L. 1992. A model of head-related transfer functions based on principal components analysis and minimum-phase reconstruction. J. Acoust. Soc. Am. 91, 1637–1647.

Kuhn, G. F. 1987. Physical Acoustics and Measurements Pertaining to Directional Hearing. In: Directional Hearing (*eds*. W. A. Yost and G. Gourevitch). Springer.

Kuwada, S., Stanford, T. R., and Batra, R. 1987. Interaural phase-sensitive units in the inferior colliculus of the unanesthetized rabbit: effects of changing frequency. J. Neurophysiol. 57, 1338–1360.

LeBeau, F. E., Malmierca, M. S., and Rees, A. 2001. Iontophoresis *in vivo* demonstrates a key role for GABA(A) and glycinergic inhibition in shaping frequency response areas in the inferior colliculus of guinea pig. J. Neurosci. 21, 7303–7312.

Le Prell, G. S., Sachs, M. B., and May, B. J. 1996. Representation of vowel-like spectra by discharge rate responses of individual auditory-nerve fibers. Aud. Neurosci. 2.

Leiman, A. L. and Hafter, E. R. 1972. Responses of inferior colliculus neurons to free field auditory stimuli. Exp. Neurol. 35, 431–449.

Levine, R. A., Abel, M., and Cheng, H. 2003. CNS somatosensory-auditory interactions elicit or modulate tinnitus. Exp. Brain Res. 153, 643–648.

Liberman, M. C., Dodds, L. W., and Pierce, S. 1990. Afferent and efferent innervation of the cat cochlea: quantitative analysis with light and electron microscopy. J. Comp. Neurol. 301, 443–460.

Lin, L. M., Bowditch, S., Anderson, M. J., May, B., Cox, K. M., and Niparko, J. K. 2006. Amplification in the rehabilitation of unilateral deafness: speech in noise and directional hearing effects with bone-anchored hearing and contralateral routing of signal amplification. Otol. Neurotol. 27, 172–182.

Lopez-Proveda, E. A. 2005. Spectral Processing by the Peripheral Auditory System: Facts and Models. In: Auditory Spectral Processing (*eds*. M. S. Malmeirca and D. R. F. Irvine), pp. 8–48. Elsevier Academic Press.

Lorente de Nó, R. 1933. Anatomy of the eighth nerve. III. General plan of structure of the primary cochlear nuclei. Laryngoscope 43, 327–350.

Ma, W. L., Hidaka, H., and May, B. J. 2006. Spontaneous activity in the inferior colliculus of CBA/J mice after manipulations that induce tinnitus. Hear Res. 212, 9–21.

Ma, W. L. and Young, E. D. 2006. Dorsal cochlear nucleus response properties following acoustic trauma: response maps and spontaneous activity. Hear. Res. 216–217, 176–188.

Malmierca, M. S., Saint Marie, R. L., Merchan, M. A., and Oliver, D. L. 2005. Laminar inputs from dorsal cochlear nucleus and ventral cochlear nucleus to the central nucleus of the inferior colliculus: two patterns of convergence. Neuroscience 136, 883–894.

Malmierca, M. S., Hernandez, O., Falconi, A., Lopez-Poveda, E. A., Merchan, M., and Rees, A. 2003. The commissure of the inferior colliculus shapes frequency response areas in rat: an *in vivo* study using reversible blockade with microinjection of kynurenic acid. Exp. Brain Res. 153, 522–529.

Masterton, B., Thompson, G. C., Bechtold, J. K., and RoBards, M. J. 1975. Neuroanatomical basis of binaural phase-difference analysis for sound localization: a comparative study. J. Comp. Physiol. Psychol. 89, 379–386.

Masterton, R. B. 1997. Neurobehavioral studies of the central auditory system. Ann. Otol. Rhinol. Laryngol. Suppl. 168, 31–34.

Masterton, R. B. and Granger, E. M. 1988. Role of the acoustic striae in hearing: contribution of dorsal and intermediate striae to detection of noises and tones. J. Neurophysiol. 60, 1841–1860.

Masterton, R. B., Granger, E. M., and Glendenning, K. K. 1994. Role of acoustic striae in hearing: mechanism for enhancement of sound detection in cats. Hear. Res. 73, 209–222.

Masterton, R. B., Jane, J. A., and Diamond, I. T. 1967. Role of brainstem auditory structures in sound localization. I. Trapezoid body, superior olive, and lateral lemniscus. J. Neurophysiol. 30, 341–359.

Masterton, R. B., Jane, J. A., and Diamond, I. T. 1968. Role of brain-stem auditory structures in sound localization. II. Inferior colliculus and its brachium. J. Neurophysiol. 31, 96–108.

May, B. J. 2000. Role of the dorsal cochlear nucleus in the sound localization behavior of cats. Hear Res. 148, 74–87.

May, B. J. and Huang, A. Y. 1996. Sound orientation behavior in cats. I. Localization of broadband noise. J. Acoust. Soc. Am. 100, 1059–1069.

May, B. J. and Huang, A. Y. 1997. Spectral cues for sound localization in cats: a model for discharge rate representations in the auditory nerve. J. Acoust. Soc. Am. 101, 2705–2719.

May, B. J., Budelis, J., and Niparko, J. K. 2004. Behavioral studies of the olivocochlear efferent system: learning to listen in noise. Arch. Otolaryngol. Head Neck Surg. 130, 660–664.

May, B. J., Huang, A., Le Prell, G. S., and Hienz, R. D. 1996. Vowel formant frequency discrimination in cats: comparison of auditory nerve representations and psychophysical thresholds. Aud. Neurosci. 3.

McPartland, J. L., Culling, J. F., and Moore, D. R. 1997. Changes in lateralization and loudness judgements during one week of unilateral ear plugging. Hear. Res. 113, 165–172.

Mehrgardt, S. and Mellert, V. 1977. Transformation characteristics of the external human ear. J. Acoust. Soc. Am. 61, 1567–1576.
Middlebrooks, J. C. 1992. Narrow-band sound localization related to external ear acoustics. J. Acoust. Soc. Am. 92, 2607–2624.
Middlebrooks, J. C. 1999a. Individual differences in external-ear transfer functions reduced by scaling in frequency. J. Acoust. Soc. Am. 106, 1480–1492.
Middlebrooks, J. C. 1999b. Virtual localization improved by scaling non-individualized external-ear transfer functions in frequency. J. Acoust. Soc. Am. 106, 1493–1510.
Middlebrooks, J. C. and Green, D. M. 1990. Directional dependence of interaural envelope delays. J. Acoust. Soc. Am. 87, 2149–2162.
Middlebrooks, J. C. and Green, D. M. 1991. Sound localization by human listeners. Annu. Rev. Psychol. 42, 135–159.
Middlebrooks, J. C. and Green, D. M. 1992. Observations on a principal components analysis of head-related transfer functions. J. Acoust. Soc. Am. 92, 597–599.
Middlebrooks, J. C., Macpherson, E. A., and Onsan, Z. A. 2000. Psychophysical customization of directional transfer functions for virtual sound localization. J. Acoust. Soc. Am. 108, 3088–3091.
Mills, A. W. 1958. On the minimum audible angle. J. Acoust. Soc. Am. 30, 237–246.
Moller, A. R. 2003. Pathophysiology of tinnitus. Otolaryngol. Clin. North. Am. 36, 249–266, v-vi.
Moore, C. N., Casseday, J. H., and Neff, W. D. 1974. Sound localization: the role of the commissural pathways of the auditory system of the cat. Brain Res. 82, 13–26.
Moore, D. R., Semple, M. N., Addison, P. D., and Aitkin, L. M. 1984. Properties of spatial receptive fields in the central nucleus of the cat inferior colliculus. I. Responses to tones of low intensity. Hear. Res. 13, 159–174.
Morimoto, M. and Ando, Y. 1982. On the Simulation of Sound Localization. In: Localization of Sound: Theory and Applications (*ed*. R. W. Gatehouse), pp. 85–89. Amphora Press.
Musicant, A. D. and Butler, R. A. 1980. Monaural localization: an analysis of practice effects. Percept. Psychophys. 28, 236–240.
Musicant, A. D. and Butler, R. A. 1984a. The influence of pinnae-based spectral cues on sound localization. J. Acoust. Soc. Am. 75, 1195–1200.
Musicant, A. D. and Butler, R. A. 1984b. The psychophysical basis of monaural localization. Hear Res. 14, 185–190.
Musicant, A. D., Chan, J. C., and Hind, J. E. 1990. Direction-dependent spectral properties of cat external ear: new data and cross-species comparisons. J. Acoust. Soc. Am. 87, 757–781.
Narayan, S. S., Temchin, A. N., Recio, A., and Ruggero, M. A. 1998. Frequency tuning of basilar membrane and auditory nerve fibers in the same cochleae. Science 282, 1882–1884.
Neff, W. D., Diamond, I. T., and Casseday, J. H. 1975. Behavioral Studies of Auditory Discrimination. In: Handbook of Sensory Physiology (*eds*. W. D. Keidel and W. D. Neff), pp. 307–400. Springer.
Nelken, I. and Young, E. D. 1994. Two separate inhibitory mechanisms shape the responses of dorsal cochlear nucleus type IV units to narrowband and wideband stimuli. J. Neurophysiol. 71, 2446–2462.
Nelken, I. and Young, E. D. 1996. Why do cats need a dorsal cochlear nucleus? J. Basic. Clin. Physiol. Pharmacol. 7, 199–220.
Oertel, D. and Young, E. D. 2004. What's a cerebellar circuit doing in the auditory system? Trends Neurosci. 27, 104–110.
Oertel, D., Wu, S. H., Garb, M. W., and Dizack, C. 1990. Morphology and physiology of cells in slice preparations of the posteroventral cochlear nucleus of mice. J. Comp. Neurol. 295, 136–154.
Oldfield, S. R. and Parker, S. P. 1986. Acuity of sound localisation: a topography of auditory space. III. Monaural hearing conditions. Perception 15, 67–81.
Oliver, D. L., Beckius, G. E., Bishop, D. C., and Kuwada, S. 1997. Simultaneous anterograde labeling of axonal layers from lateral superior olive and dorsal cochlear nucleus in the inferior colliculus of cat. J. Comp. Neurol. 382, 215–229.
Pfeiffer, R. R. 1966. Classification of response patterns of spike discharges for units in the cochlear nucleus: tone-burst stimulation. Exp. Brain Res. 1, 220–235.
Phillips, D. P., Calford, M. B., Pettigrew, J. D., Aitkin, L. M., and Semple, M. N. 1982. Directionality of sound pressure transformation at the cat's pinna. Hear Res. 8, 13–28.
Plenge, G. 1974. On the differences between localization and lateralization. J. Acoust. Soc. Am. 56, 944–951.
Poirier, P., Samson, F. K., and Imig, T. J. 2003. Spectral shape sensitivity contributes to the azimuth tuning of neurons in the cat's inferior colliculus. J. Neurophysiol. 89, 2760–2777.
Poon, P. W. and Brugge, J. F. 1993. Virtual-space receptive fields of single auditory nerve fibers. J. Neurophysiol. 70, 667–676.
Populin, L. C. and Yin, T. C. 1998a. Behavioral studies of sound localization in the cat. J. Neurosci. 18, 2147–2160.
Populin, L. C. and Yin, T. C. 1998b. Pinna movements of the cat during sound localization. J. Neurosci. 18, 4233–4243.
Pratt, C. C. 1930. The spatial character of high and low tones. J. Exp. Psychol. 13, 278–285.
Rakerd, B., Hartmann, W. M., and McCaskey, T. L. 1999. Identification and localization of sound sources in the median sagittal plane. J. Acoust. Soc. Am. 106, 2812–2820.
Ramachandran, R., Davis, K. A., and May, B. J. 1999. Single-unit responses in the inferior colliculus of decerebrate cats. I. Classification based on frequency response maps. J. Neurophysiol. 82, 152–163.
Ramachandran, R., Davis, K. A., and May, B. J. 2000. Rate representation of tones in noise in the inferior colliculus of decerebrate cats. J. Assoc. Res. Otolaryngol. 1, 144–160.
Ramachandran, R. and May, B. J. 2002. Functional segregation of ITD sensitivity in the inferior colliculus of decerebrate cats. J. Neurophysiol. 88, 2251–2261.
Rayleigh, L. (Strutt J. W.) 1907. On our perception of sound direction. Phil. Mag. 13, 214–232.
Rice, J. J., May, B. J., Spirou, G. A., and Young, E. D. 1992. Pinna-based spectral cues for sound localization in cat. Hear Res. 58, 132–152.
Rice, J. J., Young, E. D., and Spirou, G. A. 1995. Auditory-nerve encoding of pinna-based spectral cues: rate representation of high-frequency stimuli. J. Acoust. Soc. Am. 97, 1764–1776.
Rokay, E. and Penzes, L. 1988. Pathophysiological changes of the cochlea during ageing–a review. Zfa 43, 185–189.
Rosenhall, U. 1985. The influence of hearing loss on directional hearing. Scand. Audiol. 14, 187–189.
Roth, G. L., Kochhar, R. K., and Hind, J. E. 1980. Interaural time differences: implications regarding the neurophysiology of sound localization. J. Acoust. Soc. Am. 68, 1643–1651.
Ruggero, M. A., Narayan, S. S., Temchin, A. N., and Recio, A. 2000. Mechanical bases of frequency tuning and neural excitation at the base of the cochlea: comparison of basilar-membrane vibrations and auditory-nerve-fiber responses in chinchilla. Proc. Natl. Acad. Sci. U. S. A. 97, 11744–11750.
Ryugo, D. K. and Parks, T. N. 2003. Primary innervation of the avian and mammalian cochlear nucleus. Brain Res. Bull. 60, 435–456.

Sachs, M. B. and Young, E. D. 1979. Encoding of steady-state vowels in the auditory nerve: representation in terms of discharge rate. J. Acoust. Soc. Am. 66, 470–479.
Searle, C. L., Braida, L. D., Cuddy, D. R., and Davis, M. F. 1975. Binaural pinna disparity: another auditory localization cue. J. Acoust. Soc. Am. 57, 448–455.
Semple, M. N., Aitkin, L. M., Calford, M. B., Pettigrew, J. D., and Phillips, D. P. 1983. Spatial receptive fields in the cat inferior colliculus. Hear Res. 10, 203–215.
Shaw, E. A. 1974a. Transformation of sound pressure level from the free field to the eardrum in the horizontal plane. J. Acoust. Soc. Am. 56, 1848–1861.
Shaw, E. A. G. 1974b. The External Ear. In: Handbook of Sensory Physiology (*eds*. W. D. Keidel and W. D. Neff), pp. 455–490. Springer.
Shinn-Cunningham, B. G., Durlach, N. I., and Held, R. M. 1998. Adapting to supernormal auditory localization cues. I. Bias and resolution. J. Acoust. Soc. Am. 103, 3656–3666.
Slattery, W. H., 3rd and Middlebrooks, J. C. 1994. Monaural sound localization: acute versus chronic unilateral impairment. Hear Res. 75, 38–46.
Soucek, S., Michaels, L., and Frohlich, A. 1987. Pathological changes in the organ of Corti in presbyacusis as revealed by microslicing and staining. Acta Otolaryngol. Suppl. 436, 93–102.
Spirou, G. A., Davis, K. A., Nelken, I., and Young, E. D. 1999. Spectral integration by type II interneurons in dorsal cochlear nucleus. J. Neurophysiol. 82, 648–663.
Spirou, G. A., May, B. J., Wright, D. D., and Ryugo, D. K. 1993. Frequency organization of the dorsal cochlear nucleus in cats. J. Comp. Neurol. 329, 36–52.
Starch, D. 1908. The perimetry of the localization of sound. Psychol. Rev. Mon. 38 (Suppl. 9), 1–55.
Stevens, S. S. and Newman, E. B. 1936. Localization of actual sources of sound. Am. J. Psychol. 48, 297–306.
Sutherland, D. P., Glendenning, K. K., and Masterton, R. B. 1998a. Role of acoustic striae in hearing: discrimination of sound-source elevation. Hear Res. 120, 86–108.
Sutherland, D. P., Masterton, R. B., and Glendenning, K. K. 1998b. Role of acoustic striae in hearing: reflexive responses to elevated sound-sources. Behav Brain Res. 97, 1–12.
Teranishi, R. and Shaw, E. A. G. 1968. External ear acoustic models with simple geometry. J. Acoust. Soc. Am. 44, 257–263.
Tollin, D. J. and Yin, T. C. 2003. Spectral cues explain illusory elevation effects with stereo sounds in cats. J. Neurophysiol. 90, 525–530.
Tsuchitani, C. 1977. Functional organization of lateral cell groups of cat superior olivary complex. J. Neurophysiol. 40, 296–318.
Van Wanrooij, M. M. and Van Opstal, A. J. 2004. Contribution of head shadow and pinna cues to chronic monaural sound localization. J. Neurosci. 24, 4163–4171.
Van Wanrooij, M. M. and Van Opstal, A. J. 2005. Relearning sound localization with a new ear. J. Neurosci. 25, 5413–5424.
Vartanyan, I. A. and Malinina, E. S. 2004. The selectivity of neurons in the auditory zone of the mouse midbrain to the direction of movement of a spectral notch in wide-band noise. Neurosci. Behav. Physiol. 34, 159–168.
Viehweg, R. and Campbell, R. A. 1960. Localization difficulty in monaurally impaired listeners. Ann. Rhino. Laryngol. 69, 622–634.
Wenzel, E. M., Arruda, M., Kistler, D. J., and Wightman, F. L. 1993. Localization using nonindividualized head-related transfer functions. J. Acoust. Soc. Am. 94, 111–123.
Wiederhold, M. L. 1970. Variations in the effects of electric stimulation of the crossed olivocochlear bundle on cat single auditory-nerve-fiber responses to tone bursts. J. Acoust. Soc. Am 48, 966–977.
Wiener, F. M. and Ross, D. A. 1946. The pressure distribution in the auditory canal in a progressive sound field. J. Acoust. Soc. Am. 18, 401–408.
Wightman, F. L. and Kistler, D. J. 1989a. Headphone simulation of free-field listening. I. Stimulus synthesis. J. Acoust. Soc. Am. 85, 858–867.
Wightman, F. L. and Kistler, D. J. 1989b. Headphone simulation of free-field listening. II. Psychophysical validation. J. Acoust. Soc. Am. 85, 868–878.
Wightman, F. L. and Kistler, D. J. 1992. The dominant role of low-frequency interaural time differences in sound localization. J. Acoust. Soc. Am. 91, 1648–1661.
Wightman, F. L. and Kistler, D. J. 1997. Monaural sound localization revisited. J. Acoust. Soc. Am. 101, 1050–1063.
Wightman, F. L. and Kistler, D. 1998. Of vulcan ears, human ears and 'earprints'. Nat. Neurosci. 1, 337–339.
Wightman, F. L., Kistler, D. J., and Perkins, M. E. 1987. A New Approach to the Study of Human Sound Localization. In: Directional Hearing (*eds*. W. A. Yost and G. Gourevitch), Springer-Verlag.
Winslow, R. L. and Sachs, M. B. 1987. Effect of electrical stimulation of the crossed olivocochlear bundle on auditory nerve response to tones in noise. J. Neurophysiol. 57, 1002–1021.
Woodworth, R. S. 1938. Experimental Psychology. Holt. Rinehart & Winston.
Xu, L. and Middlebrooks, J. C. 2000. Individual differences in external-ear transfer functions of cats. J. Acoust. Soc. Am. 107, 1451–1459.
Young, E. D. and Davis, K. A. 2002. Circuitry and Function of the Dorsal Cochlear Nucleus. In: Integrative Functions in the Mammalian Auditory Pathway (*eds*. D. Oertel, R. R. Fay, and A. N. Popper), pp. 160–206. Springer.
Young, E. D. and Voigt, H. F. 1982. Response properties of type II and type III units in dorsal cochlear nucleus. Hear. Res. 6, 153–169.
Zakarauskas, P. and Cynader, M. 1993. A computational theory of spectral cue localization. J. Acoust. Soc. Am. 94, 1323–1331.

Further Reading

Blauert, J. 1997. Spatial Hearing. MIT Press.
Malmierca, M. and Irvine, D. R. F. 2005. Auditory Spectral Processing. Elsevier Academic Press.
Popper, A. N. and Fay, R. R. 2005. Sound Source Localization. Springer.
Rakerd, B., Vander Velde, T. J., and Hartmann, W. M. 1998. Sound localization in the median sagittal plane by listeners with presbyacusis. J. Am. Acad. Audiol. 9, 466–479.

3.38 The Bat Cochlea

M Vater, Universität Potsdam, Golm, Germany

M Kössl, Johann Wolfgang Goethe Universität, Frankfurt/Main, Germany

© 2008 Elsevier Inc. All rights reserved.

3.38.1	Echolocation Behavior	695
3.38.2	Cochlear Physiology	695
3.38.3	Cochlear Anatomy	696
3.38.4	Cochlear Development	697
3.38.5	Cochlear Mechanisms	698
References		698

3.38.1 Echolocation Behavior

Echolocation tasks differ according to the type of habitat (e.g., open space vs. dense vegetation) and behavioral goal (obstacle avoidance or localization and identification of small prey). There is a close link between sonar signals, habitat, and demands on cochlear and central auditory processing (review: Neuweiler, G., 1990; Schnitzler, H.-U. *et al.*, 2003). Brief (1–3 ms) broadband downward frequency-modulated (FM) signals or signal components provide precise references for accurate target localization based on the time differences between emitted call and returning echo. They also deliver spectral information about the fine texture of the target. Long (10–60 ms) constant-frequency (CF) signal components are advantageous in detection tasks and for analysis of relative motion. Bats employing long CF-FM calls compensate for the upward Doppler shift in the frequency of echoes that results from their own flight by lowering the frequency of the emitted call. As a consequence, returning echoes are actively clamped at a reference frequency that is slightly higher than the CF emitted at rest. The fine frequency resolution required for this task is provided by a region of strongly enhanced tuning in the audiogram. This region also serves to specifically analyze small rhythmic modulations in amplitude and frequency of the echoes that are reflected from fluttering wings of insects. Doppler-sensitive sonar was independently evolved in old-world horseshoe bats, and in one species of new-world phyllostomid bats, the mustached bat (*Pteronotus parnelli*) as an adaptation for hunting insects in dense vegetation. Remarkably, the specialized filtering mechanism for the preferred echo frequency is not a product of central auditory processing but resides in the sensory organ, the cochlea (review: Neuweiler, G., 1990; Schnitzler, H.-U. *et al.*, 2003).

3.38.2 Cochlear Physiology

Pollak G. D. *et al.* (1972) published a seminal paper on specialized cochlear processing in the mustached bat. At frequencies of about 62 kHz coinciding with the frequency range of the second harmonic CF component, there is a sharply tuned threshold minimum in the cochlear microphonic (CM) potential, and thresholds on both sides of the best frequency increase with slopes of up to 210 dB kHz^{-1}, sharper tuning than in any other vertebrate ear. At this frequency, the CM shows a pronounced nonlinearity and ringing after the offset of the acoustic stimulus (Figure 1), which is indicative of the presence of an exceptionally sharply tuned mechanical resonance. Sharp tuning and resonance were shown to be physiologically vulnerable (review: Kössl, M. and Vater, M., 1995).

Shortly after the discovery of otoacoustic emissions in humans, and the discovery of active motility of outer hair cells (OHCs) that provide the basis for the concept of an active cochlear amplifier (review: Dallos, P., 1992), it was found that the mustached bat ear routinely emits a single evoked otoacoustic emission at about 61 kHz whose amplitude is about 100 times stronger than in other mammals. Occasionally, this evoked emission becomes a strong spontaneous otoacoustic emission at the same frequency (review: Kössl, M. and Vater, M., 1995; Kössl, M., 1997). The mammalian cochlear amplifier thus is functional even at ultrasonic frequencies.

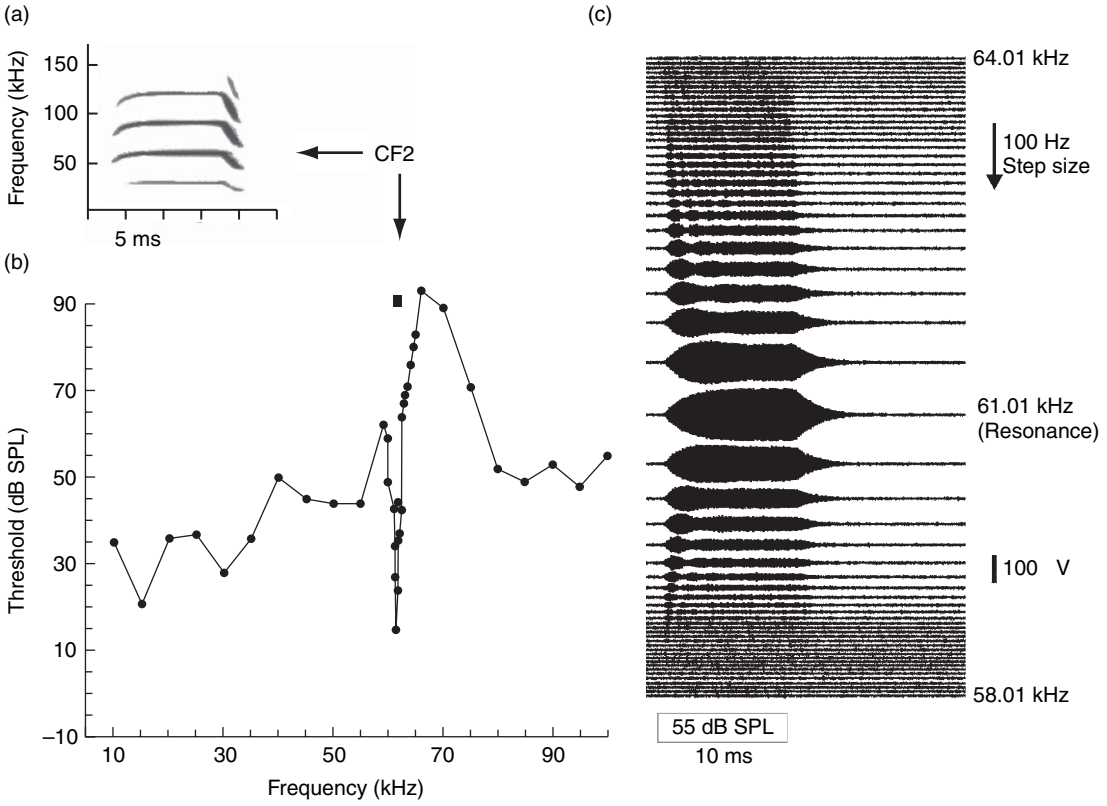

Figure 1 (a) Echolocation call of the mustached bat. (b) Cochlear microphonic threshold curve. (c) Cochlear microphonic resonance (b and c: Kössl, M. *et al.*, 2003).

CM recordings in horseshoe bats reveal sharp cochlear tuning to the CF but a less pronounced resonance, and only a weak expression of otoacoustic emissions suggesting that the specialized tuning mechanisms differ in detail. Measurements of distortion product otoacoustic emissions in CF-FM bats provide further evidence for the hydromechanical nature of sharp tuning, the contribution of nonlinear cochlear amplification, and a second filter mechanism based on filter properties of the tectorial membrane (TM) (review: Kössl, M., 1997).

With a laser diode interferometer, Kössl M. and Russell I. J. (1995) measured sensitive basilar membrane (BM) displacement in the basal cochlear turn of the mustached bat and found strong resonant oscillations at about 61 kHz that critically depended on the physiological state of the cochlea. A maximum Q10 dB value of 610 for BM tuning is a record among mammals and sharper than reported neuronal tuning in the bat.

Cochlear frequency mapping in horseshoe bats and mustached bats reveals that a narrow frequency band around the dominant CF component has an expanded representation in BM length with mapping coefficients >50 mm per octave as compared with the values of 3 mm per octave in nonspecialized mammals (Figure 2; review: Kössl, M. and Vater, M., 1995; Kössl, M., 1997). The expanded frequency representation within a cochlear region of maximal innervation density results in a vast overrepresentation of a narrow frequency band in the central auditory pathway. This frequency band contains neurons that are exceptionally sharply tuned (Q10 dB values up to 300 as compared with values of about 20 in other vertebrates). Thus, an auditory fovea is created for analysis of the biologically most important frequencies.

3.38.3 Cochlear Anatomy

Emphasizing the importance of hearing, extant microchiropteran bats are characterized by an enlarged cochlea. This character dates back at least 50 million years as evidenced by the oldest known fossil bat, *Icaronycteris index* (review: Springer, M. S. *et al.*,

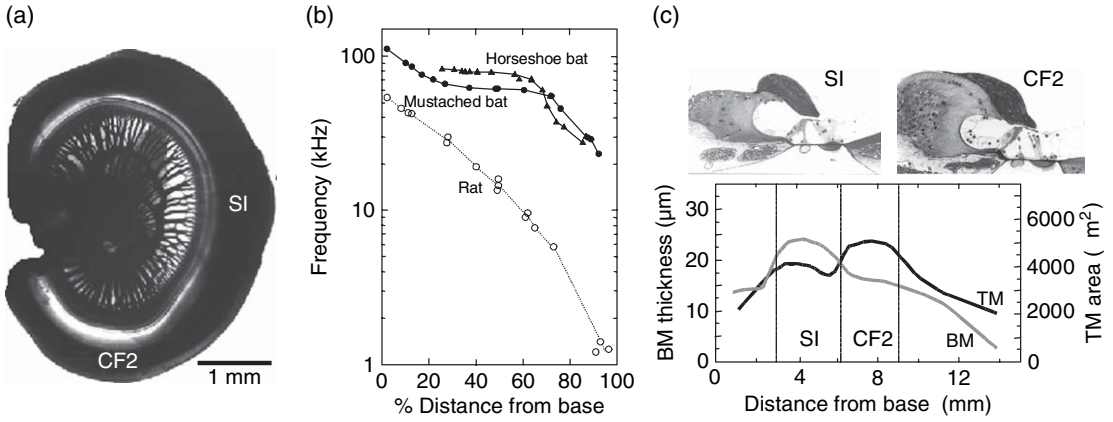

Figure 2 (a) Surface view of the basal turn of the mustached bat cochlea with densely innervated zone at the representation place of CF2 and more basally located sparsely innervated (SI) zone. (b) Cochlear frequency maps of horseshoe bats (Kössl, M. and Vater, M., 1985a; 1985b) and mustached bats (Kössl, M. and Vater, M., 1985a; 1985b) in comparison with the rat (Müller, M., 1991). (c) Cross sections of the organ of Corti in the SI and CF2 zones of the mustached bat cochlea and basoapical changes in basilar membrane (BM) thickness and tectorial membrane (TM) area (Vater, M. and Kössl, M., 1996).

2001). Cochlear size reaches maximal values in species that employ Doppler-sensitive sonar, and among different species of horseshoe bats, there is a clear correlation between the diameter of the basal cochlear turn and the frequency of the CF component (review: Kössl, M. and Vater, M., 1995; Vater, M., 1998; 2000).

The basic anatomical design of the bat cochlea follows the scheme common to all marsupial and placental mammals as evidenced by light microscopic, scanning electron, and transmission electron microscopic studies (review: Kössl, M. and Vater, M., 1995; Vater, M., 1998).

There is the same set of sensory and nonsensory structures as in nonecholocating mammals. There is one row of inner hair cells (IHCs) separated by pillar cells from the three rows of OHCs. Each OHC is supported by a Deiters' cell, and the lateral membrane of OHCs is surrounded by the spaces of Nuel. In mustached bats, the presence of prestin in OHC was demonstrated with immunocytochemical techniques. As in other mammals, IHCs receive the bulk of afferent innervation. Lateral and medial olivocochlear efferent systems are established in bats, but as a remarkable specialization, whose functional consequences still need to be resolved, OHCs of horseshoe bats completely lack efferent innervation.

Within the general mammalian scheme, bats show specializations for high-frequency hearing: short OHCs, small stereovilli, and a thick and narrow BM (review: Kössl, M. and Vater, M., 1995; Vater, M., 1998). Unlike in all other mammals, CF-FM bat cochleae have prominent maxima and minima in afferent innervation density within the basal cochlear turn, and profound specializations in the basoapical gradients in the morphology of the BM and the TM that appear to be related to exceptionally sharp tuning properties to the dominant CF signal. Bats have additional species-specific specializations. The mustached bat cochlea exhibits pronounced changes in scale volume of the basal turn, and the horseshoe bat cochlea features a specialized secondary spiral lamina.

Within the auditory fovea of the mustached bat, there are multiple morphological specializations (Figure 2). It can be subdivided into a basal and an apical part by a sharp transition (occurring within a few hundred micrometers) in morphological parameters such as innervation density and morphology of the TM and the BM. In the basal part of the fovea, innervation density is low, the BM is prominently thickened, and the TM is club shaped. In the densely innervated apical part of the fovea, the BM is not specialized, but the TM is enlarged with an extensive attachment to the spiral limbus.

3.38.4 Cochlear Development

Studies of the postnatal development of echolocation and audition in horseshoe bats (Rübsamen, R. and Schäfer, M., 1990) and mustached bats (Kössl, M. *et al.*, 2003; Russell, I. J. *et al.*, 2003) have revealed a concomitant upward shift in the frequency of the CF component and the tuning of the auditory fovea. Thus, bats seem to monitor a postnatal shift in the

cochlear frequency map in the pitch of their voice. CM recordings in young mustached bats also reveal the developmental sharpening of tuning over the first 3 postnatal weeks (Kössl, M. *et al*., 2003). Cochlear dimensions and the main morphological specializations of the BM and TM are established at birth in CF-FM bats, but subtle structural changes indicate postnatal increases in stiffness of the micromechanical system (review: Vater, M., 2000).

3.38.5 Cochlear Mechanisms

There is strong evidence for a labile, actively controlled mechanical resonator in the cochlea of the mustached bat that is tuned to 61 kHz, the frequency of the dominant component of the Doppler-shifted echo. This mechanism is superimposed on the conventional mechanisms common to all mammals. The active elements are represented by the OHCs that provide feedback to the passive mechanical system, as they do in other mammals. Unlike in other mammals, feedback through OHCs in these bats is further enhanced by a highly tuned passive resonator that is contained in the morphological specializations of BM and TM. Collating data from anatomy, frequency mapping, BM displacement measurements, and measurements of distortion product otoacoustic emissions, Russell I. J. and Kössl M. (1999) proposed a model for the mustached bat cochlea that involves (1) buildup of resonant oscillation in form of a standing wave on the TM in the basal part of the fovea; (2) transfer of resonant energy into the organ of Corti and BM of the more apical parts of the fovea, where IHCs are most densely innervated and receive a boosted 61 kHz mechanical stimulation; and (3) OHCs that are essential to enhance, fine-tune, and control the resonance.

References

Dallos, P. 1992. The active cochlea. J. Neurosci. 12, 4575–4585.

Kössl, M. 1997. Sound emission from cochlear filters and foveae – does the auditory sense organ make sense? Naturwissenschaften 84, 9–16.

Kössl, M. and Russell, I. J. 1995. Basilar membrane resonance in the cochlea of the mustached bat. Proc. Natl. Acad. Sci. U. S. A. 92, 276–279.

Kössl, M. and Vater, M. 1985a. Evoked acoustic emissions and cochlear microphonics in the mustached bat, *Pteronotus parnellii*. Hear. Res. 19, 157–170.

Kössl, M. and Vater, M. 1985b. The cochlear frequency map of the mustached bat, *Pteronotus parnellii*. J. Comp. Physiol. A 157, 687–697.

Kössl, M. and Vater, M. 1995. Cochlear Structure and Function in Bats. In: Hearing by Bats (*eds*. A. N. Popper and R. R. Fay), pp. 191–235. Springer Handbook of Auditory Research, Springer.

Kössl, M., Foeller, E., Drexl, M., Vater, M., Mora, E., Coro, F., and Russell, I. J. 2003. Postnatal development of cochlear function in the mustached bat, *Pteronotus parnellii*. J. Neurophysiol. 90, 2261–2273.

Müller, M. 1991. Frequency representation in the rat cochlea. Hear. Res. 51, 247–254.

Neuweiler, G. 1990. Auditory adaptations for prey capture in echolocating bats. Physiol. Rev. 70, 615–641.

Pollak, G. D., Henson, O. W., Jr., and Novick, A. 1972. Cochlear microphonic audiograms in the 'pure tone' bat, *Chilonycteris parnellii parnellii*. Science 176, 66–68.

Rübsamen, R. and Schäfer, M. 1990. Ontogenis of auditory fovea representation in the inferior colliculus of the Sri Lankan rufous horseshoe bat, *Rhinolophus rouxi*. J. Comp. Physiol. A 167, 757–769.

Russell, I. J. and Kössl, M. 1999. Micromechanical responses to tones in the auditory fovea of the greater mustached bats's cochlea. J. Neurophysiol. 82, 676–686.

Russell, I. J., Drexl, M., Foeller, E., Vater, M., and Kössl, M. 2003. The development of a single frequency place in the mammalian cochlea: the cochlear resonance in the mustached bat *Pteronotus parnellii*. J. Neurosci. 26, 10971–10981.

Schnitzler, H.-U., Moss, C. F., and Denzinger, A. 2003. From spatial orientation to food acquisition in echolocating bats. Trends Ecol. Evol. 18, 386–394.

Vater, M. 1998. Adaptations of the Auditory Periphery of Bats for Echolocation. In: Bats, Phylogeny, Morphology, Echolocation, and Conservation Biology (*eds*. T. H. Kunz and P. A. Racey), pp. 231–247. Smithonian Institution Press.

Vater, M. 2000. Evolutionary Plasticity and Ontogeny of the Bat Cochlea. In: Ontogeny, Functional Ecology, and Evolution of Bats (*eds*. R. A. Adams and S. C. Pedersen), pp. 137–173. Cambridge University Press.

Vater, M. and Kössl, M. 1996. Further studies on the mechanics of the cochlear partition in the mustached bat. I. Ultrastructural observations on the tectorial membrane and its attachments. Hear. Res. 94, 63–78.

Vater, M., Feng, A. S., and Betz, M. 1985. An HRP-study of the frequency-place map of the Horseshoe bat cochlea, morphological correlates of the sharp tuning to a narrow frequency band. J. Comp. Physiol. A 157, 671–686.

Further Reading

Bruns, V. 1976a. Peripheral auditory tuning for fine frequency analysis by the CF-FM bat, *Rhinolophus ferrumequinum.* II. Frequency mapping in the cochlea. J. Comp. Physiol. A 106, 87–97.

Bruns, V. 1976b. Peripheral auditory tuning for fine frequency analysis by the CF-FM bat, *Rhinolophus ferrumequinum.* I. Mechanical specializations of the cochlea. J. Comp. Physiol. A 106, 77–86.

Bruns, V. and Goldbach, M. 1980. Hair cells and tectorial membrane in the cochlea of the greater horseshoe bat. Anat. Embryol. 161, 65–83.

Bruns, V. and Schmieszek, E. 1980. Cochlear innervation in the greater Horseshoe bat, demonstration of an acoustic fovea. Hear. Res. 3, 27–43.

Dannhof, B. J., Roth, B., and Bruns, V. 1991. Length of hair cells as a measure of frequency representation in the mammalian cochlea? Naturwissenschaften 78, 570–573.

Grinnell, A. D. 1970. Comparative auditory neurophysiology of neotropical bats employing different echolocation signals. Z. Vergl. Physiol. 68, 117–153.

Habersetzer, J. and Storch, G. 1992. Cochlea size in extant chiroptera and middle eocene microchiroptera from Messel. Naturwissenschaften 79, 462–466.

Henson, O. W., Jr. 1970. The Ear and Audition. In: Biology of Bats, Vol. II (*ed*. W. A. Wimsatt), pp. 181–256. Academic Press.

Henson, M. M. 1973. Unusual nerve-fiber distribution in the cochlea of the bat *Pteronotus parnellii* (Gray). J. Acoust. Soc. Am. 53, 1739–1740.

Henson, M. M. and Henson, O. W., Jr. 1991. Specializations for sharp tuning in the mustached bat: the tectorial membrane and spiral limbus. Hear. Res. 56, 122–132.

Henson, O. W., Jr., Schuller, G., and Vater, M. 1985. A comparative study of the physiological properties of the inner ear in Doppler shift compensating bats (*Rhinolophus rouxi*, *Pteronotus parnellii*). J. Comp. Physiol. A 157, 587–597.

Huffman, R. F. and Henson, O. W., Jr. 1993. Labile cochlear tuning in the mustached bat II. Concomitant shifts in neural tuning. J. Comp. Physiol. A 171, 735–748.

Köppl, C., Manley, G. A., and Gleich, O. 1993. An auditory fovea in the barn owl cochlea. J. Comp. Physiol. A 171, 695–704.

Kössl, M. 1994a. Otoacoustic emissions from the cochlea of the 'constant frequency' bats, *Pteronotus parnellii* and *Rhinolophus rouxi*. Hear. Res. 72, 59–72.

Kössl, M. 1994b. Evidence for a mechanical filter in the cochlea of the 'constant frequency bats' *Rhinolophus rouxi* and *Pteronotus parnellii*. Hear. Res. 72, 73–80.

Kössl, M. and Vater, M. 1996a. A tectorial membrane fovea in the cochlea of the mustached bat. Naturwissenschaften 2, 89–92.

Kössl, M. and Vater, M. 1996b. Further studies on the mechanics of the cochlear partition in the mustached bat. II. A second cochlear frequency map derived from acoustic distortion products. Hear. Res. 94, 78–87.

Müller, M., Laube, B., Burda, H., and Bruns, V. 1992. Structure and function of the cochlea in the African mole rat (*Cryptomys hottentottus*), evidence for a low frequency acoustic fovea. J. Comp. Physiol. A 171, 469–476.

Neuweiler, G. 1970. Neurophysiologische Untersuchungen zum Echoortungssystem der grossen Hufeisennase Rhinolophus ferrumequinum Schreber, 1774. Z. Vergl. Physiol. 67, 273–306.

Schnitzler, H.-U. 1968. Die Ultraschallortungslaute der Hufeisen-Fledermäuse (Chiroptera-Rhinolophidae) in verschiedenen Orientierungssituationen. Z. Vergl. Physiol. 68, 25–38.

Springer, M. S. *et al.* 2001. Integrated fossil and molecular data reconstruct bat echolocation. PNAS 98, 6241–6246.

Suga, N., Simmons, J. A., and Jen, P.-H. S. 1975. Peripheral specializations for fine analysis of Doppler-shifted echoes in the auditory system of the ''CF-FM'' bat *Pteronotus parnellii*. J. Exp. Biol. 63, 161–192.

Vater, M. and Lenoir, M. 1992. Ultrastructure of the horseshoe bat's organ of Corti. I. Scanning electron microscopy. J. Comp. Neurol. 318, 367–379.

Vater, M., Lenoir, M., and Pujol, R. 1992. Ultrastructure of the horseshoe bat's organ of Corti. II. Transmission electron microscopy. J. Comp. Neurol. 318, 380–391.

Vater, M., Lenoir, M., and Pujol, R. 1997. Development of the organ of corti in horseshoe bats, scanning and transmission electron microscopy. J. Comp. Neurol. 377, 520–534.

Xie, D. H., Henson, M. M., Bishop, A. L., and Henson, O. W., Jr. 1993. Efferent terminals in the cochlea of the mustached bat. Quantitative data. Hear. Res. 66, 81–90.

Zook, J. M. and Leake, P. A. 1989. Connections and frequency representation in the auditory brainstem of the mustached bat, *Pteronotus parnellii*. J. Comp. Neurol. 290, 243–261.

3.39 Auditory Processing in the Bat Medial Superior Olive

O Behrend, Humboldt-University, Berlin, Germany

B Grothe, Ludwig-Maximilians-University, Munich, Germany

© 2008 Elsevier Inc. All rights reserved.

3.39.1	**Introduction**	701
3.39.2	**The Medial Superior Olive of Normal Low-Frequency Hearing Mammals**	703
3.39.3	**The Medial Superior Olive of Normal High-Frequency Hearing Mammals**	706
3.39.4	**The Medial Superior Olive of Bats**	708
3.39.4.1	Anatomy of the Medial Superior Olive in Bats	709
3.39.4.1.1	Frequency-modulated bats	709
3.39.4.1.2	Constant-frequency–frequency-modulated bats	709
3.39.4.2	Input Pattern and Physiology of the Medial Superior Olive in Bats	709
3.39.4.2.1	Frequency-modulated bats	709
3.39.4.2.2	Constant-frequency–frequency-modulated bats	711
3.39.4.3	Function of the Medial Superior Olive in Bats	711
3.39.4.3.1	Constant-frequency–frequency-modulated bats	711
3.39.4.3.2	Frequency-modulated bats	713
3.39.5	**Conclusions**	714
References		715

Glossary

AM Amplitude modulated.
AN Auditory nerve.
AVCN Anteroventral cochlear nucleus.
CF Constant frequency.
DMPO Dorsomedial periolivary nucleus.
DPO Dorsal periolivary nucleus.
FM Frequency modulated.
GBC Globular bushy cells.
IC Inferior colliculus.
ILD Interaural level difference.
IPD Interaural phase difference.
ITD Interaural time difference.
LNTB Lateral nucleus of the trapezoid body.
LSO Lateral superior olive.
MNTB Medial nucleus of the trapezoid body.
MSO Medial superior olive.
NL Nucleus laminaris.
SAM Sinusoidally amplitude modulated.
SBC Spherical bushy cells.
SOC Superior olivary complex.
SPN Superior paraolivary nucleus.
VCN Ventral cochlear nucleus.
VMPO Ventromedial periolivary nucleus.
VNTB Ventral nucleus of the trapezoid body.
VPO Ventral periolivary nucleus.

3.39.1 Introduction

Roughly 210–250 million years ago, three vertebrate clades had evolved means to perceive airborne sound, that is, ears that feature a tympanic membrane and a middle ear cavity. This evolutionary milestone occurred independently within anurans, reptiles (including archosaurs, the ancestors of birds), and early mammals (Clack, J. A., 1997; 2002). In order to process sensory information that derived from auditory end organs, respective central neural structures evolved in parallel. That is, either novel neural circuits were created to serve auditory computation or, alternatively, existing precursor nuclei (unspecific

or freed from serving other senses, respectively) had differentiated to support the analyses of acoustic cues (Grothe, B. *et al.*, 2004).

Evidently, the central extraction of features that indicate the nature and whereabouts (what and where) of sound sources was vital for all hearing animals. Limited acoustic cues are available to compute that source-specific information within the brain: the temporal and spectral pattern of an incoming sound, for instance, can hint to the nature of its source. The location of a sound source is reflected by level, time, and spectral disparities at the two ears that receive sound traveling along different trajectories (Irvine, D. R., 1992; Grothe, B., 2003). Within that well-defined framework of physical constraints, anurans, reptiles, and early mammals independently evolved neural solutions to process and represent acoustic objects. Consequently, auditory systems of different vertebrate classes express – particularly at early stages of the auditory pathway – striking functional, anatomical, morphological, and biophysical similarities (Grothe, B. *et al.*, 2004). A functional analogy in the context of temporal processing is reflected, for instance, by the modern avian nucleus laminaris (NL) and the mammalian medial superior olive (MSO; Figure 1). Both brainstem structures are best known for their potential to process interaural time differences (ITDs), and are characterized by regularly arranged bipolar cells with highly reminiscent input patterns, and highly specialized membrane properties (Grothe, B., 2003). In both nuclei, these principal cells receive precisely timed binaural input from bushy cells of the nucleus magnocellularis, and its mammalian equivalent, the anteroventral cochlear nucleus (AVCN), respectively. The projections were shown to promote coincident input detection within the principal cells of the NL and the MSO. So, on first glance the concepts of neural computation appeared identical within the two structures. However, recent physiological and theoretical studies (Brand, A. *et al.*, 2002; Harper, N. S. and McAlpine, D., 2004) indicate that the rules of neural processing applied within the NL and the MSO, respectively, differ. This concerns particularly inhibitory inputs that seem to be involved in shaping neural ITD functions in mammals, other than in birds where inhibitory inputs help to shunt the membrane potential in order to provide gain control (compare also Howard, M. A. *et al.*, 2007). Moreover, two different neural codes of azimuthal space were observed, a so-called place code in birds (Konishi, M., 2003) and a hemispheric population code in mammals (McAlpine, D. *et al.*, 2001), seem to be realized. The NL/MSO circuits now epitomize independently evolving neural structures that were forged by converging evolutionary pressures (Carr, C. E. and Soares, D., 2002). Research on the development of their respective rules of computation (Agmon-Snir, H. *et al.*, 1998; Cramer, K. S. *et al.*, 2002; Kapfer, C. *et al.*, 2002) further established the NL/MSO as an outstanding model system for a stringent investigation of the independent evolution of functionally analogous neural circuits on the molecular, cellular, and systemic level.

The MSO also provides, as one of very few structures, additional opportunities to study the parallel evolution within the class of mammals – by means of comparing its appearance in both acoustically specialized and nonspecialized mammalian species. Mammals have conquered a great number of ecological niches that embody a great variety of acoustic environments. But not all mammals make use of ITDs to localize low-frequency sounds. In fact, the audiogram of most mammals does not even encompass frequencies that make ITD coding useful for sound localization (i.e., in mammals, frequencies below ~2 kHz). ITD coding might therefore be considered to represent only one of several possible specializations of the MSO (in this case for low-frequency sound localization). Over a common mammalian hearing range between 4 and 40 kHz, however, interaural level differences (ILDs) are far more efficient to encode the location of a sound source (Tollin, D. J., 2003). (Note that the most primitive mammals, monotremes, which possess a middle ear strikingly similar to that of early mammals, exhibited good hearing only from 4 to 18 kHz, apparently the original mammalian range of hearing (Mills, D. M. and Shepherd, R. K., 2001) before it was extended to frequencies typically up to 40 kHz. Low-frequency hearing, therefore, has to be viewed as a late adaptation in mammals.) So it appears that the universal feature of MSO cells – whether concerned with ITD processing or not – could be precise temporal processing itself. This computational capacity, modified to various degrees, can support diverse species-specific purposes like low-frequency sound localization or high-frequency sound pattern recognition. Indeed, the MSO expresses a high degree of morphological and functional plasticity across present mammalian species (Figure 2; Grothe, B. and Neuweiler, G., 2000). Both inhibitory and excitatory inputs to the MSO seem adaptable, and reflect the structure's adjustment to individual ecological constraints (Covey, E. *et al.*, 1991; Kapfer, C. *et al.*,

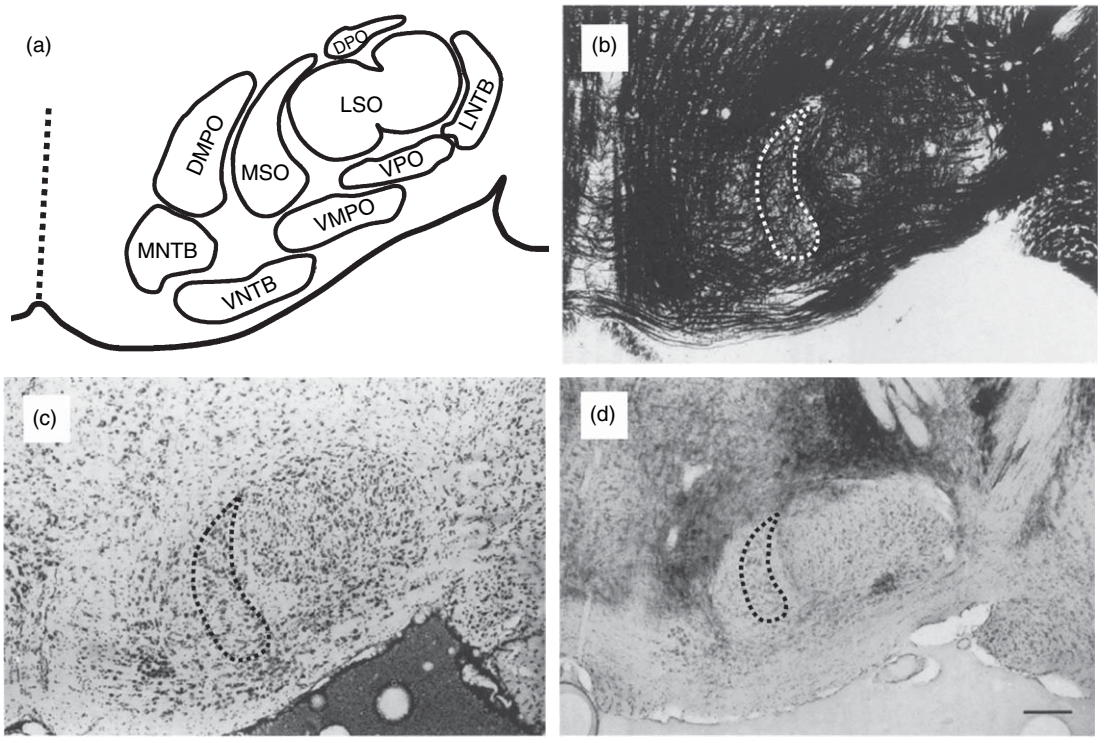

Figure 1 (a) Outline of the Mexican free-tailed bat SOC and MSO illustrated in fiber staining (b), Nissl staining (c), and acetylcholinesterase staining (d). Calibration bar = 200 μm. DMPO, dorsomedial periolivary nucleus; DPO, dorsal periolivary nucleus; LNTB, lateral nucleus of the trapezoid body; LSO, lateral superior olive; MNTB, medial nucleus of the trapezoid body; MSO, medial superior olive; SOC, superior olivary complex; VMPO, ventromedial periolivary nucleus; VNTB, ventral nucleus of the trapezoid body; VPO, ventral periolivary nucleus. Adapted from Grothe, B., Schweizer, H., Pollak, G. D., Schuller, G., and Rosemann, C. 1994. Anatomy and projection patterns of the superior olivary complex in the Mexican free-tailed bat, *Tadarida brasiliensis mexicana*. J. Comp. Neurol. 343, 630–646.

2002; Kandler, K., 2004). Acoustic constraints, in particular, are likely to have profoundly influenced the phylogenesis of the auditory brainstem of bat species with foraging strategies that rely on the auditory system. For neuroscience, therefore, the bat MSO represents a useful model system to study the evolution of a distinct neural circuit in well-defined ecological niches.

3.39.2 The Medial Superior Olive of Normal Low-Frequency Hearing Mammals

The MSO is part of the superior olivary complex (SOC; exemplified for the Mexican free-tailed bat in Figure 1) and is among the first stages in the ascending auditory pathway that integrate binaural inputs. With regard to low-frequency sound localization in dogs and cats (Goldberg, J. M. and Brown, P. B., 1969; Yin, T. C. and Chan, J. C., 1990) the MSO has traditionally been viewed as a coincidence detector that analyses ITDs: schematically, MSO cells cross-correlate phase-coupled binaural inputs, and generate a spike rate that depends on interaural phase differences (IPDs; Jeffress, L. A. and Robinson, D. E., 1962; Blauert, J. and Lindemann, W., 1986; Caird, D. and Klinke, R., 1987; Wightman, F. L. and Kistler, D. J., 1992; Macpherson, E. A. and Middlebrooks, J. C., 2002; Yin, T. C., 2002). These binaural phase disparities reflect the ITDs caused by acoustic path length differences as a sound reaches both ears, and they vary systematically with the location of a sound source relative to a listener. In agreement with Jeffress' elegant delay line model (Jeffress, L. A., 1948), a position-dependent IPD was postulated to coincidentally excite a distinct subset of MSO neurons – owing to an inverse arrangement of incoming axon path lengths. As a whole, the coincidence detector neurons demonstrated in the MSO were thought to create a place code of azimuthal space within each frequency band.

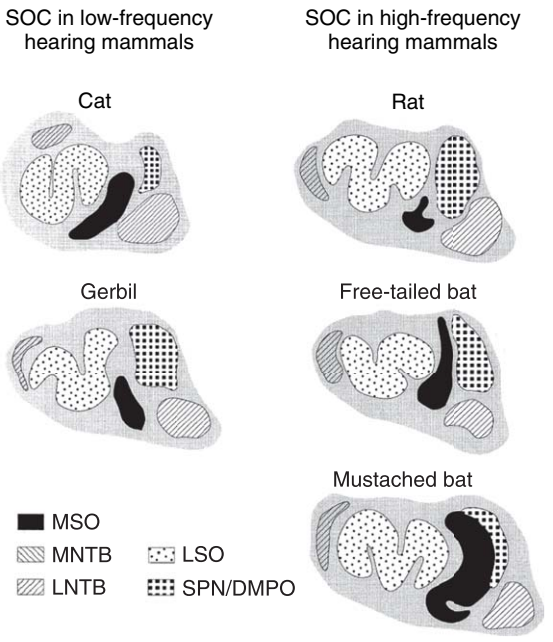

Figure 2 The outline of the MSO in several mammals as apparent from transversal sections. DMPO, dorsomedial periolivary nucleus (nonrodents); LNTB, lateral nucleus of the trapezoid body; LSO, lateral superior olive; MNTB, medial nucleus of the trapezoid body; MSO, medial superior olive; SPN, superior paraolivary nucleus (rodents). From Grothe, B. 2000. The evolution of temporal processing in the medical superior olive, an auditory brainstem structure. Prog. Neurobiol. 61, 581-610.

This view of the MSO was in line with early anatomical studies in dogs and cats that feature a prominent MSO. These animals possess bipolar principal MSO cells that are arranged in an orderly column with dendrites oriented mediolaterally (Stotler, W. A., 1953; Goldberg, J. M. and Brown, P. B., 1968). The functional significance of the MSO for sound localization was later supported by a combination of results. First, Conlee, J. W. *et al.*, (1984; 1986) typified an atrophic MSO in albino cats. Second, Heffner R. S. and Heffner H. E. (1987) gave evidence about behavioral deficits of albino cats in azimuthal sound localization. In accord with this behavioral data, a physiological study indicated a decreased ITD sensitivity within the albino cat brainstem (Yin, T. C. *et al.*, 1990). However, despite some evidence of a systematic arrangement of delay lines that could cover ITDs experienced across azimuthal space (Smith, P. H. *et al.*, 1993), the classical picture of the MSO as a pure Jeffress-type coincidence detector could neither be confirmed nor be rejected based on anatomical data.

Still, it remained conceptually fitting that the tonotopic projections to the MSO have been shown to be biased in dogs and cats, leading to a strong representation of low sound frequencies known to be predominantly localized by means of ITD (Goldberg, J. M. and Brown, P. B., 1969; Guinan, J. J. Jr., *et al.*, 1972). Also, single-unit recordings in the MSO of cats (Galambos, R. *et al.*, 1959; Caird, D. and Klinke, R., 1983; Yin, T. C. and Chan, J. C., 1990) and dogs (Goldberg, J. M. and Brown, P. B., 1969), as well as gerbils (Spitzer, M. W. and Semple, M. N., 1995; Brand, A. *et al.*, 2002), have established that most MSO neurons in low-frequency hearing animals can be excited by monaural acoustic stimulation at either ear. This response property is in line with the view of an MSO that performs neural computation on the basis of excitatory inputs from both ears. These projections augment the analysis of ITDs based on coincidence detection by maintaining or even enhancing precisely phase-coupled discharges of auditory nerve (AN) fibers (Galambos, R. and Davis, H., 1943; Kiang, N. Y. *et al.*, 1965; Rose, J. E. *et al.*, 1967; Joris, P. X. *et al.*, 1994a; 1994b), and were shown to originate in spherical bushy cells (SBC) of the ventral cochlear nucleus (VCN) (Warr, W. B., 1966; Osen, K. K., 1969; Lindsey, B. G., 1975; Smith, P. H. *et al.*, 1993; Kitzes, L. M. *et al.*, 1995).

In extension of the classical view of the MSO as a comparator structure of excitatory inputs, strong glycinergic inhibitory inputs exist that derive from the medial and lateral nuclei of the trapezoid body (MNTB; LNTB; Figure 3; Clark, G. M., 1969; Perkins, R. E., 1973; Cant, N. B., 1991; Cant, N. B. and Hyson, R. L., 1992; Kuwabara, N. and Zook, J. M., 1992). Pharmacological studies had shown that glycinergic inhibition alters the response properties of MSO neurons in gerbil slice preparations (Grothe, B. and Sanes, D. H., 1993; 1994). More recently, indirect evidence for inhibition being involved in ITD processing in the SOC came from awake rabbit recordings (Batra, R. *et al.*, 1997). In gerbils, glycinergic projections had been shown to be crucial to the MSO cells' ITD sensitivity *in vivo* (Brand, A. *et al.*, 2002). (Note gerbils are small desert rodents that depend on far-reaching low-frequency sound localization to avoid predation. To this end, extreme ITDs in the low microsecond range must suffice due to the animals' head size.)

So clearly, in low-frequency hearing mammals, the MSO encodes favorable ITDs by facilitated spike rates (Yin, T. C. and Chan, J. C., 1990; Spitzer, M. W. and Semple, M. N., 1995). Furthermore,

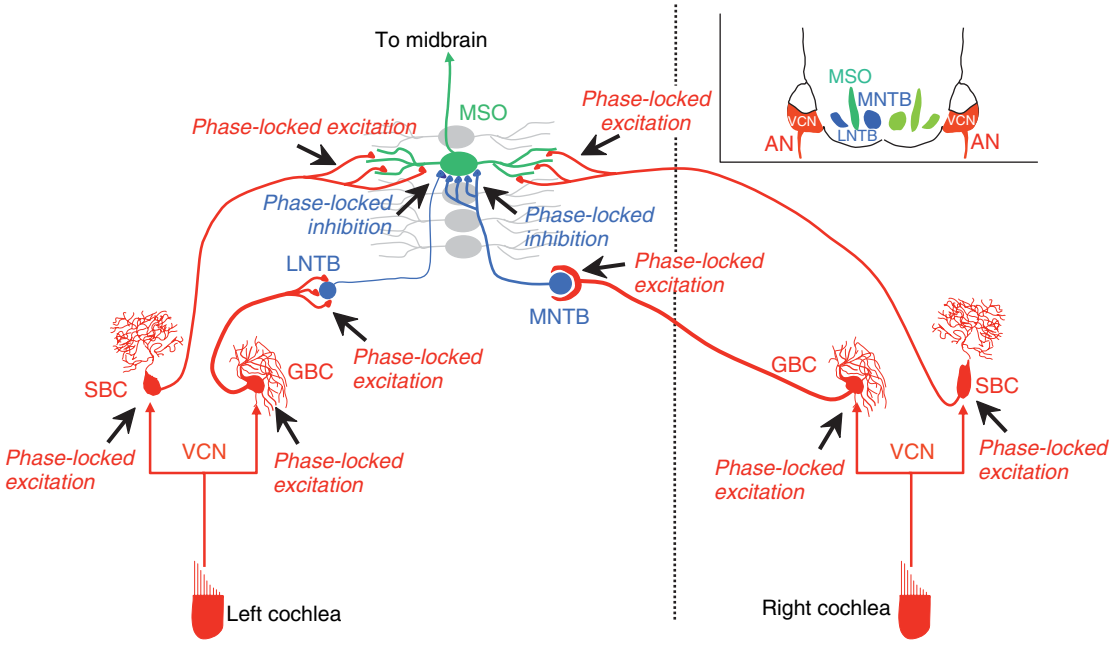

Figure 3 The mammalian ITD encoder is the MSO, an auditory brainstem structure (inset). MSO neurons are bipolar and their somata are arranged in one parasagittal plane. Excitatory projections originate from the left and right cochlea. Auditory nerve fiber discharges time-lock to the stimulus onset or phase-lock to ongoing pure tones up to about 2 kHz. They excite spherical and globular bushy cells, respectively, in the VCN. SBCs and GBCs also provide phase-locked excitation to their targets: SBCs project to the MSO on both sides, GBCs to the contralateral MNTB and the ipsilateral LNTB. The inputs to the MNTB and LNTB are specialized to preserve temporal information: the MNTB is driven by a gigantic synapse, the calyx of Held. MNTB and LNTB neurons provide phase-locked, glycinergic, hyperpolarizing inhibition to the ipsilateral MSO. MSO neurons extract the ITD from a comparison of their four inputs and project to higher auditory centers. The well-timed inhibition is crucial for adjusting the ITD sensitivity of MSO cells to the physiologically relevant range of ITDs. AN, auditory nerve; GBC, globular bushy cells; ITD, interaural intensity difference; LNTB, lateral nucleus of the trapezoid body; MNTB, medial nucleus of the trapezoid body; MSO, medial superior olive; SBC, spherical bushy cells; VCN, ventral cochlear nucleus. Adapted from Grothe, B. 2003. New roles for synaptic inhibition in sound localization. Nat. Rev. Neurosci. 4, 540–550.

several authors have demonstrated that the best IPD of an MSO unit could be predicted by the phase angle of its responses to monaural stimulation. It was also established that the best response of an MSO neuron was stable at a certain ITD across different stimulus frequencies (Figure 4(a)). All of these results support the view that the function of the MSO in low-frequency hearing mammals is to encode the azimuthal origin of low-frequency sounds by coincidence detection of binaural inputs. In remarkable contrast to avian ITD coding, however, this view had to be expanded recently in an unexpected way: The adjustment of the MSO sensitivity to the behavioral range of ITDs in gerbils seems to be accomplished by experience-driven refinement of inhibitory inputs (Brand, A. *et al.*, 2002; Kapfer, C. *et al.*, 2002; Grothe, B., 2003). During auditory maturation, the compound postsynaptic timing of these inhibitory projections is enhanced by the concentration of glycinergic synapses onto the soma of an MSO cell (Magnusson, A. K. *et al.*, 2005). As a result, binaural excitatory and mainly contralateral inhibitory inputs appear to shape a composite ITD function in MSO neurons. Interfering with this development by keeping animals in omnidirectional broadband noise for several days after hearing onset reduces the refinement of the inhibitory inputs (Kapfer, C. *et al.* 2002), and causes an abnormal ITD tuning (Seidl, A. H. and Grothe, B., 2005). One possible scenario is that inhibition precedes contralateral excitation at a given sound frequency: this phase shift determines a narrow time window during which an MSO cell can respond to coincident binaural excitation, and so tunes the maximal slope of ITD functions in the gerbil MSO to behaviorally relevant ITDs (Figure 4(b)). Therefore, a negative correlation between an MSO neuron's BF and its best ITD would result from the phase-coupled interaction of excitatory and inhibitory inputs (compare McAlpine, D. *et al.*, 2001). Analogous observations were recently made in larger

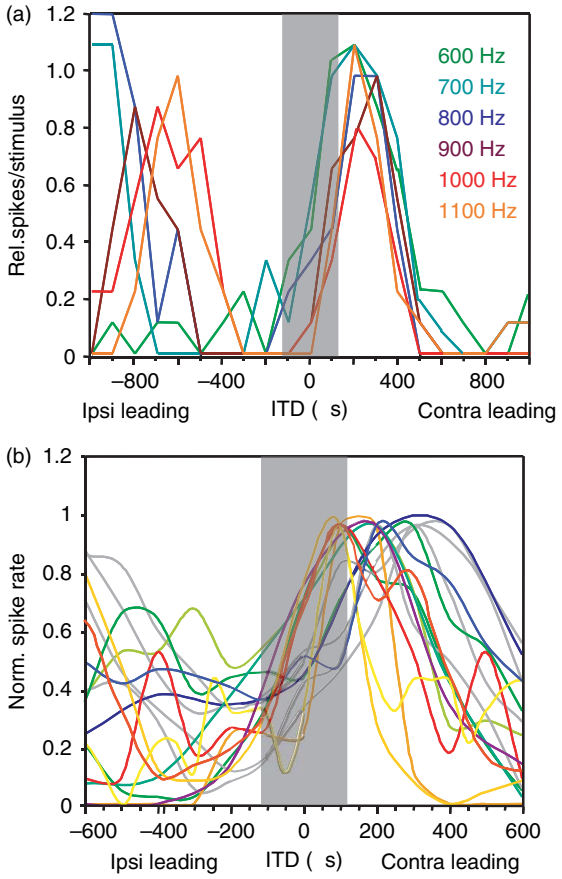

Figure 4 ITD coding in the mammalian MSO. (a) ITD function of a gerbil MSO neuron, tested with pure tones at different frequencies. As is typical, the peak ITD is independent of the stimulus frequency. The gray area indicates the physiologically relevant range for gerbils (±120 μs). (b) ITD functions of gerbil MSO neurons, each tested at its best frequency, 20 dB above threshold. Note that the peaks of ITD functions are largely outside the physiologically relevant range (gray area). The steep slopes of the ITD functions are within the relevant area. ITD, interaural time difference; MSO, medial superior olive. From Brand, A., Behrend, O., Marquardt, T., McAlpine, D., and Grothe, B. 2002. Precise inhibition is essential for microsecond interaural time difference coding. Nature 417, 543–547.

mammals with good low-frequency hearing (Hancock, K. E. and Delgutte, B., 2004). One might speculate the dazzling temporal resolution of ITDs in many low-frequency hearing mammals could be produced by similar rules of computation in an MSO that, potentially, refines coincident input detection properties by precisely adjusted and fast inhibition.

By and large, there remains little doubt about the function of the MSO as a coincidence detector that resolves ITDs in some low-frequency-hearing mammals. That said, the long-standing concept of how ITDs are neurally encoded in mammals might have to be revised in some measure to account for the role of surprisingly plastic, and potentially fast, inhibitory inputs to the MSO.

3.39.3 The Medial Superior Olive of Normal High-Frequency Hearing Mammals

Notably, even in low-frequency hearing mammals that use ITDs, up to one third of the units within the MSO do not show classical binaural excitation (Goldberg, J. M. and Brown, P. B., 1969; Yin, T. C. and Chan, J. C., 1990). Recent studies in the avian NL have indicated that this substantial neuronal subset might be overemphasized by biased sampling, since coincident detector unit activity might often remain unnoticed in extracellular recordings (Kuba, H. *et al.*, 2006). On the other hand, anatomical and physiological data on MSO cells from several bat species (discussed below) also suggest a significant presence of nonclassical MSO neurons that lack binaural excitatory input needed for the analyses of acoustic ITDs by coincidence detection. Given that the MSO had initially evolved as an ITD detector for airborne sound, such units would seem somewhat out of place. But very likely the evolutionary development of the MSO was shaped by an early auditory periphery whose transmission of low-frequency sound was limited (Mills, D. M. and Shepherd, R. K., 2001; reviews: Grothe, B., 2000; Grothe, B. *et al.* 2004). Almost certainly, the common ancestors of monotremes and therian mammals developed a three-ossicle middle ear independently from the avian one-ossicle middle ear. Whereas the latter is only suited for low-frequency hearing, the former was initially suited for rather high-frequency transmission (Fleischer, G., 1978; Mills, D. M. and Shepherd, R. K., 2001; Clack, J. A. and Allin, E., 2004; Grothe, B. *et al.*, 2004; Manley, G. A. and Clack, J. A., 2004). The middle ear structure of the early mammalian middle ear was nearly identical to that of recent monotremes or some opossums (Gregory, W. K., 1929; Rosowski, J. J., 1992), and these animals' frequency resolution could therefore approximate the auditory range postulated for early mammals (i.e., above 4–6 kHz; Frost, S. B. and Masterson, R. B., 1994; Mills, D. M. and Shepherd, R. K., 2001). This would suggest that ITD processing capacities were biologically irrelevant for

early mammals, and became relevant only after the onset of effective low-frequency sound transmission. Consequently, comparative studies on the MSO of high-frequency hearing animals were poised to yield substantial data on the origin of this neural circuit, and mechanisms of its functional evolution.

Early on, it was speculated that high-frequency hearing animals – using mainly ILDs for sound localization – do not even possess an MSO (Harrison, J. M. and Irving, R., 1966; Irving, R. and Harrison, J. M., 1967). In retrospect, this exclusive perception of the MSO as an ITD-coding structure in low-frequency-hearing mammals might have been premature: in unison with its counterpart, the lateral superior olive (LSO; Tollin, D. J., 2003), the MSO was too firmly embedded in the framework of the duplex theory of sound localization (Rayleigh, L., 1907; Masterson, B. and Diamond, I. T., 1967). Now that the resolution of low-frequency sound in itself might be viewed as a secondary adaptation in mammals, however, the classical MSO could become a rather special case. To learn more about the putative original function of early MSO cells, more comparative investigations of the MSO in high-frequency hearing animals like small opossums, rats, and mice are needed. These animals might share, to some extent, an ancient auditory system, and respective studies aptly complemented the understanding of the MSO's evolution in auditory specialists like gerbils and bats.

To date, only a few MSO-like structures have been described in normal high-frequency hearing animals, like rats (compare Figure 2; Rogowski, B. A. and Feng, A. S., 1981), opossums (Willard, F. H. and Martin, G. F., 1983; 1984), and mice (Franklin, K. B. and Paxinos, G., 1997). Interestingly, in high-frequency-hearing mammals the somata of typical bipolar MSO cells are arranged in a less orderly fashion, which indicates that the neural arrangement is rather critical to ITD specialists (Grothe, B. *et al.*, 2004). Still, a column-like arrangement of cells could be made out in rats (Feng, A. S. and Rogowski, B. A., 1980; Rogowski, B. A. and Feng, A. S., 1981). The cellular morphology of this subset of MSO units seemed nearly identical to that of bipolar fusiform principal neurons found in low-frequency hearing animals.

In line with high-frequency sound localization concepts, however, neurophysiological recordings in the albino rat MSO provided little indication that the nucleus might process ITDs, and no biologically relevant ITD sensitivity to pure tones was revealed (Inbody, S. B. and Feng, A. S., 1981). Still considerable, one half of the units in the rat MSO displayed binaural excitatory inputs, while the other half received purely inhibitory projections from the ipsilateral ear. As for the ITD-user gerbil, evidence for glycinergic inhibitory inputs to the MSO of rat and opossums was provided by Kapfer C. *et al.* (2002). This suggests that binaural excitation and inhibition (via the LNTB and the MNTB) belong to the ancient set of MSO inputs regardless of whether the animals are enabled to resolve extreme ITDs or not. A striking difference, however, concerns the refinement of glycinergic inputs to the soma of MSO cells observed in cats, ferrets, and gerbils: in the high-frequency hearing opossum and rat, glycinergic inputs do not seem to be refined but rather are distributed across the soma and dendrites.

So far, it remains open what sound parameters the MSO of opossums, rats, and mice might preferentially process. Studies on the MSO of rats indicate that the units serve functions other than ITD processing (Feng, A. S. and Rogowski, B. A., 1980; Rogowski, B. A. and Feng, A. S., 1981). The results in rats come from albinos, however, that show deficits in ITD processing (see above). Still, rat MSO neurons displayed a significant sensitivity to ILDs – a feat usually attributed to the neighboring LSO – which implies that the rat MSO could contribute to spatial integration of high-frequency sounds. As it stands, assuming that the rat MSO preserves some characteristics of an early mammalian MSO precursor, its original function could not be linked to ITD processing. Still, the classical input combination of potentially well-timed excitatory and inhibitory projections to the rat MSO suggests that the neural circuit might serve – in a more general sense – temporal computation. Note that other than pure tones, natural envelope-modulated sounds promote tightly coupled neural firing patterns that could promote acoustic pattern recognition, echo suppression, and ILD coding (Tollin, D. J., 2003). Studies on other high-frequency hearing mammals, namely bats (see below), have indicated that a principally similar MSO circuit design supports either task (Grothe, B. *et al.*, 1997; Grothe, B. and Neuweiler, G., 2000).

High-frequency hearing nonspecialists have helped to establish the anatomy, cell morphology, and inputs of an MSO that might still largely resemble a putative precursor structure in early mammals who shared similar auditory experiences (determined by, e.g., the head size, audiogram, and habitat). On the

whole, mammals without or with weakly developed low-frequency hearing that may not use ITDs for sound localization possess an anatomically less highly ordered MSO. The function of the MSO in these animals remains obscure. Even so, studies on bats have indicated putative functions of the MSO in high-frequency hearing animals, and are reviewed in the following section.

3.39.4 The Medial Superior Olive of Bats

Bats have evolved a range of hunting strategies, based in part on echolocation (Neuweiler, G., 1990). By means of auditory analysis, the animals are capable of both active and passive prey discrimination, recognition, and localization. In the bat model system behaviorally relevant auditory signals could be inferred from emitted echolocation calls and received echo patterns, respectively (Figure 5). Species-specific discrimination, recognition, and localization parameters were pinned down by psychophysical experiments (Neuweiler, G., 2000). So defined acoustic parameters could then be implemented in physiological research on the bat MSO. Thereby, stimulus paradigms were well matched to the animal's central auditory filter properties. A great amount of information was extracted with respect to MSO coding properties within bat animal models,

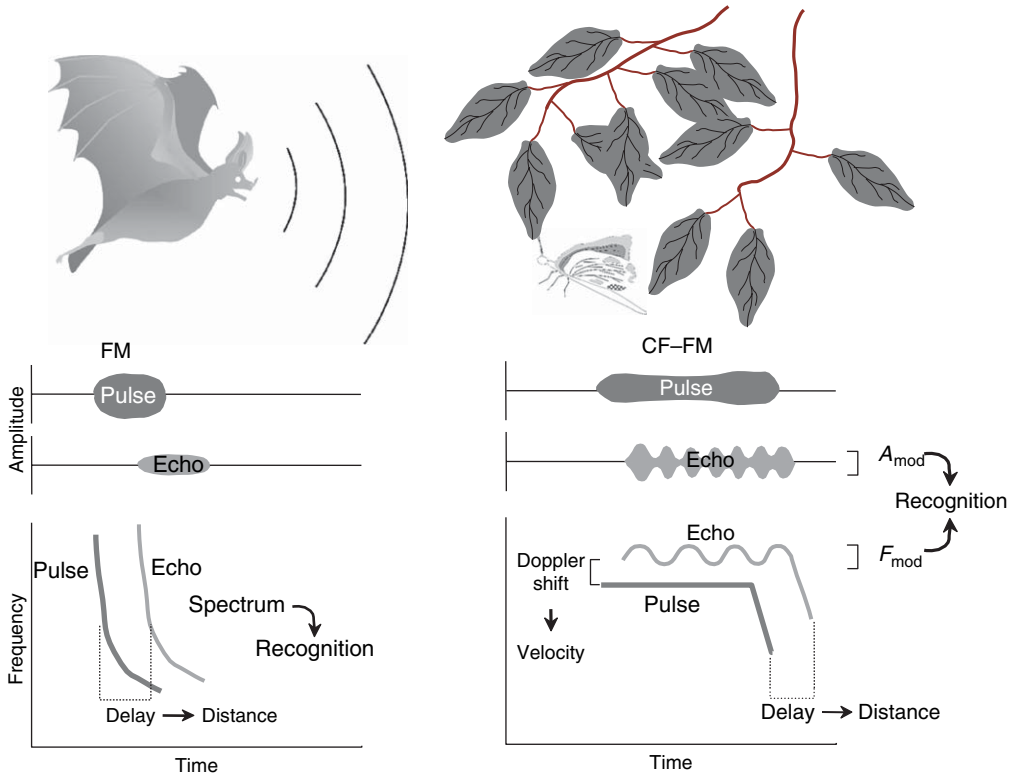

Figure 5 Two different echolocation strategies of insectivorous bats hunting for flying insects. Most bats emit downward FM sweeps of a few milliseconds' duration (left panels). Spectral changes in the echo compared to the pulse itself contain information about the object, the echo delay about the object distance. Using this echolocation call it is difficult to distinguish objects from background in dense foliage. Some bats specialized for hunting in dense foliage use a combination of an FM sweep for distance measurement and a CF component for prey recognition (right panels). CF components can last up to 80 ms. When reflected from a fluttering target the CF component in the echo is modulated in frequency and amplitude according to the insects' wing beat frequency. Doppler shifts in the CF component contain additional information about the relative velocity of the target. The upper panels give the oscillogram (time vs amplitude) of pulse (black) and echo (gray). The lower panels display the frequency changes in the echo (time vs frequency). CF, constant frequency; FM, frequency modulated. From Grothe, B. 2000. The evolution of temporal processing in the medial superior olive, an auditory brainstem structure. Prog. Neurobiol. 61, 581–610.

and the evolution of habitat-specific modifications of the MSO could be described in a number of species that showed different levels of specialization.

3.39.4.1 Anatomy of the Medial Superior Olive in Bats

3.39.4.1.1 Frequency-modulated bats

The most representative group of the microchiroptera are so-called FM bats, which use frequency-modulated (FM) echolocation calls to orient and, in most bats, catch flying insect prey. The Mexican free-tailed bat *Tadarida brasiliensis mexicana* (Grothe, B. *et al.*, 1994), the big brown bat *Eptesicus fuscus* (Covey, E. and Casseday, J. H., 1995), and the velvety free-tailed bat *Molossus ater* (Harnischfeger, G. *et al.*, 1985) were all shown to possess an MSO homologous to the MSO of normal mammals. First, the relative position of the MSO within the SOC was not altered in these species (Covey, E. and Casseday, J. H., 1995). Second, the MSO was distinct from adjacent periolivary nuclei (Schofield, B. R., 1991) by its absence of ACh-positive cells (compare Figure 1(d); Grothe, B. *et al.*, 1994). Thirdly, a low immunoreactivity for GABA and glycine has set the MSO apart from neighboring structures (Fubara, B. M. *et al.*, 1996). Fourthly, the principal cells of the MSO were of bipolar morphology, growing dendrites both medially and laterally (Grothe, B. *et al.*, 1994), although not arranged in the typical one-cell column as in low-frequency-hearing animals. In conclusion, the MSO anatomy of these bats (henceforth called *Tadarida*, *Eptesicus*, and *Molossus)* deviated little from that found in other high-frequency hearing animals. Note that not all mentioned criteria were investigated in each bat species, however.

3.39.4.1.2 Constant-frequency–frequency-modulated bats

The highly specialized CF–FM bats use echolocation calls that consist of a long constant-frequency (CF) component in combination with short initial and terminal FM sequences (compare Figure 5; Neuweiler, G., 1990). The group is typified by horseshoe bats, for instance, *Rhinolophus ferrumequinum* and *Rhinolophus rouxi* (henceforth called *Rhinolophus).* Here also, the relative location of the MSO within the SOC is comparable to the MSO position in other animals (Poljak, S., 1926; Schweizer, H., 1981; Casseday, J. H. *et al.*, 1988). Furthermore, the sheer size of the MSO in *Rhinolophus* indicated its prominent role in central auditory processing. However, the gross anatomy of the nucleus seems somehow modified. There are actually two dorsal and ventral subnuclei (dorsal medial superior olive, DMSO; ventral medial superior olive, VMSO; Casseday, J. H. *et al.*, 1988). Inspired by another CF–FM bat, *Pteronotus parnellii* (the mustached bat; henceforth called *Pteronotus*), some researchers speculated the very large MSO could have partly merged with periolivary nuclei (compare Figure 2; Zook, J. M. and Casseday, J. H., 1982a). Therefore the homology of the MSO and its neighboring periolivary structures in CF–FM bats with those of other mammals has been under debate (Casseday, J. H. *et al.*, 1988; Vater, M. and Feng, A. S., 1990). Histochemical characteristics supported the view that neural subpopulations exist within the MSO of *Pteronotus* (Zook, J. M. and Casseday, J. H., 1982a). Particularly conspicuous was the high GABA immunoreactivity in a small dorsomedial cell population of the MSO, and the apparent lack of a dorsomedial periolivary nucleus (DMPO) in *Pteronotus* (Vater, M., 1995; Winer, J. A. *et al.*, 1995). Both facts fitted the notion of merged nuclei. The principal cell type of the MSO, however, is of bipolar morphology and matched the classical characteristics of MSO cells (Zook, J. M. and Casseday, J. H., 1982a).

3.39.4.2 Input Pattern and Physiology of the Medial Superior Olive in Bats

3.39.4.2.1 Frequency-modulated bats

The input/output pattern of the MSO of *Tadarida*, *Eptesicus*, and *Molossus* fits the view that these animals possess an MSO that is, in principle, just gradually different from the classical MSO. For instance, binaural excitatory inputs to these bats' MSO originate in SBCs of the AVCN, while inhibitory inputs are relayed via the LNTB (from the ipsilateral ear), and the MNTB (from the contralateral ear; Zook, J. M. and DiCaprio, R. A., 1988; Kuwabara, N. and Zook, J. M., 1992; Grothe, B. *et al.*, 1994). Also, as usual, ascending projections from the *Tadarida* MSO mainly target the ipsilateral inferior colliculus (IC; Grothe, B. *et al.*, 1994). But the abundance of binaural neurons that display the classical connectivity of an MSO cell seems gradually reduced in *Tadarida* (whose MSO is changed the least), *Molossus* (representing an intermediate stage), and *Eptesicus* (that displays a substantial shift toward monaurally innervated units; Figure 6). The MSO of all three species exhibits a normal tonotopic arrangement with low frequencies

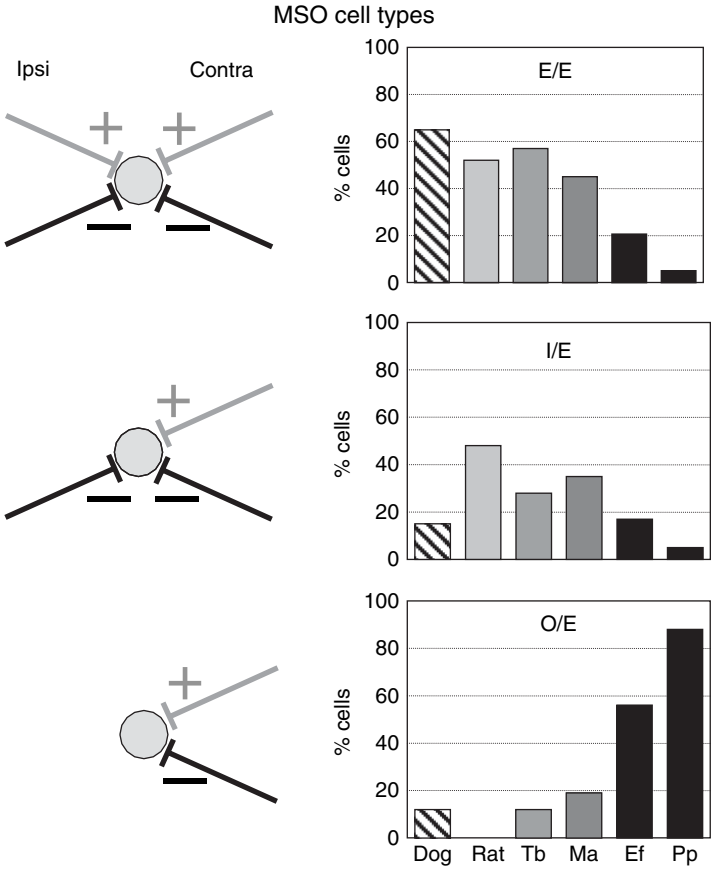

Figure 6 The distribution of projection patterns to MSO neurons in different mammals. The schematic drawings on the left show the main input patterns as suggested by anatomical and physiological studies in several mammals. The right panels show the percentage of the corresponding binaural type as derived from physiological studies. Note that the E/E classification in normal extracellular recordings does not necessarily tell whether there is an additional inhibitory input from the same side. Thus the corresponding pattern in the schematic on the left is the most likely corresponding input pattern, but not inevitably true for all neurons. Note that in all animals including dogs at least one-third of the cells apparently lack ipsilateral excitation. The mustached bat is, even among bats, the most extreme case with almost only monaural cells. Ef, *Eptesicus fuscus* (big brown bat); E, excitatory input; I, inhibitory input; Ma, *Molossus ater* (velvety free-tailed bat); MSO, medial superior olive; O, no input; Pp, *Pteronotus parnellii* (mustached bat); Tb, *Tadarida brasiliensis* (free-tailed bat). Adapted from Grothe, B. 2000. The evolution of temporal processing in the medial superior olive, an auditory brainstem structure. Prog. Neurobiol. 61, 581–610.

being represented dorsally and high frequencies ventrally (Harnischfeger, G. *et al.*, 1985; Grothe, B. *et al.*, 1997).

By the use of sinusoidally amplitude-modulated (SAM) stimuli – to the envelope of which auditory units in the AVCN and MNTB respond in a phase-coupled manner despite high-frequency carrier frequencies – it was shown that bat MSO cells can display rough ITD sensitivity (Grothe, B. *et al.*, 1997; Grothe, B. and Park, T. J., 1998). The sensitivity is likely to be generated by coincident binaural excitation, just as in low-frequency hearing animals (Yin, T. C. and Chan, J. C., 1990). But the observed neural ITD sensitivity was – by far – too broad to be of use for a small-headed animal like *Tadarida*. Its ITD sensitivity has therefore been considered to be epiphenomenal. Still, the rules of computation applied within a significant number of neurons in the MSO circuit of *Tadarida* (which is almost certainly not specialized for ITD processing) could yield usable information on the location of sound sources for animals with large head sizes.

Epiphenomenal coding of binaural disparities aside, most MSO cells of *Tadarida* and *Eptesicus* displayed low-pass filter characteristics to SAM stimuli (Grothe, B. *et al.*, 1997; 2001). A whole range of such neural filters are generated by the interaction of accurately phase-coupled excitatory and inhibitory inputs

that reach the MSO cells with various delays from the SBCs of the AVCN and the principal cells of the MNTB. Notably, it was shown for MSO cells of *Eptesicus* that the characteristic upper cutoff frequency of a neural SAM transfer function might in fact be a byproduct of pause duration filtering (Grothe, B. *et al.*, 2001). Mainly therefore, the putative function of these neurons remains under debate (discussed below; compare also CF–FM bats). In response to high-frequency pure tones, the MSO cells of *Tadarida* and *Eptesicus* predominantly exhibited transient *ON* or *OFF* discharges. These MSO response types matched expectations for interacting sustained excitatory and inhibitory inputs from the AVCN and MNTB, respectively (compare Figure 3; Grothe, B. *et al.*, 1997; 2001).

3.39.4.2.2 Constant-frequency–frequency-modulated bats

In the CF–FM bat *Pteronotus*, the MSO is very large. Just as in other mammals, ascending MSO projections mainly reach the ipsilateral IC (Zook, J. M. and Casseday, J. H., 1982b; Ross, L. S. and Pollak, G. D., 1989). Likewise, as usual, SBCs in the AVCN provide temporally precise excitatory input to the MSO of *Pteronotus*. Also, prominent inhibitory projections to the animal's MSO originate in glycinergic principal MNTB cells, and were actually first described in this animal model (Covey, E. *et al.*, 1991; Kuwabara, N. and Zook, J. M., 1992). At this point, it is helpful to recall that in low-frequency hearing animals these inhibitory projections are involved in tuning the ITD sensitivity of MSO cells (Brand, A. *et al.*, 2002; Grothe, B., 2003). In apparent contradiction, the MSO of *Pteronotus* turned out to be a predominantly monaural structure whose ipsilateral inputs are greatly reduced (compare Figure 6; Covey, E. *et al.*, 1991; Grothe, B. *et al.*, 1992). *Per se*, any substantial contribution to binaural processing was eliminated in the MSO of *Pteronotus*. The neural response of MSO cells is exclusively determined by monaural projections that consist of excitatory inputs from contralateral SBCs, and contralaterally driven inhibitory inputs from principal cells of the ipsilateral MNTB. Both sources display discharges reminiscent of AN activity, and faithfully encode the temporal structure of incoming sounds (Rhode, W. S. *et al.*, 1983; Oertel, D., 1999). Most of their target cells in the *Pteronotus* MSO differ considerably in their response to sound, however, showing transient *ON* and/or *OFF* discharges (Covey, E. *et al.*, 1991). An *in vivo* application of the glycine antagonist strychnine that reversibly blocks inhibitory inputs from the MNTB results in primary-like MSO responses (Grothe, B. *et al.*, 1992; Grothe, B., 1994). Hence, transient responses are generated by interacting excitatory and inhibitory projections. Such MSO characteristics could be used by the bats to encode sound onsets and offsets, respectively. But the implications for the function of the MSO reach beyond the generation of transient responses. By a systematic variation of the delay between excitatory and inhibitory projections, the animals could generate a bank of specific neural filters for the temporal envelope structure of sounds in the monaural MSO (Figure 7). Single-unit response properties to SAM sounds exemplified these neural filters *in vivo* (Grothe, B., 1994). Respective findings suggested that MSO neurons phase-lock to SAM rates up to 1000 Hz whenever inhibitory inputs are experimentally neutralized. Controls revealed that, naturally, MSO neurons exhibit low-pass filter functions in response to SAM stimuli (Figure 8). These filter functions are perfectly matched to amplitude and frequency-modulation rates imprinted onto the echo signals received by *Pteronotus* while preying on fluttering insects (compare Figure 5; Henson, O. W. *et al.*, 1987).

3.39.4.3 Function of the Medial Superior Olive in Bats

3.39.4.3.1 Constant-frequency–frequency-modulated bats

As mentioned above, fluttering prey objects within the emitted acoustic beam of echolocation calls do reflect echoes that are FM and amplitude modulated (AM) (Henson, O. W. *et al.*, 1987). This repetitive modulation is captured by the long-lasting CF component of the echo, and allows the detection of wing-beating insects even in dense foliage (i.e., the CF–FM bats' predominant foraging range) that creates a cluttered echo environment. Therefore, *Pteronotus*' preying strategy relies heavily on temporal pattern recognition within the CNS, and the *Pteronotus* MSO seems optimized to serve this task. To enhance the precision of temporal information, an elimination of binaural inputs to the *Pteronotus* MSO appears as a straightforward adaptation. Otherwise, the temporal analysis of an echo structure could suffer from position-dependent binaural parameters. In fact, both ITDs and ILDs affect sound-envelope coding in binaural brainstem neurons (Joris, P. X. and Yin, T. C., 1995; Grothe, B. *et al.*, 1997). In the FM bat *Tadarida* that possesses a largely binaural MSO (discussed below), ILD effects on neural SAM transfer functions were found to be significant, and rather unpredictable. Notably, temporal precision is also vital to aid

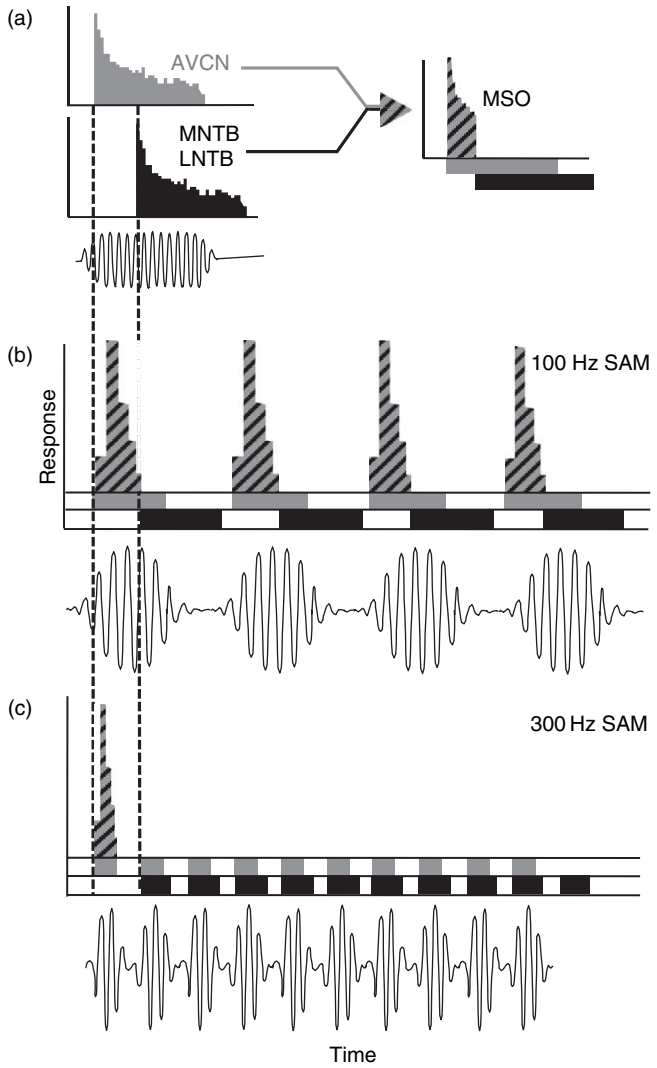

Figure 7 Schematic drawing of the monaural interaction of excitation from the AVCN (gray) and inhibition from the MNTB (black) as first described for the MSO in *Pteronotus parnellii.* (a) Pure tone stimulation leads to primary-like activity in the excitatory AVCN and the inhibitory MNTB. In most MSO neurons the inhibition is delayed by a fixed amount (-3 to $+5$ ms), leaving a small window where the cell can respond to the excitatory input before it is completely inhibited by the MNTB. The result is a phasic ON response except in a minority of cells where the inhibition arrives simultaneously or even earlier. These neurons are inhibited throughout the stimulus duration but respond with a rebound OFF. (b) The same temporal interaction of excitation and delayed inhibition will cause a phase-locked response to the envelope of SAM tones, as long as the modulation frequency is low. (c) Because of the fixed delay, the inhibition will start to overlap with the excitation in response to the following subsequent cycle when the modulation frequency reaches a certain limit (the limit depends on the actual delay of inhibition). The response to all cycles except the first would start to decrease at this modulation frequency and completely stop at even higher rates. A slightly slower time course of the inhibition (little longer duration) and some temporal summation would prevent the cell from recovering at much higher rates. AVCN, anteroventral cochlear nucleus; MNTB, medial nucleus of the trapezoid body; MSO, medial superior olive; SAM, sinusoidally amplitude modulated. Adapted from Grothe, B. 1994. Interaction of excitation and inhibition in processing of pure tone and amplitude-modulated stimuli in the medial superior olive of the mustached bat. J. Neurophysiol. 71, 706–721.

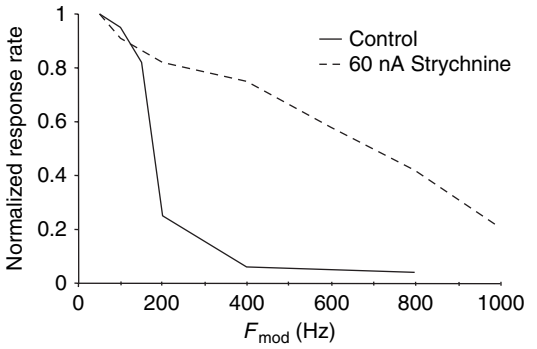

Figure 8 Normalized response rates of an MSO neuron to SAM stimuli with different modulation frequencies (modulation transfer function). The abscissa gives the modulation frequency, the ordinate the normalized response. Under control conditions the neuron responds only to modulation frequencies below 200 Hz. In the presence of strychnine, however, the neuron responds to much higher modulation frequencies. Using the 50% level as a criterion, the cutoff frequency shifts from about 180 (control) to above 700 Hz when glycinergic inhibition is blocked. MSO, medial superior olive; SAM, sinusoidally amplitude modulated. Adapted from Grothe, B. 2000. The evolution of temporal processing in the medial superior olive, an auditory brainstem structure. Prog. Neurobiol. 61, 581–610.

the distance estimation between target and bat that is calculated from the delay between the FM terminal sequence of a CF–FM call and its echo (Neuweiler, G., 1990). In this context, temporally precise *ON* and *OFF* responses to acoustic stimuli that were observed in the *Pteronotus* MSO might contribute to capture the timing of call emission and incoming echo with high acuity.

3.39.4.3.2 Frequency-modulated bats

Apart from *Pteronotus*, the putative MSO function was best studied in three bat species that exclusively use FM echolocation calls. Hence, *Tadarida*, *Molossus*, and *Eptesicus* represent species that might not be as specialized for temporal pattern recognition as *Pteronotus*. This is corroborated by the fact that all three species use less cluttered environments for foraging, meaning their potential prey objects appear more prominent in echo signals (Neuweiler, G., 1990). Nonetheless, when compared to *Pteronotus*, very similar SAM coding properties were unraveled in the MSO of *Tadarida* and *Eptesicus* (Grothe, B. *et al.*, 1997; 2001). A fundamental difference concerns the binaurality of the MSO, however, that is maintained to various degrees in *Tadarida*, *Molossus*, and *Eptesicus* (Harnischfeger, G. *et al.*, 1985; Zook, J. M. and DiCaprio, R. A., 1988; Kuwabara, N. and Zook, J. M., 1992; Grothe, B. *et al.*, 1994), but is largely reduced in *Pteronotus* (Covey, E. *et al.*, 1991). In bats that preferentially prey in open spaces rather than in dense foliage, like *Tadarida* and *Molossus*, the distribution of binaurally excited neurons in the MSO nearly matches the picture drawn for the dog and the cat MSO (Goldberg, J. M. and Brown, P. B., 1969; Yin, T. C. and Chan, J. C., 1990). The fidelity of temporal pattern analysis in *Tadarida* therefore suffers from the impact of interaural disparities on the timing of MSO inputs (Grothe, B. *et al.*, 1997). As a trade-off, binaural information is made available to integrate spatial and temporal information (Grothe, B. and Neuweiler, G., 2000). Hence, SAM filtering observed in the MSO of *Tadarida* might not reflect a pure wing beat pattern filter like in *Pteronotus*, and could merely represent a by-product of processing other temporal information. Strong indications for the MSO's role in pause duration tuning, and speculations on its part in sound duration tuning, were fuelled by a study on *Eptesicus* that demonstrated that interpulse intervals (and not modulation rates) were crucial for the sound envelope filter properties of MSO neurons (Grothe, B. *et al.*, 2001). In *Eptesicus*, the MSO input pattern rather represents a stage in between the extreme MSO variants that are embodied by *Tadarida* and *Pteronotus* (and that were linked to their individual echolocation strategies in open spaces and dense foliage, respectively). Interestingly, the intermediate anatomical status of the MSO in *Eptesicus* correlates to the variability of its species-specific echolocation calls and foraging ranges (in open and cluttered environments). During subsequent phases of its approach on flying prey, *Eptesicus* initially employs pseudo-CF echolocation calls (Simmons, J. A. and Stein, R. A., 1980) that could serve pattern-based prey recognition much like in *Pteronotus*. As the approach on prey continues, however, emitted calls of *Eptesicus* become steeply FM, and might rather serve spatial resolution in terms of distance. Pause duration tuning could assist this task, and might be supported by the typical transient ON and OFF responses in the *Eptesicus* MSO.

Taken together, the gradual variation of inputs to MSO cell populations of different bat species seems related to their habitat, and foraging strategy. Both exert pressure to process specific features of echo envelope or frequency patterns, and might enforce a physiological adjustment of MSO processing rules. Anatomical data and neural responses in

bats suggest that adjustment could be accomplished by regulating the flow of feed-forward information into the MSO.

3.39.5 Conclusions

Research on the bat MSO has taught us that gradual modifications of the MSO input could result in different ways of analyzing the temporal structure of sounds, related to behavioral strategies and habitats. In extension of the gerbil animal model (where it has been demonstrated that inhibitory projections to the MSO undergo experience-driven refinement), in bats also excitatory inputs were heavily adapted in accord with evolutionary pressures. It should be noted that MSO neurons emerge very early during ontogenesis, and thus the ancient MSO circuit is likely to represent a primitive neural configuration (Kudo, M. *et al.*, 2000). This circuit might still be little modified in some modern mammals whose hearing periphery hardly changed since the onset of hearing of airborne sound (Gregory, W. K., 1929; Rosowski, J. J., 1992; Frost, S. B. and Masterson, R. B., 1994; Mills, D. M. and Shepherd, R. K., 2001). In other mammals, some of which were reviewed here, extreme changes of the auditory system have been wrought by evolution (Grothe, B. *et al.*, 2004). As new habitats were conquered, new auditory cues became dominant and possibly vital to these developing species. The MSO has been maintained as a structure in all mammals investigated so far, and it ultimately reflects the auditory world an animal lives in by its gross anatomy, input pattern, and fine structure (Figure 9; compare also Figures 1, 2, and 6). The nucleus therefore serves well to unravel the microevolution and macroevolution of a neural circuit in the context of well-defined sensory parameters.

The distribution of MSO input patterns in bats, as well as other high- and low-frequency hearing mammals, is reconciled by an expanded concept of an ancient MSO: the text book unit of the MSO features four inputs, that is, combined inhibitory and excitatory projections from each ear. During the species-specific ontogenesis of the auditory brainstem, the initial anlage of four predominant inputs might be adjusted by axon pruning and synaptic elimination, while functional connections are facilitated (e.g., Sanes, D. H. and Friauf, E., 2000; Kapfer, C. *et al.*, 2002). In the gerbil MSO, innervation patterns were shown to undergo a combination of experience-driven and autonomous refinement processes that shift, or eliminate, the input weight of synaptic connections (Kandler, K., 2004). It remains open how developmental plasticity might be stabilized during evolution to permanently establish connectional changes that became primarily independent of sensory experience. Our scenario, however, suggests that MSO nuclei of different species might essentially encompass primordial cells at different stages of structural and functional refinement.

A monaural MSO, as it is found in *Pteronotus*, seems well adapted to pattern processing, a feature that is of great import for the foraging success of *Pteronotus* within its densely cluttered habitat. Its MSO's ability for envelope filtering in a behaviorally relevant range is based on the precise timing of tightly coupled excitation and inhibition from the contralateral ear (Covey, E. *et al.*, 1991). Reminiscent neural filters (often described as SAM filters) are also present in bats that possess a binaural MSO (Grothe, B. *et al.*, 1997; 2001). Similar response properties are maintained even in low-frequency hearing ITD-users (Behrend, O. *et al.*, 2000). The general occurrence of SAM filter units in the MSO of a number of widely unrelated species suggests that – with the possible exception of CF–FM bats – these units represent a by-product of the processing of other temporal aspects of complex sounds, for instance, of pause duration coding (Grothe, B. *et al.*, 2001). Yet the principal potential of the MSO circuit for temporal sound pattern processing shows across the range of species investigated.

The binaural MSO was linked to ITD processing by coincidence detection in low-frequency hearing mammals (Goldberg, J. M. and Brown, P. B., 1969; Yin, T. C. and Chan, J. C., 1990), and again the relative timing of the contralateral excitatory and inhibitory input has been proven to be vital – in this case to shape the ITD sensitivity within behaviorally relevant ranges (Brand, A. *et al.*, 2002). Remarkably too, the epiphenomenal ITD sensitivity of the binaural MSO of high-frequency hearing bats had established that the MSO's rules of processing promote binaural coincidence detection without any specialization for ITD coding. One might conclude that a still largely ancient MSO, as it became apparent by anatomical and physiological studies in *Tadarida*, indeed also shows a preadaptation for ITD coding.

Across the reviewed species, the MSO exemplifies that individual inputs, like the fast and precise inhibition from the contralateral MNTB, can be designated to species-specific processing

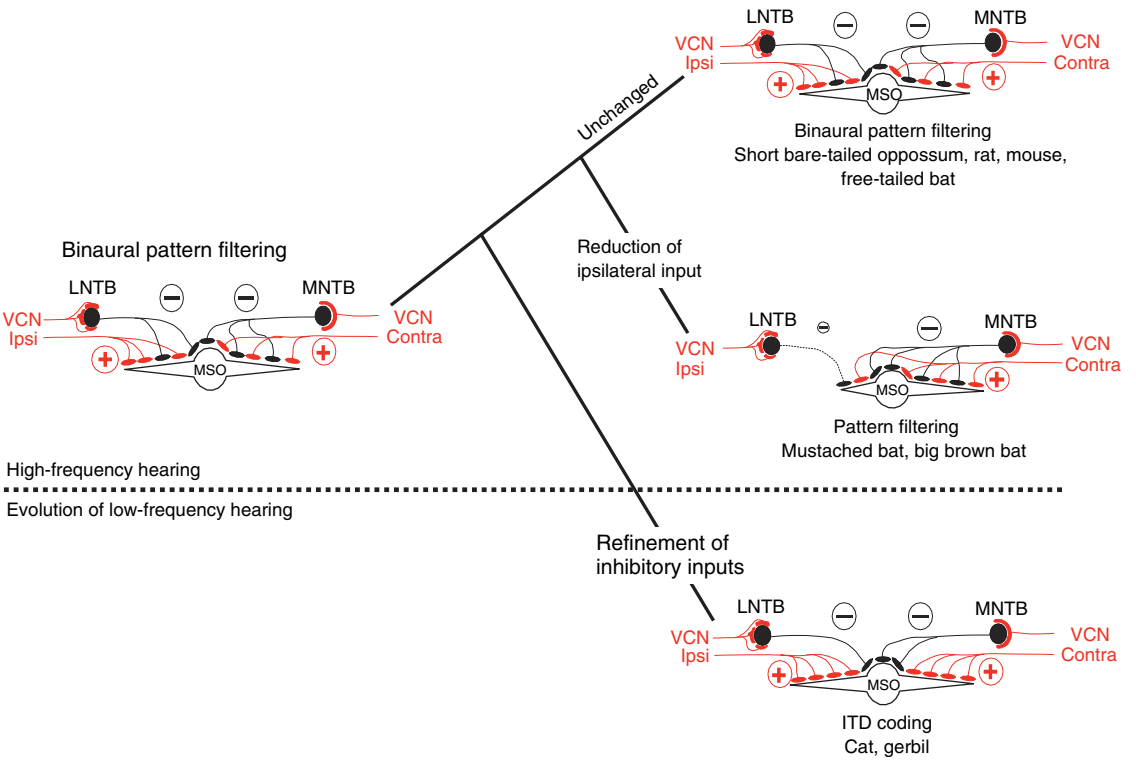

Figure 9 A scenario for the evolution of the MSO. The ancestral precursor is assumed as similar to the free-tailed bat MSO in that it showed specializations neither for pure pattern processing nor for ITD processing. This kind of MSO would have shown pattern filtering (e.g., amplitude modulation filtering). The filter characteristics were, however, influenced by binaural cues and, hence, by the position of a sound source. This MSO might be rather unchanged in most mammals that do not show any adaptations for low-frequency hearing. Some bats (like the mustached bat and partly the big brown bat) reduced the ipsilateral inputs to the MSO and, thereby, turned it into a pure pattern filter. A different direction took the evolution of the MSO in low-frequency hearing animals. Because of the preadaptation for ITD coding it has been used as the primary site for localizing low-frequency sounds in the horizontal plane. Several specializations occurred in order to improve the ITD sensitivity. One might have been a change in the inhibitory inputs by refining them to the cell somata. ITD, interaural time difference; LNTB, lateral nucleus of the trapezoid body; MNTB, medial nucleus of the trapezoid body; MSO, medial superior olive; VCN, ventral cochlear nucleus. Adapted from Grothe, B. 2000. The evolution of temporal processing in the medial superior olive, an auditory brainstem structure. Prog. Neurobiol. 61, 581–610.

demands. That is, inhibition of the MSO is likely to serve pattern recognition and spatio-temporal integration of high-frequency acoustic signals in bats – while, conversely, it supports the spatial resolution of low-frequency sound sources in gerbils. However, the epiphenomenal ITD and/or SAM sensitivity that can be observed in the MSO regardless of a species' auditory specialization suggests that the principal rules of MSO processing stay rather uniform across mammals. Only, the basic neural algorithm can be finely adjusted – by the regulation of feed-forward information (bats; Covey, E. *et al.*, 1991) and membrane properties (guinea pigs, gerbils; Smith, P. H., 1995; Magnusson, A. K. *et al.*, 2005).

Acknowledgment

This work was supported by the BMBF.

References

Agmon-Snir, H., Carr, C. E., and Rinzel, J. 1998. The role of dendrites in auditory coincidence detection. Nature 393, 268–272.

Batra, R., Kuwada, S., and Fitzpatrick, D. C. 1997. Sensitivity to interaural temporal disparities of low- and high-frequency neurons in the superior olivary complex. II. Coincidence detection. J. Neurophysiol. 78, 1237–1247.

Behrend, O., Brand, A., Breutel, G., and Grothe, B. 2000. Temporal processing in the gerbil superior olivary complex. Abstr. 23rd Meet. Assoc. Res. Otolaryngol. 5612.

Blauert, J. and Lindemann, W. 1986. Spatial mapping of intracranial auditory events for various degrees of interaural coherence. J. Acoust. Soc. Am. 79, 806–813.

Brand, A., Behrend, O., Marquardt, T., McAlpine, D., and Grothe, B. 2002. Precise inhibition is essential for microsecond interaural time difference coding. Nature 417, 543–547.

Caird, D. and Klinke, R. 1983. Processing of binaural stimuli by cat superior olivary complex neurons. Exp. Brain Res. 52, 385–399.

Caird, D. and Klinke, R. 1987. Processing of interaural time and intensity differences in the cat inferior colliculus. Exp. Brain Res. 68, 379–392.

Cant, N. B. 1991. Projections to the Lateral and Medial Superior Olivary Nuclei from the Spherical and Globular Bushy Cells of the Anteroventral Cochlear Nucleus. In: Neurobiology of Hearing: The Central Auditory System (*eds*. R. A. Altschuler, R. P. Bobbin, B. M. Clopton, and D. W. Hoffman). pp. 99–119. Raven Press.

Cant, N. B. and Hyson, R. L. 1992. Projections from the lateral nucleus of the trapezoid body to the medial superior olivary nucleus in the gerbil. Hear. Res. 58, 26–34.

Carr, C. E. and Soares, D. 2002. Evolutionary convergence and shared computational principles in the auditory system. Brain Behav. Evol. 59, 294–311.

Casseday, J. H., Covey, E., and Vater, M. 1988. Connections of the superior olivary complex in the rufous horseshoe bat *Rhinolophus rouxi*. J. Comp. Neurol. 278, 313–329.

Clack, J. A. 1997. The evolution of tetrapod ears and the fossil record. Brain Behav. Evol. 50, 198–212.

Clack, J. A. 2002. Patterns and processes in the early evolution of the tetrapod ear. J. Neurobiol. 53, 251–264.

Clack, J. A. and Allin, E. 2004. Evolution of Fish and Tetrapod Ears. In: Evolution of the Vertebrate Auditory System (*eds*. G. A. Manley, A. Geoffrey, A. N. Popper, and R. R. Fay), pp. 128–163. Springer Press.

Clark, G. M. 1969. The ultrastructure of nerve endings in the medial superior olive of the cat. Brain Res. 14, 293–305.

Conlee, J. W., Parks, T. N., and Creel, D. J. 1986. Reduced neuronal size and dendritic length in the medial superior olivary nucleus of albino rabbits. Brain Res. 363, 28–37.

Conlee, J. W., Parks, T. N., Romero, C., and Creel, D. J. 1984. Auditory brainstem anomalies in albino cats: II. Neuronal atrophy in the superior olive. J. Comp. Neurol. 225, 141–148.

Covey, E. and Casseday, J. H. 1995. The Lower Brainstem Auditory Pathway. In: Hearing by Bats. (*eds*. A. N. Popper and R. R. Fay), pp. 235–296. Springer Press.

Covey, E., Vater, M., and Casseday, J. H. 1991. Binaural properties of single units in the superior olivary complex of the mustached bat. J. Neurophysiol. 66, 1080–1094.

Cramer, K. S., Karam, S. D., Bothwell, M., Cerretti, D. P., Pasquale, E. B., and Rubel, E. W. 2002. Expression of EphB receptors and EphrinB ligands in the developing chick auditory brainstem. J. Comp. Neurol. 452, 51–64.

Feng, A. S. and Rogowski, B. A. 1980. Effects of monaural and binaural occlusion on the morphology of neurons in the medial superior olivary nucleus of the rat. Brain Res. 189, 530–534.

Fleischer, G. 1978. Evolutionary principles of the mammalian middle ear. Adv. Anat. Embryol. Cell Biol. 55, 3–70.

Franklin, K. B. and Paxinos, G. 1997. The Mouse Brain in Stereotaxic Coordinates. Academic Press.

Frost, S. B. and Masterson, R. B. 1994. Hearing in primitive mammals: *Monodelphis domestica* and *Marmosa elegans*. Hear. Res. 76, 67–72.

Fubara, B. M., Casseday, J. H., Covey, E., and Schwartz-Bloom, R. D. 1996. Distribution of $GABA_A$, $GABA_B$, and glycine receptors in the central auditory system of the big brown bat, *Eptesicus fuscus*. J. Comp. Neurol. 369, 83–92.

Galambos, R. and Davis, H. 1943. The response of single auditory nerve fibres to acoustic stimulation. J. Neurophysiol. 6, 39–57.

Galambos, R., Schwartzkopff, J., and Rupert, A. 1959. Microelectrode study of superior olivary nuclei. Am. J. Physiol. 197, 527–536.

Goldberg, J. M. and Brown, P. B. 1968. Functional organization of the dog superior olivary complex: an anatomical and electrophysiological study. J. Neurophysiol. 31, 639–656.

Goldberg, J. M. and Brown, P. B. 1969. Response of binaural neurons of dog superior olivary complex to dichotic tonal stimuli: some physiological mechanisms of sound localization. J. Neurophysiol. 32, 613–636.

Gregory, W. K. 1929. Our Face from Fish to Man. Putnams Sons, reprinted in 1965 by Capricorn.

Grothe, B. 1994. Interaction of excitation and inhibition in processing of pure tone and amplitude-modulated stimuli in the medial superior olive of the mustached bat. J. Neurophysiol. 71, 706–721.

Grothe, B. 2000. The evolution of temporal processing in the medial superior olive, an auditory brainstem structure. Prog. Neurobiol. 61, 581–610.

Grothe, B. 2003. New roles for synaptic inhibition in sound localization. Nat. Rev. Neurosci. 4, 540–550.

Grothe, B. and Neuweiler, G. 2000. The function of the medial superior olive in small mammals: temporal receptive fields in auditory analysis. J. Comp. Physiol. A. 186, 413–423.

Grothe, B. and Park, T. J. 1998. Sensitivity to interaural time differences in the medial superior olive of a small mammal, the Mexican free-tailed bat. J. Neurosci. 18, 6608–6622.

Grothe, B. and Sanes, D. H. 1993. Bilateral inhibition by glycinergic afferents in the medial superior olive. J. Neurophysiol. 69, 1192–1196.

Grothe, B. and Sanes, D. H. 1994. Synaptic inhibition influences the temporal coding properties of medial superior olivary neurons: an *in vitro* study. J. Neurosci. 14, 1701–1709.

Grothe, B., Carr, C. E., Casseday, J. H., Fritzsch, B., and Köppl, C. 2004. The Evolution of Central Pathways and Their Neural Processing Patterns. In: Evolution of the Vertebrate Auditory System (*eds*. G. A. Manley, A. Geoffrey, A. N. Popper, and R. R. Fay), pp. 289–359. Springer Press.

Grothe, B., Covey, E., and Casseday, J. H. 2001. Medial superior olive of the big brown bat: neuronal responses to pure tones, amplitude modulations, and pulse trains. J. Neurophysiol. 86, 2219–2230.

Grothe, B., Park, T. J., and Schuller, G. 1997. Medial superior olive in the free-tailed bat: response to pure tones and amplitude-modulated tones. J. Neurophysiol. 77, 1553–1565.

Grothe, B., Schweizer, H., Pollak, G. D., Schuller, G., and Rosemann, C. 1994. Anatomy and projection patterns of the superior olivary complex in the Mexican free-tailed bat, *Tadarida brasiliensis mexicana*. J. Comp. Neurol. 343, 630–646.

Grothe, B., Vater, M., Casseday, J. H., and Covey, E. 1992. Monaural interaction of excitation and inhibition in the medial superior olive of the mustached bat: an adaptation for biosonar. Proc. Natl. Acad. Sci. U. S. A. 89, 5108–5112.

Guinan, J. J., Jr., Guinan, S. S., and Norris, B. E. 1972. Single auditory units in the superior olivary complex. Part I: Responses to sounds and classifications based on physiological properties. Int. J. Neurosci. 4, 101–120.

Hancock, K. E. and Delgutte, B. 2004. A physiologically based model of interaural time difference discrimination. J. Neurosci. 24, 7110–7117.

Harnischfeger, G., Neuweiler, G., and Schlegel, P. 1985. Interaural time and intensity coding in superior olivary complex and inferior colliculus of the echolocating bat *Molossus ater*. J. Neurophysiol. 53, 89–109.

Harper, N. S. and McAlpine, D. 2004. Optimal neural population coding of an auditory spatial cue. Nature 430, 682–686.
Harrison, J. M. and Irving, R. 1966. Visual and nonvisual auditory systems in mammals. Anatomical evidence indicates two kinds of auditory pathways and suggests two kinds of hearing in mammals. Science 154, 738–743.
Heffner, R. S. and Heffner, H. E. 1987. Auditory function in albino cats. Assoc. Res. Otolaryngol. Abstr. 10, 217.
Henson, O. W., Bishop, A. L., Keating, A. W., Kobler, J. B., Henson, M. M., Wilson, B. S., and Hansen, R. 1987. Biosonar imaging of insects by *Pteronotus p. parnellii*, the mustached bat. Natl. Geogr. Res. 3, 82–101.
Howard, M. A., Burger, R. M., and Rubel, E. W. 2007. A developmental switch to GABAergic inhibition dependent on increases in Kv1-type K^+ currents. J. Neurosci. 27, 2112–2123.
Inbody, S. B. and Feng, A. S. 1981. Binaural response characteristics of single neurons in the medial superior olivary nucleus of the albino rat. Brain Res. 210, 361–366.
Irvine, D. R. 1992. Physiology of the Auditory Brainstem. In: The Mammalian Auditory Pathway: Neurophysiology (*eds*. A. N. Popper and R. R. Fay), pp. 153–231. Springer Press.
Irving, R. and Harrison, J. M. 1967. The superior olivary complex and audition: a comparative study. J. Comp. Neurol. 130, 77–86.
Jeffress, L. A. 1948. A place theory of sound localization. J. Comp. Physiol. Psychol. 41, 35–39.
Jeffress, L. A. and Robinson, D. E. 1962. Formulas for coefficient of interaural correlation for noise. J. Acoust. Soc. Am. 34, 1658–1659.
Joris, P. X. and Yin, T. C. 1995. Envelope coding in the lateral superior olive. I. Sensitivity to interaural time differences. J. Neurophysiol. 73, 1043–1062.
Joris, P. X., Carney, L. H., Smith, P. H., and Yin, T. C. 1994a. Enhancement of neural synchronization in the anteroventral cochlear nucleus. I. Responses to tones at the characteristic frequency. J. Neurophysiol. 71, 1022–1036.
Joris, P. X., Smith, P. H., and Yin, T. C. 1994b. Enhancement of neural synchronization in the anteroventral cochlear nucleus. II. Responses in the tuning curve tail. J. Neurophysiol. 71, 1037–1051.
Kandler, K. 2004. Activity-dependent organization of inhibitory circuits: lessons from the auditory system. Curr. Opin. Neurobiol. 14, 96–104.
Kapfer, C., Seidl, A. H., Schweizer, H., and Grothe, B. 2002. Experience-dependent refinement of inhibitory inputs to auditory coincidence-detector neurons. Nat. Neurosci. 5, 247–253.
Kiang, N. Y., Watanabe, T., Thomas, C., and Clark, L. F. 1965. Discharge Patterns of Single Fibres in the Cat's Auditory Nerve. MIT Press.
Kitzes, L. M., Kageyama, G. H., Semple, M. N., and Kil, J. 1995. Development of ectopic projections from the ventral cochlear nucleus to the superior olivary complex induced by neonatal ablation of the contralateral cochlea. J. Comp. Neurol. 353, 341–363.
Konishi, M. 2003. Coding of auditory space. Annu. Rev. Neurosci. 26, 31–55.
Kuba, H., Ishii, T. M., and Ohmori, H. 2006. Axonal site of spike initiation enhances auditory coincidence detection. Nature 444, 1069–1072.
Kudo, M., Sakurai, H., Kurokawa, K., and Yamada, H. 2000. Neurogenesis in the superior olivary complex in the rat. Hear. Res. 139, 144–152.
Kuwabara, N. and Zook, J. M. 1992. Projections to the medial superior olive from the medial and lateral nuclei of the trapezoid body in rodents and bats. J. Comp. Neurol. 324, 522–538.
Lindsey, B. G. 1975. Fine structure and distribution of axon terminals from the cochlear nucleus on neurons in the medial superior olivary nucleus of the cat. J. Comp. Neurol. 160, 81–103.
Macpherson, E. A. and Middlebrooks, J. C. 2002. Listener weighting of cues for lateral angle: the duplex theory of sound localization revisited. J. Acoust. Soc. Am. 111, 2219–2236.
Magnusson, A. K., Kapfer, C., Grothe, B., and Koch, U. 2005. Maturation of glycinergic inhibition in the gerbil medial superior olive after hearing onset. J. Physiol. 568, 497–512.
Manley, G. A. and Clack, J. A. 2004. An Outline of the Evolution of Vertebrate Hearing Organs. In: Evolution of the Vertebrate Auditory System (*eds*. G. A. Manley, A. Geoffrey, A. N. Popper, and R. R. Fay), pp. 1–26. Springer Press.
Masterson, B. and Diamond, I. T. 1967. Medial superior olive and sound localization. Science 155, 1696–1697.
McAlpine, D., Jiang, D., and Palmer, A. R. 2001. A neural code for low-frequency sound localization in mammals. Nat. Neurosci. 4, 396–401.
Mills, D. M. and Shepherd, R. K. 2001. Distortion product otoacoustic emission and auditory brainstem responses in the Echidna (*Tachyglossus aculeatus)*. JARO 2, 130–146.
Neuweiler, G. 1990. Auditory adaptations for prey capture in echolocating bats. Physiol. Rev. 70, 615–641.
Neuweiler, G. 2000. The Biology of Bats. Oxford University Press.
Oertel, D. 1999. The role of timing in the brain stem auditory nuclei of vertebrates. Annu. Rev. Physiol. 61, 497–519.
Osen, K. K. 1969. Cytoarchitecture of the cochlear nuclei in the cat. J. Comp. Neurol. 136, 453–484.
Perkins, R. E. 1973. An electron microscopic study of synaptic organization in the medial superior olive of normal and experimental chinchillas. J. Comp. Neurol. 148, 387–415.
Poljak, S. 1926. The connections of the acoustic nerve. J. Anat. 60, 465–469.
Rayleigh, L. 1907. On our perception of sound direction. Philos. Mag. 13, 214–232.
Rhode, W. S., Oertel, D., and Smith, P. H. 1983. Physiological response properties of cells labelled intracellularly with horseradish peroxidase in cat ventral cochlear nucleus. J. Comp. Neurol. 213, 448–463.
Rogowski, B. A. and Feng, A. S. 1981. Normal postnatal development of medial superior olivary neurons in the albino rat: a Golgi and Nissl study. J. Comp. Neurol. 196, 85–97.
Rose, J. E., Brugge, J. F., Anderson, D. J., and Hind, J. E. 1967. Phase-locked response to low-frequency tones in single auditory nerve fibers of the squirrel monkey. J. Neurophysiol. 30, 769–793.
Rosowski, J. J. 1992. Hearing in Transitional Mammals. Predictions from the Middle Ear Anatomy and Hearing Capabilities of Extant Mammals. In: The Evolutionary Biology of Hearing (*eds*. D. B. Webster, R. R. Fay, and A. N. Popper), p. 615. Springer Press.
Ross, L. S. and Pollak, G. D. 1989. Differential ascending projections to aural regions in the 60 kHz contour of the mustache bat's inferior colliculus. J. Neurosci. 9, 2819–2834.
Sanes, D. H. and Friauf, E. 2000. Development and influence of inhibition in the lateral superior olivary nucleus. Hear. Res. 147, 46–58.
Schofield, B. R. 1991. Superior paraolivary nucleus in the pigmented guinea pig: separate classes of neurons project to the inferior colliculus and the cochlear nucleus. J. Comp. Neurol. 312, 68–76.
Schweizer, H. 1981. The connections of the inferior colliculus and the organization of the brainstem auditory system in the greater horseshoe bat *(Rhinolophus ferrumequinum)*. J. Comp. Neurol. 201, 25–49.
Seidl, A. H. and Grothe, B. 2005. Development of sound localization mechanisms in the Mongolian gerbil is shaped by early auditory experience. J. Neurophysiol. 94, 1028–1036.

Simmons, J. A. and Stein, R. A. 1980. Acoustic imaging in bat sonar: echolocation signals and the evolution of echolocation. J. Comp. Physiol. 135, 61–84.

Smith, P. H. 1995. Structural and functional differences distinguish principal from nonprincipal cells in the guinea pig MSO slice. J. Neurophysiol. 73, 1653–1667.

Smith, P. H., Joris, P. X., and Yin, T. C. 1993. Projections of physiologically characterized spherical bushy cell axons from the cochlear nucleus of the cat: evidence for delay lines to the medial superior olive. J. Comp. Neurol. 331, 245–260.

Spitzer, M. W. and Semple, M. N. 1995. Neurons sensitive to interaural phase disparity in gerbil superior olive: diverse monaural and temporal response properties. J. Neurophysiol. 73, 1668–1690.

Stotler, W. A. 1953. An experimental study of the cells and connections of the superior olivary complex of the cat. J. Comp. Neurol. 98, 401–431.

Tollin, D. J. 2003. The lateral superior olive: a functional role in sound source localization. Neuroscientist 9, 127–143.

Vater, M. 1995. Ultrastructural and immunocytochemical observations on the superior olivary complex of the mustached bat. J. Comp. Neurol. 358, 155–180.

Vater, M. and Feng, A. S. 1990. Functional organization of ascending and descending connections of the cochlear nucleus of horseshoe bats. J. Comp. Neurol. 292, 373–395.

Warr, W. B. 1966. Fiber degeneration following lesions in the anterior ventral cochlear nucleus of the cat. Exp. Neurol. 14, 453–474.

Wightman, F. L. and Kistler, D. J. 1992. The dominant role of low-frequency interaural time differences in sound localization. J. Acoust. Soc. Am. 91, 1648–1661.

Willard, F. H. and Martin, G. F. 1983. The auditory brainstem nuclei and some of their projections to the inferior colliculus in the North American opossum. Neuroscience 10, 1203–1232.

Willard, F. H. and Martin, G. F. 1984. Collateral innervation of the inferior colliculus in the North American opossum: a study using fluorescent markers in a double-labeling paradigm. Brain Res. 303, 171–182.

Winer, J. A., Larue, D. T., and Pollak, G. D. 1995. GABA and glycine in the central auditory system of the mustache bat: structural substrates for inhibitory neuronal organization. J. Comp. Neurol. 355, 317–353.

Yin, T. C. 2002. Neural Mechanisms of Encoding Binaural Localization Cues in the Auditory Brainstem. In: Integrative Functions in the Mammalian Auditory Pathway (*eds*. D. Oertel, A. N. Popper, and R. R. Fay), pp. 99–159. Springer Press.

Yin, T. C. and Chan, J. C. 1990. Interaural time sensitivity in medial superior olive of cat. J. Neurophysiol. 64, 465–488.

Yin, T. C., Carney, L. H., and Joris, P. X. 1990. Interaural time sensitivity in the inferior colliculus of the albino cat. J. Comp. Neurol. 295, 438–448.

Zook, J. M. and Casseday, J. H. 1982a. Cytoarchitecture of auditory system in lower brainstem of the mustache bat, *Pteronotus parnellii*. J. Comp. Neurol. 207, 1–13.

Zook, J. M. and Casseday, J. H. 1982b. Origin of ascending projections to inferior colliculus in the mustache bat, *Pteronotus parnellii*. J. Comp. Neurol. 207, 14–28.

Zook, J. M. and DiCaprio, R. A. 1988. Intracellular labelling of afferents to the lateral superior olive in the bat, *Eptesicus fuscus*. Hear. Res. 34, 141–147.

3.40 Brain Mechanisms of Sound Localization in Barn Owls

M Konishi, California Institute of Technology, Pasadena, CA, USA

© 2008 Elsevier Inc. All rights reserved.

3.40.1	Acoustic Cues for Sound Localization	719
3.40.2	Parallel Pathways for Processing Interaural Time Difference and Interaural Intensity Difference	719
3.40.3	Detection and Coding of Interaural Time Difference	720
3.40.4	Processing of Interaural Intensity Differences	721
3.40.5	Convergence of Time and Intensity Pathways in the Midbrain	721
3.40.6	A Map of Auditory Space	721
3.40.7	A Motor Map for Sound Localization	722
References		722

3.40.1 Acoustic Cues for Sound Localization

Experiments show that the barn owl uses the interaural time difference (ITD) for determining sound azimuth and the interaural intensity difference (IID) for elevation (Moiseff, A. and Konishi, M., 1981). The ITD varies systematically as a function of sound azimuth. The maximal ITD experienced by the owl is about 170 μs and the minimal ITD is zero when sound emanates from a place equidistant to the two ears. IID is due to both the head's shadow in the sound field and the directional sensitivity of the external ears in mammals. Owls do not have any external ear, but the feather ruff that surrounds their face serves as a sound-collecting device. The facial ruff consists of left and right halves that are separated by a tall ridge of feathers along the midline of the face. In barn owls, the left ear opening is located higher in the ruff than the right one. This asymmetry and other differences between the left and right halves of the ruff make the left and right ears more sensitive to sound coming from below and above eye level, respectively. This difference in the ear's directional sensitivity causes IID to vary as a function of sound elevation. In owl species with symmetrical ears, IID does not change along the vertical plane. Given a constant size of the head and sound collectors, shorter wavelengths and thus higher frequencies produce greater intensity differences than lower frequencies. The barn owl needs relatively high frequencies (5–8 kHz) for accurate localization in elevation. Thus, to localize sound in two dimensions, the owl must be able to derive both interaural cues from the same high-frequency signal. Mammals including humans, which use both cues for azimuth, detect ITD only in low-frequency ranges and IID in high-frequency ranges (Macpherson, E. A. and Middlebrooks, J. C., 2002).

3.40.2 Parallel Pathways for Processing Interaural Time Difference and Interaural Intensity Difference

The owl's auditory system processes the two cues in two separate pathways. The owl's ear performs spectral analysis of complex sound and encodes the phase and amplitude of each frequency component. Auditory neurons phase-lock by firing at or near a particular phase of tonal stimuli. In barn owls, phase-locking occurs even in auditory neurons that are tuned to high frequencies such as 9 kHz (Köppl, C., 1997). Phase-locking is the basis for the detection of interaural phase differences from which ITDs are derived. The rate of discharge of auditory fibers encodes intensity, because it varies as a function of stimulus intensity. Birds have two anatomically separate cochlear nuclei on each side, nucleus angularis and nucleus magnocellularis, and each primary auditory fiber divides into two collaterals, one innervating nucleus angularis and the other nucleus magnocellularis. Neurons of nucleus magnocellularis phase-lock to tonal stimuli, whereas those of nucleus angularis generally do not. Thus, each cochlear nucleus is more specialized to process one cue than

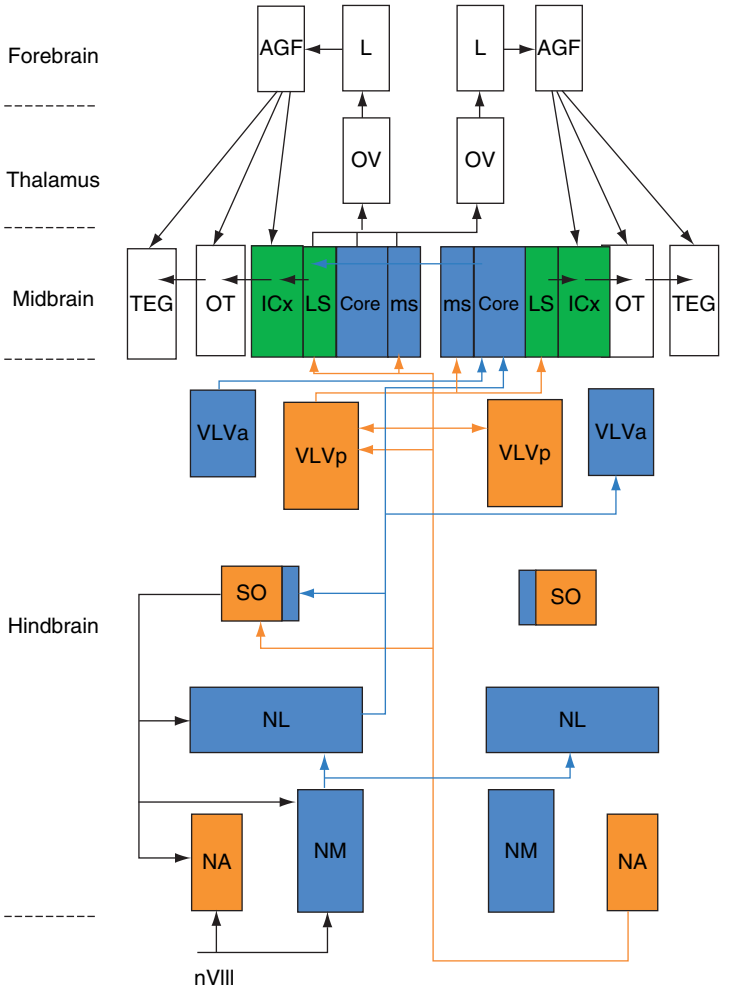

ITD and ILD are processed by parallel pathways

Figure 1 Parallel auditory pathways. The owl's brainstem auditory system consists of two parallel pathways. The blue areas indicate the nuclei of the time processing pathway and the brown areas the nuclei of the intensity processing pathway. The areas where neurons respond to both ITD and IID are indicated by green. The thick and thin arrows indicate anterograde connections, respectively, in the time and intensity pathways. The dashed lines with arrowheads on both ends represent reciprocal connections. The connections are symmetrical in two sides of the brainstem, but only one side is shown for simplicity. AGF, archistriatal gaze field Core, core of the central nucleus of the inferior colliculus; ICx, external nucleus of the inferior colliculus; L, field L; LLV, nucleus ventralis lemnisci lateralis, pars ventralis; IS, lateral shell of the central nucleus of the inferior colliculus; ms, medial shell of the central nucleus of the inferior colliculus; NA, nucleus angularis; NL, nucleus laminaris; NM, nucleus magnocellularis; nVIII, auditory nerve; OT, optic tectum; OV, nucleus ovoidalis; SO, superior olivary nucleus; TEG, tegmentum; VLVa, nucleus ventralis lemnisci lateralis, pars anterior; VLVp, nucleus ventralis lemnisci lateralis, pars posterior. Reproduced from Konishi, M. 2000. Study of sound localization by owls and its relevance to humans. Comp. Biochem. Physiol. – Part A: Mol. Integ. Physiol. 146(4), 459–469, with permission from Elsevier.

the other cue (Sullivan, W. E. and Konishi, M., 1984; Takahashi, T. *et al.*, 1984). The two pathways that start from the cochlear nuclei are anatomically separate until they converge in the inferior colliculus (Takahashi, T. and Konishi, M., 1988a; 1988b). The two channels are referred to as the time and intensity pathways (Figure 1).

3.40.3 Detection and Coding of Interaural Time Difference

Nucleus magnocellularis projects bilaterally to a third-order station, nucleus laminaris, which is presumably the avian homolog of the superior medial olivary nucleus of mammals. Thus, nucleus laminaris

is the first site of binaural convergence in the time pathway. Magnocellular and laminaris neurons form circuits for detection of ITDs by a method similar to that originally proposed by Jeffress L. A. (1948). Laminaris neurons serve as coincidence detectors which fire maximally when impulses arrive simultaneously from the left and right magnocellular nuclei. Axons of magnocellular cells convey phase-locked impulses to an array of laminaris cells with delays. These delays augment in the opposite direction for the ipsilateral and contralateral inputs, because the length of axonal paths for the two sides increases toward the opposite ends of the array (Carr, C. E. and Konishi, M., 1990). When impulses travel to a laminaris cell by a longer path on one side than on the other side, they reach the cell at different times. In general, a left–right difference in impulse arrival time (T_a) consists of an ITD in the stimulus and a difference in impulse conduction delays (T_c). Hence, $T_a = \mathrm{ITD} + T_c$. Coincidence means $T_a = 0$, which obtains when $-\mathrm{ITD} = T_c$; that is, ITD equal to T_c in magnitude but opposite in sign. Because the length of axonal paths varies systematically in both left and right inputs, T_c should also vary regularly. This argument means that neurons sensitive to different ITDs should be systematically arranged in nucleus laminaris (Peña, J. L. *et al.*, 2001).

Laminaris neurons are, however, not all or nothing coincidence detectors, for their responses decrease gradually from maximum to minimum as stimulus timing changes from perfect coincidence to out of phase by 180°. They also respond to monaural stimuli. Laminaris neurons respond best to a single interaural time difference (ITDi) which is independent of frequency. But they respond also optimally to other ITDs which vary with frequency. The relationship between these ITDs and ITDi is $\mathrm{ITDi} \pm nT$, where T is the period of the stimulus tone and n is an integer. This phenomenon, called phase ambiguity, is due to the use of phase-locked impulses for the measurement of ITD. Laminaris neurons fire maximally when they receive binaurally synchronous trains of phase-locked impulses. The coincidence of the two trains recurs every time ITD is changed by an integer multiple of the period of the stimulus tone, causing the laminaris neurons to discharge maximally. Nucleus laminaris projects both to the core of the central nucleus of the inferior colliculus (ICc) and to one of the lemniscal nuclei (VLVa). The core projects to the contralateral lateral shell of the central nucleus of the inferior colliculus (ICcl).

3.40.4 Processing of Interaural Intensity Differences

The nucleus angularis, the first station in the intensity processing pathway, projects to a lemniscal nucleus called the VLVp in which neurons are excited by sound in the contralateral ear and inhibited by sound in the ipsilateral ear. The excitatory input comes from the contralateral nucleus angularis and the inhibitory input from the other VLVp.

The louder the sound in the contralateral ear is, the greater is the response, whereas the louder the sound in the ipsilateral ear is, the greater is the degree of inhibition. Thus, the response of a VLVp neuron varies as a function of the difference in sound intensity between the two sides, even though the neuron still responds to monaural stimulation of the contralateral ear alone. Furthermore, the threshold and degree of inhibition changes systematically from the dorsal to ventral direction of VLVp (Manley, G. A. *et al.* 1988; Mogdans, J. and Knudsen, E. I., 1994). This gradient suggests a map of IIDs in this nucleus.

3.40.5 Convergence of Time and Intensity Pathways in the Midbrain

VLVp neurons project to the lateral shell of the central nucleus of the ICcl. ICcl neurons respond to narrow ranges of frequency and also to combinations of ITD and IID, indicating that the time and intensity pathways converge in each frequency band. The ICcl projects to the adjoining area called the external nucleus of the inferior colliculus (ICx) where neurons respond to broad frequency ranges (3–9 kHz). When the stimulus is a broadband signal, ICx neurons do not respond to ITD or IID alone but require specific combinations of the two cues and unfavorable combinations induce inhibition. Recent studies show that ICx neurons multiply postsynaptic potentials from the two pathways to create the combination sensitivity (Peña, J. L. and Konishi, M., 2001).

3.40.6 A Map of Auditory Space

The tuning of ICx neurons to specific pairs of ITD and IID makes these cells selective for the direction of sound propagation, because such combinations obtain only when sound comes from particular areas in an owl's auditory space. These areas are

called receptive fields and cells having such areas are called space-specific neurons. ICx neurons are systematically arranged according to the location of their receptive fields, thus forming a neural map of auditory space. The topographical representation of auditory space is due not to anatomical projections of the inner ear like the retinotopic map of the visual field but to central synthetic processes. Nevertheless, the auditory space map projects onto the retinotopic map of the optic tectum. The tectal neurons making up the bimodal map respond to both auditory and visual stimuli coming from the same area in space, that is, their auditory and visual receptive fields are mutually aligned (Knudsen, E. I., 1982). Similar maps are found in the superior colliculus of the ferret, although the mechanisms underlying these maps appear to differ from those in owls (King, J. A. and Carlile, S., 1995).

Owl species with symmetrical ears also have space-specific neurons in their ICx, but these cells map only azimuth, because their receptive fields do not have elevational boundaries, although the cells are tuned to combinations of ITD and IID (Volman, S. F. and Konishi, M., 1990). In these owls, IID does not change as a function of sound elevation, because the highest frequency audible to them is too low for this change to occur.

3.40.7 A Motor Map for Sound Localization

The overt behavior that characterizes sound localization in owls is rapid head rotation. The bimodal map of space in the optic tectum projects to a motor map for gaze control which is found in the optic lobe. Neurons of the motor map innervate the medullary nucleus involved in the control of head rotation. The tectal motor map encodes the direction, speed, and amplitude of head rotations (du Lac, S. and Knudsen, E. I., 1990). Experiments reveal that the map contains separate circuits for head rotations in azimuth and elevation (Masino, T. and Knudsen, E. I., 1990).

Both the inferior colliculus and the optic tectum are in the midbrain. Is the forebrain involved in sound localization? Lesions of the optic tectum impair sound localization, but the owl can still localize sound (Wagner, H., 1993). Ablations of both the optic tectum and the nucleus ovoidalis, the avian homolog of the medial geniculate body, completely abolish the ability of owls to localize sound (Knudsen, E. I. *et al.*, 1993). The nucleus ovoidalis receives inputs from all parts of the inferior colliculus except the ICx. Many ovoidalis neurons are tuned to combinations of ITD and IID. Nucleus ovoidalis projects to the forebrain auditory area field L which, in turn, projects to the archistriatum. This structure contains many neurons tuned to combinations of ITD and IID. But neither field L nor archistriatal neurons form an auditory space map. Focal electrical stimulation of the archistriatum induces head rotations even when the tectal motor map is disabled. Interestingly, lesions of the archistriatum cause the owl turn its head toward sound sources like an automaton. Barn owls determine and memorize sound locations before orienting toward them. When the archistriatum of a barn owl is inactivated with muscimol, the owl can no longer remember the computed sound location, even though he can still localize the sound source if it continues to emit the signal (Knudsen, E. I. and Knudsen, P. F., 1996). Thus, one of the functions of the owl's archistriatum may be storage of working memory.

References

Carr, C. E. and Konishi, M. 1990. A circuit for detection of interaural time differences in the brain stem of the barn owl. J. Neurosci. 10, 3227–3246.

du Lac, S. and Knudsen, E. I. 1990. Neural maps of head movement vector and speed in the optic tectum of the barn owl. J. Neurophysiol. 63, 131–149.

Jeffress, L. A. 1948. A place theory of sound localization. J. Comp. Physiol. Psych. 41, 35–39.

King, J. A. and Carlile, S. 1995. Neural Coding for Auditory Space. In: Cognitive Neuroscience (*ed*. M. S. Gazzaniga), pp. 279–293. MIT Press.

Konishi, M. 2000. Study of sound localization by owls and its relevance to humans. Comp. Biochem. Physiol. – Part A. Mol. Integ. Physiol. 146(4), 459–469.

Knudsen, E. I. 1982. Auditory and visual maps of space in the optic tectum of the owl. J. Neurosci. 2, 1177–1194.

Knudsen, E. I. and Knudsen, P. F. 1996. Disruption of auditory spatial working-memory by inactivation of the forebrain archistriatum in barn owls. Nature 388, 428–431.

Knudsen, E. I., Knudsen, P. F., and Masino, T. 1993. Parallel pathway mediating both sound localization and gaze control in the forebrain and midbrain of the barn owl. J. Neurosci. 13, 2837–2852.

Köppl, C. 1977. Phase locking to high frequencies in the auditory nerve and cochlear nucleus magnocellularis of the barn owl, *Tyto alba*. J. Neurosci. 17, 3312–3321.

Macpherson, E. A. and Middlebrooks, J. C. 2002. Listener weighting of cues for lateral angles: the duplex theory of sound localization revisited. J. Acoust. Soc. Am. 111, 2219–2236.

Manley, G. A., Köppl, C., and Konishi, M. 1988. A neural map of interaural intensity difference in the brainstem of the barn owl. J. Neurosci. 8, 2665–2676.

Masino, T. and Knudsen, E. I. 1990. Horizontal and vertical components of head movement are controlled by distinct neural circuits in the barn owl. Nature 345, 434–437.
Mogdans, J. and Knudsen, E. I. 1994. Representation of interaural level difference in the VLVp, the first site of binaural comparison in the barn owl auditory system. Hear. Res. 74, 148–164.
Moiseff, A. and Konishi, M. 1981. Neuronal and behavioral sensitivity to binaural time differences in the owl. J. Neurosci. 1, 40–48.
Peña, J. L. and Konishi, M. 2001. Auditory spatial receptive fields created by multiplication. Science 292, 249–252.
Peña, J. L., Viete, S., Funabiki, K., Saberi, K., and Konishi, M. 2001. Cochlear and neural delays for coincidence detection in owls. J. Neurosci. 21, 9455–9459.
Sullivan, W. E. and Konishi, M. 1984. Segregation of stimulus phase and intensity coding in the cochlear nucleus of the barn owl. J. Neurosci. 4, 1787–1799.
Takahashi, T. and Konishi, M. 1988a. Projections of the cochlear nuclei and nucleus laminaris to the inferior colliculus of the barn owl. J. Comp. Neurol. 274, 190–211.
Takahashi, T. and Konishi, M. 1988b. Projections of nucleus angularis and nucleus laminaris to the lateral lemniscal nuclear complex of the barn owl. J. Comp. Neurol. 274, 212–238.
Takahashi, T., Moiseff, A., and Konishi, M. 1984. Time and intensity cues are processed independently in the auditory system of the owl. J. Neurosci. 4, 1781–1786.
Volman, S. F. and Konishi, M. 1990. Comparative physiology of sound localization in four species of owls. Brain Behav. Evol. 36, 196–215.
Wagner, H. 1993. Sound-localization deficits induced by lesions in the barn owl's auditory space map. J. Neurosci. 13, 371–386.

Further Reading

Adolphs, R. 1993. Bilateral inhibition generates neuronal responses tuned to interaural level differences in the auditory brain-stem of the barn owl. J. Neurosci. 13, 3647–3668.
Brainard, M. S. and Knudsen, E. I. 1993. Experience-dependent plasticity in the inferior colliculus: a site for visual calibration of the neural representation of auditory space in the barn owl. J. Neurosci. 13, 4589–4608.
Knudsen, E. and Konishi, M. 1978. A neural map of auditory space in the owl. Science 200, 795–797.
Knudsen, E. I. and Knudsen, P. F. 1989. Vision calibrates sound localization in developing barn owls. J. Neurosci. 9, 3297–3305.
Knudsen, E. I. and Knudsen, P. F. 1990. Sensitive and critical periods for visual calibration of sound localization by barn owls. J. Neurosci. 10, 222–232.
Wagner, H., Takahashi, T., and Konishi, M. 1987. Representation of interaural time difference in the central nucleus of the barn owl's inferior colliculus. J. Neurosci. 7, 3105–3116.

3.41 Sound Localization in Insects

D Robert, University of Bristol, Bristol, UK

© 2008 Elsevier Inc. All rights reserved.

3.41.1	**Introduction**	725
3.41.2	**Constraints and Limitations**	726
3.41.3	**Sounds, Ears, and Directionality**	727
3.41.3.1	Directional Detection with Particle Velocity Receivers	727
3.41.3.2	Tympanal Ears as Creative Variations on One Theme	728
3.41.3.3	Directional Sound Detection Using Tympanal Ears	728
3.41.3.4	Directional Hearing Using Pressure Receivers	728
3.41.3.5	Directional Hearing Using Pressure Difference Receivers	728
3.41.3.6	Directional Hearing Using Mechanically Coupled Pressure Receivers	729
3.41.4	**Microsecond-Range Acoustic Events and Neural Responses**	730
3.41.5	**Conclusion**	731
References		731

Glossary

chordotonal organ Sensory organ found in insects and crustaceans. The name means thin structure, associated with hearing.

diffraction A collection of physical phenomena associated with wave propagation, such as the bending, spreading, and interference of waves passing by an object or an aperture that disrupt the propagation of the wave.

scolopale cell Cell that mechanically supports the geometry of a scolopidium, including the mechanosensory neurones. The scolopale cell contains rod-like structures (presumably actin) that confer mechanical rigidity and stability.

scolopidium (plural: scolopidia) Multicellular ensemble comprising one or more mechanosensory neurons, a scolopale cell, and several accessory support cells. A scolopidium is the fundamental unit of mechanoreception in insects and crustaceans.

3.41.1 Introduction

Like any of their other senses, hearing in insects is a superbly adapted and sophisticated process. In fact there is more to insect hearing than meets the eye; insect ears may be anatomically simpler and smaller than those of other animals, yet they detect and process airborne sounds with just as much accuracy and sensitivity (Robert, D. and Göpfert, M. C., 2002). While, admittedly, there are major differences in the mechanisms employed in detecting and processing sounds, some remarkable functional and structural similarities have been unveiled at the cellular and molecular levels (Eberl, D. F., 1999; Eberl, D. F. *et al.*, 2000). The process of hearing in insect is commensurate with the evolutionary diversity, ubiquity, and versatility of the class Insecta (Robert, D. and Hoy, R. R., 1998). Adapted – and adapting – to live in a multitude of habitats and move often swiftly between them, insects have rich and diverse sensory ecologies. Displaying an astonishing morphological diversity, ears have been found on almost any segment of the insect body (Fullard, J. H. and Yack, J. E., 1986; Robert, D. and Hoy, R. R., 1998). Any one auditory insect species has evolved a pair of bilateral, specialized hearing organs on one segment, with the notable exception of bladder grasshoppers which are endowed with a series of abdominal sound sensors (van Staaden, M. J. and Römer, H., 1998). It has been very astutely suggested (Meier, T. and Reichert, H., 1990; Yack, J. E. and Fullard, J. H., 1993; Yager, D. D., 1999) that such versatility in developing an ear is based on the prior presence of

the somatosensory chordotonal system distributed all over the insect's body. The mechanosensory multicellular units in that system, the scolopidia, comprising one or more ciliated neurons and accessory cells, are remarkably similar to those used in hearing organs (Field, L. H. and Matheson, T., 1998; Yack, J. E., 2004). Seemingly extreme evolutionary specialization in some insect auditory systems stands out in their functional organization.

Operationally, the process of hearing essentially amounts to detecting the amplitude, the frequency, and the timing of an incident sound wave (Lord Rayleigh, 1876). Detecting adequately each of these three acoustic physical parameters requires specific qualities of the mechanical and neuronal structures of an ear (Robert, D. and Göpfert, M. C., 2002; Hennig, M. *et al.*, 2004; Yack, J. E., 2004). The constraints imposed to fulfill these tasks are not trivial, sometimes they work against each other, and are still matter of much research. For example, the mechanical characteristics allowing auditory sensitivity, such as resonance, generally come to a cost in the temporal resolution of the system. But can an auditory system perform well at both tasks? The functional compromises and the novel mechanisms implemented to detect sound amplitude, frequency, and timing are at the heart of fundamentally understanding the process of hearing. To put it abruptly, no insect ear is good at everything, but some exhibit innovative specializations that excel at one task. The ears of auditory specialists are particularly enriching to comparative research, providing unique insights into evolutionary adaptations to common problems of acoustic detection. One such insect specialist is the fly *Ormia ochracea* and her prosternal hearing organs specialized for directional hearing.

This chapter will focus on some of the mechanisms employed by insects for sound localization. Because they are important in understanding the particularities of insect hearing, the physical constraints will be presented, using a few selected cases to illustrate how the necessity of small size fostered sensory innovation.

3.41.2 Constraints and Limitations

Like most animals, insects are endowed with bilateral symmetry. This symmetry results in the positioning of the ears on each side of the body. There are some notable exceptions, like that of the praying mantises for which the ears are still paired but are located medially, in a ventral thoracic cleft (Yager, D. D. and Hoy, R. R., 1986), or that of the tachinid parasitoid fly *Ormia*, where the ears are near the midline and are linked across it (Robert, D. *et al.*, 1996).

The diminutive size of insects together with the physical laws of sound propagation constitute a set of acute problems for the directional detection of impinging sounds. Numerous studies of acoustic communication and hearing have also shown that insects are small compared not only to other auditory animals, but also to the wavelength of the sounds that are biologically relevant (Michelsen, A., 1998; Robert, D. and Hoy, R. R., 1998). Fundamentally, symmetrically bilateral auditory receivers and their relative position on the animal's body constitute starting conditions that constrain the process of directional hearing. The fundamental problem is rather simple and has been recognized long ago (Lord Rayleigh 1876; Autrum, H., 1940). The smaller the animal, the lesser the auditory cues available for the directional detection of sound. One of the two key physical parameters used to detect the direction of an incident sound wave is the time difference in the arrival of the sound at each ears or, for continuous sounds, the difference in phase between the two auditory signals. In insects, the ears are set so close together that this temporal cue, the interaural time difference (ITD), is extremely small, also by human standard. If the distance between the ears, the interaural distance (ID), is half a millimeter, the maximum ITD is in the order of 1 μs (Robert, D. *et al.*, 1996). This is a short time for any nervous system, not only for that of a small insect (de Ruyter van Steveninck, R. R. *et al.*, 1997). Another constraint is associated with small size: the lack of diffractive conditions. In other, larger animals the size (and density) of the tissue supporting the hearing organs is large compared to the wavelength of sound resulting in diffractive interactions with impinging sounds. Diffraction results in sound pressure to vary in space, whereby, generally, the side of the diffractive structure facing the sound source experiences an increase while the other side experiences a decrease in sound pressure. The difference in sound pressure between the ears constitutes the second key cue for directional sound detection, the interaural intensity difference (IID). Very little or immeasurable diffraction, however, takes place for objects that are *c.* 10 times smaller than the wave length of incident sound waves (Morse, P. M. and Ingard, K. U., 1968, Michelsen, A., 1992; 1996, Robert, D. *et al.*, 1999). It is worth noting that some of the better known and larger ears, those of locusts and cicadas, have

tympanal membranes spanning only about 2–3 mm in diameter. Apparently, the difficulties associated with large wave length and small body sizes are also experienced by fish and their remarkable auditory diversity (Fritzsch, B., 1999).

For insects with subcentimeter body sizes frequencies lower than *c.* 7 kHz do not generate sufficient diffraction to yield measurable IIDs. In such cases, ITDs become the principal cue for directional information. For completeness, there is a third acoustic cue used by animals: the change in the spectral composition of the incident sound wave due to direction-dependent diffraction (Middlebrooks, J. C. and Green, D. M., 1991; Wightman, F. L. and Kistler, D. J., 1997). As shown above, diffraction can be limited for insects, resulting again in small, but existing, spectral variations. The capacity of insects to perform a frequency analysis – with the resolution required to detect diffraction-based spectral variations – is still not known. Frequency analysis has been documented in several insect species (Pollack, G. S., 1998; Fonseca, P. J. *et al.*, 2000). It thus becomes apparent that the constraints are multiple; to generate sufficient diffractive IIDs, insects should use higher frequencies for their acoustic communication, but this would signify a much reduced distance of propagation and reduced localization accuracy due to complex propagation paths in the usual cluttered environment (Bennet-Clark, H. C., 1998). Conversely, lower frequencies facilitate long distance propagation, but are inefficiently produced by small sound-producing structures – oscillating wings, legs, or tymbal organs – and are notoriously difficult to localize (Bennet-Clark, H. C., 1998; Michelsen, A., 1998).

Buffeted between the physics of sound propagation and small body size, how do small insects detect the direction of a sound wave?

3.41.3 Sounds, Ears, and Directionality

Insect ears can be either tympanal or flagellar (antennal). Both types are highly sensitive to airborne acoustic energy and as such are qualified as hearing organs (Tautz, J., 1977). The basic differences between these two auditory anatomies will be presented here, as they pertain to the way directional information is gathered from different physical components of the propagating sound wave. Whilst tympanal ears are sensitive to the pressure (a scalar quantity), flagellar ears are sensitive to particle velocity (a vectorial quantity). The pressure component of a sound wave propagates far from the sound source, the so-called far-field, while particle velocity dominates the overall sound energy very near to the sound source, in the near-field. Flagellar ears have thus been called near-field receivers to reflect their sensitivity to particle velocity.

3.41.3.1 Directional Detection with Particle Velocity Receivers

The capacity of insects to hear with their antennae has long been suggested (for instance in mosquitoes, Johnston, C., 1855). The directionality of the mosquito antennal ears has also been investigated (notably by Belton, P., 1974). Other forms of particle velocity receivers have been reported such as, among others, the filiform hairs borne on the body wall of caterpillars (Tautz, J., 1977), the cercal hairs of crickets (Gnatzy, W. and Tautz, J., 1980; Shimozawa, T. and Kanou, M., 1984). Particle velocity receivers are directional, a capacity due to two independent facts. First, because the physical quantity they respond to – particle velocity – is vectorial (unlike the scalar pressure component), such receivers are inherently directional. The bulk oscillations of the air particles take place in the direction of sound propagation and drive the antenna or hair in the same direction by viscous coupling (Fletcher, N. H., 1978). Thus, directional information is directly sensed by the sound-receiving structure. In the vicinity of complicated sound radiators, such as a pair of beating wings, the exact patterns of velocity vectors and how they contribute to directionality remain unknown. Second, the anatomy and mechanical responses of hair-like structures and antennae condition directionality. Any asymmetry in the flagellar structure (curvature of shaft, asymmetrical hair cover, or articulation at the base of the shaft) may alter the mobility of the entire structure. This may result in a directional sensitivity of the system oscillating in the sound field. Acting as near-field receivers, some of the filiform hairs borne on the cuticle of the caterpillar of a noctuid moth have been shown to have an inherent directional response to sound that is related to hair curvature (Tautz, J., 1977). The capacity of flagellar auditory structures to directionally respond to sound has been investigated (Belton, P., 1974), but how directional information is encoded at the neural level has not received much attention recently. An outstanding question for mosquitoes pertains to the angular

resolution of directional sensing, at the mechanical, neural, and behavioral levels. Also, because hearing is an active process in mosquitoes (Göpfert, M. C. and Robert, D., 2001; Jackson, J. C. and Robert, D., 2006), the possible role of motile sensory neurones in directional hearing is yet to be addressed.

3.41.3.2 Tympanal Ears as Creative Variations on One Theme

The morphology of tympanal ears varies greatly across insect species, yet the general construction responds to the necessity of capturing the energy conveyed in a field of acoustic pressure (Hoy, R. R. and Robert, D., 1996; Michelsen, A., 1998). Receiving acoustic pressure, for example, converting acoustic energy into mechanical motion, is done by a thin cuticular membrane backed with an air-filled cavity. The mechanical response is then sensed by mechanosensory scolopidial cells generally grouped in a chordotonal organ (Field, L. H. and Matheson, T., 1998; Yack, J. E., 2004). Sensing the direction of a sound wave is one of the essential tasks of audition and, as we shall see, insects have evolved quite original solutions to that particular problem (Michelsen, A., 1998; Robert, D. and Hoy, R. R., 1998).

3.41.3.3 Directional Sound Detection Using Tympanal Ears

For insects, the main acoustic cues for directional hearing are ITDs and IIDs.

The cues are mainly determined by the spatial separation between the ears, the ID, and their position relative to the sound source. ID can be as short as a few millimeters for crickets, grasshoppers, moths, cicadas. The shortest distance reported thus far is that of parasitoid flies of the genera *Mediosetiger* and *Ormia*, a mere 200 and 500 µm, respectively (Robert, D. and Huber, D. unpublished observation). For *Ormia*, such short ID implies ITDs no larger than 1.5 µs (Robert, D. *et al.*, 1996). The body size of these flies does not exceed 2–4 mm, a much shorter distance than the 67 mm wavelength of the biologically relevant sounds – the songs of the cricket hosts they hunt (Robert, D. *et al.*, 1992). In the absence of measurable diffraction, no IID is available as a cue. Several studies have evaluated the effects of diffraction around the body of an insect, including moths (Payne, R. *et al.*, 1966), locusts (Robert, D., 1989), grasshoppers (Michelsen, A. and Rohrseitz, K., 1995), and flies (Robert, D. *et al.*, 1999). It was thus shown that the pressure differences around the insect, and occasionally at the tympanal membranes, increase with sound frequency. The physical aspects of sound propagation and directional auditory cues as applied to insects have specifically been explored in earlier reviews (Michelsen, A., 1992; 1996; 1998; Robert, D. and Hoy, R. R., 1998). Research thus far has established the existence of three main types of tympanal receivers in insects: the pressure receivers, the pressure difference receivers, and the mechanically coupled receivers. How these different types of receivers operate will be presented in the following sections.

3.41.3.4 Directional Hearing Using Pressure Receivers

In pressure receivers, by definition, sound pressure acts only on one side of the tympanal membrane, usually the external one (Miller, L. A., 1977; Michelsen, A., 1998). Pure pressure receivers are found on insects whose bodies are large compared to the wavelength of the sound they detect. These sounds can be the high-frequency echolocation signals of hunting bats, or conspecific songs. For some bushcrickets such songs can reach frequencies above 100 kHz (Montealegre-Z, F., 2006) and can therefore generate significant diffraction around a millimeter-size animal. This way, pressure receiver ears located on each side of the animal experience interaural pressure differences that can constitute sufficient cues for directional hearing. Large diffraction-based IIDs (20–40 dB) were first measured at the ears of noctuid moths, when exposed to the ultrasonic echolocation calls of bats (30–60 kHz) (Payne, R. *et al.*, 1966). In small grasshoppers, much smaller IIDs (1–2 dB) are sufficient to elicit reliable orientation toward attractive intraspecific calling song. As stated before, diffraction-based cues decrease with decreasing frequency. This physical constraint has possibly been shaping the high-frequency calls of many insect species (Michelsen, A., 1996; Bennet-Clark, H. C., 1998). It is important to note here that the actual sound pressures at the ears have rarely been measured with high accuracy, a technical limitation due to the large size of precision microphones relative to the tympanal ear of an insect (Robert, D. *et al.*, 1999).

3.41.3.5 Directional Hearing Using Pressure Difference Receivers

Pressure difference receivers are typically found in insects with body sizes only a fraction of the

wavelength of interest. Pressure difference receivers were first proposed to be at work in locusts to endow them with directional hearing (Autrum, H., 1940). By definition, such receivers operate under the action of sound pressure on both sides of the tympanal membrane (Autrum, H., 1940; Michelsen, A., 1992). Anatomically and functionally, pressure difference receivers are more complicated than pressure receivers; they are endowed with two or more acoustic inputs. These additional inputs serve to guide sound pressure to the internal side of the tympanum. As they propagate in a thin tracheal tube and/or across air sacs, sound waves attenuate to different degrees, or get amplified, and even experience some delays (phase shifts) due to changes in the propagation velocity of sound in confined environments. The force driving the tympanal membrane is the difference between the external and internal pressures acting on the tympanal membrane. When internal and external sound pressures are identical in timing and magnitude, they cancel each other so that no driving force is exerted. When the pressures are equal but of opposite phase, the driving force is maximal, similar to the classic case of constructive (as opposed to destructive) interference between periodic functions. For some pressure difference receivers, the two, bilaterally symmetric ears are coupled by an acoustically conductive tissue, usually a large air sac. In this case, the pressure acting on the internal side of one tympanal membrane originates from the other, contralateral ear. This type of ear is at work in the locust (Miller, L. A., 1977); it operates as a pressure difference receiver for low frequencies but as a pressure receiver for high frequencies.

Bushcrickets have their tympanal ears on the tibia of the foreleg and display another type of pressure difference receivers. Bushcrickets can be much larger than the wavelengths of their usually broadly tuned calling songs. Borne on thin legs, the tympana are unlikely to experience direct and significant diffractive effects. The animal's body, however, is large and dense enough to generate diffractive effects. In this case, the tour de force has been to exploit such effects by conducting the IIDs and ITDs due to the body's presence in the sound field to the sensory cells through a set of horn-shaped tracheal tubes. This system's dominant acoustic inputs are specialized spiracles and horn-shaped atria and trachea leading to the internal side of the tympanal membranes and also to the mechanoreceptive organ (Michelsen, A., 1998). Remarkably, the pressures acting on either side of the tympanum can originate from the same side of the body. This type of pressure difference receiver has not received much biomechanical attention, and while sound amplification in the horn-shaped acoustic trachea has been characterized, the exact action of acoustic pressure on the mechanoreceptor organs is not known.

A further example of pressure difference receivers is that of the field cricket *Gryllus bimaculatus* (Michelsen, A. *et al.*, 1994). For *G. bimaculatus*, body size is less than 1 cm and the wavelength of the calling song is about 7 cm, a strong indication that the ITDs and IIDs are small in this species. The morphology of the auditory organ in field crickets is complex; it encompasses four separate inputs and one internal interaural transmission channel. The reader is encouraged to consult the original article by Michelsen A. *et al.* (1994) to appreciate the sophistication of the cricket's auditory system. In field crickets, the way mechanical energy is conducted from the tympanal system to the mechanosensory organ is not fully understood (Yack, J. E., 2004). In particular, it is unclear how tympanal vibrations determine the mechanical activation of the sensory organ in both magnitude and phase.

3.41.3.6 Directional Hearing Using Mechanically Coupled Pressure Receivers

Directional hearing in the parasitoid fly *O. ochracea* takes yet another, smaller dimension. These flies use their ears to detect, in the pressure field, the songs of their host, field crickets, upon which they deposit their larvae (Cade, W. H., 1975). In all flies of the genus *Ormia* observed to date (Huber, D. and Robert, D. unpublished) the auditory organs are situated on the prothorax, behind the head, and are smaller than 1 mm in size. In effect, the best possible ITD was measured to be 1.45 μs (SD: ±0.49, $N = 10$; Robert, D. *et al.*, 1996). For a small fly, hearing the song of a field cricket at 4.8 kHz, body size to wavelength ratio of 1:35, precludes significant diffractive effects (Robert, D. *et al.*, 1996; 1999). Several studies demonstrated, in field and laboratory conditions, that the fly locates her host, a field cricket singing its calling song or a loudspeaker (Cade, W. H., 1975), using tympanal auditory organs (Robert, D. *et al.*, 1992), and with high accuracy (Müller, P. and Robert, D., 2001). Another series of studies has established the morphology and ultrastructure of the auditory organ (Edgecomb, R. S. *et al.*, 1995) and revealed the mechanism by which directionality is achieved (Miles, R. N. *et al.*, 1995; Robert, D. *et al.*, 1996). It is

achieved by mechanically coupling two adjacent tympanal membranes (Miles, R. N. *et al.*, 1995; Robert, D. *et al.*, 1996). This is an unconventional mechanism that is known to occur only in flies (Robert, D. and Hoy, R. R., 1998). Using scanning laser Doppler vibrometry, it could be shown that mechanical coupling of tympanal membranes has the effect of amplifying tiny acoustic cues into larger interaural differences that can be processed by the nervous system. In response to the host cricket song (carrier frequency at 4.8–5 kHz), the mechanical response of this coupled tympanal system is asymmetrical, resulting from the linear combination of two resonant modes of vibration (for details see Miles, R. N. *et al.*, 1995; Robert, D. *et al.*, 1996; 1998). Remarkably, the mechanical ITD measured between the tympanal membranes is 50–60 µs and the mechanical IID is 3–12 dB for sounds delivered at 90° to the side of the animal. This mechanical ITD is thus about 40 times longer than the 1.5 µs acoustical ITD due to the ID of 520 µm. Converting time difference back into distance (owing to a 344 m s^{-1} propagation velocity of sound in air), it is as if the female tachinid *O. ochracea* had her ears set 1 cm on each side of her body.

Mechanically coupled ears are not unique to tachinid flies; they have also been described in the sarcophagid fly *Emblemasoma* spp. (Robert, D. *et al.*, 1999), an acoustic parasitoid of cicadas. This fly possesses a hearing organ on its prothorax. As a case of evolutionary convergent evolution, this auditory organ is analogous to that of the tachinid fly *O. ochracea*, but its mode of operation is not identical (Robert, D. *et al.*, 1999). The tachinid and sarcophagid auditory systems achieve directional hearing by the asymmetrical deflections of their coupled tympanal membranes. These two systems, however, present several anatomical differences that result in different mechanical responses. Yet, both types of ears give rise to interaural differences in time and amplitude that are essential cues for direction hearing (Robert, D. and Hoy, R. R., 1998). Briefly, in the tachinid system, intertympanal coupling is achieved by the presternum, an unpaired sclerite that spans the midline, where it is anchored to the immobile probasisternum. It was shown that this sclerite acts as mechanical lever coupling the two ears. The lever consists of two beams that are joined medially by a torsional spring and supported by a fulcrum that serves as an immobile pivot point. At the frequency of the cricket song, the presternum undergoes a rocking motion about the fulcrum (with some flexion at the immobile fulcrum), in such a way that one side of the lever moves much more than the other (Miles, R. N. *et al.*, 1995; Robert, D. *et al.*, 1996). The side of the coupled ears that moves more is ipsilateral to the sound source. The sarcophagid ears achieve a similar motion, yet without an immobile, median fulcrum. The tympanal membranes join at the midline of the animal and are creased horizontally, providing the rigidity necessary to the bilateral rocking motion that introduces intertympanal asymmetry (Robert, D. *et al.*, 1999). Hence, through functionally convergent but anatomically divergent evolutionary innovations, these two fly families have independently solved the problem of the directional detection of low-frequency sounds by tympanal membranes separated by a fraction (1:130) of the wavelength. In another genus of tachinid fly, *Therobia*, ears have also been described that detect the calling songs of their bush-cricket hosts singing at somewhat higher frequencies (10–15 kHz) (Lakes-Harlan, R. and Heller, K.-G., 1992). The morphology of these ears clearly indicates that mechanical coupling between tympana is also at work in *Therobia* flies.

3.41.4 Microsecond-Range Acoustic Events and Neural Responses

The capacity of insects to encode auditory information has a long history of research that is discussed in recent authoritative reviews by Pollack G. S. (1998), Hennig M. *et al.* (2004), and Hedwig B. (2006). Some information about the neuronal aspects of directional hearing is also provided in Robert D. and Göpfert M. C. (2002). It is, however, worth noting here that the coding of acoustic information is a fast process. As seen above, mechanical processing amplifies the cues available in the time domain, yet these cues remain very small, even by human standards (Middlebrooks, J. C. and Green, D. M., 1991). Even amplified by about 40 times, the mechanical ITDs are still very small (50–60 µs) and must somehow be encoded by the fly's auditory system. On the basis of neurophysiological and behavioral evidence, a study has shown that the flies can use temporal sound cues at the submicrosecond scale (Mason, A. C. *et al.*, 2001). Walking on an air-cushioned treadmill, flies could be induced to move toward a sound source off the midline by only 2°. Such small angle, given the extremely short ID of *O. ochracea* (520 µm), corresponds to acoustical ITDs of 50 ns (Mason, A. C. *et al.*, 2001). In a series of arduous experiments, the activity, and especially the exact

timing of primary afferent receptor neurons, was measured as a function of the angle of azimuth of the incident sound (Mason, A. C. *et al*., 2001; Oshinsky, M. L. and Hoy, R. R., 2002). Notably, for sounds delivered 90° off the midline, neuronal interaural time delays were measured to be about 150 μs and predicted to be 7 μs at 2° azimuth (Mason, A. C. *et al*., 2001). Importantly, the absolute time to spiking (the delay to the stimulus) was extremely regular and its variation thus remarkably small (3.164 ± 0.095 ms (SD), range 0.012–0.121 ms, $N = 7$). This indicates that the accuracy of the temporal coding is about 10 times larger than the actual neuronal ITDs for the smallest angle resolved (i.e., 0.007 ms at 2°). Entering reasonable speculation at this stage, it was proposed (Mason, A. C. *et al*., 2001) that the fly's auditory system achieves the acuity necessary by pooling a population of afferent neurons onto the first auditory interneurone. Neuroanatomically, the convergence of the fly's 50–100 sensory afferents has not been confirmed. It is known, however, that a large portion of these primary afferent neurons display highly accurate signaling, with only one single sharp and accurate spike per stimulus (Oshinsky, M. L. and Hoy, R. R., 2002). To appreciate more how this process of sensory convergence can generate hyperacute detection capacity in the time domain (de Ruyter van Steveninck, R. R. *et al*., 1977), the reader is invited to consult the articles that suggest this process for the fly *Ormia* (Mason, A. C. *et al*., 2001; Oshinsky, M. L. and Hoy, R. R., 2002) and for electric fish, notably (Rose, G. and Heiligenberg, W., 1985).

3.41.5 Conclusion

Many questions remain unanswered in insect directional hearing. Do insects possess a capacity for auditory scene analysis, which they could use to navigate within their environment in space and time? Some behavioral experiments on the fly *Ormia* (Müller, P. and Robert, D., 2001) and on crickets (Wyttenbach, R. A. and Hoy, R. R., 1997) have suggested the possibility that some insects may acquire three-dimensional auditory information about their position relative to a sound source. This capacity has not been tested in other insect species, nor have neuronal mechanisms been considered. Since the capacity for auditory space perception is generally attributed to large-brained animals (Knudsen, E. I. and Konishi, M., 1979), it would be most interesting to establish whether insect neuronal coding of directionality bears any resemblance, or convergence, to coding in vertebrate auditory specialists. More generally, research into insect sensory systems has never failed to enrich, by matter of comparison and analogy, our knowledge of the senses, including our own, inasmuch as insects have also never failed to impress the researchers with their surprisingly diverse evolutionary creativity.

References

Autrum, H. 1940. Über die Lautäusserung und Schallwahrnehmung bei Arthropoden. II. Das Richtungshören von *Locusta* und Versuch einer Hörtheorie für Tympanalorgone vom Locustidentyp. Z. vergl. Physiol. 28, 326–352.

Belton, P. 1974. An Analysis of Direction Finding in Male Mosquitoes. In: Analysis of Insect Behaviour (*ed*. L. B. Browne), pp. 139–148. Springer.

Bennet-Clark, H. C. 1998. Size and scale effects as constraints in insect sound communication. Philos. Trans. R. Soc. Lond., B. 353, 407–419.

Cade, W. H. 1975. Acoustically orienting parasitoids: fly phonotaxis to cricket song. Science 190, 1312–1313.

Eberl, D. F. 1999. Feeling the vibes: chordotonal mechanisms in insect hearing. Curr. Opin. Neurol. 9, 389–393.

Eberl, D. F., Hardy, R. W., and Kernan, M. J. 2000. Genetically similar transduction mechanisms for touch and hearing in *Drosophila*. J. Neurosci. 20, 5981–5988.

Edgecomb, R. S., Robert, D., Read, M. P., and Hoy, R. R. 1995. The tympanal hearing organ of a fly: phylogenetic analysis of its morphological origins. Cell Tissue Res. 282, 251–268.

Field, L. H. and Matheson, T. 1998. Chordotonal organs in insects. Adv. Insect Physiol. 27, 1–28.

Fletcher, N. H. 1978. Acoustical response of hair receptors in insects. J. Comp. Physiol. A 127, 185–189.

Fonseca, P. J., Münch, D., and Hennig, R. M. 2000. How cicadas interpret acoustic signals. Nature 405, 297–298.

Fritzsch, B. 1999. Hearing in Two Worlds: Theoretical and Realistic Adaptive Changes of the Aquatic and Terrestrial Ear for Sound Reception. In: Comparative Hearing: Fish and Amphibians (*eds*. A. N. Popper and R. R. Fay), pp. 15–42. Springer.

Fullard, J. H. and Yack, J. E. 1993. The evolutionary biology of insect hearing. Trends Ecol. Evol. 8, 248–252.

Gnatzy, W. and Tautz, J. 1980. Ultrastructure and mechanical properties of an insect mechanoreceptor: stimulus-transmitting structures and sensory apparatus of the cercal filiform hairs of *Gryllus*. Cell Tissue Res. 213, 441–463.

Göpfert, M. C. and Robert, D. 2001. Active auditory mechanics in mosquitoes. Proc. R. Soc. Lond., B. 268, 333–339.

Hedwig, B. 2006. Pulses, patterns and path: neurobiology of acoustic behaviour in crickets. J. Comp. Physiol. A 192, 677–689.

Hennig, M., Franz, A., and Stumpner, A. 2004. Processing of auditory information in insects. Microsc. Res. Tech. 63, 351–374.

Hoy, R. R. and Robert, D. 1996. Tympanal hearing in insects. Ann. Rev. Entomol. 41, 433–450.

Jackson, J. C. and Robert, D. 2006. Nonlinear auditory mechanism enhances female sounds for male mosquitoes. Proc. Natl. Acad. Sci. U. S. A. 103, 16734–16739.

Johnston, C. 1855. Auditory apparatus of the culex mosquito. Q. J. Microsc. Sci. 3, 97–102.

Knudsen, E. I. and Konishi, M. 1979. Mechanisms of sound localisation in the barn owl (*Tyto alba*). J. Comp. Physiol. 133, 13–21.

Lakes-Harlan, R. and Heller, K.-G. 1992. Ultrasound sensitive ears in a parasitoid fly. Naturwissenschaften 79, 224–226.

Mason, A. C., Oshinsky, M. L., and Hoy, R. R. 2001. Hyperacute directional hearing in a microscale auditory system. Nature 410, 686–690.

Meier, T. and Reichert, H. 1990. Embryonic development and evolutionary origin of the orthopteran auditory organs. J. Neurobiol. 21, 592–610.

Michelsen, A. 1992. Hearing and Sound Communication in Small Animals: Evolutionary Adaptations to the Laws of Physics. In: The Evolutionary Biology of Hearing (*eds*. D. M. Webster, A. N. Popper, and R. R. Fay), pp. 61–78. Springer.

Michelsen, A. 1996. Directional Hearing in Crickets and Other Small Animals. In: Neural Basis of Behavioural Adaptations (*eds*. K. Schildberger and N. Elsner), pp. 195–207. Fischer.

Michelsen, A. 1998. Biophysics of Sound Localization in Insects. In: Comparative Hearing: Insects (*eds*. R. R. Hoy, A. N. Popper, and R. R. Fay), pp. 18–62. Springer.

Michelsen, A. and Rohrseitz, K. 1995. Directional sound processing and interaural sound transmission in a small and a large grasshopper. J. Exp. Biol. 198, 1817–1827.

Michelsen, A., Popov, A. V., and Lewis, B. 1994. Physics of directional hearing in the cricket *Gryllus bimaculatus*. J. Comp. Physiol. 175, 153–164.

Middlebrooks, J. C. and Green, D. M. 1991. Sound localization by human listeners. Ann. Rev. Psychol. 42, 135–159.

Miles, R. N., Robert, D., and Hoy, R. R. 1995. Mechanically coupled ears for directional hearing in the parasitoid fly *O. ochracea*. J. Acoust. Soc. Am. 98, 3059–3070.

Miller, L. A. 1977. Directional hearing in the locust *Schistocerca gregaria* Forskål (Acrididae, Orthoptera). J. Comp. Physiol. 119, 85–98.

Montealegre-Z, F., Morris, G. K., and Mason, A. C. 2006. Generation of extreme ultrasonics in rainforest katydids. J. Exp. Biol. 209, 4923–4937.

Morse, P. M. and Ingard, K. U. 1968. Theoretical Acoustics, pp. 412–422. McGraw-Hill.

Müller, P. and Robert, D. 2001. A shot in the dark: the silent quest of a free-flying phonotactic fly. J. Exp. Biol. 204, 1039–1052.

Oshinsky, M. L. and Hoy, R. R. 2002. Physiology of the auditory afferents in an acoustic parasitoid fly. J. Neurosci. 22, 7254–7263.

Payne, R., Roeder, K. D., and Wallman, L. 1966. Directional sensitivity of the ears of noctuid moths. J. Exp. Biol. 44, 17–31.

Pollack, G. S. 1998. Neural Processing of Acoustic Signals. In: Comparative Hearing: Insects (*eds*. R. R. Hoy, A. N. Popper, and R. R. Fay), pp. 139–196. Springer.

Lord Rayleigh, 1876. On our perception of the direction of a sound source. Nature 14, 32–33.

Robert, D. 1989. The auditory behaviour of flying locusts. J. Exp. Biol. 147, 279–302.

Robert, D. and Göpfert, M. C. 2002. Novel schemes for hearing and acoustic orientation in insects. Curr. Opin. Neurobiol. 12, 715–720.

Robert, D. and Hoy, R. R. 1998. The evolutionary Innovation of Tympanal Hearing in Diptera. In: Comparative Hearing: Insects (*eds*. R. R. Hoy, A. N. Popper, and R. R. Fay), pp. 139–196, 197–227. Springer.

Robert, D., Amoroso, J., and Hoy, R. R. 1992. The evolutionary convergence of hearing in a parasitoid fly and its cricket host. Science 258, 1135–1137.

Robert, D., Miles, R. N., and Hoy, R. R. 1996. Directional hearing by mechanical coupling in the parasitoid fly *Ormia ochracea*. J. Comp. Physiol. 179, 29–44.

Robert, D., Miles, R. N., and Hoy, R. R. 1998. Tympanal mechanics in the parasitoid fly *Ormia ochracea*: intertympanal coupling during mechanical vibration. J. Comp. Physiol. 183, 443–452.

Robert, D., Miles, R. N., and Hoy, R. R. 1999. Tympanal hearing in the sarcophagid parasitoid fly *Emblemasoma* sp: the biomechanics of directional hearing. J. Exp. Biol. 202, 1865–1876.

Rose, G. and Heiligenberg, W. 1985. Temporal hyperacuity in electric fish. Nature 318, 178–180.

de Ruyter van Steveninck, R. R., Lewen, G. D., Strong, S., Koberle, R., and Bialek, W. 1997. Reproducibility and variability in neural spike trains. Science 275, 1805–1808.

Shimozawa, T. and Kanou, M. 1984. Varieties of filiform hairs: range fractionation by sensory afferents and cercal interneurons of a cricket. J. Comp. Physiol. A 155, 485–493.

Tautz, J. 1977. Reception of medium vibration by thoracal hairs of the caterpillar of *Barathra brassicae* L. (Lepidoptera, Noctuidae). I. Mechanical properties of the receptor hairs. J. Comp. Physiol. 118, 13–31.

van Staaden, M. J. and Römer, H. 1998. Evolutionary transition from stretch to hearing organs in ancient grasshoppers. Nature 394, 773–776.

Wightman, F. L. and Kistler, D. J. 1997. Monaural sound localization revisited. J. Acoust. Soc. Am. 101, 1050–1063.

Wyttenbach, R. A. and Hoy, R. R. 1997. Acuity of directional hearing in the cricket. J. Exp. Biol. 200, 1999–2006.

Yack, J. E. 2004. The structure and function of auditory chordotonal organs in insects. Microsc. Res. Tech. 63, 315–337.

Yack, J. E. and Fullard, J. H. 1993. What is an insect ear? Ann. Entomol. Soc. 86, 677–682.

Yager, D. D. 1999. Structure, development and evolution of insect auditory systems. Microsc. Res. Tech. 47, 380–400.

Yager, D. D. and Hoy, R. R. 1986. The cyclopean ear: a new sense for the praying mantis. Science 231, 727–729.

3.42 Inputs to the Inferior Colliculus

E Covey, University of Washington, Seattle, WA, USA

© 2008 Elsevier Inc. All rights reserved.

3.42.1	**Sources of Ascending Inputs to the Inferior Colliculus**	735
3.42.2	**Parsing the Pathways to the Inferior Colliculus**	736
3.42.2.1	Direct and Indirect Pathways	736
3.42.2.2	Binaural and Monaural Pathways	736
3.42.2.3	Gradient Systems of Pathways	737
3.42.3	**Projection Gradients in the Inferior Colliculus**	737
3.42.3.1	The Ventral Cochlear Nucleus System	737
3.42.3.2	The Dorsal Cochlear Nucleus System	739
3.42.3.3	Other Types of Gradients or Distributions	741
3.42.4	**Relationships Among Projections from Different Sources**	741
3.42.4.1	Laminar Projections Within the Anteroventral Cochlear Nucleus System	741
3.42.4.2	Relation between Dorsal Cochlear Nucleus and Ventral Cochlear Nucleus System Projections	742
3.42.5	**Relation with Intrinsic Connections**	744
3.42.6	**Biochemical Gradients**	745
3.42.7	**Evidence for Functional Gradients**	746
3.42.8	**Summary**	747
References		747

Glossary

amygdala A complex of subcortical cell groups located deep within the temporal lobe; thought to play a role in emotional responses, especially fear.

anterograde tracer A substance that, when placed in a specific region of the brain, is taken up by neuron cell bodies and transported to their axon terminals where it remains for some time. The distribution of the substance can then be visualized histologically by performing a chemical reaction that produces a colored product or through the use of fluorescence microscopy.

anteroventral cochlear nucleus (AVCN) One of two divisions of the ventral cochlear nucleus; receives direct input from the auditory nerve and provides the main ascending pathway to the principal nuclei of the superior olivary complex and the intermediate and ventral nuclei of the lateral lemniscus; also provides direct projections to the inferior colliculus.

binaural Receiving and/or responding to input from both ears.

brachium of the inferior colliculus (BIC) Bundle of fibers running from the inferior colliculus to the medial geniculate nucleus.

central nucleus of the inferior colliculus The ventromedial and central portion of the inferior colliculus that receives direct projections from the anteroventral cochlear nucleus.

cochlear nucleus The first structure in the central nervous system to receive auditory input, via the auditory nerve. The cochlear nucleus contains three complete tonotopic representations and gives rise to multiple parallel pathways in the brainstem.

corticofugal projections Projections that descend from the cortex to innervate a subcortical structure such as the medial geniculate or inferior colliculus.

cuneate nucleus Cell group in the lower brainstem that receives somatosensory input via the spinal cord.

delay lines Multiple inputs to a single target neuron, each of which has a slightly different latency (delay of response relative to stimulus onset).

dorsal cochlear nucleus (DCN) One of two major anatomical divisions of the cochlear nucleus; receives direct input from the auditory nerve as well as descending input from a variety of sources.

dorsal column nuclei Cell groups in the lower brainstem that receive somatosensory input via the dorsal column pathway of the spinal cord.

dorsal cortex of the inferior colliculus The region dorsomedial to the central nucleus.

dorsal nucleus of the lateral lemniscus (DNLL) A group of neurons located just below the inferior colliculus. The DNLL receives input from the ipsilateral medial superior olive, the lateral superior olive bilaterally, and the opposite DNLL. It projects bilaterally to the inferior colliculus.

dorsal raphe nuclei A group of cell bodies located along the midline below the periaqueductal gray. The main source of serotonergic fibers, which have diffuse and widespread projections throughout the rest of the brain.

external nucleus of the inferior colliculus The region lateral to the central nucleus.

fibrodendritic lamina An anatomical module within the inferior colliculus consisting of ascending fibers from the lower brainstem, intrinsic projections, cell bodies, and dendrites. A fibrodendritic lamina is thought to correspond to a functionally defined isofrequency contour.

frequency sweep (frequency modulation (FM)) A tonal stimulus, the frequency of which changes continuously from beginning to end.

globus pallidus Group of neuron cell bodies that is a major component of the basal ganglia system, and is involved in motor control.

inferior colliculus The principal midbrain auditory center in mammals. Integrates inputs from a variety of sources; projects to the thalamocortical system and motor-related pathways.

intermediate nucleus of the lateral lemniscus (INLL) A group of cell bodies located between the ascending fibers of the lateral lemniscus, between the dorsal and ventral nuclei of the lateral lemniscus. It receives input mainly from the contralateral anteroventral cochlear nucleus and projects to the ipsilateral inferior colliculus.

intrinsic connections (projections) Connections among neurons within a brain structure.

iontophoretic Using a small current of the same polarity as a charged molecule to eject the substance from a micropipette.

isofrequency lamina A region of an auditory structure (e.g., inferior colliculus) in which all neurons have similar best frequencies.

lateral superior olive (LSO) Cell group belonging to the superior olivary complex. LSO receives excitatory input from the ipsilateral cochlear nucleus and inhibitory input from the contralateral cochlear nucleus via a synapse in the medial nucleus of the trapezoid body; cells in LSO are sensitive to small interaural intensity differences corresponding to the location of a sound source in the horizontal plane.

locus coeruleus A group of noradrenergic cell bodies located in the dorsal and rostral part of the brainstem; provides diffuse and widespread noradrenergic projections throughout the brain.

medial geniculate body The main thalamic structure of the auditory system; receives input from the inferior colliculus and has reciprocal connections with primary auditory cortex.

medial superior olive (MSO) Cell group belonging to the superior olivary complex. In mammals with good low-frequency hearing, MSO receives excitatory input from both cochlear nuclei; cells in MSO are sensitive to small interaural time differences corresponding to the location of a sound source in the horizontal plane.

modulation rate The frequency with which a stimulus parameter is changed, usually expressed in Hz (cycles s^{-1}). Often used to describe sinusoidal frequency or amplitude modulations of a tone.

monaural Receiving and/or responding to input from one ear only.

novelty responses The property of responding exclusively, or in an enhanced manner, to a novel stimulus.

nuclei of the lateral lemniscus (NLL) A group of nuclei in the lower brainstem that includes the dorsal nucleus of the lateral lemniscus (DNLL), the intermediate nucleus of the lateral lemniscus (INLL) and the ventral nucleus of the lateral lemniscus (VNLL). The DNLL receives input from the superior olivary complex and is a binaural structure; the INLL and VNLL receive input from the contralateral cochlear nucleus and are mainly monaural structures. All divisions of the NLL project to the inferior colliculus.

nucleotopic An organization in which projections from different cell groups (nuclei) terminate in segregated areas within a single anatomically defined target structure.

nucleus incertus A group of neuron cell bodies in the ventral and caudal part of the periaqueductal gray. Possibly involved in integrating sensory input with behavioral planning and/or arousal.

periaqueductal gray (also called the central gray) Group of neuron cell bodies that surround the

cerebral aqueduct; center for integration of sensory and motor information from multiple systems.

peripeduncular nucleus Group of neuron cell bodies located adjacent to the medial geniculate nucleus; may be involved in processing sensory stimuli during emotional situations.

pontine gray A heterogeneous group of neuron cell bodies located in the rostral part of the lower brainstem; receives input from a variety of sources including the visual and auditory systems and projects to the cerebellum.

posterior intralaminar nuclei Group of neuron cell bodies located adjacent to the medial geniculate nucleus; project to auditory cortex and amygdala and may be involved in processing sensory stimuli during emotional situations.

posterior limitans nucleus Group of neuron cell bodies that is part of the posterior nuclear complex of the thalamus, and may be involved in integration of information from multiple sensory modalities.

pericentral nucleus of the inferior colliculus The regions surrounding the central nucleus.

posteroventral cochlear nucleus (PVCN) One of two divisions of the ventral cochlear nucleus. Receives direct projections from the auditory nerve and projects mainly to periolivary cell groups.

sinusoidal amplitude modulation (SAM) Periodic change in the amplitude of a stimulus according to a sine wave function.

sinusoidal frequency modulation (SFM) Periodic change in the frequency of a stimulus according to a sine wave function.

somatosensory cortex The portion of the neocortex that processes sensory information about touch, pressure, temperature, pain, and other cutaneous and somatic sensory modalities.

spinal trigeminal nucleus A group of neuron cell bodies in the lower brainstem that receive somatosensory input via the trigeminal nerve.

stimulus-specific adaptation A decrement in response to a stimulus presented repeatedly; does not generalize to other similar stimuli, provided there is a change in at least one parameter.

subparafascicular nucleus Group of neuron cell bodies in the posterior thalamus, thought to be a site for integration of auditory and nociceptive information.

substantia nigra Group of neuron cell bodies in the ventral midbrain that is part of the basal ganglia system and plays a role in motor control.

superior colliculus Midbrain center that receives input from visual system, auditory system, and other sensory systems and is involved in orienting reflexes.

superior olivary complex (SOC) A group of nuclei in the lower brainstem that includes the lateral superior olive (LSO), medial superior olive (MSO), medial nucleus of the trapezoid body (MNTB), and a number of periolivary cell groups. In most mammals the principal nuclei of the SOC (MSO and LSO) perform comparisons of sound at the two ears.

trigeminal nucleus Complex of sensory and motor neurons serving the trigeminal (fifth cranial) nerve.

ventral cochlear nucleus (VCN) One of two major anatomical divisions of the cochlear nucleus; receives direct input from the auditory nerve; comprises the anteroventral and posteroventral cochlear nuclei.

ventral nucleus of the lateral lemniscus (VNLL) A group of neuron cell bodies located between the ascending fibers of the lateral lemniscus, just ventral to the intermediate nucleus. The VNLL receives input from the contralateral anteroventral cochlear nucleus and ipsilateral medial nucleus of the trapezoid body. It projects to the ipsilateral inferior colliculus.

vestibular nuclei Groups of neuron cell bodies in the lower brainstem that receive input related to balance and acceleration from the vestibular system via the vestibular branch of the eighth cranial nerve.

3.42.1 Sources of Ascending Inputs to the Inferior Colliculus

The inferior colliculus (IC) receives a diverse assortment of inputs from multiple sources. These include monaural and binaural ascending pathways as well as intrinsic, descending, motor-related, polysensory, and modulatory inputs. The anatomical details of the main auditory pathways to the IC have been described in a number of previous reviews (e.g., Covey, E. and Casseday, J. H., 1995; Casseday, J. H. *et al.*, 2002; Cant, N. B. and Benson, C. G., 2003; Covey, E. and Carr, C. E., 2004; Cant, N. B., 2005; Saldana, E. and Merchan, M. A., 2005; Schofield, B. R., 2005; Winer, J. A., 2005), and are summarized in Figure 1. The various pathways have usually been

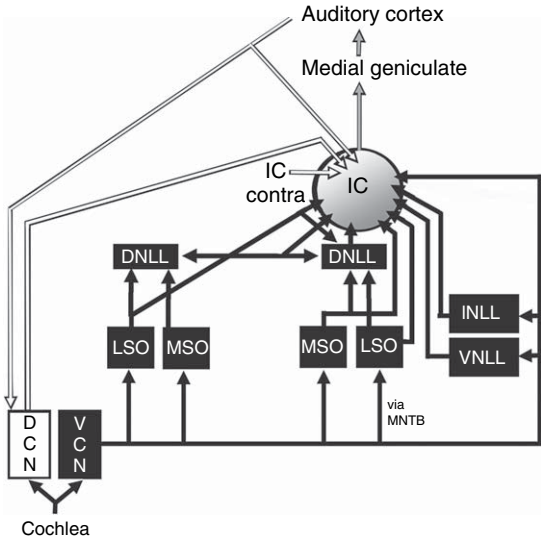

Figure 1 Block diagram illustrating the major auditory pathways to the inferior colliculus (IC). Direct and indirect pathways originating in the ventral cochlear nucleus (VCN system) are shown in black, those originating in the DCN, auditory cortex, and opposite IC (DCN system) are shown in white. Shading in the IC illustrates the dominance of the DCN system dorsally and the VCN system ventrally. DNLL, dorsal nucleus of the lateral lemniscus; INLL, intermediate nucleus of the lateral lemniscus; LSO, lateral superior olive; MNTB, medial nucleus of the trapezoid body; MSO, medial superior olive; cochlear nucleus; VNLL, ventral nucleus of the lateral lemniscus.

considered individually rather than as an integrated system, so this chapter will focus on evidence for graded patterns of input and the nature of the anatomical relationships among the various pathways. It will also briefly consider the possible functional consequences of interactions among different sources of input with graded patterns of distribution.

Although many studies in the past have been based on the hypothesis that the inputs from different sources are segregated within the IC, the evidence that has accumulated to date overwhelmingly indicates that there is at least some degree of overlap in every region of the IC, with inputs from each source forming density gradients throughout one or more spatial dimensions. The functional implication of this organizational principle is that neurons in every part of the IC have the opportunity to integrate information that originates in different pathways. In fact, such integration must be a major function of the IC (Casseday, J. H. and Covey, E., 1996). The relative contributions of all of the different pathways vary across the extent of the IC so that, functionally, each point within the IC lies at a set of coordinates in a multidimensional matrix in which the inputs from different sources have a unique ratio in terms of their strengths.

3.42.2 Parsing the Pathways to the Inferior Colliculus

The principal source of input to the IC is, of course, the ascending system of projections from the brainstem auditory nuclei (Figure 1). These include dense projections from the cochlear nucleus directly, as well as indirectly via the superior olivary complex (SOC) and nuclei of the lateral lemniscus (NLL). Because the indirect pathways via the SOC and NLL involve one or more additional synapses, it is likely that they provide a longer range of latencies than does the cochlear nucleus (Haplea, S. *et al.*, 1994).

3.42.2.1 Direct and Indirect Pathways

Because of the complexity of the ascending auditory inputs, it is possible to group these projections into different systems depending on what criterion is applied. For example, we can think of the inputs to the IC as forming direct and indirect systems of pathways in which those from the different subdivisions and cell types of the contralateral cochlear nucleus provide a fast, relatively unprocessed view of the incoming information, while those via the SOC and NLL provide a view that has been processed at one or more stages to extract information about binaural differences or specific features of temporal patterns.

3.42.2.2 Binaural and Monaural Pathways

An even more frequent way of parsing is to group ascending inputs to the IC into binaural and monaural pathways, a sort of auditory analog of the what and where pathways in the visual system, with binaural inputs originating in the SOC and dorsal nucleus of the NLL (DNLL), and monaural inputs originating in the contralateral cochlear nucleus and the intermediate and ventral nuclei of the NLL (INLL and VNLL, respectively). Both of these views are based on solid evidence, and are unquestionably valid. However, they are not without their limitations. For example, it is doubtful that the dorsal cochlear nucleus (DCN), which provides a direct pathway to the IC, conveys a simple, primarylike view of the auditory stimulus given that it receives

polysensory input as well as a significant amount of descending input from the auditory cortex (e.g., Ryugo, D. K. *et al.*, 2003). The distinction between binaural and monaural pathways is somewhat blurred for several reasons. A given pathway may be binaural or monaural depending on species, the best example being the medial superior olive (MSO), which is binaural in carnivores and rodents and monaural in some species of bats (for review, see Grothe, B. and Park, T. J., 2000). Pathways that are traditionally considered monaural are almost without exception known to receive at least some binaural input, one example being crossed projections from one anteroventral cochlear nucleus (AVCN) to the other (e.g., Schofield, B. R. and Cant, N. B., 1996).

3.42.2.3 Gradient Systems of Pathways

A different way to parse the inputs to the IC is in terms of the density gradients that they form. There is considerable evidence that the projections to the IC take the form of at least two opposing gradients approximately orthogonal to the main tonotopic progression, a DCN system in which the density of projections decreases from dorsomedial to ventrolateral, and a ventral cochlear nucleus (VCN) system, in which the density decreases from ventrolateral to dorsomedial. The following sections will present evidence for this system of gradients, review what is known about the finer grained organization of axon terminals from different sources within each system and between the two systems, and consider some of the integrative processes that might result.

3.42.3 Projection Gradients in the Inferior Colliculus

3.42.3.1 The Ventral Cochlear Nucleus System

The bulk of the projections from the different subdivisions and projecting cell types of the contralateral cochlear nucleus terminate in a partially to completely overlapping fashion in the central nucleus of the IC. Depending on species, the projections may extend to a greater or lesser extent into areas outside the central nucleus (e.g., Ryugo, D. K. *et al.*, 1981; Zook, J. M. and Casseday, J. H., 1982; Willard, F. H. and Martin, G. F., 1983; Oliver, D. L., 1984; Whitley, J. M. and Henkel, C. K., 1984; Oliver, D. L., 1985; Zook, J. M. and Casseday, J. H., 1985; Coleman, J. R. and Clerici, W. J., 1987; Zook, J. M. and Casseday, J. H., 1987; Oliver, D. L. *et al.*, 1997; Oliver, D. L. *et al.*, 1999). There is little evidence in any species that would suggest a strictly nucleotopic projection pattern, or one in which inputs are strictly segregated into different regions of the IC. Figures 2 and 3 show results of an early experiment in the mustached bat in which the distribution of projections from the VCN was compared with that of projections from the DCN (Zook, J. M. and Casseday, J. H., 1985). These authors found that although there is a small dorsal portion of the IC that receives input only from DCN, the projections from the posteroventral cochlear nucleus (PVCN), AVCN, and DCN overlap throughout most of the IC. Despite the extensive overlap, the projections from the VCN and DCN form gradients of opposite density, with the projections of DCN most dense dorsally and those from VCN most dense ventrally. This pattern has been confirmed in other mammalian species (for review see Casseday, J. H. *et al.*, 2002).

Although both VCN and DCN receive direct input from the cochlea via branches of the auditory nerve as well as some descending input from auditory nuclei higher in the central pathway, their structure, connections, and response properties are in many respects quite

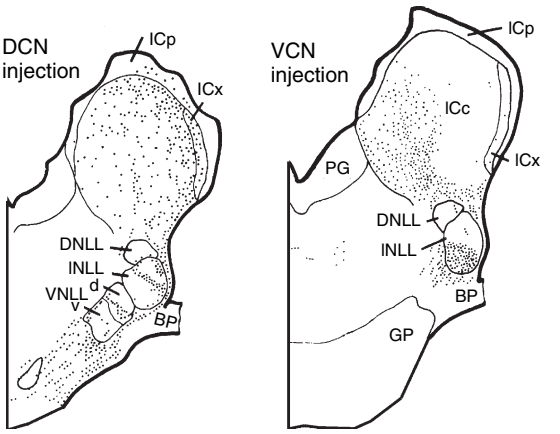

Figure 2 Distribution of label in the inferior colliculus (IC) after injections of anterograde tracers in the contralateral dorsal cochlear nucleus (DCN; left) and ventral cochlear nucleus (VCN; right). Both are frontal sections through the right side of the brain of the mustached bat, *Pteronotus parnellii*. BP, brachium pontis; DNLL, dorsal nucleus of the lateral lemniscus; GP, pontine gray; ICc, central nucleus of the IC; ICp, pericentral nucleus of the IC; ICx, external nucleus of the IC; PG, periaqueductal gray; VNLLd, dorsal division of the ventral nucleus of the lateral lemniscus; VNLLv, ventral division of the ventral nucleus of the lateral lemniscus. Adapted from Zook, J. M. and Casseday, J. H. 1985. Projections from the cochlear nuclei in the mustache bat, *Pteronotus parnellii*. J. Comp. Neurol. 237, 307–324.

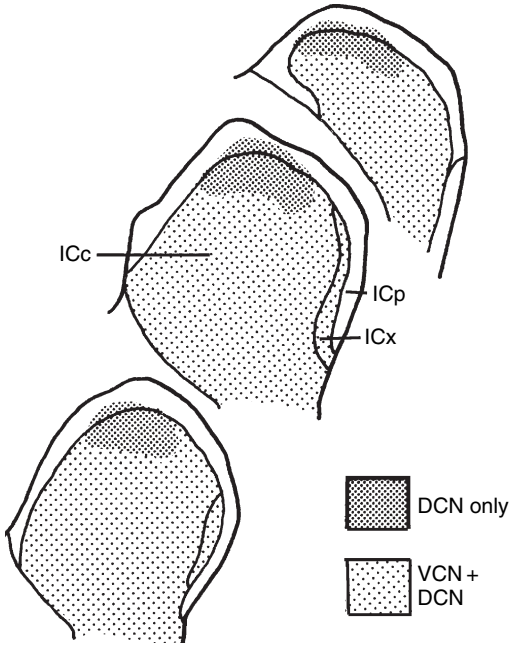

Figure 3 Summary diagram showing regions of the inferior colliculus (IC) that receive projections from both ventral cochlear nucleus (VCN) and dorsal cochlear nucleus (DCN; light shading) or DCN only (dense shading). Frontal sections through the right IC are arranged rostral to caudal, from top to bottom. ICc, central nucleus of the IC; ICp, pericentral nucleus of the IC; ICx, external nucleus of the IC. From Zook, J. M. and Casseday, J. H. 1985. Projections from the cochlear nuclei in the mustache bat, *Pteronotus parnellii*. J. Comp. Neurol. 237, 307–324.

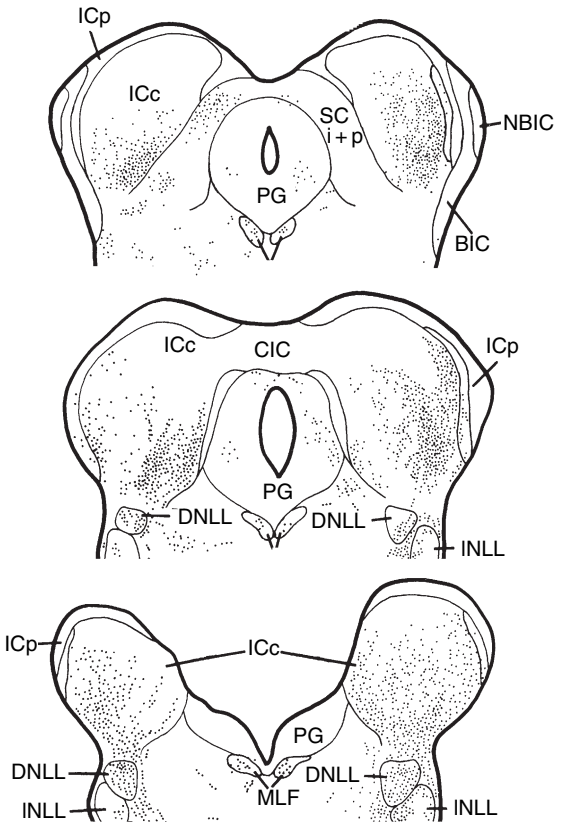

Figure 4 Distribution of anterograde label in the inferior colliculus (IC) bilaterally after an injection into part of the right medial superior olive (MSO) and lateral superior olive (LSO). Frontal sections through the brainstem of the mustached bat, arranged rostral to caudal, from top to bottom. BIC, brachium of the IC; CIC, commissure of the IC; DNLL, dorsal nucleus of the lateral lemniscus; i + p, intermediate and deep layers; ICc, central nucleus of the IC; ICp, pericentral nucleus of the IC; INLL, intermediate nucleus of the lateral lemniscus; MLF, medial longitudinal fasciculus; NBIC, nucleus of the brachium of the IC; PG, periaqueductal gray; SC, superior colliculus. Adapted from Zook, J. M. and Casseday, J. H. 1987. Convergence of ascending pathways at the inferior colliculus of the mustache bat, *Pteronotus parnellii*. J. Comp. Neurol. 261, 347–361.

different. The output of the VCN more closely reflects that of the auditory nerve than does that of the DCN, which receives descending input from the auditory cortex (Weedman, D. L. and Ryugo, D. K., 1996; Jacomme, A. V. *et al.*, 2003; Schofield, B. R. and Coomes, D. L., 2005) and the IC itself (e.g., Alibardi, L., 1999) as well as a variety of sources outside the auditory system (for a review, see Ryugo, D. K. *et al.*, 2003), including the dorsal column and cuneate nuclei, spinal trigeminal nuclei, somatosensory cortex (Itoh, K. *et al.*, 1987; Wright, D. D. and Ryugo, D. K., 1996; Li, H. and Mizuno, N., 1997; Wolff, A. and Kunzle, H., 1997; Zhou, J. and Shore, S., 2004; Haenggeli, C. A. *et al.*, 2005), vestibular nuclei (Bukowska, D., 2002), and pontine gray (Ohlrogge, M. *et al.*, 2001).

The opposing gradients in density of projections within the IC form the basis of a VCN system of projections in which density decreases from ventrolateral to dorsomedial, and a second, DCN system in which density decreases from dorsomedial to ventrolateral (Casseday, J. H. *et al.*, 2002). The inputs from the two systems overlap throughout much of the IC, albeit with different relative densities. This scheme becomes especially useful as an organizing principle when projections from other sources are added to the mix. Those structures that receive an input directly from the VCN, mainly the SOC and the NLL, all project to the IC in a gradient fashion similar to the direct projections from VCN, with the highest density ventrally (e.g., Vater, M. *et al.*, 1995; Oliver, D. L. *et al.*, 1997; Loftus, W. C. *et al.*, 2004). For easy comparison with the projections from the cochlear nucleus, Figure 4 shows an example of the pattern of labeled

terminals from a large injection of an anterograde tracer in the SOC in the mustached bat. The area containing label and the ventrolateral to dorsomedial density gradient are very similar to those seen after injections in the AVCN. Figure 5 shows an example, again from the mustached bat, of the pattern of labeled terminals resulting from an injection in the NLL. Clearly, if the label from the VCN, SOC, and NLL were superimposed, it would occupy a similar area, with a similar density gradient.

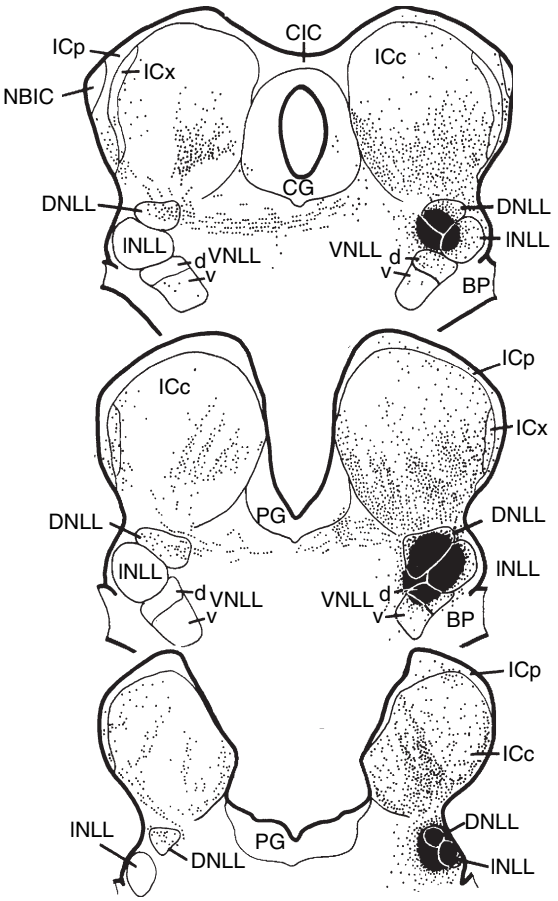

Figure 5 Distribution of anterograde label in the inferior colliculus (IC) bilaterally after an injection into part of the right nucleus of the lateral lemniscus (NLL), including the ventral nucleus of the lateral lemniscus (VNLL), intermediate nucleus of the lateral lemniscus (INLL), and dorsal nucleus of the lateral lemniscus (DNLL). Frontal sections through the brainstem of the mustached bat, arranged rostral to caudal, from top to bottom. BP, brachium pontis; CIC, commissure of the IC; DNLL, dorsal nucleus of the lateral lemniscus; ICc, central nucleus of the IC; ICp, pericentral nucleus of the IC; ICx, external nucleus of the IC; NBIC, nucleus of the brachium of the IC PG, periaqueductal gray. Adapted from Zook, J. M. and Casseday, J. H. 1987. Convergence of ascending pathways at the inferior colliculus of the mustache bat, *Pteronotus parnellii*. J. Comp. Neurol. 261, 347–361.

The current evidence suggests that the ipsilateral MSO and contralateral lateral superior olive (LSO) provide excitatory input to the IC, and the ipsilateral LSO provides glycinergic inhibitory input (e.g., Saint Marie, R. L. *et al.*, 1989; Saint Marie, R. L. and Baker, R. A., 1990; Glendenning, K. K. *et al.*, 1992; Oliver, D. L. *et al.*, 1995; see Oliver, D. L., 2000 for review). The ventral NLL (VNLL) and INLL appear to provide a mixture of excitatory projections, gamma-aminobutyric acid (GABA)ergic inhibitory projections, and glycinergic inhibitory projections, while the dorsal NLL (DNLL) provides a bilateral GABAergic projection (Gonzalez-Hernandez, T. *et al.*, 1996; Vater, M. *et al.*, 1997; Zhang, D. X. *et al.*, 1998). Therefore the VCN system alone provides ample opportunity for direct and indirect excitatory and inhibitory inputs to interact throughout most of the IC.

3.42.3.2 The Dorsal Cochlear Nucleus System

As already shown in Figures 1 and 2, the pathway from DCN terminates most densely in the dorsal part of the IC including the pericentral regions (or dorsal cortex and external nucleus, depending on the nomenclature used). Other pathways that terminate in a pattern similar to that of the DCN projections include the descending projections from multiple subdivisions of the auditory cortex (Herrera, M. *et al.*, 1994; Saldana, E. *et al.*, 1996; Druga, R. *et al.*, 1997; Winer, J. A. *et al.*, 1998; Budinger, E. *et al.*, 2000; Marsh, R. A. *et al.*, 2002; Bajo, V. M. and Moore, D. R., 2005), and the commissural projections from the opposite IC (Gonzalez-Hernandez, T. *et al.*, 1996). The dorsomedial to ventrolateral gradient of the cortical projection to the IC of the rat can be seen in Figure 6. This figure also illustrates the point that the projection does not respect the cytoarchitectural subdivisions drawn by the authors, but rather forms a set of gradients that begin densely in the dorsomedial portion of the IC, extending through the dorsal cortex, external cortex, and central nucleus, becoming less dense ventrolaterally. The corticofugal projections appear to be excitatory (e.g., Saldana, E. *et al.*, 1996), as are those from the DCN (reviewed in Cant, N. B. and Benson, C. G., 2003).

The projections from the opposite IC also form a dorsomedial to ventrolateral density gradient. Figure 7 shows an example of anterograde transport from two small injections in the right IC of the rat (Saldana, E. and Merchan, M. A., 1992). These authors make the

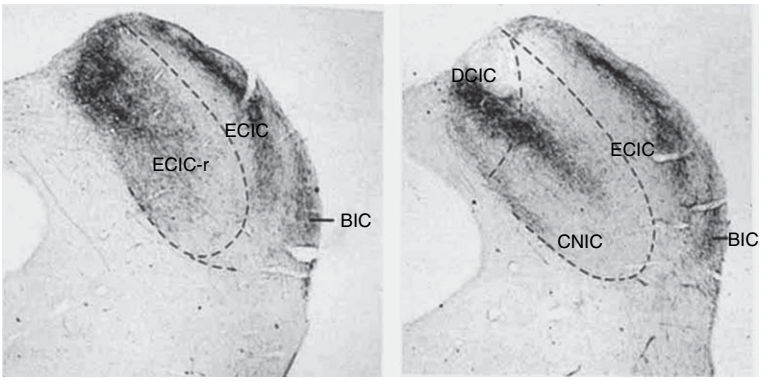

Figure 6 Photomicrographs showing distribution of anterograde label in the inferior colliculus (IC) of the rat after an injection in auditory cortex. Frontal sections through the right IC, arranged rostral to caudal from left to right. BIC, brachium of the IC; CNIC, central nucleus of the IC; DCIC, dorsal cortex of the IC; ECIC, external cortex of the IC; ECIC-r, rostral pole of the external cortex of the IC. Adapted from Saldana, E., Feliciano M., Mugnaini E. 1996. Distribution of descending projections from primary auditory neocortex to inferior colliculus mimics the topography of intracollicular projections. J. Comp. Neurol. 371, 15–40.

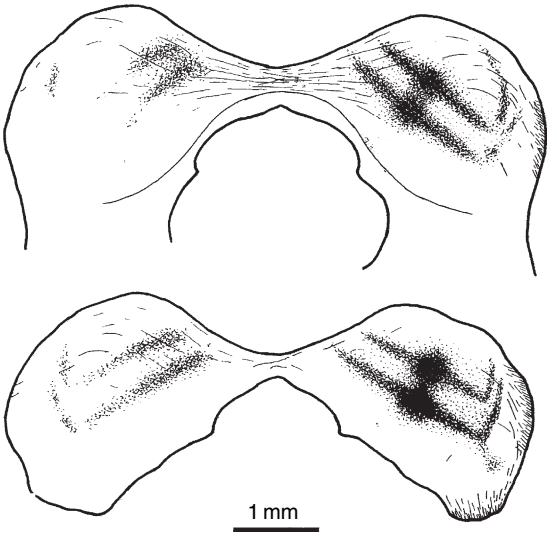

Figure 7 Drawings of frontal sections through the inferior colliculus (IC) of the rat showing 2 small tracer injections on the right side and anterograde transport on the left side. Adapted from Saldana, E. and Merchan, M. A. 1992. Intrinsic and commissural connections of the rat inferior colliculus. J. Comp. Neurol. 319, 417–437.

point that the commissural and corticofugal projections to the IC must overlap extensively. The projections from the opposite IC appear to provide a mixture of glutamatergic excitation and GABAergic inhibition (Gonzalez-Hernandez, T. *et al.*, 1996; Moore, D. R. *et al.*, 1998; Malmierca, M. S. *et al.*, 2003; 2005).

Inputs from nonauditory structures that presumably contribute a modulatory influence include serotonergic inputs from the dorsal raphe nuclei (Klepper, A. and Herbert, H., 1991; Thompson, A. M. *et al.*, 1994; Hurley, L. M. and Thompson, A. M., 2001) and noradrenergic inputs from the locus coeruleus (Klepper, A. and Herbert, H., 1991). Both serotonin and norepinephrine terminals are most dense dorsomedially and in the pericentral areas of the IC, becoming progressively less dense ventrolaterally. Figure 8 shows the distribution of fibers and terminals immmunostained for serotonin. Thus, the distribution of monoamine modulatory transmitters closely follows the DCN system pattern. Interestingly, serotonin terminal density is known to be higher in DCN than in other parts of the cochlear nucleus, suggesting that the entire DCN system of projections is more subject to modulatory influences than the VCN system.

The DCN system provides a system of inputs from areas that presumably represent relatively complex stages of processing. As in the AVCN system, these may be excitatory or inhibitory and more or less direct and, as will be seen below, there is ample opportunity for interaction between the two systems throughout much of the IC.

The IC also receives projections from thalamic regions including the medial division of the medial geniculate body, periaqueductal gray, posterior limitans nucleus, substantia nigra, peripeduncular/suprapeduncular nucleus, subparafascicular and posterior intralaminar nuclei, nucleus of the brachium of the IC, lateral tegmental/lateral mesencephalic areas, and deep layers of the superior colliculus (Winer, J. A. *et al.*, 2002), but the pattern of termination of these pathways within the IC is not clear.

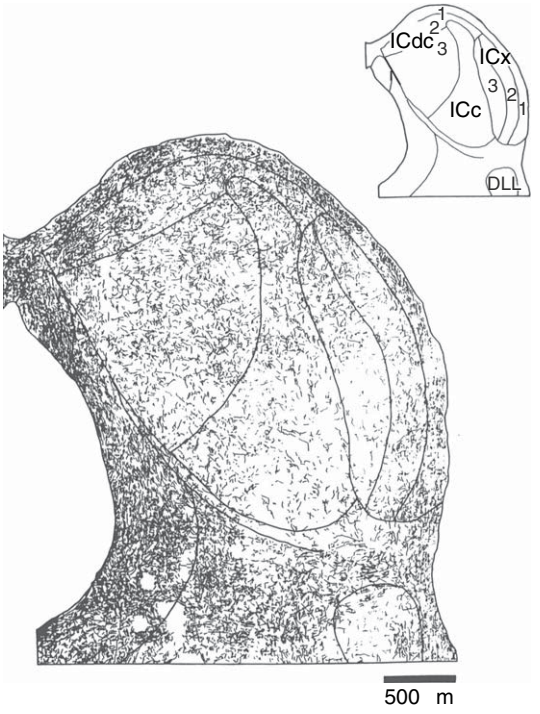

Figure 8 Distribution of immunoreactivity for serotonin in a frontal section through the right inferior colliculus (IC) of the rat. Inset shows IC subdivisions. DLL, dorsal nucleus of the laternal lemniscus; ICc, central nucleus of the IC; ICdc, dorsal cortex of the IC; ICx, external nucleus of the IC. Reproduced from Klepper, A. and Herbert, H. 1991. Distribution and origin of noradrenergic and serotonergic fibers in the cochlear nucleus and inferior colliculus of the rat. Brain Res. 557, 190–201, with permission from Elsevier.

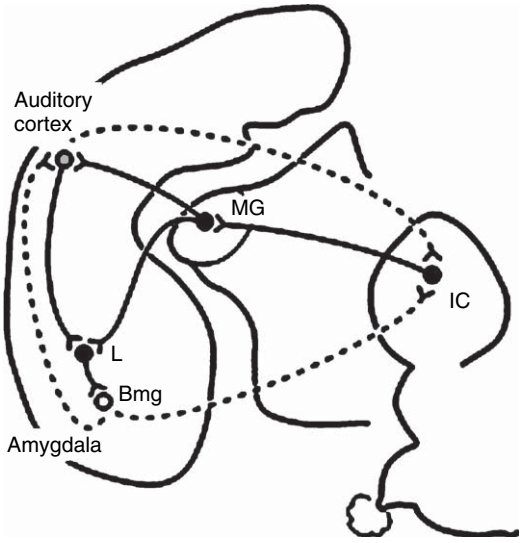

Figure 9 Connections between the inferior colliculus (IC), auditory cortex, and amygdala. Solid lines show feedforward projections, dotted lines feedback projections. L, lateral nucleus of the amygdala; Bmg, magnocellular subdivision of the basal nucleus of the amygdala; MG, medial geniculate. From Marsh, R. A., Fuzessery, Z. M., Grose, C. D., and Wenstrup, J. J. 2002. Projection to the inferior colliculus from the basal nucleus of the amygdala. J. Neurosci. 22, 10449–10460.

3.42.3.3 Other Types of Gradients or Distributions

The IC receives some inputs that do not appear to follow the DCN/VCN pattern. For example, the amygdala projects throughout virtually the entire IC, but in a gradient that is low dorsomedially and ventrolaterally, peaking somewhere near the middle (Marsh, R. A. *et al.*, 2002). Figure 9 illustrates the circuit that includes the IC, auditory cortex, and amygdala and makes the point that as in most or all of the other systems discussed here, there are direct and indirect pathways from the auditory cortex to the IC, including a widespread projection via the amygdala. This suggests that responses of neurons in the IC are subject to direct modulation by emotional state.

Other nonauditory influences on IC neurons include inputs from pathways related to motor activity and arousal. In general, these nonauditory pathways have been reported to project to the external cortex (or pericentral region) of the IC. These include the trigeminal nucleus (Kunzle, H., 1998), the globus pallidus (Shammah-Lagnado, S. J. *et al.*, 1996), the nucleus incertus, a structure thought to be involved in arousal (Olucha-Bordonau, F. E. *et al.*, 2003), and the ventrolateral tegmentum, an area that may be involved is sensory–motor integration (Herbert, H. *et al.*, 1997). It is not clear whether these projections are strictly confined to the external cortex, or whether they are simply most dense in that region.

3.42.4 Relationships Among Projections from Different Sources

3.42.4.1 Laminar Projections Within the Anteroventral Cochlear Nucleus System

Although the opposing gradient systems provide a useful general framework in which to consider the organization of the IC, within each system there are additional levels of organization that probably are important for the function of the IC. Many studies have observed that anterograde transport to the IC from injections in single structures that provide

afferent input often takes the form of bands and/or patches. This banding pattern can be seen most clearly in projections from the LSO, MSO, and DNLL, i.e., structures of the binaural system (see Figures 4 and 5). The extent of banding may vary across species, and there may be consistent differences depending on the source of the transport. For example, Shneiderman A. and Henkel C. K. (1987) found that anterograde transport from LSO in the cat formed bands of dense label about 150–200 μm thick, separated by bands of similar thickness that contained little label. The bands paralleled the fibrodendritic laminae of the IC, and presumably the isofrequency laminae. The bands originating from the ipsilateral LSO were prominent while those originating from the contralateral LSO were more diffuse. In cases in which two different anterograde tracers were used, one placed in the LSO of each side, they found that the bands from the two sides interdigitated or partly overlapped, suggesting that there was some segregation of the ipsilateral and contralateral inputs from the two sides within a lamina.

Patterns of projections from the ipsilateral MSO and contralateral LSO have also been compared in the mustached bat using different anterograde tracers (Vater, M. *et al.*, 1995; Figure 10). Projections from frequency-matched areas in the LSO and MSO terminated in much the same regions of the IC, and had a somewhat banded appearance with partial overlap of many of the bands. When viewed in a parasagittal reconstruction, low-frequency projections almost completely overlapped, but for the higher frequencies, the projections from MSO extended somewhat more dorsally and rostrally than those from LSO (Figure 11).

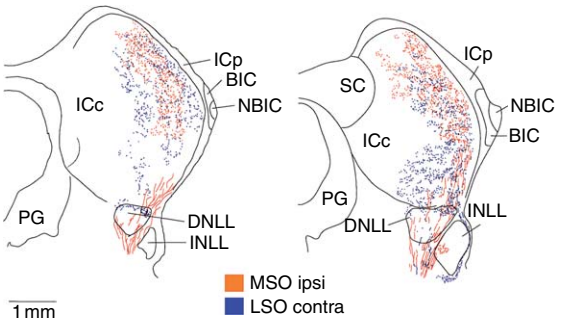

Figure 10 Comparison of the distribution of transport from injections of two anterograde tracers, one in a low-frequency region of the ipsilateral medial superior olive (MSO; orange) and another in a low frequency region of the contralateral lateral superior olive (LSO; blue). Frontal sections through the right inferior colliculus (IC) of the mustached bat, arranged caudal to rostral from left to right. BIC, brachium of the IC; DNLL, dorsal nucleus of the lateral lemniscus; ICc, central nucleus of the IC; ICp, pericentral nucleus of the IC; NBIC, nucleus of the brachium of the IC; PG, periaqueductal gray; SC, superior colliculus. Adapted from Vater, M., Casseday, J. H., and Covey, E. 1995. Convergence and divergence of ascending binaural and monaural pathways from the superior olives of the mustached bat. J. Comp. Neurol. 351, 632–646.

Loftus W. C. *et al.* (2004) added another level of complexity to the analysis of projections from the binaural pathways of the VCN system by comparing the patterns of anterograde transport from the ipsilateral MSO, ipsilateral LSO, and contralateral LSO in the cat. These authors reported that within a fibrodendritic lamina, boutons from MSO terminated mainly in the central and caudal parts of a lamina while those from LSO were more concentrated more rostrally within the lamina, and at the ventral edge of the input from MSO (Figure 12), with a denser and more clearly banded projection from the ipsilateral LSO than from the contralateral.

The projection from the DNLL of cats and ferrets is also banded (Shneiderman, A. *et al.*, 1988; Henkel, C. K. *et al.*, 2003), but in this case, the bands from the contralateral DNLL were found to be prominent while those from the ipsilateral DNLL were more diffuse. This pattern can be seen in the mustached bat in Figure 5, suggesting that it is common across species. Gabriele M. L. *et al.* (2000) found that unilateral cochlear ablation in rat pups disrupts the banded pattern of DNLL afferents in the IC, suggesting that the pattern of banded projections is determined during development by activity-dependent mechanisms.

3.42.4.2 Relation between Dorsal Cochlear Nucleus and Ventral Cochlear Nucleus System Projections

Oliver D. L. *et al.* (1997) examined the relation between projections from the contralateral LSO and DCN of the cat. As in other species, the DCN projection extended farther in the dorsomedial dimension than did that from LSO, but within the more ventral area there was considerable overlap (Figure 13). Measurements made in the regions that contained label from both sources indicated that the LSO axons were coextensive with the DCN axons about 80–90% of the time, but that there were small patches where only one projection was present. On the basis of these findings, the authors proposed a model of functional zones or modules within a fibrodendritic lamina, with DCN dominating dorsally and inputs

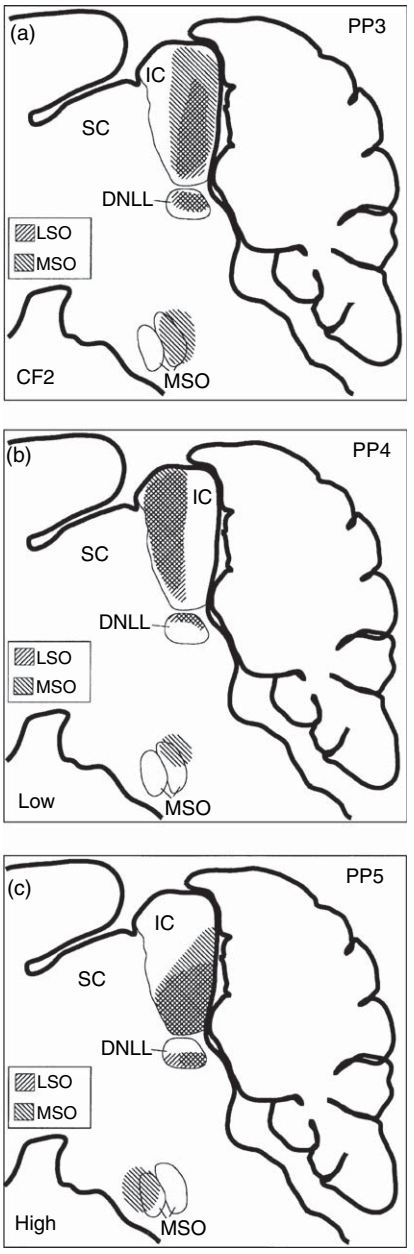

Figure 11 Parasagittal reconstructions to compare the extent of anterograde label from medial superior olive (MSO) and lateral superior olive (LSO) in three different frequency ranges in the inferior colliculus (IC) of the mustached bat. Top panel: CF2 is the frequency of the dominant harmonic of this species' echolocation call (approximately 62 kHz). This frequency occupies an expanded representation at every level of the auditory system. Low frequencies are those below CF2, and high frequencies those above CF2. DNLL, dorsal nucleus of the lateral lemniscus; SC, superior colliculus. From Vater, M., Casseday, J. H., and Covey, E. 1995. Convergence and divergence of ascending binaural and monaural pathways from the superior olives of the mustached bat. J. Comp. Neurol. 351, 632–646.

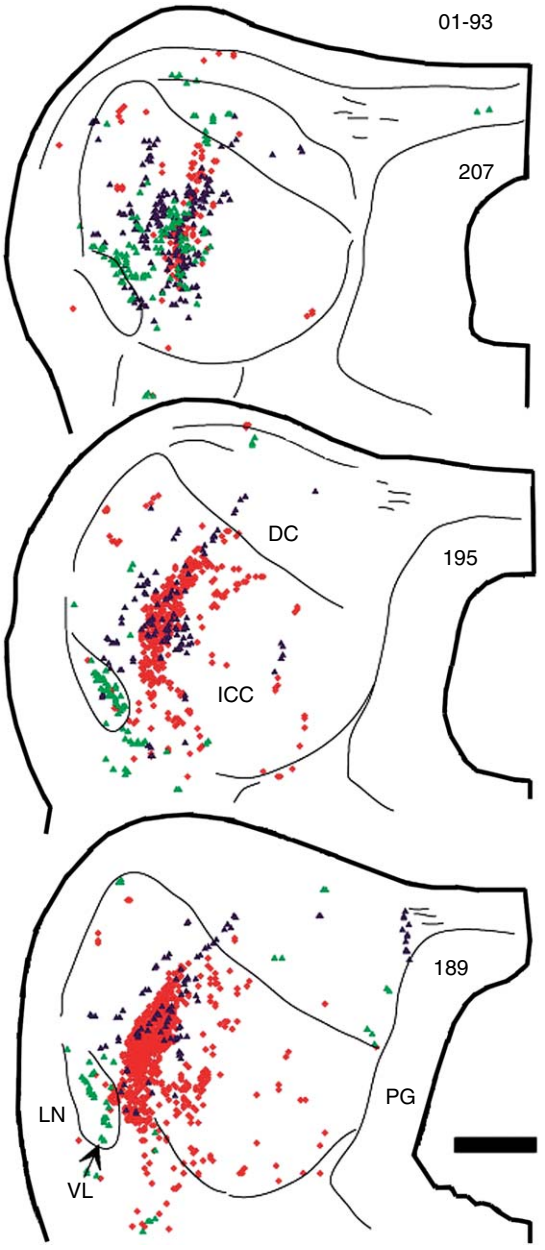

Figure 12 Frontal sections through the left inferior colliculus (IC) of the cat to compare the distribution of anterograde label from the medial superior olive (MSO; red), contralateral lateral superior olive (LSO; green) and ipsilateral LSO (blue). Sections are arranged rostral to caudal from top to bottom. DC, dorsal cortex; ICc, central nucleus of the IC; LN, lateral nucleus; PG, periaqueductal gray; VL, ventrolateral nucleus. From Loftus W. C. *et al*. (2004).

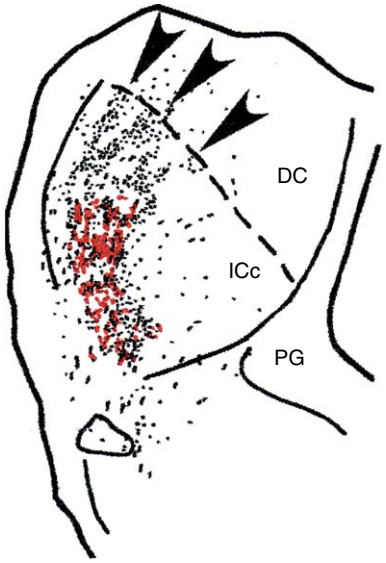

Figure 13 Frontal section through the left inferior colliculus (IC) of the cat showing the relation between anterograde transport from the contralateral lateral superior olive (LSO; red) and the contralateral dorsal cochlear nucleus (DCN) (black). Arrows point to a faint banded pattern in the central nucleus. DC, dorsal cortex; ICc, central nucleus of the IC; PG, periaqueductal gray.

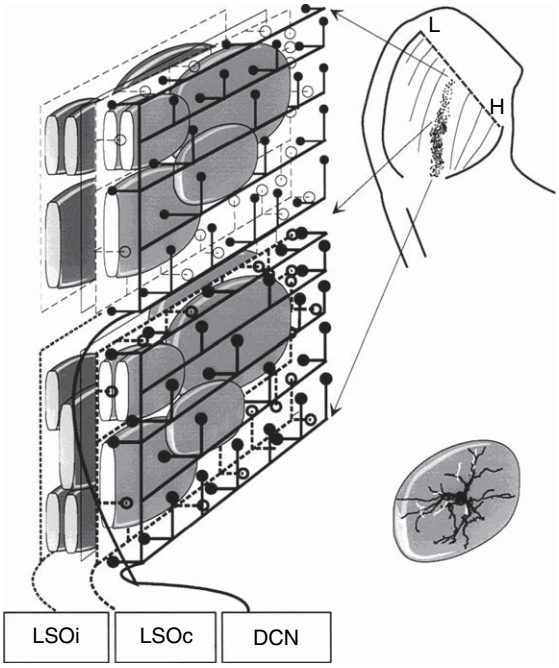

Figure 14 Model of functional zones or modules within a fibrodendritic lamina based on patterns of termination of axons from the dorsal cochlear nucleus (DCN), ipsilateral lateral superior olive (LSOi), and contralateral lateral superior olive (LSOc). The inset at the top right shows the location of the lamina that contains label within the tonotopic organization of the inferior colliculus. The small inset at the lower right shows a disk-shaped cell and its dendritic tree surrounded by a gray disk. Similar disks are used in the model to indicate the dendritic fields of individual disk-shaped neurons. The DCN axons terminate on both the dorsal and ventral parts of the lamina, but the LSO axons terminate only on the ventral part. The input from the contralateral LSO is mainly concentrated on one side of the lamina and that from the LSOi on the other side. L, low frequency; H, high frequency. From Oliver, D. L., Beckius, G. E., Bishop, D. C., and Kuwada, S. 1997. Simultaneous anterograde labeling of axonal layers from lateral superior olive and dorsal cochlear nucleus in the inferior colliculus of cat. J. Comp. Neurol. 382, 215–229.

from both sources interacting more ventrally except in a few small patches where only one input was present. In this model (Figure 14), afferents from the ipsilateral LSO are shown terminating on one side of the lamina and afferents from the contralateral LSO and DCN on the other side. The functional consequences of such a modular arrangement are unknown.

It should be kept in mind that all of the studies of this type conducted to date have examined the relationship between only two or, at most, three inputs to the IC. Given the large number of inputs that all project to the IC in a banded pattern with approximately the same spatial frequency, there must be considerable overlap among the bands from different sources as well as overlap between banded and nonbanded afferents.

3.42.5 Relation with Intrinsic Connections

The IC not only receives projections from outside sources; it also has an extensive system of intrinsic projections. Oliver D. L. *et al.* (1991) used intracellular injection of IC neurons in the cat to show that axons of IC neurons make local connections, and that at least some of them send branches both locally and to the brachium of the IC. The intrinsic projections appear to parallel the ascending projections (Saldana, E. and Merchan, M. A., 1992) as well as the crossed projections from the opposite IC (Malmierca, M. S. *et al.*, 1995). The intrinsic projections are confined to an isofrequency lamina as defined electrophysiologically, and the bulk of the projections ascend from ventrolateral to dorsomedial (Miller, K. E. *et al.*, 2005), creating a cascaded system of projections that includes progressively more multisynaptic inputs moving dorsomedially (Figure 15). Such a system would be ideally suited to create delay lines for processing temporal patterns of

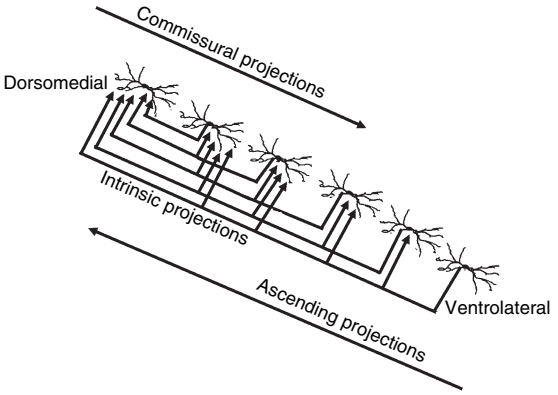

Figure 15 Schematic diagram to illustrate cascaded pattern of intrinsic projections within an isofrequency lamina of the inferior colliculus (IC). Neurons in the ventrolateral part of the lamina project to those located more dorsomedially. As a result, neurons in the dorsomedial part of the lamina have the opportunity to receive both direct and multisynaptic inputs from their more ventral counterparts. There is also opportunity for intrinsic inputs to converge with ascending inputs as well as descending and commissural inputs.

sound. The intrinsic inputs provide glutamatergic excitation (Saint Marie, R. L., 1996), and may also contain a GABAergic component (Fremouw, T. *et al.*, 1999). Because each fibrodendritic lamina has a system of intrinsic projections, there is ample opportunity for interaction of intrinsic inputs with ascending and descending inputs at every point within the lamina.

3.42.6 Biochemical Gradients

The IC receives both GABAergic and glycinergic inhibitory inputs. Because the only known sources of glycinergic input are in the lower brainstem pathways, particularly the SOC and NLL, it is not surprising that immunoreactivity for glycine and glycine receptors follows a pattern in which density is greatest ventrolaterally and lowest dorsomedially (Winer, J. A. *et al.*, 1995; Fubara, B. M. *et al.*, 1996; Casseday, J. H. *et al.*, 2003). However, instead of a continuous gradient, glycine and glycine receptor reactivity peaks in a crescent-shaped area just interior to the ventrolateral edge of the IC (Figure 16). The distribution of GABA immunoreactivity and $GABA_A$ receptors is the mirror image of the glycine distribution, with the lowest levels found in the crescent-shaped area that has the highest level of glycine (Winer, J. A. *et al.*, 1995; Casseday, J. H. *et al.*, 2003; Figure 16). $GABA_B$ receptors are most highly

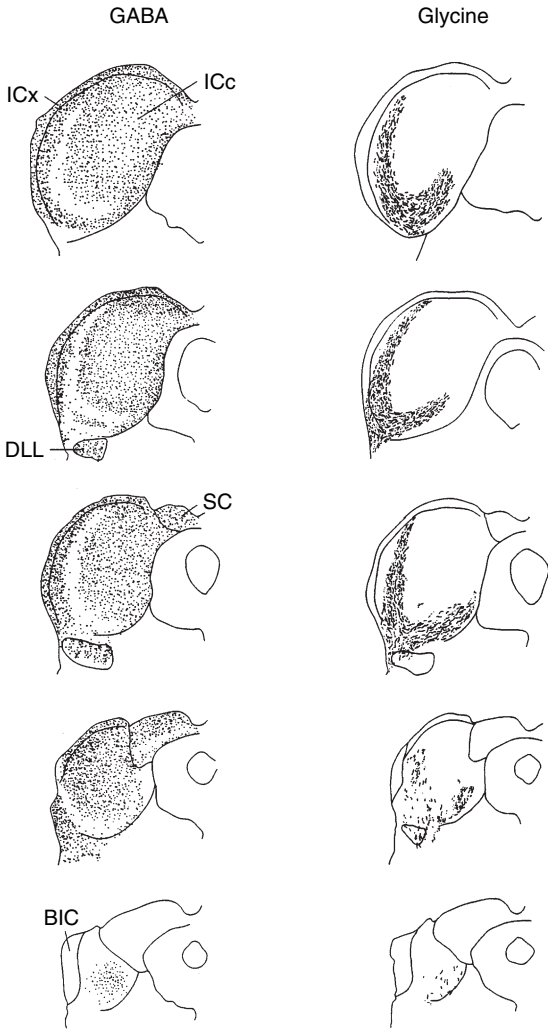

Figure 16 Distribution of immunoreactivity for gamma-aminobutyric acid (GABA; left column) and glycine (right column) in frontal sections through the left inferior colliculus (IC) of the big brown bat, *Eptesicus fuscus*. BIC, brachium of the IC; DLL, dorsal nucleus of the lateral lemniscus; ICc, central nucleus of the IC; ICx, external nucleus of the IC; SC, superior colliculus. From Casseday, J. H., Fremouw, T., and Covey, E. 2002. The Inferior Colliculus: Hub of the Auditory System. In: Springer Handbook of Auditory Research, Volume 15, Integrative Functions in the Mammalian Auditory Pathway (eds. D. Oertel, A. N. Popper, and R. R. Fay), pp. 238–318. Newyork: Springer.

expressed in the dorsomedial region of the IC where the DCN projection system terminates most densely (Fubara, B. M. *et al.*, 1996).

Serotonin has already been mentioned as being distributed in a pattern that corresponds to the DCN system gradient. Acetylcholine is also present in the IC, but its source is not entirely clear. Both of these neurotransmitters, when applied iontophoretically to

IC neurons during presentation of auditory stimuli, have effects that vary both quantitatively and qualitatively from one cell to another, suppressing responses in some and enhancing them in others (Farley, G. R. *et al.*, 1983; Habbicht, H. and Vater, M., 1996; Hurley, L. M. and Pollak, G. D., 1999). Serotonin has also been reported to change the subset of species-specific calls to which bat IC neurons responded (Hurley, L. M. and Pollak, G. D., 2005). Because of the mixed effects of the modulatory neurotransmitters, is likely that their effect depends on the other inputs that the neuron receives and on its intrinsic properties.

3.42.7 Evidence for Functional Gradients

It is clear from the anatomical evidence that there are multiple direct and indirect excitatory, inhibitory, and modulatory pathways to the IC. The multiple inputs provide different latencies, discharge patterns, tuning, thresholds, and binaural characteristics. Some subset of these pathways converge at every point throughout the IC, so there is ample opportunity for interaction of delayed and undelayed responses through direct and multisynaptic pathways, including intrinsic connections within the fibrodendritic laminae. The basic mechanisms through which multiple synaptic inputs interact have been described and reviewed elsewhere (e.g., Covey, E. *et al.*, 1996; Covey, E. and Casseday, J. H., 1998; 1999; Covey, E., 2004; Covey, E. and Faure, P. A., 2005). Because most of the inputs to the IC are not spatially homogeneous, but rather take the form of gradients, it might be expected that functional properties would vary continuously across the extent of the IC. There is some electrophysiological evidence suggesting that this is indeed the case.

There are at least a few studies that show evidence for gradients in a number of different response properties in the IC. Some of these gradients are consistent with the dorsomedial-to-ventrolateral pattern of the VCN and DCN systems, and others are not. Those that are generally consistent include discharge pattern, response latency, selectivity to modulation rate, selectivity for complex stimuli, stimulus-specific adaptation, and novelty responses.

In the mouse the proportion of transient responses is high in the dorsal part of the IC, decreasing ventrally (Reetz, G. and Ehret, G., 1999). These findings suggest that there is a stronger influence of inhibition dorsally than ventrally, or at least inhibition that would affect the later part of the response. Response latencies of IC neurons cover a broad range, from about 3 ms to more than 50 ms, and there are several studies in cats and bats that indicate that latencies are roughly organized in a dorsal-to-ventral gradient, with the longest latencies dorsally (Langner, G. 1992; Park, T. J. and Pollak, G. D., 1993; Hattori, T. and Suga, N., 1997). It might be supposed that convergence of excitatory and inhibitory inputs would lengthen latency, but blocking GABAergic and glycinergic inhibition has little effect on IC neurons' latencies (Fuzessery, Z. M. *et al.*, 2003). Even in cases where blocking inhibition causes latency to shorten, the amount of shortening is much less than would be required to produce the range of latencies seen in the IC (Casseday, J. H. *et al.*, 2000). All of these data are consistent with the idea that cascaded feedforward excitatory projections of the type seen in both the intrinsic and extrinsic projections to the IC may be the primary mechanism for progressively lengthening latencies dorsally in the IC without a need for inhibition, and for setting up delay lines that could participate in further processing of complex sounds (Miller, K. E. *et al.*, 2005).

Some IC neurons are selective for the rate of sinusoidal amplitude modulation (SAM). There is evidence in both cats and chinchillas to suggest that that there is a topographic distribution of best modulation frequencies with neurons selective for lower rates located dorsomedially and those selective for higher rates ventromedially (Schreiner, C. E. and Langner, G., 1988; Langner, G. *et al.*, 2002), again consistent with the gradients that have been described.

Moving from ventrolateral to dorsomedial an increasing proportion of neurons are selective for complex types of stimuli. For example, neurons that respond selectively to sinusoidal frequency modulations (SFM) are found mainly in the rostral and dorsal part of the IC (Casseday, J. H. *et al.*, 1997). Neurons in the dorsomedial part of the IC in the rat are more likely to show pronounced stimulus-specific adaptation and selective responses to novel stimuli (Covey, E. *et al.*, 2003).

Response–property gradients that do not directly map onto the gradients of the VCN–DCN systems include shape of neurons' frequency–response areas (Ehret, G. *et al.*, 2003). These authors report that in the mouse, the narrowest frequency–response areas are located in the central part of the IC, with broader ones more toward the outside. A similar center-outward gradient has been found in the mouse IC for frequency sweep speed and sweep direction, with selectivity for slow speeds and downward sweeps

most common in the centre of a lamina and high speeds and upward sweeps more common toward the outer edges (Hage, S. R. and Ehret, G., 2003). For response properties that follow a center-outward gradient, it may be that the center property reflects the greatest degree of convergence of the two main gradients, and the properties observed at either extreme may be characteristic of one system operating in isolation.

3.42.8 Summary

Figure 17 is a summary of the major anatomical gradient systems within the IC. The VCN–DCN gradient systems and the intrinsic projections are approximately orthogonal to the tonotopic progression, shown as an arrow from dorsolateral to ventromedial. The VCN system and DCN system provide opposing gradients in density of projections from the sources that contribute to them. At every point within the IC there is an opportunity for inputs from multiple sources to converge, and there is some evidence that at least the binaural inputs to a point along a lamina may be organized into functional domains in which one or another input predominates within a specific part of the lamina. There is evidence that at least some response properties are organized in ways that reflect the gradient structure within the IC. Given the large number of inputs to the IC, the high degree of overlap, and the complexity of the patterns of termination from different sources, it is not surprising that the IC contains multiple functional gradients, functional zones within the gradients, and other organizations of response properties, many of which remain to be investigated.

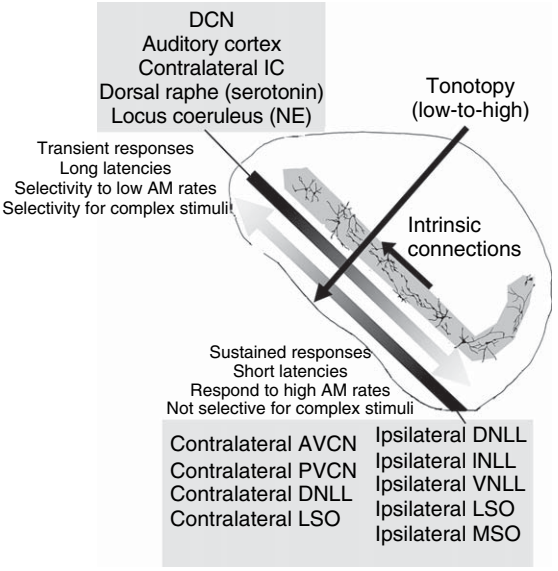

Figure 17 Summary diagram showing the two principal gradient systems within the inferior colliculus (IC) as they relate to the tonotopic organization (arrow showing tonotopy progressing from low at the dorsolateral edge to high at the ventromedial edge). AM, amplitude modulation; AVCN, anteroventral cochlear nucleus; DCN, dorsal cochlear nucleus; DNLL, dorsal nucleus of the lateral lemniscus; INLL, intermediate nucleus of the lateral lemniscus; LSO, lateral superior olive; MSO, medial superior olive; NE, norepinephrine; PVCN, posteroventral cochlear nucleus.

Acknowledgments

Supported by National Institutes of Health grants DC-00607 and DC-00287 from the National Institute on Deafness and Other Communication Disorders.

References

Alibardi, L. 1999. Fine structure, synaptology and immunocytochemistry of large neurons in the rat dorsal cochlear nucleus connected to the inferior colliculus. J. Hirnforsch. 39, 429–439.

Bajo, V. M. and Moore, D. R. 2005. Descending projections from the auditory cortex to the inferior colliculus in the gerbil, *Meriones unguiculatus*. J. Comp. Neurol. 486, 101–116.

Budinger, E., Heil, P., and Scheich, H. 2000. Functional organization of auditory cortex in the Mongolian gerbil (*Meriones unguiculatus*). IV. Connections with anatomically characterized subcortical structures. Eur. J. Neurosci. 12, 2452–2474.

Bukowska, D. 2002. Morphological evidence for secondary vestibular afferent connections to the dorsal cochlear nucleus in the rabbit. Cells Tissues Organs 170, 61–68.

Cant, N. B. 2005. Projections from the Cochlear Nuclear Complex to the Inferior Colliculus. In: The Inferior Colliculus (*eds*. J. A. Winer and C. E. Schreiner), pp. 115–131. Springer.

Cant, N. B. and Benson, C. G. 2003. Parallel auditory pathways: projection patterns of the different neuronal populations in the dorsal and ventral cochlear nuclei. Brain Res. Bull. 60, 457–474.

Casseday, J. H. and Covey, E. 1996. A neuroethological theory of the operation of the inferior colliculus. Brain Behav. Evol. 47, 311–336.

Casseday, J. H., Covey, E., and Grothe, B. 1997. Neurons specialized for periodic frequency modulations in the inferior colliculus of the big brown bat, *Eptesicus fuscus*. J. Neurophysiol. 77, 1595–1605.

Casseday, J. H., Ehrlich, D., and Covey, E. 2000. Neural measurement of sound duration: Control by excitatory-inhibitory interactions in the inferior colliculus. J. Neurophysiol. 84, 1475–1487.

Casseday, J. H., Fremouw, T., and Covey, E. 2002. The Inferior Colliculus: Hub of the Auditory System. In: Springer Handbook of Auditory Research, Volume 15, Integrative

Functions in the Mammalian Auditory Pathway (*eds*. D. Oertel, A. N. Popper, and R. R. Fay), pp. 238–318. New York Springer.

Coleman, J. R. and Clerici, W. J. 1987. Sources of projections to subdivisions of the inferior colliculus in the rat. J. Comp. Neurol. 262, 215–226.

Covey, E. 2004. Midbrain Integrative Mechanisms and Temporal Pattern Analysis in Echolocating Bats. In: Echolocation in Bats and Dolphins (*eds*. J. Thomas, C. Moss, and M. Vater), pp. 123–128. University of Chicago Press.

Covey, E. and Carr, C. E. 2004. The Inferior Colliculus in Bats and Birds. In: The Inferior Colliculus (*eds*. J. A. Winer and C. E. Schreiner), pp. 493–536. Springer.

Covey, E. and Casseday, J. H. 1995. The Lower Brainstem Auditory Pathways. In: Handbook of Auditory Research, Vol. 5, Hearing and Echolocation in Bats (*eds*. A. N. Popper, and R. R. Fay), pp. 235–295. Springer.

Covey, E. and Casseday, J. H. 1998. Brainstem Circuits for Processing Time-Varying Information. In: Psychophysical and Physiological Advances in Hearing (*eds*. A. R. Palmer, A. Rees, A. Q. Summerfield, and R. Meddis), pp. 536–545. Whurr Publishers.

Covey, E. and Casseday, J. H. 1999. Timing in the auditory system of the bat. Annu. Rev. Physiol. 61, 457–476.

Covey, E. and Faure, P. A. 2005. Neural Mechanisms for Analyzing Temporal Patterns in Echolocating Bats. In: Auditory Signal Processing: Physiology, Psychoacoustics and Models (*eds*. D. Pressnitzer, A. de Cheveigné, S. McAdams, and L. Collet), pp. 251–257. Springer.

Covey, E., Kauer, J. A., and Casseday, J. H. 1996. Whole-cell patch clamp recording reveals subthreshold sound-evoked postsynaptic currents in the inferior colliculus of awake bats. J. Neurosci. 6, 3009–3018.

Covey, E., Perez-Gonzalez, D., Hernandez, O., and Malmierca, M. 2003. Novelty units in the inferior colliculus of the rat. Neurosci. Abstr. 29.

Druga, R., Syka, J., and Rajkowska, G. 1997. Projections of auditory cortex onto the inferior colliculus in the rat. Physiol. Res. 46, 215–222.

Ehret, G., Egorova, M., Hage, S. R., and Muller, B. A. 2003. Spatial map of frequency tuning-curve shapes in the mouse inferior colliculus. Neuroreport 14, 1365–1369.

Farley, G. R., Morley, B. J., Javel, E., and Gorga, M. P. 1983. Single-unit responses to cholinergic agents in the rat inferior colliculus. Hear. Res. 11, 73–91.

Fremouw, T., Kleiser, A., Heilman, A., Casseday, J. H., and Covey, E. 1999. Intrinsic and commissural GABAergic connections in the inferior colliculus of the big brown bat. Neurosci. Abstr. 25, 1417.

Fubara, B. M., Casseday, J. H., Covey, E., and Schwartz-Bloom, R. D. 1996. Distribution of $GABA_A$, $GABA_B$ and glycine receptors in the central auditory system of the big brown bat, *Eptesicus fuscus*. J. Comp. Neurol. 369, 83–92.

Fuzessery, Z. M., Wenstrup, J. J., Hall, J. C., and Leroy, S. 2003. Inhibition has little effect on response latencies in the inferior colliculus. J. Assoc. Res. Otolaryngol. 4, 60–73.

Gabriele, M. L., Brunso-Bechtold, J. K., and Henkel, C. K. 2000. Plasticity in the development of afferent patterns in the inferior colliculus of the rat after unilateral cochlear ablation. J. Neurosci. 20, 6939–6949.

Glendenning, K. K., Baker, B. N., Hutson, K. A., and Masterton, R. B. 1992. Acoustic chiasm V: inhibition and excitation in the ipsilateral and contralateral projections of LSO. J. Comp. Neurol. 319, 100–122.

Gonzalez-Hernandez, T., Mantolan-Sarmiento, B., Gonzalez-Gonzalez, B., and Perez-Gonzalez, H. 1996. Sources of GABAergic input to the inferior colliculus of the rat. J. Comp. Neurol. 372, 309–326.

Grothe, B. and Park, T. J. 2000. Structure and function of the bat superior olivary complex. Microsc. Res. Tech. 51, 382–402.

Habbicht, H. and Vater, M. 1996. A microiontophoretic study of acetylcholine effects in the inferior colliculus of horseshoe bats: implications for a modulatory role. Brain Res. 724, 169–179.

Haenggeli, C. A., Pongstaporn, T., Doucet, J. R., and Ryugo, D. K. 2005. Projections from the spinal trigeminal nucleus to the cochlear nucleus in the rat. J. Comp. Neurol. 484, 191–205.

Hage, S. R. and Ehret, G. 2003. Mapping responses to frequency sweeps and tones in the inferior colliculus of house mice. Eur. J. Neurosci. 18, 2301–2312.

Haplea, S., Covey, E., and Casseday, J. H. 1994. Frequency tuning and response latencies at three levels in the brainstem of the echolocating bat, *Eptesicus fuscus*. J. Comp. Physiol. A 174, 671–683.

Hattori, T. and Suga, N. 1997. The inferior colliculus of the mustached bat has the frequency-vs-latency coordinates. J. Comp. Physiol. A 180, 271–284.

Henkel, C. K., Fuentes-Santamaria, V., Alvarado, J. C., and Brunso-Bechtold, J. K. 2003. Quantitative measurement of afferent layers in the ferret inferior colliculus: DNLL projections to sublayers. Hear. Res. 177, 32–42.

Herbert, H., Klepper, A., and Ostwald, J. 1997. Afferent and efferent connections of the ventrolateral tegmental area in the rat. Anat. Embryol. (Berl.) 196, 235–259.

Herrera, M., Hurtado-Garcia, J. F., Collia, F., and Lanciego, J. 1994. Projections from the primary auditory cortex onto the dorsal cortex of the inferior colliculus in albino rats. Arch. Ital. Biol. 132, 147–164.

Hurley, L. M. and Pollak, G. D. 1999. Serotonin differentially modulates responses to tones and frequency-modulated sweeps in the inferior colliculus. J. Neurosci. 19, 8071–8082.

Hurley, L. M. and Pollak, G. D. 2005. Serotonin modulates responses to species-specific vocalizations in the inferior colliculus. J. Comp. Physiol. A 191, 535–546.

Hurley, L. M. and Thompson, A. M. 2001. Serotonergic innervation of the auditory brainstem of the Mexican free-tailed bat, *Tadarida brasiliensis*. J. Comp. Neurol. 435, 78–88.

Itoh, K., Kamiya, H., Mitani, A., Yasui, Y., Takada, M., and Mizuno, N. 1987. Direct projections from the dorsal column nuclei and the spinal trigeminal nuclei to the cochlear nuclei in the cat. Brain Res. 400, 145–150.

Jacomme, A. V., Nodal, F. R., Bajo, V. M., Manunta, Y., Edeline, J. M., Babalian, A., and Rouiller, E. M. 2003. The projection from auditory cortex to cochlear nucleus in guinea pigs: an *in vivo* anatomical and *in vitro* electrophysiological study. Exp. Brain Res. 153, 467–476.

Klepper, A. and Herbert, H. 1991. Distribution and origin of noradrenergic and serotonergic fibers in the cochlear nucleus and inferior colliculus of the rat. Brain Res. 557, 190–201.

Kunzle, H. 1998. Origin and terminal distribution of the trigeminal projections to the inferior and superior colliculi in the lesser hedgehog tenrec. Eur. J. Neurosci. 10, 368–376.

Langner, G. 1992. Periodicity coding in the auditory system. Hear. Res. 60, 115–141.

Langner, G., Albert, M., and Briede, T. 2002. Temporal and spatial coding of periodicity information in the inferior colliculus of awake chinchilla (*Chinchilla laniger*). Hear. Res. 168, 110–130.

Li, H. and Mizuno, N. 1997. Collateral projections from single neurons in the dorsal column nucleus to both the cochlear nucleus and the ventrobasal thalamus: a retrograde double-labeling study in the rat. Neurosci. Lett. 222, 87–90.

Loftus, W. C., Bishop, D. C., Saint Marie, R. L., and Oliver, D. L. 2004. Organization of binaural excitatory and inhibitory

inputs to the inferior colliculus from the superior olive. J. Comp. Neurol. 472, 330–344.
Malmierca, M. S., Hernandez, O., and Rees, A. 2005. Intercollicular commissural projections modulate neuronal responses in the inferior colliculus. Eur. J. Neurosci. 21, 2701–2710.
Malmierca, M. S., Hernandez, O., Falconi, A., Lopez-Poveda, E. A., Merchan, M., and Rees, A. 2003. The commissure of the inferior colliculus shapes frequency response areas in rat: an *in vivo* study using reversible blockade with microinjection of kynurenic acid. Exp. Brain Res. 153, 522–529.
Malmierca, M. S., Rees, A., Le Beau, F. E., and Bjaalie, J. G. 1995. Laminar organization of frequency-defined local axons within and between the inferior colliculi of the guinea pig. J. Comp. Neurol. 357, 124–44.
Marsh, R. A., Fuzessery, Z. M., Grose, C. D., and Wenstrup, J. J. 2002. Projection to the inferior colliculus from the basal nucleus of the amygdala. J. Neurosci. 22, 10449–10460.
Miller, K. E., Casseday, J. H., and Covey, E. 2005. Relation between intrinsic connections and iso frequency contours in the inferior colliculus of the big brown bat, *Eptesicus fuscus*. Neuroscience 136, 895–905.
Moore, D. R., Kotak, V. C., and Sanes, D. H. 1998. Commissural and lemniscal synaptic input to the gerbil inferior colliculus. J. Neurophysiol. 80, 2229–2236.
Ohlrogge, M., Doucet, J. R., and Ryugo, D. K. 2001. Projections of the pontine nuclei to the cochlear nucleus in rats. J. Comp. Neurol. 436, 290–303.
Oliver, D. L. 1984. Dorsal cochlear nucleus projections to the inferior colliculus in the cat: a light and electron microscopic study. J. Comp. Neurol. 224, 155–172.
Oliver, D. L. 1985. Quantitative analysis of axonal endings in the central nucleus of the inferior colliculus and distribution of 3H-labeling after injections in the dorsal cochlear nucleus. J. Comp. Neurol. 237, 343–359.
Oliver, D. L. 2000. Ascending efferent projections of the superior olivary complex. Microsc. Res. Tech. 51, 355–363.
Oliver, D. L., Beckius, G. E., and Shneiderman, A. 1995. Axonal projections from the lateral and medial superior olive to the inferior colliculus of the cat: a study using electron microscopic autoradiograph. J. Comp. Neurol. 360, 17–32.
Oliver, D. L., Beckius, G. E., Bishop, D. C., and Kuwada, S. 1997. Simultaneous anterograde labeling of axonal layers from lateral superior olive and dorsal cochlear nucleus in the inferior colliculus of cat. J. Comp. Neurol. 382, 215–229.
Oliver, D. L., Kuwada, S., Yin, T. C., Haberly, L. B., and Henkel, C. K. 1991. Dendritic and axonal morphology of HRP-injected neurons in the inferior colliculus of the cat. J. Comp. Neurol. 303, 75–100.
Oliver, D. L., Ostapoff, E. M., and Beckius, G. E. 1999. Direct innervation of identified tectothalamic neurons in the inferior colliculus by axons from the cochlear nucleus. Neuroscience 93, 643–658.
Olucha-Bordonau, F. E., Teruel, V., Barcia-Gonzalez, J., Ruiz-Torner, A., Valverde-Navarro, A. A., and Martinez-Soriano, F. 2003. Cytoarchitecture and efferent projections of the nucleus incertus of the rat. J. Comp. Neurol. 464, 62–97.
Park, T. J. and Pollak, G. D. 1993. GABA shapes a topographic organization of response latency in the mustache bat's inferior colliculus. J. Neurosci. 13, 5172–5187.
Reetz, G. and Ehret, G. 1999. Inputs from three brainstem sources to identified neurons of the mouse inferior colliculus slice. Brain Res. 816, 527–543.
Ryugo, D. K., Haenggeli, C. A., and Doucet, J. R. 2003. Multimodal inputs to the granule cell domain of the cochlear nucleus. Exp. Brain Res. 153, 477–485.
Ryugo, D. K., Willard, F. H., and Fekete, D. M. 1981. Differential afferent projections to the inferior colliculus from the cochlear nucleus in the albino mouse. Brain Res. 210, 381–396.
Saint Marie, R. L. 1996. Glutamatergic connections of the auditory midbrain: selective uptake and axonal transport of D-[3H]aspartate. J. Comp. Neurol. 373, 255–270.
Saint Marie, R. L. and Baker, R. A. 1990. Neurotransmitter-specific uptake and retrograde transport of [3H]glycine from the inferior colliculus by ipsilateral projections of the superior olivary complex and nuclei of the lateral lemniscus. Brain Res. 524, 244–53.
Saint Marie, R. L., Ostapoff, E. M., Morest, D. K., and Wenthold, R. J. 1989. Glycine-immunoreactive projection of the cat lateral superior olive: possible role in midbrain ear dominance. J. Comp. Neurol. 279, 382–396.
Saldana, E. and Merchan, M. A. 1992. Intrinsic and commissural connections of the rat inferior colliculus. J. Comp. Neurol. 319, 417–437.
Saldana, E. and Merchan, M. A. 2005. Intrinsic and Commissural Connections of the Inferior Colliculus. In: The Inferior Colliculus (*eds*. J. A. Winer and C. E. Schreiner), pp. 155–181. Springer.
Saldana, E., Feliciano, M., and Mugnaini, E. 1996. Distribution of descending projections from primary auditory neocortex to inferior colliculus mimics the topography of intracollicular projections. J. Comp. Neurol. 371, 15–40.
Schofield, B. R. 2005. Superior Olivary Complex and Lateral Lemniscal Connections of the Auditory Midbrain. In: The Inferior Colliculus (*eds*. J. A. Winer and C. E. Schreiner), pp. 132–154. Springer.
Schofield, B. R. and Cant, N. B. 1996. Projections from the ventral cochlear nucleus to the inferior colliculus and the contralateral cochlear nucleus in guinea pigs. Hear. Res. 102, 1–14.
Schofield, B. R. and Coomes, D. L. 2005. Auditory cortical projections to the cochlear nucleus in guinea pigs. Hear. Res. 199, 89–102.
Schreiner, C. E. and Langner, G. 1988. Periodicity coding in the inferior colliculus of the cat. II. Topographical organization. J. Neurophysiol. 60, 1823–1840.
Shammah-Lagnado, S. J., Alheid, G. F., and Heimer, L. 1996. Efferent connections of the caudal part of the globus pallidus in the rat. J. Comp. Neurol. 376, 489–507.
Shneiderman, A. and Henkel, C. K. 1987. Banding of lateral superior olivary nucleus afferents in the inferior colliculus: a possible substrate for sensory integration. J. Comp. Neurol. 266, 519–534.
Shneiderman, A., Oliver, D. L., and Henkel, C. K. 1988. Connections of the dorsal nucleus of the lateral lemniscus: an inhibitory parallel pathway in the ascending auditory system? J. Comp. Neurol. 276, 188–208.
Thompson, G. C., Thompson, A. M., Garrett, K. M., and Britton, B. H. 1994. Serotonin and serotonin receptors in the central auditory system. Otolaryngol. Head Neck Surg. 110, 93–102.
Vater, M., Casseday, J. H., and Covey, E. 1995. Convergence and divergence of ascending binaural and monaural pathways from the superior olives of the mustached bat. J. Comp. Neurol. 351, 632–646.
Vater, M., Covey, E, and Casseday, JH 1997. The columnar region of the ventral nucleus of the lateral lemniscus in the big brown bat: synaptic arrangements and structural correlates of feedforward inhibitory function. Cell Tissue Res. 289, 223–233.
Weedman, D. L. and Ryugo, D. K. 1996. Projections from auditory cortex to the cochlear nucleus in rats: synapses on granule cell dendrites. J. Comp. Neurol. 371, 311–324.
Whitley, J. M. and Henkel, C. K. 1984. Topographical organization of the inferior collicular projection and other

connections of the ventral nucleus of the lateral lemniscus in the cat. J. Comp. Neurol. 229, 257–270.
Willard, F. H. and Martin, G. F. 1983. The auditory brainstem nuclei and some of their projections to the inferior colliculus in the North American opossum. Neuroscience 10, 1203–1232.
Winer, J. A. 2005. Three Systems of Descending Projections to the Inferior Colliculus. In: The Inferior Colliculus (*eds*. J. A. Winer and C. E. Schreiner), pp. 231–247. Springer.
Winer, J. A., Chernock, M. L., Larue, D. T., and Cheung, S. W. 2002. Descending projections to the inferior colliculus from the posterior thalamus and the auditory cortex in rat, cat, and monkey. Hear Res. 168, 181–195.
Winer, J. A., Larue, D. T., and Pollak, G. D. 1995. GABA and glycine in the central auditory system of the mustache bat: structural substrates for inhibitory neuronal organization. J. Comp. Neurol. 355, 317–353.
Winer, J. A., Larue, D. T., Diehl, J. J., and Hefti, B. J. 1998. Auditory cortical projections to the cat inferior colliculus. J. Comp. Neurol. 400, 147–174.
Wolff, A. and Kunzle, H. 1997. Cortical and medullary somatosensory projections to the cochlear nuclear complex in the hedgehog tenrec. Neurosci. Lett. 221, 125–128.
Wright, D. D. and Ryugo, D. K. 1996. Mossy fiber projections from the cuneate nucleus to the cochlear nucleus in the rat. J. Comp. Neurol. 365, 159–172.
Zhang, D. X., Li, L., Kelly, J. B., and Wu, S. H. 1998. GABAergic projections from the lateral lemniscus to the inferior colliculus of the rat. Hear Res. 117, 1–12.
Zhou, J. and Shore, S. 2004. Projections from the trigeminal nuclear complex to the cochlear nuclei: a retrograde and anterograde tracing study in the guinea pig. J. Neurosci. Res. 15, 901–907.
Zook, J. M. and Casseday, J. H. 1982. Origin of ascending projections to inferior colliculus in the mustache bat, *Pteronotus parnellii*. J. Comp. Neurol. 207, 14–28.
Zook, J. M. and Casseday, J. H. 1985. Projections from the cochlear nuclei in the mustache bat, *Pteronotus parnellii*. J. Comp. Neurol. 237, 307–324.
Zook, J. M. and Casseday, J. H. 1987. Convergence of ascending pathways at the inferior colliculus of the mustache bat, *Pteronotus parnellii*. J. Comp. Neurol. 261, 347–361.

Further Reading

Oliver, D. L. 1987. Projections to the inferior colliculus from the anteroventral cochlear nucleus in the cat: possible substrates for binaural interaction. J. Comp. Neurol. 264, 24–46.
Ostapoff, E. M., Benson, C. G., and Saint Marie, R. L. 1997. GABA- and glycine-immunoreactive projections from the superior olivary complex to the cochlear nucleus in the guinea pig. J. Comp. Neurol. 381, 500–512.
Peddicord, R. 1998. Simulation of ILD sensitive neurons in the inferior colliculus of the barn owl. Hear. Res. 123, 111–124.
Thompson, A. M. 1998. Heterogeneous projections of the cat posteroventral cochlear nucleus. J. Comp. Neurol. 390, 439–453.
Vollmer, M., Snyder, R. L., Leake, P. A., Beitel, R. E., Moore, C. M., and Rebscher, S. J. 1999. Temporal properties of chronic cochlear electrical stimulation determine temporal resolution of neurons in cat inferior colliculus. J. Neurophysiol. 82, 2883–2902.

3.43 The Nuclei of the Lateral Lemniscus: Two Functional Systems

C V Portfors, Washington State University, Vancouver, WA, USA

© 2008 Elsevier Inc. All rights reserved.

3.43.1	Introduction	751
3.43.2	Structure of the Nuclei of the Lateral Lemniscus	751
3.43.3	Role of the Dorsal Nucleus of the Lateral Lemniscus in Binaural Hearing	753
3.43.4	The Monaural Nuclei of the Lateral Lemniscus	754
3.43.4.1	General Features	754
3.43.4.2	Role of the Nuclei of the Lateral Lemniscus in Frequency Integration	754
3.43.4.3	Role of the Monaural Nuclei in Temporal Coding	755
3.43.5	Concluding Remarks	755
References		756

Glossary

afferent Movement toward a central area. Refers to neural projections going toward a particular structure.
binaural Relating to both ears.
contralateral The opposite side.
dorsal A position of an anatomical structure that is more toward the back or top in comparison to some other anatomical structure.
echolocation Method of sensory perception in which a bat or cetacean sends out a sound and uses the returning echo to orient, avoid obstacles, find food, and communicate.
ipsilateral The same side.
lateral A position that is farther from the midline of the brain.
medial A position that is closer to the midline of the brain.
monaural Relating to one ear.
spectral Frequency.
tonotopy Organization of frequency representation in a systematic manner.
ventral A position of an anatomical structure that is more toward the belly or bottom in comparison to some other anatomical structure.

3.43.1 Introduction

In between the cochlear nucleus and the inferior colliculus (IC) lies a complex set of auditory cell groups, the nuclei of the lateral lemniscus (NLL). While numerous physiological and anatomical studies have been conducted on the cochlear nucleus and the IC, the role of the NLL in detecting, localizing, and recognizing biologically relevant sounds is just beginning to emerge. What is clear, however, is that the NLL can be divided into two distinct functional systems based on the sources of afferent input and the characteristics of neural responses found in different nuclei. One functional system is part of the binaural pathways and includes the dorsal nucleus of the lateral lemniscus (DNLL). The second functional system is part of the monaural pathways and includes the intermediate nucleus of the lateral lemniscus (INLL) and the ventral nucleus of the lateral lemniscus (VNLL). The goal of this chapter is to review the characteristics of neural processing in both functional systems to better understand the role of the NLL in processing biologically relevant sounds in mammals.

3.43.2 Structure of the Nuclei of the Lateral Lemniscus

The NLL are groups of cell bodies that lie just ventral to the IC. The separation of the cell groups is highly variable across species such that in some species (e.g., rats) two groups of cell bodies are identified, whereas in other species (e.g., bats, cats, and guinea-pigs) four groups of cell bodies can be

identified. In all species, the dorsal group of cells is referred to as the DNLL. The DNLL consists of mostly fusiform cells that form clusters between dense bands of fibers in the lateral lemniscus; the fiber bundle that ascends to the IC (Figure 1). The DNLL is part of the binaural pathways as it receives afferent input from both the ipsilateral and contralateral lateral superior olivary (LSO) nucleus and from the ipsilateral medial superior olivary (MSO) nucleus (Glendenning, K. K. *et al.*, 1981); nuclei that are involved in processing interaural level differences and interaural timing differences, respectively. Electrophysiological recordings have also shown that most neurons in the DNLL are binaural (Brugge, J. F. *et al.*, 1970; Covey, E., 1993; Bajo, V. M. *et al.*, 1998). The structure and organization of the DNLL is similar across mammalian species, suggesting this is an evolutionarily conserved nucleus.

In contrast, the structure and organization of the ventral group of cell bodies is highly variable across species, possibly suggesting different sound processing needs based on different species' interactions with their environments. The ventral groups of cells are often lumped together and referred to as the VNLL or the ventral complex of the lateral lemniscus (VCLL). In this chapter, however, we will use the nomenclature derived from species (bats, cats, and guinea-pigs) in which four cell groups can be distinguished. The most dorsal group, the INLL, contains multipolar cells (guinea-pigs; Schofield, B. R. and Cant, N. B., 1997) or elongate cells (bats; Zook, J. M. and Casseday, J. H., 1982) with dendrites tending to lie mediolaterally and perpendicular to the passing lemniscal fibers. The INLL in echolocating bats tends to be very large, and in frontal sections it has a triangular outline that protrudes laterally (Figure 1(a)). This is quite distinct when compared to other species such as mouse (compare Figures 1(a) and 1(b)). It seems likely that the INLL plays an important role in the processing of echolocation signals.

Ventral to the INLL reside three distinct regions of the VNLL. Differences exist between bats and other species in which these regions are apparent. In the guinea-pig, the dorsal portion of the VNLL (VNLLd) contains mainly multipolar cells with dendrites oriented perpendicular to the lemniscal fibers. The cells in VNLLd are scattered throughout the region in no particular organization (Schofield, B. R. and Cant, N. B., 1997). More ventrally lies the ventral division of the VNLL (VNLLv). The VNLLv contains a variety of cell types including multipolar and giant cells. Most distinctive are the spherical neurons that resemble spherical bushy cells found in the

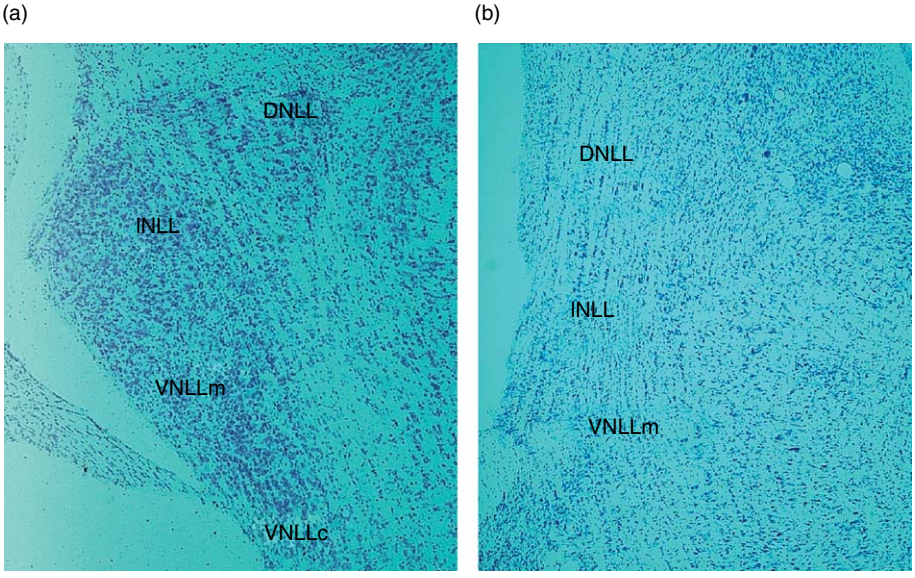

Figure 1 Photomicrographs of the NLL. Nissl staining illustrates the different nuclei. (a) Four distinct nuclei are apparent in the mustached bat. The columnar organization of VNLLc is distinct from the organization of cells in the other nuclei. The striated pattern of cell clustering in the DNLL is due to the passage of lemniscal fibers traveling to the IC. (b) Dorsal and ventral nuclei of the lateral lemniscus in the mouse are more typical of mammalian species. Divisions between nuclei are not as apparent as in the mustached bat.

cochlear nucleus. These neurons receive afferent input through endbulbs from octopus cells in the posteroventral cochlear nucleus (Vater, M. and Feng, A. S., 1990; Schofield, B. R., 1995; Adams, J. C., 1997). Finally, the VNLLa is a more anterior cluster of cells within the VNLL that contains multipolar cells. The distinctive feature of this region compared to the VNLLd is that the dendrites are oriented parallel to the lemniscal fibers.

In echolocating bats, the VNLL is hypertrophied and has a highly organized structure consisting of a columnar region (VNLLc) and a multipolar region (VNLLm). In the mustached bat (*Pteronotus parnellii*), the ventral part of the nucleus contains small, multipolar cells that are organized in densely packed columns, providing a distinct columnar appearance that is strikingly different compared to the dorsal part of the nucleus (Figure 1(a)). The VNLLm contains multipolar cells that have a variety of shapes and no distinct organization (Zook, J. M. and Casseday, J. H., 1982). The locations of the VNLLc and VNLLm in the big brown bat (*Eptesicus fuscus*) are reversed with the VNLLc dorsal to the VNLLm (Covey, E. and Casseday, J. H. 1986). The cells in the VNLLc are spherical bushy cells that receive their inputs through endbulbs and thus resemble neurons in the VNLLv of other species (Covey, E. and Casseday, J. H., 1986; Vater, M. *et al*., 1997).

Although different species show differing levels of separation and organization of the INLL and VNLL, in all species these regions receive monaural input, predominantly from the cochlear nucleus. Afferent input from monaural nuclei in the brainstem makes the INLL and VNLL part of the monaural ascending auditory pathways, and consequently the monaural NLL. In subsequent sections of this chapter, the function of the NLL is discussed in terms of the binaural and monaural functional systems.

3.43.3 Role of the Dorsal Nucleus of the Lateral Lemniscus in Binaural Hearing

Connectional, immunocytochemical, and electrophysiological studies all provide evidence for the DNLL playing an important role in binaural processing and sound localization. Neurons in the DNLL receive projections from the LSO and MSO (Glendenning, K. K. *et al*., 1981), utilize gamma-aminobutyric acid (GABA), and are inhibitory (Adams, J. C. *et al*., 1984; Vater, M. *et al*., 1997); they are also sensitive to variations in interaural intensity and/or time differences (Brugge, J. F. *et al*., 1970; Covey, E., 1993; Bajo, V. M. *et al*., 1998), which are the two major binaural cues for sound localization. Binaural responses of DNLL neurons are characterized by excitation to a contralateral sound source and inhibition to an ipsilateral sound source, creating what is referred to as an E/I response.

Neurons in the DNLL respond with sustained or transient discharge patterns. In the rat, the most common discharge pattern is a strong phasic response at the stimulus onset followed by a sustained response throughout the duration of the stimulus and an offset inhibition (Bajo, V. M. *et al*., 1998). In the DNLL of big brown bats, equal numbers of transient and sustained responses occur (Covey, E., 1993). The sustained responses have features similar to those seen in LSO neurons and most likely reflect LSO input. The transient discharge patterns likely reflect MSO input. Thus, the discharge patterns of DNLL neurons mainly reflect their inputs rather than their own membrane properties.

No clear pattern of tonotopic organization in the DNLL has resulted from physiological or anatomical studies. Neurons with similar best frequencies seem to cluster together in both bats (Covey, E. 1993) and rats (Bajo, V. M. *et al*., 1998). In rats, neurons that are responsive to high frequencies cluster in the dorsal and ventral parts of the DNLL, with neurons responsive to low frequencies located in the middle.

If DNLL neurons receive their sensitivity to interaural timing or interaural intensity differences from the MSO and LSO, and the MSO and LSO impart similar response properties directly onto IC neurons, what role does the DNLL play in binaural processing? Interestingly, the EI properties of some neurons in the IC are modified or created at the level of the IC (Faingold, C. L. *et al*., 1993). The DNLL sends bilateral inhibitory projections to the IC, and, in particular, the contralateral projection creates a novel response property in the IC that does not occur in lower binaural nuclei or in cells in the IC that do not receive a DNLL projection (Burger, R. M. and Pollak, G. D., 2001). One of the consequences of the contralateral inhibitory input is the creation of IC neurons that can process the location of a moving sound source or multiple sound sources located in different regions of space.

The inhibition elicited by ipsilateral stimulation in DNLL neurons often lasts for many milliseconds (Yang, L. and Pollak, G. D., 1998). Burger R. M. and Pollak G. D. (2001) showed that this persistent

inhibition in DNLL neurons causes normally suppressed binaural neurons in the IC to become responsive. Their argument is that if the DNLL neuron has persistent inhibition, the IC cell loses its ipsilaterally evoked inhibition and it consequently will respond to a second, or trailing, binaural sound to which it would not respond if that sound were presented alone. However, an additional consequence of this circuitry is that the sensitivity to the location of the trailing sound is reduced. These data suggest that the role of the DNLL is to change the interaural intensity sensitivity of IC cells to trailing sounds. The findings of Burger R. M. and Pollak G. D. (2001) correlate well with characteristics of the precedence effect. In the precedence effect, when two identical sounds are presented from speakers separated along the same plane in space and the second sound is slightly delayed from the first sound, the listener hears the trailing sound but cannot localize the sound (Litovsky, R.Y. *et al.*, 1999). The neural mechanism for the precedence effect may lie within the DNLL.

3.43.4 The Monaural Nuclei of the Lateral Lemniscus

3.43.4.1 General Features

In contrast to the DNLL, the INLL and VNLL have typically been considered monaural nuclei. While there is no evidence to the contrary for the INLL, the view of the VNLL as strictly monaural is slightly more controversial. While all studies in the big brown bat show neurons in both the VNLLm and VNLLc to be excited by sound at the contralateral ear and unaffected by sound at the ipsilateral ear (Covey, E. and Casseday, J. H., 1991), recent studies in the unanesthetized rabbit suggest that many neurons in the VNLLm are sensitive to interaural temporal disparities (ITDs); a major cue for sound localization (Batra, R. and Fitzpatrick, D. C., 2002). These neurons, however, respond differently than the majority of ITD sensitive cells found in traditional binaural nuclei in the auditory system, suggesting that their function may be slightly different. First, these neurons in VNLLm respond to the onset of the sound, whereas other ITD-sensitive neurons respond in a sustained manner. Second, the VNLLm neurons do not respond to dynamically changing ITDs, whereas ITD-sensitive neurons in other auditory nuclei respond vigorously to this type of stimulus. These differences suggest that the ITD-sensitive neurons in the VNLLm of unanesthetized rabbits may be specialized for detecting transient changes in ITDs (Batra, R. and Fitzpatrick, D. C., 2002). These preliminary data are intriguing and may alter the way the VNLL is viewed functionally, but it remains to be determined if neurons in the VNLL of other species are involved in any type of binaural processing or if they are strictly monaural as in echolocating bats.

Whether the monaural nuclei of the NLL exhibit a tonotopic organization is a debatable question. Some level of tonotopy has been reported in the INLL of big brown bats (Covey, E. and Casseday, J. H., 1991) and mustached bats (unpublished observations). The VNLLm of big brown bats shows a tonotopic organization, where high frequencies are represented in the center of the nucleus and lower frequencies around the core (Covey, E. and Casseday, J. H., 1991). These data fit well with the findings from anatomical studies in the rat in which retrograde tracer deposits were made in specific frequency laminae in the IC and patterns of retrogradely labeled cells in the VNLL showed a concentric organization with respect to the tonotopy in the IC (Merchan, M. A. and Berbel, P., 1996). In cats, patterns of retrogradely labeled cells in the VNLL are patchy; labeled cells after high-frequency deposits in the IC appear more laterally and more medially after low-frequency deposits (Malmierca, M. S. *et al.*, 1998). Thus, in cats there seems to be a mediolateral gradient of projections from the VNLL to the IC. However, this conclusion assumes that the projections from the VNLL to the IC are in fact tonotopic. As the IC is the first nucleus in the ascending pathway to show spectral integration properties suggesting that some cells receive nontonotopic projections from brainstem nuclei (Wenstrup, J. J. *et al.*, 1999; Portfors, C. V. and Felix, R. A., II, 2005), it is possible that the frequency response of the VNLL neurons does not match the frequency representation of the IC targets. Electrophysiological evidence of tonotopy in the VNLL in cats is lacking (Aitkin, L. M. *et al.*, 1970), questioning the interpretation of the anatomical studies.

3.43.4.2 Role of the Nuclei of the Lateral Lemniscus in Frequency Integration

The role the monaural nuclei play in processing sounds with complex frequency and temporal structures is unclear, but recent studies provide evidence as to their role in shaping response properties in the IC. Integration of spectral and temporal elements in complex sounds is essential for appropriate

representation of these sounds. Spectral integration properties such as tuning to multiple frequencies and facilitatory or inhibitory responses to the combination of two distinctly different frequency elements (combination sensitivity) occur in the IC of bats and mice (Portfors, C. V. and Wenstrup, J. J., 1999; Portfors, C. V. and Felix, R. A., II, 2005). Tuning to multiple frequencies, at least in the mustached bat, occurs to a small extent (<10% of neurons) in the NLL and VNLL. In addition, approximately 25% of neurons in the INLL show combination-sensitive response properties with most being inhibitory (Portfors, C. V. and Wenstrup, J. J., 2001). Complex responses in the INLL and VNLL occur to a far lesser extent than in the IC of the mustached bat (Portfors, C. V. and Wenstrup, J. J., 1999; 2002). This suggests that the IC plays a more substantial role in spectral integration of complex sounds than the NLL.

However, the inhibitory combination-sensitive responses in the INLL may shape responses to complex sounds in the IC. In the mustached bat, the IC contains neurons that are specialized for encoding target distance information (Portfors, C. V. and Wenstrup, J. J., 1999). These facilitatory FM-FM neurons respond to the combination of the first harmonic frequency-modulated (FM) sweep in the bat's emitted call followed by a higher FM harmonic in the returning echo. Each neuron responds best to a particular delay between the emitted call and the returning echo. Neurons that respond best to delays longer than 20 ms show a strong period of inhibition that precedes the facilitatory response. Portfors C. V. and Wenstrup J. J. (2001) found FM-FM neurons in the INLL that were inhibitory rather than facilitatory and suggested that these inhibitory FM-FM neurons could provide a dominant excitatory input to the long best delay neurons in the IC to create the prefacilitation inhibition. Support for this idea comes from a recent study by Nataraj K. and Wenstrup J. J. (2006), who found that 59% of neurons in the IC showed early inhibition that preceded facilitation and this inhibition was not eliminated with the application of bicuculline (GABAA antagonist) or strychnine (glycine antagonist). These data suggest that the inhibition resulting from the combination of two distinctly different frequency elements arises below the IC, possibly in the INLL. The key experiment to provide convincing evidence is to eliminate the combination-sensitive inhibitory responses in the INLL and test whether this eliminates the early inhibition in facilitatory neurons in the IC.

3.43.4.3 Role of the Monaural Nuclei in Temporal Coding

Many response characteristics of neurons in the INLL and VNLL make them well suited to encode temporal information in sounds: little spontaneous activity, broad frequency tuning, and short integration times (Covey, E. and Casseday, J. H., 1991). Moreover, differences in response characteristics between INLL, VNLLm, and VNLLc in echolocating bats suggest that INLL and VNLLm are involved in encoding temporal features of an ongoing sound, whereas VNLLc is involved in encoding information related to the onset of the sound (Covey, E. and Casseday, J. H., 1991).

Fundamental differences in frequency tuning, discharge pattern, and variability of first spike latency are seen in VNLLc compared to VNLLm or INLL in big brown bats (Covey, E. and Casseday, J. H., 1991). Tuning curves in VNLLc are much broader. This is important because a high level of temporal precision is gained at the expense of frequency precision. Thus, broad frequency tuning in VNLLc neurons suggests that they have better temporal precision. In addition, all neurons in VNLLc show a phasic onset discharge pattern with constant latency, whereas neurons in INLL and VNLLm show either phasic onset with variable latency or sustained discharge patterns. The ranges of latencies also differ between nuclei. Latencies tend to be shortest in VNLLc and longest in INLL (Covey, E. and Casseday, J. H., 1991; Portfors, C. V. and Wenstrup, J. J., 2001).

Neurons in the VNLLc are of special interest because of their ability to signal the onset of the sound very precisely. These neurons use the inhibitory neurotransmitter glycine (Vater, M. *et al.*, 1997) and thus send a precisely timed inhibitory input to the IC. This precise inhibitory input has been suggested to possibly play a role in resetting IC neurons to prepare them for a subsequent signal or in encoding sound duration in the IC (Casseday, J. H. *et al.*, 2002). Regardless, it is clear that neurons in the VNLLc encode very different aspects of sound than neurons in the INLL, VNLLm, and DNLL.

3.43.5 Concluding Remarks

The NLL represent a set of structures in the auditory brainstem that dramatically influence how the IC processes sound. The binaural and monaural functional systems of the NLL play unique and important

roles in transforming inputs from the lower brainstem and modifying responses in the IC. This chapter has only touched the surface on the functional importance of the NLL, but it should be clear that many more experiments are waiting to be done to better understand the NLL. For example, Bauer E. E. *et al.* (2002) recently showed that neurons in the DNLL do not show any specializations for encoding species-specific vocalizations, yet responses to species-specific vocalizations have not been tested in the monaural nuclei of the NLL. Based on temporal response properties and spectral integration properties in the INLL and VNLL, the likelihood of these nuclei showing specializations for encoding species-specific vocalizations seems higher than in the DNLL. In addition, the majority of physiological studies on the NLL have been conducted in bats. As the INLL and VNLL in bats are hypertrophied and may have evolved certain response features for echolocation behaviors, it is important to understand response characteristics in the NLL of a variety of species. Comparisons across species are vital for understanding the evolution of species-specific neural mechanisms versus mechanisms that are common across all species.

Acknowledgments

Writing of this chapter was supported by the National Institutes of Health and the National Institute on Deafness and Communication Disorders, R01 04733.

References

Adams, J. C. 1997. Projections from octopus cells of the posteroventral cochlear nucleus to the ventral nucleus of the lateral lemniscus in cat and human. Audit. Neurosci. 3, 335–350.

Adams, J. C. and Mugnaini, E. 1984. Dorsal nucleus of the lateral lemnsicus: a nucleus of GABAergic projection neurons. Brain Res. Bull. 13, 585–590.

Aitkin, L. M., Anderson, D. J., and Brugge, J. F. 1970. Tonotopic organization and discharge characteristics of single neurons in nuclei of the lateral lemniscus of the cat. J. Neurosci. 33, 421–440.

Bajo, V. M., Villa, A. E. P., de Ribaupierre, F., and Rouiller, E. M. 1998. Discharge patterns of single neurons in the dorsal nucleus of the lateral lemniscus of the rat. Brain Res. Bull. 47, 595–610.

Batra, R. and Fitzpatrick, D. C. 2002. Monaural and binaural processing in the ventral nucleus of the lateral lemniscus: a major source of inhibition to the inferior colliculus. Hear. Res. 168, 90–97.

Bauer, E. E., Klug, A., and Pollak, G. D. 2002. Spectral determination of responses to species-specific calls in the dorsal nucleus of the lateral lemniscus. J. Neurophysiol. 88, 1955–1967.

Brugge, J. F., Anderson, D. J., and Aitkin, L. M. 1970. Responses of neurons in the dorsal nucleus of the lateral lemniscus. J. Neurophysiol. 33, 441–458.

Burger, R. M. and Pollak, G. D. 2001. Reversible inactivation of the dorsal nucleus of the lateral lemnsicus reveals its role in the processing of multiple sound sources in the inferior colliculus of bats. J. Neurosci. 21, 4830–4843.

Casseday, J. H., Fremouw, T., and Covey, E 2002. The Inferior Colliculus: A Hub for the Central Auditory System. In: Integrative Functions in the Mammalian Auditory Pathway (*eds*. D. Oertel, R. Fay, and A. N. Popper), pp. 238–318. Springer.

Covey, E. 1993. Response properties of single units in the dorsal nucleus of the lateral lemniscus and paralemniscal zone of an echolocating bat. J. Neurophysiol. 69, 842–859.

Covey, E. and Casseday, J. H. 1986. Connectional basis for frequency representation in the nuclei of the lateral lemniscus of the bat Eptesicus fuscus. J. Neurosci. 6, 2926–2940.

Covey, E and Casseday, J. H. 1991. The monaural nuclei of the lateral lemniscus in an echolocating bat: parallel pathways for analyzing temporal features of sound. J. Neurosci. 11, 3456–3470.

Faingold, C. L., Anderson, C. A., and Randall, M. E. 1993. Stimulation or blockade of the dorsal nucleus of the lateral lemniscus alters binaural and tonic inhibition in contralateral inferior colliculus neurons. Hear. Res. 69, 98–106.

Glendenning, K. K., Brunso-Bechtold, J. K., Thompson, G. C., and Masterton, R. B. 1981. Ascending auditory afferents to the nuclei of the lateral lemniscus. J. Comp. Neurol. 197, 673–703.

Litovsky, R. Y., Colburn, H. S., Yost, W. A., and Guzman, S. J. 1999. The precedence effect. J. Acoust. Soc. Am. 106, 1633–1654.

Malmierca, M. S., Leergaard, T. B., Bajo, V. M., Bjaalie, J. G., and Merchan, M. A. 1998. Anatomical evidence of a three-dimensional mosaic pattern of tonotopic organization in the ventral complex of the lateral lemnsicus in cat. J. Neurosci. 18, 10603–10618.

Merchan, M. A. and Berbel, P. 1996. Anatomy of the ventral nucleus of the lateral lemniscus in rats: a nucleus with a concentric laminar organization. J. Comp. Neurol. 372, 245–263.

Nataraj, K. and Wenstrup, J. J. 2006. Roles of inhibition in creating complex auditory responses in the inferior colliculus: facilitated combination-sensitive neurons. J. Neurophysiol. 95, 2179–2192.

Portfors, C. V. and Felix, R. A., II 2005. Spectral integration in the inferior colliculus of the CBA/CaJ Mouse. Neuroscience 136, 1159–1170.

Portfors, C. V. and Wenstrup, J. J. 1999. Delay-tuned neurons in the inferior colliculus of the mustached bat: implications for analyses of target distance. J. Neurophysiol. 82, 1326–1338.

Portfors, C. V. and Wenstrup, J. J. 2001. Responses to combinations of tones in the nuclei of the lateral lemniscus. J. Assoc. Res. Otolaryngol. 2, 104–117.

Portfors, C. V. and Wenstrup, J. J. 2002. Excitatory and facilitatory frequency response areas in the inferior colliculus of the mustached bat. Hear. Res. 168, 131–138.

Schofield, B. R. 1995. Projections from the cochlear nucleus to the superior paraolivary nucleus in guinea pigs. J. Comp. Neurol. 360, 135–149.

Schofield, B. R. and Cant, N. B. 1997. Ventral nucleus of the lateral lemniscus in guinea pigs: cytoarchitecture and inputs from the cochlear nucleus. J. Comp. Neurol. 379, 363–385.

Vater, M. and Feng, A. S. 1990. Functional organization of ascending and descending connections of the cochlear nucleus in horseshoe bats. J. Comp. Neurol. 292, 373–395.

Vater, M., Covey, E., and Casseday, J. H. 1997. The columnar region of the ventral nucleus of the lateral lemniscus in the big brown bat (*Eptesicus fuscus*): synaptic arrangement and structural correlates of feedforward inhibitory function. Cell Tissue Res. 289, 223–233.

Wenstrup, J. J., Mittmann, D. H., and Grose, C. D. 1999. Inputs to combination-sensitive neurons of the inferior colliculus. J. Comp. Neurol. 409, 509–528.

Yang, L. and Pollak, G. D. 1998. Features of ipsilaterally evoked inhibition in the dorsal nucleus of the lateral lemniscus. Hear. Res. 122, 25–141.

Zook, J. M. and Casseday, J. H. 1982. Origin of ascending projections to the inferior colliculus in the mustache bat, *Pteronotus parnellii*. J. Comp. Neurol. 207, 14–28.

Further Reading

Bajo, V. M., Merchan, M. A, Malmierca, M. S., Nodal, F. R., and Bjaalie, J. G. 1999. Topographical organization of the dorsal nucleus of the lateral lemniscus in the cat. J. Comp. Neurol. 407, 349–366.

3.44 Auditory Map Plasticity in Juvenile and Adult Owls

J Bergan and E Knudsen, Stanford University School of Medicine, Stanford, CA, USA

© 2008 Elsevier Inc. All rights reserved.

3.44.1	Introduction	759
3.44.2	Synthesis of the Auditory Space Map	759
3.44.2.1	Visual Calibration of the Auditory Space Map	760
3.44.2.2	Instruction of the Auditory Space Map in the Inferior Colliculus	761
3.44.2.3	Developmental Regulation of Map Plasticity	761
3.44.3	Manipulations that Increase Auditory Plasticity in Adults	762
3.44.3.1	Training During the Juvenile Period	762
3.44.3.2	Training in Small Increments	762
3.44.3.3	Hunting Increases Map Plasticity	763
3.44.4	Conclusions	763
References		763

Glossary

interaural level difference (ILD) An important spatial cue for auditory stimuli derived from differences in sound amplitude at the two ears.

interaural timing difference (ITD) An important cue for the horizontal location of an auditory stimulus derived from relative timing differences between a sound reaching the near and far ear.

optic tectum The nonmammalian homolog to the superior colliculus, which is involved in stimulus detection and gaze control.

receptive field The area in a particular sensory space in which a neuron will respond to stimuli.

topographic A systematic anatomical arrangement, often referring to neural representations that emulate the original sensory space.

3.44.1 Introduction

Experience shapes behavior and the neural circuits that underlie behavior throughout an animal's life. In many neural circuits, the shaping influence of experience is particularly strong during early periods in development. Such sensitive periods are hallmarks of the circuits that underlie binocular vision, language acquisition, social behavior, and song learning in birds (Hensch, T. K., 2004). The barn owl midbrain auditory localization pathway also passes through a sensitive period during which visual experience calibrates auditory localization behavior, allowing individual experience to shape the relationship between auditory cues and the locations of auditory stimuli in visual space (Brainard, M. S. and Knudsen, E. I., 1998).

Early studies documented a dramatic decline in the plasticity of the auditory localization pathway as owls approached adulthood. Recent experiments, however, have demonstrated a far greater capacity for plasticity in adult owls than was previously thought. This plasticity likely maintains accurate auditory localization in the face of aging processes that alter the neural coding of binaural signals. The conditions necessary to induce plasticity in adult owls are more specific than those required in juveniles. This chapter reviews how sensory experience guides the development of aligned maps of auditory and visual space in the midbrain of the barn owl, describes how the capacity to adapt changes throughout an animal's life, and discusses ways to increase plasticity in adult owls through specific training techniques.

3.44.2 Synthesis of the Auditory Space Map

Audition and vision provide complementary information about the nature of stimuli. Sounds provide an animal with information that is not visually

accessible while vision provides accurate and precise information about the shape, size, and location of an object. Integrating auditory and visual information improves both the speed and accuracy with which stimuli are detected (Stein, B. E. and Meredith, M. A., 1993). As nocturnal predators, barn owls rely heavily on both of these senses to survive.

While information about the location of a visual stimulus is available immediately in the retina, the location of an auditory stimulus must be inferred from a variety of monaural and binaural cues. The primary cues for the horizontal location of an auditory stimulus are small timing differences between sounds arriving at the near and far ears, called interaural timing differences (ITDs). Additional cues, such as the interaural level difference (ILD), are important indicators of both the horizontal and vertical locations of stimuli.

The auditory system measures auditory cues, such as ITD and ILD, and associates particular values of these cues with the appropriate locations in space (Gutfreund, Y. and Knudsen, E. I., 2004). The initial analysis of ITD and ILD cues are carried in frequency-specific channels. However, within the midbrain, at the level of the external nucleus of the inferior colliculus (ICX), these frequency specific channels combine information to yield a map of auditory space (Figure 1). This map of auditory space is then relayed to the optic tectum (OT), where auditory and visual inputs merge and receptive fields align to create a multimodal map of space (Gutfreund, Y. and Knudsen, E. I., 2004). A primary purpose of this multimodal space map is to orient the owl's gaze towards salient stimuli regardless of the sensory modality that detected the stimulus. The alignment of auditory and visual receptive fields in the OT also makes it possible to quantify auditory plasticity at any point in the space map by measuring the difference between the observed auditory tuning and the expected auditory tuning based on the location of the visual receptive field.

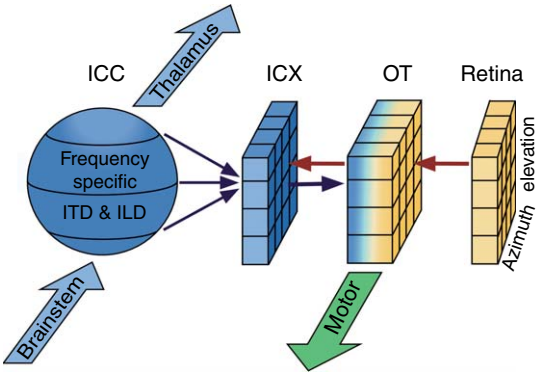

Figure 1 Sensory representations and processing in the barn owl midbrain. Auditory structures are shown in blue and visual structures are yellow. Frequency-specific interaural timing differences (ITDs) and interaural level difference (ILD) information is conveyed from brainstem nuclei to the central nucleus of the inferior colliculus (ICC). Spatial cues converge across ICC frequency laminas to form a single map of auditory space in the external nucleus of the inferior colliculus (ICX). This auditory map is then relayed forward to the optic tectum (OT) where it is aligned with a retinotopic map of visual space. Sensory activity, of either modality, within the deep layers of the OT triggers orienting head movements which bring the owl's gaze toward the location of the stimulus. A visually based spatial template projects from the OT back to the ICX. This pathway possesses many attributes necessary for instructing experience-dependent changes of auditory tuning within the ICX.

3.44.2.1 Visual Calibration of the Auditory Space Map

The first hint that the alignment of auditory and visual space maps in the OT might be guided by visual signals came from the observation that the auditory map magnifies frontal space in a manner that is predicted by the photoreceptor density in the retina, but is not predicted by properties of auditory spatial cues (Knudsen, E. I., 1982). Subsequently, the role of visual signals in calibrating auditory localization has been experimentally demonstrated in several species. For example, when owls are raised with horizontally displacing prismatic spectacles (prisms), the relationship between the locations of auditory stimuli and visual stimuli is offset by the magnitude of the prismatic displacement. Immediately after prisms are mounted on an owl, the owl's auditory orienting behavior is unchanged; however, this behavior fails to direct the animal's gaze to the source of an auditory stimulus. Over the course of several weeks, young owls recalibrate the relationship between auditory spatial cues and the locations in visual space that produce them such that they accurately fixate the source of the sound as seen through the prisms (Gutfreund, Y. and Knudsen, E. I., 1989). During this same period of time, the auditory spatial tuning of neurons in the OT changes in a manner that restores register of the auditory map with the prismatically displaced visual map (Figure 2). Axon growth, synapse formation, and changes in the gamma aminobutyric acid (GABA)ergic inhibition of native connections all contribute to the adaptive remodeling of the auditory space map (Feldman, D. E. and Knudsen, E. I., 1997; Zheng, W. and Knudsen, E. I., 1999; DeBello, W. M. *et al.*, 2001).

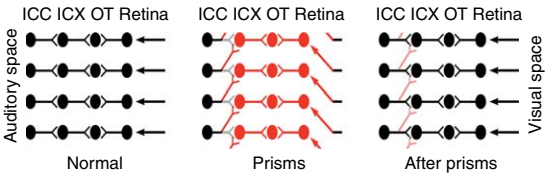

Figure 2 Anatomical changes associated with auditory plasticity. Normal: the native architecture for processing auditory and visual spatial information within the owl midbrain. Auditory spatial information is relayed from the central nucleus of the inferior colliculus (ICC) to the external nucleus of the inferior colliculus (ICX), where a map of space is formed. The space map in the ICX is then relayed to the optic tectum (OT) where it aligns with a map of visual space inherited from the retina. Prisms: the end result of prism-induced auditory plasticity. Prisms alter the horizontal trajectory of light hitting the retina, thereby shifting the visual map of space in the OT. In response to the altered visual space map, axonal growth and the formation of new synapses change the flow of auditory spatial information from the ICC to the ICX. These adaptive changes bring the auditory map of space back into alignment with the displaced visual map (red). The original anatomical projection from the ICC to the ICX remains, but the auditory responses it supports are suppressed by inhibition. After prisms: after prisms are removed the auditory space map returns to normal, however, the anatomical changes associated with prism adaptation remain (pink). This anatomical trace can be reactivated by experience in adulthood.

3.44.2.2 Instruction of the Auditory Space Map in the Inferior Colliculus

Prism-induced auditory plasticity is an example of supervised learning. While most prism experiments have focused on measuring auditory map plasticity in the OT, the ICX is the first nucleus in the midbrain auditory localization pathway to exhibit a shifted auditory space map. The auditory tuning of neurons in the lateral shell of the inferior colliculus (ICCls), one nucleus earlier in the pathway, is not affected by prism experience (Gutfreund, Y. and Knudsen, E. I., 2004). This finding raises two interesting questions. First, what is the source of instructive signals that guide auditory plasticity? Second, how does visual experience instruct auditory plasticity within a nucleus, the ICX, which is commonly regarded as a strictly auditory structure?

The instructive signal guiding auditory plasticity could either be a topographic template of visual space or it could simply indicate whether a particular head/eye movement was successful in foveating the source of an auditory stimulus. To distinguish between these two possibilities, Hyde P. S. and Knudsen E. I. (2001) raised owls with prisms that displaced only the representation of central visual space. If the instructive signal were a foveation-based signal, one would expect this manipulation to induce uniform plasticity across the entire auditory space map since all orienting movements must direct the optically displaced central gaze to the stimulus location. Alternatively, if the instructive signal were a topographic map of visual space, then one would expect this manipulation to induce plasticity only in the portion of the map that was displaced by prisms. The result was that only the auditory tuning of neurons corresponding to the prismatically displaced area of space was affected by prisms. Subsequently, the source of such a topographic instructive signal was identified as the OT: small lesions in the OT impeded auditory plasticity only in the portions of the ICX map that represented the same locations in space as lesioned in the OT (Hyde, P. S. and Knudsen, E. I., 2002).

Experiments have revealed a feedback projection from the OT to the ICX that meets all of the requirements necessary for an instructive signal (Hyde, P. S. and Knudsen, E. I., 2000; Luksch, H. *et al.*, 2000; Gutfreund, Y. *et al.*, 2002). These experiments provide two critical insights about the nature of this projection; (1) it is a point-to-point topographic projection from the OT to the ICX, and (2) it carries spatially selective visual signals that can be observed by blocking inhibition in the OT. These characteristics strongly suggest a role for this pathway in instructing adaptive auditory plasticity in the ICX. Characterizing the normal function of this potential instructive signal will be an exciting area of research.

3.44.2.3 Developmental Regulation of Map Plasticity

The plasticity of the auditory space map in the OT declines with age. This principle is illustrated by a set of experiments in which naïve owls were fitted with prisms at different ages. While prism experience led to nearly complete adaptive adjustments of the map in juvenile owls (meaning that the alignment of the auditory space map with the optically displaced visual space map was restored), the same prisms had little effect in adults (Brainard, M. S. and Knudsen, E. I., 1998). The decline in map plasticity occurs before owls are about 200 days old, which corresponds roughly to the age at which owls reach sexual maturity. Sensitive periods for auditory map development have also been described in the superior colliculus (mammalian homolog of the OT) of ferrets and guinea-pigs (King, A. J., 1999).

3.44.3 Manipulations that Increase Auditory Plasticity in Adults

The reduced plasticity observed in adult versus juvenile owls is not simply due to the same mechanisms operating more slowly in adults, since prolonging prism experience does not significantly increase adaptive plasticity. A number of factors could lead to the reduced plasticity in adult owls. For example, the system may be less plastic in adults; the signals that instruct auditory plasticity in juvenile owls may not be present, or are ignored, in adults; or the environmental and psychological factors required to induce plasticity may be more stringent in adults, and these conditions were not met in the early prism experiments. These possibilities are not mutually exclusive, and the experiments discussed below indicate that multiple factors regulate plasticity.

3.44.3.1 Training During the Juvenile Period

Adult plasticity is increased by learning during the juvenile period. When young owls are raised with prisms, they readily acquire a novel ITD map. After the prisms are removed, the auditory tuning in these owls returns to normal. Even though these owls express a functionally normal ITD map as adults, when exposed to the same prisms a second time they rapidly reacquire a shifted ITD map (Knudsen, E. I., 1998). The increased auditory plasticity in these adults is specific to the plasticity they expressed as juveniles: they are capable of adapting only to the prismatic shifts that they experienced as juveniles.

Prism adaptation physically changes the brain of young owls. The changes in ITD tuning observed in the ICX and OT are associated with an anatomical change in the axonal projection from the ICCls to the ICX. In prism-reared owls, this projection is significantly broader than in normal owls, and the broadened distribution of axon terminals in the ICX is skewed towards zones in which these terminals could support newly learned auditory responses (DeBello, W. M. *et al.*, 2001; Figure 2). Moreover, these acquired projections persist long after the prisms are removed, leaving an anatomical trace of the learning that could underlie the ability of adult owls to reacquire the alternative auditory map that was learned during the juvenile period (Linkenhoker, B. A. *et al.*, 2005; Figure 2). These results show that signals that instruct changes in auditory tuning continue to function, even though they often fail to affect auditory tuning in the adult owl.

3.44.3.2 Training in Small Increments

When adult owls are exposed to strong prisms (23° optical displacement), the auditory space map adjusts by less than 3°, even after 6 months of experience. In contrast, when owls are exposed to weak prisms (6° optical displacement), they acquire a full 6° shift of the auditory map within 3 weeks (Linkenhoker, B. A. and Knudsen, E. I., 2002). This adaptation to small prismatic shifts lays a foundation for subsequent adaptation to yet stronger prisms (Figure 3). When prismatic displacements are gradually introduced, owls eventually acquire dramatically shifted ITD maps to large (17–23°) prismatic displacements, displacements that have little effect on auditory tuning when introduced to adults as a single abrupt change in experience. Thus, a smaller difference between the desired and the existing auditory space map is more effective in altering the map of space in adult owls. Once owls have acquired a shifted ITD map through incremental training, they are able to reacquire the map in response to a single large displacement, indicating that incremental training increases the capacity for plasticity in this system.

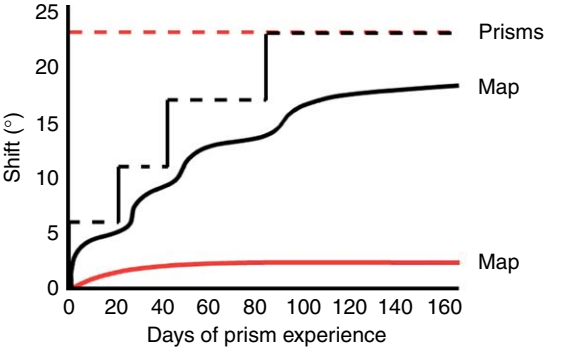

Figure 3 Incremental training increases auditory map plasticity. The ordinate represents both the prismatic shift of visual fields (Prisms; dashed lines), and the resulting shifts of the auditory space map (solid lines). Shifts in the auditory map were measured as the difference between the expected auditory tuning (based on nondisplaced visual tuning) and the observed auditory tuning. Auditory plasticity in adult owls is affected little by a single large (23°) prismatic displacement (red lines). In contrast, auditory tuning changes substantially in response to incremental increases in prismatic displacements. Black lines: adapted from Linkenhoker, B. A. and Knudsen, E. I. 2002. Incremental training increases the plasticity of the auditory space map in adult barn owls. Nature 419, 293–295.

3.44.3.3 Hunting Increases Map Plasticity

The midbrain auditory localization pathway has evolved in the context of specific types of experience. Hunting, in particular, is a crucial behavior that relies extensively on the optic tectum for directing an animal's gaze toward salient stimuli. In addition, hunting engages factors such as attention and arousal that are known to be important modulators of neural plasticity. However, in all prism experiments discussed so far, owls were not allowed to hunt live prey. Recent experiments have shown that allowing adult owls to hunt, while wearing prisms, induces five times more adaptive plasticity as compared to adult owls that are not allowed to hunt (Bergan, J. F. *et al*., 2005). One hypothesis is that experience with bimodal stimuli during periods of heightened attention and arousal underlies this effect. Another possibility is that not providing owls with the chance to perform instinctual behaviors induces a general depressed state which inhibits learning. While the mechanism by which exposure to hunting increases auditory map plasticity in adults is not yet known, it is clear that key environmental factors can have a dramatic influence on plasticity within the adult brain.

3.44.4 Conclusions

Auditory localization behavior and the underlying neural circuits are shaped by visual experience. Initially, it was thought that the influence of visual experience on auditory localization was restricted to a particular developmental window early in life. More recent experiments have shown that, although juveniles express greater plasticity than adults, adult owls maintain a substantial capacity for adaptive change. However, the experimental manipulations that elicit adaptive plasticity in adult owls are more sophisticated and reflect the kinds of experiences an adult owl might have naturally. For example, small changes in sensory experience are reminiscent of the effects of gradual aging on stimulus coding in the central auditory system, and hunting is of vital importance to an adult owl's survival. Through the growing understanding of important factors that modulate the capacity for plasticity throughout an animal's lifetime, we are becoming increasingly aware of the brain's astounding ability to acquire and maintain high performance by learning from experience.

References

Bergan, J. F., Ro, P., Ro, D., and Knudsen, E. I. 2005. Hunting increases adaptive auditory map plasticity in adult barn owls. J. Neurosci. 25, 9816–9820.

Brainard, M. S. and Knudsen, E. I. 1998. Sensitive periods for visual calibration of the auditory space map in the barn owl optic tectum. J. Neurosci. 18, 3929–3942.

DeBello, W. M., Feldman, D. E., and Knudsen, E. I. 2001. Adaptive axonal remodeling in the midbrain auditory space map. J. Neurosci. 21, 3161–3174.

Feldman, D. E. and Knudsen, E. I. 1997. An anatomical basis for visual calibration of the auditory space map in the barn owl's midbrain. J. Neurosci. 17, 6820–6837.

Gutfreund, Y. and Knudsen, E. I. 2004. Visual Instruction of the Auditory Space Map in the Midbrain. In: The Handbook of Multisensory Processes (*eds*. G. Calvert, C. Spence, and B. E. Stein), pp. 613–624. The MIT Press.

Gutfreund, Y., Zheng, W., and Knudsen, E. I. 2002. Gated visual input to the central auditory system. Sciences 297, 1556–1559.

Hensch, T. K. 2004. Critical period regulation. Annu. Rev. Neurosci. 27, 549–579.

Hyde, P. S. and Knudsen, E. I. 2000. A topographic projection from the optic tectum to the auditory space map in the inferior colliculus of the barn owl. J. Comp. Neurol. 421, 146–160.

Hyde, P. S. and Knudsen, E. I. 2001. A topographic instructive signal guides the adjustment of the auditory space map in the optic tectum. J. Neurosci. 21, 8586–8593.

Hyde, P. S. and Knudsen, E. I. 2002. The optic tectum controls visually guided adaptive plasticity in the owl's auditory space map. Nature 415, 73–76.

King, A. J. 1999. Sensory experience and the formation of a computational map of auditory space in the brain. BioEssays 21, 900–911.

Knudsen, E. I. 1982. Auditory and visual maps of space in the optic tectum of the owl. J. Neurosci. 2, 1177–1194.

Knudsen, E. I. 1998. Capacity for plasticity in the adult owl auditory system expanded by juvenile experience. Science 279, 1531–1533.

Linkenhoker, B. A. and Knudsen, E. I. 2002. Incremental training increases the plasticity of the auditory space map in adult barn owls. Nature 419, 293–295.

Linkenhoker, B. A., von der Ohe, C. G., and Knudsen, E. I. 2005. Anatomical traces of juvenile learning in the auditory system of adult barn owls. Nat. Neurosci. 8, 93–98.

Luksch, H., Gauger, B., and Wagner, H. 2000. A candidate pathway for a visual instructional signal to the barn owl's auditory system. J. Neurosci. 20, RC70.

Stein, B. E. and Meredith, M. A. 1993. The Merging of the Senses. The MIT Press.

Zheng, W. and Knudsen, E. I. 1999. Functional selection of adaptive auditory space map by GABAA-mediated inhibition. Science 284, 962–965.

Further Reading

Knudsen, E. I. 2002. Instructed learning in the auditory localization pathway of the barn owl. Nature 417, 322–328.

Knudsen, E. I. and Knudsen, P. F. 1989. Vision calibrates sound localization in developing barn owls. J. Neurosci. 9, 3306–3313.

3.45 The Functional Neuroanatomy of the Auditory Cortex

J H Kaas and T A Hackett, Vanderbilt University, Nashville, TN, USA

© 2008 Elsevier Inc. All rights reserved.

3.45.1	Introduction	765
3.45.2	Auditory Cortex in Primates	767
3.45.3	First Level of Cortical Processing: The Core Areas	767
3.45.4	Second Level of Cortical Processing: The Areas of the Auditory Belt	769
3.45.4.1	Caudolateral Area	771
3.45.4.2	Middle Lateral and Anterior Lateral Areas	771
3.45.4.3	Middle Medial and Rostromedial Areas	772
3.45.4.4	RTM and RTL Areas	772
3.45.5	Third Level of Cortical Processing: The Auditory Parabelt Areas	772
3.45.6	Levels of Auditory Processing Defined by Inputs from the Parabelt: Areas of the Fourth Level	773
3.45.7	Auditory Cortex in Humans	774
3.45.8	Auditory Cortex in Other Mammals	774
3.45.8.1	Cats and Other Carnivores	775
3.45.8.2	Rodents	776
3.45.8.3	Bats	776
3.45.9	Conclusions	777
References		778

Glossary

auditory core Those areas of auditory cortex at the first level of cortical processing. The core has the architectonic features of primary sensory cortex and distributes auditory information to other areas.

cortical area The larger functional subdivisions of cortex that are considered the organs of the cortex. They are distinguished by a unique set of anatomical and physiological features including a pattern of connections with other cortical areas and subcortical nuclei. Auditory and other sensory areas often have systematic representations of sensory receptors.

auditory belt A second level of cortical auditory processing in an array of eight proposed auditory areas surrounding the auditory core.

auditory parabelt A region of auditory cortex adjacent to the lateral auditory belt that receives inputs from belt areas and constitutes a third level of cortical processing.

dorsal and ventral streams Dosrsal core, belt, and parabelt regions are more densely interconnected with each other, as are ventral core, belt, and parabelt regions, forming the early stages of dorsal and ventral streams of auditory cortical processing The ventral stream appears to be more devoted to sound identification, while the dorsal stream is more devoted to sound localization.

3.45.1 Introduction

Auditory systems in mammals contain a large number of interconnected subcortical nuclei and cortical areas. The subcortical nuclei are thought to be highly similar across mammalian taxa (phylogenetic groups) but the subdivisions of auditory cortex vary. Thus, considerable processing of auditory stimuli occurs across five levels of nuclei in several parallel, interacting pathways before auditory cortex is reached (Figure 1).

At the level of cortex, all mammals appear to have one or more primary or primarylike auditory areas, a fringe or belt of a variable number of associated secondary areas, and perhaps one or two stages of further

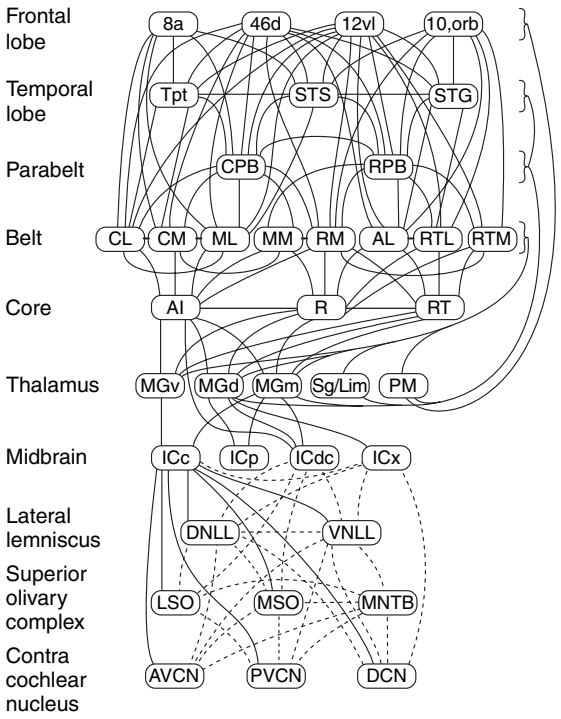

Figure 1 Subcortical and cortical connections of the auditory system in primates. Subdivisions are abbreviated within outlined ovals. Lines indicate connections between subdivisions. Dashed lines are based on studies in nonprimates that are presumed to exist in primates. Thalamic projections broadly distributed to cortical areas at a given level are indicated by brackets. Important connections of temporal lobe areas (temporoparietal (Tpt) and superior temporal sulcus (STS)) with posterior parietal areas are not included, but posterior parietal targets provide another route to the frontal cortex, especially to premotor areas. The cochlear nuclear complex includes anteroventral cochlear nuclei (AVCN), posteroventral cochlear nuclei (PVCN), and dorsal cochlear nuclei (DCN). The superior olivary complex includes the lateral superior olivary (LSO) and medial superior olivary (MSO) and nuclei, and the medial nucleus of the trapezoid body (MNTB). The lateral lemniscus includes the dorsal nucleus lateral lemniscus (DNLL) and ventral nuclear lateral lemniscus (VNLL). The inferior colliculus of the midbrain includes the inferior colliculus central nucleus (ICc), the inferior colliculus pericentral nucleus (ICp), the inferior colliculus dorsal cortex (ICdc), and the inferior colliculus external nucleus (ICx). The auditory thalamus includes the ventral medial geniculate (MGv), dorsal medial geniculate (MGd), medial (or magnocellular) geniculate (MGm) nuclei, as well as the suprageniculate (Sg) nucleus, the limitans (Lim) nucleus, and the medial pulvinar (PM) nucleus. In the cortex, the auditory core includes the primary auditory (A1) area, the rostral (R) area, and the rostrotemporal (RT) area. The auditory belt includes caudolateral (CL), caudomedial (CM), middle lateral (ML), medial middle (MM), rostromedial (RM), anterolateral (AL), rostrotemporal lateral (RTL), and rostrotemporal medial (RTM) areas. The parabelt is divided into caudal parabelt (CPB) and rostral parabelt (RPB) regions. Auditory regions of the temporal lobe include the Tpt, cortex of the STS, and cortex of the superior temporal gyrus (STG). Area 8a is periarcuate (in macaques) cortex in the region of the frontal eye field. Area 46d is prefrontal cortex for working memory in the region of the principal sulcus of macaques. Area 12vl is ventrolateral prefrontal cortex. Area 10,orb is orbitofrontal cortex and the frontal pole.

auditory processing. Auditory inputs may mix with somatosensory and visual inputs at even secondary stages of cortical processing. The organization of auditory cortex has been extensively studied in only a few species of mammals. In these species, an understanding of cortical organization has only gradually emerged, and is generally incomplete, with tentatively proposed features. Thus, it is accurate to describe current proposals as theories of cortical organization.

In this chapter we emphasize a theory of cortical organization for the auditory system of primates (Kaas, J. H. and Hackett, T. A., 2005). This theory is based on the results of over 30 years of study. Most of the information comes from studies of Old World macaque monkeys, and several species of New World monkeys, with some relevant results from prosimian galagos, and especially recently, important contributions from studies on humans. The cortical system outlined here appears to apply broadly to anthropoid primates (monkeys, apes, and humans), and at least partly to prosimian primates. The human auditory system obviously has cortical specializations

for language, and the cortical systems in the two hemispheres are not completely symmetrical. We will only briefly discuss these specializations. The evidence that cortical auditory systems are somewhat asymmetrical in apes suggests that the specializations have broader functions than language, but that the specializations increased with selection for language ability. For purposes of comparison, we will also discuss the organization of auditory cortex in rodents, carnivores, and bats, while recognizing that very little is known about the auditory cortex of the many other branches of mammalian evolution.

3.45.2 Auditory Cortex in Primates

Early concepts of the organization of auditory cortex in primates were influenced by the interpretations of early results in cats. Thus, a single primary area, A1, was defined, bordered by a second area, A2. This view was subsequently modified in that the concepts of an A2 and a single primary area were replaced by a proposed core of two or three primarylike areas, surrounded by a belt of secondary areas, and areas in several additional higher stages of cortical processing (Figure 1).

3.45.3 First Level of Cortical Processing: The Core Areas

Primary or primarylike areas of auditory cortex in mammals have several characteristic features. Most importantly, they receive dense, topographically organized projections from the principal or ventral nucleus of the medial geniculate (MGv) complex. This projection allows neurons in the primary auditory cortex to be narrowly tuned to tone frequencies so that best (threshold) or characteristic frequencies can be identified for cortical neurons, and that neurons with similar and different best frequencies are systematically arranged to form an orderly frequency map. Primary maps proceed from representing high best frequencies to low best frequencies across one dimension of the map, while best frequencies remain constant for contours across the other dimension of the map, the isofrequency contours. The terminal arbors of MGv axons in A1 and the intrinsic horizontal connections tend to be distributed along the isofrequency contours (see Ojima, H. and Takayanagi, M., 2004 for review). Primary auditory areas are also histologically specialized for having neurons with high levels of activity and constrained receptive fields. Thus, layer four of the primary auditory cortex is densely packed with small neurons, this area is usually more densely myelinated than surrounding areas, and they express high levels of the metabolic enzyme, cytochrome oxidase. In some mammals, including anthropoid primates, they also express high levels of the enzyme for deactivating the neuromodulator, acetylcholinesterase (AChE), and high levels of the calcium binding protein, parvalbumin (Hackett, T. A. *et al.*, 2001). Most or all primates appear to have three such primary areas, termed A1 (as the original primary area), R (for the area rostral to A1), and RT (for the rostrotemporal location).

The auditory core in macaque monkeys is located in the cortex of the lower bank of the lateral sulcus (Figure 2). Along the caudorostral (anteroposterior)

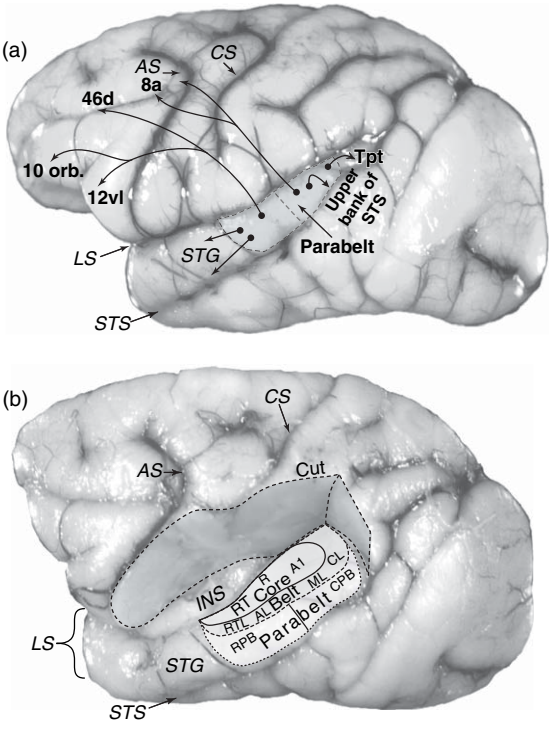

Figure 2 The locations of core, belt, and parabelt auditory fields on a lateral view of the brain of a macaque monkey. (a) An intact brain with the region of the parabelt outlined on the surface of the superior temporal gyrus (STG) located between the lateral sulcus (LS) and the superior temporal sulcus (STS). The frontal eye field is on the rostral bank of the arcuate sulcus (AS), while the central sulcus (CS) divides motor cortex from somatosensory cortex. Connections of the parabelt divisions are indicated with arrows. (b) In this view, the cortex overlying the lower bank of the LS and the insula (an island of cortex in another plane deep in the sulcus) has been exposed by cutting away (cut) the overlying portion of parietal and frontal cortex. See Figure 1 for abbreviations.

extent of the fissure, A1 is most caudal, followed by R and then RT.

The three areas form a band that is six or seven times longer than its width. Architectonically, the core is very distinct from surrounding cortex, while the three core areas are very similar. In brain sections cut parallel to the cortical surface, so that all boundaries of the core can be appreciated in a single section, sections processed for parvalbumin (Figure 3) and other markers clearly reveal the extent of the core. In general, the primarylike architectonic features are most pronounced in A1, and least pronounced in RT. A1 is the largest of the three core areas.

The position of the core varies somewhat relative to the lateral sulcus across primate species, so that in monkeys with a shallow sulcus, especially in the small marmoset monkeys, the core extends on to the surface of the temporal lobe (Aitkin, L. M. *et al.*, 1988; Luethke, L. E. *et al.*, 1989; Wang, X. M. M. *et al.*, 1995). As humans have a deep lateral fissure that contains additional fissures, the core is rotated in a manner that places A1 deepest in the fissure (Hackett, T. A. *et al.*, 2001).

The core was first divided into two areas, A1 and RL (for rostrolateral) by Merzenich M. M. and Brugge J. F. (1973), based on differences in tonotopic organization. Tones from high to low frequencies are represented in a caudomedial to rostrolateral sequence across A1, and in a reversed sequence across RL or R (Figure 4).

Later Imig T. J. *et al.* (1977) also used microelectrode recordings to identify these two fields in New World owl monkeys, while renaming RL the R area. Morel A. and Kaas J. H. (1992) subsequently defined the RT area as a third tonotopic representation, reversing the pattern in R to proceed from high to low in a caudorostral sequence. Recordings from RT have been limited, but good evidence for RT tonotopic organization has recently been obtained by Wang X. M. M. and co-workers (personal communication). In humans so far, functional magnetic resonance imaging (fMRI) data provide evidence of two tonotopic maps (Formisano, E. *et al.*, 2003) that appear to correspond to A1 and R of monkeys. As the shape of the auditory core is very similar in apes and humans to that of monkeys (Hackett, T. A. *et al.*, 2001), there is certainly room for three representations in the human core. In monkeys, MGv projects to A1, R, and RT (e.g., Morel, A. and Kaas, J. H., 1992; Morel, A. *et al.*, 1993; Hashikawa, T. *et al.*, 1995), providing further evidence of primary features for all three areas. As neurons in R remained responsive to tones after a lesion of A1 (Rauschecker, J. P. *et al.*, 1997), it is clear that A1 and R (and most likely RT) are independently activated by MGv projections.

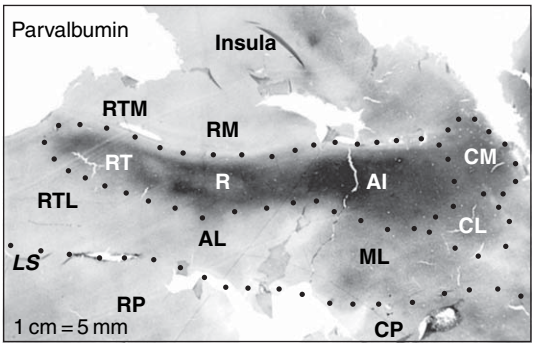

Figure 3 The core is histologically distinct from the surrounding belt and parabelt. Here the auditory region has been unfolded and flattened so that brain sections can be cut parallel to the surface. This allows all of the boundaries of the auditory cortex to be seen in a single brain section. A brain section has been processed for parvalbumin, a calcium-binding protein that is found in cortical areas of high neural activity. Although the brain section is somewhat damaged, the dark region expressing high levels of parvalbumin clearly defines the auditory core. Note that of the three core areas, RT expresses the lowest level of parvalbumin, and that belt areas CM and CL express moderate levels. The important point is that the core can be defined histologically, which both helps verify the concept of the core and aids identification in physiological studies. See Figure 1 for abbreviations. Adapted from Hackett, T. A., Stepniewska, I., and Kaas, J. H. 1998. Subdivisions of auditory cortex and ipsilateral cortical connections of the parabelt auditory cortex in macaque monkeys. J. Comp. Neurol. 394, 475–495. Wiley-Liss, with kind permission.

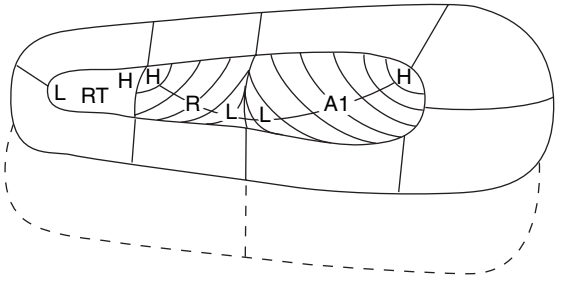

Figure 4 The tonotopic organization of A1, R, and RT of the core. A1 represents the frequencies of acoustic stimuli from high to low in a caudomedial to rostrolateral sequence across the area (compare with Figure 2). This pattern reverses in R and again in RT, providing the principle basis for dividing the core into three areas. The isofrequency contours in A1 and R are represented by curved lines. Along these contours, neurons respond best to the same frequency. RT has not been studied in enough detail to allow isofrequency contours to be depicted. See Figure 1 for abbreviations.

Neurons in the core areas project subcortically, to the adjoining auditory belt, and to matching locations

in the core of the other hemisphere (Luethke, L. E. *et al.*, 1989; Morel, A. and Kaas, J. H., 1992; Morel, A. *et al.*, 1993). Projections from each core area are most dense to adjoining portions of the belt, but sparse connections also exist between core areas and more distant belt areas. The three core areas also project to each other, most densely with the adjoining area or areas. Thus, the three core areas appear to function by modifying the signal sent by the thalamus, principally from the MGv nucleus, but also dorsal auditory thalamus (MGd) and medial (or magnocellular) auditory thalamus (MGm), and relaying the modified information in parallel to adjoining belt areas, to each other, to homologous belt areas in the other hemisphere, and via feedback connections to the MG complex and the inferior colliculus.

Quite surprisingly, there is evidence that a few neurons in the core, lateral belt and parabelt, as well as in the polysensory cortex of superior temporal sulcus (STS), project directly to portions of primary visual cortex subserving peripheral vision (Falchier, A. *et al.*, 2002; Rockland, K. S. and Ojima, J., 2003). The role of these unexpected auditory inputs to the earliest stage of visual processing is uncertain, but such presumably modulatory inputs could enhance the visual recognition, and help direct visual attention toward the source of a sound.

3.45.4 Second Level of Cortical Processing: The Areas of the Auditory Belt

The auditory belt consists of a narrow 2–3 mm fringe of cortex surrounding the core. The belt is defined as the surrounding zone with dense connections with the core. Remarkably, nearly all of the ipsilateral cortical connections of the core are with this narrow fringe of cortex: there are almost no connections with more distant cortical locations (however, see above). In this way, core auditory cortex differs from primary visual cortex (V1) in primates where V1 has dense connections with the middle temporal (MT) visual area, which is displaced from the V1 border into the upper temporal lobe, and differs from primary somatosensory cortex, area 3b, which has long connections with the second somatosensory (S2) area and the parietal ventral (PV) area in the upper bank of the lateral fissure. The belt cortex is easily distinguished from the core in that it is architectonically much less differentiated than the core, reflecting less specialization than the core for receiving relatively unprocessed sensory information and maintaining high levels of neural activity. Thus, layer four is less pronounced, the cytochrome oxidase levels of layer four are reduced, and less AChE and parvalbumin (Figure 3) are expressed. The belt receives only sparse inputs from MGv, but instead has most of its thalamic inputs coming from MGd and MGm. As neurons in the belt reflect a second level of cortical processing, these neurons are generally more depressed by anesthetics. They are also less responsive to pure tones, and more responsive to complex auditory stimuli. Nevertheless, many neurons are responsive enough to tones or frequency-centered narrow bands of noise so that best frequencies can be estimated, and frequency (tonotopic) patterns can be determined (Rauschecker, J. P. *et al.*, 1995). Such tonotopic patterns, together with patterns of cortical connections, population differences in neuron responses to auditory stimuli, and subtle differences in cortical architecture have been used to subdivide the core into as many as eight presumptive areas. For Brodmann K. (1909), a cortical area was a functionally distinct subdivision of the brain. As areas may have functionally different subunits (modules), an area should have an overall unifying feature, such as a single tonotopic map, as in A1, R, and RT. Some of the proposed subdivisions of the belt remain tentative areas because such unifying features have not been revealed yet.

Presently, there is evidence that three auditory belt areas have separate representations of cochlea. A best-frequency series for neurons across the caudorostral length of the mediolateral (ML) area parallels that of A1 and proceeds from high to low best frequencies. A reverse sequence from low to high in the anterior lateral (AL) area parallels the tonotopic organization of R. As the complete tonotopic representation in RT has only recently been determined, the possibility of frequency representations in the rostrotemporal lateral (RTL) and rostrotemporal medial (RTM) banding fields has not been explored. Likewise, little is known about the less accessible fields medial to R (RM) and medial to A1 (middle medial (MM)), but their respective association with R and A1 via dense interconnections suggests that tonotopic patterns exist. The two areas that form the caudal cap of A1 also appear to contain crude tonotopic representations in that neurons near the A1 border are more responsive to high frequencies than neurons more displaced from that border (Kajikawa, Y. *et al.*, 2005).

The cortical connections of the more accessible lateral belt areas, AL and ML, are most known (Figure 5).

ML is interconnected with all three core areas, but most densely with A1 and only sparsely with R. ML has connections with a number of belt areas, but most densely with adjoining areas AL and caudolateral (CL). Dense connections are with the adjoining caudal division of the auditory parabelt (CPB) and sparser connections are with the rostral parabelt (RPB). Other ipsilateral connections involve dorsal portions of prefrontal cortex. Callosal connections with the other hemisphere are focused in ML. AL has a similar pattern of cortical connections, with the difference that connections with R, rather than A1, are most dense and connections involve nearby belt areas, the RPB more than the CPB, a matching location in the other hemisphere and more ventral locations in the frontal lobe.

The more ventral targets in the parabelt and frontal lobe for AL and ML are part of the support for the theory that two main functional streams of interconnected areas emerge from the early levels of auditory processing in primates; a ventral stream more specialized for sound identification and a dorsal stream more specialized for localizing sound sources (what and where pathways; see Kaas, J. H. and Hackett, T. A., 1999; Romanski, L. M. *et al.*, 1999a; 1999b; Rauschecker, J. P. and Tian, B., 2000). Further evidence for these streams is discussed in subsequent sections of this chapter.

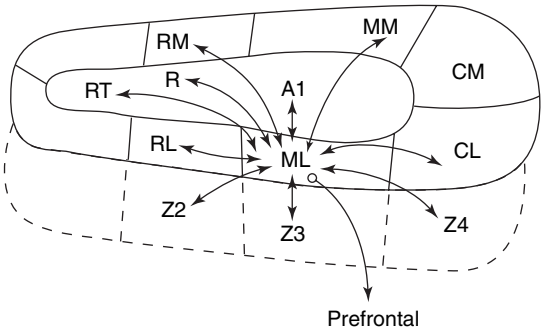

Figure 5 Cortical connections of areas of the auditory belt. Here the connections of the middle lateral (ML) area are indicated by arrows. The dashed arrows signify sparser connections. The connections of only a few of the belt areas have been determined, but they all are expected to have connections with nearby core and belt areas, as well as the parabelt. Z2–Z4 are arbitrary zones in the parabelt. Z1 (not indicated) and Z2 correspond to the rostral parabelt and Z3 and Z4 correspond to the caudal parabelt. See Figure 1 for abbreviations.

Two areas of the belt have been more extensively studied. The caudomedial (CM) area and to a lesser extent, the CL area, stand out as fields that express slightly more parvalbumin (Figure 3) and cytochrome oxidase than other belt areas, and thus appear to be somewhat corelike. Merzenich M. M. and Brugge J. F. (1973) first defined CM of macaque monkeys in roughly the position of CM as illustrated here (Figure 1). As many neurons in CM responded well to pure tones, Merzenich M. M. and Brugge J. F. determined best frequencies for neurons at enough sites in CM to suggest that the area represents high to low best frequencies in a progression away from the A1 border. This result has been confirmed by Kajikawa Y. *et al.* (2005) in an extensive comparison of neuron response properties in A1 and CM. In both areas, neurons responded well to broadband noise and to tones. As a population, neurons in CM had shorter response latencies, lower thresholds, and broader frequency tuning than neurons in A1. CM was tonotopically organized with neurons selective for middle frequencies under-represented. While the response characteristics and architectonic features of neurons suggest a close relationship to the core, CM is not included in the core because these features are muted compared to the core, and more important, CM depends greatly on inputs from A1 for activation. Rauschecker J. P. *et al.* (1997) found the responsiveness of neurons in CM to be greatly depressed by lesions to A1, providing evidence that CM is serially activated by A1. This is consistent with the anatomical evidence that MGv projects densely to A1 but only sparsely to CM (Hackett, T. A. *et al.*, 2007; Molinari, M. *et al.*, 1995; Rauschecker J. P. *et al.*, 1995; 1997). Nevertheless, some responsiveness remains in CM after A1 lesions. This responsiveness is likely mediated by MGd and MGm inputs to CM, as the responsive neurons do not have A1 qualities. The overall shorter latencies of CM neurons to sounds may be mediated by MGm inputs that involve larger diameter axons.

The most remarkable feature of CM is that it has many neurons that respond to somatosensory stimuli, especially light touch on the head and neck (Schroeder, C. E. *et al.*, 2001; Fu, K. M. *et al.*, 2003). Many neurons respond to both somatosensory and auditory stimuli. The source of this somatosensory input is presently uncertain, although CM does have connections with regions of cortex in the lateral sulcus that are likely to be somatosensory, and locations in the ventral thalamus that also could be somatosensory (de la Mothe, L. *et al.*, 2006a; 2006b; Smiley, J. F. *et al.*,

2007; Hackett, T. A., *et al.*, 2007). What is remarkable about this finding is that a second-level auditory area is highly responsive to somatosensory stimuli, and the area is clearly multisensory (or bisensory). Second-level visual or somatosensory areas are not multisensory. The significance of this early combination of somatosensory and auditory stimuli is as yet uncertain, but the ipsilateral cortical connections of CM are largely to the CPB, and the adjoining temporoparietal (Tpt) region (see below). These are considered components of the dorsal stream of auditory processing. Thus, CM may be more involved in contributing to spatial-processing stimuli, and may combine sounds and touch to focus attention toward parts of the body.

In humans, fMRI studies show that a region adjoining the auditory core is activated by both somatosensory and auditory stimuli (Foxe, J. J. *et al.*, 2002). These results support anatomical evidence that an area corresponding to CM exists in humans (Hackett, T. A. *et al.*, 2001).

3.45.4.1 Caudolateral Area

Located just lateral to CM, the CL area is a field that can be identified architectonically as it expresses less parvalbumin than adjoining areas CL and A1, but more than adjoining ML and Tpt (Figure 3). CL is also tonotopically organized as neurons near the A1 border respond better to band-passed noise bursts centered at high frequencies, while those near the caudal border prefer low frequencies (Rauschecker, J. P. *et al.*, 1995). Thus, CL and CM have parallel tonotopic organizations. Thalamic inputs are from MGd and MGm, rather than MGv (Molinari, M. *et al.*, 1995), and cortical connections are with A1, adjoining areas of the belt, the CPB, and adjoining Tpt. Neurons sensitive to the spatial locations of sounds are reported to be more common in CL than other parts of the lateral belt (Tian, B. *et al.*, 2001), but they are also found in CM (Recanzone, G. H. *et al.*, 2000b). Providing information about the locations of sound sources is a basic function of the dorsal stream of auditory cortical areas, and CL and CM have neuronal properties and cortical connections that are highly consistent with this function (Woods, T. M. *et al.*, 2006).

3.45.4.2 Middle Lateral and Anterior Lateral Areas

The portion of the lateral belt just lateral to A1 is known as the middle lateral area, ML (Rauschecker, J. P. *et al.*, 1995). The region had been previously called the lateral field, L, by Merzenich M. M. and Brugge J. F. (1973), and the posterior lateral field, PL, by Fitzpatrick K. A. and Imig T. J. (1980). ML contains a coarsely tonotopic representation of high-to-low frequencies from caudal to rostral in parallel with the representation in A1 (Merzenich, M. M. and Brugge, J. F., 1973; Morel, A. *et al.*, 1993; Rauschecker, J. P. *et al.*, 1995; Kosaki, H. *et al.*, 1997). ML has dense connections with A1, and sparse connections with R that are weakly topographical (Fitzpatrick, K. A. and Imig, T. J., 1980; Aitkin, L. M. *et al.*, 1988; Luethke, L. E. *et al.*, 1989; Morel, A. *et al.*, 1993). As for other belt areas, thalamic inputs are from MGd and MGm, rather than MGv (Morel, A. and Kaas, J. H., 1992). Other connections are with CL, MM, and AL of the belt. ML is strongly connected with the CPB. ML also has connections with cortex just rostral to the frontal eye field (Morel, A. and Kaas, J. H., 1992; Romanski, L. M. *et al.*, 1999a; 1999b). These connections may indirectly provide auditory information that directs eye movements via the frontal eye field to sound sources of interest. Thus, the frontal cortex connections, as well as those to the CPB, associate ML with the dorsal stream of processing. However, neurons in ML reportedly respond better to recorded monkey calls than energy-matched complex sounds (Rauschecker, J. P. *et al.*, 1995), and sound recognition would be a postulated feature of the ventral stream.

The AL area occupies the portion of the lateral belt that borders area R (Imig, T. J. *et al.*, 1977). Neurons in AL are broadly tuned to tone frequency, but they form a tonotopic sequence from caudal neurons preferring low frequencies to rostral neurons preferring high frequencies in parallel with the tonotopic organization of R (Imig, T. J. *et al.*, 1977; Morel, A. *et al.*, 1993; Rauschecker, J. P. *et al.*, 1995; Kosaki, H. *et al.*, 1997). Thalamic inputs are from MGm and MGd, as well as the medial pulvinar and posterior thalamus (Morel, A. and Kaas, J. H., 1992; Molinari, M. *et al.*, 1995). AL has dense connections with R, less dense connections with A1, connections with other belt areas, and more dense connections with the RPB than the CPB (Fitzpatrick, K. A. and Imig, T. J., 1980; Morel, A. and Kaas, J. H., 1992; Hackett, T. A. *et al.*, 1998). AL connections that are more distant are with lateral prefrontal cortex and orbital frontal multisensory cortex (Romanski, L. M. *et al.*, 1999a; 1999b), consistent with a proposed role in the ventral-processing stream devoted to sound recognition and evaluation. In support of this proposed role of AL, Tian B. *et al.* (2001) reported that

neurons in AL were more tuned to monkey vocalizations and less to sound source localization than neurons in CL.

3.45.4.3 Middle Medial and Rostromedial Areas

The areas of the medial belt have not been extensively explored, largely because of their less accessible position deep in the lateral sulcus. However, the MM area and the RM field receive dense projections from their respective adjoining core areas, A1 and R (Imig, T. J. *et al.*, 1977; Morel, A. and Kaas, J. H., 1992; Morel, A. *et al.*, 1993; de la Mothe, L. A. *et al.*, 2006a). This raises the possibility of crude tonotopic organization in both areas. Other connections are with belt areas CL and MM (Morel, A. *et al.*, 1993) and with the parabelt, with MM more connected with the CPB and RM more with the RPB (Hackett, T. A. *et al.*, 1998). Injections of tracers to frontal granular cortex labeled neurons in the location of MM (Romanski, L. M. *et al.*, 1999a; 1999b). Little is known about the response properties of neurons in MM and RM other than their poor response to tones (Merzenich, M. M. and Brugge, J. F., 1973). RM is expected to be more involved in ventral-stream processing and MM in dorsal-stream processing.

3.45.4.4 RTM and RTL Areas

While the evidence for a third core area, RT, is fairly solid, little is known about the proposed bordering belt areas, RTM area, and the RTL area. An injection in RT demonstrated connections with both belt areas (Morel, A. and Kaas, J. H., 1992), and both areas have connections with the auditory parabelt (Hackett, T. A. *et al.*, 1998). Unfortunately, the location of the medial belt areas in the depths of the lateral sulcus has made it difficult to determine their connections fully. As noted above, area CM has neurons that respond to touch, and some of the cortical and thalamic connections may involve somatosensory structures. Cortex adjoining the medial belt in the depths of the lateral sulcus, on the insula, and on the upper bank of the lateral sulcus is largely or completely somatosensory in function, and short interconnections could mediate bisensory (somatosensory plus auditory) functions. At least two of the proposed somatosensory areas of the lateral sulcus, the PV area and the ventral somatosensory area (see Qi, H. X. *et al.*, 2002) have neurons that respond to auditory stimuli. Area PV, at least, appears to have connections with the medial belt (Disbrow, E. *et al.*, 2003). A study of neural metabolic activity in response to auditory stimuli implicates much of somatosensory cortex of the lateral sulcus in auditory functions (Poremba, A. *et al.*, 2003).

3.45.5 Third Level of Cortical Processing: The Auditory Parabelt Areas

In monkeys, the auditory parabelt occupies much of the sector of the superior temporal gyrus (STG) that adjoins the lateral belt (Figure 1). As the lateral belt is not markedly distinct in architectonic features from most of the adjoining cortex, and there is no evidence of one or more systematic representations of any parameter of sound, such as frequency, the auditory belt is defined by a unique feature of its cortical connection pattern. Injections of tracers in any part of the parabelt label large numbers of neurons in the auditory belt, but not the core (Hackett, T. A. *et al.*, 1998). Although injections in the belt may label a few neurons in the core, a series of injections across the length of the parabelt will fill the medial and lateral belt areas with labeled neurons while labeling only the occasional neuron in the core. The dense population of labeled neurons defines the belt well while outlining the core. The obvious interpretation of this pattern of connections is that all belt areas provide the major inputs to the parabelt, but the parabelt is virtually free of a direct influence from the core. Thus, the first, second, and third levels of processing in auditory cortex of primates are clearly defined. In contrast, the more widely distributed connections of early stages of processing the visual and somatosensory systems of primates complicates the assignment of cortical areas to levels (Felleman, D. J. and Van Essen, D. C., 1991).

The size of the parabelt suggests that it may contain several functionally distinct areas, but presently there is no clear evidence of how or if the region is subdivided. Hackett T. A. *et al.* (1998) divided the parabelt into RPB and CPB regions based on differences in connections. Most notably, the RPB has its most dense connections with the rostral belt, and the CPB has its most dense connections with the caudal belt. However, the belt connection pattern shifts from rostral to caudal as the locations of injections of tracers move from caudal to rostral in the parabelt. Thus, there appears to be no sharp border between

the RPB and the CPB where the connection pattern sharply changes. Based on these connections, the parabelt may be considered a single area, two areas, or possibly three or four. For convenience, we divide the region into rostral and caudal halves. Cortex is considered to be outside the parabelt when injections of tracers fail to label more than an occasional neuron in the belt.

The outputs of the parabelt are with several cortical targets. These diverse regions constitute the fourth level of processing where various systems interact, and a strict hierarchy of fields is no longer apparent. These targets of the parabelt are discussed in a subsequent section of this chapter.

Just as the lateral parabelt is defined by connections of the belt, it seems possible that cortex in the lateral sulcus could receive inputs from the belt and thus constitute an unrecognized medial parabelt. However, this is unlikely for several reasons. Most notably, the lateral parabelt has connections with both medial and lateral belt areas. Injections in the lateral belt areas do not label regions of cortex outside the medial belt in the lateral fissure. In addition, the cortex adjoining the medial belt is dominated, largely or completely, by somatosensory inputs. Nevertheless, it does seem likely (see above) that some connections between medial belt areas and somatosensory cortex of the lateral fissure do exist, but functionally this cortex would be much different from an auditory parabelt.

3.45.6 Levels of Auditory Processing Defined by Inputs from the Parabelt: Areas of the Fourth Level

All regions of cortex with direct connections with the parabelt can be considered a diverse, distributed, fourth cortical level of auditory processing. One of these regions in macaque monkeys is the cortex of the upper bank of the STS (Seltzer, B. and Pandya, D. N., 1994; Hackett, T. A. *et al.*, 1998). Much of this STS cortex is visual as well as auditory (see Cusick, C. G., 1997 for review; Poremba, A. *et al.*, 2003), and some of this cortex may be involved in localizing visual objects that emit a sound and recognizing that a given object is producing the sound (Recanzone, G. H., 2004). This cortex may be important in the ventriloquist effect where a nearby sound is attributed to an object that appears to be the sound source. The STS cortex appears to provide feedback connections to the lateral belt and parabelt indirectly to the core where visual facial and vocal expressions of monkeys interact to enhance or suppress neural activity (Ghazanfar, A. A. *et al.*, 2005).

The parabelt also distributes connections to adjoining parts of the STGr, including more rostroventral parts that appear to be largely auditory in function, and part of the proposed ventral auditory stream related to sound identification and evaluation. The STGr region has connections with orbital parts of the frontal lobe, where multisensory neurons, including some responsive to auditory stimuli, are found. This cortex is involved in evaluating the hedonistic or rewarding value of stimuli (Rolls, E. T., 2004). Thus, primary reinforcing attributes of complex stimuli are associated with otherwise neutral aspects. The dorsocaudal tip of the gyrus, a region referred to as Tpt (or STGc), also receives parabelt inputs. Neurons in Tpt respond to auditory, visual, and somatosensory stimuli (Leinonen *et al.*, 1980). As this cortex projects to the region of the frontal eye field in the frontal lobe, a role in directing attention and eye movements toward sound sources of interest is likely (Huerta, M. F. *et al.*, 1987). This portion of the temporal lobe may also be involved in providing auditory signals to adjoining posterior parietal cortex (see Lewis, J. W. and Van Essen, D. C., 2000). Regions of posterior parietal cortex, especially those in the intraparietal sulcus of macaque monkeys are known for receiving somatosensory and visual inputs to guide reaching, eye, and other movements via connections with motor and premotor areas of the frontal lobe (see Fang, P. C. *et al.*, 2005 for review). Neurons in one of these areas, the lateral intraparietal (LIP) area respond to auditory signals after training on sound localization tasks (Grunewald, A. *et al.*, 1999). LIP is an area involved in directing eye movements toward targets. While visual signals usually guide this behavior, responses to auditory signals can be acquired.

The CPB and, to a lesser extent, the caudal belt areas are interconnected with the frontal granular cortex in the region of the principal sulcus of macaque monkeys (Hackett, T. A. *et al.*, 1999; Romanski, L. M. *et al.*, 1999a; 1999b). This region of cortex that has been implicated in short-term or working memory (e.g., Funahashi *et al.*, 1989; Constantinidis, C. *et al.*, 2001). These auditory inputs could be used to guide a reach or eye movement after a short delay.

Finally, the RPB and areas of the rostral belt contribute to the cortex of the inferior frontal lobe including the orbital and polar regions (Hackett, T. A. *et al.*, 1999; Romanski, L. M. *et al.*, 1999a; 1999b). These

areas are thought to be involved in object identification and object evaluation (Rolls, E. T., 2004). Thus, information about sounds could contribute to the multisensory identification of objects and their evaluation as tasty, rewarding, or unpleasant.

While these auditory areas of the fourth level greatly expand the proportion of cortex involved in auditory processing, additional regions of cortex show increased metabolic activity in response to auditory stimuli (Poremba, A. *et al.*, 2003), and thus are involved in audition. However, most of these regions, as well as much of auditory cortex of the fourth level, are bisensory or multisensory, and are likely not to be mainly auditory in function. As bisensory convergence occurs in the auditory cortex as early as the second level in CM, multisensory integration appears to be especially emphasized at the cortical level in the auditory system (see Schroeder, C. E. *et al.*, 2003; Ghazanfar, A. A. *et al.*, 2005).

3.45.7 Auditory Cortex in Humans

The early stages of cortical auditory processing in humans appear to be similar to those of monkeys. Thus, there is an elongated core region (Hackett, T. A. *et al.*, 2001) that appears to contain A1 and at least one other tonotopically organized area (Formisano, E. *et al.*, 2003; Talavage, T. M. *et al.*, 2004), and belt and parabelt regions have been postulated (see Hackett, T. A., 2002; Talavage, T. M. *et al.*, 2004; Sweet, R. A. *et al.*, 2005; Hackett, T. A., 2007 for review). The cortex of the lateral sulcus of humans is more complexly folded than in monkeys, creating Heschl's gyrus where the auditory core has been rotated so that A1 is deeper in the lateral fissure than presumptive R and RT. In the auditory belt of humans, a region that is activated by both touch and sounds has been identified as a probable homolog of the belt area CM of monkeys (Hackett, T. A. *et al.*, 2001; Foxe *et al.*, 2002). In monkeys, core, belt, and parabelt areas may represent, in part, preprocessing stages for the recognition of communication sounds (Rauschecker, J. P., 1998), and these three levels of processing may function in a similar role for the preprocessing of language in humans (Lewis, J. W. *et al.*, 2005). As part of the specialization of the left cerebral hemisphere for language in humans, the left Heschl's gyrus is more caudal than the right (Penhune, V. B. *et al.*, 1996). Asymmetries between the left and right hemispheres, such as in the extent and course of the lateral sulcus, have been repeatedly used as anatomical evidence for the specialization of the left cerebral hemisphere for language in humans. Interestingly, such asymmetries have been described from the skull endocasts, reflecting brain sulci, of fossil hominids, and even in macaque monkeys, arguing that hemispheric specialization in auditory function have a long history, and were not initiated by the emergence of language. In general, as brains get bigger, the cost of the long connections between hemispheres increases, and concentrating functions in one hemisphere or the other reduces the need for such long connections. In humans, a region adjoining Heschl's gyrus is enlarged in the left hemisphere (the planum temporale) and this region appears to be important in language as part of Wernicke's area. In the frontal lobe, a premotor region is larger in the left hemisphere, constituting a central part of Broca's speech area (Foundas, A. L. *et al.*, 1996). This premotor region may have emerged as a specialization of the rostral part of ventral premotor cortex of other primates (Preuss, T. M., 1995; Petrides, M. *et al.*, 2005). The region thought to be homologous to Broca's area in great apes is larger in the left than the right hemisphere (Cantalupo, C. and Hopkins, W. D., 2001). As in monkeys, what and where processing streams have been proposed for humans (e.g., Clarke, S. *et al.*, 2005). However, current understandings of the numbers and types of areas involved in auditory processing in humans are limited, and the full extent of differences in human and monkey auditory systems is not known.

3.45.8 Auditory Cortex in Other Mammals

Although an auditory core and belt seem to characterize auditory cortex in all studied mammals, auditory cortex has not been studied in detail in most mammals. However, more is known about the auditory cortex in cats, rodents, and echolocating bats. The basic features of auditory cortex organization of these mammals are outlined here for comparison with those of primates. In brief, the evidence suggests that a core of two or three areas and a belt of a number of additional areas exist in carnivores, rodents, and bats. Areas known as A1, anterior auditory field (AAF), and posterior auditory field (P; see below) may be homologous parts of the core in these mammals. As of now, homologies across mammals in belt fields, if any, remain uncertain.

3.45.8.1 Cats and Other Carnivores

Until recently, domestic cats have been the preferred research animals for investigating the cortical organization of the auditory system. As a result, much is known about auditory cortex in cats. In brief, cats have three primarylike auditory areas, named in a rostrocaudal sequence (Figure 6), the AAF, primary auditory cortex (A1), and P.

All three areas contain systematic representations of sound frequencies (see Imig, T. J. and Reale, R. A., 1980). A1 was the first of the three to be recognized (Woolsey, C. N. and Walzl, E. M., 1942), and the term A1 reflects that distinction. A1 has bands of isofrequency representation that course dorsoventrally across the area, while high-to-low frequencies are represented from rostral to caudal. A second auditory area, A2, was also proposed as the result of these early landmark studies (Woolsey, C. N. and Walzl, E. M., 1942; Woolsey, C. N., 1960). The original A2 was thought to have a reversed tonotopic organization from that of A1, but this was a misinterpretation, apparently as the result of recordings from rostral low-frequency zones in AAF and caudal high-frequency zones in P. Currently, A2 is viewed as a typical belt area with neurons more broadly tuned to frequency, and a tonotopic organization in parallel to that in A1 (high to low in a rostrocaudal direction), much as belt areas parallel the tonotopic organizations of A1 and R in monkeys (Schreiner, C. E. and Cynader, M. S., 1984). AAF has tonotopic organization from high-to-low frequencies in a caudorostral direction, to mirror A1 in organization (Knight, P. L., 1977). P extends ventrally from the caudal pole of A1 in a tonotopic pattern that reverses from that in A1 so that low tones are represented dorsally next to A1 while progressively higher tones are represented in progressively more ventral locations. All three areas have the histological features of core sensory cortex, such as a well-developed layer four with a high expression of cytochrome oxidase. A ventroposterior (VP) area reverses the tonotopic organization of P, and VP may also be part of the auditory core. Areas AAF, A1, and P all receive inputs from the MGv suggesting that they all have primarylike functions as targets of parallel projections from the auditory thalamus (Imig, T. J. and Morel, A., 1983; Lee, C. C. *et al.*, 2004). Matched tonotopic regions in the three areas are interconnected (Imig, T. J. and Reale, R. A., 1980). The core area also projects to adjoining ventral, temporal, dorsoposterior (DP), and second (A2) belt areas, and to portions of cingulate and multimodal cortex (Imig, T. J. and Reale, R. A., 1980; Lee, C. C. *et al.*, 2004). Belt cortex dorsal to A1 and AAF in the suprasylvian sulcus, called the suprasylvian fringe, also has A1 and AAF connections.

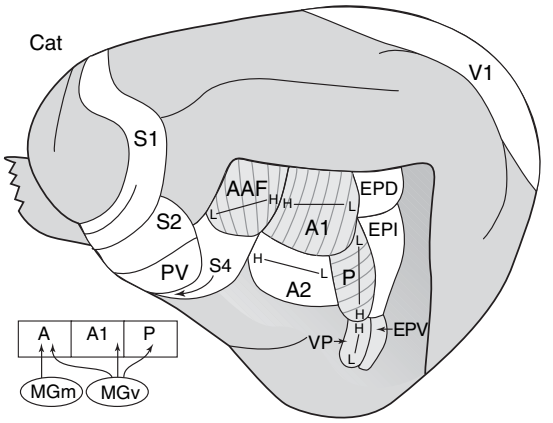

Figure 6 Proposed auditory areas in the domestic cat. Three primarylike areas include the anterior auditory field (A or AAF), the classical primary (A1) area, and the posterior (P) area. Each gets inputs from the ventral nucleus of the medial geniculate complex (MGv), although other inputs such as those from the medial (or magnocellular) geniculate nucleus (MGm), are more prevalent in A and P (see box diagram on lower left). AAF, A1, and P all have tonotopic organizations that reverse from each other at common borders. Parallel lines in these areas denote lines of isorepresentation. A2 and the ventroposterior (VP) area have crude patterns of tonotopic organization. Other auditory areas or regions include the suprasylvian fringe of auditory belt dorsal to A1 in the suprasylvian sulcus (not shown), and dorsal ectosylvian gyrus (EPD), intermediate ectosylvian gyrus (EPI), and ventral ectosylvian gyrus (EPV) sectors. The locations of somatosensory areas (primary somatosensory cortex, S1; second somatosensory area, S2; fourth somatosensory area, S4 – see arrow; parietal ventral (PV) area) and primary visual cortex (V1) are shown for reference.

Overall, cats have an auditory system that is characterized by the number of auditory areas that interconnect to form several parallel processing streams. Auditory inputs join somatosensory and visual inputs in multisensory cortex that provides an important projection to the superior colliculus to help direct eye and head movements toward stimuli of interest (Stein, B. E. *et al.*, 2004). At least superficially, the complex array of auditory areas in cats resembles that of primates, but homologies between areas are uncertain. Most notably, A1 of cats appears to have the opposite order of tonotopic representation of A1 of monkeys, where posterior A1 represents high, not low, tones. Thus, A1 of cats resembles area R of monkeys in tonotopic organization. This may be no more than a difference in rotation of the auditory

core as cortex expanded in the evolution of primates and carnivores. Uncertainties in the homologies of even A1 suggest the difficulty of postulating further homologies in cortical auditory areas in the primate and carnivore taxa. Other carnivores appear to resemble cats in the organization of auditory cortex, although relevant information is limited. Dogs have an AFF and A1 with reversed tonotopic organization as in cats, but clear evidence for a third representation in P is lacking (see Malinowska, M. and Kosmal, A., 2003). There is evidence for other fields, but they have not been well defined. Ferrets have an A1 with a tonotopic organization as in cats while two fields mirror A1 in tonotopic organization ventral to the low-frequency portion of A1 (Bizley, J. K. *et al.*, 2005). AAF of ferrets proceeds from high to low tones along the rostral border of A1 more in parallel with the progression in A1 than a reversal. Studies on these and other carnivores could usefully help identify the basic features of auditory cortex organization in carnivores.

3.45.8.2 Rodents

Rodents also have a corelike area with a surrounding belt of secondary auditory cortex. Because rodents are very convenient laboratory animals, auditory cortex has been studied in a number of rodents, including rats, mice, gerbils, guinea-pigs, squirrels, and chinchillas. However, a number of different schemes for how auditory cortex is organized have been generated, along with clear inconsistencies across schemes. Most notably, A1 has been described as having a rostrocaudal tonotopic organization from high to low tones in some rodents, and from low to high tones in other rodents. Other adjoining areas are variously named and described in rodents. One proposal with considerable experimental support is that of Scheich H. and Zuschratter W. (1995) for gerbils (Figure 7).

According to this proposal, gerbils have three areas, AAF, A1, and DP that are arranged and have tonotopic progressions much like AAF, A1, and P in cats. All three areas may be considered core areas in that they receive parallel inputs from the MGv nucleus (Budinger, E. *et al.*, 2000b), although the inclusion of DP in the core is somewhat questionable. At least ventrally, a belt of secondary areas has been defined. The interconnections of these auditory areas have been described by Budinger E. *et al.* (2000a). In other rodents, especially guinea-pigs, a dorsal belt of secondary areas has been identified (Wallace, M. N. *et al.*, 2000; Horikawa, J. *et al.*, 2001), so it is reasonable

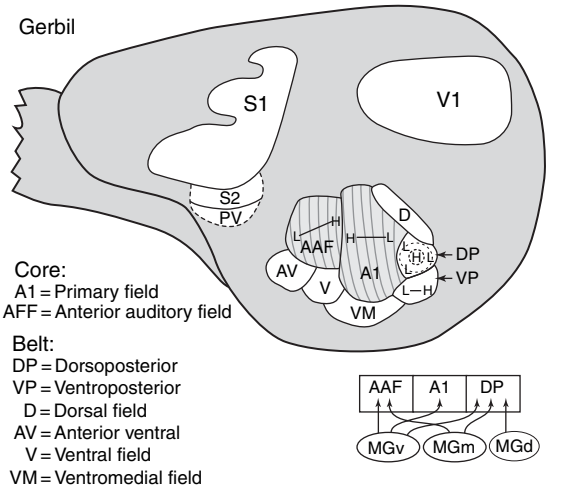

Figure 7 Proposed auditory areas in one of the more studied rodents (gerbil). In this and several other studied rodents, three primarylike areas have been identified, including a primary (A1) area with a representation of high-to-low frequencies in a rostrocaudal direction, much as in cats (Figure 6). The anterior auditory field (AAF) reverses this organization, closely resembling AAF of cats. Lines of isorepresentation are indicated in A1 and AFF. The posterior (P) area of other rodents has been divided here into dorsal (DP) and ventral (VP) components, with a more complex tonotopic organization in DP than VP. All three areas (AAF, A1, and P or DP) receive inputs from the ventral division of the medial geniculate complex (MGv), with the magnocellular division (MGm) projecting more to AAF and DP than A1, and the dorsal division (MGd) projecting more to DP (box diagram on lower right). Core and belt areas are defined in the figure. The locations of somatosensory areas S1, S2, and parietal ventral (PV) area and primary visual cortex (V1) are shown for reference. Auditory areas are based on Scheich H. and Zuschratter W. (1995).

to postulate both ventral and dorsal belts in rodents. The three corelike areas have also been identified in rats as areas A, A1, and P (Doron, N. N. *et al.*, 2002) or AV, A1, and PD (Horikawa, J. *et al.*, 1988) with each field being a mirror image of the adjoining field in tonotopic organization. Mice have at least the AAF and A1 core fields, as do chinchillas. Squirrels and guinea-pigs have at least two core fields, but their tonotopic organizations suggest that the area identified as A1 is not the same as A1 in other rodents.

3.45.8.3 Bats

The organization of auditory cortex in echolocating bats has been investigated because of great interest in the neural mechanisms of echolocation. In the

mustached bat (*Pteronotus parnellii*), Suga N. (1990) described a large A1 proceeding from representing high-to-low tones in a rostrocaudal sequence, as in A1 of cats, with a major overrepresentation of the high echolocating frequency range. In the echolocating horseshoe bat (*Rhinolophus rouxi*), Radtke-Schuller S. and Schuller G. (1995) have described an A1 again representing high-to-low frequencies in a rostrocaudal direction, and adjoining AAF and P DP fields with reversed tonotopic orders. Thus, A1 has an auditory fovea such that the relevant echolocating frequencies occupy a large part of A1. These bats also have a number of adjoining auditory areas that appear to be specialized for echolocating functions, but their relationship to auditory areas in other mammals is uncertain. In the big brown bat (*Eptesicus fuscus*; Dear, S. P. *et al*., 1993) and Seba's short-tailed bat (*Carollia perspicillata*; Esser, K. H. and Eiermann, A., 1999) a tonotopically organized area, AAF, has been described just rostral to A1 with a mirror image organization of A1. Again, there was evidence for several specialized auditory fields adjoining A1 and AAF. Connections of A1 and DP with the ventral subdivisions of the MGv suggest that at least these two areas can be considered core areas (Radtke-Schuller, S., 2004). Little is known about the cortical connections of auditory fields in bats, but a core of at least two areas and a surrounding belt would seem to characterize bats as well as primates, rodents, and carnivores.

3.45.9 Conclusions

While it would be useful to have data on a greater range of mammals, it seems likely that most mammals have a core of two or three primary areas that process auditory information in parallel from the MGv complex. These two or three core areas were likely retained from early mammal ancestors. Similarities between core areas within and across mammal groups, and differences in the tonotopy of areas given the same name (e.g., A1), suggest that mistakes in identification have been made. Such misidentifications, to the extent that they have occurred, may reflect real differences in homologous fields across taxa. Quite possibly, core areas have been differentiated and specialized in various ways in the major lines of mammalian evolution, so that homologous core areas appear different. In all mammals, the core areas distribute to adjoining secondary fields, and these fields spread auditory information even further. In monkeys and humans, there is evidence that rostral and caudal core, belt, and parabelt regions differentially distribute auditory information into a ventral stream for sound identification, and a dorsal stream for sound localization. This view is obviously an oversimplification, but different, partially overlapping arrays of areas specialized for specific types of functions are targeted by the two streams. Each stream further divides as an expanding number of cortical areas become involved in auditory processing. The functions of most of these higher order areas are not solely auditory, as multisensory processing emerges as early as in the auditory belt. While an oversimplification, the dual-stream hypothesis, which has well-established counterparts in visual and somatosensory cortex, remains a concept that is useful in directing further research. The complete connection pattern and the physiological properties of neurons of the belt areas are not yet well understood in any mammal, but considerable progress has been made in characterizing area CM of the auditory belt in monkeys. In addition, the results of a number of studies have started to inform us about the lateral belt. The medial belt is less accessible and harder to investigate, but studies of connections are ongoing, and much more will be known in the future. The concept that the parabelt has at least two divisions has usefully lead to further research, but a better understanding of the functional properties of neurons is needed, as well as evidence on how or if the parabelt is subdivided into functionally distinct parts. The broad outlines of the distribution of auditory information to higher levels and thereafter is now broadly understood, but there is much yet to learn. The sparse connections of belt and parabelt auditory areas with visual areas including V1, has only recently become apparent. The functional significance of such sparse connections is uncertain, and perhaps difficult to investigate.

Cats have an auditory system that includes a number of fields and a complex array of cortical connections. This must represent the independent evolution of a complex cortical processing system from that in primates, although a core and belt organization were probably retained from a common ancestor in lines leading to both primates and carnivores. A better understanding of the similarities and differences in auditory processing at the cortical level could be informative and interesting. Much more could be done with rats and other rodents, given the progress in outlining cortical areas in rats and other rodents. Of course, there is much to learn about

auditory cortex in understudied and unstudied mammals, and there may be surprising specializations in some of these mammals, as there are in bats. As for bats, more understanding of auditory cortex connections is needed. It remains unfortunate that auditory cortex organization in nonecholocating fruit bats has not been studied, as their less specialized cortical system could highlight the changes needed for echolocation.

References

Aitkin, L. M., Kudo, M., and Irvine, D. R. 1988. Connections of the primary auditory cortex in the common marmoset, *Callithrix jacchus jacchus*. J. Comp. Neurol. 269, 235–248.

Bizley, J. K., Nodal, F. R., Nelken, I., and King, A. J. 2005. Functional organization of ferret auditory cortex. Cereb. Cortex 15, 1637–1653.

Brodmann, K. 1909. Vergleichende Lokalizationlehre der Grosshirnrinde. Barth.

Budinger, E., Heil, P., and Scheich, H. 2000a. Functional organization of auditory cortex in the Mongolian gerbil (*Meriones unguiculatus*). III. Anatomical subdivisions and corticocortical connections. Eur. J. Neurosci. 12, 2425–2451.

Budinger, E., Heil, P., and Scheich, H. 2000b. Functional organization of auditory cortex in the Mongolian gerbil (*Meriones unguiculatus*). IV. Connections with anatomically characterized subcortical structures. Eur. J. Neurosci. 12, 2452–2474.

Cantalupo, C. and Hopkins, W. D. 2001. Asymmetric Broca's area in great apes – a region of the ape brain is uncannily similar to one linked with speech in humans. Nature 414, 505.

Clarke, S., Adriani, M., and Tardif, E. 2005. ''What'' and ''Where'' in Human Audition: Evidence from Anatomical, Activation, and Lesion Studies. In: The Auditory Cortex (*eds*. R. König, P. Heil, E. Budinger, and H. Scheich), pp. 77–94. Lawrence Erlbaum Association.

Constantinidis, C., Franowicz, M. N., and Goldman-Rakic, P. S. 2001. The sensory nature of mnemonic representation in the primate prefrontal cortex. Nat. Neurosci. 4, 311–316.

Cusick, C. G. 1997. The Superior Temporal Polysensory Region in Monkeys. In: Cerebral Cortex: Extrastriate Cortex in Primates (*ed*. K. S. Rockland), pp. 4356–4463. Plenum.

de la Mothe, L. A., Blumell, S., Kajikawa, Y., and Hackett, T. A. 2006a. Cortical connections of auditory cortex in marmoset monkeys: core and medial belt regions. J. Comp. Neurol. 496, 27–71.

de la Mothe, L. A., Blumell, S., Kajikawa, Y., and Hackett, T. A. 2006b. Thalamic connections of auditory cortex in marmoset monkeys: core and medial belt regions. J. Comp. Neurol. 496, 72–96.

Dear, S. P., Fritz, J., Haresign, T., Ferragamo, M., and Simmons, J. A. 1993. Tonotopic and functional organization in the auditory cortex of the big brown bat, *Eptesicus fuscus*. J. Neurophysiol. 70, 1988–2009.

Disbrow, E., Litinas, E., Recanzone, G. H., Padberg, J., and Krubitzer, L. 2003. Cortical connections of the second somatosensory area and the parietal ventral area in macaque monkeys. J. Comp. Neurol. 462, 382–399.

Doron, N. N., Ledoux, J. E., and Simple, M. N. 2002. Redefining the tonotopic core of rat auditory cortex: physiological evidence for a posterior field. J. Comp. Neurol. 453, 345–360.

Esser, K. H. and Eiermann, A. 1999. Tonotopic organization and parcellation of auditory cortex in the FM-bat Carollia perspicillata. Eur. J. Neurosci. 11, 3669–3682.

Falchier, A., Clavagnier, S., Barone, P., and Kennedy, H. 2002. Anatomical evidence of multimodal integration in primate striate cortex. J. Neurosci. 22, 5749–5759.

Fang, P. C., Stepniewska, I., and Kaas, J. H. 2005. Ipsilateral cortical connections of motor, premotor, frontal eye, and posterior parietal fields in a prosimian primate, *Galago garnetti*. J. Comp. Neurol. 490, 305–333.

Felleman, D. J. and Van Essen, D. C. 1991. Distributed hierarchical processing in the primate cerebral cortex. Cereb. Cortex 1, 1–47.

Fitzpatrick, K. A. and Imig, T. J. 1980. Auditory cortico-cortical connections in the owl monkey. J. Comp. Neurol. 192, 589–610.

Formisano, E., Kim, D. S., Di Salle, F., van de Moortele, P. F., Ugurbil, K., and Goebel, R. 2003. Mirror-symmetric tonotopic maps in human primary auditory cortex. Neuron 40, 859–869.

Foundas, A. L., Leonard, C. M., Gilmore, R. L., Fennell, E. B., and Heilman, K. M. 1996. Pars triangularis asymmetry and language dominance. Proc. Natl. Acad. Sci. U. S. A. 93, 719–722.

Foxe, J. J., Wylie, G. R., Martinez, A., Schroeder, C. E., Javitt, D. C., Guilfoyle, D., Ritter, W., and Murray, M. M. 2002. Auditory-somatosensory multisensory processing in auditory association cortex: an fMRI study. J. Neurophysiol. 88, 540–543.

Fu, K. M., Johnston, T. A., Shah, A. S., Arnold, L. L., Smiley, J. F., Hackett, T. A., Garraghty, P. E., and Schroeder, C. E. 2003. Auditory cortical neurons respond to somatosensory stimulation. J. Neurosci. 23, 7510–7515.

Funahashi, S., Bruce, C. J., and Goldman-Rakic, P. S. 1989. Mnemonic coding of visual space in the monkey's dorsolateral prefrontal cortex. J. Neurophysiol. 61, 331–349.

Ghazanfar, A. A., Maier, J. X., Hoffman, K. L., and Logothetis, N. K. 2005. Multisensory integration of dynamic faces and voices in rhesus monkey auditory cortex. J. Neurosci. 25, 5004–5012.

Grunewald, A., Linden, J. F., and Andersen, R. A. 1999. Responses to auditory stimuli in macaque lateral intraparietal area: I. effects of training. J. Neurophysiol. 82, 330–342.

Hackett, T. A. 2002. The Comparative Anatomy of the Primate Auditory Cortex. In: Primate Audition; Ethology and Neurobiology (*ed*. A. A. Ghazanfar), pp. 199–219. CRC Press.

Hackett, T. A. 2007. Organization and correspondence of the auditory cortex of humans and nonhuman primates. In: J. H. Kaas, *Evolution of Nervous Systems*, Vol. 4. London: Elsevier Press.

Hackett, T. A., de la Mothe, L. A., Ulbert, I., Karmos, G., Smiley, J. F., and Schroeder, C. E. 2007. Multisensory convergence in auditory cortex, II. Thalamocortical connections of the caudal superior temporal plane. J. Comp. Neurol. (in press).

Hackett, T. A., Preuss, T. M., and Kaas, J. H. 2001. Architectonic identification of the core region in auditory cortex of macaques, chimpanzees, and humans. J. Comp. Neurol. 441, 197–222.

Hackett, T. A., Stepniewska, I., and Kaas, J. H. 1998. Subdivisions of auditory cortex and ipsilateral cortical connections of the parabelt auditory cortex in macaque monkeys. J. Comp. Neurol. 394, 475–495.

Hackett, T. A., Stepniewska, I., and Kaas, J. H. 1999. Prefrontal connections of the parabelt auditory cortex in macaque monkeys. Brain Res. 817, 45–48.

Hashikawa, T., Molinari, M., Rausell, E., and Jones, E. G. 1995. Patchy and laminar terminations of medial geniculate axons in monkey auditory cortex. J. Comp. Neurol. 362, 195–208.

Horikawa, J., Hess, A., Nasu, M., Hosokawa, Y., Scheich, H., and Taniguchi, I. 2001. Optical imaging of neural activity in multiple auditory cortical fields of guinea pigs. NeuroReport 12, 3335–3339.

Horikawa, J., Ito, S. I., Hosokawa, Y., Homma, T., and Murata, K. 1988. Tonotopic representation in the rat auditory cortex. Proc. Jpn. Acad. 64, 260–267.

Huerta, M. F., Krubitzer, L. A., and Kaas, J. H. 1987. Frontal eye field as defined by intracortical microstimulation in squirrel monkeys, owl monkeys, and macaque monkeys. II. Cortical connections. J. Comp. Neurol. 265, 332–361.

Imig, T. J. and Morel, A. 1983. Organization of the thalamocortical auditory system in the cat. Ann. Rev. Neurosci. 6, 95–120.

Imig, T. J. and Reale, R. A. 1980. Patterns of cortico-cortical connections related to tonotopic maps in cat auditory cortex. J. Comp. Neurol. 192, 293–332.

Imig, T. J., Ruggero, M. A., Kitzes, L. M., Javel, E., and Brugge, J. F. 1977. Organization of auditory cortex in the owl monkey (*Aotus trivirgatus*). J. Comp. Neurol. 171, 111–128.

Kaas, J. H. and Hackett, T. A. 1999. ''What'' and ''where'' processing in auditory cortex. Nat. Neurosci. 2, 1045–1047.

Kaas, J. H. and Hackett, T. A. 2005. Subdivisions and Connections of the Auditory Cortex in Primates: A Working Model. In: The Auditory Cortex: A Synthesis of Human and Animal Research (*eds*. R. König, P. Heil, E. Budinger, and H. Scheich), pp. 7–25. Lawrence Erlbaum Association.

Kajikawa, Y., de la Mothe, L., Blumell, S., and Hackett, T. A. 2005. A comparison of neuron response properties in areas A1 and CM of the marmoset monkey auditory cortex: tones and broadband noise. J. Neurophysiol. 93, 22–34.

Knight, P. L. 1977. Representation of the cochlea within the anterior auditory field (AAF) of the cat. Brain Res. 130, 447–467.

Kosaki, H., Hashikawa, T., He, J., and Jones, E. G. 1997. Tonotopic organization of auditory cortical fields delineated by parvalbumin immunoreactivity in macaque monkeys. J. Comp. Neurol. 386, 304–316.

Lee, C. C., Imaizumi, K., Schreiner, C. E., and Winer, J. A. 2004. Concurrent tonotopic processing streams in auditory cortex. Cereb. Cortex 14, 441–451.

Leinonen, L., Hyvarinen, J., and Sovijarvi, A. R. 1980. Functional properties of neurons in the temporo-parietal association cortex of awake monkey. Exp. Brain Res. 39, 203–215.

Lewis, J. W. and Van Essen, D. C. 2000. Corticocortical connections of visual, sensorimotor, and multimodal processing areas in the parietal lobe of the macaque monkey. J. Comp. Neurol. 418, 112–137.

Lewis, J. W., Brefczynski, J. A., Phinney, R. E., Janik, J. J., and DeYoe, E. A. 2005. Distinct cortical pathways for processing tool versus animal sounds. J. Neurosci. 25, 5148–5158.

Luethke, L. E., Krubitzer, L. A., and Kaas, J. H. 1989. Connections of primary auditory cortex in the New World monkey, Saguinus. J. Comp. Neurol. 285, 487–513.

Malinowska, M. and Kosmal, A. 2003. Connections of the posterior thalamic region with the auditory ectosylvian cortex in the dog. J. Comp. Neurol. 467, 185–206.

Merzenich, M. M. and Brugge, J. F. 1973. Representation of the cochlear partition on the superior temporal plane of the macaque monkey. Brain Res. 50, 275–296.

Molinari, M., Dell'Anna, M. E., Rausell, E., Leggio, M. G., Hashikawa, T., and Jones, E. G. 1995. Auditory thalamocortical pathways defined in monkeys by calcium-binding protein immunoreactivity. J. Comp. Neurol. 362, 171–194.

Morel, A. and Kaas, J. H. 1992. Subdivisions and connections of auditory cortex in owl monkeys. J. Comp. Neurol. 318, 27–63.

Morel, A., Garraghty, P. E., and Kaas, J. H. 1993. Tonotopic organization, architectonic fields, and connections of auditory cortex in macaque monkeys. J. Comp. Neurol. 335, 437–459.

Ojima, H. and Takayanagi, M. 2004. Cortical convergence from different frequency domains in the cat primary auditory cortex. Neuroscience 126, 203–212.

Penhune, V. B., Zatorre, R. J., MacDonald, J. D., and Evans, A. C. 1996. Interhemispheric anatomical differences in human primary auditory cortex: probabilistic mapping and volume measurements from magnetic resonance scans. Cereb. Cortex 6, 661–672.

Petrides, M., Cadoret, G., and Mackey, S. 2005. Orofacial somatomotor responses in the macaque monkey homologue of Broca's area. Nature 435, 1235–1338.

Poremba, A., Saunders, R., Crane, A., Cook, M., Sokoloff, L., and Mishkin, M. 2003. Functional mapping of the primate auditory system. Science 299, 568–572.

Preuss, T. M. 1995. The Argument from Animals to Humans in Cognitive Neuroscience. In: The Cognitive Neurosciences (*ed*. M. S. Gazzaniga), pp. 1227–1241. The MIT Press.

Qi, H. X., Lyon, D. C., and Kaas, J. H. 2002. Cortical and thalamic connections of the parietal ventral somatosensory area in marmoset monkeys (*Callithrix jacchus*). J. Comp. Neurol. 443, 168–182.

Radtke-Schuller, S. 2004. Cytoarchitecture of the medial geniculate body and thalamic projections to the auditory cortex in the rufous horseshoe bat (*Rhinolophus rouxi*). I. Temporal fields. Anat. Embryol. (Berl.) 209, 59–76.

Radtke-Schuller, S. and Schuller, G. 1995. Auditory cortex of the rufous horseshoe bat. 1. Physiological response properties to acoustic stimuli and vocalizations and the topographical distribution of neurons. Eur. J. Neurosci. 7, 570–591.

Rauschecker, J. P. 1998. Mechanisms of visual plasticity: Hebb synapses, NMDA receptors, and beyond. Physiol. Rev. 71, 587–615.

Rauschecker, J. P. and Tian, B. 2000. Mechanisms and streams for processing of ''what'' and ''where'' in auditory cortex. Proc. Natl. Acad. Sci. U. S. A. 97, 11800–11806.

Rauschecker, J. P., Tian, B., and Hauser, M. 1995. Processing of complex sounds in the macaque nonprimary auditory cortex. Science 268, 111–114.

Rauschecker, J. P., Tian, B., Pons, T. P., and Mishkin, M. 1997. Serial and parallel processing in rhesus monkey auditory cortex. J. Comp. Neurol. 382, 89–103.

Recanzone, G. H. 2000b. Spatial processing in the auditory cortex of the macaque monkey. Proc. Natl. Acad. Sci. U. S. A. 97, 11829–11835.

Recanzone, G. H. 2004. Acoustic Stimulus Processing and Multimodal Interactions in Primates. In: The Cognitive Neurosciences, (*ed*. M. S. Gazzaniga), 3rd edn., pp. 359–367. The MIT Press.

Rockland, K. S. and Ojima, J. 2003. Multisensory convergence in calcarine visual areas in macaque monkey. Int. J. Psychophysiol. 50, 19–26.

Rolls, E. T. 2004. Convergence of sensory systems in the orbitofrontal cortex in primates and brain design for emotion. Anat. Rec. 281A, 1212–1225.

Romanski, L. M., Bates, J. F., and Goldman-Rakic, P. S. 1999a. Auditory belt and parabelt projections to the prefrontal cortex in the rhesus monkey. J. Comp. Neurol. 403, 141–157.

Romanski, L. M., Tian, B., Fritz, J., Mishkin, M., Goldman-Rakic, P. S., and Rauschecker, J. P. 1999b. Dual streams of auditory afferents target multiple domains in the primate prefrontal cortex. Nat. Neurosci. 12, 1131–1136.

Scheich, H. and Zuschratter, W. 1995. Mapping of stimulus features and meaning in gerbil auditory cortex with 2-deoxyglucose and c-Fos antibodies. Behav. Brain Res. 66, 195–205.
Schreiner, C. E. and Cynader, M. S. 1984. Basic functional organization of second auditory cortical field (AII) of the cat. J. Neurophysiol. 51, 1284–1305.
Schroeder, C. E., Lindsley, R. W., Specht, C., Marcovici, A., Smiley, J. F., and Javitt, D. C. 2001. Somatosensory input to auditory association cortex in the macaque monkey. J. Neurophysiol. 85, 1322–1327.
Schroeder, C. E., Smiley, J., Fu, K., McGinnis, T., O'Connell, M. N., and Hackett, T. A. 2003. Anatomical mechanisms and functional implications of multisensory convergence in early cortical processing. Int. J. Psychophysiol. 50, 5–17.
Seltzer, B. and Pandya, D. N. 1994. Parietal, temporal, and occipital projections to cortex of the superior temporal sulcus in the rhesus monkey: a retrograde tracer study. J. Comp. Neurol. 343, 445–463.
Stein, B. E., Jiang, W., and Stanford, T. R. 2004. Multisensory Integration in Single Neurons of the Midbrain. In: The Handbook of Multisensory Processes (*eds*. G. Calvert, C. Spence, and B. E. Stein), pp. 247–264. The MIT Press.
Suga, N. 1990. Biosonar and neural computation in bats. Sci. Am. 262, 60–68.
Talavage, T. M., Sereno, M. I., Melcher, J. R., Ledden, P. J., Rosen, B. R., and Dale, A. M. 2004. Tonotopic organization in human auditory cortex revealed by progressions of frequency sensitivity. J. Neurophysiol. 91, 1282–1296.
Tian, B., Reser, D., Durham, A., Kustove, A., and Rauschecker, J. P. 2001. Functional specialization in rhesus monkey auditory cortex. Science 292, 290–293.
Wallace, M. N., Rutkowski, R. G., and Palmer, A. R. 2000. Identification and localisation of auditory areas in guinea pig cortex. Exp. Brain Res. 132, 445–456.
Wang, X. M. M., Beitel, R., and Schreiner, C. E. 1995. Representation of a species-specific vocalization in the primary auditory cortex of the common marmoset: temporal and spectral characteristics. J. Neurophysiol. 74, 2685–2706.
Woods, T. M., Lopez, S. E., Long, J. H., Rahman, J. E., and Recanzone, G. H. 2006. Effects of stimulus azimuth and intensity on the single-neuron activity in the auditory cortex of the alert macaque monkey. J. Neurophysiol. 96, 3323–3337.
Woolsey, C. N. 1960. Organization of cortical auditory system: a review and synthesis. Thomas.
Woolsey, C. N. and Walzl, E. M. 1942. Topical projection of nerve fibers from local regions of the cochlea to the cerebral cortex of the cat. Bull. Johns Hopkins Hosp. 71, 315–344.

Further Reading

Funahashi, S., Bruce, C. J., and Goldman-Rakic, P. S. 2005. Mnemonic coding of visual space in the monkey's dorsolateral prefrontal cortex. J. Neurophysiol. 61, 331–349.
Hackett, T. A., Stepniewska, I., and Kaas, J. H. 1998. Thalamocortical connections of the parabelt auditory cortex in macaque monkeys. J. Comp. Neurol. 400, 271–286.
Recanzone, G. H. 2000a. Response profiles of auditory cortical neurons to tones and noise in behaving macaque monkeys. Hear. Res. 150, 104–118.
Smiley, J. F., Hackett, T. A., Ulbert, I., Karmos, G., Javitt, D. C., and Schroeder, C. E. 2007. Multisensory convergence in auditory cortex, I. Cortical connections of the caudal superior temporal plane. J. Comp. Neurol. (in press).
Sweet, R. A., Dorph-Petersen, K. A., and Lewis, D. A. 2005. Mapping auditory core, lateral belt, and parabelt cortices in the human superior temporal gyrus. J. Comp. Neurol. 491, 270–289.

3.46 Sound Localization and the Auditory Cortex

J C Middlebrooks, University of Michigan, Ann Arbor, MI, USA

I A Harrington, Augustana College, Rock Island, IL, USA

E A Macpherson, University of Michigan, Ann Arbor, MI, USA

G C Stecker, University of Washington, Seattle, WA, USA

© 2008 Elsevier Inc. All rights reserved.

3.46.1	Introduction	782
3.46.2	Spatial Sensitivity of Cortical Neurons	782
3.46.2.1	Spatial Receptive Fields in the Primary Auditory Cortex	782
3.46.2.2	Spatial Sensitivity Outside Area A1	784
3.46.2.3	Spatial Topography	786
3.46.2.4	Spatial Sensitivity in Unanesthetized Cats	786
3.46.2.5	Dynamic Spatial Sensitivity	788
3.46.2.6	Multiple Sound Sources	789
3.46.2.7	Acoustic Basis for Spatial Sensitivity	790
3.46.2.8	Nonhuman Primates	792
3.46.3	Reading the Location of a Sound Source from Patterns of Neural Activity	792
3.46.3.1	Sound Localization by Single Neurons	792
3.46.3.2	Information-Bearing Features of Spike Patterns	793
3.46.3.3	Location Signaling by Populations of Neurons	794
3.46.3.4	An Opponent Process Model	796
3.46.4	Impact of Cortical Inactivation on Localization Behavior	796
3.46.4.1	Role of the Auditory Cortex in Reflexive Orientation to Sound Sources	797
3.46.4.2	Role of the Auditory Cortex in Operant Localization of Sound Sources	797
3.46.4.3	Reversible Cortical Inactivation	798
3.46.4.4	Summary of Effects of Cortical Inactivation	799
3.46.5	Spatial Hearing and the Human Auditory Cortex	800
3.46.6	Summary and Future Directions	801
References		802

Glossary

artificial neural network A computer algorithm that has been applied to the study of cortical representation of sound-source locations. The network first is trained with examples of cortical responses to particular sound sources, and then the trained network is used to estimate the source location producing other cortical responses.

azimuth The horizontal dimension of space. In the context of this review, azimuth is the location of a sound source relative to the frontal midline measured as the angle about the vertical axis.

maximum likelihood estimator A statistical procedure that can be used to determine which of a set of stimuli is most likely to have produced a particular neural response.

precedence effect Refers to a group of phenomena in which two spatially discrete sound sources are perceived as a single source. Depending on the relative timing of the two sounds, the fused source is reported as intermediate in location between the two sources or at the location of the leading sound.

spatial receptive field The region of auditory space within which presentation of a sound elicits a criterion response from a cortical neuron.

tonotopic organization: A neural representation of the audible frequency range in which individual neu-

rons are sharply tuned for frequency and the tuning of neurons varies systematically as a function of location within a brain nucleus or cortical area.
virtual auditory space: A simulation of a spatially localized sound source produced by sounds presented through headphones. A virtual target is synthesized by filtering an arbitrary sound source with the directional filter properties of the head and external ears that have been measured previously for an actual sound source.

3.46.1 Introduction

One can say with some confidence that an intact auditory cortex is essential for normal sound localization. That assertion is based on studies of behavioral consequences of lesions and on studies of functional inactivation (reviewed in Section 3.46.4). Beyond that, however, the specific role of auditory cortex in sound localization, and more generally in spatial hearing, is not so clear. We know that acoustic cues for sound localization are encoded in patterns of activity in the two auditory nerves, we can point to specific brainstem nuclei that extract particular binaural and spectral shape cues for sound-source location, and we infer that those cues are integrated in the ascending auditory pathway to at least begin to form the neural correlates of auditory objects. Nevertheless, one cannot say with certainty how much of that integration is accomplished by the brainstem and how much remains to be done at the cortical level. Neither is it clear to what extent spatial processing might take place in a hierarchical manner among various cortical fields nor, indeed, is it clear whether any particular cortical area or areas have a special role in spatial hearing.

Although many questions remain, substantial progress has been made on these issues in the past 5–10 years, due in part to developments in virtual auditory space technology, computational algorithms for recognition of patterns of cortical activity, methods for functional inactivation of specific cortical areas, and functional imaging of the human brain. This chapter begins by reviewing the spatial sensitivity of auditory cortical neurons, including responses to stimuli that vary dynamically in space and time. We then explore how it is that the location of a sound source is written down in patterns of cortical activity and how one might read those patterns. Next, we review the behavioral consequences of destruction or inactivation of particular auditory cortical areas. We review briefly the rapidly growing body of results from studies of the human brain using functional imaging techniques. Finally, we draw some broad conclusions and list some key areas for future research.

3.46.2 Spatial Sensitivity of Cortical Neurons

The cat and, to a lesser degree, the ferret have been favored for research on cortical mechanisms of sound localization because those species have well-developed auditory cortices and because, as nocturnal predators, they have evolved accurate sound-localization behavior. We focus on the cat and the ferret, summarizing results from nonhuman primates at the end of the section.

3.46.2.1 Spatial Receptive Fields in the Primary Auditory Cortex

Early studies of the spatial sensitivity of neurons, perhaps inspired by visual cortical studies, attempted to map the borders of spatial receptive fields of neurons. Evans E. F. (1967) reported that the majority of the neurons in his sample showed a preference for the location of a handheld transient sound source and that the majority of spatially sensitive neurons preferred sound sources located on the side contralateral to the recorded cortical hemisphere. Similarly, Eisenman L. M. (1974) found a mixture of spatially sensitive and insensitive neurons, with most of the spatially sensitive neurons responding best to sounds at contralateral locations. Middlebrooks J. C. and Pettigrew J. D. (1981) mapped receptive fields using pure tones presented from a movable loudspeaker in an anechoic chamber. Stimulus levels were 10 dB above each neuron's threshold; additional levels were tested in some cases. About half of the neurons were classified as omnidirectional because they responded with at least occasional spikes to sound sources located anywhere within the 180° arc tested in front of the cat. The remaining neurons had hemifield or axial receptive fields. The hemifield receptive fields encompassed most locations contralateral to

the recording site and had borders coinciding approximately with the vertical midline. Axial receptive fields were contained entirely within the frontal contralateral quadrant of space and were centered on the acoustic axis of the pinna on the side contralateral to the recording site. The acoustic axis was defined in that study as the direction for which the pinna contributed the maximum acoustic gain at any particular frequency. Neurons with hemifield receptive fields tended to have characteristic frequencies below 12 kHz, and neurons with axial receptive fields typically were tuned to frequencies above 12 kHz. In later experiments using broadband sound sources and higher sound levels, described below, the various receptive field classes have been less distinct, tending to form a continuum from axial, through hemifield, to omnidirectional depending on the stimulus level and bandwidth and on the characteristics of particular neurons.

The results of the Middlebrooks J. C. and Pettigrew J. D. (1981) study illustrated the importance of the passive directionality of the head and external ears in shaping the directional sensitivity of cortical neurons. In that study, for example, the centers of axial receptive fields tended to vary among cats according to how the contralateral pinna was positioned, and deflection of the contralateral pinna resulted in a shift of the locations of cortical spatial receptive fields. In subsequent studies that tested multiple sound levels, sharply bounded axial receptive fields have been evident only at stimulus levels within ~10 dB of neural thresholds (Imig, T. J. *et al.*, 1990; Rajan, R. *et al.*, 1990b). Nevertheless, the imprint of pinna acoustics on spatial receptive fields is evident at levels as high as 50 dB above neural thresholds (Brugge, J. F. *et al.*, 1996; Reale, R. A. *et al.*, 2003). That most auditory spatial receptive fields are centered in front of one or the other pinna is a conspicuous difference in comparison with receptive fields in the visual and somatosensory systems. That issue will be considered further in Section 3.46.2.3.

Several groups have quantified spike rates of neurons in cat area A1 (primary auditory cortex) as a function of sound-source azimuth (i.e., the location in the horizontal dimension) and sound level (Imig, T. J. *et al.*, 1990; Rajan, R. *et al.*, 1990b; Poirier, P. *et al.*, 1997; Eggermont, J. J. and Mossop, J. E., 1998; Middlebrooks, J. C. *et al.*, 1998). As in previous qualitative studies, the distribution of spatial tuning among neurons was dominated by contralateral preferred locations. Nevertheless, a sizable number of neurons responded preferentially to sound sources near the frontal midline (17% in Imig, T. J. *et al.*, 1990) and to sources located on the ipsilateral side (23% in Imig, T. J. *et al.*, 1990). Figure 1 shows examples of an ipsilaterally tuned neuron (Figure 1(a)), a midline neuron (Figure 1(b)), and two contralaterally tuned neurons (Figures 1(c) and 1(d)). Spatial receptive fields tend to grow in size to varying degrees with increasing sound level. Rajan R. *et al.* (1990b), for instance, reported that 60% of spatially selective neurons showed receptive field borders that were constant across a 20–40 dB range of sound levels. Imig T. J. *et al.* (1990), in contrast, reported that the spatial sensitivity of only a minority of their sample was level invariant over a 40–60 dB range.

Virtual auditory space technology has been applied in several experiments for study of spatial sensitivity of neurons (e.g., Brugge, J. F. *et al.*, 1994; 1996; Mrsic-Flogel, T. D. *et al.*, 2001; 2003; 2005). In that approach, broadband sounds are presented sequentially at many locations around an animal, and the resulting sounds are recorded with miniature microphones placed in the animal's ear canals, thus capturing the direction-dependent transfer functions (DTFs) of the external ear. In a later step, arbitrary test stimuli (usually clicks or noise bursts) are filtered by the DTFs and presented to the animal's ears through sealed earphones while recording spike activity from the auditory cortex or other neural structure. The virtual auditory space technique facilitates rapid mapping of spatial sensitivity in azimuth and elevation. The majority of neurons studied with virtual auditory space techniques show receptive fields that are restricted to the contra- or ipsilateral frontal quadrant of space for sound levels no more than ~30 dB above neural thresholds. At those levels, the spatial medians of receptive fields tend to coincide with the acoustic axis of one or the other pinna. At higher sound levels, receptive fields tend to broaden, often expanding to encompass all tested locations.

Cortical neurons tend to demonstrate spatial sensitivity not only in terms of their response magnitude (i.e., their spike counts or spike probabilities) but in terms of the latencies of spikes (e.g., Middlebrooks, J. C. *et al.*, 1994; Brugge, J. F. *et al.*, 1996; Middlebrooks, J. C. *et al.*, 1998; Jenison, R. L. *et al.*, 2000; Furukawa, S. and Middlebrooks, J. C., 2002; Reale, R. A. *et al.*, 2003; Stecker, G. C. and Middlebrooks, J. C., 2003). Generally, first-spike latencies vary inversely with spike counts: sounds at preferred locations tend to elicit more spikes with shorter latencies. In some instances, however, spike latencies can show modulation by sound-source location even at high sound levels at which neurons respond with high probability to sounds at all tested locations (Reale, R. A. *et al.*, 2003). An example of spatial gradients of first-spike latencies for a neuron in cat A1 is shown in Figure 2.

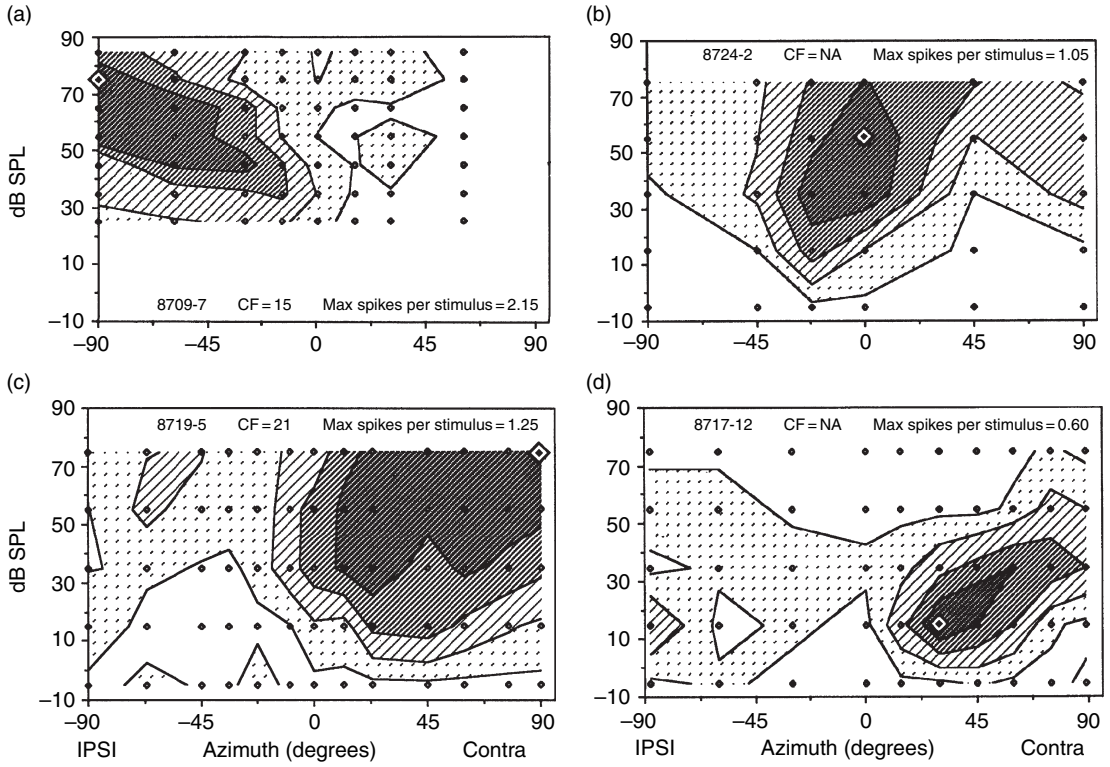

Figure 1 Spatial sensitivity of four neurons in cat area A1. In each panel, contours represent normalized spike rates as a function of sound-source azimuth (horizontal axes) and sound level (vertical axes). Contours are drawn at 5%, 25%, 50%, and 75% of maximum spike rates. The grids of small diamonds indicate stimulus locations and levels that were tested. Reproduced from Imig, T. J., Irons, W. A., and Samson, F. R. 1990. Single-unit selectivity to azimuthal direction and sound pressure level of noise bursts in cat high-frequency primary auditory cortex. J. Neurophysiol. 63, 1448–1466, used with permission from the American Physiological Society.

3.46.2.2 Spatial Sensitivity Outside Area A1

Figure 3 shows the locations of auditory cortical fields on a lateral view of the cat brain. Early studies of spatial sensitivity focused on cortical area A1, perhaps because of its central position in distributing information to other cortical area and because of demonstrations that experimental lesions in A1 result in localization deficits (e.g., Jenkins, W. M. and Merzenich, M. M., 1984). Several more-recent studies have searched beyond the bounds of A1 with the goal of identifying areas that might show enhanced spatial sensitivity. The first such studies examined two nontonotopic areas, areas AES (anterior ectosylvian nuclear area) and A2 (second auditory cortex) (Middlebrooks, J. C. *et al.*, 1994; 1998). These are auditory cortical areas in which neurons show broad frequency tuning and robust responses to broadband sounds and in which there is little or no evidence for tonotopic representation of frequency. Perceptual studies of sound localization demonstrate that localization is enhanced by broadband stimuli (reviewed by Middlebrooks, J. C. and Green, D. M., 1991), presumably indicating that listeners make effective use of location cues across multiple frequencies. The broad frequency tuning of neurons in the nontonotopic cortical areas might reflect a neural substrate for integration of multiple location cues. For that reason, the nontonotopic cortical areas might seem like a logical place to look for enhanced spatial sensitivity. Also, area AES projects to the deep layers of the superior colliculus (Meredith, M. A. and Clemo, H. R., 1989), which is known to contain a topographic map of auditory space (Middlebrooks, J. C. and Knudsen, E. I., 1984).

Despite the *a priori* speculation that areas AES and A2 might show enhanced spatial sensitivity compared with area A1, the spatial sensitivity observed in those nontonotopic areas was qualitatively similar to that observed in A1 (Middlebrooks, J. C. *et al.*, 1994; 1998; Xu, L. *et al.*, 1998; Furukawa, S. *et al.*, 2000). As in area A1, spatial receptive fields tended to broaden as sound levels were increased. Middlebrooks J. C. *et al.* (1998)

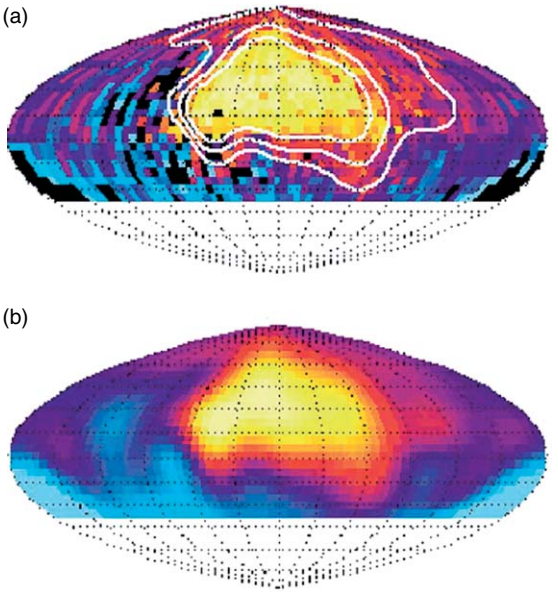

Figure 2 Spatial sensitivity of latencies for a neuron in cat area A1. Transient sounds were presented in virtual auditory space. Latency varied from 11.0 ms (yellow) to 15.0 ms (blue) as a function of virtual source location. Solid white contours are isolatency contours. These quartic authalic (equal-area) projections represent 360° of auditory space. The central vertical meridian represents the vertical midline. (a) Measured data. (b) The data from Figure 1(a) modeled as a linear combination of von Mises basis functions. Reproduced from Brugge, J. F., Reale, R. A., Jenison, R. L., and Schnupp, J. 2001. Auditory cortical spatial receptive fields. Audiol. Neurootol. 6, 173–177, with permission from S. Karger A G, Basel.

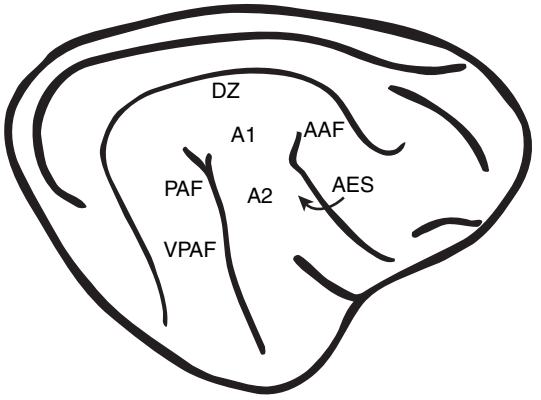

Figure 3 Lateral view of the cat brain. The following auditory areas are shown: primary auditory cortex (A1), dorsal zone of A1 (DZ), second auditory cortex (A2), anterior auditory field (AAF), anterior ectosylvian sulcus auditory area (AES), posterior auditory field (PAF), and ventral posterior auditory field (VPAF).

represented the preferred azimuths of neurons by their centroids, defined as the spike-count-weighted centers of mass of their spike-count-versus-azimuth functions. As in area A1, the centroids of the substantial majority of neurons lay in the frontal contralateral quadrant of space, near the acoustic axis of the contralateral pinna. Quantitatively, spatial sensitivity in AES and A2 appeared somewhat greater than in A1, although no direct comparison was made. Spike counts of the majority of neurons recorded in AES and A2 were modulated by >50% by changes in sound-source azimuth. Spatial tuning generally was broad in that, at sound levels >20 dB above neural thresholds, most receptive fields spanned >180° of azimuth. Although failing to demonstrate especially sharp receptive field borders in AES and A2, those studies were the first to demonstrate that spike patterns of neurons varied systematically as a function of sound-source location throughout those large receptive fields, resulting in an effectively panoramic representation of sound locations. That issue is considered further in Section 3.46.3.1.

Area A1 is surrounded by several other auditory cortical areas that are more or less tonotopically organized, including the anterior auditory field (AAF), the dorsal zone of A1 (DZ), and the posterior auditory field (PAF) (e.g., Reale, R. A. and Imig, T. J., 1980; Middlebrooks, J. C. and Zook, J. M., 1983). Recent studies of area AAF indicate that neurons there have spatial sensitivity similar to that of A1 neurons but that AAF neurons tend to show greater broadening of spatial receptive fields in response to increasing sound levels (Harrington, I. A. *et al.*, 2005). Areas DZ and PAF, however, have several features that, *a priori*, make them attractive places to search for enhanced spatial sensitivity. Area DZ was described as a band of cortex dorsal to A1 proper in which frequency tuning was conspicuously broader than in A1 and shifted somewhat to higher frequencies (Middlebrooks, J. C. and Zook, J. M., 1983). Also, in closed-field stimulus conditions, many neurons in DZ failed to respond to either ear alone but showed a strongly facilitated response to equal sounds at the two ears. That binaural response property appeared predictive of sensitivity for free-field sounds located near the midline. Area PAF has been described as having many neurons that show nonmonotonic spike-count-versus-level functions (Phillips, D. P. and Orman, S. S., 1984; Phillips, D. P. *et al.*, 1995). Nonmonotonicity is pertinent to spatial sensitivity because Imig T. J. *et al.* (1990) reported that the most spatially sensitive neurons in A1 also tended to show nonmonotonic level sensitivity. Also, neurons in PAF tend to show rather complex

frequency response areas (Loftus, W. C. and Sutter, M. L., 2001), which might reflect a sensitivity to spectral cues for sound localization.

Recordings in PAF and DZ confirmed the speculation that neurons in those areas might show enhanced spatial sensitivity (Stecker, G. C. *et al.*, 2003; 2005a). Qualitatively, there were no spatial properties that had not been seen at least in milder form in A1 (i.e., no topographic space map; no pin-point receptive fields). Nevertheless, PAF and DZ showed several quantitative differences compared with A1. Figure 4 shows examples of responses in DZ, PAF, and A1. The left column shows frequency response areas, with the typical V-shaped frequency tuning in A1 and more complex multipeaked frequency tuning in DZ and PAF. Spatial sensitivity is represented by rasters (second column) and rate-versus-azimuth functions (third column). The confusion matrices in the fourth column will be discussed in Section 3.46.3. Compared to those in area A1 (and to areas AES and A2, not shown), spike counts in PAF and DZ were modulated more strongly by sound-source location, spatial gradients were sharper, and (particularly in PAF) spatial tuning was less sensitive to changes in stimulus level. A striking finding in PAF, and to a lesser degree in DZ, was the degree of modulation of spike latencies by sound-source location. Median first-spike latencies were longer in PAF than in A1 (PAF 28.8 ms, DZ 22.0 ms, A1 17.6 ms), and the range of latencies resulting from changes in sound-source azimuth was substantially larger (median ranges: PAF 10.6 ms, DZ 8.4 ms, A1 3.1 ms). The difference between PAF and A1 in the dependence of latency on sound-source location suggests that an intracortical mechanism, as yet unidentified, might act to recode stimulus location as response latency.

3.46.2.3 Spatial Topography

Studies of spatial sensitivity in the auditory cortex consistently have failed to identify a point-to-point map of sound-source location onto cortical place. A point-to-point map would require, first, that the locations of spatial receptive fields vary continuously among neurons and, second, that receptive fields of neurons vary as a function of locations of neurons on the cortex. The first condition is largely unmet, so the second condition is moot. That is, as described above, the distribution of receptive field centroids among neurons is markedly nonuniform, with the majority of centroids located near the axis of one or the other pinna and little coverage of locations across the frontal midline. Regarding the distribution of neurons in the cortex, in A1 one can identify cortical regions on a scale of one to a few millimeters in which neurons all tend to show similar response properties, but the transition from one such region to another is abrupt (Middlebrooks, J. C. and Pettigrew, J. D., 1981; Imig, T. J. *et al.*, 1990; Rajan, R. *et al.*, 1990a; Clarey *et al.*, 1994). In AES, a quantitative test showed that there is a significant tendency of nearby neurons to have nearby receptive field locations, but there was no indication of a continuous space map (Middlebrooks, J. C. *et al.*, 1998). In DZ, there is somewhat more uniform coverage of azimuth by the distribution of centroids compared to A1 and PAF, especially a larger number of midline and ipsilaterally tuned neurons (Stecker, G. C. *et al.*, 2005a). One can find examples in DZ of sequences of neurons that show progressive shifts in centroid locations. Such sequences are the exception rather than the rule, however, and the sequences tend to terminate with abrupt shifts in centroid location. To summarize, there is no convincing evidence that auditory space is represented in the form of a point-to-point map. Instead, the data are more consistent with a highly distributed representation, as discussed in Section 3.46.3.

3.46.2.4 Spatial Sensitivity in Unanesthetized Cats

By far, the majority of previous studies of spatial sensitivity have been conducted in anesthetized animals. The use of general anesthesia almost certainly has an impact on the response patterns and on the stimulus sensitivity of cortical neurons. For that reason, there is a growing interest in cortical studies in awake animals. Mickey B. J. and Middlebrooks J. C. (2003; 2005) have used a preparation in which 16-site recording probes are implanted chronically in area A1 of cats. The cat is trained to listen to broadband noise bursts that vary in location and to release a pedal when the sound changes from a noise burst to a 200 Hz pulse train. The activity of single units and multiunit clusters is recorded simultaneously from the 16 cortical sites.

The results from recordings in area A1 in awake cats agree with the major points of the previous studies that used anesthesia. That is, spatial tuning of single neurons generally is broad, and there is no evidence for point-to-point spatial topography. Beyond that general agreement, however, the responses of neurons in the unanesthetized condition are strikingly different from those in the anesthetized condition. Examples of raster plots are shown in Figure 5. In anesthetized cats, nearly all neurons tend to respond with a burst of spikes at the onset of the sound and no continuing (tonic) response

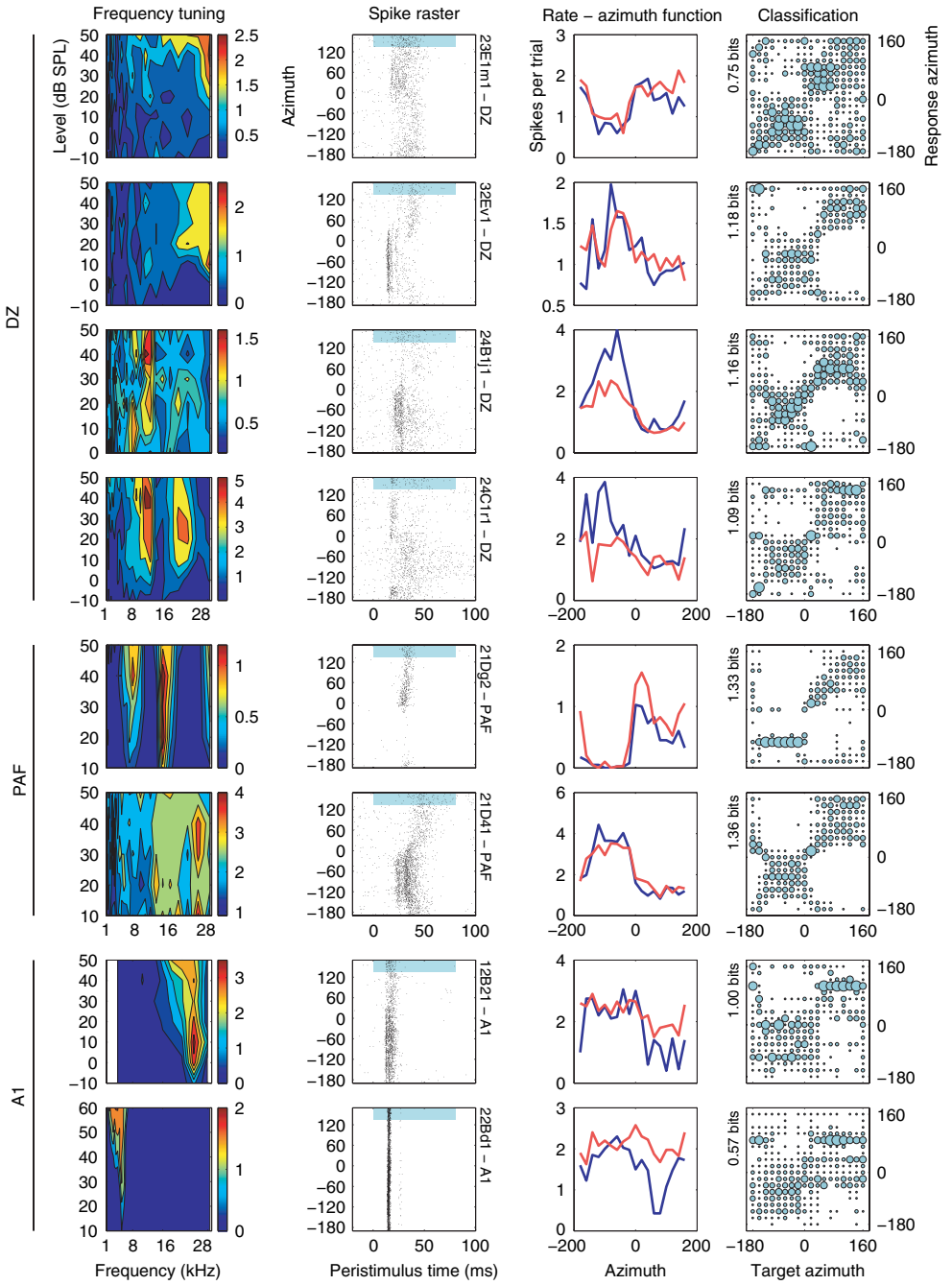

Figure 4 Examples of neural responses in cat dorsal zone of A1 (DZ), posterior auditory field (PAF), and primary auditory cortex (A1). First column: Frequency–response areas plot mean spike count as a function of stimulus frequency (horizontal axes) and level (vertical axes). Color bars indicate spikes per trial. Second column: Raster plots showing spatial sensitivity as a function of sound-source location (vertical axes). Each row of dots represents spikes resulting from one stimulus presentation. Ten repetitions are shown for each location. Time is represented on the horizontal axes. Blue shading indicates the stimulus duration. Third column: Mean spike rate sound as a function of sound-source location. Blue and red lines represent sound levels 20 and 40 dB, respectively, about neural thresholds. Fourth column: Joint stimulus–probability matrices (confusion matrices) show the accuracy of localization by neural spike patterns, as described in the text. The area of each symbol represents the proportion of trials in which a particular estimated azimuth (vertical axis) was given in response to a particular actual stimulus location (horizontal axis). Transmitted information rates computed from each matrix are given along the left axis. Reproduced from Stecker, G. C., Harrington, I. A., Macpherson, E. A., and Middlebrooks, J. C. 2005a. Spatial sensitivity in the dorsal zone (area DZ) of cat auditory cortex. J. Neurophysiol. 94, 1267–1280, used with permission from the American Physiological Society.

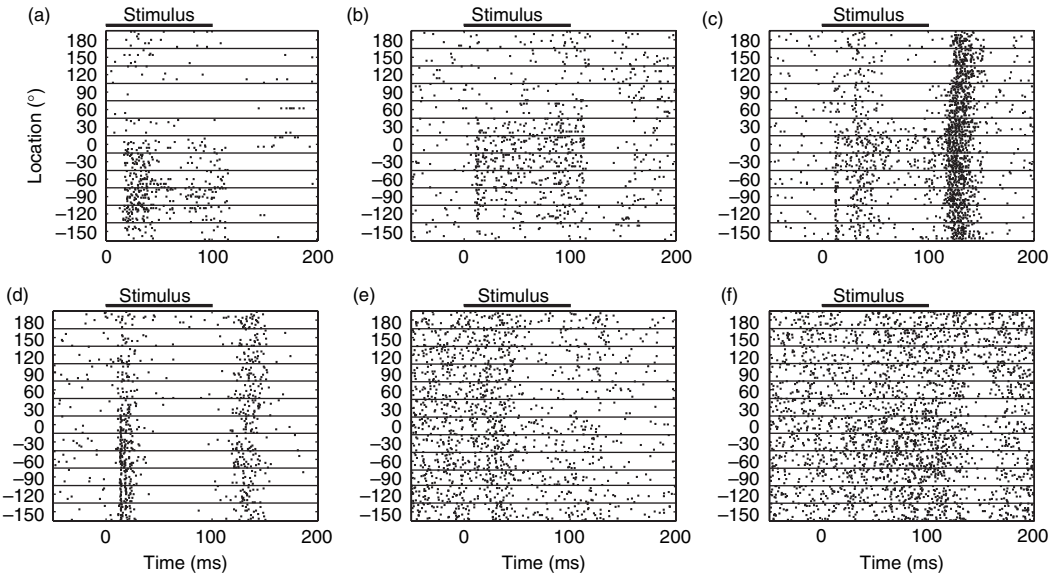

Figure 5 Spatial sensitivity of six neurons in area A1 of the awake cat. Rasters represent responses to 10 stimulus repetitions at each sound-source azimuth. The stimulus duration is given by the bar at the top of each panel. Reproduced from Mickey, B. J. and Middlebrooks, J. C. 2003. Representation of auditory space by cortical neurons in awake cats. J. Neurosci. 23, 8649–8663, with permission from the Society for Neurosciences.

(Figure 4, bottom 2 rows). In contrast, the neurons in awake animals (Figure 5) show a diversity of temporal response patterns, including onset bursts, bursts at stimulus offset, tonic responses, stimulus-related inhibition of spontaneous activity, and combinations of those patterns that vary according to stimulus location. Spatial tuning is sharper, partially due to the presence of suppression of background activity by stimuli at nonoptimal locations. Spatial sensitivity is appreciably less vulnerable to changes in sound level. Also in contrast to the anesthetized condition, the peaks of azimuth functions are distributed fairly uniformly throughout the contralateral half of space. These early results from an awake preparation offer the promise of a wealth of new understanding of spatial sensitivity of auditory cortical neurons.

3.46.2.5 Dynamic Spatial Sensitivity

The sensitivity of a cortical neural to the location of a particular sound can be influenced by preceding sounds. In this section, we will discuss effects of changes in stimulus location, more or less related to motion sensitivity. In the following section, we will consider cortical responses to pairs of sounds that could result from direct and reflected paths to the ear.

Research on the motion sensitivity of cortical neurons has been hampered by the difficulty of presenting controlled moving sound sources without introducing other extraneous sounds. One solution has been to use simulated sound motion produced by sequential activation of a series of sound sources located along some particular trajectory. Using such a technique, Poirier P. *et al.* (1997) showed that about a quarter of neurons sampled in area A1 showed direction sensitivity in the sense that their spike rate was two or more times greater for a sound moving in one direction than the same sound moving in the opposite direction. A larger proportion of neurons (88%) showed such behavior in area AES (Jiang, H. *et al.*, 2000).

A study of low-frequency neurons in area A1 of awake monkeys demonstrated dynamic sensitivity to interaural phase differences (IPDs) that could be taken as indicative of motion selectivity (Malone, B. J. *et al.*, 2002). The response of a particular neuron to a particular static IPD varied according to the IPD of a preceding sound, and the IPD of a preceding sound influenced the IPD that produced the strongest response. Moreover, neurons often showed selectivity for the direction of changing IPD, analogous to selectivity for the direction of azimuthal motion of a low-frequency sound source.

Jenison R. L. *et al.* (2001) used a form of spatial white-noise analysis to study the dynamic spatial sensitivity of neurons in area A1. Identical 10 ms noise bursts were presented from random locations in virtual

auditory space, and space–time receptive fields were computed by compiling the source locations that preceded spikes of cortical neurons. Some 14% of neurons showed receptive fields that were inseparable in that their dynamic space–time receptive fields could not be separated into independent spatial and temporal components. That is, the spatial sensitivity of a neuron at any particular time was influenced by the locations of previous sounds. This implies that neurons are sensitive to the speed and direction of sound motion. Such motion sensitivity was confirmed in tests using simulated motion trajectories.

There is some controversy in the human psychophysical literature regarding the existence of specific motion detectors in the auditory system. One possibility is that neurons in the auditory system might show motion sensitivity analogous to the motion sensitivity that is evident in the visual system. An alternative to a specific auditory motion representation would be that auditory motion is represented only in the comparison of static snapshots of the changing stimulus location (reviews: Middlebrooks, J. C. and Green, D. M., 1991; Grantham, D. W., 1997). A previous review stated: "As yet there is no compelling evidence for motion-sensitive systems in the auditory system" (Middlebrooks, J. C. and Green, D. M., 1991). Subsequent to that review, functional brain imaging has been applied to the problem, but the evidence is so far equivocal. A number of studies have found that moving stimuli activate bilateral loci in the temporal lobe (e.g., Baumgart, F. *et al.*, 1999) and in the right parietal lobe (e.g., Griffiths, T. *et al.*, 1998). The same areas, however, are activated equally well by stationary stimuli that vary randomly in spatial location (Smith, A. L. *et al.*, 2004). It is possible that these cortical areas contain both location-sensitive and motion-sensitive cells intermingled at a scale that cannot be resolved by current imaging methods.

The results discussed above from animal cortical studies showing dynamic spatial sensitivity in addition to recent psychophysical results tend to tip the balance more in favor of motion-sensitive systems. Psychophysical evidence suggests that sensitivity to source motion at relatively low velocities ($<60^\circ\ s^{-1}$) enhances the discrimination of source velocity beyond that observed when only endpoint displacement information is available, although listeners also make use of displacement cues if they are available (Grantham, D. W., 1997; Carlile, S. and Best, V., 2002). Auditory motion adaptation and aftereffect phenomena also suggest the existence of specialized motion detectors (Grantham, D. W. and Wightman, F. L., 1979; Dong, C. J. *et al.*, 1999; Neelon, M. F. and Jenison, R. L., 2004).

3.46.2.6 Multiple Sound Sources

In a typical natural environment, a listener must localize sounds in a background of other sounds and must distinguish the actual location of a sound source from multiple reflective surfaces. Several groups have begun to explore the spatial sensitivity of cortical neurons in the presence of continuous background sounds and sensitivity to the locations of leading and lagging pairs of sounds.

Brugge J. F. *et al.* (1998) examined the effect of continuous background noise on the spatial sensitivity of neurons on cat A1. Stimuli were presented in virtual auditory space, and uncorrelated noise at the two ears produced a spatially diffuse background. In the absence of a noise background, spatial receptive fields mapped with transient signals were large, typically occupying a quadrant or more of virtual auditory space. Within those large receptive fields, first-spike latencies formed functional gradients – typically, latencies were shortest for stimuli near the acoustic axis of the contralateral ear and increased with increasing separation from the axis. Introduction of background noise reduced spike counts and increased latencies throughout the receptive field, but the general structure of the receptive field, including the latency gradients, was preserved. That is, increasing the level of a background noise was largely equivalent to decreasing the level of the signal.

Furukawa S. and Middlebrooks J. C. (2001) performed a similar experiment, differing in that the stimuli were presented in a free sound field and the recordings were from area A2. In a condition of diffuse background noise, the result was the same as that obtained by Brugge J. F. *et al.* (1998). Increasing the background noise level simply decreased the effective level of the stimulus such that spike rates were reduced and spatial receptive fields narrowed. A very different result was obtained when the background noise was presented from a discrete location in the free field. In that condition, the background noise tended to mask the signal differentially according to masker location, the masking being greatest when the masker was located near the signal. That means that a masker placed at the centroid of a neuron located near the axis of the contralateral ear could suppress the response to sounds at the contralateral axis, thereby deflecting the centroid toward the axis of the ipsilateral ear. In conditions in which the spatial sensitivity of a neuron in quiet was nearly omnidirectional, the introduction of a focal background noise could suppress responses to signals

near the masker and effectively carve out a rather restricted receptive field. These results from neurons in cat area A2 are analogous to psychophysical demonstrations of spatial unmasking, in which detection of a signal in noise is enhanced by moving the signal away from the masker (Terhune, J. M. and Turnbull, S. D., 1989; Saberi, K. *et al.*, 1991). There are no analogous psychophysical demonstrations, however, suggesting that a focal continuous noise source can produce a systematic deflection of the spatial judgment of a target (Good, M. D. and Gilkey, R. H., 1996; 1997; Lorenzi, C. *et al.*, 1999).

Pairs of sounds separated in time produce in human listeners a variety of spatial percepts that differ according to the interstimulus delay (ISD). Those phenomena are referred to collectively as the precedence effect (reviewed by Litovsky, R. Y. *et al.*, 1999). Physiological analogs to those perceptual phenomena have been observed in the spatial sensitivity of cortical units. When the ISD is less than ~1 ms, a human listener will report a single auditory event that is located at a point intermediate between the two sources, biased toward the earlier source. This is summing localization. Mickey B. J. and Middlebrooks J. C. (2001) recorded responses of neurons in cat areas A1 and A2 to sound pairs that produce summing localization. They used a computer pattern-recognition algorithm to identify cortical spike patterns associated with particular locations, thus attempting to recognize the locations signaled by neurons (discussed further in Section 3.46.3). Locations recorded in that way closely followed predictions of summing localization. That is, a 1 ms ISD produced responses signaling the location of the leading stimulus, 0 ms ISDs produced responses signaling the location midway between the two sound sources, and ISDs between 0 and 1 ms produced responses signaling locations biased toward the leading source in proportion to the magnitude of the ISD.

When human listeners are presented with pairs of sounds separated by ~1–4 ms, their localization judgment is dominated by the location of the leading sound. Cortical physiology results in awake rabbits (Fitzpatrick, D. C. *et al.*, 1999) and awake or anesthetized cats (Mickey, B. J. and Middlebrooks, J. C. 2001; 2005) accord with that phenomenon in that most neurons fail to respond at all to sounds that lag a leading sound by several milliseconds. Differences between human psychophysics and animal cortical physiology appear in the ISD range of five to a few hundred milliseconds. A human listener normally can detect a lagging sound after ~5 ms and can begin to localize the lagging sound with some accuracy after ~10 ms. In contrast, the animal cortical data show that many neurons still are strongly suppressed during that time range. In a study of area A1 in the awake rabbit, for instance, the median time for 50% recovery of mean spike counts was 21.9 ms, and some neurons showed suppression out to ~300 ms (Fitzpatrick, D. C. *et al.*, 1999). In area A1 of the anesthetized cat (Reale, R. A. and Brugge, J. F., 2000), responses to lagging sounds were suppressed over an ISD range of 50–200 ms. Despite the suppression of responses to lagging sounds, however, the spatial sensitivity of neurons in that study (mapped with virtual auditory space techniques) was largely preserved. That is, spatial receptive fields of many neurons in the presence of a sound leading by 100–400 ms resembled receptive fields mapped in control conditions using a lower sound level. Similarly, spatial gradients of first-spike latencies were largely preserved.

In areas A1, A2, and PAF of anesthetized cats, most neurons responded to a leading sound with a burst of spikes followed by a period of suppression lasting 100–200 ms (Mickey, B. J. and Middlebrooks, J. C., 2005). A period of suppression also was seen in awake cats, although the recovery was somewhat faster (Mickey, B. J. and Middlebrooks, J. C., 2005). Only 12% of neurons showed discrete responses to lagging sounds at ISDs of 20 ms, a delay at which human listeners can readily detect and localize a lagging sound. In the ISD range of 1–16 ms, most neurons transmitted considerable information about the location of a leading sound, analogous to performance by human listeners. In contrast with the ability of human listeners to localize sounds at ISDs of 8–16 ms (Yang, X. and Grantham, D. W., 1997), however, there was little information transmitted in the cat cortical spike patterns about the location of the lagging sound. That is, although Reale R. A. and Brugge J. F. (2000) showed that spatial sensitivity is present at long ISDs, there is as yet no evidence for cortical coding of the locations of lagging sounds over a range of delays at which human listeners localize quite accurately.

3.46.2.7 Acoustic Basis for Spatial Sensitivity

The location of a sound source is not mapped directly at the auditory periphery but must be computed based on multiple cues provided by the interaction of the incident sound wave with the

head and external ears. Cortical neurons are well known to be sensitive to one or both of the major cues for azimuth, interaural level differences and interaural time differences. We refer the reader to other recent sources for reviews of the large literature on interaural difference sensitivity in the auditory cortex (Fitzpatrick, D. C. *et al.*, 2000; Zhang, J. *et al.*, 2004). We focus in this review on several studies that have related neuronal spatial sensitivity to the frequency sensitivity of neurons combined with the directional acoustics of the periphery.

The use of virtual auditory space techniques makes it possible to, in effect, exchange the external ear acoustics of one animal for another. That is, one can record the responses of cortical neurons in one animal to stimuli filtered with DTFs measured from another animal. For instance, Mrsic-Flogel T. D. *et al.* (2001) demonstrated that 73% of neurons studied in area A1 of the ferret showed significant changes in the shape or location of spatial receptive fields when stimulated with DTFs measured from another ferret. This approach has been used to explore the development of spatial sensitivity in the cortex (Mrsic-Flogel, T. D. *et al.*, 2003). Cortical neurons in immature ferrets (postnatal age 33–39 days) tend to be broader and to carry less information about stimulus location than do neurons in adult ferrets. When neurons in immature ferrets are tested with stimuli filtered with DTFs from mature ferrets, the spatial sensitivity sharpens. This implies that the relatively poor spatial sensitivity of cortical neurons in immature ferrets is determined by the small size and lack of development of physical structures of the head and external ears more than by immaturity of neural pathways.

Human listeners make systematic errors in vertical localization when presented with sounds that have been processed with a narrowband filter (Middlebrooks, J. C., 1992). It was hypothesized that the narrowband filter mimics an aspect of the directional filter properties of the external ears. That hypothesis was supported by a computational model that predicted localization judgments on the basis of correlation of the narrowband filter shape with the DTFs of individual listeners. An analogous procedure was tested in the cat, using recordings of neurons in area A2. The elevation sensitivity of neurons was measured using broadband and narrowband sounds presented in a free field. When tested with narrowband sounds, neural responses tended to signal particular elevations that depended on the center frequency of the stimulus, not on the actual location of the source. The computational model from the human study (Middlebrooks, J. C., 1992) was adapted to cats by applying DTFs of individual cat's ears. That model could effectively predict the spatial sensitivity of the cortical neurons, indicating a straightforward relationship between external ear acoustics and elevation sensitivity.

Schnupp J. W. H. and colleagues (Schnupp J. W. H. *et al.*, 2001; Mrsic-Flogel, T. D. *et al.*, 2005) attempted to account for the spatial sensitivity of neurons in area A1 of ferrets on the basis of a linear combination of the frequency sensitivity of the two ears and the directional acoustics of the auditory periphery. Frequency–time response fields (FTRFs) were measured using a reverse correlation analysis of responses to multiple random-frequency tone pips presented to the two ears. The FTRFs captured the frequency-dependent excitatory and inhibitory contributions of each ear. Sensitivity to interaural level differences presumably was captured by the use of stimulus sets presented simultaneously to the two ears, but sensitivity of neurons to interaural differences in temporal fine structure (i.e., IPD sensitivity) was not captured. The FTRF for each ear was multiplied by the DTF of that ear, yielding an estimate of the directional sensitivity of neuronal responses. The estimates of spatial receptive fields provided by this simple model were remarkably good for the majority of high-frequency neurons, which were said to exhibit linear processing of spatial cues. For many neurons, the procedure could estimate the growth of spatial receptive fields with increasing sound pressure level, although that estimation was more successful for neurons that receive predominantly excitatory input from the contralateral ear and inhibitory input from the ipsilateral ear (EI neurons) than for neurons that derive predominantly excitatory input from both ears (EE neurons). Performance was less satisfactory for low-frequency neurons that, presumably, derive spatial sensitivity largely from IPD cues. Also, the linear estimation procedure failed to duplicate the location dependence of first-spike latencies that commonly is observed in empirical data.

Macpherson E. A. *et al.* (2004) applied a similar linear estimation procedure to characterize elevation sensitivity of several auditory cortical fields in cats. The elevation sensitivity of neurons in areas A1 and AAF was predicted accurately by a simple linear model, but the linear model worked poorly for neurons in areas DZ and PAF. One possible explanation for those results is that neurons in DZ and PAF exhibit

greater nonlinearity than do A1 and AAF neurons, perhaps reflecting greater nonlinearity in the processes within DZ and PAF or indicating that nonlinear processes are added on in a projection from A1 to DZ and PAF. A second possibility is that spatial sensitivity in all fields incorporates similarly nonlinear processing but that the nonlinearity is not as evident in A1 and AAF neurons because those neurons tend to show relatively narrow frequency tuning.

3.46.2.8 Nonhuman Primates

In nonhuman primates, spatial sensitivity of cortical neurons has been studied in temporal lobe auditory areas and in multimodal areas of the frontal and parietal cortex. We will focus on the auditory areas and refer the reader elsewhere for a brief overview of auditory spatial sensitivity in multimodal areas (Middlebrooks, J. C., 2000). Kaas J. H. and Hackett T. A. (Chapter 3.45) review the organization of the auditory areas in primates. Briefly, there is a core area containing two or more tonotopic representations; the core area in primates is homologous to region comprising areas A1, AAF, and PAF in the cat, although homologies among specific fields are unclear. The core area in primates is bordered by medial and lateral belt areas that, in turn, are bordered by parabelt areas.

In two early studies in unanesthetized macaques, stimuli were restricted to a limited number of locations in a frontal segment of the horizontal plane (Benson, D. A. *et al.*, 1981; Ahissar, M. *et al.*, 1992). Both studies showed that the majority of neurons in area A1 responded more strongly to contralateral than to ipsilateral sounds. The Benson group reported that neurons were more active when monkeys were engaged in an auditory task than when the monkeys were idle, but few neurons showed a significant difference in neuronal responses between a sound-localization task and a simple auditory detection task. The Ahissar group reported that some neurons showed a preference for a particular direction of sound-source motion, but those researchers declined to conclude that there were separate mechanisms for localization and for motion discrimination.

Recanzone G. H. *et al.* (2000) studied the spatial sensitivity of cortical neurons in awake behaving macaques. Recordings were from area A1 and from the caudomedial (CM) area of the medial belt region. Stimuli varied in azimuth and elevation, all within 30° of the origin at 0° azimuth, 0° elevation. Most neurons in A1 and CM showed a robust response across the entire tested area. The majority of neurons in A1 and CM were spatially tuned in the sense that regression analysis showed a significant correlation of spike count with stimulus azimuth and/or elevation. A statistical procedure was performed to determine the minimum change in sound-source location that could be detected on the basis of a change in the spike counts of single neurons. Those neuronal spatial discrimination thresholds were compared with analogous behavior thresholds from the same monkeys. Generally, the thresholds of CM neurons tended to correlate more closely with the behavioral thresholds than did those of A1 neurons.

Tian B. *et al.* (2001) compared spatial sensitivity among three of the lateral belt areas in anesthetized macaques: anterolateral (AL), middle lateral (ML), and caudolateral (CL). Stimuli were a selection of monkey calls presented in 20° steps of azimuth from −60° to +60° in the frontal horizontal plane. Based on histograms of spatial-tuning widths, it appears that the majority of neurons responded with at least half-maximal spike counts across more than half of the tested locations, with the half-maximum response area extending off one or both edges of the tested range. There was no indication of any striking qualitative difference in spatial sensitivity among the three tested cortical areas, but tuning widths in CL were significantly narrower than in AL and ML.

3.46.3 Reading the Location of a Sound Source from Patterns of Neural Activity

Studies of spatial sensitivity like those described above implicitly address the question: "Given this stimulus, what is the likely neuronal response?" A question that perhaps is more relevant to perception and behavior is: "Given this neuronal response, what was the most likely stimulus?" Research by several groups has begun to address this latter question, attempting to understand how response patterns of single cortical neurons or of neural populations could signal the location of a sound source.

3.46.3.1 Sound Localization by Single Neurons

Although many cortical neurons exhibit restricted spatial receptive fields at near-threshold sound levels, receptive fields measured at moderate sound levels

typically extend throughout 180° to 360° of azimuth. Nevertheless, even within an omnidirectional receptive field, the number and latency of spikes of a single neuron can vary systematically with sound-source location. Middlebrooks J. C. *et al.* (1994) adopted an artificial neural network as a spike-pattern classifier and attempted to estimate sound-source locations by recognizing sound-location-specific spike patterns of neurons in cortical area AES of anesthetized cats. That work demonstrated that the spike patterns of neurons could signal sound-source locations with variable amounts of accuracy throughout up to 360° of azimuth. This was referred to as panoramic location coding. The accuracy with which a computer-based classifier can estimate sound localization on the basis of neural spike patterns can be taken as a measure of the information contained with those spike patterns – information that presumably could contribute to an animal's perception and behavior.

Similar analysis has subsequently been applied to cortical areas A1 (Mickey, B. J. and Middlebrooks, J. C., 2001; 2003; Stecker, G. C. *et al.*, 2003), A2 (azimuth: (Middlebrooks, J. C. *et al.*, 1998); elevation: (Xu, L. *et al.*, 1998)), PAF (Stecker, G. C. *et al.*, 2003), DZ (Stecker, G. C. *et al.*, 2005a), and AAF (Harrington, I. A. *et al.*, 2005). There have been differences in the classifiers that have been used and in other details of analysis, but the general analysis procedure has been as follows. Spike patterns are recorded in response to multiple repetitions of sounds at multiple locations. The spike patterns are divided into 'training' and 'test' sets. The training set is used to train a computer-based classifier (typically a form of artificial neural network), then the trained classifier is used to estimate the sound-source location that elicited each pattern in the test set. For convenience in presentation, we will refer to this estimation of the sound-source location as sound localization by the cortical neuron. The localization performance of each neuron is assessed either with a measure of the magnitude of errors or by a measure of transmitted information (i.e., how much information about sound-source location is transmitted by the animal's auditory system to the recording electrode in the auditory cortex).

The rightmost column of Figure 4 shows examples of sound localization by neurons in areas A1, PAF, and DZ. Each panel shows a confusion matrix in which the area of each circle indicates the proportion of spike patterns that were localized to a particular estimated location (plotted on the vertical axis) in response to a stimulus at a particular target location (horizontal axis). Correct estimates of the target location fell on the major diagonal with positive slope; the DZ unit shown in the third row is an example with many correct estimates. Points lying on one of two minor diagonals with negative slope are instances in which the estimate of the lateral position was correct but in which front and back were confused; the PAF unit shown in the sixth row shows many such front/back confusions. We note that front/back confusions often are observed in human sound-localization judgments (e.g., Middlebrooks, J. C. and Green, D. M., 1991). In some instances, neurons discriminated left targets from right fairly accurately but could not discriminate locations within one hemifield; the A1 units in the bottom two rows are examples.

Qualitatively similar sound localization by single neurons has been observed in all auditory cortical areas in which this sort of analysis has been performed. That is, there is no indication that one area is doing something dramatically different from the others. Nevertheless, one can rank the localization performance of the areas, with areas A1 and AAF showing the least accuracy, areas AES and A2 intermediate, and areas DZ and PAF showing the most accurate localization. PAF in particular exhibits localization that is least vulnerable to changes in sound-source level.

As discussed in Section 3.46.2.3, the responses of neurons are not consistent with the existence of a topographic, point-to-point, map of auditory space. That is, one cannot identify particular neurons that are watching over particular sound-source locations. Instead, all the data are consistent with a highly distributed representation, in which each neuron transmits at least partial information about nearly all source locations and the representation of each source location is distributed among most of the auditory cortical population.

3.46.3.2 Information-Bearing Features of Spike Patterns

Cortical neurons exhibit spatial sensitivity both in terms of the magnitude of responses (i.e., spike count or spike probability) and in terms of the timing of spikes, as described in Section 3.46.2 and as is clearly evident in raster plots like those in Figure 4. Response magnitude is widely accepted in sensory neuroscience as representative of the response of a neuron to a particular stimulus. The pattern classification schemes used in studies discussed in Section

3.46.3.1 potentially exploit both magnitude and timing information. In this section, we consider the relative amounts of location-related information transmitted by response magnitude and timing.

The importance of cortical spike timing for location representation can be demonstrated by reducing spike patterns to simple spike counts, thus eliminating any temporal dimension of responses. Localization by classification of spike counts of neurons in areas AES and A2 was substantially inferior to that by spike patterns that preserved spike timing (Middlebrooks, J. C. *et al*., 1994; 1998). Furukawa S. and Middlebrooks J. C. (2002) quantified the amounts of location-related information that were transmitted by intact spike patterns of neurons in area A2 and by the same patterns degraded in one of two ways. In one condition, spike times were interchanged randomly among trials, thus preserving response magnitudes but eliminating any timing information. In that condition, there was a ~35% decrease in transmitted information. In the other condition, all spikes after the first spike were deleted, thus preserving first-spike latencies and the dispersion of first-spike latencies but eliminating information from spike counts. That resulted in a decrease in transmitted information of only ~11%. In tests of information transmitted by unidimensional terms, spike count or first-spike latency, latency transmitted significantly more information than did spike count.

Similar results pertaining to spike timing, and some differences, were obtained in area A1 of awake cats (Mickey, B. J. and Middlebrooks, J. C., 2003). Complete elimination of the stimulus dependence of spike timing reduced transmission of stimulus-related information by ~50%. The awake cat A1 results differed somewhat from the results from A2 in anesthetized cats in that a substantial decrease in transmitted information was evident in the awake A1 study only when spike times were degraded on a scale of greater than ~16 ms, whereas in the anesthetized A2 study (Furukawa, S. and Middlebrooks, J. C., 2002), a substantial decrease in transmitted information was observed for degradation of timing on a scale as fine as 4 ms. Also different from the A2 study, spike count alone on average transmitted more information than did first-spike latency alone. The result likely reflects the fact that response patterns tended to be more sustained in the awake condition than in the anesthetized condition, resulting in higher spike counts and greater potential for modulation of spike counts by sound-source location.

First-spike latency typically shows a strong negative correlation with spike counts. For that reason, the amount of information transmitted in area A2 by two-dimensional vectors of spike count and spike latency is substantially less than the sum of the information transmitted by either term alone (Furukawa, S. and Middlebrooks, J. C., 2002). Location-related variation of first-spike latency is appreciably greater in area PAF than in areas A1 and A2 (Stecker, G. C. *et al*., 2003). Correlation between spike count and first-spike latency is significantly weaker in PAF, suggesting that latency contributes a greater increment in transmitted information in PAF than is the case in A1 or A2.

Estimates of transmitted information that rely on first-spike latency require knowledge of the time of onset of the sound, which is not directly available to an animal. A more biologically plausible approach would be to examine stimulus-related information that could be carried by the relative timing of spikes among neurons. Stecker G. C. and Middlebrooks J. C. (2003) compared information transmitted by patterns of spikes timed relative to stimulus onset (absolute spike times) with information transmitted by patterns of spike-time differences between pairs of spikes. When pairs of neurons were selected both from area A1 or both from PAF, information transmission by relative spike times was reduced compared to the absolute-time condition, although the relative times did transmit appreciable amounts of information. In contrast, when pairs of neurons were formed by one A1 neuron and one PAF neuron, relative and absolute spike times transmitted roughly equal amounts of information. It appears that the somewhat restricted range of spike latencies in A1 served as an adequate temporal reference by which to measure the widely varying latencies in PAF. Additional studies of information transmission by relative spike times are considered in the context of location signaling by populations of neurons, discussed in the next section.

3.46.3.3 Location Signaling by Populations of Neurons

Despite the potential for single neurons to signal sound locations throughout auditory space, no single neuron can do so accurately enough to account for the accuracy observed in behavioral trials. Hypothetically, that additional accuracy could be gained from the coordinated activity of populations of neurons. That hypothesis has been explored with

classifiers that act on simple combinations of spike patterns of multiple neurons (Furukawa, S. *et al.*, 2000; Mickey, B. J. and Middlebrooks, J. C., 2003; Stecker, G. C. *et al.*, 2003) and with classifiers that exploit some particular differential response among neurons (Jenison, R. L., 1998; 2000; 2001; Stecker, G. C. and Middlebrooks, J. C., 2003; Stecker, G. C. *et al.*, 2005b).

Furukawa S. *et al.* (2000) explored azimuth signaling by ensembles of 2–128 neurons in area A2 of anesthetized cats. Neuronal single- and multiunit data were recorded from multisite recording probes that enabled simultaneous recordings at 16 sites spaced in 100 μm intervals (i.e., all recordings were along a 1500 μm oblique line through the cortex). Ensemble spike patterns were formed either by concatenating patterns of single neurons or by compiling multiple random samples of 1–128 neural units from a pool of 377 units. Ensemble spike patterns were classified using techniques like those described in Section 3.46.3.1. Relative spike timing and spike counts among neurons were preserved by that procedure, but there was no explicit procedure to differentiate timing or count among neurons. Localization signaling performance improved rapidly with increases in the size of ensembles from 1 to about 8 or 16, then improved more slowly beyond that size. An ensemble of 128 units produced localization performance comparable to cat localization behavior (May, B. J. and Huang, A. Y., 1996). It has been noted that a substantial fraction of stimulus-related information in spike patterns is carried by spike timing (discussed in Section 3.46.3.3). The study by Furukawa and colleagues demonstrated that a similar amount of information is carried by times measured relative to the onset of the stimulus or by times measured relative to the first spike across the ensemble of neurons.

Localization signaling performance in the study by Furukawa S. *et al.* (2000) was better when units were drawn from across all recording-probe locations in multiple animals than when all units were recorded with the same 16-site probe. That suggests that localization is enhanced by neural ensembles that exhibit a greater diversity in spatial sensitivity of single units. Neurons in area PAF of anesthetized cats (Stecker, G. C. *et al.*, 2003) and A1 in awake cats (Mickey, B. J. and Middlebrooks, J. C., 2003) show substantially greater diversity of spatial sensitivity and spike patterns than do neurons in areas A1 and A2 in anesthetized cats. Analysis of location signaling by neural ensembles using procedures similar to that introduced by Furukawa and colleagues showed enhanced growth of signaling accuracy associated with increasing ensemble size in area PAF in anesthetized cats (Stecker, G. C. *et al.*, 2003) and A1 in awake cats (Mickey, B. J. and Middlebrooks, J. C., 2003) compared to areas A1 and A2 in anesthetized cats.

As noted in Section 3.46.2.1, the first-spike latencies of cortical neurons typically vary with sound-source location. Jenison R. L. *et al.* (1998) explored location signaling by the first-spike latencies of ensembles of neurons in area A1 of anesthetized cats. The spatial sensitivity of the latency of each neuron was measured with virtual auditory space techniques, then that sensitivity was modeled using a form of spherical approximation with von Mises basis functions (as in Figure 2; Jenison, R. L. and Fissel, K., 1995; 1996). A maximum-likelihood estimator then was used to estimate sound-source locations based on modeled latencies from ensembles of neurons. Performance was quantified by Monte Carlo simulations and by analytic computation of the Cramer–Rao lower bound (CRLB; Blahut, R. E., 1987), which is a measure of the variance of an unbiased estimator. Neural ensembles of varying sizes were drawn from a population of 65 single neurons studied in area A1 of anesthetized cats (Brugge, J. F. *et al.*, 1996). Performance improved rapidly with increases in ensemble size up to about 20 neurons. Asymptotic values of localization error for targets at 0° azimuth and 0° elevation were comparable to psychophysical values reported in humans (Makous, J. C. and Middlebrooks, J. C., 1990) and cats (May, B. J. and Huang, A. Y., 1996).

Jenison has extended his work in several ways. First, he showed that very similar localization performance is obtained if latencies are expressed relative to the stimulus onset (absolute latencies) or are expressed relative to the first spike in the ensemble (relative ensemble latencies) (Jenison, R. L., 2001). That result is consistent with the results of Furukawa S. *et al.* (2000) obtained with a very different form of classifier. Second, he added a sound-level term to the radial-basis-function representations of spatial receptive fields (Reale, R. A. *et al.*, 2003). Localization performance initially improved with increasing sound level, consistent with human psychophysical results (Sabin, A. T. *et al.*, 2005). Further increases in level tended to result in decreases in performance, which is not seen psychophysically except for localization of transients in elevation (Hartmann, W. M. and Rakerd, B., 1993; Macpherson, E. A. and Middlebrooks, J. C., 2000).

Finally, he demonstrated the interesting and rather unexpected result that localization by the first-spike latencies of an ensemble of neurons is enhanced by correlation among the individual neurons (Jenison, R. L., 2000).

3.46.3.4 An Opponent Process Model

Stecker G. C. *et al.* (2005b) have evaluated an opponent-process model of spatial representation. That model is based on the observation that auditory space is sampled quite nonhomogeneously by receptive fields. Indeed, as noted in Section 3.46.2, the spatial receptive fields of the large majority of neurons are centered on the acoustic axis of one or the other pinna, and few receptive fields are centered on the midline. The tendency of receptive fields to lie off the midline means that the steepest spatial gradients of neurons' spike counts or latencies tend to lie on or near the midline. The near-midline locations of steep response gradients are reflected in the tendency of spike-pattern classifiers (as in Section 3.46.3.1) to discriminate left from right with great acuity while often failing to discriminate locations within one or the other sound hemifield (e.g., see Figure 4, right column). Moreover, specific tests of the discrimination of pairs of locations by neurons in areas A1, PAF, and DZ of anesthetized cats showed that the greatest spatial acuity was for pairs of locations that straddled the frontal midline.

The opponent process model asserts that sound-source locations could be represented by the relative activity of a small number of discrete populations of neurons, as small as two, each population defined by tuning to a particular region of space. Inasmuch as the majority of neurons in each cerebral hemisphere are tuned to locations in the contralateral frontal quadrant, one might think first of a comparison of activity between left and right hemispheres. That notion is untenable, however, because it predicts that a unilateral lesion would produce a bilateral localization deficit, contrary to the largely contralateral deficits that are observed (see Section 3.46.4). Instead, Stecker G. C. *et al.* (2005b) argue that an opponent process localizer could be constituted from contralaterally tuned and the relatively few ipsilaterally tuned neurons within each hemisphere; ipsilaterally tuned neurons are particularly prevalent in area DZ (Stecker, G. C. *et al.*, 2005a). As a proof of concept, they tested a simplified model that summed normalized spike counts from contralaterally tuned neurons and subtracted them from summed counts from ipsilaterally tuned neurons. Classification of those difference terms provided localization performance that was clearly superior to classification of simple summed spike counts, particularly in conditions of varying sound levels. That test dealt only with overall levels of activation among two populations. One assumes that performance could only be better if the complexity of interconnections among neurons were to be exploited in a more realistic manner.

The opponent process model may be regarded as an extension of the panoramic coding described in Section 3.46.3.1. Results presented in that section indicate that spike patterns of many neurons can signal the locations of sound sources throughout as much as 360° of space. The opponent process model simply points out what is clear in most of the cited publications, that most of those neurons discriminate near-midline locations more accurately than they discriminate locations far off the midline. We note that the enhanced discrimination of midline locations by neurons fits with psychophysical evidence that spatial discrimination is most acute (Mills, A. W., 1958) and that localization is most accurate (Makous, J. C. and Middlebrooks, J. C., 1990; Stevens, S. S. and Newman, E. B., 1936; May, B. J. and Huang, A. Y., 1996) for near-midline targets. Furukawa S. *et al.* (2000) demonstrated that ensembles of panoramic neurons signal sound locations more accurately than do single neurons. The opponent process model extends that observation by suggesting a particular way in which information might be combined across populations – that is, as a differential between populations tuned to left or right hemifields.

3.46.4 Impact of Cortical Inactivation on Localization Behavior

The ability to localize sounds in space has long been known to depend on intact auditory cortex (e.g., Neff, W. D. *et al.*, 1956). In general, the removal or inactivation of auditory cortex in one hemisphere renders animals unable to approach, or even discriminate, the locations of sound sources in the contralateral hemifield, whereas localization performance in the ipsilateral hemifield is largely unaffected (e.g., Jenkins, W. M. and Masterton, R. B., 1982; Thompson, G. C. and Cortez, A. M., 1983; Heffner, H. E., 1997). When the auditory cortex is removed or inactivated bilaterally, the animals are rendered

unable to approach or discriminate sound sources within either lateral hemifield but generally can discriminate whether a sound source is located on the left or right, albeit with reduced acuity (Heffner, H. E. and Masterton, B., 1975; Heffner, H., 1978; Heffner, H. E. and Heffner, R. S., 1990). In what follows, we will review some of the effects of cortical lesions, as well as acute and chronic cortical inactivation, on the sound-localization behavior of species including cats, ferrets, dogs, and monkeys. It should be emphasized that although the effects of cortical lesions are similar among these species, they cannot be generalized to all species.

3.46.4.1 Role of the Auditory Cortex in Reflexive Orientation to Sound Sources

Not long after the auditory cortex was first implicated in the operant auditory spatial behavior of the cat (Neff, W. D. *et al.*, 1956; see Section 3.46.4.2), researchers began to address its role in reflexive orientation to sound sources. In the first of these studies, Riss W. (1959) observed the orienting responses of cats with bilateral auditory cortex lesions and concluded that the auditory cortex was necessary for "localizing the instantaneous position of a sound source," even when the ability was assessed in terms of reflexive orientation. Indeed, when the animals were deprived of all visual cues, their orienting responses were unrelated to the actual location of the sound source. In contrast, several later studies concluded that while the orienting responses of cats with large bilateral lesions were often abnormal, they were not entirely absent (Thompson, R. F. and Welker, W. I., 1963; Thompson, G. C. and Masterton, R. B., 1978; Beitel, R. E. and Kaas, J. H., 1993). Specifically, although most responses were generally toward the appropriate lateral hemifield, the accuracy of the final head position within that hemifield was often diminished. Indeed, in the study by Beitel and Kaas, the position of the animal's head following an orienting response was unrelated to the position of the sound source, beyond being within the appropriate hemifield. However, Thompson G. C. and Masterton R. B. (1978) observed that when the initial direction of a head turn was appropriate (e.g., turning left for a leftward source), so too was the remainder of the response. The fact that orienting responses could appear normal on one trial and aberrant on the next led those authors to suggest that the systems involved in reflexive responses to sound, although not cortical *per se*, might be under cortical control (Thompson, G. C. and Masterton, R. B., 1978). These results suggest that while bilateral lesions might impair the ability of cats to accurately orient to sound sources within a lateral hemifield, they have only a slight effect on the ability to orient appropriately to the left or the right side of the midline.

3.46.4.2 Role of the Auditory Cortex in Operant Localization of Sound Sources

In the earliest lesion study of sound localization, bilateral auditory cortex lesions impaired the ability of cats to approach a target on the left or right when it was identified by an auditory, but not a visual, cue (Neff, W. D. *et al.*, 1956). Despite their impairment, however, cats were often able to perform the task above chance levels when just two targets were used, located close to the animal on the left and right. A similar observation was later made in dogs (Heffner, H. E., 1978). Neff proposed that the deficit might reflect an inability to maintain attention between the initiation and completion of an operant response. When the target was closer to the animals, the attentional demands of the task were reduced, and performance improved. Whatever its explanation, the demonstration of an auditory localization deficit, however incomplete, supported the involvement of auditory cortex in sound-localization behavior.

Following the study by Neff W. D. *et al.* (1956), Strominger N. L. (1969a; 1969b) provided additional evidence for the preservation of left–right discrimination following bilateral lesions in cats, as well as the first evidence for an impairment following unilateral lesions (Strominger, N. L., 1969b). Cats were again trained to approach targets on the left and right. Following unilateral lesions, although some animals expressed a bias toward targets on the same side as their lesion (i.e., opposite their intact hemisphere), their behavior was otherwise unremarkable. Following bilateral lesions, however, the animals were unable to perform the discrimination except at the largest separation of 180° (Strominger, N. L., 1969b). Later studies of monkeys, dogs, and ferrets also demonstrated that while the ability to perform left–right discriminations persists following bilateral lesions, the animals' spatial resolution often was deficient and, at least in monkeys, that the degree of deficiency may be task dependent (Heffner, H. E. and Masterton, B., 1975; Heffner, H. E., 1978; Kavanagh, G. L. and Kelly, J. B., 1987; Heffner, H. E.

and Heffner, R. S., 1990). Indeed, the observation that monkeys with bilateral lesions were able to indicate whether a sound came from the left or right by making a corresponding (left or right) lever press, but not by approaching the source of the sound led to the suggestion that, "... what auditory cortex lesions seem to produce ... is an inability to demonstrate sound localization in some tasks" (Heffner, H. E. and Masterton, B., 1975; 1978, p. 742).

These and other studies suggested that cortical lesions impair but do not eliminate the ability of cats, dogs, ferrets, and monkeys to reflexively orient toward, identify, or discriminate sound sources between the left and right hemifields. It was only when animals began to be tested for the ability to localize sound sources within a lateral hemifield, however, that the severity of sound-localization deficits, particularly those that follow unilateral lesions, was made apparent. Jenkins W. M. and Masterton R. B. (1982) required cats to walk to a sound source within an array of speakers spanning 180°, a task that normal animals performed well. Following unilateral lesions, however, the accuracy of their responses was profoundly diminished in the contralesional, but not the ipsilesional, hemifield. This test procedure was later used to demonstrate contralesional deficits of tone localization that were limited to frequencies whose cortical representation in the primary field (A1) had been removed (Jenkins, W. M. and Merzenich, M. M., 1984), as well as a contralesional localization deficit in squirrel monkeys (Thompson, G. C. and Cortez, A. M., 1983). Interestingly, as with the cats tested by Strominger N. L. (1969a), when presented with a contralesional sound source, the squirrel monkeys often responded to ipsilesional sources (Thompson, G. C. and Cortez, A. M., 1983). Subsequent studies have demonstrated that monkeys and ferrets are not only unable to approach contralesional sound sources accurately, they are unable to discriminate them using simpler operant procedures (Kavanagh, G. L. and Kelly, J. B., 1987; Heffner, H. E. and Heffner, R. S., 1990).

Although each hemisphere is primarily responsible for spatial behavior in the contralateral hemifield, regions of space near the midline appear to be represented bilaterally. This ipsilateral spillover is evident when the spatial deficits that follow unilateral lesions in monkeys are mapped by fixing the location of one sound source and systematically varying the location of another sound source in a discrimination task (Heffner, H. E. and Heffner, R. S., 1990; Heffner, H. E., 1997). When both sound sources are more than 15–30° into the contralesional hemifield, they can no longer be discriminated regardless of how widely they are separated within that hemifield. In cases of bilateral lesions, discrimination fails as soon as the two sources are on the same side of the midline, again regardless of their separation (Heffner, H. E. and Heffner, R. S., 1990; Heffner, H. E., 1997). This suggests that each cerebral hemisphere represents the entire contralateral hemifield in addition to the 15–30° of the ipsilateral hemifield closest to the interaural midline. In the absence of auditory cortex in both hemispheres, the animals are only able to distinguish sounds on the left from those on the right. It is possible, however, that the animals might be performing this left–right discrimination on the basis of nonspatial cues. That is, although dogs and monkeys can learn to approach a left and right sound source with persistent training, their ability to rapidly transfer this spatial response to the discrimination of nonspatial stimulus features suggests that they may be making a spatial response to what is for them a nonspatial stimulus (Heffner, H. E., 1978).

3.46.4.3 Reversible Cortical Inactivation

Reversible inactivation techniques have emerged as a powerful tool for the investigation of brain–behavior relationships and have been used to study the role of auditory cortex in sound-localization behavior (Malhotra, S. *et al.*, 2004; Smith, A. L. *et al.*, 2004; Malhotra, S. *et al.*, 2005; Malhotra, S. and Lomber, S. G., 2007). One obvious advantage of these techniques is that the inactivation is fast-acting and reversible and thus should not lead to plastic reorganization (at least when used in the short term). They also allow for the immediate assessment of behavior during the inactivation, in contrast to lesion studies in which a period of postoperative recovery is often necessary, and allow the same experimental animals to be tested repeatedly in their normal and inactivated state (Lomber, S. G., 1999). Malhotra S. *et al.* (2004) have used cryogenic deactivation to study the involvement of individual auditory cortical fields in the localization behavior of the cat. The animals were trained to approach sound sources before, during, and after the unilateral inactivation of individual cortical fields. Of all the areas tested, only inactivation of areas A1, PAF, and AES resulted in auditory-specific localization deficits; the inactivation of two motor areas, 5L and 6m, produced modality-nonspecific deficits (Malhotra, S. *et al.*, 2004). Consistent with the effects of cortical lesions, deficits were restricted to the contralateral hemifield during

unilateral deactivations of A1, PAF, or AES (Malhotra, S. *et al.*, 2004) and were present in both hemifields during bilateral inactivations of A1, PAF, or AES (Malhotra, S. and Lomber, S. G., 2007). The latter deficits were observed following either homotopic (e.g., A1 on both sides) or heterotopic (e.g., A1 on the left and PAF on the right) inactivation. Despite their inability to accurately approach sound sources, the animals generally were able to orient toward the appropriate lateral hemifield, a finding consistent with lesion studies (e.g., Beitel, R. E. and Kaas, J. H., 1993). Thus, the deficits that occur during acute unilateral and bilateral inactivations of auditory cortex are similar to those that follow cortical lesions. It remains to be seen, however, whether the same inactivations would also impair the discrimination of sound-source locations.

Physiological results suggest that areas PAF and DZ might have particular importance for localization behavior (see Section 3.46.2.2). The expectation regarding PAF is supported by the reversible inactivation results (Malhotra, S. *et al.*, 2004). The inactivation of area A1 by Malhotra and colleagues did not distinguish the main (ventral) portion of A1 from DZ. Ongoing studies suggest that inactivation of ventral A1 alone increases the proportion of incorrect responses, whereas inactivation of DZ results in an increase in the number of very large errors (Malhotra, S. *et al.*, 2005). Physiological results do not predict the localization deficits resulting from AES inactivation in that AES neurons do not show especially strong spatial sensitivity. Those localization deficits might reflect in some way the projection from AES to the superior colliculus (Meredith, M. A. and Clemo, H. R., 1989).

Smith A. L. *et al.* (2004) have determined the effects of the longer-term chemical inactivations on the sound-localization behavior of ferrets. The animals were trained to walk to the source of a sound in a circular arena and then received unilateral or bilateral, slow-release implants over A1 that had been impregnated with the GABA agonist, muscimol. These implants produce tonic inhibition of neural activity in their immediate vicinity and can remain effective for up to 5 months. Although the animals with bilateral inactivations showed substantially decreased localization accuracy, particularly for shorter stimulus durations, their deficits were not complete and diminished with further testing. Again consistent with the contralateral control of spatial behavior evidenced by lesion and cryogenic inactivation studies (e.g., Jenkins, W. M. and Masterton, R. B., 1982; Kavanagh, G. L. and Kelly, J. B., 1987; Malhotra, S. *et al.*, 2004), animals with unilateral inactivations made larger errors in the contralateral hemifield (Smith, A. L. *et al.*, 2004). There was also a marked tendency for animals to make more front/back confusions following the bilateral inactivation of A1, leading to the suggestion that A1 may be involved in the resolution of the spectral cues that distinguish to the front/back locations of sound sources. It should be noted, however, that the accuracy of the initial head-orienting response to sound source was not affected by the chemical inactivation of A1. Indeed, the animals' initial orienting responses were not only toward the appropriate lateral hemifield but within 30° of the target, suggesting a disconnection between spatial information and certain operant spatial behaviors.

3.46.4.4 Summary of Effects of Cortical Inactivation

The auditory cortex plays a critical role in the sound-localization behavior of cats, dogs, ferrets, and monkeys (e.g., Neff, W. D. *et al.*, 1956; Heffner, H. E., 1978; Kavanagh, G. L. and Kelly, J. B., 1987; Heffner, H. E. and Heffner, R. S., 1990). Although the ability to perform left–right discriminations persists following bilateral lesions, the animals tend to have reduced spatial acuity (as evidenced by increased discrimination thresholds) and may in fact be performing what is for them a quasispatial task (Heffner, H. E., 1978; Heffner, H. E. and Heffner, R. S., 1990). In operant localization tasks, for example, the animals might simply be reinforced for trusting their reflexes, as these reflexes appear entirely sufficient to indicate the hemifield from which a sound originated (Beitel, R. E. and Kaas, J. H., 1993), or they might learn to associate location-dependent stimulus variations with appropriate behavioral responses (Heffner, H. E. and Heffner, R. S., 1990). This might also account for the observation that the left–right discrimination performance of cats and dogs is improved when the target is closer to the initial position of the animal (Neff, W. D. *et al.*, 1956; Heffner, H. E., 1978) – the proximity decreases the likelihood of the animal second-guessing its reflex. Neither of these strategies would require the animal to retain a normal appreciation of left or right or any other spatial quality for that matter. Within a lateral hemifield, however, the animals are completely unable to identify the location of a sound source, regardless of whether the ability is assessed using operant or reflexive methods

(Jenkins, W. M. and Masterton, R. B., 1982; Heffner, H. E. and Heffner, R. S., 1990; Beitel, R. E. and Kaas, J. H., 1993). Following unilateral lesions, localization deficits are restricted to the contralesional hemifield, indicating that each cerebral hemisphere is able to represent independently the contralateral spatial hemifield, as well as the 15–30° of the ipsilateral hemifield closest to the interaural midline (Heffner, H. E., 1997). The effects of acute and chronic inactivations of the auditory cortex are generally similar to the effects of lesions – unilateral inactivations produce contralateral deficits and bilateral inactivations bilateral deficits – but, particularly during longer-term inactivations, may be less severe and may resolve with time (Malhotra, S. *et al.*, 2004; Smith, A. L. *et al.*, 2004). Whether more extensive, chronic inactivations would result in more profound and permanent deficits remains to be seen. It is not surprising that lesions and inactivations produce deficits of differing severity, however, since cortical lesions also result in degeneration within the auditory thalamus and unlesioned cortical areas, thereby increasing the effective size of the manipulation.

3.46.5 Spatial Hearing and the Human Auditory Cortex

Invasive techniques for study of cortical function are only rarely applicable to humans, so the study of spatial hearing mechanisms in the human auditory cortex has emphasized different experimental techniques than are favored in animals. Classical studies in humans relied on sensory testing following cortical lesions due to stroke or trauma. With the advent of structural imaging techniques, lesion studies have been enhanced by the ability to better delineate the extents of lesions. Functional imaging studies employing positron emission tomography (PET), functional magnetic resonance imagery (fMRI), electroencephalography (EEG), and magnetoencephalography (MEG) have only recently been applied to studies of spatial hearing in humans. We will begin by considering the functional imaging results, then will compare those results with results from lesion studies. We will focus on unimodal auditory areas of the temporal lobe; the large literature covering spatial neglect and integration of auditory signals into multimodal areas of the parietal and prefrontal cortex is beyond the scope of this chapter.

The prevailing framework for much recent functional imaging work is the hypothesis that the auditory system possesses segregated what and where pathways analogous to those described in the visual system (Rauschecker, J. P. and Tian, B., 2000; Clarke, S. *et al.*, 2005). Under this model, spatially sensitive and stimulus-feature-sensitive cortical fields are thought to lie posterior and anterior, respectively, to primary auditory regions. Despite methodological differences among studies, a common finding in functional imaging studies is that posterior areas, particularly the planum temporale, are indeed preferentially stimulated by spatially varying or moving stimuli.

Preferential activation in the planum temporale has been found using fMRI and headphone presentation of ear-canal recordings of moving, free-field, amplitude-modulated noise stimuli (Pavani, F. *et al.*, 2002). In a PET imaging study, Zatorre R. J. *et al.* (2002) presented stimuli from an array of small loudspeakers surrounding the listener's head. Regardless of stimulus condition, stimuli produced activation within the superior temporal gyrus, the transverse temporal gyrus (Heschl's gyrus), and posteriorly in the planum temporale. When the source was identical on each trial, they found no cortical areas exhibiting increased activity to more spatially diverse stimulus locations, but when the stimulus varied both spatially and spectrotemporally from trial to trial, foci of activity correlated with spatial diversity were found bilaterally in posterior planum temporale. Similar findings are reported by Warren J. D. *et al.* (2002) using PET and fMRI and are interpreted by the authors as evidence that the planum temporale is involved in the separation of space-related and object-related features of stimuli. Smith A. L. *et al.* (2004) also found activation of that region, but their stimuli were unmodulated wideband noise bursts, which lacked the spectrotemporal variation found necessary by Zatorre R. J. *et al.* (2002).

Using MEG, Fujiki N. *et al.* (2002) recorded auditory mismatch fields for spatial oddball stimuli differing in azimuth or elevation from a standard and found by source analysis that stronger responses to the deviant stimuli were located posterior to those of the standards. Tata M. S. and Ward L. M. (2005), using EEG and electrical source analysis, found that spatial attention can modulate activity near the temporoparietal junction, also posterior to primary auditory areas. All of these results are at least consistent with the existence of a posterior where pathway, although some implicate the planum temporale in both spatial and nonspatial aspects of auditory processing. Hart H. C. *et al.* (2004), using fMRI, observed more

activity in the medial planum temporale for moving stimuli and more activity in the lateral planum temporale for frequency-modulated stimuli, which is suggestive of segregated what and where processing in adjacent posterior areas. In humans and other mammals possessing pinnae, information about sound-source location in the vertical plane is carried by the spectral cues generated by the direction-dependent filtering of the outer ear, but the majority of functional imaging studies have used stimuli varying only in azimuth or in the binaural interaural time- and amplitude-difference cues. Two exceptions to this are the studies by Pavani F. *et al.* (2002; fMRI) and Fujiki N. *et al.* (2002; MEG), both of which employed virtual auditory space stimuli changing location in either azimuth or elevation. The results of both studies suggest activation of similar posterior areas by location changes in either azimuth or elevation. Fujiki N. *et al.* (2002) additionally suggest, however, that monaural spectral cues affect activity more in the right hemisphere than in the left, both in terms of the level and location of activity.

Results from animal studies using electrophysiological (discussed in Sections 3.46.2 and 3.46.3) and lesion (see Section 3.46.4) techniques lead to the conclusion that the representation of each half of auditory space lies primarily in the contralateral cortical hemisphere. A contralateral representation is seen less consistently in human lesion studies (reviewed by Zattore, R. J. and Penhune, V. B., 2001). Substantial individual differences in laterality are seen, due in part to differing etiologies of cortical damage, to the difficulty exactly specifying the lesioned areas, and to possible functional reorganization following cortical damage. Nevertheless, recent well-controlled studies suggest right-hemisphere dominance for auditory spatial representation in humans. Using patients with well-characterized lesions of superior temporal cortex, Zattore R. J. and Penhune V. B. (2001) found that right temporal lobe damage was associated with localization deficits throughout auditory space, whereas similar damage on the left generally resulted in little or no reduction in localization performance. Also, that study showed disturbances in localization in patients with right temporal lobe lesions well anterior to any primary auditory areas. That finding is of course at odds with the consistent identification in imaging studies of posterior, but not anterior, areas as part of the putative where pathway.

3.46.6 Summary and Future Directions

All available data point to the necessity of intact auditory cortex for normal sound localization. The results from studies in experimental animals support the view of a contralateral cortical representation of auditory space in which most individual cortical neurons respond to sounds throughout half or more of auditory space and in which the representation of individual points in auditory space is distributed across widespread neural populations. There is no evidence that any particular cortical areas represent sound-source locations in a way that is dramatically different than in other areas, although some cortical areas seem to show quantitatively stronger spatial sensitivity or enhanced transmission of location-related information (i.e., PAF and DZ in the cat; possibly the caudal belt areas in the monkey). Sound localization by cortical neurons with accuracy comparable to behavioral performance clearly requires the coordinated activity of populations of neurons, likely involving the differential activation of neural populations within each cortical hemisphere tuned to left and right halves of auditory space.

In humans, it is clear that information about sound-source information must reach multimodal areas for spatial processing in the parietal lobe, so in that sense it is clear that there is a posterior–dorsal where stream. Whether that implies a hierarchical organization for spatial processing within the temporal lobe auditory areas remains unresolved, particularly in light of data showing localization deficits resulting from lesions in anterior auditory areas. In contrast to experimental animals, humans seem to show pronounced right-hemisphere dominance for sound localization.

The majority of physiological studies of spatial hearing have been conducted in anesthetized conditions. The few studies in awake animals show greater diversity of spatial sensitivity and greater diversity of neural response patterns than is observed in anesthetized conditions. Future studies must further explore spatial representation in awake conditions, extending studies beyond area A1 into the cortical belt areas. Also, the influence of the behavioral/attentional state of the animal is a key variable that has been largely unexplored. Most studies have used sounds presented in anechoic (or virtual anechoic) conditions. There is a need for more work on mechanisms of

sound localization in realistic environments in which most direct sounds are accompanied by later-arriving reflected sounds.

The most detailed studies of sound localization in the auditory cortex at the single-neuron level have been conducted in nonprimates, particularly in cats. Recent advances in functional imaging have begun to yield new understanding of auditory spatial representation at a more macroscopic level in the human brain. Research is needed on possible homologies between cortical areas in carnivore and primate brains so that insights from the studies in carnivores can be applied more readily toward understanding of mechanisms of spatial perception in humans.

Finally, most work on spatial hearing has focused on identification of the locations of sounds. That is an appropriate starting point because sound-source locations are readily quantified and because many experimental animals show accurate sound-localization behavior. Aspects of spatial hearing that arguably are more relevant to humans, however, are the ability to group together sounds that originate from a particular source and the ability to segregate sounds that originate from different sources. We are optimistic that future physiological studies, informed by psychophysical research, will demonstrate cortical mechanisms for grouping and segregation of sounds in complex acoustic environments.

References

Ahissar, M., Ahissar, E., Bergman, H., and Vaadia, E. 1992. Encoding of sound-source location and movement – activity of single neurons and interactions between adjacent neurons in the monkey auditory cortex. J. Neurophysiol. 67, 203–215.

Baumgart, F., Gaschler-Markefski, B., Woldorff, M. G., Heinze, H. J., and Scheich, H. 1999. A movement sensitive area in auditory cortex. Nature 4000, 724–726.

Beitel, R. E. and Kaas, J. H. 1993. Effects of bilateral and unilateral ablation of auditory cortex in cats on the unconditioned head orienting response to acoustic stimuli. J. Neurophysiol. 70, 351–369.

Benson, D. A., Hienz, R. D., and Goldstein, J. M. H. 1981. Single-unit activity in the auditory cortex of monkeys actively localizing sound sources: spatial tuning and behavioral dependency. Brain Res. 219, 249–267.

Blahut, R. E. 1987. Principles and Practice of Information Theory. Addison-Wesley.

Brugge, J. F., Reale, R. A., and Hind, J. E. 1996. The structure of spatial receptive fields of neurons in primary auditory cortex of the cat. J. Neurosci. 16, 4420–4437.

Brugge, J. F., Reale, R. A., and Hind, J. E. 1998. Spatial receptive fields of primary auditory cortical neurons in quiet and in the presence of continuous background noise. J. Neurophysiol. 80, 2417–2432.

Brugge, J. F., Reale, R. A., Hind, J. E., Chan, J. C. K., Musicant, A. D., and Poon, P. W. F. 1994. Simulation of free-field sound sources and its application to studies of cortical mechanisms of sound localization in the cat. Hear. Res. 73, 67–84.

Brugge, J. F., Reale, R. A., Jenison, R. L., and Schnupp, J. 2001. Auditory cortical spatial receptive fields. Audiol. Neurootol. 6, 173–177.

Carlile, S. and Best, V. 2002. Discrimination of sound source velocity in human listeners. J. Acoust. Soc. Am. 111, 1026–1035.

Clarey, J. C., Barone, P., and Imig, T. J. 1994. Functional organization of sound direction and sound pressure level in primary auditory cortex of the cat. J. Neurophysiol. 72, 2383–2405.

Clarke, S., Adriani, M., and Tardif, E. 2005. "What" and "Where" in Human Audition: Evidence from Anatomical, Activation, and Lesion Studies. Lawrence Erlbaum Associates.

Dong, C. J., Swindale, N. V., and Cynader, M. S. 1999. A contingent aftereffect in the auditory system. Nat. Neurosci. 2, 863–865.

Eggermont, J. J. and Mossop, J. E. 1998. Azimuth coding in primary auditory cortex of the cat. I. Spike synchrony versus spike count representations. J. Neurophysiol. 80, 2133–2150.

Eisenman, L. M. 1974. Neural encoding of sound location: an electrophysiological study in auditory cortex (AI) of the cat using free field stimuli. Brain Res. 75, 203–214.

Evans, E. F. 1967. Cortical Representation. In: Symposium on Hearing Mechanisms in Vertebrates (*eds*. A. U. S. DeReuck and J. O. E. Knight), pp. 272–287. CIBA.

Fitzpatrick, D. C., Kuwada, S., and Batra, R. 2000. Neural sensitivity to interaural time differences: beyond the Jeffress model. J. Neurosci. 20, 1605–1615.

Fitzpatrick, D. C., Kuwada, S., Kim, D. O., Parham, K., and Batra, R. 1999. Responses of neurons to click-pairs as simulated echoes: auditory nerve to auditory cortex. J. Acoust. Soc. Am. 106, 3460–3472.

Fujiki, N., Riederer, K. A., Jousmaki, V., Makela, J. P., and Hari, R. 2002. Human cortical representation of virtual auditory space: differences between sound azimuth and elevation. Eur. J. Neurosci. 16, 2207–2213.

Furukawa, S. and Middlebrooks, J. C. 2001. Sensitivity of auditory cortical neurons to locations of signals and competing noise sources. J. Neurophysiol. 86, 226–240.

Furukawa, S. and Middlebrooks, J. C. 2002. Cortical representation of auditory space: information bearing features of spike patterns. J. Neurophysiol. 87, 1749–1762.

Furukawa, S., Xu, L., and Middlebrooks, J. C. 2000. Coding of sound-source location by ensembles of cortical neurons. J. Neurosci. 20, 1216–1228.

Good, M. D. and Gilkey, R. H. 1996. Sound localization in noise: the effect of signal-to-noise ratio. J. Acoust. Soc. Am. 99, 1108–1117.

Good, M. D. and Gilkey, R. H. 1997. The Relation Between Detection in Noise and Localization in Noise in the Free Field. Erlbaum.

Grantham, D. W. 1997. Auditory Motion Perception: Snapshots Revisited. Lawrence Erlbaum Associates.

Grantham, D. W. and Wightman, F. L. 1979. Auditory motion aftereffects. Percept. Psychophys. 26, 403–408.

Griffiths, T., Rees, G., Rees, A., Green, G. G., Witton, C., and Rowe, D. 1998. Right parietal cortex is involved in the perception of sound movement in humans. Nat. Neurosci. 1, 74–78.

Harrington, I. A., Stecker, G. C., Macpherson, E. A., and Middlebrooks, J. C. 2005. Spatial sensitivity of neurons in the anterior field (AAF) of cat auditory cortex. Abst. Assoc. Res. Otolaryngol. 28, program No. 48, 2005.

Hart, H. C., Palmer, A. R., and Hall, D. A. 2004. Different areas of human non-primary auditory cortex are activated by sounds with spatial and nonspatial properties. Hum. Brain Mapp. 21, 178–190.

Hartmann, W. M. and Rakerd, B. 1993. Auditory spectral discrimination and the localization of clicks in the sagittal plane. J. Acoust. Soc. Am. 94, 2083–2092.

Heffner, H. 1978. Effect of auditory cortex ablation on localization and discrimination of brief sounds. J. Neurophysiol. 41, 963–976.

Heffner, H. E. 1997. The role of macaque auditory cortex in sound localization. Acta Otolaryngol. Suppl. 532, 22–27.

Heffner, H. E. and Heffner, R. S. 1990. Effect of bilateral auditory cortex lesions on sound localization in Japanese macaques. J. Neurophysiol. 64, 915–931.

Heffner, H. E. and Masterton, B. 1975. Contribution of auditory cortex to sound localization in the monkey (*Macaca mulatta*). J. Neurophysiol. 38, 1340–1358.

Heffner, H. E. and Masterton, B. 1978. Contribution of Auditory Cortex to Hearing in the Monkey. Academic Press.

Imig, T. J., Irons, W. A., and Samson, F. R. 1990. Single-unit selectivity to azimuthal direction and sound pressure level of noise bursts in cat high-frequency primary auditory cortex. J. Neurophysiol. 63, 1448–1466.

Jenison, R. L. 1998. Models of Direction Estimation with Spherical-Function Approximated Cortical Receptive Fields. In: Central Auditory Processing and Neural Modeling (*eds*. J. F. Brugge and P. W. F. O. E. Poon) pp. 161–174, Plenum.

Jenison, R. L. 2000. Correlated cortical populations can enhance sound localization performance. J. Acoust. Soc. Am. 107, 414–421.

Jenison, R. L. 2001. Decoding first-spike latency: a likelihood approach. Neurocomputing 38–40, 239–248.

Jenison, R. L. and Fissel, K. 1995. A comparison of the von Mises and Gaussian basis functions for approximating spherical acoustic scatter. IEEE Trans. Neural Netw. 6, 1284–1287.

Jenison, R. L. and Fissel, K. 1996. A spherical basis function neural network for modeling auditory space. Neural Comput. 8, 115–128.

Jenison, R. L., Reale, R. A., Hind, J. E., and Brugge, J. F. 1998. Modeling of auditory spatial receptive fields with spherical approximation functions. J. Neurophysiol. 80, 2645–2656.

Jenison, R. L., Schnupp, J. W. H., Reale, R. A., and Brugge, J. F. 2001. Auditory space-time receptive field dynamics revealed by spherical white-noise analysis. J. Neurosci. 21, 4408–4415.

Jenkins, W. M. and Masterton, R. B. 1982. Sound localization: effects of unilateral lesions in central auditory system. J. Neurophysiol. 47, 987–1016.

Jenkins, W. M. and Merzenich, M. M. 1984. Role of cat primary auditory cortex for sound-localization behavior. J. Neurophysiol. 52, 819–847.

Jiang, H., Lepore, F., Poirier, P., and Guillemot, J. P. 2000. Responses of cells to stationary and moving sound stimuli in the anterior ectosylvian cortex of cats. Hear. Res. 139, 69–85.

Kavanagh, G. L. and Kelly, J. B. 1987. Contribution of auditory cortex to sound localization by the ferret (*Mustela putorius*). J. Neurophysiol. 57, 1746–1766.

Litovsky, R. Y., Colburn, H. S., Yost, W. A., and Guzman, S. J. 1999. The precedence effect. J. Acoust. Soc. Am. 106, 1633–1654.

Loftus, W. C. and Sutter, M. L. 2001. Spectrotemporal organization of excitatory and inhibitory receptive fields of cat posterior auditory field neurons. J. Neurophysiol. 86, 475–491.

Lomber, S. G. 1999. The advantages and limitations of permanent or reversible deactivation techniques in the assessment of neural function. J. Neurosci. Methods 86, 109–117.

Lorenzi, C., Gatehouse, S., and Lever, C. 1999. Sound localization in noise in normal-hearing listeners. J. Acoust. Soc. Am. 105, 1810–1820.

Macpherson, E. A. and Middlebrooks, J. C. 2000. Localization of brief sounds: effects of level and background noise. J. Acoust. Soc. Am. 108, 1834–1849.

Macpherson, E. A., Stecker, G. C., Harrington, I. A., and Middlebrooks, J. C., 2004. Non-linear processing of spectral cues for sound localization in areas DZ and PAF of cat auditory cortex. *Neurosci. Abst.* 24: 529.6,2004.

Makous, J. C. and Middlebrooks, J. C. 1990. Two-dimensional sound localization by human listeners. *J. Acoust. Soc. Am.* 87, 2188–2200.

Malhotra, S. and Lomber, S. G. 2007. Sound localization during homotopic and heterotopic bilateral cooling deactivation of primary and nonprimary auditory cortical areas in the cat. J. Neurophysiol. 97, 26–43.

Malhotra, S., Hall, A. J., and Lomber, S. G. 2004. Cortical control of sound localization in the cat: unilateral cooling deactivation of 19 cerebral areas. J. Neurophysiol. 92, 1625–1643.

Malhotra, S., Hall, A. J., Stecker, G. C., Harrington, I. A., Macpherson, E. A., Middlebrooks, J. C., and Lomber, S. G. 2005. Sound localization deficits during unilateral or bilateral reversible deactivation of cat primary auditory cortex and/or the dorsal zone. Abst. Assoc. Res. Otolaryngol. 28: Program No. 670, 2005.

Malone, B. J., Scott, B. H., and Semple, M. N. 2002. Context-dependent adaptive coding of interaural phase disparity in the auditory cortex of awake macaques. J. Neurosci. 22, 4625–4638.

May, B. J. and Huang, A. Y. 1996. Sound orientation behavior in cats. I. Localization of broadband noise. J. Acoust. Soc. Am. 100, 1059–1069.

Meredith, M. A. and Clemo, H. R. 1989. Auditory cortical projection from the anterior ectosylvian sulcus (field AES) to the superior colliculus in the cat: an anatomical and electrophysiological study. J. Comp. Neurol. 289, 687–707.

Mickey, B. J. and Middlebrooks, J. C. 2001. Responses of auditory cortical neurons to pairs of sounds: correlates of fusion and localization. J. Neurophysiol. 86, 1333–1350.

Mickey, B. J. and Middlebrooks, J. C. 2003. Representation of auditory space by cortical neurons in awake cats. J. Neurosci. 23, 8649–8663.

Mickey, B. J. and Middlebrooks, J. C. 2005. Sensitivity of auditory cortical neurons to the locations of leading and lagging sounds. J. Neurophysiol. 94, 979–989.

Middlebrooks, J. C. 1992. Narrow-band sound localization related to external ear acoustics. J. Acoust. Soc. Am. 92, 2607–2624.

Middlebrooks, J. C. 2000. Cortical Representations of Auditory Space. In: New Cognitive Neurosciences, 2nd edn. (*ed*. M. S. Gazzaniga), MIT Press.

Middlebrooks, J. C. and Green, D. M. 1991. Sound localization by human listeners. Annu. Rev. Psychol. 42, 135–159.

Middlebrooks, J. C. and Knudsen, E. I. 1984. A neural code for auditory space in the cat's superior colliculus. J. Neurosci. 4, 2621–2634.

Middlebrooks, J. C. and Pettigrew, J. D. 1981. Functional classes of neurons in primary auditory cortex of the cat distinguished by sensitivity to sound location. J. Neurosci. 1, 107–120.

Middlebrooks, J. C. and Zook, J. M. 1983. Intrinsic organization of the cat's medial geniculate body identified by projections to binaural response-specific bands in the primary auditory cortex. J. Neurosci. 3, 203–224.

Middlebrooks, J. C., Clock, A. E., Xu, L., and Green, D. M. 1994. A panoramic code for sound location by cortical neurons. Science 264, 842–844.

Middlebrooks, J. C., Xu, L., Eddins, A. C., and Green, D. M. 1998. Codes for sound-source location in nontonotopic auditory cortex. J. Neurophysiol. 80, 863–881.

Mills, A. W. 1958. On the minimum audible angle. J. Acoust. Soc. Am. 30, 237–246.

Mrsic-Flogel, T. D., King, A. J., Jenison, R. L., and Schnupp, J. W. H. 2001. Listening through different ears alters spatial response fields in ferret primary auditory cortex. J. Neurophysiol. 86, 1043–1046.

Mrsic-Flogel, T. D., King, A. J., and Schnupp, J. W. 2005. Encoding of virtual acoustic space stimuli by neurons in ferret primary auditory cortex. J. Neurophysiol. 93, 3489–3503.

Mrsic-Flogel, T. D., Schnupp, J. W., and King, A. J. 2003. Acoustic factors govern developmental sharpening of spatial tuning in the auditory cortex. Nat. Neurosci. 6, 981–988.

Neelon, M. F. and Jenison, R. L. 2004. The temporal growth and decay of the auditory motion aftereffect. J. Acoust. Soc. Am. 115, 3112–3123.

Neff, W. D., Fisher, J. F., Diamond, I. T., and Yela, M. 1956. Role of auditory cortex in discrimination requiring localization of sound in space. J. Neurophysiol. 19, 500–512.

Pavani, F., Macaluso, E., Warren, J., Driver, J., and Griffiths, T. D. 2002. A common cortical substrate activated by horizontal and vertical sound movement in the human brain. Curr. Biol. 12, 1–20.

Phillips, D. P. and Orman, S. S. 1984. Responses of single neurons in posterior field of cat auditory cortex to tonal stimulation. J. Neurophysiol. 51, 147–163.

Phillips, D. P., Semple, M. N., and Kitzes, L. M. 1995. Factors shaping the tone level sensitivity of single neurons in posterior field of cat auditory cortex. J. Neurophysiol. 73, 674–686.

Poirier, P., Jiang, H., Lepore, F., and Guillemot, J. P. 1997. Positional, directional and speed selectivities in the primary auditory cortex of the cat. Hear. Res. 113, 1–13.

Rajan, R., Aitkin, L. M., and Irvine, D. R. F. 1990a. Azimuthal sensitivity of neurons in primary auditory cortex of cats. II. Organization along frequency-band strips. J. Neurophysiol. 64, 888–902.

Rajan, R., Aitkin, L. M., Irvine, D. R. F., and Mckay, J. 1990b. Azimuthal sensitivity of neurons in primary auditory cortex of cats. I. Types of sensitivity and the effects of variations in stimulus parameters. J. Neurophysiol. 64, 872–887.

Rauschecker, J. P. and Tian, B. 2000. Mechanisms and streams for processing of ''what'' and ''where'' in auditory cortex. Proc. Natl. Acad. Sci. U. S. A. 97, 11800–11806.

Reale, R. A. and Brugge, J. F. 2000. Directional sensitivity of neurons in the primary auditory (AI) cortex of the cat to successive sounds ordered in time and space. J. Neurophysiol. 84, 435–450.

Reale, R. A. and Imig, T. J. 1980. Tonotopic organization in auditory cortex of the cat. J. Comp. Neurol. 192, 265–291.

Reale, R. A., Jenison, R. L., and Brugge, J. F. 2003. Directional sensitivity of neurons in the primary auditory (AI) cortex: effects of sound-source intensity level. J. Neurophysiol. 89, 1024–1038.

Recanzone, G. H., Guard, D. C., Phan, M. L., and Su, T. K. 2000. Correlation between the activity of single auditory cortical neurons and sound-localization behaviour in the macaque monkey. J. Neurophysiol. 83, 2723–2739.

Riss, W. 1959. Effect of bilateral temporal cortical ablation on discrimination of sound direction. J. Neurophysiol. 22, 374–384.

Saberi, K., Dostal, L., Sadralodabai, T., Bull, V., and Perrott, D. R. 1991. Free-field release from masking. J. Acoust. Soc. Am. 90, 1355–1370.

Sabin, A. T., Macpherson, E. A., and Middlebrooks, J. C. 2005. Human sound localization at near-threshold levels. Hear. Res. 199, 124–134.

Schnupp, J. W. H., Mrsic-Flogel, T. D., and King, A. J. 2001. Linear processing of spatial cues in primary auditory cortex. Nature 414, 200–204.

Smith, A. L., Parsons, C. H., Lanyon, R. G., Bizley, J. K., Akerman, C. J., Baker, G. E., Dempster, A. C., Thompson, I. D., and King, A. J. 2004. An investigation of the role of auditory cortex in sound localization using muscimol-releasing Elvax. Eur. J. Neurosci. 19, 3059–3072.

Stecker, G. C. and Middlebrooks, J. C. 2003. Distributed coding of sound location in the auditory cortex. Biol. Cybern. 89, 341–349.

Stecker, G. C., Harrington, I. A., Macpherson, E. A., and Middlebrooks, J. C. 2005a. Spatial sensitivity in the dorsal zone (area DZ) of cat auditory cortex. J. Neurophysiol. 94, 1267–1280.

Stecker, G. C., Harrington, I. A., and Middlebrooks, J. C. 2005b. Location coding by opponent neural populations in the auditory cortex. PLoS Biol. 3, 520–528.

Stecker, G. C., Mickey, B. J., Macpherson, E. A., and Middlebrooks, J. C. 2003. Spatial sensitivity in field PAF of cat auditory cortex. J. Neurophysiol. 89, 2889–2903.

Stevens, S. S. and Newman, E. B. 1936. The localization of actual sources of sound. Am. J. Psychol. 48, 297–306.

Strominger, N. L. 1969a. Localization of sound in space after unilateral and bilateral ablation of auditory cortex. Exp. Neurol. 25, 521–533.

Strominger, N. L. 1969b. Subdivisions of auditory cortex and their role in localization of sound in space. Exp. Neurol. 24, 348–362.

Tata, M. S. and Ward, L. M. 2005. Spatial attention modulates activity in a posterior ''where'' auditory pathway. Neuropsychologia 43, 509–516.

Terhune, J. M. and Turnbull, S. D. 1989. Masked threshold changes associated with angular separation of noise and signal sources. Scand. Audiol. 18, 85–89.

Thompson, G. C. and Cortez, A. M. 1983. The inability of squirrel monkeys to localize sound after unilateral ablation of auditory cortex. Behav. Brain Res. 8, 211–216.

Thompson, G. C. and Masterton, R. B. 1978. Brain stem auditory pathway involved in reflexive head orientation to sound. J. Neurophysiol. 41, 1183–1202.

Thompson, R. F. and Welker, W. I. 1963. Role of auditory cortex in reflex head orientation by cats to auditory stimuli. J. Comp. Physiol. Psych. 56, 996–1002.

Tian, B., Reser, D., Durham, A., Kustov, A., and Rauschecker, J. P. 2001. Functional specialization in rhesus monkey auditory cortex. Science 292, 290–293.

Warren, J. D., Zielinski, B. A., Green, G. G. R., Rauschecker, J. P., and Griffiths, T. D. 2002. Perception of sound-source motion by the human brain. Neuron 34, 139–148.

Xu, L., Furukawa, S., and Middlebrooks, J. C. 1998. Sensitivity to sound-source elevation in nontonotopic auditory cortex. J. Neurophysiol. 80, 882–894.

Yang, X. and Grantham, D. W. 1997. Cross-spectral and temporal factors in the precedence effect: discrimination suppression of the lag sound in free-field. J. Acoust. Soc. Am. 102, 2973–2983.

Zattore, R. J. and Penhune, V. B. 2001. Spatial localization after excision of human auditory cortex. J. Neurosci. 21, 6321–6328.

Zatorre, R. J., Bouffard, P. A., and Belin, P. 2002. Where is ''where'' in the human auditory cortex? Nat. Neurosci. 5, 905–909.

Zhang, J., Nakamoto, K. T., and Kitzes, L. M. 2004. Binaural interaction revisited in the cat primary auditory cortex. J. Neurophysiol. 91, 101–117.

Further Reading

Smith, K. R., Okada, K., Saberi, K., and Hickok, G. C. A. 2004. Human cortical auditory motion areas are not motion selective. Neuroreport 15, 1523–1526.

3.47 Pitch Perception

W A Yost, Loyola University Chicago, Chicago, IL, USA

© 2008 Elsevier Inc. All rights reserved.

3.47.1	Introduction and the History of the Study of Pitch	808
3.47.2	Measuring Pitch as a Subjective Attribute of Sound	809
3.47.3	Musical Pitch	810
3.47.4	Place and Temporal Processing of Frequency (and Their Relationship to Pitch)	811
3.47.5	Pitch of Complex Sounds (Introduction to and the History of Complex Pitch Perception)	813
3.47.6	Missing Fundamental Pitch and the Pitch-Shift of the Residue	814
3.47.7	Dominance Region for Complex Pitch	816
3.47.8	Temporal Fine Structure and Complex Pitch Processing	816
3.47.9	Models and Theories of Complex Pitch Processing	818
3.47.10	Which Type of Model Provides the Better Predictions for Complex Pitch?	822
3.47.11	Pitch Strength or Pitch Saliency	823
3.47.12	Spectral Resolvability, Harmonic Number, and Pitch Perception	824
3.47.13	Neural Processing of Pitch	824
References		827

Glossary

autocorrelation (1) $x(t)x(t+\tau)\mathrm{d}t$, where $x(t)$ is a function of time, t is time, τ is a temporal lag, (2) The Fourier transform of the power spectrum, and (3) An all-order interval histogram.

dominant region for pitch The spectral region that contributes the most to determining the pitch of complex sounds, usually found to be between the second and fourth harmonics of a tonal harmonic complex.

inharmonic tonal complex a tonal harmonic complex in which one or more of the harmonics are shifted up or down in frequency by a constant frequency difference less than or equal to the frequency of the fundamental.

interval order The order of intervals between transients in a click train or neural spikes in a spike train. An *n*th-order interval is the interval between a transient or neural spike and the *n*th transient or spike that follows, for example, a second-order interval is that between every other transient or spike.

iterated rippled noise (IRN) A complex sound usually generated by repeating (through a number of iterations) a process of delaying a noise and adding the delayed noise back to the undelayed noise. The gain of the delayed noise can be adjusted relative to the undelayed noise at each stage of iteration. The pitch of IRN sounds is arguably due to its temporal fine structure and is equal to the reciprocal of the delay and the strength of IRN pitch is a function of the gain and number of stages of iteration.

matched pitch The perceptual pitch of a target sound determined by listeners adjusting the frequency or repetition rate of a comparison sound with a known pitch to match the subjective pitch of the target sound.

missing fundamental pitch The pitch of a tonal harmonic complex in which the spectral component at the fundamental frequency in the spectrum is missing.

musical pitch The perceived pitch of sound that allows a listener to determine musical melodies.

pitch of the residue The low pitch of a tonal harmonic complex that is attributed to the period of the sound's envelope that exists within the neural channels/fibers that are not able to resolve the sound's spectral structure.

pitch-shift of the residue The pitch matched to an inharmonic tonal complex. resolved spectral components Those physical spectral structures of sound that are coded in the spectral-temporal pattern of neural firings within the auditory periphery.

tonal harmonic complex A complex waveform consisting of a fundamental tonal frequency component and its higher harmonics. Sometimes the fundamental is missing.

tone chroma The pitch of a sound that remains constant when the frequency differs by an octave, that is, all of the A notes on the piano keyboard have the same pitch (i.e., pitch chroma).

tone height The pitch of sounds that vary with the fundamental frequency of the sound or by a pitch-matching procedure, for example, the A note in the lower octave of the piano keyboard has a lower pitch (i.e., pitch height) than the A note in the upper octave.

3.47.1 Introduction and the History of the Study of Pitch

From the melody of a song to the quality of one's voice to an attribute of everyday sounds, pitch is a major aspect of auditory perception. Pitch allows us to differentiate one musical melody from another, to distinguish a male talker from a female talker, and pitch differences provide a cue as to which potential sound source may have produced a sound. Pitch is a subjective perceptual attribute of sound, but sound itself does not have a pitch. Sound is characterized by vibrating objects that have physical frequency, physical intensity, and temporal properties. Each of these physical properties of sound is represented in the firing patterns of the nerves of the auditory system. The perceived pitch of sound is the nervous system's way of informing us about the physical properties of the sound sources in our world. If the frequency of a vibrating sound source changes we will usually associate that change in physical frequency as a change in subjective pitch, but as we will see in this chapter many other changes in the pattern of vibration that emanates from a vibrating sound source will also lead to a perception that the pitch of the sound has changed. This chapter attempts to highlight the key developments over the past centuries in the study of complex pitch processing. There have been several excellent reviews of pitch processing (de Boer, E., 1976; Plomp, R., 1976; Meddis, R. and Hewitt, M. J. (1991); Cohen, M. A. *et al.*, 1995; and Plack, C. *et al.*, 2005 to mention a few).

Frequency processing and the ability to perceive pitch are arguably the most informative aspects of sound. Without the ability of the nervous system to determine the frequency of sound, speech would be like Morse code, music would only be drum beats, and we would have a very difficult time telling the difference between the sound from one source and that from other sources. Pitch is nature's way of providing crucial information about the sound from the many sources that may exist in our everyday world. Thus, a major goal for understanding hearing is to understand the relationship between various changes in the physical properties of sound and pitch perception.

Pitch perception has fascinated scholars throughout recorded time (see Boring, E. G., 1942, for a history of sensation and perception). Pythagoras (*c.* 530 BC) studied the relationship between the length of strummed strings and the pitch that strings of different lengths produce. Terpander (*c.* 70 BC) and Didymos (*c.* 50 BC) added much more information about pitch and musical intervals. However, Galileo (1564–1642) is credited with first establishing a relationship between physical frequency and pitch. John Shore invented the tuning fork in about 1715 and it became one of the primary instruments for the study of pitch for almost 250 years. While Newton (1643–1727) is clearly identified with vision as a result of his work with prisms, he also studied several aspects of pitch and its relationship to physical frequency. Baron Fourier's (1822) establishment of the Fourier's theorem was developed as a part of a theory of heat, but this analytic method was quickly applied to sound by scientists such as Ohm G. S. (*c.* 1840). Fourier's theory and analysis are still major analytic tools used in the study of sound and hearing. But, perhaps, no person had a greater influence on the modern view of pitch perception than Hermann von Helmholtz. His book *On the Sensations of Tones* (von Helmholtz, H., 1877) was the classic text on pitch and hearing for almost 50 years and is still cited today.

Helmholtz proposed a theory of frequency and pitch processing that became known as a theory of hearing. Several other theories of hearing followed during the first half of the twentieth century in an attempt to account for the auditory system's ability to process sound frequency and generate a pitch perception. Eventually, there appeared to be two opposing theories. The temporal theory of processing frequency, often credited to Wever E. G. (1949) based

on his volley theory which describes how nerve impulses that are limited in firing rate by the refractory period could still code for high frequencies. The spectral or spatial theory of frequency coding was often credited to George von Bekesy (1960), based on his Nobel Prize (awarded in 1961) winning research on the biomechanical properties of the cochlea. Actually, neither von Bekesy G. nor Wever E. G. espoused that the auditory system used only one method (temporal or spectral) to process frequency, but nonetheless they are often portrayed as proposing opposing theories of frequency encoding and pitch processing. Recent studies have greatly increased our knowledge of how the temporal and spectral aspects of auditory processing help code for frequency and account for pitch processing. However, there remain today two theoretical approaches for pitch processing: spectral and temporal. Several authors (see Moore, B. C. J., 1997) have suggested that theories that combine aspects of both theories offer advantages for accounting for pitch processing. These two main theoretical approaches (temporal and spectral) will be explored in greater detail throughout a great deal of this chapter.

3.47.2 Measuring Pitch as a Subjective Attribute of Sound

As mentioned in Section 3.47.1, sound itself does not have a pitch; pitch is a subjective perceptual attribute of sound. Thus, pitch is defined in perceptual terms and measured perceptually. The standard definition of pitch is, "Pitch is that attribute of auditory sensation in terms of which sounds may be ordered on a scale extending from low to high" (American National Standards Institute, ANSI S3.20-R1978, 1978. There are three such scales that have been used to measure pitch: musical scales, the frequency scale using hertz, and the mel scale.

Musical scales will be discussed in greater detail in Section 3.47.3, but the notes of the musical scale (in Western music: A, B, C, D, E, F, G, and in some cases the sharps, #, and flats, b: Ab, Bb, F#, A#, Eb) are often used as one measure of pitch. In addition, the musical scale may be divided into octaves, and each octave into 12 equal logarithmic divisions called semitones. Each semitone has 100 cents (hence an octave has 1200 cents). Semitones and cents are also used as scales to measure pitch.

A common way to measure the pitch of a target sound is to match the pitch of a matching sound with a known pitch to that of the target sound with an unknown pitch. The physical frequency of the matching sound that is judged equal in subjective pitch to that of the target sound is used as the measure of the pitch of the target sound. Thus, if a sinusoidal matching sound is judged to have the same pitch as a target sound when the sinusoidal sound has a physical frequency of 200 Hz, the target sound is said to have a pitch of 200 Hz. Usually the matching sound is either a sinusoidal tonal sound or a periodically repeating series of impulses (clicks) or click train. The rate of the periodic pulses in the click train is expressed in hertz (e.g., 100 periodic pulses per second is 100 Hz). The click rate is adjusted so that the pitch of the click train matches that of the target sound, and the click rate expressed in hertz of the pitch-matched click train is the pitch of the target sound. Thus, the frequency scale, hertz, is a common measure of pitch.

The mel scale for pitch is not often used anymore, but it also involves a pitch-matching procedure. The standard sound in a mel pitch scaling experiment is a sinusoidal tone of 1000 Hz presented at 40 dB SPL. A listener uses a scaling procedure in which a physical variable of the target sound (e.g., its frequency) is varied until the target sound is perceived as subjectively twice, three times, four times, etc. (or conversely one-half, one-third, one-fourth, etc.) the pitch of the standard sound. A scale relating the judged ratio value to the frequency of the target sound forms the mel scale. A target sound judged to have the same pitch as the 1000 Hz, 40 dB SPL sinusoidal standard sound is defined as having a pitch of 1000 mels (i.e., a 1000 Hz, 40 dB SPL tone has a 1000 mel pitch). A sound with a pitch of 2000 mels has a perceived pitch that is twice that of the standard sound and a target sound with a pitch of 500 mels has a perceived pitch that is one-half of that of the standard sound, etc. Thus, the mel scale is a pitch scale.

Before going further it is worth mentioning that there are two other primary subjective measures of sound: loudness and timbre. Loudness as a measure of sound magnitude is not often confused with pitch, but timbre can be (although the physical magnitude of sound can influence perceived pitch). Timbral differences can also interfere with the perceptual measurement of pitch, especially when the pitch matching procedure is used. Timbre is defined by the ANSI standard (ANSI S3.20-R1978, 1978) as, "Timbre is that attribute of auditory sensation in terms of which a subject can judge that two sounds similarly presented and having the same loudness

and pitch are dissimilar." For instance, a violin and a cello each playing the same musical note for the same duration and at the same loudness generate different auditory perceptions. This difference in perceived sound quality is a difference in timbre. A sinusoidal tone has a different timbre than a click train, even if they have the same pitch, loudness, and duration. The timbre of a click train rather than that of a sinusoidal tone is often more similar to that of target stimuli, and, as such listeners are sometimes better able to make pitch matches using click trains, rather than tones, as matching stimuli. In some cases the pitch of a sound is so weak that the quality of the sound might be better described in terms of timbre rather than pitch.

3.47.3 Musical Pitch

Clearly pitch supports musical melody. Thus, any sound that can produce a musical melody has a pitch and the notes of the melody define the pitch of the sounds. However, subjects can match the pitch of sounds that support musical melody to sounds that are not very good at producing musical melodies. Thus, sounds that cannot produce a melody can have a pitch based on the matching procedure. It is also possible that some sounds that have a pitch can be subjectively judged to differ in musical interval (e.g., by a semitone), but these sounds still do not provide a good melody. Thus, there is a type of hierarchy that exists for pitch measurements. Sounds whose pitch can support melodies are accepted as having the strongest form of pitch and the pitch of these sounds is sometimes labeled musical pitch. The next strongest category of sounds that have pitch are those whose pitches can be judged to match musical intervals, but may not support good melody recognition. The weakest form of pitch arises from those sounds that have a pitch based on pitch-matching measures, but these sounds support neither good musical interval nor melody perception.

Musical pitch can mean two different things. In one case, each note on the piano keyboard has a different pitch, in that a sinusoid with a different frequency would be pitch matched to each note. Alternatively, each of the notes in one octave are often said to have same pitch as the corresponding notes in other octaves (e.g., all A notes on the keyboard have the same pitch). The perceptual similarity of pitches across octaves is one of the perceptual bases of musical transposition. Tone or pitch height is the pitch of a sound that is monotonically related to frequency, whereas tone or pitch chroma is the pitch quality shared by sounds separated by an octave. Thus, in measuring musical pitch, it is often important to differentiate between tone height and tone chroma. There are several pitch illusions (the best example is, perhaps, the Shepard Tone Illusion; Shepard, R., 1964) that are based on the perceptual aspects of tone height and tone chroma, demonstrating that these two aspects of pitch can be confused.

An octave is defined as a doubling of frequency such that the octave above 440 Hz (often the note A in the middle octave of the piano keyboard) is 880 Hz. However, different scales are used by different composers to determine the musical intervals within an octave. For instance, a musical piece played with equal temperament tuning provides that each semitone interval is 200 cents (resulting in the note A being 443 Hz). With just intonation tuning, for example, each semitone interval has a slightly different number of cents (as a result the note A is 440 Hz). Different composers and conductors prefer different types of interval tuning and they often change the tuning based on the piece of music that is to be performed. Thus, the exact pitch of the notes within a musical octave depends on what scale is used for tuning. It is also the case that some musicians prefer that the octave be slightly stretched (slightly greater than a factor of two) in order for the same note in different octaves to have the same tone chroma. Such distinctions can influence the reported pitch of sounds when musical scales of pitch are used to measure pitch.

Most listeners judge sounds whose pitches are separated by an octave to be similar indicating a strong pitch relationship to an octave spacing in pitch (Dowling, W. J. and Harwood, D. L., 1986), that is, tone chroma. A few animals also respond in ways that suggest that they too perceive a special pitch relationship for sounds whose frequencies are separated by an octave (see Blackwell, H. R. and Schlosberg, H., 1943). There is some evidence that the timing of neural spikes in the auditory nerve might reflect a different pattern when sounds have an octave (or stretched octave) relationship than when they do not (McKinney, M. F. and Delgutte, B., 1999).

The pitches produced by musical instruments range from approximately 32 Hz (Pressnitzer, D. *et al.*, 2001) up to about 2000 Hz (about a 6–7 octave range). Sounds with physical frequencies up to the

upper limit of frequency sensitivity (~20 000 Hz) can produce a pitch sensation. However, musical pitch is limited to sounds with frequencies less than approximately 2000 Hz. That is, melodies are not easily discerned when they are played at frequencies greater than 2000 Hz.

Some people have the ability to produce or recognize an exact pitch without the use of a referent sound. That is, if asked, they can sing the note A without any acoustic referent, or if an A note is played they can identify the note as A without another sound providing a referent. Such people are said to have absolute pitch (sometimes called perfect pitch, but absolute pitch is the preferred term). Most people, however, do not have such an absolute pitch ability. Many people (especially musicians) can produce or recognize one pitch relative to that of another pitch (e.g., sounds whose pitches differ by a semitone). That is, they can make relative pitch judgments and as such demonstrate relative pitch. The issue of absolute pitch; What is it? Who demonstrates this ability? Is it learned or genetically based? are questions that have been studied for decades (see for instance, Baharloo, S. *et al.*, 1998).

3.47.4 Place and Temporal Processing of Frequency (and Their Relationship to Pitch)

The elaborate biomechanical structures of the cochlea perform a frequency analysis of the vibratory pattern occurring within the inner ear caused by sound waves impinging on the outer and middle ears (see Dallos, P. *et al.*, 1996). The outcome of this cochlear frequency analysis is neurally transduced by the inner hair cells and relayed by the fibers of the auditory nerve to the brainstem. The auditory nerve, all of the ascending pathways of the auditory system, and the auditory cortex are tonotopically organized in that neural firing rate is dependent on the frequency of the sound input and each region of most neural structures responds best to a limit range of frequencies. For instance, within the auditory nerve, neurons in the middle of the bundle of auditory nerves fire best-to-low-frequency sounds, while fibers toward the outside of the nerve bundle fire best-to-high-frequency sounds. Thus, which set of nerves (i.e., which neural place) responds with the greatest firing rate provides a neural code for the frequency content of the incoming sound. The tuning of auditory nerve fibers and neurons in many other auditory centers is narrow in that only a limited range of frequencies cause the nerve fiber to fire above its spontaneous rate. It is as if the cochlea, inner hair cells, and auditory nerve provide a limited form of a Fourier analysis of the frequency content of sound and this spectral analysis is preserved throughout almost all of the auditory system. The frequency selectivity of the place code for neural frequency analysis is very good. The auditory system can code for frequency differences of less than 1% (see Weir, C. C. *et al.*, 1977).

At the same time the timing of the occurrence of neural impulses are synchronized to the temporal pattern of the vibratory sound waveform. Thus, the period of neural firings are tightly linked to the periodicity of the sound input. However, due to properties of neural transmission, nerves can only follow the temporal pattern of the sound input up to approximately 5000 Hz. Thus, the timing of neural impulses can also code for the frequency content of sound, but is limited to frequencies below 5000 Hz.

Sound can be expressed as the product of two temporal waveforms, a carrier waveform $[c(t)]$ and an envelope waveform $[e(t)]$. Thus, a complex sound $[y(t)]$, can be expressed as $y(t) = e(t)^* c(t)$, where $e(t)$ has a period that is much longer than that of $c(t)$ (see Hartmann, W. M., 1998). The auditory system codes for envelope fluctuations, carrier fine-structure fluctuations, and the spectral transform of $y(t)$, that is, the spectrum of the sound. The spectrum, $H(\omega)$, is the Fourier transform of $y(t)$. As will be discussed in more detail later, both the carrier and the envelope waveforms can produce pitch. Thus, while a neuron may not be able to follow a high carrier frequency, it could fire periodically to the envelope of the sound. As such, the perceived pitch may be that associated with the envelope of the sound, rather than the fine temporal structure of the carrier frequency. Conversely for some sounds the fine structure of the sound provides pitch information. And, the different spectral components of sound are also coded by the tonotopic properties of the auditory system and lead to various pitch perceptions.

As stated above $H(\omega)$ and $y(t)$ are transforms of each other, so knowing one function completely defines the other. That is, temporal information about the envelope, $e(t)$, and/or the carrier, $c(t)$, can be transformed into spectral information and vice versa. As such, temporal and spectral information are simple transforms of each other, and from the physical viewpoint one form of processing (temporal or spectral) is not independent of the other form.

Thus, from the stand point of physics one could not decide if a sound were processed temporally or spectrally. As we will discuss later in this chapter this basic fact of physics has made it difficult to support either a temporal or a spectral theory for how either frequency and/or pitch is processed by the auditory system.

While the physics of sound defines temporal and spectral structure of sound as a simple transform, the actual processing of sound by the auditory system places restrictions on the physical transform. For instance, at the level of the auditory periphery there are separations between the temporal and spectral coding of sound. Thus, it is possible to consider both methods of processing sound (temporal and spectral) for frequency coding and/or pitch perception. Figure 1 represents a simulation of the pattern of neural activity that is likely to occur in the bundle of auditory nerves when the auditory system is stimulated with a tonal harmonic complex consisting of a 220 Hz fundamental and its 30 equal-amplitude higher harmonics (i.e., 220, 440, 660, 880, up to 6600 Hz). Such a stimulus is like that produced by a piano key and generates a clear musical pitch of 220 Hz or the note A in the octave below the middle octave of the piano keyboard. The simulation is based on a model of the auditory periphery (Auditory Image Model of Patterson, R. D. *et al.*, 1995) which simulates the biomechanical properties of the cochlea (a gammatone filter bank, see Van Immerseel, L. and Peeters, S., 2003) and the neural properties of the hair cells (a Meddis hair cell; Meddis, R., 1986).

Figure 1 displays the neural pattern of discharges in the auditory nerve over 100 ms and for auditory fibers tuned to different frequencies – low frequencies at the bottom and high frequencies toward the top of the display. Each horizontal trace represents the histogram of neural discharges from a small set of tuned auditory nerve fibers. The spacing of the center frequency of the tuned fibers (channels) is quasilogarithmic representing an estimate of how the nerve fibers are spatially distributed within the auditory nerve bundle. As can be seen fibers tuned to a frequency region near 220, 440, 660, and up to about 1320 Hz are firing in response to the spectral

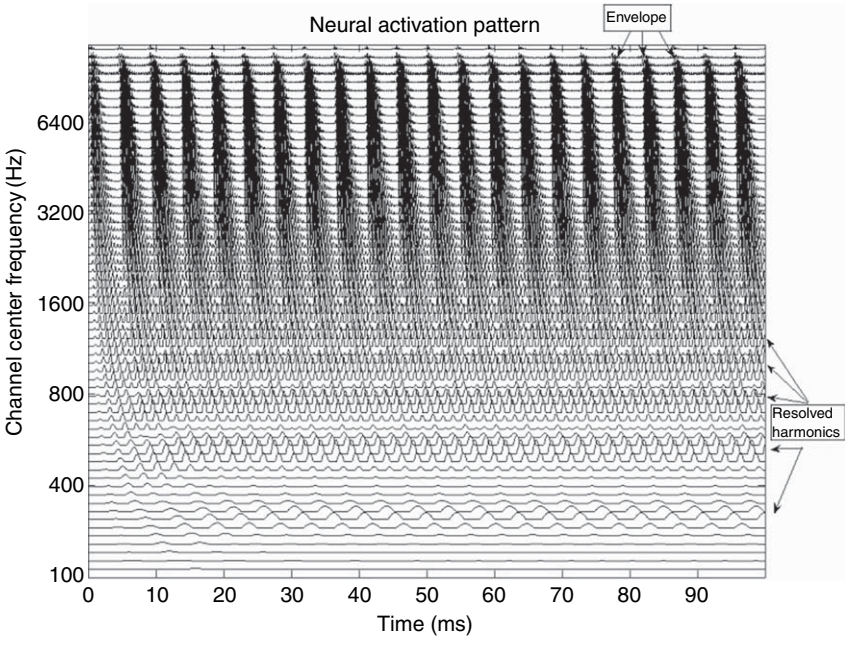

Figure 1 The simulated neural output from the auditory periphery to a tonal harmonic complex with a 220 Hz fundamental and 30 equal-amplitude harmonics. The results are from the computational AIM model (Patterson, R. D. *et al.*, 1995) with each line indicating 100 ms of a histogram of neural responses from auditory channels (fibers) tuned to narrow frequency ranges (the center frequency of the channel/fiber is shown on the *y* axis). Low-frequency channels/fibers are able to resolve the spectral components of the harmonic complex, while the higher-frequency channels/fibers cannot. The higher-frequency channels/fibers preserve the envelope of the harmonic complex and the lower-frequency channels/fibers preserve the temporal fine structure of the individual low-frequency components.

components that make up the harmonic complex. That is, the auditory periphery can resolve the 220 Hz spectral differences in these low-frequency channels. For the higher-frequency fibers (channels), the 220 Hz spacing between harmonic components cannot be resolved by the cochlea and the frequency information from several adjacent harmonics is combined within a single auditory fiber or channel. As a result these high-frequency fibers produce neural discharges that follow the envelope of the waveform. The envelope of the waveform fluctuates periodically at 220 Hz, that is, with a period of 5.5 ms, as do the neural patterns for the higher-frequency channels. In the lower-frequency channels, the neural pattern of discharges follows the temporal fine structure of the low-frequency component (e.g., in the 660 Hz channel, the neural firings occur with about a 1.5 ms period which is the period of 660 Hz), but this ability to follow temporal fine structure disappears as the tuning of the fiber increases toward higher frequencies. Thus, the spectral structure of the harmonic tone is preserved in the low-frequency region, temporal fine structure is also coded in the low-frequency channels, and the envelope of the sound is captured by high-frequency fibers. The major temporal and spectral structures of the harmonic complex are coded in the auditory nerve, but different parts of the auditory nerve code for different aspects of the waveform.

As a result of the coding performed by the auditory periphery it is usually assumed that the frequency of tonal sounds (i.e., a sinusoid) is determined by the place of neural activity for high-frequency sounds, but the tuning of auditory nerve fibers limits frequency resolution. Such a place code can also qualitatively account for the frequency processing of low-frequency tonal sounds, but the resolution of the spectral coding is too poor for low frequencies to quantitatively account for frequency discrimination, so some form of temporal processing is also usually assumed for processing low-frequency tonal sounds. Thus, the pitch of pure tones is assumed to be based on spectral coding for high frequencies and, usually, on a combination of temporal and spectral processing at low frequencies (see Moore, B. C. J., 1993). However, pure tones are not often encountered in one's everyday acoustic world. The key issue for understanding pitch processing is therefore: How are the complex sounds of everyday life processed in order to account for the pitch perceptions associated with such sounds?

3.47.5 Pitch of Complex Sounds (Introduction to and the History of Complex Pitch Perception)

An experiment by Seebeck A. (1841) is often referred to as the beginning of the controversy concerning the relationship between the physical properties of sound (envelope fluctuations, fine-structure fluctuations, and spectral characteristics) and perceived pitch. Seebeck experimented with sirens made of disks with holes in them that rotated over a device that forced air through the holes in the rotating disk. As the disk rotated, air was pulsed at a periodic rate, and the perceived pitch of the disk siren was proportional to the rotation speed (i.e., the periodic rate of air pulses). This led Seebeck to propose that it was the periodic repetition of the air pulses that caused the sensation of pitch (a temporal theory). This was in juxtaposition to Ohm's acoustic law, which said that pitch was associate with the sinusoidal components in the Fourier spectrum of the sound (a spectral theory). Helmholtz supported the spectral approach argued by Ohm and the idea that pitch was associated with the spectral components of sound dominated the pitch literature into the early twentieth century. Since, in some cases, a complex sound made be perceived as having more than one pitch, the issue concerning the processing of the pitch of a something like the disk siren was on the prominent low pitch associated with either the temporal repetition of the waveform (the temporal view) or the fundamental frequency (the lowest sinusoidal component) in the sound's spectrum (the spectral view).

The history of pitch perception and its theories is a series of experiments and theoretical developments based on altering the physical temporal and/or spectral structure of complex sounds and measuring their pitch. Each successive experiment eliminates a physical attribute that the previous experiment argued was the basis for pitch. There was a seesaw of theoretical arguments and developments based on the outcomes of the various alterations of the physical properties of complex sounds. One of the first such alterations was performed by Schouten J. F. (1938) using an optical siren in which the fundamental frequency in the sound's spectrum was missing and yet the low pitch of the siren was that of the missing fundamental. This pitch of the missing fundamental stimulus seemed at odds with the spectral theory of Ohm and Helmholtz and, thus, began the series of experiments and theories that led to our current understanding of pitch perception.

3.47.6 Missing Fundamental Pitch and the Pitch-Shift of the Residue

The optical siren used by Schouten J. F. (1938) would have a long-term spectrum like that shown in Figure 2 (the missing 220 Hz fundamental is shown as a dashed line), and would produce a peripheral neural pattern like that shown in Figure 1, except there would be no neural excitation in the 220 Hz region, since this would be the missing fundamental. Schouten J. F. (1938) found that the low pitch of the sound with and without the missing fundamental was the same. Schouten F. (1938) argued that the pitch of the lower harmonics could be heard out as separate pitches due to the spectral resolving properties of the auditory system (see Figure 1), and that the low pitch of the missing fundamental stimulus was associated with the periodic envelope fluctuations that occur at high frequencies where the harmonics could not be resolved (see Figure 1). Schouten F. (1938) argued that it was the residue pitch associated with the higher unresolved frequencies and their temporal envelope fluctuations that were the basis of the low pitch of many complex sounds.

While the missing fundamental stimulus and its low pitch associated with the frequency of the missing fundamental provided a challenge to a theory of pitch perception based on the spectral presence of the fundamental, it is possible that either the stimulus actually had energy in the spectrum at the fundamental (due to inexact control of the optical siren), or that the nonlinear properties of cochlear transduction reintroduced a spectral component at the fundamental. If a sound with the spectrum shown in Figure 2 is presented to a nonlinear system (cochlear processing is nonlinear), then a nonlinear system could produce spectral components at the difference frequencies between the existing spectral components. Since for the spectrum shown in Figure 2, the difference frequency is the missing fundamental frequency, the nonlinear properties of the cochlea could reintroduce a spectral component at the fundamental. It was well established at that time that nonlinear distortion components such as a difference tone could be detected, especially when stimuli were presented at high levels.

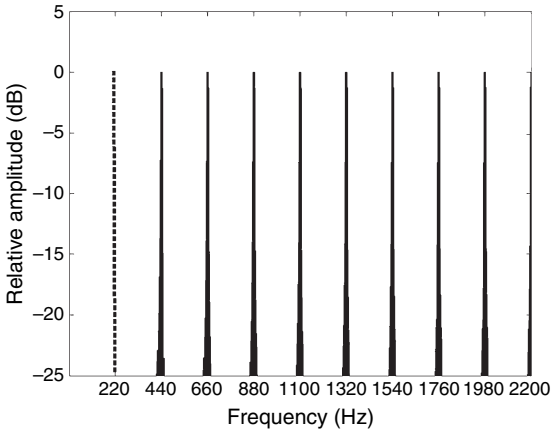

Figure 2 The amplitude spectrum of a missing fundamental tonal harmonic complex. The missing fundamental (shown as the dashed curve) is 220 Hz, and the second through tenth harmonics are present in the complex sound. The low, missing fundamental pitch for this complex sound is 220 Hz, the frequency of the missing fundamental.

Schouten J. F. (1938) showed that no beats could be detected when he added a tone to the missing-fundamental complex with a frequency that was 3 Hz different from the fundamental frequency. If there were any energy in the optical siren sound at the fundamental, one should detect a 3 Hz beat if a tone is added to the siren sound that is 3 Hz different from the fundamental. The fact that no beats were detected helped establish that the siren actually had no (or very little) energy at the fundamental. This experiment also suggests that there was not a strong nonlinear difference tone at the fundamental. Licklider J. C. R. (1955) used a low-frequency noise masker to mask the spectral region of the fundamental in a missing fundamental harmonic tone. He showed that the missing fundamental pitch was still perceived even when any nonlinear distortion products in the spectral region of the fundamental would have been masked. Other studies (e.g., Patterson, R. D., 1969) showed that the pitch of the missing fundamental was only eliminated when the noise masker was presented at a high level that actually masked the harmonics of the missing fundamental harmonic tone. Thus, by the 1960s it was well established that a harmonic tone with no fundamental frequency component produced a strong low pitch at the frequency of the missing fundamental, and this pitch is often referred to as the missing fundamental pitch.

While a spectral theory based on the pitch of complex sounds being determined by the fundamental is defeated by the missing fundamental pitch experiments, a spectral theory based on processing the frequency difference of the resolved harmonics in the missing fundamental stimulus could account for the low pitch, since the difference frequency is the perceived low pitch. That is, even though the

nonlinear distortion produced at the difference frequency is not responsible for the low pitch, some other spectral pitch mechanism could compute the spectral difference (are some form of a spectral difference) and use this as the basis of determining the missing fundamental pitch. We will describe such theories in more detail later in this chapter. Thus, there were still two possible explanations for the missing fundamental pitch: Scouten's temporal theory that it is based on the envelope fluctuations in the high, unresolved frequency region, and the spectral theory based on processing the difference frequency among the resolved harmonics.

De Boer E. (1956; 1961) performed an experiment based on some observations of Schouten J. F. (1940) that challenged both the Schouten residue theory and the spectral difference frequency theory of the missing fundamental pitch. In this experiment, de Boer used an amplitude modulation technique to create a harmonic spectrum shown in the top of Figure 3 (harmonics at 1400, 1600, 1800, 2000, 2200, 2400, and 2600 Hz). The missing fundamental of this harmonic tone is 200 Hz, and this harmonic tone had a strong 200 Hz low pitch. The frequency of each harmonic in this complex was then shifted up in frequency by an amount of Δf, where Δf was less than 200 Hz (e.g., a stimulus might have consisted of 1450, 1650, 1850, 2050, 2250, 2450, and 2650 Hz as indicated in Figure 3). The low pitch associated with such shifted spectra (producing a pitch-shift of the residue) increased noticeably, but the pitch-shifts were small (the pitch-shift of the residue for the stimulus shown in the bottom panel of Figure 3 is about 210 Hz). Since the spacing between the components in the frequency-shifted series is still 200 Hz, the spectral difference theory would predict no change in pitch, that is, the pitch would remain at 200 Hz. It is also the case that the periodicity of the envelope of the unresolved frequency components does not always match the reported pitches for the frequency shifted harmonic series. Thus, these pitch-shift of the residue experiments seemed to cast doubt on both the existing temporal and spectral theories of complex pitch.

Figure 4 shows the pitch-shift of the residue based on the work of Patterson R. D. (1973). Patterson estimated the slope of the best fitting line to the matched pitch of the pitch-shift of the residue for a stimulus with 200 Hz spacing between the 12 consecutive spectral components of a complex tonal sequence when the frequency of the lowest component was varied. Figure 4 indicates the results of these fits. For instance, the far left-hand line indicates that as the lowest spectral component increased from 100 to 300 Hz, the pitch-shift of the residue can range from about 180 to 220 Hz (when the lowest component was 200 Hz, the complex was a 12-tone harmonic complex with a 200 Hz fundamental which yields a 200 Hz matched pitch).

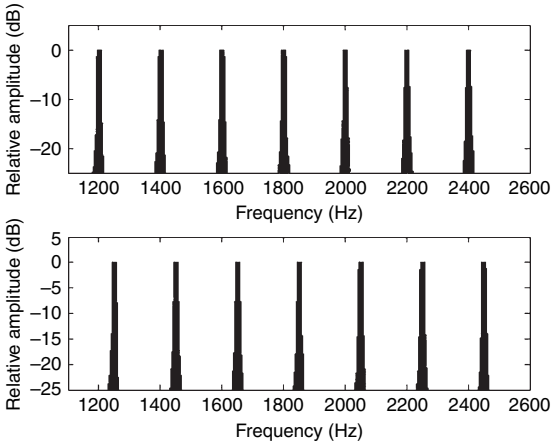

Figure 3 The top panel shows the sixth through twelfth harmonics of a tonal harmonic complex with a 200 Hz fundamental; the low, missing fundamental pitch of this complex is 200 Hz. The bottom panel depicts the case when the components of the harmonic complex shown in the top panel are each shifted up in frequency by 50 Hz. The pitch-shift of the residue for the complex sound of the bottom panel is approximately 210 Hz.

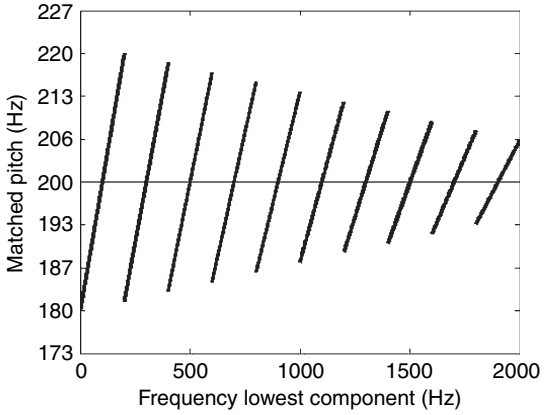

Figure 4 Best fitting straight lines (from Patterson, R. D., 1973) indicating the matched pitched for tonal harmonic complexes, with 12 consecutive tonal components spaced at 200 Hz, plotted as a function of the frequency of the lowest component. The matched pitches indicate the pitch-shift of the residue when the components of a complex sequence are each shifted up or down in frequency.

3.47.7 Dominance Region for Complex Pitch

There are a set of experiments that provide an additional key element in understanding complex pitch processing. While Schouten J. F. argued that the low pitch of the missing fundamental was due to the envelope fluctuations in the high, unresolved frequency regions of the spectrum, spectral theorists used the low-frequency resolved components to estimate a predicted pitch. So the question arises as to which spectral region is more important for the perception of the low pitch of stimuli like the missing fundamental stimulus and the complex stimuli that yield the pitch-shift of the residue. That is, does one spectral region dominate in producing complex pitch perceptions? While there have been several different types of experiments addressing this issue, the one performed by Ritsma R. J. (1962) is usually cited as the first evidence for a dominance region for complex pitch. The most often cited early study of the dominance region for pitch is one by Plomp R. (1967).

In the Plomp R. (1967) study subjects were presented with two stimuli. One stimulus was a complex harmonic tone consisting of the fundamental (ranging between 100 and 2000 Hz) and the 11 higher harmonics. The other stimulus consisted of the same basic fundamental and harmonics, but harmonics below the mth harmonic ($m = 1$–4) were shifted down in frequency by 10% and those above the mth harmonic were shifted up in frequency by 10%. The two stimuli were presented successively in random order and the subject was to indicate if the first or second stimulus was higher in pitch. The results showed that the second and higher harmonics ($m > 1$) dominated the sensation of a rising pitch. The percent of times that the pitch rose when $m = 4$ was far less than for $m < 4$. These results along with those from studies like the earlier one by Ritsma R. J. (1962) strongly suggested that the fundamental was not dominate in determining the low pitch of complex sounds, and the second through about the fourth harmonics were most dominate in determining the low pitch of complex sounds. Thus, the dominance region for complex pitch is assumed to be between the second and fourth harmonics. These results help establish the importance of resolved spectral components in forming the low pitch of complex sounds, as the second through fourth harmonics of a harmonic tone complex would be resolvable by the auditory periphery.

3.47.8 Temporal Fine Structure and Complex Pitch Processing

So far this review of history of the study of pitch processing has centered on the role of the envelope of the unresolved high-frequency components and the spectral differences among low-frequency resolved spectral components. Does the stimulus fine structure have a role in pitch processing? In a series of experiments first done by Small (see Small, A. M., Jr. and Daniloff, R. G., 1967) and then followed up by Bilsen F. A. and colleagues (see Bilsen, F. A. and Ritsam, R. J., 1970) and continued by Yost and his colleagues (see Yost, W. A., 1996a), the answer appears to be yes. A key stimulus that implicates temporal fine structure in pitch processing is rippled noise or more recently iterated rippled noise (IRN, see Yost, W. A. *et al.*, 1996).

IRN stimuli are usually generated by delaying a noise waveform by an amount, d (in ms), and adding the delayed noise (perhaps after changing the gain, g, of the delayed noise relative to the undelayed noise) back to the undelayed noise. This process can be repeated (iterated) many times resulting in an IRN stimulus. Figure 5 displays the network used to generate IRN stimuli and Figure 6 shows the time-domain waveform (top panel) and the amplitude spectrum (bottom panel) for an IRN stimulus generated with a delay of 4 ms, two iterations (as depicted in Figure 5), and when the relative gain (g) was 1 (i.e., the delayed and undelayed noises were equal in level). As can be seen in Figure 6 (top panel), the apparent envelope of the IRN stimulus appears noisy but unmodulated and there are spectral peaks at $1/d$ (250 Hz) and its higher harmonics (bottom panel). The spectrum is like a noisy version of that of a harmonic tone complex with a fundamental of 250 Hz. This IRN stimulus has a 250 Hz pitch (i.e., a pitch equal to $1/d$ which also indicates the lowest-frequency spectral peak). If the lower-frequency spectral peaks are filtered out of this IRN stimulus so that only unresolved higher frequency spectral peaks remain, the pitch of the IRN stimulus remains

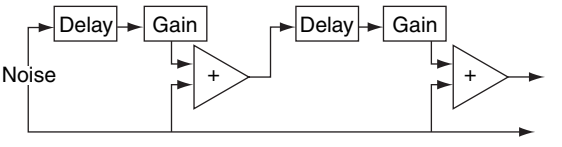

Figure 5 The delay, gain, and add circuit used to generate iterated rippled noise (IRN). Two iterations are shown.

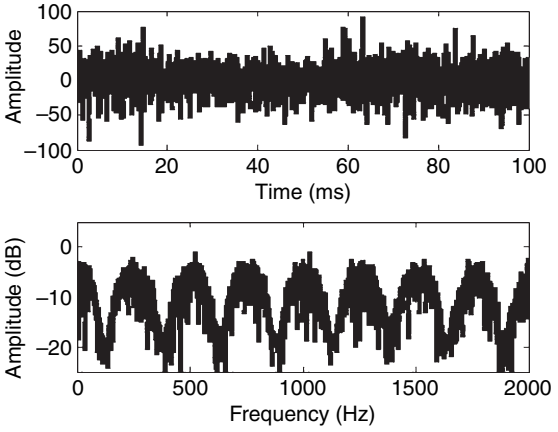

Figure 6 The time-domain waveform in the top panel for an iterated ripple noise (IRN) sound generated with a 5 ms delay, gain of one, and two iterations (see Figure 5). The bottom panel indicates the amplitude spectrum of the IRN sound, showing the noisy spectral structure with spectral peaks at 200 Hz and its higher harmonics. The pitch of this IRN sound is 200 Hz (the reciprocal of the 5 ms delay).

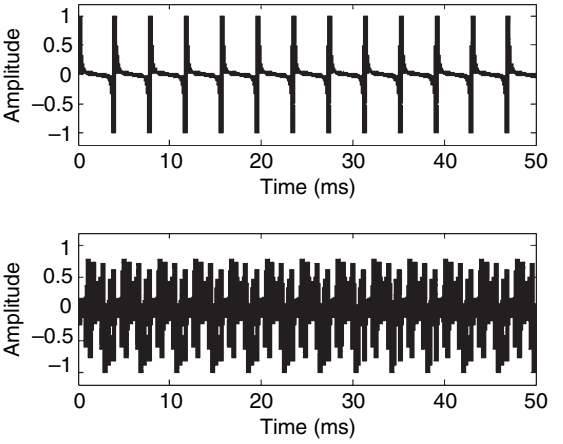

Figure 7 The time-domain plots of a tonal harmonic complex with a 250 Hz fundamental and 50 harmonics. In the top panel, the tonal components all have the same starting phase and in the bottom panel the starting phases of the components are random. Each tonal complex has a 250 Hz pitch, with the saliency of the pitch when the components are in-phase being stronger than when the tonal components are in random phase.

strong at 250 Hz (although not as strong as when the lower-frequency, resolved peaks are present; Yost, W. A., 1982). Thus, the 250 Hz pitch of the IRN stimulus does not appear to depend on resolved spectral components or on a well-defined temporal envelope. As we will discuss in more detail later on, the pitch of IRN stimuli can be explained based on temporal fine-structure processing.

The results from IRN experiments are consistent with those from other experiments in which the time-domain waveform of the complex sound is more random than that produced by a simple harmonic tone complex. Figure 7 displays the time-domain waveforms of a harmonic tonal complex in which the starting phases of each component are the same (top panel) or are randomly chosen (middle panel). Most experiments on complex pitch perception use harmonic tonal complexes with all of the starting phases of the tonal components fixed as indicated in the top panel of Figure 7. Licklider J. C. R. (1955) indicated that a random-phase harmonic tonal complex did not appear to have a missing fundamental pitch. However, several different studies (see Patterson, R. D., 1973) showed that the pitch of a tonal complex remained at the frequency of the fundamental regardless of the starting phase distribution of the harmonics (except in certain conditions, Carlyon, R. P. and Shackleton, T. M., 1994). Several studies of the pitch of harmonic tonal complexes with random starting phases indicated that while the pitch did not appear to be affected by the starting phases, the pitch sensation for a random starting phase harmonic tonal complex appeared to be less salient than that for harmonic tonal complexes generated with all components having the same starting phase (see Plomp, R., 1976). While varying the starting phases of the components in a harmonic tonal complex changes the temporal envelope of the sound, such changes do not change the amplitude spectrum and certain aspects of the temporal fine structure. There have been many studies that have investigated the complex pitch of tonal complexes generated with a variety of starting phase configurations, and it is clear in several cases that the temporal waveform that results from a particular starting phase configuration can influence the perceived pitch of tonal harmonic complexes (see Carlyon, R. P. and Shackleton, T. M., 1994).

So, perhaps complex pitch is determined by temporal fine structure. An experiment by Burns E. M. and Viemeister N. F. (1981) indicates that this is not always the case. Burns E. M. and Viemeister N. F. (1981) showed that a sinusoidally amplitude modulated wide-band noise (SAM noise) produced a very weak pitch that supports a weak form of melody recognition. Since the noise waveform has a random temporal fine structure and a random long-term spectral profile, the only possible cue for the pitch of SAM noise is its amplitude modulated envelope.

Thus, it appears as if neither spectral resolvability, nor envelope, nor temporal fine structure by themselves is necessary and sufficient to produce the pitch of complex stimuli. There is also the problem that the pitch-shift of the residue experiments appears to eliminate a spectral difference of resolved harmonics theory and the envelope of unresolved harmonics theory of complex pitch perception. In order to understand how some of these issues get partially resolved it is necessary to explain some of the models used to account for the data involving the pitch of complex sounds.

3.47.9 Models and Theories of Complex Pitch Processing

As explain above models and theories of pitch processing are either spectral, temporal, or combined spectral–temporal models. Most spectral models are based on assuming that the pitch of complex sounds is based on the best-fitting harmonic structure that can be applied to the resolved spectral components of a complex sound. The fundamental frequency of the best-fitting harmonic series to the spectrum of the complex sound is the predicted pitch of the complex sound. In the case of the missing fundamental stimulus consisting of a harmonic tonal complex without the fundamental present, the best-fitting harmonic series would be the same harmonic series as that of the entire complex, and its fundamental (i.e., the missing fundamental in the actual stimulus) would be the predicted pitch, and this, of course, is a correct prediction. In most models the fit is not done based on all of the harmonics of a complex sound, it is only done for the harmonics within the dominance region for complex pitch, that is, the fit is only made to the second to fourth harmonics of a complex sound (or the fit is weighted in favor of the dominance region for pitch). Not only does this allow the models to be consistent with the fact that there is a dominance region for complex pitch, it allows these spectral models to account for the pitch-shift of the residue effect that appeared to be in conflict with a spectral account of complex pitch.

Figure 8 is a schematic depiction of how spectral models might account for the pitch-shift of the residue. In the case shown in Figure 8 the spectral components of a 200 Hz fundamental harmonic tonal complex with six components are shifted upward 50 Hz, so that the components are at 250, 450, 650, 850, 1050, and 1250 Hz (see Figure 3). This

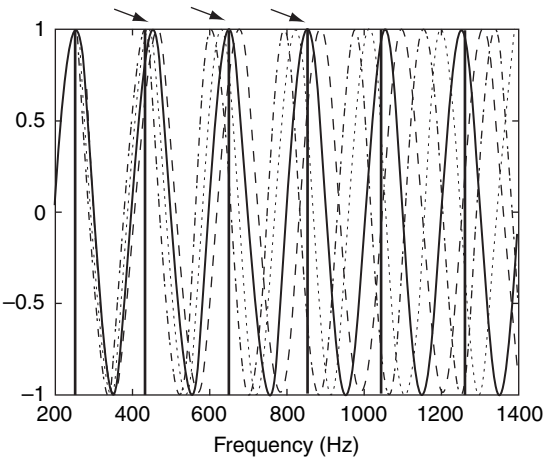

Figure 8 A schematic depiction of how spectral models estimate the pitch of a complex harmonic sound that have shifted spectral components. The spectrum of the sound is represented by the vertical lines at 250, 450, 650, 850, 1050, and 1250 Hz (see Figure 3). The four sinusoidal functions depict attempts at finding the best harmonic fit to this tonal complex that produces a pitch-shift of the residue. The solid sinusoidal function provides the best fit to the second to fourth harmonic components (marked with the arrows). The second to fourth harmonics are those in the dominant region for pitch. The frequency of this best fitting solid curve is 210 Hz, which is the pitch of the pitch-shift of the residue for this complex sound.

complex sound representing a pitch-shift of the residue condition would have a low pitch of about 210 Hz (see Patterson, R. D., 1973). That is, while the spectral spacing of the resolved low-frequency components is 200 Hz the perceived pitch is not 200 Hz, it is about 210 Hz. The spectral components of the six-component complex sound are shown as the vertical lines. The sinusoidal functions are simulations of finding a harmonic function to fit the spectral location of the six spectral components of the complex sound. The idea of most spectral models is to find a harmonic function (e.g., a sinusoid) whose second to fourth peaks best match the spectral location of the second to fourth spectral components of the complex sound (these three components are indicated with arrows in Figure 8). None of the sinusoidal functions makes a perfect fit to the second to fourth spectral components of the complex sound, but the solid sinusoidal curve comes closest to a match. The frequency of this sinusoidal fit is 210 Hz, and as such it would represent the predicted pitch for this stimulus, and 210 Hz is the pitch that most listeners would assign to this sound.

Such spectral models require several assumptions: (1) They need a process for deciding on what

constitutes a best fit. (2) They require some process that establishes the second to fourth spectral components as dominant. (3) The models must assume some sort of ability of the peripheral auditory system to resolve the spectral structure of a complex sound. (4) And, of course, they need to account for the many data that exist concerning the pitch of complex sounds. Four such formal models or theories have been proposed that are spectral approaches along the lines explained above: Wightman's (Wightman, F. L., 1973) pattern transformation model, Goldstein's (Goldstein, J. L., 1973) optimum-processor model, Terhardt's (Terhardt, E., 1974) learning-matrix model, and the Cohen M. A. *et al.* (1995) spectral-network model. Each model is able to make quantitative predictions for the pitch of most complex sounds. The spectral-network model (Cohen, M. A. *et al.*, 1995), being the most recent, is able to account for the largest amount of pitch data, but many of its assumptions and processes are derived directly from the earlier models of Wightman, F. L. *et al.*, and some of the work of Yost W. A. (1982). The learning-matrix model of Terhardt E. (1974) is a comprehensive model that also deals with several other auditory effects like consonance and dissonance. Wightman's (Wightman F. L., 1973) pattern-transformation model is actually based on the Fourier transform of the spectrally resolved amplitude spectrum of the complex sound. The Fourier transform of the amplitude spectrum is the autocorrelation function, and the pattern-transformation model uses the autocorrelation function as a means to derive spectral predictions for the pitch of complex sounds.

Most formal temporal models of complex pitch are based on Licklider's (Licklider J. C. R., 1951) original idea that autocorrelation could be used to account for pitch perception and processing. In this case the autocorrelation approach is conceived in the time-domain and the temporal features of the autocorrelation function are used to account for the pitch of complex sounds. Peaks in the autocorrelation function at particular lag times indicate high correlations of temporal regularity in the complex sound. These temporal models assume that it is this temporal regularity (either in the envelope, fine structure, or both) that accounts for the pitch of complex sounds.

Figure 9 indicates how in general autocorrelation is used to account for the pitch of complex sounds. The stimulus for this description is a 19-tone harmonic complex with a 200 Hz missing fundamental (i.e., the fundamental at 200 Hz is missing and the second through twentieth harmonics are present) and the starting phase of each of the 20 components is random. This complex sound produces a 200 Hz low pitch. The time-domain waveform is shown in the top of Figure 9. The bottom panel of Figure 9 shows the normalized autocorrelation function of this sound. As can be seen there is a large peak at a lag of 5 ms and progressively smaller peaks at lags of integer multiples of 5 ms. Some function of the reciprocal of the lag of the location of largest peak in autocorrelation function (200 Hz in this case) is used to predict the pitch of the complex sound, and the relative height of this peak has been used to account for measures of the saliency of the perceived pitch (pitch saliency or pitch strength will be discussed later in the chapter). In addition to using the peaks in the autocorrelation function, these temporal models also have processes that allow them to predict the pitch-shift of the residue effect, since additional processing of the sound is required in order for the peaks in the autocorrelation function to appear at the appropriate lags that would allow the models to account for the pitch-shift of the residue.

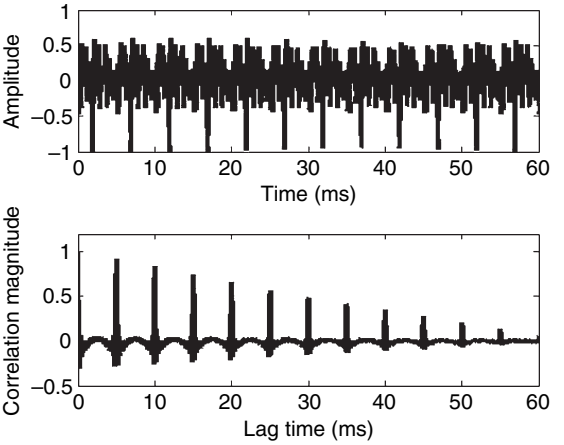

Figure 9 The top panel shows the time-domain waveform for a 19 component, 200 Hz missing fundamental complex (i.e., the spectral components are at 400–4000 Hz, every 200 Hz) generated with random starting phases for each component. This complex stimulus has a 200 Hz pitch. The bottom panel shows the normalized autocorrelation function with a major (largest) peak at 5 ms. Temporal models based on autocorrelation use the reciprocal of the delay for the major peak (200 Hz = 1/5 ms) to predict the pitch of the complex sound and the relative height of this peak to account for pitch saliency/strength.

Meddis R. and Hewitt M. J. (1991) and more recently Meddis R. and O'Mard L. (1997) developed the most complete model based on autocorrelation to account for the pitch of most of the sounds that have

been studied in the complex pitch literature. Yost and Patterson and their colleagues (see Yost, W. A. *et al.*, 1996; Patterson, R. D. *et al.*, 2000) have applied variations of this theme to deal with iterated rippled noise stimuli. De Cheveingé A. (1998) developed a variation of autocorrelation that works well in predicting some of the complex pitch data, but it has not been applied to as large a data set as the Meddis R. and Hewitt M. J. (1991) model. Cariani P. A. and Delgutte B. (1996a; 1996b), used an autocorrelation approach to analyze auditory-nerve data that accounts for a large number of perceptual pitch findings, and this approach will be discussed later in this chapter. Recently, Bernstein J. G. and Oxenham A. J. (2005) modified the model of Meddis R. and O'Mard L. (1997).

All of these autocorrelation-like approaches usually assume that the complex sound is first processed by the auditory periphery and the sound is represented in neural channels each tuned to a particular frequency region. Figures 10 and 11 indicate such an approach which is similar to that used by Meddis R. and Hewitt M. J. (1991), Yost W. A. and colleagues (1996), and Patterson R. D. *et al.* (2000). The stimulus used for Figures 10 and 11 was an IRN stimulus generated such that the spectral peaks started at 100 Hz and were spaced every 200 Hz above that (i.e., 100, 300, 500, 700, 900 Hz, etc.). This stimulus is an IRN equivalent of a pitch-shift of the residue type stimulus in that the fundamental is 100 Hz with every other (even) harmonic of 100 Hz missing (i.e., this is equivalent to shifting the spectral peaks of a 200 Hz fundamental tonal complex down by 100 Hz). In general, subjects either match the pitch (Yost, W. A., 1996a) to that of the fundamental (100 Hz in the example) and/or at about plus or minus

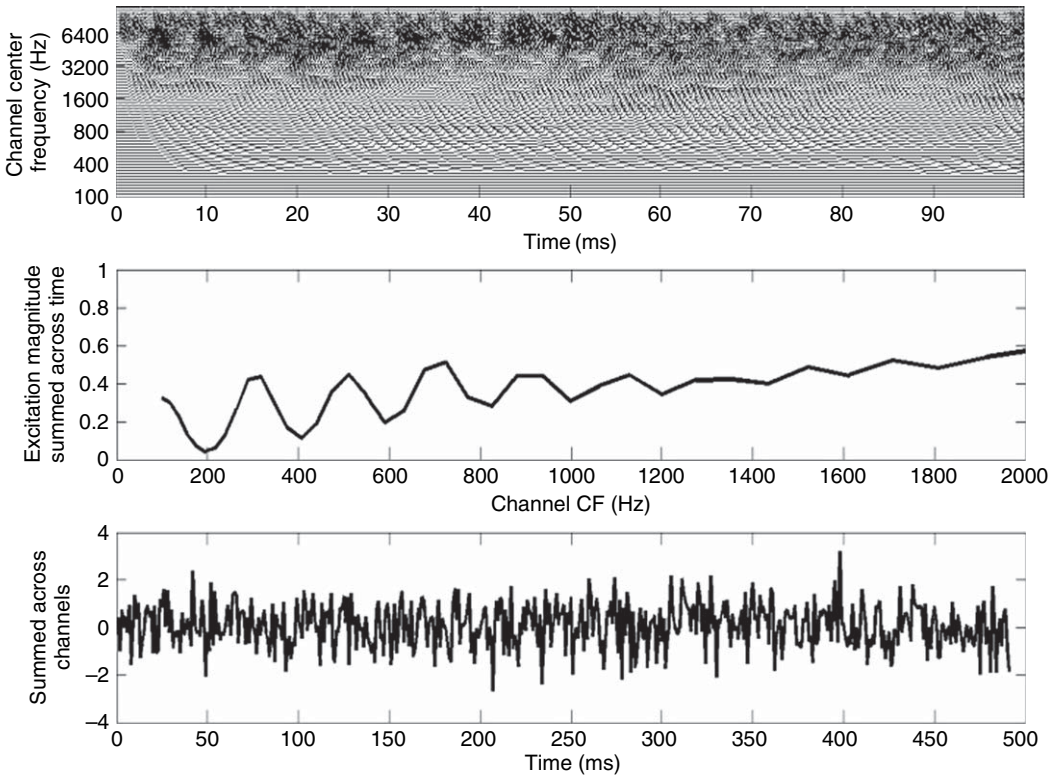

Figure 10 Three displays for an iterated ripple noise stimulus (IRN) generated such that the spectral peaks are at 100, 300, 500 Hz, etc. This IRN sound generates pitch-shift of the residue pitches, with matched pitches being at either 100 Hz, about 180 Hz, and about 220 Hz. The top panel shows the neural activation pattern using the AIM model (see Figure 1). It is difficult to see either a spectral (in the vertical direction) or a temporal structure (in the horizontal direction) to the simulated neural display for this IRN sound. The middle panel shows the auditory spectrum (excitation pattern) computed by summing over time for each frequency channel of the top display. The spectral shape of the IRN sound with resolved peaks at 100, 300, 500, 700, 900, and perhaps 1100 Hz can be seen. The bottom panel represents one view of the temporal information contained in the top display by summing across all frequency channels. None of these three displays contains information that would predict the three pitches typically matched to this IRN stimulus.

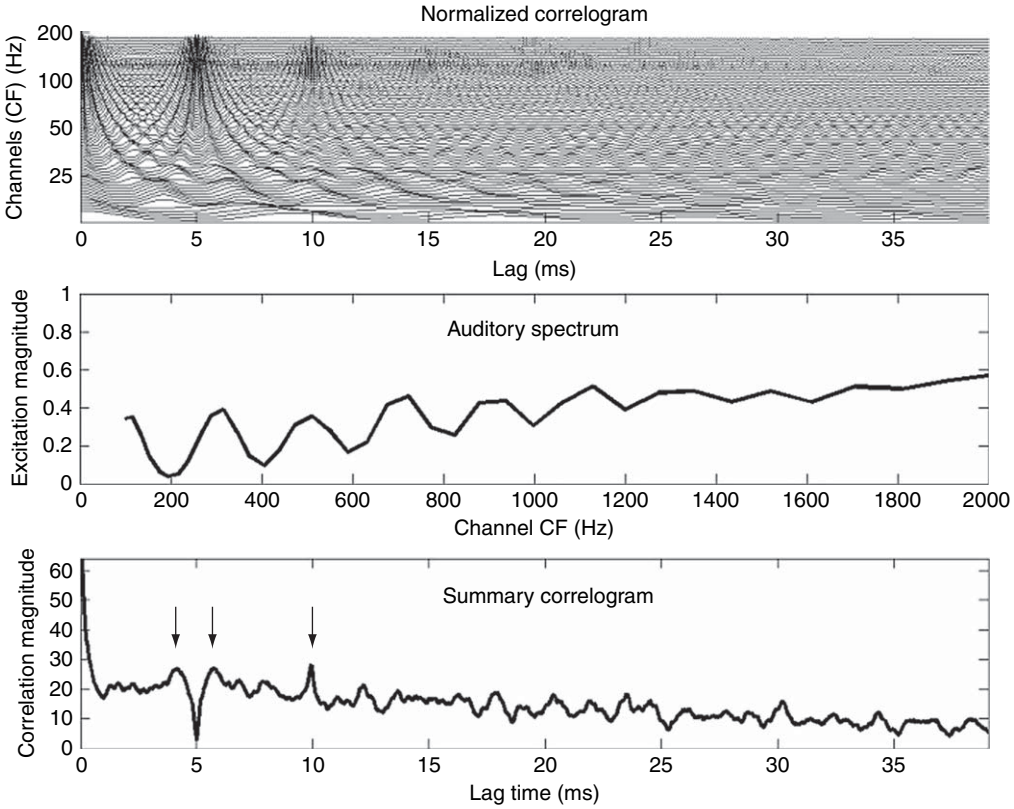

Figure 11 An autocorrelation function is applied to each channel of the display in the top panel of Figure 10 and the output of this computation is shown in the top panel of Figure 11 as a normalized correlogram. The middle panel is the same as that in Figure 10 in that the information in each frequency channel of the top display of Figure 11 is summed over time generating an auditory spectrum. In the bottom panel the autocorrelation information in the correlogram (top display) is summed across all channels generating a summary correlogram. The summary correlogram was constructed based on weighting the correlations in each channel by a function that emphasized the spectral region in the region of 300–700 Hz, which is the approximate dominant pitch region for this stimulus. The arrows point to the three largest peaks in the summary correlogram. The reciprocal of the peak at 10 ms is 100 Hz, and those of the two peaks near 5 ms are 180 and 220 Hz. These are the three matched pitches associated with this IRN stimulus.

10% of the spectral spacing of the peaks (±10% of 200 Hz; and/or 180 and/or 220 Hz in the example).

Figure 10 in the top panel displays the output of the same computational model (AIM, Patterson, R. D. *et al.*, 1995) used for Figure 1. This display is a simulation of the neural information that might flow from the cochlea to the brainstem in the auditory nerve for this IRN stimulus. In the middle panel of Figure 10, the neural activity has been summed across time for each channel and this display is a type of spectral representation (auditory spectrum or excitation pattern) that might be available to the auditory nervous system (the resolved spectral peaks in the lower frequency region can be seen, but not at high frequencies). In the bottom panel of Figure 10, the summed neural activity across channels is displayed indicating the noisy nature of the neural temporal information provided by the auditory periphery. At this level of processing, none of the three displays provides a direct prediction for the pitch(s) of this IRN stimulus.

In the top panel of Figure 11, an autocorrelation of the neural information in each channel is performed. This provides a correlogram showing the correlation of temporal regularity in each tuned channel. The middle panel in Figure 11 indicates the auditory spectrum as the sum across autocorrelation lag as shown in the middle panel of Figure 10. In the bottom panel of Figure 11, the autocorrelation functions of the correlogram shown in the top panel are summed across channels producing a summary correlogram. However, before summing across the channels the information in each spectral channel was weighted by a function that emphasizes the

spectral peaks in the dominance region for pitch (e.g., in the spectral region between 300 and 700 Hz). The weighting is similar to bandpass filtering the IRN stimulus with filter cut-offs at 300 and 700 Hz. Work by Bilsen F. A. and Ritsma R. J. (1967/1968) and Yost W. A. (1982) have shown that such dominance region weighting and filtering of IRN stimuli is important for accounting for the pitch-shift of the residue for these types of IRN stimuli. In the summary correlogram of Figure 11 there are three major peaks (indicated by the arrows). They are at lags of approximately 4.5 ms (its reciprocal is 220 Hz), 5.6 ms (its reciprocal is 180 Hz), and 10 ms (its reciprocal is 100 Hz). As indicated above, these summary correlogram peaks are consistent with the pitches of this IRN stimulus as reported in the literature (see Yost, W. A., 1982).

In addition to autocorrelation models, some researchers (see Langner, G. *et al.*, 1998) have suggested that neural circuits or units that process amplitude modulation (i.e., the envelope of sound) may also participate in pitch processing. That is, many sounds that are amplitude modulated produce a perceived pitch (as discussed previously in this chapter), and since there is evidence that neural units in the higher auditory pathway (e.g., inferior colliculus, Langner, G. and Schreiner, C. E., 1988) and auditory cortex (Schreiner, C. E. and Urbas, J. V., 1986) are selectively sensitive to different modulation rates, these units might be responsible for encoding pitch. The computational modulation filerbank model of Dau T. *et al.* (1997) has recently been applied to account for several data sets involving complex pitch. The issue of amplitude modulation and envelope as they impact complex pitch perception will be discussed later in this chapter.

3.47.10 Which Type of Model Provides the Better Predictions for Complex Pitch?

Both temporal and spectral models provide very good predictions for a great deal of the pitch data in the literature. Given the nature of the transforms between time and frequency, a temporal model can often be rewritten as a spectral model and vice versa. However, when the models are couched in terms of spectral resolvability, then such transformations are not always possible. Spectral models cannot account for the pitch of complex stimuli when the stimuli are generated in such a way that the complex stimulus's spectral structure is not resolvable by the auditory system (e.g., when a tonal harmonic complex with a low-frequency fundamental is high-passed filtered). In addition, spectral models cannot account for the pitch of amplitude modulated noises (Burns, E. M. and Viemiester, N. F., 1981).

Temporal models can often account for pitch data for stimuli with unresolved spectral structure and for modulated noise stimuli. However, the pitch of complex stimuli with unresolved spectral components is weak as is the pitch of amplitude modulated noise. In many cases the pitch of stimuli without resolved components is so weak as to not be able to support musical intervals or melodies and the quality of the sound is sometimes referred to as rattle pitch (Plomp, R., 1976) indicating that the perceptual sensation maybe more timbre like than pitch like. Thus, those stimuli that produce robust pitches are those with resolvable spectral components and these pitches can be well explained by spectral models.

Spectral models can also explain the ability of listeners to determine the pitches of the lower-frequency individual components in a tonal harmonic complex. Support for the spectral theories and their ability to account for some of the properties of the spectral theories comes from experiments with inharmonic tonal complexes. Experiments (see Moore, B. C. J. *et al.*, 1986; Lin, J. Y. and Hartmann, W. M., 1998) using tonal inharmonic complexes are often designed to determine if one tonal component in a harmonic complex is mistuned by shifting it up or down in frequency, would that tone appear perceptually as a separate pitch from that of the low pitch of the complex, and if so would the low pitch of the complex change because that tonal complex was no longer contributing to the low pitch of the complex? If, for example, the third harmonic (600 Hz) of a 200 Hz fundamental tonal harmonic complex is shifted by 8% or more (e.g., from 600 to 650 Hz), then the pitch of this tonal component (i.e., a pitch at 650 Hz) and a pitch near 200 Hz are perceived. That is, this inharmonic tonal complex with all tonal components except one (the 650 Hz mistuned tonal component) being harmonics of 200 Hz produces two pitch perceptions; one near 200 Hz and one at 650 Hz. If the pitch-shift is less than about 8%, only the 200 Hz low pitch is perceived. When the pitch of the mistuned harmonic (i.e., the 650 Hz component) is perceived separately, the low pitch is also shifted slightly from 200 Hz. These results suggest that the harmonic match used in most spectral models needs to be accurate to about 8% of the frequencies of the

harmonics in the stimulus. It is as if the harmonics of a tonal harmonic complex are passed through a spectral sieve before the harmonic structure is determined, with each sieve or channel having a spectral width of about 8%. Thus, many of the data from such inharmonic pitch studies support spectral models of pitch processing (the work of Hartmann, e.g., Lin, J. Y. and Hartmann, W. M., 1998; and Moore, e.g., Moore, B. C. J. *et al.*, 1986 should be consulted since there are several important findings from such experiments that impact the details of how these inharmonic stimuli effect pitch processing).

3.47.11 Pitch Strength or Pitch Saliency

While a wide variety of simple and complex sounds produce pitch, the saliency of the pitch varies considerably from stimuli that produce extremely strong pitches that support melody perception (e.g., an unfiltered periodic click train) to stimuli that produce pitches that are so weak that the perceptions are more like subtle timbre changes (e.g., very-high-passed filtered IRN stimuli or modulated noises). Four different techniques have been used in one way or another to estimate the strength or saliency of perceived pitches, or at least relative pitch strength. In the first technique, a few studies have used magnitude estimation to derive estimates of pitch strength (Fastl, H. and Stoll, G., 1979; Yost, W. A., 1996b; Shofner, W. P. and Seles, G., 2002). Iterated rippled noise stimuli offer the advantage of having two variables that alter the pitch strength of the IRN stimuli (i.e., the number of iterations of the add and delay network or the gain, *g*, applied to the delayed noise before it is added back to the undelayed noise, see Figure 5 and Yost, W. A. *et al.*, 1996). Listeners are asked to discriminate between IRN stimuli and noise stimuli that have no pitch and one of the parameters that varies pitch strength is changed allowing for an estimate of the parameter value that yields a threshold ability to discriminate between the noise and the IRN stimuli. In experiments in the second technique, the discrimination is between two IRN stimuli each producing a different pitch and again the variable that controls pitch strength is varied until the listener is at threshold in making the discrimination between the two IRN stimuli. In these IRN discrimination experiments the discrimination threshold value of the variable that controls pitch strength (e.g., the threshold value of the gain, *g*) is used as a measure of pitch strength. A third technique involves asking subjects to make a musical interval or musical melody judgments. When a variable that presumably controls pitch strength is varied so that an interval or melody cannot be accurately determined, the pitch is said to be too weak to support pitch perception. Pressnitzer D. *et al.* (2001) have used such a technique to measure the lower limit of pitch, which they found to be an interaction between the lowest spectral component in the sound and the duration of the temporal regularity in their complex sounds. The lowest of the lowest pitches appears to be near a temporal-regularity duration of about 30 ms or a pitch of about 33 Hz. The fourth method for estimating pitch strength or saliency is a pitch discrimination task, or since these experiments involve harmonic sequences of one sort or another the task is equivalent to a fundamental frequency (F0) discrimination task (see Carlyon, R. P. and Shackleton, T. M., 1994). Since a speech sound, like a vowel, can be simulated with a tonal harmonic sequence (the fundamental frequency simulates the frequency of vocal cord vibration), F0 discrimination is often measured for synthesized vowels (See Chapter 3.48). A great deal of the work on F0 discrimination involves the study of spectral resolvability and complex pitch which will be discussed next section.

In general, measures of pitch strength have shown that the pitch of stimuli with unresolved spectral structure is considerably weaker than the pitch of stimuli with resolved spectral structures. Some studies have shown that the pitch of complex sounds that have energy in the dominant pitch region is stronger than when the sounds do not contain spectral information in the dominant pitch region. The IRN pitch strength/discrimination experiments have supported the use of the height of the peaks in autocorrelation or summary correlogram functions as a predictor of pitch strength. There is also evidence that a 12-component tonal harmonic complex produces a stronger pitch than a six-component complex and the pitch of a tonal harmonic complex generated with random starting phases is weaker than when the starting phases are fixed (Fastl, H. and Stoll, G., 1979). Some pitch strength studies have been used to point out that in most cases there are at least two percepts associated with many complex sounds that produce a pitch (Patterson, R. D. *et al.*, 2000). There is the low-pitch and there is the timbre of the overall sound. For many stimuli the complex sound is like a mixture of two sound sources, one with a pitch mixed with one with a distinct timbre. In these cases, the

pitch strength estimate indicates the saliency of the pitch source as compared to that of the timbre source.

3.47.12 Spectral Resolvability, Harmonic Number, and Pitch Perception

There is a growing literature that indicates that pitch processing depends in several ways on either the resolved harmonics (or resolved structure) of a complex sound or on the number of lower harmonics. That is, pitch processing might not depend on spectral resolvability *per se*, but rather on the number of lower-frequency harmonics contained in the complex sound (see Bernstein, J. G. and Oxenham, A. J., 2005 for a review). A key paradigm for studying the role of the harmonic structure of complex sounds is the measurement of fundamental frequency (F0) processing for tonal harmonic complexes filtered in different ways to restrict the number of harmonics and/or to control the spectral region where the harmonics exist and/or to alter the degree to which the harmonics might be resolved by the auditory system. In several of these studies the phases of the complexes were varied in different ways to test the idea that if the spectral components of a complex are resolved, the phase of one resolved component might not interact with that of another resolved component since each resolved component is processed by a separate auditory channel or filter. However, for unresolved components that are presumably combined in one spectral channel of filter, the phases of the components would interact (see Carlyon, R. P. and Shackleton, T. M., 1994; Shackleton, T. M. and Carylon, R. P., 1994). The results from several studies indicate that F0 processing and its interaction with the phases of the components is different for resolved than for unresolved components. Some of the data suggested that for certain stimuli in which some of the components are resolved and some unresolved that neither a current spectral nor a current temporal model could account for all of the data, but a spectral model could account for some of the data and a temporal model for the remainder of the data. This suggested that there might be two pitch mechanisms, one spectral and one temporal. Subsequent experiments indicated that there were not two mechanisms and that modifications to the models, at least to the autocorrelation temporal model, could account for many of these newer data (see Bernstein, J. G. and Oxenham, A, J., 2005).

Several experiments (see Bernstein, J. G. and Oxenham, A. J., 2003) suggest that good F0 discrimination and processing that indicates good pitch processing is not determined on spectrally resolved components *per se*, but rather on the number of low-frequency harmonics that are present in the waveform. It appears that the first 10 harmonics are important for good performance in F0 processing somewhat independent on the components spectral resolvability. A summary correlogram uses all of the information from lower-frequency (resolved) and higher-frequency (unresolved) components in producing pitch predictions. Thus, a summary correlogram model should be able to predict pitch and F0 processing as a function of harmonic number. However, the summary correlogram models also include processes that account for the lack of phase locking in the high-frequency channels of the auditory system (i.e., a lack of an ability for high-frequency fibers to follow temporal fine structure). Thus, changes in the summary correlogram pitch or F0 predictions as a function of which harmonics are being processed could be a result of resolved versus unresolved spectral structure and/or a difference in the ability of different channels to phase lock to the stimulus's fine structure (see Carlyon, R. P., 1998). This ambiguity prevents the original version of the summary correlogram model from accurately predicting F0 processing for some key conditions involving F0 processing as a function of harmonic number. Bernstein J. G. and Oxenham A. J. (2005) showed that a modification to the summary correlogram models (e.g., Meddis, R. and O'Mard, L., 1997) allowed them to account for F0 processing that depends on harmonic number.

Thus, at the present time temporal models especially autocorrelation-like models do a good job of accounting for the pitch of complex sounds, especially when the sounds do not contain low-frequency spectral components. However, as we will discuss later in the next section there are some new challenges to autocorrelation accounts of pitch processing.

3.47.13 Neural Processing of Pitch

A previous section (Section 3.47.4) on spectral and temporal processing of simple sounds summarized the pitch processing that is carried out in the auditory periphery. There are several lines of evidence that complex pitch processing is preformed centrally and

not peripherally. First, complex pitch requires a comparison of the spectral and/or temporal information across the spectrum of the sound. Thus, there has to be some form of spectral and/or temporal integration or comparison in order to account for the perceived complex pitch. Such comparisons or integration are likely to occur in neural centrals central to the periphery. There is also considerable evidence that complex pitch often involves stimulation to both ears. Since only neural centers above the cochlear nucleus receive bilateral input, such binaurally generated pitches must be generated at neural locations above the level of the cochlear nucleus. Houtsma A. J. M. and Goldstein J. L. (1972) were among the first to show that if different harmonics are presented to different ears, then the reported pitch is not that predicted by the harmonic structure at either ear, but on the combined harmonic structure from both ears (see Bernstein, J. G. and Oxenham, A. J., 2003 for a more recent version of this binaural work). That is, the harmonics from each ear must be combined centrally in order to account for the perceived pitch.

Several investigators (e.g., Cramer, E. M. and Huggins, W. H., 1958; Culling, J. F. *et al.*, 1998; Yost, W. A., 1991; Bilsen, F. A. and Raatgever, J., 2000) have also showed that reversing the phases of the spectral components of a noise in a narrow frequency band in one ear relative to the phases at the other ear produces a dichotic pitch (Huggins–Cramer pitch, Cramer, E. M. and Huggins, W. H., 1958) that is associated with the narrow spectral region over which the interaural phase shift exists. Again, such dichotic pitches require some form of integration of the information between the two ears.

While the neural site at which complex pitch is processed is likely central, several studies have investigated the type of information that the auditory periphery might provide to such a central processor. Cariani P. A. and Delgutte B. (1996a; 1996b) performed several experiments showing that if the central nervous system used a form of autocorrelation then the temporal information in the firings of auditory nerve fibers contained sufficient and necessary information for an autocorrelation-like process to determine the pitch for a wide variety of complex pitch stimuli used in perceptual experiments. Their analysis suggested that it was necessary to combine neural information across auditory nerve fibers tuned to a wide range of frequencies. They also argued that an analysis like an interval histogram in which the timing between only successive neural spikes is calculated could not adequately predict the data on complex pitch. Cedolin L. and Delgutte B. (2005) have also shown that at the level of the auditory nerve neither a temporal analysis nor a spectral/place analysis (based on the ability of the auditory nerve to resolve spectral structure) of auditory nerve data can completely account for a wide range of perceptual pitch data.

In these experiments and other uses of autocorrelation to study neural responses, the autocorrelation functions are computed as all-interval histograms. The interval between each successive neural spike is considered a first-order interval and these first-order intervals are the basis of the interval histogram often used in studying the temporal properties of neuronal function. A second-order interval is one between every other neural spike, third-order interval is that between every third spike, and an *n*th-order interval is that between every *n* spikes. Autocorrelation is equivalent to an all-order interval analysis. That is, an all-order interval histogram (the proportion of times that an interval of each possible duration occurred independent of the order of the interval) is an autocorrelation function.

Kaernbach C. and Demany L. (1998) have argued that the auditory system does not calculate an all-interval analysis (i.e., an autocorrelation analysis) because they and others (see Yost, W. A. *et al.*, 2005) have shown that the auditory system seems to be less sensitive to second-order intervals as compared to first-order intervals. An autocorrelation approach does not differentiate among interval order, i.e., all interval orders make the same contribution to the autocorrelation function. Thus, these results regarding a relative insensitivity to second-order intervals suggests that an auditory analysis might be autocorrelationlike, but is not actually autocorrelation. If such processes were biased toward lower-order intervals, they might perform better in accounting for some of the pitch data than an all-interval autocorrelation approach (see Pressnitzer, D. *et al.*, 2004). It is also the case that there is no physiological evidence for any auditory neural circuits that appear to be able to form an autocorrelation analysis (e.g., there is no evidence for a coincidence network as suggested by Licklider, J. C. R., 1951, when he proposed autocorrelation as a means to calculate pitch).

Several other investigators have shown that neural units of different types in the cochlear nucleus (e.g., Shofner, W. P., 1999; Winter, I. M. *et al.*, 2003) produce all-interval autocorrelation functions that are consistent with the pitch obtained in many perceptual experiments. In several of these experiments the

units that were studied were chopperlike cells that respond robustly to the envelope of complex sounds. This suggests that envelope fluctuations may play a role in complex pitch processing. As mentioned previously, several authors (see Schreiner, C. E. and Urbas, J. V., 1986; Langner, G. *et al.*, 1998) have suggested that neural centers in the inferior colliculus and cortex that appear to be tuned to the modulation rate of the envelope of complex sound may play a significant role in complex pitch processing.

While neural units that process the envelope of complex sounds may play some role in the processing of complex pitch, it is unlikely a complex sound's envelope is the necessary and sufficient process to account for complex pitch processing. Recall that the pitch-shift of the residue is different from the pitch of the residue itself. That is, the missing fundamental pitch is that of the fundamental, whereas when the spectral components are shifted up or down in value while keeping their component spacing constant, the pitch changes. Consider for example the case cited above in which for one condition the spectral components (spectral peaks) are at 400, 600, 800 Hz, etc. In this case the pitch of the residue or missing fundamental pitch is 200 Hz. If the spectral components are at 300, 500, 700, 900 Hz, etc. (i.e., shifted up by 100 Hz from the first case), the pitch-shift of the residue is either 100 Hz or plus or minus 10% of 200 Hz (180 and/or 220 Hz), but it is never 200 Hz. The temporal envelope of these two stimuli is the same (see Yost, W. A. *et al.*, 1998). That is, shifting the components by additive amount does not alter the temporal envelope of the sound. Since the pitch of such spectrally shifted complex stimuli does change as a function of the shift but their envelope does not, the envelope cannot be used to explain the pitch-shift of the residue. The predicted pitch-shift of the residue appears to depend on either the spectrum or the temporal fine structure of a complex sound, and not the envelope.

Up until recently research investigating the neural basis of pitch has depended on physiological data from animal models used to account for human pitch perception. Several investigators (see Shofner, W. P., 2005 for a review) have shown that the behavioral responses of several different animals to missing fundamental pitch stimuli appear to be similar to the ways in which human subjects respond to these same stimuli. Shofner W. P. *et al.* (2005) have shown in several different experiments that the behavioral responses of the Chinchilla to iterated rippled noise and other harmonic stimuli are very similar to the psychophysical data obtained from human subjects (See Chapter 5.44). However, recent data suggest that the Chinchilla is perhaps more sensitive to the envelope of complex pitch-producing sounds than are human subjects (Shofner, W. P. *et al.*, 2005). Thus, different animal subjects appear to process the pitch of complex sounds in ways that are similar to that of human subjects, suggesting that the neural measures obtained from animals are relevant for understanding the neural mechanisms that underlie pitch perception.

With the use of neural imaging (e.g., positron emission tomography, functional magnetic resonance imaging, magnetencephalography, and electroencephalography) it is possible to search for neural centers in human auditory pathways (especially in auditory cortex) that might play a role in pitch processing (See Chapter 3.50). In a series of studies, Heschl's Gyrus, in the human auditory cortex, has been implicated as a cortical region that is likely significantly involved with processing pitch and, perhaps, pitch that produce melodies (see Griffiths, T. D. *et al.*, 1998; Gutschalk, A., *et al.*, 2004; Seither-Preisler, A. *et al.*, 2004). The initial work used iterated ripple noise, but further studies suggest that many different stimuli that produce complex pitch are powerful in producing neural images that are consistent with the assumption the Heschl's Gyrus is participating in processing complex pitch. These data implicated temporal processing of complex pitch. Recently Wang and colleagues (Bendor, D. and Wang, X., 2005) have shown that in a neural region of the marmoset monkey that is homologous with Heschl's Gyrus in humans (only humans have a Heschl's Gyrus) multiunit and single-unit electrophysiological recordings also suggest that this cortical region plays a significant role in complex pitch processing. They used a wide variety of stimulus conditions producing converging data implicating this cortical region as participating in pitch processing. Current speculation is that the actual computation of pitch might occur in lower brainstem centers and that Heschl's Gyrus and its homolog in primates is a pathway that reads the output of such computations (Griffiths, T. D. *et al.*, 1998).

Thus, the study of complex pitch has a rich history. After more than 100 years it is still not clear exactly how complex pitch is processed. The current view appears to be that the most parsimonious way to account for complex pitch perception is with temporal models such as ones based on autocorrelation. However, the most salient complex pitches occur in

spectral regions where the spectral structure of the sounds are resolved by the auditory periphery and where a spectral account works as well as a temporal one. In addition, there are several studies that suggest that autocorrelation may not be the appropriate temporal model. The research on complex pitch and its neural basis continues at a rapid pace, and it will probably not take another 100 years for a single well establish theory to emerge.

References

American National Standards Institute, ANSI, S3.20-R1978–1978. American National Standard on Bioacoustical Terminology. Acoustical Society of America.

Baharloo, S., Johnston, P. A., Service, S. K., Gitschier, J., and Freimer, N. B. 1998. Absolute pitch: an approach for identification of genetic and nongenetic components. Am. J. Hum. Gen. 62, 224–231.

Bendor, D. and Wang, X. 2005. The neuronal representation of pitch in primate auditory cortex. Nature 436, 1161–1165.

Bernstein, J. G. and Oxenham, A. J. 2003. Pitch discrimination of diotic and dichotic tone complexes: harmonic resolvability or harmonic number? J. Acoust. Soc. Am. 113, 3323–3334.

Bernstein, J. G. and Oxenham, A. J. 2005. An autocorrelation model with place dependence to account for the effect of harmonic number on fundamental frequency discrimination. J. Acoust. Soc. Am. 117, 3816–3831.

Bilsen, F. A. and Raatgever, J. 2000. On the dichotic pitch of simultaneously presented interaurally delayed white noises. Implications for binaural theory. J. Acoust. Soc. Am. 108, 272–284.

Bilsen, F. A. and Ritsma, R. J. 1967/1968. Repetition pitch mediated by temporal fine structure at dominant spectral regions. Acoustica 19, 114–115.

Bilsen, F. A. and Ritsma, R. J. 1970. Some parameters influencing the perception of pitch. J. Acoust. Soc. Am. 47, 469–475.

Blackwell, H. R. and Schlosberg, H. 1943. Octave generalization, pitch discrimination, and loudness thresholds in the white rat. J. Exp. Psychol. 33, 407–419.

Boring, E. G. 1942. Sensation and Perception in the History of Experimental Psychology. Appleton-Century-Crofts.

Burns, E. M. and Viemeister, N. F. 1981. Played-again SAM: further observations on the pitch of amplitude-modulated noise. J. Acoust. Soc. Am. 70, 1655–1660.

Cariani, P. A. and Delgutte, B. 1996a. Neural correlates of the pitch of complex tones. I. Pitch and pitch salience. J. Neurophysiol. 76, 1698–1716.

Cariani, P. A. and Delgutte, B. 1996b. Neural correlates of the pitch of complex tones. II. Pitch shift, pitch ambiguity, phase invariance, pitch circularity, rate pitch, and the dominance region for pitch. J. Neurophysiol. 76, 1717–1734.

Carlyon, R. P. 1998. Comments on 'A unitary model of pitch perception'. J. Acoust. Soc. Am. 102, 1811–1820.

Cedolin, L. and Delgutte, B. 2005. Pitch of complex tones: rate-place and interspike interval representations in auditory nerve. J. Neurophysiol. 94, 347–362.

Carlyon, R. P. and Shackleton, T. M. 1994. Comparing the fundamental frequencies of resolved and unresolved harmonics: evidence for two pitch mechanisms? J. Acoust. Soc. Am. 95, 3541–3554.

Cohen, M. A., Grossberg, S., and Wyse, L. L. 1995. A spectral network model of pitch perception. J. Acoust. Soc. Am. 98, 862–879.

Cramer, E. M. and Huggins, W. H. 1958. Creation of pitch through binaural interaction. J. Acoust. Soc. Am. 30, 413–417.

Culling, J. F., Summerfield, A. Q., and Marshall, D. H. 1998. Dichotic pitches as illusions of binaural unmasking I. Huggins pitch and the binaural edge pitch. J. Acoust. Soc. Am. 103, 3509–3526.

Dallos, P., Popper, A. N., and Fay, R. R. (eds.) 1996. The Cochlea. Springer.

Dau, T., Kollmeier, B., and Kohlrausch A. 1997. Modeling auditory processing of amplitude modulation. II. Spectral and temporal integration. J. Acoust. Soc. Am. 102, 2906–2919.

de Boer, E. 1956. On the 'Residue' in Hearing. Doctoral Dissertation, University of Amsterdam.

de Boer, E. 1961. A note on phase distortion and hearing. Acoustica 11, 182–184.

de Boer, E. 1976. On the ''Residue'' and Auditory Pitch Perception. In: Handbook of Sensory Physiology (*eds*. W. D. Keidel and W. D. Neff), pp. 479–583. Springer.

De Cheveigné, A. 1998. Cancellation model of pitch perception. J. Acoust. Soc. Am. 103, 1261–1271.

Dowling, W. J. and Harwood, D. L. 1986. Music Cognition. Academic Press.

Fastl, H. and Stoll, G. 1979. Scaling of pitch strength. Hear. Res. 1, 293–301.

Goldstein, J. L. 1973. An optimum processor theory for the central formation of the pitch of complex tones. J. Acoust. Soc. Am. 54, 1496–1516.

Griffiths, T. D., Beuchel, C., Frackowiak, R. S. J., and Patterson, R. D. 1998. Analysis of temporal structure in sound by the brain. Nat. Neurosci. 1, 422–427.

Gutschalk, A., Patterson, R. D., Scherg, M., Uppenkamp, S., and Rupp, A. 2004. Temporal dynamics of pitch in human auditory cortex. Neuroimage 22, 755–766.

Hartmann, W. M. 1998. Signal, Sounds and Sensation. Springer.

Houtsma, A. J. M. and Goldstein, J. L. 1972. The central origin of the pitch of pure tones: evidence from musical interval recognition. J. Acoust. Soc. Am. 51, 520–529.

Kaernbach, C. and Demany, L. 1998. Psychophysical evidence against the autocorrelation theory of auditory temporal processing. J. Acoust. Soc. Am. 104, 2298–2306.

Langner, G. and Schreiner, C. E. 1988. Periodicity coding in the inferior colliculus of the cat. I. Neuronal mechanisms. J. Neurophysiol. 60, 1799–1822.

Langner, G., Schreiner, C. E., and Biebel, U. W. 1998. Functional Implications of Frequency and Periodicity Coding in the Auditory Midbrain. In: Psychophysical and Physiological Advances in Hearing (*eds*. A. R. Palmer, A. Rees, A. Q. Summerfield, and R. Meddis), pp. 277–285. Whurr Publishers.

Licklider, J. C. R. 1951. A duplex theory of pitch perception. Experientia 7, 128–133.

Licklider, J. C. R. 1955. Influence of phase coherence upon the pitch of complex periodic sounds. J. Acoust. Soc. Am. 27, 145–151.

Lin, J. Y. and Hartmann, W. M. 1998. The pitch of a mistuned harmonic: evidence for a template model. J. Acoust. Soc. Am. 103, 2608–2613.

McKinney, M. F. and Delgutte, B. 1999. A possible neurophysiological basis of the octave enlargement. J. Acoust. Soc. Am. 106, 2679–2692.

Meddis, R. 1986. Simulation of mechanical to neural transduction in the auditory receptor. J. Acoust. Soc. Am. 79, 702–711.

Meddis, R. and Hewitt, M. J. 1991. Virtual pitch and phase sensitivity of a computer model of the auditory periphery. I: Pitch identification. J. Acoust. Soc. Am. 89, 2866–2882.
Meddis, R. and O'Mard, L. 1997. A unitary model of pitch perception. J. Acoust. Soc. Am. 102, 1811–1820.
Moore, B. C. J. 1993. Frequency Processing. In: Human Psychoacoustics (*eds*. W. A. Yost, A. N. Popper, and R. R. Fay), pp. 56–116. Springer.
Moore, B. C. J. 1997. An Introduction to the Psychology of Hearing. Academic Press.
Moore, B. C. J., Peters, R. W., and Glasberg, B. R. 1986. Thresholds for hearing mistuned partials as separate tones in harmonic complexes. J. Acoust. Soc. Am. 80, 479–483.
Patterson, R. D. 1969. Noise masking of a change in residue pitch. J. Acoust. Soc. Am. 45, 1520–1524.
Patterson, R. D. 1973. The effects of relative phase and number of components on residue pitch. J. Acoust. Soc. Am. 53, 1565–1572.
Patterson, R. D., Allerhand, M., and Giguere, C. 1995. Time-domain modeling of peripheral auditory processing: a modular architecture and a software platform. J. Acoust. Soc. Am. 98, 1890–1895.
Patterson, R. D., Yost, W. A., Handel, S., and Datta, J. A. 2000. The perceptual tone/noise ratio of merged iterated rippled noises. J. Acoust. Soc. Am. 107, 1578–1588.
Plack, C., Oxenham, A. J., Fay, R. R., and Popper, A. N. 2005. Pitch: Neural Coding and Perception. Springer.
Plomp, R. 1967. Pitch of complex tones. J. Acoust. Soc. Am. 41, 1526–1533.
Plomp, R. 1976. Aspects of Tone Sensation. Academic Press.
Pressnitzer, D., de Cheveigné, A., and Winter, I. M. 2004. Physiological correlates of the perceptual pitch shift for sounds with similar autocorrelation. Acoust. Res. Lett. 5, 1–6 (Online).
Pressnitzer, D., Patterson, R. D., and Krumbholz, K. 2001. The lower limit of melodic pitch. J. Acoust. Soc. Am. 109, 2074–2084.
Ritsma, R. J. 1962. Existence region of the tonal residue. I. J. Acoust. Soc. Am. 34, 1224–1229.
Schouten, J. F. 1938. The perception of subjective tones. Proc. Kon. Ned. Akad. Wetensch. 41, 1086–1093.
Schouten, J. F. 1940. The residue, a new component in subjective sound analysis. Proc. K. Ned. Akad. Wet. C 43, 356–365.
Schreiner, C. E. and Urbas, J. V. 1986. Representation of amplitude modulation in the auditory cortex of the cat. I. The anterior auditory field (AAF). Hear. Res. 21, 227–241.
Seebeck, A. 1841. Beobachtungen über einige Bedingungen der Entstehung von Tönen. Ann. Phys. Chem. 53, 417–436.
Seither-Preisler, A. Krumbholz, K., Patterson, R. D., Seither, A., and Lütkenhöner, B. 2004. Interaction between the neuromagnetic responses to sound energy onset and pitch onset suggests common generators. Eur. J. Neurosci. 19, 3073–3080.
Shackleton, T. M. and Carlyon, R. P. 1994. The role of resolved and unresolved harmonics in pitch perception and frequency modulation discrimination. J. Acoust. Soc. Am. 95, 3529–3540.
Shepard, R. 1964. Circularity in judgements of relative pitch. J. Acoust. Soc. Am. 36, 2346–2353.
Shofner, W. P. 1999. Responses of cochlear nucleus units in the chinchilla to iterated rippled noises: analysis of neural autocorrelograms. J. Neurophys. 81, 2662–2674.
Shofner, W. P. 2005. Comparative Aspects of Pitch Perception. In: Pitch Perception (*eds*. C. J. Plack, A. J. Oxenham, R. R. Fay, and A. N. Popper), pp. 200–245. Springer.
Shofner, W. P. and Selas, G. 2002. Pitch strength and Stevens' power law. Percept. Psychophy. 64, 437–450.
Shofner, W. P., Sparks, K., Wu, Y. E., and Pham, E. 2005. Similarity of spectral resolvability in chinchillas and human listeners based on phase discrimination. Acoust. Res. Lett. Online 6, 35–40.
Small, A. M., Jr. and Daniloff, R. G. 1967. Pitch of noise bands. J. Acoust. Soc. Am. 41, 506–512.
Terhardt, E. 1974. Pitch, consonance, and harmony. J. Acoust. Soc. Am. 55, 1061–1069.
Van Immerseel, L. and Peeters, S. 2003. Digital implementation of linear gamma tone filters: comparison of design methods. Acoust. Res. Lett. Online 4, 59–64.
von Bekesy, G. 1960. Experiments in Hearing. Reprint: Acoustical Society of America.
von Helmholtz, H. 1877. On the Sensations of Tone. Dover.
Weir, C. C., Jesteadt, W., and Green, D. M. 1977. Frequency discrimination as a function of frequency and sensation level. J. Acoust. Soc. Am. 61, 178–183.
Wever, E. G. 1949. Theory of Hearing. Wiley.
Wightman, F. L. 1973. The pattern-transformation model of pitch. J. Acoust. Soc. Am. 54, 407–416.
Winter, I. M., Palmer, A. R., Wiegrebe, L., and Patterson, R. D. 2003. Temporal coding of the pitch of complex sounds by presumed multipolar cells in the ventral cochlear nucleus. Speech Comm. 41, 135–149.
Yost, W. A. 1982. The dominance region for the pitch of ripple noise. J. Acoust. Soc. Am. 72, 416–426.
Yost, W. A. 1991. Thresholds for segregating a narrow band of broad band noise. J. Acoust. Soc. Am. 89, 834–842.
Yost, W. A. 1996a. Pitch of iterated rippled noise. J. Acoust. Soc. Am. 100, 511–519.
Yost, W. A. 1996b. Pitch strength of iterated rippled noise. J. Acoust. Soc. Am. 100, 3329–3335.
Yost, W. A., Mapes-Riordan, D., Dye, R., Sheft, S., and Shofner, W. 2005. Discrimination of first- and second-order regular intervals from random intervals as a function of highpass filter cutoff frequency. J. Acoust. Soc. Am. 117, 59–62.
Yost, W. A., Patterson, R. D., and Sheft, S. 1996. A time domain description for the pitch strength of iterated ripple noise. J. Acoust. Soc. Am. 99, 1066–1078.
Yost, W. A., Patterson, R. D., and Sheft, S. 1998. The role of the envelope in auditory processing of regular interval stimuli. J. Acoust. Soc. Am. 104, 2349–2361.

Further Reading

Boer, E. de. 1976. On the ''Residue'' and Auditory Pitch Perception. In: Handbook of Sensory Physiology (*eds*. W. D. Keidel and W. D. Neff), pp. 479–583. Springer.
Hartmann, W. M. and Zhang, P. X. 2003. Binaural models and the strength of dichotic pitches. J. Acoust. Soc. Am. 114, 3317–3326.
Plack, C., Oxenham, A., Fay, R., and Popper, A. (eds.) 2005. Pitch: Neural Coding and Perception. Springer.

3.48 Perception of Speech Sounds

K R Kluender and J M Alexander, University of Wisconsin–Madison, Madison, WI, USA

© 2008 Elsevier Inc. All rights reserved.

3.48.1	**Introduction**	831
3.48.2	**Sounds Created with Ears in Mind**	832
3.48.2.1	Speech Production	832
3.48.2.2	Linguistic Sound Systems	834
3.48.3	**Some Fundamentals of Perception**	836
3.48.3.1	The Inverse Problem	836
3.48.3.2	Why Perception Seems Veridical	837
3.48.3.3	Information for Perception	837
3.48.3.4	Sensory Systems Respond to Change (and Little Else)	839
3.48.4	**Contrast and Low-Level Speech Perception**	839
3.48.4.1	Contrast in General	839
3.48.4.2	Contrast and Perception of Co-Articulated Speech	840
3.48.4.3	Broader Spectral and Temporal Effects	843
3.48.5	**Maximizing Transmission of Speech Information with Multiple Dimensions**	845
3.48.5.1	Speech Perception Uses Multiple Sources of Information	845
3.48.5.2	Categorical Perception	846
3.48.5.2.1	Principal components analysis: an analogy	847
3.48.5.2.2	Phonemes as correlations?	848
3.48.5.2.3	Categorical perception as competing correlations	848
3.48.5.2.4	Multimodal interactions are expected	849
3.48.6	**Experience and Sound Contrasts in the Native Language**	850
3.48.6.1	Vowels	850
3.48.6.2	Consonants	851
3.48.6.3	Second-Language Perception	851
3.48.7	**To the Lexicon and Beyond**	853
3.48.7.1	Lexical Development and the Emergence of Phonemes (or Something like Them)	853
3.48.7.2	Finding Word Boundaries	854
3.48.8	**Speech in the Brain**	854
3.48.9	**Conclusion**	856
References		856

Glossary

adaptation Change in response caused by prior or continuing stimulation. Sometimes adaptation is referred to as fatigue, which can be a misnomer because sensitivity can increase (e.g., dark adaptation) as well as decrease. Instead, adaptation is a process by which absolute sensitivity adjusts in a way to enhance sensitivity to change within a given dynamic range.

affricate consonants Speech sounds produced by a complete constriction of the vocal tract that is released into a very small opening such as that for a fricative.

allophonic variation Acoustic or phonetic variants of the same phoneme; discriminably different speech sounds that are identified as the same phoneme.

alveolar stops Stop consonants /t/ and /d/ which are produced by forming a complete constriction of the vocal tract at the alveolar ridge of the hard palate.

categorical perception The phenomenon in which stimuli that are made to vary continuously along one or more dimensions are perceived discretely, rather than continuously, as distinct classes. The hallmark of categorical perception is the finding that in discrimination tasks, two stimuli that have been given the same label in an identification task are discriminated at levels near chance, while two equidistant stimuli that have been given different labels are discriminated with almost perfect accuracy.

co-articulation Articulatory overlap of adjacent speech sounds which results in a blending of acoustic features across successive speech units.

color constancy The phenomenon that the perceived color of an object stays the same despite the fact that the actual wavelength of reflected light changes with changes in the ambient lighting.

contrast effects Refers to the perceptual enhancement of a stimulus attribute when paired in time and/or space with a stimulus attribute that is to a varying extent opposite or contrastive.

dental stops Stop consonants produced by forming a complete constriction of the vocal tract behind the teeth (like the fricative th in English) as in Hindi [d̪].

dynamic range The physical range over which the biological sensors operate effectively. The difference between the stimulus levels near threshold and those where the physiological response begins to saturate.

enhancement effect A decrease in threshold, or enhanced sensitivity, for a tone in a complex when preceded by a complex in which the tone is missing.

entropy Unpredictability, randomness; entropy is directly proportional to potential information and inversely proportional to redundancy (see Shannon information theory).

formants Peaks in the speech spectrum. Frequency locations of the formants, especially the first three, are important for identifying different speech sounds and depend on the vocal tract resonances, which vary with vocal tract length.

formant transitions Monotonically increasing or decreasing changes in the frequency locations of the formants, or vocal tract resonances, associated with movements of the articulators from one speech sound to another. Some important features of formant transitions that aid in the identification of speech sounds include their onset and offset frequencies and their rate of change.

fricative consonants Speech sounds characterized by a nearly complete constriction of the vocal tract that produces noise as turbulence is created by air passing through the small opening.

fundamental frequency The lowest frequency of a periodic signal. Distance in frequency between successive harmonics in voiced speech sounds corresponding to the rate of vocal fold vibration. The harmonic spectrum consists of the fundamental frequency (first harmonic) with higher harmonics at multiples of the fundamental.

information-theoretic See Shannon information theory.

inverse projection problem The fact that it is impossible to project a given physical stimulus (e.g., acoustic or optic) back to a determinate source because multiple sources can produce the exact same physical output.

lack of invariance (problem of variability) Refers to the fact that no one acoustic or articulatory feature is both necessary and sufficient to identify a given speech sound. The lack of a simple one-to-one correspondence between attributes of speech sounds and linguistic units such as phonemes is a problem only when classifying speech sounds, but not when perceiving them.

lateral inhibition When high neural activity at one frequency region causes a reduction in the neural activity at an adjacent frequency region. In this way, the edge between regions of contrast (high and low activity) is enhanced.

lexicon The morphemes and words comprising an individual's vocabulary.

liquid Sound category for /l/ and /r/ sounds, which are produced with vocal tract constrictions that are less than those for fricative and affricates but more than those for vowels.

manner of articulation A way of classifying consonant sounds that describes how the constrictions in the vocal tract are made when they are produced.

McGurk effect Phenomenon in which the auditory perception of a syllable is influenced by the simultaneous visual presentation of a conflicting syllable. This effect is dependent on auditory stimuli that are easily confused and visual stimuli (visemes) that are easily distinguished.

morpheme The smallest unit of language that carries meaning.

nasal consonants Speech sounds characterized by a complete constriction of the oral tract accompanied with a coupling of the nasal tract through which air flow is directed.
Necker cubes An optical illusion in which a two-dimensional cube is drawn in a way that causes ambiguity when it is perceived as a three-dimensional object. Two faces of the cube appear to be in front, but not at the same time. One's perception oscillates between the two equally plausible interpretations.
perceptual constancy Functional equivalence of discriminably different physical representations of the same object.
perceptrons Single-layer artificial neural network in which multiple weighted inputs are fed into a single binary output.
phonemes Abstract linguistic categories for speech sounds that are functionally equivalent, but not necessarily acoustically equivalent.
phonetic categories See phonemes.
phonetic segments Divisions of the acoustic speech signal corresponding to consonants and vowels.
phonotactic regularities Sequences of speech sounds that tend to co-occur in a language.
pink noise Noise with an energy distribution that decreases at a rate of −3 dB per octave as frequency increases, or a halving of energy with a doubling of frequency.
place of articulation A way of classifying consonant sounds that describes where in the vocal tract the constriction is made to produce them.
retroflex stops Stop consonants produced by forming a complete constriction of the vocal tract at the hard palate (like the liquid r in English) as in Hindi [ḍ].
Shannon information theory Claude Shannon's theory of communication in which information is represented as a mathematical entity that is agnostic with respect to meaning. The potential amount of information transmitted, or entropy, is related to the number of logarithmic units (e.g., bits) needed to uniquely code the communicated message. Fewer bits are needed when the context and a receiver's prior experience make certain elements of the message redundant.
spectral contrast Contrast effect (see definition) for the frequency composition of a sound. For example, a sound with a mid-frequency peak will be perceived as relatively higher in frequency when preceded by a sound with a lower-frequency peak and will be perceived as relatively lower in frequency when preceded by a sound with a higher-frequency peak.
spectral density The distribution of energy as a function of frequency.
stop consonants Speech sounds characterized by a complete constriction of the vocal tract that is held momentarily and then released in a more or less abrupt manner.
suppression The decrease in the physiological response to a particular frequency region when another, more intense, sound at a nearby frequency region is present.
trading relations Because humans have abundant experience hearing speech sounds that co-vary along multiple attributes, a change in one attribute toward one percept can be traded or offset by a change in another attribute toward the opposite percept.
voiced Speech sounds created with the vocal folds together and in vibration.
voiceless Speech sounds created with the vocal folds apart, hence not in vibration.

3.48.1 Introduction

During the second half of the twentieth century, research concerning speech perception stood relatively distinct from the study of audition and other modalities of high-level perception such as vision. Contemporary research, however, is beginning to bridge this traditional divide. Fundamental principles that govern all perception, some known for more than a century, are shaping our understanding of perception of speech as well as other familiar sounds.

The study of speech perception traditionally consisted of attempting to explain how listeners perceive the spoken acoustic signal as a sequence of consonants and vowels, collectively referred to as phonetic segments or units. When one describes speech sounds in this way, brackets are used to surround phonetic symbols such as [y] (as in yes) and [o] (as in oh). By contrast, phonemes are abstract linguistic units that roughly correspond to letters in written language, and are transcribed enclosed by slashes (/y/ and /o/.) Morphemes are the smallest meaningful units of language, roughly corresponding to words (e.g., dog,

taste, as well as dis- and -ful) with phonemes being the smallest units that can change the meaning of a morpheme (e.g., /yo/ vs. /go/) (Trubetzkoy, N. S., 1939/1969).

Conceptualizing speech perception as a process by which phonemes are retrieved from acoustic signals is the traditional approach. Within this tradition, research in speech perception often has been focused on problems concerning segmentation and lack of invariance. The problem of segmentation refers to the fact that, if phonetic units exist, they are not like typed letters on a page. Instead, they overlap extensively in time, much like cursive handwriting. The problem of lack of invariance (or, problem of variability) is related to the segmentation problem. Because speech sounds are produced such that articulations for one consonant or vowel overlaps with production of preceding ones, and vice versa, every consonant and vowel produced in fluent connected speech is dramatically colored by its neighbors. Some of the most recalcitrant problems in the study of speech perception are the consequence of adopting discrete phonetic segments as a level of perceptual analysis. However, phonetic segments may be neither discrete nor real.

No experimental evidence clearly demonstrates that either phonetic segments or phonemes are real outside of linguistic theory (e.g., Lotto, A. J., 2000), and the intuitive appeal of phonetic segments and phonemes may arise principally from experience with alphabetic writing systems (Port, R. F., in press). One ought not be sanguine about whether speech perception really is about recognizing consonants and vowels *per se*. It is not known whether or not listeners extract phonemes preliminary to recognizing words. There may or may not be some place in the brain where phonemes reside independent of the words they comprise.

Either morphemes or words may be the first units of language that stand more or less on their own accord. It is possible, even likely, that speech perception is a series of nondiscrete processes along the way from waveforms to words. In this chapter, speech perception will be described as a continuum of processes operating on the acoustic signal with varying levels of sophistication. The consistent theme will be common principles that define how these processes work.

Before explaining perception of speech, two preliminary topics need to be addressed. First, understanding perception always requires understanding the ecology within which perceptual systems operate. If one wishes to understand speech perception, at least some knowledge of speech production proves helpful. Second, because perception of speech adheres to the same principles that govern perception of other environmental objects and events, it will be helpful to briefly review some broad principles that govern perception most broadly.

3.48.2 Sounds Created with Ears in Mind

Speech and music are somewhat distinct from most other environmental sounds because, much like visual art such as paintings and sculpture, speech and music are created with perceivers in mind. Across hundreds of generations of humans, language users have found ways to use their lungs, larynx, and mouths to produce different sounds that can transmit a wealth of information to one another.

3.48.2.1 Speech Production

There are three basic components to production of speech: respiratory (lungs), phonatory (vocal chords), and articulatory (vocal tract). First is the respiratory system through which the diaphragm pushes air out of the lungs, through the trachea, and then the larynx. At the larynx, air must pass through the two vocal folds which are made up of muscle tissue that can be adjusted to vary how freely air passes through the opening between them. In some cases, such as voiceless sounds like [p] and [s], vocal folds are apart; they do not restrict airflow and do not vibrate. For voiced speech sounds like [b] and [z], vocal folds are closer together, and the pressure of airflow causes them to vibrate at the fundamental frequency (f_0). Owing to variations in the pressure of airflow from the lungs and muscular control of vocal fold tension, talkers can vary the fundamental frequency of voiced sounds. If one were to consider the nature of speech at this point, it could be depicted as a spectrum of energy spread across frequency and concentrated at the fundamental frequency and at multiples of the fundamental (i.e., a harmonic spectrum) with decreasing energy at each successive multiple as seen in Figure 1(a).

The area above the larynx, the oral tract and the nasal tract combined, is referred to as the vocal tract. The nearly continuously varying configuration of the vocal tract is responsible for shaping the spectrum

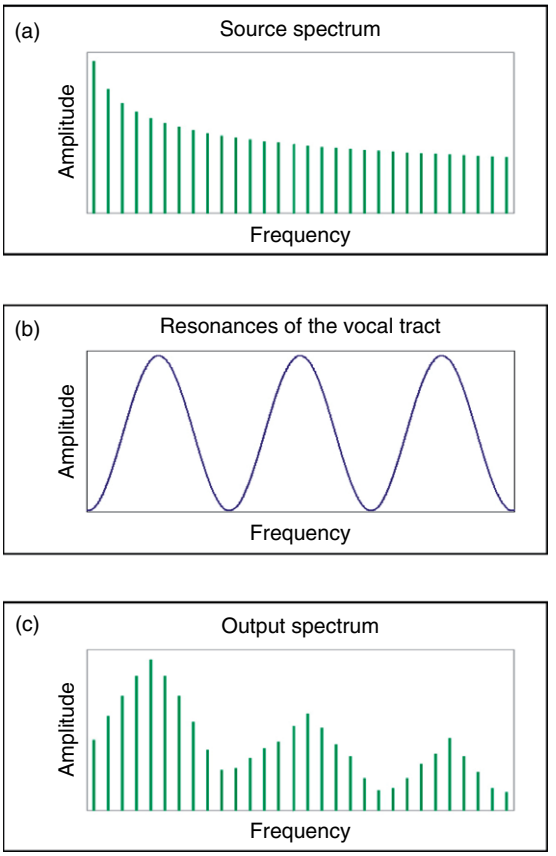

Figure 1 Harmonic spectrum of the laryngeal source (a) before passing through filtering properties (b) of the vocal tract resulting in the output spectrum with formant peaks (c).

differently for different speech sounds. There are many ways the jaw, lips, tongue body, tongue tip, velum (soft palate), and other vocal tract structures can be manipulated to shape the sounds that emanate from the mouth and nose. Widening and narrowing of points along the vocal tract selectively attenuate some frequencies while making others more prominent. Figure 1(b) illustrates the filtering effects of the vocal tract for the vowel [a] as in father. Figure 1(c) portrays the net result from passing the glottal source (a) through the vocal tract (b).

Peaks in the resultant spectrum are referred to as formants, described by number, lowest to highest (F_1, F_2, F_3,. . .). Only the first three formants are depicted in Figure 1, and for the most part, speech sounds can be identified on the basis of energy in the region of these lowest three formants. However, additional formants exist with lower amplitudes at higher frequencies (F_4, F_5, F_6, etc.), and are relatively more prominent in the speech of children.

Airflow can be channeled, constricted, or obstructed to produce different vowel and consonant sounds. Vowels are made with a relatively open unoccluded vocal tract. In terms of articulation, vowels vary mostly in how high or low and how forward (front) or back the tongue body is in the oral tract. In addition, some vowels are produced with rounded lips (e.g., [u] as in boot) or with modestly different fundamental frequencies among other variations.

In part because early linguists had greater access to their own vocal tracts than to sophisticated audio analysis, it is a general convention that speech sounds are described in terms of the articulations necessary to produce them. In addition to variation in tongue height, frontness/backness, and lip rounding as descriptions for vowels, consonants also are described by articulatory characteristics. For example, consonants are described in terms of the manner in which constrictions are introduced along the vocal tract. Stop consonants or plosives such as [b], [p], [d], [t], [g], and [k] include complete constriction such that no air may pass through. Nasal consonants such as [n], [m], and [ŋ] (as in sing) are like [b], [d], and [g], respectively, with complete constriction at some point in the oral tract, but air is allowed to escape through the nasal tract because the velum is lowered. Fricative consonants are caused by nearly complete obstruction of the vocal tract, with a noisy sound being produced by turbulence of airflow passing through a very small opening. Some examples of English fricatives are [s], [z], [š] (as in ash), and [ž] (as in azure.) Affricate consonants are produced by a combination of complete occlusion (like a stop) followed by nearly complete occlusion (like a fricative.) Examples of affricates in English are [č] (as in chug) and [ǰ] (as in jug.) The least constricted consonants in English are laterals and semivowels, such as [l], [w], [r], and [y].

Consonants also are described in terms of whether the vocal folds are close and vibrating, voiced, or further apart and not vibrating, voiceless. Thus, sounds such as [b], [d], [g], [z], [ž], [ǰ], [l], [w], [r], and [y] are voiced. And, [p], [t], [k], [s], [š], and [č] are voiceless. Finally, consonants are described on the basis of place of articulation. Constrictions can be placed along a number of places in the oral tract. In English, the three major places of articulation are bilabial (lips, [p], [b], [m]), alveolar (alveolar ridge behind teeth, [t], [d], [n]), and velar (soft palate or velum, [k], [g], [ŋ].)

3.48.2.2 Linguistic Sound Systems

The above description does not exhaust all the distinctions among the 40 or so sounds used in English, and it is a vast underdescription of variation among languages more generally. Owing primarily to unique characteristics of supralaryngeal anatomy (Lieberman, P., 1984), the adult human possesses sound-producing abilities unrivaled among other organisms. This capacity is revealed in a grand assortment of over 850 different speech sounds used contrastively by the more than 5000 distinct languages used around the world (Maddieson, I., 1984). There are more than 550 consonants and 300 vowels (including diphthongs such as [e^{y}] and [o^{y}], as in bay and boy). Such capacity dwarfs that of other animals, being more than an order of magnitude larger than the largest reported inventory of nonhuman primate calls (Cleveland, J. and Snowdon, C. T., 1982).

In contrast to this diversity in potential speech sounds, systematic inspection reveals that collections of consonants and vowels used by individual languages are anything but random. The vast majority of speech sounds are relatively rare, while a handful are extremely common. For example, all known languages have stop consonants. The overwhelming majority of languages have three places of articulation for stop consonants, typically the three described above for English. Over 80% of languages include a distinction in voicing (e.g., [p] vs. [b], [s] vs. [z]). Diversity does not imply randomness.

The structure of vowel systems is as much or more orderly than that for consonants. There is a fair amount of variety in the particular number of vowels used by languages. Some languages use as few as three vowels while others use as many as 24. English uses about 15 depending upon dialect. However, the most common number of vowels used by languages is only five, and other numbers of vowels appear to be relatively favored. Especially for the five- to nine-vowel systems that predominate across languages, particular sets of vowels are typically used. Figure 2 displays some of the more common three, five, and seven vowel systems. Although there are relatively fewer languages that use more than seven vowels, there remains a good deal of commonality among systems with the same number of vowels.

What are the forces acting upon languages that encourage the selection of some sounds and groups of sounds over others? Although the number of possible speech sounds is prodigious, one guiding factor explaining regularities is how easy some sounds are to produce either in isolation or in sequence with others. The role of articulatory ease is perhaps best evidenced by the fact that languages tend to use articulatorily simpler consonants before incorporating more complex consonants (Lindblom, B. and Maddieson, I., 1988).

Consistent with the close tethering of speech production and speech perception, languages have come to use sets of speech sounds that enhance perceptual effectiveness. Talkers expend effort for communicative robustness. For example, the tense high vowels [i] and [u] (as in beet and boot) require more effort to produce relative to their lax counterparts [I] and [U] (as in bit and book). The vowels [i] and [u], however, are acoustically more distinct, not only from each other, but also from other possible vowel sounds. And, across languages, these tense vowels [i] and [u] occur five times more frequently than lax vowels [I] and [U].

Common examples of talkers molding their utterances to the needs of the listener include instances in which conditions for communication are not optimal. Talkers speak more clearly to young or non-native listeners for whom distinctions are not obvious. When environments are noisy or reverberant, talkers strive to produce contrasts that are maximally distinctive. Most generally, speech sound repertoires of languages have developed over generations of individuals toward greater communicative effectiveness. Generations of talkers have come to capitalize upon auditory predispositions of listeners.

An obvious way that a language community achieves such robustness is by developing an inventory of phonemes so as to optimize distinctiveness acoustically and auditorily. Inspection of regularities in vowel sounds used by languages, such as those shown in Figure 2 provides some of the most illuminating examples of auditory processes operating as a driving force. Different languages use different sets of vowel sounds, and languages use subsets of vowels that are most easily discriminated from one another. In particular, those vowels favored for languages with five vowels are vowels that are as acoustically distant as possible from one another. As a general rule, the set of vowels selected by a language, whether it uses three or ten vowels, is comprised of sounds that tend toward maximal distinctiveness (Bladon, R. A. W. and Lindblom, B., 1981; Liljencrantz, J. and Lindblom, B., 1972).

There is another way that differences between speech sounds are perceptually more dependable. Every consonant and vowel is defined by multiple acoustic properties. For example, the distinction between [b] and [p] as in rabid and rapid includes

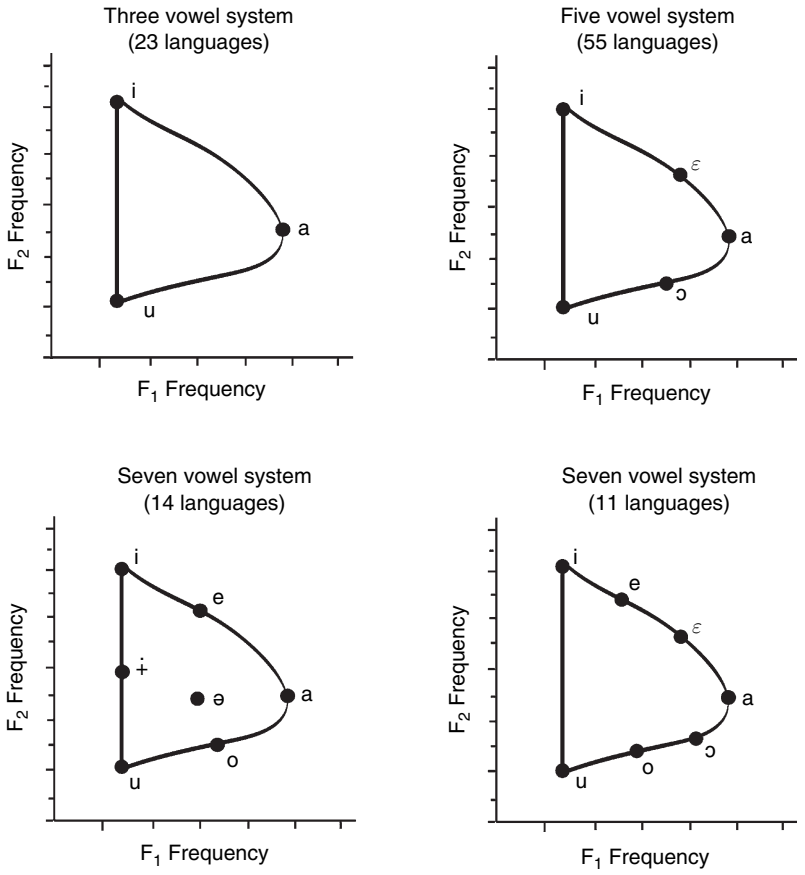

Figure 2 Common three-, five-, and seven-vowel systems used around the world as depicted in frequencies of first and second formants. Note that languages tend to use sets of vowels that are as acoustically distinct as possible within the range of vocal tract limits (solid lines.)

at least 16 different acoustic differences (Lisker, L., 1978). Further, no single acoustic attribute from these 16 is necessary to signal the distinction. Much of this redundancy in speech sounds results from the complexity of speech signal, a consequence of the fact that the structures that produce speech, the larynx and vocal tract, also are complex. Talkers morph their vocal tracts into widely varying shapes with different lengths. The surfaces inside vocal tracts vary considerably from tooth enamel to fleshy lips and soft palate, resulting in wildly varying absorption and reflection properties throughout the length of the vocal tract. Talkers produce multiple acoustic cues in a fashion that makes differences between speech sounds more perceptible (Kingston, J. and Diehl, R. L., 1994; Kluender, K. R., 1994) resulting in yet greater redundancy in the acoustic signal.

Languages have developed to be robust signaling systems, and distinctions between speech sounds do not rely upon the ability to make fine-grained discriminations bordering on thresholds of auditory systems. In this way, perception of speech bears little likeness to classic psychophysical studies of absolute thresholds and just-noticeable differences. Hearing the differences between vowels like [æ] (as in bat) and [ɛ] (as in bet), on the basis of gross spectral differences, shares little in common with psychoacoustic studies that demonstrate humans' abilities to detect changes as small as 1 Hz from a 1000 Hz sinusoid tone.

Because languages use distinctions that maximize acoustic differences and exploit auditory capacities, several observations follow. First, human infants are quite proficient at discriminating differences between speech sounds from a very early age. Three decades of studies document the impressive abilities of human infants, some less than 1 week old, to discriminate a wide variety of consonants and vowels from

across many languages (see, e.g., Jusczyk, P. W., 1981). A plethora of positive findings indicate that infants have the discriminative capacity necessary for most or all of the speech distinctions they will need to use in their language. Languages tend to use distinctions that are relatively easy to detect, and infant auditory abilities appear to be quite well developed. By 3 months of age, the human auditory system is nearly adult-like in absolute sensitivity and frequency-resolving power within the frequency range of most speech sounds (e.g., Olsho, L. W. et *al.*, 1988; 1987; Werner, L. and Gillenwater, J., 1990; Chapter Human Auditory Development).

A second observation, perhaps more telling than the first, is that discrimination of speech contrasts by nonhuman animals appears to be generally quite good. There have been a fair number of demonstrations that animals can distinguish human speech sounds with facility (see, e.g., Kluender, K. R. *et al.*, 2005). Differences between vowel sounds present no apparent difficulty for nonhuman animals. Several species have been shown to distinguish voiced from voiceless stop consonants, or to distinguish consonants on the basis of place of articulation (even beyond the basic three places described for English above). Such findings are expected on the basis of languages tending to use distinctions that are relatively easy to discriminate.

3.48.3 Some Fundamentals of Perception

To mostly ill effect, for many years much of speech perception was studied in relative isolation from the study of perception more generally. In part, this state of affairs was encouraged by the focus of language researchers (linguists and psycholinguists) seeking to know more about elemental aspects of language use. Consistent with focus on apparently unique characteristics of human language, early speech researchers were encouraged to believe that perception of speech might be as unique as language itself. For this and other historical reasons, research in speech perception was often naïve to developments in related areas of perception.

3.48.3.1 The Inverse Problem

An enduring distraction for investigators studying speech perception has concerned the extent to which articulatory gestures (e.g., Fowler, C. A., 1986; Liberman, A. M. and Mattingly, I. G., 1985), acoustic patterns, patterns of sensory stimulation (e.g., Diehl, R. L. and Kluender, K. R., 1989), or some combination (e.g., Nearey, T. M., 1997; Stevens, K. N. and Blumstein, S. E., 1981) serve as proper objects of speech perception. Controversies concerning appropriate objects of perception generated more heat than light. However, debates concerning objects of perception cannot be resolved because the question itself is ill-posed, if not outright misleading. There are no objects of perception, neither for speech nor for perception in general. There is an objective for perception, which is to maintain adequate agreement between an organism and its world in order to facilitate adaptive behavior. Success with this objective does not require objects of perception.

Within this functional framework, perceptual success does not require recovery or representations of the world *per se*. Perceivers' subjective impressions may be of objects and events in the world, and the study of perceptual processes may lead to inspection of real-world objects and events, patterns of light or sound pressure waves, transduction properties, or neural responses. By and large, however, viewing perception with a focus toward either distal or proximal properties falls short of capturing the essential functional characteristic of perception – the relationship between an organism's environment and its actions.

Much work in perception has been concerned, in one way or another, with addressing the inverse problem. The inverse problem emerges from the simple fact that information available to sensory transducers (eyes, ears, etc.) is inadequate to authentically reconstruct a unique distal state of affairs. In vision, for any two-dimensional projection, there are an infinite number of possible three-dimensional objects that could give rise to exactly the same two-dimensional (2D) retinal image (Figure 3). In audition, for any sound-pressure wave, there are an infinite number of sound producing events that could give rise to that waveform. One telling example of the difficulty of mapping from acoustics to a sound-producing event is the case of attempting to solve the inverse from waveform to simpler 2D surfaces (e.g., the shape of a drum.). Mathematicians have formally proved that even this relatively simple translation from waveform to plane geometry is impossible (Gordon, C. *et al.*, 1992).

Because multiple sound sources yield the same waveform, waveforms can never be more complex than characteristics of physical sources. Researchers within the field of speech perception have long been

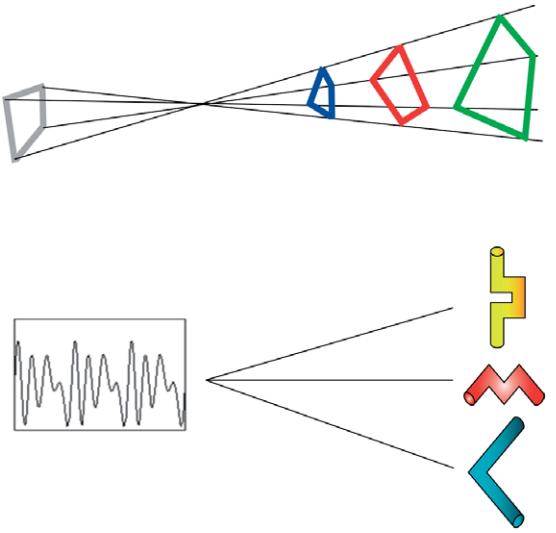

Figure 3 An infinite number of external three-dimensional objects give rise to the same two-dimensional retinal image (top, left). An infinite number of sound producing sources (characterized here as resonator shapes) give rise to the same waveform available to the ear.

familiar with appeals to perception via articulatory gestures as a simplifying construct, and there have been a series of efforts to extract gestures in order to facilitate machine speech recognition, albeit with very limited success. What physics demands, however, is that depiction of speech in terms of articulatory gestures gives only the illusion of simplicity. Because scientists are much better at measuring details of sounds than they are at measuring details of articulator activity, articulatory gestures appear simpler only because they are defined more abstractly and are measured with less precision. Because multiple resonator configurations can give rise to the same waveform, the acoustic waveform available to listeners is always less variable than articulation.

For all of the discussion that follows regarding specific issues concerning speech perception, speech typically will be described as sounds. This is not because sounds are legitimate objects of perception, but rather because, along the chain of events from creating patterns of sound pressure to encoding these patterns in some collection of neural firings to eliciting behavior, waveforms are public, easily measurable, and simpler than alternatives.

3.48.3.2 Why Perception Seems Veridical

If perceiving the true state of the world is impossible, one might ask why phenomenal experience is not fuzzy and uncertain. To effectively guide behavior and not leave the organism pondering multiple possibilities, all that is required is that the perceptual system comes to the same adaptive output every time it receives the same functional input. It is this deterministic nature of perception that prevents paralysis within a sea of alternatives. Phenomenal experience of certain reality does not depend upon authentic rendering of the world. Instead, phenomenal experience of a clear and certain world is the consequence of perceptual systems reliably arriving at deterministically unique outputs. It is this reliability that encourages certainty (Hume, D., 1748/1963), but reliability is not validity.

On rare occasions, perceptual systems do not converge upon a unique output and are left oscillating between equally fitting outputs when sensory inputs are not singly determinate (usually in response to impoverished stimuli.) Many readers are familiar with bistability when viewing Necker cubes. One such auditory experience is encountered when listening to a repeating synthesized syllable intermediate between [da] and [ta] or any other pair of similar speech sounds. When two perceptual outputs fit the input equally well, phenomenal experience oscillates between each percept (Tuller, B. *et al.*, 1994).

3.48.3.3 Information for Perception

If there are no objects of perception, how should one think about information for perception? Information for perception does not exist in the objects and events in the world, nor does it exist in the head of the perceiver. Instead, information exists in the relationship between an organism and its world. It may be useful to consider the contrast between information about and information for. When one discusses objects of perception, it is information about that is typically inferred. Implicit in such efforts is the notion that one needs to solve the inverse problem. By contrast, if the objective of a successful perceptual system is to maintain adequate agreement between an organism and its world in order to facilitate adaptive behavior, then information for successful perception is nothing more or less than information that resides in this relationship (or agreement).

This way of viewing information as a relationship is consistent with one of the fundamental characteristics of Shannon's information theory (Shannon, C. E., 1948; Weiner, N., 1948). Some readers may be familiar with Fletcher's pioneering applications of information theory to speech (Fletcher, H., 1953/1995). However,

the application here will be more akin to the approach of Attneave F. (1954; 1959) and Barlow H. B. (1961) for vision, an approach that remains highly productive (e.g., Barlow, H. B., 1997; 2001; Simoncelli, E. P. and Olshausen, B. A., 2001; Schwartz, O. and Simoncelli, E. P., 2001). One important point of Shannon's information theory is that information exists only in the relationship between transmitters and receivers; information does not exist in either *per se*, and it does not portray any essential characteristics about either transmitters or receivers. Within this information-theoretic sense, perceptual information exists in the relationship between organisms and their environments. This is the objective of perception.

Within a sea of alternative perceptual endpoints, agreement between the organism and environment aims to establish the alternative that gives rise to the most adaptive behavior. Information is transmitted when uncertainty is reduced and agreement is achieved between organism and environment. The greater the number of alternatives (uncertainty, unpredictability, variability, or entropy) there are, the greater the amount of information that potentially can be transmitted (see Figure 4(a)). There is no information when there is no variability. When there is no variability, there is total predictability and hence, no information transmitted. There is much that stays the same in the world from time to time and place to place, but there is no information in stasis. Uncertainty is reduced consequent to the perceiver's current experience (context) as well as past experiences with the environment (learning).

Although the amount of theoretical potential information transmitted is maximized at maximum entropy (total unpredictability or randomness), it is not advantageous for biological systems to shift their dynamic range as far as possible toward this maximum. In natural environments, this would result in diminishing returns if the system adjusts to register the last bits of near-random energy flux. Instead, biological systems should maximize the efficiency with which they capture information relative to the distribution of energy flux in real environments. The best estimate of statistics of natural environments is $1/f$(pink) noise (Figure 4(b)). This simple power law with a negative exponent (f^1)is scale-invariant, and it is a ubiquitous characteristic across many systems from radioactive decay to fluid dynamics, biological systems, and astronomy. As one would expect, spectral density of fluctuations in acoustic power of music and speech varies as $1/f$ (Voss, R. F. and Clarke, J.,

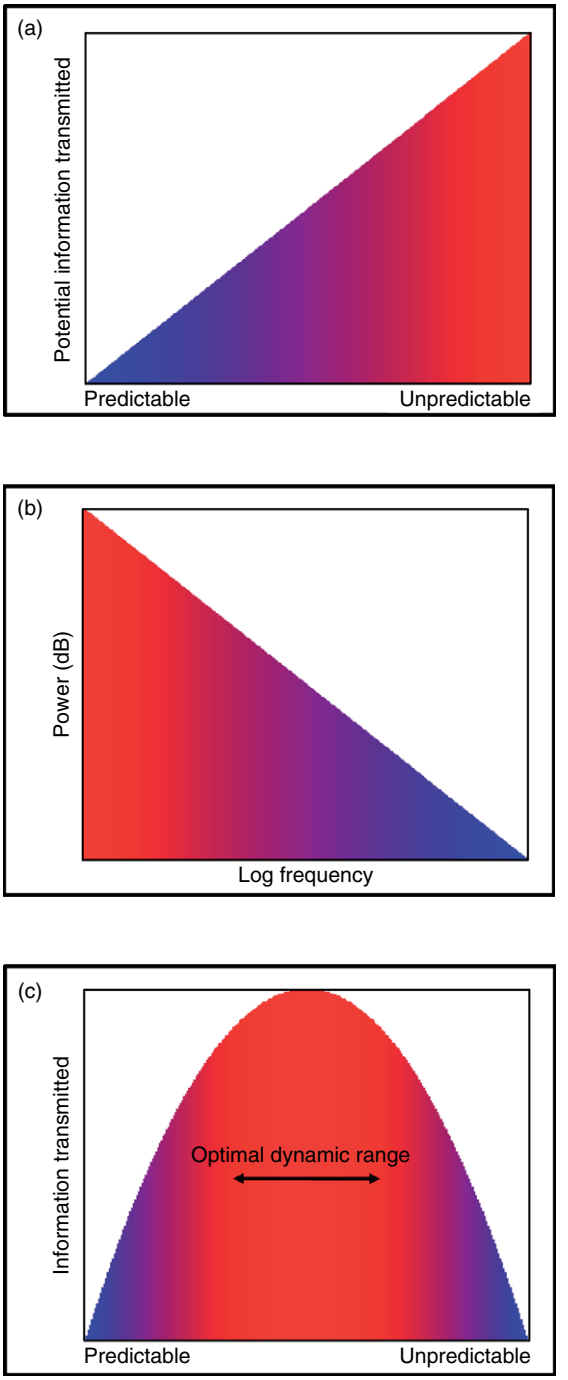

Figure 4 The greater the number of alternatives (uncertainty, unpredictability, variability, or entropy) there are, the greater the amount of information that potentially can be transmitted (a). There is no new information in what stays the same or is predictable. Relative power of energy flux in natural environments approximates 1/*f* (b). Information transmission optimized relative to energy flux in the environment (c). An ideal sensori-neural system should center dynamic range about this maximum.

1975; 1978.) Efficient information transmission for sensori-neural systems with limited dynamic range may be depicted best as the product of the positive exponential growth in information and the negative exponential of $1/f$. This yields the quadratic function shown in Figure 4(c) describing optimal transmission of information relative to energy flux in the environment.

3.48.3.4 Sensory Systems Respond to Change (and Little Else)

Given these facts about information, it is true and fortunate that sensori-neural systems operate as they do. Sensori-neural systems respond only to change relative to what is predictable or does not change. Perceptual systems do not record absolute levels whether loudness, pitch, brightness, or color. Relative change is the coin of the realm for perception, a fact known at least since Ernst Weber in the mid-eighteenth century. This has been demonstrated perceptually in every sensory domain. Humans have a remarkable ability to make fine discriminations, or relative judgments, about frequency and intensity. The number of discriminations than can be made numbers in the hundreds or thousands before full dynamic range is exhausted. Yet, most humans are capable of reliably categorizing, or making absolute judgments about only a relatively small number of stimuli regardless of physical dimension (e.g., Gardner, W.R. and Hake, H. W. 1951; Miller, G. A., 1956).

Sacrifice of absolute encoding has enormous benefits along the way to optimizing information transmission. Although biological sensors have impressive dynamic range given their evolution via borrowed parts (e.g., gill arches to middle ear bones), this dynamic range is always a fraction of the physical range of absolute levels available from the environment and essential to organisms' survival. This is true whether one is considering optical luminance or acoustic pressure. The beauty of sensory systems is that, by responding to relative change, a limited dynamic range shifts upward and downward to optimize the amount of change that can be detected in the environment at a given moment.

The simplest way that sensory systems adjust dynamic range to optimize sensitivity is via processes of adaptation. Following nothing, even a subtle sensory stimulus can trigger a strong sensation. However, when a level of sensory input is sustained over time, constant stimulation loses impact. This sort of sensory attenuation due to adaptation is ubiquitous, and has been documented in vision (Riggs, L. A. *et al.*, 1953), audition (Hood, J. D., 1950), taste (Urbantschitsch, V. 1876, cf. Abrahams, H., *et. al.*, 1937), touch (Hoagland, H., 1933), and smell (Zwaardemaker, H., 1895, Engen, T., 1982). It is not uncommon to find instances where the terms adaptation and fatigue are used interchangeably. However, this equivocation is inappropriate. Consider, for example, visual dark adaptation whereby sensitivity to light is increased. Adaptation is a process whereby dynamic range adjusts, upward or downward, to maximize sensitivity to change. There are increasingly sophisticated mechanisms supporting sensitivity to change with ascending levels of processing, and several will be discussed in this chapter. Most important for now is the fundamental principle that perception of any object or event is always relative – critically dependent on its context.

3.48.4 Contrast and Low-Level Speech Perception

3.48.4.1 Contrast in General

Because it is only change that is perceived, perception at any particular time or place always depends on temporally or spatially adjacent information. Many instances of sensitivity to change are revealed through demonstration of contrast. For example, as depicted in Figure 5, a gray region appears darker against a white background and lighter next to a black background (see, e.g., Anderson, B. L. and Winawer, J., 2005). While examples abound for all modalities, sensory contrast has been most amply demonstrated in studies of visual perception, with contrast being a fundamental process that reveals edges of objects and surfaces.

Contrast effects are ubiquitous, and of course, they exist for audition (Cathcart, E. P. and Dawson, S, 1928/1929; Christman, R. J., 1954). Forms of auditory contrast are important for several aspects of speech perception. Over the past few years, multiple studies have provided evidence that simple processes of spectral contrast contribute to solving one of the most, if not the most, difficult questions concerning speech perception, co-articulated speech. Co-articulation is the spatial and temporal overlap of adjacent articulatory activities, and it is reflected in the acoustic signal by severe context dependence. Acoustic information specifying one speech sound varies substantially depending on surrounding sounds.

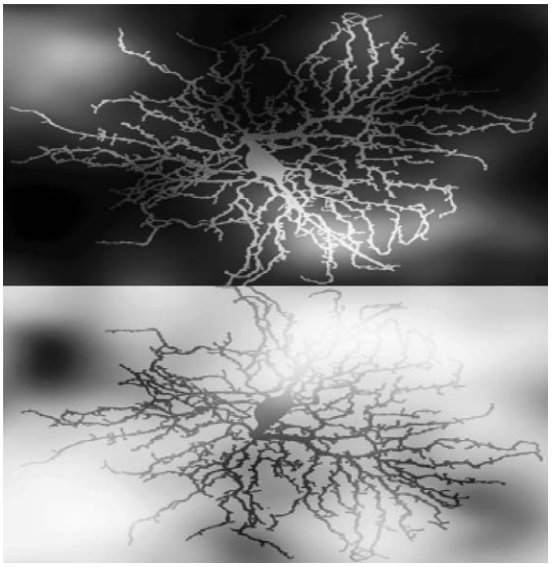

Figure 5 Contrast effects are ubiquitous in perception. For this example of lightness contrast, absolute lightness/darkness of these mirror-image neurons is identical.

3.48.4.2 Contrast and Perception of Co-Articulated Speech

The problem for speech perception is how listeners hear a speech sound such as [d] when acoustic characteristics change dramatically depending upon sounds that precede and follow (e.g., vowels [e] versus [o]) (see Figure 6). Co-articulation presents a major challenge to automatic speech recognition (ASR) systems, which largely identify speech sounds on the basis of matching stored templates. Instead of storing a single template for [d], multiple templates must be stored for [d] following all other possible speech sounds, and each of those templates must be stored multiply for every instance of [d] preceding all other possible speech sounds. For ASR, this strategy using a geometrically expanding set of templates can be made to work so long as one has sufficient memory and sufficient processing speed to sort through templates. Not surprisingly, progress in ASR over decades is closely correlated with speed of microprocessors and price of memory (Lippman, R. P., 1996).

There is a consistent pattern to co-articulation that suggests a simpler solution. Adjacent sounds always assimilate toward the spectral characteristics of one another. Owing to mass and inertia of articulators (as well as planning), articulatory movements are compromises between where articulators have been and where they are headed. Because the acoustic signal directly reflects these articulatory facts, the frequency spectrum assimilates in the same fashion that speech articulation assimilates.

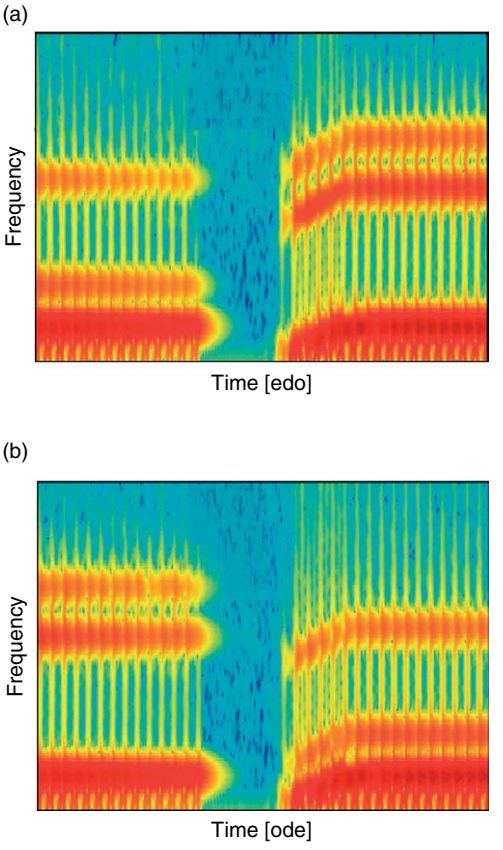

Figure 6 Schematic spectrograms of [edo] (a) and [ode] (b) Note that acoustic properties of [d] depend upon characteristics of preceding and following vowel sounds.

Lindblom B. E. F. (1963) provided some of the best early evidence concerning how context systematically influences speech production. He reported that the frequency of the second formant (F_2) was higher in the productions of [dId] (did) and [dUd] (dud) than for the vowels [ɪ] and [ʊ] in isolation, and that F_2 was lower for vowels in [bIb] and [bUb]. In both contexts, F_2 frequency approached that of flanking consonants, which are higher for [d] than for [b]. In a subsequent study, Lindblom B. E. F and Studdert-Kennedy M. (1967) demonstrated that perception of co-articulated vowels is complementary to these facts of articulation. Listeners reported hearing /ɪ/ (higher F_2) more often in [wVw] (lower F_2) context, and /ʊ/ more often in [jVj] (higher F_2) context. Consonant context affected vowel perception in a manner complementary to the assimilative effects of co-articulation. Lindblom B. E. F. and Studdert-Kennedy M. (1967) wrote: "It is worth reiterating. . .that mechanisms of perceptual analysis

whose operations contribute to *enhancing contrast* in the above-mentioned sense are precisely the type of mechanisms that seem well suited to their purpose given the fact that the slurred and sluggish manner in which human speech sound stimuli are often generated tends to reduce rather than sharpen contrast. (p. 842, italics added)"

One of the most thoroughly investigated cases for perceptual context dependence concerns the realization of [d] and [g] as a function of preceding liquid (Mann, V. A., 1980) or fricative (Mann, V. A. and Repp, B. H., 1981). Perception of /d/ as contrasted with perception of /g/, can be largely signaled by the onset frequency and trajectory of the third formant (F_3). In the context of a following [a], a higher F_3 onset encourages perception of /da/ while a lower F_3 onset results in perception of /ga/. Onset frequency of the F_3 transition varies as a function of the preceding consonant in connected speech. For example, F_3-onset frequency for [da] is higher following [al] in [alda] than when following [ar] in [arda]. The offset frequency of F_3 is higher for [al] owing to a more forward place of articulation, and is lower for [ar].

Perception of /da/ and /ga/ has been shown to be complementary to the facts of production much as it is for CVCs. Listeners are more likely to report hearing /da/ (high F_3) when preceded by the syllable [ar] (low F_3), and hearing /ga/ (low F_3) when preceded by [al] (high F_3) (Mann, V. A., 1980; Lotto, A. J. and Kluender, K. R., 1998). In subsequent studies, the effect has been found for speakers of Japanese who cannot distinguish [l] and [r] (Mann, V. A., 1986), for prelinguistic infants (Fowler, C. A. *et al.*, 1990), and for avian subjects (Lotto, A. J. *et al.*, 1997.) The same pattern of findings has been replicated for perception of /d/ and /g/ following fricatives [š] and [ʃ] such that listeners are more likely to report hearing /d/ (high F_3) following [ʃ] (lower-frequency noise) and hearing /g/ (low F_3) following [š] (higher-frequency noise) (Mann, V. A. and Repp, B. H., 1981).

Co-articulation *per se* can be dissociated from its acoustic consequences by combining synthetic speech targets with nonspeech flanking energy that captures minimal essential spectral aspects of speech. Lotto A. J. and Kluender K. R. (1998) replaced [al] and [ar] precursors with nothing more than constant-frequency sinusoids set to the offset frequencies of F_3 for [al] and [ar] syllables. Perception of following [da-ga] shifted just as it did following full-spectrum [al] and [ar] (Figure 7).

Holt L. L., *et al.*, (2000) replicated the Lindblom and Studdert-Kennedy findings (1967) with CVCs using the vowels [ɛ] and [ʌ] flanked by stop consonants [b] and [d]. They replaced flanking [b] and [d] with FM glides that tracked the center frequency of only F_2 for [b] or [d]. Again, the pattern of results for flanking nonspeech FM glides mimicked that for full-spectrum [b] and [d] syllable-initial and syllable-final transitions. Based upon the results for VCCVs (Lotto, A. J. and Kluender, K. R., 1998) and these results for CVCs, one can conclude that much of perceptual accommodation for co-articulation is not restricted to speech-like signals. All of the findings are consistent with spectral contrast, whereby the spectral composition of context serves to diminish or enhance the perceptual efficacy of spectral components for adjacent sounds.

In keeping with typical usage, the term contrast has been used in a largely descriptive way thus far. There are a large number of experimental precedents for spectral contrast – often called auditory enhancement, and these precedents provide more specific hypotheses. Summerfield Q. *et al.* (1984) established the existence of

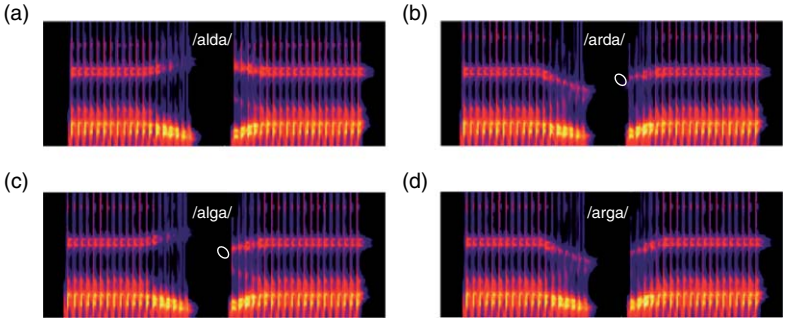

Figure 7 Due to co-articulation, acoustic properties of any speech sound become more similar to the properties of sounds preceding and following. This assimilation is a property of all fluent connected speech. Here, acoustic characteristics of [d] (e.g., F_3, marked by ellipse) following [r] are very similar to those of [g] following [l]. Listeners hear the same consonant vowel (CV) as /d/ following [ar] and as /g/ following [al].

an aftereffect in vowel perception. When a uniform harmonic spectrum was preceded by a spectrum that was complementary to a particular vowel with troughs replacing peaks and vice versa, listeners reported hearing a vowel during presentation of the uniform spectrum. The vowel percept (for the uniform spectrum) was appropriate for a spectrum with peaks at frequencies where there were troughs in the preceding spectrum.

Summerfield Q. *et al.* (1984) noted that perceiving vowel sounds in uniform spectra (following appropriate complementary spectral patterns) has a well-known precedent in psychoacoustics. This oft-reported finding is that, if just one member of a set of harmonics of equal amplitude is omitted from a harmonic series and is reintroduced, then it stands out perceptually against the background of the preexisting harmonics (Schouten, J. F., 1940; Green, D. M. *et al.*, 1959; Cardozo, B. L., 1967; Viemeister, N. F., 1980; Houtgast, T., 1972). Viemeister (1980), for example, demonstrated that the threshold for detecting a tone in a harmonic complex is 10–12 dB lower when the incomplete harmonic complex (missing the target tone) precedes the tone as compared to when the onset of the inharmonic complex is coincident with that for the target tone. This was referred to as an enhancement effect. Viemeister N. F. (1980) then examined a number of properties of this effect, finding that the complex need not be harmonic and that noise maskers or bandpass noise signals also served to enhance the detection of the tone. He also found the effect over a wide range of intensities for maskers and targets.

Summerfield Q. *et al.* (1984; 1987) suggested that their demonstration of vowel aftereffects may be rooted in peripheral sensory adaptation. One could suggest that neurons adapt, and the prominence of the added harmonic is due to the fact that neurons tuned to its frequency were not adapted prior to its onset. Alternatively, some researchers (e.g., Houtgast, T., 1974; Moore, B. C. J. and Glasberg, B. R., 1983) have suggested that rapid adaptation serves mostly to enhance onsets selectively, with suppression being a process through which differences in level of adjacent spectral regions in complex spectra (e.g., formants in speech signals) are preserved and/or enhanced.

Viemeister N. F. and Bacon S. P. (1982) showed that, not only was an enhanced target tone more detectable, the tone also served as a more effective masker of a following tone. They suggested that suppression must be included in an adaptation scenario to place it in closer accord to this finding. Different frequency components of a signal serve to suppress one another, and two-tone suppression has been cast as an instance of lateral inhibition in hearing (Houtgast, T., 1972). Investigators have argued that suppression helps to provide sharp tuning (e.g., Wightman, F. L. *et al.*, 1977; Festen, J. M. and Plomp, R., 1981), and with respect to speech perception, Houtgast T. (1974) has argued that this process serves to sharpen the neural projection of a vowel spectrum in a fashion that enhances spectral peaks.

Many neurophysiological observations bear upon enhancement effects. In particular, a number of neurophysiological studies of auditory nerve (AN) recordings (e.g., Smith, R. L. and Zwislocki, J. J., 1971; Smith, R. L., 1979; Smith, R. L. *et al.*, 1985) strongly imply a role for peripheral adaptation. Delgutte and colleagues (Delgutte, B., 1980; 1986; 1996; Delgutte, B. *et al.*, 1996; Delgutte, B. and Kiang, N. Y. S., 1984) have established the case for a much broader role of peripheral adaptation in perception of speech. Delgutte notes that peaks in AN discharge rate correspond to spectro-temporal regions that are rich in phonetic information, and that adaptation increases the resolution with which onsets are represented. He also notes neurophysiological evidence that "adaptation enhances *spectral contrast* between successive speech segments" (Delgutte, B. *et al.*, 1996, p. 3, italics added). This enhancement arises because a fiber adapted by stimulus components close to its CF is relatively less responsive to subsequent energy at that frequency, while stimulus components not present immediately prior are encoded by fibers that are unadapted – essentially the same process offered by psychoacousticians but now grounded in physiology. In addition, Delgutte notes that adaptation takes place on many timescales, and is sustained longer with increasing level in the auditory system.

Inspired by the vowel aftereffect studies by Summerfield Q. *et al.* (1984; 1987), Coady J. A. *et al.*, (2003) sought to make clearer the connections between experiments using very simple nonspeech flanking stimuli (e.g., FM glides) and Summerfield's studies using rich spectra that were complementary to those for vowel sounds. Although sine waves and FM glides have often been used as nonspeech proxies for formants, such sounds have limited resemblance to speech formants. While it is true that spectrograms illustrate formants as bands of energy, and formant transitions as bands of energy traversing frequency, such descriptions can be misleading. For example, if fundamental frequency (f_0) is constant, individual harmonics of the fundamental do not change frequency at all, and all that changes are relative amplitudes of

harmonics. Individual frequency components of the speech spectrum change frequency no more than f_0 changes.

Coady J. A. *et al.* (2003) used VCV sequences for which the initial vowel ([e] or [o]) affects perception of the following consonant (/ba/ or /da/). In addition to creating synthetic vowels [e] and [o], they created spectral complements of these vowels [∼e] and [∼o] by creating troughs where formants occurred for [e] and [o]. These precursor vowel-complements altered perception in a fashion opposite that of normal (non-complement) vowels because troughs in energy increased excitability within a frequency range for which excitability was attenuated when a frequency prominence (formant) was present in a normal vowel. In addition, they demonstrated that these perceptual effects relied substantially upon spectral characteristics of onsets.

It appears that the same underlying processes account for effects of both very simple nonspeech precursors and spectrally rich vowel-like complements. Although more complex or domain-limited theories of speech perception have been proposed to explain perception of co-articulated speech, the above patterns of perception with both simple and complex stimuli suggest that spectral contrast is an important part of the explanation for perceptual accommodation of co-articulated speech.

3.48.4.3 Broader Spectral and Temporal Effects

Contributions of spectral contrast to perception of co-articulated speech are narrowly focused in both time and frequency. Processes through which the auditory system optimizes detection of spectral change operate over durations on the order of less than 0.5 s, and spectral components of interest are relatively local (e.g., formants.) In keeping with the fundamental principle that, in the interest of maximizing transmission of new information, perceptual systems respond primarily to change, long-term signal characteristics that do not change should also alter perception in similar ways.

For vision, perceivers maintain color constancy in the face of changes in level or spectral composition of illumination, respectively. The visual system adjusts for the spectral composition of illumination (e.g., sunlight versus tungsten or fluorescent lighting), while maintaining relatively consistent perception of color under widely varying viewing conditions. Analogous challenges arise for hearing. When auditory experiments are conducted in the laboratory, experimenters typically endeavor to maintain consistent response across all frequencies through the use of high-quality audio equipment and headphones. However, in real-world listening environments, the spectrum is virtually always colored by characteristics of the listening environment. Energy at some frequencies is reinforced by reflective properties of surfaces, while energy at other frequencies is dampened by absorption properties of materials and shapes of objects in the environment. For hearing to be most effective, listeners must adapt to reliable spectral characteristics in order to be maximally sensitive to the most informative characteristics of sounds.

Kiefte M. and Kluender K. R. (in press) used vowel sounds to examine how auditory systems may adapt to predictable (redundant) spectral characteristics of the acoustic context in order to be more sensitive to information-bearing characteristics of sounds. Simple vowel sounds are useful in this application because it is known that listeners use both spectrally narrow (formant peaks) and broad properties (gross spectral tilt) to perceive vowel sounds. For example, low frequency F1 is heard as /u/ (as in boot) when accompanied by a low frequency F2, and as /i/ (as in beet) when accompanied by higher frequency F_2. In addition, gross spectral tilt, the relative balance between low- and high-frequency energy, is quite different for these vowels. The vowel [u] has more low- than high-frequency energy, resulting in a gross spectral tilt of rapidly declining energy as a function of increasing frequency. In contrast, [i] has relatively more high-frequency energy, and energy decreases much more gradually with increasing frequency. When listening to isolated vowel sounds, listeners use a combination of both formant frequencies and gross spectral tilt to identify vowels (Kiefte, M. and Kluender, K. R., 2005).

Kiefte and Kluender created a matrix of vowel stimuli that varied perceptually from /u/ to /i/ in two dimensions: center frequency of F_2 and gross spectral tilt. Along one dimension, center frequency of F_2 varied from low ([u]) to high ([i]). Along the second dimension, gross spectral tilt varied in the same stepwise fashion, from a spectral tilt characteristic of [u] to one characteristic of [i]. Listeners identified this matrix of vowel sounds preceded by a synthesized rendition of the sentence "You will now hear the vowel. . ." When long-term spectral tilt of context sentences was altered to match that of the following vowel, listeners relied virtually exclusively upon the frequency of F_2 when identifying /i/ and /u/. This pattern of performance indicates that tilt, as a predictable spectral property of

acoustic context, was effectively canceled out of perception (Figure 8).

Encoding of predictable characteristics such as spectral tilt requires only the most abstract characterization of the spectrum, with little spectral detail. Changes in spectral tilt can be due to changes in acoustic properties of the physical environment, or particular to speech, changes in emotional state or speaker identity (Klatt, D. H., 1982). Neither of these properties change rapidly and both are relatively stable across time relative to the rapid spectral changes found in speech. Kiefte and Kluender then tested whether perception also compensates for local spectral properties when these properties are stable across time.

Using the same sentence context, sentences were processed with a single-pole filter which corresponded exactly to the frequency and bandwidth of F_2 of the target, yielding intact sentences with an additional constant-frequency spectral peak added throughout. When presented with a stimulus in which F_2 was an unchanging acoustic property of the context, listeners relied largely upon global spectral characteristics (tilt) for identification of the target vowel. Effects of preceding context are not restricted to gross spectral properties. Perceptual cancellation of predictable spectral characteristics also occurs for local, relatively narrowband spectral characteristics of the acoustic context.

Perceptual cancellation of predictable acoustic context does not depend upon preceding context being speech (Holt, L. L., 2005; Stilp, C. and Kluender, K. R., 2006), nor does it depend upon the context being identical trial to trial (Kiefte, M. and Kluender, K. R., in press). Listener performance provides evidence that the auditory system is quite adept at factoring out predictable characteristics of a listening context, and is consequently more sensitive to informative changes in spectral composition across time.

Underlying mechanisms by which the auditory system calibrates for characteristics of acoustic context have not yet been extensively investigated, and are not yet understood. Some primary auditory cortex (AI) neurons encode spectral shape with respect to both broad and narrow complex spectral shapes (Barbour, D. L. and Wang, X., 2003), and neurons in AI are sensitive to the relative probabilities of pure tones of different frequencies in an extended sequence of tones (Ulanovsky, N. *et al.*, 2003). Calibrating to acoustic context in the service of enhancing sensitivity to change would have been efficacious since the very first auditory systems, even before the advent of

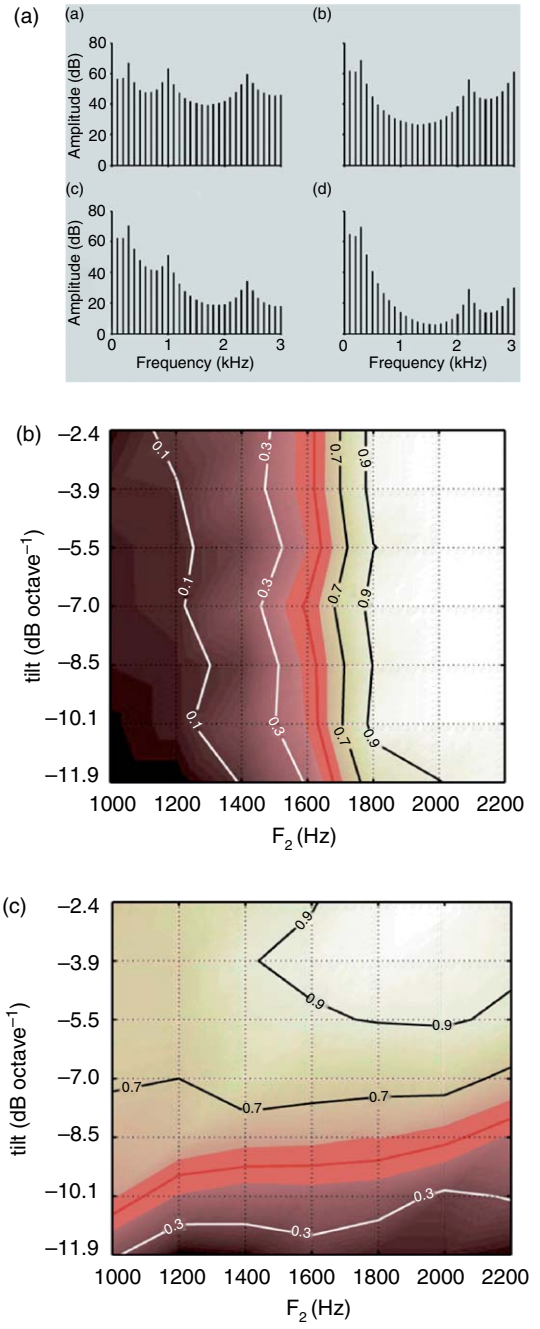

Figure 8 Spectra of vowel sounds [u] and [i] vary both in center frequency of F_2 and overall spectral tilt, and listeners use both acoustic properties to identify these vowels. Kiefte M. and Kluender K. R. (in press) created sounds that varied in each dimension independently (a). When listeners heard these vowel sounds following a precursor that was filtered to have the same spectral tilt as a target vowel, listeners used F_2 frequency exclusively when identifying the vowels (b). The complementary pattern of results, exclusive use of tilt, obtains when precursors include a constant-frequency spectral peak matching F_2 of the target sound (c).

neocortex. It is possible, or perhaps likely, that brainstem processes play an important role.

Projections from superior olive to outer hair cells, collectively called the medial olivocochlear (MOC) efferent system have been hypothesized to provide adjustments of basilar membrane tuning to improve resolution of signals against background noise. Kirk E. C. and Smith D. W. (2003), for example, hypothesized the MOC evolved as a mechanism for unmasking biologically significant acoustic stimuli. A few synapses further from the cochlea, inferior colliculus (IC) neurons adapt to structural regularities in natural sounds in a fashion that increases information transmission (Escabi, M. A. *et al.*, 2003), and stimulus specific adaptation much like that found by Ulanovsky N. *et al.* (2003) also has been demonstrated in IC (Pérez-González, D. *et al.*, 2005).

3.48.5 Maximizing Transmission of Speech Information with Multiple Dimensions

3.48.5.1 Speech Perception Uses Multiple Sources of Information

A signature property of speech perception is its extreme resilience in the face of dramatic signal degradation. For example, listeners understand speech at signal-to-noise ratios less than 0 dB, and they understand speech either when all energy is removed above 1500 Hz or when all energy is removed below 1500 Hz. Listeners can understand speech when the only information available is fluctuations in amplitude of eight or so bands of noise across frequency (Shannon, R. V. *et al.*, 1995), and some listeners can understand speech consisting of little more than sine waves that track the center frequencies of formants (Remez, R. E. *et al.*, 1981). In large part, these as well as other demonstrations of perceptual resilience can be explained by the fact that listeners can rely upon experience with speech that far exceeds experience with any other type of sounds. This power of experience rests upon the high degree of redundancy within the speech signal.

Experience with redundancy is among the reasons why performance of listeners detecting tones in quiet or detecting differences in pitch between two tones are rather poor predictors of the ability of the same listeners to understand speech. Listeners who suffer significant hearing loss can, nonetheless, manage to understand speech until the level of impairment becomes severe or there is substantial background noise competing with the speech signal. Profoundly deaf people who have received cochlear prosthetics (electrodes implanted into the cochlea) and who consequently receive extremely degraded signal via as few as one–four electrode contacts, nevertheless, can often understand speech, sometimes sufficiently well to talk on the telephone.

Redundancy does not distinguish speech from other objects and events in the world. For example, Attneave F. (1954) notes that information received by the visual system is redundant with sensory events that are highly interdependent in both space and time, and this is simply because "the world as we know it is lawful." (p. 183). Because multiple attributes are used when perceiving speech, the presence of one attribute can compensate for the absence of another, as increasing the magnitude of one source of information serves to compensate for decrease of another. There have been many demonstrations of these trading relations (e.g., Repp, B. H., 1982).

Using multiple stimulus attributes is common to perception across modalities. For example, multiple monocular and binocular cues contribute to visual perception of distance. While individual neurons rarely provide high fidelity, populations of neurons acting in concert robustly encode information even when signals are substantially degraded. Implicit to population encoding is the fact that relationships between activities of multiple neurons conspire for effective perception. It is the correlation of activity across neurons (i.e., redundancy) that makes sensorineural systems robust. Exploiting correlations among multiple attributes in speech perception provides another example of maximizing the performance of perceptual systems by extracting predictability in the service of emphasizing change. The quintessential example of combining multiple acoustic attributes is categorical perception (Figure 9).

Although rarely recognized as being so (Kluender, K. R., 1988; 1994), perceptual constancy and categorization share a great deal in common. A classic definition of categorization is that it permits treating discriminably different examples as functionally equivalent. A virtue of categorization typically is presented as efficiently directing responses to functionally equivalent objects or events. Similarly, perceptual constancy maintains when discriminably different exposures (varying with size, orientation, etc.) are treated as equivalent. For example, the apparent size of an object remains the same even when brought nearer or farther from the perceiver. And, perceived shape stays the same across rotations. The simple observation that nonhuman

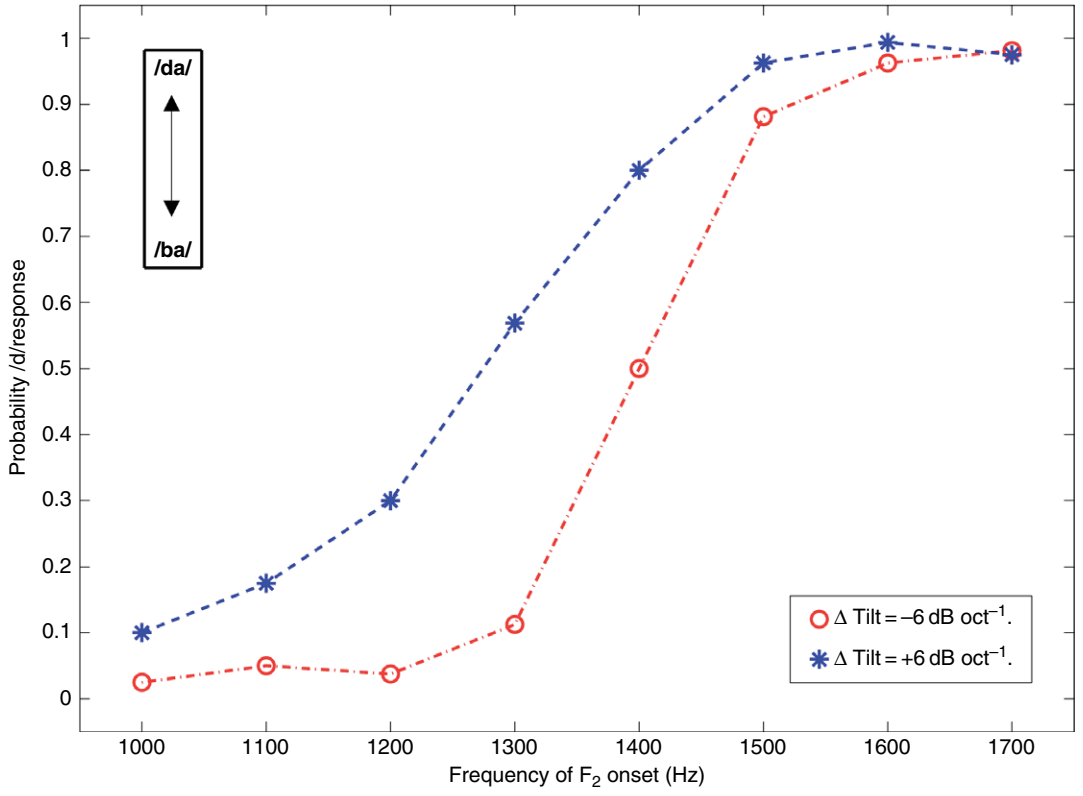

Figure 9 Listeners' use of multiple acoustic attributes is commonly demonstrated by experiments in which two attributes are independently manipulated. In this example from Alexander J. M. and Kluender K. R. (2005), when relative spectral tilt is positive (blue), listeners hear sounds with lower F_2 onset frequency as /d/. One attributes trades against another, as more of one compensates for less of another.

animals manage to navigate their worlds is ample testimony to their ability to maintain perceptual constancy. Nonhuman animals also have been shown to categorize both visual images and acoustic stimuli such as speech (Herrnstein, R. J., 1984; Kluender, K. R. *et al.*, 1987).

Confusion between perceptual constancy and perceptual categorization is common in descriptions of speech perception as somehow arriving at appropriate phonetic categories. However, there have been a fair number of instances for which researchers adopted perceptual constancy as the preferred description (see, e.g., Kuhl, P. K., 1978; 1979; 1980; 1987). Here it is proposed that categorical perception be thought of as perceptual constancy. To the extent that categorization is only a more abstract manifestation of constancy, choosing constancy may not be a particularly provocative choice. If one considers perception of speech to involve perceptual constancy, commonalities with similar perceptual achievements are revealed and surplus cognitive content typically ascribed to categorization is avoided.

3.48.5.2 Categorical Perception

Categorical perception is the most well-known pattern of perceptual performance with speech sounds. Three features define categorical perception: a sharp labeling (identification) function, discontinuous discrimination performance (near-perfect across identification boundary and near-chance to either side), and the ability to predict discrimination performance purely on the basis of labeling data (Wood, C. C., 1976). All three defining features of categorical perception arise naturally from the principle of discovering (and perceptually absorbing) predictability in the interest of maximizing sensitivity to change.

Returning to the fact that speech sounds are comprised of multiple acoustic attributes, many of which are redundant, one acoustic attribute serves to predict the occurrence of another. Through experience, perceptual processes come to absorb these correlations in a way that increases efficiency. There is no information in predictability. When perceptual systems encode correlations among attributes, there are

two consequences. First, there is a decrease in sensitivity to differences between two sounds that share the same pattern of correlation among the same set of attributes. Second, two sounds with different patterns of correlation become easier to distinguish. For speech, detection of differences between functionally different speech sounds is optimized to the extent that perceptual processes absorb redundancies across acoustic attributes that co-vary as properties of the same consonant or vowel (Figure 10).

3.48.5.2.1 Principal components analysis: an analogy

This perceptual processing can be compared with the statistical technique principal component analysis (PCA; see, e.g., Dillon, W. R. and Goldstein, M., 1984). For PCA, one begins with a correlation matrix of multiple variables, created to assess the degree to which each variable is correlated with every other variable across many observations. From this correlation matrix, it is possible to determine weighted combinations of variables, vectors, which account for as much shared variance as possible. To the extent that multiple observations reveal covariance among variables, a limited number of vectors (few relative to the number of variables) can account for a high percentage of the total variance across observations.

PCA is being used here only as analogy because it is unlikely that real neurons adhere to formal restrictions on how vectors are chosen, and the ways PCA fails as analogy are themselves illuminating. First, PCA is a linear analysis, and it is well-known that sensory processes are nonlinear. Second, PCA assumes normally distributed values, and the real world complies with this assumption only to varying extents. A related analysis, independent component analysis (ICA; see, e.g., Hyvärinen, A. and Oja, E., 2000) does permit violations of assumption of normality, and may come a bit closer to modeling neural processing. Third, PCA, but not networks of neurons, requires that vectors be ordered from most to least amount of variance accounted for, and these vectors must be uncorrelated (eigenvectors).

The issue concerning orthogonality is interesting in two ways. First, while perfect efficiency is achieved if every vector shares no variance with any other vector, achieving this goal is unlikely in a neural system. A second point is more informative. Here, perception is being construed as a cascade of processes, each working to extract redundancy from the outputs of earlier processes. To the extent that outputs of prior processes even approach orthogonality, this would seem to imply

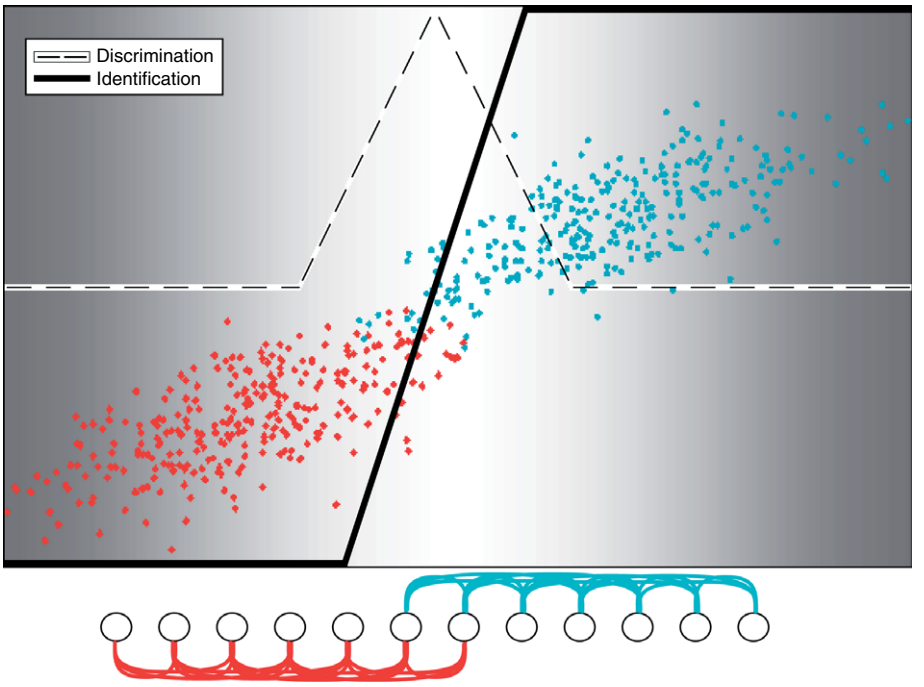

Figure 10 Categorical perception can be explained by auditory systems treating sounds with attributes that share the same correlation structure as equivalent. By this explanation, detection of differences between two complex sounds is greatest when each sound corresponds to a different pattern of experienced correlation.

that seizing upon correlation again would become increasingly implausible. The solution to this seeming dead end is that, with every successive reduction of redundancy, information over which processing operates expands in space, frequency, time, and any other dimension of interest. Thus, statistical relationships that hold relatively locally do not constrain correlations at the next coarser grain of processing. It is worthwhile to note the parallels between this statistical analogy and hierarchical organization of perceptual processing in the central nervous system.

Finally, there is a parallel between practical use of PCA and the prior argument that perceptual systems should efficiently optimize, not maximize, information transmission. Figure 4(c) depicts a sensori-neural system tuned to focus dynamic range in a way that optimizes information transmission relative to the distribution $(1/f)$ of energy flux in the environment while neglecting the last bits of potential information. At an extreme, PCA also permits characterization of all of the variance across observations when the number of eigenvectors is equal to the number of observations. However, the virtue of PCA is that the majority of, but not all, variance can be accounted for by relatively few vectors. Efficiencies are gained by capturing correlations within a few vectors. More eigenvectors are discarded than are saved, despite the fact that some snippets of information are lost.

From the analogy to PCA, it is easy to envision efficient sensori-neural encoding that extracts reliable correlations between multiple attributes across observations. This process can be instantiated in perceptrons (Rosenblat, F., 1958), the simplest connectionist networks. Most important to the analogy is that experience is encoded efficiently in a way that decreases sensitivity to differences between stimulus inputs that share the same correlation vector (or attractor) and increases sensitivity to differences between inputs that correspond to different vectors (see, e.g., Olshausen, B. A. and Field, D. J., 1997; Simoncelli, E. P. and Olshausen, B. A., 2001).

3.48.5.2.2 Phonemes as correlations?

Through experience with redundant attributes, simplified encoding of inputs as patterns of correlation serves as grist for consequent processing. It could be argued that vectors in a correlation matrix correspond to the putative linguistic units called phonemes (Kluender, K. R. and Lotto, A. J., 1999); however, the same basic principles apply continuously along the chain of processing, and such a demarcation would be artificial. The grain of synthesis steadily increases, from attributes that are spectrally and temporally local to those that extend across multiple attributes derived from preceding processing through to lexical organization. For example, Kingston J. and Diehl R. L. (1994) hypothesized intermediate perceptual properties (IPPs) may correspond to earlier analysis, and it is likely that statistical properties of acoustically simpler vowel and consonant sounds are extracted prior to those for more complex speech sounds. Further, as described below, additional reification of phoneme-like dimensions may await lexical organization.

Perhaps, no real harm may be done if one suggests that some correlations are phonemes *per se*, if only as a placeholder. However, it is important to distinguish two ways of thinking about this. The first way is common or even typical. One could suggest that the task for a listener is to identify consonants and vowels as individual psychological entities, and those entities are represented by correlations among attributes.

The second way, suggested here, is that consonants and vowels are revealed much more by what they are not than by what they are. Contrasts between sounds, not commonalities, are emphasized in speech perception. Through experience, perceptual processes become especially sensitive to acoustic differences that distinguish different consonants and vowels as a consequence ignoring differences among multiple acoustic properties that share a history of co-occurrence. What matters are distinctions between speech sounds, which are enhanced perceptually, not consonants and vowels themselves. Listeners hear the sounds of a language by virtue of learning how they are distinguished from all other consonants and vowels. This idea was most explicitly expressed by linguists Roman Jacobson and Morris Halle in their classic book *Fundamentals of Language* (1971) "All phonemes denote nothing but mere otherness" (p. 22).

3.48.5.2.3 Categorical perception as competing correlations

Returning to categorical perception, one can understand how these patterns of performance emerge naturally from perceptual systems exploiting redundancies among attributes in the service of maximizing sensitivity to change. Following experience with correlations among acoustic attributes, listeners are relatively unlikely to detect differences among complex sounds that share the same correlation structure. The fact that modest changes are perceptually neglected is consistent with the fact that listeners can understand speech when some acoustic properties

(e.g., energy above 1500 Hz) are absent. When the correlation structure is not violated too severely, perception overcomes perturbations, and even absence, of some attributes that normally contribute to the correlation. All that is required are sufficient attributes to get to the right vector.

This lack of sensitivity to perturbations among inputs accounts for the finding that discrimination performance is near chance for different instances of the same consonant or vowel. If two different stimuli fit the same correlation structure relatively well, the same perceptual consequences obtain. Complementary to this lack of discrimination for sounds that share the same correlation structure, discrimination performance is exquisite when the speech sounds to be discriminated are associated with two competing correlation structures. For these cases, discrimination is especially good because, by virtue of perceptual processes extracting redundancies within separate correlation structures, detection of change (information transmission) is optimized.

If categorical perception is only another example of perceptual constancy operating within general principles of perceptual organization, why did so many researchers believe categorical perception to be unusual? One reason is because categorical perception was routinely contrasted with psychophysical data from experiments employing very simple stimuli (typically unidimensional) of limited ecological significance. Equally important, comparisons were made to stimuli with which subjects have little or no experience before coming to the experimental session. Classic psychoacoustic experiments using pure tones, noise bursts, and inharmonic complexes have great utility for interrogating operating characteristics of sensory transduction absent content or experience. Thresholds for energy detection or sensory change are valuable things to know, but these are not as informative with respect to perception as it guides real activities in a real world.

When investigators use stimuli that are complex and familiar, signature response patterns of categorical perception are found. Categorical perception has been reported for musical intervals (Burns, E. M. and Ward, W. D. 1974; 1978; Smith, J. D. *et al.*, 1994) and tempered triads (Locke, S. and Kellar, L., 1973). Visually, humans categorically perceive human faces (Beale, J. M. and Keil, F. C., 1995) and facial expressions (Etcoff, N. L. and Magee, J. J., 1992; Calder, A. J. *et al.*, 1996; de Gelder, B. *et al.*, 1997; Young, A. W. *et al.*, 1997), as well as faces of different species (Campbell, R. *et al.*, 1997). When human observers are trained with artificial categories, they demonstrate increased perceptual sensitivity for items that are categorized differently (Goldstone, R. L., 1994). When monkeys are trained to respond differentially to clear examples of cats versus dogs (initially novel categories for monkeys), behavioral responses to stimuli along a morphed cat/dog series exhibit sharp crossovers at the series midpoint (Freedman, D. J. *et al.*, 2001). Rather than being specific to speech, categorical perception is a general property of any perceptual system consequent to experience with rich regularities of natural objects and events.

Categorical perception appears to be an emergent property of any perceptual system that is shaped by experience. Damper R. I. and Harnad S. R. (2000) reviewed evidence from human and animal listeners as well as from neural network models. They concluded that any number of generalized learning mechanisms can account for categorical perception. Models ranging from simple associative networks (e.g., Anderson, J. A., *et al.*, 1977) to back-propagation networks with no hidden units (e.g., Damper, R. I. *et al.*, 2000) exhibit categorical perception. Because categorical performance arises from a variety of simple learning algorithms that seize upon reliable statistics in their inputs, Damper R. I. and Harnad S. R. (2000) conclude that specialized processing is not necessary, and that "any general learning system operating on broadly neural principles ought to exhibit the essentials of [categorical perception]" (p. 862).

3.48.5.2.4 Multimodal interactions are expected

Thus far, and for the remainder of this contribution, discussion typically will be restricted to auditory perception of speech. This should not be taken to imply that other modalities do not contribute to understanding speech. The approach outlined here is explicitly associationist and driven by experience. The brain is opportunistic. Sensorineural systems seize upon redundancies to maximize information transmission whenever possible. Contemporary research (e.g., Bahrick, L.E. *et al.*, 2004) reveals how intersensory redundancy guides development of perception most generally. Whenever nonauditory information is redundant with speech acoustics, those correlations should contribute to efficient encoding of speech. For example, listeners have a wealth of experience simultaneously hearing speech and viewing talkers' faces, and the McGurk effect (McGurk, H. and MacDonald, J., 1976) is evidence of the profound effects visual information can have on the way speech sounds are perceived. Also, whenever people are

talking, they both hear the sounds they're producing and they experience the movements in their own vocal tracts. While ideally, this occurs less than half the time people hear speech, simultaneous activities of both hearing and talking provide exquisite conditions for extraction of correlations.

3.48.6 Experience and Sound Contrasts in the Native Language

Experience is essential for the development of every sensori-neural system. The profound role of experience is especially clear for speech perception. Infants gain significant experience with speech even before they're born. Late-term fetuses can discriminate vowel sounds (Lecanuet, J. P. *et al.*, 1986), and prenatal experience with speech sounds appears to have considerable influence on subsequent perception, as newborns prefer hearing their mother's voice (DeCasper, A., and Fifer, W., 1980). By the time French infants are 4 days old, they discriminate French from other languages (e.g., Russian) (Mehler, J. *et al.*, 1988). Perhaps most telling is the finding that newborns prefer hearing particular children's stories that were read aloud by their mothers during the third trimester (DeCasper, A. J. and Spence, M. J., 1986).

Experience plays a critical role in tuning speech perception to the distributions of sounds within one's language environment. Much, if not most, of this development as a native listener takes place during the first year of life. One of the most challenging obstacles for the infant is to use acoustic information that distinguishes one speech sound from another in the face of sometimes widely varying acoustic properties, many of which do not distinguish speech sounds in their language. Acoustic differences that convey a contrast in one language may be of little or no relevance to another language. Some of these differences simply may be unrelated (orthogonal) to distinctions used in a particular language and would not occur in a language context. In addition, clearly audible differences such as gender of talker, speaking rate, emotional state, and other factors have profound effects on the acoustic signal, yet the language learner must learn to understand speech across these variations.

3.48.6.1 Vowels

At least by the age of 6 months, infants have the ability to distinguish stimuli by vowel type even when different instances of the vowel differ considerably between presentations (Kuhl, P. K., 1983). In a reinforced head turn paradigm, Kuhl trained infants to turn their heads only when the vowel of the background stimulus changed during presentation of the closely related vowels [a] (as in tot) and [ɔ] (as in taught) spoken by a male talker. When tested on novel vowels produced by women and children (adding random variation in pitch contour in addition to shifting absolute frequencies of formants), infants provided the correct response on the first trial demonstrating that they recognized the novel instances as consistent with training vowels despite talker changes. Note that, by the shared covariance account offered above, the capacity to distinguish vowels across variation in irrelevant acoustic characteristics is a natural consequence of encoding stimuli on the basis of attributes that tend to co-occur. Attributes such as those accompanying changes in talker are irrelevant to particular consonants and vowels, so they do not play much role in phonetic distinctions.

While these studies attest to the ability of infants to respond to distinctions between vowels in the face of irrelevant variation, later studies have investigated how perception may be structured along acoustic/auditory dimensions that are directly relevant to distinguishing vowel sounds. What has become most apparent is that the degree to which infants treat acoustically different instances of the same vowel as equivalent is critically dependent upon their experience with a particular language. For example, 6-month-old infants detect differences between vowel sounds differently depending upon whether they lived in an English-speaking (Seattle) or Swedish-speaking (Stockholm) home (Kuhl, P. K., *et al.*, 1992).

Further evidence for the role of experience can be found in experiments in which performance by European starlings (*Sturnus vulgaris*), having learned statistically controlled distributions of renditions of Swedish and English vowels, was highly correlated with performance of adult human listeners (Kluender, K. R. *et al.*,1998). A simple linear association network model, exposed to the same vowels heard by the birds, accounted for 95% of the variance in avian responses. Consistent with the principle that consonants and vowels are defined mostly be what sounds they are not, both human goodness judgments (Lively, S. E., 1993) and starling response rates illustrate an anisotropy such that peak responses are skewed away from competing vowel sounds more than they are defined by centroids of vowel distributions.

3.48.6.2 Consonants

Perception of differences between consonants is similarly tuned by experience. Werkerand her colleagues (Werker, J. F. *et al*., 1981; Werker, J. F. and Logan, J. S., 1985; Werker, J. F. and Lalonde, C. E., 1988; Werker, J. F. and Tees, R. C., 1983, 1984a; 1984b) have demonstrated that, as a consequence of experience with consonants in their native language, infants' tendency to respond to differences between some consonants that are not in their language begins to attenuate. The series of studies by Werker J. F. and Lalonde C. E. (1988) permit a relatively complete description of the phenomena. They exploited the fact that speakers of English and Hindi use place of articulation somewhat differently for stop consonants. While for English, three places of articulation are used for voiced stop consonants: labial, alveolar, and velar (e.g. /b/, /d̪/, and /g/, respectively), in Hindi four places are used: labial, dental, retroflex, and velar (e.g. /b/, /d̪/, /ḍ/, and /g/, respectively.) They created a synthetic series that varied perceptually from /b/ to /d/ (for native-English speaking adults) and from /b/ to /d̪/ to /ḍ/ (for native-Hindi speaking adults) (Figure 11).

Using the same reinforced head turn procedure used by Kuhl, they found that 6- to 8-month-old infants from English-speaking families responded to changes in stimulus tokens that crossed perceptually from the English /b/ to /ḍ/ and also responded to changes between Hindi stops [d̪] and [ḍ]. A different group of infants from English speaking families aged 11- to 13-months of age responded reliably only to the English [b]-[d̪] contrast, and not to the Hindi [d̪]-[ḍ] contrast. Essentially, 6- to 8-month-old infants responded in a manner typical of native-Hindi adults, while 11- to 13-month-olds responded like native-English adults treating both dental and retroflex stops as being the same. Werker and her colleagues have found analogous results in studies using different consonant contrasts from different languages.

For vowels and consonants, perception of speech is shaped during the first year of life in ways that respect the statistics of the linguistic environment. The challenge for the infant learning the speech sound distinctions in his or her native language is precisely this. Infants must learn how acoustic/auditory attributes tend to co-occur, and those correlations among attributes define perceptual organization that optimizes sensitivity to change.

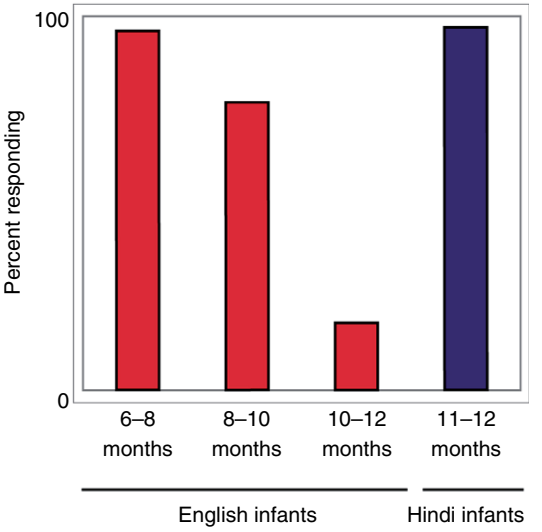

Figure 11 Perception of speech sounds is tuned by experience. As a consequence of experience with consonants in their native language, infants' tendency to respond to differences between some consonants that are not in their language begins to attenuate. Here, 6- to 8-month-old infants from English-speaking homes respond in a manner typical of native-Hindi adults and 1–12-month-old Hindi infants when hearing dental and retroflex Hindi stops. Before they are a year old, infants from English environments respond like native-English adults, treating both consonants the same. Adapted from Werker, J. F. and Lalonde, C. E., 1988 Cross-language speech perception: initial capabilities and developmental change. Dev. Psychol. 24, 672–683.

3.48.6.3 Second-Language Perception

The same principles that explain categorical perception and development of perceptual organization during the first year of life extend to predicting how difficult, or easy, it is to learn new speech contrasts in a second language. For the case of the sounds of a single language, correlated attributes distinguish each consonant or vowel from others in a fashion that optimizes sensitivity to differences. The same construct, habitual co-occurrence of acoustic attributes, constrains and predicts how listeners perceive familiar and unfamiliar sounds from a second language. There are three basic patterns of interaction between perceptual organization for the native language and the mapping of sounds from a second language.

First, acoustic attributes of two contrasting nonnative speech sounds can be equally well correlated with attributes corresponding to only a single native consonant or vowel. Consider the case for formant patterns contributing to categorization of stop consonants with varying place of articulation. For

example, both dental and retroflex stops such as those found in Hindi are acoustically realized in a manner quite similar to that for English alveolar stops. Given the range of ways English [d̪] is produced in the contexts of other speech sounds, there is ample overlap with acoustic attributes associated with both dental and retroflex stops. When [d̪] is produced in the environment of the retroflex continuant [r] as in drew, English [d̪] is shares multiple acoustic commonalities with the Hindi retroflex stop [ɖ]. Similarly, when English [d̪] is produced in the environment of a dental fricative such as [θ] in words like width, it is acoustically quite similar to the Hindi dental stop [d̪] (Polka, L., 1991). Given the facts about the distributions of acoustic attributes for alveolar stops in fluent English, attributes consistent with dental or retroflex stops are well correlated with attributes that co-occur in alveolar stops. Dental-like or retroflex-like acoustic attributes are accommodated within correlation structures for English alveolar stops via an increase in overall variance reflective of the observed variability in English alveolar stop production. Werker J. F. and Lalonde C. E.'s (1988) adult identification data are entirely consistent with this scenario. Stimuli that are identified by native-Hindi listeners as dental or retroflex are all assimilated into the set of stimuli identified as alveolar by native-English listeners. Best C. T. *et al.* (1988) referred to a similar process as single-category assimilation in her taxonomy of contrasts within an articulatory framework.

An analogous example of difficulty perceiving a distinction between two sounds is the well-known inability of native-Japanese listeners to detect the distinction between English [r] and [l] (e.g., Miyawaki, K. *et al.*, 1975). Japanese sounds include a consonant called a rhotic flap, and acoustic characteristics of these flaps overlap extensively with those of both English [r] and [l] (Sato, M. *et al.*, 2003). Consequently, acoustic attributes of [r] and [l] are equally well correlated with attributes corresponding to a single Japanese sound, and native-Japanese listeners are unable to hear, and consequently produce, the English distinction.

A related way non-native contrasts can be assimilated with native contrasts involves cases for which attributes of one sound from of a non-native contrast are very well correlated with attributes of a single native consonant or vowel, being effectively the same. Attributes of a second non-native sound fit less well with the correlation structure of the same native sound, but they do correspond better with that sound than with any other native sound. One example of this is the Farsi distinction between velar and uvular stops. Native-English listeners do not lose the ability to discriminate Farsi velars from uvulars. Instead, they perceive the Farsi voiced velar and uvular stops as being good and poor instances, respectively, of English /g/ (Polka, L., 1992). In this case, Farsi velar stops are perceived as good English velar stops because they share most or all of the acoustic/auditory attributes that comprise the correlated structure of English /g/. Farsi uvular stops share fewer attributes with those that co-occur for English [g]. Farsi uvulars somewhat, but not completely, fit the correlation structure of English [g]. A related process has been referred to as category-goodness assimilation by Best C. T. *et al.* (1988).

The third way native and non-native contrasts can interact can be found in cases where the native language does not exactly share a contrast with a non-native language, but the native language does have a similar contrast that facilitates perception of the non-native contrast. For example, French does not include a voicing distinction for dental fricatives such as /ð/-/θ/ (as in than and thank), yet native-French listeners can discriminate voiced from voiceless English fricatives by perceiving them as versions of French dental stops /d̪/ and /t̪/, respectively (Jamieson, D. G. and Morosan, D. E., 1986). Best C. T. *et al.* (1988) label this type of assimilation two-category because each sound of the non-native contrast maps more or less on to a different sound in the native language. Within the framework of correlated attributes, one would explain the fact that French listeners perceive the English fricatives as versions of French stops is because attributes of the dental fricatives are reasonably well correlated with attributes of the French dental stops as produced with typical allophonic variation in fluent speech.

This scenario leaves only those non-native distinctions that are roughly orthogonal to contrasts within the native language. Across the broad domain of possible mouth sounds, there always will remain some attributes that are not well correlated with any of attributes for any speech sounds within a given language. For example, attributes of the click sounds of Zulu are correlated with no sounds of English, and their perception should be, and is relatively unaltered by the process of learning English phonemes (Best, C. T. *et al.*, 1988). It should be noted that all of the patterns of performance above are consistent with Flege J. E.'s (1995) speech learning model (SLM) and with patterns of experience-dependent learning of speech contrasts (e.g., Flege, J. E. *et al.*, 1997; Imai, S.

et al., 2002). However, Flege's explanations of underlying processes that give rise to these patterns of performance are distinct at least in level of analysis, and he may or may not agree with specific aspects of the present authors' explanations.

3.48.7 To the Lexicon and Beyond

3.48.7.1 Lexical Development and the Emergence of Phonemes (or Something like Them)

In the introduction to this chapter, discussion of phonetic segments and phonemes as independent entities was decidedly circumspect. Throughout the foregoing, consonants and vowels have been described either as sounds or as correlations among acoustic attributes in the service of maximizing information transmission. They have not been described as inherently linguistic or as a discrete stage in processing. To borrow Angell's (Angell, J. R., 1907) dichotomy between functionalism and structuralism, discussion has been more about how and why, and less about the structuralist what of linguistic theory. Particular emphasis has been about how, and the focus now turns to why. The why of speech perception is to recognize words, and the end goal must be getting from the acoustic signal to words that have meaning. Within the information-theoretic perspective adopted here, one can construe the process of speech perception as one of successively reducing uncertainty sufficiently to arrive at words.

Over the years, some researchers have made a case that speech perception really is word perception without intermediate levels of analysis. There have been simulations of lexicons constructed directly from acoustic/auditory input *sans* phonemes (e.g., Klatt, D. H., 1980), and a number of investigators have argued for the primacy of holistic (word-size) organization in lexical development (e.g., Charles-Luce, J. and Luce, P. A., 1990; 1995; Jusczyk, P. W., 1986; Walley, A. C., 1993; Walley, A. C. *et al.*, 2003). For example, Charles-Luce and Luce (Charles-Luce, J. and Luce, P. A., 1990) argued that emergence of acoustic/auditory detail, such as consonants and vowels of words, within the lexicon is a consequence of – not antecedent to – learning more words. By such an account, as the number of words in the lexicon grows, increasing degrees of detail are required to sort each word from all the others.

Kluender K. R. and Lotto A. J. (1999), by contrast, suggested that neither words nor phonetic units may serve exclusively to structure the developing lexicon. Werker and Curtin (Werker, J. F. and Curtin, S., 2005), within their developmental framework for processing rich information from multidimensional interactive representation (PRIMIR), argue that infants have access to information for both phonetic units and the ways these units are grouped together into words. While PRIMIR is more of a framework than a detailed model, Werker and Curtin suggest that internal representations of phonemes become more firmly established and resistant to change as the lexicon grows.

The present emphasis of maximizing information transmission is consistent with concurrent development of statistical structures corresponding to consonants and vowels both preliminary to the lexicon and as an emergent property of lexical organization. In this chapter, speech perception has been described as a succession of processes operating upon the acoustic signal with varying levels of complexity. Common to all these processes is maximizing efficiency of information transmission by absorbing redundancies across inputs. For example, spectral contrast operates early, with trading relations and categorical perception operating later. Following these preliminary operations, one easily can imagine development of a nascent, but undetailed, lexicon of word forms. As a lexical space becomes increasingly populated, the covariance space becomes more complex. Predictable relationships among attributes, now with a phonetic segment-like grain, can be revealed resulting in a reduction in dimensionality of lexical items. The classic definition of phonemes is that they provide the minimal distinction between meaningful elements (morphemes) of language (Trubetzkoy, N. S., 1939/1969). Consequently, phonemes provide one of the most efficient ways to describe differences within the lexicon. Because phonemes provide efficient descriptors of lexical space, they emerge as dimensions of the developing lexical space by quite the same process that explains categorical perception, now operating over a larger time window.

One might suggest that positing phoneme-like dimensions as emergent properties of a lexical space obviates the need for anything resembling consonants and vowels preliminary to the lexicon. However, doing so violates principles of sensori-neural organization, these being that redundancies are extracted continuously with ascending levels of processing. Werker and Curtin's (Werker, J. F. and Curtin, S., 2005) proposal that phonemes become more established, and presumably increasingly tuned to

phonotactic regularities in a language, is more consistent with persistent successive absorption of redundancy in the service of maximizing sensitivity to change.

3.48.7.2 Finding Word Boundaries

One final example of auditory perception using predictability to enhance sensitivity to change is found in studies demonstrating how infants find boundaries between words. In connected speech, acoustic realization of the beginning and end of one word also overlaps with sounds of preceding and following words. Unlike white spaces between words on a page, there are no silent intervals that mark beginnings and ends of words. Interestingly, perception is at odds with this acoustic reality. When listening to someone talking, most individual words stand out quite clearly as discrete entities. But listening to someone speak in a different language is often a very different experience. Every phrase or sentence may sound like a single very long word. This is the situation faced by infants.

Saffran and colleagues (Saffran, J. R. *et al.*,1996) demonstrated that infants can use transitional probabilities between successive sounds within a speech stream as evidence for breaks between words. In their studies, they used streams of connected pseudowords, for which the probability of some sequences of consonant-vowels (CVs) was very high (1.0) while probability of other sequences was relatively low (0.33). Infants were sensitive to whether two sounds share a history of co-occurrence. When they heard successive CVs that rarely co-occurred with one another in their experience, they recognized this as a sign that there was a break between words. This discontinuity corresponds to a spike in information because one CV did not predict the occurrence of the next. Statistics of English support this emphasis upon word boundaries, as the ends of most words cannot be identified prior to the onset of the next (Luce, R. D., 1986). Infant sensitivity to boundaries is yet another example of using predictability to enhance sensitivity to change, and hence enhance transmission of information (Figure 12).

Because this is a principle of perceptual systems most broadly, one expects this use of predictability to apply most generally. Indeed, these patterns of performance extend to infants experiencing tonal sequences (Saffran, J. R. et *al.*, 1999), visual shapes (Kirkham N. Z. et *al.*, 2002), and visual-feature combinations (Fiser, J. and Aslin, R. N., 2002). In fact, even nonhuman primates (Hauser, M. D. *et al.*, 2001) exhibit this sensitivity to transitional probabilities.

3.48.8 Speech in the Brain

Given the plethora of relatively recent studies concerning speech processing using electroencephalography (EEG), magnetoencecphalography (MEG), positron emission tomography (PET), and functional magnetic resonance imaging (fMRI), extensive depiction of speech processing in cerebral cortex alone requires one or more chapters. Here, a very brief review of current understanding will be placed within the framework of information processing provided above.

Hearing sounds of any kind activates primary auditory cortex (AI). Processing of complex sounds relies upon additional areas of cortex adjacent to AI, which is functionally divided into ventral, anterior,

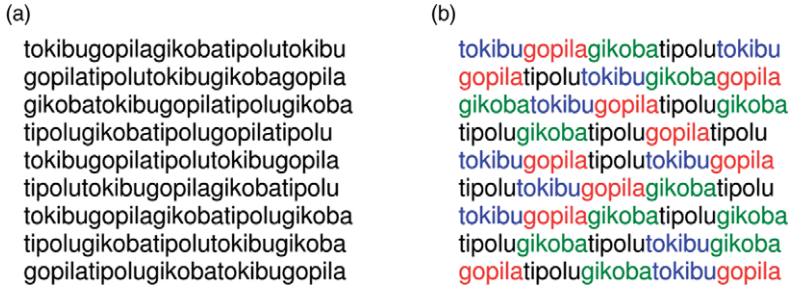

Figure 12 There are no acoustic markers between most words in a stream of fluent speech, analogous to the strings of letters on the right (a). Following minutes of experience with streams of connected speech in which probability of some sequences of consonant-vowels (CVs) is very high, while probability of other sequences was relatively low, infants are sensitive to whether two sounds share a history of co-occurrence. From Saffran, J. R. Aslin, R. N., and Newport, E. L. 1996. Statistical learning by 8-month-old infants. Science 274, 1926–1928.

and posterior sections. Neurons from AI project to the surrounding belt of cortex, and neurons from this belt synapse with neurons in the adjacent parabelt area. Just about any sound will cause activation in some part of AI. However, in the belt and parabelt areas, referred to as secondary or associational auditory areas, simple sounds such as sine waves and white noise elicit less activity, particularly if they have limited temporal structure. Thus, as in the visual system, processing proceeds from simpler to more complex stimuli farther along the auditory pathway, and there is also greater evidence of cross-modal processing (e.g., combining acoustic and optic information), particularly in parabelt areas. Of course, this general property of hierarchical organization is consistent with continuous and successive extraction of redundancy across increasing spans of space and time. As one might expect, areas beyond AI are activated when listeners hear speech and music. Further, at these early levels of cortical processing, activity in response to music, speech, and other complex sounds is relatively balanced across the two hemispheres.

When listening to speech, additional areas of both left and right superior temporal lobes along the superior temporal sulcus (STS) activate more strongly in response to speech than to nonspeech sounds such as tones and noise (e.g., Binder, J.R., 2000). While language processing is typically lateralized to one hemisphere, this activity in response to speech signals is relatively balanced across both sides of the brain when researchers have been very careful to avoid higher-level effects of language (Zatorre, R. J. and Binder, J., 2000).

At some point, however, processing of speech should become more lateralized as perceiving speech becomes part of understanding language. However, one challenge for researchers has been to create control stimuli that have all the complex properties of speech without being heard as speech. Because listeners are very good at understanding even severely distorted speech, it is very difficult to construct stimuli that are complex like speech without being heard as speech.

Liebenthal and colleagues (Liebenthal, E. *et al.*, 2005) adopted a creative way to control for acoustic complexity while varying whether sounds would be heard as speech. They synthesized speech syllables varying incrementally from [ba] to [da]. Nonspeech control stimuli were the same series of syllables, except characteristics of F_1 transitions were flipped upside down, decreasing in center frequency following syllable onset. It is impossible for a human vocal tract to create such sounds, and listeners could not identify them as consonants.

During scanning, listeners participated in a categorical perception task, discriminating pairs of stimuli from one or the other series of stimuli. For the [ba-da] speech series, performance was typical for categorical perception experiments, with stimuli that would be labeled differently (e.g., /ba/ vs. /da/) being almost perfect, while discrimination of other stimulus pairs was rather poor. For the nonspeech sounds, discrimination was above chance and pretty much the same for all pairs of stimuli. Listening to both series of stimuli resulted in increased activation in STS in both temporal lobes. When sounds were speech [ba-da] however, there was increased activation in STS superior temporal cortex, a bit anterior and ventral from activation for control stimuli and mostly in the left hemisphere. This research (Liebenthal, E. *et al.*, 2005) may have revealed a place in the left temporal lobe where experience with English [b] and [d] shapes neural activity.

This experience-dependent cortical organization for English consonants may have been predicted by previous work with visual processing of well-learned objects. In the visual system, perception of faces results in activation of the middle fusiform gyrus (or fusiform face area) of the cortex. This area is disproportionately activated when subjects view faces versus viewing other objects or scenes. Similar patterns of activation, in the same general brain region, can be found in response to other types of stimuli with which subjects are very familiar (Gauthier, I *et al.*, 1999).

A study by Scott and colleagues (Scott, S. K. *et al.*, 2000) suggest a cortical locus for the next step of processing of speech into language. They controlled for acoustic complexity while changing whether sentences were intelligible by using spectrally rotated sentences that could not be understood by listeners. Rotated speech signals were spectrographically upside down (i.e., the frequency scale was inverted). They could not be understood by listeners, but they were as complex acoustically as right-side-up sentences. Rotated stimuli activated STS comparably to intact nonrotated sentences, suggesting that auditory processing in these areas is related more to complexity than to being speech *per se.* The essential difference between cortical responses to these two types of stimuli was that, on the left temporal lobe, activation in response to intact sentences continued further anterior and ventral (including superior

temporal gyrus, STG) to the region activated by rotated sentences. Activation was a little anterior and ventral to the area in which Liebenthal and colleagues (Liebenthal, E. *et al.,* 2005) found activation for [b] and [d]. Relative left lateralization consequent to recognizability parallels findings for other environmental sounds (e.g., Lewis, J. W. *et al.*, 2004), albeit in different brain regions (Figure 13).

The extension of lateralized activation, increasingly anterior and ventral, discovered by Scott and her colleagues (Scott, S. K. *et al.,* 2000) inspires a tantalizing hypothesis concerning the next level of processing beyond speech perception to word recognition. Based upon neuropsychological data from patients, cortical areas essential to semantic memory may reside within far anterior temporal lobe (see, e.g., Rogers, T. T. *et al.*, 2004). Consider a scenario through which increasingly sophisticated redundancies are wrenched out of the speech signal, through differentiation of sounds such as [b] and [d], through detection of word boundaries, to regularities within word boundaries (i.e., words) and concomitant associations with semantic properties of words. Such a notion is clearly speculative given the present state of knowledge; however, this would be an elegant view of successive processing along increasingly anterior and ventral areas of temporal lobe.

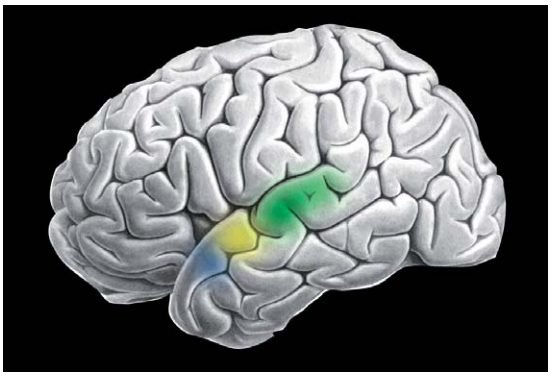

Figure 13 When listening to speech, as well as other complex sounds, cortical activity along the superior temporal sulcus (STS, green) is relatively balanced across the hemispheres. When acoustical complexity is carefully controlled, there is evidence of increased activation in STS (yellow), more anterior and mostly in the left hemisphere (Liebenthal, E. *et al.*, 2005). Cortical activation in response to recognizable sentences appears further anterior and ventral (blue), including superior temporal gyrus (STG). From Scott, S. K. Scott, S. K., Blank, C. C., Rosen, S., and Wise, R. J. S. 2000. Identification of a pathway for intelligible speech in the left temporal lobe. Brain 123, 2400–2406.

3.48.9 Conclusion

Speech perception is grounded in general principles that apply to other acoustic events and to other modalities. Classic principles that guide perception, none of which is wholly original to the authors, explain processes underlying multiple phenomena of speech perception. This information-theoretic model, operating from sensory transduction to word learning, is biologically realistic. It is intended that this framework will serve, not only to reveal processes underlying normative aspects of speech perception, but also to extend understanding of clinical conditions of speech and language processing. Finally, beyond being amenable to study like any other form of perception, speech perception holds promise as a fertile domain for research that can reveal and extend fundamental understanding of perception most generally.

Acknowledgments

Laurel Steinmeyer's and Chrsitian Stilp's assistance with figures is much appreciated. Work supported by NIDCD.

References

Alexander, J. M. and Kluender, K. R. 2005. Contributions of gross spectral properties to perception of stop consonants. J. Acoust. Soc. Am. 118(3) pt 2.

Anderson, J. A., Silverstein, J. W., Ritz, S. A., and Jones, R. S. 1977. Distinctive features, categorical perception, and probability learning: some applications of a neural model. Psychol. Rev. 84, 413–451.

Anderson, B. L. and Winawer, J. 2005. Image segmentation and lightness perception. Nature 434, 79–83.

Angell, J. R. 1907. The province of functional psychology. Psychol. Rev. 14, 61–91.

Attneave, F. 1954. Some informational aspects of visual perception. Psychol. Rev. 61, 183–193.

Attneave, F. 1959. Applications of Information Theory to Psychology: A Summary of Basic Concepts, Methods, and Results. Henry Holt and Company, Inc.

Bahrick, L. E., Lickliter, R., and Flom, R. 2004. Intersensory redundancy guides development of selective attation, perception, and cognition in infancy. Curr. Dir. in Psychol. Sci. 13, 99–102.

Barbour, D. L. and Wang, X. 2003. Contrast tuning in auditory cortex. Science 299, 1073–1075.

Barlow, H. B. 1961. Possible Principles Underlying the Transformations of Sensory Messages. In: Sensory Communication (*ed*. W. A. Rosenblith), pp. 53–85. MIT Press.

Barlow, H. B. 1997. The knowledge used in vision and where it comes from. Philos. Trans. R. Soc. Lond. B 352, 1141–1147.

Barlow, H. B. 2001. The exploitation of regularities in the environment by the brain. Behav. Brain Sci. 24, 602–607.
Beale, J. M. and Keil, F. C. 1995. Categorical effects in the perception of faces. Cognition 57, 217–239.
Best, C. T., McRoberts, G. W., and Sithole, N. M. 1988. Examination of perceptual reorganization for nonnative speech contrasts: Zulu click discrimination by English-speaking adults and infants. J. Exp. Psychol. 14, 345–360.
Binder, J. R. 2000. The neuroanatomy of speech perception (Editorial). Brain 123, 2371–2372.
Bladon, R. A. W. and Lindblom, B. 1981. Modeling the judgment of vowel quality differences 1981. J. Acuost. Soc. Am. 69, 1414–1422.
Burns, E. M. and Ward, W. D. 1974. Categorical perception of musical intervals. J. Acoust. Soc. Am. 55, 456.
Burns, E. M. and Ward, W. D. 1978. Categorical perception – phonemenon or epiphenomenon: evidence from experiments in the perception of melodic musical intervals. J. Acoust. Soc. Am. 63, 456–468.
Calder, A. J., Young, A. W., Perrett, D. I., Etcoff, N. L., and Rowland, D. 1996. Categorical perception of morphed facial expressions. Vis. Cogn. 3, 81–117.
Campbell, R., Pascalis, O., Coleman, M., Wallace, S. B., and Benson, P. J. 1997. Are faces of different species perceived categorically by human observers? Proc. R. Soc. Lond. B. Biol. Sci. 264, 1429–1434.
Cardozo, B. L. 1967. Ohm's law and masking. *IPO Annual Progress Report, Institute for Perception Research* 2, 59–64.
Cathcart, E. P. and Dawson, S. 1928/29. Persistence 2. Br. J. Psychol. 19, 343–356.
Charles-Luce, J. and Luce, P. A. 1990. Similarity neighbourhoods of words in young children's lexicons. J. Child Lang. 17, 205–215.
Charles-Luce, J. and Luce, P. A. 1995. An examination of similarity neighbourhoods in young children's receptive vocabularies. J. Child Lang. 22, 727–735.
Christman, R. J. 1954. Shifts in pitch as a function of prolonged stimulation with pure tones. Am. J. Psychol. 67, 484–491.
Cleveland, J. and Snowdon, C. T. 1982. The complex vocal repertoire of the adult cotton-top tamarin (*Saguinus oedipus oedipus*). Zeitschrift fur Tierpsychologie 58, 231–270.
Coady, J. A., Kluender, K. R., and Rhode, W. S. 2003. Effects of contrast between onsets of speech and other complex spectra. J. Acoust. Soc. Am. 114(4), 2225–2235.
Damper, R. I., Gunn, S. R., and Gore, M. O. 2000. Extracting phonetic knowledge from learning systems: perceptrons, support vector machines and linear discriminants. Appl. Intell. 12, 43–62.
Damper, R. I. and Harnad, S. R. 2000. Neural network models of categorical perception. Percept. Psychophys. 62, 843–867.
DeCasper, A. J. and Fifer, W. 1980. Of human bonding: newborns prefer their mothers' voices. Science 208, 1174–1176.
DeCasper, A. J. and Spence, M. J. 1986. Prenatal maternal speech influences newborns' perception of speech sounds. Infant Behav. Dev. 9, 133–150.
De Gelder, B., Teunisse, J. P., and Benson, P. J. 1997. Categorical perception of facial expressions: categories and their internal structure. Cogn. Emot. 11, 1–23.
Delgutte, B. 1980. Representation of speech-like sounds in the discharge patterns of auditory nerve fibers. J. Acoust. Soc. Am. 68, 843–857.
Delgutte, B. 1986. Analysis of French Stop Consonants with a Model of the Peripheral Auditory System. In: Invariance and Variability of Speech Processes (*eds*. J. S. Perkell and D. H. Klatt), pp. 131–177. Lawrence Earlbaum Associates.
Delgutte, B. 1996. Auditory Neural Processing of Speech. In: The Handbook of Phonetic Sciences (*eds*. W. J. Hardcastle and J. Laver), pp. 507–538. Blackwell.
Delgutte, B., Hammond, B. M., Kalluri, S., Litvak, L. M., and Cariani, P. A. 1996. Neural Encoding of Temporal Envelope and Temporal Interactions in Speech. In: Auditory Basis of Speech Perception (*eds*. W. Ainsworth and S. Greenberg), pp. 1–9. European Speech Communication Association.
Delgutte, B. and Kiang, N. Y. S. 1984. Speech coding in the auditory nerve IV: sounds with consonant-like dynamic characteristics. J. Acoust. Soc. Am. 75, 897–907.
Diehl, R. L. and Kluender, K. R. 1989. On the objects of speech perception. Ecol. Psychol. 1(2), 121–144.
Dillon, W. R. and Goldstein, M. 1984. Multivariate Analysis, Methods and Applications, John E Wiley and Sons.
Engen, T. 1982. The perception of odors, New York: Academic Press.
Escabi, M. A., Miller, L. M., Read, H. L., and Schreiner, C. E. 2003. Naturalistic auditory contrast improves spectrotemporal coding in the cat inferior colliculus. J. Neurosci. 23, 11489–11504.
Etcoff, N. L. and Magee, J. J. 1992. Categorical perception of facial expressions. Cognition 44, 227–240.
Festen, J. M. and Plomp, R. 1981. Relations between auditory functions in normal hearing. J. Acoust. Soc. Am. 70, 356–369.
Fiser, J. and Aslin, R. N. 2002. Statistical learning of new visual feature combinations by infants. Proc. Natl. Acad. Sci. 99, 15822–15826.
Flege, J. E. 1995. Second language speech learning: Theory, Findings and Problems. In: Speech Perception and Linguistic Experience: Issues in Cross-language Research (*eds*. W. Strange York and M. D. Timonium), pp. 233–272. York Press.
Flege, J. E., Bohn, O. S., and Jang, S. 1997. Effects of experience on non-native speakers' production and perception of English vowels. J. Phon. 25(4), 437–470.
Fletcher, H. 1953/1995. Speech and Hearing in Communication. Krieger.
Fowler, C. A. 1986. An event approach to the study of speech perception from a direct-realist perspective. J. Phon. 14, 3–28.
Fowler, C. A., Best, C. T., and McRoberts, G. W. 1990. Young infants' perception of liquid coarticulatory influences on following stop consonants. Percept. Psychophys. 48, 559–570.
Freedman, D. J., Riesenhuber, M., Poggio, T., and Miller, E. K. 2001. Categorical perception of visual stimuli in the primate prefrontal cortex. Science 291, 312–316.
Gardner, W. R. and Hake, H. W. 1951. The amount of information in absolute judgments. Psycho. Rev. 58, 446–459.
Gauthier, I., Tarr, M. J., Anderson, A. W., Skudlarski, P., and Gore, J. C. 1999. Activation of the middle fusiform 'face area' increases with expertise in recognizing novel objects. Nat. Neurosci. 2(6), 568–573.
Goldstone, R. L. 1994. Influences of categorization on perceptual discrimination. J. Exp. Psychol. General 123, 178–200.
Gordon, C., Webb, D. L., and Wolpert, S. 1992. One cannot hear the shape of a drum. Bull. Am. Math. Soc. 27, 134–138.
Green, D. M., McKey, M. J., and Licklider, J. C. R. 1959. Detection of a pulsed sinusoid in noise as a function of frequency. J. Acoust. Soc. Am., 31, 1146–1152.
Hauser, M. D., Newport, E. L., and Aslin, R. N. 2001. Segmentation of the speech stream in a non-human primate: statistical learning in cotton-top tamarins. Cognition 78, B53–B64.
Herrnstein, R. J. 1984. Objects, categories and discriminative stimuli. In: Animal Cognition, (*eds*. H. L. Roitblat, T. G. Bever, and H. S. Terrace), pp. 233–261. Erlbaum.

Hoagland, H. 1933. Quantitative aspects of cutaneous sensory adaptation I. J. Gen. Physiol. 16, 911–923.
Holt, L. L. 2005. Temporally non-adjacent non-linguistic sounds affect speech categorization. Psychol. Sci. 16, 305–312.
Holt, L. L., Lotto, A. J., and Kluender, K. R. 2000. Neighboring spectral content influences vowel identification. J. Acoust. Soc. Am. 108(2), 710–722.
Hood, J. D. 1950. Studies in auditory fatigue and adaptation. Acta Oto-Laryngol. Suppl. 92, 1–57.
Houtgast, T. 1972. Psychophysical evidence for lateral inhibition in hearing. J. Acoust. Soc. Am. 51, 1885–1894.
Houtgast, T. 1974. Auditory analysis of vowel-like sounds. Acustica 31, 320–324.
Hume, D. 1748/1963. An Enquiry Concerning Human Understanding. In: The Harvard Classics. P. F. Collier and Son Corporation (Original published in 1748 entitled My own life.) pp. 289–420.
Hyvärinen, A. and Oja, E. 2000. Independent component analysis: algorithms and applications. Neural Netw. 13, 411–430.
Imai, S., Flege, J., and Wayland, R. 2002. Perception of cross-language vowel differences: a longitudinal study of native Spanish learners of English. Acoustical Society of America Journal 111(5), 2364–2364.
Jakobson, R. and Halle, M. 1971. The Fundamentals of Language. Mouton.
Jamieson, D. G. and Morosan, D. E. 1986. Training non-native speech contrasts in adults: acquisition of English /q/-/d/ contrast by francophones. Percept. Psychophys. 40, 205–215.
Jusczyk, P. W. 1981. Infant Speech Perception: A Critical Appraisal. In: Perspectives on the Study of Speech (*eds*. P. D. Eimas and J. LMiller), pp. 113–64. Erlbaum.
Jusczyk, P. W. 1986. Towards a Model for the Development of Speech Perception. In: Invariance and Variability in Speech Processes (*eds*. J. Perkell and D. H. Klatt), pp. 1–19. Erlbaum.
Kiefte, M. and Kluender, K. R. 2005. The relative importance of spectral tilt in monophthongs and diphthongs. J. Acoust. Soc. Am. 117(3), 1395–1404.
Kiefte, M. and Kluender, K. R. (in press). Absorption of reliable spectral characteristics in auditory perception. J. Acoust. Soc. Am.
Kingston, J. and Diehl, R. L. 1994. Phonetic knowledge. Language 70, 419–454.
Kirk, E. C. and Smith, D. W. 2003. Protection from acoustic trauma is not a primary function of the medial olivocochlear efferent system. J. Assoc. Res. Otolaryngol. 4, 445–465.
Kirkham, N. Z., Slemmer, J. A., and Johnson, S. P. 2002. Visual statistical learning in infancy: evidence for a domain general learning mechanism. Cognition 83, B35–B42.
Klatt, D. H. 1980. Software for a cascade/parallel formant synthesizer. J. Acoust. Soc. Am. 67(3), 971–995.
Klatt, D. H. 1980. Speech Perception: A Model of Acoustic-Phonetic Analysis and lexical access. Perceptionand Production of Fluent Speech (*ed*. R. A. Cole), pp. 243–288. Lawrence Erlbaum Associates.
Klatt, D. H. 1982. Prediction of perceived phonetic distance from critical band spectra: a first step. Proc. ICASSP 1278–81.
Kluender, K. R. 1988. Auditory constraints on phonetic categorization: Trading relations in humans and nonhumans. Unpublished Ph.D. dissertation, University of Texas at Austin.
Kluender, K. R. 1994. Speech Perception as a Tractable Problem in Cognitive Science. In: Handbook of Psycholinguistics (*ed*. M. A. Gernsbacher), pp. 173–217. Academic.
Kluender, K. R., Diehl, R. L., and Killeen, P. R. 1987. Japanese quail can learn phonetic categories. Science 237, 1195–1197.
Kluender, K. R. and Lotto, A. J. 1999. Virtues and perils of empiricist approaches to speech perception. J. Acoust. Soc. Am. 105, 503–511.
Kluender, K. R., Lotto, A. J., and Holt, L. L. 2005. Contributions of Nonhuman Animal Models to Understanding Human Speech Perception. In: Listening to Speech: An Auditory Perspective. (*eds*. S. Greenberg and W. Ainsworth), pp. 203–220. Oxford University Press.
Kluender, K. R., Lotto, A. J., Holt, L. L., and Bloedel, S. L. 1998. Role of experience for language-specific functional mappings of vowel sounds. J. Acoust. Soc. Am. 104, 3568–3582.
Kuhl, P. K. 1978. Perceptual constancy for speech-sound categories. N.I.C.H.D. *Conference on Child Phonology: Perception, Production, and Deviation*. Bethesda, Maryland.
Kuhl, P. K. 1979. Speech perception in early infancy: perceptual constancy for spectrally dissimilar vowel categories. J. Acoust. Soc. Am. 66, 1668–1679.
Kuhl, P. K. 1980. Perceptual Constancy for Speech-Sound Categories in Early Infancy. In: Child Phonology Vol. 2: Perception (*eds*. G. H. Yeni-Komshian, J. F. Kavanagh, and C. A. Ferguson), 41–66. Academic Press.
Kuhl, P. K. 1983. Perception of auditory equivalence classes for speech in early infancy. Infant Behav. Dev. 6, 263–285.
Kuhl, P. K. 1987. Perception of Speech and Sound In Early Infancy. In: Handbook of Infant Perception Vol. 2 (*eds*. P. Salapatek and L. Cohen), pp. 257–381. Academic Press.
Kuhl, P. K., Williams, K. A., Lacerda, F., Stevens, K. N., and Lindblom, B. 1992. Linguistic experience alters phonetic perception in infants six-months of age. Science 255, 606–608.
Lecanuet, J. P., Granier-Deferre, C., Cohen, H., LeHouezec, R., and Busnel, M. C. 1986. Fetal responses to acoustic stimulation depend on heart rate variability pattern, stimulus intensity and repetition. Early Hum. Dev. 13, 269–283.
Lewis, J. W., Wightman, F., Brefczynski, J. A., Phinney, R. E., Binder, J. R., and DeYoe, E. A. 2004. Human brain regions involved in recognizing environmental sounds. Cereb. Cortex 14, 1008–21.
Lieberman, P. 1984. The Biology and Evolution of Language, Harvard University Press.
Liberman, A. M. and Mattingly, I. G. 1985. The motor theory of speech perception revisited. Cognition 21, 1–36.
Liebenthal, E., Binder, J. R., Spitzer, S. M., Possing, E. T., and Medler, D. A. 2005. Neural substrates of phonemic perception. Cereb. Cortex 15(10), 162–163.
Liljencrantz, J. and Lindblom, B. 1972. Numerical stimulation of vowel quality systems: the role of perceptual contrast. Language 48, 839–862.
Lindblom, B. E. F. 1963. Spectrographic study of vowel reduction. J. Acoust. Soc. Am. 35, 1773–1781.
Lindblom, B. and Maddieson, I 1988. Phonetic Universals in Consonant Systems. In: Language, Speech and Mind: Studies in Honour of Victoria A. Fromkin (*eds*. L. M. Hyman and C. N. Li), pp. 62–78. Routledge.
Lindblom, B. E. F. and Studdert-Kennedy, M. 1967. On the role of formant transitions in vowel recognition. J. Acoust. Soc. Am. 42, 830–843.
Lippman, R. P. 1996. Speech Perception by Humans and Machines. In: Workshop on the Auditory Basis of Speech Perception (*eds*. W. Ainsworth and S. Greenberg) pp. 309–316. Keele University.
Lisker L. 1978. Rapid versus rabid: a catalogue of acoustical features that may cue the distinction *Haskins Laboratories Status Report on Speech Research SR*-54, 127–132.
Lively, S. E. 1993. An examination of the perceptual magnet effect. J. Acoust. Soc. Am. 93, 2423.
Locke, S. and Kellar, L. 1973. Categorical perception in a non-linguistic mode. Cortex 9, 355–369.

Lotto, A. J. 2000. Reply to ''An analytical error invalidates the 'depolarization' of the perceptual magnet effect.''. J. Acoust. Soc. Am. 107, 3578–3580.
Lotto, A. J. and Kluender, K. R. 1998. General contrast effects in speech perception: effect of preceding liquid on stop consonant identification. Percept. Psychophys. 60, 602–619.
Lotto, A. J., Kluender, K. R., and Holt, L. L. 1997. Perceptual compensation for coarticulation by Japanese quail (*Coturnix coturnix japonica*). J. Accost. Soc. Am. 102, 1134–1140.
Luce, R. D. 1986. Response Times, Oxford University Press.
Maddieson, I. 1984. Patterns of Sound. Cambridge University Press.
Mann, V. A. 1980. Influence of preceding liquid in stop-consonant perception. Percept. Psychophys. 28, 407–412.
Mann, V. A. 1986. Distinguishing universal and language-dependent levels of speech perception: evidence from Japanese listeners' perception of English ''l'' and ''r''. Cognition 24, 169–196.
Mann, V. A. and Repp, B. H. 1981. Influence of preceding fricative on stop consonant perception. J. Accost. Soc. Am. 69, 548–558.
McGurk, H. and MacDonald, J. 1976. Hearing lips and seeing voices. Nature 264(5588), 746–748.
Mehler, J., Jusczyk, P., Lambertz, G., Halsted, N., Bertoncini, J., and Amiel-Tison, C. 1988. A precursor of language acquisition in young infants. Cognition 29, 143–178.
Miller, G. A. 1956. The magical number seven, plus or minus two: some limits on our capacity for processing information. Psychol. Rev. 63, 81–97.
Miyawaki, K., Strange, W., Verbrugge, R. R., Liberman, A. M., Jenkins, J. J., and Fujimura, O. 1975. An effect of linguistic experience: the discrimination of (r) and (l) by native speakers of Japanese and English. Percept. Psychophys. 18, 331–340.
Moore, B. C. J. and Glasberg, B. R. 1983. Suggested formulas for calculating auditory-filter bandwidths and excitation patterns. J. Accost. Soc. Am. 74, 750–753.
Nearey, T. M. 1997. Speech perception as pattern recognition. J. Accost. Soc. Am. 101, 3241–3254.
Olshausen, B. A. and Field, D. J. 1997. Sparse coding with an overcomplete basis set: a strategy employed by V1? Vision Res. 37, 3311–3325.
Olsho, L. W., Koch, E. G., Carter, E. A., Halpin, C. F., and Spetner, N. B. 1988. Pure-tone sensitivity of human infants. J. Acoust. Soc. Am. 84, 1316–1324.
Olsho, L. W., Koch, E. G., and Halpin, C. F. 1987. Level and age effects in infantfrequency discrimination. J. Accost. Soc. Am. 82, 454–464.
Pérez-González, D., Malmierca, M. S., and Covey, E. 2005. Novelty detector neurons in the mammalian auditory midbrain. Eur. J. Neurosci. 22, 2879–2885.
Polka, L. 1991. Cross-language speech perception in adults: phonemic, phonetic, and acoustic contributions. J. Accost. Soc. Am. 89(6), 2961–2977.
Polka, L. 1992. Characterizing the influence of native language experience on adult speech perception. Percept. Psychophys. 52(1), 37–52.
Port, R. F. (in press). The Graphical Basis of Phones and Phonemes. In: Second-Language Speech Learning: The Role Of Language Experience In: Speech Perception And Production (eds. M. Munro and O-S Bohn).
Remez, R. E., Rubin, P. E., Pisoni, D. B., and Carrell, T. D. 1981. Speech perception without traditional speech cues. Science 212, 947–950.
Repp, B. H. 1982. Phonetic trading relations and context effects: new evidence for a speech mode of perception. Psychol. Bull. 92, 81–110.
Riggs, L. A., Ratliff, F., Cornsweet, J. C., and Cornsweet, T. N. 1953. The disappearance of steadily fixated visual test objects. J. Opt. Soc. Am. 43(6), 495–501.
Rogers, T. T., Lambon Ralph, M. A., Garrard, P., Bozeat, S., McClelland, J. L., Hodges, J. R., and Patterson, K. 2004. The structure and deterioration of semantic memory: a neuropsychological and computational investigation. Psychol. Rev. 111, 205–235.
Rosenblat, F. 1958. The perceptron: a probabilistic model for information storage and organization in the brain. Psychol. Rev. 65, 386–408.
Saffran, J. R., Aslin, R. N., and Newport, E. L. 1996. Statistical learning by 8-month-old infants. Science 274, 1926–1928.
Saffran, J. R., Johnson, E. K., Aslin, R. N., and Newport, E. L. 1999. Statistical learning of tone sequences by human infants and adults. Cognition 70, 27–52.
Sato, M, Lotto, A. J., and Diehl, R. L. 2003. Patterns of acoustic variance in native and non-native phonemes. The J. Accost. Soc. Am. 114(4), 2392.
Schouten, J. F. 1940. The residue, a new component in subjective analysis. Proc. Kon. Akad. Wetensch 43, 356–365.
Schwartz, O. and Simoncelli, E. P. 2001. Natural signal statistics and sensory gain control. Nature: Neuroscience 4, 819–825.
Scott, S. K., Blank, C. C., Rosen, S., and Wise, R. J. S. 2000. Identification of a pathway for intelligible speech in the left temporal lobe. Brain 123, 2400–2406.
Shannon, C. E. 1948. A mathematical theory of communication. BSTJ 27, 379–423.
Shannon, R. V., Zeng, F. G., Wygonski, J., Kamath, V., and Ekelid, M. 1995. Speech recognition with primarily temporal cues. Science 270, 303–304.
Simoncelli, E. P. and Olshausen, B. A. 2001. Natural image statistics and neural representation. Ann. Rev. Neurosci. 24, 1193–1215.
Smith, R. L. 1979. Adaptation, saturations, and physiological masking in single auditory-nerve fibers. J. Accost. Soc. Am. 65, 166–178.
Smith, R. L., Brachman, M. L., and Frisina, R. D. 1985. Sensitivity of auditory-nerve fibers to changes in intensity: a dichotomy between decrements and increments. J. Accost. Soc. Am. 78, 1310–1316.
Smith, J. D., Kemler Nelson, D. G., Grohskopf, L. A., and Appleton, T. 1994. What child is this? What interval was that? Familiar tunes and music perception in novice listeners. Cognition 52, 23–54.
Smith, R. L. and Zwislocki, J. J. 1971. Responses of some neurons of the cochlear nucleus to tone-intensity increments. J. Accost. Soc. Am. 50, 1520–1525.
Stevens, K. N. and Blumstein, S. E. 1981. The Search for Invariant Acoustic Correlates of Phonetic Features. In: Perspectives in the Study of Speech (*eds*. P. D. Eimas and J. L. Miller), pp. 1–38. Erlbaum.
Stilp, C. and Kluender, K. R. 2006. Perceptual absorption of listening context when perceiving musical instruments. J. Accost. Soc. Am. 119, 3241.
Summerfield, Q., Haggard, M. P., Foster, J., and Gray, S. 1984. Perceiving vowels from uniform spectra: phonetic exploration of an auditory aftereffect. Percept. and Psychophys. 35, 203–213.
Summerfield, Q., Sidwell, A., and Nelson, T. 1987. Auditory enhancement of changes in spectral amplitude. J. Acoust. Soc. Amer. 81, 700–707.
Trubetzkoy, N. S. 1969. Principles of Phonology (C. Baltaxe, Trans.). University of California Press. (Original work published in 1939).
Tuller, B., Case, P., Ding, M., and Kelso, J. A. S. 1994. The nonlinear dynamics of speech categorization. J. Exp. Psychol. Hum. Percept. Perform. 20(1), 3–16.
Ulanovsky, N., Las, L., and Nelken, I. 2003. Processing of low-probability sounds by cortical neurons. Nat. Neurosci. 6, 391–398.

Urbantschitsch, V. 1876, cf. Abrahams, H., Krakauer, D., and Dallenbach, K. M. (1937). Gustatory adaptation to salt. Am. J. Psychol. 49, 462–469.
Viemeister, N. F. 1980. Adaptation of Masking. In: Psychophysical, Physiological, and Behavioral Studies in Hearing (*eds*. G. van den Brink and F. A. Bilsen), pp. 190–197. Delft: University Press.
Viemeister, N. F. and Bacon, S. P. 1982. Forward masking by enhanced components in harmonic complexes. J. Accost. Soc. Am. 71, 1502–1507.
Voss, R. F. and Clarke, J. 1975. '1/*f* noise' in music and speech. Nature 258, 317–318.
Voss, R. F. and Clarke, J. 1978. ''1/*f* noise'' in music: Music from 1/*f* noise. J. Accost. Soc. Am. 63, 258–263.
Walley, A. C. 1993. The role of vocabulary development in children's spoken word recognition and segmentation ability. Dev. Rev. 13, 286–350.
Walley, A. C., Metsala, J. L., and Garlock, V. M. 2003. Spoken vocabulary growth: its role in the development of phoneme awareness and early reading ability. Read. and Writ. 16, 5–20.
Weiner, N. 1948. Cybernetics. Wiley.
Werker, J. F. and Curtin, S. 2005. PRIMIR: a developmental framework of infant speech processing. Lang. Learn. Dev. 1(2), 197–234.
Werker, J. F., Gilbert, J. H. V., Humphrey, K., and Tees, R. C. 1981. Developmental aspects of cross-language speech perception. Child Dev. 52, 349–355.
Werker, J. F. and Lalonde, C. E. 1988. Cross-language speech perception: initial capabilities and developmental change. Dev. Psychol. 24, 672–683.
Werker, J. F. and Logan, J. S. 1985. Cross-language evidence for three factors in speech perception. Percept. and Psychophys. 37, 35–44.
Werker, J. F. and Tees, R. C. 1983. Developmental changes across childhood in the perception of non-native speech sounds. Can. J. Psychol. 37, 278–286.
Werker, J. F. and Tees, R. C. 1984a. Cross-language speech perception: evidence for perceptual reorganization during the first year of life. Infant Behav. Dev. 7, 49–63.
Werker, J. F. and Tees, R. C. 1984b. Phonemic and phonetic factors in adult cross-language speech perception. J. Accost. Soc. Am. 75, 1866–1878.
Werner, L. and Gillenwater, J. 1990. Pure-tone sensitivity of 2-to 5-week-old infants. Infant Behav. Dev. 13, 355–375.
Wightman, F. L., McGee, T., and Kramer, M. 1977. Factors Influencing Frequency Selectivity in Normal and Hearing-Impaired Listeners. In: Psychophysics and Physiology of Hearing (*eds*. E. F. Evans and J. P. Wilson), pp. 295–310. Academic Press.
Wood, C. C. 1976. Discriminability, response bias, and phoneme categories in discrimination of voice onset time. J. Accost. Soc. Am. 60, 1381–1389.
Young, A. W., Rowland, D., Calder, A. J., Etcoff, N. L, Seth, A., and Perrett, D. I. 1997. Facial expression megamix: tests of dimensional and category accounts of emotional recognition. Cognition 63, 271–313.
Zatorre, R. J. and Binder, J. 2000. Functional and Structural Imaging of the Human Auditory System, In: Brain Mapping the Systems. (*eds*. A. Toga and J. Mazziotta), pp. 365–402. Academic Press.
Zwaardemaker, H. 1895. Die physiologie des geruchs, Engelmann.

3.49 Auditory Scene Analysis

A S Bregman, McGill University, Montreal, QC, Canada

© 2008 Elsevier Inc. All rights reserved.

3.49.1	**The Problem of Mixtures**	862
3.49.1.1	How the ASA Problem Can Be Solved	863
3.49.1.1.1	The auditory stream	863
3.49.1.1.2	Regularities in acoustic mixtures	864
3.49.1.2	Grouping of Acoustic Energy Based on Acoustic Regularities	864
3.49.1.2.1	Cooperation and competition in ASA	865
3.49.1.2.2	Validity of principles in the natural world	866
3.49.2	**Sequential and Simultaneous Aspects of ASA**	866
3.49.2.1	Sequential Organization	866
3.49.2.1.1	Main findings	866
3.49.2.2	Simultaneous Organization	867
3.49.2.2.1	The ABC paradigm	867
3.49.2.2.2	Other findings	867
3.49.3	**Brain Recording and the Role of Attention in ASA**	868
3.49.4	**Animal Studies and Innate Processes of ASA**	869
3.49.5	**Summary**	869
References		870

Glossary

auditory scene analysis (ASA) Auditory scene analysis is the name for both a problem and a perceptual process. The problem is how to form mental representations of individual sounds from the summed waveform that reaches the ear of the listener. It is also the name of the brain process that accomplishes this result (with a greater or lesser degree of accuracy).

auditory stream A perceptual interpretation, produced by auditory scene analysis, of a mixed auditory input. Parts of the input are heard as separate coherent patterns evolving over time (auditory streams), and interpreted as individual acoustic sources present in the auditory environment (such as a voice, a violin, or a machine). More than one stream can be present at the same time. A stream (in ordinary conversation, we call it a sound or a sequence of sounds) is a perceptual entity, analogous to a visual object, capable of binding a cluster of properties (e.g., one sound is high in pitch, loud, and on the left, whereas the other sound is low in pitch, soft and intermittent, and straight ahead).

event-related potential (ERP) The electrical activity of the brain is measured on the scalp while external events (such as sounds) are presented to the subject. A large number of samples of the electrical recording that correspond temporally with some particular class of external event (such as an acoustic signal of a certain type) are extracted from the record of the brain activity and then aligned temporally using the start of the external event as a zero point, and averaged together. This averaging is thought to eliminate all other influences on the electrical wave except the occurrence of the event. This average wave is the ERP.

mismatch negativity (MMN) The MMN is a negative deflection in the human event-related potential recorded from frontal scalp electrodes, and is thought to originate in auditory cortex. It occurs when a change in a regularly repeating stimulus is detected by the brain, first a series of identical presentations of an auditory stimulus is presented. The repeating stimulus can be as simple as a single sound or as complex as a short pattern of sounds. Then, without a break, a change is introduced in the stimulus. The introduced change can be as simple as a single feature of the stimulus or as complex as an abstract relation between the stimuli of the repeating pattern. MMN is thought to represent the activity of an automatic process for

detecting change, since it occurs whether or not attention is directed toward the repeating stimuli.
objectrelated negativity (ORN) ORN is a component of ERPs that has a negative peak at around 150 ms relative to the onset of an acoustic signal. It occurs when the incoming spectrum is interpreted as two sounds rather than one, and is not sensitive to the involvement of attention.
stream segregation The formation of more than one auditory stream from a mixed input.
streaming A phenomenon in which a rapid sequence of tones or other acoustic units is interpreted as the co-occurrence of two or more auditory streams. The perceptual decomposition of the sequence of sounds into its component streams takes time to evolve.

3.49.1 The Problem of Mixtures

Most studies on perception, either by humans or other animals, have been done in very simplified setups, especially in the area of auditory perception. In a typical experiment in this area, listeners have been presented with an auditory signal in a background of silence, or perhaps noise, and required to judge (or, in the case of animals, to respond to) something about it: whether the signal is present, or whether it is different from a second signal in some quality such as loudness, pitch, or timbre. In the most complex case, speech signals, they may be asked to recognize the speech. This approach has given us what might be called the psychophysics of the isolated stimulus.

However, the acoustic signals we encounter in the natural world do not occur in isolation. The waves emanating from different events co-occur and overlap in time. A recording of a busy household might register a conversation, a child playing a game in an adjacent room, the clamor from a television set, and the mumble of an air conditioner, all overlapped in time. In the world of nonhuman animals in their natural environments, most of the signals are quieter than in a human household. However, these low-level signals are many: the wind, the flutter of birds' wings, insects buzzing, the chatter of small mammals, and the footsteps of larger ones. The symphony of the field is as complicated as that of the household, but with the volume turned down. In both cases, in order for listeners to recognize the signals individually, they must be able to undo the acoustic mixture. The brain process that accomplishes this has been labeled auditory scene analysis (ASA) (Bregman, A. S., 1984; 1990/1994). The critical importance of ASA can be understood by considering what would happen if the process made an error. Syllables from two different voices might be joined to make a single word. A cough in the audience might be heard as part of a piece of music. For a small animal, the noises made by the approach of a predator might simply contribute its qualities to the sound of a waterfall.

For clarity, in this discussion, we will use different terms to refer to the physical acoustic signals from those used for the mental structures and qualities to which they give rise. In the physical category, we will refer to acoustic sources and acoustic signals, or just signals, and, in the context of an experiment, stimuli. These will have properties or features, such as fundamental frequency, amplitude, spectral shape, etc. By an acoustic source, we mean any physical object or process that generates an acoustic signal by creating audible vibrations. By properties, or features, we mean physical properties (to be contrasted with perceptual qualities). Examples of acoustic sources include a person speaking, a violin playing, the wind howling, and a bird singing.

In the mental category, we will refer to sounds (not signals). These will have qualities (not properties), such as pitch, loudness, timbre, etc. So in our terminology, a signal has no pitch until the brain makes one or more sounds out of it, and assigns pitches to some of them. Timbre is a quality of a sound, not a property of a spectrum. Are these distinctions simply the product of an academic obsession with definitions? They seem to be so when we consider only the psychophysics of the isolated stimulus. However, they become essential when considering mixtures, where the qualities that emerge from the analysis depend on the particular parsing that the auditory system gives to the incoming spectrum, rather than on the way that experimenters describe the features of the physical signals that they have created. The perceived qualities of timbre, pitch, loudness, rhythm, etc., emerge from the way ASA allocates energy to individual auditory streams. A spectrum, in itself, does not

have a timbre, only a spectral composition; it may, for example, furnish the energy for two concurrent sounds, each of which has its own timbre.

Because the extracting of separate sounds usually goes on quite automatically in our own auditory systems, it is hard for us to realize how profound an accomplishment it really is. But consider the problem in physical terms. The time-varying acoustic pressure wave that reaches each of our ears is the arithmetic sum of the pressure waves emanating from the individual events that produced them. The individual events overlap in time, starting and stopping asynchronously, shaping the summed pressure wave. Yet what is needed for an appropriate response to the events around us is not a perceptual description of this happenstance mixture, but separate descriptions of the individual acoustic sources. Unfortunately, examining a short stretch of the waveform, or even its spectrum cannot tell us how the mixture was formed, since there are an enormous number of ways of decomposing it. The problem can only be solved by examining a longer window of time, analyzing the changes that occur over time, making use of some *a priori* constraints on the plausibility of particular decompositions.

3.49.1.1 How the ASA Problem Can Be Solved

We can see some of these constraints by looking at the spectrogram shown in Figure 1, of a mixture of the words, 'one, two, three', the sung syllables, 'da-da-da', a man whistling, and a computer fan. The spectrogram of the mixture is roughly what you would see if you made a spectrogram of each of these acoustic sources on separate pieces of clear plastic and superimposed them. In the audio recording from which this spectrogram was made, the individual signals are not hard for the ear to pick out.

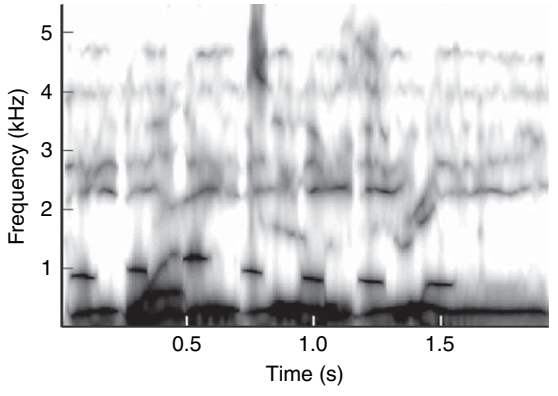

Figure 1 A spectrogram of a mixture, including the spoken words, 'one, two, three', a person singing 'da-da-da', a person whistling, and a computer fan. Adapted from Bregman, A. S. and Woszczyk, W. 2004. Controlling the Perceptual Organization of Sound: Guidelines Derived From Principles of ASA. In: Audio Anecdotes: Tools, Tips and Techniques for Digital Audio (*eds.* K. Greenebaum and R. Barzel), Vol.1, pp. 35–64. A K Peters.

The problem of using the summed spectrum to derive perceptions of the component sounds can be viewed as a problem in perceptual organization. Various parts of the energy present in this spectrum have to be allocated to form one percept and segregated from other groupings of energy that will be used to create other percepts. The difficulty is that the energy from the individual sound sources overlaps in frequency and time, and an individual frequency component may result from the summing of components from two sources. In Figure 1, we can see two dimensions of the problem, represented by the horizontal and vertical dimensions of the spectrogram.

In the horizontal dimension, listeners must group together the energy that came from the same acoustic source over time, a process called sequential organization (Bregman, A. S., 1990/1994, chapter 2). The organization across time does two things: (1) it forms each individual 'da' syllable from the moments of energy that compose it, giving it a beginning, a duration, and an end, thus making it into a temporal unit, and (2) it groups the individual 'da' syllables into a 'da-da-da' melody.

In the vertical dimension, the ASA process must allocate all the energy present at the same time to one or more concurrent sounds, each of which has emanated from a distinct acoustic source. This is called spectral organization or simultaneous organization (Bregman, A. S., 1990/1994, chapter 3).

3.49.1.1.1 The auditory stream

The mental representation of a distinct acoustic source, created by ASA, is called an auditory stream. Any acoustic input may yield a number of concurrent streams. Examples of streams include the mental representations of: (1) an individual voice, (2) a sequence of footsteps, (3) an approaching car, and so on. A stream in audition, like an object in vision, is a mental entity that is intended to correspond to an individual entity in the world, although its activities may unfold over time. Its role in perception is to act as a structure to which perceptual qualities can be bound. We say that a certain sound (the name we typically give to a stream) is loud, or nearby, or high in pitch, or voice-like, etc. There can be a number of

concurrent sounds (streams), each with its own qualities.

3.49.1.1.2 Regularities in acoustic mixtures

ASA takes advantage of regularities that cut across environments regardless of the provenance or meaning of the signal. For example, the various frequency components arising from an individual acoustic source (such as a voice or instrument) tend to start and stop at the same time. While not true without exception, this statistical regularity holds in deserts, jungles, households, in music, speech, and on Mars. The use of such general regularities by the auditory system is always useful. It is plausible that over evolutionary time, the auditory system has incorporated processes into its hard wiring that detect the general cues that signal the presence of an independent acoustic source within a mixture. These can be called primitive or built-in processes of ASA. One would expect them to be found even in young infants and in nonhuman animals.

However, the human listener is also capable of learning many regularities that apply in narrower environments. These probably include the phonetic components of one's own language and the articulations that give rise to them, the vocabulary of one's language, musical keys and scales, the sound qualities of various machines, the voice of one's own child, and so on. Humans operate in so many different environments that we possess a robust system for learning acoustic patterns, which can provide help in decomposing mixtures.

On the other hand, some nonhuman species, such as bats, operating in very specialized sonic environments and having a vital need to respond quickly to special types of acoustic signals, undoubtedly possess innate mechanisms in their perceptual systems that detect these signals even in mixtures, using the specific structure of these signals, rather than just the general regularities found in most acoustic mixtures.

3.49.1.2 Grouping of Acoustic Energy Based on Acoustic Regularities

Let us consider how the auditory system uses the general regularities to achieve sequential grouping. Going back to Figure 1, if we observe a sequence formed of spectral patterns that resemble one another, it is reasonable to assume that they may emanate from the same source. This assumption is based on the statistical regularity that most sounds change slowly if the proper timescale is chosen. The strategy derived from this regularity is: 'if patterns of spectral energy, not too far apart in time, resemble one another, they should be assigned to the same auditory stream'. This resemblance can be in terms of fundamental frequency, spectral center of gravity, spectral shape, intensity, temporal dynamics, spatial position, and perhaps other acoustic features.

Spectral or simultaneous organization also makes use of general regularities. Again we can use Figure 1 to understand them. We can see many examples in the spectrogram where energy at different frequencies starts and stops at the same time. This reflects the general fact that the components of a single sonic event tend to start and stop together. Accordingly, one of the principles used by ASA to organize simultaneous components is: 'if energy in different frequency regions or in different parts of space change in amplitude in the same direction at the same time, assign these to the same auditory stream'.

The justification for these principles and others like them derives from statistical regularities in our acoustic world. It is probable that successive wave patterns arising from the same source will resemble one another, though their properties may change slowly over time. This is not true without exception, but it is generally true, especially if you consider sufficiently short periods of time. This regularity justifies the principle of grouping a pair of signals A and B, which are close together in time and similar in properties into the same auditory stream and rejecting another dissimilar signal, C, that may occur between A and B into a different stream.

Here is another example. Many natural vibrations, including the human voice, animal calls, and insects flying, are harmonic. That is, they are formed of a fundamental frequency and many harmonics of that fundamental. The ASA system can use this as a constraint which favors the grouping of simultaneous components as parts of the same perceived sound if they appear to be harmonics of the same fundamental. Again, a regularity in the world becomes a constraint on the process of decomposing the acoustic input.

A final example has been called the old-plus-new heuristic (Bregman, A. S., 1990/1994, pp. 14, 222–227). It derives from the fact that unrelated signals rarely stop and start at the same time. Instead they overlap in time. As a signal starts, its spectrum is added to the ongoing spectrum resulting from already-present signals; so the spectrum becomes more complex and has a greater intensity.

This fact justifies the following rule in decomposing spectra: 'if a spectrum quickly changes so that it becomes more intense and more complex, do an analysis to determine whether the spectral components that were there just prior to the change are still present after the change. If they are, treat them as a continuation of the prechange spectrum and subtract them from the mixture. Treat whatever is left over as a new sound that has entered the mixture and ascertain its properties'. The moment of entry of the new sound into the mixture is an unparalleled opportunity to discover its properties since we can compare the spectrum just before and just after its entry.

3.49.1.2.1 Cooperation and competition in ASA

Despite the fact that these strategies capture important regularities in the world, and can serve as constraints in decomposing the mixture, each of them can be unreliable. For example: (1) occasionally the properties of the signal coming from a single acoustic source can change rapidly instead of slowly – think of yodeling; (2) the separate spatial origins of parts of the acoustic mixture can be unavailable if the signals are coming around a corner; or if we are listening to a monophonic broadcast or recording; and (3) the synchrony or asynchrony of onset of energy in different parts of the spectrum may be blurred in a highly reverberant environment. However, this unreliability can be dealt with by not depending too much on any individual regularity, but allowing them to collaborate and compete in determining the organization that emerges. If a process analogous to a voting system is used, so that the perceptual grouping is controlled by the greatest number of votes supplied by different strategies, the reliability of the system as a whole can be improved.

It is not just that different regularities (such as spatial proximity and fundamental frequency) compete with one another to control the parsing. Even the use of individual regularities such as separation in a frequency–time space may involve competition. Consider Figure 2. Tone B follows tone A at a certain distance in frequency and time. The question is whether A and B, as two tones in a four-tone repeating cycle, will be placed in the same stream or in different ones by ASA processes (Bregman, A. S., 1978). The answer depends on the properties of the other tones that are present. In the left panel, A and B are far from tones X and Y in frequency; so ASA isolates A and B in their own stream and X and Y in a second. The dashed lines show the resulting

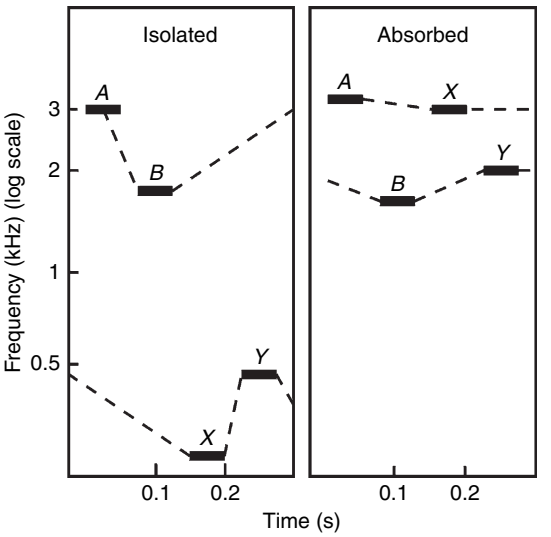

Figure 2 The stream membership of tones A and B, separated by a fixed frequency and time, depends on the context of other tones. The dashed lines show the streams that are formed. In the left panel, A and B are isolated in frequency from X and Y; so each set forms its own stream. In the right panel, X absorbs A into one stream and Y absorbs B into a second. Adapted from figure 2.27 in Bregman, A. S. 1990/1994. Auditory Scene Analysis: The Perceptual Organization of Sound. MIT Press (paperback 1994), with permission of MIT Press.

streams. The listener hears a repeating sequence AB – – AB– – ···, where the dashes represent the durations of X and Y, which appear as silences in the AB stream since they have been allocated to a stream of their own. In a lower frequency range, the listener hears – – XY – – XY···. The right panel shows how A and B can be absorbed into separate streams. Here X and Y are in the same frequency region as A and B, with X close to A, and Y close to B. Under these conditions, A and X form one stream, with the rhythm A – X – A – X ···, and B and Y form a second, with the rhythm – B – Y – B – Y···. The separation between A and B in frequency and in time are the same in the two panels. If there were a fixed separation that determined whether two sounds were assigned to the same stream, the grouping of A with B should be the same in both conditions. We can see, instead, that the frequency proximities compete, with the ASA system finding the tightest clusters that it can in the frequency–time space. Our ability to draw a picture that predicts the auditory grouping from the visual grouping encourages us to think that there are strong similarities between the grouping processes in vision and audition (Handel, S., 2006), many of which

seem to follow the principles set forth by the Gestalt psychologists (Koffka, K., 1935).

3.49.1.2.2 Validity of principles in the natural world

Simplified laboratory paradigms have been set up to study ASA. On the whole, involve the setting up of simplified stimulus patterns that can be perceived in two different ways depending on the perceptual organization, and then varying the features of parts of the stimulus pattern to see the effects on the perceived sounds. However, since the goal is to come to conclusions that are valid in the natural world, the relevance of the laboratory simplification has to be established by verifying whether the principles discovered in the laboratory are also found in the real world. To some extent this has been done by determining whether the discovered principles can be applied to music (Huron, D., 2001), to speech (Darwin, C. J., 1997, 2001), and to auditory displays (Shilling, R. and Shinn-Cunningham, B., 2002; see also Bregman, A. S., 1990/1994, chapters 5 and 6).

3.49.2 Sequential and Simultaneous Aspects of ASA

3.49.2.1 Sequential Organization

One paradigm for the experimental simplification of sequential organization is the phenomenon of stream segregation, sometimes called streaming (Bregman, A. S., 1990/1994, chapter 1) or fission (Van Noorden, L. P. A. S., 1975). Two tones of different frequencies (A and B) are played in a repeating cycle, either in the pattern ABABAB. . . , or the pattern ABA – ABA– · · · , where the gap between successive triplets is the same duration as the B tone. The latter is sometimes referred to as a galloping pattern because of its distinctive triplet rhythm. If the sequence is played rapidly, say 100 ms per tone, and if the frequencies of A and B are well separated, the sequence seems to split into two perceptual streams, a high one and a low one, each with its own timing pattern. In the case of the simple alternating ABAB. . . sequence, one hears an A stream, A – A – · · · , and a B stream, – B – B · · · , each with a rhythm at half the rate of the original integrated sequence. (Bregman, A.S., and Ahad, P. A., 1996; Van Noorden, L. P. A. S., 1975). In the case of the ABA – ABA– · · · pattern, the galloping rhythm disappears from perception and is replaced by two streams, one with the rhythm – A – A – · · · , and a slower one with the rhythm – – B – – B – – · · · In each case, the dashes represent the tone or tones lost to the other stream.

3.49.2.1.1 Main findings

The probability of segregation into two streams increases both with the time interval between the offset of one tone and the onset of the next tone of the same frequency, for example, the A-A interstimulus interval (Bregman, A. S. *et al.*, 2000) and with the frequency separation between the A's and the B's. One would think that these two facts would allow us to create a simple law relating seperation in frequency and time to stream segregation. However, segregation as a function of frequency and time is not the same for different patterns. For example, it is different for the two patterns described above, and may be different for different listeners (Van Noorden, L. P. A. S., 1975). However, the qualitative findings show that when acoustically different sounds occur in a rapid sequence, if some of the sounds are similar or identical, these will form their own stream.

The acoustic difference in the preceding example was in the frequency of pure tones. However, other differences have been shown in the laboratory to cause separate streams to emerge in rapid sequences of tones. These include differences in rise times, point of spatial origin, intensity, and the abruptness of transition between successive tones (smooth transitions favor integration of all tones into a single stream). Among complex tones, important differences include the repetition rates of their waveforms (perceived as pitch) and their spectral compositions (perceived as timbre). In sequences of bandlimited noise bursts, differences in their spectral centers on a logarithmic frequency scale (perceived as height) are important.

When substreams are created by the grouping of subsets of tones or noises, there are many effects on perception. For instance: (1) it is easier to detect the presence of a pattern of tones that is formed by the elements of one stream than one that crosses streams, (2) melodies and rhythms are formed within auditory streams, (3) judgments of timing are more precise when the time to be judged relates two sounds in the same stream then when the sounds are in different streams, (4) the continuity of synthetic speech is lost if you suddenly change the pitch of the voice, or (5) the perceived loudness of a signal can be reduced if part of its energy is interpreted by the old-plus-new heuristic as belonging to a previous sound (even if the signal is a pure tone).

3.49.2.2 Simultaneous Organization

3.49.2.2.1 The ABC paradigm

One of the simplest experimental paradigms for studying the grouping and segregation of simultaneous signals has been the ABC paradigm (Bregman, A. S. and Pinker 1978). The stimulus pattern is shown in Figure 3. We see a pure tone, A, followed by a pure tone, B, not far in frequency from A. Tone B is accompanied by another tone, C. The pattern is repeated over and over as a cycle. Its interpretation is ambiguous. B is sometimes heard as a second pure tone, grouping with A to form a sequential stream of pure tones, so that with the cyclic repetition, we hear A – B – A – · · ·. At the same time we hear a second stream, derived from C alone: – – – C – – – C· · ·. The arrows in the figure show the experimental variables. In different conditions, A may be closer or further from B in either frequency or time (Bregman, A.S. and Pinker, S., 1978; Rappold, P. W. *et al.*, 1993). As A gets closer to B, it is much more likely to capture it into an AB stream, leaving C in its own stream. The frequency and temporal position of C can also be changed in different conditions. The greater the asynchrony of onset or offset B of C, the more likely they will be allocated to separate streams. In the case of B, this means entering into an AB stream.

When B and C are both pure tones, the harmonic relation between them (e.g., whether B is exactly an octave away from C or not) has little effect. However, some experimental stimuli have been constructed in which C is not a pure tone like B but a tone with many harmonics. B and C may be aligned so that B serves as one of the harmonics in the complex tone C (that harmonic being otherwise missing from C's spectrum). If A and B are of the same frequency, B can be captured out of the C spectrum into an AB stream (Van Noorden, L. P. A. S., 1975, section 3.3). However, B is easier to capture when it is a little higher or lower in frequency than its ideal harmonic position (Hartmann, W. M., *et al.*, 1990). When it is a true harmonic of C, it seems to better able to resist the tendency to be captured by A into an AB stream. This illustrates the role played by harmonic relations in holding a set of spectral components together to form one coherent sound. Strangely enough, it is not only harmonic relations that integrate B with the components of C. Even if C is a nonharmonic set of components, but has a regularity in the spacing of its components (e.g., frequencies of 230, 430, 630, 830, . . . Hz), if B fits into this regular pattern, it seems to make it harder for it to be captured by A (Roberts, B. and Brunstrom, J. M., 1998; 2001). Why should ASA respond to this type of regularity? It is hard to think of a spectrum in nature whose components are not multiples of a common fundamental, but are nonetheless spaced regularly in some other way. The strongest possibility is that a regular, but unnatural, spectrum may trick a mechanism that has been evolved to integrate natural, harmonic components.

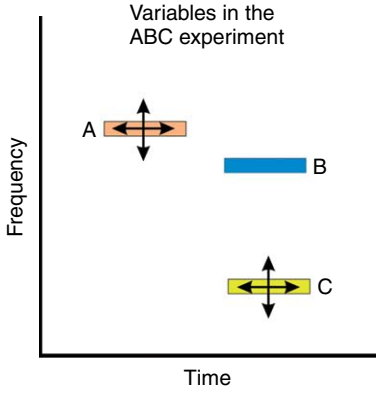

Figure 3 Stimuli for the ABC experiment. A, B, and C are pure tones. The pattern is repeated over and over as a cycle. The arrows show that both A and C may be varied in frequency or time. Adapted from figure 1.16 in Bregman, A. S. 1990/1994. Auditory Scene Analysis: The Perceptual Organization of Sound. MIT Press, (paperback 1994), with permission of MIT Press.

The ABC experiment shows that proximity in frequency and time tend to integrate a sequence of tones as parts of the same stream, just as they did in the galloping pattern of the stream segregation paradigm. It also shows that concurrent tones are better integrated into a single coherent sound when their onsets and offsets are synchronized., and when they fit into a set of frequency components that form a regular pattern in the frequency domain (the most important being the harmonic series).

3.49.2.2.2 Other findings

Other research has shown that simultaneous frequency components are somewhat more likely to be audible as separate sounds if they come from the different locations in space (Divenyi, P. L. and Oliver, S. K., 1989). This is, however, a weak effect when compared to those of asynchronous amplitude changes or the violation of harmonic relations.

Even in the integration of simultaneous components, the frequency separation of the components plays a role. This can be seen using narrow band noise bursts. The greater their frequency separation, the less likely they are to be integrated and heard as a single sound (Turgeon, M. *et al.*, 2002).

The perceptual effects of simultaneous organization are many. Whereas sequential integration forms auditory streams, the integration and segregation of simultaneous components determines which sounds are heard and their perceptual qualities. The number of sounds, their pitches, timbres, musical chord qualities, and even spatial locations depend on the organization of concurrent parts of the spectrum.

3.49.3 Brain Recording and the Role of Attention in ASA

There have been two major projects in the study of ASA using a biological approach. One has had the goal of clarifying the involvement of attention in ASA by recording the electrical activity of the brain that can be measured on the scalp. Is ASA, as claimed by (Bregman, A. S., 1990/1994) a preattentive process, or is attention involved? The advantage of brain recordings over purely behavioral testing is that it is easier to study the involvement of attention in ASA. The difficulty with trying to answer this question with behavioral research is that as soon as subjects have a task to perform with the acoustic material, they pay attention to it. With electrical recording, the subjects can be ignoring the acoustic input.

One approach has been to employ the mismatch negativity (MMN) component of auditory eventrelated potentials (ERPs) as a tool. After a series of repetitions of an unchanging short tonal pattern at a fixed rate, if some property of the pattern changes (e.g., the order of the tones in it) the ERP includes a negative component (the MMN), evoked by the detection of the change (Sussman, E. *et al.*, 1998; 1999). It is believed that this component reflects preattentive processing of the signal by the brain (Näätänen, R., 1992). MMN is found even if the subject's attention is engaged by a visual task (Näätänen, R., *et al.*, 2001). It has been possible to set up a paradigm in which the presence (or absence) of the MMN indicates that a sequence of tones has been segregated (or not segregated) into two or more auditory streams (Sussman, E. *et al.*, 1999; Sussman, E. S. *et al.*, 2005). Recent research on this topic has shown that when subjects are performing a difficult visual task and ignoring a sequence that has been made by interleaving three subsequences of tones, each occupying a distinct frequency range, three auditory streams can be formed concurrently. However, when the subjects are asked to focus their attention on one subsequence (e.g., the high tones), the MMN shows that the high-pitched stream is strengthened as a distinct perceptual entity, while the other two become weak or nonexistent (Sussman, E. *et al.*, 2005). There could be two possible explanations of this effect: (1) the ASA process requires auditory attentional resources that are being used to focus on one of the streams; therefore, it can only structure that particular stream; and (2) the absence of MMN is not due to the failure of the ASA system but rather of the MMN generating process: attention to one stream may suppress the MMN in the other streams. It is not yet clear whether either (or neither) of these explanations is correct.

A method has also been designed to use brain recordings to study the coherence of the sound resulting from multiple simultaneous components (Alain, C. *et al.*, 2001; 2002). Human subjects heard complex sounds composed of multiple harmonics, one of which could be mistuned so that it was no longer an integer multiple of the fundamental. With enough mistuning, the mistuned component stands out as a separate sound (Moore, B. C. J. *et al.*, 1986). In some conditions the subjects watched a silent movie at the same time to determine whether the mistuned component could be automatically detected. ERPs were recorded. Whenever a subject heard the mistuned component as a separate sound, a characteristic wave was obtained, first negative, peaking at about 150 ms after the onset of the sound, then positive, peaking at about 350 ms. The early negative wave, called object-related negativity (ORN) by Alain C. *et al.* (2001) was present both when the subjects were attending to the sound or watching the movie. The researchers interpreted the ORN as an index of a process that, without the involvement of attention, automatically decomposes the incoming signal into perceptual groups that can later be identified by higher processes in the brain.

These ERP studies are complemented by the work of Carlyon and his co-researchers, who studied the issue of whether ASA can go on without the involvement of attention, using behavioral tests on normal subjects and on patients with a unilateral attentional deficit (Carlyon, R. P. *et al.*, 2001). The research on normal subjects showed that the buildup of auditory streaming over time was greatly reduced or absent when they attended to a competing auditory task in the contralateral ear. Patients with an attentional neglect of the left side of space showed less stream segregation of tone sequences presented to their left than to their right ears. The researchers concluded that attention was needed for the

streaming phenomenon to occur. Presumably this research would lead one to suspect that ASA, in general, required attention.

Another question is whether attention is an indivisible mental process. The research by Sussman E. S. *et al.* (2005) cited above, suggests that auditory and visual tasks do not draw on the same pool of those particular resources that we label as attention. Performance in an engaging visual task permits three concurrent auditory streams to form; but attending to one of these streams (an exercise of auditory attention) may prevent the others from forming. Auditory attention itself may be divisible; even if ASA involves attentional resources, we still do not know whether unattended streams can be structured (perhaps by allocating a minority of attentional resources to them), in the circumstances of everyday life. It would be very useful to the animal if they could be. Then when attention was switched, it would be switched to a new partly organized auditory object, one for which an object node already existed in the nervous system, and not just to a smear of energy somewhere in the spectrum.

3.49.4 Animal Studies and Innate Processes of ASA

The study of nonhuman animals represents another approach to the biological study of ASA. If there are general regularities in the spectrum of a mixture that are present in all environments, and these regularities tell the listener how to parse it, one would expect that operations that used these regularities would be preprogrammed in the nervous systems of many species. However, one cannot assume that ASA works in the same way in all animals. For example, ASA has been studied in the echolocation of bats (e.g., Moss, C. F. and Surlykke, A., 2002). Some bats emit ultrasonic vocalizations containing frequency modulation (FM) at fairly stable rates (within 5%). They operate in a fairly complex environment in which both they and their prey are moving, and in which other bats are hunting too. Unlike humans, bats control the sounds they use for hunting; so that in order to segregate their own echoes from those of other bats, they can use strategies that go beyond the methods used by humans in ASA. It is argued that an individual bat adjusts the spectrum and sweep rate of its ultrasonic vocalizations so its own echoes will differ from those of its fellow hunters. Moss, C. F. and Surlykke, A. (2002) postulate that "the bat's perceptual system organizes acoustic information from a complex and dynamic environment into echo streams, allowing it to track spatially distributed auditory objects (sonar targets) as it flies." These streams serve the same function as those of humans – packaging a meaningful grouping of sounds (the reflections coming from a single prey animal) – but operate in an entirely different sonic environment. While the differences in how bats and humans achieve ASA is extreme because of bats' use of echolocation, even animals that do not use this method may live in acoustic worlds that are unlike the one humans inhabit. While the outcome of ASA has to be similar to that of humans, the particular cues and grouping principles may have to be different. Nevertheless, if we find a species whose ASA processes resemble those of humans, it should be possible to use physiological methods to investigate the brain structures and processes that humans may use.

3.49.5 Summary

This chapter describes some of the central issues in ASA. Considerable difficulty is involved in converting the incoming mixture of acoustic signals into separate mental representations of distinct sounds, each with its own properties. To parse the incoming spectrum, the human auditory system uses heuristic methods, based on general regularities in the world of acoustic mixtures. A set of such methods is used but no single one is decisive. They collaborate and compete to determine the final perceptual organization into distinct sounds and streams of sounds. There are two aspects of the ASA problem: how to group incoming energy over time, and how to do so over the set of components (or perhaps features) that are present concurrently. These two forms of grouping involve different regularities, but a competition for the simultaneous and successive grouping of a bit of spectral energy can occur until a final interpretation is resolved. Apart from the general regularities that are the basis for these methods, there are particular regularities in limited situations, such as in a particular language, or style of music, or type of machine, which may be learned and employed in addition to general regularities to parse the spectrum into separate overlapping auditory streams.

The role of attention in ASA is still in question and there have been some recent attempts to resolve this issue by means of brain recordings as well as behavioral studies. However, a decisive picture has

yet to emerge. Finally, it is hoped that the ASA concepts may clarify the perceptual activities of some nonhuman animals, and that having a good animal model of ASA may allow physiological explorations of the underlying processes in the central nervous system.

References

Alain, C., Arnott, S. R., and Picton, T. W. 2001. Bottom-up and top-down influences on ASA: evidence from event-related brain potentials. J. Exp. Psychology: Hum. Percept. Perf. 27, 1072–1089.

Alain, C., Schuler, B. M., and McDonald, K. L. 2002. Neural activity associated with distinguishing concurrent auditory objects. J. Acoust. Soc. Am. 111(2), 990–995.

Bregman, A. S. 1978. Auditory streaming: competition among alternative organizations. Percept. Psychophys. 23, 391–398.

Bregman, A. S. 1984. ASA. In: proceedings of the Seventh International Conference on Pattern Recognition, pp. 168–175. Silver Spring, Md. IEEE Computer Society Press (Library of Congress No. 84-80909).

Bregman, A. S. 1990/1994. Auditory Scene Analysis. The Perceptual Organization of Sound. MIT Press (paperback 1994).

Bregman, A. S. and Ahad, P. A. 1996. Demonstrations of ASA. The Perceptual Organization of Sound. (Compact disk and booklet.) Auditory Perception Laboratory, Psychology Department, McGill University. Distributed by MIT Press.

Bregman, A. S. and Pinker, S. 1978. Auditory streaming and the building of timbre. Can. J. Psychol. 32, 19–31.

Bregman, A. S. and Woszczyk, W. 2004. Controlling the Perceptual Organization of Sound: Guidelines Derived From Principles of ASA. In: Audio Anecdotes: Tools, Tips and Techniques for Digital Audio (*eds*. K. Greenebaum and R. Barzel), Vol. 1, pp. 35–64. A K Peters.

Bregman, A. S., Ahad, P. A., Crum, P. A. C., and O'Reilly, J. 2000. Effects of time intervals and tone durations on auditory stream segregation. Percept. Psychophys. 62(3), 626–636.

Carlyon, R. P., Cusack, R., Foxton, J. M., and Robertson, I. H. 2001. Effects of attention and unilateral neglect on auditory stream segregation. J. Exp. Psych. Hum. Percept. Perform. 27(1), 115–127.

Darwin, C. J. 1997. Auditory grouping. Trends Cogn. Sci. 1, 327–333.

Darwin, C. J. 2001. Auditory grouping and attention to speech (keynote paper). Proc. Inst. Acoust. 23, 165–172.

Divenyi, P. L. and Oliver, S. K. 1989. Resolution of steady-state sounds in simulated auditory space. J. Acoust. Soc. Am. 85, 2042–2052.

Handel, S. 2006. Perceptual Coherence: Hearing and Seeing, Oxford University Press.

Hartmann, W. M., McAdams, S., and Smith, B. K. 1990. Hearing a mistuned harmonic in an otherwise periodic complex tone. J. Acoust. Soc. Am. 88, 1712–1724.

Huron, D. 2001. Tone and voice: a derivation of the rules of voice-leading from perceptual principles. Mus. Percep. 19(1), 1–64.

Koffka, K. 1935. Principles of Gestalt Psychology. Harcourt, Brace and World.

Moore, B. C. J., Glasberg, B. R., and Peters, R. W. 1986. Thresholds for hearing mistuned partials as separate tones in harmonic complexes. J. Acoust. Soc. Am. 80, 479–483.

Moss, C. F. and Surlykke, A. 2002. ASA by echolocation in bats. J. Acoust. Soc. Am. 110(4), 2207–2226.

Näätänen, R. 1992. Attention and Brain Function. Erlbaum.

Näätänen, R., Tervaniemi, M., Sussman, E., Paavilainen, and Winkler, I. 2001. Pre-attentive cognitive processing (primitive intelligence) in the auditory cortex as revealed by the MMN (MMN). Trends Neurosci. 24, 283–288.

Rappold, P. W., Mendoza, L., and Collins, M. J. 1993. Measuring the strength of auditory fusion for synchronous and nonsynchronous amplitude-fluctuating, spectrally disparate narrow-bands of noise. J. Acoust. Soc. Am. 93(2), 1196–1199.

Roberts, B. and Brunstrom, J. M. 1998. Perceptual segregation and pitch shifts of mistuned components in harmonic complexes and in regular inharmonic complexes. J. Acoust. Soc. Am. 104, 2326–2338.

Roberts, B. and Brunstrom, J. M. 2001. Perceptual fusion and fragmentation of complex tones made inharmonic by applying different degrees of frequency shift and spectral stretch. J. Acoust. Soc. Am. 110, 2479–2490.

Shilling, R. and Shinn-Cunningham, B. 2002. Virtual Auditory Displays. In: Handbook of Virtual Environments: Design, Implementation, and Applications (*ed*. K. Stanney), pp. 65–92. Lawrence Erlbaum.

Sussman, E. S., Bregman, A. S., Wang, W. J., and Khan, F. J. 2005. Attentional modulation of electrophysiological activity in auditory cortex for unattended sounds within multistream auditory environments. Cogn. Affect. Behav. Neurosci. 5(1), 93–110.

Sussman, E., Ritter, W., and Vaughan, H. G. 1998. Attention affects the organization of auditory input associated with the MMN system. Brain Res. 789(1), 130–38.

Sussman, E., Ritter, W., and Vaughan, H. G. 1999. An investigation of auditory stream segregation using event-related brain potentials. Psychophysiology. 36, 22–34.

Turgeon, M., Bregman, A. S., and Ahad, P. A. 2002. Rhythmic masking release: Contribution of cues for perceptual organization to the cross-spectral fusion of concurrent narrow-band noises. J. Acoust. Soc. Am. 111(4), 1819–1831.

Van Noorden, L. P. A. S. 1975. Temporal coherence in the perception of tone sequences. Doctoral dissertation, Eindhoven University of Technology, Eindhoven, The Netherlands.

Further Reading

Divenyi, P. 2004. Speech Separation by Humans and Machines. Springer.

Relevant Websites

http://www.psych.mcgill.ca – Department of Psychology, McGill University. ASA

http://www.ebire.org – East Bay Institute for Research and Education.

http://www.aecom.yu.edu – Dr. E. Sussman, Albert Einstein College of Medicine.

3.50 Human Auditory Development

L A Werner, University of Washington, Seattle, WA, USA

© 2008 Elsevier Inc. All rights reserved.

3.50.1	**Introduction**	872
3.50.2	**Development of Primary Auditory Capacities**	873
3.50.2.1	Spectral Coding	873
3.50.2.1.1	Frequency resolution and discrimination	873
3.50.2.1.2	Pitch and timbre	875
3.50.2.2	Intensity Coding	875
3.50.2.2.1	Absolute sensitivity	876
3.50.2.2.2	Intensity discrimination	878
3.50.2.2.3	Loudness	879
3.50.2.3	Temporal Resolution	879
3.50.2.4	Spatial Resolution and Perception	880
3.50.2.4.1	Sound localization	880
3.50.2.4.2	Binaural masking level difference and spatial release from masking	881
3.50.3	**Development of Complex Perceptual Capacities**	882
3.50.3.1	Sound Source Determination	882
3.50.3.2	Auditory Attention	884
3.50.3.2.1	Attentiveness	884
3.50.3.2.2	Selective listening to relevant sound features	884
3.50.3.2.3	Ignoring irrelevant sound features	885
3.50.3.2.4	Listening to competing messages	886
3.50.4	**Summary and Conclusion**	887
References		888

Glossary

auditory brainstem response (ABR) A scalp-recorded far-field evoked potential originating in the auditory nerve and auditory brainstem nuclei. Five peaks, labeled I through V, can be identified in the response. Wave I originates in the auditory nerve and has a latency of 1–2 ms in adults; wave V originates in the inferior colliculus and has a latency of about 7 ms in adults.

auditory filter width A psychophysical measure of frequency resolution obtained by measuring the threshold for a pure tone masked by a band-reject noise. The notch in the noise spectrum is centered on the tone frequency, and the width of the notch is varied to determine the width of the auditory filter.

binaural masking level difference (BMLD) The reduction in masking that occurs when either the probe or the masker is presented dichotically. For example, threshold for a tone is reduced by as much as 15 dB when the tone is presented in opposite phase to the two ears, while the noise masker is the same in both ears. The condition in which the same masker and probe are presented to both ears is denoted N_0S_0, while the condition in which the probe is out of phase at the two ears is denoted N_0S_π.

conductive apparatus The parts of the ear that conduct sound pressure to the inner ear; the external ear and the middle ear.

critical band The band of frequencies in a broadband noise that is effective in masking a tone; conceptually equivalent to the auditory filter width.

cross-modality loudness matching A method of measuring loudness in which the listener produces a stimulus in a nonauditory modality that matches the perceived magnitude of the sound. For example, the listener might draw a line that is as long as a sound is loud.

difference limen (DL) The threshold in a discrimination experiment; the difference between two

stimuli in intensity, frequency or some other characteristic that the listener can just discriminate.

formant transition Formants are peaks in the amplitude spectrum of speech sounds. As the articulators move from the position required to produce one sound (e.g., a consonant) to the position required to produce another (e.g., a vowel), the frequency of the formants gradually changes, creating a formant transition. The direction and extent of the formant transition provide information about the identity of speech sounds.

forward masking Masking that occurs when the masker precedes the probe by 0 to about 100 ms.

gap detection A measure of temporal resolution in which the listener is asked to detect a temporal interruption in a sound.

interaural time difference The difference between the arrival times of a sound at the two ears; a cue to sound source position in space.

minimum audible angle The just noticeable difference in spatial position of a sound source, expressed as degrees of arc.

observer-based method A method for determining thresholds in infants in which an observer, blind to trial type, judges whether or not a signal was presented to the infant in a defined time period. The only information provided to the observer is the infant's behavior. Because the method does not require a particular response from the infant, it is useful in the testing of young infants who do not produce easily recorded head turns to sound sources. The method is described in detail by Werner L. A. (1995).

otoacoustic emissions (OAE) Sounds that are produced by the inner ear and that can be recorded in the ear canal with a sensitive microphone. The presence of OAE is a sign of normal hearing.

psychometric function The function that describes the relationship between performance in a psychophysical task and the value of the stimulus. For example, the function that shows the percentage of correct detections as a function of stimulus intensity is the psychometric function for detection.

psychophysical tuning curve A measure of frequency resolution in which the masker level just required to detect a fixed-frequency probe is measured for different masker frequencies. A psychophysical tuning curve resembles the tuning curve of auditory nerve fibers.

release from masking A reduction in masking resulting from a change in the probe, the masker or some other variable.

sound source determination The process by which the components of sound emanating from a single source are grouped together as an auditory object.

visual reinforcement audiometry A clinical procedure for determining thresholds in infants older than 6–7 months. The infant learns to turn her head toward a sound source; a mechanical toy or video is activated to reinforce the infant's head turn.

3.50.1 Introduction

The study of auditory development in human infants and children is relatively young. Studies of anatomical (Streeter, G. L., 1906; 1917; McKinnis, M. E., 1936; Hall, J. G., 1964; Bredberg, G., 1968), physiological (Akiyama, Y. *et al.*, 1969; Engel, R. and Young, N. B., 1969; Lenard, H. G. *et al.*, 1969), and behavioral or psychophysiological (Bartoshuk, A. K., 1962; Steinschneider, A. *et al.*, 1966; Clifton, R. K. *et al.*, 1968; Jordan, R. E. and Eagles, E. L., 1963; Eisenberg, R. B. *et al.*, 1964; Leventhal, A. and Lipsitt, L. P., 1964) development had been published prior to 1970. It was, however, only in the 1970s that interest in assessing hearing in infants became serious, with the appearance of visual reinforcement audiometry (Moore, J. M. *et al.*, 1977; Liden, G. and Kankkonen, A., 1961) and the auditory brainstem response (Salamy, A. *et al.*, 1975). The first rigorous psychophysical studies of infants and children were published in 1979 (Schneider, B. A. *et al.*, 1979), and it is only in the last 15 years that attempts have been made to relate age-related changes in auditory behavior to the underlying physiological and anatomical processes (e.g., Ponton, C. W. *et al.*, 1996; Trainor, L. J. *et al.*, 2001; Werner, L. A., 1996; 1994b). The upshot is that while we have a fairly complete description of the development of the most basic aspects of audition, less is known about complex auditory perception and about the underlying causes of auditory development.

It is generally believed that the limits on the basic aspects of audition – frequency, intensity, and temporal resolution – are established at the auditory periphery. Deficits in resolution in mature listeners generally result from peripheral damage or disease. Observations of the human fetal and neonatal inner ear indicate that the cochlea is structurally and functionally adult-like by term birth (e.g., Bredberg, G., 1968; Lavigne-Rebillard, M. and Pujol, R., 1987; Lavigne-Rebillard, M. and Bagger-Sjoback, D., 1992; Pujol, R. and Lavigne-Rebillard, M., 1992; Lasky, R. *et al.*, 1992; Brown, A. M. *et al.*, 1994; Bargones, J. Y. and Burns, E. M., 1988; Abdala, C., 1996). These observations have led to the expectation that the basic aspects of hearing will likewise be adult-like at term birth, with any apparent immaturity in auditory behavior resulting from limitations in cognition or motor processes. However, just as we now understand that some types of purely auditory dysfunction can result from deficits in the neural encoding of sound (e.g., Zeng, F. *et al.*, 2005), we understand that immaturity of the primary auditory neural pathway may lead to immaturity of frequency, intensity, or temporal resolution. Further, we must recognize that maturation of fundamentally auditory processes, such as sound source determination, may limit basic auditory sensitivities. Finally, immaturity of the so-called higher-level processes, such as attention or memory, may result in immaturity of auditory sensitivity that is functionally no different from that resulting from primary auditory immaturity. Thus, potential contributors to the development of auditory behavior include primary auditory processes at both peripheral and central levels, organizational and integrative auditory processes, and general perceptual, cognitive and motor processes.

In many ways, the methods available to describe and to understand human auditory development are limited. Few anatomical data are available and physiological indices are limited to acoustic measures, scalp-recorded far-field potentials, and recently neural imaging techniques. In addition, infants and children have limited capacities for carrying out psychophysical procedures. However, some 30 years of work honing developmental psychoacoustic procedures has resulted in what we believe to be valid and reliable measures of auditory sensitivity. The details of these procedures are beyond the scope of this chapter. The interested reader is referred to Werner L. A. and Rubel E. W. (1992).

3.50.2 Development of Primary Auditory Capacities

3.50.2.1 Spectral Coding

3.50.2.1.1 Frequency resolution and discrimination

Schneider B. A. *et al.* (1989) published the first comprehensive description of masked thresholds from infancy through adulthood. The beauty of this study is that very similar methods were used to obtain data from listeners in all age groups, 6 months to 20 years. Listeners in this study detected octave bands of noise masked by a broadband noise by identifying the speaker – left or right – that was playing the octave-band signal on each trial. Infants indicated their choice with a head turn toward the correct speaker. Older listeners pushed a button on one of the arms of their chair. This two-alternative forced-choice method also has the advantage of controlling response bias. Thresholds were estimated from psychometric functions constructed from the data of all listeners in each group. The thresholds Schneider B. A. *et al.* obtained are plotted in Figure 1 for several frequencies. Notice that masked thresholds improve with age at all frequencies. Between 6 months and adulthood the improvement is on the order of 10-12 dB, with all but a few dB of the improvement occurring prior to 8 years of age. This pattern of development was confirmed in many studies of infants or children (e.g., Bargones, J. Y. *et al.*, 1995; Berg, K. M., 1993; Berg, K. M. and Boswell, A. E., 1999; Maxon, A. B. and Hochberg, I., 1982; Nozza, R. J. and Wilson, W. R., 1984).

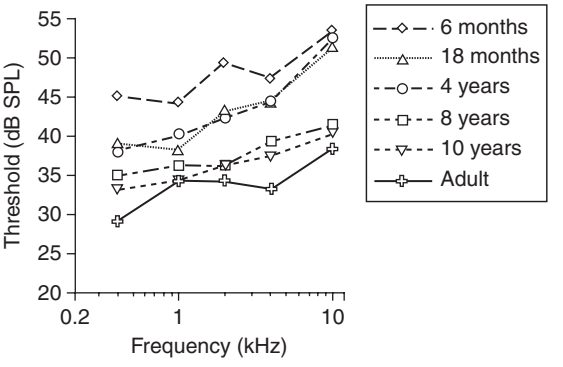

Figure 1 Thresholds for octave bands of noise masked by broadband noise, as a function of the center frequency of the noise band, for six age groups. Reproduced from Schneider, B. A., Trehub, S. E., Morrongiello, B. A., and Thorpe, L. A. 1989. Developmental changes in masked thresholds. J. Acoust. Soc. Am. 86, 1733–1742, with permission.

The observations by Schneider B. A. *et al.* (1989) provided the starting point for much of the developmental psychoacoustic research that followed. The age-related improvement in masked threshold could result from maturation of several different processes. Of course, the most obvious explanation for threshold maturation to most people is that people get better at performing psychophysical tasks as they develop. For example, listeners are better able to remain on-task and to remember what they are listening for. The consensus is that while inattentiveness or forgetting are likely responsible for young listeners' imperfect psychoacoustic performance, such processes can only account for 2–3 dB of the observed age difference in masked threshold (discussed in greater detail in Section 3.50.3; see also Schneider, B. A. and Trehub, S. E., 1992; Viemeister, N. F. and Schlauch, R. S., 1992; Werner, L. A. and Bargones, J. Y., 1992; Wightman, F. and Allen, P., 1992).

Another obvious process affecting detection in noise is frequency resolution, the precision with which the auditory system can analyze the frequency content of a complex sound. Frequency resolution improves dramatically in the period following the onset of cochlear function in mammals, and there is evidence that some neural responses continue to become more frequency selective even after cochlear tuning is well established (Sanes, D. H. and Walsh, E. J., 1998). In humans, the cochlea begins to function in the prenatal period, probably around 22 weeks of gestation (Pujol, R. *et al.*, 1990;1991). Both behavioral and brainstem evoked potentials can be recorded around 28 weeks of gestation (e.g., Birnholz, J. C. and Benacerraf, B. R., 1983; Lary, S. *et al.*, 1985). By term birth, acoustic and electrophysiological measures of cochlear function are generally reported to be adult-like (Teas, D. C. *et al.*, 1982; Abdala, C. and Chatterjee, M., 2003), save for the potential effects of conductive immaturity (discussed further ahead). Frequency resolution has been examined at the level of the brainstem using the auditory brainstem response (ABR) and masking paradigms by Folsom and his colleagues (Folsom, R. C., 1985; Folsom, R. C. and Wynne, M. K., 1987; Abdala, C. and Folsom, R. C., 1995). Their results consistently indicate mature frequency resolution at 6 months postnatal age. At 3 months, however, they report immaturity of frequency tuning, but only at frequencies above 4000 Hz.

The results of psychoacoustic studies of the development of frequency resolution are consistent with ABR results. For example, critical bandwidth (Schneider, B. A. *et al.*, 1990) and psychophysical tuning curve width (Olsho, L. W., 1985) have been reported to be adult-like in 6-month-old listeners. Spetner N. B. and Olsho L. W. (1990) conducted the only psychophysical examination of frequency resolution in infants younger than 6 months of age. These investigators reported that psychophysical tuning curve width was mature by 3 months of age at 500 and 1000 Hz, but remained immature at 4000 Hz. They also found that tuning was mature at 4000 Hz by 6 months. Several studies have examined frequency resolution in older children. While initial results indicated immature frequency resolution in 3- to 4-year-olds (Allen, P. *et al.*, 1989; Irwin, R. J. *et al.*, 1986), Hall J. W. and Grose J. H. (1991) showed that the apparent immaturity in frequency resolution in young children could be accounted for by age-related changes in perceptual decision processes. Thus, there is now general agreement that frequency resolution matures relatively early in postnatal life, and that age-related differences in masked threshold must stem from other causes. The nature of these other causes is discussed in detail in the following.

One would expect that the development of frequency discrimination would follow that of frequency resolution. The available data suggest that, in fact, high-frequency pure-tone discrimination develops along a course similar to that of frequency resolution at high frequencies: 3-month-old infants are immature in frequency discrimination from 500 to 4000 Hz, while 6- and 12-month-old infants remain immature at 500 and 1000 Hz but are close to adult-like at 4000 Hz (Olsho, L. W. *et al.*, 1987). Studies of children support this pattern of development, showing low-frequency pure-tone discrimination only reaching adult levels of performance around 10–11 years (Fischer, B. and Hartnegg, K., 2004; Maxon, A. B. and Hochberg, I., 1982). One explanation for this developmental gradient begins with the observation that low-frequency tones are discriminated on the basis of periodicity, while high-frequency tones are discriminated on the basis of excitation pattern (e.g., Moore, B. C. *et al.*, 1999). Frequency resolution and high-frequency discrimination are mature by around 6 months of age, as noted above. Immature low-frequency discrimination is consistent with immaturity of periodicity processing, either the primary representation of periodicity (i.e., phase-locking) or the ability to use that representation in the case of pure-tone frequency discrimination. Several lines of evidence point toward the latter possibility. First, the development

of evoked potentials, at least at the brainstem level (e.g., ABR), is generally complete before a child is 5 or 6 years old (Hall, J. W. III., 1992). Because evoked potential amplitude depends heavily on the existence of phase locking, this finding implies that phase locking is also mature by that age. Further, it is generally believed that more training is required to learn low-frequency discrimination, even among adults, and several studies support this belief (Olsho, L. W. *et al.*, 1988a; Harris, J. D., 1952). Soderquist D. R. and Moore M. (1970) have shown that young children can achieve adult levels of performance in low-frequency discrimination with training. Thus it appears that the periodicity information may be available even to infants, but that in the context of pure-tone frequency discrimination, listeners do not readily access that information.

3.50.2.1.2 Pitch and timbre

Complex pitch perception requires not only an adequate representation of the spectrum and periodicity of the stimulus, but some integration of temporal and spectral information across frequency regions, making it an interesting phenomenon from a developmental standpoint. Clarkson M. G. and her colleagues have conducted a series of studies examining the perception of complex pitch in 7-month-old infants. The phenomenon that defines complex pitch psychophysically is the pitch of the missing fundamental: people will assign a harmonic complex the pitch associated with its fundamental frequency, even when the fundamental frequency is not part of the complex. The perception of the pitch of the missing fundamental clearly depends on integration of the information carried by the harmonics, and Clarkson M. G. and Clifton R. K. (1985) first demonstrated that infants can learn to respond when the missing fundamental frequency of a complex changes, while ignoring other spectral changes. In many respects, infants' and adults' ability to perform this task depends on the same stimulus parameters. For example, both infants and adults continue to hear the pitch of the missing fundamental when a noise band masks the fundamental frequency, but fail to hear that pitch if the higher-frequency harmonics are masked (Montgomery, C. R. and Clarkson, M. G., 1997). Both age groups have greater difficulty categorizing the pitch of inharmonic complexes (Clarkson, M. G. and Clifton, R. K., 1995), but while adults can hear the pitch of the missing fundamental, albeit weakly, when only high-frequency harmonics are present, infants appear unable to hear this less salient pitch (Clarkson, M. G. and Rogers, E. C., 1995). Because the perception of the pitch of the missing fundamental on the basis of only high-frequency harmonics is believed to depend on the periodicity that results from unresolved harmonics, the latter observation provides additional evidence that infants may have greater problems in tasks that require the use of periodicity.

Finally, infants' ability to categorize spectrally dissimilar sounds on the basis of their common fundamental frequency would mean little if infants are unable to discriminate the spectral dissimilarity. Adults perceive these spectral changes as changes in timbre. One of the difficulties in ensuring that the listener is responding on the basis of the timbre of a complex is that the listener could listen to only a restricted frequency region of the complex and respond when the energy in that frequency region changes, regardless of the spectral shape of the complex as a whole. To prevent that from happening, studies of timbre generally vary, or rove, the overall intensity of the complex from presentation to presentation, so that the amount of energy in any frequency region is not a reliable indicator of a change in spectral shape. Several studies have reported that infants can learn to categorize sounds on the basis of spectral shape (Clarkson, M. G. *et al.*, 1988; Clarkson, M. G., 1996; Trehub, S. E. *et al.*, 1990), but infants have difficulty ignoring random changes in overall intensity (Clarkson, M. G., 1996). None of the existing studies has been able to get infants to respond to timbre changes in tonal complexes when the intensity is roved sufficiently to prevent the listener from responding on the basis of local intensity changes. Because infants are consistently able to discriminate between sounds that adults distinguish on the basis of spectral shape (e.g., vowels, Marean, G. C. *et al.*, 1992; Kuhl, P. K. and Miller, J. L., 1982) and because infants appear to have difficulty listening to a restricted frequency region (discussed in the following, Bargones, J. Y. and Werner, L. A., 1994), it is likely that they do perceive timbre in some fashion. However, a definitive demonstration remains elusive.

3.50.2.2 Intensity Coding

A difficulty in studying the development of intensity processing is that it is difficult to separate the perception of intensity from other variables that influence the efficiency with which the listener performs the task. There is no measure, like critical bandwidth or

auditory filter width that allows intensity coding to be distinguished from factors like attentiveness or memory. To date, the most fruitful approach has been to examine the effects of stimulus variables (e.g., frequency, duration) on intensity processing: the more adult-like these effects, the more likely it is that intensity processing is adult-like. A goal of future developmental research in this area, however, should be to find more definitive procedures for solving this dilemma.

3.50.2.2.1 Absolute sensitivity

To many, and certainly to audiologists, absolute sensitivity represents the most basic characterization of the auditory system. Threshold sensitivity improves dramatically in the period following the onset of cochlear function in the species that have been tested (e.g., Ehret, G., 1976; Zimmermann, E., 1993; Ehret, G. and Romand, R., 1981; Gray, L. and Rubel, E. W., 1985; Kenyon, T. N., 1996), but to date, no species has been followed systematically from the onset of hearing to adulthood in a single study. Because different methods are generally used to test the behavioral thresholds of young and adult animals, it is difficult to know how much of an age difference in threshold is due to differences in test methodology. In no case have thresholds of the oldest developing animal been found to approach adult thresholds in that species. The usual conclusion drawn from these studies, nonetheless, is that the development of threshold sensitivity is primarily due to maturation of the inner ear, although middle-ear function is also known to undergo developmental improvements early in life (e.g., Ehret, G., 1976). Neural contributions to threshold development are rarely if ever considered.

The human fetus moves in response to sound by 28 weeks of gestation. While a few attempts to measure behavioral response thresholds *in utero* have been made (reviewed by Lecanuet, J. P., 1996), the technical difficulties involved in estimating the sound pressure level *in utero*, not to mention the myriad other methodological difficulties involved in this experiment, make interpretation of the results problematic. Moreover, it is clear that whatever sound makes it to the fetus is at least partially masked by noise produced by the mother's body (e.g., Querleu, D. *et al.*, 1988; Gerhardt, K. J. *et al.*, 1990). A few studies have examined the behavioral response of preterm infants to sound. The percentage of behavioral responses to a broadband noise centered at 3000 Hz with a peak intensity of 90 dB SPL A has been reported to increase more or less systematically from about 20% to about 45% of trials between 34 and 41 weeks conceptional age (Gerber, S. E., 1985; Mencher, G. T. *et al.*, 1985), but it is, of course, difficult to know what is responsible for the increase in responsiveness to sound. If spontaneous responses to octave-band noises are considered, even in a rigorous psychophysical procedure, behavioral response thresholds in full-term newborns are on the order of 75 dB HL over the frequency range from 125 to 4000 Hz (Weir, C., 1976; 1979).

By 1 month of age, human infants are awake and alert long enough that a few attempts have been made to establish their behavioral thresholds using the observer-based approach. For example, Werner L. A. and Gillenwater J. M. (1990) estimated that 2- to 4-week-old infants' behavioral thresholds to pure tones were about 45 dB higher than adults' at 500 Hz and about 35 dB higher than adults' at 4000 Hz. Trehub S. E. *et al.* (1991) found that thresholds for a 4000 Hz octave-band noise were about 30 dB higher in 1-month-olds than in adults, and Tharpe A. M. and Ashmead D. H. (2001) reported that infants between 0 and 3 months of age had thresholds for a speech filtered noise that were about 40 dB higher than adults'. None of these studies reinforced the infants' responses to sound; Werner L. A. and Mancl L. R. (1993) reported that 1-month-olds' thresholds for pure tones were improved by about 5 dB if responses to the tones were reinforced by an audio recording of a woman reading from a children's book.

By 3 months of age, infants' behavioral thresholds improve to about 40 dB SPL at 500 Hz and to 24 dB SPL at 4000 Hz (Olsho, L. W. *et al.*, 1988b; Tharpe, A. M. and Ashmead, D. H., 2001; Trehub, S. E. *et al.*, 1991). Between 3 and 6 months, little improvement occurs in low-frequency thresholds, but thresholds are about 15 dB higher than adults' at higher frequencies (Bargones, J. Y. *et al.*, 1995; Berg, K. M. and Smith, M. C., 1983; Nozza, R. J. and Wilson, W. R., 1984; Sinnott, J. M. *et al.*, 1983; Trehub, S. E. *et al.*, 1980). Trehub S. E. *et al.* followed the development of thresholds for octave noise bands from 6 months through the school years to adulthood. They found that mature sensitivity was achieved earlier at higher frequencies, before age 5 years at 4000 and 10000 Hz, but after 10 years of age at 1000 Hz. Thus, the development of absolute sensitivity is a prolonged process, summarized in Figure 2.

The nature of these age-related changes in sensitivity have been a matter of debate. Certainly similar

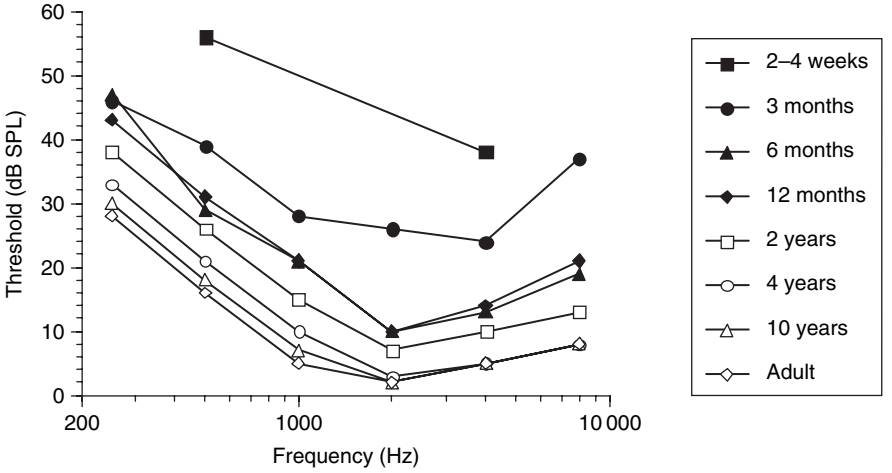

Figure 2 A summary of the development of the audibility curve, abstracted from several studies (see text).

improvements in physiological indices of sensitivity are observed in preterm and young infants. Improvements in click-evoked auditory brainstem thresholds from 40 to 10 dB nHL have been documented from about 28 to 38 weeks conceptional age on (Lary, S. *et al.*, 1985). In general, thresholds for responses generated in the inner ear or auditory nerve at term birth have been reported to be no more than 15 dB higher than those observed in adults (Engel, R. and Young, N. B., 1969; Stuart, A. *et al.*, 1993; Stevens, J. C. *et al.*, 1990; Abdala, C. *et al.*, 2006). Sininger and her colleagues (Sininger, Y. and Abdala, C., 1996; Sininger, Y. S. *et al.*, 1997) have reported that for stimuli calibrated in the ear canal, thresholds for click-evoked ABR wave V are about 20 dB higher in term neonates than in adults. This laboratory also reported that while neonates' thresholds for tone-pip-evoked ABR wave V are adult-like at 500 Hz, they are about 20 dB higher than adults' at 4000 and 8000 Hz.

One of the factors known to contribute to the improvements in absolute sensitivity with age is maturation of the conductive apparatus. Keefe D. H. and his colleagues (Keefe, D. H. *et al.*, 1993; Keefe, D. H. and Levi, E. C., 1996) have shown that the efficiency of transmission through the middle ear improves throughout infancy, and it is believed that this process continues well into childhood (Okabe, K. S. *et al.*, 1988). In 1-month-olds, as much as 20 dB less sound energy is transmitted through the middle ear at high frequencies, compared to adults. At lower frequencies, the difference in sound transmission is only 5–10 dB at 1 month. Transmission at high frequencies improves by 10 dB by 6 months of age; low-frequency transmission improves at a slower rate. Thus, it is likely that age-related threshold differences in otoacoustic emissions (OAE), ABR, and other measures of peripheral function early in infancy can be accounted for by immaturity of the conductive apparatus. Further, improvement in conductive efficiency can account for at least a portion of the improvement in behavioral thresholds observed between 1 month and 6 months of age, especially at higher frequencies. In fact, Werner L. A. and Holmer N. M. (2002) have shown that behavioral threshold at 4000 Hz is significantly correlated with middle ear admittance at that frequency among 3-month-old infants and among adults.

One of the factors unlikely to contribute to improvements in absolute sensitivity with age, at least beyond the conceptional age of 38 weeks or so, is maturation of the inner ear. On the basis of anatomical benchmarks, as well as physiological and behavioral responses, the human inner ear apparently begins to respond to sound around 22 weeks gestational age (Birnholz, J. C. and Benacerraf, B. R., 1983; Pujol, R. *et al.*, 1991). By term birth, the consensus is that the cochlea is anatomically and functionally mature (Fujimoto, S. *et al.*, 1981; Igarashi, Y. and Ishii, T., 1979a; 1979b; Igarashi, Y. *et al.*, 1978; Lavigne-Rebillard, M. and Pujol, R., 1987; 1988; 1990; Lavigne-Rebillard, M. and Bagger-Sjoback, D.; 1992, Bredberg, G., 1968; Igarashi, Y. and Ishii, T., 1980; Streeter, G. L., 1917; 1906; Lavigne-Rebillard, M. and Pujol, R., 1990; Isaacson, G. *et al.*, 1986; Shimizu, T. *et al.*, 1991; Hoshino, T., 1990; Nakai, Y., 1970; Bargones, J. Y. and Burns, E. M., 1988; Leiberman, A. *et al.*, 1973; Plinkert, P. K. *et al.*,

1990; Abdala, C., 1998; Chuang, S. W. *et al.*, 1993; Morlet, T. *et al.*, 1996; Eggermont, J. J. *et al.*, 1996; Collet, L. *et al.*, 1993).

Maturation of the primary auditory neural pathways, however, may well be involved in threshold improvements during early infancy. Werner L. A. and her colleagues (Werner, L. A. *et al.*, 1993; 1994b) have shown that behavioral threshold at 4000 and at 8000 Hz is significantly correlated with ABR threshold in the same infants, but even more strongly correlated with wave I–V interpeak latency. Improvement in ABR latencies during infancy is thought to result from changes in the length of the neural pathway, from myelination of nerve fibers, and in great part, from improvement in synaptic efficiency (Ponton, C. W. *et al.*, 1996; Moore, J. K. *et al.*, 1995; 1996; 1997; Ponton, C. W. *et al.*, 2000). It is likely that the improvement in synaptic efficiency, at least, also leads to improvements in auditory sensitivity.

3.50.2.2.2 *Intensity discrimination*

A notable property of immature auditory neurons is their limited dynamic range (Kotak, V. and Sanes, D., 1995). Thus, it would not be surprising to find that intensity discrimination undergoes postnatal development in humans. Because detection in noise is immature in infants and young children and because frequency resolution is apparently mature early in infancy, the development of masked thresholds must reflect changes in the signal-to-noise ratio required for detection. We refer to the signal-to-noise ratio required for detection as efficiency. One of the variables that determines efficiency is intensity resolution. Of course, many other factors, such as attentiveness, selective attention, motivation, and memory, also determine efficiency. Nonetheless, one would predict that the ability to detect changes in the intensity of a suprathreshold sound follows a developmental course similar to that for masked thresholds.

A summary of the development of intensity discrimination taken from several studies of infants and children is shown in Figure 3. In general, intensity discrimination has been found to be relatively immature in infants. For pure tone intensity discrimination, 6- to 9-month-old infants have been reported to have intensity difference limens (DL) on the order of 6–9 dB, compared to a DL of 1–2 dB in adults (Sinnott, J. M. and Aslin, R. N., 1985; Berg, K. M. and Boswell, A. E., 1998; Kopyar, B. A., 1997). Infants are more adult-like in intensity

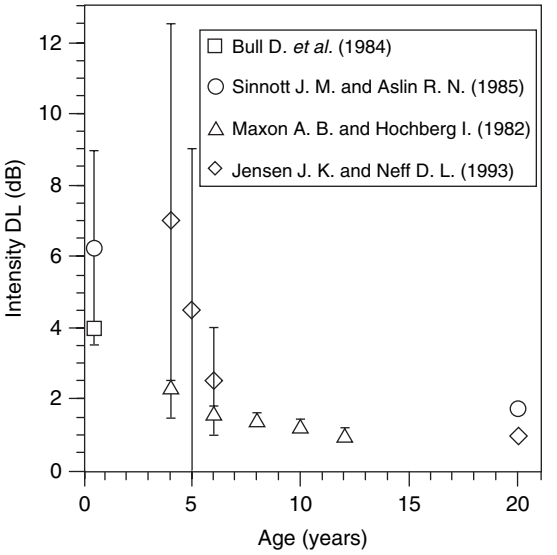

Figure 3 A summary of the development of intensity discrimination, taken from four different studies. Error bars represent ± one standard deviation. Stimuli varied across studies (see text).

discrimination of broadband than narrow band sounds (Bull, D. *et al.*, 1984; Kopyar, B. A., 1997). Although there is considerable variability in the intensity DL reported for children in different studies, there is a general trend for intensity discrimination to improve through the preschool period and to approach adult levels at 5–6 years of age (Jensen, J. K. and Neff, D. L., 1993; Maxon, A. B. and Hochberg, I., 1982; Berg, K. M. and Boswell, A. E., 2000), mirroring the age-related improvement in detection-in-noise (Schneider, B. A. *et al.*, 1989).

If the immature auditory system exhibits a sluggish growth of response with increases in intensity or if the response at a given intensity is variable, detection and discrimination will be poor. Schneider B. A. *et al.* (1989) and Schneider B. A. and Trehub S. E. (1992) discuss the role of intensity coding in the development of detection in noise, but there is little direct evidence for immaturity of intensity coding in infancy or childhood. Cochlear responses tend to grow with intensity in a similar way in neonates and adults (Abdala, C., 2000). There are few studies that have compared infants and adults in the growth of neural evoked response amplitude with intensity, although response latency appears to change with increasing intensity in an adult-like fashion even in preterm infants (Gorga, M. P. *et al.*, 1989). Several studies (Durieux-Smith, A. *et al.*, 1985; Cornacchia, L. *et al.*, 1983; Rickard, L. K., 1988) have shown that

ABR wave V amplitude grows with increasing intensity more slowly in young infants, but the age difference did not persist beyond 10 months of age. Although auditory development of cortical evoked potentials clearly continues throughout childhood (e.g., Huttenlocher, P. R., 1979; Kraus, N. *et al.*, 1985; Sharma, A. *et al.*, 1997), the effects of age on the growth of cortical potentials with stimulus intensity has not been addressed. In fact, that infants are more mature in their detection of broadband than of narrow-band sounds, in the absence of any obvious bandwidth-dependent differences in attentiveness, suggests that intensity coding is not responsible for infants' immature detection in noise (Werner, L. A. and Boike, K., 2001).

3.50.2.2.3 Loudness

Given the relatively prolonged development of intensity discrimination performance, it is surprising that direct measures of loudness growth show few developmental effects beyond infancy (Bond, B. and Stevens, S. S., 1969; Collins, A. A. and Gescheider, G. A., 1989; Dorfman, D. D. and Megling, R., 1966). For example, Collins A. A. and Gescheider G. A. found that preschool children could not only perform a cross-modality loudness matching procedure, but that their results were quite similar to those of adults. It should be noted that this observation argues against immaturity of intensity processing in general, at least during the preschool period.

Interestingly, there is limited evidence for immaturity of loudness perception among infants. Leibold L. J. and Werner L. A. (2002) showed that infants, like adults, respond more quickly to a more intense tone. They found, further, that the rate at which response latency decreased with increasing tone intensity was greater in infants than it was in adults. In other words, loudness growth appeared to be more rapid in infants than in adults. This finding is difficult to reconcile with the idea that the neural response is growing more slowly with increasing intensity in young listeners. It is consistent with the idea that infants listen in a high level of internal noise: loudness grows more rapidly in external noise among adult listeners.

3.50.2.3 Temporal Resolution

Again, several observations of early auditory development in nonhuman species suggest that age-related changes in temporal resolution occur in the course of human development. Immature auditory neurons, for example, do not sustain response to continuous stimulation and demonstrate prolonged recovery from prior stimulation (e.g., Brugge, J. F. *et al.*, 1978). Whether the corresponding developmental period in humans occurs in the postnatal period is not clear.

Estimates of temporal resolution in infancy are heavily dependent on the measure used to assess temporal resolution. A popular measure has been the gap detection threshold, the shortest interruption in ongoing sound that can just be detected by the listener. Werner L. A. *et al.* (1992) measured gap detection thresholds in 3-, 6-, and 12-month-old infants and in adults for broadband noise and for low-pass noises with varying high-frequency cutoffs. Infants' gap detection thresholds were quite poor, on the order of 40–50 ms in the broadband noise condition. Gap detection threshold did not improve between 3 and 12 months of age, but changed with the frequency of the stimulus in a manner similar to that seen in adults. In subsequent experiments, Werner L. A. and her colleagues reported the same poor gap detection thresholds using a different method to estimate thresholds (Werner, L. A. *et al.*, 1994a) and showed that the effect of changing the stimulus frequency from gap onset to gap offset had similar effects on infants and adults (Werner, L. A. *et al.*, 1994a). Trehub S. E. *et al.* (1995) found that infants were better at detecting a gap between two Gaussian-shaped tone bursts than gaps in noise, but their gap thresholds were still far from adult-like. Studies of preschool children, on the other hand, generally indicated mature gap detection thresholds by 4 or 5 years of age (Wightman, F. *et al.*, 1989; Trehub, S. E. *et al.*, 1995).

Studies employing other measures of temporal resolution suggest a quite different pattern of development. Duration discrimination, for example, has been shown to be immature in infants and to remain immature in young children (Morrongiello, B. A. and Trehub, S. E., 1987; Elfenbein, J. L. *et al.*, 1993). Werner L. A. (1999), in contrast, reported that forward masking was adult-like by 6 months of age. While Buss E. *et al.* (1999) reported improvements in forward masked thresholds between 5 and 11 years, the improvement in masked threshold just paralleled the improvement seen in threshold in quiet. Thus, the amount of forward masking demonstrated at each age was about the same as that seen in adults. Finally, two developmental studies of the temporal modulation transfer function (TMTF) have been conducted. The TMTF shows the depth of modulation required to detect amplitude

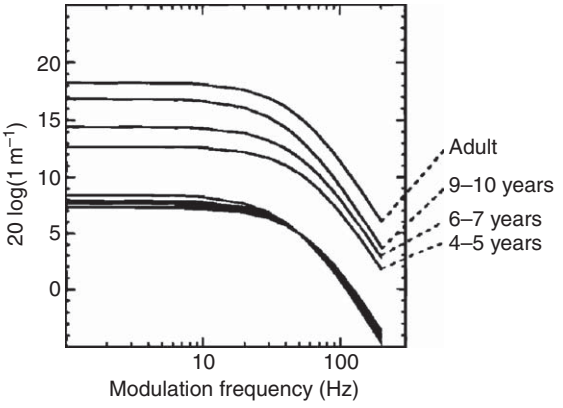

Figure 4 Temporal modulation transfer functions fit to the modulation detection data of four age groups. The functions are superimposed at the bottom of the panel to emphasize the similarity in shape. Reproduced from Hall, J. W. and Grose, J. H. 1994. Development of temporal resolution in children as measured by the temporal modulation transfer function. J. Acoust. Soc. Am. 96, 150–154, with permission.

modulation as a function of the modulation frequency. The TMTF has a low-pass characteristic and its cutoff frequency is a measure of temporal resolution (Viemeister, N. F., 1979). Both 3-month-old infants and 4- to 5-year-old children (Figure 4) appear to have adult-like TMTF (Hall, J. W. and Grose, J. H., 1994; Werner, L. A., 2006).

What conclusion can be drawn about the development of temporal resolution? On the basis of the TMTF, the gold standard of measures of temporal resolution, one would conclude that temporal resolution is mature quite early in life. This conclusion is consistent with several developmental physiological studies of temporal resolution: forward masking and gap detection in the ABR (Lasky, R. E., 1991; 1993; Werner, L. A. *et al.*, 2001) and in the mismatch negativity, a cortical evoked potential (Trainor, L. J. *et al.*, 2001) appear to be adult-like by 3 months postnatal age. An unanswered question is why infants and children have greater difficulty dealing with other temporally based tasks.

3.50.2.4 Spatial Resolution and Perception

3.50.2.4.1 Sound localization

Of all auditory capacities, spatial resolution would seem to be the most likely to undergo clear improvements with age because it depends on the size of the external ear and the head. Infants will certainly have a smaller range of interaural differences to work with, even if peripheral coding and the central circuits that calculate interaural differences are adult-like. In addition, the resonance of the small external ear will limit the frequencies that infants can use to localize sounds in elevation or to make front–back distinctions.

In fact, spatial resolution has been found to improve systematically with age, but to an extent that cannot be accounted for by peripheral immaturity alone. Newborn infants turn toward a sound source on their left or right (Clifton, R. K. *et al.*, 1981; Muir, D. and Field, T., 1979), but the minimum audible angle (MAA) at birth has been estimated at around 30° in azimuth (Morrongiello, B. A. *et al.*, 1994). The MAA in azimuth has been examined in infants and children in several laboratories; it has been reported to decrease from 30° at birth to about 14° at 7 months to adult levels at 5 years (Morrongiello, B. A. and Rocca, P. T., 1987a; 1990; Morrongiello, B. A. *et al.*, 1994; Litovsky, R. Y. and Ashmead, D. H., 1997; Clifton, R. K., 1992; Clarkson, M. G., 1995; Ashmead, D. H. *et al.*, 1987). However, sound localization probably continues to develop beyond the preschool period; for example, 5-year-olds' sound localization may be disrupted by the presence of sound reflections more than adults' (Litovsky, R., 1993).

Sound localization in elevation has been less well studied, although one laboratory has reported that the MAA in elevation for an 8–12 kHz noise band improved from nearly 16° at 6 months to about 6° at 18 months (Morrongiello, B. A. and Rocca, P. T., 1987c; 1987b). An interesting observation in these studies is that infants never achieve 75% correct in detecting a change in the position of a 4–8 kHz noise band or a 4 kHz low-pass noise. Adults also perform better in elevation discrimination if the stimulus contains frequencies above 4–5 kHz, but it appears that infants are more heavily dependent on frequencies above 8 kHz, which would be consistent with their smaller pinnas.

By 7 months of age, infants appear to discriminate differences in the distance to a sound source. Clifton R. K. and her colleagues (1991) developed a clever procedure to allow infants to demonstrate their ability to judge the distance of a sounding object. After allowing the infant to play with a sounding object in the light, these researchers presented the same sounding object to infants at varying distances in the dark. Infants were found to reach more often for the object when it was within their reach than when it was beyond their reach. Litovsky R. and Clifton R. K. (1992) subsequently showed that infants did not

depend solely on the sound pressure level arriving at their head to perform this discrimination; they continued to reach more to within-reach than to beyond-reach objects even when the intensity of sound was varied randomly. Interestingly, adult subjects tested in a similar situation appeared to be more heavily dependent on sound pressure level in making distance judgments.

Several attempts have been made to explicate the mechanisms responsible for age-related improvements in sound localization. Potential candidates include acoustic cues, peripheral coding, neural calculation of interaural differences and spectral shape, and the central mapping of acoustic cues onto positions in space. Clifton R. K. *et al.* (1988) addressed the issue of changes in the acoustic cues available for localization by directly measuring interaural distance and head circumference in neonates and 22-week-olds. From these measurements, they estimated that the maximum interaural time difference (ITD) available to infants would increase from 400 to 500 μs over this age period. If infants depended only on interaural time differences to locate sounds in azimuth, they should be able to achieve an MAA less than 10° at this age, compared to the 20° observed (Ashmead D. H. *et al.*, 1987). Ashmead D. H. *et al.* (1991) followed the development of ITD discrimination from 16 to 28 weeks of age. ITD discrimination thresholds were on the order of 50–75 μs, were never poor enough to account for the infant's immature MAA, and did not improve with age as the MAA does. This suggests that maturation of neither the precision of temporal information provided by the ear nor the function of the neural circuits involved in ITD calculation can entirely account for the maturation of spatial resolution in azimuth. Gray L. (1992) has argued that changes in chicks' responses to changes in the location of a sound source in the first few days after hatching reflect the acquisition of an organized representation of auditory space. Observations of humans who are congenitally deprived of binaural input support the idea that this mapping process is an important aspect of the development of sound localization. These individuals achieve respectable performance in ITD discrimination when surgical intervention makes binaural hearing possible for them, but they continue to have quite poor abilities to identify the location of a sound source in space (Wilmington D. *et al.*, 1994). These observations in humans are consistent with many studies of the effects of abnormal binaural experience on the development of spatial hearing in other species (e.g., Moore D. R., 1983; Knudsen, E. I., 1988; Binns, K. E. *et al.*, 1995).

3.50.2.4.2 Binaural masking level difference and spatial release from masking

One advantage of binaural hearing is the improvement in sensitivity to target sounds that results when target and competing sounds are perceived as coming from different spatial locations. In the laboratory, one form of this advantage, the binaural masking level difference (BMLD), has been extensively studied. Compared to the condition in which the same masker and tone are presented under earphones to both ears (designated N_0S_0), threshold for a tone presented in a broadband masker is as much as 15 dB lower when the same masker is presented to both ears, while the tone is presented 180° out of phase at one ear relative the other (designated N_0S_π). The BMLD is the threshold improvement observed under such dichotic conditions.

Given the dramatic improvement in auditory spatial resolution during infancy and early childhood, it is of some interest whether similar improvements are evident in the BMLD. To the extent that the same mechanisms are involved in calculating the interaural time difference that underlies both sound localization and the BMLD, one might predict that the two follow similar developmental courses. At first blush, this appears to be the case. Nozza R. J. (1987) and Nozza R. J. *et al.* (1988) have reported, that under conditions that produce a BMLD of about 11 dB for adults, 7-month-old infants have a BMLD of only 5 dB. Nozza R. J. *et al.* concluded that preschool children were probably adult-like in BMLD, but Hall J.W. and Grose J. H. (1990) subsequently found that while 6-year-old children had adult-like BMLD, 4- to 5-year-old children still had somewhat smaller BMLD than adults. In all cases, the reduced BMLD resulted from a relatively higher threshold in the N_0S_π condition, suggesting immaturity of binaural processing.

In several studies, however, Hall J.W., Grose J. H. and colleagues (Grose, J. H. *et al.*, 1997; Hall, J. W. and Grose, J. H., 1990; Hall, J. W. *et al.*, 2004) have found that while school-age children have adult-like BMLD for a broadband masker, they have significantly smaller BMLD for narrow-band maskers. Adults seem to be able to take advantage of low-energy segments of the fluctuating envelope of a narrow-band masker in binaural detection (i.e., by listening in the dips). One explanation for the

developmental trend observed in the BMLD for narrow-band maskers is that children are less able than adults to use this additional information. This idea is consistent with an observation by Litovsky R. Y. (2005) that school-age children were unable to take advantage of spatial separation of speech target and masker in free field when the masker is the voice of a single speaker, although they did show spatial release from masking in other masking conditions. In the single-speaker masking condition, listeners have a particular opportunity to use gaps in the masker to hear the target.

Thus, infants appear to have immature binaural processing. Given little evidence that intensity or temporal coding is immature at 7 months, this finding is consistent with a central processing immaturity. By age 5 or 6 years, children appear capable of using binaural information under many conditions, but under more difficult listening conditions, adults are able to access additional cues that children do not.

3.50.3 Development of Complex Perceptual Capacities

Mature processing of complex sounds in real environments requires more than a simple representation of the spectral and temporal characteristics of the acoustic stimulus. Because sound from multiple sources is generally present, the listener is required to group the components of each complex sound according to its source and to select the sound from the appropriate source for further processing. Furthermore, within the complex arising from any one source, some frequency bands or temporal segments may be more informative than others, and thus be more heavily weighted in the process of recognition or identification. An important point is that immaturity of processes such as sound source determination, selective attention, and listening to relevant sound features is likely to manifest itself in many ways, including apparent immaturity of intensity resolution or listening efficiency. Because primary auditory processes appear to be relatively mature during infancy, we tend to believe that it is these complex, higher-level auditory processes that limit the performance of infants and children, even in simple listening tasks.

The idea that infants and children are just not as good as adults in performing psychophysical tasks is one that occurs to even the casual student of sensory development. In psychophysical terms, infants and children are inefficient listeners. Efficiency is influenced by primary auditory processes, but also by a variety of factors such as memory, attention, and motivation. Both resolution and efficiency influence sensitivity. An inefficient listener is less sensitive to a tone in noise, and one would expect that inefficiency to carry over into the perception of any sound in a noisy background. Many investigators have suggested that infants and children are inefficient listeners compared to adults (Allen, P. and Wightman, F., 1994; Bargones, J. Y. *et al.*, 1995; Hartley, D. E. H. *et al.*, 2000; Werner, L. A. and Boike, K., 2001). The sources of early immature efficiency, however, are not well understood. In this section, possible contributions of higher-level perceptual processes to the development of auditory sensitivity are considered.

3.50.3.1 Sound Source Determination

By sound source determination is meant the process by which a listener segregates the components of complex sound into different auditory objects. For example, listeners are able to take sound emanating simultaneously from the voice of a conversant, a barking dog, and a passing car and to parse the complex into three different sound sources despite the fact that there is spectral and temporal overlap among the three sounds. Listeners use many types of information to accomplish this task, considering common temporal modulation, location, and harmonicity among others. In the lab, a common approach to studying sound source determination is auditory streaming, in which a listener is asked to report the number of separate sound sources heard in a complex sound and sometimes to describe each source. Because infants and young children have difficulty understanding such procedures, researchers have had to develop more indirect measures of sound source determination in young listeners.

It is clear that infants can segregate sound sources under some conditions. Newman R. S. and Jusczyk P. W. (1996) exposed 7- to 8-month-old infants to two superimposed voices, one male and one female. The female voice spoke a series of words with exaggerated intonation, while the male voice recited text from the methods section of a journal article. Following 30 s exposure, infants were presented with a list of words spoken by the same female voice whenever they looked at a flashing light. On some trials, the words were the same words spoken in the initial exposure; on others, the words were novel.

If infants looked longer for one list of words than the other, it was concluded that the infants recognized the words they had heard in competition with the male voice. If the female voice was presented at a level 5 or 10 dB greater than that of the male voice, infants looked longer for the word list previously presented, but if the levels of the two voices were equal, they showed no evidence of recognizing the words. This study certainly indicates that under some circumstances, infants are capable of segregating two competing voices. However, it suggests that even when the two voices differ in fundamental frequency, timing, and intonation, infants have difficulty segregating the two voices without an additional intensity difference. Because adult's speech reception thresholds under similar conditions would be well below 0 dB signal-to-noise ratio (e.g., Litovsky R. Y., 2005), the acoustic components of the target words were presumably audible to both infants and adults. Beyond that, infants' failure to respond differentially to the familiar words at 0 dB signal-to-noise ratio could result from a failure of sound source determination, a failure of selective attention, or both. Although it does not resolve this issue, a recent study by Hollich G. *et al.* (2005) showed that infants did recognize the words in the target voice when the competing voice was of equal intensity, if presentation of the voices was accompanied by a video of the talker's face.

Several investigators have attempted to study auditory streaming in infants using other approaches. Adult listeners have difficulty judging the relative order of elements of sound that are perceived in separate auditory streams. Thus, if the order of sounds in a sequence is reversed, the listener's ability to discriminate the change in order will depend on whether or not the sounds are heard in the same auditory stream (Figure 5). Demany, L (1982), Fassbender C. (1993), and McAdams S. and Bertoncini J. (1997) have all demonstrated that infants' ability to discriminate a change in the order of a sound sequence changes in a way that is consistent with adults' stream segregation. However, the limits of the infants' ability to form auditory streams and the relative importance of different acoustic cues in determining how infants form streams remain unexplored.

It is curious that auditory streaming experiments with older children have not been reported, because it is quite possible that even preschool children would be able to perform some version of the auditory streaming task. The question of sound source determination in children has been addressed indirectly in studies of co-modulation masking release (CMR). Adults detect a tone at a lower intensity if intensity fluctuations in sounds in frequency bands away from the tone frequency match the fluctuations in the intensity of a masker centered on the signal frequency. Adults' thresholds for the tone are actually

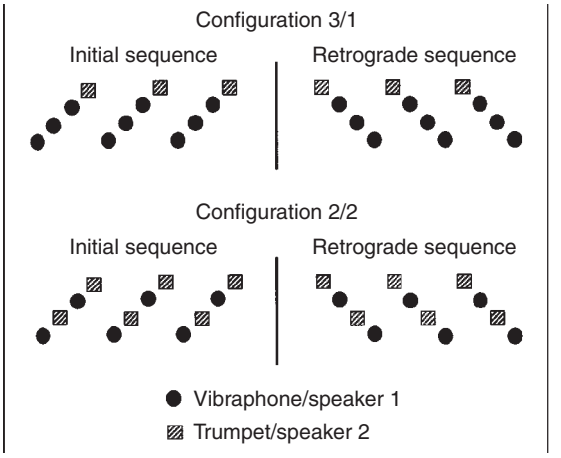

Figure 5 Examples of stimulus sequences used in an auditory streaming experiment with infant subjects. The vertical dimension in each panel is fundamental frequency. The circles represent synthetic vibraphone tones that were played from a speaker to one side of the infant's head. The squares represent trumpet tones that were played from a speaker on the opposite side of the infant's head. Adults listening to both sequences reported hearing two auditory streams. In the top panel, a slowly repeated trumpet tone was heard in one stream, while, in the other, a descending ('initial sequence') or ascending ('retrograde sequence') series of faster vibraphone tones was heard. In the bottom panel, a series of alternating high and low vibraphone tones was heard in one stream, while, in the other, a slightly lower alternating high and low sequence of trumpet tones was heard. When the initial sequence in the top panel was played in reverse, adults could discriminate the change. In the bottom panel, if adults had heard the sound as a single stream, they would be able to discriminate the initial sequence from its reverse, because the pitch would now decrease, rather than increase, across each repetition of the four-tone sequence. However, when the adults heard the stimulus as two streams, the same alternating high–low sequence could be heard whether the sequence was played forward or backward. Infants listening to these two stimulus configurations discriminated the initial sequence in the top panel from its retrograde, but showed no evidence of discriminating the initial sequence in the bottom panel from its retrograde. The latter result suggests that infants heard the sequence in the bottom panel as two auditory streams, as adults did. Reproduced from McAdams, S. and Bertoncini, J. 1997. Organization and discrimination of repeating sound sequences by newborn infants. J. Acoust. Soc. Am. 102, 2945–2953, with permission.

higher if no sounds other than the masker centered on its frequency are present. This phenomenon is referred to as CMR (Hall, J. W., 1987). CMR is thought to reflect processes important to sound source determination: the signal tone may be more audible if the on-signal masker is perceptually grouped with the other flanking noise bands. Grose J. H. *et al.* (1993) reported that 4-year-old children showed the same threshold improvement from adding off-frequency, co-modulated frequency bands as adults do. Hall J.W. *et al.* (1997) found that slightly older children also exhibited adult-like CMR, but reported that when the masker band centered on the signal frequency and the off-frequency co-modulated bands were slightly asynchronous, adults' CMR was reduced while children's CMR was eliminated or became negative. One possible explanation for this result is that temporal synchrony is a more important grouping factor for children than it is for adults.

3.50.3.2 Auditory Attention

The development of two varieties of attention is considered here. The first is attentiveness, often referred to as sustained attention. By attentiveness is meant the ability to remain 'on task' and to acquire information about the stimulus. The other, probably more important sort of attention will be referred to as selective attention. Once incoming sound has been parsed into separate auditory objects, a listener must frequently choose the sound from one source for further processing while ignoring others. Further, some features of sound from a single source may be processed while others are not. These processes require auditory selective attention. It should be noted that any complex listening task involves the basic analytic processes that underlie all hearing. Then the components belonging to a single source must be identified and integrated, and finally, one source selected for processing. Failure to selectively process a sound, then, will occur if any of these processes – analysis, sound source determination, selective attention – is immature. On the basis of the studies reviewed above, we conclude that the basic analytic processes are mature by 6 or 7 months of age, but while several studies have attempted to study selective auditory attention, immature sound source determination could well have influenced children's performance in these studies.

3.50.3.2.1 Attentiveness

An obvious reason that infants and children perform rather poorly in some psychophysical tasks is that they have difficulty sustaining attention to the task. Inattentiveness may prevent them from having any idea whether or not a tone was presented on some trials, for example. Several investigators have argued that while infants and children are undoubtedly inattentive at some points during testing, the effects of inattentiveness would not be expected to be large enough to account for the observed age differences in auditory sensitivity (Schneider, B. A. and Trehub, S. E., 1992; Viemeister, N. F. and Schlauch, R. S., 1992; Werner, L. A. and Bargones, J. Y., 1992; Wightman, F. and Allen, P., 1992). In studies that have examined the psychometric function for detection, the upper asymptote of the function has been reported to be less than 1 for many infants and children (Allen, P. and Wightman, F., 1994; Bargones, J. Y. *et al.*, 1995; Werner, L. A. and Boike, K., 2001). This is consistent with inattentive listening: even when the sound is audible, young listeners respond incorrectly on some trials. If one assumes that the listener has no information about the stimulus on inattentive trials and that on such trials the listener guesses whether or not a signal occurred, then the rate of inattention would be twice the difference between 1 and the observed upper asymptote. In infants, the inattention rate is estimated at about 30% in a variety of conditions (Bargones, J. Y. *et al.*, 1995; Werner, L. A. and Boike, K., 2001), and, in children, it appears to range from 0% to 25% (Allen, P. and Wightman, F., 1994). Further analyses show, however, that even an inattention rate of 30% would shift the observed threshold for detecting a tone by only 2–3 dB. Similarly small effects would be expected in other tasks. In no case is the effect of inattentiveness sufficient to account for the observed difference between adults and infants and children.

3.50.3.2.2 Selective listening to relevant sound features

Another explanation for early immature psychoacoustic performance is immature listening strategies. Adults tend to listen at expected frequencies and at times when a sound could be presented. Adults quickly discover and focus on the most informative cues in a complex stimulus. Infants, on the other hand, may listen in a less selective fashion. Werner L. A. and Bargones J. Y. (1991), for example, showed that 7-month-old infants' threshold for a tone were elevated by the presence of a higher frequency

masker well removed from the frequency region of the tone. Adults tested under the same condition demonstrated little or no masking. Bargones J. Y. and Werner L. A. (1994) subsequently showed that while adults were more sensitive to a frequency they expected to hear than to other unexpected frequencies, infants were equally sensitive to expected and unexpected frequencies. Thus, adults appear to restrict listening to the frequency band around the signal they are trying to detect, while infants listen broadly across frequencies regardless of the signal to be detected. It has been estimated that failure to monitor the frequency band around the to-be-detected signal would increase threshold by about 7 dB (Dai, H. *et al.*, 1991), which would account for a large portion of the difference between infants' and adults' thresholds for a tone in noise (Werner, L. A. and Boike, K., 2001).

Preschool children have not yet become consistently selective listeners. Stellmack M. A. *et al.* (1997) asked 5-year-olds and adults to discriminate changes in intensity in one component of a three-component complex. If the level of the 'distractor' components was lower than that of the target, both children and adults were able to listen selectively to the target component. In contrast, if the target and distractors were equal in level, only the adults were able to continue to listen selectively to the target. It should be noted, however, that even when the task was to discriminate overall intensity differences between three-component complexes, 5-year-olds needed larger intensity differences to perform the task than adults did, despite the fact that selective listening was not the optimal strategy (Willihnganz, M. S. *et al.*, 1997).

Even infants may be able to listen selectively in time, however. Parrish H. K. and Werner L. A. (2004) tested infants' ability to detect a tone that occurred following a short noise burst that indicated the beginning of a trial. On most trials, the tone occurred 500 ms after the noise burst, but on a small proportion of trials, the tone occurred 200 or 800 ms after the noise burst. Under these conditions, both infants and adults detected the tone at 500 ms better than the tone at 200 or at 800 ms, and the effect of presentation time was no different for the two age groups. Thus, it would appear that listening broadly over time does not contribute to infant–adult threshold differences.

Another developmental effect that may be important in somewhat more complex listening situations is a shift in the cues used to detect or discriminate sounds. One example is the observation of Hall J.W. and Grose J. H. (2004) discussed above, that children do not take advantage of temporal fluctuations in the level of a masker to detect a signal. Similarly, infants and children may focus on salient aspects of a sound, but ignore additional cues that may allow them to discriminate between sounds under more difficult listening conditions. For example, Lacerda F. (1992) found that infants younger than 5 months of age were more likely to respond to a change in a formant transition in a CV syllable, while adults labeled the syllables primarily on the basis of vowel quality. Nittrouer S. and her colleagues (Nittrouer, S. and Studdert-Kennedy, M., 1987; Nittrouer, S. and Boothroyd, A., 1990; Nittrouer S., 1996; Nittrouer, S. and Miller, M. E., 1997; Nittrouer, S. and Crowther, C. S., 1998; 2001; Nittrouer, S. *et al.*, 1998) have completed a series of studies of preschool and school-age children that demonstrate that they, too, are more influenced by formant transitions than by static cues in identifying consonants. Recently, Nittrouer S. (2005) has suggested that young children's differential attention to dynamic cues in speech may make it more difficult for them to identify speech in noise.

3.50.3.2.3 Ignoring irrelevant sound features

Informational masking is defined here as a reduction in the audibility or discriminability of one sound that results from the presence of another sound, beyond that accounted for by overlap of the excitation patterns of the two sounds in the auditory periphery. Although there is currently some controversy over the meaning of informational masking (e.g., Durlach, N. I. *et al.*, 2003), this definition captures the generally agreed upon features of the phenomenon. In a paradigm that has been used in many subsequent studies, Neff D. L. and Green D. M. (1987) showed that detection threshold for a tone was elevated over quiet threshold when the frequencies of a competing multicomponent complex varied randomly from trial to trial, even though the frequencies in the competing complex were well outside the auditory filter centered on the target frequency. Essentially, informational masking results from a failure to ignore the resolvable competing components (Lutfi, R. A. *et al.*, 2003). There are large individual differences among adults in the amount of informational masking demonstrated, but in general, the greatest amount of masking is seen with ten-component competing complexes (e.g., Neff, D. L. and Callaghan, B. P., 1988). Allen P. and Wightman F. (1995) first demonstrated

that preschool children's threshold for a pure tone in noise was increased by more than 24 dB if one other random frequency tone was presented simultaneously, compared to 11 dB for adults. Moreover, half of the children Allen P. and Wightman F. tested were unable to detect the target tone at an intensity less than 90 dB.

Oh E. L. *et al.* (2001) obtained thresholds for a 1000 Hz tone from preschoolers and adults in broadband noise and in the presence of tonal complexes with 2–1000 randomly drawn components. Children demonstrated somewhat more masking than adults in the broadband noise masker, but 25–35 dB more masking than adults when the masker components varied randomly. Children were qualitatively similar to adults in that they demonstrated the most informational masking in the ten-component masker condition, but were more likely than adults to exhibit significant masking in the presence of a two-component masker. The results were well described by a model (Lutfi, R. A., 1993) in which children monitor a greater number of auditory filters than adults do, consistent with previous studies of infants and children (Allen, P. and Wightman, F., 1994; Bargones, J. Y. and Werner, L. A., 1994; Bargones, J. Y. *et al.*, 1995; Werner, L. A. and Boike, K., 2001).

Leibold L. J. and Werner L. A. (2006) compared 7–9-month-olds' and adults' detection of a 1000 Hz tone in the presence of three different maskers, a broadband noise, a random-frequency two-tone complex and a fixed-frequency two-tone complex. Neither of the two-tone complexes had energy around 1000 Hz. Adults' thresholds were 15 dB higher, while infants' thresholds were 23 dB higher, with the random frequency masker than with the broadband noise masker, suggesting more informational masking with the random frequency masker. It is not clear why children appear to perform more poorly than infants, relative to adults, in informational masking (cf., Oh, E. L. *et al.*, 2001 described earlier). Interestingly, adults' thresholds were 37 dB higher, while infants' thresholds were just 33 dB higher, with the fixed-frequency two-tone masker than with the random-frequency two-tone masker. On this basis, it is not clear at all that infants are more susceptible to random-frequency masking effects than adults are.

A related question is whether manipulations that reduce informational masking in adults have similar effects on children. For example, gating a random-frequency masker prior to the onset of the target tone tends to reduce the amount of informational masking, as does repeating the target several times while the random-frequency masker varies (Hall, J. W. *et al.*, 2005; Kidd, G. *et al.*, 1994). Hall J. W. *et al.* reported that children tended to derive less benefit in detection from such manipulations than adults do, but it was not clear whether the ability to do so improved between 5 and 9 years of age. Another manipulation that reduces informational masking in adults is a spatial difference between the random-frequency masker and the target tone, for example, by presenting the masker and target to different ears or to speakers located in different spatial positions (Neff, D. L., 1995; Kidd, J., G. *et al.*, 1998; Arbogast, T. L. *et al.*, 2002). Two different laboratories have now demonstrated that 4- to 9-year-old children do not show a spatial release from informational masking and may even show increased masking when the masker and target are presented dichotically (Hall, J. W. *et al.*, 2005; Wightman, F. *et al.*, 2003).

3.50.3.2.4 Listening to competing messages

Dichotic listening is the classic paradigm for the study of selective auditory attention (Cherry, E. C., 1953): a listener is presented with two sound sequences. In one condition, the sequences are presented simultaneously to the same ear(s). In the other, one sound sequence is presented to one ear and a different sound sequence to the other. The sound sequences are typically speech. The listener is asked to report the sound presented in one sequence, while ignoring the other. Maccoby E. E. and Konrad K. W. (1966) tested kindergarten, second-grade, and fourth-grade children in such a selective listening task. In the dichotic condition, a male voice spoke words in one ear, while a female voice spoke words in the other. In the diotic condition, both voices were presented to both ears. Children were instructed to report the word spoken by either the male or female voice. Performance in the diotic condition was rather poor overall, but improved from 18% to 33% correct between kindergarten and fourth grade. In the dichotic condition, performance was uniformly better at all ages, but still improved from 35% to 52% correct over the age range tested. Doyle A.-B. (1973) reported that the improvement in performance in the diotic competing message condition continued to a lesser extent between 8 and 14 years of age. The results of more recent studies are consistent with this pattern, and indicate that differences between event-related potentials evoked by attended and unattended stimuli increase in parallel with performance in

dichotic listening tasks (Bartgis, J. *et al.*, 2003; Berman, S. and Friedman, D., 1995; Coch, D. *et al.*, 2005).

Recent studies of children disentangling competing messages have produced a wide range of results. For example, Litovsky R. Y. (2005) asked 4- to 7-year-olds and adults to identify spondees in the presence of 1- or 2-talker speech or of speech-shaped noise modulated with the 1- or 2-talker speech envelope. Children's thresholds were higher than adults' in all conditions, but: (1) the amount of masking exhibited by children and adults was similar in all conditions; (2) both children and adults had higher speech reception thresholds in modulated speech-shaped noise than in speech; and (3) children and adults showed equivalent release from masking when the spondee was presented from the speaker in front of the listener and the competing sound was presented to a speaker on the listener's right. Fallon M. *et al.* (2000) reported that 5-year-olds were as good as adults in identifying words in a background of multitalker babble, as long as age differences in masked thresholds were taken into account. Hall J.W. *et al.* (2002), in contrast, found that while adults' spondee identification was about the same with two-talker and noise maskers, 5- to 9-year-old children's spondee identification was worse with a two-talker masker than with a noise masker, particularly when the speech masker was presented continuously throughout the session. Finally, Wightman F. and Kistler D. (2005) asked children and adults to identify speech in a paradigm developed by Brungart, D. S. and his colleagues (Brungart, D. S., 2001). Listeners heard a target sentence along with a competing sentence in one ear, and in one condition, an additional competing sentence or a modulated speech-shaped noise was presented in the other ear. Listeners ranging in age from 4.6 to 30 years were tested with a female-talker distracter. The youngest children, 4.6–5.7 years old, needed a 23 dB greater signal-to-distracter ratio than 20- to 30-year-olds to identify a word in the target sentence when no contralateral distracter was presented. Adding noise to the contralateral ear had little effect at any age, but adding speech to the contralateral ear had a greater effect on the youngest children than on other age groups. Older children seemed to be affected by the presence of contralateral speech to about the same extent as adults.

It is difficult to draw conclusions about the development of selective attention from these studies. Several variables seem to be important in determining whether children will be able to attend selectively to one of several competing messages. One of these is the extent to which the target and distracters are synchronized in time. In the Wightman F. and Kistler D. (2005) experiment, for example, the words in the target and distracter stimuli were precisely aligned. Temporal synchrony is one variable that makes it difficult for listeners to segregate sound sources (Yost, W. A., 1991).

It is interesting that in the speech studies in which the words in the target and distracter sentences were not precisely aligned, children are generally able to take advantage of differences in spatial location to improve performance, while in informational masking studies where target and distracter are temporally aligned, they are not. This suggests a problem with sound source segregation rather than with selective attention. The precise characteristics of the distracter also seem to be important. For example, if children are less able than adults to take advantage of periods of low distracter energy to process the target, then more modulated distracters (e.g., single-talker versus multitalker) will put children at a relative disadvantage compared to adults. Finally, it does appear that children may less easily ignore the semantic content of the distracter than adults. Hall J.W. *et al.* (2002) reported that children's spondee identification was more disrupted by continuous speech (in which the listener might follow the meaning) than by gated speech (in which the semantic content would be disrupted by gating), while gating the distracter made little difference to adult performance. A similar result was reported by Cherry E. C. (1981). Considerably more research will obviously be needed to understand the development of auditory attention.

3.50.4 Summary and Conclusion

Postnatal auditory development in humans appears to occur in two stages. In the first six months of life, maturation of the conductive apparatus and of the primary neural pathways results in substantial improvement in absolute sensitivity and frequency resolution, especially at high frequencies. The challenge for future research in this area is to develop approaches that allow us to understand the nature of these early changes and their impact on early perceptual learning.

After six months of age, perceptual performance remains immature, however, despite the fact that intensity, frequency, and temporal processing are

nearly adult-like. Auditory perception continues to improve into childhood and adolescence. Development over this prolonged period involves maturation of perceptual organization and attentional processes, but also learning about the important features of sound through experience. The challenge in understanding development in this later period is to develop approaches that will allow us to disentangle the effects of the many perceptual processes involved.

References

Abdala, C. 1996. Distortion product otoacoustic emission (2f1-f2) amplitude as a function of f2/f1 frequency ratio and primary tone level separation in human adults and neonates. J. Acoust. Soc. Am. 100, 3726–3740.

Abdala, C. 1998. A developmental study of distortion product otoacoustic emission (2f1- f2) suppression in humans. Hear. Res. 121, 125–138.

Abdala, C. 2000. Distortion product otoacoustic emission (2f1-f2) amplitude growth in human adults and neonates. J. Acoust. Soc. Am. 107, 446–456.

Abdala, C. and Chatterjee, M. 2003. Maturation of cochlear nonlinearity as measured by distortion product otoacoustic emission suppression growth in humans. J. Acoust. Soc. Am. 114, 932–943.

Abdala, C. and Folsom, R. C. 1995. The development of frequency resolution in humans as revealed by the auditory brain–stem response recorded with notched-noise masking. J. Acoust. Soc. Am. 98, 921–930.

Abdala, C., Oba, S., and Keefe, D. H. 2006. DPOAE ipsilateral suppression from birth through six months of age. Paper presented at the meeting of the American Auditory Society, Scottsdale, AZ.

Akiyama, Y., Schulte, F. J., Schultz, M. A., and Parmelee, A. H. 1969. Acoustically evoked responses in premature and full term newborn infants. Electroencephalogr. Clin. Neurophysiol. 26, 371–380.

Allen, P. and Wightman, F. 1994. Psychometric functions for children's detection of tones in noise. J. Speech Hear. Res. 37, 205–215.

Allen, P. and Wightman, F. 1995. Effects of signal and masker uncertainty on children's detection. J. Speech Hear. Res. 38, 503–511.

Allen, P., Wightman, F., Kistler, D., and Dolan, T. 1989. Frequency resolution in children. J. Speech Hear. Res. 32, 317–322.

Arbogast, T. L., Mason, C. R., and Kidd, G. 2002. The effect of spatial separation on informational and energetic masking of speech. J. Acoust. Soc. Am. 112, 2086–2098.

Ashmead, D. H., Clifton, R. K., and Perris, E. E. 1987. Precision of auditory localization in human infants. Dev. Psychol. 23, 641–647.

Ashmead, D. H., Davis, D., Whalen, T., and Odom, R. 1991. Sound localization and sensitivity to interaural time differences in human infants. Child Dev. 62, 1211–1226.

Bargones, J. Y. and Burns, E. M. 1988. Suppression tuning curves for spontaneous otoacoustic emissions in infants and adults. J. Acoust. Soc. Am. 83, 1809–1816.

Bargones, J. Y. and Werner, L. A. 1994. Adults listen selectively; infants do not. Psychol. Sci. 5, 170–174.

Bargones, J. Y., Werner, L. A., and Marean, G. C. 1995. Infant psychometric functions for detection: mechanisms of immature sensitivity. J. Acoust. Soc. Am. 98, 99–111.

Bartgis, J., Lilly, A. R., and Thomas, D. G. 2003. Event-related potential and behavioral measures of attention in 5-, 7-, and 9-year-olds. J. Gen. Psychol. 130, 311–335.

Bartoshuk, A. K. 1962. Human neonatal cardiac acceleration to sound: habituation and dishabituation. Percept. Mot. Skills 15, 15–27.

Berg, K. M. 1993. A comparison of thresholds for 1/3-octave filtered clicks and noise bursts in infants and adults. Percept. Psychphys. 54, 365–369.

Berg, K. M. and Boswell, A. E. 1998. Infants' detection of increments in low- and high-frequency noise. Percept. Psychophys. 60, 1044–1051.

Berg, K. M. and Boswell, A. E. 1999. Effect of masker level on infants' detection of tones in noise. Percept. Psychophys. 61, 80–86.

Berg, K. M. and Boswell, A. E. 2000. Noise increment detection in children 1 to 3 years of age. Percept. Psychophys. 62, 868–873.

Berg, K. M. and Smith, M. C. 1983. Behavioral thresholds for tones during infancy. J. Exp. Child Psychol. 35, 409–425.

Berman, S. and Friedman, D. 1995. The development of selective attention as reflected by event-related brain potentials. J. Exp. Child Psychol. 59, 1–31.

Binns, K. E., Withington, D. J., and Keating, M. J. 1995. The developmental emergence of the representation of auditory azimuth in the external nucleus of the inferior colliculus of the guinea-pig: the effects of visual and auditory deprivation. Brain Res. Dev. Brain Res. 85, 14–24.

Birnholz, J. C. and Benacerraf, B. R. 1983. The development of human fetal hearing. Science 222, 516–518.

Bond, B. and Stevens, S. S. 1969. Cross-modality matching of brightness to loudness by 5-year-olds. Percept. Psychophys. 6, 337–339.

Bredberg, G. 1968. Cellular pattern and nerve supply of the human organ of Corti. Acta Otolaryngol. Suppl. (Stockh) 236, 1–135.

Brown, A. M., Sheppard, S. L., and Russell, P. 1994. Acoustic distortion products (ADP) from the ears of term infants and young adults using low stimulus levels. Br. J. Audiol. 28, 273–280.

Brugge, J. F., Javel, E., and Kitzes, L. M. 1978. Signs of functional maturation of peripheral auditory system in discharge patterns in anteroventral cochlear nucleus of kittens. J. Neurophysiol. 41, 1557–1579.

Brungart, D. S. 2001. Evaluation of speech intelligibility with the coordinate response measure. J. Acoust. Soc. Am. 109, 2276–2279.

Bull, D., Eilers, R. E., and Oller, D. K. 1984. Infants' discrimination of intensity variation in mulitsyllabic stimuli. J. Acoust. Soc. Am. 76, 13–17.

Buss, E., Hall, J. W., Grose, J. H., and Dev, M. B. 1999. Development of adult-like performance in backward, simultaneous, and forward masking. J. Speech Lang. Hear. Res. 42, 844–849.

Cherry, E. C. 1953. Some experiments on the recogntion of speech, with one ear and with two ears. J. Acoust. Soc. Am. 25, 975–979.

Cherry, R. S. 1981. Development of selective auditory attention skills in children. Percept. Mot. Skills 52, 379–385.

Chuang, S. W., Gerber, S. E., and Thornton, A. R. 1993. Evoked otoacoustic emissions in preterm infants. Int. J. Pediatr. Otorhinolaryngol. 26, 39–45.

Clarkson, M. G. 1995. Psychophysical measures of auditory localization in human infants. Abstracts of the Association for Research in Otolaryngology 18, 57.

Clarkson, M. G. 1996. Infants' intensity discrimination; spectral profiles. Infant Beh. Dev. 19, 181–190.

Clarkson, M. G. and Clifton, R. K. 1985. Infant pitch perception: evidence for responding to pitch categories and the missing fundamental. J. Acoust. Soc. Am. 77, 1521–1528.
Clarkson, M. G. and Clifton, R. K. 1995. Infants' pitch perception: inharmonic tonal complexes. J. Acoust. Soc. Am. 98, 1372–1379.
Clarkson, M. G., Clifton, R. K., and Perris, E. E. 1988. Infant timbre perception: discrimination of spectral envelopes. Percept. Psychophys. 43, 15–20.
Clarkson, M. G. and Rogers, E. C. 1995. Infants require low-frequency energy to hear the pitch of the missing fundamental. J. Acoust. Soc. Am. 98, 148–154.
Clifton, R. K. 1992. The Development of Spatial Hearing in Human Infants. In: Developmental Psychoacoustics (*eds*. L. A. Werner and E. W. Rubel), pp. 135–157. American Psychological Association.
Clifton, R. K., Graham, F. K., and Hatton, H. M. 1968. Newborn heart-rate response and response habituation as a function of stimulus duration. J. Exp. Child Psychol. 6, 265–278.
Clifton, R. K., Gwiazda, J., Bauer, J., Clarkson, M., and Held, R. 1988. Growth in head size during infancy: implications for sound localization. Dev. Psychol. 24, 477–483.
Clifton, R. K., Morrongiello, B. A., Kulig, J. W., and Dowd, J. M. 1981. Developmental Changes in Auditory Localization in Infancy. In: Development of Perception (*eds*. R. Aslin, J. Alberts, and M. R. Petersen), pp. 141–160. Academic Press.
Clifton, R. K., Perris, E. E., and Bullinger, A. 1991. Infants' perception of auditory space. Dev. Psychol. 27, 187–197.
Coch, D., Sanders, L., and Neville, H. 2005. An event-related potential study of selective auditory attention in children and adults. J. Cogn. Neurosci. 17, 605–622.
Collet, L., Garner, M., Veuillet, E., Moulin, A., and Morgon, A. 1993. Evoked and spontaneous otoacoustic emissions: a comparison of neonates and adults. Brain Dev. 15, 249–252.
Collins, A. A. and Gescheider, G. A. 1989. The measurement of loudness in individual children and adults by absolute magnitude estimation and cross-modality matching. J. Acoust. Soc. Am. 85, 2012–2021.
Cornacchia, L., Martini, A., and Morra, B. 1983. Air and bone conduction brain stem responses in adults and infants. Audiol. 22, 430–437.
Dai, H., Scharf, B., and Buus, S. 1991. Effective attenuation of signals in noise under focused attention. J. Acoust. Soc. Am. 89, 2837–2842.
Demany, L. 1982. Auditory stream segregation in infancy. Infant Beh. Dev. 5, 261–276.
Dorfman, D. D. and Megling, R. 1966. Comparison of magnitude estimation of loudness in children and adults. Percept. Psychophys. 1, 239–241.
Doyle, A.-B. 1973. Listening to distraction: a developmental study of selective attention. J. Exp. Child Psychol. 15, 100–115.
Durieux-Smith, A., Edwards, C. G., Picton, T. W., and Mcmurray, B. 1985. Auditory brainstem responses to clicks in neonates. J. Otolaryngol. 14, 12–18.
Durlach, N. I., Mason, C. R., Kidd, G., Arbogast, T. L., Colburn, H. S., and Shinn-Cunningham, B. G. 2003. Note on informational masking (L). J. Acoust. Soc. Am. 113, 2984–2987.
Eggermont, J. J., Brown, D. K., Ponton, C. W., and Kimberley, B. P. 1996. Comparison of distortion product otoacoustic emission (DPOAE) and auditory brainstem response (ABR) traveling wave delay measurements suggests frequency-specific synapse maturation. Ear Hear. 17, 386–394.
Ehret, G. 1976. Development of absolute auditory thresholds in the house mouse (mus musculus). J. Am. Audiol. Soc. 1, 179–184.
Ehret, G. and Romand, R. 1981. Postnatal development of absolute auditory thresholds in kittens. J. Comp. Physiol. Psychol. 95, 304–311.
Eisenberg, R. B., Griffin, E. J., Coursin, D. B., and Hunter, M. A. 1964. Auditory behavior in the human neonate: a preliminary report. J. Speech Hear. Res. 7, 233–244.
Elfenbein, J. L., Small, A. M., and Davis, M. 1993. Developmental patterns of duration discrimination. J. Speech Hear. Res. 36, 842–849.
Engel, R. and Young, N. B. 1969. Calibrated pure tones audiograms in normal neonates based on evoked electroencephalographics responses. Orig. Articles 1, 149–160.
Fallon, M., Trehub, S. E., and Schneider, B. A. 2000. Children's perception of speech in multitalker babble. J. Acoust. Soc. Am. 108, 3023–3029.
Fassbender, C. (1993). Auditory Grouping and Segregation Processes in Infancy. Kaste Verlag.
Fischer, B. and Hartnegg, K. 2004. On the development of low-level auditory discrimination and deficits indyslexia. Dyslexia. 10, 105–118.
Folsom, R. C. 1985. Auditory brain stem responses from human infants: pure tone masking profiles for clicks and filtered clicks. J. Acoust. Soc. Am. 78, 555–562.
Folsom, R. C. and Wynne, M. K. 1987. Auditory brain stem responses from human adults and infants: wave V tuning curves. J. Acoust. Soc. Am. 81, 412–417.
Fujimoto, S., Yamamoto, K., Hayabuchi, I., and Yoshizuka, M. 1981. Scanning and transmission electron microscope studies on the organ of corti and stria vascularis in human fetal cochlear ducts. Arch. Histol. Jap. 44, 223–235.
Gerber, S. E. 1985. Stimulus, response, and state variables in the testing of neonates. Ear Hear. 6, 15–19.
Gerhardt, K. J., Abrams, R. M., and Oliver, C. C. 1990. Sound environment of the fetal sheep. Am. J. Obstet. Gynecol. 162, 282–287.
Gorga, M. P., Kaminski, J. R., Beauchaine, K. L., Jesteadt, W., and Neely, S. T. 1989. Auditory brainstem responses from children three months to three years of age: normal patterns of response II. J. Speech Hear. Res. 32, 281–288.
Gray, L. 1992. Interactions between Sensory and Nonsensory Factors in the Responses of Newborn Birds to Sound. In: Developmental Psychoacoustics (*eds*. L. A. Werner and E. W. Rubel), pp. 89–112. American Psychological Association.
Gray, L. and Rubel, E. W. 1985. Development of absolute thresholds in chickens. J. Acoust. Soc. Am. 77, 1162–1172.
Grose, J. H., Hall, J. W., and Dev, M. B. 1997. MLD in children: effects of signal and masker bandwidths. J. Speech Lang. Hear. Res. 40, 955–959.
Grose, J. H., Hall, J. W., and Gibbs, C. 1993. Temporal analysis in children. J. Speech Hear. Res. 36, 351–356.
Hall, J. G. 1964. The cochlea and the cochlear nuclei in neonatal asphyxia. Acta Otolaryngol. Suppl. (Stockh) 194, 8–93.
Hall, J. W. 1987. Experiments on Comodulation Masking Release. In: Auditory Processing of Complex Sounds (*eds*. W. A. Yost and C. S. Watson), pp. 57–66. Erlbaum.
Hall, J. W., Buss, E., and Grose, J. H. 2005. Informational masking release in children and adults. J. Acoust. Soc. Am. 118, 1605–1613.
Hall, J. W., Buss, E., Grose, J. H., and Dev, M. B. 2004. Developmental effects in the masking-level difference. J. Speech Lang. Hear. Res. 47, 13–20.
Hall, J. W. and Grose, J. H. 1990. The masking level difference in children. J. Am. Acad. Audiol. 1, 81–88.
Hall, J. W. and Grose, J. H. 1991. Notched-noise measures of frequency selectivity in adults and children using fixed-masker-level and fixed-signal-level presentation. J. Speech Hear. Res. 34, 651–660.

Hall, J. W. and Grose, J. H. 1994. Development of temporal resolution in children as measured by the temporal modulation transfer function. J. Acoust. Soc. Am. 96, 150–154.
Hall, J. W., Grose, J. H., Buss, E., and Dev, M. B. 2002. Spondee recognition in a two-talker masker and a speech-shaped noise masker in adults and children. Ear Hear. 23, 159–165.
Hall, J. W., Grose, J. H., and Dev, M. B. 1997. Auditory development in complex tasks of comodulation masking release. J. Speech Lang. Hear. Res. 40, 946–954.
Hall, J. W. III. (1992) Handbook of Auditory Evoked Responses. Allyn and Bacon.
Harris, J. D. 1952. Pitch discrimination. J. Acoust. Soc. Am. 24, 750–755.
Hartley, D. E. H., Wright, B. A., Hogan, S. C., and Moore, D. R. 2000. Age-related improvements in auditory backward and simultaneous masking in 6- to 10-year-old children. J. Speech Lang. Hear. Res. 43, 1402–1415.
Hoshino, T. 1990. Scanning electron microscopy of nerve fibers in human fetal cochlea. J. Electron Microsc. 15, 104–114.
Hollich, G., Newman, R. S., and Jusczyk, P. W. 2005. Infants' use of synchronized visual information to separate streams of speech. Child Dev. 76, 598–613.
Huttenlocher, P. R. 1979. Synaptic density in human frontal cortex – developmental changes and effects of aging. Brain Res. 163, 195–205.
Igarashi, Y. and Ishii, T. 1979a. Development of organ of corti and stria vascularis in human fetus. Audiol. (Jap.) 22, 459–460.
Igarashi, Y. and Ishii, T. 1979b. Development of the cochlear and the blood-vessel-network in the fetus: a transmission electrographic observation. Audiol. (Jap.) 22, 459–460.
Igarashi, Y. and Ishii, T. 1980. Embryonic development of the human organ of corti: electron microscopic study. Int. J. Ped. Otorhinolaryngol. 2, 51–62.
Igarashi, Y., Yamazaki, H., and Mitsui, T. 1978. An electronographic study of inner/outer haircells of human fetuses. Audiol. (Jap.) 21, 375–377.
Irwin, R. J., Stillman, J. A., and Schade, A. 1986. The width of the auditory filter in children. J. Exp. Child Psychol. 41, 429–442.
Isaacson, G., Mintz, M. C., and Sasaki, C. T. 1986. Magnetic resonance imaging of the fetal temporal bone. Laryngoscope 96, 1343–1346.
Jensen, J. K. and Neff, D. L. 1993. Development of basic auditory discrimination in preschool children. Psychol. Sci. 4, 104–107.
Jordan, R. E. and Eagles, E. L. 1963. Hearing sensitivity and related factors in children. Monogr. Laryngoscope 143.
Keefe, D. H., Bulen, J. C., Arehart, K. H., and Burns, E. M. 1993. Ear-canal impedance and reflection coefficient in human infants and adults. J. Acoust. Soc. Am. 94, 2617–2638.
Keefe, D. H. and Levi, E. C. 1996. Maturation of the middle and external ears: acoustic power-based responses and reflectance typmanometry. Ear Hear. 17, 1–13.
Kenyon, T. N. 1996. Ontogenetic changes in the auditory sensitivity of damselfishes (pomacentridae). J. Comp. Physiol. A 179, 553–561.
Kidd, G., Mason, C. R., Deliwala, P. S., Woods, W. S., and Colburn, H. S. 1994. Reducing informational masking by sound segregation. J. Acoust. Soc. Am. 95, 3475–3480.
Kidd, J. G., Mason, C. R., Rohtla, T. L., and Deliwala, P. S. 1998. Release from masking due to spatial separation of sources in the identification of nonspeech auditory patterns. J. Acoust. Soc. Am. 104, 422–431.
Knudsen, E. I. 1988. Experience Shapes Sound Localization and Auditory Unit Properties during Development in the Barn Owl. In: Auditory Function: Neurobiological Bases of Hearing (*eds*. G. M. Edelman, W. E. Gall, and W. M. Cowan), pp. 137–149. John Wiley & Sons.
Kopyar, B. A. 1997. Intensity discrimination abilities of infants and adults: implications for underlying processes. Doctoral dissertation, University of Washington, Seattle, Washington.
Kotak, V. and Sanes, D. 1995. Synaptically evoked prolonged depolarizations in the developing auditory system. J. Neurophsyiol. 74, 1611–1620.
Kraus, N., Smith, D., Reed, N. L., Stein, L. K., and Cartee, C. 1985. Auditory middle latency responses in children: effects of age and diagnostic category. Electroencephal. Clin. Neurophysiol. 62, 343–351.
Kuhl, P. K. and Miller, J. L. 1982. Discrimination of auditory target dimensions in the presence or absence of variation in a second dimension by infants. Percept. Psychophys. 31, 279–292.
Lacerda, F. 1992. Young Infants' Discrimination of Confusable Speech Signals. In: The Auditory Processing of Speech: From Sound to Words (*ed*. M. E. H. Schouten), pp. 229–238. Mouton de Gruyter.
Lary, S., Briassoulis, G., De Vries, L., Dubowitz, L. M. S., and Dubowitz, V. 1985. Hearing threshold in preterm and term infants by auditory brainstem response. J. Pediatr. 107, 593–599.
Lasky, R., Perlman, J., and Hecox, K. 1992. Distortion-product otoacoustic emissions in human newborns and adults. Ear Hear. 103, 430–441.
Lasky, R. E. 1991. The effects of rate and forward masking on human adult and newborn auditory evoked response thresholds. Dev. Psychobiol. 24, 21–64.
Lasky, R. E. 1993. The effect of forward masker duration, rise/fall time, and integrated pressure on auditory brain stem evoked responses in human newborns and adults. Ear Hear. 14, 95–103.
Lavigne-Rebillard, M. and Bagger-Sjoback, D. 1992. Development of the human stria vascularis. Hear. Res. 64, 39–51.
Lavigne-Rebillard, M. and Pujol, R. 1987. Surface aspects of the developing human organ of corti. Acta Otolaryngol. (Stockh.) 436, 43–50.
Lavigne-Rebillard, M. and Pujol, R. 1988. Hair cell innervation in the fetal human cochlea. Acta Otolaryngol. (Stockh.) 105, 398–402.
Lavigne-Rebillard, M. and Pujol, R. 1990. Auditory hair cells in human fetuses: synaptogenesis and ciliogenesis. J. Electron. Microsc. Tech. 15, 115–122.
Lecanuet, J. P. 1996. Fetal sensory competencies. Eur. J. Obstet. Gynecol. 68, 1–23.
Leiberman, A., Sohmer, H., and Szabo, G. 1973. Cochlear audiometry (Electro-cochleography) during the neonatal period. Dev. Med. Child Neurol. 15, 8–13.
Leibold, L. J. and Werner, L. A. 2002. Relationship between intensity and reaction time in normal hearing infants and adults. Ear Hear. 23, 92–97.
Leibold, L. J. and Werner, L. A. 2006. The effect of masker-frequency variability on the detection performance of infants and adults. J. Acoust. Soc. Am. 119, 3960–3970.
Lenard, H. G., Bernuth, H. V., and Hutt, S. J. 1969. Acoustic evoked responses in newborn infants: the influence of pitch and complexity of the stimulus. Electroencephal. Clin. Neurophsyiol. 27, 121–127.
Leventhal, A. and Lipsitt, L. P. 1964. Adaptation, pitch discrimination and sound localization in the neonate. Child Dev. 35, 759–767.
Liden, G. and Kankkonen, A. 1961. Visual reinforcement audiometry. Acta Otolaryngol. (Stockh.) 67, 281–292.
Litovsky, R. 1993. The influence of the precedence effect on developmental changes in sound localization precision. J. Acoust. Soc. Am. 94, 1–31.

Litovsky, R. Y. 2005. Speech intelligibility and spatial release from masking in young children. J. Acoust. Soc. Am. 117, 3091–3099.
Litovsky, R. Y. and Ashmead, D. H. 1997. Development of Binaural and Spatial Hearing in Infants and Children. In: Binarual and Spatial Hearing in Real and Virtual Environments (*eds*. R. H. Gilkey and T. R. Anderson), pp. 571–592. Lawrence Erlbaum Associates.
Litovsky, R. Y. and Clifton, R. K. 1992. Use of sound-pressure level in auditory distance discrimination by 6-month-old infants and adults. J. Acoust. Soc. Am. 92, 794–802.
Lutfi, R. A. 1993. A model of auditory pattern analysis based on component-relative-entropy. J. Acoust. Soc. Am. 94, 748–758.
Lutfi, R. A., Kistler, D. J., Oh, E. L., Wightman, F. L., and Callahan, M. R. 2003. One factor underlies individual differences in auditory informational masking within and across age groups. Percept. Psychophys. 65, 396–406.
Maccoby, E. E. and Konrad, K. W. 1966. Age trends in selective listening. J. Exp. Child Psychol. 3, 113–122.
Marean, G. C., Werner, L. A., and Kuhl, P. K. 1992. Vowel categorization by very young infants. Dev. Psychol. 28, 396–405.
Maxon, A. B. and Hochberg, I. 1982. Development of psychoacoustic behavior: sensitivity and discrimination. Ear Hear. 3, 301–308.
McAdams, S. and Bertoncini, J. 1997. Organization and discrimination of repeating sound sequences by newborn infants. J. Acoust. Soc. Am. 102, 2945–2953.
Mckinnis, M. E. 1936. The number of ganglion cells in dorsal root ganglia of the second and third cervical nerves in human fetuses of various ages. Anat. Rec. 65, 255–259.
Mencher, G. T., Mencher, L. S., and Rohland, S. L. 1985. Maturation of behavioral response. Ear Hear. 6, 10–14.
Montgomery, C. R. and Clarkson, M. G. 1997. Infants' pitch perception: masking by low- and high-frequency noises. J. Acoust. Soc. Am. 102, 3665–3672.
Moore, B. C., Peters, R. W., and Glasberg, B. R. 1999. Effects of frequency and duration on psychometric functions for detection of increments and decrements in sinusoids in noise. J. Acoust. Soc. Am. 106, 3539–3552.
Moore, D. R. 1983. Development of Inferior Colliculus and Binaural Audition. In: Development of Auditory and Vestibular Systems (*ed*. R. Romand), pp. 121–166. Academic Press.
Moore, J. K., Guan, Y. L., and Shi, S. R. 1997. Axogenesis in the human fetal auditory system, demonstrated by neurofilament immunohistochemistry. Anat. Embryol. (Berl.) 195, 15–30.
Moore, J. K., Perazzo, L. M., and Braun, A. 1995. Time course of axonal myelination in human brainstem auditory pathway. Hear. Res. 87, 21–31.
Moore, J. K., Ponton, C. W., Eggermont, J. J., Wu, B. J., and Huang, J. Q. 1996. Perinatal maturation of the auditory brain stem response: changes in path length and conduction velocity. Ear Hear. 17, 411–418.
Moore, J. M., Wilson, W. R., and Thompson, G. 1977. Visual reinforcement of head-turn responses in infants under 12 months of age. J. Speech Hear. Disord. 42, 328–334.
Morlet, T., Perrin, E., Durrant, J. D., Lapillonne, A., Ferber, C., Duclaux, R., Putet, G., and Collet, L. 1996. Development of cochlear active mechanisms in humans differs between gender. Neurosci. Lett. 220, 49–52.
Morrongiello, B. A., Fenwick, K. D., Hillier, L., and Chance, G. 1994. Sound localization in newborn human infants. Dev. Psychobiol. 27, 519–538.
Morrongiello, B. A. and Rocca, P. T. 1987a. Infants' localization of sounds in the horizontal plane: effects of auditory and visual cues. Child Dev. 58, 918–927.
Morrongiello, B. A. and Rocca, P. T. 1987b. Infants' localization of sounds in the median sagittal plane: effects of signal frequency. J. Acoust. Soc. Am. 82, 900–905.
Morrongiello, B. A. and Rocca, P. T. 1987c. Infants' localization of sounds in the median vertical plane: estimates of mimimal audible angle. J. Exp. Child Psychol. 43, 181–193.
Morrongiello, B. A. and Rocca, P. T. 1990. Infants' localization of sounds within hemifields: estimates of minimum audible angle. Child Dev. 61, 1258–1270.
Morrongiello, B. A. and Trehub, S. E. 1987. Age-related changes in auditory temporal perception. J. Exp. Child Psych. 44, 413–426.
Muir, D. and Field, T. 1979. Newborn infants orient to sounds. Child Dev. 50, 431–436.
Nakai, Y. 1970. An electron microscopic study of the human fetus cochlea. Pract. Otol. Rhinol. Laryngol. 32, 257–267.
Neff, D. L. 1995. Signal properties that reduce masking by simultaneous, random-frequency maskers. J. Acoust. Soc. Am. 98, 1909–1920.
Neff, D. L. and Callaghan, B. P. 1988. Effective properties of multicomponent simultaneous maskers under conditions of uncertainty. J. Acoust. Soc. Am. 83, 1833–1838.
Neff, D. L. and Green, D. M. 1987. Masking produced by spectral uncertainty with multicomponent maskers. Percept. Psychophys. 41, 409–415.
Newman, R. S. and Jusczyk, P. W. 1996. The cocktail party effect in infants. Percept. Psychophys. 58, 1145–1156.
Nittrouer, S. 1996. Discriminability and perceptual weighting of some acoustic cues to speech perception by 3-year-olds. J. Speech Hear. Res. 39, 278–297.
Nittrouer, S. 2005. Age-related differences in weighting and masking of two cues to word-final stop voicing in noise. J. Acoust. Soc. Am. 118, 1072–1088.
Nittrouer, S. and Boothroyd, A. 1990. Context effects in phoneme and word recognition by young children and older adults. J. Acoust. Soc. Am. 87, 2705–2715.
Nittrouer, S. and Crowther, C. S. 1998. Examining the role of auditory sensitivity in the developmental weighting shift. J. Speech Lang. Hear. Res. 41, 809–818.
Nittrouer, S. and Crowther, C. S. 2001. Coherence in children's speech perception. J. Acoust. Soc. Am. 110, 2129–2140.
Nittrouer, S., Crowther, C. S., and Miller, M. E. 1998. The relative weighting of acoustic properties in the perception of s +stop clusters by children and adults. Percept. Psychophys. 60, 51–64.
Nittrouer, S. and Miller, M. E. 1997. Predicting developmental shifts in perceptual weighting schemes. J. Acoust. Soc. Am. 101, 3353–3366.
Nittrouer, S. and Studdert-Kennedy, M. 1987. The role of coarticulatory effects in the perception of fricatives by children and adults. J. Speech Hear. Res. 30, 319–329.
Nozza, R. J. 1987. The binaural masking level difference in infants and adults: developmental change in binaural hearing. Infant Beh. Dev. 10, 105–110.
Nozza, R. J., Wagner, E. F., and Crandell, M. A. 1988. Binaural release from masking for a speech sound in infants, preschoolers, and adults. J. Speech Hear. Res. 31, 212–218.
Nozza, R. J. and Wilson, W. R. 1984. Masked and unmasked pure-tone thresholds of infants and adults: development of auditory frequency selectivity and sensitivity. J. Speech Hear. Res. 27, 613–622.
Oh, E. L., Wightman, F., and Lutfi, R. A. 2001. Children's detection of pure-tone signals with random multitone maskers. J. Acoust. Soc. Am. 109, 2888–2895.
Okabe, K. S., Tanaka, S., Hamada, H., Miura, T., and Funai, H. 1988. Acoustic impedance measured on normal ears of children. J. Acoust. Soc. Jap. 9, 287–294.
Olsho, L. W. 1985. Infant auditory perception: tonal masking. Infant Beh. Dev. 7, 27–35.

Olsho, L. W., Koch, E. G., and Carter, E. A. 1988a. Nonsensory factors in infant frequency discrimination. Infant Beh. Dev. 11, 205–222.

Olsho, L. W., Koch, E. G., Carter, E. A., Halpin, C. F., and Spetner, N. B. 1988b. Pure-tone sensitivity of human infants. J. Acoust. Soc. Am. 84, 1316–1324.

Olsho, L. W., Koch, E. G., and Halpin, C. F. 1987. Level and age effects in infant frequency discrimination. J. Acoust. Soc. Am. 82, 454–464.

Parrish, H. K. and Werner, L. A. 2004. Listening windows in infants and adults. *Paper presented at the meeting of the American Auditory Society Meeting*, Scottsdale, AZ.

Plinkert, P. K., Sesterhenn, G., Arold, R., and Zenner, H. P. 1990. Evaluation of otoacoustic emisssions in high-risk infants by using an easy and rapid objective auditory screening method. Eur. Arch. Otorhinolaryngol. 247, 356–360.

Ponton, C. W., Eggermont, J. J., Kwong, B., and Don, M. 2000. Maturation of human central auditory system activity: evidence from multi-channel evoked potentials. Clin. Neurophysiol. 111, 220–236.

Ponton, C. W., Moore, J. K., and Eggermont, J. J. 1996. Auditory brain stem response generation by parallel pathways: differential maturation of axonal conduction time and synaptic transmission. Ear Hear. 17, 402–410.

Pujol, R. and Lavigne-Rebillard, M. 1992. Development of neurosensory structures in the human cochlea. Acta Otolaryngol. (Stockh.) 112, 259–264.

Pujol, R., Lavigne-Rebillard, M., and Uziel, A. 1990. Physiological correlates of development of the human cochlea. Semin. Perinatol. 14, 275–280.

Pujol, R., Lavigne-Rebillard, M., and Uziel, A. 1991. Development of the human cochlea. Acta Otolaryngol. (Stockh.) Suppl 482, 7–12.

Querleu, D., Renard, X., Versyp, F., Paris-Delrue, L., and Crepin, G. 1988. Fetal hearing. Eur. J. Ob. Gyn. Repro. Biol. 29, 191–212.

Rickard, L. K. 1988. Auditory brainstem responses from infants and adults to extended high-frequency tone pips. Masters thesis, University of Washington, Seattle, WA.

Salamy, A., Mckean, C. M., and Buda, F. B. 1975. Maturational changes in auditory transmission as reflected in human brain stem potentials. Brain Res. 96, 361–366.

Sanes, D. H. and Walsh, E. J. 1998. The Development of Central Auditory Function. In: Development of the Auditory System (*eds*. E. W. Rubel, R. R. Fay, and A. N. Popper), pp. 271–314. Springer Verlag.

Schneider, B. A., Morrongiello, B. A., and Trehub, S. E. 1990. The size of the critical band in infants, children, and adults. J. Exp. Psych. [Hum. Percept. Perform.] 16, 642–652.

Schneider, B. A. and Trehub, S. E. 1992. Sources of Developmental Change in Auditory Sensitivity. In: Developmental Psychoacoustics (*eds*. L. A. Werner and E. W. Rubel), pp. 3–46. American Psychological Association.

Schneider, B. A., Trehub, S. E., and Bull, D. 1979. The development of basic auditory processes in infants. Can. J. Psychol. 33, 306–319.

Schneider, B. A., Trehub, S. E., Morrongiello, B. A., and Thorpe, L. A. 1989. Developmental changes in masked thresholds. J. Acoust. Soc. Am. 86, 1733–1742.

Sharma, A., Kraus, N., McGee, T., and Nicol, T. 1997. Developmental changes in P1 and N1 central auditory responses elicited by consonant-vowel syllables. Evoked Potentials Electroenceph. Clin. Neurophysiol. 104, 540–545.

Shimizu, T., Salvador, L., Allanson, J., Hughes-Benzie, R., and Nimrod, C. 1991. Ultrasonographic measurements of the fetal ear. Obstet. Gynecol. 80, 381–384.

Sininger, Y. and Abdala, C. 1996. Auditory brainstem response thresholds of newborns based on ear canal levels. Ear Hear. 17, 395–401.

Sininger, Y. S., Abdala, C., and Cone-Wesson, B. 1997. Auditory threshold sensitivity of the human neonate as measured by the auditory brainstem response. Hear. Res. 104, 1–22.

Sinnott, J. M. and Aslin, R. N. 1985. Frequency and intensity discrimination in human infants and adults. J. Acoust. Soc. Am. 78, 1986–1992.

Sinnott, J. M., Pisoni, D. B., and Aslin, R. M. 1983. A comparison of pure tone auditory thresholds in human infants and adults. Infant Beh. Dev. 6, 3–17.

Soderquist, D. R. and Moore, M. 1970. Effect of training on frequency discrimination in primary school children. J. Aud. Res. 10, 185–192.

Spetner, N. B. and Olsho, L. W. 1990. Auditory frequency resolution in human infancy. Child Dev. 61, 632–652.

Steinschneider, A., Lipton, E. L., and Richmond, J. B. 1966. Auditory sensitivity in the infant: effect of intensity on cardiac and motor responsivity. Child Dev. 37, 233–252.

Stellmack, M. A., Willihnganz, M. S., Wightman, F. L., and Lutfi, R. A. 1997. Spectral weights in level discrimination by preschool children: analytic listening conditions. J. Acoust. Soc. Am. 101, 2811–2821.

Stevens, J. C., Webb, H. D., Smith, M. F., and Buffin, J. T. 1990. The effect of stimulus level on click evoked oto-acoustic emissions and brainstem responses in neonates under intensive care. Br. J. Audiol. 24, 293–300.

Streeter, G. L. 1906. On the development of the membranous labyrinth and the acoustic and facial nerves in the human embryo. Am. J. Anat. 6, 139–165.

Streeter, G. L. 1917. The development of the scala tympani, scala vestibuli and perioticular cistern in the human embryo. Am. J. Anat. 21, 299–320.

Stuart, A., Yang, E. Y., Stenstroml, R., and Reindorp, A. G. 1993. Auditory brainstem response thresholds to air and bone conducted clicks in neonates and adults. Am. J. Otol. 14, 176–182.

Teas, D. C., Klein, A. J., and Kramer, S. J. 1982. An analysis of auditory brainstem responses in infants. Hear. Res. 7, 19–54.

Tharpe, A. M. and Ashmead, D. H. 2001. A longitudinal investigation of infant auditory sensitivity. Am. J. Audiol. 10, 104–112.

Trainor, L. J., Samuel, S. S., Desjardins, R. N., and Sonnadara, R. R. 2001. Measuring temporal resolution in infants using mismatch negativity. Neuroreport 12, 2443–2448.

Trehub, S. E., Endman, M. W., and Thorpe, L. A. 1990. Infants' perception of timbre: classification of complex tones by spectral structure. J. Exp. Child. Psychol. 49, 300–313.

Trehub, S. E., Schneider, B. A., and Endman, M. 1980. Developmental changes in infants' sensitivity to octave-band noises. J. Exp. Child Psychol. 29, 282–293.

Trehub, S. E., Schneider, B. A., and Henderson, J. 1995. Gap detection in infants, children, and adults. J. Acoust. Soc. Am. 98, 2532–2541.

Trehub, S. E., Schneider, B. A., Thorpe, L. A., and Judge, P. 1991. Observational measures of auditory sensitivity in early infancy. Dev. Psychol. 27, 40–49.

Viemeister, N. F. 1979. Temporal modulation transfer functions based upon modulation thresholds. J. Acoust. Soc. Am. 66, 1364–1380.

Viemeister, N. F. and Schlauch, R. S. 1992. Issues in infant Psychoacoustics. In: Developmental Psychoacoustics (*eds*. L. A. Werner and E. W. Rubel), pp. 191–210. American Psychological Association.

Weir, C. 1976. Auditory frequency sensitivity in the neonate: a signal detection analysis. J. Exp. Child Psychol. 21, 219–225.

Weir, C. 1979. Auditory frequency sensitivity of human newborns: some data with improved acoustic and behavioral controls. Percept. Psychophys. 26, 287–294.

Werner, L. A. 1995. Observer-Based Approaches to Human Infant Psychoacoustics. In: Methods in Comparative Psychoacoustics (*eds*. G. M. Klump, R. J. Dooling, R. R. Fay, and W. C. Stebbins), pp. 135–146. Birkhauser Verlag.

Werner, L. A. 1996. The development of auditory behavior (or what the anatomists and physiologists have to explain). Ear Hear. 17, 438–446.

Werner, L. A. 1999. Forward masking among infant and adult listeners. J. Acoust. Soc. Am. 105, 2445–2453.

Werner, L. A. 2006. Preliminary observations on the temporal modulation transfer functions of infants and adults. Paper presented at the meeting of the American Auditory Society, Scottsdale, AZ.

Werner, L. A. and Bargones, J. Y. 1991. Sources of auditory masking in infants: distraction effects. Percept. Psychophys. 50, 405–412.

Werner, L. A. and Bargones, J. Y. 1992. Psychoacoustic Development of Human Infants. In: Advances in Infancy Research (*eds*. C. Rovee-Collier and L. Lipsitt), pp. 103–145. Ablex.

Werner, L. A. and Boike, K. 2001. Infants' sensitivity to broadband noise. J. Acoust. Soc. Am. 109, 2101–2111.

Werner, L. A., Constantino, J. C., and Mancl, L. R. 1994a. Gap detection by human infants. J. Acoust. Soc. Am. 95, 2940.

Werner, L. A., Folsom, R. C., and Mancl, L. R. 1993. The relationship between auditory brainstem response and behavioral thresholds in normal hearing infants and adults. Hear. Res. 68, 131–141.

Werner, L. A., Folsom, R. C., and Mancl, L. R. 1994b. The relationship between auditory brainstem response latencies and behavioral thresholds in normal hearing infants and adults. Hear. Res. 77, 88–98.

Werner, L. A., Folsom, R. C., Mancl, L. R., and Syapin, C. 2001. Human auditory brainstem response to temporal gaps in noise. J. Speech Lang. Hear. Res. 44, 737–750.

Werner, L. A. and Gillenwater, J. M. 1990. Pure-tone sensitivity of 2- to 5-week-old infants. Infant Beh. Dev. 13, 355–375.

Werner, L. A. and Holmer, N. M. 2002. Infant hearing thresholds measured in the ear canal. *Paper presented at the meeting of the American Auditory Society*, Scottsdale, AZ.

Werner, L. A. and Mancl, L. R. 1993. Pure-tone thresholds of 1-month-old human infants. J. Acoust. Soc. Am. 93, 2367.

Werner, L. A., Marean, G. C., Halpin, C. F., Spetner, N. B., and Gillenwater, J. M. 1992. Infant auditory temporal acuity: gap detection. Child Dev. 63, 260–272.

Werner, L.A. and Rubel, E.W. (eds.) (1992). Developmental Psychoacoustics. American Psychological Association.

Wightman, F. and Allen, P. 1992. Individual Differences in Auditory Capability Among Preschool Children. In: Developmental Psychoacoustics (*eds*. L. A. Werner and E. W. Rubel), pp. 113–133. American Psychological Association.

Wightman, F., Allen, P., Dolan, T., Kistler, D., and Jamieson, D. 1989. Temporal resolution in children. Child Dev. 60, 611–624.

Wightman, F., Callahan, M. R., Lutfi, R. A., Kistler, D. J., and Oh, E. 2003. Children's detection of pure-tone signals: informational masking with contralateral maskers. J. Acoust. Soc. Am. 113, 3297–3305.

Wightman, F. L. and Kistler, D. J. 2005. Informational masking of speech in children: effects of ipsilateral and contralateral distracters. J. Acoust. Soc. Am. 118, 3164–3176.

Willihnganz, M. S., Stellmack, M. A., Lutfi, R. A., and Wightman, F. L. 1997. Spectral weights in level discrimination by preschool children: synthetic listening conditions. J. Acoust. Soc. Am. 101, 2803–2810.

Wilmington, D., Gray, L., and Jahrsdorfer, R. 1994. Binaural processing after corrected congenital unilateral conductive hearing loss. Hear. Res. 74, 99–114.

Yost, W. A. 1991. Auditory image perception and analysis: the basis for hearing. Hear. Res. 56, 8–18.

Zeng, F., Kong, Y., Michalewski, H., and Starr, A. 2005. Perceptual consequences of disrupted auditory nerve activity, J. Neurophysiol. 93, 3050–3063.

Zimmermann, E. 1993. Behavioral measures of auditory thresholds in developing tree shrews (*Tupaia belageri*). J. Acoust. Soc. Am. 94, 3071–3075.

3.51 Sleep and Memory Consolidation in Audition

D Margoliash and K M Fenn, University of Chicago, Chicago, IL, USA

© 2008 Elsevier Inc. All rights reserved.

3.51.1	**Introduction**	896
3.51.2	**Sleep and Memory Consolidation in Humans**	896
3.51.2.1	Consolidation in Generalized Learning	897
3.51.2.2	Auditory Memory Consolidation	897
3.51.2.3	Multiple Processes of Memory Consolidation in Humans	898
3.51.3	**Sleep and Memory Consolidation in Animals**	898
3.51.3.1	Bird Song Learning	898
3.51.3.2	The Role of Sleep in Song Learning: Circadian Deconsolidation during Vocal Development	899
3.51.3.3	Implications of Circadian Deconsolidation for Models of Song Learning	900
3.51.4	**Mechanisms of Sleep and Memory Consolidation in Humans**	900
3.51.4.1	Evidence for Reactivation during Sleep in Humans	900
3.51.4.2	Changes in Cortical Representations of Memory After Sleep	901
3.51.4.3	Slow Wave Activity Effects on Consolidation	901
3.51.5	**Mechanisms of Sleep and Memory Consolidation in Vocal Learning**	901
3.51.5.1	Auditory Pathways Leading to the Song System	902
3.51.5.1.1	Physiological specificity within the auditory pathways	902
3.51.5.1.2	Behavioral and neural plasticity in the auditory pathways	903
3.51.5.2	State-Dependent Auditory Processing in the Song System of Awake Birds	903
3.51.5.2.1	Neuromodulatory processing in the song system of awake birds	904
3.51.5.3	Replay and Plasticity during Sleep	905
3.51.5.3.1	Site and form of the replay phenomenon	905
3.51.5.3.2	Plasticity in Robust Nucleus of Archopallium replay – spontaneous and auditory activity	906
3.51.5.3.3	Sleep-mediated developmental plasticity in Robust Nucleus of Archopallium	907
3.51.6	**Conclusions and Future Directions**	908
References		908

Glossary

auditory feedback The sound perceived of one's own vocalization.

consolidation An active offline process that serves to increase the stability of a memory.

declarative memory Explicit memory, such as for facts or concepts.

deconsolidation An active offline process that serves to decrease the stability of a memory.

generalized learning Deriving categories from learning explicit items/instances, hence applying the learning to categorize newly encountered items/instances.

nondeclarative memory Implicit memory such as procedural memory.

offline processing Information processing related to a task that occurs after the task and associated feedback are completed.

procedural memory A memory for performing a task.

neuronal replay Neural activity, typically emitted spontaneously in the absence of a behavior, that nevertheless matches the neural activity observed during the behavior.

sensorimotor learning Motor learning that involves sensory feedback.

tutor song The song that a juvenile bird commits to memory as a guide for further song development.

3.51.1 Introduction

The role of the unconscious, specifically the impact of dreaming, on our conscious life has been the subject of speculation through millennia of human thought. Sleep provides a state during which information acquired during the day may be reprocessed without competition from other stimuli, and this processing may reflect the consolidation of memory. Empirical evidence that waking events are replayed during dreaming (Stickgold, R. *et al.*, 2000b) and theoretical work on learning and unlearning in neural networks (Crick, F. and Mitchison, G., 1983; Hinton, G. E. *et al.*, 1995) provides support for this view. Although there remains considerable ignorance concerning the functional significance of sleep stages, as well as considerable controversy regarding specific hypotheses such as the rapid eye movement (REM)-consolidation hypothesis (Siegel, J. M., 2001), it is now well established that sleep makes a significant contribution to a broad range of learning tasks (Walker, M. P. and Stickgold, R., 2006). In animals, the neurophysiological mechanisms of how sleep influences natural behavior is being elaborated (Sutherland, G. R. and McNaughton, B., 2000). In this chapter, we review how sleep interacts with several forms of memory acquisition. Our principal focus is on auditory tasks in humans and animals.

Sleep is thought to influence learning through its effect on memory consolidation, the processing of the memory trace after its initial formation (memory acquisition) but while the memory remains in a labile state. Sleep was traditionally believed to passively to protect memory against loss, a quiescent state preventing new information from interfering with prior learning (retroactive interference) (Jenkins, J. M. and Dallenbach, K. M., 1924). However, neither sleep nor memory formation is a unitary process, indicating that consolidation must describe a broad range of phenomena. For example, there is compelling evidence that the action of sleep to deconsolidate vocal behavior is a regular feature of vocal development (Deregnaucourt, S. *et al.*, 2005), a major focus of this chapter.

Sleep is one of several physiological states during which offline processing occurs. Offline processing comprises the processing of information after the completion of a task (i.e., changes in representations) and after explicit feedback regarding the task has occurred, and cannot occur when an animal is engaged in another task (Foster, D. J. and Wilson, M. A., 2006). Thus, resting wakeful states (Gottselig, J. M. *et al.*, 2004) and naps (Mednick, S. C. *et al.*, 2002; 2003; Gomez, R. L. *et al.*, 2006) should also contribute to memory consolidation.

3.51.2 Sleep and Memory Consolidation in Humans

The way in which sleep affects memory depends on the type of memory being studied. Memory is traditionally divided into two systems, declarative and nondeclarative, or procedural, memory (Squire, L., 1987). The formation of declarative memory, or memory for facts, concepts, or information that can be explicitly recalled, is mediated by medial temporal lobe structures, particularly the hippocampus and surrounding areas (Mishkin, M. 1978; Zola-Morgan, S. *et al.*, 1993). A role of sleep in declarative memory consolidation has been elusive (Smith, C., 2001) and has been only recently elucidated with the demonstration that memory for paired associated word lists is enhanced more after a period of slow wave sleep (SWS) than an equal duration of REM sleep or waking (Plihal, W. and Born, J., 1997; Gais, S. and Born, J., 2004). After sleep, memory is less susceptible to retroactive interference than after an equal interval of waking (Ellenbogen, J. M. *et al.*, 2006), suggesting that sleep normally protects memories formed 1 day from associative interference of new information acquired on subsequent days.

Nondeclarative memory is memory for a procedure for accomplishing a task, and also includes simple habituation, sensitization, or conditioning. Formation of nondeclarative memory generally relies on task-dependent cortical and subcortical structures and does not always involve the hippocampus or medial temporal lobe (Milner, B., 1965). There is considerable evidence that sleep enhances nondeclarative memory consolidation in simple task acquisition. In a rote motor sequence-tapping task, performance improved after sleep but not after an equivalent period of waking (Walker, M. P. *et al.*, 2002; 2003). In a visual texture discrimination task, performance declined throughout training; improvement over baseline was seen only after sleep and was blocked by sleep deprivation followed training (Stickgold, R. *et al.*, 2000a; 2000c). REM sleep is essential for nondeclarative learning in the visual texture discrimination task: REM sleep deprivation following learning prevents performance improvement, whereas SWS deprivation has no effect on learning (Karni, A. *et al.*, 1994). Thus, sleep has two distinct effects on nondeclarative memory. Either,

performance improves after training and remains stable throughout the day, with additional performance gains are found following a night of sleep (cf. Walker, M. P., 2005a; 2005b), or performance declines throughout training and improvement over baseline performance requires sleep (cf. Stickgold, R., 2000a; 2000c). The origin of these disparate effects remains unclear.

3.51.2.1 Consolidation in Generalized Learning

Whereas the declarative/nondeclarative distinction is a useful way to divide memory, recent research has identified additional dimensions relevant to memory formation and consolidation. Memory may record specific details of an experience but retrieval may bring forth either the particular or some level of abstraction (e.g., McClelland, J. L. and Rumelhart, D. E., 1985). Learning may produce improved performance on particular items as in rote memory or may enable generalization to new items that have not been encountered. Generalized learning is a hallmark of adaptive behavior.

Sleep interacts with generalized learning. When individuals were given a relatively complex algorithm that could be solved using a hidden rule, the ability to generalize information to apply this rule was more likely to appear after sleep than after a day (or night) awake (Wagner, U. *et al.*, 2004). Learning can promote faster performance on each individual step or it can lead to the discovery of hidden rules that promote faster performance on the entire problem (but does not affect performance on the individual steps). Finding hidden rules requires the ability to flexibly use the information given during training to develop an alternate solution. After sleep, the memory representation has been restructured to produce this abstraction.

In generalized sensorimotor learning, sleep both inoculates memory against subsequent loss and also restores performance levels that were reduced at the end of a waking interval. Individuals trained in a video game task showed improved performance, but a waking interval resulted in a loss of some of this learning that was then restored by sleep (Brawn, T. *et al.*, 2006). Sleep shortly after training prevented the loss. It remains unclear which aspects of the learning are lost by the end of the day and whether sleep restores the aspects of learning that are lost during the day or improves performance on different aspects of the task.

3.51.2.2 Auditory Memory Consolidation

The diverse effects of sleep on memory have been observed in a variety of auditory tasks. In rote tone discrimination memory, a waking interval stabilizes performance gains achieved after training. Sleep enhances this memory, with additional improvement appearing after a night of sleep (Gaab, N. *et al.*, 2004). Whereas this pattern of waking stabilization and sleep-dependent enhancement is similar to that found for rote motor memory, it is not found for generalized auditory learning or for other rote auditory tasks. For example, performance in an auditory tone sequence learning task significantly improved both after sleep and after an equal period of quiet waking in which no external stimuli were administered. However, performance did not improve if new information was presented in the waking interval, illuminating its susceptibility to retroactive interference (Gottselig, J. M. *et al.*, 2004). Similar waking-consolidation effects were also found for an auditory oddball paradigm. This task required the detection of a deviant tone sequence within a series of repetitions of a standard sequence. The two eight-tone sequences differed only in the frequency of the sixth tone. In this task, continued behavioral enhancement occurred for three nights following training, even if sleep-deprivation occurred on the first night (Atienza, M. *et al.*, 2004), further demonstrating consolidation without sleep.

Consolidation in generalized auditory memory shows a similar pattern to consolidation of complex sensorimotor learning (Fenn, K. M. *et al.*, 2003). In a perceptual language learning task, subjects were trained and tested on monosyllabic words that were produced by a speech synthesizer. Learning to generalize linguistic categories from the novel acoustic patterns (as was required by the experimental design) was robustly consolidated by sleep (Figure 1). After a relatively brief period of training, performance increased from about one-third words correctly identified to about one-half of words correctly identified. For subjects trained in the morning, roughly half of the performance increase was lost by the evening, but remarkably the original level of posttraining performance was restored after a night's sleep. Performance degradation did not occur on subsequent days.

Sleep has been shown to affect generalization in a linguistic task in infants. Using a statistical learning paradigm (cf. Saffran, J. R. *et al.*, 1996) in which auditory strings adhering to a simple rule were presented, a nap was found to qualitatively change the memory representation such that the infants generalized

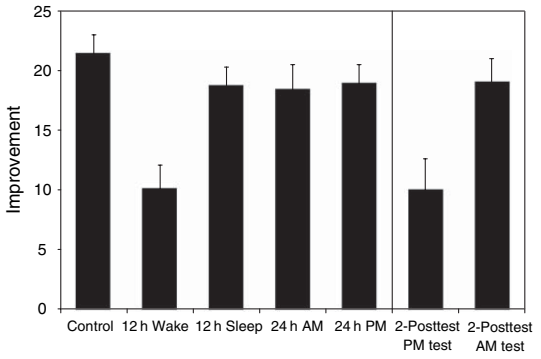

Figure 1 Effects of sleep on generalized speech learning. Change in percent correct from pretest to posttest in a generalized speech learning task when tested immediately after training (Control), after a 12 h waking interval (12 h Wake), after a 12 h interval that included a regular sleep phase (12 h Sleep), or after a 24 h interval with testing in the morning (24 h AM) or evening (24 h PM). The final two bars represent data from the same group of subjects, replicating the effects observed in the between-subjects comparison. The first bar indicates amount of improvement after a 12 h waking interval and the second bar indicates improvement when tested 12 h later, after a regular sleep phase.

beyond the trained stimuli. In this task, the stimuli were three-element spoken sequences in which the initial and final elements were predictive of one another, whereas the middle item could vary. Learning could be achieved by remembering either the exact sequences experienced during training or a general rule between initial and final words that could be applied to novel stimuli. A waking interval stabilized memory for the trained information, but did not produce generalization to new stimuli, whereas after sleep, infants could recognize novel stimuli that followed the same pattern (Gomez, R. L. *et al.*, 2006). When sleep was delayed, the generalization to new stimuli did not occur (Hupbach, A. *et al.*, submitted). Infant memory may be too unstable to benefit except from immediate consolidation during sleep, which implies an adaptive value to the considerable sleep that infants engage in.

3.51.2.3 Multiple Processes of Memory Consolidation in Humans

These data indicate that human auditory memory is subject to several different forms of consolidation or offline processing. Evidence for offline processing is manifest most often after sleep but also occurs during the wake state. This processing serves to stabilize, enhance, or even restore memory that could not be demonstrated after a waking interval. It is unclear whether the variety of consolidation effects results from differences in tasks or because the tasks involve different neuronal systems. The most consistent pattern of consolidation entails memory stabilization during a waking interval and memory enhancement after sleep. This pattern is found in rote motor and auditory memory and declarative memory for associated word pairs but is somewhat different in a visual rote memory task where fatigue plays a factor.

For generalized learning, a distinct pattern of consolidation emerges. A generalized sensorimotor task and a generalized spoken language learning task show both that a waking interval degrades performance from initial performance gains but that a subsequent sleep period restores memory that was inaccessible and that sleep inoculates the memory against waking degradation. Thus, within the class of nondeclarative learning tasks, the pattern of consolidation for generalized learning differs markedly from consolidation effects found acquiring simpler nondeclarative skills. We hypothesize that complex generalized skills recruit a broader network of cortical and subcortical structures than do simple skills, and sleep-dependent learning of complex generalized skills involves interaction between a diverse set of brain regions. This latter theme is taken up next as we consider animal studies.

3.51.3 Sleep and Memory Consolidation in Animals

Sleep and memory consolidation has been studied more in humans than in animals. There is still no paradigm comparing simple skill with generalized learning in adult animals. Laboratory studies directed toward neurophysiological investigation of sleep and learning have focused on naturalistic behavior (Dave, A. S. and Margoliash, D., 2000; Poe, G. R. *et al.*, 2000; Frank, M. G. *et al.*, 2001).

3.51.3.1 Bird Song Learning

The study of bird song learning takes advantage of attributes of the auditory modality for naturalistic studies. The behavioral context of species-specific vocalizations can give insights into the potential significance of neuronal stimulus selectivity (Margoliash, D. and Konishi, M., 1985) and vocal behavior is amenable to study, in that the auditory signal itself is the referent both for production and for perception

(Marler, P., 1970a; Tchernichovski, O. *et al.*, 2001). Furthermore, for sleep research, audition has advantage over vision, in that natural stimuli can be presented without special consideration during sleep (Dave, A. S. *et al.*, 1998).

Birdsong also shares deep similarities with speech and language acquisition in humans (Marler, P., 1970b; Doupe, A. J. and Kuhl, P. K., 1999), which extends to the role of sleep in vocal learning (Margoliash, D., 2003). Typically, true songbirds (oscine passerine birds, hereafter songbird) become sensitive to exposure to adult male songs at approximately the time they fledge, with the duration of this sensory phase being highly variable across species and environmentally sensitive (Kroodsma, D. E. and Pickert, R., 1980). The song memories formed during this phase have been described as an acquired sensory template that guides subsequent sensorimotor learning. Sensorimotor interactions are implicated in song learning, in that auditory feedback is necessary for normal vocal development (Konishi, M., 1985) and, for some species, also for adult song maintenance (Nottebohm, F. *et al.*, 1976; Nordeen, K. W. and Nordeen, E. J., 1992; Okanoya, K. and Yamaguchi, A., 1997; Leonardo, A. and Konishi, M., 1999). Furthermore, although audition is the principal medium that guides song learning, social interactions can moderate (Payne, R. B., 1983; Baptista, L. F. and Petrinovich, L., 1986) and in some special cases even directly guide song acquisition (West, M. J. and King, A. P., 1988). Thus, the separate but linked processes of perception and production in birds mimic the basic features of ontogeny of human speech and language. There are *c.* 3500 species of oscine birds that exhibit a broad variety of learning and singing strategies but no primate species other than humans with highly plastic vocal behavior. Passerines therefore represent a treasure trove of biological richness whose exploration has barely begun.

3.51.3.2 The Role of Sleep in Song Learning: Circadian Deconsolidation during Vocal Development

In the long history of research in birdsong learning, the potential of sleep to influence the learning process has only recently been considered (Margoliash, D., 2002). In the traditional instructional model, the environment directly guides song development (Konishi, M. 1965; 1978). In a proposed selectional model, the environment biases choices of innately specified sensory or motor patterns (Marler, P., 1998). In both cases, feedback has been envisioned as acting directly and immediately, either being compared with the template or enhancing matching internal representations. In such systems, the memory required for the feedback signal is short, perhaps only long enough to resolve the temporal credit assignment problem (Sutton, R. S. and Barto, A. G., 1998) – the delay between when neuronal commands are formed and feedback from the resulting gestures return to the brain.

Recent behavioral results have challenged this perspective. Analysis of song variability throughout ontogeny has demonstrated that vocal development of zebra finches shows a strong sleep-dependent effect (Deregnaucourt, S. *et al.*, 2005). Sleep acts to deteriorate song production in juveniles, which is then reversed by subsequent daytime singing, a process that has been termed deconsolidation. Syllable production before and after sleep shows greater variation than when compared during the morning and afternoon (Figure 2). Importantly, individual variation in the magnitude of the fluctuations predicts the degree of learning. Birds with the largest fluctuations are those that ultimately produce the most faithful copies of the tutor songs (Deregnaucourt, S. *et al.*, 2005). Deconsolidation is related to sleep itself and is dissociated from a purely circadian effect. For example, a similar pattern is also observed when

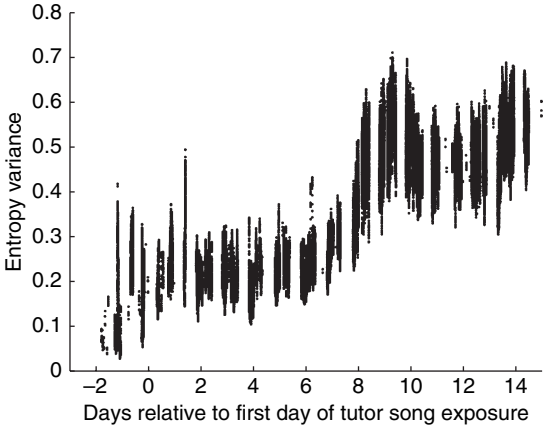

Figure 2 Analysis of song development. An example of the circadian variation in the entropy variance for one cluster (roughly representing one or more syllables) from 2 days prior to the first day of tutoring to 14 days after tutoring onset. The magnitude of the circadian variation increases following the onset of tutoring. This analysis was performed using the Song Analysis software (Tchernichovski, O. *et al.*, 2001).

sleep is artificially induced. Birds that are housed in the laboratory in the morning and precluded from experiencing intense singing until the afternoon also show the same pattern. Furthermore, juveniles raised in isolation from tutor songs show little variation in singing after sleep.

Humans and some bird species including zebra finches also rely on auditory feedback to maintain adult vocalizations. Modifying feedback in adult birds, either by deafening (Nordeen, K. W. and Nordeen, E. J., 1992) or via a syllable-triggered delay procedure during production (Leonardo, A. and Konishi, M., 1999), causes song degradation. Adult song maintenance has been used as a surrogate for song development, under the assumption that similar plastic mechanisms are involved. Small circadian fluctuations in adult singing occur over short periods of time and throughout the day (Chi, Z. and Margoliash, D., 2001; Glaze, C. M. and Troyer, T. W., 2006). A role of sleep in these circadian fluctuations, or during song degradation, has yet to be reported.

3.51.3.3 Implications of Circadian Deconsolidation for Models of Song Learning

A heuristic for evaluating deconsolidation during song learning comes from consideration of artificial neural networks. In a high-dimensional space, an effective search algorithm is to add energy to the system, thereby escaping from local minima. Slowly cooling the system (reducing energy) helps to achieve stabilization at a better (lower energy) solution. Adding too little energy constrains the search space, which could result in poorer learning. This heuristic views sleep as performing a random search of the space of solutions (Deregnaucourt, S. *et al.*, 2005). Below, we suggest an alternate hypothesis.

Because the quality of juvenile song is regulated in part by a mechanism expressed during sleep, this could suggest that the effects of sleep are related to motor processing (a nondeclarative task). An alternate hypothesis is that the acquired sensory template for song learning is itself modified on a circadian basis. The copy accuracy of the template may degrade each night because of passage of time without reinforcement. This hypothesis, however, is hard to reconcile with the observations that song learning can proceed with only minimal exposure to tutor songs. Isolated zebra finches learn best when only exposed to approximately 20 songs per day throughout the developmental period (Tchernichovski, O. *et al.*, 1999), and in European nightingales, just a few days exposure to tutor songs can result in veridical song learning (Hultsch, H. and Todt, D., 1989). Alternatively, auditory feedback could be modifying the sensory template during the day, and the effects on the sensory template could be expressed in nighttime activity. Notably, this implies that activity during sleep is better described by a directed, not random, search. The language abstraction results in human infants (Gomez, R. L. *et al.*, 2006), and the prior results showing sleep effects on speech perceptual learning (Fenn, K. M. *et al.*, 2003) help to emphasize the point that sleep may be acting in concert with sensory structures.

3.51.4 Mechanisms of Sleep and Memory Consolidation in Humans

We now turn to the neuronal mechanisms that might be associated with memory consolidation during sleep, first considering the data for humans. The diverse set of behavioral results in humans indicates that the consolidation process may differ across types of memory (e.g., declarative vs. nondeclarative) or forms of learning (e.g., rote vs. generalized). In recent years, neuroimaging experiments have yielded insight into the mechanisms underlying these processes.

3.51.4.1 Evidence for Reactivation during Sleep in Humans

Neuroimaging techniques used in a range of human studies have observed changes in brain activation both during and after a period of sleep. One central observation is that brain regions active during a task can be reactivated during sleep (Maquet, P. *et al.*, 2000; Peigneux, P. *et al.*, 2004). Hippocampal activity elicited during a virtual spatial navigation task is replayed during subsequent SWS, and activation in task-related areas in a serial reaction time task (SRT) is replayed during REM sleep (Maquet, P. *et al.*, 2000). Furthermore, the amount of reactivation in spatial learning in humans is positively correlated with performance (Peigneux, P. *et al.*, 2004). Whether the difference in sleep stage-specific effects of reactivation is related to different mechanisms of consolidation remains unresolved. Of course, it is important to note that reactivation in humans refers to localized changes in brain activity, whereas

reactivation in experimental animals is defined by examining spatial/temporal patterns of activity in individual neurons or populations of neurons.

3.51.4.2 Changes in Cortical Representations of Memory After Sleep

In humans, replay acts as a form of offline practice of information. Similar to waking practice, as the amount of offline practice increases, performance benefits also increase. Offline processing could act to simply strengthen the patterns of connections (memory representations) established during the initial learning phase. In addition, offline processing could act to change those patterns of connections, changing the way the memory is represented or accessed. While there are no studies that have looked both at reactivation during sleep and subsequent neural processing of the same information in humans, the behavioral evidence suggests that sleep strengthens the cortical representations of a memory and also changes the functional connectivity of the memory.

In skill learning, sleep has been found to produce an expansion of the cortical representation of the memory in primary sensory or motor cortices and also to change the functional connectivity in subcortical and higher-level cortical areas (Walker, M. P. *et al*., 2005a; 2005b). These changes are first observed after a period of sleep and are not produced after a waking interval. However, they persist and continue to evolve over a period of several days or weeks, and perhaps longer (Karni, A. *et al*., 1995; Pascual-Leone, A. *et al*., 1995). The neural plastic changes are associated with behavioral plasticity; performance after a period of sleep is significantly better than after a waking interval.

Neurophysiological changes resulting from consolidation are found not only in the quantity of neural activity elicited by a task but also in qualitative changes in event-related potentials (ERPs). Behavioral improvement in an auditory discrimination task continues for at least 48 h after training and changes in various ERP components also evolve over this time course, in the absence of additional task exposure (Atienza, M. *et al*., 2002). In particular, the amplitude of the mismatch negativity (MMN), which is thought to underlie automatic detection of an auditory change, is significantly enhanced 36 h after training. This is accompanied by a decrease in reaction time and similar to the effects found in functional neuroimaging; the amplitude of the MMN was found to be strongly, though insignificantly, correlated with reaction time.

3.51.4.3 Slow Wave Activity Effects on Consolidation

Reactivation and changes in cortical representations interact with the backdrop of transitions through sleep stages during consolidated sleep in humans. These interactions are integral to the consolidation process. For example, it has been proposed that SWS is important to memory consolidation and that the slow oscillating waves may reflect the transfer of information from the hippocampus to the neocortex (Buzsaki, G., 1998). Recently, it was found that boosting these oscillations via transcranial stimulation enhances declarative memory. The amount of memory enhancement exceeds that found after normal, undisturbed, SWS (Marshall, L. *et al*., 2006). This is particularly strong evidence to suggest that synchronous activation of populations of neurons as reflected in slow wave activity (SWA) plays a causal role in declarative, hippocampal-dependent memory.

Substantively altering electroencephalography (EEG) patterns during SWS is one approach to unraveling the effect of SWS on memory, but if SWA is indeed important for consolidation, it follows that the formation of a memory may alter patterns of SWA in subsequent sleep, reflective of consolidation. Indeed, after learning a motor adaptation task, localized increases in the amount of SWA are found in parietal cortices (Huber, R. *et al*., 2004) implicated during waking task performance. The increase in SWA is not found globally over all of cortex but is restricted to task-related areas. Moreover, the amount of SWA during sleep is correlated with subsequent performance. This lends additional support to the existence of a link between SWA and memory consolidation.

3.51.5 Mechanisms of Sleep and Memory Consolidation in Vocal Learning

The two principle animal neurophysiological models of sleep effects on learning have focused on naturalistic behaviors – spatial navigation by rats and vocal learning by songbirds. The former is considered a form of declarative memory and the latter a form of nondeclarative memory, but each behavior may have elements of both. For example, a rat may have an internal map of extrapersonal space and follow a procedure (path) to a target, and a songbird (especially one with a multiple song repertoire) may have labels attached to each song type. In both cases, the

associated learning mechanisms are complex and require integration across multiple modalities. Here we focus on vocal learning in songbirds. The results from nondeclarative learning experiments in humans would predict that sleep would have a significant, and complex, interaction with vocal learning.

3.51.5.1 Auditory Pathways Leading to the Song System

An extensive set of pathways that contribute to song learning have been elucidated over the past 30 years (Figure 3). Principally, these include a forebrain ascending auditory pathway, a forebrain descending vocal motor pathway, an ascending brainstem vocal-respiratory pathway, and an anterior forebrain pathway which forms a separate major loop connecting nuclei of the descending vocal motor pathway. Neuromodulatory inputs to the song system have also been identified. The modern reinterpretation of the avian forebrain as being mostly pallial has facilitated our understanding of the song learning pathways (Reiner, A. *et al.*, 2004). The organization of the avian forebrain has been related to mammalian cortical organization, including elements of the auditory pathway and descending motor pathway (Karten, H. J., 1997). The anterior forebrain pathway has homology with the corticobasal ganglia pathway in mammals. The neuromodulatory systems of birds and mammals are apparently homologous.

In the forebrain, the ascending auditory pathways include a thalamorecipient Field L (Karten, H., 1968), and its projections to secondary auditory areas including the caudal medial nidopallium (NCM) and the caudal mesopallium (CM). NCM projects to the caudomedial mesopallium (CMM) and CMM projects to the caudolateral mesopallium (CLM). Most connections within Field L and between areas are unilateral and reciprocal (Mello, C. V. *et al.*, 1998). In many ways, the organization of these pathways resembles that for mammalian auditory forebrain (Kass, this volume). CLM projects to the nucleus interface of the nidopallium (NIf) (Mello, C. V. *et al.*, 1998). Physiological observations indicate that this pathway may serve as the principal auditory input to the song system (Janata, P. and Margoliash, D., 1999; Coleman, M. J. and Mooney, R., 2004).

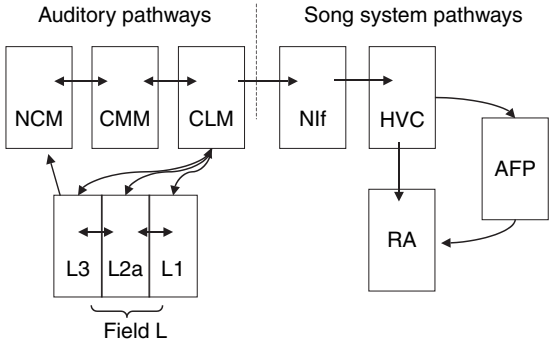

Figure 3 A highly simplified representation of the forebrain auditory and song system pathways in songbirds. Field L receives thalamic input. Auditory input to the song system arises through the projection of CLM to NIf. RA is the principal forebrain output of the song system. The AFP comprises three nuclei (not shown). Auditory responses are found in all the song system nuclei but are distinguished from auditory pathway nuclei by the selective responses to the bird's own song.

3.51.5.1.1 Physiological specificity within the auditory pathways

The hierarchical anatomical relations of the forebrain auditory pathways correlate with a number of physiological properties of these pathways. Neurons in the granular layer L2a in Field L have simple response properties. They typically respond vigorously to tone bursts and often to broadband noise bursts and have a narrow range of frequencies that elicit excitation often with inhibitory frequency surrounds. Within field L, tonotopic organization is most robust in L2a.

In contrast, neurons in the surrounding L1 and L3 regions of Field L have more complex response properties. L1 and L3 neurons often respond less vigorously or not at all to tone bursts. A greater number of L1 and L3 neurons respond more selectively to a repertoire of species-specific and other complex natural vocalizations, and responses for some neurons are based on multiple spectral features of species-specific vocalizations (Leppelsack, H.-J. and Vogt, M., 1976; Bonke, D. *et al.*, 1979).

Neurons in the secondary auditory nuclei can have particularly complex and selective responses. For example, many neurons in the starling CMM respond highly selectively when presented a repertoire of songs (Stripling, R. *et al.*, 1997; Gentner, T. Q. and Margoliash, D., 2003; Terleph, T. A. *et al.*, 2006). Quantitative analysis of input–output transfer functions of single neurons also supports these conclusions, showing a hierarchical relation comparing L2a with other Field L subdivisions and CM (Sen, K. *et al.*, 2001; Theunissen, F. E. *et al.*, 2004).

3.51.5.1.2 Behavioral and neural plasticity in the auditory pathways

Studies of adult animals using a variety of techniques indicate that the secondary auditory areas express plasticity throughout life that could contribute to memory formation. A remarkable form of plasticity has been described with gene expression studies. The immediate early gene (IEG) *zenk* shows a complex pattern of expression in NCM and CM in response to auditory stimulation (Mello, C. V. *et al.*, 1992; Mello, C. V. and Clayton, D. F., 1994; Terpstra, N. J. *et al.*, 2005). This includes sensitivity to acoustic features of conspecific songs, heightened response to conspecific vs. heterospecific songs, and lack of expression to simple stimuli such as tone bursts. If the same conspecific song is presented multiple times, *zenk* expression drops and remains at suppressed levels until the bird is presented with a novel song (Chew, S. J. *et al.*, 1995; Mello, C. *et al.*, 1995). Single and multicell recordings also demonstrate some evidence of habituation (Stripling, R. *et al.*, 1997; Gentner, T. Q. and Margoliash, D., 2003; Terleph, T. A. *et al.*, 2006), although the relation between *zenk* and electrophysiological habituation is complex.

In adult starlings trained on an operant song recognition task, the population of CMM neurons as assessed by sequential, single-cell recordings was found to be biased toward the songs birds had learned to discriminate (Gentner, T. Q. and Margoliash, D., 2003). A large proportion of the neurons exhibited strong, selective responses to one or a limited number of songs and much weaker responses to unfamiliar songs. The strength of response was related not only to familiarity but also to behavioral valence: in a Go-Nogo paradigm, neurons exhibited much stronger responses to the Go stimulus than to the Nogo stimulus, but stronger responses to the Nogo stimulus than to unfamiliar songs. Thus, both IEG expression studies and extracellular recordings indicate that secondary auditory pathways participate in the formation of long-term memories in adult animals.

The conspecific songs birds commit to memory early in life drive vocal learning. IEG expression studies have examined tutor song representations, searching for long-term memory for tutor songs in adult zebra finches. Exposure of adult males to song they were tutored with as juveniles elicited expression of *zenk* and *c-fos* (Bolhuis, J. J. *et al.*, 2000). In female zebra finches, levels of Zenk protein product in CMM were significantly higher when birds were re-exposed as adults to their tutor songs than when exposed to novel songs (Terpstra, N. J. *et al.*, 2006). This design removes the confound that males engage in self-stimulation with a close copy of the tutor song when they sing, because female zebra finches do not sing. These results are also supported by multiunit studies of habituation in NCM, which show greater (and significant) habituation in adults exposed to tutor songs than in adults exposed to unfamiliar songs, and a correlation between the degree of habituation and the degree of song copying (Phan, M. L. *et al.*, 2006). When tested with playback of the bird's own song (BOS), the correlation with habituation strength is not observed. This implies that the observed correlations do not result from similarity between tutor and own songs.

In summary, converging data from behavior, electrophysiological, and gene expression studies indicate that secondary auditory areas in songbirds exhibit plasticity throughout life, with some populations of single neurons exhibiting selective responses to learned, behaviorally relevant stimuli. The effect of behavioral state has been extensively examined from the perspective of the strong habituation to familiar songs observed in gene expression and neuronal activity. The habituation phenomenon may focus attention on new songs, and attendant neural plasticity may elicit rapid representational reorganization, allowing songbirds to acquire and perhaps retain multiple song memories throughout life. In young birds in the process of acquiring songs, these memories could represent a component of the long-hypothesized template for birdsong learning. The impact of the conclusions regarding developmental mechanisms is tempered by the principal limitation that relatively few observations have been made in juvenile birds (Jin, H. and Clayton, D. F., 1997; Stripling, R. *et al.*, 2001; Bailey, D. J. and Wade, J., 2003; 2005). This identifies a path for future research.

3.51.5.2 State-Dependent Auditory Processing in the Song System of Awake Birds

In the songbird forebrain, auditory responses are expressed extensively throughout the song system, with numerous properties reflecting the sensorimotor nature of singing. In adult birds, song system neurons exhibit strong preference for playback of BOS (Margoliash, D. and Konishi, M., 1985; Doupe, A. J., 1997). In zebra finches, with a single song repertoire, the response to song playback shows a consistent pattern of complex temporal dynamics throughout HVC (Sutter, M. L. and Margoliash, D., 1994),

which is also seen in other song system nuclei. In song sparrows, with a multiple song repertoire, there is more local variability in response to song playback (Nealen, P. M. and Schmidt, M. F., 2006). Auditory responses of HVC neurons are exquisitely tuned to features of BOS (Margoliash, D., 1983; Theunissen, F. E. and Doupe, A. J., 1998), including sensitivity to temporal sequences of song syllables (Margoliash, D., 1983; Doupe, A. J., 1997). The structuring of auditory responses in the song system by features of BOS differentiates auditory responses in the forebrain auditory pathways from those in the song system and emphasizes the role of auditory feedback in song learning and maintenance.

The auditory responses of song system neurons are also strongly modulated by behavioral state, with large differences observed across species. Early studies using chronic multiunit recordings in awake canaries and white-crowned sparrows observed robust HVC auditory responses (McCasland, J. S. and Konishi, M., 1981; Margoliash, D., 1986), which has also been confirmed in the HVC of song sparrows (Nealen, P. M. and Schmidt, M. F., 2006). In contrast, auditory responses in the song system including HVC are suppressed in awake zebra finches (Dave, A. S. *et al.*, 1998; Schmidt, M. F. and Konishi, M., 1998) but in a complex pattern involving some but not all classes of HVC neurons (Rauske, P. L. *et al.*, 2003). Responses in awake white-crowned sparrows varied according to behavioral state such that weaker responses and loss of bursting activity were observed just prior to periods of arousal, although this was observed anecdotally (Margoliash, D., 1986). In a controlled study, the responses of HVC in zebra finches showed similar properties, with stable, BOS selective responses in sedated birds and far more variable, arousal-dependent, and less BOS selective responses in awake birds (Cardin, J. A. and Schmidt, M. F., 2003). The species differences in song system auditory responses in awake birds might reflect ecological aspects of social organization, such as comparing territorial and gregarious species, but this remains speculative.

3.51.5.2.1 Neuromodulatory processing in the song system of awake birds

Both cholinergic and adrenergic systems have been implicated in state-dependent processing in the song system. In birds, as in mammals, neuromodulatory systems access forebrain neurons, and there is varying and in some cases substantial evidence of cholinergic and adrenergic input to nucleus uvaeformis (Uva), NIf, HVC, and RA. HVC is the principal source of auditory input to robust nucleus of archopallium (RA) and to the anterior forebrain pathway (Doupe A. J. and Konishi, M., 1991). Injection of cholinergic agonists and antagonists into HVC, and in the presence of stimulation of the cholinergic basal forebrain, indicates strong cholinergic regulation at the level of HVC, with different classes of cholinergic receptors regulating auditory output to RA and to the anterior forebrain pathway (Shea, S. D. and Margoliash, D., 2003). This may give rise to differential expression of auditory activity in the forebrain song system, with complete suppression of auditory responses in RA (Dave, A. S. *et al.*, 1998) but not in the anterior forebrain pathway. Lesioning the cholinergic basal forebrain results in rapid song deterioration, in some cases followed by substantial recovery of song structure (Levin, T. *et al.*, 2005). NIf neurons may be the first in the song system to show selectivity for BOS and may give rise to the principal source of auditory input to the song system (Janata, P. and Margoliash, D., 1999; Coleman, M. J. and Mooney, R., 2004; Cardin, J. A. *et al.*, 2005). Auditory activity in NIf is strongly regulated by noradrenergic mechanisms (Cardin, J. A. and Schmidt, M. F., 2004), as is auditory activity in HVC (Dave, A. S. *et al.*, 1998). Uva, which has been implicated in regulating singing (Coleman, M. J. and Vu, E. T., 2005), receives cholinergic input from the habenula (Akutagawa, E. and Konishi, M., 2005).

Collectively, these data imply that cholinergic and noradrenergic systems have powerful influence on sensory activity in the song system and that the cholinergic system has powerful influence on singing behavior. Neuromodulatory input to Uva and HVC might be recruited to release song pattern generators. Neuromodulatory systems could also act to regulate auditory input to the song system. In awake quiescent birds, this could help regulate the flow of auditory information to the anterior forebrain pathway, which has been implicated in song recognition behavior (Brenowitz, E. A., 1991; Burt, J. M. *et al.*, 2000). In singing birds, this could help regulate the flow of auditory feedback to the anterior forebrain pathway (AFP) and the descending motor system. In developing birds, neuromodulatory systems might help focus attention on the songs of potential adult tutors. Finally, these same neuromodulatory mechanisms could have particularly profound effects during sleep, when the functional properties of the song system are dramatically altered. This possibility is considered in the next section.

3.51.5.3 Replay and Plasticity during Sleep

As an adult bird begins to sing, RA neurons transition from a highly regular spontaneous tonic firing mode to a bursting firing mode superimposed over complete inhibition of spontaneous activity. The tonic firing mode is characterized by single mode, Gaussian-shaped inter-spike interval (ISI) histograms (Figure 4(a)). The bursting firing mode is characterized by individual spike bursts that are exceptionally reliable and well structured (Yu, A. C. and Margoliash, D., 1996). Combined, this results in a bimodal ISI distribution. In virtually all cases, each burst of spikes can be assigned a unique identity, with a typical neuron emitting circa 20 different burst types during a motif of song (Figure 5). The dictionary is unique for each neuron, that is, the timing and structure of a given burst cannot be predicted for a given neuron, but knowing that dictionary one can reliably read off the singing behavior just by examining the activity pattern of a single RA neuron (Yu, A. C. and Margoliash, D., 1996). Converging feed-forward excitation from sparse-firing, HVC-RAn has been posited as dominating the firing properties of RA neurons (Leonardo, A. and Fee, M. S., 2005).

3.51.5.3.1 Site and form of the replay phenomenon

During sleep, state transitions are observed that mimic those associated with daytime singing (Dave, A. S. *et al*., 1998; Dave, A. S. and Margoliash, D., 2000). ISI histograms obtained during sleep are bimodal. A short-duration ISI mode (corresponding to bursting) has a similar structure to that obtained for singing. The peak may be shifted toward longer ISIs, reflecting the higher-frequency bursting obtained during singing than during sleep, and the shape of the short-duration ISI mode reflects the greater variability in bursting observed during singing. A long-duration ISI mode may be anisotropic, corresponding to the combination of regular firing mode activity with long inter-burst intervals from the bursting firing mode activity. The peak of the long-duration ISI mode is also shifted toward longer ISIs, reflecting slower spontaneous activity during sleep than in awake birds. ISIs obtained from anesthetized birds are similar to those obtained during sleep (Figure 4(b)).

The similarity of the short-duration ISI mode obtained from RA neurons in singing and sleeping birds results from bursts emitted during sleep that have similar patterns to those bursts emitted during singing (Dave, A. S. and Margoliash, D., 2000). This

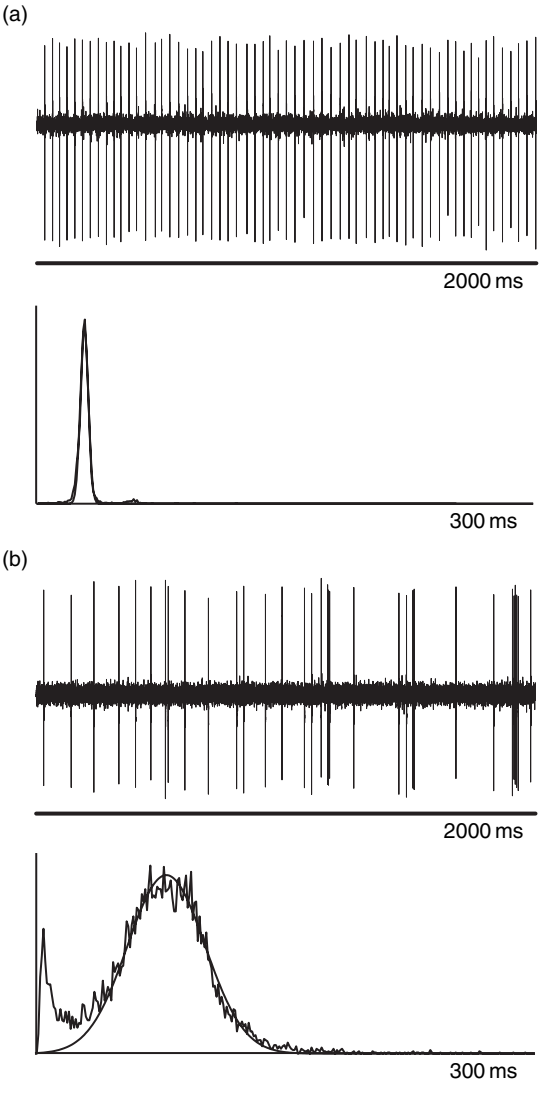

Figure 4 Spontaneous discharge in RA neurons in an awake quiescent bird (a) and in a urethane anesthetized bird (b). In each part, the top panel shows a raw record and the bottom panel shows an ISI histogram fitted with a Gaussian. The fit is excellent for (a) but only for the long-duration ISI peak in (b), because in anesthetized (and sleeping) birds, there are short ISIs associated with bursting.

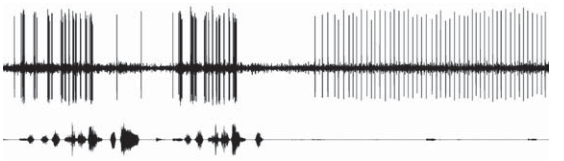

Figure 5 Activity of RA neuron (top trace) during singing (oscillograph, bottom trace); traces are 5 s in duration. Note the bursting activity and recovery of regular firing pattern after postsong inhibition.

represents a replay (reactivation) phenomenon, one that is observed at the level of single cells. In comparison, reactivation in the hippocampus is related to ensemble patterns (Wilson, M. A. and McNaughton, B. L., 1994; Skaggs, W. E. and McNaughton, B. L., 1996). In the zebra finch, comparing only on a burst-by-burst basis, only approximately 15% of bursts show a statistically significant match. This number is likely to be an underestimate because it fails to consider sequences of bursts that are also observed during sleep. Nevertheless, it is important to emphasize that many bursts during sleep may not match or may only poorly match the structure of bursting during singing. This implies that variability exists during sleep that could be the substrate for plasticity.

The replay phenomena as described above relies on comparison of bursting activity during singing and during spontaneous sleep in the same neurons, which is a technically difficult experiment. By this definition of replay, replay in the song system has been confirmed only for RA neurons. However, several structures show similar firing properties in both wake and sleep. Neuronal activity in HVC of sleeping birds shares similarities with activity observed in awake birds, with RA-projecting HVC neurons (HVC-RAn) and Area X-projecting HVC neurons (HVC-Xn) exhibiting sparse firing and interneurons exhibiting tonic firing (Hahnloser, R. H. *et al.*, 2002; Rauske, P. L. *et al.*, 2003). In sleeping birds, NIf neurons show bursts that are correlated with HVC bursts, and silencing NIf stops HVC sleep bursting (Hahnloser, R. H. and Fee, M. S., 2007). The overall levels of NIf activity are higher in fully awake than lightly sedated birds (Cardin, J. A. and Schmidt, M. F., 2004), but bursting statistics are not altered in sleeping birds (Hahnloser, R. H. and Fee, M. S., 2007). Overall burst rates are similar in RA-projecting LMAN neurons (LMAN-RAn) in sleeping zebra finches (Hahnloser, R. H. *et al.*, 2006), but during singing, bursts in LMAN are not time-locked to song syllables (though some spikes are) (Leonardo, A. 2004).

Collectively, these data suggest that replay is limited to the descending motor pathway, but for HVC (and possibly Uva), the existence of replay has yet to be directly confirmed. Whereas analysis of bursting in sleeping birds can give insight into the mechanisms generating bursting, the fidelity of replay – variability of bursting during sleep as compared to bursting during singing – has yet to be assessed. If variability of activity during sleep is important for plastic mechanisms during sleep, as we argue below, this attribute will be important problem to address in future work. The other implication is that replay will be particularly difficult to assess in juvenile birds, because song is plastic (variable) as are the bursting properties of song system neurons. This implies the need to acquire a larger data set to achieve statistical significance comparing singing and sleeping bursting, a challenging task.

3.51.5.3.2 Plasticity in Robust Nucleus of Archopallium replay – spontaneous and auditory activity

The replay phenomenon exhibited by RA neurons opens the possibility that neuronal activity patterns change during sleep and that these changes are part of a plasticity mechanism associated with song learning in juvenile birds and song maintenance in adult birds. The exceptional precision of RA bursting during singing in zebra finches was exploited to search for such adaptive changes. Single neuron recordings commenced while the animal sang near the end of its normal diurnal phase and continued through a period of sleep and a bout of singing immediately upon wakening. A principal observation was that consistent if subtle changes in the patterns of spike bursting were observed comparing activity during singing before and after a period of sleep (Rauske, P. L. *et al.*, 2001). Such changes also were observed during daytime singing, but at a much lower frequency of occurrence. In this small data set, it was difficult to associate the neuronal changes directly with behavioral vocal plasticity. Nevertheless, these observations establish that long-term changes in the structure of neuronal bursting can be mediated via changes occurring during sleep.

As well as changes in spontaneous discharge properties, during sleep, song system neurons acquire heightened sensory responses (Dave, A. S. *et al.*, 1998; Dave, A. S. and Margoliash, D., 2000; Cardin, J. A. and Schmidt, M. F., 2003; Rauske, P. L. *et al.*, 2003). The most dramatic changes observed to date are for zebra finch forebrain RA neurons, which exhibit vigorous responses to BOS playback during sleep and no response while awake. A systematic analysis of the degree of variation in BOS playback that RA neurons will tolerate during sleep has yet to be reported, but the neurons exhibit high selectivity of response. In general, conspecific songs elicit no response or inhibition, compared to exceptionally robust responses to BOS.

The structure of the response to playback during sleep shows visually compelling and statistically significant similarity to the structure of activity of the same neurons during daytime singing (Figure 6). This is observed comparing both the timing and the

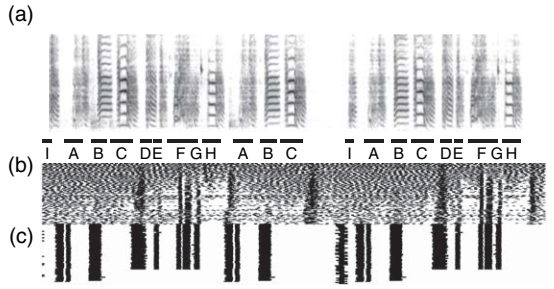

Figure 6 Activity of a single RA neuron in relation to song shown in (a); (b) response of the neuron to song playback while the bird sleeps; (c) premotor activity of the same neuron while the bird is singing (b) and while it is listening (auditory response) to playback of its own song auditory response (c) in relation to the song (a). The letters under the spectrograph in (a) identify syllables that are repeated multiple times in the song.

structure of individual bursts emitted during BOS playback and during singing, although there tend to be fewer spikes in the bursts stimulated by BOS. It is common, however, that neurons participate throughout more of song during singing than they do when stimulated by BOS playback during sleep so that neurons exhibit ongoing discharge to some syllables of BOS playback (Figure 6). Furthermore, during singing RA neurons are premotor, their discharge leads and predicts the notes and syllables that will follow. During BOS playback, nonlinear integration over preceding syllables releases RA responses.

Thus, there are similarities to the structure of spike bursts spontaneously emitted during sleep, or spike bursts emitted during song playback, as compared with spike bursts emitted during singing. Nevertheless, the patterns of activity are not the same. The variability in the structure and timing of spontaneous bursting during sleep could serve to drive sleep-induced changes, which is predicted by the song developmental studies. The upregulation during sleep of auditory activity in the descending motor system suggests the possibility that the system enters a plastic state, where memories of auditory feedback can drive changes in premotor networks.

3.51.5.3.3 Sleep-mediated developmental plasticity in Robust Nucleus of Archopallium

Virtually, all the data acquired with regard to replay have been collected in adult birds or in late juvenile birds (Dave, A. S. and Margoliash, D., 2000; Kozhevnikov, A. and Fee, M. S., 2007). In a recent study, the spontaneous activity of RA neurons was examined in sleeping juvenile birds in the nights before and after the birds first gained access to tutor songs at circa 42 days of age (Shank, S. and Margoliash, D., 2006). Prior to being exposed to a tutor song, RA neurons exhibited little spontaneous bursting, and ISI histograms had a unimodal peak centered at long intervals. A dramatic change was observed starting the night of the first day the birds were exposed to tutor songs. RA neurons exhibited greatly increased spontaneous bursting. ISI histograms had bimodal peaks, with the second peak centered at short intervals. In contrast, the number of spontaneously emitted bursts in RA normally emerges slowly during development (Adret, P. and Margoliash, D., 2002). The sudden emergence of bursting correlated with the first days of tutoring, however, demonstrates that tutoring strongly influences the structure of sleep activity in the descending motor system. Furthermore, the structure of the ISIs was dependent on which tutor song the birds were exposed to. Thus, the effects of tutoring are not nonspecific, but rather parameters of the tutor songs (as of yet unknown) are encoded in the nighttime spontaneous activity of RA neurons. This provides the strongest evidence to date linking auditory activity in the motor system for song and the sensory phase of song acquisition.

The data from juvenile RA support a new hypothesis regarding song learning. Activity at night is an active process reflecting auditory memories. The principle memory represented is that of the song tutor model. We assume that this memory representation of the song tutor model is modified during development by RA network properties acquired in relation to daytime singing. Thus, song development can be viewed as a circadian iterative process of bringing two types of representations into conjunction, auditory memories expressed at night and singing activity expressed during the day. Activity at night modifies the premotor network and affects singing the following day; activity during singing stores information in the form of auditory feedback. Song is most variable in the hours immediately after waking because the influence of the auditory memories (i.e., interactions between two disparate representations, for auditory memory and singing) is strongest in the morning and is largely – but not entirely – erased by the afternoon following hours of singing. The strength of the influence of auditory memory should be reflected in the depth of circadian song disruption, hence birds with greater circadian variation in song ultimately achieve better copies (Deregnaucourt, S. *et al.*, 2005). This formulation

differs from the suggestion that circadian song deterioration during development results from song replay during sleep unaccompanied by auditory feedback (Deregnaucourt, S. *et al.*, 2005). It shares at least superficial similarities with the wake–sleep algorithm (Hinton, G. E. *et al.*, 1995).

If two representations interact, then they must be expressed by different populations of interacting neurons or by the same population in different states. If the same RA (and other song system) neurons are active during singing, then where are auditory memories stored? Altering auditory feedback in adult (Nordeen, K. W. and Nordeen, E. J., 1992; Leonardo, A. and Konishi, M., 1999) or juvenile (Fukushima, M. and Margoliash, D., 2006) birds disrupts song, but clear effects emerge only after 2 or more weeks. To date, recordings from song system neurons during singing in altered feedback conditions have failed to identify an auditory component in the activity patterns (Leonardo, A. 2004; Kozhevnikov, A. and Fee, M. S., 2007). One possibility is that in zebra finches, the auditory feedback component is small so that the effect of feedback perturbation is expressed only over long intervals and the signal is hard to detect in electrophysiology. None of the experiments rule out the possibility that feedback changes the representation of auditory memories of song, stored for example in secondary auditory pathways, and in turn these memories drive changes at night in motor behavior. The analysis of neuronal replay during sleep has provided support for this hypothesis. Thus, in some sense, with regard to vocal behavior, zebra finches may be hearing themselves more at night than during the day.

3.51.6 Conclusions and Future Directions

Converging behavioral and neurophysiological evidence strongly suggests that during sleep, active processing of newly learned material changes the memory representation. This processing can change the functional connectivity of the memory. In several of the examples described here, endogenous oscillatory patterns produced during SWS have been shown to improve memory. The data further provide some support for the hypothesis that the nature of the consolidation process varies based on task or modality, approximating the behavioral evidence reviewed earlier in this chapter, but this remains speculative.

We have conjectured that the outcomes of memory consolidation are not only divided along traditional memory subsystems, such as declarative and nondeclarative memory. Behavioral outcomes of consolidation also differ for simple, rote memory tasks and complex, generalized memory. We conjecture that the neurophysiological mechanisms of consolidation are distinct for simple memory and complex memory and that reactivation recruits neural networks of different extents in simple and complex tasks. We assume that learning a complex task is associated with establishing a pattern of coordinated recruitment across a larger set of cortical structures than for simple learning. The distributed memory trace of the complex task would make it more vulnerable to unrelated daytime activity, whereas perhaps a more focal representation associated with a simple task would make it more vulnerable to similar daytime activity (i.e., interference effects). Since any given replay exemplar during sleep only approximates the corresponding waking activity, coordinated replay distributed across multiple cortical and subcortical regions would carry additional (mutual) information about the complex task. This model predicts the reciprocal patterns of interactions between sleep and task learning that have been observed for complex but not simple learning.

The data from the bird song system support and extend this model. Similar to hippocampal-dependent spatial learning in rats, vocal learning involves coordination across multiple systems not only during waking behavior but also during sleep. Sleep reactivation is often described as a random walk. The recent observation that spontaneous activity in the song system is influenced by song tutoring implies that this view of reactivation is incomplete because nighttime activity may be supervised or structured by tutor song representations and possibly auditory feedback during singing. The potential contribution of sleep as a mechanism to bring disparate motor and sensory representations into congruence during vocal development helps to highlight that sleep contribution to learning is not a unitary phenomenon. Rather, sleep can be recruited in a variety of ways in service of a broad range of task requirements.

References

Adret, P. and Margoliash, D. 2002. Metabolic and neural activity in the song system nucleus robustus archistriatalis: effect of age and gender. J. Comp. Neurol. 454, 409–423.

Akutagawa, E. and Konishi, M. 2005. Connections of thalamic modulatory centers to the vocal control system of the zebra finch. Proc. Natl. Acad. Sci. U. S. A. 102, 14086–14091.

Atienza, M., Cantero, J. I., and Dominguez-Marin, E. 2002. The time course of neural changes underlying auditory perceptual learning. Learn. Mem. 9, 138–150.

Atienza, M., Cantero, J. I., and Stickgold, R. 2004. Posttraining sleep enhances automaticity in perceptual discrimination. J. Cogn. Neurosci. 16, 53–64.

Bailey, D. J. and Wade, J. 2003. Differential expression of the immediate early genes FOS and ZENK following auditory stimulation in the juvenile male and female zebra finch. Brain Res. 116, 147–154.

Bailey, D. J. and Wade, J. 2005. FOS and ZENK responses in 45-day-old zebra finches vary with auditory stimulus and brain region, but not sex. Behav. Brain Res. 162, 108–115.

Baptista, L. F. and Petrinovich, L. 1986. Song development in the white-crowned sparrow: social factors and sex differences. Anim. Behav. 34, 1359–1371.

Bolhuis, J. J., Zijlstra, G. G., den Boer-Visser, A. M., and Van Der Zee, E. A. 2000. Localized neuronal activation in the zebra finch brain is related to the strength of song learning. Proc. Natl. Acad. Sci. U. S. A. 97, 2282–2285.

Bonke, D., Scheich, H., and Langner, G. 1979. Responsiveness of units in the auditory neostriatum of the Guinea fowl (*Numida meleagris*) to species-specific calls and synthetic stimuli. I. Tonotopy and functional zones. J. Comp. Physiol. 132, 243–255.

Brawn, T., Fenn, K., Nusbaum, H., and Margoliash, D. 2006. Consolidation during sleep of complex sensorimotor skill learning. Soc. Neurosci. Abstr. 32, 365.315.

Brenowitz, E. A. 1991. Altered perception of species-specific song by female birds after lesions of a forebrain nucleus. Science 251, 303–305.

Burt, J. M., Lent, K. L., Beecher, M. D., and Brenowitz, E. A. 2000. Lesions of the anterior forebrain song control pathway in female canaries affect song perception in an operant task. J. Neurobiol. 42, 1–13.

Buzsaki, G. 1998. Memory consolidation during sleep: a neurophysiological perspective. J. Sleep Res. 7, 17–23.

Cardin, J. A. and Schmidt, M. F. 2003. Song system auditory responses are stable and highly tuned during sedation, rapidly modulated and unselective during wakefulness, and suppressed by arousal. J. Neurophysiol. 90, 2884–2899.

Cardin, J. A. and Schmidt, M. F. 2004. Noradrenergic inputs mediate state dependence of auditory responses in the avian song system. J. Neurosci. 24, 7745–7753.

Cardin, J. A., Raksin, J. N., and Schmidt, M. F. 2005. Sensorimotor nucleus NIf is necessary for auditory processing but not vocal motor output in the avian song system. J. Neurophysiol. 93, 2157–2166.

Chew, S. J., Mello, C., Nottebohm, F., Jarvis, E., and Vicario, D. S. 1995. Decrements in auditory responses to a repeated conspecific song are long-lasting and require two periods of protein synthesis in the songbird forebrain. Proc. Natl. Acad. Sci. U. S. A. 92, 3406–3410.

Chi, Z. and Margoliash, D. 2001. Temporal precision and temporal drift in brain and behavior of zebra finch song. Neuron 32, 899–910.

Coleman, M. J. and Mooney, R. 2004. Synaptic transformations underlying highly selective auditory representations of learned birdsong. J. Neurosci. 24, 7251–7265.

Coleman, M. J. and Vu, E. T. 2005. Recovery of impaired songs following unilateral but not bilateral lesions of nucleus uvaeformis of adult zebra finches. J. Neurobiol. 63, 70–89.

Crick, F. and Mitchison, G. 1983. The function of dream sleep. Nature 304, 111–114.

Dave, A. S. and Margoliash, D. 2000. Song replay during sleep and computational rules for sensorimotor vocal learning. Science 290, 812–816.

Dave, A. S., Yu, A. C., and Margoliash, D. 1998. Behavioral state modulation of auditory activity in a vocal motor system. Science 282, 2250–2254.

Deregnaucourt, S., Mitra, P. P., Feher, O., Pytte, C., and Tchernichovski, O. 2005. How sleep affects the developmental learning of bird song? Nature 433, 710–716.

Doupe, A. J. 1997. Song- and order-selective neurons in the songbird anterior forebrain and their emergence during vocal development. J. Neurosci. 17, 1147–1167.

Doupe, A. J. and Konishi, M. 1991. Song-selective auditory circuits in the vocal control system of the zebra finch. Proc. Natl. Acad. Sci. U. S. A. 88, 11339–11343.

Doupe, A. J. and Kuhl, P. K. 1999. Birdsong and human speech: common themes and mechanisms. Annu. Rev. Neurosci. 22, 567–631.

Ellenbogen, J. M., Hulbert, J. C., Stickgold, R., Dinges, D. F., and Thompson-Schill, S. L. 2006. Interfering with theories of sleep and memory: sleep, declarative memory, and associative interference. Curr. Biol. 16, 1290–1294.

Fenn, K. M., Nusbaum, H. C., and Margoliash, D. 2003. Consolidation during sleep of perceptual learning of spoken language. Nature 425, 614–616.

Foster, D. J. and Wilson, M. A. 2006. Reverse replay of behavioural sequences in hippocampal place cells during the awake state. Nature 440, 680–683.

Frank, M. G., Issa, N. P., and Stryker, M. P. 2001. Sleep enhances plasticity in the developing visual cortex. Neuron 30, 275–287.

Fukushima, M. and Margoliash, D. 2006. Song development with delayed auditory feedback. Soc. Neurosci. Abstr. 32, 818.811.

Gaab, N., Paetzold, M., Becker, M., Walker, M. P., and Schlaug, G. 2004. The influence of sleep on auditory learning – a behavioral study. Neuroreport 15, 731–734.

Gais, S. and Born, J. 2004. Declarative memory consolidation: mechanisms acting during sleep. Learn. Mem. 11, 679–685.

Gentner, T. Q. and Margoliash, D. 2003. Neuronal populations and single cells representing learned auditory objects. Nature 424, 669–674.

Glaze, C. M. and Troyer, T. W. 2006. Temporal structure in zebra finch song: implications for motor coding. J. Neurosci. 26, 991–1005.

Gomez, R. L., Bootzin, R. R., and Nadel, L. 2006. Naps promote abstraction in language-learning infants. Psychol. Sci. 17, 670–674.

Gottselig, J. M., Hofer-Tinguely, G., Borbely, A. A., Regel, S. J., Landolt, H.-P., Revety, J. V., and Achermann, P. 2004. Sleep and rest facilitate auditory learning. Neuroscience 127, 557–561.

Hahnloser, R. H. and Fee, M. S. 2007. Sleep-related spike bursts in HVC are driven by the nucleus interface of the nidopallium. J. Neurophysiol. 97, 423–435.

Hahnloser, R. H., Kozhevnikov, A. A., and Fee, M. S. 2002. An ultra-sparse code underlies the generation of neural sequences in a songbird. Nature 419, 65–70.

Hahnloser, R. H., Kozhevnikov, A. A., and Fee, M. S. 2006. Sleep-related neural activity in a premotor and a basal-ganglia pathway of the songbird. J. Neurophysiol. 96, 794–812.

Hinton, G. E., Dayan, P., Frey, B. J., and Neal, R. M. 1995. The ''wake–sleep'' algorithm for unsupervised neural networks. Science 268, 1158–1161.

Huber, R., Ghilardi, M. F., Massimini, M., and Tononi, G. 2004. Local sleep and learning. Nature 430, 78–81.

Hultsch, H. and Todt, D. 1989. Memorization and reproduction of songs in nightingales (*Luscinia megarhynchos*): evidence for package formation. J. Comp. Physiol. A 165, 197–203.

Hupbach, A., Gomez, R. L., Bootzin, R. R., and Nadel, L. Nap-dependent learning in infants. (submitted).

Janata, P. and Margoliash, D. 1999. Gradual emergence of song selectivity in sensorimotor structures of the male zebra finch song system. J. Neurosci. 19, 5108–5118.
Jenkins, J. M. and Dallenbach, K. M. 1924. Obliviscence during sleep and waking. Am. J. Psychol. 35, 605–612.
Jin, H. and Clayton, D. F. 1997. Localized changes in immediate-early gene regulation during sensory and motor learning in zebra finches. Neuron 19, 1049–1059.
Karni, A., Meyer, G., Jezzard, P., Adams, M. M., Turner, R., and Ungerleider, L. G. 1995. Functional MRI evidence for adult motor cortex plasticity during motor skill learning. Nature 377, 155–158.
Karni, A., Tanne, D., Rubenstein, B. S., Askenasy, J. J. M., and Sagi, D. 1994. Dependence on REM sleep of overnight perceptual skill. Science 265, 679–682.
Karten, H. 1968. The ascending auditory pathway in the pigeon (*Columba livia*). II. Telencephalic projections of the nucleus ovoidalis thalami. Brain Res. 11, 134–153.
Karten, H. J. 1997. Evolutionary developmental biology meets the brain: the origins of mammalian cortex. Proc. Natl. Acad. Sci. U. S. A. 94, 2800–2804.
Konishi, M. 1965. The role of auditory feedback in the control of vocalization in the white-crowned sparrow. Z. Tierpsychol. 22, 770–783.
Konishi, M. 1978. Auditory Environment and Vocal Development in Birds. In: Perception and Experience (*eds*. R. D. Walk and H. L. J. Pick), pp. 105–118. Plenum.
Konishi, M. 1985. Birdsong: from behavior to neuron. Ann. Rev. Neurosci. 8, 125–170.
Kozhevnikov, A. and Fee, M. S. 2007. Singing-related activity of identified HVC neurons in the zebra finch. J. Neurophysiol. 97(6), 4271–4283.
Kroodsma, D. E. and Pickert, R. 1980. Environmentally dependent sensitive periods for avian vocal learning. Nature 288, 477–479.
Leonardo, A. 2004. Experimental test of the birdsong error-correction model. Proc. Natl. Acad. Sci. U. S. A. 101, 16935–16940.
Leonardo, A. and Fee, M. S. 2005. Ensemble coding of vocal control in birdsong. J. Neurosci. 25, 652–661.
Leonardo, A. and Konishi, M. 1999. Decrystallization of adult birdsong by perturbation of auditory feedback. Nature 399, 466–470.
Leppelsack, H.-J. and Vogt, M. 1976. Responses of auditory neurons in the forebrain of a songbird to stimulation with species-specific sounds. J. Comp. Physiol. 107, 263–274.
Levin, T., Shea, S., and Margoliash, D. 2005. Cholinergic basal forebrain regulation of bird song production. Soc. Neurosci. Abstr. 31, 1002.1002.
Maquet, P., Laureys, S., Peigneux, P., Fuchs, S., Petiau, C., Phillips, C., Aerts, J., and Del Fiore, G. 2000. Experience-dependent changes in cerebral activation during human REM sleep. Nat. Neurosci. 3, 831–836.
Margoliash, D. 1983. Acoustic parameters underlying the responses of song-specific neurons in the white-crowned sparrow. J. Neurosci. 3, 1039–1057.
Margoliash, D. 1986. Preference for autogenous song by auditory neurons in a song system nucleus of the white-crowned sparrow. J. Neurosci. 6, 1643–1661.
Margoliash, D. 2002. Evaluating theories of bird song learning: implications for future directions. J. Comp. Physiol. A Neuroethol. Sens. Neural Behav. Physiol. 188, 851–866.
Margoliash, D. 2003. Offline Learning and the Role of Autogenous Speech: New Suggestions From Birdsong Research. In: Speech (*ed*. S. B. Commun), pp. 165–178. Elsevier.
Margoliash, D. and Konishi, M. 1985. Auditory representation of autogenous song in the song-system of white-crowned sparrows. Proc. Natl. Acad. Sci. U. S. A. 82, 5997–6000.
Marler, P. 1970a. A comparative approach to vocal learning: song development in white-crowned sparrows. J. Comp. Physiol. Psychol. 71(2), Pt 21–25.
Marler, P. 1970b. Birdsong and speech development: could there be parallels? Am. Sci. 58, 669–673.
Marler, P. 1998. Three models of song learning: evidence from behavior. J. Neurobiol. 33, 501–516.
Marshall, L., Helgadottir, H., Moole, M., and Born, J. 2006. Boosting slow oscillations during sleep potentiates memory. Nature 444, 610–613.
McCasland, J. S. and Konishi, M. 1981. Interaction between auditory and motor activities in an avian song control nucleus. Proc. Natl. Acad. Sci. U. S. A. 78, 7815–7819.
McClelland, J. L. and Rumelhart, D. E. 1985. Distributed memory and the representation of general and specific information. J. Exp. Psychol. Gen. 114, 159–188.
Mednick, S. C., Nakayama, K., Cantero, J. L., Atienza, M., Levin, A. A., Pathak, N., and Stickgold, R. 2002. The restorative effect of naps on perceptual deterioration. Nat. Neurosci. 5, 677–681.
Mednick, S. C., Nakayama, K., and Stickgold, R. 2003. Sleep-dependent learning: a nap is as good as a night. Nat. Neurosci. 6, 697–698.
Mello, C. V. and Clayton, D. F. 1994. Song-induced ZENK gene expression in auditory pathways of songbird brain and its relation to the song control system. J. Neurosci. 14, 6652–6666.
Mello, C., Nottebohm, F., and Clayton, D. 1995. Repeated exposure to one song leads to a rapid and persistent decline in an immediate early gene's response to that song in zebra finch telencephalon. J. Neurosci. 15, 6919–6925.
Mello, C. V., Vates, G. E., Okuhata, S., and Nottebohm, F. 1998. Descending auditory pathways in the adult male zebra finch (*Taeniopygia guttata*). J. Comp. Neurol. 395, 137–160.
Mello, C. V., Vicario, D. S., and Clayton, D. F. 1992. Song presentation induces gene expression in the songbird forebrain. Proc. Natl. Acad. Sci. U. S. A. 89, 6818–6822.
Millner, B. 1965. Visually-guided maze learning in man: effects of bilateral hippocampal, bilateral frontal, and unilateral cerebral lesions. Neuropsychologia 3, 317–338.
Mishkin, M. 1978. Memory in monkeys severely impaired by combined but not by separate removal of amygdala and hippocampus. Nature 273, 297–298.
Nealen, P. M. and Schmidt, M. F. 2006. Distributed and selective auditory representation of song repertoires in the avian song system. J. Neurophysiol. 96, 3433–3447.
Nordeen, K. W. and Nordeen, E. J. 1992. Auditory feedback is necessary for the maintenance of stereotyped song in adult zebra finches. Behav. Neural Biol. 57, 58–66.
Nottebohm, F., Stokes, T. M., and Leonard, C. M. 1976. Central control of song in the canary, *Serinus canarius*. J. Comp. Neurol. 165, 457–486.
Okanoya, K. and Yamaguchi, A. 1997. Adult Bengalese finches (*Lonchura striata var. domestica*) require real-time auditory feedback to produce normal song syntax. J. Neurobiol. 33, 343–356.
Pascual-Leone, A., Nguyet, D., Cohen, L., Brasil-Neto, J., Cammarota, A., and Hallett, M. 1995. Modulation of muscle responses evoked by transcranial magnetic stimulation during the acquisition of new fine motor skills. J. Neurophysiol. 74, 1037–1045.
Payne, R. B. 1983. The social context of song mimicry: song-matching dialects in indigo buntings (*Passerina cyanea*). Anim. Behav. 31, 788–805.
Peigneux, P., Laureys, S., Fuchs, S., Collette, F., Perrin, F., Reggers, J., Phillips, C., Degueldre, C., Del Fiore, G., Aerts, J., *et al.* 2004. Are spatial memories strengthened in

the human hippocampus during slow wave sleep?. Neuron 44, 535–545.
Phan, M. L., Pytte, C. L., and Vicario, D. S. 2006. Early auditory experience generates long-lasting memories that may subserve vocal learning in songbirds. Proc. Natl. Acad. Sci. U. S. A. 103, 1088–1093.
Plihal, W. and Born, J. 1997. Effects of early and late nocturnal sleep on declarative and procedural memory. J. Cogn. Neurosci. 9, 534–547.
Poe, G. R., Nitz, D. A., McNaughton, B. L., and Barnes, C. A. 2000. Experience-dependent phase-reversal of hippocampal neuron firing during REM sleep. Brain Res. 855, 176–180.
Rauske, P. L., Dave, A. S., and Margoliash, D. 2001. Sleep in adult zebra finches functionally rewires the song system nucleus RA. Soc. Neurosci. Abstr. 27, 381.383.
Rauske, P. L., Shea, S. D., and Margoliash, D. 2003. State and neuronal class-dependent reconfiguration in the avian song system. J. Neurophysiol. 89, 1688–1701.
Reiner, A., Perkel, D. J., Bruce, L. L., Butler, A. B., Csillag, A., Kuenzel, W., Medina, L., Paxinos, G., Shimizu, T., Striedter, G., *et al.* 2004. Revised nomenclature for avian telencephalon and some related brainstem nuclei. J. Comp. Neurol. 473, 377–414.
Saffran, J. R., Aslin, R. N., and Newport, E. L. 1996. Statistical learning by 8-month-old infants. Science 274.
Schmidt, M. F. and Konishi, M. 1998. Gating of auditory responses in the vocal control system of awake songbirds. Nat. Neurosci. 1, 513–518.
Sen, K., Theunissen, F. E., and Doupe, A. J. 2001. Feature analysis of natural sounds in the songbird auditory forebrain. J. Neurophysiol. 86, 1445–1458.
Shank, S. and Margoliash, D. 2006. Song tutoring onset precedes rapid modification of nighttime sleep activity in a premotor nucleus of the juvenile zebra finch. Soc. Neurosci. Abstr. 32, 579.516.
Shea, S. D. and Margoliash, D. 2003. Basal forebrain cholinergic modulation of auditory activity in the zebra finch song system. Neuron 40, 1213–1226.
Siegel, J. M. 2001. The REM sleep – memory consolidation hypothesis. Science 294, 1058–1063.
Skaggs, W. E. and McNaughton, B. L. 1996. Replay of neuronal firing sequences in rat hippocampus during sleep following spatial experience. Science 271, 1870–1873.
Smith, C. 2001. Sleep states and memory processes in humans: procedural versus declarative memory systems. Sleep Med. Rev. 5, 491–506.
Squire, L. 1987. Memory and Brain. Oxford University Press.
Stickgold, R., James, L., and Hobson, J. A. 2000a. Visual discrimination learning requires sleep after training. Nat. Neurosci. 3, 1237–1238.
Stickgold, R., Malia, A., Maguire, D., Roddenberry, D., and O'Connor, M. 2000b. Replaying the game: hypnagogic images in normals and amnesics. Science 290, 350–353.
Stickgold, R., Whidbee, D., Schirmer, B., Patel, V., and Hobson, J. A. 2000c. Visual discrimination task improvement: a multi-step process occurring during sleep. J. Cogn. Neurosci. 12, 246.
Stripling, R., Kruse, A. A., and Clayton, D. F. 2001. Development of song responses in the zebra finch caudomedial neostriatum: role of genomic and electrophysiological activities. J. Neurobiol. 48, 163–180.
Stripling, R., Volman, S. F., and Clayton, D. F. 1997. Response modulation in the zebra finch neostriatum: relationship to nuclear gene regulation. J. Neurosci. 17, 3883–3893.
Sutherland, G. R. and McNaughton, B. 2000. Memory trace reactivation in hippocampal and neocortical neuronal ensembles. Curr. Opin. Neurobiol. 10, 180–186.
Sutter, M. L. and Margoliash, D. 1994. Global synchronous response to autogenous song in zebra finch HVc. J. Neurophysiol. 72, 2105–2123.
Sutton, R. S. and Barto, A. G. 1998. Reinforcement Learning: An Introduction. MIT Press.
Tchernichovski, O., Lints, T., Mitra, P. P., and Nottebohm, F. 1999. Vocal imitation in zebra finches is inversely related to model abundance. Proc. Natl. Acad. Sci. U. S. A. 96, 12901–12904.
Tchernichovski, O., Mitra, P. P., Lints, T., and Nottebohm, F. 2001. Dynamics of the vocal imitation process: how a zebra finch learns its song. Science 291, 2564–2569.
Terleph, T. A., Mello, C. V., and Vicario, D. S. 2006. Auditory topography and temporal response dynamics of canary caudal telencephalon. J. Neurobiol. 66, 281–292.
Terpstra, N. J., Bolhuis, J. J., Den Boer-Visser, A. M., and Ten Cate, C. 2005. Neuronal activation related to auditory perception in the brain of a non-songbird, the ring dove. J. Comp. Neurol. 488, 342–351.
Terpstra, N. J., Bolhuis, J. J., Riebel, K., van der Burg, J. M., and den Boer-Visser, A. M. 2006. Localized brain activation specific to auditory memory in a female songbird. J. Comp. Neurol. 494, 784–791.
Theunissen, F. E. and Doupe, A. J. 1998. Temporal and spectral sensitivity of complex auditory neurons in the nucleus HVc of male zebra finches. J. Neurosci. 18, 3786–3802.
Theunissen, F. E., Amin, N., Shaevitz, S. S., Woolley, S. M., Fremouw, T., and Hauber, M. E. 2004. Song selectivity in the song system and in the auditory forebrain. Ann. N. Y. Acad. Sci. 1016, 222–245.
Wagner, U., Gais, S., Haider, H., Verleger, R., and Born, J. 2004. Sleep inspires insight. Nature 427, 352–355.
Walker, M. P. 2005. A refined model of sleep and the time course of memory formation. Behav. Brain Sci. 28, 51–104.
Walker, M. P. and Stickgold, R. 2006. Sleep, memory, and plasticity. Annu. Rev. Psychol. 57, 139–166.
Walker, M. P., Brakefield, T., Morgan, A., Hobson, J. A., and Stickgold, R. 2002. Practice with sleep makes perfect: sleep-dependent motor skill learning. Neuron 35, 205–211.
Walker, M. P., Brakefield, T., Seidman, J., Morgan, A., Hobson, J. A., and Stickgold, R. 2003. Sleep and the time course of motor skill learning. Learn Mem. 275–284.
Walker, M. P., Stickgold, R., Alsop, D., Gaab, N., and Schlaug, G. 2005a. Sleep-dependent motor memory plasticity in the human brain. Neuroscience 133, 911–917.
Walker, M. P., Stickgold, R., Jolesz, F. A., and Seung-Schik, Y. 2005b. The functional anatomy of sleep-dependent visual skill learning. Cereb. Cortex 15, 1666–1675.
West, M. J. and King, A. P. 1988. Female visual displays affect the development of male song in the cowbird. Nature 334, 244–246.
Wilson, M. A. and McNaughton, B. L. 1994. Reactivation of hippocampal ensemble memories during sleep. Science 265, 676–679.
Yu, A. C. and Margoliash, D. 1996. Temporal hierarchical control of singing in birds. Science 273, 1871–1875.
Zola-Morgan, S., Squire, L. M., Clower, R. P., and Rempel, N. L. 1993. Damage to the perhinal cortex exacerbates memory impairment following lesions to the hippocampal formation. J. Neurosci. 13, 251–265.

4.01 Phylogeny of Chemical Sensitivity

B W Ache, University of Florida, Gainesville, FL, USA

J M Young, Fred Hutchinson Cancer Research Center, Seattle, WA, USA

© 2008 Elsevier Inc. All rights reserved.

4.01.1	**Introduction**	1
4.01.2	**Chemical Signals**	2
4.01.2.1	Nature of Chemical Signals	2
4.01.2.2	Dynamics of Chemical Signals	4
4.01.3	**Chemoreceptor Proteins**	5
4.01.3.1	Receptor Expression Patterns	5
4.01.3.2	Receptor Structure	7
4.01.3.3	Receptor–Ligand Pairings	7
4.01.3.4	Receptor Gene Family Evolution	8
4.01.4	**Peripheral Chemoreceptor Cells**	10
4.01.4.1	Receptor Cell Morphology	10
4.01.4.2	Receptor Cell Turnover	10
4.01.4.3	Signal Transduction	11
4.01.5	**Perireceptor Processes**	13
4.01.5.1	Mechanical Processes	13
4.01.5.2	Biochemical Processes	14
4.01.6	**Processing of Chemosensory Information**	15
4.01.6.1	Central Neural Organization	15
4.01.6.2	Quality Coding	16
4.01.7	**Chemosensory-Mediated Behavior and Plasticity**	18
4.01.8	**Overview**	20
References		20

4.01.1 Introduction

> Smells are surer than sounds and sights to make your heart-strings crack.
>
> Rudyard Kipling

It is difficult for humans, being the visually oriented creatures we are, to appreciate the fundamental importance of chemical sensitivity to life. The ability to detect and respond in an adaptive manner to chemical signals serves as the primary window to the sensory world for most species of animals. Chemical sensitivity is present even in the simplest of the extant life forms: bacteria, slime molds, and protozoans. Indeed, all living cells are irritable to chemicals. This predisposition of cells to be perturbed by chemicals led to the eventual evolution of specific receptor proteins to detect chemical signals and, ultimately, to specific chemosensory organs. The fundamental importance of chemical sensitivity to life and health was recognized by the award of the 2004 Nobel Prize in Physiology or Medicine to Drs. Linda Buck and Richard Axel for their pioneering discovery of olfactory receptor proteins and the understanding of olfactory organization these groundbreaking findings allowed.

Most of our detailed knowledge of chemical sensitivity comes from relatively few, but evolutionary distant species of animals that allow for phylogenetic comparison, including nematodes, insects, crustaceans, fish, frogs, mouse, and rat. Insights gained from rapid advances in molecular biology greatly facilitate this comparison, especially using the experimental model organisms *Caenorhabditis elegans*, *Drosophila*, zebrafish, and mice. Comparison across phylogenetically distant animals can be difficult, however. Even the most fundamental of distinctions such as that between smell and taste can blur when one considers, for example, that lobsters and fish have anatomically distinct olfactory systems that even sniff. Yet odors for these animals are sapid molecules in solution, not unlike

the context in which tastants activate vertebrate taste receptor cells. The distinction between smell and taste is further obscured by the presence of taste receptor cells in fish that respond to the same molecules as fish olfactory receptor cells and with greater sensitivity than the olfactory receptor cells. Comparison across animals as phylogenetically distant as nematodes, flies, fish, and mice inevitably requires caution when even basic terminology such as olfaction and taste can be called into question. At the same time, understanding the phylogeny of chemical sensitivity can produce important new insight into how we detect smells and tastes. From the two examples just mentioned, for example, we learn that the fundamental difference between smell and taste must be based on something other than the signaling medium, the nature of the ligands, and the threshold of sensitivity – the descriptors traditionally used to distinguish these two chemosensory modalities in terrestrial vertebrates. We are challenged to understand what really is unique about the chemosensory modality we call olfaction. In addition to comparative studies leading to new questions and insights into chemical sensitivity, animal models provide the opportunity to perform experiments designed to answer those questions.

In this chapter, we take a broad view, trying to look through species-dependent differences in an attempt to reveal broad principles of chemical sensitivity. We conclude that, even though the details differ between phylogenetically diverse animals, general principles of chemical signal detection are shared by most species. Citations throughout are only representative and are not intended to be exhaustive.

4.01.2 Chemical Signals

4.01.2.1 Nature of Chemical Signals

Animals use chemical stimuli to communicate in an amazingly diverse array of behavioral contexts, many of which are hard to appreciate because the action of chemosensory cues is often subtle and difficult for humans to even envision. Chemical stimuli emanating from other species of organisms, known collectively as allelochemics (Whittaker, R. H. and Feeny, P. P., 1971), control prey localization, homing, symbiotic associations, territorial marking, predator deterrence and avoidance, metamorphosis and growth, and pollination, to name just a few examples. Other chemical stimuli of conspecific origin, known collectively as pheromones (Shorey, H. H., 1976), act far beyond their now well-known role as sex attractants, a function which has been described in most animal phyla. For example, recognition pheromones denote the identity of individuals, social status, social group, and place; aggregation pheromones mediate feeding, sex, and aggression; dispersion pheromones maintain individual spacing and minimize predation; and reproductive pheromones trigger courtship displays and postures. In addition to these triggering functions, pheromones also serve priming functions in equally diverse contexts, in which the chemical stimulus additionally or alternately initiates longer term changes in the state of the recipient animal rather than just triggering immediate, overt responses (Vandenburg, J. G., 1983). The many, diverse behavioral roles chemical stimuli serve in phylogenetically diverse animals underscore the extreme importance of chemical sensitivity.

Many classes of molecules fall within the theoretical limits of molecular size and type for signal function, especially when one considers that these limits expand for chemical signals that can travel by bulk flow in aqueous media and that signals are not restricted to volatile molecules that can diffuse through air. The enormous information content inherent in having such a large number of potential signal molecules is one of the hallmarks of chemosensory communication. Given the great diversity of potential signal molecules, one might expect a given molecule to acquire signal function only occasionally in evolution. However, it is not uncommon to find that members of the same class of molecule or even the same molecular species have signal function in phylogenetically diverse animals. The role of purine nucleotides as chemosensory signals epitomizes this point. Guanosine 5′-monophosphate (GMP) synergizes the perceived intensity of monosodium glutamate in human taste, and methyl xanthenes, compounds that inhibit adenosine receptors, enhance sweet taste (Rifkin, B. and Bartoshuk, L. M., 1980). GMP and other purine nucleotides also increase the binding of glutamate to its receptors isolated from bovine taste papillae by several fold (Torii, K. and Cagan, R. H., 1980). Slime molds use adenosine 5′-monophosphate as an aggregating signal (Mato, J. M. *et al.*, 1978), while adenosine 5′-triphosphate (ATP) in mammalian blood triggers gorging by blood-feeding insects (Friend, W. G. and Smith, J. J. B., 1982). Finally, lobsters recognize food sources in part based on the ratio of ATP to other adenosine nucleotides in their food (Zimmer-Faust, R. K. *et al.*, 1988), and inosine 5′-monophosphate (IMP)

activates gustatory receptors in marine flatfish (Mackie, A. M. and Adron, J. W., 1978). It is not clear whether such diversity of signaling roles for a single class of molecules reflects the early evolution and retention of specific receptor types, or convergent evolution of different receptor types to recognize especially biologically relevant ligands. Such questions can now be addressed as more chemoreceptor proteins are cloned and functionally expressed (see Section 4.01.3).

Chemical signals are rarely, if ever, single compounds in real-world situations. Rather, they are complex mixtures of compounds, where related signals can contain many of the same components in different ratios (Figure 1). Single chemical compounds can elicit physiological and behavioral responses and are used routinely in the laboratory to experimentally dissect chemosensory function. However, complete biological activity inevitably requires stimulation with complex, multicomponent

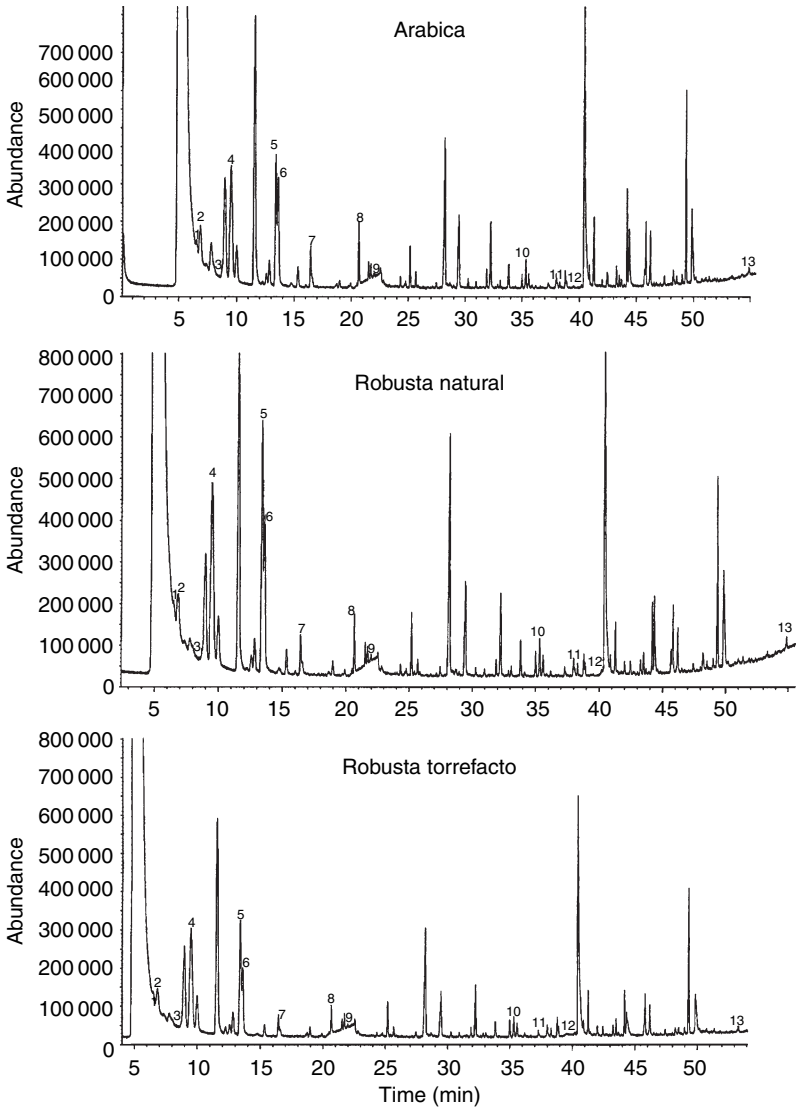

Figure 1 Natural odorants are complex, often highly redundant mixtures. Plots show GC–MS chromatograms of the aroma volatiles of three varieties of espresso coffee: Arabica, Robusta natural, and Robusta torrefacto. Ordinate, absorbance, measuring relative abundance. Abscissa, time in minutes. Similarly numbered peaks in each chromatogram reflect the same compound. Adapted with permission from Maeztu, L., Sanz, C., Andueza, S., Paz De Pena, M., Bello, J., and Cid, C. 2001. Characterization of espresso coffee aroma by static headspace GC-MS and sensory flavor profile. J. Agric. Food. Chem. 49, 5437–5444. Copyright 2001 American Chemical Society.

mixtures of chemical compounds. This generalization holds across phylogenetically diverse species. Relatively simple animals such as cnidarians, jellyfish and sea anemones, can capture and ingest their prey in response to single chemical compounds: glutathione elicits feeding in *Hydra* (Lenhoff, H. M. and Lindstedt, K. J., 1974). But even for these relatively simple animals, discharge of the prey-capturing organs, the cnidia, is regulated by at least two classes of receptors, one for amino and imino acids and another for N-acetylated sugars (Thorington, G. U. and Hessinger, D. A., 1988). Although insect pheromones were originally thought to be silver bullet odorants, as single chemical compounds can attract male to female moths in the field, natural insect pheromones also turn out to be mixtures. For example, the cabbage looper flies upwind in response to major components of the natural pheromone blend, but at least six other components of the female's pheromone gland are required to evoke the full behavioral response of male moths to virgin females (Bjostad, L. B. *et al.*, 1984). Indeed, it is often only subtle differences in the blend ratios of insect pheromones that keep sympatric insect species isolated. Mammals also use complex blends of compounds in pheromone secretions. Here, too, while single putative pheromone components can activate rodent vomeronasal (pheromone) chemoreceptor cells (Leinders-Zufall, T. *et al.*, 2000), it can be difficult to assign behavioral function to individual compounds due to the complexity of mammalian pheromonal secretions and the relatively small contribution of any one component. The scent secretions of tamarins, for example, lack marked differences in the qualitative composition of the marks of individuals of different gender or subspecies, suggesting that this level of behavioral discrimination must be encoded by subtle quantitative differences in the composition of scent mixtures (Belcher, A. M. *et al.*, 1988). Dissecting multicomponent stimulus blends can be daunting due to possible interactions among co-activated elements in the chemosensory pathway. When these interactions are inhibitory, for instance, removal of any one component from a mixture can result in expansion of the relative stimulus strength of the remaining components, masking the ability to detect the component's contribution to the stimulus capacity of the mixture.

4.01.2.2 Dynamics of Chemical Signals

Another hallmark of chemosensory signaling is that the signal is usually intermittent. Indeed, intermittency is fundamental to chemosensation, if not to sensory perception in general, by serving to offset adaptation and sharpen the onset of the signal (Dethier, V. G., 1987). Intermittency is an inherent property of the stimulus field or plume for many animals. Microbes and the smallest of eukaryotes that live within the viscous sublayer of the boundary zone of surfaces, and even those microorganisms that live suspended in the water column, experience stimulus spread that is dominated by diffusion and therefore concentration increases or decreases continuously. All larger animals, however, experience turbulent air or water flow; hence local currents and eddies dominate and perturb stimulus clouds emanating from point sources. Earlier models of odor plumes described the turbulent mixing of the chemical signal into the surrounding water or air as a diffusion process, producing homogeneous clouds with concentration that decreases with distance from the source. However, measurement of stimulus plumes on the scale at which they are encountered by most macroscopic animals in both water and air shows the plumes to be highly discontinuous (Koehl, M. A. R. *et al.*, 2001). As a result, chemoreceptors are only intermittently exposed to the stimulus as the animal moves through the medium or the medium moves over the animal (Figure 2). The specific parameters of the plume structure are medium-dependent and presumably contribute to shaping the dynamic aspects of chemical sensitivity

Figure 2 Odor plumes are highly discontinuous in space and time. Photograph of an odor field in a flume flowing from right to left past the antennule of a lobster. The odorant is a fluorescent dye illuminated by a laser sheet that penetrates the water mass in the plane of the organ. Note the scale of the discontinuities relative to the size of the olfactory organ, the tuft of sensilla on the distal end of the antennule (arrow). Unpublished photograph courtesy of M. Koehl.

in different animals. In addition to intermittency inherent in the stimulus field, animals often actively control the release of chemical signals in a pulsatile manner so as to enhance the intermittency of the stimulus field, further underscoring the fundamental importance of intermittency to chemical sensitivity. This phenomenon typically occurs in association with the release of pheromones, intraspecific chemical signals in which the sender and the receiver of the signal are coevolving. Intermittent release occurs in animals as phylogenetically diverse as slime molds (Mato, J. M. *et al.*, 1978) and insects (Christensen, T. A. *et al.*, 1994). In addition to intermittency inherent in the signal itself, active processes often intermittently gate access of the stimulus to the receptor organ, as considered in Section 4.01.5.2.

4.01.3 Chemoreceptor Proteins

Recognition of this diverse assortment of chemical signals is achieved largely using G-protein-coupled receptors (GPCRs), seven-transmembrane domain proteins that activate G-protein-based signaling cascades when activated by their ligands. Members of the GPCR superfamily recognize a wide range of both external and endogenous chemical signals including general odorants, pheromones, and tastants, as well as endogenous peptide, lipid, neurotransmitter, and nucleotide signals (Vassilatis, D. K. *et al.*, 2003). Several independent expansions of ancestral GPCRs have resulted in a number of sizeable, distantly related chemosensory gene families.

In 1991, Linda Buck and Richard Axel identified a large, diverse family of GPCRs expressed in the rat olfactory epithelium (Buck, L. and Axel, R., 1991) and proposed that they function as odorant receptors (commonly referred to as olfactory receptors, as distinct from a subsequently identified family proposed to be receptors for pheromonal odorants – but see below). This landmark discovery opened the door to the subsequent identification of a number of other chemosensory GPCR families, including insect olfactory and gustatory receptors (Clyne, P. J. *et al.*, 1999; Scott, K. *et al.*, 2001), nematode chemoreceptors (Troemel, E. R. *et al.*, 1995), the V1R and V2R families of mammalian pheromone receptors (Dulac, C. and Axel, R., 1995; Matsunami, H. and Buck, L. B, 1997), and the T1R and T2R families of mammalian taste receptors (Hoon, M. A. *et al.*, 1999; Chandrashekar, J. *et al.*, 2000). With the recent availability of almost complete genome sequences for a variety of species, there has been an explosion in papers describing entire families of chemosensory GPCRs (Table 1). These vast quantities of sequence data allow systematic, in-depth studies of many aspects of chemosensory coding: evolution, receptor–ligand interactions, expression patterns, etc. The size of these chemosensory families varies greatly, from only three GPCRs in the entire yeast proteome (GPR1, a nutritional sensor, and the STE2 and STE3 pheromone receptors) and three receptors in the mammalian T1R family (Liao, J. and Schultz, P. G., 2003) to over 1000 functional members in the rodent olfactory receptor repertoires, comprising up to ~6% of all genes in the genome (Young, J. M. *et al.*, 2003; Rat Genome Sequencing Project Consortium, 2004).

4.01.3.1 Receptor Expression Patterns

In many cases, the function of these gene families was initially postulated based only on expression in the appropriate chemosensory organ. A common assumption has been that the olfactory epithelium and the odorant receptor family expressed therein recognize general (nonpheromonal) odorants and that the vomeronasal organ and its receptor families recognize pheromones. Recent data show that this may be an oversimplification: the vomeronasal organ appears to recognize some compounds which have no known pheromonal activity (Sam, M. *et al.*, 2001) and some pheromones can be recognized after ablation of the vomeronasal organ, perhaps by the nose (Brennan, P. A. and Keverne, E. B., 2004). Additional proof of chemosensory receptor function has been provided for some members of these gene families, for example, by demonstrating functional expression in heterologous cell lines (e.g., Krautwurst, D. *et al.*, 1998), knockout and transgenic rescue experiments (e.g., Mueller, K. L. *et al.*, 2005), or by correlating natural sequence variation with phenotypic variation in chemosensory abilities (e.g., Chandrashekar, J. *et al.*, 2000).

However, the expression pattern of many other genes in these families remains untested, and their functional assignment should be considered tentative as it is based only on sequence similarity. Some systematic studies have been performed to confirm chemosensory expression of subsets of these genes (e.g., Scott, K. *et al.*, 2001) but are not comprehensive. Indeed, expression of some chemosensory receptors has been demonstrated outside the tissue that would

Table 1 Size of selected chemosensory receptor gene families

	No.of genes[a]	*No. of pseudogenes*[a]	*Reference*
Olfactory receptors			
Human	388	414	(1)
Mouse	~1200	~300	(2)
Rat	~1430	~640	(3)
Dog	~1070	~230	(4)
Chicken	82	476	(5)
Frog	410	478	(5)
Zebrafish	102	35	(5)
V1R pheromone receptors			
Human	2	115	(6)
Mouse	165	165	(6)
Rat	106	110	(6)
Dog	8	54	(6)
Cow	32	41	(7)
Opossum	49	53	(7)
Zebrafish	1	0	(8)
V2R pheromone receptors			
Rat		~100 (total)	(9)
T1R taste receptors			
Human, mouse, rat	3	n.d.	(10)
T2R bitter taste receptors			
Human	25	11	(11)
Rat, mouse	36	7	(12)
Zebrafish	≥2	n.d.	(8)
Chicken	3	n.d.	(13)
Invertebrate chemoreceptors			
Fly olfactory	60	Few	(14)
Fly gustatory	68	Few	(14)
Mosquito olfactory	79	n.d.	(15)
Mosquito gustatory	76	n.d.	(15)
Nematode worm		~1100 (total)	(16)

[a]Most numbers represent lower bound estimates of gene numbers, as genome assemblies are incomplete, and draft assemblies can contain sequencing errors that mean some intact genes appear as pseudogenes. Many gene families have been reported in several studies; for brevity, a single representative report is cited (in general, more recent reports are chosen as they are based on best available genomic data); apologies are due to other authors.

n.d, not determined.

(1) Niimura Y. and Nei M. (2003); (2) Young J. M. *et al.* (2003); (3) Rat Genome Sequencing Project Consortium (2004); (4) Quignon P. *et al.* (2003); (5) Niimura Y. and Nei M. (2005); (6) Young J. M. *et al.* (2005); (7) Grus W. E. *et al.* (2005); (8) Pfister P. and Rodriguez I. (2005); (9) Herrada G. and Dulac C. (1997); (10) Hoon M. A. *et al.* (1999), Montmayeur J. P. *et al.* (2001), Liao J. and Schultz P. G. (2003); (11) Go Y. *et al.* (2005); (12) Wu S. V. *et al.* (2005); (13) Hillier L. W. *et al.* (2004); (14) Robertson H. M. *et al.* (2003); (15) Hill C. A. *et al.* (2002); (16) Robertson H. M. (2001).

be expected based on their family membership. For example, one human pheromone receptor gene appears to be expressed in the olfactory epithelium rather than the vomeronasal organ (Rodriguez, I. *et al.*, 2000), some mammalian olfactory receptors are expressed in nonolfactory tissues, principally the testis (Parmentier, M. *et al.*, 1992), and some bitter taste receptors are expressed in the nose (Finger, T. E. *et al.*, 2003) and gastrointestinal tract (Wu, S. V. *et al.*, 2002). It is possible that some of these reports may reflect promiscuous, irrelevant transcriptional activity, but a recent study provides convincing evidence that the human olfactory receptor hOR17-4 is expressed in testis as well as the nose, responds to the chemical bourgeonal, and allows sperm to undergo chemotaxis toward bourgeonal sources (Spehr, M. *et al.*, 2003). Given their ability to detect a diverse range of ligands, it is perhaps unsurprising that chemosensory receptors have been co-opted to perform other functions.

Within a chemosensory organ, members of some chemosensory gene families exhibit a remarkable and mysterious expression pattern. For example, each neuron in the mammalian olfactory epithelium

probably expresses only one allele of one of the thousand or more genes in the family (Chess, A. *et al.*, 1994; Malnic, B. *et al.*, 1999; Serizawa, S. *et al.*, 2000), although it is still possible that this model is only partially correct (Mombaerts, P., 2004b). This one-neuron, one-gene expression regime ensures that responses to different ligands are segregated into different neurons, allowing fine discrimination between molecules. Axons of neurons expressing the same olfactory receptor converge at a limited number of locations in the olfactory bulb in the brain, thus integrating signals from functionally identical neurons (Mombaerts, P. *et al.*, 1996). Vomeronasal neurons probably follow a similar expression regime (Rodriguez, I. *et al.*, 1999), as do fruitfly olfactory neurons. Most fruitfly neurons each express two receptors: one, Or83b, that is broadly expressed in many olfactory neurons and a second receptor (or occasionally a pair of receptors) selected from among the rest of the gene family (Larsson, M. C. *et al.*, 2004; Goldman, A. L. *et al.*, 2005). The mechanism ensuring singular expression of olfactory receptors is still unclear, although negative feedback may be operating to ensure that once one receptor gene is chosen for expression, no other genes of the family are expressed (Serizawa, S. *et al.*, 2003).

Other families of chemosensory GPCRs, however, are expressed under a less strictly controlled regime. Each mammalian bitter taste receptor cell expresses many or all of the ~30 members of the T2R bitter taste receptor family and is thus broadly tuned to detect a wide range of bitter tastants (Mueller, K. L. *et al.*, 2005). Likewise, each of the nematode worm's 32 chemosensory neurons expresses multiple receptors (Troemel, E. R. *et al.*, 1995). Very few cell types are therefore needed to detect a broad range of chemicals, with the corresponding disadvantage that discrimination between different ligands may be impossible without additional input from other chemosensory modalities. The specificity of neuronal tuning and wiring is discussed further in Section 4.01.6.2.

4.01.3.2 Receptor Structure

It is assumed that regions of the chemoreceptor proteins that vary between members of a family are involved in ligand specification and that regions that are conserved between family members are important for functions common to all members, such as signaling through the G protein (Buck, L. and Axel, R., 1991). Elucidating the three-dimensional structure of many of these GPCRs has proved difficult, as they are transmembrane proteins and in some cases difficult to express in heterologous cell lines. However, distant similarity to rhodopsin, whose crystal structure is known, has allowed some groups to model the structure of a few olfactory receptors (e.g., Floriano, W. B. *et al.*, 2000). Functional studies utilizing these models have been slow to appear, but one study shows that structural considerations can successfully predict which residues are important in determining ligand specificity (Katada, S. *et al.*, 2005).

It has recently become clear that dimerization (both heterodimerization and homodimerization) is important for many GPCRs to function correctly. Dimerization can help achieve proper cell-surface expression, as well as being involved in signal transduction and in determining ligand specificity (Bouvier, M., 2001). The role of dimerization is still largely unknown for the chemosensory receptors, except for the mammalian T1R taste receptor family. This family has three members, T1R1, T1R2, and T1R3; cells expressing T1R1 and T1R3 (presumably functioning as a heterodimer) recognize L-amino acids (Nelson, G. *et al.*, 2002), whereas cells expressing T1R2 and T1R3 recognize sweet tastes (Nelson, G. *et al.*, 2001). The coexpression of olfactory receptor OR83b with other receptors in fruitflies (Larsson, M. C. *et al.*, 2004) and of its ortholog in silk moths (Nakagawa, T. *et al.*, 2005) suggests that these receptors may also function as heterodimers. Heterodimerization among members of the mammalian olfactory and pheromone receptor families is unlikely, as each neuron appears to express only a single gene of the family. There is, however, some evidence to suggest that these receptors dimerize with other GPCR or non-GPCR molecules (Loconto, J *et al.*, 2003; Hague, C. *et al.*, 2004; Saito, H. *et al.*, 2004).

4.01.3.3 Receptor–Ligand Pairings

With the availability of vast numbers of chemosensory receptor sequences, it would be very useful to know which chemical ligand or ligands each receptor responds to. A few general principles emerge from what we know so far about receptor–ligand pairing: receptors may be broadly tuned (each olfactory receptor recognizes multiple odorants) or finely tuned to recognize a single ligand, like the pheromone receptors (Malnic, B. *et al.*, 1999; Leinders-Zufall, T. *et al.*, 2000). In addition, each ligand may activate multiple receptors, each to a different extent. Section 4.01.6.2 discusses these issues in more detail. Several different approaches have been taken to

deciphering receptor–ligand pairings, including coupling expression in heterologous cell lines with functional assays (e.g., Krautwurst, D. *et al.*, 1998), correlating natural or engineered genetic variation in chemosensory receptors with phenotypic variation in chemosensory abilities (Montmayeur, J. P. *et al.*, 2001) and measuring ligand responsiveness of chemosensory neurons expressing particular receptors (Malnic, B. *et al.*, 1999; Bozza, T. *et al.*, 2002; Hallem, E. A. *et al.*, 2004). The success of these approaches has varied between the chemosensory receptor families (Mombaerts, P., 2004a). Many ligands have been identified for mammalian taste receptors and insect olfactory receptors. Unfortunately, heterologous expression (the approach which seems most promising for large-scale identification of receptor–ligand relationships) of many olfactory receptors has proved remarkably difficult. Three recent studies have identified proteins that interact with olfactory or pheromone receptors to facilitate cell-surface expression (Loconto, J. *et al.*, 2003; Hague, C. *et al.*, 2004; Saito, H. *et al.*, 2004). Use of these proteins may allow a much larger number of receptor–ligand pairs to be identified in the near future, findings that are likely to be of great interest and commercial value (Gilbert, A. N. and Firestein, S., 2002).

4.01.3.4 Receptor Gene Family Evolution

As well as greatly informing our knowledge of how chemicals are sensed, the chemosensory families provide fascinating case studies of gene family evolution. Although some chemosensory gene families have remained static over time (e.g., the mammalian T1R family has three members in both human and mouse, and each mouse gene clearly corresponds to a single human gene: Liao, J. and Schultz, P. G., 2003), others have changed greatly even between closely related species. A number of processes have shaped and continue to change these gene families: gene duplication increases the number of family members; accumulation of sequence changes in new gene duplicates creates novel ligand-binding capabilities; deletions and inactivating mutations cause gene loss; and gene conversion erases sequence divergence and/or creates new combinations of sequence variants (Sharon, D. *et al.*, 1999; Young, J. M. *et al.*, 2002). The net result of these ongoing processes is that different species can have very different functional receptor repertoires (Table 1). Figure 3 illustrates how some of these processes have shaped the modestly sized human and mouse T2R bitter taste receptor families.

Differences between species in chemosensory receptor families may be driven by differences in the biological needs of the species – for example, some authors suggest that the loss of functional genes and accumulation of pseudogenes in the primate olfactory and perhaps pheromone receptor families were coincident with the acquisition of trichromatic vision (Zhang, J. and Webb, D. M., 2003; Gilad, Y. *et al.*, 2004), implying that our increased reliance on visual cues made chemosensation at least partially obsolete. For most single-copy genes in a genome, it is possible to identify a unique equivalent in other organisms, a fact that motivates the use of animal models to learn about human biology. The dramatic evolutionary change seen in some of these chemosensory families, together with the fact that even very minor changes in amino acid sequence can alter ligand-binding specificities (Katada, S. *et al.*, 2005), means that studies on individual chemoreceptors may not be particularly applicable across species.

The V1R pheromone receptor family provides perhaps the most striking example of evolutionary change in the chemosensory gene families. Recent studies (Grus, W. E. *et al.*, 2005; Young, J. M. *et al.*, 2005) have shown that rodents have over a hundred functional V1R genes, cows have 30 or more, and opossum at least 49, while dogs have only 8, and humans and chimps close to none. The lack of functional V1Rs in humans and chimps is in keeping with the finding that one of the downstream signaling components, Trp2β, is a pseudogene (Liman, E. R. *et al.*, 1999) and that the vomeronasal organ is absent or vestigial in these species (Trotier, D. *et al.*, 2000). Even between two closely related species, rat and mouse, V1R repertoires reveal dramatic species-specific expansions in some subfamilies, with as many as 23 mouse genes in a V1R subfamily that contains only one rat pseudogene (Grus, W. E. and Zhang, J., 2004; Young, J. M. *et al.*, 2005). It is possible that as two lineages separate during evolution, changes in pheromone receptor gene families establish or reinforce speciation barriers through their role in determining mating behaviors.

These genome-altering processes are ongoing, resulting in polymorphism between different individuals both in receptor sequences and in gene copy number. There are at least 26 human sequence polymorphisms where one variant encodes an apparently functional olfactory receptor and the other variant encodes a pseudogene (Menashe, I. *et al.*, 2003). The

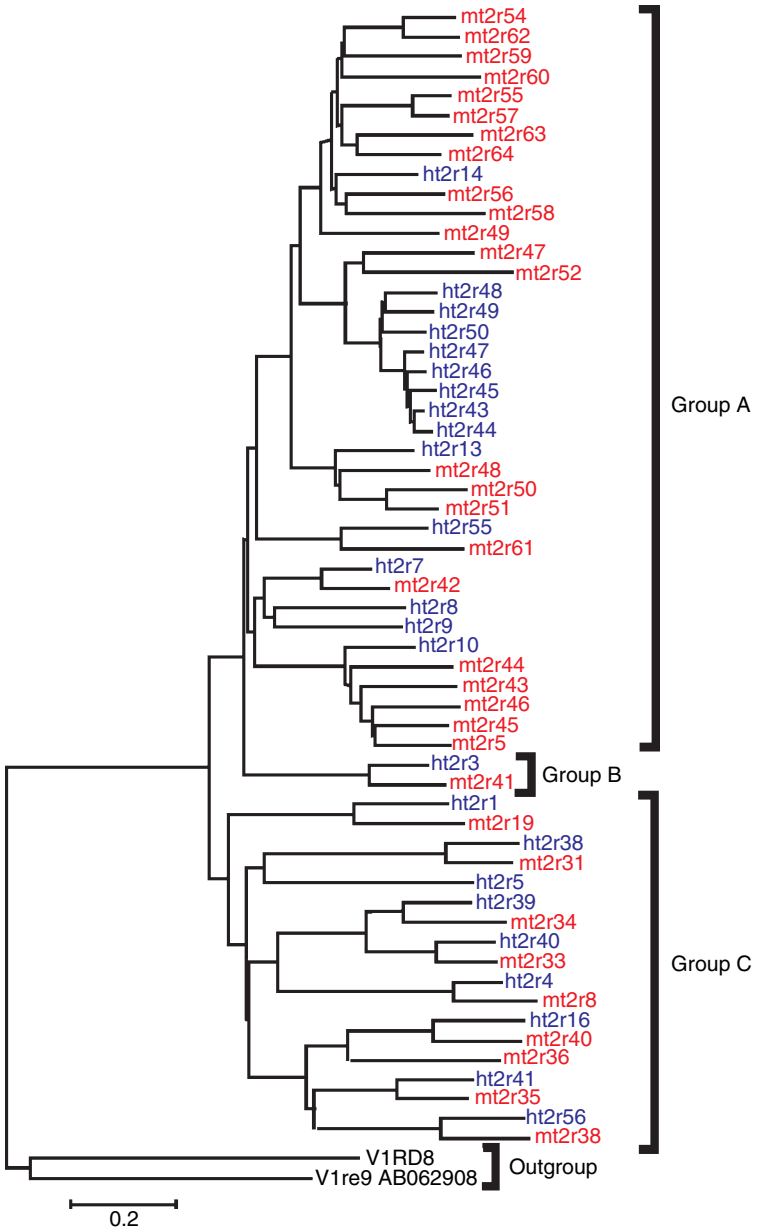

Figure 3 Chemosensory receptor gene families are evolving dynamically. Phylogenetic tree comparing 58 putatively functional human (blue) and mouse (red) bitter taste receptor genes showing that in some branches of the tree (groups B and C) many pairs of one-to-one human–mouse equivalents can be identified, suggesting that these genes have remained stable since the human and rodent lineages diverged. In other branches of the tree (group A), some genes have duplicated several times since the lineages diverged, resulting in clusters of very similar genes and loss of simple, one-to-one equivalence relationships. Stable genes may recognize tastants important to both species, whereas recently duplicated genes might be responsible for the differences between humans and rodents in their gustatory abilities. Adapted from Shi, P., Zhang, J., Yang, H., and Zhang, Y.-P. 2003. Adaptive diversification of bitter taste receptor genes in mammalian evolution. Mol. Biol. Evol. 205, 805–814, with permission from Oxford University Press.

functional implications of some individuals having many more functional olfactory receptors than others are not known, but could be significant. Many other sequence polymorphisms cause a single amino acid change whose functional consequences are currently unknown (e.g., Zhang, X. *et al.*, 2004). Copy number polymorphism of a group of human olfactory receptors has also been described. A recent duplication of a

sequence block found near the ends of several human chromosomes results in different individuals having between 7 and 11 copies of one functional receptor and two pseudogenes, with many copies showing subtle differences in amino acid sequence (Trask, B. J. *et al.*, 1998). Such variation can be difficult to detect; future studies will undoubtedly uncover additional examples of chemosensory receptor gene copy number polymorphism.

One can imagine two possible selective advantages to retaining duplicates of chemosensory receptors. Sequence changes accumulating in a new gene copy might result in novel ligand-binding specificities, providing a selective advantage to an individual who can now detect additional chemical signals. Alternatively, an increase in gene copy number of a given chemosensory receptor might increase the relative number of sensory cells choosing to express that receptor, resulting in increased sensitivity to the corresponding ligand. Evolutionary selective pressures favoring novel amino acid sequence variants are often described as positive selection: when sequence changes are not tolerated, selection is said to be purifying. Initial studies looking at orthologous receptor genes in different species, at paralogous genes within a species, and at polymorphisms between members of the same species are suggestive of positive selection acting on a subset of olfactory receptors (e.g., Hughes, A. L. and Hughes, M. K., 1993; Gilad, Y. *et al.*, 2000), pheromone receptors (Emes, R. D. *et al.*, 2004; Lane, R. P. *et al.*, 2004), nematode chemosensory receptors (Thomas, J. H. *et al.*, 2005), and mammalian bitter taste receptors (Shi, P. *et al.*, 2003). It will be fascinating to learn whether the signs of positive selection observed in these genes correlate with the emergence of novel ligand-binding capabilities.

The functional consequences of changes in the chemosensory receptor families (both in copy number and in amino acid sequence) are mostly unclear at the moment, although some progress is being made in correlating sequence differences and changes in ligand responsiveness. A number of studies describe differential sensitivity to various odorants and tastants, for example, musk, isovaleric acid, and asparagus metabolites (Whissell-Buechy, D. and Amoore, J. E., 1973; Lison, M. *et al.*, 1980; Pourtier, L. and Sicard, G., 1990), but the underlying sequence differences have been identified in only a few cases. Polymorphisms between mouse strains in the gene encoding T1R3 govern their sensitivity to several sweet tastants including saccharin and sucrose (Montmayeur, J. P. *et al.*, 2001). Variation in the mouse mT2R-5 bitter taste receptor affects cycloheximide sensitivity (Chandrashekar, J. *et al.*, 2000), and variation in one of the human T2R genes determines whether the bitter compound phenylthiocarbamide can be tasted (Kim, U. K. *et al.*, 2003).

4.01.4 Peripheral Chemoreceptor Cells

4.01.4.1 Receptor Cell Morphology

The evolution of multicellularity allowed for specialization of cellular function and the appearance of cells dedicated to the detection of chemical cues. Some chemosensory input is mediated by free nerve endings, as in the case of vertebrate trigeminal chemoreceptor neurons, but typically animals have evolved more specialized chemoreceptor cells. Chemoreceptor cells occur both internally, for example, in blood vessels and the gastrointestinal tract, where they monitor the internal milieu, and externally. The general morphology of specialized chemoreceptor cells, whether internal or external, is strikingly similar among species and systems, notwithstanding species-specific differences in their detailed morphology. With one main exception, chemoreceptor cells tend to be primary bipolar neurons in which the dendritic membrane terminates in a filamentous array generally assumed to increase the surface area for stimulus capture, and the axon extends without synapsing to the central nervous system (CNS). Comparing the morphology of olfactory receptor cells in vertebrates and insects and receptor cells in the nematode amphid organ demonstrates this point (Figure 4). Vertebrate taste cells, however, along with their probably evolutionarily related counterparts, solitary chemoreceptor cells (Finger, T. E. *et al.*, 2003), are not bipolar neurons, but secondary-type sensory cells of epithelial origin that make synaptic contact with afferent nerve fibers in the periphery. These cells, too, terminate in filamentous extensions of the plasma membrane. The filamentous extensions of chemoreceptor cells can be either ciliary or microvillar in origin.

4.01.4.2 Receptor Cell Turnover

Chemosensory cells are necessarily exposed to the environment and therefore subject to environmental onslaught. Presumably in response to this stress, they have evolved the ability to turn over and replace

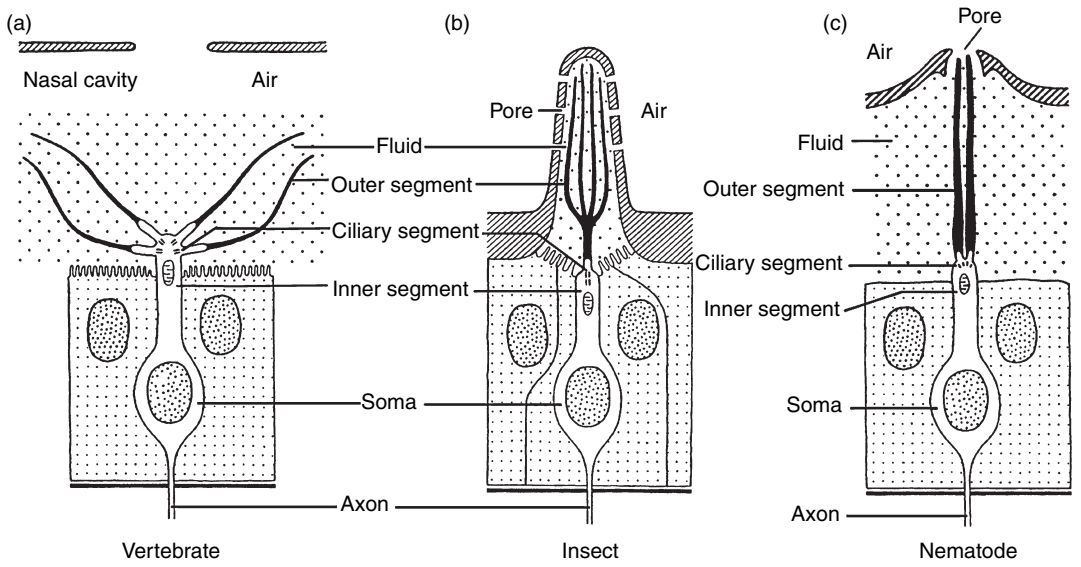

Figure 4 Comparison of primary chemoreceptor neurons in vertebrates, insects, and nematodes. Diagrams compare primary chemoreceptor neurons in the vertebrate olfactory epithelium (a), an insect olfactory sensillum (b), and the nematode amphid organ (c), all drawn to the same size. Note that all are small, bipolar neurons that terminate in a ciliary arbor and send their axon without branching to the CNS. Reproduced from Ache, B. W. 1991. Phylogeny of Smell and Taste. In: Smell and Taste in Health and Disease (*eds.* T. V. Getchell, *et al.*), pp. 3–18. Raven Press. © 1991 Lippincot Williams & Wilkins, with permission.

themselves throughout the life of the animal. Both olfactory and taste receptor cells in all vertebrates are characterized by well-established cycles of birth, maturation, and death (Graziadei, P. P. C. and Monti-Graziadei, G. A., 1978). Given that the olfactory receptor cells are neurons, this feature is remarkable, in that adult neurons generally are not considered to undergo neurogenesis. Receptor cell turnover is not limited to more complex animals, however. The same pulse-labeling technique used to document turnover in vertebrate olfactory receptor neurons shows that chemoreceptor neurons in the anterior tentacles (olfactory organs) of snails also turn over (Chase, R. and Rieling, J., 1986). Lobster olfactory receptor cells (aesthetascs) also turn over, moving from birth, to maturation, to senescence distally along the length of the olfactory organ as the animal grows and adds new segments to the olfactory organ (Steullet, P. *et al.*, 2000). While data are lacking for other species, functional constancy in three such phylogenetically diverse groups of animals argues that turnover is an adaptive property of specialized chemosensory cells that can be expected to occur more generally.

4.01.4.3 Signal Transduction

In addition to detecting the stimulus, chemosensitive cells need to transduce the signal by coupling it to one or more downstream effector molecules. Prokaryotes such as bacteria sense chemical stimuli such as sugars and amino acids differently than most eukaryotes, using transmembrane methyl-accepting chemotaxis proteins (MCPs) linked to a cytoplasmic histidine-aspartate phosphorylating (HAP) system (Wadhams, G. H. and Armitage, J. P., 2004). HAP systems rely on autophosphorylation of a histidine residue and subsequent transfer of a phosphoryl group to an aspartate residue on an associated regulatory protein to generate a response. As detailed in the previous section, eukaryotic chemoreceptor proteins are typically GPCRs that couple to downstream effectors through heteromeric GTP-binding proteins and intracellular second messengers. The second messenger typically targets ion channels that when activated alter the membrane potential of the cell and generate a graded, voltage-dependent response. In multicellular animals with specialized chemoreceptor cells, this leads to the generation of all-or-none electrical signals (action potentials or spikes) that propagate to the CNS with a frequency that is proportional to the magnitude of the graded change in membrane potential. Action potentials are generated within the sensory cell in the case of primary sensory receptor neurons or through synaptic coupling to a neuron in the case of secondary sensory receptor cells.

Two main intracellular signaling pathways are used in eukaryotic cells, utilizing cyclic nucleotides and phosphoinositide-derived signals. Both pathways seem to operate in a diverse range of species, with no clear evolutionary trend in the use of one signaling cascade over the other. Cyclic nucleotide signaling in chemosensory transduction is best understood in vertebrate olfactory receptor neurons (Figure 5(a)). The target of cyclic nucleotide signaling in these cells is the olfactory cyclic nucleotide-gated ion channel

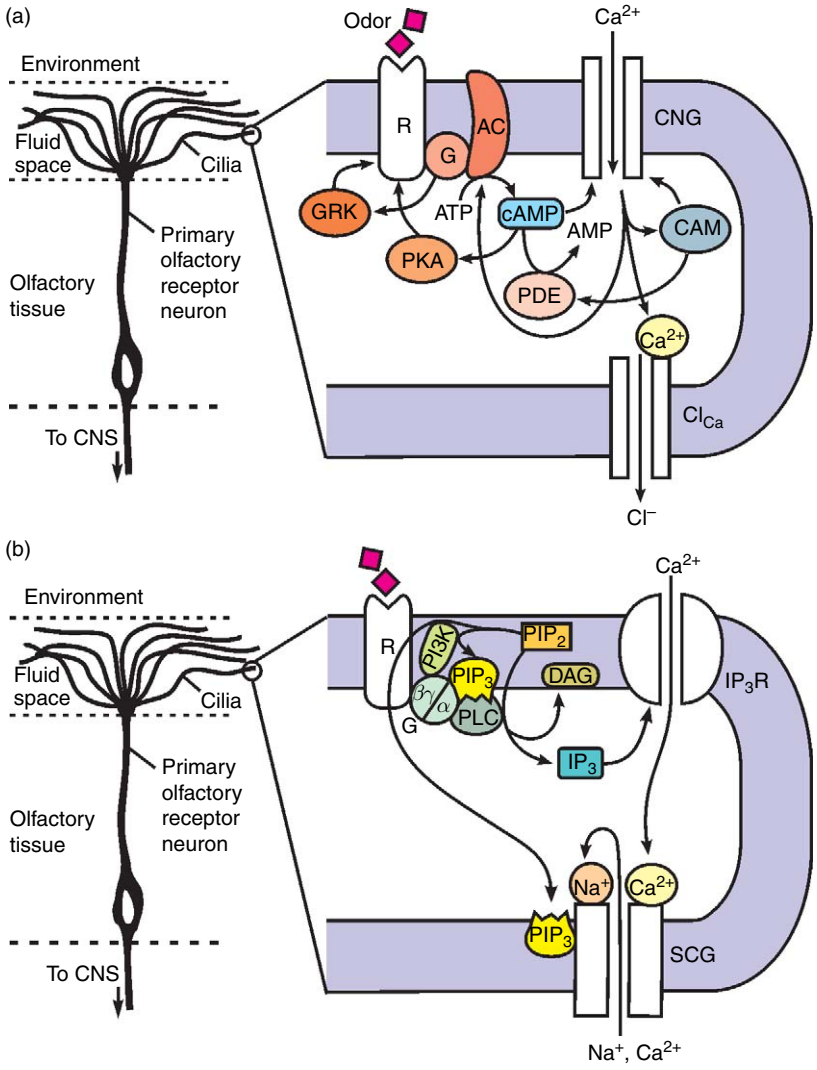

Figure 5 Two intracellular signaling cascades implicated in chemosensory transduction. (a) Diagram of cyclic nucleotide signaling in the transduction compartment (olfactory cilia) of vertebrate olfactory receptor neurons. Odorant molecules bind to a receptor protein (R) coupled to an olfactory specific G_s-protein (G) and activate a type III adenylyl cyclase (AC), increasing intracellular cAMP levels. cAMP targets an olfactory-specific cyclic-nucleotide gated ion channel (CNG), a nonselective cation channel that increases intracellular calcium and secondarily activates a calcium-activated chloride channel thought to carry the majority of the transduction current. Other regulatory pathways are also shown. (b) Diagram of phosphoinositide signaling as currently understood in the transduction compartment (outer dendrite) of lobster olfactory receptor neurons. Odorant molecules bind to a receptor protein (R) coupled to a G_q-protein and activate both phospholipase-C (PLC) and phosphoinositide 3-OH kinase (PI3K) to generate diacylglycerol (DAG) and inositol 1,4,5-trisphosphate (IP_3), and phosphatidylinositol 3,4,5-trisphosphate (PIP_3), respectively, from phosphatidylinositol 4,5-bisphosphate (PIP_2). PIP_3 in concert with release of extracellular calcium from a plasma membrane IP_3 receptor (IP_3R) targets a lobster homolog of a transient receptor potential channel, a nonselective cation channel that is modulated by both sodium and calcium (SGC) and is thought to carry the majority of the transduction current. Details of these pathways vary in other receptor cells and other species.

(Zufall, F. *et al.*, 1994), activation of which allows calcium entry into the cell that secondarily activates a calcium-activated chloride current in a two-step activation cascade. The latter current generates much of the excitatory receptor potential (Reisert, J. *et al.*, 2003). Cyclic nucleotide signaling also appears to operate in chemosensory transduction in slime molds (Newell, P. C. *et al.*, 1988), protozoans (*Paramecium*, Yang, W. Q. *et al.*, 1997), nematodes (*C. elegans*, Komatsu, H. *et al.*, 1999), and arthropods (lobster, Boekhoff, I. *et al.*, 1994). The role of phosphoinositide signaling in chemosensory transduction is less well established than that of cyclic nucleotide signaling and is perhaps best understood in mediating excitation of crustacean olfactory receptor cells (Figure 5(b)). There, the target of phosphoinositide signaling is a calcium-sensitive presumptive lobster homolog of the TRP family of ion channels (Bobkov, Y. V. and Ache, B. W., 2005). Odorants activate both the PLC- and the PI3K-mediated arms of this signaling cascade, allowing the channel to be targeted directly by 3-phosphoinositides and/or indirectly via gating of extracellular calcium from an associated plasma membrane $InsP_3$ receptor (Munger, S. *et al.*, 2000). Phosphoinositide signaling has also been implicated at least indirectly in chemosensory transduction in other, phylogenetically diverse species, including slime molds (Newell, P. C. *et al.*, 1988), nematodes (Colbert, H. A. *et al.*, 1997), insects (Boekhoff, I. *et al.*, 1990), fish (Bruch, R. C. and Teeter, J. H., 1989), mammalian vomeronasal receptor cells (Lucas, P. *et al.*, 2003), and receptor cells in the main olfactory epithelium of mammals (Spehr, M. *et al.*, 2002).

A question that has been the subject of some controversy, for example, in taste transduction in mammals (Zhang, Y. *et al.*, 2003), is whether individual receptor cells use both cyclic nucleotide and phosphoinositide signaling cascades for chemosensory transduction. There is no *a priori* need for a receptor cell to utilize multiple signaling cascades to encode the magnitude of receptor binding. However, when coupled to different receptors or to different sites on the same receptor in a ligand-specific manner, multiple signaling cascades can allow receptor cells to integrate responses to multiple chemical stimuli with potentially important consequences for quality coding (see Section 4.01.6.2). Many diverse species appear to utilize both signaling pathways, including slime molds (Newell, P. C. *et al.*, 1988), arthropods (lobster, Boekhoff, I. *et al.*, 1994), and mammalian olfactory (Spehr, M. *et al.*, 2002), and taste (Gilbertson, T. A. *et al.*, 2000) receptor cells, suggesting that having both signaling pathways in the same cell may serve a fundamental role in chemosensory signaling, although one that is still being resolved.

Sensitivity to some chemicals can be mediated through non-GPCR-based pathways. Odor- or taste-gated ion channels have been proposed as a potential mechanism of chemosensory transduction in a small number of cases (e.g., Teeter, J. H. *et al.*, 1990), although ionotropic chemoreceptors do not appear to play a major role in chemosensory transduction. The best understood exceptions to the involvement of GPCRs in chemosensory signaling involve direct action of the stimulus on the cell without the need for cell-surface receptors. Ions such as Na^+ and protons serve as salt and sour stimuli, respectively, in mammalian taste. These ions are thought to permeate through steady-state ion channels and alter the membrane potential directly without the involvement of downstream signaling cascades (Gilbertson, T. A. *et al.*, 2000). While ions might act similarly in other species, this question has not received the same degree of attention as it has in mammalian taste receptor cells. It is known, however, that ammonia can penetrate the cell membrane of protozoans such as the ciliate, *Paramecium*, and alter chemotaxis through alkalization of the cytoplasm (Van Houten, J. L., 1998), suggesting that nonreceptor-mediated chemical sensitivity can work in parallel with receptor-mediated chemosensitivity in diverse species.

4.01.5 Perireceptor Processes

Activation and adaptation of chemoreceptor cells can be influenced by mechanical and biochemical events in the vicinity of the receptor cells. By modulating or filtering the chemical signal that actually reaches the site of transduction, these so-called perireceptor processes are essential components of chemosensory systems (Carr, W. E. *et al.*, 1990a). The importance of perireceptor processes in chemical sensitivity is still being appreciated, but these processes, too, appear to be conserved in diverse species, suggesting that they are fundamentally important in chemical signal detection.

4.01.5.1 Mechanical Processes

As noted earlier, chemoreceptor cells are seldom, if ever, continuously exposed to the stimulus, and the

resulting intermittency of stimulation is fundamental to how they operate. In addition to the signal itself being intermittent, active processes often result in intermittent access of the stimulus to the receptor cells. Receptors within the taste papillae on the surface of the tongue, for example, are only intermittently contacted by the stimulus, the food bolus, when food is actively moved around the oral cavity by tongue movements and mastication. Perhaps the best known example of active intermittent sampling is sniffing in mammalian olfaction, a process that has an integral effect on odor processing in the olfactory bulb and lateral hypothalamus (Macrides, F. and Chorover, S. L., 1972) and that optimizes the perception of odor intensity in humans (Laing, D. G., 1985). A diverse range of active processes in other vertebrate and invertebrate species gate access of stimulus to their respective olfactory organs. Snakes flick their tongue, periodically bringing airborne volatiles to the vomeronasal organ (Kubie, J. and Halpern, M., 1975). Salamanders actively ventilate their olfactory and vomeronasal receptor cavities at 1–2 Hz (Kauer, J. S. and Shepherd, G. M., 1977). Octopus (Chase, R. and Wells, M. J., 1986) and cyclosmate fish like flounders (Doving, K. B. and Thommesen, G., 1977) actively pump water through their siphons or nasal chamber, respectively. Moths fan their wings to enhance air penetration through their olfactory sensillae (Loudon, C. and Koehl, M. A. R., 2000) and decapod crustaceans flick their olfactory organ (Schmitt, B. C. and Ache, B. W., 1979). The ubiquity of active gating suggests that time-locked intermittency is somehow fundamental to the recognition and discrimination of chemosensory signals. Indeed, the dynamic properties of downstream elements in the transduction cascade as well as the kinetics of synaptic interactions in the CNS may be tuned to such intermittency.

4.01.5.2 Biochemical Processes

The apical ends of chemoreceptor cells typically do not project into the environment directly, but instead into a fluid-filled compartment that in turn contacts the environment. This holds even for aquatic animals where desiccation and/or osmotic challenge would not necessarily be a problem. The composition of the fluid bathing the receptor cells is actively regulated by the organism and can contain enzymes, buffers, and other molecules capable of interacting with and potentially modifying the chemical signal (Pelosi, P., 1996). Best known of these are the so-called odorant-binding proteins (OBPs), small soluble dimeric proteins that bind hydrophilic odorants. OBPs have been characterized in human olfactory mucus (Briand, L. *et al.*, 2002), as well as in most terrestrial animals, including sheep, pigs, cows, rats, frogs, insects, snails (Pelosi, P. and Maida, R., 1990), and elephants (Lazar, J. *et al.*, 2002). The common molecular properties and the occurrence of OBPs in such a phylogenetically diverse range of terrestrial animals suggest they played an important role in the terrestrialization of olfaction. OBPs in moth and rat are not homologous, suggesting the common molecular properties of at least these OBPs evolved convergently (Pevsner, J. *et al.*, 1988). Given the homology of mammalian OBPs to the lipocalin superfamily of proteins (Tegoni, M. *et al.*, 2000), it has often been assumed that OBPs serve to bind and transport hydrophobic ligands through the aqueous perireceptor environment. However, OBPs have also been proposed to serve other functions, including serving as molecular filters to specify and perhaps facilitate stimulus access to receptors (Vogt, R. G. *et al.*, 1990). Another family of proteins, pheromone-binding proteins (PBPs), helps deliver volatile pheromone compounds. Some OBPs and PBPs are similar in sequence, suggesting that members of the OBP family may serve as molecular filters for pheromones rather than for general odors (Pelosi, P., 2001). However, the function of OBPs remains unclear for any type of odorant.

The perireceptor fluid also contains degradative enzymes that could deactivate the stimulus (Carr, W. E. S. *et al.*, 1990b). These, too, occur in phylogenetically diverse species. Slime molds, for example, aggregate in response to the pulsatile release of cAMP from calling amoeboid cells. Both membrane-associated and soluble phosphodiesterases rapidly inactivate cAMP in the vicinity of the source, thereby sharpening the chemotaxic gradient (Janssens, P. M. W. and Van Haastert, P. J. M., 1987). An esterase (Vogt, R. G. *et al.*, 1985) and an aldehyde oxidase (Rybczynski, R. *et al.*, 1989) that rapidly degrade pheromones have been identified in the perireceptor fluid or lymph of insect olfactory receptor cells. Ectonucleotidases in the lobster olfactory organ progressively dephosphorylate adenosine nucleotides (feeding cues) into nonstimulatory adenosine (Trapido-Rosenthal, H. G. *et al.*, 1987). Finally, the mammalian olfactory epithelium contains many catabolic enzymes that could potentially degrade various classes of odorants, including an olfactory-specific homolog of uridine

diphosphate-glucuronosyl transferase (Dahl, A., 1988) and several isoforms of cytochrome P450 enzymes. Lower levels of cytochrome P450 are also found in the mammalian vomeronasal organ (Gu, J. *et al.*, 1999). It remains to be determined whether such degradative enzymes act on the signal *per se*, that is, whether they rapidly terminate the signal and therefore alter its dynamic properties or whether they serve to maintain the perireceptor space over longer intervals of time by minimizing the background levels of stimuli and/or removing potentially toxic environmental compounds.

4.01.6 Processing of Chemosensory Information

4.01.6.1 Central Neural Organization

Chemosensory organs are sometimes associated with a peripheral nerve net or plexus, as occurs, for example, in mollusks, resulting in an afferent signal that already reflects some degree of integration. Such peripheral chemosensory integration is best characterized in the vertebrate taste system, where groups of taste receptor cells, supporting cells, and their associated neural elements form a distinct end organ, the taste bud, with synaptic and ephaptic connections suggestive of interactions among the cells reminiscent of those in the vertebrate retina (Huang, Y. J. *et al.*, 2005). Accordingly, afferent taste nerves transmit an integrated signal to the CNS. The more common organizational plan of chemosensory pathways, however, is for the primary chemosensory afferents to project without synapsing to the CNS, shifting the majority of signal processing to the brain. We are only just beginning to understand how the brain processes chemosensory information, but new molecular and imaging approaches to studying the CNS are poised to rapidly increase our level of understanding of the central neural substrates for molecular recognition (e.g., Zou, Z. *et al.*, 2001).

One system that has been particularly well studied in several, phylogenetically diverse animals is the first olfactory relay – the vertebrate olfactory bulb and its functional equivalent in arthropods, the insect antennal lobe, and the crustacean olfactory lobe. The rather striking analogy of the vertebrate olfactory bulb and the insect antennal lobe was noted by neuroanatomists as early as 1883 (Belloncei, G., 1883), even though some differences are apparent. The mammalian olfactory bulb is laminarly organized with neurons integral to the neuropil, the synaptic-containing region of the bulb (Figure 6(a)), while the

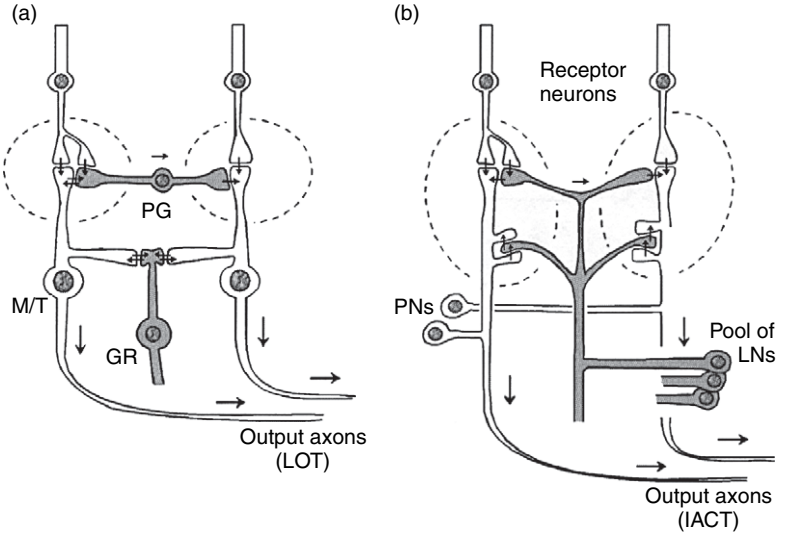

Figure 6 Comparison of the first olfactory relay in insects and mammals. (a) Diagram of the mammalian olfactory bulb showing receptor cells contacting mitral/tufted (M/T) and periglomerular (PG) cells in glomerularly organized neuropil (dashed circles), creating parallel output pathways in the lateral olfactory tract (LOT), transected by two levels of lateral inhibitory connections, one formed by the PG cells and the other by granular (GR) cells. (b) Diagram of the insect antennal lobe drawn in the same format as (a) showing essentially the same overall organization of the projection neurons (PNs) and various types of local interneurons (LNs). From Christensen, T. A. and White, J. 2000. Representation of Olfactory Information in the Brain. In: The Neurobiology of Taste and Smell, 2nd edn. (*eds.* T. E. Finger, W. L. Silver, and D. Restrepo), pp. 201–232. Wiley-Liss, Inc. Copyright 2000 John Wiley, Reprinted with permission of Wiley-Liss, Inc., a subsidiary of John Wiley & Sons, Inc.

insect antennal lobe lacks laminar organization, and its neurons are peripheral to the neuropil, with the synapses confined to the glomeruli (Figure 6(b)). To see the organizational similarity emerge, one has to look through these characteristic differences in the organization of vertebrate and invertebrate neuropil (Christensen, T. A. and White, J., 2000). Doing so shows that in both the olfactory bulb and the antennal lobe, the primary olfactory afferents strongly converge into glomerularly organized neuropil where they branch profusely and terminate on both projection neurons and local interneurons. As mentioned above, glomeruli are formed by the convergence of olfactory neurons that have chosen to express the same receptor and thus integrate signals from functionally identical neurons. Glomeruli in both structures contain the same complex, serial reciprocal synapses (Pinching, A. J. and Powell, T. P. S., 1971; Tolbert, L. P. and Hildebrand, J. G., 1981). The projection neurons take the output of one or a few (depending on the species) glomeruli directly to the next synaptic level, the olfactory cortex in mammals and the corpora pedunculata in arthropods. Local interneurons inherent to the neuropil create two levels of lateral connectivity across the afferent fiber-projection neuron throughput pathway. Interestingly, while most of the olfactory glomeruli tend to be morphologically uniform, one glomerulus in each structure, the modified glomerular complex in mammals (Teicher, M. H. *et al.*, 1980) and the macroglomerular complex in some insects (Matsumoto, S. G. and Hildebrand, J. G., 1981), is greatly enlarged and processes input from pheromone receptors. Many of these organizational features also occur in the first olfactory relay in terrestrial snails, the protocerebral lobe (Chase, R. and Tolloczko, B., 1986), further underscoring the potential utility of this organizational plan to olfactory signal detection.

The apparent conservation between species in the anatomical organization of the first olfactory relay suggests it has important functions in olfactory signal detection. Clearly, the synaptic connections within and among glomeruli are integral to the way olfactory information is processed at this level of the olfactory pathway, and molecular and imaging approaches are actively being used in both vertebrate and invertebrate models to decipher the role(s) of olfactory glomeruli in odor recognition (e.g., Bozza, T. *et al.*, 2004). While the functional role(s) of the first olfactory relay still remain to be understood, some conserved functional features can be identified. One such conserved feature is presynaptic afferent inhibition (PAI), in which the terminals of the primary afferent fibers are contacted by inhibitory local interneurons. One distinct subpopulation of the local interneurons that laterally connect olfactory glomeruli mediates PAI in animals as diverse as mammals (Hayar, A. *et al.*, 2004) and lobsters (Wachowiak, M. *et al.*, 1997). There is functional evidence for PAI in lobsters, turtles, and rodents, and in both vertebrates and invertebrates, this involves paired neurotransmitters (Wachowiak, M. *et al.*, 2002). As is commonly the case in phylogenetic comparisons, the cellular mechanism differs even though the principal holds. PAI in lobsters reflects ionotropic receptor-mediated changes in membrane potential, while in the turtle, PAI reflects metabotropic receptor-mediated changes in intracellular calcium (Wachowiak, M. and Cohen, L. B., 1999).

4.01.6.2 Quality Coding

The question of how the molecular identity of a chemical stimulus is coded by the nervous system is fundamental to understanding chemical sensitivity. In spite of recent progress, however, the answer remains elusive for both smell and taste. The central argument is whether the identity or quality of the chemical signal is coded by labeled lines, in which the particular cell type that is activated specifies or labels the stimulus, or whether the quality of the stimulus is not inherent in any particular cell type but rather is represented by the pattern of activation across a population of cells with relatively broad overlapping response spectra in a combinatorial manner (Figure 7). Operationally, labeled line or combinatorial coding is often considered in reference to a particular level of a chemosensory pathway, e.g., the tuning or range of ligands that activate individual receptor cells, but the concept ultimately applies more to the overall coding strategy for the sensory modality in question. In that regard, labeled line and combinatorial coding are not mutually exclusive and could be integrated within a given level or across levels of a chemosensory pathway, as seen in the coding of odor mixtures in the lobster olfactory pathway (Derby, C. D., 2000). Both strategies appear to be used in a wide range of species. The choice of coding strategy may be more closely tied to the informational importance of the stimulus than the phylogenetic position of the species. Labeled line coding is expensive as it requires dedicated neural space and therefore may serve to detect stimuli of

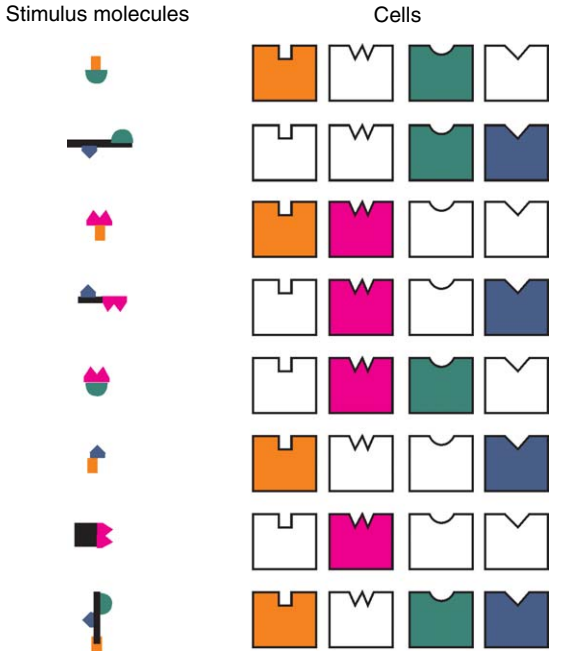

Figure 7 Combinatorial coding. Diagram of hypothetical stimulatory molecules with some shared as well as some different molecular features (left) and the different patterns of neural activity each molecule would elicit across a hypothetical population of four receptor cells each expressing one receptor protein tuned to a particular molecular feature (right). The cells that are activated by each molecule are colored. Note that many molecules activate multiple receptors, and each molecule generates a unique pattern of activity across the population of receptor cells. Reproduced from Malnic, B., Hirono, J., Sato, T., and Buck, L. B. 1999. Combinatorial receptor codes for odors. Cell 96, 713–723, with permission from Elsevier.

especially strong adaptive value, for example, the detection of salt in terrestrial mammals, or of pheromones in short-lived insects that hatch, mate, and die.

It is now generally agreed that odorants are coded in a combinatorial manner. This long-standing idea received strong support from recent evidence that individual mammalian olfactory receptor cells expressing a single, identified receptor protein can be activated by multiple different odorants and that individual odorants activate multiple receptor cells expressing different receptor proteins (Malnic, B. *et al.*, 1999). Similar findings for the olfactory receptors of insects (Hallem, E. A. *et al.*, 2004) and fish (Luu, P. *et al.*, 2004) suggest that combinatorial coding has been conserved in the evolution of olfaction. Combinatorial coding is also used in other chemosensory systems, as demonstrated by the hundreds of receptor proteins expressed in the nematode *C. elegans*, which has only 32 chemoreceptor cells in the entire adult worm (Bargmann, C. I. and Kaplan, J. M., 1998).

Chemosensory receptor cells can have two (bipolar) modes of signaling, excitation and inhibition. Such flexibility adds to the combinatorial possibilities in chemosensory coding and has been observed in a phylogenetically diverse range of species. Odors inhibit as well as excite olfactory receptor cells in mollusks (squid, Lucero, M. T. *et al.*, 1992), arthropods (insects, lobsters, McClintock, T. S. and Ache, B. W., 1989; De Bruyne, M. *et al.*, 2001), fish (Kang, J. and Caprio, J., 1995), amphibians (frogs, Sanhueza, M. *et al.*, 2000), and mammals (rats, Duchamp-Viret, P. *et al.*, 1999). The cellular mechanism(s) that mediate this opponent input are still being explored, but as noted earlier, this phenomenon can be explained in at least some species by ligand-directed activation of opposing intracellular signaling pathways. Different chemical stimuli attract and repel even single-celled organisms such as *Paramecium* by polarizing the cell in opposite directions (Van Houten, J. L., 1998).

How tastants are coded has focused mainly on the mammalian gustatory system, where the ability to distinguish the so-called basic tastes – sweet, sour, bitter, salt, and amino acids – spawned the search for cell types coding for these qualities. Recent evidence suggests that bitter, sweet, and amino acid tastes are coded by labeled lines, at least at the level of the receptor cells (Zhang, Y. *et al.*, 2003; Mueller, K. L. *et al.*, 2005). It is possible, for example, to induce a sweet response, that is, attraction, to bitter stimuli that otherwise evoke aversion by genetically engineering a mouse to drive the expression of a bitter receptor in taste receptor cells that normally express sweet receptors. This finding implies that taste cells that normally express sweet taste receptors are hardwired to elicit attraction independently of what receptors or ligands are present. Consistent with this interpretation, some cells in the taste nerve as well as in the second gustatory relay in rodents, the parabranchial nucleus (PBN), are best for, that is, respond most strongly to, specific taste qualities and could be considered to function as labeled lines for those qualities (Smith, D. V., 1985). However, the labeled line principle may not exclusively hold. Smith and others found that no one cell type in the PBN can distinguish similar-tasting compounds and that other, more broadly tuned cells contribute to a combinatorial code for taste quality. In multivariate analyses, he found, for example, that sweet-best PBN neurons can distinguish sweet tasting compounds in a

panel of tastants, but neither these nor the more broadly tuned cells by themselves were able to differentiate sweet from, say, bitter tasting compounds. Only both types of cells together contained sufficient information to differentiate sweet from bitter. These and other findings argue that, like odorants, tastants are coded in a combinatorial manner. Unfortunately, little additional insight into taste coding is available from other vertebrates or invertebrates, in large part due to the difficulty inherent in defining taste quality in nonmammalian species. In an extensive analysis of phytophagous caterpillar species with differing types of food preference, it was not possible to identify specific taste receptor cell types that could account for food preference, even in strict monophagous species, arguing that food preference was not based on a labeled line code (Dethier, V. G. and Crnjar, R. M., 1982). On the other hand, a distinct set of neurons in the main taste organ of flies, the labellum, exhibit potential hallmarks of a labeled line for sweet taste. These neurons express a receptor for trehalose, project to a distinct brain region, and mediate responsiveness to sweet (as defined by mammalian behavioral responses) compounds, while being unresponsive to bitter compounds (Thorne, N. *et al.*, 2004). Whether tastants are coded using a common strategy or whether coding strategy is context- and/or species-dependent remains an open question.

4.01.7 Chemosensory-Mediated Behavior and Plasticity

As noted earlier, phylogenetically diverse animals use chemical stimuli to communicate in an amazingly diverse array of behavioral contexts. The ability of pheromones to convey remarkably specific information about gender, status, and individuality is just one particularly noteworthy example. Primate secretions are sufficiently complex to allow social information to be communicated by unique blends of the major and minor constituents of these secretions (Epple, G. *et al.*, 1989). Chemosensory-mediated social recognition in mammals is better understood in mice, where genes of the major histocompatibility complex (MHC), the genes controlling immunological identity, have been known for some time to determine pheromone-mediated mating preference (Yamaguchi, M. *et al.*, 1981; Yamazaki, K. *et al.*, 1989). Recently, MHC class I peptides in the urine of mice, the peptides that mediate individual recognition in pregnancy block, were shown to activate a subset of vomeronasal chemoreceptor cells (Leinders-Zufall, T. *et al.*, 2004). Pheromones also mediate individual recognition in cnidarians – the jellyfish, corals, and sea anemones. These animals can reproduce asexually by budding and form large colonies or mats of genetically identical individuals. Clear borders between mats of such sea anemone individuals are actively maintained by intraspecific aggression (Francis, L., 1973). This behavior is triggered when distinct chemoreceptors on the tentacles contact foreign individuals in neighboring mats as the animals wave about (Lubbock, R., 1980), suggesting this is a chemosensory-mediated behavior. Thomas L. (1974) proposed the existence of a fundamental similarity between immunorecognition and chemical sensitivity, suggesting that the histocompatibility genes on which immunorecognition is based evolved to protect the integrity of the individual organism, for example from invasion of potential symbionts, by strategies such as imparting a characteristic odor to each individual. The presence of individual-specific pheromones in animals as phylogenetically diverse as coelenterates and mammals gives credence to his hypothesis.

All animals must adapt to changing environments, so it is not surprising that plasticity is a hallmark of chemosensory-mediated behavior. Behavioral plasticity encompasses a broad range of phenomena that do not necessarily share a common neural substrate. These phenomena range from simple alterations in levels of responsiveness such as sensitization and habituation to imprinting, to more complex forms of associative leaning. One type of plasticity of particular relevance to chemical sensitivity is food aversion learning, the long-term retention of experience gained from a single association between ingestion and subsequent illness that most humans have experienced at one time or another. This phenomenon is also well documented in other mammals, especially in coyotes and rats where it has been studied in the context of bait shyness (Garcia, J. *et al.*, 1974). Food aversion also occurs in blue jays after eating toxic monarch butterflies. They subsequently seize but no longer consume monarchs due to the distinctively bitter taste of the toxic cardiac glycosides the butterflies sequester from the plants on which they feed (Brower, L. P. and Glazier, S. C., 1975). Food aversion even occurs in mollusks, where a single meal of carrot followed by exposure to quinidine sulfate, an irritant, causes the terrestrial slug, *Limax*, to reduce its preference for carrots (Gelperin, A., 1975). Interestingly, food aversion in slugs shows all

the classical characteristics of food aversion in mammals, including rapid onset, the need for only a single pairing of the conditioned (CS) and unconditioned (US) stimulus, a long CS–US interval, persistence without reinforcement, association restricted to a specific CS, and enhancement through co-association with odor cues. Thus, even complex, associative chemosensory-mediated behavior, and possibly its underlying neural circuitry, can transcend broad species differences.

The early stages of olfactory processing are involved in experience-dependent behavioral modification in animals as phylogenetically diverse as mammals and mollusks. Early odor experience in rat pups, for example, dramatically enhances later responses of the animals to the familiar odor, a phenomenon that is accompanied by specific physiological and morphological changes in the circuitry of the olfactory bulb (Coopersmith, R. and Leon, M., 1984). Similarly, the gastropod mollusk, *Limax*, can also be behaviorally conditioned to odors. Indeed, it is possible to condition the brain after it has been isolated from the animal and placed in a recording chamber using the same paradigm used to condition the intact animal (Gelperin, A., 1986), allowing direct access to the altered neural circuitry for biochemical and biophysical analyses. The network of olfactory interneurons in the protocerebral lobe of the slug shows coherent oscillations in local field potentials (LFPs) that can be modified by odor input, not unlike similar coherent LFP oscillations observed in insects and a wide array of vertebrates (Figure 8). The

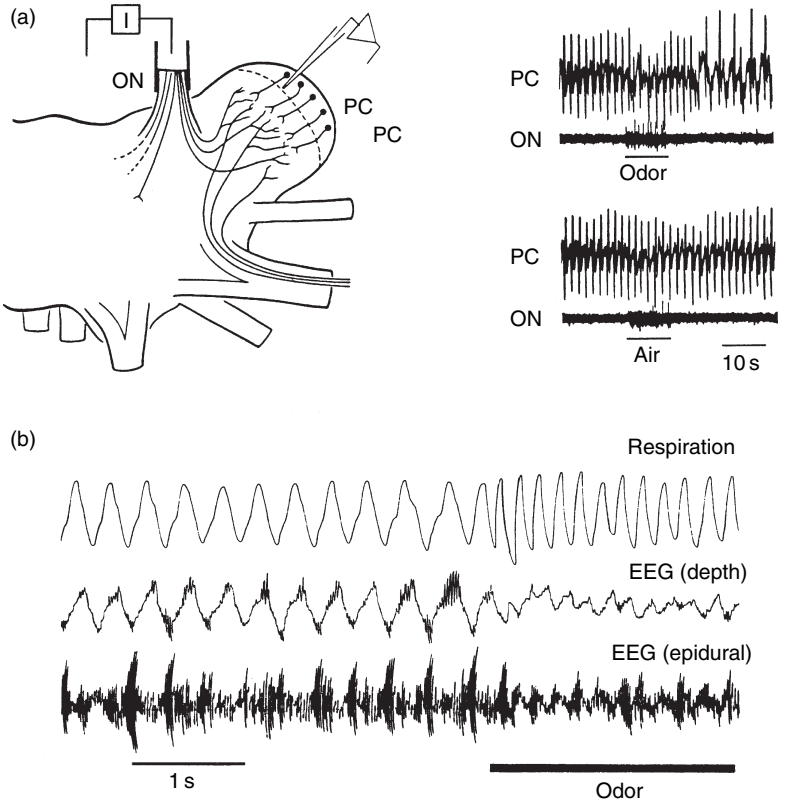

Figure 8 Dynamical structure of neural activity in the first olfactory relay implicated in odor discrimination and memory. (a) Left panel: diagram of the cerebral ganglion of a terrestrial slug showing a recording electrode in the protocerebral lobe (PC) and a stimulating electrode on the olfactory nerve (ON, shown here cut for electrical stimulation but normally intact). Right panel: recordings of neural oscillations from the preparation showing responses to potato odor (upper pair of traces) and clean air (lower pair of traces). Note the odor-induced changes in the waveform and frequency of the PC lobe oscillations. (b) Recordings from the rabbit olfactory bulb showing the 3–7 Hz respiratory rhythm (upper trace) and 40–80 Hz oscillatory EEGs recorded at depth (middle trace) and on the surface (bottom trace) of the bulb. Note the odor-induced changes in the waveform and frequency of the oscillatory field potentials. Reproduced from Ache, B. W. 1991. Phylogeny of Smell and Taste. In: Smell and Taste in Health and Disease (*eds.* T. V. Getchell, *et al.*), pp. 3–18. Raven Press. © 1991 Lippincot Williams & Wilkins, with permission.

presence of neural circuitry at the same synaptic level of the olfactory pathway with similar dynamical structure in animals as phylogenetically diverse as mollusks, insects, and mammals suggests that local circuit oscillations or the coherent neural activity that underlies them play a fundamental role in odor discrimination (Laurent, G., 2002). Odor memory has been shown to be associated with olfactory network dynamics in both insects (locusts, Stopfer, M. and Laurent, G., 1999) and mollusks (slugs, Gelperin, A., 1999). This research is leading to testable predictions as to how oscillatory dynamics may influence the acquisition and storage of odor memory.

4.01.8 Overview

In this chapter, we focus on features shared by different chemosensory systems and different species to reveal the guiding principles of chemical detection. Evolutionary conservation of these shared features presumably reflects the use of a common solution to the common need that all species have to interact with their chemical environment. The rather striking similarities seen in the organization of some of these chemosensory systems, especially olfaction, across a broad range of species suggest there is an optimal solution to the problem of detecting and discriminating chemosensory signals. Either this solution evolved relatively early and was subsequently retained or, more likely, different species convergently evolved the same or similar solutions to the chemosensory problem. As a result, the biological strategy for odor recognition, for example, should be worth emulating in designing biosensors to detect chemical compounds of importance in biomedicine, biosafety, and biodefense. Such biosensors need to detect multicomponent chemical signatures in the complex, dynamic chemical backgrounds that form real-world chemosensory environments. The utility of imitating this biological strategy to develop biosensors provides just one example of how one can learn from a broad, evolutionary approach to understanding chemical sensitivity.

The similarities seen between humans and other species in structural and functional elements of chemical sensing supports the continued use of animal models to investigate chemosensation. As noted by Dethier V. G. (1981), animal studies can tell us not only about those species but also about ourselves, provided we are careful to avoid the dual pitfalls of anthropomorphism and zoomorphism. Even knowing the extent to which chemical sensing in animals differs from that in humans cannot help but reveal something about ourselves.

Acknowledgments

B.W.A. gratefully acknowledges the contribution of his many students and postdoctoral associates over the years to the insight and ideas presented here. J.M.Y. thanks Barbara Trask and colleagues in the Trask laboratory for support, stimulating discussions, and explorations of the literature. The authors thank the National Institute of Deafness and Other Communication Disorders for support (DC05995 and DC04209). We also thank Ms M.L. Milstead for assistance with the illustrations and Ms J. Tulsian for assistance with the bibliography.

References

Ache, B. W. 1991. Phylogeny of Smell and Taste. In: Smell and Taste in Health and Disease (*eds*. T. V. Getchell, *et al.*), pp. 3–18. Raven Press.

Bargmann, C. I. and Kaplan, J. M. 1998. Signal transduction in the *Caenorhabditis elegans* nervous system. Annu. Rev. Neurosci. 21, 279–308.

Belcher, A. M., Epple, G., Kuderling, I., and Smith III A. B. 1988. Volatile components of scent material from the cotton-top tamarin (*Saguinus o*. *oedipus*): a chemical and behavioral study. J. Chem. Ecol. 14, 1367–1384.

Bjostad, L. B., Linn, C. E., Du, J. W., and Roelofs, W. L. 1984. Identification of new sex pheromone components in *Trichoplusia ni* predicted from biosynthetic precursors. J. Chem. Ecol. 10, 1309–1323.

Bobkov, Y. V. and Ache, B. W. 2005. Pharmacological properties and functional role of a TRP-related ion channel in lobster olfactory receptor neurons. J. Neurophysiol. 93, 1372–1380.

Boekhoff, I., Michel, W. C., Breer, H., and Ache, B. W. 1994. Single odors differentially stimulate dual second messenger pathways in lobster olfactory receptor cells. J. Neurosci. 14, 3304–3309.

Boekhoff, I., Raming, K., and Breer, H. 1990. Pheromone-induced stimulation of inositol-trisphophate formation in insect antennae is mediated by G-proteins. J. Comp. Physiol. B 160, 99–103.

Belloncei, G. 1883. Sur la structure et les rapports des lobes olfactifs dans les arthropods superieurs et les vertebras. Arch. Ital. Biol. 3, 191–196.

Bouvier, M. 2001. Oligomerization of G-protein-coupled transmitter receptors. Nat. Rev. Neurosci. 2, 274–286.

Bozza, T., Feinstein, P., Zheng, C., and Mombaerts, P. 2002. Odorant receptor expression defines functional units in the mouse olfactory system. J. Neurosci. 22, 3033–3043.

Bozza, T., McGann, J. P., Mombaerts, P., and Wachowiak, M. 2004. *In vivo* imaging of neuronal activity by targeted expression of a genetically encoded probe in the mouse. Neuron 42, 9–21.

Brennan, P. A. and Keverne, E. B. 2004. Something in the air? New insights into mammalian pheromones. Curr. Biol. 14, R81–R89.

Briand, L., Eliot, C., Nespoulous, C., Bezirard, V., Huet, J.-C., Henery, C., Blon, F., Trotier, D., and Pernollet, J.-C. 2002. Evidence of an odorant-binding protein in the human olfactory mucus: location, structural characterization, and odorant-binding properties. Biochemistry 41, 7241–7252.

Brower, L. P. and Glazier, S. C. 1975. Localization of heart poisons in the monarch butterfly. Science 208, 753–755.

Bruch, R. C. and Teeter, J. H. 1989. Second-Messenger Signaling Mechanisms in Olfaction. In: Chemical Senses: Vol. 1, Receptor Events and Transduction in Taste and Olfaction (*eds*. J. G. Brand, J. H. Teeter, R. H. Cagan, and M. R. Kare), pp. 283–298. Marcel Dekker.

Buck, L. and Axel, R. 1991. A novel multigene family may encode odorant receptors: a molecular basis for odor recognition. Cell 65, 175–187.

Carr, W. E., Gleeson, R. A., and Trapido-Rosenthal, H. G. 1990a. The role of perireceptor events in chemosensory processes. Trends Neurosci. 13, 212–215.

Carr, W. E. S., Trapido-Rosenthal, H. G., and Gleeson, R. A. 1990b. The role of degradative enzymes in chemosensory processes. Chem. Senses 15, 181–190.

Chandrashekar, J., Mueller, K. L., Hoon, M. A., Adler, E., Feng, L., Guo, W., Zuker, C. S., and Ryba, N. J. 2000. T2Rs function as bitter taste receptors. Cell 100, 703–711.

Chase, R. and Rieling, J. 1986. Autoradiographic evidence for receptor cell renewal in the olfactory epithelium of a snail. Brain Res. 384, 232–239.

Chase, R. and Tolloczko, B. 1986. Synaptic glomeruli in the olfactory system of a snail, *Achatina fulica*. Cell Tiss. Res. 246, 567–573.

Chase, R. and Wells, M. J. 1986 Chemotactic behavior in *Octopus*. J. Comp. Physiol. A 158, 375–381.

Chess, A., Simon, I., Cedar, H., and Axel, R. 1994. Allelic inactivation regulates olfactory receptor gene expression. Cell 78, 823–834.

Christensen, T. A. and White, J. 2000. Representation of Olfactory Information in the Brain. In: The Neurobiology of Taste and Smell, 2nd edn. (*eds*. T. E. Finger, W. L. Silver, and D. Restrepo), pp. 201–232. Wiley-Liss, Inc.

Christensen, T. A., Laskbrook, J. M., and Hildebrand, J. G. 1994. Neural activation of the sex pheromone gland in the moth *Manduca sexta*: real-time measurement of pheromone release. Physiol. Entomol. 19, 265–270.

Clyne, P. J., Warr, C. G., Freeman, M. R., Lessing, D., Kim, J., and Carlson, J. R. 1999. A novel family of divergent seven-transmembrane proteins: candidate odorant receptors in *Drosophila*. Neuron 22, 327–338.

Colbert, H. A., Smith, T. L., and Bargmann, C. I. 1997. OSM-9, a novel protein with structural similarity to channels is required for olfaction, mechanosensation, and olfactory adaptation in *Caenorhabditis elegans*. J. Neurosci. 17, 8259–8269.

Coopersmith, R. and Leon, M. 1984. Enhanced neural response to familiar olfactory cues. Science 225, 849–851.

Dahl, A. 1988. The Effect of Cytochrome P-450-Dependent Metabolism and Other Enzymes Activities on Olfaction. In: Molecular Neurobiology of the Olfactory System (*eds*. F. L. Margolis and T. V. Getchell), pp. 51–70. Plenum Press.

De Bruyne, M., Foster, K., and Carlson, J. 2001. Odor coding in the *Drosophila* antenna. Neuron 30, 537–552.

Derby, C. D. 2000. Learning from spiny lobsters about chemosensory coding of mixtures. Physiol. Behav. 69, 203–209.

Dethier, V. G. 1981. Fly, rat, and man: the continuing quest for an understanding of behavior. Proc. Am. Philos. Soc. 125, 460–466.

Dethier, V. G. 1987. Sniff, flick, and pulse: an appreciation of interruption. Proc. Am. Philos. Soc. 131, 159–176.

Dethier, V. G. and Crnjar, R. M. 1982. Candidate codes in the gustatory system of caterpillars. J. Gen. Physiol. 79, 549–569.

Doving, K. B. and Thommesen, G. 1977. Some Properties of the Fish Olfactory System. In: Olfaction and Taste, (*eds*. J. LeMagnen and P. MacLeod), Vol. 6, pp. 175–183. Information Retrieval.

Duchamp-Viret, P., Chaput, M., and Duchamp, A. 1999. Odor response properties of rat olfactory receptor neurons. Science 284, 2171–2174.

Dulac, C. and Axel, R. 1995. A novel family of genes encoding putative pheromone receptors in mammals. Cell 83, 195–206.

Emes, R. D., Beatson, S. A., Ponting, C. P., and Goodstadt, L. 2004. Evolution and comparative genomics of odorant- and pheromone-associated genes in rodents. Genome Res. 14, 591–602.

Epple, G., Belcher, A., Greenfield, K. L, Kuderling, I., Nordstrom, K., and Smith III A. B. 1989. Scent Mixtures Used as Social Signals in Two Primate Species: *Saguinus fuscicollis* and *Saguinus o*. *oedipus*. In: Perception of Complex Smells and Tastes (*eds*. D. G. Laing, W. S. Cain, R. L. McBride, and B. W. Ache), pp. 1–26. Academic Press.

Finger, T. E., Bottger, B., Hansen, A., Anderson, K. T., Alimohammadi, H., and Silver, W. L. 2003. Solitary chemoreceptor cells in the nasal cavity serve as sentinels of respiration. Proc. Natl. Acad. Sci. U. S. A. 100, 8981–8986.

Floriano, W. B., Vaidehi, N., Goddard, W. A., III, Singer, M. S., and Shepherd, G. M. 2000. Molecular mechanisms underlying differential odor responses of a mouse olfactory receptor. Proc. Natl. Acad. Sci. U. S. A. 97, 10712–10716.

Francis, L. 1973. Intraspecific aggression and its effect on the distribution of *Anthopleura elegantissima* and some related sea anemones. Biol. Bull. 144, 73–92.

Friend, W. G. and Smith, J. J. B. 1982. ATP analogs and other phosphate compounds as gorging stimulants for *Rhodnius prolixus*. J. Insect Physiol. 28, 371–376.

Garcia, J., Hankins, W. G., and Rusiniak, K. W. 1974. Behavioral regulation of the milieu interne in man and rat. Science 185, 824–831.

Gelperin, A. 1975. Rapid food-aversion learning by a terrestrial mollusk. Science 189, 567–570.

Gelperin, A. 1986. Complex associative learning in small neural networks. Trends Neurosci. 9, 323–368.

Gelperin, A. 1999. Oscillatory dynamics and information processing in olfactory systems. J. Exp. Biol. 202, 1855–1864.

Gilad, Y., Segre, D., Skorecki, K., Nachman, M. W., Lancet, D., and Sharon, D. 2000. Dichotomy of single-nucleotide polymorphism haplotypes in olfactory receptor genes and pseudogenes. Nat. Genet. 26, 221–224.

Gilad, Y., Wiebe, V., Przeworski, M., Lancet, D., and Paabo, S. 2004. Loss of olfactory receptor genes coincides with the acquisition of full trichromatic vision in primates. PLoS Biol. 2, E5.

Gilbert, A. N. and Firestein, S. 2002. Dollars and scents: commercial opportunities in olfaction and taste. Nat. Neurosci 5(Suppl. 1), 1043–1045.

Gilbertson, T. A., Damak, S., and Margolskee, R. F. 2000. The molecular physiology of taste transduction. Curr. Opin. Neurobiol. 10, 519–527.

Go, Y., Satta, Y., Takenaka, O., and Takahata, N. 2005. Lineage-specific loss of function of bitter taste receptor genes in humans and nonhuman primates. Genetics 170, 313–326.

Goldman, A. L., Van der Goes van Naters, W., Lessing, D., Warr, C. G., and Carlson, J. R. 2005. Coexpression of two functional odor receptors in one neuron. Neuron 45, 661–666.

Graziadei, P. P. C. and Monti-Graziadei, G. A. 1978. Continuous Nerve Cell Renewal in the Olfactory System. In: Handbook of Sensory Physiology (*ed*. M. Jacobson), Vol. 9, pp. 55–83. Springer.

Grus, W. E. and Zhang, J. 2004. Rapid turnover and species-specificity of vomeronasal pheromone receptor genes in mice and rats. Gene 340, 303–312.

Grus, W. E., Shi, P., Zhang, Y. P., and Zhang, J. 2005. Dramatic variation of the vomeronasal pheromone receptor gene repertoire among five orders of placental and marsupial mammals. Proc. Natl. Acad. Sci. U. S. A. 102, 5767–5772.

Gu, J., Dudley, C., Su, Tt., Spink, D. C., Zhang, Q.-Y., Moss, R. L., and Ding, X. 1999. Cytochrome P450 and steroid hydroxylase activity in mouse olfactory and vomeronasal mucose. Biochem. Biophys. Res. Comm. 266, 262–267.

Hague, C., Uberti, M. A., Chen, Z., Bush, C. F., Jones, S. V., Ressler, K. J., Hall, R. A., and Minneman, K. P. 2004. Olfactory receptor surface expression is driven by association with the beta2-adrenergic receptor. Proc. Natl. Acad. Sci. U. S. A. 101, 13672–13676.

Hallem, E. A., Ho, M. G., and Carlson, J. R. 2004. The molecular basis of odor coding in the *Drosophila* antenna. Cell 117, 965–979.

Hayar, A., Karnup, S., Ennis, M., and Shipley, M. T. 2004. External tufted cells: a major excitatory element that coordinates glomerular activity. J. Neurosci. 24, 6676–6685.

Herrada, G. and Dulac, C. 1997. A novel family of putative pheromone receptors in mammals with a topographically organized and sexually dimorphic distribution. Cell 90, 763–773.

Hill, C. A., Fox, A. N., Pitts, R. J., Kent, L. B., Tan, P. L., Chrystal, M. A., Cravchik, A., Collins, F. H., Robertson, H. M., and Zwiebel, L. J. 2002. G protein-coupled receptors in *Anopheles gambiae*. Science 298, 176–178.

Hillier, L. W., Miller, W., Birney, E., Warren, W., Hardison, R. C., Ponting, C. P., Bork, P., Burt, D. W., Groenen, M. A., Delany, M. E., *et al.* 2004. Sequence and comparative analysis of the chicken genome provide unique perspectives on vertebrate evolution. Nature 432, 695–716.

Hoon, M. A., Adler, E., Lindemeier, J., Battey, J. F., Ryba, N. J., and Zuker, C. S. 1999. Putative mammalian taste receptors: a class of taste-specific GPCRs with distinct topographic selectivity. Cell 96, 541–551.

Huang, Y. J., Maruyama, Y., Lu, K. S., Pereira, E., Plonsky, I., Baur, J. E., Wu, D., and Roper, S. D. 2005. Mouse taste buds use serotonin as a neurotransmitter. J. Neurosci. 25, 843–847.

Hughes, A. L. and Hughes, M. K. 1993. Adaptive evolution in the rat olfactory receptor gene family. J. Mol. Evol. 36, 249–254.

Janssens, P. M. W. and Van Haastert, P. J. M. 1987. Molecular basis of transmembrane signal transduction in *Dictyostelium discoideum*. Microbiol. Rev. 51, 396–418.

Kang, J. and Caprio, J. 1995. *In vivo* responses of single olfactory receptor neurons in the channel catfish, *Ictalurus punctatus*. J. Neurophysiol. 73, 172–177.

Katada, S., Hirokawa, T., Oka, Y., Suwa, M., and Touhara, K. 2005. Structural basis for a broad but selective ligand spectrum of a mouse olfactory receptor: mapping the odorant-binding site. J. Neurosci. 25, 1806–1815.

Kauer, J. S. and Shepherd, G. M. 1977 Analysis of the onset phase of olfactory bulb unit responses to odour pulses in the salamander. J. Physiol. (Lond.) 272, 495–516.

Kim, U. K., Jorgenson, E., Coon, H., Leppert, M., Risch, N., and Drayna, D. 2003. Positional cloning of the human quantitative trait locus underlying taste sensitivity to phenylthiocarbamide. Science 299, 1221–1225.

Koehl, M. A. R., Koseff, J. R., Crimaldi, J. P., McCay, M. G., Cooper, T., Wiley, M. B., and Moore, P. A. 2001. Lobster sniffing: antennule design and hydrodynamic filtering of information in an odor plume. Science 294, 1948–1951.

Komatsu, H., Jin, Y. H., L'Etoile, N., Mori, I., Bargmann, C. I., Akaike, N., and Ohshima, Y. 1999. Functional reconstitution of a heteromeric cyclic nucleotide-gated channel of *Caenorhabditis elegans* in cultured cells. Brain Res. 821, 160–168.

Krautwurst, D., Yau, K. W., and Reed, R. R. 1998. Identification of ligands for olfactory receptors by functional expression of a receptor library. Cell 95, 917–926.

Kubie, J. and Halpern, M. 1975. Laboratory observations of trailing behavior in garter snakes. J. Comp. Physiol. Psychol. 89, 667–674.

Laing, D. G. 1985. Optimum perception of odor intensity by humans. Physiol. Behav. 34, 569–574.

Lane, R. P., Young, J., Newman, T., and Trask, B. J. 2004. Species specificity in rodent pheromone receptor repertoires. Genome Res. 14, 603–608.

Larsson, M. C., Domingos, A. I., Jones, W. D., Chiappe, M. E., Amrein, H., and Vosshall, L. B. 2004. Or83b encodes a broadly expressed odorant receptor essential for *Drosophila* olfaction. Neuron 43, 703–714.

Laurent, G. 2002. Olfactory network dynamics and the coding of multidimensional signals. Nat. Rev. Neurosci. 3, 884–895.

Lazar, J., Greenwood, D. R., Rasmussen, L. E., and Prestwich, G. D. 2002. Molecular and functional characterization of an odorant binding protein of the Asian elephant, *Elephas maximus*: implications for the role of lipocalins in mammalian olfaction. Biochemistry 41, 11786–11794.

Lenhoff, H. M. and Lindstedt, K. J. 1974. Chemoreception in Aquatic Invertebrates with Special Emphasis on the Feeding Behavior of Coelenterates. In: Chemoreception in Marine Organisms (*eds*. P. T. Grant and A. M. Mackie), pp. 143–175. Academic Press.

Leinders-Zufall, T., Brennan, P., Widmayer, P., Prashanth-Chandramani, S., Maul-Pavicic, A., Jager, M., Li, X. H., Breer, H., Zufall, F., and Boehm, T. 2004. MHC class I peptides as chemosensory signals in the vomeronasal organ. Science 306, 1033–1037.

Leinders-Zufall, T., Lane, A. P., Puche, A. C., Ma, W., Novotny, M. V., Shipley, M. T., and Zufall, F. 2000. Ultrasensitive pheromone detection by mammalian vomeronasal neurons. Nature 405, 792–796.

Liao, J. and Schultz, P. G. 2003. Three sweet receptor genes are clustered in human chromosome 1. Mamm. Genome 14, 291–301.

Liman, E. R., Corey, D. P., and Dulac, C. 1999. TRP2: a candidate transduction channel for mammalian pheromone sensory signaling. Proc. Natl. Acad. Sci. U. S. A. 96, 5791–5796.

Lison, M., Blondheim, S. H., and Melmed, R. N. 1980. A polymorphism of the ability to smell urinary metabolites of asparagus. Br. Med. J. 281, 1676–1678.

Loconto, J., Papes, F., Chang, E., Stowers, L., Jones, E. P., Takada, T., Kumanovics, A., Lindahl, K. F., and Dulac, C. 2003. Functional expression of murine V2R pheromone receptors involves selective association with the M10 and M1 families of MHC class Ib molecules. Cell 112, 607–618.

Loudon, C. and Koehl, M. A. R. 2000. Sniffing by a silkworm moth: wing fanning enhances air penetration through and pheromone interception by antennae. J. Exp. Biol. 203, 2977–2990.

Lubbock, R. 1980. Clone-specific cellular recognition in a sea anemone. Proc. Natl. Acad. Sci. U. S. A. 77, 6667–6669.

Lucas, P., Ukhanov, K., Leinders-Zufall, T., and Zufall, F. 2003. A diacylglycerol-gated cation channel in vomeronasal neuron dendrites is impaired in *TRPC2* mutant mice: mechanism of pheromone transduction. Neuron 40, 551–561.

Lucero, M. T., Horrigan, F. T., and Gilly, W. F. 1992. Electrical responses to chemical-stimulation of squid olfactory receptor-cells. J. Exp. Biol. 162, 231–249.

Luu, P., Acher, F., Bertrand, H. O., Fan, J., and Ngai, J. 2004. Molecular determinants of ligand selectivity in a vertebrate odorant receptor. J. Neurosci. 24, 10128–10137.

Mackie, A. M. and Adron, J. W. 1978. Identification of inosine and inosine 5′-monophosphate as the gustatory feeding stimulants for the turbot, *Scophthalmus maximus*. Comp. Biochem. Physiol. A 60, 79–83.

Macrides, F. and Chorover, S. L. 1972. Olfactory bulb units: activity correlated with inhalation cycles and odor quality. Science 175, 84–87.

Maeztu, L., Sanz, C., Andueza, S., Paz De Pena, M., Bello, J., and Cid, C. 2001. Characterization of espresso coffee aroma by static headspace GC-MS and sensory flavor profile. J. Agric. Food. Chem. 49, 5437–5444.

Malnic, B., Hirono, J., Sato, T., and Buck, L. B. 1999. Combinatorial receptor codes for odors. Cell 96, 713–723.

Mato, J. M., Jastorff, B., Morr, M., and Konijn, T. M. 1978. A model for cyclic AMP-chemoreceptor interaction in *Dictyostelium discoideum*. Biochem. Biophys. Acta 544, 309–314.

Matsumoto, S. G. and Hildebrand, J. G. 1981. Olfactory mechanisms in the moth *Manduca sexta*: response characteristics and morphology of central neurons in the antennal lobes. Proc. R. Soc. Lond., B 213, 249–277.

Matsunami, H. and Buck, L. B. 1997. A multigene family encoding a diverse array of putative pheromone receptors in mammals. Cell 90, 775–784.

McClintock, T. S. and Ache, B. W. 1989. Hyperpolarizing receptor potentials in lobster olfactory receptor cells: implications for transduction and mixture suppression. Chem. Senses 14, 637–647.

Menashe, I., Man, O., Lancet, D., and Gilad, Y. 2003. Different noses for different people. Nat. Genet. 34, 143–144.

Mombaerts, P. 2004a. Genes and ligands for odorant, vomeronasal and taste receptors. Nat. Rev. Neurosci. 5, 263–278.

Mombaerts, P. 2004b. Odorant receptor gene choice in olfactory sensory neurons: the one receptor-one neuron hypothesis revisited. Curr. Opin. Neurobiol. 14, 31–36.

Mombaerts, P., Wang, F., Dulac, C., Chao, S. K., Nemes, A., Mendelsohn, M., Edmondson, J., and Axel, R. 1996. Visualizing an olfactory sensory map. Cell 87, 675–686.

Montmayeur, J. P., Liberles, S. D., Matsunami, H., and Buck, L. B. 2001. A candidate taste receptor gene near a sweet taste locus. Nat. Neurosci. 4, 492–498.

Mueller, K. L., Hoon, M. A., Erlenbach, I., Chandrashekar, J., Zuker, C. S., and Ryba, N. J. 2005. The receptors and coding logic for bitter taste. Nature 434, 225–229.

Munger, S., Gleeson, R. A., Aldrich, H. C., Rust, N. C., Ache, B. W., and Greenberg, R. M. 2000. Characterization of a phosphoinositide-mediated odor transduction pathway reveals plasma membrane localization of an inositol 1,4,5-trisphosphate receptor in lobster olfactory receptor neurons. J. Biol. Chem. 275, 20450–20457.

Newell, P. C., Europe-Finner, G. N., Small, N. V., and Liu, G. 1988. Inositol phosphates, G-proteins and *ras* genes involved in chemotactic signal transduction in *Dictyostelium discoideum*. J. Cell. Sci. 96, 669–673.

Nakagawa, T., Sakurai, T., Nishioka, T., and Touhara, K. 2005. Insect sex-pheromone signals mediated by specific combinations of olfactory receptors. Science 307, 1638–1642.

Nelson, G., Chandrashekar, J., Hoon, M. A., Feng, L., Zhao, G., Ryba, N. J., and Zuker, C. S. 2002. An amino-acid taste receptor. Nature 416, 199–202.

Nelson, G., Hoon, M. A., Chandrashekar, J., Zhang, Y., Ryba, N. J., and Zuker, C. S. 2001. Mammalian sweet taste receptors. Cell 106, 381–390.

Niimura, Y. and Nei, M. 2003. Evolution of olfactory receptor genes in the human genome. Proc. Natl. Acad. Sci. U. S. A. 100, 12235–12240.

Niimura, Y. and Nei, M. 2005. Evolutionary dynamics of olfactory receptor genes in fishes and tetrapods. Proc. Natl. Acad. Sci. U. S. A. 102, 6039–6044.

Parmentier, M., Libert, F., Schurmans, S., Schiffmann, S., Lefort, A., Eggerickx, D., Ledent, C., Mollereau, C., Gerard, C., Perret, J., *et al.* 1992. Expression of members of the putative olfactory receptor gene family in mammalian germ cells. Nature 355, 453–455.

Pelosi, P. 1996. Perireceptor events in olfaction. J. Neurobiol. 30, 3–19.

Pelosi, P. 2001. The role of perireceptor events in vertebrate olfaction. Cell Mol. Life Sci. 58, 503–509.

Pelosi, P. and Maida, R. 1990. Odorant-binding proteins in vertebrates and insects: similarities and possible common function. Chem. Senses 15, 205–215.

Pevsner, J., Reed, R. R., Feinstein, P. G., and Snyder, S. H. 1988. Molecular cloning of odorant-binding protein: member of a ligand carrier family. Science 241, 336–339.

Pfister, P. and Rodriguez, I. 2005. Olfactory expression of a single and highly variable V1r pheromone receptor-like gene in fish species. Proc. Natl. Acad. Sci. U. S. A. 102, 5489–5494.

Pinching, A. J. and Powell, T. P. S. 1971. The neuropil of the glomeruli of the olfactory bulb. J. Cell Sci. 9, 347–377.

Pourtier, L. and Sicard, G. 1990. Comparison of the sensitivity of C57BL/6J and AKR/J mice to airborne molecules of isovaleric acid and amyl acetate. Behav. Genet. 20, 499–509.

Quignon, P., Kirkness, E., Cadieu, E., Touleimat, N., Guyon, R., Renier, C., Hitte, C., Andre, C., Fraser, C., and Galibert, F. 2003. Comparison of the canine and human olfactory receptor gene repertoires. Genome Biol. 4, R80.

Rat Genome Sequencing Project Consortium. 2004. Genome sequence of the Brown Norway rat yields insights into mammalian evolution. Nature 428, 493–521.

Reisert, J., Bauer, P. J., Yau, K. W., and Frings, S. 2003. The Ca-activated Cl channel and its control in rat olfactory receptor neurons. J. Gen. Physiol. 122, 349–363.

Rifkin, B. and Bartoshuk, L. M. 1980. Taste synergism between monosodium glutamate and disodium 5′-guanylate. Physiol. Behav. 24, 1169–1172.

Robertson, H. M. 2001. Updating the str and srj (stl) families of chemoreceptors in *Caenorhabditis nematodes* reveals frequent gene movement within and between chromosomes. Chem. Senses 26, 151–159.

Robertson, H. M., Warr, C. G., and Carlson, J. R. 2003. Molecular evolution of the insect chemoreceptor gene superfamily in *Drosophila melanogaster*. Proc. Natl. Acad. Sci. U. S. A. 100 Suppl. 2, 14537–14542.

Rodriguez, I., Feinstein, P., and Mombaerts, P. 1999. Variable patterns of axonal projections of sensory neurons in the mouse vomeronasal system. Cell 97, 199–208.

Rodriguez, I., Greer, C. A., Mok, M. Y., and Mombaerts, P. 2000. A putative pheromone receptor gene expressed in human olfactory mucosa. Nat. Genet. 26, 18–19.

Rybczynski, R., Reagan, J., and Lerner, M. R. 1989. A pheromone-degrading aldehyde oxidase in the antennae of the moth *Manduca sexta*. J. Neurosci. 9, 1341–1353.

Saito, H., Kubota, M., Roberts, R. W., Chi, Q., and Matsunami, H. 2004. RTP family members induce functional expression of mammalian odorant receptors. Cell 119, 679–691.

Sam, M., Vora, S., Malnic, B., Ma, W., Novotny, M. V., and Buck, L. B. 2001. Odorants may arouse instinctive behaviors. Nature 412, 142.

Sanhueza, M., Schmachtenberg, O., and Bacigalupo, J. 2000. Excitation, inhibition, and suppression by odors in isolated

toad and rat olfactory receptor neurons. J. Exp. Biol. 203, 253–262.
Schmitt, B. C. and Ache, B. W. 1979. Olfaction: responses of a decapod crustacean are enhanced by flicking. Science 205, 204–206.
Scott, K., Brady, R., Jr., Cravchik, A., Morozov, P., Rzhetsky, A., Zuker, C., and Axel, R. 2001. A chemosensory gene family encoding candidate gustatory and olfactory receptors in *Drosophila*. Cell 104, 661–673.
Serizawa, S., Ishii, T., Nakatani, H., Tsuboi, A., Nagawa, F., Asano, M., Sudo, K., Sakagami, J., Sakano, H., Ijiri, T., *et al.* 2000. Mutually exclusive expression of odorant receptor transgenes. Nat. Neurosci. 3, 687–693.
Serizawa, S., Miyamichi, K., Nakatani, H., Suzuki, M., Saito, M., Yoshihara, Y., and Sakano, H. 2003. Negative feedback regulation ensures the one receptor–one olfactory neuron rule in mouse. Science 302, 2088–2094.
Sharon, D., Glusman, G., Pilpel, Y., Khen, M., Gruetzner, F., Haaf, T., and Lancet, D. 1999. Primate evolution of an olfactory receptor cluster: diversification by gene conversion and recent emergence of pseudogenes. Genomics 61, 24–36.
Shi, P., Zhang, J., Yang, H., and Zhang, Y.-P. 2003. Adaptive diversification of bitter taste receptor genes in mammalian evolution. Mol. Biol. Evol. 205, 805–814.
Shorey, H. H. 1976. Animal Communication by Pheromones. Academic Press.
Smith, D. V. 1985. Brainstem Processing of Gustatory Information. In: Taste, Olfaction, and the Central Nervous System (*ed*. D. W. Pfaff), pp. 151–177. Rockefeller University Press.
Spehr, M., Wetzel, C. H., Hatt, H., and Ache, B. W. 2002. 3-Phosphoinositides modulate cyclic nucleotide signaling in olfactory receptor neurons. Neuron 33, 731–739.
Spehr, M., Gisselmann, G., Poplawski, A., Riffell, J. A., Wetzel, C. H., Zimmer, R. K., and Hatt, H. 2003. Identification of a testicular odorant receptor mediating human sperm chemotaxis. Science 299, 2054–2058.
Steullet, P., Cate, H. S., and Derby, C. D. 2000. A spatiotemporal wave of turnover and functional maturation of olfactory receptor neurons in the spiny lobster *Panulirus argus*. J. Neurosci. 20, 3282–3294.
Stopfer, M. and Laurent, G. 1999. Short-term memory in olfactory network dynamics. Nature 402, 664–668.
Teeter, J. H, Brand, J. G., and Kumazawa, T. 1990. A stimulus-activated conductance in isolated taste epithelial membranes. Biophys. J. 58, 253–259.
Teicher, M. H., Stewart, W. B., Kauer, J. S., and Shepherd, G. M. 1980. Suckling pheromone stimulation of a modified glomerular region in the developing rat olfactory bulb revealed by the 2-deoxy glucose method. Brain Res. 194, 530–535.
Tegoni, M., Pelosi, P., Vincent, F., Spinelli, S., Campanacci, V., Grolli, S., Ramoni, R., and Cambillau, C. 2000. Mammalian odorant binding proteins. Biochem. Biophys. Acta 1482, 229–240.
Thomas, J. H., Kelley, J. L., Robertson, H. M., Ly, K., and Swanson, W. J. 2005. Adaptive evolution in the SRZ chemoreceptor families of *Caenorhabditis elegans* and *Caenorhabditis briggsae*. Proc. Natl. Acad. Sci. U. S. A. 102, 4476–4481.
Thomas, L. 1974. The Lives of a Cell: Notes of a Biology Watcher. The Viking Press.
Thorne, N., Chromey, C., Bray, S., and Amrein, H. 2004. Taste perception and coding in *Drosophila*. Curr. Biol. 14, 1065–1079.
Thorington, G. U. and Hessinger, D. A. 1988. Control of cnidia discharge: I, Evidence for two classes of chemoreceptor. Biol. Bull. 174, 163–171.
Tolbert, L. P. and Hildebrand, J. G. 1981. Organization and synaptic ultrastructure of glomeruli in the antennal lobes of the moth *Manduca sexta*: a study using thin sections and freeze-fracture. Proc. R. Soc. Lond. B 213, 279–301.
Torii, K. and Cagan, R. H. 1980. Biochemical studies of taste sensation, IX, Enhancement of L-[3H] glutamate binding to bovine taste papillae by 5′-ribonucleotides. Biochem. Biophys. Acta 627, 313–323.
Trapido-Rosenthal, H. G., Carr, W. E. S., and Gleeson, R. A. 1987. Biochemistry of an olfactory purinergic system: dephosphorylation of excitatory nucleotides and uptake of adenosine. J. Neurochem. 49, 1174–1182.
Trask, B. J., Friedman, C., Martin-Gallardo, A., Rowen, L., Akinbami, C., Blankenship, J., Collins, C., Giorgi, D., Iadonato, S., Johnson, F., *et al.* 1998. Members of the olfactory receptor gene family are contained in large blocks of DNA duplicated polymorphically near the ends of human chromosomes. Hum. Mol. Genet. 7, 13–26.
Troemel, E. R., Chou, J. H., Dwyer, N. D., Colbert, H. A., and Bargmann, C. I. 1995. Divergent seven transmembrane receptors are candidate chemosensory receptors in *C. elegans*. Cell 83, 207–218.
Trotier, D., Eloit, C., Wassef, M., Talmain, G., Bensimon, J. L., Doving, K. B., and Ferrand, J. 2000. The vomeronasal cavity in adult humans. Chem. Senses 25, 369–380.
Vandenburg, J. G. 1983. Pheromones and Reproduction in Mammals. Academic Press.
Van Houten, J. L. 1998. Chemosensory transduction in *Paramecium*. Eur. J. Protistol. 34, 301–307.
Vassilatis, D. K., Hohmann, J. G., Zeng, H., Li, F., Ranchalis, J. E., Mortrud, M. T., Brown, A., Rodriguez, S. S., Weller, J. R., Wright, A. C., *et al.* 2003. The G protein-coupled receptor repertoires of human and mouse. Proc. Natl. Acad. Sci. U. S. A. 100, 4903–4908.
Vogt, R. G., Riddiford, L. M., and Prestwich, G. D. 1985. Kinetic measurements of a sex pheromone-degrading enzyme: the sensillar esterase of *Antheraea polyphemus*. Proc. Natl. Acad. Sci. U. S. A. 82, 8827–8831.
Vogt, R. G., Rybczynski, R., and Lerner, M. R. 1990. The Biochemistry of Odorant Reception and Transduction. In: Chemosensory Information Processing (*ed*. D. Schild), pp. 33–76. Springer.
Wachowiak, M. and Cohen, L. B. 1999. Presynaptic inhibition of primary olfactory afferents mediated by different mechanisms in lobster and turtle. J. Neurosci. 19, 8808–8817.
Wachowiak, M., Cohen, L. B., and Ache, B. W. 2002. Presynaptic inhibition of olfactory receptor neurons in crustaceans. Micro. Res. Tech. 58, 365–375.
Wachowiak, M., Diebel, C. E., and Ache, B. W. 1997. Local interneurons define functionally distinct regions within lobster olfactory glomeruli. J. Exp. Biol. 200, 989–1001.
Wadhams, G. H. and Armitage, J. P. 2004. Making sense of it all: bacterial chemotaxis. Nat. Rev. Mol. Cell Biol. 5, 1024–1037.
Whissell-Buechy, D. and Amoore, J. E. 1973. Odour-blindness to musk: simple recessive inheritance. Nature 242, 271–273.
Whittaker, R. H. and Feeny, P. P. 1971. Allelochemics: chemical interactions between species. Science 171, 757–770.
Wu, S. V., Chen, M. C., and Rozengurt, E. 2005. Genomic organization, expression and function of bitter taste receptors (T2R) in mouse and rat. Physiol. Genomics 22, 139–149.
Wu, S. V., Rozengurt, N., Yang, M., Young, S. H., Sinnett-Smith, J., and Rozengurt, E. 2002. Expression of bitter taste receptors of the T2R family in the gastrointestinal tract and enteroendocrine STC-1 cells. Proc. Natl. Acad. Sci. U. S. A. 99, 2392–2397.
Yamaguchi, M., Yamazaki, K., Beauchamp, G. K., Bard, J., Thomas, L., and Boyse, E. A. 1981. Distinctive urinary odors

governed by the major histocompatibility locus of the mouse. Proc. Natl. Acad. Sci. U. S. A. 78, 5817–5820.
Yamazaki, K., Beauchamp, G. K., Bard, J., and Boyse, E. A. 1989. Sex-chromosomal odor types influence the maintenance of early pregnancy in mice. Proc. Natl. Acad. Sci. U. S. A. 86, 9399–9401.
Yang, W. Q., Braun, C., Plattner, H., Purvee, J., and Van Houten, J. L. 1997. Cyclic nucleotides in glutamate chemosensory signal transduction of *Paramecium*. J. Cell Sci. 110, 2567–2572.
Young, J. M., Friedman, C., Williams, E. M., Ross, J. A., Tonnes-Priddy, L., and Trask, B. J. 2002. Different evolutionary processes shaped the mouse and human olfactory receptor gene families. Hum. Mol. Genet. 11, 535–546.
Young, J. M., Shykind, B. M., Lane, R. P., Tonnes-Priddy, L., Ross, J. A., Walker, M., Williams, E. M., and Trask, B. J. 2003. Odorant receptor expressed sequence tags demonstrate olfactory expression of over 400 genes, extensive alternate splicing and unequal expression levels. Genome Biol. 4, R71.
Young, J. M., Kambere, M., Trask, B. J., and Lane, R. P. 2005. Divergent V1R repertoires in five species: amplification in rodents, decimation in primates, and a surprisingly small repertoire in dogs. Genome Res. 15, 231–240.
Zimmer-Faust, R. K., Gleeson, R. A., and Carr, W. E. S. 1988. The behavioral response of spiny lobsters to ATP: evidence for mediation by P2-like chemosensory receptors. Biol. Bull. 175, 167–174.
Zhang, J. and Webb, D. M. 2003. Evolutionary deterioration of the vomeronasal pheromone transduction pathway in catarrhine primates. Proc. Natl. Acad. Sci. U. S. A. 100, 8337–8341.
Zhang, X., Rodriguez, I., Mombaerts, P., and Firestein, S. 2004. Odorant and vomeronasal receptor genes in two mouse genome assemblies. Genomics 83, 802–811.
Zhang, Y., Hoon, M. A., Chandrashekar, J., Mueller, K. L., Cook, B., Wu, D., Zuker, C. S., and Ryba, N. J. P. 2003. Coding of sweet, bitter, and umami tastes: different receptor cells sharing similar signaling pathways. Cell 112, 293–301.
Zou, Z., Horowitz, L. F., Montmayeur, J. P., Snapper, S., and Buck, L. B. 2001. Genetic tracing reveals a stereotyped sensory map in the olfactory cortex. Nature 414, 173–179.
Zufall, F., Firestein, S., and Shepherd, G. M. 1994. Cyclic nucleotide-gated ion channels and sensory transduction in olfactory receptor neurons. Ann. Rev. Biophys. Biomol. Struct. 23, 577–607.

Further Reading

Hildebrand, J. G. and Shepherd, G. M. 1997. Mechanisms of olfactory discrimination: converging evidence for common principles across phyla. Ann. Rev. Neurosci. 20, 595–631.
Van Houten, J.l. 1994. Chemosensory transduction in eukaryotic microorganisms: trends for neuroscience? Trends Neurosci. 17, 62–71.

4.02 Chemistry of Gustatory Stimuli

G E DuBois, The Coca-Cola Company, Atlanta, GA, USA

J DeSimone and V Lyall, Virginia Commonwealth University, Richmond, VA, USA

© 2008 Elsevier Inc. All rights reserved.

4.02.1	**Introduction**	28
4.02.2	**Sweet-Tasting Stimuli**	29
4.02.2.1	Biochemistry of Sweet Taste	29
4.02.2.2	Sweetener Structure–Activity Relationship	31
4.02.2.2.1	Carbohydrate caloric, partially caloric and noncaloric sweeteners	32
4.02.2.2.2	Synthetic noncaloric sweeteners	36
4.02.2.2.3	Natural noncaloric sweeteners	42
4.02.2.2.4	Sweet-tasting minerals	48
4.02.2.3	Sensory Properties of Sweeteners	49
4.02.2.3.1	Concentration/response functions	49
4.02.2.3.2	Flavor profiles	49
4.02.2.3.3	Temporal profiles	49
4.02.2.3.4	Adaptation	50
4.02.3	**Bitter-Tasting Stimuli**	50
4.02.3.1	Biochemistry of Bitter Taste	50
4.02.3.2	Bitterant Structure–Activity Relationship	53
4.02.4	**Umami-Tasting Stimuli**	56
4.02.4.1	Biochemistry of Umami Taste	56
4.02.4.2	Umami Tastant Structure–Activity Relationship	57
4.02.5	**Sour-Tasting Stimuli**	58
4.02.5.1	Biochemistry of Sour Taste	59
4.02.5.2	Acidulant Structure–Activity Relationship	62
4.02.6	**Salty-Tasting Stimuli**	64
4.02.6.1	Biochemistry of Salty Taste	64
4.02.6.2	Salty Tastant Structure–Activity Relationship	66
References		68

Glossary

adaptation The phenomenon of taste desensitization which occurs on iterative exposure to a taste stimulus over a short period of time, a phenomenon believed to be a consequence of receptor phosphorylation by kinases specific for action on G-protein-coupled receptors.

concentration/response function A function which describes the relationship between tastant response (R) and stimulus concentration (C). Generally, C/R functions take the form of the law of mass action $R = R_m C/(k_d + C)$, where R_m is maximal response and k_d is the apparent receptor/tastant dissociation constant.

epithelial sodium channel A multi-subunit ion channel protein, usually referred to as ENaC, believed to be the principal initiator in the activation of salt-sensitive taste bud cells.

flavor profile A graphical description of the quality of the taste of a stimulus in terms of the relative intensities of multiple sensory attributes such as sweet, bitter, umami, sour, and salty.

G-protein Heterotrimeric guanosine triphosphate (GTP)-binding proteins constituted of α, β, and γ subunits which transduce the activation of G-protein-coupled receptors into cellular activation.

G-protein-coupled receptor A membrane protein receptor, usually referred to as a GPCR, which signals the presence of an extracellular ligand to an intracellular signaling protein known as a G protein, thus leading to cellular activation. GPCRs are constituted of extracellular ligand-binding domains and intracellular G-protein-binding domains connected by seven α-helical transmembrane segments.

gustatory stimuli Chemical compounds which initiate responses from taste bud cells and are perceived as sweet, bitter, umami, sour, or salty in quality of taste.

inositol trisphosphate receptor A protein receptor, present on intracellular calcium storage vesicles in sweet-, bitter-, and umami-sensitive taste bud cells, which is activated by its ligand inositol trisphosphate (IP_3) to promote the release of calcium ions into the cytoplasm, free calcium being a key element in the cascade of reactions leading to cellular excitation.

phospholipase $C_{\beta 2}$ An enzyme present in sweet-, bitter-, and umami-sensitive taste bud cells which communicates receptor and G-protein activation by action on the membrane lipid phosphatidylinositol to produce inositol trisphosphate (IP_3) and diacylglycerol (DAG), where IP_3, and possibly DAG, are key elements in the cascade of reactions involved in excitation of taste bud cells.

polycystic-kidney-disease-like ion channel An ion channel protein of the transient receptor potential family thought to mediate the excitation of sour-sensitive taste bud cells.

T1R1/T1R3 The heterodimeric G-protein-coupled receptor constituted of the two proteins T1R1 and T1R3 which initiates the responses of umami-sensitive taste bud cells to monosodium glutamate and other savory stimulants.

T1R2/T1R3 The heterodimeric G-protein-coupled receptor constituted of the two proteins T1R2 and T1R3 which initiates the responses of sweet-sensitive taste bud cells to sweeteners.

T2R A member of the family of G-protein-coupled receptors (25 in humans) which initiates the responses of bitter-sensitive taste bud cells to bitterants.

temporal profile A graphical description of the temporal characteristics of a taste experience which includes quantification of the rate of taste onset and the rate of taste extinction.

transient receptor potential channel M5 An ion channel protein, usually referred to as TRPM5, which is activated by intracellular calcium and mediates the activation of sweet-, bitter-, and umami-sensitive taste bud cells through membrane depolarization.

transient receptor potential channel V1 An ion channel protein, usually referred to as TRPV1 and known to be the receptor for vanilloid trigeminal nerve stimulants including capsaicin, thought to work together with the epithelial sodium channel in excitation of salt-sensitive taste bud cells.

4.02.1 Introduction

All chemical compounds, whether organic, inorganic, or organometallic, exhibit taste and therefore are potential gustatory stimuli. This is a fundamental premise for the discussion to follow. In order to exhibit taste, however, compounds must be in solution and some compounds that appear to be tasteless are probably not really tasteless, but rather are insufficiently soluble to reach their thresholds for activation of any of the gustatory sensor systems. In this chapter, we undertake the challenge of developing a coherent picture of the relationship between chemical structure and biological activity for each of the common modalities of taste. Understanding the structure–activity relationship (SAR) within series of biologically active chemical compounds is the never-ending and elusive vision for medicinal, flavor and fragrance, and agricultural chemists. The reason for the elusive nature of this vision is made clear by a quotation of Melvin Calvin, 1961, Nobel laureate in chemistry:

> It's no trick to get the right answer when you have all the data. The real creative trick is to get the right answer when you have only half the data in hand and half of it is wrong. And you don't know which half.

Thus, as we challenge ourselves to understand the chemistry of gustatory stimuli, it is important to recognize that some of the data that we are trying to make sense out of are misleading at best and, in some cases, just wrong. With this fact in mind, we proceed.

What is taste? In the lexicon of the consumer, taste is the total sensory experience that results from a

superimposition of gustatory, olfactory, and chemesthetic sensory inputs to the central nervous system which occurs on sampling a food or beverage. And it can be argued that even the senses of vision and audition contribute significantly. In this Chapter, only gustatory stimuli are considered. Historically, it has been generally accepted that the sense of gustation is made up of the four modalities: sweet, bitter, sour, and salty. We now know that savory, often referred to by the Japanese word *umami*, is a fifth gustatory modality. In this Chapter, the relationship between chemical structure and gustatory activity, or gustatory SAR, for each of these five taste modalities is discussed. In each case, current understandings of the biochemical mechanisms are summarized first since without such a background, little sense can be made of SAR.

4.02.2 Sweet-Tasting Stimuli

Sweet taste is clearly a very important sensation as evidenced by the fact that wars have been fought and people enslaved over sugar, the prototypical sweet stimulus (Mintz, S. W., 1985). More sweeteners, principally sugar but also syrups derived from starch as well as a variety of noncaloric sweeteners, are added to foods and beverages than any other ingredient type. Human liking of sweet taste is innate as has been demonstrated by Steiner J. E. (1994). He studied the behavioral responses of newborns and clearly showed that they exhibit strong liking for sweettasting stimuli. As a consequence of the importance of sweet taste in the human diet, more research has been conducted on elucidating the biochemical pathways which mediate it and on the discovery and commercial development of noncaloric sweeteners than on bitter, umami, sour, and salty tastes combined. For this rationale, we discuss sweet-tasting stimuli first and in considerable detail.

4.02.2.1 Biochemistry of Sweet Taste

In spite of the importance of sweet taste to our daily enjoyment of life, until the late 1980s, the biochemical pathway which mediates it was largely unknown. Then, evidence began to accumulate that it must be G-protein-coupled receptor (GPCR) mediated. More specifically, sweet taste was thought to be the result of activation of several GPCRs since the findings of biochemical, electrophysiological, and psychophysical experiments could only be easily explained by a plurality of receptors (Faurion, A., 1987; DuBois, G. E., 1997). And this expectation was supported by the fact that multiple subtypes of GPCRs commonly exist for other important signal molecules (e.g., acetylcholine, norepinephrine, dopamine, serotonin, etc.).

In the early 2000s, a breakthrough occurred dramatically improving our understanding of sweet taste. In 2001, a collaborative team from the laboratories of Charles Zuker (University of California, San Diego) and Nicholas Ryba (US National Institutes of Health) reported the discovery of the rat sweetener receptor (Nelson, G. *et al.*, 2001). In a functional assay, they showed that all substances that rats generalize to sucrose taste appear to be mediated by a single receptor which their observations suggested to be a heterodimer of two 7-transmembrane domain (TMD) proteins which they named T1R2 and T1R3. This heterodimeric sweetener receptor is usually written as T1R2/T1R3. Both T1R2 and T1R3 are members of the small family of class C GPCRs. The most studied members of the class C GPCRs are the 8 homodimeric metabotrophic glutamate, single heterodimeric gamma-aminobutyric acid type B, and single homodimeric extracellular calcium receptors which have recently been reviewed (Pin, J.-P. *et al.*, 2003). This rat receptor discovery was quickly followed by the report by Li X. *et al.* (2002) of Senomyx (La Jolla, CA) of parallel findings for the human system. Again, as in the rodent, the results were most consistent with human sweet taste initiation by the single heterodimeric receptor T1R2/T1R3. Heterologous cells (i.e., HEK-293 cells), in which both human T1R2 and human T1R3 were expressed, responded to all structural types of sweeteners tested in a manner consistent with expectation from sensory experiments. Thus, at the present time, there is a general consensus that the heterodimer T1R2/T1R3 is the sweetener receptor. Evidence has been presented for the mouse by the Zuker and Ryba laboratories that a T1R3-only receptor, perhaps a homodimer, is functional as a carbohydrate (CHO)-only sweetener receptor (Zhao, G. Q. *et al.*, 2003). However, no evidence has yet been reported on such a receptor in humans or other animal models. At about the same time as the pioneering work by the Zuker and Ryba laboratories, several other laboratories also identified the T1R3 component of the receptor (Bachmanov, A. A. *et al.*, 2001; Max, M. *et al.*, 2001; Montmayeur, J.-P. *et al.*, 2001; Sainz, E. *et al.*, 2001).

Class C GPCRs are unique in that they possess very large N-terminal Venus flytrap-like domains (VFDs). For the case of the metabotrophic glutamate receptor mGluR1, Kunishima N. *et al.* (2000) demonstrated that its VFD closes on binding glutamate, hence the analogy to a Venus flytrap. This precedent, and the fact that the sweetener receptor and the umami receptor, shown in parallel work by Li and co-workers to be the GPCR heterodimer T1R1/T1R3, contain the common subunit T1R3 lead to the expectation that sweeteners likely bind in the VFD of T1R2. Subsequent work by Li and co-workers (Xu, H. *et al.*, 2004) probed the fundamental question of sweetener-binding locus with the finding that, while some sweeteners do bind in the VFD of T1R2 (e.g., aspartame and neotame), at least one sweetener (i.e., cyclamate) does not, but rather binds within the 7-TMD of T1R3. The binding of cyclamate to the TMD of T1R3 was corroborated by Robert Margolskee and associates of Mt Sinai School of Medicine (Jiang, P. *et al.*, 2005) with site-directed mutagenesis studies which provided significant detail on the interactions of cyclamate with T1R3. Other work by Margolskee and associates on brazzein, a natural protein sweetener, showed that its locus of binding is in the cysteine-rich domain (CRD) of T1R3, a subunit of the protein which connects VFD and TMD domains (Jiang, P. *et al.*, 2004). The human sweetener receptor is the first Class C GPCR demonstrated to have multiple agonist-binding loci (orthosteric sites).

A topic of considerable controversy in the field of taste research has been that of taste quality coding. Taste bud cells (TBCs) are known to be innervated by nerve fibers of three gustatory nerves: the chorda tympani (CT), the glossopharyngeal, and the superpetrosal nerves. Each of these nerves is a bundle of many individual fibers and some have argued that taste quality is coded by a cross-fiber pattern of activity and others have argued that individual fibers are specific for activity. Evidence for taste quality coding due to modality-specific fibers was provided by electrophysiological studies in chimpanzees by Goran Hellekant and Yuzo Ninomiya. They carried out single fiber recordings and demonstrated that some fibers responded only to sweeteners (Hellekant, G. and Ninomiya, Y., 1991) and other fibers responded only to bitterants (Hellekant, G. and Ninomiya, Y., 1994a; 1994b) leading them to conclude that taste quality is coded at the level of the TBC. In other words, they argued that individual TBCs are specific sensors for sweet, bitter, umami, sour, or salty. Further convincing evidence that taste quality coding occurs at the level of the TBC comes from recent work of the Zuker and Ryba laboratories. Early in 2003, working with $PLC_{\beta 2}$ knockout mice, they engineered mice in which they selectively rescued $PLC_{\beta 2}$ function in bitter receptor expressing cells (Zhang, Y. *et al.*, 2003) and found that these mice responded normally to bitterants but still exhibited no responses to sweet or umami stimuli. Later, working with T_1R knockout mice that gave no responses to sweet or umami stimuli, they engineered mice in which human T1R2 function was added to T1R3-expressing TBCs (Zhao, G. Q. *et al.*, 2003) and found that these mice responded to aspartame, a compound sweet to humans but inactive in mice. They also selectively introduced an opioid receptor into sweet-sensing TBCs and observed that these mice now responded with attraction to opioid agonists. In summary, the evidence is now strong that taste quality is coded at the level of the TBC.

The recent identification of the sweetener receptor and elucidation of the mechanism of sweet taste coding was preceded by the discovery of specific G proteins that mediate sweet taste. In 1992, Robert Margolskee, then at Roche Institute of Molecular Biology, and associates reported that a G protein closely related to transducin is critical for sweet taste (McLaughlin, S. K. *et al.*, 1992). They called this G-protein gustducin but noted that low levels of transducin are also present in TBCs. And, in addition, very recently, Guy Servant and co-workers (Senomyx) obtained evidence showing that the sweetener receptor can also functionally interact with $G_{\alpha i(o)}$ proteins (Ozeck, M. *et al.*, 2004). $G_{i(2)}$ is a favored $G_{\alpha i(o)}$ candidate as it was shown to be the most highly expressed $G_{\alpha i(o)}$ in TBCs. Other key elements of the sweet taste transduction cascade were identified by Margolskee and associates (Pérez, C. A. *et al.*, 2002) and by the Zuker and Ryba team (Zhang, Y. *et al.*, 2003). They found that phospholipase $C_{\beta 2}$ ($PLC_{\beta 2}$), the inositol trisphosphate (IP_3) receptor (IP_3R), and the transient receptor potential (TRP) channel m5 (TRPM5) are key effector elements in sweet taste transduction. Thus, at this time, evidence exists for the participation of one receptor (T1R2/T1R3), as many as three G proteins (gustducin, transducin, and possibly $G_{i(2)}$), one enzyme ($PLC_{\beta 2}$), a second messenger receptor (IP_3R), and an ion channel (TRPM5) in the activation of sweet-sensing TBCs. Recognition of (1) the relatively high concentrations of noncaloric sweeteners (i.e., millimolar levels) commonly employed in foods and beverages, (2) the fact that noncaloric

sweeteners are commonly lipophilic, and (3) the fact that such lipophilic molecules are generally absorbed into cells led to speculation (DuBois, G. E., 1997) that sweeteners may initiate their activity at intracellular elements of the transduction cascade. Support for this idea is provided by the work of Michael Naim and associates (Hebrew University) who reported that some noncaloric sweeteners have the capability to directly activate G proteins (Naim, M. *et al.*, 1994). And further support is provided by recent work from the Naim group through studies showing that several noncaloric sweeteners are rapidly taken up into TBCs (Zubare-Samuelov, M. *et al.*, 2005). However, in view of the finding that every sweetener tested by Senomyx investigators activated HEK-293 cells in which the T1R2/T1R3 receptor is expressed, while otherwise identical control cells, lacking only the T1R2/T1R3 receptor, are unaffected, it remains to be demonstrated that any sweeteners do actually act at downstream elements in the sweet-sensing TBC activation cascade. Further, since we now know that bitter and umami taste stimuli initiate their sensations at the TBC level through the same effectors which mediate sweet taste signaling (i.e., gustducin, $PLC_{\beta 2}$, IP_3R, and TRPM5), if any sweeteners do initiate their activities at intracellular components of TBCs, then they should also simultaneously activate bitter- and umami-sensitive TBCs resulting in mixed modality (i.e., sweet/bitter/umami) compounds. And while sweet/bitter compounds are known, no compounds with sweet/umami or sweet/bitter/umami taste have been reported, thus leading to the overall conclusion that initiation of sweet taste activity at intracellular targets of TBCs seems unlikely. Nonetheless, since Naim and co-workers have demonstrated that small molecules including some sweeteners are readily taken up into TBCs, it is logical to expect that some such compounds may exist.

In summary, transduction of sweet taste is generally accepted as proceeding via activation of the heterodimeric sweetener receptor T1R2/T1R3 with subsequent activation of the G protein gustducin (and/or transducin and possibly $G_{i(2)}$). In this generally accepted transduction pathway, the gustducin $G_\beta G_\gamma$ subunit activates $PLC_{\beta 2}$ to act on membrane phosphatidylinositol to produce IP_3, which acts at its receptor IP_3R on intracellular Ca^{2+} storage sites to release Ca^{2+}. And finally, Ca^{2+} gates the TRPM5 ion channel enabling the inward flow of Na^+, depolarizing the sweet-sensing TBC, and initiating signaling to the CNS. Evidence from the Zuker and Ryba laboratories argues that this gustducin $G_\beta G_\gamma$ pathway is the only sweet taste transduction pathway since mice in which the TRPM5 gene was partially deleted were observed to lack all behavioral and nerve responses to sweeteners (Zhang, Y. *et al.*, 2003). Earlier work, however, argues for a gustducin G_α pathway in sweet taste transduction, where G_α is the gustducin subunit which communicates with intracellular effectors (Varkevisser, B. and Kinnamon, S. C., 2000; Margolskee, R. F., 2002). And very recent work from the Margolskee laboratory (Damak, S. *et al.*, 2006), in which TRPM5 gene expression in the mouse was fully blocked, continues to argue for a sweet taste transduction pathway not mediated by TRPM5. In this work, the TRPM5 knockout mice continue to exhibit weak responses to sweeteners. And, in the electrophysiological component of this work, glossopharyngeal nerve responses were observed while the CT nerve responses were not, thus suggesting that transduction pathway may vary between TBCs innervated by the two different nerve systems. Thus, at this time, while we have a general consensus that the primary pathway for sweet taste transduction is the gustducin $G_\beta G_\gamma/PLC_{\beta 2}/IP_3R/$ TRPM5 pathway, it appears too early to conclude that it is the exclusive pathway.

4.02.2.2 Sweetener Structure–Activity Relationship

Since the early 1800s, chemists have discovered hundreds of synthetic and natural sweeteners and by the 1980s, at least 50 structural classes of sweet-tasting organic compounds were known. In an effort to make sense of this structural diversity, models were developed in an attempt to rationalize the relationship between structure and taste activity. These are pharmacophore models and the most well known of them is the so-called A-H/B model (Shallenberger, R. S. and Acree, T. E., 1967). In this model, it was hypothesized that all sweeteners contain H-bond donor and H-bond acceptor groups separated by not <2.5 or >4.0 Å. In effort to better explain empirical observations, many improved pharmacophore models have been developed since the A-H/B model (Kier, L. B., 1972; van der Heijden, A. *et al.*, 1985a; 1985b; Douglas, A. J. and Goodman, M. 1991; Rohse, H. and Belitz, H.-D., 1991; Temussi, P. A. *et al.*, 1991; Tinti, J.-M. and Nofre, C., 1991; Bassoli, A. *et al.*, 2002). An assumption implicit in all of these models is that sweetness is initiated following the binding of a sweetener to a single site

(i.e., orthosteric site) on a single receptor. However, recent studies on the mapping of sweetener-binding loci to the sweetener receptor (Jiang, P. *et al.*, 2004; Xu, H. *et al.*, 2004) have demonstrated that the human sweetener receptor contains at least three orthosteric sites and thus the A-H/B model as well as all of the other pharmacophore models, while perhaps correct within structural classes of sweeteners, are not correct in the general sense. In summary, it appears that human sweetness is substantially, and perhaps exclusively, initiated by activation of a single receptor, the GPCR heterodimer T1R2/T1R3, at a plurality (i.e., $\geq$3) of orthosteric sites. And therefore $\geq$3 pharmacophore models are required to characterize the relationship between chemical structure and sweet taste. The first model consistent with this logic was developed at The NutraSweet Company for the aspartame orthosteric site (Culberson, J. C. and Walters, D. E., 1991). Later, an enhancement of this aspartame pharmacophore model, employing comparative molecular field analysis to provide quantitative predictive power, was developed at The Coca-Cola Company (D'Angelo, L. and Iacobucci, G., 1995).

Over the last 200 years, chemists have identified and characterized many, many sweet-tasting chemical compounds. Many of these compounds are synthetic but also many of them have been found in nature. The most common sweeteners, present in ordinary fruits and vegetables, are CHO sweeteners. However, health concerns related to obesity and diabetes led to the commercial development of noncaloric sweeteners found either in the chemist's laboratory or in nature. In Sections 4.02.2.2.1–4.02.2.2.4 of this discussion on sweeteners is given a representative sampling of chemical compounds found to exhibit sweet taste. Numerous reviews on sweetener SAR are available (e.g., Lee, C.-K., 1987; Marie, S. and Piggott, J. R., 1991; Shallenberger, R. S., 1993; O'Brien Nabors, L., 2001; Kim, N.-C. and Kinghorn, A. D., 2002). In this review, all commercially developed sweeteners are discussed. Chemical structures, empirical formulas, molecular weights, and, to the extent available, sweetness potencies (P) are provided. In Section 4.02.2.2.5 of this section on sweet-tasting stimuli, important information on differences in sensory characteristics of sweeteners is presented. As explained, P values for CHO sweeteners are constants, independent of sucrose reference concentration, while for synthetic and natural noncaloric sweeteners, they are variable with a strong dependence on sucrose reference concentration. Thus, P values for synthetic and natural noncaloric sweeteners are given relative to a sucrose reference and are on a weight basis (P_w). P_w values can easily be converted to molar basis potencies (P_m) by multiplication by the factor $M_{compound}/M_{sucrose}$ (i.e., the ratio of the molecular weights of a compound and of sucrose). Sweetness potencies for the synthetic and natural noncaloric sweeteners are expressed as $P_w(X)$ where X is the sucrose reference concentration (% w/v). Ideally, all P_w values would be provided relative to a common sucrose reference, determined by a common protocol and be at a sucrose use level relevant to food and beverage applications (e.g., 10% sucrose). However, synthetic and natural noncaloric sweeteners have variable maximal responses that in many cases are much less than 10% sucrose sweetness equivalency. And oftentimes, literature sweetness potencies are reported without sucrose reference information. Such unreferenced sweetness potencies are reported here as P_w(ur). As a consequence of these and other complexities, the comparison of sweetness potencies for sweeteners reported by different authors using different protocols is difficult at best.

4.02.2.2.1 Carbohydrate caloric, partially caloric and noncaloric sweeteners

CHOs are generally considered to be aldehyde- or ketone-containing polyhydroxylic compounds which most commonly exist in hemiacetal, acetal, hemiketal, or ketal forms. In nature, CHOs exist predominantly in polymeric form. Principal among the natural CHO polymers are starch and cellulose, both of which are glucose polymers, and chitin, a polymer of 2-acetamido-2-deoxyglucose. Polymeric CHOs are not sweet. At the same time, all low molecular weight CHOs are sweet-tasting compounds. Some low molecular weight CHOs are also bitter, but all are sweet with P_w values within a factor of 0.1–2 of that of sucrose. In the author's (GED) experience, reports in the literature to the contrary are incorrect. The most common of the CHO sweeteners is sucrose, a disaccharide constituted of glucose and fructose monosaccharide subunits. Sucrose is produced on a very large scale with 2005 world production forecast at 144.8×10^6 MT. In acidic foods and beverages, sucrose hydrolyzes to a 1/1 mixture of glucose and fructose as illustrated in Figure 1. This 1/1 glucose/fructose mixture is prepared on a commercial scale from sucrose and is called invert sugar. Other glucose/fructose mixtures are manufactured from starch on a very large scale. These products are known as high fructose starch syrups (HFSSs) and are available as

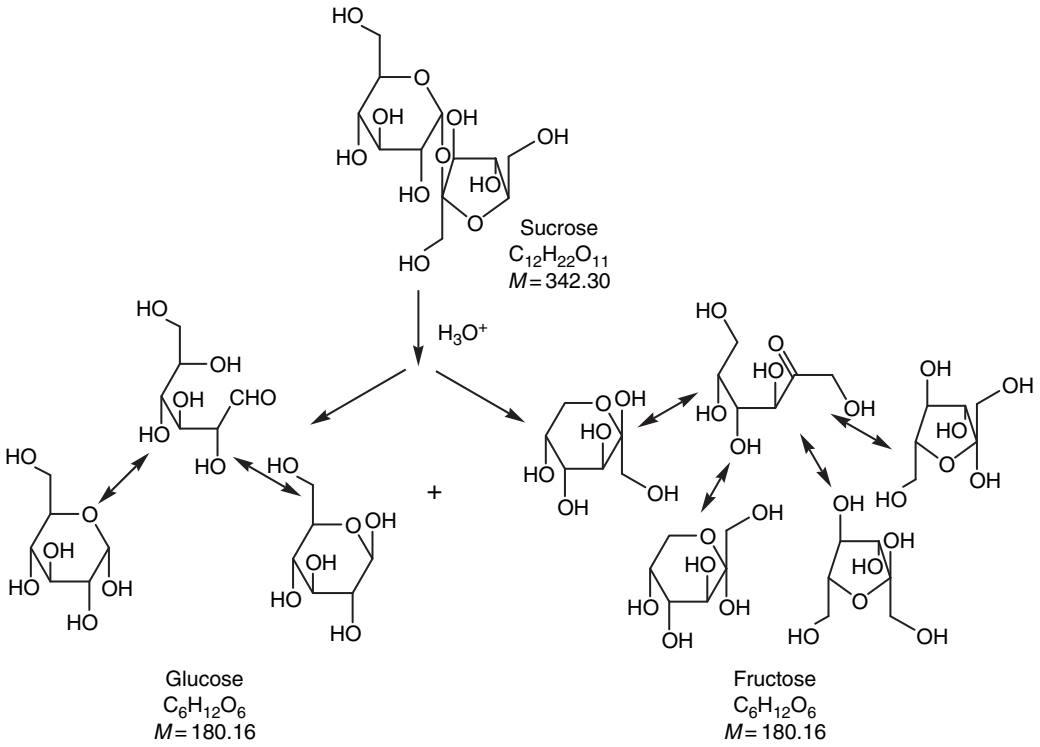

Figure 1 The hydrolysis of sucrose to glucose and fructose.

42% fructose (HFSS-42), 55% fructose (HFSS-55), and 90% fructose (HFSS-90). It is important to recognize that, while sucrose is a single chemical entity, glucose is a mixture of three tautomeric forms and fructose, a mixture of five tautomeric forms, the tautomeric forms of each monosaccharide being in rapid equilibrium with each other. And thus, in acidic foods or beverages sweetened with sucrose, the active sweetener system is a mixture of three compounds, with two of them present in eight tautomeric forms, all present simultaneously. Efforts have been made to determine the relative sweetness potencies of the different tautomeric forms of glucose and fructose. However, since these tautomers are in rapid equilibrium, the published sweetness potencies are highly speculative.

A great many other low molecular weight CHOs are known and all are sweet to humans. A sampling of mono-, di-, and oligosaccharides, intended to illustrate the diversity of sweet-tasting CHOs, is provided in Figures 2 and 3 along with their sweetness potencies where available. No attempt has been made to be comprehensive in this listing. The examples given are provided simply to illustrate the breadth of the SAR among CHO sweeteners. Some low molecular weight CHOs are reported to be bitter rather than sweet. As example, gentiobiose is reported to be bitter (Pfeilsticker, K. *et al.*, 1978). However, as a 25% solution, a commercial sample was observed to exhibit both sweet and bitter tastes (DuBois, G. E. *et al.*, 1994). In work on synthetic analogs of natural CHOs, many of them, even at high states of purity, exhibit bitterness (DuBois, G. E., 1997). However, in general, further purification resulted in purely sweet samples. It seems likely that the bitter tastes reported for many CHOs may be due to potent bitter contaminants.

The simplest monosaccharide CHOs, glycolaldehyde (**1**) and glyceraldehyde (**2**), cannot form monomeric cyclic acetals or ketals and are reported to exist primarily in dimeric form and thus their active pharmacophores are believed to be their dimeric hemiacetals. All of the higher molecular weight monosaccharide CHOs illustrated exist almost exclusively as cyclic hemiacetal or hemiketal tautomeric forms. And thus it is believed that their active pharmacophores are the cyclic tautomers. A very surprising finding among the monosaccharide CHOs is the total absence of enantiospecificity in some enantiomeric pairs. Thus Shallenberger R. S. *et al.* (1969) reported complete inability of human

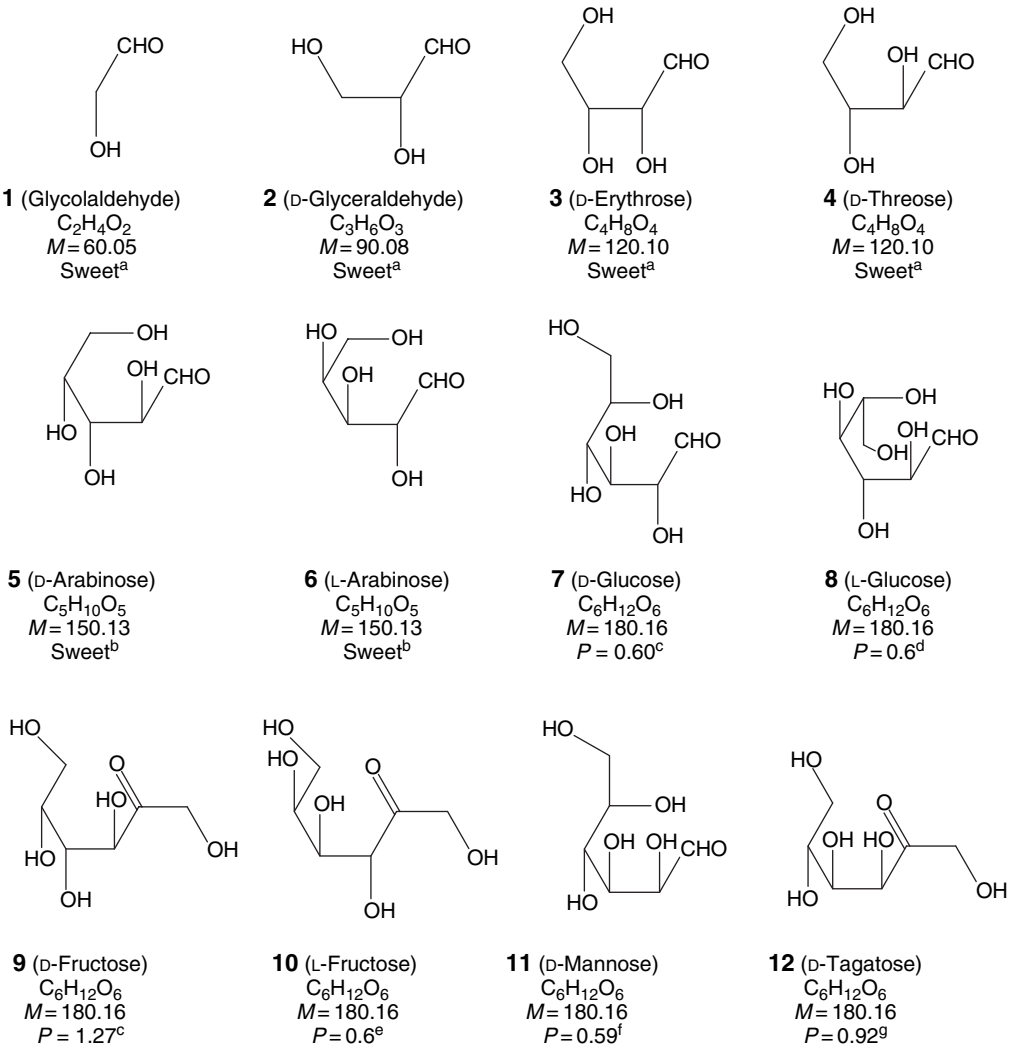

Figure 2 Examples of monosaccharide CHO sweeteners. [a]Shallenberger R. S. (1993); [b]Birch G. G. *et al*. (1996); [c]DuBois G. E. *et al*. (1991); [d]DuBois G. E. and Singer N. (1984); [e]DuBois G. E. (1995); [f]Schutz H. G. and Pilgrim F. J. (1957); and [g]Bertelsen H. *et al*. (2001).

subjects to differentiate D- and L-enantiomers for several sugars. Birch G. G. *et al.* (1996) corroborated the Shallenberger report for the case of D- and L-arabinose, **5** and **6**. And the author (GED) and Singer N. (1984) corroborated the Shallenberger report for the case of D- and L-glucose, **7** and **8**. In both the arabinose and the glucose enantiomeric pairs, identical tastes are observed when tasted at equal concentrations. In contrast, however, D- and L-fructose are quite different, with the natural D enantiomer being approximately twice as potent as the L enantiomer (DuBois, G. E., 1995). Given that CHO sweeteners are thought to activate the sweetener receptor T1R2/T1R3 through a binding interaction, it is to be expected that enantiomers should differ in their binding effectiveness and thus the observed difference in potencies for the fructose enantiomers is expected. However, identical sweetness potencies within the D/L arabinose and D/L glucose enantiomeric pairs are very surprising.

It seems very unlikely that each enantiomer in a pair of CHO sweeteners should bind with equal affinity to the receptor and this reasoning led to the suggestion that CHOs as well as other highly hydrophilic compounds may activate the receptor via a nonbinding mechanism (DuBois, G. E., 1997). The binding sites for the natural agonists for family C GPCRs are known to be in the VFDs

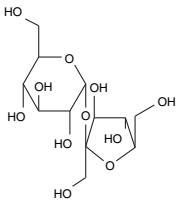

13 (Sucrose)
$C_{12}H_{22}O_{11}$
$M = 342.30$
$P = 1.00$[a]

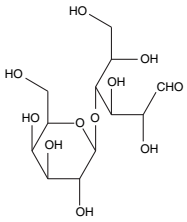

14 (Lactose)
$C_{12}H_{22}O_{11}$
$M = 342.30$
$P = 0.30$[b]

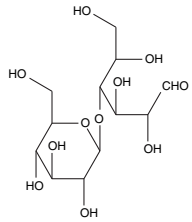

15 (Cellobiose)
$C_{12}H_{22}O_{11}$
$M = 342.30$
Sweet[c]

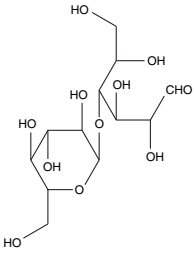

16 (Maltose)
$C_{12}H_{22}O_{11}$
$M = 342.30$
$P = 0.46$[b]

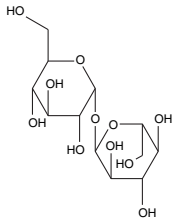

17 (Trehalose)
$C_{12}H_{22}O_{11}$
$M = 342.30$
$P = 0.14$[b]

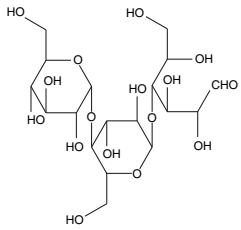

18 (Maltotriose)
$C_{18}H_{32}O_{16}$
$M = 504.44$
Sweet[d]

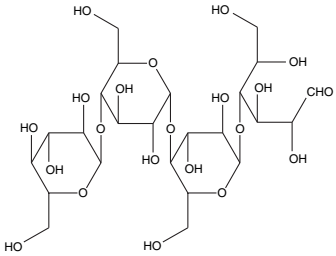

19 (Maltotetraose)
$C_{24}H_{42}O_{21}$
$M = 666.58$
Sweet[d]

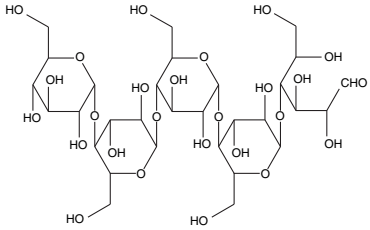

20 (Maltopentaose)
$C_{30}H_{52}O_{26}$
$M = 828.72$
Sweet[d]

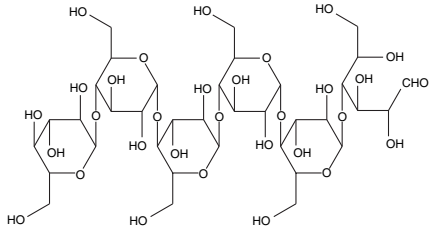

21 (Maltohexaose)
$C_{36}H_{62}O_{31}$
$M = 990.86$
Sweet[d]

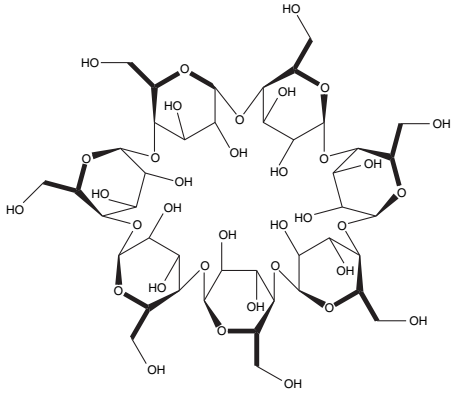

22 (β-Cyclodextrin)
$C_{42}H_{70}O_{35}$
$M = 1134.98$
$P = 0.70$[e]

Figure 3 Examples of disaccharide and oligosaccharide CHO sweeteners. [a]DuBois G. E. *et al*. (1991); [b]Schutz H. G. and Pilgrim F. J. (1957); [c–e]DuBois G. E. and D'Angelo L. L. (1996).

and these agonists are believed to activate the receptor by causing the VFD to adopt a closed conformation. And recent work on an analog of the $GABA_B$ family C GPCR, engineered to exist exclusively in a closed conformation (Kniazeff, J. *et al* 2004), shows that the closed conformation is fully active. The binding site for aspartame has been shown to be in the VFD of the T1R2 component of the T1R2/T1R3 receptor (Xu, H. *et al*., 2004) and recent evidence (Nie, Y. *et al*., 2005) suggests that sucrose binds in the VFDs of both T1R2 and T1R3. Thus, it appears that CHO sweeteners most likely modulate the equilibrium between the open (inactive) and closed (active) conformations of the VFD of T1R2 and perhaps T1R3 as well. If this is the case, it seems reasonable that the open/closed equilibria could be altered in two ways. The first possibility is that CHO sweeteners, like other family C GPCR agonists, bind to a site within the VFD. A second possibility, however, is that CHO sweeteners activate the receptor by a nonbinding mechanism where they simply alter the VFD open/closed equilibrium in favor of the closed conformation by a general solvent effect. Solution equilibria of all types are well known to be solvent dependent and a change in the open/closed equilibria for T1R2 and T1R3 to favor the closed forms that is promoted by a change in solvent from normal saliva to a concentrated CHO sweetener solution should not be a surprise. Thus, it could well be that CHO sweeteners showing no enantiospecificity (i.e., D/L arabinose and D/L glucose) may activate the receptor exclusively by a nonbinding mechanism and that CHO sweeteners which do show enantiospecificity (i.e., D/L fructose) activate the receptor by both binding and nonbinding mechanisms. If this nonbinding pathway for sweetener receptor activation does exist, then it is to be expected that all sweeteners acting by this pathway should exhibit similar levels of activity. And they do, as is made clear with the examples to follow.

The aldehyde or ketone moieties present in the CHO sweeteners in Figure 2 are not prerequisites for sweet taste. Simple alcohols as well as CHO reduction products, often referred to as polyols, are also sweet in taste. An exemplary list of polyol sweeteners is provided in Figure 4.

Within the last 20–30 years, due to the increased interest in reduced-calorie food and beverage products, substantial interest has been expended on the commercial development of reduced-calorie CHOs and polyols. Among naturally occurring CHOs and polyols already mentioned which are reduced in bioavailable energy content are the naturally occurring *meso*-erythritol and D-tagatose. In the United States, the FDA has accepted bioavailable calorie levels of 0.2 and 1.5 kcal g^{-1} for erythritol and D-tagatose, respectively, although, in Japan, an energy content for erythritol of 0.0 kcal g^{-1} is accepted. A number of semisynthetic reduced-calorie CHOs and polyols have been commercially developed. These compounds are listed in Figure 5.

A survey of the relationship between structure and activity for the CHO sweeteners shown above leads to the expectation that any polyhydroxylic organic compound may be sweet. In food applications, sucrose, the most common CHO sweetener, provides functionality beyond sweetness including freezing point depression (frozen desserts) and starch gelatinization point elevation (baked goods). These properties are colligative in nature and thus the ideal noncaloric CHO sweetener should have molecular weight comparable to that of sucrose. In addition, the quality of taste of CHO sweeteners was noted to be dependent on the ratio of hydroxyl groups to carbon atoms. This logic led the author (GED) and a team at The NutraSweet Company to the synthesis of a diverse group of approximately 100 CHO-like noncaloric sweeteners (DuBois, G. E. *et al*., 1992). Compounds **35–38**, illustrated in Figure 6, are exemplary of this work and all are noncaloric and exhibit clean sweet tastes. At about the same time, Adam Mazur and co-workers (Procter & Gamble Company) reported the synthetic lactitol derivative **39** to be sweet and noncaloric.

4.02.2.2.2 Synthetic noncaloric sweeteners

The field of organic chemistry really had its beginning in the nineteenth century. Many new chemical reactions were discovered and novel chemicals synthesized. These new chemical compounds were characterized by techniques available at the time which included physical description (i.e., solid, liquid, crystalline form, etc.), color, boiling point, melting point, odor, and, of particular reference to this discussion, taste. The routine tasting of novel chemical compounds by chemists continued well into the twentieth century. And in this way, synthetic sweeteners were discovered among many structural classes of compounds. Examples of 21 structural classes of synthetic noncaloric sweeteners, along with chemical structures, molecular weights,

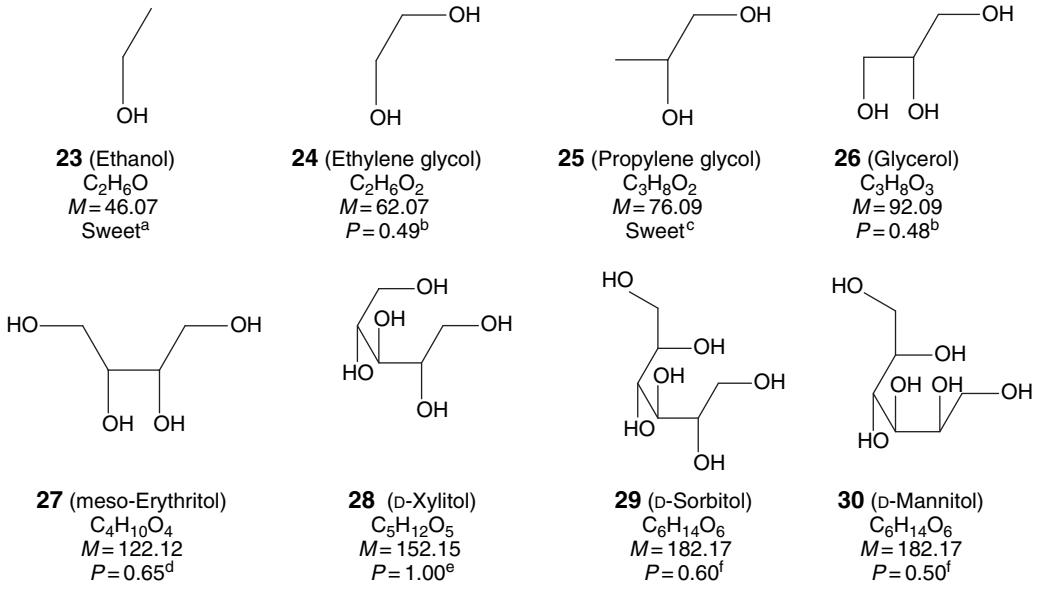

Figure 4 Examples of common polyol sweeteners. [a]Scinska A. *et al*. (2000); [b]Shallenberger R. S. (1993); [c,d]Embuscado M. E. and Patil S. K. (2001); [e]Olinger P. M. and Pepper T. (2001); and [f]Le A. S. and Bowe Mulderrig K. (2001).

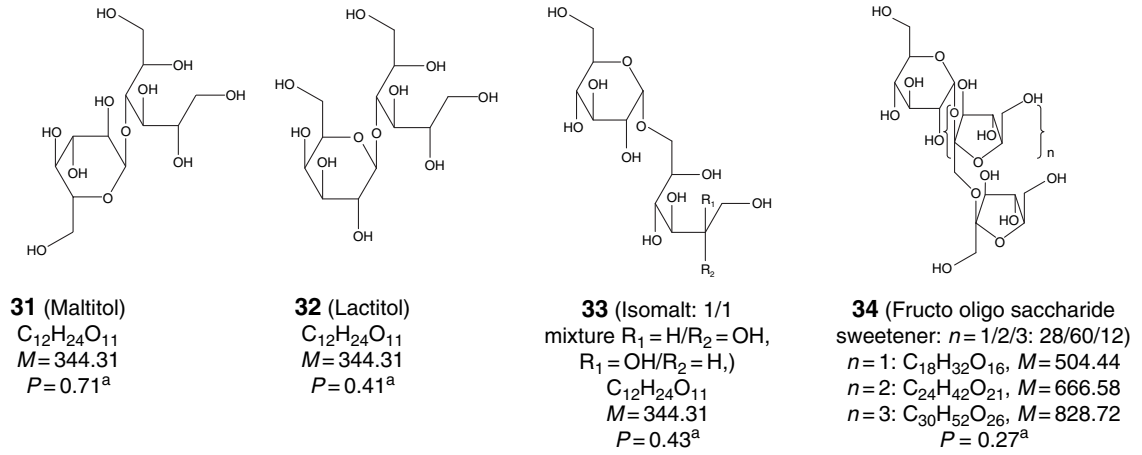

Figure 5 Commercially developed reduced-calorie CHO and polyol sweeteners. [a]DuBois G. E. *et al.* (1991).

empirical formulas, and sweetness potency information, are provided in Figures 7 and 8. Generic and common names are provided for sweeteners which have been commercially developed. The sweeteners are listed in the approximate order of their discovery. Additional information on the discoveries of each of these classes of sweeteners is as follows:

1. *Nitroanilines.* Muspratt J. and Hofmann A. (1846) reported sweet taste for *m*-nitroaniline (**40**) and this is the earliest report, of which the author (GED) is aware, of a compound more potent than common CHO sweeteners. Nearly a century later, the very potent analog P-4000 (**41**) was reported by Blanksma J. J. and van der Weyden P. W. M. (1940) of the Rijks-Universiteit (Leiden, The Netherlands). For many years, P-4000 was the most potent sweetener known.
2. *N-Sulfonyl amides.* Saccharin (**42**) is the first sweetener of this structural type. The sweetness of saccharin was discovered by Constantine Fahlberg in the laboratory of Ira Remsen at Johns Hopkins University (Fahlberg, C. and Remsen, I., 1879) and was commercialized in the United States as the first product of the Monsanto Chemical Company. Much

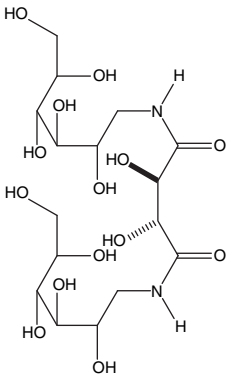

35
$C_{16}H_{32}N_2O_{14}$
$M = 476.43$
$P = 0.46$[a]

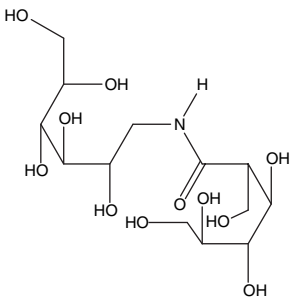

36
$C_{13}H_{27}NO_{11}$
$M = 373.35$
$P = 0.46$[a]

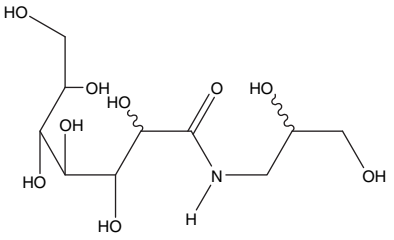

37
$C_{10}H_{21}NO_9$
$M = 299.28$
$P = 0.36$[a]

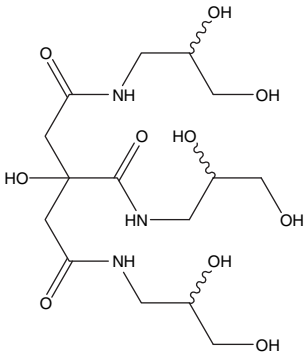

38
$C_{15}H_{29}N_3O_{10}$
$M = 411.40$
$P = 0.36$[a]

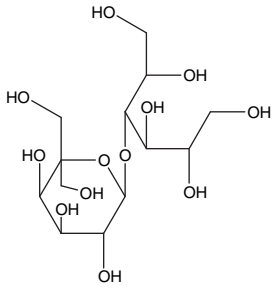

39
$C_{13}H_{26}O_{12}$
$M = 374.34$
$P = 0.50$[b]

Figure 6 Synthetic noncaloric CHO-like sweeteners. [a]DuBois G. E. *et al.* (1992) and [b]Mazur A. W. and Mohlenkamp M. J. (1997).

later, the structurally similar oxathiazinone class of sweeteners was discovered by chemists Clauss K. and Jensen H. (1973) of Hoechst AG and acesulfame (**43**) selected for commercial development. Both saccharin (Na and Ca salts) and acesulfame (K salt) have broad approvals for use in foods and beverages. Also, both sweeteners exhibit significant bitter/metallic off tastes and, for this reason, are almost always blended with other sweeteners.

3. *Aryl ureas.* Berlinerblau J. (1883), in the laboratory of R. Schmitt of Polytechnikum Dresden (Germany), reported the discovery of a series of sweet-tasting aryl ureas. Dulcin (**44**) is the best representative of this structural class of sweeteners which is the third structural class of synthetic sweeteners to be reported. Dulcin was evaluated as a candidate for commercial development but, following the finding of significant toxicity in rat studies at 0.1% of the diet, was not further considered (Fitzhugh, O. G. *et al.*, 1951).
4. *Oximes.* Many oximes have been found to be sweet. The first example was reported by Furukawa S. and Tomizawa Z. (1920). This compound is the oxime (**45**) of perillaldehyde. It was reported to exhibit a sweetness potency of 3400 relative to 9% glucose. Since glucose is 0.6× sucrose in sweetness potency, its sucrose basis sweetness potency is calculated to be $P_w(5.4) = 3400$.
5. *2-Carboxyalkyl benzimidazoles.* Chatterjee B. (1929) of the University of Manchester (Manchester, UK)

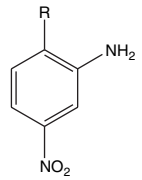

40 (R = H): $C_6H_6N_2O_2$;
M = 138.12; Sweet[a]
41 (R = O-n-Pr; P-4000):
$C_9H_{12}N_2O_2$;
M =180.20; $P_w(1) = 4100$[b]

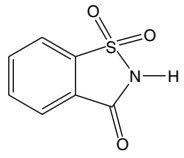

42 (Saccharin)
$C_7H_5NO_3S$
M = 183.18
$P_w(8) = 180$[c]

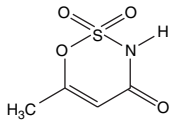

43 (Acesulfame)
$C_4H_5NO_4S$
M = 163.15
$P_w(8) = 76$[c]

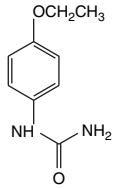

44 (Dulcin)
$C_9H_{12}N_2O_2$
M = 180.20
$P_w(3) = 250$[d]

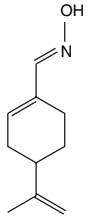

45 (Perillartine)
$C_{10}H_{15}NO$
M = 165.23
$P_w(5.4) = 3400$[e]

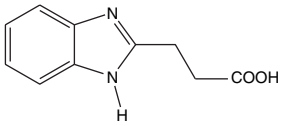

46
$C_{10}H_{10}N_2O_2$
M = 190.20
"Very sweet taste"[f]

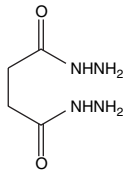

47
$C_4H_{10}N_4O_2$
M = 146.15
Sweet[g]

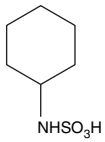

48 (Cyclamic acid)
$C_6H_{13}NO_3S$
M = 179.24
$P_w(8) = 23$[c]

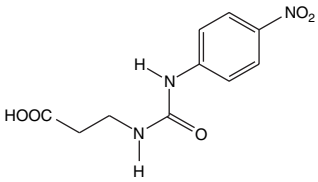

49 (Suosan)
$C_{10}H_{11}N_3O_5$
M = 253.21
Sweet[h]

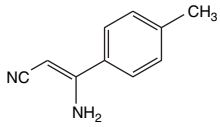

50
$C_{10}H_{10}N_2$
M = 158.20
$P_w(ur) = 700$[i]

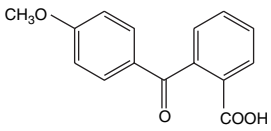

51
$C_{15}H_{12}O_4$
M = 256.25
$P_w(ur) = 150$[j]

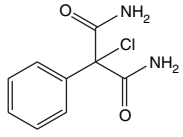

52
$C_9H_9ClN_2O_2$
M = 212.63
$P_w(ur) = 400$[k]

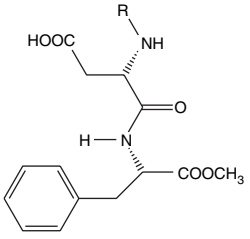

53 (R = H: Aspartame):
$C_{14}H_{18}N_2O_5$;
M = 294.30; $P_w(8)$ = 140[c]

54 (R = $(CH_2)_2C(CH_3)_3$:
Neotame): $C_{20}H_{30}N_2O_5$;
M = 378.46; $P_w(10)$ = 10,000[l]

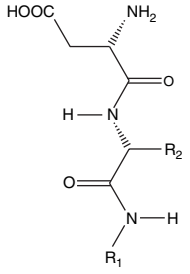

55 (R_1 = c-$(CHC(CH_3)_2SC(CH_3)_2)$,
$R_2 = CH_3$: Alitame):
$C_{14}H_{25}N_3O_4S$; M = 331.43;
$P_w(8) = 2350$[c]

56 (R_1 = (S)-$CH(Ph)CH_2CH_3$,
$R_2 = CH_2CH_3$): $C_{16}H_{23}N_3O_4$;
M = 321.37; $P_w(10) = 2500$[c]

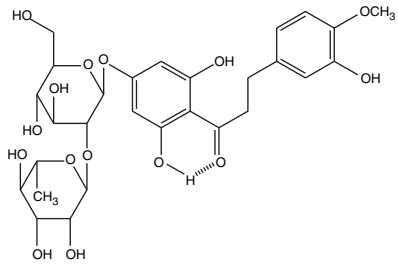

57 (Neohesperidin dihydrochalcone)
$C_{28}H_{36}O_{15}$
M = 612.58
$P_w(8) = 240$[c]

Figure 7 Synthetic noncaloric sweeteners and analogs discovered in the nineteenth and early twentieth centuries. [a]Muspratt J. T. and Hofmann A. W. (1846); [b]Blanksma J. J. and van der Weyden P. W. M. (1940); [c]DuBois G. E. (2000); [d]Berlinerblau J. (1883); [e]Furukawa S. and Tomizawa Z. (1920); [f]Chatterjee B. (1929); [g]DeGraaf H. (1930); [h]Petersen S. and Müller E. (1948); [i]Dornow A. *et al*. (1949); [j]Runti C. and Galimberti S. (1957); [k]Runti C. and Collino F. (1964); and [l]Nofre C. and Tinti J.-M. (2000).

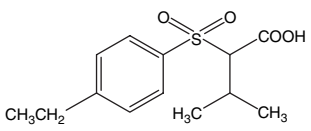

58
$C_{13}H_{18}O_4S$
$M = 270.34$
$P_w(ur) = 220$[a]

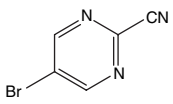

59
$C_5H_2BrN_3$
$M = 183.99$
Sweet[b]

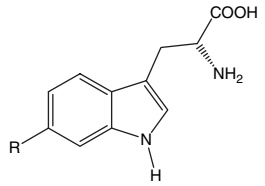

60 (R = H; D-Tryptophan):
$C_{11}H_{12}N_2O_2$; $M = 204.23$;
$P_w(ur) = 35$[c]

61 (R = Cl): $C_{11}H_{11}ClN_2O_2$;
$M = 238.67$; $P_w(10) = 270$[d]

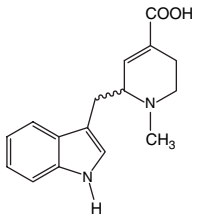

62
$C_{16}H_{18}N_2O_2$
$M = 270.33$
Sweet[e]

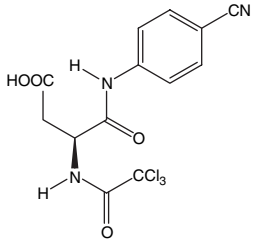

63
$C_{13}H_{10}Cl_3N_3O_4$
$M = 378.60$
$P_w(2) = 3\,000$[f]

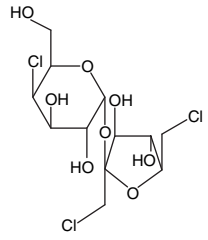

64 (Sucralose)
$C_{12}H_{19}Cl_3O_8$
$M = 397.63$
$P_w(5) = 500$[g]

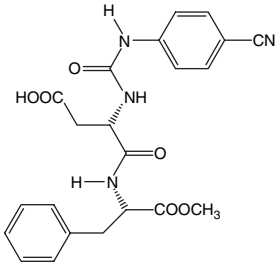

65 (Superaspartame)
$C_{22}H_{22}N_4O_6$
$M = 438.43$
$P_w(2) = 14\,000$[h]

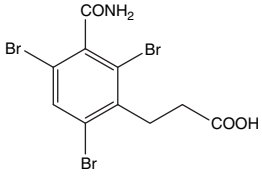

66
$C_{10}H_8Br_3NO_3$
$M = 429.89$
$P_w(5) = 6000–7000$[i]

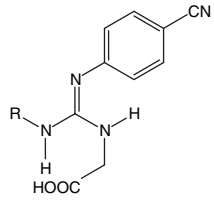

67 (R = (S)-CH(CH$_3$)Ph; SC-45647): $C_{18}H_{18}N_4O_2$;
$M = 322.36$; $P_w(2) = 28\,000$[j]

68 (R = c-C_9H_{17}; Sucrononic acid): $C_{19}H_{26}N_4O_2$;
$M = 342.44$; $P_w(2) = 200\,000$[h]

69 (R = CH(Ph)$_2$); $C_{23}H_{20}N_4O_2$;
$M = 384.43$; $P_w(2) = 200\,000$[k]

Figure 8 Synthetic noncaloric sweeteners and analogs discovered in the late twentieth century. [a]Cram D. J. and Ratajczak A. (1971); [b]Budesinsky Z. and Vavrina J. (1972); [c]Solms J. (1965); [d]Suarez T. *et al*. (1975); [e]Hofmann A. (1972); [f]Lapidus M. and Sweeney M. (1973); [g]Hough L. and Phadnis S. P. (1976); [h]Tinti J.-M. and Nofre C. (1991); [i]Gries H. and Mützel W. (1985); [j]Nofre C. *et al.* (1990); and [k]Nagarajan S. *et al.* (1992).

reported that members of this structural class of compounds show very sweet taste. Exemplary is 2-carboxyethylbenzimidazole (**46**).

6. *Hydrazides*. Simple carboxylic acid hydrazides were discovered to be sweet in taste by DeGraaf H. (1930). Exemplary is the dihydrazide derivative of succinic acid (**47**).
7. *Sulfamates*. The discovery of sweet taste in this structural type of compounds was made by Michael Sveda in the laboratory of Professor L.

Audrieth at the University of Illinois (Audrieth, L. F. and Sveda, M., 1944). The best known sweetener of this structural class is *N*-cyclohexylsulfamic acid (**48**), commercially developed in the sodium and calcium salt forms which are well known as cyclamates. Cyclamates have been widely used in foods and beverages, usually in blends with other noncaloric sweeteners.

8. *Carboxyalkyl aryl ureas*. The discovery of sweet taste in this class of compounds was reported by Petersen S. and Müller E. (1948) of Farbenfabriken Bayer (Leverkusen, Germany). Later, a substantial number of sweet analogs were reported by Tinti J.-M. *et al.* (1982) of the Université Claude Bernard (Lyon, France).
9. *β-Amino cinnamonitriles*. Dornow A. *et al.* (1949) of Institut für Organische Chemie der Technischen Hochschule (Hanover, Germany) reported this structural class of sweeteners which is best exemplified by **50**.
10. *Carboxy benzophenones*. Runti C. and Galimberti S. (1957) of the University of Trieste reported this structural class of sweeteners which is best exemplified by **51**.
11. *Halogenated malonamides*. Runti C. and Collino F. (1964) of the University of Trieste reported this structural class of sweeteners which is best exemplified by **52**.
12. *Dipeptide esters and amides*. This is the structural class of noncaloric sweeteners of greatest commercial significance and is best exemplified by aspartame (**53**). The sweet taste of aspartame was serendipitously discovered in 1965 by James Schlatter in the laboratory of Robert Mazur of Searle Pharmaceutical Company (Mazur, R. H. *et al.*, 1969). Aspartame is unique among synthetic sweeteners as its metabolism leads only to natural amino acids and methanol, all of which are ingested in much higher amounts on consumption of common foods. Neotame (**54**), an analog of aspartame with substantially increased potency, was reported recently by Nofre C. and Tinti J.-M. (2000) of the Université Claude Bernard. It has also been commercially developed. Many dipeptide class sweeteners have been identified since the pioneering work by Mazur and co-workers. Included among such discoveries are the related dipeptide amides, exemplified by alitame (**55**) by Brennan T. M. and Hendrick M. E. (1983) of Pfizer Pharmaceutical Company, and **56** by Sweeny J. G. *et al.* (1995) of The Coca-Cola Company. Alitame has also been commercially developed.
13. *Dihydrochalcones*. Horowitz R. M. and Gentili B. (1969), of the USDA Laboratory (Pasadena, CA), reported the discovery of a series of sweet-tasting dihydrochalcones. The discovery of sweet taste in this series of compounds was particularly unexpected since it was made in a study of bitter taste SAR within flavanoid glycosides which are well known to exhibit potent bitterness. Neohesperidin dihydrochalcone (**57**), the preferred compound in the series, has been commercially developed but has only seen limited use because of sweetness which is noticeably delayed in onset and which lingers very significantly.
14. *Sulfones*. The discovery of sweet taste in this class of compounds, exemplified by **58**, was made by Aleksander Ratajczak in the laboratory of Donald Cram at UCLA (Cram, D. J. and Ratajczak, A., 1971). This class of sweeteners has been described in detail by Polanski J. and Ratajczak A. (1993).
15. *Pyrimidines*. The discovery of potent sweet taste among substituted pyrimidines, exemplified by **59**, was reported by Budesinsky Z. and Vavrina J. of the Research Institute for Pharmacy and Biochemistry (Prague, Czechoslovakia) in 1972.
16. *D-Amino acids*. Many D-amino acids are sweet with the most potent being D-tryptophan (**60**) (Solms, J. *et al.*, 1965). Much more potent substituted analogs were reported by Suarez T. *et al.* (1975) of Eli Lilly Pharmaceutical Company including **61**. And, at about the same time, in a study of lysergic acid derivatives by Hofmann A. (1972) of Sandoz AG (Basel, Switzerland), **62** was reported to be twice as sweet as saccharin.
17. *N′-Acyl-aspartyl-anilides*. The discovery of this structural class of sweeteners, exemplified by **63**, which is clearly related to the carboxyalkyl aryl ureas, was reported by Lapidus M. and Sweeney M. (1973) of Wyeth Laboratories (Philadelphia, PA).
18. *Halogenated sugars*. The discovery of substantial elevation in sweetness potency of sucrose by halogen substitution of sugar hydroxyl groups was first reported by Hough L. and Phadnis S. P. (1976) of the University of London. The most well-known member of this structural class is sucralose (**64**) which has been commercially developed.
19. *Dipeptide ester/carboxyalkyl aryl urea hybrids*. Tinti J.-M. and Nofre C. (1991) of Université Claude Bernard (Lyon, France) reported the discovery

of highly potent hybrids of the dipeptide ester and carboxyalkyl aryl urea classes of sweeteners. Exemplary of such hybrid sweeteners is a compound that they named superaspartame (**65**). This finding strongly suggests that these two classes of sweeteners bind to the sweetener receptor at contiguous and overlapping sites.

20. *Halogenated carboxyalkyl benzamides*. Gries H. and Mützel W. (1985) of Schering Pharmaceutical Company AG (Berlin, Germany) reported the discovery of a highly potent class of substituted benzamides best exemplified by **66**.
21. *Guanidinoacetic acids*. In the mid-1980s, based on modeling made possible by their superaspartame discovery, Nofre C. *et al.* (1990) of the Université Claude Bernard (Lyon, France) discovered the guanidino-acetic acid class of sweeteners. This class is exemplified by SC-45647 (**67**) which has proven useful in mechanistic studies of sweet taste because of its activity in common animal models. It is further exemplified by the more potent sucrononic acid (**68**), also discovered by Nofre and co-workers and **69** discovered by Nagarajan S. *et al.* (1996) of The NutraSweet Company who were in collaboration with the Université Claude Bernard team.

4.02.2.2.3 Natural noncaloric sweeteners

As organic chemists discovered sweet taste in many novel synthetic compounds, they also elucidated the chemical structures of many sweet-tasting compounds found in nature. Natural product structure elucidation was a very difficult process up until the second half of the twentieth century. Although in very significant part, the difficulty in structure elucidation of natural noncaloric sweeteners was due to their structural complexity, the difficulty was also due to the absence of modern spectroscopic and chromatographic methods that now make such structure elucidations routine. What was impossible, or a very challenging task 50 years ago, can now usually be accomplished within a few days. Examples of noncaloric sweeteners found in nature are illustrated in Figures 9–12. Two research groups in particular have been active, beginning in the mid-1970s and continuing up until the mid-1990s, in the elucidation of the structures of natural noncaloric sweeteners. One was an American group led by A. Douglas Kinghorn of the University of Illinois at Chicago. And the second was a Japanese group led by Osamu Tanaka of Hiroshima University. Both groups made major contributions to our understanding of the diversity of potently sweet chemical compounds which exist in nature. The increase in structural complexity between the natural noncaloric sweeteners discussed here and the synthetic noncaloric sweeteners discussed above is noteworthy. A high percentage of the natural noncaloric sweeteners are glycosylated terpenoids or flavanoids, many times with unusual sugars, and still others are proteins. As a result of this structural complexity, economical preparation of natural noncaloric sweeteners by synthetic methods is quite unlikely. Examples of 21 structural classes of natural noncaloric sweeteners along with chemical structures, molecular weights, empirical formulas, and sweetness potency information are provided in Figures 9–12. Information on six protein sweeteners is provided below without structure. Common names are used for sweeteners which have been commercially developed or which, for other reasons, are best known by such names. The sweeteners are listed according to structural class (i.e., terpenoids, flavanoids, etc.). Additional information on the discoveries of each of these natural noncaloric sweeteners is as follows:

1. *Hernandulcin (**70**)*. The only nonglycosylated sweet-tasting sesquiterpenoid identified in nature to date is hernandulcin. Kinghorn and associates (Compadre, C. M. *et al.*, 1987) reported the isolation of hernandulcin from the Mexican plant *Lippia dulcis* Trev. (Verbenaceae).
2. *Pine rosin diterpenoid (**71**)*. One sweet-tasting nonglycosylated diterpenoid natural product has also been reported. Tahara A. *et al.* (1971) of The Institute of Physical and Chemical Research (Saitama-ken, Japan) reported elucidation of the structure of **71**, a potently sweet compound present in pine tree rosin.
3. *Mukuroziosides (**72**)*. A glycosylated sesquiterpenoid exhibiting sweet taste was first identified in *Sapindus mukurossi* Gaertn. (Sapindaceae) by Tanaka and co-workers (Kasai, R. *et al.*, 1986). It is present at high levels in the fruits of this plant and is responsible for its sweetness.
4. *Stevioside (**73**) and rebaudioside A (**74**)*. A total of eight sweet-tasting glycosides of an entkaurene-type diterpenoid known as steviol have been isolated from the plant *Stevia rebaudiana* (Bertoni), indigenous to Paraguay. In the common variety of the plant, stevioside is the most abundant, and rebaudioside A, the second most abundant, steviol glycoside. Several groups have participated in elucidation of the structures of the steviol glycosides

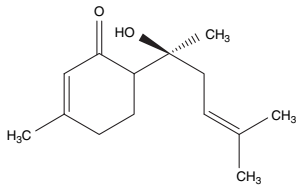

70 (Hernandulcin)
$C_{14}H_{22}O_2$
$M = 222.32$
$P_w(8.6) = 1800$[a]

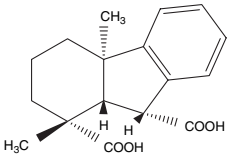

71
$C_{17}H_{20}O_4$
$M = 288.34$
$P_w(1) = 1600$[b]

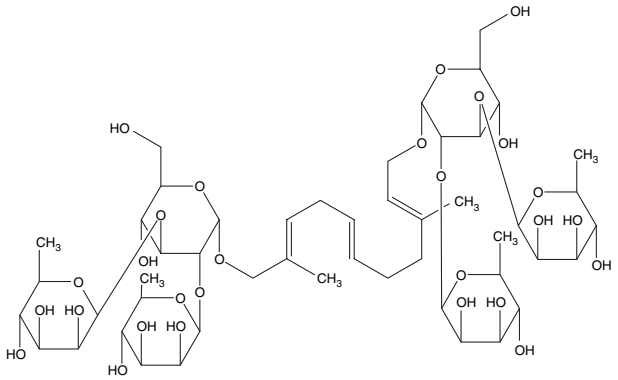

72 (Mukurozioside)
$C_{50}H_{84}O_{27}$
$M = 1117.19$
$P_w(2) = 1$[c]

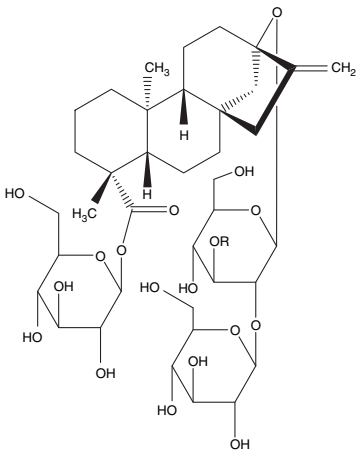

73 (R = H: Stevioside): $C_{38}H_{60}O_{18}$; $M = 804.87$; $P_w(5) = 120$[d]

74 (R = β-D-Glu: Rebaudioside A): $C_{44}H_{70}O_{23}$; $M = 967.01$; $P_w(5) = 250$[d]

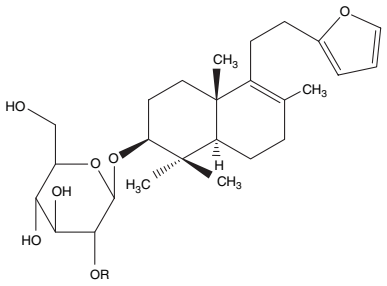

75 (R = β-D-Xyl: Baiyunoside): $C_{31}H_{48}O_{11}$; $M = 596.71$; $P_w(\text{ur}) = 500$[e]

76 (R = α-L-Rham: Phlomisoside I): $C_{32}H_{50}O_{11}$; $M = 610.73$; $P_w(\text{ur}) = 500$[e]

Figure 9 Sesquiterpenoid and diterpenoid natural noncaloric sweeteners. [a]Compadre C. M. *et al.* (1987); [b]Tahara A. *et al.* (1971); [c]Kasai R. *et al.* (1986); [d]DuBois G. E. (2000); and [e]Tanaka T. *et al.* (1983).

and these efforts have been reviewed (Crammer, B. and Ikan, R., 1987; Phillips, K. C., 1987).

5. *Baiyunoside (75) and phlomisoside I (76).* Two sweet-tasting labdane-type diterpenoid glycosides known as baiyunoside and phlomisoside were isolated from the Chinese plant *Phlomis betonicoides* Diels (Labiatae) by Tanaka T. *et al.* (1983; 1985).
6. *Glycyrrhizic acid (77).* The structure elucidation of the sweet-tasting triterpenoid glycoside known as glycyrrhizic acid, isolated from the European and central Asian shrub *Glycyrrhiza glabra* L. (Fabaceae), was completed by Lythgoe B. and Trippett S. (1950) of Cambridge University. The crude extract of this plant is known as licorice.

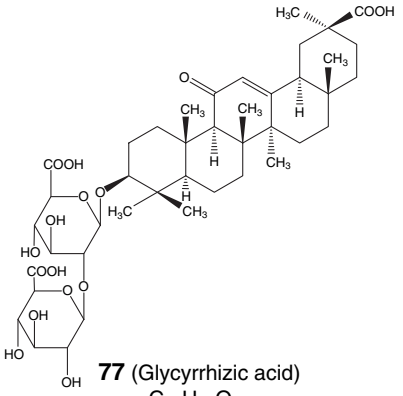

77 (Glycyrrhizic acid)
$C_{42}H_{62}O_{16}$
$M = 822.93$
$P_w(10) = 33$[a]

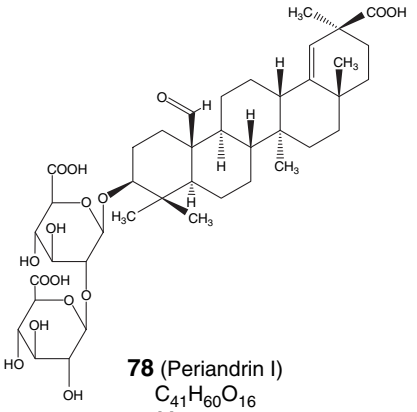

78 (Periandrin I)
$C_{41}H_{60}O_{16}$
$M = 808.91$
$P_w(0.9) = 90$[b]

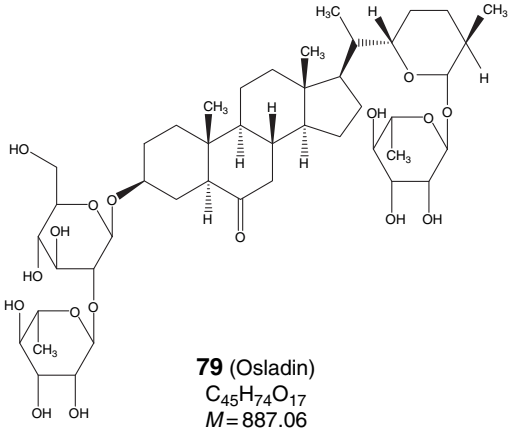

79 (Osladin)
$C_{45}H_{74}O_{17}$
$M = 887.06$
$P_w(ur) = 500$[c]

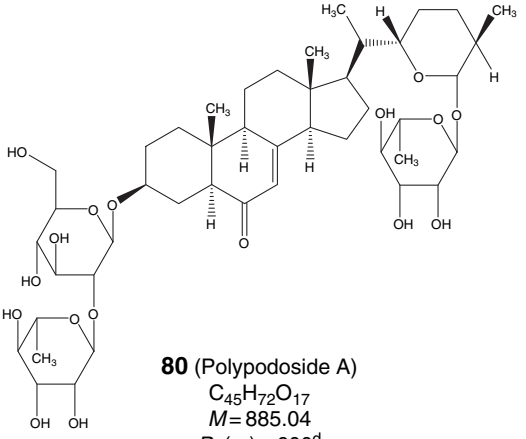

80 (Polypodoside A)
$C_{45}H_{72}O_{17}$
$M = 885.04$
$P_w(ur) = 600$[d]

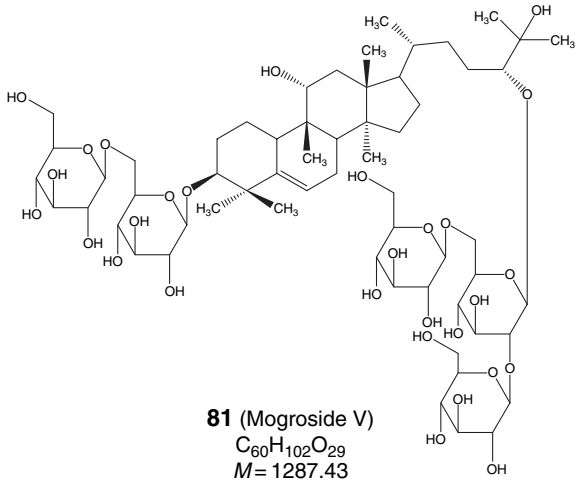

81 (Mogroside V)
$C_{60}H_{102}O_{29}$
$M = 1287.43$
$P_w(ur) = 250\text{-}425$[e]

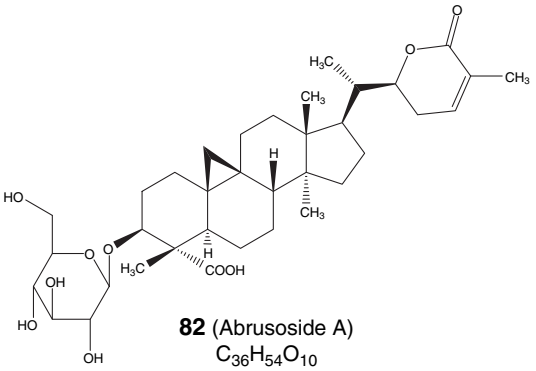

82 (Abrusoside A)
$C_{36}H_{54}O_{10}$
$M = 646.81$
$P_w(2) = 30$[f]

Figure 10 (Continued)

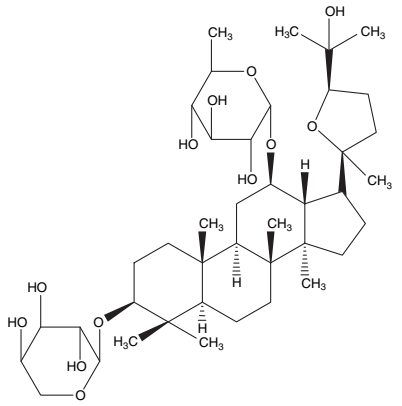

83 (Cyclocarioside I)
$C_{41}H_{70}O_{12}$
$M = 754.99$
$P_w(ur) = 250$[g]

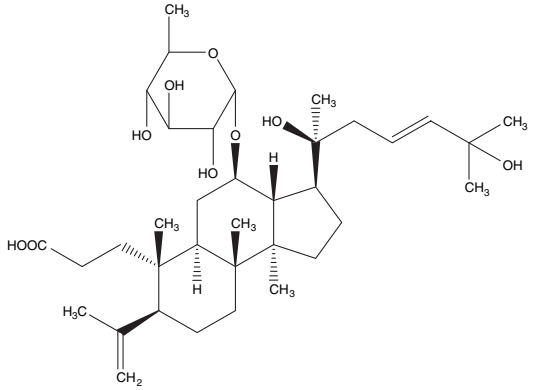

84 (Pterocaryoside A)
$C_{36}H_{60}O_9$
$M = 636.86$
$P_w(ur) = 50$[h]

Figure 10 Triterpenoid natural noncaloric sweeteners. [a]DuBois G. E. (2000); [b]Hashimoto Y. *et al.* (1980); [c]Nishizawa M. and Yamada H. (1996); [d]Kim J. *et al.* (1988); [e]Kasai R. *et al.* (1989); [f]Choi Y.-H. *et al.* (1989); [g]Shu R. G. *et al.* (1995); and [h]Kennelly E. J. *et al.* (1995).

Glycyrrhizic acid is commercially available as the monoammonium salt and is characterized as exhibiting sweetness with a notable delay in onset and with a long linger. Glycyrrhizic acid and its salts have approval for use as flavors in the United States.

7. *Periandrin I (**78**).* The structure elucidation of the sweet-tasting triterpenoid glycosides known as the periandrins I–IV, isolated from the Brazilian plant *Periandra dulcis* Mart. (Leguminosae), was completed by Hashimoto Y. *et al.* (1980) of Kobe Women's College of Pharmacy in the early 1980s. The taste properties of the periandrins are similar to those of glycyrrhizic acid.
8. *Osladin (**79**).* The structure elucidation of the sweet-tasting triterpenoid glycoside known as osladin, isolated from the rhizomes of the fern *Polypodium vulgare* L. (Polypodiaceae), was only completed recently following an X-ray crystal structure determination by Nishizawa M. and Yamada H. (1996).
9. *Polypodoside A (**80**).* The structure elucidation of the sweet-tasting triterpenoid glycosides polypodosides A and B isolated from the North American fern *Polypodium glycyrrhiza* DC. Eaton (Polypodiaceae) was completed by Kinghorn and co-workers (Kim, J. *et al.*, 1988).
10. *Mogroside V (**81**).* The structure elucidation of the sweet-tasting cucurbitane-type triterpenoid glycosides mogrosides IV and V isolated from the Chinese medicinal plant known as Luo Han Guo (*Siraitia grosvenorii* (Swingle) C. Jeffrey) was completed by Tanaka and co-workers in the late 1980s (Kasai, R. *et al.*, 1989; Matsumoto, K. *et al.*, 1990). Extracts of this plant are in common use in China and recently, a concentrate from the fruit of this plant has been commercially developed by Procter & Gamble for use in formulation of reduced-calorie beverages.
11. *Abrusoside A (**82**).* The structure elucidation of the sweet-tasting cycloartenol-type triterpenoid glycoside abrusoside A isolated from *Abrus precatorius* L. (Leguminosae) was completed by Kinghorn and co-workers (Choi, Y.-H. *et al.*, 1989).
12. *Cyclocarioside I (**83**).* The structure elucidation of the sweet-tasting dammarane-type triterpenoid glycoside cyclocarioside I, isolated from the leaves of the Chinese plant *Cyclocarya paliurus* Batal. Iljinsk (Juglandaceae) was completed by Shu R. G. *et al.* (1995) of Jiangxi College of Traditional Chinese Medicine. This plant is said to be used in China for the treatment of diabetes.
13. *Pterocaryoside A (**84**).* The structure elucidation of the sweet-tasting secodammarane-type triterpenoid glycosides pterocaryosides A and B, isolated from the leaves of *Pterocarya paliurus* Batal. (Juglandaceae) was reported by Kinghorn and co-workers (Kennelly, E. J. *et al.*, 1995). The leaves of this plant are used in China to sweeten foods.

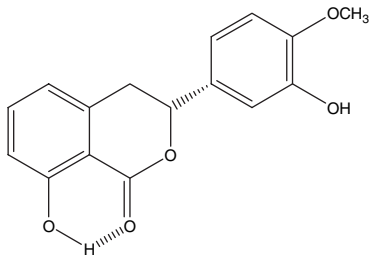

85 (Phyllodulcin)
$C_{16}H_{14}O_5$
$M = 286.28$
$P_w(3) = 400$[a]

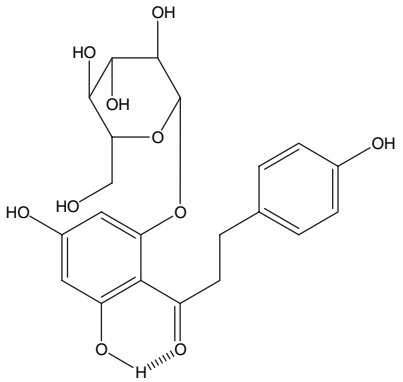

86 (Phloridzin)
$C_{21}H_{24}O_{10}$
$M = 436.41$
Sweet[b]

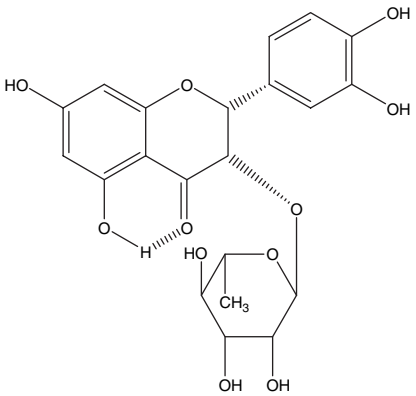

87 (Neoastilbin)
$C_{21}H_{22}O_{11}$
$M = 450.39$
Sweet[c]

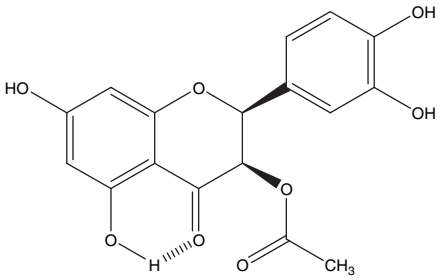

88
$C_{17}H_{14}O_8$
$M = 346.29$
$P_w(2) = 80$[d]

Figure 11 Naturally occuring dihydroisocoumarin, dihydrochalcone, and flavanone noncaloric sweeteners. [a]Arakawa H. and Nakazaki M. (1959); [b]Tanaka T. *et al.* (1982); [c]Kasai R. *et al.* (1988); and [d]Nanayakkara N. P. D. *et al.* (1988).

14. *Phyllodulcin (85).* The structure elucidation of the sweet-tasting 3,4-dihydroisocoumarin-type polyketide isolated from the leaves of *Hydrangea macrophylla* Seringe var. *thunbergii* (Siebold) Makino (Saxifragaceae) was completed by Arakawa H. and Nakazaki M. (1959) of Osaka City University. Extracts of the leaves of this plant are used in Japan to make a sweet tea at a festival known as Hamatsuri, a celebration of Buddha's birth.
15. *Phloridzin (86).* The sweet-tasting dihydrochalcone glycoside phloridzin is present in many parts of apple trees except for the mature fruit. Its structure was elucidated and first isolated from the leaves of *Symplocos lancitolia* Sieb. by Tanaka T. *et al.* (1982).
16. *Neoastilbin (87).* The flavanone glycoside neoastilbin is reported to be the sweet-tasting component in the leaves of *Engelhardtia chrysolepis* Hance (Juglandaceae), a tree which grows in a subtropical region of China. Its structure was elucidated by Tanaka and co-workers (Kasai, R. *et al.*, 1988).
17. *[2(R),3(R)]-Dihydroquercetin-3-O-acetate (88).* The structure elucidation of this sweet-tasting flavanone, isolated from *Tessaria dodoneifolia* (Hook

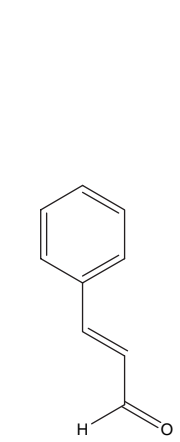

89 (Cinnamaldehyde)
C_9H_8O
$M = 132.16$
Sweet[a]

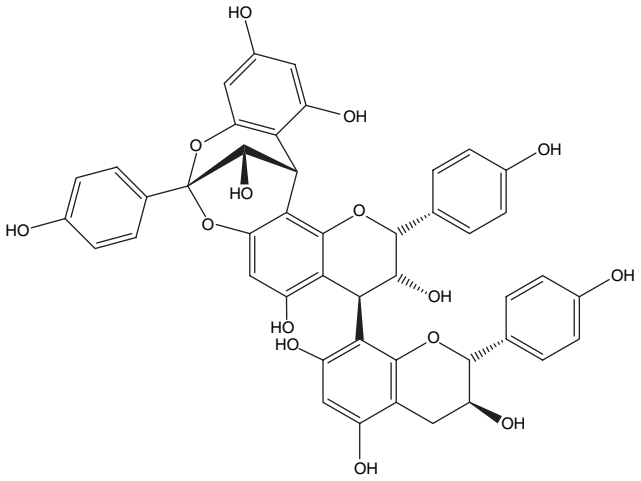

90 (Selligueain A)
$C_{45}H_{36}O_{15}$
$M = 816.76$
$P_w(2) = 35$[b]

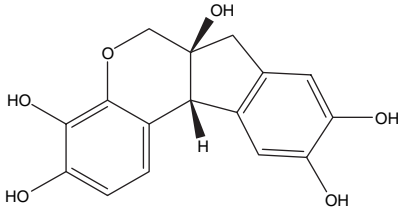

91 (Hematoxylin)
$C_{16}H_{14}O_6$
$M = 302.28$
$P_w(3) = 120$[c]

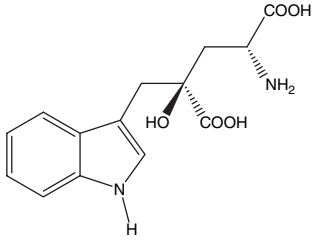

92 ((2R, 4R)-Monatin)
$C_{14}H_{16}N_2O_5$
$M = 292.29$
$P_w(5) = 2700$[d]

Figure 12 Phenylpropanoid, proanthocyanidin, benzo-[*b*]-indeno-[*1,2-d*]-pyran, and amino acid natural noncaloric sweeteners. [a]Hussain R. A. (1990); [b]Baek N.-I. *et al.* (1993); [c]Masuda H. *et al.* (1991); and [d]Bassoli A. *et al.* (2005).

and Arn.) Cabrera (Compositae), a plant indigenous to Paraguay, was reported by Kinghorn and co-workers (Nanayakkara, N. P. D. *et al.*, 1988).

18. *Cinnamaldehyde (**89**).* *trans*-Cinnamaldehyde was identified as the sweet-tasting component in *Cinnamomum osmophloeum* Kanehira (Lauraceae) by Kinghorn and co-workers (Hussain, R. A. *et al.*, 1990).
19. *Selligueain A (**90**).* The structure elucidation of the sweet-tasting proanthocyanidin selligueain A, following isolation from the rhizomes of the Indonesian fern *Selliguea feei* Bory (Polypodiaceae), was reported by Kinghorn and co-workers (Baek, N.-I. *et al.*, 1993).
20. *Hematoxylin (**91**).* The benzo[*b*]indeno[1,2-*d*]pyran hematoxylin is reported to be the sweet-tasting component in an extract of the heartwood of *Haematoxylon campechianum* L. (Leguminosaeae). Its structure was elucidated by Tanaka and co-workers (Masuda, H. *et al.*, 1991). This compound had been used as a microbiological staining agent but was not previously recognized to be sweet.
21. *Monatin (**92**).* The sweet-tasting amino acid monatin was isolated from the roots of the African plant *Schlerochiton ilicifolius* A. Meeuse (Acanthaceae). The structure of monatin was reported by Louis Ackerman and co-workers of the University of Pretoria (Pretoria, South Africa) (Vleggaar, R. *et al.*, 1992). In later work by Bassoli A. *et al.* (2005) of the University of Milan, it was found that all four stereoisomers are present in an extract

of the natural source, that all four stereoisomers exhibit sweetness, but that the most potent stereoisomer is the 2*R*/4*R* form.

22. *Thaumatin (93).* The sweet-tasting component in the berries of the West African plant *Thaumatococcus danielli* Benth, locally known as katempfe berries, was first isolated by van der Wel H. (1972) at Unilever and shown to be a protein. This protein called thaumatin was later shown to be a mixture of at least four similar 207 amino acid proteins. Thaumatin I, one of the two major forms, has $M = 22\,206$. The crystal structure of thaumatin was determined by Sung-Hou Kim and co-workers at the University of California at Berkeley (de Vos, A. M. *et al.*, 1985). Thaumatin exhibits potent sweetness [$P_w(10) = 1600$] with a notable delay in onset and with a very pronounced sweetness linger (DuBois, G. E., 2000).
23. *Monellin (94).* The sweet-tasting component in the berries of the West African plant *Dioscoreophyllum cumminsii*, also known as the serendipity berry, was first isolated by Morris J. A. and Cagan R. H. (1972) at Monell Chemical Senses Center and shown to be a protein. Monellin consists of two separate peptide chains, the A chain of 45 and the B chain of 50 amino acid residues, which are associated noncovalently with each other and has $M = 11\,086$. And the crystal structure was determined by Sung-Hou Kim and co-workers at the University of California at Berkeley (Ogata, C. *et al.*, 1987). Like thaumatin, monellin exhibits potent sweetness [$P_w(\text{ur}) = 3000$] with a notable delay in onset and with a very pronounced sweetness linger.
24. *Mabinlin (95).* The sweet-tasting component in the seeds of the Chinese plant *Capparis masaikai* Levl. (Capparidaceae) was shown to be a mixture of two proteins known as mabinlins I and II. In work by Masanori Kohmura and Yasuo Ariyoshi of Ajinomoto Company (1998), mabinlin II was determined to be composed of an A chain (33 amino acids) and a B chain (72 amino acids) which are connected via disulfide linkages. It was determined to have $M = 12\,441$ and sweetness recognition threshold of 0.1%. Since the threshold for sucrose sweetness recognition is *c.* 0.5%, it is only slightly more potent than sucrose.
25. *Brazzein (96).* The sweet-tasting component in the fruits of the African climbing vine *Pentadiplandra brazzeana* Baillon (Pentadiplandraceae) was demonstrated by Ming D. and Hellekant G. (1994) of the University of Wisconsin to be a 54 amino acid residue protein with $M = 6473$ and $P_w(2) = 2000$.
26. *Miraculin (97).* A protein isolated from the fruits of the African plant *Richardella dulcifica* (Schum. et Thonn.) Baehni (Sapotaceae), often referred to as miracle fruit, is known as miraculin and was first shown to be a protein by Kurihara K. and Beidler L. (1968) of Florida State University. This protein, having $M = c.\ 24\,000$, is not sweet at all but, interestingly, causes sour solutions to taste sweet.
27. *Curculin (98).* The sweet-tasting component in the fruit of the Malaysian plant *Curculigo latifolia* was shown by Yoshie Kurihara and co-workers of Yokohama University to be a dimer of a 114 amino acid polypeptide ($M = 24\,734$) (Yamashita, H. *et al.*, 1990). They named this protein curculin. Curculin, in addition to being a sweetener, causes sour solutions to taste sweet and also causes water to taste sweet. Curculin exhibits $P_w(6.8) = 550$.

4.02.2.2.4 Sweet-tasting minerals

Sweet taste is not limited to organic chemicals. Many inorganic salts are also known to exhibit sweet taste. Since the late 1800s, there have been many reports of sweet taste among inorganic salts and this topic has been reviewed by Shallenberger R. S. (1993). Sweet taste has been generally reported for alkali metal salts. As example, for NaCl, von Skramlik E. reported (1926) that its taste changes from tasteless at 9 mM, to slightly sweet at 10 mM, to sweet at 20 mM, to strongly sweet at 30 mM, to salty sweet at 40 mM to salty at 50 mM. In more recent work on the sweet taste of NaCl, Bartoshuk L. M. *et al.* (1978) of Yale University confirmed the presence of sweet taste but found that its observation is dependent on adaptation of the sensory system to water before tasting. Work in the author's laboratory (GED) is in general agreement with the reports of sweet taste for NaCl and other salts except that the sweetness observed is only weak before saltiness dominates the overall taste quality. Many other salts are known to exhibit sweet taste including beryllium (II) and lead (II) salts. Little analysis of the sweetness potencies of these salts appears to have been done, no doubt because of their significant toxicities. Rare earth salts, specifically $LaCl_3$, $TbCl_3$, and $EuCl_3$, have been observed to be potently sweet in the author's laboratory. All exhibit similar sweetness potencies [$P_w(5) = c.\ 100$] but are disadvantaged in that they

are strongly astringent as well as bitter in taste (DuBois, G. E., 2003).

4.02.2.3 Sensory Properties of Sweeteners

As is clear from the discussion above in II. A-D, many, many chemical compounds exhibit sweet taste. However, because of their natural occurrence in common fruits and vegetables, CHO sweeteners, and sucrose in particular, have become the consumer's standards for sweet taste. And it has been found that the synthetic and natural noncaloric sweeteners exhibit sweet tastes that differ from the tastes of CHO sweeteners in several ways. Principal differences include the following:

4.02.2.3.1 Concentration/response functions

Over the years, it has become common practice to define the sweetness potencies of sweeteners relative to sucrose as a reference. In doing so, the author (GED) *et al.* (1990) of The NutraSweet Company reported the finding that CHO sweetener potencies are independent of sucrose reference concentration while, in contrast, all synthetic and natural noncaloric sweeteners are strongly dependent on sucrose reference concentration. And it was demonstrated that the concentration/response (C/R) functions, where R is in units of percent sucrose equivalents, for all synthetic and natural noncaloric sweeteners are well modeled by the law of mass action $R = R_m C/(k_d + C)$, where R_m is the maximal response and k_d is the apparent sweetener/receptor dissociation constant. From these findings, the conclusion was drawn that all CHO sweeteners have a common R_m while all synthetic and natural noncaloric sweeteners have lower R_ms. Although other interpretations are possible, the data are consistent with the idea that all noncaloric sweeteners are partial agonists relative to CHO sweeteners. Exemplary of C/R function behavior of noncaloric sweeteners are the C/R functions for sodium saccharin and sodium cyclamate which are illustrated in Figure 13.

4.02.2.3.2 Flavor profiles

In general, CHO sweeteners exhibit clean sweet tastes without bitter, sour, salty, or savory taste attributes. This is not generally the case, however, for synthetic and natural noncaloric sweeteners. In fact, clean sweet taste is the exception rather than the rule for noncaloric sweeteners. Bitter off taste is a common off taste among noncaloric sweeteners and is particularly noticeable in saccharin. It has now been demonstrated that the bitter off taste of saccharin is due to activation of specific bitterant receptors (Pronin, A. N. *et al.*, 2004). Exemplary of flavor profiles for noncaloric sweeteners are the flavor profiles for sodium saccharin and sodium cyclamate which are illustrated in Figure 14.

4.02.2.3.3 Temporal profiles

CHO sweeteners exhibit rapid onset of sweet taste and sweetness which dissipates relatively quickly. In general, all synthetic and natural noncaloric sweeteners exhibit sweet tastes which develop more slowly and which then dissipate more slowly, oftentimes very slowly. In a very recent report, Michael Naim and co-workers of Hebrew University speculate that the lingering sweetness character of many noncaloric sweeteners may be due to inhibition of a specific G-protein receptor kinase which is responsible for termination of receptor signaling (Zubare-Samuelov, M. *et al.*, 2005). Although this is a possible explanation, the cause of the atypical temporal profiles of noncaloric sweeteners remains to be determined with certainty.

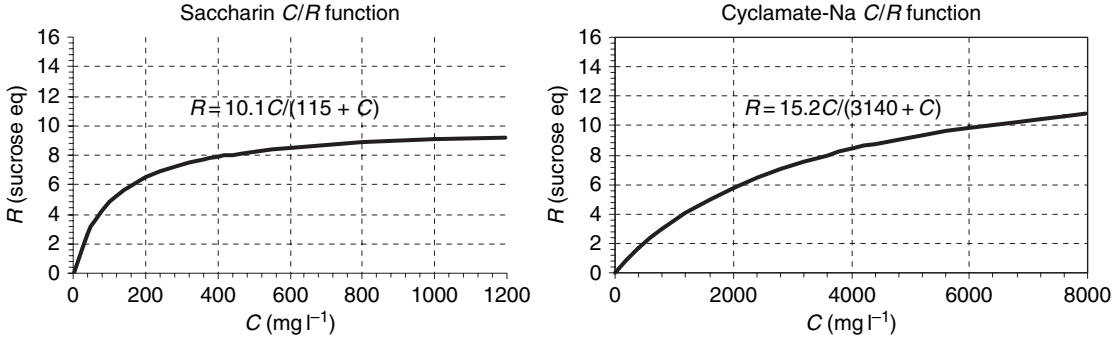

Figure 13 Concentration/response functions for sodium saccharin and sodium cyclamate.

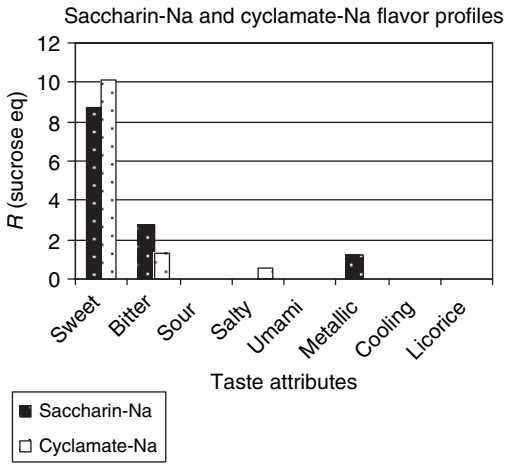

Figure 14 Comparison of flavor profiles of sodium saccharin and sodium cyclamate.

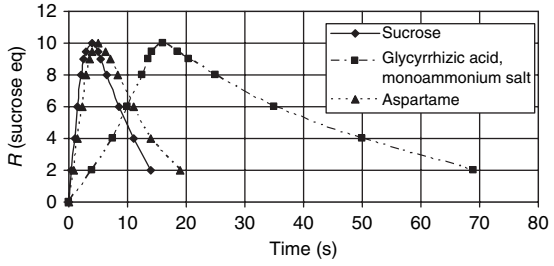

Figure 15 Comparison of temporal profiles of sucrose, aspartame, and monoammonium glycyrrhizinate.

Exemplary of temporal profiles for noncaloric sweeteners are the temporal profiles for sucrose, aspartame, and monoammonium glycyrrhizinate which are illustrated in Figure 15.

4.02.2.3.4 Adaptation

If a CHO sweetener is tasted iteratively over a short period of time, little change in sweetness intensity is noted. However, synthetic and natural noncaloric sweeteners exhibit significant decrements in perceived sweetness. The sensory system appears to desensitize to the noncaloric sweeteners to a much greater extent than is the case for CHO sweeteners. It is generally true that signaling from GPCRs is terminated by receptor phosphorylation by specific intracellular kinases. However, even if this is the case with the sweetener receptor, it is not clear as to why the desensitization following receptor activation with noncaloric sweeteners should exceed that promoted by CHO sweeteners. Exemplary of the desensitization differences between CHO sweeteners and noncaloric sweeteners are the sensory panel estimates of sweetness intensity on iterative tasting of cola beverages sweetened with HFSS, aspartame, and an aryl urea type sweetener as is illustrated in Figure 16.

4.02.3 Bitter-Tasting Stimuli

It is generally accepted that the sense of bitter taste evolved as a mechanism whereby potentially toxic substances could be avoided. In fact, a great many natural and synthetic chemical compounds which exhibit toxicity are bitter in taste at some concentration. It is not apparent, however, that thresholds for bitter taste correlate well with thresholds for toxicity. And many perfectly safe naturally occurring compounds exhibit bitterness (e.g., caffeine and quinine) and provide desirable sensory attributes to foods and beverages. Still other bitter compounds (e.g., vitamins, minerals, and bioflavonoids) provide nutritional benefits. Another confounding factor is that some very toxic compounds (e.g., lead salts and beryllium salts) are not bitter and, to the contrary, are sweet. As a bottom line, bitter taste sensation, at best, may only be considered as a first line of defense against ingestion of toxic chemical compounds.

4.02.3.1 Biochemistry of Bitter Taste

A great deal of work has been done to elucidate the biochemical pathways that mediate the sense of bitter taste. And while a historical summary of this work is beyond the scope of this review, a few key discoveries will be pointed out preliminarily to a concise discussion of the current understanding of the biochemistry of bitter taste. Many reviews of the older literature are available and included among them are Belitz H. D. *et al.* (1985), Shallenberger R. S. (1993), Beauchamp G. K. (1994), and Roy G. (1997). In our view, the SAR for bitter-tasting compounds can only be appreciated after the mechanistic pathways that mediate bitter taste are understood.

Chemists have long been fascinated with the very high level of structural diversity among bitter-tasting chemical compounds. And, at least in part, because of this extraordinary diversity, Spielman A. I. *et al.*, (1992) had already concluded by the early 1990s that multiple mechanistic pathways must be involved. Also in the early 1990s, support was provided that bitter taste, at least for

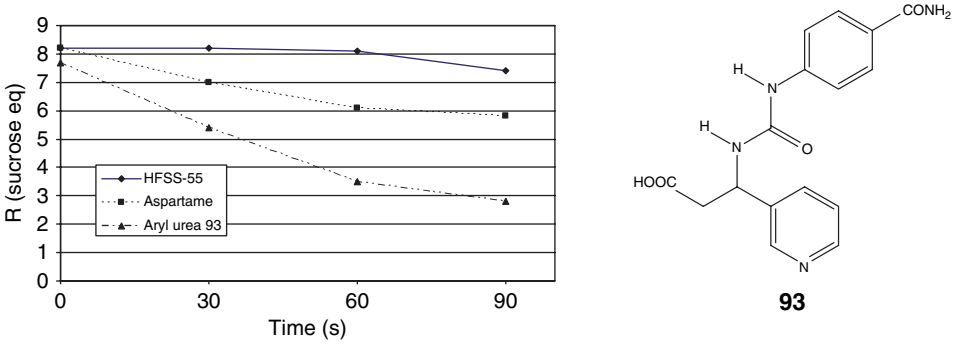

Figure 16 Comparison of the rates of sensory desensitization to HFSS-55, aspartame, and *N*-(4-carboxamidophenyl)-*N*′-(1-(3-pyridyl)-2-carboxy)-ethyl-urea (**93**) in a cola beverage system.

many compounds, must be mediated by one or more GPCRs. The support for GPCR involvement was the discovery of the G-protein gustducin and the demonstration that mice lacking gustducin could not detect common bitterants (Margolskee, R. L., 2004). The major breakthrough in understanding the biochemistry of bitter taste did not occur, however, until 2000. At this time, mouse and human genomic analysis led to the discovery of families of GPCRs referred to as T2Rs and these receptors were shown to be mediators of bitter taste signaling (Adler, E. *et al.*, 2000; Chandrashekar, J. *et al.*, 2000; Matsunami, H. *et al.*, 2000). More recently, comprehensive analysis of the human genome led to the conclusion that human bitter taste is mediated by a family of 25 T2Rs which are all expressed in the same subset of TBCs (Pronin, A. N. *et al.*, 2004). And, at the present time, substantial efforts are in place to identify the ligands which activate these 25 T2Rs, a process commonly referred to as deorphanization. Results to date include the finding (Bufe, B. *et al.*, 2002) that T2R16 mediates the activities of bitter glucopyranosides such as salicin and that T2R10 mediates the activity of strychnine. Additional findings (Pronin, A. N. *et al.*, 2004) include that T2R44 is activated by denatonium chloride and 6-nitrosaccharin and that T2R61 is activated by 6-nitrosaccharin. Extensive work is underway at this time to deorphanize all of the bitterant receptors. The finding that T2R44 responds to bitterants as diverse in structure as 6-nitrosaccharin and denatonium chloride, however, merits comment. It seems highly likely that bitter compounds will activate multiple receptors and the exception will be that a particular bitterant will activate a single T2R. And, in this sense, the bitter taste system may be similar to the olfactory system where individual odorants typically activate multiple members of the set of 350–400 human olfactory receptors. The T2Rs and olfactory receptors are similar in structure, all being family A GPCRs, and are thought to bind their ligands at conserved agonist binding sites within the TMD. It should also be noted that while the primary structures of the T2Rs are known, the structures of the functional bitterant receptors are not. The principal complication is that many GPCRs exist in dimeric and perhaps even oligomeric forms (Breitwieser, G. E., 2004). If the bitterant receptors are dimeric, are they limited to homodimers or are they heterodimeric as well? If they are only homodimeric, then 25 T2Rs will enable formation of 25 $(T2R)_2$ receptors. If, however, all possible heterodimeric receptors form as well, the number of functional receptors will be 325. In view of the highly diverse relationship between chemical structure and bitter taste, such a large number of bitterant receptors would not be a surprise.

So, it appears that the dominant pathway for initiation of the bitter taste signaling process is activation of one or more T2Rs. The next question is how do activated T2Rs excite TBCs? As already noted, the G-protein gustducin is required for TBC responses to bitterants. And so, the question really is, how does activated gustducin lead to TBC excitation? The answer began to emerge in 2002 in work done in the Margolskee laboratory (Pérez, C. A. *et al.*, 2002). In differential cDNA screening experiments in mouse TBCs, they found the common expression of several transduction elements including the α subunit of gustducin ($G_{\alpha gust}$), the G-protein subunit $G_{\gamma 13}$, the enzyme phospholipase $C_{\beta 2}$ ($PLC_{\beta 2}$), the inositol 1,4,5-trisphosphate (IP_3) receptor type III (IP_3R3), and the TRP m5

ion channel (TRPM5). And they proposed that activated gustducin initiates a cascade of reactions as follows:

1. activation of $PLC_{\beta 2}$ to convert phosphatidylinositol to IP_3,
2. action by IP_3 at its intracellular receptor IP_3R3 to promote release of Ca^{2+} from intracellular storage vesicles, and
3. Ca^{2+} binding to an intracellular site on the ion channel TRPM5 causing the channel to open allowing cations to enter the cell, thus causing the depolarization requisite for TBC excitation.

Strong support for this proposal was provided by a collaborative team from the Charles Zuker and Nicholds Ryba laboratories (Zhang, Y. *et al.*, 2003) that developed strains of mice in which expression of $PLC_{\beta 2}$ and TRPM5, respectively, were knocked out. The strain lacking $PLC_{\beta 2}$ was demonstrated to be incapable of responding to any of bitter, sweet, or umami taste stimuli. The same finding was made with the strain lacking TRPM5. This work demonstrated that responses to sweet, bitter, and umami stimuli are transduced by a common pathway and suggested that their signaling must be initiated by separate subsets of TBCs. This was demonstrated to be the case by developing a strain of mice from a $PLC_{\beta 2}$ knockout strain in which $PLC_{\beta 2}$ function was restored only in bitterant receptor expressing cells. These mice were found to have sensitivity to bitter stimuli but not to sweet or umami stimuli. Thus, it appears that coding of taste quality occurs at the cellular level. And therefore, some TBCs are sweetener sensors, some bitterant sensors and some umami sensors. This finding is consistent with work by Hellekant G. *et al.* (1997) showing that chimpanzee single CT nerve fibers emanating from taste buds show strong taste modality specificity. In general, fibers responding to the bitterants caffeine, quinine HCl, and denatonium benzoate were unresponsive to sucrose and fructose (sweet), citric acid (sour), NaCl (salty), and monosodium glutamate (umami). So, as a bottom line, some TBCs are bitterant-specific and they communicate with the brain via labeled lines so as to preserve their sensory quality coding.

Given that bitter taste may result from activation of any of 25, or even as many as 325, bitterant receptors in the bitter-sensitive subset of TBCs, it is obvious that a very broad bitterant SAR is to be expected. A finding that leads to the expectation of an even more diverse bitterant SAR is the observation that at least some bitter-tasting compounds readily cross the membranes of TBCs on a time scale consistent with the taste experience (Naim, M. *et al.*, 2002). Specifically the bitterants quinine and c-(Leu-Trp) were shown to readily accumulate at significant levels in TBCs within 1–2 s. As a result of these findings, Naim and coworkers speculated that many bitterants may initiate their effects at intracellular sites in the bitter-sensitive TBC activation cascade. In support of this idea, further work with TRPM5 (Damak, S. *et al.*, 2006) and $PLC_{\beta 2}$ (Dotson *et al.*, 2005) knockout mice indicates that other sites could be involved in bitter signaling as these mice show some aversive responses at high concentrations of bitter compounds. In summary, for bitter taste, we have 25 bitterant receptors and at least 4 major intracellular components (i.e., gustducin, $PLC_{\beta 2}$, IP_3R3, and TRPM5) that, in principle, may be sites of action for bitter-tasting chemical compounds. Without any knowledge of the SAR of bitterant compounds, the biochemistry of bitterant taste leads to the expectation of an extraordinarily diverse SAR.

As has already been noted, the bitterant SAR is an extraordinary diverse relationship as may be understood now based on the biochemistry of bitter taste. Volumes could be filled with the chemical structures of compounds reported to exhibit bitter taste. As a bottom line, it appears that bitter taste is the default taste. Thus as a general rule, if a compound's taste is not sweet, umami, sour, or salty, it will be bitter. The only factor in question is bitterness potency. Clearly, since bitterness is mediated by a family of membrane receptors, and probably by intracellular effectors as well, some bitterants will have high receptor affinities and some will not, thus resulting in a range of potencies. While this general rule is consistent with empirical observations on taste, poorly soluble compounds may appear to be exceptions. Clearly, in order to activate receptors, compounds must be in solution at sufficiently high concentration to reach their taste detection thresholds. And some apparently tasteless compounds are probably tasteless only because they are insufficiently soluble to initiate a threshold level of receptor activation. In such series of compounds, analogs of the poorly soluble compounds with higher solubility always exhibit taste and, almost always, it is bitter taste.

Interestingly, for some compounds thought to be purely sweet in taste, desensitization to sweet taste leads to bitterness perception (DuBois, G., 1985). It seems possible that signaling by sweet-sensitive

TBCs may be able to inhibit bitter-sensitive TBC signaling, an inhibition effect that is eliminated following desensitization of sweet-sensitive TBCs. Thus, for example, iterative tasting of a high concentration of aspartame results in aspartame exhibiting pronounced bitterness. Other highly hydrophilic sweeteners (e.g., sucrose, fructose, glucose) exhibit no bitterness at all even after attempted desensitization. Thus, it appears that some threshold hydrophobicity must be necessary for organic compounds to stimulate bitter-sensitive TBCs. Organic compounds that are too hydrophilic appear incapable of activating bitter-sensitive TBCs. Yet many inorganic compounds which are extremely hydrophilic are capable of activating bitter-sensitive TBCs. Many organic compounds are known which exhibit both sweet and bitter tastes. Typically such compounds exhibit only sweetness when evaluated at concentrations just above their taste thresholds, but at higher concentrations exhibit both sweet and bitter tastes. In such cases, it appears that sweet-sensitive TBCs are not able to inhibit activities of bitter-sensitive TBCs. It could be that the inhibitory effect of sweet-sensitive TBCs on bitter-sensitive cells only occurs when there is a wide difference between sweetness and bitterness potencies for compounds.

4.02.3.2 Bitterant Structure–Activity Relationship

An objective of this review is to summarize the SAR of bitter stimuli. However, given the extraordinary diversity of bitterant SAR, it would be of little value to provide a comprehensive listing of chemical compounds which have been reported to exhibit bitter taste. So, rather than attempt such a feat, a listing is provided of common bitter compounds that are either used in research or are present in common foods. Chemical structures, empirical formulas, and molecular weights are provided. Bitterant potencies are not generally available as is the case for sweetener potencies. Bitter taste has generally been a taste that food, beverage, and pharmaceutical manufacturers have tried to eliminate or minimize. And for this reason, there has not been a great deal of research in which bitterant potencies have been systematically determined as has been the case in the sweetener field. In some cases, bitter taste recognition thresholds (BRTs) have been reported as has been summarized by Glendinning J. I. (1994a; 1994b) and Belitz H.-D. and Wieser H. (1985).

A listing of ten common naturally occurring bitterants **94–103**, selected to illustrate the extraordinary diversity of bitterant SAR, with structures, molecular weights, empirical formulas, and BRT information provided in Figure 17, is as follows:

1. *Urea (94)*. Ureas in general are bitter in taste with the simplest member of the series exhibiting bitterness and bitterness potency increasing 100-fold on substitution with hydrophobic groups.
2. *Potassium chloride (95)*. KCl is commonly employed as a salt substitute by people suffering from hypertension. Its use is limited, however, by the presence of pronounced bitterness in addition to saltiness. Many other inorganic salts also exhibit bitter taste.
3. *Nicotine (96)*. Alkaloids, in general, are bitter in taste with nicotine being one of the simplest members of this class of compounds. It is the physiologically active and addictive component present in tobacco smoke.
4. *Caffeine (97)*. Caffeine is a fully methylated purine base present in many natural products including coffee beans, tea leaves and cola nuts. It, like other purine and pyrimidine bases, exhibits bitter taste.
5. *Catechin (98)*. Catechin is a flavanoid commonly found in tea.
6. *Quinine (99)*. Quinine is the most abundant alkaloid in the bark of the cinchona tree which is indigenous to South America. It was originally commercialized as an antimalarial but today is commonly employed as a bitterant in foods and beverages.
7. *Humulone (100)*. Humulone and related compounds are the bitter principles in hops which are key ingredients in beer.
8. *Limonin (101)*. Limonin is a member of the triterpenoid class of natural products and is the primary bitter principle in lemon and some other citrus fruit. It is a member of a group of natural products referred to as limonoids, all of which are bitter in taste.
9. *Naringin (102)*. Naringin is a member of a class of natural products known as flavanoid glycosides and is the principal bitter component present in the peel of grapefruit.
10. *Digitoxin (103)*. Digitoxin is a steroidal cardiac glycoside present in the plant *Digitalis purpurea* and is representative of a great many triterpenoid glycoside natural products, nearly all of which exhibit potent bitter taste.

A listing of ten bitterants, **104–113**, principally of synthetic origin, selected to further illustrate the

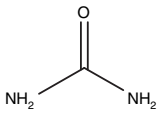

94 (Urea)
M = 60.06
CH_4N_2O
[a]BRT = 60–70 μM

KCl

95 (Potassium chloride)
M = 74.55
KCl
[b]BRT = >21 000 μM

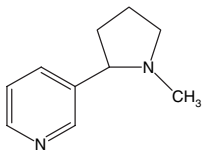

96 (Nicotine)
M = 162.23
$C_{10}H_{14}N_2$
[c]BRT = 19 μM

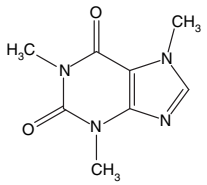

97 (Caffeine)
M = 194.19
$C_8H_{10}N_4O_2$
[c]BRT = 700 μM

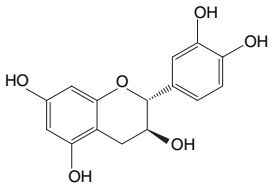

98 (Catechin)
M = 290.27
$C_{15}H_{14}O_6$
[d]BRT = 1000 μM

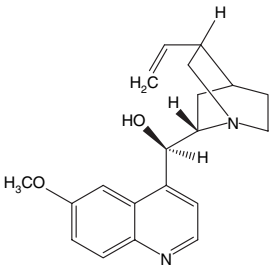

99 (Quinine)
M = 324.42
$C_{20}H_{24}N_2O_2$
[c]BRT = 30 μM (HCl salt)

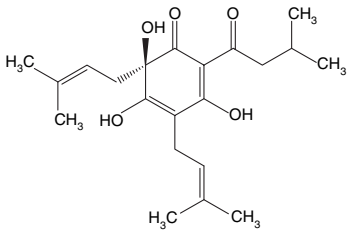

100 (Humulone)
M = 362.46
$C_{21}H_{30}O_5$

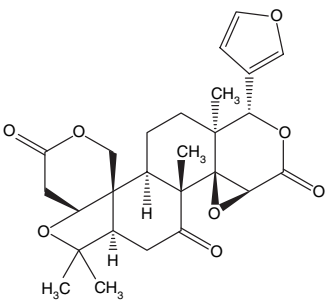

101 (Limonin)
M = 470.51
$C_{26}H_{30}O_8$
[c]BRT = 75 μM

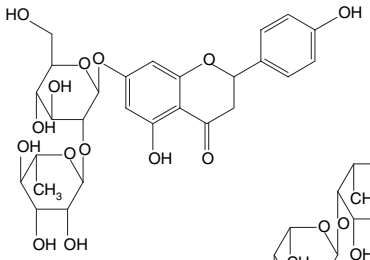

102 (Naringin)
M = 580.53
$C_{27}H_{32}O_{14}$
[c]BRT = 170 μM

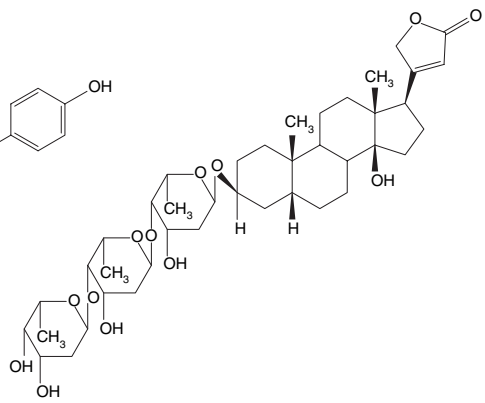

103 (Digitoxin)
M = 764.94
$C_{41}H_{64}O_{13}$
[c]BRT = 98 μM

Figure 17 Chemical structures, molecular weights, empirical formulas, and bitterness recognition thresholds of some naturally occurring bitter-tasting chemical compounds. [a]Belitz H.-D. and Wieser H. (1985); [b]Henkin R. I. *et al.* (1963); [c]Glendinning J. I. (1994a; 1994b); and [d]Stark T. *et al.* (2005).

extraordinary diversity of bitterant SAR, with structures, molecular weights, empirical formulas, and BRT information provided in Figure 18, is as follows:

1. *Cyclohexylamine (**104**).* Aliphatic amines in general are bitter-tasting compounds with bitterness potency increasing with the size of the aliphatic substituent. Interestingly, on sulfamation (i.e., R-NH_2 → R-$NHSO_3^-$ Na^+) the bitter-tasting cyclohexylamine is converted into a sweet-tasting sulfamate salt commonly known as sodium cyclamate.
2. *Ethylpyrazine (**105**).* Pyrazines are important flavor compounds exhibiting nutty and coffee-like aromatic characters. As a class of compounds,

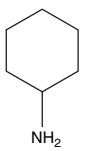

104 (Cyclohexylamine)
$M = 99.17$
$C_6H_{13}N$
[a]BRT = 1500–2000 μM

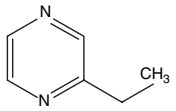

105 (Ethylpyrazine)
$M = 108.14$
$C_6H_8N_2$
[a]BRT = 4000–6000 μM

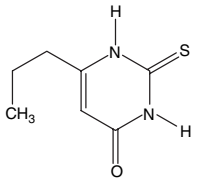

106 (6-Propylthiouracil)
$M = 170.23$
$C_7H_{10}N_2OS$
[b]BRT = <180 μM (tasters)

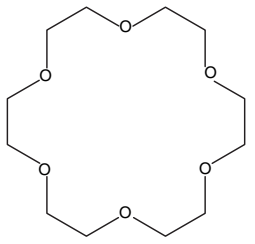

107 (18-Crown-6)
$M = 264.32$
$C_{12}H_{24}O_6$
[a]BRT = 500–700 μM

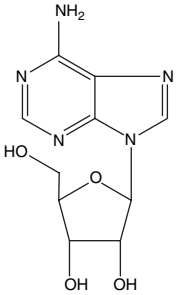

108 (Adenosine)
$M = 267.24$
$C_{10}H_{13}N_5O_4$
[a]BRT = 3000–6000 μM

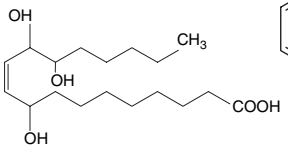

109 (*cis*-9,12,13-Trihydroxyoct-10-enoic acid)
$M = 330.46$; $C_{18}H_{34}O_5$
[a]BRT = 600–900 μM

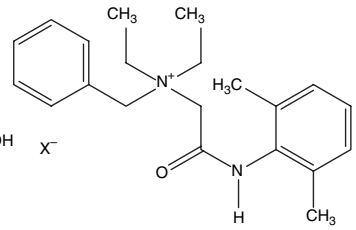

110 (Denatonium salts)
X = Cl: $M = 360.92$;
$C_{21}H_{29}ClN_2O$;
X = Benzoate: $M = 446.58$
$C_{28}H_{34}N_2O_3$; [c]BRT = 0.0064 μM

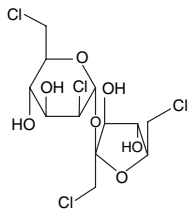

111 (2.6,1′,6′-Tetrachloro-2,6,1′,6′-tetradeoxymannosucrose) $M = 416.08$
$C_{12}H_{18}Cl_4O_7$
BRT = ca. 30 μM

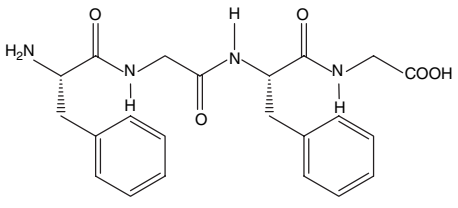

112 (Phe-Gly-Phe-Gly)
$M = 426.47$
$C_{22}H_{26}N_4O_5$
[a]BRT = 1000–1500 μM

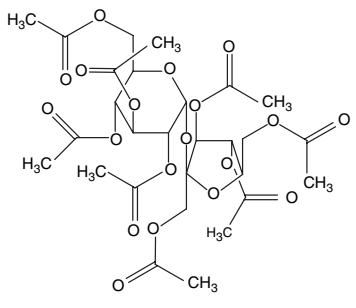

113 (Sucrose octaacetate)
$M = 678.59$
$C_{28}H_{38}O_{19}$
[d]BRT = 4 μM

Figure 18 Chemical structures, molecular weights, empirical formulas, and bitterness recognition thresholds of some synthetic bitter-tasting chemical compounds. [a]Belitz H.-D. and Wieser H. (1985); [b]Chang W. I. *et al.* (2006); [c]Saroli A. (1986); and [d]Boughter J. D. and Whitney G. (1993).

however, they are generally bitter in taste with bitterness potency increasing with hydrophobicity.

3. *6-n-Propylthiouracil (PROP) (106).* Thioureas are quite generally bitter in taste. PROP is a compound of substantial interest in that people exhibit a bimodal distribution in sensitivity to its bitterness with some individuals highly sensitive to its bitterness and some only sensitive to it at much higher concentrations. This difference in sensitivity has been demonstrated to have a genetic origin and is believed to be due to a mutation in T2R4 (Chandrashekar, J. *et al.*, 2000).

4. *18-Crown-6 (**107**).* Crown ethers are uniformly bitter in taste with bitterness potency increasing with hydrophobicity.
5. *Adenosine (**108**).* Purine and pyrimidine nucleosides as well as their bases are generally bitter, where the deoxyribosides are more potently bitter than the ribosides and nucleotides are generally not bitter. As in other series of compounds, bitterness potency increases with hydrophobicity.
6. *cis-9,12,13-Tri-hydroxyoct-10-enoic acid (**109**).* Hydroxylated fatty acids are common products of lipolysis and lipoxidation and are uniformly bitter. Such fat degradation products are responsible for the bitter off taste of many cereal and soy-based products.
7. *Denatonium salts (**110**).* Quaternary ammonium salts in general are bitter in taste, although the most potent bitterants reported are denatonium salts as reported by Saroli A. (1986). Denatonium salts are commonly employed bitter stimulants employed in mechanistic studies in animal models.
8. *2,6,1′,6′-Tetrachloro-2,6,1′,6′-tetradeoxy-mannosucrose (**111**).* Many halogenated deoxy sucrose derivatives are potently sweet compounds. Of particular note are 4,1′,6′-trichlorotrideoxygalactosucrose (sucralose) and 4,6,1′,6′-tetrachloro-galactosucrose which are potent sweeteners. Interestingly, a few halogenated deoxy sucrose derivatives are potently bitter, with some such as **111** matching quinine in bitterness potency.
9. *(L)-Phenylalanyl-glycyl-(L)-phenylalanyl-glycine (**112**).* Peptides, quite generally, are bitter as are hydrophobic amino acids. The exceptions are a few amino acids (e.g., glycine, D- and L-alanine, D-phenylalanine, and D-tryptophan) and a few peptide derivatives (e.g., aspartame) which are sweet in taste. And, as is the general trend, bitterness potency in such series of compounds increases with hydrophobicity. Many foods acquire bitter tastes due to the formation of bitter peptides on enzymatic breakdown of proteins. Tetrapeptide **112** is just one of the many bitter peptides which have been reported.
10. *Sucrose octaacetate (**113**).* Acetylated sugars in general exhibit bitter taste, and sucrose octaacetate has been used extensively in the study of bitter taste in humans and animal model systems.

4.02.4 Umami-Tasting Stimuli

Until the close of the twentieth century, for many, taste was considered to be one of the five senses which may be subdivided into four basic tastes: sweet, sour, salty, and bitter. Even though this is the case, evidence began to accumulate for a fifth basic taste, savory taste. The first claim for savory taste was by Ikeda K. (1909) who isolated glutamic acid from a seaweed source and argued that its taste was unique. As the monosodium salt, the taste is savory and was given the Japanese word *umami* which means delicious. The literature on umami taste has been reviewed quite comprehensively by Kawamura Y. and Kare M. R. (1987) and more recently by Bellisle F. (1999).

4.02.4.1 Biochemistry of Umami Taste

At the beginning of the twenty-first century, conclusive evidence that umami taste is a fifth basic taste began to accumulate. First, Nirupa Chaudhari and associates (2000) at the University of Miami obtained evidence suggesting that the umami taste receptor is a truncated form of the metabotrophic glutamate receptor mGluR4. Shortly thereafter, a collaborative team from the laboratories of Charles Zuker and Nicholas Ryba reported discovery of a mouse amino acid receptor (Nelson, G. *et al.*, 2002). In a functional assay in HEK-293 cells, they showed that glutamic acid activity, as well as the activities of many other L-amino acids, is mediated by a single receptor, apparently a heterodimer of two 7-TMD proteins which they named T1R1 and T1R3, often written as T1R1/T1R3. Both T1R1 and T1R3 are members of the small family of class C GPCRs and T1R3 is the same 7-TMD protein present in the sweetener receptor T1R2/T1R3 already discussed. The rat amino acid receptor discovery was quickly followed by a report by Li X. *et al.* (2002) of Senomyx (La Jolla, CA) on parallel findings for the human system. HEK-293 cells, in which both human T1R1 and T1R3 were expressed, responded to L-glutamic acid in a manner consistent with expectation from sensory experiments. L-Aspartic acid was also active but all other amino acids tested were essentially inactive. Thus, while the rodent receptor is a general L-amino acid receptor, the human receptor is specific for glutamate and aspartate. In addition, inosine monophosphate (IMP) and other nucleotides, which appear synergistic with monosodium glutamate in

taste tests, exhibited strong enhancements *in vitro*. On further analysis, it was learned that, in the absence of glutamate, these nucleotides are inactive. And therefore, they are not synergistic with glutamate. They are really enhancers of glutamate taste activity and likely function at the receptor as positive allosteric modulators. Positive and negative allosteric modulators of agonist activity are now known for many family C GPCRs as has been reviewed (Goudet, C. *et al.*, 2004).

Family C GPCRs are generally thought to bind their agonists within their large extracellular VFDs. Since the umami receptor is a heterodimeric receptor and since the umami and sweetener receptors contain the common subunit T1R3, it is thought, though not yet proven, that the glutamate binding site is most likely in the VFD of T1R1. Many other umami taste agonists have been identified as are reviewed below. Do they all bind in the glutamate binding site? In view of the finding that the closely related sweetener receptor T1R2/T1R3 binds agonists at no less than three sites, it seems likely that umami taste agonists also initiate their activities at a plurality of binding sites on T1R1/T1R3.

Sweet, bitter, and umami tastes are transduced by a common biochemical pathway. Experiments with gustducin and transducin knockout mice demonstrate that both of these G proteins mediate umami taste (He, W. *et al.*, 2004). Other work with $PLC_{\beta 2}$ and TRPM5 knockout mice demonstrates the critical role for both of these effectors in umami taste (Zhang, Y. *et al.*, 2003). In summary, while the role of the truncated mGluR4 receptor is not yet clear, there is a general consensus that umami taste is primarily mediated by a receptor T1R1/T1R3 as well as several intracellular effectors (i.e., gustducin, $PLC_{\beta 2}$, IP_3R, and TRPM5). It is also known that umami taste quality is coded at the cellular level, just as is the case for sweet and bitter taste qualities. Thus, within the taste bud, some TBCs are specific sensors for umami taste stimuli. They differ from the sweet- and bitter-sensitive TBCs in that they uniquely express the umami taste receptor T1R1/T1R3, while not expressing the sweetener receptor T1R2/T1R3 or bitterant T2R receptors.

4.02.4.2 Umami Tastant Structure–Activity Relationship

An objective of this review is to summarize the SAR of umami taste stimuli. Efforts aimed at discovery of novel umami tastants have not received the same intensity of focus as efforts to find novel sweeteners or to determine the structures of natural sweeteners or bitterants. Nonetheless, some umami tastant discovery work has been carried out in recent years and eight umami tastants **114**–**121**, with structures, molecular weights, empirical formulas, and umami taste potency information provided, are illustrated in Figure 19. Some di-, tri-, and tetra-peptides including Glu-Asp, Glu-Glu, Asp-Glu, Thr-Glu, Asp-Glu-Ser, Glu-Gly-Ser, Asp-Asp-Asp-Asp, and even the octapeptide Lys-Gly-Asp-Glu-Glu-Ser-Leu-Ala have been reported in the literature to exhibit umami taste. However, recent studies, as reviewed by Beksan E. *et al.* (2003), do not support the presence of umami taste in any of these compounds.

The purine nucleotides IMP (**122**), guanosine monophosphate (GMP (**123**)), and adenosine monophosphate (AMP (**124**)), as well as many synthetic analogs, have been reported to exhibit umami taste, as has been reviewed by Yamaguchi S. (1979). The chemical structures, empirical formulas, molecular weights, and relative umami taste activities are provided in Figure 20. In addition to exhibiting umami tastes themselves, these compounds are claimed to be strongly synergistic with monosodium glutamate. However, in the *in vitro* studies on the rat umami receptor carried out by Nelson G. *et al.* (2002) and on the human umami receptor carried out by Li X. *et al.* (2002), it was demonstrated that these purine nucleotides are inactive at the umami receptor if evaluated in the absence of glutamate or other amino acids with umami taste. Normally, in the *in vitro* receptor assays carried out in heterologous cell systems, the extracellular fluid contains low levels of amino acids. And, under these conditions, purine nucleotides were observed to exhibit activity. However, to ensure that the activity observed was due to the purine nucleotides rather than an enhancement effect of endogenous amino acids, the cell preparations were washed with amino acid free saline immediately before assay. Under these conditions, purine nucleotides give no responses while glutamate still exhibits its typical activity. Control cell preparations lacking the umami taste receptor are also unresponsive to purine nucleotides even without the cell washing step, thus providing evidence that the enhancement effect of purine nucleotides is receptor-mediated. In summary, it appears that purine nucleotides are not umami receptor agonists but are enhancers, presumably positive allosteric modulators, of glutamate and other amino acids. An observation consistent with

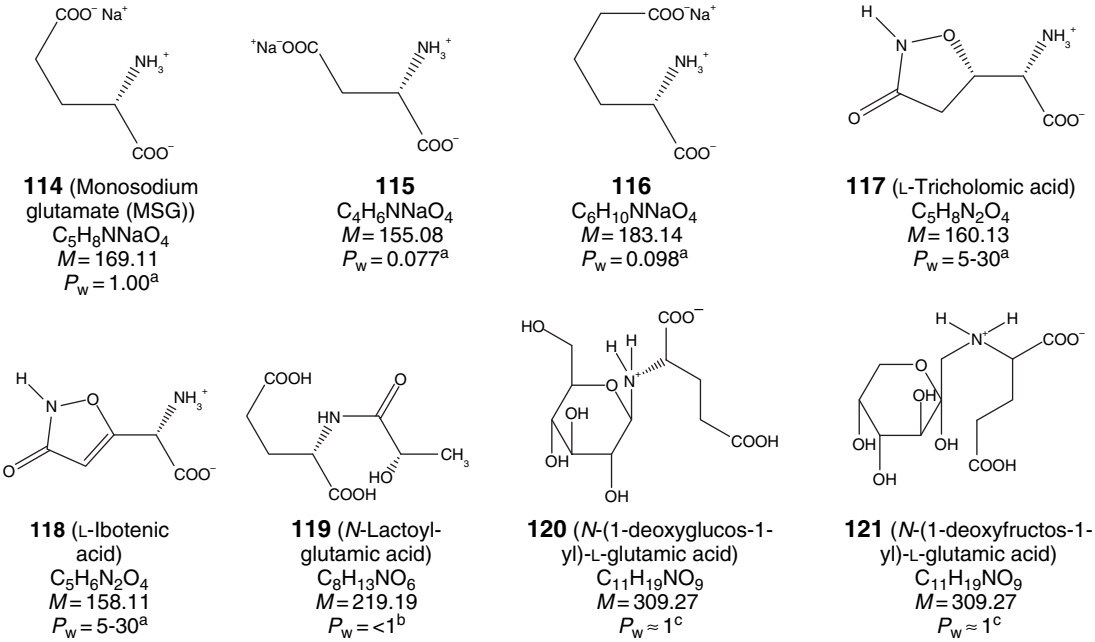

114 (Monosodium glutamate (MSG))
$C_5H_8NNaO_4$
$M = 169.11$
$P_w = 1.00$[a]

115
$C_4H_6NNaO_4$
$M = 155.08$
$P_w = 0.077$[a]

116
$C_6H_{10}NNaO_4$
$M = 183.14$
$P_w = 0.098$[a]

117 (L-Tricholomic acid)
$C_5H_8N_2O_4$
$M = 160.13$
$P_w = 5\text{-}30$[a]

118 (L-Ibotenic acid)
$C_5H_6N_2O_4$
$M = 158.11$
$P_w = 5\text{-}30$[a]

119 (*N*-Lactoyl-glutamic acid)
$C_8H_{13}NO_6$
$M = 219.19$
$P_w = <1$[b]

120 (*N*-(1-deoxyglucos-1-yl)-L-glutamic acid)
$C_{11}H_{19}NO_9$
$M = 309.27$
$P_w \approx 1$[c]

121 (*N*-(1-deoxyfructos-1-yl)-L-glutamic acid)
$C_{11}H_{19}NO_9$
$M = 309.27$
$P_w \approx 1$[c]

Figure 19 Chemical structures, molecular weights, empirical formulas, and umami taste potencies of some chemical compounds with umami taste. [a]Yamaguchi S. (1979); [b]Frérot E. and Escher S. D. (1997); and [c]Beksan E. *et al*. (2003).

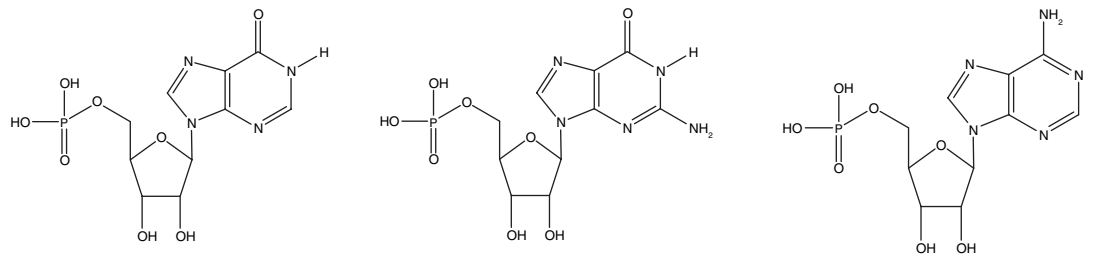

122 (Inosine monophosphate)[a]
$C_{10}H_{13}N_4O_8P$
$M = 348.21$
Enhancement potency: 1.0

123 (Guanosine monophosphate)[a]
$C_{10}H_{14}N_5O_8P$
$M = 363.22$
Enhancement potency: 2.3

124 (Adenosine monophosphate)[a]
$C_{10}H_{14}N_5O_7P$
$M = 347.22$
Enhancement potency: 0.18

Figure 20 Chemical structures, molecular weights, empirical formulas, and umami enhancement activities of purine nucleotides. [a]Yamaguchi S. (1979).

this conclusion is that, while 0.1 mM IMP exhibits a weak umami taste, no increase in umami taste intensity is observed for 1.0 and 10.0 mM solutions (DuBois, G. E. and San Miguel, R. S., 2005). It appears that 0.1 mM IMP is sufficient to maximally enhance the umami taste of the glutamate endogenous to saliva and thus increased IMP levels are without effect. Since purine nucleotides are not umami taste agonists, the umami taste activities provided for the examples in Figure 20 are really metrics for their relative potencies as enhancers of the umami taste of umami agonists (i.e., glutamate and aspartate) in human saliva. It is noteworthy that IMP, GMP, and AMP exhibit quite significant differences in activity as would be expected for a receptor-mediated effect.

4.02.5 Sour-Tasting Stimuli

Sour taste has always been accepted as one of the primary tastes and is very important to the enjoyment of many foods and beverages, especially those with sweet tastes. Here we provide a review of the current understanding of the cellular pathways which

mediate sour taste followed by a review of knowledge on the taste of acids that are commonly used in foods and beverages.

4.02.5.1 Biochemistry of Sour Taste

There is no question that sour taste is a unique and primary taste, but yet, in spite of its importance to our daily enjoyment of foods and beverages, until quite recently, the biochemical pathways which mediate it were largely unknown. Then, evidence began to accumulate that it must be an ion channel-mediated activation pathway in specific subsets of TBCs. Sour taste is the response to acids. All acidic chemical compounds are sour in taste. Here we discuss pH homeostasis in the body and the role that sour taste sensation plays in it, the biochemical mechanisms for excitation of acid-sensitive TBCs, and the rationale for difference in sour taste for different acids.

pH homeostasis and sour taste. A unique characteristic of living organisms is that they maintain their internal milieu at constant pH. Even small deviations from the physiological pH can be life threatening for most organisms. Therefore, organisms have developed efficient cellular mechanisms to detect the presence of H^+ or acid equivalents in their immediate environment and to limit acid entry into their internal milieu. However, if some acid is absorbed into the internal milieu, it is immediately buffered and ultimately excreted. For the detection of acid in their environment most animal species rely on sour taste, and to a lesser extent on the sense of smell. Sour taste is elicited by acidic stimuli and is detected by a subset of specialized TBCs in the oral cavity referred to as acid-sensing TBCs. Many of the foods, juices, and beverages that humans consume are acidic in nature (Feldman, M. and Barnett, C.,1995). In humans, sour taste evokes an innate rejection response to extremely acidic or sour stimuli, limiting the *ad libitum* ingestion of acid (Beauchamp, G. K. *et al.*, 1991; Scott, T. R. and Plata-Salaman, C. R., 1991). In this regard, along with the lungs and kidneys, which are the primary organs for acid secretion, acid-sensing TBCs in the oral cavity, by restricting the intake of acid, function as part of a multiorgan system to maintain acid–base homeostasis.

Acid-sensing. Since most acids decrease extracellular pH (pH_o), it would seem reasonable to think that a decrease in the pH_o in the oral cavity should be the signal for sour taste transduction. However, if that were the case, one would expect all acids at the same pH_o to taste equally sour. In our everyday experience and in animal model systems, different acids at same pH_o do not elicit the same neural responses or give the same perception of sourness (Beidler, L. M., 1967; Beidler, L. M. and Gross, G. W., 1971; Ogiso, K. *et al.*, 2000). In animal models it is well recognized that acetic acid at a fixed pH is always a more potent sour stimulus than an equivalent pH strong acid, such as HCl (Lyall, V. *et al.*, 2001). This indicates that a decrease in pH_o is not the signal for sour taste transduction. However, changes in intracellular pH (pH_i) of TBCs have been shown to correlate extremely well with the neural responses, indicating that it is the decrease in pH_i that is the proximate signal for sour taste transduction (Lyall, V. *et al.*, 2001; 2002a; 2002b; 2004; 2006).

Mechanisms for acid entry to TBCs. Acid transduction begins with the entry of H^+ or acid equivalents across the apical membrane of TBCs that causes a decrease in intracellular pH (pH_i) of acid-sensing TBCs. Acids exist in two forms: fully dissociated strong acids (e.g., HCl) and weak organic acids (e.g., acetic acid or citric acid) or dissolved CO_2, the precursor of carbonic acid. Accordingly, there are acid entry mechanisms for both strong and weak acids in the apical membrane of TBCs. For strong acids, acid entry involves H^+ flux through an apical proton channel that is blocked by divalent metal ions Zn^{2+} or Cd^{2+} (Lyall, V. *et al.*, unpublished observations). This channel is amiloride- and Ca^{2+}-insensitive but is activated by an increase in intracellular adenosine 3′,5′-cyclic monophosphate (cAMP) (Lyall, V. *et al.*, 2002a; 2004). However, there is some evidence to suggest that H^+-gated channels, such as the acid-sensing ion channel (ASIC) in the apical membrane and both ASIC (Ugawa S., *et al.*, 1998; Lin, W. *et al.*, 2002) and hyperpolarization-activated channels (HCN) (Stevens, D. R. *et al.*, 2001) in the basolateral membrane of TRCs, and TASK-2, a two pore domain K^+ channel (Lin, W. *et al.*, 2004; Richter, T. A. *et al.*, 2004a), may also play a role in sour taste transduction. These channels in the basolateral membrane could be activated if H^+ can cross tight junctions and decrease pH in the basolateral compartment. In mice, ASIC2 is not required for acid taste (Richter, T. A. *et al.*, 2004b) suggesting that at least in mice, ASIC channels do not play a major role in acid-sensing.

In contrast, weak organic acids do not seem to have apical membrane receptors. They enter TBCs across the apical membrane by passive diffusion as lipid-soluble undissociated neutral molecules. Once inside the

cell they dissociate to generate H^+ intracellularly and decrease TBC pH_i (Lyall, V. *et al.*, 2001). For example, in the case of dissolved CO_2, the CO_2 molecules passively enter TBCs across the apical membrane and combine with H_2O in a reaction catalyzed by intracellular carbonic anhydrases to form carbonic acid (H_2CO_3), which then dissociates to yield $H^+ + HCO_3^-$.

Taste receptor cells also contain NPPB (**125**) sensitive stretch-activated Cl^- channels (Gilbertson, T. A., 2002). The presence of an NPPB-sensitive Cl^- channel activated by acid was demonstrated in mouse taste cells (Miyamoto, T., *et al.*, 1998), suggesting a role for Cl^- channels in acid taste transduction. In addition to Cl^- channels, there is also evidence that an NPPB-insensitive poorly selective cationic conductance in the apical receptive membranes of mouse TBCs may also be involved in sour taste transduction (Miyamoto, T., *et al.*, 1998). In summary, sour taste transduction is mediated via multiple pathways. Similarly, in the case of other acid-sensitive cells, such as the central chemosensitive neurons, a multiple factors model has been proposed for acid signaling (Putnam, R. W. *et al.*, 2004).

Neural responses to acidic stimuli. A decrease in TBC pH_i is responsible for the neural response profiles to acidic stimuli. Acidic stimuli elicit both CT and glossopharyngeal taste nerve responses that are composed of two components with distinct temporal characteristics. A rapid transient increase in the phasic neural response slowly declines to a quasi-steady state, defined as the tonic phase of the neural response. Treating rat tongue with specific membrane permeable blockers of carbonic anhydrases MK-417 (**126**) or MK-507 (**127**) inhibits both the phasic and tonic components of the CT response to CO_2 (Lyall, V. *et al.*, 2001; 2002b). This indicates that an acid-induced decrease in TBC pH_i is necessary to elicit both the phasic and the tonic components of the CT response to acid stimulation.

Following a decrease in pH_i, the proximate sour stimulus, the downstream transduction mechanisms for the phasic and tonic components of the CT response to acid stimulation follow distinct and separate pathways. An acid-induced decrease in pH_i of acid-sensing TBCs alters the cell cytoskeleton by shifting the F- to G-actin equilibrium toward G-actin resulting in cell shrinkage and by titrating the mean charge of the intracellular membrane-impermeant anions (which could include elements of the cytoskeleton) (Fraser, J. A. *et al.*, 2005). The pH_i-induced decrease in cell volume activates a flufenamic acid (**128**) sensitive shrinkage-activated nonselective cation channel (SANSCC) in the basolateral membrane of TRCs. The entry of one or more monovalent cations through SANSCC depolarizes the receptor potential and is the basis for the phasic component of the CT response to acidic stimuli. Loading TBCs *in vivo* with the Ca^{2+}-chelator, BAPTA (**129**), did not affect the phasic part of the CT response to acids (Figure 21), indicating that phasic response is indifferent to changes in cytosolic Ca^{2+} (Lyall, V. *et al.*, 2006).

In acid-sensing TBCs a decrease in pH_i is followed by an increase in intracellular Ca^{2+} ($[Ca^{2+}]_i$) (Liu, L. and Simon, S. A., 2001a; 2001b; Richter, T. A. *et al.*, 2003). An increase in TBC $[Ca^{2+}]_i$ activates basolateral Na^+-H^+-exchanger-1 (NHE-1) and results in cell volume recovery and the neural adaptation to both strong and weak acid stimuli (Lyall, V. *et al.*, 2002a; 2004; Vinnikova, A. K. *et al.*, 2004; Lyall, V. *et al.*, 2006). Neural adaptation is related to the tonic part of the CT response to acidic stimuli (Figure 22). Therefore, a primary decrease in TBC pH_i, followed by a secondary increase in $[Ca^{2+}]_i$, and the subsequent activation of basolateral NHE-1 are specific events related to the tonic part of the neural response only (Figure 23).

One unexpected outcome from work on the identity of the molecular taste receptors for sweet, bitter, and umami taste is that the molecular receptors for each of these modalities are segregated in separate subsets of receptor cells (Zhang, Y. *et al.*, 2003). Recent work on sour taste shows that this modality is also expressed uniquely in a separate

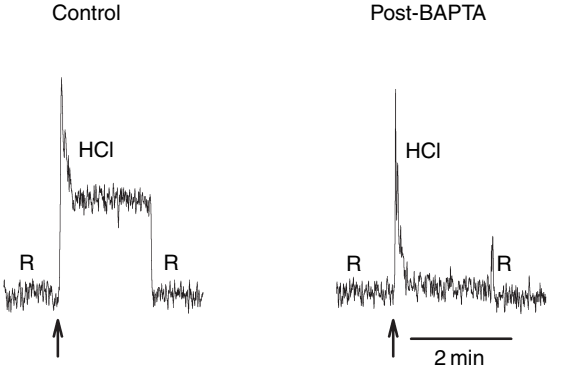

Figure 21 Loading fungiform TRCs with BAPTA *in vivo* eliminates tonic responses to HCl. Adapted from Lyall, V., Pasley, H., Phan, T-H. T., Mummalaneni, S., Heck, G. L., Vinnikova, A. K., and DeSimone, J. A. 2006. Intracellular pH modulates taste receptor volume and the phasic part of the chorda tympani response to acids. J. Gen. Physiol. 127, 15–34 with permission.

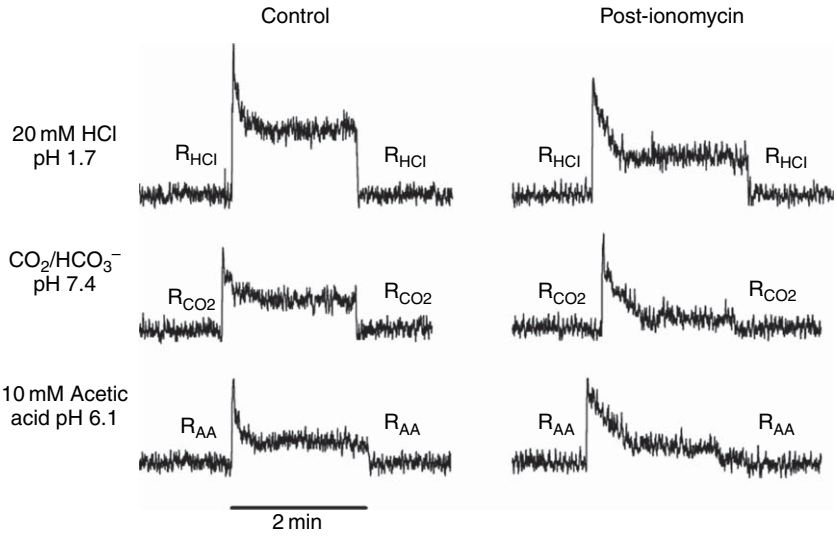

Figure 22 Effect of increasing TRC $[Ca^{2+}]_i$ by ionomycin on the tonic part of the CT response to acidic stimuli. CT responses were recorded before and after topical lingual application of 150 μM ionomycin (**130**). An increase in $[Ca^{2+}]_i$ increases the rate of adaptation to acidic stimuli. Adapted from Lyall, V., Heck, G. L., Vinnikova, A. K., Ghosh, S., Phan, T. H., Alam, R. I., Russell, O. F., Malik, S. A., Bigbee, J. W., and DeSimone, J. A. 2004. The mammalian amiloride-insensitive non-specific salt taste receptor is a vanilloid receptor-1 variant. J. Physiol. 558, 147–159 with permission.

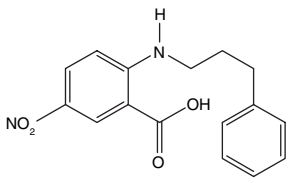

125 (5-Nitro-2-(3-phenyl-propylamino) benzoic acid (NPPB)
$C_{16}H_{16}N_2O_4$
$M = 300.31$

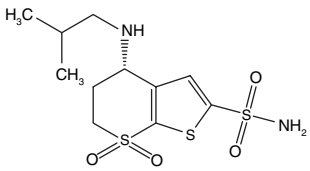

126 (MK-417)
$C_{11}H_{18}N_2O_4S_3$
$M = 338.47$

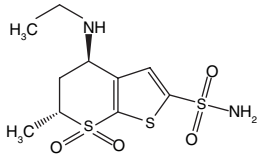

127 (MK-507)
$C_{10}H_{16}N_2O_4S_3$
$M = 324.44$

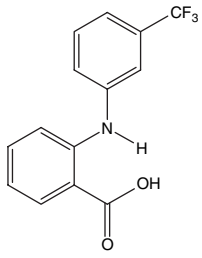

128 (Flufenamic acid)
$C_{10}H_{14}F_3NO_2$
$M = 281.23$

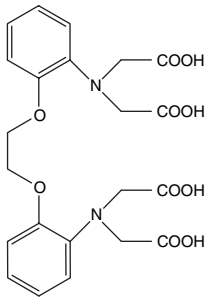

129 (BAPTA)
$C_{22}H_{24}N_2O_{10}$
$M = 476.43$

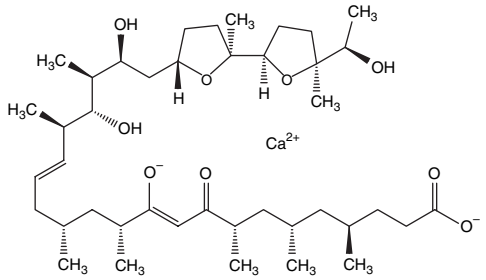

130 (Ionomycin)
$C_{41}H_{70}CaO_9$
$M = 747.07$

Figure 23 Molecular tools employed in the study of sour taste.

subset of taste receptor cells in the fungiform, circumvallate, and foliate papillae, and taste buds of the palate (Huang, A. L. *et al.*, 2006; Ishimaru, Y. *et al.*, 2006; Lopez-Jimenez, N. D. *et al.*, 2006). In the taste buds of the circumvallate and foliate papillae, this subset of cells expresses two unique TRP proteins, designated PKD2L1 and PKD1L3, in each cell of the subset. In fungiform and palatal taste buds,

only PKD2L1 is expressed in each of the cells of the subset. PKD2L1 and PKD1L3 localize preferentially in the apical regions of the taste receptor cells. When PKD2L1 and PKD1L3 are coexpressed in HEK cells they respond to the presence of citric acid and HCl by causing an increase in intracellular calcium concentration (Ishimaru, Y. *et al.*, 2006). It is unclear, however, if these proteins behave as calcium-conducting channels *in vivo*. That PKD2L1 containing cells are involved in sour taste is elegantly demonstrated in genetic ablation studies in which mice are engineered such that cells that would normally express PKD2L1 are destroyed by attenuated diphtheria toxin (Huang, A. L. *et al.*, 2006). In such mice, CT responses to acids were completely absent while responses to the other taste modalities remained intact. The fact that taste receptor cells lacking PKD2L1 fail to respond to weak and strong acids alike suggests that these proteins may be part of the intracellular pH-sensing system in sour taste receptor cells and in some central nervous system neurons where PKD2L1 is also expressed.

Neurotransmitter: TBCs detect the presence of acid in the oral cavity and elicit taste nerve responses. This implies that acid-induced changes in TBC pH_i, Ca^{2+}, cell shrinkage, and/or depolarization are communicated to the taste nerve fibers innervating TBCs via one or more neurotransmitters. Recent studies suggest the possible role for serotonin (**131**) (Kaya, N. *et al.*, 2004; Huang, Y. J. *et al.*, 2005) and ATP (**132**) (Finger, T. E., *et al.*, 2005). Serotonin, also known as 5-hydroxytryptamine (5-HT), is suggested to act on the 5-HT_3 receptor on the taste nerve fibers. However, the 5-HT_{3A} knockout mice did not show any differences in their neural response to taste stimuli, including acids (Finger, T. E., *et al.*, 2005), indicating that serotonin may not be the taste neurotransmitter. In contrast to 5-HT_{3A} knockout mice, in a double knockout mouse model lacking ionotropic purinergic P2X receptor units $P2X_2$ and $P2X_3$, no neural taste responses in CT or glossopharyngeal nerve were observed for salty, bitter, sweet, umami, and acidic stimuli. This suggests that ATP may be the taste-specific neurotransmitter that transmits information from TBCs to taste nerves (Figure 24).

4.02.5.2 Acidulant Structure–Activity Relationship

As already noted, all acids exhibit sour taste. The proximate event for signaling by acid-sensing TBCs is a drop in intracellular pH. Strong mineral acids (e.g., HCl, H_2SO_4, H_3PO_4) reduce intracellular pH by the diffusion of hydronium ions through an apical proton channel. Organic acids (e.g., citric acid, malic acid, tartaric acid), however, while modulating intracellular pH by the hydronium ion/apical proton channel pathway to some degree, principally reduce intracellular pH following diffusion through the TBC membrane. This mechanistic rationale suggests that mineral acids at constant pH should exhibit equal sourness while the sournesses of organic acids should not be strongly correlated with pH but should be dependent on efficiencies of diffusion into the TBC. This expectation is consistent with observations. Exemplary listings of common mineral acids and organic acids, as well as their empirical formulas, molecular weights, and pK_as, are provided in Figures 25 and 26.

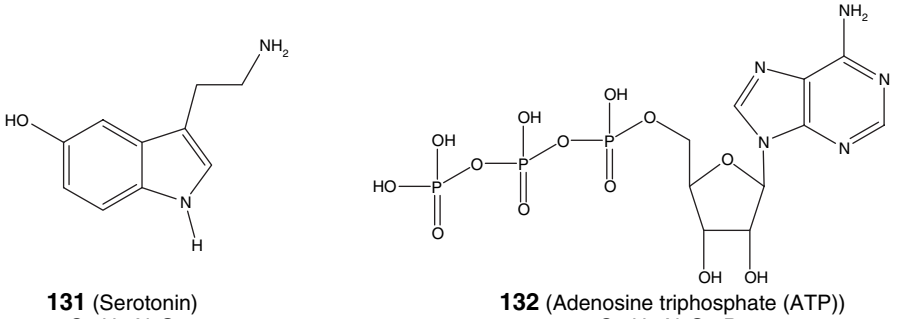

131 (Serotonin)
$C_{10}H_{12}N_2O$
$M = 176.22$

132 (Adenosine triphosphate (ATP))
$C_{10}H_{16}N_5O_{13}P_3$
$M = 507.18$

Figure 24 Possible taste neurotransmitters.

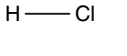

133 (Hydrochloric acid)
HCl
$M = 36.46$
$pK_a = -6.1$[a]

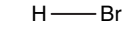

134 (Hydrobromic acid)
HBr
$M = 80.91$
$pK_a = -9$[a]

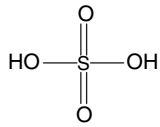

135 (Sulfuric acid)
H_2O_4S
$M = 98.08$
$pK_{a1} = -3$; $pK_{a2} = 1.99$[a]

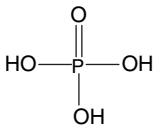

136 (Phosphoric acid)
H_3O_4P
$M = 98.00$
$pK_{a1} = 2.15$; $pK_{a2} = 7.20$; $pK_{a3} = 12.38$[a]

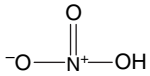

137 (Nitric acid)
HNO_3
$M = 63.01$
$pK_a = -1.38$[a]

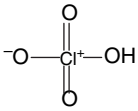

138 (Perchloric acid)
$HClO_4$
$M = 100.46$
$pK_a = -\infty$[a]

Figure 25 Chemical structures, empirical formulas, molecular weights, and pK_a constants for some common mineral acids.
[a]Dean J. A. (1985).

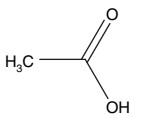

139 (Acetic acid)
$C_2H_4O_2$
$M = 60.05$
$pK_a = 4.76$[a]

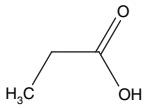

140 (Propionic acid)
$C_3H_6O_2$
$M = 74.08$
$pK_a = 4.87$[a]

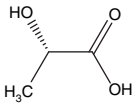

141 ((S)-Lactic acid)
$C_3H_6O_3$
$M = 90.08$
$pK_a = 3.86$[a]

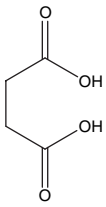

142 (Succinic acid)
$C_4H_6O_4$
$M = 118.09$
$pK_{a1} = 4.21$; $pK_{a2} = 5.64$[a]

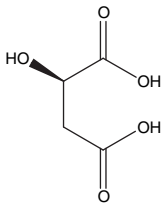

143 (Malic acid)
$C_4H_6O_5$
$M = 134.09$
$pK_{a1} = 3.40$; $pK_{a2} = 5.05$[a]

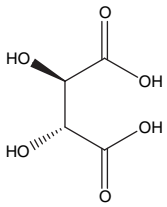

144 (L-Tartaric acid)
$C_4H_6O_6$
$M = 150.09$
$pK_{a1} = 3.04$; $pK_{a2} = 4.37$[a]

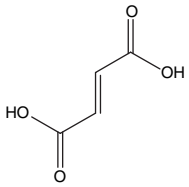

145 (Fumaric acid)
$C_4H_4O_4$
$M = 116.07$
$pK_{a1} = 3.10$; $pK_{a2} = 4.60$[a]

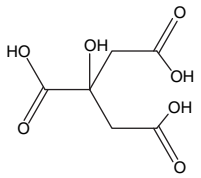

146 (Citric acid)
$C_6H_8O_7$
$M = 192.12$
$pK_{a1} = 3.13$; $pK_{a2} = 4.76$; $pK_{a3} = 6.40$[a]

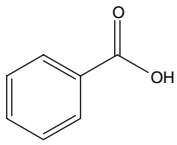

147 (Benzoic acid)
$C_7H_6O_2$
$M = 122.12$
$pK_a = 4.20$[a]

Figure 26 Chemical structures, empirical formulas, molecular weights, and pK_a constants for some common organic acids.
[a]Dean J. A. (1985).

4.02.6 Salty-Tasting Stimuli

Salty taste has always been accepted as one of the primary tastes and is very important to the enjoyment of many foods, especially foods with umami tastes. In fact, until the recent identification of the umami receptor, many held the belief that umami taste was a superimposition of salty and sweet tastes. In umami taste, the presence of a cation (e.g., Na^+) is critical as without it, even the prototypical umami agonist monosodium glutamate does not exhibit umami taste. Here we provide a review of the current understanding of the biochemistry of salty taste followed by a review of observations on the taste of NaCl and a few other common salts.

4.02.6.1 Biochemistry of Salty Taste

Salty taste is a unique and primary taste and in spite of its importance to our daily enjoyment of foods, until quite recently, the biochemical pathways which mediate it were largely unknown. Then, evidence began to accumulate that it must be mediated by ion channels present in specific subsets of TBCs. Salty taste is the response to NaCl, the prototypical salty taste stimulus, as well as a number of other salts. Here we discuss the biological mechanisms which mediate salt homeostasis, the ion channels which mediate the excitation of salt-sensitive TBCs and the biochemical explanation for the differences in tastes between salts of differing composition.

Sodium balance and sodium appetite. Tight regulation of the ionic composition and osmotic pressure of the extracellular fluid compartment of terrestrial mammals is fundamental to their survival. This is accomplished, in part, through the agency of the regulatory hormone, aldosterone, which increases Na^+ transport across epithelial cells from the lumina of the renal collecting duct and colon (Rossier, B. C. *et al.*, 2002). Aldosterone action, therefore, reduces Na^+ excretion in urine and feces. On the input side, changes in Na^+ balance depend on the subject's eating behavior which in turn is influenced by the sense of taste and the subject's endocrine status as determined by current Na^+ balance (Denton, D. A., 1967). For example, in Na^+-replete rats, NaCl concentrations near isotonicity tend to be preferred over water while those in the hypertonic range are increasingly less palatable (Richter, C. P., 1936; Fregly, M. J. and Rowland, N. E., 1986). Na^+-deprived and adrenalectomized rats, on the other hand, prefer even hypertonic NaCl solutions over water (Richter, C. P., 1936; Fregly, M. J. and Rowland, N. E., 1986; Scott, T. R. and Plata-Salaman, C. R., 1991). Increased salt preference has also been reported for human subjects taking diuretics on a Na^+-restricted diet (Beauchamp, G. K. *et al.*, 1990). Na^+-deficient wild rabbits taste and then readily consume Na^+ from salt licks while tasting and then rejecting nearby licks of nonsodium salts (Denten, D. A., 1967). These and other data indicate a connection between Na^+-specific taste and an animal's current interstitial fluid Na^+ levels and mineralocorticoid status.

Among the Na^+ transporters upregulated by aldosterone is the epithelial sodium channel (ENaC). ENaC is present in the membranes of various types of epithelial cells, including taste receptor cells of rats (Kretz, O. *et al.*, 1999; Lin, W. *et al.*, 1999). As such, ENaC would appear to be an excellent candidate for the Na^+-specific salt taste receptor. For the rat and other rodents, the preponderance of evidence indicates that this is the case.

Sodium taste and ENaC pharmacology. Na^+ transport across epithelia, including lingual epithelia, involves the passive flux of Na^+ from the luminal compartment (oral cavity for dorsal lingual epithelia) into the epithelial cells (for taste, receptor cells in taste buds and some surrounding nontaste epithelia) through apical membrane ENaC. Na^+ is then pumped across the basolateral membranes of the epithelial cells by the Na^+-K^+-ATPase (Verrey, F. *et al.*, 2000). Transepithelial Na^+ transport can be inhibited at the cell apical membrane by adding amiloride (**148**) or one of its analogs to the luminal solution, thereby reducing the Na^+ permeability of ENaC (Verrey, F. *et al.*, 2000). For the species in which transepithelial ion transport has been studied across the dorsal lingual epithelium, viz., dog (DeSimone, J. A. *et al.* 1984; Mierson, S. *et al.*, 1985; Simon, S. A. and Garvin, J. L., 1985), rat (Heck, G. L. *et al.*, 1984; Garvin, J. L. *et al.*, 1988; Mierson, S. *et al.*, 1988; Gilbertson, T. A. and Zhang, H., 1998), rabbit (Simon, S. A. *et al.*, 1986), and hamster (Gilbertson, T. A. and Zhang, H., 1998), the Na^+ transport paradigm appears to apply. The most compelling evidence that ENaC or some ENaC variants are indeed Na^+-specific salt taste receptor proteins is that the taste nerve response to NaCl is significantly inhibited by amiloride and its analogs in a variety of species. Taste responses to NaCl recorded in the

afferent CT or in the nucleus of the solitary tract of rat (Schiffman, S. S. *et al.*, 1983; Heck, G. L. *et al.*, 1984; Brand, J. G. *et al.*, 1985; Hill, D. L. and Bour, T. C., 1985; Yoshii, K. *et al.*, 1986; Ninomiya, Y. and Funakoshi, M., 1988; Scott, T. R. and Giza, B. K., 1990; St. John, S. J. and Smith, D. V., 2000), hamster (Hettinger, T. P. and Frank, M. E., 1990), some mouse strains (Ninomiya, Y. *et al.*, 1989), and gerbil (Schiffman, S. S. *et al.*, 1990) are significantly inhibited by amiloride without effect on responses to stimuli of other taste modalities. Amiloride sensitivity is observed in single CT units of the chimpanzee that respond strongly to Na^+ and Li^+ salts, but not in units sensitive to both Na^+ and K^+ (Hellekant, G. *et al.*, 1997). Whole cell patch clamp studies on isolated rat and hamster taste buds show that amiloride blocks a Na^+ current across taste cell membranes, consistent with a role for ENaC in Na^+ taste reception (Avenet, P. and Lindemann, B., 1988; 1991; Gilbertson, T. A. *et al.*, 1993). Taken together the data are consistent with the conclusion that ENaC is the Na^+-specific salt taste receptor in many species including many rodents and nonhuman primates. In rats the amiloride-sensitive part of the response accounts for 75–80% of the total response to 100 mM NaCl(see Figure 23). Surprisingly, ENaC appears to play less of a role in human salt taste (Smith, D. V. and Ossebaard, C. A., 1995).

In rats, ENaC appears to be functional only in the taste buds innervated by the CT, that is, principally those in fungiform papillae. Behavioral studies convincingly show that the rat's ability to discriminate between NaCl and KCl depends on taste information from the CT and this ability is progressively lost with the NaCl solutions containing increasing amiloride concentrations (Spector, A. C. *et al.*, 1996). This behavioral change correlates perfectly with the amiloride concentration dependence of the diminution of the response to NaCl in Na^+-sensitive single units of the nucleus of the solitary tract. The cumulative molecular, immunocytochemical, electrophysiological, and behavioral evidence indicates, therefore, that ENaC is a Na^+-specific salt taste receptor, and most likely the only Na^+-specific receptor.

Amiloride-insensitive salt taste reception. As seen in Figure 27, after inhibition of the NaCl response by benzamil (**149**), a significant neural response remains. Analysis of single CT units in rats (Frank, M. E. *et al.*, 1983), hamsters (Frank, M. E. *et al.*, 1988), and chimpanzees (Hellekant, G. *et al.*, 1997) suggests the existence of a salt taste receptor type that is

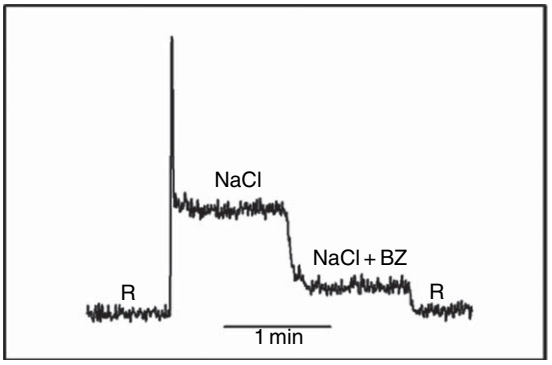

Figure 27 Integrated rat chorda tympani response to 100 mM NaCl followed by a response to 100 mM NaCl + 5 μM benzamil (**149;** Bz). R denotes the rinse solution (10 mM KCl). The NaCl response above baseline response (R) minus the NaCl + Bz response is the amiloride-sensitive part of the NaCl response (about 75% of the NaCl response).

cation-nonselective in addition to one that is Na^+-specific. Accordingly, one obvious candidate for such a taste receptor would be a nonselective cation channel. Unfortunately this fact alone does little to limit the number of possibilities, given the plethora of nonselective cation channels that have been described. One possibly fruitful approach is to seek pharmacological probes that might restrict the number of possible candidate receptor types, that is, an approach analogous to that leading to the discovery of ENaC as the Na^+-specific taste receptor through the action of its pharmacological inhibitor, amiloride. In this manner it has been shown that the amiloride-insensitive part of the NaCl CT response, as well as the responses to KCl, NH_4Cl, and $CaCl_2$, are enhanced by the vanilloids, resiniferatoxin (**150**; RTX), and capsaicin (**151**) (Lyall, V. *et al.*, x). At higher vanilloid concentrations the salt-evoked CT responses are inhibited. The amiloride-insensitive part of the NaCl CT response is completely inhibited by the vanilloid receptor-1 (VR1 or TRPV1) inhibitor, SB366971 (**152**) (Lyall, V. *et al.*, 2004). These results have led to the hypothesis that TRPV1, a nonselective cation channel, or more likely, one of its splice variants, is the nonselective cation salt taste receptor. Additional data in support of this are as follows (cf. Lyall, V. *et al.*, 2004):

1. The amiloride-insensitive part of the NaCl CT response increases with temperature and the effects of temperature and vanilloids are additive, similar to TRPV1.

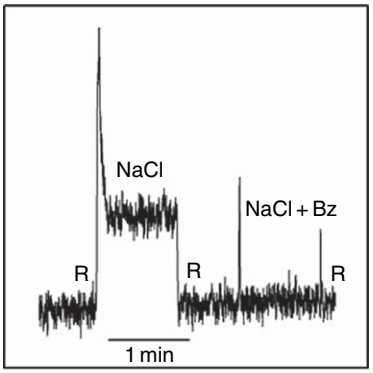

Figure 28 Integrated chorda tympani response to 100 mM NaCl and 100 mM NaCl + 5 μM benzamil (**148**; Bz) in a TRPV1 knockout mouse. Note there is no amiloride-insensitive response (i.e., no response to NaCl + Bz). Wildtype mice show an amiloride-insensitive NaCl response. This shows that the amiloride-insensitive response to NaCl depends on the expression of the TRPV1 gene.

2. Increases in temperature and vanilloid concentration, in turn, increase the response conductance (slope of the normalized CT response with voltage applied to the anterior lingual receptive field), that is, the taste receptor has ion channel characteristics *in situ*.
3. Vanilloids, external pH, and ATP lower the temperature threshold of the response.
4. A TRPV1 mRNA transcript common to several channels in the TRP receptor family was detected in rat fungiform TBCs (see also Liu, L. and Simon, S. A., 2001a; 2001b).
5. TRPV1 knockout mice lack an amiloride-insensitive NaCl CT response (see Figure 28) while control mice show an intact response.
6. Ethanol is an agonist of the amiloride-insensitive salt taste response (Lyall, V. *et al.*, 2005) similar to its agonist effect on cloned TRPV1 (Trevisani *et al.*, 2002).

These results suggest that the amiloride-insensitive nonselective cation salt taste receptor in the taste cells of fungiform papillae is a TRPV1 variant (TRPV1t). Two reasons indicating that TRPV1t differs from TRPV1 are as follows:

1. TRPV1t is constitutively active, while TRPV1 must be activated by temperature, pH, or vanilloids, and
2. Unlike TRPV1, TRPV1t is not affected by a drop in pH alone.

A vanilloid must be present for TRPV1t to show pH dependence. At present it is not known what structural differences between TRPV1t and TRPV1 account for these important functional differences. Also it is not known if TRPV1t accounts for the nonselective cation salt sensitivity in the glossopharyngeal nerve (i.e., whether or not TRPV1t is also present in circumvallate taste cells) (Figure 29).

Differences in taste for salts with common cations. Why is NaCl a more potent salty stimulus than Na_2SO_4 or Na_3PO_4? Based on the foregoing discussion on the involvement of ENaC and TRPV1 in human salty taste, these three sodium salts should be equivalent in salty taste at common Na^+ concentration. However, this is not the case. NaCl is the most potent of the Na^+ salts and the diminished potencies of other Na^+ salts have long puzzled investigators in gustation research. An explanation for this apparent paradox began to emerge in the 1980s with the work of Harry Harper at Rockefeller University (1987), the author (JD) and co-workers at Virginia Commonwealth University (Ye, Q. *et al.*, 1991), and Sid Simon and co-workers at Duke University (Elliot, E. J. and Simon, S. A. 1990; Simon, S. A. *et al.*, 1993). It was proposed that NaCl and other Na^+ salts are able to passively diffuse through the tight junctions between TBCs and that, for salts with small counterions (e.g., Cl^-), both cation and anion are able to diffuse through the tight junctions at comparable rates. On the other hand, it was recognized that, while this is the case for small anions, for Na^+ salts with large anions, the rates of diffusion for the anions would be lower than that for the Na^+ ion and that therefore, for such salts, a hyperpolarizing field potential would be imposed on salt-sensitive TBCs which would inhibit the diffusion of Na^+ ions through ion channels in the apical membrane. The net result of this differential ionic diffusion is that Na^+ salts with large anions are expected to be less potent in salty taste than are salts with small anions and this is exactly what is observed.

4.02.6.2 Salty Tastant Structure–Activity Relationship

As already discussed, salt (i.e., NaCl) is the prototypical salty stimulus. However, for reasons that are now clear based on an understanding of the biochemistry of salty taste, many other salts exhibit

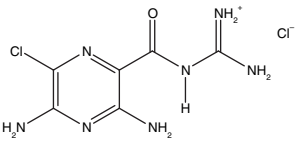

148 (Amiloride HCl)
$C_6H_9Cl_2N_7O$
$M = 266.09$

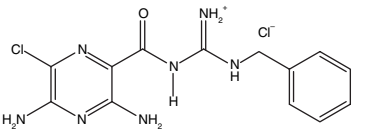

149 (Benzamil HCl)
$C_{13}H_{15}Cl_2N_7O$
$M = 356.21$

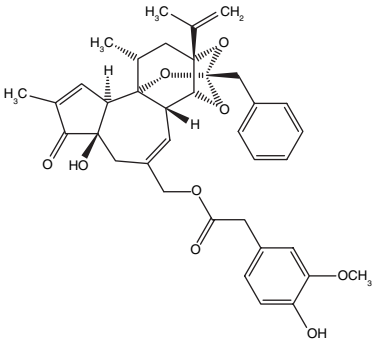

150 (Resiniferatoxin (RTX))
$C_{37}H_{40}O_9$
$M = 628.71$

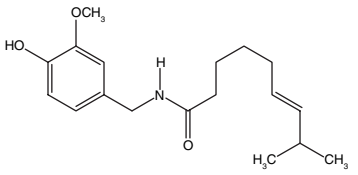

151 (Capsaicin)
$C_{18}H_{27}NO_3$
$M = 305.41$

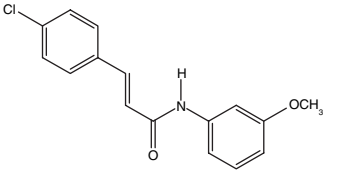

152 (SB360971)
$C_{16}H_{14}ClNO_2$
$M = 287.74$

Figure 29 Molecular tools employed in the study of salty taste.

salty taste. In general, salts exhibit multiple qualities of taste with sweet and bitter tastes being particularly common and even sourness observed for some (Shallenberger, R. S., 1993). Thus, as example, NaCl is perceived as sweet at low concentrations, salty and sweet at midrange concentrations, and only salty at higher concentrations. Bartoshuk L. M. *et al.* at Yale University (1978) noted that the observation of sweet taste for NaCl was protocol-dependent and required rinsing with water immediately before tasting the salt solution. KCl exhibits salty, sweet, and bitter qualities of taste. Thus, at low concentrations, KCl is weakly sweet and salty; at midrange concentrations, salty and weakly bitter; and at very high concentrations, only bitter. LiCl exhibits salty, sweet, and sour tastes. Thus, at low concentrations, LiCl is weakly sweet and salty, and at high concentrations, salty and weakly sour. K_2SO_4 exhibits salty, sweet, sour, and bitter tastes. Thus, at low concentrations, K_2SO_4 is sweet and bitter; at midrange concentrations, sweet, salty, and bitter; and at high concentrations, salty, bitter, and sour. As a bottom line, the presence of salty taste is common in salts of many different types even though the purest salty taste is exhibited by NaCl. The saltiness potencies for a number of salts were determined by von Skramlik E. (1926) and have been reviewed by Beets M. G. J. (1978). These potencies, recalculated so as to place them on a scale where 1 M NaCl is defined as having a potency of 1.00, are given in Figure 30 along with empirical formulas and formula weights.

NaCl **153** (Sodium chloride) ClNa FW = 58.44 P_m (1) = 1.00	NaBr **154** (Sodium bromide) BrNa FW = 102.89 P_m (1) = 1.00	NaI **155** (Sodium iodide) INa FW = 149.89 P_m (1) = 0.77	Na_2SO_4 **156** (Sodium sulfate) Na_2O_4S FW = 142.04 P_m (1) = 1.25	$NaNO_3$ **157** (Sodium nitrate) $NaNO_3$ FW = 84.99 P_m (1) = 0.17
$NaHCO_3$ **158** (Sodium bicarbonate) $CHNaO_3$ FW = 84.01 P_m (1) = 0.21	LiCl **159** (Lithium chloride) ClLi FW = 42.39 P_m (1) = 0.44	LiBr **160** (Lithium bromide) BrNa FW = 86.84 P_m (1) = 0.79	LiI **161** (Lithium iodide) INa FW = 133.85 P_m (1) = 0.57	$LiNO_3$ **162** (Lithium nitrate) $LiNO_3$ FW = 68.95 P_m (1) = 0.23
KCl **163** (Potassium chloride) ClK FW = 74.55 P_m (1) = 1.36	KBr **164** (Potassium bromide) BrK FW = 119.00 P_m (1) = 1.16	KI **165** (Potassium iodide) IK FW = 166.00 P_m (1) = 0.54	K_2SO_4 **166** (Potassium sulfate) K_2O_4S FW = 174.26 P_m (1) = 0.26	KNO_3 **167** (Potassium nitrate) KNO_3 FW = 101.10 P_m (1) = 0.14
$KHCO_3$ **168** (Potassium bicarbonate) $CHKO_3$ FW = 100.12 P_m (1) = 0.23	NH_4Cl **169** (Ammonium chloride) H_4ClN FW = 53.49 P_m (1) = 2.83	NH_4Br **170** (Ammonium bromide) H_4BrN FW = 97.94 P_m (1) = 1.83	NH_4I **171** (Ammonium iodide) H_4IN FW = 144.94 P_m (1) = 2.44	$(NH_4)_2SO_4$ **172** (Ammonium sulfate) $H_8N_2O_4S$ FW = 132.14 P_m (1) = 1.26
NH_4NO_3 **173** (Ammonium nitrate) $H_4N_2O_3$ FW = 80.04 P_m (1) = 1.03	$CaCl_2$ **174** (Calcium chloride) $CaCl_2$ FW = 110.98 P_m (1) = 1.23	$MgCl_2$ **175** (Magnesium chloride) Cl_2Mg FW = 95.21 P_m (1) = 0.20	Mg_2SO_4 **176** (Magnesium sulfate) MgO_4S FW = 120.37 P_m (1) = 0.01	

Figure 30 Empirical formulas, formula weights, and saltiness potencies of 24 common salts (Beets, M. G. J., 1978).

References

Arakawa, H. and Nakazaki, M. 1959. Absolute configuration of phyllodulcin. Chem. Ind. (Lond.), 671.

Audrieth, L. F. and Sveda, M. 1944. Preparation and properties of some *N*-substituted sulfamic acids. J. Org. Chem. 9, 89–101.

Avenet, P. and Lindemann, B. 1988. Amiloride-blockable sodium currents in isolated taste receptor cells. J. Membr. Biol. 105, 245–255.

Avenet, P. and Lindemann, B. 1991. Noninvasive recording of receptor cell action potentials and sustained currents from single taste buds maintained in the tongue: the response to mucosal NaCl and amiloride. J. Membr. Biol. 124, 33–41.

Bachmanov, A. A., Li, X., Reed, D. R., Ohmen, J. D., Li, S., Chen, Z., Tordoff, M. G., de Jong, P. J., Wu, C., West, D. B., Chatterjee, A., Ross, D. A., and Beauchamp, G. K. 2001. Positional cloning of the mouse saccharin preference (*Sac)* locus. Chem. Senses 26, 925–933.

Baek, N.-I., Chung, M.-S., Shamon, L., Kardono, L. B. S., Tsauri, S., Padmawinata, K., Pezzuto, J. M., Soejarto, D. D., and Kinghorn, A. D. 1993. Potential sweetening agents of plant origin. 29. Studies on Indonesian medicinal plants. 6. Selligueain A, a novel highly sweet proanthocyanidin from the rhizomes of *Selliguea feei*. J. Nat. Prod. 56, 1532–1538.

Bartoshuk, L. M., Murphy, C., and Cleveland, C. T. 1978. Sweet taste of dilute NaCl: psychophysical evidence for a sweet stimulus. Physiol. Behav. 21, 609–613.

Bassoli, A., Borgonovo, G., Busnelli, G., Morini, G., and Drew, M. G. B. 2005. Monatin and its stereoisomers: chemoenzymatic synthesis and taste properties. Eur. J. Org. Chem 1652–1658.

Bassoli, A., Drew, M. G. B., Merlini, L., and Morini, G. 2002. General pseudoreceptor model for sweet compounds: a semiquantitative prediction of binding affinity for sweet-tasting molecules. J. Med. Chem. 45, 4402–4409.

Beauchamp, G. K. (*ed*.) 1994. Kirin International Symposium on Bitter Taste, Elsevier Science.

Beauchamp, G. K., Bertino, M., Burke, D., and Engelman, K. 1990. Experimental sodium depletion and salt taste in normal human volunteers. Am. J. Clin. Nutr. 51, 881–889.

Beauchamp, G. K, Cowart, B., and Schmidt, H. J. 1991. Development of Chemosensitivity and Preference. In: Smell and Taste in Health and Disease (*ed*. T. V. Getchell, R. L. Doty, L. M. Bartoshuk, and J. B. Snow), pp. 405–416. Raven Press.

Beets, M. G. J. 1978. Structure–Activity Relationships in Human Chemoreception. Applied Science Publishers.

Beidler, L. M. 1967. Anion Influences on Taste Receptor Responses. In: Olfaction and Taste II (*ed*. T. Hayashi), pp. 509–534. Pergamon Press.

Beidler, L. M. and Gross, G. W. 1971. The Nature of Taste Receptor Sites. In: Contributions to Sensory Physiology (*ed*. W. D. Neff), pp. 97–127. Academic Press.

Beksan, E., Schieberle, P., Robert, F., Blank, I., Fay, L. B., Schlictherle-Cerny, H., and Hofmann, T. 2003. Synthesis and sensory characterization of novel umami-tasting glutamate glycoconjugates. J. Agric. Food Chem. 51, 5428–5436.

Belitz, H.-D. and Wieser, H. 1985. Bitter compounds: occurrence and structure–activity relationships. Food Rev. Int. 1(2), 271–354.

Bellisle, F. 1999. Glutamate and the UMAMI taste: sensory, metabolic, nutritional and behavioural considerations. A review of the literature published in the last 10 years. Neurosci. Biobehav. Rev. 23, 423–438.

Berlinerblau, J. 1883. Über die einwirkung von chlorcyan auf ortho- und auf para-amidophenetol. Journal für Praktische Chemie 30, 97–115.

Bertelsen, H., Hansen, S. J., Laursen, R. S., Saunders, J., and Eriknauer, K. 2001. Tagatose. In: Alternative Sweeteners, 3rd edn (*ed*. L. O'BrienNabors), pp. 105–127. Marcel Dekker.

Birch, G. G., Parke, S., Siertsema, R., and Westwell, J. M. 1996. Specific volumes and sweet taste. Food Chem. 56(3), 223–230.

Blanksma, J. J. and van der Weyden, P. W. M. 1940. Relationship between taste and structure in some derivatives of meta-nitraniline. Recueil des Travaux Chimiques des Pays-Bas 59, 629–632.

Boughter, J. D., Jr. and Whitney, G. 1993. Human taste thresholds for sucrose octaacetate. Chem. Senses 18(4), 445–448.

Brand, J. G., Teeter, J. H., and Silver, W. L. 1985. Inhibition by amiloride of chorda tympani responses evoked by monovalent salts. Brain Res. 334, 207–214.

Breitwieser, G. E. 2004. G protein-coupled receptor oligomerization: implications for G protein activation and cell signaling. Circ. Res. 94, 17–27.

Brennan, T. M. and Hendrick, M. E., US Patent 4 411 925 (October 25, 1983) (To Pfizer, Inc).

Budesinsky, Z. and Vavrina, J. 1972. Nucleophilic substitutions in the 2-methylsulfonyl pyrimidine series. Collection Czechoslov. Chem. Commun. 37, 1721–1733.

Bufe, B., Hofmann, T., Krautwurst, D., Raguse, J. D., and Meyerhof, W. 2002. The human TAS2R16 receptor mediates bitter taste in response to α-glucopyranosides. Nature Genet. 32, 397–401.

Chandrashekar, J., Mueller, K. L., Hoon, M. A., Adler, E., Feng, L., Guo, W., Zuker, C. S., and Ryba, N. J. P. 2000. T2RT2RSsT2RSsT2RSs function as bitter taste receptors. Cell 100, 703–711.

Chang, W.-I., Chung, J.-W., Kim, Y.-K., Chung, S.-C., and Kho, H.-S. 2006. The relationship between phenylthiocarbamide (PTC) and 6-n-propylthiouracil (PROP) taster status and taste thresholds for sucrose and quinine. Arch Oral Bio 51, 427–432.

Chatterjee, B. 1929. Attempts to find new anti-malarials. Part IV. β-Benziminazolylethylamine and β-5(or 6)-ethoxybenziminazolylethylamine. J. Chem. Soc. 2965–2968.

Chaudhari, N., Landin, A. M., and Roper, S. D. 2000. A metabotropic glutamate receptor variant functions as a taste receptor. Nat Neurosci 3, 113–119.

Choi, Y.-H., Kinghorn, A. D., Shi, X., Zhang, H., and Teo, B. K. 1989. Abrusoside A: a new type of highly sweet triterpene glycoside. J. Chem. Soc., Chem. Commun. 887–888.

Clauss, K. and Jensen, H. 1973. Oxathiazinone dioxides, a novel group of sweetening agents. Angew. Chem. Int. Ed. Engl. 12, 869–876.

Compadre, C. M., Hussain, R. A., Lopez de Compadre, R. L., Pezzuto, J. M., and Kinghorn, A. D. 1987. The intensely sweet herb sesquiterpene hernandulcin: isolation, synthesis, characterization and preliminary safety evaluation. J. Agric. Food Chem., 35, 273–279.

Cram, D. J. and Ratajczak, A. 1971. 1-(Phenylsulfonyl)-cyclopropanecarboxylic acids. US Patent 3 598 868 (August 10, 1971; to The Regents of the University of California, Berkeley, CA, USA).

Crammer, B. and Ikan, R. 1987. Progress in the Chemistry and Properties of Rebaudiosides. In: Developments in Sweeteners-3 (*ed*. T. H. Grenby), pp. 45–64. Elsevier Applied Science.

Culberson, J. C. and Walters, D. E. 1991. Three-Dimensional Model for the Sweet Taste Receptor: Development and Use, Chapter 16. In: Sweeteners: Discovery, Molecular Design and Chemoreception (*ed*. D. E. Walters, F. T. Orthoefer, and G. E. DuBois), ACS Symposium Series 450, 214–223. American Chemical Society.

Damak, S., Rong, M., Yasumatsu, K., Kokrashvili, Z., Perez, C. A., Shigemura, N., Yoshida, R., Mosinger, B., Jr., Glendinning, J. I., Ninomiya, Y., and Margolskee, R. F. 2006. Trpm5 null mice respond to bitter, sweet and umami compounds. Chem. Senses 31, 253–264.

D'Angelo, L. L. and Iacobucci, G. A. 1995. QSAR studies of a group of structurally diverse sweeteners using CoMFA and design of a new series of aspartame analogs. *Presented at the 210th National Meeting of the American Chemical Society*, Chicago, IL, USA, August 20–24. Book of Abstracts, Pt 1, COMP-083, American Chemical Society.

Dean, J. A. (*ed*.). 1985. Lange's Handbook of Chemistry, 13th edn. McGraw-Hill Book Company.

DeGraaf, H. 1930. The relationship between taste and the constitution in the dihydrazides of dicarboxylic acids and their derivatives, Diss., Leiden, 138; Chem. Abstr. 24, 5723.

Denten, D. A. 1967. Salt Appetite. In: Handbook of Physiology, Section 6. Vol. 1 (*eds*. C. F. Code and W. Heidel), p. 433. American Physiological Society.

DeSimone, J. A., Heck, G. L., Mierson, S., and DeSimone, S. K. 1984. The active ion transport properties of canine lingual epithelia *in vitro.* Implications for gustatory transduction. J. Gen. Physiol. 83, 633–656.

Dornow, A., Kühlcke, I., and Baxmann, F. 1949. Über einige derivate der benzoylessigsäure, Chemische Berichte 82, 254–257.

Dotson, C. D., Roper, S. D., and Spector, A. C. 2005. PLC$_{\beta 2}$-Independent Behavioral Avoidance of Prototypical Bitter-Tasting Ligands. Chem. Senses 30, 593–600.

Douglas, A. J. and Goodman, M. 1991. Molecular Basis of Taste: A Stereoisomeric Approach, Chapter 10. In: Sweeteners: Discovery, Molecular Design and Chemoreception (*ed*. D. E. Walters, F. T. Orthoefer, and G. E. DuBois), pp. 128–142. ACS Symposium Series 450, American Chemical Society.

DuBois, G. E. 1985. Unpublished Results. G. D. Searle Pharmaceutical Company Skokie, IL, USA.

DuBois, G. E. 1995. Unpublished Results, The Coca-Cola Company, Atlanta, GA, USA.

DuBois, G. E. 1997. New Insights on the Coding of the Sweet Taste Message in Chemical Structure. In: Firmenich Jubilee Symposium Olfaction and Taste: A Century for the Senses 1895–1995 (*ed*. G. Salvadori), pp. 32–95, Allured Publishing Corp.

DuBois, G. E. 2000. Nonnutritive Sweeteners. In: Encyclopedia of Food Science & Technology (*ed*. Frederick J Francis), pp. 2245–2265. John Wiley & Sons,.

DuBois, G. E. 2003. Unpublished Results, The Coca-Cola Company, Atlanta, GA.

DuBois, G. E. and D'Angelo, L. L. 1996. Current thoughts on the workings of polyol sweeteners. *Oral Presentation, International Sweetener Symposium*, Jerusalem, Israel.
DuBois, G. E. and San Miguel, R. S. 2005. Unpublished Results, The Coca-Cola Company, Atlanta, GA, USA.
DuBois, G. E. and Singer, N. 1984. Unpublished Results, G. D. Searle Pharmaceutical Company, Skokie, IL, USA.
DuBois, G. E., D'Angelo, L. L., and King, G. A. 1994. Unpublished Results, The Coca-Cola Company, Atlanta, GA, USA.
DuBois, G. E., Walters, D. E., Schiffman, S. S., Warwick, Z. S., Booth, B. J., Pecore, S. D., Gibes, K., Carr, B. T., and Brands, L. M. 1991. Concentration–response relationships of sweeteners (*eds*. D. E. Walters, F. T. Orthoefer, and G. E. DuBois), pp. 261–276. ACS Symposium Series 450, American Chemical Society.
DuBois, G. E., Zhi, B., Roy, G. M., Stevens, S. Y., and Yalpani, M. 1992. New non-ionic polyol derivatives with sucrose-mimetic properties. J. Chem. Soc. Chem. Commun. 1604–1605.
Elliot, E. J. and Simon, S. A. 1990. The anion in salt taste: a possible role for paracellular pathways. Brain Res. 535(1), 9–17.
Embuscado, M. E. and Patil, S. K. 2001. Erythritol. In: Alternative Sweeteners, 3rd edn (*ed*. L. O'Brien Nabors), pp. 235–254. Marcel Dekker.
Fahlberg, C. and Remsen, I. 1879. Über die oxydation des orthotoluolsulfamids. Chem. Ber. 2, 469–473.
Faurion, A. 1987. Physiology of the Sweet Taste. In: Progress in Sensory Physiology, Vol. 8 (*eds*. H. Autrum, D. Ottoson, E. R. Perl, R. F. Schmidt, H. Suimazu, and W. D. Willis), pp. 129–201. Springer.
Feldman, M. and Barnett, C. 1995. Relationship between the acidity and osmolarity of popular beverages and reported postprandial heartburn. Gastroenterology 108, 125–131.
Finger, T. E., Danilova, V., Barrows, J., Bartel, D. L., Vigers, A. J., Stone, L., Hellekant, G., and Kinnamon, S. C. 2005. ATP signaling is crucial for communication from taste buds to gustatory nerves. Science 310, 1495–1499.
Fitzhugh, O. G., Nelson, A. A., and Frawley, J. P. 1951. A comparison of the chronic toxicities of synthetic sweetening agents. J. Am. Pharm. Assoc. 40, 583–586.
Frank, M. E., Bieber, S. L., and Smith, D. V. 1988. The organization of taste sensibilities in hamster chorda tympani nerve fibers. J. Gen. Physiol. 91, 861–896.
Frank, M. E., Contreras, R. J., and Hettinger, T. P. 1983. Nerve fibers sensitive to ionic taste stimuli in chorda tympani of the rat. J. Neurophysiol. 50, 941–960.
Fraser, J. A., Middlebrook, C. E., Usher-Smith, J. A., Schwiening, C. J., and Huang, C. L. 2005. The effect of intracellular acidification on the relationship between cell volume and membrane potential in amphibian skeletal muscle. J. Physiol. 563, 745–764.
Fregly, M. J. and Rowland, N. E. 1986. Hormonal and neural mechanisms of sodium appetite. NIPS 1, 51–54.
Frérot, E. and Escher, S. D. 1997. Flavoured products and method for preparing the same. WO 97/04667.
Furukawa, S. and Tomizawa, Z. 1920. J. Chem. Ind. Tokyo, 23, 342; Chem. Abstr. 1920, 14, 2839.
Garvin, J. L., Robb, R., and Simon, S. A. 1988. Spatial map of salts and saccharides on dog tongue. Am. J. Physiol. 255, R117–122.
Gilbertson, T. A. 2002. Hypoosmotic stimuli activate a chloride conductance in rat taste cells. Chem. Senses 27, 383–394.
Gilbertson, T. A. and Zhang, H. 1998. Self inhibition in amiloride-sensitive sodium channels in taste receptor cells. J. Gen. Physiol. 111, 667–677.
Gilbertson, T. A., Roper, S. D., and Kinnamon, S. C. 1993. Proton currents through amiloride-sensitive Na^+ channels in isolated hamster taste cells: enhancement by vasopressin and cAMP. Neuron 10, 931–942.
Glendinning, J. I. 1994a. Is the Bitter Rejection Response Always Adaptive? In: Kirin International Symposium on Bitter Taste (*ed*. G. K. Beauchamp), pp. 1217–1222. Elsevier Science.
Glendinning, J. I. 1994b. Is the bitter rejection response always adaptive? Physiol. Behav. 56(6), 1217–1227.
Goudet, C., Binet, V., Prezeau, L., and Pin, J.-P. 2004. Allosteric modulators of class-C G-protein-coupled receptors open new possibilities for therapeutic application. Drug Discov. Today: New Strategies 1(1), 125–133.
Gries, H. and Mützel, W. 1985. 3-Substituted 2,4,6-trihalogenated benzamides as sweetening agents, US Patent 4 522 839 (June 11, 1985).
Harper, H. W. 1987. A diffusion potential model of salt taste receptors. Ann. N. Y. Acad. Sci. 510, 349–351.
Hashimoto, Y., Ishizone, H., and Ogura, M. 1980. Periandrin II and IV, triterpenoid glycosides from *Periandra dulcis*. Phytochemistry 19, 2411–2415.
He, W., Yasumatsu, K., Varadarajan, V., Yamada, A., Lem, J., Ninomiya, Y., Margolskee, R. F., and Damak, S. 2004. Umami taste responses are mediated by alpha-transducin and alpha-gustducin. J. Neurosci. 24, 7674–7680.
Heck, G. L., Mierson, S., and DeSimone, J. A. 1984. Salt taste transduction occurs through an amiloride-sensitive sodium transport pathway. Science 223, 403–405.
Hellekant, G. and Ninomiya, Y. 1991. On the taste of umami in chimpanzee. Physiol. Behav. 49, 927–934.
Hellekant, G. and Ninomiya, Y. 1994a. Bitter Taste in Single Chorda Tympani Taste Fibers from Chimpanzee. In: Kirin International Symposium on Bitter Taste (*ed*. G. K. Beauchamp), pp. 1185–1188. Elsevier Science.
Hellekant, G. and Ninomiya, Y. 1994b. Bitter taste in single chorda tympani taste fibers from chimpanzee. Physiol. Behav. 56(6), 1185–1188.
Hellekant, G., Ninomiya, Y., and Danilova, V. 1997. Taste in chimpanzees II: single chorda tympani fibers. Physiol. Behav. 61, 829–841.
Henkin, R. I., Gill, J. R., Jr., and Bartter, F. C. 1963. Studies on taste thresholds in normal man and in patients with adrenal cortical insufficiency: the role of adrenal cortical steroids and of serum sodium concentration. J. Clinical Invest. 42, 727–735.
Hettinger, T. P. and Frank, M. E. 1990. Specificity of amiloride inhibition of hamster taste responses. Brain Res. 513, 24–34.
Hill, D. L. and Bour, T. C. 1985. Addition of functional amiloride-sensitive components to the receptor membrane: a possible mechanism for altered taste responses during development. Brain Res. 352, 310–313.
Hofmann, A. 1972. Ein neuer süssstoff aus der indolreihe. Helv. Chim. Acta 55, 2934–2940.
Horowitz, R. M. and Gentili, B. 1969. Taste and structure in phenolic glycosides. J. Agric. Food Chem. 17, 696–700.
Hough, L. and Phadnis, S. P. 1976. Enhancement in the sweetness of sucrose. Nature 263, 800.
Huang, A. L., Chen, X., Hoon, M. A., Chandrashekar, J., Guo, W., Trankner, D., Ryba, N. J., and Zuker, C. S. 2006. The cells and logic for mammalian sour taste detection. Nature 442, 934–938.
Huang, Y. J., Maruyama, Y., Lu, K. S., Pereira, E., Plonsky, I, Baur, J. E., Wu, D., and Roper, S. D. 2005. Using biosensors to detect the release of serotonin from taste buds during taste stimulation. Arch. Ital. Biol. 143, 87–96.
Hussain, R. A., Poveda, L. J., Pezzuto, J. M., Soejarto, D. D., and Kinghorn, A. D. 1990. Sweetening agents of plant origin: phenylpropanoid constituents of seven sweet-tasting plants. Econ. Bot. 44(2), 174–182.
Ikeda, K. 1909. On a new seasoning. J. Tokyo Chem. Soc. 30, 820–836.

Ishimaru, Y., Inada, H., Kubota, M., Zhuang, H., Tominaga, M., and Matsunami, H. 2006. Transient receptor potential family members PKD1L3 and PKD2L1 form a candidate sour taste receptor. Proc. Natl. Acad. Sci. U. S. A. 103, 12569–12574.

Jiang, P., Cui, M., Zhao, B., Snyder, L. A., Benard, B. M. J., Osman, R., Max, M., and Margolskee, R. F. 2005. Identification of the cyclamate interaction site within the transmembrane domain of the human sweet taste receptor subunit T_1R_3T1R3. J. Biol. Chem. 280, 34296–34305.

Jiang, P., Ji, Q., Liu, Z., Snyder, L. A., Bernard, M. J., Margolskee, R. F., and Max, M. 2004. The cysteine-rich region of T_1R_3T1R3 determines responses to intensely sweet proteins. J. Biol. Chem. 279, 45068–45075.

Kasai, R., Fujino, H., Kuzuki, T., Wong, W.-H., Goto, C., Yata, N., Tanaka, O., Yasuhara, F., and Yamaguchi, S. 1986. Acyclic sesquiterpene oligoglycosides from pericarps of *Sapindus mukurossi*. Phytochemistry 25, 871–876.

Kasai, R., Hirono, S., Chou, W.-H., Tanaka, O., and Chen, F.-H. 1988. Sweet dihydroflavanol rhamnoside from leaves of *Engelhardtia shrysolepis*, a Chinese folk medicine, Chem. Pharm. Bull. 36, 4167–4170.

Kasai, R., Nie, R.-L., Nashi, K., Ohtani, K., Zhou, J., Tao, G.-D., and Tanaka, O. 1989. Sweet cucurbitane glycosides from fruits of *Siraitia siamensis* (chi-zi luo-han-guo), a Chinese folk medicine. Agric. Biol. Chem., 53, 3347–3349.

Kawamura, Y. and Kare, M. R. (*eds.).* 1987. Umami: A Basic Taste, Marcel Dekker.

Kaya, N., Shen, T., Lu, S. G., Zhao, F. L., and Herness, S. 2004. A paracrine signaling role for serotonin in rat taste buds: expression and localization of serotonin receptor subtypes. Am. J. Physiol. Regul. Integr. Comp. Physiol. 286, R649–658.

Kennelly, E. J., Cai, L., Long, L., Shamon, L., Zaw, K., Zhou, B.-N., Pezzuto, J. M., and Kinghorn, A. D. 1995. Novel highly sweet secodammarane glycosides from *Pterocarya paliurus*. J. Agric. Food Chem. 43, 2602–2607.

Kier, L. B. 1972. Molecular theory of sweet taste. J. Pharm. Sci. 61, 1394–1397.

Kim, N.-C. and Kinghorn, A. D. 2002. Sweet-Tasting and Sweetness-Modifying Constituents of Plants. In: Studies in Natural Products Chemistry, Vol. 27 (*ed*. Atta-ur-Rahman), pp. 3–57, Elsevier Science B. V.

Kim, J., Pezzuto, J. M., Soejarto, D. D., Lang, F. A., and Kinghorn, A. D. 1988. Polypodoside A, an intensely sweet constituent of the rhizomes of polypodium glycyrrhiza<NET>. J. Nat. Prod. 51, 1166–1172.

Kniazeff, J., Saintot, P.-P., Goudet, C., Liu, J., Charnet, A., Guillon, G., and Pin, J.-P. 2004. Locking the $GABA_B$ G-protein-coupled receptor in its active state. J. Neurosci. 24(2), 370–377.

Kohmura, M. and Ariyoshi, Y. 1998. Chemical synthesis and characterization of the sweet protein mabinlin II. Biopolymers 46, 215–223.

Kretz, O., Barbry, P., Bock, R., and Lindemann, B. 1999. Differential expression of RNA and protein of the three pore-forming subunits of the amiloride-sensitive epithelial sodium channel in taste buds of the rat. J. Histochem. Cytochem. 47, 51–64.

Kunishima, N., Shimada, Y., Tsuji, Y., Sato, T., Yamamoto, M., Kumasaka, T., Nakanishi, S., Jingami, H., and Morikawa, K. 2000. Structural basis of glutamate recognition by a dimeric metabotrophic glutamate receptor. Nature 407, 971–977.

Kurihara, K. and Beidler, L. M. 1968. Taste-modifying protein from miracle fruit. Science 161, 1241–1243.

Lapidus, M. and Sweeney, M. 1973. L-4′-Cyano-3-(2,2,2-trifluoroacetamido)-succinanilic acid and related synthetic sweetening agents. J. Med. Chem. 16, 163–166.

Le, A. S. and Bowe Mulderrig, K. 2001. Sorbitol and Mannitol. In: Alternative Sweeteners, 3rd edn (*ed*. L. O'Brien Nabors), pp. 317–334. Marcel Dekker.

Lee, C.-K. 1987. The Chemistry and Biochemistry of the Sweetness of Sugars. In: Advances in Carbohydrate Chemistry and Biochemistry, Vol. 45 (*eds*. R. S. Tipson and D. Horton),pp. 199–351.. Academic Press.

Li, X., Staszewski, L., Xu, H., Durick, K., Zoller, M., and Adler, E. 2002. Human receptors for sweet and umami taste. PNAS 99, 4692–4696.

Lin, W., Burks, C. A., Hansen, D. R., Kinnamon, S. C., and Gilbertson, T. A. 2004. Taste receptor cells express pH-sensitive leak K^+ channels. J. Neurophysiol. 92, 2909–2919.

Lin, W., Finger, T. E., Rossier, B. C., and Kinnamon, S. C. 1999. Epithelial Na^+ channel subunits in rat taste cells: localization and regulation by aldosterone. J. Comp. Neurol. 405, 406–420.

Lin, W., Ogura, T., and Kinnamon, S. C. 2002. Acid-activated cation currents in rat vallate taste receptor cells. J. Neurophysiol. 88, 133–141.

Liu, L. and Simon, S. A. 2001a. Acidic stimuli activate two distinct pathways in taste receptor cells from rat fungiform papillae. Brain Res. 923, 58–70.

Lopez-Jimenez, N. D, Cavenagh, M. M, Sainz, E., Cruz-Ithier, M. A., Battey, J. F., and Sullivan, S. L. 2006. Two members of the TRPP family of ion channels, Pkd1l3 and Pkd2l1, are co-expressed in a subset of taste receptor cells. J. Neurochem. 98, 68–77.

Lyall, V., Alam, R. I., Malik, S. A., Phan, T-H. T., Vinnikova, A. K., Heck, G. L., and DeSimone, J. A. 2004. Basolateral Na^+-H^+ exchanger-1 in rat taste receptor cells is involved in neural adaptation to acidic stimuli. J. Physiol. 556, 159–173.

Lyall, V., Alam, R. I., Phan, D. Q., Ereso, G. L., Phan, T-H. T., Malik, S. A., Montrose, M. H., Chu, S., Heck, G. L., Feldman, G. M., and DeSimone, J. A. 2001. Decrease in rat taste receptor cell intracellular pH is the proximate stimulus in sour taste transduction. Am. J. Physiol. Cell Physiol. 281, C1005–C1013.

Lyall, V., Alam, R. I., Phan, T-H. T., Phan, D. Q., Heck, G. L., and DeSimone, J. A. 2002a. Excitation and adaptation in the detection of hydrogen ions by taste receptor cells: a role for cAMP and Ca^{2+}. J. Neurophysiol. 87, 399–408.

Lyall, V., Alam, R. I., Phan, T-H. T., Russell, O. F., Malik, S. A., Heck, G. L., and DeSimone, J. A. 2002b. Modulation of rat chorda tympani NaCl responses and intracellular Na^+ activity in polarized taste receptor cells by pH. J. Gen. Physiol. 120, 793–815.

Lyall, V., Heck, G. L., Phan, T. H., Mummalaneni, S., Malik, S. A., Vinnikova, A. K., and DeSimone, J. A. 2005. Ethanol modulates the VR-1 variant amiloride-insensitive salt taste receptor. II. Effect on chorda tympani salt responses. J. Gen. Physiol. 125, 587–600.

Lyall, V., Heck, G. L., Vinnikova, A. K., Ghosh, S., Phan, T. H., Alam, R. I., Russell, O. F., Malik, S. A., Bigbee, J. W., and DeSimone, J. A. 2004. The mammalian amiloride-insensitive non-specific salt taste receptor is a vanilloid receptor-1 variant. J. Physiol. 558, 147–159.

Lyall, V., Pasley, H., Phan, T-H. T., Mummalaneni, S., Heck, G. L., Vinnikova, A. K., and DeSimone, J. A. 2006. Intracellular pH modulates taste receptor volume and the phasic part of the chorda tympani response to acids. J. Gen. Physiol. 127, 15–34.

Lythgoe, B. and Trippett, S. 1950. The constitution of the disaccharide of glycyrrhinic acid. J. Chem. Soc., 1983–1990.

Margolskee, R. F. 2002. Molecular mechanisms of bitter and sweet taste transduction. J. Biol. Chem. 277, 1–4.

Margolskee, R. L. 2004. Insights into Taste Transduction and Coding from Molecular, Biochemical, and Transgenic

Studies. In: Challenges in Taste Chemistry and Biology, ACS Symposium Series 867 (*eds*. T. Hofmann, C. -T. Ho, and W. Pickenhagen), pp. 26–44. American Chemical Society.
Marie, S. and Piggott, J. R. (*eds*.) 1991. Handbook of Sweeteners. Blackie & Son.
Masuda, H., Ohtani, K., Mizutani, K., Ogawa, S., Kasai, R., and Tanaka, O. 1991. Chemical study on *Haematoxylon campechianum*: a sweet principle and new dibenz-[*b*,*d*]-oxocin derivatives. Chem. Pharm. Bull. 39, 1382–1384.
Matsumoto, K., Kasai, R., Ohtani, K., and Tanaka, O. 1990. Minor cucurbitane glycosides from fruits of *Siraitia grosvenori* (Cucurbitaceae). Chem. Pharm. Bull. 38, 2030–2032.
Matsunami, H., Montmayeur, J. P., and Buck, L. B. 2000. A family of candidate taste receptors in human and mouse. Nature 404, 601–604.
Max, M., Gopi Shanker, Y., Huang, L., Rong, M., Liu, Z., Campagne, F., Weinstein, H., Damak, S., and Margolskee, R. F. 2001. *Tas1r3*, encoding a new candidate taste receptor, is allelic to the sweet responsiveness locus *Sac*. Nat. Genet. 28, 58–63.
Mazur, A. W. and Mohlenkamp, M. J. 1997. Small, Non-nutritive Carbohydrates as Sucrose Substitutes for Foods. In: New Technologies for Healthy Foods & Nutraceuticals (*ed*. M. Yalpani), pp. 124–142. ATL Press.
Mazur, R. H., Schlatter, J. M., and Goldkamp, A. H. 1969. Structure–taste relationships of some dipeptides, J. Am. Chem. Soc. 91, 2684–2691.
McLaughlin, S. K., Mckinnon, P. J., and Margolskee, R. F. 1992. Gustducin is a taste-cell-specific G-protein closely related to the transducins, Nature 357, 563–569.
Mierson, S., Heck, G. L., DeSimone, S. K., Biber, T. U., and DeSimone, J. A. 1985. The identity of the current carriers in canine lingual epithelium *in vitro*. Biochim. Biophys. Acta. 816, 283–293.
Mierson, S., Welter, M. E., Gennings, C., and DeSimone, J. A. 1988. Lingual epithelium of spontaneously hypertensive rats has decreased short-circuit current in response to NaCl. Hypertension 11, 519–522.
Ming, D. and Hellekant, G. 1994. Brazzein, a new high-potency thermostable sweet protein from *Pentadiplandra brazzeana* B. FEBS Lett. 355, 106–108.
Mintz, S. W. 1985. Sweetness and Power: The Place of Sugar in Modern History. Penguin Books.
Miyamoto, T., Fujiyama, R., Okada, Y., and Sato, T. 1998. Sour transduction involves activation of NPPB-sensitive conductance in mouse taste cells. J. Neurophysiol. 80, 1852–1859.
Montmayeur, J.-P., Liberles, S. D., Matsunami, H., and Buck, L. B. 2001. A candidate taste receptor gene near a sweet taste locus. 2001. Nat. Neurosci. 4(5), 492–498.
Morris, J. A. and Cagan, R. H. 1972. Purification of monellin, sweet principle in *Dioscoreophyllum cuminsii*, Biochim. Biophys. Acta 261, 114–122.
Muspratt, J. T. and Hofmann, A. W. 1846. Über das nitranilin, ein neues zersetzungsprodukt des dinitrobenzols. Ann. Chem. 57, 201–224.
Nagarajan, S., Kellogg, M. S., DuBois, G. E., Williams, D. S., Gresk, C. J., and Markos, C. S. 1992. Understanding the mechanism of sweet taste: synthesis of tritium labeled guanidineacetic acids. J. Labelled Comp. Radiopharm. 31(8), 599–607.
Naim, M., Nir, S., Spielman, A. I., Noble, A. C., Peri, I., Rodin, S., and Samuelov-Zubare, M. 2002. Hypothesis of Receptor-Dependent and Receptor-Independent Mechanisms for Bitter and Sweet Taste Transduction: Implications for Slow Taste Onset and Lingering Aftertaste. In: Chemistry of Taste: Mechanisms, Behaviors and Mimics (*eds*. P. Given and D. Paredes), pp. 1–17. ACS Symposium Series 825, American Chemical Society.
Naim, M., Seifert, R., Nürnberg, B., Grünbaum, L., and Schultz, G. 1994. Some taste substances are direct activators of G-proteins, Biochem. J. 297, 451–454.
Nanayakkara, N. P. D., Hussain, R. A., Pezzuto, J. M., Soejarto, D. D., and Kinghorn, A. D. 1988. An intensely sweet dihydroflavonol derivative based on a natural product lead compound, J. Med. Chem. 31, 1250–1253.
Nelson, G., Chandrashekar, J., Hoon, M. A., Feng, L., Zhao, G., Ryba, N. J. P., and Zuker, C. S. 2002. An amino-acid taste receptor. Nature 416, 199–202.
Nelson, G., Hoon, M. A., Chandrashekar, J., Zhang, Y., Ryba, N. J. P., and Zuker, C. S. 2001. Mammalian sweet taste receptors. Cell 106, 381–390.
Nie, Y., Vigues, S., Hobbs, J. R., Conn, Graeme, L., and Munger, S. D. 2005. Distinct contributions of T1R2T1R2 and T1R3T1R3 taste receptor subunits to the detection of sweet stimuli, Curr. Biol. 15(21), 1948–1952.
Ninomiya, Y. and Funakoshi, M. 1988. Amiloride inhibition of responses of rat single chorda tympani fibers to chemical and electrical tongue stimulations. Brain Res. 451, 319–325.
Ninomiya, Y., Sako, N., and Funakoshi, M. 1989. Strain differences in amiloride inhibition of NaCl responses in mice, *Mus musculus*. J. Comp. Physiol. 166, 1–5.
Nishizawa, M. and Yamada, H. 1996. Intensely Sweet Saponin Osladin: Synthetic and Structural Study. In: Saponins Used in Food and Agriculture (*eds*. G. R. Waller and K. Yamasaki), pp. 25–36. Plenum Press.
Nofre, C. and Tinti, J.-M. 2000. Neotame: discovery, properties and utility. Food Chem, 69(3), 245–257.
Nofre, C., Tinti, J.-M., and Ouar Chatzopoulos, F. 1990. Sweetening Agents, US Patent 4 921 939 (May 1, 1990), (to Universite Claude Bernard, Lyon, France).
O'Brien Nabors, L. (*ed*.) 2001. Alternative Sweeteners, 3rd edn, Marcel Dekker.
Ogata, C., Hatada, M., Tomlinson, G., Shin, W.-C., and Kim, S.-H. 1987. Crystal structure of the intensely sweet protein monellin, Nature (Lond.) 328, 739–742.
Ogiso, K., Shimizu, Y., Watanabe, K., and Tonasaki, K. 2000. Possible involvement of undissociated acid molecules in the acid response of the chorda tympani nerve of the rat. J. Neurophysiol. 83, 2776–2779.
Olinger, P. M. and Pepper, T. 2001. Xylitol. In: Alternative Sweeteners, 3rd edn (*ed*. L. O'Brien Nabors), pp. 335–365. Marcel Dekker.
Ozeck, M., Brust, P., Xu, H., and Servant, G. 2004. Receptors for bitter, sweet and umami taste couple to inhibitory G protein signaling pathways. Eur. J. Pharmacol. 489, 139–149.
Pérez, C. A., Huang, L., Rong, M., Kozak, J. A., Preuss, A. K., Zhang, H., Max, M., and Margolskee, R. F. 2002. Transient receptor potential channel expressed in taste receptor cells. Nat. Neurosci. 5(11), 1–8.
Petersen, S. and Müller, E. 1948. Über eine neue gruppe von süssstoffen. Chem. Ber. 81, 31–38.
Pfeilsticker, K., Ruffler, I., Engel, C., and Rehage, C. 1978. Relation between bitter taste and positive surface tension of pure substances in aqueous solutions. Lebensm. Wiss. Technol. 11(6), 323–329.
Phillips, K. C. 1987. Stevia: Steps in Developing a New Sweetener. In: Developments in Sweeteners, 3 (*ed*. T. H. Grenby), pp. 1–43. Elsevier Applied Science.
Pin, J.-P., Galvez, T., and Prezeau, L. 2003. Evolution, structure, and activation mechanism of family 3/C G-protein-coupled receptors. Pharmacol. Ther. 98, 325–354.
Polanski, J. and Ratajczak, A. 1993. A Structure–Taste Study of a New Class of Artificial Sweeteners, Arylsulphonylalkanoic Acids, Chapter 11. In: Sweet-Taste Chemoreception

(*eds*. M. Mathlouthi, J. A. Kanters, and G. G. Birch), pp. 185–203. Elsevier Applied Science.
Pronin, A. N., Tang, H., Connor, J., and Keung, W. 2004. Identification of ligands for two bitter T2RT2RS receptors. Chem. Senses 29, 583–593.
Putnam, R. W., Filosa, J. A., and Ritucci, N. A. 2004. Cellular mechanisms involved in CO_2 and acid signaling in chemosensitive neurons. Am. J. Physiol. 287, C1493–C1526.
Richter, C. P. 1936. Increased salt appetite of adrenalectomized rats. Am. J. Physiol. 115, 155–161.
Richter, T. A., Caicedo, A., and Roper, S. D. 2003. Sour taste stimuli evoke Ca^{2+} and pH responses in mouse taste cells. J. Physiol. 547, 475–483.
Richter, T. A., Dvoryanchikov, G. A., Chaudhari, N., and Roper, S. D. 2004a. Acid-sensitive two-pore domain potassium (K_2P) channels in mouse taste buds. J. Neurophysiol. 92, 1928–1936.
Richter, T. A., Dvoryanchikov, G. A., Roper, S. D., and Chaudhari, N. 2004b. Acid-sensing ion channel-2 is not necessary for sour taste in mice. J. Neuroscience 24, 4088–4091.
Rohse, H. and Belitz, H.-D. 1991. Shape of Sweet Receptors Studied by Computer Modeling, Chapter 13. In: Sweeteners: Discovery, Molecular Design and Chemoreception (*eds*. D. E. Walters, F. T. Orthoefer, and G. E. DuBois), pp. 176–192. ACS Symposium Series 450, American Chemical Society.
Rossier, B. C., Pradervand, S., Schild, L., and Hummler, E. 2002. Epithelial sodium channel and the control of sodium balance: interaction between genetic and environmental factors. Annu. Rev. Physiol. 64, 877–897.
Roy, G. (*ed*.) 1997. Modifying Bitterness: Mechanism, Ingredients and Applications, Technomic Publishing AG.
Runti, C. and Collino, F. 1964. Relations between chemical constitution and sweet taste. Derivatives of *p*-methoxybenzoylbenzoic acid and of malonic acid diamides. XII, Ann. Chim. (Rome) 54, 431–440.
Runti, C. and Galimberti, S. 1957. The relations between chemical constitutions and sweet taste. Derivatives of *p*-methoxybenzoylbenzoic acid. Ann. Chim. (Rome) 47, 250–259.
Sainz, E., Korley, J. N., Battey, J. F., and Sullivan, S. L. 2001. Identification of a novel member of the T_1R family of putative taste receptors. J. Neurochem. 77, 896–903.
Saroli, A. 1986. Structure-activity relationship of bitter compounds related to denatonium chloride and dipeptide methyl esters. Zeitschrift für Lebensmittel-Untersuchung und Forschung 182, 118–120.
Schiffman, S. S., Gatlin, L. A., Sattely-Miller, E. A., Graham, B. G., Heiman, S. A., Stagner, W. C., and Erickson, R. P. 1994. The effect of sweeteners on bitter taste in young and elderly adults. Brain Res. Bull. 35(3), 189–204.
Schiffman, S. S., Lockhead, E., and Maes, F. W. 1983. Amiloride reduces the taste intensity of Na^+ and Li^+ salts and sweeteners. Proc. Natl. Acad. Sci. U. S. A. 80, 6136–6140.
Schiffman, S. S., Suggs, M. S., Cragoe, E. J., Jr., and Erickson, R. P. 1990. Inhibition of taste responses to Na^+ salts by epithelial Na^+ channel blockers in gerbil. Physiol. Behav. 47, 455–459.
Schutz, H. G. and Pilgrim, F. J. 1957. Sweetness of various compounds and its measurement. Food Res. 22, 206–213.
Scinska, A., Koros, E., Habrat, B., Kukwa, A., Kostowski, W., and Bienkowski, P. 2000. Bitter and sweet components of ethanol taste in humans. Drug and alcohol dependence 60(2), 199–206.
Scott, T. R. and Giza, B. K. 1990. Coding channels in the taste system of the rat. Science 249, 1585–1587.
Scott, T. R. and Plata-Salaman, C. R. 1991. Coding of Taste Quality. In: Smell and Taste in Health and Disease (*eds*. T. V. Getchell, R. L. Doty, L. M. Bartoshuk, and J. B. Snow), pp. 345–368. Raven Press.
Shallenberger, R. S. 1993. Taste Chemistry. Blackie Academic & Professional.
Shallenberger, R. S. and Acree, T. E. 1967. Molecular Theory of Sweet Taste. Nature (Lond.) 216, 480–482.
Shallenberger, R. S., Acree, T. E., and Lee, C. Y. 1969. Sweet taste of D- and L-sugars and amino acids and the steric nature of their chemoreceptor site. Nature (Lond.) 221, 555–556.
Shu, R. G., Xu, C. R., and Li, L. N. 1995. Studies on the sweet principles from the leaves of *Cyclocarya paliurus* (Batal.) Iljinsk. Acta Pharmaceutica Sinica 30, 757–761.
Simon, S. A. and Garvin, J. L. 1985. Salt and acid studies on canine lingual epithelium. Am. J. Physiol. 249, C398–408.
Simon, S. A., Holland, V. F., Benos, D. J., and Zampighi, G. A. 1993. Transcellular and paracellular pathways in lingual epithelia and their influence in taste transduction. Microsc. Res. Tech. 26(3), 196–208.
Simon, S. A., Robb, R., and Garvin, J. L. 1986. Epithelial responses of rabbit tongues and their involvement in taste transduction. Am. J. Physiol. 251, R598–608.
von Skramlik, E. 1926. Handbuch der Physiologie der niederen sinne: Band I. Die physiologie des geruchs-und geschmacksinnes. G. Thieme.
Smith, D. V. and Ossebaard, C. A. 1995. Amiloride suppression of the taste intensity of sodium chloride: evidence from direct magnitude scaling. Physiol. Behav. 57, 773–777.
Solms, J. 1969. Taste of amino acids, peptides and proteins. Int. z. vitaminforsch. 39, 320–322.
Spector, A. C., Guagliardo, N. A., and St. John, S. J. 1996. Amiloride disrupts NaCl versus KCl discrimination performance: implications for salt taste coding in rats. J. Neurosci. 16, 8115–8122.
Spielman, A. I., Huque, T., Whitney, G., and Brand, J. G. 1992. The Diversity of Bitter Taste Mechanisms. In: Sensory Transduction (*eds*. D. Corey and S. D. Roper), pp. 307–324. Rockefeller University Press.
St. John, S. J. and Smith, D. V. 2000. Neural representation of salts in the rat solitary nucleus: brain stem correlates of taste discrimination. J. Neurophysiol. 84, 628–638.
Stark, T., Bareuther, S., and Hofmann, T. 2005. Sensory-guided decomposition of roasted cocoa nibs (*Theobroma cacao*) and structure determination of taste-active polyphenols. J. Agric. Food Chem. 53, 5407–5418.
Steiner, J. E. 1994. Behavior Manifestations Indicative of Hedonics and Intensity in Chemosensory Experience. In: Olfaction and Taste XI, Proceedings of the 11th International Symposium on Olfaction and Taste and of the 27th Japanese Symposium on Taste and Smell (*eds*. K. Kurihara, N. Suzuki, and H. J. Ogawa), pp. 284–287. Springer-Verlag.
Stevens, D. R., Seifert, R., Bufe, B., Muller, F., Kremmer, E., Gauss, R., Meyerhof, W., Kaupp, U. B., and Lindemann, B. 2001. Hyperpolarization-activated channels HCN1 and HCN4 mediate responses to sour stimuli. Nature 413, 631–635.
Suarez, T., Kornfeld, E. C., and Sheneman, J. M. 1975. Sweetening Agent. US Patent 3 899 592 (August 12, 1975).
Sweeny, J. G., D'Angelo, L. L., Ricks, E. A., and Iacobucci, G. A. 1995. Discovery and synthesis of a new series of high-potency L-aspartyl-D-α-aminoalkanoyl-(*S*)-α-alkylbenzylamide sweeteners. J. Agric. Food. Chem. 43(8), 1969–1976.
Tahara, A., Nakata, T., and Ohtsuka, Y. 1971. New type of compound with strong sweetness. Nature (Lond.), 233–619.
Tanaka, T., Kawamura, K., Kohda, H., Yamasaki, K., and Tanaka, O. 1982. Glycosides of the leaves of *Symplocos* spp. (Symplocaceae), Chem. Pharm. Bull. 30, 2421–2423.
Tanaka, T., Tanaka, O., Lin, Z.-W., and Zhou, J. 1985. Sweet and bitter glycosides of the Chinese plant drug, Bai-Yun-

Shen: revision of the assignment of the source plant and isolation of two new diterpene glycosides. Chem. Pharm. Bull. 33, 4275–4280.
Tanaka, T., Tanaka, O., Lin, Z.-W., Zhou, J., and Ageta, H. 1983. Sweet and bitter glycosides of the Chinese plant drug, Bai-Yun-Shen (Roots of *Salvia Digitaloides)*. Chem. Pharm. Bull. 31, 780–783.
Temussi, P. A., Lelj, F., and Tancredi, T. 1991. Structure–Activity Relationship of Sweet Molecules, Chapter 11. In: Sweeteners: Discovery, Molecular Design and Chemoreception (*eds*. D. E. Walters, F. T. Orthoefer, and G. E. DuBois), pp. 143–161. ACS Symposium Series 450, American Chemical Society.
Tinti, J.-M. and Nofre, C. 1991. Why Does a Sweetener Taste Sweet? A New Model. In: Sweeteners: Discovery, Molecular Design and Chemoreception (*eds*. D. E. Walters, F. T. Orthoefer, and G. E. DuBois), pp. 206–213. ACS Symposium Series 450, American Chemical Society.
Tinti, J.-M., Nofre, C., and Peytavi, A.-M. 1982. Interaction of suosan with the sweet taste receptor. Z. Lebensm.-Unters. -Forsch. 175, 266–268.
Trevisani, M., Smart, D., Gunthorpe, M. J., Tognetto, M., Barbieri, M., Campi, B., Amadesi, S., Gray, J., Jerman, J. C., Brough, S. J., Owen, D., Smith, G. D., Randall, A. D., Harrison, S., Bianchi, A., Davis, J. B., and Geppetti, P. 2002. Ethanol elicits and potentiates nociceptor responses via the vanilloid receptor-1. Nat. Neurosci. 5, 546–551.
Ugawa, S., Minami, Y., Guo, W., Saishin, Y., Takatsuji, K., Yamamoto, T., Tohyama, M., and Shimada, S. 1998. Receptor that leaves a sour taste in the mouth. Nature 395, 555–556.
van der Heijden, A., van der Wel, H., and Peer, H. G. 1985a. Structure–activity relationships in sweeteners. I. Nitroanilines, sulphamates, oximes, isocoumarins and dipeptides, Chem. Senses 10, 57–72.
van der Heijden, A., van der Wel, H., and Peer, H. G. 1985b. Structure–activity relationships in sweeteners. II. Saccharins, acesulfames, chlorosugars, tryptophans and ureas. Chem. Senses 10, 73–88.
van der Wel, H. 1972. Isolation and characterization of thaumatin I and II, the sweet tasting proteins from *Thaumatococcus danielli* (Benth), Eur. J. Biochem. 31, 221–225.
Varkevisser, B. and Kinnamon, S. C. 2000. Sweet taste transduction in hamster: role of protein kinases. J. Neurophysiol. 83(5), 2526–2532.
Verrey, F., Hummler, E., Schild, L., and Rossier, B. C. 2000. Control of Na Transport by Aldosterone. In: The Kidney: Physiology and Pathophysiology, Vol. 1 (*eds*. D. W. Seldin and G. Giebisch), pp. 1441–1471. Lippincott.
Vinnikova, A. K., Alam, R. I., Malik, S. A., Ereso, G. L., Feldman, G. M., McCarty, J. M., Knepper, M. A., Heck, G. L., DeSimone, J. A., and Lyall, V. 2004. Na^+–H^+ exchange activity in taste receptor cells. J. Neurophysiol. 91, 1297–1313.
Vleggaar, R., Ackerman, L. G. J., and Steyn, P. S. 1992. Structure elucidation of monatin, a high-intensity sweetener isolated from the plant *Schlerochiton ilicifolius*. J. Chem. Soc. Perkin Trans. I Organic and Bio-Organic Chemistry 3095–3098.
de Vos, A. M., Hatada, M., van der Wel, H., Krabbendam, H., Peerdemann, A. F., and Kim, S.-H. 1985. Three dimensional structure of thaumatin I, an intensely sweet protein, Proc. Natl. Acad. Sci. U. S. A. 82, 1406–1409.
Xu, H., Staszewski, L., Tang, H., Adler, E., Zoller, M., and Li, X. 2004. Different functional roles of T1R subunits in the heteromeric taste receptors. Proc. Natl. Acad. Sci. U. S. A. 101, 14258–14263.
Yamaguchi, S. 1979. The Umami Taste. In: (*ed*. J. C. Boudreau), pp. 33–51, ACS Symposium Series 115, American Chemical Society.
Yamashita, H., Theerasilp, S., Aiuchi, T., Nakaya, K., Nakamura, Y., and Kurihara, Y. 1990. Purification and complete amino acid sequence of a new type of sweet protein with taste-modifying activity, curculin. J. Biol. Chem. 265, 15770–15775.
Ye, Q., Heck, G. L., and DeSimone, J. A. 1991. The anion paradox in sodium taste reception: resolution by voltage clamp studies. Science 254, 724–726.
Yoshii, K., Kiyomoto, Y., and Kurihara, K. 1986. Taste receptor mechanism of salts in frog and rat. Comp. Biochem. Physiol. A. 85, 501–507.
Zhang, Y., Hoon, M. A., Chandrashekar, J., Mueller, K. L., Cook, B., Wu, D., Zuker, C. S., and Ryba, N. J. P. 2003. Coding of sweet, bitter, and umami tastes: different receptor cells sharing similar signaling pathways. Cell 112, 293–301.
Zhao, G. Q., Zhang, Y., Hoon, M. A., Chandrashekar, J., Erlenbach, I., Ryba, N. J. P., and Zuker, C. S. 2003. The receptors for mammalian sweet and umami taste. Cell 115, 255–266.
Zubare-Samuelov, M., Shaul, M. E., Peri, I., Aliluiko, A., Tirosh, O., and Naim, M. 2005. Inhibition of signal termination-related kinases by membrane-permeant bitter and sweet tastants: potential role in taste signal termination. Am. J. Physiol. Cell Physiol. 289, C483–C492.

Further Reading

Economic and Social Department, Food and Agriculture Organization of the United Nations (2004). Food Outlook No. 4, Sugar, http://www.fao.org//docrep/007/j3877e/j3877e/j3877e12.htm.
Hashimoto, Y., Ishizone, H., Saganuma, M., Ogura, M., Nakatsu, K., and Yoshioka, H. 1983. Periandrin I, a sweet triterpene glycoside from *Periandra dulcis*. Phytochemistry 22, 259–264.
Hashimoto, Y., Ohta, Y., Ishizone, H., Kuriyama, M., and Ogura, M. 1982. Periandri III, a novel sweet triterpene glycoside from *Periandra dulcis*. Phytochemistry 21, 2335–2337.

4.03 Insect Gustatory Systems

John I Glendinning, Barnard College, Columbia University, New York, NY, USA

© 2008 Elsevier Inc. All rights reserved.

4.03.1	**Introduction**	75
4.03.2	**Organization of the Peripheral Gustatory System**	76
4.03.3	**Responses of Taste Cells to Food-Related Chemical Stimuli**	77
4.03.3.1	Bitter Compounds	77
4.03.3.2	Carbohydrates	80
4.03.3.3	Salts	81
4.03.3.4	Amino Acids	82
4.03.3.5	Acids	82
4.03.3.6	Miscellaneous Compounds	83
4.03.4	**Organization of the Central Gustatory System**	83
4.03.5	**Central Processing of Gustatory Input**	84
4.03.5.1	Coding Mechanisms	85
4.03.6	**Taste–Mixture Interactions**	86
4.03.7	**Factors that Modulate Gustatory Responsiveness**	87
4.03.7.1	Physical Changes in Taste Sensilla	87
4.03.7.2	Nutrient Levels in Blood	87
4.03.7.3	Dietary Experience Effects	88
4.03.7.3.1	Short-term sensory adaptation	88
4.03.7.3.2	Habituation	88
4.03.7.3.3	Long-term adaptation	88
4.03.7.3.4	Induced food preferences	89
4.03.7.4	Health Status	89
4.03.8	**Future Directions**	89
References		90

4.03.1 Introduction

The sense of taste is vital to invertebrates. It helps them avoid noxious chemicals (White, P. R. and Chapman, R. F., 1990: Schoonhoven, L. M. *et al.*, 1992; Glendinning, J. I., 2002), select host plants and oviposition sites (Ma, W.-C. and Schoonhoven, L. M., 1973; Städler, E. *et al.*, 1995), and identify and discriminate food-related chemical stimuli (Dethier, V. G., 1976; Bernays, E. A. and Chapman, R. F., 1994; Glendinning, J. I. *et al.*, 2002). Taste also helps invertebrates coordinate digestion by stimulating salivation during meals (Friend, W. G. and Smith, J. J., 1971; Ribeiro, J. M. C. and Garcia, E. S., 1980; Watanabe, H. and Mizunami, M., 2006) and determining whether ingested food is directed to the midgut for digestion or the crop for storage (Schmidt, J. M. and Friend, W. G., 1991).

I will examine several features of taste function: (1) the organization of the peripheral and central gustatory system; (2) responses of taste cells to food-related stimuli; (3) central processing of gustatory input; (4) taste–mixture interactions; and (5) factors that modulate gustatory responses. I will limit discussion to insects because this is the invertebrate taxon whose gustatory system has been studied most extensively. Further, because this chapter focuses on the mechanisms by which taste modulates feeding of insects, I will not review comprehensively the literature on insect gustatory receptor (Gr) genes and associated signaling pathways. Detailed reviews of these topics can be found elsewhere (Clyne, P. J. *et al.*, 2000; Glendinning, J. I. *et al.*, 2000a; Ishimoto, H. *et al.*, 2000; Dahanukar, A. *et al.*, 2001; Scott, K. *et al.*, 2001; Robertson, H. M. *et al.*, 2003; Chyb, S., 2004; Hallem, E. A. *et al.*, 2006; Robertson, H. M. and Wanner, K. W., 2006).

4.03.2 Organization of the Peripheral Gustatory System

Insect taste cells are bipolar sensory neurons, which are housed in peg-shaped uniporous structures called basiconic sensilla (or taste sensilla) (Figure 1(a)). These taste sensilla can occur inside the oral cavity, on mouthpart appendages, and/or on the thorax, ovipositor, antennae, wing margins, and/or legs (Chapman, R. F., 1982; Hansen-Delkeskamp, E., 1992; Stocker, R. F., 1994; Schoonhoven, L. M. and van Loon, J. J. A., 2002; Shuichi Haupt, S., 2004). Owing to the external location of many taste sensilla, insects can taste foods simply by contacting them. The taste sensilla are innervated by the single, unbranched dendrites of two to six taste cells, which terminate near the distal tip of the sensillum (Figure 1(b)). The cell body of each cell is located

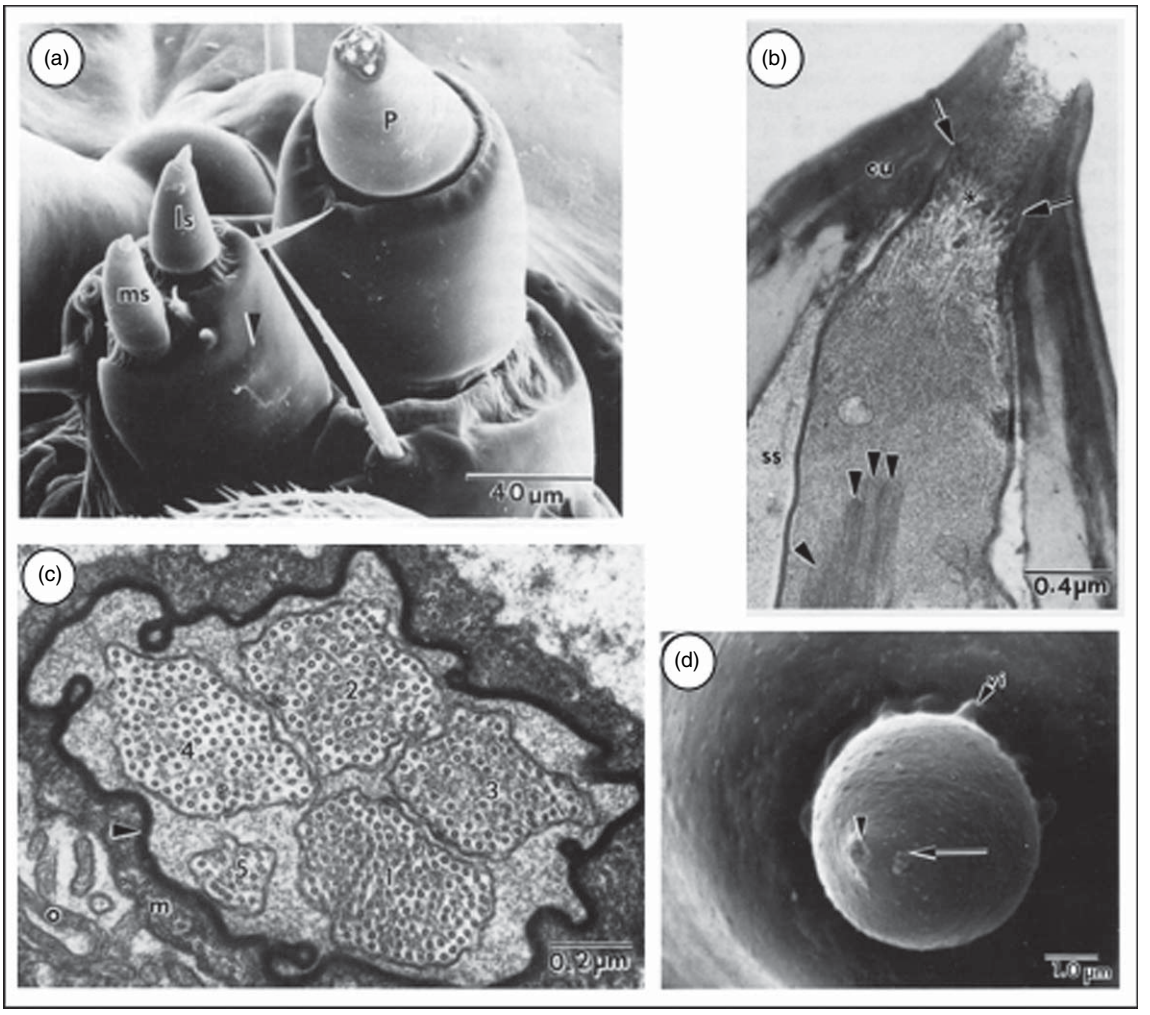

Figure 1 SEM micrographs of a taste sensillum from a caterpillar (*Mamestra configurata*, Lepidoptera: Noctuidae). (a) Left maxilla of caterpillar with lateral (*ls*) and medial (*ms*) styloconic sensilla, and a maxillary palp (*P*). (b) Longitudinal section of a lateral styloconic sensillum. At the top of the image, one can see the tip of the pore, which contains a plug of fenestrated fibirils (asterisk), and the dendritic sheath (arrows), which is fused with the cuticular wall of the sensillum. Four distal dendrites, each from different taste cells (arrowheads), can be seen near the bottom of the image; they are enclosed by the dendritic sheath. *cu*, cuticle; *ss*, sensillar sinus. (c) Proximal cross-section of a medial styloconic sensillum, showing four taste cells (*1–4*) and a mechanosensory neuron (*5*). All neurons are enclosed by a dendritic sheath (arrowhead), which is surrounded by a densely granulated intermediate sheath cell (m). *o*, outer sheath cell. (d) Apical view of the tip of a lateral styloconic sensillum with the terminal pore (arrowhead). These micrographs are from Shields, V. D. C. 1994. Ultrastructure of the uniporous sensilla on the galea of larval *Mamestra configurata* (Walker) (Lepidoptera: Noctuidae). Can. J. Zool. 72, 2016–2031.

near the base of the taste sensillum, and the axon extends directly to the central nervous system. In addition to taste cells, there is usually a single mechanosensory neuron in each taste sensillum (Figure 1(c)). The total number of taste sensilla per insect, and the distribution of these sensilla across the body surface, varies greatly among insect species (Chapman, R. F., 1982). Our ability to explore the membrane properties and intracellular signaling mechanisms of taste cells was increased by a recently developed method for isolating dissociated taste cells from pupal blowflies, *Phormia regina* (Murata, Y. *et al*., 2006).

Taste transduction begins when a chemical stimulus encounters the pore at the tip of a taste sensillum, diffuses through a mucopolysaccharide substance in the pore, and then dissolves into the fluid surrounding the dendrites (Figures 1(b) and 1(d)). This fluid (or receptor lymph) constitutes the outer ionic milieu for the dendritic process of each taste cell. Once the chemical stimulus encounters the distal dendritic membrane, it is thought to interact with specific receptor proteins and/or ionic channels, leading to changes in membrane conductance (Morita, H., 1992). The changes induce an inward current that flows through the transduction ion channels and down to the base of the dendritic process, where current outflow causes depolarization. While the receptor lymph provides some of the driving electromotive force for this taste cell current, most of the force appears to come from a +40 to +60 mV potential difference between the receptor lymph space and the blood (or hemolymph), called the transepithelial voltage (Thurm, U. and Küppers, J., 1980; Kijima, H. *et al*., 1995). The transepithelial voltage is established by electrogenic ion pumps located in the folded membrane of the tormogen and trichogen cells, which surround the taste cells.

4.03.3 Responses of Taste Cells to Food-Related Chemical Stimuli

Insect physiologists typically classify taste cells according to their best taste stimuli – that is, the stimuli that generate the strongest excitatory response. Accordingly, a taste cell that responds best to salts is called salt-sensitive, and a taste cell that responds best to compounds that humans describe as bitter is called bitter-sensitive. There are two caveats associated with this terminology. First, because most insect taste cells have been tested with only a limited number of taste stimuli, it is conceivable that the best stimulus for a taste cell has not yet been discovered. Second, the categorization of a taste cell as salt sensitive implies that stimulation of that taste cell generates a perception akin to saltiness in humans. At this point, we do not even know whether insects perceive distinct taste qualities like salty and sweet (see Section 4.03.5). For the sake of simplicity, I will use the conventional terminology for categorizing the taste cells, keeping in mind the above-stated caveats.

4.03.3.1 Bitter Compounds

Many of the compounds that taste bitter in humans also elicit an aversive response in insects (e.g., rapid cessation of feeding). Because virtually all naturally occurring poisons taste bitter to humans, the aversive response to these bitter compounds is thought to represent an evolved mechanism for limiting ingestion of toxic foods (Bate-Smith, E. C., 1972; Garcia, J. and Hankins, W. G., 1975; Brower, L. P., 1984; Brieskorn, C. H., 1990). The effectiveness of this taste-mediated poison detection system is limited by the fact that even though most poisons taste bitter, the opposite is not always true – that is, many compounds with a bitter taste are harmless (Bernays, E. A. and Chapman, R. F., 1987; Bernays, E. A., 1990; Rouseff, R. L., 1990; Bernays, E. A., 1991; Glendinning, J. I., 1994). Given that many nutritious plant tissues contain bitter compounds, insects (particularly herbivorous ones) would benefit from gustatory mechanisms that discriminate harmful and harmless bitter compounds.

Insects have several preingestive and postingestive mechanisms for detecting potentially toxic compounds in foods (Glendinning, J. I., 2002). The primary mechanism, however, is gustation. Insects have numerous taste cells that respond selectively to bitter compounds and elicit an aversive response when activated (Dethier, V. G., 1980; Schoonhoven, L. M. *et al*., 1992). These bitter-sensitive taste cells have been discovered in Orthopterans (White, P. R. and Chapman, R. F., 1990; Chapman, R. F. *et al*., 1991), Dipterans (Meunier, N. *et al*., 2003), Lepidopterans (Schoonhoven, L. M. *et al*., 1992), and some but not all Coleopterans (Mitchell, B. K., 1987; Messchemdorp, L. *et al*., 1998). To illustrate the response properties of bitter-sensitive taste cells, I will feature the caterpillar of *Manduca sexta* (Lepidoptera: Sphingidae). This insect has a total of 62 taste cells distributed across five classes of bilaterally paired taste sensilla: one lateral styloconic, one medial styloconic, one epipharyngeal, and five maxillary palp sensilla (Figure 2(a)).

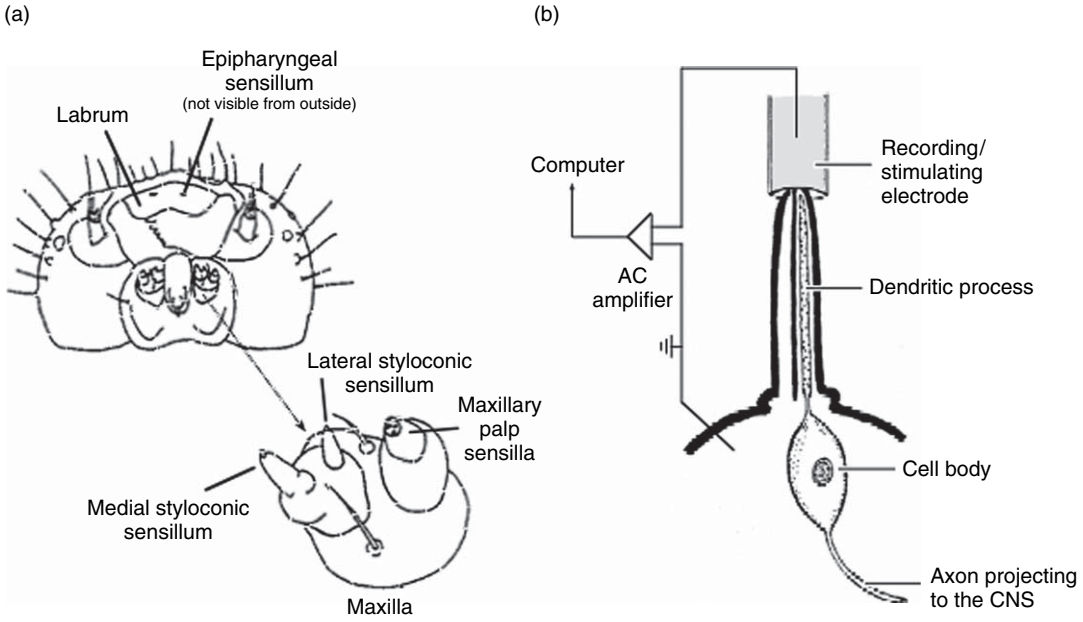

Figure 2 (a) Cartoon of the head of a *Manduca sexta* caterpillar, as viewed from below. An enlargement of the maxilla (indicated with an arrow) is provided to clarify the location of the medial and lateral styloconic sensilla. The epipharyngeal sensilla are located underneath the labrum, and thus are not visible in this diagram. (b) Illustration of the tip recording method, which was used to record excitatory responses of individual taste cells located within a taste sensillum. During a tip recording (Hodgson, E. S. *et al.*, 1955), the tip of a taste sensillum is inserted into the end of a glass recording/stimulating electrode, which is filled with a taste stimulus dissolved in an electrolyte solution (0.1 M KCl in deionized water). The taste stimulus solution diffuses through a pore in the tip of the sensillum and activates transduction mechanism(s) on the distal end of a taste cell's dendritic process; the electrode detects the ensuing action potentials. For clarity, only one taste cell is indicated. Note that the taste cell's axonal process projects directly to the central nervous system without synapsing. (a) This cartoon was adapted from Bernays, E. A. and Chapman, R. F. 1994. Host-Plant Selection by Phytophagous Insects. Chapman and Hall, their Figure 3.4.

Given that each taste sensillum contains one bitter-sensitive taste cell, *M. sexta* has a total of eight bilateral pairs of bitter-sensitive taste cells. Using the tip recording technique (Figure 2(b)), investigators have characterized the response of each bitter-sensitive taste cell to a structurally diverse range of substances that elicit immediate aversive responses: salicin, caffeine, aristolochic acid, *Canna* extract, and *Grindelia* extract (Figure 3). These recordings illustrate that the bitter-sensitive taste cell in the (1) epipharyngeal sensilla responds vigorously to salicin, caffeine, aristolochic acid, and *Canna* extract, (2) lateral styloconic sensilla responds vigorously to salicin, caffeine, aristolochic acid, and weakly to *Canna* extract, (3) medial styloconic sensilla responds vigorously to aristolochic acid and *Canna* extract, and weakly to caffeine and salicin, and (4) maxillary palp sensilla responds vigorously to *Grindelia* extract only (Glendinning, J. I. *et al.*, 2002). Behavioral studies have revealed that any bilateral pair of taste sensilla that responds vigorously to a particular bitter compound is also sufficient to mediate an aversive response to that compound (Glendinning, J. I. *et al.*, 1999a; 2002; Glendinning, J. I., unpublished data). Taken together, these studies show that *M. sexta* possesses a heterogeneous population of bitter-sensitive taste cells – some with identical molecular receptive ranges (MRRs), others with partially overlapping MRRs, and yet others with unique MRRs. The adaptive significance of this taste cell diversity is that it facilitates the detection and discrimination of bitter taste stimuli.

To determine whether two bitter taste stimuli (e.g., caffeine and salicin) activate the same taste cell, one can examine the neural response of a taste cell to each compound, both alone and in binary mixture. In Figure 4(a), we show the response of the bitter-sensitive taste cell in the lateral styloconic sensillum to caffeine alone, salicin alone, and the binary mixture of both. Because the binary mixture caused the bitter-sensitive taste cell to generate approximately twice as many spikes as did caffeine or salicin alone, we infer that caffeine and salicin activated the same bitter-sensitive taste cell. In Figure 4b, we show the response of the bitter-sensitive taste cell in the lateral

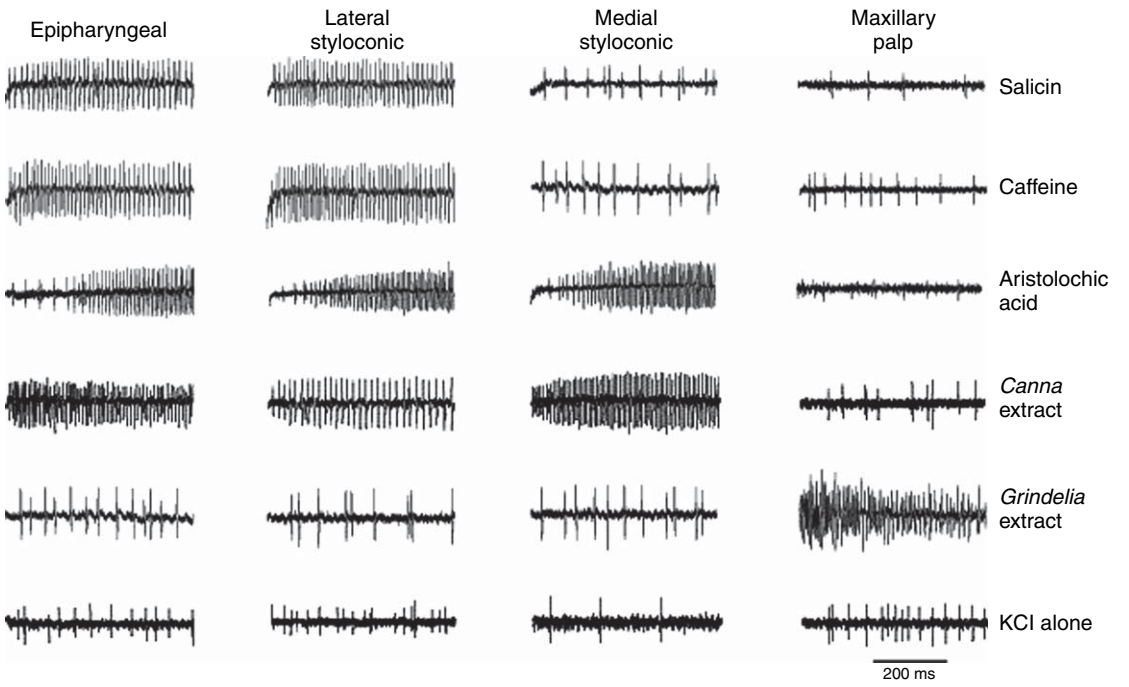

Figure 3 Typical excitatory responses of the four different classes of taste sensilla to five bitter taste stimuli: salicin, caffeine, aristolochic acid, *Canna* extract, and *Grindelia* extract (see Glendinning, J. I. *et al.*, 2002, for exact concentrations of each taste stimulus). The onset of stimulation occurred at the beginning of each trace, and each vertical line reflects the occurrence of an action potential. In most of the traces containing a large number of action potentials, there is a single taste cell (the bitter-sensitive taste cell) firing regularly, and another taste cell (the salt-sensitive taste cell) firing sporadically. The only exception is the multiunit response of the maxillary palp sensilla to the *Grindelia* extract, which probably contains action potentials from several bitter-sensitive taste cells. Because all bitter taste stimuli were presented in a 0.1 M KCl solution, we also show representative responses of each sensillum to the electrolyte solution alone for comparison (see bottom row of traces). Note that each bitter taste stimulus selectively activates bitter-sensitive taste cells in a subset of the taste sensilla (e.g., the *Grindelia* extract only stimulated bitter-sensitive taste cells in the maxillary palp). These traces are from Glendinning, J. I., Davis, A., and Ramaswamy, S. 2002. Contribution of different taste cells and signaling pathways to the discrimination of "bitter" taste stimuli by an insect. J. Neurosci. 22, 7281–7287.

styloconic sensillum to caffeine alone, *myo*-inositol alone, and the binary mixture of both. Because the response to the binary mixture consisted of two taste cells discharging out of phase with one another, and at the same rate as when each component was presented alone, we infer that each taste stimulus activated a different taste cell.

Several recent observations in adult *Drosophila* offer an explanation for why the bitter-sensitive taste cells in *Drosophila* (Meunier, N. *et al.*, 2003) and perhaps *M. sexta* (Figure 4) express distinct MRRs. The first observation is that the bitter-sensitive taste cells that express Gr66a (a presumed bitter taste receptor) respond to a diversity of bitter taste stimuli (Wang, Z. *et al.*, 2004; Marella, S. *et al.* 2006), and that silencing the Gr66a-expressing taste cells attenuates the aversive response to many bitter compounds (Wang, Z. *et al.*, 2004). The second observation is that knocking out the Gr66a receptor attenuates the responses of the bitter-sensitive taste cells to caffeine and theophylline, but spares responses to most other bitter taste stimuli (Moon, S. J. *et al.*, 2006). Taken together, these observations indicate (1) that there are many different bitter taste receptors, (2) that each receptor has a relatively narrow and distinct MRR; and (3) that each class of bitter-sensitive taste cell expresses different combinations of the receptors.

A final gustatory mechanism for limiting ingestion of bitter and potentially toxic compounds is activated when insects encounter foods that contain mixtures of nutrients and bitter compounds. For instance, the labellar taste sensilla in some flies appear to lack bitter-sensitive taste cells *per se*. However, the excitatory response of the sugar-, salt-, and water-sensitive taste cells to their respective ligands is inhibited by the presence of bitter compounds (Morita, H., 1959; Dethier, V. G. and Bowdan, E., 1989; Meunier, N. *et al.*, 2003). This inhibition effectively eliminates the gustatory input that would normally stimulate feeding

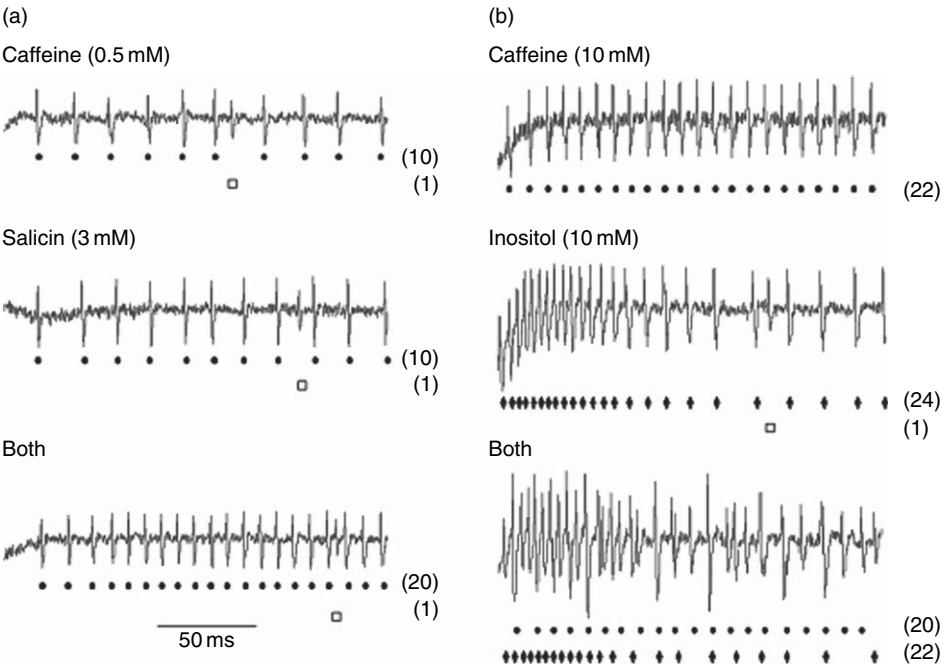

Figure 4 Excitatory responses of taste cells within a lateral styloconic sensillum of *Manduca sexta* caterpillars to single-component taste stimuli and binary mixtures. (a) Response of a bitter-sensitive taste cell to 0.5 mM caffeine alone, 3 mM salicin alone, and the binary mixture of both. Underneath each neural trace, we indicate the response of the bitter-sensitive taste cell (closed circle) and that of the salt-sensitive taste cell to the 0.1 mM KCl solvent (open square). We also indicate the total number of spikes assigned to each taste cell in parentheses. It is apparent that the bitter-sensitive taste cell generated twice as many spikes in response to the binary mixture than it did to either component alone. These traces are from Glendinning, J. I. and Hills, T. T. 1997. Electrophysiological evidence for two transduction pathways within a bittersensitive taste receptor. J. Neurophysiol. 78, 734–745. (b) Response of a bitter-sensitive taste cell to 10 mM caffeine, an inositol-sensitive taste cell to 10 mM *myo*-inositol alone, and both taste cells to the binary mixture of both taste stimuli. Underneath each neural trace, we indicate the response of the bitter-sensitive taste cell (closed circle), the response of the inositol-sensitive taste cell (closed diamonds), and the salt-sensitive taste cell (to the 0.1 mM KCl solvent) (open square). It is apparent that the bitter-sensitive taste cell and the inositol-sensitive taste cells each responded equally vigorously to their respective ligands, irrespective of whether they occurred alone or in binary mixture. Further, note that the response to the binary mixture contains two taste cells firing independently of one another; the unusually high-amplitude spikes reflect superpositions (i.e., instances when the two taste cells fired simultaneously). These traces are from Glendinning, J. I., Nelson, N., and Bernays, E. A. 2000b. How do inositol and glucose modulate feeding in *Manduca sexta* caterpillars? J. Exp. Biol. 203, 1299–1315.

(Dethier, V. G. and Bowdan, E., 1992). One limitation of this detection mechanism is that it is relatively nonselective – e.g., bitter stimuli that differ greatly in toxicity all produce a similar degree of inhibition (Dethier, V. G. and Bowdan, E., 1992).

4.03.3.2 Carbohydrates

Carbohydrates are strong feeding stimulants for many insects (Dethier, V. G., 1976; Bernays, E. A., 1985; Scheiner, R., 2004; Wang, Z. *et al.*, 2004). Most insects possess taste cells that respond selectively to saccharides (e.g., glucose, sucrose, fructose, and trehalose) and/or sugar alcohols (e.g., sorbitol, mannitol, and *myo*-inositol). Whereas Dipterans have carbohydrate-sensitive taste cells that respond both to saccharides and to sugar alcohols, most Lepidopterans have separate taste cells for saccharides and sugar alcohols (Dethier, V. G., 1976; Schoonhoven, L. M. and van Loon, J. J. A., 2002).

The taste system of adult *Drosophila* is notable because it contains the only deorphaned sweet taste receptor in insects: Gr5a. Using a combination of molecular, physiological, and behavioral approaches, investigators demonstrated that Gr5a is encoded by the *Gr5a* gene, and that it is tuned specifically to trehalose, an abundant metabolic byproduct of yeast and an important food source for *Drosophila* (Tanimura, T. *et al.*, 1982; 1988; Dahanukar, A. *et al.*, 2001; Ueno, K. *et al.*, 2001; Chyb, S. *et al.*, 2003; Inomata, N. *et al.*, 2004). Although mutation of Gr5a attenuated the responsiveness of the sugar-sensitive taste cells to trehalose, it had no impact on responsiveness of the same taste cells to

sucrose (Tanimura, T. *et al.*, 1982; 1988; Dahanukar, A. *et al.*, 2001; Ueno, K. *et al.*, 2001; Chyb, S. *et al.*, 2003; Inomata, N. *et al.*, 2004). In addition, two laboratories developed methods for selectively silencing the *Gr5a*-expressing taste cells in adult *Drosophila*; they did so by causing them to produce either tetanus (Thorne, N. *et al.*, 2004) or diphtheria (Wang, Z. *et al.*, 2004) toxin. Using the genetically modified flies, the laboratories demonstrated that flies expressing the toxins under the *Gr5a* driver showed an attenuated appetitive response to trehalose, but normal appetitive response to sucrose. Taken together, these molecular findings indicate that individual carbohydrate-sensitive taste cells express multiple taste receptors for sugars, each of which has a unique MRR. This inference is supported by electrophysiological studies showing that different classes of sensilla in *Drosophila* exhibit different response profiles for sugars (Hiroi, M. *et al.*, 2002).

Prior to the discovery of Gr5a, most work on sugar transduction focused on two hypothetical receptor sites: one that responds to pyranose sugars (e.g., glucose and sucrose) and another to furanose sugars (e.g., fructose) (Morita, H., 1992). The existence of these separate receptor sites was based on the following lines of evidence. Treating the sugar-sensitive taste cell with *p*-chloromercuribenzonate (a specific sulphydryl reagent) almost completely eliminated the response to pyranose sugars, but had no impact on the response to furanose sugars (Shimada, I. *et al.*, 1974). Conversely, treating the sugar-sensitive taste cell with amiloride abolished its response to furanose sugars, but not pyranose sugars (Liscia, A. *et al.*, 1997). Finally, Ozaki and her colleagues used affinity electrophoresis to isolate two putative taste receptor molecules; each of these proteins exhibited sugar-binding affinities and specificities that were consistent with separate pyranose- and furanose-binding sites (Ozaki, M. *et al.*, 1993). More work is needed to integrate these hypothetical receptor sites with our growing molecular understanding of insect gustation.

Based on sequence data from *Drosophila*, the 68 putative gustatory receptor genes (including *Gr5a*) are predicted to encode G-protein-coupled receptors (Robertson, H. M. *et al.*, 2003). In support of this prediction, several recent studies have reported that two G-protein subunits, Gsα and Gγ1, are both required for sugar detection in *Drosophila* (Ishimoto, H. *et al.*, 2005; Ueno, K. *et al.*, 2006). These G-protein subunits, in turn, appear to activate an IP_3 signaling pathway (Usui-Aoki, K. *et al.*, 2005). Other signaling molecules proposed to mediate sugar transduction include Gq-α (Seno, K. *et al.*, 2005b), nitric oxide (Schuppe, H. *et al.*, 2006), and calmodulin (Seno, K. *et al.*, 2005a).

4.03.3.3 Salts

Virtually all taste sensilla contain at least one salt-sensitive taste cell. Monovalent inorganic cations are the most effective stimulants for these taste cells (Dethier, V. G., 1976). Cations differ, however, in their stimulatory effectiveness (e.g., in the fleshfly, *Boettcherisca peregrina*, $Li^+ < Na^+ < Cs^+ < Rb^+ < K^+$) (den Otter, C. J., 1972). den Otter speculated that this order of stimulatory effectively does not vary as a function of ionic size or mobility because each cation interacts differentially with negative groups (probably phosphates) on the surface of the taste cells.

Flies show an appetitive response to low NaCl concentrations (5–10 mM) and aversive response to high NaCl concentrations ($\geq$500 mM) (Dethier, V. G., 1968; Hiroi, M. *et al.*, 2004). This concentration-dependent change in affective response to salts is thought to have evolved because low concentrations of salts satisfy nutritional needs, whereas higher concentrations threaten osmotic equilibrium. To explain the mechanistic basis of this behavior, Wang Z. *et al.* (2004) silenced the sugar-sensitive taste cells of *Drosophila* that express *Gr5a*. When these flies were offered a range of NaCl concentrations, they exhibited an attenuated appetitive response to the 5 mM concentration, but a normal aversive response to concentrations $\geq$500 mM. These latter findings, together with those of Hiroi M. *et al.* (2004), indicate that NaCl stimulates two different classes of taste cell – low concentrations stimulate a taste cell that elicits an appetitive response (presumably the so-called sugar-sensitive taste cell) and high concentrations stimulate a taste cell that elicits an aversive response (presumably a salt-sensitive taste cell).

In *Drosophila*, the aversive response to high (i.e., $\geq$500 mM) concentrations of NaCl is mediated in part by the *dpr* gene. This inference is based on behavioral studies with wildtype and *dpr*-knockout flies (Nakamura, M. *et al.*, 2002). The proboscis extension reflex was strongly inhibited by high NaCl concentrations in wildtype flies, but not in *dpr*-knockout flies. This *dpr* gene is thought to encode a protein with a single transmembrane domain and two Ig repeats, and to be expressed in a subset of taste cells (Nakamura, M. *et al.*, 2002).

An important, but unexplained, observation is that some insects can discriminate between different types of salts (Arms, K. *et al.*, 1974; Maes, F. W. and Bijpost,

S. C. A., 1979; Miyakawa, Y., 1981; 1982). In laboratory rats, the ability to discriminate Na^+ and K^+ salts appears to be mediated by differential input from Na^+-specific (amiloride-sensitive) and Na^+-nonspecific (amiloride-insensitive) cation channels (Spector, A. C. and Grill, H. J., 1992; Smith, D. V. *et al.*, 2000). The question of whether insects use a similar mechanism is unresolved. A recent study reported that *Drosophila* expresses a Na^+-nonspecific (amiloride-sensitive) cation channel (DEG/ENaC) in taste cells within the gustatory terminal organ (in larvae) and taste sensilla on the labellum, legs, and wing margins (in adults) (Liu, L. *et al.*, 2003). The inference that this channel is Na^+ nonspecific was based on the observation that disruption of the genes for DEG/ENaC (*ppk11* and *ppk19*) diminished behavioral and taste cell responsiveness to low (i.e., 10 mM) concentrations of both KCl and NaCl (Liu, L. *et al.*, 2003). Given that the gustatory response to 10 mM KCl in the genetically disrupted flies was still robust (i.e., ~50% of that observed in wildtype flies), it is likely that *Drosophila* also has a DEG/ENaC-independent mechanism for detecting salts. Accordingly, differential input from the DEG/ENaC-dependent and DEG/ENaC-independent mechanisms could mediate the discrimination of Na^+ and K^+ salts.

4.03.3.4 Amino Acids

Amino acids stimulate feeding in many species of insect, but the behavioral responsiveness to any given amino acid varies considerably across species (Bernays, E. A., 1985; Albert, P. J. and Parisella, S., 1988; Hirao, T. and Ariai, N., 1990; Kim, J. H. and Mullin, C. A., 1998). A positive feeding response to amino acids may serve two adaptive functions. First, amino acids could be used as a proxy for protein content of foods, given that plant tissues with relatively high protein concentrations should, on average, have relatively high concentrations of free amino acids. If so, then amino acid-sensitive taste cells could help insects identify protein-rich plant tissues. Second, because some amino acids (e.g., phenylalanine) are considered limiting nutrients for plant-feeding insects (Bernays, E. A., 1982), amino acid-sensitive taste cells could help the insect maintain nutritional homeostasis.

In caterpillars, amino acids often stimulate specific taste cells (Dethier, V. G., 1973; Schoonhoven, L. M. and van Loon, J. J. A., 2002). For example, two closely related species of *Pieris* possess an amino acid-sensitive taste cell that shows concentration-dependent increases in response to ecologically relevant concentrations of 12 L-amino acids (Dethier, V. G., 1973; van Loon, J. J. A. and van Eeuwijk, F. A., 1989). Other species of caterpillar (e.g., *Grammia geneura*) detect amino acids with multiple taste cells (Bernays, E. A. and Chapman, E. A., 2001b). One of the amino acid-sensitive taste cells in *G. geneura* is unusual in that it responds to a diverse array of phagostimulants present in the insect's preferred food plants, including seven amino acids, three sugars, and a secondary plant compound (catalpol, an iridoid glycoside) (Bernays, E. A. *et al.*, 2000).

Dipterans use a variety of gustatory mechanisms for detecting amino acids. On the one hand, the tsetse fly (*Flossina fuscipes fuscipes*) has an amino acid-sensitive taste cell that responds selectively and vigorously 11 of the 20 L-amino acids present in animal proteins (van der Goes van Naters, W. M. and den Otter, C. J., 1998). On the other hand, the blowfly (*P. regina*), fleshfly (*B. peregrina*), and hoverfly (*Eristalis tenax*) all lack taste cells that respond to amino acids (Wolbarsht, M. L. and Hanson, F. E., 1965; Shiraishi, A. and Kuwabara, M., 1970; Goldrich, N. R., 1973; Wacht, S. *et al.*, 2000). Instead, these flies detect amino acids in more complex ways. For instance, when the labellar sensilla of blowflies and fleshflies were stimulated with each of 19 L-amino acids, the ensuing neural response fell into one of four categories. The amino acids (1) inhibited the excitatory response of all taste cells (aspartic acid, glutamic acid, histidine, arginine, and lysine); (2) stimulated the salt-sensitive taste cells (proline and hydroxyproline); (3) stimulated the sugar-sensitive taste cell (valine, leucine, isoleucine, methionine, phenylalanine, and tryptophan); or (4) failed to stimulate or inhibit any taste cell (glycine, alanine, serine, threonine, cysteine, and tyrosine) (Shiraishi, A. and Kuwabara, M., 1970; Goldrich, N. R., 1973). The behavioral significance of these neural responses is unclear because the same taste stimuli fail to elicit normal appetitive responses – that is, proboscis extension reflexes (Wolbarsht, M. L. and Hanson, F. E., 1965).

4.03.3.5 Acids

In humans, acids elicit the perception of sourness. Although organic acids tend to be more sour than inorganic acids (at the same pH), the intensity of sourness generally increases with proton concentration. Little is known about the behavioral responses of insects to low pH foods, however. There is one report showing that ascorbic acid stimulates feeding in *Pieris*

brassicae caterpillars, but only when it is presented in binary mixture with sucrose (Ma, W.-C., 1972).

Organic acids occur in all plant tissues, and their concentrations can reach levels over 100 mM (e.g., citric acid from the Krebs cycle) (Harborne, J. B., 1973). Another nutritionally significant organic acid, ascorbic acid, occurs in plant tissues at concentrations of 1–10 mM (Schultz, J. C. and Lechowicz, M. J., 1986). The fact that ascorbic acid is an essential vitamin for most herbivorous insects may explain why caterpillars show an appetitive response to ascorbic acid when it co-occurs with sugars. On the other hand, the fact that acidic substances can be toxic and/or depress pH of the midgut may explain why many insects display an aversive response to highly acidic foods.

Ground beetles (Coleoptera, Carabidae) are the only known taxon of insects with taste cells that show pH-dependent changes in excitatory response. In these taste cells, the higher the pH, the higher the firing rate (Millius, M. *et al.*, 2006). For most other taxa of insects, acids appear to play a modulatory role – that is, alter the responsiveness of specific taste cells to their best stimuli. For example, at low concentrations, acids inhibit the responsiveness of salt-sensitive taste cells, whereas at higher concentrations, they inhibit the responsiveness of sugar- and inositol-sensitive taste cells and stimulate bitter-sensitive taste cells (Dethier, V. G. and Kuch, J. H., 1971; Bernays, E. A. *et al.*, 1998). These modulatory effects of acids are due to pH and not to specific effects of any particular acidic compound.

4.03.3.6 Miscellaneous Compounds

In addition to the taste stimuli described above, insect taste cells have been found to respond to chemicals not traditionally studied by taste physiologists. Below are four examples. First, the sugar-sensitive taste cells of blood-feeding insects (e.g., the fleshfly, *B. peregrina*) discharge in response to nucleotides in the blood of hosts (e.g., ADP and GDP) (Furuyama, A. *et al.*, 1999). Second, several herbivorous insects possess taste cells that respond to phytoecdysteroids in plant tissues (Ma, W.-C., 1969; Tanaka, Y. *et al.*, 1994; Marion-Poll, F. and Descoins, C., 2002; Calas, D. *et al.*, 2007). Stimulation of these taste cells elicits an aversive response. This response is thought to have evolved because phytoecdysteroids are found in about 6% of all land plant species, and their consumption can interfere with ecdysis. Third, some plant compounds, which are bitter and poisonous to mammals, actually stimulate feeding in herbivorous insects. For example, several species of insect, which depend on pyrrolizidine alkaloids (PAs) for reproduction and chemical defense against predators, possess taste cells specifically tuned to PAs (Bernays, E. A. *et al.*, 2002; 2003). These PA-sensitive taste cells are thought to facilitate the location and consumption of PA-containing plants. Fourth, given the ease at which insects desiccate, it is not surprising that they have evolved taste cells tuned to water (Dethier, V. G., 1976). A recent study identified water-sensitive taste cells in adult *Drosophila* and showed that these taste cells project to a region of the subesophageal ganglion (SOG) that is distinct from that of the sugar- and bitter-sensitive taste cells (Inoshita, T. and Tanimura, T., 2006).

4.03.4 Organization of the Central Gustatory System

The SOG is considered the first relay center for taste processing because it is where the axons of most taste cells terminate (Kent, K. S. and Hildebrand, J. G., 1987; Mitchell, B. K. and Itagaki, H., 1992; Stocker, R. F., 1994; Mitchell, B. K. *et al.*, 1999; Thorne, N. *et al.*, 2004; Wang, Z. *et al.*, 2004). Exceptions to this pattern include instances where (1) taste cells in the legs of Orthopterans project to thoracic ganglia (Rogers, S. M. and Newland, P. L., 2002); and (2) a subpopulation of taste cells in the mouthpart sensilla of Lepidopterans project to the tritocerebrum (Kent, K. S. and Hildebrand, J. G., 1987; Jørgensen, K. *et al.*, 2006).

Several lines of evidence indicate that taste cells can directly activate feeding control circuits in the SOG. First, taste cell axons intermingle with (or occur in close apposition to) arborizations from the mouthpart motor neurons (Altman, J. S. and Kien, J., 1987). Second, some SOG interneurons have branches that occur in neuropil with both sensory and motor terminals (Altman, S. and Kien, J., 1987). Third, stimulating taste cells with plant extracts directly modulates the output of the mouthpart motor neurons (Griss, C. *et al.*, 1991). In addition to exerting effects within the SOG, afferent gustatory information appears to be relayed via the subesophageal-calycal tract to higher processing centers in the calyces of the mushroom body, which are important neuropils for learning and memory (Schröter, U. and Menzel, R., 2003).

To gain insight into the organization of the SOG, investigators initially used anatomical and cobalt-filling techniques, together with activity-dependent

staining of single neurons, to determine the projection sites of axons from taste cells. These studies revealed that taste cells from different gustatory organs, different taste sensilla, or even the same sensillum can project to spatially distinct regions of the SOG (Kent, K. S. and Hildebrand, J. G., 1987; Shanbhag, S. R. and Singh, R. N., 1992; Stocker, R. F., 1994; Pollack, G. S. and Balakrishnan, R., 1997; Jørgensen, K. *et al.*, 2006).

Using molecular tools, investigators have been able to define more precisely the central projection patterns of taste cells. For example, work in *Drosophila* has shown that taste receptor expression can be used to characterize axonal projections from different classes of taste cell. Several investigators have shown that axonal projections to the SOG are segregated spatially according to both taste cell type (e.g., sugar sensitive versus bitter sensitive) and gustatory organ (proboscis, mouthparts, and legs) (Figure 5) (Thorne, N. *et al.*, 2004; Wang, Z. *et al.*, 2004; Inoshita, T. and Tanimura, T., 2006). These findings reveal that the SOG is organized according to a chemotopic and somatotopic organizational plan – i.e., the spatial pattern of activation reflects both the class of taste cell that was stimulated and the location of the taste stimulus on the body.

4.03.5 Central Processing of Gustatory Input

Mammals categorize taste stimuli according to three orthogonal dimensions: intensity, hedonics, and quality (Grill, H. J. and Berridge, K. C., 1985; Spector, A. C.,

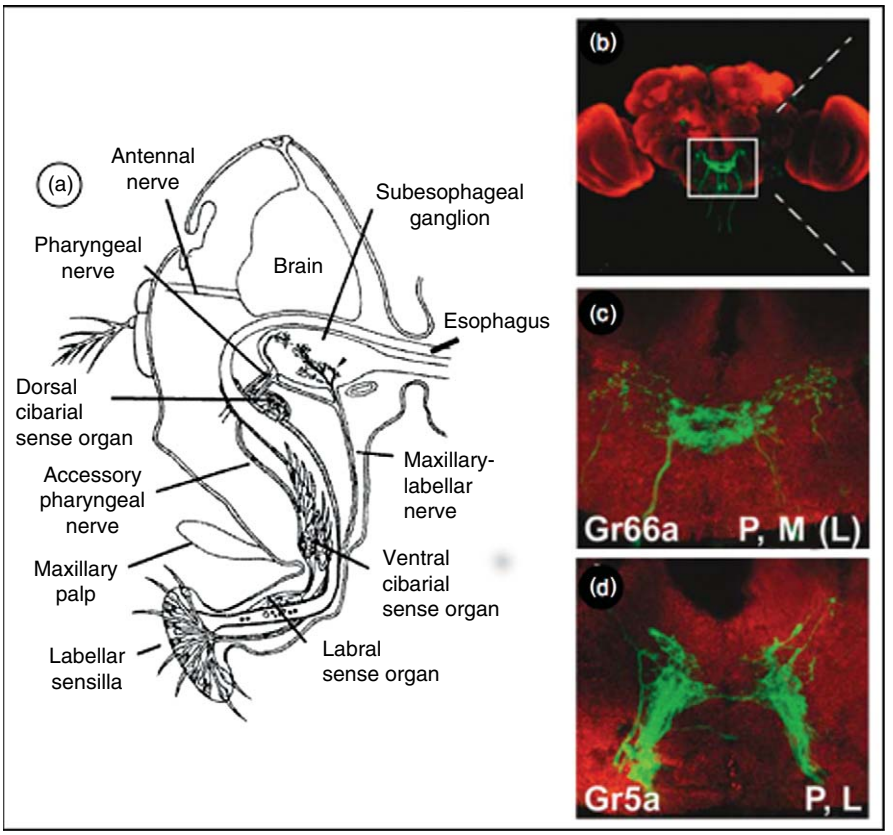

Figure 5 (a) Ultrastructure of the head, feeding apparatus, and central nervous system of an adult fruit fly *Drosophila melanogaster* (from Stocker, R. F. and Schorderet, M. 1981. Cobalt filling of sensory projections from internal and external mouthparts in *Drosophila*. Cell Tissue Res. 216, 513–523). (b) A whole-mount of the brain of *D. melanogaster*, showing axonal projects from taste cells (labeled with anti-GFP immunohistochemistry). The white box indicates the region of the SOG depicted in (c)–(d). (c–d) The green axons are from taste cells expressing a presumed bitter taste receptor, Gr66a (c), and the trehalose taste receptor, Gr5a (d). It is notable that the projection sites for taste cells expressing Gr66a are spatially distinct from those expressing Gr5a. (b)–(d) Are from Wang, Z., Singhvi, A., Kong, P., and Scott, K. 2004. Taste representations in the *Drosophila* brain. Cell 117, 981–991.

2000). Do insects use these three taste dimensions as well? Behavioral studies provide clear support for use of the intensity and hedonic dimensions. With regard to intensity, there are several reports of insects (1) exhibiting concentration-dependent changes in taste-mediated behavioral responsiveness to specific taste stimuli (Dethier, V. G., 1968; Bowdan, E., 1995; Glendinning, J. I. and Gonzalez, N. A., 1995; Glendinning, J. I. *et al*., 1999a; Wang, Z. *et al*., 2004), and (2) discriminating different intensities (i.e., concentrations) of salts in a classical conditioning paradigm (Maes, F. W. and Bijpost, S. C. A., 1979). With regard to hedonics, there are numerous reports of insects showing a taste-mediated preference or aversion to chemical stimuli (Harley, K. L. S. and Thorsteinson, A. J., 1967; Dethier, V. G., 1968; 1976; Bernays, E. A. and Chapman, R. F., 1994; Bowdan, E., 1995; Glendinning, J. I. and Gonzalez, N. A., 1995; Glendinning, J. I. *et al*., 1999a; Wang, Z. *et al*., 2004). The question of whether insects categorize taste stimuli into different qualities, however, has not been examined systematically.

To demonstrate that taste stimuli are grouped into different qualities (e.g., sweet, salty, sour, bitter, and umami), one cannot simply observe unconditioned behavioral responses. This is because taste stimuli with different taste qualities can elicit similar behavioral responses (Spector, A. C., 2000). For example, in many insects, high concentrations of bitter or salty taste stimuli elicit an aversive response. In the mammal literature, the most commonly used paradigm for determining whether two stimuli elicit distinct taste qualities is the conditioned taste aversion (CTA) (Frank, M. E. and Nowlis, G. H., 1989; Wiggins, L. L. *et al*., 1989). In brief, one creates a CTA to a reference taste stimulus (e.g., quinine), and then asks whether the CTA generalizes to an isostimulatory concentration of another taste stimulus (e.g., NaCl). If the animal does not generalize the CTA, then one infers that the two taste stimuli have distinct taste qualities. On the other hand, if the animal does generalize the CTA, then one infers that the animal could not distinguish the two taste stimuli because they produce a common taste quality. While this CTA-generalization procedure has been used successfully in mammals, I am unaware of its application to insects. Given that insects are capable of forming CTAs (Gelperin, A., 1968; Lee, J. C. and Bernays, E. A., 1990), the CTA-generalization paradigm should provide a powerful tool for analyzing taste qualities in insects. If not, then an alternative approach would be to generate a conditioned taste preference (CTP) to one taste stimulus (Gerber, B. *et al*., 2004; Hendel, T. *et al*., 2005.), and then test for generalization of the CTP to another taste stimulus.

The question of how gustatory input is processed is complicated by the observation that many taste-responsive neurons in the SOG respond to tactile input (Mitchell, B. K. and Itagaki, H., 1992; Rogers, S. M. and Simpson, S. J., 1999). This tactile input is derived from touch receptors within the taste sensilla, which generate action potentials when the taste sensilla are bent (e.g., while contacting food items). Even though tactile input from taste sensilla may provide critical proprioceptive feedback about the position of the chemosensilla relative to a food item, one might predict that the convergence of taste and tactile input on the same SOG interneurons would complicate taste processing. The insect may be able to reduce the contribution of tactile input, however, by limiting the strength of contact between the taste sensilla and food item (Rogers, S. M. and Simpson, S. J., 1999).

A recent study of *Drosophila* larvae revealed the power of applying molecular tools to the study of central taste processing (Melcher, C. and Pankratz, M. J., 2005). Using microarray analysis, the authors discovered a neuropeptide gene, *hugin* (*hug*), which is expressed in about 20 interneurons within the SOG. The axons of these interneurons project to the pharyngeal muscles, the ring gland (a central neuroendocrine organ), and the protocerebrum. On the other hand, the dendrites of the *hug*-expressing neurons receive input from taste cells and pharyngeal chemosensory cells. When the authors blocked synaptic transmission of the *hug*-expressing neurons, they altered the initiation of feeding in the larvae. Taken together, these observations suggest that the *hug*-expressing neurons are part of a neural circuit that modulates taste-mediated feeding responses.

4.03.5.1 Coding Mechanisms

The nature of the neural code for insect taste is unresolved. As in mammalian systems, there is debate over the relative importance of three different coding frameworks: labeled lines, ensemble (i.e., across fiber) patterns, and temporal patterns of spiking. The labeled-line framework hypothesizes that tastant identity is represented by neural activity in a limited subset of gustatory neurons. According to this model, activation of the sugar-sensitive taste cells would stimulate neural circuits within the SOG that initiate biting, whereas activation of a bitter-sensitive taste

cell would inhibit the same neural circuits. Further, the behavioral response to a mixture of sugars and bitter taste stimuli should reflect the algebraic sum of the inputs from the carbohydrate- and bitter-sensitive taste cells, respectively (Schoonhoven, L. M. and Blom, F., 1988; Simmonds, M. S. J. and Blaney, W. M., 1991). A recent study (Marella, S. *et al.*, 2006) provided strong evidence that *Drosophila* uses labeled-line coding. The investigators genetically engineered two types of flies (e.g., A and B). Type A flies expressed a capsaicin receptor (VR1E600K) in the taste cells that express the Gr5a receptor (i.e., the sugar-sensitive taste cells), whereas type B flies expressed the same capsaicin receptor in taste cells that express the Gr66a receptor (i.e., the bitter-sensitive taste cells). Then, they showed that when offered a capsaicin-treated agar, the type A flies exhibited an appetitive response, while the type B flies exhibited an aversive response. This remarkable result shows that the nature of an insect's ingestive response to a chemical stimulus (i.e., appetitive or aversive) is not determined by the chemical itself; rather, it is determined by the specific class of taste cell (or labeled line) that is activated.

The ensemble coding framework hypothesizes that tastant identity is represented by the spatial pattern of activity across large populations of neurons (Schoonhoven, L. M. *et al.*, 1992; Smith, D. V. *et al.*, 2000). According to this framework, discriminable taste stimuli should each elicit different ensemble patterns (i.e., different magnitudes of discharge across the population of taste cells). Ensemble coding was evaluated in a study that sought to determine how *M. sexta* caterpillars discriminate the taste of three different host plants (Dethier, V. G. and Crnjar, R. M., 1982). After evaluating the three potential coding frameworks, the authors concluded that ensemble pattern provided the most parsimonious discrimination mechanism. Elsewhere, another study (Glendinning, J. I. *et al.*, 2002) demonstrated that *M. sexta* uses ensemble coding to discriminate between two aversive taste stimuli (salicin and *Grindelia* leaf extract), which activate different classes of bitter-sensitive taste cell.

While the labeled-line and ensemble coding frameworks focus on which neurons are activated within the gustatory neuraxis, the temporal coding framework focuses on how neurons are activated. The latter framework hypothesizes that tastant identity is represented by the precise temporal pattern of spiking within a neuron or across populations of neurons (Dethier, V. G. and Crnjar, R. M., 1982; Katz, D. B. *et al.*, 2002; Katz, D. B., 2005). Support for this hypothesis comes from a recent study of *M. sexta* caterpillars (Glendinning, J. I. *et al.*, 2006). Several of the bitter-sensitive taste cells in this caterpillar generate a decelerating temporal pattern of spiking when stimulated by caffeine and salicin, and an accelerating temporal pattern of spiking when stimulated by aristolochic acid. The authors showed that the caterpillars use the distinct temporal patterns of spiking generated by salicin and aristolochic acid as a basis for discrimination.

It is important to emphasize two caveats associated with the coding frameworks discussed above. First, the three frameworks are not mutually exclusive. In fact, they probably function together in a complimentary manner within the same insect, as suggested by Dethier V. G. and Crnjar R. M. (1982). Second, given the profound effects of taste–mixture interactions, physiological state, and experience on responsiveness of individual taste cells to their respective ligands (see Sections 4.03.6 and 4.03.7), central processing of the peripheral signal is probably more dynamic than hitherto appreciated.

4.03.6 Taste–Mixture Interactions

Most studies of insect taste focus on single-component stimuli. While this approach offers many experimental advantages, it has limited ecological relevance because most foods contain complex mixtures of taste stimuli. Below I discuss our current (and admittedly, incomplete) understanding of taste–mixture interactions.

Four different types of taste–mixture interactions have been described in the peripheral taste system of insects. First, some compounds fail to produce any stimulatory effects on their own, but nevertheless inhibit the response of specific taste cells to their best stimulus (Dethier, V. G. and Bowdan, E., 1989; Bernays, E. A. and Chapman, R. F., 2000). Second, complex mixtures of taste stimuli can produce inhibitory effects in which the total number of impulses generated by the mixture is less than the algebraic sum of impulses generated by each of the mixture components alone (Ishikawa, S., 1967; Schoonhoven, L. M., 1978; Bernays, E. A. and Chapman, R. F., 2001a). Third, activation of one taste cell can inhibit the response of another taste cell to its own best stimulus (Mitchell, B. K., 1987; Blaney, W. M. and Simmonds, M. S. J., 1990; Chapman, R. F. *et al.*, 1991;

Schoonhoven, L. M. *et al*., 1992; Shields, V. D. C. and Mitchell, B. K., 1995; Bernays, E. A. and Chapman, R. F., 2000). Fourth, taste mixtures can produce synergistic interactions – for example, simultaneous activation of two taste cells by their respective best stimuli can cause a single taste cell to discharge at a rate substantially higher than expected based on tests with each taste stimulus alone (Dethier, V. G., 1971; Dethier, V. G. and Kuch, J. H., 1971).

The mechanistic basis for peripheral mixture interactions is unclear. Some interactions may involve direct electrical communication between taste cells via gap junctions. In support of this suggestion, two studies have found what appear to be gap junctions between taste cells in flies (Isidoro, N. *et al*., 1993) and thermo/hygrosensory neurons in a moth (Steinbrecht, R. A., 1989). However, another study failed to observe any evidence for gap junctions between taste cells in a caterpillar (Shields, V. D. C., 1994). A second possibility is that stimulation of one taste cell influences the responsiveness of others within the same taste sensillum through centrifugal feedback from the central nervous system. A third possibility is that activity in one taste cell may inhibit activity in a nearby cell through an ephaptic interaction (Jefferys, J. G., 1995; Bokil, H. *et al*., 2001). A final possibility is that that a single taste cell could express two signaling pathways, and activation of one pathway inhibits (or enhances) the response of the other (Dethier, V. G. and Bowdan, E., 1989).

Taste–mixture interactions have also been observed in the central gustatory system. For instance, caffeine normally elicits a taste-mediated aversive response in *M. sexta* caterpillars (Glendinning, J. I. *et al*., 1999a). However, when caffeine is presented in binary mixture with *myo*-inositol, the aversive response is completely attenuated (Glendinning, J. I. *et al*., 2000b). Recordings from the peripheral taste system of this insect revealed that the bitter-sensitive taste cells exhibited the same response to caffeine, irrespective of whether the caffeine was presented alone or in binary mixture with *myo*-inositol; likewise, the inositol-sensitive taste cells exhibited the same response to *myo*-inositol, irrespective of whether the myo-inositol was presented alone or in binary mixture with caffeine (Glendinning, J. I. *et al*., 2000b). The most parsimonious interpretation of these findings is that input from the inositol-sensitive taste cells inhibited the neural circuit in the central nervous system that mediates the aversive response to caffeine.

4.03.7 Factors that Modulate Gustatory Responsiveness

One of the most remarkable features of the insect taste system is its plasticity. To illustrate this point, I discuss below four factors known to increase (or decrease) the responsiveness of the gustatory system to specific taste stimuli.

4.03.7.1 Physical Changes in Taste Sensilla

In order for a chemical to stimulate a taste cell, it must first diffuse through the pore at the tip of a taste sensillum (see Figure 1). Although this terminal pore remains permanently open in many insect species, it opens and closes in Orthopterans (Bernays, E. A. *et al*., 1972). The functional significance of terminal pore closure was revealed by a series of experiments in locusts, *Locusta migratoria* (Bernays, E. A. and Chapman, R. F., 1972). When the foregut of the locust becomes distended (e.g., after a meal), stretch receptors in the wall of the foregut are activated and send afferent signals to the brain via the posterior pharyngeal nerves and frontal connectives. These afferent signals stimulate the release of a diuretic hormone from the corpora cardiaca, which in turn cause pore closure in many of the taste sensilla. The functional effect of terminal pore closure is that it contributes to meal termination by eliminating phagostimulatory input from the peripheral taste system.

4.03.7.2 Nutrient Levels in Blood

Several investigators have discovered that changes in the concentration of specific nutrients in the blood (e.g., amino acids or trehalose) directly modulate the responsiveness of taste cells in grasshoppers and caterpillars to the same chemicals (Simmonds, M. S. J. *et al*., 1992; Simpson, S. J. and Simpson, C. L., 1992; Bernays, E. A. *et al*., 2004). In locusts, when blood levels of amino acids are low and sugars high, the responsiveness of the taste cells to amino acids is high and that to sugars is low (Simpson, S. J. and Simpson, C. L., 1992). In contrast, when blood levels of amino acids are high and sugars low, the responsiveness of the taste cells to amino acids is low and that to sugars is high. Because these modulatory effects of blood nutrients on taste cell responsiveness occur in the absence of neural or humoral links between the central nervous system and taste cells, they must be mediated peripherally. A recent study indicates that nutrient

levels in the blood may modulate secretion of nitric oxide from glandular cells surrounding the taste cells, which in turn modulates the responsiveness of taste cells to their respective ligands (Schuppe, H. *et al.*, 2006).

4.03.7.3 Dietary Experience Effects

When insects are exposed repeatedly to the same taste stimulus (e.g., within and across successive meals), the responsiveness of their gustatory system to these stimuli can increase or decrease. The time scale over which these changes occur varies from seconds to days. Below, I discuss four ways that dietary experience modifies taste.

4.03.7.3.1 Short-term sensory adaptation

A common feature of all sensory receptor cells is that their firing rate diminishes over time in response to continuous stimulation (i.e., adapts), but recovers rapidly upon removal of the stimulus (i.e., disadapts). Adaptation and disadaptation occur over a period of milliseconds to seconds. To illustrate this process, we show adaptation curves for two taste cells in the lateral styloconic sensillum of *M. sexta* caterpillars (Figure 6). It is apparent that the response (as indicated by impulses per 100 ms) of the inositol-sensitive taste cell to 1 mM *myo*-inositol diminished by >50% over 500 ms, whereas that of the bitter-sensitive taste cell to 5 mM caffeine diminished by <10% over the same time period.

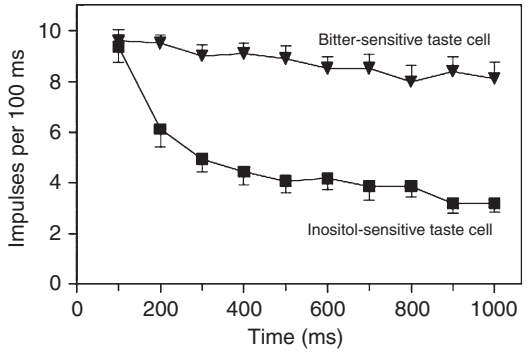

Figure 6 Adaptation rates of three different taste cells in the lateral styloconic sensillum of *Manduca sexta* caterpillars (as indicated by the number of spikes during each of 10 consecutive 100 ms bins). We show adaptation of the bitter-sensitive taste cell to 5 mM caffeine and the inositol-sensitive taste cell to 1 mM *myo*-inositol. Symbols indicate mean ±SE; $N = 10$ sensilla, each from different fifth instar caterpillars. These data are from Glendinning, J. I., Nelson, N., and Bernays, E. A. 2000b. How do inositol and glucose modulate feeding in *Manduca sexta* caterpillars? J. Exp. Biol. 203, 1299–1315.

The finding that bitter-sensitive taste cells are more resistant to adaptation than nutrient-sensitive taste cells has been reported for other insects as well (Schoonhoven, L. M., 1977). From a functional standpoint, this finding indicates that the relative amount of afferent input from different taste cells during a meal may not be constant, with the relative amount of input from the bitter-sensitive taste cells increasing over time. The extent to which these adaptation processes contribute to feeding during a meal is unclear, however, because insect gustatory organs do not remain in continuous contact with foods throughout a meal. Some gustatory organs make a series of drumming movements, resulting in intermittent contacts lasting only 100–200 ms (Blaney, W. M. and Duckett, A. M., 1975; Devitt, B. D. and Smith, J. J. B., 1985). These drumming movements could serve to minimize the effects of short-term adaptation in the taste cells and effectively increase the level of sensory input from taste cells over time (Blaney, W. M. and Duckett, A. M., 1975).

4.03.7.3.2 Habituation

When an animal is presented with a stimulus repeatedly across a sequence of trials, its responsiveness to that stimulus usually wanes (Hinde, R. A., 1970). This phenomenon is referred to as habituation if it meets several criteria – for example, it must be mediated centrally, recover spontaneously, generalize to related stimuli, and develop more readily in response to weak than intense stimuli (Thompson, R. F. and Spencer, W. A., 1966). For instance, fruit flies and bees normally exhibit a proboscis extension reflex for 5% sucrose, but this reflex extinguishes following 20 consecutive stimulations within a 5 min period (Duerr, J. S. and Quinn, W. G., 1982; Braun, G. and Bicker, G., 1992; Scheiner, R., 2004; Scheiner, R. *et al.*, 2004). This exposure-induced response decrement for sucrose was considered habituation because it met at least two of Thompson and Spencer's habituation criteria.

4.03.7.3.3 Long-term adaptation

When herbivorous insects are offered a diet containing an unpalatable but harmless compound as their only source of water and nutrients, they will usually sample the diet repeatedly. After ~24 h of such sampling, the insects eventually adapt their aversive response. This long-term adaptation phenomenon has been reported in several species of herbivorous

insect (Jermy, T. *et al.*, 1982; Simmonds, M. S. J. and Blaney, W. M., 1983; Szentesi, A. and Bernays, E. A., 1984; Blaney, W. M. and Simmonds, M. S. J., 1987; Usher, B. F. *et al.*, 1988; Glendinning, J. I. and Gonzalez, N. A., 1995; Bernays, E. A. *et al.*, 2004), but has been examined most extensively in caterpillars of *M. sexta* (Schoonhoven, L. M., 1969; 1978; Glendinning, J. I. *et al.*, 1999b; 2001a; 2001b; 2002). For example, 24 h of dietary exposure to a caffeine diet eliminates the aversive response to caffeine. The long-term adaptation phenomenon appears to be mediated peripherally because the dietary exposure regime profoundly desensitizes all of the bitter-sensitive taste cells to caffeine. Twenty-four hours of dietary exposure to a salicin diet also eliminates the aversive response to salicin. However, this latter adaptation phenomenon must be mediated centrally because there is no associated reduction in responsiveness of the bitter-sensitive taste cells. Taken together, these results indicate that the peripheral and central gustatory system of *M. sexta* each have independent mechanisms for overcoming the aversive response to harmless bitter compounds.

Because the long-term adaptation to salicin is mediated by the central gustatory system, and because it generalizes to related taste stimuli (Glendinning, J. I. *et al.*, 2001a; 2002), it can be viewed as a type of habituation. It is important to note, however, that the onset latency for the habituation to salicin (in *M. sexta*) is about 24 h, whereas that to sucrose (in flies and bees) is $\leq$5 min (Duerr, J. S. and Quinn, W. G., 1982; Braun, G. and Bicker, G., 1992; Scheiner, R., 2004; Scheiner, R. *et al.*, 2004). Further work is needed to determine whether these different onset latencies reflect (1) species differences, (2) greater difficulty habituating to aversive taste stimuli, and/or (3) the existence of multiple habituation mechanisms.

4.03.7.3.4 Induced food preferences

After feeding on a particular plant species for 1–2 days, many species of herbivorous insect induce a strong preference for that plant species (review in Szentesi, A. and Jermy, T., 1990). Despite the widespread occurrence of this phenomenon, the underlying physiological mechanisms are poorly understood. In all likelihood, a variety of mechanisms are activated, depending on the chemical constituents of the plant tissue and the insect species – e.g., induction of detoxification enzymes, changes in gustatory and/or olfactory responsiveness, and conditioned preferences (Bernays, E. A. and Weiss, M. R., 1996).

That taste contributes to induced food preferences was established recently in a study of *M. sexta* caterpillars, which are facultative specialists on plants in the family Solanaceae. When these caterpillars were reared on solanaceous foliage, they induced a strong and exclusive preference for the same foliage (Hanson, F. E. and Dethier, V. G., 1973; Yamamoto, R. T., 1974; de Boer, G. and Hanson, F. E., 1987; del Campo, M. L. and Renwick, J. A. A., 2000). A team of investigators discovered that indioside D (a steroidal glycoside) is one of the chemicals in the solanaceous foliage to which the caterpillars induce their preference (del Campo, M. L. *et al.*, 2001). These investigators also presented evidence that the taste cells in the caterpillar's styloconic sensilla become tuned to indioside D over the course of the induction process, and that this chemosensory tuning process is sufficient to explain the induced preference for solanaceous leaves (del Campo, M. L. *et al.*, 2001; del Campo, M. L. and Miles, C. I., 2003). According to the chemosensory tuning hypothesis, the taste cells sensitive to indioside D maintain their normal responsiveness, while those sensitive to other plant chemicals (e.g., sugars, salts, and bitter taste stimuli) become less responsive.

4.03.7.4 Health Status

A recent study demonstrated that peripheral gustatory sensitivity of two species of caterpillar changes in response to endoparasitic infection (Bernays, E. A. and Singer, M. S., 2005). More specifically, the investigators discovered that endoparasitic infections cause specific taste cells in the caterpillars to respond more vigorously to specific host plant compounds (i.e., PAs). Given that activation of the PA-sensitive taste cells stimulates increased feeding, it follows that an elevated responsiveness of the PA-sensitive taste cells would promote intake of PA-containing plant tissues. This sequence of events should benefit the caterpillars because PAs are toxic to the endoparasites and thus may help the caterpillars control (or even eliminate) the endoparasitic infection.

4.03.8 Future Directions

Despite all of the recent molecular advances in insect taste (review in Amrein, H. and Thorne, N., 2005), we still have a relatively simplistic understanding of how taste contributes to the control of feeding. This reflects a number of complicating factors. One is that

investigators have distributed their efforts over a wide range of insect species. While this approach has offered important comparative insights, it has prevented a detailed analysis of the taste system in any one species. At this point, the insect species with the best-characterized taste system include adult blowflies (*P. regina*), adult *Drosophila melanogaster*, and larval *M. sexta*. By focusing future efforts on these species, investigators will be able to build a substantial body of knowledge, and ask even more sophisticated questions.

A second factor that has limited progress on insect taste is the widespread use of long-term feeding assays to assess taste function – for example, preference tests that span 2–6 h. Given that secondary plant compounds (and nutrients) can inhibit feeding in <5 min through postoral mechanisms (Reynolds, S. E., 1990; Timmins, W. A. and Reynolds, S. E., 1992; Glendinning, J. I. and Slansky Jr., F., 1994; Glendinning, J. I., 1996), it is likely that the results from feeding tests lasting ≥2 h will reflect contributions of both oral and postoral response mechanisms. The contribution of postoral mechanisms can confound the interpretation of behavioral assays that seek to isolate taste-mediated responses. Another problem with the use of long-term feeding assays is that they weaken attempts to link neural responses of the taste system to behavior. Because electrophysiological studies usually focus on the initial milliseconds (or seconds) of response, one cannot easily extrapolate these transient neural processes to behavioral processes that span 2–6 h. A more rational approach would be to determine the operative time frame for the feeding behavior of interest, and then to examine the neural responses that occur over that time frame. For instance, given that caterpillars and flies can discriminate taste stimuli in less than 1 s (Dethier, V. G., 1968; Dethier, V. G. and Crnjar, R. M., 1982), one should focus electrophysiological analyses of discrimination on the initial 1 s of neural response. To this end, investigators could use well-established techniques for measuring immediate taste-mediated responses – for example, the proboscis extension reflex in flies and bees (Dethier, V. G., 1976) or initial biting responses in caterpillars and beetles (Dethier, V. G. and Crnjar, R. M., 1982; Frazier, J. L., 1986; Sperling, J. L. and Mitchell, B. K., 1991; Glendinning, J. I. *et al*., 2006).

A final factor that has hampered progress on insect taste is the absence of a framework for integrating taste into more generalized feeding control mechanisms. Such a framework has been developed for mammals (Spector, A. C., 2000) and has been of enormous value in helping understand how taste input modulates different aspects of the ingestive process. In mammals, taste processing has been grouped into three categories. Stimulus identification involves the discrimination of ecologically relevant taste stimuli, and the association of these taste stimuli with specific events or outcomes. These associative processes encompass both innate and conditioned responses. Ingestive motivation involves the central gustatory mechanisms that promote or inhibit the consumption of foods, and thereby represents the hedonic component of taste (i.e., whether an animal prefers or avoids a food). Digestive preparation involves the mechanisms by which taste activates feedforward mechanisms that aid in the digestive process. Application of this integrative framework to studies of insect taste would significantly enhance our ability to identify and analyze the central neuropils involved in different aspects of taste processing and better characterize phenotypic effects of genetic manipulations.

References

Albert, P. J. and Parisella, S. 1988. Feeding preferences of eastern spruce budworm larvae in two-choice tests with extracts of mature foliage and with pure amino acids. J. Chem. Ecol. 14, 1649–1656.

Altman, J. S. and Kien, J. 1987. Functional Organization of the Subesophageal Ganglion in Arthropods. In: Arthropod Brain: Its Evolution, Development, Structure and Functions (*ed*. A. P. Gupta), pp. 265–301. John-Wiley and Sons.

Amrein, H. and Thorne, N. 2005. Gustatory perception and behavior in *Drosophila melanogaster*. Curr. Biol. 15, R673–R684.

Arms, K., Feeny, P., and Lederhouse, R. C. 1974. Sodium: stimulus for puddling behavior by tiger swallowtail butterflies, *Papilio glaucus*. Science 185, 372–374.

Bate-Smith, E. C. 1972. Attractants and Repellents in Higher Animals. In: Phytochemical Ecology: Proceedings of the Phytochemical Society Symposium (*ed*. J. B. Harborne), pp. 45–56. Academic Press.

Bernays, E. A. 1982. The Insect on the Plant – a Closer Look. In: Proceedings of the 5th international symposium on insect-plant relationships (*eds*. J. H. Visser and A. K. Minks), pp. 3–17. Pudoc, Wageningen.

Bernays, E. A. 1985. Regulation of Feeding Behaviour. In: Comprehensive Insect Physiology, Biochemistry and Pharmacology, Vol. 4 (*eds*. G. A. Kerkut and L. I. Gilbert), pp. 1–32. Pergamon Press.

Bernays, E. A. 1990. Plant secondary compounds deterrent but not toxic to the grass specialist acridid *Locusta migratoria*: implications for the evolution of graminivory. Entomol. Exper. Appl. 54, 53–56.

Bernays, E. A. 1991. Relationship between deterrence and toxicity of plant secondary metabolites for the grasshopper *Schistocerca americana*. J. Chem. Ecol. 17, 2519–2526.

Bernays, E. A. and Chapman, R. F. 1972. The control of changes in peripheral sensilla associated with feeding in *Locusta migratoria* (L.). J. Exp. Biol. 57, 755–763.

Bernays, E. A. and Chapman, R. F. 1987. The Evolution of Deterrent Responses in Plant-Feeding Insects. In: Perspectives in Chemoreception and Behavior (*eds*. R. F. Chapman, E. A. Bernays, and J. G. Stoffolano, Jr.), pp. 159–173. Springer-Verlag.

Bernays, E. A. and Chapman, R. F. 1994. Host–Plant Selection by Phytophagous Insects. Chapman and Hall.

Bernays, E. A. and Chapman, R. F. 2000. A neurophysiological study of sensitivity to a feeding deterrent in two sister species of *Heliothis* with different diet breadths. J. Insect Physiol. 46, 905–912.

Bernays, E. A. and Chapman, R. F. 2001a. Taste cell responses in a polyphagous arctiid: towards a general pattern for caterpillars. J. Insect Physiol. 47, 1029–1043.

Bernays, E. A. and Chapman, R. F. 2001b. Electrophysiological responses of taste cells to nutrient mixtures in the polyphagous caterpillar of *Grammia geneura*. J. Comp. Physiol. A 187, 205–213.

Bernays, E. A. and Singer, M. S. 2005. Taste alteration and endoparasites. Nature 436, 476.

Bernays, E. A. and Weiss, M. R. 1996. Induced food preferences in caterpillars: the need to identify mechanisms. Entomol. Exper. Appl. 78, 1–8.

Bernays, E. A., Blaney, W. M., and Chapman, R. F. 1972. Changes in the chemoreceptor sensilla on the maxillary palps of *Locusta migratoria* in relation to feeding. J. Exp. Biol. 57, 745–753.

Bernays, E. A., Chapman, R. F., and Hartmann, T. 2002. A taste receptor neurone dedicated to the perception of pyrrolizidine alkaloids in the medial galeal sensillum of two polyphagous arctiid caterpillars. Physiol. Entomol. 27, 312–321.

Bernays, E. A., Chapman, R. F., Lamunyon, C. W., and Hartmann, T. 2003. Taste receptors for pyrrolizidine alkaloids in a monophagous caterpillar. J. Chem. Ecol. 29, 1709–1722.

Bernays, E. A., Chapman, R. F., and Singer, M. S. 2000. Sensitivity to chemically diverse phagostimulants in a single gustatory neuron of a polyphagous caterpillar. J. Comp. Physiol. A 186, 13–19.

Bernays, E. A., Chapman, R. F., and Singer, M. S. 2004. Changes in taste receptor cell sensitivity in a polyphagous caterpillar reflect carbohydrate but not protein imbalance. J. Comp. Physiol. A 190, 39–48.

Bernays, E. A., Glendinning, J. I., and Chapman, R. F. 1998. Plant acids modulate chemosensory responses in *Manduca sexta* larvae. Physiol. Entomol. 23, 193–201.

Blaney, W. M. and Duckett, A. M. 1975. The significance of palpation by the maxillary palps of *Locusta migratoria* (L.): an electrophysiological and behavioural study. J. Exp. Biol. 63, 701–712.

Blaney, W. M. and Simmonds, M. S. J. 1987. Experience: a Modifier of Neural and Behavioural Sensitivity. In: Insects–Plants (*eds*. V. Labeyrie, G. Fabres, and D. Lachaise), pp. 237–241. Dr. W. Junk Publishers.

Blaney, W. M. and Simmonds, M. S. J. 1990. A behavioural and electrophysiological study of the role of tarsal chemoreceptors in feeding by adults of *Spodoptera*, *Heliothis virescens* and *Helicoverpa armigera*. J. Insect Physiol. 36, 743–756.

Bokil, H., Laaris, N., Blinder, K., Ennis, M., and Keller, A. 2001. Ephaptic interactions in the mammalian olfactory system. J. Neurosci. 21, RC173.

Bowdan, E. 1995. The effects of a phagostimulant and a deterrent on the microstructure of feeding by *Manduca sexta* caterpillars. Entomologia Experimentalis et Applicata 77, 297–306.

Braun, G. and Bicker, G. 1992. Habituation of an appetitive reflex in the honeybee. J. Neurophysiol. 67, 588–598.

Brieskorn, C. H. 1990. Physiological and Therapeutic Aspects of Bitter Compounds. In: Bitterness in Foods and Beverages (*ed*. R. L. Rouseff), pp. 15–33. Elsevier.

Brower, L. P. 1984. Chemical Defense in Butterflies. In: The Biology of Butterflies (*eds*. R. I. Vane-Wright and P. R. Ackery), pp. 109–134. Academic Press.

Calas, D., Thiéry, D., and Marion-Poll, F. 2007. 20-Hydroxyecdysone deters oviposition and larval feeding in the European grapevine moth, *Lobesia botrana*. J. Chem. Ecol. 32, 2443–2454.

Chapman, R. F. 1982. Chemoreception: the significance of sensillum numbers. Adv. Insect Physiol. 16, 247–356.

Chapman, R. F., Ascoli-Christensen, A., and White, P. R. 1991. Sensory coding for feeding deterrence in the grasshopper *Schistocerca americana*. J. Exp. Biol. 158, 241–259.

Chyb, S. 2004. *Drosophila* gustatory receptors: from gene identification to functional expression. J. Insect Physiol. 50, 469–477.

Chyb, S., Dahanukar, A., and Carlson, J. R. 2003. *Drosophila* Gr5a encodes a taste receptor tuned to trehalose. Proc. Natl. Acad. Sci. U. S. A. 100(Suppl. 2), 14526–14530.

Clyne, P. J., Warr, C. G., and Carlson, J. R. 2000. Candidate taste receptors in *Drosophila*. Science 287, 1830–1834.

Dahanukar, A., Foster, K., van der Goes van Naters, W. M., and Carlson, J. R. 2001. A Gr receptor is required for response to the sugar trehalose in taste neurons of *Drosophila*. Nat. Neurosci. 4, 1182–1186.

de Boer, G. and Hanson, F. E. 1987. Differentiation of roles of chemosensory organs in food discrimination among host and non-host plants by larvae of the tobacco hornworm, *Manduca sexta*. Physiol. Entomol. 12, 387–398.

del Campo, M. L. and Miles, C. I. 2003. Chemosensory tuning to a host recognition cue in the facultative specialist larvae of the moth *Manduca sexta*. J. Exp. Biol. 206, 3979–3990.

del Campo, M. L. and Renwick, J. A. A. 2000. Induction of host specificity in larvae of *Manduca sexta*: chemical dependence controlling host recognition and developmental rate. Chemoecology 10, 115–121.

del Campo, M. L., Miles, C. I., Schroeder, F. C., Muellerk, C., Booker, R., and Renwick, J. A. 2001. Host recognition by the tobacco hornworm is mediated by a host plant compound. Nature 411, 186–189.

den Otter, C. J. 1972. Differential sensitivity of insect chemoreceptors to alkali cations. J. Insect Physiol. 18, 109–131.

Dethier, V. G. 1968. Chemosensory input and taste discrimination in the blowfly. Science 161, 389–391.

Dethier, V. G. 1971. A surfeit of stimuli: a paucity of receptors. Am. Sci. 59, 706–715.

Dethier, V. G. 1973. Electrophysiological studies of gustation in Lepidopterous larvae. II. Taste spectra in relation to food-plant discrimination. J. Comp. Physiol. 82, 103–134.

Dethier, V. G. 1976. The Hungry Fly: A Physiological Study of the Behavior Associated with Feeding. Harvard University Press.

Dethier, V. G. 1980. Evolution of receptor sensitivity to secondary plant substances with special reference to deterrents. Am. Nat. 115, 45–66.

Dethier, V. G. and Bowdan, E. 1989. The effect of alkaloids on the sugar receptors of the blowfly. Physiol. Entomol. 14, 127–136.

Dethier, V. G. and Bowdan, E. 1992. Effects of alkaloids on feeding by *Phormia regina* confirm the critical role of sensory inhibition. Physiol. Entomol. 17, 325–330.

Dethier, V. G. and Crnjar, R. M. 1982. Candidate codes in the gustatory system of caterpillars. J. Gen. Physiol. 79, 549–569.

Dethier, V. G. and Kuch, J. H. 1971. Electrophysiological studies of gustation in lepidopterous larvae. I. Comparative sensitivity to sugars, amino acids, and glycosides. Z. Vergl. Physiol. 72, 343–363.

Devitt, B. D. and Smith, J. J. B. 1985. Action of mouthparts during feeding in the dark-sided cutworm, *Euoxa messoria* (Lepidoptera: Noctuidae). Can. Entomol. 117, 343–349.

Duerr, J. S. and Quinn, W. G. 1982. Three *Drosophila* mutations that block associative learning also affect habituation and sensitization. Proc. Natl. Acad. Sci. U. S. A. 79, 3646–3650.

Frank, M. E. and Nowlis, G. H. 1989. Learned aversions and taste qualities in hamsters. Chem. Senses 14, 379–394.

Frazier, J. L. 1986. The Perception of Plant Allelochemicals that Inhibit Feeding. In: Molecular Aspects of Insect–Plant Interactions (*eds*. L. B. Brattsten and S. Ahmad), pp. 1–42. Plenum Press.

Friend, W. G. and Smith, J. J. 1971. Feeding in *Rhodnius prolixus*: mouthpart activity and salivation, and their correlation with changes of electrical resistance. J. Insect Physiol. 17, 233–243.

Furuyama, A., Koganezawa, M., and Shimida, I. 1999. Multiple receptor sites for nucleotide reception in the labellar taste receptor cells of the fleshfly *Boettcherisca peregrina*. J. Insect Physiol. 45, 249–255.

Garcia, J. and Hankins, W. G. 1975. The Evolution of Bitter and the Acquisition of Toxiphobia. In: Olfaction and Taste. V. Proceedings of the 5th International Symposium in Melbourne, Australia (*eds*. D. A. Denton and J. P. Coghlan), pp. 39–45. Academic Press.

Gelperin, A. 1968. Feeding behaviour of the praying mantis: a learned modification. Nature 217, 399–400.

Gerber, B., Scherer, S., Neuser, K., Michels, B., Hendel, T., Stocker, R. F., and Heisenberg, M. 2004. Visual learning in individually assayed *Drosophila* larvae. J. Exp. Biol. 207, 179–188.

Glendinning, J. I. 1994. Is the bitter rejection response always adaptive? Physiol. Behav. 56, 1217–1227.

Glendinning, J. I. 1996. Is chemosensory input essential for the rapid rejection of toxic foods? J. Exp. Biol. 199, 1523–1534.

Glendinning, J. I. 2002. How do herbivorous insects cope with noxious secondary plant compounds in their diet? Entomologia Experimentatlis et Applicata 104, 15–25.

Glendinning, J. I. and Gonzalez, N. A. 1995. Gustatory habituation to deterrent compounds in a grasshopper: concentration and compound specificity. Anim. Behav. 50, 915–927.

Glendinning, J. I. and Hills, T. T. 1997. Electrophysiological evidence for two transduction pathways within a bitter-sensitive taste receptor. J. Neurophysiol. 78, 734–745.

Glendinning, J. I. and Slansky, F., Jr. 1994. Interactions of allelochemicals with dietary constituents: effects on deterrency. Physiol. Entomol. 19, 173–186.

Glendinning, J. I., Brown, H., Capoor, M., Davis, A., Gbedemah, A., and Long, E. 2001b. A peripheral mechanism for behavioral adaptation to specific ''bitter'' taste stimuli in an insect. J. Neurosci. 21, 3688–3696.

Glendinning, J. I., Chaudhari, N., and Kinnamon, S. C. 2000a. Taste Transduction and Molecular Biology. In: The Neurobiology of Taste and Smell (*eds*. T. Finger, W. L. Silver, and D. Restrepo), 2nd edn., pp. 315–351. Wiley-Liss.

Glendinning, J. I., Davis, A., and Rai, M. 2006. Temporal coding mediates discrimination of ''bitter'' taste stimuli by an insect. J. Neurosci. 26, 8900–8908.

Glendinning, J. I., Davis, A., and Ramaswamy, S. 2002. Contribution of different taste cells and signaling pathways to the discrimination of ''bitter'' taste stimuli by an insect. J. Neurosci. 22, 7281–7287.

Glendinning, J. I., Domdom, S., and Long, E. 2001a. Selective adaptation to noxious foods by an insect. J. Exp. Biol. 204, 3355–3367.

Glendinning, J. I., Ensslen, S., Eisenberg, M. E., and Weiskopf, P. 1999b. Diet-induced plasticity in the taste system of an insect: localization to a single transduction pathway in an identified taste cell. J. Exp. Biol. 202, 2091–2102.

Glendinning, J. I., Nelson, N., and Bernays, E. A. 2000b. How do inositol and glucose modulate feeding in *Manduca sexta* caterpillars?. J. Exp. Biol. 203, 1299–1315.

Glendinning, J. I., Tarre, M., and Asaoka, K. 1999a. Contribution of different bitter-sensitive taste cells to feeding inhibition in a caterpillar (*Manduca sexta*). Behav. Neurosci. 113, 840–854.

Goldrich, N. R. 1973. Behavioral responses of *Phormia regina* (Meigen) to labellar stimulation with amino acids. J. Gen. Physiol. 61, 74–88.

Grill, H. J. and Berridge, K. C. 1985. Taste reactivity as a measure of the neural control of palatability. Prog. Psychobiol. Physiol. Psychol. 11, 1–61.

Griss, C., Simpson, S. J., Rohrbacher, J., and Rowell, C. H. F. 1991. Localization in the central nervous system of larval *Manduca sexta* (Lepidoptera: Sphingidae) of areas responsible for aspects of feeding behavior. J. Insect Physiol. 37, 477–482.

Hallem, E. A., Dahanukar, A., and Carlson, J. R. 2006. Insect odor and taste receptors. Annu. Rev. Entomol. 51, 113–135.

Hansen-Delkeskamp, E. 1992. Functional characterizaion of antennal contact chemoreceptors in the cockroach, *Periplaneta americana*. J. Insect Physiol. 38, 813–822.

Hanson, F. E. and Dethier, V. G. 1973. Role of gustation and olfaction in food plant discrimination in the tobacco hornworm, *Manduca sexta*. J. Insect Physiol. 19, 1019–1034.

Harborne, J. B. 1973. Phytochemical Methods. Chapman and Hall.

Harley, K. L. S. and Thorsteinson, A. J. 1967. The influence of plant chemicals on the feeding behavior, development, and survival of the two-striped grasshopper, *Melanoplus bivittatus* (Say), Acrididae: Orthoptera. Can. J. Zool. 45, 305–319.

Hendel, T., Michels, B., Neuser, K., Schipanski, A., Kaun, K., Sokolowski, M. B., Marohn, F., Michel, R., Heisenberg, M., and Gerber, B. 2005. The carrot, not the stick: appetitive rather than aversive gustatory stimuli support associative olfactory learning in individually assayed *Drosophila* larvae. J. Comp. Physiol. A 191, 265–278.

Hinde, R. A. 1970. Behavioural Habituation. In: Short-Term Changes in Neural Activity and Behaviour (*eds*. G. Horn and R. A. Hinde), pp. 3–40. Cambridge University Press.

Hirao, T. and Ariai, N. 1990. Gustatory and feeding responses to amino acids in the silkworm, *Bombyx mori*. Jpn. J. Appl. Entomol. Zool. 35, 73–76.

Hiroi, M., Marion-Poll, F., and Tanimura, T. 2002. Differentiated response to sugars among labellar chemosensilla in *Drosophila*. Zool. Sci. 19, 1009–1018.

Hiroi, M., Meunier, N., Marion-Poll, F., and Tanimura, T. 2004. Two antagonistic gustatory receptor neurons responding to sweet-salty and bitter taste in *Drosophila*. J. Neurobiol. 61, 333–342.

Hodgson, E. S., Lettvin, J. Y., and Roeder, K. D. 1955. Physiology of a primary chemoreceptor unit. Science 122, 417–418.

Inomata, N., Goto, H., Itoh, M., and Isono, K. 2004. A single amino-acid change of the gustatory receptor gene, *Gr5a*, has a major effect on trehalose sensitivity in a natural population of *Drosophila melanogaster*. Genetics 168, 1449–1458.

Inoshita, T. and Tanimura, T. 2006. Cellular identification of water gustatory receptor neurons and their central projection pattern in *Drosophila*. Proc. Natl. Acad. Sci. U. S. A. 103, 1094–1099.

Ishikawa, S. 1967. Maxillary Chemoreceptors in the Silkworm. In: Olfaction and Taste 2 (*ed*. T. Hayashi), pp. 761–777. Pergamon Press.

Ishimoto, H., Matsumoto, A., and Tanimura, T. 2000. Molecular identification of a taste receptor gene for trehalose in *Drosophila*. Science 289, 116–119.

Ishimoto, H., Takahashi, K., Ueda, R., and Tanimura, T. 2005. G-protein gamma subunit 1 is required for sugar reception in *Drosophila*. EMBO J. 24, 3259–3265.

Isidoro, N., Solinar, M., Baur, R., Roessingh, P., and Städler, E. 1993. Functional morphology of a tarsal sensillum of *Delia radicum* L (Diptera, Anthomyiidae) sensitive to important host-plant compounds. Int. J. Insect Morphol. Embryol. 39, 275–281.

Jefferys, J. G. 1995. Nonsynaptic modulation of neuronal activity in the brain: electric currents and extracellular ions. Physiol. Rev. 75, 689–723.

Jermy, T., Bernays, E. A., and Szentesi, A. 1982. The Effect of Repeated Exposure to Feeding Deterrents on Their Acceptability to Phytophagous Insects. In: Proceedings of the 5th International Symposium on Insect–Plant Relationships (*eds*. H. Visser and A. Minks), pp. 25–32. PUDOC.

Jørgensen, K., Kvello, P., Jørgen Almaas, T., and Mustaparta, H. 2006. Two closely located areas in the subesophageal ganglion and the tritocerebrum receive projections from gustatory receptor neurons located on the antennae and the proboscis in the moth *Heliothis virescens*. J. Comp. Neurol. 496, 121–134.

Katz, D. B. 2005. The many flavors of temporal coding in the gustatory cortex. Chem. Senses 30(Suppl. 1), 80–81.

Katz, D. B., Nicolelis, M. A., and Simon, S. A. 2002. Gustatory processing is dynamic and distributed. Curr. Opin. Neurobiol. 12, 448–454.

Kent, K. S. and Hildebrand, J. G. 1987. Cephalic sensory pathways in the central nervous system of larval *Manduca sexta* (Lepidoptera: Sphingidae). Philos. Trans. R. Soc. Lond. B Biol. Sci. 315, 1–36.

Kijima, H., Okada, Y., Oiki, S., Goshima, S., Nagata, N., and Kazawa, T. 1995. Free ion concentration in receptor lymph and a role of transepithelial voltage in the fly labellar taste receptor. J. Comp. Physiol. A 177, 123–133.

Kim, J. H. and Mullin, C. A. 1998. Structure-phagostimulatory relationships for amino acids in adult western corn rootworm, *Diabrotica virgifera virgifera*. J. Chem. Ecol. 24, 1499–1511.

Lee, J. C. and Bernays, E. A. 1990. Food tastes and toxic effects: Associative learning by the phytophagous grasshopper *Schistocerca americana* (Drury) (Orthoptera: Acrididae). Anim. Behav. 39, 163–173.

Liscia, A., Solari, P., Majone, R., Tomassini-Barbarossa, I., and Crnjar, R. 1997. Taste reception mechanisms in the blowfly: evidence of amiloride-sensitive and insensitive sites. Physiol. Behav. 62, 875–879.

Liu, L., Soren Leonard, A., Price, M. P., Johnson, W. A., and Welsh, M. J. 2003. Contribution of *Drosophlia* DEG/ENaC genes to salt taste. Neuron 39, 133–149.

Ma, W.-C. 1969. Some properties of gustation in the larvae of *Pieris brassicae*. Entomologia Experimentalis et Applicata 12, 584–590.

Ma, W.-C. 1972. Dynamics of feeding responses in *Pieris brassicae* Linn as a function of chemosensory input: a behavioral and electrophysiological study. Meded. Laudbouwhoge school Wageningen 72–11, 1–162.

Ma, W.-C. and Schoonhoven, L. M. 1973. Tarsal contact chemoreception hairs of the large white butterfly *Pieris brassicae* and their possible role in oviposition behavior. Entomologia Experimentatlis et Applicata 16, 343–357.

Maes, F. W. and Bijpost, S. C. A. 1979. Classical conditioning reveals discrimination of salt taste quality in the blowfly *Calliphora vicina*. J. Comp. Physiol. 133, 53–62.

Marella, S., Fischler, W., Kong, P., Asgarian, E., and Scott, K. 2006. Imaging taste responses in the fly brain reveals a functional map of taste category and behavior. Neuron 49, 285–295.

Marion-Poll, F. and Descoins, C. 2002. Taste detection of phytoecdysteriods in larvae of *Bombyx mori*, *Spodoptera littoralis* and *Ostrinia nubilalis*. J. Insect Physiol. 48, 467–476.

Melcher, C. and Pankratz, M. J. 2005. Candidate gustatory interneurons modulating feeding behavior in the *Drosophila* brain. PLoS Biol. 3, 1618–1628.

Messchemdorp, L., Smid, H. M., and Loon, J. J. A.v. 1998. The role of an epipharyngeal sensillum in the perception of feeding deterrents by *Leptinotarsa decemlineata* larvae. J. Comp. Physiol. A 183, 255–264.

Meunier, N., Marion-Poll, F., Rospars, J. P., and Tanimura, T. 2003. Peripheral coding of bitter taste in *Drosophila*. J. Neurobiol. 56, 139–152.

Millius, M., Merivee, E., Williams, I., Luik, A., Mänd, M., and Must, A. 2006. A new method for electrophysiological identification of antennal pH receptor cells in ground beetles: the example of *Pterostichus aethiops* (Panzer, 1796) (Coleoptera, Carabidae). J. Insect Physiol. 52, 960–967.

Mitchell, B. K. 1987. Interactions of alkaloids with galeal chemosensory cells of Colorado potato beetle. J. Chem. Ecol. 13, 2009–2022.

Mitchell, B. K. and Itagaki, H. 1992. Interneurons of the subesophageal ganglion of *Sarcophaga bullata* responding to gustatory and mechanosensory stimuli. J. Comp. Physiol. A 171, 213–230.

Mitchell, B. K., Itagaki, H., and Rivet, M.-P. 1999. Peripheral and central structures involved in insect gustation. Microsc. Res. Tech. 47, 401–415.

Miyakawa, Y. 1981. Bimodal response in a chemotactic behaviour of *Drosophila* larvae to monovalent salts. J. Insect Physiol. 27, 387–392.

Miyakawa, Y. 1982. Behavioural evidence for the existence of sugar, salt and amino acid taste receptor cells and some of their properties in *Drosophila* larvae. J. Insect Physiol. 28, 405–410.

Moon, S. J., Köttgen, M., Jiao, Y., Xu, H., and Montell, C. 2006. A taste receptor required for the caffeine response in vivo. Curr. Biol. 16, 1812–1817.

Morita, H. 1959. Initiation of spike potentials in contact chemosensory hairs of insects. III. D. C. stimulation and generator potential of labellar chemoreceptor of *Calliphora*. J. Cell Comp. Physiol. 54, 189–204.

Morita, H. 1992. Transduction process and impulse initiation in insect contact chemoreceptor. Zool. Sci. 9, 1–16.

Murata, Y., Ozaki, M., and Nakamura, T. 2006. Primary culture of gustatory receptor neurons from the Blowfly, *Phormia regina*. Chem. Senses 31, 497–504.

Nakamura, M., Baldwin, D., Hannaford, S., Palka, J., and Montell, C. 2002. Defective proboscus extension response (DPR), a member of the Ig superfamily required for the gustatory response to salt. J. Neurosci. 22, 3463–3472.

Ozaki, M., Amakawa, T., Ozaki, K., and Tokunaga, F. 1993. Two types of sugar-binding protein in the labellum of the fly. Putative taste receptor molecules for sweetness. J. Gen. Physiol. 102, 201–216.

Pollack, G. S. and Balakrishnan, R. 1997. Taste sensilla of flies: function, central neuronal projections, and development. Microsc. Res. Tech. 39, 532–546.

Reynolds, S. E. 1990. Feeding in Caterpillars: Maximizing or Optimizing Food Acquisition? In: Animal Nutrition and Transport Processes. I. Nutrition in Wild and Domestic Animals. Comparative Physiology, Vol. 5 (*ed*. J. Mellinger), pp. 106–118. Karger.

Ribeiro, J. M. C. and Garcia, E. S. 1980. The salivary and crop apyrase activity of *Rhodnius prolixus*. J. Insect Physiol. 26, 303–307.

Robertson, H. M. and Wanner, K. W. 2006. The chemoreceptor superfamily in the honey bee, *Apis mellifera*: expansion of the odorant, but not gustatory, receptor family. Genome Res. 16, 1395–1403.

Robertson, H. M., Warr, C. G., and Carlson, J. R. 2003. Molecular evolution of the insect chemoreceptor gene superfamily in *Drosophila melanogaster*. Proc. Natl. Acad. Sci. U. S. A. 100(Suppl. 2), 14537–14542.

Rogers, S. M. and Newland, P. L. 2002. Gustatory processing in thoracic local circuits of locusts. J. Neurosci. 22, 8324–8333.

Rogers, S. M. and Simpson, S. J. 1999. Chemo-discriminatory neurons in the sub-oesophageal ganglion of *Locusta migratoria*. Entomol. Exper. Appl. 91, 19–28.

Rouseff, R. L. 1990. Bitterness in Foods and Beverages. Elsevier Science Publishers.

Scheiner, R. 2004. Responsiveness to sucrose and habituation of the proboscis extension response in honey bees. J. Comp. Physiol. A 190, 727–733.

Scheiner, R., Sokolowski, M. B., and Erber, J. 2004. Activity of cGMP-dependent protein kinase (PKG) affects sucrose responsiveness and habituation in *Drosophila melanogaster*. Learn. Mem. 11, 303–311.

Schmidt, J. M. and Friend, W. G. 1991. Ingestion and diet destination in the mosquito *Culiseta inornata*: effects of carbohydrate configuration. J. Insect Physiol. 37, 817–828.

Schoonhoven, L. M. 1969. Sensitivity changes in some insect chemoreceptors and their effect on food selection behavior. Proc. Kon. Ned. Akad. Wet. Amsterdam. Ser. C 72, 491–498.

Schoonhoven, L. M. 1977. On the individuality of insect feeding behavior. Proceedings of the Koninklijke Nederlandse Akademie van Wetenschappen (Series C) 80, 341–350.

Schoonhoven, L. M. 1978. Long-term sensitivity changes in some insect taste receptors. Drug Res. 28, 2367.

Schoonhoven, L. M. and Blom, F. 1988. Chemoreception and feeding behavior in a caterpillar: towards a model of brain functioning in insects. Entomologia Experimentalis et Applicata 49, 123–129.

Schoonhoven, L. M. and van Loon, J. J. A. 2002. An inventory of taste in caterpillars: each species is its own key. Acta Zool. Acad. Sci. Hung. 48 (Suppl. 1), 215–263.

Schoonhoven, L. M., Blaney, W. M., and Simmonds, M. S. J. 1992. Sensory Coding of Feeding Deterrents in Phytophagous Insects. In: Insect–Plant Interactions, Vol. IV (*ed*. E. A. Bernays), pp. 59–79. CRC Press.

Schröter, U. and Menzel, R. 2003. A new ascending sensory tract to the calyces of the honeybee mushroom body, the subesophageal-caclcal tract. J. Comp. Neurol. 465, 168–178.

Schultz, J. C. and Lechowicz, M. J. 1986. Host–plant, larval age, and feeding behavior influence midgut pH in the gypsy moth (*Lymantria dispar*). Oecologia 71, 133–137.

Schuppe, H., Cuttle, M., and Newland, P. L. 2006. Nitric oxide modulates sodium taste via a cGMP-independent pathway. J. Neurobiol. 67, 219–232.

Scott, K., Brady, R., Jr., Cravchik, A., Morozov, P., Rzhetsky, A., Zuker, C., and Axel, R. 2001. A chemosensory gene family encoding candidate gustatory and olfactory receptors in *Drosophila*. Cell 104, 661–673.

Seno, K., Fujikawa, K., Nakamura, T., and Ozaki, M. 2005b. Gq-alpha subunit mediates receptor site-specific adaptation in the sugar taste receptor cell of the blowfly, *Phormia regina*. Neurosci. Lett. 377, 200–205.

Seno, K., Nakamura, T., and Ozaki, M. 2005a. Biochemical and physiological evidence that calmodulin is involved in the taste response of the sugar receptor cells of the blowfly, *Phormia regina*. Chem. Senses 30, 497–504.

Shanbhag, S. R. and Singh, R. N. 1992. Functional implications of the projections of neurons from individual labellar sensillum of *Drosophila melanogaster* as revealed by neuronal-marker horseradish peroxidase. Cell Tissue Res. 267, 273–282.

Shields, V. D. C. 1994. Ultrastructure of the uniporous sensilla on the galea of larval *Mamestra configurata* (Walker) (Lepidoptera: Noctuidae). Can. J. Zool. 72, 2016–2031.

Shields, V. D. C. and Mitchell, B. K. 1995. The effect of phagostimulant mixtures on deterrent receptor(s) in two crucifer-feeding lepidopterous species. Philos. Trans. R. Soc. Lond. B 347, 459–464.

Shimada, I., Shiraishi, A., Kijima, H., and Morita, H. 1974. Separation of two receptor sites in a single labellar sugar receptor of the flesh-fly by treatment with *p*-chloromercuribenzoate. J. Insect Physiol. 20, 605–621.

Shiraishi, A. and Kuwabara, M. 1970. The effect of amino acids on the labellar hair chemosensory cells of the fly. J. Gen. Physiol. 56, 768–782.

Shuichi Haupt, S. 2004. Antennal sucrose perception in the honey bee (*Apis mellifera* L.): behaviour and electrophysiology. J. Comp. Physiol. A 190, 735–745.

Simmonds, M. S. J. and Blaney, W. M. 1983. Some Neurophysiological Effects of Azadirachtin on Lepidopterous Larvae and their Feeding Response. In: Proceedings of the Second International Neem Conference (*eds*. H. Schmutterer and K. R. S. Ascher), pp. 163–180. Deutsche Gesellschaft für Technische Zusammernarbeit (GTZ) GmbH.

Simmonds, M. S. J. and Blaney, W. M. 1991. Gustatory codes in lepidopterous larvae. Symposia Biologica Hungarica 39, 17–27.

Simmonds, M. S. J., Simpson, S. J., and Blaney, W. M. 1992. Dietary selection behaviour in *Spodoptera littoralis*: The effects of conditioning diet and conditioning period on neural responsiveness and selection behavior. J. Exp. Biol. 162, 73–90.

Simpson, S. J. and Simpson, C. L. 1992. Mechanisms controlling modulation by haemolymph amino acids of gustatory responsiveness in the locust. J. Exp. Biol. 168, 269–287.

Smith, D. V., St. John, S. J., and Boughter, J. D. 2000. Neuronal cell types and taste quality coding. Physiol. Behav. 69, 77–85.

Spector, A. C. 2000. Linking gustatory neurobiology to behavior in vertebrates. Neurosci. Biobehav. Rev. 24, 391–416.

Spector, A. C. and Grill, H. J. 1992. Salt taste discrimination after bilateral section of the chorda tympani or glossopharyngeal nerves. Am. J. Physiol. (Regul. Integr. Comp. Physiol.) 263, R169–R176.

Sperling, J. L. and Mitchell, B. K. 1991. A comparative study of host recognition and the sense of taste in *Leptinotarsa*. J. Exp. Biol. 157, 439–459.

Städler, E., Renwick, J. A. A., Radke, C. D., and Sachdev-Gupta, K. 1995. Tarsal contact chemoreceptor response to glucosinolates and cardenolides mediating ovipositioning in *Pieris rapae*. Physiol. Entomol. 20, 175–187.

Steinbrecht, R. A. 1989. The fine structure of thermohygrosensitive sensilla in the silkmoth *Bombyx mori*: receptor membrane structure and sensory cell contacts. Cell Tissue Res. 255, 49–57.

Stocker, R. F. 1994. The organization of the chemosensory system in *Drosophila melanogaster*: a review. Cell Tissue Res. 275, 3–26.

Stocker, R. F. and Schorderet, M. 1981. Cobalt filling of sensory projections from internal and external mouthparts in *Drosophila*. Cell Tissue Res. 216, 513–523.

Szentesi, A. and Bernays, E. A. 1984. A study of behavioural habituation to a feeding deterrent in nymphs of *Schistocerca gregaria*. Physiol. Entomol. 9, 329–340.

Szentesi, A. and Jermy, T. 1990. The role of experience in host plant choice by phytophagous insects. In: Insect–Plant

Interactions (*ed*. E. A. Bernays), Vol. 2, pp. 39–74. CRC Press.

Tanaka, Y., Asaoka, K., and Takeda, S. 1994. Different feeding and gustatory responses to ecdysone and 20-hydroxyecdysone by larvae of the silkworm, *Bombyx mori*. J. Chem. Ecol. 20, 125–133.

Tanimura, T., Isono, K., Takamura, T., and Shimada, I. 1982. Genetic dimorphism in the taste sensitivity to trehalose in *Drosophila melanogaster*. J. Comp. Physiol. 147, 433–437.

Tanimura, T., Isono, K., and Yamamoto, M. 1988. Taste sensitivity to trehalose and its alteration by gene dosage in *Drosophila melanogaster*. Genetics 119, 399–406.

Thompson, R. F. and Spencer, W. A. 1966. Habituation: a model phenomenon for the study of neuronal substrates of behavior. Psychol. Rev. 73, 16–43.

Thorne, N., Chromey, C., Bray, S., and Amrein, H. 2004. Taste perception and coding in *Drosophila*. Curr. Biol. 14, 1065–1079.

Thurm, U. and Küppers, J. 1980. Epithelial Potential of Insect Sensilla. In: Insect Biology of the Future (*eds*. M. Locke and D. Smith), pp. 735–763. Academic Press.

Timmins, W. A. and Reynolds, S. E. 1992. Physiological mechanisms underlying the control of meal size in *Manduca sexta* larvae. Phyisol. Entomol. 17, 81–89.

Ueno, K., Kohatsu, S., Clay, C., Forte, M., Isono, K., and Kidokoro, Y. 2006. Gsα is involved in sugar perception in *Drosophila melanogaster*. J. Neurosci. 26, 6143–6152.

Ueno, K., Ohta, M., Morita, H., Mikuni, Y., Nakajima, S., Yamamoto, K., and Isono, K. 2001. Trehalose sensitivity in *Drosophila* correlates with mutations in and expression of the gustatory receptor gene Gr5a. Curr. Biol. 11, 1451–1455.

Usher, B. F., Bernays, E. A., and Barbehenn, R. V. 1988. Antifeedant tests with larvae of *Pseudaletia unipuncta*: variability of behavioral response. Entomol. Exper. Appl. 48, 203–212.

Usui-Aoki, K., Matsumoto, K., Koganezawa, M., Kohatsu, S., Isono, K., Matsubayashi, H., and Yamamoto, M.-T. 2005. Targeted expression of IP3 sponge and IP3 dsRNA impairs sugar taste sensation in *Drosophila*. J. Neurogenet. 19, 123–141.

van der Goes van Naters, W. M. and den Otter, C. J. 1998. Amino acids as taste stimuli for tsetse flies. Physiol. Entomol. 23, 278–284.

van Loon, J. J. A. and van Eeuwijk, F. A. 1989. Chemoreception of amino acids in larvae of two species of *Pieris*. Physiol. Entomol. 14, 459–469.

Wacht, S., Lunau, K., and Hansen, K. 2000. Chemosensory control of pollen ingestion in the hoverfly *Eristalis tenax* by labellar taste hairs. J. Comp. Physiol. A 186, 193–203.

Wang, Z., Singhvi, A., Kong, P., and Scott, K. 2004. Taste representations in the *Drosophila* brain. Cell 117, 981–991.

Watanabe, H. and Mizunami, M. 2006. Classical conditioning of activities of salivary neurons in the cockroach. J. Exp. Biol. 209, 766–779.

White, P. R. and Chapman, R. F. 1990. Tarsal chemoreception in the polyphagous grasshopper *Schistocerca americana*: behavioural assays, sensilla distributions and electrophysiology. Physiol. Entomol. 15, 105–121.

Wiggins, L. L., Frank, R. A., and Smith, D. V. 1989. Generalization of learned taste aversions in rabbits: similarities among gustatory stimuli. Chem. Senses 14, 103–119.

Wolbarsht, M. L. and Hanson, F. E. 1965. Electrical and Behavioral Responses to Amino Acid Stimulation in the Blowfly. In: Olfaction and Taste, II (*ed*. T. Hayashi), pp. 749–760. Oxford.

Yamamoto, R. T. 1974. Induction of host plant specificity in the tobacco hornworm, *Manduca sexta*. J. Insect Physiol. 20, 641–650.

4.04 Aquatic Animal Models in the Study of Chemoreception

J Caprio, Louisiana State University, Baton Rouge, LA, USA

C D Derby, Georgia State University, Atlanta, GA, USA

© 2008 Elsevier Inc. All rights reserved.

4.04.1	**Introduction**	99
4.04.2	**Olfactory Transduction**	100
4.04.2.1	Introduction	100
4.04.2.2	Fish	100
4.04.2.3	Crustaceans	101
4.04.2.4	Overview	102
4.04.3	**Properties of the Peripheral Chemical Detectors**	102
4.04.3.1	Introduction	102
4.04.3.2	Fish	102
4.04.3.2.1	Specificity of single olfactory receptor neurons	102
4.04.3.2.2	Correlation between olfactory receptor neuron type, transduction process, and odorant sensitivity	103
4.04.3.3	Crustaceans	104
4.04.3.3.1	Organization	104
4.04.3.3.2	Sensitivity	105
4.04.3.3.3	Temporal properties	106
4.04.3.4	Processing Chemical Information by Single Peripheral Chemoreceptor Neurons of Crustaceans	106
4.04.3.5	Overview	107
4.04.4	**Organization of Central Olfactory Pathways**	107
4.04.4.1	Introduction	107
4.04.4.2	Fish	107
4.04.4.2.1	Organization of the olfactory bulb	107
4.04.4.2.2	Extrabulbar pathway	108
4.04.4.2.3	Odotopic representation of odorants in the teleost olfactory bulb	108
4.04.4.2.4	Odorant specificity of single olfactory bulb neurons	109
4.04.4.2.5	Olfactory forebrain	111
4.04.4.3	Crustaceans	112
4.04.4.3.1	Organization of the olfactory lobes	112
4.04.4.3.2	Organization of other chemosensory neuropils	113
4.04.4.3.3	Higher-order processing centers	114
4.04.4.3.4	Other chemoreceptor neuron processing centers	114
4.04.4.4	Overview	114
4.04.5	**Neurogenesis and Turnover of Olfactory Neurons in Adult Crustaceans**	114
4.04.6	**Taste in Fish**	115
4.04.6.1	Peripheral Taste Anatomy	115
4.04.6.2	Taste Cell Physiology and Transduction	116
4.04.6.3	Peripheral Nerve Taste Responses	116
4.04.6.4	Processing Taste Information by Single Peripheral Taste Fibers	117
4.04.6.5	Taste and Tactile Input to the Central Nervous System (Medulla)	118
4.04.7	**Processing of Mixtures**	119
4.04.7.1	Introduction	119
4.04.7.2	Fish	119
4.04.7.2.1	Introduction	119
4.04.7.2.2	Responses of single units	120

4.04.7.2.3	Behavioral discrimination	121
4.04.7.3	Crustaceans	121
4.04.7.3.1	Electrophysiology	121
4.04.7.3.2	Behavior	122
4.04.7.4	Overview	123
4.04.8	**Behavioral Roles of Olfaction and Taste**	123
4.04.8.1	Introduction	123
4.04.8.2	Fish	123
4.04.8.3	Crustaceans	124
4.04.8.4	Overview	124
References		125

Glossary

accessory lobes (ALs) The paired deutocerebral neuropils in crustaceans that are connected to the olfactory lobes through interneurons but do not receive direct input from primary chemoreceptor neurons.

accessory olfactory bulb (AOB) The initial portion of the vertebrate central nervous system that processes information arriving from the vomeronasal organ.

aesthetasc sensilla Also called olfactory sensilla, they are the cuticular sensory structures of crustaceans that are located on the distal end of the lateral flagellum of the antennule and contain only olfactory receptor neurons that project only to the olfactory lobes.

antennal lobes The paired deutocerebral neuropils of insects that process odor information arriving from olfactory receptor neurons on the antennae; analogous to the vertebrate olfactory bulbs and the crustacean olfactory lobes.

antennules The first pair of antennae of crustaceans that are composed of basal segments at the proximal end and two flagella (lateral and medial) at the distal end.

chemoreceptor neuron (CRN) First-order neurons that detect environmental chemicals and transmit that information via their axonal projections into the central nervous system.

deutocerebrum The midbrain of arthropods (positioned between the protocerebrum and the tritocerebrum), which receives sensory information from the antenna; in crustaceans, the deutocerebrum includes the olfactory lobes, ALs, and lateral antennular neuropils.

facial lobe (FL) The primary gustatory nucleus of the medulla in teleosts that receives input from the facial taste nerve (cranial nerve VII) that innervates taste buds on the external body surface, lips, and rostral oral cavity.

lateral antennular neuropils (LANs) The paired deutocerebral neuropils of crustaceans that receive input from the CRNs and mechanoreceptor neurons that innervate the nonaesthetasc sensilla on the lateral and medial flagella of the antennules.

median antennular neuropil (MAN) The unpaired deutocerebral neuropil of crustaceans that receives input from the CRNs and mechanoreceptor neurons that innervate the nonaesthetasc sensilla of the antennules.

nonolfactory chemosensilla Also called nonaesthetasc chemosensilla, they are a diverse assortment of cuticular sensory structures located on the antennule of crustaceans, which project into the LANs and MAN.

olfactory bulb (OB) The initial portion of the central nervous system in vertebrates that processes odor information arriving from olfactory receptor neurons.

olfactory lobe (OL) In teleosts, the portion of the forebrain that receives input from the olfactory tract, the axons of mitral cells, the output neurons of the OB. In crustaceans, the deutocerebral neuropil that receives input from the axons of olfactory receptor neurons of the aesthetasc sensilla of the lateral flagellum of the antennule.

olfactory receptor (OR) Molecules, typically G-protein-coupled receptors, located on CRNs, to

which odorant molecules bind to initiate the olfactory transduction process.

olfactory receptor neuron (ORN) Primary receptor neurons whose dendrites contain the molecular ORs and whose axons project via the olfactory nerve into the olfactory region of the brain; in fish, the olfactory nerve is cranial nerve I projecting to the OB, and in crustaceans, it is a tract of the antennular nerve projecting to the OL.

perireception Events occurring around the olfactory and taste receptors that influence the chemical environment and the reception of chemical stimuli.

vagal lobe (VL) The primary gustatory nucleus of the medulla in teleosts that receives input from taste activity transmitted by the vagal taste nerve (cranial nerve X) that innervates taste buds within the oral cavity caudal to the first gill arch.

4.04.1 Introduction

The aim of this chapter is to provide a basic understanding of the chemosensory structures and mechanisms found in aquatic animals. Because of the vast literature on such an enormous topic, we have had to narrow considerably the scope of our review. First, we focus only on the major aquatic animal models in the study of chemoreception. We have selected two groups, representing the vertebrates and the invertebrates: the teleosts (bony fishes) and decapod crustaceans (spiny lobsters, clawed lobsters, crayfish, and crabs). Second, we focus on topics more aligned with biomedical than ecological issues: general structure of the chemosensory cells and their organization, and mechanisms of chemosensory transduction and the neural processing of chemical stimuli. Due to space limitations, topics such as pheromones (Stacey, N. E. and Sorensen, P. W., 2002; 2005) and the chemosensory basis of homing behavior (Døving, K. B., 1996; Døving, K. B. and Stabell, O. B., 2003) in fishes are not discussed. This chapter is also not an encyclopedic listing of how chemicals may influence various behaviors of aquatic organisms but focuses on chemosensory behaviors where there is better understanding of the neurophysiological substrate. Due to the necessary selection of research reports to include in this chapter from the numerous research articles that have allowed the field of aquatic chemoreception to progress to date, we take this opportunity to apologize to our coworkers whose work was not given the treatment that it deserves. Previously published excellent reviews in this field include Kleerekoper H. (1969), Hara T. J. (1982; 1992), Atema J. *et al.* (1989), Carr W. E. S. *et al.* (1990), Sandeman D. C. *et al.* (1992), Derby C. D. (2000), Weissburg M. J. (2000), Zimmer R. K. and Butman C. A. (2000), McClintock T. S. and Xu F. (2001), Ache B. W. (2002), Schachtner J. *et al.* (2005), Ache B. W. and Young J. M. (2005), Moore P. A. and Berman D. A. (2005), and Atema J. and Steinbach M. A. (2007).

For terrestrial animals including mammals and insects, olfaction and taste are neatly distinguished based on the physical medium in which they operate. Olfaction is for volatile molecules that are delivered in air to the receptor epithelium, and taste is for water-soluble molecules that are delivered in an aqueous medium to the receptors. For fish and most crustaceans, which live in aquatic environments and whose chemosensory world is limited to water-soluble rather than to volatile chemical stimuli, this distinction between olfaction and taste is nonsensical.

Olfaction and taste are also distinguished within the vertebrates based on anatomical organization, regardless of the media in which the animals live. Olfaction is mediated by the olfactory nerve (cranial nerve (CN) I), and taste is mediated by modified epithelial (taste) cells innervated by CN VII (facial), IX (glossopharyngeal), or X (vagal), regardless of whether the animal is a human living in air, a fish living in water, or a frog that lives in both worlds. Yet this anatomical distinction, which works for vertebrates, is not instructive for the other ~97% of the animals – that is, the invertebrates.

A third way of distinguishing olfaction and taste is a functional one. Taste mediates more simple, reflexive behaviors – grabbing, biting, and swallowing (i.e., consummatory behavior), whereas olfaction mediates more complex behaviors, that is, search for chemicals from a distance, courtship behavior, and learning about odors (Atema, J. 1977; 1995); however, taste in some fish like catfishes mediates searching for distant food (i.e., appetitive behavior).

Another way to identify olfaction, at least for vertebrates and arthropods, is the organization of the first-order processing regions in the brains that receive the

peripheral chemosensory input. This region – the olfactory bulb (OB) of vertebrates, the antennal lobe of insects, and the olfactory lobe of crustaceans – is organized into glomeruli, which contain the synapses between the olfactory receptor neurons (ORNs) and second-order neurons. Furthermore, there is an odotopic organization to these glomeruli, in which odorants of different chemical categories generate distinctive activation patterns across the glomeruli.

In this chapter, olfaction and taste in fish is distinguished according to the vertebrate-specific pattern of nerve innervation, which is consistent with the olfaction-has-glomeruli model. For crustaceans, the glomerular definition of olfaction, and thus their olfactory pathway, is defined as the aesthetasc–olfactory lobe pathway (as described below). However, distinguishing between olfaction and taste creates a binary categorization that does not adequately describe the diversity of chemical senses of any animal, including fish and crustaceans. For example, this categorization applied to fish combines the oropharyngeal pathway and the extraoral pathway, even though they differ in cranial innervation (IX/X versus VII) and function – the former controlling reflexive swallowing (consummatory behavior) and the latter for locating distant food and taking it into the mouth (appetitive behavior). In addition, this categorization does not include the solitary chemoreceptor cells, which individually are anatomically similar to taste cells, but they are not organized into bud-like structures and they synapse with taste, trigeminal, or spinal nerves (Kapoor, B. G. and Finger, T. E., 2003). For crustaceans, this binary classification results in identifying all nonaesthetasc chemoreceptive neurons (CRNs) as taste, even though they are extremely diverse in how they are packaged into functional units, how they connect to the central nervous system (CNS), their organization within the CNS, and the behaviors they mediate (see below). Combining them into a single taste category is too simplistic and restrictive, and thus, in this chapter they are termed nonaesthetasc or nonolfactory chemosensors.

4.04.2 Olfactory Transduction

4.04.2.1 Introduction

ORNs of teleosts and crustaceans have served as important models not only for understanding the specifics of transduction in these species but also for elucidating fundamental and general principles of olfactory transduction (Ache, B. W. and Zhainazarov, A. B., 1995; Bruch, R. C., 1996; Ache, B. W. 2002; Ache, B. W. and Young, J. M. 2005). Transduction processes that are well characterized and that we describe in this section include perireception (in crustaceans), molecular biology of receptor molecules (in fish), second messengers, ion channels, and kinases. Much has been learned about chemoreception in fishes from only a few animal models of the more than 25 000 extant teleost species. These model species include catfishes, zebrafish, goldfish, and salmonids. For crustaceans, the spiny lobster *Panulirus argus* and the clawed lobster *Homarus americanus* are the models of choice for studying olfactory transduction.

4.04.2.2 Fish

Genes for putative olfactory receptors (ORs) are identified from several teleosts (Ngai, J. *et al.*, 1993; Byrd, C. A. *et al.*, 1996; Cao, Y. *et al.*, 1998; Sun, H. *et al.*, 1999; Kondo, R. *et al.*, 2002). These ORs are G-protein-coupled receptors, although they are structurally highly dissimilar from the ORs of mammals and other vertebrates.

OR activation by odorants results in the formation of second messengers – cAMP and/or inositol 1,4,5-trisphosphate (IP_3)/diacylglycerol (DAG). These second messengers lead to the depolarization of ORNs via the gating of (1) cyclic nucleotide-gated (CNG) channels and subsequently Ca^{2+}-activated Cl^- channels (for the cAMP pathway), which amplifies the odor-activated signal (Schild, D. and Restrepo, D., 1998), (2) ciliary IP_3 channels (Bruch, R. C., 1996; Schild, D. and Restrepo, D., 1998), or (3) TRPC2 (transient receptor potential) channels (Sato, Y. *et al.*, 2005), leading in all three cases to increasing intracellular Ca^{2+}. Although excitatory conductances have only been described to date, ORNs of teleosts also exhibit odorant-induced suppression (Kang, J. and Caprio, J., 1995b), but little definitive information is known in fish about the responsible mechanisms. The cAMP pathway is the generally accepted excitatory mechanism for the ciliated ORNs (cORNs) of tetrapods, especially mammals (Gold, G. H., 1999), although recent evidence suggests that odor transduction in mammals likely also involves a cAMP-independent pathway (Lin, W. *et al.*, 2004). However, in microvillous receptor neurons of the vomeronasal system, a DAG transduction pathway was recently implicated (Lucas, P. *et al.*, 2003). Fish, however, do not possess a vomeronasal

system, and both cORNs and microvillous ORNs (mORNs) are present in the main olfactory epithelium. Recent evidence from teleosts suggests that specific odorants activate ORs and the cAMP second messenger system in cORNs (Sato, K. and Suzuki, N., 2000; Hansen, A. *et al*., 2003; Schmachtenberg, O. and Bacigalupo, J., 2004; Sato, Y. *et al*., 2005), whereas other odorants activate members of the V2R gene family and the IP_3 (and possibly the diacyl glycerol) pathway of mORNs (Speca, D. J. *et al*., 1999; Hansen, A. *et al*., 2003; Sato, Y. *et al*., 2005).

A recent molecular modeling study identified key amino acid residues that are involved in ligand binding and selectivity for the L-arginine OR (a V2R olfactory receptor) in goldfish (Luu, P. *et al*., 2004). Identified was a key residue, methionine 389, in goldfish OR 5.24 that provides OR selectivity to basic amino acids, and another residue, lysine 386, in zebrafish that is critical for OR selectivity to acidic amino acids. Although neither the odorant nor receptor types are known for crypt ORNs, the transduction mechanism in channel catfish likely utilizes $G\alpha_o$ (Hansen, A. *et al*., 2003), whereas in goldfish the same crypt ORN expresses both $G\alpha_o$ and $G\alpha_q$ (Hansen, A. *et al*., 2004).

4.04.2.3 Crustaceans

The importance of perireceptor events, which influence the odorant environment around the receptors, has been well studied in spiny lobsters. Flicking of the olfactory organ leads to periodic loading and unloading of chemical stimuli around the densely packed aesthetascs (Schmitt, B. C. and Ache, B. W., 1979; Koehl, M. A. R. *et al*., 2001). Lobsters, fish, and other aquatic animals do not appear to have odorant-binding proteins, whose function in terrestrial animals may include delivery of odorants to receptors or even be more directly central to receptor activation (Vogt, R. G., 2005; Xu, P. *et al*., 2005). Lobsters, however, do have several perireceptor elements that are involved in inactivating or removing odorants from the receptor environment. These include ectoenzymes, such as ectonucleotidases, to convert the excitatory compounds AMP and ATP into non-excitatory adenosine, and transporters for odorants such as taurine, adenosine, and glutamate (Carr, W. E. S. *et al*., 1990).

Despite the fact that genes for ORs are not yet identified in any crustacean, other lines of inquiry, including biochemical, molecular, and physiological, reveal much about the nature of these receptors and their role in transduction. Patch clamp (Hatt, H. and Ache, B. W., 1994), binding studies (Olson, K. S. *et al*., 1992), and transmission electron microscopy (Blaustein, D. N. *et al*., 1993) demonstrate odorant-binding receptors on the dendritic membrane of ORNs. Furthermore, biochemical analysis of receptor–ligand binding shows that high (nM to pM) and low (μM) affinity sites for taurine, AMP, glutamate, and arginine receptors on the ORN dendrites (Olson, K. S. *et al*., 1992; Michel, W. C. *et al*., 1993; Olson, K. S. and Derby, C. D., 1995).

These receptors are G-protein-coupled receptors, as demonstrated by physiological, biochemical, and molecular studies. Odor-activated physiological responses of ORNs are affected in predictable ways by blockers or activators of G proteins (Fadool, D. A. *et al*., 1995). In addition, several G-protein subunits ($G\alpha_i$, $G\alpha_s$, $G\alpha_q$, and $G\beta$), phospholipase C-β (PLC-β), and a G-protein-coupled receptor kinase are identified from cDNA libraries of the antennules of lobsters (*Homarus*) (McClintock, T. S. and Xu, F., 2001). Furthermore, functional assays demonstrate a role for these molecules in either activation or desensitization of odorant responses (McClintock, T. S. and Xu, F., 2001).

Lobster ORNs have two distinct G-protein-coupled second messenger pathways (Ache, B. W., 2002). One of these is excitatory, mediated by phosphoinositol signaling. In this pathway, $InsP_3$ activates a cation-selective channel, leading to an inward conductance that normally depolarizes the cell. The other G-protein pathway is inhibitory, mediated by cyclic nucleotide signaling. In this pathway, cAMP activates an outward conductance, carried by K^+ through a CNG K^+ channel (Michel, W. C. and Ache, B. W., 1992), and suppresses a steady-state Cl^- channel (Doolin, R. E. *et al*., 2001; Doolin, R. E. and Ache, B. W., 2005a). Both excitatory and inhibitory pathways are present in the same ORN, as revealed by electrophysiological recordings from both individual cells (McClintock, T. S. and Ache, B. W., 1989; Michel, W. C. *et al*., 1991) and from patches of ORN dendritic membranes (Hatt, H. and Ache, B. W., 1994).

A given odorant can be excitatory to some ORNs and inhibitory to others (Michel, W. C. *et al*., 1991) and can activate either the inward or the outward conductance (Doolin, R. E. and Ache, B. W., 2005b). Furthermore, it appears that the two inhibitory conductances, Cl^- and K^+, are not odor specific (Doolin, R. E. and Ache, B. W., 2005b). Thus, no odorant is exclusively excitatory or inhibitory across cells, and

no receptor exclusively mediates excitation or inhibition.

These two second messenger-mediated pathways are the first step in odor activation, and this is followed by a second step that amplifies this signal and sets the gain of the ORN (Ache, B. W., 2002). This amplification involves a nonselective cation channel, which is a member of the TRP channel family (Zhainazarov, A. B. *et al.*, 2001; Bobkov, Y. V. and Ache, B. W., 2005) and may be functionally similar to the Ca^{2+}-activated Cl^- channel that participates in odor detection in mammals (Kleene, S. J., 1997).

These and other results lead to the conclusion that individual ORNs of spiny lobsters contain a rich diversity of transduction molecules. Together, these diverse intracellular pathways allow ORNs to do substantial processing and integration (Ache, B. W. *et al.*, 1998). In addition, ORN responsiveness can be modulated by gamma-aminobutyric acid ($GABA_A$) receptors on the soma (Zhainazarov, A. B., *et al.*, 1999) and by centrifugal synaptic inhibition at their axonal terminals (Wachowiak, M. *et al.*, 2002). An important question is, whether having ORNs with such complex integration properties is a feature of simpler animals (i.e., invertebrates), which have fewer ORNs than vertebrates, or whether vertebrate ORNs are similarly complex. Although this topic is hotly debated, recent evidence indicates that mammalian ORNs have both cAMP and IP_3 pathways that can interact in complex ways (Spehr, M. *et al.*, 2002; Zhainazarov, A. B. *et al.*, 2004).

4.04.2.4 Overview

Olfactory transduction in teleosts and crustaceans has many commonalities with each other and with other characterized ORNs. ORs are G-protein-coupled receptors linked via second messenger pathways to ion channels. A diversity of olfactory transduction cascades that lead to the activation of CNG, IP_3, and/or TRPC2 channels exist. Other channels are secondarily activated, which in turn amplify the signal. Single ORNs of teleosts and lobsters can have more than one second messenger pathway. In lobsters, these include specific excitatory and inhibitory pathways. For teleosts, dual excitatory ORN pathways are identified, but it is currently unknown whether odorant-induced suppression requires an additional inhibitory transduction pathway, or whether specific odorants can affect the resident pathways to result in suppression (Hallem, E. A. *et al.*, 2004). Multiple transduction cascades in individual cells can enhance the diversity of odor responses generated by ORNs. Perireceptor events are important to aquatic animals – for example, ectoenzymes and transporters clean up the odor environment around the ORs – but other perireceptor processes not relevant to aquatic animals are absent – for example, no odorant-binding proteins.

4.04.3 Properties of the Peripheral Chemical Detectors

4.04.3.1 Introduction

Peripheral chemosensory systems have the task of extracting biologically important information about the type, amount, and temporal dynamics of environmental chemicals and sending this information to the CNS. In this section, we review the organization of peripheral olfactory systems of fish and crustaceans and describe how they perform these important tasks.

4.04.3.2 Fish

4.04.3.2.1 Specificity of single olfactory receptor neurons

Although numerous studies in fishes tested amino acids as odorant stimuli, few investigations focused primarily on the odorant specificities of individual ORNs (Mac Leod, N. K., 1976; Meredith, M. and Moulton, D. G., 1978; Meredith, M., 1981; Restrepo, D. *et al.*, 1990; Ivanova, T. T. and Caprio, J., 1993; Kang, J. and Caprio, J., 1995a; 1995b; 1997; Sato, K. and Suzuki, N., 2001; Friedrich, R. W. and Laurent, G., 2004). Electrophysiological studies in the channel catfish indicated that single ORNs had ongoing spontaneous activity ($\sim$5 spikes s^{-1}) that could be elevated or suppressed in response to amino acids (Kang, J. and Caprio, J., 1995b; 1997); furthermore, response suppression (25%) was the dominant response type (13% excited; 62% nonresponsive). A few single ORNs showed excitation to some amino acids and suppression to others. In an innovative study to reveal odor-induced spike activity of single ORNs whose responses were likely to have been shunted from an extracellular recording electrode due to the high ionic content of the pond water bathing the olfactory organ, the olfactory organ of bullhead catfish was bathed in water of low ionic content (Valentinčič, T. *et al.*, 2005). ORNs having low or no spontaneous activity were excited by specific amino acids. That excitation is the major type of

response to amino acids in teleost ORNs was also reported for zebrafish where only 4% (3 of 76 ORNs) were suppressed by an amino acid (Friedrich, R. W. and Laurent, G., 2004). None of these reports provided evidence for the existence of specific neuron types that were excited by particular amino acids.

Current unpublished data (Nikonov A. A. and Caprio J.), however, indicate the existence of ORNs that are highly specific to basic and neutral amino acids, respectively, similar to those reported for group I neurons in the OB (see section 4.04.4.2.4) and FB (see Nikonov, A. A. and Caprio, J., 2007).

4.04.3.2.2 Correlation between olfactory receptor neuron type, transduction process, and odorant sensitivity

Several morphological types of ORNs occur in the olfactory epithelium of teleosts: ciliated (c), microvillous (m), and crypt (cp) (Figure 1). However, controversy exists as to whether these different cell types process specific types of odorants (see Eisthen, H. L., 2004, for a review). A whole-cell patch clamp study of isolated ORNs from rainbow trout indicated, however, that mORNs responded specifically to amino acids, whereas cORNs were more broadly tuned, responding to a wide variety of odorants including amino acids (Sato, K. and Suzuki, N., 2001). That mORNs also respond to amino acids was indicated via activity-dependent labeling by the ion channel permeant probe, agmatine, in zebrafish (Lipschitz, D. L. and Michel, W. C., 2002). Additional evidence to suggest that mORNs respond to amino acids was obtained in the goldfish where a V2R receptor for L-arginine was shown to couple to PLC and IP_3 production and be expressed in ORNs whose cell bodies were located superficially in the olfactory epithelium, a characteristic of mORNs (Speca, D. J. *et al.*, 1999). Evidence that cORNs also respond to amino acids, as reported above for rainbow trout, comes from a perforated patch study of isolated cORNs in a marine fish, the Cabinza grunt (*Isacia conceptionis*). cORNs in this marine species responded to amino acids through the activation of CNG channels and calcium-activated conductances (Schmachtenberg, O. and Bacigalupo, J., 2004), confirming a similar report for cORNs in rainbow trout (Sato, K. and Suzuki, N., 2000).

The recent determination of the odotopic organization within the OB of a few species of teleosts also provided the pathway to link odorant type with receptor cell morphology. By placing DiI, a postmortem retrograde tracer, into select and discrete regions of the teleost OB shown to be excited by specific classes of odorants, a direct link between ORN morphology and the type of odorant detected was recently derived from studies in crucian carp, channel catfish, and goldfish. For crucian carp, the evidence suggests that mORNs respond to food odors (Hamdani, E. H. *et al.*, 2001a), whereas cORNs are involved in the detection of alarm substances (Hamdani, E. H. and Døving, K. B., 2002). For channel catfish, the combination of a variety of experimental procedures (light and electron microscopy, *in situ* hybridization, immunocytochemistry, electrophysiology, and pharmacology) provided the necessary information to link the specific anatomical type of ORN with the type of molecular OR, its specificity for odorant type, and its probable mechanism of transduction (Hansen, A. *et al.*, 2003). In channel catfish, bile salt odorants (possible socially relevant cues in teleosts; Sorensen, P. W. and Caprio, J., 1998), are detected primarily by ORs expressed within cORNs and transduced via the $G\alpha_{olf}$/cAMP cascade, whereas nucleotides are detected by V2Rs expressed in mORNs but transduced via an unknown (neither $G\alpha_{olf}$/cAMP nor $G\alpha_{q/11}$/PLC) cascade; however, recent evidence in zebrafish suggests that nucleotides possibly activate TRPC2 channels expressed in mORNs (Sato, Y. *et al.*, 2005). Amino acid odorants in channel catfish activate both cORNs (expressing ORs) and mORNs (expressing V2Rs) but via different transduction pathways in the two types of ORNs (Hansen, A. *et al.*, 2003). For goldfish, cORNs also express ORs and $G\alpha_{olf}$, and mORNs express V2R genes but are primarily immunoreactive for $G\alpha_o$; however, $G\alpha_{i-3}$ and $G\alpha_q$ are also indicated for mORNs that are shorter and that possess more stiff microvilli than other mORNs (Hansen, A. *et al.*, 2004). Independent pharmacological evidence in goldfish also indicated that bile salt odorants and some amino acids are detected via the cAMP pathway and that amino acids also utilize the IP_3 transduction pathway (Rolen, S. H. *et al.*, 2003), which is consistent with previous molecular investigations (Bruch, R. C., 1996).

Sex pheromones in teleosts are gonadal steroids and prostoglandins (Sorensen, P. W. and Caprio, J., 1998). Recent evidence in crucian carp indicate that axons of cp neurons project to the ventral OB where they synapse with mitral cells whose axons form the lateral bundle of the medial olfactory tract and mediate sexual behavior (Hamdani, E. H. and Døving, K. B., 2006; Lastein, S. *et al.*, 2006; Weltzien, F. *et al.*, 2003).

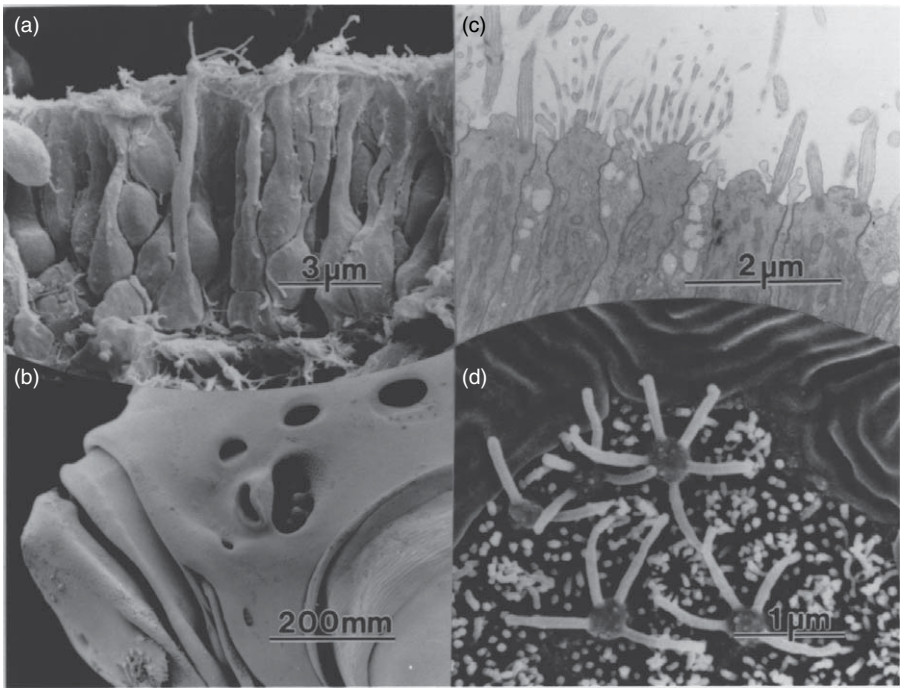

Figure 1 Teleost olfactory epithelia. (a) Scanning electron micrograph (SEM) of the adult sensory epithelium of a zebrafish, *Danio rerio*, showing some receptor cells with long dendrites, and some round receptor cells with short dendrites. (b) SEM of the olfactory organ of a zebrafish showing the organ, lateral line canals, and eye. (c) Transmission electron micrograph (TEM) of an apical longitudinal section of the olfactory epithelium of a goldfish, *Carassius auratus*, showing microvillous and ciliated olfactory receptor cells separated by supporting cells with vesicles. (d) SEM of the Indo-Pacific catfish, *Plotosus lineatus*, showing apical knobs of ciliated and microvillous receptor neurons. Reprinted from Sorensen, P. W. and Caprio, J. 1998. Chemoreception. In: The Physiology of Fishes (ed. D.H. Evans), 375–405. CRC Press LLC, by courtesy of Taylor and Francis Group, LLC. Courtesy: Eckart Zeiske and Anne Hanson.

4.04.3.3 Crustaceans

4.04.3.3.1 Organization

Being arthropods, crustaceans have an exoskeletal covering. Consequently, their chemosensory neurons are packaged into thin extensions of the cuticle, called setae or sensilla. A rich diversity of sensilla exists, which can be classified into olfactory and nonolfactory chemosensilla.

4.04.3.3.1.(i) Olfactory sensilla The olfactory sensilla, called aesthetascs, have been recognized in many crustacean taxa (Grünert, U. and Ache, B. W., 1988; Hallberg, E. *et al.*, 1992). Aesthetascs are distinguished by their peripheral structure and central connections. They are the only sensilla known to be innervated solely by chemosensory neurons and are typically richly innervated (hundreds of ORNs in some species such as spiny lobsters) (Derby, C. D. *et al.*, 2003). Aesthetascs are located on the paired first antennae (antennules) but only on the distal end of the lateral flagellum of the antennule (Figure 2). Chemical stimuli pass through the porous cuticle of the aesthetascs and bind to receptor sites on the ORN dendrites. Each mature aesthetasc contains representatives of each of the functional types of ORNs, and thus, aesthetascs appear to be functional units of olfaction (Steullet, P. *et al.*, 2000b). The axons of the aesthetasc ORNs project ipsilaterally to the olfactory lobes (Schmidt, M. and Ache, B. W., 1996b) (see Section 4.04.4). Although aesthetascs are present in many crustacean taxa, they differ in their structure in functionally significant ways. For example, the organization of aesthetascs differs in aquatic, semiterrestrial, and terrestrial species (Ghiradella, H. *et al.*, 1968; Stensmyr, M. C. *et al.*, 2005). Aesthetasc sensilla contain not only sensory neurons but also supporting cells, which have functional overlap with supporting cells in insect and vertebrate olfactory organs. For example, supporting cells include (1) secretory cells associated with glands that produce a substance that likely coats the external surface of the aesthetasc cuticle (Schmidt, M. and Derby, C. D., 2005); (2) cells that secrete the sensillar cuticle; and (3) cells that produce ectoenzymes and

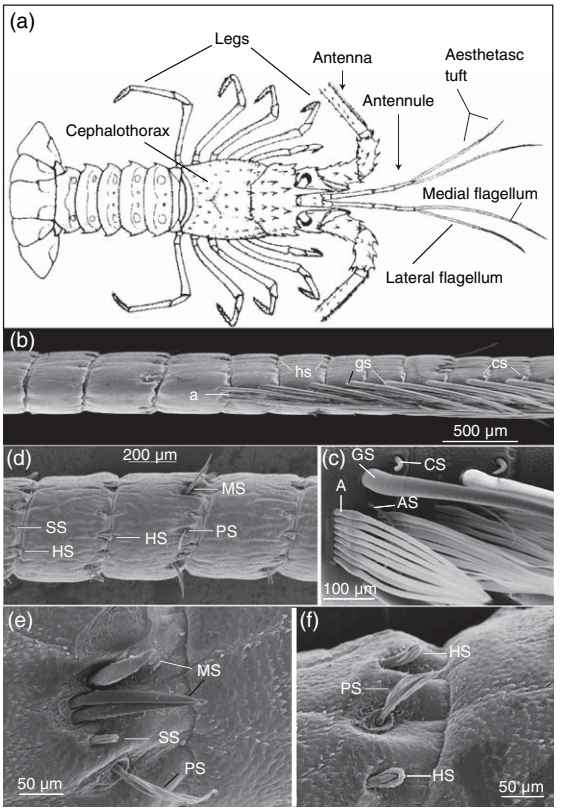

Figure 2 Peripheral chemosensory structures in spiny lobsters. (a) Drawing of a spiny lobster, *Panulirus argus*, showing the chemosensory organs. Each of the antennules (first antennae) has a medial flagellum and lateral flagellum. The sensory neurons are packaged into sensilla. The aesthetasc tuft, which contains aesthetasc sensilla and other associated sensilla (shown in the right half of b and in c), is located on the ventral side of the distal half of the lateral flagellum. Chemoreceptor neurons that innervate sensilla other than aesthetascs are called nonaesthetasc or nonolfactory chemoreceptor neurons. (b–f) Scanning electron micrographs of antennular sensilla. (b) The lateral flagellum at the boundary of the aesthetasc tuft. The aesthetasc tuft is to the right in this figure. The flagellum is divided into annuli, 12 of which are shown here. Each annulus in the aesthetasc region bears a similar complement of sensilla (shown in c), and each annulus in the nonaesthetasc region bears a similar complement of setae (shown in d–f). (c) Tuft region of the lateral flagellum. (d) Nontuft region of the lateral flagellum; the medial flagellum has similar types and organization of sensilla to this region. (e, f) High magnification views of nonaesthetasc regions of the lateral flagellum, showing four types of nonaesthetasc sensilla. A, aesthetasc sensillum; AS, asymmetric sensillum; CS, companion sensillum; GS, guard sensillum; HS, hooded sensillum; MS, medium-length simple sensillum; PS, plumose sensillum; SS, setuled sensillum. From figure 1 of Steullet, P., Dudar, O., Flavus, T., Zhou, M., and Derby, C. D. 2001. Selective ablation of antennular sensilla on the Caribbean spiny lobster *Panulirus argus* suggests that dual antennular chemosensory pathways mediate odorant activation of searching and localization of food. J. Exp. Biol. 204, 4259–4269, used with permission.

transporters that regulate the chemical environment of the fluid bathing the sensory cells (Carr, W. E. S. *et al.*, 1990; Gleeson, R. A. *et al.*, 1992).

4.04.3.3.1.(ii) Nonolfactory chemosensilla Nonolfactory sensilla are on all appendages and most of the body surface. Some of these, such as those on the mouthparts, are clearly gustatory in function, in that they control the ingestion of food (Derby, C. D. and Atema, J., 1982; Garm, A. *et al.*, 2005). Others are found on the legs, antennules, antennae, and general body surface (Derby, C. D., 1982; Schmidt, M. and Gnatzy, W., 1984; Cate, H. S. and Derby, C. D., 2001; 2002; Schmidt, M. and Derby, C. D., 2005), and consequently, these have many different functions. The nonolfactory chemosensilla are morphologically diverse, but they do have several common features. They are at least bimodally innervated, containing not only chemosensory neurons but also mechanosensory neurons (Schmidt, M. and Gnatzy, W., 1984; Cate, H. S. and Derby, C. D., 2002; Garm, A. *et al.*, 2005). Nonolfactory sensilla are more sparsely innervated than aesthetascs, typically with two or three mechanoreceptor neurons and fewer than 20 CRNs. Their cuticle is thick and not porous, and thus, chemicals enter through a terminal pore. The chemosensory neurons of these sensilla do not project to the olfactory lobe but rather to other neuropils in the CNS. This occurs even for nonolfactory antennular chemosensory neurons, which project ipsilaterally to the lateral antennular neuropils (LANs) and to the median antennular neuropil (MAN) (Schmidt, M. and Ache, B. W., 1996a) (see Section 4.04.4).

4.04.3.3.2 Sensitivity

4.04.3.3.2.(i) Response thresholds Olfactory and nonolfactory receptor neurons often differ in sensitivity. For *P. argus*, the sensitivity of antennular CRNs is much greater than for mouthpart CRNs (Thompson, H. A. and Ache, B. W., 1980; Derby, C. D. *et al.*, 1991; Garm, A. *et al.*, 2005). For example, thresholds for antennular CRNs (which include aesthetasc ORNs) are typically nanomolar and sometimes lower, whereas mouthpart CRNs have micromolar thresholds.

4.04.3.3.2.(ii) Tuning Crustaceans are sensitive to chemicals associated with most biologically important items, including food stimuli, social and sexual pheromones, settlement factors, and defensive compounds (Atema, J., 1988; Carr, W. E. S., 1988; Zimmer, R. K. and Butman, C. A., 2000; Kicklighter, C. E. *et al.*, 2005). Differences in sensitivity among species are partly

attributable to the habitat in which they live. For example, for aquatic crustaceans, all sensors, including olfactory, are stimulated by water-soluble compounds. For terrestrial crustaceans, the antennules are sensitive to volatile chemicals, whereas the legs and mouthparts are sensitive to water-soluble stimuli (Rittschof, D. and Sutherland, J. P., 1986; Wellins, C. A. *et al.*, 1989; Stensmyr, M. C. *et al.*, 2005). Trophic level also accounts for interspecific differences in sensitivity. For example, carnivores such as *Panulirus* and *Homarus* have CRNs that respond to small, nitrogen-containing compounds – amino acids, amines, nucleotides, and peptides – that are prevalent in tissues of their animal prey and are relatively insensitive to carbohydrates and sugars (Zimmer-Faust, R. K. and Case, J. F., 1982a; Carr, W. E. S., 1988; Derby, C. D. and Atema, J., 1988; Zimmer-Faust, R. K., 1993). Herbivores and omnivores, such as fiddler crabs (Weissburg, M. J. and Zimmer-Faust, R. K., 1991), ghost crabs (Robertson, J. R. *et al.*, 1981; Trott, T. J. and Robertson, J. R., 1984), kelp crabs (Zimmer-Faust, R. K. and Case, J. F., 1982b), and crayfish (Ashby, E. A. and Larimer, J. L., 1965), often are sensitive to sugars common to plants, bacteria, and diatoms, as well as to some amino acids.

4.04.3.3.2.(iii) Specificity The CRNs of crustaceans tend to be narrowly tuned, responding with high specificity to one compound or a set of structurally related compounds. Examples include CRNs of *H.americanus* tuned to predominantly to taurine, hydroxy-L-proline, or L-glutamate (Voigt, R. and Atema, J., 1992), and antennular CRNs of *P.argus* tuned primarily to taurine, glutamate, AMP, ATP, or ammonium (Derby, C. D. *et al.*, 1991; Derby, C. D., 2000). In the crayfish *Austropotamobius torrentium*, leg CRNs are less narrowly tuned but still have specificity to one of the following classes of compounds – amino acids, pyrimidines, or amines (Bauer, U. and Hatt, H., 1980; Bauer, U. *et al.*, 1981).

Within a species, there may be differences in specificity of CRNs in different organs. For example, in *P. argus*, individual antennular CRNs have narrower response profiles than mouthpart chemoreceptors (Garm, A. *et al.*, 2005).

Physiological studies of CRNs suggest that there are as many as a dozen types of molecular receptors that are heterogeneously distributed across the CRNs. Do single cells express a single receptor type, or more than one? It is often stated that ORNs of mammals and *Drosophila* express only one type of receptor, but this idea is being questioned in the face of new data (Mombaerts, P., 2004; Goldman, A. L. *et al.*, 2005), and it certainly is not true for CRNs in other animals such as *C. elegans* (Troemel, E. R., 1999). Although genes for chemoreceptors have not been identified in any crustacean, physiological studies strongly suggest that a given cell type has multiple receptor types, each coupled to either an excitatory or an inhibitory transduction cascade (see Section 4.04.2). However, the density of the receptor types on a CRN may vary, thus creating high response specificity (Cromarty, S. and Derby, C., 1997).

4.04.3.3.3 Temporal properties

Chemical stimuli in nature, even those released at a constant rate from a single odor source, are patchy and discontinuous. This is due to turbulence, which is ever-present though at different degrees in different environments. The temporal features of chemical stimuli influence the response pattern of a cell and consequently an animal's ability to find an odor source (Atema, J., 1995; Weissburg, M. J., 2000; Zimmer, R. K. and Butman, C. A., 2000; Koehl, M. A. R. *et al.*, 2001). Since the ability of CRNs to resolve temporal fluctuations determines the animal's ability to respond to them, it is important to identify these properties. The frequency following of CRNs is dependent on adaptation and disadaptation rates (Atema, J., 1995). Many crustacean CRNs have phasotonic response profiles, although this varies across cells (Borroni, P. F. and Atema, J., 1988; 1989; Weissburg, M. J. and Derby, C. D., 1995; Garm, A. *et al.*, 2005). CRNs on *Homarus* antennules can follow 4–5 odor pulses per second (Gomez, G. and Atema, J., 1996a; 1996b; Gomez, G. *et al.*, 1999). Since temporal variability of this magnitude is common in aquatic environments (see the above references), this ability to follow such pulses is obviously adaptive.

4.04.3.4 Processing Chemical Information by Single Peripheral Chemoreceptor Neurons of Crustaceans

To summarize our knowledge of neural coding by crustacean peripheral CRNs using a parallel construction with the section Processing Taste Information by Single Peripheral Taste Fibers by single peripheral taste fibers, we offer the following points:

1. Information about different classes of chemical stimuli can be transmitted to the CNS by different groups or types of CRNs; for example, the antennules, legs, and mouthparts of spiny lobsters and American lobsters have some CRNs most sensitive

to one or several amino acids, others most sensitive to one or several adenine nucleotides, and others most sensitive to ammonium ions (Voigt, R. and Atema, J., 1992; Derby, C. D., 2000; Garm, A. *et al.*, 2005).

2. The specificity of single CRNs is not limited to a particular class of chemical stimuli, although the strongest stimulus is usually several orders of magnitude more stimulatory than other stimuli; for example, taurine-best cells on antennules of spiny lobsters may also be sensitive to other amino acids, AMP, and ammonium, although the thresholds for taurine are 100–10 000 lower than for the other stimuli (Cromarty, S. and Derby, C., 1997).
3. Different CRNs having widely different tuning to members of the same class of chemicals can exist within the sensory appendage; for example, populations of CRNs with different amino acid specificities occur on the antennules, legs, and mouthparts of lobsters (Derby, C. D. *et al.*, 1991; Voigt, R. and Atema, J., 1992; Derby, C. D., 2000).
4. CRNs in different sensory appendages within the same species can have different chemical specificities; for example, in the American lobster, CRNs highly sensitive to hydroxy-L-proline are more abundant on the antennule than the legs or mouthparts (Voigt, R. and Atema, J., 1992).
5. The proportion and types of CRNs in different sensory appendages can vary within the same species. For example, cells with best responses to either hydroxy-L-proline, taurine, L-arginine, L-glutamate, betaine, and ammonium chloride occur in the antennules, legs, and mouthparts of the American lobster but in different proportions (Voigt, R. and Atema, J., 1992).
6. L-Amino acids are much more stimulatory than their respective D-isomers, but receptors for some D-isomers do exist (Michel, W. C. *et al.*, 1993).
7. Stimulus quantity appears to be coded by the frequency of action potentials generated. For individual CRNs, some have a dynamic concentration–response range of 5–6 log units of stimulus concentration, while others have more truncated concentration–response relationships. The absolute concentrations to which cells are responsive can differ widely (Derby, C. D. and Atema, J., 1988; Borroni, P. F. and Atema, J., 1988; 1989; Derby, C. D. *et al.*, 1991; Cromarty, S. and Derby, C., 1997).
8. Except for one report (Hatt, H., 1986), CRNs are not known to be sensitive to mechanical stimulation. However, they can respond to temperature and salinity changes (Schmidt, M., 1989).

4.04.3.5 Overview

Fish and crustaceans have a diversity of peripheral chemoreceptors. In teleosts, three types of ORNs have been identified: ciliated, microvillous, and crypt, which differ in their mode of transduction. The crustacean olfactory organ has many types of chemosensory neurons packaged into units called sensilla, but one of these sensillar types – the aesthetascs – is an olfactory sensillum based on its organization and central projections. The ability of fish and crustacean ORNs to detect and identify the type, amount, and temporal dynamics of chemical stimuli is well understood. ORNs generally have low spontaneous spiking activity, which is more usually increased but sometimes decreased by chemical stimulation. The population of ORNs on an olfactory organ responds to many chemicals, with small nitrogenous compounds, such as amino acids, amines, and nucleotides being the most effective. However, individual ORNs differ in their response specificities, which can be quite narrow. The response of ORNs increases in a concentration-dependent manner. Crustacean ORNs can follow pulses of chemicals up to at least 4–5 per second.

4.04.4 Organization of Central Olfactory Pathways

4.04.4.1 Introduction

The organization of the olfactory pathway of fishes and crustaceans has many elements common with that of other vertebrates, arthropods, and even other taxa. This section examines the connectivity between the olfactory periphery and CNS, the organization of the olfactory CNS, and how odor responses from the periphery are shaped by synaptic interactions within the olfactory CNS.

4.04.4.2 Fish

4.04.4.2.1 Organization of the olfactory bulb

Although the general anatomical organization of the olfactory system is similar across the vertebrates, the structure of the neural connections within the OB can be different between fish and mammals (reviewed in Dryer, L. and Graziadei, P. P. C., 1994). In contrast to mammals where a single mitral cell generally projects a single primary dendrite to a single large (50–200 μm in diameter), well-defined

glomerulus, mitral cells in the fish OB can project primary dendrites to several different, small (10–20 μm in diameter), and less well-defined glomeruli (Mori, K., 1995). However, the organization of the teleost OB may not be that radically different than in some mammals, since ~20% of the mitral cells in the main OB in rabbits possess multiple primary dendrites (Mori, K. *et al.*, 1983).

The anatomical organization in the teleost OB is similar to that observed in the accessory olfactory bulb (AOB) of the vomeronasal system in tetrapods where AOB mitral cells also have multiple apical dendrites, each of which innervates a small glomerulus (Satou, M., 1990; Takami, S. and Graziadei, P. P. C., 1991). This organization suggests that mitral cells in both the fish OB and the tetrapod AOB integrate odorant information from different types of ORNs (i.e., those expressing different molecular receptors) that provide input to the different glomeruli. A recent tracing study in the mouse, however, indicated that AOB mitral cells innervate glomeruli that only receive input from the same receptor type (i.e., a homotypic connectivity) (Del Punta, K. *et al.*, 2002). It is currently unknown whether such a homotypic connectivity is characteristic of the teleost OB (Satou, M. *et al.*, 1983; Riddle, D. R. and Oakley, B., 1992). Depending on the particular species of teleost, the anatomical organization within the OB can vary. For example, a recent investigation of the zebrafish OB indicated that the majority (~80%) of the mitral cells observed possessed a single primary apical dendrite (Fuller, C. L. *et al.*, 2005).

The dendritic field of a single mitral cell in fish can extend for more than 300–400 μm from the soma (Kosaka, T. and Hama, K., 1982b; Oka, Y., 1983) and terminate either in discrete tufts or in diffuse, brush-like ending (Kosaka, T. and Hama, K., 1982b; Riddle, D. R. and Oakley, B., 1992). However, in spite of this extensive dendritic field, the neuronal activities on one side of the OB are not influenced much by those in the opposite side (Satou, M., 1990), suggesting that there is little crossing of dendritic fields to opposite sides of the bulb. The recent evidence for odotopy within the OB of channel catfish (Nikonov, A. A. and Caprio, J., 2001) supports the functional isolation between right and left OB. In other aspects, mitral cells within fish lack basal dendrites, and thus, lateral interactions between mitral cells occur at the bases of their primary dendrites (Ichikawa, M., 1976; Kosaka, T. and Hama, K., 1982a; Oka, Y., 1983). Furthermore, axons of fish mitral cells arise not only from cell bodies but from thick dendrites (Dryer, L. and Graziadei, P. P. C., 1994). Ruffed neurons, a cell type not observed in tetrapods, are also located within the mitral cell layer in teleosts. These cells synapse with granule cells but not with ORNs (Kosaka, T. and Hama, K., 1979; 1981). Tufted and periglomerular cells are apparently lacking in the teleost OB (Satou, M., 1990; Dryer, L. and Graziadei, P. P. C., 1994).

4.04.4.2.2 Extrabulbar pathway

Although the vast majority of axons of ORNs project to the OB, in some teleosts, a small subset ORN axons pass through the OB and project directly to the ventromedial telencephalon (Bazer, G. T. *et al.*, 1987; Honkanen, T. and Ekstrom, P., 1990; Szabo, T. *et al.*, 1991; Riddle, D. R. and Oakley, B., 1992; Becerra, M. *et al.*, 1994; Hofmann, M. H. and Meyer, D. L., 1995). Little functional information is known about this extrabulbar primary olfactory pathway (Fujita, I. *et al.*, 1991), but it is distinct from that of the terminal nerve (CN 0) whose axons also pass through the OB and connect to specific forebrain (FB) nuclei (Demski, L. S. and Northcutt, R. G., 1983).

4.04.4.2.3 Odotopic representation of odorants in the teleost olfactory bulb

Indication that the teleost OB is divided into different zones, each processing a specific class of biologically relevant odor, was initially indicated by Thommesen G. (1978), based on the recording of local field potentials in salmonids. This study showed that the lateral OB was highly responsive to amino acids, whereas the medial OB was more selective to bile acids/salts. Other evidence came from anatomical studies also in a salmonid (rainbow trout) that olfactory information arriving at the OB from the olfactory epithelium was likely sorted chemotopically (Riddle, D. R. *et al.*, 1993) and not topographically (Riddle, D. R. and Oakley, B., 1991). More direct evidence for the existence of an odotopic map in the teleost OB was derived from additional investigations of field potential in salmonids (Døving, K. B. *et al.*, 1980; Hara, T. J. and Zhang, C., 1996), calcium (Friedrich, R. W. and Korsching, S. I., 1997; Fuss, S. H. and Korsching, S. I., 2001) and voltage (Friedrich, R. W. and Korsching, S. I., 1998) imaging of olfactory nerve terminals within the OB of zebrafish, and a single-unit study in the OB of the channel catfish (Nikonov, A. A. and Caprio, J., 2001). The exceptional optical imaging study of odor responses to amino acids of olfactory receptor terminals within glomeruli of the lateral OB in zebrafish (Friedrich, R. W. and Korsching, S. I., 1997) provided the direct evidence that both odor identity and concentration

are encoded by combinatorial glomerular activity patterns (Buck, L. B., 1996). Although some variations exist across the species of teleosts investigated, the general results of these studies indicate that food-related odors (i.e., amino acids and nucleotides) are mapped in OB regions (generally in the lateral OB) distinct from those of more socially relevant odors (bile salts, bile acids, and pheromones), which are mapped generally in the medial OB (Sorensen, P. W. *et al.*, 1991; Nikonov, A. A. and Caprio, J., 2001).

The medial–lateral distinction in odotopy within the teleost OB is consistent with mitral cell axons of the medial and lateral OB, respectively, projecting into the medial and lateral olfactory tracts (OTs) (Sheldon, R. E., 1912; Satou, M., 1990). The neuronal activities on one side of the fish OB are not influenced much by those on the opposite side, which is explained by limited dendritic fields of neurons in each part of the OB (Satou, M., 1990). In this respect, electrical stimulation experiments of distinct bundles of the OT in salmonids (Døving, K. B. *et al.*, 1980) and goldfish (Stacey, N. E. and Kyle, A. L., 1983; Demski, L. S. and Dulka, J. G., 1984) and behavioral investigations in crucian carp that had selected transections of different OT bundles (Hamdani, E. H. *et al.*, 2000; 2001a; 2001b; Weltzien, F. *et al.*, 2003) also support the previous evidence for a functional (food-related versus socially related) division between the medial and the lateral OB. This functional separation between types of odorants processed in medial and lateral OB is in sharp contrast to the two mirror-symmetric glomerular maps that exist in rodents (Lodovichi, C. *et al.*, 2003).

4.04.4.2.4 Odorant specificity of single olfactory bulb neurons

Electrophysiological investigations within the OB of the channel catfish (Nikonov, A. A. and Caprio, J., 2004) and zebrafish (Friedrich, R. W. and Laurent, G., 2004) provided information concerning the excitatory response spectrum to amino acids of single neurons (likely mitral cells) at the first synaptic level in the teleost olfactory system. Since the axons of ORNs expressing like ORs converge in the OB onto specific target glomeruli (Ressler, K. J. *et al.*, 1994; Vassar, R. *et al.*, 1994; Mombaerts, P. *et al.*, 1996; Strotmann, J. *et al.*, 2000), it is likely even in fish that the mitral cells whose apical dendrites innervate the respective glomeruli are tuned to odorants similarly as the ORNs that provide the input, but modified by intraglomerular circuitry (Yokoi, M. *et al.*, 1995; Sachse, S. and Galizia, G., 2002).

Two groups of neurons were recently identified in the OB of the channel catfish that were excited by amino acids. Group I OB neurons ($n = 91$ (37%)) were highly specific to the type of amino acid, that is, excited by acidic, basic, or neutral (those possessing short and long side chains, respectively) amino acids, and group II OB neurons ($n = 154$ (63%)) were also excited by a second amino acid but only at $\geq$10 times higher odorant concentration (Nikonov, A. A. and Caprio, J., 2004). Tested with an expanded series of amino acids, a subset of the group I OB units that were selective for neutral amino acids also distinguished neutral amino acids possessing long linear side chains from those with branched side chains. With increasing stimulus concentration, however, responses broadened such that single OB neurons responded selectively to neutral amino acids having either linear or branched side chains, but not to amino acids with either acidic or basic side chains. These results are consistent with the identification of relatively independent molecular ORs for acidic, basic, and neutral amino acids that were previously indicated in teleosts from electrophysiological cross-adaptation (Caprio, J. and Byrd, R. P., Jr. 1984; Caprio, J., *et al.* 1989; Sveinsson, T. and Hara, T. J., 1990; Michel, W. C. and Derbidge, D. S., 1997), biochemical binding (Cagan, R. H. and Zeiger, W. N., 1978; Brown, S. B. and Hara, T. J., 1981; Rhein, L. D. and Cagan, R. H., 1983; Rehnberg, B. G. and Schreck, C. B. 1986; Lo, Y. H. *et al.*, 1991), and calcium imaging (Friedrich, R. W. and Korsching, S. I., 1997; Fuss, S. H. and Korsching, S. I., 2001) studies. Relatively independent ORs for neutral amino acids with short and long side chains, respectively, were also reported (Caprio, J. and Byrd, R. P., Jr. 1984; Bruch, R. C. and Rulli, R. D., 1988; Sveinsson, T. and Hara, T. J., 1990).

It is rather intriguing that recent electrophysiological data obtained in zebrafish also provide evidence for OB unit selectivity to the type of amino acid prior to a reported declustering of odor representations that occurred over the first 800 ms of the response (Friedrich, R. W. and Laurent, G., 2001; Laurent, G. *et al.*, 2001). However, a similar effect was not observed in OB unit responses in channel catfish analyzed over a 3 s response period (Nikonov, A. A. and Caprio, J., 2004). Of 78 group I units analyzed from the OB of the channel catfish (i.e., those that were originally determined to be selectively responsive to only Met, Ala, Arg, or Glu over 3 s of response), 81% and 85% were similarly classified when analyzing the first and third seconds of the responses, respectively (Nikonov, A. A. and Caprio, J., 2004). A reanalysis (Caprio, J., unpublished data) was performed of zebrafish OB unit responses over the initial 400 ms of the response as reported in Figure 3 of Friedrich R. W. and Laurent

(a) Antennular olfactory pathway

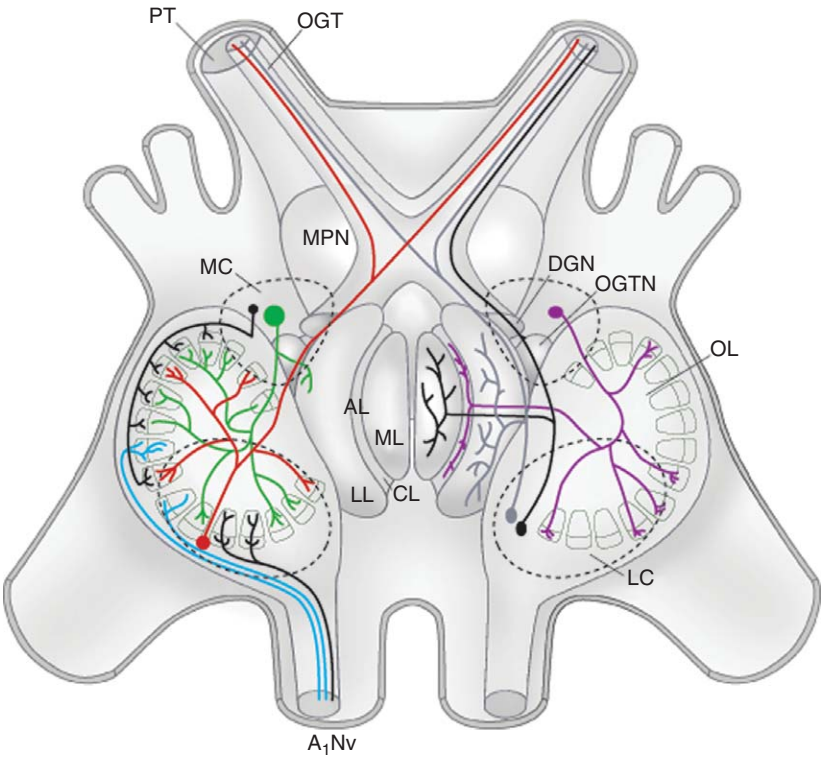

(b) Antennular nonolfactory chemosensory pathway

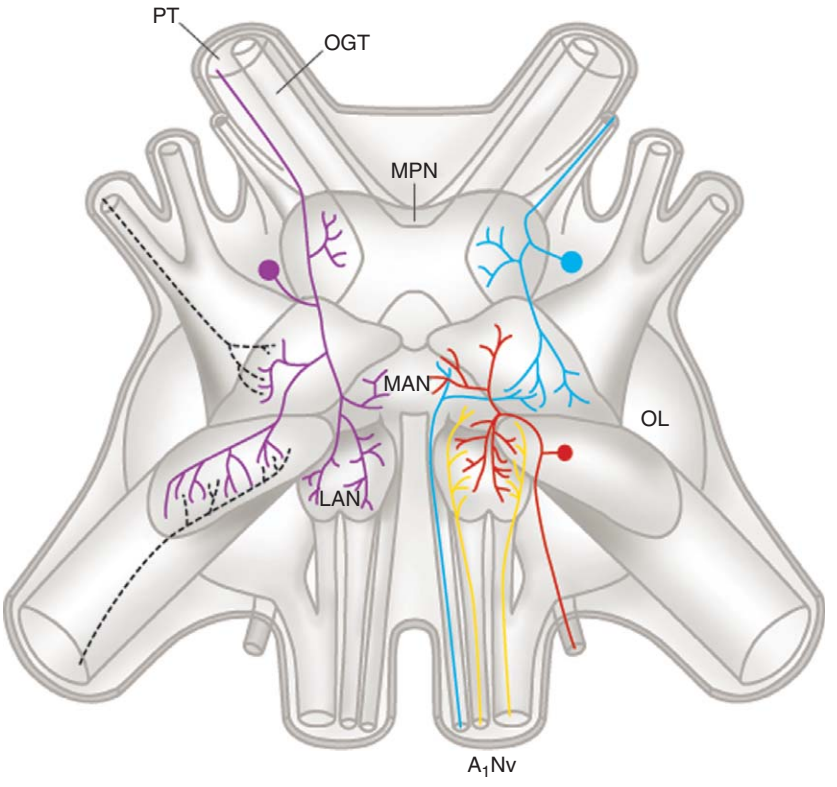

G. (2004) using the catfish scheme of identifying different groups of units by their selected excitatory responses to a specific type of amino acid. The results of this analysis suggested that 49 of the 58 units (84%) could be arranged into the same groups as had been reported for catfish – that is, those units that were preferentially excited by acidic, basic, short-chain neutral, and long-chain neutral amino acids. In addition, a fifth group emerged that was not detected in the channel catfish, those responsive to aromatic amino acids. Of these 49 zebrafish OB units, 63% were similarly classified when analyzing their responses over the first 1 s of the response, and 45% were similarly classified when the analysis time included 1.4 s of the response. These results suggest that there were not profound changes in responses of mitral cells in the zebrafish to the type of amino acid over response time and that the gradual dissolution of responses to types of amino acids over response time is possibly due to adaptational processes. For the zebrafish studies, however, the interpretation of the data is that responses of the population of mitral cells change over time in a stimulus-specific manner, thus providing a mechanism for the behavioral discrimination of individual amino acids (Friedrich, R. W. and Laurent, G., 2001). At present, the two different interpretations of the experimental results remain disputable.

Recently, the specificity of single OB units in the channel catfish to bile salts was reported (Rolen, S. H. and Caprio, J., 2007). OB neurons were identified that were excited selectively by taurine-conjugated bile salts and nonconjugated bile salts, respectively. A third type of OB neuron was rather nonselective and was excited by at least one member of each of three types of bile salts: taurine-conjugated, glycine-conjugated, and nonconjugated.

4.04.4.2.5 Olfactory forebrain

The OB odotopic maps of the aforementioned species of teleosts provide a blueprint for investigation of the organization of odor processing at the next ascending synaptic level in the olfactory system. The axons of the output neurons of the OB (i.e., mitral and ruffed cells) constitute the medial and lateral OTs, which terminate in the cerebral lobes of the olfactory FB. A critical question is whether an odor map exists in the FB, and if so, whether its organization is based on odorant structure as it is in the OB and the antennal lobe of insects. An alternate possibility is that an FB map is not based on odorant quality but on odorant function (e.g., feeding or social odorant cues), or even, that due to the apparent extensive overlap of medial and lateral OT projections, a chemotopic map may not exist in the FB.

Recent experiments performed to visualize FB neurons in mice (Zou, Z. *et al.*, 2001; 2005) and mushroom body and lateral horn neurons of the protocerebrum in *Drosophila* (Wong, A. M. *et al.*, 2002; Marin, E. C. *et al.*,

Figure 3 Antennular chemosensory pathways in the brain of spiny lobsters. (a) Summary diagram of the olfactory (aesthetasc) pathway, which is a ventral view of the brain. The olfactory lobe (OL) receives input from aesthetasc olfactory receptor neurons (ORNs) via the main antennular nerve (A_1Nv). ORNs typically terminate in a single glomerulus (blue), though there may be multiglomerular ORNs (black). The OL has two general types of interneurons: projection neurons (PNs), with their somata in the lateral somata cluster (LC); and local neurons (LNs), with their somata in the medial somata cluster (MC). Three types of OL interneurons are shown, distinguished according to color (red, black, and gray). In red is a PN with multiglomerular innervation in the OL and an axon that bifurcates and extends via the olfactory globular tracts (OGTs) to higher-order neuropils. Two types of OL LNs are shown (purple and green). The accessory lobe (AL) is organized into three regions: medial lobe (ML), central lobe (CL), and lateral lobe (LL). The AL receives no direct sensory input from receptor neurons, but it does receive input from the OL via LNs. AL LNs (purple), similar to those of the OL, have somata in the MC. The AL has PNs (black and gray), which are similar to PNs of the OL in having somata in the LC and bifurcated processes that exit the brain via the OGTs. The deutocerebral commissure neuropil (DCN) and olfactory globular tract neuropil (OGTN) are also innervated by processes from OL interneurons. (b) Summary diagram of the nonolfactory (nonaesthetasc) pathway, which is a dorsal view of the brain. Nonaesthetasc antennular chemoreceptor neurons (CRNs) and antennular mechanoreceptor neurons (yellow) project via the antennular nerve (A_1Nv) into the ipsilateral LAN. The LAN has two regions: a lateral lobe and a medial lobe. There is a general topotopy, in that receptor neurons from the antennular lateral flagellum innervate the lateral lobe of the LAN, and receptor neurons from the antennular medial flagellum innervate the medial lobe of the LAN. These receptor neuron terminals overlap with arborization of the antennular motor neurons (red). The MAN receives mechanoreceptor input via the A_1Nv from the statocyst (blue), an organ for maintaining equilibrium. PNs of the LAN leave the brain via the protocerebral tract (PT). The tegumentary neuropil (TN) and antennal neuropil (AnN) receive sensory input (dashed black) from the second antenna (A_{II}Nv). (a) is adapted from Schmidt, M. and Ache, B. W. 1996b. Processing of antennular input in the brain of the spiny lobster, *Panulirus argus.* II. The olfactory pathway. J. Comp. Physiol. A 178, 605–628. (b) is adapted from Schmidt, M. and Ache, B. W. 1996a. Processing of antennular input in the brain of the spiny lobster, *Panulirus argus.* I. Non-olfactory chemosensory and mechanosensory pathway of the lateral and median antennular neuropils. J. Comp. Physiol. A 178, 579–604. Courtesy: Amy Horner.

2002) that receive input from specific glomeruli of the OB (mice) or antennal lobe (*Drosophila*) provided a consistent picture of the general organization of OT projection patterns and suggested the possible logic for olfactory information processing in these brain structures. Common to both mice and *Drosophila* was a stereotypic projection of secondary olfactory projection neurons from specific glomerular modules of the OB or antennal lobe that terminate with considerable overlap in their multiple brain target areas. The recent findings that projection classes with similar axon terminal fields in the lateral horn in *Drosophila* tended to receive input from neighboring glomeruli (Marin, E. C. *et al.*, 2002) and that structurally similar odorants in the honeybee (Sachse, S. *et al.*, 1999), zebrafish (Friedrich, R. W. and Korsching, S. I., 1997), and rodents (Tsuboi, A. *et al.*, 1999; Malnic, B. *et al.*, 1999; Strotmann, J. *et al.*, 2000; Uchida, N. *et al.*, 2000) likely activate adjacent and overlapping glomeruli of the OB or antennal lobe suggest an odotopic organization in these central olfactory processing centers. However, recent studies indicated that this map in higher-order olfactory centers is different from that within the OB or antennal lobe (Zou, Z. *et al.*, 2001; 2005; Marin, E. C. *et al.*, 2002; Wong, A. M. *et al.*, 2002). Thus, in contrast to the OB, axonal arborizations in FB are diffuse and extensive, and projections from different OB glomeruli often overlap to varying degrees. This anatomical organizational pattern suggests that third-order neurons in the olfactory pathway integrate odor information arriving from multiple OB glomeruli, which possibly codes for odorant quality and which may also relate to the odor's behavioral significance (e.g., food or pheromones) (Johnson, D. M. G. *et al.*, 2000; Haberly, L. B., 2001; Wang, Y. *et al.*, 2001; Zou, Z. *et al.*, 2001; Marin, E. C. *et al.*, 2002; Wong, A. M. *et al.*, 2002).

For channel catfish, an FB odotopic map resembling somewhat that present in the OB was recently determined (Nikonov, A. A. *et al.*, 2005; Nikonov, A. A. and Caprio, J., 2007). Both the medial–lateral distinction between excitatory responses to bile salts and amino acids and the rostrocaudal distinction between excitatory responses to amino acids and nucleotides reflect a similar topographical organization within the OB of the same species. The amino acid-responsive terminal field appears homologous to the olfactory cortex and perhaps the olfactory tubercle, whereas the bile salt-responsive region, the medial terminal field, is possibly homologous to portions of the amygdala in amniote vertebrates (Wullimann, M. F. and Rink, E., 2002; Wullimann, M. F. and Mueller, T., 2004; Nikonov, A. A. *et al.*, submitted). Furthermore, as suggested by the previous anatomical investigations of possible convergence within the FB of OT fibers emanating from different OB glomeruli, cell types not previously observed within the OB were evident. These included units that were excited by both amino acids and nucleotides and others excited by both neutral and basic amino acids; however, there was no evidence of the convergence of odor information arriving via the separate medial and lateral OTs. Thus, convergence occurred between OT fibers providing input of food-related odorants, but not between food-relevant and socially relevant chemical signals.

4.04.4.3 Crustaceans

4.04.4.3.1 Organization of the olfactory lobes

CRNs of the antennules are packaged into a diversity of types of sensilla (see Section 4.04.3). One of these types is specialized as the olfactory sensilla – the aesthetascs. The ORNs of the aesthetascs project ipsilaterally to the paired OL (Schmidt, M. and Ache, B. W., 1996b) (Figure 3). The OLs are thought to receive input almost exclusively from aesthetasc ORNs (Schmidt, M. and Ache, B. W., 1992; 1996b; Sandeman, D. C. *et al.*, 1992).

The OLs have a glomerular organization (Figure 3), generally similar to first-order olfactory neuropils of other animals – the antennal lobes of insects and the OBs of vertebrates (Hildebrand, J. G. and Shepherd, G. M., 1997; Strausfeld, N. J. and Hildebrand, J. G., 1999; Eisthen, H. L., 2002; Schachtner, J. *et al.*, 2005). The neuronal components of the OL glomeruli are also generally similar to that of the olfactory neuropils of vertebrates and insects. Besides the primary afferent input from the aesthetasc ORNs, there are projection interneurons (PNs), several classes of local interneurons (LNs), and centrifugal neurons. The location of the somata associated with these neurons is precise: the LNs have their somata in the medial cluster (cluster 9), and the PNs have their somata in the lateral cluster (cluster 10). The OL glomeruli have clear subdivisions: cap, subcap, and basal regions. These regions contain different neuronal types and synaptic interactions (Schmidt, M. and Ache, B. W., 1996b; Wachowiak, M. *et al.*, 1997). Most ORNs branch in only one glomerulus, primarily in the cap and subcap regions (Schmidt, M. and Ache, B. W., 1992). PNs have multiglomerular projections, with dense innervation in a few glomeruli and sparse

innervation in many (Schmidt, M. and Ache, B. W., 1996b). The centrifugal fibers synapse on the somata of OL interneurons and are probably modulatory in function (Schmidt, M., 1997). The glomerular cap region is innervated by only two types of neurons: ORNs and multiglomerular GABAergic LNs. This implies that there are synapses between these neuronal types. This is probably the basis for the presynaptic inhibition from LNs onto ORNs (Wachowiak, M. *et al.*, 2002). Presynaptic inhibition in the OB also occurs in the vertebrates (Wachowiak, M. *et al.*, 2002).

Inhibition within the OL is mediated through at least two overlapping but functionally distinct inhibitory pathways (Wachowiak, M. and Ache, B. W., 1997). These are based on GABA and histamine, which shape the odor responses of OL units (Wachowiak, M. and Ache, B. W., 1998). These inhibitory circuits may have functional correlates with lateral inhibitory pathways in antennal lobe of insects and OB of vertebrates (Ache, B. W., 2002).

The number of OL glomeruli drastically varies across crustaceans, ranging from about 150 to 1300. The basis for this range is not obviously related to the number of aesthetascs, the animal's habitat, or phylogeny (Beltz, B. S. *et al.*, 2003).

Additionally, no clear sexually dimorphism in OLs is known, unlike has been described in some insects (e.g., the macroglomerular complex). This is in spite of the fact that sex pheromones are known in many crustaceans and their reception is mediated by aesthetascs (Gleeson, R. A., 1991; Kamio, M. *et al.*, 2002). It is possible that the OL possesses pheromone-specific glomeruli, but they are not morphologically distinct at a gross level.

Given findings that the glomerular organization in insects and vertebrates reflects odotopic mapping, it might be expected that the crustacean OL also has odotopic maps. There is indirect evidence for this, based on the fact that each aesthetasc expresses a diversity of ORNs (Steullet, P. *et al.*, 2000b) and the axons of ORNs from a single aesthetasc projects to many if not most glomeruli (Mellon, D. Jr. and Munger, S. D., 1990; Mellon, D. Jr. and Alones, V., 1993). The relationship between the number of ORNs and number of OL interneurons is instructive. For example, in spiny lobsters, each aesthetasc has ~300 ORNs (Derby, C. D. *et al.*, 2003). Aesthetascs appear to be functional units, with similar sets of ORNs in each aesthetasc (Steullet, P. *et al.*, 2000b); however, the number of different types of OR genes or ORNs is not known. Even assuming that there are 300 different types of ORs or ORNs, more than one type of ORN must innervate each glomerulus. However, direct tests of this hypothesis are lacking. Additionally, there is extensive convergence, given that there young adult spiny lobsters have about 300 000 ORNs per antennule projecting into 1200 glomeruli containing about 200 000 PNs and 100 000 LNs (Schmidt, M. and Ache, B. W., 1996b; Schachtner, J. *et al.*, 2005).

Closely associated with the OL, but lacking any primary sensory input, are the paired accessory lobes (ALs), olfactory globular tract neuropils, and deutocerebral commissure neuropils (Wachowiak, M. *et al.*, 1996; 1997; Sandeman, D. and Mellon, D., 2001; Ache, B. W., 2002; Schachtner, J. *et al.*, 2005) (Figure 3). The ALs are notable because of their large size in lobsters and crayfish and their glomerular organization. However, the AL glomeruli are smaller, more numerous, and of different synaptic organization than the OL glomeruli (Wachowiak, M. *et al.*, 1996; Schmidt, M. and Ache, B. W., 1996b). ALs have three regions – medial, central, and lateral – and each with specific synaptic connections (Wachowiak, M. *et al.*, 1996; Ache, B. W., 2002). For example, the medial and lateral regions have PNs, and the central region has interneurons connecting the AL to the OL as well as connection to the medial and lateral regions of the AL through LNs. The function of the AL is unknown, though its variance in size in different groups of crustaceans provides some grounds for speculation (Sandeman, D. C. *et al.*, 1993; Ache, B. W., 2002).

4.04.4.3.2 Organization of other chemosensory neuropils

All other antennular CRNs besides those in the aesthetascs, which include those on both the lateral and medial flagella of the antennules, project ipsilaterally to the paired LANs and to the unpaired MAN (Schmidt, M. and Ache, B. W., 1996a) (Figure 3). The LANs and MAN have a laminated organization, not glomerular. Unlike the OLs, the LANs and MAN also receive projections of mechanosensory neurons and antennular motor neurons. This organization is suggestive of topotopic maps, where space along the antennule is mapped topographically onto these neuropils (Schmidt, M. and Ache, B. W., 1993; 1996a; Schachtner, J. *et al.*, 2005); however, critical data are lacking.

4.04.4.3.3 Higher-order processing centers

The output interneurons from the OLs, ALs, and LANs project via the olfactory–globular tract (Figure 3) to a region of the protocerebrum called the terminal medulla and hemiellipsoid bodies, which are probably functionally equivalent to the mushroom bodies and lateral horn of insects (Schachtner, J. *et al.*, 2005). But the interneurons from the OLs, LANs, and ALs terminate in different regions of these neuropils, with phylogenetically diverse patterns of connection (Sullivan, J. M. and Beltz, B. S., 2004; 2005). The functional significance of these different projections and the activity of neurons in these higher-order neuropils are being explored (Sandeman, D. and Mellon, D., Jr. 2001; McKinzie, M. E. *et al.*, 2003).

4.04.4.3.4 Other chemoreceptor neuron processing centers

Virtually nothing is known about central processing of CRNs from the legs or mouthparts, except the identity of the regions into which their receptors project (e.g., Weissburg, M. J. *et al.*, 2001). While it is appreciated that the leg and mouthpart pathways control different behaviors than do the antennules (Derby, C. D., 2000; Horner, A. J. *et al.*, 2004; Garm, A. *et al.*, 2005), the mechanisms responsible for these differences remain largely unexplored.

4.04.4.4 Overview

The first-order olfactory processing center in both fishes and crustaceans, as with other vertebrates and arthropods, is glomerular in organization. These are the OB and AOB of fish, and the OL of crustaceans. The glomeruli are clusters of neuropil that contain the synapses between inputs (ORNs), outputs (mitral cells in fishes, projection neurons in crustaceans), and local interneurons. ORNs have ipsilateral projections, most being uniglomerular. The glomerular organization reflects an odotopy, with the odorants, at least food-related odorants, being represented across the glomeruli in a combinatorial fashion. Synaptic interactions within the OB and OL, which include inhibitory lateral connections, shape neuronal responses such that the output neurons of the OB and OL have different quality and temporal and response characteristics.

4.04.5 Neurogenesis and Turnover of Olfactory Neurons in Adult Crustaceans

Many crustaceans, fortunately including the model organisms for chemosensory research such as spiny lobsters, clawed lobsters, and crayfish, have indeterminate growth and add new ORNs to their olfactory organ and local and output interneurons to the OLs in the brain, throughout life including as adults (Steullet, P. *et al.*, 2000a; Harzsch, S., 2001; Derby, C. D. *et al.*, 2001a; Harrison, P. J. H. *et al.*, 2001a; Schmidt, M. 2001; Beltz, B. S. and Sandeman, D. C., 2003; Sandeman, R. and Sandeman, D., 2003).

Olfactory neurogenesis is highly flexible. Its rate can be modulated in adaptive ways by many variables. For example, following damage to the antennule, ORN neurogenesis increases dramatically so as to quantitatively compensate for the damage (Harrison, P. J. H. *et al.*, 2001a; 2003; 2004). As well, damage to the antennule modulates the rate of neurogenesis of olfactory interneurons (Sandeman, R. *et al.*, 1998; Hansen, A. and Schmidt, M., 2001; Sandeman, R. and Sandeman, D., 2003). Neurogenesis can also vary with internal factors, such as molt stage that is controlled by steroid hormones (Harrison, P. J. H. *et al.*, 2001a; 2001b), and environmental factors, such as circadian cycle (Goergen, E. M. *et al.*, 2002), season (Hansen, A. and Schmidt, M., 2004), environmental richness (Sandeman, R. and Sandeman, D., 2000), and social experience (Beltz, B. S. and Sandeman, D. C., 2003; Sandeman, R. and Sandeman, D., 2003; Song, C.-K. *et al.*, 2004).

In addition to continuous neurogenesis, olfactory neurons in the antennule, and to some extent in the brain, continuously turn over (Sandeman, R. and Sandeman, D. C., 1996; Steullet, P. *et al.*, 2000a; Schmidt, M., 2001; Harrison, P. J. H. *et al.*, 2001a; 2001b; 2003; 2004). The functional impact of this is that the olfactory organ completely turns over its ORNs after approximately four to five molts; the time for this depends on factors such as size of animal and environmental conditions, but for a young adult spiny lobster, this is approximately 1 year (Steullet, P. *et al.*, 2000a; Harrison, P. J. H. *et al.*, 2001a). The antennule is fully functional at any time, although the most proximal (newest) and distal (oldest) regions of aesthetascs have fewer aesthetascs and, at least in the case of the proximal (immature) aesthetascs, are not or less responsive to odors (Steullet, P. *et al.*, 2000a; 2000b). ORNs may be immature for several weeks or

more after their birth (Steullet, P. *et al.*, 2000a; Harrison, P. J. H. *et al.*, 2001a), and olfactory interneurons may be immature (defined by typical expression of neurochemicals) for several months (Schmidt, M., 2001).

The fact that the site of proliferation of new ORNs is in a very small area of the olfactory organ gives experimental advantages of using crustacean models over others in exploring aspects of olfactory neurogenesis. For example, candidate molecules involved in ORN proliferation can be identified by using techniques such as representational difference analysis to identify transcripts that are enriched in the region of ORN proliferation compared to regions of mature ORNs. Initial analyses of this kind have identified interesting candidates (Stoss, T. D. *et al.*, 2004). These include (1) one whose expression levels also increase following damage, which also upregulates neurogenesis; (2) a member of the same protein family as follistatin, which is an antagonist of GDF 11, and GDF 11 is expressed by progenitors of mammalian ORNs and whose absence prevents proliferation of ORNs (Wu, H.-H. *et al.*, 2003); and (3) a growth factor of the PDGF/VEGF family. RT–PCR approaches (Chien, H. *et al.*, 2005) have also identified *splash*, a spiny lobster homologue of achaete-scute genes, and which is expressed in regions of ORN neurogenesis in the olfactory organ. Since the mammalian achaete-scute homologue, MASH, is involved in differentiation of ORNs in rodents, *splash* is an interesting initial candidate in the exploration of molecular mechanisms of control and modulation of olfactory neurogenesis in crustaceans.

4.04.6 Taste in Fish

4.04.6.1 Peripheral Taste Anatomy

Taste buds in teleosts are located generally on the lips and within the oral cavity, including high densities on the gill rakers (Jakubowski, M. and Whitear, M., 1990; Sorensen, P. W. and Caprio, J., 1998; Finger, T. E., and Simon, S. A., 2000; Hansen, A. and Reutter, K., 2004) (Figure 4). The buds can be elevated on epidermal hillocks, be flush with the surrounding epidermis, or sunken. Taste buds are also found on the external body surface, primarily on the face and in some species, such as catfishes, along the entire external body surface (Reutter, K., 1978). This increase in extraoral taste buds is thought not to result directly in an increase in sensitivity but in a greater ability to localize a taste source (Bardach, J. E. *et al.*, 1967). Taste bud densities can vary tremendously depending on the species, the location of the receptive field, and the size of the specimen. In some fishes, such as minnows and certain cyprinids, up to ~300 taste buds mm^{-2} were estimated (Gomahr, H. *et al.*, 1992). Teleost taste

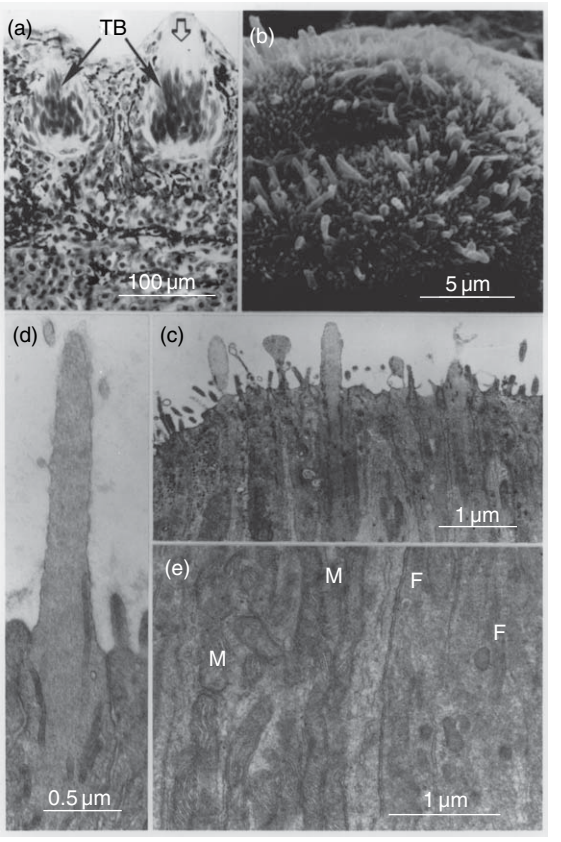

Figure 4 Teleost taste buds. (a) Light micrograph of a longitudinal section through two maxillary barbell taste buds of the bullhead catfish, *Ameiurus nebulosus*. TB indicates two taste buds and cells within; these taste buds are of the elevated type (unfilled arrow). At the lower portion of each taste bud, basal cells are observed. (b) Scanning electron micrograph (SEM) of a portion of the surface of a catfish (*Ameiurus*) taste bud showing numerous small and fewer large receptor microvilli. (c) Transmission electron micrograph (TEM) of the apical portion of an *Ameiurus* taste bud in longitudinal section. The apical portion of the light cells forms a single large receptor villus of a light cell and a small villus of an adjacent dark cell in longitudinal section from a *Silurus glanis* (European Wels catfish) taste bud. (e) Detail of the supranuclear region of a longitudinally sectioned *Silurus* taste bud that shows numerous mitochondria (M) within a light cell (left) and bundles of intermediate filaments (F) in a dark cell (right). Reprinted from Sorensen, P. W. and Caprio, J. 1998. Chemoreception. In: The Physiology of Fishes (ed. D.H. Evans), pp. 375–405. CRC Press LLC, by courtesy of Taylor and Francis Group, LLC. Courtesy: Klaus Reutter.

buds contain up to ~100 cells that are generally divided into three types: light, dark, and basal cells (Reutter, K., 1978; Jakubowski, M. and Whitear, M., 1990). Light cells, considered the actual taste cell, possess a single large (0.5 µm thick, 1.5–3 µm long) club-shaped microvillus at its apical surface, whereas dark cells, which partially wrap light cells, have at their apical surface numerous small (0.1–0.2 µm thick, 0.5–1.0 µm long) microvilli and are considered supporting cells. However, dark cells in some species (e.g., ictalurid catfishes) form synapses with basal cells and may function also as taste cells (Reutter, K., 1978). Serotonin-rich basal cells, which resemble Merkel cells, number up to ~5 per taste bud, are oriented transversely to the longitudinal axis of the taste bud at the basal pole and form synaptic contacts with presumed taste cells. As in land vertebrates, taste cells undergo turnover. However, since teleosts are poikilothermic, the rate of turnover is dependent on the ambient water temperature. At temperatures of 14, 18, 22, and 30 °C, taste cells in channel catfish have an average life span of 40, 30, 15, and 12 days, respectively (Raderman-Little, R., 1979). Also, as in other vertebrates, taste buds, depending on their location, are innervated by branches of either the VII, IX, or X CN. In addition to taste cells located within taste buds, teleosts can possess solitary chemosensory cells (SCCs), which resemble taste receptor cells that reach densities in excess of $100\,000\,\mathrm{mm}^{-2}$ and, depending on the location on the fish, form synaptic contact with different afferent nerve fibers (V, VII, and spinal) (Kotrschal, K., 1991; 1993; Finger, T. E., 1997; Hansen, A. and Reutter, K., 2004). Furthermore, there can be considerable overlap between input to the CNS of both SCC and gustatory neurons as in rocklings *Ciliata* and *Gaidropsarus* (Teleostei: Gadidae), or the SCC input via spinal nerves can be quite distinct from the taste system as in searobins (*Prionotus carolinus*) (Finger, T. E., 1982; Kotrschal, K. and Finger, T. E., 1996). These anatomical differences in central connections suggest that the SCCs of rocklings and searobins are not homologous. Physiological studies on SCCs are scant, but they suggest that SCCs in rocklings respond primarily to body mucus of heterospecific fish (Peters, R. C. *et al.*, 1991).

4.04.6.2 Taste Cell Physiology and Transduction

The major class of taste stimuli studied in a wide variety of fish species is amino acids, although additional gustatory stimuli investigated in particular species include small peptides, nucleotides, bile salts and acids, aliphatic acids, quaternary ammonium compounds, and steroids (Marui, T. and Caprio, J., 1992; Hara, T. J., 1993). High-affinity taste receptor sites for L-alanine (dissociation constant (K_D) of 1.5 µM) and L-arginine (two affinity states: K_D values of 18 nM and 1.3 µM), respectively (Caprio, J., *et al.*, 1993), are located primarily on different taste cells within the same taste bud (Finger, T. E. *et al.*, 1996). The existence of independent gustatory receptor sites for L-alanine and L-arginine in channel catfish was determined previously from both electrophysiological and biochemical studies; a low-affinity receptor site for L-proline was also indicated (Caprio, J. *et al.*, 1993). Current evidence suggests that these three major classes of amino acid taste receptors in the channel catfish are coupled to activation of the taste receptor cells by two different mechanisms. At micromolar concentrations, L-alanine activates a G-protein-dependent increase in IP_3 or cAMP, but with a more rapid IP_3 production (Kalinoski, D. L. *et al.*, 1989). In contrast, both L-arginine and L-proline appear to be directly coupled to the activation of nonselective, but independent, cation channels (Kumazawa, T. *et al.*, 1998; Grosvenor, W. *et al.*, 2004). Further evidence of nonrandom expression of these amino acid taste receptors on taste cells is from electrophysiological studies of single taste fibers in the channel catfish, which has identified fiber types in the facial taste system that are highly responsive to L-alanine and L-arginine, respectively (Kohbara, J. *et al.*, 1992), and fiber types highly responsive to L-alanine, L-arginine, and L-proline, respectively, in the glossopharyngeal taste system (Ogawa, K. and Caprio, J., unpublished data).

Specific information concerning the molecular nature of taste receptors in vertebrates and the identification of their ligands has recently become available. As in mammals (Zhang, Y. *et al.*, 2003), fishes express two families of G-protein-coupled receptors, T1Rs and T2Rs in separate taste cells (Ishimaru, Y. *et al.*, 2005). T1Rs, members of class C GPCRs that possess an extensive N-terminus, exist as dimers. T1R dimers in fish detect amino acids (either T1R1/3 or multiple T1R2/3s), whereas T2Rs, which possess a short extracellular N-terminus and have not been shown to exist as dimers, detect bitter tastants (Oike, H. *et al.*, 2007).

4.04.6.3 Peripheral Nerve Taste Responses

Among the fishes tested electrophysiologically with amino acids, two groups were identified (Hara, T. J.

and Zielinski, B., 1989; Hara, T. J., 1993): (1) those whose facial taste system (those taste buds innervated by facial (CN VII) nerve fibers) responded to a number of different amino acids (i.e., wide response range) as demonstrated by channel catfish (Caprio, J., 1975; 1978) and (2) those whose facial taste systems were more selective (i.e., limited response range) as seen in salmonids (Hara, T. J. and Zielinski, B., 1989; Hara, T. J. *et al.*, 1999). Furthermore, multiunit recordings demonstrate that different branches of the facial nerve innervating different populations of taste buds located in different anatomical locations on the body of the fish have similar response properties and selectivities (Caprio, J., 1978; Davenport, C. J. and Caprio, J., 1982; Kanwal, J. S. *et al.*, 1987). The data are usually analyzed by comparing the magnitude of the integrated neural taste responses to the different chemicals at the same concentration. The relative magnitude of the integrated taste responses obtained even from different CNs can be similar as observed in rainbow trout (Kohbara, J. and Caprio, J., 2001). However, in other species such as channel catfish, taste responses between facial and glossopharyngeal/vagal nerves can be quite distinct (Kanwal, J. S. and Caprio, J., 1983; Kohbara, J. *et al.*, 1992). Facial taste thresholds for specific amino acids ranged generally between nano- and micromolar. Furthermore, depending on the species studied, taste thresholds of IX/X nerve fibers to specific amino acids can be either similar or higher than that determined for facial taste responses (Kanwal, J. S. and Caprio, J., 1983; Kohbara, J. and Caprio, J., 2001). Taste thresholds estimated from recordings from IX and/or X nerves in channel catfish were higher than those for VII, which is logical considering that high taste sensitivity of taste buds within the oropharyngeal cavity is not essential because of the higher stimulus concentrations present in the mouth once food intake occurs (Kanwal, J. S. and Caprio, J., 1987). The L-isomer of an amino acid was significantly more stimulatory than its D-isomer. However, a population of facial taste fibers in the sea catfish, *Arius felis*, was described that was more responsive to D- than to L-alanine (Michel, W. and Caprio, J., 1991) (see next section). In some fishes, sensitivity to a particular non-amino acid stimulus may even be greater than it is to amino acids. For example, the facial taste system of the rainbow trout to a bile salt, taurolithocholate, approaches picomolar concentrations, which is 4 log units lower than for L-proline, the most stimulatory amino acid (Hara, T. J. *et al.*, 1984; Yamashita, S. *et al.*, 2006).

4.04.6.4 Processing Taste Information by Single Peripheral Taste Fibers

Since taste receptor cells are secondary receptors, they must synapse with afferent nerve fibers (VII, IX, or X) to transmit gustatory information to the primary gustatory nucleus of the medulla. A single taste fiber may synapse with multiple taste cells, not all of which are necessarily located in the same taste bud. For example, in channel catfish, the number of taste buds innervated by a single taste fiber of the recurrent facial nerve that innervates taste buds on the flank increases with the size of the fish, from two taste buds per axon in small fish (~5 cm in length) to nearly 14 taste buds per axon profile in larger fish (37–40 cm) (Finger, T. E. *et al.*, 1991). Information on the processing of taste information by peripheral nerve fibers in teleosts is extremely limited and is based primarily on quantitative analyses of responses of facial taste fibers in only a few species. The data obtained with amino acid stimuli from these species, however, indicate that there is sufficient similarity in the tuning characteristics of gustatory neurons to justify the existence of different fiber types.

Although single-unit studies of the taste specificity of teleosts were accomplished in only a few species of the more than 25 000 that exist, some tentative generalizations can be drawn:

1. Taste information concerning different classes of taste stimuli can be transmitted to the medulla by different groups (i.e., types of facial taste fibers); for example, the facial taste system of Japanese puffer fish (*Fugu pardalis*) consists of different populations of taste fibers with specificities to amino acids, nucleotides, and an inorganic acid, respectively (Kiyohara, S. *et al.*, 1985).
2. The specificity of a single taste fiber is not limited to a particular class of chemical stimuli; for example, one taste fiber type in the yellowtail flounder is highly responsive to both a nucleotide (uridine-5′-monophosphate) and an amino acid (L-tryptophan) (Zeng, C. and Hidaka, I., 1990).
3. Different taste fiber types having widely different tuning to members of the same class of chemicals can exist within the same CN of a particular species; for example, populations of facial taste fibers with different amino acid specificities occur in channel catfish (Kohbara, J. *et al.*, 1992; Caprio, J., *et al.*, 1993), sea catfish (Michel, W. and Caprio, J., 1991), Japanese puffer (Kiyohara, S. *et al.*, 1985), and yellowtail (Zeng, C. and Hidaka, I., 1990).
4. Taste fibers of different CNs (VII versus IX and X) within the same species can have different chemical

specificities; for example, a population of taste fibers highly responsive to L-proline occurs for the IX but not VII taste system in channel catfish (Ogawa, K. and Caprio, J., unpublished data).

5. The proportion and types of taste fibers comprising different CNs can vary within the same species; for example, the population of L-alanine taste fibers within the IX taste nerve in channel catfish was reduced by 55% compared with VII.
6. In addition to the existence of populations of taste fibers that are highly responsive to particular L-amino acids, taste fibers for D-amino acids may also exist; for example, 38% of the single facial taste fibers analyzed from the sea catfish, *Arius felis*, were most responsive to D-alanine (Michel, W. and Caprio, J., 1991). However, this fiber type also responded to L-alanine, and the L-alanine fiber type responded to D-alanine. High concentrations of D-amino acids occur in the tissues of soft-bodied invertebrates (Preston, R. L. 1987), potential prey items of the sea catfish. In contrast, only 3% of the single facial taste fibers in the freshwater channel catfish were most responsive to D-alanine (Kohbara, J. *et al.*, 1992).
7. Irrespective of the of the chemical specificity of the particular taste fiber types occurring in a species, stimulus quantity appears to be coded by the frequency of action potentials generated. For individual taste fibers, some have a dynamic response range of 5–6 log units of stimulus concentration, whereas other fibers, even in the same fish, have more truncated dose–response relations (Michel, W. and Caprio, J., 1991; Kohbara, J. *et al.*, 1992).
8. Some peripheral taste fibers in a particular species may be bimodal, that is, they respond to both taste and mechanical stimuli as in catfish (Davenport, C. J. and Caprio, J., 1982; Ogawa, K. *et al.*, 1997), whereas in other species, such as the Japanese puffer, this does not appear to be the case (Kiyohara, S. *et al.*, 1985).

4.04.6.5 Taste and Tactile Input to the Central Nervous System (Medulla)

Chapter 10 in this volume and a previous report (Kanwal, J. S. and Finger, T. E., 1992) provide excellent reviews of the gustatory pathways within the CNS of teleosts. This section is thus limited to a brief summary of the topographical manner in which taste and tactile information is represented in the primary gustatory nucleus of the medulla of catfishes since much of the limited information on the processing of taste information was derived from these teleosts known for their elaborate gustatory system. Limited electrophysiological information also exists concerning taste and tactile activity in higher-order, that is, pontine (Lamb, C. F. IV and Caprio, J., 1992) and diencephalic (Lamb, C. F. IV and Caprio, J., 1993), gustatory nuclei in catfish but is beyond the scope of this review.

Taste and tactile information (see point 8 above) arriving via VII and IX/X terminates in register and in a somatotopic and viscerotopic manner, respectively, within the special visceral sensory column of the rostral medulla that is equivalent to the gustatory portion of the nucleus of the solitary tract in mammals. Both taste and tactile information from the external body surface and rostral oral cavity in catfishes is processed within the facial lobe (FL) of the medulla and that within the more posterior oral cavity and gill rakers by the glossopharyngeal nucleus (possibly a small lobe in some species) and vagal lobe (VL) (Finger, T. E., 1976; Kanwal, J. S. and Caprio, J., 1987). There is, however, a disproportionate representation of structures (e.g., an enlarged volume of medulla for the representation of barbels and gill rakers), which is indicative of their relative functional importance for taste and tactile input. The FL, through its input from external body taste buds and its interconnections to the spinal cord and medullary reticular formation, is involved in localization of a stimulus and controlling swimming behavior (Kanwal, J. S. and Finger, T. E., 1997). As such, the FL map is well defined and precise. The glossopharyngeal and vagal systems, which receive input from taste buds within the oral cavity, in contrast connects with brainstem nuclei in the control of swallowing and oropharyngeal movements (Atema, J., 1971; Finger, T. E. and Morita, Y., 1985). The VL map is not so important for the localization of food and is thus more diffuse than that of the FL (Kanwal, J. S. and Caprio, J., 1988).

For teleosts that possess specialized taste and tactile structures, such as barbels, the special visceral column can be subdivided into two to three lobes (Kanwal, J. S. and Finger, T. E., 1992). Within each lobe a finer representation of body parts (e.g., barbels and gill arches) can be represented in lobules (Kanwal, J. S. and Caprio, J., 1987; Hayama, T. and Caprio, J., 1989; Kiyohara, S. and Caprio, J., 1996). For catfishes, taste and tactile inputs from each of the different barbels project to a different lobule within the FL (Kiyohara, S. *et al.*, 1986; Kanwal, J. S. and Caprio, J., 1988; Marui, T. *et al.*, 1988). In addition to

the existence of peripheral bimodal (taste and tactile) fibers, mechanosensory input into the primary gustatory nucleus also occurs via mechanosensory-only facial (Davenport, C. J. and Caprio, J., 1982; Kiyohara, S. *et al.*, 1985) and trigeminal (Kiyohara, S. *et al.*, 1986) fibers. Medullary neurons responsive to taste stimuli (i.e., amino acids) were limited to smaller areas of the electrode tracks than neurons sensitive to touch alone (Marui, T., 1977; Marui, T. and Funakoshi, M., 1979; Marui, T. and Caprio, J., 1982; Kanwal, J. S. and Caprio, J., 1988). The overlap of taste and tactile maps is interesting from a neuroethological aspect as both types of input are involved in the detection and selective food ingestion in catfish and are likely processed simultaneously prior to activation of the respective motor neurons.

4.04.7 Processing of Mixtures

4.04.7.1 Introduction

In all natural environments, including aquatic, olfactory and gustatory receptor cells rarely encounter single pure chemicals as are usually presented in experimental studies. The composition of many biologically relevant mixtures in aquatic environments, particularly of food, is well characterized (Carr, W. E. S., 1988). Behavioral studies demonstrate the high potency of animal extracts and mixtures of amino acids to fishes and crustaceans. Additionally, however, the magnitude of the response to a chemical mixture is poorly predicted from knowledge of the responses to the individual components – revealing mixture interactions. These are either mixture suppression or mixture enhancement, in which the response to the mixture is less or greater, respectively, than expected. Obviously then, defining the expected response to a mixture becomes the critical issue. To do so for a CRN, it is critical to know several of its features: Does a CRN have both excitatory and inhibitory transduction pathways? Does a CRN have more than one type of receptor? If so, how are these coupled to the excitatory and/or inhibitory transduction pathways? Which mixture components interact with each receptor and transduction pathway? How do those components interact with the receptors – that is, are they agonists or antagonists, and is their action competitive or noncompetitive?

The more completely characterized is the cell, the more accurate is the predicted response to a mixture. In other words, mixture interactions are a consequence of an incomplete understanding of the above processes.

Fish and crustaceans, especially catfish and spiny lobsters, serve as model organisms to understand how mixtures are processed. These studies are built largely on electrophysiological and biochemical studies that have defined the diversity of receptor types and transduction pathways at the cellular level. Arguably, our understanding of how the sensory systems of animals detect, process, and ultimately lead to the discrimination and perception of mixtures is as complete for catfish and lobsters as it is for any animal. (And sadly, we still have a long way to go!) This section summarizes our understanding of mixture processing in these systems.

4.04.7.2 Fish

4.04.7.2.1 Introduction

Electrophysiological studies in teleosts attempted to predict the global response, that is, olfactory EOG (electro-oculography) and olfactory and gustatory integrated neural activity (Hidaka, I. *et al.*, 1976; Caprio, J., *et al.* 1989; Kohbara, J. and Caprio, J., 1996; Ogawa, K. and Caprio, J., 2000) to simple (binary and ternary) mixtures of amino acids. Additionally, a single olfactory electrophysiological investigation studied responses to complex mixtures (up to 10 components) of amino acids (Kang, J. and Caprio, J., 1991). The overall results of these investigations indicated that knowledge of the relative independence of the receptors for the component stimuli in a mixture, obtained from receptor binding and/or electrophysiological cross-adaptation experiments, was essential to successfully predict the magnitude of the electrophysiological response. Mixtures whose components showed little competition or cross-adaptation generated responses greater than those whose components were indicated to compete with a common receptor or with receptors having highly overlapping specificities. There was little evidence for mixture suppression. That mixture interactions are weak in the peripheral olfactory system in teleosts was also indicated in the zebrafish (Tabor, R. *et al.*, 2004). For olfaction, where single ORNs express one or at most a few ORs (Ngai, J. *et al.*, 1993; Mombaerts, P. 2004), the greater response to a mixture of amino acids was likely due to the activation of multiple populations of ORNs, each ORN within a specific population expressing one of the receptors for a particular component in the mixture. The greater response to mixtures observed in the peripheral taste system was also likely due to the activation of different receptors wherever expressed; for this effect observed in single taste fibers in the channel catfish (Ogawa, K. and Caprio, J., 1999) and Japanese puffer (Hidaka, I. *et al.*,

1976), the different receptors could theoretically be located on individual cells within a single taste bud or on different taste cells in different taste buds innervated by the single taste fiber. These studies also indicated for both olfactory and gustatory systems that the greater responses to mixtures are more likely due to the simultaneous activation of different receptors by the individual components of the mixture than by stimulus binding at the same total concentration to a single receptor. The greater response to a mixture whose components bind to relatively independent receptors than to a single or highly cross-reactive receptors may be the electrophysiological correlate of the behavioral observations that mixtures are often more stimulatory than individual components, even in cases when the concentration of the individual component is higher than the total concentration of the multiple-component stimuli within the mixture.

4.04.7.2.2 Responses of single units

4.04.7.2.2.(i) Olfaction There are few quantitative physiological studies of how single olfactory neurons in fishes respond to stimulus mixtures – primarily amino acids. For teleosts, only in the channel catfish was a quantitative study of single ORNs performed to stimulus mixtures (Kang, J. and Caprio, J., 1997), whereas responses of single OB neurons to stimulus mixtures were investigated in both the channel catfish (Kang, J. and Caprio, J., 1995b; 1997; Tabor, R. *et al.*, 2004) and zebrafish (Tabor, R. *et al.*, 2004). For channel catfish, the types of responses of single ORNs and OB neurons to binary mixtures comprising components that were either both excitatory, both suppressive, or both nonresponsive were similar (based on response type) to those of the components in 80% (for ORNs) and 82% (for OB neurons) of the trials. These results are comparable to a similar study in rats where 75% of the responses of single OB neurons to binary mixtures evoked similar response patterns as the components of the binary mixtures (Giraudet, P. *et al.*, 2002). Overall, these results indicate that profound mixture interactions are rare in simple mixtures where the components evoke similar responses.

For simple binary mixtures where the responses to the components were different (i.e., excitatory (E) and nonresponsive (N); suppressive (S) and N; E + S, respectively), responses of catfish OB neurons to the mixture were often similar in 94% of the trials to that for one of the components (Kang, J. and Caprio, J., 1995b). For example, in a binary mixture of an excitatory and a suppressive component, the response of an OB neuron to the mixture was either excitatory or suppressive in 94% of the trials – in only 6% of the trials was the mixture nonresponsive. For catfish ORNs, responses to the mixtures were similar to that for one of the components in 82% of the trials for E + S mixtures and 100% for both E + N and S + N mixtures (Kang, J. and Caprio, J., 1997). In a comparable study in the OB of the rat, units evoked a similar pattern of response, as did one of the components in the mixture in 83% of the trials (Giraudet, P. *et al.*, 2002). For zebrafish OB units, where binary mixtures of amino acids comprised an excitatory and a suppressive component ($n = 18$), the response to the binary mixture was dominated (in 85% of the cases) by the excitatory response, whereas the suppressive component occurred in the remaining 17% of the trials. In additional experiments, the component responses and those to the binary mixtures were complex, differing primarily in their temporal patterns (Tabor, R. *et al.*, 2004). In contrast, for OB units in channel catfish where excitatory and suppressive responses to the mixture components tested were equivalent (29%; 42% null), the response to the binary mixture was excitatory in 34%, suppressive in 41%, and null (no response significantly different from control) in 25% of the trials ($n = 32$) (Kang, J. and Caprio, J., 1995b). Mixture suppression or masking, where a component reduced or concealed the neuron's excitatory or inhibitory response to the other component, however, was observed with single ORN and OB neurons in catfish and single OB neurons in rat. This effect was observed when there was no significant response to a binary mixture composed of an effective stimulus (evoking either an E or S response) and a nonstimulatory component. Such mixture suppression occurred in 62% (for E + N components) and 68% (for S + N components) of these trials in catfish ORNs, 43% in catfish OB neurons, and 46% in rat OB neurons (when analyzing firing rates).

4.04.7.2.2.(ii) Taste Electrophysiological responses of integrated and single-unit facial taste responses to binary mixtures of amino acids in the channel catfish (Ogawa, K. and Caprio, J., 1999) were consistent with previous olfactory results obtained in the same species (see above). These reports collectively indicate that the magnitude of multiunit responses to binary and more complex olfactory and gustatory stimulus mixtures is greater if the component stimuli bind to relatively independent receptor sites than to the same or highly cross-reactive sites. The study also indicated that the greater taste activity observed to the mixture was not significantly different, whether

recording the taste activity in a multifiber or a single--unit preparation. This finding is noteworthy in indicating that greater taste activity is not exclusively the result of the components in a binary mixture simultaneously activating different fiber types (i.e., having different chemical specificities); that is, the greater response also occurred by the activation of different taste receptors on taste cells innervated by the same single taste fiber. Also indicated was that the magnitude in enhanced taste activity could be significantly different across the different responding gustatory fiber types. In the Japanese puffer, *F. pardalis*, the amino acid derivative betaine (*N*-trimethyl glycine) enhanced taste activity of facial taste fibers to particular amino acids (Hidaka, I. *et al.*, 1976).

4.04.7.2.3 Behavioral discrimination

Fish are similar to humans in that components of binary mixtures are discriminable. Humans can identify up to approximately three components in either taste (Laing, D. G. *et al.*, 2002) or olfactory mixtures (Laing, D. G. and Francis, G. W., 1989). Whether a binary mixture of amino acids is detected by fishes as a unique odor or whether the qualities of the individual components are retained within the mixture was investigated in catfish (Valentinčič, T. *et al.*, 2000a). It was previously determined for catfish that the discrimination of chemicals is based on olfaction and not on taste (Valentinčič, T. *et al.*, 1994). Catfish conditioned to a binary mixture initially treat the mixture as the component eliciting the greater physiological response (based on the magnitude of the EOG in response to each component). This result is similar to that for humans, where binary odor mixtures are perceived as the more stimulatory component (Laing, D. G. and Willcox, M. E., 1983). Additional discrimination training in catfish, however, facilitates the discrimination of the less potent component in a binary mixture – that is, the binary mixture is no longer detected as its more stimulatory component. Thus, with enough training, catfish are able to elementally process mixtures (i.e., identify the separate components of the mixture).

4.04.7.3 Crustaceans

4.04.7.3.1 Electrophysiology

Electrophysiological studies of processing of mixtures by crustaceans have been performed exclusively using single cells rather than global responses such as EOGs. Thus, explanations are possible at the single-cell level as well as at the system level through analysis of populations of these single cells.

Single CRNs of crustaceans have multiple transduction pathways, including excitatory and inhibitory pathways and including more than one receptor type in the excitatory pathway (see Section 4.04.2). Thus, when trying to understand the response to a mixture, even a simple one such as a binary mixture, the magnitude and direction of the response (i.e., increase or decrease from spontaneous spiking rate) will depend on whether the components of a mixture activate the excitatory or the inhibitory pathway and on whether they activate the same or different receptor sites in a given pathway. As a consequence, responses to mixtures can be either more or less than the more excitatory component. The following are some examples.

If a CRN has both excitatory and inhibitory transduction pathways, and one chemical activates the excitatory pathway and another chemical activates the inhibitory pathway, then we would expect that a mixture of these two chemicals would generate a response less than excitatory chemical and greater than the inhibitory chemical. This has been observed from intracellular whole-cell patch clamp recording from lobster CRNs (Michel, W. C. and Ache, B. W., 1992). This type of effect can explain some cases of mixture suppression identified from extracellular measurement of spiking activity of single-unit recordings from lobster CRNs. These CRNs often have very low levels of spontaneously spiking activity – often much less than 1 spike per second – so that if a compound activates an inhibitory transduction pathway, this inhibition is not expressed as a reduction in spiking activity. If only spiking activity were being recorded, this would lead to an identification of mixture suppression. Yet knowing the transduction cascades activated by these components of a mixture leads to a predicted response that matches that observed.

If a CRN has two receptors types, each coupled to an excitatory transduction pathway as seems to be the case for many CRNs of crustaceans (see Section 4.04.2), then it is important to know how the components of a mixture interact with these receptor types. The predicted responses are different if the mixture components bind primarily to the same receptor or bind to different receptors. If the components compete for the same receptor, then whether they are competitive agonists or antagonists will influence the response generated by the mixture. The clearest demonstration of this is in a study by Cromarty S. and Derby C. (1997). This study examined responses

of taurine-sensitive CRNs to binary mixtures of excitatory compounds, either competitive agonists (taurine and structural analogues of taurine) or noncompetitive agonists (taurine and structurally dissimilar molecules). Responses to binary mixtures of competitive agonists were significantly lower than responses to mixtures of noncompetitive agonists, but they were exactly that expected from a competitive model. Knowing how these compounds bind to receptors and how these receptors are coupled to transduction cascades allowed accurate predictions of responses to mixtures; without this, mixture interactions would be suggested to have occurred.

As described in the next section, behavioral studies suggest that spiny lobsters can use elemental processing to analyze mixtures, such that the mixture is perceived as a set of identifiable components (Livermore, A. *et al.*, 1997). This behavioral finding has implications on how mixtures are processed by the peripheral olfactory system. It suggests that a mixture and its components should generate different neural response profiles and that the response profile of the mixture should have features in common with its components. In addition, if one component of a mixture dominates the perception of a mixture, then the neural profile generated by the mixture should be more similar to that of the dominant component. These ideas were tested using different blend ratios of binary mixtures (Steullet, P. and Derby, C. D., 1997). The results suggest that for the neural profiles generated in the peripheral olfactory system of spiny lobsters, the qualities of individual compounds are maintained when the compounds are mixed to form blends. This result suggests a neural explanation of the ability of spiny lobsters to elementally process an odor mixture.

4.04.7.3.2 Behavior

Mixture interactions have been examined at the behavioral level in some detail in several crustacean species, including the glass shrimp *Palaemonetes pugio* (Carr, W. E. S. and Derby, C. D., 1986a; 1986b), the Caribbean spiny lobster *P. argus* (Derby, C. D. *et al.*, 1989; Daniel, P. C. and Derby, C. D., 1991), the California spiny lobster *Panulirus interruptus* (Zimmer-Faust, R. K. *et al.*, 1984; Zimmer-Faust, R. K., 1987; 1993), and the American lobster *H. americanus* (Borroni, P. F. *et al.*, 1986; Atema, J. *et al.*, 1989). In these studies, typically the magnitude of the behavioral response (usually an appetitive response) to a mixture is compared to that of the responses to that mixture's components. The response magnitudes are then compared to each other and to the predicted responses calculated on a variety of models that fall into two classes: (1) those that assume the components interact with the same transduction pathways and (2) those that assume the components activate independent transduction pathways. The outcomes of these studies differ. For the glass shrimp, mixture enhancement or synergism, in which the mixture response was significantly greater than expected, was common. Compounds that by themselves had no activity, when mixed with each other or with compounds that were moderately active, generated very strong responses. Using an antennular flicking assay on the Caribbean spiny lobster and binary mixtures of compounds, mixture suppression was much more common, in which the response to a binary mixture was less than expected. In the California spiny lobster, adding a repellent compound (ammonium) to an attractive compound (ATP) predictably produced a response to the mixture that was less than that to the attractant alone (Zimmer-Faust, R. K. *et al.*, 1984; Zimmer-Faust, R. K., 1987; 1993). From these results, it is clear that predicting responses to mixtures based only on responses to components is unreliable. We have argued earlier that with detailed knowledge of the transduction pathways within an ORN and the chemical stimuli that activate each of them, accurate predictions of mixture responses are possible. But of course for behavior, many neuronal levels exist between ORNs and motor output, including complex synaptic interactions. For example, some mixture interactions occur at the level of the CNS, independent of the ORNs (Derby, C. D. *et al.*, 1985). Thus, generating a better understanding of processing of chemical information in the CNS is essential for understanding the behavior of animals to mixtures.

The ability of lobsters to discriminate among chemical stimuli is known from studies using aversive paradigms similar to those used on other animals. Such associative conditioning generates an aversive response to one chemical stimulus, even one previously attractive, and then animals can be examined for response generalization to other stimuli (Fine-Levy, J. B. *et al.*, 1988). This procedure was used for several sets of stimuli that were also used in electrophysiological studies of mixture processing (see below). These include single compounds; binary mixtures that differ only in blend ratios, and their components; and complex mixtures of 29–35 components that mimic their natural food (crab, shrimp, oyster, and mullet). These results show that lobsters show the greatest generalization between stimuli that are closest in composition. For example,

lobsters show much more generalization between crab mixture and shrimp mixture than between other mixtures, and this is highly correlated with the degree of similarity in the blend ratios of these mixtures (Fine-Levy, J. B. *et al.*, 1988; 1989; Fine-Levy, J. B. and Derby, C. D., 1991).

Behavioral studies also showed that spiny lobsters perceive chemical mixtures in different ways, depending on the salience of the components. They can learn them as a set of elemental cues if the salience of the components during learning is sufficiently high. In addition, they can also learn them as a configural cue (i.e., as a mixture-unique entity) if the salience of the individual components is not emphasized (Livermore, A. *et al.*, 1997; Derby, C. D., 2000).

4.04.7.4 Overview

Catfish and spiny lobsters are two of the more intensely studied animals regarding the neural processing and behavioral responses to chemical mixtures, and as such, they provide excellent case studies. Behavioral studies show that both catfish and spiny lobsters perceive the components of binary and even larger mixtures as discriminable elements, if the salience or relevance of those components is emphasized. This implies elemental processing. If the salience of the components is not emphasized, then mixtures are perceived as a configural (i.e., mixture-unique) cue. This leads to the conclusion that each discriminable component of a mixture should generate a unique neural profile, at least at early processing levels. Electrophysiological studies on catfish and lobsters support this conclusion. Individual studies identified examples of mixture interactions, in which the response to the mixture is different from that expected from the response to the mixture's components. However, the body of work on catfish and spiny lobsters demonstrates that the more completely characterized is a cell or a system, the more accurate is the predicted response to a mixture. If one knows the receptor types, the transduction cascades, how receptor types are coupled to those cascades, and which chemical stimuli interact with each receptor type and transduction cascade, then by using rigorous experimental procedures, responses to mixtures are highly predictable. A few studies on catfish and lobsters demonstrate this (Caprio, J., *et al.*, 1989; Kang, J. and Caprio, J., 1991; Cromarty, S. and Derby, C., 1997). The challenge is of course to build a detailed understanding of all of these molecular pathways. Since mixtures are the biologically relevant stimuli for animals, this is more than a worthy endeavor, as difficult as it is.

4.04.8 Behavioral Roles of Olfaction and Taste

4.04.8.1 Introduction

The chemical senses are involved to some degree in many behaviors of fishes and crustaceans. These include finding food, mates, habitat, and shelter, avoiding predators, social interactions, and homing. Although many studies investigated the chemosensory behavior of different species to chemical stimuli, the vast majority did not determine which chemosensory systems – olfaction, taste, or others – were primarily responsible for the behavioral results. Since both olfactory and taste systems for particular species of fishes and crustaceans can be highly sensitive to specific classes (e.g., amino acids) of chemical stimuli (Caprio, J., 1978; Goh, Y. and Tamura, T., 1980; Hara, T. J., 1994), without the appropriate controls, it can be confusing as to which system or systems are responsible for releasing a specific behavioral response.

4.04.8.2 Fish

Olfaction is involved in the detection and search for food and is uniquely implicated in the detection of pheromones and other chemicals that provide information concerning sex, social interactions, alarm, and homing. Taste, on the other hand, is also associated with food-related behaviors, but those that are more of a reflexive nature, such as ingestion, biting, and swallowing of food; for catfishes, taste also participates directly in the localization of the food source (Hara, T. J., 1993; Sorensen, P. W. and Caprio, J., 1998).

Typical feeding stimulants of fishes are amino acids, and both the olfactory and gustatory systems are generally highly stimulated by amino acids. However, the chemical specificity and the specific functions of the two chemosensory systems to these compounds can be quite distinct (Caprio, J., 1977; Goh, Y. and Tamura, T., 1980; Kohbara, J. *et al.*, 1992; Nikonov, A. A. and Caprio, J., 2004), and the feeding behaviors controlled by the two are not identical but are overlapping. For a generic fish (i.e., one without an elaborate extraoral taste system) such as rainbow trout, both olfactory (Hara, T. J., 1973) and gustatory (Marui, T. *et al.*, 1983) systems can be highly sensitive to amino acids. However, anosmic

rainbow trout are incapable of initiating feeding in response to these chemical cues, in spite of a fully functioning taste system (Valentinčič, T. and Caprio, J., 1997). In contrast, for catfishes, which possess extensive extraoral and oral taste systems and a concomitant increase in the neural circuitry of the medulla facial and VLs to process gustatory information, both food search and ingestion are released in anosmic specimens (Bardach, J. E. *et al.*, 1967; Valentinčič, T. and Caprio, J., 1994). Olfaction in catfishes, however, is essential for the discrimination of different amino acid stimuli in a learning paradigm (Valentinčič, T. *et al.*, 1994; 2000b; Valentinčič, T., 2004).

4.04.8.3 Crustaceans

There are differences, as well as some overlap, in those behaviors controlled by olfaction (aesthetascs) and taste. In spiny lobsters, the antennules drive detection of and orientation to distant, attractive chemicals, including food-related chemicals and intraspecific chemicals such as aggregation pheromones and alarm pheromones (Derby, C. D. *et al.*, 2001b; Horner, A. J. *et al.*, 2004; Shabani, S. and Derby, C. D., 2006) and pheromones (aggregation cue and alarm cues) (Horner, A. J. and Derby, C. D., 2005; Shabani, S. and Derby, C. D., 2006). Interestingly, either the aesthetasc (olfactory) pathway alone or the nonaesthetasc antennular pathway alone is sufficient to mediate the animal's response to food odors (Horner, A. J. and Derby, C. D., 2005; Shabani, S. and Derby, C. D., 2006). In addition, both of these pathways can mediate discrimination of and learning about food-related chemicals, be they single compounds, simple mixtures, or complex mixtures. Thus, there is considerable redundancy between the aesthetasc and the nonaesthetasc antennular pathways. However, differences in the functions of the aesthetasc and nonaesthetasc antennular pathways have been identified as well. For example, only the aesthetasc pathway, and not the nonaesthetasc antennular pathway or extra-antennular chemosensory pathway, mediates attraction to aggregation pheromones or alarm pheromones (Horner, A. J. *et al.*, 2004; Horner, A. J. and Derby, C. D., 2005; Shabani, S. and Derby, C. D., 2006). "Aesthetases are also necessary for the response of clawed lobsters to social odors (Johnson, M. E. and Atema, J., 2005)". Thus, the aesthetascs uniquely possess detectors of aggregation and alarm cues.

It must be emphasized that although we have placed the nonaesthetasc antennular sensors in a single category, they differ not only structurally but also functionally. On the antennular flagella, there are nine different types of nonaesthetasc sensilla (Cate, H. S. and Derby, C. D., 2001). Although they all are bimodally innervated by chemosensory neurons and mechanosensory neurons that project to the LANs, they differ in setal structure and organization and in location on the antennule (Cate, H. S. and Derby, C. D., 2001; 2002). They also differ in function. For example, the asymmetric sensilla are uniquely responsible for mediating chemically activated antennular grooming behavior (Schmidt, M. and Derby, C. D., 2005).

Chemosensors on the legs of lobsters differ structurally and functionally from antennular sensory. In lobsters, they direct local searches to food chemicals, and when the leg touches the source of the chemicals, that item is grabbed and transferred to the mouthparts (Derby, C. D. and Atema, J., 1982).

Mouthpart chemoreceptors, with their high threshold and broad tuning (Garm, A. *et al.*, 2005), control whether food should be eaten (Derby, C. D. and Atema, J., 1982). Presumably they are checking the quality of the prey, such as determining whether feeding stimulants are present and deterrents are absent.

The hierarchy of control of behaviors by the different chemosensors as described above for lobsters may not apply completely to all crustaceans. For example, in the blue crab *Callinectes sapidus*, leg chemoreceptors can also play a role in orientation to distant cues (Keller, T. A. *et al.*, 2003).

Crustaceans demonstrate several types of learning involving their chemical senses, including habituation and aversive associative learning (Derby, C. D., 2000), one-trial flavor avoidance learning (hermit crab), and other important behaviors though less well-defined mechanistically (Caldwell, R. and Dingle, J., 1985; Wight, K. *et al.*, 1990). Aversive associative learning has been used to study spiny lobster's ability to discriminate chemical stimuli, including single-odorant compounds and different blend ratios of the same binary or complex mixtures (Derby, C. D., 2000). The associative task is learning to avoid a previously attractive food stimulus. Since this task is controlled by the antennules, expression of this learned task depends on the presence of fully functional antennules. But it does not require aesthetascs: either the aesthetasc (olfactory) pathway or the nonaesthetasc antennular pathway can mediate discrimination and learning about chemical stimuli (Steullet, P. *et al.*, 2001; 2002).

4.04.8.4 Overview

The chemical senses of fish and crustaceans control or modulate many of their behaviors. There are overlaps

and differences in the behaviors that are mediated by the different chemosensory systems, including olfaction and taste. Both olfactory and nonolfactory systems can mediate orientation to distant food-related chemicals. Olfactory systems tend to control detection of pheromones and thus cues associated with intraspecific interactions. Some of the behaviors controlled by olfaction include learning about chemicals involved in discrimination. Taste and other nonolfactory systems are uniquely associated with chemically activated biting and swallowing of food and other more reflexive behaviors.

Acknowledgment

We also thank NIH and NSF for their support over the years, currently from NIH DC00312, NIH DC-03792, NSF IBN-0321444, and NSF IBN-0314970.

References

Ache, B. W. 2002. Crustaceans as Animal Models for Olfactory Research. In: Crustacean Experimental Systems in Neurobiology (*ed*. K. Wiese), pp. 189–199. Springer.

Ache, B. W. and Young, J. M. 2005. Olfaction: diverse species, conserved principles. Neuron 48, 417–430.

Ache, B. W. and Zhainazarov, A. B. 1995. Dual second-messenger pathways in olfactory transduction. Curr. Opin. Neurobiol. 5, 461–466.

Ache, B. W., Munger, S., and Zhainazarov, A. 1998. Organizational complexity in lobster olfactory receptor cells. Ann. N. Y. Acad. Sci. 855, 194–198.

Ashby, E. A. and Larimer, J. L. 1965. Modification of cardiac and respiratory rhythms in crayfish following carbohydrate chemoreception. J. Cell. Comp. Physiol. 65, 373–380.

Atema, J. 1971. Structures and functions of the sense of taste in the catfish, *Ictalurus natalis*. Brain Behav. Evol. 4, 273–294.

Atema, J. 1977. Functional Separation of Smell and Taste in Fish and Crustacea. In: Olfaction and Taste VI (*eds*. J. Le Magnen and P. Mac Leod), pp. 165–174. Information Retrieval Ltd

Atema, J. 1988. Distribution of Chemical Stimuli. In: Sensory Biology of Aquatic Animals (*eds*. J. Atema, R. R. Fay, A. N. Popper, and W. N. Tavolga), pp. 29–56. Springer.

Atema, J. 1995. Chemical signals in the marine environment: dispersal, detection, and temporal signal analysis. Proc. Natl. Acad. Sci. U. S. A. 92, 62–66.

Atema, J. and Steinbach, M. A. 2007. Chemical Communication in the Social Behavior of the lobster, *Homarus americanus*, and Other Decapod Crustacea. In: Ecology and Evolution of Social Behavior: Crustaceans as Model Systems (*eds*. E. Duffy and M. Thiel), Oxford University Press.

Atema, J., Borroni, P., Johnson, B., Voigt, R., and Handrich, L. 1989. Adaptation and Mixture Interactions in Chemoreceptor Cells: Mechanisms for Diversity and Contrast Enhancement. In: Perception of Complex Smells and Tastes (*eds*. D. G. Laing, W. S. Cain, R. L. McBride, and B. W. Ache), pp. 83–100. Academic Press.

Bardach, J. E., Todd, J. H., and Crickmer, R. 1967. Orientation by taste in fish of the genus *Ictalurus*. Science 155, 1276–1278.

Bauer, U. and Hatt, H. 1980. Demonstration of three different types of chemosensitive units in the crayfish claw using a computerized evaluation. Neurosci. Lett. 17, 209–214.

Bauer, U., Dudel, J., and Hatt, H. 1981. Characteristics of single chemoreceptive units sensitive to amino acids and related substances in the crayfish leg. J. Comp. Physiol. A 144, 67–74.

Bazer, G. T., Ebbesson, S. O. E., Reynolds, J. B., and Bailey, R. P. 1987. A cobalt-lysine study of primary olfactory projections in king salmon fry (*Oncorhynchus tshawytscha* Walbaum). Cell Tissue Res. 248, 499–503.

Becerra, M., Manso, M. J., Rodriguez-Moldes, I., and Anadón, R. 1994. Primary olfactory fibers project to the ventral telencephalon and preoptic region of trout (*Salmo trutta)*: a developmental immunocytochemical study. J. Comp. Neurol. 342, 131–143.

Beltz, B. S. and Sandeman, D. C. 2003. Regulation of life-long neurogenesis in the decapod crustacean brain. Arthropod Struct. Dev. 32, 39–60.

Beltz, B. S., Kordas, K., Lee, M. M., Long, J. B., Benton, J. L., and Sandeman, D. C. 2003. Ecological, evolutionary, and functional correlates of sensilla number and glomerular density in the olfactory system of decapod crustaceans. J. Comp. Neurol. 455, 260–269.

Blaustein, D. N., Simmons, R. B., Burgess, M. F., Derby, C. D., Nishikawa, M., and Olson, K. S. 1993. Ultrastructural localization of 5′AMP odorant receptor sites on the dendrites of olfactory receptor neurons of the spiny lobster. J. Neurosci. 13, 2821–2828.

Bobkov, Y. V. and Ache, B. W. 2005. Pharmacological properties and functional role of a TRP-related ion channel in lobster olfactory receptor neurons. J. Neurophysiol. 93, 1372–1380.

Borroni, P. F. and Atema, J. 1988. Adaptation in chemoreceptor cells. I. Self-adapting backgrounds determine threshold and cause parallel shift of response function. J. Comp. Physiol. A 164, 67–74.

Borroni, P. F. and Atema, J. 1989. Adaptation in chemoreceptor cells. II. The effects of cross-adapting backgrounds depend on spectral tuning. J. Comp. Physiol. A 165, 669–677.

Borroni, P. F., Handrich, L. S., and Atema, J. 1986. The role of narrowly tuned taste cell populations in lobster (*Homarus americanus*) feeding behavior. Behav. Neurosci. 100, 206–212.

Brown, S. B. and Hara, T. J. 1981. Accumulation of chemostimulatory amino acids by a sedimentable fraction isolated from olfactory rosettes of rainbow trout (*Salmo gairdneri*). Biochem. Biophys. Acta 675, 149–162.

Bruch, R. C. 1996. Phosphoinositide second messengers in olfaction. Comp. Biochem. Physiol. 113B, 451–459.

Bruch, R. C. and Rulli, R. D. 1988. Ligand binding specificity of a neutral L-amino acid olfactory receptor. Comp. Biochem. Physiol. 91B, 535–540.

Buck, L. B. 1996. Information coding in the vertebrate olfactory system. Annu. Rev. Neurosci. 19, 517–544.

Byrd, C. A., Jones, J. T., Quattro, J. M., Rogers, M. E., Brunjes, P. C., and Vogt, R. G. 1996. Ontogeny of odorant receptor gene expression in zebrafish, *Danio rerio*. J. Neurobiol. 29, 445–458.

Cagan, R. H. and Zeiger, W. N. 1978. Biochemical studies of olfaction: binding specificity of radioactivity labeled stimuli to an isolated olfactory preparation from rainbow trout (*Salmo gairdneri*). Proc. Natl. Acad. Sci. U. S. A. 75, 4679–4683.

Caldwell, R. and Dingle, J. 1985. A test of individual recognition in the stomatopod *Gonodactylus festae*. Anim. Behav. 33, 101–106.

Cao, Y., Oh, B. C., and Stryer, L. 1998. Cloning and localization of two multigene receptor families in goldfish olfactory epithelium. Proc. Natl. Acad. Sci. U. S. A. 95, 11987–11992.

Caprio, J. 1975. High sensitivity of catfish taste receptors to amino acids. Comp. Biochem. Physiol. 52A, 247–251.
Caprio, J. 1977. Electrophysiological distinctions between the taste and smell of amino acids in catfish. Nature 266, 850–851.
Caprio, J. 1978. Olfaction and taste in the channel catfish: an electrophysiological study of the responses to amino acids and derivatives. J. Comp. Physiol. A 123, 357–371.
Caprio, J. and Byrd, R. P., Jr. 1984. Electrophysiological evidence for acidic, basic, and neutral amino acid olfactory receptor sites in the catfish. J. Gen. Physiol. 84, 403–422.
Caprio, J., Brand, J. G., Teeter, J. H., Valentinčič, T., Kalinoski, D. L., Kohbara, J., Kumazawa, T., and Wegert, S. 1993. The taste system of the channel catfish: from biophysics to behaviour. Trends Neurosci. 16, 192–197.
Caprio, J., Dudek, J., and Robinson, J. J., II 1989. Electro-olfactogram and multiunit olfactory receptor responses to binary and trinary mixtures of amino acids in the channel catfish, *Ictalurus punctatus*. J. Gen. Physiol. 93, 245–262.
Carr, W. E. S. 1988. The Molecular Nature of Chemical Stimuli in the Aquatic Environment. In: Sensory Biology of Aquatic Animals (*eds*. J. Atema, R. R. Fay, A. N. Popper, and W. N. Tavolga), pp. 3–27. Springer.
Carr, W. E. S. and Derby, C. D. 1986a. Behavioral chemoattractants for the shrimp, *Palaemonetes pugio*: identification of active components in food extracts and evidence of synergistic mixture interactions. Chem. Senses 11, 49–64.
Carr, W. E. S. and Derby, C. D. 1986b. Chemically stimulated feeding behavior in marine animals: importance of chemical mixtures and involvement of mixture interactions. J. Chem. Ecol. 12, 989–1011.
Carr, W. E. S., Gleeson, R. A., and Trapido-Rosenthal, H. G. 1990. The role of perireceptor events in chemosensory processes. Trends Neurosci. 13, 212–215.
Cate, H. S. and Derby, C. D. 2001. Morphology and distribution of setae on the antennules of the Caribbean spiny lobster *Panulirus argus* reveal new types of bimodal chemo-mechanosensilla. Cell Tissue Res. 304, 439–454.
Cate, H. S. and Derby, C. D. 2002. Ultrastructure and physiology of the hooded sensillum, a bimodal chemo-mechanosensillum of lobsters. J. Comp. Neurol. 442, 293–307.
Chien, H., Liu, H., Schmidt, M., Tai, P. C., and Derby, C. D. 2005. Molecular cloning and characterization of proneural genes in the olfactory organ of spiny lobsters. Chem. Senses 30, A91–A92.
Cromarty, S. and Derby, C. 1997. Multiple excitatory receptor types on individual olfactory neurons: implications for coding of mixtures in the spiny lobster. J. Comp. Physiol. A 180, 481–491.
Daniel, P. C. and Derby, C. D. 1991. Mixture suppression in behavior: the antennular flick response in the spiny lobster towards binary odorant mixtures. Physiol. Behav. 49, 591–601.
Davenport, C. J. and Caprio, J. 1982. Taste and tactile recordings from the ramus recurrens facialis innervating flank taste buds in the catfish. J. Comp. Physiol. A 147, 217–229.
Del Punta, K., Puche, A., Adams, N. C., Rodriguez, I., and Mombaerts, P. 2002. A divergent pattern of sensory axonal projections is rendered convergent by second-order neurons in the accessory olfactory bulb. Neuron 35, 1057–1066.
Demski, L. S. and Dulka, J. G. 1984. Functional-anatomical studies on sperm release evoked by electrical stimulation of the olfactory tract in goldfish. Brain Res. 291, 241–247.
Demski, L. S. and Northcutt, R. G. 1983. The terminal nerve: a new chemosensory system in vertebrates? Science 220, 435–437.
Derby, C. D. 1982. Structure and function of cuticular sensilla of the lobster *Homarus americanus*. J. Crust. Biol. 2, 1–21.
Derby, C. D. 2000. Learning from spiny lobsters about chemosensory coding of mixtures. Physiol. Behav. 69, 203–209.
Derby, C. D. and Atema, J. 1982. The function of chemo- and mechanoreceptors in lobster (*Homarus americanus)* feeding behaviour. J. Exp. Biol. 98, 317–327.
Derby, C. D. and Atema, J. 1988. Chemoreceptor Cells in Aquatic Invertebrates: Peripheral Mechanisms of Chemical Signal Processing in Decapod Crustaceans. In: Sensory Biology of Aquatic Animals (*eds*. J. Atema, R. R. Fay, A. N. Popper, and W. N. Tavolga), pp. 365–385. Springer.
Derby, C. D., Ache, B. W., and Kennel, E. W. 1985. Mixture suppression in olfaction: electrophysiological evaluation of the contribution of peripheral and central neural components. Chem. Senses 10, 301–316.
Derby, C. D., Cate, H. S., Steullet, P., and Harrison, P. J. H. 2003. Comparison of turnover in the olfactory organ of early juvenile stage and adult Caribbean spiny lobsters. Arthropod Struct. Dev. 31, 297–311.
Derby, C. D., Girardot, M.-N., and Daniel, P. C. 1991. Responses of olfactory receptor cells of spiny lobsters to binary mixtures. I. Intensity mixture interactions. J. Neurophysiol. 66, 112–130.
Derby, C. D., Girardot, M.-N., Daniel, P. C., and Fine-Levy, J. B. 1989. Olfactory Discrimination of Mixtures: Behavioral, Electrophysiological, and Theoretical Studies Using the Spiny Lobster *Panulirus Argus*. In: Perception of Complex Smells and Tastes (*eds*. D. G. Laing, W. S. Cain, R. L. McBride, and B. W. Ache), pp. 65–81. Academic Press.
Derby, C. D., Steullet, P., Cate, H. S., and Harrison, P. J. H. 2001a. A Compound Nose: Functional Organization and Development of Aesthetasc Sensilla. In: The Crustacean Nervous System (*ed*. K. Wiese), pp. 346–358. Springer.
Derby, C. D., Steullet, P., Horner, A. J., and Cate, H. S. 2001b. The sensory basis to feeding behavior in the Caribbean spiny lobster *Panulirus Argus*. Mar. Freshw. Res. 52, 1339–1350.
Doolin, R. E. and Ache, B. W. 2005a. Cyclic nucleotide signaling mediates an odorant-suppressible chloride conductance in lobster olfactory receptor neurons. Chem. Senses 30, 127–135.
Doolin, R. E. and Ache, B. W. 2005b. Specificity of odorant-evoked inhibition in lobster olfactory receptor neurons. Chem. Senses 30, 105–110.
Doolin, R. E., Zhainazarov, A. B., and Ache, B. W. 2001. An odorant-suppressed Cl^- conductance in lobster olfactory receptor cells. J. Comp. Physiol. A 187, 477–487.
Døving, K. B. 1996. Homing of Fish and the Nervous Pathways for Kin Recognition. In: Fish Pheromones. Origins and Mode of Action (*eds*. A. V. M. Canario and D. M. Power), pp. 98–109. University of Algarve.
Døving, K. B. and Stabell, O. B. 2003. Trails in Open Waters: Sensory Cues in Salmon Migration. In: Sensory Processing in the Aquatic Environment (*eds*. S. P. Collin and N. J. Marshall), pp. 39–52. Springer.
Døving, K. B., Selset, R., and Thommesen, G. 1980. Olfactory sensitivity to bile acids in salmonid fishes. Acta Physiol. Scand. 108, 123–131.
Dryer, L. and Graziadei, P. P. C. 1994. Mitral cell dendrites: a comparative approach. Anat. Embryol. (Berlin) 189, 91–106.
Eisthen, H. L. 2002. Why are olfactory systems of different animals so similar? Brain Behav. Evol. 59, 273–293.
Eisthen, H. L. 2004. The goldfish knows: olfactory receptor cell morphology predicts receptor gene expression. J. Comp. Neurol. 477, 341–346.
Fadool, D. A., Estey, S. J., and Ache, B. W. 1995. Evidence that a Gq-protein mediates excitatory odor transduction in lobster olfactory receptor neurons. Chem. Senses 20, 489–498.

Fine-Levy, J. B. and Derby, C. D. 1991. Effects of stimulus intensity and quality on discrimination of odorant mixtures by spiny lobsters in an associative learning paradigm. Physiol. Behav. 49, 1163–1168.

Fine-Levy, J. B., Daniel, P. C., Girardot, M., and Derby, C. D. 1989. Behavioral resolution of quality of odorant mixtures by spiny lobsters: differential aversive conditioning of olfactory responses. Chem. Senses 14, 503–524.

Fine-Levy, J. B., Girardot, M., Derby, C. D., and Daniel, P. C. 1988. Differential associative conditioning and olfactory discrimination in the spiny lobster *Panulirus argus*. Behav. Neural Biol. 49, 315–331.

Finger, T. E. 1976. Gustatory pathways in the bullhead catfish I. Connections of the anterior ganglion. J. Comp. Neurol. 165, 513–526.

Finger, T. E. 1982. Somatotopy in the representation of the pectoral fin and free fin rays in the spinal cord of the sea robin, *Prionotus carolinus*. Biol. Bull. 163, 154–161.

Finger, T. E. 1997. Evolution of taste and solitary chemoreceptor cell systems. Brain Behav. Evol. 50, 234–243.

Finger, T. E. and Morita, Y. 1985. Two gustatory systems: facial and vagal gustatory nuclei have different brainstem connections. Science 227, 776–778.

Finger, T. E. and Simon, S. A. 2000. Cell Biology of Taste Epithelium. In: The Neurobiology of Taste and Smell (*eds*. T. E. Finger, W. L. Silver, and D. Restrepo), pp. 287–314. Wiley-Liss Inc

Finger, T. E., Bryant, B. P., Kalinoski, D. L., Teeter, J. H., Bottger, B., Grosvenor, W., Cagan, R. H., and Brand, J. G. 1996. Differential localization of putative amino acid receptors in taste buds of the channel catfish *Ictalurus punctatus*. J. Comp. Neurol. 373, 129–138.

Finger, T. E., Drake, S. K., Kotrschal, K., Womble, M., and Dockstader, K. C. 1991. Postlarval growth of the peripheral gustatory system in the channel catfish, *Ictalurus punctatus*. J. Comp. Neurol. 314, 55–66.

Friedrich, R. W. and Korsching, S. I. 1997. Combinatorial and chemotopic odorant coding in the zebrafish olfactory bulb visualized by optical imaging. Neuron 18, 737–752.

Friedrich, R. W. and Korsching, S. I. 1998. Chemotopic, combinatorial, and noncombinatorial odorant representations in the olfactory bulb revealed using a voltage-sensitive axon tracer. J. Neurosci. 18, 9977–9988.

Friedrich, R. W. and Laurent, G. 2001. Dynamic optimization of odor representations by slow temporal patterning of mitral cell activity. Science 291, 889–894.

Friedrich, R. W. and Laurent, G. 2004. Dynamics of olfactory bulb input and output activity during odor stimulation in zebrafish. J. Neurophysiol. 91, 2658–2669.

Fujita, I., Sorensen, P. W., Stacey, N. E., and Hara, T. J. 1991. The olfactory system, not the terminal nerve, functions as the primary chemosensory pathway mediating responses to sex pheromones in male goldfish. Brain Behav. Evol. 38, 313–321.

Fuller, C. L., Ruthel, G., Warfield, K. L., Swenson, D. L., Basio, C. M., Aman, M. J., and Bavari, S. 2006. Mitral cells in the olfactory bulb of adult zebrafish (Danio rerio): morphology and distribution. J. Comp. Neurol. 499, 218–230.

Fuss, S. H. and Korsching, S. I. 2001. Odorant feature detection: activity mapping of structure response relationships in the zebrafish olfactory bulb. J. Neurosci. 21, 8396–8407.

Garm, A., Shabani, S., Hoeg, J. T., and Derby, C. D. 2005. Chemosensory neurons in the mouthparts of the spiny lobsters *Panulirus argus* and *Panulirus interruptus* (Crustacea: Decapoda). J. Exp. Mar. Biol. Ecol. 314, 175–186.

Ghiradella, H., Case, J. F., and Cronshaw, J. 1968. Structure of aesthetascs in selected marine and terrestrial decapods: chemoreceptor morphology and environment. Am. Zool. 8, 603–621.

Giraudet, P., Berthommier, F., and Chaput, M. 2002. Mitral cell temporal response patterns evoked by odor mixtures in the rat olfactory bulb. J. Neurophysiol. 88, 829–838.

Gleeson, R. A. 1991. Intrinsic Factors Mediating Pheromone Communication in the Blue Crab, *Callinectes sapidus*. In: Crustacean Sexual Biology (*eds*. R. T. Bauer and J. W. Martin), pp. 17–32. Columbia University Press.

Gleeson, R. A., Trapido-Rosenthal, H. G., McDowell, L. M., Aldrich, H. C., and Carr, W. E. S. 1992. Ecto-ATPase/phosphatase activity in the olfactory sensilla of the spiny lobster, *Panulirus argus*: localization and characterization. Cell Tissue Res. 269, 439–445.

Goergen, E. M., Bagay, L. A., Rehm, K., Benton, J. L., and Beltz, B. S. 2002. Circadian control of neurogenesis. J. Neurobiol. 53, 90–95.

Goh, Y. and Tamura, T. 1980. Olfactory and gustatory responses to amino acids in two marine teleosts – red sea bream and mullet. Comp. Biochem. Physiol. 66C, 217–224.

Gold, G. H. 1999. Controversial issues in vertebrate olfactory transduction. Annu. Rev. Physiol. 61, 857–871.

Goldman, A. L., Van der Goes van Naters, W., Lessing, D., Warr, C. G., and Carlson, J. R. 2005. Coexpression of two functional odor receptors in one neuron. Neuron 45, 661–666.

Gomahr, H., Palzenberger, M., and Kotrschal, K. 1992. Density and distribution of external taste buds in cyprinids. Environ. Biol. Fish. 33, 125–134.

Gomez, G. and Atema, J. 1996a. Temporal resolution in olfaction: stimulus integration time of lobster chemoreceptor cells. J. Exp. Biol. 199, 1771–1779.

Gomez, G. and Atema, J. 1996b. Temporal resolution in olfaction. II. Time course of recovery from adaptation in lobster chemoreceptor cells. J. Neurophysiol. 76, 1340–1343.

Gomez, G., Voigt, R., and Atema, J. 1999. Temporal resolution in olfaction. III. Flicker fusion and concentration-dependent synchronization with stimulus pulse trains of antennular chemoreceptor cells in the American lobster. J. Comp. Physiol. A 185, 427–436.

Grosvenor, W., Kaulin, Y., Spielman, A. I., Bayley, D. L., Kalinoski, D. L., Teeter, J. H., and Brand, J. G. 2004. Biochemical enrichment and biophysical characterization of a taste receptor for L-arginine from the catfish, *Ictalurus punctatus*. BMC Neurosci. 5, 25p.

Grünert, U. and Ache, B. W. 1988. Ultrastructure of the aesthetasc (olfactory) sensilla of the spiny lobster, *Panulirus argus*. Cell Tissue Res. 251, 95–103.

Haberly, L. B. 2001. Parallel-distributed processing in olfactory cortex: new insights from morphological and physiological analysis of neuronal circuitry. Chem. Senses 26, 551–576.

Hallberg, E., Johansson, K. U. I., and Elofsson, R. 1992. The aesthetasc concept: structural variations of putative olfactory receptor cell complexes in Crustacea. J. Microsc. Res. Tech. 22, 325–335.

Hallem, E. A., Ho, M. G., and Carlson, J. R. 2004. The molecular basis of odor coding in the *Drosophila* antenna. Cell 117, 965–979.

Hamdani, E. H. and Døving, K. B. 2006. Specific projection of the sensory crypt cells in the olfactory system in crucian carp, *Carassius carassius*. Chem. Senses 31, 63–67.

Hamdani, E. H., Alexander, G., and Døving, K. B. 2001a. Projection of sensory neurons with microvilli to the lateral olfactory tract indicates their participation in feeding behaviour in crucian carp. Chem. Senses 26, 1139–1144.

Hamdani, E. H., Kasumyan, A., and Døving, K. B. 2001b. Is feeding behaviour in crucian carp mediated by the lateral olfactory tract? Chem. Senses 26, 1133–1138.

Hamdani, E. H., Stabell, O. B., Alexander, G., and Døving, K. B. 2000. Alarm reaction in the crucian carp is mediated by the medial bundle of the medial olfactory tract. Chem. Senses 25, 103–109.

Hansen, A. and Reutter, K. 2004. Chemosensory Systems in Fish: Structural, Functional and Ecological Aspects. In: The Senses of Fish: Adaptations for the Reception of Natural Stimuli (*eds*. G. von der Emde, J. Mogdans, and B. G. Kapoor), pp. 55–89. Narosa Publishing House Pvt. Ltd.

Hansen, A. and Schmidt, M. 2001. Neurogenesis in the central olfactory pathway of the adult shore crab *Carcinus maenas* is controlled by sensory afferents. J. Comp. Neurol. 441, 223–233.

Hansen, A. and Schmidt, M. 2004. Influence of season and environment on adult neurogenesis in the central olfactory pathway of the shore crab, *Carcinus maenas*. Brain Res. 1025, 85–97.

Hansen, A., Anderson, K., and Finger, T. E. 2004. Differential distribution of olfactory receptor neurons in goldfish: structural and molecular correlates. J. Comp. Neurol. 477, 347–359.

Hansen, A., Rolen, S. H., Anderson, K., Morita, Y., Caprio, J., and Finger, T. E. 2003. Correlation between olfactory receptor cell type and function in the channel catfish. J. Neurosci. 23, 9328–9339.

Hara, T. J. 1973. Olfactory responses to amino acids in rainbow trout, *Salmo gairdneri*. Comp. Biochem. Physiol. 44A, 407–416.

Hara, T. J. 1982. Chemoreception in Fishes. Elsevier.

Hara, T. J. 1992. Fish Chemoreception. Chapman & Hall.

Hara, T. J. 1993. Chemoreception. In: The Physiology of Fishes (*ed*. D. H. Evans), pp. 191–218. CRC Press.

Hara, T. J. 1994. Olfaction and gustation in fish: an overview. Acta Physiol. Scand. 152, 207–217.

Hara, T. J. and Zhang, C. 1996. Spatial projections to the olfactory bulb of functionally distinct and randomly distributed primary neurons in salmonid fishes. Neurosci. Res. 26, 65–74.

Hara, T. J. and Zielinski, B. 1989. Structural and functional development of the olfactory organ in teleosts. Trans. Am. Fish. Soc. 118, 183–194.

Hara, T. J., Carolfeld, J., and Kitamura, S. 1999. The variability of the gustatory sensibility in salmonids, with special reference to strain differences in rainbow trout, *Oncorhynchus mykiss*. Can. J. Fish. Aquat. Sci. 56, 13–24.

Hara, T. J., Macdonald, S., Evans, R. E., Marui, T., and Arai, S. 1984. Morpholine, Bile Acids and Skin Mucus as Possible Chemical Cues in Salmonid Homing: Electrophysiological Re-evaluation. In: Mechanisms of Migration in Fishes (*eds*. J. D. McCleave, G. P. Arnold, J. D. Dodson, and W. H. Neill), pp. 363–378. Plenum Publishing Corporation.

Harrison, P. J. H., Cate, H. S., and Derby, C. D. 2004. Localized ablation of olfactory receptor neurons induces both localized regeneration and widespread replacement of neurons in spiny lobsters. J. Comp. Neurol. 471, 72–84.

Harrison, P. J. H., Cate, H. S., Steullet, P., and Derby, C. D. 2001a. Structural plasticity in the olfactory system of adult spiny lobsters: postembryonic development permits life-long growth, turnover, and regeneration. Mar. Freshw. Res. 52, 1357–1365.

Harrison, P. J. H., Cate, H. S., Steullet, P., and Derby, C. D. 2003. Amputation-induced activity of progenitor cells leads to rapid regeneration of olfactory tissue in lobsters. J. Neurobiol. 55, 97–114.

Harrison, P. J. H., Cate, H. S., Swanson, E. S., and Derby, C. D. 2001b. Postembryonic proliferation in the spiny lobster antennular epithelium: rate of genesis of olfactory receptor neurons is dependent on molt stage. J. Neurobiol. 47, 51–66.

Harzsch, S. 2001. From Stem Cell to Structure: Neurogenesis in the CNS of Decapod Crustaceans. In: The Crustacean Nervous System (*ed*. K. Wiese), pp. 417–432. Springer.

Hatt, H. 1986. Responses of a bimodal neuron (chemo- and vibration-sensitive) on the walking legs of the crayfish. J. Comp. Physiol. A 159, 611–617.

Hatt, H. and Ache, B. W. 1994. Cyclic nucleotide- and inositol phosphate-gated ion channels in lobster olfactory receptor neurons. Proc. Natl. Acad. Sci. U. S. A. 91, 6264–6268.

Hayama, T. and Caprio, J. 1989. Lobule structure and somatotopic organization of the medullary facial lobe in the channel catfish *Ictalurus punctatus*. J. Comp. Neurol. 285, 9–17.

Hidaka, I., Nyu, N., and Kiyohara, S. 1976. Gustatory response in the puffer-IV effects of mixtures of amino acids and betaine. Bull. Fac. Fish. Mie Univ. 3, 17–28.

Hildebrand, J. G. and Shepherd, G. M. 1997. Mechanisms of olfactory discrimination: converging evidence for common principles across phyla. Annu. Rev. Neurosci. 20, 595–631.

Hofmann, M. H. and Meyer, D. L. 1995. The extrabulbar olfactory pathway: primary olfactory fibers bypassing the olfactory bulb in bony fishes? Brain Behav. Evol. 46, 378–388.

Honkanen, T. and Ekstrom, P. 1990. An immunocytochemical study of the olfactory projections in the three-spined stickleback, *Gasterosteus aculeatus*, L. J. Comp. Neurol. 292, 65–72.

Horner, A. J. and Derby, C. D. 2005. Chemical signals and chemosensory pathways involved in spiny lobster sheltering behavior. Chem. Senses 30, A97p.

Horner, A. J., Weissburg, M. J., and Derby, C. D. 2004. Dual antennular chemosensory pathways can mediate orientation by Caribbean spiny lobsters in naturalistic flow conditions. J. Exp. Biol. 207, 3785–3796.

Ishimaru, Y., Okada, S., Naito, H., Nagai, T., Yasuoka, A., Matsumoto, I., and Abe, K. 2005. Two families of candidate taste receptors in fishes. Mech. Develop. 122, 1310–1321.

Ivanova, T. T. and Caprio, J. 1993. Odorant receptor activated by amino acids in sensory neurons of the channel catfish *Ictalurus punctatus*. J. Gen. Physiol. 102, 1085–1105.

Jakubowski, M. and Whitear, M. 1990. Comparative morphology and cytology of taste buds in teleosts. Z. mikrosk.-anat. Forsch (Leipzig) 104, 529–560.

Johnson, M. E. and Atema, J. 2005. The olfactory pathway for individual recognition in the American lobster *Homarus americanus*. J. Exp. Biol. 208, 2865–2872.

Johnson, D. M. G., Illig, K. R., Behan, M., and Haberly, L. B. 2000. New features of connectivity in piriform cortex visualized by intracellular injection of pyramidal cells suggest that ''primary'' olfactory cortex functions like ''association'' cortex in other sensory systems. J. Neurosci. 20, 6974–6982.

Kalinoski, D. L., Huque, T., LaMorte, V. J., and Brand, J. G. 1989. Second-Messenger Events in Taste. In: Chemical Senses. Vol. 1: Receptor Events and Transduction in Taste and Olfaction (*eds*. J. G. Brand, J. H. Teeter, R. H. Cagan, and M. R. Kare), pp. 85–101. Marcel Dekker, Inc

Kamio, M., Matsunaga, S., and Fusetani, N. 2002. Copulation pheromone in the crab *Telmessus cheiragonus* (Brachyura: Decapoda). Mar. Ecol. Prog. Ser. 234, 183–190.

Kang, J. and Caprio, J. 1991. Electro-olfactogram and multiunit olfactory receptor responses to complex mixtures of amino acids in the channel catfish, *Ictalurus punctatus*. J. Gen. Physiol. 98, 699–721.

Kang, J. and Caprio, J. 1995a. Electrophysiological responses of single olfactory bulb neurons to binary mixtures of amino acids in the channel catfish, *Ictalurus punctatus*. J. Neurophysiol. 74, 1435–1443.

Kang, J. and Caprio, J. 1995b. In vivo responses of single olfactory receptor neurons in the channel catfish, *Ictalurus punctatus*. J. Neurophysiol. 73, 172–177.

Kang, J. and Caprio, J. 1997. In vivo responses of single olfactory receptor neurons of channel catfish to binary mixtures of amino acids. J. Neurophysiol. 77, 1–8.

Kanwal, J. S. and Caprio, J. 1983. An electrophysiological investigation of the oro-pharyngeal (IX-X) taste system in the channel catfish, *Ictalurus punctatus*. J. Comp. Physiol. A 150, 345–357.

Kanwal, J. S. and Caprio, J. 1987. Central projections of the glossopharyngeal and vagal nerves in the channel catfish, *Ictalurus punctatus*: clues to differential processing of visceral inputs. J. Comp. Neurol. 264, 216–230.

Kanwal, J. S. and Caprio, J. 1988. Overlapping taste and tactile maps of the oropharynx in the vagal lobe of the channel catfish, *Ictalurus punctatus*. J. Neurobiol. 19, 211–222.

Kanwal, J. S. and Finger, T. E. 1992. Central Representation and Projections of Gustatory Systems. In: Fish Chemoreception (*ed*. T. J. Hara), pp. 79–102. Chapman & Hall.

Kanwal, J. S. and Finger, T. E. 1997. Parallel medullary gustatospinal pathways in a catfish: possible neural substrates for taste-mediated food search. J. Neurosci. 17, 4873–4885.

Kanwal, J. S., Hidaka, I., and Caprio, J. 1987. Taste responses to amino acids from facial nerve branches innervating oral and extra-oral taste buds in the channel catfish, *Ictalurus punctatus*. Brain Res. 406, 105–112.

Kapoor, B. G. and Finger, T. E. 2003. Taste and Solitary Chemoreceptor Cells. In: Catfishes: Vol. 2 (*eds*. G. Arratia, B. G. Kapoor, M. Chardon, and R. Diogo), pp. 753–769. Science Publishers, Inc

Keller, T. A., Powell, I., and Weissburg, M. J. 2003. Role of appendages in chemically mediated orientation of blue crabs. Mar. Ecol. Prog. Ser. 261, 217–231.

Kicklighter, C. E., Shabani, S., Johnson, P. M., and Derby, C. D. 2005. Sea hares use novel antipredatory chemical defenses. Curr. Biol. 15, 549–554.

Kiyohara, S. and Caprio, J. 1996. Somatotopic organization of the facial lobe of the sea catfish *Arius felis* studied by transganglionic transport of horseradish peroxidase. J. Comp. Neurol. 368, 121–135.

Kiyohara, S., Hidaka, I., Kitoh, J., and Yamashita, S. 1985. Mechanical sensitivity of the facial nerve fibers innervating the anterior palate of the puffer, *Fugu pardalis*, and their central projection to the primary taste center. J. Comp. Physiol. A 157, 705–716.

Kiyohara, S., Houman, H., Yamashita, S., Caprio, J., and Marui, T. 1986. Morphological evidence for a direct projection of trigeminal nerve fibers to the primary gustatory center in the sea catfish, *Plotosus anguillaris*. Brain Res. 379, 353–357.

Kleene, S. J. 1997. High-gain, low-noise amplification in olfactory transduction. Biophys. J. 73, 1110–1117.

Kleerekoper, H. 1969. Olfaction in Fishes. Indiana University Press.

Koehl, M. A. R., Koseff, J. R., Crimaldi, J. P., McCay, M. G., Cooper, T., Wiley, M. B., and Moore, P. A. 2001. Lobster sniffing: antennule design and hydrodynamic filtering of information in an odor plume. Science 294, 1948–1951.

Kohbara, J. and Caprio, J. 1996. Taste responses to binary mixtures of amino acids in the sea catfish, *Arius felis*. Chem. Senses 21, 45–53.

Kohbara, J. and Caprio, J. 2001. Taste responses of the facial and glossopharyngeal nerves to amino acids in the rainbow trout. J. Fish Biol. 58, 1062–1072.

Kohbara, J., Michel, W., and Caprio, J. 1992. Responses of single facial taste fibers in the channel catfish, *Ictalurus punctatus*, to amino acids. J. Neurophysiol. 68, 1012–1026.

Kondo, R., Kaneko, S., Sun, H., Sakaizumi, M., and Chigusa, S. I. 2002. Diversification of olfactory receptor genes in the Japanese medaka fish, *Oryzias latipes*. Gene 282, 113–120.

Kosaka, T. and Hama, K. 1979. Ruffed cell: a new type of neuron with a distinctive initial unmyelinated portion of the axon in the olfactory bulb of the goldfish (*Carassius auratus*). J. Comp. Neurol. 186, 301–320.

Kosaka, T. and Hama, K. 1981. Ruffed cell: a new type of neuron with a distinctive initial unmyelinated portion of the axon in the olfactory bulb of the goldfish (*Carassius auratus*). III. Three-dimensional structure of the ruffed cell dendrite. J. Comp. Neurol. 201, 571–587.

Kosaka, T. and Hama, K. 1982a. Structure of the mitral cell in the olfactory bulb of the goldfish (*Carassius auratus*). J. Comp. Neurol. 212, 365–384.

Kosaka, T. and Hama, K. 1982b. Synaptic organization in the teleost olfactory bulb. J. Physiol. (Paris) 78, 707–719.

Kotrschal, K. 1991. Solitary chemosensory cells – taste, common chemical sense or what? Rev. Fish Biol. Fish. 1, 3–22.

Kotrschal, K. 1993. Sampling and behavioral evidence for mucus detection in a unique chemosensory organ: the anterior dorsal fin in rocklings. Zool. Jb. Physiol. 97, 47–67.

Kotrschal, K. and Finger, T. E. 1996. Secondary connections of the dorsal and ventral facial lobes in a teleost fish, the rockling (*Ciliata mustela*). J. Comp. Neurol. 370, 415–426.

Kumazawa, T., Brand, J. G., and Teeter, J. H. 1998. Amino acid-activated channels in the catfish taste system. Biophys. J. 75, 2757–2766.

Laing, D. G. and Francis, G. W. 1989. The capacity of humans to identify odors in mixtures. Physiol. Behav. 32, 809–814.

Laing, D. G. and Willcox, M. E. 1983. Perception of components in binary odour mixtures. Chem. Senses 7, 249–264.

Laing, D. G., Link, C., and Hutchinson, I. 2002. The limited capacity of humans to identify the components of taste mixtures and taste-odor mixtures. Perception 31, 617–635.

Lamb, C. F., IV and Caprio, J. 1992. Convergence of oral and extraoral information in the superior secondary gustatory nucleus of the channel catfish. Brain Res. 588, 201–211.

Lamb, C. F., IV and Caprio, J. 1993. Taste and tactile responsiveness of neurons in the posterior diencephalon of the channel catfish. J. Comp. Neurol. 337, 419–430.

Lastein, S., Hamdani, E. H., and Doving, K. B. 2006. Gender distinction in neural discrimination of sex pheromones in the olfactory bulb of crucian carp, *Carassius carassius*. Chem. Senses 31, 69–77.

Lin, W., Arellano, J., Slotnick, B., and Restrepo, D. 2004. Odors detected by mice deficient in cyclic nucleotide-gated channel subunit A2 stimulate the main olfactory system. J. Neurosci. 24, 3703–3710.

Lipschitz, D. L. and Michel, W. C. 2002. Amino acid odorants stimulate microvillar sensory neurons. Chem. Senses 27, 277–286.

Livermore, A., Hutson, M., Ngo, V., Hadjisimos, R., and Derby, C. D. 1997. Elemental and configural learning and the perception of odorant mixtures by the spiny lobster *Panulirus argus*. Physiol. Behav. 62, 169–174.

Lo, Y. H., Bradley, T. M., and Rhoads, D. E. 1991. L-Alanine binding sites and Na^+,K^+-ATPase in cilia and other membrane fractions from olfactory rosettes of Atlantic salmon. Comp. Biochem. Physiol. 98B, 121–126.

Lodovichi, C., Belluscio, L., and Katz, L. C. 2003. Functional topography of connections linking mirror-symmetric maps in the mouse olfactory bulb. Neuron 38, 265–276.

Lucas, P., Ukhanov, K., Leinders-Zufall, T., and Zufall, F. 2003. A diacylglycerol-gated cation channel in vomeronasal neuron dendrites is impaired in TRPC2 mutant mice: mechanism of pheromone transduction. Neuron 40, 551–561.

Luu, P., Achner, F., Bertrand, H.-O., Fan, J., and Ngai, J. 2004. Molecular determinants of ligand selectivity in a vertebrate odorant receptor. J. Neurosci. 24, 10128–10137.

Mac Leod, N. K. 1976. Spontaneous activity of single neurons in the olfactory bulb of the rainbow trout (*Salmo gairdneri*) and its modulation by olfactory stimulation with amino acids. Exp. Brain Res. 25, 267–278.

Malnic, B., Hirono, J., Sato, T., and Buck, L. 1999. Combinatorial receptor codes for odors. Cell 96, 712–723.

Marin, E. C., Jefferis, G. S. X. E., Komiyama, T., Zhu, H., and Luo, L. 2002. Representation of the glomerular olfactory map in the *Drosophila*. brain. Cell 109, 243–255.

Marui, T. 1977. Taste responses in the facial lobe of the carp, *Cyprinus carpio*. L. Brain Res. 130, 287–298.

Marui, T. and Caprio, J. 1982. Electrophysiological evidence for the topographical arrangement of taste and tactile neurons in the facial lobe of the channel catfish. Brain Res. 231, 185–190.

Marui, T. and Caprio, J. 1992. Teleost Gustation. In: Fish Chemoreception (*ed*. T. J. Hara), pp. 171–198. Chapman & Hall, Ltd

Marui, T. and Funakoshi, M. 1979. Tactile input to the facial lobe of the carp, *Cyprinus carpio* L. Brain Res. 177, 479–488.

Marui, T., Caprio, J., Kiyohara, S., and Kasahara, Y. 1988. Topographical organization of taste and tactile neurons in the facial lobe of the sea catfish, *Plotosus lineatus*. Brain Res. 446, 178–182.

Marui, T., Evans, R. E., Zielinski, B. S., and Hara, T. J. 1983. Gustatory responses of the rainbow trout (*Salmo gairdneri*) palate to amino acids and derivatives. J. Comp. Physiol. A 153, 423–433.

McClintock, T. S. and Ache, B. W. 1989. Hyperpolarizing receptor potentials in lobster olfactory receptor cells: implications for transduction and mixture suppression. Chem. Senses 14, 637–647.

McClintock, T. S. and Xu, F. 2001. Molecular Physiology of G-Proteins in Olfactory Transduction and CNS Neurotransmission in the Lobster. In: The Crustacean Nervous System (*ed*. K. Wiese), pp. 359–366. Springer.

McKinzie, M. E., Benton, J. L., Beltz, B. S., and Mellon, D. 2003. Parasol cells of the hemiellipsoid body in the crayfish *Procambarus clarkii*: dendritic branching patterns and functional implications. J. Comp. Neurol. 462, 168–179.

Mellon, D., Jr. and Alones, V. 1993. Cellular organization and growth-related plasticity of the crayfish olfactory midbrain. Microsc. Res. Tech. 24, 231–259.

Mellon, D., Jr. and Munger, S. D. 1990. Nontopographic projection of olfactory sensory neurons in the crayfish brain. J. Comp. Neurol. 296, 253–262.

Meredith, M. 1981. The analysis of response similarity in single neurons of the goldfish olfactory bulb using amino-acids as odor stimuli. Chem. Senses 6, 277–293.

Meredith, M. and Moulton, D. G. 1978. Patterned response to odor in single neurons of goldfish olfactory bulb: influence of odor quality and other stimulus parameters. J. Gen. Physiol. 71, 615–643.

Michel, W. C. and Ache, B. W. 1992. Cyclic nucleotides mediate an odor-evoked potassium conductance in lobster olfactory receptor cells. J. Neurosci. 12, 3979–3984.

Michel, W. and Caprio, J. 1991. Responses of single facial taste fibers in the sea catfish, *Arius felis*, to amino acids. J. Neurophysiol. 66, 247–260.

Michel, W. C. and Derbidge, D. S. 1997. Evidence of distinct amino acid and bile salt receptors in the olfactory system of the zebrafish, *Danio rerio*. Brain Res. 764, 179–187.

Michel, W. C., McClintock, T. S., and Ache, B. W. 1991. Inhibition of lobster olfactory receptor cells by an odor-activated potassium conductance. J. Neurophysiol. 65, 446–453.

Michel, W. C., Trapido-Rosenthal, H. G., Chao, E. T., and Wachowiak, M. 1993. Stereoselective detection of amino acids by lobster olfactory receptor neurons. J. Comp. Physiol. A 171, 705–712.

Mombaerts, P. 2004. Odorant receptor gene choice in olfactory sensory neurons: the one receptor-one neuron hypothesis revisited. Curr. Opin. Neurobiol. 14, 31–36.

Mombaerts, P., Wang, F., Dulac, C., Chao, S. K., Nemes, A., Mendelsohn, M., Edmondson, J., and Axel, R. 1996. Visualizing an olfactory sensory map. Cell 87, 675–686.

Moore, P. A. and Bergman, D. A. 2005. The smell of success and failure: the role of intrinsic and extrinsic chemical signals on the social behavior of crayfish. Integr. Comp. Biol. 45, 650–657.

Mori, K. 1995. Relation of chemical structure to specificity of response in olfactory glomeruli. Curr. Opin. Neurobiol. 5, 467–474.

Mori, K., Kishi, K., and Ojima, H. 1983. Distribution of dendrites of mitral, displaced mitral, tufted, and granule cells in the rabbit olfactory bulb. J. Comp. Neurol. 219, 339–355.

Ngai, J., Dowling, M. M., Buck, L., Axel, R., and Chess, A. 1993. The family of genes encoding odorant receptors in the channel catfish. Cell 72, 657–666.

Nikonov, A. A. and Caprio, J. 2001. Electrophysiological evidence for a chemotopy of biologically relevant odors in the olfactory bulb of the channel catfish. J. Neurophysiol. 86, 1869–1876.

Nikonov, A. A. and Caprio, J. 2004. Odorant specificity of single olfactory bulb neurons to amino acids in the channel catfish. J. Neurophysiol. 92, 123–134.

Nikonov, A. A. and Caprio, J. 2007. Responses of olfactory forebrain units to amino acids in the channel catfish. J. Neurophysiol. 97, 2490–2498.

Nikonov, A. A., Finger, T. E., and Caprio, J. 2005. Beyond the olfactory bulb: An odotopic map in forebrain. Proc. Natl. Acad. Sci. U.S.A 102, 18688–18693.

Ogawa, K. and Caprio, J. 1999. Facial taste responses of the channel catfish to binary mixtures of amino acids. J. Neurophysiol. 82, 564–569.

Ogawa, K. and Caprio, J. 2000. Glossopharyngeal taste responses of the channel catfish to binary mixtures of amino acids. Chem. Senses 25, 501–506.

Oike, H., Nagai, T., Furuyama, A., Okada, S., Aihara, Yoshiko, Ishimaru, Y, Marui, T., Matsumoto, I., Misaka, T., and Abe, K. 2007. Characterization of ligands for fish taste receptors. J. Neurosci. 27, 5584–5592.

Oka, Y. 1983. Golgi, electron microscopic and combined Golgi-electron microscopic studies of the mitral cells in the goldfish olfactory bulb. Neuroscience 8, 723–742.

Olson, K. S. and Derby, C. D. 1995. Inhibition of taurine 5′AMP olfactory receptor sites of the spiny lobster *Panulirus argus* by odorant compounds and mixtures. J. Comp. Physiol. A 176, 527–540.

Olson, K. S., Trapido-Rosenthal, H. G., and Derby, C. D. 1992. Biochemical characterization of independent olfactory receptor sites for 5′-AMP and taurine in the spiny lobster. Brain Res. 583, 262–270.

Peters, R. C., Kotrschal, K., and Krautgartner, W. 1991. Solitary chemoreceptor cells of *Ciliata mustela* (Gadidae, Teleostei) are tuned to mucoid stimuli. Chem. Senses 16, 31–42.

Preston, R. L. 1987. Occurrence of D-amino acids in higher organisms: a survey of the distribution of D-amino acids in marine invertebrates. Comp. Biochem. Physiol. 87B, 55–62.

Raderman-Little, R. 1979. The effect of temperature on the turnover of taste bud cells in catfish. Cell. Tissue Kinet. 12, 269–280.

Rehnberg, B. G. and Schreck, C. B. 1986. The olfactory L-serine receptor in coho salmon: biochemical specificity and behavioral response. J. Comp. Physiol. A 159, 61–67.

Ressler, K. J., Sullivan, S. L., and Buck, L. B. 1994. Information coding in the olfactory system: evidence for a stereotyped and highly organized epitope map in the olfactory bulb. Cell 79, 1245–1255.

Restrepo, D., Miyamoto, T., Bryant, B. P., and Teeter, J. H. 1990. Odor stimuli trigger influx of calcium into olfactory neurons of the channel catfish. Science 249, 1166–1168.

Reutter, K. 1978. Taste organ in the bullhead (Teleostei). Adv. Anat. Embryol. Cell Biol. 55, 1–98.

Rhein, L. D. and Cagan, R. H. 1983. Biochemical studies of olfaction: binding specificity of odorants to cilia preparation from rainbow trout olfactory rosettes. J. Neurochem. 41, 569–577.

Riddle, D. R. and Oakley, B. 1991. Evaluation of projection patterns in the primary olfactory system of rainbow trout. J. Neurosci. 11, 3752–3762.

Riddle, D. R. and Oakley, B. 1992. Immunocytochemical identification of primary olfactory afferents in rainbow trout. J. Comp. Neurol. 324, 575–589.

Riddle, D. R., Wong, L. D., and Oakley, B. 1993. Lectin identification of olfactory receptor neuron subclasses with segregated central projections. J. Neurosci. 13, 3018–3033.

Rittschof, D. and Sutherland, J. P. 1986. Field studies on chemically mediated behavior in land hermit crabs: volatile and nonvolatile odors. J. Chem. Ecol. 12, 1273–1284.

Robertson, J. R., Fudge, J. A., and Vermeer, G. K. 1981. Chemical and live feeding stimulants of the sand fiddler crab, *Uca pugilator* (Bose). J. Exp. Mar. Biol. Ecol. 53, 47–64.

Rolen, S. H. and Caprio, J. 2007. Processing of bile salt odor information by single olfactory bulb neurons in the channel cat fish. J. Neurophysiol. 97, 4058–4068.

Sachse, S. and Galizia, G. 2002. Role of inhibition for temporal and spatial odor representation in olfactory output neurons: a calcium imaging study. J. Neurophysiol. 87, 1106–1117.

Sachse, S., Rappert, A., and Galizia, C. G. 1999. The spatial representation of chemical structures in the antennal lobe of honeybees: steps towards the olfactory code. Eur. J. Neurosci. 11, 3970–3982.

Sandeman, D. and Mellon, D., Jr. 2001. Olfactory Centers in the Brain of Freshwater Crayfish. In: The Crustacean Nervous System (*ed*. K. Wiese), pp. 386–404. Springer.

Sandeman, R. and Sandeman, D. C. 1996. Pre- and postembryonic development, growth and turnover of olfactory receptor neurones in crayfish antennules. J. Exp. Biol. 199, 2409–2418.

Sandeman, R. and Sandeman, D. 2000. ''Impoverished'' and ''enriched'' living conditions influence the proliferation and survival of neurons in crayfish brain. J. Neurobiol. 45, 215–226.

Sandeman, R. and Sandeman, D. 2003. Development, growth, and plasticity in the crayfish olfactory system. Microsc. Res. Tech. 60, 266–277.

Sandeman, R., Clarke, D., Sandeman, D., and Manly, M. 1998. Growth-related and antennular amputation-induced changes in the olfactory centers of crayfish brain. J. Neurosci. 18, 6195–6206.

Sandeman, D. C., Sandeman, R. E., Derby, C. D., and Schmidt, M. 1992. Morphology of the brain of crayfish, crabs, and spiny lobsters: a common nomenclature for homologous structures. Biol. Bull. 183, 304–326.

Sandeman, D. C., Scholtz, G., and Sandeman, R. E. 1993. Brain evolution in decapod Crustacea. J. Exp. Zool. 265, 112–133.

Sato, K. and Suzuki, N. 2000. The contribution of a Ca^{2+}-activated Cl^{-} conductance to amino-acid-induced inward current responses of ciliated olfactory neurons of the rainbow trout. J. Exp. Biol. 203, 253–262.

Sato, K. and Suzuki, N. 2001. Whole-cell response characteristics of ciliated and microvillous olfactory receptor neurons to amino acids, pheromone candidates and urine in rainbow trout. Chem. Senses 26, 1145–1156.

Sato, Y., Miyasaka, N., and Yoshihara, Y. 2005. Mutually exclusive glomerular innervation by two distinct types of olfactory sensory neurons revealed in transgenic zebrafish. J. Neurosci. 25, 4889–4897.

Satou, M. 1990. Synaptic organization, local neuronal circuitry, and functional segregation of the teleost olfactory bulb. Prog. Neurobiol. 34, 115–142.

Satou, M., Fujita, I., Ichikawa, M., Yamaguchi, K., and Ueda, K. 1983. Field potential and intracellular potential studies of the olfactory bulb in the carp: evidence for a functional separation of the olfactory bulb into lateral and medial subdivisions. J. Comp. Physiol. A 152, 319–333.

Schachtner, J., Schmidt, M., and Homberg, U. 2005. Organization and evolutionary trends of primary olfactory brain centers in Tetraconata (Crustacea + Hexapoda). Arthrop. Struct. Devel. 34, 257–299.

Schild, D. and Restrepo, D. 1998. Transduction mechanisms in vertebrate olfactory receptor cells. Physiol. Rev. 78, 429–458.

Schmachtenberg, O. and Bacigalupo, J. 2004. Olfactory transduction in ciliated receptor neurons of the Cabinza grunt, *Isacia conceptionis* (Teleostei: Haemulidae). Eur. J. Neurosci. 20, 3378–3386.

Schmidt, M. 1989. The hair-peg organs of the shore crab, *Carcinus maenas* (Crustacea, Decapoda): ultrastructure and functional properties of sensilla sensitive to changes in seawater concentration. Cell Tissue Res. 257, 609–621.

Schmidt, M. 1997. Distribution of presumptive chemosensory afferents with FMRFamide- or substance P-like immunoreactivity in decapod crustaceans. Brain. Res. 746, 71–84.

Schmidt, M. 2001. Neuronal differentiation and long-term survival of newly generated cells in the olfactory midbrain of the adult spiny lobster, *Panulirus argus*. J. Neurobiol. 48, 181–203.

Schmitt, B. C. and Ache, B. W. 1979. Olfaction: responses of a decapod crustacean are enhanced by flicking. Science 205, 204–206.

Schmidt, M. and Ache, B. W. 1992. Antennular projections to the midbrain of the spiny lobster. II. Sensory innervation of the olfactory lobe. J. Comp. Neurol. 318, 291–303.

Schmidt, M. and Ache, B. W. 1993. Antennular projections to the midbrain of the spiny lobster. III. Central arborizations of motoneurons. J. Comp. Neurol. 336, 583–594.

Schmidt, M. and Ache, B. W. 1996a. Processing of antennular input in the brain of the spiny lobster, *Panulirus argus.* I. Non-olfactory chemosensory and mechanosensory pathway of the lateral and median antennular neuropils. J. Comp. Physiol. A 178, 579–604.

Schmidt, M. and Ache, B. W. 1996b. Processing of antennular input in the brain of the spiny lobster, *Panulirus argus.* II. The olfactory pathway. J. Comp. Physiol. A 178, 605–628.

Schmidt, M. and Derby, C. D. 2005. Non-olfactory chemoreceptors in asymmetric setae activate antennular grooming behavior in the Caribbean spiny lobster *Panulirus argus*. J. Exp. Biol. 208, 233–248.

Schmidt, M. and Gnatzy, W. 1984. Are the funnel-canal organs the ''campaniform sensilla'' of the shore crab, *Carcinus maenas* (Decapoda, Crustacea)? II. Ultrastructure. Cell Tissue Res. 237, 81–93.

Shabani, S., Kamio, M., and Derby, C. D. 2006. Chemicals released by injured or disturbed conspecifics mediate defensive behaviors via the aesthetasc pathway in the spiny lobster *Panulirus argus*. Chem. Senses 31, A81–A82.

Sheldon, R. E. 1912. The olfactory tracts and centers in teleosts. J. Comp. Neurol. 22, 177–339.

Song, C.-K., Johnstone, L. M., Schmidt, M., Derby, C. D., and Edwards, D. H. 2004. Social experience decreases the rate of postembryonic neurogenesis in the olfactory system of juvenile *Procambarus clarkii*. Soc. Neurosci. Abstr. 754.12.

Sorensen, P. W. and Caprio, J. 1998. Chemoreception. In: The Physiology of Fishes (*ed*. D. H. Evans), pp. 375–405. CRC Press LLC.

Sorensen, P. W., Hara, T. J., and Stacey, N. E. 1991. Sex pheromones selectively stimulate the medial olfactory tracts of male goldfish. Brain Res. 558, 343–347.

Speca, D. J., Lin, D. M., Sorensen, P. W., Isacoff, E. Y., Ngai, J., and Dittman, A. 1999. Functional identification of a goldfish odorant receptor. Neuron 23, 487–498.

Spehr, M., Wetzel, C. H., Hatt, H., and Ache, B. W. 2002. 3-Phosphoinositides modulate cyclic nucleotide signaling in olfactory receptor neurons. Neuron 33, 731–739.

Stacey, N. E. and Kyle, A. L. 1983. Effects of olfactory tract lesions on sexual and feeding behavior in the goldfish. Physiol. Behav. 30, 621–628.

Stacey, N. E. and Sorensen, P. W. 2002. Fish Hormonal Pheromones. In: Hormones, Brain, and Behavior, Vol. 2 (*eds*. D. W. Pfaff, A. P. Arnold, S. Etgen, S. Fahrbach, and R. Rubin), pp. 375–435. Academic Press.

Stacey, N. E. and Sorensen, P. W. 2005. Hormones, Pheromones, and Reproductive Behaviors. In: Behaviour: Interactions with Fish Physiology (*eds*. K. A. Sloman, S. Balshine, and R. W. Wilson), Vol. 24 in Fish Physiology (series editors W. S. Hoar, D. J. Randall, and A.P. Farrell), Chap. 9, pp. 359–412. Academic Press, New York.

Stensmyr, M. C., Erland, S., Hallberg, E., Wallen, R., Greenaway, P., and Hansson, B. S. 2005. Insect-like olfactory adaptations in the terrestrial giant robber crab. Curr. Biol. 15, 116–121.

Steullet, P. and Derby, C. D. 1997. Coding of blend ratios of binary mixtures by olfactory neurons in the Florida spiny lobster, *Panulirus argus*. J. Comp. Physiol. A 180, 123–135.

Steullet, P., Cate, H. S., and Derby, C. D. 2000a. A spatiotemporal wave of turnover and functional maturation of olfactory receptor neurons in the spiny lobster *Panulirus argus*. J. Neurosci. 20, 3282–3294.

Steullet, P., Cate, H. S., Michel, W. C., and Derby, C. D. 2000b. Functional units of a compound nose: aesthetasc sensilla house similar populations of olfactory receptor neurons on the crustacean antennule. J. Comp. Neurol. 418, 270–280.

Steullet, P., Dudar, O., Flavus, T., Zhou, M., and Derby, C. D. 2001. Selective ablation of antennular sensilla on the Caribbean spiny lobster *Panulirus argus* suggests that dual antennular chemosensory pathways mediate odorant activation of searching and localization of food. J. Exp. Biol. 204, 4259–4269.

Steullet, P., Kruetzfeldt, D. R., Hamidani, G., Flavus, T., Ngo, V., and Derby, C. D. 2002. Dual parallel antennular chemosensory pathways mediate odor-associative learning and odor discrimination in the Caribbean spiny lobster *Panulirus argus*. J. Exp. Biol. 205, 851–867.

Stoss, T. D., Nickell, M. D., Hardin, H., Derby, C. D., and McClintock, T. S. 2004. Inducible transcript expressed by reactive epithelial cells at sites of olfactory sensory neuron proliferation. J. Neurobiol. 58, 355–368.

Strausfeld, N. J. and Hildebrand, J. G. 1999. Olfactory systems: common design, uncommon origins? Curr. Opin. Neurobiol. 9, 634–639.

Strotmann, J., Conzelmann, S., Beck, A., Feinstein, P., Breer, H., and Mombaerts, P. 2000. Local permutations in the glomerular array of the mouse olfactory bulb. J. Neurosci. 20, 6927–6938.

Sullivan, J. M. and Beltz, B. S. 2004. Evolutionary changes in the olfactory projection neuron pathways of eumalacostracan crustaceans. J. Comp. Neurol. 470, 25–38.

Sullivan, J. M. and Beltz, B. S. 2005. Integration and segregation of inputs to higher-order neuropils of the crayfish brain. J. Comp. Neurol. 481, 118–126.

Sun, H., Kondo, R., Shima, A., Naruse, K., Hori, H., and Chigusa, S. I. 1999. Evolutionary analysis of putative olfactory receptor genes of medaka fish, *Oryzias latipes*. Gene 231, 137–145.

Sveinsson, T. and Hara, T. J. 1990. Multiple olfactory receptors for amino acids in Arctic char (*Salvelinus alpinus*) evidenced by cross-adaptation experiments. Comp. Biochem. Physiol. 97A, 289–293.

Szabo, T., Blahser, S., Denizot, J. P., and Ravaille-Veron, M. 1991. Extensive primary olfactory projections beyond the olfactory bulb in teleost fish. Neurobiology 312, 555–560.

Tabor, R., Yaksi, E., Weislogel, J.-M., and Friedrich, R. W. 2004. Processing of odor mixtures in the zebrafish olfactory bulb. J. Neurosci. 24, 6611–6620.

Takami, S. and Graziadei, P. P. C. 1991. Light microscopic Golgi study of mitral/tufted cells in the accessory olfactory bulb of the adult rat. J. Comp. Neurol. 311, 65–83.

Thommesen, G. 1978. The spatial distribution of odour induced potentials in the olfactory bulb of char and trout (Salmonidae). Acta Physiol. Scand. 102, 205–217.

Thompson, H. A. and Ache, B. W. 1980. Threshold determination for olfactory receptors of the spiny lobster. Mar. Behav. Physiol. 7, 249–260.

Troemel, E. R. 1999. Chemosensory signaling in *C. elegans*. BioEssays 21, 1011–1020.

Trott, T. J. and Robertson, J. R. 1984. Chemical stimulants of cheliped flexion behavior by the western Atlantic ghost crab *Ocypode quadrata* (Fabricius). J. Exp. Mar. Biol. Ecol. 78, 237–252.

Tsuboi, A., Yoshihara, Y., Yamazaki, N., Kasai, H., Asai-Tsuboi, H., Komatsu, M., Serizawa, S., Ishii, T., Matsuda, Y., Nagawa, F., and Sakano, H. 1999. Olfactory neurons expressing closely linked and homologous odorant receptor genes tend to project their axons to neighboring glomeruli on the olfactory bulb. J. Neurosci. 19, 8409–8418.

Uchida, N., Takahashi, Y. K., Tanifuji, M., and Mori, K. 2000. Odor maps in the mammalian olfactory bulb: domain organization and odorant structural features. Nat. Neurosci. 3, 1035–1043.

Valentinčič, T. 2004. Taste and Olfactory Stimuli and Behavior in Fishes. In: The Senses of Fish (*eds*. G. von derEmde, J. Mogdans, and B. G. Kapoor), pp. 90–108. Narosa Publishing House.

Valentinčič, T. and Caprio, J. 1994. Consummatory feeding behavior to amino acids in intact and anosmic channel catfish *Ictalurus punctatus*. Physiol. Behav. 55, 857–863.

Valentinčič, T. and Caprio, J. 1997. Visual and chemical release of feeding behavior in adult rainbow trout. Chem. Senses 22, 375–382.

Valentinčič, T., Kralj, J., Stenovec, M., Koce, A., and Caprio, J. 2000a. The behavioral detection of binary mixtures of amino acids and their individual components by catfish. J. Exp. Biol. 203, 3307–3317.

Valentinčič, T., Metelko, J., Ota, D., Pirc, V., and Blejec, A. 2000b. Olfactory discrimination of amino acids in brown bullhead catfish. Chem. Senses 25, 21–29.

Valentinčič, T., Miklavc, P., Dolensek, J., and Plibersek, K. 2005. Correlations between olfactory discrimination, olfactory receptor neuron responses and chemotopy of amino acids in fishes. Chem. Senses 30(Suppl. 1), i312–i314.

Valentinčič, T., Wegert, S., and Caprio, J. 1994. Learned olfactory discrimination versus innate taste responses to amino acids in channel catfish, *Ictalurus punctatus*. Physiol. Behav. 55, 865–873.

Vassar, R., Chao, S. K., Sitcheran, R., Nuñez, J. M., Vosshall, L. B., and Axel, R. 1994. Topographic organization of sensory projections to the olfactory bulb. Cell 79, 981–991.

Vogt, R. G. 2005. Molecular Basis of Pheromone Detection in Insects. In: Comprehensive Insect Physiology, Biochemistry, Pharmacology and Molecular Biology. Vol. 3. Endocrinology (*eds*. L. I. Gilbert, K. Iatro, and S. Gill), pp. 753–804. Elsevier, London.

Voigt, R. and Atema, J. 1992. Tuning of chemoreceptor cells of the second antenna of the American lobster (*Homarus*

americanus) with a comparison of four of its other chemoreceptor organs. J. Comp. Physiol. A 171, 673–683.
Wachowiak, M. and Ache, B. W. 1997. Dual inhibitory pathways mediated by GABA- and histaminergic interneurons in the lobster olfactory lobe. J. Comp. Physiol. A 180, 357–372.
Wachowiak, M. and Ache, B. W. 1998. Multiple inhibitory pathways shape odor-evoked responses in lobster olfactory projection neurons. J. Comp. Physiol. A 182, 425–434.
Wachowiak, M., Cohen, L. B., and Ache, B. W. 2002. Presynaptic inhibition of olfactory receptor neurons. Microsc. Res. Tech. 58, 365–375.
Wachowiak, M., Diebel, C. E., and Ache, B. W. 1996. Functional organization of olfactory processing in the accessory lobe of the spiny lobster. J. Comp. Physiol. A 178, 211–226.
Wachowiak, M., Diebel, C. E., and Ache, B. W. 1997. Local interneurons define functionally distinct regions within lobster olfactory glomeruli. J. Exp. Biol. 200, 989–1001.
Wang, Y., Wright, N. J. D., Guo, H.-F., Xie, Z., Svoboda, K., Malinow, R., Smith, D. P., and Zhong, Y. 2001. Genetic manipulation of the odor-evoked distributed neural activity in the *Drosophila* mushroom body. Neuron 29, 267–276.
Weissburg, M. J. 2000. The fluid dynamical context of chemosensory behavior. Biol. Bull. 198, 188–202.
Weissburg, M. J. and Derby, C. D. 1995. Regulation of sex-specific feeding behavior in fiddler crabs: physiological properties of chemoreceptor neurons in claws and legs of males and females. J. Comp. Physiol. A 176, 513–526.
Weissburg, M. J. and Zimmer-Faust, R. K. 1991. Ontogeny *versus* phylogeny in determining patterns of chemoreception: initial studies with fiddler crabs. Biol. Bull. 181, 205–215.
Weissburg, M. J., Derby, C. D., Johnson, O., McAlvin, B., and Moffett, J. M., Jr. 2001. Transsexual limb transplants in fiddler crabs and expression of novel sensory capabilities. J. Comp. Neurol. 440, 311–320.
Wellins, C. A., Rittschof, D., and Wachowiak, M. 1989. Location of volatile odor sources by ghost crab *Ocypode quadrata* (Fabricius). J. Chem. Ecol. 15, 1161–1169.
Weltzien, F., Hoglund, E., Hamdani, E. H., and Døving, K. B. 2003. Does the lateral bundle of the medial olfactory tract mediate reproductive behavior in male crucian carp? Chem. Senses 28, 293–300.
Wight, K., Francis, L., and Eldridge, D. 1990. Food aversion learning by the hermit crab *Pagurus granosimanus*. Biol. Bull. 178, 205–209.
Wong, A. M., Wang, J. W., and Axel, R. 2002. Spatial representation of the glomerular map in the *Drosophila* protocerebrum. Cell 109, 229–241.
Wu, H.-H., Ivkovic, S., Murray, R. C., Jaramillo, S., Lyons, K. M., Johnson, J. E., and Calof, A. L. 2003. Autoregulation of neurogenesis by GDF 11. Neuron 37, 197–207.
Wullimann, M. F. and Mueller, T. 2004. Teleostean and mammalian forebrains contrasted: evidence from genes to behavior. J. Comp. Neurol. 475, 143–162.
Yamashita, S., Yamada, T., and Hara, T. J. 2006. Gustatory responses to feeding- and non-feeding-stimulant chemicals, with an emphasis on amino acids, in rainbow trout. J. Fish Biol. 68, 783–800.
Xu, P., Atkinson, R., Jones, D. N., and Smith, D. P. 2005. Drosophila OBP LUSH is required for activity of pheromone-sensitive neurons. Neuron 45, 193–200.
Yokoi, M., Mori, K., and Nakanishi, S. 1995. Refinement of odor molecule tuning by dendrodendritic synaptic inhibition in the olfactory bulb. Proc. Natl. Acad. Sci. U. S. A. 3371–3375.
Zeng, C. and Hidaka, I. 1990. Single fiber responses in the palatine taste nerve of the yellowtail *Seriola quinqueradiata*. Nippon Suisan Gakkai Shi 56, 1611–1618.
Zhainazarov, A. B., Doolin, R. E., and Ache, B. W. 2001. Properties and Functional Role of a Sodium-Activated Nonselective Cation Channel in Lobster Olfactory Receptor Neurons. In: The Crustacean Nervous System (*ed*. K. Wiese), pp. 367–375. Springer.
Zhainazarov, A. B., Doolin, R. E., Hoegg, R., and Ache, B. W. 1999. GABA-mediated inhibition of primary olfactory receptor neurons. Biol. Signals Recept. 8, 348–359.
Zhang, Y., Hoon, M. A., Chandrashekar, J., Mueller, K. L., Cook, B., Wu, D., Zuker, C. S., and Ryba, N. J. 2003. Coding of sweet, bitter, and umami tastes: different receptor cells sharing similar signaling pathways. Cell 112, 293–301.
Zimmer, R. K. and Butman, C. A. 2000. Chemical signaling processes in the marine environment. Biol. Bull. 198, 168–187.
Zimmer-Faust, R. K. 1987. Crustacean chemical perception: towards a theory on optimal chemoreception. Biol. Bull. 172, 10–29.
Zimmer-Faust, R. K. 1993. ATP: a potent prey attractant evoking carnivory. Limnol. Oceanogr. 38, 1271–1275.
Zimmer-Faust, R. K. and Case, J. F. 1982a. Odors influencing foraging behavior of the California spiny lobster, *Panulirus interruptus*, and other decapod Crustacea. Mar. Behav. Physiol. 9, 35–58.
Zimmer-Faust, R. K. and Case, J. F. 1982b. Organization of food search in the kelp crab, *Pugettia producta* (Randall). J. Exp. Mar. Biol. Ecol. 57, 237–255.
Zimmer-Faust, R. K., Tyre, J. E., Michel, W. C., and Case, J. F. 1984. Chemical mediation of appetitive feeding in a marine decapod crustacean: the importance of suppression and synergism. Biol. Bull. 167, 339–353.
Zou, Z., Horowitz, L. F., Montmayeur, J.-P., Snapper, S., and Buck, L. B. 2001. Genetic tracing reveals a stereotyped sensory map in the olfactory cortex. Nature 414, 173–179.
Zou, Z., Li, F., and Buck, L. B. 2005. Odor maps in the olfactory cortex. Proc. Natl. Acad. Sci. U. S. A. 102, 7724–7729.

4.05 Ultrastructure of Taste Buds

J C Kinnamon and R Yang, University of Denver, Denver, CO, USA

© 2008 Elsevier Inc. All rights reserved.

4.05.1	**Introduction**	136
4.05.2	**History**	136
4.05.3	**A Classic Taste Bud: The Rabbit Foliate Taste Bud**	138
4.05.3.1	General Morphological Features of Rabbit Foliate Taste Buds	138
4.05.3.2	Primary Foliate Taste Bud Cell Types	139
4.05.3.2.1	Type I cells	139
4.05.3.2.2	Type II cells	140
4.05.3.2.3	Type III cells	140
4.05.3.2.4	Synaptic connections	143
4.05.4	**Rodent Taste Buds**	143
4.05.4.1	Innervation	143
4.05.4.2	General Morphological Features	143
4.05.4.3	Primary Taste Bud Cell Types	143
4.05.4.3.1	Type I cells	144
4.05.4.3.2	Type II cells	145
4.05.4.3.3	Type III cells	146
4.05.4.3.4	Type IV cells (basal cells)	146
4.05.4.4	Taste Cell Synapses	147
4.05.4.5	Putative Nonsynaptic Connections	148
4.05.4.5.1	Subsurface cisternae of smooth endoplasmic reticulum	148
4.05.4.5.2	Atypical mitochondria	148
4.05.5	**Concluding Remarks**	149
References		150

Glossary

a-gustducin Alpha subunit of G protein-coupled receptor for bitter and sweet taste transduction pathways.

atypical mitochondria Large mitochondria with twisted-energized or swollen cristae found in Type II taste cells.

chorda tympani nerve Branch of the facial nerve (VIIth cranial) that innervates taste buds in the anterior two-thirds of the tongue.

circumvallate papillae Large, dome-shaped gustatory papillae located in the posterior one-third of the tongue; innervated by the glossopharyngeal nerve (IXth cranial).

facial nerve (Cranial nerve VII) Innervates taste buds fungiform and foliate papillae in the anterior two-thirds of the tongue.

foliate papillae Rows of gustatory papillae located on the sides of the posterior of the tongue; innervated by both the chorda tympani and glossopharyngeal nerve in rodents.

fungiform papillae Mushroom-shaped papillae located in the anterior two-thirds of the tongue; innervated by the chorda tympani nerve.

fusiform Spindle-shaped, with a wider center and tapered ends.

glossopharyngeal nerve Cranial nerve IX, which controls taste sensation in the posterior one-third of the tongue.

innervated Supplied with nerves.

intragemmal Located within the taste bud.

neurotropic Having an affinity for neural tissue, as in a neurotropic stain.

perigemmal Nerves that are found on the periphery of the taste bud.

pore substance Electron-dense material located in the taste pore of a taste bud.

subsurface cisternae Flat membranous stacks of smooth endoplasmic reticulum.

sustentacular taste cells Provides support or sustains.

umami Japanese word for delicious to describe the taste sensation when consuming amino acids such as glutamate.

vagus nerve Cranial nerve X, which innervated taste buds in the pharynx.

4.05.1 Introduction

Taste buds are onion-shaped end organs containing 50–150 cells that are specialized for detecting aqueous chemical stimuli. The taste bud is a dynamic system in which new taste cells (=taste bud cells) are continually being born, maturing, performing their sensory functions, eventually going into senescence, and ultimately dying – all within a period of from 10 days to 2 weeks (Beidler, L. and Smallman, R., 1965). However, recent evidence suggests that taste buds contain both long- and short-lived taste cells (Hamamichi, R. *et al.*, 2006). At the same time, the nervous system is believed to sprout new nerve processes and form synaptic connections with developing taste cells, while retracting synapses from old cells. Intragemmal taste cells are located within the taste bud proper, while perigemmal taste cells are located at the periphery of the taste bud. The goal of the present review is to provide the reader with a basic understanding of taste bud morphology.

Taste buds are surrounded by a relatively electron-dense, nongustatory epithelium replete with desmosomes, from which intermediate filaments project into the cytoplasm of the epithelial cells. The appearance of the nongustatory epithelial cells and the filamentous material is less organized near the basal region of the taste bud, making it more difficult to distinguish the basal region of the taste bud from the surrounding nongustatory epithelium. A typical mammalian taste bud is innervated by sensory nerve processes that enter at the base and ramify throughout the basal two-thirds of the taste bud. Nerve processes within a taste bud are termed intragemmal fibers. The intragemmal fibers originate from either the VII (facial), IX (glossopharyngeal), or the X (vagus) nerves (Figure 1). A small subset of taste cells form synapses onto the intragemmal nerve processes. Another set of nerve processes envelop but do not penetrate the taste bud; these are termed perigemmal nerves (however, see Nagy, J. *et al.*, 1982; Finger, T., 1986).

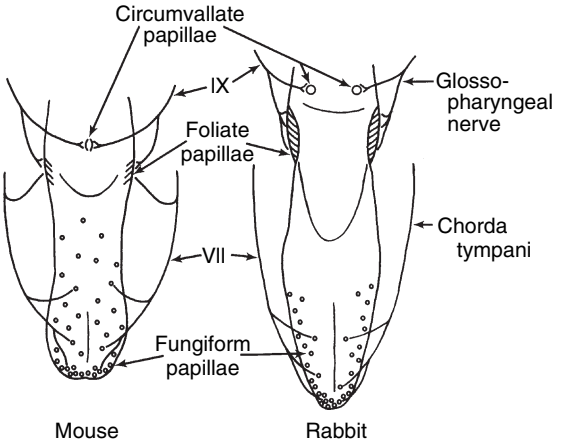

Figure 1 Innervation of rabbit and rat taste buds.

Although taste buds occur throughout the oral cavity, this review deals only with taste buds located on the foliate papillae of the rabbit and circumvallate taste buds of murines (rat and mouse). The rabbit foliate taste bud was selected because it was the first mammalian taste bud to be studied extensively and is the progenitor of the current system of taste cell classification. Taste buds of the rat and mouse were selected because these animals are the species of choice for physiological and molecular biology studies.

4.05.2 History

Taste bud structure has been studied for over a century, yet there is still considerable controversy concerning the classification of taste cells and an understanding of their functions (for reviews see Scalzi, H., 1967; Murray, R., 1973; Kinnamon, J., 1987; Roper, S., 1989; Reutter, K. and Witt, M., 1993; Miller, I., 1995; Finger, T., 1997; Pumplin, D. *et al.*, 1997; Finger, T. and Simon, S., 2000; Lindemann, B., 2001; Finger, T., 2005; Chandrashekar, J. *et al.*, 2006; Roper, S., 2006). The first descriptions of taste buds were in fish (Leydig, F., 1851). Mammalian taste buds were first studied by Schwalbe G. (1868) and Loven C. (1868). In the

nineteenth century taste on cells were named, classified, and ascribed functions based on their staining properties, especially to neurotropic stains such as methylene blue (e.g., Wilson, J. and Edin, M., 1905). Electron microscopy was first used to characterize taste bud ultrastructure over five decades ago (Engstrom, H. and Rytzner, C., 1956a; 1965b). Since then there have been numerous studies on taste bud ultrastructure of mammalian and nonmammalian species (Table 1). Ultrastructural criteria have been used to classify taste cells into various types, including undifferentiated peripheral cells, type I (dark) cells, type II (light) cells, type III (receptor) cells, type IV (basal) cells, and intermediate cells. Traditionally, the morphological criteria used to classify taste cells have included:

1. electron density of the cytoplasm;
2. nuclear shape;
3. types and distribution of nuclear chromatin;
4. accumulations of specific organelles (e.g., polyribosomes, granular and smooth endoplasmic reticulum, and Golgi bodies);
5. number, types, and arrangement of apical microvilli; and
6. presence of synapses onto nerve processes.

Some newer criteria include the presence of subsurface cisternae (SSCs) of smooth endoplasmic reticulum and large, atypical mitochondria with tubular cristae (Royer, S. and Kinnamon, J., 1988; 1994; Clapp, T. *et al.*, 2004).

Table 1 Studies on taste bud ultrastructure of mammalian and nonmammalian species

Species	*References*
Axolotl	Fährmann W. (1967), Fährmann W. and Schuchardt E. (1967), Toyoshima K. *et al.* (1987), Wistuba J. *et al.* (1999).
Bird	Ganchrow D. *et al.* (1991; 1993; 1994; 1995; 1998), Stornelli M. *et al.* (2000), Witt M. *et al.* (2000).
Cat	Yoshie S. *et al.* (1997).
Cow	Tabata S. *et al.* (2003).
Dog	Baradi A. (1965), Kanazawa H. (1993).
Fish	Trujillo-Cenóz O. (1961), Hirata Y. (1966), Uga S. and Hama K. (1967), Welsch U. and Storch V. (1969), Kapoor B. *et al.* (1975), Grover-Johnson N. and Farbman A. (1976), Ovalle W. and Shinn S. (1977), Joyce E. and Chapman G. (1978), Reutter K. (1978; 1982; 1987; 1992), Fujimoto S. and Yamamoto K. (1980), Ono R. (1980), Toyoshima K. *et al.* (1984), Sbarbati A. *et al.* (1988a; 1998b; 1993; 2006), Witt M. and Reutter K. (1990), Reuter K. and Witt M. (1993, 2004), Boudriot F. and Reutter K. (2001).
Frog	Uga S. (1966), Uga S. and Hama K. (1967), Graziadei P. and DeHan R. (1971), Witt M. (1993), Witt M. *et al.* (2000).
Guinea-pig	Yoshie S. *et al.* (1990; 1991), Huang Y. *et al.* (2003).
Hamster	Miller R. and Chaudhry A. (1976).
Human	Graziadei P. (1969), Mattern C. *et al.* (1970), Takeda M. (1972), Paran N. *et al.* (1975), Azzali G. (1997), Witt M. and Reutter K. (1997), Witt M. *et al.* (2000).
Lamb	Sweazey R. *et al.* (1994).
Monkey	Murray R. and Murray A. (1960), Cottler-Fox M. *et al.* (1980, 1987), Ide C. and Munger B. (1980), Zahm D. and Munger B. (1983a; 1983b; 1985), Farbman A. *et al.* (1985).
Mouse	Mattern C. and Paran N. (1974), Takeda M. (1976; 1977), Akisaka T. and Oda M. (1978), Takeda M. and Kitao K. (1980), Takeda M. *et al.* (1981; 1985; 1988; 1989), Kinnamon J. *et al.* (1985; 1988), Delay R. *et al.* (1986), Royer S. and Kinnamon J. (1988; 1994), Esses B. *et al.* (1988), Kudoh M. (1988), Murray R. (1993), Sekerkova G. *et al.* (2005).
Mud puppy	Farbman A. and Yonkers J. (1971), Cummings T. *et al.* (1987), Delay R. and Roper S. (1988), Delay R. *et al.* (1993).
Rabbit	Trujillo-Cenóz O. (1957), De Lorenzo (1958; 1960; 1963), Iriki T. (1960), Nemetschek-Gansler H. and Ferner H. (1964), Murray R. and Murray A. (1967), Scalzi H. (1967), Jeppsson P. (1969), Murray R. 1969; 1973; 1986), Murray R. *et al.* (1969), Iwayama T. (1970), Fujimoto S. and Murray R. (1970), Sangiacomo C. (1970), Nada O. and Hirata K. (1975), Jahnke K. and Baur P. (1979), Toyoshima K. and Tandler B. (1989), Royer S. and Kinnamon J. (1991; 1994).
Rat	Farbman A. (1965a; 1965b; 1967), Gray E. and Watkins K. (1965), Beidler L. (1969), Uga S. (1969), Takeda M. and Hoshino T. (1975), Akisaka T. and Oda M. (1977; 1978), Graziadei P. and Graziadei M. (1978), Akisaka T. (1980), Toyoshima K. and Shimamura A. (1982), Kobayashi T. and Tomita H. (1986), Endo Y. (1988), Finger T. *et al.* (1990), Montavon P. *et al.* (1996), Yoshie S. *et al.* (1996), Sbarbati A. *et al.* (1998a; 1998b), Sakai H. *et al.* (1999), Yang R. *et al.* (2000a; 2000b; 2004; 2007), Yee C. *et al.* (2001), Seta *et al.* (2003), Clapp T. *et al.* (2004), Ma *et al.* (2007).
Squirrel	Popov V. *et al.* (1999).

4.05.3 A Classic Taste Bud: The Rabbit Foliate Taste Bud

The first ultrastructural studies on rabbit taste buds were carried out by Engstrom H. and Rytzner C. (1956a; 1956b) on foliate taste buds. They observed that taste cells had varying morphologies and staining properties, but found it difficult to classify the cells into different types. Because there appeared to be a continuum of cellular morphologies, Engstrom and Rytzner postulated that the different cell types represented stages of development of a single cell line. Since then the rabbit has been used extensively for ultrastructural studies on taste buds, most notably by Raymond Murray and coworkers (Murray, A., 1961; Murray, R. and Murray, A., 1966; 1967; Murray, R., 1969; Murray, R. *et al.*, 1969; Murray, R. and Murray, A., 1970; Murray, R., 1971; Murray, R. and Murray, A., 1971; Murray, R., 1973; Murray, R., 1986; Murray, R., 1993). The foliate papillae of a rabbit reside on both sides of the posterior tongue and contain numerous taste buds. These taste buds are innervated by branches of the glossopharyngeal nerve (IXth cranial nerve) (Murray, R. and Murray, A., 1971) as shown in Figure 1. This contrasts with the innervation of foliate papillae of the rat, which are innervated by branches of both the glossopharyngeal nerve and the chorda tympani branch of the facial nerve (VIIth cranial nerve) (Whiteside, B., 1927; Oakley, B., 1967).

As stated above, Engstrom H. and Rytzner C. (1956a; 1956b) did not classify rabbit foliate taste cells into specific types, postulating that the differing cellular morphologies represented stages of development of a single cell type. Later investigators began to classify rabbit taste cells into different types. Trujillo-Cenóz O. (1957) referred to neuroepithelial cells while De Lorenzo A. (1958; 1960; 1963) described receptor and sustentacular cells in rabbit foliate taste buds. Iriki T. (1960) classified taste cells from rabbit foliate taste buds as either gustatory or sustentacular. Murray A. (1961) observed two morphological cell types but eschewed the terms gustatory or sustentacular, instead proposing that both morphological cells types were gustatory in nature. Scalzi H. (1967), like Engstrom and Rytzner, supported the notion that there was most likely a single taste cell line in rabbit foliate taste buds, with cells differentiating from one cell type to another. This was reflected in the system of taste cell classification proposed by Scalzi, which included pregustatory, type Ia, type Ib, and type Ic taste cells. Murray R. and Murray A. (1967) described dark and light cells in rabbit foliate papillae, based primarily on the electron density of the cytoplasm. At that time, the light cell was believed to be the most likely candidate for being the gustatory receptor cell, but the dark cell was not completely excluded. Jeppsson P. (1969) adopted the dark and light cell nomenclature of Murray. In 1969 Murray and coworkers modified their system of classification for rabbit taste bud cells to include dark cells, light cells and introduced a new cell type – the type III or sensory cell (Murray, R., 1969; Murray, R. *et al.*, 1969; Murray, R., 1971). In addition, they adopted the type IV or basal cell proposed by Farbman A. (1965a) for rat taste buds. Following the nomenclature proposed by Farbman A. (1965a), Murray and coworkers referred to dark cells as type I cells, and light cells as type II cells. Iwayama T. (1970) and Fujimoto S. and Murray R. (1970) each carried out separate degeneration/regeneration studies on rabbit foliate taste buds and reached antipodal conclusions. Whereas Iwayama concluded that there was a single cell line that differentiated from dark (type I) to intermediate to light (type II) cells, Fujimoto S. and Murray R. (1970) concluded that the different cell types arose from separate cell lines. The same year Sangiacomo C. (1970) described type I, type II, and neurosecretory cells in rabbit foliate taste buds. Today, most investigators have adopted the nomenclature of Farbman A. (1965a) and Murray and co-workers (type I, type II, type III, and type IV) for most mammalian taste buds (see Murray, R., 1973).

4.05.3.1 General Morphological Features of Rabbit Foliate Taste Buds

A longitudinal section through a rabbit foliate taste bud reveals a broad, onion-shaped structure that rests on the basal lamina (Figure 2). The taste bud extends from the basal lamina to the surface of the lingual epithelium (Figure 2). The lamina propria underlying the basal lamina contains connective tissue, vasculature, and nerve processes. Rabbit foliate taste buds range from 30 to 70 μm in width and 50–60 μm in height (Murray, R., 1973; Royer, S. and Kinnamon, J., 1991). The intragemmal taste cells (=cells located within the taste bud proper) display a range of morphologies. Most of the taste cell nuclei are located in the bottom half to two-thirds of the taste bud. Taste cells are joined together at their apices by

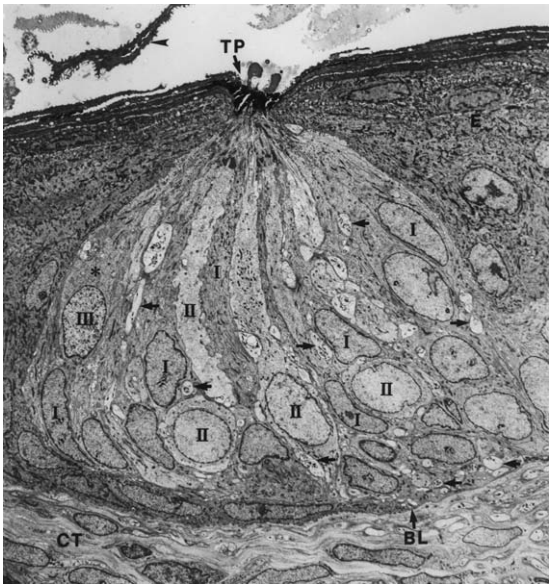

Figure 2 High-voltage electron micrograph (HVEM) of a longitudinal section through a rabbit foliate taste bud. The nucleus and part of the apical process (*) of a type III cell (III) appear at the left margin of this taste bud. Several nuclei and apical processes of type I and II cells are also present. Intragemmal nerve fibers are indicated by arrows. Two plumes of electron-dense pore substance extend above the taste pore (TP). Note the sloughing of the surface layer of the epithelium (E) at the upper left (arrowhead). BL, basal lamina; CT, connective tissue. ×2250. From Royer, S. and Kinnamon J. 1991. HVEM serial-section analysis of rabbit foliate taste buds: I. Type III cells and their synapses. J. Comp. Neurol. 306, 49–72.

tight junctions and by desmosomes elsewhere. Although there is considerable variability in cellular morphology within a taste bud, most taste cells are fusiform to spindle-shaped structures with centrally positioned nuclei. In favorable sections a few taste cells can be seen extending from the base of the taste bud to the taste pit, where apical microvilli from the taste cells project into a cavity below the epithelial surface. The taste pit opens into the oral cavity at the taste pore. The taste pore is typically filled with an electron-dense pore substance. It is not uncommon for foliate taste buds of the rabbit to possess multiple taste pores (Royer, S. and Kinnamon, J., 1991).

Prominent intercellular spaces have been described in taste buds (Nemetschek-Gansler, H. and Ferner, H., 1964; Baradi, A., 1965; Scalzi, H., 1967). Murray R. (1973) noted the high variability of intragemmal intercellular spaces and suggested these spaces were probably artifacts of specimen preparation. Our experience is similar; manipulation of the osmolarity of the fixative can alter the size and shape of intercellular spaces within taste buds. Nerve processes ramify throughout the basal two-thirds of the taste bud. Synapses can be seen from type III cells onto nerve processes (Figure 5). We have used the following criteria to identify synapses (Royer, S. and Kinnamon, J., 1991):

1. a thickening of the presynaptic membrane, with a 15–20 nm cleft separating the parallel membranes;
2. clustering of vesicles adjacent to the membrane thickening; and
3. the appearance of this configuration in at least two consecutive 0.25 μm-thick sections.

When compared with taste cells of rodents, rabbit foliate taste cells are more distinctive and easier to classify into cell types. We have not observed any intermediate or transitional cell types in rabbit foliate taste buds.

4.05.3.2 Primary Foliate Taste Bud Cell Types

4.05.3.2.1 Type I cells

Type I cells (previously termed, dark cells), are slender cells with moderately expanded nuclear regions (Figures 2 and 3). No synaptic connections associated with type I cells have been observed. The type I cell has been referred to as being sustentacular by most investigators, implying that this cell type does not perform a sensory function, although one may wonder about the function of the apical microvilli of these cells. Both basal and apical processes are present, with the apical process terminating in approximately 30–40 long, slender, microvilli varying in length from 1 to 2 μm (Murray, R., 1973). In cross section, the microvilli possess hexagonally arranged electron-dense filamentous material (Scalzi, H., 1967), which is most likely actin. Unlike other cell types, type I cells also possess finger- or sheet-like cytoplasmic processes that separate and envelop type II cells, type III cells, and intragemmal nerve fibers in a Schwann cell-like manner (Murray, R., 1973; Royer, S. and Kinnamon, J., 1994). These processes can best be seen in transverse sections (Figure 3).

The cytoplasmic ground substance of a type I cell varies from intensely electron-dense to electron-lucent. The apical cytoplasm also contains varying amounts of granular and/or smooth endoplasmic reticulum. Perhaps the most distinguishing ultrastructural feature of the type I cell is the presence of numerous

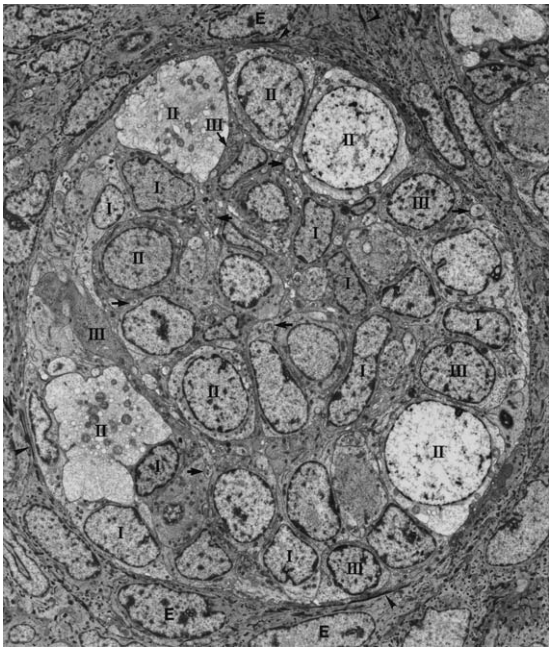

Figure 3 High-voltage electron micrograph (HVEM) of a transverse section through the nuclear region of a rabbit foliate taste bud. Cells of type I, type II, and type III are indicated. Several nerve fiber profiles are labeled with arrows. Note that the nuclei of three of the five type III cells in this taste bud lie along the right edge of the bud. The basal processes of the other two type III cells are located close to the left and top edges, respectively. One of these (at the center left) exhibits densely stained cytoplasm. The taste bud is surround by epithelial cells (E) containing numerous bundles of cytokeratin filaments (arrowheads). ×3900. From Royer, S. and Kinnamon J. 1991. HVEM serial-section analysis of rabbit foliate taste buds: I. Type III cells and their synapses. J. Comp. Neurol. 306, 49–72.

apical, electron-dense granules varying in size from 100 to 400 nm (Murray, R., 1973; Royer, S. and Kinnamon, J., 1994). The similarity of the contents of these granules to the pore substance found in the taste pore suggests that the pore substance is produced by the exocytosis of the apical granules in type I cells (Murray, R. and Murray, A., 1971).

The nuclei of type I cells are irregular in shape but generally are more slender when compared with the round-to-ovoid nuclei of type II cells. The nuclear matrix of a type I cell is considerably more electron-dense than the matrix of a type II or type III cell (Figure 3). Type I cell nuclei are more elongate than type II cell nuclei and contain patchy heterochromatin distributed throughout the nuclear matrix. Clumps of heterochromatin can also be seen adherent to the inner leaflet of the nuclear membrane.

4.05.3.2.2 Type II cells

Type II cells, previously termed, light cells, have a pronounced fusiform appearance, with a noticeably expanded nuclear region (Murray, R., 1973; Royer, S. and Kinnamon, J., 1994) (Figures 2 and 3). At low magnifications, type II cells are distinguished from type I and type III cells by the presence of large, round-to-ovoid nuclei in the type II cells. The nuclear matrix of a type II cell is more uniform in appearance, lacking much of the patchy heterochromatin present in the nuclei of type I cells.

The cytoplasmic ground substance of a type II cell is variable in appearance, but generally more electron-lucent than observed in a type I cell. Type II cells lack the enveloping, sheet-like cytoplasmic processes associated with type I cells, as well as the apical, dense granules characteristic of type I cells. The apical cytoplasm of type II cells often contains swollen or dilated cisternae of smooth endoplasmic reticulum and numerous mitochondria. The apical process of a type II cell terminates in several microvilli of generally uniform length, giving a brush-like appearance. In addition to conventional type II cells, we have observed a subset with large, round, lightly staining nuclei, and extremely electron-lucent, highly vesiculate cytoplasm, which we termed type II-VL (for very light) (Royer, S. and Kinnamon, J., 1994). These cells are primarily found at the periphery of the taste bud (e.g., Figure 3).

4.05.3.2.3 Type III cells

Early descriptions of cell types in rabbit foliate taste buds described only dark and light cells. A third cell type, termed the gustatory receptor, was described by Murray, R. *et al.*, in 1969. Type III cells are spindle-shaped with apical and basal processes and constitute approximately 5% of the cells within a rabbit foliate taste bud (5–15%: Murray, R. *et al.*, 1969; 5–7%: Royer, S. and Kinnamon, J., 1994). The type III cell is the only cell type in foliate taste buds of the rabbit that has been observed to form synaptic connections with nerve processes (Figures 4 and 5). Thus, the type III cell was considered to be the receptor cell (Murray, R., 1973). We found type III cells to be concentrated around the periphery of the taste bud (Figure 3; see also Figure 9: Royer, S. and Kinnamon, J., 1991). This contrasts with Murray's observation that type III cells are centrally placed (Murray, R., 1971). The apical region of the type III cell terminates in a single, blunt microvillus approximately 0.5–0.6 μm in diameter at its base and up to 4–5 μm in length (Royer, S. and Kinnamon, J., 1994). This contrasts

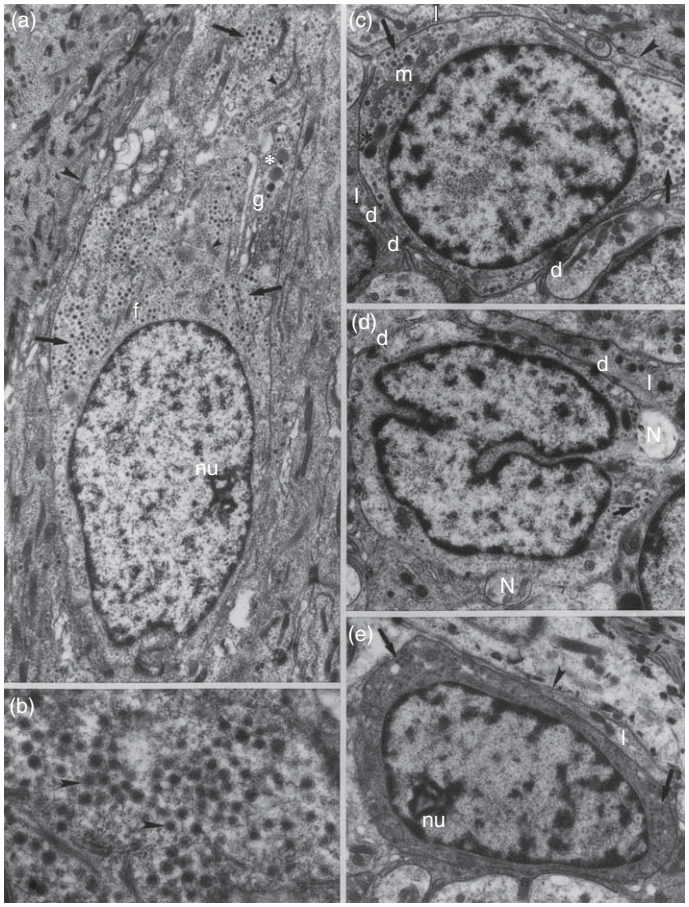

Figure 4 (a) Longitudinal section through the nucleus and apical process of a type III cell (also shown in Figure 2). The cytoplasm of the apical process contains abundant dense-cored vesicles (arrows), Golgi complex (g), lysosome-like dense bodies (*), granular endoplasmic reticulum (small arrowheads), and filaments (f). Nucleolus (nu). The margin of the taste bud indicated by the large arrowhead (cf. Figure 2). ×9600. (b) Higher magnification view of dense-cored vesicles located in the apical process of the type III cell shown in Figures 2 and a. The electron-lucent halo around the dense core is apparent in some of the vesicles (arrowhead). ×28 500. (c) Transverse section through the perikaryal region of a type III cell. A thin type I cell process (l) separates this cell from the border of the taste bud (arrowhead). The cytoplasm of the type III cell contains numerous dense-cored vesicles (arrows), several mitochondria (m), and a dense lysosome-like body (*). Desmosomes (d) attach the type III cell to adjacent type I cells. ×12 700. (d) Transverse section through the parikaryal region of a type III cell. The nuclear membrane displays two deep invaginations. Nerve fibers (N), desmosomes (d). ×11 300. (e) Transverse section through the perikaryal region of a type III cell located at the margin of a taste bud (arrowhead) and separated from surrounding cells by a thin type I cell process. Although the cytoplasm of this cell is quite electron-dense, groups of dense-cored vesicle can still be distinguished (arrows). ×13 100. From Royer, S. and Kinnamon J. 1991. HVEM serial-section analysis of rabbit foliate taste buds: I. Type III cells and their synapses. J. Comp. Neurol. 306, 49–72.

with the multiple microvilli at the apices of both type I and type II cells. In the upper third of the taste bud, type III cells are often separated from other cells by the cytoplasmic processes of type I cells, but may contact each other in the basal region. As with other taste cells, type III cells are joined to adjacent cells by desmosomes. Radiating from the desmosomes are numerous intermediate filaments that project into the cytoplasm.

The cytoplasm of a type III cell is variable, but usually moderately electron-dense (Royer, S. and Kinnamon, J., 1994). Scattered throughout the cytoplasm are mitochondria, granular and smooth endoplasmic reticulum, free ribosomes, and polyribosomes. The cytoplasmic ground substance of a small subset of type III cells is significantly more electron-dense (e.g., Figures 3 and 4). These cells have been termed dark type III cells (Murray R.,

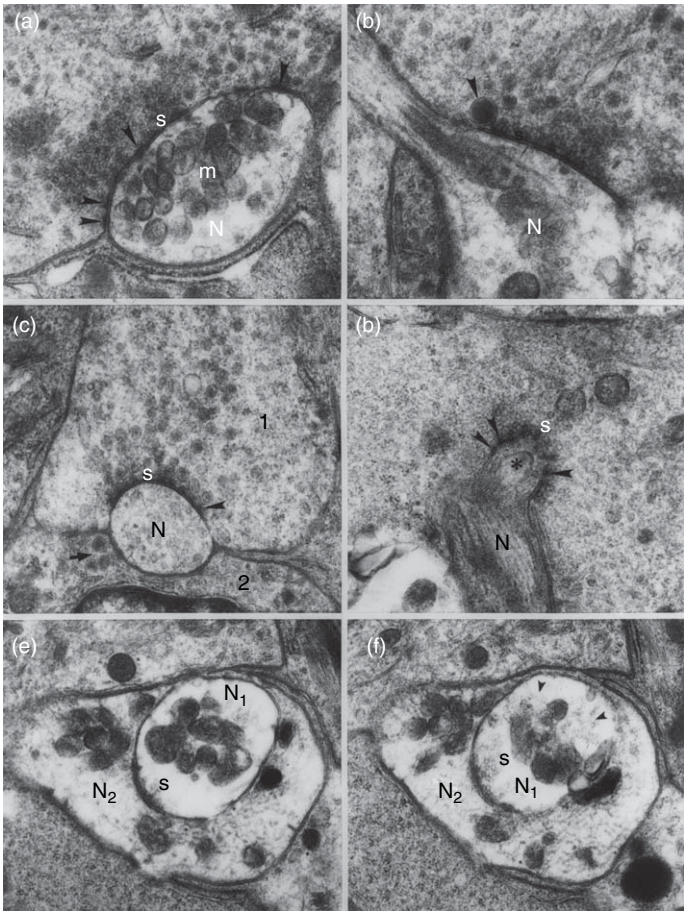

Figure 5 (a) Synapse (s) between a type III cell and a nerve process (N). Note the dense cloud of small, clear-cored vesicles as well as several large, dense-cored vesicles at the presynaptic site and presynaptic dense projections (arrowheads). The nerve fiber contains numerous mitochondria (m). ×36 900. (b) Synapse (s) from a type III cell onto an enlarged nerve process (N). Note the synaptic cleft and the very large dense-cored vesicle (arrowhead) adjacent to the synapse. ×44 600. (c) A small nerve fiber (N) lying between two adjacent type III cells (1 and 2) is postsynaptic to one of these cells (cell 1). Numerous dense-cored vesicles and presynaptic dense projections (arrowhead) are evident. The arrow points to a small group of dense-cored vesicles in cell 2 near its contact with the nerve fiber. ×29 900. (d) Synapse (s) from a type III cell onto a finger-like projection (*) of a nerve fiber (N). Presynaptic dense projections are indicated by arrowheads. ×37 900. (e, f) An axoaxonal synapse (s) between two nerve fibers. N_1 is presynaptic to N_2 and contains a cluster of clear vesicles adjacent to the presynaptic membrane. Dense material adheres to the postsynaptic membrane in N_2. Arrowheads in F indicate groups of clear vesicles in N_1. (e) ×32 600. (f) ×29 000. From Royer, S. and Kinnamon J. 1991. HVEM serial-section analysis of rabbit foliate taste buds: I. Type III cells and their synapses. J. Comp. Neurol. 306, 49–72.

and Murray, A., 1971). Murray R. (1986) speculated that dark type III cells might be developing or degenerating type III cells. A distinguishing feature of the type III cell is the presence of large, dense-cored vesicles (80–140 nm) with prominent electron-lucent halos (Figure 4). These vesicles are especially numerous in the cytoplasm surrounding the nucleus. These vesicles are distributed throughout the cytoplasm and should not be confused with the small, clear vesicles (40–60 nm) located at the presynaptic regions (see below).

The nuclei of type III cells are situated in the lower half of the taste bud. These nuclei are intermediate in appearance between the nuclei of type I and type II cells (Figures 2 and 3). Type III cell nuclei are ovoid to round in cross section, similar to type II cell nuclei, but elongate in longitudinal section like type I cell nuclei. The density of the nuclear matrix of a type III cell is intermediate between that of a type I and a type II cell. Like type I cells, the nuclei of type III cells possess prominent nuclear invaginations (Figures 3 and 4). Another similarity

between the nuclei of type III cells and type I cells is the presence of clumps of heterochromatin scattered throughout the nuclear matrix, some of which are adherent to the nuclear membrane.

4.05.3.2.4 Synaptic connections

Type III cells are the only cells that have been observed to form synapses with intragemmal nerve fibers (Murray, R. and Murray, A., 1970; 1971; Murray, R., 1971; 1973; Royer, S. and Kinnamon, J., 1991; 1994). It is curious that both type I and type II cells possess apical microvilli – putative sites for sensory transduction – yet neither cell type forms conventional chemical synapses with nerve processes. We found that some type III cells had divergent synaptic connections with synapses from a single type III cell onto a maximum of six nerve processes. Convergence of input from two to three type III cells onto a single nerve process was also a common observation. Most synapses are located on the basolateral region of the type III cell. These synapses are usually asymmetrical with electron-dense presynaptic thickenings, often including presynaptic dense projections (Figure 5). Type III cell synapses in rabbit foliate taste buds are especially well developed when compared with synapses in taste buds of rodents. Round, clear vesicles (40–60 nm) of varying numbers are associated with the presynaptic active zone (Royer, S. and Kinnamon, J., 1991; 1994). Dense-cored vesicles can also be present at these synapses. In some instances, only a few dense-cored vesicles are interspersed among the clear vesicles. At other synapses dense-cored vesicles are the predominant vesicle type. Thus, there may be more than one type of synapse associated with type III cells, as well as more than one neurotransmitter/neuromodulator. On rare occasions we have observed neuroneuronal synapses in taste buds (e.g., Figures 5(e) and 5(f)).

4.05.4 Rodent Taste Buds

4.05.4.1 Innervation

Lingual taste buds in rodents are innervated by branches of the facial (VII cranial) and glossopharyngeal (IX cranial) nerves (Whiteside, B., 1927; Oakley, B., 1967; Beidler, L., 1969; Farbman, A. and Hellekant, G., 1978; Bradley, R. 1971; Whitehead, M. *et al*., 1985) (Figure 1). Fungiform and anterior foliate taste buds of rodents are innervated by the chorda tympani branch of the VII cranial nerve. This differs from innervation of rabbit foliate taste buds, which are innervated only by the glossopharyngeal (IX) nerve. Taste buds in the vallate and posterior foliate papillae of rodents are innervated by the fibers of the lingual–tonsillar branch of the glossopharyngeal cranial nerve (IX) (Whiteside, B., 1927; Oakley, B., 1967).

4.05.4.2 General Morphological Features

Recent evidence indicates that taste cells in rodents are epithelial in origin (Stone, L. and Finger, T., 1994; Stone, L. *et al*., 1995). The classic study on taste cell turnover in the rat was carried out by Beidler L. and Smallman R. (1965), who found that taste cells were replaced approximately every 10 days to 2 weeks. Rodent taste buds are onion-shaped structures with spindle-shaped cells that span the entire length of the taste bud from the basal lamina up to the taste pore. Taste cell nuclei are usually located in the lower third of the taste bud. Based on their staining characteristics and ultrastructural features, taste cells are currently classified into type I (dark), II (light), type III, and type IV (basal) cells. The type I, type II, and type III cells extend their microvilli into the taste pore (Figure 7). The structural features of the microvilli are distinctive for each of the taste cell types (Figure 7). Electron-dense pore substance is present in the taste pore, although its function is unclear. Basal cells are found near the base of the bud, but these cells lack apical processes. Nerve fibers are abundant in the connective tissue underlying the taste buds and penetrate the taste bud at its base and course throughout the bud. Most nerve fibers terminate in the lower half of the taste bud, where they may receive synaptic contacts from taste cells.

4.05.4.3 Primary Taste Bud Cell Types

Farbman A. (1965a) introduced the nomenclature type I and type II taste cells and classified taste cells in rat taste buds into four types: peripheral, basal (type IV), type I (dark), and type II (light) cells (Figure 8). The type III cell was first described in the rat by Takeda M. and Hoshino T. (1975) and in circumvallate taste buds of the mouse by Takeda M. (1976). Type III cells were considered to be sensory cells because they were the only cell type forming synaptic contacts onto nerve processes in rodent taste buds (Takeda, M. and Hoshino, T., 1975; Takeda, M., 1976). Using ultrastructural criteria, we classified taste cells in mouse circumvallate taste buds into

dark cells (type I), intermediate cells, light cells (type II), basal cells, and undifferentiated peripheral cells (Scalzi, H. 1967; Iwayama, T., 1970; Kinnamon, J. *et al.*, 1985; Delay, R. *et al.*, 1986; Kinnamon, J. *et al.*, 1988). Dark cells, intermediate cells, and light cells all appeared to form synaptic contacts with nerve processes (Kinnamon, J. *et al.*, 1985; 1988). Recent studies using immunofluorescence and immunoelectron microscopy with antisera markers for different taste cell types indicate that cells originally classified as intermediate cells in mouse circumvallate taste buds should properly be classified as type III cells (Yang, R. *et al.*, 2000a; Yee, C. *et al.*, 2001; Clapp, T. *et al.*, 2004; Yang, R. *et al.*, 2004). Thus, type III cells in rat circumvallate taste buds are believed to be the only cell type that forms classical synapses onto nerve processes (Yang, R. *et al.*, 2000b; Yee, C. *et al.*, 2001; Yang, R. *et al.*, 2004). Type II cells do not form classical synapses with nerve fibers. Instead, at the points of contact with nerve fibers, type II cells exhibit SSCs of smooth endoplasmic reticulum (Royer, S. and Kinnamon, J., 1988; Clapp, T. *et al.*, 2004), that suggest a functional contact with nerve processes.

4.05.4.3.1 Type I cells

Farbman A. (1965a) built upon the dark cell and light cell nomenclature of Murray and coworkers, referring to dark cells as type I cells and light cells as type II cells. Type I cells (Figures 6 and 8), are the most numerous taste cells (50–60%), usually located peripherally in the taste bud (Farbman, A. 1965a; Murray, R., 1973; Kinnamon, J. *et al.*, 1985; Delay, R. *et al.*, 1986). These cells are slender with electron-dense cytoplasm and elongate, electron-dense nuclei with, prominent, distinguishing nuclear invaginations. These cells span the entire length of the taste bud from the basal lamina to the taste pore (Figure 6). The apical end of a type I cell terminates in several long and slender microvilli (Figure 7). Perhaps the most distinguishing feature of type I cells involves the numerous dense-cored granules (100–400 nm in diameter) located in the apical cytoplasm (Figures 7 and 8). These dense-cored granules, which are conspicuously absent in type II cells, are present in the apical cytoplasm of type I cells in both mouse and rat foliate and circumvallate taste buds. This is not the case, however, with fungiform taste buds. Several investigators have reported that the apical cytoplasm of type I cells in fungiform taste buds lacks the dense-cored granules (Farbman, A. 1965a; Murray, R., 1973; Kinnamon, J. *et al.*, 1988; Royer, S. and Kinnamon, J., 1991; Kinnamon, J. *et al.*, 1993; Reutter, K. and Witt, M., 1993; Miller, I., 1995). Other investigators have observed dense-cored granules in the type I cells of rat fungiform taste buds, but those granules were rod-shaped, only moderately electron-dense, and few in number. This contrasts with the circular, electron-dense apical vesicles observed in type I cells of circumvallate taste buds (Takeda, M. and Hoshino, T., 1975). These apical granules are believed to be secretory precursors of the dense substance in the taste pore (Murray, R. and Murray, A., 1967; Scalzi, H., 1967). The function of the dense pore substance is unknown, however, it may play an important role in facilitating and modifying the response of taste receptor cells to sapid stimuli (Murray, R. and Murray, A., 1970). Type I cells have irregular cytoplasmic processes that surround type II or type III taste cells. Thus, type I cells may function like

Figure 6 Longitudinal section through a taste bud from a rat circumvallate papilla. A type I cell (I) or dark cell contains electron-dense cytoplasm and a slender nucleus. Dense-cored granules (arrows) are present in the apical cytoplasm. A type II (II) or light cell has a large, circular nucleus and an electron-lucent cytoplasm. Taste pore (TP); nerve process (arrow); epithelium (E). ×4500. Adapted from Yang, R., Crowley, H., Rock, M. and Kinnamon, J. 2000a. Taste cells with synapses in rat circumvallate papillae display SNAP-25-like immunoreactivity. J. Comp. Neurol. 424, 205–215.

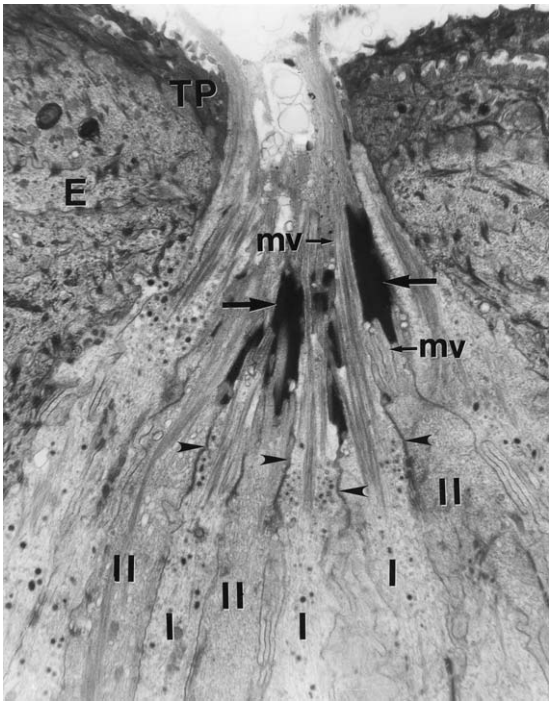

Figure 7 Longitudinal section through the taste pore region from a rat circumvallate taste bud. type I cells (I) are characterized by the presence of apical dense-cored granules (arrowheads) and several long, slender microvilli, whereas the apical microvilli of the type II cells (II) are brush-like, i.e., short and uniform in length. The most distinguishing ultrastructural feature of the type III cell (III) is the presence of a single, large, blunt microvillus that extends onto taste pore. The taste cells are joined by tight junctions (arrowheads). Microvilli (MV); pore substance (arrows); taste pore (TP); nongustatory epithelium (E). ×21 000.

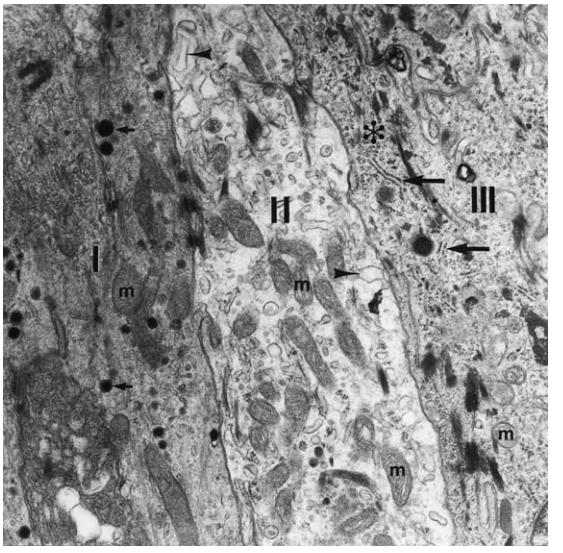

Figure 8 Longitudinal section showing the apical cytoplasm of three taste cells (I, II, and III) from a mouse taste bud. The electron-dense cytoplasm of the type I cell (I) contains numerous dense-cored granules (small arrows). The cytoplasm of the type I cell is rich in filaments and contains mitochondria and free ribosomes. The cytoplasm of the type II cell (II) is electron-lucent with numerous mitochondria (m) and swollen cisternae of agranular endoplasmic reticulum (arrowheads). Type III cells (III) exhibit electron density intermediate between that of type I (I) and type II (II) cells. The cytoplasm of type III cells contains numerous free ribosomes and rough endoplasmic reticulum. ×35 000.

glial cells in terms of isolation and nutrition (Reutter, K. and Witt, M., 1993; Pumplin, D. *et al.*, 1997). Although type I cells possess apical microvilli and are in direct contact with nerve processes, no synaptic contacts are believed to be present between type I cells and nerve processes (Farbman, A., 1965a; Murray, R., 1973; Reutter, K. and Witt, M., 1993). Although early studies suggested that type I cells might function as sensory receptors, it is generally accepted that they are restricted to a supportive or sustentacular role (Murray, R. and Murray, A., 1971; Murray, R., 1986; Lindemann, B., 1996; Lawton, D. *et al.*, 2000; Bartel, D. *et al.*, 2006).

The dark appearance of type I cell cytoplasm (Figure 8) results from an electron-dense ground substance, close packing of free ribosomes and polyribosomes, scattered cisternae of rough endoplasmic reticulum, and bundles of filamentous material surrounding the nucleus. The cytoplasm of type I cells also contains numerous mitochondria with densely staining matrices and lamellar cristae. These mitochondria are rod-shaped or elongate and randomly distributed throughout the cytoplasm. The Golgi bodies of type I cells typically consist of stacks of flattened cisternae, which are expanded only at their edges (Kinnamon, J. *et al.*, 1988).

The nuclei of type I cells are variable in profile. Compared with type II taste cells, the nuclei of type I cells are small, irregular, and electron-dense (Figure 6) (Kinnamon, J. *et al.*, 1985). The nuclei often contain one or more poorly defined nucleoli or aggregations of heterochromatin adhering to the inner leaflet of nuclear membrane (Kinnamon, J. *et al.*, 1988). The invaginations of type I cell nuclei are smaller than the deep prominent invaginations of type III cell nuclei.

4.05.4.3.2 Type II cells

The type II cell, initially termed light cell, constitutes approximately 15–30% of the cells in a taste bud

(Farbman, A., 1965a; Murray, R., 1973; Kinnamon, J. *et al.*, 1985; Delay, R. *et al.*, 1986) (Figures 6 and 8). Most type II cells extend the entire length of the taste bud from the basal lamina to the taste pore. A small subset of these cells, however, are located in the upper third of the taste bud and possess no apparent basal processes. These cells have a triangular profile in longitudinal sections. A typical type II cell possesses an electron-lucent cytoplasm and large circular or ovoid nuclei (Farbman, A., 1965a; Murray, R., 1973; Kinnamon, J. *et al.*, 1985; Delay, R. *et al.*, 1986; Kinnamon, J. *et al.*, 1988; Royer, S. and Kinnamon, J., 1988; Royer, S. and Kinnamon, J., 1991; Kinnamon, J. *et al.*, 1993; Royer, S. and Kinnamon, J., 1994; Pumplin, D. *et al.*, 1997). In contrast with the type I cell, the apical portion of a type II cell is wider than the type I cell and lacks the apical dense granules characteristic of the type I cells. The apical microvilli of a type II cell are numerous, short, and uniform in length, giving a brush-like appearance (Figure 7). Type II cells lack classical chemical synapses with nerve processes (Farbman, A., 1965a; Murray, R., 1973; Yee, C. *et al.*, 2001; Yang, R. *et al.*, 2004). However, other type II cell–nerve process contacts, such as SSCs of smooth endoplasmic reticulum and atypical mitochondria have been found at close appositions between taste cells and nerve processes (Farbman, A. 1965a; Fujimoto, S. and Murray, R., 1970; Murray, R., 1971; Takeda, M., 1976; Ide, C. and Munger, B., 1980; Royer, S. and. Kinnamon, J., 1988). Results from our laboratory suggest that SSCs are found exclusively at close appositions between type II cells and nerve processes in rat circumvallate taste buds (Clapp, T. *et al.*, 2004).

The cytoplasm of a type II cell contains an abundance of mitochondria, vesicles, and vacuoles (Farbman, A., 1965a) (Figure 6). The supranuclear region of a type II cell is rich in microchrondia, and more apically, the cytoplasm is replete with swollen vesicles of agranular endoplasmic reticulum. The cytoplasm also contains rough endoplasmic reticulum, free ribosmes, and intermediate filaments.

The nuclei of type II cells are large with a round-to-ovoid profiles. These nuclei are generally electron-lucent with a homogeneous nuclear matrix containing one to a few nucleoli (Kinnamon, J. *et al.*, 1985; Delay, R. *et al.*, 1986; Kinnamon, J. *et al.*, 1988; Reutter, K. and Witt, M., 1993) (Figure 6). In contrast with type I cell nuclei, the nuclei of type II cells generally lack invaginations and have fewer aggregations of heterochromatin and electron-dense material.

4.05.4.3.3 Type III cells

Type III cells (Figure 8) were first described in the foliate papillae of rabbits (Murray, R., 1973), but this cell type is present in other species as well, including the mouse (Takeda, M., 1976; 1977; Takeda, M. and Kitao, K., 1980; Takeda, M. *et al.*, 1981), rat (Takeda, M. and Hoshino, T., 1975; Yee, C. *et al.*, 2001; Yang, R. *et al.*, 2004), monkey (Farbman, A. *et al.*, 1985), and guinea-pig (Yoshie, S. *et al.*, 1990). Type III cells represent of the smallest proportion (5–15%) of taste cells in taste buds (Delay, R. *et al.*, 1986; Reutter, K. and Witt, M., 1993; Kinnamon, 1997). Type III cells are slender cells with a moderately electron-lucent cytoplasm. These cells span the entire length of taste buds from basal lamina to taste pore with a cytoplasm containing numerous ribosomes and cisternae of granular endoplasmic reticulum (Takeda, M. and Hoshino, T., 1975; Kinnamon, J. *et al.*, 1985; 1988; Reutter, K. and Witt, M., 1993; Kinnamon, J. 1987). The nuclei are intermediate in appearance between the nuclei of type I and type II cells (Takeda, M. and Hoshino, T., 1975; Yang, R. *et al.*, 2004; 2007). Type III cells in the mouse and rat taste buds lack the large dense-cored vesicles seen in the nuclear region of the cytoplasm of type III cells in rabbit foliate taste buds. The primary distinguishing features of type III cells in mouse and rat taste buds are as follows:

1. an elongate nucleus with large prominent invaginations;
2. a single, large, blunt microvillus that extends into the taste pore;
3. synapses onto nerve processes (Takeda, M. and Hoshino, T., 1975; Takeda, M., 1976; Royer, S. and Kinnamon, J., 1991); and
4. dense-cored vesicles (90–120 nm in diameter) and numerous clear vesicles (40–70 nm in diameter) are present at presynaptic sites (Kinnamon J. *et al.*, 1985; 1988; Yang, R. *et al.*, 2000a; 2004; 2007) (Figures 7, 9, and 10).

4.05.4.3.4 Type IV cells (basal cells)

Type IV cells lie in the basolateral region of taste buds. These cells are small, irregular, and similar to peripheral cells in morphology. but do not exend apical processes to the taste pore (Farbman, A., 1965a; 1965b; Reutter, K. and Witt, M., 1993). The most distinguishing feature of basal cells is the presence of intermediate filaments attached to the nuclear envelope (Delay, R. *et al.*, 1986). These cells

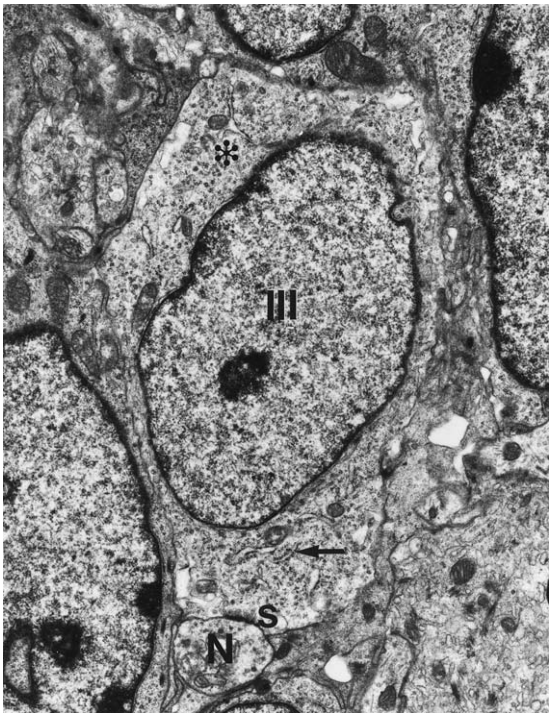

Figure 9 A low-magnification micrograph showing a mouse circumvallate type III taste cell (III) with a synapse (S) onto a nerve process. The cytoplasm of the taste cell contains numerous polyribosomes ribosomes (asterisk) and rough endoplasmic reticulum (arrow). The nucleus contains a small invagination and a prominent nucleolus. A group of small, clear synaptic vesicles are aggregated at the active zone of the synapse. The postsynaptic element, a nerve process (N) contains several mitochondria. ×15 000. Adapted from Kinnamon, J., Taylor, B., Delay, R. and Roper, S. 1985. Ultrastructure of mouse vallate taste buds. I. Taste cells and their associated synapses. J. Comp. Neurol. 235, 48–60.

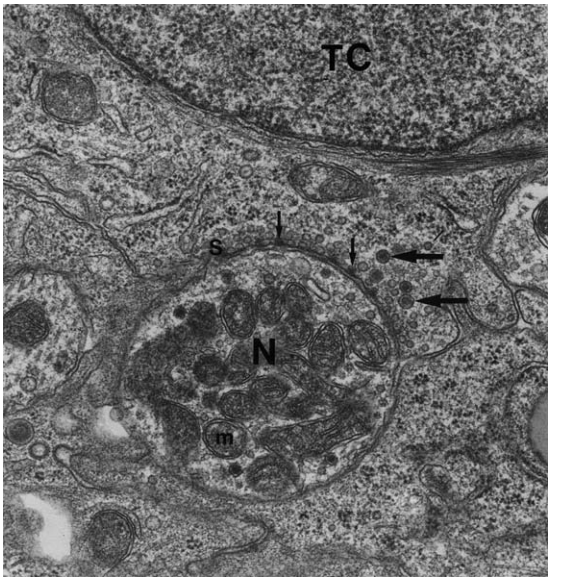

Figure 10 High magnification micrograph showing a macular synapse (S) from a mouse circumvallate taste cell (TC) onto a nerve process (N). Several small clear synaptic vesicles (40–70 nm) and a few large dense-cored vesicles (90–120 nm) (large arrows) are present at the presynaptic zone. Presynaptic dense projections (small arrows) can be seen at the synapse. The nerve process is replete with mitochondria (m), dense-cored vesicles and small clear vesicles. ×38 000. Adapted from Kinnamon, J., Sherman, T. and Roper, S. 1988. Ultrastructure of mouse vallate taste buds: III. Patterns of synaptic connectivity. J. Comp. Neurol. 270, 48–60.

are considered to be the precursor cells for other taste cell types in taste buds (Beidler, L. and Smallman, R., 1965; Conger, A. and Wells, M., 1969, Farbman, A., 1980, Stone *et al.*, 2002).

4.05.4.4 Taste Cell Synapses

De Lorenzo A. (1960) suggested that nerve fibers are in continual state of flux, forming synapses with new taste cells and retracting synapses from dying taste cells. Ultrastructural correlates of synapses in taste buds were first observed five decades ago (De Lorenzo, A. 1960; 1963; Gray, E. and Watkins, K., 1965; Hirata, Y., 1966), although Trujillo-Cenóz (1961) described contacts between taste cells and nerve fibers in catfish barbels. The presence or absence of synapses often has been used as a criterion for sensory function in taste cells (Hirata, Y., 1966; Uga, S. and Hama, K., 1967; Murray, R., 1969; 1973; Takeda, M. and Hoshino, T., 1975; Takeda, M., 1976; Ide, C. and Munger, B., 1980; Zahm, D. and Munger, B., 1983a; 1983b; Kinnamon, J. *et al.*, 1985; 1988; 1993). Most investigators now consider the type III cell to be the chemoreceptor cell. In the mouse approximately 20% of the taste cells have synapses onto nerve processes in circumvallate taste buds (Kinnamon, J. *et al.*, 1985). Synapses in fungiform taste buds are fewer, but contain more vesicles than synapses in either circumvallate or foliate taste buds (Kinnamon, J. *et al.*, 1993). Virtually, all synapses in mammalian taste buds are from taste cells onto nerve fibers (Murray, R. and Murray, A., 1967; Scalzi, H., 1967; Beidler, L., 1969; Murray, R., 1969; Takeda, M. and Hoshino, T., 1975; Takeda, M., 1976; Miller, R. and Chaudhry, A., 1976; Takeda, M. *et al.*, 1981; Kinnamon, J. *et al.*, 1985; 1988; Royer, S. and Kinnamon, J., 1988; Kinnamon, J. *et al.*, 1993; Yang, R. *et al.*, 2000a; Yee, C. *et al.*, 2001; Yang, R. *et al.*, 2004). Taste cell synapses are generally located near the

nuclear region of the presynaptic taste cell (Figure 9). The synaptic structure varies from macular to finger-like (Kinnamon, J. *et al.*, 1985; Yang, R. *et al.*, 2000a; 2004). The macular synapses are punctate and usually flat (Figure 10). A typical finger-like synapse, however, consists of a process from a postsynaptic nerve fiber protruding into an invagination of the presynaptic taste cell (Kinnamon, J. *et al.*, 1985). Synapses between intragemmal nerve processes are commonly observed during taste bud development (Kinnamon, J. *et al.*, 2005), but only rarely in taste buds of adult animals (however, see Graziadei, P. 1969; Royer, S. and Kinnamon, J., 1988; 1994). The function of neuroneuronal synapses in taste buds is not well understood.

4.05.4.5 Putative Nonsynaptic Connections

It is generally accepted that type II cells are important in the transduction of bitter, sweet, and umami taste, yet these cells do not form synapses onto nerve fibers. Other specialized contacts between taste cells and nerve processes have been observed that may be part of the transduction pathway, including SSCs of smooth endoplasmic reticulum and atypical mitochondria (Figures 11–13).

4.05.4.5.1 Subsurface cisternae of smooth endoplasmic reticulum

SSCs are narrow sacs of agranular endoplasmic reticulum that lie adjacent to the cytoplasmic leaflet of taste cell membranes at sites of close apposition with nerve processes (Figure 11) (Royer, S. and Kinnamon, J., 1988). The outer membranes of the cisternae are separated from the inner leaflet of the taste cell membrane by a narrow gap averaging 15 nm in width. The close apposition between the cisternae and cell membrane may extend for a distance up to 2–3 μm (Figure 11). SSCs have been reported in rat fungiform taste buds (Farbman, A., 1965a), rabbit foliate taste buds (Fujimoto, S. and Murray, R., 1970; Murray, R., 1971), mouse vallate and foliate (Takeda, M., 1976; Royer, S. and Kinnamon, J., 1988), and monkey laryngeal taste buds (Ide, C. and Munger, B., 1980). SSCs have been found at the close appositions between the plasma membrane of type II taste cells and nerve processes (Clapp, T. *et al.*, 2004). Although the function of SSCs is unclear, we speculate that the type II cells may communicate to the nerve processes via SSCs (Romanov, R. *et al.*, 2007).

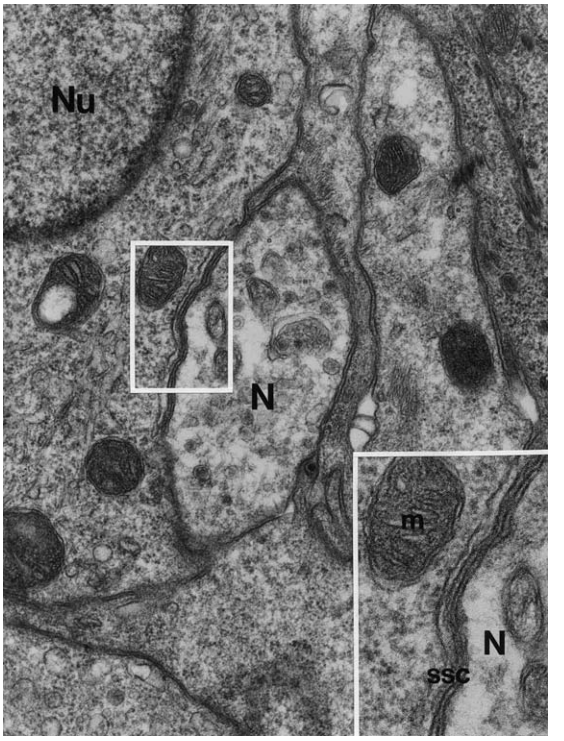

Figure 11 Electron micrograph showing a subsurface cisterna in close apposition to the junction of a taste cell (TC) with a nerve process (N). ×40 000. Inset: High magnification of the subsurface cisterna as it abuts the taste cell membrane. ×90 000. Adapted from Royer, S. and Kinnamon, J. 1988. Ultrastructure of mouse foliate taste buds: synaptic and nonsynaptic interactions between taste cells and nerve fibers. J. Comp. Neurol. 270, 11–24.

4.05.4.5.2 Atypical mitochondria

Most mitochondria in taste cells are elongate, slender structures with lamellar cristae rarely exceeding 0.3 μm in diameter (Royer, S. and Kinnamon, J., 1988) (Figure 12). At sites of close apposition between taste cells and nerve fibers, we occasionally observe unusually large, atypical microchondria (Figure 12). These atypical mitochondria are found only at the close appositions with nerve processes. The atypical mitochondria that we have observed have diameters two to three times larger and do not possess the lamellar or baffle cristae of conventional mitochondria. The cristae of the atypical mitochondria exhibit a twisted-energized or swollen twisted-energized configuration (Figure 12) (Korman, E. *et al.*, 1970; Williams, C. *et al.* 1970), presenting the impression of electron-dense sacs or tubules within the mitochondrion. The outer membranes of the mitochondria are separated from the taste cell membrane by a gap of approximately 20 nm. In favorable

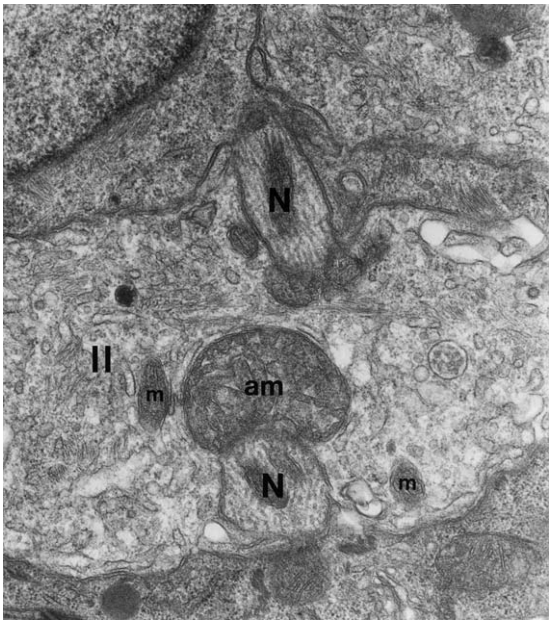

Figure 12 An atypical mitochondrion (AM) between a type II cell (II) and two nerve processes (N). The AM has a diameter two to three times larger than conventional mitochondria. The cristae of the atypical mitochondria exhibit a twisted-energized or swollen twisted-energized configuration. ×30 000. Adapted from Royer, S. and Kinnamon, J. 1988. Ultrastructure of mouse foliate taste buds: synaptic and nonsynaptic interactions between taste cells and nerve fibers. J. Comp. Neurol. 270, 11–24.

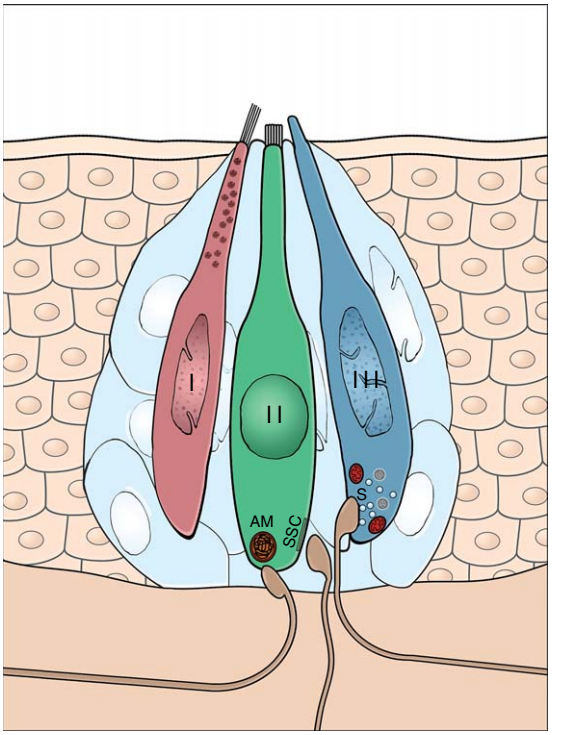

Figure 13 Diagram of a rat circumvallate taste bud showing a type I cell (I), a type II cell (II), and a type III cell (III). The type I cell has an electron-dense cytoplasm and a slender, elongate nucleus with invaginations and clumpy heterochromatin. The apical region of the type I cell contains dense granules and several long, slender microvilli. The type II cell is spindle-shaped with an electron-lucent cytoplasm. The nucleus of a type II cell is round to ovoid with a homogeneous nuclear matrix containing little heterochromatin. Subsurface cisternae (SSC) of smooth endoplasmic reticulum or atypical mitochondria (AM) are sometimes present at junctions with nerve processes. The apical cytoplasm of a type I cell often contains swollen cisternae of smooth endoplasmic reticulum. Several short, apical microvilli of uniform length give a brush-like appearance. The type III cell is slender with cytoplasm that is intermediate in electron density between a type I and type II cell. The slender nucleus contains patchy heterochromatin and pronounced invaginations. A single large, blunt, apical microvillus extends into the taste pore. Type III cells form synapses onto nerve processes. The presynaptic region of the type III cell contains numerous small, clear vesicles and a few large, dense-cored vesicles.

profiles, an electron-dense, wispy material can be seen connecting the mitochondrion to the inner leaflet of the taste cell plasma membrane. Because of their large size, the atypical mitochondria at taste cell–nerve fiber contacts would seem to be significant energy reservoirs and as such would be ready sources of ATP (Royer, S. and Kinnamon, J., 1988; Romanov, R. *et al.*, 2007). This is supported by recent results which demonstrate the importance of ATP as a neurotransmitter in taste buds (Finger, T., 2005).

4.05.5 Concluding Remarks

There is general agreement concerning the ultrastructure of circumvallate taste buds of rodents (Figure 13). The three most significant cell types are type I, type II, and type III cells. Features of type I (dark) cells: (1) slender cells with electron-dense cytoplasm, (2) elongate, electron-dense nuclei with prominent invaginations, (3) dense granules in the apical cytoplasm, and (4) several, long, slender microvilli projecting into the taste pore. Type I (dark) cells are believed to perform a glial function and to isolate other taste cells, but are not thought to be receptor cells. Features of type II (light) cells: (1) these cells are spindle-shaped with an expanded nuclear region and an electron-lucent cytoplasm, (2) type II cell have round-to-ovoid nuclei with a homogeneous, electron-lucent nuclear matrix,

(3) there are several short, apical microvilli of the same length, giving a brush-like appearance, and (4) recent electrophysiological and molecular biological studies indicate that type II cells are chemoreceptors. Although type II cells lack classical chemical synapses, they do possess specialized junctions with nerve processes involving SSCs of smooth endoplasmic reticulum or large, atypical mitochondria. Features of type III cells: (1) type III cells are slender and possess a moderately electron-lucent cytoplasm, (2) the nuclei are slender and contain prominent nuclear invaginations, (3) there is a single, blunt apical microvillus, and (4) type III cells have classical chemical synapses onto nerve processes with small, clear vesicles and large, dense-cored vesicles.

Our understanding of taste bud structure and function has increased greatly over the past 20 years. Knowledge of the ultrastructural features of a taste bud helps to understand the structural basis for taste function, but is not an explanation of taste cell function. Previously, investigators have made well-meaning attempts to infer taste cell function based solely on structural features. Several new approaches now make it possible to elucidate the function of taste cells and correlate this information with the structural features of taste cells. Immunohistochemistry and immunoelectron microscopy using markers for taste cells types and transduction pathways have provided significant indirect data that have enhanced our understanding of taste cell function. The use of the patch clamp recording technique has made it possible to characterize the electrophysiological properties of individual taste cells. Molecular and genetic approaches have made it possible to learn more about taste cell function by using transgenic and knockout mice. Recent studies have led to the identification of two families of G protein-coupled receptors (GPCRs) in taste cells: the T1Rs (T1R1, T1R2, and T1R3) (Hoon, M. *et al*., 1999; Nelson, G. *et al*., 2001; Sainz, E. *et al*., 2001) and T2Rs (Adler, E. *et al*., 2000). T1R1 is primarily expressed in the receptor cells of fungiform taste buds, and T1R2 is expressed in the receptor cells of circumvallate and foliate taste buds. T1R3, however, is broadly expressed in all lingual taste buds (Hoon, M. *et al*., 1999; Sainz, E. *et al*., 2001). T1R1 and T1R2 are expressed in separate taste cells and localize in the taste pore where the microvilli of the taste receptor cells exposed to taste stimuli. T1R1 and T1R3 are believed to function in the transduction of amino acid (umami) stimuli (Nelson, G. *et al*., 2002; Li, X. *et al*., 2002), whereas T1R2 and T1R3 transduce sweet stimuli (Nelson, G. *et al*., 2001; Li, X. *et al*., 2002). The three T1Rs taste receptors are rarely coexpressed with α-gustducin in taste cells in circumvallate and foliate taste buds (Kim, M. *et al*., 2003; Stone, L. *et al*., 2007). T2Rs are exclusively expressed in taste receptor cells that contain gustducin, a G protein α subunit, implying that T2Rs are associated with bitter transduction (Adler, E. *et al*., 2000; Chandrashekar, J. *et al*., 2000; Matsunami, H. *et al*., 2000). T1Rs and T2Rs are almost completely coexpress with TRMP5 and PLCβ2. Sweet, amino acid, and bitter reception are abolished inPLCβ2 knockout mice (Zhang, Y. *et al*., 2003). T1Rs and T2Rs are believed to present in different subsets of type II taste cells. Most or all T2Rs are expressed in a particular subset of taste receptor cells that do not express T1Rs (Chandrashekar, J. *et al*., 2000). Using combinations of the techniques described above it is now possible to truly begin to correlate structure with function in the taste cell and taste bud.

References

Adler, E., Hoon, M., Mueller, K., Chandrashekar, J., Ryba, N., and Zuker, C. 2000. A novel family of mammalian taste receptors. Cell 100, 693–702.

Akisaka, T. 1980. Morphological and functional aspect of the rat taste bud by means of electron microscope. J. Osaka Dent. Univ. 14, 1–28.

Akisaka, T. and Oda, M. 1977. The fine structural localization of adenosine triphosphatase activity on the taste bud in the fungiform papillae of the rat. Arch. Histol. Jpn. 41, 87–98.

Akisaka, T. and Oda, M. 1978. Taste buds in the vallate papillae of the rat studied with freeze-fracture preparation. Arch. Histol. Jpn. 41, 87–98.

Azzali, G. 1997. Ultrastructure and immunocytochemistry of gustatory cells in man. Ann. Anat. 179, 37–44.

Baradi, A. 1965. Intragemmal spaces in taste buds. Z. Zellforsch. 65, 313–318.

Bartel, D., Sullivan, S., Lavoie, E., Sevigny, J., and Finger, T. 2006. Nucleoside triphosphate diphosphohydrolase-2 is the ecto-ATPase of type I cells in taste buds. J. Comp. Neurol. 497, 1–12.

Beidler, L. and Smallman, R. 1965. Renewal of cells within taste buds. J. Cell. Biol. 27, 263–272.

Beidler, L. 1969. Innervation of Rat Fungiform Papilla. In: *Olfaction and Taste III (ed*. C. Pfaffmann), pp. 354–369. Rockefeller University Press.

Boudriot, F. and Reutter, K. 2001. Ultrastructure of the taste buds in the blind cave fish *Astyanax jordani* (''Anoptichthys'') and the sighted river fish *Astyanax mexicanus* (Teleostei, Characidae). J. Comp. Neurol. 434, 428–444.

Bradley, R. 1971. Tongue Topography. In: *Handbook of Sensory Physiology (ed*. L. Beidler), pp. 1–30. Springer-Verlag.

Chandrashekar, J., Hoon, M., Ryba, N., and Zuker, C. 2006. The receptors and cells for mammalian taste. Nature 444, 288–294.

Chandrashekar, J., Mueller, K., Hoon, M., Adler, E., Feng, L., Guo, W., Zuker, C., and Ryba, N. 2000. T2Rs function as bitter taste receptors. Cell 100, 703–711.

Clapp, T., Yang, R., Stoick, C., Kinnamon, S., and Kinnamon, J. 2004. Morphologic characterization of rat taste receptor cells that express components of the phospholipase C signaling pathway. J. Comp. Neurol. 468, 311–321.

Conger, A. and Wells, M. 1969. Radiation and aging effect on taste structure and function. Radiat. Res. 37, 31–49.

Cottler-Fox, M., Arvidson, K., and Friberg, U. 1980. On the occurrence of dark and light cells in the fungiform taste buds. J. Dent. Res. 59, 191.

Cottler-Fox, M., Arvidson, K., Hammarlund, E., and Friberg, U. 1987. Fixation and occurrence of dark and light cells in taste buds of fungiform papillae. Scand. J. Dent. Res. 95, 417–427.

Cummings, T., Delay, R., and Roper, S. 1987. Ultrastructure of apical specializations of taste cells in the mudpuppy, *Necturus maculosus*. J. Comp. Neurol. 261, 604–615.

Delay, R. and Roper, S. 1988. Ultrastructure of taste cells and synapses in the mudpuppy *Necturus maculosus*. J. Comp. Neurol. 277, 268–280.

Delay, R., Kinnamon, J., and Roper, S. 1986. Ultrastructure of mouse vallate taste buds: II. Cell types and cell lineage. J. Comp. Neurol. 253, 242–252.

Delay, R., Taylor, R., and Roper, S. 1993. Merkel-like basal cells in *Necturus* taste buds contain serotonin. J. Comp. Neurol. 335, 606–613.

De Lorenzo, A. 1958. Electron microscopic observations on the taste buds of the rabbit. J. Biophys. Biochem. 4, 143–148.

De Lorenzo, A. 1960. Electron microscopy of the olfactory and gustatory pathways. Ann. Otol. Laryngol. 69, 410–420.

De Lorenzo, A. 1963. Studies on the Ultrastructure and Histophysiology of Cell Membranes, Nerve Fibers and Synaptic Junctions in Chemoreceptors. In: Olfaction and Taste (*ed*. Y. Zotterman), pp. 5–17. Pergamon.

Endo, Y. 1988. Exocytotic release of neurotransmitter substances from nerve endings in the taste buds of rat circumvallate papillae. Arch. Histol. Cytol. 51, 489–494.

Engstrom, H. and Rytzner, C. 1956a. The fine structure of taste buds and taste fibres. Ann. Otol. Rhinol. Laryngol. 65, 361–375.

Engstrom, H. and Rytzner, C. 1956b. The structure of taste buds. Acta Otolaryngol. 46, 361–367.

Esses, B., Jafek, B., Hommel, D., and Eller, P. 1988. Histological and ultrastructural changes of the murine taste bud following ionizing irradiation. Ear Nose Throat J. 67, 478–484.

Farbman, A. 1965a. Fine structure of the taste bud. J. Ultrastruct. Res. 12, 328–350.

Farbman, A. 1965b. Electron microscopy study of the developing taste bud in rat fungiform papilla. Dev. Biol. 11, 110–135.

Farbman, A. 1967. A particle–membrane complex in developing rat taste buds. J. Ultrastruct. Res. 19, 514–521.

Farbman, A. 1980. Renewal of taste bud cells in rat circumvallate papillae. Cell Tissue Kinet. 13, 349–357.

Farbman, A. and Hellekant, G. 1978. Quantitative analysis of the fiber population in rat chorda tympani nerves and fungiform papillae. Am. J. Anat. 153, 509–522.

Farbman, A. and Yonkers, J. 1971. Fine structure of the taste bud in the mud puppy, *Necturus maculosus*. Am. J. Anat. 131, 353–370.

Farbman, A., Hellekant, G., and Nelson, A. 1985. Structure of taste buds in foliate papillae of the rhesus monkey, *Macaca mulatta*. Am. J. Anat. 172, 41–56.

Fährmann, W. 1967. Licht- und elektronenmikroskopiche Befunde an den Geschmacksknospen der Axolotleunge. Z. Mikr. Anat. Forsch. 77, 117–152.

Fährmann, W. and Schuchardt, E. 1967. Light and electron microscope observations on the taste buds of the axolotl tongue (German). Experientia 23, 657–659.

Finger, T. 1986. Peptide immunohistochemistry demonstrates multiple classes of perigemmal nerve fibers in the circumvallate papilla of the rat. Chem Senses 11, 135–144.

Finger, T. 1997. Evolution of taste and solitary chemoreceptor cell systems. Brain Behav. Evol. 50, 234–243.

Finger, T. 2005. Cell types and lineages in taste buds. Chem. Senses 30 (Suppl. 1), i54–i55.

Finger, T. and Simon, S. 2000. Cell Biology of Taste Epithelium. In: The Neurobiology of Taste and Smell (*eds*. T. Finger, W. Silver, and D. Restrepo), pp. 287–314. Wiley-Liss.

Finger, T., Womble, M., Kinnamon, J., and Ueda, T. 1990. Synapsin I-like immunoreactivity in nerve fibers associated with lingual taste buds of the rat. J. Comp. Neurol. 292, 283–290.

Fujimoto, S. and Murray, R. 1970. Fine structure of degeneration and regeneration in denervated rabbit vallate taste buds. Anat. Rec. 168, 393–414.

Fujimoto, S. and Yamamoto, K. 1980. Electron microscopy of terminal buds on the barbels of the silurid fish, *Corydoras paleatus*. Anat. Rec. 197, 133–141.

Ganchrow, D., Ganchrow, J., and Goldstein, R. 1991. Ultrastructure of palatal taste buds in the perihatching chick. Am. J. Anat. 192, 69–78.

Ganchrow, D., Ganchrow, J., Gross-Isseroff, R., and Kinnamon, J. 1995. Taste bud cell generation in the perihatching chick. Chem. Senses 20, 19–28.

Ganchrow, D., Ganchrow, J., Romano, R., and Kinnamon, J. 1994. Ontogenesis and taste bud cell turnover in the chicken. I. Gemmal cell renewal in the hatchling. J. Comp. Neurol. 345, 105–114.

Ganchrow, D., Ganchrow, J., Royer, S., Dovidpor, S., and Kinnamon, J. 1998. Identified taste bud cell proliferation in the perihatching chick. Chem. Senses 23, 333–341.

Ganchrow, J., Ganchrow, D., Royer, S., and Kinnamon, J. 1993. Aspects of vertebrate gustatory phylogeny: morphology and turnover of chick taste bud cells. Microsc. Res. Tech. 26, 6–19.

Gray, E. and Watkins, K. 1965. Electron microscopy of taste buds of the rat. Z. Zellforsch 66, 583–595.

Graziadei, P. 1969. The Ultrastructure of Vertebrate Taste Buds. In: Olfaction and Taste III (*ed*. C. Pfaffmann), pp. 315–330. Rockefeller University Press.

Graziadei, P. and DeHan, R. 1971. The ultrastructure of frogs' taste organs. Acta Anat. (Basel) 180, 563–603.

Graziadei, P. and Graziadei, G. 1978. Observations on the ultrastructure of ganglion cells in the circumvallate papilla of rat and mouse. Acta Anat. (Basel) 100, 289–305.

Grover-Johnson, N. and Farbman, A. 1976. Fine structure of taste buds in the barbel of the catfish, *Ictalurus punctatus*. Cell Tissue Res. 169, 395–403.

Hamamichi, R., Asano-Miyoshi, M., and Emori, Y. 2006. Taste bud contains both short-lived and long-lived cell populations. Neuroscience 141, 2129–2138.

Hirata, Y. 1966. Fine structure of the terminal buds on the barbels of some fishes. Arch. Histol. Jpn. 26, 507–523.

Hoon, M., Adler, E., Lindemeier, J., Battey, J., Ryba, N., and Zuker, C. 1999. Putative mammalian taste receptors: a class of taste-specific GPCRs with distinct topographic selectivity. Cell 96, 541–551.

Huang, Y., Wu, Y., and Lu, K. 2003. Immunoelectron microscopic studies on protein gene product 9.5 and calcitonin gene-related peptide in vallate taste cells and related nerves in the guinea pig. Microsc. Res. Tech. 62, 383–395.

Ide, C. and Munger, B. 1980. The cytologic composition of primate laryngeal chemosensory corpuscles. Am. J. Anat. 158, 193–209.

Iriki, T. 1960. Electron micrscopic observation of the taste buds of the rabbit. Acta Med. Univ. Kagoshima 2, 78–94.

Iwayama, T. 1970. Changes in the cell population of taste buds during degeneration and regeneration of their sensory innervation. Z. Zellforsch. 110, 487–495.

Jahnke, K. and Baur, P. 1979. Freeze-fracture study of taste bud pores in the foliate papillae of the rabbit. Cell Tissue Res. 200, 245–256.

Jeppsson, P. 1969. Studies on the structure and innervation of taste buds. An experimental and clinical investigation. Acta Otolaryngol. Suppl. 259, 50–99.

Joyce, E. and Chapman, G. 1978. Fine structure of the nasal barbel of the channel catfish, *Ictalurus punctatus*. J. Morphol. 158, 109–154.

Kanazawa, H. 1993. Fine structure of the canine taste bud with special reference to gustatory cell functions. Arch. Histol. Cytol. 56, 533–548.

Kapoor, B., Evans, H., and Pevzner, R. 1975. The gustatory system in fish. Adv. Mar. Biol. 13, 53–108.

Kim, M., Kusakabe, Y., Miura, H., Shindo, Y., Ninomiya, Y., and Hino, A. 2003. Regional expression patterns of taste receptors and gustducin in the mouse tongue. Biochem. Biophys. Res. Commun. 312, 500–506.

Kinnamon, J. 1987. Organization and Innervation of Taste Buds. In: Neurobiology of Taste and Smell (*eds*. T. Finger and W. Silver), pp. 277–297. John Wiley & Sons.

Kinnamon, J., Dunlap, M., and Yang, R. 2005. Synaptic connections in developing and adult rat taste buds. Chem. Senses 30(Suppl I), 60–61.

Kinnamon, J., Henzler, D., and Royer, S. 1993. HVEM ultrastructural analysis of mouse fungiform taste buds, cell types, and associated synapses. Microsc. Res. Tech. 26, 142–156.

Kinnamon, J., Sherman, T., and Roper, S. 1988. Ultrastructure of mouse vallate taste buds: III. Patterns of synaptic connectivity. J. Comp. Neurol. 270, 48–60.

Kinnamon, J., Taylor, B., Delay, R., and Roper, S. 1985. Ultrastructure of mouse vallate taste buds. I. Taste cells and their associated synapses. J. Comp. Neurol. 235, 48–60.

Kobayashi, T. and Tomita, H. 1986. Electron microscopic observation of vallate taste buds of zinc-deficient rats with taste disturbance. Auris Nasus Larynx 13(Suppl. 1), S25–S31.

Korman, E., Addink, A., Wakabayashi, T., and Green, D. 1970. A unified model of mitochondrial morphology. Bioenergetics 1, 9–32.

Kudoh, M. 1988. Ultrastructural and histochemical localization of acetylcholinesterase in the taste bud of mouse vallate papilla. Fukushima J. Med. Sci. 34, 27–44.

Lawton, D., Furness, D., Lindemann, B., and Hackney, C. 2000. Localization of the glutamate-aspartate transporter, GLAST, in rat taste buds. Eur. J. Neurosci. 12, 3163–3171.

Leydig, F. 1851. Ueber die aussere Haut einiger Susswasserfische. Z. Wiss. Zool. 3, 1–12.

Li, X., Staszewski, L., Xu, H., Durick, K., Zoller, M., and Adler, E. 2002. Human receptors for sweet and umami taste. Proc. Natl. Acad. Sci. U. S. A. 99, 4692–4696.

Lindemann, B. 1996. Chemoreception: tasting the sweet and bitter. Curr. Biol. 6, 1234–1237.

Lindemann, B. 2001. Receptors and transduction in taste. Nature 413, 219–225.

Loven, C. 1868. Beitrage zur Kenntnis vom Bau der Geschmackswarzchen der Zunge. Arch. Mikrosk. Anat. 4, 96–110.

Matsunami, H., Montmayeur, J., and Buck, L. 2000. A family of candidate taste receptors in human and mouse. Nature 404, 601–604.

Mattern, C. and Paran, N. 1974. Evidence of a contractile mechanism in the taste bud of the mouse fungiform papilla. Exp. Neurol. 44, 461–469.

Mattern, C., Daniel, W., and Henkin, R. 1970. The ultrastructure of the human circumvallate papilla. I. Cilia of the papillary crypt. Anat. Rec. 167, 175–181.

Ma, H., Yang, R., Thomas, S., and Kinnamon, J. 2007. Qualitative and quantitative differences between taste buds of the rat and mouse. BMC. Neurosci. 8, 5.

Miller, I. 1995. Anatomy of the Peripheral Taste System. In: *Handbook of Olfaction and Gustation (ed*. R. Doty), pp. 521–547. Marcel Dekker.

Miller, R. and Chaudhry, A. 1976. An ultrastructural study on the development of vallate taste buds of the golden Syrian hamster. Acta Anat. (Basel) 95, 190–206.

Montavon, P., Hellekant, G., and Farbman, A. 1996. Immunohistochemical, electrophysiological, and electron microscopical study of rat fungiform taste buds after regeneration of chorda tympani through the non-gustatory lingual nerve. J. Comp. Neurol. 367, 491–502.

Murray, A. 1961. Two gustatory types in rabbit taste buds. Anat. Rec. 139, 331.

Murray, R. 1969. Cell Types in Rabbit Taste Buds. In: Olfaction and Taste, III (*ed*. C. Pfaffmann), pp. 331–344. Rockefeller University Press.

Murray, R. 1971. Ultrastructure of Taste Receptors. In: Handbook of Sensory Physiology, Vol. IV (*ed*. L. M. Beidler), pp. 31–50. Springer-Verlag.

Murray, R. 1973. The Ultrastructure of Taste Buds. In: *The Ultrastructure of Sensory Organs (ed*. I. Friedmann), pp. 1–81. North-Holland.

Murray, R. 1986. The mammalian taste bud type III cell: A critical analysis. J. Ultrastruct. Molec. Struct. Res. 95, 175–188.

Murray, R. 1993. Cellular relations in mouse circumvallate taste buds. Microsc. Res. Tech. 26, 209–224.

Murray, R. and Murray, A. 1960. The fine structure of the taste buds of rhesus and cynomalgus monkeys. Anat. Rec. 138, 211–219.

Murray, R. and Murray, A. 1966. Fine Structure of Rabbit Taste Buds. In: Proceedings of the 6th International Congress on Electron Microscopy Vol. 2, (*ed*. R. Ueda), pp. 484–486. Maruzen.

Murray, R. and Murray, A. 1967. Fine structure of taste buds of rabbit foliate papillae. J. Ultrastruct. Res. 19, 327–353.

Murray, R. and Murray, A. 1970. The Anatomy and Ultrastructure of Taste Endings. In: Taste and Smell in Vertebrates (*eds*. G. Wolstenhome and J. Knight), pp. 3–30. J. & A. Churchill.

Murray, R. and Murray, A. 1971. Relations and possible significance of taste bud cells. Contrib. Sens. Physiol. 5, 47–95.

Murray, R., Murray, A., and Fujimoto, S. 1969. Fine structure of gustatory cells in rabbit taste buds. J. Ultrastruct. Res. 27, 444–461.

Nada, O. and Hirata, K. 1975. The occurrence of the cell type containing a specific monoamine in the taste bud of the rabbit's foliate papilla. Histochemistry 43, 237–240.

Nagy, J., Goedert, M., Hunt, S., and Bond, A. 1982. The nature of the substance P-containing nerve fibres in taste papillae of the rat tongue. Neuroscience 7, 3137–3151.

Nelson, G., Chandrashekar, J., Hoon, M., Feng, L., Zhao, G., Ryba, N., and Zuker, C. 2002. An amino-acid taste receptor. Nature 416, 199–202.

Nelson, G., Hoon, M., Chandrashekar, J., Zhang, Y., Ryba, N., and Zuker, C. 2001. Mammalian sweet taste receptors. Cell 106, 381–390.

Nemetschek-Gansler, H. and Ferner, H. 1964. Uber die ultrastruktur der geschmacksknospen. Z. Zellforsch 63, 155–178.

Oakley, B. 1967. Altered temperature and taste responses from cross-regenerated sensory nerves in the rat's tongue. J. Physiol. 188, 353–371.

Ono, R. 1980. Fine structure and distribution of epidermal projections associated with taste buds on the oral papillae in some loricariid catfishes Siluroidei: Loricariidae. J. Morphol. 164, 139–159.

Ovalle, W. and Shinn, S. 1977. Surface morphology of taste buds in catfish barbels. Cell Tissue Res. 178, 375–384.

Paran, N., Mattern, C., and Henkin, R. 1975. Ultrastructure of the taste bud of the human fungiform papilla. Cell Tissue Res. 161, 1–10.

Popov, V., Ignat'ev, D., and Lindemann, B. 1999. Ultrastructure of taste receptor cells in active and hibernating ground squirrels. J. Electron. Microsc. (Tokyo) 48, 957–969.

Pumplin, D., Yu, C., and Smith, D. 1997. Light and dark cells of rat vallate taste buds are morphologically distinct cell types. J. Comp. Neurol. 378, 389–410.

Reutter, K. 1978. Taste organ in the bullhead Teleostei. Anat. Embryol. Cell. Biol. 55, 1–98.

Reutter, K. 1982. Taste Organ in the Barbel of the Bullhead. In: Chemoreception in Fishes (*ed*. T. Hara), pp. 77–91. Elsevier.

Reutter, K. 1987. Specialized receptor villi and basal cells within the taste bud of the European silurid fish, *Silurus glanis* Teleostei. Ann. N. Y. Acad. Sci. 510, 570–573.

Reutter, K. 1992. Structure of the Peripheral Gustatory Organ, Represented by the Siluroid Fish *Plotosus lineatus* Thunberg. In: *Fish Chemoreception (ed*. T. Hara), pp. 60–78. Chapman & Hall.

Reutter, K. and Witt, M. 1993. Morphology of Vertebrate Taste Organs and Their Nerve Supply. In: *Mechanisms of Taste Transduction (eds*. S. Simon and S. Roper), pp. 29–82. CRC Press.

Reutter, K. and Witt, M. 2004. Are there efferent synapses in fish taste buds? J. Neurocytol. 33, 647–656.

Romanov, R., Rogachevskaja, O., Bystrova, M., Jiang, P., Margolskee, R., and Kolesnikov, S. 2007. Afferent neurotransmission mediated by hemichannels in mammalian taste cells. EMBO J. 26, 657–656.

Roper, S. 1989. The cell biology of vertebrate taste receptors. Annu. Rev. Neurosci. 12, 329–353.

Roper, S. 2006. Cell communication in taste buds. Cell Mol. Life Sci. 63, 1494–1500.

Royer, S. and Kinnamon, J. 1988. Ultrastructure of mouse foliate taste buds: synaptic and nonsynaptic interactions between taste cells and nerve fibers. J. Comp. Neurol. 270, 11–24.

Royer, S. and Kinnamon, J. 1991. HVEM serial-section analysis of rabbit foliate taste buds: I. Type III cells and their synapses. J. Comp. Neurol. 306, 49–72.

Royer, S. and Kinnamon, J. 1994. Application of serial sectioning and three-dimensional reconstruction to the study of taste bud ultrastructure and organization. Microsc. Res. Tech. 29, 381–407.

Sainz, E., Korley, J., Battey, J., and Sullivan, S. 2001. Identification of a novel member of the T1R family of putative taste receptors. J. Neurochem. 77, 896–903.

Sakai, H., Kaidoh, T., Morino, S., and Inoue, T. 1999. Three-dimensional architecture of the keratin filaments in epithelial cells surrounding taste buds in the rat circumvallate papilla. Arch. Histol. Cytol. 62, 375–381.

Sangiacomo, C. 1970. Neurosecretory cell types in normal taste bud. Experientia 26, 289–290.

Sbarbati, A., Benati, D., Crescimanno, C., and Osculati, F. 1998a. Membrane-bounded intratubular bodies in rat taste buds. J. Neurocytol. 27, 157–161.

Sbarbati, A., Franceschini, F., Zancanaro, C., Cecchini, T., Ciaroni, S., and Osculati, F. 1988b. The fine morphology of the basal cell in the frog's taste organ. J. Submicrosc. Cytol. Pathol. 20, 73–79.

Sbarbati, A., Merigo, F., Benati, D., Bernardi, P., Tizzano, M., Fabene, P., Crescimanno, C., and Osculati, F. 2006. Axon-like processes in type III cells of taste organs. Anat. Rec. A Discov. Mol. Cell Evol. Biol. 288, 276–279.

Sbarbati, A., Zancanaro, C., Ferrara, P., Franceschini, F., Accordini, C., and Osculati, F. 1993. Freeze-fracture characterization of cell types at the surface of the taste organ of the frog, *Rana esculenta*. J. Neurocytol. 22, 118–127.

Scalzi, H. 1967. The cytoarchitecture of gustatory receptors from the rabbit foliate papillae. Z. Zellforsch. 80, 413–435.

Schwalbe, G. 1868. Ueber die Geschmacksorgane der Saugethiere und des Menschen. Arch. Mikrosk. Anat. Entwickl. 4, 154–189.

Sekerkova, G., Freeman, D., Mugnaini, E., and Bartles, J. 2005. Espin cytoskeletal proteins in the sensory cells of rodent taste buds. J. Neurocytol. 34, 171–182.

Seta, Y., Seta, C., and Barlow, L. A. 2003. Notch-associated gene expression in embryonic and adult taste papillae and taste buds suggests a role in taste cell lineage decisions. J. Comp. Neurol. 464, 49–61.

Stone, L. and Finger, T. 1994. Mosaic analysis of the embryonic origin of taste buds. Chem. Senses 19, 725–735.

Stone, L., Barrows, J., Finger, T., and Kinnamon, S. 2007. Expression of T1Rs and gustducin in palatal taste buds of mice. Chem Senses. 32, 255–262.

Stone, L., Finger, T., Tam, P., and Tan, S. 1995. Taste receptor cells arise from local epithelium, not neurogenic ectoderm. Proc. Natl. Acad. Sci. U. S. A. 92, 1916–1920.

Stone, L., Tan, S., Tam, P., and Finger, T. 2002. Analysis of cell lineage relationships in taste buds. J. Neurosci. 22, 4522–29.

Stornelli, M., Lossi, L., and Giannessi, E. 2000. Localization, morphology and ultrastructure of taste buds in the domestic duck (*Cairina moschata* domestica L.) oral cavity. Ital. J. Anat. Embryol. 105, 179–188.

Sweazey, R., Edwards, C., and Kapp, B. 1994. Fine structure of taste buds located on the lamb epiglottis. Anat. Rec. 238, 517–527.

Tabata, S., Wada, A., Kobayashi, T., Nishimura, S., Muguruma, M., and Iwamoto, H. 2003. Bovine circumvallate taste buds: taste cell structure and immunoreactivity to alpha-gustducin. Anat. Rec. A Discov. Mol. Cell. Evol. Biol. 271, 217–224.

Takeda, M. 1972. Fine structure of developing taste buds in human fetal circumvallate papillae. Kaibogaku Zasshi. 47, 325–337.

Takeda, M. 1976. An electron microscopic study on the innervation in the taste buds of the mouse circumvallate papillae. Arch. Histol. Jpn. 39, 257–269.

Takeda, M. 1977. Uptake of 5-hydroxytryptophan by gustatory cells in the mouse taste bud. Arch. Histol. Jpn. 40, 243–250.

Takeda, M. and Hoshino, T. 1975. Fine structure of taste buds in the rat. Arch. Histol. Jpn. 37, 395–413.

Takeda, M. and Kitao, K. 1980. Effect of monoamines on the taste buds in the mouse. Cell Tissue Res. 210, 71–78.

Takeda, M., Obara, N., and Suzuki, Y. 1988. Intermediate filaments in mouse taste bud cells. Arch. Histol. Cytol. 51, 99–108.

Takeda, M., Obara, N., and Suzuki, Y. 1989. Cytoskeleton in the apical region of mouse taste bud cells. Shika Kiso Igakkai Zasshi 31, 317–323.

Takeda, M., Shishido, Y., Kitao, K., and Suzuki, Y. 1981. Biogenic monoamines in developing taste buds of mouse circumvallate papillae. Arch. Histol. Jpn. 44, 485–495.

Takeda, M., Suzuki, Y., and Shishido, Y. 1985. Effects of colchicine on the ultrastructure of mouse taste buds. Cell Tissue Res. 242, 409–416.

Toyoshima, K. and Shimamura, A. 1982. Virus-like particles in the taste buds of the circumvallate papilla of the rat. J. Electron Microsc. (Tokyo) 31, 273–275.

Toyoshima, K. and Tandler, B. 1989. Dense-cored vesicles and unusual lamellar bodies in type III gustatory cells in taste

buds of rabbit foliate papillae. Acta Anat. (Basel) 135, 365–369.
Toyoshima, K., Miyamoto, K., and Shimamura, A. 1987. Fine structure of taste buds in the tongue, palatal mucosa and gill arch of the axolotl, *Ambystoma mexicanum*. Okajimas Folia Anat. Jpn. 64, 99–109.
Toyoshima, K., Nada, O., and Shimamura, A. 1984. Fine structure of monoamine-containing basal cells in the taste buds on the barbels of three species of teleosts. Cell Tissue Res. 235, 479–484.
Trujillo-Cenóz, O. 1957. Electron microscope study of the rabbit gustatory bud. Z. Zellforsch 46, 272–280.
Trujillo-Cenóz, O. 1961. Electron microscope observations on chemo- and mechano-receptor cells of fishes. Z. Zellforsch. 34, 654–676.
Uga, S. 1966. The fine structure of gustatory receptors and their synapses in frog's tongue. Symp. Cell Chem. 16, 75–85.
Uga, S. 1969. A study on the cytoarchitecture of taste buds of rat cirumvallate papillae. Arch. Histol. Jpn. 31, 59–72.
Uga, S. and Hama, K. 1967. Electron microscopic studies on the region of the taste organ of carps and frogs. J. Electron Microsc. 16, 269–276.
Welsch, U. and Storch, V. 1969. Die Feinstruktur der Geschmacksknospen von Welsen [*Clarias batrachus* L. und *Kryptopterus bicirrhis* Cuvier et Valenciennes]. Z. Zellforsch. 100, 552–559.
Whiteside, B. 1927. Nerve overlap in the gustatory apparatus of the rat. J. Comp. Neurol. 44, 363–377.
Whitehead, M., Beeman, C., and Kinsella, B. 1985. Distribution of taste and general sensory nerve ending in fungiform papillae of the hamster. Am. J. Anat. 173, 185–202.
Williams, C., Vail, W., Harris, R., Caldwell, M., Green, D., and Valdivia, E. 1970. Conformational basis of energy transduction in membrane systems. VII. Configurational changes of mitochondria *in situ* and *in vitro*. Bioenergetics 1, 147–180.
Wilson, J. and Edin, M. 1905. The structure and function of the taste-buds in the larynx. Brain 28, 339–351.
Wistuba, J., Opolka, A., and Clemen, G. 1999. The epithelium of the tongue of *Ambystoma mexicanum*. Ultrastructural and histochemical aspects. Ann. Anat. 181, 523–536.
Witt, M. 1993. Ultrastructure of the taste disc in the red-bellied toad *Bombina orientalis* (Discoglossidae, Salientia). Cell Tissue Res. 272, 59–70.
Witt, M. and Reutter, K. 1990. Electron microscopic demonstration of lectin binding sites in the taste buds of the European catfish *Silurus glanis* (Teleostei). Histochemistry 94, 617–628.
Witt, M. and Reutter, K. 1997. Scanning electron microscopical studies of developing gustatory papillae in humans. Chem. Senses 22, 601–612.
Witt, M., Reutter, K., Ganchrow, D., and Ganchrow, J. 2000. Fingerprinting taste buds: intermediate filaments and their implication for taste bud formation. Philos. Trans. R. Soc. Lond. B Biol. Sci. 335, 1233–1237.
Yang, R., Crowley, H., Rock, M., and Kinnamon, J. 2000a. Taste cells with synapses in rat circumvallate papillae display SNAP-25-like immunoreactivity. J. Comp. Neurol. 424, 205–215.
Yang, R., Ma, H., Thomas, S., and Kinnamon, J. 2007. Immunocytochemical analysis of syntaxin-1 in rat circumvallate taste buds. J. Comp. Neurol., 502, 883–93.
Yang, R., Stoick, C., and Kinnamon, J. 2004. Synaptobrevin-2-like immunoreactivity is associated with vesicles at synapses in rat circumvallate taste buds. J. Comp. Neurol. 471, 59–71.
Yang, R., Tabata, S., Crowley, H., Margolskee, R., and Kinnamon, J. 2000b. Immunocytochemical localization of gustducin immunoreactivity in microvilli of type II taste cells of the rat. J. Comp. Neurol. 425, 139–151.
Yee, C., Yang, R., Böttger, B., Finger, T., and Kinnamon, J. 2001. "Type III" cells of rat taste buds: immunohistochemical and ultrastructural studies of neuron-specific enolase, protein gene product 9.5, and serotonin. J. Comp. Neurol. 440, 97–108.
Yoshie, S., Kanazawa, H., and Fujita, T. 1996. A possibility of efferent innervation of the gustatory cell in the rat circumvallate taste bud. Arch. Histol. Cytol. 59, 479–484.
Yoshie, S., Kanazawa, H., Nishida, Y., and Fujita, T. 1997. Occurrence of subtypes of gustatory cells in cat circumvallate taste buds. Arch. Histol. Cytol. 60, 421–426.
Yoshie, S., Wakasugi, C., Teraki, Y., and Fujita, T. 1990. Fine structure of the taste bud in guinea pigs. I. Cell characterization and innervation patterns. Arch. Histol. Cytol. 53, 103–119.
Yoshie, S., Wakasugi, C., Teraki, Y., Iwanaga, T., and Fujita, T. 1991. Fine structure of the taste bud in guinea pigs. II. Localization of spot 35 protein, a cerebellar Purkinje cell-specific protein, as revealed by electron-microscopic immunocytochemistry. Arch. Histol. Cytol. 54, 113–118.
Zahm, D. and Munger, B. 1983a. Fetal development of primate chemosensory corpuscles. I. Synaptic relationships in late gestation. J. Comp. Neurol. 213, 146–162.
Zahm, D. and Munger, B. 1983b. Fetal development of primate chemosensory corpuscles. I. Synaptic relationships in early gestation. J. Comp. Neurol. 219, 36–50.
Zahm, D. and Munger, B. 1985. The innervation of the primate fungiform papilla – development, distribution and changes following selective ablation. Brain Res. Rev. 9, 147–186.
Zhang, Y., Hoon, M., Chandrashekar, J., Mueller, K., Cook, B., Wu, D., Zuker, C., and Ryba, N. 2003. Coding of sweet, bitter, and umami tastes: different receptor cells sharing similar signaling pathways. Cell 112, 293–301.

Further Reading

Beidler, L. and Smallman, R. 1963. Dynamics of taste cells. In: Olfaction and Taste (*ed*. Y. Zotterman), pp. 133–148. Pergamon Press.
Bigiani, A. and Roper, D. 1995. Estimation of the junctional resistance between electrically coupled receptor cells in *Necturus* taste buds. J. Gen. Physiol. 106, 705–725.
Finger, T., Danilova, V., Barrows, J., Bartel, D., Vigers, A., Stone, L., Hellekant, G., and Kinnamon, S. 2005. ATP signaling is crucial for communication from taste buds to gustatory nerves. Science 310, 1495–1499.
Fish, H., Malone, P., and Richter, C. 1944. The anatomy of the tongue of the domestic Norway rat. Anat. Rec. 89, 429–440.
Gilbertson, T., Damak, S., and Margolskee, R. 2000. The molecular physiology of taste transduction. Curr. Opin. Neurobiol. 10, 519–527.
Gomez-Ramos, P. and Rodriguez-Echandia, E. 1979. The fine structural effect of sialectomy on the taste bud cells in the rat. Tissue Cell 11, 19–29.
Kinnamon, S. and Margolskee, R. 1996. Mechanisms of taste transduction. Curr. Opinion Neurobiol. 6, 506–513.
Miller, I. and Bartoshuk, L. 1991. Taste Bud Distribution and Spatial Relationships. In: *Smell* and Taste in Health and Disease (*eds*. T. Getchell, R. Doty, L. Bartoshuk, and J. Snow), pp. 205–231. Raven Press.
Pumplin, D., Getschman, E., Boughter, J., Yu, C., and Smith, D. 1999. Differential expression of carbohydrate blood-group antigens on rat taste-bud cells: relation to the functional marker alpha-gustducin. J. Comp. Neurol. 415, 230–239.
Roper, S. 1992. The microphysiology of peripheral taste organs. J. Neurosci. 12, 1127–1134.

Travers, S. and Nicklas, K. 1990. Taste bud distribution in the rat pharynx and larynx. Anat. Rec. 227, 373–379.
Witt, M. and Reutter, K. 1996. Embryonic and early fetal development of human taste buds: a transmission electron microscopical study. Anat. Rec. 246, 507–523.
Yamasaki, H., Kubota, Y., Tagagi, H., and Tohyama, M. 1984. Immunoelectron-microscopic study on the fine structure of substance-P-containing fibers in the taste buds of the rat. J. Comp. Neurol. 227, 380–392.
Yang, J. and Roper, S. 1987. Dye-coupling in taste buds in the mudpuppy, *Necturus maculosus*. J. Neurosci. 7, 3561–3565.
Yoshii, K. 2005. Gap junctions among taste bud cells in mouse fungiform papillae. Chem. Senses 30(Suppl. i), 35–36.

4.06 Development of the Taste System

R F Krimm, University of Louisville School of Medicine, Louisville, KY, USA

L A Barlow, University of Colorado School of Medicine, Aurora, CO, USA

© 2008 Elsevier Inc. All rights reserved.

4.06.1	Introduction	157
4.06.2	The Taste Periphery: Of Buds and Bumps	158
4.06.3	Development of the Taste Periphery: How Does Taste Bud Pattern Arise?	159
4.06.3.1	Taste Bud Development in Axolotls	160
4.06.3.2	Taste Bud Development in Rodents	161
4.06.3.3	Molecular Mechanisms of Taste Patterning	162
4.06.3.4	Tests of Gene Function in Taste Organ Formation and Patterning	164
4.06.4	Development of the Circumvallate Papilla, a Specialized Structure in Mammals	164
4.06.5	Taste Bud Cell Lineage and Turnover	165
4.06.6	Development of Gustatory Innervation	166
4.06.6.1	Development of the Sensory Neurons of the Gustatory Ganglia	167
4.06.6.2	Development of Peripheral Taste Innervation	167
4.06.6.3	Development of Projections of Gustatory Neurons to the Central Nervous System	171
4.06.6.4	Survival and Maintenance of Gustatory Neurons and Taste Buds	172
4.06.7	Postnatal Plasticity in Taste Bud Innervation	174
4.06.8	Plasticity of Central Taste Connections	174
4.06.9	Conclusion	175
References		175

4.06.1 Introduction

At birth, all vertebrates possess a functional taste system. This sensory system is key for young animals to survive in a new world, in which they must avoid noxious and potentially lethal substances, yet ingest nutritionally valuable foods. From a developmental biologist's perspective, the taste system comprises four basic elements which arise in locations remote from one another and must connect accurately during embryogenesis. Specifically these components are: (1) taste buds arrayed within the mouth and pharynx; (2) sensory neurons residing within the cranial nerve ganglia which connect taste buds to (3) discrete gustatory regions of the hindbrain, which in turn connect to (4) upstream nuclei within the brain. This organization is already intricate from an anatomical perspective (see Chapter Gustatory Pathways in Fish and Mammals), but is truly a marvel of complexity when one considers its embryonic development. Taste buds develop *in situ* within the epithelia lining the oral and pharyngeal cavities, quite far from the developing brain. Likewise the sensory neurons destined to innervate taste buds also arise from neurogenic precursors outside of the brain. Finally, populations of hindbrain and higher order central neurons arise directly from specific regions of the forming neural tube. As we will review here, these elements each arise initially quite independently of, and at great distance from, the others, yet subsequently manage to connect to one another to produce a coordinated, fully functional taste system at birth (Figure 1).

In addition to these dynamic embryonic events, the taste system continues to develop postnatally. The cells within taste buds are constantly renewed throughout adult life, and the connections between the taste periphery and central targets remain plastic and modifiable by environmental influences. Despite this flexibility, we experience no alterations in our ability to taste.

In the past decade or so, studies of taste system development have been invigorated in large part by an expansion of experimental studies focused on embryonic development, as well as by use of transgenic mouse models in both embryonic and postnatal settings. These new approaches have provided new answers to major questions in the field: what are the molecular,

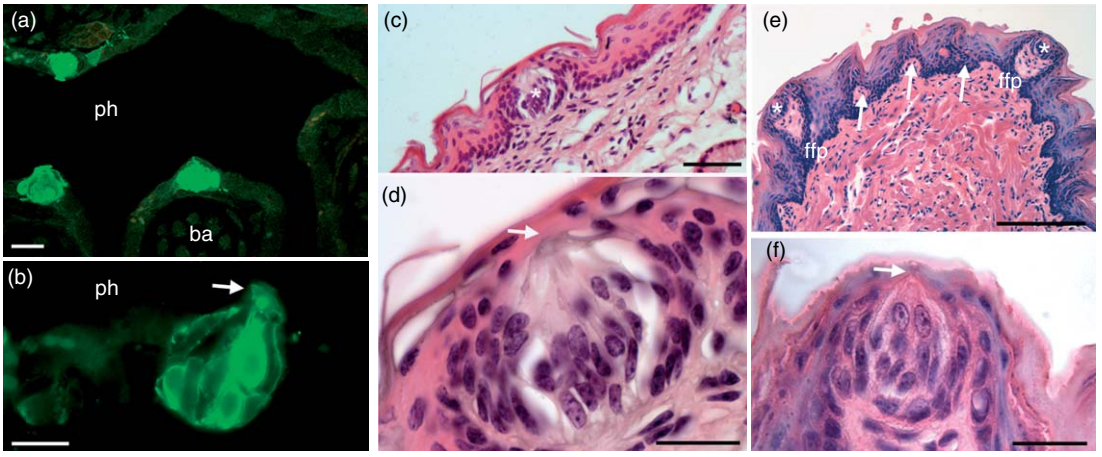

Figure 1 Depending upon the species or the location of taste buds within the oral cavity, taste buds can occur as discrete organs within the general epithelium or within more complex epithelial specializations. (a, b): Taste buds of juvenile axolotls (an aquatic salamander) are embedded directly in the oral and pharyngeal epithelia (ph; pharyngeal cavity). In these transverse sections through the pharyngeal region (dorsal is up), a subset of taste cells have been immunofluorescently stained (green) with antiserum against calretinin (Barlow, L. A. *et al.*, 1996). Note the characteristic onion shape of the taste organs and the narrow apical regions extruding into the pharyngeal cavity (arrow in b). (c, d): In mice, palatal taste buds are large and readily recognized as discrete organs within the epithelium. Again, these taste buds are found within the general epithelium, are onion-shaped (* in c), and narrow apically in the vicinity of the taste pore (arrow in d). (e, f): In contrast, taste buds on the mouse tongue are housed in elaborate papillae, including the fungiform papillae shown here (ffp). A single taste bud (* in e) sits in the apical papillary epithelium, while each papilla comprises an evaginated epithelium with a mesenchymal core. The fungiform papillae are interspersed with numerous, heavily keratinized filiform papillae (arrows in e). Despite their localization to fungiform papillae, the taste buds therein have the common onion shape and terminate apically in a narrow taste pore (arrow in f). Scale bars = 50 μm (a, c); 25 μm (b); 20 μm (d); 100 μm (e); 40 μm (f). (a, b, e, f) Transverse sections, dorsal is up. (c, d) Transverse sections, dorsal is down.

cellular, and tissue level interactions involved in taste organ development and patterning; how do sensory neurons come to innervate specifically both peripheral taste bud and central hindbrain targets; what types of cellular and molecular mechanisms maintain the mature taste system; and how well conserved are these developmental mechanisms in vertebrate evolution? These topics are thus the focus of our review.

4.06.2 The Taste Periphery: Of Buds and Bumps

To date, all vertebrate animals possess taste buds within the mouth and pharynx (although some fishes have external taste buds, see Gomahr, A. *et al.*, 1992; Reutter, K. and Witt, M., 1993; Hansen, A. *et al.*, 2002; Northcutt, R. G., 2005). These multicellular receptor organs are each composed of a mixed population of roughly 100 fusiform cells, which taper both apically and somewhat basally, to create an onion-shaped aggregate (Figure 2; and see Chapter Ultrastructure of Taste Buds). While this is the common organization for vertebrate taste buds, there is an extremely wide variety in the morphology of epithelial structures associated with taste buds proper. In their most simplified state, taste buds occur within the general epithelium, and are not associated with any specialized epithelial appendages or structures (Figure 2). This is the case for aquatic salamanders, such as the axolotl (Fährmann, W., 1967; Toyoshima, K. *et al.*, 1987; Northcutt, R. G. *et al.*, 2000), where taste buds are readily detected in the oropharyngeal epithelium simply by their multicellularity and classic onion shape. In mammals, taste buds in the palate, pharynx, and larynx are also simple and onion shaped, residing directly within the epithelia (Mistretta, C. M., 1972; Belecky, T. L. and Smith, D. V., 1990; Zhang, C. and Oakley, B., 1996). However, in numerous instances, taste buds occur in the epithelium of specialized structures. For example, in catfish and zebrafish, individual taste buds are associated with taste hillocks (Gomahr, A. *et al.*, 1992; Reutter, K. and Witt, M., 1993; Hansen, A. *et al.*, 2002; Northcutt, R. G., 2005), which are slight epithelial elevations with small mesenchymal cores (Figure 2). On the tongues of mammals, taste buds are restricted to elaborate

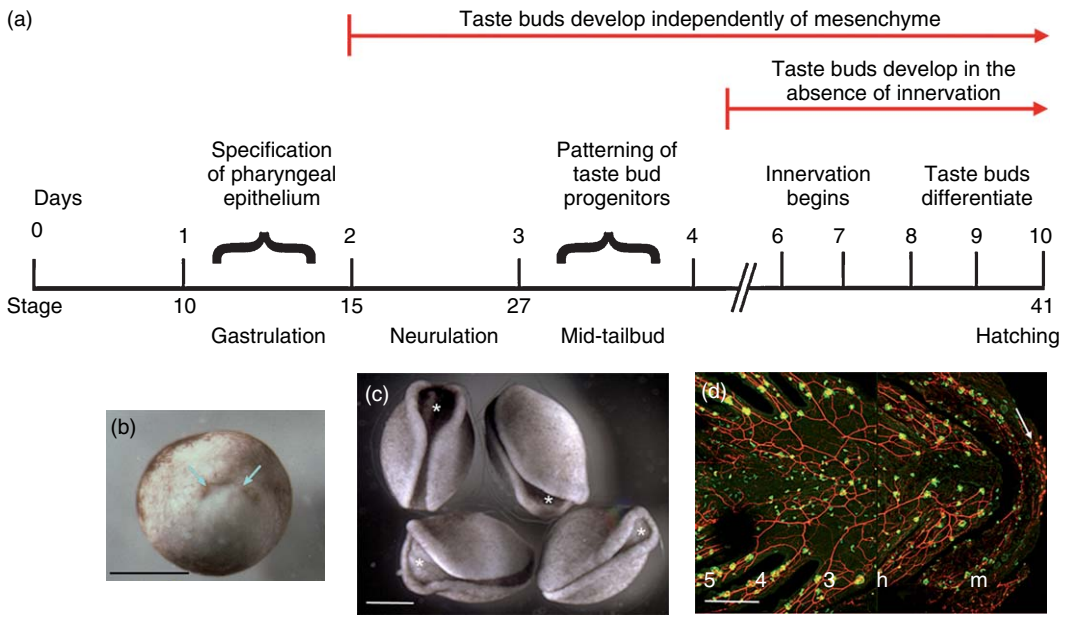

Figure 2 Time line of the experimental dissection of tissue level mechanisms governing taste bud development in axolotls. (a): Axolotl embryos develop from fertilization (day 0) to hatching (stage 41) over 10 days. Taste buds differentiate within a day of hatching, while the epithelium has already received innervation by 6 days. Nonetheless, taste buds develop in the absence of innervation (short red arrow; see text for full details). Further, taste buds develop in epithelium devoid of contact with cranial mesenchyme (long red arrow; see text). In fact, pharyngeal epithelium is specified by signals it receives during gastrulation and is patterned by tissue-intrinsic signaling during tailbud stages (horizontal brackets; see text). (b): At the onset of gastrulation, the dorsal blastopore lip is evident as a pigmented depression in the dorsal vegetal surface of an axolotl embryo (blue arrows; vegetal view). (c): During neurulation, the paired neural folds rise up from the dorsal surface of each axolotl embryo, and in this micrograph, the folds have approached the dorsal midline to fuse and form the neural tube. The anterior region (*s) will give rise to the forebrain and midbrain, while the more posterior folds produce the hindbrain and spinal cord. (d): At hatching, both differentiated taste buds and their extensive innervation are evident in the internal pharyngeal surface of the lower jaw of axolotls. Using confocal microscopy on a larval axolotl head processed in whole mount for double immunofluorescence, taste buds (green) are revealed with antiserum against calretinin, and antiacetylated tubulin allows detection of nerves (red). m: mandible; h: hyoid arch; 3, 4, 5: third, fourth, and fifth branchial arches. Scale bars = 1 mm (b–d). Image acquired by Mark A. Parker.

structures, termed taste papillae (Mistretta, C. M., 1972). These appendages are composed of epithelial evaginations and/or invaginations, surrounding substantial mesenchymal cores (Figure 2). Taste buds reside in the epithelia of gustatory papillae, and taste cells within each bud extrude their apical microvilli into the lumen of a tightly arranged taste pore. The number of taste buds housed in these papillae can vary from 1 to 3 per papilla, as is the case for the smaller fungiform papillae in the anterior tongue, to several hundred per papillae as is the case for the large, posterior foliate and circumvallate papillae (Figure 2). In sum, while the morphology of taste buds is quite similar among vertebrates, ancillary epithelial structures associated with taste buds differ widely. This latter variability may reflect different selective pressures on taste epithelium, including tasting in air versus in water, and the types of foods ingested by different animals.

Because aquatic salamanders have a taste bud organization uncomplicated by association with specialized epithelial structures, they perhaps can serve as a model for the most basic mechanisms driving the development of this system. Thus, that is where this review of new data on taste system development begins in earnest.

4.06.3 Development of the Taste Periphery: How Does Taste Bud Pattern Arise?

Recently, a number of studies providing insight into how taste buds develop have utilized either

amphibian (axolotl) or mammalian (mouse and rat) embryos. And therefore, we will first review the insights into taste periphery development gleaned from studies of axolotls, then present the new findings in rodents that speak to these same issues.

4.06.3.1 Taste Bud Development in Axolotls

Axolotls are a species of aquatic salamander native to the high altitude lakes in the vicinity of Mexico City (Smith, H. M., 1969), and embryos of this species and those of its close relatives have been an important tool in studies of embryogenesis for nearly a century (e.g., Vogt, W., 1929; Mangold, O., 1931; Nieuwkoop, P. D. and Ubbels, G. A., 1972; Slack, J. M. and Forman, D., 1980; Armstrong, J. B. and Malacinski, G. M., 1989). In the last decade, we have taken advantage of the ease of microsurgical manipulation of these embryos at virtually any stage of development to explore tissue-level and cellular mechanisms regulating taste bud formation.

Although taste buds are first evident morphologically in the oral cavity as axolotl larvae hatch and begin to feed (Barlow, L. A. and Northcutt, R. G., 1995), the oral and pharyngeal epithelia are innervated by gustatory nerve fibers long before, during mid- to late embryonic stages. This sequence of events, innervation followed by taste bud differentiation, is common to all vertebrates examined to date (Landacre, F. L., 1907; Stone, L. S., 1940; Farbman, A. I., 1965; Bradley, R. M. and Stern, I. B., 1967; Reutter, K. and Witt, M., 1993; Whitehead, M. C. and Kachele, D. L., 1994; Barlow, L. A. *et al.*, 1996; Witt, M. and Reutter, K., 1996; Northcutt, R. G., 2005); and when combined with studies employing adult vertebrates demonstrating that maintenance of mature taste bud morphology is dependent upon intact innervation (e.g., Vintschgau, M. and Honigschmied, J., 1876; Torrey, T. W., 1934; Poritsky, R. and Singer, M., 1963; but see Whitehead, M. C. *et al.*, 1987), has led to a neural induction model for taste bud formation. Specifically, this model posits that during development, early arriving nerve fibers induce taste buds to form from an otherwise homogeneous local epithelium.

Over 10 years ago, expanding on ectopic grafting studies first published by Stone L. S. (1932; 1940), the neural induction model was tested using axolotl embryos and modern immunocytochemical methods to detect all nerve fibers (Barlow, L. A. *et al.*, 1996). The oropharyngeal epithelium of amphibian embryos, destined to give rise to taste buds (Barlow, L. A. and Northcutt, R. G., 1995), was removed prior to innervation and cultured in isolation. Despite the complete absence of nerve contact, the explanted epithelia generated taste buds in appropriate densities and with a time course identical to that of intact embryos. Thus, at least in these amphibians, innervation is not required for taste bud formation.

Since taste buds are not induced by nerves, they might instead be induced by contact with cranial mesenchyme. This latter cell population contacts the oral epithelium during embryogenesis and is a known inducer of other tissues within the oral cavity, including teeth (Kollar, E. J., 1983; Lumsden, A. G. S., 1987; 1988) and cartilage (Graveson, A. C. and Armstrong, J. B., 1987). However, when oropharyngeal epithelia of early axolotl embryos are removed and cultured prior to and without subsequent contact with embryonic mesenchyme, taste buds still form in epithelial explants at the appropriate developmental stage, some 10 days later (Barlow, L. A., and Northcutt, R. G., 1997). Thus, taste bud development is independent of both nerves and cranial mesenchyme. Logically then, since no other tissues contact the oropharyngeal epithelium during embryogenesis, formation of taste buds is an intrinsic feature of this epithelium, one that is acquired early in embryonic development. In fact, this predisposition or specification (see Slack, J. M. W., 1991) to a taste bud-bearing fate is acquired during gastrulation and is due to signals from the embryonic notochord (Barlow, L. A., 2001). The implication here is that molecular signals from the notochord induce changes in the oropharyngeal epithelium such that the latter produces taste buds which differentiate 10 days later.

One unanticipated aspect of these results was how early the tissue-level interactions that set the stage for epithelium-intrinsic taste bud formation occurred – so much earlier than taste bud differentiation at the end of embryonic development. Given the large expanse of developmental time between the completion of gastrulation and taste bud differentiation 10 days later, how does this early intrinsic property transform into the patterned array of taste buds in the mouth? To address this question, we proposed that local cell–cell interactions were mediating pattern formation of presumed taste bud progenitor cells (Barlow, L. A. and Northcutt, R. G., 1998; Northcutt, R. G. and Barlow, L. A., 1998). To test if and when this was occurring, intercellular contacts were disrupted transiently in oropharyngeal epithelial explants at progressive developmental

stages. These studies reveal a critical 12 h window, again long before taste bud differentiation and innervation of the epithelium, during which cell–cell communication is crucial for determining taste bud pattern when intercellular signals are interrupted during this phase, the total number and size of individual taste buds is dramatically increased (Parker, M. A. *et al.*, 2004). This result has led to our hypothesis that a population of distributed taste bud progenitor cells is induced at this earlier stage, which later goes on to divide and give rise to taste bud cells proper, a hypothesis that remains to be tested.

4.06.3.2 Taste Bud Development in Rodents

In broad overview, the development of taste buds in mice and rats is quite comparable to that of axolotls. Taste buds arise directly from the oral epithelium (Stone, L. M. *et al.*, 1995; 2002) and do not differentiate until perinatal stages, the precise timing depending upon their location. The sequence of taste bud formation has been best studied in the tongue because the future location of these organs can be discerned quite early in development via changes in the morphology of subsets of cells within the lingual epithelium. For example, in the anterior two-thirds of the tongue, fungiform papillae are first evident as two parasagittal rows of columnar epithelial foci (Mistretta, C. M., 1972; Farbman, A. I. and Mbiene, J.-P., 1991). These epithelial thickenings are termed placodes, which grow and invaginate to surround and create the mesenchymal core of each papilla. At birth, an onion-shaped aggregate of immature taste cells is present in the apex of each papilla, which subsequently differentiates fully into a mature taste bud sometime within the first postnatal week. Key to this designation of full differentiation is the postnatal formation of a definitive taste pore, which is the gold standard for a functional taste bud (Hosley, M. A. *et al.*, 1987; Farbman, A. I. and Mbiene, J.-P., 1991; Harada, S. *et al.*, 2000).

Intriguingly, lingual taste buds of the fungiform, foliate, and circumvallate papillae are not fully differentiated at birth in rodents (Mistretta, C. M., 1972; Oakley, B. *et al.*, 1991; Sbarbati, A. *et al.*, 1999), yet newborn mice and rats suckle almost immediately, inferring that they must possess a functional taste system. In fact, it is likely that the taste buds residing in the epithelium of the palate subserve this early requirement for sweet taste sensation in rodent pups (Harada, S. *et al.*, 1997; Sollars, S. I. and Hill, D. L., 2005). Palatal taste buds, as a population, differentiate prior to birth, in that over half of them possess pores, compared to ~15–20% of fungiform taste buds in newborns (Harada, S. *et al.*, 2000; Zhang, G. H. *et al.*, 2006). This result has been corroborated employing immunocytochemistry for a marker of a subtype of differentiated taste cells (Boughter, J. D. *et al.*, 1997; Yang, R. *et al.*, 2000). Using antiserum against alpha-gustducin, the majority of palatal taste buds have gustducin-immunoreactive taste cells at birth (El-Sharaby, A. *et al.*, 2001a; 2001b), while gustducin immunoreactivity is not detected in lingual taste buds until later, during the first postnatal week (El-Sharaby, A. *et al.*, 2001b; Zhang, G. H. *et al.*, 2006).

Regardless of location, and as in axolotls, however, taste bud differentiation occurs well after nerves contact the developing epithelium (Farbman, A. I., 1965; Farbman, A. I. and Mbiene, J.-P., 1991; Mbiene, J.-P. and Mistretta, C. M., 1997; Mbiene, J.-P., 2004; Sharaby, A. E. *et al.*, 2006), consistent with a neural induction model.

The neural induction hypothesis has now also been tested explicitly in rodents via lingual explant culture. Several groups have shown that the formation of fungiform placodes is independent of innervation. When lingual primordia are removed prior to placode formation and then cultured in the absence of innervation, these explants first develop placodes, which then begin papillary morphogenesis (Farbman, A. I. and Mbiene, J.-P., 1991; Mbiene, J.-P. *et al.*, 1997; Nosrat, C. A. *et al.*, 2001; Hall, J. M. *et al.*, 2003; Mistretta, C. M. *et al.*, 2003; Liu, H. X. *et al.*, 2004). Unfortunately, these cultures do not survive long enough to allow taste bud differentiation, and thus the precise relationship between placodes, papillae, and the late developing taste buds is unclear. While a number of studies have examined the impact of loss of sensory neurons via a neurotrophin knockout strategy in mice, this approach has shown primarily that innervation is required postnatally for taste bud maintenance rather than for testing the role of nerves in taste organ formation. These results will be addressed fully later on.

Currently, the accepted model for taste organ development is that placodes arise independently of innervation and, in turn, form rudimentary papillae in the absence of nerves. Shortly before birth, taste bud progenitor cells are organized within a small region of the papillary epithelium, and this latter process is thought to be nerve dependent (Farbman, A. I. and Mbiene, J.-P., 1991; Oakley, B. and Witt, M., 2004; Mistretta, C. M. and Liu, H. X., 2006). A counterview is that placodes actually represent taste bud progenitors (Mbiene, J.-P. and Roberts,

J. D., 2003). Thus the taste progenitor pool arises in a nerve-independent fashion, while full differentiation of these cells is again thought to rely on innervation; however, this early progenitor interpretation is controversial (see Oakley, B. and Witt, M., 2004).

Regardless of the identity of the taste placode cells, that is, progenitors for papillae or for taste buds, it is generally believed that taste papilla development is governed via epithelial–mesenchymal interactions. This assumption is based on similarities with other epithelial specializations, such as hair follicles, teeth, and feathers (Mistretta, C. M., 1998; Yu, M. *et al.*, 2002; Pispa, J. and Thesleff, I., 2003), yet until very recently, experimental tests of this idea were lacking. Through a series of elegant epithelial/mesenchymal recombination experiments employing embryonic lingual explants, Kim J. Y. *et al.* (2003) have shown that there are indeed signals between the epithelium and mesenchyme during early papilla morphogenesis. Moreover, the pattern of placode formation appears to reside within the lingual epithelium, while papillary morphogenesis requires general signals from mesenchyme. This latter finding suggests, as has been shown in axolotls (Parker, M. A. *et al.*, 2004), that taste organ pattern in rodent embryos is set up initially via cell–cell interactions intrinsic to the lingual epithelium. Consistent with a role for intercellular communication, disruption of gap junctional contacts in cultured mouse tongues results in alterations in taste placode pattern (Kim, J. Y. *et al.*, 2005).

4.06.3.3 Molecular Mechanisms of Taste Patterning

In addition to experimental tests of tissue and cellular interactions, there has been an expansion of molecular investigations of developing taste buds. A number of groups have shown that genes belonging to powerful developmental signaling pathways are expressed in the embryonic tongue and taste organs. The pathways investigated include: Sonic Hedgehog (Shh), Bone Morphogenetic Protein (BMP), Wnt/β-catenin, fibroblast growth factor (FGF), and Notch. All of these pathways are key regulators of numerous aspects of embryonic development, as well as of adult tissue homeostasis (Shh: Chuong, C. M. *et al.*, 2000; Marti, E. and Bovolenta, P., 2002; BMP: Tanabe, Y. and Jessell, T. M., 1996; Botchkarev, V. A. and Sharov, A. A., 2004; Wnt: Wodarz, A. and Nusse, R., 1998; Ciani, L. and Salinas, P. C., 2005; FGF: Cornell, R. A. and Eisen, J. S., 2005; Dvorak, P. *et al.*, 2006; Notch: Blanpain, C. *et al.*, 2007).

In terms of taste organ patterning in rodent embryos, the Shh pathway is the most heavily studied to date. Shh is a secreted factor which is recognized by the transmembrane protein, Patched (Ptc) (see Athar, M. *et al.*, 2006). When Shh binds Ptc, this releases Smoothened (Smo), another transmembrane protein, from Ptc inhibition and activates an intracellular cascade, which in turn activates gene transcription. In particular, Shh signaling results in upregulation of Ptc and of the Glil transcription factor. Thus, Glil and Ptc expression are good indicators of active Shh signaling. In embryos, Shh ligand is present throughout the lingual epithelium as the tongue first forms from bilateral lingual swellings and becomes restricted to the columnar placodal epithelial cells as placodes arise. This focal Shh expression persists in papillae as they undergo morphogenesis (Bitgood, M. J. and McMahon, A. P., 1995; Hall, J. M. *et al.*, 1999; Jung, H. S. *et al.*, 1999; Mistretta, C. M. *et al.*, 2003; Liu, H. X. *et al.*, 2004). *Ptc* and *Gli1* are detected similarly throughout the lingual epithelium commencing with tongue formation but, unlike Shh, are also expressed in the subepithelial mesenchyme (Hall, J. M. *et al.*, 1999). Both epithelial and mesenchymal expression of *Ptc* and *Gli1* become progressively limited to the forming taste papillae, until both of these genes are detected in the epithelium in rings surrounding the Shh-expressing cells, as well as within the mesenchymal core of each papilla. In sum, these expression patterns are consistent in time and place with an important role for Shh signaling in taste organ development.

Expression of the BMP pathway has also been examined in the developing tongue of rodent embryos (Jung, H. S. *et al.*, 1999; Hall, J. M. *et al.*, 2003; Nie, X., 2005). BMPs comprise a small subfamily belonging to the large transforming growth factor-β (TGFβ) family of secreted factors (Kingsley, D. M., 1994). BMP ligands bind to heterodimeric BMP receptors which, through a series of transphosphorylations, result in activation of SMAD transcription factors, and thus of target gene transcription (Balemans, W. and Van Hul, W., 2002). BMP signaling is tightly regulated by a host of native, secreted antagonists, of which Noggin was the founding member (Zimmerman, L. B. *et al.*, 1996). When mRNA or protein for several BMP ligands is examined, low-level expression appears to commence throughout the epithelium and mesenchyme of the tongue rudiment as it forms (Jung, H. S. *et al.*, 1999; Zhou, Y. *et al.*, 2006). Expression, especially of *BMP4*,

then consolidates within the developing placodal epithelium, coincident with Shh expression. In fact, there is a one-to-one correspondence between placodal cells expressing BMP4 and those expressing Shh (Hall, J. M. *et al.*, 2003). BMP4 protein is also detected within the subepithelial mesenchyme as papillae develop, whereas its mRNA is not, suggesting that the epithelial cells of the papillae are the source for the diffusible BMP4 found in the mesenchyme (Zhou, Y. *et al.*, 2006). Expression of most other genes of the BMP pathway has yet to be examined in the developing tongue, with the exception of Noggin, a secreted BMP2, 4, and 7 antagonist; Noggin-immunoreactivity is detected in a pattern similar to that described above for the BMP ligand (Zhou, Y. *et al.*, 2006). Like Shh, the timing and pattern of BMP expression is consistent with a role in taste organ formation and patterning.

Most recently, expression of the Wnt/β-catenin pathway has been explored in the developing taste periphery of mouse embryos. Wnts are secreted ligands, comprising 19 members to date (see Relevant Website section). The Wnt signal is transduced by several distinct, yet likely interacting, intracellular pathways (Moon, R. T. *et al.*, 2002; Bejsovec, A., 2005; Widelitz, R., 2005). Of these, the β-catenin pathway is the best studied (Wodarz, A. and Nusse, R., 1998). In the Wnt/β-catenin signaling cascade, Wnt ligands bind Frizzled receptors, which complex with intracellular proteins to inhibit the action of the GSK3β protein kinase. In the absence of Wnt, GSK3β phosphorylates β-catenin, thus targeting the latter for degradation. When Wnt is present, however, β-catenin is not degraded, and accumulates to sufficient levels to translocate to the nucleus and contribute to a transcriptional activating complex with TCF and LEF transcription factors. In this way, Wnt-responsive target genes are activated.

Wnt expression is evident in developing mouse tongues coincident with the appearance of taste placodes. In particular, *Wnt10b* is restricted to placodal epithelium, while *Wnt10a* is found broadly throughout the lingual epithelium as taste placodes form (Iwatsuki, K. *et al.*, 2007; Liu, F. *et al.*, 2007). Similarly, *Lef1*, a downstream transcription factor of the Wnt/β-catenin pathway is expressed in taste placodes and later in taste papilla epithelium (Iwatsuki, K. *et al.*, 2007). Via use of mice expressing a Wnt/β-catenin reporter transgene (TOPGAL transgenic strain; DasGupta, R. and Fuchs, E., 1999), the location of Wnt-responsive cells has also been determined. The TOPGAL gene reveals active Wnt/β-catenin signaling in the lingual epithelium commencing as taste placodes form, and consistent with *Wnt10b* focal expression (Okubo, T. *et al.*, 2006; Iwatsuki, K. *et al.*, 2007; Liu, F. *et al.*, 2007). However, TOPGAL expression is also evident at these early stages in the intervening epithelial cells destined to give rise to filiform, that is, nongustatory, papillae of the lingual surface (Liu, F. *et al.*, 2007). Intriguingly, TOPGAL expression becomes increasingly restricted in the lingual epithelium, such that immediately prior to birth, it is detected only in immature taste buds in the apices of the fungiform papillae (Liu, F. *et al.*, 2007). Thus, Wnt/β-catenin signaling is implicated in taste organ formation, and possibly taste bud differentiation, by virtue of its spatiotemporal pattern of expression.

Compared with the extensive data on Shh, BMP, and recently Wnts, there is far less information on the expression of the FGF and Notch pathways in developing tongues. The FGF family comprises 22 genes to date, with numerous splice variants, which bind to FGF receptors (FGFRs 1–4; Itoh, N. and Ornitz, D. M., 2004). mRNA for several FGF ligands and a variety of FGFRs have been detected in the developing tongues of mice (Jung, H. S. *et al.*, 1999; Nie, X., 2005). *Fgf8*, which is known to function in early branchial arch patterning (Abu-Issa, R. *et al.*, 2002; Crump, J. G. *et al.*, 2004), is expressed in the lingual epithelium and subepithelial mesenchyme in the lateral lingual swellings prior to their fusion into the tongue rudiment (Jung, H. S. *et al.*, 1999). By the time the tongue proper has formed and taste placodes begin to appear, however, *Fgf8* expression is lost, suggesting that FGF8 functions in tongue formation, but does not have a direct role in taste placode formation.

The Notch pathway has numerous roles in cell fate decisions throughout embryonic development. Notch is a transmembrane receptor, which recognizes several transmembrane ligands, including Delta-like (Dll) and Jagged (or Serrate), in adjacent cells. When the Notch receptor is activated, gamma secretases cleave N, generating the N intracellular domain (N_{ICD}), which translocates to the nucleus and affects target gene transcription (Artavanis-Tsakonas, S., 1988; Cornell, R. A. and Eisen, J. S., 2005). In particular, in the developing nervous system and in neural stem cells, activated Notch signaling turns on transcription of Hes transcription factor genes and these cells assume a glial fate or remain undifferentiated; while cells in which Notch is not active transcribe neurogenic genes, such as Mash1, and assume a neural fate (Gaiano, N. and Fishell, G., 2002). In the developing tongue, Notch gene expression is not detected until well after Wnt,

Shh, and BMP expression have become focal within developing papillae (Seta, Y. *et al.*, 2003). As the papillae undergo morphogenesis, several Notch receptors and ligands are expressed broadly in the papillary epithelium. The transcription factors, *Mash1* and *Hes6,* by contrast, are expressed in small numbers of epithelial cells during papillary development (Seta, Y. *et al.*, 2003). Thus, while Shh, Wnt, and BMP expression are coincident with placode formation, Notch signaling appears to function later on, during papillary morphogenesis, and thus may regulate cell fate decisions within taste papillae.

4.06.3.4 Tests of Gene Function in Taste Organ Formation and Patterning

Recent tests of Wnt, Shh, and BMP function have revealed roles for each of these pathways in early taste organ development, as was predicted based upon the spatiotemporal expression of these genes. Perhaps the most complete studies have come from manipulation of Wnt/β-catenin, where the levels of signaling by this pathway have been altered genetically *in vivo* and via pharmacological manipulation *ex vivo* (Iwatsuki, K. *et al.*, 2007; Liu, F. *et al.*, 2007).

Using tissue-specific and inducible transgenic mouse lines, Wnt/β-catenin signaling was completely abolished within the lingual epithelium of mouse embryos, commencing just prior to the onset of taste placode formation. In these knockdown and knockout embryos, placodes are not evident, nor are evaginated papillae present at birth (Liu, F. *et al.*, 2007). Similarly, papillae are reduced, although not lost, in both Lef1$^{-/-}$ and Wnt10b$^{-/-}$ mice (Iwatsuki, K. *et al.*, 2007), implying that these two genes are not the only Wnt signaling genes involved in taste placode and papillary development. Conversely, when β-catenin is stabilized, that is, genetic alteration having rendered β-catenin resistant to degradation throughout the embryonic lingual epithelium, the entire lingual surface is transformed into taste papillae. Moreover, filiform papillae are absent, and taste buds within the taste papillae appear to have accelerated development (Liu, F. *et al.*, 2007).

Wnt/β-catenin signaling also appears to function as an initiator signal for taste placode formation, as it is upstream, at least genetically, of both Shh and BMPs. When Wnt/β-catenin signaling is lost, *Shh* is not expressed in the lingual epithelium, consistent with the observed loss of placodes. Similarly, *BMP4* is not expressed in the lingual epithelium of mouse embryos with epithelial loss of Wnt/β-catenin function (Liu, F. *et al.*, 2007). Moreover, in the gain-of-function genetic manipulation, as well as *ex vivo* when Wnt/β-catenin signaling is increased pharmacologically, *Shh* expression is increased, in that *Shh* placodal expression is expanded (Iwatsuki, K. *et al.*, 2007; Liu, F. *et al.*, 2007). Wnt/β-catenin is also upstream of Sox2, a transcription factor recently shown to be required for taste organ development (Okubo, T. *et al.*, 2006); elevation of Wnt/β-catenin signaling in cultured tongue explants increases Sox2-expressing taste placodes.

The role of Wnt/β-catenin as a positive regulator of Shh signaling, however, appears to be reciprocal, in that manipulation of Shh in cultured tongue explants alters expression of Wnt activity, as monitored by the TOPGAL reporter gene (Iwatsuki, K. *et al.*, 2007). Substantial data also implicate a key role for Shh in taste placode formation. When Shh is blocked in cultured tongue explants, taste placodes increase in number and size and occur closer together (Hall, J. M. *et al.*, 2003; Mistretta, C. M. *et al.*, 2003), while Shh ligand blocks papillary formation (Iwatsuki, K. *et al.*, 2007). These effects are clearly indirect, however, as blocking Shh causes placodal Shh expression to expand, as do taste papillae, while increasing Shh signaling *in vitro* causes loss of Shh expression just as taste papillae are lost. Moreover, Shh also regulates BMP4; Shh inhibition *in vitro* increases the number and size of BMP4-expressing placodes (Hall, J. M. *et al.*, 2003). Recently, BMPs have also been implicated in regulation of Shh in developing taste papillae (Zhou, Y. *et al.*, 2006). Again, using a culture approach, antagonizing BMP in lingual explants results in more and larger papillae, with commensurate increases in Shh expression, while exposure to BMPs reduces papillae and Shh expression. In sum, these functional data suggest that the molecular regulation of taste placode formation relies upon a network of interactions of at least the Wnt/β-catenin, Shh, and BMP pathways, which are likely integrated by additional intracellular and extracellular mechanisms.

4.06.4 Development of the Circumvallate Papilla, a Specialized Structure in Mammals

Until now, this review has focused on development of fungiform papillae and their resident taste buds, which arise as a distributed array on the anterior two-thirds of the tongue. However, mammals possess additional lingual taste buds housed in complex, and

large, papillae at the posterior portion of the lingual tongue; these are the circumvallate and foliate papillae. In adult rodents, each of these structures possesses hundreds of taste buds embedded in the epithelia lining the trenches and folds of the circumvallate and foliate papillae, respectively. The circumvallate papilla in particular is known to have a number of additional anatomical specializations. von Ebner's glands (also known as posterior deep lingual glands) empty directly into the circumvallate trenches (Sbarbati, A. *et al.*, 2002; Lee, M. J. *et al.*, 2006; Suzuki, Y., 2006). Additionally, the mesenchymal core of the circumvallate is associated with a circumvallate ganglion (Graziadei, P. P. and Graziadei, G. A., 1978; Sbarbati, A. *et al.*, 2000). Thus, the development of the circumvallate papilla involves the coordinated formation of a complex taste organ, in concert with glandular and ganglionic components.

The circumvallate papilla of rodents begins to develop quite early, as the lateral lingual swellings of the tongue first fuse at the midline. At this time point, the epithelium of the future circumvallate has already begun to thicken (Jitpukdeebodintra, S. *et al.*, 2002). Shortly thereafter, it is recognizable as a broad epithelial thickening or placode, also visible on the dorsal surface of the tongue, coincident with the appearance of fungiform placodes (Paulson, R. B. *et al.*, 1985; AhPin, P. *et al.*, 1989; Wakisaka, S. *et al.*, 1996; Mbiene, J.-P. and Roberts, J. D., 2003). Subsequently, the lateral walls of the presumptive papillae invaginate and grow ventrally, surrounding a large mesenchymal core, which is invaded by neuroblasts of the papillary ganglion. Trench invagination continues, due to cell proliferation localized primarily to the growing tips of the trench epithelium (Lee, M. J. *et al.*, 2006), for the remainder of embryogenesis and into postnatal stages (Mistretta, C. M., 1972; Sbarbati, A. *et al.*, 2000; Jitpukdeebodintra, S. *et al.*, 2002). The trenches are thought to give rise to the von Ebner's glands via branching morphogenesis commencing late in embryonic development (Jitpukdeebodintra, S. *et al.*, 2002; Lee, M. J. *et al.*, 2006). The taste buds first differentiate within the circumvallate epithelium several days after birth (Mistretta, C. M., 1972; Oakley, B. *et al.*, 1991), although onion-shaped aggregates of cells considered to be immature taste buds are evident at birth in rodents (Mistretta, C. M., 1972).

Given the complex nature of the circumvallate papilla, are the molecular mechanisms governing its formation similar to those involved in fungiform development? At first glance, they may not be. Although both *Shh* and BMP4 are expressed in the developing circumvallate papilla (Hall, J. M. *et al.*, 1999; 2003; Lee, M. J. *et al.*, 2006), alterations in Shh signaling *in vitro* do not appear to affect circumvallate morphology or Shh expression therein (Hall, J. M. *et al.*, 2003; Mistretta, C. M. *et al.*, 2003; Liu, H. X. *et al.*, 2004). BMP2 and BMP4 do not appear to be expressed in the developing circumvallate, nor does manipulating BMP signaling in tongue explants appear to affect this papilla (Zhou, Y. *et al.*, 2006). Further, evidence of Wnt/β-catenin signaling was not observed by us in the developing circumvallate papilla (Liu, F. *et al.*, unpublished observation), suggesting that Wnt/β-catenin may not be active in this taste structure during embryogenesis. Thus, it appears that molecular mechanisms distinct from those involved in fungiform placode formation likely regulate circumvallate development. This dichotomy may be due to the increased complexity of this posterior taste papilla or may reflect an endodermal origin (Zhang, C. and Oakley, B., 1996).

Specifically, the oral cavity marks the boundary between the surface ectoderm and the foregut endoderm, although precisely where the border lies in rodents has been a topic of conjecture. One possibility, based on differential cytokeratin expression, is that the circumvallate lies in the endodermal epithelium, while the fungiform taste buds arise from ectoderm covering the anterior portion of the tongue (Zhang, C. and Oakley, B., 1996). Another molecular correlate of this supposition is that cytokeratin 14 (K14) is expressed in the epithelium of the anterior two-thirds of the embryonic tongue, encompassing the fungiform domain, yet is absent from the posterior third of the lingual epithelium where the circumvallate forms (Liu, F. *et al.*, 2007). This difference in K14 expression may indicate that each region arises from a different germ layer, fungiform from ectoderm, circumvallate from endoderm, or may simply reflect different molecular regulation of anterior versus posterior taste organs due to differences in their complexity.

4.06.5 Taste Bud Cell Lineage and Turnover

Postnatal taste buds comprise a heterogeneous population of approximately 100 cells, divided into roughly three cell types, I, II, and III, based upon ultrastructure and molecular markers (see Chapters Ultrastructure of Taste Buds and Taste Receptors). Briefly, type I cells are thought to function as glia,

while types II and III are taste receptor cells. Type II cells express numerous bitter, sweet, and umami receptors and lack clear morphological synapses. In contrast, type III cells possess synapses and the transduction machinery for sour tastants. However, the intrigue from a developmental biologist's perspective in investigating mature taste buds is that the cells within each bud are continually replaced at a rapid pace, raising the questions of how taste cells are related to one another within a bud, and what is the nature of the cell lineage(s) that produces taste bud cells. Our current knowledge of taste cell turnover is limited primarily to birthdating studies for differentiated taste cell types.

Immature taste cells are thought to arise as a result of asymmetric division of between 7 and 13 putative stem or progenitor cells per taste bud (Beidler, L. M. and Smallman, R. L., 1965; Farbman, A. I., 1980; Stone, L. M. *et al.*, 2002). After ~3 days, taste cells differentiate, expressing appropriate cell type immuno-markers (Zhang, C. *et al.*, 1995; Cho, Y. K. *et al.*, 1998; Hirota, M. *et al.*, 2001). The relationship among cells of each bud is unclear, although type I cells likely represent a distinct lineage (Farbman, A. I., 1980). In terms of types II and III cells, either these are distinct cell lineages (Hamamichi, R. *et al.*, 2006), or a subset of type III cells may also give rise to type II cells (Miura, H. *et al.*, 2005; Ueda, K. *et al.*, 2006). Finally, taste cells are relatively short lived, as they die, via programmed cell death, on average 10 days after birth (Beidler, L. M. and Smallman, R. L., 1965; Farbman, A. I., 1980; Delay, R. J. *et al.*, 1986). However, it appears that not all taste cells have equivalent residence times in the taste bud. For example, in Farbman's tritiated thymidine birthdating study, he found that while the average lifespan for a likely type I or glial cell was 9 days, the persistence of type II receptor cells could be detected for as long as 25 days (Farbman, A. I., 1980). More recently, this finding has been confirmed using BrdU birthdating in combination with taste cell-type markers for types II and III (Hamamichi, R. *et al.*, 2006). A very short-lived population of cells is detected in taste buds with an average life span of 2 days, while a small proportion of type II and III cells are long-lived residents in the taste bud, detectable after 21 days. This perdurance of type II and III cells may reflect more elaborate differentiation and functional requirements for receptor cells compared with glial cells; the latter might be replaced on a shorter time frame. Alternatively, the very short lived cells may be immature taste cells of all three types and indicate that taste bud stem cells continually produce an overabundance of immature cells to quickly accommodate injury or any errors in cell lineage decisions.

While it is well recognized that taste buds continually turn over, the molecular regulation of this process is unknown. Certainly a large number of regulatory genes and transcription factors are expressed in subsets of adult taste cells, implying that these factors function in taste cell turnover and lineage decisions within buds. For example, several embryonic signaling pathways persist in adult taste buds. *Shh* is expressed in a small number of rounded cells in the basal compartment of each taste bud, while the Shh receptor, *Ptc1*, localizes to cells surrounding the bud (Miura, H. *et al.*, 2001; 2003). Elements of the Notch pathway are also found in adult taste buds, including Notch receptors and ligands, as well as downstream transcription factors (Kusakabe, Y. *et al.*, 2002; Suzuki, Y. *et al.*, 2002; Miura, H. *et al.*, 2003; Seta, Y. *et al.*, 2003; Hamamichi, R. *et al.*, 2006; Seta, Y. *et al.*, 2006). In addition, a number of other signaling pathways not well described in embryonic taste organ development are present in adult taste buds, including the EGF pathway (McLaughlin, S. K., 2000; Sun, H. and Oakley, B., 2002) and the insulin-like growth factor (IGF) pathway (Suzuki, Y. *et al.*, 2005). Consistent also with a role in taste cell turnover, loss of expression of many of these gene products occurs when taste buds are denervated in nerve injury experiments, which are known to cause a transitory loss of taste buds, including *Shh* (Miura, H. *et al.*, 2004), *Mash*1(Seta, Y. *et al.*, 1999), and NeuroD, a transcription factor in the Notch pathway (Suzuki, Y. *et al.*, 2002). In each of these cases, as the nerve regenerates, taste buds reappear, as does the expression of these factors. However, these data are correlative. To elucidate the function of these gene pathways in taste cell turnover and to perhaps gain insight into the lineage relationships of taste cells within buds, inducible genetic manipulations will have to be employed.

Innervation is also known to regulate taste bud differentiation and maintenance, and this topic will be considered fully in a later section.

4.06.6 Development of Gustatory Innervation

The other major focus of this review is to discuss the development of the gustatory sensory neurons which contact taste buds in the lingual epithelium and

convey taste information to the gustatory centers of the hindbrain. As mentioned in the introduction, the neurons that reside in the gustatory cranial ganglia arise embryonically from two neurogenic tissues that form both outside of the developing neural tube and distant from the oral epithelium. These two populations of developing sensory neurons must first locate one another and coalesce into a ganglion. They then send out both peripheral and central neurites to pathfind to the proper targets and make appropriate synaptic connections with taste buds and hindbrain neurons, respectively.

4.06.6.1 Development of the Sensory Neurons of the Gustatory Ganglia

Sensory neurons of the VII, IX, and X cranial nerve ganglia convey gustatory information from the mouth, pharynx, and larynx to the brain. Neurons of each of these ganglia arise from two discrete embryonic regions: the epibranchial placodes and a subset of the cranial neural crest (Narayanan, C. H. and Narayanan, Y., 1980; D'Amico-Martel, A. and Noden, D. M., 1983; Barlow, L. A. and Northcutt, R. G., 1995; Northcutt, R. G. and Brändle, K., 1995; Gross, J. B. *et al.*, 2003). Epibranchial placodes are a series of epithelial thickenings, which form in the ectoderm just dorsal to the branchial arches as the neural tube fuses. These placodes are neurogenic, in that they are mitotically active, producing immature neuroblasts which then migrate to assemble into portions of cranial ganglia VII, IX, and X (Webb, J. F. and Noden, D. M., 1993; Baker, C. V. and Bronner-Fraser, M., 2001; Begbie, J. and Graham, A., 2001a; Begbie, J. *et al.*, 2002; Schlosser, G., 2006). The cranial neural crest is a migratory population of cells, which gives rise to a broad variety of derivatives, including a portion of the sensory neurons and all of the glial cells of the VII, IX, and X cranial ganglia (Le Douarin, N. M. and Kalcheim, C., 1999).

Based primarily upon descriptive studies in catfish, it has been proposed that the epibranchial placodes give rise to the gustatory neurons of each ganglion. Catfish are rather unique with respect to the taste system; they have thousands of external taste buds distributed in the skin covering their head and trunk (Landacre, F. L., 1907; Atema, J., 1971; Reutter, K. *et al.*, 1974; Caprio, J. *et al.*, 1993). Regardless of location, these external taste buds are all innervated by a recurrent branch of the VII cranial nerve, and the ganglion for this nerve is greatly enlarged in catfish (Herrick, C. J., 1903; Kohbara, J. *et al.*, 1992). In examining the developing epibranchial placode of the VII ganglion, Landacre found that it was also enlarged, and its size correlated with the size of the VII ganglion itself and with the vast number of taste buds this nerve innervates in catfish (Landacre, F. L., 1907; 1910). More recently, using grafting and transgenic technology in axolotls, we find that indeed epibranchial placodes give rise to sensory neurons that exclusively innervate taste buds (Harlow, D. and Barlow, L. A., in preparation). Moreover, neural crest-derived sensory neurons in these same ganglia provide only somatosensory innervation to the oral and pharyngeal epithelium, and never innervate taste buds. Thus despite coalescence of these two cell populations within the ganglia providing gustatory innervation to the oral cavity, the mature function of these neurons is determined by their embryonic origin.

Once these sensory neurons have come together to form the nascent cranial ganglia, these cells begin to send out processes both distally and proximally to pathfind to their peripheral taste bud and central nervous system (CNS) targets.

4.06.6.2 Development of Peripheral Taste Innervation

In rodents, fungiform taste buds and taste papillae are innervated by the chorda tympani (gustatory) branch of the VII nerve and the lingual (somatosensory) branch of the V nerve, while the circumvallate receives both gustatory and somatosensory innervation from the glossopharyngeal (IX) nerve. Fungiform innervation commences shortly after ganglion formation as the chorda tympani and lingual nerve fibers penetrate the base of the developing tongue rudiment (Mbiene, J.-P. and Mistretta, C. M., 1997; Scott, L. and Atkinson, M. E., 1998; Mbiene, J.-P., 2004), while the glossopharyngeal nerve enters the tongue 1 day later (Mbiene, J.-P. and Mistretta, C. M., 1997). Almost immediately after entering the tongue, the chorda tympani and lingual nerves, which have thus far traveled into the tongue as a unitary bundle, now defasciculate, and branches of each nerve extend toward the dorsal epithelial surface (Mbiene, J.-P., 2004). During this initial sensory innervation, the bulk of sensory fiber growth into the tongue in both rats and mice is from the chorda tympani nerve; growth of lingual fibers appears to follow the chorda tympani into the tongue (Rochlin, M. W. and Farbman, A. I., 1998; Mbiene, J.-P., 2004). As chorda tympani axons approach the epithelial surface they branch profusely. However, even 1 day prior to target

innervation (at E13.5 in mice), only a few nerve bundles are specifically directed toward developing fungiform placodes (Mbiene, J.-P., 2004). In mice at this age, many nerve bundles have been described as having brush-like endings with numerous filopodia (Mbiene, J.-P., 2004). If so, these endings could be sampling the local environment to locate molecular cues that then guide the fiber bundles to individual fungiform placodes. Once chorda tympani fiber bundles are close to the epithelial surface they begin to grow toward taste placodes. Although lingual nerve bundles branch as they near the epithelial surface, growth of lingual fibers is not directed toward fungiform placodes (Mbiene, J.-P., 2004).

The initial progression of chorda tympani and lingual innervation in the tongue varies considerably among species, even between different rodents. In rats and mice, the chorda tympani is the first nerve to enter the tongue followed by the lingual fibers, while in hamsters, the lingual nerve is the first to enter the tongue and provides the bulk of its innervation (Whitehead, M. C. and Kachele, D. L., 1994). Also, unlike lingual innervation in rats and mice, the lingual nerve bundles in hamsters are actually directed toward fungiform papillae, with chorda tympani nerve bundles following (Whitehead, M. C. and Kachele, D. L., 1994).

By E14 in hamster, E14.5 in mouse, and E16 in rat, chorda tympani fibers have entered the core of the fungiform papillae and are clearly associated primarily with gustatory organs (Figure 3(a); Farbman, A. I. and Mbiene, J.-P., 1991; Whitehead, M. C. and Kachele, D. L., 1994; Mbiene, J.-P., 2004). By E16.5–E17 in rat and E14.5–E15 in mouse, chorda tympani fibers first penetrate the epithelium of individual taste papillae (Farbman, A. I., 1965; Farbman, A. I. and Mbiene, J.-P., 1991; Hall, J. M. *et al.*, 1999; Mbiene, J.-P. and Roberts, J. D., 2003). Initial innervation is sparse, but additional fibers continue to invade the epithelium at later embryonic ages. Synapse-like structures between gustatory afferents and fungiform taste buds are first observed several days after the initial innervation of fungiform papillae (Mbiene, J.-P. and Farbman, A. I., 1993). The sequence of events is comparable for the circumvallate papilla; glossopharyngeal fibers invade the circumvallate papilla core by mid-gestation and occasionally penetrate the epithelial surface (Figure 5(b); Mbiene, J.-P. and Mistretta, C. M., 1997). Circumvallate taste buds appear within the epithelial trenches and develop synapses during early postnatal development (Kinnamon, J. C. *et al.*, 2005). During this time, a robust neural plexus surrounds the taste bud; in addition to afferent synapses, this neural plexus contains neuroneuronal synapses. The role of this neural plexus is unclear, but it could be important for organizing initial taste bud–neuron connectively.

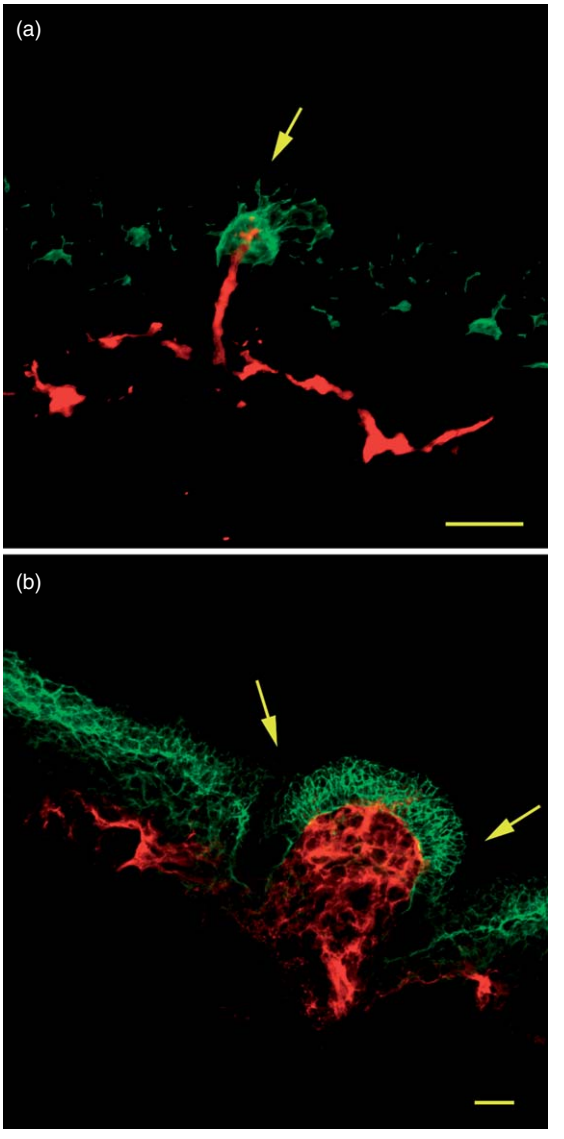

Figure 3 By E14.5 in the mouse, developing gustatory epithelia (anti-Shh; green) are associated with nerve fibers (anti-GAP43; red). Innervation has penetrated the epithelia of the developing fungiform papillae (a. arrow), although a neural bud is not yet present. The core of the developing circumvallatc papillae is filled with nerve fibers (b, between arrows). Scale bar = 20 μm.

Because chorda tympani nerve bundles are already associated with newly formed fungiform papillae by E14.5, the accuracy of initial targeting can be quantified at this age (Figure 4; Lopez, G. F. and Krimm, R. F., 2006b). This early targeting is incredibly accurate

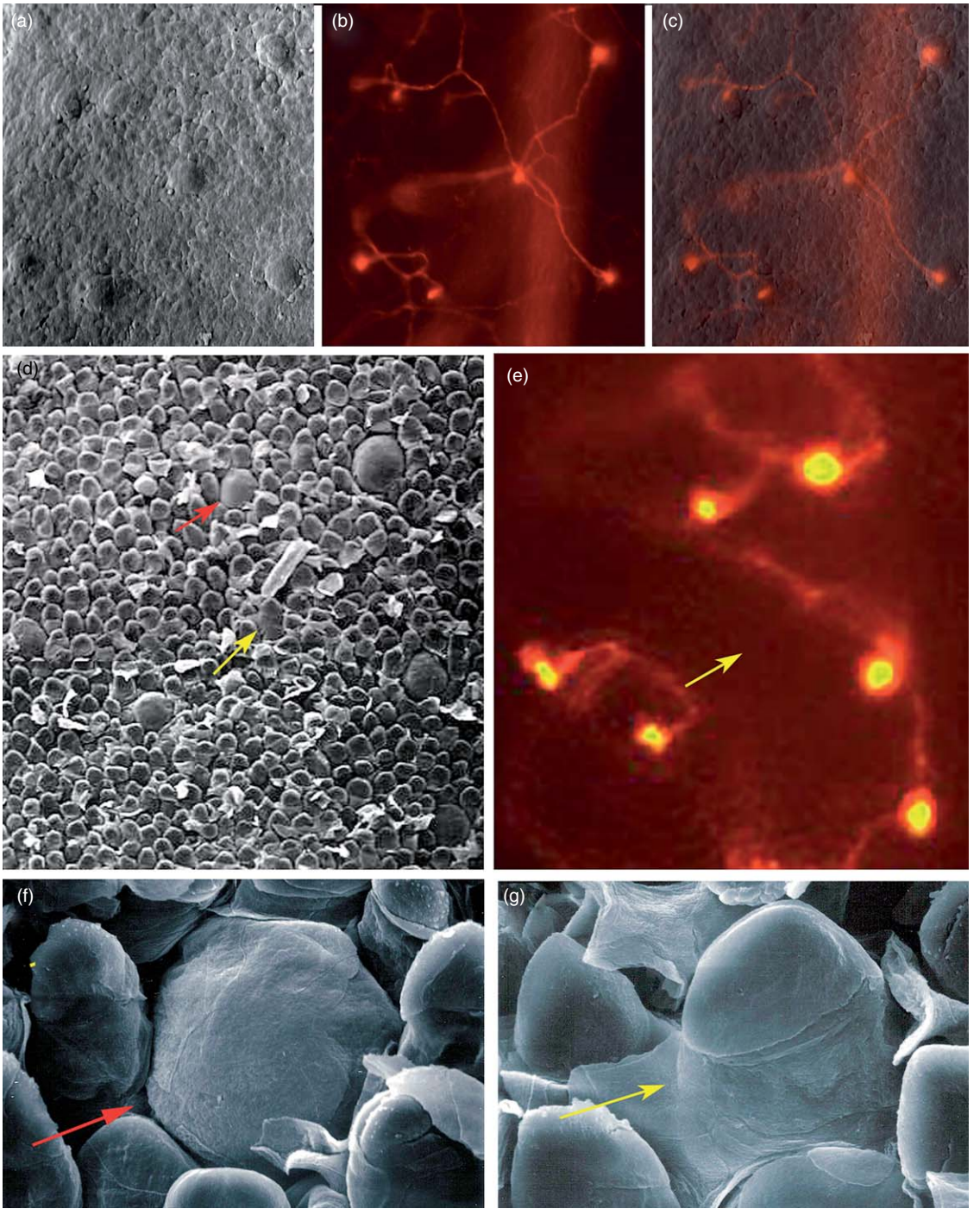

Figure 4 The locations of fungiform papillae (a,d) and innervation patterns (b,e) can be visualized in the same tongues by labeling first with DiI and then processing for scanning electron microscopy. Most fungiform papillae are innervated at both E14.5 (a,b,c) and E18.5 (d,e,f,g), although a few remain uninnervated. By E18.5, any uninnervated papillae (yellow arrow in d,g) have begun to adopt a morphology more similar to surround filiform papillae. Innervated papillae (red arrow in d and f) have a normal appearance.

in that most fungiform papillae are innervated and most fiber bundles are associated with a fungiform papilla. However, a few fungiform papillae are lacking innervation, and the chorda tympani innervates a few regions of the tongue that have no papillae. Between E14.5 and E18.5, most fungiform papillae previously lacking innervation now receive innervation, and any aberrant fiber bundles withdraw from nongustatory epithelium. Thus, a period of embryonic plasticity and rearrangement follows initial innervation.

Although the path gustatory axons take to their final destination is well described, axon guidance mechanisms are less clear. *In vitro*, initial axon outgrowth from gustatory ganglia requires addition of a neurotrophin to the culture media (Rao, H. *et al.*, 1997; Rochlin, M. W. *et al.*, 2000; Wiklund, P. and Ekstrom, P. A., 2000). Neurotrophins are a group of structurally and functionally related growth factors that exert a major influence on numerous aspects of sensory and sympathetic neuron development. The neurotrophins, brain-derived neurotrophic factors (BDNFs), neurotrophin-4 (NT4), and glial-derived neurotrophic factors (GDNFs) are capable of supporting neurite outgrowth of geniculate ganglion (VII) neurons, while neurotrophin-3 (NT3) and nerve growth factor (NGF) are not (Rao, H. *et al.*, 1997; Rochlin, M. W. *et al.*, 2000). Interestingly, removal of BDNF or NT4 does not disrupt the ability of chorda tympani axons to reach the tongue (Lopez, G. F. and Krimm, R. F., 2006a), indicating that neurotrophins are also functionally redundant for supporting initial axonal outgrowth *in vivo*.

Because the growth of chorda tympani axon bundles appears to follow predetermined pathways (Mbiene, J.-P. and Mistretta, C. M., 1997), the chorda tympani is probably guided by molecular cues in the environment. It is likely that multiple chemoattractive and chemorepulsive cues are required to direct gustatory axons from the geniculate (nVII) and petrosal (nIX) ganglia to the tongue and then to individual fungiform and circumvallate placodes (Tessier-Lavigne, M. and Goodman, C. S., 1996). For example, one factor produced by the tongue mesenchyme may encourage initial tongue innervation. A second factor produced by early gustatory epithelia may allow chorda tympani fibers to distinguish gustatory from surrounding epithelium. Finally, multiple chemorepulsive cues likely prevent chorda tympani axons from invading areas prematurely, from exiting the appropriate axonal pathway prematurely, and from innervating nongustatory regions of the epithelium.

One chemorepulsive factor important during both trigeminal and gustatory axon guidance is semaphorin 3A (Sema3A; Rochlin, M. W. and Farbman, A. I., 1998; Rochlin, M. W. *et al.*, 2000), which is expressed in developing tongue (Giger, R. *et al.*, 1996). Sema3A expression decreases medially to laterally across the tongue surface and prevents premature and aberrant growth of trigeminal and gustatory fibers into the tongue mid-region (Rochlin, M. W. and Farbman, A. I., 1998; Rochlin, M. W. *et al.*, 2000). In addition, as geniculate fibers near the epithelial surface, Sema3A may prevent premature penetration of the epithelium (Vilbig, R. *et al.*, 2004).

The lingual epithelium also produces chemoattractants (Gross, J. B. *et al.*, 2003; Vilbig, R. *et al.*, 2004). Axons of gustatory neurons isolated from the epibranchial placodes of axolotl are attracted to the pharyngeal endoderm (Gross, J. B. *et al.*, 2003). In addition, tongue explants from rats attract geniculate ganglion axons in culture (Vilbig, R. *et al.*, 2004). The chemoattractive factor emanating from the tongue epithelium has not yet been identified; however, it is probably not a neurotrophin because its chemoattractive properties are not blocked by the addition of high concentrations of neurotrophic factors to the culture media (Vilbig, R. *et al.*, 2004). This unidentified factor may be responsible for encouraging initial gustatory axon growth into the tongue and/or may direct chorda tympani branches to grow toward the dorsal tongue epithelia.

Although neurotrophins are not required to attract gustatory axons to the tongue, *in vitro* and *in vivo* studies support a chemotropic role for neurotrophins in the developing taste system. Growth cones reorient and grow toward a neurotrophin source (Ming, G. *et al.*, 1997; Paves, H. and Saarma, M., 1997; Ming, G. *et al.*, 1999; Tucker, K. L. *et al.*, 2001) and axons of the geniculate ganglion are attracted to beads containing BDNF (Rochlin, M. W. *et al.*, 2006). In the tongue, BDNF is located in gustatory epithelium while the surrounding somatosensory epithelium primarily expresses NT3 (Nosrat, C. A. and Olson, L., 1995; Nosrat, C. A. *et al.*, 1996; Nosrat, C. A., 1998; Fan, L. *et al.*, 2004). Thus, BDNF and NT3 are in the correct locations to direct gustatory fibers to fungiform papillae and somatosensory fibers to nongustatory epithelium. Consistent with these possible roles for BDNF and NT3, the disruption of the normal BDNF expression pattern *in vivo* prevents chorda tympani innervation of fungiform papillae (Ringstedt, T. *et al.*, 1999; Krimm, R. F. *et al.*, 2001; Lopez, G. F. and Krimm, R. F., 2006a). Specifically, overexpression of BDNF throughout the lingual epithelium, under the control of a keratin 14

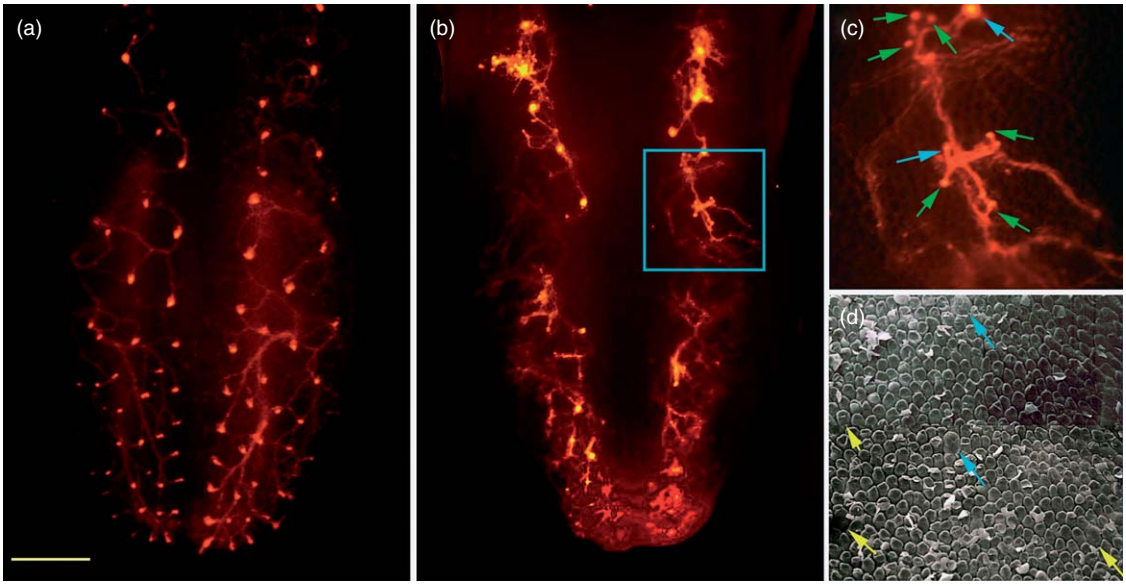

Figure 5 Innervation patterns are disrupted in BDNF-OE mice (b) compared with wild type mice (a). Fibers from the chorda tympani branch as they near the tongue surface in wild type mice (a) and innervate specific regions of the epithelium. In BDNF-OE mice (b), many thin processes are present near the epithelial surface; however, most fail to innervate fungiform papillae. The apparent disorganization of gustatory innervation can be seen more clearly in higher magnification of the tongue mid-region (c) along with scanning electron microscopy of the same region (d). While some of fungiform papillae appear to be innervated (blue arrows in c,d), some regions of the tongue epithelium are innervated by gustatory fibers even though no fungiform papillae are near by (green arrows in c). In addition, some fungiform papillae clearly remain uninnervated (yellow arrows in d). Scale bar in (a) = 500 μm and applies to (a) and (b).

promoter, disrupts the initial innervation of fungiform papillae and alters the normal morphology of gustatory sensory neurons (Figure 5; Krimm, R. F. *et al.*, 2001; Lopez, G. F. and Krimm, R. F., 2006a). BDNF overexpression also increases branching and attracts gustatory innervation to inappropriate regions of the taste epithelium. Finally, BDNF overexpression in both muscle and gustatory neurons disrupts chorda tympani target innervation (Ringstedt, T. *et al.*, 1999). Importantly, removal of functional BDNF also disrupts normal targeting (Lopez, G. F. *et al.*, 2006). In $BDNF^{-/-}$ mice, geniculate axons enter the tongue and grow toward the lingual epithelium normally, but once they near the epithelial surface, they grow wildly in the lamina propria and fail to penetrate the developing gustatory epithelia. Taken together, these findings indicate hat the chemoattractant properties of BDNF allow chorda tympani fibers to select and penetrate fungiform placodes as their appropriate target. It is still not clear whether NT3 is required to direct somatosensory afferents toward the nongustatory lingual epithelium, but NT3 expression patterns are consistent ith this possibility (Nosrat, C. A. and Olson, L., 1998).

4.06.6.3 Development of Projections of Gustatory Neurons to the Central Nervous System

The central axons of all cranial ganglion sensory neurons, including those of gustatory ganglia, project to the hindbrain. In axolotl, projections from early forming ganglia reach both peripheral and central targets earlier than later forming ganglia (Fritzsch, B. *et al.*, 2005). Each cranial ganglion forms its central and peripheral projections simultaneously, ruling out the possibility that innervation of peripheral targets directs central innervation and vice versa. Instead, the central and peripheral targets for these ganglia appear to be selected as the ganglia develop, with more ventrally located ganglia developing first and innervating central and peripheral targets that form early. More dorsally located ganglia develop later and innervate peripheral and central targets that develop later, thus suggesting that early molecular cues for ganglion differentiation may also influence the selection of central targets.

In rat CNS, geniculate ganglion axons begin to invade the first central nucleus of the gustatory system in the hindbrain, the nucleus of the solitary tract

(NTS), at E15 (Zhang, L. L. and Ashwell, K. W., 2001), the same age that peripheral fiber bundles arrive at fungiform papillae (Farbman, A. I. and Mbiene, J.-P., 1991). Thus, similar to axolotl, rat CNS projections from gustatory ganglia develop at the same time as peripheral projections. Consequently, peripheral connections with fungiform papillae probably do not control CNS targeting. Rather, as in axolotl, molecular cues for timing ganglia differentiation may also direct CNS targeting. Consistent with this idea, in mammals, the same transcription factor (e.g., Phox2b) regulates the development of geniculate and petrosal ganglia and their CNS target, the NTS, thus coordinating visceral sensory circuitry (Dauger, S. *et al.*, 2003).

Centrally projecting taste afferents find their way to the hindbrain by following the path of migrating neuroglial neural crest from the hindbrain (Begbie, J. and Graham, A., 2001b). When the neural crest is ablated prior to migration, gustatory ganglion neurons fail to migrate internally from the epibranchial placodes. Central processes of these neurons form aberrant connections, frequently with adjacent ganglia, and fail to project toward the hindbrain. Thus, early developmental events such as the timing of ganglion differentiation, transcription factors, and migrating neural crest cells function together to regulate the initial growth of gustatory projections to the NTS.

4.06.6.4 Survival and Maintenance of Gustatory Neurons and Taste Buds

In addition to their demonstrated role in targeting of gustatory afferents, neurotrophins are also important for gustatory neuron survival. The traditional view of neurotrophic function is that sensory neuron targets regulate the number of surviving neurons by secreting limited amounts of neurotrophic compounds. BDNF may function as an important target-derived factor in the taste system, influencing neuronal survival after initial innervation of gustatory epithelium. BDNF mRNA is expressed in cells of the developing gustatory epithelium and taste buds (Nosrat, C. A. and Olson, L., 1995; Nosrat, C. A. *et al.*, 1996), and BDNF expression begins prior to, and occurs independently of, gustatory innervation (Nosrat, C. A. and Olson, L., 1995; Nosrat, C. A. *et al.*, 2001). The geniculate ganglion also produces BDNF (Schecterson, L. C. and Bothwell, M., 1992), which may influence neuronal survival through an autocrine or paracrine mechanism (Acheson, A. *et al.*, 1995; Acheson, A. and Lindsay, R. M., 1996). The central target of geniculate and petrosal neurons, the NTS, also produces BDNF, which may regulate survival of gustatory neurons (Acheson, A. *et al.*, 1995).

Regardless of its source, BDNF is an important regulator of gustatory neuron number. $BDNF^{-/-}$ mice lose approximately half of their geniculate and nodose/petrosal ganglion neurons during development (Conover, J. C. *et al.*, 1995; Liu, X. *et al.*, 1995; Erickson, J. T. *et al.*, 1996; Liebl, D. J. *et al.*, 1997). Although both of these ganglia innervate taste and nontaste regions, many of the neurons lost in $BDNF^{-/-}$ mice probably innervate taste buds. Taste buds, in turn, require gustatory innervation for their continued maintenance (Hosley, M. A. *et al.*, 1987; Nagato, T. *et al.*, 1995; Sollars, S. I., 2005), and it is well established that fungiform and circumvallate taste buds are lost by birth in $BDNF^{-/-}$ mice (Nosrat, C. A. *et al.*, 1997; Zhang, C. *et al.*, 1997; Cooper, D. and Oakley, B., 1998; Oakley, B. *et al.*, 1998; Mistretta, C. M. *et al.*, 1999; Sun, H. and Oakley, B., 2002). The most likely explanation for these findings is that BDNF produced in either taste papillae, gustatory ganglia, or NTS is required for the survival of gustatory neurons, which in turn maintain taste buds. Therefore, the neurons lost in $BDNF^{-/-}$ mice are most likely gustatory neurons; however, retrograde labeling has not yet been used to determine the number of gustatory neurons that are lost in $BDNF^{-/-}$ mice.

Geniculate neurons are first lost in $BDNF^{-/-}$ mice between E12.5 and E14.5, indicating these neurons are first lost just before or as they innervate gustatory epithelia (Patel, A. V. and Krimm, R. F., 2005). However, geniculate neuron loss continues after E14.5, indicating the BDNF is required to support geniculate neuron survival throughout embryonic development.

BDNF is not the only neurotrophin that regulates taste system development. In addition, NT4 is expressed in tongue, taste buds, and geniculate ganglion neurons (Cho, T. T. and Farbman, A. I., 1999; Farbman, A. I. *et al.*, 2004b; Takeda, M. *et al.*, 2005a), and $NT4^{-/-}$ mice lose approximately half of their geniculate and nodose/petrosal ganglion neurons during development (Conover, J. C. *et al.*, 1995; Liu, X. *et al.*, 1995; Erickson, J. T. *et al.*, 1996). Moreover, double $BDNF^{-/-}/NT4^{-/-}$ null mutants lose $\geq$90% of geniculate and petrosal neurons (Conover, J. C. *et al.*, 1995; Liu, X. *et al.*, 1995; Erickson, J. T. *et al.*, 1996), indicating that NT4- and BDNF-dependent neurons may represent two separate populations. Fungiform papillae are lost by birth in $NT4^{-/-}$ mice (Liebl, D. J. *et al.*, 1999), but circumvallate

taste buds are not, indicating that at least some of the NT4-dependent neurons in the geniculate ganglion are gustatory, while those in the petrosal ganglion are not. In $NT4^{-/-}$ mice, neurons are lost earlier than in $BDNF^{-/-}$ mice before E12.5, which is before target innervation (Patel, A. V. and Krimm, R. F., 2005). Also in $NT4^{-/-}$ mice, there is a separate wave of neuron loss between E14.5 and E16.5, distinct from neuronal loss in $BDNF^{-/-}$ mice. Thus, it is likely that NT4 plays two distinct roles at different stages of geniculate neuron development.

In addition to BDNF and NT4, NT3 may also play a regulatory role in gustatory neuron development. There is an abundance of NT3 in the tongue (Nosrat, C. A. *et al.*, 1996; Nosrat, C. A. and Olson, L., 1998; Fan, L. *et al.*, 2004) and ~45% of geniculate and nodose/petrosal neurons are lost in $NT3^{-/-}$ mice (Liebl, D. J. *et al.*, 1997). Oddly, while no fungiform papillae are lost in $NT3^{-/-}$ mice, double $BDNF^{-/-}/NT3^{-/-}$ null mutants lose more fungiform papillae than $BDNF^{-/-}$ mice (Nosrat, C. A. *et al.*, 2004), suggesting that NT3-supported trigeminal neurons maintain taste buds in the absence of BDNF. Alternatively, NT3 could function in conjunction with BDNF to support gustatory neurons, or NT3 could have a direct, nerve-independent, influence on taste bud maintenance.

The neurotrophins, BDNF and NT4, function via the same receptors, TrkB, a member of the tyrosine kinase family, and p75, a pan-neurotrophin receptor. All mouse geniculate neurons express the TrkB receptor early in development (Yamout, A. *et al.*, 2005). While some geniculate neurons in rat continue to express TrkB postnatally and into adulthood, most express other neurotrophin receptors (Cho, T. T. and Farbman, A. I., 1999; Farbman, A. I. *et al.*, 2004a; 2004b). Expression of neurotrophin receptors in the geniculate ganglion may vary across rodent species; however, more likely, TrkB is downregulated postnatally. Mice lacking TrkB lose geniculate neurons by E12.5 (Fritzsch, B. *et al.*, 1997), and by E13.5, neuronal loss is greater in $TrkB^{-/-}$ mice than in $NT4^{-/-}$ or $BDNF^{-/-}$ mice, indicating that both neurotrophins regulate survival via TrkB. Because most geniculate and nodose/petrosal neurons are lost in $TrkB^{-/-}$ mice, taste buds may not receive gustatory innervation in $TrkB^{-/-}$ mice. Some fungiform taste buds are present at birth in $TrkB^{-/-}$ mice (Fritzsch, B. *et al.*, 1997); however, taste bud number has not been quantified, so how many remain is unclear.

Other factors are also required to maintain gustatory neurons and taste buds. Disruption of dystonin, a molecule important for cytoskeletal organization, causes a loss of petrosal ganglion neurons and a loss of circumvallate taste buds (Ichikawa, H. *et al.*, 2006). Although dystonin regulates neuronal cytoskeletal organization, only some subpopulations of neurons, primarily sensory neurons, are effected by its removal. There is a possible link between dystonin function and neuronal dependence on the neurotrophins NT3 and GDNF, in that the somatosensory neurons that are most sensitive to disruption of dystonin also tend to depend on either NT3 or GDNF for survival (Carlsten, J. A. *et al.*, 2001). Possible roles of NT3 in gustatory neuron development/maintenance have already been discussed. Currently, it is unclear whether GDNF plays a role in gustatory development. GDNF is expressed by the developing tongue (Nosrat, C. A. *et al.*, 1998) and adult taste buds (Takeda, M. *et al.*, 2004; 2005b) and geniculate neurons express GDNF receptors (Yamout, A. *et al.*, 2005). Furthermore, removal of GDNF reduces the number of petrosal ganglion neurons (Erickson, J. T. *et al.*, 1996). Thus a role for GDNF in gustatory system development or maintenance remains likely.

In addition to the known factors, an unidentified factor produced by gustatory neurons acts to maintain taste buds during development and into adulthood (Hosley, M. A. *et al.*, 1987; Oakley, B. *et al.*, 1990; Nagato, T. *et al.*, 1995; Sollars, S. I. *et al.*, 2002; Sollars, S. I., 2005). It is reasonable to hypothesize that this unknown factor is a growth factor, and growth factors typically function via tyrosine kinase receptors. With this possibility in mind, McLaughlin S. K. (2000) amplified both receptor and nonreceptor tyrosine kinases from a cDNA library to identify tyrosine kinases expressed in taste buds. The tyrosine kinase receptors, ErbB1 (the epithelial growth factor receptor, (Egfr)), ErbB2, ErbB3, and c-kit tyrosine kinase receptors are all preferentially expressed in taste buds (McLaughlin, S. K., 2000). ErbB2 typically functions as a coreceptor, but ErbB1 and ErbB3 have ligand-binding abilities. ErbB1/ErbB1 and ErbB1/ErbB2 heterodimers typically bind EGF, TGFα, and amphiregulin. Fungiform papillae and/or taste buds are lost and malformed in mice lacking Egfr/ErbB1 (Miettinen, P. J. *et al.*, 1995; Threadgill, D. W. *et al.*, 1995), but sensory innervation is unaffected (Sun, H. and Oakley, B., 2002). Thus, Egfr/ErbB1 signaling is important for the maintenance of taste buds.

One ligand of this receptor, EGF, is expressed in the tongue where it influences early fungiform placode development (Mistretta, C. M. *et al.*, 2005), indicating that taste bud loss in $ErbB1^{-/-}$ mice could be due to disruption of early placode development. Another

intriguing possibility is that EGF in saliva maintains taste buds and fungiform papillae via ErbB1 (Morris-Wiman, J. *et al.*, 2000). Consistent with this interpretation, taste buds in circumvallate and foliate papillae are unaffected by either mutation of Egfr/ErbB1 or salivary gland removal (Morris-Wiman, J. *et al.*, 2000; Sun, H. and Oakley, B., 2002). Also, the addition of EGF to drinking water rescues the taste bud loss seen with salivary gland removal (Morris-Wiman, J. *et al.*, 2000). Lastly, it is possible that gustatory neurons produce an Erb ligand that is important for taste bud maintenance. This would be consistent with the role of other Erb ligands in the maintenance of sensory receptors (Hippenmeyer, S. *et al.*, 2002). Thus, while Erb receptor ligands may function to maintain taste buds, the exact function and source of these ligands is unclear. Equally elusive is the nature of the factor(s) produced by gustatory neurons that serves to support both taste bud differentiation during development and taste bud maintenance in adulthood.

4.06.7 Postnatal Plasticity in Taste Bud Innervation

Taste buds continue to develop postnatally, to turn over, and to reestablish connections with innervating neurons even into adulthood (Beidler, L. M. and Smallman, R. L., 1965). Changes in peripheral gustatory innervation patterns are related to, and may even regulate, changes in taste bud development. In adult rats, taste bud size is correlated with the number of geniculate ganglion neurons that innervate it (Krimm, R. F. and Hill, D. L., 1998b). This relationship develops over a prolonged period of postnatal development and is not observed until postnatal day 40 (PN40). Between PN10 and PN40, geniculate ganglion cells rearrange their peripheral connections (Krimm, R. F. and Hill, D. L., 2000), withdrawing innervation from certain taste buds, then innervating others. This constant rearrangement of peripheral connectivity does not appear to establish the relationship between taste bud size and geniculate neuron number. That is, individual ganglion neurons do not remove innervation from small taste buds in favor of larger taste buds. Instead, the number of neurons that innervate a given taste bud at PN10 predicts taste bud size at PN40. Thus, the number of neurons innervating a given taste bud is established early in development and taste buds grow to match the number of neurons innervating them.

Taste buds grow between PN10 and PN40 by adding taste cells (Hendricks, S. J. *et al.*, 2004). Taste cells are constantly turning over, undergoing a continuous process of differentiation followed by death (Beidler, L. M. and Smallman, R. L., 1965). Postnatal differences in taste cell proliferation, differentiation, or life span could all increase the number of taste bud cells. The approximate 10-day life span of taste cells appears to remain constant during development (Hendricks, S. J. *et al.*, 2004) as does the proliferation rate of basal cells. However, the rate of taste cell addition accelerates. It is unclear what factor(s) controls the addition of new taste cells. Because taste buds increase in size in proportion to the amount of neural innervation they receive (Krimm, R. F. and Hill, D. L., 2000), the critical factor may be neuronal. Alternatively, factor(s) produced in fungiform papillae could regulate both the rate of taste cell addition and the number of neurons innervating the taste bud.

The number of geniculate neurons that typically innervate a fungiform taste bud varies considerably across rodent species. Rat taste buds are innervated by 3–14 ganglion neurons (Krimm, R. F. and Hill, D. L., 1998a; Shuler, M. G. *et al.*, 2004) while mouse taste buds are innervated by substantially fewer (2–7) (Zaidi, F. N. and Whitehead, M. C., 2006). Hamster fungiform taste buds are innervated by many more geniculate neurons (5–35) than either rat or mouse taste buds (Whitehead, M. C. *et al.*, 1999; Zaidi, F. N. and Whitehead, M. C., 2006). Differences in peripheral branching characteristics of ganglion cells (Zaidi, F. N. and Whitehead, M. C., 2006), rather than differences in the ratio of fungiform taste buds to geniculate neurons, appear to account for species variation. That is, geniculate neurons branch more and innervate more taste buds in hamsters than in mice (Zaidi, F. N. and Whitehead, M. C., 2006). It is unclear whether postnatal plasticity also diverges across species as a reflection of geniculate neuron branching.

4.06.8 Plasticity of Central Taste Connections

As discussed earlier, initial projection of gustatory axons to the NTS is dictated by early developmental cues, whereas further refinement occurs over a protracted developmental period after birth. The combined terminal field of the chorda tympani and the greater superficial petrosal (GSP) afferents steadily increases between PN7 and PN25 (Lasiter, P. S. and Bulcourf, B. B., 1995), illustrating that terminal field development is not complete until late postnatal

stages. The terminal field of the chorda tympani nerve increases until PN15, then decreases in size (Sollars, S. I. *et al*., 2006) before becoming adult-like at PN35. Postsynaptic neurons in the gustatory NTS also undergo remodeling between PN22 and PN28 (Liu, Y. S. *et al*., 2000). For example, dendritic fields of salt-sensitive geniculate ganglion neurons decrease during this postnatal period. Because NTS connections are refined during late postnatal development, remodeling of these connections may be influenced by sensory experiences in the taste system.

In most sensory systems, including the taste system, blocking normal sensory experiences alters the development of central connections (Hubel, D. H. and Wiesel, T. N., 1970; Cummings, D. M. and Brunjes, P. C., 1997; Fox, K. *et al*., 2002). Similarly, fungiform papillae/taste bud damage at PN2 stunts the terminal field expansion of the combined chorda tympani/GSP nerves in the NTS (Lasiter, P. L. and Kachele, D. L., 1990). The underlying mechanisms are unclear but may include injury-induced expression of numerous growth and/or immune factors or the loss of primary sensory afferents.

Developmental sodium restriction also influences later sensory experiences. Maternal sodium restriction during embryonic development specifically blocks postnatal development of chorda tympani nerve responses to sodium salts (Hill, D. L. and Przekop, P. R., 1988) and substantially alters the CNS projections of gustatory neurons. Chorda tympani and glossopharyngeal terminal fields within the rostral NTS are enlarged (King, C. T. and Hill, D. L., 1991; Krimm, R. F. and Hill, D. L., 1997; May, O. L. and Hill, D. L., 2006; Sollars, S. I. *et al*., 2006) because connections are not refined and eliminated between PN25 and PN35, resulting in adult projections with an early developmental morphology (Sollars, S. I. *et al*., 2006). Interestingly, unlike for the chorda tympani nerve, sodium responses in the GSP nerve are unaffected by sodium deprivation as is the size of the terminal field (Sollars, S. I. and Hill, D. L., 2000; May, O. L. and Hill, D. L., 2006). Alterations due to sodium restriction are not limited to the terminal fields of the affected primary afferents; postsynaptic neurons are also affected. Dendritic arbors of putative projection neurons in the gustatory NTS are longer in sodium-restricted rats than in controls (King, C. T. and Hill, D. L., 1993). The mechanisms through which sodium deprivation influences gustatory CNS development are not yet clear. Probably, the failure of the chorda tympani nerve to develop sodium sensitivity reduces total postnatal chorda tympani activity, thus preventing postnatal refinement of the terminal field.

4.06.9 Conclusion

The general organization of the taste system is conserved across vertebrate species, from fish to humans: bipolar sensory neurons of the VII, IX, and X cranial ganglia convey taste information from aggregates of spindle-shaped cells, taste buds, located in the oral and pharyngeal epithelia to the first relay nucleus, the NTS, in the hindbrain. We propose that this conservation of anatomy is reflected in a conserved and basic plan for the development of elements of the taste system. Taste bud progenitors arise from the local epithelium and are induced and patterned via epithelium-intrinsic intercellular communication. While little is known specifically about the development of the NTS, it is clear that these cells arise from the hindbrain in all vertebrates. Gustatory neurons arise from epibranchial placodes and pathfind simultaneously to innervate both peripheral and central targets, allowing formation of a functional taste system.

Of course, there are variations in this theme, when one examines the details of development within several species. Chief among the differences encountered is the role of innervation in the differentiation of taste buds. In amphibians, taste buds differentiate fully in the complete absence of nerves, while full cytodifferentiation likely depends upon innervation in rodents. Additionally, the development of taste buds in many species, including mammals, is interwoven with the development of specialized epithelial structures, such as taste papillae. Thus, the interconnectedness of buds and papillae may obscure our ability to readily detect commonalities in taste organ developmental mechanisms across species.

However, by continuing to explore taste system development in a number of vertebrates, perhaps expanding to employ additional developmental models, such as zebrafish and chick, we will gain a clearer view of the basic mechanisms underlying development of this key sensory system.

References

Abu-Issa, R., Smyth, G., Smoak, I., Yamamura, K., and Meyers, E. N. 2002. Fgf8 is required for pharyngeal arch and cardiovascular development in the mouse. Development 129(19), 4613–4625.

Acheson, A. and Lindsay, R. M. 1996. Non target-derived roles of the neurotrophins. Philos. Trans. R. Soc. Lond. B Biol. Sci. 351(1338), 417–422.

Acheson, A., Conover, J. C., Fandl, J. P., DeChiara, T. M., Russell, M., Thadani, A., Squinto, S. P., Yancopoulos, G. D., and Lindsay, R. M. 1995. A BDNF autocrine loop in adult sensory neurons prevents cell death. Nature 374(6521), 450–453.

AhPin, P., Ellis, S., Arnott, C., and Kaufman, M. H. 1989. Prenatal development and innervation of the circumvallate papilla in the mouse. J. Anat. 162, 33–42.

Armstrong, J. B. and Malacinski, G. M. 1989. Developmental Biology of the Axolotl, p. 327. Oxford University Press.

Artavanis-Tsakonas, S. 1988. The molecular biology of the *Notch* locus and the fine tuning of differentiation in *Drosophila*. Trends Gen. 4, 95–100.

Atema, J. 1971. Structures and functions of the sense of taste in the catfish (*Ictalurus natalis*). Brain Behav. Evol. 4, 273–294.

Athar, M., Tang, X., Lee, J. L., Kopelovich, L., and Kim, A. L. 2006. Hedgehog signalling in skin development and cancer. Exp. Dermatol. 15(9), 667–677.

Baker, C. V. and Bronner-Fraser, M. 2001. Vertebrate cranial placodes I. embryonic induction. Dev. Biol. 232(1), 1–61.

Balemans, W. and Van Hul, W. 2002. Extracellular regulation of BMP signaling in vertebrates: a cocktail of modulators. Dev. Biol. 250(2), 231.

Barlow, L. A. 2001. Specification of pharyngeal endoderm is dependent on early signals from axial mesoderm. Development 128(22), 4573–4583.

Barlow, L. A. and Northcutt, R. G. 1995. Embryonic origin of amphibian taste buds. Dev. Biol. 169, 273–285.

Barlow, L. A. and Northcutt, R. G. 1997. Taste buds develop autonomously from endoderm without induction by cephalic neural crest or paraxial mesoderm. Development 124, 949–957.

Barlow, L. A. and Northcutt, R. G. 1998. The role of innervation in the development of taste buds: insights from studies of amphibian embryos. Ann. N. Y. Acad. Sci. 855, 58–69.

Barlow, L. A, Chien, C.-B., and Northcutt, R. G. 1996. Embryonic taste buds develop in the absence of innervation. Development 122, 1103–1111.

Begbie, J. and Graham, A. 2001a. The ectodermal placodes: a dysfunctional family. Philos. Trans. R. Soc. Lond. B Biol. Sci. 356(1414), 1655–1660.

Begbie, J. and Graham, A. 2001b. Integration between the epibranchial placodes and the hindbrain. Science 294(5542), 595–598.

Begbie, J., Ballivet, M., and Graham, A. 2002. Early steps in the production of sensory neurons by the neurogenic placodes. Mol. Cell Neurosci. 21(3), 502–511.

Beidler, L. M. and Smallman, R. L. 1965. Renewal of cells within taste buds. J. Cell Biol. 27, 263–272.

Bejsovec, A. 2005. Wnt pathway activation: new relations and locations. Cell 120(1), 11–14.

Belecky, T. L. and Smith, D. V. 1990. Postnatal development of palatal and laryngeal taste buds in the hamster. J. Comp. Neurol. 293, 646–654.

Bitgood, M. J. and McMahon, A. P. 1995. Hedgehog and Bmp genes are coexpressed at many diverse sites of cell–cell interaction in the mouse embryo. Dev. Biol. 172, 126–138.

Blanpain, C., Horsley, V., and Fuchs, E. 2007. Epithelial stem cells: turning over new leaves. Cell 128(3), 445–458.

Botchkarev, V. A. and Sharov, A. A. 2004. BMP signaling in the control of skin development and hair follicle growth. Differentiation 72(9-10), 512–526.

Boughter, J. D., Jr., Pumplin, D. W., Yu, C., Christy, R. C., and Smith, D. V. 1997. Differential expression of alpha-gustducin in taste bud populations of the rat and hamster. J. Neurosci. 17(8), 2852–2858.

Bradley, R. M. and Stern, I. B. 1967. The development of the human taste bud during the foetal period. J. Anat. 101, 743–752.

Caprio, J., Brand, J. G., Teeter, J. H., Valentincic, T., Kalinoski, D. L., Kohbara, J., Kumazawa, T., and Wegert, S. 1993. The taste system of the channel catfish: from biophysics to behavior. Trends Neurosci. 16, 192–197.

Carlsten, J. A., Kothary, R., and Wright, D. E. 2001. Glial cell line-derived neurotrophic factor-responsive and neurotrophin-3-responsive neurons require the cytoskeletal linker protein dystonin for postnatal survival. J. Comp. Neurol. 432(2), 155–168.

Cho, T. T. and Farbman, A. I. 1999. Neurotrophin receptors in the geniculate ganglion. Brain Res. Mol. Brain Res. 68(1–2), 1–13.

Cho, Y. K., Farbman, A. I., and Smith, D. V. 1998. The timing of alpha-gustducin expression during cell renewal in rat vallate taste buds. Chem. Senses 23(6), 735–742.

Chuong, C. M., Patel, N., Lin, J., Jung, H. S., and Widelitz, R. B. 2000. Sonic hedgehog signaling pathway in vertebrate epithelial appendage morphogenesis: perspectives in development and evolution. Cell Mol. Life Sci. 57(12), 1672–1681.

Ciani, L. and Salinas, P. C. 2005. WNTs in the vertebrate nervous system: from patterning to neuronal connectivity. Nat. Rev. Neurosci. 6(5), 351–362.

Conover, J. C., Erickson, J. T., Katz, D. M., Bianchi, L. M., Poueymirou, W. T., McClain, J., Pan, L., Helgren, M., Ip, N. Y., Boland, P., Friedman, B., Weigand, S., Vejsada, R., Kato, A., Dechiara, T. M., and Yancopoulos, G. D. 1995. Neuronal deficits, not involving motor neurons, in mice lacking BDNF and/or NT4. Nature 375(6528), 235–238.

Cooper, D. and Oakley, B. 1998. Functional redundancy and gustatory development in bdnf null mutant mice. Brain Res. Dev. Brain Res. 105(1), 79–84.

Cornell, R. A. and Eisen, J. S. 2005. Notch in the pathway: the roles of Notch signaling in neural crest development. Semin. Cell Dev. Biol. 16(6), 663–672.

Crump, J. G., Maves, L., Lawson, N. D., Weinstein, B. M., and Kimmel, C. B. 2004. An essential role for Fgfs in endodermal pouch formation influences later craniofacial skeletal patterning. Development 131(22), 5703–5716.

Cummings, D. M. and Brunjes, P. C. 1997. The effects of variable periods of functional deprivation on olfactory bulb development in rats. Exp. Neurol. 148(1), 360–366.

D'Amico-Martel, A. and Noden, D. M. 1983. Contributions of placodal and neural crest cells to avian cranial peripheral ganglia. Am. J. Anat. 166, 445–468.

DasGupta, R. and Fuchs, E. 1999. Multiple roles for activated LEF/TCF transcription complexes during hair follicle development and differentiation. Development 126(20), 4557–4568.

Dauger, S., Pattyn, A., Lofaso, F., Gaultier, C., Goridis, C., Gallego, J., and Brunet, J. F. 2003. Phox2b controls the development of peripheral chemoreceptors and afferent visceral pathways. Development 130(26), 6635–6642.

Delay, R. J., Kinnamon, J. C., and Roper, S. D. 1986. Ultrastructure of mouse vallate taste buds: II. Cell types and cell lineage. J. Comp. Neurol. 253(2), 242–252.

Dvorak, P., Dvorakova, D., and Hampl, A. 2006. Fibroblast growth factor signaling in embryonic and cancer stem cells. FEBS Lett. 580(12), 2869–2874.

El-Sharaby, A., Ueda, K., Kurisu, K., and Wakisaka, S. 2001a. Development and maturation of taste buds of the palatal epithelium of the rat: histological and immunohistochemical study. Anat. Rec. 263(3), 260–268.

El-Sharaby, A., Ueda, K., and Wakisaka, S. 2001b. Differentiation of the lingual and palatal gustatory epithelium

of the rat as revealed by immunohistochemistry of alpha-gustducin. Arch. Histol. Cytol. 64(4), 401–409.
Erickson, J. T., Conover, J. C., Borday, V., Champagnat, J., Barbacid, M., Yancopoulos, G., and Katz, D. M. 1996. Mice lacking brain-derived neurotrophic factor exhibit visceral sensory neuron losses distinct from mice lacking NT4 and display a severe developmental deficit in control of breathing. J. Neurosci. 16(17), 5361–5371.
Fährmann, W. 1967. Licht- und electronenmikroskopische Untersuchungen an der Geschmacksknospe des neotenen Axolotls (*Siredon mexicanum* Shaw). Zeit Microsk Anat Forsch. 77, 117–152.
Fan, L., Girnius, S., and Oakley, B. 2004. Support of trigeminal sensory neurons by nonneuronal p75 neurotrophin receptors. Brain Res. Dev. Brain Res. 150(1), 23–39.
Farbman, A. I. 1965. Electron microscope study of the developing taste bud in rat fungiform papilla. Dev. Biol. 11, 110–135.
Farbman, A. I. 1980. Renewal of taste bud cells in rat circumvallate papillae. Cell Tissue Kinet. 13(4), 349–357.
Farbman, A. I. and Mbiene, J.-P. 1991. Early development and innervation of taste bud-bearing papillae on the rat tongue. J. Comp. Neurol. 304, 172–186.
Farbman, A. I., Brann, J. H., Rozenblat, A., Rochlin, M. W., Weiler, E., and Bhattacharyya, M. 2004a. Developmental expression of neurotrophin receptor genes in rat geniculate ganglion neurons. J. Neurocytol. 33(3), 331–343.
Farbman, A. I., Guagliardo, N., Sollars, S. I., and Hill, D. L. 2004b. Each sensory nerve arising from the geniculate ganglion expresses a unique fingerprint of neurotrophin and neurotrophin receptor genes. J. Neurosci Res. 78(5), 659–667.
Fox, K., Wallace, H., and Glazewski, S. 2002. Is there a thalamic component to experience-dependent cortical plasticity? Philos. Trans. R. Soc. Lond. B Biol. Sci. 357(1428), 1709–1715.
Fritzsch, B., Gregory, D., and Rosa-Molinar, E. 2005. The development of the hindbrain afferent projections in the axolotl: evidence for timing as a specific mechanism of afferent fiber sorting. Zoology (Jena) 108(4), 297–306.
Fritzsch, B., Sarai, P. A., Barbacid, M., and Silos-Santiago, I. 1997. Mice lacking the neurotrophin receptor trkB lose their specific afferent innervation but do develop taste buds. Int. J. Dev. Neurosci. 15, 563–576.
Gaiano, N. and Fishell, G. 2002. The role of notch in promoting glial and neural stem cell fates. Annu. Rev. Neurosci. 25, 471–490.
Giger, R., Wolfer, D. P., De Wit, G. M., and Verhaagen, J. 1996. Anatomy of rat semaphorin III/collapsin-1 mRNA expression and relationship to developing nerve tracts during neuroembryogenesis. J. Comp. Neurol. 375, 378–392.
Gomahr, A., Palzenberger, M., and Kotrschal, K. 1992. Density and distribution of external taste buds in cyprinids. Environ. Biol. Fishes 33, 125–134.
Graveson, A. C. and Armstrong, J. B. 1987. Differentiation of cartilage from cranial neural crest in the axolotl (*Ambystoma mexicanum*). Differentiation 35(1), 16–20.
Graziadei, P. P. and Graziadei, G. A. 1978. Observations on the ultrastructure of ganglion cells in the circumvallate papilla of rat and mouse. Acta Anat. (Basel) 100(3), 289–305.
Gross, J. B., Gottlieb, A. A., and Barlow, L. A. 2003. Gustatory neurons derived from epibranchial placodes are attracted to, and trophically supported by, taste bud-bearing endoderm *in vitro*. Dev. Biol. 264(2), 467–481.
Hall, J. M., Bell, M. L., and Finger, T. E. 2003. Disruption of sonic hedgehog signaling alters growth and patterning of lingual taste papillae. Dev. Biol. 255(2), 263–277.
Hall, J. M., Hooper, J. E., and Finger, T. E. 1999. Expression of sonic hedgehog, patched, and Gli1 in developing taste papillae of the mouse. J. Comp. Neurol. 406(2), 143–155.
Hamamichi, R., Asano-Miyoshi, M., and Emori, Y. 2006. Taste bud contains both short-lived and long-lived cell populations. Neuroscience 141(4), 2129–2138.
Hansen, A., Reutter, K., and Zeiske, E. 2002. Taste bud development in the zebrafish, *Danio rerio*. Dev. Dyn. 223(4), 483–496.
Harada, S., Yamaguchi, K., Kanemaru, N., and Kasahara, Y. 2000. Maturation of taste buds on the soft palate of the postnatal rat. Physiol. Behav. 68(3), 333–339.
Harada, S., Yamamoto, T., Yamaguchi, K., and Kasahara, Y. 1997. Different characteristics of gustatory responses between the greater superficial petrosal and chorda tympani nerves in the rat. Chem. Senses 22(2), 133–140.
Hendricks, S. J., Brunjes, P. C., and Hill, D. L. 2004. Taste bud cell dynamics during normal and sodium-restricted development. J. Comp. Neurol. 472(2), 173–182.
Herrick, C. J. 1903. On the phylogeny and morphological position of the terminal buds of fishes. J. Comp. Neurol. 13, 121–138.
Hill, D. L. and Przekop, P. R. 1988. Influences of dietary sodium on functional taste receptor development: a sensitive period. Science 241, 1826–1827.
Hippenmeyer, S., Shneider, N. A., Birchmeier, C., Burden, S. J., Jessell, T. M., and Arber, S. 2002. A role for neuregulin1 signaling in muscle spindle differentiation. Neuron 36(6), 1035–1049.
Hirota, M., Ito, T., Okudela, K., Kawabe, R., Hayashi, H., Yazawa, T., Fujita, K., and Kitamura, H. 2001. Expression of cyclin-dependent kinase inhibitors in taste buds of mouse and hamster. Tissue Cell. 33(1), 25–32.
Hosley, M. A., Hughes, S. E., Morton, L. L., and Oakley, B. 1987. A sensitive period for the neural induction of taste buds. J. Neurosci. 7(7), 2075–2080.
Hubel, D. H. and Wiesel, T. N. 1970. The period of susceptibility to the physiological effects of unilateral eye closure in kittens. J. Physiol. 206(2), 419–436.
Ichikawa, H., De Repentigny, Y., Kothary, R., and Sugimoto, T. 2006. The survival of vagal and glossopharyngeal sensory neurons is dependent upon dystonin. Neuroscience 137(2), 531–536.
Itoh, N. and Ornitz, D. M. 2004. Evolution of the Fgf and Fgfr gene families. Trends Genet. 20(11), 563–569.
Iwatsuki, K., Liu, H. X., Gronder, A., Singer, M. A., Lane, T. F., Grosschedl, R., Mistretta, C. M., and Margolskee, R. F. 2007. Wnt signaling interacts with Shh to regulate taste papilla development. Proc. Natl Acad. Sci. U. S. A. 104(7), 2253–2258.
Jitpukdeebodintra, S., Chai, Y., and Snead, M. L. 2002. Developmental patterning of the circumvallate papilla. Int. J. Dev. Biol. 46(5), 755–763.
Jung, H. S., Oropeza, V., and Thesleff, I. 1999. Shh, Bmp-2, Bmp-4 and Fgf-8 are associated with initiation and patterning of mouse tongue papillae. Mech. Dev. 81(1–2), 179–182.
Kim, J. Y., Cho, S. W., Lee, M. J., Hwang, H. J., Lee, J. M., Lee, S. I., Muramatsu, T., Shimono, M., and Jung, H. S. 2005. Inhibition of connexin 43 alters Shh and Bmp-2 expression patterns in embryonic mouse tongue. Cell Tissue Res. 320(3), 409–415.
Kim, J. Y., Mochizuki, T., Akita, K., and Jung, H. S. 2003. Morphological evidence of the importance of epithelial tissue during mouse tongue development. Exp. Cell Res. 290(2), 217–226.
King, C. T. and Hill, D. L. 1991. Dietary sodium chloride deprivation throughout development selectively influences the terminal field organization of gustatory afferent fibers projecting to the rat nucleus of the solitary tract. J. Comp. Neurol. 303(1), 159–169.
King, C. T. and Hill, D. L. 1993. Neuroanatomical alterations in the rat nucleus of the solitary tract following early maternal

NaCl deprivation and subsequent NaCl repletion. J. Comp. Neurol. 333, 531–542.
Kingsley, D. M. 1994. The TGF-beta superfamily: new members, new receptors, and new genetic tests of function in different organisms. Genes Dev. 8(2), 133–146.
Kinnamon, J. C., Dunlap, M., and Yang, R. 2005. Synaptic connections in developing and adult rat taste buds. Chem. Senses 30(Suppl. 1), i60–i61.
Kohbara, J., Michel, W., and Caprio, J. 1992. Responses of single facial taste fibers in the channel catfish, *Ictalurus punctatus*, to amino acids. J. Neurophysiol. 68(4), 1012–1026.
Kollar, E. J. 1983. Epithelial–Mesenchymal Interactions in the Mammalian Integument: Tooth Development as a Model for Instructive Induction. In: Epithelial–Mesenchymal Interactions in Development (*eds*. R. H. Sawyer and J. F. Fallon), pp. 27–49. Praeger Publishers.
Krimm, R. F. and Hill, D. L. 1997. Early prenatal critical period for chorda tympani nerve terminal field development. J. Comp. Neurol. 378(2), 254–264.
Krimm, R. F. and Hill, D. L. 1998a. Innervation of single fungiform taste buds during development in rat. J. Comp. Neurol. 398(1), 13–24.
Krimm, R. F. and Hill, D. L. 1998b. Quantitative relationships between taste bud development and gustatory ganglion cells. Ann. N. Y. Acad. Sci. 855, 70–75.
Krimm, R. F. and Hill, D. L. 2000. Neuron/target matching between chorda tympani neurons and taste buds during postnatal rat development. J. Neurobiol. 43(1), 98–106.
Krimm, R. F., Miller, K. K., Kitzman, P. H., Davis, B. M., and Albers, K. M. 2001. Epithelial overexpression of BDNF or NT4 disrupts targeting of taste neurons that innervate the anterior tongue. Dev. Biol. 232(2), 508–521.
Kusakabe, Y., Miura, H., Hashimoto, R., Sugiyama, C., Ninomiya, Y., and Hino, A. 2002. The neural differentiation gene Mash-1 has a distinct pattern of expression from the taste reception-related genes gustducin and T1R2 in the taste buds. Chem. Senses 27(5), 445–451.
Landacre, F. L. 1907. On the place of origin and method of distribution of taste buds in *Ameiurus melas*. J. Comp. Neurol. 17, 1–66.
Landacre, F. L. 1910. The origin of the cranial ganglia in *Ameiurus*. J. Comp. Neurol. 20, 309–411.
Lasiter, P. S. and Bulcourf, B. B. 1995. Alterations in geniculate ganglion proteins following fungiform receptor damage. Dev. Brain Res. 89, 289–306.
Lasiter, P. L. and Kachele, D. L. 1990. Effects of early postnatal receptor damage on development of gustatory recipient zones within the nucleus of the solitary tract. Dev. Brain Res. 55, 57–71.
Le Douarin, N. M. and Kalcheim, C. 1999. The Neural Crest, p. 445. Cambridge University Press.
Lee, M. J., Kim, J. Y., Lee, S. I., Sasaki, H., Lunny, D. P., Lane, E. B., and Jung, H. S. 2006. Association of Shh and Ptc with keratin localization in the initiation of the formation of circumvallate papilla and von Ebner's gland. Cell Tissue Res. 325(2), 253–261.
Liebl, D. J., Mbiene, J. P., and Parada, L. F. 1999. NT4/5 mutant mice have deficiency in gustatory papillae and taste bud formation. Dev. Biol. 213(2), 378–389.
Liebl, D. J., Tessarollo, L., Palko, M. E., and Parada, L. F. 1997. Absence of sensory neurons before target innervation in brain-derived neurotrophic factor-, neurotrophin 3-, and TrkC-deficient embryonic mice. J. Neurosci. 17(23), 9113–9121.
Liu, F., Thirumangalathu, S., Gallant, N. M., Yang, S. H., Stoick-Cooper, C. L., Reddy, S. T., Andl, T., Taketo, M. M., Dlugosz, A. A., Moon, R. T., Barlow, L. A., and Millar, S. E. 2007. Wnt-beta-catenin signaling initiates taste papilla development. Nat. Genet. 39(1), 106–112.
Liu, H. X., Maccallum, D. K., Edwards, C., Gaffield, W., and Mistretta, C. M. 2004. Sonic hedgehog exerts distinct, stage-specific effects on tongue and taste papilla development. Dev. Biol. 276(2), 280–300.
Liu, X., Ernfors, P., Wu, H., and Jaenisch, R. 1995. Sensory but not motor neuron deficits in mice lacking NT4 and BDNF. Nature 375(6528), 238–241.
Liu, Y. S., Schweitzer, L., and Renehan, W. E. 2000. Development of salt responsive neurons in the nucleus of the solitary tract. J. Comp. Neurol. 425, 219–232.
Lopez, G. F. and Krimm, R. F. 2006a. Epithelial overexpression of BDNF and NT4 produces distinct gustatory axon morphologies that disrupt initial targeting. Dev. Biol. 292(2), 457–468.
Lopez, G. F. and Krimm, R. F. 2006b. Refinement of innervation accuracy following initial targeting of peripheral gustatory fibers. J. Neurobiol.
Lopez, G. F., Pa, V., and Krimm, R. F. 2006. The regulation of neural targeting in the developing gustatory system. Chem. Senses 154.
Lumsden, A. G. S. 1987. The Neural Crest Contribution to Tooth Development in the Mammalian Embryo. In: Developmental and Evolutionary Aspects of the Neural Crest (*ed*. P. F. A. Maderson), pp. 261–300. Wiley.
Lumsden, A. G. S. 1988. Spatial organization of the epithelium and the role of neural crest cells in the initiation of the mammalian tooth germ. Development 103(Suppl. 103), 155–169.
Mangold, O. 1931. Versuche zur Analyse der Entwicklung des Haftfadens beir Urodelen; ein Beispiel für die Inducktion artfrmeder Organe. Naturwissenschaften 45, 905–911.
Marti, E. and Bovolenta, P. 2002. Sonic hedgehog in CNS development: one signal, multiple outputs. Trends Neurosci. 25(2), 89–96.
May, O. L. and Hill, D. L. 2006. Gustatory terminal field organization and developmental plasticity in the nucleus of the solitary tract revealed through triple-fluorescence labeling. J. Comp. Neurol. 497(4), 658–669.
Mbiene, J.-P. 2004. Taste placodes are primary targets of geniculate but not trigeminal sensory axons in mouse developing tongue. J. Neurocytol. 33(6), 617–629.
Mbiene, J.-P. and Farbman, A. I. 1993. Evidence for stimulus access to taste cells and nerves during development: an electron microscopic study. Microsc. Res. Tech. 26(2), 94–105.
Mbiene, J.-P. and Mistretta, C. M. 1997. Initial innervation of embryonic rat tongue and developing taste papillae: nerves follow distinctive and spatially restricted pathways. Acta Anat. 160, 139–158.
Mbiene, J.-P. and Roberts, J. D. 2003. Distribution of keratin 8-containing cell clusters in mouse embryonic tongue: evidence for a prepattern for taste bud development. J. Comp. Neurol. 457(2), 111–122.
Mbiene, J.-P., MacCallum, D. K., and Mistretta, C. M. 1997. Organ cultures of embryonic rat tongue support tongue and gustatory papilla morphogenesis *in vitro* without intact sensory ganglia. J. Comp. Neurol. 377, 324–340.
McLaughlin, S. K. 2000. Erb and c-Kit receptors have distinctive patterns of expression in adult and developing taste papillae and taste buds. J. Neurosci. 20(15), 5679–5688.
Miettinen, P. J., Berger, J. E., Meneses, J., Phung, Y., Pedersen, R. A., Werb, Z., and Derynck, R. 1995. Epithelial immaturity and multiorgan failure in mice lacking epidermal growth factor receptor. Nature 376(6538), 337–341.
Ming, G., Lohof, A. M., and Zheng, J. Q. 1997. Acute morphogenic and chemotropic effects of neurotrophins on

cultured embryonic *Xenopus* spinal neurons. J. Neurosci. 17(20), 7860–7871.
Ming, G., Song, H., Berninger, B., Inagaki, N., Tessier-Lavigne, M., and Poo, M. 1999. Phospholipase C-gamma and phosphoinositide 3-kinase mediate cytoplasmic signaling in nerve growth cone guidance. Neuron 23(1), 139–148.
Mistretta, C. M. 1972. Topographical and Histological Study of the Developing Rat Tongue, Palate and Taste Buds. In: Third Symposium on Oral Sensation and Perception the Mouth of the Infant (*ed*. J. F. Bosma), pp. 163–187. Charles C. Thomas.
Mistretta, C. M. 1998. The role of innervation in induction and differentiation of taste organs: introduction and background. Ann. N. Y. Acad. Sci. 855, 1–13.
Mistretta, C. M. and Liu, H. X. 2006. Development of fungiform papillae: patterned lingual gustatory organs. Arch. Histol. Cytol. 69(4), 199–208.
Mistretta, C. M., Goosens, K. A., Farinas, I., and Reichardt, L. F. 1999. Alterations in size, number, and morphology of gustatory papillae and taste buds in BDNF null mutant mice demonstrate neural dependence of developing taste organs. J. Comp. Neurol. 409(1), 13–24.
Mistretta, C. M., Grigaliunas, A., and Liu, H. X. 2005. Development of gustatory organs and innervating sensory ganglia. Chem. Senses 30(Suppl. 1), i52–i53.
Mistretta, C. M., Liu, H. X., Gaffield, W., and MacCallum, D. K. 2003. Cyclopamine and jervine in embryonic rat tongue cultures demonstrate a role for Shh signaling in taste papilla development and patterning: fungiform papillae double in number and form in novel locations in dorsal lingual epithelium. Dev. Biol. 254(1), 1–18.
Miura, H., Kato, H., Kusakabe, Y., Ninomiya, Y., and Hino, A. 2005. Temporal changes in NCAM immunoreactivity during taste cell differentiation and cell lineage relationships in taste buds. Chem Senses 30(4), 367–375.
Miura, H., Kato, H., Kusakabe, Y., Tagami, M., Miura-Ohnuma, J., Ninomiya, Y., and Hino, A. 2004. A strong nerve dependence of sonic hedgehog expression in basal cells in mouse taste bud and an autonomous transcriptional control of genes in differentiated taste cells. Chem. Senses 29(9), 823–831.
Miura, H., Kusakabe, Y., Kato, H., Miura-Ohnuma, J., Tagami, M., Ninomiya, Y., and Hino, A. 2003. Co-expression pattern of Shh with Prox1 and that of Nkx2.2 with Mash1 in mouse taste bud. Gene Expr. Patterns 3(4), 427–430.
Miura, H., Kusakabe, Y., Sugiyama, C., Kawamatsu, M., Ninomiya, Y., Motoyama, J., and Hino, A. 2001. Shh and Ptc are associated with taste bud maintenance in the adult mouse. Mech. Dev. 106(1–2), 143–145.
Moon, R. T., Bowerman, B., Boutros, M., and Perrimon, N. 2002. The promise and perils of Wnt signaling through beta-catenin. Science 296(5573), 1644–1646.
Morris-Wiman, J., Sego, R., Brinkley, L., and Dolce, C. 2000. The effects of sialoadenectomy and exogenous EGF on taste bud morphology and maintenance. Chem. Senses 25(1), 9–19.
Nagato, T., Matsumoto, K., Tanioka, H., Kodama, J., and Toh, H. 1995. Effect of denervation on morphogenesis of the rat fungiform papilla. Acta Anat. (Basel) 153(4), 301–309.
Narayanan, C. H. and Narayanan, Y. 1980. Neural crest and placodal contributions in the development of the glossopharyngeal–vagal complex in the chick. Anat. Rec. 196, 71–82.
Nie, X. 2005. Apoptosis, proliferation and gene expression patterns in mouse developing tongue. Anat. Embryol. (Berl.) 210(2), 125–132.
Nieuwkoop, P. D. and Ubbels, G. A. 1972. The formation of the mesoderm in Urodelean amphibians. IV. Qualitative evidence for the purely ''ectodermal'' origin of the entire mesoderm and of the pharyngeal endoderm. Wilhelm Roux's Arch. 169, 185–199.
Northcutt, R. G. 2005. Taste bud development in the channel catfish. J. Comp. Neurol. 482(1), 1–16.
Northcutt, R. G. and Barlow, L. A. 1998. Amphibians provide new insights into taste bud development. Trends Neurosci. 21(1), 38–42.
Northcutt, R. G. and Brändle, K. 1995. Development of branchiomeric and lateral line nerves in the axolotl. J. Comp. Neurol. 355, 427–454.
Northcutt, R. G., Barlow, L. A., Braun, C. B., and Catania, K. C. 2000. Distribution and innervation of taste buds in the axolotl. Brain Behav. Evol. 56(3), 123–145.
Nosrat, C. A. 1998. Neurotrophic factors in the tongue: expression patterns, biological activity, relation to innervation and studies of neurotrophin knockout mice. Ann. N. Y. Acad. Sci. 855, 28–49.
Nosrat, C. A. and Olson, L. 1995. Brain-derived neurotrophic factor mRNA is expressed in the developing taste bud-bearing tongue papillae of rat. J. Comp. Neurol. 360(4), 698–704.
Nosrat, C. A. and Olson, L. 1998. Changes in neurotrophin-3 messenger RNA expression patterns in the prenatal rat tongue suggest guidance of developing somatosensory nerves to their final targets. Cell Tissue Res. 292(3), 619–623.
Nosrat, C. A., Blomlof, J., ElShamy, W. M., Ernfors, P., and Olson, L. 1997. Lingual deficits in BDNF and NT3 mutant mice leading to gustatory and somatosensory disturbances, respectively. Development 124(7), 1333–1342.
Nosrat, C. A., Ebendal, T., and Olson, L. 1996. Differential expression of brain-derived neurotrophic factor and neurotrophin 3 mRNA in lingual papillae and taste buds indicates roles in gustatory and somatosensory innervation. J. Comp. Neurol. 376(4), 587–602.
Nosrat, C. A., MacCallum, D. K., and Mistretta, C. M. 1998. Early molecular events in gustatory papilla development are independent of nerve fibers. Chem. Senses. 23, 603–604.
Nosrat, C. A., MacCallum, D. K., and Mistretta, C. M. 2001. Distinctive spatiotemporal expression patterns for neurotrophins develop in gustatory papillae and lingual tissues in embryonic tongue organ cultures. Cell Tissue Res. 303(1), 35–45.
Nosrat, I. V., Agerman, K., Marinescu, A., Ernfors, P., and Nosrat, C. A. 2004. Lingual deficits in neurotrophin double knockout mice. J. Neurocytol. 33(6), 607–615.
Oakley, B. and Witt, M. 2004. Building sensory receptors on the tongue. J. Neurocytol. 33(6), 631–646.
Oakley, B., Brandemihl, A., Cooper, D., Lau, D., Lawton, A., and Zhang, C. 1998. The morphogenesis of mouse vallate gustatory epithelium and taste buds requires BDNF-dependent taste neurons. Brain Res. Dev. Brain Res. 105(1), 85–96.
Oakley, B., LaBelle, D. E., Riley, R. A., Wilson, K., and Wu, L.-H. 1991. The rate and locus of development of rat vallate taste buds. Dev. Brain Res. 58, 215–221.
Oakley, B., Wu, L. H., Lawton, A., and deSibour, C. 1990. Neural control of ectopic filiform spines in adult tongue. Neuroscience 36(3), 831–838.
Okubo, T., Pevny, L. H., and Hogan, B. L. 2006. Sox2 is required for development of taste bud sensory cells. Genes Dev. 20(19), 2654–2659.
Parker, M. A., Bell, M., and Barlow, L. A. 2004. Cell contact-dependent mechanisms specify taste bud number and size during a critical period early in embryonic development. Dev. Dyn. 230, 630–642.
Patel, A. V. and Krimm, R. F. 2005. BDNF and NT4 regulate geniculate ganglion neuron number at different

developmental time points. Soc. Neurosci. Abst. Program # 252.17 (Online).
Paulson, R. B., Hayes, T. G., and Sucheston, M. E. 1985. Scanning electron microscope study of tongue development in the CD-1 mouse fetus. J. Craniofac. Genet. Dev. Biol. 5(1), 59–73.
Paves, H. and Saarma, M. 1997. Neurotrophins as *in vitro* growth cone guidance molecules for embryonic sensory neurons. Cell Tissue Res. 290(2), 285–297.
Pispa, J. and Thesleff, I. 2003. Mechanisms of ectodermal organogenesis. Dev. Biol. 262(2), 195–362.
Poritsky, R. and Singer, M. 1963. The fate of taste buds in tongue transplants to the orbit in the urodele *Triturus*. J. Exp. Zool. 153, 211–218.
Rao, H., Xu, Z., MacCallum, D. K., and Mistretta, C. M. 1997. BDNF and NGF differ in promoting neurite outgrowth from cultured embryonic rat geniculate and trigeminal ganglia. Chem. Senses 22, 775.
Reutter, K. and Witt, M. 1993. Morphology of Vertebrate Taste Organs and Their Nerve Supply. In: Mechanisms of Taste Transduction (*eds*. S. A. Simon and S. D. Roper), pp. 29–82. CRC Press.
Reutter, K., Breipohl, W., and Bijvank, G. J. 1974. Taste bud types in fishes II. Scanning electron microscopical investigations on *Xiphophorus helleri* Heckel (Poeciliidae, Cyprinodontiformes, Teleostei). Cell Tissue Res. 153, 151–165.
Ringstedt, T., Ibanez, C. F., and Nosrat, C. A. 1999. Role of brain-derived neurotrophic factor in target invasion in the gustatory system. J. Neurosci. 19(9), 3507–3518.
Rochlin, M. W. and Farbman, A. I. 1998. Trigeminal ganglion axons are repelled by their presumptive targets. J. Neurosci. 18(17), 6840–6852.
Rochlin, M. W., Egwiekhor, A., Vatterott, P., and Spec, A. 2006. BDNF attracts geniculate neurites, NT4 does not. Neurosci. Abstr. Program # 501.5 (Online).
Rochlin, M. W., O'Connor, R., Giger, R. J., Verhaagen, J., and Farbman, A. I. 2000. Comparison of neurotrophin and repellent sensitivities of early embryonic geniculate and trigeminal axons. J. Comp. Neurol. 422(4), 579–593.
Sbarbati, A., Crescimanno, C., Bernardi, P., Benati, D., Merigo, F., and Osculati, F. 2000. Postnatal development of the intrinsic nervous system in the circumvallate papilla–vonEbner gland complex. Histochem. J. 32(8), 483–488.
Sbarbati, A., Crescimanno, C., Bernardi, P., and Osculati, F. 1999. Alpha-gustducin-immunoreactive solitary chemosensory cells in the developing chemoreceptorial epithelium of the rat vallate papilla. Chem. Senses 24(5), 469–472.
Sbarbati, A., Merigo, F., Bernardi, P., Crescimanno, C., Benati, D., and Osculati, F. 2002. Ganglion cells and topographically related nerves in the vallate papilla/von Ebner gland complex. J. Histochem. Cytochem. 50(5), 709–718.
Schecterson, L. C. and Bothwell, M. 1992. Novel roles for neurotrophins are suggested by BDNF and NT-3 mRNA expression in developing neurons. Neuron 9(3), 449–463.
Schlosser, G. 2006. Induction and specification of cranial placodes. Dev. Biol. 294(2), 303–351.
Scott, L. and Atkinson, M. E. 1998. Target pioneering and early morphology of the murine chorda tympani. J. Anat. 192(Pt 1), 91–98.
Seta, Y., Seta, C., and Barlow, L. A. 2003. Notch-associated gene expression in embryonic and adult taste papillae and taste buds suggests a role in taste cell lineage decisions. J. Comp. Neurol. 464(1), 49–61.
Seta, Y., Stoick-Cooper, C. L., Toyono, T., Kataoka, S., Toyoshima, K., and Barlow, L. A. 2006. The bHLH transcription factors, Hes6 and Mash1, are expressed in distinct subsets of cells within adult mouse taste buds. Arch. Histol. Cytol. 69(3), 189–198.
Seta, Y., Toyono, T., Takeda, S., and Toyoshima, K. 1999. Expression of Mash1 in basal cells of rat circumvallate taste buds is dependent upon gustatory innervation. FEBS Lett. 444, 43–46.
Sharaby, A. E., Ueda, K., Honma, S., and Wakisaka, S. 2006. Initial innervation of the palatal gustatory epithelium in the rat as revealed by growth-associated protein-43 (GAP-43) immunohistochemistry. Arch. Histol. Cytol. 69(4), 257–272.
Shuler, M. G., Krimm, R. F., and Hill, D. L. 2004. Neuron/target plasticity in the peripheral gustatory system. J. Comp. Neurol. 472(2), 183–192.
Slack, J. M. W. 1991. The concepts of experimental Embryology In: From Egg to Embryo (*eds*. P. W. Barlow, D. Bray, P. B. Green, and J. M. W. Slack), pp. 9–33. Cambridge University Press
Slack, J. M. and Forman, D. 1980. An interaction between dorsal and ventral regions of the marginal zone in early amphibian embryos. J. Embryol. Exp. Morphol. 56, 283–299.
Smith, H. M. 1969. The Mexican axolotl: some misconceptions and problems. Bioscience 19(7), 593–597.
Sollars, S. I. 2005. Chorda tympani nerve transection at different developmental ages produces differential effects on taste bud volume and papillae morphology in the rat. J. Neurobiol. 64(3), 310–320.
Sollars, S. I. and Hill, D. L. 2000. Lack of functional and morphological susceptibility of the greater superficial petrosal nerve to developmental dietary sodium restriction. Chem. Senses 25(6), 719–727.
Sollars, S. I. and Hill, D. L. 2005. *In vivo* recordings from rat geniculate ganglia: taste response properties of individual greater superficial petrosal and chorda tympani neurones. J. Physiol. 564(Pt 3), 877–893.
Sollars, S. I., Smith, P. C., and Hill, D. L. 2002. Time course of morphological alterations of fungiform papillae and taste buds following chorda tympani transection in neonatal rats. J. Neurobiol. 51(3), 223–236.
Sollars, S. I., Walker, B. R., Thaw, A. K., and Hill, D. L. 2006. Age-related decrease of the chorda tympani nerve terminal field in the nucleus of the solitary tract is prevented by dietary sodium restriction during development. Neuroscience 137(4), 1229–1236.
Stone, L. M., Finger, T. E., Tam, P. P. L., and Tan, S.-S. 1995. Both ectoderm and endoderm give rise to taste buds in mice. Chem. Senses 20, 785–786.
Stone, L. M., Tan, S.-S., Tam, P. P. L., and Finger, T. E. 2002. Analysis of cell lineage relationships in taste buds. J. Neurosci. 22(11), 4522–4529.
Stone, L. S. 1932. Independence of taste organs with respect to their nerve fibers demonstrated in living salamanders. Proc. Soc. Exp. Biol. Med. 30, 1256–1257.
Stone, L. S. 1940. The origin and development of taste organs salamanders observed in the living condition. J. Exp. Zool. 83, 481–506.
Sun, H. and Oakley, B. 2002. Development of anterior gustatory epithelia in the palate and tongue requires epidermal growth factor receptor. Dev. Biol. 242(1), 31–43.
Suzuki, Y. 2006. Expression of IGFBPs in the developing mouse submandibular and von Ebner's glands. Anat. Embryol. (Berl.) 211(3), 189–196.
Suzuki, Y., Takeda, M., and Obara, N. 2002. Expression of NeuroD in the mouse taste buds. Cell Tissue Res. 307(3), 423–428.
Suzuki, Y., Takeda, M., Sakakura, Y., and Suzuki, N. 2005. Distinct expression pattern of insulin-like growth factor family in rodent taste buds. J. Comp. Neurol. 482(1), 74–84.
Takeda, M., Suzuki, Y., Obara, N., and Tsunekawa, H. 2005a. Immunohistochemical detection of neurotrophin-3 and -4, and their receptors in mouse taste bud cells. Arch. Histol. Cytol. 68(5), 393–403.

Takeda, M., Suzuki, Y., Obara, N., Uchida, N., and Kawakoshi, K. 2004. Expression of GDNF and GFR alpha 1 in mouse taste bud cells. J. Comp. Neurol. 479(1), 94–102.

Takeda, M., Suzuki, Y., Obara, N., Uchida, N., and Kawakoshi, K. 2005b. Expression of glial cell line-derived neurotrophic factor (GDNF) and GDNF family receptor alpha1 in mouse taste bud cells after denervation. Anat. Sci. Int. 80(2), 105–110.

Tanabe, Y. and Jessell, T. M. 1996. Diversity and pattern in the developing spinal cord. Science 274, 1115–1123.

Tessier-Lavigne, M. and Goodman, C. S. 1996. The molecular biology of axon guidance. Science 274, 1123–1133.

Threadgill, D. W., Dlugosz, A. A., Hansen, L. A., Tennenbaum, T., Lichti, U., Yee, D., LaMantia, C., Mourton, T., Herrup, K., Harris, R. C., Barnard, J. A., Yuspa, S. H., Coffey, R. J., and Magnuson, T. 1995. Targeted disruption of mouse EGF receptor: effect of genetic background on mutant phenotype. Science 269(5221), 230–234.

Torrey, T. W. 1934. The relation of taste buds to their nerve fibers. J. Comp. Neurol. 59, 203–220.

Toyoshima, K., Miyamoto, K., and Shimamura, A. 1987. Fine structure of taste buds in the tongue, palatal mucosa and gill arch of the axolotl, *Ambystoma mexicanum*. Okajimas Folia Anat. Jpn. 64, 99–110.

Tucker, K. L., Meyer, M., and Barde, Y. A. 2001. Neurotrophins are required for nerve growth during development. Nat. Neurosci. 4(1), 29–37.

Ueda, K., Ichimori, Y., Okada, H., Honma, S., and Wakisaka, S. 2006. Immunolocalization of SNARE proteins in both type II and type III cells of rat taste buds. Arch. Histol. Cytol. 69(4), 289–296.

Vilbig, R., Cosmano, J., Giger, R., and Rochlin, M. W. 2004. Distinct roles for Sema3A, Sema3F, and an unidentified trophic factor in controlling the advance of geniculate axons to gustatory lingual epithelium. J. Neurocytol. 33(6), 591–606.

Vintschgau, M. and Honigschmied, J. 1876. Nervus glossopharyngeus und Schmeckbecher. Arch. Gesamte Physiol. 14, 443–448.

Vogt, W. 1929. Gestaltungsanalyse am Amphibienkeim mit örtlicher Vitalfärbung. II. Gastrulation und Mesodermbildung bei Urodelen und Anuren. Wilhelm Roux's Arch. Entwicklungmech Org. 120, 385–706.

Wakisaka, S., Miyawaki, Y., Youn, S. H., Kato, J., and Kurisu, K. 1996. Protein gene-product 9.5 in developing mouse circumvallate papilla: comparison with neuron-specific enolase and calcitonin gene-related peptide. Anat. Embryol. (Berl.) 194(4), 365–372.

Webb, J. F. and Noden, D. M. 1993. Ectodermal placodes: contributions to the development of the vertebrate head. Am. Zool. 33(4), 434–447.

Whitehead, M. C. and Kachele, D. L. 1994. Development of fungiform papillae, taste buds, and their innervation in the hamster. J. Comp. Neurol. 340(4), 515–530.

Whitehead, M. C., Frank, M. E., Hettinger, T. P., Hou, L.-T., and Nah, H.-D. 1987. Persistence of taste buds in denervated fungiform papillae. Brain Res. 405, 192–195.

Whitehead, M. C., Ganchrow, J. R., Ganchrow, D., and Yao, B. 1999. Organization of geniculate and trigeminal ganglion cells innervating single fungiform taste papillae: a study with tetramethylrhodamine dextran amine labeling. Neuroscience 93(3), 931–941.

Widelitz, R. 2005. Wnt signaling through canonical and non-canonical pathways: recent progress. Growth Factors 23(2), 111–116.

Wiklund, P. and Ekstrom, P. A. 2000. Axonal outgrowth from adult mouse nodose ganglia *in vitro* is stimulated by neurotrophin-4 in a Trk receptor and mitogen-activated protein kinase-dependent way. J. Neurobiol. 45(3), 142–151.

Witt, M. and Reutter, K. 1996. Embryonic and early fetal development of human taste buds: a transmission electron microscopical study. Anat. Rec. 246, 507–523.

Wodarz, A. and Nusse, R. 1998. Mechanisms of Wnt signaling in development. Annu. Rev. Cell Dev. Biol. 14, 59–88.

Yamout, A., Spec, A., Cosmano, J., Kashyap, M., and Rochlin, M. W. 2005. Neurotrophic factor receptor expression and *in vitro* nerve growth of geniculate ganglion neurons that supply divergent nerves. Dev. Neurosci. 27(5), 288–298.

Yang, R., Tabata, S., Crowley, H. H., Margolskee, R. F., and Kinnamon, J. C. 2000. Ultrastructural localization of gustducin immunoreactivity in microvilli of type II taste cells in the rat. J. Comp. Neurol. 425(1), 139–151.

Yu, M., Wu, P., Widelitz, R. B., and Chuong, C. M. 2002. The morphogenesis of feathers. Nature 420(6913), 308–312.

Zaidi, F. N. and Whitehead, M. C. 2006. Discrete innervation of murine taste buds by peripheral taste neurons. J. Neurosci. 26(32), 8243–8253.

Zhang, C. and Oakley, B. 1996. The distribution and origin of keratin 20-containing taste buds in rat and human. Differentiation 61(2), 121–127.

Zhang, C., Brandemihl, A., Lau, D., Lawton, A., and Oakley, B. 1997. BDNF is required for the normal development of taste neurons *in vivo*. Neuroreport 8(4), 1013–1017.

Zhang, C., Cotter, M., Lawton, A., Oakley, B., Wong, L., and Zeng, Q. 1995. Keratin 18 is associated with a subset of older taste cells in the rat. Differentiation 59(3), 155–162.

Zhang, G. H., Deng, S. P., Li, L. L., and Li, H. T. 2006. Developmental change of alpha-gustducin expression in the mouse fungiform papilla. Anat. Embryol. (Berl.).

Zhang, L. L. and Ashwell, K. W. 2001. The development of cranial nerve and visceral afferents to the nucleus of the solitary tract in the rat. Anat. Embryol. (Berl.) 204(2), 135–151.

Zhou, Y., Liu, H. X., and Mistretta, C. M. 2006. Bone morphogenetic proteins and noggin: Inhibiting and inducing fungiform taste papilla development. Dev. Biol. 297(1), 198–213.

Zimmerman, L. B., De Jesus-Escobar, J. M., and Harland, R. M. 1996. The Spemann organizer signal noggin binds and inactivates bone morphogenetic protein 4. Cell 86(4), 599–606.

Relevant Website

http://www.stanford.edu – Stanford University.

4.07 The Sweet Taste of Childhood

J A Mennella, Monell Chemical Senses Center, Philadelphia, PA, USA

© 2008 Elsevier Inc. All rights reserved.

4.07.1	Introduction	183
4.07.2	Ontogeny of Sweet Preferences	183
4.07.2.1	Fetal Life and Infancy	183
4.07.2.2	Childhood and Adolescence	184
4.07.2.3	Early Experiences and Contextual Learning about Sweets	185
4.07.3	Pain-Reducing Properties of Sweet Tastes	185
4.07.3.1	Infancy	185
4.07.3.2	Childhood	185
4.07.4	Concluding Remarks	186
References		186

4.07.1 Introduction

Since the nineteenth century, sweet-tasting candies have been the first purchase children make with their own money (Woloson, W. A., 2002). The liking for all that tastes sweet is universal and a hallmark of development. Although strong evidence is lacking, it has been suggested that such preferences evolved to solve a basic nutritional problem of attracting children to sources of high energy during periods of maximal growth (Simmen, B. and Hladik, C. M., 1998; Beauchamp, G. K., 1999; Coldwell, S. E. and Oswald, T. K., 2004).

In this essay, the scientific literature that documents the innate and heightened preferences that children have for sweet-tasting foods and beverages when compared to adults will be reviewed. This review serves as a foundation for a discussion on the pain-reducing properties of sugars which, along with heightened sweet preferences, may be an identifying feature of childhood.

4.07.2 Ontogeny of Sweet Preferences

4.07.2.1 Fetal Life and Infancy

The preference for sweet tastes is present early in ontogeny and remarkably well conserved phylogenetically (Steiner, J. E. *et al.*, 2001). Although each measure has its limitations, the convergence of findings from the scientific literature suggests that from birth, infants are quite sensitive to and prefer sweet tastes. This ability to detect sweet tastes and, in turn, the efficacy of sweets to modulate a variety of behaviors may be evidenced as early as fetal life. It should be emphasized that although the response of human fetuses to sweet taste has never been directly investigated, indirect evidence from albeit methodologically flawed studies (see Mistretta, C. M. and Bradley, R. M., 1977), suggests that that prenatal monitoring of taste stimuli dissolved in amniotic fluid is possible during late gestation. That is, two studies reported increased fetal swallowing following the injection of sweet stimuli such as saccharin (De Snoo, K., 1937; Liley, A. W., 1972) into the amniotic fluid of pregnant women and decrease swallowing following the injection of a bitter-tasting substance (Liley, A. W., 1972).

Stronger evidence that the fetus can respond to taste stimuli comes from research on premature infants. To overcome methodological limitations and because premature infants often have immature suck–swallow coordination, innovative methods were developed that avoided the risk of fluid aspiration by embedding the taste substance in a nipple-shaped gelatin medium that released small amounts of the sweet substance when mouthed or sucked. Infants born preterm and tested between 33 and 40 weeks postconception produced stronger and more frequent sucking responses when offered the sucrose-sweetened nipple compared with a latex nipple (Maone, T. R. *et al.*, 1990).

After birth, the liking for sweet tastes is unequivocal. Newborns are sweet connoisseurs. They respond to even dilute sweet tastes, differentiate varying degrees of sweetness, and will consume more of a sugar solution when compared to water (Desor, J. A.

et al., 1973; Nowlis, G. H. and Kessen, W., 1976). When a sweet solution is placed in the oral cavity, the infant's face relaxes, resembling an expression of satisfaction which may be followed by a smile (Steiner, J. E., 1977; Rosenstein, D. and Oster, H., 1988). That the positive facial expressions elicited by sweet-tasting sugars are reflexlike is supported by the finding that single response components, such as tongue movements, can be reliably elicited in newborns by sweet tastes in a concentration-dependent manner (e.g., Nowlis, G. H. and Kessen, W., 1976; Weiffenbach, J. M., 1977). Moreover, neonates born with severe developmental malformations of the central nervous system (e.g., anencephalic infants) react to sweet tastes, as well as other tastants, like normal, term infants (Steiner, J. E., 1977).

Newborns also respond to sweet stimulation with changes in autonomic response (e.g., Crook, C. K. and Lipsitt, L. P., 1976; Lipsitt, L. P. *et al.*, 1976; Lipsitt, L. P., 1977; Haouari, N. *et al.*, 1995; Rao, M. *et al.*, 1997; Blass, E. M. and Watt, L. B., 1999), but the behavioral state of the infant modifies the direction of the change. For example, heart rate increased proportionally when increasing concentrations of sucrose were placed in the mouths of nonagitated infants (Ashmead, D. H. *et al.*, 1980). Conversely, heart rate decreased when sweet tastes were introduced to infants who were agitated, resulting in overall calmness (e.g., Blass, E. M. and Watt, L. B., 1999). Furthermore, electroencephalographic recordings of 2–3-day-old newborns revealed that infants respond to sucrose administration with an asymmetry of brain electrical activity, a response which is usually associated with hedonically positive emotional reactions or approach behavior (Fox, N. A. and Davidson, R. J., 1986).

4.07.2.2 Childhood and Adolescence

The preference for sweet taste is universal and evident among children around the world (e.g., Brazil (Tomita, N. E. *et al.*, 1999); France (Bellisle, F. *et al.*, 1990); Iraq (Jamel, H. A. *et al.*, 1997); Israel (Steiner, J. E. *et al.*, 1984); Mexico (Vazquez, M. *et al.*, 1982); The Netherlands (De Graaf, C. and Zandstra, E. H., 1999); and North America (Desor, J. A. *et al.*, 1975; Beauchamp, G. K. and Cowart, B. J., 1987; Liem, D. G. and Mennella, J. A., 2002). Both cross-sectional and longitudinal studies revealed that the preference for sweets remains heightened throughout childhood (Beauchamp, G. K. and Moran, M., 1984; Mennella, J. A. *et al.*, 2005; Pepino, M. Y. and Mennella, J. A., 2005a) and early adolescence (Desor, J. A. *et al.*, 1975) and declines to adult levels during late adolescence (Desor, J. A. and Beauchamp, G. K., 1987).

The level of sucrose that children prefer, as measured in the laboratory, is significantly related to children's preferences for sweet-tasting foods such as cereals (Liem, D. G. and Mennella, J. A., 2002; Mennella, J. A. *et al.*, 2005) and beverages (Olson, C. M. and Gemmill, K. P., 1981; Mennella, J. A. *et al.*, 2005). Sweet taste can clearly drive consumption such that adding sugar to beverages such as Kool Aid™ (Beauchamp, G. K. and Moran, M., 1984) and solid foods such as spaghetti (Filer, L. J., 1978), ricotta, and jicama (Sullivan, S. A. and Birch, L. L., 1990) increased both liking and acceptance by children.

What causes the developmental shift in sweet preferences and consumption between childhood and adulthood remains a mystery, but this age-related decline in sweet preference has been observed in other mammals (Wurtman, J. J. and Wurtman, R. J., 1979; Bertino, M. and Wehmer, F., 1981; Marlin, N. A., 1983). Two hypotheses, not mutually exclusive, are presented here. First, children may be less sensitive to sweet tastes, thereby requiring larger amounts of sugars to obtain optimal sweetness. However, there is no strong evidence that the heightened sweet preference evidenced during infancy and childhood is due to decreased sensitivity to sweet tastes (see Cowart, B. J., 1981 for review). Whereas some investigators may report that children are more sensitive than adults when small regions of the anterior tongue are stimulated with sucrose (Stein, N. *et al.*, 1994), others found that taste sensitivity during childhood does not differ from that during adulthood (Cowart, B. J., 1981). Second, the heightened sweet preferences early in life may be linked to the growing child's need for calories (Drewnowski, A., 2000). Recent findings support this hypothesis. In brief, 11–15-year-old children were divided into sweet likers and dislikers based on their sucrose preferences (Coldwell, S. E. and Oswald, T. K., 2004). Although there were no differences between these two groups in measures such as sucrose detection thresholds, age, body mass index, percent of body fat, and pubertal development, growth rate was significantly lower in dislikers when compared to sweet likers suggesting that the age-related decline in sucrose preferences may be related to the cessation of growth.

4.07.2.3 Early Experiences and Contextual Learning about Sweets

Although the scientific evidence supports the hypothesis that sweet taste liking is innate and present at birth, if not earlier, the degree to which early experiences alter or modulate the development of sweet preferences later in life is largely unknown. Longitudinal studies revealed that babies who were routinely fed sweetened water (e.g., water sweetened with table sugar, Karo syrup or honey) during the first months of life exhibited a greater preference for sweetened water when tested at 6 months (Beauchamp, G. K. and Moran, M., 1982) and then again at 2 years of age (Beauchamp, G. K. and Moran, M., 1984) when compared to those who had little or no experience with sweetened water. Similarly, a more recent cross-sectional study on 6–10-year-old children revealed that such feeding practices may have longer-term effects on the preference for sweetened water than previously realized (Pepino, M. Y. and Mennella, J. A., 2005a).

Whether early experience with sweetened water modifies overall liking for sweetened foods is less uncertain. In fact, there is no compelling data suggesting that repeated exposure to sugar water results in a generalized heightened hedonic response to sweetness (Beauchamp, G. K. and Moran, M., 1984). Moreover, 4–7-year-old children whose mothers reported adding sugar to their foods on a routine basis were significantly more likely to prefer apple juices with added sugar and cereals with higher sugar contents than similar age children whose mothers reported never adding sugar to the foods at home (Liem, D. G. and Mennella, J. A., 2002). These data support the hypothesis that the context in which the taste experience occurred is an important factor and through familiarization, children develop a sense of what should, or should not, taste sweet (Beauchamp, G. K. and Cowart, B. J., 1985).

4.07.3 Pain-Reducing Properties of Sweet Tastes

4.07.3.1 Infancy

The pioneering research of Elliott Blass, Ronald Barr, and their colleagues revealed, more than a decade ago, that tasting a sweet substance modified crying behaviors and certain physiological responses in infants. A small amount of a sweet solution placed on the tongue of a crying newborn exerts a rapid, calming effect that persists for several minutes (Blass, E. M. and Hoffmeyer, L. B., 1991; Barr, R. G. *et al.*, 1994). Sweet tastes can also blunt expressions of pain, and calm both preterm and full-term infants who have been subjected to painful events such as heel stick or circumcision (see Stevens, B. *et al.*, 2004 for review). That sucrose attenuated a negative electroencephalographic response to a painful procedure (Fernandez, M. *et al.*, 2003) suggests that sucrose blocks pain afferents which, in turn, diminish stress and cardiac changes. Because noncaloric sweet substances such as aspartame mimic the calming effects of sucrose (Barr, R. G. *et al.*, 1999; Bucher, H. U. *et al.*, 2000) and because the administration of sucrose by direct stomach loading is not effective (Ramenghi, L. A. *et al.*, 1999), afferent signals from the mouth, rather than gastric or metabolic changes, appear to be responsible for the analgesic properties of sweet tastes.

Other flavors and orosensory components also reduce pain in infants and may act synergistically with sweet tastes. These include the flavor of mother's milk (Upadhyay, A. *et al.*, 2004) and some of its constituents (i.e., fat, protein; Blass, E. M., 1997). Orotactile stimulation from a pacifier (Blass, E. M. and Hoffmeyer, L. B., 1991; Carbajal, R. *et al.*, 1999), maternal skin-to-skin contact (Gray, L. *et al.*, 2000), or being held before and during the painful procedure (Gormally, S. *et al.*, 2001) also produce the analgesic effect, but the effects are transient when compared to when sweet taste is in the oral cavity (Smith, B. A. *et al.*, 1990). Although the use of sterile sugar water to reduce pain in infants is now routine practice in several hospital nurseries because of its natural simplicity, viability and efficacy (Anand, K. J. S., 2001), we caution that more research is needed to determine sweet taste's efficacy in reducing pain after repeated administrations (Stevens, B. *et al.*, 2004).

4.07.3.2 Childhood

The ability of sweet tastes to reduce pain continues during childhood as evidenced by the finding that the presence of sucrose, but not water, in the oral cavity delayed 8–11-year-old children's reporting of pain onset when undergoing a cold-induced pain stimulus test (Miller, A. *et al.*, 1994; Pepino, M. Y. and Mennella, J. A., 2005b). Sucrose's efficacy in reducing pain is related to the hedonic value of sweet taste for the child (Pepino, M. Y. and Mennella, J. A., 2005b). The more children like

sucrose, the better it works in increasing pain tolerance.

Less certain is whether sweet taste continues to be an analgesic during adulthood. While some studies suggested no effects (Miller, A. *et al*., 1994; Mercer, M. E. and Holder, M. D., 1997), others reported increased tolerance to mechanical pain following consumption of palatable sweet food in women but not in men (Blass, E. *et al*., 1987; Mercer, M. E. and Holder, M. D., 1997). From these observations, it can be postulated that if the analgesic response to intraoral sucrose is present during adulthood, it is less robust than that during childhood. The absence or diminution of an analgesic response to sucrose in adults is apparently not due to the lowered sucrose preference observed in adults overall (Miller, A. *et al*., 1994) and is consistent with animal model studies that revealed that sweet-induced analgesia progressively declines during development and is absent by the third week of life in rats (Anseloni, V. C. *et al*., 2002).

4.07.4 Concluding Remarks

The research discussed herein revealed that, as a group, children prefer significantly higher concentrations of sugars in foods and liquids than do adults. Nevertheless, there are striking individual and group differences in the levels of sweetness preferred (Desor, J. A. *et al*., 1975; Beauchamp, G. K. and Moran, M., 1982; Pepino, M. Y. and Mennella, J. A., 2005a). The recent identification of some taste receptor genes (e.g., Drayna, D. *et al*., 2003; Kim, U. K. *et al*., 2003) has enabled us to explore the contribution of genetic variation (see McDaniel A. H. and Reed D. R., 2004). Alleles of the bitter-taste receptor *TAS2R38* gene explained much of the phenotypic variation in the sensitivity to the bitter compound, propylthiouracil, and partially explained individual differences in children's sweet preferences (Mennella, J. A. *et al*., 2005; see also Keller, K. L. and Tepper, B. J., 2004). The future promises more research on how variation in other taste receptor genes, particularly those involved in sweet taste perception, contribute to individual differences in preferences and food habits. More knowledge about the factors that contribute to preferences for sweet-tasting foods and beverages in children, a generation who will struggle with obesity and diabetes, may suggest population-based strategies to overcome diet-induced disease and promote healthy eating habits.

Acknowledgments

Preparation of this manuscript was supported in part by NIH grants AA09523 and HD37119.

References

Anand, K. J. S. 2001. Consensus statement for the prevention and management of pain in the newborn. Arch. Pediatr. Adolesc. Med. 155, 173–180.

Anseloni, V. C., Weng, H. R., Terayama, R., Letizia, D., Davis, B. J., Ren, K., Dubner, R., and Ennis, M. 2002. Age-dependency of analgesia elicited by intraoral sucrose in acute and persistent pain models. Pain 97, 93–103.

Ashmead, D. H., Reilly, B. M., and Lipsitt, L. P. 1980. Neonates' heart rate, sucking rhythm, and sucking amplitude as a function of the sweet taste. J. Exp. Child Psychol. 29, 264–281.

Barr, R. G., Pantel, M. S., Young, S. N., Wright, J. H., Hendricks, L. A., and Gravel, R. 1999. The response of crying newborns to sucrose: is it a ''sweetness'' effect? Physiol. Behav. 66, 409–417.

Barr, R. G., Quek, V. S., Cousineau, D., Oberlander, T. F., Brian, J. A., and Young, S. N. 1994. Effects of intra-oral sucrose on crying, mouthing and hand–mouth contact in newborn and six-week-old infants. Dev. Med. Child Neurol. 36, 608–618.

Beauchamp, G. K. 1999. Factors Affecting Sweetness. In: Low-Calorie Sweeteners: Present and Future (*ed*. A. Corti), pp. 10–17. Karger. World Rev. Nutr. Diet.

Beauchamp, G. K. and Cowart, B. J. 1985. Congenital and experiential factors in the development of human flavor preferences. Appetite 6, 357–372.

Beauchamp, G. K. and Cowart, B. J. 1987. Development of Sweet Taste. In: Sweetness (*ed*. J. Dobbing), pp. 127–138. Springer.

Beauchamp, G. K. and Moran, M. 1982. Dietary experience and sweet taste preference in human infants. Appetite 3, 139–152.

Beauchamp, G. K. and Moran, M. 1984. Acceptance of sweet and salty tastes in 2-year-old children. Appetite 5, 291–305.

Bellisle, F., Dartois, A. M., Kleinknecht, C., and Broyer, M. 1990. Perceptions of and preferences for sweet taste in uremic children. J. Am. Diet. Assoc. 90, 951–954.

Bertino, M. and Wehmer, F. 1981. Dietary influence on the development of sucrose acceptability in rats. Dev. Psychobiol. 14, 19–28.

Blass, E., Fitzgerald, E., and Kehoe, P. 1987. Interactions between sucrose, pain and isolation distress. Pharmacol. Biochem. Behav. 26, 483–489.

Blass, E. M. 1997. Milk-induced hypoalgesia in human newborns. Pediatrics 99, 825–829.

Blass, E. M. and Hoffmeyer, L. B. 1991. Sucrose as an analgesic for newborn infants. Pediatrics 87, 215–218.

Blass, E. M. and Watt, L. B. 1999. Suckling- and sucrose-induced analgesia in human newborns. Pain 83, 611–623.

Bucher, H. U., Baumgartner, R., Bucher, N., Seiler, M., and Fauchere, J. C. 2000. Artificial sweetener reduces nociceptive reaction in term newborn infants. Early Hum. Dev. 59, 51–60.

Carbajal, R., Chauvet, X., Couderc, S., and Olivier-Martin, M. 1999. Randomised trial of analgesic effects of sucrose, glucose, and pacifiers in term neonates. BMJ 319, 1393–1397.

Coldwell, S. E. and Oswald, T. K. 2004. Growth-rate differs between children with adult-like versus child-like sugar preference. J. Dent. Res. 83 (Spec. Issue A), Abst. 0740.

Cowart, B. J. 1981. Development of taste perception in humans: sensitivity and preference throughout the life span. Psychol. Bull. 90, 43–73.

Crook, C. K. and Lipsitt, L. P. 1976. Neonatal nutritive sucking: effects of taste stimulation upon sucking rhythm and heart rate. Child Dev. 47, 518–522.

De Graaf, C. and Zandstra, E. H. 1999. Sweetness intensity and pleasantness in children, adolescents, and adults. Physiol. Behav. 67, 513–520.

De Snoo, K. 1937. Das trinkende kind im uterus [The drinking child in utero]. Monatsschr. Geburtsh Gynaekol. 105, 88–97.

Desor, J. A. and Beauchamp, G. K. 1987. Longitudinal changes in sweet preferences in humans. Physiol. Behav. 39, 639–641.

Desor, J. A., Greene, L. S., and Maller, O. 1975. Preferences for sweet and salty in 9- to 15-year-old and adult humans. Science 190, 686–687.

Desor, J. A., Maller, O., and Turner, R. E. 1973. Taste in acceptance of sugars by human infants. J. Comp. Phys. Psychol. 496–501.

Drayna, D., Coon, H., Kim, U. K., Elsner, T., Cromer, K., Otterud, B., Baird, L., Peiffer, A. P., and Leppert, M. 2003. Genetic analysis of a complex trait in the Utah Genetic Reference Project: a major locus for PTC taste ability on chromosome 7q and a secondary locus on chromosome 16p. Hum. Genet. 112, 567–572.

Drewnowski, A. 2000. Sensory control of energy density at different life stages. Proc. Nutr. Soc. 59, 239–244.

Fernandez, M., Blass, E. M., Hernandez-Reif, M., Field, T., Diego, M., and Sanders, C. 2003. Sucrose attenuates a negative electroencephalographic response to an aversive stimulus for newborns. J. Dev. Behav. Pediatr. 24, 261–266.

Filer, L. J. 1978. Studies of taste perception in infancy and childhood. Pediatr. Basics 5–9.

Fox, N. A. and Davidson, R. J. 1986. Taste-elicited changes in facial signs of emotion and the asymmetry of brain electrical activity in human newborns. Neuropsychologia 24, 417–422.

Gormally, S., Barr, R. G., Wertheim, L., Alkawaf, R., Calinoiu, N., and Young, S. N. 2001. Contact and nutrient caregiving effects on newborn infant pain responses. Dev. Med. Child Neurol. 43, 28–38.

Gray, L., Watt, L., and Blass, E. M. 2000. Skin-to-skin contact is analgesic in healthy newborns. Pediatrics 105, e14.

Haouari, N., Wood, C., Griffiths, G., and Levene, M. 1995. The analgesic effect of sucrose in full term infants: a randomised controlled trial. BMJ 310, 1498–1500.

Jamel, H. A., Sheiham, A., Watt, R. G., and Cowell, C. R. 1997. Sweet preference, consumption of sweet tea and dental caries; studies in urban and rural Iraqi populations. Int. Dent. J. 47, 213–217.

Keller, K. L. and Tepper, B. J. 2004. Inherited taste sensitivity to 6-*n*-propylthiouracil in diet and body weight in children. Obes. Res. 12, 904–912.

Kim, U. K., Jorgenson, E., Coon, H., Leppert, M., Risch, N., and Drayna, D. 2003. Positional cloning of the human quantitative trait locus underlying taste sensitivity to phenylthiocarbamide. Science 299, 1221–1225.

Liem, D. G. and Mennella, J. A. 2002. Sweet and sour preferences during childhood: role of early experiences. Dev. Psychobiol. 41, 388–395.

Liley, A. W. 1972. Disorders of Amniotic Fluid. In: Pathophysiology of Gestation, Vol. II, Fetal-placental Disorders (*ed*. N. S. Assali), pp. 157–206. Academic Press.

Lipsitt, L. P. 1977. Taste in Human Neonates: its Effects on Sucking and Heart Rate. In: Taste and Development: The Genesis of Sweet Preference (*ed*. J. M. Weiffenbach), pp. 125–142. U.S. Government Printing Office.

Lipsitt, L. P., Reilly, B. M., Butcher, M. J., and Greenwood, M. M. 1976. The stability and interrelationships of newborn sucking and heart rate. Dev. Psychobiol. 9, 305–310.

Maone, T. R., Mattes, R. D., Bernbaum, J. C., and Beauchamp, G. K. 1990. A new method for delivering a taste without fluids to preterm and term infants. Dev. Psychobiol. 23, 179–191.

Marlin, N. A. 1983. Early exposure to sugars influences the sugar preference of the adult rat. Physiol. Behav. 31, 619–623.

McDaniel, A. H. and Reed D. R. 2004. The Human Sweet Tooth and its Relationship to Obesity. In: Genomics and Proteomics in Nutrition (*eds*. N. Moustaid-Moussa and C. Berdanier), pp. 49–67. Dekker.

Mennella, J. A., Pepino, M. Y., and Reed, D. R. 2005. Genetic and environmental determinants of bitter perception and sweet preferences. Pediatrics 115, e216–e222.

Mercer, M. E. and Holder, M. D. 1997. Antinociceptive effects of palatable sweet ingesta on human responsivity to pressure pain. Physiol. Behav. 61, 311–318.

Miller, A., Barr, R. G., and Young, S. N. 1994. The cold pressor test in children: methodological aspects and the analgesic effect of intraoral sucrose. Pain 56, 175–183.

Mistretta, C. M. and Bradley, R. M. 1977. Taste in Utero: Theoretical Considerations. In: Taste and Development: The Genesis of Sweet Preference (*ed*. J. M. Weiffenbach), DHEW Publication No. NIH 77-1068, pp. 51–69. U.S. Government Printing Office.

Nowlis, G. H. and Kessen, W. 1976. Human newborns differentiate differing concentrations of sucrose and glucose. Science 191, 865–866.

Olson, C. M. and Gemmill, K. P. 1981. Association of sweet preference and food selection among four to five year old children. Ecol. Food Nutr. 11, 145–150.

Pepino, M. Y. and Mennella, J. A. 2005a. Factors contributing to individual differences in sucrose preference. Chem. Senses 30 (Suppl 1), i319–i320.

Pepino, M. Y. and Mennella, J. A. 2005b. Sucrose-induced analgesia is related to sweet preferences in children but not adults. Pain 119 , 210–218.

Ramenghi, L. A., Evans, D. J., and Levene, M. I. 1999. ''Sucrose analgesia'': absorptive mechanism or taste perception? Arch. Dis. Child Fetal Neonatal Ed. 80, F146–F147.

Rao, M., Blass, E. M., Brignol, M. M., Marino, L., and Glass, L. 1997. Reduced heat loss following sucrose ingestion in premature and normal human newborns. Early Hum. Dev. 48, 109–116.

Rosenstein, D. and Oster, H. 1988. Differential facial responses to four basic tastes in newborns. Child Dev. 59, 1555–1568.

Simmen, B. and Hladik, C. M. 1998. Sweet and bitter taste discrimination in primates: scaling effects across species. Folia Primatol. 69, 129–138.

Smith, B. A., Fillion, T. J. and Blass, E. M. 1990. Orally mediated sources of calming in 1 to 3-day-old human infants. Dev. Psychol. 26, 731–737.

Stein, N., Laing, D. G., and Hutchinson, I. 1994. Topographical differences in sweetness sensitivity in the peripheral gustatory system of adults and children. Brain Res. Dev. Brain Res. 82, 286–292.

Steiner, J. E. 1977. Facial expressions of the neonate infant indicating the hedonics of food-related chemical stimuli. In: Taste and Development: the Genesis of Sweet Preference (*ed*. J. M. Weiffenbach), pp. 173–188. U.S. Government Printing Office.

Steiner, J. E., Glaser, D., Hawilo, M. E., and Berridge, K. C. 2001. Comparative expression of hedonic impact: affective reactions to taste by human infants and other primates. Neurosci. Biobehav. Rev. 25, 53–74.

Steiner, J. E., Sgan-Cohen, H. D., and Nahas, J. 1984. Sweet preference and dental caries among Bedouin youth in Israel. Commun. Dent. Oral Epidemiol. 12, 386–389.

Stevens, B., Yamada, J., and Ohlsson, A. 2004. Sucrose for analgesia in newborn infants undergoing painful procedures. Cochrane Database Syst. Rev. Issue 3, CD001069.

Sullivan, S. A. and Birch, L. L. 1990. Pass the sugar, pass, the salt: experience dictates preference. Dev. Psychol. 26, 546–551.

Tomita, N. E., Nadanovsky, P., Vieira, A. L., and Lopes, E. S. 1999. Taste preference for sweets and caries prevalence in preschool children. Rev. Saude Publica 33, 542–546.

Upadhyay, A., Aggarwal, R., Narayan, S., Joshi, M., Paul, V. K., and Deorari, A. K. 2004. Analgesic effect of expressed breast milk in procedural pain in term neonates: a randomized, placebo-controlled, double-blind trial. Acta Paediatr. 93, 518–522.

Vazquez, M., Pearson, P. B., and Beauchamp, G. K. 1982. Flavor preferences in malnourished Mexican infants. Physiol. Behav. 28, 513–519.

Weiffenbach, J. M. 1977. Sensory mechanisms of the newborn's tongue. In: Taste and Development: the Genesis of Sweet Preference (*ed*. J. M. Weiffenbach), pp. 205–234. U.S. Government Printing Office.

Woloson, W. A. 2002. Refined Tastes: Sugar, Confectionery, and Consumers in Nineteenth-Century America. The Johns Hopkins University Press.

Wurtman, J. J. and Wurtman, R. J. 1979. Sucrose consumption early in life fails to modify the appetite of adult rats for sweet foods. Science 205, 321–322.

4.08 Taste Analgesia in Newborns

V Anseloni, University of Maryland Dental School, Baltimore, MD, USA

M Ennis, University of Tennessee Health Science Center, Memphis, TN, USA

© 2008 Elsevier Inc. All rights reserved.

4.08.1	Taste Analgesia in Human Infants	189
4.08.2	Taste Analgesia in Rodents	190
4.08.2.1	General Properties	190
4.08.2.2	Oral Cavity versus Postingestional/Absorptive Mechanism?	191
4.08.2.3	Neurochemical Mechanisms – Opioid Mediation	191
4.08.3	Outstanding Issues and Recent Developments	191
4.08.3.1	Ontogeny of Taste-Analgesia and Efficacy for Inflammatory Pain	192
4.08.3.2	Neural Circuitry	193
4.08.4	Future Directions	194
References		195

Glossary

allodynia A painful response to a previously non-painful or subthreshold stimulus. Typically occurs after tissue injury and/or inflammation.

hyperalgesia A state characterized by enhanced sensation of pain. Typically occurs after tissue injury and/or inflammation.

mid-collicular transection A surgical procedure used to sever connections between the forebrain and the hindbrain.

von Frey filaments Filaments of various bending forces used to measure responses to mechanical cutaneous stimulation.

4.08.1 Taste Analgesia in Human Infants

Decades of studies have reported the analgesic and calming effects following intraoral infusion of sweet tastants (sucrose, glucose, fructose, aspartame), mother's milk, commercial formula, protein (provomin), fat (coconut, corn, and soy oil), and carbohydrates (polycose) on human infants (Blass, E. M. and Smith, B. A., 1992; Blass, E. M., 1997a; 1997c; Graillon, A. *et al.*, 1997; Blass, E. M. and Miller, L. W., 2001; Akman, I. *et al.*, 2002). Surprisingly, neither lactose nor colostrum has proven to produce analgesic or calming effects (Blass, E. M. and Smith, B. A., 1992; Blass, E. M., 1997a; 1997c; Blass, E. M. and Miller, L. W., 2001). Instead, the most potent taste analgesia is that triggered by sucrose.

The effects of sucrose have been well characterized in human infants. Analgesic and calming effects of taste analgesia are immediate and endure at least 5 min after sucrose termination (Blass, E. M. *et al.*, 1989; Smith, B. A. *et al.*, 1990; Blass, E. M. and Shah, A., 1995). When delivered repetitively (up to three times daily) over a 7-day period, there appears to be little or no tolerance to the analgesic effects of intraoral sucrose (Johnston, C. C. *et al.*, 2002). Intraoral infusion of microliter volumes (100–200 µl) of sucrose over a dose-range of 12–50% produce a flat dose–response relationship (Blass, E. M. *et al.*, 1989; Blass, E. M., 1997b; Overgaard, C. and Knudsen, A., 1999; Smith, B. A. *et al.*, 1990; Blass, E. M. and Hoffmeyer, L. B., 1991; Blass, E. M. and Smith, B. A., 1992).

Sucrose markedly diminishes crying in response to painful standard hospital procedures such as circumcision or blood collection via heel prick (Blass, E. M. and Hoffmeyer, L. B., 1991; Kaufman, G. E. *et al.*, 2002). In those studies, crying, grimacing, and heart rate have been the main assessments of nociception and calming in human newborns. The use of sucrose-coated pacifiers is currently recommended as a behavioral approach in the guidelines for managing pain in human newborns (Anand, K. J., 2001). However, despite the well-documented analgesic effects of

sucrose, a clinically relevant question remains open for investigation: does repetitive administration of sucrose, especially in a neonatal intensive care unit (NICU) preterm infant, have long-term developmental consequences? A study by Johnston C. C. *et al.* (2002) reported that infants receiving intraoral sucrose up to three times daily for 1 week exhibited subsequent impairments in motor development and vigor. The cause of these deficits is unclear, but it is possible that the withdrawal of sucrose may render the infant more susceptible to subsequent pain.

Both preterm (Taddio, A. *et al.*, 2003) and full-term human infants of either cesarean section or vaginal deliveries readily exhibit analgesic and calming effects of sweet tastants. The age range of full term in those studies varied from few hours after birth (Blass, E. M. and Miller, L. W., 2001; Gray, L. *et al.*, 2002) to 2–6-week-old infants (Barr, R. G., *et al.*, 1994; Zeifman, D. *et al.*, 1996). Although rat studies have already unveiled the age-dependency of sucrose-induced analgesia, the age-dependency in human infants remains unclear. One major difference is that sucrose is effective in preterm human newborns, whereas in rats sucrose effects emerge between postnatal (P) day 2 and 3 (Anseloni, V. C. *et al.*, 2002). While the human developmental period over which intraoral sucrose is analgesic has not been systemically studied, it appears to be analgesic in 5–10-year-old children but not adults (Pepino, M. Y. and Mennella, J. A., 2005). Interestingly, this same study showed that analgesia elicited by sucrose correlates with sweet preferences in 5–10-year-old children but not adults. The more the children liked sucrose, the higher its analgesic efficacy. Therefore, the hedonic value of sucrose is reported to be a major component in triggering sucrose effects. It is unknown if there are gender-based differences in taste analgesia in human infants.

In agreement with animal studies discussed below, there is evidence that taste analgesia in human infants is mediated by central opioid mechanisms. Blass E. M. and Ciaramitaro V. (1994) reported that babies born to women who were maintained on methadone during pregnancy did not quiet to the taste of sucrose. This suggests an opioid mediation in the calming, and perhaps the analgesic, effects elicited by intraoral tastants. Taddio A. *et al.* (2003) reported that intraoral administration of sucrose in preterm infants does not lead to an increase in serum β-endorphin concentrations. However, synaptic release of opioid in the central nervous system (CNS) may not translate to increases in the periphery.

4.08.2 Taste Analgesia in Rodents

4.08.2.1 General Properties

Studies in rodents have revealed remarkable similarities of the properties of taste analgesia to those in human infants. As in human infants, intraoral infusion (20–140 µl) of dairy milk or half-and-half produces analgesia in P0 or P10 rats (Blass, E. M. *et al.*, 1991; Blass, E. M., 1997c). The analgesia develops rapidly ($\leq$15 s) and persists for 0.5 min to at least 4 min after termination of infusion (Blass, E. M. *et al.*, 1991; Blass, E. M., 1997c). Milk infusions also reduced ultrasonic vocalizations, similar to its quieting effect in human infants (Blass, E. M. and Fitzgerald, E., 1988). Similar analgesic and quieting effects lasting up to 5 min were obtained by infusion of polycose or corn oil (Shide, D. J. and Blass, E. M., 1989).

Intraoral infusion (0.18 ml) of several sugars present in human and rat mother's milk were also shown to be analgesic in P10 rat pups (Blass, E. M. and Shide, D. J., 1994). Infusion of 0.22 M fructose, sucrose, or glucose reduced spontaneous ultrasonic vocalizations and increased paw withdrawal latencies to a conductive thermal stimulus. By contrast, lactose was ineffective. The rank-order of potencies was sucrose > glucose > fructose, paralleling findings in human infants. Testing of additional sugar concentrations (0.44 and 0.66 M) produced a flat dose–response relationship; that is, no additional effects were observed with higher concentrations. The reason for the flat dose–response function is unclear. Behavioral and electrophysiological studies demonstrate graded responses to these sugars over this concentration range in juvenile rodents. In P14–P20 hamsters, graded responses of the chorda tympani nerve are observed in response to sugars from 0.2 to 0.6 M, although these responses are of smaller amplitude than in adult animals (Hill, D. L., 1988). It is possible that the analgesic mechanisms (e.g., opioid release) activated by the sugars are saturated (i.e., ceiling effect) at 0.2 M and that a graded analgesic effect might be observed only with lower concentrations. Hill D. L. (1988) also reported that the chorda tympani responses to lactose (0.2–0.5 M) were essentially similar to those of fructose and glucose at identical concentrations. Extrapolating to rats, it is thus unclear why fructose and glucose produce analgesia, while lactose does not. One possibility is that central neural responses to lactose may be considerably less than the other sugars. Unfortunately, there is a relative paucity of information on the

development of central gustatory neuronal responses to sugars during early postnatal development in rats.

Are the calming and analgesic effects of intraoral infusion explained by mechanical, somatosensory stimulation of tastant infusion? A number of studies have addressed this question, finding that intraoral infusion of distilled water, saline, or other salt stimuli do not reduce vocalizations and do not produce analgesia (Blass, E. M. *et al.*, 1987; Shide, D. J. and Blass, E. M., 1989; Blass, E. M. *et al.*, 1991; Blass, E. M. and Shide, D. J., 1994; Ren, K. *et al.*, 1997; Anseloni, V. C. *et al.*, 2002; 2005). Thus, the effects of intraoral infusion are not due to somatosensory stimulation from the cannula or fluid movement in the oral cavity, nor are they due to gustatory stimulation of other taste qualities (i.e., salt).

4.08.2.2 Oral Cavity versus Postingestional/Absorptive Mechanism?

An important question is if the quieting and analgesic effects of intraoral sucrose are mediated by stimulation of taste receptors in the oral cavity or to postingestional or absorptive mechanisms? The rapid onset (i.e., within seconds) of the effects of intraoral tastants suggest that they are triggered by oral cavity taste receptors. The contribution of postingestional mechanisms has not been directly examined in animal studies. However, this question was addressed in human infants. Ramenghi L. A. *et al.* (1999) found that while intraoral sucrose reduced crying and behavioral responses indicative of pain following heel lancing, direct stomach loading via a nasogastric tube was without effect. This suggests that stimulation of taste buds in the oral cavity by sucrose is necessary to induce analgesia.

Given that taste analgesia is due to stimulation of taste receptors in the oral cavity, it is of interest to determine which of the various taste-related cranial nerve branches are involved. Taste receptors are topographically distributed throughout the oral cavity and are innervated by three cranial nerves. The chorda tympani and the greater superficial petrosal branches of the facial nerve (VII) innervate the taste receptors of the anterior tongue and palate, respectively. In rats, receptors responsive to sweet stimuli are located primarily on the palate, consistent with observations that greater petrosal nerve fibers are more responsive to sugars than chorda tympani fibers. Taste receptors in the circumvallate and foliate papillae on the posterior tongue are innervated by the lingual branch of the glossopharyngeal nerve (IX), and those in the oropharynx are innervated by superior laryngeal branch of the vagus nerve (X). Gustatory fibers of VII, IX, and X terminate in a rostral–caudal sequence in the rostral, gustatory portion of the nucleus tractus solitarius (rNTS; reviewed in Travers, S. P., 1993). Unfortunately, the contribution of these cranial nerves to taste analgesia has not been investigated. Additional studies are needed to clarify the roles of the gustatory cranial nerves in taste analgesia.

4.08.2.3 Neurochemical Mechanisms – Opioid Mediation

A number of rodent studies have investigated the neurochemical mechanisms underlying taste analgesia. The effects of oral sucrose are similar to those of opioid narcotics such as morphine. Morphine is analgesic, calming, and decreases vocalizations. Blass E. M. *et al.* (1991) reported that the analgesic effect of a single 20 µl intraoral bolus of milk was comparable in magnitude to that elicited by systemic injection of a moderate dose of the morphine ($0.125\ mg\ kg^{-1}$). Other studies showed that the analgesic and quieting effects of intraoral milk and sugars were blocked by systemic injections of the nonselective opioid receptor antagonists naloxone or naltrexone (Blass, E. M. *et al.*, 1987; Blass, E. M. and Fitzgerald, E., 1988; Shide, D. J. and Blass, E. M., 1989; Blass, E. M. *et al.*, 1991). Taken together, these findings demonstrate that the calming and analgesic effects of intraoral fats and sugars are mediated by release of endogenous opioids.

Interestingly, additional studies showed that calming effects of intraoral tastants may also involve the gastrointestinal peptide, cholecystokinin (CCK). Calming effects, as measured by reductions in ultrasonic vocalizations, are elicited by systemic injection of CCK (Weller, A. and Blass, E. M., 1988). In the same study, CCK had no effect on pain thresholds. CCK receptor antagonists were subsequently found to block the calming effects of intraoral milk or corn oil, but not milk (Blass, E. M. and Shide, D. J., 1993; Weller, A. and Gispan, I. H., 2000). These studies indicate that the calming, but not the analgesic, effects of intraoral tastant involve a CCK component.

4.08.3 Outstanding Issues and Recent Developments

Sucrose-induced analgesia in rats and humans develops within seconds, lasts for minutes, is prevented by

systemic injection of opiate receptor antagonists, and is compromised in human infants born to opiate-dependent mothers. Thus, the mechanisms appear to be remarkably well conserved phylogenetically and involve central opioid systems. A number of critical questions about taste analgesia remain unanswered. The rodent work summarized above was confined to the early postnatal period (P0–P10). Does taste analgesia exhibit a critical period in which intraoral tastants are effective? In other words, is this phenomenon developmentally transient? The pain-relieving effects of intraoral tastants were assayed in acute pain tests using primarily noxious thermal stimuli. Are intraoral tastant equally effective for other types of nociceptive stimuli, such as mechanical stimuli? Persistent inflammatory pain is a major consequence of tissue injury. Are intraoral tastants effective in attenuating hyperalgesia and allodynia associated with tissue injury? The neural circuits by which taste stimuli engage central opioid analgesic mechanisms are not known. The remainder of this chapter summarizes recent studies from our laboratories that have begun to address these questions.

4.08.3.1 Ontogeny of Taste-Analgesia and Efficacy for Inflammatory Pain

We investigated the effects of intraoral sucrose (7.5%) on nocifensive withdrawal responses to thermal and mechanical stimuli in naive rat pups and in pups in which Complete Freund's adjuvant (CFA) was injected in a fore- or hindpaw to produce inflammation (Anseloni, V. C. *et al.*, 2002). Pain thresholds were tested using conductive thermal and mechanical (von Frey filaments) stimuli from P0 (the day of birth) to P21. In noninflamed animals, for noxious thermal stimuli, sucrose-induced analgesia for the hindpaw emerged at P3, peaked at P7–P10, then progressively declined and was absent at P17 (Figure 1). For mechanical forepaw stimuli, sucrose-induced analgesia emerged, and was maximal at ~P10, then declined and was absent at P17. By contrast, maximal sucrose-induced analgesia for mechanical hindpaw stimuli was delayed (P13) compared to that for the forepaw, although it was also absent at P17. In inflamed animals, sucrose reduced hyperalgesia and allodynia assessed with mechanical stimuli (Figure 2). Sucrose-induced analgesia in inflamed animals was initially present at P3 for the forepaw and P13 for the hindpaw, and was absent by P17 for both limbs. Intraoral sucrose produced significantly greater effects on responses in fore- and

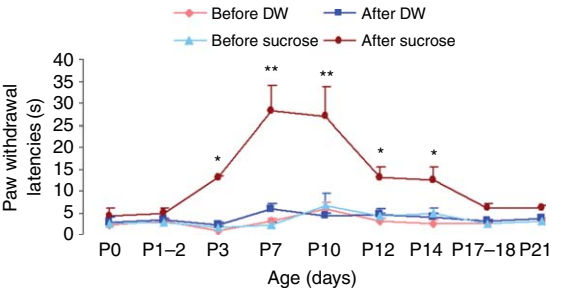

Figure 1 Effects of intraoral sucrose infusion of forepaw withdrawal latencies to thermal stimuli from P0 to P21. Infusion of distilled water (DW) did not influence paw withdrawal latencies ($P > 0.05$) and baseline withdrawal latencies were similar across P0–P21. Sucrose infusion did not significantly influence paw withdrawal latencies at P0–P2 or P17–P21. However, sucrose infusion significantly elevated withdrawal latencies from P3 to P14. Each time point includes a minimum of eight animals. Data are expressed as mean ± standard error of the mean paw withdrawal latency. $^{*}P < 0.01$; $^{**}P < 0.001$.

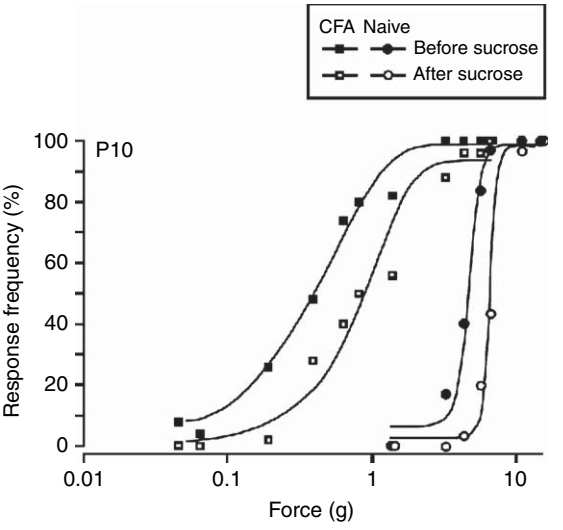

Figure 2 Stimulus–response function curves illustrating the effects of intraoral sucrose on response frequency of the forepaw to mechanical stimuli in noninflamed (naive) and inflamed (CFA) rats at P10; see text for details. Note the leftward shift in the stimulus–response function in inflamed rats compared to naive rats. After inflammation, rats respond to stimuli that are subthreshold in naive rats, indicating the development of inflammation-induced allodynia. There is also an increased response to suprathreshold stimuli, indicating the development of inflammation-induced hyperalgesia. Note that sucrose infusion (open symbols) diminished the response frequency, resulting in a significant rightward shift of the curves for both naive and inflamed rats ($P < 0.001$). Reprinted from Anseloni, V. C., Weng, H. R., Terayama, R., Letizia, D., Davis, B. J., Ren, K., Dubner, R., and Ennis, M. 2002. Age-dependency elicited by intraoral sucrose in acute and persistent pain models. Pain 97, 93–103, with permission from IASP.

hindpaws in inflamed rats than in naive rats indicating that it reduces hyperalgesia and allodynia beyond its effects on responses in naive animals.

The preceding study demonstrated that sucrose-induced analgesia is age-dependent and maximal at P10–P13, and is limited to the preweaning period (<P17) in rats. After P10–P13, the analgesic effect of intraoral sucrose progressively subsides as weaning approaches, and is absent at the approximate time of weaning (P17–P21). Extrapolating to humans, P7 in rats correlates to full-term human newborns and the range of P0–P20 in rats corresponds approximately to 24 weeks of gestation and the toddler stage, respectively, in human infants (Helmuth, L., 2000). Sucrose-induced analgesia in rats thus disappears at a neonatal age when locomotor activity is sufficiently developed for the animal to generate organized escape from noxious stimuli. The age-dependency of sucrose-induced analgesia and its differential maturation for the fore- and hindpaw may be due to developmental changes in endogenous analgesic mechanisms and developmental modulation of the interaction between gustatory and pain modulatory pathways (for review see Anseloni, V. C. *et al.*, 2002). The findings above support the hypothesis that sucrose has a selective influence on analgesic mechanisms and that an enhanced sucrose effect takes place in hyperalgesic, inflamed animals as compared to naive animals. These results indicate that intraoral sucrose alleviates transient pain in response to thermal and mechanical stimuli, and also effectively reduces inflammatory hyperalgesia and allodynia.

The absence of an analgesic effect of sucrose infusion at P0–P2 was surprising given previous reports that intraoral milk infusion was analgesic in P0 pups delivered by cesarean section (Blass, E. M. *et al.*, 1991). The reason for the difference between the two studies is unclear. Stress or changes in opioid mechanisms as a result of natural delivery may compromise the ability of milk and/or sucrose to produce analgesia for the first few postnatal days. Milk also contains a number of individual analgesic sugars and fats, and the combination of these, but not sucrose alone, may be sufficient to produce analgesia immediately after birth. Further studies are needed to address these questions.

4.08.3.2 Neural Circuitry

As reviewed above, the characteristics of sucrose-induced analgesia have been well established in rat pups and human infants. By contrast, nothing is known about the neurobiological substrate underlying this phenomenon. The ability of a small intraoral bolus of sucrose to trigger opiate-mediated analgesia suggests that there are connections from sweet taste-responsive brain neurons to the descending antinociceptive systems. In this regard, it is noteworthy that several gustatory areas have been reported to be involved in analgesia, including the parabrachial nucleus (Bester, H. *et al.*, 1995), insular cortex (Burkey, A. R. *et al.*, 1996), central nucleus of the amygdala (Kalivas, P. W. *et al.*, 1982; Oliveras, J. L. and Besson, J. M., 1988), and lateral hypothalamus. Additionally, tract tracing studies have demonstrated that several gustatory areas project to two major brainstem antinociceptive sites involved in opiate-receptor-dependent analgesia: the midbrain periaqueductal gray (PAG) and the rostroventromedial medullary region that includes nucleus raphe magnus (RMG). For example, the parabrachial nucleus, insular cortex, central nucleus of the amygdala, and lateral hypothalamus densely innervate the PAG and some of these areas directly project to the RMG area (Behbehani, M. M. *et al.*, 1988; Krukoff, T. L. *et al.*, 1993; Behbehani, M. M., 1995; Hermann, D. M. *et al.*, 1997). Thus, there is considerable overlap among, as well as numerous potential anatomical linkages between, components of gustatory pathway and sites known to be involved in centrally mediated analgesia.

To begin to assess these circuits, we used mid-collicular transections as well as immunohistochemistry for the protein product of the immediate early gene c-*fos*, to identify sites involved in the analgesic effect of sucrose in neonatal rats. Previous studies have shown that certain functions of the taste system do not require processing or feedback from higher-order gustatory structures. Adult animals exhibit appropriate motor and discriminative responses to taste stimuli following mid-collicular transections that isolate the parabrachial nucleus (PBN) from the taste thalamus and other forebrain gustatory structures. For example, rats will ingest palatable sweet taste solutions or milk and reject unpalatable bitter taste solutions following mid-collicular transections (Kornblith, C. L. and Hall, W. G., 1979; Grill, H. J. and Norgren, R., 1978; Grill, H. J. and Berridge, K., 1985). Thus, the discriminatory and basic motor aspects of taste behavior are retained in the brainstem caudal to the level of the PBN. Given these findings, we asked whether the neural circuitry necessary for mediating sucrose-induced analgesia in neonatal rats also resides within the brainstem and spinal cord. To assess this, mid-collicular transections that isolated

the PBN, as well as more caudal structures, from mid- and forebrain components of the gustatory pathway were performed (Anseloni, V. C. *et al.*, 2005). Also present posterior to the transection were several structures involved in antinociception, including the caudal PAG and RMG. We found that in the transected pups, the analgesic actions of intraoral sucrose infusion persisted. Moreover, sucrose-induced analgesia was enhanced compared to its actions in the sham pups. This suggested that descending projections from the mid- or forebrain may tonically facilitate central responses to noxious somatosensory input. Consistent with this, transection alone produced a decrease in withdrawal responses to noxious mechanical stimuli, resulting in behavioral hypoalgesia. However, a simple shift in baseline responses did not appear to account for the persistence of sucrose's analgesic effect in the transected pups. Transection alone increased the baseline withdrawal responses to roughly the same degree (30–40%) as did sucrose in the sham animals (40–50%). By contrast, sucrose produced a significantly greater increase (173%) following mid-collicular transection (Figure 3).

The preceding findings indicate that the neural circuitry underlying sucrose-induced analgesia resides within the brainstem and spinal cord. We next assessed c-fos activity elicited by brief intraoral infusion (90 µl in 90 s) of sucrose (0.2 M) or ammonium chloride (a salt stimulus, 0.1 M) to identify candidate brainstem neurons involved in this circuitry (Anseloni, V. C. *et al.*, 2005). Compared to control groups (intact, cannula, distilled water), both sucrose and ammonium chloride induced Fos expression in the rNTS, the first relay in the ascending gustatory pathway. Sucrose also elicited Fos expression in several brainstem areas associated with centrally mediated analgesia, including the PAG and the RMG. Taken together, these findings demonstrate that analgesia elicited by intraoral sucrose does not require involvement of the forebrain. Intraoral sucrose activates neurons in the PAG and RMG, two key brainstem sites critically involved in descending pain modulation.

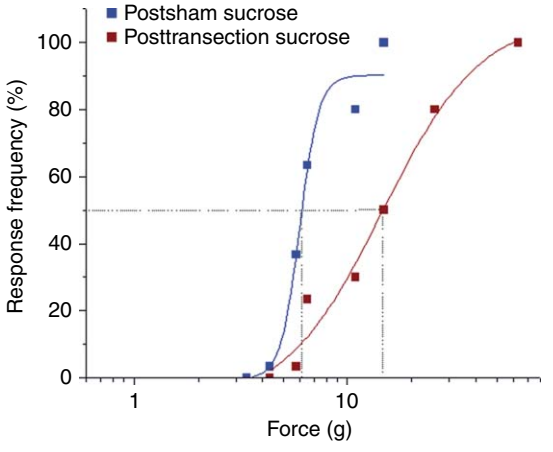

Figure 3 Stimulus–response function curves comparing the effects of intraoral sucrose on response frequency of the hindpaw to mechanical stimuli following sham and mid-collicular transection surgeries in P10–P12 rats. Sucrose after transection had an enhanced analgesic effect compared to sucrose in sham animals, as illustrated by the significant rightward shift in the stimulus–response curve ($P < 0.001$); see text for details.

Previous studies have shown that activation of the PAG and RMG produce analgesia and are two key brain substrates involved in the analgesic actions of opioids. RMG neurons are the main source of descending projections (via the dorsolateral funiculus) to the dorsal horn of the spinal cord. RMG stimulation, or morphine administration, inhibits dorsal horn neurons involved in pain transmission (Fields, H. L. *et al.*, 1991; Behbehani, M. M., 1995). If, as suggested above by the study of Anseloni V. C. *et al.* (2005), intraoral sucrose produces analgesia via activation of RMG neurons, then intraoral sucrose should, similar to direct stimulation of RMG, inhibit spinal cord neuronal responses to nociceptive stimuli. Ren K. *et al.* (1997) found that intraoral sucrose markedly diminished Fos expression in the spinal cord elicited by inflammation of the forepaw. Thus, the effects of intraoral sucrose are similar to those of morphine, in that both blunt dorsal horn neuronal responses to noxious somatosensory input.

4.08.4 Future Directions

Despite our increased understanding of the neurobiological underpinnings and properties of taste analgesia in humans and rodents, significant questions remain. What mechanisms are responsible for the ontogeny and developmentally transient nature of this phenomenon? Where are the specific links where gustatory information accesses central analgesic circuits? What opioid neurotransmitters (e.g., enkephalin, dynorphin) and opiate receptor subtypes are involved, and where are they located? These will be difficult questions to answer, as opioids and opiate receptors are located in numerous components in both the ascending gustatory pathway and

descending antinociceptive circuits. Might analgesia elicited by nursing provide a natural neuroprotective function for the developing nervous system? The ability of natural stimuli to produce analgesia may have important consequences beyond transient or brief pain relief in developing infants. Preterm and certain high-risk infants undergo repeated clinical procedures which produce cutaneous inflammation accompanied by hyperalgesia lasting for several hours or even days (Anand, K. J., 1999). Recent studies have shown that tissue injury during the first few postnatal weeks produces changes in the long-term development of nociceptive circuits and pain thresholds that persist in adult animals (Ruda, M. A. *et al*., 2000; Lidow, M. S. *et al*., 2001; Ren, K. *et al*., 2004). Thus, analgesia produced by natural stimuli during the preweaning period may protect against the deleterious effects of tissue injury and inflammation on the development and/or maturation of nociceptive circuits.

Acknowledgments

Supported by PHS grants DC03895 and NS41384.

References

Akman, I., Ozek, E., Bilgen, H., Ozdogan, T., and Cebeci, D. 2002. Sweet solutions and pacifiers for pain relief in newborn infants. J. Pain 3, 199–202.

Anand, K. J. 2001. International evidence-based group for neonatal pain. Consensus statement for the prevention and management of pain in the newborn. Arch. Pediatr. Adolesc. Med. 155, 173–180.

Anand, K. J., Coskun, V., Thrivikraman, K. V., Nemeroff, C. B., and Plotsky, P. M. 1999. Long-term behavioral effects of repetitive pain in neonatal rat pups. Physiol. Behav. 66, 627–637.

Anseloni, V. C., Ren, K., Dubner, R., and Ennis, M. 2005. A brainstem substrate for analgesia elicited by intraoral sucrose. Neuroscience 133, 231–243.

Anseloni, V. C., Weng, H. R., Terayama, R., Letizia, D., Davis, B. J., Ren, K., Dubner, R., and Ennis, M. 2002. Age-dependency elicited by intraoral sucrose in acute and persistent pain models. Pain 97, 93–103.

Barr, R. G., Quek, V. S., Cousineau, D., Oberlander, T. F., Brian, J. A., and Young, S. N. 1994. Effects of intra-oral sucrose on crying, mouthing and hand–mouth contact in newborn and six-week-old infants. Dev. Med. Child. Neurol. 36(7), 608–618.

Behbehani, M. M. 1995. Functional characteristics of the midbrain periaqueductal gray. Prog. Neurobiol. 46, 575–605.

Behbehani, M. M., Park, M. R., and Clement, M. E. 1988. Interactions between the lateral hypothalamus and the periaqueductal gray. J. Neurosci. 8, 2780–2787.

Bester, H., Menendez, L., Besson, J. M., and Bernard, J. F. 1995. Spino (trigemino) parabrachiohypothalamic pathway: electrophysiological evidence for an involvement in pain processes. J. Neurophysiol. 73, 568–585.

Blass, E. M. 1997a. Infant formula quiets crying human newborns. J. Dev. Behav. Pediatr. 18, 162–165.

Blass, E. M. 1997b. Interactions between contact and chemosensory mechanisms in pain modulation in 10-day-old rats. Behav. Neurosci. 111, 147–154.

Blass, E. M. 1997c. Milk-induced hypoalgesia in human newborns. Pediatrics 99, 825–829.

Blass, E. M. and Ciaramitaro, V. 1994. A new look at some old mechanisms in human newborns: taste and tactile determinants of state, affect, and action. Monogr. Soc. Res. Child Dev. 59, 1–81.

Blass, E. M. and Fitzgerald, E. 1988. Milk-induced analgesia and comforting in 10-day-old rats: opioid mediation. Pharmacol. Biochem. Behav. 29, 9–13.

Blass, E. M. and Hoffmeyer, L. B. 1991. Sucrose as an analgesic for newborn infants. Pediatrics 87, 215–218.

Blass, E. M. and Miller, L. W. 2001. Effects of colostrum in newborn humans: dissociation between analgesic and cardiac effects. J. Dev. Behav. Pediatr. 22, 385–390.

Blass, E. M. and Shah, A. 1995. Pain-reducing properties of sucrose in human newborns. Chem. Senses 20, 29–35.

Blass, E. M. and Shide, D. J. 1993. Endogenous cholecystokinin reduces vocalizations in isolated 10-day-old rats. Behav. Neurosc. 107, 488–492.

Blass, E. M. and Shide, D. J. 1994. Some comparisons among the calming and pain-relieving effects of sucrose, glucose, fructose and lactose in infant rats. Chem. Senses 19, 239–249.

Blass, E. M. and Smith, B. A. 1992. Differential effects of sucrose, fructose, glucose, and lactose on crying in 1- to 3-day-old human infants: qualitative and quantitative considerations. Dev. Psych. 28, 804–810.

Blass, E. M., Fillion, T. J., Rochat, P., Hoffmeyer, L. B., and Metzger, M. A. 1989. Sensorimotor and motivational determinants of hand–mouth coordination in 1–3-day-old human infants. Dev. Psych. 25, 963–975.

Blass, E. M., Fitzgerald, E., and Kehoe, P. 1987. Interactions between sucrose, pain and isolation distress. Pharmacol. Biochem. Behav. 26, 483–489.

Blass, E. M., Jackson, A. M., and Smotherman, W. P. 1991. Milk-induced, opioid-mediated antinociception in rats at the time of cesarean delivery. Behav. Neurosci. 105, 677–686.

Burkey, A. R., Carstens, E., Wenniger, J. J., Tang, J., and Jasmin, L. 1996. An opioidergic cortical antinociception triggering site in the agranular insular cortex of the rat that contributes to morphine antinociception. J. Neurosci. 16, 6616–6623.

Fields, H. L., Heinricher, M. M., and Mason, P. 1991. Neurotransmitters in nociceptive medullary circuits. Ann. Rev. Neurosci. 14, 219–245.

Graillon, A., Barr, R. G., Young, S. N., Wright, J. H., and Hendricks, L. A. 1997. Differential response to intraoral sucrose, quinine and corn oil in crying human newborns. Physiol. Behav. 62, 317–325.

Gray, L., Miller, L. W., Philipp, B. L., and Blan, E. M. 2002. Breastfeeding is analgeric in healthy newborns. Pediatrics 109(4), 590–593.

Grill, H. J. and Berridge, K. 1985. Taste reactivity as a measure of neural control of palatability. Prog. Psychobiol. Physiolog. Psychol. 11, 1–61.

Grill, H. J. and Norgren, R. 1978. Chronically decerebrate rats demonstrate satiation but not bait shyness. Science 201, 267–269.

Helmuth, L. 2000. Early insult rewires pain circuits. Science 289, 521–522.

Hermann, D. M., Luppi, P. H., Peyron, C., Hinckel, P., and Jouvet, M. 1997. Afferent projections to the rat nuclei raphe

magnus, raphe pallidus and reticularis gigantocellularis pars alpha demonstrated by iontophoretic application of choleratoxin (subunit b). J. Chem. Neuroanat. 13, 1–21.
Hill, D. L. 1988. Development of chorda tympani nerve taste responses in the hamster. J. Comp. Neurol. 268, 346–356.
Johnston, C. C., Filion, F., Snider, L., Majnemer, A., Limperopoulos, C., Walker, C. D., Veilleux, A., Pelausa, E., Cake, H., Stone, S., Sherrard, A., and Boyer, K. 2002. Routine sucrose analgesia during the first week of life in neonates younger than 31 weeks' postconceptional age. Pediatrics 110, 523–528.
Kalivas, P. W., Gau, B. A., Nemeroff, C. B., and Prange, A. J. 1982. Antinociception after microinjection of neurotensin into the central amygdaloid nucleus of the rat. Brain Res. 243, 279–286.
Kaufman, G. E., Cimo, S., Miller, L. W., and Blass, E. M. 2002. An evaluation of the effects of sucrose on neonatal pain with 2 commonly used circumcision methods. Am. J. Obstet. Gynecol. 186, 564–568.
Kornblith, C. L. and Hall, W. G. 1979. Brain transections selectively alter ingestion and behavioral activation in neonatal rats. J. Comp. Physiol. Psychol. 93, 1109–1117.
Krukoff, T. L., Harris, K. H., and Jhamandas, J. H. 1993. Efferent projections from the parabrachial nucleus demonstrated with the anterograde tracer *Phaseolus vulgaris* leucoagglutinin. Brain Res. Bull. 30, 163–172.
Lidow, M. S., Song, Z. M., and Ren, K. 2001. Long-term effects of short-lasting early local inflammatory insult. Neuroreport 12, 399–403.
Oliveras, J. L. and Besson, J. M. 1988. Stimulation-produced analgesia in animals: behavioral investigations. Prog. Brain Res. 77, 141–157.
Overgaard, C. and Knudsen, A. 1999. Pain-relieving effect of sucrose in newborns during heel prick. Biol. Neonate 75, 279–284.
Pepino, M. Y. and Mennella, J. A. 2005. Sucrose-induced analgesia is related to sweet preferences in children but not adults. Pain 119, 210–218.
Ramenghi, L. A., Evans, D. J., and Levene, M. I. 1999. ''Sucrose analgesia'': absorptive mechanism or taste perception? Arch. Dis. Child. Fetal Neonatal Ed. 80, F146–F147.
Ren, K., Anseloni, V., Zou, S. P., Wade, E. B., Novikova, S. I., Ennis, M., Traub, R. J., Gold, M. S., Dubner, R., and Lidow, M. S. 2004. Characterization of basal and re-inflammation-associated long-term alteration in pain responsivity following short-lasting neonatal local inflammatory insult. Pain 110, 588–596.
Ren, K., Blass, E. M., Zhou, Q., and Dubner, R. 1997. Suckling and sucrose ingestion suppress persistent hyperalgesia and spinal cord Fos expression after forepaw inflammation in infant rats. Proc. Natl. Acad. Sci. U. S. A. 94, 1471–1475.
Ruda, M. A., Ling, Q. D., Hohmann, A. G., Peng, Y. B., and Tachibana, T. 2000. Altered nociceptive neuronal circuits after neonatal peripheral inflammation. Science 289, 628–631.
Shide, D. J. and Blass, E. M. 1989. Opioidlike effects of intraoral infusions of corn oil and polycose on stress reactions in 10-day-old rats. Behav. Neurosci. 103, 1168–1175.
Smith, B. A., Fillion, T. J., and Blass, E. M. 1990. Orally mediated sources of calming in 1- to 3-day-old human infants. Dev. Psych. 26, 731–737.
Taddio, A., Shah, V., Shah, P., and Katz, J. 2003. Beta-endorphin concentration after administration of sucrose in preterm infants. Arch. Pediatr. Adolesc. Med. 157, 1071–1074.
Travers, S. P. 1993. Orosensory Processing in Neural Systems of the Nucleus of the Solitary Tract. In: Mechanisms of Taste Transduction (*eds*. S. A. Simon and S. D. Roper), pp. 339–394. CRC Press.
Weller, A. and Blass, E. M. 1988. Behavioral evidence for cholecystokinin-opiate interactions in neonatal rats. Am. J. Physiol. 255, R5901–R5907.
Weller, A. and Gispan, I. H. 2000. A cholecystokinin receptor antagonist blocks milk-induced but not maternal-contact-induced decrease of ultrasonic vocalization in rat pups. Dev. Psychobiol. 37, 35–43.
Zeifman, D., Delaney, S., and Blass, E. M. 1996. Sweet taste, looking, and calm in a 2- and 4-week-old infants: the eyes have it. Dev. Psych. 32, 1090–1099.

4.09 Taste Receptors

M Max, Mount Sinai School of Medicine, New York, NY, USA

W Meyerhof, German Institute of Human Nutrition Potsdam-Rehbruecke, Nuthetal, Germany

© 2008 Elsevier Inc. All rights reserved.

4.09.1	**Introduction**	197
4.09.2	**Bitter-Taste Receptors**	198
4.09.2.1	Discovery of TAS2Rs	198
4.09.2.2	Molecular Evolution of *TAS2R* Genes	199
4.09.2.3	Expression of *TAS2R* Genes in Oral and Extraoral Tissues	199
4.09.2.3.1	Expression of TAS2R genes in oral tissues	199
4.09.2.3.2	Expression of TAS2R genes in extraoral tissues	200
4.09.2.4	Functional Properties of Bitter Receptors	200
4.09.2.4.1	Tuning of TAS2Rs to their agonists	200
4.09.2.4.2	Activation of TAS2Rs by agonists	201
4.09.2.4.3	G-protein coupling	202
4.09.2.5	Polymorphisms and Functional Heterogeneity of TAS2Rs	203
4.09.2.6	Implications for Nutrition	204
4.09.3	**Sweet-Taste Receptors**	204
4.09.3.1	Tas1Rs	204
4.09.3.1.1	Tas1Rs belong to family C G-protein-coupled receptors	204
4.09.3.1.2	Structure–function studies of family C receptors' venus flytrap module	204
4.09.3.1.3	Cysteine-rich domain structure	205
4.09.3.1.4	Role of the transmembrane domain in family C G-protein-coupled receptors	205
4.09.3.2	Discovery of Tas1Rs	206
4.09.3.2.1	Orphan receptors Tas1R1 and Tas1R2	206
4.09.3.2.2	ID of possible umami receptors: truncated mGluR4, mGluR1	206
4.09.3.2.3	Identification of Sac locus GPCR Tas1R3 – Tas1R3 is Sac	206
4.09.3.2.4	Are there other Tas1Rs?	207
4.09.3.3	Functional Identification of Tas1Rs	207
4.09.3.3.1	Tas1R2 + Tas1R3 is the primary sweet receptor	207
4.09.3.4	Ligand-Binding Sites on Tas1Rs	207
4.09.3.4.1	Orthosteric binding site within the VFTM of Tas1R2	208
4.09.3.4.2	Activity assays map the sweet receptor aspartame interaction site to the VFTM of hTas1R2	208
4.09.3.4.3	Mutational analysis of the aspartame interaction site within the venus flytrap module of hTas1R2	209
4.09.3.4.4	The expressed venus flytrap modules of both mTas1R2 and mTas1R3 bind sugars and sucralose	210
4.09.3.4.5	The cysteine-rich domain of Tas1R3	210
4.09.3.4.6	The transmembrane domain of Tas1R3	212
4.09.4	**Future Studies/Unanswered Questions**	212
References		214

4.09.1 Introduction

Bitter taste has been considered to be part of a warning system designed by nature to prevent organisms from ingesting poisonous substances. Bitter transduction, therefore, appears to be associated with neural networks involved in avoidance behavior. In marked contrast, sweet and amino acid taste (also referred to as umami taste) are thought to act as calorie detectors and consequently elicit attractive behavioral patterns

that promote intake. It turned out recently that in the periphery taste receptor cells form separate populations, one for each taste modality (Chandrashekar, J., 2006). It is apparently not important how a taste receptor cell population is stimulated to elicit the sensation of umami, sweet or bitter, it is only important that it is exited (Zhang, Y. *et al.*, 2003; Mueller, K. L. *et al.*, 2005). In this scenario, the taste receptors fulfill the task to convert a chemical structure into a biochemical response that is propagated to the cerebral cortex, where the activities of neurons reflect the cognitive perception. This chapter focuses on the receptors for sweet, umami, and bitter tastes. During the last ~7 years enormous progress has been in elucidating many of the receptor properties. But still the field is in dynamic expansion. The accumulated knowledge will be summarized with reference to the current problems and to identify future directions.

4.09.2 Bitter-Taste Receptors

4.09.2.1 Discovery of TAS2Rs

A number of reasonable assumptions provided the basis of cloning the bitter-taste receptor genes. First, the observation that the G-protein subunit α-gustducin plays a major role in bitter taste (McLaughlin, S. K. *et al.*, 1992; Wong, G. T. *et al.*, 1996a; 1996b; Ming, D. *et al.*, 1998; 1999; Ruiz-Avila, L. *et al.*, 2000) suggested that bitter receptors are G-protein-coupled receptors (GPCRs). Second, it has been hypothesized that a family of receptors must exist that allows detection of the numerous bitter compounds (Belitz, H. D. and Wieser, H., 1985). Third, it has been anticipated that the receptor genes are linked to chromosomal loci that have previously been demonstrated to influence the sensitivities for various bitter-tasting substances (Lush, I. E., 1981; 1984; 1986; Lush, I. E. and Holland, G., 1988). Searching the human genome data base ultimately led to the identification of the first members of a gene family encoding a new class of GPCRs termed T2Rs (Adler, E. *et al.*, 2000) or TRBs (Matsunami, H. *et al.*, 2000). With the gene sequences at hand several other groups subsequently isolated additional members of this gene family from humans, mice, rats, and various primate species (Bufe, B. *et al.*, 2002; Conte, C. *et al.*, 2002; 2003; Shi, P. *et al.*, 2003; Parry, C. M. *et al.*, 2004; Fischer, A. *et al.*, 2005; Go, Y. *et al.*, 2005). Today the complete repertoire of bitter receptor genes has been identified in humans, mice, rats, dogs, cows, opossums, chickens, frogs, and several fish (Conte, C. *et al.*, 2002; 2003; Go, Y., 2006; Shi, P. and Zhang, J., 2006). Twenty-three of the 25 human *TAS2R* genes are present in two extended clusters on chromosomes 7q34-35 and 12p13.31-13.2, while one each is located on chromosome 5p15.31 and 7q31.32 (Adler, E. *et al.*, 2000; Matsunami, H. *et al.*, 2000; Bufe, B. *et al.*, 2004). In mice, all but two genes are found in two clusters on chromosome 6, the two exceptions being located on chromosomes 2 and 15. Due to the simultaneous cloning in different laboratories the nomenclature of bitter receptor genes is confusing. In this review article the authors use the nomenclature of Bufe B. *et al.* (2002), that has been approved by the human genome project nomenclature committee.

Like many other GPCRs, the coding regions of TAS2Rs are not interrupted by introns (Adler, E. *et al.*, 2000; Matsunami, H. *et al.*, 2000; Bufe, B. *et al.*, 2002; Conte, C. *et al.*, 2002; 2003) and likely fold into seven transmembrane regions with the corresponding intracellular and extracellular domains (Floriano, W. B. *et al.*, 2006; Miguet, L. *et al.*, 2006). TAS2Rs lack, however, any sequence relationship to other members of the GPCR superfamily, but do show sequence relationship among themselves. They also lack the typical signatures of other GPCRs, such as the DRY motif close to transmembrane domain (TMD) 3 and the two conserved cysteine residues in extracellular loops 2 and 3 thought to form disulphide bridges in other GPCRs. TAS2Rs also miss N-linked glycosylation consensus sequences in the N-terminal domain. TAS2Rs are characterized by short N- and C-terminal domains and a well conserved N-linked glyco-sylation consensus sequence in extracellular loop 2. They are therefore considered to form a separate class of GPCRs. Even within a species sequence identities amongst TAS2Rs vary greatly ranging from less then 20% for some members to more than 80% for others. The extracellular parts of the TAS2Rs and the parts of the transmembrane segments facing the extracellular space are less conserved than the intracellular domains and the parts of the transmembrane segments close to the cytoplasm. This is consistent with the idea that the former regions form heterogeneous binding pockets for the numerous bitter compounds, whereas the latter regions engage in G-protein activation that is likely less variable (Meyerhof, W., 2005). The C-terminal domain, which also shows little sequence conservation, could reflect differences in receptor trafficking and/or regulation.

4.09.2.2 Molecular Evolution of *TAS2R* Genes

The available TAS2R repertoires reveal different numbers of genes in humans, mice, rats, dogs, cows, opossums, chickens, frogs, and fish. Whereas chickens have only three genes, their number in mammals and amphibian is in the range of 20–50 (Go, Y., 2006; Shi, P. and Zhang, J., 2006). The high numbers of TAS2Rs in frogs are surprising as most bitter substances are of plant origin and frogs mostly feed on animals. It has been proposed that the TAS2R gene repertoires evolved from multiple ancestors in the lineage leading to teleosts and tetrapods by frequent gene duplications and deactivations with expansions in mammals and amphibia and contraction in chickens. Another characteristic of the TAS2R repertoires across species is a one-to-one orthology for some genes whereas others are lineage or species specific. The lineage specific TAS2Rs appear to be duplicated lately in evolution as their sequences are comparably well conserved and the genes are closely spaced on the chromosomes. These genes may be under positive selection driven by adaptation of species to changing nutritional habits during phylogenetic evolution and detect species specific bitter substances (Bufe, B. *et al.*, 2002; Shi, P. *et al.*, 2003). The *TAS2R* genes with a one-to-one orthology appear to be under more selective constraints and have been proposed to detect bitter compounds encountered by various species (Shi, P. *et al.*, 2003).

Evidence for reduced selective pressure of primate *TAS2R* genes compared with their rodent counterparts comes from the increasing number of pseudogenes from rodents to apes and human and from similar proportions of synonymous to nonsynonymous substitutions (Fischer, A. *et al.*, 2005; Go, Y. *et al.*, 2005). In the hominid lineage, the reduced functional constraints may have been arisen by diminished necessity to detect bitter substances due to decreased consumption of plant food, increased consumption of animal meat and detoxification of food through the controlled use of fire (Wang, X. *et al.*, 2004). Positive selection has also been shown to shape *TAS2R* genes. A sensitive allele of the human glucopyranoside receptor, TAS2R16, was generated during the Paleolithic and, with the migration of *Homo* out of Africa, spread all over the world while the original low sensitivity allele is only found in Africa (Soranzo, N. *et al.*, 2005). It has been proposed that increased sensitivity for frequent toxic glycosides allowed ancient humans to establish healthier diets with low contents of such plant secondary metabolites exerting a selective advantage in carriers of the sensitive allele. The low-sensitivity allele, restricted to Africa with a distribution similar to those of known anti-Malaria alleles, may have been associated with a higher intake of cyanogenic glycosides. A possible consequence could be chronic cyanide poisoning and sickle cell anemia. This provides a selective advantage to carriers of the low sensitivity allele as sickle cell anemia protects against malaria infection (Soranzo, N. *et al.*, 2005). In addition to loss of functional constraints and positive selection, balancing natural selection has been shown as an evolutionary force. It maintains functional nontaster alleles of the phenylthiocarbamide receptor, TAS2R38 (Kim, U. K. *et al.*, 2003; Bufe, B. *et al.*, 2005), in the human but not in the chimpanzee population (Wooding, S. *et al.*, 2004, Wooding, S. *et al.*, 2006).

4.09.2.3 Expression of *TAS2R* Genes in Oral and Extraoral Tissues

4.09.2.3.1 Expression of TAS2R genes in oral tissues

Fully consistent with their role as taste receptor genes, TAS2R messenger ribonucleic acids (mRNAs) have been found by reverse-transcriptase polymerase chain reaction (RT-PCR) and *in situ* hybridization in taste bud cells of all three types of lingual papillae in rodents and humans (Adler, E. *et al.*, 2000; Matsunami, H. *et al.*, 2000; Ueda, T. *et al.*, 2001; Bufe, B. *et al.*, 2002; Kim, M. R. *et al.*, 2003; Behrens, M. *et al.*, 2004; Kuhn, C. *et al.*, 2004; Bufe, B. *et al.*, 2005). TAS2R expression did not overlap with that of TAS1Rs supporting the finding that separate taste receptor cell populations exist for the different taste modalities (Zhang, Y. *et al.*, 2003; Mueller, K. L. *et al.*, 2005; Huang, A. L. *et al.*, 2006). From the number of cells labeled by *in situ* hybridization probes it has been estimated that some 15% of rodent taste bud cells express TAS2Rs (Adler, E. *et al.*, 2000). Based on a smaller set of data a similar estimate has been achieved in humans (Meyerhof, W. *et al.*, 2005). The proportion of TAS2R-positive cells in taste buds was similar for all types of taste papillae (Adler, E. *et al.*, 2000). Differences in TAS2R expression, however, were seen across papillae. Whereas almost all foliate and vallate taste buds contain TAS2R-positive cells, only less than 10% of the fungiform papillae do so (Adler, E. *et al.*, 2000). As gustatory information of fungiform papillae is largely transmitted by the chorda tympani nerve, while

responses from foliate and vallate papillae are transmitted by the glossopharyngeal nerve the question arises whether or not the TAS2R expression pattern generates a chemotopic map. Although this question cannot be answered definitely, it is important to note that for some but not all bitter compounds glossopharyngeal responses differed from those of the chorda tympani (Dahl, M. *et al.*, 1997; Danilova, V. and Hellekant, G., 2003; 2004).

From *in situ* hybridization experiments in rodents with single and mixed TAS2R probes Adler E. *et al.* (2000) concluded that a large number of TAS2R genes, possibly the full repertoire, is expressed in the same subset of taste receptor cells that therefore form a uniform population of bitter-taste cells which could explain the uniformity of bitter taste. This conclusion was supported in phospholipase C-β2 knockout mice that lost their responses to bitter stimuli. When phospholipase C-β2 expression was rescued under the control of various *TAS2R* gene promoters, the animals acquired nerve and behavioral responses to many bitter stimuli (Mueller, K. L. *et al.*, 2005). However, this conclusion is challenged by another *in situ* hybridization study in mice that did not reveal the same degree of homogeneity amongst bitter-taste cells (Matsunami, H. *et al.*, 2000) and by physiological recordings in mouse taste tissues that revealed clear heterogeneity across bitter cells by demonstrating that taste cells responded only to one or two out of a collection of five different bitter compounds (Caicedo, A. and Roper, S. D., 2001). A nonuniform population of bitter receptor cells would be a prerequisite for mammals to discriminate among bitter stimuli. However, this ability has also been disputed (Whitney, G. and Harder, D. B., 1994; Dahl, M. *et al.*, 1997; Delwiche, J. F. *et al.*, 2001; Spector, A. C. and Kopka, S. L., 2002). Perhaps mammals categorize compounds into but can discriminate amongst them within taste modalities.

4.09.2.3.2 Expression of TAS2R genes in extraoral tissues

The recent observation that *TAS2R* gene expression and expression of taste-signaling molecules has been detected in extraoral tissues challenged the role of TAS2Rs as taste receptors. As long as the complete TAS2R repertoire has not been demonstrated to be present in taste tissues, some of them may not function as taste sensors but fulfill other specific tasks. Nevertheless, extraorally expressed TAS2Rs likely exert additional functions. Sites of extraoral TAS2R expression were the solitary chemoreceptor cells in the respiratory epithelium. Irrigation of the respiratory epithelium with bitter compounds elicited trigeminal responses and pronounced respiratory effects (Finger, T. E. *et al.*, 2003). These results indicate that, similar to their oral function to prevent intoxication, nasal bitter receptors could protect mammals from the aspiration of noxious substances. Other sites of TAS2R expression were gastrointestinal cells and the testes (Wu, S. V. *et al.*, 2002; Behrens, M. *et al.*, 2006) suggesting that they may be involved in metabolic and reproductive functions.

4.09.2.4 Functional Properties of Bitter Receptors

4.09.2.4.1 Tuning of TAS2Rs to their agonists

Most of the known properties of TAS2Rs have been uncovered in heterologous expression assays using mammalian and insect cell lines (Chandrashekar, J. *et al.*, 2000; Bufe, B. *et al.*, 2002; Sainz, E. *et al.*, 2007). Usually the recombinant receptors are expressed as chimeras containing N-terminally located domains of bovine rhodopsin (Chandrashekar, J. *et al.*, 2000; Sainz, E. *et al.*, 2007) or rat somatostatin type 3 receptor (Bufe, B. *et al.*, 2002) that serve as cell surface-targeting modules. For some receptors such targeting motifs can be omitted if auxiliary proteins of the receptor transport protein or receptor expression enhancing protein families are coexpressed (Saito, H. *et al.*, 2004; Behrens, M. *et al.*, 2006). Receptor activation is monitored by fluorometric detection of bitter compound-induced changes in cytosolic calcium concentrations in cell lines expressing the promiscuously coupling G-protein subunit Gα15 (Chandrashekar, J. *et al.*, 2000; Bufe, B. *et al.*, 2002) or chimeras of α-gustducin and Gα16 (Ueda, T. *et al.*, 2003; Behrens, M. *et al.*, 2004; Kuhn, C. *et al.*, 2004; Bufe, B. *et al.*, 2005). Alternative approaches rely on the incorporation of radiolabeled GTPγS into purified G-protein α-subunits added to membranes containing the recombinant TAS2Rs (Chandrashekar, J. *et al.*, 2000; Sainz, E. *et al.*, 2007).

With these assays, the cognate bitter compounds for a number of TAS2Rs have been identified (Table 1) and a number of important conclusions have been drawn from the experiments. First, the identified compounds taste bitter confirming the role of TAS2Rs as bitter receptors. Second, TAS2Rs are broadly tuned to detect numerous substances. Some of them are activated by compounds with common substructures. Human TAS2R16 for instance detects numerous β-glucopyranosides and hTAS2R38 various thioamides (Bufe, B.

Table 1 Cognate bitter compounds for TAS2Rs

TAS2R	*Cognate compounds*	*Reference*
hTAS2R4	Denatonium benzoate, PTC	Chandrashekar J. (2006)
mTAS2R5	Cycloheximide, lidocaine	Pronin A. N. *et al*. (2004); Chandrashekar J. (2006)
mTAS2R8	Denatonium benzoate	Chandrashekar J. (2006)
hTAS2R7	Atropine, chloroquine, papaverine, quinacrine, strychnine	Sainz E. *et al*. (2007)
hTAS2R10	Strychnine	Bufe B. *et al*. (2002)
hTAS2R14	Aristolochic acid, α-thujone, picrotin, naphtoic acid	Behrens M. *et al*. (2004); Sainz E. *et al*. (2007)
hTAS2R16	Numerous β-glucopyranosides	Bufe B. *et al*. (2002)
hTAS2R38	Numerous thioamides including PROP and PTC	Kim U. K. *et al*. (2003); Bufe B. *et al*. (2005)
hTAS2R43	Saccharin, acesulfame K, aristolochic acid, 6-nitrosaccharin	Kuhn C. *et al*. (2004)
hTAS2R44	Saccharin, acesulfame K, aristolochic acid	Kuhn C. *et al*. (2004); Pronin A. N. *et al*. (2004)
hTAS2R47	Denatonium benzoate, 6-nitrosaccharin	Pronin A. N. *et al*. (2004)

PROP, 6-*n*-propylthiouracil; PTC, phenylthiocarbamide

et al., 2002; 2005). Human TAS2R7 and TAS2R14 are even more promiscuous and responded to chemically extremely diverse compounds (Behrens, M. *et al*., 2004; Sainz, E. *et al*., 2007). It has been proposed that during evolution different functional constraints shaped bitter-taste receptors to fulfill different tasks. More selective TAS2Rs could detect the prominent plant toxins in a familiar environment, whereas the promiscuous TAS2Rs may be important for accessing novel habitats (Behrens, M. *et al*., 2004). Nevertheless, if the broad tuning is a property of all TAS2Rs, it would easily explain how mammals detect the numerous bitter substances in their environment with a small repertoire of bitter receptors. Third, it appears that the sensitivity of TAS2Rs for their agonists recorded *in vitro* corresponds reasonably well to the sensory performance of mice or human subjects (Chandrashekar, J. *et al*., 2000; Bufe, B. *et al*., 2002; Bufe, B. *et al*., 2005) suggesting that the biochemical properties of the receptors determine perceptive performance. This assumption is impressively supported by experiments in transgenic mice. Wild-type mice are indifferent to β-glucopyranosides. However, if the human *TAS2R16* gene is expressed as a transgene in mice bitter receptor cells the animals acquire sensitivity toward these compounds with parameters similar to those seen in human subjects and hTAS2R16 receptor assays (Mueller, K. L. *et al*., 2005). Fourth, although not examined specifically, it appears from Table 1 that some redundancy exists in TAS2R tuning. For instance, hTAS2R44 shares agonists with hTAS2R43 and hTAS2R14; hTAS2R10 with hTAS2R7; and hTAS2R4 with hTAS2R47. The physiological consequences, if there are any, are unknown. We may speculate here that, possibly, bitter taste would have a backup system at its disposal in the case mutations silence TAS2Rs or that compounds activating several receptors would have greater bitterness than compounds with only one receptor or that compounds with multiple receptors could be detected over a wider concentration range than those with only one.

4.09.2.4.2 Activation of TAS2Rs by agonists

The broad tuning of TAS2Rs immediately raises the question of how these receptors accommodate their ligands. In contrast to neurotransmitter or peptide hormone receptors, which have affinities in the nanomolar or picomolar range for their receptors (Olias, G. *et al*., 2004), TAS2Rs respond to micromolar and millimolar concentrations of their agonists (see references in Table 1). We may imagine that TAS2Rs have loosely fitting binding pockets in which the agonists are accommodated in a relatively unspecific fashion. Or, TAS2Rs may exhibit separate or overlapping highly specific binding sites for their agonists. Considerations about the structure-activities of bitter compounds at their TAS2Rs would support the latter conjecture. Human TAS2R16, for instance, specifically detects β-glucopyranosides but is not activated by β-galactopyranosides or α-glucopyranosides. Variations in the size and hydrophobicity of the aglycon influence critically the potencies of glucopyranosides at hTAS2R16. These data argue for specific interactions of molecular groups of the agonists with definite amino acid residues of the receptor. (Bufe, B. *et al*., 2002). Analogous observations

that have been made with hTAS2R38 support this conclusion (Bufe, B. *et al.*, 2005).

Unfortunately, the molecular architecture of TAS2Rs remained largely unknown. Only one report addressed this question experimentally by mutational analysis and provided limited insight into the interaction of the TAS2Rs with their agonists (Pronin, A. N. *et al.*, 2004). Analyses of domain swapping experiments and chimeras made of the closely related receptors, TAS2R43, which responded to 6-nitrosaccharin, and TAS2R44, which is sensitive to *N*-isopropyl-2-methyl-5-nitrobenzenesulfonamide (IMNB), suggested that amino acid residues responsible for selective receptor activation by IMNB are present in extracellular loop 1 but not 2. Both loops and other parts of the receptor, however, contain residues important for activation of hTAS2R43 by 6-nitrosaccharin. Further analysis uncovered the importance of residue G92 in the extracellular loop of hTAS2R44. Exchange of this residue for the corresponding asparagine of hTAS2R43 made the mutant receptor responsive to both ligands, whereas the reciprocal mutation in hTAS2R43 impaired the activation properties of this receptor. This residue was also of importance for denatonium activation of hTAS2R47, the corresponding mutants N92G and N92A being unresponsive. Also a tryptophan residue present at position 88 of these receptors and conserved in 21 out of 25 human TAS2Rs was critical for agonist activation of hTAS2R43, hTAS2R44, and hTAS2R47. Although these findings are of great importance and interest, they do not allow precise conclusions to be drawn about the binding motifs of TAS2Rs. The analyzed residues may be involved in ligand binding, activation mechanisms, or globally alter the structure of the receptors (Meyerhof, W., 2005).

4.09.2.4.3 G-protein coupling

There are ~20 different Gα subunits falling into four major classes Gαs, Gαi, Gα12, and Gαq (Gudermann, T. *et al.*, 1997). α-Gustducin, a Gαi-type protein closely related to visual transducin, has originally been identified as a lingual G protein present in a subset of taste receptor cells and been suggested to transduce taste stimuli (McLaughlin, S. K. *et al.*, 1992). Biochemical, physiological, and genetic studies since then confirmed that α-gustducin is critically involved in bitter transduction (Wong, G. T. *et al.*, 1996a; 1996b; Ming, D. *et al.*, 1998; Ming, D. *et al.*, 1999; Wong, G. T. *et al.*, 1999; Caicedo, A. *et al.*, 2003). Direct proof was finally obtained by showing that agonist activation of recombinant mT2R5 in insect cell membranes resulted in GDP/GTPγS exchange in exogenously added purified α-gustducin in the presence of purified β/γ G-protein subunits (Chandrashekar, J. *et al.*, 2000).

However, these results do not rule out the possibility that TAS2Rs may couple to other G-protein α-subunits. In fact, in human embryonic kidney cells previously transfected with DNA for mTAS2R5 that do not express α-gustducin, cycloheximide stimulation activated extracellular signal-regulated kinase activity in a pertussis toxin sensitive fashion, suggesting that this bitter receptor also couples to Gi/o-type G-proteins (Ozeck, M. *et al.*, 2004). This suggestion has been confirmed by reconstituting signal transduction of recombinant mTAS2R5, hTAS2R7, hTAS2R14, hTAS2R43, and hTAS2R47 in insect cell membranes in the presence of purified G-protein subunits (Sainz, E. *et al.*, 2007). None of the receptors coupled to Gαs or Gαq. These experiments demonstrated that members of the TAS2R family are capable of signaling through multiple Gαi subunits, including transducin, Gαi, and Gαo, but not through Gαs- and Gαq-type G-proteins. The findings are also in line with observations made in α-gustducin gene-targeted mice showing that bitter responses were clearly impaired but not abolished (Caicedo, A. *et al.*, 2003; Wong, G. T. *et al.*, 1996a) and with findings showing that transducin is present in taste tissue, partially rescues gustucin null mice, and functionally couples to bitter-taste receptors (He, H. T. *et al.*, 1990; Ruiz-Avila, L. *et al.*, 1995; Yang, H. *et al.*, 1999).

TAS2Rs activate phospholipase C-β2 but not through Gαq suggesting that they do so via β/γ G-protein subunits (Sainz, E. *et al.*, 2007). Searches for such subunits that are involved in bitter taste identified Gγ13 which colocalizes with α-gustducin in taste receptor cells and physically interacts with Gβ1, a subunit also expressed in taste cells (Huang, L. *et al.*, 1999). Blocking experiments with specific antibodies led to the proposal that the heterotrimeric G-protein may be composed of α-gustducin and Gβ1/γ13 or Gβ3/γ13 (Huang, L. *et al.*, 1999; Rossler, P. *et al.*, 2000). Reconstitution experiments with membranes containing recombinant receptors and purified G-protein subunits demonstrated that mTAS2R5, hTAS2R7, and hTAS2R47 indeed couple to Gβ1/γ13 but also to Gβ3/γ13 (Sainz, E. *et al.*, 2007). Together, the available data suggest that complex rules govern TAS2R-G-protein coupling and that coupling is influenced by the precise concentrations of subunits of all three classes and their individual affinities for each other and for the receptors.

4.09.2.5 Polymorphisms and Functional Heterogeneity of TAS2Rs

Genetically determined differences in bitter-taste sensitivity for various compounds have been seen in mice and mapped to specific chromosomal loci (Lush, I. E., 1981; 1984; 1986; Lush, I. E. and Holland, G., 1988). One of these loci encodes the bitter-taste receptor TAS2R5 of which strain specific functionally distinct variants exist that determine taste sensitivities for cycloheximide in strains of mice (Chandrashekar, J. *et al.*, 2000). Thus, there is a molecular basis for explaining taste sensitivity ranging from genotype to receptor properties and sensory performance. In humans, inherited differences in bitter-taste sensitivity are known for some 70 years when it has been discovered that there are genetically determined pronounced individual differences in tasting phenylthiocarbamide (PTC; Blakeslee, A. F., 1931; 1932; Fox, A. L., 1932). PTC-tasters have been reported to taste PTC and chemically related compounds, such as propylthiouracil, at micromolar concentrations, whereas nontasters are taste-blind to these compounds even when they were exposed to them at several 100-fold higher concentrations (Bufe, B. *et al.*, 2005). Eventually, positional cloning identified the *hTAS2R38* gene as a receptor for PTC and showed that three nonsynonymous single nucleotide polymorphisms, SNPs, define different hTAS2R38 haplotypes (Figure 1), of which two are frequent (Kim, U. K. *et al.*, 2003). Depending on the amino acids present in the positions affected by the SNPs, the so-called PAV haplotype is associated with high sensitivity for PTC, whereas the AVI haplotype is linked to nontaster status (Kim, U. K. *et al.*, 2003). A subsequent study then demonstrated that the different hTAS2R38 haplotypes encode functionally distinct hTAS2R38 variants and their sensitivities monitored *in vitro* determine perceptual performance of human subjects (Bufe, B. *et al.*, 2005). Thus, also in humans we have a clear indication that the TAS2R genotype determines the functional properties of the encoded bitter receptor and, these in turn, are crucial for the sensory abilities of subjects.

A comprehensive evaluation of sequence and haplotype variation in the human *TAS2R* gene repertoire identified substantial coding sequence diversity. In a worldwide population sample of 55 individuals, more than four variant amino acid positions were found on average per *TAS2R* gene. Together, the 25 *hTAS2R* genes encode 151 different protein-coding haplotypes, yet some show translational stop codons (Kim, U. *et al.*, 2005). It is reasonable to assume that many of the variant receptors differ in their functional properties toward ligands by showing no responses, or altered ligand spectra, or modified sensitivities for agonists. This has already been shown for the alleles specifying hTAS2R16-N172 and

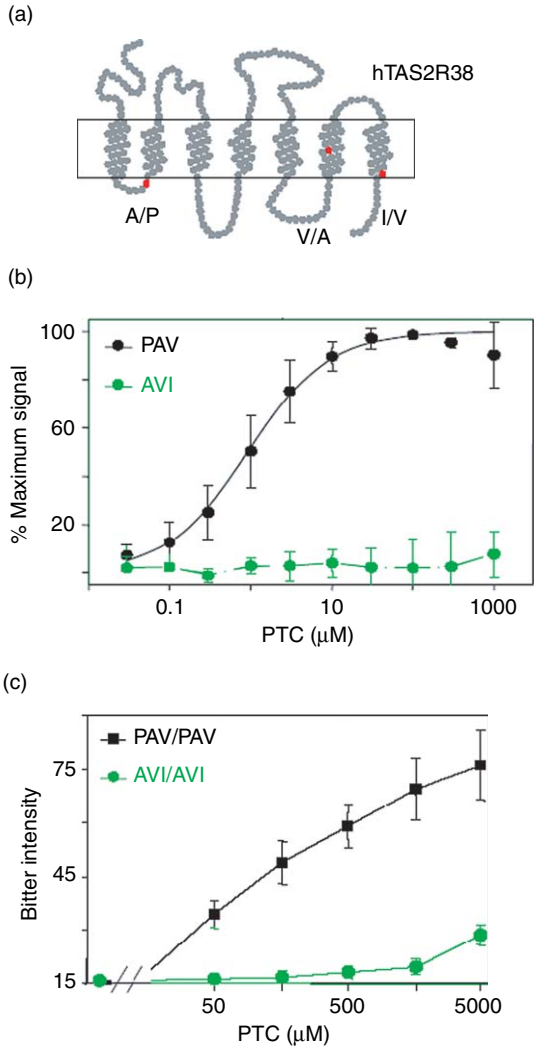

Figure 1 Molecular basis of tasting phenylthiocarbamide. (a) Schematic representation of TAS2R38. Each circle represents an amino acid residue. Amino acid residues in positions 49, 262, and 296 that are affected by single nucleotide polymorphisms are depicted in red and the specific amino acids present in these positions are indicated. (b) Postthreshold bitter intensity ratings of subject groups genotyped to be PAV or AVI homozygous. Please note the pronounced differences in taste sensitivity. (c) functional responses of hTAS2R38-PAV and hTAS2R38-AVI variants recorded in transfected cell lines. The differences in receptor activation closely resemble those seen in the taste experiment shown in (b). Data from Kim, M. R. *et al.* (2003) and Bufe, B. *et al.* (2005).

hTAS2R16-K172 (Soranzo, N. *et al.*, 2005). We may also expect that the functional differences of TAS2Rs translate into perceptual differences in the population. This conclusion is supported by the observed differences in tasting chloramphenicol, strychnine, and quinine across subjects (Blakeslee, A. F., 1935; Sugino, Y. *et al.*, 2002).

4.09.2.6 Implications for Nutrition

It is still a matter of speculation to what extent, if at all, differences in taste sensitivities, particularly bitter sensitivity influences nutritional behavior. Food choice is determined by many parameters with the taste of food being crucial (Drewnowski, A., 1997; 2001). However, a mechanistic explanation is currently unavailable. It has been pointed out that bitter taste contributes to the enjoyment of food and beverages (Drewnowski, A., 2001). In contrast, moderate or strong bitter taste may lead to rejection of healthy compounds (Drewnowski, A. and Gomez-Carneros, C., 2000). Based on the finding that individual TAS2Rs mediate bitter taste for specific compounds and on the conjecture that TAS2R variants determine interindividual bitter-taste sensitivities, we have reason to expect that rejection of bitter substances occurs more easily in subjects carrying high-sensitivity haplotypes than in carriers of low-sensitivity haplotypes. Many studies have been carried out that aimed at associating PTC taster status or hTAS2R38 genotypes with intake behavior and risks for diseases (Drewnowski, A., 2004; Duffy, V. B. *et al.*, 2004b). Indeed such associations have been reported in some studies for preferences for vegetables, fruits, fats, alcohol, and sweeteners (Bartoshuk, L. M., 1979; Drewnowski, A. and Rock, C. L., 1995; Tepper, B. J. and Nurse, R. J., 1997) and risks for goiter, alcoholism, cancer, and depression (Harris, H. *et al.*, 1949; Facchini, F. *et al.*, 1990; Pelchat, M. L. and Danowski, S., 1992; Duffy, V. B. *et al.*, 2004a; Joiner, T. E., Jr. and Perez, M., 2004) while another study did not find such associations (Timpson, N. J. *et al.*, 2005). Also for the hTAS2R16-K172 low-sensitvity allele an association with risk for alcoholism has been detected (Hinrichs, A. L. *et al.*, 2006). Perhaps, all these studies may be biased by the fact that the food items monitored, i.e., vegetables or fruits in general, contain numerous bitter compounds while hTAS2R38 detects only thioamides. Future association studies should look into foods that are rich in hTAS2R38 agonists. To the authors' knowledge, to date only one preliminary study is available, which showed that PTC tasters avoided intake of plant-derived food containing possible hTAS2R38 agonists (Sandell, M. A. and Breslin, P. A., 2006).

4.09.3 Sweet-Taste Receptors

4.09.3.1 Tas1Rs

4.09.3.1.1 Tas1Rs belong to family C G-protein-coupled receptors

The receptors for sweet (Tas1R2 + Tas1R3 function as a sweet receptor) and umami (Tas1R1 + Tas1R3 also function as an umami receptor) taste qualities are GPCRs that, by their protein sequence and homology to other GPCRs, can be assigned to family C. This family has the typical 7TM spanning domain as seen in family A (rhodospinlike GPCRs) but also contains a large extracellular domain that is known to be the orthosteric endogenous ligand-binding domain. Other family members include the metabotropic glutamate binding receptors (mGluRs), calcium-sensing receptors, metabotropic gamma-aminobutyric acid (GABA) receptors and several putative odorant receptors. Although it is now thought that most GPCRs dimerize along their TM domains, family C receptors are known to be obligate dimers that dimerize along their extracellular domains as well as their TM domains. The Tas1 receptors are variously called Tas1R, Tas1R, and Tas1R. At the amino acid level Tas1Rs are 26–34% identical with each other, and ~22–25% identical with mGluRs. The similarity of the Tas1Rs to mGluRs is much higher, ranging from 36% to 43%, making them members of GPCR family C. Family C GPCRs include the mGluRs, calcium-sensing receptors, metabotropic GABA receptors, and a variety of odorant (fish) and pheromone-sensing receptors. A truncated taste-expressed variant of mGluR4 (taste-mGluR4) is present in ~40–70% of taste buds and may also function as an umami receptor (Chaudhari, N. *et al.*, 2000). Below we review what is known about the structure of family C receptors from crystal studies of mGluRs.

4.09.3.1.2 Structure–function studies of family C receptors' venus flytrap module

In addition to the heptihelical TMD common to GPCRs from family A, family C GPCRs have large extracellular region composed of two domains: the venus flytrap module (VFTM, ~500 residues) and the cysteine-rich domain (CRD, ~70 residues; Jingami, H. *et al.*, 2003). The VFTM is a two-lobed clamshell-like structure. The CRD lies between the VFTM and the heptahelical TMD. The CRD has nine highly conserved cysteines within its span of ~70 residues. Based

on extensive structure–function studies of family C receptors, the crystal structure of mGluR1, mGluR2, and mGluR3 (see below), and homology to periplasmic sugar and amino acid transporters, it is highly likely that the VFTM is the receptor's primary ligand-binding domain (Hermans, E. and Challiss, R. A., 2001). It is thought that ligand binding occurs independently to one or both monomers of each dimeric receptor. The ligand-binding site for the endogenous ligand lies in a cleft between the two prominent lobes, with the ligand fitting like a pearl inside a closed oyster. Family C GPCRs are obligate homodimers or heterodimers that dimerize via a discontinuous set of contacts in lobe 1 of the VFTM.

There are a number of structures of the VFTM (mGluR1) and VFTM + CRD (mGluR3) (Kunishima, N. *et al.*, 2000; Tsuchiya, D. *et al.*, 2002; Muto, T. *et al.*, 2007). The crystal structure of the homodimeric mGluR1–3 VFTM consists of two asymmetrical mirror-image monomers. Each VFTM monomer has two lobes that together form a clamshell. The two monomers dimerize by interacting along each lobe 1; the two lobes 2 have no part in the dimerization (Kunishima, N. *et al.*, 2000). Lobe 1 and lobe 2 of each monomer approach each other and their intersection forms the cleft that binds ligand. The ligand-bound, closed conformation of the monomer is the active form. Upon ligand binding and closure of the cleft, the dimer interface rotates upon itself, which brings the two lobes 2 within closer proximity. In mGluR1 the majority of ligand-contacting residues in lobe 1 make direct hydrogen bonds with glutamate, while those in lobe 2 make water-mediated hydrogen bonds and salt bridges (Jingami, H. *et al.*, 2003).

Tas1Rs and other family C GPCRs are expected to dimerize and to bind ligands in a manner similar to mGluR1. Comparing Tas1R and mGluR VFTMs (independently of the receptors' CRDs and TMDs) reveals amino acid identities of ~25% and similarities ~41%. The predicted secondary structures of helices and β-strands of the extracellular domains of Tas1Rs match that of the crystal structure of mGluR1 at nearly every point. The conformational change in family C GPCRs that takes place upon ligand binding appears to be transmitted from the VFTM and CRD to the TMD helical bundle, then onward to the cytoplasmic surface, where it contacts and activates the G protein.

4.09.3.1.3 Cysteine-rich domain structure

Recently a crystal structure of mGluR3 VFTM + CRD was published showing for the first time the structure of the CRD (Muto, T. *et al.*, 2007), which contains three β-sheets composed of two antiparallel β-strands. Eight of the nine conserved cysteines formed four structurally stabilizing disulphide bonds within the structure. A ninth cysteine forms a disulphide bond with a conserved cysteine at the bottom of lobe 2 of the same monomer VFTM. This structure is likely to hold for all the family C receptors except for the GABA receptors, which do not have the conserved cysteines in its linker domain. The CRD, with its connection to the motion of lobe 2 of the VFTM via the disulphide linkage is likely to be critical for transmittal of the conformational change from the ligand-binding VFTM to the TMD. The structure of the CRD suggests that there is a reorientation of the ends of the CRD from 104–126 Å to 46–90 Å apart between the resting and the active state of the VFTM. This suggests an activation mechanism that involves movements of the two TMDs relative to one another upon receptor activation (Muto, T. *et al.*, 2007). However, it is currently unknown how the VFTMs communicate with the TMDs and to what extent intra-TMD versus inter-TMD conformational change contributes to receptor activity.

4.09.3.1.4 Role of the transmembrane domain in family C G-protein-coupled receptors

A hallmark of GPCRs is that they have seven transmembrane helices constituting a TMD. Another key feature of GPCRs is that they mediate their intracellular actions via coupling to and activation of G proteins. Thus, activation of family A receptors by binding of ligand within the TMD is transmitted to the G protein by cytoplasmic loops adjacent to the TMD, whereas, activation of family C receptors by ligand binding within the VFTM is transmitted to the TMD and then by cytoplasmic loops to the G protein. The solved crystal structures of bovine rhodopsin have been widely used as a structural templates to construct homology models of diverse GPCRs using comparative modeling techniques (Visiers, I. *et al.*, 2000; 2002; Malherbe, P. *et al.*, 2003; Miedlich, S. U. *et al.*, 2004; Petrel, C. *et al.*, 2004). The crystal structures of bovine rhodopsin are at present the only solved structures of any GPCRs that include the heptahelical TMD (Palczewski, K. *et al.*, 2000; Teller, D. C. *et al.*, 2001; Okada, T. *et al.*, 2002). The supposition that the general topology of the TMD of rhodopsin is shared by most or all other types of GPCRs, including family C receptors, is supported by the following two points. First, numerous

studies indicate that allosteric binding sites of several family C receptors are within their TMDs. For example, several noncompetitive antagonists and agonists bind within the TMDs of mGluR1, mGluR5, and the calcium-sensing receptor (Pagano, A. *et al.*, 2000; Malherbe, P. *et al.*, 2003; Petrel, C. *et al.*, 2004). Second, although the overall sequence homology of TMDs between GPCRs in families A and C is low, key residues that define the TM helices are conserved in rhodopsin and in family C GPCRs.

4.09.3.2 Discovery of Tas1Rs

4.09.3.2.1 Orphan receptors Tas1R1 and Tas1R2

The taste receptors Tas1R1 and Tas1R2 were first identified in taste cell-specific libraries (Hoon, M. A. *et al.*, 1999). It was originally proposed that mTas1R2 might be a bitter-responsive receptor and that mTas1R1 might be a sweet-responsive taste receptor; the rationale being that Tas1R1 is expressed at the front of the tongue (which is sometimes thought to be more sensitive to sweet) and that Tas1R1 gene maps nearer to the *sac* locus at the distal end of mouse chromosome 4 (Hoon, M. A. *et al.*, 1999). While it is true that both Tas1R1 and Tas1R2 map to the distal end of mouse chromosome 4, refined mapping studies indicated that Tas1R1 and Tas1R2 are several centimorgans away from the *sac* locus, much too far to be the *sac* gene itself (Li, X. *et al.*, 2001).

The taste cell-specific expression of Tas1R1 and Tas1R2 suggested that both receptors might play roles in taste transduction. *In situ* hybridization showed that Tas1R1 and Tas1R2 have different expression patterns in rat taste tissue: rTas1R1 is localized to geschmackstreifen (taste stripe) and fungiform papillae, and rTas1R2 is localized primarily to circumvallate and foliate papillae. The significance of this regional expression pattern is unclear, since it does not correspond to any known pattern of tastant sensitivity in rodents (Lindemann, B., 1999; Sako, N. *et al.*, 2000). Prior to the discovery of Tas1R3, the function of the Tas1R1 and Tas1R2 orphan receptors could not be studied in heterologous cells because as was later shown, Tas1R1 and Tas1R2 form obligate heterodimers with Tas1R3 to function, hindering identification of their natural ligands.

4.09.3.2.2 ID of possible umami receptors: truncated mGluR4, mGluR1

A truncated taste-expressed variant of mGluR4 (taste-mGluR4) was proposed to function as an umami receptor. By *in situ* hybridization, this receptor is present in ~40–70% of the taste buds examined (Chaudhari, N. *et al.*, 2000). Taste mGluR4 displays the characteristics of an umami receptor, with sensitivity to glutamate in the millimolar range, consistent with concentrations known to elicit the sensation of umami. Heterologously expressed taste-mGluR4 shows two other hallmarks of the umami response: it is activated by L-AP4, which elicits a taste similar to L-glutamate in rats, and it is potentiated by 5′-ribonucleotides.

Upon identification of Tas1R3, it became possible to show that the combination of Tas1R1 + Tas1R3 gave rise to a receptor that was sensitive to a variety of L-amino acids including monosodium glutamate suggesting that this combination of Tas1Rs was an umami receptor (Li, X. *et al.*, 2002a; Zhao, G. Q. *et al.*, 2003).

4.09.3.2.3 Identification of Sac locus GPCR Tas1R3 – Tas1R3 is Sac

Inbred strains of mice vary widely in their behavioral and electrophysiological responses to saccharin, sucrose and other compounds that humans perceive as sweet. The *sac* locus was identified as the primary genetic determinant in mice of preference for saccharin and other sweet compounds, distinguishing taster strains (e.g., C57BL/6) from nontasters (e.g., DBA/2; Fuller, J. L., 1974; Lush, I. E., 1989; Lush, I. E. *et al.*, 1995; Blizard, D. A. *et al.*, 1999). To identify candidates for the *sac* gene we searched the sequence of the distal end of mouse chromosome 4 (to which *sac* maps) for genes that might encode GPCRs and other signal transduction elements. This search yielded Tas1R3, a previously unknown GPCR located within 20 kbp of the genetic marker closest to *sac* (Max, M. *et al.*, 2001). Tas1R3 is the third member of the Tas1R taste receptor family, and is most closely related to Tas1R1 and Tas1R2. *In situ* hybridization and immunohistochemistry showed that Tas1R3 is expressed selectively in a subset of taste receptor cells. Sequence analysis of mTas1R3 from eight independently derived strains of mice identified specific polymorphisms (T55A and I60T) that assort between taster and nontaster strains (Max, M. *et al.*, 2001). Other laboratories also identified Tas1R3 by RT-PCR or genomics-based approaches (Bachmanov, A. A. *et al.*, 2001; Kitagawa, M. *et al.*, 2001; Montmayeur, J. P. *et al.*, 2001; Nelson, G. *et al.*, 2001; Sainz, E. *et al.*, 2001). Transgenic expression of the taster form of Tas1R3 converted nontaster mice into tasters, demonstrating that Tas1R3 is

indeed *sac* (Nelson, G. *et al.*, 2001; Damak, S., personal communication).

4.09.3.2.4 Are there other Tas1Rs?

A fourth related gene known as GPRC6A is related to Tas1R1-3 by 20–24% identity. It has been speculated that this gene might be a taste receptor gene by several groups; however, convincing expression in taste cells has not been found to date. Other studies identify this receptor as either an amino acid receptor or a second calcium-sensing receptor with important function in bone (Pi, M. *et al.*, 2005; Christiansen, B. *et al.*, 2006). The latter work is particularly compelling because there is extensive expression of this receptor in bone and it shows responses to calcium, calcium mimetics, and to an important bone peptide, osteocalcin. It remains to be seen if there is a role for this receptor in taste although as this juncture it appears unlikely.

4.09.3.3 Functional Identification of Tas1Rs

4.09.3.3.1 Tas1R2 + Tas1R3 is the primary sweet receptor

Damak S. *et al.* (2003) found that knockout mice lacking Tas1R3 showed no behavioral or nerve response to noncaloric sweeteners, and diminished responses to sugars and umami compounds. Zhao G. Q. *et al.* (2003) observed that knockout mice lacking both Tas1R2 and Tas1R3 had no responses to sweet compounds; mice lacking both Tas1R1 and Tas1R3 had no responses to umami compounds. Zhao G. Q. *et al.* (2003) also showed that mice expressing human Tas1R2 as a transgene were responsive to human-specific sweeteners such as aspartame and thaumatin that are detected by humans but not mice.

Calcium-imaging assays of HEK 293 cells transfected with Tas1R2, Tas1R3, and a reporter G-protein showed responses to a wide range of sweet ligands (Nelson, G. *et al.*, 2001; Li, X. *et al.*, 2002a; Jiang, P. *et al.*, 2004). If either Tas1R2 or Tas1R3 was omitted from the transfection no responses to sweet compounds were detected, leading to the conclusion that the combination of Tas1R2 + Tas1R3 is a broadly responding sweet receptor. In contrast, cells transfected with Tas1R1, Tas1R3, and the reporter G protein responded to amino acids, but not to sweeteners, indicating that the combination of Tas1R1 + Tas1R3 is an umami receptor (Nelson, G. *et al.*, 2001; Li, X. *et al.*, 2002b; Nelson, G. *et al.*, 2002). Apparently, Tas1R3 provides a common element necessary for the proper function of both sweet and umami receptors. Initially, it was thought that ligand-binding determinants would be present only in Tas1R1 and Tas1R2, but not in Tas1R3; however, it appears that Tas1R3 also contributes to the ligand-binding process (see below). Although, heterologous expression of Tas1R1 or Tas1R2 alone yielded no responses to either sweet or umami compounds, expression of Tas1R3 alone yielded responses to trehalose, but not to other sweeteners (Ariyasu, T. *et al.*, 2003; Jiang, P., personal communication) although high concentrations of natural sweeteners appear to be sensed by homodimers of Tas1R3. Like other family C GPCRs, the Tas1Rs probably function as dimers (heterodimers, and in some cases homodimers).

HEK cells expressing hTas1R2 + hTas1R3 respond to all sweet-taste stimuli tested: sugars (sucrose, fructose, galactose, glucose, etc.); amino acids (glycine and D-tryptophan); sweet proteins (brazzein, monellin, and thaumatin); and synthetic sweeteners (cyclamate, saccharin, ace K, aspartame, dulcin, neotame, and sucralose; Nelson, G. *et al.*, 2001; Jiang, P. *et al.*, 2004; Xu, H. *et al.*, 2004). All of these responses are inhibited by the sweet-taste inhibitor lactisole, which acts on the TMD of Tas1R3 (Xu, H. *et al.*, 2004; Jiang, P. *et al.*, 2005a; Winnig, M. *et al.*, 2005). These results, along with the observation that human perception of sweet taste is inhibited by lactisole (Sclafani, A. and Perez, C., 1997). Schiffman S. S. *et al.* (1999) argue that Tas1R2 + Tas1R3 is the primary or the only sweet-taste receptor although that knockout Tas1R3 mice still respond to natural sweeteners suggests that there may be some alternative sugar-sensing mechanism that remains in the absence of the sweet receptor.

4.09.3.4 Ligand-Binding Sites on Tas1Rs

The sweet receptor appears to have multiple sites of interaction for sugars and sweet-tasting artificial compounds. The orthosteric site for sugars is likely to be the closed cleft of the VFTM Tas1R2, and perhaps the cleft of the VFTM of Tas1R3. Artificial sweeteners may also interact with the closed cleft of the VFTM of Tas1R2 in sites overlapping that of the orthosteric site for natural sugars as well as an allosteric site within the TMD of Tas1R3. We have proposed that the larger, noncarbohydrate-containing, naturally occurring peptide sweeteners found in some plants may interact with both the CRD of Tas1R3 and the VFTM of Tas1R2 (Jiang, P. *et al.*, 2004; Maillet, E., personal communication) although other groups have suggested that these proteins interact with the open

cleft of both VFTMs (Morini, G. *et al.*, 2005; Walters, D. E. and Hellekant, G., 2006).

4.09.3.4.1 Orthosteric binding site within the VFTM of Tas1R2

Work from our laboratory indicates that the VFTM of Tas1R2 is one orthosteric binding site for natural sugars as well as forming a binding site for dipeptide and several other artificial sweeteners. We concluded this from studies where we mutated numerous amino acids that line the VFTM cleft and tested the resulting receptors for specific defects in the receptors ability to be activated by a variety of sweeteners (Maillet, E., personal communication). We have also employed receptors composed partly of human and partly of mouse sequences (chimeric receptors) to show which domains of the receptor are required for specific responses to sweeteners that only humans and other primates can taste (dipeptide sweeteners, cyclamate, brazzein, monellin, and others).

4.09.3.4.2 Activity assays map the sweet receptor aspartame interaction site to the VFTM of hTas1R2

Scientists in our laboratory assayed the effects of sweeteners on heterologously expressed mismatched receptors from mouse and human. While mTas1R2 + mTas1R3 responded to D-tryp, saccharin, and sucrose, but not to the human-specific sweeteners (i.e., aspartame, monellin, and brazzein), the interspecies pairing hTas1R2 + mTas1R3 responded to aspartame and most other sweeteners, but not brazzein. These results indicate that responsiveness to aspartame requires the human form of Tas1R2, but does not require the human form of Tas1R3.

A chimeric receptor with the VFTM of human Tas1R2 and the rest from mouse Tas1R2 paired with mTas1R3 (i.e., hVFTM-CRD/mTMDT1R2 + mT1R3) gave responses to aspartame (Figure 2(a)). This indicates that responsiveness to aspartame requires human residues within the VFTM–CRD of Tas1R2, and not human residues within the TMD of Tas1R2. To localize the residues of hTas1R2 required for responsiveness to aspartame better we made additional mouse/human and human/mouse chimeras within the VFTM–CRD of TAS1R2 (Figure 2(b)) and coexpressed them with mTas1R3. The pairing of human/mouse chimeras h1-468/mT1R2 or h1-577/mT1R2 with mT1R3 gave normal responses to aspartame and neotame (Figure 2(b)). This indicated that responsiveness to aspartame and neotame requires human residues within residues 1–468 of the VFTM of hTas1R2 – the rest of Tas1R2 and all of Tas1R3 can be from mouse and still support responses to these human-specific dipeptide sweeteners. The pairing of mouse/

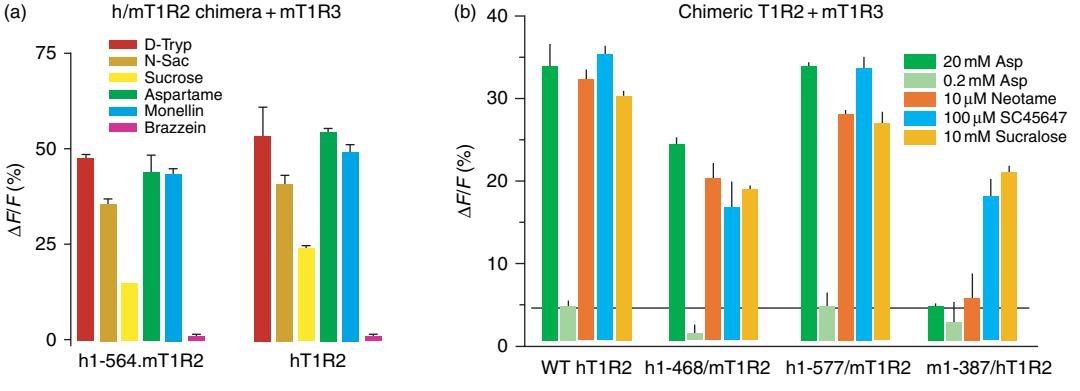

Figure 2 Sweet-receptor responsiveness to aspartame (Asp) and neotame requires human-specific residues within the venus flytrap module (VFTM) of TAS1R2. (a) HEK293E cells transiently transfected with the human/mouse chimera h.1–564.mTas1R2, mTas1R3, and Gα16-i3 were assayed for calcium mobilization in response to the indicated sweet ligands (see methods for details). h1–564.mTas1R2 Contains the extracellular domain of hTas1R2 and the transmembrane region of mTas1R2. Its response profile is comparable to that of hTas1R2. (b) Human/mouse and mouse/human chimeras of Tas1R2 were constructed and coexpressed in HEK cells along with mTas1R3 and Gα16-i3. SC45647 and sucralose served as positive controls for activity. By our naming convention h1-468/mTas1R2 contains residues 1–468 from hTas1R2 and the remainder from mTas1R2. Tas1R2 chimeras with residues 1–468 (VFTM) or 1–577 (VFTM plus part of cysteine-rich domain) from hTas1R2 were responsive to both aspartame and neotame. A Tas1R2 chimera containing mouse residues 1–387 (amino terminal two-thirds of VFTM) from mTas1R2 and the remainder from human Tas1R2 did not respond to aspartame or neotame. We conclude that specific human residues within the VFTM of hasS1R2 are required for responsiveness to aspartame and neotame. ΔF/F, the change of fluorescence at peak over the baseline fluorescence.

human chimera m1-387/hT1R2 with mTas1R3 gave no responses to aspartame or neotame (Figure 2(b)), indicating that one or more residues in the amino terminal two-thirds of the VFTM of hTAS1R2 are necessary for responsiveness toward aspartame and neotame. Based on mapping the interaction of aspartame and neotame to the VFTM of Tas1R2 and the overall homology of the Tas1Rs to mGlurR1, we reasoned that aspartame might bind within the cleft of the VFTM in a manner similar to that of glutamate in mGluR1.

To test this idea, scientists in our laboratory used homology modeling, automatic docking, chimeric and mutant receptors, and activity assays with heterologously expressed receptors to identify the potential binding site(s) within the VFTM of hTas1R2 for aspartame and neotame (Figure 3). We constructed models of Tas1R2 + Tas1R3 based upon the crystal structures of mGluR1 and used them to dock various sweeteners. For aspartame and neotame, our docking studies predicted that the NH^{3+} of aspartame and NH^{2+} of neotame interact through salt bridges with the negatively charged carbonyl groups of Tas1R2 Asp278 and Asp307, and through hydrogen bonds with a backbone oxygen atom of Ser303. The negatively charged carbonyl groups (COO–) of aspartame and neotame are proposed to interact through hydrogen bonds with the NH backbone atoms of Tas1R2 Arg383 and Val384. The phenyl groups of aspartame and neotame are proposed to interact through pi-pi interactions with Tas1R2 Tyr215, and through hydrophobic interactions with Pro277. Morini G. *et al.* (2005) have also modeled the structure of the sweet receptor VFTMs (based on the structure of the VFTM of the mGluR1), and proposed that aspartame could bind within the VFTMs of both TAS1R2 and TAS1R3. The predictions of our model and theirs are in general agreement with regard to the interaction of aspartame with the VFTM of TAS1R2 (both models identified S165, E302, and Y215 as potential interactions), although, our model makes more extensive predictions of potential contacts for aspartame in the VFTM of TAS1R2. Furthermore, based on our activity assays with hTAS1R3 homodimers (unpublished data) we think it unlikely, although theoretically possible, that aspartame binds to the VFTM of TAS1R3.

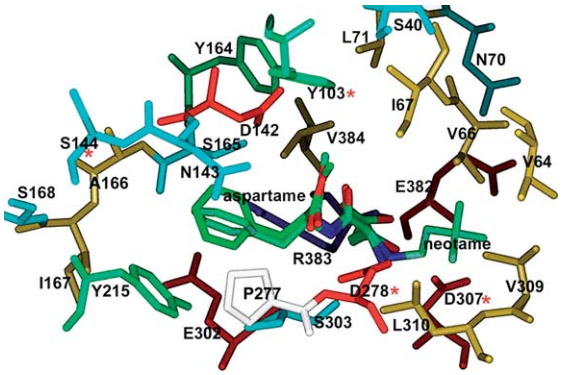

Figure 3 Model of cleft between lobes 1 and 2 of the venus flytrap module (VFTM) of hTas1R2 with docked aspartame and neotame. The metabotropic glutamate binding receptor (mGluR1; PDB:1EWK) crystal structure was used to model the VFTM of Tas1R2, then aspartame and neotame were individually docked onto the structure. Our model predicts that aspartame and neotame forms hydrogen bonds with the side chains of D278, D307, and S303, and makes hydrophobic interactions with the side chains of Y215, Y103, P277, and with the backbones of R383, V384, D142, and L279.

4.09.3.4.3 Mutational analysis of the aspartame interaction site within the venus flytrap module of hTas1R2

Our models of docked aspartame and neotame suggested that there is a good possibility that the VFTM of Tas1R2 contains a cleft between its lobes 1 and 2 that could serve as a small molecule-binding site for sugars and/or dipeptides akin to the canonical glutamate binding site of mGluR1. Using our identification of residues within the presumptive small molecule binding cleft of hTas1R2 we carried out alanine scan mutagenesis to determine which, if any, of residues do indeed contribute to a binding pocket for aspartame and other dipeptide sweeteners. In a few cases of interest (e.g., D307) we followed up with more conservative replacements. We have tested these mutants for their responses to aspartame and neotame (and cyclamate – our control for overall efficacy of mutant receptors) (Figure 4). Some mutations had similar effects on responsiveness to both aspartame and cyclamate (e.g., R383A, D307A, E302A, Y215A, D142A, and I67A), suggesting that they had altered general responsiveness of the receptor, or altered coupling between the VFTM of Tas1R2 and the TMD of Tas1R3. Other mutations had relatively specific effects on the response to aspartame (e.g., D307N, D278A, S144A, and Y103A), suggesting that they might be part of the aspartame-binding site. These residues are implicated by our model as being part of the binding site for aspartame within the VFTM of hTas1R2.

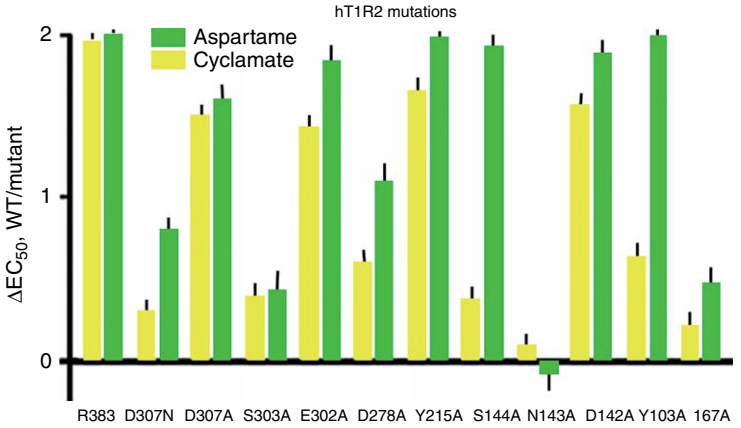

Figure 4 Effects of alanine scan mutations in the venus flytrap module (VFTM) of hTAS1R2 on responses to aspartame. Residues within a potential aspartame binding site of the VFTM of hTas1R2, predicted by homology with the metabotropic glutamate binding receptor binding site and by homology models of hTas1R2, were individually mutated to alanine (and in one case to asparagine (D307N)). Mutants were coexpressed with hTas1R3 and tested for responsiveness to aspartame and cyclamate. Some mutations had similar effects on responsiveness to both aspartame and cyclamate (e.g., R383A, D307A, E302A, Y215A, D142A, and I67A), suggesting that they altered general responsiveness of the receptor, or altered coupling between the VFTM of Tas1R2 and the TMD of TAS1R3. Other mutations had relatively specific effects on the response to aspartame (e.g., D307N, D278A, S144A, and Y103A), suggesting that they might be part of the aspartame binding site. ΔEC_{50}, the change in the effective concentration to produce 50% response; WT, wild type.

4.09.3.4.4 The expressed venus flytrap modules of both mTas1R2 and mTas1R3 bind sugars and sucralose

Work in Munger's laboratory, using direct physical binding assays, also shows that the expressed VFTMs of Tas1R2 and Tas1R3 react with sugars and sucralose as shown by changes in intrinsic fluorescence. The peak intrinsic tryptophan fluorescence of the mTas1R VFTM proteins was monitored and then the concentration–response relationship for this fluorescence was determined upon titration of VFTM with sweet ligands. Glucose, sucrose, and sucralose decreased the peak fluorescence intensity of $mTas1R3VFTM_{B6}$, exhibiting K_d values of 7.3 ± 0.7 mM, 2.9 ± 0.4 mM, and 0.9 ± 0.1 mM, respectively (Nie, Y. *et al.*, 2005), indicating binding of these ligands to the VFTM of mTas1R3. Ligand binding is known to stabilize a conformational change in the VFTMs of other class C GPCRs (Kunishima, N. *et al.*, 2000; Pin, J. P. *et al.*, 2003). A synchrotron radiation circular dichroism (SRCD) spectroscopy, assay was used to determine if Tas1R VFTMs undergo a ligand binding-dependent change in conformation. Addition of 5 mM glucose and sucrose were shown to produce large changes in the SRCD spectrum of the mTas1R2 and mTas1R3 VFTMs, although the changes seen differed between Tas1R2 and Tas1R3 VFTMs. These results demonstrate that the VFTMs of both Tas1R3 and Tas1R2 undergo a conformational change upon ligand binding, supporting roles for each subunit in response to binding sweet ligands. Using these two techniques, Nie Y. *et al.* (2005) showed that a naturally occurring variant in mouse Tas1R3 VFTM, *sac* (I60T), which renders the mice less sensitive to sweeteners was shown to alter the function of the sweet-taste receptor in two important ways: (1) by decreasing affinity for sweet ligands and (2) by inhibiting the subunit's ability to undergo a conformational change upon ligand binding. The diminished sweet preference displayed by nontaster mice is likely due to the decreased ability of Tas1R3 to bind ligand and/or undergo a conformational change that may be involved in signal transduction (Nie, Y. *et al.*, 2005).

4.09.3.4.5 The cysteine-rich domain of Tas1R3

In 2004 we determined that the CRD of hTas1R3 contains residues critical for the sweet receptor's interaction with the sweet protein brazzein (Jiang, P. *et al.*, 2004). Brazzein is sweet to humans, but not to mice. Using mismatched pairs and chimeric receptors from mouse and human, we identified a small region of the CRD of hTAS1R3 that was required for the response to brazzein (residues 535–545).

Within this region of the CRD of TAS1R3 there are only five amino acids that differ between mTAS1R3 and hTAS1R3 (see figure 3a of Jiang, P. *et al.*, 2004). Starting with hTAS1R3 we individually mutated each of these five amino acids to their mouse counterparts (a loss-of-function experiment; see figure 3b of Jiang, P. *et al.*, 2004). In this way we identified hTAS1R3 A537 and F540 as contributing to brazzein's activity. To identify additional residues of the CRD of hTAS1R3 involved in responsiveness to brazzein we made a series of alanine-scan mutations within the CRD (Jiang, P. *et al.*, personal communication). Analysis of these mutants showed that D535A selectively abolished sweet receptor responsiveness to brazzein (Figure 5). The adjacent substitution, D534A, had no effect on sweet receptor responses to brazzein or the other sweeteners in our panel. Substituting glutamine for aspartate at position 535 (D535Q) also blocked responsiveness to brazzein (Jiang, P. *et al.*, personal communication, data not shown).

A new crystal structure of mGluR3 that includes the CRD region was recently published (Muto, T. *et al.*, 2007). We have constructed a homology model of the heterotrimer hTas1R2 + hTas1R3 based on this new structure (Figure 6). In this structure we see that D535, A537, and F540 lie on a single face of the CRD, making it an attractive site of interaction for a site on brazzein. In addition, evidence suggests that brazzein also makes contact with the VFTM of Tas1R2, suggesting that this protein sweetener acts by stabilizing an active conformation of the receptor by binding to multiple domains simultaneously.

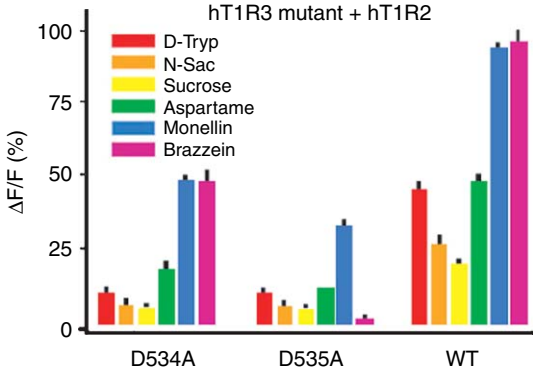

Figure 5 The D535A mutation in the cysteine-rich domain (CRD) of hTAS1R3 specifically abolishes sweet receptor responses to brazzein. Several residues within the CRD of hTas1R3 were individually mutated to alanine. Ala-scan mutants were coexpressed with hTas1R2 in HEK 293 cells along with a G-protein reporter, then tested for responsiveness to brazzein and a panel of sweeteners. D535A, but not D534A, showed a selective deficit in responsiveness to brazzein. D535 may participate in, or be close to the brazzein binding site in the CRD of hTas1R3.

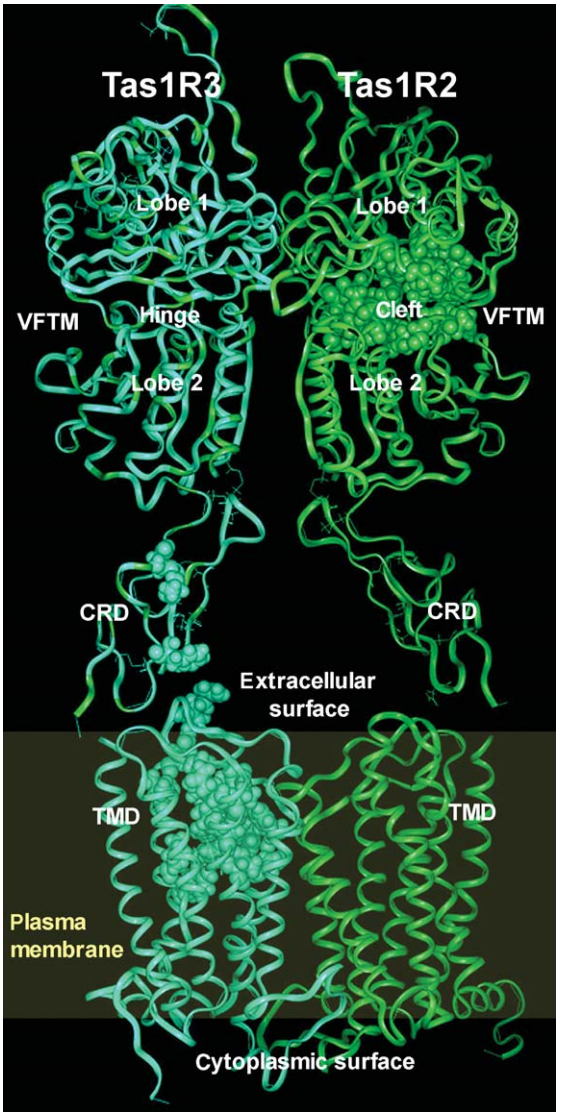

Figure 6 The homology model of all six domains of the sweet receptor (Tas1R2 + Tas1R3). The extracellular component of our model is based on the metabotropic glutamate binding receptor (mGluR3) venus flytrap module (VFTM) plus cysteine-rich domain (CRD) in the closed:closed configuration (2E4U). The two transmembrane domains are based on the crystal structure of rhodopsin (1HZX). The dimer interface between opposing helices 4 and 5 was chosen to best optimize the continuance of the CRD structure into that of TM helix 1 and is entirely speculative. The model is represented as a ribbon structure with only those residue side chains represented in Corey–Pauling–Koltun space filling representation. (CPK) that we have mutated and which alter receptor function in response to ligands. ΔF/F, the change of fluorescence at peak over the baseline fluorescence.

Other workers (Morini, G. *et al.*, 2005; Walters, D. E. and Hellekant, G., 2006) have independently used molecular modeling to dock the protein sweeteners, brazzein and monellin, to the open cleft of both Tas1R2 and Tas1R3 using a docking strategy that relies heavily on electrostatics as its primary basis for fitting ligand to binding site. It seems unlikely, however, that these protein sweeteners could activate the receptor by interacting with it in an open cleft conformation given the likelihood that the sweet receptor's mode of activation is similar to that of the mGluRs and calcium-sensing receptor which are known to require the closed state of the VFTM for activity.

4.09.3.4.6 The transmembrane domain of Tas1R3

The transmembrane portion of the sweet receptor is composed of one TMD from Tas1R2 and one from Tas1R3. It is presumed that these TMDs dimerize as has recently been shown for family A receptors although the specific contact interface(s) have yet to be determined. Like family A receptors, family C receptors have intra-TMD binding sites for small molecules that can act as either agonists or antagonists or as enhancers. From a series of human/mouse chimeras of Tas1R3 it was determined that it is the TMD of hTas1R3 that is required for sweet receptor responsiveness to cyclamate and lactisole (Jiang, P. *et al.*, 2005b; summarized in Figure 7). More refined chimeras and the generation of mutants (human-to-mouse loss of function and mouse-to-human gain of function) led us to identify specific residues within TM helices 5 (A733) and 7 (L798), and extracellular loop 3 (R790) that were required for the receptor to interact with cyclamate and lactisole.

These findings suggested that both lactisole and cyclamate bind within the TMD of the sweet receptor in a manner similar to that seen with other ligands binding to family A GPCRs (e.g., catecholamines bound within the TMD of the β-adrenergic receptor, or retinal bound within the TMD of rhodopsin). An alignment of the TMD of hTas1R3 with that of rhodopsin was used to identify 17 residues forming a candidate ligand-binding pocket within the TMD of hTas1R3. Alanine was substituted for each of these 17 residues and tested for responsiveness to a variety of sweeteners and lactisole. This produced seven receptors that responded to no tested sweetener, two receptors that were reduced specifically in their response to cyclamate, one receptor that was specifically reduced in their response to lactisole, and three receptors that had altered responsiveness to both cyclamate and lactisole. These results suggest that the binding pockets for cyclamate and latisole overlap within the TMD of hTas1R3 (Figure 8).

4.09.4 Future Studies/Unanswered Questions

Many questions remain to be answered about the sweet receptor. Of primary interest is mapping the various binding sites for ligands that lead to its active

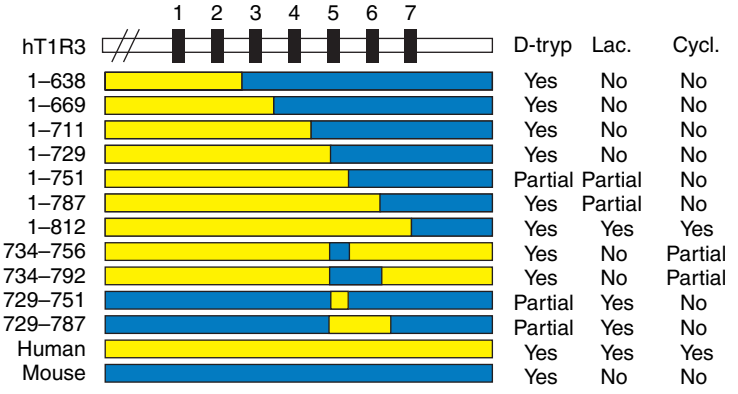

Figure 7 Schematic diagram showing responses of m/hTas1R3 chimeras to D-tryptophan, lactisole, and cyclamate. mTas1R3 portions are colored blue, hTas1R3 portions are yellow. Responsiveness of dimers of hTas1R2 + m/hTas1R3 chimeras to D-tryptophan (D-tryp), D-tryp + lactisole (Lac), or cyclamate (Cycl) are shown to the right. Chimeras containing mTas1R3 TM helix 5 did not respond to lactisole. The response to cyclamate by chimeras is more complicated and appears to require human residues in TM helices 5 and 7.

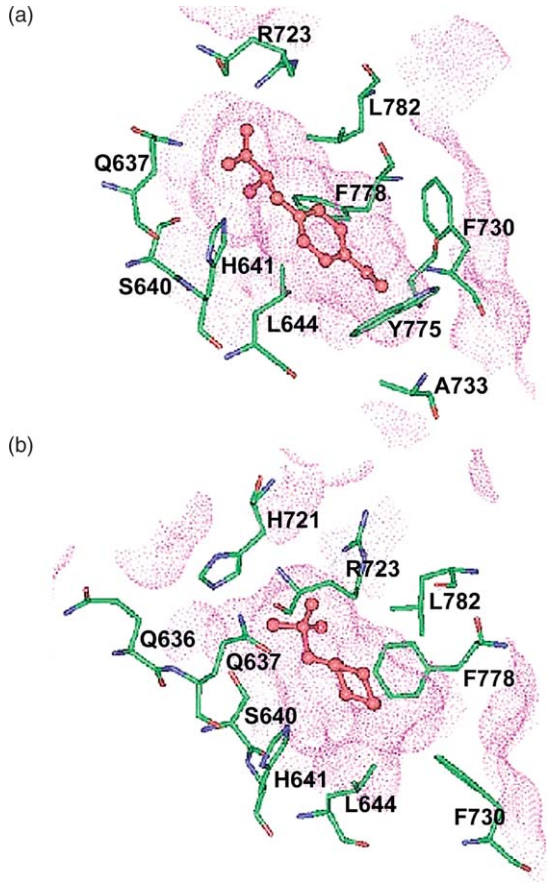

Figure 8 Models of the transmembrane domains (TMD) of the ligand-binding pocket of hTas1R3. (a) Lactisole docked within the TMD pocket. Lactisole's negatively charged propionic acid moiety is near H641 (TM helix 3). Lactisole's phenyl ring is predicted to form pi–pi interactions with F778 (TM helix 6). Lactisole's methoxyl group extends into a hydrophobic pocket and faces A733 (TM helix 5). (b) Cyclamate docked within the TMD pocket. The sulfamate group of cyclamate extends toward the top part of the pocket formed by TM helix 3 and extracellular loop 2. Residues Q637, S640, H641, H721, and R723 are in proximity to form ionic or hydrogen bonds with cyclamate's sulfamate group. Residues L644, F730, and F778 are predicted to form a hydrophobic pocket around cyclamate's cyclohexanyl group. Note that the binding pockets for the two ligands overlap but are not identical.

conformation. That there are over 50 molecules that taste sweet to humans that vary in structure from small molecule natural sugars, artificial sweeteners of multiple classes and even small proteins as well as at least one antagonist, suggests a great complexity to the receptor. Our work and that of others has demonstrated that there are multiple binding sites in at least four domains (VFTMs of Tas1R2 and Tas1R3 and the CRD and TMD of Tas1R3) and with overlapping binding sites for various ligands in each. New work from Jay Slack at Givaudan (personal communication, data not shown) suggests that the TMD of Tas1R2 may also be a binding site for perillartine (an aldoxime-type sweetener). An understanding of binding sites for sweeteners might well lead to a rational design for artificial sweeteners with better taste profiles. Binding-site studies along with investigations that use them to understand domain:domain interactions that lead to receptor activation may eventually give us the ability to rationally design better more potent sweeteners. Of even more interest, we might discover ways to enhance the sweetness of natural sugars with compounds that have no taste of their own.

An active area of investigation, not only of the sweet receptor but of all family C receptors is the conformational changes that the receptors undergo that leads to activation of G protein. Of particular interest is whether the monomer, the dimer or some larger grouping of receptors provides maximal activity in response to sweeteners. Of interest in this regard is the observation that many artificial sweeteners, while more potent than natural sugars, are none-the-less, at best, only partial agonists. Studies investigating additivity or synergy between sweeteners that bind to different domains of the receptor will be particularly important in our understanding of signal transmission within the sweet receptor.

Some of the knowledge gathered for sweet-taste receptors is still lacking for bitter-taste receptors. This applies in particular to the molecular architecture of TAS2Rs. Complex mutational analyses along with molecular modeling approaches are required. Clearly for a complete understanding of bitter-taste coding the cognate bitter substances for all TAS2Rs need to be identified, although this will be a never-ending project in light of the numerous bitter compounds and the extensive species differences. In humans, it emerges that there are pronounced variations among *TAS2R* genes, a fact that is expected to affect eating behavior. Uncovering the underlying mechanisms is scientifically interesting and of great potential medical and social importance for eating disorders, obesity, and their consequences. In this context, pharmacological treatment of taste in patients suffering from eating disorders with compounds developed by aid of *in vitro* receptor assay could be a therapeutic option. Another important

development in the field would be the elucidation of how bitter receptor cells communicate with the nervous system and how bitter transmission proceeds and is processed in relation to the other taste modalities. With some optimism we can await the future which will us bring exciting discoveries.

References

Adler, E., Hoon, M. A., Mueller, K. L., Chandrashekar, J., Ryba, N. J., and Zuker, C. S. 2000. A novel family of mammalian taste receptors [see comments]. Cell 100, 693–702.

Ariyasu, T., Matsumoto, S., Kyono, F., Hanaya, T., Arai, S., Ikeda, M., and Kurimoto, M. 2003. Taste receptor T1R3 is an essential molecule for the cellular recognition of the disaccharide trehalose. In Vitro Cell Dev. Biol. Anim. 39, 80–88.

Bachmanov, A. A., Li, X., Reed, D. R., Ohmen, J. D., Li, S., Chen, Z., Tordoff, M. G., de Jong, P. J., Wu, C., West, D. B., Chatterjee, A., Ross, D. A., and Beauchamp, G. K. 2001. Positional cloning of the mouse saccharin preference (Sac) locus. Chem. Senses 26, 925–933.

Bartoshuk, L. M. 1979. Bitter taste of saccharin related to the genetic ability to taste the bitter substance 6-*n*-propylthiouracil. Science 205, 934–935.

Behrens, M., Bartelt, J., Reichling, C., Winnig, M., Kuhn, C., and Meyerhof, W. 2006. Members of RTP and REEP gene families influence functional bitter taste receptor expression. J. Biol. Chem. 281, 20650–20659.

Behrens, M., Brockhoff, A., Kuhn, C., Bufe, B., Winnig, M., and Meyerhof, W. 2004. The human taste receptor hTAS2R14 responds to a variety of different bitter compounds. Biochem. Biophys. Res. Commun. 319, 479–485.

Belitz, H. D. and Wieser, H. 1985. Bitter compounds: occurrence and structure–activity relationship. Food Rev. Int. 1, 271–354.

Blakeslee, A. F. 1931. Genetics of sensory thresholds: taste for pheny thio carbamide. Science 74, 607.

Blakeslee, A. F. 1932. Genetics of sensory thresholds: taste for pheny thio carbamide. Proc. Natl. Acad. Sci. U. S. A. 18, 120–130.

Blakeslee, A. F. 1935. A dinner demonstration of threshold differences in taste and smell. Science 81, 504–507.

Blizard, D. A., Kotlus, B., and Frank, M. E. 1999. Quantitative trait loci associated with short-term intake of sucrose, saccharin and quinine solutions in laboratory mice. Chem. Senses 24, 373–385.

Bufe, B., Breslin, P. A., Kuhn, C., Reed, D. R., Tharp, C. D., Slack, J. P., Kim, U. K., Drayna, D., and Meyerhof, W. 2005. The molecular basis of individual differences in phenylthiocarbamide and propylthiouracil bitterness perception. Curr. Biol. 15, 322–327.

Bufe, B., Hofmann, T., Krautwurst, D., Raguse, J. D., and Meyerhof, W. 2002. The human TAS2R16 receptor mediates bitter taste in response to beta-glucopyranosides. Nat. Genet. 32, 397–401.

Bufe, B., Schöley-Pohl, E., Krautwurst, D., Hofmann, T., and Meyerhof, W. 2004. Identification of human bitter taste receptors. Am. Chem. Soc. 45–59.

Caicedo, A. and Roper, S. D. 2001. Taste receptor cells that discriminate between bitter stimuli. Science 291, 1557–1560.

Caicedo, A., Pereira, E., Margolskee, R. F., and Roper, S. D. 2003. Role of the G-protein subunit alpha-gustducin in taste cell responses to bitter stimuli. J, Neurosci. 23, 9947–9952.

Chandrashekar, J. 2006. The receptors and cells for mammalian taste. Nature 444, 288–294.

Chandrashekar, J., Mueller, K. L., Hoon, M. A., Adler, E., Feng, L., Guo, W., Zuker, C. S., and Ryba, N. J. 2000. T2Rs function as bitter taste receptors. Cell 100, 703–711.

Chaudhari, N., Landin, A. M., and Roper, S. D. 2000. A metabotropic glutamate receptor variant functions as a taste receptor. Nat. Neurosci. 3, 113–119.

Christiansen, B., Wellendorph, P., and Brauner-Osborne, H. 2006. Known regulators of nitric oxide synthase and arginase are agonists at the human G-protein-coupled receptor GPRC6A. Br. J. Pharmacol. 147, 855–863.

Conte, C., Ebeling, M., Marcuz, A., Nef, P., and Andres-Barquin, P. J. 2002. Identification and characterization of human taste receptor genes belonging to the TAS2R family. Cytogenet. Genome Res. 98, 45–53.

Conte, C., Ebeling, M., Marcuz, A., Nef, P., and Andres-Barquin, P. J. 2003. Evolutionary relationships of the Tas2r receptor gene families in mouse and human. Physiol. Genomics 14, 73–82.

Dahl, M., Erickson, R. P., and Simon, S. A. 1997. Neural responses to bitter compounds in rats. Brain Res. 756, 22–34.

Damak, S., Rong, M., Yasumatsu, K., Kokrashvili, Z., Varadarajan, V., Zou, S., Jiang, P., Ninomiya, Y., and Margolskee, R. F. 2003. Detection of sweet and umami taste in the absence of taste receptor T1r3. Science 301, 850–853.

Danilova, V. and Hellekant, G. 2003. Comparison of the responses of the chorda tympani and glossopharyngeal nerves to taste stimuli in C57BL/6J mice. BMC Neurosci. 4, 5.

Danilova, V. and Hellekant, G. 2004. Sense of taste in a New World monkey, the common marmoset. II. Link between behavior and nerve activity. J. Neurophysiol. 92, 1067–1076.

Delwiche, J. F., Buletic, Z., and Breslin, P. A. 2001. Covariation in individuals' sensitivities to bitter compounds: evidence supporting multiple receptor/transduction mechanisms. Percept. Psychophys. 63, 761–776.

Drewnowski, A. 1997. Taste preferences and food intake. Annu. Rev. Nutr. 17, 237–253.

Drewnowski, A. 2001. The science and complexity of bitter taste. Nutr. Rev. 59, 163–169.

Drewnowski, A. 2004. 6-n-Propylthiouracil Sensitivity, Food Choices, and Food Consumption. In: Genetic Variation in Taste Sensitivity (*eds*. J. Presscott and B. J. Tepper), pp. 179–194. Marcel.

Drewnowski, A. and Gomez-Carneros, C. 2000. Bitter taste, phytonutrients, and the consumer: a review. Am. J. Clin. Nutr. 72, 1424–1435.

Drewnowski, A. and Rock, C. L. 1995. The influence of genetic taste markers on food acceptance. Am. J. Clin. Nutr. 62, 506–511.

Duffy, V. B., Davidson, A. C., Kidd, J. R., Kidd, K. K., Speed, W. C., Pakstis, A. J., Reed, D. R., Snyder, D. J., and Bartoshuk, L. M. 2004a. Bitter receptor gene (TAS2R38), 6-*n*-propylthiouracil (PROP) bitterness and alcohol intake. Alcohol Clin. Exp. Res. 28, 1629–1637.

Duffy, V. B., Lucchina, L. A., and Bartoshuk, L. M. 2004b. Genetic Variation in Taste: Potential Biomarker for Cardiovascular Disease Risk? In: Genetic Variation in Taste Sensitivity (*eds*. J. Prescott and B. J. Tepper), pp. 195–228. Marcel.

Facchini, F., Abbati, A., and Campagnoni, S. 1990. Possible relations between sensitivity to phenylthiocarbamide and goiter. Hum. Biol. 62, 545–552.

Finger, T. E., Bottger, B., Hansen, A., Anderson, K. T., Alimohammadi, H., and Silver, W. L. 2003. Solitary chemoreceptor cells in the nasal cavity serve as sentinels of respiration. Proc. Natl. Acad. Sci. U. S. A. 100, 8981–8986.

Fischer, A., Gilad, Y., Man, O., and Paabo, S. 2005. Evolution of bitter taste receptors in humans and apes. Mol. Biol. Evol. 22, 432–436.

Floriano, W. B., Hall, S., Vaidehi, N., Kim, U., Drayna, D., and Goddard, W. A., 3rd. 2006. Modeling the human PTC bitter-taste receptor interactions with bitter tastants. J. Mol. Model. 12, 931–941.

Fox, A. L. 1932. The Relationship between chemical constitution and taste. Proc. Nat. Acad. Sci. U. S. A. 18, 115–120.

Fuller, J. L. 1974. Single-locus control of saccharin preference in mice. J. Hered. 65, 33–36.

Go, Y. 2006. Lineage-specific expansions and contractions of the bitter taste receptor gene repertoire in vertebrates. Mol. Biol. Evol. 23, 964–972.

Go, Y., Satta, Y., Takenaka, O., and Takahata, N. 2005. Lineage-specific loss of function of bitter taste receptor genes in humans and non-human primates. Genetics 170, 313–326.

Gudermann, T., Schoneberg, T., and Schultz, G. 1997. Functional and structural complexity of signal transduction via G-protein-coupled receptors. Annu. Rev. Neurosci. 20, 399–427.

Harris, H., Kalmus, H., and Trotter, W. R. 1949. Taste sensitivity to phenylthiourea in goitre and diabetes. Lancet 2, 1038.

He, H. T., Rens-Domiano, S., Martin, J. M., Law, S. F., Borislow, S., Woolkalis, M., Manning, D., and Reisine, T. 1990. Solubilization of active somatostatin receptors from rat brain. Mol. Pharmacol. 37, 614–621.

Hermans, E. and Challiss, R. A. 2001. Structural, signalling and regulatory properties of the group I metabotropic glutamate receptors: prototypic family C G-protein-coupled receptors. Biochem. J. 359, 465–484.

Hinrichs, A. L., Wang, J. C., Bufe, B., Kwon, J. M., Budde, J., Allen, R., Bertelsen, S., Evans, W., Dick, D., Rice, J., Foroud, T., Nurnberger, J., Tischfield, J. A., Kuperman, S., Crowe, R., Hesselbrock, V., Schuckit, M., Almasy, L., Porjesz, B., Edenberg, H. J., Begleiter, H., Meyerhof, W., Bierut, L. J., and Goate, A. M. 2006. Functional variant in a bitter-taste receptor (hTAS2R16) influences risk of alcohol dependence. Am. J. Hum. Genet. 78, 103–111.

Hoon, M. A., Adler, E., Lindemeier, J., Battey, J. F., Ryba, N. J., and Zuker, C. S. 1999. Putative mammalian taste receptors: a class of taste-specific GPCRs with distinct topographic selectivity. Cell 96, 541–551.

Huang, A. L., Chen, X., Hoon, M. A., Chandrashekar, J., Guo, W., Trankner, D., Ryba, N. J., and Zuker, C. S. 2006. The cells and logic for mammalian sour taste detection. Nature 442, 934–938.

Huang, L., Shanker, Y. G., Dubauskaite, J., Zheng, J. Z., Yan, W., Rosenzweig, S., Spielman, A. I., Max, M., and Margolskee, R. F. 1999. Ggamma13 colocalizes with gustducin in taste receptor cells and mediates IP3 responses to bitter denatonium. Nat. Neurosci. 2, 1055–1062.

Jiang, P., Cui, M., Zhao, B., Liu, Z., Snyder, L. A., Benard, L. M., Osman, R., Margolskee, R. F., and Max, M. 2005a. Lactisole interacts with the transmembrane domains of human T1R3 to inhibit sweet taste. J. Biol. Chem. 280, 15238–15246.

Jiang, P., Cui, M., Zhao, B., Snyder, L. A., Benard, L. M., Osman, R., Max, M., and Margolskee, R. F. 2005b. Identification of the cyclamate interaction site within the transmembrane domain of the human sweet taste receptor subunit T1R3. J. Biol. Chem. 280, 34296–34305.

Jiang, P., Ji, Q., Liu, Z., Snyder, L. A., Benard, L. M., Margolskee, R. F., and Max, M. 2004. The cysteine-rich region of T1R3 determines responses to intensely sweet proteins. J. Biol. Chem. 279, 45068–45075.

Jingami, H., Nakanishi, S., and Morikawa, K. 2003. Structure of the metabotropic glutamate receptor. Curr. Opin. Neurobiol. 13, 271–278.

Joiner, T. E., Jr. and Perez, M. 2004. Phenylthiocarbamide tasting and family history of depression, revisited: low rates of depression in families of supertasters. Psychiatry Res. 126, 83–87.

Kim, M. R., Kusakabe, Y., Miura, H., Shindo, Y., Ninomiya, Y., and Hino, A. 2003. Regional expression patterns of taste receptors and gustducin in the mouse tongue. Biochem. Biophys. Res. Commun. 312, 500–506.

Kim, U., Wooding, S., Ricci, D., Jorde, L. B., and Drayna, D. 2005. Worldwide haplotype diversity and coding sequence variation at human bitter taste receptor loci. Hum. Mutat. 26, 199–204.

Kim, U. K., Jorgenson, E., Coon, H., Leppert, M., Risch, N., and Drayna, D. 2003. Positional cloning of the human quantitative trait locus underlying taste sensitivity to phenylthiocarbamide. Science 299, 1221–1225.

Kitagawa, M., Kusakabe, Y., Miura, H., Ninomiya, Y., and Hino, A. 2001. Molecular genetic identification of a candidate receptor gene for sweet taste. Biochem. Biophys. Res. Commun. 283, 236–242.

Kuhn, C., Bufe, B., Winnig, M., Hofmann, T., Frank, O., Behrens, M., Lewtschenko, T., Slack, J. P., Ward, C. D., and Meyerhof, W. 2004. Bitter taste receptors for saccharin and acesulfame K. J. Neurosci. 24, 10260–10265.

Kunishima, N., Shimada, Y., Tsuji, Y., Sato, T., Yamamoto, M., Kumasaka, T., Nakanishi, S., Jingami, H., and Morikawa, K. 2000. Structural basis of glutamate recognition by a dimeric metabotropic glutamate receptor. Nature 407, 971–977.

Li, X., Inoue, M., Reed, D. R., Huque, T., Puchalski, R. B., Tordoff, M. G., Ninomiya, Y., Beauchamp, G. K., and Bachmanov, A. A. 2001. High-resolution genetic mapping of the saccharin preference locus (Sac) and the putative sweet taste receptor (T1R1) gene (Gpr70) to mouse distal Chromosome 4. Mamm. Genome 12, 13–16.

Li, X., Staszewski, L., Xu, H., Durick, K., Zoller, M., and Adler, E. 2002a. Human receptors for sweet and umami taste. Proc. Natl. Acad. Sci. U. S. A. 99, 4692–4696.

Li, X., Staszewski, L., Xu, H., Durick, K., Zoller, M., and Adler, E. 2002b. Human receptors for sweet and umami taste. Proc. Natl. Acad. Sci. U. S. A. 99, 4692–4696.

Lindemann, B. 1999. Receptor seeks ligand: on the way to cloning the molecular receptors for sweet and bitter taste. Nat. Med. 5, 381–382.

Lush, I. E. 1981. The genetics of tasting in mice. I. Sucrose octaacetate. Genet. Res. 38, 93–95.

Lush, I. E. 1984. The genetics of tasting in mice. III. Quinine. Genet. Res. 44, 151–160.

Lush, I. E. 1986. The genetics of tasting in mice. IV. The acetates of raffinose, galactose and beta-lactose. Genet. Res. 47, 117–123.

Lush, I. E. 1989. The genetics of tasting in mice. VI. Saccharin, acesulfame, dulcin and sucrose. Genet. Res. 53, 95–99.

Lush, I. E. and Holland, G. 1988. The genetics of tasting in mice. V. Glycine and cycloheximide. Genet. Res. 52, 207–212.

Lush, I. E., Hornigold, N., King, P., and Stoye, J. P. 1995. The genetics of tasting in mice. VII. Glycine revisited, and the chromosomal location of Sac and Soa. Genet. Res. 66, 167–174.

Malherbe, P., Kratochwil, N., Zenner, M. T., Piussi, J., Diener, C., Kratzeisen, C., Fischer, C., and Porter, R. H. 2003. Mutational analysis and molecular modeling of the binding pocket of the metabotropic glutamate 5 receptor negative modulator 2-methyl-6-(phenylethynyl)-pyridine. Mol. Pharmacol. 64, 823–832.

Matsunami, H., Montmayeur, J. P., and Buck, L. B. 2000. A family of candidate taste receptors in human and mouse [see comments]. Nature 404, 601–604.

Max, M., Shanker, Y. G., Huang, L., Rong, M., Liu, Z., Campagne, F., Weinstein, H., Damak, S., and

Margolskee, R. F. 2001. Tas1r3, encoding a new candidate taste receptor, is allelic to the sweet responsiveness locus Sac. Nat. Genet. 28, 58–63.

McLaughlin, S. K., McKinnon, P. J., and Margolskee, R. F. 1992. Gustducin is a taste-cell-specific G protein closely related to the transducins. Nature 357, 563–569.

Meyerhof, W. 2005. Elucidation of mammalian bitter taste. Rev. Physiol. Biochem. Pharmacol. 154, 37–72.

Meyerhof, W., Behrens, M., Brockhoff, A., Bufe, B., and Kuhn, C. 2005. Human bitter taste perception. Chem. Senses 30 Suppl 1, i14–i15.

Miedlich, S. U., Gama, L., Seuwen, K., Wolf, R. M., and Breitwieser, G. E. 2004. Homology modeling of the transmembrane domain of the human calcium sensing receptor and localization of an allosteric binding site. J. Biol. Chem. 279, 7254–7263.

Miguet, L., Zhang, Z., and Grigorov, M. G. 2006. Computational studies of ligand-receptor interactions in bitter taste receptors. J. Recept. Signal Transduct. Res. 26, 611–630.

Ming, D., Ninomiya, Y., and Margolskee, R. F. 1999. Blocking taste receptor activation of gustducin inhibits gustatory responses to bitter compounds. Proc. Natl. Acad. Sci. U. S. A. 96, 9903–9908.

Ming, D., Ruiz-Avila, L., and Margolskee, R. F. 1998. Characterization and solubilization of bitter-responsive receptors that couple to gustducin. Proc. Natl. Acad. Sci. U. S. A. 95, 8933–8938.

Montmayeur, J. P., Liberles, S. D., Matsunami, H., and Buck, L. B. 2001. A candidate taste receptor gene near a sweet taste locus. Nat. Neurosci. 4, 492–498.

Morini, G., Bassoli, A., and Temussi, P. A. 2005. From small sweeteners to sweet proteins: anatomy of the binding sites of the human T1R2–T1R3 receptor. J. Med. Chem. 48, 5520–5529.

Mueller, K. L., Hoon, M. A., Erlenbach, I., Chandrshekar, J., Zuker, C. S., and Ryba, N. J. P. 2005. The receptors and coding logic for bitter taste. Nature 434, 225–229.

Muto, T., Tsuchiya, D., Morikawa, K., and Jingami, H. 2007. Structures of the extracellular regions of the group II/III metabotropic glutamate receptors. Proc. Natl. Acad. Sci. U. S. A. 104, 3759–3764.

Nelson, G., Chandrashekar, J., Hoon, M. A., Feng, L., Zhao, G., Ryba, N. J., and Zuker, C. S. 2002. An amino-acid taste receptor. Nature 416, 199–202.

Nelson, G., Hoon, M. A., Chandrashekar, J., Zhang, Y., Ryba, N. J., and Zuker, C. S. 2001. Mammalian sweet taste receptors. Cell 106, 381–390.

Nie, Y., Vigues, S., Hobbs, J. R., Conn, G. L., and Munger, S. D. 2005. Distinct contributions of T1R2 and T1R3 taste receptor subunits to the detection of sweet stimuli. Curr. Biol. 15, 1948–1952.

Okada, T., Fujiyoshi, Y., Silow, M., Navarro, J., Landau, E. M., and Shichida, Y. 2002. Functional role of internal water molecules in rhodopsin revealed by X-ray crystallography. Proc. Natl. Acad. Sci. U. S. A. 99, 5982–5987.

Olias, G., Viollet, C., Kusserow, H., Epelbaum, J., and Meyerhof, W. 2004. Regulation and function of somatostatin receptors. J. Neurochem. 89, 1057–1091.

Ozeck, M., Brust, P., Xu, H., and Servant, G. 2004. Receptors for bitter, sweet and umami taste couple to inhibitory G protein signaling pathways. Eur. J. Pharmacol. 489, 139–149.

Pagano, A., Ruegg, D., Litschig, S., Stoehr, N., Stierlin, C., Heinrich, M., Floersheim, P., Prezeau, L., Carroll, F., Pin, J. P., Cambria, A., Vranesic, I., Flor, P. J., Gasparini, F., and Kuhn, R. 2000. The non-competitive antagonists 2-methyl-6-(phenylethynyl)pyridine and 7-hydroxyiminocyclopropan[b]chromen-1a-carboxylic acid ethyl ester interact with overlapping binding pockets in the transmembrane region of group I metabotropic glutamate receptors. J. Biol. Chem. 275, 33750–33758.

Palczewski, K., Kumasaka, T., Hori, T., Behnke, C. A., Motoshima, H., Fox, B. A., Le Trong, I., Teller, D. C., Okada, T., Stenkamp, R. E., Yamamoto, M., and Miyano, M. 2000. Crystal structure of rhodopsin: A G protein-coupled receptor. Science 289, 739–745.

Parry, C. M., Erkner, A., and le Coutre, J. 2004. Divergence of T2R chemosensory receptor families in humans, bonobos, and chimpanzees. Proc. Natl. Acad. Sci. U. S. A. 101, 14830–14834.

Pelchat, M. L. and Danowski, S. 1992. A possible genetic association between PROP-tasting and alcoholism. Physiol. Behav. 51, 1261–1266.

Petrel, C., Kessler, A., Dauban, P., Dodd, R. H., Rognan, D., and Ruat, M. 2004. Positive and negative allosteric modulators of the Ca^{2+}-sensing receptor interact within overlapping but not identical binding sites in the transmembrane domain. J. Biol. Chem. 279, 18990–18997.

Pi, M., Faber, P., Ekema, G., Jackson, P. D., Ting, A., Wang, N., Fontilla-Poole, M., Mays, R. W., Brunden, K. R., Harrington, J. J., and Quarles, L. D. 2005. Identification of a novel extracellular cation-sensing G-protein-coupled receptor. J. Biol. Chem. 280, 40201–40209.

Pin, J. P., Galvez, T., and Prezeau, L. 2003. Evolution, structure, and activation mechanism of family 3/C G-protein-coupled receptors. Pharmacol. Ther. 98, 325–354.

Pronin, A. N., Tang, H., Connor, J., and Keung, W. 2004. Identification of Ligands for Two Human Bitter T2R Receptors. Chem. Senses 29, 583–593.

Rossler, P., Boekhoff, I., Tareilus, E., Beck, S., Breer, H., and Freitag, J. 2000. G protein betagamma complexes in circumvallate taste cells involved in bitter transduction. Chem. Senses 25, 413–421.

Ruiz-Avila, L., McLaughlin, S. K., Wildman, D., McKinnon, P. J., Robichon, A., Spickofsky, N., and Margolskee, R. F. 1995. Coupling of bitter receptor to phosphodiesterase through transducin in taste receptor cells. Nature 376, 80–85.

Ruiz-Avila, L., Ming, D., and Margolskee, R. F. 2000. An In vitro assay useful to determine the potency of several bitter compounds. Chem. Senses 25, 361–368.

Sainz, E., Cavenagh, M. M., Gutierrez, J., Battey, J. F., Northup, J. K., and Sullivan, S. L. 2007. Functional characterization of human bitter taste receptors. Biochem. J. 403, 537–543.

Sainz, E., Korley, J. N., Battey, J. F., and Sullivan, S. L. 2001. Identification of a novel member of the T1R family of putative taste receptors. J. Neurochem. 77, 896–903.

Saito, H., Kubota, M., Roberts, R. W., Chi, Q., and Matsunami, H. 2004. RTP family members induce functional expression of mammalian odorant receptors. Cell 119, 679–691.

Sako, N., Harada, S., and Yamamoto, T. 2000. Gustatory information of umami substances in three major taste nerves. Physiol. Behav. 71, 193–198.

Sandell, M. A. and Breslin, P. A. 2006. Variability in a taste-receptor gene determines whether we taste toxins in food. Curr. Biol. 16, R792–794.

Schiffman, S. S., Booth, B. J., Sattely-Miller, E. A., Graham, B. G., and Gibes, K. M. 1999. Selective inhibition of sweetness by the sodium salt of +/−2-(4-methoxyphenoxy)propanoic acid. Chem Senses 24, 439–447.

Sclafani, A. and Perez, C. 1997. Cypha [propionic acid, 2-(4-methoxyphenol) salt] inhibits sweet taste in humans, but not in rats. Physiol. Behav. 61, 25–29.

Shi, P. and Zhang, J. 2006. Contrasting modes of evolution between vertebrate sweet/umami receptor genes and bitter receptor genes. Mol. Biol. Evol. 23, 292–300.

Shi, P., Zhang, J., Yang, H., and Zhang, Y. P. 2003. Adaptive diversification of bitter taste receptor genes in Mammalian evolution. Mol. Biol. Evol. 20, 805–814.

Soranzo, N., Bufe, B., Sabeti, P. C., Wilson, J. F., Weale, M. E., Marguerie, R., Meyerhof, W., and Goldstein, D. B. 2005. Positive selection on a high-sensitivity allele of the human bitter-taste receptor TAS2R16. Curr. Biol. 15, 1257–1265.

Spector, A. C. and Kopka, S. L. 2002. Rats fail to discriminate quinine from denatonium: implications for the neural coding of bitter-tasting compounds. J. Neurosci. 22, 1937–1941.

Sugino, Y., Umemoto, A., and Mizutani, S. 2002. Insensitivity to the bitter taste of chloramphenicol: an autosomal recessive trait. Genes Genet. Syst. 77, 59–62.

Teller, D. C., Okada, T., Behnke, C. A., Palczewski, K., and Stenkamp, R. E. 2001. Advances in determination of a high-resolution three-dimensional structure of rhodopsin, a model of G-protein-coupled receptors (GPCRs). Biochemistry 40, 7761–7772.

Tepper, B. J. and Nurse, R. J. 1997. Fat perception is related to PROP taster status. Physiol. Behav. 61, 949–954.

Timpson, N. J., Christensen, M., Lawlor, D. A., Gaunt, T. R., Day, I. N., and Smith, G. D. 2005. TAS2R38 (phenylthiocarbamide) haplotypes, coronary heart disease traits, and eating behavior in the British Women's Heart and Health Study. Am. J. Clin. Nutr. 81, 1005–1011.

Tsuchiya, D., Kunishima, N., Kamiya, N., Jingami, H., and Morikawa, K. 2002. Structural views of the ligand-binding cores of a metabotropic glutamate receptor complexed with an antagonist and both glutamate and Gd^{3+}. Proc. Natl. Acad. Sci. U. S. A. 99, 2660–2665.

Ueda, T., Ugawa, S., Ishida, Y., Shibata, Y., Murakami, S., and Shimada, S. 2001. Identification of coding single-nucleotide polymorphisms in human taste receptor genes involving bitter tasting. Biochem. Biophys. Res. Commun. 285, 147–151.

Ueda, T., Ugawa, S., Yamamura, H., Imaizumi, Y., and Shimada, S. 2003. Functional interaction between T2R taste receptors and G-protein α-subunits expressed in taste receptor cells. J. Neurosci. 23, 7376–7380.

Visiers, I., Ballesteros, J. A., and Weinstein, H. 2002. Three-dimensional representations of G protein-coupled receptor structures and mechanisms. Methods Enzymol. 343, 329–371.

Visiers, I., Braunheim, B. B., and Weinstein, H. 2000. Prokink: a protocol for numerical evaluation of helix distortions by proline. Protein Eng. 13, 603–606.

Walters, D. E. and Hellekant, G. 2006. Interactions of the sweet protein brazzein with the sweet taste receptor. J. Agric. Food Chem. 54, 10129–10133.

Wang, X., Thomas, S. D., and Zhang, J. 2004. Relaxation of selective constraint and loss of function in the evolution of human bitter taste receptor genes. Hum. Mol. Genet. 13, 2671–2678.

Whitney, G. and Harder, D. B. 1994. Genetics of bitter perception in mice. Physiol. Behav. 56, 1141–1147.

Winnig, M., Bufe, B., and Meyerhof, W. 2005. Valine 738 and lysine 735 in the fifth transmembrane domain of rTas1r3 mediate insensitivity towards lactisole of the rat sweet taste receptor. BMC Neurosci 6, 22.

Wong, G. T., Gannon, K. S., and Margolskee, R. F. 1996a. Transduction of bitter and sweet taste by gustducin. Nature 381, 796–800.

Wong, G. T., Ruiz-Avila, L., and Margolskee, R. F. 1999. Directing gene expression to gustducin-positive taste receptor cells. J. Neurosci. 19, 5802–5809.

Wong, G. T., Ruiz-Avila, L., Ming, D., Gannon, K. S., and Margolskee, R. F. 1996b. Biochemical and transgenic analysis of gustducin's role in bitter and sweet transduction. Cold Spring Harb. Symp. Quant. Biol. 61, 173–184.

Wooding, S., Bufe, B., Grassi, C., Howard, M. T., Stone, A. C., Vazquez, M., Dunn, D. M., Meyerhof, W., Weiss, R. B., and Bamshad, M. J. 2006. Independent evolution of bitter-taste sensitivity in humans and chimpanzees. Nature 440, 930–934.

Wooding, S., Kim, U. K., Bamshad, M. J., Larsen, J., Jorde, L. B., and Drayna, D. 2004. Natural selection and molecular evolution in PTC, a bitter-taste receptor gene. Am. J. Hum. Genet. 74, 637–646.

Wu, S. V., Rozengurt, N., Yang, M., Young, S. H., Sinnett-Smith, J., and Rozengurt, E. 2002. Expression of bitter taste receptors of the T2R family in the gastrointestinal tract and enteroendocrine STC-1 cells. Proc. Natl. Acad. Sci. U. S. A. 99, 2392–2397.

Xu, H., Staszewski, L., Tang, H., Adler, E., Zoller, M., and Li, X. 2004. Different functional roles of T1R subunits in the heteromeric taste receptors. Proc. Natl. Acad. Sci. U. S. A. 101, 14258–14263.

Yang, H., Wanner, I. B., Roper, S. D., and Chaudhari, N. 1999. An optimized method for in situ hybridization with signal amplification that allows the detection of rare mRNAs. J. Histochem. Cytochem 47, 431–446.

Zhang, Y., Hoon, M. A., Chandrashekar, J., Mueller, K. L., Cook, B., Wu, D., Zuker, C. S., and Ryba, N. J. 2003. Coding of sweet, bitter, and umami tastes. Different receptor cells sharing similar signaling pathways. Cell 112, 293–301.

Zhao, G. Q., Zhang, Y., Hoon, M. A., Chandrashekar, J., Erlenbach, I., Ryba, N. J., and Zuker, C. S. 2003. The receptors for mammalian sweet and umami taste. Cell 115, 255–266.

4.10 Taste Transduction

S C Kinnamon, Colorado State University, Fort Collins, CO, USA

R F Margolskee, Mount Sinai School of Medicine, New York, NY, USA

© 2008 Elsevier Inc. All rights reserved.

4.10.1	**Introduction**	219
4.10.1.1	Taste Qualities	220
4.10.1.2	Taste Buds, Taste Cell Types, and Afferent Innervation	220
4.10.1.3	Taste Receptor Cell Properties	221
4.10.2	**Quality Specific Transduction**	221
4.10.2.1	Salt Taste	221
4.10.2.1.1	Amiloride-sensitive versus amiloride-insensitive mechanisms	222
4.10.2.1.2	ENaC – the amiloride-sensitive salt taste receptor	222
4.10.2.1.3	Amiloride-insensitive mechanisms	223
4.10.2.2	Sour Taste	224
4.10.2.2.1	Intracellular versus extracellular pH as a stimulus	224
4.10.2.2.2	Proton-permeable ion channels	224
4.10.2.2.3	Proton-gated ion channels	224
4.10.2.2.4	Proton-blocked K^+ channels	225
4.10.2.2.5	PKD1L3 and PKD2L1	225
4.10.2.2.6	Downstream signaling effectors in sour taste	226
4.10.2.3	Transduction Mechanisms Common to Bitter, Sweet, and Umami Taste Qualities	226
4.10.2.3.1	G proteins	226
4.10.2.3.2	Effector enzymes	227
4.10.2.3.3	PLCβ2 knockout mice	228
4.10.2.3.4	Target channels	228
4.10.2.4	Transduction Elements Specific to Particular Taste Qualities	229
4.10.3	**Other Transduction Mechanisms**	229
4.10.3.1	Fat Taste	229
4.10.3.1.1	Fatty acid modulation of taste cells	229
4.10.3.1.2	Fatty acid taste receptors	230
4.10.3.2	Water Taste	230
4.10.4	**Signaling to Afferent Nerve Fibers and Adjacent Taste Cells**	230
4.10.4.1	Adenosine Triphosphate as a Transmitter	230
4.10.4.2	Serotonin and Other Neuroactive Modulators	231
4.10.4.3	Other Candidate Transmitters	232
References		232

4.10.1 Introduction

During the past decade considerable progress has been made in revealing the basic mechanisms of taste transduction and signaling. This explosion of information is due in large part to the sequencing of the rodent and human genomes, allowing identification of the taste receptors, downstream signaling molecules, and effector ion channels involved in taste transduction. Further, these discoveries have led to the production of gene-targeted and transgenic mice, where the role of individual signaling proteins can be assessed *in vivo*. Here we review recent progress in quality-specific transduction, focusing primarily on mammalian taste cells. In addition, we discuss the identity and potential roles of neurotransmitters in taste cells and how taste information is communicated to afferent nerve fibers. Detailed information

about G-protein-coupled taste receptors (GPCRs) is covered in Chapter Taste Receptors.

4.10.1.1 Taste Qualities

The sense of taste affords organisms the ability to discriminate nutritionally important substances from potentially harmful ones. The gustatory system detects and discriminates nonvolatile stimuli representing five basic taste qualities – sweet, salty, sour, bitter, and umami. Sweet, salty, and umami stimuli are generally appetitive, because they represent chemicals required for proper nutrition. These include sugars for energy production, sodium (Na^+) for ionic homeostasis, and amino acids as a source for protein synthesis. Bitter and sour stimuli are naturally aversive and warn against ingestion of potentially toxic or poisonous substances.

Recently obtained evidence suggests that fat and water may each constitute additional primary taste qualities. In the case of fat, it is well established that mammals prefer lipid enriched foods. However, until recently, this preference for fat was presumed to be due only to its pleasant textural qualities (mouth feel). New data suggest that specific fatty acid receptors and fatty acid-modulated ion channels are expressed in taste receptor cells, where they may be involved in the detection of fatty acids as taste stimuli (for review, Laugerette, F. *et al.*, 2007). Similarly, water-permeable ion channels were recently found on the apical membrane of taste cells, suggesting they may be the source of the gustatory neural response to water (Watson, K. J. *et al.*, 2007). However, whether water represents a specific taste or whether it is involved in volume regulation of taste cells is not known.

4.10.1.2 Taste Buds, Taste Cell Types, and Afferent Innervation

Taste buds are the transducing elements of gustatory sensation. A typical taste bud is an onion shaped end organ comprising 50–100 spindle shaped cells that extend from the basal lamina to the surface of the tongue. The apical portion of each taste cell contains microvilli, which protrude through an opening in the epithelium called the taste pore. The basolateral membrane makes synaptic contacts with afferent nerve fibers, which project taste information to the brain. Four types of cells can be distinguished based on morphological and functional criteria. Type I cells, also known as dark cells, make up about 50% of the cells in a taste bud. These cells are generally considered to have a support function, and are not likely to be involved directly in transducing taste stimuli, although their apical membranes do reach the taste pore. The membranes of type I cells wrap around other cells in a glial-like fashion, and they express transporters and enzymes for uptake and inactivation of transmitters (Lawton, D. M. *et al.*, 2000; Bartel, D. L. *et al.*, 2006; Figure 1.) Type II cells, also known as light cells, make up about 30% of the taste bud. These cells express the taste receptors and downstream signaling elements implicated in responses to bitter, sweet, and umami taste stimuli. These cells associate with afferent nerve fibers, but do not form definitive synapses with pre- and postsynaptic specializations (Clapp, T. R. *et al.*, 2004; 2006). Type III cells, also known as intermediate cells, make up about 20% of cells in the

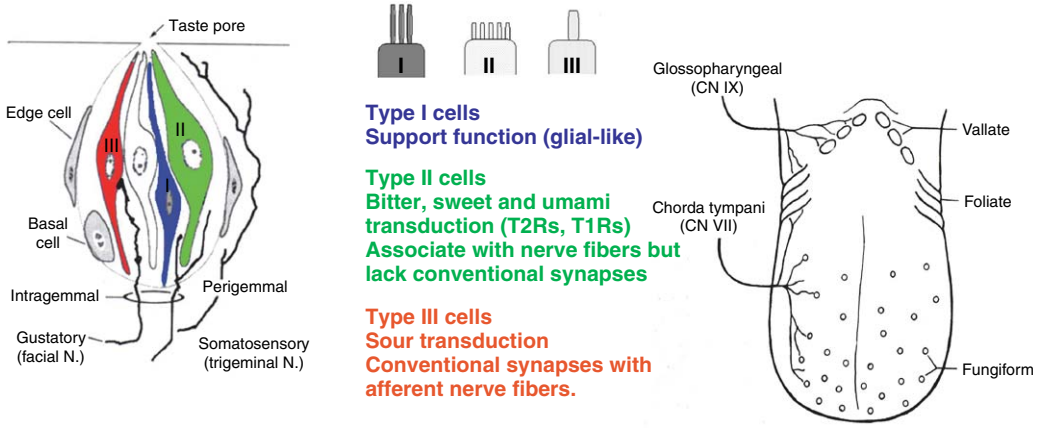

Figure 1 Cell types and innervation of taste buds. Type II taste cells are coded green, while Type III taste cells are coded red in subsequent figures. (Modified, with permission, from Finger and Simon, 2000).

taste bud. Recent evidence suggests that type III cells are the transducers of acidic (sour) stimuli (Richter, T. A. *et al.*, 2003; Kataoka, S. *et al.*, 2007). These cells form prominent synapses with afferent nerve fibers and may also be involved in cell-to-cell signaling in the taste bud (Herness, S. *et al.*, 2005; Roper, S. D., 2006). Proliferative basal cells are also found in the basolateral regions of the taste bud. These spherical cells divide to form new taste cells, which turn over every 10 days to 2 weeks. Ultrastructural features of these cell types are reviewed in Chapter Ultrastructure of Taste Buds.

Lingual taste buds are housed in connective tissue papillae. The anterior two-thirds of the tongue contains fungiform papillae, each of which contain one or two taste buds. These taste buds are innervated by the chorda tympani branch of the facial nerve (CN VII). The posterior region of the tongue contains the circumvallate and foliate papillae, each of which contain hundreds of taste buds. These taste buds are innervated primarily by the glossopharyngeal nerve (CN IX), but the anterior foliate taste buds are innervated by a branch of the chorda tympani nerve. Taste buds are also located on the soft palate, where they are innervated by the greater superficial petrosal nerve, a branch of CN VII, and on the larynx and esophagus, where they are innervated by a branch of the vagus nerve (CN X).

4.10.1.3 Taste Receptor Cell Properties

Simple taste stimuli, such as salts and acids, act on apically located ion channels, while more complex stimuli, such as sugars and plant alkaloids, bind to GPCRs and activate intracellular second messenger signaling cascades. In all cases, transduction appears to result in membrane depolarization and action potential initiation. Action potentials in taste cells were first observed over two decades ago, using intracellular recordings from mudpuppy taste cells (Roper, S., 1983). Action potentials are now known to be a general property of type II and type III rodent taste cells and they are generated regularly in response to most taste stimuli (Avenet, P. and Lindemann, B., 1991; Gilbertson, T. A. *et al.*, 1992; Cummings, T. A. *et al.*, 1993; Yoshida, R. *et al.*, 2006). Underlying action potential generation are tetrodotoxin-sensitive Na^+ channels (Herness, M. S. and Sun, X. D., 1995), a variety of potassium (K^+) channels (Chen, Y. *et al.*, 1996; Liu, L. *et al.*, 2005), and voltage-gated Ca^{2+} channels (Behe, P. *et al.*, 1990). Recent data obtained from specific taste cell types indicated that while both type II and type III cells express voltage-gated Na^+ and K^+ channels, only type III taste cells express voltage-gated Ca^{2+} channels (Medler, K. F. *et al.*, 2003; Clapp, T. R. *et al.*, 2006; DeFazio, R. A. *et al.*, 2006). The role of action potentials in the transduction process has been unclear, since taste cells are short receptor cells that should be capable of transmitter release without requiring action potentials. Recent data using cell attached recordings from a polarized, semi intact preparation show that the breadth of tuning of individual taste cells in response to taste stimuli is nearly identical to the breadth of tuning of single afferent nerve fibers, suggesting that action potentials may be required for transmitter release (Yoshida, R. *et al.*, 2006).

4.10.2 Quality Specific Transduction

During the past 10–15 years several candidate taste transduction elements have been identified in taste receptor cells. Validation of candidates as confirmed taste transduction elements requires their presence in taste cells along with the demonstration of their involvement, from *in vivo* and/or *in vitro* studies, in specific taste transduction pathways underlying particular taste qualities.

4.10.2.1 Salt Taste

Ingestion of salts, particularly NaCl, is critical for the maintenance of ionic homeostasis. The cation of the salt is the main component detected, and several cations, including Na^+, Li^+, K^+, Ca^{2+}, and NH_4^+ contribute to salty taste perception. When salts are present in sufficient concentration in the oral cavity, cations permeate ionic channels in the apical membrane of the taste cells, causing cationic influx and membrane depolarization. Monovalent cations also permeate the tight junctions at the apex of the taste bud, where they interact with the basolateral membrane of taste cells and generate a hyperpolarizing field potential (Ye, Q. *et al.*, 1991). This paracellular shunt pathway reduces the magnitude of the receptor potential and attenuates the perception of saltiness. The magnitude of the paracellular shunt is strongly influenced by the anion of the salt. Small anions such as chloride (Cl^-) diffuse readily into the paracellular space, where they blunt the hyperpolarizing field potential produced by the cations. In contrast, large anions such as gluconate and acetate fail to permeate the paracellular pathway. Thus, salts with large

anions are perceived to be less salty than equivalent concentrations of salts with small anions (Elliott, E. J. and Simon, S. A., 1990; Ye, Q. *et al.*, 1994).

4.10.2.1.1 Amiloride-sensitive versus amiloride-insensitive mechanisms

Salt taste transduction mechanisms vary in different species, depending on the ionic composition of the diet (Boudreau, J. C. *et al.*, 1985). Herbivores and other mammals on a low Na^+ diet have a Na^+-specific appetite, mediated by highly Na^+-specific channels that are inhibited by the diuretic drug amiloride. Amiloride-sensitive Na^+ channels were originally proposed as a salt transduction mechanism by John DeSimone and colleagues, who observed that the chorda tympani response to NaCl in rats is sensitive to amiloride (Heck, G. L. *et al.*, 1984). Whole cell patch-clamp studies have confirmed the presence of amiloride-sensitive Na^+ currents in hamster (Gilbertson, T. A. *et al.*, 1992; 1993; Gilbertson, T. A. and Fontenot, D. T., 1998), rat (Doolin, R. E. and Gilbertson, T. A., 1996), and mouse (Miyamoto, T. *et al.*, 2001) fungiform taste cells. However, other mechanisms for salt transduction exist, because about 20% of the chorda tympani response and the entire glossopharyngeal response to NaCl is amiloride-insensitive in rodents (Ninomiya, Y. *et al.*, 1989; Gannon, K. S. and Contreras, R. J., 1995; Ninomiya, Y., 1998). Amiloride-insensitive mechanisms appear to predominate in species with adequate dietary Na^+ levels, including humans, although both mechanisms exist to some extent in most species. While amiloride-sensitive mechanisms are highly Na^+ selective, amiloride-insensitive mechanisms do not discriminate between cations. Indeed, when the chorda tympani nerve is transected, or when amiloride is present, rats lose the ability to discriminate Na^+ from K^+ in behavioral discrimination assays (Spector, A. C. *et al.*, 1996). Amiloride-sensitive and -insensitive mechanisms are likely distributed in different taste cells, because NaCl responses in single chorda tympani nerve fibers are either inhibited completely by amiloride, or unaffected by amiloride (Figure 2). Fibers that are inhibited by amiloride are narrowly tuned to NaCl (i.e., N fibers), while amiloride-insensitive fibers are broadly tuned to several salts as well as acids (i.e., H fibers; for a recent review, see Spector, A. C. and Travers, S. P., 2005).

4.10.2.1.2 ENaC – the amiloride-sensitive salt taste receptor

The epithelial Na^+ channel ENaC is now believed to be the Na^+-specific, amiloride-sensitive salt taste receptor. ENaC was first cloned from colon epithelium, but is expressed widely in many Na^+-transporting epithelial tissues (for review, see Garty, H. and Palmer, L. G., 1997). The functional channel is composed of three homologous subunits, α, β, and γ. Expression studies in heterologous cells suggest that all three subunits are required for normal function (Canessa, C. M. *et al.*, 1994). In taste cells,

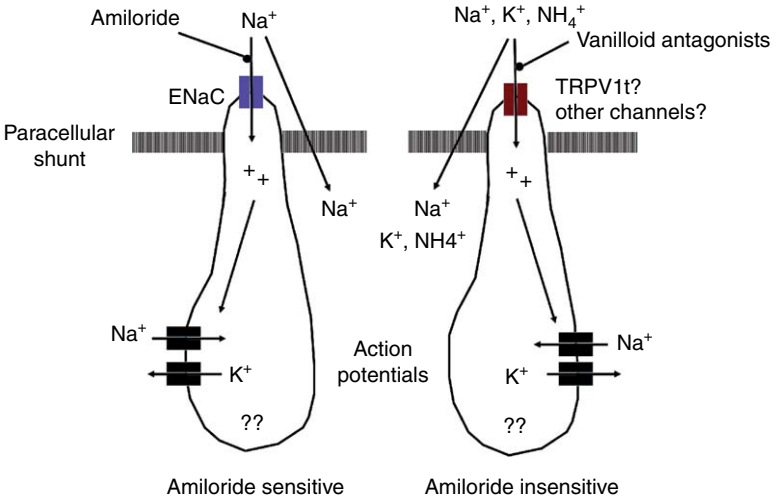

Figure 2 Salt transduction. The epithelial Na^+ channel ENaC is the amiloride-sensitive, Na^+ specific salt taste receptor. Other apical channels, including a variant of the capsaicin receptor TRPV1, mediate the amiloride-insensitive salt response, which is non-selective for cations. These mechanisms appear to be expressed in different populations of taste cells, but in neither case is it clear which taste cell type (II or III) mediates the response.

molecular and immunocytochemical studies indicate that α-, β-, and γ-ENaC are expressed in a large fraction of rat taste cells in all papilla. However, the density of expression of β- and γ-ENaC is significantly lower in foliate and circumvallate taste cells compared to fungiform taste cells (Kretz, O. *et al.*, 1999; Lin, W. *et al.*, 1999). This differential expression is consistent with the presence of functional amiloride-sensitive Na^+ currents in fungiform, but not in vallate or foliate taste cells (Doolin, R. E. and Gilbertson, T. A., 1996). ENaC in taste cells shares electrophysiological and pharmacological properties with ENaC in other tissues, including a high sensitivity to amiloride, high selectivity for Na^+ over K^+, significant permeability to protons, and self-inhibition by extracellular Na^+ (Gilbertson, T. A. *et al.*, 1993; Doolin, R. E. and Gilbertson, T. A., 1996; Gilbertson, T. A. and Zhang, H., 1998). Further, the same hormones that regulate Na^+ transport in epithelial cells regulate ENaC expression in taste cells. Both aldosterone and vasopressin increase the number of functional channels in the apical membrane (Herness, M. S., 1992; Gilbertson, T. A. *et al.*, 1993; Lin, W. *et al.*, 1999), while atrial natriuretic peptide (ANP) and oxytocin decrease them (Lindemann, B. *et al.*, 1999). Vasopressin acts via the V_2 receptor to increase the density of existing channels, probably via cAMP-dependent phosphorylation, while aldosterone likely acts to increase transcription of the channel, as it does in other tissues. Interestingly, aldosterone treatment of rats causes upregulation of both β- and γ-ENaC in taste cells, resulting in a larger density of amiloride-sensitive currents in fungiform taste cells. In vallate and foliate taste cells, which are normally unresponsive to amiloride, aldosterone treatment induces a small amiloride-sensitive Na^+ current in about half of the taste cells (Lin, W. *et al.*, 1999).

4.10.2.1.3 Amiloride-insensitive mechanisms

In contrast to the amiloride-sensitive mechanism, much less is known about the basis of amiloride-insensitive salt mechanisms, and multiple mechanisms are likely to contribute. The amiloride-insensitive mechanism was originally believed to be solely a consequence of the paracellular shunt pathway. Na^+ and other monovalent cations penetrate the tight junctions and come into contract with the basolateral membrane of taste cells. However, amiloride is impermeable and therefore inaccessible to basolateral Na^+ channels. Although ENaC channels are restricted to the apical membrane in most transporting epithelia, some studies have suggested basolateral amiloride-sensitive Na^+ channels are present in taste cells. Ussing chamber studies in rat showed that amiloride inhibited a Na^+ current in the basolateral regions of taste epithelia, but these channels were less sensitive to amiloride than were apical channels ($K_i = 52\,\mu M$ compared to $0.2\,\mu M$), and less highly selective for Na^+ (Mierson, S. *et al.*, 1996). Whether this mechanism contributes significantly to the amiloride-insensitive Na^+ response is not clear. The concentration of Na^+ in the extracellular space near taste cells is at least 140 mM, and it is difficult to conceive how salt taste stimuli could achieve sufficient concentrations in the paracellular space to create a driving force for Na^+ to enter the cells.

Recent studies suggest that, in addition to the paracellular pathway, apical nonselective cation channels may contribute to the amiloride-insensitive mechanism. Evidence for apical nonselective cation channels was first obtained from whole cell recordings in polarized mouse taste cells, where apical NaCl stimulation was shown to elicit both amiloride-sensitive and amiloride-insensitive inward currents (Miyamoto, T. *et al.*, 2001). Further evidence for apical nonselective cation channels was obtained by the use of a novel pharmacological probe, cetylpyridinium chloride (CPC). When applied to the rat tongue, CPC selectively modulates the amiloride-insensitive component of the chorda tympani response to NaCl as well as responses to KCl and NH_4Cl, suggesting that the conductance may be a nonselective cation channel (Lyall, V. *et al.*, 2001). CPC is chemically related to the vanilloid family of modulators, which suggested that the channel may be related to the vanilloid family of TRP channels, the TRPVs. Indeed, a variant of TRPV1, called TRPV1t, is expressed in fungiform taste receptor cells (Lyall, V. *et al.*, 2004b). Several lines of evidence suggested a role of TRPV1t in the amiloride-insensitive salt response. First, other vanilloid modulators, including resiniferatoxin and capsaicin, selectively modulate the amiloride-insensitive chorda tympani response, and the response is temperature-sensitive, as is characteristic of TRPV channels. Further, blockers of TRPV1, including capsazepine and SB-366791, inhibit the amiloride-insensitive response. Finally, TRPV1 knockout mice appear to be lack the amiloride-insensitive chorda tympani response to NaCl (Lyall, V. *et al.*, 2004b). However, a more detailed analysis of chorda tympani responses in the knockout mice revealed that although the tonic portion of the

amiloride-insensitive salt response is missing, some phasic response remains in the knockout (Treesukosol, Y. *et al.*, 2007). Further, behavioral studies revealed nearly identical detection thresholds for NaCl in knockout and wild-type mice, even in the presence of amiloride (Ruiz, C. *et al.*, 2006; Treesukosol, Y. *et al.*, 2007). Two bottle preference tests showed that TRPV1 knockout mice prefer NaCl at concentrations normally avoided by wild-type mice, suggesting that TRPV1t may play a role in the avoidance of high concentrations of salt (Ruiz, C. *et al.*, 2006), but this must be confirmed with brief access tests to rule out post ingestive effects. What these behavioral data imply is that additional mechanisms must contribute to the amiloride-insensitive salt response. Further studies are needed, particularly on circumvallate and foliate taste buds, where the amiloride-insensitive response predominates.

4.10.2.2 Sour Taste

Acidic stimuli elicit sour taste, a naturally aversive taste quality that likely evolved to prevent ingestion of strong acids, spoiled foods, and unripe fruit. As is the case with salt transduction, sour taste transduction mechanisms likely involve both apical and paracellular pathways, and mechanisms vary considerably in different species. Generally, however, weak organic acids produce larger nerve responses and taste more sour than strong highly dissociated acids at equivalent pH (for recent review, see DeSimone, J. A. and Lyall, V., 2006). Thus, extracellular protons are unlikely to be the effective stimulus in sour transduction.

4.10.2.2.1 Intracellular versus extracellular pH as a stimulus

A preponderance of data suggests that intracellular pH (pH_i), is the proximate stimulus mediating sour taste transduction. Similar concentrations of buffered and unbuffered acids produce equivalent chorda tympani nerve responses and equivalent decreases in pH_i, even though their pH_o levels are vastly different. Direct evidence for the role of intracellular pH in sour transduction was obtained recently by exposing the rat tongue to nigericin, a K^+-H^+ exchanger that equilibrates pH_i with pH_o when high extracellular K^+ is present. Under these conditions, intracellular pH can be controlled rather precisely simply by varying the pH of extracellular solution. In the presence of nigericin and K^+, the threshold for eliciting a chorda tympani response decreases from pH 4.5 to pH 6.5 (Lyall, V. *et al.*, 2007). It is proposed that neutral acids, such as citric or acetic acid readily permeate the plasma membrane of taste cells in their undissociated form. Once inside the cell they dissociate, resulting in a decreased pH_i (Lyall, V. *et al.*, 2001). CO_2 also readily crosses the membrane, where it is converted intracellularly to H_2CO_3 by carbonic anhydrase. Strong acids also decrease intracellular pH, likely by permeation of proton channels, but lower pH values are required for equivalent effects. In addition to proton permeable channels, several proton-modulated ion channels are expressed in taste cells and these may also contribute to sour transduction, by depolarizing taste cells and activating voltage-gated Ca^{2+} channels. The identity of channels proposed to be involved in sour taste is summarized below.

4.10.2.2.2 Proton-permeable ion channels

In mice and rats, evidence exists for two types of apical proton channels. The chorda tympani response to HCl, but not to weak acids or CO_2, is decreased by several proton channel blockers, including Zn^{2+}, Cd^{2+} and diethylpolycarbonate (DEPC; DeSimone, J. A. *et al.*, 2007). The pharmacology of the response suggests that the proton influx may occur via the NADPH oxidase-linked proton channel, $gp91^{phox}$. This hypothesis was recently tested with $gp91^{phox}$ knockout mice, in which approximately 60% of the chorda tympani response to HCl was diminished. The remaining response was insensitive to specific modulators of $gp91^{phox}$, but was enhanced by membrane permeant analogs of cAMP (Lyall, V. *et al.*, 2002; DeSimone, J. A. *et al.*, 2007). The identity of the cAMP-modulated proton channel is not known.

The epithelial Na channel ENaC is also permeable to H^+ in the absence of extracellular Na^+. In hamsters, where salivary Na^+ is very low, ENaC appears to contribute to sour transduction (Gilbertson, T. A. *et al.*, 1992; 1993; Gilbertson, D. M. and Gilbertson, T. A., 1994). However, amiloride has no effect on acid responses in mice (Miyamoto, T. *et al.*, 2000; Richter, T. A. *et al.*, 2003) or rats (DeSimone, J. A. *et al.*, 1995), suggesting that this mechanism may be unique to hamsters.

4.10.2.2.3 Proton-gated ion channels

A number of proton-gated cation channels are expressed in taste cells and several have been suggested to serve as sour receptors or modulators. However, none is known definitively to contribute to sour transduction *in vivo*. Acid-sensing ion channels (ASICs), which are proton-gated cation channels that mediate pain perception accompanying tissue acidosis

(Waldmann, R. *et al.*, 1999), have been proposed as sour receptors. ASIC2a and 2b are co-expressed in many rat taste cells (Ugawa, S. *et al.*, 1998; 2003), and when heterologously expressed, the channels mediate a transient, amiloride-sensitive inward current in response to a decrease in extracellular pH. In a subset of isolated rat taste cells, pH 4.5 similarly elicits a transient inward current that is partially sensitive to high concentrations of amiloride (Lin, W. *et al.*, 2002). However, ASIC2 knockout mice have normal behavioral and electrophysiological responses to low pH, suggesting that the acid-gated inward current is likely mediated by a different mechanism, at least in mice (Kinnamon, S. C. *et al.*, 2000; Richter, T. A. *et al.*, 2004b). Again, species differences may be involved here, since much less ASIC2 mRNA is present in mouse taste cells compared to those of rat (Richter, T. A. *et al.*, 2004b).

The hyperpolarization-activated channels HCN1 and HCN4 are expressed in a subset of rat taste cells. These channels were suggested to serve as sour receptors, because, when expressed in heterologous cells, they are activated by low external pH (Stevens, D. R. *et al.*, 2001). However, Cs^+, a specific blocker of HCN channels, has no effect on acid-induced Ca^{2+} responses in mouse taste cells (Richter, T. A. *et al.*, 2003), suggesting that HCN channels may play other roles in the taste bud.

In polarized mouse taste cells, apically applied citric acid elicits an inward current that is sensitive to NPPB, a Cl^- channel blocker (Miyamoto, T. *et al.*, 1998). These data suggest that an acid-gated Cl^- channel may be involved in sour transduction. Two acid-sensitive Cl^- channels have been identified in taste cells, CIC-4 and its splice variant, CIC-4A (Huang, L. *et al.*, 2005). Whether either of these channels is directly involved in acid detection remains to be determined.

4.10.2.2.4 Proton-blocked K^+ channels

Most K^+ channels are inhibited by a decrease in pH_o. K^+ channel block could conceivably contribute to acid-induced depolarization, if the K^+ channels were localized to the apical membrane and conductive at the resting potential. In mudpuppy, voltage-gated K^+ channels are restricted to the apical membrane, where they are blocked directly by protons to depolarize the membrane (Kinnamon, S. C. *et al.*, 1988; Roper, S. D. and McBride, D. W., Jr., 1989). However, in mammals, several studies have indicated that K^+ channels appear to be absent from the apical membrane, at least in fungiform taste cells (Miyamoto, T. *et al.*, 1996; Furue, H. and Yoshii, K., 1997; Miyamoto, T. *et al.*, 1998). Thus, this mechanism is unlikely to contribute to sour transduction in mammals. Basolateral K^+ channels could contribute to sour transduction, if they are inhibited by a decrease in intracellular pH. Several members of the two-pore domain K^+ channels (K_{2P} or KCNK) are expressed in rat taste cells, including TWIK 1, TASK 1-2, TREK 1-2, and TRAAK 1 (Lin, W. *et al.*, 2004; Richter, T. A. *et al.*, 2004a). Some of these channels can be modulated by intracellular acidification, however whether they are located in the taste cells that communicate sour information to the nervous system is unknown.

4.10.2.2.5 PKD1L3 and PKD2L1

Recently, two members of the TRPP family of transient receptor potential (TRP) channels, PKD1L3 and PKD2L1, were identified in taste cells by expression screening. These channels are expressed in a specific subset of taste cells, distinct from the type II taste cells involved in bitter, sweet, and umami transduction (Huang, A. L. *et al.*, 2006; Ishimaru, Y. *et al.*, 2006; LopezJimenez, N. D. *et al.*, 2006). When coexpressed in heterologous cells, PKD2L1 and PKD1L3 respond to low pH_o with an increase in intracellular Ca^{2+}. The increase in intracellular Ca^{2+} occurs with a delay, suggesting that intracellular, rather than extracellular pH may be mediating the effect (Ishimaru, Y. *et al.*, 2006). Recent immunocytochemical studies using antibodies directed against PKD2L1 show that although the channel is located in the apical third of the taste bud, most channels appear to be located basolateral to the tight junctions, where they would be more likely to respond to changes in intracellular pH. Further, the channel is expressed exclusively in the type III taste cells, those cells that express voltage-gated Ca^{2+} channels (Kataoka, S. *et al.*, 2007). These data agree well with Richter T. A. *et al.* (2003), who show that apically applied acids elicit a decrease in intracellular pH in most taste cells, but only those taste cells with voltage-gated Ca^{2+} channels show a concomitant increase in intracellular Ca^{2+} (Richter, T. A. *et al.*, 2003). These data suggest that the taste cells with voltage-gated Ca^{2+} channels are the cells that communicate sour taste information to the nervous system.

Further evidence for a role of PKD channels in sour taste came from molecular studies of the Zuker laboratory. Targeted expression of diphtheria toxin (DTA) was used to ablate those taste cells which expressed PKD2L1. These mice completely lack chorda tympani responses to all acids, both weak and strong, but have normal responses to other taste

stimuli (Huang, A. L. *et al.*, 2006). These data suggest that the same taste cells transduce both strong and weak acids, and that the sour transducing taste cells are likely to be a unique subset of taste cells. However, PKD channel knockouts will be needed to determine if any of the PKD proteins are involved in sour transduction (Figure 3).

4.10.2.2.6 Downstream signaling effectors in sour taste

The DeSimone laboratory has combined single cell imaging with chorda tympani nerve recording to investigate sour transduction downstream of the decrease in intracellular pH (for review, DeSimone, J. A. and Lyall, V., 2006). They have found that the phasic part of the chorda tympani response to both strong and weak acids is mediated by different mechanisms than is the tonic portion of the response. The phasic part of the response is associated with a rapid, pH_i-mediated decrease in taste cell volume, caused by a change in the equilibrium between F-actin and G-actin. This in turn activates a flufenamic acid-sensitive shrinkage-activated cation channel on the basolateral membrane. Blocking either the conversion of F-actin to G-actin, or the cation channel completely suppresses the phasic portion of the chorda tympani, with no effect on the tonic portion of the response (Lyall, V. *et al.*, 2006). In contrast, the tonic portion of the response appears to be Ca^{2+}-dependent. It is likely that the decrease in pH_i activates a cation channel, possibly PKD2L1, which results in membrane depolarization and activation of voltage-gated Ca^{2+} channels, mediating transmitter release. The increase in intracellular Ca^{2+} not only mediates the tonic part of the chorda tympani response to acids but also causes adaptation to acids, by activating a basolateral Na^+-H^+ exchanger, NHE1 (Lyall, V. *et al.*, 2004a; Vinnikova, A. K. *et al.*, 2004). This exchanger likely attenuates the decrease in pH_i, which would cause adaptation of the inward induced by acid stimulation. Indeed, acid stimulation induces a rapidly adapting current in taste cells (Lin, W. *et al.*, 2002), but further studies will be required to determine if the adaptation phase is dependent on NHE1.

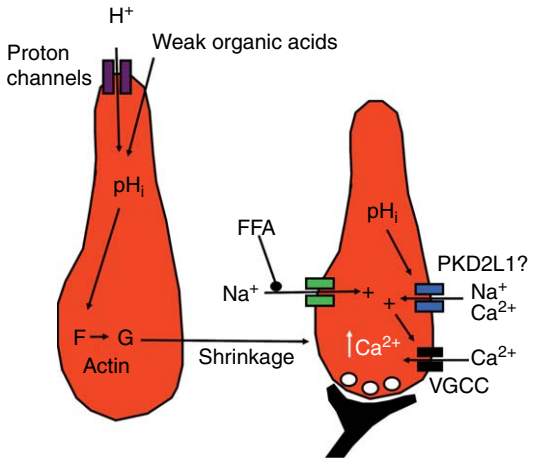

Figure 3 Sour transduction. Proton channels mediate the response to strong acids, while weak organic acids permeate the cell membrane in the undissociated state. Both mechanisms are present in the same taste cells, and both lead to decreases in intracellular pH, which is the proximate stimulus for sour transduction. The decrease in pHi leads to a change in the equilibrium between F and G actin, causing the taste cell to shrink in volume. The shrinkage activates a flufenamic-sensitive cation channel, which elicits the phasic portion of the afferent nerve response. The tonic portion of the nerve response is also mediated by the decrease in pHi, which activates a proton-gated non-selective cation channel, possibly PKD2L1. This causes membrane depolarization and activation of voltage-gated Ca^{2+} channels, presumably in Type III taste cells, since these are the only taste cells that express voltage gated Ca^{2+} channels.

4.10.2.3 Transduction Mechanisms Common to Bitter, Sweet, and Umami Taste Qualities

Although different GPCRs have been shown to underlie the initial detection of bitter, sweet and umami tastants (see Chapter Taste Receptors), there are several transduction elements that are common to pathways underlying all three taste qualities. As is typical of signaling pathways in sensory and nonsensory systems, specific GPCRs couple through their associated G proteins to initiate signaling cascades involving effector enzymes, second messengers and second messenger-activated/inhibited ion channels and other end targets.

4.10.2.3.1 G proteins

The first taste signaling element identified was α-gustducin, an α-transducin-like G protein α-subunit selectively expressed in ~25% of taste cells, specifically of type II (McLaughlin, S. K. *et al.*, 1992; Boughter, J. D., Jr. *et al.*, 1997). In *in vitro* assays gustducin heterotrimers couple to isolated native bitter receptors (Ruiz-Avila, L. *et al.*, 2000) and heterologously expressed bitter-responsive T2R receptors (Chandrashekar, J. *et al.*, 2000). Heterotrimers containing α-gustducin chimeras

capable of promoting calcium mobilization (to monitor receptor activity) also couple to heterologously expressed sweet-responsive T1R2 + T1R3 receptors and umami-responsive T1R1 + T1R3 receptors (Nelson, G. *et al.*, 2001; Li, X. *et al.*, 2002; Nelson, G. *et al.*, 2002). Studies of α-gustducin knockout mice have demonstrated gustducin's key role *in vivo* in bitter, sweet and umami taste transduction (Wong, G. T. *et al.*, 1996; Ming, D. *et al.*, 1998; Ruiz-Avila, L. *et al.*, 2001; Ruiz, C. J. *et al.*, 2003; Glendinning, J. I. *et al.*, 2005; Danilova, V. *et al.*, 2006). That α-gustducin knockout mice have markedly reduced, but not entirely absent, behavioral and nerve responses to the bitter, sweet and umami compounds suggests that other taste cell-expressed G proteins may couple to these GPCRs normally or in the absence of gustducin. Consistent with this inference is the observation that transgenic expression of a dominant-negative version of α-gustducin in the α-gustducin knockout background further diminished taste responses to bitter and sweet (Ruiz-Avila, L. *et al.*, 2001).

In addition to α-gustducin the following G α-subunits are known to be expressed in taste cells: Gαs, Gαq, Gα14, Gα15, Gαi2, Gαi3, α-transducin (McLaughlin, S. K. *et al.*, 1992; Ruiz-Avila, L. *et al.*, 1995; Boughter, J. D., Jr. *et al.*, 1997; Kusakabe, Y. *et al.*, 1998). Heterologously expressed mT2R5 selectively coupled to α-gustducin over the other G proteins examined (αi, αs, αo, or αq) (Chandrashekar, J. *et al.*, 2000). Although α-transducin knockouts had no effect on taste responses, double knockouts lacking α-transducin and α-gustducin showed that α-transducin is involved in umami taste, but not in bitter or sweet (He, W. *et al.*, 2004).

Upon activation, heterotrimeric G proteins such as gustducin dissociate into α and $\beta\gamma$ components, each capable of carrying a signal to one or more downstream effectors. Gβ1, Gβ3, and Gγ13 are expressed with α-gustducin and Gαi2 in type II taste cells (Huang, L. *et al.*, 1999; Clapp, T. R. *et al.*, 2001). α-Gustducin expressing taste cells are a subset of those which express Gγ13 and Gαi2 (Huang, L. *et al.*, 1999; Adler, E. *et al.*, 2000; Matsunami, H. *et al.*, 2000; Clapp, T. R. *et al.*, 2001). The T2R bitter receptors are only expressed in a subset of gustducin-positive type II taste cells (Adler, E. *et al.*, 2000; Matsunami, H. *et al.*, 2000; Kim, M. R. *et al.*, 2003) and likely couple preferentially to gustducin over any other G proteins in those same taste cells. Marked regional differences in coexpression of gustducin and taste receptors have been noted: in posterior fields (i.e., circumvallate papillae) gustducin was typically found along with T2Rs, while in anterior fields (fungiform papillae and palatal taste buds) gustducin is more often seen coexpressed with T1Rs (Huang, L. *et al.*, 1999; Adler, E. *et al.*, 2000; Matsunami, H. *et al.*, 2000; Clapp, T. R. *et al.*, 2001; Stone, L. M. *et al.*, 2007). This pattern is consistent with gustducin's involvement in responses to bitter, sweet, and umami taste stimuli.

4.10.2.3.2 Effector enzymes

Phospholipase β2 (PLCβ2), phospholipase A2, cNMP phosphodiesterase (PDE), and adenylyl cyclase (AC) type 8 have been identified in type II taste cells as candidate effector enzymes to mediate G protein-dependent taste responses (Ruiz-Avila, L. *et al.*, 1995; Rossler, P. *et al.*, 1998; Oike, H. *et al.*, 2006a; Trubey, K. R. *et al.*, 2006). α-Gustducin and α-transducin activate retinal and taste PDEs (Ruiz-Avila, L. *et al.*, 1995), whereas gustducin's $\beta\gamma$ complex activates taste PLCβ2 (Huang, L. *et al.*, 1999; Matsunami, H. *et al.*, 2000; Yan, W. *et al.*, 2001). In *in vitro* assays antibodies against α-gustducin, but not those against gustducin's β subunits, blocked stimulation of taste tissue PDE activity by native bitter taste receptors (Yan, W. *et al.*, 2001). Conversely, antibodies against Gβ3 or Gγ13 blocked the IP_3 response of taste tissue receptors to bitters, but had no effect on cNMP levels (Huang, L. *et al.*, 1999; Yan, W. *et al.*, 2001). Thus, heterotrimeric gustducin interacts with two different effectors to effect two responses in taste cells: 1. hydrolysis of cNMPs via α-subunit activation of PDE, and 2. generation of IP_3 and DAG via $\beta\gamma$ activation of PLCβ2. The subsequent steps in the PLCβ2 pathway are activation of IP_3 receptors (type III IP_3 receptors are selectively expressed in the same type II taste cells that express PLCβ2 (Clapp, T. R. *et al.*, 2001) and release of Ca^{2+} from internal stores followed by activation of the calcium-activated cation channel Trpm5 (see below). Arachidonic acid generated by taste cell-expressed phospholipase A2 (Oike, H. *et al.*, 2006a) may activate Trpm5 (Oike, H. *et al.*, 2006b). The subsequent steps in the cNMP pathway are presently unclear: decreased cNMPs may act on protein kinases which in turn may regulate taste cell ion channel activity, or cNMP levels may regulate directly the activity of cNMP-gated and cNMP-inhibited ion channels expressed in taste cells (Kolesnikov, S. S. and Margolskee, R. F., 1995; Misaka, T. *et al.*, 1997; 1998; 1999).

Both PLCβ2 and AC have been implicated in sweet taste transduction (reviewed in (Kinnamon, S.

C. and Margolskee, R. F., 1996; Lindemann, B., 1996; Herness, M. S. and Gilbertson, T. A., 1999). In both biochemical and physiological studies taste responses to sugars differ from those to artificial sweeteners. In biochemical studies with taste tissue, sucrose elicits an elevation of cAMP, while certain artificial sweeteners lead to the generation of IP_3 (reviewed in Kinnamon, S. C. and Margolskee, R. F., 1996; Lindemann, B., 1996; Herness, M. S. and Gilbertson, T. A., 1999). In physiological studies with rat taste cells, sucrose led to Ca^{2+} influx, while the artificial sweeteners saccharin and SC45647 elevated Ca^{2+} via release from internal stores (Bernhardt, S. J. *et al.*, 1996). Although a single heterodimeric sweet receptor (T1R2 + T1R3) mediates responses to both natural and artificial sweeteners (see Chapter Taste Receptors), it appears that activation by different types of sweet compounds elicits differential activation of downstream effectors, presumably by promoting activation of one or another G protein coupled to the sweet receptor.

4.10.2.3.3 PLCβ2 knockout mice

PLCβ2 knockout mice were reported to lack all nerve and behavioral responses to bitter, sweet and umami compounds (Zhang, Y. *et al.*, 2003; Damak, S. *et al.*, 2006). In a subsequent behavioral study it was shown that these knockout mice displayed aversive responses to high concentrations of the bitter compounds quinine and denatonium (Dotson, C. D. *et al.*, 2005). Although the PLCβ2 knockout mice showed no appetitive lick responses to sucrose at even the highest concentrations, their aversive responses to high concentrations of bitters were shifted to about a tenfold higher threshold (Dotson, C. D. *et al.*, 2005). This indicates that at least for bitters there are PLCβ2-independent mechanisms that come to bear at high concentrations.

4.10.2.3.4 Target channels

Trpm5 is a transient receptor potential ion channel subtype that is selectively expressed in type II taste cells along with α-gustducin, Gγ13 and PLCβ2 (Clapp, T. R. *et al.*, 2001; Perez, C. A. *et al.*, 2002). Trpm5 is cation selective and in heterologous expression systems can be activated by IP_3 or intracellular Ca^{2+} (Hofmann, T. *et al.*, 2003; Liu, D. and Liman, E. R., 2003; Prawitt, D. *et al.*, 2003) or arachidonic acid (Oike, H. *et al.*, 2006b). Recent studies with caged IP_3 and caged Ca^{2+} show that native Trpm5 in excised taste cell patches is gated directly by Ca^{2+} (Zhang, Y. *et al.*, 2007). Similarly to PLCβ2 knockout mice, Trpm5 knockout mice have pronounced deficits in their nerve and behavioral responses to bitter, sweet and umami compounds (Zhang, Y. *et al.*, 2003; Damak, S. *et al.*, 2006). However, Trpm5-independent transduction mechanisms contributing to bitter, sweet and umami were revealed by the reduced but not absent nerve and behavioral responses observed with Trpm5 knockout mice (Damak, S. *et al.*, 2006; Figure 4). It was noted that the effects of knocking

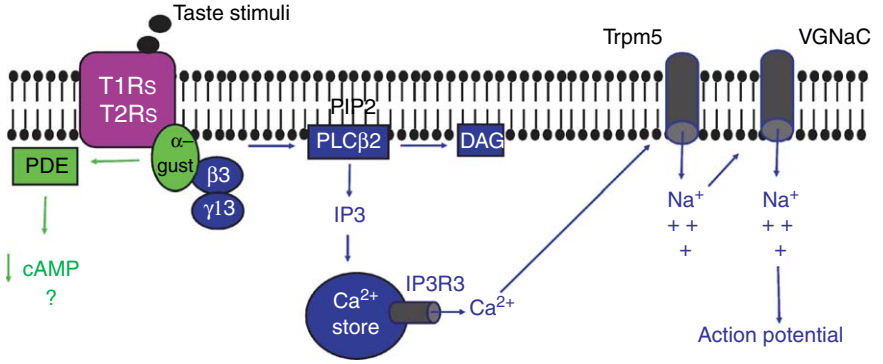

Figure 4 Transduction of bitter, sweet, and umami taste stimuli. Although different receptors are involved (T2Rs for bitter and T1Rs for sweet and umami stimuli), all utilize similar downstream signaling effectors in Type II taste cells. Receptor binding leads to activation of a heterotrimeric G protein, gustducin. The α subunit activates phosphodiesterase (PDE) to decrease intracellular cAMP, while the $\beta\gamma$ partners stimulate phospholipase Cβ2 (PLCβ2) to produce the second messengers IP3 and diacylglycerol (DAG). The IP3 binds to the Type III IP3 receptor (IP3R3), causing release of Ca^{2+} from intracellular stores and subsequent Ca^{2+}-dependent activation of a monovalent cation channel, TRPM5. This causes membrane depolarization, activation of voltage-gated Na^+ channels (VGNaC), and action potentials, which are believed to be required for transmitter release. Knockout of PLCβ2, TRPM5, or α-gustducin compromises responses to bitter, sweet, and umami taste stimuli. The role of the decrease in intracellular cAMP is not known, but it may regulate phosphorylation of downstream signaling effectors or target cyclic nucleotide modulated ion channels.

out Trpm5 varied with the taste field and type of taste quality examined: with bitter compounds, glossopharyngeal nerve responses were greatly diminished while chorda tympani nerve responses were normal; with umami compounds, glossopharyngeal nerve responses were intact while chorda tympani responses were greatly diminished. That target channels in addition to Trpm5 may exist in taste cells comes from the detection of another Ca^{2+}-activated cation conductance in excised taste cell patches from Trpm5 knockout mice (Zhang, Y. *et al.*, 2007). Thus Trpm5 is the primary target channel for the taste cell phosphoinositide signaling pathway: activation of PLCβ2 by Gγ13 would generate IP_3 to activate IP_3RIII, released intracellular Ca^{2+} would activate Trpm5 leading to cation influx and taste cell depolarization. In addition there may be other targets of this pathway as well as other target channels in other pathways.

4.10.2.4 Transduction Elements Specific to Particular Taste Qualities

Although several elements are common to the transduction of bitter, sweet, and umami taste qualities, the only transduction element, aside from the receptors themselves, that is involved in one but not all three taste qualities is α-transducin. As noted above, α-transducin knockouts had a specific effect on umami responses, however, this was only revealed in the α-gustducin knockout background – single knockouts lacking only α-transducin had no effect on bitter sweet or umami (He, W. *et al.*, 2004). That the closely related G protein α-subunits, α-transducin and α-gustducin are not interchangeable in taste signaling comes from studies in which α-transducin was added back as a transgene in α-gustducin knockout mice (He, W. *et al.*, 2002).

That umami transduction might employ unique transduction elements not in common with those of the other GPCR-dependent taste qualities might stem from the multiplicity of receptors and channels implicated in umami. As is further discussed in Chapter Taste Receptors both GPCRs and ion channels have been implicated as umami receptors. Amongst the GPCRs implicated in umami responses are ionotropic glutamate receptors (Lin, W. and Kinnamon, S. C., 1999; Caicedo, A. *et al.*, 2000b), metabotropic glutamate receptors (mGluRs) (Monastyrskaia, K. *et al.*, 1999; Chaudhari, N. *et al.*, 2000), and the heterodimer of T1R1 and T1R3 (Nelson, G. *et al.*, 2001; Li, X. *et al.*, 2002).

4.10.3 Other Transduction Mechanisms

4.10.3.1 Fat Taste

Preference for fatty foods is ubiquitous among mammals. This is not surprising, since lipids represent a significant source of energy and have appealing orosensory qualities (for recent review, see Laugerette, F. *et al.*, 2007). However, whether fat is actually detected as a taste stimulus has been controversial. If fat is detected as a taste stimulus, long chain fatty acids appear to mediate the effect. Rodents prefer long chain fatty acids to either triglycerides or medium-chain fatty acids in preference assays (Fukuwatari, T. *et al.*, 1997) and conditioned taste aversion tests show that rats can specifically detect long chain fatty acids (McCormack, D. N. *et al.*, 2006). Long chain fatty acids are produced from triglycerides by the action of lingual lipase, an enzyme that has been identified in the secretion of von Ebner's glands, which bathe the circumvallate taste buds. In mice, inhibition of this enzyme reduced preference for triglycerides, but not for free fatty acids (Kawai, T. and Fushiki, T., 2003).

4.10.3.1.1 Fatty acid modulation of taste cells

The first evidence for a direct effect of fatty acids was obtained from whole-cell recordings showing fatty acids block delayed rectifier K^+ channels in rat taste cells (Gilbertson, T. A. *et al.*, 1997). These channels are blocked directly by long chain polyunsaturated fatty acids in fungiform taste buds, and by monounsaturated fatty acids in vallate and foliate taste buds. The fatty acid inhibition of K^+ channels depolarizes taste cells and is hypothesized to modulate sensitivity to conventional taste stimuli. In support of this model, low concentrations of linoleic acid augmented preference for subthreshold concentrations of saccharin in two bottle preference tests (Gilbertson, T. A. *et al.*, 2005). Further, licking rates of rats to suprathreshold concentrations of prototypical sweet, salty, sour, and bitter compounds were altered by addition of linoleic and oleic acids to the taste stimuli. Licking rates to sweet stimuli were augmented by the fatty acids, while licking rates to bitter, sour, and salty stimuli were decreased (Pittman, D. W. *et al.*, 2006). Similar psychophysical studies in humans, however, have failed to show a significant effect of fatty acids on either detection thresholds or intensity ratings of

taste stimuli (Mattes, R. D., 2007), suggesting fatty acid modulation of taste may be less important in humans.

4.10.3.1.2 Fatty acid taste receptors

Evidence was obtained recently for a fatty acid transporter that may serve as a specific taste receptor for fat (Fukuwatari, T. *et al.*, 1997; Laugerette, F. *et al.*, 2005). CD36, a lipid-binding protein, is expressed in the apical region of taste cells in both mice and rats. It is highly expressed in circumvallate papillae, but less so in foliate and fungiform papillae. The role of CD36 as a fatty acid transducer is supported by its predicted structure. The protein contains a large extracellular hydrophobic pocket and a C terminal sequence that associates with Src kinases, suggesting a role in intracellular signaling (Laugerette, F. *et al.*, 2005). More definitive evidence for its role in fat sensing came from studies in CD36 knockout mice. These mice lack preference for long chain fatty acids, but have normal preference for other taste stimuli. Further, these mice lack a lipid-induced cephalic phase response normally present in wild-type mice (Laugerette, F. *et al.*, 2005). These data provide the strongest evidence to date that fat may be the sixth primary taste. However, further work is necessary to determine how CD36 activation is converted into a taste signal, which taste cells detect fat, and how fat information is encoded in the nervous system with respect to other taste qualities. Also, it will be important to determine if CD36 is expressed in human taste cells, where it could serve as a substrate to modulate fat intake.

Some evidence also exists for GPCRs for fat. GPR 120 is a fatty acid receptor expressed in enteroendocrine cells of the colon. mRNA for GPR 120 was recently found in circumvallate taste buds, and immunocytochemistry showed intense labeling in the apical region of a subset of rat taste cells (Matsumura, S. *et al.*, 2007). Thus, its expression pattern is consistent with a potential role in fat sensing, but definitive evidence must await knockout of the gene.

4.10.3.2 Water Taste

Although water is not classically considered to have a taste, it is well established that gustatory nerve fibers respond to water applied to the tongue (for review, see Gilbertson, T. A. *et al.*, 2006). The mechanisms involved in the water response are only now beginning to be understood. Gilbertson T. A. (2002) showed that hypo-osmotic solutions lead to an increase in cell capacitance accompanied by activation of a Cl^- conductance. This conductance is similar physiologically and pharmacologically to the well studied swelling-activated Cl^- current observed in other cell types (Jentsch, T. J., 1996). Such a current likely plays a role in regulating taste cell volume in response to varying osmotic taste stimuli. Recently, the water-permeable ion channels involved in the hypo-osmotic swelling were identified (Watson, K. J. *et al.*, 2007). Several aquaporins (AQPs) are expressed in taste cells, including AQP1 and AQP2, which label predominately the basolateral membrane, and AQP5, which labels both apical and basolateral membranes. Whole-cell recording showed that a specific AQP inhibitor significantly reduces hypo-osmotic-induced Cl^- currents in taste cells, suggesting that AQPs are the source of the water influx. Further studies are needed to determine how this leads to the well-characterized water response in afferent nerve fibers.

4.10.4 Signaling to Afferent Nerve Fibers and Adjacent Taste Cells

Taste cells communicate sensory information to afferent nerve fibers as well as to adjacent cells within taste buds (for review, see Herness, S. *et al.*, 2005; Roper, S. D., 2006). Many transmitters have been proposed to contribute to chemical communication in the taste bud, including serotonin, adenosine triphosphate (ATP), glutamate, acetylcholine, norepinephrine, gamma-aminobutyric acid (GABA), and various peptides. Indeed, evidence exists for expression of each of these neuroactive compounds or their receptors in taste buds, but to date only two, ATP and serotonin, have met all the criteria required to be considered as a taste cell transmitter or modulator. By analogy to the nervous system, these criteria include: (1) presence in the presynaptic cell, (2) release upon stimulation, (3) activation of the postsynaptic cell, usually through specific receptors, and (4) mechanism for termination of transmitter action.

4.10.4.1 Adenosine Triphosphate as a Transmitter

ATP is now believed to be the primary transmitter that links taste cells to activation of gustatory afferent

fibers (Finger, T. E. *et al.*, 2005). The first clue that ATP might serve as a taste cell transmitter was the observation that the ionotropic purinergic receptors P2X2 and P2X3 are abundantly expressed on gustatory afferent terminals (Bo, X. *et al.*, 1999). Definitive evidence for a role of P2X2 and P2X3 was obtained from P2X2/P2X3 double knockout mice, which lack behavioral and afferent nerve responses to most taste stimuli (Finger, T. E. *et al.*, 2005). Further, taste stimuli evoke release of ATP from taste cells (Finger, T. E. *et al.*, 2005; Huang, L. *et al.*, 2007; Romanov, R. A. *et al.*, 2007), and the released ATP is likely degraded by NTPDase2, an ecto ATPase abundantly expressed on the membranes of type I (support) taste cells (Bartel, D. L. *et al.*, 2006). Thus, ATP appears to fit all the criteria required to serve as a transmitter in the taste bud. The released ATP also binds to G-protein-coupled P2Y receptors on taste cell membranes (Kataoka, S. *et al.*, 2004; Bystrova, M. F. *et al.*, 2006; Huang, L. *et al.*, 2007), suggesting that ATP may also serve as an autocrine or paracrine modulator in the taste bud. Recent studies using sensitive biosensor cells expressing purinergic receptors have shown that either taste stimuli (Huang, L. *et al.*, 2007) or membrane depolarization (Romanov, R. A. *et al.*, 2007) can evoke ATP release from single type II taste cells, likely via gap junction hemichannels composed of pannexin 1 or connexin 43. Release can be evoked in the absence of Ca^{2+} (Romanov, R. A. *et al.*, 2007), which may explain the curious observation that although type II taste cells generate action potentials, they lack voltage-gated Ca^{2+} channels and conventional synapses with the nervous system (Clapp, T. R. *et al.*, 2004; 2006; DeFazio, R. A. *et al.*, 2006).

4.10.4.2 Serotonin and Other Neuroactive Modulators

Serotonin (5-HT) was originally believed to be the primary taste cell transmitter, since it is widely expressed in taste buds of a variety of species from fish to mammals (Kim, D. J. and Roper, S. D., 1995). In nonmammalian vertebrates serotonin is expressed in Merkel-like basal cells, where it appears to serve as a paracrine modulator in the taste bud (Delay, R. J. *et al.*, 1997). In mammalian taste cells, it is expressed in a subpopulation of type III taste cells (Yee, C. L. *et al.*, 2001). Recent studies show that serotonin is released from single type III cells in response to membrane depolarization and from intact taste buds in response to bitter taste stimuli, presumably in response to ATP released from type II taste cells (Huang, L. *et al.*, 2007). Enzymes for serotonin biosynthesis (DeFazio, R. A. *et al.*, 2006; Ortiz-Alvarado, R. *et al.*, 2006; Seta, Y. *et al.*, 2007) and reuptake (Ren, Y. *et al.*, 1999) are expressed in taste buds, as well as specific serotonin receptors. Both 5-HT_{1A} and 5-HT_3 were amplified by RT-PCR from RNA extracts of taste buds (Kaya, N. *et al.*, 2004). Immunocytochemical labeling showed that 5-HT_{1A} is expressed on the membranes of nonserotonergic taste cells, where it likely mediates the effects of serotonin as a paracrine neuromodulator (Figure 5). 5-HT_{1A} receptor agonists modulate taste cells by inhibiting calcium-activated K^+ currents and voltage-dependent Na^+ currents, suggesting that serotonin affects the membrane excitability of taste cells (Herness, M. S. and Chen, Y., 1997; Herness, S. and Chen, Y., 2000). In contrast, taste cell membranes lack expression of 5-HT_3 receptors, suggesting it may be present on afferent nerve terminals (Kaya,

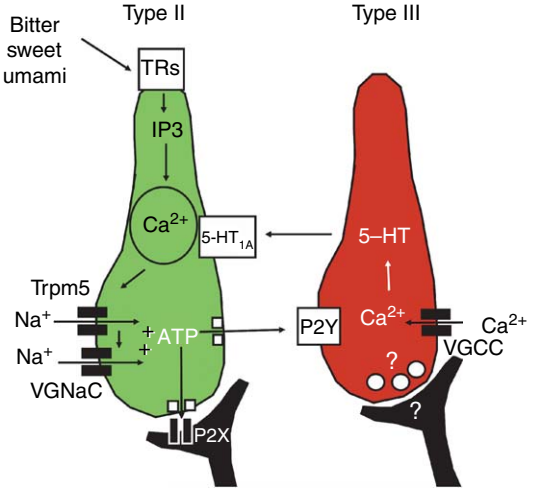

Figure 5 Proposed role of ATP and serotonin in afferent signaling. Bitter, sweet, and umami taste stimuli evoke ATP release from Type II taste cells. The ATP subsequently binds to the ionotropic purinergic receptors P2X2 and P2X3, which are abundantly expressed on afferent nerve fibers. Recent data suggest that the release of ATP is nonvesicular, involving voltage- and Ca^{2+}-gated gap junction hemichannels. ATP also binds to G protein-coupled purinergic receptors (P2Y) on the membranes of Type III taste cells, causing them to release serotonin (5-HT). The 5-HT likely binds to 5-HT_{1A} receptors on Type II taste cells, modulating their sensitivity to sweet and bitter taste stimuli. A major unanswered question is the identity and role of the transmitter at the prominent synapses between Type III taste cells and nerve fibers, but it is not believed to be 5-HT, because 5-HT3 knockout mice have normal behavioral responses to taste stimuli.

N. *et al.*, 2004). However, mice lacking 5-HT_3 receptors have normal behavioral responses to taste stimuli (Finger, T. E. *et al.*, 2005), indicating that serotonin is not likely to be involved in direct activation of afferent fibers. Recent behavioral data suggest a role of serotonin in modulation of taste thresholds in humans. Serotonin reuptake inhibitors, which increase the life time of serotonin in the synaptic cleft, enhance sensitivity to sweet and bitter taste stimuli in healthy adult human subjects (Heath, T. P. *et al.*, 2006). Further studies will be required to determine if 5-HT_{1A} receptors play a role in this modulation.

Norepinephrine (noradrenaline) and its receptors are expressed in subsets of taste cells, suggesting a role in cell-to-cell communication. α- and β-adrenoceptor agonists inhibit outward K^+ currents in taste cells, and multiple α- and β-adrenoceptors are expressed in lingual epithelium (Herness, S. *et al.*, 2002). However, which taste cell types are involved, and whether norepinephrine is an autocrine or paracrine modulator has not been determined. As is the case with serotonin, norepinephrine reuptake inhibitors enhance taste sensitivity in humans, suggesting a role for norepinephrine in modulating human taste thresholds (Heath, T. P. *et al.*, 2006).

Several neuropeptides are expressed in taste buds, including cholecystokinin (CCK), vasoactive intestinal peptide (VIP), and neuropeptide Y (NPY; Shen, T. *et al.*, 2005; Zhao, F. L. *et al.*, 2005). These peptides are all members of the brain-gastrointestinal tract family of peptides, which modulate feeding circuits in the brain. Thus, it is of interest that they are also expressed in taste receptor cells, the gateway to food intake. All three peptides are largely coexpressed with gustducin in circumvallate taste buds, suggesting that they are expressed primarily in bitter sensitive taste cells. Interestingly, NPY and CCK both modulate an inwardly rectifying K^+ current in taste cells, but in opposite directions – NPY enhances the current to hyperpolarize taste cells, while CCK inhibits it, resulting in taste cell depolarization.

4.10.4.3 Other Candidate Transmitters

While it is clear that ATP released from type II cells activates purinergic receptors on gustatory nerve fibers, the identity of the transmitter at the prominent synapse between type III taste cells and nerve fibers remains enigmatic. Investigators have failed to detect ATP release from type III taste cells (Huang, L. *et al.*, 2007; Romanov, R. A. *et al.*, 2007), and serotonin is unlikely to directly activate nerve fibers, as discussed above. These synapses are normally associated with clusters of clear vesicles (see Chapter Ultrastructure of Taste Buds), suggesting they may contain a conventional transmitter. Glutamate has long been proposed as a transmitter in taste buds, due to the expression of the glial glutamate transporter GLAST in type I taste cells (Lawton, D. M. *et al.*, 2000), and the expression of ionotropic glutamate receptors on the basolateral membranes of taste cells (Caicedo, A. *et al.*, 2000a). Another conventional transmitter candidate is acetylcholine, which modulates taste cells via muscarinic receptors (Ogura, T., 2002; Ogura, T. and Lin, W., 2005). However, the source of acetylcholine is still unclear. Recently, GAD67, involved in the synthesis of GABA, was shown to be expressed exclusively in type III cells (DeFazio, R. A. *et al.*, 2006), suggesting GABA may play a role at this synapse. Further studies are necessary to determine if type III taste cells release any of these potential transmitter candidates.

References

Adler, E., Hoon, M. A., Mueller, K. L., Chandrashekar, J., Ryba, N. J., and Zuker, C. S. 2000. A novel family of mammalian taste receptors. Cell 100, 693–702.

Avenet, P. And and Lindemann, B. 1991. Noninvasive recording of receptor cell action potentials and sustained currents from single taste buds maintained in the tongue: the response to mucosal NaCl and amiloride. J. Membr. Biol. 124, 33–41.

Bartel, D. L., Sullivan, S. L., Lavoie, E. G., Sevigny, J., and Finger, T. E. 2006. Nucleoside triphosphate diphosphohydrolase-2 is the ecto-ATPase of type I cells in taste buds. J. Comp. Neurol. 497, 1–12.

Behe, P., DeSimone, J. A., Avenet, P., and Lindemann, B. 1990. Membrane currents in taste cells of the rat fungiform papilla. Evidence for two types of Ca currents and inhibition of K currents by saccharin. J. Gen. Physiol. 96, 1061–1084.

Bernhardt, S. J., Naim, M., Zehavi, U., and Lindemann, B. 1996. Changes in IP3 and cytosolic Ca^{2+} in response to sugars and non-sugar sweeteners in transduction of sweet taste in the rat. J. Physiol. 490, 325–336.

Bo, X., Alavi, A., Xiang, Z., Oglesby, I., Ford, A., and Burnstock, G. 1999. Localization of ATP-gated P2X2 and P2X3 receptor immunoreactive nerves in rat taste buds. Neuroreport 10, 1107–1111.

Boudreau, J. C., Sivakumar, L., Do, L. T., White, T. D., Oravec, J., and Hoang, N. K. 1985. Neurophysiology of geniculate ganglion (facial nerve) taste systems: species comparisons. Chem. Senses 10, 89–127.

Boughter, J. D., Jr., Pumplin, D. W., Yu, C., Christy, R. C., and Smith, D. V. 1997. Differential expression of alpha-gustducin in taste bud populations of the rat and hamster. J. Neurosci. 17, 2852–2858.

Bystrova, M. F., Yatzenko, Y. E., Fedorov, I. V., Rogachevskaja, O. A., and Kolesnikov, S. S. 2006. P2Y isoforms operative in mouse taste cells. Cell Tissue Res. 323, 377–382.

Caicedo, A., Jafri, M. S., and Roper, S. D. 2000a. *In situ* Ca^{2+} imaging reveals neurotransmitter receptors for glutamate in taste receptor cells. J. Neurosci. 20, 7978–7985.

Caicedo, A., Kim, K. N., and Roper, S. D. 2000b. Glutamate-induced cobalt uptake reveals non-NMDA receptors in rat taste cells. J. Comp. Neurol. 417, 315–324.

Canessa, C. M., Schild, L., Buell, G., Thorens, B., Gautschi, I., Horisberger, J. D., and Rossier, B. C. 1994. Amiloride-sensitive epithelial Na^+ channel is made of three homologous subunits. Nature 367, 463–467.

Chaudhari, N., Landin, A. M., and Roper, S. D. 2000. A metabotropic glutamate receptor variant functions as a taste receptor. Nat. Neurosci. 3, 113–119.

Chandrashekar, J., Mueller, K. L., Hoon, M. A., Adler, E., Feng, L., Guo, W., Zuker, C. S., and Ryba, N. J. 2000. T2Rs function as bitter taste receptors. Cell 100, 703–711.

Chen, Y., Sun, X. D., and Herness, S. 1996. Characteristics of action potentials and their underlying outward currents in rat taste receptor cells. J. Neurophysiol. 75, 820–831.

Clapp, T. R., Medler, K. F., Damak, S., Margolskee, R. F., and Kinnamon, S. C. 2006. Mouse taste cells with G protein-coupled taste receptors lack voltage-gated calcium channels and SNAP-25. BMC Biol. 4, 7.

Clapp, T. R., Stone, L. M., Margolskee, R. F., and Kinnamon, S. C. 2001. Immunocytochemical evidence for co-expression of Type III IP3 receptor with signaling components of bitter taste transduction. BMC Neurosci. 2, 6.

Clapp, T. R., Yang, R., Stoick, C. L., Kinnamon, S. C., and Kinnamon, J. C. 2004. Morphologic characterization of rat taste receptor cells that express components of the phospholipase C signaling pathway. J. Comp. Neurol. 468, 311–321.

Cummings, T. A., Powell, J., and Kinnamon, S. C. 1993. Sweet taste transduction in hamster taste cells: evidence for the role of cyclic nucleotides. J. Neurophysiol. 70, 2326–2336.

Damak, S., Rong, M., Yasumatsu, K., Kokrashvili, Z., Perez, C. A., Shigemura, N., Yoshida, R., Mosinger, B., Jr., Glendinning, J. I., Ninomiya, Y., and Margolskee, R. F. 2006. Trpm5 null mice respond to bitter, sweet, and umami compounds. Chem. Senses 31, 253–264.

Danilova, V., Damak, S., Margolskee, R. F., and Hellekant, G. 2006. Taste responses to sweet stimuli in α-gustducin knockout and wild-type mice. Chem. Senses 31, 573–580.

DeFazio, R. A., Dvoryanchikov, G., Maruyama, Y., Kim, J. W., Pereira, E., Roper, S. D., and Chaudhari, N. 2006. Separate populations of receptor cells and presynaptic cells in mouse taste buds. J. Neurosci. 26, 3971–3980.

Delay, R. J., Kinnamon, S. C., and Roper, S. D. 1997. Serotonin modulates voltage-dependent calcium current in Necturus taste cells. J. Neurophysiol. 77, 2515–2524.

DeSimone, J. A. and Lyall, V. 2006. Taste receptors in the gastrointestinal tract III. Salty and sour taste: sensing of sodium and protons by the tongue. Am. J. Physiol. Gastrointest. Liver Physiol. 291, G1005–1010.

DeSimone, J. A., Callaham, E. M., and Heck, G. L. 1995. Chorda tympani taste response of rat to hydrochloric acid subject to voltage-clamped lingual receptive field. Am. J. Physiol. 268, C1295–1300.

DeSimone, J. A., Phan, T. H., Heck, G. L., Mummalaneni, S., Sturz, G. R., and Lyall, V. 2007. Proton flux through NADPH oxidase-linked H^+ channel ($gp91^{phox}$) is involved in eliciting chorda tympani (CT) taste nerve responses to strong acids. Chem. Senses Abstract. (in press).

Doolin, R. E. and Gilbertson, T. A. 1996. Distribution and characterization of functional amiloride-sensitive sodium channels in rat tongue. J. Gen. Physiol. 107, 545–554.

Dotson, C. D., Roper, S. D., and Spector, A. C. 2005. PLCbeta2-independent behavioral avoidance of prototypical bitter-tasting ligands. Chem. Senses 30, 593–600.

Elliott, E. J. and Simon, S. A. 1990. The anion in salt taste: a possible role for paracellular pathways. Brain Res. 535, 9–17.

Finger, T. E., Danilova, V., Barrows, J., Bartel, D. L., Vigers, A. J., Stone, L., Hellekant, G., and Kinnamon, S. C. 2005. ATP signaling is crucial for communication from taste buds to gustatory nerves. Science 310, 1495–1499.

Fukuwatari, T., Kawada, T., Tsuruta, M., Hiraoka, T., Iwanaga, T., Sugimoto, E., and Fushiki, T. 1997. Expression of the putative membrane fatty acid transporter (FAT) in taste buds of the circumvallate papillae in rats. FEBS Lett. 414, 461–464.

Furue, H. and Yoshii, K. 1997. In situ tight-seal recordings of taste substance-elicited action currents and voltage-gated Ba currents from single taste bud cells in the peeled epithelium of mouse tongue. Brain Res. 776, 133–139.

Gannon, K. S. and Contreras, R. J. 1995. Sodium intake linked to amiloride-sensitive gustatory transduction in C57BL/6J and 129/J mice. Physiol. Behav. 57, 231–239.

Garty, H. and Palmer, L. G. 1997. Epithelial sodium channels: function, structure, and regulation. Physiol. Rev. 77, 359–396.

Gilbertson, D. M. and Gilbertson, T. A. 1994. Amiloride reduces the aversiveness of acids in preference tests. Physiol. Behav. 56, 649–654.

Gilbertson, T. A. 2002. Hypoosmotic stimuli activate a chloride conductance in rat taste cells. Chem. Senses 27, 383–394.

Gilbertson, T. A. and Fontenot, D. T. 1998. Distribution of amiloride-sensitive sodium channels in the oral cavity of the hamster. Chem. Senses 23, 495–499.

Gilbertson, T. A. and Zhang, H. 1998. Self-inhibition in amiloride-sensitive sodium channels in taste receptor cells. J. Gen. Physiol. 111, 667–677.

Gilbertson, T. A., Avenet, P., Kinnamon, S. C., and Roper, S. D. 1992. Proton currents through amiloride-sensitive Na channels in hamster taste cells. Role in acid transduction. J. Gen. Physiol. 100, 803–824.

Gilbertson, T. A., Baquero, A. F., and Spray-Watson, K. J. 2006. Water taste: the importance of osmotic sensing in the oral cavity. J. Water Health 4(Suppl 1), 35–40.

Gilbertson, T. A., Fontenot, D. T., Liu, L., Zhang, H., and Monroe, W. T. 1997. Fatty acid modulation of K^+ channels in taste receptor cells: gustatory cues for dietary fat. Am. J. Physiol. 272, C1203–C1210.

Gilbertson, T. A., Liu, L., Kim, I., Burks, C. A., and Hansen, D. R. 2005. Fatty acid responses in taste cells from obesity-prone and -resistant rats. Physiol. Behav. 86, 681–690.

Gilbertson, T. A., Roper, S. D., and Kinnamon, S. C. 1993. Proton currents through amiloride-sensitive Na^+ channels in isolated hamster taste cells: enhancement by vasopressin and cAMP. Neuron 10, 931–942.

Glendinning, J. I., Bloom, L. D., Onishi, M., Zheng, K. H., Damak, S., Margolskee, R. F., and Spector, A. C. 2005. Contribution of alpha-gustducin to taste-guided licking responses of mice. Chem. Senses 30, 299–316.

He, W., Danilova, V., Zou, S., Hellekant, G., Max, M., Margolskee, R. F., and Damak, S. 2002. Partial rescue of taste responses of alpha-gustducin null mice by transgenic expression of alpha-transducin. Chem. Senses 27, 719–727.

He, W., Yasumatsu, K., Varadarajan, V., Yamada, A., Lem, J., Ninomiya, Y., Margolskee, R. F., and Damak, S. 2004. Umami taste responses are mediated by alpha-transducin and alpha-gustducin. J. Neurosci. 24, 7674–7680.

Heath, T. P., Melichar, J. K., Nutt, D. J., and Donaldson, L. F. 2006. Human taste thresholds are modulated by serotonin and noradrenaline. J. Neurosci. 26, 12664–12671.

Heck, G. L., Mierson, S., and DeSimone, J. A. 1984. Salt taste transduction occurs through an amiloride-sensitive sodium transport pathway. Science 223, 403–405.

Herness, M. S. 1992. Aldosterone increases the amiloride-sensitivity of the rat gustatory neural response to NaCl. Comp. Biochem. Physiol. Comp. Physiol. 103, 269–273.
Herness, M. S. and Chen, Y. 2000. Serotonergic agonists inhibit calcium-activated potassium and voltage-dependent sodium currents in rat taste receptor cells. J. Membr. Biol. 173, 127–138.
Herness, M. S. and Gilbertson, T. A. 1999. Cellular mechanisms of taste transduction. Annu. Rev. Physiol. 61, 873–900.
Herness, M. S. and Sun, X. D. 1995. Voltage-dependent sodium currents recorded from dissociated rat taste cells. J. Membr. Biol. 146, 73–84.
Herness, S. and Chen, Y. 1997. Serotonin inhibits calcium-activated K^+ current in rat taste receptor cells. Neuroreport 8, 3257–3261.
Herness, S., Zhao, F. L., Kaya, N., Lu, S. G., Shen, T., and Sun, X. D. 2002. Adrenergic signalling between rat taste receptor cells. J. Physiol. 543, 601–614.
Herness, S., Zhao, F. L., Kaya, N., Shen, T., Lu, S. G., and Cao, Y. 2005. Communication routes within the taste bud by neurotransmitters and neuropeptides. Chem. Senses 30(Suppl 1), i37–i38.
Hofmann, T., Chubanov, V., Gudermann, T., and Montell, C. 2003. TRPM5 is a voltage-modulated and Ca(2+)-activated monovalent selective cation channel. Curr. Biol. 13, 1153–1158.
Huang, A. L., Chen, X., Hoon, M. A., Chandrashekar, J., Guo, W., Trankner, D., Ryba, N. J., and Zuker, C. S. 2006. The cells and logic for mammalian sour taste detection. Nature 442, 934–938.
Huang, L., Cao, J., Wang, H., Vo, L. A., and Brand, J. G. 2005. Identification and functional characterization of a voltage-gated chloride channel and its novel splice variant in taste bud cells. J. Biol. Chem. 280, 36150–36157.
Huang, L., Shanker, Y. G., Dubauskaite, J., Zheng, J. Z., Yan, W., Rosenzweig, S., Spielman, A. I., Max, M., and Margolskee, R. F. 1999. Ggamma13 colocalizes with gustducin in taste receptor cells and mediates IP3 responses to bitter denatonium. Nat. Neurosci. 2, 1055–1062.
Huang, Y. J., Maruyama, Y., Dvoryanchikov, G., Pereira, E., Chaudhari, N., and Roper, S. D. 2007. The role of pannexin 1 hemichannels in ATP release and cell–cell communication in mouse taste buds. Proc. Natl. Acad. Sci. U. S. A. 104, 6436–6441.
Ishimaru, Y., Inada, H., Kubota, M., Zhuang, H., Tominaga, M., and Matsunami, H. 2006. Transient receptor potential family members PKD1L3 and PKD2L1 form a candidate sour taste receptor. Proc. Natl. Acad. Sci. U. S. A. 103, 12569–12574.
Jentsch, T. J. 1996. Chloride channels: a molecular perspective. Curr. Opin. Neurobiol. 6, 303–310.
Kataoka, S., Hansen, A., Matsunami, H., and Finger, T. E. 2007. The sour taste receptor PKD2L1 is expressed by Type III taste cells in the mouse. Chem. Senses Abst. In press.
Kataoka, S., Toyono, T., Seta, Y., Ogura, T., and Toyoshima, K. 2004. Expression of P2Y1 receptors in rat taste buds. Histochem. Cell Biol. 121, 419–426.
Kawai, T. and Fushiki, T. 2003. Importance of lipolysis in oral cavity for orosensory detection of fat. Am. J. Physiol. Regul. Integr. Comp. Physiol. 285, R447–R454.
Kaya, N., Shen, T., Lu, S. G., Zhao, F. L., and Herness, S. 2004. A paracrine signaling role for serotonin in rat taste buds: expression and localization of serotonin receptor subtypes. Am. J. Physiol. Regul. Integr. Comp. Physiol. 286, R649–R658.
Kim, D. J. and Roper, S. D. 1995. Localization of serotonin in taste buds: a comparative study in four vertebrates. J. Comp. Neurol. 353, 364–370.
Kim, M. R., Kusakabe, Y., Miura, H., Shindo, Y., Ninomiya, Y., and Hino, A. 2003. Regional expression patterns of taste receptors and gustducin in the mouse tongue. Biochem. Biophys. Res. Commun. 312, 500–506.
Kinnamon, S. C. and Margolskee, R. F. 1996. Mechanisms of taste transduction. Curr. Opin. Neurobiol. 6, 506–513.
Kinnamon, S. C., Dionne, V. E., and Beam, K. G. 1988. Apical localization of K^+ channels in taste cells provides the basis for sour taste transduction. Proc. Natl. Acad. Sci. U. S. A. 85, 7023–7027.
Kinnamon, S. C., Price, M. P., Stone, L. M., Lin, W., and Welsh, M. J. 2000. The acid-sensing ion channel BNC1 is not required for sour taste transduction; 2000; Brighton, UK. p. 80.
Kolesnikov, S. S. and Margolskee, R. F. 1995. A cyclic-nucleotide-suppressible conductance activated by transducin in taste cells. Nature 376, 85–88.
Kretz, O., Barbry, P., Bock, R., and Lindemann, B. 1999. Differential expression of RNA and protein of the three pore-forming subunits of the amiloride-sensitive epithelial sodium channel in taste buds of the rat. J. Histochem. Cytochem. 47, 51–64.
Kusakabe, Y., Yamaguchi, E., Tanemura, K., Kameyama, K., Chiba, N., Arai, S., Emori, Y., and Abe, K. 1998. Identification of two α-subunit species of GTP-binding proteins, Gα15 and Gαq, expressed in rat taste buds. Biochim. Biophys. Acta 1403, 265–272.
Laugerette, F., Gaillard, D., Passilly-Degrace, P., Niot, I., and Besnard, P. 2007. Do we taste fat? Biochimie 89, 265–269.
Laugerette, F., Passilly-Degrace, P., Patris, B., Niot, I., Febbraio, M., Montmayeur, J. P., and Besnard, P. 2005. CD36 involvement in orosensory detection of dietary lipids, spontaneous fat preference, and digestive secretions. J. Clin. Invest. 115, 3177–3184.
Lawton, D. M., Furness, D. N., Lindemann, B., and Hackney, C. M. 2000. Localization of the glutamate–aspartate transporter, GLAST, in rat taste buds. Eur. J. Neurosci. 12, 3163–3171.
Li, X., Staszewski, L., Xu, H., Durick, K., Zoller, M., and Adler, E. 2002. Human receptors for sweet and umami taste. Proc. Natl. Acad. Sci. U. S. A. 99, 4692–4696.
Lin, W. and Kinnamon, S. C. 1999. Physiological evidence for ionotropic and metabotropic glutamate receptors in rat taste cells. J. Neurophysiol. 82, 2061–2069.
Lin, W., Burks, C. A., Hansen, D. R., Kinnamon, S. C., and Gilbertson, T. A. 2004. Taste receptor cells express pH-sensitive leak K^+ channels. J. Neurophysiol. 92, 2909–2919.
Lin, W., Finger, T. E., Rossier, B. C., and Kinnamon, S. C. 1999. Epithelial Na^+ channel subunits in rat taste cells: localization and regulation by aldosterone. J. Comp. Neurol. 405, 406–420.
Lin, W., Ogura, T., and Kinnamon, S. C. 2002. Acid-activated cation currents in rat vallate taste receptor cells. J. Neurophysiol. 88, 133–141.
Lindemann, B. 1996. Taste reception. Physiol. Rev. 76, 718–766.
Lindemann, B., Gilbertson, T. A., and Kinnamon, S. C. 1999. Amiloride-sensitive sodium channels in taste. Curr. Topics Membr. 47, 315–336.
Liu, D. and Liman, E. R. 2003. Intracellular Ca^{2+} and the phospholipid PIP2 regulate the taste transduction ion channel TRPM5. Proc. Natl. Acad. Sci. U. S. A. 100, 15160–15165.
Liu, L., Hansen, D. R., Kim, I., and Gilbertson, T. A. 2005. Expression and characterization of delayed rectifying K^+ channels in anterior rat taste buds. Am. J. Physiol. Cell Physiol. 289, C868–C880.
LopezJimenez, N. D., Cavenagh, M. M., Sainz, E., Cruz-Ithier, M. A., Battey, J. F., and Sullivan, S. L. 2006. Two members of the TRPP family of ion channels, Pkd1l3 and Pkd2l1, are co-expressed in a subset of taste receptor cells. J. Neurochem. 98, 68–77.

Lyall, V., Alam, R. I., Malik, S. A., Phan, T. H., Vinnikova, A. K., Heck, G. L., and DeSimone, J. A. 2004a. Basolateral Na^+-H^+ exchanger-1 in rat taste receptor cells is involved in neural adaptation to acidic stimuli. J. Physiol. 556, 159–173.

Lyall, V., Alam, R. I., Phan, D. Q., Ereso, G. L., Phan, T. H., Malik, S. A., Montrose, M. H., Chu, S., Heck, G. L., Feldman, G. M., and DeSimone, J. A. 2001. Decrease in rat taste receptor cell intracellular pH is the proximate stimulus in sour taste transduction. Am. J. Physiol. Cell Physiol. 281, C1005–C1013.

Lyall, V., Alam, R. I., Phan, T. H., Phan, D. Q., Heck, G. L., and DeSimone, J. A. 2002. Excitation and adaptation in the detection of hydrogen ions by taste receptor cells: a role for cAMP and Ca^{2+}. J. Neurophysiol. 87, 399–408.

Lyall, V., Heck, G. L., Vinnikova, A. K., Ghosh, S., Phan, T. H., Alam, R. I., Russell, O. F., Malik, S. A., Bigbee, J. W., and DeSimone, J. A. 2004b. The mammalian amiloride-insensitive non-specific salt taste receptor is a vanilloid receptor-1 variant. J. Physiol. 558, 147–159.

Lyall, V., Pasley, H., Phan, T. H., Mummalaneni, S., Heck, G. L., Vinnikova, A. K., and DeSimone, J. A. 2006. Intracellular pH modulates taste receptor cell volume and the phasic part of the chorda tympani response to acids. J. Gen. Physiol. 127, 15–34.

Lyall, V., Sturz, G. R., Phan, T. T., Heck, G. L., Mummalaneni, S., and DeSimone, J. A. 2007. Nigericin shifts the pH threshold for the chorda tympani (CT) taste nerve response from 4.5 to 6.5. Chem. Senses Abstract. (in press).

Matsumura, S., Mizushige, T., Yoneda, T., Iwanaga, T., Tsuzuki, S., Inoue, K., and Fushiki, T. 2007. GPR expression in the rat taste bud relating to fatty acid sensing. Biomed. Res. 28, 49–55.

Matsunami, H., Montmayeur, J. P., and Buck, L. B. 2000. A family of candidate taste receptors in human and mouse. Nature 404, 601–604.

Mattes, R. D. 2007. Effects of linoleic acid on sweet, sour, salty and bitter taste thresholds and intensity ratings of adults. Am. J. Physiol. Gastrointest. Liver Physiol. 292, G 1243–G 1248.

McCormack, D. N., Clyburn, V. L., and Pittman, D. W. 2006. Detection of free fatty acids following a conditioned taste aversion in rats. Physiol. Behav. 87, 582–594.

McLaughlin, S. K., McKinnon, P. J., and Margolskee, R. F. 1992. Gustducin is a taste-cell-specific G protein closely related to the transducins. Nature 357, 563–569.

Medler, K. F., Margolskee, R. F., and Kinnamon, S. C. 2003. Electrophysiological characterization of voltage-gated currents in defined taste cell types of mice. J. Neurosci. 23, 2608–2617.

Mierson, S., Olson, M. M., and Tietz, A. E. 1996. Basolateral amiloride-sensitive Na^+ transport pathway in rat tongue epithelium. J. Neurophysiol. 76, 1297–1309.

Ming, D., Ruiz-Avila, L., and Margolskee, R. F. 1998. Characterization and solubilization of bitter-responsive receptors that couple to gustducin. Proc. Natl. Acad. Sci. U. S. A. 95, 8933–8938.

Misaka, T., Ishimaru, Y., Iwabuchi, K., Kusakabe, Y., Arai, S., Emori, Y., and Abe, K. 1999. A gustatory cyclic nucleotide-gated channels CNGgust, is expressed in the retina. Neuroreport 10, 743–746.

Misaka, T., Kusakabe, Y., Emori, Y., Arai, S., and Abe, K. 1998. Molecular cloning and taste bud-specific expression of a novel cyclic nucleotide-gated channel. Ann. N. Y. Acad. Sci. 855, 150–159.

Misaka, T., Kusakabe, Y., Emori, Y., Gonoi, T., Arai, S., and Abe, K. 1997. Taste buds have a cyclic nucleotide-activated channel, CNGgust. J. Biol. Chem. 272, 22623–22629.

Miyamoto, T., Fujiyama, R., Okada, Y., and Sato, T. 1998. Sour transduction involves activation of NPPB-sensitive conductance in mouse taste cells. J. Neurophysiol. 80, 1852–1859.

Miyamoto, T., Fujiyama, R., Okada, Y., and Sato, T. 2000. Acid and salt responses in mouse taste cells. Prog. Neurobiol. 62, 135–157.

Miyamoto, T., Miyazaki, T., Fujiyama, R., Okada, Y., and Sato, T. 2001. Differential transduction mechanisms underlying NaCl- and KCl-induced responses in mouse taste cells. Chem. Senses 26, 67–77.

Miyamoto, T., Miyazaki, T., Okada, Y., and Sato, T. 1996. Whole-cell recording from non-dissociated taste cells in mouse taste bud. J. Neurosci. Methods 64, 245–252.

Monastyrskaia, K., Lundstrom, K., Plahl, D., Acuna, G., Schweitzer, C., Malherbe, P., and Mutel, V. 1999. Effect of the umami peptides on the ligand binding and function of rat mGlu4a receptor might implicate this receptor in the monosodium glutamate taste transduction. Br. J. Pharmacol. 128, 1027–1034.

Nelson, G., Chandrashekar, J., Hoon, M. A., Feng, L., Zhao, G., Ryba, N. J., and Zuker, C. S. 2002. An amino-acid taste receptor. Nature 416, 199–202.

Nelson, G., Hoon, M. A., Chandrashekar, J., Zhang, Y., Ryba, N. J., and Zuker, C. S. 2001. Mammalian sweet taste receptors. Cell 106, 381–390.

Ninomiya, Y. 1998. Reinnervation of cross-regenerated gustatory nerve fibers into amiloride-sensitive and amiloride-insensitive taste receptor cells. Proc. Natl. Acad. Sci. U. S. A. 95, 5347–5350.

Ninomiya, Y., Sako, N., and Funakoshi, M. 1989. Strain differences in amiloride inhibition of NaCl responses in mice, Mus musculus. J. Comp. Physiol. A 166, 1–5.

Ogura, T. 2002. Acetylcholine increases intracellular Ca^{2+} in taste cells via activation of muscarinic receptors. J. Neurophysiol. 87, 2643–2649.

Ogura, T. and Lin, W. 2005. Acetylcholine and acetylcholine receptors in taste receptor cells. Chem. Senses 30 (Suppl 1), i41.

Oike, H., Matsumoto, I., and Abe, K. 2006a. Group IIA phospholipase A(2) is coexpressed with SNAP-25 in mature taste receptor cells of rat circumvallate papillae. J. Comp. Neurol. 494, 876–886.

Oike, H., Wakamori, M., Mori, Y., Nakanishi, H., Taguchi, R., Misaka, T., Matsumoto, I., and Abe, K. 2006b. Arachidonic acid can function as a signaling modulator by activating the TRPM5 cation channel in taste receptor cells. Biochim. Biophys. Acta 1761, 1078–1084.

Ortiz-Alvarado, R., Guzman-Quevedo, O., Mercado-Camargo, R., Haertle, T., Vignes, C., and Bolanos-Jimenez, F. 2006. Expression of tryptophan hydroxylase in developing mouse taste papillae. FEBS Lett. 580, 5371–5376.

Perez, C. A., Huang, L., Rong, M., Kozak, J. A., Preuss, A. K., Zhang, H., Max, M., and Margolskee, R. F. 2002. A transient receptor potential channel expressed in taste receptor cells. Nat. Neurosci. 5, 1169–1176.

Pittman, D. W., Labban, C. E., Anderson, A. A., and O'Connor, H. E. 2006. Linoleic and oleic acids alter the licking responses to sweet, salt, sour, and bitter tastants in rats. Chem. Senses 31, 835–843.

Prawitt, D., Monteilh-Zoller, M. K., Brixel, L., Spangenberg, C., Zabel, B., Fleig, A., and Penner, R. 2003. TRPM5 is a transient Ca^{2+}-activated cation channel responding to rapid changes in $[Ca]_i^{2+}$. Proc. Natl. Acad. Sci. U. S. A. 100, 15166–15171.

Ren, Y., Shimada, K., Shirai, Y., Fujimiya, M., and Saito, N. 1999. Immunocytochemical localization of serotonin and serotonin transporter (SET) in taste buds of rat. Brain Res. Mol. Brain Res. 74, 221–224.

Richter, T. A., Caicedo, A., and Roper, S. D. 2003. Sour taste stimuli evoke Ca^{2+} and pH responses in mouse taste cells. J. Physiol. 547, 475–483.

Richter, T. A., Dvoryanchikov, G. A., Chaudhari, N., and Roper, S. D. 2004a. Acid-sensitive two-pore domain potassium (K2P) channels in mouse taste buds. J. Neurophysiol. 92, 1928–1936.

Richter, T. A., Dvoryanchikov, G. A., Roper, S. D., and Chaudhari, N. 2004b. Acid-sensing ion channel-2 is not necessary for sour taste in mice. J. Neurosci. 24, 4088–4091.

Romanov, R. A., Rogachevskaja, O. A., Bystrova, M. F., Jiang, P., Margolskee, R. F., and Kolesnikov, S. S. 2007. Afferent neurotransmission mediated by hemichannels in mammalian taste cells. Embo J. 26, 657–667.

Roper, S. 1983. Regenerative impulses in taste cells. Science 220, 1311–1312.

Roper, S. D. 2006. Cell communication in taste buds. Cell Mol. Life Sci. 63, 1494–1500.

Roper, S. D. and McBride, D. W., Jr. 1989. Distribution of ion channels on taste cells and its relationship to chemosensory transduction. J. Membr. Biol. 109, 29–39.

Rossler, P., Kroner, C., Freitag, J., Noe, J., and Breer, H. 1998. Identification of a phospholipase C beta subtype in rat taste cells. Eur. J. Cell. Biol. 77, 253–261.

Ruiz, C., Gutknecht, S., Delay, E., and Kinnamon, S. 2006. Detection of NaCl and KCl in TRPV1 knockout mice. Chem. Senses 31, 813–820.

Ruiz, C. J., Wray, K., Delay, E., Margolskee, R. F., and Kinnamon, S. C. 2003. Behavioral evidence for a role of alpha-gustducin in glutamate taste. Chem. Senses 28, 573–579.

Ruiz-Avila, L., McLaughlin, S. K., Wildman, D., McKinnon, P. J., Robichon, A., Spickofsky, N., and Margolskee, R. F. 1995. Coupling of bitter receptor to phosphodiesterase through transducin in taste receptor cells. Nature 376, 80–85.

Ruiz-Avila, L., Ming, D., and Margolskee, R. F. 2000. An *in vitro* assay useful to determine the potency of several bitter compounds. Chem. Senses 25, 361–368.

Ruiz-Avila, L., Wong, G. T., Damak, S., and Margolskee, R. F. 2001. Dominant loss of responsiveness to sweet and bitter compounds caused by a single mutation in alpha-gustducin. Proc. Natl. Acad. Sci. U. S. A. 98, 8868–8873.

Seta, Y., Kataoka, S., Toyono, T., and Toyoshima, K. 2007. Immunohistochemical localization of aromatic L: -amino acid decarboxylase in mouse taste buds and developing taste papillae. Histochem. Cell Biol. 127, 415–422.

Shen, T., Kaya, N., Zhao, F. L., Lu, S. G., Cao, Y., and Herness, S. 2005. Co-expression patterns of the neuropeptides vasoactive intestinal peptide and cholecystokinin with the transduction molecules alpha-gustducin and T1R2 in rat taste receptor cells. Neuroscience 130, 229–238.

Spector, A. C. and Travers, S. P. 2005. The representation of taste quality in the mammalian nervous system. Behav. Cogn. Neurosci. Rev. 4, 143–191.

Spector, A. C., Guagliardo, N. A., and St John, S. J. 1996. Amiloride disrupts NaCl versus KCl discrimination performance: implications for salt taste coding in rats. J. Neurosci. 16, 8115–8122.

Stevens, D. R., Seifert, R., Bufe, B., Muller, F., Kremmer, E., Gauss, R., Meyerhof, W., Kaupp, U. B., and Lindemann, B. 2001. Hyperpolarization-activated channels HCN1 and HCN4 mediate responses to sour stimuli. Nature 413, 631–635.

Stone, L. M., Barrows, J., Finger, T. E., and Kinnamon, S. C. 2007. Expression of T1Rs and gustducin in palatal taste buds of mice. Chem. Senses 32, 255–262.

Treesukosol, Y., Lyall, V., Heck, G. L., Desimone, J. A., and Spector, A. C. 2007. A psychophysical and electrophysiological analysis of salt taste in Trpv1 null mice. Am. J. Physiol. Regul. Integr. Comp. Physiol. 292, R 1799–1809.

Trubey, K. R., Culpepper, S., Maruyama, Y., Kinnamon, S. C., and Chaudhari, N. 2006. Tastants evoke cAMP signal in taste buds that is independent of calcium signaling. Am. J. Physiol. Cell. Physiol. 291, C237–244.

Ugawa, S., Minami, Y., Guo, W., Saishin, Y., Takatsuji, K., Yamamoto, T., Tohyama, M., and Shimada, S. 1998. Receptor that leaves a sour taste in the mouth. Nature 395, 555–556.

Ugawa, S., Yamamoto, T., Ueda, T., Ishida, Y., Inagaki, A., Nishigaki, M., and Shimada, S. 2003. Amiloride-insensitive currents of the acid-sensing ion channel-2a (ASIC2a)/ ASIC2b heteromeric sour-taste receptor channel. J. Neurosci. 23, 3616–3622.

Vinnikova, A. K., Alam, R. I., Malik, S. A., Ereso, G. L., Feldman, G. M., McCarty, J. M., Knepper, M. A., Heck, G. L., DeSimone, J. A., and Lyall, V. 2004. Na^{+}-H^{+} exchange activity in taste receptor cells. J. Neurophysiol. 91, 1297–1313.

Waldmann, R., Champigny, G., Lingueglia, E., De Weille, J. R., Heurteaux, C., and Lazdunski, M. 1999. H(+)-gated cation channels. Ann. N. Y. Acad. Sci. 868, 67–76.

Watson, K. J., Kim, I., Baquero, A. F., Burks, C. A., Liu, L., and Gilbertson, T. A. 2007. Expression of aquaporin water channels in rat taste buds. Chem. Senses. 32, 411–421.

Wong, G. T., Gannon, K. S., and Margolskee, R. F. 1996. Transduction of bitter and sweet taste by gustducin. Nature 381, 796–800.

Yan, W., Sunavala, G., Rosenzweig, S., Dasso, M., Brand, J. G., and Spielman, A. I. 2001. Bitter taste transduced by PLC-beta(2)-dependent rise in IP(3) and alpha-gustducin-dependent fall in cyclic nucleotides. Am. J. Physiol. Cell Physiol. 280, C742–C751.

Ye, Q., Heck, G. L., and DeSimone, J. A. 1991. The anion paradox in sodium taste reception: resolution by voltage-clamp studies. Science 254, 724–726.

Ye, Q., Heck, G. L., and DeSimone, J. A. 1994. Effects of voltage perturbation of the lingual receptive field on chorda tympani responses to Na^{+} and K^{+} salts in the rat: implications for gustatory transduction. J. Gen. Physiol. 104, 885–907.

Yee, C. L., Yang, R., Bottger, B., Finger, T. E., and Kinnamon, J. C. 2001. ''Type III'' cells of rat taste buds: immunohistochemical and ultrastructural studies of neuron-specific enolase, protein gene product 9.5, and serotonin. J. Comp. Neurol. 440, 97–108.

Yoshida, R., Yasumatsu, K., Shigemura, N., and Ninomiya, Y. 2006. Coding channels for taste perception: information transmission from taste cells to gustatory nerve fibers. Arch. Histol. Cytol. 69, 233–242.

Zhang, Y., Hoon, M. A., Chandrashekar, J., Mueller, K. L., Cook, B., Wu, D., Zuker, C. S., and Ryba, N. J. 2003. Coding of sweet, bitter, and umami tastes: different receptor cells sharing similar signaling pathways. Cell 112, 293–301.

Zhang, Z., Zhao, Z., Margolskee, R. F., and Liman, E. R. 2007. The transduction channel TRPM5 is gated by intracellular calcium in taste cells. J. Neurosci. 27, 5777–5786.

Zhao, F. L., Shen, T., Kaya, N., Lu, S. G., Cao, Y., and Herness, S. 2005. Expression, physiological action, and coexpression patterns of neuropeptide Y in rat taste-bud cells. Proc. Natl. Acad. Sci. U. S. A. 102, 11100–11105.

4.11 Gustatory Pathways in Fish and Mammals

M C Whitehead, University of California, San Diego, La Jolla, CA, USA

T E Finger, University of Colorado School of Medicine, Aurora, CO, USA

© 2008 Elsevier Inc. All rights reserved.

4.11.1	**Introduction and Overview**	238
4.11.1.1	Functional Organization of the Taste System in Vertebrates	238
4.11.1.1.1	Primary sensory nuclei	239
4.11.1.1.2	Local reflex pathway	240
4.11.1.1.3	The gustatory lemniscus	240
4.11.1.2	Visceral–Limbic Connections	240
4.11.1.3	The Gustatory Sense as a Visceral Modality	241
4.11.2	**Gustatory Centers in Fish: A Comparative Viewpoint**	241
4.11.2.1	Primary Gustatory Nuclei	242
4.11.2.1.1	Facial nerve specializations	242
4.11.2.1.2	Vagus nerve specializations	244
4.11.2.2	Brainstem Reflex Connections	244
4.11.2.3	Second-Order Gustatory Nuclei	245
4.11.2.4	Ascending Fiber System	246
4.11.3	**Gustatory Pathways in Mammals**	246
4.11.3.1	Primary Sensory Nucleus	246
4.11.3.1.1	Primary afferent inputs	247
4.11.3.1.2	Subdivisions and cell types	248
4.11.3.2	Brainstem Reflex Connections	250
4.11.3.2.1	Topography of taste quality	253
4.11.3.3	Lemniscal Pathway	254
4.11.3.3.1	Second-order (parabrachial) nucleus	255
4.11.3.3.2	Third-order (thalamic) nucleus and gustatory cortex	255
4.11.3.4	Basal Forebrain and Descending Pathways	255
4.11.4	**Conclusion**	256
References		256

Glossary

alar plate A sensory region located dorsally in the embryonic spinal cord and hindbrain.

barbels Whisker-like, taste bud-bearing organs located near the mouth in some fishes, for example catfish.

basal plate A motor region located ventrally in the embryonic spinal cord and hindbrain.

bauplan Building plan: In taxonomy, the common properties of the members of a systematic group of animals.

brachium conjunctivum A white matter landmark in the pons consisting of axon bundles exiting the cerebellum.

Golgi stain A specialized stain showing cell bodies, dendrites and axons of a small, random subset of neurons in a histological section.

lemniscal pathway A sensory pathway that ascends from the spinal cord or brainstem, through the thalamus, to the cerebral cortex, that is from first-order to second-order to third-order nuclei, etc.

limbic Brain regions and functions concerned with visceral processes, e.g., the emotional or homeostatic status of the organism.

Nissl stain A routine stain showing all neuronal cell bodies in a histological section.

nucleus ambiguus A group of motor neurons that innervate pharyngeal muscles.

parabrachial nucleus A group of neurons surrounding the brachium conjunctivum in the dorsal pons.
primary sensory nucleus A brain region first activated by peripheral inputs; the neuronal group in the medulla receiving direct connections from peripheral nerves.
second-order sensory nucleus A brain region, located rostral to the medulla, that receives input from a primary sensory nucleus.
somatotopic A spatial representation that maps the sensory surface of an organism within the nervous system.
telencephalic Related to the forebrain.
teleost A group of bony, ray-finned, fishes with movable upper jaws.
third-order sensory nucleus A brain region that receives input from a second-order nucleus.

4.11.1 Introduction and Overview

The sense of taste in all complex animals begins with specialized chemoreceptors located in and around the mouthparts. These receptor organs are crucial in determining the palatability of potential food items and in orchestrating the appropriate ingestive or avoidance reactions. The organization of the neural centers activated by the receptors is the topic of this chapter, which presents a comparative perspective. Comparison of invertebrate and vertebrate systems may be instructive in terms of recognizing general principles of processing or organization, but data from one group is not likely to be directly applicable to the other group. For example, taste receptor organs in invertebrates involve sensory neurons with axons directly extending into the central nervous system. In the vertebrates, taste receptor organs (taste buds) consist of modified epithelial cells, not neurons. The taste bud cells connect with the primary taste neurons which lie in remote cranial ganglia, and it is the central processes of these ganglion cells that convey the taste message into the central nervous system. Thus, the taste system in invertebrates, for example, leech, fruit fly, is analogous, but not homologous to the taste system in vertebrates although commonalities do exist, probably through convergence (Finger, T. E., 2006). In contrast, the taste system in the different vertebrates is homologous (derived from a common ancestral condition), and so similarities in organization and mechanism are likely. Many such homologies are apparent when comparing the taste systems of different groups within vertebrates.

The general structure and organization of the taste system in vertebrates suggest that this system evolved in the earliest vertebrates and therefore is part of the common bauplan of all vertebrates. Taste buds are present in all vertebrates including lampreys, elasmobranches, bony fishes, amphibia, and amniotes including mammals. Comparison of the organization of the taste systems in various vertebrates contributes to an understanding of which features are part of the common organizational plan and which features may be derived for particular species or groups. This chapter first describes the general organizational plan for the central representation of taste within the brains of vertebrates. Then it examines in more detail the neuroanatomical organization of the taste system in two well-studied vertebrate groups: teleost fish and mammals, especially rodents.

4.11.1.1 Functional Organization of the Taste System in Vertebrates

Taste buds serve as sentinels for the digestive tract. They are positioned to allow the animal to assess the chemical composition of potential food items before they are given entrance to the alimentary canal. Not surprisingly then, stimulation of taste buds can evoke either ingestive or rejection reflexes. Yet taste does more than to merely serve as a go/no-go switch for foods. The sense of taste offers a conscious awareness of the composition of foods and is used to preferentially ingest particular substances according to past experience. Concomitant with a role in feeding, the sense of taste is involved in triggering digestive reflexes appropriate to the items ingested.

The roles for the gustatory system can be divided into three broad functional domains: (1) local brainstem pathways – reflexive action involving oropharyngeal muscles and digestive processes, (2) lemniscal pathways – mediating conscious awareness of what is being eaten, and (3) basal forebrain (limbic) pathways – visceral functions relating to hunger

status, homeostasis, and drive state. Accordingly, it is not surprising that taste inputs to the brain ultimately influence centers associated with each of these functions, respectively: (1) oromotor and visceromotor nuclei of the brainstem, (2) a lemniscal system conveying information to specific gustatory areas of the forebrain, for example, gustatory cortex, and (3) basal forebrain regions, for example, the hypothalamus and amygdala, areas that are interconnected with the gustatory brainstem and typically associated with drive states, emotions, and homeostasis.

4.11.1.1.1 Primary sensory nuclei

In all vertebrates, taste information is conveyed to the central nervous system via three cranial nerves: the facial (CN VII), glossopharyngeal (CN IX), and vagus (CN X) nerves. The taste fibers in these nerves project to a restricted portion of the visceral sensory column of the medulla, an area situated dorsolateral to the sulcus limitans, a groove in the lateral wall of the ventricle. In the embryo, this sulcus separates alar plate from basal plate, and therefore separates sensory nuclei dorsally, from motor nuclei ventrally. In the medulla, the embryonic neural tube spreads apart dorsally to form the fourth ventricle so that the alar plate comes to lie dorsolateral of the basal plate. The visceral sensory column lies along the medioventral margin of the alar plate, where it is adjacent to the basal plate (Figure 1).

The viscerosensory column (Herrick, C. J., 1922) is, however, not a single homogeneous structure any

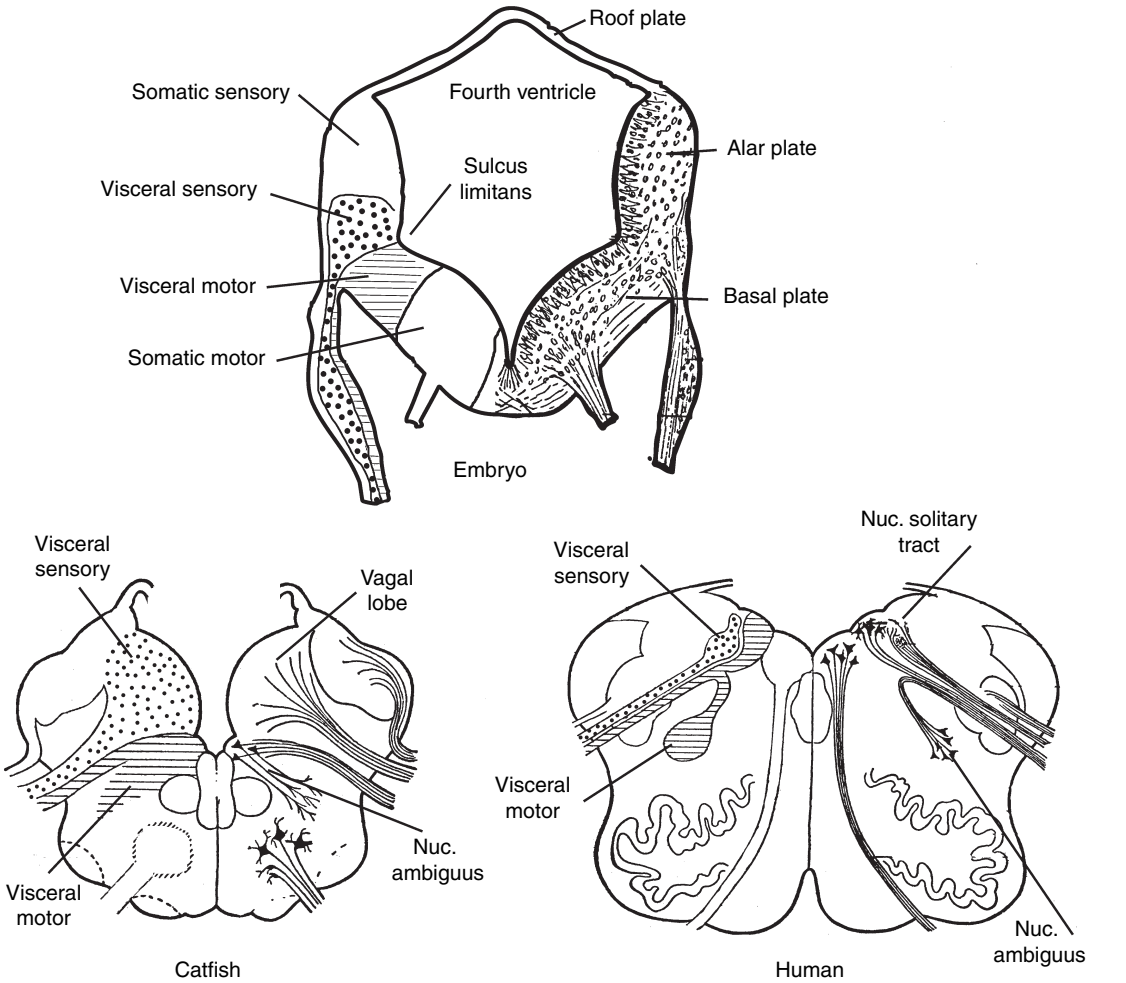

Figure 1 Semischematic diagrams showing the situation of the visceral sensory and motor columns in cross sections of the medulla in the embryo (above), the adult catfish (lower left) and adult human (lower right). In all situations, the visceral sensory column lies immediately dorsal to the sulcus limitans, while the visceral motor column lies immediately ventral. This same relationship holds in the adult brain of all vertebrate species. Adapted from Herrick, C. J. 1922. An Introduction to Neurology. W.B. Saunders Co.

more than the dorsolaterally adjacent somatic sensory column is a unitary structure. The somatic sensory column, for example, contains special somatic components: cochlear nuclei and vestibular nuclei, as well as general somatic components, i.e., trigeminal nuclei. Similarly, the visceral sensory column contains special visceral components for taste, and general visceral components for interoceptive functions carried on the vagus nerve including those mediated by digestive, cardiac, and respiratory afferent fibers. The taste portion of the visceral sensory column lies rostral and lateral to the general visceral components. In amniote vertebrates, the visceral sensory column is represented by the nucleus of the solitary tract (NST), containing separable gustatory and general visceral subdivisions. In fishes, the visceral sensory column is grossly divisible into lobes or lobules which protrude dorsally into the fourth ventricle. These lobules form clear anatomical boundaries between the gustatory and general visceral components of the nuclear complex. The gustatory lobes in the medulla in fishes are homologous to the gustatory portion of the NST in other vertebrates.

The gustatory and general visceral portions of the visceral sensory complex differ not only in terms of inputs but also in terms of connectivity with the rest of the brain. The general visceral components of the visceral complex maintain intimate reflex interconnections with the subjacent dorsal motor nucleus of the vagus, a preganglionic parasympathetic nucleus (Rogers, R. C. and McCann, M. J., 1993) and areas of the reticular formation that influence autonomic outflow (Ross, C. A. *et al.*, 1985). In addition, the general visceral subnuclei are extensively interconnected with limbic structures such as hypothalamus and amygdala (Ricardo, J. A. and Koh, E. T., 1978). The gustatory nuclei not only have interconnections with these limbic areas but possess unique connections as well. The reflex connections of the gustatory subnuclei involve oromotor centers and salivatory nuclei much more so than they do the dorsal motor nucleus of the vagus (Cunningham, E. T. and Sawchenko, P. E., 2000). In addition, the gustatory nuclei give rise to a unique lemniscal system conveying gustatory information to the thalamus and thence to a primary gustatory region of the cerebrum (e.g., gustatory cortex in mammals).

4.11.1.1.2 Local reflex pathway

Activation of the gustatory system will result in oropharyngeal movements (whether they be ingestion and swallowing or gagging and rejection) as well as reflex salivation and activation of the GI tract. The gustatory nuclei have reflex connections ending on oromotor nuclei (trigeminal motor nuc., nuc. ambiguus, hypoglossal nuc.) and in the adjacent premotor reticular formation. The more rostral gustatory nuclei tend to have more connections with reticular formation and anterior oromotor centers, while more caudal gustatory nuclei have more substantial connections with oropharyngeal motoneurons of the nucleus ambiguus. Homologous reflex pathways in fish and mammals will be described.

4.11.1.1.3 The gustatory lemniscus

Like other special senses, the gustatory system maintains a chain of connections within the brain with an ultimate target in the telencephalon. A labeled-line sensory pathway that ascends from the medulla to the thalamus and finally to cerebral cortex is known as a lemniscus. In mammals, the ultimate target of the gustatory lemniscus is primary gustatory cortex. In nonmammalian vertebrates, the telencephalic target is a restricted area within the dorsal telencephalon.

The gustatory lemniscus starts from the primary gustatory nuclei of the medulla to reach a specific thalamic relay nucleus. The ascending fibers proceed along two routes. Some percentage of the fibers more in some species (e.g., monkey) fewer in others (e.g., rat) ascend through the brainstem directly to reach the ipsilateral taste nucleus of the thalamus. Other fibers from the primary sensory nuclei ascend only as far as the ipsilateral secondary viscerosensory nucleus of the dorsal pons (i.e., pontine taste area (Norgren, R. and Leonard, C. M., 1973), parabrachial nuc. (Norgren, R. and Pfaffmann, C., 1975), in mammals, superior secondary gustatory nuc. (Herrick, C. J., 1905) in fish. The secondary viscerosensory nucleus of the pons, like the primary viscerosensory column of the medulla, contains distinct gustatory and general visceral components. The gustatory component of the secondary viscerosensory nucleus projects to the ipsilateral thalamic taste nucleus that is targeted by the direct ascending gustatory lemniscal system. The thalamic gustatory nucleus relays taste information to the telencephalic gustatory target which, in mammals, is gustatory cortex.

4.11.1.2 Visceral–Limbic Connections

The gustatory system, consistent with its visceral sensory nature, has extensive interconnection with the portions of the limbic system involved in

regulation of homeostatic functions and drive states. The gustatory modality is crucial in the selection of particular foods. The choice of preferred foods changes according to an animal's physiological state (specific appetites, e.g., sodium appetite) and past experience. For example, a sodium-deprived rat will specifically seek out sodium salts in preference to other salts. Similarly, an animal that has fallen ill after ingesting a novel food will develop a strong aversion to the taste associated with that food (conditioned taste aversion). Both the specific appetites and conditioned taste aversions require coordination of limbic areas (hypothalamus and amygdala) with incoming gustatory information. Hence it is not surprising to find that ascending gustatory information reaches these limbic areas as well as the thalamocortical system.

4.11.1.3 The Gustatory Sense as a Visceral Modality

The gustatory sense has a unique location at the boundary between the external environment and the internal milieu. In some vertebrates (and even young children!), the gustatory system is used as an exteroceptive sense to gather information about the external world. But in all vertebrates, the gustatory modality is used to monitor intake of substances into the alimentary tract and to protect the airways from foreign substances, for example, laryngal taste buds which line the airway side of the larynx detect food or liquid that might be inhaled (Dickman, J. D. and Smith, D. V., 1988). The farther posterior a taste bud lies in the oropharynx, the more it serves as a visceral sensory organ; the more anterior a taste bud lies (e.g., tip of the tongue; barbels and lips of fishes), the more it is used as an exteroceptive special sense.

The most posterior taste buds are innervated by the vagus nerve, a mixed nerve containing some fibers which convey taste from these buds, while other fibers convey multiple general visceral modalities from interoceptive chemoreceptive end organs. These general visceral modalities, for example, information on blood gases, cardiac functions, upper GI tract functions, project into caudal portions of the brainstem viscerosensory complex (nuc. solitary tract). These inputs are relayed to brainstem visceromotor centers, to the pontine viscerosensory relay (parabrachial complex), and to the limbic areas of the forebrain including hypothalamus and amygdala. These limbic connections are highly reminiscent of the limbic relays for taste information, which they parallel to a large extent; their organization reflects the visceral nature of the gustatory system.

4.11.2 Gustatory Centers in Fish: A Comparative Viewpoint

This section will describe how taste information is represented in the brains of nonmammalian vertebrates and especially teleost (bony) fishes. Understanding the organization of the gustatory system across vertebrates is important in two ways. First, it allows us to abstract general organizational principles that are evolutionarily conserved and which are likely to underlie the central organization of taste systems in mammals including humans. Second, the gustatory system is comparatively large in many fishes, and so the central taste nuclei represent a much larger portion of the brain, thus making the system more amenable to study. The basic connectivity of the brain is preserved through evolution, so understanding these pathways in fish will shed light on the basic organization of these systems in mammals.

What are the major features of the central gustatory system that can be discerned in these comparative studies? First, the primary principle of organization of the primary visceral nuclei, including the taste nuclei, is a somatotopic, or organotopic, representation. In the taste nuclei of fishes, a fine-grained topography is a recurrent theme across species, with particular sensory appendages or specializations being represented in elaborate corresponding central structures. This detailed somatotopic arrangement is mirrored in the primary general visceral nuclei in both fish and amniote vertebrates (Katz, D. M. and Karten, H. J., 1983; Altschuler, S. M. *et al.*, 1989) where different organs of the digestive and respiratory systems target specific subnuclei of the primary visceral sensory complex. Second, reflex systems arising from the different parts of the gustatory nuclear complex are different according to the end organ or part of the oral cavity innervated. Accordingly, facial taste information, which arises from more distal sensory fields, has connectivity more related to movements of the body, head, or tongue, whereas vagal taste information, arising from the posterior part of the oral cavity, has connectivity with motor systems driving swallowing. Third, despite the elaborate detail of the primary gustatory nuclei, the second-order nuclei do not mirror this somatotopic encoding of the information. The implication is

that either the somatotopic information is encoded in some other fashion as it is relayed to higher centers or else the somatotopic information is utilized for processing in the primary sensory nuclei but is less important higher in the neuraxis. Nonetheless, despite the loss of the fine-grain somatotopy (Marui, T., 1981), the secondary nucleus does maintain the gross separation of facial and vagal gustatory information (Morita, Y. *et al.*, 1980) as well as gustatory and general visceral functions (Finger, T. E. and Kanwal, J. S., 1992).

4.11.2.1 Primary Gustatory Nuclei

A great deal of diversity exists in terms of the relative size and complexity of the taste system in the 20 000 species of teleost fishes. Some, for example, zebrafish, have a relatively undistinguished gustatory system encompassing both intraoral and external taste buds. Other fishes, including catfishes (order: siluriformes), many carps (family: cyprinidae) including goldfish, goatfish (family: Mullidae), and *Heterotis*, an unusual African fish unrelated to the mainstream teleosts, have elaborate taste bud arrays and central specializations. Because of the diverse species exhibiting such gustatory specializations, the elaboration of the system must have occurred independently several times during evolution. Despite these independent enlargements of the system in some species, numerous similarities still exist, and these must point to the underlying organizational scheme that formed early in vertebrate evolution. Such traits are likely to be consistent throughout all groups from fishes to amniote vertebrates including humans.

In all vertebrates, taste inputs arrive on three cranial nerves: CN VII (facial), CN IX (glossopharyngeal), and CN X (vagus). The facial nerve innervates taste buds situated farthest from the esophagus. In mammals, these are on the tip of the tongue, but in most fishes, taste buds occur on the external epithelium as well as in the oral cavity. Those taste buds lying outside of the oral cavity are always innervated by branches of the facial nerve. In fishes with specialized taste appendages (barbels), for example, catfish (Atema, J., 1971) and goatfish (Kiyohara, S. *et al.*, 2002), there is a concomitant relative enlargement of the facial taste system. Conversely, other fish species exhibit a relative enlargement and specialization of the vagal taste system which innervates elaborations of palatal or branchial taste organs (Braford, M. R. J., 1986; Finger, T. E., 1988).

As in other vertebrates, the three taste nerves enter the medulla to terminate in the viscerosensory column of nuclei extending along the wall of the fourth ventricle from near the obex to the level of the pontomedullary junction. The facial nerve terminates most rostrally in this column while the vagus nerve ends most caudally; the glossopharyngeal zone occupies an intermediate position. Even in fishes lacking an elaborately derived gustatory system, this overall organization is obvious. The three taste nerves terminate in serial order: facial terminals most anterior, glossopharyngeal terminals in the middle, and vagal taste inputs most posterior of the three. In all fishes, the general visceral components of the vagus nerve (e.g., innervating gut) terminate still more posteriorly in the viscerosensory column (Morita, Y. and Finger, T. E., 1985b; 1987).

Because the facial nerve taste system and the vagal nerve taste system innervate different populations of taste buds and terminate in clearly different lobes of the medulla, straightforward lesion experiments have been feasible to determine functional and behavioral differences between these systems. Atema J. (1971) ablated either the facial or vagal lobe in catfish to show that the facial taste system is involved in food localization, while the vagal taste system is necessary for ingestion and swallowing. The reflex connections arising from each of the gustatory lobes are commensurate with the behaviors and movements driven by each of these subsystems. The facial lobe is connected to premotor reticular formation that is involved in orientation to external food sources (Finger, T. E. and Morita, Y., 1985; Morita, Y. and Finger, T. E., 1985a); the vagal lobe has a tight reflex connection to the nuc. ambiguus motoneurons necessary for swallowing of identified food items.

4.11.2.1.1 Facial nerve specializations

The peripheral gustatory organs are especially numerous in those species with elaborate external gustatory appendages used to find food in the environment. Such species include catfishes, goatfishes, and gadids (cods and their relatives). These species are not closely related, emphasizing that gustatory specializations have evolved numerous times during fish phylogeny. Nonetheless, in each of these forms, the elaboration of the external, facially innervated taste periphery results in elaboration of the rostral part of the gustatory sensory column. In fish with an elaborate gustatory periphery, the rostral part of the viscerosensory column bulges medially and dorsally into the fourth ventricle to form an obvious facial lobe (Figure 2).

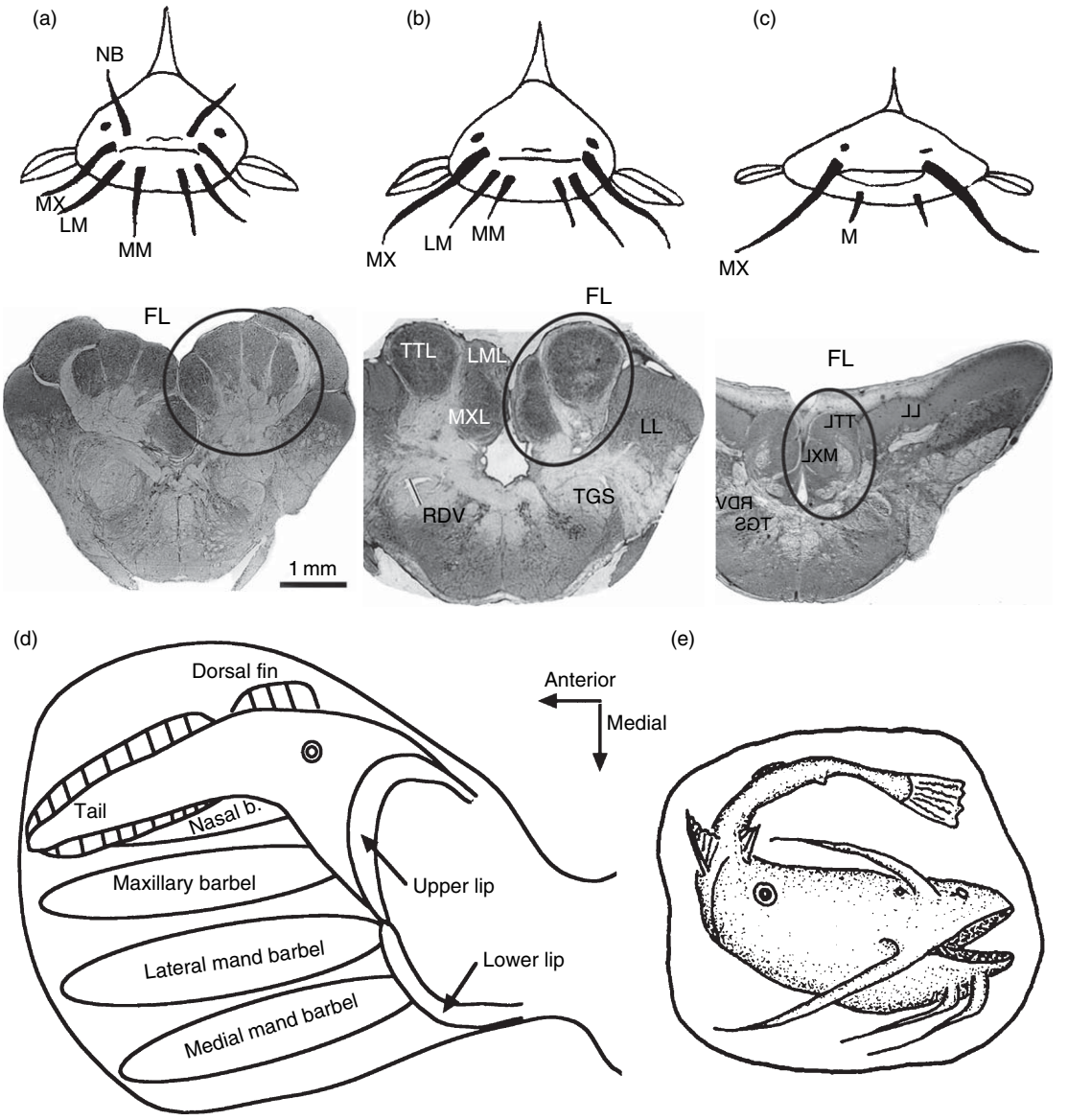

Figure 2 (a–c) The relationship between the number of barbels and the number of lobules in the facial lobe can be appreciated in these matched front views of the fish and cross sections of the rostral medulla in three different species of catfishes. (a) *Plotosus lineatus* has four barbels on each side and four lobules to the facial lobe. (b) *Arius felis* has three barbels and three lobules. (c) *Silurus asotus* has only two barbels and two lobules. (d, e) Semischematic diagrams of the piscunculus in the facial lobes of two species of catfish. A piscunculus is a distorted map of the receptor surface in the brain similar to the somatosensory homunculus drawn for the representation of touch in human somatosensory cortex. (d) The detailed somatotopic organization of the facial lobe of *Plotosus lineatus* can be seen in this figure. The seemingly disproportionate size of the barbels is related to the high density of taste buds on these organs. Representation in the facial lobe is in proportion to amount of taste input and not physical size of the receptor organ. (e) A more fanciful piscunculus projected onto the facial lobe of the bullhead catfish, *Ictalurus nebulosus*. (a, c) Parts of this figure were reprinted from Kiyohara, S. and Caprio, J. 1996. Somatotopic organization of the facial lobe of the sea catfish *Arius felis* studied by transganglionic transport of horseradish peroxidase. J. Comp. Neurol. 368, 121–135, with permission of Wiley Press. (d) Reprinted with permission from Kiyohara, S. and Tsukahara, J. 2005. Barber Taste System in Catfish and Goatfish. In: Fish chemosenser (*eds.* K. Reutter and B. G. Kapoor), pp. 175–211. Science Publishers. (e) Reprinted with permission from Wiley Press from Finger, T. E. 1978. Gustatory pathways in the bullhead catfish. II. Facial lobe connections. J. Comp. Neurol. 180, 691–705.

The structure and complexity of the facial lobe in each species match well the peripheral elaborations present on the animal. In catfishes, the number of lobules present exactly corresponds to the number of peripheral barbels the fish has (Kiyohara, S. and Caprio, J., 1996). In goatfish, the elongate single barbel is represented in a recurved tubular neuropil that maintains a precise somatotopic map of the peripheral end organ (Kiyohara, S. *et al.*, 2002). In codfish, with a simple single barblet, the facial lobe is present but is not particularly elaborate.

4.11.2.1.2 Vagus nerve specializations

Some fishes have an elaborate intra-oral food-sorting apparatus innervated by the vagus nerve. In carps, this mechanism involves the gill arches and palate (Sibbing, F. A. *et al.*, 1986; Osse, J. W. *et al.*, 1997). In the unrelated Osteoglossmorph, *Heterotis,* the food sorting is accomplished in a specialization of the gill chamber (Braford, M. R. J., 1986). In both cases, the vagal taste information enters an elaborate, laminated vagal lobe. In goldfish (and probably *Heterotis*), the taste periphery is represented in a fine-grain orototopic fashion, matching the structure of the peripheral end organ: spiraled in *Heterotis*, a hemisphere in goldfish (Morita, Y. and Finger, T. E., 1985b) (Figure 3).

4.11.2.2 Brainstem Reflex Connections

The gustatory lobes in fishes give rise to local connections to adjacent nuclei and reticular formation

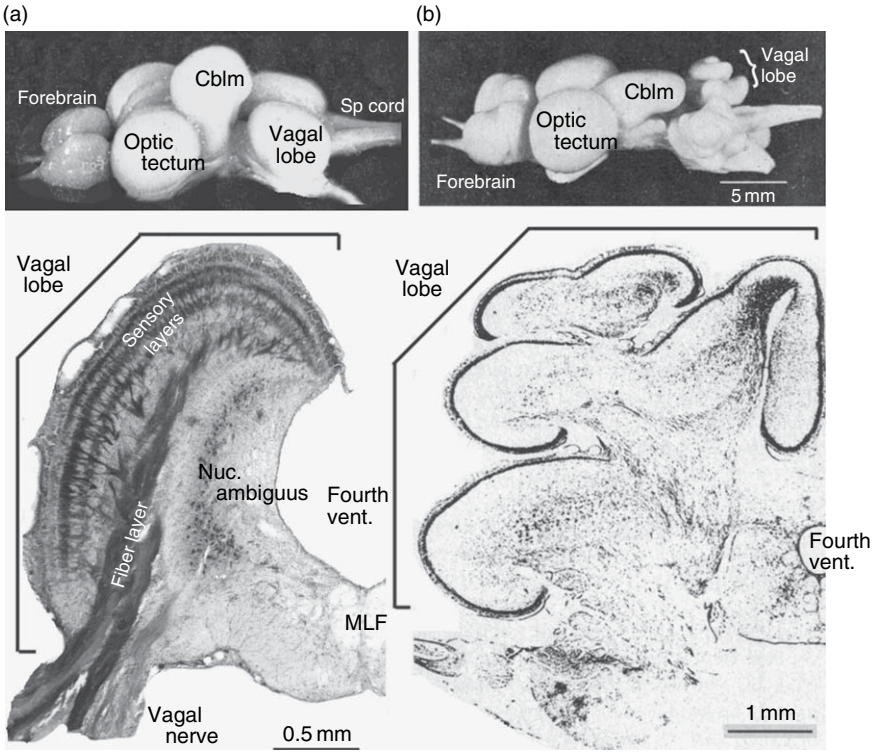

Figure 3 In some fish species, the vagal lobe, which is homologous to the vagal portion of the NST, is quite elaborate and may constitute nearly 20% of the entire brain mass. (a) In the common goldfish, *Carassius auratus*, the vagal lobe is a large, laminated hemisphere protruding from the dorsolateral surface of the medulla. Above: Lateral view of the brain. The large size of the vagal lobe can be appreciated in relation to the rest of the brain. Below: Cross section of the medulla through the vagal lobe, showing the left half of the brain (medial to the right). The laminated nature of the vagal lobe in goldfish is readily apparent in this preparation in which the vagus nerve was filled with the tracer horseradish peroxidase (HRP). The sensory layers lie along the outer half of the lobe overlying the fiber layer. The sensory layers are homologous to the vagal taste part of the NST. The motoneurons that innervate the palate, part of the nuc. ambiguus (visceral motor column) lie deeper in the lobe and are retrogradely labeled by HRP in this preparation. (b) In the African fish, *Heterotis niloticus*, the vagal lobe assumes a spiral shape matching a spiraled food-sorting organ of the branchial cavity (Braford, M. R. J., 1986). Above: The vagal lobe corkscrews dorsolaterally outward from the medulla. Below: Cross section of the medulla through the vagal lobe showing the left side of the brain. Three turns of the spiral can be seen in section. The superficial layer of small closely packed cells is similar to the superficial layer of the vagal lobe in goldfish (left).

areas of the medulla as well as ascending and descending connections (Herrick, C. J., 1905; Finger, T. E., 1978; Finger, T. E. and Morita, Y., 1985). The distinct nature of these reflex connections is more evident in these fishes than it is in mammals, but the same principle obtains. Reflex connections from each division of the visceral sensory column are appropriate for the particular organ or system represented (Figure 4). Thus, for example, general visceral sensory nuclei (GVM) have reflex connections with the general visceral motor nuclei (DMNX) that drive the autonomic nervous system (Altschuler, S. M. *et al*, 1989; Goehler, L. E. and Finger, T. E., 1992; Rogers, R. C. and McCann, M. J., 1993). Within the brainstem gustatory complex itself, distinct reflex channels are evident according to the particular peripheral organ innervated. Thus the subnucleus representing the pharynx (GVL) maintains reflex connections with the motoneurons that drive the pharyngeal musculature (nAphar). Similarly, the areas representing the palate (VLs) have reflex connections with motoneurons driving the palate (nApal – the motor layer of the vagal lobe). Finally, the areas representing taste buds on the lips and external body surface are connected to the subjacent reticular formation which provides coordinated output to the motor nuclei necessary to drive movements of the body and head (Kanwal, J. S. and Finger, T. E., 1997).

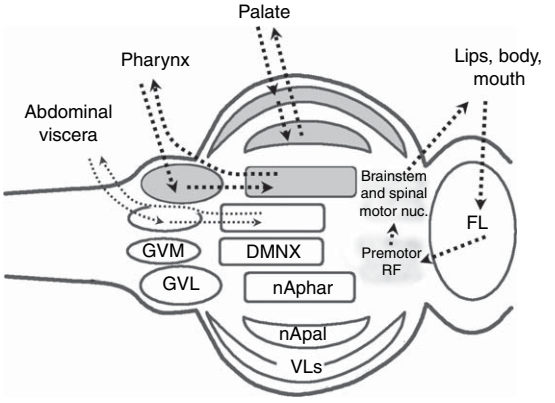

Figure 4 Schematic diagram of a dorsal view of the medulla of a goldfish, anterior to the right. The different reflex systems for the four visceral subsystems are illustrated. The abdominal viscera are innervated by the general visceral branch of the vagus nerve which projects centrally to the medial division of the general visceral nucleus (GVM) and commissural nucleus of Cajal. As in mammals, these maintain an intimate reflex system with the dorsal motor nucleus of the vagus (DMNX). Three semi-independent taste reflex systems also can be identified (shaded in gray): (1) pharyngeal, (2) palatal and caudal oral cavity, and (3) taste buds on the lips and external body surface. Each is connected to a different motor subsystem. The pharyngeal sensory nucleus (GVL) has reflex connections to the pharyngeal motor pool (nAphar). The sensory layers of the vagal lobe (VLs) have a topographically organized reflex connection with the pool of nuc. ambiguus neurons that extend into the vagal lobe motor layer (nApal). The facial lobe gustatory system, which drives complex movements of the body and head for orientation to external food sources, has connections to the premotor reticular formation. DMNX, dorsal motor nucleus of the vagus; FL, facial lobe; GVL, general visceral nucleus, lateral component; GVM, general visceral nucleus medial component; nApal, palatal portion of the nucleus ambiguus (=motor layers of the vagal lobe); nAphar, pharyngeal portion of nucleus ambiguus; VLs, sensory layers of the vagal lobe. Adapted from Goehler L. E. and Finger T. E. (1992) and Kanwal J. S. and Finger T. E. (1997).

4.11.2.3 Second-Order Gustatory Nuclei

The principal target for the ascending secondary gustatory fiber systems is the superior secondary gustatory nucleus (Herrick, C. J., 1905) which is homologous to the pontine taste area or parabrachial nuclear complex in mammals (Norgren, R. and Leonard, C. M., 1973; Norgren, R. and Pfaffmann, C., 1975). In fishes, as in mammals, the superior secondary gustatory nucleus lies in the dorsal pons adjacent to the superior cerebellar peduncle, or brachium conjunctivum. Whereas in mammals, the gustatory portion of the parabrachial complex is a small, poorly differentiated region; in fishes with large gustatory systems, the superior secondary gustatory nucleus is a large well-differentiated nucleus clearly divided into three or more compartments (Finger, T. E., 1978; Morita, Y. *et al*., 1980; Finger, T. E. and Kanwal, J. S., 1992). The facial lobe (taste) projects to the most medial subnucleus; the vagal lobe (taste) projects laterally, and the commissural nucleus of Cajal and associated general visceral nuclei project to a superior secondary general visceral nucleus, ventral and anterior of the secondary gustatory nuclei (Morita, Y. *et al*., 1980; Finger, T. E. and Kanwal, J. S., 1992; Yoshimoto, M. *et al*., 1998). The secondary gustatory and general visceral nuclei exhibit distinct histochemical differences as well as the differences in connectivity (Finger, T. E. and Kanwal, J. S., 1992). A substantial bilateral projection exists so that the superior secondary gustatory nucleus receives information from both sides of the body and mouth (Figure 5).

Although the superior secondary gustatory nucleus in fishes is often very large and well differentiated, the fine topography so evident in the primary gustatory centers appears largely lost in the

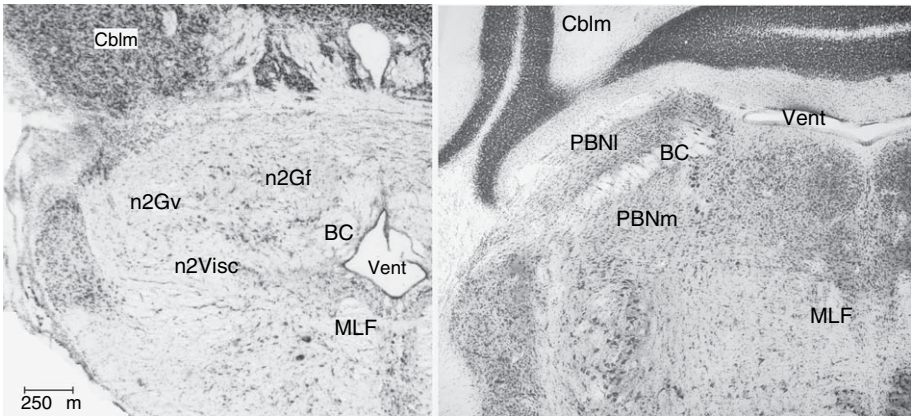

Figure 5 The secondary gustatory nuclei of the pons in (left) a catfish (*Ictalurus punctatus*) and (right) a mouse shown at the same magnification. In fishes, this nucleus is the superior secondary gustatory nucleus (n2G) whereas in mammals, it is called the parabrachial nucleus (PBN) or pontine taste area. In these species, as in all other vertebrates, the secondary gustatory nuclei lie adjacent or surrounding the Brachium conjunctivum (BC) which carries the ascending output from the cerebellum. In fishes, the n2G is divisible into a general visceral zone (n2visc) and a gustatory zone, itself divisible into a facial taste relay (n2Gf) and a vagal taste relay (n2Gv). The parabrachial complex also contains several subdivisions, the most prominent being a lateral subnucleus (PBNl) dorsolateral to the BC and a medial subnucleus (PBNm) ventral to the BC. BC, brachium conjunctivum; Cblm, cerebellum; MLF, medial longitudinal fasciculus; vent, ventricle (rostral end of fourth ventricle).

second-order nucleus. Receptive fields are large rather than discrete (Marui, T., 1981; Lamb, C. F. and Caprio, J., 1992), and small injections of tracer into the primary gustatory nuclei label widespread terminals throughout large areas of the secondary gustatory complex.

4.11.2.4 Ascending Fiber System

As mentioned above, ascending gustatory information targets two different sorts of nuclei in the forebrain. The first is a specific taste lemniscal pathway with an ultimate telencephalic target. The second is a more diffuse ascending system targeting a variety of limbic structures including the hypothalamus and amygdala.

In mammals, the telencephalic target of the gustatory lemniscus is gustatory cortex; the thalamic relay is VPMpc (parvocellular subnucleus of the ventroposteriomedial nucleus of the thalamus). Forebrain organization in fish is still being debated, but the clearest formulation names the third-order thalamic gustatory target as the preglomerular tertiary gustatory nucleus (Wullimann, M. F., 1988; Rink, E. and Wullimann, M. F., 1998; Yoshimoto, M. *et al.*, 1998). This tertiary gustatory nucleus relays taste information to a caudal, medial portion of the dorsal forebrain (dDm) (Kanwal, J. S. *et al.*, 1988; Yoshimoto, M. *et al.*, 1998). Based on connectivity and physiology, the gustatory part of dDm appears homologous to gustatory cortex.

The secondary gustatory nucleus also gives rise to a more diffuse ascending fiber system. In mammals, the system extends from the parabrachial nucleus (PBN) and terminates in various limbic structures including hypothalamus and amygdala (Nomura, S. *et al.*, 1979; Halsell, C. B., 1992). Likewise in fishes, the superior secondary gustatory nucleus projects broadly to limbic forebrain areas including the hypothalamus and probable amygdalar equivalent zones (Lamb, C. F. and Finger, T. E., 1996; Yoshimoto, M. *et al.*, 1998; Folgueira, M. *et al.*, 2003).

4.11.3 Gustatory Pathways in Mammals

This section describes the taste and general viscerosensory systems in mammals and highlights the many features of the organization of these systems in mammals which are comparable to those described for fish in the last section.

4.11.3.1 Primary Sensory Nucleus

The central sensory nucleus that receives taste input from the periphery, in mammals, is the NST. The nucleus is an extensive viscerosensory cell grouping that is small in the dorsoventral and mediolateral

planes, but long rostrocaudally. In fact, the NST extends throughout nearly the entire length of the medulla, from the level of the cochlear nucleus rostrally, where it is positioned somewhat laterally beneath the vestibular nuclei, to the spinal-medullary junction caudally, where it is positioned on the midline below the area postrema. The NST has, embedded laterally within it, the histologically distinct, rostrocaudally running solitary tract, the structure that gives the nucleus its name.

4.11.3.1.1 Primary afferent inputs

The solitary tract contains all the axons of the cranial nerves that provide input to the NST from the periphery. Thus, afferent axons from cranial nerves VII, IX, and X all travel in the tract and give off terminal branches that synapse in the NST. These inputs, which include both taste (special viscerosensory) and general viscerosensory axons (e.g., from the gastrointestinal organs), are arranged topographically in the nucleus (Figure 6). This topography is primarily

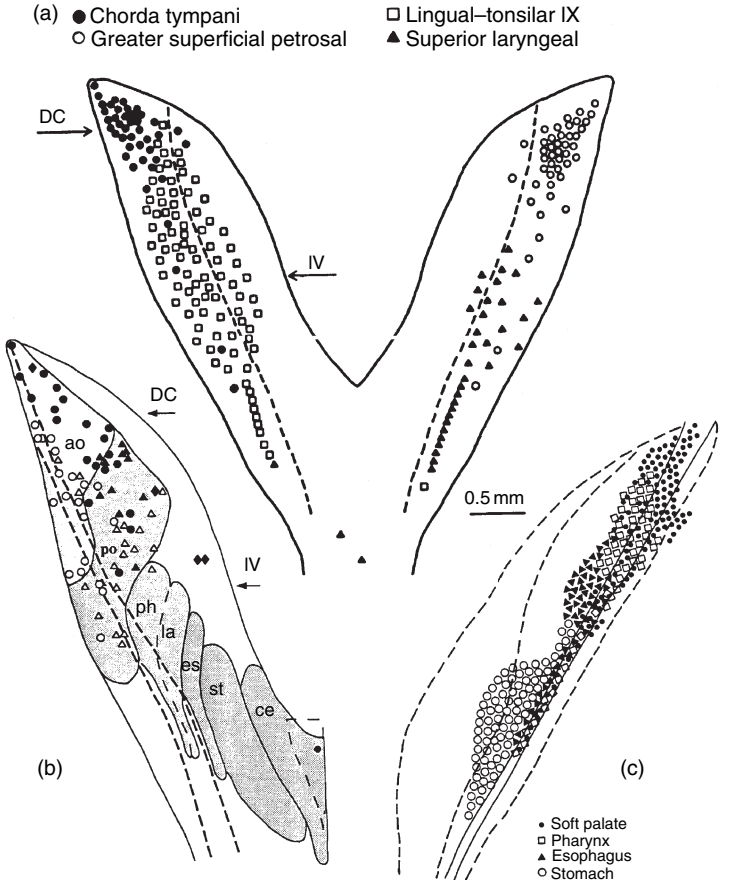

Figure 6 Horizontal depiction of the entire nucleus of the solitary tract in rat showing the topography of primary afferent inputs and of responses to oral and alimentary tract stimulation. Rostral is at the top of the figures. (a) Distribution of terminals of the peripheral gustatory nerves. Chorda tympani and greater superficial petrosal terminals, both of the seventh nerve, overlap and are located rostral to the ninth (lingual-tonsilar IX) nerve and the tenth (superior laryngeal) nerve. (b) Distribution of electrophysiological responses to oral stimulation. Taste responses from the anterior oral cavity (ao), closed circles; taste responses from the posterior oral cavity (po), closed triangles; taste responses from the whole mouth, closed diamonds; responses to mechanical stimulation of the anterior oral cavity, open circles; responses to mechanical stimulation of the posterior oral cavity, open triangles. Caudal shaded areas indicate primary afferent terminals from the pharynx (ph), larynx (la), esophagus (es), stomach (st), and cecum (ce). (c) Differential, but overlapping terminations from the soft palate, closed circles; pharynx, open squares; esophagus, closed triangles; and stomach, open circles. The dashed line in (a) represents a parcellation of the NST into medial and lateral regions. DC and IV arrows indicate, respectively, the level of the dorsal cochlear nucleus, and union of the NST with the fourth ventrical medially. Reproduced from Norgren, R. 1995. Gustatory System. In: The Rat Nervous System (*ed.* G. Paxinos), pp. 751–771. Academic Press, with permission from Elsevier, as adapted from Travers, S. P. 1993. Orosensory Processing in Neural Systems of the Nucleus of Solitary Tract. In: Mechanisms of Taste Transduction (*eds.* S. A. Simon and S. D. Roper), pp. 339–424. CRC press.

in the rostrocaudal plane reflecting the different medullary entry points of the NST's cranial nerve inputs, from the rostral-most VII to the caudal-most X. Moreover, the pattern of gustatory inputs defines an oropharyngeal topography within the NST wherein the taste buds of different regions of the oropharyngeal cavity are represented centrally in a somatotopic arrangement. Cranial nerve VII-innervated buds are on the anterior tongue and on the apposing palate, the central endings of the nerve branches innervating these two fields are largely coincident and located at the rostral pole of the NST. Cranial nerve IX-innervated buds are on the posterior tongue, the nerve's gustatory endings are overlapping but immediately caudal to those of CN VII (Whitehead, M. C., 1988a; 1988b in hamster; May, O. L. and Hill, D. L., 2006, in rat). Cranial nerve X-innervated buds are farthest posterior (on the larynx), the nerve's endings are located farthest caudal in the gustatory NST.

Primary afferent inputs are also arranged with a gross modality-specific topography in that gustatory axons synapse in rostral levels of the NST, while general visceral ones synapse caudally. This rostrocaudal arrangement is related to the differential representation of these two broad functional categories of axon types in VII, IX, and X. Thus, for example, VII which contains taste but no general visceral axons synapses rostrally, X with some taste, but predominant general viscerosensory axons synapses caudally. At any particular rostrocaudal level of the NST, primary afferent endings are concentrated in some cell groups of the nucleus, light or absent in others, indicating that there are subdivisions within the nucleus that can be defined on the basis of cytoarchitecture and inputs (Figure 7). Taste primary afferent synapses, in particular, are concentrated in a centrally located cell grouping in the rostral half of the NST, termed the rostral central subdivision. They synapse to a lesser extent also in the rostral lateral subdivision. These two subdivisions, and others involved in higher order, lemniscal connections of the taste pathways, are characterized by differences in the densities, sizes, and shapes of constituent neurons. The functional segregation within the NST further extends to the general visceral inputs themselves, with different visceral organs being represented in different longitudinal domains (i.e., subdivisions) within the NST (Katz, D. M. and Karten, H. J., 1983; Altschuler, S. M. *et al.*, 1989).

4.11.3.1.2 Subdivisions and cell types

Cells of the NST, generally, are smaller than those that surround the nucleus, for example, in the vestibular nuclei above, or the reticular formation below. This feature and the nucleus' felt-like neuropil, evident in silver stains and as differentially heterochromatic Nissl staining, allow the boundaries of the NST to be readily drawn (Whitehead, M. C., 1988a; 1988b). Cell groupings within the NST give the nucleus a heterogeneous cytological organization (Figure 8). A number of investigators have subdivided the nucleus based on routine cell staining with the Nissl method. Most studies recognize medial and lateral differences in cell packing and have simply divided the nucleus at every rostrocaudal level into two parts, medial and lateral (see, e.g., Torvik, A., 1956 in rat; Beckstead, R. M. and Norgren, R., 1979 in monkey; Hamilton, R. B. and Norgren, R., 1984 in rat). In hamster, additional staining methods, most notably, the Golgi stain which shows the dendrites and axons of cells, provided evidence for a third area, the central subdivision, that is cytologically distinct and interposed between the medial and lateral subdivisions (Whitehead, M. C., 1988a; 1988b). Subsequent studies in rat have similarly identified the rostral central subdivision as the prominent zone of neural activation by gustatory inputs from the periphery (e.g., Harrer, M. I. and Travers, S. P., 1996; Travers, S. P. and Hu, H., 2000). This central area coincides with parts of the lateral and medial subdivisions of earlier parcellation schemes (Torvik, A., 1956; Beckstead, R. M. and Norgren, R., 1979).

The central subdivision of the NST is distinguished by cells that are relatively small and densely packed and that exhibit three types of dendritic morphologies (Figure 9). Elongate cells have ovoid cell bodies and dendrites that extend in the mediolateral plane. Tufted neurons have dendrites or dendritic branches with one predominant orientation, usually dorsally or ventrally. Stellate cells have rounded or polygonal cell bodies and dendrites that radiate in all directions. A variety of small stellate cell with lumpy, irregular dendrites and a very short, locally arborizing axons, i.e., a local circuit neuron, is also present. The dendrites of all three cell types bear spiny or pedunculated appendages.

Correlating the cytoarchitectonic subdivisions with the locations of taste nerve endings, labeled by application of tracers to gustatory branches of the facial (CN VII), glossopharyngeal (CN IX), and vagus (CN X) nerves, established that the taste primary afferent termination zone coincides with the

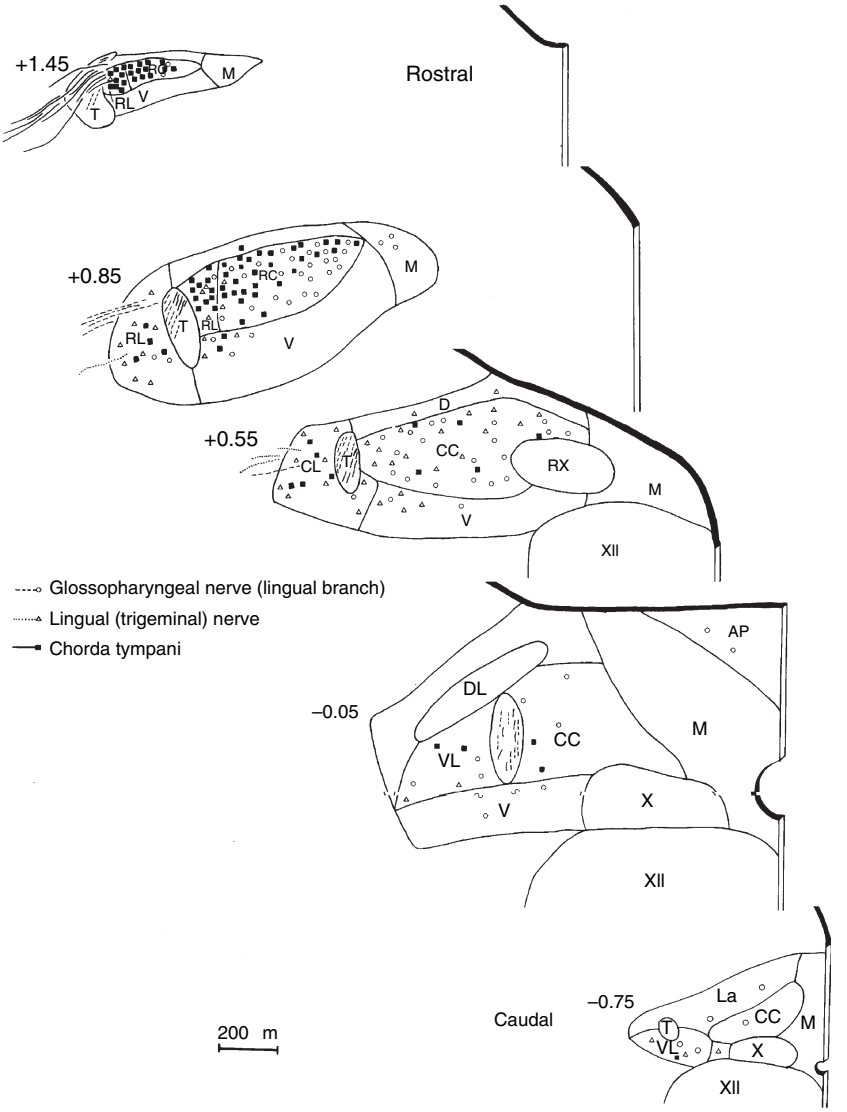

Figure 7 The NST in transverse sections showing the relationship of oral cavity inputs to cytoarchitectonic subdivisions in hamster (see Figure 8 for abbreviations). Taste afferent terminals from the anterior tongue (chorda tympani, closed squares) are concentrated in the rostral central subdivision; terminals from the posterior tongue (glossopharyngeal nerve, lingual branch, open circles) overlap but are densest more caudal than chorda ones in the rostral central subdivision. Nontaste, trigeminal inputs from the anterior tongue (lingual nerve, open triangles) overlap taste inputs but are concentrated in the rostral lateral subdivision. Numbers at left indicate distance (in mm) of each section from the obex. Reproduced from Whitehead M. C. (1988a; 1988b).

rostral central subdivision (Figure 7). The rostral lateral subdivision also received many taste endings, with fewer and fewer endings in the caudal central and caudal lateral subdivisions, respectively. Considering the entire extent and outlines of the NST, the distribution of all taste endings is to rostral and lateral regions of the nuclear complex.

The synaptic organization of taste inputs within the rostral central subdivision has been defined for the hamster (Whitehead, M. C., 1986; Brining, S. K. and Smith, S. K., 1996). Taste afferent endings, labeled with the marker horseradish peroxidase, were found to synapse *via* round vesicle-containing endings and asymmetrical membrane specializations primarily with small caliber dendrites and dendritic spines (Figure 10). Synapses of this type are likely excitatory. The taste afferent endings synapse in association with other, presumably nonprimary, endings. Some of

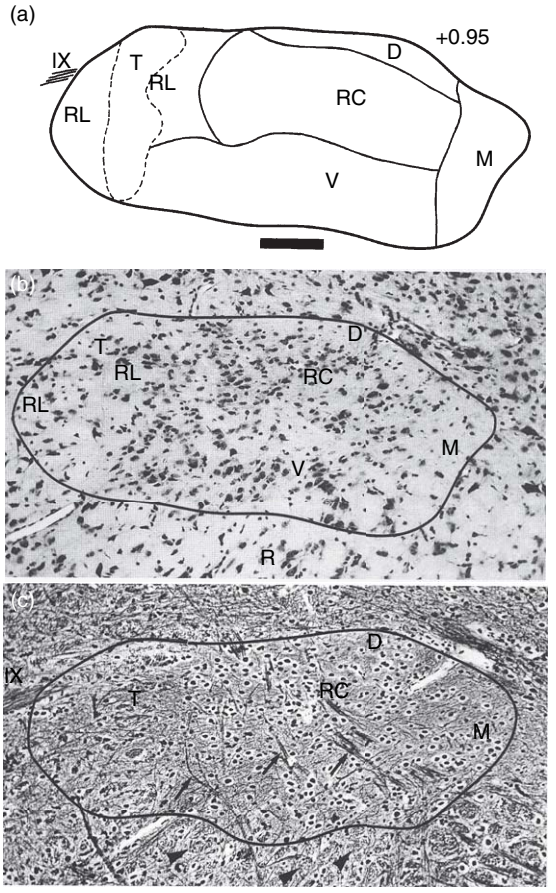

Figure 8 Cytoarchitectonic subdivisions of the NST in transverse sections at the level of the glossopharyngeal sensory nerve root in hamster (level similar to the second from the top in Figure 7). (a) Drawing of the outlines of subdivisions in the Nissl-stained section (b) The rostral central subdivision (RC) is characterized by smaller, densely packed, round, oval, and elongate cells; the medial subdivision (M) is sparsely cellular; the ventral subdivision (V) has larger somewhat clustered cells; the rostral lateral subdivision is moderately cellular and has the solitary tract (T) embedded within it. (c) Reduced silver-stained section adjacent to that in (b) showing the felt-like neuropil of the NST and thick fibers of passage arcing from the vestibular nuclei dorsal to the NST through the rostral central (RC) and ventral (V) subdivisions. Number at upper right indicates distance (in mm) of the sections from the obex. Reproduced from Whitehead M. C. (1988a; 1988b).

these nonprimary endings contain flat vesicles and engage in symmetrical synaptic junctions indicative of inhibitory synapses. The presence of presumed inhibitory endings is consistent with the identification of GABA-ergic cells and endings in the rostral NST (Lasiter, P. S. and Kachele, D. L., 1988; King, M. S., 2003) and similar small neurons in the rostral central subdivision that have locally arborizing axons, that is, inhibitory local circuit neurons. The complex synaptic milieu of taste endings on second-order neuronal dendrites, distant from their cell bodies, allows for modulation of taste-elicted activity in the afferent endings themselves or in the second-order neurons by other inputs, including interneuronal ones.

Other subdivisions border the rostral central subdivision (see, e.g., Figure 8). They differ in the extent to which they are involved in taste-related pathways (Whitehead, M. C., 1988a; 1988b). Thus, there are ventral and medial subdivisions bordering the rostral central subdivision which receive sparse taste afferent input (Figure 7). Similarly, caudally in the NST, subdivisions include caudal central, ventral medial, and ventrolateral which receive sparse taste input, but receive other inputs including general visceral primary afferent axonal endings from internal organs (Figure 6). These caudal areas of the NST project to the rostral areas and allow for interoceptive (e.g., gastrointestinal) and oral (taste) interactions within the NST (Karimnamazi, H. *et al.*, 2002).

4.11.3.2 Brainstem Reflex Connections

Taste stimulation elicits highly stereotyped oromotor behaviors that effect ingestion of palatable compounds (e.g., licking of sweet tastants) and rejection of aversive tastes (e.g., tongue protrusion and gaping to eject bitter, potentially poisonous, compounds) (Grill, H. J. and Norgren, R., 1978a; 1978b). These motor behaviors result from activation and modulation of local gustatory sensory–motor reflex pathways involving short distance connections confined within the medulla. These local, intramedullary pathways and the neurons they engage have, to some level of detail, been defined anatomically and functionally. The rostral (gustatory) NST projects heavily to the nearby, subjacent reticular formation (Travers, J. B., 1988; Beckman, M. E. and Whitehead, M. E., 1991) (Figures 11 and 12). The reticular formation, in turn, projects to motor nuclei involved in oromotor behaviors (Travers, J. B. and Norgren, R., 1983) (Figures 12 and 13). These include the hypoglossal nucleus for tongue movements, the trigeminal motor nucleus for jaw movements, the facial motor nucleus for facial movements, and nucleus ambiguus for pharyngeal movements associated with swallowing. Though less well studied because of the small size of the NST and the difficulty of mapping short connections, there are intranuclear connections that ultimately influence reticular and oromotor neuronal responses to tastes. These intranuclear

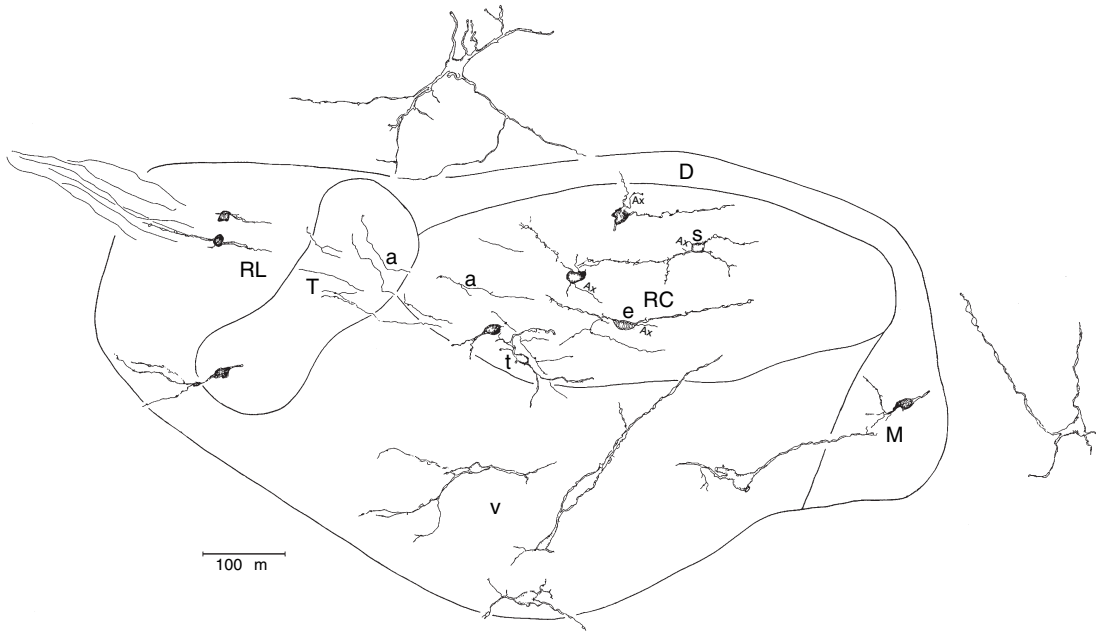

Figure 9 Cell types and axons (Golgi-Cox method) of the rostral NST in hamster at the level of the glossopharyngeal nerve root (fibers at upper left) (level similar to that in Figure 8). Primary afferent axons of the nerve root and solitary tract (a) parallel the dendrites of elongate cells in the rostral lateral subdivision and in the rostral central subdivision (e). A stellate cell (s) also has mediolaterally oriented dendrites; t, tufted neuron. Cells of the ventral subdivision are larger with longer dendrites than those of other subdivisions. Larger still, with more elaborate dendritic branching, are the cells dorsal (vestibular) and medial to the NST which are drawn for comparison. (Abbreviations of subdivisions as in Figure 8.) Reproduced from Whitehead M. C. (1988a; 1988b).

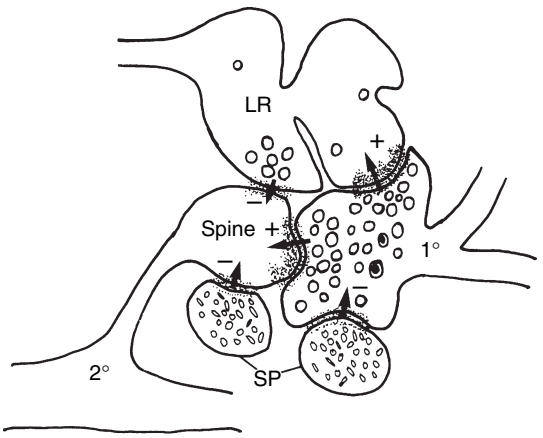

Figure 10 A synaptic circuit for taste (facial, including chorda tympani) primary afferent endings in the rostral central subdivision of the NST in hamster. Taste endings (1°) synapse on dendritic spines of second-order neurons (2°) and on other (possibly dendritic) endings (LR), which in turn influence transmission by means of LR (dendro?)-dendritic synapse. Transmission through the taste axon-second-order neuron circuit is also modulated pre- and postsynaptically by SP axonal endings with flat vesicles and symmetrical synaptic junctions. The signs (+) and (−) indicate possible excitatory and inhibitory influences. Reproduced from Whitehead, M.C. 1986. Anatomy of the gustatory system in the hamster: synaptology of facial afferent terminals in the solitary nucleus. J. Comp. Neurol. 244, 72–85.

connections appear to differentially involve the cytoarchitectonic subdivisions.

Small neuroanatomical tracer injections confined to the rostral NST and heavily involving the rostral central subdivision demonstrate that there are intra-NST projections from this taste-afferent recipient region to ventral and medial portions of the NST at more caudal levels. Thus, the medial and ventral subdivisions at intermediate rostrocaudal levels of the nucleus receive heavy input from the rostral central NST. Outside the NST, heavy axonal projections terminate in the parvicellular medullary reticular formation immediately ventral to the NST (Beckman, M. E. and Whitehead, M. C., 1991) (Figures 11 and 12). The injection sites yielding these local projections, while small, invariably include the ventral subdivision, so it is difficult to resolve all the possible short distance connections. Nevertheless, the evidence to date is consistent with a pathway whereby neurons in the rostral central subdivision are activated by taste-elicited impulses arriving from primary afferent synapses (Figure 12). In turn, many of these first-order central neurons project to other regions of the NST, including to the ventral subdivision. The ventral subdivision (and, perhaps, the rostral central

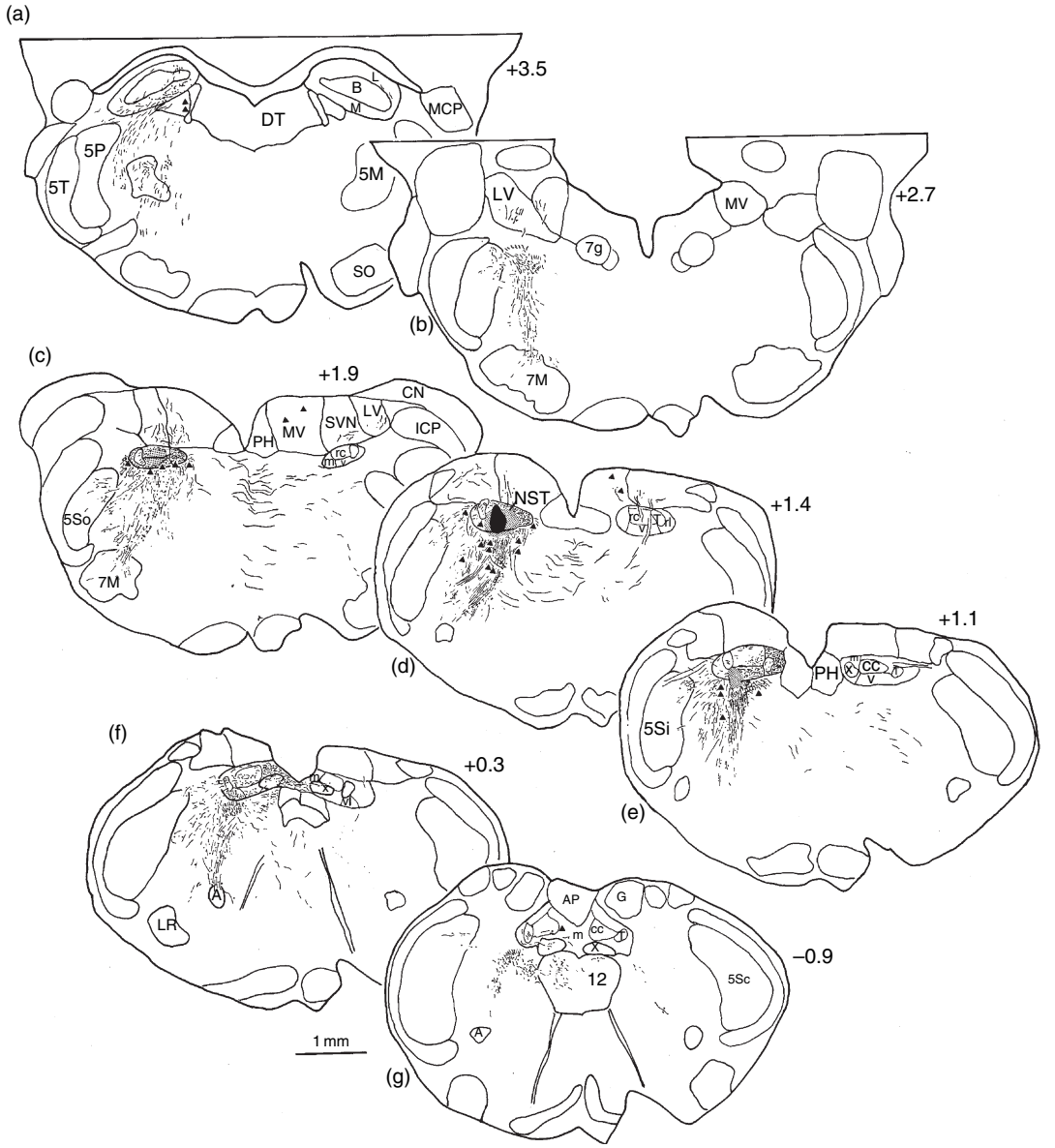

Figure 11 Ascending (lemniscal) projections and local (reflex) projections from the rostral NST in hamster seen after an injection of neuroanatomical tracer (HRP) into the gustatory domain (center of injection site at same level as in Figure 8, includes rostral central and ventral subdivisions). Letters identifying nuclei are shown on the right side of the brain in order to best see labeled endings (dots) on the right. Ascending axons from the NST terminate rostrally in the medial PBN (B-M) and sparsely in the trigeminal motor nucleus (5M). Local and caudally directed labeled axons terminate in the reticular formation (RF) ventral to the NST and lateral to the hypoglossal nucleus (12) and, sparsely, within the hypoglossal, vagal (X) and facial (7M) motor nuclei. Nucleus ambiguus (A). Intra-NST label extends caudally to the level of the area postrema (AP) and is concentrated in the medial (m) and ventral (v) subdivisions. Triangles indicate retrogradely labeled neuronal cell bodies. Numbers at right indicate distance (in mm) of each section from the obex. Reproduced from Beckman, M. E. and Whitehead, M. C. 1991. Intramedullary connections of the nucleus of the solitary tract in the hamster. Brain Res. 557, 265–279, with permission from Elsevier.

subdivision, directly) projects heavily to the parvocellular reticular formation (Beckman, M. E. and Whitehead, M. C., 1991) which, in turn, projects heavily to all the oromotor nuclei (Travers, J. B. and Norgren, R., 1983; Travers, J. B., 1988).

Combining Fos labeling during taste stimulation with neuroanatomical retrograde labeling of cells that project to the parvocellular reticular formation revealed a pattern consistent with a role for ventrally projecting neurons and of the ventral NST

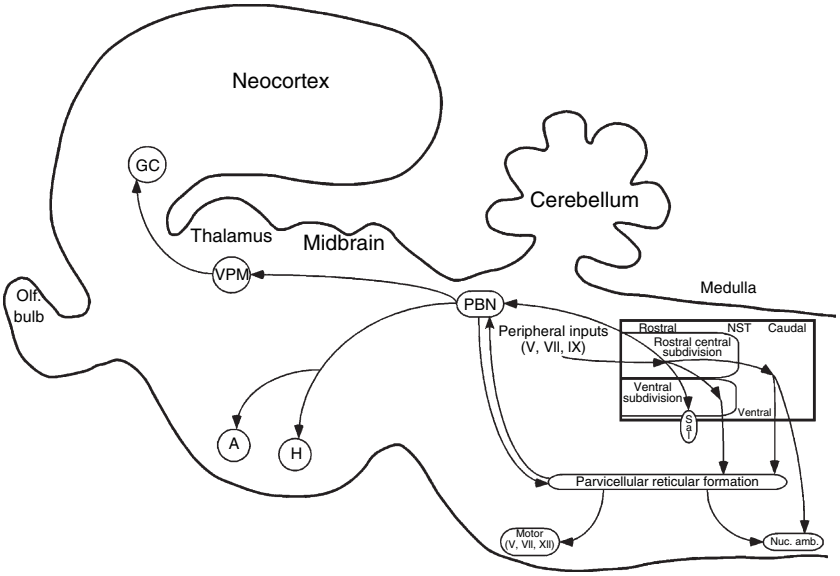

Figure 12 Local and ascending pathways of the mammalian central gustatory system diagrammed on a sagittal view of the brain. The local (reflex) pathway involves cells in the rostral central subdivision of the NST that receive input from primary afferent peripheral fibers. These cells can project to the ventral subdivision of the NST either directly or via the caudal NST. The ventral subdivision, in turn, projects to the reticular formation. Finally, the parvicellular reticular formation projects to nucleus ambiguus and the oral motor nuclei (motor V, VII, XII). Local projections also involve the salivatory nuclei (Sal). The major ascending (lemniscal) pathway involves cells of the rostral central subdivision that project to the parabrachial nucleus of the pons (PBN) which, in turn, projects to the parvocellular ventroposteromedial nucleus of the thalamus (VPM). This gustatory part of the thalamus projects to agranular insular cortex (GC). A second ascending pathway involves a projection from the PBN to the basal forebrain (principally to the lateral hypothalamus (H), amygdala (A), and bed nucleus of the stria terminalis (not shown).

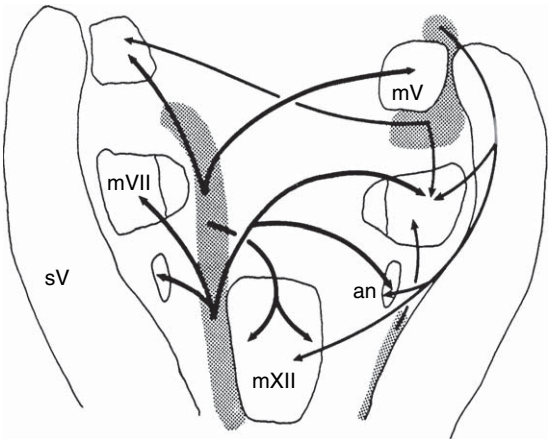

Figure 13 Diagram (horizontal plane) of the regions of the reticular formation (in gray cross-hatching) that project to the oral motor nuclei in rat. The reticular-motor projection neurons are located throughout the length of the medulla, including the area below the NST as in Figure 11. Projections are to nucleus ambiguus (an), the hypoglossal nucleus (mXII), the facial (mVII), and trigeminal (mV) motor nuclei bilaterally. Reproduced from Travers, J. B., and Norgren, R. 1983. Afferent projections to the oral motor nuclei in the rat. J. Comp. Neurol. 220, 280–298.

subdivision in influencing premotor reticular formation neurons (Travers, S. P. and Hu, H., 2000). Electrical stimulation of the second-order gustatory nucleus (the PBN, in rat) activates cells in the ventral NST and elicits oromotor behaviors, illustrating an influence of descending impulses from the second-order taste center on the medullary reflex pathway (King, M. S. *et al.*, 2003).

4.11.3.2.1 Topography of taste quality

Functional evidence that the rostral central and lateral subdivisions of the rostral NST are principally involved in taste information processing derives from experiments seeking to determine whether taste quality is represented topographically in the NST. Electrophysiological recordings, either single or multiunit methods, have not, despite many investigations, revealed a consistent or clear-cut chemotopic organization (e.g., Pfaffmann, C. *et al.*, 1961; Scott, T. R. *et al.*, 1986; Mistretta, C. M., 1988). Nevertheless, reconstructions of sites of taste-activated neurons in relation to subdivisions of the NST localize most of them, in hamster, to the rostral central and rostral lateral subdivisions (McPheeters, M. *et al*, 1990;

Whitehead, M. C. *et al.*, 1993). More recently, anatomical localization of NST cells activated by particular taste stimuli was accomplished with immunocytochemistry for Fos, the protein product of the c-fos gene. Fos-positive cells attributable to taste stimulation were differentially concentrated in the rostral central subdivision (Harrer, M. I. and Travers, S. P., 1996, in rat). Although no straightforward chemotopography was evident and sucrose and quinine activated cells were intermingled, the latter were concentrated medially within the central subdivision evidence for a crude chemotopography as has been suggested in earlier electrophysiological studies (Halpern, B. P. and Nelson, L. M. 1965) (Figure 14). This crude chemotopy may reflect the differential distribution of different taste receptors within the oral cavity (Chandrashekar, J. *et al.*, 2006) making it difficult to distinguish a chemotopic map from an orotopic one.

4.11.3.3 Lemniscal Pathway

The lemniscal pathway in the mammalian gustatory system extends from the NST through the thalamus to the cerebral cortex for perception (Figure 12). In rodents, but not primates, all information ascending to the thalamocortical system undergoes an obligatory synaptic interruption in the PBN of the pons. The PBN is also a site of synaptic interruption in the pathway leading to the basal forebrain (see Section 4.11.3.4).

The projection from the NST to the PBN is massive and involves axons originating from cells in rostral and caudal levels of the medullary nucleus (Norgren, R. and Leonard, C. M., 1973; Norgren, R., 1978; Beckstead, R. M. *et al.*, 1980; Travers, J. B., 1988). Thus, both taste and general viscerosensory impulses project to the pons. The pontine representations of taste and nontaste (e.g., gastric) signals are separated among the subdivisions of the PBN (Karimnamazi, H. *et al.*, 2002). The gustatory PBN projection neurons of the NST have been identified and are predominantly located in the rostral central subdivision, the same region receiving densest taste inputs from the periphery (Whitehead, M. C., 1990). Specific cell types in the rostral central subdivision that project to the PBN, in hamster, are the elongate and stellate cells. These projection neurons, back-

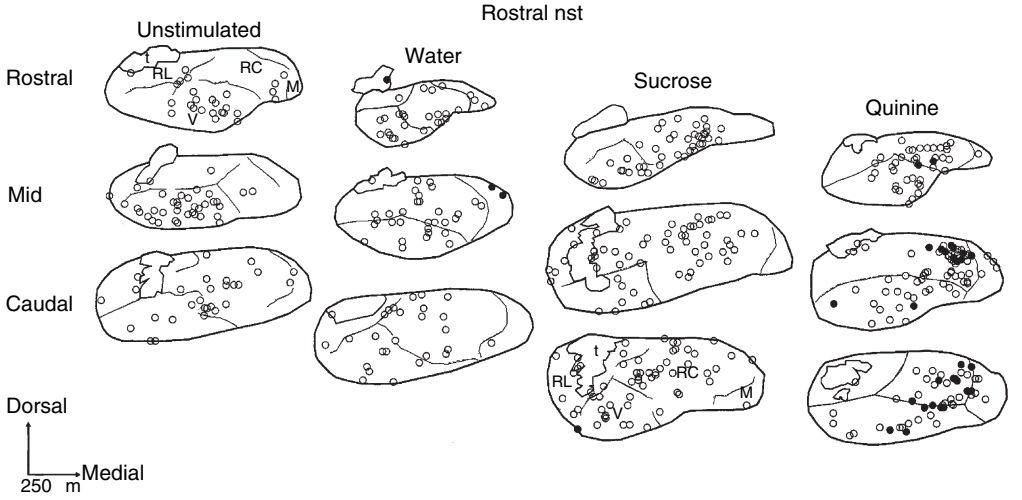

Figure 14 Distribution of cells immuno-positive for Fos elicited by two qualitatively and hedonically distinct taste stimuli, sucrose and quinine, within the rostral nucleus of the solitary tract of rat. Three anteroposterior levels in the transverse plane are shown for one animal from each of four stimulus conditions. Thin lines depict boundaries of cytoarchitectonic subdivisions (abbreviations as in Figure 8). Filled and open circles indicate intensely and moderately stained nuclei, respectively, of Fos-positive cells. Taste-stimulated animals had more numerous Fos-positive cells than the water and unstimulated animals, particularly in the rostral central subdivision. Within the central subdivision, Fos-positive neurons following quinine stimulation were concentrated medially; positive neurons following sucrose stimulation were distributed more evenly along the mediolateral axis. Despite their differential distribution, sucrose- and quinine-activated neurons were intermingled. Reproduced from Harrer, M. I. and Travers, S .P. 1996. Topographic organization of Fos-like immunoreactivity in the rostral nucleus of the solitary tract evoked by gustatory stimulation with sucrose and quinine. Brain Res. 711, 125–137, with permission from Elsevier.

filled with neuroanatomical markers, have been analyzed with the electron microscope to establish that they receive primary-like synaptic inputs (Whitehead, M. C., 1993). Therefore, the NST–PBN gustatory projection neurons correspond to first-order central neurons that are contacted directly by taste afferent endings from the periphery.

4.11.3.3.1 Second-order (parabrachial) nucleus

The PBN is a complex of different cytoarchitectonic subdivisions that surround the brachium conjunctivum (Fulwiler, C. E. and Saper, C. B., 1984; Halsell, C. B. and Frank, M. E., 1989). These subdivisions are generally grouped into either the lateral division, dorsal and lateral to the brachium conjunctivum and bordering the external surface of the pons, or the medial division, medial to the brachium. Gustatory-responsive neurons have been localized predominantly in the medial division, while general viscerosensory neurons have been localized in the lateral division. Anatomical studies support this functional parcellation: the medial PBN receives input from the rostral, gustatory NST; the lateral PBN receives input from the caudal, viscerosensory NST. In particular, the medial PBN, predominantly its caudal and ventral parts, receives projections from cells of the rostral central and rostral lateral subdivisions of the NST. The lateral PBN, predominantly its intermediate and rostral–dorsal parts, receives projections from the caudal central and medial subdivisions of the NST (Whitehead, M. C., 1990). PBN projection cells of the rostral NST, that is, gustatory cells of the ascending viscerosensory system, are more numerous than PBN projection cells of the caudal NST, that is, general viscerosensory cells. The pontine projections are predominantly ipsilateral, although a small minority of NST neurons project to the contralateral PBN. The most prominent subdivision within the PBN receiving input from the gustatory NST is the medial subdivision, especially at caudal levels of the nucleus. Gustatory projections also extend, but lightly, into the medial part of the lateral subdivision. Within the gustatory PBN neurons responsive to anterior and posterior regions of the oral cavity are located in different cytoarchitectonic subdivisions, evidence for at least a gross orotopy at this second-order level of the ascending taste system in mammals (Halsell, C. B. and Travers, S. P., 1997), just as in fish (see Section 4.11.3.2).

4.11.3.3.2 Third-order (thalamic) nucleus and gustatory cortex

In contrast with other lemniscal sensory systems in which the thalamus receives input directly from the medulla, in the taste system, excepting for Old World monkeys (Hamilton, R. B. *et al.*, 1985), the thalamus receives input from second-order central neurons in the PBN (Figure 12). The PBN-thalamus projection terminates in a small medial-most sliver of the ventroposteromedial thalamic nucleus (VPM) (Norgren, R. and Leonard, C. M., 1973). The VPM generally processes information about somatosensation of the face relayed rostrally from first-order central neurons in the trigeminal sensory nucleus of the brainstem. The gustatory-specific thalamic nucleus, the VPMgus parvocellularis (pc), is the medial-most part of the VPM. Thus, functions are topographically represented; third-order taste neurons lie just medial to second-order general sensory neurons processing, for example, touch and temperature information from the face, mouth, and tongue. Indeed, taste and lingual touch neurons occur side by side in the VPM. The VPMgus pc projects to gustatory neocortex (Figure 12).

Gustatory neocortex lies in the insular region, dorsal to the rhinal fissure. This region, identified as taste-responsive (Kosar, E. *et al.*, 1986 in rat, Wehby, R. G. and London, J. A., 1995 in hamster), is characterized cytoarchitectonically as being agranular or dysgranular, that is, lacking a well-defined layer IV (Kosar, E. *et al.*, 1986) As in thalamus, somatotopy is evident in the cortical taste area. Taste neurons are located in a region bordering (ventral to) somatosensory primary cortical neurons representing the tongue, which in turn are just ventral to mouth and face representations (Norgren, R. and Wolf, G., 1975).

4.11.3.4 Basal Forebrain and Descending Pathways

In addition to the thalamocortical gustatory pathway, there are dense ascending taste projections to the basal forebrain (Figure 12). Axons from cells in the NST and PBN terminate heavily in the lateral hypothalamus, the amygdala, and the bed nucleus of the stria terminalis (Saper, C. B., 1982; Halsell, C. B., 1992; Nakashima, M. *et al.*, 2000; Pritchard, T. C. *et al.*, 2000). These limbic projections likely mediate autonomic functions related to activation of the taste system and hedonic aspects of feeding. These limbic regions, together with the pontine and

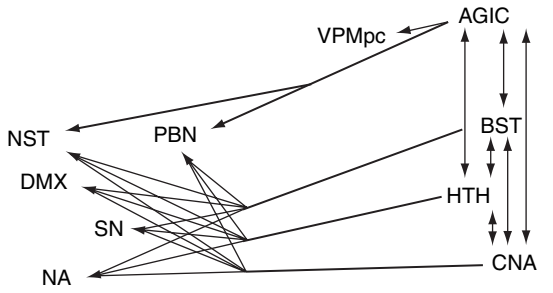

Figure 15 Descending pathways of the mammalian gustatory system schematically represented in the sagittal plane (rostral is at the right). Lines with single arrowheads indicate major long, descending forebrain projections to the hindbrain. Forebrain regions include agranular insular (gustatory) cortex (AGIC), the bed nucleus of the stria terminalis (BST), the hypothalamus (HTH), and the central nucleus of the amygdala (CNA). Hindbrain nuclei that receive terminals from the forebrain gustatory-related areas are the NST, the PBN, the dorsal motor vagal nucleus (DMX), the salivatory nuclei (SN) and nucleus ambiguus (NA). Double arrows indicate local forebrain reciprocal interconnections. Reproduced from Norgren, R. 1985. Taste and the autonomic nervous system. Chem. Senses 10, 143 –161, by permission of Oxford University Press.

thalamocortical areas, are reciprocally interconnected with each other (Figure 15).

Descending axons from forebrain, taste-related areas also synapse in the NST (Figure 15). Projections from gustatory cortex to the taste region of the NST are particularly dense and terminate heavily in the rostral central subdivision, the same subnuclear zone that contains primary afferent synapse and PBN projection neurons (Whitehead, M. C. *et al.*, 2000). Thus, descending impulses from cortex are positioned to influence the first central taste area. In addition, there are descending connections from gustatory cortex to the amygdala, the hypothalamus, and the PBN (Reep, R. L. and Winans, S. S., 1982). These areas, therefore, interconnect both the gustatory NST and the gustatory neocortex. The interconnections are quite precise and related to gustatory functions (Karimnamazi, H. and Travers, J. B., 1998; Cho, Y. K. *et al.*, 2003). Thus, gustatory cortex receives projections from the lateral hypothalamus, the same region that sends descending axons to the rostral NST. Cortical connections with the PBN are reciprocal and most heavily involve the medial PBN, the major termination site for axons ascending from the rostral NST, and a site originating projections back to the rostral NST. The gustatory cortex projects heavily to the central amygdaloid nucleus, a site of origin of amygdalofugal axons that project to the rostral NST. The anterior and basolateral amygdala are also reciprocally connected with gustatory cortex (Reep, R. L. and Winans, S. S., 1982; Whitehead, M. C. *et al.*, 2000). By these connections, the forebrain, particularly the limbic system, has access to both taste information and regions involved in autonomic outflow, for example, for energy and hydromineral regulation (Norgren, R., 1985; Grill, H. J. and Kaplan, J. M., 2002).

4.11.4 Conclusion

In summary, the general organization of the central gustatory pathways is similar in mammals and teleost fishes. This implies that this organizational scheme evolved early in vertebrate phylogeny. Not only are the broad patterns of connectivity similar between these disparate groups but also the details of connectivity and neurotransmitters. For example, glutamate acting on ionotropic glutamate receptors is the neurotransmitter at the first synapse of the system within the medullary gustatory nuclei (Bradley, R. M. *et al.*, 1996; Smeraski, C. A. *et al.*, 1996; Li, C. S. and Smith, D. V., 1997; Smeraski, C. A. *et al.*, 1998; 1999). Different cell populations in the primary taste relay give rise to the reflex connections and the ascending fiber systems (Finger, T. E., 1978; Whitehead, M. C., 1990; Halsell, C. B. *et al.*, 1996; Gill, C. F. *et al.*, 1999). In addition, neurons of the secondary gustatory nucleus can either project widely to both lemniscal and limbic targets or may show more restricted projections to the lemniscal nuclei only (Nomura, S. *et al.*, 1979; Halsell, C. B., 1992; Lamb, C. F. and Finger, T. E., 1996). Taken together, these findings indicate that the basic organization of the central gustatory system is phylogenetically old and stable through evolution. This stability may reflect the crucial nature of this system for survival.

References

Altschuler, S. M., Bao, X. M., Bieger, D., Hopkins, D. A., and Miselis, R. R. 1989. Viscerotopic representation of the upper alimentary tract in the rat: sensory ganglia and nuclei of the solitary and spinal trigeminal tracts. J. Comp. Neurol. 283, 248–268.

Atema, J. 1971. Structures and functions of the sense of taste in the catfish (*Ictalurus natalis*). Brain Behav. Evol. 4, 273–294.

Beckman, M. E. and Whitehead, M. C. 1991. Intramedullary connections of the nucleus of the solitary tract in the hamster. Brain Res. 557, 265–279.

Beckstead, R. M. and Norgren, R. 1979. An autoradiographic examination of the central distribution of the trigeminal, facial, glossopharyngeal, and vagal nerves in the monkey. J. Comp. Neurol. 184, 455–472.

Beckstead, R. M., Morse, J. R., and Norgren, R., 1980. The nucleus of the solitary tract in the monkey: projections to the thalamus and brain stem nuclei. J. Comp. Neurol. 190, 259–282.

Bradley, R. M., King, M. S., Wang, L., and Shu, X. 1996. Neurotransmitter and neuromodulator activity in the gustatory zone of the nucleus tractus solitarius. Chem. Senses 21, 377–385.

Braford, M. R. J. 1986. *De Gustibus Non Est Disputandem*: a spiral center for taste in the brain of the teleost fish, *Heterotis niloticus*. Science 232, 489–491.

Brining, S. K. and Smith, D. V. 1996. Distribution and synaptology of glossopharyngeal afferent nerve terminals in the nucleus of the solitary tract of the hamster. J. Comp. Neurol. 365, 556–574.

Chandrashekar, J., Hoon, M. A., Ryba, N. J., and Zuker, C. S. 2006. The receptors and cells for mammalian taste. Nature 444, 288–294.

Cho, Y. K., Li, C. S., and Smith, D. V. 2003. Descending influences from the lateral hypothalamus and amygdala converge onto medullary taste neurons. Chem. Senses 28, 155–171.

Cunningham, E. T. and Sawchenko, P. E., Jr. 2000. Dorsal medullary pathways subserving oromotor reflexes in the rat: implications for the central neural control of swallowing. J. Comp. Neurol. 417, 448–466.

Dickman, J. D. and Smith, D. V. 1988. Response properties of fibers in the hamster superior laryngeal nerve. Brain Res. 45, 25–38.

Finger, T. E. 1978. Gustatory pathways in the bullhead catfish. II. Facial lobe connections. J. Comp. Neurol. 180, 691–705.

Finger, T. E. 1988. Sensorimotor mapping and oropharyngeal reflexes in goldfish, *Carassius auratus.* Brain Behav. Evol. 31, 17–24.

Finger, T. E. 2006. Evolution of Taste. In: Evolution of the Nervous System: Non-mammalian Vertebrates (*eds*. J. Kaas, G. Striedter, T. Bullock, T. Preuss, J. Rubenstein, and L. Krubitzer), pp. 423–441. Elsevier.

Finger, T. E. and Kanwal, J. S. 1992. Ascending general visceral pathways within the brainstems of two teleost fishes: *Ictalurus punctatus* and *Carassius auratus*. J. Comp. Neurol. 320, 509–520.

Finger, T. E. and Morita, Y. 1985. Two gustatory systems: facial and vagal gustatory nuclei have different brainstem connections. Science 227, 776–778.

Folgueira, M., Anadon, R., and Yanez, J. 2003. Experimental study of the connections of the gustatory system in the rainbow trout, *Oncorhynchus mykiss*. J. Comp. Neurol. 465, 604–619.

Fulwiler, C. E. and Saper, C. B. 1984. Subnuclear organization of the efferent connections of the parabrachial nucleus in the rat. Brain Res. Rev. 7, 229–259.

Gill, C. F., Madden, J. M., Roberts, B. P., Evans, L. D., and King, M. S. 1999. A subpopulation of neurons in the rat rostral nucleus of the solitary tract that project to the parabrachial nucleus express glutamate-like immunoreactivity. Brain Res. 821, 251–262.

Goehler, L. E. and Finger, T. E. 1992. Functional organization of vagal reflex systems in the brain stem of the goldfish, *Carassius auratus*. J. Comp. Neurol. 319, 463–478.

Grill, H. J. and Kaplan, J. M. 2002. The neuroanatomical axis for control of energy balance. Front Neuroendocrinol. 23, 2–40.

Grill, H. J. and Norgren, R. 1978a. The taste reactivity test. I. Mimetic responses to gustatory stimuli in neurologically normal rats. Brain Res. 143, 263–79.

Grill, H. J. and Norgren, R. 1978b. The taste reactivity test. II. Mimetic responses to gustatory stimuli in chronic thalamic and chronic decerebrate rats. Brain Res. 143, 281–97.

Halpern, B. P. and Nelson, L. M. 1965. Bulbar gustatory responses to anterior and to posterior tongue stimulation in the rat. Am. J. Physiol. 209, 105–110.

Halsell, C. B. 1992. Organization of parabrachial nucleus efferents to the thalamus and amygdala in the golden hamster. J. Comp. Neurol. 317, 57–78.

Halsell, C. B. and Frank, M. E. 1989. Cytoarchitecture of the pontine taste area in the golden hamster. Chem. Senses 14, 707.

Halsell, C. B. and Travers, S. P. 1997. Anterior and posterior oral cavity responsive neurons are differentially distributed among parabrachial subnuclei in rat. J. Neurophysiol. 78, 920–38.

Halsell, C. B., Travers, S. P., and Travers, J. B. 1996. Ascending and descending projections from the rostral nucleus of the solitary tract originate from separate neuronal populations. Neuroscience 72, 185–197.

Hamilton, R. B. and Norgren, R. 1984. Central projections of gustatory nerves in the rat. J. Comp. Neurol. 222, 560–577.

Hamilton, R. B., Pritchard, T. C., and Norgren, R. 1985. Projections to the gustatory thalamus of new world primates. Soc. Neurosci. Abstr. 11, 1259.

Harrer, M. I. and Travers, S. P. 1996. Topographic organization of Fos-like immunoreactivity in the rostral nucleus of the solitary tract evoked by gustatory stimulation with sucrose and quinine. Brain Res. 711, 125–137.

Herrick, C. J. 1905. The central gustatory paths in the brains of bony fishes. J. Comp. Neurol. 15, 375–456.

Herrick, C. J. 1922. An Introduction to Neurology. W.B. Saunders Co.

Kanwal, J. S. and Finger, T. E. 1997. Parallel medullary gustatospinal pathways in a catfish: possible neural substrates for taste-mediated food search. J. Neurosci. 17, 4873–4885.

Kanwal, J. S., Finger, T. E., and Caprio, J. 1988. Forebrain connections of the gustatory system in ictalurid catfishes. J. Comp. Neurol. 278, 353–376.

Karimnamazi, H. and Travers, J. B. 1998. Differential projections from gustatory responsive regions of the parabrachial nucleus to the medulla and forebrain. Brain Res. 813, 283–302.

Karimnamazi, H., Travers, S. P., and Travers, J. B. 2002. Oral and gastric input to the parabrachial nucleus of the rat. Brain Res. 957, 193–206.

Katz, D. M. and Karten, H. J. 1983. Visceral representation within the nucleus of the tractus solitarius in the pigeon, *Columba livia*. J. Comp. Neurol. 218, 42–73.

King, M. S. 2003. Distribution of immunoreactive GABA and glutamate receptors in the gustatory portion of the nucleus of the solitary tract in rat. Brain Res. Bull. 60, 241–54.

King, M. S., Smith, M. T., Jani, K. P., and King, C. T. 2003. The locations of Fos-immunoreactive neurons following electrical stimulation of the gustatory parabrachial nucleus in conscious rats. Soc. Neurosci. Abstr. 594. 8.

Kiyohara, S. and Caprio, J. 1996. Somatotopic organization of the facial lobe of the sea catfish *Arius felis* studied by transganglionic transport of horseradish peroxidase. J. Comp. Neurol. 368, 121–135.

Kiyohara, S. and Tsukahara, J. 2005. Barbel Taste System in Catfish and Goatfish. In: Fish chemosenser (*eds*. K. Reutter and B. G. Kapoor), pp. 175–211. Science Publishers.

Kiyohara, S., Sakata, Y., Yoshitomi, T., and Tsukahara, J. 2002. The 'goatee' of goatfish: innervation of taste buds in the barbels and their representation in the brain. Proc. R. Soc. B. Biol. Sci. 269, 1773–1780.

Kosar, E., Grill, H. J., and Norgren, R. 1986. Gustatory cortex in the rat. I. Physiological properties and cytoarchitecture. Brain Res. 379, 329–241.

Lamb, C. F. and Caprio, J. 1992. Convergence of oral and extraoral information in the superior secondary gustatory nucleus of the channel catfish. Brain Res. 588, 201–211.

Lamb, C. F. and Finger, T. E. 1996. Axonal projection patterns of neurons in the secondary gustatory nucleus of channel catfish. J. Comp. Neurol. 365, 585–593.

Lasiter, P. S. and Kachele, D. L. 1988. Organization of GABA and GABA-transaminase containing neurons in the gustatory zone of the nucleus of the solitary tract. Brain Res. Bull. 21, 623–636.

Li, C. S. and Smith, D. V. 1997. Glutamate receptor antagonists block gustatory afferent input to the nucleus of the solitary tract. J. Neurophysiol. 77, 1514–1525.

Marui, T. 1981. Taste responses in the superior secondary gustatory nucleus of the carp, *Cyprinus carpio* L. Brain Res. 217, 59–68.

May, O. L. and Hill, D. L. 2006. Gustatory terminal field organization and developmental plasticity in the nucleus of the solitary tract revealed through triple-fluorescence labeling. J. Comp. Neurol. 497, 658–669.

McPheeters, M., Hettinger, T. P., Nuding, S. C., Savoy, L. D., Whitehead, M. C., and Frank, M. E. 1990. Taste-responsive neurons and their locations in the solitary nucleus of the hamster. Neuroscience 34, 745–758.

Mistretta, C. M. 1988. How the anterior tongue and taste responses are mapped onto the NST in fetal and perinatal sheep. Chem. Senses 13, 719–720.

Morita, Y. and Finger, T. E. 1985a. Reflex connections of the facial and vagal gustatory systems in the brainstem of the bullhead catfish, *Ictalurus nebulosus*. J. Comp. Neurol. 231, 547–558.

Morita, Y. and Finger, T. E. 1985b. Topographic and laminar organization of the vagal gustatory system in the goldfish, *Carassius auratus*. J. Comp. Neurol. 238, 187–201.

Morita, Y. and Finger, T. E. 1987. Topographic representation of the sensory and motor roots of the vagus nerve in the medulla of goldfish, *Carassius auratus*. J. Comp. Neurol. 264, 231–249.

Morita, Y., Ito, H., and Masai, H. 1980. Central gustatory paths in the crucian carp, *Carassius carassius*. J. Comp. Neurol. 191, 119–132.

Nakashima, M., Uemura, M., Yasui, K., Ozaki, H. S., Tabata, S., and Taen, A. 2000. An anterograde and retrograde tract-tracing study on the projections from the thalamic gustatory area in the rat: distribution of neurons projecting to the insular cortex and amygdaloid complex. Neurosci. Res. 36, 297–309.

Nomura, S., Mizuno, N., Itoh, K., Matsuda, K., Sugimoto, T., and Nakamura, Y. 1979. Localization of parabrachial nucleus neurons projecting to the thalamus or the amygdala in the cat using horseradish peroxidase. Exp. Neurol. 64, 375–385.

Norgren, R. 1978. Projections from the nucleus of the solitary tract in the rat. Neuroscience 3, 207–218.

Norgren, R. 1985. Taste and the autonomic nervous system. Chem. Senses 10, 143–161.

Norgren, R. 1995. Gustatory System. In: The Rat Nervous System (*ed*. G. Paxinos), pp. 751–771. Academic Press.

Norgren, R. and Leonard, C. M. 1973. Ascending central gustatory pathways. J. Comp. Neurol. 150, 217–237.

Norgren, R. and Pfaffmann, C. 1975. The pontine taste area in the rat. Brain Res. 91, 99–117.

Norgren, R. and Wolf, G. 1975. Projections of thalamic gustatory and lingual areas in the rat. Brain Res. 92, 123–129.

Osse, J. W., Sibbing, F. A., and van den Boogaart, J. G. 1997. Intra-oral food manipulation of carp and other cyprinids: adaptations and limitations. Acta Physiol. Scand. Suppl. 638, 47–57.

Pfaffmann, C., Erickson, R. O., Frommer, G. P., and Halpern, B. P. 1961. Gustatory Discharges in the Rat Medulla and Thalamus. In: Sensory Communication (*ed*. W. A. Rosenblith), pp. 455–473. Wiley.

Pritchard, T. C., Hamilton, R. B., and Norgren, R. 2000. Projections of the parabrachial nucleus in the old world monkey. Exp. Neurol. 165, 101–117.

Reep, R. L. and Winans, S. S. 1982. Afferent connections of dorsal and ventral agranular insular cortex in the hamster. Neuroscience 7, 1265–1288.

Ricardo, J. A. and Koh, E. T. 1978. Anatomical evidence of direct projections from the nucleus of the solitary tract to the hypothalamus, amygdala, and other forebrain structures in the rat. Brain Res. 153, 1–26.

Rink, E. and Wullimann, M. F. 1998. Some forebrain connections of the gustatory system in the goldfish *Carassius auratus* visualized by separate DiI application to the hypothalamic inferior lobe and the torus lateralis. J. Comp. Neurol. 394, 152–170.

Rogers, R. C. and McCann, M. J. 1993. Intramedullary connections of the gastric region in the solitary nucleus: a biocytin histochemical tracing study in the rat. J. Auton. Nerv. Syst. 42(2), 119–130.

Ross, C. A., Ruggiero, D. A., and Reis, D. J. 1985. Projections from the nucleus tractus solitarii to the rostral ventrolateral medulla. J. Comp. Neurol. 242, 511–534.

Saper, C. B. 1982. Convergence of autonomic and limbic connections in the insular cortex of the rat. J. Comp. Neurol. 210, 163–173.

Scott, T. R., Yazley, S., Sienkiewicz, J., and Rolls, E. T. 1986. Gustatory responses in the nucleus tractus solitarius of the alert cynomolgus monkey. J. Neurophysiol. 55, 182–200.

Sibbing, F. A., Osse, J. M. W., and Terlouw, A. 1986. Food handling in the carp (*Cyrinus carpio)*: its movement patterns, mechanisms, and limitations. J. Zool. 210, 161–203.

Smeraski, C. A., Dunwiddie, T. V., Diao, L., and Finger, T. E. 1998. Excitatory amino acid neurotransmission in the primary gustatory nucleus of the goldfish *Carassius auratus*. Ann. N. Y. Acad. Sci. 855, 442–449.

Smeraski, C. A., Dunwiddie, T. V., Diao, L., and Finger, T. E. 1999. NMDA and non-NMDA receptors mediate responses in the primary gustatory nucleus in goldfish. Chem. Senses 24, 37–46.

Smeraski, C. A., Dunwiddie, T. V., Diao, L. H., Magnusson, K. R., and Finger, T. E. 1996. Glutamate receptors mediate synaptic responses in the primary gustatory nucleus in goldfish. Soc. Neurosci. Abstr. 22.

Torvik, A. 1956. Afferent connections to the sensory trigeminal nuclei, the nucleus of the solitary tract and adjacent structure. J. Comp. Neurol. 106, 51–132.

Travers, J. B. 1988. Efferent projections from the anterior nucleus of the solitary tract of the hamster. Brain Res. 457, 1–11.

Travers, S. P. 1993. Orosensory Processing in Neural Systems of the Nucleus of Solitary Tract. In: Mechanisms of Taste Transduction (*eds*. S. A. Simon and S. D. Roper), pp. 339–424. CRC press.

Travers, J. B. and Norgren, R. 1983. Afferent projections to the oral motor nuclei in the rat. J. Comp. Neurol., 220, 280–298.

Travers, S. P. and Hu, H. 2000. Extranuclear projections of rNST neurons expressing gustatory-elicited Fos. J. Comp Neurol. 427, 124–138.

Wehby, R. G. and London, J. A. 1995. Cyto-, myelo-, and chemoarchitecture of the insular cortex of the Syrian golden hamster. AChems. Abstr. 17, 251.

Whitehead, M. C. 1986. Anatomy of the gustatory system in the hamster: synaptology of facial afferent terminals in the solitary nucleus. J. Comp. Neurol. 244, 72–85.

Whitehead, M. C. 1988a. Neuroanatomy of the gustatory system. Gerodontics 4, 239–243.
Whitehead, M. C. 1988b. Neuronal architecture of the nucleus of the solitary tract in the hamster. J. Comp. Neurol., 276, 547–572.
Whitehead, M. C. 1990. Subdivisions and neuron types of the nucleus of the solitary tract that project to the parabrachial nucleus in the hamster. J. Comp. Neurol. 301, 554–574.
Whitehead, M. C. 1993. Distribution of synapses on identified cell types in a gustatory subdivision of the nucleus of the solitary tract. J. Comp. Neurol. 332, 326–340.
Whitehead, M. C., Bergula, A., and Holliday, K. 2000. Forebrain projections to the rostral nucleus of the solitary tract in the hamster. J. Comp. Neurol. 422, 429–447.
Whitehead, M. C., McPheeters, M., Savoy, L. D., and Frank, M. E. 1993. Morphological types of neurons located at taste-responsive sites in the solitary nucleus of the hamster. Microsc. Res. Tech. 26, 245–359.
Wullimann, M. F. 1988. The tertiary gustatory center in sunfishes is not nucleus glomerulosus. Neurosci. Lett. 86, 6–10.
Yoshimoto, M., Albert, J. S., Sawai, N., Shimizu, M., Yamamoto, N., and Ito, H. 1998. Telencephalic ascending gustatory system in a cichlid fish, *Oreochromis* (Tilapia) *niloticus*. J. Comp. Neurol. 392, 209–226.

Further Reading

Mistretta, C. M. 1998. How the anterior tongue and taste responses are mapped onto the NST in fetal and perinatal sheep. Chem. Senses. 13, 719–720.

4.12 Neurotransmitters in the Taste Pathway

R M Bradley, University of Michigan, Ann Arbor, MI, USA

© 2008 Elsevier Inc. All rights reserved.

4.12.1	Introduction	261
4.12.2	Neurotransmitters in the Sensory Ganglia Involved in Transmission of Taste Information	261
4.12.3	Neurotransmitters in the Rostral Nucleus of the Solitary Tract Involved in Processing of Taste Information	262
4.12.4	Neurotransmitters in the Parabrachial Nucleus Involved in Processing of Taste Information	265
4.12.5	Role of Neurotransmitters in Brainstem Taste-Initiated Reflex Activity	266
4.12.5.1	Gusto-Salivary Reflex Activity	266
4.12.5.2	Synaptic Effects of Neuromodulators Known to have Profound Effects on Feeding Behavior on rNST Neurons	266
4.12.6	Conclusions	267
References		268

4.12.1 Introduction

In general there are two groups of investigators studying the nucleus of the solitary tract (NST). The largest group investigates the caudal nucleus that is involved in control of the digestive, cardiovascular, and respiratory systems. A much smaller cadre of investigators study the rostral nucleus (rNST) that forms the first central relay in the central taste pathway. Gustatory, tactile, and thermal information is relayed from the oral cavity via the chorda tympani and greater superficial petrosal branches of the facial nerve and the lingual branch of the glossopharyngeal nerve to the rNST, sometimes referred to as the gustatory NST. From there information either passes to rostral brain areas or to brainstem motor systems involved in facial and masticatory movements or the secretion of saliva.

Synaptic processing is involved at all stages of the pathway and investigators of both the rostral and caudal NST have extensively studied the synapses using anatomical, neurophysiological, and immunocytochemical techniques. The present review is restricted to the current knowledge of the neurotransmitters involved in the taste pathway which has been the focus of reviews (Bradley, R. M. *et al.*, 1996; Bradley, R. M. and Grabauskas, G., 1998; Smith, D. V. *et al.*, 1998). Neurotransmitters involved in the caudal NST have been extensively reviewed (Van Giersbergen, P. L. M. *et al.*, 1992; Andresen, M. C. and Kunze, D. L., 1994; Lawrence, A. J. and Jarrott, B., 1996) and whereas there are similarities between both the rostral and caudal divisions of the NST there are significant differences. While these differences often reflect true differences in neurotransmitter expression, they may also be due to the fact that investigators studying a particular neurotransmitter restrict the investigation to either the caudal or rostral division. Moreover it is not always possible in investigations using coronal sections to determine how far rostral in the NST the sections are studied (e.g., see Ambalavanar, R. *et al.*, 1998; Saha, S. *et al.*, 2001) even though the title of the reports implies that the whole NST is being investigated. When investigators use horizontal sections of the entire extent of the NST differences in neurotransmitter distribution become evident (see Davis, B. J. and Jang, T., 1988).

4.12.2 Neurotransmitters in the Sensory Ganglia Involved in Transmission of Taste Information

Gustatory information derived from taste receptor cells is conveyed to the first central relay in the taste pathway via afferent sensory fibers. The cell bodies of these fibers are collected in peripheral sensory ganglia which include the geniculate (GG, facial nerve VII), petrosal (PG, glossopharyngeal IX), and nodose ganglia (NG, vagus nerve X). The neurotransmitter composition of the PG and NG has been studied using immunocytochemical techniques and these ganglia contain glutamate, substance P (SP), tyrosine hydroxylase, vasoactive intestinal polypeptide, calcitonin gene-related peptide, galanin, and aspartate

(Helke, C. J. and Hill, K. M., 1988; Helke. C. J. and Niederer, A. J., 1990; Czyzyk-Kreska, M. F. *et al.*, 1991; Helke, C. J. and Rabchevsky, A., 1991; Ichikawa, H. *et al.*, 1991; Finley, J. C. W. *et al.*, 1992; Okada, J. and Miura, M., 1992). No similar immunocytochemical survey has been undertaken for the GG. However, because afferent sensory neurons with cell bodies in the PG and GG supply a heterogeneous population of receptors, retrograde tracing techniques have been used to isolate the neurons that innervate taste buds for detailed investigation. Neurons in the GG and PG supplying the tongue, fluorescently labeled with either Fluorogold or true blue, were immunoreacted for glutamate receptors (Caicedo, A. *et al.*, 2004) or acutely dissociated and analyzed with patch-clamp recording (King, M. S. and Bradley, R. M., 2000; Koga, T. and Bradley, R. M., 2000). The pharmacological properties of neurons of the NG innervating laryngeal taste buds have not been determined.

There were significant differences in the response of PG and GG gustatory neurons to the application of acetylcholine (ACh), serotonin (5-HT), SP, and gamma-aminobutyric acid (GABA). Whereas PG neurons responded to ACh, serotonin, SP, and GABA, GG neurons only responded to SP and GABA (Koga, T. and Bradley, R. M., 2000; Figure 1).

Gustatory neurons of the GG have been examined for their expression and response to glutamate receptor agonists. Ionotropic glutamate receptors are divided into two major groups based on their sensitivity to the agonists *N*-methyl-D-aspartate (NMDA) and α-amino-3-hydroxy-5-methyl-4-isoxazoleproprionic acid (AMPA). Dissociated GG taste neurons responded to application of both agonists (King, M. S. and Bradley, R. M., 2000; Figure 2). By using antibodies to NMDA and AMPA receptor subunits, Caicedo A. *et al.* (2004) were able to demonstrate that gustatory neurons in the GG were strongly immunoreactive for GluR2/3, GluR4, and NR1 subunits suggesting that putative AMPA receptors are mainly composed of GluR3 and GluR4 subunits while NMDA receptors consist of NR1 receptor subunits.

4.12.3 Neurotransmitters in the Rostral Nucleus of the Solitary Tract Involved in Processing of Taste Information

Both anatomical and electrophysiological techniques have been used to define the neurotransmitters and neuromodulators and their receptors within the rNST. Glutamate and GABA have been shown to play a role in synaptic transmission in the rNST. Glutamate is the afferent excitatory transmitter released from gustatory afferent terminals (Wang, L. and Bradley, R. M., 1995; Li, C. S. and Smith, D. V., 1997) and is contained in neurons of the rNST (Sweazey, R. D., 1995). GABA immunoreactivity is present in the rNST, primarily contained in small ovoid neurons (Lasiter, P. S. and Kachele, D. L., 1988; Davis, B. J., 1993; Sweazey, R. D., 1996; Leonard, N. L. *et al.*, 1999). Electrophysiological recordings in brain slices indicate that neuron of the rNST express both AMPA and NMDA receptors as well as $GABA_A$ and $GABA_B$ receptors (Liu, H. *et al.*, 1993; Wang, L. and Bradley, R. M., 1993; Bradley, R. M. *et al.*, 1996; Li, C. S. and Smith, D. V., 1997; Figure 2). The brainstem slice experiments all suggest that rNST neurons are under tonic GABAergic inhibition. This was directly tested *in vivo* on taste-responsive neurons in which the spontaneous activity was suppressed in a concentration-dependent manner by microinjection of GABA (Smith, D. V. and Li, C. S., 1998).

The distribution of glutamate and GABA receptors in the rNST is not uniform. AMPA and NMDA receptors are concentrated in the rostral central division of the rNST which receives most of the primary afferent input (Whitehead, M. C., 1988). In contrast, GABA is more uniformly distributed throughout the rNST (King, M. S., 2003). These differences in distribution of the glutamate and GABA receptors are thought to represent their different roles in gustatory processing, glutamate being involved in excitatory input from afferent taste fibers, and GABA mediating generalized tonic inhibition of the whole rNST.

Study of rNST synaptic potentials reveals that they consist of a complex mixture of excitatory and inhibitory potentials. The synaptic potentials result from excitatory afferent input mediated by glutamate and inhibitory transmission is mediated primarily at $GABA_A$ synapses (Grabauskas, G. and Bradley, R. M., 1996). By eliminating the excitatory component with glutamate receptor blockers the inhibitory component can be isolated, allowing the study of pure inhibitory postsynaptic potentials (IPSPs) in rNST. In addition, instead of using single-shock stimuli to investigate synaptic potentials, trains of stimuli (tetanic stimulation) that mimic the frequency of afferent input to the rNST evoked by gustatory stimulation reveals additional characteristics of inhibitory activity in the rNST. Tetanic stimulation at frequencies of 10–30 Hz resulted in sustained hyperpolarizing IPSPs that could be blocked by the $GABA_A$

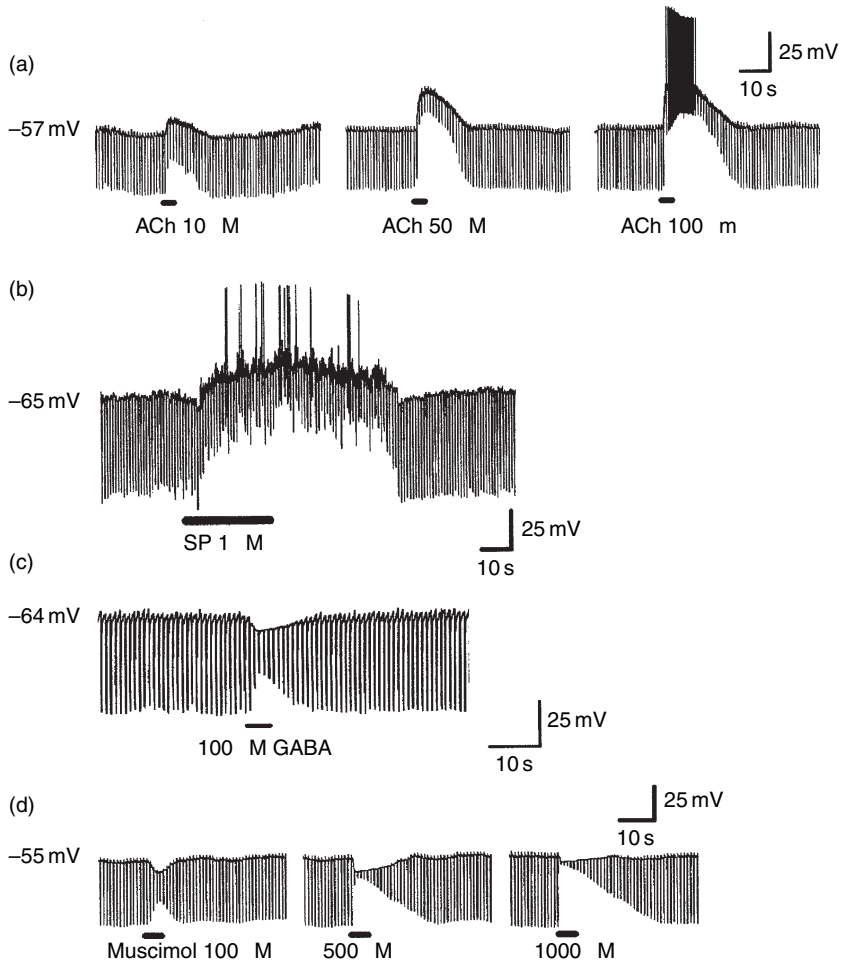

Figure 1 Voltage responses recorded from petrosal (PG) and geniculate ganglion (GG) neurons innervating the tongue to hyperpolarizing injections of −100 pA, 100 ms current pulses. (a) Membrane responses of a PG neuron to a 5 s application (bar) of increasing concentrations of acetylcholine (ACh). The ACh application induced membrane depolarization accompanied by a decrease in input resistance. The response is dose-dependent and returns to control levels within 30 s after termination of application. The depolarization resulting from the highest concentration of ACh initiated a burst of action potentials. (b) Membrane response of a PG neuron to a 5 s application (bar) of substance P (SP). In this neuron SP application depolarized the neuron and initiated the production of action potentials. (c) Membrane response of a GG neuron to a 5 s application (bar) of gamma-aminobutyric acid (GABA). In this neuron GABA application hyperpolarized the neuron with a decrease in input resistance. (d) Membrane responses of a PG neuron to a 5 s application (bar) of increasing concentrations of the $GABA_A$ receptor agonist muscimol. The mucimol application induced dose-dependent membrane hyperpolarization accompanied by a decrease in input resistance. Reproduced from Koga T. and Bradley R. M. 2000. Biophysical properties and responses to neurotransmitters of petrosal and geniculate ganglion neurons innervating the tongue. J. Neurophysiol. 84, 1404–1413, used with permission from the American Physiological Society.

antagonist bicuculline. Because afferent sensory information to the rNST consists of relatively high-frequency spike trains, these short-term changes in inhibitory synaptic activity could potentially play a key role in taste processing by facilitating synaptic integration (Grabauskas, G. and Bradley, R. M., 1998).

A single tetanic stimulation results in potentiation of single stimulus shock-evoked IPSPs for a considerable time. This potentiation can last over 30 min (Figure 3). Tetanic stimulation results in activation of all postsynaptic $GABA_A$ receptors and induces long-lasting changes in the presynaptic GABAergic neuron. These long-lasting changes of the presynaptic neuron facilitate the release of GABA during single stimulus shock and, as a consequence, more postsynaptic receptors are activated during a single stimulus shock. Long-term potentiation of inhibition in the gustatory relay nucleus has the capability to profoundly alter transmission of

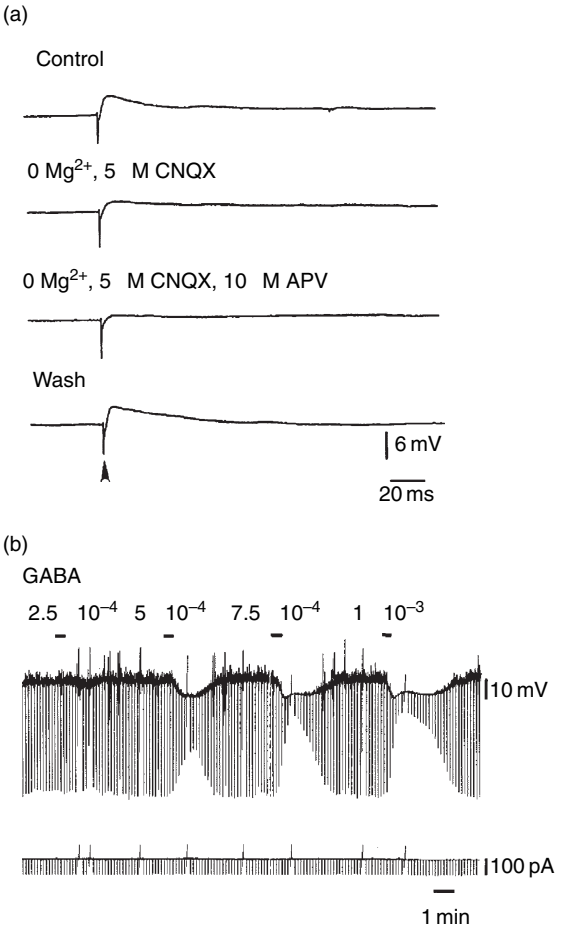

Figure 2 (a) Effect of glutamate receptor antagonists on excitatory postsynaptic potential (EPSP) recorded from a rostal nucleus of the solitary tract (rNST) neuron in a brain slice preparation superfused with physiological saline that did not contain magnesium. The EPSPs were initiated (arrowhead) by electrical stimulation of the solitary tract. Mean of 10 EPSPs under control conditions and after application of CNQX (an α-amino-3-hydroxy-5-methyl-4-isoxazoleproprionic acid (AMPA)/kinate glutamate receptor antagonist) alone and CNQX and APV (an *N*-methyl-D-aspartate (NMDA) glutamate receptor blocker). CNQX reduced the EPSP leaving a CNQX-resistant component. The CNQX resistant component was blocked by application of APV. (b) Voltage responses recorded from an rNST neuron in a brain slice preparation to hyperpolarizing injections of −100 pA, 100 ms current pulses. The neuron was exposed to increasing 5 s (bar) concentrations of gamma-aminobutyric acid (GABA) interspersed with control saline rinses. GABA hyperpolarizes the neuron in a concentration-dependent manner accompanied by a decrease in input resistance. (a) Reproduced from Wang L. and Bradley R. M. 1995. *In vitro* study of afferent synaptic transmission in the rostral gustatory zone of the rat nucleus of the solitary tract. Brain Res. 702, 188–198, with permission from Elsevier. (b) Reproduced from Wang L. and Bradley R. M. 1993. Influence of GABA on neurons of the gustatory zone of the rat nucleus of the solitary tract. Brain Res. 616, 144–153, with permission from Elsevier.

taste information and therefore may be of significance in the mechanism of taste-related learning phenomena (Grabauskas, G. and Bradley, R. M., 1999).

The postnatal development of inhibition in rNST has also been examined (Grabauskas, G. and Bradley, R. M., 2001). All IPSPs recorded in postnatal rats were hyperpolarizing, but the rise and decay time constants of the single stimulus shock-evoked IPSPs decreased, and the inhibition response–concentration function to the GABA antagonist bicuculline shifted to the left during development. In postnatal 0 (P0)–P14, but not older animals, the IPSPs had a bicuculline insensitive component that was sensitive to block by picrotoxin, suggesting a transient expression of $GABA_C$ receptors. These developmental changes in inhibitory synaptic activity may operate to shape synaptic activity in early development of the rat gustatory system during a time of maturation of taste preferences and aversions (Grabauskas, G. and Bradley, R. M., 2001).

Other neurotransmitters and neuropeptides have been identified in the gustatory NST including SP, enkephalin, and catecholamines (Davis, B. J. and Jang, T., 1988; Davis, B. J. and Kream, R. M., 1993; Davis, B. J. and Smith, H. M., 1999). SP immunoreactivity is found within the glossopharyngeal nerve (Cuello, A. C. and Kanazawa, I., 1978; Helke, C. J. and Hill, K. M., 1988) as well as within the rNST (Cuello, A. C. and Kanazawa, I., 1978; Jacquin, T. *et al.*, 1989). Application of SP to neurons of the rNST in an *in vitro* brain slice preparation depolarized the majority of the neurons studied (68%) in a dose-dependent manner (King, M. S. *et al.*, 1993). The excitatory effect of SP was the result of direct postsynaptic action on the neurons (King, M. S. *et al.*, 1993). Similar results were reported when SP was microinjected onto rNST neurons in an *in vivo* preparation (Davis, B. J. and Smith, D. V., 1997). In this study, SP excited 48% of the neurons and enhanced the response of the rNST neurons to stimulation of the tongue with taste stimuli. In both the *in vitro* and *in vivo* studies a small number of neurons were inhibited by SP application demonstrated by membrane hyperpolarization or suppression of taste responses, respectively. Thus, SP effectively modulates the activity of gustatory neurons in rNST.

Opioids also modulate the activity of gustatory neurons in rNST (Li, C. S. *et al.*, 2003). During extracellular recording from rNST neurons, met-enkephalin was microinjected resulting in the suppression of taste initiated responses in 24% of the recorded neurons. The opioid antagonist naltrexone effectively blocked the inhibitory effect

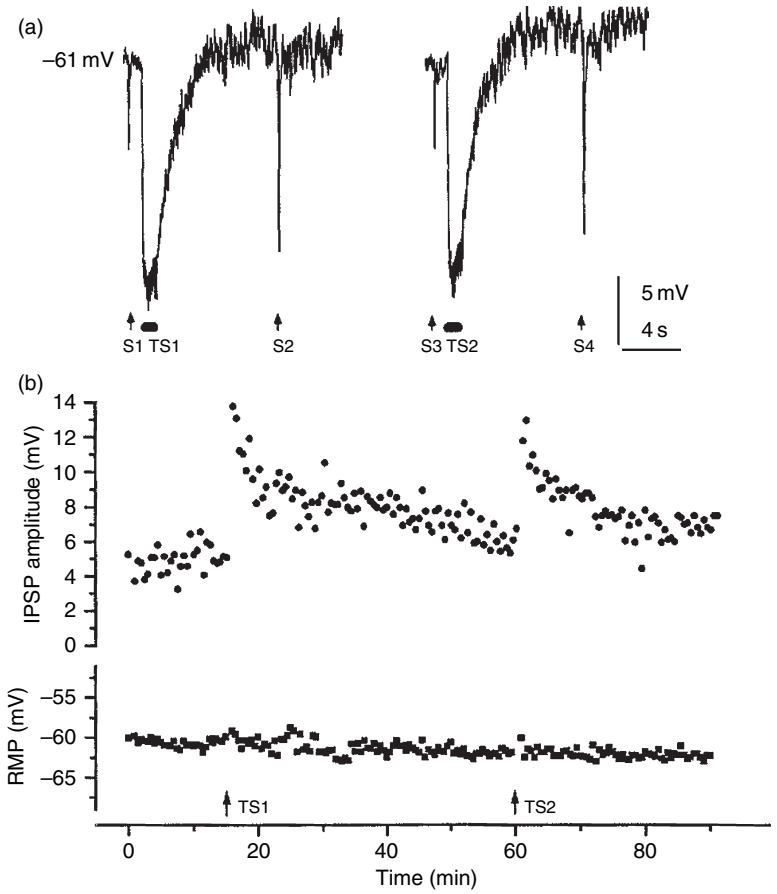

Figure 3 Effect of tetanic stimulation on inhibitory postsynaptic potentials (IPSPs) recorded from a rostal nucleus of the solitary tract (rNST) neuron in a brain slice preparation. IPSPs were isolated by chronic application of glutamate receptor blockers and elicited by electrical stimulation of the rNST. (a) After eliciting a control IPSP (S1) a tetanic stimulation (TS1) evoked potentiation of the amplitude of a subsequent IPSP (S2). Forty-five minutes after the initial potentiation the IPSP returns to control levels (S3). A second tetanic stimulation (TS2) results in potentiation again (S4). (b) Tetanic stimulation (TS1) potentiates the IPSP amplitude (●) for a considerable length of time. Tetanic stimulation does not change the resting potential (■). Once the IPSP returns to control levels a second tetanic stimulation (TS2) results in potentiation again. RMP, resting membrane potential. Reproduced from Grabauskas G. and Bradley R. M. 1999. Potentiation of GABAergic synaptic transmission in the rostral nucleus of the solitary tract. Neuroscience 94, 1173–1182, with permission from Elsevier.

of met-enkephalin suggesting that opiates maintain a tonic inhibitory action on a subpopulation of taste responsive neurons in rNST.

4.12.4 Neurotransmitters in the Parabrachial Nucleus Involved in Processing of Taste Information

In rodents and lagomorphs, gustatory information processed at the brainstem level ascends and relays in the parabrachial nucleus (PBN) in the dorsal pons (Norgren, R., 1978; Travers, J. B., 1988; Whitehead, M. C., 1990). Taste-responsive PBN neurons also have descending connections to the rNST as well as to medullary motor nuclei (Karimnamazi, H. and Travers, J. B., 1998). These connections imply that the PBN plays a significant role in taste processing by transmitting information in both a rostral and caudal direction.

The PBN has been dived into a number of major regions (Fulwiler, C. E. and Saper, C. B., 1984) with the central medial (CM), ventrolateral (VL), and waist area (W) being important in taste processing because these areas have been shown to receive input from the rNST and neurons in these areas respond to taste stimuli flowed over the tongue (Norgren, R. and Pfaffmann, C., 1975). Synaptic input from the rNST

to the PBN is mostly excitatory and mediated by glutamate since this neurotransmitter has been shown to be contained in a subset of rNST neurons that project to the PBN (Chamberlin, N. L. and Saper, C. B., 1995; Gill, C. F. *et al.*, 1999). Glutamate receptors have been shown to be present throughout the PBN but neurons in the W express AMPA (Chamberlin, N. L. and Saper, C. B., 1995; Guthmann, A. and Herbert, H., 1999c), NMDA receptors (Zidichouski, J. A. *et al.*, 1996; Guthman, A. and Herbert, H., 1999b) as well as metabotropic glutamate receptors (Zidichouski, J. A. *et al.*, 1996; Guthman, A. and Herbert, H., 1999a).

Investigators have also demonstrated that PBN neurons receive inhibitory input from the NST (Granata, A. R. and Kitai, S. T., 1989; Jhamandas, J. H. and Harris, K. H., 1992; Suemori, K. *et al.*, 1994). Based on the results of injections of GABA agonists and antagonists into the PBN this inhibition has been demonstrated to be GABAergic (Christie, M. J. and North, R. A., 1988; Mollace, V. *et al.*, 1991). The effect of GABA was studied on gustatory PBN neurons *in vitro* indicating that GABA functions as an inhibitory neurotransmitter in the gustatory PBN, mediated principally by $GABA_A$ receptors (Kobashi, M. and Bradley, R. M., 1998). At present no specific information is available on other neurotransmitters active on neurons in the gustatory PBN or on other synaptic relays in the ascending gustatory pathway.

4.12.5 Role of Neurotransmitters in Brainstem Taste-Initiated Reflex Activity

4.12.5.1 Gusto-Salivary Reflex Activity

Saliva is essential in the initial stages of taste transduction, acting as a solvent for taste stimuli, as a transport medium of the dissolved stimuli, and a possible source of ions that pass through taste receptor apical ion channels to depolarize or hyperpolarize the taste cell (Bradley, R. M., 1991). In concert, stimulation of taste receptors reflexly initiates saliva flow (Matsuo, R., 1999a). This reflex pathway involves afferent input to the rNST that then synapses with parasympathetic secretomotor neurons innervating the salivary glands. The parasympathetic neurons are collected in a column of brainstem neurons termed salivatory nuclei that are closely associated with the medial border of the rNST. Dendrites of the salivatory neurons penetrate into the rNST (Kim, M. *et al.*, 2004) facilitating synaptic contacts.

Recordings from identified neurons of the salivatory nuclei have demonstrated that the postsynaptic potentials initiated by stimulation of the solitary tract or adjacent neuropil are a mixture of excitation and inhibition (Mitoh, Y. *et al.*, 2004; Bradley, R. M. *et al.*, 2005). Application of synaptic agonists and antagonists have revealed that the excitatory component is mediated by NMDA and AMPA receptors and that inhibition results from stimulation of $GABA_A$ receptors (Mitoh, Y. *et al.*, 2004; Suwabe, T. and Bradley, R. M., 2005). Glycinergic receptors have been demonstrated on some salivatory neurons also (Mitoh, Y. *et al.*, 2004). Somata and dendrites of salivatory neurons receive symmetric synapses from glutamatergic, GABA, and glycine immunoreactive varicosities (Kobayashi, M. *et al.*, 1997). Salivatory nucleus neuron somata were shown to be strongly positive for the glutamate receptor subtypes NR1, NR2A, and either unlabeled or weakly positive for other glutamate receptor subtypes indicating that postsynaptic activity is mediated principally by NMDA receptors (Kim, M. *et al.*, 2005; Figure 4). Based on the neurophysiological measures these excitatory and inhibitory synapses are either monosynaptic connections between primary afferent fibers or involve polysynaptic connections via neurons in the rNST (Suwabe, T. and Bradley, R. M., 2005).

The salivary reflex is also influenced by descending input from higher brain centers (Matsuo, R., 1999b) and a number of neuropeptides have been hypothesized to be involved in this descending modulation of secretion as demonstrated by strong immunoreactivity for SP, serotonin, neuropeptide Y, somatostatin, tyrosine hydroxylase, vasoactive intestinal peptide, and calcitonin gene-related peptide (Nemoto, T. *et al.*, 1995). Of these neuropeptides, SP and serotonin have been shown to excite salivatory neurons in a concentration-dependent manner (Suwabe, T. and Bradley, R. M., 2007).

4.12.5.2 Synaptic Effects of Neuromodulators Known to have Profound Effects on Feeding Behavior on rNST Neurons

Injection of the benzodiazepine (BZ) receptor agonist diazepam into the fourth ventricle enhances food palatability and intake (Berridge, K. C. and Peciña, S., 1995), and it has been hypothesized that this phenomenon results from the action of diazepam on rNST neurons. BZs facilitate GABA-induced IPSPs

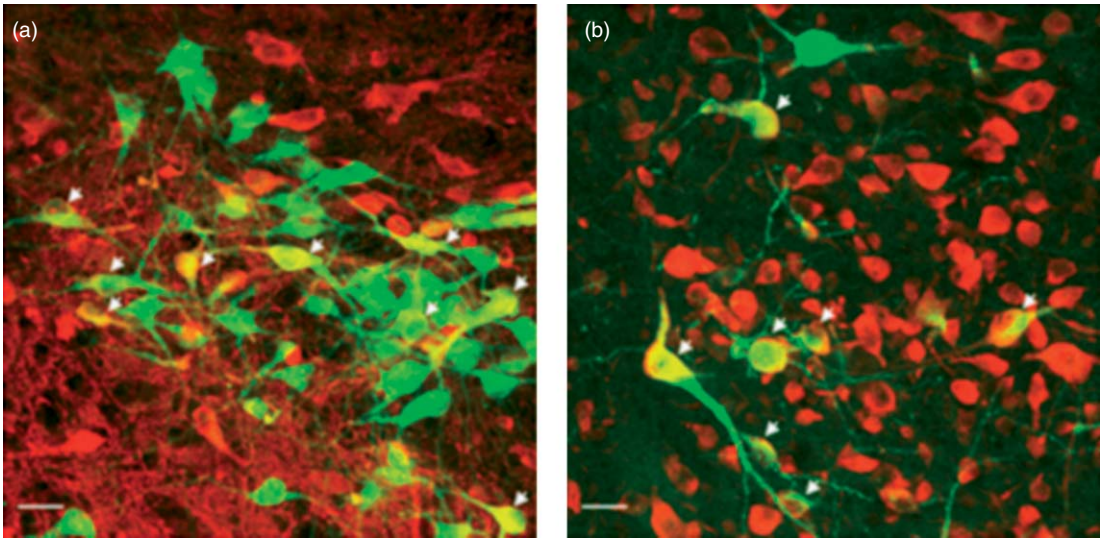

Figure 4 Glutamate receptor immunoreactivity of identified neurons of the salivatory nucleus. Parasympathetic secretomotor neurons of the inferior salivatory nucleus were identified by retrograde transport of a fluorescent marker. Horizontal sections of the medulla were subsequently immunoreacted for glutamate receptor subunits tagged with a fluorescent label. The resulting sections were examined using confocal microscopy. (a) Brainstem neurons labeled with antibodies to NR1 receptors (red) and retrogradely labeled neurons of the inferior salivatory nucleus (green). Doubled labels neurons appear yellow and are indicated by white arrows. (b) Brainstem neurons labeled with antibodies to NR2A receptors (red) and retrogradely labeled neurons of the inferior salivatory nucleus (green). Doubled labels neurons appear yellow and are indicated by white arrows. Note that many neurons in the brainstem are strongly labeled with the receptor antibody, but not all the salivatory neurons express the glutamate receptor. Scale bar = 25 μm.

in postsynaptic neurons that have $GABA_A$ receptors by modulating chloride channel activity. In brain slices maintained at body temperature, pharmacologically isolated IPSPs are diazepam sensitive demonstrating that rNST neurons express $GABA_A$ receptors with BZ binding sites. It is possible, therefore, that application of BZ into the fourth ventricle influences food intake by potentiation of GABAergic neurotransmission in the rNST (Grabauskas, G. and Bradley, R. M., 2000).

Cholecystokinin (CCK), a peptide secreted by gastrointestinal tract-lining cells, plays an important role in digestion. CCK has also been shown to cause satiety by acting centrally (Baile, C. A. *et al.*, 1986) and neurons immunoreactive for CCK have been located in the NST (Kubota, Y. *et al.*, 1983) and the PBN, including the W (Kubota, Y. *et al.*, 1983; Block, C. H. and Hoffman, G., 1987; Sutin, E. L. and Jacobowitz, D. M., 1988; Herbert, H. and Saper, C. B., 1990; Födor, M. *et al.*, 1992). Thus, CCK is present in the NST and taste-responsive area of the PBN suggesting that this neuropeptide may have a role in taste processing. While investigators using electrophysiological methods have demonstrated that CCK can modulate the excitatory response initiated by vagal stimulation (Saleh, T. M. and Cechetto, D. F., 1996) there are no similar studies on taste-responsive neurons in the PBN.

4.12.6 Conclusions

The essence of neural processing involves synaptic interactions and synaptic interactions involve neurotransmitters. Investigators studying taste processing have only recently turned their attention to the role of neurotransmitters at each relay in the taste pathway. In the review by Travers J. B. *et al.* (1987) on gustatory neural processing in the hindbrain, neurotransmitters are not even mentioned. Since that time a number of investigators have demonstrated both anatomically and physiologically the role neurotransmission plays in taste processing. They have determined that glutamate is the excitatory transmitter between afferent taste fibers and neurons of the rNST. They have demonstrated that inhibition mediated principally by $GABA_A$ receptors is an important factor in modulating the afferent input and that neurons of the rNST are under tonic GABA inhibition. Moreover, a form of long-term

inhibition must also be factored into gustatory processing by rNST circuits. It is important to also remember that afferent information is distributed to a number of destinations after arriving at the brainstem and that each of these circuits may use different neurotransmitters. Other neurotransmitters are also important as well, and some of these have been characterized, particularly SP. Besides neurotransmitters active in the ascending pathway other neurotransmitters are found in the descending pathways from more rostral brain areas. While much more information remains to be acquired it is evident from the current state of knowledge that the apparent complexity of synaptic interactions at all levels of the taste pathway should be taken into account when the subject of central taste coding is discussed.

References

Ambalavanar, R., Ludlow, C. L., Wenthold, R. J., Tanaka, Y., Damirjian, M., and Petralia, R. S. 1998. Glutamate receptor subunits in the nucleus of the tractus solitarius and other regions of the medulla oblongata in the cat. J. Comp. Neurol. 402, 75–92.

Andresen, M. C. and Kunze, D. L. 1994. Nucleus tractus solitarius – gateway to neural circulatory control. Annu. Rev. Physiol. 56, 93–116.

Baile, C. A., McLaughlin, C. L., and Della-Fera, M. A. 1986. Role of cholecystokinin and opioid peptides in control of food intake. Physiol. Rev. 66, 172–234.

Berridge, K. C. and Peciña, S. 1995. Benzodiazepines, appetite, and taste palatability. Neurosci. Biobehav. Rev. 19, 121–131.

Block, C. H. and Hoffman, G. 1987. Neuropeptides and monoamine components of the parabrachial pontine complex. Peptides 8, 267–283.

Bradley, R. M. 1991. Salivary Secretion. In: Smell and Taste in Health and Disease (*eds*. T. V. Getchel, R. L. Doty, L. M. Bartoshuk, and J. B. J. Snow), pp. 127–144. Raven Press.

Bradley, R. M. and Grabauskas, G. 1998. Neural Circuits for Taste – Excitation, Inhibition, and Synaptic Plasticity in the Rostral Gustatory Zone of the Nucleus of the Solitary Tract. In: Olfaction and Taste XII (*ed*. C. Murphy), pp. 467–474. New York Academy of Sciences.

Bradley, R. M., Fukami, H., and Suwabe, T. 2005. Neurobiology of the gustatory-salivary reflex. Chem. Senses 30, i70–i71.

Bradley, R. M., King, M. S., Wang, L., and Shu, X. Q. 1996. Neurotransmitter and neuromodulatory activity in the gustatory zone of the nucleus tractus solitarius. Chem. Senses 21, 377–385.

Chamberlin, N. L. and Saper, C. B. 1995. Differential distribution of AMPA-selective glutamate receptor subunits in the parabrachial nucleus of the rat. Neuroscience 68, 435–443.

Caicedo, A., Zucchi, B., Pereira, E., and Roper, S. D. 2004. Rat gustatory neurons in the geniculate ganglion express glutamate receptor subunits. Chem. Senses 29, 463–471.

Christie, M. J. and North, R. A. 1988. Agonist at m-opioid, M_2-muscarinic and $GABA_B$-receptors increase the same potassium conductances in rat lateral parabrachial neurones. Br. J. Pharmacol. 95, 896–902.

Cuello, A. C. and Kanazawa, I. 1978. The distribution of substance P immunoreactive fibers in the rat central nervous system. J. Comp. Neurol. 178, 129–156.

Czyzyk-Kreska, M. F., Bayliss, D. A., Seroogy, K. B., and Millhorn, D. E. 1991. Gene expression for peptides in neurons of the petrosal and nodose ganglia in rat. Exp. Brain Res. 83, 411–418.

Davis, B. J. 1993. GABA-like immunoreactivity in the gustatory zone of the nucleus of the solitary tract in the hamster: light and electron microscopic studies. Brain Res. Bull. 30, 69–77.

Davis, B. J. and Jang, T. 1988. Tyrosine hydroxylase-like and dopamine beta-hydroxylase-like immunoreactivity in the gustatory zone of the nucleus of the solitary tract in the hamster: light- and electron-microscopic studies. Neuroscience 27, 949–964.

Davis, B. J. and Kream, R. M. 1993. Distribution of tachykinin- and opioid-expressing neurons in the hamster solitary nucleus: An immuno- and *in situ* hybridization histochemical study. Brain Res. 616, 6–16.

Davis, B. J. and Smith, D. V. 1997. Substance P modulates taste responses in the nucleus of the solitary tract of the hamster. Neuroreport 8, 1723–1727.

Davis, B. J. and Smith, H. M. 1999. Neurokinin-1 receptor immunoreactivity in the nucleus of the solitary tract in the hamster. Neuroreport 10, 1003–1006.

Finley, J. C. W., Polak, J., and Katz, D. M. 1992. Transmitter diversity in carotid body afferent neurons: dopaminergic and peptidergic phenotypes. Neuroscience 51, 973–987.

Födor, M., Gorcs, T. J., and Plakovits, M. 1992. Immunohistochemical study on the distribution of neuropeptides within the pontine tegmentum-particularly the parabrachial nucleus and the locus coeruleus of the human brain. Neuroscience 46, 891–908.

Fulwiler, C. E. and Saper, C. B. 1984. Subnuclear organization of the efferent connections of the parabrachial nucleus in the rat. Brain Res. Rev. 7, 229–256.

Gill, C. F., Madden, J. M., Roberts, B. P., Evans, L. D., and King, M. S. 1999. A subpopulation of neurons in the rat rostral nucleus of the solitary tract that project to the parabrachial nucleus express glutamate-like immunoreactivity. Brain Res. 821, 251–262.

Grabauskas, G. and Bradley, R. M. 1996. Synaptic interactions due to convergent input from gustatory afferent fibers in the rostral nucleus of the solitary tract. J. Neurophysiol. 76, 2919–2927.

Grabauskas, G. and Bradley, R. M. 1998. Tetanic stimulation induces short-term potentiation of inhibitory synaptic activity in the rostral nucleus of the solitary tract. J. Neurophysiol. 79, 595–604.

Grabauskas, G. and Bradley, R. M. 1999. Potentiation of GABAergic synaptic transmission in the rostral nucleus of the solitary tract. Neuroscience 94, 1173–1182.

Grabauskas, G. and Bradley, R. M. 2000. Effect of diazepam on inhibitory postsynaptic potentials in nucleus of the solitary tract of neonatal rats is temperature dependent. Chem. Senses 25, 678.

Grabauskas, G. and Bradley, R. M. 2001. Postnatal development of inhibitory synaptic transmission in the rostral nucleus of the solitary tract. J. Neurophysiol. 85, 2203–2212.

Granata, A. R. and Kitai, S. T. 1989. Intracellular study of nucleus parabrachialis and nucleus tractus solitarii interconnections. Brain Res. 492, 281–292.

Guthmann, A. and Herbert, H. 1999a. Distribution of metabotropic glutamate receptor subunits in the parabrachial and kölliker-fuse nuclei of the rat. Neuroscience 89, 873–881.

Guthmann, A. and Herbert, H. 1999b. Expression on N-methyl-D-aspartate receptor subunits in the rat parabrachial and

kölliker-fuse nuclei of the rat and in selected ponuomedullary brainstem nuclei. J. Comp. Neurol. 415, 501–517.
Guthmann, A. and Herbert, H. 1999c. *In situ* hybridization analysis of flip/flop splice variants of AMPA-type glutamate receptor subunits in the rat parabrachial and kölliker-fuse nuclei. Mol. Brain Res. 74, 145–157.
Helke, C. J. and Hill, K. M. 1988. Immunohistochemical study of neuropeptides in vagal and glossopharyngeal afferent neurons in the rat. Neuroscience 26, 539–551.
Helke, C. J. and Niederer, A. J. 1990. Studies on the coexistance of substance P with other putative neurotransmitters in the nodose and petrosal ganglia. Synapse 5, 144–151.
Helke, C. J. and Rabchevsky, A. 1991. Axotomy alters putative neurotransmitters in visceral sensory neurons of the nodose and petrosal ganglia. Brain Res. 551, 44–51.
Herbert, H. and Saper, C. B. 1990. Cholecystokinin-, galanin-, and corticotropin-releasing factor-like immunoreactive projections from the nucleus of the solitary tract to the parabrachial nucleus in the rat. J. Comp. Neurol. 293, 581–598.
Ichikawa, H., Jacobowitz, D. M., Winsky, L., and Helke, C. J. 1991. Calretinin-immunoreactivity in vagal and glossopharyngeal sensory neurons of the rat. Distribution and coexistence with putative transmitter agents. Brain Res. 557, 316–321.
Jacquin, T., Denavit-Saubié, M., and Champagnat, J. 1989. Substance P and serotonin mutually reverse their excitatory effects in the rat nucleus tractus solitarius. Brain Res. 502, 214–222.
Jhamandas, J. H. and Harris, K. H. 1992. Influence of nucleus tractus solitarius stimulation and baroreceptor activation on rat parabrachial neurons. Brain Res. Bull. 28, 565–571.
Karimnamazi, H. and Travers, J. B. 1998. Differential projections from gustatory responsive regions of the parabrachial nucleus to the medulla and forebrain. Brain Res. 813, 283–302.
Kim, M., Chiego, D. J., and Bradley, R. M. 2005. Characterization of the gusto-salivary reflex: ionotropic glutamate receptor expression in preganglionic neurons of the rat inferior salivatory nucleus. Program No. 281. 4, Abstract viewer/Itinerary Planner. Society for Neuroscience.
King, M. S. 2003. Distribution of immunoreactive GABA and glutamate receptors in the gustatory portion of the nucleus of the solitary tract in rat. Brain Res. Bull. 60, 241–254.
King, M. S. and Bradley, R. M. 2000. Biophysical properties and responses to glutamate receptor agonists of identified subpopulations of rat geniculate ganglion neurons. Brain Res. 866, 237–246.
King, M. S., Wang, L., and Bradley, R. M. 1993. Substance P excites neurons in the gustatory zone of the rat nucleus tractus solitarius. Brain Res. 619, 120–130.
Kobashi, M. and Bradley, R. M. 1998. Effects of GABA on neurons of the gustatory and visceral zones of the parabrachial nucleus in rats. Brain Res. 799, 323–328.
Kobayashi, M., Nemoto, T., Nagata, H., Konno, A., and Chiba, T. 1997. Immunohistochemical studies on glutamatergic, GABAergic and glycinergic axon viscosities presynaptic to parasympathetic preganglionic neurons in the superior salivatory nucleus of the rat. Brain Res. 766, 72–82.
Koga, T. and Bradley, R. M. 2000. Biophysical properties and responses to neurotransmitters of petrosal and geniculate ganglion neurons innervating the tongue. J. Neurophysiol. 84, 1404–1413.
Kubota, Y., Inagaki, S., Shiosaka, S., Cho, H. J., Tateishi, K., Hasimura, E., Hamaoka, T., and Tohyama, M. 1983. The distribution of cholecystokinin octapeptide-like structures in the lower brain stem of the rat: an immunohistochemical analysis. Neuroscience 9, 587–604.
Lasiter, P. S. and Kachele, D. L. 1988. Organization of GABA and GABA-transaminase containing neurons in the gustatory zone of the nucleus of the solitary tract. Brain Res. Bull. 21, 623–636.
Lawrence, A. J. and Jarrott, B. 1996. Neurochemical modulation of cardiovascular control in the nucleus tractus solitarius. Prog. Neurobiol. 48, 21–53.
Leonard, N. L., Renahan, W. E., and Schweitzer, L. 1999. Structure and function of gustatory neurons in the nucleus of the solitary tract. IV. The morphology and synaptology of GABA-immunoreactive terminals. Neuroscience 92, 151–162.
Li, C. S. and Smith, D. V. 1997. Glutamate receptor antagonists block gustatory afferent input to the nucleus of the solitary tract. J. Neurophysiol. 77, 1514–1525.
Li, C. S., Davis, B. J., and Smith, D. V. 2003. Opioid modulation of taste responses in the nucleus of the solitary tract. Brain Res. 965, 21–34.
Liu, H., Behbehani, M. M., and Smith, D. V. 1993. The influence of GABA on cells in the gustatory region of the hamster solitary nucleus. Chem. Senses 18, 285–305.
Matsuo, R. 1999a. Interrelation of Taste and Saliva. In: Neural Mechanisms of Salivary Gland Secretion (*eds*. J. R. Garrett, J. Ekström, and L. C. Anderson), pp. 185–195. Karger.
Matsuo, R. 1999b. Central Connections for Salivary Innervation and Efferent Impulse Formation. In: Neural Mechanisms of Salivary Secretion (*eds*. J. R. Garrett, J. Ekström, and L. C. Anderson), pp. 26–43. Karger.
Mitoh, Y., Funahashi, M., Kobashi, M., and Matsuo, R. 2004. Excitatory and inhibitory postsynaptic currents of the superior salivatory nucleus innervating the salivary glands and tongue in the rat. Brain Res. 999, 62–72.
Mollace, V., De Francesco, E. A., Fersini, G., and Nistico, G. 1991. Age-dependent changes in cardiovascular responses induced by muscimol infused into the nucleus tractus solitarii and nucleus parabrachialis in rats. Br. J. Pharmacol. 103, 1802–1806.
Nemoto, T., Konno, A., and Chiba, T. 1995. Synaptic contact of neuropeptide- and amine-containing axons on parasympathetic preganglionic neurons in the superior salivatory nucleus of the rat. Brain Res. 685, 33–45.
Norgren, R. 1978. Projections from the nucleus of the solitary tract in the rat. Neuroscience 3, 207–218.
Norgren, R. and Pfaffmann, C. 1975. The pontine taste area in the rat. Brain Res. 91, 99–117.
Okada, J. and Miura, M. 1992. Transmitter substances contained in the petrosal ganglion cells determined by a double-labeling method in the rat. Neurosci. Lett. 146, 33–36.
Saha, S., Sieghart, W., Fritschy, J. M., McWilliam, P. N., and Batten, T. F. 2001. γ-Aminobutyric acid receptor ($GABA_A$) subunits in rat nucleus tractus solitarii (NTS) revealed by polymerase chain reaction (PCR) and immunohistochemistry. Mol. Cell. Neurosci. 17, 241–257.
Saleh, T. M. and Cechetto, D. F. 1996. Peptide changes in the parabrachial nucleus following cervical vagal stimulation. J. Comp. Neurol. 366, 390–405.
Smith, D. V. and Li, C. S. 1998. Tonic GABAergic inhibition of taste-responsive neurons in the nucleus of the solitary tract. Chem. Senses 23, 159–169.
Smith, D. V., Li, C. S., and Davis, B. J. 1998. Excitatory and Inhibitory Modulation of Taste Responses in the Hamster Brainstem. In: Olfaction and Taste XII (*ed*. C. Murphy), pp. 450–456. New York Academy of Sciences.
Suemori, K., Kobashi, M., and Adachi, A. 1994. Effects of gastric distension and electrical stimulation of dorsomedial medulla on neurons in parabrachial nucleus of rats. J. Auton. Nerv. Syst. 48, 221–229.
Sutin, E. L. and Jacobowitz, D. M. 1988. Immunocytochemical localization of peptides and other neurochemicals in the rat

laterodorsal nucleus and adjacent area. J. Comp. Neurol. 270, 243–270.
Suwabe, T. and Bradley, R. M. 2005. Characterization of the gusto-salivary reflex: excitatory postsynaptic potentials recorded from identified rat inferior salivatory neurons. Program No. 281. 3, Abstract viewer/Itinerary Planner. Society for Neuroscience.
Suwabe, T. and Bradley, R. M. 2007. Effects of 5-hydroxytryptamine and substance P on neurons of the inferior salivatory nucleus. J. Neurophysiol. 97, 2605–2611.
Sweazey, R. D. 1995. Distribution of aspartate and glutamate in the nucleus of the solitary tract of the lamb. Exp. Brain Res. 105, 241–253.
Sweazey, R. D. 1996. Distribution of GABA and glycine in the lamb nucleus of the solitary tract. Brain Res. 737, 275–286.
Travers, J. B. 1988. Efferent projections from the anterior nucleus of the solitary tract of the hamster. Brain Res. 457, 1–11.
Travers, J. B., Travers, S. P., and Norgren, R. 1987. Gustatory neural processing in the hindbrain. Annu. Rev. Neurosci. 10, 595–632.
Van Giersbergen, P. L. M., Palkovits, M., and de Jong, W. 1992. Involvement of neurotransmitters in the nucleus tractus solitarii in cardiovascular regulation. Physiol. Rev. 72, 789–824.
Wang, L. and Bradley, R. M. 1993. Influence of GABA on neurons of the gustatory zone of the rat nucleus of the solitary tract. Brain Res. 616, 144–153.
Wang, L. and Bradley, R. M. 1995. *In vitro* study of afferent synaptic transmission in the rostral gustatory zone of the rat nucleus of the solitary tract. Brain Res. 702, 188–198.
Whitehead, M. C. 1988. Neuronal architecture of the nucleus of the solitary tract in the hamster. J. Comp. Neurol. 276, 547–572.
Whitehead, M. C. 1990. Subdivisions and neuron types of the nucleus of the solitary tract that project to the parabrachial nucleus in the hamster. J. Comp. Neurol. 301, 554–574.
Zidichouski, J. A., Easaw, J. C., and Jhamandas, J. H. 1996. Glutamate receptor subtypes mediate excitatory synaptic responses of rat lateral parabrachial neurons. Am. J. Physiol. Heart Circ. Physiol. 270, H1557–H1567.

4.13 Functional Magnetic Resonance Imaging Study of Taste

A Faurion, Neurobiologie Sensorielle, NOPA-NBS, INRA, Jouy en Josas, France

T Kobayakawa, National Institute of Advanced Industrial Science and Technology (AIST), Tsukuba, Japan

B Cerf-Ducastel, San Diego State University, San Diego, CA, USA

© 2008 Elsevier Inc. All rights reserved.

4.13.1	History of Functional Magnetic Resonance Imaging Applied to the Study of Task-Dependent Cerebral Activation	271
4.13.2	Mapping Brain Activity in Response to Taste Stimulation	272
4.13.3	The Insular/Opercular Area and the Role of Anterior Inferior Insula	273
4.13.4	Timing of Activation: Magnetoencephalography Experiments	274
4.13.5	Intensity Coding, Absence of Chemotopy	275
4.13.6	Imagination of Taste versus Perception of Taste	275
4.13.7	Learning by Familiarization	275
4.13.8	Orbitofrontal Cortex, an Integrative Area Contributing to Hedonic Valence and Food Reward	275
4.13.9	Amygdala Involved in Hedonic Valence and Memorization	276
4.13.10	Other Areas	276
4.13.11	Conclusive Remarks	277
References		277

Glossary

chemotopy Similar to tonotopy or somatotopy. For taste, still an hypothesis: the different chemicals would elicit an activation in a given localization of the primary projection area in the cortex.

EGM Electrogustometry. The application of a very low current on the tongue moves the saliva cations toward the microvillosities of the taste pores; detection thresholds are easily and precisely measured varying the current.

finger span A technique for perceived intensity evaluation. The forefinger is attached to the cursor of a potentiometer, while the thumb is fixed at the end of the resistor: the distance between both finger tips, a reflect of the articulation opening, measures the perceived intensity.

fMRI Functional magnetic resonance imaging, a brain imaging technique.

MEG Magnetoencephalography, a brain imaging technique.

NMR Nuclear magnetic resonance.

TEP Tomography by emission of positrons, a brain imaging technique.

T–I Time–intensity. The perception profile is continuously measured during the stimulation or even after the stimulation has ended, during a persisting aftertaste.

4.13.1 History of Functional Magnetic Resonance Imaging Applied to the Study of Task-Dependent Cerebral Activation

Roy C. W. and Sherrington C. S. (1890) were the first to suggest that an increase of the local blood flow may signal an increased neuronal activity, which is now possibly visualized using nuclear magnetic resonance (NMR) imaging (Lauterbur, P. C., 1973). Neural activity results in an increased blood flow with a relative decrease in deoxyhemoglobin and an increase in oxyhemoglobin. Many efforts were developed to map brain tissue and brain activity (Le Bihan, D. *et al.*, 1986; Belliveau *et al.*, 1991; Kwong, K. K. *et al.*, 1992; Ogawa, S. *et al.*, 1992), leading to the first observation of

an increased oxygen content in the visual area under stimulation. Functional magnetic resonance imaging (fMRI) uses the magnetic resonance of protons in living tissues. Spins carried by molecules are labeled by gradient pulses. During the relaxation time after a first pulse, a second one is applied which will result in a net phase shift. A relative decrease in deoxyhemoglobin (blood oxygenated level-dependent effect, BOLD) is reflected as an increase in the relaxation time, hence, as an increase of the magnetic resonance signal. The signal is an indirect reflect of the neural activity. Fundamental research in fMRI imaging is still under development to record signals that should be as close as possible from the neuronal activity.

After stimulating the spins, echoes are collected to form an image of the moving spins. With single-shot brain images that typically last between 25 and 100 ms (for example in echo-planar imaging, EPI), the technique allows powerful statistics and minimizes motion artifacts, offering a high spatial resolution of 1 mm or better. New statistical developments now care for naturally different amplitudes of the signal for repeated stimuli (in event-related experiments). The most important breakthrough brought by fMRI is that averaging data across brains is not necessary as in positron emission tomography (PET), thus allowing interpretation of individual brain activity and the study of interindividual differences (functional inter-individual differences). After a brilliant start with visual, counting, finger tapping, speech and memory tasks, chemoreception was a new challenge with the difficulty of mastering stimulation from a distance. A whole body magnet puts the subject's mouth at a minimum of 1.60 m from the outside of the machine, and every apparatus including magnetic parts must be localized outside of the shielded room, some 8 m apart.

But, as for PET, the temporal resolution is limited by the timing of the physiological event actually recorded, which is not the electrical activity of neurons but the delayed hemodynamic response, between 5 and 8 s. The temporal data acquisition is *de facto* averaged with this time constant. For a better time resolution, magnetoencephalography (MEG), directly recording the brain electrical activity, is a complementary choice. Magnetic fields are measured using SQUID sensors on the whole scalp. The signal emitted by active regions of the brain is collected in each sensor, sampled, and filtered. A number of trials (30–40) are summated. The magnitude of the neuromagnetic field at each sensor is compared to a magnitude calculated at the same sensor based on a theoretical model by the Grynszpan–Geselowitz equation (Grynszpan, F. and Geselowitz, D. B., 1973). The difference observed at each sensor results from the neuronal activity, the localization of which is to be found by mathematically resolving the inverse problem. The number of activated foci responsible for the signal is arbitrarily determined by the experimenter, and their localization, at first putative, is confirmed by the minimization algorithm. The advantage of the technique is that the recorded signal is directly generated by the electrical activity of neurones with a temporal precision of 1 ms.

Associating both fMRI and MEG techniques enables researchers to look at firing foci in individual brains with the precision of 1 ms and 1 mm, provided the experimental paradigm records enough psychophysical data for the interpretation of the function of the task-activated foci. Not only similarities but also differences of results may be informative as both techniques look at physiological events through different time windows.

4.13.2 Mapping Brain Activity in Response to Taste Stimulation

The pioneering work imaging brain activation for taste was from Kinomura S. with PET in 1994 showing thalamus, insular cortex, anterior cingulate gyrus, parahippocampal gyrus, lingual gyrus, caudate nucleus, and temporal gyrus activation (Kinomura, S. *et al.*, 1994). The same year, we started experimenting with fMRI in the 3T of the Service Frédéric Joliot (CEA) at Orsay, Director D. Le Bihan. We developed a stimulating method in order to suppress somatic information, sensory adaptation, and head movements consecutive to swallowing, using a continuous flow alternating water and stimulus in an on–off paradigm (Cerf, B. *et al.*, 1996; 1998). Small bolus (100 µl) was repetitively sent to the subject's mouth, through 2 m long silicone tubes every 3 s to minimize adaptation (pulsatile stimulation). This procedure ensured a negligible increase of the volume of fluid in the mouth with respect to saliva. Subjects were allowed to swallow *ad libitum*; hence no mouth movement could be correlated with the stimulation paradigm. The time–intensity (T–I) perception profile, which was recorded with the finger-span technique using a linear potentiometer, was used as a template to correlate to the NMR signal of each pixel or voxel. This template allowed visualizing more numerous activated clusters of pixels (+400%) than the convolution (Bandettini, P. A., *et al.*, 1993) of the stimulation paradigm waveform with a standard 6 s time-constant filter. For example, the correlation between the NMR

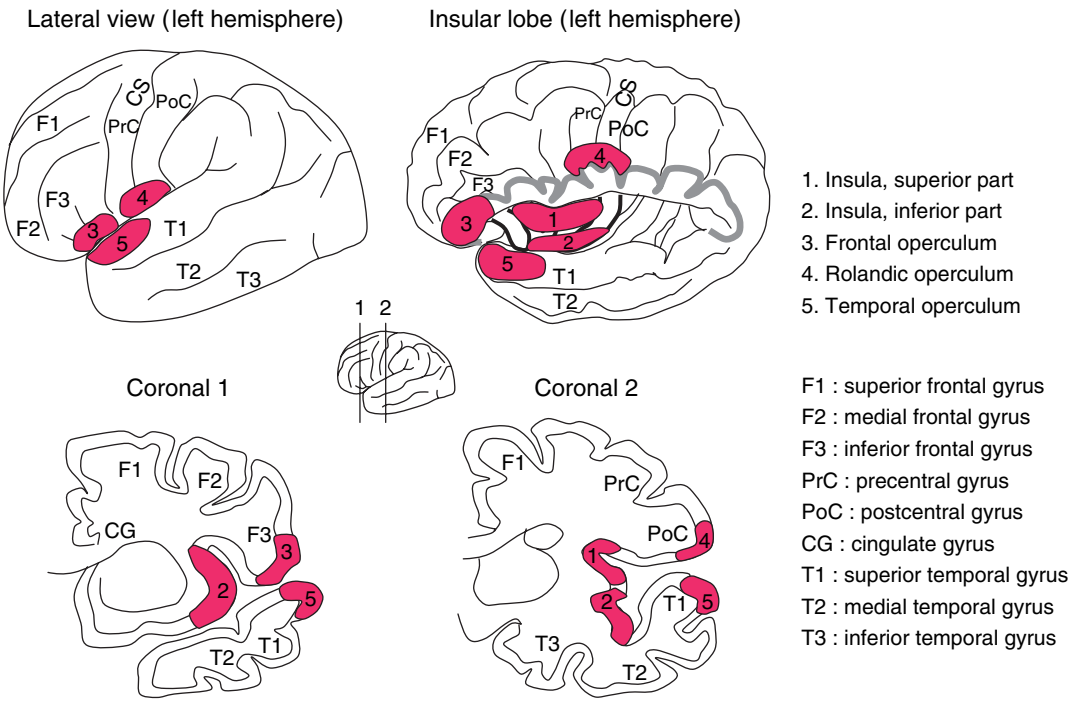

Figure 1 Brain areas activated by taste stimuli, observed with fMRI in human subjects. From Cerf, B. 1998. Doctoral dissertation, Paris.

signal and the T–I perception profile was above 0.6 in 30% of cases (thresholded at 0.4) and above 0.7 in 10% of cases instead of below 0.6 in standard conditions (Cerf, B. *et al.*, 1996; Van de Moortele, P.-F. *et al.*, 1997). The explanation comes from the waveform of recorded profiles which confirmed a slow rate of rise of the taste perception in these conditions (usually above 6 s time constant), which could vary with the stimulus and also with the subject who however individually exhibited a high reproducibility across sessions. Introducing the T–I perception measurement in the magnet enabled finding out pure taste activation that was barely detected otherwise (so-called taste is usually associated with somatosensory and retro-olfactory converging information). Hence, associating quantitative psychophysical evaluation to functional brain imaging is an important factor of success and an important factor for interpreting results. Besides, it provides a control of the stimulation. This recording of perception could also be run off-line, out of the magnet, for control sessions.

Using these conditions, and single subject analysis rather than group analysis, taste areas were localized (Figure 1) in various parts of the insula and in frontal, temporal, rolandic opercula, including pre- and postcentral gyri (Cerf, B. *et al.*, 1998; Faurion, A. *et al.*, 1999; Cerf-Ducastel, B. *et al.*, 2001) as expected from electrophysiological recordings in the monkey (Ruch, T. C. and Patton, H. D., 1946; Bagshaw, M. H. and Pribram, K. H., 1953; Benjamin, R. M. and Burton, H., 1968; Ogawa, H. *et al.*, 1985; Pritchard, T. C. *et al.*, 1986; Yaxley, S. *et al.*, 1990; Scott, T. R. *et al.*, 1991; Ogawa, H., 1994; Kadohisa, M. *et al.*, 2005) or clinical observations in humans (Bornstein, W. S., 1940; Lewey, F. H., 1943; Penfield, W. and Faulk, M. E., 1955; Motta, T. A., 1959; Hausser-Hauw, C. and Bancaud, J., 1987). Other localizations of activation of lower occurrence were not all mentioned at that time. More interestingly, a bilateral projection was found at the superior part of insula, whereas a small location in the anterior inferior insular area was found activated in the left hemisphere for strict right-handers and in the right hemisphere for left-handers (Faurion, A. *et al.*, 1999).

4.13.3 The Insular/Opercular Area and the Role of Anterior Inferior Insula

The activations due to pure taste and somatosensory or trigeminal oral stimuli, such as strong acid or potassium aluminate, were studied comparatively in the same subjects and experimental sessions. They were shown to appear in the same regions of the brain

of 12 right-handed subjects (Cerf-Ducastel, B. *et al.*, 2001). However, it was possible to make out both senses on the basis of the coactivation of areas across experiments, such as the rolandic operculum for somatosensory stimuli and the anterior inferior insula for taste. Factor analysis of the table of activated brain areas across experiments showed that the right and left rolandic operculum were discriminated from all other regions when experiments included somatosensory stimuli, whereas the right and left anterior inferior insula were discriminated from all other regions when experiments included only pure taste. It appears that multidimensional analysis sorted out the somatosensory projection area for the tongue for strong acid and astringent stimuli as an internal control of the experiment and, on the contrary, the anterior inferior insula appeared taste specific. For taste stimuli, the anterior inferior insular area was not only found again activated in the left hemisphere for right-handers but also statistically coactivated with the left angular gyrus (Cerf-Ducastel, B. *et al.*, 2001), a structure that is known to be related to comprehension of language in the dominant hemisphere of these right-handers. Furthermore, it was shown with MEG (Kobayakawa, T. *et al.*, in preparation) that this very region was the latest one to be activated, between 800 and 1400 ms for saccharin, after all other regions and after the most prominent brain activation had been recorded between 200 and 500 ms. This set of results suggests an integrative function for the inferior insula with special functions related to semantics for taste in the dominant hemisphere of right-handers, and an initial activation in the bilateral upper part of insula. A controversy remains concerning the first location of activation in this upper part of the insula, either anterior for some authors or posterior for other ones. For studying initial activation, MEG is a preferred technique, *vide infra*: timing of activation.

A much clearer picture of brain activation was obtained looking at the spatiotemporal pattern of activation. The time course of brain image formation was different for experiments including NaCl and saccharin in MEG studies, as expected from electrophysiological recordings of taste nerves in rodents. Moreover, both the temporal dimension given by the apparition of different dipoles in various places successively in the brain and the movement of each dipole we can follow during a few dozens of milliseconds helped visualizing the cross-talk activity between different brain areas and within each area during the first second of stimulation. In many behavioral experiments, this period is fairly sufficient to identify the signification of the stimulus.

Using electrogustometric stimulation at low current intensities for taste which excludes tingling sensation, in right-handed subjects, Barry M. A. *et al.* (2001) could not show a simple relationship between the side of the stimulus applied and the side where the activation was found in insular and opercular areas at individual level. However, on the group analysis, they found a predominant right activation in the frontal opercular area. Finally, in this study, taste appears to project more to the right hemisphere than lingual touch. May be the group analysis averaged different results in different subjects, or a more complex data treatment is already performed prior to this projection. By comparison, and except in the inferior anterior insula, we observed an alternated right–left prevalence depending on anteriority, with equal left and right projection in the anterior insula/opercular area at $20 < y < 30$ and a more pronounced right insular activation at $0 < y < 10$ (less anterior), which may also look subject dependent. The electrogustometric (EGM) stimulation at low current is an interesting technique to confirm that actual taste and not somatosensory responses were found in this study in the postcentral gyrus: taste (saliva cations being applied iontophoretically) elicited activation at a more ventral location of the postcentral gyrus than in Pardo J. V. *et al.* (1997) where both taste and somatosensory senses were recruited. A recent clinical study tended to show a predominantly ipsilateral projection for taste and a more prominent contralateral projection for lingual touch information (Berlucchi, G. *et al.*, 2004). Taking together their results and ours, Barry *et al.*, looking more precisely at insula, which they divided into nine parts (i.e., anterior, middle, posterior x superior, central, inferior), concluded that taste-evoked activation in the superior part seems to predominate in the right-hand side, that activation in the central part appears bilateral and that activation in the inferior part is in the dominant left hemisphere of right-handers.

4.13.4 Timing of Activation: Magnetoencephalography Experiments

MEG is the best technique to locate the first temporal activation (primary taste area). Kobayakawa T. *et al.* (1996; 1999; 2005) showed an initial activation in the most posterior superior region of insula and

rolandic operculum at onset latencies below 100 ms for salt and about 120–140 ms for saccharin. A complementary argument to assess this area was the first one to be activated came from EEG simultaneously recorded (Mizoguchi, C. *et al.*, 2002). Using electrogustometric stimulation, Yamamoto C. *et al.* (2003) showed, with MEG, a more anterior insular early projection, close to frontal operculum as shown in electrophysiological studies in primates. These discrepancies might refer to different experimental conditions.

4.13.5 Intensity Coding, Absence of Chemotopy

In the insula, Small D. M. *et al.* (2003) with fMRI and Kobayakawa T. *et al.* (2005) with MEG found indication of the coding of intensity of taste. O'Doherty J. P. *et al.* (2002) and De Araujo I. E. T. *et al.* (2003) confirmed, with fMRI, the existence of unimodal neuronal activity for taste in the anterior superior insula ($y = 3$ to 14) and frontal operculum.

O'Doherty J. *et al.* (2001) looked for topography of taste quality, but they found no trace of different localization of activation for glucose and salt: neither group analysis nor single subject analysis did provide any evidence of chemical topography in either insula or opercula. This result is not unexpected and matches well with (1) the indication of great interindividual differences of quality perception by subjects: any averaging of eventually different chemotopies would fail showing different locations for different taste qualities and with (2) the existence a continuum of numerous tastes, each stimulus being coded by a different neuronal pattern of activation, which is its signature.

4.13.6 Imagination of Taste versus Perception of Taste

Kobayashi M. *et al.* (2004) showed that the left insula was activated by gustatory imagery tasks and that the middle and superior frontal gyri which are occasionally found activated in taste experiments seemed to play an important role in the generation of hallucination of taste (top-down information, evoked imagery without the stimulus) rather than in taste perception due to the stimulus (bottom-up information).

4.13.7 Learning by Familiarization

Faurion A. *et al.* (1998; 2002) showed plasticity on repetitive imaging of subjects submitted to a protocol of familiarization to novel tastes: the number of pixels significantly changed in the insular/opercular area between the first fMRI session in which the subject tasted the novel stimuli for the first time and the second fMRI session which occurred after a heavy psychophysics session in which subjects evaluated the intensity of the novel stimuli about 120 times. The number of pixels did not change any more in the third fMRI session run after 10 more psychophysics sessions. When looking for a psychophysical parameter correlated with this pixel number variation, it was shown that the group of experiments showing an increase of the pixel number was the same as the group of experiments showing an increase of the hedonic evaluation with familiarization and that the group of experiments showing a decrease of the pixel number was the same as the group of experiments showing a decrease of the hedonic evaluation with familiarization. This result pointed to some relationship in the insular/opercular area between the evolution of the number of activated pixels and the direction of the evolution of the hedonic assessment in process of familiarization to foods, a situation that frequently occurs in everyday life for taste.

4.13.8 Orbitofrontal Cortex, an Integrative Area Contributing to Hedonic Valence and Food Reward

In the literature, the orbitofrontal cortex (OFC) is thought to be the region where the reward value of the food is expressed. If they did not find chemotopy in the insula, O'Doherty J. *et al.* (2001) showed that considering subjects taken individually, the areas activated for glucose (pleasant) and for salt (slightly unpleasant) were separated and only slightly overlapping. Averaging subjects tended to blur these interindividual differences. Hence the OFC responds to affectively positive and affectively negative taste stimuli in topographically different locations.

Small D. M. *et al.* (2003) found pleasant/aversive value in the anterior part of insula extending to the OFC. Similarly, De Araujo I. E. T. *et al.* (2003) mapped three distinct functions in the continuous region extending from the far anterior insula toward

and including the orbitofrontal cortex. They looked at taste and olfactory convergence in relation with pleasantness of flavor. If unimodal neurones for taste were found in the anterior superior insula and frontal operculum, taste and olfaction seem to converge at the far anterior (inferior) insula where it joins the OFC (MNI coordinates: 45, 15, −9), in a region even more caudal than the caudal OFC (ventral forebrain) and in the nearby cingulate gyrus, which seems to respond to the mere association of both sensations. Small D. M. *et al.* (2004) proposed that the OFC together with the insula and the anterior cingulate gyrus constitute the key components of the network underlying flavor perception, which is in agreement with electrophysiological recordings: this region is known in the primate to receive olfactory input and secondary taste projection from the primary taste area.

In the lateral anterior OFC, a positive intermodality synergistic interaction appeared as the activation in this region seems to be more pronounced for the stimulation with the mixture of sucrose taste and strawberry odor (flavor) than by the sum of the activation to each stimulus separately.

In a more medial part of the anterior OFC appeared information relevant to taste and smell subjectively matching together (judgment of congruence between taste and smell). This region was also shown to respond to pleasant odors (Zald, D. H. and Pardo, J. V., 1997) and pleasant touch (Rolls, E. T. *et al.*, 2003).

Finally, a region responding to anticipation of pleasant and unpleasant taste was found only in the OFC where regions responding to expectation of reward and reward receipt were separated (O'Doherty, J. P. *et al.*, 2002), whereas other areas in striatum (putamen, nucleus accumbens) and amygdala responded to both. The OFC appears as the key structure for efficient and rapid stimulus reinforcement of an association learning between visual or olfactory stimulus and a positive or negative reinforcer such as taste or touch (Rolls, E. T., 2004).

For the sake of comparison, Cerf, Kobayakawa, and Faurion together showed a complex long-lasting integration process including semantics and taste in the dominant hemisphere in the anterior inferior insula (-45 ± 4; 7 ± 11; -3 ± 5 and 39 ± 10; 28 ± 6; -5 ± 3), a region that is nearby the frontal operculum and the caudal OFC, and this region may be the same as, or very close to, areas that were shown to be activated by taste (38; 20; −4; −32; 22; 0) in Kringelbach M. L. *et al.* (2004), by sucrose and strawberry odor (−31; 22; 0) in de Araujo I. E. T. *et al.* (2003), by glucose (−33; 17; 2) in O'Doherty J. *et al.* (2001), and unpleasant taste (−39; 27; −3) in Small D. M. *et al.* (2003).

4.13.9 Amygdala Involved in Hedonic Valence and Memorization

In amygdala, Small D. M. *et al.* (2003) found intensity of taste, as well as aversive value. O'Doherty J. *et al.* (2001) suggested that amygdala may signal as well aversive taste and affectively positive taste. Slightly different was the result of Zald D. H. *et al.* (2002) showing that the amygdala would respond preferentially to the aversive quinine and poorly to nonaversive stimulus such as sucrose. O'Doherty J. P. *et al.* (2002) showed that the OFC and not the amygdala responded to changes in pleasantness associated with eating (satiety effect). The authors propose that flavor novelty might be expressed in the amygdala on the basis of match/mismatch association of odor and flavor. These results are confirmed by Small D. M. *et al.* (2003). It could be hypothesized that in amygdala, novelty triggers some memorization mechanisms and recall memories with cultural clues. Activation for unpleasant taste may be more pronounced than for mild pleasant taste as unpleasant taste is more impressive and probably triggers more actively the memorization circuits. Zald D. H. (2003), in a very comprehensive review, points to the fact that the amplitude of pleasantness and unpleasantness for stimuli presented is usually not equivalent, a factor that may obscure the role of the amygdala with respect to positive hedonic valence stimuli. The author stresses the importance of dissociating the arousal value from the emotional value of the stimulus presented. Another interesting point for amygdala is that it seems to be activated for low-intensity subliminal stimuli which do not elicit conscious perception. Based on animal literature, a direct fast connection between thalamus and amygdala may be the source of behavioral responses related to nonperceived subliminal though emotionally relevant stimuli.

4.13.10 Other Areas

The anterior cingulate is known to be related to emotion. De Araujo I. E. and Rolls E. T. (2004) showed an activation in the anterior cingulum for

fat independent of viscosity and for glucose, suggesting a response to the hedonic positive somatosensory aspect of fat. Small D. M. *et al.* (2004) found also activation in the anterior cingulate for congruent odor taste combination, activation depending on previous experience with taste/smell combinations.

Also the precentral gyrus at various z coordinates is often activated at various z coordinates during taste stimulation; its contribution to taste the function of which in taste is still to be determined.

Other locations were found in various studies which were at first not considered as they were either seldom or not expected from previous electrophysiological studies. As their roles were not easily interpreted, they could have been taken as putative artifacts. However, they repetitively appear in recently published studies, the number of which, although still low, now significantly increases (from one in 1994 to more than 10 in 2004) (e.g., the ventral and medial part of the thalamus, the lingual gyrus in the visual area, and the cerebellum). More numerous studies might confirm the validity of these activated areas as relevant to the taste stimulus.

Finally, Kringelbach M. L. *et al.* (2004) showed that not only the anterior insula, the frontal operculum, and the caudal OFC do respond to taste, but that taste activation is also found in the dorsolateral prefrontal cortex at a rather high level ($z = 36$). This region is already known to be implicated in response selection, working memory, attention, and integration (i.e., executive control).

4.13.11 Conclusive Remarks

So far, one of the key points for interpreting images remains that the examined areas benefit from being identified by eye recognition in anatomical images, coordinates being only indicative as they can be different from one imaging technique to another one and from one subject to another one (anatomical differences). Second, different imaging techniques (PET, fMRI, or MEG) or different stimulation protocols may identify different locations responding to taste in a given area; for example, MEG studies (Kobayakawa, T. *et al.*, 1996; 1999) did not find middle insula activation and PET studies find also more posterior activation in insula (Frey, S. and Petrides, M., 1999; Small, D. M. *et al.*, 1999) than fMRI experiments do, which also show anterior superior insular activation. The different time windows of the techniques resulting in different temporal averaging might be responsible for focusing on different regions, or the tasks given to subjects were different and accounted for different responses.

Complementary studies with MEG and fMRI associating both high temporal and spatial resolutions allow observing the dynamics of activation in the brain in response to a given tastant, with dipoles flashing as questions and answers in and toward various regions alternately, a cross-talk pattern which is specific of the quality and contextual properties of the stimulus. Such results confirm (1) the specific signature of each single tastant and (2) a widespread representation of taste information across various regions of the brain. Reliable tools are now available for mapping the individual coding of taste sensation and its relevant cultural signification, for example, for thoroughly investigating innate and acquired interindividual differences in taste perception.

References

Bagshaw, M. H. and Pribram, K. H. 1953. Cortical organization in gustation (*Macaca mulatta*). J. Neurophysiol. 16, 499–508.

Bandettini, P. A., Jesmanowicz, A., Wong, E. C., and Hyde, J. S. 1993. Processing strategies for functional MRI of the human brain. Magn. Reson. Med. 30, 161–173.

Barry, M. A., Gatenby, J. C., Zeiger, J. D., and Gore, J. C. 2001. Hemispheric dominance of cortical activity evoked by focal electrogustometry stimuli. Chem. Senses 26, 471–782.

Belliveau, J. W., Kennedy, D. N., McKinstry, R. C., Buchbinder, B. R., Weisskoff, R. M., Cohen, M. S., Verea, J. M., Brady, T. J., and Rosen, B. R. 1991. Functional mapping of the human visual cortex by magnetic resonance imaging. Science 254, 716–719.

Benjamin, R. M. and Burton, H. 1968. Projection of taste nerve afferents to anterior opercular-insular cortex in squirrel monkey (*Saimiri sciureus*). Brain Res. 7, 221–231.

Berlucchi, G., Moro, V., Guerrini, C., and Aglioti, S. M. 2004. Dissociation between taste and tactile extinction on the tongue after right brain damage. Neuropsychologia 42, 1007–1016.

Bornstein, W. S. 1940. Cortical representation of taste in man and monkey. II. The localization of the cortical taste area in man and a method of measuring impairment of taste in man. Yale J. Biol. Med. 13, 133–156.

Cerf, B., Mac Leod, P., Van de Moortele, P.-F., Le Bihan, D., and Faurion, A. 1998. Functional lateralization of human gustatory cortex related to handedness disclosed by MRI study. Ann. N. Y. Acad. Sci. 855, 575–578.

Cerf, B., Van de Moortele, P.-F., Giacomini, E., Mac Leod, P., Faurion, A., and Le Bihan, D. 1996. Correlation of perception to temporal variations of fMRI signal: a taste study. Proc. Int. Soc. Magn. Reson. Med. (ISMRM), 280.

Cerf-Ducastel, B., Van de Moortele, P.-F., Mac Leod, P., Le Bihan, D., and Faurion, A. 2001. Interaction of gustatory and lingual somatosensory perceptions at the cortical level in the human: a functional magnetic resonance imaging study. Chem. Senses 26, 371–383.

De Araujo, I. E. and Rolls, E. T. 2004. Representation in the human brain of food texture and oral fat. J. Neurosci. 24(12), 3086–3093.

De Araujo, I. E. T., Rolls, E. T., Kringelbach, M. L., McGlone, F., and Phillips, N. 2003. Taste-olfactory convergence, and the representation of the pleasantness of flavour, in the human brain, Eur. J. Neurosci. 18, 2059–2068.

Faurion, A., Cerf, B., Le Bihan, D., and Pillias, A. M. 1998. fMRI study of taste cortical areas in humans (activations observed in relation to the hedonic and semantic status of the stimulus). Ann. N. Y. Acad. Sci. 585, 535–545.

Faurion, A., Cerf, B., Van de Moortele, P.-F., Lobel, E., Mac Leod, P., and Le Bihan, D. 1999. Human taste cortical areas studied with functional magnetic resonance imaging: evidence of functional lateralization related to handedness. Neurosci. Lett. 277, 189–192.

Faurion, A. B., Cerf, A. M., Pillias, N., and Boireau, N. 2002. Increased Taste Sensitivity by Familiarization to ''Novel'' Stimuli. Psychophysics, fMRI and Electrophysiological Techniques Suggest Modulations at Peripheral and Central Levels. In: Olfaction, Taste and Cognition (*eds*. C. Rouby, B. Schaal, D. Dubois, R. Gervais, and A. Holley), pp. 350–366. Cambridge University Press.

Frey, S. and Petrides, M. 1999. Re-examination of the human taste region: a positron emission tomography. Eur. J. Neurosci. 11, 2985–2988.

Grynszpan, F. and Geselowitz, D. B. 1973. Model studies of the magnetocardiogram. Biophys. J. 13(9), 911–925.

Hausser-Hauw, C. and Bancaud, J. 1987. Gustatory hallucinations in epileptic seizures. Electrophysiological, clinical and anatomical correlates. Brain 110, 339–359.

Kadohisa, M., Rolls, E. T., and Verhagen, J. V. 2005. Neuronal representations of stimuli in the mouth: The primate insular taste cortex, orbitofrontal cortex and amygdala. Chem. Senses 30, 1–19.

Kinomura, S., Kawashima, K., Yamada, S., Ono, M., Itoh, S., Yoshioka, T., Yamaguchi, H., Matsui, H., Itoh, R., Goto, T., Fujiwara, K., Satoh, K., and Fukuda, H. 1994. Functional anatomy of taste perception in the human brain studied with positron emission tomography, regional cerebral blood flow, taste stimulation, insular cortex, cingulate cortex, parahippocampal gyrus, human brain. Brain Res. 659, 263–266.

Kobayakawa, T., Endo, H., Ayabe-Kanamura, S., Kumagai, T., Yamaguchi, Y., Kikuchi, Y., Takeda, T., Saito, S., and Ogawa, H. 1996. The primary gustatory area in human cerebral cortex studied by magnetoencephalography. Neurosci. Lett. 212, 155–158.

Kobayakawa, T., Ogawa, H., Kaneda, H., Ayabe-Kanamura, S., Endo, H., and Saito, S. 1999. Spatio-temporal analysis of cortical activity evoked by gustatory stimulation in human. Chem. Senses 24, 201–209.

Kobayakawa, T., Wakita, M., Saito, S., Gotow, N., Sakai, N., and Ogawa, H. 2005. Location of the primary gustatory area in humans and its properties studied by magnetoencephalography. Chem. Senses 30(Suppl.1), i226–i227.

Kobayashi, M., Takeda, M., Hattori, N., Fukunaga, M., Sasabe, T., Inoue, N., Nagai, Y., Sawada, T., Sadato, N., and Watanabe, Y. 2004. Functional imaging of gustatory perception and imagery: ''top-down'' processing of gustatory signals. Neuroimage 23(4), 1271–1282.

Kringelbach, M. L., de Araujo, I. E. T., and Rolls, E. T. 2004. Taste-related activity in the human dorsolateral prefrontal cortex. Neuroimage 21, 781–788.

Kwong, K. K., *et al.* 1992. Dynamic magnetic resonance imaging of human brain activity during primary sensory stimulation. Proc. Natl. Acad. Sci. U. S. A. 89, 5675–5679.

Lauterbur, P. C. 1973. Image formation by induced local interaction. Examples employing nuclear magetic resonance imaging Nature 241, 190–191.

Le Bihan, D., *et al.* 1986. MR imaging of intravoxel incoherent motions: application to diffusion and perfusion in neurologic disorders. Radiology 161, 401–407.

Lewey, F. H. 1943. Aura of taste preceding convulsions associated with a lesion of the parietal operculum: report of a case. Arch. Neurol. Psychiatr. 50, 575–578.

Mizoguchi, C., Kobayakawa, T., Saito, S., and Ogawa, H. 2002. Gustatory evoked cortical activity in humans studied by simultaneous EEG and MEG recording. Chem. Senses. 27(7), 629–634.

Motta, T. A. 1959. G. I centri corticali del gusto. Bulletino delle Scienze Mediche 131, 480–493.

O'Doherty, J. P., Deichmann, R., Critchley, H. D., and Dolan, R. J. 2002. Neural responses during anticipation of a primary taste reward. Neuron 33(5), 815–826.

O'Doherty, J., Rolls, E. T., Francis, S., Bowtell, R., and McGlone, F. 2001. Representation of pleasant and aversive taste in the human brain. J. Neurophysiol. 85, 1315–1321.

Ogawa, H. 1994. Gustatory cortex of primates: anatomy and physiology. Neurosci. Res. 20, 1–13.

Ogawa, H., Ito, S. I., and Nomura, T. 1985. Two distinct projection areas from tongue nerves in the frontal operculum of macaque monkeys as revealed with evoked potential mapping. Neurosci. Res. 2, 447–459.

Ogawa, S., *et al.* 1992. Intrinsic signal changes accompanying sensory stimulation: functional brain mapping with magnetic resonance imaging. Proc. Natl. Acad. Sci. U. S. A. 89, 5951–5955.

Pardo, J. V., Wood, T. D., Costello, P. A., Pardo, P. J., and Lee, J. T. 1997. PET study of the localization and laterality of lingual somatosensory processing in humans. Neurosci. Lett. 234, 23–26.

Penfield, W. and Faulk, M. E. 1955. The insula. Further observations on its function. Brain 78(4), 445–470.

Pritchard, T. C., Hamilton, R. B., Morse, J. R., and Norgren, R. 1986. Projections of thalamic gustatory and lingual areas in the monkey, *Macaca fascicularis*. J. Comp. Neurol. 244, 213–228.

Rolls, E. T. 2004. The functions of the orbitofrontal cortex. Brain Cogn. 55(1), 11–29. Review.

Rolls, E. T., O'Doherty, J., Kringelbach, M. L., Francis, S., Bowtell, R., and McGlone, F. 2003. Representations of pleasant and painful touch in the human orbitofrontal and cingulate cortices. Cereb. Cortex 13(3), 308–17.

Roy, C. W. and Sherrington, C. S. 1890. On the regulation of the blood supply of the brain. J. Physiol. 11, 85–108.

Ruch, T. C. and Patton, H. D. 1946. The relation of the deep opercular cortex to taste. Fed. Proc. 5, 89–90.

Scott, T. R., Plata-Salaman, C. R., Smith, V. L., and Giza, B. K. 1991. Gustatory neural coding in the monkey cortex: stimulus intensity. J. Neurophysiol. 65(1), 76–86.

Small, D. M., Gregory, M. D., Mak, Y. E., Gitelman, D., Mesulam, M. M., and Parish, T. 2003. Dissociation of neural representation of intensity and affective valuation in human gustation. Neuron 39, 701–711.

Small, D. M., Voss, J., Mak, Y. E., Simmons, K. B., Parrish, T., and Gitelman, D. 2004. Experience-dependent neural integration of taste and smell in the human brain. J. Neurophysiol. 92(3), 1892–1903.

Small, D. M., Zald, D. H., Jones-Gotman, M., Zatorre, R. J., Pardo, J. V., Frey, S., and Petrides, M. 1999. Human cortical gustatory areas: a review of functional neuroimaging data. Neuroreport 10, 7–14.

Van de Moortele, P.-F., Cerf, B., Lobel, E., Paradis, A.-L., and Faurion, A. 1997. Latencies in fMRI time-series: effect of slice acquisition order and perception. NMR Biomed. 10, 230–236.

Yamamoto, C., Takehara, Morikawa, K., Nakagawa, S., Yamaguchi, M., Iwaki, S., Tonoike, M., and Yamamoto, T. 2003. Magnetoencephalographic study of cortical activity evoked by electrogustatory stimuli. Chem. Senses 28, 245–251.
Yaxley, S., Rolls, E. T., and Sienkiewicz, Z. J. 1990. Gustatory responses of single neurons in the insula of the macaque monkey. J. Neurophysiol. 63(4), 689–700.
Zald, D. H. 2003. The human amygdala and the emotional evaluation of sensory stimuli. Brain Res. Brain Res. Rev. 41(1), 88–123.
Zald, D. H. and Pardo, J. V. 1997. Emotion, olfaction, and the human amygdala: amygdala activation during aversive olfactory stimulation. Proc. Natl. Acad. Sci. U. S. A. 94(8), 4119–4124.
Zald, D. H., Hagen, M. C., and Pardo, J. V. 2002. Neural correlates of tasting concentrated quinine and sugar solutions. J. Neurophysiol. 87, 1067–1075.

Relevant Website

http://www.madic.org/index.php – For technical aspects.

4.14 Amiloride-Sensitive Ion Channels

J A DeSimone and V Lyall, Virginia Commonwealth University, Richmond, VA, USA

© 2008 Elsevier Inc. All rights reserved.

4.14.1	**Epithelial Na^+ Channel**	281
4.14.1.1	Epithelial Na^+ Channel Function	281
4.14.1.2	Epithelial Na^+ Channel Structure	282
4.14.1.3	Epithelial Na^+ Channel Regulation	283
4.14.2	**Amiloride-Sensitive Salt Taste Receptor**	284
4.14.2.1	Hormonal Regulation of Epithelial Na^+ Channel and Salt Taste	284
4.14.2.2	Regulation of Epithelial Na^+ Channel by cAMP and Salt Taste	284
4.14.2.3	Regulation of Epithelial Na^+ Channel by Intracellular pH and Salt Taste	284
4.14.2.4	Regulation of Epithelial Na^+ Channel by Intracellular Ca^{2+} and Salt Taste	284
4.14.2.5	Regulation of Epithelial Na^+ Channel by Osmolarity and Salt Taste	285
4.14.2.6	Regulation of Epithelial Na^+ Channel by Temperature and Salt Taste	286
4.14.2.7	Regulation of Epithelial Na^+ Channel by Proteases and Salt Taste	286
4.14.2.8	Na^+ Self-Inhibition of Epithelial Na^+ Channel and Salt Taste	287
4.14.3	**Summary and Conclusions**	287
References		287

Glossary

pS Picosiemens, a conductance unit (10^{-12} siemens).

rENaC Rat ENaC, ENaC cloned from rat tissue.

TRPV1t Taste variant of TRPV1, transient receptor potential cation channel, subfamily V, member 1

4.14.1 Epithelial Na^+ Channel

4.14.1.1 Epithelial Na^+ Channel Function

Sodium (Na^+) absorption across many epithelial tissues depends on the epithelial Na^+ channel (ENaC), an apical membrane integral protein. Net absorption of Na^+ from the luminal side of the tissue to the submucosal side can occur when the luminal Na^+ concentration is equal to or less than the interstitial fluid Na^+ concentration, that is, Na^+ transport across epithelial cells is overall active, that is, coupled to metabolic energy sources (Ussing, H. H. and Zerahn, K., 1951; Verrey, F. *et al.*, 2000). However, the initial influx of Na^+ from lumen to cell occurs by passive electrodiffusion down both the Na^+ concentration gradient and the apical membrane electrical potential gradient. Cell Na^+ is then actively extruded across the basolateral membrane through sodium–potassium (Na^+-K^+) pumps (Horisberger, J. D., 2004). Net Na^+ transport can be pharmacologically blocked by either adding ouabain to the basolateral side to inhibit the Na^+-K^+ pumps or with amiloride on the apical side to reduce the Na^+ conductance of ENaC (Verrey, F. *et al.*, 2000). Before the structure of ENaC was determined, the potent effect of amiloride as a Na^+-transport blocker proved to be a reliable indication of the channel's presence, hence its much cited earlier name: amiloride-sensitive epithelial Na^+ channel. Transepithelial Na^+ transport can be monitored *in vitro* in a variety of tissues as the major component of the short-circuit current (I_{sc}) across the epithelium mounted as a tissue sheet between a pair of Ussing chambers allowing solutions with ionic composition approximating extracellular fluid to bathe both apical and basolateral tissue surfaces (Ussing, H. H. and Zerahn, K., 1951). If Na^+ enters the epithelial cells exclusively through apical membrane ENaC, then amiloride or its analogs will significantly inhibit the I_{sc} (Will, P. C. *et al.*, 1985). If Na^+ is the major ion actively absorbed, as in the

case of amphibian urinary bladder, then I_{sc} will be reduced nearly to zero (Palmer, L. G. *et al.*, 1982).

Mammalian tissues, for which the presence of ENaC has either been directly demonstrated or inferred from electrophysiological, pharmacological, or immunocytochemical studies include: the distal convoluted tubule and collecting tubules of the kidney, colon, trachea, sweat and salivary glands, and dorsal lingual epithelium including taste receptor cells (Garty, H. and Palmer, L. G., 1997). The single channel biophysical properties of Na^+-transporting ion channels obtained from patch clamp recordings from rat cortical collecting tubules and the A6 cell line from *Xenopus* kidney correspond well with those of cloned ENaC expressed in *Xenopus* oocytes (Canessa, C. M. *et al.*, 1994). Based on such comparisons the consensus opinion is that the Na^+-transporting properties of most epithelia derive from ENaC. First, ion transport in epithelia and through cloned ENaC is selective for Na^+ over K^+ with a Na^+:K^+ permeability ratio in excess of 20 (Garty, H. and Palmer, L. G., 1997; Rossier, B. C. *et al.*, 2002). Epithelial and cloned ENaC demonstrate a unitary conductance of 5 pS, an open probability of 0.5, and a dissociation constant for amiloride binding of 0.1–1.0 μM (Garty, H. and Palmer, L. G., 1997). The aldosterone-responsive epithelia of the kidney and colon are critical in the control of blood volume, blood pressure, and Na^+ balance. Consequently, in humans loss-of-function mutations in ENaC result in pseudohypoaldosteronism type 1, a severe salt wasting disease, and gain-of-function mutations cause pseudoaldosteronism, a form of salt-sensitive hypertension (Rossier, B. C. *et al.*, 2002). Na^+ consumption, in which Na^+ taste plays a role, is a factor in overall Na^+ balance. All three ENaC subunits are expressed in rat taste buds (Kretz, O. *et al.*, 1999). It is perhaps not surprising, therefore, that in mammals utilizing ENaC as a Na^+-specific taste receptor, that ENaC levels in taste cells are also modulated by aldosterone (Lin, W. *et al.*, 1999). The sensory consequence of this is that the amiloride-sensitive component of the chorda tympani taste nerve response to sodium chloride (NaCl) in rats increases following aldosterone treatment (Herness, M. S., 1992).

4.14.1.2 Epithelial Na^+ Channel Structure

ENaC is an integral membrane protein composed of three subunits, designated α, β, and γ, each of which is comprised of about 650–700 amino acids (Canessa, C. M. *et al.*, 1994). Evidence suggests the native channel consists of two α, one β, and one γ subunit (Firsov, D. *et al.*, 1998; Kosari, F. *et al.*, 1998; Figure 1).

The essential Na^+-conducting properties of ENaC are found only in the α subunit. While the β and γ subunits have no intrinsic channel function, their coexpression with the α subunit enhanced its amiloride-sensitive conductance by more than 100-fold (Canessa, C. M. *et al.*, 1994). Each subunit has just two membrane-spanning domains. Both the N- and C-termini are relatively short and located on the cytoplasmic side while the extracellular domain consists of a loop, containing nearly 70% of each subunit's amino acids, connecting the membrane-spanning hydrophobic segments (Benos, D. J. and Stanton, B. A., 1999). Evidence suggests that the major amiloride binding sites in rat ENaC involve a six amino acid residue track (α-278-283, WYRFHY), within the extracellular domain of α-rENaC (Kieber-Emmons, T. *et al.*, 1995). Histidine at α-282 appears to provide an essential electropositive moiety because mutagenesis of it to negative aspartic acid resulted in a 40-fold increase in the binding dissociation constant between amiloride and ENaC, while substitution with positive arginine decreased the dissociation constant by sixfold (Lin, C. *et al.*, 1994). The extracellular domain may also bind an accessory protein that is the site of action of serine proteases. The action of channel activating protease 1 (CAP1, prostasin), an endogenous serine protease, increases the Na^+ flux through ENaC, an effect that can be reproduced with trypsin using ENaC expressed in *Xenopus* oocytes (Chraïbi, A. *et al.*, 1998) and in rat taste receptors (see Section 4.14.2.7). Deletion of the N-terminal region of each subunit eliminates channel activity suggesting that it

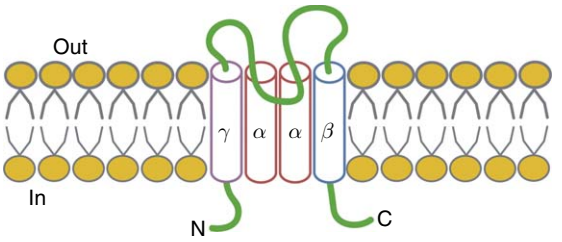

Figure 1 Model of epithelial Na^+ channel illustrating the stoichiometry among the subunits. Each subunit has two transmembrane domains (not shown) with C- and N-terminal regions in the cytoplasmic domain as shown. Reprinted, with permission, from the Annual Review of Physiology, Volume 64 © 2002 by Annual Reviews.

is important in regulating channel gating and proper assembly of functional ENaC from its subunits (Chalfant, M. L. *et al.*, 1999a). Point substitutions of serine for glycine in the N-terminus at G95 of (α-rENaC) rat ENaC, G37 of β-rENaC, or G40 of γ-rENaC significantly decrease ENaC conductance by decreasing the channel open probability (Grunder, S. *et al.*, 1997). The significance of the serine for glycine substitution at G37 of β-rENaC is evident from the fact that it is responsible for pseudohypoaldosteronism type 1. The second membrane-spanning region (M2) of each subunit and part of the pre-M1 domain contain the channel selectivity filter, sites responsible for conductance inhibition by divalent cations, and further sites involved in amiloride inhibition (Benos, D. J. and Stanton, B. A., 1999). The C-terminal region of each subunit is the most variable, and probably accounts for species and tissue differences in some of ENaC's regulatory properties, such as sensitivity to cyclic AMP (cAMP). In airway cells (Kunzelmann, K. *et al.*, 2000), renal collecting duct cells (Handler, J. S. and Orloff, J., 1981), and taste cells (Gilbertson, T. A. *et al.*, 1993; see Figure 1) cAMP stimulates amiloride-sensitive Na^+ transport through ENaC, while in mammalian colon and urinary bladder cAMP has no effect (Garty, H. and Palmer, L. G., 1997). Point mutations in a proline-rich region in the β- and γ-subunit C-termini of ENaC are sufficient to produce the gain-of-function disease, pseudoaldosteronism. This proline-rich region is important for normal internalization of ENaC from the plasma membrane and its absence results in overexpression of ENaC and a gain-of-function disease resulting in severe hypertension.

4.14.1.3 Epithelial Na^+ Channel Regulation

Salt and water balance in terrestrial mammals is tightly regulated by the hormone, aldosterone which exerts stimulatory effects on ENaC, Na^+-K^+ pumps, and various membrane ion exchangers in cells of the renal collecting duct and colon (Rossier, B. C. *et al.*, 2002). Aldosterone-sensitive Na^+ transport occurs in the duct cells of salivary and sweat glands and in the taste cells (Herness, M. S., 1992; Lin, W. *et al.*, 1999). Following a latent period of 0.5–1.0 h, the aldosterone early response, which lasts from 1.5 to 3.0 h, consists of activation of preexisting Na^+ channels and pumps. The late response (at 6–24 h) is characterized by *de novo* synthesis of ENaC and Na^+-K^+ pumps. In rat colon (Lingueglia, E. *et al.*, 1994) and rat taste cells (Lin, W. *et al.*, 1999) aldosterone increases the expression of β- and γ-ENaC without effect on α-ENaC. A second hormone, vasopressin, also increases Na^+ transport through its effects on ENaC activity. The effect is well studied in amphibian skin, urinary bladder, and amphibian-derived A6 cells (Li, J. H. Y. *et al.*, 1982). In mammals vasopressin acts on renal collecting duct cells and on taste cells (Gilbertson, T. A. *et al.*, 1993). Vasopressin binds to the membrane receptor, V_2, which in turn activates adenylyl cyclase resulting in an increased cell cAMP concentration. When cell cAMP levels are elevated pharmacologically in vasopressin-responsive epithelia, including taste cells (Gilbertson, T. A. *et al.*, 1993), the effect mimics vasopressin. cAMP increases the Na^+ conductance of epithelia by increasing the apical membrane density of ENaC without changing the channel open time probability (Morris, R. G. and Schafer, J. A., 2002). The flux of Na^+ through ENaC is observed to be locally downregulated over a range of increasing apical Na^+ concentrations, a process referred to as Na^+ self-inhibition (Lindemann, B., 1984). Na^+ self-inhibition is one of many processes by which cells resist excessive increase in osmotic pressure. This self-regulatory process has been demonstrated in rat taste cells showing amiloride sensitivity (Gilbertson, T. A. and Zhang, H., 1998). Na^+ self-inhibition can itself be inhibited by a range of compounds including: sulfhydryl reagents, organic cations, cadmium (Cd^{2+}), and zinc (Zn^{2+}). An inhibitory effect of *p*-hydroxymercuribenzoate on Na^+ self-inhibition has been shown in rat fungiform taste cells (Gilbertson, T. A. and Zhang, H., 1998). The inhibitory effect of Zn^{2+} on Na^+ self-inhibition can be demonstrated by an enhanced rat chorda tympani response to NaCl in the presence of Zn^{2+} (see Section 4.14.2.8). Intracellular calcium (Ca^{2+}) and intracellular pH exert potent regulatory effects on ENaC under physiological conditions. An increase in intracellular Ca^{2+} inhibits the Na^+ flux through ENaC (Ishikawa, T. *et al.*, 1998) as does a decrease in intracellular pH (Palmer, L. G. and Frindt, G., 1987; Chalfant, M. L. *et al.*, 1999b). These inhibitory effects of intracellular Ca^{2+} and pH can be demonstrated in the taste system in recordings of the rat chorda tympani response to NaCl (see Sections 4.14.2.3 and 4.14.2.4). In ENaC-expressing oocytes, an increase in the extracellular osmotic pressure due to nonelectrolytes such as mannitol at hyperosmotic concentrations, will also increase the Na^+ conductance of ENaC (Ji, H. L. *et al.*, 1998). This effect of hyperosmotic mannitol can be observed under

physiological conditions in recordings of the NaCl chorda tympani response (Lyall, V. *et al.*, 1999; see Section 4.14.2.5). The temperature dependence of the ENaC conductance is unusual in that it is greater at lower temperature than at higher (Chraïbi, A. and Horisberger, J. D., 2002). This appears to be due to a decrease in the channel open probability with increasing temperature. This accounts for the striking inhibition of the amiloride-sensitive part of the chorda tympani response to NaCl with increasing temperature (see Section 4.14.2.6). Proteases can eliminate the inhibitory effect of increased temperature and also can block Na^+ self-inhibition (Chraïbi, A. and Horisberger, J. D., 2002), which indicates that the temperature effect is connected with the mechanism of Na^+ self-inhibition and that proteases modulate ENaC conductance by blocking that mechanism.

4.14.2 Amiloride-Sensitive Salt Taste Receptor

4.14.2.1 Hormonal Regulation of Epithelial Na^+ Channel and Salt Taste

In rats, where ENaC plays a major role in the animal's behavior toward Na^+ salts versus non-Na^+ salts (Spector, A. C. *et al.*, 1996), data support a role for both aldosterone and vasopressin in taste cell function. Injection of Sprague-Dawley rats with aldosterone increased apical immunoreactivity to β- and γ-ENaC, increased the number of amiloride-sensitive fungiform taste cells, and enhanced the magnitude of the Na^+ current (Lin, W. *et al.*, 1999). The sensory consequence of this is that following aldosterone injection the amiloride-sensitive component of the rat chorda tympani response to NaCl was significantly increased (Herness, M. S., 1992). Vasopressin and its associated second messenger, cAMP, increased the amiloride-sensitive Na^+ current in hamster fungiform taste cells (Gilbertson, T. A. *et al.*, 1993), suggesting a role for vasopressin in taste nerve activity toward Na^+ salts. It should be emphasized that these hormonal influences are likely to be less of a factor in human salt taste because the amiloride-sensitive NaCl-taste response in humans represents the smaller component of the two salt taste-sensing mechanisms (Schiffman, S. S. *et al.*, 1983; Smith, D. V. and Ossebaard, C. A., 1995; Lyall, V. *et al.*, 2004a).

4.14.2.2 Regulation of Epithelial Na^+ Channel by cAMP and Salt Taste

While no data are available on the action of vasopressin on the chorda tympani response to NaCl, topical application of 8-(4-chlorophenylthio)-cAMP (CPT-cAMP), a membrane permeable analog of cAMP, to the rat tongue significantly enhances the response to NaCl as seen in Figure 2(a) (Russell, O. F. *et al.*, 2002). The increased response is amiloride-sensitive (data not shown) indicating that cAMP increased ENaC activity, which is consistent with its well-studied action in Na^+-transporting epithelia.

The effect of cAMP on the chorda tympani response to NaCl also suggests a possible mechanism for taste mixture interaction at the cellular level. If a subset of ENaC-containing taste cells is also responsive to tastants that modulate intracellular cAMP, it is clear that tastant-evoked modulation of cAMP can also affect cell responsiveness to NaCl as part of a stimulus mixture.

4.14.2.3 Regulation of Epithelial Na^+ Channel by Intracellular pH and Salt Taste

The decrease in the Na^+ conductance of ENaC with decreasing intracellular pH, observed in a variety of Na^+-transporting epithelia and in ENaC-expressing oocytes, also occurs in ENaC-containing taste cells (Lyall, V. *et al.*, 2002). A decrease in intracellular pH in rat taste cells decreases the Na^+ flux across the apical membranes and this pH-induced modulation of ENaC conductance in taste cells significantly affects the chorda tympani response to NaCl (Lyall, V. *et al.*, 2002; Figure 2(b)). Figure 2(b) shows the effect of extracellular pH on the neural response to 100 mM NaCl. Data show, however, that the pH regulatory site is intracellular, and that extreme extracellular pH variation (e.g., pH 2 or 10.3) produces intracellular pH changes of only a few tenths of a unit (Lyall, V. *et al.*, 2002). These changes are, however, sufficient to produce a strong effect on the Na^+ conductivity of ENaC and, therefore, account for the mixture suppression of ENaC-based salt taste by low pH and its mixture enhancement at high pH.

4.14.2.4 Regulation of Epithelial Na^+ Channel by Intracellular Ca^{2+} and Salt Taste

An increase in intracellular Ca^{2+} due to an increase in TRPM5 cation conductance occurs in taste cells during transduction for the sweet, bitter, and

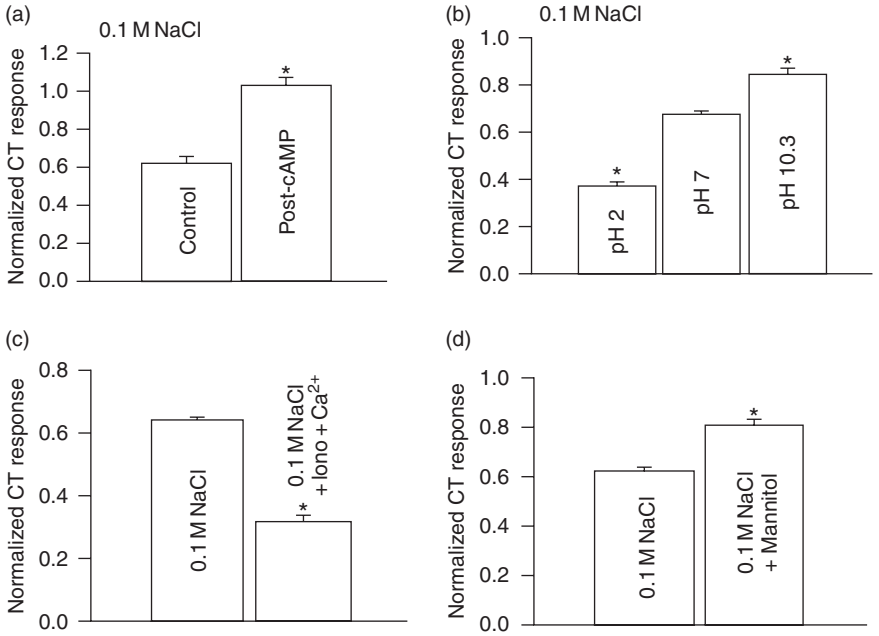

Figure 2 (a) Tonic rat chorda tympani (CT) response to 0.1 M sodium chloride (NaCl) normalized to the response to 0.3 M ammonium chloride (NH_4Cl) before (control) and following treatment of the tongue with chlorophenylthio-cAMP (CPT-cAMP) for 20 min. The increase in response due to cyclic AMP (cAMP) is consistent with an enhancement of the Na^+ flux through epithelial Na^+ channel (ENaC; cf. Russell, O. F. *et al.*, 2002). (b) Normalized CT response to 0.1 M NaCl as a function of solution pH. Results illustrate that the inhibitory effect of decreasing pH on Na^+ transport by ENaC is reflected in the neural response to NaCl (cf. Lyall, V. *et al.*, 2002). (c) Normalized CT response to 0.1 M NaCl before (control, contains 10 mM calcium chloride ($CaCl_2$)) and following treatment of the rat tongue with 150 μM ionomycin (iono) plus 10 mM $CaCl_2$. Increasing the intracellular Ca^{2+} concentration of ENaC-containing taste cells causes a decrease in the neural response to NaCl, which is consistent with the observed decrease in Na^+ conductance of ENaC due to increasing cytosolic Ca^{2+} (cf. Russell, O. F. *et al.*, 2002). (d) Normalized CT response to 0.1 M NaCl (control) and 0.1 M NaCl plus 1 M mannitol. The effect of hyperosmotic mannitol on the neural response is consistent with the observed increase in the Na^+ conductance of ENaC due to hyperosmotic mannitol. Each bar represents the mean ± standard error ($n = 3$; cf. Lyall, V. *et al.*, 1999). (b) Reproduced from The Journal of General Physiology, 2002, 120: 793–815. Copyright 2002 The Rockefeller University Press. (d) Reproduced from Lyall, V., Heck, G. L., DeSimone, J. A., and Feldman, G. M. 1999. Effects of osmolarity on taste receptor cell size and function. Am. J. Physiol. 277, C800–C813, used with permission from the American Physiological Society.

umami taste qualities (Zhang, Y. *et al.*, 2003). Sour taste also involves an increase in intracellular Ca^{2+} that both sustains transduction (Liu, L. and Simon, S. A., 2001; Richter, T. A. *et al.*, 2003) and serves as a potent stimulus for the activation of the Na^+-H^+ exchanger isoform 1, the major cellular sour taste adaptation mechanism (Lyall, V. *et al.*, 2004b; Vinnikova, A. K. *et al.*, 2004). As already discussed, ENaC conductance is reduced by an increase in intracellular Ca^{2+}. As Figure 2(c) shows, increasing taste cell intracellular Ca^{2+} using the Ca^{2+} ionophore, ionomycin, significantly suppresses the chorda tympani response to NaCl (Russell, O. F. *et al.*, 2002). Thus, any subset of cells expressing both ENaC and a second transduction or adaptation mechanism resulting in an increase in intracellular Ca^{2+}, will lead to a suppression of the cells responsiveness to NaCl.

4.14.2.5 Regulation of Epithelial Na^+ Channel by Osmolarity and Salt Taste

As mentioned above (Section 4.14.1.3), hyperosmotic mannitol increases ENaC conductance. On this basis one would expect hyperosmotic mannitol to increase the chorda tympani response to NaCl and the increased response to be abolished by amiloride significantly. This is in fact what is observed (Lyall, V. *et al.*, 1999; Figure 2(d)). Thus, ENaC-based salt taste reception is enhanced in a hyperosmotic stimulus mixture. This osmotic effect accounts for some of the taste properties in rats and hamsters of the short-chain polysaccharide, polycose. During polycose preparation low levels of salt are added which, due to the osmotic effect of the saccharide, add a detectable salt taste component to polycose solutions (Lyall, V. *et al.*, 1999). This may account, in part,

for the fact that polycose stimulates salt-sensitive units in the rat nucleus of the solitary tract and the strong behavioral preference rats show for polycose solutions (Giza, B. K. *et al.*, 1991).

4.14.2.6 Regulation of Epithelial Na^+ Channel by Temperature and Salt Taste

In oocytes expressing ENaC, the steady-state amiloride-sensitive current due to 100 mM NaCl at 36 °C was less than 50% of the current at 27 °C (Chraïbi, A. and Horisberger, J. D., 2002). This unusual inhibitory effect of increasing temperature on ENaC conductance is reflected in the amiloride-sensitive part of the chorda tympani response to NaCl. As Figure 3(c) shows the amiloride-sensitive part of the chorda tympani response to 100 mM NaCl decreased about 50% from 30.0 to 36.8 °C and rapidly decreased to zero at 43.0 °C. By contrast the amiloride-insensitive part of the NaCl response increased with temperature reaching a maximum at 43.0 °C and then declined slowly with temperature. This temperature dependence is one of many properties that indicate that the amiloride-insensitive NaCl response is mediated through a variant of the vanilloid receptor 1 (TRPV1t; Lyall, V. *et al.*, 2004a). It is clear that most of the taste sensitivity to salt at temperatures above 37 °C is not due to ENaC but rather to TRPV1t.

4.14.2.7 Regulation of Epithelial Na^+ Channel by Proteases and Salt Taste

ENaC conductance is modulated by endogenous proteases, an effect that can be mimicked using low concentrations of exogenous trypsin (Chraïbi, A. *et al.*, 1998). Trypsin, as might be anticipated, has an enhancing effect on the chorda tympani response to NaCl. As seen in Figure 3(a) the effect is specific for

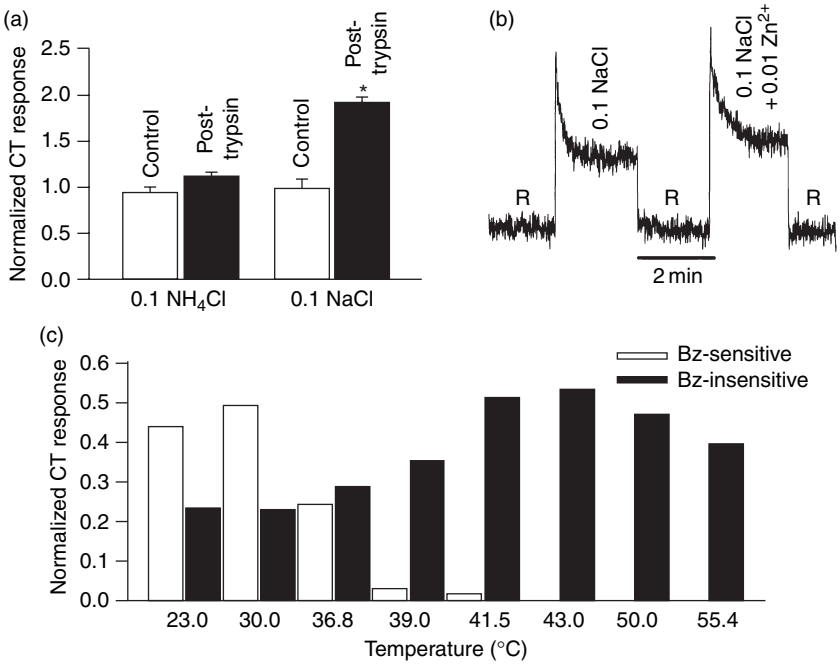

Figure 3 (a) Normalized rat chorda tympani (CT) responses to 0.1 M ammonium chloride (NH_4Cl) and 0.1 M sodium chloride (NaCl). For each salt white bars indicate control responses and black bars indicate responses following treatment of the rat tongue with 20 $\mu g\,ml^{-1}$ trypsin for 20 min. Note trypsin had no effect on the response to NH_4Cl, but increased the tonic response to NaCl by 100%. This is consistent with the observed enhancing effect of trypsin and other proteases on the Na^+ conductance of epithelial Na^+ channel (ENaC). Each bar represents the mean ± standard error ($n = 3$). (b) Chorda tympani response to 30 mM NaCl relative to a baseline response in 10 mM potassium chloride (KCl) followed by a response to 30 mM NaCl plus 10 mM zinc chloride ($ZnCl_2$). The 10 mM $ZnCl_2$ does not give a neural response above baseline. The increase in the response to NaCl by Zn^{2+} is consistent with the observed inhibitory action of Zn^{2+} on the Na^+ self-inhibition property of ENaC. (c) The amiloride-sensitive component of the chorda tympani response to 0.1 M NaCl (white bars) and the amiloride-insensitive component (black bars) as a function of temperature. Note that the amiloride-sensitive component rapidly diminishes above 30 °C, a property consistent with the observed temperature dependence of ENaC. In contrast the amiloride-insensitive component increases with temperature to a maximum at 43 °C and then slowly diminishes with increasing temperature.

responses to NaCl which is consistent with a mechanism involving ENaC and protease blockage of Na^+ self-inhibition.

4.14.2.8 Na^+ Self-Inhibition of Epithelial Na^+ Channel and Salt Taste

A wide variety of substances interfere with Na^+ self-inhibition of ENaC. Zn^{2+} concentrations too low to give a chorda tympani response in the rat, can nonetheless significantly enhance the response to NaCl. Figure 3(b) shows the chorda tympani response to 30 mM NaCl relative to a baseline in 10 mM KCl. A subsequent stimulation with 30 mM NaCl plus 10 mM $ZnCl_2$ shows a significantly enhanced response. This is consistent with Zn^{2+}-induced blockage of Na^+ self-inhibition that is in turn consistent with the effect of temperature and trypsin shown in Figures 3(c) and 3(a), respectively.

4.14.3 Summary and Conclusions

The demonstration of ENaC in rat fungiform taste receptor cells, the close conformity of the rat amiloride-sensitive neural response to NaCl, and the properties of ENaC expressed in oocytes, and the results of rat salt taste behavioral studies leave no doubt that ENaC is the Na^+-specific salt taste receptor located in the anterior tongue. All three ENaC subunits are found in fungiform taste cells in the anterior tongue, but only α-ENaC is found in abundance in the circumvallate taste cells of the posterior tongue. This may explain why amiloride sensitivity is found in the chorda tympani response to NaCl (anterior tongue), but not in the glossopharyngeal nerve response (posterior tongue) (Kretz, O. *et al.*, 1999). It should be noted, however, that treatment of rats with aldosterone induced an amiloride-sensitive Na^+ current in cells of the circumvallate papillae that normally do not have amiloride sensitivity (Lin, W. *et al.*, 1999). This suggests that perhaps aldosterone increases the targeting of ENaC subunits to the apical membrane of taste cells. A definitive answer requires, however, the cloning of each ENaC subunit from both fungiform and circumvallate taste receptor cells, a task not yet completed. Until that is accomplished it remains unclear whether the ENaC subunits in taste cells share 100% homology with complementary subunits in colon or kidney collecting tubules. While ENaC is a major salt taste receptor in rodents and other mammals, it is much less important in humans. For that reason the amiloride-insensitive salt taste receptor is beginning to receive more attention especially now that some progress has been made in its characterization (Lyall, V. *et al.*, 2004a).

References

Benos, D. J. and Stanton, B. A. 1999. Functional domains within the degenerin/epithelial sodium channel (Deg/ENaC) superfamily of ion channels. J. Physiol. 520, 631–644.

Canessa, C. M., Schild, L., Buell, G., Thorens, B., Gautschi, I., Horisberger, J. D., and Rossier, B. C. 1994. Amiloride-sensitive epithelial Na^+ channel is made of three homologous subunits. Nature 367, 463–467.

Chalfant, M. L., Denton, J. S., Berdiev, B. K., Ismailov, I. I., Benos, D. J., and Stanton, B. A. 1999b. Intracellular H^+ regulates the α subunit of ENaC, the epithelial Na^+ channel. Am. J. Physiol. 276, C477–C486.

Chalfant, M. L., Denton, J. S., Langloh, A. L., Karlson, K. H., Loffing, J., Benos, D. J., and Stanton, B. A. 1999a. The NH_2 terminus of the epithelial sodium channel contains an endocytic motif. J. Biol. Chem. 274, 32889–32896.

Chraïbi, A. and Horisberger, J. D. 2002. Na self inhibition of human epithelial Na channel: temperature dependence and effect of extracellular proteases. J. Gen. Physiol. 120, 133–145.

Chraïbi, A., Vallet, V., Firsov, D., Hess, S. K., and Horisberger, J. D. 1998. Protease modulation of the activity of the epithelial sodium channel expressed in *Xenopus* oocytes. J. Gen. Physiol. 111, 127–138.

Firsov, D., Gautschi, I., Merillat, A. M., Rossier, B. C., and Schild, L. 1998. The heterotetrameric architecture of the epithelial sodium channel (ENaC). EMBO J. 17, 344–352.

Garty, H. and Palmer, L. G. 1997. Epithelial sodium channels: function, structure, and regulation. Physiol. Rev. 77, 359–396.

Gilbertson, T. A. and Zhang, H. 1998. Self-inhibition in amiloride-sensitive sodium channels in taste receptor cells. J. Gen. Physiol. 111, 667–677.

Gilbertson, T. A., Roper, S. D., and Kinnamon, S. C. 1993. Proton currents through amiloride-sensitive Na^+ channels in isolated hamster taste cells: enhancement by vasopressin and cAMP. Neuron 10, 931–942.

Giza, B. K., Scott, T. R., Sclafani, A., and Antonucci, R. F. 1991. Polysaccharides as taste stimuli: their effect in the nucleus tractus solitarius of the rat. Brain Res. 555, 1–9.

Grunder, S., Firsov, D., Chang, S. S., Jaeger, N. F., Gautschi, I., Schild, L., Lifton, R. P., and Rossier, B. C. 1997. A mutation causing pseudohypoaldosteronism type 1 identifies a conserved glycine that is involved in the gating of the epithelial sodium channel. EMBO J. 16, 899–907.

Handler, J. S. and Orloff, J. 1981. Antidiuretic hormone. Annu. Rev. Physiol. 43, 611–624.

Herness, M. S. 1992. Aldosterone increases the amiloride-sensitivity of the rat gustatory neural response to NaCl. Comp. Biochem. Physiol. 103A, 269–273.

Horisberger, J. D. 2004. Recent insights into the structure and the mechanism of the sodium pump. Physiology 19, 377–387.

Ishikawa, T., Marunaka, Y., and Rotin, D. 1998. Electrophysiological characterization of the rat epithelial Na^+ channel (rENaC) expressed in MDCK cells. Effects of Na^+ and Ca^{2+}. J. Gen. Physiol. 111, 825–846.

Ji, H. L., Fuller, C. M., and Benos, D. J. 1998. Osmotic pressure regulates $\alpha\beta\gamma$-rENaC expressed in *Xenopus* oocytes. Am. J. Physiol. 275, C1182–C1190.

Kieber-Emmons, T., Lin, C., Prammer, K. V., Villalobos, A., Kosari, F., and Kleyman, T. R. 1995. Defining topological similarities among ion transport proteins with anti-amiloride antibodies. Kidney Int. 48, 956–964.

Kosari, F., Sheng, S., Li, J., Mak, D. O., Foskett, J. K., and Kleyman, T. R. 1998. Subunit stoichiometry of the epithelial sodium channel. J. Biol. Chem. 273, 13469–13474.

Kretz, O., Barbry, P., Bock, R., and Lindemann, B. 1999. Differential expression of RNA and protein of the three pore-forming subunits of the amiloride-sensitive epithelial sodium channel in taste buds of the rat. J. Histochem. Cytochem. 47, 51–64.

Kunzelmann, K., Schreiber, R., Nitschke, R., and Mall, M. 2000. Control of epithelial Na^+ conductance by the cystic fibrosis transmembrane conductance regulator. Pfluegers Arch. 440, 193–201.

Li, J. H., Palmer, L. G., Edelman, I. S., and Lindemann, B. 1982. The role of sodium-channel density in the natriferic response of the toad urinary bladder to an antidiuretic hormone. J. Membr. Biol. 64, 77–89.

Lin, C., Kieber-Emmons, T., Villalobos, A. P., Foster, M. H., Wahlgren, C., and Kleyman, T. R. 1994. Topology of an amiloride-binding protein. J. Biol. Chem. 269, 2805–2813.

Lin, W., Finger, T. E., Rossier, B. C., and Kinnamon, S. C. 1999. Epithelial Na^+ channel subunits in rat taste cells: localization and regulation by aldosterone. J. Comp. Neurol. 405, 406–420.

Lindemann, B. 1984. Fluctuation analysis of sodium channels in epithelia. Annu. Rev. Physiol. 46, 497–515.

Lingueglia, E., Renard, S., Waldmann, R., Voilley, N., Champigny, G., Plass, H., Lazdunski, M., and Barbry, P. 1994. Different homologous subunits of the amiloride-sensitive Na^+ channel are differently regulated by aldosterone. J. Biol. Chem. 269, 13736–13739.

Liu, L. and Simon, S. A. 2001. Acidic stimuli activate two distinct pathways in taste receptor cells from rat fungiform papillae. Brain Res. 923, 58–70.

Lyall, V., Alam, R. I., Malik, S. A., Phan, T. H., Vinnikova, A. K., Heck, G. L., and DeSimone, J. A. 2004b. Basolateral Na^+-H^+ exchanger-1 in rat taste receptor cells is involved in neural adaptation to acidic stimuli. J. Physiol. 556, 159–173.

Lyall, V., Alam, R. I., Phan, T. H., Russell, O. F., Malik, S. A., Heck, G. L., and DeSimone, J. A. 2002. J. Gen. Physiol. 120, 793–815.

Lyall, V., Heck, G. L., DeSimone, J. A., and Feldman, G. M. 1999. Effects of osmolarity on taste receptor cell size and function. Am. J. Physiol. 277, C800–C813.

Lyall, V., Heck, G. L., Vinnikova, A. K., Ghosh, S., Phan, T. H., Alam, R. I., Russell, O. F., Malik, S. A., Bigbee, J. W., and DeSimone, J. A. 2004a. The mammalian amiloride-insensitive non-specific salt taste receptor is a vanilloid receptor-1 variant. J. Physiol. 558, 147–159.

Morris, R. G. and Schafer, J. A. 2002. cAMP increases density of ENaC subunits in the apical membrane of MDCK cells in direct proportion to amiloride-sensitive Na^+ transport. J. Gen. Physiol. 120, 71–85.

Palmer, L. G. and Frindt, G. 1987. Effects of cell Ca and pH on Na channels from rat cortical collecting tubule. Am. J. Physiol. 253, F333–F339.

Palmer, L. G., Li, J. H., Lindemann, B., and Edelman, I. S. 1982. Aldosterone control of the density of sodium channels in the toad urinary bladder. J. Membr. Biol. 64, 91–102.

Richter, T. A., Caicedo, A., and Roper, S. D. 2003. Sour taste stimuli evoke Ca^{2+} and pH responses in mouse taste cells. J. Physiol. 547, 475–483.

Rossier, B. C., Pradervand, S., Schild, L., and Hummler, E. 2002. Epithelial sodium channel and the control of sodium balance: interaction between genetic and environmental factors. Annu. Rev. Physiol. 64, 877–897.

Russell, O. F., Phan, T. T., Alam, R. I., Heck, G. L., Lyall, V., and DeSimone, J. A. 2002. Acute regulation of rat NaCl taste responses by cAMP and calcium. Chem. Senses 27, 661–671.

Schiffman, S. S., Lockhead, E., and Maes, F. W. 1983. Amiloride reduces the taste intensity of Na^+ and Li^+ salts and sweeteners. Proc. Natl. Acad. Sci. U. S. A. 80, 6136–6140.

Smith, D. V. and Ossebaard, C. A. 1995. Amiloride suppression of the taste intensity of sodium chloride: evidence from direct magnitude scaling. Physiol. Behav. 57, 773–777.

Spector, A. C., Guagliardo, N. A., and St. John, S. J. 1996. Amiloride disrupts NaCl versus KCl discrimination performance: implications for salt taste coding in rats. J. Neurosci. 16, 8115–8122.

Ussing, H. H. and Zerahn, K. 1951. Active transport of sodium as the source of electric current in the short-circuited frog skin. Acta Physiol. Scand. 23, 110–127.

Verrey, F., Hummler, E., Schild, L., and Rossier, B. C. 2000. Control of Na Transport by Aldosterone. In: (*eds*. D. W. Seldin and G. Giebisch),The Kidney: Physiology and Pathophysiology Vol. 1, pp. 1441–1471.. Lippincott.

Vinnikova, A. K., Alam, R. I., Malik, S. A., Ereso, G. L., Feldman, G. M., McCarty, J. M., Knepper, M. A., Heck, G. L., DeSimone, J. A., and Lyall, V. 2004. Na^+-H^+ exchange activity in taste receptor cells. J. Neurophysiol. 91, 1297–1313.

Will, P. C., Cortright, R. N., DeLisle, R. C., Douglas, J. G., and Hopfer, U. 1985. Regulation of amiloride-sensitive electrogenic sodium transport in the rat colon by steroid hormones. Am. J. Physiol. 248, G124–G132.

Zhang, Y., Hoon, M. A., Chandrashekar, J., Mueller, K. L., Cook, B., Wu, D., Zuker, C. S., and Ryba, N. J. 2003. Coding of sweet, bitter, and umami tastes: different receptor cells sharing similar signaling pathways. Cell 112, 293–301.

4.15 Central Neural Processing of Taste Information

D V Smith[†], The University of Tennessee College of Medicine, Memphis, TN, USA

S P Travers, The Ohio State University, Columbus, OH, USA

© 2008 Elsevier Inc. All rights reserved.

4.15.1	**Introduction**	289
4.15.2	**Properties of Brainstem Gustatory Neurons**	292
4.15.2.1	Neuron Types in the Nucleus of the Solitary Tract and Parabrachial Nuclei	292
4.15.2.1.1	Morphological cell types	292
4.15.2.1.2	Cell types based on biophysical properties	293
4.15.2.1.3	Cell types based on gustatory responsiveness	294
4.15.2.2	Neural Processing Through the Brainstem	297
4.15.2.2.1	Breadth of tuning of nucleus of the solitary tract and parabrachial nuclei neurons	297
4.15.2.2.2	Convergence, orotopy, and oral somatosensory responsiveness	298
4.15.2.2.3	Modulation of gustatory responsiveness	300
4.15.2.2.4	Neurotransmitters and neuromodulators in the nucleus of the solitary tract	303
4.15.2.2.5	Descending pathways from forebrain targets: modulation of nucleus of the solitary tract and parabrachial nuclei	305
4.15.3	**Gustatory Responsiveness of Forebrain Neurons**	308
4.15.3.1	Taste Cortex	308
4.15.3.1.1	Organization and relationship to other sensory modalities	308
4.15.3.1.2	Gustatory cell types and processing	312
4.15.3.1.3	Neurotransmitters and neuromodulators in the insular cortex	313
4.15.3.2	Limbic Forebrain	317
4.15.4	**Conclusions**	318
References		319

4.15.1 Introduction

The sense of taste has a critical role throughout the animal kingdom because it detects and discriminates key chemicals in the animal and plant matter, which constitutes potential foodstuff. Diet varies among species and the gustatory systems of different animals exhibit important specializations. Nevertheless, mammalian species, the topic of the present chapter, possess the ubiquitous ability to sense nutritive carbohydrates and amino acids, as well as electrolytes such as sodium. Similarly, mammals distinguish potential corrosive or toxic substances including acids and alkyloids. These different groups of stimuli are described by human subjects as having distinctive qualities: most carbohydrates are sweet, acids are sour, alkaloids and other toxins are bitter, and sodium is salty; other electrolytes have mixed tastes. Amino acid taste is less well understood, but in humans, L-glutamate seems to have a special potency for activating a selective amino acid receptor (Li, X. *et al.*, 2002b) and is often assumed to have a unique taste, best known as umami. In rodents, a larger variety of L-amino acids appear to share a common transduction mechanism (Nelson, G. *et al.*, 2002), though at least glutamate is probably closely aligned perceputally with carbohydrates (Yamamoto, T. *et al.*, 1991; Stapleton, J. R. *et al.*, 1999).

Making distinctions between tastants is vital for maintaining a diet that promotes homeostasis and avoids harmful substances. The structure and function of the G-protein-coupled receptors and ion channels with the requisite specificity for this discrimination have been described in elegant detail in the last decade (reviewed in Chandrashekar, J. *et al.*, 2006). Agreement is mounting that these receptors are distributed in a relatively segregated manner (Nelson, G. *et al.*, 2001; Huang, A. L. *et al.*, 2006), such that different taste receptor cells are specialized for detecting particular classes of chemicals (Yoshida, R. *et al.*, 2006). Similarly, a notable degree of specificity is maintained

†Deceased

in the individual gustatory nerve fibers that innervate taste receptor cells, and carry this information into the brain (e.g., Frank, M., 1973; Frank, M. E. *et al.*, 1983; Frank, M. E., 1991). Thus, much of the peripheral code for taste quality is arguably sparse with just a few different groups of receptor cells and their innervating fibers comprising labeled lines. However, there is not unanimous agreement on this coding scheme, and there are important caveats particularly with regard to the code for sodium versus acids, as many peripheral nerve fibers are broadly responsive across these classes of chemicals (e.g., Frank, M., 1973; Frank, M. E. *et al.*, 1983; Frank, M. E., 1991, #241). Further, in the central nervous system, convergence of primary afferents (Ogawa, H. *et al.*, 1982; Travers, S. P. *et al.*, 1986; Sweazey, R. D. and Smith, D. V., 1987; Vogt, M. B. and Mistretta, C. M., 1990) and complex integrative processing within central circuits, gives rise to neurons with heterogeneous tuning curves, and although some neurons remain narrowly tuned (e.g., Nishijo, H. and Norgren, R., 1990; Geran, L. C. and Travers, S. P., 2006); many are broad (e.g., Nishijo, H. and Norgren, R., 1990; Di Lorenzo, P. M. and Victor, J. D., 2003; Lemon, C. H. and Smith, D. V., 2005; Geran, L. C. and Travers, S. P., 2006), as summarized in Spector A. C. and Travers S. P. (2005). As a consequence, whether any aspect of central coding employs dedicated pathways, or whether central coding relies entirely upon comparison across neurons is still a topic of considerable debate (see Chapter A Perspective on Chemosensory Quality Coding). Furthermore, there is growing interest in the possibility of a contribution of temporal coding to making distinctions among tastes (see Chapter Neural Ensembles in Taste Coding).

Overlaid on any scheme for taste quality coding are additional, equally important aspects of gustatory processing. Foods possess not only taste, but also texture, thermal, and olfactory components. These multiple characteristics are integrated largely through central circuits to produce flavor. In addition, though some taste preferences and aversions are innate, they are not hardwired. The central nervous system plays a key role in providing the requisite plasticity to meet changing homeostatic states and environmental demands. Thus, the desirability of even the most delectable dessert is suppressed by satiety. Limited specific mechanisms appear to be present to accommodate particular changes in homeostatic state. Satiety has a more pronounced impact on palatable, for example, sweet substances (Foster, L. A. *et al.*, 1996), and a sodium deficit leads to an increased preference for this specific ion (Contreras, R. and Hatton, G., 1975). However, deficits in other micro- or macronutrients, for example, vitamins or essential amino acids, are not associated with such predetermined changes in gustatory responsiveness. Instead, organisms learn to associate the flavor of a particular food with the correction of a deficit (Markison, S. *et al.*, 1999; 2000). Learning is also essential to assure that an animal will avoid contaminated food sources that do not have an innately aversive taste (Garcia, J. *et al.*, 1970).

This chapter presents data on the functional characteristics of central gustatory neurons. We consider the topographic organization of the system, as well as several key features of neurons including their tuning curves, receptive field organization, and inputs from other modalities. In addition, the plasticity of these circuits as evidenced by the impact of homeostatic state, learning, neurotransmitters and neuromodulators, and interactions between different regions of the gustatory neuraxis, is discussed. The study of the cellular basis of these features had lagged behind a systems level analysis; but significant information is now available at the level of the first-order relay, the rostral nucleus of the solitary tract (rNST). Some key ideas regarding taste quality coding are presented in the subsections following the current chapter. For a fuller perspective, the reader is referred to several recent reviews that present divergent opinions (Spector, A. C. and Travers, S. P., 2005; Chandrashekar, J. *et al.*, 2006; Jones, L. M. *et al.*, 2006; Simon, S. A. *et al.*, 2006; Hallock, R. M. and Di Lorenzo, P. M., 2006).

A schematic diagram of gustatory system organization highlighting those regions and connections discussed in this review is presented in Figure 1. Further details regarding anatomical organization can be found in the chapter in this volume by Whitehead and Finger. Classic decerebration studies by Grill H. J. and Norgren R. (1978b) established important hierarchical features of the system. When transections are made just rostral to the midbrain, the existing brainstem circuitry still possesses impressive regulatory capacity. Decerebrate rats do not voluntarily eat or drink but if fluids are introduced into their mouths, stereotyped oral behaviors, virtually identical to those observed in intact animals, assure that sweet substances are ingested and that bitter substances are rejected. Similar behaviors are observed in anencephalic human infants, establishing phylogenetic generality (Steiner, J. E., 1973). Moreover, this restricted component of the system possesses some degree of modifiability by homeostatic state, as filling the stomach with liquid food shortens bouts of licking

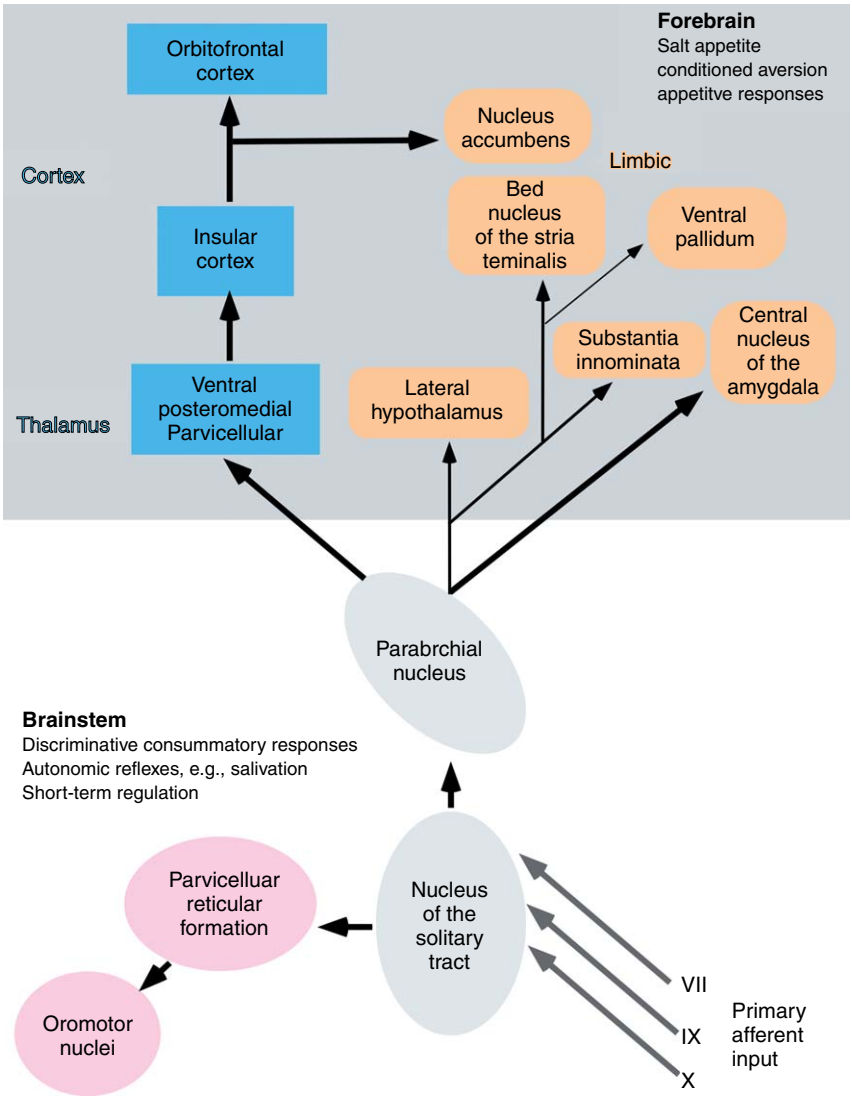

Figure 1 Schematic diagram depicting primary afferent input, and the major, direct connections of the gustatory system in rodents. Line thickness gives a rough indication of the strength of a given connection. Primate gustatory pathways are similar, despite some notable differences that are discussed in the text. The diagram also indicates two main functional divisions within the system: brainstem and forebrain, with each division associated with different behavioral repertoires. Importantly, however, there are extensive reciprocal connections between the forebrain and brainstem (see Figure 2), indicating important interactions between these two major divisions. Likewise, the gustatory forebrain can be loosely divided into thalamocortical and limbic divisions, which are differentially associated with perceptual and motivational function; however, again there are extensive anatomical connections between these networks (not shown), forming a substrate for functional interactions.

elicited by intraoral infusions of sucrose, just as it does in normal rats (Grill, H. J. and Norgren, R., 1978a). However, without the forebrain, critical aspects of modifiability are lost. Thus, longer-term changes in homeostatic state, such as that induced by food (Seeley, R. J. *et al.*, 1994; Kaplan, J. M. *et al.*, 2000) or sodium (Grill, H. J. *et al.*, 1986) deprivation cause modifications in the intake of different tasting substances in the intact, but not decerebrate rat. Finally, the effects of learning are not expressed in decerebrate animals. In intact animals, when a novel taste is paired with gastrointestinal malaise, the animal subsequently rejects that taste, a phenomenon known as conditioned taste aversion (Garcia, J. *et al.*, 1970); decerebrate rats do not exhibit this switch in behavior. Although the system is arranged hierarchically, this is not to say that the components of the system operate in isolation to perform these different functions.

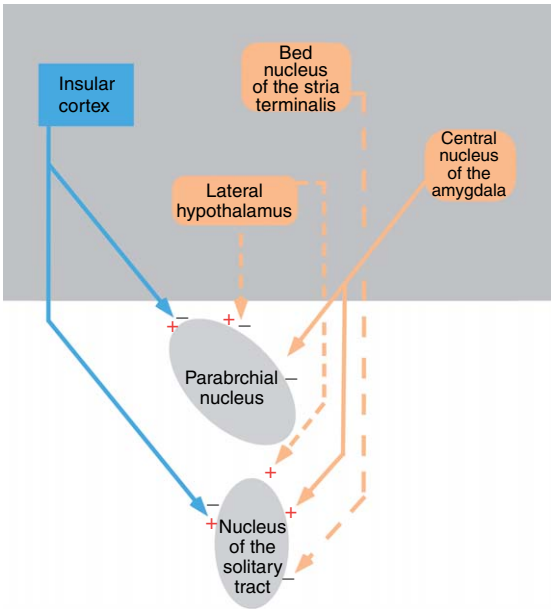

Figure 2 Major, direct, descending pathways from forebrain to brainstem, which have been documented both anatomically and physiologically. Note that all of these regions also receive ascending gustatory input, as shown in Figure 1. The most prevalent effects of electrical stimulation or glutamate activation of each forebrain structure on gustatory responses are also shown. Some effects are mixed, some largely excitatory, and others largely inhibitory.

Instead, the connections shown in Figure 2 comprise a substrate indicative of a high degree of interaction between the forebrain and hindbrain, and there are a multitude of other interactions, particularly between various regions of the forebrain.

4.15.2 Properties of Brainstem Gustatory Neurons

Taste information is processed through two brainstem nuclei on its way to the forebrain (Figure 1). Gustatory axons from the VII, IX, and X cranial nerves terminate first within the rNST, from which axons arise to project predominantly to the parabrachial nuclei (PbN) of the pons, but also to synaptic targets within the medulla, including the subadjacent reticular formation and indirectly and in some cases directly to oral motor nuclei. Cells within the nucleus of the solitary tract (NST) and PbN are also targeted by descending axons from all gustatory-responsive areas of the forebrain, providing a substrate for the modulation of taste activity in response to physiological need and prior experience. Attempts to understand the neural substrate for gustatory processing have addressed the morphology and physiology of cells within these brainstem nuclei.

4.15.2.1 Neuron Types in the Nucleus of the Solitary Tract and Parabrachial Nuclei

Progress in our understanding of many sensory or motor systems has come from a thorough description of the cells comprising the networks involved. In the gustatory brainstem, there have been numerous attempts to categorize neurons on the basis of their morphologies, intrinsic membrane properties, and taste responsiveness.

4.15.2.1.1 Morphological cell types

Neurons within the NST have been examined using a variety of anatomical techniques in an attempt to classify them on the basis of their morphologies. Purely anatomical studies have shown several prominent cell types, including multipolar (stellate), elongate (fusiform), and small ovoid cells. Several different parameters have been used to classify these cells. One of the earliest schemes grouped hamster NST cells according to their size and the invagination of their nuclei, resulting in four groups: large and small cells with or without nuclear invaginations (Davis, B. J. and Jang, T., 1986). In Nissl-stained material, Whitehead M. C. (1988) described three major cell types in the hamster NST: elongate, ovoid, and round, based on the shape of the soma, which he quantified by measuring each cell's form factor. Form factor is a measure of roundness, given by the formula $ff = 4\pi\text{area}/\text{perimeter}^2$, ranging from 1.0 for a perfectly round cell to 0.0 for a straight line. Elongate cells were those with $ff < 0.7$, ovoid with ff between 0.7 and 0.9, and round with $ff > 0.9$. Elongate cells were more common in the rostral lateral subdivision of the NST, whereas those cells within the ventral subdivision were typically larger cells. Throughout the NST, ovoid cells were the most common. Lasiter P. S. and Kachele D. L. (1988) described similar cell types in the rat NST and further demonstrated that the ovoid cells had smaller cross-sectional areas than other cell types.

Later studies used Golgi impregnation to examine cells in the hamster NST. Davis B. J. and Jang T. (1988a) described two cell types:

1. large, fusiform cells with two or three relatively unbranched primary dendrites and
2. smaller, stellate cells with more numerous and more highly branched dendrites.

Using Golgi methods (Whitehead, M. C., 1988) also described elongate and stellate cells and another class he termed tufted cells, which were large neurons with several dendrites, one of which exhibited many branches. There are some discrepancies between these studies in what constitutes large versus small or medium neurons and a thorough description of these neuronal classification studies and their limitations was provided in a later review article (Schweitzer, L. *et al.*, 1995).

Immunocytochemical studies have demonstrated that many of the small ovoid neurons express the inhibitory neurotransmitter gamma-aminobutyric acid (GABA), suggesting that these numerous cells comprise a network of inhibitory interneurons within the NST (Lasiter, P. S. and Kachele, D. L., 1988). In addition, tract-tracing experiments have demonstrated that the majority of NST neurons projecting to the PbN are elongate and stellate cells (Whitehead, M. C., 1990). Further, some of these larger neurons expressed tyrosine hydroxylase or dopamine-β-hydroxylase (Davis, B. J. and Jang, T., 1988b). Overall, the idea that there are numerous small ovoid cells serving as interneurons and elongate cells and large multipolar cells comprising the PbN projection neurons within the NST is fairly well accepted. That scheme was used by King M. S. and Bradley R. M. (1994) in their attempt to relate the biophysical properties of rat NST neurons to their morphology. These investigators grouped rat NST neurons that were labeled with biocytin during *in vitro* slice recording experiments into ovoid, elongate and multipolar cells, although they admitted that such a straightforward classification was not always easy. Nevertheless, the 58 neurons that they reconstructed were divided into 9 elongate, 21 multipolar, and 28 ovoid cells. These cell types, however, were not clearly related to the biophysical properties of the neurons (see below). A similar attempt to correlate electrophysiology and morphology was made by Renehan W. E. *et al.* (1994; 1996), who labeled rat NST cells with biocytin *in vivo* after recording their responses to gustatory stimulation. Although there was some indication that cells responding to quinine were smaller than those responding to sucrose, NaCl or HCl and that some cells had greater or lesser dendritic dimensions, there was little or no relationship between gustatory responsiveness and cell classification into elongate, multipolar, or ovoid neurons. These authors actually used a hierarchical cluster analysis to classify rat NST neurons based on their morphologies, but the resultant six classifications did not relate clearly to taste responsiveness either. Thus, cells in the NST are classifiable into groups based on morphology, as is common in many areas of the brain, but so far the functional significance of such a classification is not apparent.

4.15.2.1.2 Cell types based on biophysical properties

With the advent of brain slice techniques, it has become possible to characterize many of the intrinsic membrane properties of brainstem gustatory neurons, particularly those in the rostral portion of the NST. In pioneering work on rat medullary slices, Bradley R. M. and Sweazey R. D. (1990; 1992) demonstrated four different groups of NST neurons based on their responses to injected current (Figure 3). Three groups of cells (groups I–III) exhibited regular firing in whole-cell recordings in response to a 1200 ms, 100 pA depolarizing current injection. These groups were separable on the basis of the effects of a preceding hyperpolarization on this firing pattern produced by a 150 ms, 200 pA hyperpolarizing pulse. The firing of group I cells was severely disrupted by hyperpolarization, whereas those of group III were completely unaffected by hyperpolarizing the membrane. Group II cells showed regular firing to a depolarizing current step after an initial delay produced by the preceding hyperpolarization; this delay was produced by activation of a potassium A current (I_{KA}) (Tell, F. and Bradley, R. M., 1994) as it was this current that was blocked by 4-aminopyridine. Cells of group IV showed only a brief, rapid burst of action potentials to depolarization, which was variably affected by prior hyperpolarization. These different groups of neurons would be expected to respond differently to excitatory and inhibitory influences in the processing of gustatory information.

In a more recent study of rat NST neurons, a group of cells was identified that exhibited a depolarizing response to hyperpolarization, known as I_h current (Uteshev, V. V. and Smith, D. V., 2006). In response to hyperpolarizing current steps, these cells exhibit a nonohmic response in which the membrane potential depolarizes during the hyperpolarization, due to hyperpolarization-activated cation channels. This current is blocked by 1 mM CsCl applied to the bath. These cells were largely a different subset than those showing I_A current and were differentially distributed within the rNST. Cells with I_A current were

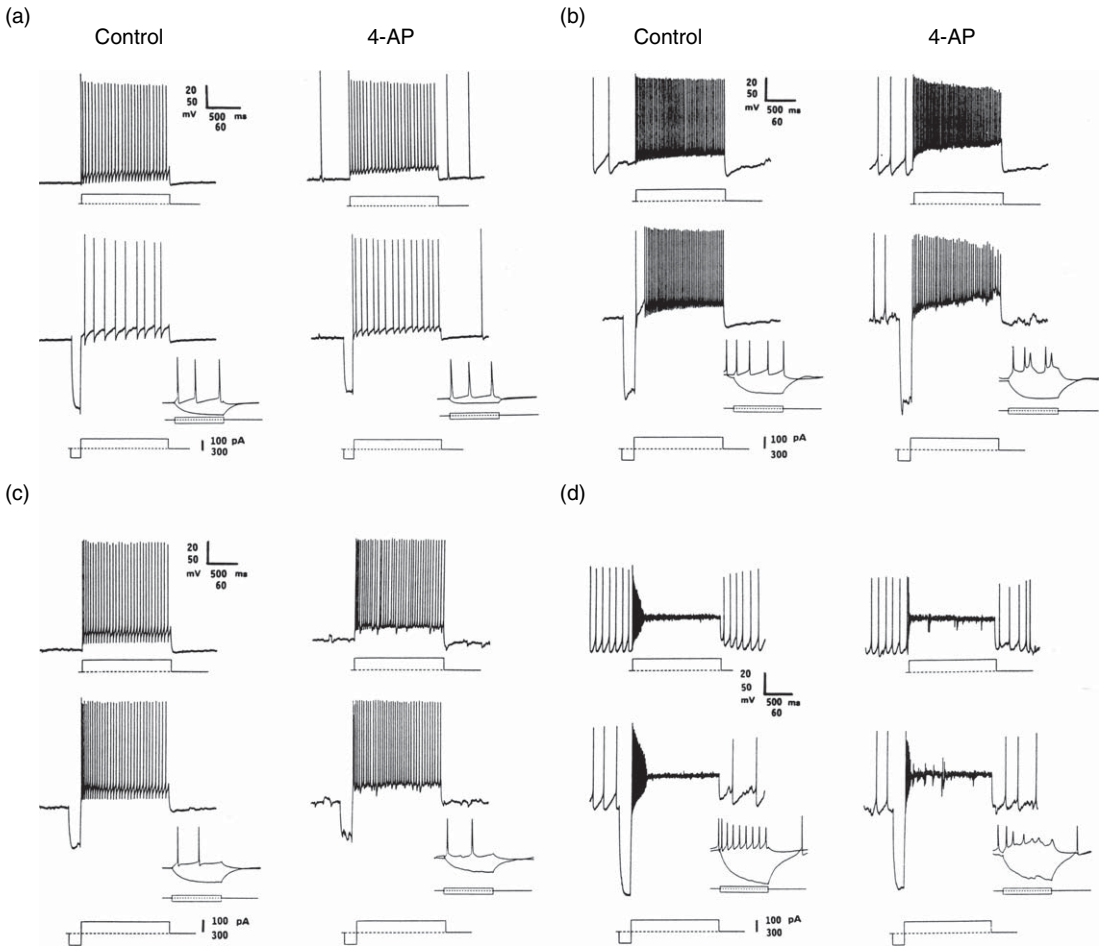

Figure 3 Types of rostral nucleus of the solitary tract (rNST) neurons defined based on membrane properties demonstrated in *in vitro* preparations. Types I–IV are shown in panels (a)–(d), respectively. Groups I–III exhibit repetitive firing throughout a depolarizing current pulse; group IV only a brief train of action potentials. Groups I–IV differ according to the effect of a preceding hyperpolarizing current pulse. Group III neurons are little affected. However, type I neurons respond with a more irregular and reduced firing and type II with a delay in the initiation of the response. Although not present in this example, a preceding hyperpolarizing pulse often shortens the burst of action potentials exhibited by type IV neurons. The response delay observed in type III neurons is eliminated by 4-aminopyridine (4-AP), indicating that a hyperpolarization elicited A-current is responsible for the delay. From Tell, F. and Bradley, R. M. 1994. Whole-cell analysis of ionic currents underlying the firing pattern of neurons in the gustatory zone of the nucleus tractus solitarii. J. Neurophysiol. 71, 479–492, with permission.

found in the medial half of the NST, where the majority of neurons projecting to the PbN are located (Halsell, C. B. *et al.*, 1996). On the other hand, those neurons expressing I_h were predominantly located in the lateral half (Uteshev, V. V. and Smith, D. V., 2006), where most of the cells project into oral motor circuits through the subadjacent reticular formation (Halsell, C. B. *et al.*, 1996). Although NST neurons can be grouped according to their responses to injected current (Bradley, R. M. and Sweazey, R. D., 1992) or by the presence of I_A or I_h current (Uteshev, V. V. and Smith, D. V., 2006), there does not appear to by any clear relationship between such classifications and cell morphology (King, M. S. and Bradley, R. M., 1994; Uteshev, V. V. and Smith, D. V., 2006).

4.15.2.1.3 Cell types based on gustatory responsiveness

A direct way to understand gustatory processing by the brainstem would be to categorize neurons on the basis of their taste responsiveness. Such an effort has

been made by almost all investigators working in this area, but the most pervasive of these classifications are the best-stimulus categories first described by Frank M. (1973) for taste-responsive fibers of the chorda tympani nerve. Chorda tympani fibers were classified into groups (S-, N-, H-, or Q-best) based on which of four basic taste stimuli: sucrose, NaCl, HCl, or quinine were most effective when presented to the anterior tongue at midrange concentrations.

A best-stimulus categorization based simply on the basis of identifying the most effective among four stimuli is subject to criticism because it is nearly a foregone conclusion that at least one stimulus will be nominally more effective than the others. However, what is more compelling is that, within a best-stimulus group, the cells are relatively similar in their overall pattern of responsiveness. Thus, when the four stimuli were ordered along the abscissa from most to least preferred (i.e., S, N, H, and Q), chorda tympani fibers peaked at a single point, with profiles indicative of S-, N-, or H-best fibers. Q-best fibers (except for one) were not evident in the hamster chorda tympani nerve, but are common in the glossopharyngeal nerve of both hamsters (Hanamori, T. *et al.*, 1988) and rats (Frank, M. E., 1991). In fact, this similarlity between members of a group holds up to the challenge of applying more stimuli and to categorizing response profiles in a more quantitative fashion; for example, by using hierarchical cluster analysis, which is a numerical taxonomic procedure (e.g., Rodieck, R. W. and Brening, R. K., 1982). When such an analysis is applied to the responses of hamster chorda tympani fibers to 13 stimuli, three groups of neurons emerge (Frank, M. E. *et al.*, 1988), which almost without exception correspond to the S-, N-, and H-best classifications. This analysis demonstrates that neurons within a group are more similar to one another than to members of other groups and provides a quantitative basis for classifying neurons in this system. In a series of experiments on the hamster brainstem, Smith and his co-workers showed that a best-stimulus classification worked well to categorize neurons of the NST (Travers, J. B. and Smith, D. V., 1979) and PbN (Van Buskirk, R. L. and Smith, D. V., 1981). Further, multivariate analyses of the response profiles of these cells, even including responses from as many as 18 stimuli, resulted in classifications that were, to a large extent, predicted from the best stimulus (Smith, D. V. *et al.*, 1983). Similar analyses of rat NST (Nakamura, K. and Norgren, R., 1993; Lemon, C. H. and Smith, D. V., 2005; Geran, L. C. and Travers, S. P., 2006) or PbN (Nishijo, H. and Norgren, R., 1990) neurons also show such neural groups, but only if taste stimuli are applied to receptors responsive to sweet stimuli. Earlier studies in rats, in which stimuli were not applied to the palate, did not present clear evidence for neural groups based on hierarchical clustering (Woolston, D. C. and Erickson, R. P., 1979) and, in fact, argued against the existence of functional neural groups. Examples from a recent study that included neurons responsive to inputs from the anterior tongue, palate, and posterior tongue are depicted in Figure 4. As a result of including neurons with inputs from the posterior foliate papillae, this study described groups of cells with optimal responses to bitter stimuli as well as to sweeteners (and amino acids), sodium, and acids. Thus, cells within the gustatory brainstem are readily classified into groups based on similarities and differences in their responses to taste stimulation.

When a classification scheme can be supported by biological parameters, it increases the confidence one places in such a categorization. An example of such support is the funneling of input from amiloride-sensitive epithelial sodium channels (ENaCs) on the taste receptor cells into a single class of neurons in the peripheral and central nervous system. Fibers of the chorda tympani nerve that respond best to NaCl exhibit responses to NaCl that are blockable in a dose-dependent fashion by lingual application of the diuretic drug amiloride (Ninomiya, Y. and Funakoshi, M., 1988; Hettinger, T. P. and Frank, M. E., 1990). The substantial response to NaCl in HCl-best fibers is much less affected by amiloride treatment. This segregation of amiloride-sensitive input to the NaCl- but not the HCl-best neurons is maintained in the NST (Scott, T. R. and Giza, B. K., 1990; Giza, B. K. and Scott, T. R., 1991). Application of amiloride to the tongue disrupts performance of rats on a two-lever operant task in which they have been taught to discriminate NaCl from KCl, implicating amiloride-sensitive NaCl-best neurons as an important contributor to the rat's ability to discriminate these two salts (Spector, A. C. *et al.*, 1996; see also Hill, D. L. *et al.*, 1990).

Another systematic relationship between chemosensitivity and a biological parameter has been described for neurons optimally responsive to bitter tasting stimuli. In a study including electrical stimulation of the PbN to test for antidromic invasion, Cho Y. K. *et al.* (2002a) found a substantial group of quinine-best neurons based on responses of the anterior tongue to equally effective concentrations of the basic stimuli: 0.032 M

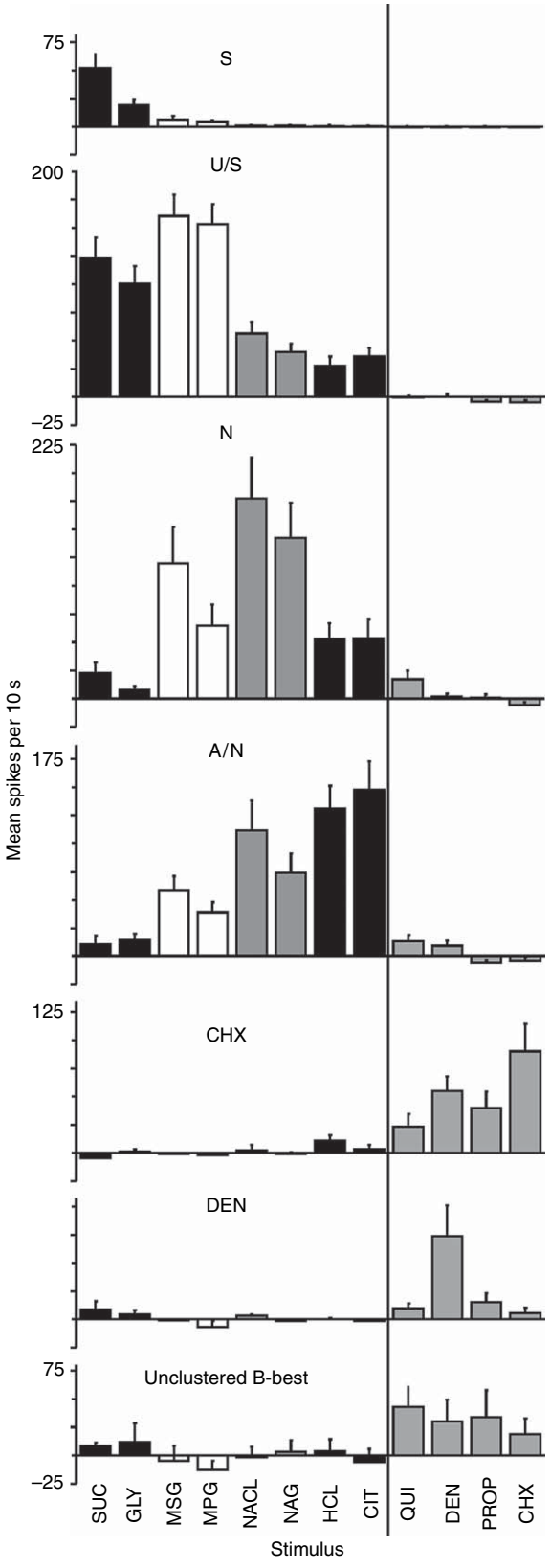
75
S
200
U/S
–25
225
N
175
A/N
125
CHX
DEN
75
Unclustered B-best
–25
Mean spikes per 10 s
SUC
GLY
MSG
MPG
NACL
NAG
HCL
CIT
QUI
DEN
PROP
CHX
Stimulus

sucrose, 0.032 M NaCl, 0.0032 M citric acid, and 0.032 M QHCl (quinine-HCl). When this strong concentration of QHCl is used, QHCl-best neurons are readily evident in the hamster NST following stimulation of the anterior tongue. Interestingly, all 23 QHCl-best neurons in this sample that projected axons to the PbN had conduction velocities that were less than 25% of those of the other neurons. In other words, this best-stimulus classification identified a subset of small, slowly conducting neurons. This finding corresponds well with those of Renehan W. E. *et al.* (1995) , who found that neurons responding specifically to QHCl in the rat NST were significantly smaller than other cells, and of Geran L. C. and Travers S. P. (2006) who also found that bitter-best rat NST neurons had very slow conduction velocities.

Overall, numerous studies of the responsiveness of central gustatory neurons have described groups of cells based on their best stimulus. This classification scheme corresponds well to those categories derived from more quantitative techniques such as hierarchical cluster analysis, even those based on responses to many different stimuli. To some extent, because of the relatively broader tuning of central taste neurons in comparison to peripheral gustatory fibers, the correspondence between a best-stimulus classification and a hierarchical cluster solution is not quite as tight as for peripheral fibers (Smith, D. V. *et al.*, 1983). It is also clear that changes in relative stimulus concentrations can result in changes in best-stimulus classification, as concentration–response functions for different stimuli are not always parallel (e.g., see Smith, D. V. and Travers, J. B., 1979). Nevertheless, although to some extent dependent on stimulus concentration, receptive field stimulated, and species, best-stimulus groups exhibit remarkable consistencies between laboratories and the use of such a classification scheme encompasses an important organizing principle in this system.

4.15.2.2 Neural Processing Through the Brainstem

Taste fibers traveling in the chorda tympani and greater superficial petrosal branches of the VII nerve, the lingual–tonsillar branch of the IX nerve, and the internal branch of the superior laryngeal nerve send their axons into the NST in an orderly rostral to caudal distribution (Contreras, R. J. *et al.*, 1982; Hamilton, R. B. and Norgren, R., 1984). However, the terminations of these nerves also exhibit significant overlap, giving rise to convergence between axons within the same nerve (Vogt, M. B. and Mistretta, C. M., 1990) and between inputs from completely separate receptor fields (Travers, S. P. *et al.*, 1986; Travers, S. P. and Norgren, R., 1991).

4.15.2.2.1 Breadth of tuning of nucleus of the solitary tract and parabrachial nuclei neurons

One parameter that is important in every sensory system is the tuning profile of afferent neurons. In taste, early studies described this feature by tabulating the number of stimuli among those representing the basic taste qualities that evoked activity in a recorded neuron; that is, the breadth of tuning of gustatory fibers and central neurons was simply described in terms of how many stimuli produced responses (e.g., Frank, M. and Pfaffmann, C., 1969; Perrotto, R. S. and Scott, T. R., 1976). However, such an approach depends heavily on the definition of a response, which varies across laboratories. In

Figure 4 Examples of central neuron types (rat nucleus of the solitary tract (NST)) based on chemosensitive response profiles. Types were identified using cluster analysis, and generally corresponded to a best-stimulus classification. The response types resemble those in other studies, though additional features are apparent, based on including neurons responsive to the posterior tongue, as well as including L-glutamate in the stimulus array. Two neuron types were robustly responsive to sucrose including a small group of posterior tongue responsive neurons with a relatively specific response to sucrose (S neurons), and a larger group comprised mainly of anterior oral cavity responsive neurons. The latter group also responded well to glycine, and in fact responded nominally better to glutamate (U/S neurons). Two groups responded best to sodium salts (N neurons) or acids. As is common, acid-best neurons were also robustly responsive to sodium salts, and thus named A/N neurons. Finally, there were neurons with posterior tongue receptive fields optimally and relatively specifically responsive to bitter-tasting chemicals. The multiple types of bitter-best neurons provide preliminary evidence for heterogeneous processing of different (ionic vs. nonionic) bitter tastants. SUC, 300 mM sucrose; GLY, 300 mM glycine; MSG, 30 mM monosodium glutamate + 3 mM inosine monophosphate; MPG, 30 mM monopotassium L-glutamate + 3 mM inosine monophosphate; NACL, 100 mM NaCl; NAG, 100 mM NaGluconate; HCL, 10 mM HCl; CIT, 30 mM citric acid; QUI, 3 mM quinine hydrochloride; DEN, 10 mM denatonium benzoate; PROP, 7 mM propylthiouracil; CHX, 0.01 mM cycloheximide. From Geran, L. C. and Travers, S. P. 2006. Single neurons in the nucleus of the solitary tract respond selectively to bitter taste stimuli. J. Neurophysiol. 96, 2513–2527, with permission.

1979, Smith D. V. and Travers J. B. introduced the entropy measure as a way to quantify the breadth of tuning of gustatory neurons. This measure is given by the equation:

$$H = -K \sum p_i(\log p_i), \quad i = 1, n$$

where H is the breadth of responsiveness, K is a scaling constant, and p_i is the proportional response to each of n stimuli. The p_i's for each cell are derived by converting the neural response profile for that cell to a proportional profile, the response to each stimulus being expressed as a proportion of the total response to all four stimuli. This manipulation maintains the relative response to all stimuli and does not depend upon a response criterion. Therefore, a cell might be considered broadly responsive if it responds well to its best stimulus and strongly to one other or weakly to two or three others. An $H = 1.0$ indicates a cell that is equally responsive to all four stimuli, whereas an $H = 0.0$ indicates a cell responding exclusively to one stimulus of the four. This measure has seen extensive use over the past 25 years in the study of both peripheral and central gustatory neurons (see Spector, A. C. and Travers, S. P., 2005 for a thorough review of this literature). Recently, Spector A. C. and Travers S. P. (2005) have proposed an additional measure of response tuning, which they termed the noise-to-signal measure, which takes into account the relative magnitudes of the responses to the most and second most effective stimuli. Using this approach, a cell with a large second response would be considered more broadly tuned than one with responses to all three other stimuli if their responses were smaller. Both approaches together can provide a good description of the breadth of tuning of gustatory neurons.

Comparing the breadth of tuning across levels of the gustatory system is difficult, even with a standard way of measuring response breadth. Different laboratories often use different stimuli and concentrations, and also study neurons receiving input from different regions of the mouth, all of which can impact how broadly tuned the cells appear. For example, Figure 4 depicted bitter-best neurons with relatively narrow tuning to bitter stimuli and posterior tongue receptive fields. However, another recent study, which concentrated on the anterior mouth-responsive portion of NST, and which used different concentrations of electrolytes and different bitter tastants, reported that bitter-responsive neurons responded nearly equally to salty and sour stimuli (Lemon, C. H. and Smith, D. V., 2005) (Figure 5).

To avoid such complications, a direct comparison of hamster chorda tympani, NST, and PbN responses was made using the same stimuli and concentrations. The results demonstrated that cells within the brainstem are more broadly tuned than peripheral gustatory axons (Van Buskirk, R. L. and Smith, D, V., 1981). Among chorda tympani fibers, the sucrose-best neurons are the most narrowly tuned (mean $H = 0.386$, compared to 0.587 for NaCl-best and 0.668 for HCl-best neurons). At the level of the NST, sucrose-best neurons are significantly more broadly responsive ($H = 0.586$) and this breadth increases again at the level of the PbN ($H = 0.743$). Thus, the one neuron type in the periphery which stands out for its narrow tuning becomes systematically more broadly tuned as information converges onto neurons in the medulla and pons of the hamster. In fact, at the level of the pons, sucrose-best neurons are more broadly tuned than the broadly tuned HCl-best fibers of the chorda tympani nerve. There is a wealth of data on several species and several levels of the nervous system about the breadth of responsiveness of gustatory neurons (summarized in Spector, A. C. and Travers, S. P., 2005). Overall, many cells in the central nervous system are relatively broadly responsive to stimuli representing different taste qualities; however, some neurons with more specific tuning profiles can also be observed.

4.15.2.2.2 Convergence, orotopy, and oral somatosensory responsiveness

Fibers of the chorda tympani nerve typically innervate taste cells in multiple fungiform papillae, although the sensitivities of each branch appear to be highly similar, suggesting that taste axons are guided to make connections to particular receptors (Oakley, B. *et al.*, 1979; see also Ninomiya, Y., 1998). Thus convergence of separate axonal branches within the tongue does not appreciably increase the breadth of a neuron's responsiveness. On the other hand, when recordings are made from neurons in the NST, separate receptive fields are seen to converge (Vogt, M. B. and Mistretta, C. M., 1990), resulting in greater breadth of responsiveness. Further, axons from completely separate receptor populations have been shown to converge on NST neurons in the rat (Ogawa, H. and Hayama, T., 1984), particularly between the palate and anterior tongue (Travers, S. P. *et al.*, 1986; Travers, S. P. and Norgren, R., 1991). These neurons often responded best to NaCl applied to the anterior tongue and sucrose applied to the

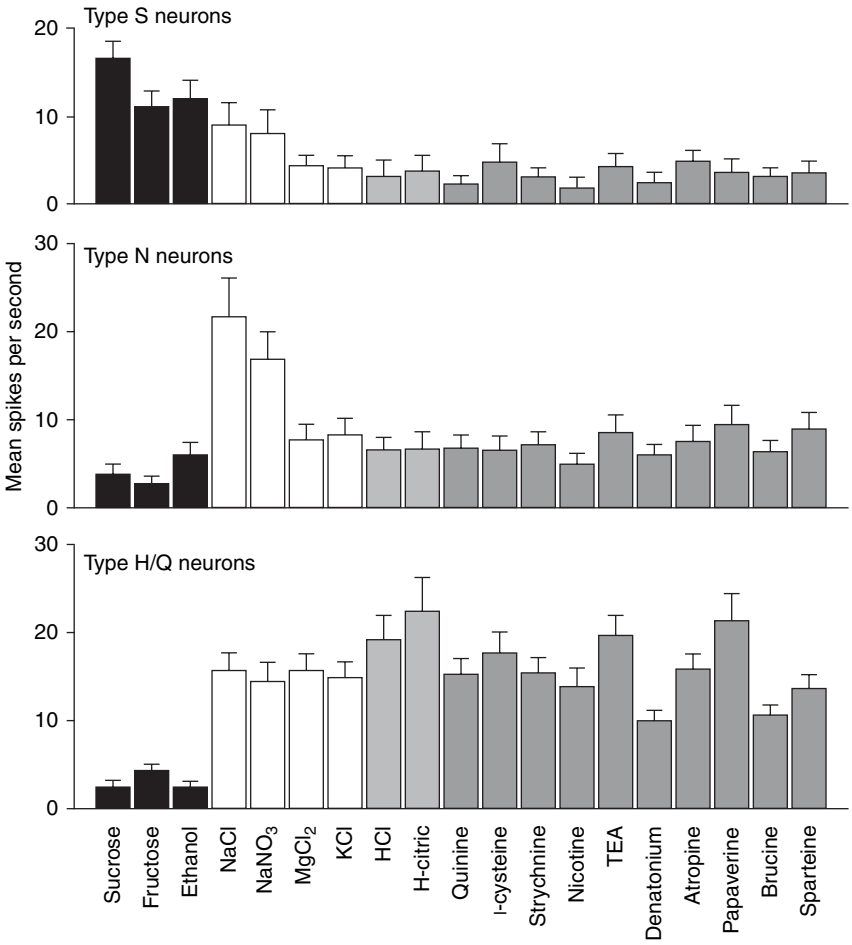

Figure 5 Further examples of rat nucleus of the solitary tract (NST) neuron types based on chemosensitive response profiles. The N neurons strongly resemble the N neurons in Figure 4, and the S neurons are similar to the S/U neurons in Figure 4. However, neurons with selective responses to bitter tastants were not apparent. Instead, neurons with optimal responses to acids responded nearly as well to salts and bitter stimuli. Stimuli: 320 mM sucrose, 500 mM fructose, 40% ethanol, 10 mM NaCl, 8 mM $NaNO_3$, 3 mM HCl, 5 mM citric acid, 10 mM $MgCl_2$, 5 mM KCl, 15 mM denatonium benzoate, 3 mM L-cysteine, 1 mM nicotine, 5 mM strychnine, 40 mM tetraethylammonium, 30 mM atropine, 5 mM brucine, 30 mM papaverine, 9 mM sparteine, 7 mM quinine hydrochloride. From Lemon, C. H. and Smith, D. V. 2005. Neural representation of bitter taste in the nucleus of the solitary tract. J. Neurophysiol. 94, 3719–3729 with permission.

palate. Convergence from different parts of the oral cavity onto cells in the hamster NST has also been described (Sweazey, R. D. and Smith, D. V., 1987). Convergence of peripheral axons onto neurons of the NST is probably responsible for the increased breadth of responsiveness seen in NST neurons over peripheral fibers. Although there are little or no data on whether sucrose-best fibers of the chorda tympani nerve exhibit amiloride-sensitive responses to NaCl, responses to NaCl in sucrose-best neurons in the NST are blocked by amiloride (Boughter, J. D., Jr. and Smith, D. V., 1998; St. John, S. J. and Smith, D. V., 2000), probably reflecting convergence between peripheral NaCl-best and sucrose-best chorda tympani axons onto cells of the NST. At the level of the PbN, in addition to an increase in the breadth of tuning of sucrose-best neurons (Van Buskirk, R. L. and Smith, D .V., 1981), there is direct evidence that inputs from the anterior and posterior oral cavity converge onto single neurons (Halsell, C. B. and Travers, S. P., 1997).

As a result of the diverse anatomical distribution of taste buds across the tongue, palate, and oropharyngeal and laryngeal epithelia and their innervation by three different cranial nerves, the central representation of gustatory input is arranged in an orotopic fashion (Contreras, R. J. *et al.*, 1982; Hamilton, R. B. and Norgren, R., 1984; Travers, S. P. and Norgren, R.,

1995). Within the medulla, afferent neurons of the VII nerve, including those within the chorda tympani and the greater superficial petrosal nerves, terminate in the most rostral pole of the NST. Overlapping this distribution but extending more caudally is the input from the IX nerve and this distribution is overlapped and extended more caudally still by afferent terminals of the gustatory axons of the X nerve. Consequently, the oral cavity is roughly represented spatially within the NST, with input from the anterior tongue and palate most rostral and that from the epiglottis most caudal within the nucleus. In rodents there are some differences in responsiveness to different stimuli across the various receptor fields, most notably a greater sensitivity to quinine and other bitter stimuli on the posterior tongue. This difference is reflected in the responsiveness of cells in different regions of the NST (Sweazey, R. D. and Smith, D. V., 1987; Geran, L. C. and Travers, S. P., 2006). In the PbN, gustatory input to the external lateral–inner subdivision is exclusively from the posterior oral cavity, whereas both posterior and anterior oral inputs are comingled in the central medial and ventral lateral subdivisions (Halsell, C. B. and Travers, S. P., 1997). In fact, orotopy is observed all the way to the cortex, where input from the VII and IX nerves is still somewhat segregated (e.g., Benjamin, R. M. and Akert, K., 1959). Thus input from the posterior and anterior oral cavities is partially segregated at all levels of the gustatory system. Functionally, gustatory information carried in the VII nerve, but not the IX, appears to be critical for taste discrimination (Spector, A. C. and Grill, H. J., 1992; Spector, A. C. *et al.*, 1997; St. John, S. J. and Spector, A. C., 1998), whereas aversive taste reactivity (e.g., gapes) depends upon IX nerve input (Travers, J. B. *et al.*, 1987; Grill, H. J. *et al.*, 1992). These data suggest that gustatory input carried by different cranial nerves may subserve somewhat different functional roles, as is seen quite clearly in fish, where the VII nerve is involved in food seeking and the IX in ingestion (Bardach, J. E. *et al.*, 1967; Atema, J., 1971). Although the degree of anatomical overlap between cranial nerve inputs in mammals makes such a relationship more difficult to discern, a similar functional dichotomy between VII and IX nerve gustatory function may exist.

In addition to processing gustatory information, the rNST also receives notable inputs from oral somatosensensory receptors. Somatosensory input arising from the anterior mouth reaches the nucleus though projections of oral divisions of the trigeminal nerve; and that from the posterior mouth through the IX nerve (Beckstead, R. M. and Norgren, R., 1979; Contreras, R. J. *et al.*, 1982; Hamilton, R. B. and Norgren, R., 1984). Neurons that are unresponsive to taste, but instead responsive to nonnociceptive mechanical stimulation of the oral mucosa are also arranged in an orderly orotopic fashion, laterally adjacent to the location of taste-responsive neurons (Travers, S. P. and Norgren, R., 1995). In addition, a number of gustatory-responsive neurons can also be activated by mechanical stimulation of the mouth, with such responses stronger and more prevalent in posterior-responsive neurons receiving inputs from the IX nerve (Travers, S. P. and Norgren, R., 1995).

4.15.2.2.3 Modulation of gustatory responsiveness

Gustatory neurons in the rodent PbN send projections to two distinct forebrain systems: thalamocortical and limbic (Figure 1). Double-labeling experiments have shown that some PbN neurons project to the ventral posterior medial nucleus, parvicellularis (VPMpc) of the thalamus, whereas others project to the central nucleus of the amygdala (CeA) (Voshart, K. and van der Kooy, D., 1981). From the VPMpc, gustatory information is transmitted to the gustatory insular cortex. PbN neurons also project to the lateral hypothalamus, bed nucleus of the stria terminalis, and the substantia innominata (Norgren, R., 1974; 1976). Although the precise route may be different (see below), taste information in the primate also reaches limbic, as well as thalamocortical forebrain sites. These various areas of the limbic forebrain pathway have been implicated in food and water regulation, sodium appetite, taste aversion learning, and the response to stress, suggesting a substrate through which taste activity interfaces with motivated behavior. Both the insular cortex and many of these limbic areas have feedback projections to the NST and PBN (Figure 2) (van der Kooy, D. *et al.*, 1984; Veening, J. G. *et al.*, 1984; Moga, M. M. *et al.*, 1990b; Halsell, C. B., 1998; Whitehead, M. C. *et al.*, 2000), providing a mechanism by which higher-level processing can impact taste responses at the initial stages of the pathway.

4.15.2.2.3.(i) Physiological alterations The first indications of a modulatory effect of the forebrain on taste activity came from studies on decerebrate rats, which demonstrated that taste responses in brainstem nuclei were changed by severing the connections with the forebrain (Hayama, T. *et al.*, 1985; Di Lorenzo, P. M., 1988; Mark, G. P. *et al.*, 1988). Further experiments

using reversible lesions of the insular cortex with procaine demonstrated both increased and decreased responding to taste stimulation in the PbN (Di Lorenzo, P.M. and Monroe, S., 1990) as well as the NST (Di Lorenzo, P. M. and Monroe, S., 1995). These data demonstrated that the responsiveness of gustatory neurons in the brainstem are not simply the result of the integration of afferent inputs, but are modifiable by descending circuits. Several kinds of experiments have illustrated that physiological and experiential factors may modulate the responsiveness of taste neurons in the brainstem; descending modulation presumably makes a key contribution to these influences, though local circuits most likely play a role as well.

4.15.2.2.3.(ii) Homeostatic mechanisms: feeding and appetite Gustatory input is critical to the initiation and control of ingestive behavior, guiding the choice of nutritive foods, and promoting the avoidance of toxic substances. A number of studies have shown that manipulations that alter an animal's state of satiety can have an influence on the responses of gustatory neurons in the brainstem. For example, hyperglycemia produced by intravenous infusion of glucose decreased responses to orally applied glucose in cells of the rat NST by an average of 43% (Giza, B. K. and Scott, T. R., 1983) Responses to NaCl and HCl were considerably less affected (20% and 16%, respectively) by blood glucose levels and those to QHCl (3%) not at all. Similarly, rats decreased their preference for glucose following an intravenous glucose load, which had no effect on their behavioral responses to quinine (Giza, B. K. and Scott, T. R., 1987). Therefore, when blood sugar levels are elevated, gustatory responses in the brain are decreased and the intake of glucose is concomitantly reduced. Intravenous infusion of other satiety factors, including insulin and pancreatic glucagon, also decreased NST multiunit responses to glucose, although cholecystokinin (CCK) had no effect on taste activity (Giza, B. K. *et al.*, 1992). Similarly, gastric distension has been shown to decrease the responsiveness of NST neurons to taste stimulation (Glenn, J. F. and Erickson, R. P., 1976). These factors, all of which can be signals contributing to satiety, appear to decrease gustatory sensitivity to nutritive taste stimuli.

It is generally believed that in the short-term regulation of feeding behavior, the sensory components of food play a dominant role (Smith, G. P., 1996). In sham-feeding experiments in which orosensory stimulation is isolated from any postingestive effects, fat infusions into the duodenum decrease food intake (e.g., Greenberg, D. *et al.*, 1990; Foster, L. A. *et al.*, 1996). Electrophysiological evidence indicates that intraduodenal infusion of lipid reversibly decreases the responsiveness of PbN taste neurons to sucrose and somewhat to NaCl, with no effect on responses to acid or quinine (Figure 6, Hajnal, A. *et al.*, 1999).

The effects were also differential for neuron type, indicating a further specialization for this modulation. Sucrose responses were most affected in sucrose-best neurons, and in particular those with the most specific responses to sucrose. These effects were rapid, beginning within 5–10 min, and reversible within about 40 min after the beginning of a 10 min lipid infusion. These data demonstrate that fat introduced into the duodenum has a specific effect on taste mechanisms, providing for decreased taste sensitivity to stimuli that signal nutritional value.

Another area in which nutritional need results in altered gustatory responsiveness is sodium appetite. Normal rats behaviorally choose to ingest NaCl at concentrations that maintain sodium homeostasis. Thus an isotonic concentration of about 0.15 M is avidly consumed, whereas lower concentrations are less preferred and higher concentrations become increasingly avoided; indeed rats can voluntarily mix NaCl and water to maintain isotonic levels of intake (Rinaman, L. *et al.*, 1993). However, when plasma sodium concentration declines, a condition known as hyponatremia, there are two mechanisms for returning sodium to normal levels. One is to conserve sodium through activation of the renin–antiotensin–aldosterone system to increase sodium resorption and the other is to increase the ingestion of sodium by creating a specific sodium appetite (see McCaughey, S. A. and Scott, T. R., 1998). Like most other mammals, rats that are made sodium deficient will exhibit a sodium appetite that is characterized by an increase in the intake of sodium salts, such as NaCl (Jalowiec, J. E. and Stricker, E. M., 1970; Contreras, R. and Hatton, G., 1975), which is ingested at concentrations that are normally behaviorally neutral or avoided. Investigation of the responsiveness of gustatory neurons following sodium deficiency demonstrates that the responsiveness to NaCl is decreased, particularly in those neurons most responsive to sodium salts (i.e., those with amiloride-sensitive input) in both peripheral chorda tympani axons (Contreras, R. J., 1977; Contreras, R. J. and Frank, M., 1979) and in neurons of the NST (Jacobs, K. M. *et al.*, 1988) and PbN (Shimura, T. *et al.*, 1997a). These results have been interpreted to

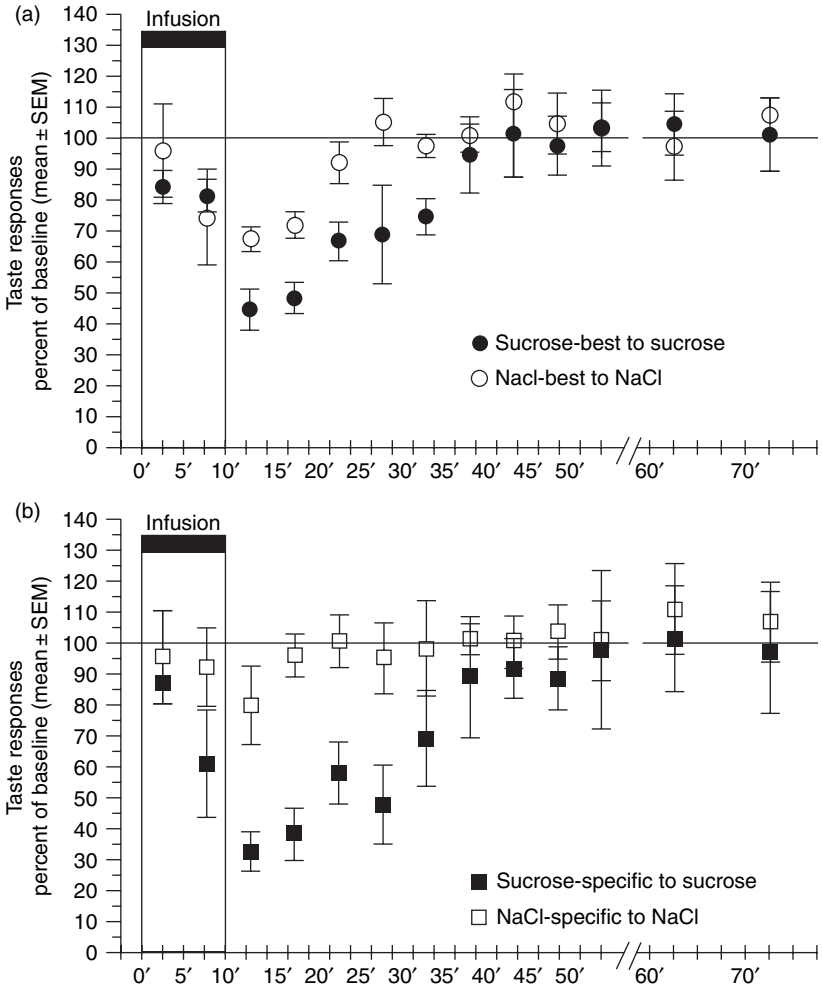

Figure 6 Effects of intraduodenal lipid infusion on taste responses in parabrachial nuclei (PbN) neurons. (a) Mean responses to sucrose in sucrose-best neurons, and mean responses to NaCl in NaCl-best neurons before and at different times after the infusion. Both the responses to sucrose and NaCl were suppressed rapidly, but the sucrose response was much more profoundly affected. (b) The sucrose effect was more pronounced in the subset of sucrose-best neurons that were most selectively tuned to this tastant; the opposite was true for the suppression of the NaCl response; lipids infusion was less effective in suppressing the NaCl response of NaCl-specific neurons. From Hajnal, A., Takenouchi, K., and Norgren, R. 1999. Effect of intraduodenal lipid on parabrachial gustatory coding in awake rats. J. Neurosci. 19, 7182–7190, with permission.

mean that a sodium-deprived rat would require greater ingestion of NaCl to establish the same level of sensory input as a normal rat (Contreras, R. J. and Frank, M., 1979). Whether or not this decrease in the sodium responsiveness is actually required for the expression of sodium appetite is unclear, however, since varying the way in which sodium appetite is induced can actually lead to opposite changes; that is, increases in brainstem taste responses (Tamura, R. and Norgren, R., 1997), even though the animal still consumes more sodium. Thus, the relationship between changes in taste responsiveness and changes in ingestive behavior do not appear simple.

4.15.2.2.3.(iii) Learning: conditioned preferences and aversions Palatable taste stimuli that are associated with gastrointestinal illness become aversive, a learning phenomenon known as conditioned taste aversion (CTA), first described by Garcia J. *et al.* (1970) . When rats are made ill following exposure to a novel stimulus, they associate the resulting illness with the taste of the stimulus and thereafter are averse to it and to other stimuli with a similar taste (Nachman, M., 1963; Halpern, B. P. and Tapper, D. N., 1971). Such behavior has survival value for the animal by helping it to avoid the ingestion of food that contains toxic substances. The generalization of CTA has been used as a

psychophysical tool to assess the similarity in quality among gustatory stimuli in experimental animal models (e.g., Smith, D. V. and Travers, J. B., 1979; Smith, D. V. *et al.*, 1979; Nowlis, G. H. *et al.*, 1980), as animals will avoid other stimuli in proportion to the perceived similarity to the conditioned stimulus (CS) (Smith, D. V. and Theodore, R. M., 1984). Several studies have shown that such conditioning alters the responsiveness of gustatory neurons, generally by making the CS a somewhat more effective stimulus. For example, Chang F. C. and Scott T. R. (1984) demonstrated that a CTA to saccharin increased the responsiveness to the CS in those neurons most responsive to sweet substances. Similarly, conditioning an aversion to NaCl resulted in an increased response to the CS in NaCl-best neurons of the rat PbN (Shimura, T. *et al.*, 1997b). Such an increase is restricted to those neurons receiving amiloride-sensitive sodium input, but this increase in responsiveness was not evident in decerebrate animals (Tokita, K. *et al.*, 2004). Thus, as shown above, sodium need leads to a decreased neural response to NaCl and increased consumption, whereas CTA leads to an increased neural response to NaCl and decreased consumption. On the other hand, when the CS was a normally nonpreferred HCl solution, the effects of CTA were the opposite: PbN responses to the CS were reduced (Shimura, T. *et al.*, 2002). When rats are conditioned to prefer a $MgCl_2$ or citric acid solution, there were slight shifts in neural responses in the rat NST, making the CS more distinct from other nonpreferred solutions, but these effects were much less robust than the effects of CTA (Giza, B. K. *et al.*, 1997).

4.15.2.2.4 Neurotransmitters and neuromodulators in the nucleus of the solitary tract

Recently, significant progress has been made in identifying the neurotransmitters and neuromodulators along the gustatory pathway, and defining their roles in gustatory information processing. In the brainstem, most is known about the NST.

4.15.2.2.4.(i) Excitatory amino acids Much of the excitatory transmission in the central nervous system is mediated by excitatory amino acids (EAAs), such as glutamate (Mayer, M. L. and Westbrook, G. L., 1987). In the visceral portions of the NST, several EAA agonists had been shown to elicit cardiovascular responses when injected into the medial NST, mimicking the effects of stimulation of baroreceptor afferent fibers, and these responses are blocked by both *N*-methyl-D-aspartic acid (NMDA) and non-NMDA antagonists (Guyenet, P. G. *et al.*, 1987; Kubo, T. and Kihara, M., 1988a; 1988b). Synaptic transmission between primary vagal afferent fibers and second-order cells of the caudal NST appears to be mediated by glutamate (Drewe, J. A. *et al.*, 1990; Glaum, S. R. *et al.*, 1992; Vardhan, A. *et al.*, 1993; Andresen, M. and Yang, M., 1994). In studies done *in vitro* on rat brainstem slices, the responses of cells in the gustatory region of the rNST to electrical stimulation of the solitary tract are reduced or blocked by antagonists of both NMDA and α-amino-3-hydroxy-5-methyl-4-isoxazolepropionic acid (AMPA)/kainate receptors (Wang, L. and Bradley, R. M., 1995), suggesting that both NMDA and non-NMDA receptors may mediate transmission between primary gustatory fibers and second-order neurons of the NST. The direct involvement of EAA receptors in the transmission of gustatory information was shown in an *in vivo* experiment, in which gustatory responses in individual cells of the hamster NST were blocked by EAA receptor antagonists (Li, C. S. and Smith, D. V., 1997). Microinjection of kynurenic acid, a broad-spectrum EAA antagonist, into the vicinity of taste-responsive neurons of the NST completely and reversibly blocked their activity. In these *in vivo* experiments, the AMPA/kainate receptor antagonist 6-cyano-7-nitroquinoxaline-2,3-dione (CNQX) also completely and reversibly blocked these responses, although the NMDA antagonist DL-2-amino-5-phosphonovalerate (APV) was less effective. All gustatory responses in the NST were blocked by CNQX, regardless of the type of cell or nature of the gustatory stimulus (Li, C. S. and Smith, D. V., 1997). Because the *in vitro* experiments had shown colocalization of NMDA and non-NMDA receptors on many of the same NST neurons (Wang, L. and Bradley, R. M., 1995), it is likely that the NMDA receptors play a secondary role which is not easily revealed *in vivo*.

4.15.2.2.4.(ii) Gamma-aminobutyric acid, tonic inhibition There are many small ovoid neurons within the NST that express the inhibitory neurotransmitter GABA in both rats (Lasiter, P. S. and Kachele, D. L., 1988) and hamsters (Davis, B. J., 1993). Slice experiments on the rNST had suggested that cells within the gustatory NST could be inhibited by GABA and excited by the $GABA_A$ receptor antagonist, bicuculline methodide (BICM), suggesting a tonic GABAergic inhibitory network within this region (Liu, H. *et al.*, 1993; Wang, L. and Bradley, R. M., 1993). When GABA was microinjected into the hamster NST *in vivo*, taste-responsive neurons showed a dose-dependent inhibition of spontaneous

and evoked activity and their responses to taste stimulation were enhanced in a dose-dependent manner by BICM; 63% of the taste-responsive cells in the NST were modulated by GABAergic mechanisms in these experiments (Smith, D. V. and Li, C. S., 1998). The responses of all tastants were enhanced by BICM administration, showing that particular neurons, but not particular stimuli, are modulated by GABAergic inhibitory circuits. The result of the removal of GABAergic inhibition was an increase in the breadth of responsiveness of NST neurons to gustatory stimulation as the cells became more responsive to all stimuli, similar to the effects on tuning seen in other sensory systems following BICM (Kyriazi, H. T. *et al.*, 1996; Lazareva, N. A. *et al.*, 1997).

One source of inhibition of NST gustatory neurons arises from the gustatory cortex (GC), which sends descending connections to the NST (van der Kooy, D. *et al.*, 1984). Stimulation of GC results in both excitation and inhibition of the activity of taste neurons in the NST (Di Lorenzo, P. M. and Monroe, S., 1995). Both electrical stimulation of the GC and excitation produced by the glutamate analog DL-homocysteic acid (DLH) produced either excitation or inhibition in about 34% of taste-responsive cells in the hamster NST (Smith, D. V. and Li, C., 2000). The inhibition produced by GC stimulation was blocked by infusion of BICM into the vicinity of the recorded cell in the NST. Of the eight cells inhibited by GC stimulation, seven were most responsive to NaCl, suggesting that cortical-evoked inhibition of NST activity may be somewhat stimulus-specific (Smith, D. V. and Li, C., 2000), although the effects of GC stimulation on the responses to NaCl themselves were not tested in this study. Gustatory neurons in both the PbN (Kobashi, M. and Bradley, R. M., 1998) and insular cortex (Ogawa, H. *et al.*, 1998) are also modulated by GABAergic mechanisms.

4.15.2.2.4.(iii) Peptides: substance P and opioids

Immunocytochemical studies show that there are substance P (SP)-containing neurons and fiber terminals within the rNST (South, E. H. and Ritter, R. C., 1986; Davis, B. J. and Kream, R. M., 1993). In experiments on *in vitro* brainstem slices in rats (King M. S. *et al.*, 1993), SP transiently depolarized 80 of 117 (68%) rNTS neurons in a dose-dependent manner. Submicromolar concentrations of SP had potent excitatory effects, and the half-maximal response occurred at 0.6 μM. The depolarizing effect of SP was accompanied by an increase in input resistance in 81% of the responsive neurons and persisted in low Ca^{2+} and high Mg^{2+} saline as well as in the presence of tetrodotoxin (TTX), suggesting direct postsynaptic action of SP on the recorded neurons. SP also hyperpolarized four neurons (4%) and had no effect on 33 cells (28%). When gustatory neurons were recorded *in vivo* from hamster NST, about 48% were excited by microinjection of SP into the nucleus, whereas 9% were inhibited (Davis, B. J. and Smith, D. V., 1997). In this experiment, only NaCl was used as a taste stimulus, so it is as yet unclear whether SP produces differential effects according to stimulus. However, the responses to NaCl were clearly enhanced by SP.

Endogenous opiates have been implicated in gustatory palatability (e.g., Rideout, H. J. and Parker, L. A., 1996) and earlier studies had shown that systemic administration of morphine resulted in inhibition of taste-evoked multiunit activity in the rat PbN (Hermann, G. E. and Novin, D., 1980) Injection of naltrexone (NLTX), a nonselective opioid receptor antagonist, into the NST blocks feeding induced by neuropeptide Y administration into the paraventricular nucleus (Kotz, C. M. *et al.*, 1997), implicating an opioid-mediated influence within the NST. Further, μ-opioid receptors are expressed by rNST neurons that receive synaptic input from neurons in the central nucleus of the amygdala (Pickel, V. M. and Colago, E. E., 1999), an area known to provide modulatory input to the gustatory NST (Li, C. S. *et al.*, 2002a). Within the gustatory portion of the rNST, there are both nerve fibers and cell bodies expressing methionine enkephalin (met-ENK) immunoreactivity (Davis, B. J. and Kream, R. M., 1993). In neurons recorded *in vivo* from the hamster NST, microinjection of met-ENK reversibly reduced the responses of 39 of 165 (23.6%) taste-responsive neurons in a dose-dependent manner (Li, C. S. *et al.*, 2003). This inhibition was blocked by NLTX, although NLTX alone had no effect, suggesting that opioid inhibition in these neurons is not tonic. Thus, along with GABAergic mechanisms, opioids exert an inhibitory effect on gustatory processing in the NST.

4.15.2.2.4.(iv) Other neurotransmitters: dopamine, acetylcholine, and nitric oxide

Less is known about the function of other neurotransmitters in the gustatory NST, although there is some evidence for dopaminergic, cholinergic, and nitrergic mechanisms. Within the gustatory portion of the hamster NST, neurons expressing tyrosine hydroxylase and dopamine-β-hydroxylase have been described (Davis, B. J. and Jang, T., 1988b). In electron micrographic studies,

(Davis, B. J., 1998) demonstrated that NST neurons expressing tyrosine hydroxylase received synaptic input directly from chorda tympani nerve axons, suggesting that these neurons are second-order gustatory cells. The rNST also contains neurons that express nitric oxide synthase (NOS), the synthetic enzyme for nitric oxide and stain for NADPH diaphorase (NADPHd), a marker for NOS (Ruggiero, D. A. *et al.*, 1996; Travers, S. P. and Travers, J. B., 2006). In fact, about 15–20% of the neurons that express Fos-like immunoreactivity in response to gustatory stimulation with quinine or citric acid are double-labeled for NADPHd suggesting that nitric oxide may be a transmitter in a subset of taste cells. Further, many of these Fos neurons intermingle with NOS fibers, implying that nitric oxide could modulate taste responses (Travers, S. P. and Travers, J. B., 2006). However, to date, there are no functional data showing a role for dopamine or nitric oxide in gustatory processing. On the other hand, application of acetylcholine (ACh) to cells recorded in rat brain slices through the rNST show that many of these neurons are modulated by ACh, mediated through both nicotinic and muscarinic ACh receptors (Uteshev, V. V and Smith, D. V., 2006). Nicotinic responses, which were always excitatory, were mediated by either $\alpha 7$ or non-$\alpha 7$ nicotinic AChRs and comprised about 66% (50/76) of the cells examined. Responses mediated by muscarinic AChRs were seen in 42% (31/73) neurons tested. These responses were inhibitory near the resting potential, resulting in a block of evoked spikes. Extensive acetylcholinesterase (AChE) immunostaining is closely associated with the terminal fields of both the chorda tympani and glossopharyngeal nerves in the rNST (Barry, M. A. *et al.*, 2001) and there are neurons expressing choline actetyltransferease (ChAT) in the medial portion of the rNST (Ruggiero, D. A. *et al.*, 1990). These latter neurons are part of the parasympathetic preganglionic neurons of the inferior salivatory nucleus (Contreras, R. J. *et al.*, 1980), which could conceivably modulate taste activity as a consequence of parasympathetic activity. There are as yet no data on cholinergic modulation of taste responses *in vivo*, nor is it clear whether all of the cholinergic input to this area is derived from these parasympathetic neurons.

4.15.2.2.5 Descending pathways from forebrain targets: modulation of nucleus of the solitary tract and parabrachial nuclei

As delineated above, decerebration has been shown to modulate brainstem gustatory activity, indicating that the responsiveness of brainstem gustatory neurons reflects not only sensory input from the taste receptors, but descending influences from forebrain circuits. There are direct descending projections from the GC, the lateral hypothalamus, the central nucleus of the amygdala, and the bed nucleus of the stria terminalis to both the NST and PbN gustatory regions (van der Kooy, D. *et al.*, 1984; Moga, M. M. *et al.*, 1990b; Allen, G. V. *et al.*, 1991; Halsell, C. B., 1998). A series of recent experiments on both rats and hamsters has demonstrated that each of these forebrain targets of the gustatory system provides modulatory control over taste-responsive neurons in the NST and PbN (Figure 2).

4.15.2.2.5.(i) Gustatory cortex

When the activity of GC was blocked by local infusion of procaine, both increases and decreases in the taste responses were recorded from the rat NST (Di Lorenzo, P. M. and Monroe, S., 1995) and PbN (Di Lorenzo, P. M., 1990), showing that these cells can be either facilitated or inhibited by cortical influences. Similar results were seen as a result of electrical or chemical stimulation of the GC in hamsters (Smith, D. V. and Li, C., 2000). Of 50 neurons recorded from the hamster NST, 17 (34%) were modulated by ipsilateral cortical stimulation. About half of these (9/17) were excited and half (8/17) were inhibited. Although the excitatory effects were distributed across different cell types, the inhibitory effects were significantly more common in NST cells responding best to NaCl. In a more recent experiment, in which stimulating electrodes were implanted bilaterally in the GC, a slightly greater influence of the contralateral cortex was noted: 16 of 50 cells (32%) were modulated ipsilaterally, whereas 20 of 50 (40%) responded to contralateral stimulation (Smith, D. V. *et al.*, 2004). Eleven of these neurons received converging input from both sides of the cortex, so that among the 50 cells recorded, 25 (50%) were modulated by one or both sides. A similar experiment on the rat showed that taste-responsive neurons in the PbN are also modulated by GC stimulation, with both inhibitory and excitatory responses (Lundy, R. F., Jr. and Norgren, R., 2004a). Both of these stimulation studies are compatible with the earlier studies in which the cortex was anesthetized with procaine, which resulted in both increased and decreased taste responses in PbN and NST (Di Lorenzo, P. M., 1990).

4.15.2.2.5.(ii) Lateral hypothalamus

Cells within the lateral hypothalamus respond to taste stimuli

applied to the oral cavity (Norgren, R., 1970; Yamamoto, T. *et al.*, 1989a) or alter their activity during food ingestion (Sasaki, K. *et al.*, 1984; Ono, T. *et al.*, 1986). There are descending projections from the lateral hypothalamus to both the PbN and NST (van der Kooy, D. *et al.*, 1984; Moga, M. M. *et al.*, 1990a). Earlier studies had suggested that stimulation of the lateral hypothalamus enhanced the responses of rat NST neurons evoked by chorda tympani nerve stimulation (Bereiter, D. *et al.*, 1980) or by electrical stimulation of the tongue (Matsuo, R. *et al.*, 1984). Electrical and chemical stimulation of the lateral hypothalamus in hamsters produced orthodromic modulation of half (49/99) of NST taste-responsive neurons (Cho, Y. K. *et al.*, 2002b) (Grossman, S. P. *et al.*, 1978; Frank, R. A. and Stutz, R. M., 1982). Most of these effects (44/99) were excitatory, as shown in the example in Figure 7.

Thus about half the taste-responsive cells of the NST are modulated (mostly excited) by the lateral hypothalamus. Stimulation of this region of the brain induces feeding behavior and, conversely, lateral hypothalamic lesions reduce food intake (Grossman, S. P. *et al.*, 1978; Frank, R. A. and Stutz, R. M., 1982), and tthese effects have been shown to interact with taste-guided behavior (Murzi, E. *et al.*, 1986; Touzani, K. *et al.*, 1990; Conover, K. L. and Shizgal, P., 1994). Thus, it is interesting to speculate that the lateral hypothalamus could enhance the signal-to-noise ratio in NST taste neurons during bouts of feeding (Cho, Y. K. *et al.*, 2002b). Lateral hypothalamic stimulation has also been shown to modulate taste activity in neurons of the rat PbN, although the excitatory and inhibitory influences were equal (Lundy, R. F., Jr. and Norgren, R., 2004a).

4.15.2.2.5.(iii) Central nucleus of the amygdala

The central nucleus of the amygdala contains neurons that respond differentially to hedonically positive and negative taste stimuli (Nishijo, H. *et al.*, 1998) and both the central nucleus and basolateral amygdala are involved in CTA learning (Yamamoto, T. *et al.*, 1994). The central nucleus of the amygdala provides a direct descending projection to both the NST and PbN (Norgren, R., 1976; Veening, J. G. *et al.*, 1984; Halsell, C. B., 1998). When stimulating electrodes were implanted bilaterally in the hamster central nucleus, 36 of 109 NST taste-responsive neurons (33%) were orthodromically modulated; 33 of these cells were excited and 3 were inhibited. Interestingly, those neurons that were modulated by the central nucleus of the amygdala had a significantly smaller response to taste stimuli than those that were not modulated. However, like the modulation of cells by the lateral hypothalamus, there was no specific effect on any one stimulus or cell type within the NST. On the other hand, in the PbN, Lundy R. F., Jr. and Norgren R. (2001) reported that stimulation of the central nucleus of the amygdala in the rat produced mostly suppressive effects, with an overall effect of enhancing the salience of the response to NaCl, suggesting that descending control from the amygdala could play a role in the mechanisms of sodium appetite. Stimulation of the central nucleus of the amygdala also produced more inhibition than excitation in another experiment (Tokita, K. *et al.*, 2004), in which it was shown that alterations in PbN neuronal responses to NaCl following CTA are eliminated by decerebration. These authors argued that descending influences from the central nucleus are important for the gustatory changes seen in the PbN following conditioning. Thus, one of the roles of the descending influence of the central nucleus of the amygdala on both the PbN and NST may be to produce alterations in brainstem responding following CTA, such as changes in taste reactivity seen, for example, to sucrose following aversive conditioning (Grill, H. J., 1985).

In both the NST (Cho, Y. K. *et al.*, 2003) and PbN (Lundy, R. F., Jr. and Norgren, R., 2004a), taste-responsive cells are often modulated by more than one forebrain structure. For example, of 113 cells in the hamster NST that were modulated by stimulation of either the lateral hypothalamus or central nucleus of the amygdala, 52 were responsive to stimulation of both sites. In the rat PbN, 60 neurons were tested for their responses to stimulation of the GC, central nucleus of the amygdale and lateral hypothalamus and 53 of them were modulated; 37 of them responded to more than one of these sites, with 17 neurons influenced by two sites and 20 by all three. In both the NST and PbN studies, the influence of different sites was most often similar, although there were cells that were excited by one site and inhibited by another. In a recent study of the effects of CeA and LH stimulation on neurons of the hamster PbN, most cells of the PbN were antidromically activated by stimulation of these sites (Li, C. S. *et al.*, 2005), which are synaptic targets of output neurons of the PbN (Norgren, R., 1976). Of 101 neurons tested in this study, 83 were antidromically driven by either the lateral hypothalamus or central nucleus of the amygdala and 57 of these by both, indicating a direct projection from the PbN to both of these areas. Only a small number of cells were

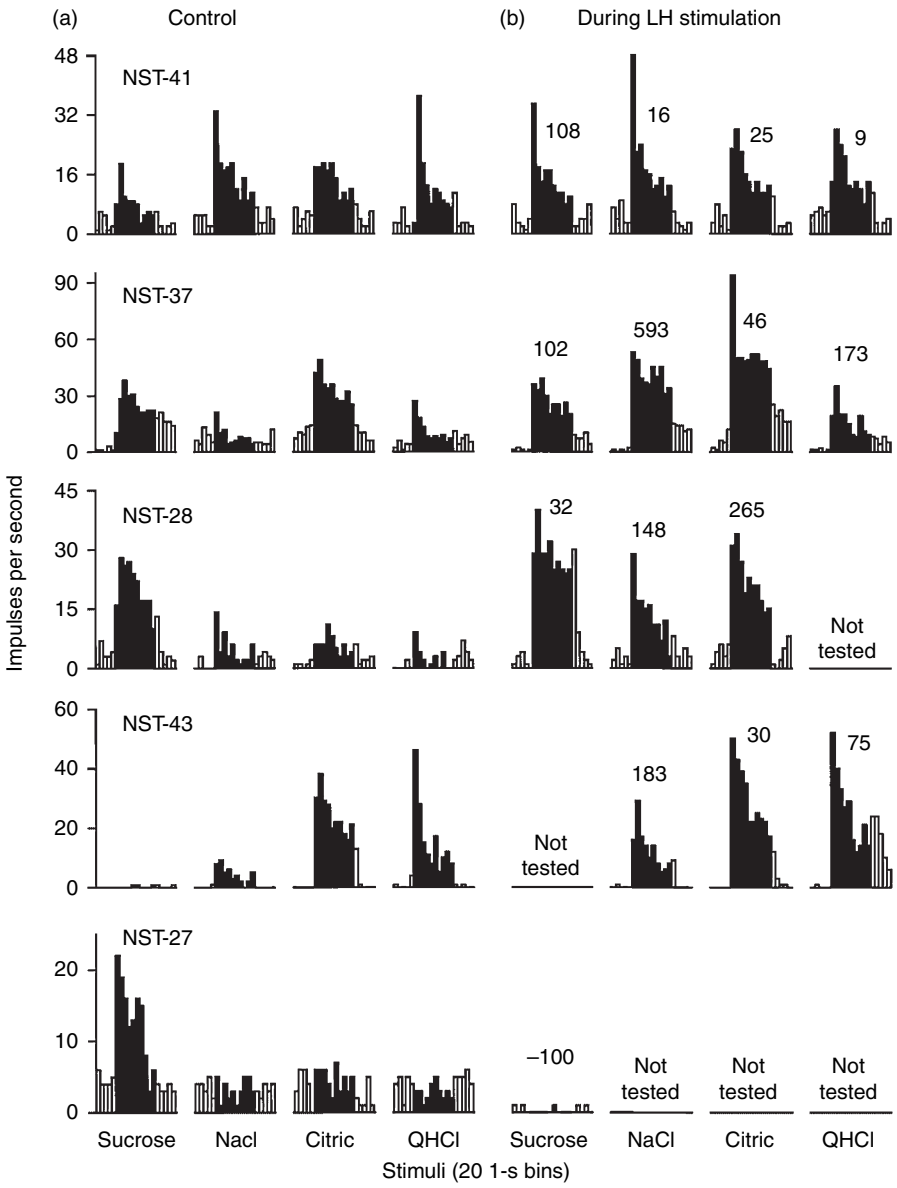

Figure 7 Effects of electrical stimulation of the lateral hypothalamus (LH) on taste-evoked responses in the rostral nucleus of the solitary tract (NST). Left: Gustatory responses in five neurons in the absence of LH stimulation. Right: Taste-evoked activity of these same neurons during concurrent stimulation (100 Hz, 0.2 ms pulses) using an intensity that was just subthreshold for altering spontaneous activity. As was typical for the entire population, the taste responses of most (4/5) of these neurons were amplified by activation of the LH. From Cho, Y. K. *et al.*, 2002b. Taste responses of neurons of the hamster solitary nucleus are enhanced by lateral hypothalamic stimulation. J. Neurophysiol. 87, 1981–1992, with permission.

orthodromically modulated, with five cells excited and eight inhibited by one of these forebrain areas. Clearly, there are complex descending influences on the gustatory responses of cells in both the NST and PbN.

4.15.2.2.5.(iv) Bed nucleus of the stria terminalis

In addition to the ventral projection of the PbN to the lateral hypothalamus and central nucleus of the amygdala, there is also a projection to the dorsolateral bed nucleus of the stria terminalis (Norgren, R., 1976), although to date there are no electrophysiological data showing gustatory responsiveness in this area. Nevertheless, the bed nucleus sends a descending projection to both the NST and the PbN (van der Kooy, D. *et al.*, 1984; Moga, M. M. *et al.*, 1990b; Whitehead, M. C. *et al.*, 2000). Stimulation of the

bed nucleus of the stria terminalis inhibited 29 of 101 hamster NST taste neurons, whereas only 7 were excited. All cell types were affected, although the number of NaCl-best neurons were fewer and citric acid-best greater among the modulated cells than expected by chance. Although we know that various subnuclei of the bed nucleus of the stria terminalis are implicated in a number of neural systems, including those involved in responses to stress (Morley, J. E. and Levine, A. S., 1980; Herman, J. P. and Cullinan, W. E., 1997; Cecchi, M. *et al.*, 2002), and in motivation, reward, and drug addition (Walker, J. R. *et al.*, 2000; Macey, D. J. *et al.*, 2003), how it plays a role in taste processing is not clear. Descending feedback from this region could conceivably be involved in the effects of stress on eating behavior (Morley, J. E. and Levine, A. S., 1980; Fullerton, D. T. *et al.*, 1985; Walker, J. R. *et al.*, 2000; Hagan, M. M. *et al.*, 2003; Macey, D. J. *et al.*, 2003).

These kinds of stimulation experiments have demonstrated extensive centrifugal modulation of brainstem gustatory activity, in both the NST and PbN. Essentially, every forebrain target of the gustatory system, including the GC, lateral hypothalamus, central nucleus of the amygdala, and bed nucleus of the stria terminalis exerts a descending modulatory influence on the processing of taste information. The hypothalamus and amygdala have predominantly an excitatory effect on the NST, whereas the cortex and bed nucleus produce significant inhibition of medullary taste responses. This extensive neural substrate no doubt underlies the modulation of taste activity by physiological and experiential factors and further research should be directed toward determining how these pathways are engaged by alterations in blood glucose, gastric distension, CTA, and other physiological conditions known to alter taste activity.

4.15.3 Gustatory Responsiveness of Forebrain Neurons

Although we know a great deal about the responsiveness of brainstem gustatory neurons, there are also data on gustatory areas beyond the pons, including the gustatory thalamic area, the taste cortex, and some regions of the limbic forebrain, including the lateral hypothalamus, central nucleus of the amygdala, nucleus accumbens, and ventral pallidum. The types of cells seen in brainstem areas, that is, sucrose-best, NaCl-best, etc., are also evident in more rostral nuclei. However, cells that appear to be tuned to stimulus palatability more than taste quality *per se* are also evident, especially in the limbic regions. Whereas the data on brainstem taste responses are almost exclusively from the rodent, and with notable exceptions (Nakamura, K. and Norgren, R., 1991; Nishijo, H. and Norgren, R., 1991; Nishijo, H. *et al.*, 1991; Nakamura, K. and Norgren, R., 1993), mostly from anesthetized preparations, much of the forebrain data is from primates, and regardless of species, frequently studies utilize awake, behaving preparations. Studies based on functional imaging in humans further provide a novel perspective for studying forebrain gustatory function. Due to space constraints, we will concentrate on cortical and limbic processing of taste information.

4.15.3.1 Taste Cortex

4.15.3.1.1 Organization and relationship to other sensory modalities

As discussed in Chapter Gustatory Pathways in Fish and Mammals, primary GC in both rodents and primates is located in insular cortex (Pritchard, T. C. *et al.*, 1986; Kosar, E. *et al.*, 1986a; 1986b). In primates, the gustatory insular cortex is buried in the Sylvian fissure but the primary gustatory area extends from the insula onto the opercular cortex (Pritchard, T. C. *et al.*, 1986). In both rodents and primates, gustatory signals reach the insular cortex via a relay in the most medial part of the ventroposteromedial nucleus of the thalamus (VPMpc). However, in rodents taste information reaches the thalamus only after making a synapse in the parabrachial nucleus (Norgren, R. and Leonard, C. M., 1971; 1973); in primates there is a direct rNST–thalamic pathway (Beckstead, R. M. *et al.*, 1980). Although a gustatory relay in the primate PBN was initially considered unlikely, recent human imaging studies hint that a pontine relay may be a possibility in these species as well (Small, D. M. *et al.*, 2003; Topolovec, J. C. *et al.*, 2004). However, because the rostral pole of the monkey NST does not project to the PBN (Beckstead, R. M. *et al.*, 1980), nor are anterior tongue taste responses apparent in the pons (Pritchard, T. C. *et al.*, 2000), any gustatory PBN representation in primates is likely to arise from posterior tongue or pharyngeal taste buds (discussed in Travers, S. P., 1993).

In primates, taste-responsive neurons are also located in the orbitofrontal cortex and this area has typically been considered to constitute secondary GC (Baylis, L. L. *et al.*, 1995); taste-related activity

has recently been reported in an analogous region in rodents as well (Gutierrez, R. *et al.*, 2006). Further, emerging data, including human imaging studies, suggest that there is a high degree of complexity in cortical processing such that multiple hierarchical gustatory relays may be located within both the insular and orbitofrontal cortex (discussed in Pritchard, T. C. and Norgren, R., 2004). In addition to confirming the involvement of insular/opercular and orbitofrontal cortex in representing gustatory information in humans, imaging studies implicate other cortical areas, most consistently the cingulate, but also the posterior parietal or prefrontal, in processing some aspects of the gustatory signal (e.g., Small, D. M. *et al.*, 2003; 2004).

Cortical taste representation is complex with regard to its gustatory orotopic organization and relationship to the representation of innocuous somatosensation, visceral sensation, pain, and olfactory signals. Consistent with lower levels of the neuraxis, at least in subprimates, taste inputs to the cortex are arranged orotopically. Based on electrically stimulating the chorda tympani and glossopharyngeal nerves and recording evoked potentials (Benjamin, R. M. and Pfaffmann, C., 1955; Yamamoto, T. and Kawamura, Y., 1975; Yamamoto, T. *et al.*, 1980) or single units (Hanamori, T. *et al.*, 1997), information from the anterior oral cavity is located more anteriorly; that from the posterior oral cavity more posteriorly. A recent experiment using intrinsic optical imaging suggests that taste quality may also have a systematic topographic organization along the anterior–posterior axis in cortex. Although not exhibiting complete segregation, activity elicited by sweet and salty tastants (sucrose and NaCl) was located more anteriorly than that produced by stimulation with sour or bitter stimuli (citric acid and quinine) (Accolla, R. *et al.*, 2007).

4.15.3.1.1.(i) Taste–visceral relationships

Gustatory orotopy is actually part of a more extensive orderly topography in insular cortex, again mirroring the brainstem and thalamic organizations. The representation of inputs arising from the postoral gastrointestinal tract and other visceral organs extends posteriorly from the posterior oral cavity gustatory representation (Cechetto, D. F. and Saper, C. B., 1987; Squire, L. R. *et al.*, 2003). The degree of segregation or overlap between taste signals and visceral signals has not been thoroughly explored, but some degree of convergence onto single neurons in rodents seems likely (Yamamoto, T. *et al.*, 1989b; Hanamori, T. *et al.*, 1998a; 1998b; but see Cechetto, D. F. and Saper, C. B., 1987). In nonhuman primates, single-unit responses in the insula evoked by visceral stimulation have mostly been assessed indirectly, by noting how satiety affects gustatory responses. In the insular cortex, feeding a monkey to satiety does not alter the magnitude of gustatory responses (Yaxley, S. *et al.*, 1988), suggesting segregation between gustatory and visceral signals in this region. However, this segregation in the primary GC seems to be a major difference between monkeys and rodents, as in rodents, taste and visceral signals converge even at brainstem levels (e.g., Giza, B. K. *et al.*, 1992; Hajnal, A. *et al.*, 1999; Baird, J. P. *et al.*, 2001). In monkeys, convergence of taste and visceral signals has been reported to be a higher-level function first observed in the orbitofrontal cortex (Rolls, E. T. *et al.*, 1989; Pritchard, T. C. *et al.*, 2005), and is reflected in a decline of taste responses coincident with the onset of satiety. Interestingly, the decline in gustatory responsiveness is limited to the stimulus used to induce satiation, and this neural change parallels a specific change in behavior, a phenomenon termed sensory-specific satiety (Rolls, B. J. *et al.*, 1981; 1986). Human imaging studies further demonstrate that gustatory-evoked activity in the orbitofrontal cortex is altered by satiety (Kringelbach, M. L. *et al.*, 2003), although, in contrast to the monkey, insular responses also seem to be affected (Kringelbach, M. L. *et al.*, 2003; Smeets, P. A. *et al.*, 2006; Uher, R. *et al.*, 2006).

4.15.3.1.1.(ii) Taste–somatosensory relationships

As with lower levels of the neuraxis, gustatory responses in primary taste cortex have a proximate relationship with the representation of oral somatosensory, as well as visceral sensory inputs. The primary somatosensory cortex (S1) is comprised of somatosensory-specific neurons. In primates, S1 is located in Brodmann's areas 3a, 3b, 1, and 2. S1 in rodents is in a homologous location. In both species, S1 is medial to the primary gustatory representation in insular cortex. The somatotopy in S1 is arranged such that the oral representation is most lateral and abuts the gustatory-responsive zone (Squire, L. R. *et al.*, 2003). The extent to which there is a segregated region, comprised only of taste-responsive neurons, remains an unanswered question. There is evidence for an orderly medial-to-lateral progression of oral tactile, thermal, and gustatory responses, suggestive of a certain degree of segregation (Kosar, E. *et al.*, 1986a). However, other data indicate that cells responsive to oral mechanical stimulation are intermingled with taste cells in this region. Further, a large subset of

gustatory cortical neurons also respond to oral mechanical stimuli (Katz, D. B. *et al.*, 2001; Ogawa, H. and Wang, X. D., 2002; Wang, X. and Ogawa, H., 2002). In fact, taste cells with oral mechanical RF's have also been reported to receive additional inputs from remote regions of the glaborous skin of the body (Wang, X. and Ogawa, H., 2002). Thus it is tempting to conclude that nearly all cortical taste neurons also have a tactile input. However, as recently pointed out by Lundy R. F., Jr. and Norgren R. (2004b), only a few studies have actually tested responsiveness of insular neurons to both modalities, particularly in a quantitative fashion. Thus, though convergence seems pervasive, the relative magnitudes of taste and somatosensory responses within individual neurons are unclear (Wang, X. and Ogawa, H., 2002). Furthermore, since some converging somatosensory responses appear nociceptive since they require high pressures or pinch (Ogawa, H. and Wang, X. D., 2002), a more thorough examination is required to rule out nonspecific effects, such as arousal. Nevertheless, the apparent multimodal nature of many neurons in primary taste cortex raises the question of how these neurons are able to clearly code the presence of a taste apart from somatosensory stimuli. A proposed solution to this conundrum is the interesting suggestion that the different modalities are coded by temporally distinct components of the response; that is, the initial 0.5 s of the response codes somatosensory events and the subsequent response codes gustatory-specific information (Katz, D. B. *et al.*, 2001).

A novel hypothesis regarding the relationship of gustatory to somatosensory cortex was recently suggested by Kaas J. H. (2005) . Observations in primates have revealed an ever-expanding region for somatosensory cortex, indicating that it is much more extensive than evident in the original descriptions. Neurophysiological mapping studies indicate that multiple, higher-level somatosensory maps extend laterally from areas 3a, 3b, and 1 into the insula. These regions receive spinal and extraoral trigeminal, in addition to an intraoral representation, and arguably encompass what has classically been considered primary GC (e.g., Jain, N. *et al.*, 2001). These findings prompted Kaas J. H. to propose the provocative idea that there may be no pure primary GC, but instead, that the insular taste area is an integral part of the intraoral representations embedded in higher-order somatosensory zones. He further speculates that this may account for the common observation that single-unit studies observe only a small fraction of neurons in the insular GC that actually respond to taste stimulation (e.g., Scott, T. R. *et al.*, 1986; Plata-Salaman, C. R. *et al.*, 1996; Wang, X. and Ogawa, H., 2002). Although such a radical restructuring of the concept of primary GC is intriguing, further experiments are required for verification. Another possibility is that it is simply difficult to precisely locate the relatively small region receiving direct inputs from the gustatory thalamus (Pritchard, T. C. *et al.*, 1986), making it equally plausible that there is a small, more purely taste core adjacent to a larger area with mixed inputs.

The complexity of the insular region is also highlighted by discoveries about the nociceptive pathway. Neuroanatomical (Jasmin, L. *et al.*, 2004), neurophysiological (Ito, S. I., 1998; Hanamori, T. *et al.*, 1998b; Gauriau, C. and Bernard, J. F., 2004), and functional imaging studies (Petrovic, P. *et al.*, 2002; Bingel, U. *et al.*, 2003; Schweinhardt, P. *et al.*, 2006) in humans have identified the insular cortex as a major locus for processing pain information. These signals reach the insula via multiple pathways, including a spinoparabrachial pathway that relays through the ventroposteromedial and nearby regions of the thalamus (Menendez, L. *et al.*, 1996; Bester, H. *et al.*, 1999; Krout, K. E. and Loewy, A. D., 2000; Jasmin, L. *et al.*, 2004), and in primates through an additional evolutionarily newer direct spinal–thalamic–insular pathway that synapses in a posteriorly adjacent distinct nucleus in the thalamus, the posterior portion of the ventromedial nucleus (Craig, A. D., 2004). In fact, these pathways appear to carry not only nociceptive signals, but also thermal signals (Craig, A. D. *et al.*, 2000; Craig, A. D., 2003a; 2003b). The representation of pain, thermal, visceral, and taste information in the insular cortex has led to the suggestion that it is a region unified for processing the homeostatic state of the body (Craig, A. D., 2003a; 2003b).

4.15.3.1.1.(iii) Taste–olfactory relationships

Because the everyday appreciation of food and drink does not rely on taste alone, but rather on the combination of taste with oral somatosensory and olfactory sensations, it is especially important to understand where these two types of chemical signals converge centrally. The first point of convergence appears to be in the forebrain, but neither the initial site of convergence nor the responsible pathway(s) is entirely clear. Furthermore, species differences are likely. In the rodent, anatomical data suggest that olfactory information can impact the insular cortex via a least two routes, a direct projection from the olfactory bulb (Shipley, M. T. and Geinisman, Y., 1984), or a connection from the endopyriform

nucleus (Behan, M. and Haberly, L. B., 1999; Fu, W. *et al.*, 2004). However, whether the insular area described in these studies is actually gustatory is not certain, nor is it clear that olfactory signals actually converge on a significant proportion of taste cells in rodent insular cortex. Other sites of forebrain convergence are also possible. A recent optical imaging/recording brain slice study demonstrated that signals from the pyriform (olfactory) and dysgranular (probably taste) insular cortex both reach the endopyriform nucleus, and converge on single cells (Fu, W. *et al.*, 2004). In addition, another forebrain region, the amygdalopyriform transition area, seems to receive relatively direct olfactory and gustatory information over a different route (Santiago, A. C. and Shammah-Lagnado, S. J., 2005). In this case, the olfactory inputs arise from neurons in the pyriform cortex, whereas putative gustatory inputs arise from the parabrachial nucleus. That the parabrachial input is gustatory seems quite likely because the cells of origin depicted in photomicrographs are centered in precisely the same part of the waist region where electrophysiological studies routinely report taste responses (e.g., Norgren, R. and Pfaffmann, C., 1975). There has not been a systematic neurophysiological investigation of gustatory–olfactory convergence in the rodent forebrain, although one report did document a few such convergent cells in insular cortex (Yamamoto, T. *et al.*, 1989b). In contrast, in the monkey, responses to both taste and olfactory stimulation have been recorded from significant populations of single neurons in the lateral orbitofrontal cortex (Rolls, E. T. and Baylis, L. L., 1994), although such convergence has not been observed in the insula. However, it may be premature to rule out taste–olfactory convergence in the insula. Indeed, as summarized by Small, D. M. and Prescott, J. (2005), human imaging studies reveal that olfactory stimuli activate the same insular and orbitofrontal regions as do tastants, although the obverse is not true for primary olfactory cortex. Imaging studies also indicate other cortical regions where taste and smell interact or overlap, with the anterior cingulate being particularly notable. Importantly, the human imaging studies point to critical integrative features of this convergence; that is, synergy between taste and olfactory signals occurs prominently with retronasal but not orthonasal olfactory signals (Small, D. M. *et al.*, 2005) and further requires that the taste and olfactory signals are congruent (Figure 8). Thus a

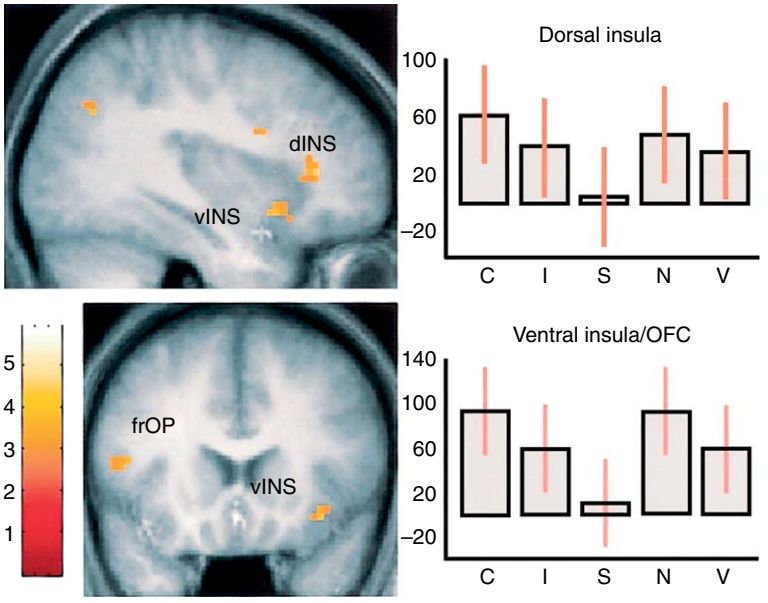

Figure 8 Functional magnetic resonance imaging (fMRI) activation of the insular region following presentation of a sweet stimulus (0.18 M sucrose) mixed with vanilla. Both the dorsal insula (primary gustatory cortex) and the ventral insula, a higher-order processing region, are activated in a supra-additive fashion by this congruent, familiar mixture. The graphs on the right depict these results quantitatively and compare the sucrose–vanilla congruent mixture (C), with an incongruent mixture (NaCl–vanilla, I), and with each of the components alone. S, sucrose; N, NaCl; V, vanilla. (a) From Small, D. M., Voss, J., Mak, Y. E., Simmons, K .B., Parrish, T., and Gitelman, D. 2004. Experience-dependent neural integration of taste and smell in the human brain. J. Neurophysiol. 92, 1892–1903, with permission.

familiar olfactory–taste pair, vanilla–sweet, yielded superadditive functional magnetic resonance imaging (fMRI) responses in the insula and several other forebrain regions but an unfamiliar, incongruent pair, vanilla–salty, did not (Small, D. M. *et al.*, 2004).

4.15.3.1.2 Gustatory cell types and processing

4.15.3.1.2.(i) Response profiles and firing rates

Compared to other sensory systems, the transformation of gustatory information by cortical circuits at first glance seems subtle. Some differences have been reported, for example, a minority of insular neurons in the rat appeared to code palatability rather than quality (Yamamoto, T. *et al.*, 1989b). Nevertheless, in both rodents (Yamamoto, T. *et al.*, 1985; 1989b; Ogawa, H. *et al.*, 1992) and primates (Yaxley, S. *et al.*, 1990), many studies of primary GC have yielded reports of best-stimulus neurons quite similar to those in peripheral nerves and brainstem. The same is true for neurons in caudolateral (secondary) GC (Baylis, L. L. and Rolls, E. T., 1991) though, as noted above, more modulation by satiety and interaction with other modalities probably occurs in this higher-order cortex. On the face of it, the lack of an obvious transformation at the cortical level is not due to using restricted stimulus arrays, or suppressed cortical activity in anesthetized preparations. A significant number of these studies used large numbers of tastants (e.g., Smith-Swintosky, V. L. *et al.*, 1991; Plata-Salaman, C. R. *et al.*, 1992; 1993; Scott, T. R. *et al.*, 1994; Plata-Salaman, C. R. *et al.*, 1995; Scott, T. R. *et al.*, 1999), included taste mixtures (Miyaoka, Y. and Pritchard, T. C., 1996; Plata-Salaman, C. R. *et al.*, 1996), and many were carried out in awake preparations.

Though the relative response profiles appear similar to those at lower levels of the neuraxis, it is notable that lower response rates are often characteristic of cortical taste cells. In addition, in contrast to the concentrated populations of taste neurons found in the brainstem, gustatory cortical neurons often appear to be intermingled with a larger population of nongustatory cells (e.g., Scott, T. R. *et al.*, 1986; Plata-Salaman, C. R. *et al.*, 1996; Wang, X. and Ogawa, H., 2002). The reason for this apparent sparseness is not known. As discussed above, Kaas J. H. (2005) suggests that one possibility is that multiple gustatory cortical regions are intertwined with secondary somatosensory cortex; that is, there is no pure GC. Another possibility is suggested by the findings of Pritchard T. C. *et al.* (2005). These investigators recently explored a different cortical area in monkey, the medial orbitofrontal cortex, a region implicated in taste function by anatomical experiments. In this previously unexplored area, the proportion of taste cells was markedly higher than in many other cortical studies. A careful reconstruction of recording sites showed that the incidence of gustatory cells was highly dependent upon the exact recording location; the concentrated core of taste-responsive neurons was very restricted. This suggests that some apparent sparseness in other studies could be due to the inherent technical difficulties in precisely targeting gustatory cortical regions, particularly in chronic recording studies. Interestingly, this study hints at another possible reason for sparseness since 24% of the neurons did not respond significantly to any of the four standard tastants but did respond to another (but unspecified) taste stimulus. This finding emphasizes that much remains to be learned about what constitutes the optimal stimulus configuration for cortical cells. Thus, cortical neurons may require more specific taste stimuli, combinations of taste stimuli or gustatory stimulation coincident with inputs from other modalities. For example, some taste cells may require particular combinations of learned taste and olfactory stimuli, as suggested by the human imaging studies (Small, D. M. *et al.*, 2004), or more speculatively, other learned combinations such as mixtures of different tastes, or of specific taste/texture combinations.

4.15.3.1.2.(ii) Breadth of tuning As discussed above, central neurons are, on average, more broadly tuned than those in the periphery. However, there are divergent reports concerning whether there is a systematic trend for tuning to broaden (Stapleton, J. R. *et al.*, 2006), sharpen (Scott, T. R. *et al.*, 1986; Rolls, E. T. *et al.*, 1990), or remain unchanged in cortex, compared to the brainstem (summarized in Spector, A. C. and Travers, S. P., 2005). At present, it is difficult to resolve this issue, in part, due to the variety of animal models (rodent, primate), types of preparation (acute anesthetized, chronic awake), recording procedures (single-unit sharp electrode; microwire bundles), and analytic techniques (summed activity, time course) used in the cortical experiments. Chronic, awake preparations arguably provide the most powerful tool for revealing the full range of responsiveness of central sensory neurons. This is particularly true for the cortex, because of the profound anesthetic suppression of sensory responses at this level of the nervous system (Sloan, T. B., 1998), as well as the active behaviors

sometimes required for revealing cortical response properties (e.g., Krupa, D. J. *et al.*, 2004). However, even when consideration is limited to awake preparations, varied tuning curves are apparent between studies. For example, although both groups of investigators recorded from a similar cortical region with microwire bundles, Stapleton, J. R. *et al.* (2006) reported an *H* value of 0.97, indicating that different stimuli evoked responses of roughly equal magnitude, whereas Yamamoto T. *et al.* (1989b) reported an average *H* value of 0.54, indicating much more specificity. In fact, although they tend to be more consistent, varied tuning curves can be observed within studies; in a typical instance, Pritchard T. C. *et al.* (2005) reported *H* values that ranged from 0.28 to 0.98. Thus, one conclusion emphasized in another recent review is that central tuning curves are inherently heterogeneous, including both narrowly and broadly tuned neurons best suited to subserve distinct functions, such as perception, motivation, and learning (Spector, A. C. and Travers, S. P., 2005).

4.15.3.1.2.(iii) Response time course, behavioral context Other more recent perspectives for devising a taste code involve alternate analyses which take time course and behavioral context into account (Katz, D. B. *et al.*, 2001; 2002; Hallock, R. M. and Di Lorenzo, P. M., 2006; Stapleton, J. R. *et al.*, 2006). In one experiment that analyzed just the initial 150 ms of the response, firing rates alone indicated almost no stimulus specificity, but when time course was considered, more specificity emerged (Stapleton, J. R. *et al.*, 2006). Another report of insular neurons not only observed very broadly tuned cells, but further found that the tuning curves of many neurons changed during a single experimental session, in parallel with decreases in the animal's attentional state (Fontanini, A. and Katz, D. B., 2006). Thus, unlike most previous studies, these recent reports provide little evidence for the classic best stimulus categories of neurons based on differential response magnitudes. Instead, they focus on the complex dynamic features of gustatory cortical responses and the key influence of behavioral state. It is important to point out, however, that the differences apparent in these more recent studies are probably due not only to differences in the type of analysis or behavioral paradigm, but also from differences in sampled populations. Although earlier studies similarly used awake animals, they also typically tested each stimulus on just a few trials and used simple response measures of summed activity; thus, taste responses were defined on the basis of relatively obvious changes in response rate (e.g., Scott, T. R. *et al.*, 1986; Yamamoto, T. *et al.*, 1989b; Rolls, E. T. *et al.*, 1990; Pritchard, T. C. *et al.*, 2005). In contrast, many current studies that take time course into account also tend to perform many repeated trials, a combination that adds a great deal of statistical power for identifying variations in neuronal firing. Such approaches extend the taste-responsive population to neurons that formerly would not have been considered to be gustatory (Katz, D. B. *et al.*, 2001). To what extent they include those neurons with more obvious responses is not entirely clear. Furthermore, the advantage conferred by this increased statistical power makes it important to demonstrate that these relatively subtle, but statistically demonstrable changes in time course or magnitude are behaviorally meaningful, as well as to attend to potential contributions from nearby oral thermal and tactile neurons. Nevertheless, it is clear that studies in behaving animals that use more complex behavioral paradigms and more powerful analytic techniques have great potential.

A particularly intriguing study has shed additional light on the function of rodent orbitofrontal cortex as it relates to rewarding tastes and voluntary ingestive behavior (Gutierrez, R. *et al.*, 2006; Travers, J. B., 2006). Neurons in this area of the cortex exhibited clear modulations of activity predictive of the beginning, occurrence, or end of a licking bout (Figure 9), and were more subtly modified depending on whether the rat was drinking sucrose or water. Thus, similar to what has been suggested for primate (Rolls, E. T. and Scott, T. R., 2003), rodent orbitofrontal cortex appears to monitor the reward value of tastes, and play a direct role in controlling reward-seeking behavior. Indeed, temporary inactivation of the rat orbitofrontal cortex with a $GABA_A$ agonist, muscimol, altered the microstructure of licking behavior. Overall intake remained relatively stable, but ingestion occurred in shorter bouts, indicative of a disruption of appetitive behavior (Gutierrez, R. *et al.*, 2006).

4.15.3.1.3 Neurotransmitters and neuromodulators in the insular cortex

4.15.3.1.3.(i) Excitatory amino acids In GC, a large variety of neurotransmitters, modulators, and their receptors comprise a rich substrate for processing sensory information. Taste responses in the majority of rat insular cortex neurons are dependent on glutamatergic input acting via non-NMDA, as well as NMDA receptors (Otawa, S. *et al.*, 1995), implying that

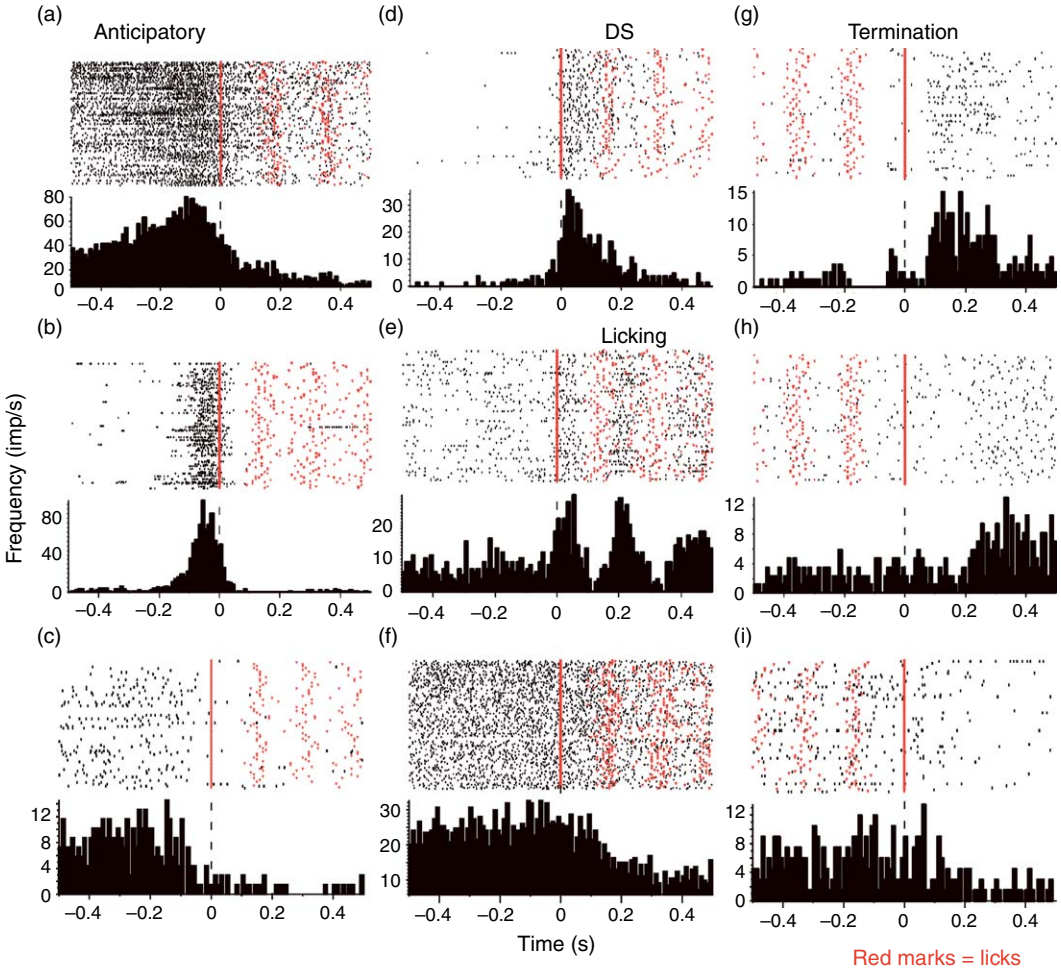

Figure 9 Responses of orbitofrontal cortex neurons prior to, during, and after bouts of licking 0.4 M sucrose. Each graph shows a different neuron, and depicts raster displays for multiple trials above a summed perievent histogram. The red dashes indicate licks. Each neuron exhibits a unique response pattern, but each column shows a given type based on whether the neuron alters its firing rate prior to a licking bout (Anticipatory), during the licking bout/stimulus (DS), or after the termination of the bout (Termination). From Gutierrez, R., Carmena, J. M., Nicolelis, M. A., and Simon, S. A. 2006. Orbitofrontal ensemble activity monitors licking and distinguishes among natural rewards. J. Neurophysiol. 95, 119–133, with permission.

glutamate is a key transmitter in the thalamocortical projection. Interestingly, in distinct contrast to the NST, NMDA receptor antagonists were as potent at reducing taste responses as non-NMDA antagonists, perhaps reflecting the greater plasticity inherent in cortical regions (Otawa, S. *et al.*, 1995). Ogawa and his group further demonstrated that both spontaneous and taste-evoked activity in the insular cortex is modulated by inhibitory amino acids, ACh, and peptides (Ogawa, H. *et al.*, 1998; 2000; Hasegawa, K. and Ogawa, H., 2007). These neurotransmitter systems likely play a major role in taste processing as 40–60% of insular cells were sensitive to iontophoresis of their antagonists and agonists.

4.15.3.1.3.(ii) Gamma-aminobutyric acid Similar to the NST, gustatory cortical neurons appear to be under tonic inhibition (Ogawa, H. *et al.*, 1998). Iontophoresis of the $GABA_A$ antagonist, bicuculline, onto insular cortical neurons yielded increases in spontaneous rate in 69% of the taste neurons sampled. Interestingly, only 51% of the entire population of insular cortical neurons (taste and nontaste combined) exhibited such an effect, suggesting that gustatory neurons may be subject to a greater degree of tonic inhibition than surrounding cells. Bicuculline exerted an effect on the taste responses themselves in a somewhat smaller (38%) but still significant proportion of neurons. As expected, taste responses

usually increased following bicuculline application; however, a more surprising outcome was that the increases were stimulus specific. These differential effects produced marked alterations in response profiles, including changes of best-stimulus and breadth of tuning (Figure 10).

Similar to the effects of bicuculline in the somatosensory cortex (Dykes, R. W. *et al.*, 1984; Tremere, L. *et al.*, 2001), receptive field size of gustatory neurons also increased when $GABA_A$ inhibition was removed. Before drug application most neurons had receptive fields restricted to the anterior tongue, but after bicuculline, inputs from the posterior tongue and palate became apparent. A particularly dramatic outcome was the recruitment of previously silent neurons that lacked both spontaneous and evoked activity; after bicuculline, these neurons became responsive to taste stimuli.

4.15.3.1.3.(iii) Acetylcholine ACh also affected taste responses in a substantial proportion (63%) of insular neurons but spontaneous rate was affected less often (17%; Hasegawa, K. and Ogawa, H., 2007). In contrast to bicuculline, iontophoresis of ACh both increased and decreased gustatory responses, though the action was usually in the same direction for different stimuli in a given cell. Nevertheless, within cells, responses to different

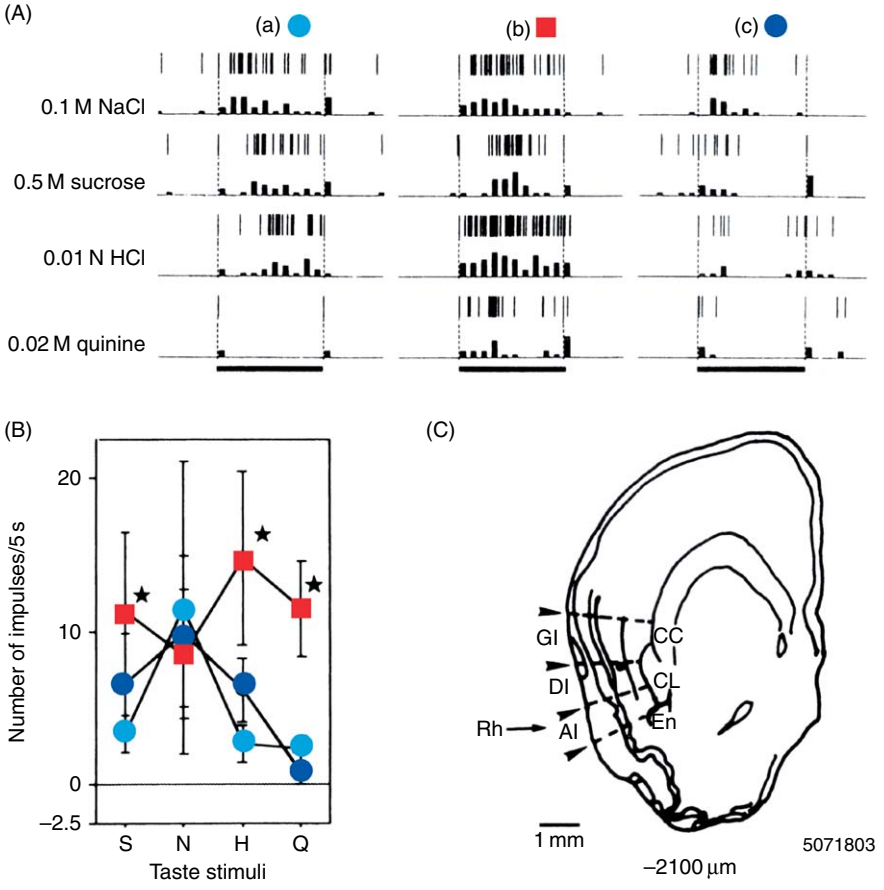

Figure 10 Example of an insular cortical neuron in which taste responses were increased in a stimulus-specific manner by the gamma-aminobutyric acid ($GABA_A$) antagonist, bicuculline. (A) Perievent histograms of a single trial (a) before, (b) during, and (c) after iontophoresis of bicuculline. (B) Mean responses for 5 s summed activity before (dark blue circles), during (red squares), and after (light blue circles). Before application of the $GABA_A$ antagonist, the neuron responded most robustly to NaCl but weakly to quinine. Following bicuculline, all of the responses, except that to NaCl, were significantly increased (asterisks), resulting in a best-stimulus change from NaCl to HCl, and an increase in breadth of tuning. (C) Location of the recorded cell in dysgranular insular (DI) cortex adapted from Ogawa, H., Hasegawa, K., Otawa, S., and Ikeda, I. 1998. GABAergic inhibition and modifications of taste responses in the cortical taste area in rats. Neurosci. Res. 32, 85–95, with permission.

stimuli were affected to varying extents, producing a net change in the chemosensitive profile, rather than a simple change in the overall level of responsiveness. Indeed the best stimulus changed in nearly half (19/43) of the cells. In contrast to other sensory cortical areas where ACh seems to sharpen tuning profiles (e.g., Sillito, A. M. and Kemp, J. A., 1983), ACh effects in taste cortex were more complex, and could give rise to either increases or decreases in neuronal selectivity. In about 2/3 of the cases, atropine antagonized the actions of ACh, suggesting a muscarinic basis; however, the remaining third of the effects were presumably nicotinic.

4.15.3.1.3.(iv) Peptides Consistent with the presence of SP and calcitonin gene-related peptide (CGRP) fibers in insular cortex, (Mantyh, P. W. and Hunt, S. P., 1984; Yasui, Y. *et al.*, 1989; Yamamoto, T. *et al.*, 1990), both peptides altered spontaneous rate, as well as taste responses in gustatory cells (Ogawa, H. *et al.*, 2000). Spontaneous rate was affected in 40% of neurons and the effects were largely (~86%) facilitory, consistent with the known cellular actions of the NK1 and CGRP receptors (Strand, F., 1999). Somewhat surprisingly, although these peptides also altered taste responses in a large proportion of insular neurons (~50%), the effects were mainly suppressive; that is, opposite to the effects on spontaneous rate, suggestive of an indirect effect through inhibitory interneurons. Furthermore, these peptides modulated responses to various taste stimuli to different degrees within individual neurons. Thus, for the three neurotransmitter systems evaluated so far, each is associated with unique net effects on spontaneous and evoked activity. However, all produce stimulus-specific alterations, which give rise to changes in response profiles in individual neurons. These diverse actions seem well suited to provide the substrate for cortical plasticity, such as those instances that have been observed during alterations of attentional state and homeostasis discussed above.

4.15.3.1.3.(v) Neurochemical substrate for conditioned taste aversion Analysis of the insular substrate important for conditioned taste aversion provides additional insights into the functions of the various neurotransmitters in taste cortex. Insular infusions of muscarinic antagonists blunt the acquisition of a conditioned taste aversion, but only if they are given prior to taste exposure, suggesting that that ACh impacts critical aspects of processing the taste signal (Ferreira, G. *et al.*, 2002). However, the effect is not simply on taste perception since infusions prior to retrieval are ineffective (Naor, C. and Dudai, Y., 1996; Berman, D. E. *et al.*, 2000). Interestingly, novel taste stimuli are much more potent in establishing an aversion, and microdialysis experiments have revealed that novel but not familiar taste stimuli elicit ACh release in the insular cortex (Miranda, M. I. *et al.*, 2000). There appears to be a complex relationship between stimulus novelty and muscarinic action in the insula, however, as muscarinic antagonists interfere only with the attenuation of neophobia, but do not abolish neophobia itself (reviewed in Bermudez-Rattoni, F. *et al.*, 2004). NMDA antagonists also blunt the acquisition of a conditioned taste aversion (Rosenblum, K. *et al.*, 1997; Gutierrez, H. *et al.*, 1999; Ferreira, G. *et al.*, 2002), but unlike muscarinic agonists, have effects when injected either before or after the presentation of the taste stimulus (Ferreira, G. *et al.*, 2002). Beta adrenergic antagonists also interfere with acquisition of a conditioned taste aversion, and unlike NMDA or muscarinic receptors, interfere with extinction once the aversion is established (Berman, D. E. and Dudai, Y., 2001). Thus multiple cortical transmitter systems have specific effects on this learned behavior. Although some of these effects may be due to short-term modulations of taste or visceral responses and second messenger systems, it is clear that long-term retention of conditioned taste aversion requires protein synthesis in insular cortex (Rosenblum, K. *et al.*, 1993). The immediate-early gene, c-fos, is a transcription factor that is differentially upregulated in the insular cortex upon exposure to novel taste stimuli (Koh, M. T. and Bernstein, I. L., 2005) and appears to serve as a critical intermediary, at least for protein synthesis required for conditioned taste aversion retention (Yasoshima, Y. *et al.*, 2006). The downstream targets of this gene are unknown, but an earlier report suggested that the amount of CGRP in insular cortex was higher after exposure to aversive compared to preferred stimuli, including a previously preferred stimulus, to which a conditioned taste aversion had been given (Yamamoto, T. *et al.*, 1990). Although this discussion focuses on the role of insular cortex in conditioned taste aversion, this does not imply that the cortex is the sole substrate for this behavior. Instead, interactions between cortical (e.g., Schafe, G. E. and Bernstein, I. L., 1998), subcortical (e.g., Schafe, G. E. and Bernstein, I. L., 1996), and brainstem sites (e.g., Reilly, S. *et al.*, 1993) are critical.

4.15.3.2 Limbic Forebrain

Structures in the limbic forebrain and hypothalamus are intimately involved in motivated behaviors, including ingestion. To maintain homeostasis, a complex neural network must integrate a wide variety of internal and external signals with past experience. Although the final consummatory sequences of eating and drinking are characterized by relatively fixed, species-specific patterns of oromotor movements, the appetitive behaviors necessary to reach this endpoint must be flexible in order to accommodate changing environmental demands. The ventral forebrain receives all the relevant information to accomplish this task, including gustatory signals.

The highly interconnected nature of forebrain circuits suggests that taste has the potential to influence a large number of limbic and hypothalamic structures. As shown in Figure 1, in the rodent, anatomical tracing experiments have demonstrated direct projections from the taste-responsive regions in the parabrachial nucleus to the central nucleus of the amygdala and the bed nucleus of the stria terminalis, as well to a contiguous ventral region including the lateral hypothalamus, substantia innominata, fundus striatum, and ventral pallidum (Norgren, R. and Leonard, C. M., 1973; Norgren, R., 1974; 1976; Bernard, J. F. *et al.*, 1993; Alden, M. *et al.*, 1994; Karimnamazi, H. and Travers, J. B., 1998). In the primate, gustatory information reaches many of these same structures, but the most direct route is likely through connections from the GC (discussed in Pritchard, T. C. and Norgren, R., 2004). In addition to this anatomical evidence, antidromic activation has been used to verify that some of the projections to the rodent lateral hypothalamus, substantia innominata, and amygdala do carry taste information (Norgren, R., 1974; 1976); this has not yet been demonstrated for the other sites. Besides this direct pathway from the PBN, there are a number of potential indirect pathways to these regions, and others. Of particular note is the projection from the insular cortex to the nucleus accumbens (Reynolds, S. M. and Zahm, D. S., 2005), a structure with a prominent role in motivational processes. However, the insular–accumbens projection does not appear to be from the primary taste cortex, that is, it is not from the dysgranular region, which receives a direct projection from the gustatory thalamus (Kosar, E. *et al.*, 1986b), nor the surrounding granular cortex, where taste responses have also been recorded (Ogawa, H. *et al.*, 1992), but rather from the ventrally adjacent agranular insular cortex (Reynolds, S. M. and Zahm, D. S., 2005). However, the dysgranular insular cortex projects to the agranular (Shi, C. J. and Cassell, M. D., 1998), providing a potential pathway for taste information to reach nucleus accumbens.

Taste responses in the limbic forebrain have been studied most frequently in the lateral hypothalamus (Burton, M. J. *et al.*, 1976; Ono, T. *et al.*, 1986; Rolls, E. T. *et al.*, 1986; Schwartzbaum, J. S., 1988) and amygdala, with an emphasis on the central nucleus (Yan, J. and Scott, T. R., 1996; Nishijo, H. *et al.*, 1998). A more recent focus has been on the nucleus accumbens (Roitman, M. F. *et al.*, 2005; Taha, S. A. and Fields, H. L., 2005) and ventral pallidum (Tindell, A. J. *et al.*, 2004; 2006). Virtually all of the recording preparations assessing gustatory responsiveness in the limbic forebrain utilize awake, behaving animals, presumably because such responses would be difficult to detect in anesthetized preparations (but see Azuma, S. *et al.*, 1984). Ample evidence for a taste influence on the limbic forebrain is provided from a score of reports of presumptive taste responses observed in the context of food or fluid rewards obtained in operant tasks. Often, these same cells are influenced by other unconditioned sensory stimuli like olfaction, or other aspects of the task, including the onset or offset of the conditioned stimulus or operant responding (e.g., Rolls, E. T. *et al.*, 1979; Sanghera, M. K. *et al.*, 1979; Schwartzbaum, J. S., 1988; Yamamoto, T. *et al.*, 1989a; Oomura, Y. *et al.*, 1991; Williams, G. V. *et al.*, 1993; Tindell, A. J. *et al.*, 2004). There is less information on the detailed nature of gustatory processing in these circuits. In the lateral hypothalamus and central nucleus of the amygdala, it is clear that taste influences just a limited proportion of encountered neurons (Schwartzbaum, J. S., 1988; Yan, J. and Scott, T. R., 1996; Nishijo, H. *et al.*, 2000), suggesting that they are a specialized population. In the nucleus accumbens and ventral pallidum, a larger proportion of neurons seems to be active during taste stimulation (Tindell, A. J. *et al.*, 2004; Roitman, M. F. *et al.*, 2005; Taha, S. A. and Fields, H. L., 2005; Tindell, A. J. *et al.*, 2006), but since different testing paradigms have been used in the various areas, direct comparisons are difficult. Compared to what is known about the thalamocortical pathway, gustatory-modulated neurons in all of the limbic-related regions appear to have a wider variety of nongustatory inputs (Oomura, Y. *et al.*, 1991; Karadi, Z. *et al.*, 1992; Nishijo, H. *et al.*, 1998), and frequently exhibit marked decrements, as well as increments in firing, in response to taste stimuli (Schwartzbaum, J. S., 1988; Oomura, Y. *et al.*, 1991; Roitman, M. F. *et al.*, 2005). Although single neurons

in the lateral hypothalamus (Yan, J. and Scott, T. R., 1996) and amygdala (Scott, T. R. *et al.*, 1993; Nishijo, H. *et al.*, 1998), respond differentially to different tastants, they do not appear to code for quality, *per se*. A systematic comparison of amygdalar and PBN taste responses in the rat instead suggested that the distinctions that amygdalar neurons make are more simply related to binary palatability decisions than those in the PBN, which make additional distinctions between different tastants (Nishijo, H. *et al.*, 1998); a detailed study in the monkey came to a similar conclusion (Scott, T. R. *et al.*, 1993). The pervasive influence of satiety on taste responses in the lateral hypothalamus and amygdala suppots a primary role for these cells in coding palatability (Burton, M. J. *et al.*, 1976; Rolls, E. T. *et al.*, 1986; Yan, J. and Scott, T. R., 1996).

Likewise, palatability appears to be a critical stimulus dimension for neurons in the nucleus accumbens and ventral pallidum. Previous studies had suggested that nucleus accumbens neurons responded to rewarding stimuli, including sweet tastes but the apparent gustatory responses had been observed during operant tasks (e.g., Nicola, S. M. *et al.*, 2004), making it unclear whether they were were innate or instead required learning and/or a more complex behavioral context. In addition, little attention had been paid to stimuli at the opposite end of the spectrum. A recent study that utilized stimulus delivery via intraoral cannulas indeed demonstrated that the hedonically negative taste stimulus, quinine, as well as hedonically positive sucrose, could drive accumbens neurons and that the responses were apparent when the animal initially encountered the gustatory stimuli; that is, learning was not required (Roitman, M. F. *et al.*, 2005). Further, different neurons responded to sucrose and quinine. Over the course of several trials, these taste cells in accumbens also developed distinctive responses to the conditioned visual and auditory stimuli that signaled tastant delivery. Similar to the unconditioned responses to the tastants themselves, neurons that responded to the sucrose cue were mostly separate from those responsive to the quinine cue although the relationships between the conditioned and unconditioned responses were complicated. This study also suggested that, for the most part, sucrose- and quinine-responsive neurons responded differentially, that is, with response decrements and increments, respectively. Another description of accumbens taste responses provides a different perspective on the significance of the excitatory and inhibitory responses (Taha, S. A. and Fields, H. L., 2005). These investigators observed accumbens activity while water-deprived rats licked water and varying concentrations of sucrose. Similar to what Roitman and coworkers observed, most responses to sucrose were inhibitory. However, these inhibitory responses appeared most directly related to the licking behavior, *per se*. Decrements did not vary as a function of sucrose concentration, and licking to water or even a dry spout resulted in similar decreases in firing rate. However, in agreement with the other report, these investigators also observed a small population of sucrose-driven responses, which exhibited positive concentration–response functions. Furthermore, the excitatory responses were modulated by context, since a given concentration of sucrose elicited larger responses when paired with water, than with a higher concentration of sugar. Such a contrast paradigm is well-known to change the reward value of a gustatory stimulus (Flaherty, C. F. *et al.*, 1994).

The ventral pallidum, a target of accumbens projections (reviewed in Zahm, D. S., 2000) also contains gustatory-responsive neurons whose firing rates are modulated by the hedonic nature of the stimulus (Tindell, A. J. *et al.*, 2004; 2006). An experiment which tracked pallidal taste responses before, during, and after induction of a salt appetite is particularly illuminating in this regard (Tindell, A. J. *et al.*, 2006) (Figure 11).

Prior to and following sodium deprivation, ventral pallidal neurons responded more robustly to a highly preferred concentration of sucrose (0.5 M) than to a highly aversive, hypertonic (1.5 M) concentration of sodium chloride. Following deprivation, this same concentration of salt elicited parallel increases in positively hedonic behaviors and firing in ventral pallidal neurons. In fact, firing rates to sodium were now equivalent to those elicited by sucrose. Interestingly, deprivation also caused pallidal neurons to become more broadly tuned, at least with regard to the limited number of taste qualities tested. When neurons were classified as a function of responsiveness to sucrose, salt, and water, the largest proportion of neurons responded to one of the stimuli prior to deprivation, in contrast to all three during the deprived state. These results provide a rather dramatic example of gustatory malleability in the face of changing homeostatic demands.

4.15.4 Conclusions

The critical role of the gustatory system in guiding feeding behavior is accomplished by a network characterized by a high degree of discriminative and

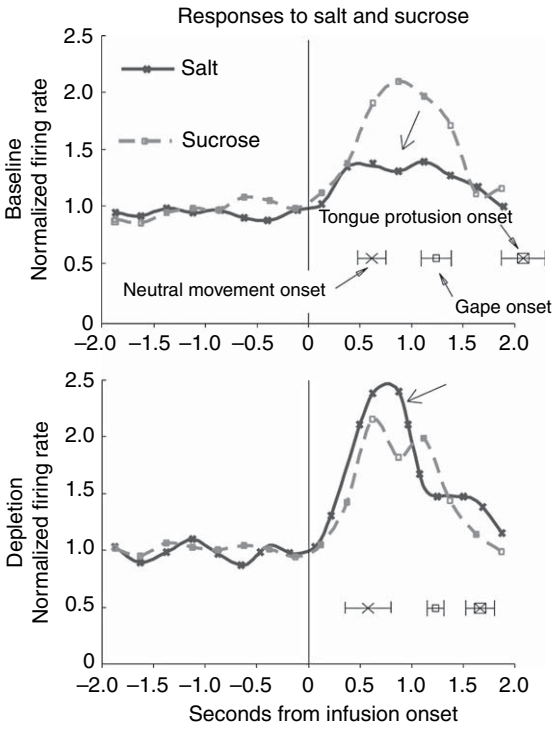

Figure 11 Mean firing rate of ventral pallidum neurons during infusions of 0.5 M sucrose (dotted line) and 1.5 M NaCl (solid line) during a normal homeostatic state (top graph) and during sodium deprivation (bottom graph). In the normal state, palatable sucrose induces a brief, twofold increase in firing rate but NaCl elicits a much smaller response. Under the sodium deprivation condition, when NaCl is as palatable as sucrose, both stimuli elicit similar increases in the activity of ventral pallidal neurons. The symbols beneath the neural responses indicate the onset of the oromotor responses elicited by these stimuli. The onset of the neural response precedes licking or gaping, but is not tightly coupled to these behaviors. From Tindell, A. J., Smith, K. S., Pecina, S., Berridge, K. C. and Aldridge, J. W. 2006. Ventral pallidum firing codes hedonic reward: when a bad taste turns good. J. Neurophysiol. 96, 2399–2409, with permission.

integrative capacity, and an equally high degree of plasticity necessary to meet shifting environmental and homeostatic demands. The operations of this system have become increasingly clarified, but key questions remain unanswered. First, the central code(s) for taste quality remains an area of active investigation (see Chapters Neural Ensembles in Taste Coding and A Perspective on Chemosensory Quality Coding). The broad tuning of many central neurons is suggestive of an ensemble code, but its precise nature, including the size and dynamic aspects of the necessary ensemble, are just now coming to light. In addition, there is a subset of more narrowly tuned central neurons. It is unclear whether such cells simply comprise part of an ensemble code, or instead are a specialized subpopulation that uses a sparse code to accomplish particular functions. It has become increasingly apparent that single central taste neurons also can respond to olfactory and somatosensory stimuli. The likely function of such convergence is to give rise to the compound sensation of flavor. Human imaging studies further suggest that integration between modalities not only requires special combinations of stimuli, but also relies upon learning. However, the way in which single gustatory neurons combine these multiple aspects of a compound flavor stimulus signals requires much more scrutiny. Similarly, the list of manipulations that can modify taste responses, including changes in homeostatic state, learning, modulation by neurotransmitters, and activiation of other neural structures, is continuing to grow. The challenge is to be able to define how these changes relate mechanistically to one another, and which changes in neural responsiveness comprise the critical alternations that drive adaptive behavior.

References

Accolla, R., Bathellier, B., Petersen, C. C. H., and Carleton, A. 2007. Differential spatial representation of taste modalities in the rat gustatory cortex. J. Neurosci. 27, 1396–1404.

Alden, M., Besson, J. M., and Bernard, J. F. 1994. Organization of the efferent projections from the pontine parabrachial area to the bed nucleus of the stria terminalis and neighboring regions: a PHA-L study in the rat. J. Comp. Neurol. 341, 289–314.

Allen, G. V., Saper, C. B., Hurley, K. M., and Cechetto, D. F. 1991. Organization of visceral and limbic connections in the insular cortex of the rat. J. Comp. Neurol. 311, 1–16.

Andresen, M. and Yang, M. 1994. Excitatory Amino Acid Receptors and Afferent Synaptic Transmission in The Nucleus Tractus Solitarius. In: Nucleus of the Solitary Tract (*ed*. I. Barraco), pp. 187–192. CRC Press.

Atema, J. 1971. Structures and functions of the sense of taste in the catfish (*Ictalurus natalis*). Brain Behav. Evol. 4, 273–294.

Azuma, S., Yamamoto, T., and Kawamura, Y. 1984. Studies on gustatory responses of amygdaloid neurons in rats. Exp. Brain Res. 56, 12–22.

Baird, J. P., Travers, S. P., and Travers, J. B. 2001. Integration of gastric distension and gustatory responses in the parabrachial nucleus. Am. J. Physiol. Regul. Integr. Comp. Physiol. 281, R1581–R1593.

Bardach, J. E., Todd, J. H., and Crickmer, R. 1967. Orientation by taste in fish of the genus Ictalurus. Science 155, 1276–1278.

Barry, M. A., Haglund, S., and Savoy, L. D. 2001. Association of extracellular acetylcholinesterase with gustatory nerve terminal fibers in the nucleus of the solitary tract. Brain Res. 921, 12–20.

Baylis, L. L. and Rolls, E. T. 1991. Responses of neurons in the primate taste cortex to glutamate. Physiol. Behav. 49, 973–979.

Baylis, L. L., Rolls, E. T., and Baylis, G. C. 1995. Afferent connections of the caudolateral orbitofrontal cortex taste area of the primate. Neuroscience 64, 801–812.

Beckstead, R. M. and Norgren, R. 1979. An autoradiographic examination of the central distribution of the trigeminal, facial, glossopharyngeal, and vagal nerves in the monkey. J. Comp. Neurol. 184, 455–472.

Beckstead, R. M., Morse, J. R., and Norgren, R. 1980. The nucleus of the solitary tract in the monkey: projections to the thalamus and brain stem nuclei. J. Comp. Neurol. 190, 259–282.

Behan, M. and Haberly, L. B. 1999. Intrinsic and efferent connections of the endopiriform nucleus in rat. J. Comp. Neurol. 408, 532–548.

Benjamin, R. M. and Akert, K. 1959. Cortical and thalmic areas involved in taste discrimination in the albino rat. J. Comp. Neurol. 111, 231–259.

Benjamin, R. M. and Pfaffmann, C. 1955. Cortical localization of taste in albino rat. J. Neurophysiol. 18, 56–64.

Bereiter, D., Berthoud, H. R., and Jeanrenaud, B. 1980. Hypothalamic input to brain stem neurons responsive to oropharyngeal stimulation. Exp. Brain Res. 39, 33–39.

Berman, D. E. and Dudai, Y. 2001. Memory extinction, learning anew, and learning the new: dissociations in the molecular machinery of learning in cortex. Science 291, 2417–2419.

Berman, D. E., Hazvi, S., Neduva, V., and Dudai, Y. 2000. The role of identified neurotransmitter systems in the response of insular cortex to unfamiliar taste: activation of ERK1-2 and formation of a memory trace. J. Neurosci. 20, 7017–7023.

Bermudez-Rattoni, F., Ramirez-Lugo, L., Gutierrez, R., and Miranda, M. I. 2004. Molecular signals into the insular cortex and amygdala during aversive gustatory memory formation. Cell Mol. Neurobiol. 24, 25–36.

Bernard, J. F., Alden, M., and Besson, J. M. 1993. The organization of the efferent projections from the pontine parabrachial area to the amygdaloid complex: a *Phaseolus vulgaris* leucoagglutinin (PHA-L) study in the rat. J. Comp. Neurol. 329, 201–229.

Bester, H., Bourgeais, L., Villanueva, L., Besson, J. M., and Bernard, J. F. 1999. Differential projections to the intralaminar and gustatory thalamus from the parabrachial area: a PHA-L study in the rat. J. Comp. Neurol. 405, 421–449.

Bingel, U., Quante, M., Knab, R., Bromm, B., Weiller, C., and Buchel, C. 2003. Single trial fMRI reveals significant contralateral bias in responses to laser pain within thalamus and somatosensory cortices. Neuroimage 18, 740–748.

Boughter, J. D., Jr and Smith, D. V. 1998. Amiloride blocks acid responses in NaCl-best gustatory neurons of the hamster solitary nucleus. J. Neurophysiol. 80, 1362–1372.

Bradley, R. M. and Sweazey, R. D. 1990. *In vitro* intracellular recordings from gustatory neurons in the rat solitary nucleus. Brain Res. 508, 168–171.

Bradley, R. M. and Sweazey, R. D. 1992. Separation of neuron types in the gustatory zone of the nucleus tractus solitarii on the basis of intrinsic firing properties. J. Neurophysiol. 67, 1659–1668.

Burton, M. J., Rolls, E. T., and Mora, F. 1976. Effects of hunger on the responses of neurons in the lateral hypothalamus to the sight and taste of food. Exp. Neurol. 51, 668–677.

Cecchi, M., Khoshbouei, H., Javors, M., and Morilak, D. A. 2002. Modulatory effects of norepinephrine in the lateral bed nucleus of the stria terminalis on behavioral and neuroendocrine responses to acute stress. Neuroscience 112, 13–21.

Cechetto, D. F. and Saper, C. B. 1987. Evidence for a viscerotopic sensory representation in the cortex and thalamus in the rat. J. Comp. Neurol. 262, 27–45.

Chandrashekar, J., Hoon, M. A., Ryba, N. J., and Zuker, C. S. 2006. The receptors and cells for mammalian taste. Nature 444, 288–294.

Chang, F. C. and Scott, T. R. 1984. Conditioned taste aversions modify neural responses in the rat nucleus tractus solitarius. J. Neurosci. 4, 1850–1862.

Cho, Y. K., Li, C. S., and Smith, D. V. 2002a. Gustatory projections from the nucleus of the solitary tract to the parabrachial nuclei in the hamster. Chem. Senses 27, 81–90.

Cho, Y. K., Li, C. S., and Smith, D. V. 2002b. Taste responses of neurons of the hamster solitary nucleus are enhanced by lateral hypothalamic stimulation. J. Neurophysiol. 87, 1981–1992.

Cho, Y. K., Li, C. S., and Smith, D. V. 2003. Descending influences from the lateral hypothalamus and amygdala converge onto medullary taste neurons. Chem. Senses 28, 155–171.

Conover, K. L. and Shizgal, P. 1994. Competition and summation between rewarding effects of sucrose and lateral hypothalamic stimulation in the rat. Behav. Neurosci. 108, 537–548.

Contreras, R. J. 1977. Changes in gustatory nerve discharges with sodium deficiency: a single unit analysis. Brain Res. 121, 373–378.

Contreras, R. J. and Frank, M. 1979. Sodium deprivation alters neural responses to gustatory stimuli. J. Gen. Physiol. 73, 569–594.

Contreras, R. and Hatton, G. 1975. Gustatory adaptation as an explanation for dietary-induced sodium appetite. Physiol. Behav. 15, 569–576.

Contreras, R. J., Beckstead, R. M., and Norgren, R. 1982. The central projections of the trigeminal, facial, glossopharyngeal and vagus nerves: an autoradiographic study in the rat. J. Auton. Nerv. Syst. 6, 303–322.

Contreras, R. J., Gomez, M. M., and Norgren, R. 1980. Central origins of cranial nerve parasympathetic neurons in the rat. J. Comp. Neurol. 190, 373–394.

Craig, A. D. 2003a. Interoception: the sense of the physiological condition of the body. Curr. Opin. Neurobiol. 13, 500–505.

Craig, A. D. 2003b. Pain mechanisms: labeled lines versus convergence in central processing. Annu. Rev. Neurosci. 26, 1–30.

Craig, A. D. 2004. Distribution of trigeminothalamic and spinothalamic lamina I terminations in the macaque monkey. J. Comp. Neurol. 477, 119–148.

Craig, A. D., Chen, K., Bandy, D., and Reiman, E. M. 2000. Thermosensory activation of insular cortex. Nat. Neurosci. 3, 184–190.

Davis, B. J. 1993. GABA-like immunoreactivity in the gustatory zone of the nucleus of the solitary tract in the hamster: light and electron microscopic studies. Brain Res. Bull. 30, 69–77.

Davis, B. J. 1998. Synaptic relationships between the chorda tympani and tyrosine hydroxylase-immunoreactive dendritic processes in the gustatory zone of the nucleus of the solitary tract in the hamster. J. Comp. Neurol. 392, 78–91.

Davis, B. J. and Jang, T. 1986. The gustatory zone of the nucleus of the solitary tract in the hamster: light microscopic morphometric studies. Chem. Senses 11, 213–228.

Davis, B. J. and Jang, T. 1988a. A Golgi analysis of the gustatory zone of the nucleus of the solitary tract in the adult hamster. J. Comp. Neurol. 278, 388–396.

Davis, B. J. and Jang, T. 1988b. Tyrosine hydroxylase-like and dopamine beta-hydroxylase-like immunoreactivity in the gustatory zone of the nucleus of the solitary tract in the

hamster: light- and electron-microscopic studies. Neuroscience 27, 949–964.
Davis, B. J. and Kream, R. M. 1993. Distribution of tachykinin- and opioid-expressing neurons in the hamster solitary nucleus: an immuno- and *in situ* hybridization histochemical study. Brain Res. 616, 6–16.
Davis, B. J. and Smith, D. V. 1997. Substance P modulates taste responses in the nucleus of the solitary tract of the hamster. Neuroreport 8, 1723–1727.
Di Lorenzo, P. M. 1988. Taste responses in the parabrachial pons of decerebrate rats. J. Neurophysiol. 59, 1871–1887.
Di Lorenzo, P. M. 1990. Corticofugal influence on taste responses in the parabrachial pons of the rat. Brain Res. 530, 73–84.
Di Lorenzo, P. M. and Monroe, S. 1990. Taste responses in the parabrachial pons of ovariectomized rats. Brain Res. Bull. 25, 741–748.
Di Lorenzo, P. M. and Monroe, S. 1995. Corticofugal influence on taste responses in the nucleus of the solitary tract in the rat. J. Neurophysiol. 74, 258–272.
Di Lorenzo, P. M. and Victor, J. D. 2003. Taste response variability and temporal coding in the nucleus of the solitary tract of the rat. J. Neurophysiol. 90, 1418–1431.
Drewe, J. A., Miles, R., and Kunze, D. L. 1990. Excitatory amino acid receptors of guinea pig medial nucleus tractus solitarius neurons. Am. J. Physiol. 259, H1389–H1395.
Dykes, R. W., Landry, P., Metherate, R., and Hicks, T. P. 1984. Functional role of GABA in cat primary somatosensory cortex: shaping receptive fields of cortical neurons. J. Neurophysiol. 52, 1066–1093.
Ferreira, G., Gutierrez, R., De La Cruz, V., and Bermudez-Rattoni, F. 2002. Differential involvement of cortical muscarinic and NMDA receptors in short- and long-term taste aversion memory. Eur. J. Neurosci. 16, 1139–1145.
Flaherty, C. F., Turovsky, J., and Krauss, K. L. 1994. Relative hedonic value modulates anticipatory contrast. Physiol. Behav. 55, 1047–1054.
Fontanini, A. and Katz, D. B. 2006. State-dependent modulation of time-varying gustatory responses. J. Neurophysiol. 96, 3183–3193.
Foster, L. A., Nakamura, K., Greenberg, D., and Norgren, R. 1996. Intestinal fat differentially suppresses sham feeding of different gustatory stimuli. Am. J. Physiol. 270, R1122–R1125.
Frank, M. 1973. An analysis of hamster afferent taste nerve response functions. J. Gen. Physiol. 61, 588–618.
Frank, M. and Pfaffmann, C. 1969. Taste nerve fibers: a random distribution of sensitivities to four tastes. Science 164, 1183–1185.
Frank, M. E. 1991. Taste-responsive neurons of the glossopharyngeal nerve of the rat. J. Neurophysiol. 65, 1452–1463.
Frank, R. A. and Stutz, R. M. 1982. Behavioral changes induced by basolateral amygdala self-stimulation. Physiol. Behav. 28, 661–665.
Frank, M. E., Bieber, S. L., and Smith, D. V. 1988. The organization of taste sensibilities in hamster chorda tympani nerve fibers. J. Gen. Physiol. 91, 861–896.
Frank, M. E., Contreras, R. J., and Hettinger, T. P. 1983. Nerve fibers sensitive to ionic taste stimuli in chorda tympani of the rat. J. Neurophysiol. 50, 941–960.
Fu, W., Sugai, T., Yoshimura, H., and Onoda, N. 2004. Convergence of olfactory and gustatory connections onto the endopiriform nucleus in the rat. Neuroscience 126, 1033–1041.
Fullerton, D. T., Getto, C. J., Swift, W. J., and Carlson, I. H. 1985. Sugar, opioids and binge eating. Brain Res. Bull. 14, 673–680.
Garcia, J., Kovner, R., and Green, K. 1970. Cue properties vs palatability of flavors in avoidance learning. Psychon. Sci. 20, 313–314.
Gauriau, C. and Bernard, J. F. 2004. Posterior triangular thalamic neurons convey nociceptive messages to the secondary somatosensory and insular cortices in the rat. J. Neurosci. 24, 752–761.
Geran, L. C. and Travers, S. P. 2006. Single neurons in the nucleus of the solitary tract respond selectively to bitter taste stimuli. J. Neurophysiol. 96, 2513–2527.
Giza, B. K. and Scott, T. R. 1983. Blood glucose selectively affects taste-evoked activity in rat nucleus tractus solitarius. Physiol. Behav. 31, 643–650.
Giza, B. K. and Scott, T. R. 1987. Blood glucose level affects perceived sweetness intensity in rats. Physiol. Behav. 41, 459–464.
Giza, B. K. and Scott, T. R. 1991. The effect of amiloride on taste-evoked activity in the nucleus tractus solitarius of the rat. Brain Res. 550, 247–256.
Giza, B. K., Ackroff, K., McCaughey, S. A., Sclafani, A., and Scott, T. R. 1997. Preference conditioning alters taste responses in the nucleus of the solitary tract of the rat. Am. J. Physiol. 273, R1230–R1240.
Giza, B. K., Scott, T. R., and Vanderweele, D. A. 1992. Administration of satiety factors and gustatory responsiveness in the nucleus tractus solitarius of the rat. Brain Res. Bull. 28, 637–639.
Glaum, S. R., Slater, N. T., Rossi, D. J., and Miller, R. J. 1992. Role of metabotropic glutamate (ACPD) receptors at the parallel fiber-Purkinje cell synapse. J. Neurophysiol. 68, 1453–1462.
Glenn, J. F. and Erickson, R. P. 1976. Gastric modulation of gustatory afferent activity. Physiol. Behav. 16, 561–568.
Greenberg, D., Smith, G. P., and Gibbs, J. 1990. Intraduodenal infusions of fats elicit satiety in sham-feeding rats. Am. J. Physiol. 259, R110–R118.
Grill, H. J. 1985. Introduction: physiological mechanisms in conditioned taste aversions. Ann. N. Y. Acad. Sci. 443, 67–88.
Grill, H. J. and Norgren, R. 1978a. Chronically decerebrate rats demonstrate satiation but not bait shyness. Science 201, 267–269.
Grill, H. J. and Norgren, R. 1978b. The taste reactivity test. II. Mimetic responses to gustatory stimuli in chronic thalamic and chronic decerebrate rats. Brain Res. 143, 281–297.
Grill, H. J., Schulkin, J., and Flynn, F. W. 1986. Sodium homeostasis in chronic decerebrate rats. Behav. Neurosci. 100, 536–543.
Grill, H. J., Schwartz, G. J., and Travers, J. B. 1992. The contribution of gustatory nerve input to oral motor behavior and intake-based preference. I. Effects of chorda tympani or glossopharyngeal nerve section in the rat. Brain Res. 573, 95–104.
Grossman, S. P., Dacey, D., Halaris, A. E., Collier, T., and Routtenberg, A. 1978. Aphagia and adipsia after preferential destruction of nerve cell bodies in hypothalamus. Science 202, 537–539.
Gutierrez, R., Carmena, J. M., Nicolelis, M. A., and Simon, S. A. 2006. Orbitofrontal ensemble activity monitors licking and distinguishes among natural rewards. J. Neurophysiol. 95, 119–133.
Gutierrez, H., Hernandez-Echeagaray, E., Ramirez-Amaya, V., and Bermudez-Rattoni, F. 1999. Blockade of *N*-methyl-D-aspartate receptors in the insular cortex disrupts taste aversion and spatial memory formation. Neuroscience 89, 751–758.
Guyenet, P. G., Filtz, T. M., and Donaldson, S. R. 1987. Role of excitatory amino acids in rat vagal and sympathetic baroreflexes. Brain Res. 407, 272–284.
Hagan, M. M., Chandler, P. C., Wauford, P. K., Rybak, R. J., and Oswald, K. D. 2003. The role of palatable food and hunger as trigger factors in an animal model of stress induced binge eating. Int. J. Eat Disord. 34, 183–197.
Hajnal, A., Takenouchi, K., and Norgren, R. 1999. Effect of intraduodenal lipid on parabrachial gustatory coding in awake rats. J. Neurosci. 19, 7182–7190.

Hallock, R. M. and Di Lorenzo, P. M. 2006. Temporal coding in the gustatory system. Neurosci. Biobehav. Rev. 30, 1145–1160.

Halpern, B. P. and Tapper, D. N. 1971. Taste stimuli: quality coding time. Science 171, 1256–1258.

Halsell, C. B. 1998. Differential distribution of amygdaloid input across rostral solitary nucleus subdivisions in rat. Ann. N. Y. Acad. Sci. 855, 482–485.

Halsell, C. B. and Travers, S. P. 1997. Anterior and posterior oral cavity responsive neurons are differentially distributed among parabrachial subnuclei in rat. J. Neurophysiol. 78, 920–938.

Halsell, C. B., Travers, S. P., and Travers, J. B. 1996. Ascending and descending projections from the rostral nucleus of the solitary tract originate from separate neuronal populations. Neuroscience 72, 185–197.

Hamilton, R. B. and Norgren, R. 1984. Central projections of gustatory nerves in the rat. J. Comp. Neurol. 222, 560–577.

Hanamori, T., Kunitake, T., Kato, K., and Kannan, H. 1997. Convergence of afferent inputs from the chorda tympani, lingual–tonsillar and pharyngeal branches of the glossopharyngeal nerve, and superior laryngeal nerve on the neurons in the insular cortex in rats. Brain Res. 763, 267–270.

Hanamori, T., Kunitake, T., Kato, K., and Kannan, H. 1998a. Neurons in the posterior insular cortex are responsive to gustatory stimulation of the pharyngolarynx, baroreceptor and chemoreceptor stimulation, and tail pinch in rats. Brain Res. 785, 97–106.

Hanamori, T., Kunitake, T., Kato, K., and Kannan, H. 1998b. Responses of neurons in the insular cortex to gustatory, visceral, and nociceptive stimuli in rats. J. Neurophysiol. 79, 2535–2545.

Hanamori, T., Miller, I. J., Jr, and Smith, D. V. 1988. Gustatory responsiveness of fibers in the hamster glossopharyngeal nerve. J. Neurophysiol. 60, 478–498.

Hasegawa, K. and Ogawa, H. 2007. Effects of acetylcholine on coding of taste information in the primary gustatory cortex in rats. Exp Brain Res. 179, 97–109

Hayama, T., Ito, S., and Ogawa, H. 1985. Responses of solitary tract nucleus neurons to taste and mechanical stimulations of the oral cavity in decerebrate rats. Exp. Brain Res. 60, 235–242.

Herman, J. P. and Cullinan, W. E. 1997. Neurocircuitry of stress: central control of the hypothalamo-pituitary-adrenocortical axis. Trends Neurosci. 20, 78–84.

Hermann, G. E. and Novin, D. 1980. Morphine inhibition of parabrachial taste units reversed by naloxone. Brain Res. Bull. 5(Suppl. 4), 169–173.

Hettinger, T. P. and Frank, M. E. 1990. Specificity of amiloride inhibition of hamster taste responses. Brain Res. 513, 24–34.

Hill, D. L., Formaker, B. K., and White, K. S. 1990. Perceptual characteristics of the amiloride-suppressed sodium chloride taste response in the rat. Behav. Neurosci. 104, 734–741.

Huang, A. L., Chen, X., Hoon, M. A., Chandrashekar, J., Guo, W., Trankner, D., Ryba, N. J., and Zuker, C. S. 2006. The cells and logic for mammalian sour taste detection. Nature 442, 934–938.

Ito, S. I. 1998. Possible representation of somatic pain in the rat insular visceral sensory cortex: a field potential study. Neurosci. Lett. 241, 171–174.

Jacobs, K. M., Mark, G. P., and Scott, T. R. 1988. Taste responses in the nucleus tractus solitarius of sodium-deprived rats. J. Physiol. (Lond.) 406, 393–410.

Jain, N., Qi, H. X., Catania, K. C., and Kaas, J. H. 2001. Anatomic correlates of the face and oral cavity representations in the somatosensory cortical area 3b of monkeys. J. Comp. Neurol. 429, 455–468.

Jalowiec, J. E. and Stricker, E. M. 1970. Restoration of body fluid balance following acute sodium deficiency in rats. J. Comp. Physiol. Psychol. 70, 94–102.

Jasmin, L., Burkey, A. R., Granato, A., and Ohara, P. T. 2004. Rostral agranular insular cortex and pain areas of the central nervous system: a tract-tracing study in the rat. J. Comp. Neurol. 468, 425–440.

Jones, L. M., Fontanini, A., and Katz, D. B. 2006. Gustatory processing: a dynamic systems approach. Curr. Opin. Neurobiol. 16, 420–428.

Kaas, J. H. 2005. The future of mapping sensory cortex in primates: three of many remaining issues. Philos. Trans. R. Soc. Lond. B. Biol. Sci. 360, 653–664.

Kaplan, J. M., Roitman, M., and Grill, H. J. 2000. Food deprivation does not potentiate glucose taste reactivity responses of chronic decerebrate rats. Brain Res. 870, 102–108.

Karadi, Z., Oomura, Y., Nishino, H., Scott, T. R., Lenard, L., and Aou, S. 1992. Responses of lateral hypothalamic glucose-sensitive and glucose- insensitive neurons to chemical stimuli in behaving rhesus monkeys. J. Neurophysiol. 67, 389–400.

Karimnamazi, H. and Travers, J. B. 1998. Differential projections from gustatory responsive regions of the parabrachial nucleus to the medulla and forebrain. Brain Res. 813, 283–302.

Katz, D. B., Simon, S. A., and Nicolelis, M. A. 2001. Dynamic and multimodal responses of gustatory cortical neurons in awake rats. J. Neurosci. 21, 4478–4489.

Katz, D. B., Simon, S. A., and Nicolelis, M. A. 2002. Taste-specific neuronal ensembles in the gustatory cortex of awake rats. J. Neurosci. 22, 1850–1857.

King, M. S. and Bradley, R. M. 1994. Relationship between structure and function of neurons in the rat rostral nucleus tractus solitarii. J. Comp. Neurol. 344, 50–64.

King, M. S., Wang, L., and Bradley, R. M. 1993. Substance P excites neurons in the gustatory zone of the rat nucleus tractus solitarius. Brain Res. 619, 120–130.

Kobashi, M. and Bradley, R. M. 1998. Effects of GABA on neurons of the gustatory and visceral zones of the parabrachial nucleus in rats. Brain Res. 799, 323–328.

Koh, M. T. and Bernstein, I. L. 2005. Mapping conditioned taste aversion associations using c-Fos reveals a dynamic role for insular cortex. Behav. Neurosci. 119, 388–398.

van der Kooy, D., Koda, L. Y., McGinty, J. F, Gerfen, C. R., and Bloom, F. E. 1984. The organization of projections from the cortex, amygdala, and hypothalamus to the nucleus of the solitary tract in rat. J. Comp. Neurol. 224, 1–24.

Kosar, E., Grill, H. J., and Norgren, R. 1986a. Gustatory cortex in the rat. I. Physiological properties and cytoarchitecture. Brain Res. 379, 329–341.

Kosar, E., Grill, H. J., and Norgren, R. 1986b. Gustatory cortex in the rat. II. Thalamocortical projections. Brain Res. 379, 342–352.

Kotz, C. M., Billington, C. J., and Levine, A. S. 1997. Opioids in the nucleus of the solitary tract are involved in feeding in the rat. Am. J. Physiol. 272, R1028–R1032.

Kringelbach, M. L., O'Doherty, J., Rolls, E. T., and Andrews, C. 2003. Activation of the human orbitofrontal cortex to a liquid food stimulus is correlated with its subjective pleasantness. Cereb. Cortex 13, 1064–1071.

Krout, K. E. and Loewy, A. D. 2000. Parabrachial nucleus projections to midline and intralaminar thalamic nuclei of the rat. J. Comp. Neurol. 428, 475–494.

Krupa, D. J., Wiest, M. C., Shuler, M. G., Laubach, M., and Nicolelis, M. A. 2004. Layer-specific somatosensory cortical activation during active tactile discrimination. Science 304, 1989–1992.

Kubo, T. and Kihara, M. 1988a. Evidence for gamma-aminobutyric acid receptor-mediated modulation of the aortic baroreceptor reflex in the nucleus tractus solitarii of the rat. Neurosci. Lett. 89, 156–160.

Kubo, T. and Kihara, M. 1988b. *N*-methyl-D-aspartate receptors mediate tonic vasodepressor control in the caudal ventrolateral medulla of the rat. Brain Res. 451, 366–370.

Kyriazi, H. T., Carvell, G. E., Brumberg, J. C., and Simons, D. J. 1996. Quantitative effects of GABA and bicuculline methiodide on receptive field properties of neurons in real and simulated whisker barrels. J. Neurophysiol. 75, 547–560.

Lasiter, P. S. and Kachele, D. L. 1988. Organization of GABA and GABA-transaminase containing neurons in the gustatory zone of the nucleus of the solitary tract. Brain Res. Bull. 21, 623–636.

Lazareva, N. A., Shevelev, I. A., Eysel, U. T., and Sharaev, G. A. 1997. Bicuculline and orientation tuning of neurons of the visual cortex. Neurophysiology 27, 42–49.

Lemon, C. H. and Smith, D. V. 2005. Neural representation of bitter taste in the nucleus of the solitary tract. J. Neurophysiol. 94, 3719–3729.

Li, C. S. and Smith, D. V. 1997. Glutamate receptor antagonists block gustatory afferent input to the nucleus of the solitary tract. J. Neurophysiol. 77, 1514–1525.

Li, C. S., Cho, Y. K., and Smith, D. V. 2002a. Taste responses of neurons in the hamster solitary nucleus are modulated by the central nucleus of the amygdala. J. Neurophysiol. 88, 2979–2992.

Li, C. S., Cho, Y. K., and Smith, D. V. 2005. Modulation of parabrachial taste neurons by electrical and chemical stimulation of the lateral hypothalamus and amygdala. J. Neurophysiol. 93, 1183–1196.

Li, C. S., Davis, B. J., and Smith, D. V. 2003. Opioid modulation of taste responses in the nucleus of the solitary tract. Brain Res. 965, 21–34.

Li, X., Staszewski, L., Xu, H., Durick, K., Zoller, M., and Adler, E. 2002b. Human receptors for sweet and umami taste. Proc. Natl. Acad. Sci. U. S. A. 99, 4692–4696.

Liu, H., Behbehani, M. M., and Smith, D. V. 1993. The influence of GABA on cells in the gustatory region of the hamster solitary nucleus. Chem. Senses 18, 285–305.

Lundy, R. F., Jr. and Norgren, R. 2001. Pontine gustatory activity is altered by electrical stimulation in the central nucleus of the amygdala. J. Neurophysiol. 85, 770–783.

Lundy, R. F., Jr. and Norgren, R. 2004a. Activity in the hypothalamus, amygdala, and cortex generates bilateral and convergent modulation of pontine gustatory neurons. J. Neurophysiol. 91, 1143–1157.

Lundy, R. F., Jr. and Norgren, R. 2004b. Gustatory System. In: The Rat Nervous System (*ed*. G. Paxinos), pp. 890–911. Elsevier Academic Press.

Macey, D. J., Smith, H. R., Nader, M. A., and Porrino, L. J. 2003. Chronic cocaine self-administration upregulates the norepinephrine transporter and alters functional activity in the bed nucleus of the stria terminalis of the rhesus monkey. J. Neurosci. 23, 12–16.

Mantyh, P. W. and Hunt, S. P. 1984. Neuropeptides are present in projection neurones at all levels in visceral and taste pathways: from periphery to sensory cortex. Brain Res. 299, 297–312.

Mark, G. P., Scott, T. R., Chang, F. C., and Grill, H. J. 1988. Taste responses in the nucleus tractus solitarius of the chronic decerebrate rat. Brain Res. 443, 137–148.

Markison, S., Gietzen, D. W., and Spector, A. C. 1999. Essential amino acid deficiency enhances long-term intake but not short-term licking of the required nutrient. J. Nutr. 129, 1604–1612.

Markison, S., Thompson, B. L., Smith, J. C., and Spector, A. C. 2000. Time course and pattern of compensatory ingestive behavioral adjustments to lysine deficiency in rats. J. Nutr. 130, 1320–1328.

Matsuo, R., Shimizu, N., and Kusano, K. 1984. Lateral hypothalamic modulation of oral sensory afferent activity in nucleus tractus solitarius neurons of rats. J. Neurosci. 4, 1201–1207.

Mayer, M. L. and Westbrook, G. L. 1987. The physiology of excitatory amino acids in the vertebrate central nervous system. Prog. Neurobiol. 28, 197–276.

McCaughey, S. A. and Scott, T. R. 1998. The taste of sodium. Neurosci. Biobehav. Rev. 22, 663–676.

Menendez, L., Bester, H., Besson, J. M., and Bernard, J. F. 1996. Parabrachial area: electrophysiological evidence for an involvement in cold nociception. J. Neurophysiol. 75, 2099–2116.

Miranda, M. I., Ramirez-Lugo, L., and Bermudez-Rattoni, F. 2000. Cortical cholinergic activity is related to the novelty of the stimulus. Brain Res. 882, 230–235.

Miyaoka, Y. and Pritchard, T. C. 1996. Responses of primate cortical neurons to unitary and binary taste stimuli. J. Neurophysiol. 75, 396–411.

Moga, M. M., Herbert, H., Hurley, K. M., Yasui, Y., Gray, T. S., and Saper, C. B. 1990a. Organization of cortical, basal forebrain, and hypothalamic afferents to the parabrachial nucleus in the rat. J. Comp. Neurol. 295, 624–661.

Moga, M. M., Saper, C. B., and Gray, T. S. 1990b. Neuropeptide organization of the hypothalamic projection to the parabrachial nucleus in the rat. J. Comp. Neurol. 295, 662–682.

Morley, J. E. and Levine, A. S. 1980. Stress-induced eating is mediated through endogenous opiates. Science 209, 1259–1261.

Murzi, E., Hernandez, L., and Baptista, T. 1986. Lateral hypothalamic sites eliciting eating affect medullary taste neurons in rats. Physiol. Behav. 36, 829–834.

Nachman, M. 1963. Learned aversion to the taste of lithium chloride and generalization to other salts. J. Comp. Physiol. Psychol. 56, 343–349.

Nakamura, K. and Norgren, R. 1991. Gustatory responses of neurons in the nucleus of the solitary tract of behaving rats. J. Neurophysiol. 66, 1232–1248.

Nakamura, K. and Norgren, R. 1993. Taste responses of neurons in the nucleus of the solitary tract of awake rats: an extended stimulus array. J. Neurophysiol. 70, 879–891.

Naor, C. and Dudai, Y. 1996. Transient impairment of cholinergic function in the rat insular cortex disrupts the encoding of taste in conditioned taste aversion. Behav. Brain Res. 79, 61–67.

Nelson, G., Chandrashekar, J., Hoon, M. A., Feng, L., Zhao, G., Ryba, N. J., and Zuker, C. S. 2002. An amino-acid taste receptor. Nature 416, 199–202.

Nelson, G., Hoon, M. A., Chandrashekar, J., Zhang, Y., Ryba, N. J., and Zuker, C. S. 2001. Mammalian sweet taste receptors. Cell 106, 381–390.

Nicola, S. M., Yun, I. A., Wakabayashi, K. T., and Fields, H. L. 2004. Firing of nucleus accumbens neurons during the consummatory phase of a discriminative stimulus task depends on previous reward predictive cues. J. Neurophysiol. 91, 1866–1882.

Ninomiya, Y. 1998. Reinnervation of cross-regenerated gustatory nerve fibers into amiloride-sensitive and amiloride-insensitive taste receptor cells. Proc. Natl. Acad. Sci. U. S. A. 95, 5347–5350.

Ninomiya, Y. and Funakoshi, M. 1988. Amiloride inhibition of responses of rat single chorda tympani fibers to chemical and electrical tongue stimulations. Brain Res. 451, 319–325.

Nishijo, H. and Norgren, R. 1990. Responses from parabrachial gustatory neurons in behaving rats. J. Neurophysiol. 63, 707–724.

Nishijo, H. and Norgren, R. 1991. Parabrachial gustatory neural activity during licking by rats. J. Neurophysiol. 66, 974–985.

Nishijo, H., Ono, T., and Norgren, R. 1991. Parabrachial gustatory neural responses to monosodium glutamate ingested by awake rats. Physiol. Behav. 49, 965–971.

Nishijo, H., Ono, T., Uwano, T., Kondoh, T., and Torii, K. 2000. Hypothalamic and amygdalar neuronal responses to various

tastant solutions during ingestive behavior in rats. J. Nutr. 130, 954S–959S.
Nishijo, H., Uwano, T., Tamura, R., and Ono, T. 1998. Gustatory and multimodal neuronal responses in the amygdala during licking and discrimination of sensory stimuli in awake rats. J. Neurophysiol. 79, 21–36.
Norgren, R. 1970. Gustatory responses in the hypothalamus. Brain Res. 21, 63–77.
Norgren, R. 1974. Gustatory afferents to ventral forebrain. Brain Res. 81, 285–295.
Norgren, R. 1976. Taste pathways to hypothalamus and amygdala. J. Comp. Neurol. 166, 17–30.
Norgren, R. and Leonard, C. M. 1971. Taste pathways in rat brainstem. Science 173, 1136–1139.
Norgren, R. and Leonard, C. M. 1973. Ascending central gustatory pathways. J. Comp. Neurol. 150, 217–237.
Norgren, R. and Pfaffmann, C. 1975. The pontine taste area in the rat. Brain Res. 91, 99–117.
Nowlis, G. H., Frank, M. E., and Pfaffmann, C. 1980. Specificity of acquired aversions to taste qualities in hamsters and rats. J. Comp. Physiol. Psychol. 94, 932–942.
Oakley, B., Jones, L. B., and Kaliszewski, J. M. 1979. Taste responses of the gerbil IXth nerve. Chem. Senses 4, 79–87.
Ogawa, H. and Hayama, T. 1984. Receptive fields of solitario-parabrachial relay neurons responsive to natural stimulation of the oral cavity in rats. Exp. Brain Res. 54, 359–366.
Ogawa, H. and Wang, X. D. 2002. Neurons in the cortical taste area receive nociceptive inputs from the whole body as well as the oral cavity in the rat. Neurosci. Lett. 322, 87–90.
Ogawa, H., Hasegawa, K., and Murayama, N. 1992. Difference in taste quality coding between two cortical taste areas, granular and dysgranular insular areas, in rats. Exp. Brain Res. 91, 415–424.
Ogawa, H., Hasegawa, K., and Nakamura, T. 2000. Action of calcitonin gene-related peptide (CGRP) and substance P on neurons in the insular cortex and the modulation of taste responses in the rat. Chem. Senses 25, 351–359.
Ogawa, H., Hasegawa, K., Otawa, S., and Ikeda, I. 1998. GABAergic inhibition and modifications of taste responses in the cortical taste area in rats. Neurosci. Res. 32, 85–95.
Ogawa, H., Hayama, T., and Ito, S. 1982. Convergence of input from tongue and palate to the parabrachial nucleus neurons of rats. Neurosci. Lett. 28, 9–14.
Ono, T., Sasaki, K., Nishino, H., Fukuda, M., and Shibata, R. 1986. Feeding and diurnal related activity of lateral hypothalamic neurons in freely behaving rats. Brain Res. 373, 92–102.
Oomura, Y., Nishino, H., Karadi, Z., Aou, S., and Scott, T. R. 1991. Taste and olfactory modulation of feeding related neurons in behaving monkey. Physiol. Behav. 49, 943–950.
Otawa, S., Takagi, K., and Ogawa, H. 1995. NMDA and non-NMDA receptors mediate taste afferent inputs to cortical taste neurons in rats. Exp. Brain Res. 106, 391–402.
Perrotto, R. S. and Scott, T. R. 1976. Gustatory neural coding in the pons. Brain Res. 110, 283–300.
Petrovic, P., Kalso, E., Petersson, K. M., and Ingvar, M. 2002. Placebo and opioid analgesia – imaging a shared neuronal network. Science 295, 1737–1740.
Pickel, V. M. and Colago, E. E. 1999. Presence of mu-opioid receptors in targets of efferent projections from the central nucleus of the amygdala to the nucleus of the solitary tract. Synapse 33, 141–152.
Plata-Salaman, C. R., Scott, T. R., and Smith-Swintosky, V. L. 1992. Gustatory neural coding in the monkey cortex: L-amino acids. J. Neurophysiol. 67, 1552–1561.
Plata-Salaman, C. R., Scott, T. R., and Smith-Swintosky, V. L. 1993. Gustatory neural coding in the monkey cortex: the quality of sweetness. J. Neurophysiol. 69, 482–493.
Plata-Salaman, C. R., Scott, T. R., and Smith-Swintosky, V. L. 1995. Gustatory neural coding in the monkey cortex: acid stimuli. J. Neurophysiol. 74, 556–564.
Plata-Salaman, C. R., Smith-Swintosky, V. L., and Scott, T. R. 1996. Gustatory neural coding in the monkey cortex: mixtures. J. Neurophysiol. 75, 2369–2379.
Pritchard, T. C. and Norgren, R. 2004. Gustatory System. In: The Human Nervous System. Chap. 31 (*eds*. G. Paxinos and J. Mai), Elsevier.
Pritchard, T. C., Edwards, E. M., Smith, C. A., Hilgert, K. G., Gavlick, A. M., Maryniak, T. D., Schwartz, G. J., and Scott, T. R. 2005. Gustatory neural responses in the medial orbitofrontal cortex of the old world monkey. J. Neurosci. 25, 6047–6056.
Pritchard, T. C., Hamilton, R. B., Morse, J. R., and Norgren, R. 1986. Projections of thalamic gustatory and lingual areas in the monkey, *Macaca fascicularis*. J. Comp. Neurol. 244, 213–228.
Pritchard, T. C., Hamilton, R. B., and Norgren, R. 2000. Projections of the parabrachial nucleus in the old world monkey. Exp. Neurol. 165, 101–117.
Reilly, S., Grigson, P. S., and Norgren, R. 1993. Parabrachial nucleus lesions and conditioned taste aversion: evidence supporting an associative deficit. Behav. Neurosci. 107, 1005–1017.
Renehan, W. E., Jin, Z., Zhang, X., and Schweitzer, L. 1994. Structure and function of gustatory neurons in the nucleus of the solitary tract. I. A classification of neurons based on morphological features. J. Comp. Neurol. 347, 531–544.
Renehan, W. E., Jin, Z., Zhang, X., and Schweitzer, L. 1996. Structure and function of gustatory neurons in the nucleus of the solitary tract: II. Relationships between neuronal morphology and physiology. J. Comp. Neurol. 367, 205–221.
Renehan, W. E., Zhang, X., Beierwaltes, W. H., and Fogel, R. 1995. Neurons in the dorsal motor nucleus of the vagus may integrate vagal and spinal information from the GI tract. Am. J. Physiol. 268, G780–G790.
Reynolds, S. M. and Zahm, D. S. 2005. Specificity in the projections of prefrontal and insular cortex to ventral striatopallidum and the extended amygdala. J. Neurosci. 25, 11757–11767.
Rideout, H. J. and Parker, L. A. 1996. Morphine enhancement of sucrose palatability: analysis by the taste reactivity test. Pharmacol. Biochem. Behav. 53, 731–734.
Rinaman, L., Verbalis, J. G., Stricker, E. M., and Hoffman, G. E. 1993. Distribution and neurochemical phenotypes of caudal medullary neurons activated to express cFos following peripheral administration of cholecystokinin. J. Comp. Neurol. 338, 475–490.
Rodieck, R. W. and Brening, R. K. 1982. On classifying retinal ganglion cells by numerical methods. Brain Behav. Evol. 21, 42–46.
Roitman, M. F., Wheeler, R. A., and Carelli, R. M. 2005. Nucleus accumbens neurons are innately tuned for rewarding and aversive taste stimuli, encode their predictors, and are linked to motor output. Neuron 45, 587–597.
Rolls, E. T. and Baylis, L. L. 1994. Gustatory, olfactory, and visual convergence within the primate orbitofrontal cortex. J. Neurosci. 14, 5437–5452.
Rolls, E. T. and Scott, T. R. 2003. Central Taste Anatomy and Physiology. In: Handbook of Olfaction and Gustation. Chap. 33 (*ed*. R. L. Doty), Marcel Dekker.
Rolls, E. T., Murzi, E., Yaxley, S., Thorpe, S. J., and Simpson, S. J. 1986. Sensory-specific satiety: food-specific reduction in responsiveness of ventral forebrain neurons after feeding in the monkey. Brain Res. 368, 79–86.

Rolls, B. J., Rolls, E. T., Rowe, E. A., and Sweeney, K. 1981. Sensory specific satiety in man. Physiol. Behav. 27, 137–142.

Rolls, E. T., Sanghera, M. K., and Roper-Hall, A. 1979. The latency of activation of neurones in the lateral hypothalamus and substantia innominata during feeding in the monkey. Brain Res. 164, 121–135.

Rolls, E. T., Sienkiewicz, Z. J., and Yaxley, S. 1989. Hunger modulates the responses to gustatory stimuli of single neurons in the caudolateral orbitofrontal cortex of the macaque monkey. Eur. J. Neurosci. 1, 53–60.

Rolls, E. T., Yaxley, S., and Sienkiewicz, Z. J. 1990. Gustatory responses of single neurons in the caudolateral orbitofrontal cortex of the macaque monkey. J. Neurophysiol. 64, 1055–1066.

Rosenblum, K., Berman, D. E., Hazvi, S., Lamprecht, R., and Dudai, Y. 1997. NMDA receptor and the tyrosine phosphorylation of its 2B subunit in taste learning in the rat insular cortex. J. Neurosci. 17, 5129–5135.

Rosenblum, K., Meiri, N., and Dudai, Y. 1993. Taste memory: the role of protein synthesis in gustatory cortex. Behav. Neural Biol. 59, 49–56.

Ruggiero, D. A., Giuliano, R., Anwar, M., Stornetta, R., and Reis, D. J. 1990. Anatomical substrates of cholinergic–autonomic regulation in the rat. J. Comp. Neurol. 292, 1–53.

Ruggiero, D. A., Mtui, E. P., Otake, K., and Anwar, M. 1996. Central and primary visceral afferents to nucleus tractus solitarii may generate nitric oxide as a membrane-permeant neuronal messenger. J. Comp. Neurol. 364, 51–67.

Sanghera, M. K., Rolls, E. T., and Roper-Hall, A. 1979. Visual responses of neurons in the dorsolateral amygdala of the alert monkey. Exp. Neurol. 63, 610–626.

Santiago, A. C. and Shammah-Lagnado, S. J. 2005. Afferent connections of the amygdalopiriform transition area in the rat. J. Comp. Neurol. 489, 349–371.

Sasaki, K., Ono, T., Muramoto, K., Nishino, H., and Fukuda, M. 1984. The effects of feeding and rewarding brain stimulation on lateral hypothalamic unit activity in freely moving rats. Brain Res. 322, 201–211.

Schafe, G. E. and Bernstein, I. L. 1996. Forebrain contribution to the induction of a brainstem correlate of conditioned taste aversion: I. The amygdala. Brain Res. 741, 109–116.

Schafe, G. E. and Bernstein, I. L. 1998. Forebrain contribution to the induction of a brainstem correlate of conditioned taste aversion. II. Insular (gustatory) cortex. Brain Res. 800, 40–47.

Schwartzbaum, J. S. 1988. Electrophysiology of taste, feeding and reward in lateral hypothalamus of rabbit. Physiol. Behav. 44, 507–526.

Schweinhardt, P., Glynn, C., Brooks, J., McQuay, H., Jack, T., Chessell, I., Bountra, C., and Tracey, I. 2006. An fMRI study of cerebral processing of brush-evoked allodynia in neuropathic pain patients. Neuroimage 32, 256–265.

Schweitzer, L., Jin, Z., Zhang, X., and Renehan, W. E. 1995. Cell types in the rostral nucleus of the solitary tract. Brain Res. Brain Res. Rev. 20, 185–195.

Scott, T. R. and Giza, B. K. 1990. Coding channels in the taste system of the rat. Science 249, 1585–1587.

Scott, T. R., Giza, B. K., and Yan, J. 1999. Gustatory neural coding in the cortex of the alert cynomolgus macaque: the quality of bitterness. J. Neurophysiol. 81, 60–71.

Scott, T. R., Karadi, Z., Oomura, Y., Nishino, H., Plata-Salaman, C. R., Lenard, L., Giza, B. K., and Aou, S. 1993. Gustatory neural coding in the amygdala of the alert macaque monkey. J. Neurophysiol. 69, 1810–1820.

Scott, T. R., Plata-Salaman, C. R., and Smith-Swintosky, V. L. 1994. Gustatory neural coding in the monkey cortex: the quality of saltiness. J. Neurophysiol. 71, 1692–1701.

Scott, T. R., Yaxley, S., Sienkiewicz, Z. J., and Rolls, E. T. 1986. Gustatory responses in the frontal opercular cortex of the alert cynomolgus monkey. J. Neurophysiol. 56, 876–890.

Seeley, R. J., Grill, H. J., and Kaplan, J. M. 1994. Neurological dissociation of gastrointestinal and metabolic contributions to meal size control. Behav. Neurosci. 108, 347–352.

Shi, C. J. and Cassell, M. D. 1998. Cortical, thalamic, and amygdaloid connections of the anterior and posterior insular cortices. J. Comp. Neurol. 399, 440–468.

Shimura, T., Komori, M., and Yamamoto, T. 1997a. Acute sodium deficiency reduces gustatory responsiveness to NaCl in the parabrachial nucleus of rats. Neurosci. Lett. 236, 33–36.

Shimura, T., Tanaka, H., and Yamamoto, T. 1997b. Salient responsiveness of parabrachial neurons to the conditioned stimulus after the acquisition of taste aversion learning in rats. Neuroscience 81, 239–247.

Shimura, T., Tokita, K., and Yamamoto, T. 2002. Parabrachial unit activities after the acquisition of conditioned taste aversion to a non-preferred HCl solution in rats. Chem. Senses 27, 153–158.

Shipley, M. T. and Geinisman, Y. 1984. Anatomical evidence for convergence of olfactory, gustatory, and visceral afferent pathways in mouse cerebral cortex. Brain Res. Bull. 12, 221–226.

Sillito, A. M. and Kemp, J. A. 1983. Cholinergic modulation of the functional organization of the cat visual cortex. Brain Res. 289, 143–155.

Simon, S. A., de Araujo, I. E., Gutierrez, R., and Nicolelis, M. A. 2006. The neural mechanisms of gustation: a distributed processing code. Nat. Rev. Neurosci. 7, 890–901.

Sloan, T. B. 1998. Anesthetic effects on electrophysiologic recordings. J. Clin. Neurophysiol. 15, 217–226.

Small, D. M. and Prescott, J. 2005. Odor/taste integration and the perception of flavor. Exp. Brain Res. 166, 345–357.

Small, D. M., Gerber, J. C., Mak, Y. E., and Hummel, T. 2005. Differential neural responses evoked by orthonasal versus retronasal odorant perception in humans. Neuron 47, 593–605.

Small, D. M., Gregory, M. D., Mak, Y. E., Gitelman, D., Mesulam, M. M., and Parrish, T. 2003. Dissociation of neural representation of intensity and affective valuation in human gustation. Neuron 39, 701–711.

Small, D. M., Voss, J., Mak, Y. E., Simmons, K. B., Parrish, T., and Gitelman, D. 2004. Experience-dependent neural integration of taste and smell in the human brain. J. Neurophysiol. 92, 1892–1903.

Smeets, P. A., de Graaf, C., Stafleu, A., van Osch, M. J., Nievelstein, R. A., and van der Grond, J. 2006. Effect of satiety on brain activation during chocolate tasting in men and women. Am. J. Clin. Nutr. 83, 1297–1305.

Smith, G. P. 1996. The direct and indirect controls of meal size. Neurosci Biobehav. Rev. 20, 41–46.

Smith, D. V. and Li, C. S. 1998. Tonic GABAergic inhibition of taste-responsive neurons in the nucleus of the solitary tract. Chem. Senses 23, 159–169.

Smith, D. V. and Li, C. 2000. GABA-mediated corticofugal inhibition of taste-responsive neurons in the nucleus of the solitary tract [In Process Citation]. Brain Res. 858, 408–415.

Smith, D. V. and Theodore, R. M. 1984. Conditioned taste aversions: generalization to taste mixtures. Physiol. Behav. 32, 983–989.

Smith, D. V. and Travers, J. B. 1979. A metric for the breadth of tuning of gustatory neurons. Chem. Senses 4, 215–229.

Smith, D. V., Li, C. S., and Cho, Y. C. 2004. Forebrain modulation of brainstem gustatory processing. Chem. Senses 30(Suppl. 1), i176–i177.

Smith, D. V., Travers, J. B., and Van Buskirk, R. L. 1979. Brainstem correlates of gustatory similarity in the hamster. Brain Res. Bull. 4, 359–372.

Smith, D. V., Van Buskirk, R. L., Travers, J. B., and Bieber, S. L. 1983. Gustatory neuron types in hamster brain stem. J. Neurophysiol. 50, 522–540.

Smith-Swintosky, V. L., Plata-Salaman, C. R., and Scott, T. R. 1991. Gustatory neural coding in the monkey cortex: stimulus quality. J. Neurophysiol. 66, 1156–1165.

South, E. H. and Ritter, R. C. 1986. Substance P-containing trigeminal sensory neurons project to the nucleus of the solitary tract. Brain Res. 372, 283–289.

Spector, A. C. and Grill, H. J. 1992. Salt taste discrimination after bilateral section of the chorda tympani or glossopharyngeal nerves. Am. J. Physiol. 263, R169–R176.

Spector, A. C. and Travers, S. P. 2005. The representation of taste quality in the mammalian nervous system. Behav. Cogn. Neurosci. Rev. 4, 143–191.

Spector, A. C., Markison, S., St. John, S. J., and Garcea, M. 1997. Sucrose vs. maltose taste discrimination by rats depends on the input of the seventh cranial nerve. Am. J. Physiol. 272, R1210–R1218.

Spector, A. C., Redman, R., and Garcea, M. 1996. The consequences of gustatory nerve transection on taste-guided licking of sucrose and maltose in the rat. Behav. Neurosci. 110, 1096–1109.

Squire, L. R., Bloom, F. E., McConnell, S. K., Roberts, J. L., Spitzer, N. C., and Zigmond, M. J. 2003. Fundamental Neuroscience, Academic Press.

St. John, S. J. and Smith, D. V. 2000. Neural representation of salts in the rat solitary nucleus: brain stem correlates of taste discrimination. J. Neurophysiol. 84, 628–638.

St. John, S. J. and Spector, A. C. 1998. Behavioral discrimination between quinine and KCl is dependent on input from the seventh cranial nerve: implications for the functional roles of the gustatory nerves in rats. J. Neurosci. 18, 4353–4362.

Stapleton, J. R., Lavine, M. L., Wolpert, R. L., Nicolelis, M. A., and Simon, S. A. 2006. Rapid taste responses in the gustatory cortex during licking. J. Neurosci. 26, 4126–4138.

Stapleton, J. R., Roper, S. D., and Delay, E. R. 1999. The taste of monosodium glutamate (MSG), L-aspartic acid, and *N*-methyl-D-aspartate (NMDA) in rats: are NMDA receptors involved in MSG taste? Chem. Senses 24, 449–457.

Steiner, J. E. 1973. The gustofacial response: observation on normal and anencephalic newborn infants. Symp. Oral Sens. Percept. 4, 254–278.

Strand, F. 1999. Neuropeptides: Regulators of Physiological Processes. MIT Press.

Sweazey, R. D. and Smith, D. V. 1987. Convergence onto hamster medullary taste neurons. Brain Res. 408, 173–184.

Taha, S. A. and Fields, H. L. 2005. Encoding of palatability and appetitive behaviors by distinct neuronal populations in the nucleus accumbens. J. Neurosci. 25, 1193–1202.

Tamura, R. and Norgren, R. 1997. Repeated sodium depletion affects gustatory neural responses in the nucleus of the solitary tract of rats. Am. J. Physiol. 273, R1381–R1391.

Tell, F. and Bradley, R. M. 1994. Whole-cell analysis of ionic currents underlying the firing pattern of neurons in the gustatory zone of the nucleus tractus solitarii. J. Neurophysiol. 71, 479–492.

Tindell, A. J., Berridge, K. C., and Aldridge, J. W. 2004. Ventral pallidal representation of pavlovian cues and reward: population and rate codes. J. Neurosci. 24, 1058–1069.

Tindell, A. J., Smith, K. S., Pecina, S., Berridge, K. C., and Aldridge, J. W. 2006. Ventral pallidum firing codes hedonic reward: when a bad taste turns good. J. Neurophysiol. 96, 2399–2409.

Tokita, K., Karadi, Z., Shimura, T., and Yamamoto, T. 2004. Centrifugal inputs modulate taste aversion learning associated parabrachial neuronal activities. J. Neurophysiol. 92, 265–279.

Topolovec, J. C., Gati, J. S., Menon, R. S., Shoemaker, J. K., and Cechetto, D. F. 2004. Human cardiovascular and gustatory brainstem sites observed by functional magnetic resonance imaging. J. Comp. Neurol. 471, 446–461.

Touzani, K., Ferssiwi, A., and Velley, L. 1990. Localization of lateral hypothalamic neurons projecting to the medial part of the parabrachial area of the rat. Neurosci. Lett. 114, 17–21.

Travers, J. B. 2006. Organization and expression of reward in the rodent orbitofrontal cortex. Focus on ''orbitofrontal ensemble activity monitors licking and distinguishes among natural rewards. J. Neurophysiol. 95, 14–15.

Travers, S. P. (*ed*.) 1993. *Orosensory Processing in Neural Systems of the Nucleus of the Solitary Tract pp. 339–394. CRC Press.*

Travers, S. P. and Norgren, R. 1991. Coding the sweet taste in the nucleus of the solitary tract: differential roles for anterior tongue and nasoincisor duct gustatory receptors in the rat. J. Neurophysiol. 65, 1372–1380.

Travers, S. P. and Norgren, R. 1995. Organization of orosensory responses in the nucleus of the solitary tract of rat. J. Neurophysiol. 73, 2144–2162.

Travers, S. P. and Travers, J. B. 2006. Taste-evoked Fos expression in nitrergic neurons in the nucleus of the solitary tract and reticular formation of the rat. J. Comp. Neurol. 500, 746–760.

Travers, S. P., Pfaffmann, C., and Norgren, R. 1986. Convergence of lingual and palatal gustatory neural activity in the nucleus of the solitary tract. Brain Res. 365, 305–320.

Travers, J. B. and Smith, D. V. 1979. Gustatory sensitivities in neurons of the hamster nucleus tractus solitarius. Sens. Processes 3, 1–26.

Travers, J. B., Grill, H. J., and Norgren, R. 1987. The effects of glossopharyngeal and chorda tympani nerve cuts on the ingestion and rejection of sapid stimuli: an electromyographic analysis in the rat. Behav. Brain Res. 25, 233–246.

Tremere, L., Hicks, T. P., and Rasmusson, D. D. 2001. Expansion of receptive fields in raccoon somatosensory cortex *in vivo* by GABA(A) receptor antagonism: implications for cortical reorganization. Exp. Brain Res. 136, 447–455.

Uher, R., Treasure, J., Heining, M., Brammer, M. J., and Campbell, I. C. 2006. Cerebral processing of food-related stimuli: effects of fasting and gender. Behav. Brain Res. 169, 111–119.

Uteshev, V. V. and Smith, D. V. 2006. Cholinergic modulation of neurons in the gustatory region of the nucleus of the solitary tract. Brain Res. 1084, 38–53.

Van Buskirk, R. L. and Smith, D. V. 1981. Taste sensitivity of hamster parabrachial pontine neurons. J. Neurophysiol. 45, 144–171.

Vardhan, A., Kachroo, A., and Sapru, H. N. 1993. Excitatory amino acid receptors in the nucleus tractus solitarius mediate the responses to the stimulation of cardio-pulmonary vagal afferent C fiber endings. Brain Res. 618, 23–31.

Veening, J. G., Swanson, L. W., and Sawchenko, P. E. 1984. The organization of projections from the central nucleus of the amygdala to brainstem sites involved in central autonomic regulation: a combined retrograde transport-immunohistochemical study. Brain Res. 303, 337–357.

Vogt, M. B. and Mistretta, C. M. 1990. Convergence in mammalian nucleus of solitary tract during development and functional differentiation of salt taste circuits. J. Neurosci. 10, 3148–3157.

Voshart, K. and van der Kooy, D. 1981. The organization of the efferent projections of the parabrachial nucleus of the forebrain in the rat: a retrograde fluorescent double-labeling study. Brain Res. 212, 271–286.

Walker, J. R., Ahmed, S. H., Gracy, K. N., and Koob, G. F. 2000. Microinjections of an opiate receptor antagonist into the bed nucleus of the stria terminalis suppress heroin self-administration in dependent rats. Brain Res. 854, 85–92.

Wang, L. and Bradley, R. M. 1993. Influence of GABA on neurons of the gustatory zone of the rat nucleus of the solitary tract. Brain Res. 616, 144–153.

Wang, L. and Bradley, R. M. 1995. *In vitro* study of afferent synaptic transmission in the rostral gustatory zone of the rat nucleus of the solitary tract. Brain Res. 702, 188–198.

Wang, X. and Ogawa, H. 2002. Columnar organization of mechanoreceptive neurons in the cortical taste area in the rat. Exp. Brain Res. 147, 114–123.

Whitehead, M. C. 1988. Neuronal architecture of the nucleus of the solitary tract in the hamster. J. Comp. Neurol. 276, 547–572.

Whitehead, M. C. 1990. Subdivisions and neuron types of the nucleus of the solitary tract that project to the parabrachial nucleus in the hamster. J. Comp. Neurol. 301, 554–574.

Whitehead, M. C., Bergula, A., and Holliday, K. 2000. Forebrain projections to the rostral nucleus of the solitary tract in the hamster. J. Comp. Neurol. 422, 429–447.

Williams, G. V., Rolls, E. T., Leonard, C. M., and Stern, C. 1993. Neuronal responses in the ventral striatum of the behaving macaque. Behav. Brain Res. 55, 243–252.

Woolston, D. C. and Erickson, R. P. 1979. Concept of neuron types in gustation in the rat. J. Neurophysiol. 42, 1390–1409.

Yamamoto, T. and Kawamura, Y. 1975. Cortical responses to electrical and gustatory stimuli in the rabbit. Brain Res. 94, 447–463.

Yamamoto, T., Matsuo, R., Fujimoto, Y., Fukunaga, I., Miyasaka, A., and Imoto, T. 1991. Electrophysiological and behavioral studies on the taste of umami substances in the rat. Physiol. Behav. 49, 919–925.

Yamamoto, T., Matsuo, R., Ichikawa, H., Wakisaka, S., Akai, M., Imai, Y., Yonehara, N., and Inoki, R. 1990. Aversive taste stimuli increase CGRP levels in the gustatory insular cortex of the rat. Neurosci. Lett. 112, 167–172.

Yamamoto, T., Matsuo, R., and Kawamura, Y. 1980. Localization of cortical gustatory area in rats and its role in taste discrimination. J. Neurophysiol. 44, 440–455.

Yamamoto, T., Matsuo, R., Kiyomitsu, Y., and Kitamura, R. 1989a. Response properties of lateral hypothalamic neurons during ingestive behavior with special reference to licking of various taste solutions. Brain Res. 481, 286–297.

Yamamoto, T., Matsuo, R., Kiyomitsu, Y., and Kitamura, R. 1989b. Taste responses of cortical neurons in freely ingesting rats. J. Neurophysiol. 61, 1244–1258.

Yamamoto, T., Shimura, T., Sako, N., Yasoshima, Y., and Sakai, N. 1994. Neural substrates for conditioned taste aversion in the rat. Behav. Brain Res. 65, 123–137.

Yamamoto, T., Yuyama, N., Kato, T., and Kawamura, Y. 1985. Gustatory responses of cortical neurons in rats. II. Information processing of taste quality. J. Neurophysiol. 53, 1356–1369.

Yan, J. and Scott, T. R. 1996. The effect of satiety on responses of gustatory neurons in the amygdala of alert cynomolgus macaques. Brain Res. 740, 193–200.

Yasoshima, Y., Sako, N., Senba, E., and Yamamoto, T. 2006. Acute suppression, but not chronic genetic deficiency, of c-fos gene expression impairs long-term memory in aversive taste learning. Proc. Natl. Acad. Sci. U. S. A. 103, 7106–7111.

Yasui, Y., Saper, C. B., and Cechetto, D. F. 1989. Calcitonin gene-related peptide immunoreactivity in the visceral sensory cortex, thalamus, and related pathways in the rat. J. Comp. Neurol. 290, 487–501.

Yaxley, S., Rolls, E. T., and Sienkiewicz, Z. J. 1988. The responsiveness of neurons in the insular gustatory cortex of the macaque monkey is independent of hunger. Physiol. Behav. 42, 223–229.

Yaxley, S., Rolls, E. T., and Sienkiewicz, Z. J. 1990. Gustatory responses of single neurons in the insula of the macaque monkey. J. Neurophysiol. 63, 689–700.

Yoshida, R., Shigemura, N., Sanematsu, K., Yasumatsu, K., Ishizuka, S., and Ninomiya, Y. 2006. Taste responsiveness of fungiform taste cells with action potentials. J. Neurophysiol. 96, 3088–3095.

Zahm, D. S. 2000. An integrative neuroanatomical perspective on some subcortical substrates of adaptive responding with emphasis on the nucleus accumbens. Neurosci. Biobehav. Rev. 24, 85–105.

4.16 Neural Ensembles in Taste Coding

A Fontanini, S E Grossman, B A Revill, and D B Katz, Brandeis University, Waltham, MA, USA

© 2008 Elsevier Inc. All rights reserved.

4.16.1	Introduction	329
4.16.2	Population Coding and Neural Interactions	330
4.16.3	Functional Implications of Interactive Population Coding	331
4.16.4	The Purposes of Neural Interactions in Taste	333
4.16.5	Conclusions	334
References		334

Glossary

coherence The state of sticking together, here meaning neurons firing (or changing firing) at the same times.

context A set of variables having to do with the environment, either internal or external.

ensembles Groups of neurons recorded simultaneously.

forebrain The rostral-most portion of the brain, including the thalamus, hypothalamus, basal ganglia, limbic system, and of course cerebral cortex.

hierarchy Classification for a system containing a series of levels, each of which does a particular job or set of jobs.

interactions Activity in one element (here, a neuron or brain region) having an impact on activity in another.

pattern completion A property of a neural network architecture, whereby the act of setting a small subset of units into a state reflecting a particular global pattern causes, through time, the rest of the network to complete this global pattern.

receptive field The range of stimuli to which a neuron responds.

taste space A theoretical organization of the relative similarities between the stimuli within a particular modality.

top-down Interregional interactions reflecting the influence of a higher level of a hierarchy on a lower level of the same hierarchy.

4.16.1 Introduction

Two main theories of taste coding, the labeled-line (LL) and across-neuron pattern (ANP) hypotheses, dominate research in gustation. The two theories are similar, in that both explain taste coding in terms of activity in populations of neurons. They differ in only one regard: according to the LL theory, a particular subgroup of neurons communicates information for a particular taste, and therefore a reduction in firing among one subgroup (say, sucrose-best neurons) codes a reduction in that taste (sweetness); according to the ANP theory, the entire population of taste-responsive neurons participates in all codes, and therefore a reduction in the response of sucrose-best neurons is expected to code both a reduction in sweetness and an increase in some other taste quality (which is coded, in part, by specifically low firing rates in sucrose-best neurons).

It is not our intent to pursue these distinctions here. Excellent pro-LL (Scott, K., 2004) and pro-ANP (Smith, D. V. and St. John, S. J., 1999) reviews have been written in the last 10 years. Instead, we will discuss a basic aspect of neural population function that is largely lacking from debates over taste coding. In this essay, we will suggest that coding in distributed neural populations is intrinsically interactive, and that future advances in our theories of gustatory population coding will therefore require an accounting of such interactions. We will present data demonstrating that such interactions occur in sensory systems, including the gustatory system. This will lead to a discussion of the spatial and temporal structures that such interactions introduce

into population activity, and finally to our suggestion that dynamic population codes may be best thought of not as coding stimuli themselves, but rather as driving the transformation of sensory-related activity into action-related activity. Guided by seminal theorizing about perception and action (Gibson, J. J., 1966; Erickson, R., 1984) and by data from taste and other sensory systems, we will argue that the time has come to think about gustatory population coding in a way that is orthogonal to the LL–ANP debate.

4.16.2 Population Coding and Neural Interactions

While the LL and ANP hypotheses both refer to activity in populations of neurons, neither suggests a specific role for interactions between the neurons. Such interactions, embodied at the simplest level by concepts such as lateral or reciprocal inhibition and excitation, would in fact introduce complications into the decoding of a LL or ANP code, because such interactions cause neural activity to be modulated through time (see below). In fact, any purely spatial coding scheme (such as both LL and ANP) proposed to function in a network in which neurons interact must include specification of the operative time period during which the spatial code will be polled for content.

By comparison, most conceptions of neural population function explicitly rely on convergence and/or feedback between nodes (see, for instance, Nagai, T. *et al.*, 1992; van Vreeswijk, C. and Sompolinsky, H., 1998; Nagai, T., 2000; Masuda, N. and Aihara, K., 2003). The earliest neural network models, founded on basic neuroscientific principles but developed before researchers had the means to do ensemble electrophysiology, suggested that population coding relies on information transfer among an entire set of neural elements (McClelland, J. L. and Rumelhart, D. E., 1981). No individual group of neurons in these models (save the input and output nodes) is profitably described as coding any particular stimulus. Instead, processing is a function of the interactions between neurons. Input to such models – even LL input – is transformed by interconnected neural networks into dynamic patterns in which individual neural elements seldom code stimulus attributes independently of their neighbors (see, for instance, Lumer, E. D. *et al.*, 1997; Rabinovich, M. I. *et al.*, 2000; Sporns, O. *et al.*, 2000).

Data collected in the light of such neural network modeling has suggested that real brain systems engage in exactly this sort of population coding. A variety of vertebrate and invertebrate sensory, cognitive, and motor systems may make explicit use of interactions between neurons (see below). These interactions introduce considerable complexity into single-neuron behavior and do processing work in neural systems. And while most of this work has been done in the visual, auditory, somatosensory, and olfactory systems, it now appears that the same can be said of the gustatory system – neuronal interactions occur both within and between brain regions in the taste neuroaxis. We will now briefly discuss those anatomical and physiological data.

Interactive processing within single brain regions can be revealed in cross-correlogram (CCG) and cross-coherence peaks, which indicate that one neuron produces action potentials in a consistent temporal relationship to those of another (Brody, C. D., 1999). When that correlated activity is specific to particular stimuli, it suggests that neural coding may involve population interactions. Such coding has been observed to occur in the somatosensory (Roy, S. and Alloway, K. D., 1999), auditory (e.g., Eggermont, J. J., 1994; DeCharms, R. C. and Merzenich, M. M., 1996; Eggermont, J. J., 2000), visual (e.g., Brosch, M. *et al.*, 1997; Lampl, I. *et al.*, 1999; Bretzner, F. *et al.*, 2001; Yoshimura, Y. *et al.*, 2005), and olfactory (e.g., Wehr, M. and Laurent, G., 1996; Christensen, T. A. *et al.*, 2003) systems, and similar findings have been reported in the frontal cortex of monkeys performing a GO NO-GO task (Vaadia, E. *et al.*, 1995) and in motor cortex (Hatsopoulos, N. G. *et al.*, 2003).

In the taste system as well, pairs of cortical neurons produce correlated spike patterns during the presentation of particular subsets of tastes (Yokota, T. *et al.*, 1996; Nakamura, T. and Ogawa, H., 1997; Yokota, T. and Satoh, T., 2001; Katz, D. B. *et al.*, 2002b). Taste administration recruits taste-specific but overlapping neuronal ensembles, including some neurons that are broadly tuned and some that according to classic single-neuron analyses cannot even be identified as taste responsive, that is, neurons with flat or unremarkable responses to taste administration may still be involved in taste-specific cross-correlations (Katz, D. B. *et al.*, 2002b). Taste-specific cross-correlations have also been observed in the nucleus of the solitary tract (NTS, Adachi, M. *et al.*, 1989) and in the pontine parabrachial nuclei (PbN, Yamada, S. *et al.*, 1990; Adachi, M., 1991). Patterns of

neural interactions appear to provide an additional source of taste-related information not inherent in single-unit spike trains, suggesting that taste neurons are embedded in interactive ensembles.

Of course, these intraregional ensembles are themselves embedded in larger interactive networks. Various dye-labeling techniques have demonstrated the existence of reciprocal connections among taste-responsive nuclei in brainstem, thalamic, limbic, and cortical regions. Just as injections of horse-radish peroxidase into PbN have revealed two parallel ascending taste pathways in rodents – a parabrachio-thalamo-cortical and parabrachio-amygdaloid pathway (Halsell, C. B., 1992) – similar methods have revealed descending pathways back to the brainstem (van der Kooy, D. *et al.*, 1984; Huang, T. *et al.*, 2003). Reciprocal connections have been shown to exist between various pairs of taste regions, including gustatory cortex (GC) and thalamus (Nakashima, M. *et al.*, 2000), GC and amygdala (McDonald, A. J. and Jackson, T. R., 1987), and amygdala and PbN (Takeuchi, Y. *et al.*, 1982). These data suggest that taste information is processed in a distributed system of information exchange involving ascending and descending pathways.

Interregional connectivity in the taste system is both convergent and functional (Di Lorenzo, P. M. and Monroe, S., 1997), just as it is in other systems (e.g., Kay, L. M. *et al.*, 1996; Alonso, J. M. *et al.*, 2001; Alloway, K. D. and Roy, S. A., 2002; Villalobos, M. E. *et al.*, 2005). For example, stimulation of GC, amygdala, or hypothalamus modifies single-neuron PbN responses to lingual application of the four basic tastes (Lundy, R. F. and Norgren, R., 2004; Li, C. S. *et al.*, 2005). A large percentage of the PbN taste neurons that receive any sort of feedback receive it from at least two forebrain sites, suggesting that multiple feedback loops may converge upon single brainstem taste neurons. Modulation of neurons in NTS, the very first central taste relay, via manipulation of both central amygdala and lateral hypothalamus, produces similar results (Cho, Y. K. *et al.*, 2003).

The specific function of feedback from forebrain to brainstem has been suggested to be a sharpening of receptive field (i.e., forebrain stimulation typically reduces the number of stimuli to which brainstem neurons respond, see Lundy, R. F. and Norgren, R., 2004). It might be tempting to conclude that the ultimately sharpened responses are evidence for a LL code, but in fact these data compellingly demonstrate that feed-forward projections are relatively broadly tuned (reflecting either broadly receptive transduction mechanisms or very early mixing of pathways), and that the apparent labeling of brainstem neurons represents an interactive network effect, in which the broad responses are tuned up by forebrain populations.

4.16.3 Functional Implications of Interactive Population Coding

The existence of interactive ensembles has strong implications for neural network function. Specifically, within- and between-region interactions affect neural activity by introducing structure – both spatial and temporal – into spontaneous and evoked neural activity. Through such imposition of structure, interneuronal interactions imbue neural activity with contextual and behavioral specificity. We will now discuss studies demonstrating that these phenomena are prominent in many neural systems and, to the extent that they have been studied, in the taste system as well.

Classical analysis of sensory neural coding relies on the tacit assumption that spontaneous, prestimulus neural activity is random and uncorrelated – noise with which stimulus-evoked signals must compete. In populations of interacting neural elements, however, spontaneous activity is far from random. Hallmark phenomena of interactive processing, such as pattern completion (Rumelhart, D. E. and McClelland, J. L., 1986), ensure that spontaneous activity can drive a network into preferred coherent states.

Little work on this topic has yet been done in the taste neuroaxis, but visual cortex has been shown to spontaneously attain spatially coherent global states (Arieli, A. *et al.*, 1996). Images of intrinsic V1 signals, keyed to the spontaneous firing of individual neurons, are nearly identical to the maps produced when those neurons' best stimuli are presented (Tsodyks, M. *et al.*, 1999; Kenet, T. *et al.*, 2003). Analogously, motor cortical networks have been suggested to attain states, referred to as preshapes, that predict population codes for particular movements well in advance of such movements (Bastian, A. *et al.*, 1998; 2003). Cortex can produce best-stimulus responses both in the presence and absence of these stimuli.

The complementary result has also been shown: cortex produces surprisingly variable responses to static stimuli. In fact, the specific spatial structure of cortical responses is less dependent on the exact

physical stimulus than on the cognitive context, that is, the animal's interpretation of the stimulus at a particular moment. In the visual system, for example, attention modulates the magnitude of sensory activity, enhancing responses to the attended object and suppressing responses to unattended ones (e.g., Fischer, B. and Boch, R., 1985; Reynolds, J. H. and Chelazzi, L., 2004). In situations in which a stimulus is bistable (e.g., the figure-ground illusion), meanwhile, cortical neurons shift firing rates in direct relation to changes in perception, despite the fact that the actual sensory stimulus is static (Leopold, D. A. and Logothetis, N. K., 1996; Otterpohl, J. R. *et al.*, 2000). Cognitive states also influence the correlations between neurons responding to simultaneously presented stimuli, modifying spatial patterns of neural interactions in cortical regions (Hatsopoulos, N. G. *et al.*, 1998; 2003), and thereby tagging the ensembles recruited to code particular real-world objects; the visual responses to disconnected line segments that are perceived to be part of a single occluded rod fire in synchrony, for instance, while responses to identical line segments that do not present the percept of an occluded rod do not (Singer, W., 1993; see also Harris, K. D., 2005).

In the taste system, as well, attentional variables affect cortical coding: when a rat ceases to pay attention to taste stimuli, the responses of 40% of the neurons in taste cortex suddenly change their receptive fields (Fontanini, A. and Katz, D. B., 2006). These changes are not random, but rather represent an interpretable modulation of perceptual taste space – specifically, an increase in the salience of the palatability dimension. Changes in orofacial responses to the tastes (Grill, H. J. and Norgren, R., 1978; Berridge, K. C., 2000) confirm this interpretation (Fontanini, A. and Katz, D. B., 2006). Such placing of coherent responses into a meaningful context has been suggested to have its source in feedback from higher neural centers (Engel, A. K. *et al.*, 2001; Buffalo, E. A. *et al.*, 2005). In other words, inclusion of multiple brain regions in the coding population places the neural code into the motivational and cognitive context, such that sensory responses reflect the meaning of stimuli, and not simply their physical makeup.

While it has not yet been shown that taste networks organize into analogous spatial coherence (but see Yoshimura, H. *et al.*, 2004), it is becoming clear that neural responses to taste administration, like those to other stimuli (e.g., Golomb, D. *et al.*, 1994; Vaadia, E. *et al.*, 1995; MacLeod, K, and Laurent, G., 1996; Seidemann, E. *et al.*, 1996; Compte, A. *et al.*, 2000; Kirkland, K. L. *et al.*, 2000; Bazhenov, M. *et al.*, 2001; Miller, P. *et al.*, 2005), do have temporal structure. Such temporal structure has been extensively described in both brainstem (Di Lorenzo, P. M. and Schwartzbaum, J. S., 1982; Erickson, R. P. *et al.*, 1994; Di Lorenzo, P. M. and Victor, J. D., 2003) and cortex (Katz, D. B. *et al.*, 2001; see also Tabuchi, E. *et al.*, 2002). The use of chronic recordings in active, tasting rats has allowed us to observe not only slower dynamics but also oscillations (Fontanini, A. and Katz, D. B., 2005) in taste cortex, a region rife with inhibitory cross-talk (Ogawa, H. *et al.*, 1998). These cortical dynamics have been directly linked to network functioning (Katz, D. B. *et al.*, 2002b), a finding that is consistent with paired-pulse studies showing that two identical inputs, separated by just long enough to allow the processing of information from the first input to begin, cause reliably distinct patterns of response in NTS neurons (Lemon, C. H. and Di Lorenzo, P. M., 2002; Di Lorenzo, P. M. *et al.*, 2003). Gustatory responses are clearly dynamic, as predicted by interactive population models (but not by either the LL or ANP model).

Analogous to the above findings on spatial coherence, perceptual relevance emerges in the temporal structure of cortical taste responses, much as it does in other systems (Sugase, Y. *et al.*, 1999; Friedrich, R. W. and Laurent, G., 2001). While data from primates have suggested that only prefrontal cortical activity is affected by important changes in state (i.e., satiety, Rolls, E. T. *et al.*, 1989), rat primary cortical responses clearly contain both sensory and cognitive components. These responses can be divided in three epochs, each of which reflects a particular stage of gustatory processing – somatosensation, chemosensation, and palatability (Katz, D. B. *et al.*, 2001). Attention-related changes in stimulus palatability are preferentially expressed in changes in late-epoch coding (Fontanini, A. and Katz, D. B., 2006), a fact that reinforces the conclusion that the three epochs represent genuine temporal coding, rather than trivially reflecting the outcome of processing.

The evolution of activity during these three epochs could be the result of interactions/reverberations between the gustatory system and other high-order areas known to code palatability, such as the amygdala (Nishijo, H. *et al.*, 1998). It has also recently been shown that even later aspects of cortical responses in rats change as a taste becomes familiar (Bahar, A. S. *et al.*, 2004). Thus, cognitive processes are apparent both in the spatial and temporal

structures of sensory responses, as one expects when examining a system functioning via interacting populations of neurons.

4.16.4 The Purposes of Neural Interactions in Taste

It is clear that the behavior of neurons in primary GC must be interpreted in terms of context – both the physical context of the networks (of neurons and brain areas) into which the neuron is connected and the cognitive context of the task. Primary GC is not a passive receiver, but rather a dynamic processor of information constantly engaged in a behaviorally dependent interplay with other regions; taste neurons in cortex interact with populations of neurons throughout the taste neuroaxis in the process of stimulus coding. A fundamental issue that remains to be addressed, however, is the definition of the term coding. Put another way, the question is: what kind of processes are interacting populations of taste neurons involved in?

It has been suggested that neural ensembles may interact for the purposes of binding and/or effective signal transmission, collapsing neurons into a functional, synchronous ensemble in order that this ensemble may code a context-embedded percept. Intraregional connectivity is thought to allow flexible assembly of a broad range of possible ensembles, while longer-range connections modulate that assembly according to global (cognitive) states (Brosch, M. *et al.*, 1997). This hypothesis has been further extended to consider time-varying responses, wherein distinct subpopulations of neurons fire synchronously at different times during the response (Vaadia, E. *et al.*, 1995; Wehr, M. and Laurent, G., 1996).

Synchrony is potentially powerful, because synchronous input can be decoded by coincidence-detecting readout cells whose firing represents a synthetic and sparsened version of the input. Perhaps the most well-studied example comes from the insect olfactory system. Kenyon cells in the mushroom body of the locust and fly receive complex, time-varying inputs from populations of projecting neurons in the antenna lobe (Laurent, G. *et al.*, 2001; Lei, H. *et al.*, 2004; Wilson, R. I. *et al.*, 2004) and respond to this very complex input with relatively few – and very reliable – action potentials following the arrival of synchronous inputs (Perez-Orive, J. *et al.*, 2002). The attractiveness of the synchronization hypothesis lies in the ease with which it fits into an overall vision of the brain as a coding–decoding device: every area codes the input according to some rules and feeds its output to a higher level area that synthesizes it into a sparser representation. In this framework the brain is treated as a linear hierarchical system, where the output of a level is sent to the next, and where the highest level decodes a fully contextualized percept.

The evidence collected thus far, however, does not provide strong support for such a model of gustatory function. As described above, information traversing the gustatory system is hierarchical only to a first approximation – for every ascending pathway between brainstem and forebrain there is matching feedback. In the context of this recurrent organization it is hard to identify the putative decoding zone in which convergence and sparsening might occur. Recordings confirm that the taste selectivity of neural responses does not increase by a great deal as one ascends through the system (Yamamoto, T. *et al.*, 1985; Ogawa, H. *et al.*, 1990; Nishijo, H. *et al.*, 1998), and there is not much evidence for synchrony or oscillations during gustatory processing. In fact, while oscillations occur prominently in gustatory cortex, they specifically occur when rats are not engaged in taste processing (Fontanini, A. and Katz, D. B., 2005). Significant CCGs between pairs of neurons separated by more than 100 μm, meanwhile, appear to reflect simultaneous changes of firing rate, rather than synchronous firing of action potentials (Katz, D. B. *et al.*, 2002b).

Alternative theories avoid the coding–decoding issue entirely, simply by suggesting that processing of a sensory stimulus can be accomplished in the absence of coding of the sensory stimulus. Several researchers and philosophers (see, for instance, Varela, F. J. *et al.*, 1991; van Gelder, T., 1992; Eggermont, J. J., 1998; Engel, A. K. *et al.*, 2001), including more than one chemosensory scientist (Freeman, W. J. and Skarda, C. A., 1994; Halpern, B. P., 2000), have suggested that coding and representation may be constructs with more relevance to computer function than to brain function. Such a notion is *prima facie* attractive, because all extant concepts of taste coding run into trouble over the fact of the wide range of response latencies produced in gustatory behavior – the fact that some taste responses can be produced as little as 200 ms following taste administration, while others take well over 1 s (Halpern, B. P., 2005). Furthermore, it makes sense from an ecological prospective, in that the function of gustation is to provide information for

the crucial decision of ingesting or rejecting food (Gibson, J. J., 1966). Taste is therefore intimately linked to orofacial motor behavior – a linkage that is explicit in the fact that the brainstem taste relays are almost directly connected into orofacial motor-neuron pools (Travers, J. B. and Norgren, R., 1983; Travers, J. B. *et al.*, 2000). It may be reasonably argued that the job of populations of neurons in the gustatory neuroaxis is not to code tastes at all, but rather to transform taste input into motor output. In such a scheme, the spatial hierarchy in which each successive brain region contains more highly processed information is replaced by a temporal hierarchy in which successive time points contain more highly processed information.

This, then, would be the function of interacting neural populations – to transform input, through poststimulus time, into a form adequate for driving behavior. Stimulus-related input does not get represented by neural firing (or even by neural synchrony) for any particular finite time, but rather sets in motion a dynamic process of population interaction (Harris, K. D., 2005). This is consistent not only with the recent data on temporal coding and cross-correlations in taste (Katz, D. B. *et al.*, 2002a), but also with data from other systems showing: (1) action-oriented responses in early sensory relays (Kay, L. M. and Laurent, G., 1999, Shuler, M. G. and Bear, M. F., 2006); (2) emergence of perceptual information through time (Sugase, Y. *et al.*, 1999); and (3) intriguing new data suggesting that visual input merely perturbs active processes already underway in V1 (Fiser, J. *et al.*, 2004).

4.16.5 Conclusions

These are necessarily speculative musings, because the study of interactive population coding in taste cortex and the larger taste neuroaxis is still in its infancy. We do not write this review in an attempt to resolve the debate between LL and ANP theories – both theories have their adherents, both can be thought to receive support from data, and as of now neither can be disproved in the central nervous system. Our suggestion is that we will need a more explicit account of interacting populations, perhaps adapted from research in other systems, if we are to provide the necessary framework for a complete understanding of the functioning of taste networks. These interactions exist in the taste system, as they do in other, more extensively examined systems and in realistic neural models. The extant theory and data suggest that they may be central to sensory function – function that may conceivably have more to do with transforming input smoothly into motor output than with actual coding of the stimulus *per se*. It will likely be years before these issues can be completely resolved.

References

Adachi, M. 1991. The mechanism of taste quality discrimination in rat pontine parabrachial nucleus. Aichi Gakuin Daigaku Shigakkai Shi 29, 283–299.

Adachi, M., Ohshima, T., Yamada, S., and Satoh, T. 1989. Cross-correlation analysis of taste neuron pairs in rat solitary tract nucleus. J. Neurophysiol. 62, 501–509.

Alloway, K. D. and Roy, S. A. 2002. Conditional cross-correlation analysis of thalamocortical neurotransmission. Behav. Brain Res. 135, 191–196.

Alonso, J. M., Usrey, W. M., and Reid, R. C. 2001. Rules of connectivity between geniculate cells and simple cells in cat primary visual cortex. J. Neurosci. 21, 4002–4015.

Arieli, A., Sterkin, A., Grinvald, A., and Aertsen, A. 1996. Dynamics of ongoing activity: explanation of the large variability in evoked cortical responses. Science 273, 1868–1871.

Bahar, A. S., Dudai, Y., and Ahissar, E. 2004. Neural signature of taste familiarity in the gustatory cortex of the freely behaving rat. J. Neurophysiol. 92, 3298–3308.

Bastian, A., Riehle, A., Erlhagen, W., and Schoner, G. 1998. Prior information preshapes the population representation of movement direction in motor cortex. Neuroreport 9, 315–319.

Bastian, A., Schoner, G., and Riehle, A. 2003. Preshaping and continuous evolution of motor cortical representations during movement preparation. Eur. J. Neurosci. 18, 2047–2058.

Bazhenov, M., Stopfer, M., Rabinovich, M., Abarbanel, H. D., Sejnowski, T. J., and Laurent, G. 2001. Model of cellular and network mechanisms for odor-evoked temporal patterning in the locust antennal lobe. Neuron 30, 569–581.

Berridge, K. C. 2000. Measuring hedonic impact in animals and infants: microstructure of affective taste reactivity patterns. Neurosci. Biobehav. Rev. 24, 173–198.

Bretzner, F., Aitoubah, J., Shumikhina, S., Tan, Y. F., and Molotchnikoff, S. 2001. Modulation of the synchronization between cells in visual cortex by contextual targets. Eur. J. Neurosci. 14, 1539–1554.

Brody, C. D. 1999. Disambiguating different covariation types. Neural Comput. 11, 1527–1535.

Brosch, M., Bauer, R., and Eckhorn, R. 1997. Stimulus-dependent modulations of correlated high-frequency oscillations in cat visual cortex. Cereb. Cortex 7, 70–76.

Buffalo, E. A., Bertini, G., Ungerleider, L. G., and Desimone, R. 2005. Impaired filtering of distracter stimuli by TE neurons following V4 and TEO lesions in macaques. Cereb. Cortex 15, 141–151.

Cho, Y. K., Li, C. S., and Smith, D. V. 2003. Descending influences from the lateral hypothalamus and amygdala converge onto medullary taste neurons. Chem. Senses 28, 155–171.

Christensen, T. A., Lei, H., and Hildebrand, J. G. 2003. Coordination of central odor representations through transient, non-oscillatory synchronization of glomerular

output neurons. Proc. Natl. Acad. Sci. U. S. A. 100, 11076–11081.
Compte, A., Brunel, N., Goldman-Rakic, P. S., and Wang, X. J. 2000. Synaptic mechanisms and network dynamics underlying spatial working memory in a cortical network model. Cereb. Cortex 10, 910–923.
DeCharms, R. C. and Merzenich, M. M. 1996. Primary cortical representation of sounds by the coordination of action-potential timing. Nature 381, 610–613.
Di Lorenzo, P. M. and Monroe, S. 1997. Transfer of information about taste from the nucleus of the solitary tract to the parabrachial nucleus of the pons. Brain Res. 763, 167–181.
Di Lorenzo, P. M. and Schwartzbaum, J. S. 1982. Coding of gustatory information in the pontine parabrachial nuclei of the rabbit: temporal patterns of neural response. Brain Res. 251, 245–257.
Di Lorenzo, P. M. and Victor, J. D. 2003. Taste response variability and temporal coding in the nucleus of the solitary tract of the rat. J. Neurophysiol. 90, 1418–1431.
Di Lorenzo, P. M., Lemon, C. H., and Reich, C. G. 2003. Dynamic coding of taste stimuli in the brainstem: effects of brief pulses of taste stimuli on subsequent taste responses. J. Neurosci. 23, 8893–8902.
Eggermont, J. J. 1994. Neural interaction in cat primary auditory cortex II. Effects of sound stimulation. J. Neurophysiol. 71, 246–270.
Eggermont, J. J. 1998. Is there a neural code? Neurosci. Biobehav. Rev. 22, 355–370.
Eggermont, J. J. 2000. Sound-induced synchronization of neural activity between and within three auditory cortical areas. J. Neurophysiol. 83, 2708–2722.
Engel, A. K., Fries, P., and Singer, W. 2001. Dynamic predictions: oscillations and synchrony in top-down processing. Nat. Rev. Neurosci. 2, 704–716.
Erickson, R. 1984. On the neural bases of behavior. Am. Sci. 72, 233–241.
Erickson, R. P., Di Lorenzo, P. M., and Woodbury, M. A. 1994. Classification of taste responses in brain stem: membership in fuzzy sets. J. Neurophysiol. 71, 2139–2150.
Fischer, B. and Boch, R. 1985. Peripheral attention versus central fixation: modulation of the visual activity of prelunate cortical cells of the rhesus monkey. Brain Res. 345, 111–123.
Fiser, J., Chiu, C., and Weliky, M. 2004. Small modulation of ongoing cortical dynamics by sensory input during natural vision. Nature 431, 573–578.
Fontanini, A. and Katz, D. B. 2005. 7 to 12 Hz activity in rat gustatory cortex reflects disengagement from a fluid self-administration task. J. Neurophysiol. 93, 2832–2840.
Fontanini, A. and Katz, D. B. 2006. State-dependent modulation of time-varying gustatory responses. J. Neurophysiol. 96, 3183–3193.
Freeman, W. J. and Skarda, C. A. 1994. Representations: Who Needs Them? In: Brain Organization and Memory: Cells, Systems, and Circuits (*eds*. J. L. McGaugh, N. Weinberger, and G. Lynch), pp. 375–380. Oxford University Press.
Friedrich, R. W. and Laurent, G. 2001. Dynamic optimization of odor representations by slow temporal patterning of mitral cell activity. Science 291, 889–894.
van Gelder, T. 1992. What might cognition be if not computation? J. Philo. 91, 345–381.
Gibson, J. J. 1966. The Senses Considered as Perceptual Systems. Houghton Mifflin.
Golomb, D., Wang, X. J., and Rinzel, J. 1994. Synchronization properties of spindle oscillations in a thalamic reticular nucleus model. J. Neurophysiol. 72, 1109–1126.
Grill, H. J. and Norgren, R. 1978. The taste reactivity test. I. Mimetic responses to gustatory stimuli in neurologically normal rats. Brain Res. 143, 263–279.
Halpern, B. P. 2000. Sensory coding, decoding, and representations. Unnecessary and troublesome constructs? Physiol. Behav. 69, 115–118.
Halpern, B. P. 2005. Temporal characteristics of human taste judgements as calibrations for gustatory event-related potentials and gustatory magnetoencephalographs. Chem. Senses 30(Suppl. 1), i228–i229.
Halsell, C. B. 1992. Organization of parabrachial nucleus efferents to the thalamus and amygdala in the golden hamster. J .Comp. Neurol. 317, 57–78.
Harris, K. D. 2005. Neural signatures of cell assembly organization. Nat. Rev. Neurosci. 6, 399–407.
Hatsopoulos, N. G., Ojakangas, C. L., Paninski, L., and Donoghue, J. P. 1998. Information about movement direction obtained from synchronous activity of motor cortical neurons. Proc. Natl. Acad. Sci. U. S. A. 95, 15706–15711.
Hatsopoulos, N. G., Paninski, L., and Donoghue, J. P. 2003. Sequential movement representations based on correlated neuronal activity. Exp. Brain. Res. 149, 478–486.
Huang, T., Yan, J., and Kang, Y. 2003. Role of the central amygdaloid nucleus in shaping the discharge of gustatory neurons in the rat parabrachial nucleus. Brain Res. Bull. 61, 443–452.
Katz, D. B., Nicolelis, M. A., and Simon, S. A. 2002a. Gustatory processing is dynamic and distributed. Curr. Opin. Neurobiol. 12(4), 448–454.
Katz, D. B., Simon, S. A., and Nicolelis, M. A. 2001. Dynamic and multimodal responses of gustatory cortical neurons in awake rats. J. Neurosci. 21, 4478–4489.
Katz, D. B., Simon, S. A., and Nicolelis, M. A. 2002b. Taste-specific neuronal ensembles in the gustatory cortex of awake rats. J. Neurosci. 22, 1850–1857.
Kay, L. M. and Laurent, G. 1999. Odor- and context-dependent modulation of mitral cell activity in behaving rats. Nat. Neurosci. 2, 1003–1009.
Kay, L. M., Lancaster, L. R., and Freeman, W. J. 1996. Reafference and attractors in the olfactory system during odor recognition. Int. J. Neural Syst. 7, 489–495.
Kenet, T., Bibitchkov, D., Tsodyks, M., Grinvald, A., and Arieli, A. 2003. Spontaneously emerging cortical representations of visual attributes. Nature 425, 954–956.
Kirkland, K. L., Sillito, A. M., Jones, H. E., West, D. C., and Gerstein, G. L. 2000. Oscillations and long-lasting correlations in a model of the lateral geniculate nucleus and visual cortex. J. Neurophysiol. 84, 1863–1868.
van der Kooy, D., Koda, L. Y., McGinty, J. F., Gerfen, C. R., and Bloom, F. E. 1984. The organization of projections from the cortex, amygdala, and hypothalamus to the nucleus of the solitary tract in rat. J. Comp. Neurol. 224, 1–24.
Lampl, I., Reichova, I., and Ferster, D. 1999. Synchronous membrane potential fluctuations in neurons of the cat visual cortex. Neuron 22, 361–374.
Laurent, G., Stopfer, M., Friedrich, R. W., Rabinovich, M. I., Volkovskii, A., and Abarbanel, H. D. 2001. Odor encoding as an active, dynamical process: experiments, computation, and theory. Annu. Rev. Neurosci. 24, 263–297.
Lei, H., Christensen, T. A., and Hildebrand, J. G. 2004. Spatial and temporal organization of ensemble representations for different odor classes in the moth antennal lobe. J. Neurosci. 24, 11108–11119.
Lemon, C. H. and Di Lorenzo, P. M. 2002. Effects of electrical stimulation of the chorda tympani nerve on taste responses in the nucleus of the solitary tract. J. Neurophysiol. 88, 2477–2489.
Leopold, D. A. and Logothetis, N. K. 1996. Activity changes in early visual cortex reflect monkeys' percepts during binocular rivalry. Nature 379, 549–553.
Li, C. S., Cho, Y. K., and Smith, D. V. 2005. Modulation of parabrachial taste neurons by electrical and chemical

stimulation of the lateral hypothalamus and amygdala. J. Neurophysiol. 93, 1183–1196.
Lumer, E. D., Edelman, G. M., and Tononi, G. 1997. Neural dynamics in a model of the thalamocortical system. I. Layers, loops and the emergence of fast synchronous rhythms. Cereb. Cortex 7, 207–227.
Lundy, R. F., Jr. and Norgren, R. 2004. Activity in the hypothalamus, amygdala, and cortex generates bilateral and convergent modulation of pontine gustatory neurons. J. Neurophysiol. 91, 1143–1157.
MacLeod, K. and Laurent, G. 1996. Distinct mechanisms for synchronization and temporal patterning of odor-encoding neural assemblies. Science 274, 976–979.
Masuda, N. and Aihara, K. 2003. Duality of rate coding and temporal coding in multilayered feedforward networks. Neural Comput. 15, 103–125.
McClelland, J. L. and Rumelhart, D. E. 1981. An interactive activation model of context effects in letter perception. Part 1. An account of basic findings. Psychol. Rev. 88, 375–407.
McDonald, A. J. and Jackson, T. R. 1987. Amygdaloid connections with posterior insular and temporal cortical areas in the rat. J. Comp. Neurol. 262, 59–77.
Miller, P., Brody, C. D., Romo, R., and Wang, X. J. 2005. A recurrent network model of somatosensory parametric working memory in the prefrontal cortex. Cereb. Cortex 15, 679.
Nagai, T. 2000. Artificial neural networks estimate the contribution of taste neurons to coding. Physiol. Behav. 69, 107–113.
Nagai, T., Yamamoto, T., Katayama, H., Adachi, M., and Aihara, K. 1992. A novel method to analyse response patterns of taste neurons by artificial neural networks. Neuroreport 3, 745–748.
Nakamura, T. and Ogawa, H. 1997. Neural interaction between cortical taste neurons in rats: a cross-correlation analysis. Chem. Senses 22, 517–528.
Nakashima, M., Uemura, M., Yasui, K., Ozaki, H. S., Tabata, S., and Taen, A. 2000. An anterograde and retrograde tract-tracing study on the projections from the thalamic gustatory area in the rat: distribution of neurons projecting to the insular cortex and amygdaloid complex. Neurosci. Res. 36, 297–309.
Nishijo, H., Uwano, T., Tamura, R., and Ono, T. 1998. Gustatory and multimodal neuronal responses in the amygdala during licking and discrimination of sensory stimuli in awake rats. J. Neurophysiol. 79, 21–36.
Ogawa, H., Hasegawa, K., Otawa, S., and Ikeda, I. 1998. GABAergic inhibition and modifications of taste responses in the cortical taste area in rats. Neurosci. Res. 32, 85–95.
Ogawa, H., Ito, S., Murayama, N., and Hasegawa, K. 1990. Taste area in granular and dysgranular insular cortices in the rat identified by stimulation of the entire oral cavity. Neurosci. Res. 9, 196–201.
Otterpohl, J. R., Haynes, J. D., Emmert-Streib, F., Vetter, G., and Pawelzik, K. 2000. Extracting the dynamics of perceptual switching from 'noisy' behaviour: an application of hidden Markov modelling to pecking data from pigeons. J. Physiol. Paris 94, 555–567.
Perez-Orive, J., Mazor, O., Turner, G. C., Cassenaer, S., Wilson, R. I., and Laurent, G. 2002. Oscillations and sparsening of odor representations in the mushroom body. Science 297, 359–365.
Rabinovich, M. I., Huerta, R., Volkovskii, A., Abarbanel, H. D., Stopfer, M., and Laurent, G. 2000. Dynamical coding of sensory information with competitive networks. J. Physiol. Paris 94, 465–471.
Reynolds, J. H. and Chelazzi, L. 2004. Attentional modulation of visual processing. Annu. Rev. Neurosci. 27, 611–647.
Rolls, E. T., Sienkiewicz, Z. J., and Yaxley, S. 1989. Hunger modulates the responses to gustatory stimuli of single neurons in the caudolateral orbitofrontal cortex of the macaque monkey. Eur. J. Neurosci. 1, 53–60.
Roy, S. and Alloway, K. D. 1999. Synchronization of local neural networks in the somatosensory cortex: a comparison of stationary and moving stimuli. J. Neurophysiol. 81, 999–1013.
Rumelhart, D. E. and McClelland, J. L. 1986. Parallel Distributed Processing: Explorations in the Microstructure of Cognition, MIT Press.
Scott, K. 2004. The sweet and the bitter of mammalian taste. Curr. Opin. Neurobiol. 14, 423–427.
Seidemann, E., Meilijson, I., Abeles, M., Bergman, H., and Vaadia, E. 1996. Simultaneously recorded single units in the frontal cortex go through sequences of discrete and stable states in monkeys performing a delayed localization task. J. Neurosci. 16, 752–768.
Shuler, M. G. and Bear, M. F. 2006. Reward timing in the Primary Visual Cortex. Science 311, 1606–1609.
Singer, W. 1993. Synchronization of cortical activity and its putative role in information processing and learning. Annu. Rev. Physiol. 55, 349–374.
Smith, D. V. and St. John, S. J. 1999. Neural coding of gustatory information. Curr. Opin. Neurobiol. 9, 427–435.
Sporns, O., Tononi, G., and Edelman, G. M. 2000. Connectivity and complexity: the relationship between neuroanatomy and brain dynamics. Neural Netw. 13, 909–922.
Sugase, Y., Yamane, S., Ueno, S., and Kawano, K. 1999. Global and fine information coded by single neurons in the temporal visual cortex. Nature 400, 869–873.
Tabuchi, E., Yokawa, T., Mallick, H., Inubushi, T., Kondoh, T., Ono, T., and Torii, K. 2002. Spatio-temporal dynamics of brain activated regions during drinking behavior in rats. Brain Res. 951, 270–279.
Takeuchi, Y., McLean, J. H., and Hopkins, D. A. 1982. Reciprocal connections between the amygdala and parabrachial nuclei: ultrastructural demonstration by degeneration and axonal transport of horseradish peroxidase in the cat. Brain Res. 239, 583–588.
Travers, J. B. and Norgren, R. 1983. Afferent projections to the oral motor nuclei in the rat. J. Comp. Neurol. 220, 280–298.
Travers, J. B., DiNardo, L. A., and Karimnamazi, H. 2000. Medullary reticular formation activity during ingestion and rejection in the awake rat. Exp. Brain Res. 130, 78–92.
Tsodyks, M., Kenet, T., Grinvald, A., and Arieli, A. 1999. Linking spontaneous activity of single cortical neurons and the underlying functional architecture. Science 286, 1943–1946.
Vaadia, E., Haalman, I., Abeles, M., Bergman, H., Prut, Y., Slovin, H., and Aertsen, A. 1995. Dynamics of neuronal interactions in monkey cortex in relation to behavioural events. Nature 373, 515–518.
Varela, F. J., Thompson, E. T., and Rosch, E. 1991. The Embodied Mind: Cognitive Science and Human Experience. MIT Press.
Villalobos, M. E., Mizuno, A., Dahl, B. C., Kemmotsu, N., and Muller, R. A. 2005. Reduced functional connectivity between V1 and inferior frontal cortex associated with visuomotor performance in autism. Neuroimage 25, 916–925.
van Vreeswijk, C. and Sompolinsky, H. 1998. Chaotic balanced state in a model of cortical circuits. Neural Comput. 10, 1321–1371.
Wehr, M. and Laurent, G. 1996. Odour encoding by temporal sequences of firing in oscillating neural assemblies (w/ commentary). Nature 384, 162–166.
Wilson, R. I., Turner, G. C., and Laurent, G. 2004. Transformation of olfactory representations in the *Drosophila* antennal lobe. Science 303, 366–370.
Yamada, S., Ohshima, T., Oda, H., Adachi, M., and Satoh, T. 1990. Synchronized discharge of taste neurons recorded

simultaneously in rat parabrachial nucleus. J. Neurophysiol. 63, 294–302.
Yamamoto, T., Yuyama, N., Kato, T., and Kawamura, Y. 1985. Gustatory responses of cortical neurons in rats. II. Information processing of taste quality. J. Neurophysiol. 53, 1356–1369.
Yokota, T. and Satoh, T. 2001. Three-dimensional estimation of the distribution and size of putative functional units in rat gustatory cortex as assessed from the inter-neuronal distance between two neurons with correlative activity. Brain Res. Bull. 54, 575–584.
Yokota, T., Eguchi, K., and Satoh, T. 1996. Correlated discharges of two neurons in rat gustatory cortex during gustatory stimulation. Neurosci. Lett. 209, 204–206.
Yoshimura, Y., Dantzker, J. L., and Callaway, E. M. 2005. Excitatory cortical neurons form fine-scale functional networks. Nature 433, 868–873.
Yoshimura, H., Sugai, T., Fukuda, M., Segami, N., and Onoda, N. 2004. Cortical spatial aspects of optical intrinsic signals in response to sucrose and NaCl stimuli. Neuroreport 15, 17–20.

4.17 A Perspective on Chemosensory Quality Coding

M E Frank, University of Connecticut Health Center, Farmington, CT, USA

© 2008 Elsevier Inc. All rights reserved.

4.17.1	**The Sweet–Salty–Sour–Bitter Decision**	340
4.17.2	**Stimulus and Perceptual Domains**	340
4.17.2.1	Nonchemosensory	340
4.17.2.1.1	Pitch	340
4.17.2.1.2	Color	340
4.17.2.2	Chemosensory	341
4.17.2.2.1	Taste	341
4.17.2.2.2	Smell	341
4.17.3	**Processing of Chemosensory Quality Signals**	342
4.17.3.1	Mixtures	342
4.17.3.2	Chemosensory Quality Constancy	342
4.17.4	**Conclusion**	343
References		343

Glossary

Dedicated sensory neurons They are activated by single or multiple chemosensory receptors to directly and separately code each chemosensory quality.

Discrete stimuli They are separate entities that may share parts and sizes. Chemosensory stimuli are examples; each chemosensory receptor has a discrete molecular domain.

Dynamic chemosensory coding It promotes brief identification of the strong and novel in a complex chemical mixture by combining mixture suppression and rapid sensory adaptation.

Hedonic valence It is positive when a chemosensory stimulus is perceived as good; negative when a chemosensory stimulus is perceived as bad.

Odor notes They are distinct perceptual olfactory qualities; there are hundreds, grouped as object-like (e.g., flower, fruit, animal) or process-like (e.g., spoiled, excreted, burned).

Perceptual continua They are constructed for color and pitch by red-green and blue-yellow opponent cells for each retinal position and multicell frequency maps, respectively.

Quality constancy This occurs if a chemosensory quality remains the same in different contexts, allowing chemosensory stimulus recognition.

Quality tuning They may be broad or fine, depending on how stimuli are biologically detected and species-selective perceptual requirements. An example of broad tuning is the tripartite cellular code for color carried by three pigments, each found in a dedicated retinal cone. An example of fine receptor tuning is the best-frequency cellular code for pitch carried by hundreds of cochlear hair cells.

Somatotopic neural maps These represent distinct touch, pain, warm, and cold senses side by side for each bodily place: for example, on legs, arms, head, nose, mouth, and tongue.

Sound space This is coded in interaural time differences but visual space is coded by positions in images projected on the retina.

Spectral stimuli They are continuous and unidimensional; examples are the visible spectrum of electromagnetic waves and the audible spectrum of airborne pressure waves.

Taste qualities They are distinct perceptual gustatory qualities; there are few; primarily sweet, salty, sour, and bitter.

4.17.1 The Sweet–Salty–Sour–Bitter Decision

In humans, the essence of most tastes is described by a handful of distinct qualities. There are hundreds of odor qualities. The logic of chemosensory coding must take into account the hundreds of different olfactory receptors (ORs) (Axel, R., 2005; Buck, L. B., 2005) compared to the many fewer receptors implicated in taste reception (Chandrashekar, J. *et al.*, 2006), both of which are now being characterized for a multiple mammalian species.

For tastes, besides quality, that is, the sweet–salty–sour–bitter decision, there is a good–bad decision (Nowlis, G. H. and Frank, M. E., 1981), as there is for smells (Anderson, A. K. *et al.*, 2003). The gustatory and olfactory systems code hedonic attributes that are associated with the water-soluble and airborne chemicals that they, respectively, detect. The good–bad decision about tastes and smells can be changed with experience (Cain, W. S. and Johnson, F., 1978; Palmerino, C. C. *et al.*, 1980). In contrast, the sweet–salty–sour–bitter and odor note decision, although it may be enhanced or dulled via intensity shifts (Contreras, R. J. and Lundy, R. F. 2000), appears unchanged and recoverable. The neural basis for sweet–salty–sour–bitter decisions, like odor-quality decisions, persists intact throughout the brain. This is consistent with taste-quality (Frank, M. E. *et al.*, 2003) and odor-quality (Goyert, H. F. *et al.*, 2007) constancy. The constancies are necessary and sufficient for chemosensory stimulus recognition, and instruct us on the logic of chemosensory coding in the central nervous system (CNS).

4.17.2 Stimulus and Perceptual Domains

It would simplify the study of sensory systems if all systems detected stimuli and coded perceptions in one way (Erickson, R. P., 1985). However, by their nature, different kinds of stimuli do not fall along comparable stimulus dimensions (Frank, M. E. and Hettinger, T. P., 2005). It may be convenient to use well-studied senses such as visual color or auditory pitch as model systems, but is it productive? Color and pitch are spectral senses in which stimuli fall on convenient physical continua that can be sampled with a frequency sweep. Sampling chemosensory stimuli, in contrast, is discrete; there is no single stimulus dimension to sweep across.

4.17.2.1 Nonchemosensory

4.17.2.1.1 Pitch

Pitches, like tastes and smells, neither define external space, like color, nor identify stimulation sites, like the somatotopic body senses. The stimulus domain of pitch is temporal, a spectrum of molecular pressure waves. In the cochlea, these waves are transformed to a cellular continuum. The waves localize according to frequency from the apex to the base of the basilar membrane (Békésy, G. von, 1970). Pitch is detected mechanically by multiple individual receptor cells (inner hair cells) located at multiple points along the vibrating membrane. The activated cells create a neuronal continuum in cranial nerve (CN) VIII that is transmitted to the neurons in the brainstem cochlear nucleus. CN VIII fibers mostly connect one to one to inner hair cells, a connectivity that sets the fibers' quite specific best-frequency tuning (Goldstein, E. B., 2007). This is fine tuning.

Thus, a temporal stimulus domain is translated into an intercellular domain to code pitch in the auditory nerve. In the CNS, frequency is mapped multiple times from cochlear nucleus to auditory cortex, and, as a consequence, pitch information is present in the form of maps everywhere in the auditory CNS. Taste quality information is also found throughout the gustatory CNS but does not appear to be in the form of sweet–salty–sour–bitter maps; rather, tastes and other oral senses originating from the same regions may be aligned (Chapter 4.15; McPheeters, M. *et al.*, 1990; Lundy, R. F. and Norgren, R., 2004; Kaas, J. H., 2005). Odor-quality signals detected by the subsets of olfactory sensory neurons (OSNs), each exclusively expressing a single OR variant, converge onto a few particular glomeruli in the olfactory bulb; but this stereotyped OR-based representation is neither somatotopic nor recapitulated elsewhere in the brain (Buck, L. B., 2005).

4.17.2.1.2 Color

The most popular model used to instruct studies of chemosensory systems is color vision (Erickson, R. P., 1985; Shepherd, G. M., 2005). Colors are parts of every discrete spot of every image in the visual field. In that sense, color, unlike pitch, is a spectral percept distributed in external space. Color stimuli are electromagnetic waves within a continuous visible spectrum and spectral sensitivity

is species-dependent (Glosmann, M. and Anhelt, P. K., 2002). The continuum of visible frequencies is partitioned by a few chemical pigment chromophores. In humans each chromophore is located exclusively in one of the three subsets of cone receptor cells in the retina. The three human cones contain all our color information. Each cone pigment absorbs light across the entire visible spectrum, with absorbance peaking at different frequencies. This is a broad tuning, characteristic of pigment absorbance.

Thus, a visible spectral wavelength continuum is reduced to a tripartite cellular code present in separate cells: so-called red (L), green (M), and blue (S) cones. Within the retina, the three cone spectra are combined to yield blue-yellow (L + M) and red-green opponent retinal ganglion cells associated with every spot on the retina, and these two opponents are represented in neurons distributed throughout the visual system from thalamus to visual cortex (Goldstein, E. B., 2007). Exactly how the continuity of colors that we perceive localized to each spot in our visual experience is reconstructed from absorbance differences of several pigments by the brain is unknown (Lennie, P., 2000). In the gustatory system there are peripheral and central neurons that respond antagonistically to good–bad stimulus pairs. (Chapter 4.15; McPheeters, M. *et al.*, 1990; Formaker, B. K. *et al.*, 1997).

4.17.2.2 Chemosensory

In contrast to the spectral senses of color and pitch, chemosensory stimulus detection in mammals involves discrete stimulus–receptor biochemical interactions, reactions with specified chemosensory molecular ranges (Bargman, C. L., 2006). Not needing to first convert spectral information to chemical or mechanical information in order to activate cells, the chemical senses coding logic can be more direct and represents phyletically early sensing systems. Candidate G protein-coupled receptors (GPCRs) have been discovered for (1) sweet taste; (2) mostly unidentified, species-specific, bitter tastes (Chandrashekar, J., *et al.*, 2006); and (3) multiple, mostly unidentified, species-specific odors (Axel, R., 2005; Buck, L. B., 2005). In nearly all the cases, the environmental ligands that match the receptors are unknown.

4.17.2.2.1 Taste

The perceptual simplicity of taste has facilitated the identification of a single heterodimeric GPCR taste receptor (TR) for sweet compounds (Tas1r2–Tas1r3), which has a molecular range coincident with compounds that taste sweet to humans (Li, X. *et al.*, 2002). The molecular range is species-selective. Tas1r2 is not expressed in cats (Li, X. *et al.*, 2005) and, consequently, cats do not detect sweet stimuli. Just as each OR is expressed in a dedicated set of OSNs, the single sweet TR is found in a subset of taste receptor cells (TRCs) likely dedicated for signaling sweet stimuli (Chandrashekar, J. *et al.*, 2006).

An alternate arrangement has been implicated for bitter taste. Multiple candidate bitter receptors have been discovered, but all 30 T2Rs may be expressed in each cell of a subset of TRCs. Similar arrangements have been seen for nematode chemosensory receptors (Bargman, C. L., 2006). Each T2R receptor of a given species would detect distinct dangerous chemicals, possibly produced by other competing species. (Hettinger, T. P. *et al.*, 2007). In contrast to sweet, no single TR could service the chemical diversity of bitters with appropriate specificity. However, this tentative bitter coding logic fails to account for the fact that all bitter stimuli do not necessarily elicit a unitary sensation. Rodent chorda tympani and glossopharyngeal nerves, both of which may innervate TRCs containing T2Rs, carry distinct information about aversive stimuli to the brain (St. John, S. J. and Spector, A. C., 1998; King, C. T. *et al.*, 2000) and code for several distinct aversive perceptions (Frank, M. E. *et al.*, 2004; Hettinger, T. P. *et al.*, 2007) that have perhaps been reduced to a single bitter in humans.

4.17.2.2.2 Smell

In comparison to TRCs, identification of the function of particular dedicated OSNs has been a struggle, likely for the same reason that odor qualities have not been satisfactorily classified (Cain, W. S., 1978): there are so many odors and many may be sensed only by a few related species (Niimura, Y. and Nei, M., 2006). Just like tastes, odors are not distinguished merely as feature detectors of stimulus functional groups, shapes, or sizes. Rather, TRs and ORs likely evolved to make distinctions among particular whole molecules important for survival, some sharing functional groups, and with as much specificity as required for recognition (Bargman, C. L., 2006; Mori, T. *et al.*, 2006; Goyert, H. F. *et al.*, 2007).

Thus, like the body senses (McBurney, D. H. and Gent, J. F., 1979), there is a distinctly possible direct coupling of TR or OR with a discrete chemosensory quality, taste, or odor. Deconstruction of stimulus

dimensions and their reconstruction into perceptual dimensions by the brain (Buck, L. B., 2005) may be appropriate for continuous spectral senses partitioned by a few receptor cell types like color. However, deconstruction and subsequent reconstruction (Turin, L., 2006) may be unnecessary for multiple discrete chemosensory domains.

4.17.3 Processing of Chemosensory Quality Signals

Although processing can potentially occur among the TRCs within taste buds (Kaya, N. *et al.*, 2004; Roper, S. D., 2006), recent findings strongly suggest that perceptual taste categories are isomorphic with TR specificity (Chandrashekar, J. *et al.*, 2006). This is consistent with modular specificities defined by single taste-fiber neural responses transmitted to the CNS (Frank, M. E., 2000; Frank, M. E. *et al.*, 2005).

4.17.3.1 Mixtures

Sweet–salty–sour–bitter is a set of distinct taste perceptions that is not transformed in stimulus mixtures (Frank, M. E. *et al.*, 2003). Figure 1 demonstrates this with the specificity of intake suppression driven by conditioned taste aversions, which do not alter the sweet–salty–sour–bitter decision (Hettinger, T. P. *et al.*, 2007). The taste of NaCl is recognized by hamsters in the binary mixtures of NaCl and sucrose, or NaCl and quinine, or the ternary mixture of NaCl and sucrose and quinine. The mixture percepts contain salt-like components. There are specific adjustments in intensity, however. One example is the suppression of quinine recognition in the presence of NaCl (Figure 1); but it can be recovered by an increase in quinine concentration (Nowlis, G. H. and Frank, M. E., 1981). There is also a mixture suppression of intensity in ternary mixtures (e.g., sucrose results in Figure 1). Mixture suppression, seen in humans (Bartoshuk, L. M., 1975), focuses mixture perception on the stronger mixture components.

In taste, mixture processing begins in the taste bud (Formaker, B. K. *et al.*, 1997), perhaps between the multiple TRCs containing cells expressing receptors for distinct qualities, and may continue within the brainstem nucleus of the solitary tract, which, like the olfactory bulb, contains ample inhibitory interneurons within its circuitry (Chapter 4.15; Bradley, R. M., 2006). In chemosensory mixtures, stronger stimuli suppress the weaker one more than the weaker

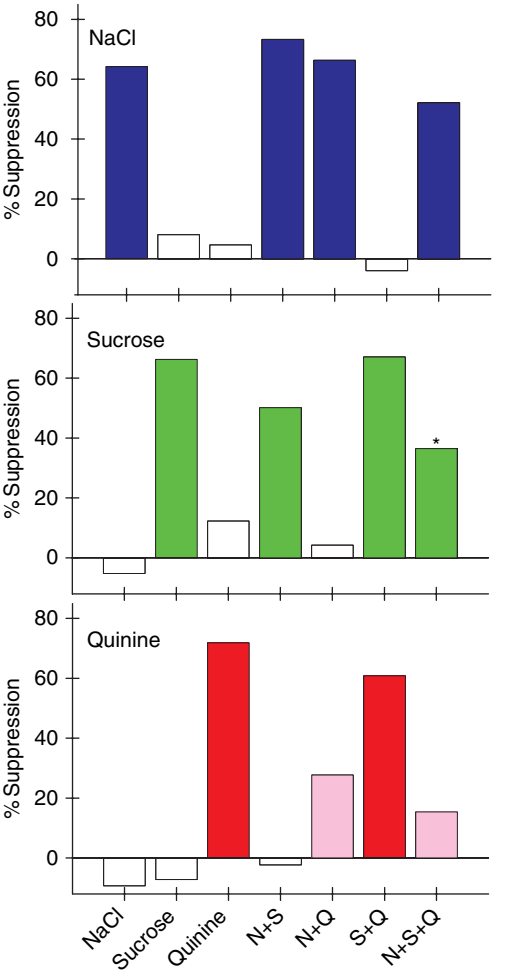

Figure 1 Recognition of components of binary and ternary taste mixtures by hamsters. The percentage suppression of intake measures stimulus recognition. NaCl (100 mM) was recognized (blue bars) in mixtures containing NaCl (N). Sucrose (100 mM) was recognized (green bars) in mixtures containing sucrose (S). Quinine (1 mM, Q) was recognized (red bars) in sucrose–quinine mixtures but not in NaCl–quinine mixtures (pink bars). *Sucrose recognition was weaker for the ternary S+N+Q mixture than for sucrose alone. Data are from Frank, M. E., Formaker, B. K., and Hettinger, T. P. 2003. Taste responses to mixtures: analytic processing of taste quality. Behav. Neurosci. 117, 228–235.

suppress the stronger (Laing, D. G. *et al.*, 1984). In this context, there is also an important temporal process to consider, rapid sensory adaptation.

4.17.3.2 Chemosensory Quality Constancy

Quality tuning of brainstem and forebrain taste neurons appear, on average, to broaden when compared

to tuning of receptors or taste nerve fibers (Chapter 4.15). Explanations of how tuning profiles change at different levels of the nervous system should lead to a greater understanding of the roles of identified CNS neurons with distinct inputs and projections (Bradley, R. M., 2006). Likely some CNS transformations serve to stabilize a compound's taste or odor quality in a complex labile chemical environment. Stimuli that we usually experience are not pure or equally strong but are combinations of multiple compounds that wax and wane in time. In both taste and smell, identification of mixture components falls off rapidly with decreases in intensity and with increases in the number of components (Laing, D. H. *et al.*, 1984; Livermore, A. and Laing, D. H. 1998; Laing, D. H. *et al.*, 2002). In odor mixtures, rapid adaptation and mixture suppression determine which characteristic odors will be identified at a given moment (Goyert, H. F. *et al.*, 2007). Unlike taste for which taste buds are potential sites of TRC interaction, OSN interactions are initiated in the complex layered olfactory bulb via well-defined inhibitory circuitry (Yokoi, M. *et al.*, 1995) before they are transmitted to higher central levels.

Figure 2 shows correct identification of four characteristic odors by people. Each odor is recognized more often if other mixture components are sniffed for a few seconds right before (solid color bars) and less often if the test component itself is sniffed right before (diagonal striped bars). Instead of cross-adapting, the other odors release mixture suppression among the signals for the four compounds. For example, the odor of vanillin, labeled vanilla, is recognized more frequently in two-, three-, and four-component mixtures when the other mixture components, isopropyl alcohol, menthol (labeled mint), and phenethyl alcohol (labeled rose), are sniffed first. Vanillin recognition is poorer after it is sampled. The dynamic coding mechanisms of mixture suppression and rapid adaptation promote recognition of characteristic odors of newly introduced and stronger chemosensory stimuli. Chemosensory circuits may have evolved to focus our attention on the recognition of chemicals that we need to know are there in the environment or the mouth: serious new opportunities for, or dangers to, our survival.

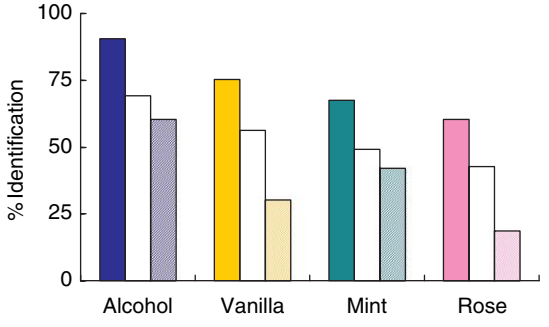

Figure 2 Identification of components in two-, three-, and four-component mixtures. The stimuli (labels) were 1 M isopropyl alcohol (alcohol), 5 mM vanillin (vanilla), 1 mM *l*-menthol (mint), and 0.5 mM phenethyl alcohol (rose). Correct component identification was greatest following sniffing other mixture components (solid color bars) for a few seconds and poorest following sniffing stimuli containing the indicated component (striped color bars). White bars are controls. Data are from Goyert, H. F., Frank, M. E., Gent, J. F., and Hettinger, T. P. 2007. Characteristic component odors emerge from mixtures after selective adaptation. Brain Res. Bull. 72, 1–9.

4.17.4 Conclusion

Stimuli that we usually encounter are not pure chemicals but combinations of varying amounts of multiple compounds that come and go. In such shifting contexts, a few taste or odor qualities are identified at a time. This dynamic chemosensory coding (Goyert, H. F. *et al.*, 2007) warrants further study in peripheral taste neurons, which transmit signals to the CNS after they are processed by taste buds, and in mitral and tufted cells, which transmit the processed signals from the olfactory bulb to the olfactory cortex. The taste or odor perceived is typically characteristic of the pure component, a chemosensory quality constancy: the objective of quality coding. The Pied Beauty described in G. M. Hopkins' poem (Nowlis, G. H. and Frank, M. E., 1981) for chemosensory perceptions may not be appreciated all at once, except in our memories.

Acknowledgment

This cameo is supported by NIH grant DC004099.

References

Anderson, A. K., Christoff, K., Stappen, I., Panitz, D., Ghahremani, D. G., Glover, G., Gabrieli, J. D., and Sobel, N. 2003. Dissociated neural representations of intensity and valence in human olfaction. Nature Neurosci. 6, 196–202.

Axel, R. 2005. Scents and sensibility: a molecular logic of olfactory perception (Nobel lecture). Angew. Chem. Int. Ed. 44, 6111–6127.

Bargman, C. I. 2006. Comparative chemosensation from receptors to ecology. Nature 444, 295–301.

Bartoshuk, L. M. 1975. Taste mixtures: is mixture suppression related to compression? Physiol. Behav. 14, 643–649.

Békésy, G. von. 1970. Travelling waves as frequency analysers in the cochlea. Nature 225, 1207–1209.

Bradley, R. M. 2006. rNST Circuits. In: The Role of the Nucleus of the Solitary Tract in Gustatory Processing (*ed*. R. M. Bradley), Chapter 7, pp. 137–151. CRC Press.

Buck, L. B. 2005. Unraveling the sense of smell (Nobel lecture). Angew. Chem. Int. Ed. 44, 6128–6140.

Cain, W. S. 1978. History of Research on Smell. In: Handbook of Perception, Vol. VIA, Tasting and Smelling (*eds*. E. C. Carterette and M. P. Friedman), pp. 197–229. Academic Press.

Cain, W. S. and Johnson, F., Jr. 1978. Lability of odor pleasantness: influence of mere exposure. Perception 7, 459–465.

Chandrashekar, J., Hoon, M. A., Ryba, N. J., and Zuker, C. S. 2006. The receptors and cells for mammalian taste. Nature 444, 288–294.

Contreras, R. J. and Lundy, R. F., Jr. 2000. Gustatory neuron types in the periphery: a functional perspective. Physiol. Behav. 69, 41–52.

Erickson, R. P. 1985. Definitions: A Matter of Taste. In: Taste, Olfaction, and the Central Nervous System (*ed*. D. W. Pfaff), pp. 129–150. Rockefeller University Press.

Formaker, B. K., MacKinnon, B. I., Hettinger, T. P., and Frank, M. E. 1997. Opponent effects of quinine and sucrose on single fiber taste responses of the chorda tympani nerve. Brain Res. 772, 239–242.

Frank, M. E. 2000. Neuron types, receptors, behavior, and taste quality. Physiol. Behav. 69, 53–62.

Frank, M. E. and Hettinger, T. P. 2005. What the tongue tells the brain about taste. Chem. Senses 30(Suppl. 1), i68–i69.

Frank, M. E., Bouverat, B. P., MacKinnon, B. I., and Hettinger, T. P. 2004. The distinctiveness of ionic and nonionic bitter stimuli. Physiol. Behav. 80, 421–431.

Frank, M. E., Formaker, B. K., and Hettinger, T. P. 2005. Peripheral gustatory processing of sweet stimuli by golden hamsters. Brain Res. Bull. 66, 70–84.

Frank, M. E., Formaker, B. K., and Hettinger, T. P. 2003. Taste responses to mixtures: analytic processing of taste quality. Behav. Neurosci. 117, 228–235.

Glosmann, M. and Anhelt, P. K. 2002. A mouse-like retinal cone in the Syrian hamster: S opsin coexpressed with M opsin in a common cone photoreceptor. Brain Res. 929, 139–146.

Goldstein, E. B. 2007. Sensation and Perception, 7th edn. Thomson Wadsworth.

Goyert, H. F., Frank, M. E., Gent, J. F., and Hettinger, T. P. 2007. Characteristic component odors emerge from mixtures after selective adaptation. Brain Res. Bull. 72, 1–9.

Hettinger, T. P., Formaker, B. K., and Frank, M. E. 2007. Cycloheximide: no ordinary bitter stimulus. Behav. Brain Res.180, 4–17.

Kaas, J. H. 2005. The future or mapping sensory cortex in primates: three of the remaining issues. Philos. Trans. R. Soc. Lond. B 360, 653–664.

Kaya, N., Shen, T., Lu, S. G., Zhao, F. L., and Herness, S. 2004. A paracrine signaling role for serotonin in rat taste buds: expression and localization of serotonin receptor subtypes. Am. J. Physiol. Regul. Integr. Comp. Physiol. 286, R649–R658.

King, C. T., Garcea, M., and Spector, A. C. 2000. Glossopharyngeal nerve regeneration is essential for the complete recovery of quinine-stimulated oromotor rejection behaviors and central patterns of neuronal activity in the nucleus of the solitary tract in the rat. J. Neurosci. 20, 8426–8434.

Laing, D. G., Link, C., Jinks, A. L., and Hutchinson, I. 2002. The limited capacity of humans to identify the components of taste mixtures and taste–odour mixtures. Perception 31, 617–635.

Laing, D. G., Panhuber, H., Willcox, M. E., and Pittman, E. A. 1984. Quality and intensity of binary odor mixtures. Physiol. Behav. 33, 309–319.

Lennie, P. 2000. Color Vision. In: Principles of Neural Science, 4th edn. (*eds*. E. R. Kandel, J. H. Schwartz, and T. M. Jessell), pp. 572–589. McGraw-Hill.

Li, X., Li, W., Wang, H., Cao, J., Maehashi, K., Huang, L., Bachmanov, A. A., Reed, D. R., Legrand-Defretin, V., Beauchamp, G. K., and Brand, J. G. 2005. Pseudogenization of a sweet-receptor gene accounts for cats' indifference toward sugar. PloS Genet. 1, 27–35.

Li, X., Staszewski, L., Xu, H., Durick, K., Zoller, M., and Adler, E. 2002. Human receptors for sweet and umami taste. Proc. Natl. Acad. Sci. U. S. A. 99, 4692–4696.

Livermore, A. and Laing, D. G. 1998. The influence of odor type on the discrimination and identification of odorants in multicomponent odor mixtures. Physiol. Behav. 65, 311–320.

Lundy, R. F., Jr. and Norgren, R. 2004. Gustatory System. In: The Rat Nervous System (*ed*. G. Paxinos), pp. 891–921. Elsevier Academic Press.

McBurney, D. H. and Gent, J. F. 1979. On the nature of taste qualities. Psychol. Bull. 86, 151–167.

McPheeters, M., Hettinger, T. P., Nuding, S. C., Savoy, L. D., Whitehead, M. C., and Frank, M. E. 1990. Taste-responsive neurons and their locations in the solitary nucleus of the hamster. Neuroscience 34, 745–758.

Mori, K., Takahashi, Y. K., Igarashi, K. M., and Yamaguchi, M. 2006. Maps of odorant molecular features in the mammalian olfactory bulb. Physiol. Rev. 86, 409–433.

Niimura, Y. and Nei, M. 2006. Evolutionary dynamics of olfactory and other chemosensory receptor genes in vertebrates. J. Hum. Genet. 51, 505–517.

Nowlis, G. H. and Frank, M. E. 1981. Quality Coding in Gustatory Systems of Rats and Hamsters. In: Perception of Behavioral Chemicals (*ed*. D. M. Norris), pp. 59–80. Elsevier/North Holland Biomedical Press.

Palmerino, C. C., Rusiniak, K. W., and Garcia, J. 1980. Flavor-illness aversions: the peculiar roles of odor and taste in memory for poison. Science 208, 753–755.

Roper, S. D. 2006. Cell communication in taste buds. Cell Mol. Life Sci. 63, 1494–1500.

Shepherd, G. M. 2005. Outline of a theory of olfactory processing and its relevance to humans. Chem. Senses 30(Suppl. 1), i3–i5.

St. John, S. J. and Spector, A. C. 1998. Behavioral discrimination between quinine and KCl is dependent on input-from the seventh cranial nerve: implications for the functional roles of the gustatory nerves in rats. J. Neurosci. 18, 4353–4362.

Turin, L. 2006. The Secret of Scent: Adventures in Perfume and the Science of Smell. HarperCollins.

Yokoi, M., Mori, K., and Nakanishi, S. 1995. Refinement of odor molecule tuning by dendrodendritic synaptic inhibition in the olfactory bulb. Proc. Natl. Acad. Sci. U. S. A. 92, 3371–3375.

4.18 Oral Chemesthesis and Taste

C T Simons, Global Research and Development Center, Cincinnati, OH, USA

E Carstens, University of California, Davis, CA, USA

© 2008 Elsevier Inc. All rights reserved.

4.18.1	Oral Chemesthesis: Anatomy	346
4.18.2	Oral Chemesthesis: Physiology	350
4.18.3	Chemoirritation: Temporal Phenomena	353
4.18.4	Irritant–Taste Interactions	356
4.18.4.1	Peripheral Interactions	358
4.18.4.2	Central Interactions – Nucleus of the Solitary Tract	361
4.18.4.3	Cognitive Interactions	362
4.18.5	Perspectives	363
References		363

Glossary

adaptation Reduction in the response magnitude of a sensory neuron during a maintained stimulus.

chemesthesis Sensations of a burning, stinging, tingling, or anesthetic quality elicited by chemical stimulation of the mucosa or skin.

desensitization (tachyphylaxis) Reduction in response to reapplication of a stimulus. Self-desensitization refers to a reduced response to reapplication of the same stimulus, and cross-desensitization is a reduction in the expected magnitude of a response to one stimulus when preceded by a different conditioning stimulus.

masking Inability or reduced ability to detect a stimulus in the presence of another stimulus, usually of a higher intensity.

nociceptor Sensory receptor innervating skin, mucosa, or other tissues that respond to noxious (potentially or overtly damaging) stimulation.

noxious Of sufficient intensity to threaten or overtly damage tissue.

pain An unpleasant sensory and emotional experience associated with actual or potential tissue damage, or described in terms of such damage.

sensitization Progressive increase in perceived sensory intensity during repeated application of a fixed stimulus (also refers to increased response of a sensory neuron following a noxious conditioning stimulus).

stimulus-induced recovery After desensitization, repeated reapplication of the stimulus induces a progressive increase in response that eventually reaches the same level as before desensitization.

TRP Transient receptor potential class of ion channels, some of which respond to chemicals or temperature changes.

Oral somatosensation provides important information regarding the texture, temperature, and pungency associated with oral stimuli. These stimuli are detected, respectively, by the presence of mechanosensitive, thermosensitive, and nociceptive neurons that are dispersed throughout the oral epithelium (Nagy, J. I. *et al.*, 1982; Whitehead, M. C. and Frank, M. E., 1983; Ito, J. and Oyagi, S., 1995). Whereas mechanosensitive neurons have receptor endings specialized to detect specific mechanically evoked sensations (e.g., vibration), thermosensitive neurons and nociceptors are thinly (Aδ-fibers) or unmyelineated (C-fibers) and are believed to have free nerve endings that respond to non-noxious heat and cold or various types of noxious stimuli including those of thermal, mechanical, or chemical origin (Dubner, R. and Bennett, G. J., 1983; Sessle, B. J., 1987; Willis, W. D. and Westlund, K. N., 1997; Millan, M. J., 1999). Although nociceptors are specifically tuned to convey sensations of pain, it is currently unclear whether

nociceptors responsive to a particular class of noxious stimuli exist (e.g., chemonociceptors) (Schmidt, R. *et al.*, 1995). Sensitivity to chemical irritants serves to protect organisms against exposure to potentially harmful compounds. This specialized sense, defined in the early 1900s (Parker, G. H., 1912) as the common chemical sense, is mediated by chemonociceptive nerve fibers and is separate from the system that provides chemosensitivty to taste and smell molecules (although at high concentrations, salts and acids can evoke sensations of pain; Carstens, E. *et al.*, 1998; Dessirier, J. M. *et al.*, 2000a; 2001b). More recently, objections to the term common chemical sense has resulted in the term chemesthesis being used to describe the sensations resulting from chemical activation of somatosensory pathways (Green, B. G. *et al.*, 1990). Chemesthesis refers to the ability to detect and respond to potentially noxious chemical stimuli across the entire body, not just in the oral or nasal mucosa. Whereas mucosal membranes (such as the cornea and oral and nasal epithelium) are generally more sensitive to chemical irritants, the mechanisms that subserve the detection of noxious chemicals are likely the same as those occurring in skin. The important feature which differentiates oral chemesthesis from generalized chemesthesis relates to its contribution to flavor. The pungency associated with horseradish, the burn of hot chili peppers, and the tingle induced by carbonated beverages all result from the activation of neural pathways sensitive to specific chemicals. In fact, along with taste and smell, oral chemesthesis is often considered to be one of the three main contributors to food and beverage flavor profiles. As such, increasing attention has been paid to oral chemesthesis and its impact on taste and flavor perception.

4.18.1 Oral Chemesthesis: Anatomy

The detection of oral irritants is achieved primarily by the activation of the trigeminal nerve, although the glossopharyngeal and vagus nerves also participate (Figure 1). The trigeminal nerve, as the name suggests, is comprised of three divisions that innervate the whole of the orofacial region. The mandibular and maxillary divisions are responsible for conveying somatosensory information from the oral cavity, whereas the ophthalmic division, via the ciliary and ethmoid nerves, innervates the cornea and nasal epithelium, respectively. The mandibular branch is the largest of the three divisions and innervates the anterior tongue and mandibular dental pulp. Unlike the maxillary and ophthalmic divisions, the mandibular division is a mixed nerve and contains both afferent and efferent fibers (Shankland, W. E., 2001b). Of particular importance for detecting oral irritants, trigeminal innervation of the anterior tongue occurs via the lingual nerve (Sostman, A. L. and Simon, S. A., 1991; Wang, Y. *et al.*, 1993). Although nociceptive fibers are found across the entire lingual surface, they terminate most densely in close proximity to taste buds (Nagy, J. I. *et al.*, 1982; Finger, T., 1986; Whitehead, M. C. and Kachele, D. L., 1994; Whitehead, M. C. *et al.*, 1999). This so-called perigemmal pattern of innervation is different from that of gustatory fibers which make intragemmal (within taste bud) synaptic contact with taste receptor cells. The midfacial region is innervated by the maxillary division of the trigeminal nerve. The maxillary division is a sensory nerve comprised exclusively of afferent fibers (Shankland, W. E., 2001a). The maxillary branch innervates many important structures for the detection of oral irritants including the soft and hard palate, the tonsils, and the nasopharyngeal mucosa (Shankland, W. E., 2001a). Although not involved in oral chemesthesis, the ophthalmic division of the trigeminal nerve is important in nasal irritation (Silver, W. L. and Moulton, D. G., 1982). The ethmoid nerve conveys afferent signals from the nasal mucosa, and sensitivity to nasal irritants has been linked to sick-building syndrome (Shusterman, D., 2003) and other disorders including seasonal allergic rhinitis (Shusterman, D., 2002).

In addition to the trigeminal nerve, the glossopharyngeal and vagus nerves also contribute to oral chemosensitivity by responding to oral irritants, as well as tastants, delivered to the posterior oral cavity. Specifically, the glossopharyngeal nerve responds to chemoirritants delivered to the posterior tongue (Barry, M. A. *et al.*, 1993; Hayakawa, T. *et al.*, 2005) as well as the soft palate (Hayakawa, T. *et al.*, 2005) and upper oropharynx (Hayakawa, T. *et al.*, 2005). The vagus nerve is activated by irritants delivered to the lower pharynx and the epiglottis (Boucher, Y. *et al.*, 2003).

Primary afferent somatosensory fibers from the oral cavity and throat project, in a topographical manner, to central relays in the brainstem. Trigeminal afferents carry information to the brainstem trigeminal complex where there appears to be some segregation in the processing of different types of somatosensory inputs. Nociceptive and thermally sensitive fibers project to superficial layers (I–II) of

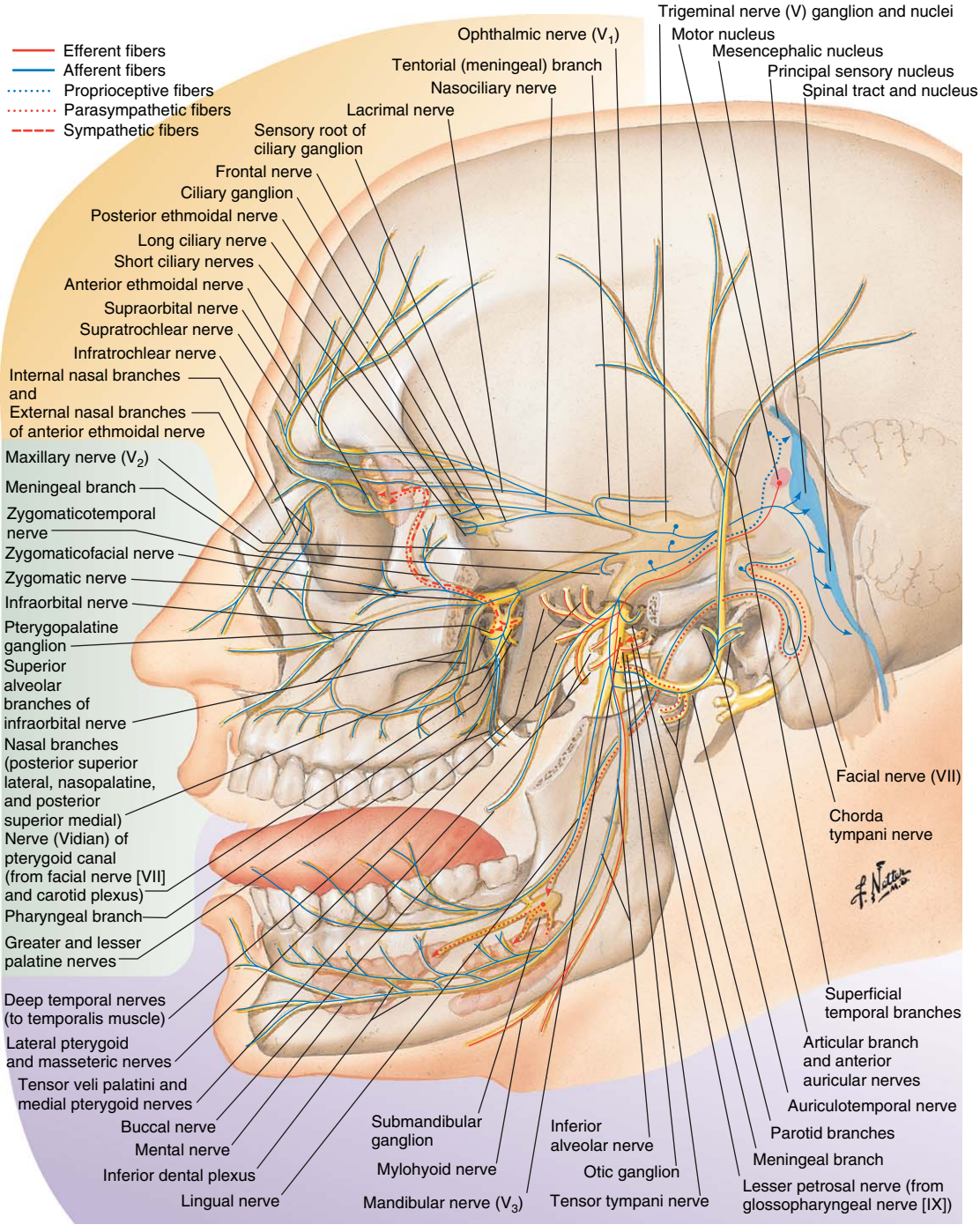

Figure 1 Anatomy of the trigeminal nerve, its innervation territory, and central connections. From Netter, with permission.

the trigeminal complex, whereas innocuous low-threshold mechanical stimuli activate neurons in superficial as well as deeper (III–IV) trigeminal layers (Hu, J. W. *et al.*, 2005). As the majority of studies investigating oral chemesthesis have focused on lingual sensitivity, more is known regarding the topographical organization of lingual inputs compared to other nerve inputs (however, see Rentmeister-Bryant, H. and Green, B. G. 1997; Green, B. G. 1998). In particular, it has been shown

that lingual nociceptors project to the superficial layers of the trigeminal subnucleus caudalis (Vc) (Hayashi, H., 1985; Jacquin, M. F. *et al.*, 1986; Komai, M. and Bryant, B. P., 1993; Strassman, A. M. and Vos, B. P., 1993; Coimbra, F. and Coimbra, A., 1994). There they form synaptic connections with second-order neurons involved in relaying nociceptive information to higher centers (Kruger, L. and Michel, F., 1962; Yokota, T., 1975; Amano, N. *et al.*, 1986; Strassman, A. M. and Vos, B. P., 1993; Carstens, E. *et al.*, 1995; Raboisson, P. *et al.*, 1995; Carstens, E. *et al.*, 1998; Simons, C. T. *et al.*, 1999; Dessirier, J. M. *et al.*, 2000b; Simons, C. T. *et al.*, 2000; Carstens, E. *et al.*, 2002a). Although Vc has been the most extensively studied (for review see Sessle, B. J. and Greenwood, L. F., 1976; Hu, J. W. *et al.*, 1981; Dubner, R. and Bennett, G. J., 1983), the more rostral trigeminal subnuclei interpolaris and oralis are also involved with processing and relaying oral pain information (Greenwood, L. F. and Sessle, B. J., 1976; Sessle, B. J. and Greenwood, 1976; Nord, S. G. and Young, R. F., 1979; Hu, J. W. *et al.*, 1981; Hayashi, H. *et al.*, 1984; Hu, J. W. and Sessle, B. J., 1984; Hayashi, H. and Tabata, T., 1989; Dallel, R. *et al.*, 1990; Jacquin, M. F. and Rhoades, R. W., 1990; Raboisson, P. *et al.*, 1991; Hu, J. W. *et al.*, 1992; Ohya, A., 1992; Ohya, A. *et al.*, 1993; Dallel, R. *et al.*, 1996).

Oral somatosensory information conveyed by non-trigeminal nerve fibers also project topographically to brainstem nuclei. Both, the glossopharyneal nerve and the vagus nerve project to the nucleus of the solitary tract (NTS). *c-fos* studies of nicotine-induced throat irritation have shown that vagal afferents project to the most caudal aspects of the NTS (Boucher, Y. *et al.*, 2003). The glossopharyngeal nerve, on the other hand, projects more rostrally (Hamilton, R. B. and Norgren, R., 1984). Importantly, although both nerves encode the quality and intensity of oral somatosensory and taste stimuli, the processing of such information is segregated and distributed to different parts of the NTS. Taste processing occurs in rostral medial NTS, whereas somatosensory processing occurs more laterally (Barry, M. A. *et al.*, 1993). Interestingly, collateral branches from trigeminal afferents also project to rostromedial NTS, providing a substrate by which trigeminal–taste interactions might occur (Jacquin, M. F. *et al.*, 1982; Whitehead, M. C. and Frank, M. E., 1983; Marfurt, C. F. and Rajchert, D. M. 1991; Boucher, Y. *et al.*, 2003).

Two classes of second-order nociceptive neurons reside in Vc and NTS. The majority tend to be of the wide-dynamic-range (WDR) type and respond, in graded fashion, to both innocuous and noxious somatosensory stimuli (Dubner, R. and Bennett, G. J., 1983; Sessle, B. J., 1987). The existence of WDR cells is possible due to the convergence of nociceptive and non-nociceptive peripheral afferents onto second-order cells. As the stimulus intensity increases from innocuous to noxious, the second-order cell integrates the afferent volleys first from non-nocicepive cells and then from nociceptors as well. Thus, an innocuous stimulus elicits a low level of activity from WDR cells relative to a noxious stimulus that will evoke larger responses. The other class of second-order nociceptor includes those that respond exclusively to high-intensity, noxious stimuli. These nociceptive-specific (NS) cells receive input exclusively from peripheral C- or Aδ- fibers (Villanueva, L. *et al.*, 1988). Electrophysiolgical studies have revealed that relative to the numbers of WDR-type cells, NS cells tend to be less prevalent, at least in Vc (see, e.g., Carstens, E. *et al.*, 1998). Nociceptors sensitive to chemical irritants exist in both classes of cells (Hu, J. W., 1990; Carstens, E. *et al.*, 1998; Simons, C. T. *et al.*, 1999; Dessirier, J. M. *et al.*, 2000b). Interestingly, both neuron types exhibit similar response characteristics to chemical stimuli. Specifically, they tend to be broadly tuned, with a given Vc neuron capable of responding to a variety of noxious chemicals (Carstens, E. *et al.*, 1998; Simons, C. T. *et al.*, 1999; Dessirier, J. M. *et al.*, 2000b) (Figure 2). This suggests that either peripheral nociceptors express receptor mechanisms to a broad range of irritant chemicals or, alternatively nocieptors in the periphery are specifically tuned, but convergence of these neurons in Vc broadens the tuning characteristic of central neurons. The former explanation is most parsimonious with peripheral fiber and trigeminal ganglion studies in which a single nociceptive fiber or ganglion cell responds to multiple chemical irritants (Wang, Y. *et al.*, 1993; Bryant, B. P. and Moore, P. A., 1995; Liu, L. and Simon, S. A., 1996a; 1996c; Liu, L. *et al.*, 1997; Liu, L. and Simon, S. A., 1997; 1998; Steen, K. H. *et al.*, 1999).

From the first central relay in the trigeminal complex or NTS, oral somatosensory information remains segregated as it is conveyed to third-order sites. In humans, the dorsal column pathway transmits tactile information from layers III–IV of the trigeminal complex to the contralateral ventroposteriomedial (VPM) thalamus (Kandel, E. R. *et al.*, 2000). The anterolateral tract conveys thermal and nociceptive signals from superficial layers to a more lateral thalamic region, the contralateral

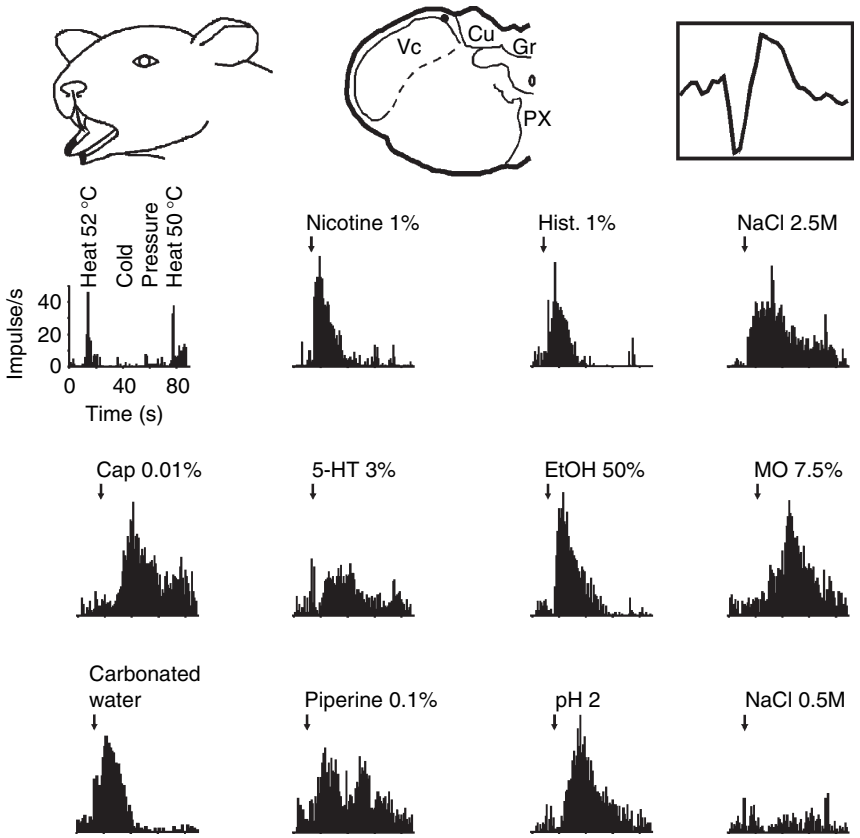

Figure 2 Nonselective responses of Vc neuron to different oral irritants. The figurines in the upper row show, from left to right, a drawing of the rat's face with the receptive field of this neuron on the tongue and chin (black), a cross-section of the medulla showing the recording site (dot) in the superficial part of dorsomedial Vc, and the action potential waveform. The lower three rows show peristimulus–time histograms (PSTHs, bin width 1 s) of responses to various stimuli. Calibrations given in left-hand PSTH, second row. Cap, capsaicin; Cu, cunate n.; EtOH, ethanol; Gr, gracile n.; Hist., histamine; 5-HT, serotonin; MO, mustard oil; pH2, HCl at pH of 2. PX, pyramidal decussation; Vc, trigeminal subnucleus caudalis. Reproduced from Carstens, E., Iodi Carstens, M., Dessirier, J. M., O'Mahony, M., Simons, C. T., Sudo, M., and Sudo, S. 2002. It hurts so good: oral irritation by spices and carbonated drinks and the underlying neural mechanisms. Food Qual. Pref. 13, 431–443, with permission from Elsevier; adapted from Carstens, E., Kuenzler, N., and Handwerker, H. O. 1998. Activation of neurons in rat trigeminal subnucleus caudalis by different irritant chemicals applied to oral or ocular mucosa. J. Neurophysiol. 80, 4654–4692.

ventroposteriolateral (VPL) thalamus (Kandel, E. R. *et al.*, 2000). In rodents, where many of the functional anatomical studies have been completed, ascending somatosensory information has an obligatory relay in the contralateral pontine parabrachial nucleus (Feil, K. and Herbert, H., 1995). From the parabrachial nucleus, somatosensory projections are to the appropriate regions of the ventroposterior thalamus.

Following thalamic processing, ascending anterolateral tract and dorsal column pathways project to the somatosensory (SI) cortex, an area found in the postcentral gyrus of the anterior parietal lobe. Somatosensory projections from the thalamus are organized such that a representation of the body is mapped onto the cortex (Kandel, E. R. *et al.*, 2000). This map, known as a homunculus, is arranged so that body regions having greater sensory acuity occupy a larger region of the SI cortex. Thus, oral structures (lips, teeth, tongue, and pharynx) occupy a relatively large region of lateral SI cortex compared to legs and trunk, which occupy a smaller region of medial SI cortex. Projections from SI are directed toward secondary cortical areas in the parietal lobe (LaMotte, R. H. and Mountcastle, V. B., 1979) and tertiary areas in the insula and orbitofrontal cortex (Verhagen, J. V. *et al.*, 2003; Kadohisa, M. *et al.*, 2004; 2005). Oral somatosensory inputs into the insula and orbitofrontal cortex are of particular interest to taste and flavor interactions. The primary gustatory cortex is found in the insula (Yaxley, S. *et al.*, 1990; Small, D. M.

et al., 1999; Stapleton, J. R. *et al.*, 2006), and the orbitofrontal cortex receives converging taste, smell, somatosensory, and visual information to encode stimulus valence (Rolls, E. T. and Baylis, L. L., 1994; Critchley, H. D. and Rolls, E. T., 1996).

4.18.2 Oral Chemesthesis: Physiology

The role of chemonociceptive neurons in the oral cavity is to signal the presence of stimuli that are potentially or overtly damaging prior to ingestion. However, not all stimuli that activate nociceptors are damaging. For example, capsaicin, the pungent principle in chili peppers, binds to the vanilloid-1 receptor (TRPV1 or VR-1) expressed in nociceptors (Caterina, M. J. *et al.*, 1997; Tominaga, M. *et al.*, 1998; Caterina, M. J. *et al.*, 1999; Nagy, I. and Rang, H. P., 1999; Caterina, M. J. *et al.*, 2000) to elicit a burning sensation that, in some cuisines, is highly sought after. Capsaicin, however, is relatively benign and TRPV1 is ordinarily present in nociceptors to detect the presence of noxious thermal or acidic stimuli (Tominaga, M. *et al.*, 1998; Cesare, P. *et al.*, 1999; Nagy, I. and Rang, H. P., 1999; Jordt, S. E. *et al.*, 2000).

The process of detecting chemesthetic stimuli is initiated at the receptor level. In the oral cavity, trigeminal ganglion neurons express a variety of receptors that are activated by the presence of chemical irritants (Wang, Y. *et al.*, 1993; Bryant, B. P. and Moore, P. A., 1995; Liu, L. and Simon, S. A., 1996a; 1996c; 1997; Liu, L. *et al.*, 1997; Liu, L. and Simon, S. A., 1998; Steen, K. H. *et al.*, 1999). A variety of methods, including patch-clamp techniques and calcium imaging, have been used to study the response characteristics of trigeminal ganglion neurons to oral irritants, and in the last decade, a wealth of information has been generated regarding the receptor and cellular mechanisms underlying irritant chemical detection. The great majority of known chemoirritant receptors are of the transient receptor potential (TRP) superfamily (for review see Clapham, D. E., 2003; Wang, H. and Woolf, C. J., 2005) of cation channels. All mammalian TRP channels are 6-transmembrane polypeptides that assemble as tetramers to form cation channels (Clapham, D. E., 2003). To date, TRP channels have been shown to transduce and discriminate a large variety of sensations ranging from taste (sweet, bitter, and umami) (Perez, C. A. *et al.*, 2002; Zhang, Y. *et al.*, 2003) to temperature (Caterina, M. J. *et al.*, 1997; 1999; McKemy, D. D. *et al.*, 2002; Peier, A. M. *et al.*, 2002b; Smith, G. D. *et al.*, 2002; Xu, H. *et al.*, 2002), pressure (Mizuno, A. *et al.*, 2003; Suzuki, M. *et al.*, 2003), and noxious chemicals (Caterina, M. J. *et al.*, 1997; Tominaga, M. *et al.*, 1998; Trevisani, M. *et al.*, 2002; Yang, B. H. *et al.*, 2003; Bandell, M. *et al.*, 2004; Jordt, S. E. *et al.*, 2004; Bautista, D. M. *et al.*, 2005; Macpherson, L. J. *et al.*, 2005; Moqrich, A. *et al.*, 2005). Interestingly, most of the chemosensitive TRP channels identified thus far are also responsive to other noxious stimuli. For instance, the first channel to be identified as chemosensitive, TRPV1, has been shown to be activated by noxious heat (>43 °C) in addition to the irritants capsaicin, acids (Caterina, M. J. *et al.*, 1997; Tominaga, M. *et al.*, 1998), ethanol (Trevisani, M. *et al.*, 2002), eugenol (Yang, B. H. *et al.*, 2003), and camphor (Xu, H. *et al.*, 2005) (see Table 1).

The chemosensitive TRP channels come from three different subfamilies. The TRPV family is characterized primarily by its thermosensitvity (Clapham, D. E., 2003). Of the six members in this subfamily, four appear to be thermosensitive and three express chemosensitivity (Table 1). In addition to TRPV1's well-known sensitivity to noxious heat, capsaicin (Caterina, M. J. *et al.*, 1997), acidic stimuli (Tominaga, M. *et al.*, 1998), and ethanol (Trevisani, M. *et al.*, 2002), TRPV3, responds to innocuous warmth (>30 °C) (Peier, A. M.

Table 1 Thermo- and chemosensitive transient receptor potentials (TRPs)

	Temperature sensitivity	*Chemical sensitivity*
TRPV1 (VR1)	>43 °C	Capsaicin, acid, ethanol, eugenol camphor
TRPV2 (VRL-1)	>52 °C	
TRPV3	>30 °C	Camphor, carvacol, eugenol, thymol
TRPV4	>24 °C	Acid
TRPM8	<25 °C	Menthol, icilin
TRPA1	<18 °C	Allyl isothiocyanate (mustard oil), cinnamic aldehyde, methyl salicylate (wintergreen oil), eugenol (clove oil), gingerol (ginger), allicin (garlic)

et al., 2002b; Smith, G. D. *et al.*, 2002; Xu *et al.*, 2002) as well as camphor (Moqrich, A. *et al.*, 2005), carvacol, eugenol, and thymol (Xu, H. *et al.*, 2006). TRPV4 is responsive to pressure (Mizuno, A. *et al.*, 2003; Suzuki, M. *et al.*, 2003), innocuous warming (>24 °C) (Guler, A. D. *et al.*, 2002), and low pH (Suzuki, M. *et al.*, 2003).

Like the TRPV subfamily, the TRPM and TRPA receptor subfamilies display sensitivity to multiple stimuli (Table 1). In regard to chemesthesis, TRPM8 and TRPA1 (ANKTM1) are well characterized. TRPM8 has been shown to respond to cold (<25 °C) as well as the cooling agents menthol and icillin (McKemy, D. D. *et al.*, 2002; Peier, A. M. *et al.*, 2002a; Andersson, D. A. *et al.*, 2004; Chuang, H. H. *et al.*, 2004). At high concentrations, menthol has been shown to evoke activity in nociceptive neurons (Xing, H. *et al.*, 2006) and elicit sensations of both cooling and irritation when applied to humans (Green, B. G. 1992; Cliff, M. A. and Green, B. G., 1994; Dessirier, J. M. *et al.*, 2001a). Initial studies indicated that TRPA1 was responsive to noxious cold (<18 °C) (Story, G. M. *et al.*, 2003), although this has been challenged (Jordt, S. E. *et al.*, 2004) and it was recently reported that knockout mice lacking TRPA1 do not exhibit any deficit in responsiveness to noxious cold (Bautista, D. M. *et al.*, 2006). Subsequently, TRPA1 has been shown to additionally respond to pungent compounds including mustard oil, cinnamic aldehyde, wintergreen oil, clove oil, ginger, and garlic (Bandell, M. *et al.*, 2004; Jordt, S. E. *et al.*, 2004; Bautista, D. M. *et al.*, 2005; Macpherson, L. J. *et al.*, 2005) (see Table 1).

Additional receptor families have been implicated for the detection of other oral irritants. For instance, in addition to TRPV1, acid-sensitive ion channels (ASICs) have been shown to be present in trigeminal ganglion cells (Olson, T. H. *et al.*, 1998) and respond to low pH (Lingueglia, E. *et al.*, 1997; Waldmann, R. *et al.*, 1997; Price, M. P. *et al.*, 2001). Similarly, nicotinic acetylcholinergic receptors signal the presence of nicotine irritation (Liu, L. and Simon, S. A. 1996d; Dessirier, J. M. *et al.*, 1998; Liu, L. *et al.*, 1998; Marubio, L. M. *et al.*, 1999).

Electrophysiological recordings elicited by lingual application of chemesthetic stimuli have been made along the entire neural pathway. Remarkably, there is great correspondence between the patterns of activity generated at different levels of the neuraxis. Unlike other systems, activity generated in the periphery seems to be faithfully transmitted to higher brain levels, thus providing a solid foundation for studying the neural correlates of irritant sensation.

Lingual nerve recordings have been made in response to application of a variety of chemesthetic stimuli including acids (Sostman, A. L. and Simon, S. A., 1991; Komai, M. and Bryant, B. P., 1993), vanilloids (Wang, Y. *et al.*, 1993), menthol (Wang, Y. *et al.*, 1993; Lundy, R. F., Jr. and Contreras, R. J., 1994; 1995), ethanol (Danilova, V. and Hellekant, G. 2002), and astringent (Shiffman, S. S., *et al.*, 1992) and tingling (Bryant, B. P. and Mezine, I., 1999) compounds. The difficulty in isolating single C- and Aδ-fibers makes this technique extremely labor intensive and, consequently, whole-nerve recordings are often made. Despite these technical limitations, when combined with patch-clamp and calcium-imaging studies of trigeminal ganglion cells, important information has been gathered detailing cellular processes and coding mechanisms. Indeed, increasing numbers of studies suggest that the processing of chemoirritant information remains segregated from the processing of non-nociceptive chemically evoked sensations. For instance, chemical irritants (e.g., capsaicin, pentanoic acid, and mustard oil) tend to activate the same population of chemosensitive trigeminal cells, whereas menthol, when delivered at a low, nonirritating dose, activates a different population (Jordt, S. E. *et al.*, 2004; Abe, J. *et al.*, 2005; Kobayashi, K. *et al.*, 2005). Some of the overlap in chemical sensitivity is the result of a specific receptor being activated by multiple irritants as is the case with TRPV1 which is activated by vanilloids (Caterina, M. J. *et al.*, 1997), protons (Tominaga, M. *et al.*, 1998; Jordt, S. E. *et al.*, 2000), and ethanol (Trevisani, M. *et al.*, 2002). Additionally, multiple studies have shown individual trigeminal ganglion cells or fibers to respond to a diverse sample set of chemical irritants, suggesting that multiple receptor mechanisms are coexpressed in the same cell. The fact that TRPM8 is expressed in a population of neurons separate from those expressing TRPV1 or TRPA1 (Jordt, S. E. *et al.*, 2004; Abe, J. *et al.*, 2005; Kobayashi, K. *et al.*, 2005) provides a mechanism by which chemically evoked irritant and thermal sensations are kept separate. If the pungency associated with high menthol concentrations can be attributed to activation of TRPA1, then a chemesthetic model supporting the separate processing of irritant and thermal stimuli can be developed. However, to date, rodent TRPA1 has not been shown to be menthol sensitive.

Centrally, *c-fos* immunohistochemistry has been used to show that similar populations of neurons in superficial Vc are activated by lingual application of a variety of chemical irritants including nicotine,

capsaicin, piperine, histamine, acids, and high salt concentrations (Carstens, E. *et al.*, 1995; Simons, C. T. *et al.*, 1999; Dessirier, J. M. *et al.*, 2000; Carstens, E. *et al.*, 2001; Sudo, S. *et al.*, 2003). However, immunohistochemical studies are static representations of neural activity and cannot show whether a given neuron responds to multiple chemical stimuli. Thus, electrophysiological recordings of Vc neural activity are necessary to delineate the response properties of chemosensitive neurons. To date, extracellular recordings suggest that Vc neurons respond to multiple classes of chemoirritants (Carstens, E. *et al.*, 1998; Simons, C. T. *et al.*, 1999; Dessirier, J. M. *et al.*, 2000; Sudo, S. *et al.*, 2002; Simons, C. T. *et al.*, 2003c; Sudo, S. *et al.*, 2003; Simons, C. T. *et al.*, 2004) (Figure 2). Recent studies indicate that neurons in superficial laminae of Vc that respond to noxious tongue cooling also respond to menthol, and that the large majority of these additionally respond to noxious heat, capsaicin, mustard oil, and other irritant chemicals (Carstens, E. *et al.*, 2005) (Figure 3). This multiple sensitivity is true for WDR and NS cell types. Thus, although in the periphery, chemoirritation may be coded along labeled lines, at the level of the first central synapse, this specificity appears to be lost.

Few studies have looked at the chemosensitivity of neurons residing in thalamus or somatosensory cortex. Injections of capsaicin under the skin of the lip in rat increased spontaneous firing rate of thalamocortical neurons within 15 min and resulted in reorganization of VPM and SI whisker receptive fields within 1 h (Katz, D. B. *et al.*, 1999). These findings are in contrast to studies at the brainstem and spinal level wherein capsaicin induces immediate increases in neuronal firing (e.g., Carstens, E. *et al.*, 1998; Dessirier, J. M. *et al.*, 2000), and the time course for capsaicin-induced reorganization is significantly shorter (Simone, D. A. *et al.*, 1991; Pettit, M. J. and Schwark, H. D., 1996; Chiang, C. Y. *et al.*, 1997). Capsaicin has been shown to activate neurons in higher cortical levels including the orbitofrontal cortex and amygdala (Rolls, E. T. *et al.*, 2003; Kadohisa, M. *et al.*, 2004; 2005). Of the population of macaque orbitofrontal neurons responding to taste, temperature, or viscosity, nearly 16% also responded to capsaicin (Kadohisa, M. *et al.*, 2004). Notably, the response characteristics of neurons in orbitofrontal cortex activated by thermal stimuli were different from those activated by capsaicin, indicating that the representation of capsaicin in this region is different from other somatosensory stimuli such as temperature.

Perceptually, chemesthetic sensations elicited by various irritant chemicals are often verbalized using the same descriptor. Typically, these sensations are described as burning or pungent regardless of whether the stimulus is, for example, capsaicin or menthol. However, it is unknown whether these chemically diverse compounds all elicit sensations that are qualitatively identical or, alternatively, whether the compounds evoke qualitatively different sensations that are described as similar due to a limited vocabulary. Neurophysiological evidence has shown that a single nociceptor can express multiple receptor subtypes and respond to a variety of chemoirritants. However, subjects can easily discriminate the irritant

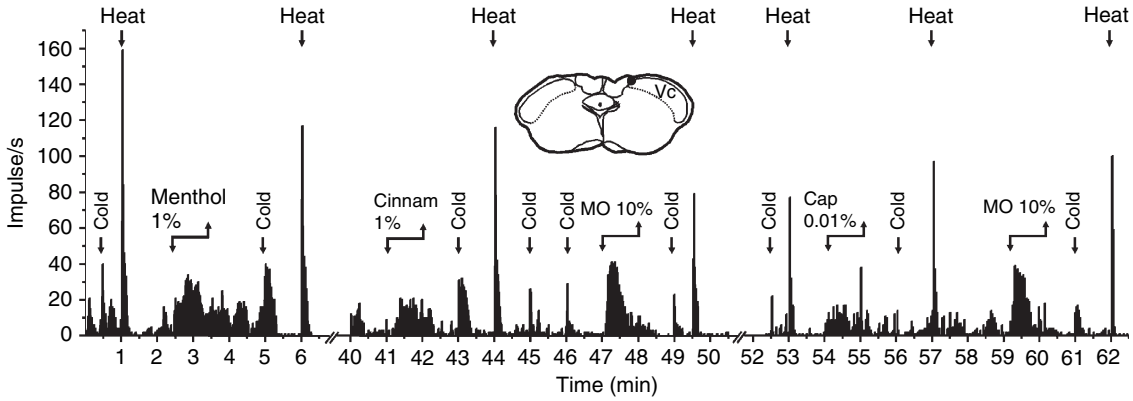

Figure 3 Representative individual example of cold- and menthol-responsive Vc unit that additionally responded to noxious heat and other irritant chemicals. Shown are peristimulus–time histograms (PSTHs; bin width 1 s) of activity. Arrows indicate time of application of noxious cold (0–3 °C water) or heat (53 °C water) stimuli, and bars with downward and upward arrows indicate start and end of chemical application. Cinnam: cinnamaldehyde; MO, mustard oil; Cap, capsaicin. Inset shows recording site (dot).

sensation evoked from different chemical compounds. Certainly, temporal cues assist subjects in this discrimination task. For instance, some compounds, such as allyisothiocyanate, have a quick onset and relatively short duration, whereas others have a slower onset (nicotine) or longer duration (capsaicin). Further studies are needed to delineate whether chemesthetic submodalities exist. Further advances in neuroimaging techniques might allow investigators to determine the neural underpinnings that allow subjects to differentiate chemical irritants.

4.18.3 Chemoirritation: Temporal Phenomena

Most sensory systems maintain sensitivity to conditions of repeated or prolonged stimulation by a process called adaptation. Adaptation is a specialized cellular response that results in a decreased number of evoked action potentials despite a maintained stimulus. Cellular adaptation results in the loss of the conscious perception of a constant stimulus. Unique to the chemesthetic sense, irritant stimuli often evoke patterns of sensation that do not conform to the classic models of adaptation. Indeed the sensation elicited by irritant stimuli can increase or decrease with repeated stimulation depending upon chemical compound and the interstimulus interval (ISI).

Sensitization is the phenomenon encountered when a chemesthetic stimulus elicits an irritant sensation of progressively increasing magnitude when applied repeatedly to the tongue (Stevens, D. A. and Lawless, H. T., 1987; Green, B. G., 1989; Cliff, M. A. and Green, B. G., 1996; Prescott, J. and Stevenson, R. J., 1996b; Dessirier, J. M. *et al.*, 1997; Dessirier, J. M. *et al.*, 1999; Prescott, J. and Swain-Campbell, N., 2000). The most well-studied sensitizing irritant is the vanilloid capsaicin. Numerous investigators have noted that when capsaicin is applied to the oral mucosa at ISIs of less than 3 min, the perceived irritant sensation grows (Figure 4(a), left). However, following a short hiatus of greater than 3 min, a condition of self-desensitization (Figure 4, right) develops where further capsaicin applications are perceived as less irritating (Green, B. G., 1989; Geppetti, P. *et al.*, 1993; Cliff, M. A. and Green, B. G., 1996; Green, B. G., 1998; Green, B. G. and Rentmeister-Bryant, H., 1998). With continued application, the perceived irritation builds up again to eventually reach the same level obtained prior to

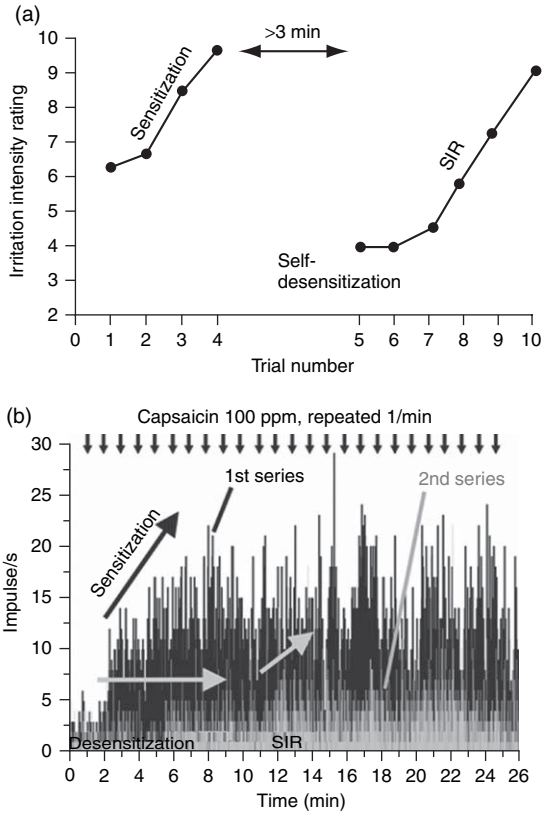

Figure 4 Capsaicin sensitization, desensitization, and stimulus-induced recovery. (a) Graph plots human psychophysical intensity ratings of irritation elicited by repeated application of capsaicin (10 ppm) to the tongue at 1-min interstimulus intervals. (b) Example of response of Vc neuron to repeated application of capsaicin (at arrows). Black histogram shows the response to initial series of capsaicin applications and gray histogram shows the response to second series of applications 30 min after the end of the first series. Note the progressive increase in response to the first series of applications (sensitization), the absence of response to the initial capsaicin applications in the second series (desensitization) with a delayed increased (stimulus-induced recovery = SIR). (a) Data adapted from Green, B. G. 1996. Rapid recovery from capsaicin desensitization during recurrent stimulation. Pain 68, 245–253. (b) Adapted from Dessirier, J. M., Simons, C. T., Sudo, M., Sudo, S., and Carstens, E. 2000b. Sensitization, desensitization and stimulus-induced recovery of trigeminal neuronal responses to oral capsaicin and nicotine. J. Neurophysiol. 84, 1851–1862.

desensitization (Figure 4(a), right); this condition has been termed stimulus-induced recovery (SIR) (Green, B. G., 1996; Green, B. G. and Rentmeister-Bryant, H., 1998). Other vanilloids, including piperine (Stevens, D. A. and Lawless, H. T., 1987; Green, B. G., 1996; Dessirier, J. M. *et al.*, 1999), acids (Green, B. G., 1996; Dessirier, J. M. *et al.*, 2000a), and high concentrations of salt (Dessirier, J. M. *et al.*, 2001b),

elicit patterns of irritation similar to those evoked by capsaicin. Allylisothiocyanate (Simons, C. T. *et al.*, 2003b), nicotine (Dessirier, J. M. *et al.*, 1999), menthol (Cliff, M. A. and Green, B. G., 1994; 1996; Green, B. G. and McAuliffe, B. L., 2000; Dessirier, J. M. *et al.*, 2001a), zingerone (Prescott, J. and Stevenson, R. J., 1996a), cinnamaldehyde (Prescott, J. and Swain-Campbell, N., 2000), and ethanol (Prescott, J. and Swain-Campbell, N., 2000), however, show a pronounced desensitization with repeated application. Figure 5(a) shows desensitization with menthol. Furthermore, reapplication of the same chemical

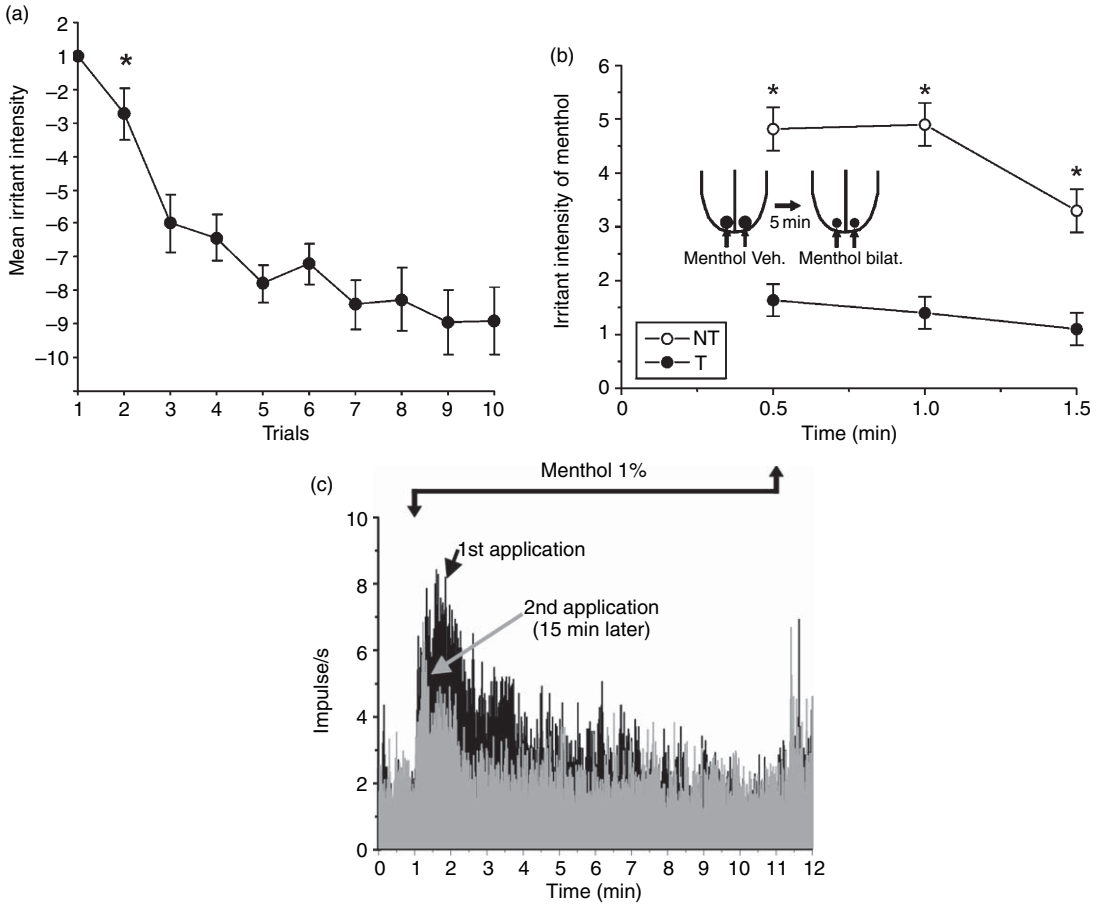

Figure 5 Menthol desensitization. (a) Mean irritant intensity reported 25 s following stimulus onset as a function of trials of menthol (19.2 mM) delivered sequentially at 1 min intervals. Intensity ratings were made using a bipolar category scale in which the magnitude of irritation elicited by the initial stimulus is rated 1; increasingly negative numbers indicate weaker intensity compared to the first trial. Error bars: SE *: significantly different from initial rating ($P < 0.05$, ANOVA). (b) Menthol self-desensitization, assessed using half-tongue two-alternative forced-choice procedure. Menthol was applied to one side of the tongue and vehicle to the other (left-hand inset showing figurine of tongue), followed 5 min later by bilateral application of menthol (right-hand inset). Graph plots the mean irritant intensity for the menthol-treated (T, filled circles) and nontreated (NT, open circles) side of the tongue vs. time following bilateral application of menthol. Note the significant self-desensitization. Error bars: SE Asterisks indicate significant difference between T and NT ($P < 0.05$, *t*-test). (c) Desensitization of responses of Vc neurons to menthol. Black peristimulus–time histogram (PSTH, bin width 1 s) shows averaged responses of 14 Vc neurons to the first application of menthol to the dorsal tongue for 10 min by constant flow (downward and upward arrows denote onset and cessation of menthol application). Note the initial increase in response followed by a decline to baseline levels (desensitization) despite continued menthol, similar to the psychophysical ratings (a). Gray PSTH shows averaged response of the same group of Vc neurons to a second application of menthol 15 min later. Note that the response was smaller compared to the first menthol application (self-desensitization), also similar to the psychophysical findings (b). (a) From Dessirier, J. M., O'Mahony, M., and Carstens, E. 2001a. Oral irritant properties of menthol: sensitizing and desensitizing effects of repeated application and cross-desensitization to nicotine. Physiol. Behav. 73, 25–36. (b) From Dessirier, J. M., O'Mahony, M., and Carstens, E. 2001a. Oral irritant properties of menthol: sensitizing and desensitizing effects of repeated application and cross-desensitization to nicotine. Physiol. Behav. 73, 25–36.

following a hiatus elicits weaker irritation. An example of this self-desensitization with menthol is shown in Figure 5(b).

In addition to sensitization, desensitization, and SIR, many compounds cross-interact to influence another irritant's temporal properties. Information from these studies sheds important light on the transduction and coding mechanisms underlying chemesthesis. For instance, following a hiatus from capsaicin application, the irritant sensation evoked by either piperine (Green, B. G., 1996), nicotine (Dessirier, J. M. *et al.*, 1997), mustard oil (Simons, C. T. *et al.*, 2003b), citric acid (Dessirier, J. M. *et al.*, 2000a), or carbonated water (Dessirier, J. M. *et al.*, 2001c) is reduced. Similar results have been obtained with menthol and nicotine (Dessirier, J. M. *et al.*, 2001a). This phenomenon has been termed cross-desensitization. Cross-sensitization and cross-SIR have been noted for NaCl–capsaicin (Dessirier, J. M. *et al.*, 2001b) and citric acid–capsaicin (Dessirier, J. M. *et al.*, 2000a), respectively. When the temporal chemesthetic properties of an irritant are influenced by the application of a different irritant, several conclusions can be drawn. For instance, the results can be used to suggest that the two irritants share a common receptor mechanism as has been shown with capsaicin and piperine or ethanol. Similarly, for irritant compounds that activate different receptors, like capsaicin and mustard oil or nicotine and menthol, cross-interactions suggest that the same nociceptive cells or neural pathways are involved in the processing of the chemesthetic information.

The different patterns of sensation (i.e., sensitization, desensitization, and SIR) most likely reflect competing cellular mechanisms that differentially dominate during the continued application of the chemical irritant. To date, there is no evidence that sensitization occurs within a single isolated trigeminal ganglion cell. In fact, with repeated application of capsaicin, tachyphylaxis has been observed whereby the size of the evoked inward current decreases (Cholewinski, A. *et al.*, 1993; Liu, L. and Simon, S. A. 1996b; Koplas, P. A. *et al.*, 1997). Thus, the mechanism proposed to mediate sensitization is one of spatial summation (Carstens, E. *et al.*, 2002). In this model (Figure 6), a chemoirritant applied to the tongue is believed to diffuse into the lingual tissue where it accesses previously quiescent nociceptive cells. As long as the pool of irritant stimuli is maintained, sensitization is believed to continue until the rate of diffusion is equaled by the rate at which the stimulus is broken down or absorbed into the blood stream. When the diffusion rate equals the absorption rate, the perceived irritant is hypothesized to plateau and when the absorption rate is greater than the diffusion rate, mechanisms subserving tachyphylaxis dominate, and a state of desensitization results.

Electrophysiological studies in rat Vc neurons have indicated that a remarkable correlation exists between their chemical responsivity and the sensations perceived in human psychophysical studies. Capsaicin, when applied with a short ISI to the rat tongue, elicits activity in Vc neurons that progressively increases over time to reach a plateau approximately 7 min following stimulus administration (Figure 4(b)) (Dessirier, J. M. *et al.*, 2000b). When capsaicin is reapplied following a

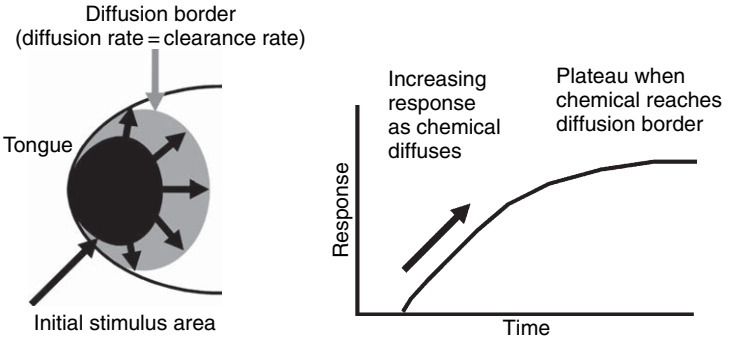

Figure 6 Spatial recruitment of lingual nociceptors to explain sensitization. Left-hand drawing shows initial area (black) of chemical stimulus applied to the tongue. With repeated application, the area increases to a maximum diffusion border (gray) where the rate of chemical diffusion equals the rate of clearance. As the chemical diffuses, it progressively excites more nociceptors by spatial recruitment, causing a progressive rise in sensation (right-hand graph) that plateaus as the chemical reaches its diffusion border.

hiatus of 15 min, evoked activity is significantly delayed; however, further administration causes the firing rate to eventually increase (Figure 4(b)). These data are suggestive of desensitization and SIR, respectively. Conversely, menthol and other chemicals elicit a desensitizing pattern of irritation in human psychophysical studies (see above) which is also reflected in the response pattern of Vc neurons. When applied to the tongue of anesthetized rats, menthol (Carstens, E. *et al.*, 2005), nicotine (Dessirier, J. M. *et al.*, 2000b), and allylisothiocyanate (Simons, C. T. *et al.*, 2004) have been shown to evoke activity in Vc neurons that decreases with continued application. An example with menthol is shown in Figure 5(c) (black histogram). Note that when menthol was reapplied after a 15 min hiatus, it elicited a weaker response (Figure 5(c), gray histogram) consistent with human psychophysical studies (Figure 5(b)).

4.18.4 Irritant–Taste Interactions

Foods containing irritant chemicals continue to gain in popularity in the United States and elsewhere. However, despite the increasing consumption of spicy foods, few studies have looked at irritation–taste interactions. From a nutritional perspective, taste is a major contributor to diet selection (Scott, T. R. and Verhagen, J. V., 2000). Thus, alterations in perceptions of taste resulting from the presence of irritant stimuli could impact nutritional status. Moreover, the existence of irritant–taste interactions could alter the way sensory methodologies are utilized within the food industry. Many irritant chemicals evoke sensitizing or desensitizing patterns of irritation (see above). If these chemicals similarly modulate sensations of taste, new precautions or methodologies must be developed to ensure that the sensory data obtained from spicy products are useful.

Once thought to be tasteless, vanilloids (capsaicin, piperine, and zingerone), as well as menthol, have recently been shown to evoke a bitter taste from a subpopulation of individuals when applied directly to taste papillae (Green, B. G. and Schullery, M. T., 2003; Green, B. G. and Hayes, J. E., 2003; 2004). For those subjects sensitive to the taste quality of capsaicin and zingerone, the intensity appears to be stronger when applied to circumavallate as opposed to fungiform papillae. The mechanism appears to be vanilloid activation of taste receptor cells. However, whether these compounds activate TRPV1 or a particular receptor from the T2R bitter family is still unclear.

Despite the recent observations that most, if not all, irritants evoke a sensation of taste, anecdotal evidence suggests that these same pungent chemicals modify the gustatory qualities of many foods (Prescott, J. *et al.*, 1993). Subjects often report not liking pungent spices (e.g., chili peppers) because the irritant quality blocks or masks the normal taste quality of the food they want to enjoy. A number of psychophysical studies have attempted to quantify the effects reported anecdotally. Most investigations examined the impact of vanilloids (capsaicin and piperine) on taste perception (Szolcsányi, J., 1977; Lawless, H. T. and Stevens, D. A., 1984; Lawless, H. T. *et al.*, 1985; Cowart, B. J., 1987; Prescott, J. *et al.*, 1993; Karrer, T. and Bartoshuk, L., 1995; Prescott, J. and Stevenson, R. J., 1995; Stevenson, R. J. and Prescott, J., 1997, Simons, C. T. *et al.*, 2002); however, CO_2 has also been addressed (Cometto-Muñiz, J. E. *et al.*, 1987; Cowart, B. J., 1998).

Initial studies reported that recognition thresholds of taste stimuli were not affected by rinsing with aqueous solutions of capsaicin (Szolcsányi, J., 1977). However, recognition thresholds are notoriously inconsistent and often show great intraindividual variability (O'Mahony, M. *et al.*, 1976). At suprathreshold concentrations of taste stimuli, the effects of capsaicin appear to be variable. Following this initial study, Lawless H. T. and Stevens D. A. (1984) noted modest-to-significant reductions in the perceived intensity of sour, bitter, and sweet stimuli following a whole-mouth capsaicin rinse. The effect of piperine was more pronounced with a significant suppression noted of all taste qualities. Similarly, evaluated as sucrose– or NaCl–capsaicin mixtures, perceived sweet intensity was decreased, whereas there was minimal impact on perceived saltiness (Prescott, J. *et al.*, 1993). These findings were confirmed in a subsequent study (Stevenson, R. J. and Prescott, J., 1997). Most recently, capsaicin pretreatment was found to suppress the perceived intensity of sucrose-induced sweetness, quinine-induced bitterness, and glutamate-induced umami (Simons, C. T. *et al.*, 2002). It is tempting to speculate that across these studies, the taste sensations that consistently show suppression when capsaicin irritation is present are those that typically involve G-protein-coupled receptors (GPCRs); however, it should be emphasized that quinine is thought to have a mode of action that is independent of GPCRs (Chen, Y. and Herness, M. S., 1997).

Some of this interstudy variability can be attributed to the method of capsaicin/tastant delivery as evidence suggests that pretreating the oral cavity with irritants prior to evaluating tastes results in a greater apparent reduction in taste intensity compared to rinsing with irritant–tastant mixtures (Cowart, B. J., 1987). Moreover, confounding influences of solution concentrations and temperature have not always been controlled. However, despite these methodological differences, pretreating the oral cavity with capsaicin or piperine appears to consistently suppress the intensity of perceived sweetness.

Several studies also investigated the effect of capsaicin desensitization on taste perception (Gilmore, M. M. and Green, B. G., 1993; Karrer, T. and Bartoshuk, L., 1995; Simons, C. T. *et al.*, 2002). Capsaicin desensitization reduced the sensation elicited by citric acid and NaCl, but this effect was minimized when controlling for context effects (Gilmore, M. M. and Green, B. G., 1993). In fact, when controlling for context effect, only the sensations elicited by the highest levels of NaCl or citric acid were reduced. At high concentrations, both citric acid and NaCl evoke irritant sensations that are difficult to separate from the taste sensations. The reduction in sensation reported at the high tastant concentrations, therefore, might be due to capsaicin's ability to cross-desensitize the irritation elicited by NaCl or citric acid as opposed to desensitizing taste sensation *per se*. Similar results were found using a different methodology (Simons, C. T. *et al.*, 2002). Self-desensitization evoked by low capsaicin concentrations (1.5 or ppm) had no effect on the taste sensations elicited by sucrose, quinine, monosodium glutamate, NaCl, or citric acid. However, at high capsaicin concentrations (100 ppm or more), self-desensitization led to a reduction in the perceived bitter intensity elicited by propthiouracil or quinine as well as the saltiness and sourness of NaCl and citric acid solutions (Karrer, T. and Bartoshuk, L., 1995). However, at lower capsaicin concentrations (10 ppm), these same authors saw no effect of capsaicin desensitization on perceived intensity of taste solutions (Karrer, T. and Bartoshuk, L., 1995).

The presence of CO_2 appears to variably modulate the perceived intensity of taste solutions. When added to aqueous solutions of sucrose, citric acid, NaCl, or quinine, CO_2 was found to slightly increase the perceived intensity of salty and sour sensations (Cometto-Muñiz, J. E. *et al.*, 1987). However, these results were not interpreted as a CO_2 enhancement of saltiness or sourness, but instead attributed to subject confusion between the sensation elicited by low concentrations of NaCl or citric acid with the pungent sensation elicited by CO_2. In a subsequent experiment (Cowart, B. J., 1998), carbonation was found to have no effect on total taste intensity of model taste solutions, but increased the intensity of the sweet and salty subcomponents of the stimulus. On the surface, it is surprising that CO_2 would increase the perceived intensity of some tastants, whereas vanilloids tend to have a suppressive effect. However, CO_2, being an acid, is sour and would therefore be expected to increase the perceived intensity of some taste sensations.

Despite the psychophysical evidence for irritant–taste interactions, it is not clearly understood where they occur. Clearly, in the case of vanilloid-evoked taste sensations (Green, B. G. and Schullery, M. T., 2003; Green, B. G. and Hayes, J. E., 2003; 2004), the compound is acting to excite taste receptor cells. However, in the case of irritant modulation of taste sensations, there are a number of potential sites and mechanisms. For instance, it is possible that irritants and tastants interact at the cognitive level as has been proposed for gustation and olfaction. Given the distinct anatomical separation of the olfactory and gustatory neural pathways, this scenario makes sense. However, in the case of oral irritants and tastants, the two chemical modalities stimulate neurons located within the same oral tissue, most notably the tongue. This provides a substrate by which chemicals (i.e., substance P, calcitonin gene-related peptide (CGRP)) released locally from trigeminal nerve endings in response to a noxious stimulus might modulate the activity of taste receptor cells or gustatory neurons (Wang, Y. *et al.*, 1995; Osada, K. *et al.*, 1997; Simon, S. A. *et al.*, 2003). Therefore, it is possible that intermodality communication occurs peripherally. Other potential sites of interaction also exist. Trigeminal primary afferent neurons project not only to brainstem nuclei involved in processing nociceptive information but also send collateral branches to the gustatory NTS (Beckstead, R. M. and Norgren, R., 1979). Similarly, second-order projections from Vc have also been identified in the NTS (Menétrey, D. and Basbaum, A. I., 1987). Therefore, oral irritant and taste information might converge onto second-order neurons residing in the taste nucleus. Nociceptive input could, therefore, directly modulate NTS gustatory neurons or, alternatively, excite inhibitory gamma-amino-*n*-butyric acid (GABA)-ergic or opioidergic interneurons that have been identified within this area (Lynch, W. C.

et al., 1985; Davis, B. J., 1993; Davis, B. J. and Kream, R. M., 1993). Either mechanism of central interaction could suppress the activity of gustatory cells resulting in alterations to taste perception.

4.18.4.1 Peripheral Interactions

Several investigations have addressed the possibility that trigeminal and gustatory interactions occur in the periphery. In particular, three studies have looked directly at the consequence of lingual nerve stimulation on the response of chorda tympani fibers (Wang, Y. *et al.*, 1995; Osada, K. *et al.*, 1997; Simon, S. A. *et al.*, 2003). In the first (Wang, Y. *et al.*, 1995), chorda tympani responses to NaCl were recorded before, during, and after electrical stimulation of the lingual nerve. It was found that the NaCl-induced activity in these fibers was significantly depressed during simultaneous lingual nerve stimulation (Figure 7). The effect was presumed to be due to the release of neuroactive peptides from the peripheral terminals of trigeminal nociceptive nerve endings that directly affected the responses of gustatory neurons to NaCl. Anatomical studies have shown that taste receptor cells or perigemmal neurons express receptors for a variety of neuropeptides including substance P (Chang, G. Q. *et al.*, 1996) and CGRP (van Rossum, D. *et al.*, 1997), both of which are released from C-fiber terminals following electrical stimulation or via an axon reflex (Holzer, P., 1998).

In the second study (Osada, K. *et al.*, 1997), chorda tympani responses to NaCl or KCl were recorded in the presence or absence of capsaicin. The majority of responses to NaCl and KCl were depressed when capsaicin was presented simultaneously with the gustatory stimulus (Figure 8). Interestingly, in a subpopulation of neurons, capsaicin treatment significantly enhanced the NaCl or KCl response. As in the previous study, the attenuated gustatory response was attributed to the presence of neuroactive peptides released in response to capsaicin.

However, with the completion of more recent studies, alternative explanations are possible. For instance, studies suggest that the amiloride-insensitive pathway mediating NaCl sensitivity involves a TRPV1 variant (Lyall, V. *et al.*, 2004; 2005) that responds to the TRPV1 agonists resiniferatoxin and capsaicin. As such, the possibility exists that simultaneous capsaicin application may directly gate the TRPV1 variant to evoke a heightened NaCl or KCl response. Similarly, if the TRPV1 variant has altered desensitization kinetics, capsaicin application might be speculated to result in attenuated NaCl responses. In addition to the potential modulation of the TRPV1 variant, recent studies confirm that capsaicin inhibits voltage-sensitive ion channels expressed in taste receptor cells (Park, K. *et al.*, 2003, Costa, R. M. *et al.*, 2005). The conductance of outwardly rectifying K-channels was found to be completely inhibited in the presence of 500 nM capsaicin (Park, K. *et al.*, 2003), suggesting a mechanism by which capsaicin could enhance gustatory responses of taste receptor cells. In a similar set of experiments, 30 μM capsaicin was found to inhibit both the peak inward current and the peak outward current by 20% and 30%, respectively (Costa, R. M. *et al.*, 2005). Attenuation of the voltage-sensitive inward current would result in decreased sensitivity to any gustatory stimulus. Interestingly, support for a non-TRPV1-mediated mechanism was observed in a behavioral experiment where the preference for sucrose exhibited by TRPV1-knockout mice was abolished in the presence of capsaicin (Costa, R. M. *et al.*, 2005).

Substance P and CGRP are released from the peripheral terminals of nociceptive nerve endings in response to an activating noxious stimulus (Holzer, P., 1998). The close proximity of nociceptive free nerve endings to taste receptor cells suggests that peptides released might modulate gustatory signaling. To specifically address the direct effect of neuropeptides on gustatory signaling, Simon S. A. *et al.* (2003) recorded chorda tympani taste responses in the presence and

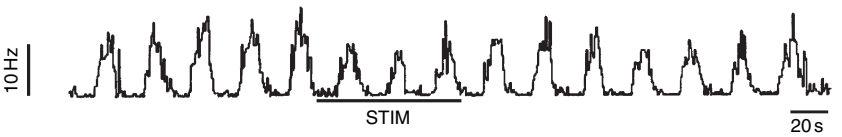

Figure 7 Peripheral trigeminal modulation of taste nerve activity. Shown are responses (in PSTH format) of a single chorda tympani fiber to repeated application of 0.1 M NaCl to the tongue, without and during electrical stimulation of the lingual nerve (0.5 ms biphasic pulses at 15 Hz and 5 V). Note the depressant effect of lingual nerve stimulation on tastant-evoked responses. From Wang, Y., Erickson, R. P., and Simon, S. A. 1995. Modulation of rat chorda tympani nerve activity by lingual nerve stimulation. J. Neurophysiol. 73, 1468–1483, figure 8B, with permission.

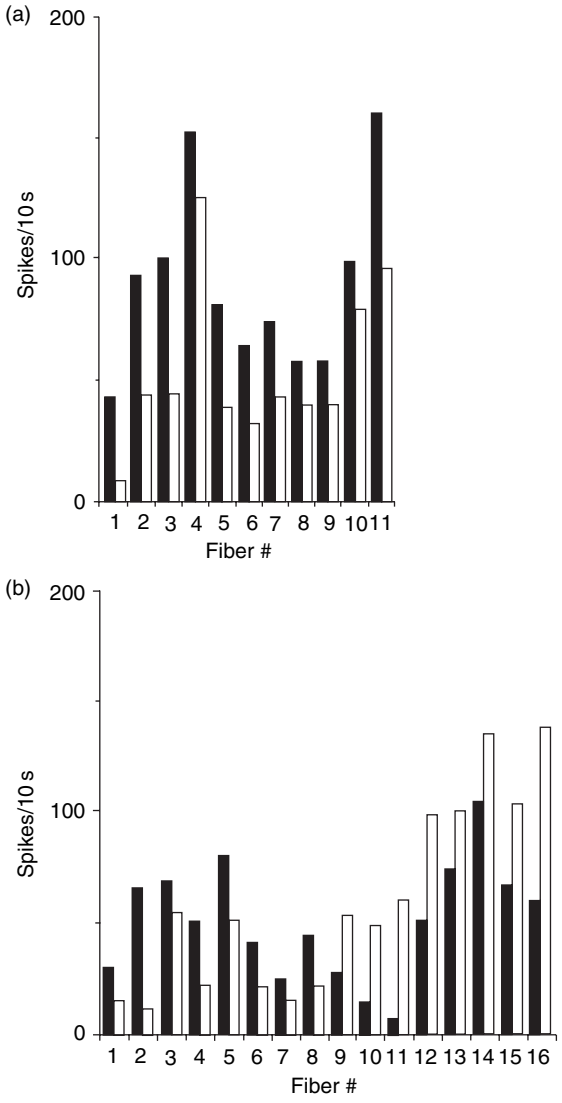

Figure 8 Capsaicin modulation of taste nerve responses. Graphs plot the responses of single N-type (a: responsive to sodium salts) and E-type (b: broadly responsive to cations) chorda tympani fibers. Filled bars show responses to 100 mM NaCl. Open bars show responses to 100 mM NaCl plus 100 ppm capsaicin. Note that responses of N-type fibers were depressed in the presence of capsaicin, while responses of some E-type fibers were depressed and others enhanced in the presence of capsaicin. From Osada, K., Komai, M., Bryant, B. P., Suzuki, H., Goto, A., Tsunoda, K., Kimura, S., and Furukawa, Y. 1997. Capsaicin modifies responses of rat chorda tympani nerve fibers to NaCl. Chem. Senses 22, 249–255, figure 4, with permission.

absence of substance P and CGRP. Whole-nerve recordings in response to lingual NaCl, HCl, quinine HCl, and sucrose were made from the chorda tympani of rats. Simultaneously, substance P or CGRP was infused into the ipsilateral lingual artery. Infusion of CGRP reduced the chorda tympani response to NaCl and HCl to about 80% of preinfusion levels (Figure 9). Importantly, these effects were shown to be independent of any vasoactive or thermal change induced by neuropeptide infusion. Conversely, substance P injection had no noticeable effect on NaCl or HCl when injected at concentrations that did not induce vasodilation or increased lingual temperature. In addition, neither substance P nor CGRP had any apparent effect on sucrose- or quinine-evoked responses. However, for these two taste responses, methodological limitations were thought to have mitigated the reliable detection of possible neuropeptide effects.

Results from central gustatory recordings corroborate the existence of peripheral interactions between the trigeminal and gustatory systems. Responses to sucrose, quinine HCl, monosodium glutamate, NaCl, and citric acid recorded from taste cells in the NTS were shown to be significantly suppressed following prolonged (7 min) lingual capsaicin (100 μM) application (Figure 10) (Simons, C. T. *et al.*, 2003a). Across all tastants, capsaicin suppressed the evoked response to approximately 57% of precapsaicin levels. Interestingly, the same level of capsaicin suppression was observed after bilateral trigeminal ganglionectomy, indicating that an intact trigeminal pathway is not required for capsaicin attenuation of taste responses (Simons, C. T. *et al.*, 2003a).

Anatomical studies further support a peripheral effect of capsaicin (Simons, C. T. *et al.*, 2003a). In addition to the direct effects of neuroactive peptides mentioned previously, substance P and CGRP have potent vasoactive properties that induce changes in the permeability of the vascular wall leading to a localized inflammatory response including plasma extravasation and edema. Tests for plasma extravasation typically involve the systemic injection of dye into the bloodstream followed by a noxious stimulus. When plasma extravasation occurs, dye that has leaked out of the vasculature is found to have stained surrounding tissue. Following lingual capsaicin application, plasma extravasation was found to be localized to the intragemmal space of taste papillae (Figure 11), and this effect was seen in both intact and ganglionectomized animals. This finding provides additional evidence that neuropeptides act in close proximity to taste receptor cells and suggests that edema localized to the taste bud may also play a role in capsaicin-induced taste suppression.

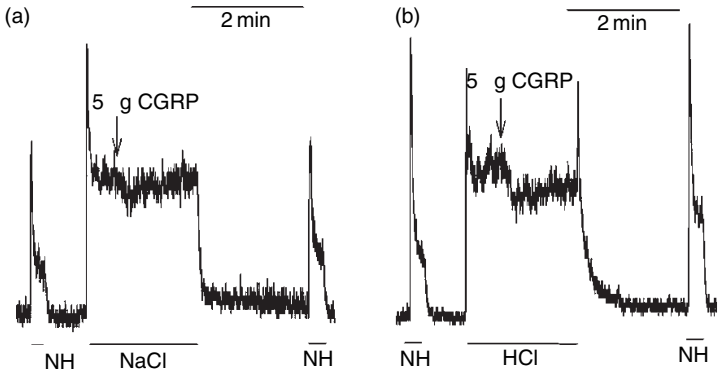

Figure 9 Depressant effects of calcitonin gene-related peptide (CGRP) on chorda tympani fiber responses to tastants. Shown are the effects of lingual artery perfusion of 5 μg CGRP in 100 μl KH buffer (arrows). Responses to 0.1 M NH_4Cl bracket each trial. (a) CGRP (at arrow) decreased the tonic responses to 0.1 M NaCl. (b) CGRP (arrow) decreased response to 10 mM HCl. From Simon, S. A., Liu, L., and Erickson, R. P. 2003. Neuropeptides modulate rat chorda tympani responses. Am. J. Physiol. (Regul. Integr. Comp. Physiol.) 284, R1494–R1505, figure 7.

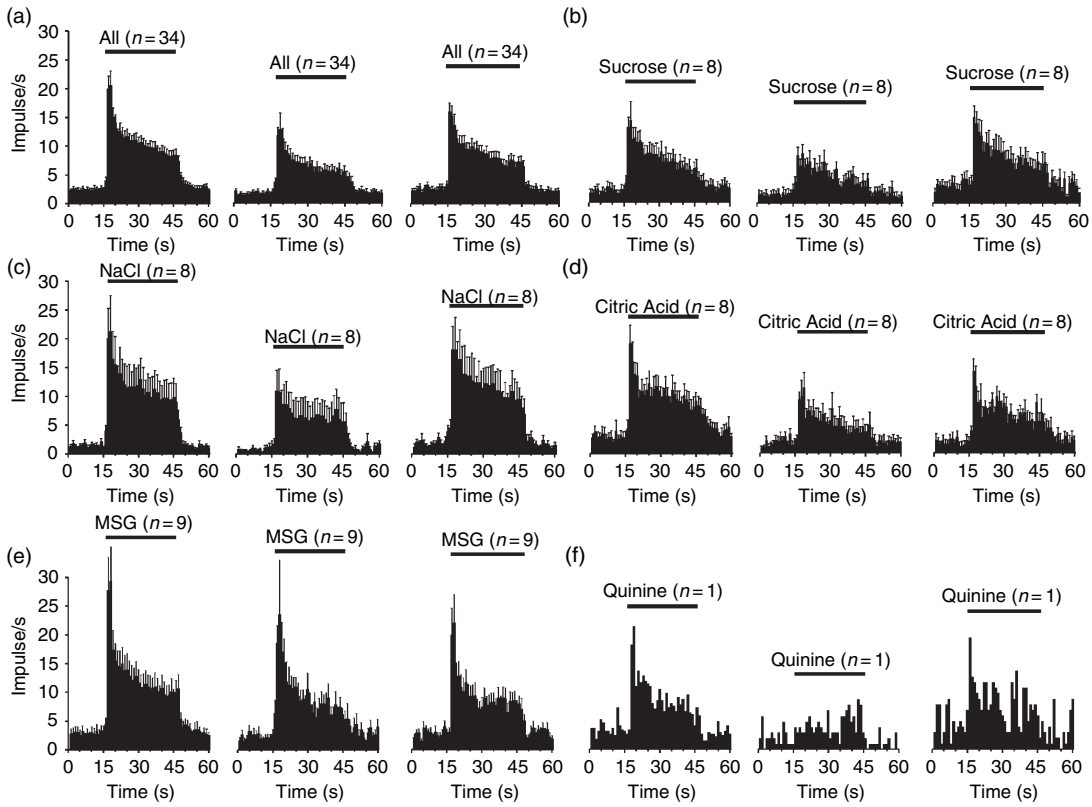

Figure 10 Suppression of tastant-evoked responses of nucleus of the solitary tract (NTS) units by oral capsaicin. Each triad of panels shows averaged peristimulus–time histograms (PSTHs) of NTS unit responses to the indicated tastant, before capsaicin (left PSTHs), immediately after cessation of capsaicin (middle PSTHs), and 12 min after cessation of capsaicin (right PSTHs). Horizontal bars indicate 30 s duration of tastant stimulus. Error bars indicate SEM. (a) Data from all 34 units were pooled to show averaged responses to the best tastant. Note suppression of response (middle panel; to 57%) immediately after capsaicin with recovery (right panel). (b) Sucrose. Note suppression (middle panel; to 63%) immediately after capsaicin with recovery (right panel). (c) NaCl. Note suppression (middle panel; to 44%) immediately after capsaicin with recovery (right panel). (d), Citric acid. Note suppression (middle panel; to 50%) immediately after capsaicin with partial recovery (right panel). (e) Monosodium glutamate (MSG). Note suppression (middle panel; to 73%) immediately after capsaicin with little or no recovery (right panel). (f), Quinine; individual example showing that the response of the unit to quinine (left panel) was depressed immediately after capsaicin (middle panel) with recovery (right panel). From Simons, C. T., Boucher, Y., and Carstens, E. 2003a. Suppression of central taste transmission by oral capsaicin. J. Neurosci. 23, 978–985, figure 2, with permission.

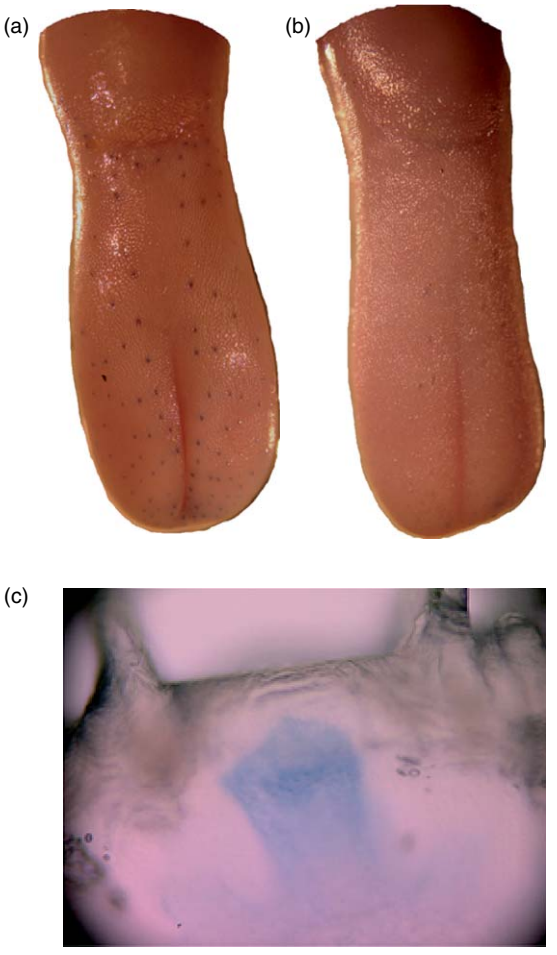

Figure 11 Capsaicin-induced plasma extravasation. (a) Photograph of rat tongue treated previously with topical capsaicin. Note accumulation of blue dye within taste papillae across the lingual surface. (b) Photograph of rat tongue pretreated with ethanol. Note absence of punctuate dye extravasation. (c), Photomicrograph of section through fungiform papillae (100× magnification). The black arrowhead indicates the dorsal lingual surface, whereas the white arrowhead shows a filliform papilla. Note that blue dye accumulates within the taste bud, with little or none in surrounding tissues. From Simons, C. T., Boucher, Y., and Carstens, E. 2003a. Suppression of central taste transmission by oral capsaicin. J. Neurosci. 23, 978–985, figure 6, with permission.

4.18.4.2 Central Interactions – Nucleus of the Solitary Tract

Several investigators have found that second-order neurons located in the caudal portion of the gustatory nucleus respond not only to sapid stimuli but also to touch and temperature (Ogawa, H. and Hayama, T., 1984; Ogawa, H. *et al.*, 1984; 1988; Halsell, C. B. *et al.*, 1993; Travers, S. P. and Norgren, R., 1995). Although the chorda tympani nerve is well known to respond to tastants as well as to mechanical and thermal stimuli (Ogawa, H. *et al.*, 1968; Robinson, P. P., 1988), these findings nevertheless give rise to the possibility that gustatory and somatosensory (including nociceptive) information converge onto cells located within the gustatory NTS. Anatomic evidence additionally provides support. Primary afferent trigeminal fibers have been shown to send collateral branches into the NTS (Beckstead, R. M. and Norgren, R., 1979), and second-order neurons originating in Vc similarly project onto the same region (Davis, B. J. and Kream, R. M., 1993). Moreover, trigeminal afferent fibers projecting to the NTS contain the neuromodulator substance P (South, E. H. and Ritter, R. C., 1986), and dense neurokinin 1 (substance P receptor) labeling has been observed in the same dorsomedial and dorsolateral subnuclei (Davis, B. J and Smith, D. V., 1997). Physiological findings confirm that substance P has a modulatory effect on gustatory cellular activity. Whole-cell patch-clamp recordings in rat brainstem slices showed the intrinsic activity of NTS units was influenced by the application of substance P (0.1–4 μM) to the bathing medium (King, M. S. *et al.*, 1993). Indeed, substance P induced a transient (~7 min) depolarization in 70% of the tested neurons that was accompanied by an increase in the input resistance. In contrast, only 4% of neurons exhibited a hyperpolarization following substance P exposure. These findings suggest that substance P has primarily an excitatory effect that is mediated by the closure of ion channels. Similar results were obtained from whole animal recordings where microinjection of substance P into the hamster NTS was found to modulate the responses to electrical or NaCl stimulation of the tongue (Davis, B. J and Smith, D. V. 1997). In 60% of the neurons tested, substance P injection increased the activity evoked by electrical stimulation. In the remaining 40%, substance P substantially reduced (to approximately 50%) the electrically evoked response. Correspondingly, nearly 50% of the NaCl-evoked responses were increased following injection of substance P into the NTS. However, in contrast to the electrical stimulus, only 9% of NaCl-evoked responses were inhibited by substance P. Thus, substance P appears to be a potent and varied modulator of central gustatory cells, although it is still speculative this effect is mediated by trigeminal activity.

Dense innervation of the NTS by inhibitory GABAergic and opioidergic neurons (Lynch, W. C.

et al., 1985; Davis, B. J, 1993; Davis, B. J. and Kream, R. M., 1993) suggests another mechanism of inhibitory modulation. Noxious stimuli directed at the oral cavity could activate trigeminal nociceptors that further excite inhibitory interneurons to directly suppress tastant-evoked activity in NTS.

Functional studies directly testing the hypothesis that trigeminal activity modulates central gustatory responses have recently been completed (Boucher, Y. *et al.*, 2003; Simons, C. T. *et al.*, in press). Single-cell gustatory responses were recorded from rats before and after trigeminal ganglionectomy (Boucher, Y. *et al.*, 2003). Ganglioectomy *per se* did not modulate taste responses, suggesting that trigeminally mediated excitatory or inhibitory processes are not tonically active. However, with simultaneous electrical activation of the central cut end of the mandibular nerve, 64% of gustatory responses were modulated relative to prestimulation levels. Indeed, approximately 21% of the gustatory responses were inhibited by simultaneous mandibular nerve stimulation, whereas 43% of the responses were enhanced (Boucher, Y. *et al.*, 2003). Consistent with a peripheral mode of suppression, central gustatory responses were attenuated when the peripheral cut end of the mandibular nerve was stimulated.

Nicotine activation of trigeminal afferents has a similar effect (Simons, C. T. *et al.*, in press). Topical application of nicotine to the tongue for a period of 4 min suppressed taste responses recorded in NTS. This effect was dose dependent. Whereas low nicotine concentrations (0.84 mM) had no effect, higher doses (8.4 mM or 600 mM) suppressed taste-evoked responses to 54% and 27%, respectively. The attenuation was nearly equal for all taste qualities. Mecamylamine was shown to reduce the nicotine's suppressive effect of taste responses, suggesting the involvement of nicotinic cholinergic receptors. Interestingly, following bilateral ganglionectomy, nicotine application had no effect on taste responses, indicating that nicotine suppression of taste occurs centrally and is mediated through the trigeminal system. This is in marked contrast to capsaicin which was shown to have a peripheral mechanism of suppression.

4.18.4.3 Cognitive Interactions

In addition to the possible peripheral and central mechanisms discussed above, high-level interactions occurring in the cortex might contribute to the effect of oral irritants on taste perception. The convergence of somatosensory and taste pathways into the insular and orbitofrontal cortex provides the neural substrate for these interactions to occur (Cerf-Ducastel, B. *et al.*, 2001). Several studies have identified neurons in the orbitofrontal cortex that respond to gustatory as well as to somatosensory stimuli (Rolls, E. T. *et al.*, 1999; 2003; Verhagen, J. V. *et al.*, 2003; Kadohisa, M. *et al.*, 2004; 2005). In particular, neurons were identified that responded to taste but also to the texture (Rolls, E. T. *et al.*, 1999; 2003; Verhagen, J. V. *et al.*, 2003) and temperature (Kadohisa, M. *et al.*, 2004; 2005) of a stimulus as well as the presence of capsaicin (Kadohisa, M. *et al.*, 2004; 2005). These studies indicate that areas involved in high-level stimulus processing can be modulated by a variety of multimodal inputs to impact both perception and palatability.

There are several possible ways that higher-order somatosensory–taste interactions can result in altered perceptual responses. It is well known that attention is a primary determinant of perception (Marks, L. E. and Wheeler, M. E., 1998; Driver, J. and Frackowiak, R. S., 2001). Attending to a stimulus brings it into the consciousness where it can be evaluated and processed. It is plausible, under some paradigms, that the presence of oral irritation draws attention away from the gustatory stimulus such that it is perceived as less intense. Similarly, context effects have often been shown to impact perceived stimulus intensity. Any evaluation of stimulus strength is made in the context of other stimuli. When a given stimulus is evaluated in the presence of a stronger stimulus, intensity of the first stimulus is often reported as much less than when that same stimulus is evaluated alone or in the presence of a weaker stimulus. Changes to intensity judgments due to context have been explained by Parducci's range–frequency theory (Parducci, A., 1965). Two studies assessed the context effect in regard to the mechanism by which trigeminal irritants modulate taste perceptions (Gilmore, M. M. and Green, B. G., 1993; Simons, C. T. *et al.*, 2002).

In one study (Simons, C. T. *et al.*, 2002), context effect was minimized by using a half-tongue methodology in which capsaicin was applied unilaterally but taste intensity was evaluated bilaterally. In this condition, context effect would be expected to affect perceived taste on both sides equally not just the side receiving capsaicin pretreatment (Simons, C. T. *et al.*, 2002). Moreover, context effect is a generalized phenomenon and would not be expected to impact only specific taste qualities. However, these results were not observed. In fact, capsaicin irritation suppressed

only the perceived intensity of sweetness, bitterness, and umami sensations. Another study noted that context effect plays a role in the suppression of salt and sour tastes following zingerone desensitization as well as playing lesser role following capsaicin desensitization (Gilmore, M. M. and Green, B. G., 1993). Thus, psychological mechanisms including attention and context effect may contribute to the chemesthetic suppression of taste observed both anecdotally and experimentally, and this is a factor that should be controlled for.

Masking is another mechanism by which the presence of oral irritants might impact the perception of gustatory stimuli. Masking is a phenomenon that occurs when the presence of one stimulus obscures the presence of another. In most cases, masking can be achieved simply by increasing the intensity of a second stimulus. In the food and beverage industry, off-notes related to a particular ingredient can be masked by increasing the concentration of a more desirable ingredient. Thus, the presence of a bitter stimulus is often masked by increasing the level of sucrose or other palatable substance. There are limitations as to how effective masking can be. For instance, it is often difficult to mask very intense stimuli. Additionally, often masking agents have a concentration at which they are most effective. Going beyond that level can result in additional undesirable attributes. Capsaicin might serve as a masking agent. The perception of an irritating sensation could mask the sensation evoked by gustatory stimuli. The convergence of taste and somatosensory information in the orbitofrontal cortex (Kadohisa, M. *et al.*, 2004; 2005) provides a mechanism by which a chemoirritants can modulate gustatory information. However, as with context effects, masking is a general phenomena, and it would not be expected to impact only select taste qualities.

4.18.5 Perspectives

The study of the chemical senses is beginning to flourish. In particular, chemesthesis research is attracting the attention of a greater number of investigators. Light is beginning to be shed on questions that were unresolved just a few years ago. However, to further the knowledge of chemesthesis, a multidisciplinary approach using genetic, molecular, physiological, and perceptual methods will be needed. Unlike many sensory systems, chemesthetic information appears to be transmitted relatively faithfully from the periphery to higher centers of the brain. This provides an ideal opportunity to link perceptual endpoints to the neural and molecular correlates that drive them. As the era of molecular biology continues to unfold, undoubtedly additional receptors will be identified that contribute to chemesthetic perception. It will be imperative to understand how these receptors are distributed across trigeminal neurons and how they contribute to the sensations elicited by chemical stimuli. In addition, further studies are needed to delineate whether qualitative differences exist between the sensations elicited by different chemoirritants. The cross-modal interactions occurring between chemesthesis and taste are deserving of more attention. It is clear that multiple mechanisms contribute to the ability of oral irritants to suppress gustatory processing. However, to date, only a few of the many chemesthetic stimuli have been evaluated for effects on taste. It will be interesting to determine whether taste suppression is a phenomenon common to all oral irritants or, alternatively, if only select compounds have this capacity.

References

Abe, J., Hosokawa, H., Okazawa, M., Kandachi, M., Sawada, Y., Yamanaka, K., Matsumura, K., and Kobayashi, S. 2005. TRPM8 protein localization in trigeminal ganglion and taste papillae. Brain Res. Mol. Brain Res. 136, 91–98.

Amano, N., Hu, J. W., and Sessle, B. J. 1986. Responses of neurons in feline trigeminal subnucleus caudalis (medullary dorsal horn) to cutaneous, intraoral, and muscle afferent stimuli. J. Neurophysiol. 55, 227–243.

Andersson, D. A., Chase, H. W., and Bevan, S. 2004. TRPM8 activation by menthol, icilin, and cold is differentially modulated by intracellular pH. J. Neurosci. 24, 5364–5369.

Bandell, M., Story, G. M., Hwang, S. W., Viswanath, V., Eid, S. R., Petrus, M. J., Earley, T. J., and Patapoutian, A. 2004. Noxious cold ion channel TRPA1 is activated by pungent compounds and bradykinin. Neuron 41, 849–857.

Barry, M. A., Halsell, C. B., and Whitehead, M. C. 1993. Organization of the nucleus of the solitary tract in the hamster: acetylcholinesterase, NADH dehydrogenase, and cytochrome oxidase histochemistry. Microsc. Res. Tech. 26, 231–244.

Bautista, D. M., Jordt, S.-V., Nikai, T., Tsuruda, P. R., Read, A. J., Poblete, J., Yamoah, E. N., Basbaum, A. I., and Julius, D. 2006. TRPA1 mediates the inflammatory actions of environmental irritants and proalgesic agents. Cell 124(6), 1269–1282.

Bautista, D. M., Movahed, P., Hinman, A., Axelsson, H. E., Sterner, O., Hogestatt, E. D., Julius, D., Jordt, S. E., and Zygmunt, P. M. 2005. Pungent products from garlic activate the sensory ion channel TRPA1. Proc. Natl. Acad. Sci. U. S. A. 102, 12248–12252.

Beckstead, R. M. and Norgren, R. 1979. An autoradiographic examination of the central distribution of the trigeminal,

facial, glossopharyngeal, and vagal nerves in the monkey. J. Comp. Neurol 184, 455–472.
Boucher, Y., Simons, C. T., Cuellar, J. M., Jung, S. W., Carstens, M. I., and Carstens, E. 2003. Activation of brain stem neurons by irritant chemical stimulation of the throat assessed by c-fos immunohistochemistry. Exp. Brain Res. 148, 211–218.
Bryant, B. P. and Mezine, I. 1999. Alkylamides that produce tingling paresthesia activate tactile and thermal trigeminal neurons. Brain Res. 842, 452–460.
Bryant, B. P. and Moore, P. A. 1995. Factors affecting the sensitivity of the lingual trigeminal nerve to acids. Am. J. Physiol. 268, R58–65.
Carstens, E., Iodi Carstens, M., Dessirier, J. M., O'Mahony, M., Simons, C. T., Sudo, M., and Sudo, S. 2002. It hurts so good: oral irritation by spices and carbonated drinks and the underlying neural mechanisms. Food Qual. Pref. 13, 431–443.
Carstens, E., Kuenzler, N., and Handwerker, H. O. 1998. Activation of neurons in rat trigeminal subnucleus caudalis by different irritant chemicals applied to oral or ocular mucosa. J. Neurophysiol. 80, 4654–4692.
Carstens, E., Merrill, A. W., Zanotto, K., and Iodi Carstens, M. 2005 Cold- and menthol-sensitive neurons in superficial trigeminal subnucleus caudalis (Vc). Program No. 747.4. 2005 Abstract Viewer/Itinerary Planner. Society for Neuroscience.
Carstens, E., Saxe, I., and Ralph, R. 1995. Brainstem neurons expressing c-Fos immunoreactivity following irritant chemical stimulation of the rat's tongue. Neuroscience 69, 939–953.
Carstens, E., Simons, C. T., Dessirier, J.-M., Iodi-Carstens, M., and Jinks, S. L. 2001. Role of neuronal nicotinic acetylcholine receptors in the activation of neurons in the trigeminal subnucleus caudalis by nicotine delivered to the oral mucosa. Exp. Brain Res. 132, 375–383.
Caterina, M. J., Leffler, A., Malmberg, A. B., Martin, W. J., Trafton, J., Petersen-Zeitz, K. R., Koltzenburg, M., Basbaum, A. I., and Julius, D. 2000. Impaired nociception and pain sensation in mice lacking the capsaicin receptor [see comments]. Science 288, 306–313.
Caterina, M. J., Rosen, T. A., Tominaga, M., Brake, A. J., and Julius, D. 1999. A capsaicin-receptor homologue with a high threshold for noxious heat. Nature 398, 436–441.
Caterina, M. J., Schumacher, M. A., Tominaga, M., Rosen, T. A., Levine, J. D., and Julius, D. 1997. The capsaicin receptor: a heat-activated ion channel in the pain pathway [see comments]. Nature 389, 816–824.
Cerf-Ducastel, B., Van de Moortele, P. F., MacLeod, P., Le Bihan, D., and Faurion, A. 2001. Interaction of gustatory and lingual somatosensory perceptions at the cortical level in the human: a functional magnetic resonance imaging study. Chem. Senses 26, 371–383.
Cesare, P., Moriondo, A., Vellani, V., and McNaughton, P. A. 1999. Ion channels gated by heat. Proc. Natl. Acad. Sci. U.S.A. 96, 7658–7563.
Chang, G. Q., Vigna, S. R., and Simon, S. A. 1996. Localization of substance P NK-1 receptors in rat tongue. Regul. Pept. 63, 85–89.
Chen, Y. and Herness, M. S. 1997. Electrophysiological actions of quinine on voltage-dependent currents in dissociated rat taste cells. Pflugers Arch. 434, 215–226.
Chiang, C. Y., Hu, J. W., and Sessle, B. J. 1997. NMDA receptor involvement in neuroplastic changes induced by neonatal capsaicin treatment in trigeminal nociceptive neurons. J. Neurophysiol. 78, 2799–2803.
Cholewinski, A., Burgess, G. M., and Bevan, S. 1993. The role of calcium in capsaicin-induced desensitization in rat cultured dorsal root ganglion neurons. Neuroscience 55, 1015–1023.
Chuang, H. H., Neuhausser, W. M., and Julius, D. 2004. The super-cooling agent icilin reveals a mechanism of coincidence detection by a temperature-sensitive TRP channel. Neuron 43, 859–869.
Clapham, D. E. 2003. TRP channels as cellular sensors. Nature 426, 517–524.
Cliff, M. A. and Green, B. G. 1994. Sensory irritation and coolness produced by menthol: evidence for selective desensitization of irritation. Physiol. Behav. 56, 1021–1029.
Cliff, M. A. and Green, B. G. 1996. Sensitization and desensitization to capsaicin and menthol in the oral cavity: interactions and individual differences. Physiol. Behav. 59, 487–494.
Coimbra, F. and Coimbra, A. 1994. Dental noxious input reaches the subnucleus caudalis of the trigeminal complex in the rat, as shown by c-fos expression upon thermal or mechanical stimulation. Neurosci. Lett. 173, 201–204.
Cometto-Muñiz, J. E., García-Medina, M. R., Calviño, A. M., and Noriega, G. 1987. Interactions between CO_2 oral pungency and taste. Perception 16, 629–640.
Costa, R. M., Liu, L., Nicolelis, M. A., and Simon, S. A. 2005. Gustatory Effects of capsaicin that are independent of TRPV1 receptors. Chem. Senses 30, i198–i200.
Cowart, B. J. 1987. Oral chemical irritation: does it reduce perceived taste intensity? Chem. Senses 12, 467–479.
Cowart, B. J. 1998. The addition of CO_2 to traditional taste solutions alters taste quality. Chem. Senses 23, 397–402.
Critchley, H. D. and Rolls, E. T. 1996. Hunger and satiety modify the responses of olfactory and visual neurons in the primate orbitofrontal cortex. J. Neurophysiol. 75, 1673–1686.
Dallel, R., Luccarini, P., Molat, J. L., and Woda, A. 1996. Effects of systemic morphine on the activity of convergent neurons of spinal trigeminal nucleus oralis in the rat. Eur. J. Pharmacol. 314, 19–25.
Dallel, R., Raboisson, P., Woda, A., and Sessle, B. J. 1990. Properties of nociceptive and non-nociceptive neurons in trigeminal subnucleus oralis of the rat. Brain Res. 521, 95–106.
Danilova, V. and Hellekant, G. 2002. Oral sensation of ethanol in a primate model III: responses in the lingual branch of the trigeminal nerve of *Macaca mulatta*. Alcohol 26, 3–16.
Davis, B. J. 1993. GABA-like immunoreactivity in the gustatory zone of the nucleus of the solitary tract in the hamster: light and electron microscopic studies. Brain Res. Bull. 30, 69–77.
Davis, B. J. and Kream, R. M. 1993. Distribution of tachykinin- and opioid-expressing neurons in the hamster solitary nucleus: an immuno- and in situ hybridization histochemical study. Brain Res. 616, 6–16.
Davis, B. J. and Smith, D. V. 1997. Substance P modulates taste responses in the nucleus of the solitary tract of the hamster. Neuroreport 8, 1723–1727.
Dessirier, J. M., Nguyen, N., Sieffermann, J. M., Carstens, E., and O'Mahony, M. 1999. Oral irritant properties of piperine and nicotine: psychophysical evidence for asymmetrical desensitization effects. Chem. Senses 24, 405–413.
Dessirier, J. M., O'Mahony, M., and Carstens, E. 1997. Oral irritant effects of nicotine: psychophysical evidence for decreased sensation following repeated application and lack of cross-desensitization to capsaicin. Chem. Senses 22, 483–492.
Dessirier, J. M., O'Mahony, M., and Carstens, E. 2001a. Oral irritant properties of menthol: sensitizing and desensitizing effects of repeated application and cross-desensitization to nicotine. Physiol. Behav. 73, 25–36.

Dessirier, J. M., O'Mahony, M., Iodi-Carstens, M., and Carstens, E. 2000a. Sensory properties of citric acid: psychophysical evidence for sensitization, self-desensitization, cross-desensitization and cross-stimulus-induced recovery following capsaicin. Chem. Senses 25, 769–780.

Dessirier, J. M., O'Mahony, M., Iodi-Carstens, M., Yao, E., and Carstens, E. 2001b. Oral irritation by sodium chloride: sensitization, self-desensitization, and cross-sensitization to capsaicin. Physiol. Behav. 72, 317–324.

Dessirier, J. M., O'Mahony, M., Sieffermann, J. M., and Carstens, E. 1998. Mecamylamine inhibits nicotine but not capsaicin irritation on the tongue: psychophysical evidence that nicotine and capsaicin activate separate molecular receptors. Neurosci. Lett. 240, 65–68.

Dessirier, J. M., Simons, C. T., O'Mahony, M., and Carstens, E. 2001c. The oral sensation of carbonated water: cross-desensitization by capsaicin and potentiation by amiloride. Chem. Senses 26, 639–643.

Dessirier, J. M., Simons, C. T., Sudo, M., Sudo, S., and Carstens, E. 2000b. Sensitization, desensitization and stimulus-induced recovery of trigeminal neuronal responses to oral capsaicin and nicotine. J. Neurophysiol. 84, 1851–1862.

Driver, J. and Frackowiak, R. S. 2001. Neurobiological measures of human selective attention. Neuropsychologia 39, 1257–1262.

Dubner, R. and Bennett, G. J. 1983. Spinal and trigeminal mechanisms of nociception. Annu. Rev. Neurosci. 6, 381–418.

Feil, K. and Herbert, H. 1995. Topographic organization of spinal and trigeminal somatosensory pathways to the rat parabrachial and Kolliker–Fuse nuclei. J. Comp. Neurol. 353, 506–528.

Finger, T. 1986. Peptide immunohistochemistry demonstrates multiple classes of perigemmal nerve fibers in the circumvallate papilla of the rat. Chem. Senses 11, 135–144.

Geppetti, P., Tramontana, M., Del Bianco, E., and Fusco, B. M. 1993. Capsaicin-desensitization to the human nasal mucosa selectively reduces pain evoked by citric acid. Br. J. Clin. Pharmacol. 35, 178–183.

Gilmore, M. M. and Green, B. G. 1993. Sensory irritation and taste produced by NaCl and citric acid: effects of capsaicin desensitization. Chem. Senses 18, 257–272.

Green, B. G. 1989. Capsaicin sensitization and desensitization on the tongue produced by brief exposures to a low concentration. Neurosci. Lett. 107, 173–178.

Green, B. G. 1992. The sensory effects of l-menthol on human skin. Somatosens. Mot. Res. 9, 235–244.

Green, B. G. 1996. Rapid recovery from capsaicin desensitization during recurrent stimulation. Pain 68, 245–253.

Green, B. G. 1998. Capsaicin desensitization and stimulus-induced recovery on facial compared to lingual skin. Physiol. Behav. 65, 517–523.

Green, B. G. and Hayes, J. E. 2003. Capsaicin as a probe of the relationship between bitter taste and chemesthesis. Physiol. Behav. 79, 811–821.

Green, B. G. and Hayes, J. E. 2004. Individual differences in perception of bitterness from capsaicin, piperine and zingerone. Chem. Senses 29, 53–60.

Green, B. G. and McAuliffe, B. L. 2000. Menthol desensitization of capsaicin irritation. Evidence of a short-term anti-nociceptive effect. Physiol. Behav. 68, 631–639.

Green, B. G. and Rentmeister-Bryant, H. 1998. Temporal characteristics of capsaicin desensitization and stimulus-induced recovery in the oral cavity. Physiol. Behav. 65, 141–149.

Green, B. G. and Schullery, M. T. 2003. Stimulation of bitterness by capsaicin and menthol: differences between lingual areas innervated by the glossopharyngeal and chorda tympani nerves. Chem. Senses 28, 45–55.

Green, B. G., Mason, J. R., and Kare, M. R. 1990. General Discussion. In: Chemical Senses, Irritation, (*eds*. B. G. Green, J. R., Mason, and M. R. Kare), Vol. 2. pp. 325–340. Dekker.

Greenwood, L. F. and Sessle, B. J. 1976. Inputs to trigeminal brain stem neurones from facial, oral, tooth pulp and pharyngolaryngeal tissues: II. Role of trigeminal nucleus caudalis in modulating responses to innocuous and noxious stimuli. Brain Res. 117, 227–238.

Guler, A. D., Lee, H., Iida, T., Shimizu, I., Tominaga, M., and Caterina, M. 2002. Heat-evoked activation of the ion channel, TRPV4. J. Neurosci. 22, 6408–6414.

Halsell, C. B., Travers, J. B., and Travers, S. P. 1993. Gustatory and tactile stimulation of the posterior tongue activate overlapping but distinctive regions within the nucleus of the solitary tract. Brain Res. 632, 161–173.

Hamilton, R. B. and Norgren, R. 1984. Central projections of gustatory nerves in the rat. J. Comp. Neurol. 222, 560–577.

Hayakawa, T., Maeda, S., Tanaka, K., and Seki, M. 2005. Fine structural survey of the intermediate subnucleus of the nucleus tractus solitarii and its glossopharyngeal afferent terminals. Anat. Embryol. (Berl.) 210, 235–244.

Hayashi, H. 1985. Morphology of terminations of small and large myelinated trigeminal primary afferent fibers in the cat. J. Comp. Neurol. 240, 71–89.

Hayashi, H. and Tabata, T. 1989. Physiological properties of sensory trigeminal neurons projecting to mesencephalic parabrachial area in the cat. J. Neurophysiol. 61, 1153–1160.

Hayashi, H., Sumino, R., and Sessle, B. J. 1984. Functional organization of trigeminal subnucleus interpolaris: nociceptive and innocuous afferent inputs, projections to thalamus, cerebellum, and spinal cord, and descending modulation from periaqueductal gray. J. Neurophysiol. 51, 890–905.

Holzer, P. 1998. Neurogenic vasodilatation and plasma leakage in the skin. General Pharmacol. 30, 5–11.

Hu, J. W. 1990. Response properties of nociceptive and non-nociceptive neurons in the rat's trigeminal subnucleus caudalis (medullary dorsal horn) related to cutaneous and deep craniofacial afferent stimulation and modulation by diffuse noxious inhibitory controls. Pain 41, 331–345.

Hu, J. W. and Sessle, B. J. 1984. Comparison of responses of cutaneous nociceptive and nonnociceptive brain stem neurons in trigeminal subnucleus caudalis (medullary dorsal horn) and subnucleus oralis to natural and electrical stimulation of tooth pulp. J. Neurophysiol. 52, 39–53.

Hu, J. W., Dostrovsky, J. O., and Sessle, B. J. 1981. Functional properties of neurons in cat trigeminal subnucleus caudalis (medullary dorsal horn). I. Responses to oral-facial noxious and nonnoxious stimuli and projections to thalamus and subnucleus oralis. J. Neurophysiol. 45, 173–192.

Hu, J. W., Sessle, B. J., Raboisson, P., Dallel, R., and Woda, A. 1992. Stimulation of craniofacial muscle afferents induces prolonged facilitatory effects in trigeminal nociceptive brain-stem neurones. Pain 48, 53–60.

Hu, J. W., Sun, K. Q., Vernon, H., and Sessle, B. J. 2005. Craniofacial inputs to upper cervical dorsal horn: implications for somatosensory information processing. Brain Res. 1044, 93–106.

Ito, J. and Oyagi, S. 1995. Localization of trigeminal sensory innervation to the tongue and pharynx of the cat using horseradish peroxidase as tracer. Eur. Arch. Otorhinolaryngol. 252, 172–175.

Jacquin, M. F. and Rhoades, R. W. 1990. Cell structure and response properties in the trigeminal subnucleus oralis. Somatosens. Mot. Res. 7, 265–288.

Jacquin, M. F., Renehan, W. E., Mooney, R. D., and Rhoades, R. W. 1986. Structure–function relationships in rat medullary and cervical dorsal horns. I. Trigeminal primary afferents. J. Neurophysiol. 55, 1153–1186.

Jacquin, M. F., Semba, K., Rhoades, R. W., and Egger, M. D. 1982. Trigeminal primary afferents project bilaterally to dorsal horn and ipsilaterally to cerebellum, reticular formation, and cuneate, solitary, supratrigeminal and vagal nuclei. Brain Res. 246, 285–291.

Jordt, S. E., Bautista, D. M., Chuang, H. H., McKemy, D. D., Zygmunt, P. M., Hogestatt, E. D., Meng, I. D., and Julius, D. 2004. Mustard oils and cannabinoids excite sensory nerve fibres through the TRP channel ANKTM1. Nature 427, 260–265.

Jordt, S. E., Tominaga, M., and Julius, D. 2000. Acid potentiation of the capsaicin receptor determined by a key extracellular site. Proc. Natl. Acad. Sci. U. S. A. 97, 8134–8139.

Kadohisa, M., Rolls, E. T., and Verhagen, J. V. 2004. Orbitofrontal cortex: neuronal representation of oral temperature and capsaicin in addition to taste and texture. Neuroscience 127, 207–221.

Kadohisa, M., Rolls, E. T., and Verhagen, J. V. 2005. Neuronal representations of stimuli in the mouth: the primate insular taste cortex, orbitofrontal cortex and amygdala. Chem. Senses 30, 401–419.

Kandel, E. R., Schwartz, J. H., and Jessell, T. A. 2000. Principles of Neural Science, 4th edn. McGraw-Hill.

Karrer, T. and Bartoshuk, L. 1995. Effects of capsaicin desensitization on taste in humans. Physiol. Behav. 57, 421–429.

Katz, D. B., Simon, S. A., Moody, A., and Nicolelis, M. A. 1999. Simultaneous reorganization in thalamocortical ensembles evolves over several hours after perioral capsaicin injections. J. Neurophysiol. 82, 963–977.

King, M. S., Wang, L., and Bradley, R. M. 1993. Substance P excites neurons in the gustatory zone of the rat nucleus tractus solitarius. Brain Res. 619, 120–130.

Kobayashi, K., Fukuoka, T., Obata, K., Yamanaka, H., Dai, Y., Tokunaga, A., and Noguchi, K. 2005. Distinct expression of TRPM8, TRPA1, and TRPV1 mRNAs in rat primary afferent neurons with adelta/c-fibers and colocalization with trk receptors. J. Comp. Neurol. 493, 596–606.

Komai, M. and Bryant, B. P. 1993. Acetazolamide specifically inhibits lingual trigeminal nerve responses to carbon dioxide. Brain Res. 612, 122–129.

Koplas, P. A., Rosenberg, R. L., and Oxford, G. S. 1997. The role of calcium in the desensitization of capsaicin responses in rat dorsal root ganglion neurons. J. Neurosci. 17, 3525–3537.

Kruger, L. and Michel, F. 1962. A single neuron analysis of buccal cavity representation in the sensory trigeminal complex of the cat. Arch. Oral Biol. 7, 491–503.

LaMotte, R. H. and Mountcastle, V. B. 1979. Disorders in somesthesis following lesions of parietal lobe. J. Neurophysiol. 42, 400–419.

Lawless, H. T. and Stevens, D. A. 1984. Effects of oral chemical irritation on taste. Physiol. Behav. 32, 995–998.

Lawless, H. T., Rozin, P., and Shenker, J. 1985. Effect of oral capsaicin on gustatory, olfactory and irritant sensations and flavor identification in humans who regularly or rarely consume chili pepper. Chem. Senses 10, 579–589.

Lingueglia, E., de Weille, J. R., Bassilana, F., Heurteaux, C., Sakai, H., Waldmann, R., and Lazdunski, M. 1997. A modulatory subunit of acid sensing ion channels in brain and dorsal root ganglion cells. J. Biol. Chem. 272, 29778–29783.

Liu, L. and Simon, S. A. 1996a. Capsaicin and nicotine both activate a subset of rat trigeminal ganglion neurons. Am. J. Physiol. 270, C1807–C1814.

Liu, L. and Simon, S. A. 1996b. Capsaicin-induced currents with distinct desensitization and Ca2+ dependence in rat trigeminal ganglion cells. J. Neurophysiol. 75, 1503–1514.

Liu, L. and Simon, S. A. 1996c. Similarities and differences in the currents activated by capsaicin, piperine, and zingerone in rat trigeminal ganglion cells. J. Neurophysiol. 76, 1858–1869.

Liu, L. and Simon, S. A. 1996d. Capsaicin and nicotine both activate a subset of rat trigeminal ganglion neurons. Am. J. Physiol. (Cell. Physiol.) 270, C1807–C1814.

Liu, L. and Simon, S. A. 1997. Capsazepine, a vanilloid receptor antagonist, inhibits nicotinic acetylcholine receptors in rat trigeminal ganglia. Neurosci. Lett. 228, 29–32.

Liu, L. and Simon, S. A. 1998. The influence of removing extracellular Ca^{2+} in the desensitization responses to capsaicin, zingerone and olvanil in rat trigeminal ganglion neurons. Brain Res. 809, 246–252.

Liu, L., Chang, G. Q., Jiao, Y. Q., and Simon, S. A. 1998. Neuronal nicotinic acetylcholine receptors in rat trigeminal ganglia. Brain Res. 809, 238–245.

Liu, L., Lo, Y., Chen, I., and Simon, S. A. 1997. The responses of rat trigeminal ganglion neurons to capsaicin and two nonpungent vanilloid receptor agonists, olvanil and glyceryl nonamide. J. Neurosci. 17, 4101–4111.

Lundy, R. F., Jr. and Contreras, R. J. 1994. Neural responses of thermal-sensitive lingual fibers to brief menthol stimulation. Brain Res. 641, 208–216.

Lundy, R. F., Jr. and Contreras, R. J. 1995. Tongue adaptation temperature influences lingual nerve responses to thermal and menthol stimulation. Brain Res. 676, 169–177.

Lyall, V., Heck, G. L., Vinnikova, A. K., Ghosh, S., Phan, T. H., Alam, R. I., Russell, O. F., Malik, S. A., Bigbee, J. W., and DeSimone, J. A. 2004. The mammalian amiloride-insensitive non-specific salt taste receptor is a vanilloid receptor-1 variant. J. Physiol. 558, 147–159.

Lyall, V., Heck, G. L., Vinnikova, A. K., Ghosh, S., Phan, T. H., and Desimone, J. 2005. A novel vanilloid receptor-1 (VR-1) variant mammalian salt taste receptor. Chem. Senses 30, i42–i43.

Lynch, W. C., Watt, J., Krall, S., and Paden, C. M. 1985. Autoradiographic localization of kappa opiate receptors in CNS taste and feeding areas. Pharmacol. Biochem. Behav. 22, 699–705.

Macpherson, L. J., Geierstanger, B. H., Viswanath, V., Bandell, M., Eid, S. R., Hwang, S., and Patapoutian, A. 2005. The pungency of garlic: activation of TRPA1 and TRPV1 in response to allicin. Curr. Biol. 15, 929–934.

Marfurt, C. F. and Rajchert, D. M. 1991. Trigeminal primary afferent projections to ''non-trigeminal'' areas of the rat central nervous system. J. Comp. Neurol. 303, 489–511.

Marks, L. E. and Wheeler, M. E. 1998. Attention and detectability of weak taste stimuli. Chem. Senses 23, 19–29.

Marubio, L. M., del Mar Arroyo-Jimenez, M., Cordero-Erausquin, M., Lena, C., Le Novere, N., de Kerchove d'Exaerde, A., Huchet, M., Damaj, M. I., and Changeux, J. P. 1999. Reduced antinociception in mice lacking neuronal nicotinic receptor subunits. Nature 398, 805–810.

McKemy, D. D., Neuhausser, W. M., and Julius, D. 2002. Identification of a cold receptor reveals a general role for TRP channels in thermosensation. Nature 416, 52–58.

Menétrey, D. and Basbaum, A. I. 1987. Spinal and trigeminal projections to the nucleus of the solitary tract: a possible substrate for somatovisceral and viscerovisceral reflex activation. J. Comp. Neurol. 255, 439–450.

Millan, M. J. 1999. The induction of pain: an integrative review. Prog. Neurobiol. 57, 1–164.

Mizuno, A., Matsumoto, N., Imai, M., and Suzuki, M. 2003. Impaired osmotic sensation in mice lacking TRPV4. Am. J. Physiol. (Cell. Physiol.) 285, C96–C101.

Moqrich, A., Hwang, S. W., Earley, T. J., Petrus, M. J., Murray, A. N., Spencer, K. S., Andahazy, M., Story, G. M., and Patapoutian, A. 2005. Impaired thermosensation in mice lacking TRPV3, a heat and camphor sensor in the skin. Science 307, 1468–1472.

Nagy, I. and Rang, H. P. 1999. Similarities and differences between the responses of rat sensory neurons to noxious heat and capsaicin. J. Neurosci. 19, 10647–10655.

Nagy, J. I., Goedert, M., Hunt, S. P., and Bond, A. 1982. The nature of the substance P-containing nerve fibres in taste papillae of the rat tongue. Neuroscience 7, 3137–3151.

Nord, S. G. and Young, R. F. 1979. Effects of chronic descending tractotomy on the response patterns of neurons in the trigeminal nuclei principalis and oralis. Exp. Neurol. 65, 355–372.

Ogawa, H. and Hayama, T. 1984. Receptive fields of solitario-parabrachial relay neurons responsive to natural stimulation of the oral cavity in rats. Exp. Brain Res. 54, 359–366.

Ogawa, H., Hayama, T., and Yamashita, Y. 1988. Thermal sensitivity of neurons in a rostral part of the rat solitary tract nucleus. Brain Res. 454, 321–331.

Ogawa, H., Imoto, T., and Hayama, T. 1984. Responsiveness of solitario-parabrachial relay neurons to taste and mechanical stimulation applied to the oral cavity in rats. Exp. Brain Res. 54, 349–358.

Ogawa, H., Sato, M., and Yamashita, S. 1968. Multiple sensitivity of chorda typani fibres of the rat and hamster to gustatory and thermal stimuli. J. Physiol. 199, 223–240.

Ohya, A. 1992. Responses of trigeminal subnucleus interpolaris neurons to afferent inputs from deep oral structures. Brain Res. Bull. 29, 773–781.

Ohya, A., Tsuruoka, M., Imai, E., Fukunaga, H., Shinya, A., Furuya, R., Kawawa, T., and Matsui, Y. 1993. Thalamic- and cerebellar-projecting interpolaris neuron responses to afferent inputs. Brain Res. Bull. 32, 615–621.

Olson, T. H., Riedl, M. S., Vulchanova, L., Ortiz-Gonzalez, X. R., and Elde, R. 1998. An acid sensing ion channel (ASIC) localizes to small primary afferent neurons in rats. Neuroreport 9, 1109–1113.

O'Mahony, M., Kingsley, L., Harji, A., and Davies, M. 1976. What sensation signals the salt taste threshold? Chem. Senses Flavor 2, 177–188.

Osada, K., Komai, M., Bryant, B. P., Suzuki, H., Goto, A., Tsunoda, K., Kimura, S., and Furukawa, Y. 1997. Capsaicin modifies responses of rat chorda tympani nerve fibers to NaCl. Chem. Senses 22, 249–255.

Parducci, A. 1965. Category judgment: a range-frequency model. Psychol. Rev. 72, 407–418.

Park, K., Brown, P. D., Kim, Y. B., and Kim, J. S. 2003. Capsaicin modulates K+ currents from dissociated rat taste receptor cells. Brain Res. 962, 135–143.

Parker, G. H. 1912. The relation of smell, taste and the common chemical sense in vertebrates. J. Acad. Natl. Sci. 15, 221–234.

Peier, A. M., Moqrich, A., Hergarden, A. C., Reeve, A. J., Andersson, D. A., Story, G. M., Earley, T. J., Dragoni, I., McIntyre, P., Bevan, S., and Patapoutian, A. 2002a. A TRP channel that senses cold stimuli and menthol. Cell 108, 705–715.

Peier, A. M., Reeve, A. J., Andersson, D. A., Moqrich, A., Earley, T. J., Hergarden, A. C., Story, G. M., Colley, S., Hogenesch, J. B., McIntyre, P., Bevan, S., and Patapoutian, A. 2002b. A heat-sensitive TRP channel expressed in keratinocytes. Science 296, 2046–2049.

Perez, C. A., Huang, L., Rong, M., Kozak, J. A., Preuss, A. K., Zhang, H., Max, M., and Margolskee, R. F. 2002. A transient receptor potential channel expressed in taste receptor cells. Nat. Neurosci. 5, 1169–1176.

Pettit, M. J. and Schwark, H. D. 1996. Capsaicin-induced rapid receptive field reorganization in cuneate neurons. J. Neurophysiol. 75, 1117–1125.

Prescott, J. and Stevenson, R. J. 1995. Effects of oral chemical irritation on tastes and flavors in frequent and infrequent users of chili. Physiol. Behav. 58, 1117–1127.

Prescott, J. and Stevenson, R. J. 1996a. Desensitization to oral zingerone irritation: effects of stimulus parameters. Physiol. Behav. 60, 1473–1480.

Prescott, J. and Stevenson, R. J. 1996b. Psychophysical responses to single and multiple presentations of the oral irritant zingerone: relationship to frequency of chili consumption. Physiol. Behav. 60, 617–624.

Prescott, J. and Swain-Campbell, N. 2000. Responses to repeated oral irritation by capsaicin, cinnamaldehyde and ethanol in PROP tasters and non-tasters. Chem. Senses 25, 239–246.

Prescott, J., Allen, S., and Stephens, L. 1993. Interactions between oral chemical irritation, taste and temperature. Chem. Senses 18, 389–404.

Price, M. P., McIlwrath, S. L., Xie, J., Cheng, C., Qiao, J., Tarr, D. E., Sluka, K. A., Brennan, T. J., Lewin, G. R., and Welsh, M. J. 2001. The DRASIC cation channel contributes to the detection of cutaneous touch and acid stimuli in mice. Neuron 32, 1071–1083.

Raboisson, P., Bourdiol, P., Dallel, R., Clavelou, P., and Woda, A. 1991. Responses of trigeminal subnucleus oralis nociceptive neurones to subcutaneous formalin in the rat. Neurosci. Lett. 125, 179–182.

Raboisson, P., Dallel, R., Clavelou, P., Sessle, B. J., and Woda, A. 1995. Effects of subcutaneous formalin on the activity of trigeminal brain stem nociceptive neurones in the rat. J. Neurophysiol. 73, 496–505.

Rentmeister-Bryant, H. and Green, B. G. 1997. Perceived irritation during ingestion of capsaicin or piperine: comparison of trigeminal and non-trigeminal areas. Chem. Senses 22, 257–266.

Robinson, P. P. 1988. The characteristics and regional distribution of afferent fibres in the chorda tympani of the cat. J. Physiol. 406, 345–357.

Rolls, E. T. and Baylis, L. L. 1994. Gustatory, olfactory, and visual convergence within the primate orbitofrontal cortex. J. Neurosci. 14, 5437–5452.

Rolls, E. T., Critchley, H. D., Browning, A. S., Hernadi, I., and Lenard, L. 1999. Responses to the sensory properties of fat of neurons in the primate orbitofrontal cortex. J. Neurosci. 19, 1532–1540.

Rolls, E. T., Verhagen, J. V., and Kadohisa, M. 2003. Representations of the texture of food in the primate orbitofrontal cortex: neurons responding to viscosity, grittiness, and capsaicin. J. Neurophysiol. 90, 3711–3724.

van Rossum, D., Hanisch, U. K., and Quirion, R. 1997. Neuroanatomical localization, pharmacological characterization and functions of CGRP, related peptides and their receptors. Neurosci. Biobehav. Rev. 21, 649–678.

Schiffman, S. S., Suggs, M. S., Sostmon, A. C., and Simon, S. A. 1992. Chorda tympani and lingual nerve responses to astringent compounds in rodents. Physiol. Behav. 51, 55–63.

Schmidt, R., Schmelz, M., Forster, C., Ringkamp, M., Torebjork, E., and Handwerker, H. 1995. Novel classes of responsive and unresponsive C nociceptors in human skin. J. Neurosci. 15, 333–341.

Scott, T. R. and Verhagen, J. V. 2000. Taste as a factor in the management of nutrition. Nutrition 16, 874–885.

Sessle, B. J. 1987. The neurobiology of facial and dental pain: present knowledge, future directions. J. Dent. Res. 66, 962–981.

Sessle, B. J. and Greenwood, L. F. 1976. Inputs to trigeminal brain stem neurones from facial, oral, tooth pulp and pharyngolaryngeal tissues: I. Responses to innocuous and noxious stimuli. Brain Res. 117, 211–226.

Shankland, W. E., II. 2001a. The trigeminal nerve. Part iii: the maxillary division. Cranio 19, 78–83.

Shankland, W. E., II. 2001b. The trigeminal nerve. Part IV: the mandibular division. Cranio 19, 153–161.

Shusterman, D. 2002. Review of the upper airway, including olfaction, as mediator of symptoms. Environ. Health Perspect. 110, 649–653.

Shusterman, D. 2003. Toxicology of nasal irritants. Curr. Allergy Asthma Rep. 3, 258–265.

Silver, W. L. and Moulton, D. G. 1982. Chemosensitivity of rat nasal trigeminal receptors. Physiol. Behav. 28, 927–931.

Simon, S. A., Liu, L., and Erickson, R. P. 2003. Neuropeptides modulate rat chorda tympani responses. Am. J. Physiol. (Regul. Integr. Comp. Physiol.) 284, R1494–R1505.

Simone, D. A., Sorkin, L. S., Oh, U., Chung, J. M., Owens, C., LaMotte, R. H., and Willis, W. D. 1991. Neurogenic hyperalgesia: central neural correlates in responses of spinothalamic tract neurons. J. Neurophysiol. 66, 228–246.

Simons, C. T., Boucher, Y., and Carstens, E. 2003a. Suppression of central taste transmission by oral capsaicin. J. Neurosci. 23, 978–985.

Simons, C. T., Boucher, Y., Iodi Carstens, M., and Carstens, E. (2006) Nicotine suppression of gustatory neurons in the nucleus of the solitary tract. J. Neurophysiol. 96, 1877–1886.

Simons, C. T., Carstens, M. I., and Carstens, E. 2003b. Oral irritation by mustard oil: self-desensitization and cross-desensitization with capsaicin. Chem. Senses 28, 459–465.

Simons, C. T., Dessirier, J. M., Carstens, M. I., O'Mahony, M., and Carstens, E. 1999. Neurobiological and psychophysical mechanisms underlying the oral sensation produced by carbonated water. J. Neurosci. 19, 8134–8144.

Simons, C. T., Dessirier, J.-M., Carstens, M. I., O'Mahony, M., and Cartens, E. 2000. The Tingling Sensation of Carbonated Drinks is Mediated by a Carbonnic Anhydrase-Dependent Excitation of Trigeminal Nociceptive Neurons. In: Proceedings of the 9th World Congress on Pain, Vol. 16. (*eds*. M. Devor, M. C. Rowbotham, and Z. Wiesenfeld-Hallin). IASP Press.

Simons, C. T., O'Mahony, M., and Carstens, E. 2002. Taste suppression following lingual capsaicin pre-treatment in humans. Chem. Senses 27, 353–365.

Simons, C. T., Sudo, S., Sudo, M., and Carstens, E. 2003c. Mecamylamine reduces nicotine cross-desensitization of trigeminal caudalis neuronal responses to oral chemical irritation. Brain Res. 991, 249–253.

Simons, C. T., Sudo, S., Sudo, M., and Carstens, E. 2004. Mustard oil has differential effects on the response of trigeminal caudalis neurons to heat and acidity. Pain 110, 64–71.

Small, D. M., Zald, D. H., Jones-Gotman, M., Zatorre, R. J., Pardo, J. V., Frey, S., and Petrides, M. 1999. Human cortical gustatory areas: a review of functional neuroimaging data. Neuroreport 10, 7–14.

Smith, G. D., Gunthorpe, M. J., Kelsell, R. E., Hayes, P. D., Reilly, P., Facer, P., Wright, J. E., Jerman, J. C., Walhin, J. P., Ooi, L., Egerton, J., Charles, K. J., Smart, D., Randall, A. D., Anand, P., and Davis, J. B. 2002. TRPV3 is a temperature-sensitive vanilloid receptor-like protein. Nature 418, 186–190.

Sostman, A. L. and Simon, S. A. 1991. Trigeminal nerve responses in the rat elicited by chemical stimulation of the tongue. Arch. Oral Biol. 36, 95–102.

South, E. H. and Ritter, R. C. 1986. Substance P-containing trigeminal sensory neurons project to the nucleus of the solitary tract. Brain Res. 372, 283–289.

Stapleton, J. R., Lavine, M. L., Wolpert, R. L., Nicolelis, M. A., and Simon, S. A. 2006. Rapid taste responses in the gustatory cortex during licking. J. Neurosci. 26, 4126–4138.

Steen, K. H., Wegner, H., and Reeh, P. W. 1999. The pH response of rat cutaneous nociceptors correlates with extracellular [Na+] and is increased under amiloride. Eur. J. Neurosci. 11, 2783–2792.

Stevens, D. A. and Lawless, H. T. 1987. Enhancement of responses to sequential presentation of oral chemical irritants. Physiol. Behav. 39, 63–65.

Stevenson, R. J. and Prescott, J. 1997. Judgments of chemosensory mixtures in memory. Acta Psychol. 95, 195–214.

Story, G. M., Peier, A. M., Reeve, A. J., Eid, S. R., Mosbacher, J., Hricik, T. R., Earley, T. J., Hergarden, A. C., Andersson, D. A., Hwang, S. W., McIntyre, P., Jegla, T., Bevan, S., and Patapoutian, A. 2003. ANKTM1, a TRP-like channel expressed in nociceptive neurons, is activated by cold temperatures. Cell 112, 819–829.

Strassman, A. M. and Vos, B. P. 1993. Somatotopic and laminar organization of fos-like immunoreactivity in the medullary and upper cervical dorsal horn induced by noxious facial stimulation in the rat. J. Comp. Neurol. 331, 495–516.

Sudo, S., Sudo, M., Simons, C. T., Dessirier, J. M., and Carstens, E. 2002. Sensitization of trigeminal caudalis neuronal responses to intraoral acid and salt stimuli and desensitization by nicotine. Pain 98, 277–286.

Sudo, S., Sudo, M., Simons, C. T., Dessirier, J. M., Iodi Carstens, M., and Carstens, E. 2003. Activation of neurons in trigeminal caudalis by noxious oral acidic or salt stimuli is not reduced by amiloride. Brain Res. 969, 237–243.

Suzuki, M., Mizuno, A., Kodaira, K., and Imai, M. 2003. Impaired pressure sensation in mice lacking TRPV4. J. Biol. Chem. 278, 22664–22668.

Szolcsányi, J. 1977. A pharmacological approach to elucidation of the role of different nerve fibres and receptor endings in mediation of pain. J. Physiol. 73, 251–259.

Tominaga, M., Caterina, M. J., Malmberg, A. B., Rosen, T. A., Gilbert, H., Skinner, K., Raumann, B. E., Basbaum, A. I., and Julius, D. 1998. The cloned capsaicin receptor integrates multiple pain-producing stimuli. Neuron 21, 531–543.

Travers, S. P. and Norgren, R. 1995. Organization of orosensory responses in the nucleus of the solitary tract of rat. J. Neurophysiol. 73, 2144–2162.

Trevisani, M., Smart, D., Gunthorpe, M. J., Tognetto, M., Barbieri, M., Campi, B., Amadesi, S., Gray, J., Jerman, J. C., Brough, S. J., Owen, D., Smith, G. D., Randall, A. D., Harrison, S., Bianchi, A., Davis, J. B., and Geppetti, P. 2002. Ethanol elicits and potentiates nociceptor responses via the vanilloid receptor-1. Nat. Neurosci. 5, 546–551.

Verhagen, J. V., Rolls, E. T., and Kadohisa, M. 2003. Neurons in the primate orbitofrontal cortex respond to fat texture independently of viscosity. J. Neurophysiol. 90, 1514–1525.

Villanueva, L., Bouhassira, D., Bing, Z., and Le Bars, D. 1988. Convergence of heterotopic nociceptive information onto subnucleus reticularis dorsalis neurons in the rat medulla. J. Neurophysiol. 60, 980–1009.

Waldmann, R., Champigny, G., Bassilana, F., Heurteaux, C., and Lazdunski, M. 1997. A proton-gated cation channel involved in acid-sensing. Nature 386, 173–177.

Wang, H. and Woolf, C. J. 2005. Pain TRPs. Neuron 46, 9–12.

Wang, Y., Erickson, R. P., and Simon, S. A. 1993. Selectivity of lingual nerve fibers to chemical stimuli. J. Gen. Physiol. 101, 843–866.

Wang, Y., Erickson, R. P., and Simon, S. A. 1995. Modulation of rat chorda tympani nerve activity by lingual nerve stimulation. J. Neurophysiol. 73, 1468–1483.
Whitehead, M. C. and Frank, M. E. 1983. Anatomy of the gustatory system in the hamster: central projections of the chorda tympani and the lingual nerve. J. Comp. Neurol. 220, 378–395.
Whitehead, M. C. and Kachele, D. L. 1994. Development of fungiform papillae, taste buds, and their innervation in the hamster. J. Comp. Neurol. 340, 515–530.
Whitehead, M. C., Ganchrow, J. R., Ganchrow, D., and Yao, B. 1999. Organization of geniculate and trigeminal ganglion cells innervating single fungiform taste papillae: a study with tetramethylrhodamine dextran amine labeling. Neuroscience 93, 931–941.
Willis, W. D. and Westlund, K. N. 1997. Neuroanatomy of the pain system and of the pathways that modulate pain. J. Clin. Neurophysiol. 14, 2–31.
Xing, H., Ling, J., Chen, M., and Gu, J. G. 2006. Chemical and cold sensitivity of two distinct populations of TRPM8-expressing somatosensory neurons. J. Neurophysiol. 95, 1221–1230.
Xu, H., Blair, N. T., and Clapham, D. E. 2005. Camphor activates and strongly desensitizes the transient receptor potential vanilloid subtype 1 channel in a vanilloid-independent mechanism. J. Neurosci. 25, 8924–8937.
Xu, H., Delling, M., Jun, J. C., and Clapham, D. E. 2006. Oregano, thyme and clove-derived flavors and skin sensitizers activate specific TRP channels. Nat. Neurosci. 9, 628–635.
Xu, H., Ramsey, I. S., Kotecha, S. A., Moran, M. M., Chong, J. A., Lawson, D., Ge, P., Lilly, J., Silos-Santiago, I., Xie, Y., DiStefano, P. S., Curtis, R., and Clapham, D. E. 2002. TRPV3 is a calcium-permeable temperature-sensitive cation channel. Nature 418, 181–186.
Yang, B. H., Piao, Z. G., Kim, Y. B., Lee, C. H., Lee, J. K., Park, K., Kim, J. S., and Oh, S. B. 2003. Activation of vanilloid receptor 1 (VR1) by eugenol. J. Dent. Res. 82, 781–785.
Yaxley, S., Rolls, E. T., and Sienkiewicz, Z. J. 1990. Gustatory responses of single neurons in the insula of the macaque monkey. J. Neurophysiol. 63, 689–700.
Yokota, T. 1975. Excitation of units in marginal rim of trigeminal subnucleus caudalis elicited by tooth pulp stimulation. Brain Res. 95, 154–158.
Zhang, Y., Hoon, M. A., Chandrashekar, J., Mueller, K. L., Cook, B., Wu, D., Zuker, C. S., and Ryba, N. J. 2003. Coding of sweet, bitter, and umami tastes: different receptor cells sharing similar signaling pathways. Cell 112, 293–301.

Further Reading

Brand, G. and Jacquot, L. 2002. Sensitization and desensitization to allyl isothiocyanate (mustard oil) in the nasal cavity. Chem. Senses 27, 593–598.
Carstens, E., Simons, C. T., Dessirier, J.-M., Sudo, M., Sudo, S., Iodi Carstens, M., and Jinks, S. L. 2002. Activation of Neurons in Trigeminal Subnucleus Caudalis (Vc) by Irritant Chemical Stimulation: Extracellular Single-Unit Recording and c-fos Immunohistochemical Methods. In: Methods in Chemosensory Research (*eds*. S. A. Simon and M. A. L. Nicolelis), pp. 267–292. CRC Press.
Dessirier, J. M., Simons, C. T., Carstens, M. I., O'Mahony, M., and Carstens, E. 2000. Psychophysical and neurobiological evidence that the oral sensation elicited by carbonated water is of chemogenic origin. Chem. Senses 25, 277–284.

4.19 Genetics and Evolution of Taste

J D Boughter, Jr., University of Tennessee Health Science Center, Memphis, TN, USA

A A Bachmanov, Monell Chemical Senses Center, Philadelphia, PA, USA

© 2008 Elsevier Inc. All rights reserved.

4.19.1	**Taste Is a Complex Trait**	372
4.19.2	**Genetic Approaches to Taste Behavior**	372
4.19.2.1	Assessing Taste Behavior	372
4.19.2.2	Behavioral Genetic Techniques	373
4.19.3	**Bitter Taste**	376
4.19.3.1	Phenylthiocarbamide Taste in Man and Mouse	376
4.19.3.2	Genetics of Taste Responses to Other Bitter Compounds in Mice	376
4.19.3.3	Bitter Taste Loci and Receptors	377
4.19.3.4	Evolution of the T2R Receptors	377
4.19.4	**Sweet and Umami Taste**	379
4.19.4.1	Strain Differences in Responses to Sweet-Tasting Stimuli	379
4.19.4.2	Mapping and Identification of Sweet Taste Receptor Genes	380
4.19.4.3	Umami Taste Genetics	380
4.19.4.4	Evolution of T1R Receptors	382
4.19.5	**Salt and Sour Taste**	383
4.19.6	**Taste and Other Complex Phenotypes**	383
4.19.6.1	Taste and Diet	383
4.19.6.2	Taste and Drug Intake	384
4.19.7	**Conclusions**	384
References		385

Glossary

complex trait A trait influenced by multiple factors, including effects of genes, environment, and their interactions.

congenic strain A strain that is identical to one of the progenitor inbred strains (inbred partner or background strain) except for a particular locus of interest that originates from the other progenitor strain (donor strain). Traditional congenic strains are produced through a series of at least 10 lineal backcrosses. Marker-assisted selective breeding of congenic strains (speed congenics) requires a smaller number of backcross generations.

conserved synteny Correspondence in order of chromosomal locations of orthologous genes in different species.

inbred strain A strain that has been bred using brother–sister matings for at least 20 consecutive generations. Same-sex individuals within an inbred strain are considered to be ~99% identical genetically.

haplotype Haploid genotype; a combination of linked alleles at an individual chromosome; may refer to a set of linked genes or to a set of sequence variants within a gene.

locus A location in the genome. It may correspond to a gene, an anonymous DNA segment (marker), or a genomic region linked to a phenotypical variation (qualitative or quantitative trait locus).

ortholog Genes or proteins in different species that have similar sequences, which suggests that they have originated from a common ancestral gene.

paralog Genes in the same species with similar sequence, which suggests that they originated from a common ancestral gene.

phenotype The observable characteristics of an organism, as determined by both genetic makeup and environmental influences.

recombinant inbred strains A set of independently derived strains, all of which originate from

the same two inbred progenitor strains. The two inbred progenitor strains are outcrossed to produce F_1 hybrids, which are intercrossed to produce F_2 hybrids, followed by consecutive generations of brother–sister matings. After 20 generations of brother–sister mating, mice within each recombinant inbred strain are genetically nearly identical.

segregating cross A cross between inbred strains, in which alleles of polymorphic markers or genes segregate among subgroups of the cross with different genotypes. Commonly produced segregating crosses are hybrids of the second filial (F_2) or a backcross (N_2) generation.

4.19.1 Taste Is a Complex Trait

Behavioral genetic approaches have been instrumental in the discovery of genes that influence taste phenotypes. The investigation of genetic bases of taste began early in the twentieth century with the description of human differences in sensitivity to the bitter-tasting chemical phenylthiocarbamide (PTC) (Fox, A. L., 1931; 1932). In the years following this discovery, behavioral genetic approaches conducted predominately in mice identified considerable variation in taste responses among inbred strains. Chromosomal mapping of genetic loci influencing preferences for sweet- and bitter-tasting stimuli led to the identification of families of G-protein-coupled receptors (GPCR) for sweet and bitter taste. However, the search for genes influencing taste function is not necessarily limited to receptors. Situated at the beginning of the alimentary canal, the gustatory system is a key player in homeostatic systems dealing with both fluid and food intake. In fact, taste and feeding are linked in terms of reciprocal connectivity between brain regions, and taste detection has been shown to be heavily modulated by postingestive feedback, including neural and hormonal factors (e.g., Scott, T. R., 2001; Bloomgarden, Z. T., 2006). Additionally, evidence indicates that taste sensitivity is modifiable by environmental factors such as diet and experience (Duffy, V. B. and Bartoshuk, L. M., 2000; Tichansky, D. S. *et al.*, 2006). This interactivity implies that taste sensitivity is a complex trait, and as such taste-related behavior phenotypes are likely to be determined by multiple genes and factors (Figure 1). This review will focus primarily on the study of rodent taste behavior genetics, as human genetic approaches are reviewed elsewhere (Chapter Propylthiouracil (PROP) Taste). However, an evolutionary perspective on taste receptor genes will include both vertebrate and invertebrate species.

Traditionally, the five major taste qualities have been described using terms that reflect human perceptual experience (sweet, salty, bitter, sour, and umami). Although there are many studies indicating that the mechanisms underlying perception of different taste qualities are similar in humans and nonhuman species, one should use caution when applying human descriptors to animal sensory function. It is perhaps more accurate to describe taste quality perception by nonhuman animals using chemical names of taste stimuli (e.g., sodium taste or sucrose-like taste), but for brevity the human descriptors are used throughout this review.

4.19.2 Genetic Approaches to Taste Behavior

4.19.2.1 Assessing Taste Behavior

Taste ability includes multiple aspects such as quality, intensity, and hedonic value. In addition, taste behavior may be influenced by nongustatory sensory factors such as olfaction and somatosensation. Early studies of human genetic variation of taste sensitivity concentrated on either responses to a single concentration of a stimulus (i.e., tasters vs. nontasters of PTC) or measurement of detection thresholds (Harris, H. and Kalmus, H., 1949; Wooding, S., 2006). More recent studies have utilized psychophysical methods such as suprathreshold magnitude estimation (Bartoshuk, L. M. *et al.*, 1994) to evaluate additional aspects of taste perception. In rodents, the majority of behavioral genetic studies have been conducted using 48 h two-bottle preference test, where an animal is presented with two bottles in the home cage, one containing water, and one containing a taste solution. After 24 h, the position of the bottles is switched to control for side preference (Richter, C., 1932). In these tests, the taste quality and intensity of the stimulus are inferred based

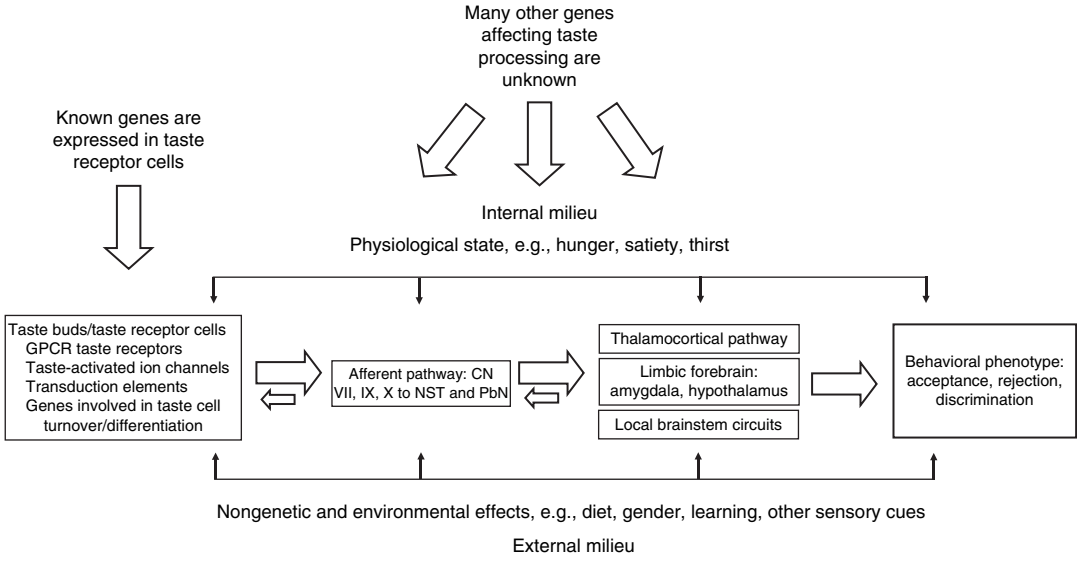

Figure 1 Components of the taste system and its associated genes. The search for the genetic basis of taste has primarily focused on taste receptors and other components of the taste signaling pathway expressed in peripheral taste receptor cells, and their relationship to taste behavior phenotypes. Other genes must play a role in complex interactions between peripheral mechanisms, brain taste centers, and behavioral outcomes. All of these steps in taste processing are subject to modulation by factors associated with the internal and external milieu, including physiological systems involved in food and fluid intake, and by other, nongenetic factors such as diet, learning, and exteroceptory cues like odors or visual stimuli. CN, cranial nerve; NST, nucleus of the solitary tract; PbN, parabrachial nucleus.

on level of avoidance or preference for the solution bottle. Such tests are relatively simple to conduct, and offer a considerable advantage in that one may conduct simultaneous testing of large groups of animals that are required for the genetic analysis. Tests involving multiple stimulus bottles are also useful (Tordoff, M. G. and Bachmanov, A. A., 2003). However, behavior over this relatively long time frame may be influenced not only by an animal's perception of a stimulus, but also by postingestive consequences. Taste-salient, brief-access tests minimize postingestive cues by restricting sampling times to short durations (<30 s). Such tests have been recently modified for use in high-throughput screening of taste function in mouse populations (Boughter, J. D., Jr. *et al.*, 2002; Glendinning, J. I. *et al.*, 2002). Behavioral test methods for animals are reviewed extensively in Chapter Behavioral Analysis of Taste Function in Rodent Models.

4.19.2.2 Behavioral Genetic Techniques

The goal of behavioral genetics is to understand how genes influence individual differences. Usually, a starting point for discerning genetic effects on behavior in rodents is the use of inbred strains. After 20 generations of inbreeding, same-sex individuals within a given strain are considered to be ~99% identical genetically. When individuals from multiple inbred strains are compared on a particular behavior or phenotype, the mean difference among these strains means is considered to be due to genetic factors. Commonly used strains in biomedical research include C57BL/6 (B6), DBA, 129, and BALB. Indeed, early studies with inbred mice indicated substantial strain differences in solution intake for various taste qualities (McClearn, G. E. and Rodgers, D., 1959; 1961; Hoshishima, K. *et al.*, 1962). Since then, inbred strains have been extensively characterized with regards to taste ability using not only intake tests, but also taste-salient behavioral tasks, taste nerve and central nervous system (CNS) physiology, and anatomical methods (e.g., Ninomiya, Y. *et al.*, 1984; Shingai, T. and Beidler, L. M., 1985; Ninomiya, Y. and Funakoshi, M., 1989; Kachele, D. L. and Lasiter, P. S., 1990; Lush, I. E., 1991; Eylam, S. and Spector, A. C., 2004; Inoue, M. *et al.*, 2004a; Boughter, J. D., Jr. *et al.*, 2005; McCaughey, S. A., 2007). Inbred strains of rats have not been used as commonly, although rat strains differ in salt and sweet taste responses (Sollars, S. I. *et al.*, 1990; Goodwin, F. L. and Amit, Z., 1998).

Differences between strains serve as the starting point for genetic mapping studies. Using Mendelian

crosses of parental strains (i.e., F_1 and F_2 hybrids, and backcrosses) the investigator may estimate the relative size and number of genetic factors contributing to the behavior (Figure 2). Individuals from a segregating generation such as F_2 can be both phenotyped with respect to taste behavior, and genotyped using a set of genetic markers such as single nucleotide polymorphisms (SNPs). Significant association between phenotype and marker results in the identification of qualitative or quantitative trait loci (QTL) that pinpoint regions of the genome where genes influencing the trait of interest reside. For example, QTL studies conducted in an F_2 cross of B6 (high sweetener preferring) and 129 (low preferring)

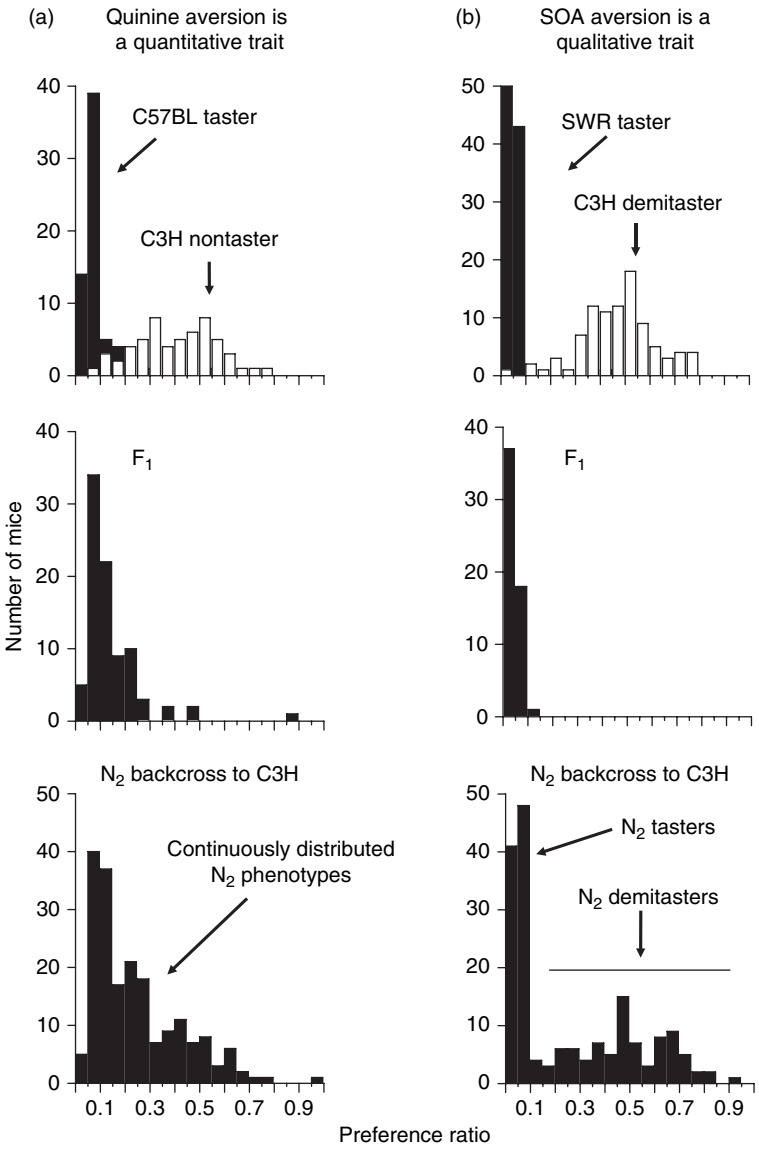

Figure 2 Examples of quantitative and qualitative traits for bitter taste aversion. Graphs show individual distributions of preference ratios for quinine (a) or sucrose octaacetate (SOA) (b) solutions. For quinine (a), there is overlap in the distributions between C57BL/6 (taster) and C3H/HeB (nontaster) progenitor inbred strains. An F_1 generation consists primarily of phenotypic tasters, whereas the N_2 backcross to C3H is comprised of a continuous distribution of phenotypes ranging from taster to nontaster. This continuous distribution is consistent with control by more than one quantitative trait locus. For SOA (b), there is almost no overlap in the distributions of SWR (taster) and C3H (demitaster) progenitor inbred strains. The F_1 distribution is comprised of phenotypic tasters. The N_2 backcross distribution is bimodal, consisting of about half tasters, half demitasters. Unlike the case for quinine, this distribution is consistent with expectations from a single locus model. SOA aversion is therefore a qualitative trait. Data from Boughter J. D. Jr., *et al*. (1992) and Boughter J. D. Jr., and Whitney G. (1995).

mouse strains demonstrate loci linked to both behavioral and physiological responses to sweeteners (Inoue, M. *et al.*, 2004b). Recombinant inbred (RI) strains (Figure 3) have also been used to identify QTLs influencing behavioral or neural phenotypes, including the frequently used BXD set, derived from B6 and DBA/2 mice (Peirce, J. L. *et al.*, 2004). Notably, BXDs have been used to map QTLs influencing sweet and bitter taste in mice (Lush, I. E. and Holland, G., 1988; Nelson, T. M. *et al.*, 2005). Finally, congenic strains (Figure 4) have been used extensively in taste behavioral genetic research (Whitney, G. *et al.*, 1989; Boughter, J. D., Jr. and Whitney, G., 1995; Bachmanov, A. A. *et al.*, 2001a; Li, X. *et al.*, 2001). A congenic strain is one that is identical to a progenitor inbred strain except for the substitution of a particular locus of interest (Flaherty, L., 1981). This is accomplished through a series of (at least 10) lineal backcrosses. The newly created mice are used to evaluate an allelic variant against a particular strain background. For example, 129.B6 congenics (created from 129P3 and B6 mice) were used to localize the *Sac* locus influencing sweetener preference in mice (Li, X. *et al.*, 2001).

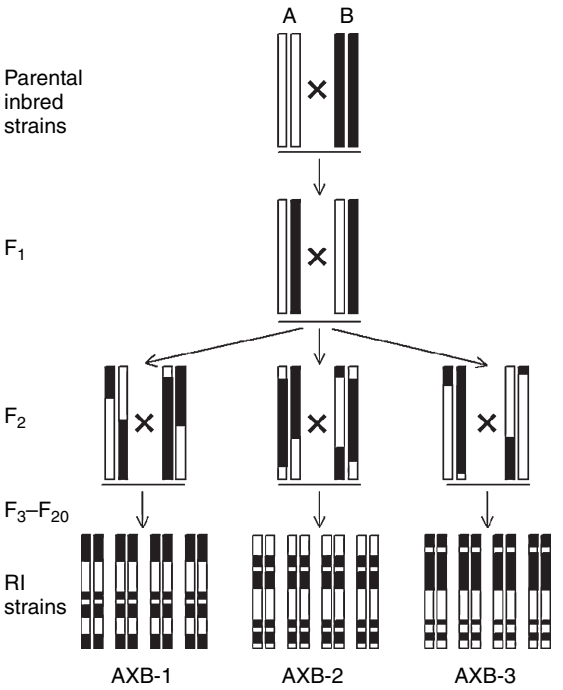

Figure 3 Production of recombinant inbred (RI) strains. A pair of homologous autosomes is shown in different generations of RI strains production. Genetic material of two hypothetical progenitor inbred strains, A and B, is shown in white and black respectively. Recombinant chromosomes (combining parts from both progenitor strains) are first observed in the F_2 generation. Randomly chosen F_2 mice are mated, and their offspring is maintained by brother–sister mating for at least another 18 generations. In the subsequent generations of breeding, additional chromosomal recombinations occur, and mice of each RI strain become genetically more similar. After 20 generations of brother–sister mating, mice within each RI strain are genetically nearly identical (illustrated by chromosomal pairs of four mice from thee hypothetical RI strains).

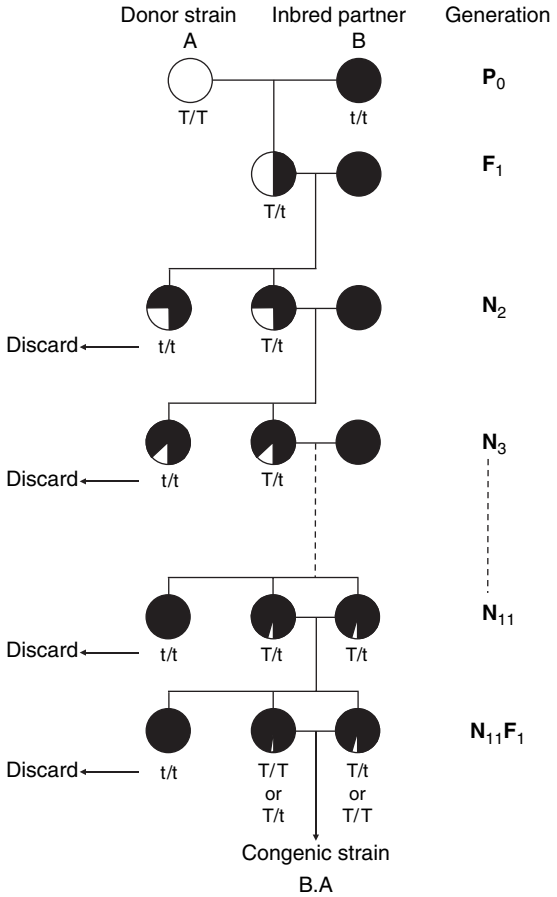

Figure 4 Backcross protocol for congenic strain development involving transfer of an autosomal dominant taster allele T from a donor strain (strain A; white circle) onto the genomic background of an inbred partner (strain B; black circle) with a recessive nontaster allele t. F_1 heterozygote offspring from the parent strains are mated to mice from the partner strain. Only phenotypic taster offspring (T/t) from subsequent generations are selected for backcrossing to the partner strain. With each backcross generation, one-half of the remaining genetic material from the donor strain is lost, except for material closely linked on the chromosome bearing the locus of interest. By generation N_{11}, the introgressed chromosome segment is isolated on a ~99% genomic background from the partner strain. Tasters from generation N_{11} and subsequent generations are sib intercrossed.

4.19.3 Bitter Taste

A large and diverse array of molecules evoke the sensation of bitterness, and the ability to detect and avoid these stimuli is assumed to have evolved as a mechanism to prevent ingestion of toxins (Spielman, A. I. *et al.*, 1992). In fact, a strong correlation exists in the animal kingdom between bitter sensitivity and tolerance to toxic compounds (Glendinning, J. I., 1994). It has long been appreciated that there is substantial variation among mouse strains in regard to intake and aversion of bitter-tasting compounds. The discovery of genetic loci influencing bitter sensitivity led to the identification of a family of GPCR genes, dubbed *Tas2r*s. These receptors are characterized by a short N-terminus with a potential transmembrane ligand-binding domain. To date, about 25 human and 36 mouse bitter taste receptor genes have been identified, although only a handful have known ligands.

4.19.3.1 Phenylthiocarbamide Taste in Man and Mouse

Variation in taste sensitivity for the bitter goitrogenic compound PTC is a classic example of an inherited trait in humans. It has been the source of much genetic and sensory research since the 1930s (see Chapter Propylthiouracil (PROP) Taste). It is now known that up to 85% of the variation in PTC sensitivity among humans is accounted for by allelic variation of a single bitter taste receptor gene on chromosome 7q, dubbed *TAS2R38* (Kim, U. K. *et al.*, 2003; Kim, U. K. and Drayna, D., 2005). Spurred on by the early discovery of human variation in PTC sensitivity, investigators sought a parallel finding in animal models. There was some evidence for a PTC dimorphism in chimpanzees (Fischer, R. A. *et al.*, 1939), suggesting that taste polymorphisms were not restricted to humans. Richter C. and Clisby K. H. (1941) reported individual variation in PTC avoidance thresholds of rats, although the genetic analysis of this was not pursued. Mice from a BALB strain displayed greater aversion of PTC in two-bottle tests than mice from other strains, including B6, although this difference required 10–12 consecutive days of testing to develop (Klein, T. W. and DeFries, J. C., 1970; Whitney, G. and Harder, D. B., 1986a). Several intercross and backcross generations created from BALB and B6 strains yielded segregation ratios consistent with phenotypic control by a single autosomal locus, with a dominant taster allele. It was suggested that this effect reflects other variables in addition to sensory ability, such as sensitivity to postingestive effects of PTC, which is extremely toxic to mice. A direct comparison of intake tests and brief-access procedures demonstrated that differential avoidance of PTC among inbred strains depends on the amount of stimulus consumed, and not necessarily on immediate orosensory or taste cues (Nelson, T. M. *et al.*, 2003). Furthermore, PTC has been shown to be nearly as effective as LiCl in serving as the unconditioned stimulus in a conditioned taste aversion (CTA) experiment (St. John, S. J. *et al.*, 2005). Although sensitivity to PTC and the chemically related compound 6-*n*-propylthiouracil (PROP) is highly correlated among human subjects, aversions to these compounds do not correlate among mice (Barnicot, N. *et al.*, 1951; Whitney, G. and Harder, D. B., 1994). In summary, an ortholog to the human PTC receptor *TAS2R38* has not yet been described in mice, a finding perhaps not surprising in light of species-specific differences in the bitter taste gene family (Shi, P. *et al.*, 2003).

4.19.3.2 Genetics of Taste Responses to Other Bitter Compounds in Mice

The genetic basis of differences in taste sensitivity to other bitter compounds has been studied throughout the last several decades. Inbred mouse strains have been found to differ in aversion to a large number of both toxic and nontoxic bitter stimuli, including (but not limited to) quinine, strychnine, acetylated sugars, $MgCl_2$, cycloheximide, denatonium benzoate, isohumulone, quinine, and sucrose octaacetate (SOA) (Warren, R. P. and Lewis, R. C., 1970; Lush, I. E., 1981; 1982; 1984; 1986; Lush, I. E. and Holland, G., 1988; Whitney, G. and Harder, D. B., 1994; Bachmanov, A. A. *et al.*, 1996a; Boughter, J. D., Jr. and Whitney, G., 1998; Nelson, T. M. *et al.*, 2003). Aversion of the acetylated sugar SOA among mice is predominantly due to variation at a single qualitative trait locus, *Soa*, although SOA aversion may also be influenced by additional loci and environment. Aversion ratios among segregating generations of mice were consistent with variation at a single autosomal locus (*Soa*), with the taster allele dominant over either a demitaster (partial sensitivity) or nontaster allele (Figure 2; Lush, I. E., 1981; Whitney, G. and Harder, D. B., 1986b; Harder, D. B. *et al.*, 1992; Boughter, J. D., Jr. and Whitney, G., 1995). Results of both taste-salient brief-access behavioral tests and peripheral taste nerve physiology yielded concentration-by-concentration similarity with two-bottle data and

confirmed that the strain difference was gustatory in nature (Inoue, M. *et al.*, 2001a; Boughter, J. D., Jr. *et al.*, 2002). However, at least one other study has found evidence for polygenic control of SOA aversion (Le Roy, I. *et al.*, 1999). The aversion phenotype is subject to environmental modulation: unlike control tasters, taster mice raised on drinking water adulterated with a normally avoided concentration of SOA display only minimal avoidance of SOA in a two-bottle test with water (Harder, D. B. *et al.*, 1989). Unlike SOA avoidance, aversion to quinine and PROP in two-bottle tests has been demonstrated to be under polygenic control in segregating crosses or RI strains (Figure 2; Boughter, J. D., Jr. *et al.*, 1992; Bachmanov, A. A. *et al.*, 1996a; Harder, D. B. and Whitney, G., 1998). Interestingly, strain differences in intake of bitter-tasting drugs such as nicotine have been shown (Robinson, S. F. *et al.*, 1996; Butt, C. M. *et al.*, 2005), but it is not known whether these differences are related to taste or postingestive effects of these drugs.

4.19.3.3 Bitter Taste Loci and Receptors

Using a segregating cross of mice, Capeless C. G. *et al.* (1992) mapped a single locus influencing SOA sensitivity, *Soa*, to a region on distal mouse chromosome 6. This locus overlapped with the *Prp* genes encoding salivary proteins (Bachmanov, A. A. *et al.*, 2001a); although these genes were considered as candidates for the *Soa* locus, they have been shown not to influence SOA taste (Harder, D. B. *et al.*, 2000). Studies with RI and congenic strains linked aversion to a number of other bitter compounds, including quinine, cycloheximide, and PROP, to this same region (Lush, I. E. and Holland, 1988; Lush, I. E. *et al.*, 1995; Boughter, J. D., Jr. and Whitney, G., 1998; Blizard, D. A. *et al.*, 1999). Subsequent genome mining studies discovered a cluster of GPCR bitter taste receptor genes (*Tas2rs*) at this location (Adler, E. *et al.*, 2000; Chandrashekar, J. *et al.*, 2000; Matsunami, H. *et al.*, 2000). Recent characterization of the *Tas2r* receptor gene family in mice indicates 36 genes distributed into two clusters on distal chromosome 6 and one on chromosome 15, including 24 genes at the *Soa-Qui* locus that collectively comprise a large haplotype for bitter taste sensitivity (Wu, S. V. *et al.*, 2005; Nelson, T. M. *et al.*, 2005; Shi, P. *et al.*, 2003). It is likely that allelic variation of these receptors is responsible for phenotypical variation in sensitivity to different bitter tastants linked to the *Soa-Qui* locus.

Analysis of *Tas2r* sequences in strains of quinine taster (B6) and nontaster (DBA/2) mice reveals considerable variation across the *Tas2r* genes (Nelson, T. M. *et al.*, 2005). Among bitter receptors in the mouse, only two have been deorphanized thus far with respect to ligand, one responding exclusively to cycloheximide (encoded by the *Tas2r105* gene), the other to PROP and denatonium (encoded by *Tas2r108*) (Chandrashekar, J. *et al.*, 2000; Conte, C. *et al.*, 2006; Mueller, K. L. *et al.*, 2005). In contrast, several human T2R receptors (aside from T2R38) have been characterized with respect to ligand binding, including T2R16 which responds rather narrowly to a class of bitter chemicals known as β-glucopyranosides, T2R14 that responds to a variety of bitter stimuli, and T2R43 and T2R44 that respond to the bitter aftertaste of saccharin (Bufe, B. *et al.*, 2002; Behrens, M. *et al.*, 2004; Kuhn, C. *et al.*, 2004).

4.19.3.4 Evolution of the T2R Receptors

The study of taste receptor gene evolution has provided key insights into the dynamic process of adaptation of different species to their feeding ecology and environment. Invertebrates such as insects possess aversive responses to bitter-tasting or deterrents chemicals (Glendinning, J. I. and Hills, T. T., 1997; Glendinning, J. I. *et al.*, 1998). A Drosophila *Gr66a* taste receptor responsible for aversive response to caffeine (Moon, S. J. *et al.*, 2006), a compound that tastes bitter to humans, is unrelated to vertebrate T2R genes. This suggests that receptors for detection of aversive taste evolved independently in vertebrate and invertebrate species.

Fish and chickens have a small number of the T2R genes (ten or less; Table 1) and no pseudogenes. Mammals and frogs have much larger numbers of the T2R genes (21–64) and a high proportion of T2R pseudogenes (15–44%). An analysis of relatedness of the T2R genes in different species suggests a complex evolution of this gene family. The common ancestor of tetrapods and teleost fish already had multiple T2Rs. This initial expansion in the common ancestor of tetrapods was followed by additional independent expansions in frogs and mammals and contraction in birds (Go, Y., 2006; Shi, P. and Zhang, J., 2006).

These evolutionary changes likely reflect adaptation to different diets. It appears that the number of functional T2R genes in mammals correlates with levels of toxic compounds in different types of food. Toxic bitter compounds are more common in plant than in animal tissues (Glendinning, J. I., 1994). Correspondingly, omnivores (potentially exposed to the largest number of toxic compounds) have the

Table 1 Numbers of T1R and T2R genes in vertebrate

Species	*T1R genes*			*T2R genes*	
	T1R1 genes	*T1R2 genes*	*T1R3 genes*	*Functional and putatively functional genes*	*Pseudogenes*
Human (*Homo sapiens*)	1	1	1	28	16
Mouse (*Mus musculus*)	1	1	1	36	7
Rat (*Rattus norvegicus*)	1	1	1	37	7
Cow (*Bos taurus*)	Unknown	Unknown	Unknown	19	15
Dog (*Canis familiaris*)	1	1	1	16	5
Cat (*Felis catus*)[a]	1	0	1	Unknown	Unknown
Opossum (*Monodelphis domestica*)	1	1	1	29	5
Chicken (*Gallus gallus*)	1	0	1	3	0
Frog (*Xenopus tropicals*)	0	0	0	52	12
Fugu fish (*Takifugu rubripes*)	1	2	1	4	0
Puffer fish (*Tetraodon nigroviridis*)	1	3	1	6	0
Zebra fish (*Danio rerio*)	1	2	1	10	0
Medaka fish (*Oryzias latipes*)	1	3	1	0	0

[a]Cat *Tas1r2* and *Tas1r3* data from Li X. *et al*. (2005); cat Tas1r1 is based on a cat genome sequence (GenBank accession AANG01000989) with a corresponding predicted protein 90% identical to dog T1R1.
Data from Li X. *et al.* (2005), Shi P. and Zhang J. (2006), Liao J. and Schultz P.G. (2003), Shi P. *et al.* (2003), Go Y. *et al.* (2005), Li X. *et al.* (2002a; 2002b; 2002c), Hoon M. A. *et al.* (1999), Bachmanov A. A. *et al.* (2001), Lagerstrom M. C. *et al.* (2006), Adler E. *et al.* (2000), Ishimaru Y. *et al.* (2005), Go Y. (2006), Conte C. *et al.* (2002; 2003a; 2003b), Wang X. *et al.* (2004), Wu S. U. *et al.* (2005), Bjarnadottir T. K. *et al.* (2005; 2006), Fischer R. A. *et al.* (2005), and Parry C. M. *et al.* (2004). When different sources indicated different numbers of genes, the highest estimate is shown.

largest number of T2R genes, carnivores (potentially exposed to the smallest number of toxic compounds) seem to have the smallest number of T2R genes, and herbivores are intermediate (Shi, P. and Zhang, J., 2006) (see also Table 1).

The repertoire of the T2R genes is highly conserved between the mouse and rat (Wu, S. V. *et al*., 2005) and among primate species, including humans (Fischer, A. *et al*., 2005; Go, Y. *et al*., 2005; Parry, C. M. *et al*., 2004). Primates have a smaller number of intact T2R genes and a higher number and proportion of pseudogenes compared with rodents (Conte, C. *et al*., 2003a; Go, Y. *et al*., 2005) (Table 1). Comparison of T2R sequences in rodents and primates showed that several major groups of these genes were present prior to divergence of their lineages (Conte, C. *et al*., 2003a). Consistent with this, mouse and human T2R genes reside in chromosomal regions with conserved synteny, indicating that major duplication events occurred prior to the separation of primates and rodents (Bufe, B. *et al*., 2002). Approximately 1/4 of the T2R genes have 1:1 mouse–human orthology, nearly 1/4 showed expansion in humans, and ~1/2 showed expansion in mice (Shi, P. *et al*., 2003; Bjarnadottir, T. K. *et al*., 2005). T2R gene families in rodents and primates appear to have undergone a complex combination of local and interchromosomal duplications, deletions, pseudogenization, and positive selection driving divergence of paralogous T2Rs (Conte, C. *et al*., 2003b; Shi, P. *et al*., 2003; Liman, E. R., 2006; Shi, P. and Zhang, J., 2006). The role of tandem gene duplication in evolution of the T2R genes is supported by clustering of these genes in a few chromosomal regions (Fredriksson, R. *et al*., 2003; Shi, P. *et al*., 2003).

Current literature provides conflicting views on evolution of the T2R genes in primates. Several studies suggested reduced selective constraint and neutral evolution of T2R genes in primates compared with rodents (Wang, X. *et al*., 2004; Fischer, A. *et al*., 2005; Go, Y. *et al*., 2005). These conclusions were based on analyses of rates of synonymous and nonsynonymous nucleotide substitutions, higher number of pseudogenes in primates compared with rodents, and allelic segregation of pseudogenes in humans (Conte, C. *et al*., 2003b; Kim, U. K. *et al*., 2004; Wang, X. *et al*., 2004; Fischer, A. *et al*., 2005; Go, Y. *et al*., 2005; Meyerhof, W., 2005). On the other hand, several other studies have detected signs of natural selection of the T2R genes in humans, as is likely the case with other species (Shi, P. *et al*., 2003; Wooding, S. *et al*., 2004; Soranzo, N. *et al*., 2005; Shi, P. and Zhang, J., 2006). For example, signs of positive selection were found for human *TAS2R16* gene, which encodes a receptor for β-glucopyranosides. Its ancestral allele

associated with lower sensitivity to β-glucopyranosides is under positive selection only in central Africa, while in the rest of the world the evolutionarily derived allele associated with an increased sensitivity to β-glucopyranosides is under positive selection. It was suggested that that the global pattern of allelic variation of the *TAS2R16* gene depends on selective pressures of protection against malaria in Africa and protection against toxins in malaria-free zones (Soranzo, N. *et al.*, 2005). Taster and nontaster alleles of the *TAS2R38* gene encoding a PTC taste receptor are maintained in different human populations under balancing selection. It was hypothesized that the *TAS2R38* nontaster allele encodes a functional receptor responsive to toxic bitter substances other than PTC, so that *TAS2R38* heterozygotes gain a fitness advantage because of their ability to perceive and avoid a larger number of bitter toxins compared with homozygotes (Wooding, S. *et al.*, 2004).

Evidence for both neutral evolution and natural selection of T2R genes in primates may reflect adaptation to their feeding ecology. If primates are exposed to a smaller number of toxins than their ancestors were, this may result in loss of selective pressure for some *TAS2R* genes. However, receptors involved in detection of toxins to which primates are still exposed would remain under stabilizing, balancing, or positive selection.

4.19.4 Sweet and Umami Taste

Sweetness is evoked by a diversity of chemicals, including simple carbohydrates, and in most species the sweet taste is associated with appetitive consummatory behavior (Bachmanov, A. A., 2008). Umami is a unique taste quality, described by humans as meaty or brothy, evoked by the amino acid glutamate (e.g., monosodium glutamate or MSG) and some other L-type amino acids and purine 5′-nucleotides (Lindemann, B., 2000) These two distinct taste qualities are linked because their function depends on shared GPCR proteins from the T1R family. In the mouse, three T1R-encoding genes, *Tas1r1*, *Tas1r2*, and *Tas1r3*, are located on chromosome 4 (Hoon, M. A. *et al.*, 1999; Kitagawa, M. *et al.*, 2001; Max, M. *et al.*, 2001; Montmayeur, J. P. *et al.*, 2001; Nelson, G. *et al.*, 2001; Sainz, E. *et al.*, 2001; Reed, D. R. *et al.*, 2004). The three corresponding receptor proteins, T1R1, T1R2, and T1R3, comprise a small family of class C GPCRs. This class includes also the metabotropic glutamate and extracellular calcium-sensing receptors, all of which have a large N-terminal extracellular domain. When T1R3 is coexpressed in a heterologous system with T1R2, it functions as a broad-spectrum sweet taste receptor (Nelson, G. *et al.*, 2001; Li, X. *et al.*, 2002b; Nelson, G. *et al.*, 2002). In contrast, a heterodimer of T1R1 and T1R3 proteins functions as an umami taste receptor in humans, and is more broadly tuned in rodents to respond to L-amino acids (Li, X. *et al.*, 2002c; Nelson, G. *et al.*, 2002; Damak, S. *et al.*, 2003; Zhao, G. Q. *et al.*, 2003).

4.19.4.1 Strain Differences in Responses to Sweet-Tasting Stimuli

Taste sensitivity to compounds classified as tasting sweet, such as sugars, certain amino acids, and artificial sweeteners, varies among human individuals and there is evidence this may be determined genetically (e.g., Greene, L. S. *et al.*, 1975; Gent, J. F. and Bartoshuk, L. M, 1983; Reed, D. R. *et al.*, 1997). Genetic variation in sweet taste responsiveness exists also among inbred mouse strains. In early studies, C57BL mice displayed a significantly greater avidity for sucrose than did DBA/2 mice (McClearn, G. E. and Rodgers, D., 1959; 1962). Fuller J. L. (1974) noted that DBA/2 mice were indifferent to certain concentrations of sodium saccharin in two-bottle tests, whereas B6 mice strongly preferred it. Segregation ratios in a cross of these strains were reported to be consistent with a single locus, two-allele model. An autosomal gene (*Sac*) was proposed to explain this variation, with a dominant Sac^b allele in the B6 strain and a recessive Sac^d allele in the DBA/2 strain. Fuller proposed that this genetic variation affected a hedonic-based response rather than sensory threshold. Subsequent studies by Lush I. E. (1989) suggested that the *Sac* locus also influenced preference to other synthetic sweeteners, including acesulfame and dulcin. Consistent with this, earlier reports had noted that saccharin and sucrose intakes correlated among inbred strains (Pelz, W. E. *et al.*, 1973; Ramirez, I. and Fuller, J. L., 1976). Thus, early studies were supportive of a common genetic basis and single taste receptor underlying sweet taste in mice.

A detailed analysis of sweet taste behavior has been conducted with mice from the B6 and 129 strains. Compared with 129 mice, B6 mice display a higher preference for a large number of sweeteners, including sugars (sucrose and maltose) sweet-tasting amino acids (glycine, D-phenylalanine, D-tryptophan, L-proline, and L-glutamine), and several but not all noncaloric sweeteners (saccharin, acesulfame, dulcin, sucralose, and SC-45647) (Lush, I. E., 1989; Belknap, J. K. *et al.*, 1993; Capeless, C. G. and Whitney, G., 1995; Lush, I. E.

et al., 1995; Bachmanov, A. A. *et al.*, 2001d). This phenotypic difference is not due to a generalized difference in taste responsiveness or differences in appetite, but is rather specific to variation in sweet taste responsiveness (Bachmanov, A. A. *et al.*, 1996b; 2001c). Differences between these strains in preference for a sweet-tasting amino acid, glycine (Bachmanov, A. A. *et al.*, 2001d) appeared to depend on mechanisms distinct from those affecting responses to many other sweeteners. Both B6 and 129 mice generalized CTA between glycine and several other sweeteners, demonstrating that they perceive the sucrose-like taste of glycine. Thus, the lack of a strong glycine preference by 129 mice cannot be explained by their inability to perceive its sweetness (Manita, S. *et al.*, 2006). Despite differences in glycine intakes and preferences, chorda tympani (CT) responses to glycine are similar in mice from both strains (Inoue, M. *et al.*, 2001b). Neither behavioral nor neural responses to glycine are influenced by the *Tas1r3* genotype (Eylam, S. and Spector, A. C., 2004; Inoue, M. *et al.*, 2004b), suggesting that variation in taste responses to glycine depends on other genes.

4.19.4.2 Mapping and Identification of Sweet Taste Receptor Genes

Linkage studies conducted with BXD RI strains, or in crosses with B6 and DBA/2 or 129 strains, detected at least one to two loci on mouse chromosome 4 influencing sweetener preferences (Lush, I. E., 1989; Belknap, J. K. *et al.*, 1992; Phillips, T. J. *et al.*, 1994; Lush, I. E. *et al.*, 1995; Blizard, D. A. *et al.*, 1999). Bachmanov A. A. *et al.* (1997) reported the existence of two distinct loci on chromosome 4 (including *Sac*) in a B6 by 129 cross that collectively accounted for more than 50% of the genetic variability in sucrose intake; these loci were also shown to affect the magnitude and threshold of the CT response to sucrose. A subsequent positional cloning study demonstrated that the *Sac* locus in the subtelomeric region of chromosome 4 corresponded to the *Tas1r3* taste receptor gene (Figure 5) (Bachmanov, A. A. *et al.*, 2001b; Li, X. *et al.*, 2002a).

Polymorphisms of *Tas1r3* have been linked to sweet taste responses attributed to allelic variants of the *Sac* locus (Figure 5). A comprehensive quantitative analysis of *Tas1r3* sequence variants associated with saccharin preference using 30 inbred mouse strains yielded association at a haplotype including the amino acid substitution of isoleucine to threonine at position 60 (Ile60Thr) (Reed, D. R. *et al.*, 2004). A subsequent *in vitro* study showed that a corresponding site-directed mutation changes binding affinity of the T1R3 protein to several sweeteners (Nie, Y. *et al.*, 2005).

The T1R2 + T1R3 sweet receptor responds to a broad variety of ligands in both humans and rodents (although there are species differences), including sugars, artificial sweeteners, and sweet-tasting amino acids (Nelson, G. *et al.*, 2001; Li, X. *et al.*, 2002b; Nelson, G. *et al.*, 2002). There is also evidence that T1R3 functions as a low-affinity sugar receptor alone, probably as a homodimer (Zhao, G. Q. *et al.*, 2003).

Aside from the *Tas1r* family, there may be other genes that affect sweet taste. Multigenic inheritance of sweetener preferences was shown in a number of studies (Ramirez, I. and Fuller, J. L., 1976; Phillips, T. J. *et al.*, 1994; Capeless, C. G. and Whitney, G., 1995; Lush, I. E. *et al.*, 1995; Bachmanov, A. A. *et al.*, 1996a). Mice lacking T1R3 have detection thresholds for sucrose identical to wild types, and can discriminate among sweet and savory stimuli (Delay, E. R. *et al.*, 2006). In F_2 hybrids produced from B6 and 129 strains, intake and neural response of the sweet amino acid glycine was not linked to *Tas1r3* (Inoue, M. *et al.*, 2004b), suggesting the possibility of a non-T1R mechanism. One of the genetic loci affecting sweet taste responses is *dpa* (D-phenylalanine aversion), which affects ability of mice to generalize CTA between D-phenylalanine and sucrose, inferring that *dpa* affects ability to detect sweetness of D-phenylalanine. The *dpa* locus also affects responses of sweet-sensitive fibers of the CT nerve to D-phenylalanine. B6 mice carry a dominant allele of *dpa* that determines an ability to recognize the sweetness of D-phenylalanine, whereas BALB/c mice carry a recessive *dpa* allele conferring inability to detect D-phenylalanine sweetness. The *dpa* locus was mapped to proximal chromosome 4, a region distinct from the subtelomeric chromosome 4 harboring the *Tas1r* genes (Ninomiya, Y. *et al.*, 1987; 1991; 1992; Shigemura, N. *et al.*, 2005). A locus on proximal chromosome 4, in the *dpa* region, was found to be suggestively linked to consumption of, and CT responses to, sucrose (Bachmanov, A. A. *et al.*, 1997). An epistatic interaction between effects on sucrose intake of this locus and the *Tas1r3* locus suggests that these two loci may encode interacting components of sweet taste transduction (Bachmanov, A. A. *et al.*, 1997).

4.19.4.3 Umami Taste Genetics

Little is known about genetic variation in umami taste responses. Humans appear to differ in perception of glutamate taste (Lugaz, O. *et al.*, 2002), but it is not

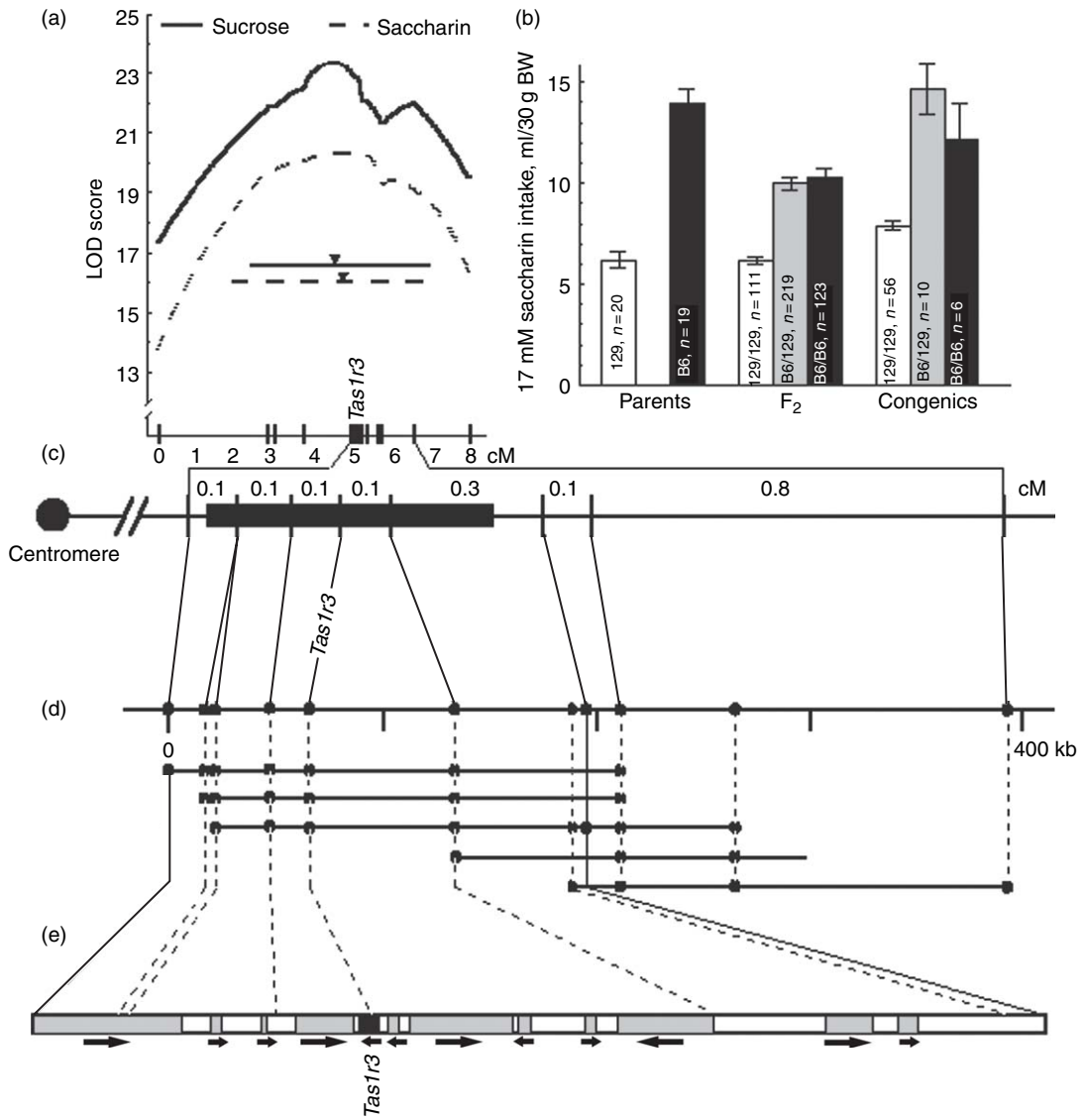

Figure 5 Positional identification of the *Sac* (saccharin preference) locus. (a) Linkage map of mouse distal chromosome 4 based on data from the B6 × 129 F_2 intercross. The *X*-axis shows distances between markers in recombination units (cM). The *Y*-axis shows the logarithm of the odds ratio (LOD) scores for sucrose and saccharin consumption. The LOD score peaks (indicated by black triangles) and confidence intervals (solid horizontal line for sucrose, 4.5 cM, and dotted horizontal line for saccharin, 5.3 cM) define the genomic region of the *Sac* locus. (b) Average daily 17 mM saccharin consumption by mice from parental 129 and B6 strains (left), B6 × 129 F_2 hybrids (center), and congenic 129.B6-*Sac* mice (right) in 96 h two-bottle tests with water (means ± SE). *Tas1r3* genotypes of the F_2 and congenic mice and mouse numbers are indicated on the bars. Differences between parental strains and among the F_2 and congenic genotypes were significant ($p < 0.0001$, ANOVA). F_2 and congenic B6 homozygotes and heterozygotes for *Tas1r3* did not differ from each other, and had higher saccharin intakes compared with 129 homozygotes ($p < 0.0001$, posthoc tests). (c) Linkage map of the *Sac*-containing region defined based on the size of the donor fragment in the 129.B6-*Sac* congenic strain (black box). Distances between markers were estimated based on the B6 × 129 F_2 intercross (see panel a). (d) A contig of bacterial artificial chromosome (BAC) clones and physical map of the *Sac* region. BAC clones are represented by horizontal lines. Dots indicate marker content of the BAC clones. (e) Genes within the *Sac*-containing interval. Filled areas indicate predicted genes. Arrows indicate the predicted direction of transcription. Reproduced from Bachmanov, A. A., Reed, D. R., Li, X., and Beauchamp, G. K. 2002. Genetics of sweet taste preferences. Pure Appl. Chem. 74, 1135–1140, with permission from IUPAC.

known whether this variation has a genetic basis. Genetically determined differences in responses to umami taste stimuli were shown in mice: in two-bottle tests, B6 mice display higher consumption of MSG and inosine monophosphate than do mice from the 129 strain (Bachmanov, A. A. *et al.*, 2000). These strain differences seem to be specific for umami stimuli and are not associated with variation in sweet or salty tastes (Bachmanov, A. A. *et al.*, 1996a; 1998; 2000).

A heterodimer of the T1R1 and T1R3 proteins is thought to function as a receptor for umami taste stimuli. Consistent with this, disruption of the *Tas1r1* and/or *Tas1r3* genes diminishes behavioral or neural responses of knockout mice to umami taste stimuli (Nelson, G. *et al.*, 2002; Damak, S. *et al.*, 2003; Zhao, G. Q. *et al.*, 2003). However, natural allelic variation of the *Tas1r3* gene does not affect umami taste responses in mice: an analysis of the F_2 hybrids between the B6 and 129 inbred mouse strains has shown that the *Tas1r3* allelic variants are not associated with behavioral or neural taste responses to umami stimuli (Inoue, M. *et al.*, 2004b). Therefore, although the T1R3 receptor is involved in transduction of umami taste, the B6/129 sequence variants affecting its sensitivity to sweeteners do not affect its sensitivity to umami compounds. Recent studies of umami taste transduction indicate the existence of more than one receptor responding to this class of stimuli (Chaudhari, N. *et al.*, 2000; Maruyama, Y. *et al.*, 2006); allelic variation of these genes might underlie genetic differences in umami taste.

4.19.4.4 Evolution of T1R Receptors

Numbers of the T1R genes in different vertebrate species range from complete absence in the frog to five in the puffer fish and medaka fish (Table 1). With the exception of the frog, all vertebrates have single T1R1 and T1R3 genes, but the number of the T1R2 genes varies: the chicken and Felidae species (domestic cat, tiger, and cheetah; Li, X. *et al.*, 2005) lack functional T1R2 genes, but several fish species have two to three T1R2 genes. The vertebrate T1R receptors are not found in invertebrates (Bjarnadottir, T. K. *et al.*, 2005) and are not related to a Drosophila taste receptor for a sugar trehalose encoded by the *Gr5a* gene (Dahanukar, A. *et al.*, 2001; Ueno, K. *et al.*, 2001; Chyb, S. *et al.*, 2003; Inomata, N. *et al.*, 2004; Isono, K. *et al.*, 2005; Hallem, E. A. *et al.*, 2006).

These data allow us to establish changes in the T1R repertoire during evolution. Although many vertebrate and invertebrate animals detect the taste of sugars and avidly consume them, receptors for sugars evolved independently in these two lineages. Most vertebrates have three clades of T1R genes, suggesting that all three evolved before separation of tetrapods and teleosts (Shi, P. and Zhang, J., 2006). However, another group concluded from a similar analysis that fish and mammalian T1R1 and T1R3 genes are orthologs, but fish and mammalian T1R2 evolved independently (Ishimaru, Y. *et al.*, 2005). It appears that after separation of tetrapods and teleosts, duplication of the T1R2 gene occurred in the evolution of different fish species. Several Felidae species (Li, X. *et al.*, 2005) and the chicken (Lagerstrom, M. C. *et al.*, 2006; Shi, P. and Zhang, J., 2006) lost the T1R2 gene, and the tongueless western clawed frog lost all three T1R genes. Thus, pseudogenization of the T1R2 gene occurred multiple times in evolution.

Loss of the T1R2 gene in cats and chickens must result in the absence of the T1R2 + T1R3 sweet taste receptor, which corresponds to the lack of taste responses to sweeteners in these species (Kare, M. R., 1961; Halpern, B. P., 1962; Bartoshuk, L. M *et al.*, 1975; Beauchamp, G. K. *et al.*, 1977; Ganchrow, J. R. *et al.*, 1990). Interestingly, some birds recognize sugar taste (Matson, K. D. *et al.*, 2000; 2001), suggesting that they may have a functional T1R2. The T1R2 pseudogenization and lack of sweet taste responsiveness in cats are probably results of these animals being obligate carnivores that do not seek sugars in their food, and thus do not have a selective advantage of having a functional sweet taste receptor that recognizes sugars. Dogs, which are carnivores from the Canidae family, have a functional T1R2 gene structure (Li, X. *et al.*, 2005; Shi, P. and Zhang, J., 2006) and are attracted to sugars (Grace, J. and Russek, M., 1969). Thus, loss of the T1R2 gene in cats and chickens may be a consequence of their feeding behavior that does not require a sweet taste receptor for proper food choice. However, a reverse causative relationship cannot be excluded, when a loss-of-function mutation in the T1R2 gene resulted in loss of sweet taste sensation, which in turn altered feeding behavior of these animals.

The role of natural selection in evolution of the T1R genes was shown in several studies involving comparisons of the paralogous genes and analyses of their within-species variation. Sequence divergence among the paralogous T1R genes appears to be governed by positive selection (Shi, P. and Zhang, J., 2006). Most of the inferred positively selected sites are located in the N-terminal extracellular domains of the T1R proteins (Shi, P. and Zhang, J., 2006),

which participate in ligand binding (Xu, H. *et al.*, 2004; Jiang, P. *et al.*, 2005a, Nie, Y. *et al.*, 2005). Analysis of within-species *TAS1R* sequence variation among humans suggested that *TAS1R* variants have come to their current frequencies under positive natural selection during population growth, which implies that the coding sequence variants affect receptor function (Kim, U. K. *et al.*, 2006).

Results of these studies suggest that the evolutionary changes of the T1R receptors are likely to affect their ligand binding properties. This is consistent with currently available data on species differences in ligand specificity of the T1R1 + T1R3 and T1R2 + T1R3 receptors (Nelson, G. *et al.*, 2001; 2002; Li, X. *et al.*, 2002c; Winnig, G. *et al.*, 2005). Several studies have shown that sequence variation between the T1R orthologs underlies species differences in responses to several amino acids, sweeteners and sweet taste blockers. T1R variants that determine species differences in ligand binding were found in the cysteine-rich region of the extracellular N-terminal domain (Jiang, P. *et al.*, 2004) and in the transmembrane domains (Jiang, P. *et al.*, 2005a; 2005b; Winnig, G. *et al.*, 2005).

Although ligands for the T1R receptors have been experimentally confirmed only for humans and rodents, it is likely that their orthologs in other species have similar ligand specificities. This would make sense because sugars and amino acids, the main natural T1R ligands, are important nutrients for animals of many different species. This explains the lower diversity and slower evolution of the T1R genes compared with the T2R genes involved in bitter taste (Shi, P. and Zhang, J., 2006). Nevertheless, variation in the T1R genes among species may reflect species differences in diets, for example the amino acid composition of food or presence of sweet proteins in some tropical fruits.

4.19.5 Salt and Sour Taste

Ionic taste stimuli such as H^+ or Na^+ are thought to be transduced primarily via apically located ion channels. A large portion of NaCl or salt taste is thought to be dependent on the influx of sodium through epithelial sodium channels, members of the degenerin/ENaC superfamily of ion channels. ENaC is blocked by the diuretic compound amiloride. Taste receptor cells (TRCs) express Na^+-selective channels that are also blocked by amiloride and share a number of other physiological properties with the ENaCs (for a review, see Boughter, J. D., Jr. and Gilbertson, T. A., 1999; Gilbertson, T. A. *et al.*, 2000). Entry of the sodium ion through these channels depolarizes the taste cell. However, the specific identity of these channels, as well as the mechanisms by which salty taste of non-sodium salts is transduced, are not well understood (Chandrashekar, J. *et al.*, 2006). Sour-tasting (acid) stimuli also depolarize TRCs either by activating cation channels, or by direct permeation of protons through ion channels, including ENaC (Gilbertson, T. A. *et al.*, 1992; Gilbertson, T. A. and Boughter, J. D., Jr., 2003). Additionally, transient receptor potential (TRP) channels have been shown to be involved in acid taste (Huang, A. L. *et al.*, 2006; Ishimaru, Y. *et al.*, 2006).

Comparatively few studies have reported genetic variation affecting taste responses to salty or sour substances. Inbred strain differences have been reported for NaCl preferences in both mice (Hoshishima, K. *et al.*, 1962; Ninomiya, Y. *et al.*, 1989; Beauchamp, G. K., 1990; Lush, I. E., 1991; Bachmanov, A. A. *et al.*, 2002; Tordoff, M. G. *et al.*, 2007) and rats (Midkiff, E. E. *et al.*, 1985). Among commonly used strains, B6 and BALB are NaCl avoiding, and their CT response to NaCl is amiloride sensitive, whereas DBA/2, C3H/He, and 129 mice are NaCl-tolerant and their CT response to NaCl is amiloride-insensitive (Ninomiya, Y. *et al.*, 1989; Gannon, K. and Contreras, R. J., 1993; Ninomiya, Y., 1996). Experiments using isolated taste buds indicated that the strain difference might be due to a difference in the density of functional amiloride-sensitive Na^+ channels on taste cells (Miyamoto, T. *et al.*, 1999). Although B6 and DBA/2 mice differ in terms of the amiloride sensitivity of their CT response to NaCl (Ninomiya, Y. *et al.*, 1989), these strains do not differ in detection or discrimination of salts, and these behaviors are attenuated by amiloride in a similar fashion in both strains (Eylam, S. and Spector, A. C., 2003; 2005). More studies are needed to determine whether there is a relationship between amiloride sensitivity of neural responses to NaCl, and NaCl preference. The genetic variation in voluntary NaCl consumption may also depend on a variety of other factors in addition to peripheral taste responsiveness.

4.19.6 Taste and Other Complex Phenotypes

4.19.6.1 Taste and Diet

Taste sensitivity is associated with food choice and intake, and taste preferences are a predictor of propensity to consume sweet or high-fat foods (e.g., Bartoshuk, L., 1980; Drewnowski, A. *et al.*, 1985; Anliker, J. A. *et al.*, 1991; Drewnowski, A. J. *et al.*, 1998; Salbe, A. D. *et al.*,

2004). At least some of this association is underlied by allelic variation of taste receptor genes (Mennella, J. A. *et al*., 2005; Dinehart, M. E. *et al*., 2006; Reed, D. R. and McDaniel, A. H., 2006; Sandell, M. A. and Breslin, P. A., 2006). Unexpectedly, haplotypes at the *TAS2R38* gene encoding the PTC receptor were significantly related to children's to preference for sucrose and sweet-tasting foods and beverages: Those possessing taster alleles tended to be sweet preferrers; the authors speculate that the PTC gene may be in linkage disequilibrium with sweet taste genes (Mennella, J. A. *et al*., 2005). Other studies have shown that *TAS2R38* genotype or PROP taster status affects perception of bitterness of vegetables, such as broccoli, turnips, or Brussels sprouts, and hence may influence dietary selection (Dinehart, M. E. *et al*., 2006; Sandell, M. A. and Breslin, P. A., 2006). It is furthermore possible that there is a relationship between genetic determinates of taste sensitivity and obesity (Bartoshuk, L. M *et al*., 2006).

There is a strong relationship between taste and feeding (Scott, T. R., 2001), and future taste-related gene discovery may focus on the interaction of taste processing with homeostatic systems involved in the regulation of feeding, appetite, fluid balance, reward, and drug administration.

4.19.6.2 Taste and Drug Intake

It has long been appreciated that a consistent predictor of alcohol (ethanol) drinking in rodents is avidity for consumption of sweet-tasting compounds. Positive correlations between ethanol and sweetener intake have been noted in multiple strains of rats and mice, and a common genetic basis is strongly supported by a robust association of these phenotypes in both selected lines and segregating populations (McClearn, G. E. and Rodgers, D., 1959; Belknap, J. K. *et al*., 1993; Overstreet, D. H. *et al*., 1993; Bachmanov, A. A. *et al*., 1996b; Dess, N. K. *et al*., 1998; Stewart, R. B. *et al*., 2003). There is also substantial evidence for an association between alcohol drinking and sweet taste in humans (Yamamoto, M. E. *et al*., 1991; Kampov-Polevoy, A. *et al*., 1997; 2003; 2004). *Tas1r3* knockout mice do not prefer ethanol unlike their wild-type controls, strongly arguing for a direct role of the sweet taste receptor in mediating ethanol intake (Blednov, Y. A. *et al*., 2007). In rats, ethanol applied to the tongue selectively activates a subpopulation of sweet-responsive taste neurons in the CNS, and this activity is blocked by lingual application of gurmarin, a peripheral antagonist of sweet taste (Lemon, C. H. *et al*., 2004).

There is also an association of bitter taste sensitivity with alcohol, caffeine and nicotine use (Hall, M. J. *et al*., 1975; Mela, D. J., 1989; Mela, D. J. *et al*., 1992; Mattes, R. D., 1994; Enoch, M. A. *et al*., 2001; Snedecor, S. M. *et al*., 2006). This association may be due to individual variation in bitter taste receptors. For example, subjects possessing nontaster haplotypes at the *TAS2R38* locus rate alcoholic beverages as less bitter, and more preferred (Duffy, V. B. *et al*., 2004; Lanier, S. A. *et al*., 2005). Similarly, there is a greater percentage of bitter-insensitive individuals among smokers than nonsmokers, suggesting these nontasters may be at risk for nicotine addiction (Enoch, M. A. *et al*., 2001). Because there is a strong relationship between smoking and alcohol use in humans (Pomerleau, C. S. *et al*., 2004) it is reasonable to assume taste may be a common factor in both addictions. However, oral somatosensory factors may also play a role because both nicotine and ethanol are trigeminal irritants (e.g., Carstens, E. *et al*., 1998). In addition, causative relationships between taste and drug intake may be more complex, as drug intake may influence taste sensitivity. There is evidence that long-term smoking or oral tobacco use may contribute to a decrement in overall taste acuity (Sato, K. *et al*., 2002; Khan, G. J. *et al*., 2003), and taste detection thresholds for caffeine are elevated in habitual caffeine drinkers relative to nonusers (Mela, D. J. *et al*., 1992).

4.19.7 Conclusions

Historically, behavioral genetic studies of taste and intake behaviors have been instrumental in the eventual discovery of G-protein-coupled taste receptors. In particular, the discovery of the PTC polymorphism in humans stimulated research into the genetics basis of taste behavior. In rodents, strain differences in responsiveness to bitter- and sweet-tasting stimuli, primarily in two-bottle tests, provided linkages to chromosome regions later found to harbor taste receptor genes. However, the balance of evidence suggests that taste-related behaviors are under polygenic control, and other genes have yet to be elucidated. Within- and between-species differences in the T1R and T2R genes are associated with variation in taste-related behaviors. The evolution of the T1R and T2R gene families reflects adaptation strategies of different species to their chemical environments and feeding ecology.

References

Adler, E., Hoon, M. A., Mueller, K. L., Chandrashekar, J., Ryba, N. J. P., and Zuker, C. S. 2000. A novel family of mammalian taste receptors. Cell 100, 693–702.

Anliker, J. A., Bartoshuk, L., Ferris, A. M., and Hooks, L. D. 1991. Children's food preferences and genetic sensitivity to the bitter taste of 6-*n*-propylthiouracil (PROP). Am. J. Clin. Nutr. 54, 316–320.

Bachmanov, A. A. 2008. Genetic Architecture of Sweet Taste. In: Sweetness and Sweeteners: Biology, Chemistry and Psychophysics. ACS Symposium Series (*eds*. D. K. Weerasinghe and G. E. Dubois), Oxford University Press.

Bachmanov, A. A., Beauchamp, G. K., and Tordoff, M. G. 2002. Voluntary consumption of NaCl, KCl, $CaCl_2$, and NH_4Cl solutions by 28 mouse strains. Behav. Genet. 32, 445–457.

Bachmanov, A. A., Li, X., Li, S., Neira, M., Beauchamp, G. K., and Azen, E. A. 2001a. High-resolution genetic mapping of the sucrose octaacetate taste aversion (Soa) locus on mouse Chromosome 6. Mamm. Genome 12, 695–699.

Bachmanov, A. A., Li, X., Reed, D. R., Ohmen, J. D., Li, S., Chen, Z., Tordoff, M. G., De Jong, P. J., Wu, C., West, D. B., Chatterjee, A., Ross, D. A., and Beauchamp, G. K. 2001b. Positional cloning of the mouse saccharin preference (Sac) locus. Chem. Senses 26, 925–933.

Bachmanov, A. A., Reed, D. R., Li, X., and Beauchamp, G. K. 2002. Genetics of sweet taste preferences. Pure Appl. Chem. 74, 1135–1140.

Bachmanov, A. A., Reed, D. R., Ninomiya, Y., Inoue, M., Tordoff, M. G., Price, R. A., and Beauchamp, G. K. 1997. Sucrose consumption in mice: major influence of two genetic loci affecting peripheral sensory responses. Mamm. Genome 8, 545–548.

Bachmanov, A. A., Reed, D. R., Tordoff, M. G., Price, R. A., and Beauchamp, G. K. 1996a. Intake of ethanol, sodium chloride, sucrose, citric acid, and quinine hydrochloride solutions by mice: a genetic analysis. Behav. Genet. 26, 563–573.

Bachmanov, A. A., Reed, D. R., Tordoff, M. G., Price, R. A., and Beauchamp, G. K. 2001c. Nutrient preference and diet-induced adiposity in C57BL/6ByJ and 129P3/J mice. Physiol. Behav. 72, 603–613.

Bachmanov, A. A., Tordoff, M. G., and Beauchamp, G. K. 1996b. Ethanol consumption and taste preferences in C57BL/6ByJ and 129/J mice. Alcoholism: Clin. Exp. Res. 20, 201–206.

Bachmanov, A. A., Tordoff, M. G., and Beauchamp, G. K. 1998. Voluntary sodium chloride consumption by mice: Differences among five inbred strains. Behav. Genet. 28, 117–124.

Bachmanov, A. A., Tordoff, M. G., and Beauchamp, G. K. 2000. Intake of umami-tasting solutions by mice: a genetic analysis. J. Nutr. 130, 935S–941S.

Bachmanov, A. A., Tordoff, M. G., and Beauchamp, G. K. 2001d. Sweetener preference of C57BL/6ByJ and 129P3/J mice. Chem. Senses 26, 905–913.

Barnicot, N., Harris, H., and Kalmus, H. 1951. Taste thresholds of further eighteen compounds and their correlation with PTC thresholds. Ann. Eugenics 16, 119–128.

Bartoshuk, L. 1980. Influence of chemoreception and psychologic state on food selection. Int. J. Obesity 4, 351–355.

Bartoshuk, L. M., Duffy, V. B., Hayes, J. E., Moskowitz, H. R., and Snyder, D. J. 2006. Psychophysics of sweet and fat perception in obesity: problems, solutions and new perspectives. Phil. Trans. R. Soc. Lond. B Biol. Sci. 361, 1137–1148.

Bartoshuk, L. M., Duffy, V. B., and Miller, I. J. 1994. PTC/PROP tasting: anatomy, psychophysics, and sex effects. Physiol. Behav. 56, 1165–1171.

Bartoshuk, L. M., Jacobs, H. L., Nichols, T. L., Hoff, L. A., and Ryckman, J. J. 1975. Taste rejection of nonnutritive sweeteners in cats. J. Comp. Physiol. Psychol. 89, 971–975.

Beauchamp, G. K. 1990. Genetic control over salt preference in inbred strains of mice. Chem. Senses 15, 551.

Beauchamp, G. K., Maller, O., and Rogers, J. G. 1977. Flavor preferences in cats (*Felis catus* and Panthera sp.). J. Comp. Physiol. Psychol. 91, 1118–1127.

Behrens, M., Brockhoff, A., Kuhn, C., Bufe, B., Winnig, M., and Meyerhof, W. 2004. The human taste receptor hTAS2R14 responds to a variety of different bitter compounds. Biochem. Biophys. Res. Commun. 319, 479–485.

Belknap, J. K., Crabbe, J. C., Plomin, R., Mcclearn, G. E., Sampson, K. E., O'Toole, L. A., and Gora-Maslak, G. 1992. Single-locus control of saccharin intake in BXD/Ty recombinant inbred (RI) mice: some methodological implications for RI strain analysis. Behav. Genet. 22, 81–100.

Belknap, J. K., Crabbe, J. C., and Young, E. R. 1993. Voluntary consumption of ethanol in 15 inbred mouse strains. Psychopharmacology (Berl.) 112, 503–510.

Bjarnadottir, T. K., Fredriksson, R., and Schioth, H. B. 2005. The gene repertoire and the common evolutionary history of glutamate, pheromone (V2R), taste(1) and other related G protein-coupled receptors. Gene 362, 70–84.

Blednov, Y. A., Walker, D., Martinez, M., Levine, M., Damak, S., and Margolskee, R. F. 2007. Perception of sweet taste is important for voluntary alcohol consumption in mice. Genes Brain Behav. doi: 10.1111/j.1601-183X.2007.00309.X.

Blizard, D. A., Kotlus, B., and Frank, M. E. 1999. Quantitative trait loci associated with short-term intake of sucrose, saccharin and quinine solutions in laboratory mice. Chem. Senses 24, 373–385.

Bloomgarden, Z. T. 2006. Gut hormones and related concepts. Diabetes Care 29, 2319–2324.

Boughter, J. D., Jr. and Gilbertson, T. A. 1999. From channels to behavior: an integrative model of NaCl taste. Neuron 22, 213–215.

Boughter, J. D., Jr. and Whitney, G. 1995. C3.SW-Soa[a] heterozygous congenic taster mice. Behav. Genet. 25, 233–237.

Boughter, J. D., Jr. and Whitney, G. 1998. Behavioral specificity of the bitter taste gene Soa. Physiol. Behav. 63, 101–108.

Boughter, J. D., Jr., Harder, D. B., Capeless, C. G., and Whitney, G. 1992. Polygenic determination of quinine sensitivity among mice. Chem. Senses 17, 427–434.

Boughter, J. D., Jr., Raghow, S., Nelson, T. M., and Munger, S. D. 2005. Inbred mouse strains C57BL/6J and DBA/2J vary in sensitivity to a subset of bitter stimuli. BMC Genet. 6, 36.

Boughter, J. D., Jr., St. John, S. J., Noel, D. T., Ndubuizu, O., and Smith, D. V. 2002. A brief-access test for bitter taste in mice. Chem. Senses 27, 133–142.

Bufe, B., Hofmann, T., Krautwurst, D., Raguse, J. D., and Meyerhof, W. 2002. The human TAS2R16 receptor mediates bitter taste in response to beta-glucopyranosides. Nat. Genet. 32, 397–401.

Butt, C. M., King, N. M., Hutton, S. R., Collins, A. C., and Stitzel, J. A. 2005. Modulation of nicotine but not ethanol preference by the mouse Chrna4 A529T polymorphism. Behav. Neurosci. 119, 26–37.

Capeless, C. G. and Whitney, G. 1995. The genetic basis of preference for sweet substances among inbred strains of mice: preference ratio phenotypes and the alleles of the *Sac* and *dpa* loci. Chem. Senses 20, 291–298.

Capeless, C. G., Whitney, G., and Azen, E. A. 1992. Chromosome mapping of Soa, a gene influencing gustatory sensitivity to sucrose octaacetate in mice. Behav. Genet. 22, 655–663.

Carstens, E., Kuenzler, N., and Handwerker, H. O. 1998. Activation of neurons in rat trigeminal subnucleus caudalis

by different irritant chemicals applied to oral or ocular mucosa. J. Neurophysiol. 80, 465–492.
Chandrashekar, J., Hoon, M. A., Ryba, N. J., and Zuker, C. S. 2006. The receptors and cells for mammalian taste. Nature. 444, 288–294.
Chandrashekar, J., Mueller, K. L., Hoon, M. A., Adler, E., Feng, L., Guo, W., Zuker, C. S., and Ryba, J. P. 2000. T2Rs function as bitter taste receptors. Cell 100, 703–711.
Chaudhari, N., Landin, A. M., and Roper, S. D. 2000. A metabotropic glutamate receptor variant functions as a taste receptor. Nat. Neurosci. 3, 113–119.
Chyb, S., Dahanukar, A., Wickens, A., and Carlson, J. R. 2003. Drosophila Gr5a encodes a taste receptor tuned to trehalose. Proc. Natl. Acad. Sci. U. S. A. 100(Suppl. 2), 14526–14530.
Conte, C., Ebeling, M., Marcuz, A., and Andres-Barquin, P. J. 2003a. Identification of the T2R repertoire of taste receptor genes in the rat genome sequence. Genome Lett. 2, 155–161.
Conte, C., Ebeling, M., Marcuz, A, Nef, P., and Andres-Barquin, P. J. 2002. Identification and characterization of human taste receptor genes belonging to the TAS2R family. Gene Mapp. Clon. Seq. 98, 45–53.
Conte, C., Ebeling, M., Marcuz, A., Nef, P., and Andres-Barquin, P. J. 2003b. Evolutionary relationships of the Tas2r receptor gene families in mouse and human. Physiol. Genomics 14, 73–82.
Conte, C., Guarin, E., Marcuz, A., and Andres-Barquin, P. J. 2006. Functional expression of mammalian bitter taste receptors in *Caenorhabditis elegans*. Biochimie. 88, 801–806.
Dahanukar, A., Foster, K., Van der Goes Van Naters, W. M., and Carlson, J. R. 2001. A Gr receptor is required for response to the sugar trehalose in taste neurons of Drosophila. Nat. Neurosci. 4, 1182–1186.
Damak, S., Rong, M., Yasumatsu, K., Kokrashvili, Z., Varadarajan, V., Zou, S., Jiang, P., Ninomiya, Y., and Margolskee, R. F. 2003. Detection of sweet and umami taste in the absence of taste receptor T1r3. Science 301, 850–853.
Delay, E. R., Hernandez, N. P., Bromley, K., and Margolskee, R. F. 2006. Sucrose and monosodium glutamate taste thresholds and discrimination ability of T1R3 knockout mice. Chem. Senses. 31, 351–357.
Dess, N. K., Badia-Elder, N. E., Thiele, T. E., Kiefer, S. W., and Blizard, D. A. 1998. Ethanol consumption in rats selectively bred for differential saccharin intake. Alcohol 16, 275–278.
Dinehart, M. E., Hayes, J. E., Bartoshuk, L. M., Lanier, S. L., and Duffy, V. B. 2006. Bitter taste markers explain variability in vegetable sweetness, bitterness, and intake. Physiol. Behav. 87, 304–313.
Drewnowski, A., Henderson, S. A., and Barratt-Fornell, A. 1998. Genetic sensitivity to 6-*n*-propylthiouracil and sensory responses to sugar and fat mixtures. Physiol. Behav. 63, 771–777.
Drewnowski, A. J., Brunzell, J. D., Sande, K., Iverius, P. H., and Greenwood, M. R. 1985. Sweet tooth reconsidered: taste responsiveness in human obesity. Physiol. Behav. 35, 617–622.
Duffy, V. B. and Bartoshuk, L. M. 2000. Food acceptance and genetic variation in taste. J. Am. Dietetic Assoc. 100, 647–655.
Duffy, V. B., Davidson, A. C., Kidd, J. R., Kidd, K. K., Speed, W. C., Pakstis, A. J., Reed, D. R., Snyder, D. J., and Bartoshuk, L. M. 2004. Bitter receptor gene (TAS2R38), 6-*n*-propylthiouracil (PROP) bitterness and alcohol intake. Alcoholism: Clin. Exp. Res. 28, 1629–1637.
Enoch, M. A., Harris, C. R., and Goldman, D. 2001. Does a reduced sensitivity to bitter taste increase the risk of becoming nicotine addicted? Addictive Behav. 26, 399–404.
Eylam, S. and Spector, A. C. 2003. Oral amiloride treatment decreases taste sensitivity to sodium salts in C57BL/6J and DBA/2J mice. Chem. Senses 28, 447–458.
Eylam, S. and Spector, A. C. 2004. Stimulus processing of glycine is dissociable from that of sucrose and glucose based on behaviorally measured taste signal detection in Sac 'taster' and 'non-taster' mice. Chem. Senses 29, 639–649.
Eylam, S. and Spector, A. C. 2005. Taste discrimination between NaCl and KCl is disrupted by amiloride in inbred mice with amiloride-insensitive chorda tympani nerves. Am. J. Physiol. Regul. Integr. Comp. Physiol. 288, R1361–R1368.
Fischer, A., Gilad, Y., Man, O., and Paabo, S. 2005. Evolution of bitter taste receptors in humans and apes. Mol. Biol. Evol. 22, 432–436.
Fischer, R. A., Ford, E. B., and Huxley, J. 1939. Taste testing the anthropoid apes. Nature 144, 750.
Flaherty, L. 1981. Congenic Strains. In: The Mouse in Biomedical Research. Vol. 1. History, Genetics, and Wild Mice (*eds*. H. L. Foster, J. D. Small, and J. G. Fox), pp. 215–222. Academic Press.
Fox, A. L. 1931. Six in ten ''tasteblind'' to bitter chemical. Sci. News Lett. 9, 249.
Fox, A. L. 1932. The relationship between chemical constituion and taste. Proc. Natl. Acad. Sci. U. S. A. 18, 115–120.
Fredriksson, R., Lagerstrom, M. C., Lundin, L. G., and Schioth, H. B. 2003. The G-protein-coupled receptors in the human genome form five main families. Phylogenetic analysis, paralogon groups, and fingerprints. Mol. Pharmacol. 63, 1256–1272.
Fuller, J. L. 1974. Single-locus control of saccharin preference in mice. J. Heredity 65, 33–36.
Ganchrow, J. R., Steiner, J. E., and Bartana, A. 1990. Behavioral reactions to gustatory stimuli in young chicks (*Gallus gallus domesticus*). Dev. Psychobiol. 23, 103–117.
Gannon, K. and Contreras, R. J. 1993. Sodium intake linked to amiloride-sensitive gustatory transduction in C57BL/6J and 129/J mice. Physiol. Behav. 57, 231–239.
Gent, J. F. and Bartoshuk, L. M. 1983. Sweetness of sucrose, neohesperidin dihydrochalcone, and saccharin is related to genetic ability to taste the bitter substance 6-*n*-propylthiouracil. Chem. Senses 7, 265–272.
Gilbertson, T. A. and Boughter, J. D., Jr. 2003. Taste transduction: appetizing times in gustation. NeuroReport 14, 905–911.
Gilbertson, T. A., Avenet, P., Kinnamon, S. C., and Roper, S. D. 1992. Proton currents through amiloride-sensitive Na channels in hamster taste cells: role in acid transduction. J. Gen. Physiol. 100, 803–824.
Gilbertson, T. A., Damak, S., and Margolskee, R. F. 2000. The molecular physiology of taste transduction. Curr. Opin. Neurobiol. 10, 519–527.
Glendinning, J. I. 1994. Is the bitter rejection response always adaptive? Physiol. Behav. 56, 1217–1227.
Glendinning, J. I. and Hills, T. T. 1997. Electrophysiological evidence for two transduction pathways within a bitter-sensitive taste receptor. J. Neurophysiol. 78, 734–745.
Glendinning, J. I., Gresack, J., and Spector, A. C. 2002. A high-throughput screening procedure for identifying mice with aberrant taste and oromotor function. Chem. Senses 27, 461–474.
Glendinning, J. I., Valcic, S., and Timmermann, B. N. 1998. Maxillary palps can mediate taste rejection of plant allelochemicals by caterpillars. J. Comp. Physiol. A 183, 35–43.
Go, Y. 2006. Lineage-specific expansions and contractions of the bitter taste receptor gene repertoire in vertebrates. Mol. Biol. Evol. 23, 964–972.
Go, Y., Satta, Y., Takenaka, O., and Takahata, N. 2005. Lineage-specific loss of function of bitter taste receptor genes in humans and nonhuman primates. Genetics 170, 313–1326.

Goodwin, F. L. and Amit, Z. 1998. Do taste factors contribute to the mediation of ethanol intake? Ethanol and saccharin–quinine intake in three rat strains. Alcoholism: Clin. Exp. Res. 22, 837–844.

Grace, J. and Russek, M. 1969. The influence of previous experience on the taste behavior of dogs toward sucrose and saccharin. Physiol. Behav. 4, 553–558.

Greene, L. S., Desor, J. A., and Maller, O. 1975. Heredity and experience: their relative importance in the development of taste preference in man. J. Comp. Physiol. Psychol. 89, 279–284.

Hall, M. J., Bartoshuk, L. M., Cain, W. S., and Stevens, J. C. 1975. PTC taste blindness and the taste of caffeine. Nature 253, 442–443.

Hallem, E. A., Dahanukar, A., and Carlson, J. R. 2006. Insect odor and taste receptors. Annu. Rev. Entomol. 51, 113–135.

Halpern, B. P. 1962. Gustatory nerve responses in the chicken. Am. J. Physiol. 203, 541–544.

Harder, D. B. and Whitney, G. 1998. A common polygenic basis for quinine and PROP avoidance in mice. Chem. Senses 23, 327–332.

Harder, D. B., Azen, E. A., and Whitney, G. 2000. Sucrose octaacetate avoidance in nontaster mice is not enhanced by two type-A Prp transgenes from taster mice. Chem. Senses 25, 39–45.

Harder, D. B., Capeless, C. G., Maggio, J. C., Boughter, J. D., Gannon, K. S., Whitney, G., and Azen, E. A. 1992. Intermediate sucrose octa-acetate sensitivity suggests a third allele at mouse bitter taste locus *Soa* and *Soa-Rua* identity. Chem. Senses 17, 391–401.

Harder, D. B., Maggio, J. C., and Whitney, G. 1989. Assessing gustatory detection capabilities using preference procedures. Chem. Senses 14, 547–564.

Harris, H. and Kalmus, H. 1949. The measurement of taste sensitivity to phenylthiourea (P.T.C.). Ann. Eugenics 15, 24–31.

Hoon, M. A., Adler, E., Lindemeier, J., Battey, J. F., Ryba, N. J., and Zuker, C. S. 1999. Putative mammalian taste receptors: a class of taste-specific GPCRs with distinct topographic selectivity. Cell 96, 541–551.

Hoshishima, K., Yokoyama, S., and Seto, K. 1962. Taste sensitivity in various strains of mice. Am. J. Physiol. 202, 1200–1204.

Huang, A. L., Chen, X., Hoon, M. A., Chandrashekar, J., Guo, W., Trankner, D., Ryba, N. J., and Zuker, C. S. 2006. The cells and logic for mammalian sour taste detection. Nature 442, 934–938.

Inomata, N., Goto, H., Itoh, M., and Isono, K. 2004. A single-amino-acid change of the gustatory receptor gene, Gr5a, has a major effect on trehalose sensitivity in a natural population of *Drosophila melanogaster*. Genetics 167, 1749–1758.

Inoue, M., Beauchamp, G. K., and Bachmanov, A. A. 2004a. Gustatory neural responses to umami taste stimuli in C57BL/6ByJ and 129P3/J mice. Chem. Senses 29, 789–795.

Inoue, M., Li, X., Mccaughey, S. A., Beauchamp, G. K., and Bachmanov, A. A. 2001a. Soa genotype selectively affects mouse gustatory neural responses to sucrose octaacetate. Physiol. Genomics 5, 181–186.

Inoue, M., McCaughey, S. A., Bachmanov, A. A., and Beauchamp, G. K. 2001b. Whole nerve chorda tympani responses to sweeteners in C57BL/6ByJ and 129P3/J mice. Chem. Senses 26, 915–923.

Inoue, M., Reed, D. R., Li, X., Tordoff, M. G., Beauchamp, G. K., and Bachmanov, A. A. 2004b. Allelic variation of the *Tas1r3* taste receptor gene selectively affects behavioral and neural taste responses to sweeteners in the F_2 hybrids between C57BL/6ByJ and 129P3/J mice. J. Neurosci. 24, 2296–2303.

Ishimaru, Y., Inada, H., Kubota, M., Zhuang, H., Tominaga, M., and Matsunami, H. 2006. Transient receptor potential family members PKD1L3 and PKD2L1 form a candidate sour taste receptor. Proc. Natl. Acad. Sci. U. S. A. 103, 12569–12574.

Ishimaru, Y., Okada, S., Naito, H., Nagai, T., Yasuoka, A., Matsumoto, I., and Abe, K. 2005. Two families of candidate taste receptors in fishes. Mech. Dev. 122, 1310–1321.

Isono, K., Morita, H., Kohatsu, S., Ueno, K., Matsubayashi, H., and Yamamoto, M. T. 2005. Trehalose sensitivity of the gustatory receptor neurons expressing wild-type, mutant and ectopic Gr5a in Drosophila. Chem. Senses 30(Suppl.1), i275–i276.

Jiang, P., Cui, M., Ji, Q., Snyder, L., Liu, Z., Benard, L., Margolskee, R. F., Osman, R., and Max, M. 2005a. Molecular mechanisms of sweet receptor function. Chem. Senses 30(Suppl. 1), i17–i18.

Jiang, P., Cui, M., Zhao, B., Snyder, L. A., Benard, L. M., Osman, R., Max, M., and Margolskee, R. F. 2005b. Identification of the cyclamate interaction site within the transmembrane domain of the human sweet taste receptor subunit T1R3. J. Biol. Chem. 280, 34296–34305.

Jiang, P., Ji, Q., Liu, Z., Snyder, L. A., Benard, L. M., Margolskee, R. F., and Max, M. 2004. The cysteine-rich region of T1R3 determines responses to intensely sweet proteins. J. Biol. Chem. 279, 45068–45075.

Kachele, D. L. and Lasiter, P. S. 1990. Murine strain differences in taste responsivity and organization of the rostral nucleus of the solitary tract. Brain Res. Bull. 24, 239–247.

Kalmus, H. 1971. Genetics of Taste. In: Handbook of Sensory Physiology (*ed*. L. M. Beidler), pp. 165–179. Springer.

Kampov-Polevoy, A. B., Eick, C., Boland, G., Khalitov, E., and Crews, F. T. 2004. Sweet liking, novelty seeking, and gender predict alcoholic status. Alcoholism: Clin. Exp. Res. 28, 1291–1298.

Kampov-Polevoy, A., Garbutt, J. C., and Janowsky, D. 1997. Evidence of preference for a high-concentration sucrose solution in alcoholic men. Am. J. Psychiatry 154, 269–270.

Kampov-Polevoy, A. B., Garbutt, J. C., and Khalitov, E. 2003. Family history of alcoholism and response to sweets. Alcoholism: Clin. Exp. Res. 27, 1743–1749.

Kare, M. R. 1961. Comparative Aspects of the Sense of Taste. In: Physiological and Behavioral Aspects of Taste (*eds*. M. R. Kare and B. P. Halpern). The University of Chicago Press.

Khan, G. J., Mehmood, R., Salah Ud, D., and Ihtesham Ul, H. 2003. Effects of long-term use of tobacco on taste receptors and salivary secretion. J. Ayub Med. College Abbottabad 15, 15, 37–39.

Kim, U. K. and Drayna, D. 2005. Genetics of individual differences in bitter taste perception: lessons from the PTC gene. Clin. Genet. 67, 275–280.

Kim, U. K., Breslin, P. A., Reed, D., and Drayna, D. 2004. Genetics of human taste perception. J. Dental Res. 83, 448–453.

Kim, U. K., Jorgenson, E., Coon, H., Leppert, M., Risch, N., and Drayna, D. 2003. Positional cloning of the human quantitative trait locus underlying taste sensitivity to phenylthiocarbamide. Science 299, 1221–1225.

Kim, U. K., Wooding, S., Riaz, N., Jorde, L. B., and Drayna, D. 2006. Variation in the human TAS1R taste receptor genes. Chem. Senses 31, 599–611.

Kitagawa, M., Kusakabe, Y., Miura, H., Ninomiya, Y., and Hino, A. 2001. Molecular genetic identification of a candidate receptor gene for sweet taste. Biochem. Biophys. Res. Commun. 283, 236–242.

Klein, T. W. and Defries, J. C. 1970. Similar polymorphism of taste sensitivity to PTC in mice and men. Nature 225, 555–557.

Kuhn, C., Bufe, B., Winnig, M., Hofmann, T., Frank, O., Behrens, M., Lewtschenko, T., Slack, J. P., Ward, C. D., and Meyerhof, W. 2004. Bitter taste receptors for saccharin and acesulfame K. J. Neurosci. 24, 10260–10265.

Lagerstrom, M. C., Hellstrom, A. R., Gloriam, D. E., Larsson, T. P., Schioth, H. B., and Fredriksson, R. 2006. The G protein-coupled receptor subset of the chicken genome. PLoS Comput. Biol. 2, e54.

Lanier, S. A., Hayes, J. E., and Duffy, V. B. 2005. Sweet and bitter tastes of alcoholic beverages mediate alcohol intake in of-age undergraduates. Physiol. Behav. 83, 821–831.

Le Roy, I., Pager, J., and Roubertoux, P. L. 1999. Genetic dissection of gustatory sensitivity to bitterness (sucrose octaacetate) in mice. C. R. Acad. Sci. Série III 322, 831–836.

Lemon, C. H., Brasser, S. M., and Smith, D. V. 2004. Alcohol activates a sucrose-responsive gustatory neural pathway. J. Neurophysiol. 92, 536–544.

Li, X., Bachmanov, A. A., Li, S., Chen, Z., Tordoff, M. G., Beauchamp, G. K., De Jong, P. J., Wu, C., Chen, L., West, D. B., Ross, D. A., Ohmen, J. D., and Reed, D. R. 2002a. Genetic, physical, and comparative map of the subtelomeric region of mouse Chromosome 4. Mamm. Genome 13, 5–19.

Li, X., Inoue, M., Reed, D. R., Huque, T., Puchalski, R. B., Tordoff, M. G., Ninomiya, Y., Beauchamp, G. K., and Bachmanov, A. A. 2001. High-resolution genetic mapping of the saccharin preference locus (Sac) and the putative sweet taste receptor (T1R1) gene (Gpr70) to mouse distal Chromosome 4. Mamm. Genome 12, 13–16.

Li, X., Li, W., Wang, H., Cao, J., Maehashi, K., Huang, L., Bachmanov, A. A., Reed, D. R., Legrand-Defretin, V., Beauchamp, G. K., and Brand, J. G. 2005. Pseudogenization of a sweet-receptor gene accounts for cats' indifference toward sugar. PLoS Genet. 1, 27–35.

Li, X., Staszewski, L., Xu, H., Durick, K., Zoller, M., and Adler, E. 2002b. Human receptors for sweet and umami taste. Proc. Natl. Acad. Sci. U. S. A. 99, 4692–4696.

Liao, J. and Schultz, P. G. 2003. Three sweet receptor genes are clustered in human chromosome 1. Mamm. Genome 14, 291–301.

Liman, E. R. 2006. Use it or lose it: molecular evolution of sensory signaling in primates. Pflugers Arch. 453, 125–131.

Lindemann, B. 2000. A taste for umami. Nat. Neurosci. 3, 99–100.

Lugaz, O., Pillias, A. M., and Faurion, A. 2002. A new specific ageusia: some humans cannot taste L-glutamate. Chem. Senses 27, 105–115.

Lush, I. E. 1981. The genetics of tasting in mice. I. Sucrose octaacetate. Genet. Res. 38, 93–95.

Lush, I. E. 1982. The genetics of tasting in mice. II. Strychnine. Chem. Senses 7, 93–98.

Lush, I. E. 1984. The genetics of tasting in mice. III. Quinine. Genet. Res. 44, 151–160.

Lush, I. E. 1986. The genetics of tasting in mice. IV. The acetates of raffinose, galactose and beta-lactose. Genet. Res. 47, 117–123.

Lush, I. E. 1989. The genetics of tasting in mice. VI. Saccharin, acesulfame, dulcin and sucrose. Genet. Res. 53, 95–99.

Lush, I. E. 1991. The Genetics of Bitterness, Sweetness, and Saltiness in Strains of Mice. In: Genetics of Perception and Communication (*eds*. C. J. Wysocki and M. R. Kare). Dekker.

Lush, I. E. and Holland, G. 1988. The genetics of tasting in mice. V. Glycine and cycloheximide. Genet. Res. 52, 207–212.

Lush, I. E., Hornigold, N., King, P., and Stoye, J. P. 1995. The genetics of tasting in mice. VII. Glycine revisited, and the chromosomal location of Sac and Soa. Genet. Res. 66, 167–174.

Manita, S., Bachmanov, A. A., Li, X., Beauchamp, G. K., and Inoue, M. 2006. Is glycine ''sweet'' to mice? Mouse strain differences in perception of glycine taste. Chem. Senses 31, 785–793.

Maruyama, Y., Pereira, E., Margolskee, R. F., Chaudhari, N., and Roper, S. D. 2006. Umami responses in mouse taste cells indicate more than one receptor. J. Neurosci. 26, 2227–2234.

Matson, K. D., Millam, J. R., and Klasing, K. C. 2000. Taste threshold determination and side-preference in captive cockatiels (*Nymphicus hollandicus*). Appl. Anim. Behav. Sci. 69, 313–326.

Matson, K. D., Millam, J. R., and Klasing, K. C. 2001. Thresholds for sweet, salt, and sour taste stimuli in cockatiels (*Nymphicus hollandicus*). Zoo Biol. 20, 1–13.

Matsunami, H., Montmayeur, J. P., and Buck, L. B. 2000. A family of candidate taste receptors in human and mouse. Nature 404, 601–604.

Mattes, R. D. 1994. Influences on acceptance of bitter foods and beverages. Physiol. Behav. 56, 1229–1236.

Max, M., Shanker, Y. G., Huang, L., Rong, M., Liu, Z., Campagne, F., Weinstein, H., Damak, S., and Margolskee, R. F. 2001. Tas1r3, encoding a new candidate taste receptor, is allelic to the sweet responsiveness locus Sac. Nat. Genet. 28, 58–63.

McCaughey, S. A. 2007. Taste-evoked responses to sweeteners in the nucleus of the solitary tract differ between C57BL/6ByJ and 129P3/J mice. J. Neurosci. 27, 35–45.

McClearn, G. E. and Rodgers, D. 1961. Genetic factors in alcohol preference of laboratory mice. J. Comp. Physiol. Psychol. 54, 116–119.

McClearn, G. E. and Rodgers, D. A. 1959. Differences in alcohol preference among inbred strains of mice. Q. J. Stud. Alcohol 20, 691–695.

Mela, D. J. 1989. Gustatory function and dietary habits in users and nonusers of smokeless tobacco. Am. J. Clin. Nutr. 49, 482–489.

Mela, D. J., Mattes, R. D., Tanimura, S., and Garcia-Medina, M. R. 1992. Relationships between ingestion and gustatory perception of caffeine. Pharmacol. Biochem. Behav. 43, 513–521.

Mennella, J. A., Pepino, M. Y., and Reed, D. R. 2005. Genetic and environmental determinants of bitter perception and sweet preferences. Pediatrics 115, e216–222.

Meyerhof, W. 2005. Elucidation of mammalian bitter taste. Rev. Physiol. Biochem. Pharmacol. 154, 37–72.

Midkiff, E. E., Bernstein, I. L., Fitts, D. A., and Simpson, J. B. 1985. Salt preference and salt appetite of Fischer-344 rats. Chem. Senses 10, 446.

Miyamoto, T., Fujiyama, R., Okada, Y., and Sato, T. 1999. Strain difference in amiloride-sensitivity of salt-induced responses in mouse non-dissociated taste cells. Neurosci. Lett. 277, 13–16.

Montmayeur, J. P., Liberles, S. D., Matsunami, H., and Buck, L. B. 2001. A candidate taste receptor gene near a sweet taste locus. Nat. Neurosci. 4, 492–498.

Moon, S. J., Kottgen, M., Jiao, Y., Xu, H., and Montell, C. 2006. A taste receptor required for the caffeine response *in vivo*. Curr. Biol. 16, 1812–1817.

Mueller, K. L., Hoon, M. A., Erlenbach, I., Chandrashekar, J., Zuker, C. S., and Ryba, N. J. P. 2005. The receptors and coding logic for bitter taste. Nature 434, 225–229.

Nelson, G., Chandrashekar, J., Hoon, M. A., Feng, L., Zhao, G., Ryba, N. J., and Zuker, C. S. 2002. An amino-acid taste receptor. Nature 416, 199–202.

Nelson, G., Hoon, M. A., Chandrashekar, J., Zhang, Y., Ryba, N. J., and Zuker, C. S. 2001. Mammalian sweet taste receptors. Cell 106, 381–390.

Nelson, T. M., Munger, S. D., and Boughter, J. D., Jr. 2003. Taste sensitivities to PROP and PTC vary independently in mice. Chem. Senses 28, 695–704.

Nelson, T. M., Munger, S. D., and Boughter, J. D., Jr. 2005. Haplotypes at the Tas2r locus on distal chromosome 6 vary with quinine taste sensitivity in inbred mice. BMC Genet. 6, 32.

Nie, Y., Vigues, S., Hobbs, J. R., Conn, G. L., and Munger, S. D. 2005. Distinct contributions of T1R2 and T1R3 taste receptor

subunits to the detection of sweet stimuli. Curr. Biol. 15, 1948–1952.
Ninomiya, Y. 1996. Salt taste responses of mouse chorda tympani neurons: evidence for existence of two different amiloride-sensitive receptor components for NaCl with different temperature dependencies. J. Neurophysiol. 76, 3550–3554.
Ninomiya, Y. and Funakoshi, M. 1989. Behavioural discrimination between glutamate and the four basic taste substances in mice. Comp. Biochem. Physiol. 92, 365–370.
Ninomiya, Y., Higashi, T., Mizukoshi, T., and Funakoshi, M. 1987. Genetics of the ability to perceive sweetness of D-phenylalanine in mice. Ann. N. Y. Acad. Sci. 510, 527–529.
Ninomiya, Y., Mizukoshi, T., Higashi, T., Katsukawa, H., and Funakoshi, M. 1984. Gustatory neural responses in three different strains of mice. Brain Res. 302, 305–314.
Ninomiya, Y., Nomura, T., and Katsukawa, H. 1992. Genetically variable taste sensitivity to D-amino acids in mice. Brain Res. 596, 349–352. Dekker.
Ninomiya, Y., Sako, N., and Funakoshi, M. 1989. Strain differences in amiloride inhibition of NaCl responses in mice, *Mus musculus*. J. Comp. Physiol. 166, 1–5.
Ninomiya, Y., Sako, N., Katsukawa, H., and Funakoshi, M. 1991. Taste Receptor Mechanisms Influenced by a Gene on Chromosome 4 in Mice. In: Genetics of Perception and Communication (*eds*. C. J. Wysocki and M. R. Kare), pp. 267–278.
Overstreet, D. H., Kampov-Polevoy, A. B., Rezvani, A. H., Murelle, L., Halikas, J. A., and Janowsky, D. S. 1993. Saccharin intake predicts ethanol intake in genetically heterogeneous rats as well as different rat strains. Alcoholism: Clin. Exp. Res. 17, 366–369.
Parry, C. M., Erkner, A., and Le Coutre, J. 2004. Divergence of T2R chemosensory receptor families in humans, bonobos, and chimpanzees. Proc. Natl. Acad. Sci. U. S. A. 101, 14830–14834.
Peirce, J. L., Lu, L., Gu, J., Silver, L. M., and Williams, R. W. 2004. A new set of BXD recombinant inbred lines from advanced intercross populations in mice. BMC Genet. 5, 7.
Pelz, W. E., Whitney, G., and Smith, J. C. 1973. Genetic influences on saccharin preference of mice. Physiol. Behav. 10, 263–265.
Phillips, T. J., Crabbe, J. C., Metten, P., and Belknap, J. K. 1994. Localization of genes affecting alcohol drinking in mice. Alcoholism: Clin. Exp. Res. 18, 931–941.
Pomerleau, C. S., Marks, J. L., Pomerleau, O. F., and Snedecor, S. M. 2004. Relationship between early experiences with tobacco and early experiences with alcohol. Addictive Behav. 29, 1245–1251.
Ramirez, I. and Fuller, J. L. 1976. Genetic influence on water and sweetened water consumption in mice. Physiol. Behav. 16, 163–168.
Reed, D. R., Bachmanov, A. A., Beauchamp, G. K., Tordoff, M. G., and Price, R. A. 1997. Heritable variation in food preferences and their contribution to obesity. Behav. Genet. 27, 373–387.
Reed, D. R., Li, S., Li, X., Huang, L., Tordoff, M. G., Starling-Roney, R., Taniguchi, K., West, D. B., Ohmen, J. D., Beauchamp, G. K., and Bachmanov, A. A. 2004. Polymorphisms in the taste receptor gene (*Tas1r3*) region are associated with saccharin preference in 30 mouse strains. J. Neurosci. 24, 938–946.
Reed, D. R. and McDaniel, A. H. 2006. The human sweet tooth. BMC Oral Health 6(Suppl. 1), S17.
Richter, C. 1932. Mineral appetite of parathyroidectomized rats. Am. J. Med. Sci. 9, 9.
Richter, T. A. and Clisby, K. H. 1941. Phenylthiocarbamide taste thresholds of rats and human beings. Am. J. Physiol. 134, 157–164.
Robinson, S. F., Marks, M. J., and Collins, A. C. 1996. Inbred mouse strains vary in oral self-selection of nicotine. Psychopharmacology (Berl.) 124, 332–339.
Rodgers, D. A. and McClearn, G. E. 1962. Mouse strain differences in preference for various concentrations of alcohol. Q. J. Stud. Alcohol 23, 26–33.
Sainz, E., Korley, J. N., Battey, J. F., and Sullivan, S. L. 2001. Identification of a novel member of the T1R family of putative taste receptors. J. Neurochem. 77, 896–903.
Salbe, A. D., Delparigi, A., Pratley, R. E., Drewnowski, A., and Tataranni, P. A. 2004. Taste preferences and body weight changes in an obesity-prone population. Am. J. Clin. Nutr. 79, 372–378.
Sandell, M. A. and Breslin, P. A. 2006. Variability in a taste-receptor gene determines whether we taste toxins in food. Current Biol. 16, R792–R794.
Sato, K., Endo, S., and Tomita, H. 2002. Sensitivity of three loci on the tongue and soft palate to four basic tastes in smokers and non-smokers. Acta Otolaryngol. 2002, 74–82.
Scott, T. R. 2001. The role of taste in feeding. Appetite 37, 111–113.
Shi, P. and Zhang, J. 2006. Contrasting modes of evolution between vertebrate sweet/umami receptor genes and bitter receptor genes. Mol. Biol. Evol. 23, 292–300.
Shi, P., Zhang, J., Yang, H., and Zhang, Y. P. 2003. Adaptive diversification of bitter taste receptor genes in mammalian evolution. Mol. Biol. Evol. 20, 805–814.
Shigemura, N., Yasumatsu, K., Yoshida, R., Sako, N., Katsukawa, H., Nakashima, K., Imoto, T., and Ninomiya, Y. 2005. The role of the dpa locus in mice. Chem. Senses 30(Suppl. 1), i84–i85.
Shingai, T. and Beidler, L. M. 1985. Interstrain differences in bitter taste responses in mice. Chem. Senses 10, 51–55.
Snedecor, S. M., Pomerleau, C. S., Mehringer, A. M., Ninowski, R., and Pomerleau, O. F. 2006. Differences in smoking-related variables based on phenylthiocarbamide ''taster'' status. Addictive Behav. 31, 2309–2312.
Sollars, S. I., Midkiff, E. E., and Bernstein, I. L. 1990. Genetic transmission of NaCl aversion in the Fisher-344 rat. Chem. Senses 15, 521–527.
Soranzo, N., Bufe, B., Sabeti, P. C., Wilson, J. F., Weale, M. E., Marguerie, R., Meyerhof, W., and Goldstein, D. B. 2005. Positive selection on a high-sensitivity allele of the human bitter-taste receptor TAS2R16. Curr. Biol. 15, 1257–1265.
Spielman, A. I., Huque, T., Whitney, G., and Brand, J. G. 1992. The diversity of bitter taste signal transduction mechanisms. Soc. Gen. Physiol. Ser. 47, 307–324.
St. John, S. J., Pour, L., and Boughter, J. D., Jr. 2005. Phenylthiocarbamide produces conditioned taste aversions in mice. Chem. Senses 30, 377–382.
Stewart, R. B., Bice, P., Foroud, T., Lumeng, L., Li, T. K., and Carr, L. G. 2003. Correlation of saccharin and ethanol intake in the F2 progeny of HAD2 and LAD2 crosses. Alcoholism: Clin. Exp. Res. 27, 49A.
Tichansky, D. S., Boughter, J. D., Jr., and Madan, A. K. 2006. Taste change after laparoscopic Roux-en-Y gastric bypass and laparoscopic adjustable gastric banding. Surg. Obes. Relat. Dis. 2, 440–444.
Tordoff, M. G. and Bachmanov, A. A. 2003. Mouse taste preference tests: why only two bottles? Chem. Senses 28, 315–324.
Tordoff, M. G., Bachmanov, A. A., and Reed, D. R. 2007. Forty mouse strain survey of water and sodium intake. Physiol. Behav. Apr. 1 (Epub ahead of print).
Ueno, K., Ohta, M., Morita, H., Mikuni, Y., Nakajima, S., Yamamoto, K., and Isono, K. 2001. Trehalose sensitivity in

Drosophila correlates with mutations in and expression of the gustatory receptor gene Gr5a. Curr. Biol. 11, 1451–1455.
Wang, X., Thomas, S. D., and Zhang, J. 2004. Relaxation of selective constraint and loss of function in the evolution of human bitter taste receptor genes. Hum. Mol. Genet. 13, 2671–2678.
Warren, R. P. and Lewis, R. C. 1970. Taste polymorphism in mice involving a bitter sugar derivative. Nature 227, 77–78.
Whitney, G. and Harder, D. B. 1986a. PTC preference among laboratory mice: understanding of a previously ''unreplicated'' report. Behav. Genet. 16, 409–416.
Whitney, G. and Harder, D. B. 1986b. Single locus control of sucrose octaacetate tasting among mice. Behav. Genet. 16, 559–574.
Whitney, G. and Harder, D. B. 1994. Genetics of bitter perception in mice. Physiol. Behav. 56, 1141–1147.
Whitney, G., Harder, D. B., and Gannon, K. S. 1989. The B6.SW bilineal congenic sucrose octaacetate (SOA)-taster mice. Behav. Genet. 19, 409–416.
Winnig, M., Bufe, B., and Meyerhof, W. 2005. Valine 738 and lysine 735 in the fifth transmembrane domain of rTas1r3 mediate insensitivity towards lactisole of the rat sweet taste receptor. BMC Neurosci. 6, 22.
Wooding, S. 2006. Phenylthiocarbamide: a 75-year adventure in genetics and natural selection. Genetics 172, 2015–2023.
Wooding, S., Kim, U. K., Bamshad, M. J., Larsen, J., Jorde, L. B., and Drayna, D. 2004. Natural selection and molecular evolution in PTC, a bitter-taste receptor gene. Am. J. Hum. Genet. 74, 637–646.
Wu, S. V., Chen, M. C., and Rozengurt, E. 2005. Genomic organization, expression, and function of bitter taste receptors (T2R) in mouse and rat. Physiol. Genomics 22, 139–149.
Xu, H., Staszewski, L., Tang, H., Adler, E., Zoller, M., and Li, X. 2004. Different functional roles of T1R subunits in the heteromeric taste receptors. Proc. Natl. Acad. Sci. U. S. A. 101, 14258–14263.
Yamamoto, M. E., Block, G. D., and Ishii, E. 1991. Food patterns among adolescents: influence of alcohol consumption. Alcoholism: Clin. Exp. Res. 15, 359.
Zhao, G. Q., Zhang, Y., Hoon, M. A., Chandrashekar, J., Erlenbach, I., Ryba, N. J., and Zuker, C. S. 2003. The receptors for mammalian sweet and umami taste. Cell 115, 255–266.

Relevant Websites

http://www.ensembl.org – Ensemble browser of sequenced genomes.
http://www.ncbi.nlm.nih.gov/gquery – Entrez (National Center for Biotechnology Information cross-database search).
http://www.ncbi.nlm.nih.gov/Genbank – GenBank.
http://gdbwww.gdb.org/gdb – Human Genome Database.
http://www.monell.org/MMTPP – Monell Mouse Taste Phenotyping Project.
http://www.informatics.jax.org – Mouse Genome Database.
http://www.jax.org/phenome – Mouse Phenome Database.
http://www.ncbi.nlm.nih.gov/mapview – National Center for Biotechnology Information browser of sequenced genomes.
http://rgd.mcw.edu – Rat Genome Database.
http://genome.ucsc.edu – University of California Santa Cruz browser of sequenced genomes.

4.20 Propylthiouracil (PROP) Taste

D J Snyder, Yale University, New Haven, CT, USA

V B Duffy, University of Connecticut, Storrs, CT, USA

J E Hayes, Brown University, Providence, RI, USA

L M Bartoshuk, University of Florida, Gainesville, FL, USA

© 2008 Elsevier Inc. All rights reserved.

4.20.1	Discovery of Taste Blindness	392
4.20.2	New Psychophysical Methods and the Discovery of Supertasters	392
4.20.2.1	Visual Analog Scales and Category Scales: Invalid for Across-Group Psychophysical Comparisons	392
4.20.2.2	Magnitude Matching	393
4.20.2.3	Supertasting, Oral Burn, and Oral Touch	394
4.20.2.4	Pathology	394
4.20.2.5	How Are Supertasters Defined?	394
4.20.2.6	Supertasters and Flavor	396
4.20.3	Implications of Oral Sensory Variation for Nutrition and Health	396
4.20.3.1	Cancer Risk	396
4.20.3.2	Cardiovascular Disease Risk	397
4.20.3.3	Alcohol Intake	397
4.20.3.4	Smoking	397
4.20.3.5	Future Interventions?	397
References		397

Glossary

category scale A method of rating perceived intensity in which subjects place ratings in categories (e.g., a 9-point scale, in which 1 = very weak, 5 = medium, and 9 = very strong).

chorda tympani A branch of the facial nerve (cranial nerve VII) that carries taste information from the mobile, anterior two-thirds of the tongue.

flavor The combined sensations of taste, oral somatosensation, and retronasal olfaction.

gLMS General labeled magnitude scale, a method of rating perceived intensity. The scale is a numbered line running from 0 = no sensation to 100 = strongest imaginable sensation of any kind with intermediate labels: 1.4 = barely detectable, 6 = weak, 16 = moderate, 35 = strong, and 53 = very strong. This spacing of labels gives the scale ratio properties, that is, a rating of 40 denotes a perceived intensity twice as strong as a rating of 20.

magnitude matching A method of rating-perceived intensity that permits valid comparisons across groups. This technique depends on the ability of subjects to match the intensities of different types of sensations. Subjects rate the perceived intensities of stimuli of interest relative to an unrelated standard. By assuming that variability in the intensity of the standard is equivalent across two or more groups, magnitude matching permits group comparisons of the stimulus of interest.

orthonasal olfaction Odor sensations arising from environmental stimuli that are sniffed.

PROP 6-*n*-Propylthiouracil, a compound that binds to the T2R38 receptor and to which some individuals are taste blind.

PTC Phenylthiocarbamide, a compound that binds to the T2R38 receptor and to which some individuals are taste blind.

retronasal olfaction Odor sensations arising from foods in the mouth; these are pumped into the nasal cavity via the rear of the throat during chewing and swallowing.

supertaster An individual who experiences the most intense oral sensations (i.e., taste, oral burn, oral touch) and the most intense retronasal olfactory sensations.
tastant A substance that evokes a taste sensation.
VAS Visual analog scale, a method of rating-perceived intensity in which subjects mark a line labeled with the minimum and maximum intensities possible for a given sensory experience.

4.20.1 Discovery of Taste Blindness

Taste blindness was discovered by accident in 1931. Arthur Fox, a chemist working for DuPont de Nemours, synthesized some phenylthiocarbamide (PTC), and when he attempted to put the compound into a bottle, some of it escaped. One of his colleagues, Dr. C. R. Noller, an eminent organic chemist, noticed a bitter taste; Fox did not. Testing co-workers (Fox, A. L., 1931) revealed that the majority tasted PTC as bitter. When Fox and a prominent geneticist of the day asked 2550 attendees at a meeting of the American Association for the Advancement of Science to vote on the quality of taste from PTC crystals (Blakeslee, A. F. and Fox, A. L., 1932), they confirmed that most tasted bitter (tasters) but a substantial number (28%) did not (nontasters). When *The Journal of Heredity* published these data, the editor had small pieces of filter paper impregnated with PTC inserted into the journal. Readers could purchase these PTC papers which facilitated testing of a variety of groups (e.g., the Dionne quintuplets were all tasters; Ford, N. and Mason, A. D., 1941). Family studies (Snyder, L. H., 1931) suggested that nontasting was recessive.

The informal testing of that era was displaced by more quantitative threshold methodology (Harris, H. and Kalmus, H., 1949) that produced the now-familiar bimodal distribution of PTC thresholds. Evaluation of a series of compounds showed that those containing the N–C═S group (including PTC and 6-*n*-propylthiouracil (PROP)) produced the bimodal distribution. Studies in this early era focused on assessing percentages of tasters by race, sex, and various disease states.

Fischer brought new insights to taste blindness. He stopped using PTC and switched to PROP because it lacked the sulfurous odor of PTC. In addition, he added an assessment for quinine; he reasoned that PROP thresholds assessed a specific sensitivity while quinine thresholds assessed a general ability to taste (Fischer, R., 1967). He began to consider the implications of sensory variation for behavior relevant to health; he found associations between taste thresholds (PROP and quinine) and food preferences, alcohol abuse, cigarette smoking, and body weight.

Most recently, Drayna's group found that the gene for PTC/PROP tasting is located on chromosome 7 (Kim, U. K. *et al.*, 2003). Those individuals with nontaster thresholds (PROP threshold > 0.0002 M) were homozygous for the recessive allele; those with taster thresholds (PROP threshold < 0.0001 M) were either homozygous for the dominant allele or were heterozygous. The human genome project has resulted in the discovery of a variety of other taste-related genes as well (e.g., Mombaerts, P., 2004). In the future, the elucidation of ligands for the receptors expressed by those genes and the development of more accurate methods for oral sensory genotype/phenotype analysis will make possible more detailed studies of the associations between oral sensation and health.

4.20.2 New Psychophysical Methods and the Discovery of Supertasters

4.20.2.1 Visual Analog Scales and Category Scales: Invalid for Across-Group Psychophysical Comparisons

Fischer lacked the psychophysical tools we have today, but his speculations on health outcomes associated with genetic differences in taste foreshadowed the results that are now emerging. With the new tools that modern scaling studies provide, the magnitude of the associations between sensation and behavior can finally be quantified.

The search for associations between diet, smoking, alcohol intake, and the ability to taste PROP requires comparisons between the sensations

experienced by nontasters and tasters. Unfortunately, many of the studies searching for these associations used labeled scales (e.g., visual analog scale (VAS) and category scales like the Natick 9-point scale or the labeled magnitude scale (Green, B. G. *et al.*, 1993)). Comparisons across nontasters and tasters cannot be made with these scales. That is, these scales are valid for making within-subject comparisons or making comparisons across groups where the group members are randomly selected, but they are invalid for making across-group comparisons. The explanation will be briefly reviewed here but the interested reader is referred to more complete treatments of the issue (Bartoshuk, L. M. 2002; Bartoshuk, L. M. *et al.*, 2002; Bartoshuk, L. M. *et al.*, 2004a; 2005b; Snyder, D. J. *et al.*, 2004; Bartoshuk, L. M. *et al.*, 2006b).

VAS and category scales are usually anchored in terms of the minimum and maximum of the sensation to be measured. For example, a VAS used to assess sweetness was a line labeled "not at all" at one end and "extremely" at the other end (Salbe, A. D. *et al.*, 2004); similarly, a 9-point category scale for sweetness was labeled 1 = "not at all" and 9 = "extremely" (Drewnowski, A. *et al.*, 1997). Intermediate values on category scales may be labeled as well; another 9-point category scale was labeled 1 = "none," 3 = "slight," 5 = "moderate," 7 = "strong," and 9 = "extreme" (Kamen, J., 1959).

Unfortunately, the intensity labels on these scales do not denote the same perceived intensities to all. Suppose that groups of nontasters and tasters were presented with a series of sucrose solutions varying in concentration from near threshold to very concentrated and asked to select one they would describe as strong. In this situation, nontasters and tasters would select similar concentrations. However, if they were then asked to don earphones and set the loudness of a tone to match the sweetness of the sucrose they had selected, the two groups would behave differently. The nontasters would match the sweetness they experienced to a lower tone intensity than would the tasters. Since we have no reason to believe that nontasters and tasters hear differently, this result shows that nontasters experienced less sweetness than did the tasters even though both groups described the sweetness as strong (e.g., see Bartoshuk, L. M. and Snyder, D. J. 2004 or Snyder, D. J. *et al.*, 2004 for the data on which this example was based).

In other words, intensity descriptors are relative. The mental intensity ruler that we apply to sensations behaves as if it were printed on elastic; this ruler expands or contracts with the sensory domain of interest, the physiological capacity of that domain, and the individual's experience. The relativity of intensity descriptors was captured in a dramatic quote from Stevens S. S. (1958, p. 633): "Mice may be called large or small, and so may elephants, and it is quite understandable when someone says it was a large mouse that ran up the trunk of the small elephant."

Invalid comparisons have been discussed periodically throughout the history of scale development (e.g., Aitken, R. C. B. 1969; Narens, L. and Luce, R. D. 1983; Biernat, M. and Manis, M. 1994; Birnbaum, M. H. 1999). These errors most often result in the failure to see real differences, but occasionally they will produce erroneous differences that appear to go in the wrong direction (e.g., see the results for KCl taste in Schifferstein, H. N. J. and Frijters, J. E. R., 1991 and NaCl taste in Drewnowski, A. *et al.*, 1997). Most of the early failures to find differences between nontasters and tasters can be attributed to this measurement error.

4.20.2.2 Magnitude Matching

The sweetness experiment above demonstrates a serious problem with sensory measurement, but it also suggests a solution. When two groups apply the same intensity descriptor to a given sensory experience, this does not mean that the two groups are experiencing the same perceived intensity. In order to reveal differences in perceived intensities between two groups, members of those groups should be asked to compare the sensation of interest to an unrelated standard. There will be variation in the perception of the standard within each of the two groups, but if the standard is unrelated to the sensation of interest, that variation will be roughly the same for both groups. The use of an unrelated standard led to the formalization of the method of magnitude matching (Hall, M. J. *et al.*, 1975; Marks, L. E. and Stevens, J. C., 1980; Stevens, J. C. and Marks, L. E., 1980; Marks, L. E. *et al.*, 1988). Magnitude matching is feasible using any ratio method (e.g., magnitude estimation (Stevens, S. S., 1969), general labeled magnitude scale (Bartoshuk, L. M. *et al.*, 2004b), general VAS (Bartoshuk, L. M. *et al.*, 2005b)) that permits assessments of both sensations of interest and independent standards on the same scale. Recent work shows that these standards need not be actual stimuli, but may include remembered sensations (e.g., the brightest light ever seen, the loudest sound ever heard, the

strongest sensation of any kind ever experienced) (Bartoshuk, L. M. *et al.*, 2005b).

4.20.2.3 Supertasting, Oral Burn, and Oral Touch

As data collected with magnitude matching accumulated, significant differences among tasters became apparent. A subgroup of tasters were found to experience not only the greatest bitterness from PROP but also the greatest taste intensities from all other tastants as well. These supertasters also experienced the most intense burn from oral irritants (e.g., chili peppers) as well as the most intense oral tactile sensations (e.g., fats) (Duffy, V. B. *et al.*, 1996; Tepper, B. J. and Nurse, R. J. 1997; Prutkin, J. M. *et al.*, 2000; Hayes, J. E. *et al.*, 2007).

Insights from Miller's anatomical studies help to explain these associations. Miller, I. J. and Whitney G. (1989) discovered a relationship between taste intensity and taste bud density in mice, and they suggested that a similar relationship could explain human variation in taste intensity. They were correct; the density of fungiform papillae (i.e., structures that contain taste buds on the anterior tongue) shows great variability in humans. Moreover, the taste buds on fungiform papillae are surrounded by nerve fibers that mediate oral burn/pain sensations, and other areas on fungiform papillae are innervated by fibers that mediate oral touch sensations (e.g., see Bartoshuk, L. M. *et al.*, 2006a for a discussion). Thus, the more fungiform papillae an individual has, the more intense the experiences of taste, oral burn, and oral touch.

4.20.2.4 Pathology

Inhibition among brain regions mediating oral sensation also contributes to individual differences (e.g., Bartoshuk, L. M. *et al.*, 2005c). While widespread oral sensory damage compromises perceived taste intensity, damage to a localized part of this system can release inhibition in other parts, producing paradoxical increases in perceived taste intensity. Further, the presence of central interactions between the taste and trigeminal systems means that taste damage may intensify nontaste oral sensations. In short, oral sensory variation is the joint result of genetic, anatomical and pathological variation. One of the major goals of modern research into associations between sensory experience and health is to assess the degree of variance explained by each of these sources and their interactions (e.g., Dinehart, M. E. *et al.*, 2006).

Oral sensory pathology cannot be assessed without testing function at individual nerve fields in the mouth, mainly because disinhibition maintains the constancy of whole-mouth perception, thus masking local pathology. We assess regional oral sensation with a spatial test using scaling methodology that includes an unrelated standard (e.g., Dinehart, M. E. *et al.*, 2006).

4.20.2.5 How Are Supertasters Defined?

As our understanding of taste blindness has evolved, so too has our ability to assess oral sensory function accurately. The discovery of taste blindness involved a binary question: does PTC taste bitter or not (Fox, A. L., 1931)? Threshold testing (Fischer, R. and Griffin, F., 1964) subsequently led to quantitative criteria to classify subjects as nontasters or tasters of PROP, while the development of suprathreshold scaling methods subdivided tasters into supertasters and medium tasters (Bartoshuk, L. M. *et al.*, 1994). PROP supertasters proved to be supertasters in general – that is, they experience the most intense tastes from non-PROP tastants – and super-perceivers of oral burn and oral touch. Recent advances in anatomical and genetic assessment have added further complexity, but for historical and practical reasons, we believe that psychophysical criteria are the most important determinants of oral sensory function; after all, taster status should reflect how people actually experience taste.

We initially suspected that taste blindness arose from a single gene (i.e., supertasters = homozygous dominant, medium tasters = heterozygous, nontasters = recessive), but the discovery that fungiform papilla density correlates with suprathreshold PROP bitterness (Bartoshuk, L. M. *et al.*, 1994) suggested another possibility: supertasters of PROP might be tasters (homozygous or heterozygous) bearing the largest number of fungiform papillae. Fortunately, the identification of a gene (*T2R38*) encoding a PTC/PROP taste receptor (Kim, U. K. *et al.*, 2003) permitted further resolution. The most common alleles for this gene are distinguished by specific amino acid differences at crucial positions – Ala49Pro, Val262Ala, and Ile296Val – with the two most common haplotypes noted as PAV and AVI. Nontasters carry two recessive alleles (AVI/AVI), while tasters are heterozygous (PAV/AVI) or carry two dominant alleles (PAV/PAV). Genotype analysis

alone, however, is insufficient for classification, mainly because *T2R38* genotypes associate with threshold measures of PTC/PROP bitterness (Kim, U. K. *et al*., 2003), but not with suprathreshold measures. Individuals expressing PAV/PAV perceive slightly more suprathreshold PROP bitterness than do those expressing PAV/AVI, but the difference is too small to account for psychophysical measures of supertasting (Duffy, V. B. *et al*., 2004a).

Figure 1 demonstrates the utility of using only suprathreshold perceived intensity to define taster status. Threshold measures (left panel) divide subjects into the two groups identified in early studies (i.e., nontasters and tasters). But a different picture emerges when both of these groups are subdivided by suprathreshold PROP intensity (right panel). Consistent with our previous work, we separated subjects with taster thresholds (i.e., PAV/PAV or PAV/AVI) into those who perceive the least bitterness (i.e., medium tasters) and those who perceive the most (i.e., supertasters), resulting in greater group differences across a wider intensity range. When we separated subjects with nontaster thresholds (i.e., AVI/AVI) in the same fashion, we found that some of these individuals produce a suprathreshold function that classifies them as medium tasters. In other words, genetic analysis of *T2R38* fails to identify supertasters and includes among nontasters those who experience considerable bitterness from PROP.

Why is this? Recently, Hayes and Duffy (Hayes, J. E., 2007) showed that fungiform papilla density is largely independent of *T2R38* genotype. We previously reported (Bartoshuk, L. M. *et al*., 1994) that nontasters tend to have the fewest fungiform papillae, but that finding was an artifact caused by classifying subjects by both threshold and suprathreshold PROP bitterness. In fact, we excluded subjects with discordant results, such as those with nontaster thresholds who tasted PROP as fairly bitter, but we now know that those AVI/AVI individuals with the most fungiform papillae taste PROP as fairly bitter. These individuals are supertasters for many oral stimuli, but not for those that bind to T2R38 (e.g., PTC/PROP). *T2R38* variation fails to account for differences in perceived intensity because it fails to account for differences in oral anatomy.

The term supertaster was originally applied to those individuals who perceived the most intense taste sensations from a variety of taste stimuli, including PROP. We continue to support this view; taster status should reflect responses to multiple oral sensory cues. Because many oral sensations are influenced by anatomy, it might seem that anatomy is more accurate than PROP bitterness for classification, but pathology complicates the picture because damage to the taste system can alter oral perception while leaving fungiform papillae intact. In truth, anatomy, genetics and pathology help us to determine the underlying basis of oral sensation, but psychophysical assessment of perceived intensity remains the critical measure of oral sensory function – and the only way to identify supertasters. PROP

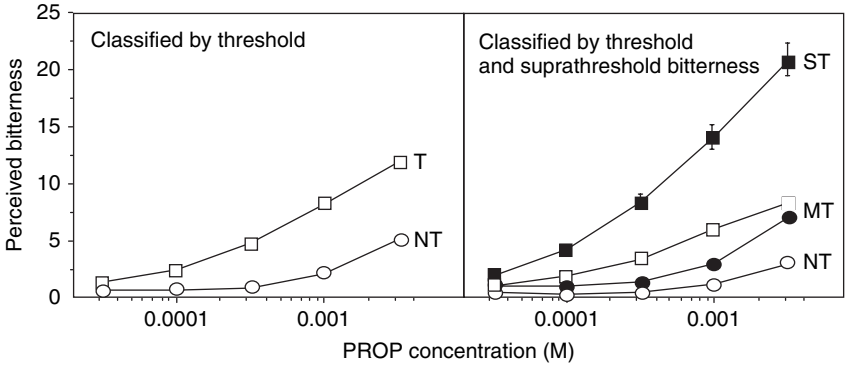

Figure 1 Bitterness of PROP (±SE) assessed with magnitude matching (i.e., magnitude estimation relative to a tone standard). The left panel shows the PROP functions for individuals with PROP thresholds > 0.0002 M (i.e., nontasters, NT, indicated by circles) and those with thresholds < 0.0001 M (i.e., tasters, T, indicated by squares). PROP thresholds strongly reflect different *T2R38* genotypes: NTs express AVI/AVI; Ts express PAV/AVI or PAV/PAV. The right panel shows the same groups subdivided into two groups each: those who tasted the least bitterness from PROP (open symbols) and those who tasted the most bitterness from PROP (filled symbols). The resulting intermediate function (i.e., medium tasters, MT) reflects a combination of PAV/PAV, PAV/AVI, and AVI/AVI genotypes. Data from Bartoshuk, L. M. 2000. Comparing sensory experiences across individuals: recent psychophysical advances illuminate genetic variation in taste perception. Chem. Senses 25, 447–460.

bitterness may provide only one picture of oral sensation, but it is quite a good picture because it represents the combined influences of *T2R38* genotype, fungiform papilla density, and disease. Oral sensation may be influenced by additional factors with uncertain impact (e.g., hormones, trophic factors, other taste/tactile genes), but PROP bitterness has proven valuable in identifying relationships between taste intensity, dietary choice, and long-term health outcomes (see below). That said, there is nothing intrinsically special about PTC/PROP except that it is a probe stimulus – one that elicits highly variable responses that often show strong agreement with other oral stimuli.

Because the functions of PROP bitterness across concentration diverge (right panel), the most accurate way to sort individuals based on PROP bitterness is to use the highest practical concentration; consistent with Figure 1, we typically use a 0.0032 M solution. An alternative to testing with PROP solutions is to use impregnated filter papers, similar to those used by Blakeslee A. F. and Fox A. L. (1932). To produce the most intense bitter taste possible with a paper test, we soak small pieces of filter paper (3 cm diameter, Whatman #1) in a saturated PROP solution (e.g., Bartoshuk, L. M. *et al.*, 2002), yielding ~1.6 mg PROP per paper. These PROP papers produce similar variability in perceived bitterness as a solution of 0.0032 M PROP.

4.20.2.6 Supertasters and Flavor

When food is consumed, the sensations we know as flavor result from mixtures of taste and oral somatosensory cues, as well as olfactory sensations produced when chewing and swallowing force food odors behind the palate and into the nasal cavity. These odor sensations are called retronasal to distinguish them from environmental odors that are sniffed, or orthonasal olfaction. Although both types of odor cues stimulate the same olfactory receptors high in the nasal cavity, retronasal olfaction is perceptually localized to the mouth and orthonasal olfaction to the nose; the two are processed in related but distinct brain regions (Small, D. M. and Jones-Gotman, M., 2001). For many years, the localization of retronasal olfaction to the mouth was thought to be mediated by oral touch (Hollingworth, H. L. and Poffenberger, A. T., 1917), but we now know that taste plays a critical role as well. If the chorda tympani taste nerve is anesthetized on one side of the mouth, retronasal olfactory cues are less intense and appear to arise from the unanesthetized side of the mouth (Fast, K. *et al.*, 2000; Snyder, D. J. *et al.*, 2001). This association explains a curious clinical phenomenon: some patients with compromised taste and oral touch report a normal ability to smell, yet they claim that flavors are diminished or absent. The brain appears to rely on the simultaneous presence of multiple cues to determine how to process incoming olfactory information – odor + sniffing = orthonasal olfaction; odor + taste + oral touch + oromotor activity = retronasal olfaction. In patients with normal smell but damaged innervation of the oral cavity, food-related odors may fail to be discriminated as retronasal because the concomitant oral cues that identify odor input as coming from the mouth are absent or reduced.

Connections between taste and retronasal olfaction suggest that perceptual differences associated with oral sensory genetics, anatomy, and pathology should extend to flavor perception; not surprisingly, supertasters perceive more intense flavors than do nontasters (Duffy, V. B. *et al.*, 2003; Bartoshuk, L. M. *et al.*, 2005a). This finding helps to explain interesting curiosities (e.g., chefs are more likely to be supertasters than chance would predict; Bartoshuk, L. M. *et al.*, 2004a), but more importantly, it contributes to robust differences in food behavior.

4.20.3 Implications of Oral Sensory Variation for Nutrition and Health

Food preferences influence food intake. Because diet is an important risk factor for a variety of chronic diseases, we have found that oral sensory variation is associated with several of these diseases. The methodological advances we have described enabled the discovery of these associations.

4.20.3.1 Cancer Risk

Links between PTC/PROP tasting and cancer first appeared some years ago (e.g., Milunicová, A. *et al.*, 1969), but more recent studies have specifically targeted oral sensory variation as a potential contributor to cancer risk. The bitter tastes of phytonutrients with cancer-preventive properties can be a barrier to their intake (Drewnowski, A. and Gomez-Carneros, C., 2000). PROP tasting is associated with reduced vegetable intake (Basson, M. D. *et al.*, 2005; Dinehart, M. E. *et al.*, 2006; Bell, K. I. and Tepper, B. J., 2006; Sandell, M. A. and Breslin, P. A., 2006). Those

who taste PROP as most bitter reported the lowest preferences for traditionally disliked vegetables (e.g., Brussels sprouts, kale) because they taste more bitter and less sweet (Dinehart, M. E. *et al.*, 2006). One of the risk factors for colon cancer is low vegetable intake (McCullough, M. L. *et al.*, 2003), and data from routine colonoscopies show that men who tasted PROP as most bitter had the most colonic polyps (Basson, M. D. *et al.*, 2005).

4.20.3.2 Cardiovascular Disease Risk

Body mass (BMI) is an important risk factor for cardiovascular disease. The first data linking BMI to PROP tasting came from Fischer (Fischer, R. *et al.*, 1966), who used thresholds for PTC and quinine to show that thinner individuals tended to be tasters. Recent work supports this early observation and suggests that those who taste less bitterness from PROP and other compounds have dietary preferences that support increased energy intake (e.g., higher preferences for fats, sweets, alcohol). For example, overweight (but not obese) middle-aged and elderly individuals tend to find PROP less bitter (Lucchina, L. *et al.*, 1995; Tepper, B. J. and Ullrich, N. V., 2001; Duffy, V. B. *et al.*, 2004b; Duffy, V. B., 2004; Goldstein, G. L. *et al.*, 2005).

Taste pathology appears to interact with genetic variability to affect BMI over time. Diminished bitter taste on the anterior tongue suggests damage to the chorda tympani taste nerve; both are associated with higher BMI (Lanier, S. A. *et al.*, 2005a). Severe middle ear infections may permanently damage the chorda tympani nerve as it traverses the middle ear, and prior histories of such infection are associated with increased BMI, especially in PROP supertasters (Tanasescu, M. *et al.*, 2000; Snyder, D. J. *et al.*, 2003; Bartoshuk, L. M. *et al.*, 2006a).

4.20.3.3 Alcohol Intake

Suggestions that PTC/PROP nontasters are most likely to abuse alcohol date back many years (e.g., Driscoll, K. E. *et al.*, 2006). The sensory properties of alcohol vary with PROP status: supertasters perceive the most intense bitterness and oral burn from alcoholic beverages, and so they like and consume them least (Bartoshuk, L. M., 1993; Duffy, V. B. *et al.*, 2004a; 2004c). Similar to the results observed with vegetables, supertasters find alcoholic beverages more bitter and less sweet than do nontasters (Lanier, S. A. *et al.*, 2005b).

4.20.3.4 Smoking

As with so many health associations related to PTC/PROP, nontasting was first associated with tobacco use by Fischer (Fischer, R. *et al.*, 1963). Modern studies support these early observations (e.g., Snedecor, C. M. *et al.*, 2006), suggesting that supertasters smoke the least (Snyder, D. J. *et al.*, 2005).

4.20.3.5 Future Interventions?

Taste blindness appears to explain some of the widespread variation in food choice. Accordingly, dietary recommendations that account for differences in oral sensation may promote food enjoyment and healthier dietary habits. While supertasters may benefit from oral sensory hindrances to overconsuming alcohol, sweets, and fats, they may have less desire to consume recommended intakes of vegetables. Manipulations that reduce vegetable bitterness (e.g., bitterness inhibition; Ming, D. *et al.*, 1999) may increase preferences for these important foods. Meanwhile, nontasters experience fewer negative sensory experiences from vegetables, but may benefit from dietary counseling to curb alcohol and carbohydrate intake, consume healthful dietary fats, and balance energy intake with physical activity. In short, understanding the behavioral implications of oral sensory variation permits us to discover effective interventions for improved health.

References

Aitken, R. C. B. 1969. Measurement of feelings using visual analogue scales. Proc. R. Soc. Med. 62, 989–993.

Bartoshuk, L. M. 1993. The biological basis of food perception and acceptance. Food Qual. Preference 4, 21–32.

Bartoshuk, L. M. 2000. Comparing sensory experiences across individuals: recent psychophysical advances illuminate genetic variation in taste perception. Chem. Senses 25, 447–460.

Bartoshuk, L. M. 2002. Self reports and across-group comparisons: a way out of the box. APS Obs. 15(7), 26–28.

Bartoshuk, L. M. and Snyder, D. J. 2004. Psychophysical Measurement of Human Taste Experience. In: Handbook of Behavioral Neurobiology (*eds*. E. Stricker and S. Woods), pp. 89–107. Plenum.

Bartoshuk, L. M., Christensen, C. M., Duffy, V., Sheridan, K., Small, D. M., and Synder, D. 2005a. PROP and retronasal olfaction. Chem. Senses 30, A236.

Bartoshuk, L. M., Duffy, V. B., Chapo, A. K., Fast, K., Yiee, J. H., and Hoffman, H. J. 2004a. From psychophysics to the clinic: missteps and advances. Food Qual. Pref. 15, 617–632.

Bartoshuk, L. M., Duffy, V. B., Green, B. G., Hoffman, H. J., Ko, C.-W., Lucchina, L. A., Marks, L. E., Snyder, D. J., and Weiffenbach, J. 2004b. Valid across-group comparisons

with labeled scales: the gLMS vs magnitude matching. Physiol. Behav. 82, 109–114.
Bartoshuk, L. M., Duffy, V. B., Fast, K., Green, B. G., Prutkin, J. M., and Snyder, D. J. 2002. Labeled scales (e.g., category, Likert, VAS) and invalid across-group comparisons. What we have learned from genetic variation in taste. Food Qual. Pref. 14, 125–138.
Bartoshuk, L. M., Duffy, V. B., Hayes, J. E., Moskowitz, H., and Snyder, D. J. 2006a. Psychophysics of sweet and fat perception in obesity: problems, solutions and new perspectives. Philos. Trans. R. Soc. Biol. Sci. 361, 1137–1148.
Bartoshuk, L. M., Duffy, V. B., and Miller, I. J. 1994. PTC/PROP tasting: anatomy, psychophysics, and sex effects. Physiol. Behav. 56, 1165–1171.
Bartoshuk, L. M., Fast, K., and Snyder, D. 2005b. Differences in our sensory worlds: Invalid comparisons with labeled scales. Curr. Dir. Psychol. Sci. 14, 122–125.
Bartoshuk, L. M., Snyder, D. J., and Duffy, V. B. 2006b. Hedonic gLMS: valid comparisons for food liking/disliking across obesity, age, sex and PROP status. Chem. Senses 31, A50.
Bartoshuk, L. M., Snyder, D. J., Grushka, M., Berger, A. M., Duffy, V. B., and Kveton, J. F. 2005c. Taste damage: previously unsuspected consequences. Chem. Senses 30(Suppl. 1), (suppl. 1) i218–i219.
Basson, M. D., Bartoshuk, L. M., Dichello, S. Z. L. P., Weiffenbach, J., and Duffy, V. B. 2005. Association between 6-*n*-propylthiouracil (PROP) bitterness and colonic neoplasms. Dig. Dis. Sci. 50, 483–489.
Bell, K. I. and Tepper, B. J. 2006. Short-term vegetable intake by young children classified by 6-*n*-propylthiouracil bitter-taste phenotype. Am. J. Clin. Nutr. 84, 245–251.
Biernat, M. and Manis, M. 1994. Shifting standards and stereotype-based judgements. J. Person. Soc. Psychol. 66, 5–20.
Birnbaum, M. H. 1999. How to show that 9>221: collect judgements in a between-subjects design. Psychol. Meth. 4, 243–249.
Blakeslee, A. F. and Fox, A. L. 1932. Our different taste worlds. J. Hered. 23, 97–107.
Dinehart, M. E., Hayes, J. E., Bartoshuk, L. M., Lanier, S. L., and Duffy, V. B. 2006. Bitter taste markers explain variability in vegetable sweetness, bitterness, and intake. Physiol. Behav. 87, 304–313.
Drewnowski, A. and Gomez-Carneros, C. 2000. Bitter taste, phytonutrients, and the consumer: a review. Am. J. Clin. Nutr. 72, 1424–1435.
Drewnowski, A., Henderson, S. A., Shore, A. B., and Barratt-Fornell, A. 1997. Nontasters, tasters, and supertasters of 6-*n*-propylthiouracil (PROP) and hedonic response to sweet. Physiol. Behav. 62, 649–655.
Driscoll, K. E., Perez, M., Cukrowicz, K. C., Butler, M., and Joiner, T. E. 2006. Associations of phenythiocarbamide tasting to alcohol problems and family history of alcoholism differ by gender. Psychiatry Res. 143, 21–27.
Duffy, V. B. 2004. Associations between oral sensation, dietary behaviors and risk of cardiovascular disease (CVD). Appetite 43, 5–9.
Duffy, V. B., Bartoshuk, L. M., Lucchina, L. A., Snyder, D. J., and Tym, A. 1996. Supertasters of PROP (6-*n*-propylthiouracil) rate the highest creaminess to high-fat milk products. Chem. Senses 21, 598.
Duffy, V. B., Chapo, A. K., Hutchins, H. L., and Bartoshuk, L. M. 2003. Retronasal olfactory intensity: associations with taste. Chem. Senses 28, A33.
Duffy, V. B., Davidson, A. C., Kidd, J. R., Kidd, K. K., Speed, W. C., and Pakstis, A. J. 2004a. Bitter receptor gene (TAS2R38), 6-*n*-propylthiouracil (PROP) bitterness and alcohol intake. Alcohol. Clin. Exp. Res. 28, 1629–1637.
Duffy, V. B., Lucchina, L. A., and Bartoshuk, L. M. 2004b. Genetic Variation in Taste: Potential Biomarker for Cardiovascular Disease Risk? In: Genetic Variations in Taste Sensitivity: Measurement, Significance and Implications (*eds*. J. Prescott and B. J. Tepper), pp. 195–228. Dekker.
Duffy, V. B., Peterson, J. M., and Bartoshuk, L. M. 2004c. Associations between taste genetics, oral sensation and alcohol intake. Physiol. Behav. 82, 435–445.
Fast, K., Tie, K., Bartoshuk, L. M., Kveton, J. F., and Duffy, V. B. 2000. Unilateral anesthesia of the chorda tympani nerve suggests taste may localize retronasal olfaction. Chem. Senses 25, 614–615.
Fischer, R. 1967. Genetics and Gustatory Chemoreception in Man and Other Primates. In: The Chem. Senses and Nutrition (*eds*. M. R. Kare and O. Maller), pp. 621–681. John Hopkins Press.
Fischer, R. and Griffin, F. 1964. Pharmacogenetic aspects of gustation. Drug Res. 14, 673–686.
Fischer, R., Griffin, F., and Kaplan, A. R. 1963. Taste thresholds, cigarette smoking, and food dislikes. Med. Exp. 9, 151–167.
Fischer, R., Griffin, F., and Rockey, M. A. 1966. Gustatory chemoreception in man: multidisciplinary aspects and perspectives. Perspect. Biol. Med. 9, 549–577.
Ford, N. and Mason, A. D. 1941. Taste reactions of the Dionne quintuplets. J. Hered. 10, 365–368.
Fox, A. L. 1931. Six in ten ''tasteblind'' to bitter chemical. Sci. News Lett. 9, 249.
Goldstein, G. L., Daun, H., and Tepper, B. J. 2005. Adiposity in middle-aged women is associated with genetic taste blindness to 6-*n*-propylthiouracil. Obes. Res. 13, 1017–1023.
Green, B. G., Shaffer, G. S., and Gilmore, M. M. 1993. A semantically-labeled magnitude scale of oral sensation with apparent ratio properties. Chem. Senses 18, 683–702.
Hall, M. J., Bartoshuk, L. M., Cain, W. S., and Stevens, J. C. 1975. PTC taste blindness and the taste of caffeine. Nature 253, 442–443.
Harris, H. and Kalmus, H. 1949. The measurement of taste sensitivity to phenylthiourea (P.T.C.). Ann. Eugen. 15, 24–31.
Hayes, J. E. 2007. Statistical modeling of taste markers, food preference and intake, and anthropometrics. PhD dissertation, University of Connecticut.
Hayes, J. E., Bartoshuk, L. M., Kidd, J. R., and Duffy, V. B. 2007. TAS2R38 genotype, fungiform papillae and suprathreshold taste response. Chem. Senses 32 (in press).
Hollingworth, H. L. and Poffenberger, A. T. 1917. The Sense of Taste. Moffat, Yard and Company.
Kamen, J. 1959. Interaction of sucrose and calcium cyclamate on perceived intensity of sweetness. J. Food Sci. 24, 279–282.
Kim, U. K., Jorgenson, E., Coon, H., Leppert, M., Risch, N., and Drayna, D. 2003. Positional cloning of the human quantitative trait locus underlying taste sensitivity to phenylthiocarbamide. Science 299, 1221–1225.
Lanier, S. A., Hutchins, H., and Duffy, V. B. 2005a. Taste and dietary predictors of central adipositiy in adult females. Chem. Senses 30, A34.
Lanier, S. A., Hayes, J. E., and Duffy, V. B. 2005b. Sweet and bitter tastes of alcoholic beverages mediate alcohol intake in of-age undergraduates. Physiol. Behav. 83, 821–831.
Lucchina, L., Bartoshuk, L. M., Duffy, V. B., Marks, L. E., and Ferris, A. M. 1995. 6-*n*-Propylthiouracil perception affects nutritional status of independent-living older females. Chem. Senses 20, 735.
Marks, L. E. and Stevens, J. C. 1980. Measuring Sensation in the Aged. In: Aging in the 1980's: Psychological Issues (*ed*. L. W. Poon), pp. 592–598. American Psychological Association.

Marks, L. E., Stevens, J. C., Bartoshuk, L. M., Gent, J. G., Rifkin, B., and Stone, V. K. 1988. Magnitude matching: the measurement of taste and smell. Chem. Senses 13, 63–87.
McCullough, M. L., Robertson, A. S., Chao, A., Jacobs, E. J., Stampfer, M. J., Jacobs, D. R., Diver, W. R., Calle, E. E., and Thun, M. J. 2003. A prospective study of whole grains, fruits, vegetables and colon cancer risk. Cancer Causes Control 14, 959–970.
Miller, I. J. and Whitney, G. 1989. Sucrose octaacetate-taster mice have more vallate taste buds than non-tasters. Neurosci. Lett. 100, 271–275.
Milunicová, A., Jandová, A., Laurová, L., Novotná, J., and Skoda, V. 1969. Hereditary blood and serum types, PTC test and level of the fifth fraction of serum lactatedehydrogenase in females with gyneological cancer (II. Communication). Neoplasma 16, 311–316.
Ming, D., Ninomiya, Y., and Margolskee, R. F. 1999. Blocking taste receptor activation of gustducin inhibits gustatory responses to bitter compounds. Proc. Natl. Acad. Sci. U. S. A. 17, 9903–9908.
Mombaerts, P. 2004. Genes and ligands for odorant, vomeronasal and taste receptors. Nat. Rev. Neurosci. 5, 263–278.
Narens, L. and Luce, R. D. 1983. How we may have been misled into believing in the interpersonal comparability of utility. Theor. Decis. 15, 247–260.
Prutkin, J. M., Duffy, V. B., Etter, L., Fast, K., Gardner, E., and Lucchina, L. A. 2000. Genetic variation and inferences about perceived taste intensity in mice and men. Physiol. Behav. 69, 161–173.
Salbe, A. D., DelParigi, A., Pratley, R. E., Drewnowski, A., and Tataranni, P. A. 2004. Taste preferences and body weight changes in an obesity-prone population. Am. J. Clin. Nutr. 79, 372–378.
Sandell, M. A. and Breslin, P. A. 2006. Variability in a taste-receptor gene determines whether we taste toxins in food. Curr. Biol. 16, R792–R794.
Schifferstein, H. N. J. and Frijters, J. E. R. 1991. The perception of the taste of KCl, NaCl, and quinine HCl is not related to PROP-sensitivity. Chem. Senses 16, 303–317.
Small, D. M. and Jones-Gotman, M. 2001. Neural substrates of taste/smell interactions and flavour in the human brain. Chem. Senses 26, 1034.
Snedecor, C. M., Pomerleau, C. S., Mehringer, A. M., Ninowski, R., and Pomerleau, O. F. 2006. Differences in smoking-related variables based on phenylthiocarbamide 'taster' status. Addict. Behav. 31, 2309–2312.
Snyder, L. H. 1931. Inherited taste deficiency. Science 74, 151–152.
Snyder, D. J., Davidson, A. C., Kidd, J. R., Kidd, K. K., Speed, W. C., Pakstis, A. J., Cubells, J. F., O'Malley, S. S., and Bartoshuk, L. M. 2005. Oral sensation influence tobacco use: genetic and psychophysical evidence. Presented at the Annual Meetings of the Society for Research on Nicotine and Tobacco, Prague, Czech Republic.
Snyder, D. J., Duffy, V. B., Chapo, A. K., Cobbett, L. E., and Bartoshuk, L. M. 2003. Childhood taste damage modulates obesity risk: effects on fat perception and preference. Obes. Res. 11(Suppl), A147.
Snyder, D. J., Dwivedi, N., Mramor, A., Bartoshuk, L. M., and Duffy, V. B. 2001. Taste and touch may contribute to the localization of retronasal olfaction: unilateral and bilateral anesthesia of cranial nerves V/VII. Paper presented at the Society of Neuroscience Abstract, San Diego, CA, USA.
Snyder, D. J., Fast, K., and Bartoshuk, L. M. 2004. Valid comparisons of suprathreshold stimuli. J. Conscious. Stud. 11, 40–57.
Stevens, J. C. and Marks, L. E. 1980. Cross-modality matching functions generated by magnitude estimation. Percept. Psychophys. 27, 379–389.
Stevens, S. S. 1969. Sensory scales of taste intensity. Percept. Psychophys. 6, 302–308.
Stevens, S. S. 1958. Adaptation-level vs the relativity of judgment. Am. J. Psychol. 71, 633–646.
Tanasescu, M., Ferris, A. M., Himmelgreen, D. A., Rodriguez, N., and Perez-Escamilla, R. 2000. Biobehavioral factors are associated with obesity in Puerto Rican children. J. Nutrit. 130, 1734–1742.
Tepper, B. J. and Nurse, R. J. 1997. Fat perception is related to PROP taster status. Physiol. Behav. 61, 949–954.
Tepper, B. J. and Ullrich, N. V. 2001. Influence of genetic taste sensitivity to 6-*n*-propylthiouracil (PROP), dietary restraint and disinhibition on body mass index in middle-aged women. Physiol. Behav. 75, 305–312.

Further Reading

Hayes, J. and Duffy, V. B. 2007. Revisiting sucrose-fat mixtures: sweetness and creaminess vary with phenotypic markers of oral sensation. Chem. Senses, in press.
Snyder, D. J., Prescott, J., and Bartoshuk, L. M. 2006. Modern Psychophysics and the Assessment of Human Oral Sensation. In: Taste and Smell: An Update (*eds*. T. Hummel and A. Welge-Lüssen). Karger.
Trock, B. J., Lanza, E., and Greenwald, P. 1990. High fiber diet and colon cancer: a critical review. Prog. Clin. Biol. Res. 346, 145–157.

4.21 Salt Taste

G K Beauchamp and L J Stein, Monell Chemical Senses Center, Philadelphia, PA, USA

© 2008 Elsevier Inc. All rights reserved.

4.21.1	**What Makes Salt Taste Salty?**	401
4.21.2	**Why Do We Like the Taste of Salt?**	402
4.21.2.1	Liking for Salt: Sodium Need	402
4.21.2.2	Liking for Salt: Need-Free Consumption	403
4.21.3	**What Are the Functions of Salt in Food?**	404
4.21.4	**What Can Be Done to Reduce Salt Consumption?**	405
4.21.5	**Final Comment**	406
References		406

Glossary

KCl Potassium chloride.
LiCl Lithium chloride.
Na Sodium.
NaCl Sodium chloride; salt.

Sodium chloride (NaCl: herein referred to as salt unless otherwise noted) has played a central role in human society throughout history. As a highly valued commodity, wars have been fought to control salt access and availability, and it has served as a major basis for taxation for millennia (see Gandhi, M., 1930 for example). People have been paid in salt (salaries) and salt has been transported, sometimes requiring considerable effort and expense, across long distances (reviews: Denton, D., 1982; Kurlansky, M., 2002).

Until recently, a major problem for many people has been to obtain sufficient salt, both for themselves and also for their domestic animals, especially herbivorous ones that cannot obtain sufficient quantities of sodium (Na) from most plants. Times have changed, however, and the salt problem in much of today's world is not one of insufficiency, but of excess.

In this essay, we do not address health implications of high salt consumption; these are covered in numerous reviews and commentaries (e.g., Taubes, G., 1998; Sacks, F. M. *et al.*, 2001; Alderman, M. H., 2002; Hooper, L. *et al.*, 2002; De Wardener, H. E. *et al.*, 2004; Karppanen, H. and Mervaalo, E., 2006). The consensus is that intake of too much salt – exactly what constitutes too much for any given individual likely depends on many factors – is unhealthy for at least some proportion of the population. Consequently, achieving a more thorough understanding of salt taste, including how it is detected, the role it plays in food palatability, and how salt intake may be modified, carries public health implications. A better understanding of all aspects of salt taste is thus a necessity.

In what follows, we discuss four topics. First, we focus on how salt in the mouth evokes the sensation of saltiness. As will be shown, our knowledge of this area has advanced greatly over the past years but remains incomplete. Second, we discuss why people seem to like salt so much. This section considers both innate and acquired factors. In the third part, we consider the varied reasons for adding salt to human foods. Although these sections primarily address human salt taste and consumption, issues relevant to other animals will sometimes be raised. The final section provides an overview of strategies that might be employed to address the public health mandate to reduce salt intake.

4.21.1 What Makes Salt Taste Salty?

NaCl and LiCl (lithium chloride) are the only two substances that taste almost purely salty, lacking virtually any bitter, sour, sweet, or umami quality. Of the sodium salts, several, such as Na-acetate, are predominantly salty but weakly so, while most others

taste salty and something else, usually bitter. A few other compounds are salty with additional taste characteristics. For example, KCl is quite salty but also bitter, particularly so to some people. A small number of amino acids have a salty taste component. Nevertheless, it is striking how few salty compounds exist, and of these, how even fewer are purely salty. This paucity of salty stimuli contrasts starkly with bitter and even sweet taste, for each of which there are numerous and diverse molecular stimulants. These observations suggest a highly specific mechanism for salty taste detection. And since the primary ion in salty taste is thought to be Na (Bartoshuk, L. M., 1980), this mechanism must be specific to sodium.

A major advance in our understanding of salt taste mechanisms was made independently in the early 1980s by Schiffman S. and colleagues (Schiffman, S. S. *et al.*, 1983) and DeSimone J. and colleagues (DeSimone, J. A. *et al.*, 1981). These investigators hypothesized that the Na taste recognition mechanism might be the same or very similar to mechanisms for sodium recognition in other parts of the body, particularly the kidneys. Following this logic, dissociated Na dissolved in saliva was postulated to activate a Na-specific ion channel. Over the ensuing 25 years, this important insight has received a substantial body of support from biophysical, physiological, and sensory studies that employed mainly animal models such as rats, mice, and dogs. Particularly telling support came from studies demonstrating that a major component of salt taste transduction is inhibited by amiloride, a diuretic that blocks sodium channels. However, most of these studies also indicated the additional existence of a nonamiloride-suppressible component to salt taste transduction (see, e.g., Geran, L. C. and Spector, A. C., 2000). The nature of this second element remains obscure, although it might involve a nonspecific vanilloid receptor-1 analog (Lyall, V. *et al.*, 2004).

The sodium ion channel scenario is elegant in its simplicity and intuitive appeal. In particular, it can account for the specificity of Na as the main component of saltiness perception. Moreover, sodium ion channels have been implicated in the salt taste perception of animal models ranging from sheep to rats to flies (e.g., Liu, L. *et al.*, 2003). Nevertheless, the hypothesis is not completely compelling. Although some of the original data from human psychophysical studies showed that amiloride reduced human perception of salty taste, subsequent studies have been inconsistent. Indeed, in an extremely thorough review of this literature, Halpern concluded that amiloride has little or no effect on human perception of NaCl saltiness (Halpern, B. P., 1998). These human data are quite puzzling in the face of the overwhelming evidence for an amiloride effect to reduce salt taste perception in other animal models.

Perhaps this should not be so surprising; species differences are common for other taste transduction mechanisms, as they are in many other biological areas. Yet given the fundamental nature of salt taste, along with the widespread evidence for involvement of a sodium channel in so many species, it seems implausible that humans would possess a completely novel mechanism for detecting NaCl. Perhaps the channel is sufficiently altered in humans that amiloride is ineffective; this would account for the fact that some human sodium channels are not amiloride blockable. What is needed to fully understand human salt taste is a comprehensive explanation of the molecular mechanisms that underlie its detection. While this is not yet available, it is likely to be forthcoming quite soon.

As noted above, salt taste transduction also includes an amiloride-insensitive component, which again is not well understood (Halpern, B. P., 1998). Activation of this component, which is not specific to sodium, may not be perceived as fully or even partially salty. Nevertheless, identification of this mechanism and its function will be necessary for a full understanding of the molecular basis for salt taste.

4.21.2 Why Do We Like the Taste of Salt?

Attempts to answer this complicated question are generally addressed at two levels: one involving true physiological salt need and the second involving need-free salt intake.

4.21.2.1 Liking for Salt: Sodium Need

It is widely assumed that the very existence of a mechanism to specifically detect Na is due to the special role Na plays in animal biology. This rationale has been thoroughly reviewed elsewhere (Denton, D., 1982) and includes the importance of Na in nerve conduction, energy release, and acid–base balance. Moreover, since Na is not evenly distributed in nature and is present in very low concentrations in many plants, it is assumed that a

specific means to detect its presence would be highly adaptive. These theoretical arguments are supported by the widespread existence across species of mechanisms for detecting salt, by salt taste's apparent status as one of a small group of basic tastes in many organisms, and by the motivating effects of salt taste, particularly when Na is scarce (McBurney, D. H. and Gent, J. F., 1979).

This last point requires elaboration. A tremendous number of observational and experimental studies (again reviewed with great scholarship by Denton, D., 1982; for a more recent review see Schulkin, J., 1991) demonstrate that a sodium-deficient animal, especially an herbivore or omnivore, will go to great lengths to obtain Na, using salty taste to detect sources of Na. This need-based search for and consumption of salt has provided a model system that demonstrates innate and specific mechanisms for detecting Na and has identified some of the hormonal substrates that underlie need-based salt appetite. This vast area of research is difficult to summarize, but apparently Na depletion elicits changes in hormones and central neural system organization that over time alter avidity for the taste of salt. Indeed, the taste quality elicited by salt may change as a function of sodium depletion and hence need (for review, see McCaughey, S. A. and Scott, T. R., 1998). A peripheral component may also contribute to increased avidity for Na in the face of need, as Na depletion may alter salt taste transduction mechanisms (Contreras, R. J. and Frank, M., 1979) in addition to central mechanisms regulating the avidity for salt. Put simply, Na depletion seems to make salt taste both better and different in animal models such as rodents and sheep.

Once again, species differences are apparent. As might be anticipated based on a meat diet naturally rich in sodium, carnivores may not respond physiologically or behaviorally to Na depletion in the same ways that omnivores and herbivores do. Perhaps carnivores such as dogs and cats never experience the consequences of Na depletion. As meat-eating animals, they either ingest sufficient food to survive, consequently ensuring adequate Na, or they die of starvation.

A more puzzling species difference again involves humans. The evidence that Na depletion in adult humans stimulates a specific, intense desire for the taste of salt is weak (Beauchamp, G. K., 1991). Although some human experimental studies indicate that Na loss is followed by an elevation in salt liking, this does not truly mimic the responses of animal models, where extreme avidity follows depletion. A partial explanation may be that human experimental studies cannot induce the same degree of depletion routinely employed in animal model studies.

In one area, species differences may not exist. When Na depletion occurs very early in human life as a result of varied clinical conditions, a profound elevation in the desire for salt occurs, similar to that seen in experimental rodent models. For obvious reasons, there are no experimental studies of early Na depletion in humans; however, the weight of clinical evidence (Beauchamp, G. K. *et al.*, 1991) indicates that such heightened avidity is remarkably persistent. This observation is mirrored in some animal model studies (e.g., Thaw, A. K. *et al.*, 2000), demonstrating a permanent elevation of salt taste avidity following early Na depletion. The relative roles of central and peripheral changes in modulating this effect remain unknown.

4.21.2.2 Liking for Salt: Need-Free Consumption

Although it makes some evolutionary sense that many species would develop mechanisms to enable detection of environmental Na and facilitate ingestion under conditions of depletion, why do they consume it avidly when not deficient? More specifically, why do humans in almost all developed societies, who are probably never truly sodium deficient, so like their food with substantial added salt?

Two explanations have been proffered. The first suggests that herbivores and some omnivores have an innate liking for the taste of salt. According to this rationale, it is to an organism's benefit to consume salt when it is available. There is no cost for this behavior, with the exception of some adult-onset diseases, as excess sodium is easily removed by the kidneys. Furthermore, it has been hypothesized that high Na intake may reflect evolutionary pressure to protect against sudden dehydration (Fessler, D. M. T., 2003). A problem with this line of argument centers on the fact that sodium cannot be stored. What then is the advantage of consuming salt in excess whenever it is available? Perhaps, this behavior allows animals learn its location so as to be able to quickly locate it in preparation, from an evolutionary perspective, for later deficits. Indeed, sodium-deprived rats do use learned associations between environmental cues and salt taste to guide them to locations where they have previously ingested salt (Stouffer, E. M. and White, N. M., 2005).

The second explanation is that individual exposure to salt, particularly early exposure, results in a heightened desire or avidity (e.g., Smirga, M. *et al.*, 2002). This is a commonly-held belief among nutritionists, dieticians, physicians, and others (e.g., MacGregor, G. A. and de Wardener, H. E., 1998). But this explanation raises yet another question. Why should a taste experienced in infancy or even adulthood take on heightened value? This is often called taste imprinting but, unlike classic imprinting where the animal learns important characteristics of its parent, the adaptive value of taste imprinting is obscure, particularly for omnivorous species like humans or rats.

Experimental studies in animal models and humans provide several examples of effects of early dietary exposure to salt on subsequent perception and preference. As noted previously, sodium depletion early in life may cause an elevation of salt preference. The opposite – high sodium consumption early in life – also has been reported to have modest effects in heightening later preferences (Contreras, R. J. and Kosten, T., 1983). Furthermore, amniotic fluid, saliva, and milk all contain sodium, consumption of which could establish or heighten a preference, and many studies with rodent models, particularly rats, demonstrate that salt solutions around isotonicity are avidly consumed on first presentation.

As with most arguments pitting innateness versus learning, this dichotomy is almost assuredly false. Liking for salt and salty foods is surely the result of an interaction between innate and acquired information. Human infants at birth are either indifferent to salt or reject it, particularly at hypertonic concentrations (Beauchamp, G. K. *et al.*, 1986). By approximately 4–6 months of age, infants show a preference (relative to plain water) for low-to-moderate saline solutions around the level of isotonicity. This age-related hedonic shift may represent in part the maturation of an innate transductive or neurological mechanism. Some rodent studies have shown the ability to detect salty taste matures postnatally (for review, see Hill, D.L. and Mistretta, C.M., 1990); this may also be the case for humans. Prior exposure to foods containing salt may modulate this developmental change (e.g., Harris, G. and Booth, D. A., 1985). We have recently found (Stein, L. J. *et al.*, in preparation) that infants fed starchy foods between months 2 and 6 of life show heightened salt preferences relative to infants not exposed to these foods. Since one characteristic accompanying ingestion of starchy foods is likely a substantial exposure to salt, it is possible that this difference represents effects of prior exposure to salt. Perhaps, salt exposure during a critical period of receptive element maturation permanently alters peripheral and/or central structures and is thereby particularly potent in establishing childhood and perhaps even adult habits of intake. Alternatively, the heightened salt preference could reflect a shift in response to increased salt in the diet, similar to what is observed in adults (Bertino, M. *et al.*, 1986; see also discussion below). This is surely an area that should be investigated since it has major public health implications.

Although liking for salt in foods by children and adults is virtually universal, there are substantial individual differences. The degree to which genetic differences in salt taste perception could underlie these differences is unknown, but as the human salt taste mechanism(s) becomes better characterized, the influence of genetic variation will simultaneously become more clear.

In addition to probable effects of early exposure, environmental factors play a major role in determining salt avidity and consumption. The existence of societies where salt intake is very low has been interpreted to indicate that higher intake, such as that of Western societies, is the result of habit and commercial interests (e.g., MacGregor, G. A. and de Wardener, H. E., 1998). However, in most of these societies, low salt intake reflects low availability; wherever salt is inexpensive and widely available, it is noteworthy that most cultures consume roughly the same amount (see data in Intersalt Cooperative Research Group, 1988). This observation leads one to wonder whether there remains an unidentified (physiological?) explanation for human salt consumption. This question was raised many years ago (Bunge, G., 1902; Kaunitz, H., 1956) and remains worthy of consideration, particularly in light of calls for substantial population-wide reduction in salt consumption.

4.21.3 What Are the Functions of Salt in Food?

In the foregoing, it has been implicitly assumed that the proximate reason humans avidly consume Na is because we like the experience of the salty taste. This is undoubtedly part of the reason for modern human salt consumption, but surely not the only one, for salt plays many other roles in human food and nutrition.

Virtually all the salt people consume is in or on food; very few individuals eat pure salt outside that

Table 1 Number of recipes for which salt is called for in La Cuisine de France (Turgeon, C., 1964)

Food group	*Number of recipes*	*Number calling for salt*	*Number calling for other salty ingredients*	*% calling for salt*
Vegetables	142	131	11	100
Soups	51	51	0	100
Sauces	26	26	0	100
Starches (potato, rice, pasta, etc.)	59	57	2	100
Pastry[a]	136	70	10	58

[a]Many of the pastry recipes are for frosting-like items that are mainly sugar.
Note: Not tabulated are entrees, eggs, fish, poultry and game, meat, salads, desserts, and wine. Many of these use or are served with the items in the table.

context. In foods, salt has several technical functions (Man, C. M. D., 2007). It is an excellent preservative, preventing bacterial growth. It also serves structural functions during cooking and food processing by interacting with other ingredients to affect the texture and color of food. In addition to salt's functional benefits, it has a very significant additional strong point for both industry and the home cook: it is cheap. Consequently, any acceptable salt alternative must not only taste good and function as well as salt, but must also be inexpensive.

In addition to these functional features that make salt so important in foods, salt plays a sensory role over and above making food taste salty. Consider again bread and bread products. The salt in these makes up the single largest source of sodium consumed in the US diet; yet, we typically do not perceive bread as salty. Bread without salt tastes insipid or bad; when salt is added, the flavor is enhanced without making the bread taste salty. Thus salt, when added to food, must have functions other than adding saltiness. What are they?

One supposition is that the sense of taste imparts not only a quality, but also a sensation of quantity, amount, or bulk. It is difficult to know how to experimentally approach this concept; something similar to mouthfeel might be involved. It is as if taste stimuli (umami and sweet perhaps having some of the same characteristics as salt) might also interact with tactile fibers or other chemosensory structures to give a sense that the food has substance.

If this idea of mouthfeel is hard to encompass, yet another function of salt is better established. Sodium is an outstanding inhibitor of certain bitter-tasting compounds (Breslin, P. A. S. and Beauchamp, G. K., 1995). We have shown (Breslin, P. A. S. and Beauchamp, G. K., 1997) that a sodium salt added to a mixture of bitter and sweet suppresses the bitterness, thereby releasing the sweet from inhibition. The overall sensory effect in the three-component model system is to enhance sweetness. We suggest that this can help explain why salt is added to so many foods when the intent is not to add saltiness: the salt suppresses off tastes and enhances good ones. Indeed, in a survey of recipes from one traditional French cook book (Turgeon, C., 1964) (Table 1), we found that most included either salt or a condiment-like olives that is high in salt. Clearly, the value of salt to food is demonstrated by its frequent use both by the home cook and by the multinational food companies.

4.21.4 What Can Be Done to Reduce Salt Consumption?

If salt reduction is the goal, what reasonable strategies are possible? There appear to be two approaches to reducing sodium consumption. In both salt is removed from foods; in the first, it is claimed that people would adjust to or at least tolerate the changes in taste (if the nontaste functions could be accounted for by other means), whereas in the second, an alternative taste-active substance is added to offset the loss of salt.

Consider the first strategy, which assumes that excess intake (relative to known physiological need) is due to habit and that habits can be changed. Clinical and anecdotal literature (see Beauchamp, G. K., 1991) reveal that when people undertake a low-sodium diet, the immediate response is misery. However, the lower sodium diet eventually becomes accepted, and in fact, foods containing the previous amount of salt are perceived as too salty (e.g., Stefansson, V., 1946). Many years ago, we provided experimental evidence to support this observation

(Bertino, M. *et al.*, 1983). After assuming a diet with about a 50% reduction in sodium content for 2–3 months, volunteers came to prefer their food with lower salt levels. They acclimated to this diet. We also showed (Bertino, M. *et al.*, 1986) that preference could be moved in the other direction: when people were put on a higher salt diet, they began to like more concentrated salt in their foods.

This evidence supports the view that if somehow we were to all undertake a low sodium diet, it would soon come to be the norm and no one would notice or feel deprived. But is this really possible? One widely recommended strategy is for food suppliers to gradually reduce the salt in foods so that the change is not noticed. Indeed, it appears that one can reduce the salt in some foods as much as 25% without consumers being aware (Girgis, S. *et al.*, 2003). But if people do not notice the reduction, will their taste preference change? And without a change in preference, can significant reductions really be obtained? Another issue that has not been experimentally addressed is whether one could lower the expected level of salt in one segment of the diet (e.g., commercial soups) and not the remainder of the foods. Would people come to prefer a lowered salt level in the single food if the overall levels were not correspondingly lowered or would they just choose not to eat as much soup (or add salt to it)? I am aware of no research that bears on this point. Finally, how would one deal with the nontaste functions of salt discussed above?

In summary, there is reason to believe that sodium intake could be successfully lowered through a unified dietary reduction in salt (assuming that the drive to consume salt in excess of need referred to in the previous section does not exist), but many practical difficulties need to be addressed.

Diabetics should not consume sugar in excess. Until fairly recently, this meant that they could not have sweeteners in their diet. Then came the introduction of saccharin and other alternative sweeteners. Could there be a saccharin or aspartame or sucralose for salt? Unlike the many molecules that function as alternative sweeteners, very few purely salty compounds have been identified. Indeed, given what we know about the receptor mechanisms for sweet and salty taste, it is quite likely that few or no such compounds will be found. Sweet taste recognition involves a classical seven-transmembrane G-coupled receptor system. It acts similarly to a lock and key, and apparently any molecule having the key's features will taste sweet (see Nelson, G. *et al.*, 2001; reviews: Margolskee, R. R., 2002; Kim, U.-K. *et al.*, 2004). In marked contrast, as discussed above, the high specificity of the sodium channel involved in salt taste transduction may mandate that no sodium-free salt taste substitutes exist.

Amiloride studies inform us that it is possible to modify the intensity of saltiness (at least in animal models). This leads to the question: If saltiness can be inhibited, can it also be enhanced? Might it be possible to find a compound or compounds that, when added to a reduced sodium food, make that food taste acceptably salty? Some amino acids and amino acid salts have this property, thus demonstrating proof of principle (Tamura, M. *et al.*, 1989; Lee, T. D., 1992; Riha III, W. E. *et al.*, 1997). What is needed is a concerted effort, most efficiently using the (yet unidentified) human salt receptor as a screening device, to search for such molecules. Of course, if one is found, many practical problems will arise. Is it safe? Does it have the other functions of salt, for example the bitter blocking activity? Is it sufficiently inexpensive? Will people accept a new chemical in their food? In spite of these problems, the search for a salt enhancer is worthwhile and has promise.

4.21.5 Final Comment

There is still much to learn about how salt taste is perceived and what factors are responsible for preferences for salt in foods. Given the apparent role of excess salt intake in human disease, primarily essential hypertension, it is imperative that this gap in our knowledge be closed.

References

Alderman, M. H. 2002. Salt, blood pressure and health: a cautionary tale. Int. J. Epidemiol. 31, 311–315.

Bartoshuk, L. M. 1980. Sensory Analysis of the Taste of NaCl. In: Biological and Behavioral Aspects of Salt Intake (*eds*. M. R. Kare, M. J. Fregly, and R. A. Bernard), pp. 83–98. Academic Press.

Beauchamp, G. K. 1991. Salt Preference in Humans. In: Encyclopedia of Human Biology, Vol. 6, p. 715. Academic Press.

Beauchamp, G. K., Bertino, M., and Engelman, K. 1991. Human Salt Appetite. In: Chemical Senses, Appetite and Nutrition (*eds*. M. I. Friedman, M. G. Tordoff, and M. R. Kare), pp. 85–107. Dekker.

Beauchamp, G. K., Cowart, B. J., and Moran, M. 1986. Developmental changes in salt acceptability in human infants. Dev. Psychobiol. 19, 75–83.

Bertino, M., Beauchamp, G. K., and Engelman, K. 1983. Long-term reduction in dietary sodium alters the taste of salt. Am. J. Clin. Nutr. 36, 1134–1144.
Bertino, M., Beauchamp, G. K., and Engelman, K. 1986. Increasing dietary salt alters salt taste. Physiol. Behav. 38, 203–213.
Breslin, P. A. S. and Beauchamp, G. K. 1995. Suppression of bitterness by sodium: variation among bitter stimuli. Chem. Senses 20, 609–623.
Breslin, P. A. S. and Beauchamp, G. K. 1997. Sodium salts potentiate flavour by suppressing bitterness. Nature 287, 563.
Bunge, G. 1902. Textbook of Physiological and Pathological Chemistry, 2nd edn. Blakison.
Contreras, R. J. and Frank, M. 1979. Sodium deprivation alters neural responses to gustatory stimuli. J. Gen. Physiol. 73, 569–594.
Contreras, R. J. and Kosten, T. 1983. Prenatal and early postnatal sodium chloride intake modifies the solution preferences of adult rats. J. Nutr. 113, 1051–1062.
Denton, D. 1982. The Hunger for Salt. Springer-Verlag, Inc.
DeSimone, J. A., Heck, G. L., and DeSimone, S. K. 1981. Active ion transport in dog tongue: a possible role in taste. Science 214, 1039–1041.
De Wardener, H. E., He, F. J., and MacGregor, G. A. 2004. Plasma sodium and hypertension. Kidney Int. 66, 2454–2466.
Fessler, D. M. T. 2003. An evolutionary explanation of the plasticity of salt preferences: prophylaxis against sudden dehydration. Med. Hypotheses 61(3), 412–415.
Gandhi, M. 1930. Monograph on Common Salt. Federation of Indian Chambers of Commerce and Industry.
Geran, L. C. and Spector, A. C. 2000. Sodium taste detectability in rats is independent of anion size: the psychophysical characteristics of the transcellular sodium taste transduction pathway. Behav. Neurosci. 114(6), 1229–1238.
Girgis, S., Prescott, N. B., Prendergast, J., Dumbrell, S., Turner, C., and Woodward, M. 2003. A one-quarter reduction in the salt content of bread can be made without detection. Eur. J. Clin. Nutr. 57(4), 616–620.
Halpern, B. P. 1998. Amiloride and vertebrate gustatory responses to NaCl. Neurosci.. Biobehav. Rev. 23, 5–47.
Harris, G. and Booth, D. A. 1985. Sodium preference in food and previous dietary exposure in 6-month-old infants. IRCS Med. Sci. 13, 1178–1179.
Hill, D. L. and Mistretta, C. M. 1990. Developmental neurobiology of salt taste sensation. Trends Neurosci. 13, 188–195.
Hooper, L., Bartlett, C., Smith, G. D., and Ebrahim, S. 2002. Systematic review of long term effects of advice to reduce dietary salt in adults. BMJ 325, 1–9.
Intersalt Cooperative Research Group. 1988. An international study of electrolyte excretion and blood pressure: Results for 24 hour urinary sodium and potassium excretion. Br. Med. J. 297, 319–328.
Karppanen, H. and Mervaala, E. 2006. Sodium intake and hypertension. Prog. Cardiovase. Dis. 49(2), 59–75.
Kaunitz, H. 1956. Causes and consequences of salt consumption. Nature 178, 1141–1144.
Kim, U.-K., Breslin, P. A. S., and Drayna, D. 2004. Genetics of human taste perception. J. Dent. Res. 83(6), 448–453.
Kurlansky, M. 2002. Salt: A World History, 484 pp. Walker and Company.
Lee, T. D., inventor; Kraft General Foods Inc., assignee. Seasoned food product with a salt enhancer. US Patent 5 176 934. April 16, 1992.
Liu, L., Leonard, A. S., Motto, D. G., Feller, M. A., Price, M. P., Johnson, W. A., and Welsh, M. J. 2003. Contribution of drosophila DEG/ENaC genes to salt taste. Neuron 39(1), 133–146.
Lyall, V., Heck, G. L., Ninnikova, A. K., Shosh, S., Phan, T-H. T., Alan, R. I., Russell, O. F., Makik, S. A., Bigbee, J. W., and DeSimone, J. A., 2004. The mammalian amiloride-insensitive non-specific salt taste receptor is a vanilloid receptor-1 variant. J. Physiol. 558(1), 147–159.
MacGregor, G. A. and de Wardener, H. E. 1998. Salt, Diet and Health, 227 pp. Cambridge University Press.
Man, C. M. D. 2007. Technological Functions of Salt in Food Products. In: Reducing Salt in Foods: Practical Strategies (*eds*. D. Kilcast and F. Angus), pp. 157–173. Woodhead Publishing and CRC Press.
Margolskee, R. R. 2002. Molecular mechanisms of bitter and sweet taste transduction. J. Biol. Chem. 277(1), 1–4.
McBurney, D. H. and Gent, J. F. 1979. On the nature of taste qualities. Psychol. Bull. 86, 151–167.
McCaughey, S. A. and Scott, T. R. 1998. The taste of sodium. Neurosci. Biobehav. Rev. 22, 663–676.
Nelson, G., Hoon, M. A., Chandrashekar, J., Zhang, Y., Ryba, N. J. P., and Zuker, C. S. 2001. Mammalian sweet taste receptors. Cell 106, 381–390.
Riha, III,W. E., Brand, J. G., and Breslin, P. A. S. 1997. Salty taste enhancement with amino acids. Chem. Senses 22, 778.
Sacks, F. M., Svetkey, P., Vollmer, W. M., Appel, L., Bray, G. A., Harsha, D., Obarzanek, E., Conlin, P. R., Miller, III, E. R., Simons-Morton, D. G., Karanja, N., and Lin, P.-H. 2001. Effects on blood pressure of reduced dietary sodium and the dietary approaches to stop hypertension (DASH) diet. 2001. N. Engl. J. Med. 344(1), 3–10.
Schiffman, S. S., Lockhead, E., and Maes, F. W. 1983. Amiloride reduces the taste intensity of Na and Li salts and sweeteners. Proc. Natl. Acad. Sci. U. S. A. 80, 6136–6140.
Schulkin, J. 1991. Sodium Hunger: The Search for a Salty Taste. Cambridge University Press.
Smriga, M., Kameishi, M., and Torii, K. 2002. Brief exposure to NaCl during early postnatal development enchances adult intake of sweet and salty compounds. Neuroreport. 13(18), 2565–2569.
Stefansson, V. 1946. Not by Bread Alone. Macmillan.
Stouffer, E. M. and White, N. M. 2005. A latent cue preference based on sodium depletion in rats. Learn. Mem. 12, 549–552.
Tamura, M., Seki, T., Yoshihiro, K., Tada, M., Kikuchi, E., and Okai, H. 1989. An enhancing effect on the saltiness of sodium chloride of added amino acids and their esters. Agric. Biol. Chem. 53, 1625–1633.
Taubes, G. 1998. The political history of salt. Science 281, 898–907.
Thaw, A. K., Frankmann, S., and Hill, D. L. 2000. Behavioral taste responses of developmentally NaCl-restricted rats to various concentrations of NaCl. Behav. Neurosci. 114, 437–441.
Turgeon, C. 1964. La Cuisine de France, Mapie, the Countess de Toulouse-Lautrec, Edited and translated by Charlotte Turgeon, 763 pp. The Orion Press.

Further Reading

Appel, L. J., Moore, T. J., Obarzanek, E., Vollmer, W. M., Svetkey, L. P., Sacks, F. M., Bray, G. A., Vogt, T. M., Cutler, J. A., Windhauser, M. M., Lin, P.-H, and Karanja, N. 1997. A clinical trial of the effects of dietary patterns on blood pressure. N. Engl. J. Med. 336(16), 1117–1124.

Beauchamp, G. K. and Cowart, B. 1990. Preference for high salt concentrations among children. Dev. Psychol. 26, 539–545.

Beauchamp, G. K., Bertino, M., Burke, D., and Engelman, K. 1990. Experimental sodium depletion and salt taste in normal human volunteers. Am. J. Clin. Nutr. 51, 881–889.

He, F. J. and MacGregor, G. A. 2003. How far should salt intake be reduced? Hypertension 42, 1093–1099.

Zinner, S. H., McGarvey, S. T., Lipsitt, L. P., and Rosner, B. 2002. Neonatal blood pressure and salt taste responsiveness. Hypertension 40, 280–285.

4.22 Behavioral Analysis of Taste Function in Rodent Models

S J St. John, Rollins College, Winter Park, FL, USA

A C Spector, The Florida State University, Tallahassee, FL, USA

© 2008 Elsevier Inc. All rights reserved.

4.22.1	**Introduction**	409
4.22.2	**Domains of Taste Function**	410
4.22.3	**Behavioral Assessment of Taste Function**	411
4.22.3.1	Two-Bottle Preference Test	411
4.22.3.1.1	Procedure	411
4.22.3.1.2	Strengths	413
4.22.3.1.3	Limitations	413
4.22.3.2	Brief-Access Taste Test	414
4.22.3.2.1	Procedure	414
4.22.3.2.2	Strengths	414
4.22.3.2.3	Limitations	414
4.22.3.3	Oromotor Taste Reactivity Test	415
4.22.3.3.1	Procedure	415
4.22.3.3.2	Strengths	415
4.22.3.3.3	Limitations	415
4.22.3.4	Progressive Ratio Taste Reinforcer Efficacy Test	415
4.22.3.4.1	Procedure	415
4.22.3.4.2	Strengths	415
4.22.3.4.3	Limitations	415
4.22.3.5	Conditioned Taste Aversion	416
4.22.3.5.1	Procedure	416
4.22.3.5.2	Strengths	416
4.22.3.5.3	Limitations	416
4.22.3.6	Operantly Conditioned Taste Detection and Discrimination	416
4.22.3.6.1	Procedure	416
4.22.3.6.2	Strengths	417
4.22.3.6.3	Limitations	417
4.22.4	**Use of Multiple Behavioral Assays Can Provide Rich Insight into the Organization of the Gustatory System**	417
4.22.4.1	Peripheral Mechanisms of Salt Taste	417
4.22.4.2	Use of Behavioral Procedures to Study the Functional Neuroanatomy of the Central Gustatory System	419
4.22.4.2.1	Taste reactivity in decerebrate rats	420
4.22.4.2.2	Taste function after lesions in the gustatory nuclei	420
4.22.5	**Final Comments**	422
References		422

4.22.1 Introduction

Researchers studying sensation and perception face the daunting task of making inferences about the internal experience of the subject without the benefit of direct measurement. In humans, perception is sometimes inferred through verbal report. This is not possible in nonhuman animals, from which the primary neurobiological database derives. Consequently, perceptual processes must be assessed through other behavioral means. This poses significant methodological and conceptual challenges, but is an absolutely

essential component in any attempt to understand the neural principles underlying perception. Indeed, the strategic use of well-designed and complementary behavioral procedures, coupled with theoretically relevant manipulations of the nervous system, can lead to rich insights into the relatively concealed workings of our own sensory machinery.

Comparisons of the consequences of neural manipulations on the performance of animals tested on diverse behavioral tasks have historically provided powerful breakthroughs in understanding sensory function. A vivid example of this was the use of multiple visual tasks to better define the blindness caused by tectal lesions in hamsters (Schneider, G. E., 1969). Following such lesions, hamsters located food only by touch and smell, and did not orient their heads to motion, but did learn to associate a visual cue with the availability of water. In contrast, animals with lesions of the primary visual cortex located food by sight and oriented their heads in response to moving stimuli, but did not learn to associate a visual cue with water if the stimulus was sufficiently complex. This study, and others like it, highlights the danger of misinterpreting functional deficits, or lack thereof, following neural manipulations, if the scope of the behavioral analysis is limited. In other words, if only a single behavioral task had been employed to assess the effects of the lesion, different conclusions may have been reached regarding the functional use of sight. Without question, such experiments helped refine the concept of blindness and have contributed greatly to our view of the brain as a parallel processor.

In this vein, the purpose of this chapter is to discuss some basic interpretive properties of standard behavioral tasks that have been, and can be, used to infer the taste capabilities of nonhuman animal subjects and to provide some examples of how several of these paradigms have been successfully used in efforts to reveal the functional organization of the gustatory system.

4.22.2 Domains of Taste Function

Taste function can be heuristically divided into at least three domains (see Pfaffmann, C. *et al.*, 1979; Norgren, R., 1985; Scott, T. R. and Mark, G. P., 1986; Spector, A. C., 2000). The sensory-discriminative domain refers to the processes that allow animals to discriminate between taste compounds. This function can be subdivided into intensity, providing information regarding the amount of the stimulus, and quality, providing information about the identity of the stimulus. The motivational domain refers to processes that promote or discourage ingestion of chemical substances. This function can be subdivided into an appetitive/avoidance component, which refers to actions that bring the animal closer to, or take the animal further from, the stimulus, and a consummatory/rejection component, which refers to reflex-like oromotor movements that lead to the ingestion or expulsion of stimuli contacting taste receptors (Craig, W., 1918; see also Grill, H. J. *et al.*, 1987; Berridge, K. C., 2004). Finally, the physiological domain refers to the ability of taste stimuli to trigger autonomic responses such as salivation (e.g., Pavlov, I. P., 1902).

In mammals, taste buds are distributed throughout the oral cavity in distinct fields each innervated by a different branch of three cranial nerves (Bradley, R. M., 1971; Miller, I. J., Jr., 1977; Travers, S. P. and Nicklas, K., 1990). In the central nervous system, gustatory projections form two divergent pathways as they ascend from the caudal brainstem to the forebrain – a thalamocortical pathway, characteristic of many sensory systems, and a ventral forebrain pathway, involving the amygdala, hypothalamus, and other structures (see Norgren, R., 1992; Travers, S. P., 1993; Norgren, R., 1995). Thus, the anatomical organization of the gustatory system invites speculation regarding the functional significance of these neural circuits. One effective strategy that has been used to uncover the relationship between nervous system structures and gustatory function is to alter the flow of information along these pathways and assess the consequences on taste-related behavioral tasks. Several decades of such experiments have taught us that a single behavioral measure is not sufficient to capture the full impact of a given manipulation on gustatory function. Just as blindness can be a relative term, so can aguesia. Competence or impairment on one behavioral task involving taste stimuli does not necessarily predict the same level of performance on another after a given experimental manipulation of the nervous system.

Some examples of such functional dissociations can be found in the following pages. The remainder of Section 4.22.3 will briefly review some of the methodological and interpretive properties of various behavioral paradigms used to assess gustatory processes in animal models, and Section 4.22.4 will illustrate the successful use of such procedures in neurobiological studies.

4.22.3 Behavioral Assessment of Taste Function

The assessment of taste function in animals requires careful consideration of the methodological features of the behavioral procedures used. Performance in some behavioral paradigms reflects the outcome of processes involving more than one functional domain (Table 1). These behavioral paradigms differ in some fundamental ways.

Procedures that involve the measurement of intake over prolonged periods of stimulus presentation (e.g., two-bottle preference test) are governed partly by the affective potency of the stimulus, but are also vulnerable to the influence of postingestive events (e.g., McCleary, R. A., 1953; Shuford, E., Jr., 1959; Mook, D. G., 1963; Rabe, E. F. and Corbit, J. D., 1973; Weingarten, H. P. and Watson, S. D., 1982; Nissenbaum, J. W. and Sclafani, A., 1987a). Intake tests involving the use of the sham drinking preparation (in which the ingested content flows out of an open gastric cannula) provide greater confidence that taste processing – or at least orosensory processing – guides behavior (e.g., Davis, J. D. and Campbell, C. S., 1973; Weingarten, H. P. and Watson, S. D., 1982; Schneider, L. H. *et al.*, 1986; Nissenbaum, J. W. and Sclafani, A., 1987a). Similarly, the presentation of fluids in brief-access trials, which minimize the influence of postingestive receptor systems during the response, can be used to assess the motivational characteristics (i.e., affective potency) of taste stimuli (see Young, P. T., 1952; Young, P. T. and Madsen, C. H., Jr., 1963; Grill, H. J. and Berridge, K. C., 1985). These procedures involve both an appetitive/avoidance component and a consummatory/rejection component. Other tasks allow investigators to assess the appetitive/avoidance component (e.g., a progressive ratio procedure) independent of the consummatory/rejection component and vice versa (e.g., an oromotor taste reactivity procedure).

In still other procedures, taste compounds are used as discriminative stimuli in operant-conditioning procedures or as conditioned stimuli in classical conditioning paradigms (e.g., Koh, S. D. and Teitelbaum, P., 1961; Morrison, G. R. and Norrison, W. 1966; Morrison, G. R., 1967; Slotnick, B. M., 1982; Spector, A. C. *et al.*, 1990b; Stapleton, J. R. *et al.*, 2002). These tasks provide a means by which sensory-discriminative taste function can be assessed separately from the affective properties of a stimulus. For example, hydrochloric acid or citric acid, quinine, and high concentrations of sodium chloride (NaCl), are all avoided by rats in intake and brief-access taste tests, but rats can be trained to discriminate these compounds in operant or classical conditioning paradigms (Morrison, G. R., 1967; Nowlis, G. H. *et al.*, 1980).

Regardless of the behavioral procedure employed, the potential for nongustatory cues associated with other chemosensory receptor systems must be considered. Perhaps the most vexing of these signals arises from stimulation of the trigeminal and olfactory systems, particularly at higher stimulus concentrations. For example, the viscosity of sugar solutions or the irritant properties of salts and acids (e.g., Gilmore, M. M. and Green, B. G., 1993) produce trigeminal sensations that could potentially affect behavioral responses. Although many prototypical taste compounds have very low vapor pressures and are thus suboptimal olfactory stimuli, there is evidence that rats can detect the smell of some taste solutions (Miller, S. D. and Erickson, R. P., 1966; Van Buskirk, R. L., 1981; Rhinehart-Doty, J. A. *et al.*, 1994; Capaldi, E. D. *et al.*, 2004). In contrast, at least with certain types of stimulus delivery designs (e.g., Spector, A. C. *et al.*, 1990a), it is clear that odor cues, if present, are insufficient at maintaining normal performance in some taste-related tasks when certain gustatory nerves are transected – a neural manipulation unlikely to have any direct effect on the olfactory system (e.g., Spector, A. C. *et al.*, 1990b; Slotnick *et al.*, 1991; Spector, A. C. *et al.*, 1996b; St. John, S. J. and Spector, A. C., 1996; St. John, S. J. and Spector, A. C., 1998). In any event, such concerns often necessitate empirical assays of the contribution of extragustatory sensory cues to behavior.

4.22.3.1 Two-Bottle Preference Test

4.22.3.1.1 Procedure

In the two-bottle preference test, animals are presented with two bottles usually placed on their cages for ~24 h. One bottle contains a taste solution and the other contains water (or some other taste solution). The relative intake of the two solutions is calculated and then the bottles are refilled, the positions reversed, and the test repeated. The repetition of the test with the bottles reversed serves to offset the appearance of a solution preference that may instead reflect a position preference. The determination of preference is based on the 48 h values. If the animals are unfamiliar with having access to two bottles or to bottles of the type used for the experiment, it is advisable to present habituation trials consisting of only water in advance of the experimental tests.

In most applications of this procedure, it is the outcome of the behavioral response, intake, which is

Table 1 Functional features of behavioral taste tests

Behavioral procedure	*Taste quality measure*	*Intensity measure*	*Hedonic measure*	*Appetitive/ avoidance component*	*Consummatory/ reflex component*	*Postingestive influence*	*Deprivation necessary*
Unconditioned two-bottle preference test	No[a]	Yes	Yes	Yes	Yes[b]	Yes[c]	Variable[d,e]
Unconditioned brief-access taste test	No[a]	Yes	Yes	Yes	Yes[f]	Minimized	Variable[d]
Unconditioned oromotor taste reactivity test	No[a]	Yes	Yes	No	Yes	Minimized	No
Unconditioned sham drinking test	No[a]	Yes	Yes	Yes	Yes[b]	No[g]	Variable[d]
Progressive ratio taste reinforcer efficacy test	No[a]	Yes	Yes	Yes	No	Minimized	Variable[d]
Conditioned taste preference/aversion: two-bottle preference test	Yes	Yes	Yes	Yes	Yes[b]	Yes[c]	Variable[e]
Conditioned taste preference/aversion: brief-access taste test	Yes	Yes	Yes	Yes	Yes[f]	Minimized	Yes
Conditioned taste preference/aversion: oromotor taste reactivity test	Yes	Yes	Yes	No	Yes	Minimized	No
Conditioned taste preference/aversion: progressive ratio test	Yes	Yes	Yes	Yes	No	Minimized	Yes
Operantly conditioned taste detection	No	Yes	No	No	No	Minimized	Yes
Operantly conditioned taste intensity discrimination	No	Yes	No	No	No	Minimized	Yes
Operantly conditioned taste discrimination	Yes	No	No[h]	No	No	Minimized	Yes

[a]Because of the specificity of responses to sodium salts in sodium-depleted animals, this test could be considered as a sensory measure of taste quality under certain conditions.
[b]Though not explicitly measured. If this test is coupled with a licking pattern analysis, then burst of licks could be considered as reflecting a strong consummatory component.
[c]The extent depends upon the duration of the test.
[d]Deprivation is not always required for unconditionally reinforcing stimuli (like sucrose).
[e]Deprivation is not required for long-duration tests (24 h, overnight, etc.).
[f]Though not explicitly measured. Trials initiated would be considered a pure appetitive measure, but the licks taken on a trial in some sense represents both appetitive and consummatory responses.
[g]Or virtually none. There is some evidence of some small amounts of nutrients passing into the duodenum during sham drinking.
[h]There may be some stimulus pairs (e.g., sucrose vs. quinine) where hedonically based taste discriminations could be possible.

measured. However, in some cases, investigators have measured licking behavior itself and have thus been able to reconstruct the pattern of drinking (e.g., LeMagnen, J. and Devos, M., 1980; Smith, J. C. and Foster, D. F., 1980; Spector, A. C. and Smith, J. C., 1984; Davis, J. D., 1989; Davis, J. D. and Smith, G. P., 1992; Davis, J. D., 1996; Spector, A. C. and St. John, S. J., 1998). When this is done in rodents, it is clear that drinking occurs in bursts of licks separated by pauses. A collection of bursts followed by a long pause could be construed as an ingestive bout or a meal if the solution is caloric. The number of bursts represents a relatively pure assessment of the appetitive behavior (i.e., initiations of drinking) and the size of a burst is heavily influenced by consummatory processes (e.g., swallowing). Thus, more refined measurement of behavior during a two-bottle preference test can provide meaningful information regarding the effects of taste on the components of motivated action.

4.22.3.1.2 Strengths

The two-bottle preference test has a long history, and thus a large body of normative data exists using this procedure. It is also relatively inexpensive, requires no customized equipment, and does not involve complicated training protocols for either animals or the staff. It is also usually amenable to testing a large number of subjects simultaneously.

4.22.3.1.3 Limitations

This test has been used to assess unconditioned and conditioned taste preferences and aversions. When used to measure unconditioned responses to taste compounds it does not provide any explicit information about the discriminative qualitative features of the stimulus (i.e., an animal might avoid both hydrochloric acid and quinine relative to water, but a similar level of avoidance does not preclude that that animal could discriminate these tastes from one another). The two-bottle preference test can provide some information about intensity, but it is difficult to discern the intensity of the stimulus independent of its hedonic characteristics because it is the latter that help drive the intake. For example, Eylam S. and Spector A. C. (2002) found that the NaCl detection thresholds measured with an operant-conditioning procedure (discussed below) were well below the concentration at which the same mice started to reliably avoid the stimulus in a two-bottle preference test. Thus, although mice could detect low concentrations of NaCl, they apparently displayed no consistent preference or aversion for them (Figure 1). In contrast, detection thresholds for

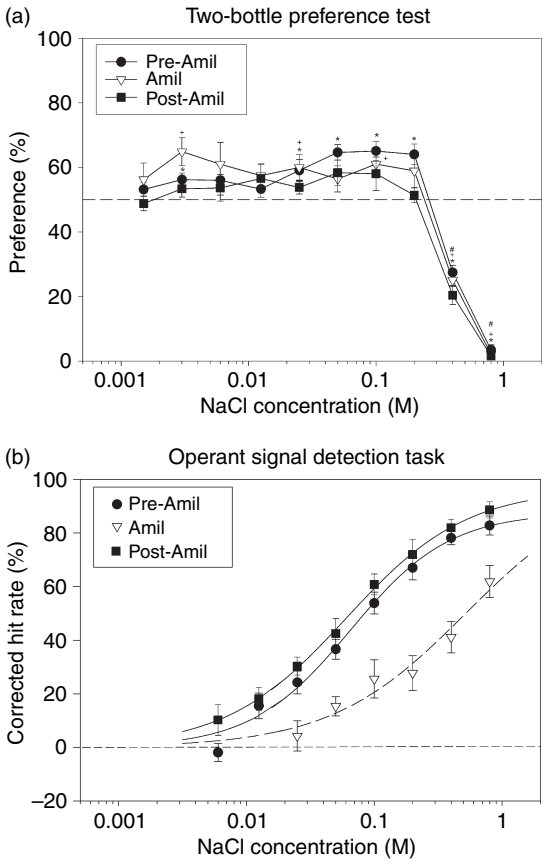

Figure 1 (a) Mean (± standard error of the mean) percentage NaCl intake by C57BL/6J mice ($n = 7$) in a 48 h two-bottle preference test in which ascending concentrations of NaCl were pitted against water in three series of tests with (Amil, open triangles) and without (preAmil, closed circles; post-Amil, closed squares) 100 μM amiloride serving as the solvent. Significant differences from 50%: * for pre-Amil, + for Amil, and # for post-Amil. These mice had been previously tested for detection thresholds in an operant signal detection task (see (b)). (b) Mean (± standard error of the mean) percentage hits on NaCl trials corrected for false alarms on water trials in an operant signal detection task as a function of NaCl concentration. The mice were tested in three phases of sessions. In the first (preAmil, filled circles) and third phase (post-Amil, filled squares), the NaCl was dissolved in water. In the second phase of sessions (Amil, open triangles), the NaCl was dissolved in 100 μM amiloride. In comparing (a) and (b) note that the preference-avoidance function is relatively flat until the concentration exceeds 0.2 M, whereas the dynamic range of responsiveness in the operant signal detection task occurs at lower concentrations. Also, amiloride had little effect on NaCl preference in these mice, but had a striking effect on NaCl detectability in the operant task. Adapted with permission from Eylam, S. and Spector, A. C. The effect of amiloride on operantly conditioned performance in an NaCl taste detection task and NaCl preference in C57BL/6J mice. Behav. Neurosci. 116, 149–159, 2002, Copyright 2002, American Psychological Association.

sucrose and glucose in mice correspond reasonably well with preference thresholds reported in the literature in mice (Bachmanov, A. A. *et al.*, 2001) likely because the affective value of these stimuli grows sharply once they are detected (see Eylam, S. and Spector, A. C., 2004). It is prudent to use the term preference threshold to indicate the concentration that subjects treat differently than water in two-bottle preference tests, and reserve the term detection threshold for concentrations discriminated from water in assays (like operant-conditioning procedures) where behavior is not dependent on hedonic evaluations.

As mentioned above, one principal shortcoming of the long-term two-bottle preference test is that postingestive events can influence intake and thus can complicate the interpretation of taste effects. For example, St. John S. J. *et al.* (2005) recently demonstrated that the dramatic increased avoidance of phenylthiocarbamide with ascending concentration in certain mouse strains was most likely due to the formation of a conditioned aversion to that compound over successive intake tests, rather than the expression of unconditioned avoidance due to its taste.

4.22.3.2 Brief-Access Taste Test

4.22.3.2.1 Procedure

In the brief-access taste test, animals are presented with very brief access to taste solutions, on the order of a few seconds, during which licking responses are measured (e.g., Young, P. T. and Trafton, C. L., 1964; Davis, J. D., 1973; Yamamoto, T. and Asai, K., 1986; Krimm, R. F. *et al.*, 1987; Smith, J. C. *et al.*, 1992; Breslin, P. A. *et al.*, 1993b; Spector, A. C. *et al.*, 1993a; 1993b; O'Keefe, G. B. *et al.*, 1994; St. John, S. J. *et al.*, 1994; Contreras, R. J. *et al.*, 1995; Markison, S. *et al.*, 1995; Spector, A. C. *et al.*, 1996b; Boughter, J. D. *et al.*, 2002; Glendinning, J. I. *et al.*, 2002; Zhang, Y. *et al.*, 2003; Dotson, C. D. and Spector, A. C., 2004). Many trials are presented during a session and responses to a variety of different solutions varying in concentration and/or solute can be tested. For normally preferred compounds, the test can be conducted in nondeprived animals, but for normally avoided compounds, the test must be conducted in fluid-deprived animals so that the subjects are highly motivated to sample the stimuli in search of water.

4.22.3.2.2 Strengths

Because immediate responses to small volumes of taste stimuli are measured, this test minimizes the influence of postingestive events on the behavior. Furthermore, the brief-access taste test can measure changes in responsiveness past the point at which preference tests reach asymptote as the concentration is raised. Because many trials are presented in a single session, full concentration–response functions can be obtained in a single test session. Random presentation minimizes order effects which are sometimes present in concentration series of longer-duration intake tests. In general, very orderly concentration–response functions are derived in the brief-access taste test, although the dynamic range of responsiveness is biased toward the higher concentrations (i.e., as with the two-bottle preference test, the concentration at which the lick rate differs from water may or may not be closely related to the detection threshold).

4.22.3.2.3 Limitations

First, like the two-bottle preference test, the brief-access taste procedure relies on the hedonic characteristics of the stimulus to drive responses and thus does not provide explicit information regarding the discriminative qualitative features of a taste compound. For example, animals will avoid licking both NaCl and quinine in a concentration-dependent manner even though they can discriminate between these stimuli in several other tasks (e.g., Morrison, G. R., 1967; Nowlis, G. H. *et al.*, 1980; Spector, A. C. *et al.*, 1993a; Cauthon, R. *et al.*, 1994; St. John, S. J. *et al.*, 1994; Spector, A. C., 1995b; Boughter, J. D. *et al.*, 2002; Glendinning, J. I. *et al.*, 2002; Geran, L. C. *et al.*, 2004).

Second, although concentration–response functions using this method are highly reliable within a given context, the context can affect the outcome. For example, the concentration–response function can be shifted to the left when an animal is tested with only one concentration per session pitted against water, rather than randomly presenting all concentrations on each day of testing (Glendinning, J. I. *et al.*, 2005).

Third, the brief-access taste test provides a measure of the affective potency of a taste stimulus, but does not clearly differentiate between appetitive/avoidance and consummatory/rejection responses. The former behavior is associated with the animal approaching the drinking spout and the latter behavior is reflexively triggered by the contact of the oral receptors with the stimulus. Although it may be possible to reconstruct the pattern of licking behavior during a trial to try to distinguish these processes, the very brief duration of the observation period (usually 5–10 s) places limitations on such an analysis. In contrast, trials initiated could be considered a measure of appetitive behavior, but this datum is also

under the influence of the postingestive properties of the stimulus and the physiological state of the animal. For example, it is likely that the more fluid-deprived an animal is, the more trials it will initiate.

Finally, and unlike a long-term preference test, the brief-access taste test must be conducted differently for normally preferred and normally avoided stimuli. Animals will not initiate trials to nonpreferred stimuli unless they are water-deprived; in contrast, water-deprived rats will lick all concentrations of preferred substances at a maximal rate (a ceiling effect). Depending on the overall goals of the research, the physiological state of testing may constrain interpretation.

4.22.3.3 Oromotor Taste Reactivity Test

4.22.3.3.1 Procedure

Chronic indwelling cannulae can be surgically implanted into the oral cavity through which taste solutions can be infused at a rate and pattern under the control of the experimenter. Oral motor and somatic responses can then be monitored (Grill, H. J. and Norgren, R., 1978c; 1978d; Grill, H. J. *et al.*, 1987; Spector, A. C. *et al.*, 1988; Brining, S. K. *et al.*, 1991; Berridge, K. C., 1996). Animals can swallow or expel the infused fluid. Ingestive responses elicited by normally preferred stimuli include tongue protrusions and low-amplitude mouth movements. Aversive responses elicited by normally avoided stimuli include gapes, chin rubs, head shakes, and forelimb flails. Generally the responses are videotaped or measured with electromyographic (EMG) electrodes placed in relevant oromotor muscles (e.g., Travers, J. *et al.*, 2000).

4.22.3.3.2 Strengths

Orofacial responses are triggered by the stimulus contacting the oral receptors and no appetitive action is necessary for stimulus delivery making the test useful for assessing consummatory/rejection behavior almost purely. In addition, because the experimenter initiates stimulation directly, there is no need for food or water deprivation to promote stimulus sampling.

The test is typically very short, on the order of a minute, precluding any substantial postingestive influence.

4.22.3.3.3 Limitations

As with the other tests described thus far, taste reactivity is dependent on the affective properties of the stimulus, and thus does not indicate the relative discriminability of stimuli or provide high-fidelity information about detection thresholds. Unlike most behavioral assays, this procedure requires a surgical procedure, albeit one that rodents tolerate well. Also, unlike most behavioral assays, the dependent variable cannot be automatically counted (e.g., by a lickometer circuit) unless EMG electrodes are surgically implanted (see Travers, J. B. *et al.*, 1997). Thus, time and training are required of the experimenter to score videotapes frame by frame.

4.22.3.4 Progressive Ratio Taste Reinforcer Efficacy Test

4.22.3.4.1 Procedure

In the progressive ratio taste reinforcer efficacy test, animals are trained to execute a specific operant response, such as lever pressing or dry-spout licking, to receive a small volume of a taste solution. Initially, the number of responses required to produce the taste reinforcer is low, but the requirement is progressively raised as the session continues until the animal reaches a breakpoint and ceases to respond further (Hodos, W., 1961; Hodos, W. and Kalman, G., 1963; Reilly, S., 1999; Reilly, S. and Trifunovic, R., 1999; Sclafani, A. and Ackroff, K., 2003). The breakpoint is thought to reflect the efficacy of the reinforcer and thus can be construed as a measure of the affective potency of a taste stimulus.

4.22.3.4.2 Strengths

Once trained, deprivation states are unnecessary for normally preferred stimuli (e.g., sucrose), but water deprivation is required to test normally avoided stimuli (e.g., quinine). In the latter case, the motivation to rehydrate is pitted against the aversive characteristics of the taste stimulus. Depending on the step-size schedule, the actual total amount of reinforcer delivered can be kept relatively small, thus attenuating the influence of postingestive factors and satiation. Just as the oromotor taste reactivity test is a pure measure of consummatory/rejection responses, the progressive ratio is a pure measure of appetitive behavior. This is because the behavior, which leads to the presentation of the taste reinforcer, is produced without the stimulus contacting the receptors.

4.22.3.4.3 Limitations

This procedure has the same limitations as some of the other procedures discussed in that the responses are driven by the affective evaluation of the stimulus.

4.22.3.5 Conditioned Taste Aversion

4.22.3.5.1 Procedure

Typically, when ingestion of a specific taste stimulus is followed by injection of a viscerally aversive agent (e.g., lithium chloride (LiCl); see Garcia, J. *et al.*, 1955; Nachman, M. and Ashe, J. H., 1973; Domjan, M., 1980; Barker, L. M. *et al.*, 1999), often after only a single conditioning trial (depending on the dose of the aversive agent), animals will display robust avoidance and rejection behavior in response to the conditioned taste stimulus. Because animals will generalize their conditioned responses to some taste compounds but not others, this procedure has been useful for making inferences about the degree of qualitative similarity between taste stimuli (e.g., Nachman, M., 1963; Tapper, D. N. and Halpern, B. P., 1968; Nowlis, G. H. *et al.*, 1980; Smith, D. V. and Theodore, R. M., 1984).

4.22.3.5.2 Strengths

To the extent that taste aversion generalization paradigms provide information about the sensory-discriminative features of taste solutions, the taste aversion methodology is technically simpler than operant discrimination paradigms. In addition, training is usually effective after a single conditioning trial. If a gustometer is used to measure conditioned avoidance responses, a variety of test compounds can be included in the stimulus array and generalization profiles can be obtained in a single test session.

4.22.3.5.3 Limitations

From a practical perspective, one must be concerned with the possibility of extinction effects that can occur with continued testing that involve the conditioned stimulus or compounds that bear some qualitative similarity to it. This places limits on the number of test sessions and test stimuli that can be included in the design. From a conceptual perspective, conditioned taste aversions are functionally complex measures in that the quality, intensity, hedonics, and even physiological responses (e.g., Berridge, K. *et al.*, 1981) are all potentially involved. These procedures are designed to change the hedonic properties of a specific stimulus identified by its quality. Like all conditioning processes the concentration of the taste stimuli must be considered because generalization can take place along the intensity dimension (Hagstrom, E. C. and Pfaffmann, C., 1959; Tapper, D. N. and Halpern, B. P., 1968; Nowlis, G. H., 1974; Scott, T. R. and Giza, B. K., 1987; Spector, A. C. and Grill, H. J., 1988). Accordingly, a given experimental manipulation of the gustatory system can affect behavioral outcomes in this paradigm by influencing function in one of several of these domains.

Second, it must be remembered that generalization and discrimination, while related, are distinct psychological concepts. For example, taste aversions to sucrose generalize to maltose (e.g., Nissenbaum, J. W. and Sclafani, A., 1987b; Spector, A. C. and Grill, H. J., 1988) and glutamate (Heyer, B. R. *et al.*, 2003), but sucrose can also be discriminated from these compounds on the basis of gustatory cues (Spector, A. C. *et al.*, 1997; Stapleton, J. R. *et al.*, 2002; Heyer, B. R. *et al.*, 2004).

4.22.3.6 Operantly Conditioned Taste Detection and Discrimination

4.22.3.6.1 Procedure

Operantly conditioned taste detection and discrimination tasks have a well-established history of use in the psychophysical examination of a variety of sensory systems in animals (see Blough, D. and Blough, P., 1977; Stebbins, W. C. and Berkley, M. A., 1990). In the study of gustatory processes, generally a taste stimulus is used as a cue for responding in a specific way (see Carr, W. J., 1952; Harriman, A. E. and MacLeod, R. B., 1953; Koh, S. D. and Teitelbaum, P., 1961; Morrison, G. R. and Norrison, W., 1966; Morrison, G. R., 1967; Shaber, G. S. *et al.*, 1970; Slotnick, B. M., 1982; Brosvic, G. M. and Slotnick, B. M., 1986; Spector, A. C. *et al.*, 1990b; Willner, P. *et al.*, 1990; Thaw, A. K. and Smith, J. C., 1992; St. John, S. J. *et al.*, 1997; Stapleton, J. R. *et al.*, 2002; Spector, A. C., 2003). If the response is correctly executed the behavior can be reinforced (e.g., the animal is rewarded); if the response is incorrectly executed, the animal can be punished. For instance, a thirsty rat can be trained to press a left-hand lever if a five-lick stimulus sample is NaCl and a right-hand lever if the sample is water. A correct response can lead to access to 20 licks of water (which is rewarding because the animal is on a water-restriction schedule) and an incorrect response can lead to a 30 s time-out, further delaying the opportunity to receive water. The concentration of the NaCl stimulus can be varied across trials until it reaches a low enough value that the animal does not differentially respond between the taste and water stimulus; thus a detection threshold can be measured. If the water stimulus in the prior example is replaced with a second taste

stimulus (e.g., potassium chloride (KCl)), then the procedure can be used to measure the degree of discriminability between the two taste compounds being tested.

4.22.3.6.2 Strengths

These procedures possess some of the same benefits as the brief-access taste test in that small stimulus samples are used and immediate responses are measured curtailing the influence of postingestive events on responses. In addition, the taste compounds serve as signals for other events (reward or punishment) and, thus, the responses are under the control of the reinforcement contingencies established and not the inherent motivational characteristics of the sapid stimuli.

4.22.3.6.3 Limitations

Under ideal circumstances, the strength of this procedure is that it allows a relatively pure assay of the sensory-discriminative aspects of the tastant. However, animals working for reinforcement may use whatever cues are available. If all of the concentrations of one stimulus are more reinforcing or more aversive than all of the concentrations of the comparison stimulus, then discrimination might arguably take place along a hedonic dimension. For example, if rats were trained to discriminate sucrose from quinine, it is conceivable that such a discrimination could be guided by the hedonic valence of the stimuli as opposed to their qualitative characteristics. In general, because the hedonic potency of a taste stimulus often covaries with its concentration, and several concentrations of each stimulus are presented within a session, there is likely overlap in the affective valence of the discriminated compounds such that the hedonic properties of the stimuli are rendered irrelevant cues. Nevertheless, there may be some stimulus pairs (e.g., sucrose vs. quinine) where hedonically based taste discriminations could be possible.

An additional consideration in the use of discrimination procedures is that it remains possible that animals might use taste cues that are not strictly related to the perceptual quality of the compounds to guide their performance. For example, perhaps compounds evoking similar qualities might vary in their kinetics of reaching or activating receptors such that they differ in the rise and/or decay times of the sensation. Potentially, that information could be used by the animal to competently discriminate between the two stimuli. Although such a possibility remains speculative, it is difficult to entirely dismiss. Because animals potentially have a variety of taste cues not strictly related to the quality of the stimulus per se to guide performance, a failure for an animal to discriminate between two compounds is an interpretively powerful result, provided that learning and motivational factors can be discounted.

4.22.4 Use of Multiple Behavioral Assays Can Provide Rich Insight into the Organization of the Gustatory System

As noted in the introduction, the use of multiple behavioral assays is critical to gain a comprehensive understanding of sensory function; no single behavioral procedure provides a gold standard test. A given assay may reveal taste deficits after a particular experimental manipulation, but other assays may indicate normal function. This is because each behavioral paradigm is influenced by various aspects of taste processing as summarized in Table 1. An experimental manipulation may affect one aspect of taste function (e.g., quality) but not another (e.g., hedonic), and whether performance in a task is affected will depend on the degree to which the behavior in the assay is dependent on the relevant function. Some examples are provided below.

4.22.4.1 Peripheral Mechanisms of Salt Taste

Decades ago, Pfaffmann and Beidler (Pfaffmann, C., 1941; Beidler, L. M., 1953; 1954; Pfaffmann, C., 1955) showed that the chorda tympani (CT) nerve of the rat was exceptionally responsive to sodium salts. Thus, although this nerve innervating the anterior tongue transmits afferent information from a minority of taste buds (in the rat, less than 15% of the total), the electrophysiological data promoted the rational expectation that transection of the CT nerve would severely impair taste sensitivity to salt. Pfaffmann C. (1952) tested this hypothesis by using the two-bottle preference test and comparing salt preference in intact rats, rats with CT nerve transection, and rats with combined transection of both the CT and glossopharyngeal (GL, innervates posterior tongue) nerves (denervating >70% of the total taste buds). To his surprise, none of these transections had an effect on salt preference; an outcome reported by others using similar behavioral paradigms (Richter, C. P., 1939; Akaike, N. *et al.*, 1965; Vance, W. B., 1967;

Grill, H. J. and Schwartz, G. J., 1992; Grill, H. J. *et al.*, 1992). Although some or all of this maintained responsiveness in the neurotomized rats may have been due to the influence of the NaCl on postlaryngeal receptors, a similar lack of effect on salt responsiveness has been observed even when a brief-access taste test, which minimizes the contribution of postingestive events, was used as an assay (Cauthon, R. *et al.*, 1994).

Adulteration of NaCl solutions with the epithelial sodium channel blocker amiloride also has little or no effect on NaCl preference measured in a two-bottle preference test in either C57BL/6 (B6) mice (Figure 1) or F-344 rats (Chappell, J. P. *et al.*, 1998; Eylam, S. and Spector, A. C., 2002). Like the lack of effect of CT nerve transection on NaCl preference, the ineffectiveness of amiloride to alter ingestive behavior in this test was unexpected because the drug notably suppresses CT and greater superficial petrosal (GSP) responses to NaCl in most rodents (e.g., Heck, G. I. *et al.*, 1984; Brand, J. G. *et al.*, 1985; DeSimone, J. A. and Ferrell, F., 1985; Herness, M. S., 1987; Ninomiya, Y. *et al.*, 1989; Hettinger, T. P. and Frank, M. E., 1990; Simon, S. A. *et al.*, 1993; Ye, Q. *et al.*, 1993; Doolin, R. E. and Gilbertson, T. A., 1996; Sollars, S. I. and Hill, D. L., 1998; Lindemann, B. *et al.*, 1999).

One seemingly straightforward conclusion consistent with these behavioral data is that the CT and the epithelial sodium channels in taste receptor cells are not critical in the maintenance of taste sensitivity to NaCl, but such a verdict would be premature. Responsiveness in both the two-bottle preference test and the brief-access taste test are driven by the hedonic characteristics of the stimulus. Moreover, the former procedure is vulnerable to postingestive events and the latter procedure does not have optimal sensitivity in the low concentration range. Neither procedure provides explicit information on the qualitative characteristics of the taste stimulus. Thus, to conclude that rodents had normal salt taste perception following these manipulations in the peripheral gustatory system would be akin to concluding that hamsters are visually normal after visual cortex lesions based on the results of one or only a few behavioral assays.

As it turns out, suppression of the amiloride-sensitive salt transduction pathway or removal of the afferent input from the CT has severe consequences on sodium taste discriminability. When operant conditioning procedures are used to train rats to respond differentially to NaCl and water and the concentration of the stimulus is varied, the resulting detection threshold is shifted 1–2 orders of magnitude by transection of the CT (Spector, A. C. *et al.*, 1990b; Slotnick, B. M. *et al.*, 1991; Kopka, S. L. and Spector, A. C., 2001). When the nerve regenerates, the NaCl detection threshold returns to normal (Kopka, S. L. and Spector, A. C., 2001). Likewise, stimulus adulteration with amiloride, which appears to be tasteless to rats and mice (Markison, S. and Spector, A. C., 1995; Eylam, S. *et al.*, 2003), raises detection thresholds for NaCl and sodium gluconate, but not KCl, measured in operantly trained rats and mice (Geran, L. C. *et al.*, 1999; Geran, L. C. and Spector, A. C., 2000a; 2000b; Eylam, S. and Spector, A. C., 2002; 2003). It is important to note, however, that while CT transection raises the NaCl detection threshold measured in operant conditioning procedures, when a similar task was used to assess NaCl difference thresholds (i.e., just noticeable differences between NaCl concentrations) at mid-range concentrations, CT (or GL) transection had little effect (Colbert, C. L. *et al.*, 2004). Apparently, the input from the remaining gustatory nerves is sufficient in maintaining the ability of rats to make normal intensity discriminations within the NaCl concentration range that is detectable after CT transection.

Thus, amiloride treatment and CT transection decrease the sensitivity of some rodents to NaCl. But do these manipulations have any effect on the qualitative nature of NaCl taste? Rats can be trained to discriminate between salts in operant-conditioning paradigms. In these designs, concentration is varied so that intensity cues are irrelevant. Interestingly, performance of rats in an NaCl versus KCl operant discrimination task is significantly impaired by CT transection, but is unaffected by GL transection (Spector, A. C. and Grill, H. J., 1992; St. John, S. J. *et al.*, 1997; Kopka, S. L. *et al.*, 2000). Combined transection of the CT and GSP, removing all of the taste input of cranial nerve VII, drops performance on either an NaCl versus NH_4Cl or on an NH_4Cl versus KCl taste discrimination task to chance levels, but GL transection is without effect (Geran, L. C. and Spector, A. C., 2002; Geran, L. C. *et al.*, 2002b).

Stimulus adulteration with amiloride also leads to chance performance on a NaCl versus KCl discrimination task in rats and mice (Spector, A. C. *et al.*, 1996a; Eylam, S. and Spector, A. C., 2005). In these experiments, animals had many more errors on NaCl trials than on KCl trials suggesting that when the stimuli are mixed with amiloride, NaCl tastes more similar to KCl than to unadulterated NaCl. In support of this conclusion, taste aversions conditioned to

NaCl mixed with amiloride generalize to nonsodium salts in a brief-access taste test (Hill, D. L. *et al.*, 1990). In contrast, when unadulterated NaCl is used as a conditioned stimulus, rats (and other rodents) will specifically avoid NaCl and LiCl but not nonsodium salts (Nowlis, G. H. *et al.*, 1980; Hill, D. L. *et al.*, 1990; see also Nachman, M., 1963).

Another way in which CT transection and amiloride treatment have been shown to affect the taste quality of NaCl is through procedures that take advantage of the physiological and behavioral mechanisms that apparently evolved to protect herbivores and some omnivores from dangerous deficiencies in body sodium. When rats are acutely depleted of sodium, hormonal mechanisms are engaged that facilitate the reabsorption of sodium and trigger neural circuits that potentiate appetitive and consummatory behavior promoting the search for and ingestion of sodium salts (see Denton, D., 1982; Schulkin, J., 1991). Sodium-depleted rats will display increased intake of NaCl in brief-access, short- and long-term drinking tests (Richter, C. P., 1936; Handal, P. J., 1965; Jalowiec, J. E. and Stricker, E. M., 1970; Wolf, G., 1982; Epstein, A. N., 1984; Bernstein I. L. and Hennessy C. J., 1987; Rowland, N. E. and Fregly, M. J., 1992; Breslin, P. A. *et al.*, 1993a; O'Keefe, G. B. *et al.*, 1994; Brot, M. D. *et al.*, 2000), will enhance their licking response for sodium salts over nonsodium salts in brief-access taste tests (Breslin, P. A. *et al.*, 1993b; 1995; Markison, S. *et al.*, 1995; Geran, L. C. and Spector, A. C., 2004), and will show increased ingestive oral motor consummatory responses to NaCl (Berridge, K. C. *et al.*, 1984; Grill, H. J. and Berridge, K. C., 1985; Grill, H. J. and Bernstein, I. L., 1988). The appetite is specific for salts with a sodium cation; the only exception is lithium which is treated as if it is sodium. Transection of the CT compromises, and amiloride treatment eliminates, the vigor and cation-specificity of depletion-induced sodium appetite in rats (Bernstein I. L. and Hennessy C. J., 1987; McCutcheon, N. B., 1991; Sollars, S. I. and Bernstein, I. L., 1992; Breslin, P. A. *et al.*, 1993b; Sollars, S. I. and Bernstein, I. L., 1994; Breslin, P. A. *et al.*, 1995; Markison, S. *et al.*, 1995; Frankmann, S. P. *et al.*, 1996; Roitman, M. F. and Bernstein, I. L., 1999; Brot, M. D. *et al.*, 2000; Geran, L. C. and Spector, A. C., 2004).

Collectively, the findings from these various behavioral procedures in rats indicate that absolute sensitivity to NaCl, as well as the perceived quality of this salt stimulus, is partially dependent on the input of the CT nerve that likely derives from the activation of the amiloride-sensitive salt transduction pathway. This is consistent with the fact that the rat CT has narrowly tuned fibers that respond to NaCl and LiCl but do not respond well to other salts or acids (Frank, M. E. *et al.*, 1983; Ninomiya, Y. and Funakoshi, M., 1988; Lundy, R. F., Jr. and Contreras, R. J., 1999; Sollars, S. I. and Hill, D. L., 2005). Moreover, the sodium responsiveness of these fibers is significantly suppressed by lingual amiloride treatment (Ninomiya, Y. and Funakoshi, M., 1988). There are, however, other sodium-responsive fibers in the CT and in other gustatory nerves that are not affected by the application of amiloride on their receptor fields (Ninomiya, Y. and Funakoshi, M., 1988; Formaker, B. K. and Hill, D. L., 1991; Kitada, Y. *et al.*, 1998; Sollars, S. I. and Hill, D. L., 2005). It would appear that these amiloride-insensitive fibers are sufficient at providing input that can maintain normal unconditioned avoidance responses to salt. This is presumably one reason why the two-bottle preference test and the brief-access taste test, when used to assess unconditioned responses to NaCl, reveal normal function after CT transection or amiloride treatment. Thus, many of the procedures listed in Table 1 have nicely complemented each other and have collectively provided insight into the principles and peripheral mechanisms associated with salt taste in the rodent model.

4.22.4.2 Use of Behavioral Procedures to Study the Functional Neuroanatomy of the Central Gustatory System

Some of the behavioral procedures in Table 1 have been used to assess taste function after production of experimental lesions in central gustatory structures. Interpretation of the behavioral effects following manipulations of the brain is always challenging because any resulting impairments might have a variety of functional origins. Furthermore, any behavioral deficit following a lesion may not be due to the disruption of processing in the damaged brain site, but might be due to the interruption of information flow to brain regions anatomically downstream. Nevertheless, the complementary use of different behavioral procedures combined with theoretically relevant anatomical manipulations of the brain has offered insight into the functional organization of the central gustatory system in at least the rat model. Some examples are provided below.

4.22.4.2.1 Taste reactivity in decerebrate rats

Gustatory signals from the periphery are transmitted to the rostral one-third of the nucleus of the solitary tract (NST) by branches of cranial nerves VII, IX, and X. In rodents, the main ascending gustatory pathway begins with the projections of the second-order neurons in the NST to third-order taste-responsive neurons in the parabrachial nucleus (PBN). The projections of the third-order neurons in the PBN form two pathways destined for forebrain sites. The first terminates in the parvicellular subdivision of the ventral posteromedial nucleus of the thalamus, which, in turn, projects to the insular cortex. The second pathway terminates in several ventral forebrain regions including the lateral hypothalamus, the central nucleus of the amygdala, and the substantia innominata (see Norgren, R. and Leonard, C. M., 1973; Norgren, R., 1974; 1976; Hamilton, R. B. and Norgren, R., 1984; Halsell, C. B., 1992; Travers, S. P., 1993; Norgren, R., 1995).

About 30 years ago, Grill H. J. and Norgren R. (1978d) made a remarkable discovery that began to shed light on the functional significance of hindbrain and forebrain gustatory circuits. They developed the taste reactivity test procedure (see Section 4.22.3.3) to test the responsiveness of supracollicular decerebrate rats to prototypical taste stimuli (Grill, H. J. and Norgren, R., 1978c). In this neural preparation, the forebrain is neurally isolated from the rest of the nervous system. Animals that survive this procedure do not spontaneously eat and drink and have impairments in body temperature regulation, but they can nonetheless be chronically maintained by gavage feeding and close control of environmental conditions (Grill, H. J. and Norgren, R., 1978b). Despite the fact that these animals are severely compromised behaviorally, they display relatively normal concentration-dependent oral motor responses to taste stimuli (Grill, H. J. and Norgren, R., 1978d). Intraoral infusions of quinine elicit gapes and intraoral infusions of sucrose elicit tongue protrusions and mouth movements. These findings provide convincing evidence that the neural circuits of the caudal brainstem are sufficient to support taste-elicited oral motor reflexes.

In intact rats, taste reactivity can be modified by learning. If the intraoral delivery of a palatable fluid is followed by visceral malaise, animals will display aversive oral motor responses to this normally palatable sugar stimulus when tested on subsequent occasions (e.g., Grill, H. J. and Norgren, R., 1978a; Grill, H. J. and Berridge, K. C., 1985; Spector, A. C. *et al.*, 1988). Grill H. J. and Norgren R. (1978a) went onto show that even though decerebrate rats display relatively normal unconditioned taste reactivity, these animals do not change their response profile even after several pairings of the taste stimulus with a malaise-inducing LiCl injection. Regardless of the functional basis for the impairment, it is clear that the forebrain is necessary for this particular form of taste-related learning to be expressed. The taste reactivity paradigm is the only type of taste-related behavioral measure from Table 1 that can be used in the examination of decerebrate rats. However, its application in the assessment of both unconditioned and conditioned responses to taste stimuli led to fundamental insights concerning the functional significance of caudal brainstem versus forebrain gustatory circuits.

4.22.4.2.2 Taste function after lesions in the gustatory nuclei

One limitation of the decerebration strategy is that it involves a very crude and expansive neural manipulation affecting many different sensory, motor, and autonomic systems. Thus, while functions that survive this substantial neural insult are conceptually meaningful, not much can be said of behaviors that are impaired or eliminated. The interpretative significance of any lesion-induced behavioral deficit depends heavily on the anatomical specificity of the neural manipulation. For close to 50 years, researchers have targeted brain sites along the gustatory pathway and have assessed the degree of behavioral competence following the production of lesions. The early work generally involved large lesions and almost the exclusive use of intake tests to assess taste function (Patton, H. D. *et al.*, 1944; Benjamin, R. M., 1955a; 1955b; Benjamin, R. M. and Akert, K., 1958; Oakley, B. and Pfaffmann, C., 1962; Blomquist, A. J. and Antem, A., 1967; Loullis, C. C. *et al.*, 1978; Braun, J. J. *et al.*, 1982; Hill, D. L. and Almli, C. R., 1983; Lasiter, P. S., 1985; see also, Spector, A. C., 1995a; Reilly, S., 1998). Later investigations involved more anatomically precise lesions often placed with electrophysiological guidance and incorporated more diverse behavioral paradigms (but see Oakley, B. and Pfaffmann, C., 1962; Oakley, B., 1965). Rather than review the entire spectrum of results from such studies, it is worth noting a few findings that highlight the interpretive power of comprehensive behavioral analyses.

The consequences of lesions directed toward the second central relay in the rodent gustatory system, the PBN, provide an interpretive complement to the findings from experiments involving supracollicular transections described in Section 4.22.4.2.1. Overall, a PBN lesion is considerably less drastic than decerebration, but at the same time is anatomically more severe in terms of interrupting gustatory neural circuits. Decerebration presumably leaves intact the NST and PBN as well as connections between these areas and medullary nuclei, including those involved in orofacial motor and physiological reflexes (see Travers, J. B. *et al.*, 1999). Lesions in the gustatory zone of the dorsal pons, in contrast, should limit gustatory processing to the NST and its local connections, to the extent that the PBN is an obligate relay for forebrain taste projections.

From that perspective, it is noteworthy that electrophysiologically guided lesions in the PBN have relatively little effect on the intake of a variety of prototypical taste stimuli by rats (in contrast to the complete suppression of appetitive behavior in the decerebrate). Nonetheless, intake is not normal following this manipulation; investigators have reported overconsumption of several prototypical taste stimuli (e.g., Flynn, F. W. *et al.*, 1991b). Converging evidence for an alteration in taste processing comes from brief-access taste testing (see Section 4.22.3.2). Substantial changes in behavioral responses to quinine, sucrose, and NaCl have been reported in rats with bilateral PBN lesions (Spector, A. C. *et al.*, 1993a; 1995) collectively suggesting that rats are made hypoguesic by this lesion. The simplest explanation is that PBN lesion reduces the perceived intensity of gustatory stimuli, but these data also suggest that hedonic processing and possibly stimulus identification remain intact. For example, although the effective concentration range is shifted to higher concentrations, rats with PBN lesion nonetheless avoid quinine and NaCl in a concentration-dependent manner, and increase licking of sucrose in a concentration-dependent manner.

The simple explanation of hypoguesia (weakened taste intensity) is complicated by another study which demonstrated that detection thresholds measured using operant procedures sometimes were not altered following PBN lesion (Spector, A. C. *et al.*, 1995). That is, individual animals with PBN lesion showed elevated detection thresholds in some cases and not in others. Importantly, all of these animals failed to express a learned taste aversion to either sucrose or NaCl after multiple conditioning trials, a finding that served as functional confirmation of the PBN lesion. Similar individual animal variability has also been reported in operant discrimination procedures; rats with PBN lesion that fail to form conditioned taste aversions are in some cases unable to discriminate NaCl from KCl in an operantly trained discrimination task, but in other cases show near-normal discrimination performance (Spector, A. C., 1995a). Whether the individual differences are related to prelesion training differences, the exact locus and extent of the lesion, or differences in the plasticity of pre-PBN circuitry is unknown. What is clear from this work is that rats with lesions centered in the taste-responsive zone of the dorsal pons are not aguesic, and that their gustatory competence can, in some cases, emulate that of intact rats depending on the task.

Importantly, this residual competence is informative in interpretation of other effects of PBN lesion. As noted, a hallmark of PBN lesion is that, like decerebration, this neural manipulation prevents the formation of conditioned taste aversions (DiLorenzo, P. M., 1988; Ivanova, S. F. and Bures, J., 1990; Flynn, F. W. *et al.*, 1991a; Yamamoto, T. and Fujimoto, Y., 1991; Spector, A. C. *et al.*, 1992; Reilly, S. *et al.*, 1993; Scalera, G. *et al.*, 1995; Spector, A. C. *et al.*, 1995; Grigson, P. S. *et al.*, 1997; 1998; Sclafani, A. *et al.*, 2001) Such a deficit would be expected if PBN lesions rendered the rat aguesic or severely hypoguesic to taste solutions; likewise, rats would not be able to express taste aversions if PBN lesions prevented the identification of a specific taste solution. However, work cited above converges on the conclusion that although some deficits in detection thresholds, suprathreshold sensitivity, and taste discriminability can be seen, those deficits do not always occur and are not severe enough to explain the deficits in taste aversion acquisition. Indeed, if the taste aversion is conditioned presurgically, rats with PBN lesions display normal avoidance of the conditioned taste stimulus, but are unable to learn an aversion to a novel sapid compound (Grigson, P. S. *et al.*, 1997). Clearly, the use of multiple behavioral tests has provided considerable interpretive power in diagnosing the role of the PBN in taste aversion learning and leads to the conclusion that the taste-responsive portion of this nucleus must remain intact for taste signals to be conditionally associated with visceral malaise (see Spector, A. C. *et al.*, 1992; Spector, A. C., 1995a; Norgren, R. and Grigson, P. S., 1996; Grigson, P. S. *et al.*, 1997; 1998).

Likewise, PBN lesions eliminate the expression of a salt appetite (Flynn, F. W. *et al*., 1991a; Scalera, G. *et al*., 1995), impair the formation of a conditioned flavor preference (Sclafani, A. *et al*., 2001), and prevent the avoidance of diets deficient in amino acids or protein (Fromentin, G. *et al*., 2000). Against the backdrop of the behavioral work discussed so far, the interpretation of the cause of these deficits would not rely on the animal failing to taste NaCl, the conditioned stimulus, or the deficient diet. Rather, like with taste aversion, the PBN or its downstream processing targets appear to be indispensable for behaviors that require the integration of taste and viscerosensory signals.

4.22.5 Final Comments

This chapter has provided an overview of the behavioral techniques that have been used to assess taste function in animal, primarily rodent, models. We have attempted to show how these various paradigms can complement each other leading to a more comprehensive interpretation of the effects of experimental manipulations on the gustatory system, be they anatomical, pharmacological, or genetic. Greater coordination in the application of behavioral, neurobiological, and genetic techniques, all of which are evolving rapidly, should ultimately lead to a better understanding of the neural mechanisms underlying taste function and provide a logical bridge potentially connecting findings based on animal models to the study of human gustation.

References

Akaike, N., Hiji, Y., and Yamada, K. 1965. Taste preference and aversion in rats following denervation of the chorda tympani and IXth nerve. Kumamoto Med. J. 18, 108–109.

Bachmanov, A. A., Tordoff, M. G., and Beauchamp, G. K. 2001. Sweetener preference of C57BL/6ByJ and 129P3/J mice. Chem. Senses 26, 905–913.

Barker, L. M., Best, M. R., and Domjan, M. 1999. Learning Mechanisms in Food Selection. Baylor University Press.

Beidler, L. M. 1953. Properties of chemoreceptors of tongue of rat. J. Neurophysiol. 16, 595–607.

Beidler, L. M. 1954. A theory of taste stimulation. J. Gen. Physiol. 38, 133–139.

Benjamin, R. M. 1955a. Cortical taste mechanisms studied by two different test procedures. J. Comp. Physiol. Psychol. 48, 119–122.

Benjamin, R. M. 1955b. The effect of fluid deprivation on taste deficits following cortical lesions. J. Comp. Physiol. Psychol. 48, 502–505.

Benjamin, R. M. and Akert, K. 1958. Cortical and thalamic areas involved in taste discrimination in the albino rat. J. Comp. Neurol. 111, 231–260.

Bernstein I. L. and Hennessy C. J. 1987. Amiloride-sensitive sodium channels and expression of sodium appetite in rats. Am. J. Physiol. Regul. Integr. Comp. Physiol. 253, R371–R374.

Berridge, K., Grill, H. J., and Norgren, R. 1981. Relation of consummatory responses and preabsorptive insulin release to palatability and learned taste aversions. J. Comp. Physiol. Psychol. 95, 363–382.

Berridge, K. C. 1996. Food reward: brain substrates of wanting and liking. Neurosci. Biobehav. Rev. 20, 1–25.

Berridge, K. C. 2004. Motivation concepts in behavioral neuroscience. Physiol. Behav. 81, 179–209.

Berridge, K. C., Flynn, F. W., Schulkin, J., and Grill, H. J. 1984. Sodium depletion enhances salt palatability in rats. Behav. Neurosci. 98, 652–660.

Blomquist, A. J. and Antem, A. 1967. Gustatory deficits produced by medullary lesions in the white rat. J. Comp. Physiol. Psychol. 63, 439–443.

Blough, D. and Blough, P. 1977. Animal Psychophysics. In: Handbook of Operant Behavior (*eds*. W. K. Honig and J. E. R. Straddon), pp. 514–539. Prentice-Hall.

Boughter, J. D., St. John, S. J., Noel, D. T., Ndubuizu, O., and Smith, D. V. 2002. A brief-access test for bitter taste in mice. Chem. Senses 27, 133–142.

Bradley, R. M. 1971. Tongue Topography. In: Taste (*ed*. Beidler, L. M.), pp. 1–30. Springer.

Brand, J. G., Teeter, J. H., and Silver, W. L. 1985. Inhibition by amiloride of chorda tympani responses evoked by monovalent salts. Brain Res. 334, 207–214.

Braun, J. J., Lasiter, P. S., and Kiefer, S. W. 1982. The gustatory neocortex of the rat. Physiol. Psychol. 10, 13–45.

Breslin, P. A., Kaplan, J. M., Spector, A. C., Zambito, C. M., and Grill, H. J. 1993a. Lick rate analysis of sodium taste-state combinations. Am. J. Physiol. 264, R312–R318.

Breslin, P. A., Spector, A. C., and Grill, H. J. 1993b. Chorda tympani section decreases the cation specificity of depletion-induced sodium appetite in rats. Am. J. Physiol. 264, R319–R323.

Breslin, P. A., Spector, A. C., and Grill, H. J. 1995. Sodium specificity of salt appetite in Fischer-344 and Wistar rats is impaired by chorda tympani nerve transection. Am. J. Physiol. 269, R350–R356.

Brining, S. K., Belecky, T. L., and Smith, D. V. 1991. Taste reactivity in the hamster. Physiol. Behav. 49, 1265–1272.

Brosvic, G. M. and Slotnick, B. M. 1986. Absolute and intensity-difference taste thresholds in the rat: evaluation of an automated multi-channel gustometer. Physiol. Behav. 38, 711–717.

Brot, M. D., Watson, C. H., and Bernstein, I. L. 2000. Amiloride-sensitive signals and NaCl preference and appetite: a lick-rate analysis. Am. J. Physiol. Regul. Integr. Comp. Physiol. 279, R1403–R1411.

Capaldi, E. D., Hunter, M. J., and Privitera, G. J. 2004. Odor of taste stimuli in conditioned ''taste'' aversion learning. Behav. Neurosci. 118, 1400–1408.

Carr, W. J. 1952. The effect of adrenalectomy upon the NaCl taste threshold in rat. J. Comp. Physiol. Psychol. 45, 377–380.

Cauthon, R., Garcea, M., and Spector, A. C. 1994. Taste-guided unconditioned licking to suprathreshold sodium chloride solutions is unaffected by selective lingual denervation. Chem. Senses 19, 452.

Chappell, J. P., St. John, S. J., and Spector, A. C. 1998. Amiloride does not alter NaCl avoidance in Fischer-344 rats. Chem. Senses 23, 151–157.

Colbert, C. L., Garcea, M., and Spector, A. C. 2004. Effects of selective lingual gustatory deafferentation on suprathreshold

taste intensity discrimination of NaCl in rats. Behav. Neurosci. 118, 1409–1417.
Contreras, R. J., Carson, C. A., and Pierce, C. E. 1995. A novel psychophysical procedure for bitter taste assessment in rats. Chem. Senses 20, 305–312.
Craig, W. 1918. Appetites and aversions as constituents of instincts. Biol. Bull. 34, 91–107.
Davis, J. D. 1973. The effectiveness of some sugars in stimulating licking behavior in the rat. Physiol. Behav. 11, 39–45.
Davis, J. D. 1989. The Microstructure of Ingestive Behavior. In: The Psychobiology of Human Eating Disorders (*eds*. L. H. Schneider, S. J. Cooper, and K. A. Halmi), pp. 106–121. Annals of the New York Academy of Sciences.
Davis, J. D. 1996. Deterministic and probabilistic control of the behavior of rats ingesting liquid diets. Am. J. Physiol. Regul. Integr. Comp. Physiol. 270, R793–R800.
Davis, J. D. and Campbell, C. S. 1973. Peripheral control of meal size in the rat: effect of sham feeding on meal size and drinking rate. J. Comp. Physiol. Psychol. 83, 379–387.
Davis, J. D. and Smith, G. P. 1992. Analysis of the microstructure of the rhythmic tongue movements of rats ingesting maltose and sucrose solutions. Behav. Neurosci. 106, 217–228.
Denton, D. 1982. The Hunger for Salt. Springer.
DeSimone, J. A. and Ferrell, F. 1985. Analysis of amiloride inhibition of chorda tympani taste response of rat to NaCl. Am. J. Physiol. Regul. Integr. Comp. Physiol. 249, R52–R61.
DiLorenzo, P. M. 1988. Long-delay learning in rats with parabrachial pontine lesions. Chem. Senses 13, 219–229.
Domjan, M. 1980. Ingestional Aversion Learning: Unique and General Processes. In: Advances in the Study of Behavior, vol. 2 (*eds*. J. Rosenblatt, R. Hinde, C. Beer, and M. Busnel), pp. 215–336. Academic Press.
Doolin, R. E. and Gilbertson, T. A. 1996. Distribution and characterization of functional amiloride-sensitive sodium channels in rat tongue. J. Gen. Physiol. 107, 545–554.
Dotson, C. D. and Spector, A. C. 2004. The relative affective potency of glycine, L-serine and sucrose as assessed by a brief-access taste test in inbred strains of mice. Chem. Senses 29, 489–498.
Epstein, A. N. 1984. The dependence of the salt appetite of the rat on the hormonal consequences of sodium deficiency. J. Physiol. 79, 494–498.
Eylam, S. and Spector, A. C. 2002. The effect of amiloride on operantly conditioned performance in an NaCl taste detection task and NaCl preference in C57BL/6J mice. Behav. Neurosci. 116, 149–159.
Eylam, S. and Spector, A. C. 2003. Oral amiloride treatment decreases taste sensitivity to sodium salts in C57BL/6J and DBA/2J mice. Chem. Senses 28, 447–458.
Eylam, S. and Spector, A. C. 2004. Stimulus processing of glycine is dissociable from that of sucrose and glucose based on behaviorally measured taste signal detection in Sac 'taster' and 'non-taster' mice. Chem. Senses 29, 639–649.
Eylam, S. and Spector, A. C. 2005. Taste discrimination between NaCl and KCl is disrupted by amiloride in inbred mice with amiloride-insensitive chorda tympani nerves. Am. J. Physiol. Regul. Integr. Comp. Physiol. 288, R1361–R1368.
Eylam, S., Tracy, T., Garcea, M., and Spector, A. C. 2003. Amiloride is an ineffective conditioned stimulus in taste aversion learning in C57BL/6J and DBA/2J mice. Chem. Senses 28, 681–689.
Flynn, F. W., Grill, H. J., Schulkin, J., and Norgren, R. 1991a. Central gustatory lesions: II. Effects on sodium appetite, taste aversion learning, and feeding behaviors. Behav. Neurosci. 105, 944–954.
Flynn, F. W., Grill, H. J., Schwartz, G. J., and Norgren, R. 1991b. Central gustatory lesions: I. Preference and taste reactivity tests. Behav. Neurosci. 105, 933–943.
Formaker, B. K. and Hill, D. L. 1991. Lack of amiloride sensitivity in SHR and WKY glossopharyngeal taste responses to NaCl. Physiol. Behav. 50, 765–769.
Frank, M. E., Contreras, R. J., and Hettinger, T. P. 1983. Nerve fibers sensitive to ionic taste stimuli in chorda tympani of the rat. J. Neurophysiol. 50, 941–960.
Frankmann, S. P., Sollars, S. I., and Bernstein, I. L. 1996. Sodium appetite in the sham-drinking rat after chorda tympani nerve transection. Am. J. Physiol. Regul. Integr. Comp. Physiol. 271, R339–R345.
Fromentin, G., Feurte, S., Nicolaidis, S., and Norgren, R. 2000. Parabrachial lesions disrupt responses of rats to amino acid devoid diets, to protein-free diets, but not to high-protein diets. Physiol. Behav. 70, 381–389.
Garcia, J., Kimeldorf, D. J., and Koelling, R. A. 1955. Conditioned aversion to saccharin resulting from exposure to gamma radiation. Science 122, 157–158.
Geran, L. C. and Spector, A. C. 2000a. Amiloride increases sodium chloride taste detection threshold in rats. Behav. Neurosci. 114, 623–634.
Geran, L. C. and Spector, A. C. 2000b. Sodium taste detectability in rats is independent of anion size: the psychophysical characteristics of the transcellular sodium taste transduction pathway. Behav. Neurosci. 114, 1229–1238.
Geran, L. C. and Spector, A. C. 2002. Glossopharyngeal nerve transection does not compromise chloride salt discrimination in the rat. Chem. Senses 27, A78.
Geran, L. C. and Spector, A. C. 2004. Anion size does not compromise sodium recognition by rats after acute sodium depletion. Behav. Neurosci. 118, 178–183.
Geran, L. C., Garcea, M., and Spector, A. C. 2004. Nerve regeneration-induced recovery of quinine avoidance after complete gustatory deafferentation of the tongue. Am. J. Physiol. Regul. Integr. Comp. Physiol. 287, R1235–R1243.
Geran, L. C., Garcea, M., and Spector, A. C. 2002. Transecting the gustatory branches of the facial nerve impairs NH(4)Cl vs. KCl discrimination in rats. Am. J. Physiol. Regul. Integr. Comp. Physiol. 283, R739–R747.
Geran, L. C., Guagliardo, N. A., and Spector, A. C. 1999. Chorda tympani nerve transection, but not amiloride, increases the KCl taste detection threshold in rats. Behav. Neurosci. 113, 185–195.
Gilmore, M. M. and Green, B. G. 1993. Sensory irritation and taste produced by NaCl and citric acid: effects of capsaicin desensitization. Chem. Senses 18, 257–272.
Glendinning, J. I., Bloom, L. D., Onishi, M., Zheng, K. H., Damak, S., Margolskee, R. F., and Spector, A. C. 2005. Contribution of α-gurtducin to taste-guided licking responses of mice. Chem. Senses 30, 299–316.
Glendinning, J. I., Gresack, J., and Spector, A. C. 2002. A high-throughput screening procedure for identifying mice with aberrant taste and oromotor function. Chem. Senses 27, 461–474.
Grigson, P. S., Reilly, S., Shimura, T., and Norgren, R. 1998. Ibotenic acid lesions of the parabrachial nucleus and conditioned taste aversion: further evidence for an associative deficit in rats. Behav. Neurosci. 112, 160–171.
Grigson, P. S., Shimura, T., and Norgren, R. 1997. Brainstem lesions and gustatory function. 3. The role of the nucleus of the solitary tract and the parabrachial nucleus in retention of a conditioned taste aversion in rats. Behav. Neurosci. 111, 180–187.
Grill, H. J. and Bernstein, I. L. 1988. Strain differences in taste reactivity to NaCl. Am. J. Physiol. Regul. Integr. Comp. Physiol. 255, R424–R430.

Grill, H. J. and Berridge, K. C. 1985. Taste reactivity as a measure of the neural control of palatability. Prog. Psychobiol. Physiol. Psychol. 11, 1–61.

Grill, H. J. and Norgren, R. 1978a. Chronic decerebrate rats demonstrated satiation, but not bait shyness. Science 201, 267–269.

Grill, H. J. and Norgren, R. 1978b. Neurological tests and behavioral deficits in chronic thalamic and chronic decerebrate rats. Brain Res. 143, 299–312.

Grill, H. J. and Norgren, R. 1978c. The taste reactivity test. I. Mimetic responses to gustatory stimuli in neurologically normal rats. Brain Res. 143, 263–279.

Grill, H. J. and Norgren, R. 1978d. The taste reactivity test. II. Mimetic responses to gustatory stimuli in chronic thalamic and chronic decerebrate rats. Brain Res. 143, 281–297.

Grill, H. J. and Schwartz, G. J. 1992. The contribution of gustatory nerve input to oral motor behavior and intake-based preference. II. Effects of combined chorda tympani and glossopharyngeal nerve section in the rat. Brain Res. 573, 105–113.

Grill, H. J., Schwartz, G. J., and Travers, J. B. 1992. The contribution of gustatory nerve input to oral motor behavior and intake-based preference. I. Effects of chorda tympani or glossopharyngeal nerve section in the rat. Brain Res. 573, 95–104.

Grill, H. J., Spector, A. C., Schwartz, G. J., Kaplan, J. M., and Flynn, F. W. 1987. Evaluating Taste Effects on Ingestive Behavior. In: Techniques in the Behavioral and Neural Sciences, vol. 1: Feeding and Drinking (*eds*. F. Toates and N. Rowland), pp. 151–188. Elsevier.

Hagstrom, E. C. and Pfaffmann, C. 1959. The relative taste effectiveness of different sugars for the rat. J. Comp. Physiol. Psychol. 59, 259–262.

Halsell, C. B. 1992. Organization of parabrachial nucleus efferents to the thalamus and amygdala in the golden hamster. J. Comp. Neurol. 317, 57–78.

Hamilton, R. B. and Norgren, R. 1984. Central projections of gustatory nerves in the rat. J. Comp. Neurol. 222, 560–577.

Handal, P. J. 1965. Immediate acceptance of sodium salts by sodium deficient rats. Psychon. Sci. 3, 315–316.

Harriman, A. E. and MacLeod, R. B. 1953. Discriminative thresholds of salt for normal and adrenalectomized rats. Am. J. Psychol. 66, 465–471.

Heck, G. I., Mierson, S., and DeSimone, J. A. 1984. Salt taste transduction occurs through an amiloride-sensitive sodium transport pathway. Science 223, 403–405.

Herness, M. S. 1987. Effect of amiloride on bulk flow and iontophoretic taste stimuli. J. Comp. Physiol. A 160, 281–288.

Hettinger, T. P. and Frank, M. E. 1990. Specificity of amiloride inhibition of hamster taste responses. Brain Res. 513, 24–34.

Heyer, B. R., Taylor-Burds, C. C., Mitzelfelt, J. D., and Delay, E. R. 2004. Monosodium glutamate and sweet taste: discrimination between the tastes of sweet stimuli and glutamate in rats. Chem. Senses 29, 721–729.

Heyer, B. R., Taylor-Burds, C. C., Tran, L. H., and Delay, E. R. 2003. Monosodium glutamate and sweet taste: generalization of conditioned taste aversion between glutamate and sweet stimuli in rats. Chem. Senses 28, 631–641.

Hill, D. L. and Almli, C. R. 1983. Parabrachial nuclei damage in infant rats produces residual deficits in gustatory preferences/aversions and sodium appetite. Dev. Psychobiol. 16, 519–533.

Hill, D. L., Formaker, B. K., and White, K. S. 1990. Perceptual characteristics of the amiloride-suppressed sodium chloride taste response in the rat. Behav. Neurosci. 104, 734–741.

Hodos, W. 1961. Progressive ratio as a measure of reward strength. Science 134, 943–944.

Hodos, W. and Kalman, G. 1963. Effects of increment size and reinforcer volume on progressive ratio performance. J. Exp. Anal. Behav. 6, 387–392.

Ivanova, S. F. and Bures, J. 1990. Acquisition of conditioned taste aversion in rats is prevented by tetrodotoxin blockade of a small midbrain region centered around the parabrachial nuclei. Physiol. Behav. 48, 543–549.

Jalowiec, J. E. and Stricker, E. M. 1970. Restoration of body fluid balance following acute sodium deficiency in rats. J. Comp. Physiol. Psychol. 70, 94–102.

Kitada, Y., Mitoh, Y., and Hill, D. L. 1998. Salt taste responses of the IXth nerve in Sprague-Dawley rats: lack of sensitivity to amiloride. Physiol. Behav. 63, 945–949.

Koh, S. D. and Teitelbaum, P. 1961. Absolute behavioral taste thresholds in the rat. J. Comp. Physiol. Psychol. 54, 223–229.

Kopka, S. L. and Spector, A. C. 2001. Functional recovery of taste sensitivity to sodium chloride depends on regeneration of the chorda tympani nerve after transection in the rat. Behav. Neurosci. 115, 1073–1085.

Kopka, S. L., Geran, L. C., and Spector, A. C. 2000. Functional status of the regenerated chorda tympani nerve as assessed in a salt discrimination task. Am. J. Physiol. Regul. Integr. Comp. Physiol. 278, R720–R731.

Krimm, R. F., Nejad, M. S., Smith, J. C., Miller, I. J., Jr., and Beidler, L. M. 1987. The effect of bilateral sectioning of the chorda tympani and the greater superficial petrosal nerves on the sweet taste in the rat. Physiol. Behav. 41, 495–501.

Lasiter, P. S. 1985. Thalamocortical relations in taste aversion learning: II. Involvement of the medial ventrobasal thalamic complex in taste aversion learning. Behav. Neurosci. 99, 477–495.

LeMagnen, J. and Devos, M. 1980. Parameters of the meal pattern in rats: their assessment and physiological significance. Neurosci. Biobehav. Rev. 4, 1–11.

Lindemann, B., Gilbertson, T. A., and Kinnamon, S. C. 1999. Amiloride-Sensitive Sodium Channels in Taste. Academic Press.

Loullis, C. C., Wayner, M. J., and Jolicoeur, F. B. 1978. Thalamic taste nuclei lesions and taste aversion. Physiol. Behav. 20, 653–655.

Lundy, R. F., Jr. and Contreras, R. J. 1999. Gustatory neuron types in rat geniculate ganglion. J. Neurophysiol. 82, 2970–2988.

Markison, S. and Spector, A. C. 1995. Amiloride is a poor conditioned stimulus in taste aversion. Chem. Senses 20, 739–740.

Markison, S., St. John, S. J., and Spector, A. C. 1995. Glossopharyngeal nerve transection does not compromise the specificity of taste-guided sodium appetite in rats. Am. J. Physiol. Regul. Integr. Comp. Physiol. 269, R215–R221.

McCleary, R. A. 1953. Taste and post-ingestion factors in specific-hunger behavior. J. Comp. Physiol. Psychol. 46, 411–420.

McCutcheon, N. B. 1991. Sodium deficient rats are unmotivated by sodium chloride solutions mixed with the sodium channel blocker amiloride. Behav. Neurosci. 105, 764–766.

Miller, I. J., Jr. 1977. Gustatory Receptors of the Palate. In: Food Intake and Chemical Senses (*eds*. Y. Katsuki, M. Sato, S. Takagi, and Y. Oomura), pp. 173–186. University of Tokyo Press.

Miller, S. D. and Erickson, R. P. 1966. The odor of taste solutions. Physiol. Behav. 1, 145–146.

Mook, D. G. 1963. Oral and postingestional determinants of the intake of various solutions in rats with esophageal fistulas. J. Comp. Physiol. Psychol. 56, 645–659.

Morrison, G. R. 1967. Behavioral response patterns to salt stimuli in the rat. Can. J. Psychol. 21, 141–152.

Morrison, G. R. and Norrison, W. 1966. Taste detection in the rat. Can. J. Psychol. 20, 208–217.
Nachman, M. 1963. Learned aversion to the taste of lithium chloride and generalization to other salts. J. Comp. Physiol. Psychol. 56, 343–349.
Nachman, M. and Ashe, J. H. 1973. Learned taste aversions in rats as a function of dosage, concentration, and route of administration of LiCl. Physiol. Behav. 10, 73–78.
Ninomiya, Y. and Funakoshi, M. 1988. Amiloride inhibition of responses of rat single chorda tympani fibers to chemical and electrical tongue stimulations. Brain Res. 451, 319–325.
Ninomiya, Y., Sako, N., and Funakoshi, M. 1989. Strain differences in amiloride inhibition of NaCl responses in mice, Mus Musculus. J. Comp. Physiol. A 166, 1–5.
Nissenbaum, J. W. and Sclafani, A. 1987a. Sham-feeding response of rats to polycose and sucrose. Neurosci. Biobehav. Rev. 11, 215–222.
Nissenbaum, J. W. and Sclafani, A. 1987b. Qualitative differences in polysaccharide and sugar tastes in the rat: a two-carbohydrate taste model. Neurosci. Biobehav. Rev. 11, 187–196.
Norgren, R. 1974. Gustatory afferents to ventral forebrain. Brain Res. 81, 285–295.
Norgren, R. 1976. Taste pathway to hypothalamus and amygdala. J. Comp. Neurol. 166, 17–30.
Norgren, R. 1985. Taste and the autonomic nervous system. Chem. Senses 10, 143–161.
Norgren, R. 1992. The central gustatory and visceral afferent systems arising from the nucleus of the solitary tract. Adv. Physiol. Sci. 16, 359–366.
Norgren, R. 1995. Gustatory System. In: The Rat Nervous System (*ed*. G. Paxinos), pp. 751–771. Academic Press.
Norgren, R. and Grigson, P. S. 1996. The Role of the Central Gustatory System in Learned Taste Aversions. In: Perception, Memory and Emotion: Frontiers in Neuroscience (*eds*. T. Ono, B. McNaughton, S. Molotchnikoff, E. Rolls, and H. Nishijo), pp. 479–497. Pergamon.
Norgren, R. and Leonard, C. M. 1973. Ascending central gustatory pathways. J. Comp. Neurol. 150, 217–238.
Nowlis, G. H. 1974. Conditioned stimulus intensity and acquired alimentary aversions in the rat. J. Comp. Physiol. Psychol. 86, 1173–1184.
Nowlis, G. H., Frank, M. E., and Pfaffmann, C. 1980. Specificity of acquired aversions to taste qualities in hamsters and rat. J. Comp. Physiol. Psychol. 94, 932–942.
O'Keefe, G. B., Schumm, J., and Smith, J. C. 1994. Loss of sensitivity to low concentrations of NaCl following bilateral chorda tympani nerve sections in rats. Chem. Senses 19, 169–184.
Oakley, B. 1965. Impaired operant behavior following lesions of the thalamic taste nucleus. J. Comp. Physiol. Psychol. 59, 202–210.
Oakley, B. and Pfaffmann, C. 1962. Electrophysiologically monitored lesions in the gustatory thalamic relay of the albino rat. J. Comp. Physiol. Psychol. 55, 155–160.
Patton, H. D., Ruch, T. C., and Walker, A. E. 1944. Experimental hypoguesia from Horsley-Clarke lesions of the thalamus in *Macaca mulatta*. J. Neurophysiol. 7, 171–184.
Pavlov, I. P. 1902. The Work of the Digestive Glands. Charles Griffin.
Pfaffmann, C. 1941. Gustatory afferent impulses. J. Cell Comp. Physiol. 17, 243–258.
Pfaffmann, C. 1952. Taste preference and aversion following lingual denervation. J. Comp. Physiol. Psychol. 45, 393–400.
Pfaffmann, C. 1955. Gustatory nerve impulses in rat, cat, and rabbit. J. Neurophysiol. 18, 429–440.
Pfaffmann, C., Frank, M., and Norgren, R. 1979. Neural mechanisms and behavioral aspects of taste. Ann. Rev. Psychol. 30, 283–325.
Rabe, E. F. and Corbit, J. D. 1973. Postingestional control of sodium chloride solution drinking in the rat. J. Comp. Physiol. Psychol. 84, 268–274.
Reilly, S. 1998. The role of the gustatory thalamus in taste-guided behavior. Neurosci. Biobehav. Rev. 22, 883–901.
Reilly, S. 1999. Reinforcement value of gustatory stimuli determined by progressive ratio performance. Pharmacol. Biochem. Behav. 63, 301–311.
Reilly, S. and Trifunovic, R. 1999. Progressive ratio performance in rats with gustatory thalamus lesions. Behav. Neurosci. 113, 1008–1019.
Reilly, S., Grigson, P. S., and Norgren, R. 1993. Parabrachial nucleus lesions and conditioned taste aversion: evidence supporting an associative deficit. Behav. Neurosci. 107, 1005–1017.
Rhinehart-Doty, J. A., Schumm, J., Smith, J. C., and Smith, G. P. 1994. A non-taste cue of sucrose in short-term taste tests in rats. Chem. Senses 19, 425–431.
Richter, C. P. 1936. Increased salt appetite in adrenalectomized rats. Am. J. Physiol. Regul. Integr. Comp. Physiol. 115, 155–161.
Richter, C. P. 1939. Transmission of taste sensation in animals. Trans. Am. Neurol. Assoc. 65, 49–50.
Roitman, M. F. and Bernstein, I. L. 1999. Amiloride-sensitive sodium signals and salt appetite: multiple gustatory pathways. Am. J. Physiol. 276, R1732–R1738.
Rowland, N. E. and Fregly, M. J. 1992. Repletion of acute sodium deficit in rats drinking either low or high concentrations of sodium chloride solution. Am. J. Physiol. Regul. Integr. Comp. Physiol. 262, R419–R425.
Scalera, G., Spector, A. C., and Norgren, R. 1995. Excitotoxic lesions of the parabrachial nuclei prevent conditioned taste aversions and sodium appetite in rats. Behav. Neurosci. 109, 997–1008.
Schneider, G. E. 1969. Two visual systems. Science 163, 895–902.
Schneider, L. H., Gibbs, J., and Smith, G. P. 1986. D-2 selective receptor antagonists suppress sucrose sham feeding in the rat. Brain Res. Bull. 17, 605–611.
Schulkin, J. 1991. Sodium Hunger: the Search for a Salty Taste. Cambridge University Press.
Sclafani, A. and Ackroff, K. 2003. Reinforcement value of sucrose measured by progressive ratio operant licking in the rat. Physiol. Behav. 79, 663–670.
Sclafani, A., Azzara, A. V., Touzani, K., Grigson, P. S., and Norgren, R. 2001. Parabrachial nucleus lesions block taste and attenuate flavor preference and aversion conditioning in rats. Behav. Neurosci. 115, 920–933.
Scott, T. R. and Giza, B. K. 1987. A measure of taste intensity discrimination in the rat through conditioned taste aversion. Physiol. Behav. 41, 315–320.
Scott, T. R. and Mark, G. P. 1986. Feeding and taste. Prog. Neurobiol. 27, 293–317.
Shaber, G. S., Brent, R. L., and Rumsey, J. A. 1970. Conditioned suppression taste thresholds in the rat. J. Comp. Physiol. Psychol. 73, 193–201.
Shuford, E., Jr. 1959. Palatability and osmotic pressure of glucose and sucrose solutions as determinants of intake. J. Comp. Physiol. Psychol. 52, 150–153.
Simon, S. A., Holland, V. F., Benos, D. J., and Zampighi, G. A. 1993. Transcellular and paracellular pathways in lingual epithelia and their influence in taste transduction. Microsc. Res. Tech. 26, 196–208.
Slotnick, B. M. 1982. Sodium chloride detection threshold in the rat determined using a simple operant taste discrimination task. Physiol. Behav. 28, 707–710.
Slotnick, B. M., Sheelar, S., and Rentmeister-Bryant, H. 1991. Transection of the chorda tympani and insertion of ear pins

for stereotaxic surgery: equivalent effects on taste sensitivity. Physiol. Behav. 50, 1123–1127.
Smith, D. V. and Theodore, R. M. 1984. Conditioned taste aversions: generalization to taste mixtures. Physiol. Behav. 32, 983–989.
Smith, J. C. and Foster, D. F. 1980. Some determinants of intake of glucose + saccharin solutions. Physiol. Behav. 25, 127–133.
Smith, J. C., Davis, J. D., and O'Keefe, G. B. 1992. Lack of an order effect in brief contact taste tests with closely spaced test trials. Physiol. Behav. 52, 1107–1111.
Sollars, S. I. and Bernstein, I. L. 1992. Sodium appetite after transection of the chorda tympani nerve in Wistar and Fischer 344 rats. Behav. Neurosci. 106, 1023–1027.
Sollars, S. I. and Bernstein, I. L. 1994. Gustatory deafferentation and desalivation: effects of NaCl preference of Fischer 344 rats. Am. J. Physiol. Regul. Integr. Comp. Physiol. 266, R510–R517.
Sollars, S. I. and Hill, D. L. 1998. Taste responses in the greater superficial petrosal nerve: substantial sodium salt and amiloride sensitivities demonstrated in two rat strains. Behav. Neurosci. 112, 991–1000.
Sollars, S. I. and Hill, D. L. 2005. *In vivo* recordings from geniculate ganglia: taste response properties of individual greater superficial petrosal and chorda tympani neurones. J. Physiol. 564, 877–893.
Spector, A. C. 1995a. Gustatory function in the parabrachial nuclei: implications from lesion studies in rats. Rev. Neurosci. 6, 143–175.
Spector, A. C. 1995b. Gustatory parabrachial lesions disrupt taste-guided quinine responsiveness in rats. Behav. Neurosci. 109, 79–90.
Spector, A. C. 2000. Linking gustatory neurobiology to behavior in vertebrates. Neurosci. Biobehav. Rev. 24, 391–416.
Spector, A. C. 2003. Psychophysical Evaluation of Taste Function in Non-Human Mammals. In: Handbook of Olfaction and Gustation (*ed*. R. L. Doty), pp. 861–879. Marcel Dekker.
Spector, A. C. and Grill, H. J. 1988. Differences in the taste quality of maltose and sucrose in rats: issues involving the generalization of conditioned taste aversions. Chem. Senses 13, 95–113.
Spector, A. C. and Grill, H. J. 1992. Salt taste discrimination after bilateral section of the chorda tympani or glossopharyngeal nerves. Am. J. Physiol. Regul. Integr. Comp. Physiol. 263, R169–R176.
Spector, A. C. and Smith, J. C. 1984. A detailed analysis of sucrose drinking in the rat. Physiol. Behav. 33, 127–136.
Spector, A. C. and St. John, S. J. 1998. Role of taste in the microstructure of quinine ingestion by rats. Am. J. Physiol. 274, R1687–R1703.
Spector, A. C., Andrews-Labenski, J., and Letterio, F. C. 1990a. A new gustometer for psychophysical taste testing in the rat. Physiol. Behav. 47, 795–803.
Spector, A. C., Breslin, P., and Grill, H. J. 1988. Taste reactivity as a dependent measure of the rapid formation of conditioned taste aversion: a tool for the neural analysis of taste-visceral associations. Behav. Neurosci. 102, 942–952.
Spector, A. C., Grill, H. J., and Norgren, R. 1993a. Concentration-dependent licking of sucrose and sodium chloride in rats with parabrachial gustatory lesions. Physiol. Behav. 53, 277–283.
Spector, A. C., Guagliardo, N. A., and St. John, S. J. 1996a. Amiloride disrupts NaCl versus KCl discrimination performance: implications for salt taste coding in rats. J. Neurosci. 16, 8115–8122.
Spector, A. C., Markison, S., St. John, S. J., and Garcea, M. 1997. Sucrose vs. maltose taste discrimination by rats depends on the input of the seventh cranial nerve. Am. J. Physiol. Regul. Integr. Comp. Physiol. 41, R1210–R1228.
Spector, A. C., Norgren, R., and Grill, H. J. 1992. Parabrachial gustatory lesions impair taste aversion learning in rats. Behav. Neurosci. 106, 147–161.
Spector, A. C., Redman, R., and Garcea, M. 1996b. The consequences of gustatory nerve transection on taste-guided licking of sucrose and maltose in the rat. Behav. Neurosci. 110, 1096–1109.
Spector, A. C., Scalera, G., Grill, H. J., and Norgren, R. 1995. Gustatory detection thresholds after parabrachial nuclei lesions in rats. Behav. Neurosci. 109, 939–954.
Spector, A. C., Schwartz, G. J., and Grill, H. J. 1990b. Chemospecific deficits in taste detection after selective gustatory deafferentation in rats. Am. J. Physiol. Regul. Integr. Comp. Physiol. 258, R820–R826.
Spector, A. C., Travers, S. P., and Norgren, R. 1993b. Taste receptors on the anterior tongue and nasoincisor ducts of rats contribute synergistically to behavioral responses to sucrose. Behav. Neurosci. 107, 694–702.
St. John, S. J. and Smith, D. V. 2000. Neural representation of salts in the rat solitary nucleus: brain stem correlates of taste discrimination. J. Neurophysiol. 84, 628–638.
St. John, S. J. and Spector, A. C. 1996. Combined glossopharyngeal and chorda tympani nerve transection elevates quinine detection thresholds in rats (*Rattus norvegicus*). Behav. Neurosci. 110, 1456–1468.
St. John, S. J. and Spector, A. C. 1998. Behavioral discrimination between quinine and KCl is dependent on input from the seventh cranial nerve: implications for the functional roles of the gustatory nerves in rats. J. Neurosci. 18, 4353–4362.
St. John, S. J., Garcea, M., and Spector, A. C. 1994. Combined, but not single, gustatory nerve transection substantially alters taste-guided licking behavior to quinine in rats. Behav. Neurosci. 108, 131–140.
St. John, S. J., Markison, S., Guagliardo, N. A., Hackenberg, T. D., and Spector, A. C. 1997. Chorda tympani transection and selective desalivation differentially disrupt two-lever salt discrimination performance in rats. Behav. Neurosci. 111, 450–459.
St. John, S. J., Pour, L., and Boughter, J. D., Jr. 2005. Phenylthiocarbamide produces conditioned taste aversions in mice. Chem. Senses 30, 377–382.
Stapleton, J. R., Luellig, M., Roper, S. D., and Delay, E. R. 2002. Discrimination between the tastes of sucrose and monosodium glutamate in rats. Chem. Senses 27, 375–382.
Stebbins, W. C. and Berkley, M. A. 1990. Comparative Perception: Complex Signals. John Wiley & Sons.
Tapper, D. N. and Halpern, B. P. 1968. Taste stimuli: a behavioral categorization. Science 161, 708–710.
Thaw, A. K. and Smith, J. C. 1992. Conditioned suppression as a method of detecting taste thresholds in the rat. Chem. Senses 17, 211–223.
Travers, J. B., DiNardo, L. A., and Karimnamazi, H. 1997. Motor and premotor mechanisms of licking. Neurosci. Biobehav. Rev. 21, 631–647.
Travers, J. B., Urbanek, K., and Grill, H. J. 1999. Fos-like immunoreactivity in the brain stem following oral quinine stimulation in decerebrate rats. Am. J. Physiol. Regul. Integr. Comp. Physiol. 277, R384–R394.
Travers, J., DiNardo, L., and Karimnamazi, H. 2000. Medullary reticular formation activity during ingestion and rejection in the awake rat. Exp. Brain Res. 130, 78–92.
Travers, S. P. 1993. Orosensory Processing in Neural Systems of the Nucleus of the Solitary Tract. In: Mechanisms of Taste Transduction (*eds*. S. A. Simon and S. D. Roper), pp. 339–393. CRC Press.
Travers, S. P. and Nicklas, K. 1990. Taste bud distribution in the rat pharynx and larynx. Anatom. Rec. 227, 373–379.

Van Buskirk, R. L. 1981. The role of odor in the maintenance of flavor aversion. Physiol. Behav. 27, 189–193.
Vance, W. B. 1967. Hypogeusia and taste preference behavior in the rat. Life Sci. 6, 743–748.
Weingarten, H. P. and Watson, S. D. 1982. Sham feeding as a procedure for assessing the influence of diet palatability on food intake. Physiol. Behav. 28, 401–407.
Willner, P., Papp, M., Phillips, G., Maleeh, M., and Muscat, R. 1990. Pimozide does not impair sweetness discrimination. Psychopharmacology 102, 278–282.
Wolf, G. 1982. Refined salt appetite methodology for rats demonstrated by assessing sex differences. J. Comp. Physiol. Psychol. 96, 1016–1021.
Yamamoto, T. and Asai, K. 1986. Effects of gustatory deafferentation on ingestion of taste solutions as seen by licking behavior in rats. Physiol. Behav. 37, 299–305.
Yamamoto, T. and Fujimoto, Y. 1991. Brain mechanisms of taste aversion learning in the rat. Brain Res. Bull. 27, 403–406.
Ye, Q., Heck, G. L., and DeSimone, J. A. 1993. Voltage dependence of the rat chorda tympani response to Na^+ salts: implications for the functional organization of taste receptor cells. J. Neurophysiol. 70, 167–178.
Young, P. T. 1952. The role of hedonic processes in the organization of behavior. Psychol. Rev. 59, 249–257.
Young, P. T. and Madsen, C. H., Jr. 1963. Individual isohedons in sucrose-sodium chloride and sucrose-saccharin gustatory areas. J. Comp. Physiol. Psychol. 56, 903–909.
Young, P. T. and Trafton, C. L. 1964. Activity contour maps as related to preference in four gustatory stimulus areas of the rat. J. Comp. Physiol. Psychol. 58, 68–75.
Zhang, Y., Hoon, M. A., Chandrashekar, J., Mueller, K. L., Cook, B., Wu, D., Zuker, C. S., and Ryba, N. J. 2003. Coding of sweet, bitter, and umami tastes: different receptor cells sharing similar signaling pathways. Cell 112, 293–301.

4.23 Flavor Aversion Learning

I L Bernstein, University of Washington, Seattle, WA, USA

© 2008 Elsevier Inc. All rights reserved.

4.23.1	General Description	429
4.23.2	Conditioned Taste Aversion: The Conditioned Stimulus	430
4.23.2.1	Salience of Taste Cues	430
4.23.2.2	Salience of Novel Tastes	431
4.23.3	Conditioned Taste Aversions: The Unconditioned Stimulus	431
4.23.3.1	Neural Mediation of Food Aversion Learning	431
4.23.4	Food Aversions in Humans	432
4.23.5	Clinical Implications	433
References		434

Glossary

c-Fos protein Product of immediate early gene *c-fos*, regulates the induction of downstream target genes as a transcription factor.

conditioned stimulus (CS) A neutral stimulus which comes to be associated, after training, with an unconditioned stimulus.

emetic Causing nausea and/or vomiting.

latent inhibition A process by which preexposure to a stimulus without consequence retards the learning of subsequent conditioned associations with that stimulus.

N-methyl-D-aspartate (NMDA) receptors One class of glutamate receptors which potentiates synapses in several neural pathways and is believed to be importantly involved in neural plasticity.

phosphorylation The addition of a phosphate to a protein or a small molecule which can switch on or off cellular regulatory events.

protein kinase A cAMP-dependent protein kinase, also known as protein kinase A (PKA), refers to a family of enzymes whose activity is dependent on the level of cyclic AMP (cAMP) in the cell.

unconditioned stimulus (US) A stimulus used in classical conditioning which produces an unconditioned response without any learning.

Flavor cues such as taste, odor, and texture, are critical to food selection. These cues contribute to the palatability of food but they also play a protective role by discouraging the consumption of dangerous edibles. Flavor aversion refers to the avoidance of foods or fluids based on these cues. Aversions can be innate or they can be learned. Innate aversions, as exemplified by bitter avoidance, do not require prior experience, probably evolved to deter consumption of toxic chemicals that could be detected by their taste, and tend to be shared by members of a species. Learned aversions are those that are based on experience, such as consumption of a food prior to a bout of illness or discomfort. In such cases, illness can be a consequence of ingestion or coincidentally associated with it, such as a food eaten just before the onset of a bout of gastroenteritis (stomach flu). Among humans learned aversions tend to be idiosyncratic; that is, individuals differ from one another with respect to the foods that happen to become associated with the malaise.

The topic of this chapter is the sort of aversions which are acquired; those commonly referred to as learned taste aversions. A brief description of the distinctive characteristics of this learning, a review of what is known about the neural mechanisms that underlie it, and a summary of some clinical implications will be provided.

4.23.1 General Description

Animals and humans learn to avoid foods which may have made them sick, and they do this with remarkable facility. This learning is a form of associative conditioning in which an individual comes to avoid a

taste (conditioned stimulus (CS)) which has previously been paired with a treatment that produces transient illness (unconditioned stimulus (US)). Taste aversion learning is unusually robust and has clear adaptive advantages, particularly for omnivorous species which must select from a range of nutrients, some of which may be toxic. However, conditioned taste aversions (CTAs) can also be maladaptive, as in the case where safe, nutritious foods are avoided because of a chance association with symptoms of nausea or malaise. In cases such as gastroenteritis or cancer chemotherapy, the symptoms are not causally related to the food in question but the association and consequent distaste develops anyway (Bernstein, I. L. and Borson, S., 1986).

Several features of taste aversion learning are striking when they are compared to other learning paradigms (Riley, A. L., 2005). CTAs occur rapidly and potently under conditions that could not support other types of learning. Virtually every other conditioning paradigm requires close temporal proximity between presentation of CS and US. CTAs are routinely acquired after delays of several minutes or an hour between exposure to CS taste and US illness (Garcia, J. *et al.*, 1966). When one considers that long delay learning of taste aversions is often displayed after only one conditioning trial, the unusual potency of this learning is quite impressive. The requirement for temporal contiguity, with an optimal range being 500 ms to 2 s is so common a feature of associate learning paradigms that it has been used to build models of the types of cellular signaling processes that might underlie plasticity (Abrams, T. W. and Kandel, E. R., 1988). In this regard taste aversion learning is clearly an anomaly. This raises the question of how neural signaling in CTA circuits bridge a CS–US intervals of minutes and hours (Koh, M. T. *et al.*, 2003). The degree to which similar or unique mechanisms of neural plasticity are recruited and/or modified for this task remains to be determined.

The robustness of food aversion learning is also underscored by the findings of Roll D. L. and Smith J. C. (1972) that rats will acquire aversions even when they are completely anesthetized during and after the time when the US is administered. These findings, replicated and extended by Bermúdez-Rattoni F. *et al.* (1988), imply that these associations can be formed while unconscious.

In the laboratory, taste aversion learning has most often been studied in rats. This is likely to have been a fortuitous choice since rats have proven to be remarkably good at taste aversion learning. This may be due to two characteristics of this species; first, they are omnivores and opportunistic foragers which means that in their natural environment they frequently sample new foods and are thus at risk for encountering toxins. Second, they are unable to vomit which means that once they eat something toxic they cannot dispose of it easily. For these reasons, this species may have been under particularly strong selective pressure to develop a robust and efficient taste aversion conditioning mechanism as a means of toxin avoidance. But rats are certainly not unique in this ability. Taste aversion learning has been demonstrated in an enormous range of animal species, from the very simple, such as the garden slug, *limax* (Sahley, C. L. *et al.*, 1981), to the complex, such as humans (Garb, J. L. and Stunkard, A. J., 1974; Bernstein, I. L., 1978; Logue, A. W. *et al.*, 1981; Midkiff, E. E. and Bernstein, I. L., 1985; Bernstein, I. L. and Borson, S., 1986).

4.23.2 Conditioned Taste Aversion: The Conditioned Stimulus

4.23.2.1 Salience of Taste Cues

Typical CTA training consists of the presentation of a palatable taste solution, such as dilute saccharin, followed by the injection of a nonlethal toxin. In untrained rats saccharin is highly preferred and consumed with enthusiasm. This makes the behavior of the conditioned animals particularly striking, because they avoid the saccharin and appear to actually be disgusted by it.

The earliest characterizations of taste aversion learning emphasized the ease with which taste cues were associated with subsequent illness, and the relative difficulty of associating cues in other sensory modalities (e.g., sounds and sights) with illness (Garcia, J. *et al.*, 1974). This makes sense from an adaptive perspective as foods, and the sensations associated with their ingestion, are the most likely culprits when unpleasant gastrointestinal consequences arise. This left open the question of the salience of other food-related sensations, especially olfaction. When we commonly refer to the flavors of foods and fluids, we conflate taste and odor cues so that taste aversions may actually be flavor aversions, aversions to both the taste and odor of a food. In the laboratory, the contribution of these two modalities can be assessed independently. In rats, odor cues, presented without tastes, are much less effective than taste cues as CSs in aversion conditioning (Palmerino, C. C. *et al.*, 1980). In contrast, if an odor is conditioned in compound with a taste a

phenomenon referred to as taste potentiation of odor is observed. That it, after conditioning the compound (taste plus odor), when the odor is tested in isolation, it is clear that it has become a highly potent cue for avoidance. Under most normal circumstances, then, odors may be important cues in aversion conditioning. Furthermore, it should be noted that reliance on odor cues allows animals to actually avoid ingestion of a toxic or suspicious substance, whereas reliance on taste cues require some sampling and that can be risky.

4.23.2.2 Salience of Novel Tastes

The robust and rapid CTA acquisition which has been described relies heavily on a CS taste characteristic that has not been mentioned yet, that is, the novelty of the taste. Aversions arise extremely rapidly if a CS food or taste is novel, but if an organism has had prior, safe exposure to the food, conditioning is significantly retarded (Revusky, S. H. and Bedarf, E. W., 1967; Garcia, J. *et al.*, 1974) or prevented completely (Koh, M. T. and Bernstein, I. L., 2005). In the laboratory, one or two safe exposures to a taste prior to conditioning can dramatically attenuate learning.

This characteristic of taste aversion learning is dramatic but not unique. An analogous phenomenon has been described in other associative conditioning paradigms and the general process whereby CS preexposure retards conditioning is referred to as latent inhibition (Lubow, R. E., 1973). CTA acquisition shares additional characteristics with other associative learning paradigms. Conditioning strength is positively correlated with CS intensity, US intensity, and number of CS–US pairings. CTAs display generalization and, although very durable, CTAs are subject to extinction (Riley, A. L., 2005).

4.23.3 Conditioned Taste Aversions: The Unconditioned Stimulus

Laboratory studies of taste aversion learning commonly involve administration of a drug, such as lithium chloride (LiCl), as the US. LiCl, and many other US drugs, are known to act as emetics. This might lead one to assume that if a treatment is capable of acting as a US in taste aversion conditioning it probably causes nausea, or at least produces unpleasant symptoms. This is almost certainly not the case. Instead, the CTA literature yields a remarkably varied list of drugs and other treatments which are effective USs in conditioning (Riley, A. L., 2005). Careful examination of these treatments does not reveal particular feature(s) that they have in common (Gamzu, E. *et al.*, 1985). Although emetic drugs are highly effective as USs, many drugs that are not emetic can be effective (Grant, V. L., 1987; Goudie, 1979). Even more puzzling, some effective drugs do not appear to be particularly aversive. A striking demonstration of this is the fact that drugs which humans and animals will self-administer (Hunt, T. and Amit, Z., 1987) can support CTAs. So the claim that taste aversion conditioning can serve as a behavioral assay of aversiveness or toxicity should be met with skepticism.

Although it is clear that nausea is not necessary for the development of food aversions, there is compelling evidence that nausea may play a unique and particularly potent role in this learning. Evidence both from humans and rats (Pelchat, M. L. and Rozin, P., 1982; Pelchat, M. *et al.*, 1983) suggests that the prototypical learned food aversion, where the food becomes genuinely distasteful, generally is associated with symptoms of nausea. One demonstration of this point emerged from a survey undertaken by Pelchat M. L. and Rozin P. (1982) of people who suffered from food allergies. When allergic symptoms included nausea, subjects reported not only that they avoided the food, but that they actually disliked the taste. In contrast, when the allergic response included symptoms such as mouth sores or hives, subjects avoided the food but reported no change in the food's hedonic rating. In other words these subjects avoided eating the food because it would cause unpleasant symptoms, not because they actually found it distasteful. Thus, Pelchat M. L. and Rozin P. (1982) argue that nausea is not only sufficient for the establishment of a taste aversion but is actually necessary for the development of hedonic shifts or distaste toward foods. It is this shift in the hedonic or incentive value of a taste that, some believe, constitutes a genuine learned taste aversion.

4.23.3.1 Neural Mediation of Food Aversion Learning

When humans develop aversions as a result of the coincidental association between consumption of a food and chemotherapy or symptoms of gastroenteritis, the aversions appear to defy cognition. That is, strong aversions arise despite a person's awareness that the target food was not actually the cause of their illness. These findings suggest that food aversion learning is based on relatively primitive associative

mechanisms perhaps involving neural integration occurring in lower brain areas such as the brainstem.

Taste and visceral information converge in the brain stem, within the nucleus of the solitary tract (NTS) although there is little or no overlap between the regions responsive to gustatory and visceral input (Travers, J. B. *et al.*, 1987). Gustatory neurons from the facial, glossopharyngeal, and vagus nerves terminate in the rostral portion of the NTS. The NTS would, therefore, appear to be a critical part of the pathway mediating taste aversion learning. However, Grigson P. S. *et al.* (1997a) found that rats with extensive lesions of the rostral (gustatory) zone of the NTS demonstrated normal taste aversion learning. Since reception of gustatory information would appear to be obligatory to taste aversion learning, one might assume the NTS lesions, though extensive, did not completely eliminate incoming gustatory signals and that a degraded signal is sufficient for the learning.

In contrast to the rather limited role indicated for NTS, the next site in the ascending gustatory and visceral relay, the pontine parabrachial nucleus (PBN), appears to be crucial for taste aversion acquisition. Rats with lesions of the PBN are unable to acquire a CTA (Reilly, S. *et al.*, 1993). This deficit appears to be quite specific. It does not appear to be due to an inability to taste the CS or experience the US but rather to an inability to associate the two stimuli at the time of conditioning. Also, if conditioning occurs prior to lesioning, PBN lesions do not disrupt CTA expression (Grigson, P. S. *et al.*, 1997b). Thus, the PBN appears necessary for taste aversion acquisition but not expression.

Although taste and visceral information converge within the brainstem and pons, these regions do not appear to be sufficient for the integration needed for taste aversion learning. The chronic decerebrate rat has been shown to be incapable of forming the associations necessary for taste aversion learning (Grill, H. J. and Norgren, R., 1978) which suggests that integration of taste and visceral inputs within the brainstem of the rat is insufficient to support the acquisition or expression of taste aversions. A variety of studies indicate that forebrain structures within the ascending gustatory projection are involved in taste aversion learning (Chambers, K. C., 1990; Yamamoto, T. and Fujimoto, Y., 1991). Two regions of particular interest are the amygdala and gustatory (insular) cortex.

Studies examining the effects of amygdala lesions on taste aversion learning have been somewhat inconsistent. Some of the inconsistency may be attributable to differences in lesion method as well as details of the conditioning protocol (Schafe, G. E. *et al.*, 1998; Morris, R. *et al.*, 1999). Overall, a role for the amygdala in CTA acquisition and expression has been supported by lesion studies as well as studies using methods which lack the interpretational limitations of the lesion approach (Schafe, G. E. and Bernstein, I. L., 1996; Koh, M. T. *et al.*, 2003; Koh, M. T. and Bernstein, I. L., 2005). For example, inhibition of immediate early gene expression and protein kinase A signaling within the amygdala has been demonstrated to interfere with CTA acquisition (Lamprecht, R. and Dudai, Y., 1996; Koh, M. T. *et al.*, 2002).

Like the amygdala, the insular cortex (IC) has strong reciprocal connections with NTS and PBN (Saper, C. B., 1982) and lesion studies have been quite consistent in demonstrating attenuation of taste aversion learning after destruction of this area (Lasiter, P. S. and Glanzman, D. L., 1982; 1985; Bermúdez-Rattoni, F. and McGaugh, J. L., 1991). Furthermore, reversible interference with cholinergic function or blockade of *N*-methyl-D-aspartate (NMDA) receptors in rat IC disrupts taste aversion learning (Naor, C. and Dudai, Y., 1996), and protein tyrosine phosphorylation is altered in the IC following training (Rosenblum, K. *et al.*, 1995). Combining IC lesions or inactivation with staining for c-Fos protein also provides evidence for a dynamic role for the IC in CTA learning. Collectively, results support an important role for this region in taste memory and taste aversion learning.

Thus, lesion studies and new molecular techniques, as well as neuroanatomical approaches, have begun to define the pathways involved in processing taste and visceral signals, and in forming the durable associations between them which are the basis of a CTA. The cellular mechanisms which underlie these associations have also begun to be identified. A recent review provides an intriguing theoretical perspective on these processes (Bermúdez-Rattoni, F., 2004).

4.23.4 Food Aversions in Humans

Food aversion learning in humans has been examined principally through the use of survey methods (Garb, J. L. and Stunkard, A. J., 1974; Logue, A. W. *et al.*, 1981; Midkiff, E. E. and Bernstein, I. L., 1985). Characteristics of food aversions reported by humans are generally similar to those observed in laboratory studies of rats. Acquisition often occurs in a single trial, frequently with long delays interposed between tasting the food and experiencing illness. Aversions

were more likely to develop to less familiar as well as less preferred foods. Extinction was reported to be more effective at reducing aversions than forgetting. This raises the question of what role this powerful and primitive learning plays in human food choice.

The extent to which food aversions, learned as a consequence of the association of specific foods with gastrointestinal symptoms, contribute to overall food choice is not simple to determine. Some who have evaluated this issue have concluded that the role of aversion conditioning is minor. They base this on the following reasoning. Many studies have shown that a majority of people surveyed report having experienced the development of a food aversion at some time in their life. However, if the number of people reporting existing food aversions and the number of foods they avoid due to these experiences are calculated, this number is small relative to the large number of foods people seem to dislike which leaves a vast number of food aversions unaccounted for in terms of their cause (Rozin, P. and Vollmecke, T. A., 1986).

Another line of reasoning leads to a different conclusion. There are good reasons to believe that verbal reports of learned food aversions underestimate the actual number of such aversions. Memory researchers distinguish between implicit and explicit memories (Squire, L. R. *et al.*, 1993). Explicit memories are those you are aware of consciously while implicit memories are those you have but are not consciously aware of. Since classical conditioning is more likely to generate implicit than explicit memories, most food aversion learning experiences in humans may form implicit, not explicit, memories. Research indicates that implicit memory formation is less susceptible to anesthesia (Andrade, J., 1995) which might explain the resistance of food aversion learning to anesthesia (Roll, D. L. and Smith, J. C., 1972; Bermúdez-Rattoni, F. *et al.*, 1988). Thus, if all but the most severe learned food aversions form implicit not explicit memories, subjects' recall of taste aversion experiences may not be the most sensitive way to assess aversion conditioning. If this is true then conditioned food aversions may affect food choices and hedonic responses to foods unconsciously and such conditioning may play a significant role in human food choice but this role would be quite difficult to assess methodologically. Also some people who are chronically ill, prone to motion sickness, or otherwise vulnerable to experiencing unpleasant gastrointestinal symptoms may be at a much higher risk of developing these aversions and having them limit their acceptable food choices (Bernstein, I. L. and Borson, S., 1986).

4.23.5 Clinical Implications

As previously noted, learned taste aversions often arise when the consumption of a food or drink is followed by nausea or gastrointestinal malaise. Sometimes the illness is actually caused by the food or beverage consumed, but it is frequently the case that the food and illness are only coincidentally associated. An example of aversions in which there is indeed a causal relationship between CS and US is the common occurrence of aversions to specific alcoholic beverages, such as bourbon or tequila, which were consumed in excess and which led to nausea and vomiting. Aversions to specific alcoholic beverages frequently appear in surveys done with college students, for obvious reasons (Logue, A. W. *et al.*, 1981; Midkiff, E. E. and Bernstein, I. L., 1985). Another situation in which food aversions develop is in patients receiving cancer chemotherapy (Bernstein, I. L., 1978). Drugs used to treat cancer, while frequently effective in halting the growth of tumor cells, can have severe side effects including nausea and vomiting. Cancer patients often develop aversions to specific foods they consume before these treatments, despite their recognition that their chemotherapy and not their lunch was the cause of these symptoms (Bernstein, I. L. and Borson, S., 1986). Recognition that cancer patients are at risk for the development of learned food aversions and that this can affect their appetite and nutritional status has led to interventions which can prevent the development of these aversions (Broberg, D. J. and Bernstein, I. L., 1987).

The rapid acquisition and robustness of learned taste aversions have made them an attractive tool in therapeutic efforts to modify problem behaviors such as alcoholism and smoking. In point of fact, a natural consequence of excessive alcohol consumption is illness, including severe nausea and vomiting. As noted above, these symptoms are effective in inducing aversions to specific alcoholic beverages in many college students. Do alcoholics fail to acquire such aversions? If they acquire such aversions, how do the aversions subsequently affect their drinking? A survey of alcoholics in a treatment facility indicated that alcoholics do acquire taste aversions to alcoholic beverages as a consequence of overconsumption. However, when a taste aversion to a specific alcoholic beverage was acquired, alcoholics avoided that particular beverage, choosing some other alcoholic beverages instead (Logue, A. W. *et al.*, 1983). Chemical aversion therapy involves the use of drugs, such as emetine, to induce nausea and vomiting after alcohol consumption. This

form of therapy has been incorporated into a range of alcoholism treatment packages. Available outcome data from a number of these programs indicate that the effectiveness of their treatment packages in promoting abstinence is quite good. However, the contribution of chemical aversion therapy, *per se*, to the effectiveness of the entire treatment package has not been explicitly evaluated and therefore it remains unknown. Aversion therapy has also been used as an aid to smoking cessation. This involves a rapid smoking procedure which conforms to the taste aversion learning paradigm in that it involves pairing the flavor cues associated with smoking cigarettes with aversive symptoms such as nausea and headache. This procedure has been reported to be effective in producing aversions to the taste and smell of cigarettes and to improve abstinence rates in smoking cessation programs.

References

Abrams, T. W. and Kandel, E. R. 1988. Is contiguity detection in classical conditioning a system or a cellular property? Learning in Aplysia suggests a possible molecular site. Trends Neurosci. 11, 128–135.

Andrade, J. 1995. Learning during anaesthesia: a review. Br. J. Psychol. 86, 479–506.

Bermúdez-Rattoni, F. 2004. Molecular mechanisms of taste-recognition memory. Nat. Rev. Neurosci. 5, 209–217.

Bermúdez-Rattoni, F. and McGaugh, J. L. 1991. Insular cortex and amygdala lesions differentially affect acquisition on inhibitory avoidance and conditioned taste aversion. Brain Res. 549, 165–170.

Bermúdez-Rattoni, F., Forthman, D. L., Sanchez, M. A., Perez, J. L., and Garcia, J. 1988. Odor and taste aversions conditioned in anesthetized rats. Behav. Neurosci. 102, 726–732.

Bernstein, I. L. 1978. Learned taste aversions in children receiving chemotherapy. Science 200, 1302–1303.

Bernstein, I. L. and Borson, S. 1986. Learned food aversion: a component of anorexia syndromes. Psychol. Rev. 93, 462–472.

Broberg, D. J. and Bernstein, I. L. 1987. Candy as a scapegoat in the prevention of food aversions in children receiving chemotherapy. Cancer 60, 2344–2347.

Chambers, K. C. 1990. A neural model for conditioned taste aversions. Annu. Rev. Neurosci. 13, 373–385.

Gamzu, E., Vincent, G., and Boff, E. 1985. A pharmacological perspective of drugs used in establishing conditioned food aversions. Ann. N. Y. Acad. Sci. 443, 231–249.

Garb, J. L. and Stunkard, A. J. 1974. Taste aversions in man. Am. J. Psychiatry 131, 1204–1207.

Garcia, J., Ervin, R. R., and Koelling, R. A. 1966. Learning with prolonged delay of reinforcement. Psychon. Sci. 5, 121–122.

Garcia, J., Hankins, W. G., and Rusiniak, K. W. 1974. Behavioral regulation of the milieu interne in man and rat. Science 185, 824–831.

Goudie, A. J. 1979. Aversine stimulus properties of drugs. Neuropharmacology 18, 971–979.

Grant, V. L. 1987. Do conditioned taste aversions result from activation of emetic mechanisms? Psychopharmacology 93, 405–415.

Grigson, P. S., Shimura, T., and Norgren, R. 1997a. Brainstem lesions and gustatory function: II. The role of the nucleus of the solitary tract in NA+ appetite, conditioned taste aversion and conditioned odor aversion in rats. Behav. Neurosci. 111, 169–179.

Grigson, P. S., Shimura, T., and Norgren, R. 1997b. Brainstem lesions and gustatory function: III. The role of the nucleus of the solitary tract and the parabrachial nucleus in retention of a conditioned taste aversion in rats. Behav. Neurosci. 111, 180–187.

Grill, H. J. and Norgren, R. 1978. Chronically decerebrate rats demonstrate satiation but not bait shyness. Science 201, 267–269.

Hunt, T. and Amit, Z. 1987. Conditioned taste aversion induced by self-administered drugs: paradox revisited. Neurosci. Biobehav. Rev. 11, 107–130.

Koh, M. T. and Bernstein, I. L. 2005. Mapping conditioned taste aversion associations using c-fos reveals a dynamic role for insular cortex. Behav. Neurosci. 119, 388–398.

Koh, M. T., Thiele, T. E., and Bernstein, I. L. 2002. Inhibition of protein kinase A activity interferes with long-term, but not short-term, memory of conditioned taste aversions. Behav. Neurosci. 116, 1070–1074.

Koh, M. T., Wilkins, E. E., and Bernstein, I. L. 2003. Novel taste elevates c-fos expression in the central amygdala and insular cortex: implication for taste aversion learning. Behav. Neurosci. 117, 1416–1422.

Lamprecht, R. and Dudai, Y. 1996. Transient expression of c-fos in rat amygdala during training is required for encoding conditioned taste aversion memory. Learn. Memory 3, 31–41.

Lasiter, P. S. and Glanzman, D. L. 1982. Cortical substrates of taste aversion learning: dorsal prepiriform (insular) lesions disrupt taste aversion learning. J. Comp. Physiol. Psychol. 96, 376–392.

Lasiter, P. S. and Glanzman, D. L. 1985. Cortical substrates of taste aversion learning: Involvement of dorsolateral amygdaloid nuclei and temporal neocortex in taste aversion learning. Behav. Neurosci. 99, 257–276.

Logue, A. W., Logue, K. R., and Strauss, K. E. 1983. The acquisition of taste aversions in humans with eating and drinking disorders. Behav. Res. Ther. 21, 275–289.

Logue, A. W., Ophir, I., and Strauss, K. E. 1981. The acquisition of taste aversions in humans. Behav. Res. Ther. 19, 319–333.

Lubow, R. E. 1973. Latent inhibition. Psychol. Bull. 79, 398–407.

Midkiff, E. E. and Bernstein, I. L. 1985. Targets of learned food aversions in humans. Physiol. Behav. 34, 839–841.

Morris, R., Frey, S., Kasambira, T., and Petrides, M. 1999. Ibotenic acid lesions of the basolateral, but not the central, amygdala interfere with conditioned taste aversion: evidence from a combined behavioral and anatomical tract-tracing investigation. Behav. Neurosci. 113, 291–302.

Naor, C. and Dudai, Y. 1996. Transient impairment of cholinergic function in the rat insular cortex disrupts the encoding of taste in conditioned taste aversion. Behav. Brain Res. 79, 61–67.

Palmerino, C. C., Rusiniak, K. W., and Garcia J. 1980. Flavor illness aversions: the peculiar role of odor and taste in memory for poison. Science 208, 753–755.

Pelchat, M. L. and Rozin, P. 1982. The special role of nausea in the acquisition of food dislikes by humans. Appetite 3, 341–351.

Pelchat, M., Grill, H. J., Rozin, P., and Jacobs, J. 1983. Quality of acquired responses to tastes by *Rattus norvegicus* depends upon type of associated discomfort. J. Comp. Physiol. Psychol. 97, 140–153.

Reilly, S., Grigson, P. S., and Norgren, R. 1993. Parabrachial nucleus lesions and conditioned taste aversion: evidence supporting an associative deficit. Behav. Neurosci. 107, 1005–1017.

Revusky, S. H. and Bedarf, E. W. 1967. Association of illness with prior ingestion of novel foods. Science 155, 219–220.

Riley, A. L. 2005. Conditioned Taste Aversion: An Annotated Bibliography. http://ctalearning.com.
Roll, D. L. and Smith, J. C. 1972. Conditioned Taste Aversion in Anesthetized Rats. In: Biological Boundaries of Learning (*eds*. M. E. P. Seligman and J. L. Hager), pp. 98–102. Appleton-Century-Crofts.
Rosenblum, K., Schul, R., Meiri, N., Hadari, Y. R., Zick, Y., and Dudai, Y. 1995. Modulation of protein tyrosine phosphorylation in rat insular cortex after conditioned taste aversion training. Proc. Natl. Acad. Sci. U. S. A. 92, 1157–1161.
Rozin, P. and Vollmecke, T. A. 1986. Food likes and dislikes. Annu. Rev. Nutr. 6, 433–456.
Sahley, C. L., Gelperin, A., and Rudy, J. 1981. One-trial associative learning modifies food odor preferences of a terrestrial mollusc. Proc. Natl. Acad. Sci. U. S. A. 78, 640–642.
Saper, C. B. 1982. Reciprocal parabrachial-cortical connections in the rat. Brain Res. 52, 91–97.
Schafe, G. E. and Bernstein, I. L. 1996. Forebrain contribution to the induction of a brainstem correlate of conditioned taste aversion: I. The amygdala. Brain Res. 741, 109–116.
Schafe, G. E., Thiele, T. E., and Bernstein, I. L. 1998. Conditioning method dramatically alters the role of amygdala in taste aversion learning. Learn. Memory 15, 481–492.
Squire, L. R., Knowlton, B., and Musen, G. 1993. The structure and organization of memory. Annu. Rev. Psychol. 44, 453–495.
Travers, J. B., Travers, S. P., and Norgren, R. 1987. Gustatory neural processing in the hindbrain. Annu. Rev. Neurosci. 10, 595–632.
Yamamoto, T. and Fujimoto, Y. 1991. Brain mechanisms of taste aversion learning in the rat. Brain Res. Bull. 27, 403–406.

Further Reading

Bernstein, I. L. 1991. Flavor Aversion. In: Smell and Taste in Health and Disease (*eds*. T. V. Getchell, R. L. Doty, L. M. Bartoshuk, and J. B. Snow), pp. 417–428. Raven Press.
Yamamoto, T., Shimura, T., Sako, N., Yasoshima, Y., and Sakai, N. 1994. Neural substrates for conditioned taste aversion in the rat. Behav. Brain Res. 65, 123–137.

4.24 Roles of Taste in Feeding and Reward

T Yamamoto and T Shimura, Osaka University, Osaka, Japan

© 2008 Elsevier Inc. All rights reserved.

4.24.1	**Central Pathways Involved in Hedonic Evaluation**	438
4.24.1.1	Inputs from the Gustatory Pathway to Reward System and Feeding Center	438
4.24.1.2	Central Representation of Flavor	438
4.24.1.3	Taste-Mediated Reflexes	439
4.24.1.4	Salivary Secretion	439
4.24.1.5	Somatic Motor Responses	439
4.24.2	**Substances Related to Palatability**	440
4.24.2.1	Benzodiazepine	440
4.24.2.2	Opioids	442
4.24.2.3	Cannabinoid	443
4.24.2.4	Substances Related to Negative Hedonics	443
4.24.3	**Role of the Reward System in Taste-Mediated Behavior**	444
4.24.3.1	What is the Reward System?	444
4.24.3.2	The Role of Dopamine in Food Reward	444
4.24.3.3	The Nucleus Accumbens	445
4.24.4	**Role of Taste in Feeding**	446
4.24.4.1	Feeding Behavior to Palatable and Aversive Foods	446
4.24.4.2	Learning and Memory Related to Feeding Behavior	448
4.24.4.3	Preference Learning	448
4.24.4.4	Aversion Learning	448
4.24.4.5	Orexigenic Substances	450
4.24.5	**Brain Imaging Study on Hedonic Evaluation in Humans**	450
References		452

Glossary

conditioned taste aversion (CTA) Avoidance and aversion to a substance after an association learning between the ingestion of the substance (CS) and subsequent malaise (US) with gastrointestinal disorders and nausea. Animals remember the taste for a long time and reject its ingestion at subsequent exposures. CTA has unique characteristics such that strong and long-lasting memory can be acquired by a single pairing of the CS and US even with a long (up to several hours) CS–US interval.

When we take a bite of our favorite food, we experience a variety of sensations, and almost simultaneously we will smile and perceive it to be delicious. We will then be motivated to have more bites, the jaws and tongue move rhythmically with salivary secretion and active gastrointestinal functions to ingest the food. Eventually, the ingestive behavior finishes with the satisfaction of feeling full. Sometimes if something is palatable, we will overeat. Some of our favorite foods may have been innately determined, e.g., cakes and chocolates with innately preferred sweet tastes, but others are acquired after good experiences, or as a more specific example, on the basis of association learning between taste perception and nutritive postingestional effects. Conversely, even favorite foods can become aversive and avoided as a consequence of an unpleasant experience including postingestional malaise. Such taste-mediated behaviors can be commonly observed in everyone. In this chapter, we review the literature regarding these different aspects of pleasantness and rewarding eating behavior and discuss the underlying anatomy, neural substrates, and chemical mediators in the brain, learning and memory processes, and finally the activation patterns in the human brain.

4.24.1 Central Pathways Involved in Hedonic Evaluation

4.24.1.1 Inputs from the Gustatory Pathway to Reward System and Feeding Center

Central gustatory pathways have been well studied and documented in monkeys (Rolls, E. T., 2004) and rodents, especially rats (Norgren, R., 1995). Figure 1 shows a schematic diagram of some of the gustatory pathways in rats. Branches of the facial, glossopharyngeal, and vagus nerves, which synapse with receptor cells in the taste buds, convey taste messages to the first relay nucleus, the rostral part of the nucleus tractus solitarius (NTS). The second relay nucleus for ascending taste inputs is the parabrachial nucleus (PBN) of the pons. The third relay nucleus is the medial parvocellular component of the ventrobasal complex of the thalamus (VPMpc). This thalamic nucleus projects to the gustatory cortex (GC), the cortical gustatory area in the insular cortex (IC). Other ascending projections from the PBN are to the lateral hypothalamus (LH) (not shown in Figure 1), the central nucleus of the amygdala, and the bed nucleus of the stria terminalis (not shown in Figure 1). In monkeys, however, ascending fibers of neurons in the gustatory area of the NTS directly reach the VPMpc, bypassing the PBN (Beckstead, R. M. *et al.*, 1980). It is known that general visceral inputs also project in a similar fashion to the brain regions in parallel with the gustatory projections described above.

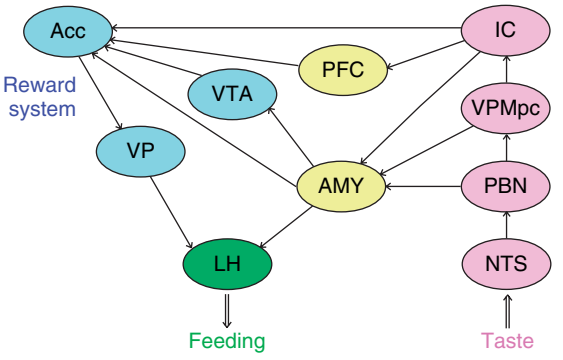

Figure 1 Diagram of connections from the taste system to reward system and feeding center. NTS, nucleus of tractus solitarius; PBN, parabrachial nucleus; VPMpc, parvocellular part of the ventralis posteromedial thalamic nucleus; IC, insular cortex; PFC, prefrontal cortex; AMY, amygdala; VTA, ventral tegmental area; Acc, nucleus of accumbens; VP, ventral pallidum; LH, lateral hypothalamic area. Note that this diagram does not include all of the connections.

The neural pathway of the brain reward system has also been studied and documented (Berridge, K. C. and Robinson, T. E., 1998; Wise, R. A., 2002 for reviews). As shown in Figure 1 and described in more detail in the following sections in this chapter, the essential components are the ventral tegmental area (VTA) in the midbrain, the origin of the mesolimbic dopamine system, the nucleus accumbens (Acc), an essential interface between motivation (e.g., palatability) and action (e.g., feeding), and the ventral pallidum (VP) situated between the Acc and LH, known as the feeding center.

When we consider the roles of taste in feeding and reward, we have to make clear how the taste system interacts with the reward and feeding systems. However, this has not yet been well clarified. The amygdala (AMY), the prefrontal cortex (PFC) including the ventrolateral (or anterior sulcal) and dorsomedial cortices, and IC are the candidates for the interfaces between the two systems. The gustatory insular cortex sends axons to the PFC (Saper, C. B., 1982; Shi, C.-J. and Cassell, M. D., 1998), and the dorsomedial PFC neurons actually respond to gustatory stimuli (Lukáts, B. *et al.*, 2002; Karádi, Z. *et al.*, 2005). Among other structures, the PFC is interconnected with the feeding-related subcortical areas such as the basal forebrain (Divac, I. *et al.*, 1978), amygdala (Pérez-Jaranay, J. M. and Vives, F., 1991), LH (Kita, H. and Oomura, Y., 1981), VTA (Divac, I. *et al.*, 1978; Kosobud, A. E. *et al.*, 1994), and Acc (Brog, J. S. *et al.*, 1993). Behavioral studies have shown that the PFC is associated with various mechanisms in the central control of feeding, for example, lesions of the dorsomedial PFC result in finickiness (Kolb, B. and Nonneman, A. J., 1975) and impairment of conditioned taste aversion (CTA) (Hernádi, I. *et al.*, 2000; Karádi, Z. *et al.*, 2005), while lesion and electrical stimulation of the ventrolateral PFC induce feeding disturbances (Kolb, B. and Nonneman, A. J., 1975; Brandes, J. S. and Johnson, A. K., 1978) and feeding (Bielajew, C. and Trzcinska, M., 1994), respectively.

4.24.1.2 Central Representation of Flavor

It is widely accepted that flavor is the integrated sensation of taste and odor, and often the somatic sensations of texture and temperature are included (Bartoshuk, L. M. and Beauchamp, G. K., 1994 for a review). Flavor contributes significantly to hedonic evaluation of food and feeding behavior. The brain sites involved in flavor evaluation are thought to be the regions where taste and other sensory inputs are

integrated. In rodents, although neurons in the NTS, PBN, and VPMpc are more or less responsive to taste, tactile, and thermal stimulation of the tongue, more intense overlapping activation including olfactory and visceral inputs are in regions of the GC (Shipley, M. T. and Geinisman, Y., 1984; Yamamoto, T. *et al*., 1989a), amygdala (Azuma, S. *et al*., 1984; Nishijo, H. *et al*., 1998c), and hypothalamus (Yamamoto, T. *et al*., 1989b). In monkeys, single-neuron recording studies have identified neurons responsive to both taste and smell in the insula/operculum, the primary GC (Scott, T. R. and Plata-Salaman, C. R., 1999 for a review), and orbitofrontal cortex (Rolls, E. T. and Baylis, L. L., 1994). Some neurons in the monkey orbitofrontal cortex receive visual (Rolls, E. T. and Baylis, L. L., 1994) and somatosensory inputs related to fat-like texture (Rolls, E. T. *et al*., 1999) and viscosity of the texture (Rolls, E. T. *et al*., 2003) in the mouth. Neurons in the amygdala also respond to different sensory inputs (Nishijo, H., *et al*., 1988a; 1988b). In a recent neuroimaging study in humans, Small D. M. *et al*. (2004) suggest that the insula, orbitofrontal cortex, and anterior cingulate cortex are key components of the network underlying flavor perception and that taste–smell integration is dependent on the mode of olfactory delivery, the orthonasal or retronasal routes, and previous experience with taste and smell combinations.

4.24.1.3 Taste-Mediated Reflexes

Taste stimuli evoke a variety of autonomic and hormonal reflex responses including salivary secretion, increases in gastric motility and gastric acid, exocrine pancreatic secretion, and endocrine secretions (Pavlov, I. P., 1902; Janowitz, H. D. *et al*., 1950; Novis, B. H. *et al*., 1971; Fischer, U. *et al*., 1972; Steffens, A. B., 1976; Nicolaidis, S., 1977; Ohara, I. *et al*., 1988; Niijima, A., 1991; Ohara, I. *et al*., 1996). In addition to these responses, taste stimuli elicit somatic motor responses involving mainly lingual and oral-facial muscles (Steiner, J. E., 1973; Grill, H. J. and Norgren, R. 1978a). Cephalic phase insulin release is a reflexly induced secretion elicited by oral stimulation with taste stimuli especially including sweet- (Steffens, A. B., 1976; Berthoud, H. R. *et al*., 1980) and umami-tasting (Niijima, A. *et al*., 1990) substances. Such a taste quality-specific reflex can also be seen for salivary secretion, as shown below.

4.24.1.4 Salivary Secretion

Salivary secretion occurs when sapid foods are put in the mouth, termed the gustatory-salivary reflex. The volume and chemical composition of saliva reflexly induced by taste stimulation are markedly different depending on the quality (Baxter, H., 1933; Kerr, A. C., 1961; Newbrun, E., 1962; Funakoshi, M. and Kawamura, Y., 1967; Gantt, W. H., 1973) and nature of the gustatory stimulus. Dry bread induces a copious serous saliva and meat elicits a small amount of mucous saliva (Pavlov, I. P., 1902). Gjorstrup P. (1980) found that sweet stimuli regularly produced a large increase in the amylase secretion from the parotid gland of conscious rabbits, salty stimuli had a small effect, and sour and bitter stimuli had a negligibly small effect.

It is generally known that the most copious salivary secretion is induced by sour (or acid) stimulation (Kerr, A. C., 1961; Emmelin, N. and Holmberg, J., 1967; Funakoshi, M. and Kawamura, Y., 1967) and that the amount of secretion increases with the stimulus concentration (Feller, R. P. *et al*., 1965; Chauncey, H. H. and Feller, R. P., 1967). The gustatory-salivary reflex has been studied in anesthetized decerebrate animals (Yamamoto, T. and Kawamura, Y., 1977; Kawamura, Y. and Yamamoto, T., 1978; Matsuo, R. and Yamamoto, Y., 1989; Matsuo, R. *et al*., 1989; 2001) where taste neurons in the lower brainstem (NTS and/or PBN) and the salivatory nuclei are involved. These studies have shown that the magnitude of response of the gustatory afferent neurons to taste stimulation is correlated with the volume of salivary secretion regardless of the taste quality, except for copious secretions to strong acids (Kawamura, Y. and Yamamoto, T., 1978) and bitter tastes accompanying rejection behaviors (Matsuo, R. *et al*., 2001). According to Matsuo R. *et al*. (2001), aversive taste information from the PBN reaches the salivatory secretory center via the reticular formation ventral to the PBN with a slight contribution of the connection between the NTS and the salivatory nuclei.

Since the amount of salivary secretion elicited by taste stimulation is markedly reduced after lesions of the cortical taste area in conscious dogs (Funakoshi, M. *et al*., 1972), higher central nervous system structures may also be involved in the modulation of activity of the reflex arc in conscious animals.

4.24.1.5 Somatic Motor Responses

Animals as well as humans accept and ingest sweet and slightly salty substances (e.g., sucrose and NaCl),

while they reject very sour and bitter substances (e.g., HCl and quinine), accompanied by particular oral-facial movements. The possibility that such acceptance or rejection behaviors based on the hedonics of taste are determined in the brainstem without higher cortical involvement was first noticed by Miller F. R. and Sherrington C. R. (1916).

Effects of taste stimuli on tongue motility have been reported in human neonates. For example, Weiffenbach J. M. and Thach B. T. (1973) reported that a drop of glucose solution, but not water, to the tongue elicited lateral tongue movement toward the site of the sapid stimulation. Nowlis G. H. (1973) has pointed out that human newborn infants are capable of eliciting differential tongue movements depending on the quality of gustatory stimuli. Moreover, Steiner J. E. (1973) observed that human newborn infants showed active and differential oral-facial expression based on the hedonic dimension of gustatory stimuli. The responses to sugar (sweet taste) and quinine (bitter taste) were characterized by expressions of pleasure (or relaxation and acceptance) and displeasure (or rejection), respectively. He concluded that the neural substrate of such hedonic behavior is located at the brainstem level, because essentially identical features of facial expression were observed in anencephalic and hydroanencephalic neonates.

Taste-elicited behavioral displays were also investigated in rats (Grill, H. J. and Norgren, R., 1978a; 1978b) and newborn rabbit pups (Ganchrow, J. R. *et al.*, 1979). Grill H. J. and Norgren R. (1978a) analyzed the pattern of tongue, jaw, and body movements in normal and decerebrate rats in response to an injection of a small amount of taste solution into the oral cavity and showed that sucrose, NaCl, and HCl solutions elicited a response sequence beginning with rhythmic mouth movements followed by rhythmic tongue protrusions and then lateral tongue movements, while quinine induced a response beginning with gaping followed by various characteristic body responses. These behavioral experiments on animals again show that taste-elicited behaviors can be grouped into acceptance and rejection based on hedonics of tastes, and these behaviors depend only on the lower brainstem.

When taste solutions were infused into the mouth, c-*fos* was strongly expressed in the lateral and intermediate zones of the medullary reticular formation, which includes premotor neurons of masticatory, facial and tongue motor systems (DiNardo, L. A. and Travers, J. B., 1994; Travers, J. B. *et al.*, 1999). This area receives inputs from the taste areas of the NTS (Shammah-Lagnado, S. J. *et al.*, 1992; Halsell, C. B. *et al.*, 1996) and PBN (Herbert, H. *et al.*, 1990; Karimnamazi, H. and Travers, J. B., 1998). These findings suggest that taste information reaches the motor nuclei through the medullary reticular formation to generate well-organized taste-elicited motor reactions.

4.24.2 Substances Related to Palatability

This section describes several neurochemicals that appear to be related to taste hedonics, especially to palatability. We discuss the possible involvement of dopamine with palatability in the next section.

4.24.2.1 Benzodiazepine

Benzodiazepines such as chlordiazepoxide and diazepam are widely prescribed for the treatment of anxiety disorders. A considerable body of evidence has indicated that benzodiazepine agonists, which facilitate the opening of Cl^- channels in response to $GABA_A$ receptor activation, promote food intake (Berridge, K. C. and Peciña, S., 1995 for a review). Although in most studies, this hyperphagic effect has been shown in rodents, benzodiazepines also enhances food intake in rhesus monkeys (Foltin, R. W. *et al.*, 1985), baboons (Foltin, R. W. *et al.*, 1989), and humans (Haney, M. *et al.*, 1997).

Because of their well-known anxiolytic and sedative actions, the facilitatory effect of benzodiazepines on food intake was once interpreted as an indirect consequence (Poschel, B. P. H., 1971). However, the following results suggest that benzodiazepine-induced hyperphagia is not due to secondary effects of benzodiazepine on anxiety or arousal. First, benzodiazepine agonists increase food intake in rats under nonstressful conditions of the home cage (McLaughlin, C. L. and Baile, C. A., 1979; Cole, S. O., 1983). Second, while sedative effects are rapidly reduced by repeated treatments with benzodiazepine, tolerance to the hyperphagic effects slowly develops (Wise, R. A. and Dawson, V., 1974). Third, while some partial agonists of benzodiazepine (Ro16-6028, Ro17-1812, Ro23-0364) facilitate food intake, these drugs do not produce a strong sedative effect (Cooper, S. J. and Green, A. E., 1993). Other types of benzodiazepines (CGS 9895 and CGS 9896) diminish behavioral expressions of anxiety and arousal

without facilitating food intake (Cooper, S. J. and Yerbury, R. E., 1986). Thus, the benzodiazepine neural systems that modulate anxiety are thought to be separable from those that increase feeding.

In earlier studies, the hyperphagic effect of benzodiazepines was considered to be due to an antisatiety effect (Margules, D. L. and Stein, L., 1967) or to a hunger-inducing effect (Wise, R. A. and Dawson, V., 1974). Several lines of evidence, however, strongly suggest that benzodiazepines specifically enhance the hedonic palatability of food (Cooper, S. J. and Estall, L. B., 1985; Berridge, K. C. and Peciña, S., 1995). For example, systemic administration of benzodiazepines selectively increase the intake of preferred foods such as cookies, sweetened foods, and saccharin solution, but not the intake of regular chow or plain water (Cooper, S. J. and McClelland, A., 1980; Cooper, S. J., 1987; Cooper, S. J. and Yerbury, R. E., 1988; Parker, L. A., 1991).

Since these studies used the volume (g or ml) of food or fluid consumed as a measure for pharmacological modulation of feeding, some factors other than intraoral taste stimulation might have affected the results. Cooper S. J. *et al.* (1988) reported that a benzodiazepine agonist facilitated, and an antagonist reduced, sucrose sham feeding in the gastric-fistulated rat, suggesting that benzodiazepine-induced hyperphagia is not due to postingestional factors.

Although the hedonic aspect of the taste of food and fluid is one of the most important factors that affect feeding, it is difficult to determine the perceived palatability in animals from the volume of food or fluid consumed. Grill H. J. and Norgren R. (1978a) developed a more direct method to quantify palatability (termed taste reactivity), which measures a characteristic set of orofacial and somatic responses that rats display when taste solutions are infused directly into their mouths. For example, sucrose solution elicits an ingestive taste reactivity pattern of tongue protrusions, paw licking, and mouth movements, while bitter quinine solution elicits an aversive taste reactivity pattern such as gaping, chin rubbing, and paw pushing. Mildly aversive taste solutions elicit predominantly passive drips. Using the taste reactivity test, Berridge K. C. and Treit D. (1986) have showed that systemic injection of chlordiazepoxide, a benzodiazepine agonist, selectively facilitates positive hedonic responses to sucrose infusions into the mouth. In contrast, chlordiazepoxide has little or no effect on aversive reactions elicited by quinine. Since such a selective enhancement of hedonic reactivity patterns by benzodiazepine agonists is blocked by benzodiazepine antagonist Ro 15-1788 (Treit, D. *et al.*, 1987), the effects of benzodiazepines on taste palatability are benzodiazepine receptor specific. Similar enhancements of positive palatability to taste stimuli induced by benzodiazepines have been reported by several studies using the taste reactivity test (Gray, R. W. and Cooper, S. J., 1995; Söderpalm, A. H. and Hansen, S., 1998). In addition to taste reactivity, Higgs S. and Cooper S. J. (1997; 1998a) showed that benzodiazepines increased bouts of licking for highly palatable solutions by a microstructural analysis of licking behavior in a brief contact test in the rat.

Aside from these behavioral and pharmacological evaluations, it is important to identify the site(s) in the central nervous system on which benzodiazepines act to enhance palatability. The distribution of benzodiazepine receptors is relatively greater in the forebrain than in the lower brainstem (Richards, J. G. and Mohler, H., 1984). Nevertheless, recent evidence strongly suggests that benzodiazepines act on the particular receptors in the lower brainstem and enhance taste palatability. In an attempt to determine a possible site of benzodiazepine action, Berridge K. C. (1988) examined taste reactivity in chronic decerebrate rats that are known to demonstrate normal affective taste reactivity (Grill, H. J. and Norgren, R., 1978b). Systemic benzodiazepine injection facilitated the positive taste reactivity in response to normally preferred taste solutions, indicating that the midbrain and/or hindbrain seem to contain the minimum benzodiazepine receptors and neural circuitry required to enhance positive hedonic reactions to taste. The notion is supported by the result that in normal rats, benzodiazepine is more effective at eliciting feeding (Higgs, S. and Cooper, S. J., 1996a) and enhancing positive hedonic reactions to oral sucrose (Peciña, S. and Berridge, K. C., 1996) when microinjections are made in the fourth ventricle (lower brainstem) than in the lateral ventricle (forebrain). Furthermore, direct administration of the benzodiazepine agonist midazolam into the PBN increases the consumption of palatable food (Higgs, S. and Cooper, S. J., 1996b) and positive taste reactivity (Söderpalm, A. H. and Berridge, K. C., 2000), suggesting that the PBN is the most probable region on which benzodiazepines act to influence food intake. Because the PBN is the second gustatory relay, it is likely that benzodiazepines act on specific receptors in the PBN to modify taste information so as to enhance taste palatability and facilitate consumption of food.

Some results suggest that the enhancement of palatability induced by intra-PBN injection of benzodiazepine is mediated by $GABA_A$ receptors in the PBN. It is well known that benzodiazepines act on the $GABA_A$ receptor to increase its affinity for GABA. In fact, GABA functions as an inhibitory neurotransmitter in both gustatory and visceral part of the PBN, mediated in part, by $GABA_A$ receptors (Kobashi, M. and Bradley, R. M., 1998). Shimura T. *et al.* (2004) found that systemic injection of midazolam increased the intake of a sucrose solution in wildtype mice but not in mice deficient in the 65-kDa isoform of glutamate decarboxylase (GAD65), a GABA synthetic enzyme in the central nervous system. The results indirectly suggest that GAD65-generated GABA is necessary for benzodiazepines to enhance taste palatability in the PBN. Nevertheless, greater understanding of the physiological significance of benzodiazepines for taste palatability awaits further investigation.

4.24.2.2 Opioids

Various endogenous opioids and their receptor subtypes are found in diverse brain regions, particularly within sites involved in emotion, pain and stress, and endocrine function and feeding (Mansour, A. *et al.*, 1987). Long before the discovery of endogenous opioids, it had been demonstrated that systemic morphine administrations increase food intake in rats (Flowers, S. H. *et al.*, 1929; Martin, W. R. *et al.*, 1963). Since the demonstrations that opioid antagonists reduce food intake at appropriate dosages (Holtzman, S. G., 1974; Brown, D. R. and Holtzman, S. G., 1979), many studies have examined the involvement of opioids in the regulation of food intake (Glass, M. J. *et al.*, 1999 for a review). In general, opioid agonists facilitate and antagonists diminish food consumption. Although precise mechanisms are still unclear, evidence supports the hypothesis that opioids modulate food and taste palatability, leading to increased food intake (Cooper, S. J. and Kirkham, T. C., 1993 for a review). One reason for this hypothesis is that the hyperphagic effect is selective to normally preferred food and tastes. For example, the preference for sweet solutions over water is abolished by systemic administration of opioid antagonist naloxone in rats (Le Magnen, J. *et al.*, 1980). Naltrexone, an opioid antagonist, does not modify the energy intake in control rats receiving ordinary chow but suppresses hyperphagia induced by a highly palatable diet (Apfelbaum, M. and Mandenoff, A., 1981). Both naloxone and naltrexone abolish the preference for a highly palatable saccharin solution in water-deprived rats due to a selective decrease in the consumption of the saccharin solution, with no effect on water intake (Cooper, S. J., 1983).

Studies with the taste reactivity test show that systemic morphine administrations selectively increase positive hedonic reactions to a mixture of sucrose and quinine solution without enhancing aversive reactions (Doyle, T. G. *et al.*, 1993), suggesting that opioid-induced feeding is at least partly mediated by increased palatability of food. Since opioid receptor antagonists reduce sucrose sham feeding in the gastric-fistulated rat (Kirkham, T. C. and Cooper, S. J., 1988), intraoral but not postingestional factors seem to affect opioid-induced modification of feeding. In addition, using a microstructural analysis of licking pattern for sucrose or fat emulsion, Higgs S. and Cooper S. J. (1998b) showed that palatability is modulated by opioids.

In fact, blood levels of β-endorphin levels increase after the consumption of palatable sweeteners and decrease following the intake of aversive quinine in thirsty rats (Yamamoto, T. *et al.*, 2000). β-Endorphin levels in the cerebrospinal fluid, on the other hand, increase after water consumption by thirsty rats. The difference in β-endorphin levels between blood and cerebrospinal fluid suggests that two opiate systems separately function during the intake of fluid.

Experimental work in humans also supports the notion that the modification of feeding produced by opioid agonists and antagonists is mediated by a hedonic shift in the palatability of food and fluid. Fantino M. *et al.* (1986) showed that naltrexone produces a significant decrease on a subjective pleasure scale for sweetened solution in normal human subjects. Naloxone reduces taste preferences for sweet high-fat foods such as cookies or chocolate in both binge eaters and controls (Drewnowski, A. *et al.*, 1992).

Intracerebroventricular as well as systemic administration of opioid agonists facilitates food intake (Gosnell, B. A., 1987). Moreover, the opioid antagonist naloxone causes a reduction in food intake when injected intracerebroventricularly at a dose that is ineffective when administered peripherally (Gosnell, B. A., 1987). Morphine administrations into the lateral ventricle increase both positive hedonic taste reactivity patterns and feeding (Peciña, S. and Berridge, K. C., 1995). These results favor the notion that opioids act centrally to modify food intake.

Although opioids are believed to affect multiple feeding systems (Glass, M. J. *et al.*, 1999), recent evidence strongly suggests that the nucleus accumbens and its associated circuitry are primarily involved in palatability-dependent feeding (Kelley, A. E. *et al.*, 2002 for a review). We describe several lines of evidence that support this hypothesis in the next section.

The hypothalamus is known to be an important region of opioid action for food intake. Microinjections of β-endorphin into the ventromedial nucleus (Grandison, L. and Guidotti, A., 1977) or the paraventricular nucleus (McLean, S. and Hoebel, B. G., 1983) of the hypothalamus facilitates food intake in satiated rats. On the contrary, localized injections of naloxone into the paraventricular nucleus of the hypothalamus significantly reduces food intake (Woods, J. S. and Leibowitz, A. F., 1985). However, these studies suggest that opioids in the hypothalamus are involved in energy needs rather than the palatability of food.

The gustatory relays in the lower brainstem also appear to be sites on which opioids act to facilitate feeding. Infusion of the selective mu-opioid receptor agonist [d-Ala2,N-Me-Phe4,Gly5-ol]enkephalin (DAMGO) into the lateral PBN increases food intake and naloxone antagonizes DAMGO-induced feeding (Wilson, J. D. *et al.*, 2003) Injection of DAMGO into the NTS, the first gustatory relay, stimulates food intake, whereas injection of either the delta or kappa receptor agonist has no effect (Kotz, C. M. *et al.*, 1997). Microinfusion of methionine-enkephalin into the NTS suppresses both spontaneous and evoked activity of more than 20% of taste responsive neurons (Li, C. S. *et al.*, 2003). These effects are blockable by naltrexone, which alone is without effect, suggesting that opioids play some role in processing of taste information in the NTS.

4.24.2.3 Cannabinoid

Recent evidence suggests that the endocannabinoid system is involved in the control of food intake mainly by modulating food and taste palatability (Cooper, S. J., 2004 for a review). The psychoactive effects of marijuana are largely attributable to a constituent called THC (delta-9-tetrahydrocannabinol). Various cannabinoids which are chemicals of the same class as THC may also be psychoactive (Kephalas, T. A. *et al.*, 1976). Since the discovery of a specific receptor in the brain for cannabinoids and endogenous ligands (Devane, W. A. *et al.*, 1992), increasing attention has been directed to possible behavioral functions of endocannabinoids, including a role in feeding. Although earlier studies had suggested that marijuana facilitates appetite and food intake in humans (Abel, E. L., 1971; Foltin, R. W. *et al.*, 1986), a hyperphagic effect had not been demonstrated clearly in animal studies until recently. Several recent studies have shown that endocannabinoids can facilitate food intake under certain conditions. For example, both the exogenous cannabinoid THC and the endocannabinoid arachidonoyl ethanolamide (anandamide) stimulate eating in presatiated rats, with a marked reduction in latency to feed (Williams, C. M. and Kirkham, T. C., 2002). Microstructural analyses of licking reveal that THC and anandamide significantly increase both the total number of licks and bout duration (Higgs, S. *et al.*, 2003). These results suggest that cannabinoids promote eating by increasing the incentive value of food.

Microinjection of 2-arachidonoyl glycerol (2-AG) into the nucleus accumbens shell robustly increases food intake (Kirkham, T. C. *et al.*, 2002). Since subcutaneous administration of a cannabinoid receptor antagonist blocked the hyperphagic response, cannabinoids in the nucleus accumbens appear to be involved in the facilitation of food intake. Microinjection of the cannabinoid receptor agonist CP55,940 into the fourth, but not lateral, ventricle increases consumption of highly palatable sweetened condensed milk (Miller, C. C. *et al.*, 2004), suggesting that cannabinoids can act on the hindbrain to enhance food intake. Nevertheless, our knowledge about behavioral mechanisms of cannabinoid-induced hyperphagia is still quite limited. Further studies are needed to conclude that endogenous cannabinoids directly affect palatability leading to food intake.

4.24.2.4 Substances Related to Negative Hedonics

While studies of substances related to negative hedonics of taste are quite limited, Yamamoto T. *et al.* (1990) showed that the calcitonin gene-related peptide (CGRP)-like immunoreactivity levels in the gustatory insular cortex were increased by aversive taste stimuli such as quinine and even by palatable stimuli such as NaCl and sucrose, if animals had been trained to avoid them by conditioning. The results suggest that CGRP in the GC is implicated in rejection or avoidance behaviors to aversive taste stimuli.

Recent evidence suggests that diazepam-binding inhibitor (DBI), the only known endogenous ligand of the benzodiazepine receptor, is related to negative hedonics of taste. DBI-like peptide is released by aversive quinine stimuli (Manabe, Y. *et al.*, 2000). Injection of a DBI fragment into the fourth ventricle suppressed the intake of 5% sucrose solution and water and increased the aversive taste reactivity to NaCl in mice (Manabe, Y. *et al.*, 2001). In contrast with the facilitatory effect of exogenous benzodiazepine agonists for positive palatability, the possible role of the endogenous DBI for negative hedonics is of interest.

Histamine, which is widely distributed in the mammalian central nervous system as a neurotransmitter or neuromodulator, also seems to be related to negative hedonics of taste. Intraoral infusions of quinine-HCl increase hypothalamic histamine release, but infusions of sucrose or saccharin produced a decrease in histamine levels, suggesting that histamine plays a role in the behavioral expression to aversive taste stimuli (Treesukosol, Y. *et al.*, 2005).

4.24.3 Role of the Reward System in Taste-Mediated Behavior

4.24.3.1 What is the Reward System?

Rats (Olds, J. and Milner, P. M., 1954), humans (Bishop, M. P. *et al.*, 1963), and many other species will perform a response, such as pressing a lever, in order to obtain direct electrical stimulation to specific sites in their own brains. Originally, Olds and Milner argued that the specific brain sites that mediate self-stimulation are those that normally mediate the pleasurable effects of natural rewards (e.g., food, water, and sex). Although there have been numerous debates for a relatively long period, the current consensus seems to be that the circuits mediating intracranial self-stimulation phenomena are reward circuits. Similarly, it is well documented that the brain reward systems are neural substrates for the rewarding effects of addictive drugs. The mesolimbic dopamine system, arising from dopaminergic neurons in the VTA of the midbrain to terminate in the nucleus accumbens, has been shown to play a particularly important role in natural as well as drug rewards (Wise, R. A., 2002 for a review).

Many studies have shown that activation of dopamine systems is triggered in animals by encounters with food, sex, drugs of abuse, and intracranial self-stimulation (Berridge, K. C. and Robinson, T. E., 1998 for a review). In humans, a functional MRI study also reported that presentation of rewards such as cocaine to cocaine-dependent subjects modulated activity in dopamine target sites including the nucleus accumbens (Breiter, H. C. *et al.*, 1997).

4.24.3.2 The Role of Dopamine in Food Reward

It is well known that dopamine affects feeding behavior (Blackburn, J. R. *et al.*, 1992 for a review). Systemic administration of pimozide, a dopamine receptor antagonist, attenuates lever pressing and running for food reward in hungry rats (Wise, R. A. *et al.*, 1978). Pimozide also suppresses the consumption of a saccharin-glucose solution in a dose-related manner (Xenakis, S. and Sclafani, A., 1981; Geary, N. and Smith, G. P., 1985). These early studies favor the view that dopamine receptor blockade reduces the rewarding impact of palatable stimuli, including food (Wise, R. A., 1982). However, taste reactivity analyses have shown that dopamine is less likely involved in modifying palatability. Berridge and his colleagues (Berridge, K. C. *et al.*, 1989; Berridge, K. C., 1996) injected 6-hydroxydopamine (6-OHDA), a selective neurotoxin for dopamine, bilaterally into the ascending dopaminergic bundle, at a point in the LH where fibers join together from midbrain A9 and A10 sites on their way to the neostriatum and nucleus accumbens. In these rats, dopamine was depleted by 95–99% in both the neostriatum and nucleus accumbens and rats became aphagic. However, positive hedonic reactions to sucrose were not suppressed relative to control levels even in these aphagic rats. Aversive reactions to bitter solutions were also unaltered by these selective dopaminergic lesions.

Electrophysiological experiments also suggest that dopamine neurons in the mesolimbic system are less related to the evaluation of taste palatability. Dopamine neurons in the midbrain including the VTA of the monkey show short, phasic activation in a rather homogenous fashion after the presentation of liquid and food rewards, and visual or auditory stimuli that predict reward, suggesting that these dopamine neurons preferentially report rewarding events (Schultz, W. and Romo, R., 1990). However, these dopamine neurons appear to encode a discrepancy between the prediction of reward (a reward prediction error) rather than reward per se (Ljungberg, T. *et al.*, 1992). Recently, we have found that more than half of the neurons recorded in the

VTA of freely behaving rats change their firing during licking of liquid reward (Shimura, T. *et al.*, 2005). Since there is no difference in the responsiveness to taste solutions and water, these neurons may be involved in fluid reward rather than the hedonic impact of taste.

Shimura T. *et al.* (2002a) showed evidence that the mesolimbic dopaminergic system interacts with the benzodiazepine and/or opioid systems to exhibit the normal intake pattern for palatable fluid. Electrolytic or 6-OHDA lesions of the VTA suppress the consumption of a preferred sucrose or NaCl solution without influencing the intake of other tastes or water. Systemic injections of the benzodiazepine agonist midazolam significantly facilitates the consumption of a preferred sucrose in sham control but not in VTA-lesioned rats. Midazolam does not affect the consumption of an aversive quinine solution in either lesioned or sham animals. Moreover, while systemic administration of morphine, an opioid agonist, selectively increases the consumption of sucrose solution in control rats without affecting the consumption of quinine solution, the intake of both sucrose and quinine solutions remains unchanged by morphine injections in VTA-lesioned rats. These results suggest that the dopaminergic mediation is required for the normal expression of both benzodiazepine- and opioid-induced overconsumption of palatable fluid. According to the current concept that food reward contains distinguishable functional components, liking (palatability) and wanting (incentive motivation) (Berridge, K. C., 1996), the mesolimbic dopamine system seems to mediate wanting rather than liking for food and fluid reward. In fact, hyperdopaminergic dopamine transporter-knockdown mutant mice have higher wanting for a sweet reward in a runway task (Peciña, S. *et al.*, 2003). But sucrose taste fails to elicit higher orofacial liking reactions from mutant mice in an affective taste reactivity test. On the other hand, since sucrose sham feeding increases dopamine levels in the nucleus accumbens in a concentration-dependent manner (Hajnal, A. *et al.*, 2004), the mesolimbic dopamine system seems to be implicated in a reward effect of taste palatability.

4.24.3.3 The Nucleus Accumbens

The nucleus accumbens has long been considered to be an essential interface between motivation and action (Mogenson, G. J. *et al.*, 1980). Neuroanatomical and histochemical studies have revealed that the accumbens is composed of two major subregions, the core, and the shell extending medially, ventrally, and laterally around the core. The functions of core and shell subregions are thought to be different on the basis of distinctive anatomical profiles (Heimer, L. *et al.*, 1991). Considerable evidence has indicated that the nucleus accumbens is critically involved in palatability-induced feeding behavior. The hyperphagic effect of opioids described in the previous section has been shown to be most prominent when opioids are injected into the nucleus accumbens, especially into the shell subdivision. For example, microinjections of DAMGO induce a robust, dose-dependent increase in food intake that is blocked by coadministration of naltrexone (Bakshi, V. P. and Kelley, A. E., 1993). It is noted that the hyperphagic effects of DAMGO are selective to highly palatable taste stimuli such as a high-fat diet (Zhang, M. *et al.*, 1998; Zhang, M. and Kelley, A. E., 2000), sucrose solution (Zhang, M. and Kelley, A. E., 1997), saccharin, NaCl, and ethanol solutions (Zhang, M. and Kelley, A. E., 2002). In addition, morphine microinjections into the nucleus accumbens shell not only facilitates feeding but also selectively increases positive hedonic patterns of behavioral affective reaction elicited by oral sucrose, using the taste reactivity test of hedonic palatability (Peciña, S. and Berridge, K. C., 2000).

The nucleus accumbens receives afferent inputs from corticolimbic and thalamic structures, which are primarily mediated by excitatory amino acids (Robinson, T. G. and Beart, P. M., 1988). Microinjections of 6,7-dinitroquinoxaline-2,3-dione (DNQX), a glutamatergic α-amino-3-hydroxy-5-methylisoxazole-4-propionic acid (AMPA) receptor antagonist, but not the NMDA antagonist 2-amino-5-phosphonopentanoic acid (AP-5), into the medial shell subregion resulted in a pronounced feeding response (Maldonado-Irizarry, C. S. *et al.*, 1995). DNQX significantly facilitates intake of solid and liquid food, but does not significantly affect water intake or gnawing behavior, suggesting that DNQX is acting on a system specifically involved with the regulation of food intake (Stratford, T. R. *et al.*, 1998). Moreover, the feeding response is completely inhibited by concurrent infusion of the $GABA_A$ agonist muscimol into the LH, a major projection area of the accumbens shell (Maldonado-Irizarry, C. S. *et al.*, 1995). These findings demonstrate a selective role for non-NMDA receptors in the nucleus accumbens shell in ingestive behavior and suggest an important functional link between the nucleus accumbens and the LH.

The majority of cells projecting from the accumbens shell are medium spiny neurons that use GABA as a neurotransmitter (Meredith, G. E. *et al.*, 1993). Acute inhibition of cells in the accumbens shell by administration of the $GABA_A$ receptor agonist muscimol or the $GABA_B$ receptor agonist baclofen elicits intense, dose-related feeding without altering water intake (Stratford, T. R. and Kelley, A. E., 1997). Moreover, injections of muscimol into the accumbens shell greatly increase the number of cells exhibiting Fos-like immunoreactivity in the LH (Stratford, T. R. and Kelley, A. E., 1999). Immunohistochemical results show that intra-accumbens shell muscimol treatment increases the percentage of orexin/hypocretin-containing neurons expressing Fos in the lateral hypothalamic area (Baldo, B. A. *et al.*, 2004). The same treatment fails to increase Fos expression in melanin concentrating hormone-containing neurons in the LH. These results suggest that extensive reciprocal interaction between the nucleus accumbens shell and LH regulates feeding behavior.

The VP is a main output target of the GABAergic neuron in the nucleus accumbens. From the VP, GABAergic efferents project to the LH (Groenewegen, H. J. *et al.*, 1993). Thus, the VP is anatomically interposed between neurons in the nucleus accumbens and those in the LH that are known to be intimately related to feeding behavior. Blockade of $GABA_A$ receptors in the VP with bicuculline elicits a strong feeding response in satiated rats without affecting water intake (Stratford, T. R. *et al.*, 1999). Recently, we have found that microinjection of bicuculline into the VP enhances the intake of a preferred saccharin but not quinine solution and water in dehydrated rats, suggesting that the overconsumption produced by GABA blockade in the VP is specific to palatable tastes (Shimura, T. *et al.*, 2006).

Compared to evidence concerning the efferent connections of the nucleus accumbens that may mediate food intake, the role of afferent inputs that convey taste and visceral information to the accumbens are poorly understood. Some anatomical evidence shows that the accumbens receives taste and visceral information through direct input from the NTS in the medulla (Ricardo, J. A. and Koh, E. T., 1978; Saper, C. B., 1982). The accumbens also receives taste information from the insular GC (Brog, J. S. *et al.*, 1993). The amygdala is likely an important source of information about taste and visceral functions to the nucleus accumbens. Taste information received by the central nucleus of the amygdala via the NTS and PBN projects caudally to the VTA, then arrives at the nucleus accumbens. The insular GC – basolateral amygdala – accumbens pathway is also suggested in rats (McDonald, A. J. and Jackson, T. R., 1987; McDonald, A. J. *et al.*, 1999). Because of these afferent as well as efferent connections, the nucleus accumbens appears to be well suited to regulate food intake. Although increasing evidence suggests that the nucleus accumbens shell has a key role for palatability-induced consumption as described above, the precise mechanism for processing of taste palatability in the accumbens is not yet understood.

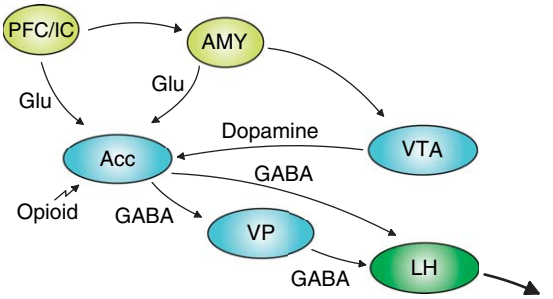

Figure 2 Diagram of reward system responsible for palatability-induced feeding. Glu, glutamate. Other abbreviations are the same as those in Figure 1.

The role of the reward system in palatability-induced feeding is summarized in Figure 2. Taste relays in the lower brainstem are responsible for the palatability shift mediated primarily by benzodiazepines, at least in rodents. Converging corticolimbic input of taste and visceral information to the nucleus accumbens shell is likely involved in mediation of palatability-induced food intake. The GABAergic efferents from the nucleus accumbens shell project to the LH, partly via the VP, so as to regulate the intake of food that is hedonically desirable. Opioid mechanisms in the ventral striatum, especially in the nucleus accumbens, are critically involved in the enhancement of taste palatability. The dopaminergic projection arising from the VTA to the nucleus accumbens is implicated in wanting rather than liking for food and liquid reward.

4.24.4 Role of Taste in Feeding

4.24.4.1 Feeding Behavior to Palatable and Aversive Foods

Substances and liquids with sweet taste, umami taste, and salty taste of hypotonic and isotonic sodium salts are palatable and preferred, while those with sour

taste and bitter taste are aversive and are rejected. Such taste-mediated behaviors have been shown by organisms through the long history of evolution so that sweetness is a signal for energy sources; umami, a signal for protein; saltiness, a signal for minerals; sourness, for rotten food; bitterness, for poisons. These relationships are innately common among different species of animals, that is, human newborn babies show ingestive behavior with mild facial expressions to sweeteners and rejective behavior with aversive expressions to acids and bitter substances, whereas rats show the characteristic oral-lingual movements and body reactions as described in the previous section of this chapter and show a very similar preference–aversion pattern of intake to different sapid solutions as do humans (Figure 3)

The neural substrates for taste-mediated ingestion are basically located in the brainstem without the involvement of higher centers of the gustatory system since similar hedonic reactions to taste stimuli can be seen in anencephalic or hydroanencephalic human infants (Steiner, J. E., 1973) and decerebrate rats (Grill, H. J. and Norgren, R., 1978b). The possible existence of anatomical segregation of taste-responsive neurons in both the qualitative and hedonic aspects of taste at the brainstem level (Yamamoto, T. *et al.*, 1994a) may serve an efficient basis of eliciting quality-specific and hedonic-oriented gustatory reflexes. Other lines of evidence through c-*fos* immunohistological and electrophysiological studies suggest that there are dual separate pathways for sensory and hedonic aspects of taste in each station of the ascending gustatory route including the NTS, PBN, and VPMpc, and in the GC (Sewards, T. V., 2004, for a review).

It is also necessary to add that higher brain centers which may not be directly involved in the processing of gustatory quality discrimination play important roles in evaluation of hedonic values of foods and tastes. As is described in detail in the following sections of this chapter, such regions include the amygdala, orbitofrontal cortex, cingulate cortex, reward system, and hypothalamus.

Besides the innate preference or aversion behaviors, nutrients or minerals that are essential for living organisms will become very palatable, preferred, and craved when those substances are deficient. The well-known and documented instances are salt appetite and amino acid deficiency. When animals are deficient in body sodium, they ingest excessive amounts of salt solutions at high concentrations which are normally avoided. They also increase their intake of lower salt concentrations. The mean response of neurons to NaCl is reduced in the NTS of sodium-deprived rats (Jacobs, K. M. *et al.*, 1988; Nakamura, K. and Norgren, R., 1995). It has further been demonstrated that sodium depletion causes not only lowered responses to NaCl but also an alteration in the neural representation of NaCl (Jacobs, K. M.

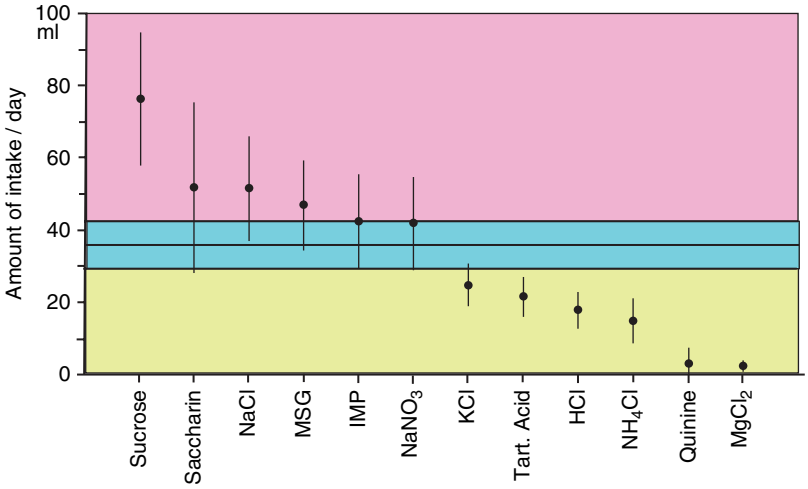

Figure 3 Amount of fluid intake/day for 12 different taste stimuli with the single bottle method in rats. Each value with a vertical line and a horizontal bar with upper and lower horizontal bars (water intake, blue belt) indicates means ± SEs ($n = 15$). The chemicals on the abscissa are arranged from left to right in the order of most to least preferred. If the amount of intake of a stimlus is over the blue belt (within the pink area), the stimulus is preferable, and if within the yellow area, the stimulus is aversive. Adapted from Yamamoto, T., Yuyama, N., Kato, T., and Kawamura, Y. 1985b Gustatory responses of cortical neurons in rats. III. Neural and behavioral measures compared. J. Neurophysiol. 53, 1370–1386.

et al., 1988). As for PBN neurons (Shimura, T. *et al.*, 1997a), taste responses to 0.3 and 0.5 M solutions of NaCl were significantly lower in the sodium-deprived rats than in controls, and correlation coefficients of responses among sodium salts and those between 0.5 M NaCl and sweeteners were larger in the sodium-deprived rats than in controls. These results suggest that PBN neurons in sodium-deprived rats are critically implicated in induction of quantitative and qualitative changes of gustatory sense to sodium salts. Rats display a preference for a particular amino acid when they are deprived of the amino acid. For example, when rats were fed with a lysine-deficient diet, the order of preference was lysine > saline > monosodium glutamate > glycine > threonine > water > arginine > histidine, while in control rats, arginine > saline > monosodium glutamate > glycine > water > threonine > histidine > lysine (Tabuchi, E. *et al.*, 1991). These investigators found that some neurons in the LH responded specifically to lysine when the animals were lysine deficient, suggesting that the LH is involved in mediating the preference for deficient amino acids.

4.24.4.2 Learning and Memory Related to Feeding Behavior

Feeding behavior can be modified by learning through gustatory experience associated with pleasant or unpleasant consequences.

4.24.4.3 Preference Learning

There are two types of learned taste preference: (1) attenuation of neophobia and (2) conditioned taste preference (CTP). When an animal ingests a harmless new substance or liquid, it shows neophobia (see the left in Figure 4) and it increases the consumption at subsequent exposures after learning that the substance is safe to consume (see the upper-right in Figure 4). Through this process of the attenuation of neophobia (or learned safety), foods can be classified as familiar-safe (Nachman, M. and Jones, D. R., 1974; Domjan, M., 1976). Although each part of the gustatory pathway may be concerned with neophobia, since lesions of only one of these parts attenuate neophobia (Yamamoto, T. *et al.*, 1995), a recent study (Bahar, A. *et al.*, 2004) shows that the GC plays an important role in the recognition of whether the taste is familiar or novel. Gutiérrez R. *et al.* (2003) show that cortical muscarinic receptors are important during a 2- to 4-h continuous period in which noxious consequences of food ingestion are absent for the formation and consolidation of learned safety.

When ingestion of a neutral or mildly aversive food is associated with good postingestive visceral sensation, those foods become hedonically positive, or rewarding and preferred. This phenomenon is referred to as CTP (Fanselow, G. and Birk, J., 1982). CTP is attained gradually but more strongly via a flavor conditioning process. Previous studies demonstrated that rats could learn to prefer a taste solution paired with intragastric nutrient infusion (Elizalde, G. and Sclafani, A., 1990), opiate administration (Mucha, R. F. and Herz, A., 1986), and intracranial self-stimulation (Olds, J. and Milner, P. M., 1954). Nutrients can have positive postingestive actions that influence food selection and increase consumption (Sclafani, A., 2004). Giza B. K. *et al.* (1997) showed that the consumption of even an innately aversive $MgCl_2$ solution could be preferred by pairing with a nutrient, polycose, in rats. The rewarding properties of food that promote eating and influence food choice result from the central integration of orosensory and viscerosensory stimuli. The central neural mechanism of association of taste with postingestive food reward is not fully understood. The PBN and LH may play some important roles in flavor preference learning (Sclafani, A. *et al.*, 2001; Touzani, K. and Sclafani, A., 2001). The central dopamine system may also have a critical role in flavor learning (Azzara, A. V. *et al.*, 2001), whereas the involvement of opioid systems is less certain (Azzara, A. V. *et al.*, 2000).

4.24.4.4 Aversion Learning

When ingestion of a substance is followed by malaise such as gastrointestinal discomfort and nausea, associative learning between the ingested substance and internal consequences is quickly established; animals remember the taste for a long time and reject its ingestion on subsequent exposure (see the lower-right in Figure 4). This phenomenon is called a CTA or taste aversion learning.

CTA has the following characteristics, which are distinguished from classical conditioning (Bures, J. *et al.*, 1988): (1) Strong and long-lasting CTAs to novel taste stimuli can be established in a single learning procedure, that is, after one pairing of conditioned stimulus (CS) and unconditioned stimulus (US). (2) Successful CTAs can develop to the CS after delays of as long as 4–12 h between exposure to the CS and delivery of the US. CTA can be considered as a kind of

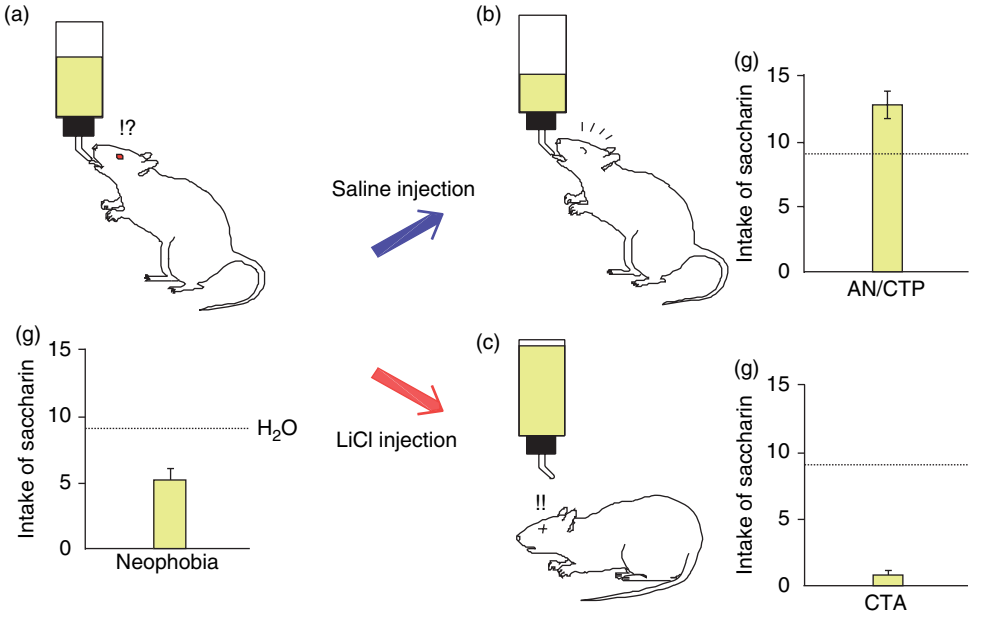

Figure 4 Schematic drawing of neophobia, attenuation of neophobia (AN), conditioned taste preference (CTP), and conditioned taste aversion (CTA). The magnitude of saccharin intake in each graph is taken from Yamamoto, T., Fujimoto, Y., Shimura, T., and Sakai, N. 1995. Conditioned taste aversion in rats with excitotoxic brain lesions. Neurosci. Res. 22, 31–49.

fear learning and serves as a defense mechanism of the organism to avoid ingestion of harmful substances. CTA is easily acquired in humans as well, for example, our survey (unpublished) for Osaka University students shows that a significant proportion of their food dislikes is based on CTA acquired before the middle grade of the elementary school (or below 10 years old). After the acquisition of CTA to an artificial sweetener, saccharin, this sweet and palatable substance still tastes sweet but changes to an aversive stimulus. Taste quality may not change, but the hedonic aspect changes drastically. This fact may indicate the existence of separate neural representations of the sensory aspects and the hedonic aspects of taste in the gustatory pathway (Sewards, T. V., 2004 for a review). Although the neural substrate and the molecular mechanisms of CTA have recently been well studied (Yamamoto, T. *et al.*, 1994b; Bures, J. *et al.*, 1998; Yamamoto, T. *et al.*, 1998; Bermúdez-Rattoni, F., 2004; Yamamoto, T., 2007 for reviews), a detailed discussion of the contribution of the different brain regions to formation of the CTA is outside the scope of this review except for the following few topics.

Electrophysiological studies of unit activity in GC neurons in freely ingesting and anesthetized rats have revealed that the GC processes multiple aspects of taste-related responses including sensory and hedonic responses (Yamamoto, T. *et al.*, 1989a), convergent responses (Yamamoto, T. *et al.*, 1988; 1989a; Hanamori, T. *et al.*, 1998), temporal responses (Katz, D. B. *et al.*, 2001), anticipation (Yamamoto, T. *et al.*, 1988), and familiarity (Bahar, A. *et al.*, 2004). These response characteristics of GC neurons may not only contribute to the acquisition and retention of CTA but may be actively involved in the formation of CTA as revealed by occurrence of short-term and long-term potentiated responses to the CS after pairing its ingestion with the US (LiCl) (Yamamoto, T. *et al.*, 1989a; Yasoshima, Y. and Yamamoto, T. 1998). The amygdala is one of the most important areas in the integration of the CS and US. Yamamoto T. *et al.* (1994b), Yamamoto T. *et al.* (1995), and Yasoshima Y. *et al.* (2006) found that the basolateral nucleus was more important in the acquisition and retention of CTA in comparison with the central nucleus of the amygdala. Electrical stimulation of the central nucleus enhanced the responsiveness of the PBN neurons that responded best to the CS (Tokita, K. *et al.*, 2004). Taking these results together with those from other literature, it is plausible that the basolateral amygdala, which is involved in the formation of fear learning (Maren, S. and Fanselow, M. S., 1996 for a review), is important in the hedonic shift from palatable to aversive, and that the central nucleus,

which is known to receive taste inputs together with other sensory inputs, contributes to the enhancement of gustatory responses to the CS (Shimura, T. *et al.*, 1997b; 2002b; Tokita, K. *et al.*, 2004), which facilitates detecting and avoiding the harmful substance.

4.24.4.5 Orexigenic Substances

Palatability is one of the most important factors that regulates food and fluid intake. Animals usually prefer innately palatable sweet-tasting substances, and their consumption often exceeds the need for homeostatic repletion. The effects of palatable food on feeding behavior may be related to functions of the newly identified chemical mediators that regulate appetite, for example, orexins (orexin-A and -B), melanin-concentrating hormone (MCH), agouti-related protein (AgRP), ghrelin, and neuropeptideY (NPY), all of which are known to stimulate feeding and thus, to function as orexigenic peptides (Inui, A., 2000; Schwartz, M. W. *et al.*, 2000). These peptides are produced in the hypothalamus and are well studied in terms of feeding, energy homeostasis, and obesity. Among these peptides, Furudono Y. *et al.* (2006) have suggested that orexin-A, NPY, and MCH are involved, in this order of effectiveness, in palatability-induced ingestion on the bases of the following. Administration of orexin-A into the lateral ventricle in rats increased both water and saccharin intake compared to vehicle administration. Similarly, administration of MCH increased the intake of both fluids. However, NPY injections enhanced only the intake of saccharin. These results suggest that orexin-A, MCH, and NPY are related to the facilitation of drinking. On the other hand, ghrelin and AgRP had no effects on fluid intake. When the changes in mRNA levels for orexin, NPY, and MCH in the hypothalamus were examined after drinking saccharin or water, saccharin, but not water, facilitated an increase in the orexin and NPY mRNA levels. MCH mRNA levels did not differ between saccharin and water intake and remained stable. Increased ingestion may be closely related to enhanced digestive functions. To address this issue, Kobashi M. *et al.* (2003) examined the effects of intraventricular injections of orexin-A on gastric motility. They measured the motility changes as alterations in intragastric pressure, by means of two balloons in the proximal and distal parts of the stomach (Kobashi, M. *et al.*, 2000). The proximal stomach is known to function as a reservoir, whereas the distal stomach's main function is to stir and drain gastric contents. Orexin-A induced strong rhythmical gastric motility in the distal stomach, while the vehicle had no effect. Since the function of the distal stomach is to stir and discharge gastric contents, gastric motility induced by orexin-A may facilitate digestive function. In the proximal stomach, orexin-A induced relaxation, while the vehicle had no effect. It is suggested that the relaxation of the proximal stomach enables it to accept more food, and the facilitation of phasic contractions of the distal stomach accelerates draining of the increased gastric contents. Thus, it is plausible that the orexigenic action of orexin-A accompanies the activation of digestive function. These results may answer a common question about why you can eat palatable sweet-tasting foods faster and in larger amount than neutral or unpalatable foods.

4.24.5 Brain Imaging Study on Hedonic Evaluation in Humans

When we wish to analyze the role of taste in feeding and reward in humans, the most suitable method now available is the noninvasive brain imaging techniques such as functional magnetic resonance imaging (fMRI), positron emission tomography (PET), and magnetoencephalography (MEG).

A single chemical solution placed into the mouth can elicit both sensory (or qualitative) perception and hedonic (preferred or aversive) feeling, for example, sucrose is sweet and palatable, while 1 M NaCl is salty and aversive and quinine hydrochloride is bitter and aversive. Therefore, we can analyze sensory and/or hedonic aspects when these taste stimuli are used.

A number of researchers have identified the primary taste area (PTA) in the opercular-insular cortex by using fMRI (Faurion, A. *et al.*, 1999; O'Doherty, J. *et al.*, 2001; Schoenfeld, M. A. *et al.*, 2004), PET (Kinomura, S. *et al.*, 1994; Small, D. M. *et al.*, 1999 for a review), and MEG (Kobayakawa, T. *et al.*, 1996; Yamamoto, C. *et al.*, 2003; 2006). One of the issues in the PTA concerning taste quality representation is the existence of chemotopy, that is, topographic arrangement of taste responsiveness to each of the five basic tastes: sweet, umami, salty, sour, and bitter. In spite of the limitations of analysis due to the anatomical position and small size of the PTA, Schoenfeld M. A. *et al.* (2004) used the fMRI method and showed the possible existence of chemotopy with a high interindividual variability, although with some considerable overlap. They reported that

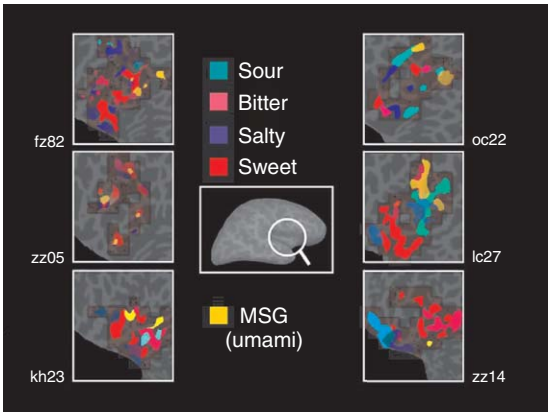

Figure 5 The functional magnetic resonance imaging (fMRI) analysis of the topography of hemodynamic activity elicited by citric acid (sour), caffeine (bitter), NaCl (salty), sucrose (sweet), and monosodium glutamate (umami) on the flattened cortical surfaces of the insular/opercular cortex (encircled area in the center of the figure) of the right hemisphere of six human subjects. Each panel corresponding to each subject shows a composite pattern of responses to multiple stimulations with each of the five taste stimuli denoted by the different colors. Note the different patterns of hemodynamic activity for the five tastes with considerable overlap and a high interindividual topographical variability. Taste-specific patterns, however, were stable over time in each subject. From Schoenfeld, M. A., Neuer, G., Tempelmann, C., Schüßler, K., Noesselt, T., Hopf, J. M., and Heinze, H. J. 2004. Functional magnetic resonance tomography correlates of taste perception in the human primary taste cortex. Neuroscience 127, 347–353.

the taste-specific patterns as shown in Figure 5 were stable over time in each subject. The existence of chemotopy and implication of its importance in taste quality discrimination have been implicated in the rat GC (Yamamoto, T. *et al.*, 1985a; 1985b; 1989a; Yoshimura, H. *et al.*, 2005; Accolla, R. *et al.*, 2007) and suggested in the monkey PTA (Scott, T. R. *et al.*, 1986).

The PTA is involved not only in receiving and processing of taste inputs for qualitative and quantitative discrimination of taste stimuli but also in gustatory imagery by recalling gustatory memories. According to Kobayashi M. *et al.* (2004) in fMRI study, there is an asymmetrical topography of activation in the insula: the left insula is predominantly activated by gustatory imagery tasks, while the right insula, by actual gustatory stimulation in the mouth.

Recent fMRI and PET studies have shown that human amygdala responds specifically to negative emotion, especially to facial expressions of anger, fear, or sorrow (Hyman, S. E., 1988). There is a report, however, that the left amygdala is activated by a facial expression of fear and right amygdala is activated by an expression of happiness (Morris, J. S. *et al.*, 1996). Unpleasant odor stimulation also activates the amygdala. Zald D. H. and Pardo J. V. (1997) showed that strong unpleasant odor of sulfate compounds activated the bilateral amygdala and left orbitofrontal cortex. There are high correlations among the left amygdala, left orbitofrontal cortex, and perceived aversive feeding, indicating strong functional interactions between the amygdala and orbitofrontal cortex and important roles in emotional evaluation of odor.

Concerning the activation of the amygdala by taste stimulation in humans, Zald D. H. *et al.* (1998) reported in a PET study that 1 M NaCl, a strong and aversive taste stimulus, activated the right amygdala and neutral water and palatable chocolate induced no response in the amygdala, suggesting that the amygdala is responsive to aversive stimuli. Further, Zald D. H. *et al.* (2002) showed in a PET study that bitter and aversive quinine (0.02 M), but not sweet and palatable sucrose (30%), induced big responses in the left amygdala. Both quinine and sucrose excited the right posterior part of the orbitofrontal cortex, but the left inferior frontal pole and the anterior part of the orbitofrontal cortex were activated only by quinine stimulation. On the other hand, O'Doherty J. *et al.* (2001) found in fMRI study that both pleasant (1 M glucose) and unpleasant (0.1 M NaCl) taste stimuli evoked responses in the amygdala and orbitofrontal cortex, but the areas activated were different between the two stimuli. Thus, the activated areas are not consistent among researchers.

As already described, a flavor, taste-odor integration is very important in the sensory evaluation of foods. Small D. M. *et al.* (1997) in a PET study found that mismatched combinations such as salty and strawberry, sour and coffee, sweet and soy sauce, bitter and grapefruit, in contrast to the matched combinations such as salty and soy sauce, bitter and coffee, sour and grapefruit, sweet and strawberry, induced stronger activation in the left amygdala and the bilateral forebrain basal area. From these results, they suggest that these areas are important in processing of neophobic or unpleasant taste stimuli. In a further study using fMRI technique, Small D. M. *et al.* (2004) observed superadditive responses during the perception of the congruent flavor (vanilla/sweet) compared with the sum of its constituents in the anterior cingulate cortex, dorsal insular, anterior ventral insular extending into the caudal orbitofrontal cortex, frontal operculum, ventral lateral PFC, and posterior parietal cortex. Taken together with

previous findings in the literature (O'Doherty, J. *et al*., 2001; Small, D. M. *et al*., 2001; Zald, D. H. *et al*., 2002), their results suggest that the insular, orbitofrontal, and anterior cingulate cortices are key components of the network underlying flavor perception.

Acknowledgments

The preparation of the manuscript for this chapter and some of the work reported herein was supported in part by the Grant-in Aid for 21st Century COE program.

References

Abel, E. L. 1971. Effects of marijuana on the solution of anagrams, memory and appetite. Nature 231, 260–261.

Accolla, R., Bathellier, B., Petersen, C. C. H., and Carleton, A. 2007. Differential spatial representation of taste modalities in the rat gustatory cortex. J. Neurosci. 27, 1396–1404.

Apfelbaum, M. and Mandenoff, A. 1981. Naltrexone suppresses hyperphagia induced in the rat by a highly palatable diet. Pharmacol. Biochem. Behav. 15, 89–91.

Azuma, S., Yamamoto, T., and Kawamura, Y. 1984. Studies on gustatory responses of amygdaloid neurons in rats. Exp. Brain Res. 56, 12–22.

Azzara, A. V., Bodnar, R. J., Delamater, A. R., and Sclafani, A. 2000. Naltrexone fails to block the acquisition or expression of a flavor preference conditioned by intragastric carbohydrate infusions. Pharmacol. Biochem. Behav. 67, 545–557.

Azzara, A. V., Bodnar, R. J., Delamater, A. R., and Sclafani, A. 2001. D_1 but not D_2 dopamine receptor antagonism blocks the acquisition of a flavor preference conditioned by intragastric carbohydrate infusions. Pharmacol. Biochem. Behav. 68, 709–720.

Bahar, A., Dudai, Y., and Ahissar, E. 2004. Neural signature of taste familiarity in the gustatory cortex of the freely behaving rat. J. Neurophysiol. 92, 3298–3308.

Bakshi, V. P. and Kelley, A. E. 1993. Feeding induced by opioid stimulation of the ventral striatum: role of opiate receptor subtypes. J. Pharmacol. Exp. Ther. 265, 1253–1260.

Baldo, B. A., Gual-Bonilla, L., Sijapati, K., Daniel, R. A., Landry, C. F., and Kelley, A. E. 2004. Activation of a subpopulation of orexin/hypocretin-containing hypothalamic neurons by GABAA receptor-mediated inhibition of the nucleus accumbens shell, but not by exposure to a novel environment. Eur. J. Pharmacol. 19, 376–386.

Bartoshuk, L. M. and Beauchamp, G. K. 1994. Chemical senses. Annu. Rev. Psychol. 45, 419–449.

Baxter, H. 1933. Variations in the inorganic constituents of mixed and parotid gland saliva activated by reflex stimulation in the dog. J. Biol. Chem. 102, 203–217.

Beckstead, R. M., Morse, J. R., and Norgren, R. 1980. The nucleus of the solitary tract in the monkey: projections to the thalamus and brain stem nuclei. J. Comp. Neurol. 190, 259–282.

Bermúdez-Rattoni, F. 2004. Molecular mechanisms of taste-recognition memory. Nat. Rev. Neurosci. 5, 209–217.

Berridge, K. C. 1988. Brainstem systems mediate the enhancement of palatability by chlordiazepoxide. Brain Res. 447, 262–268.

Berridge, K. C. 1996. Food reward: brain substrates of wanting and liking. Neurosci. Biobehav. Rev. 20, 1–25.

Berridge, K. C. and Peciña, S. 1995. Benzodiazepines, appetite, and taste palatability. Neurosci. Biobehav. Rev. 19, 121–131.

Berridge, K. C. and Robinson, T. E. 1998. What is the role of dopamine in reward: hedonic impact, reward learning, or incentive salience? Brain Res. Rev. 28, 309–369.

Berridge, K. C. and Treit, D. 1986. Chlordiazepoxide directly enhances positive ingestive reactions in rats. Pharmacol. Biochem. Behav. 24, 217–221.

Berridge, K. C., Venier, I. L., and Robinson. T. E. 1989. Taste reactivity analysis of 6-hydroxydopamine-induced aphagia: implications for arousal and anhedonia hypotheses of dopamine function. Behav. Neurosci. 103, 36–45.

Berthoud, H. R., Trimble, E. R., Siegel, E. G., Bereiter, D. A., and Jeanrenaud, B. 1980. Cephalic-phase insulin secretion in normal and pancreatic islet-transplanted rats. Am. J. Physiol. 238, E336–E340.

Bielajew, C. and Trzcinska, M. 1994. Characteristics of stimulation-induced feeding sites in the sulcal prefrontal cortex. Behav. Brain Res. 61, 29–35.

Bishop, M. P., Elder, S. T., and Heath, R. G. 1963. Intracranial self-stimulation in man. Science 140, 394–396.

Blackburn, J. R., Pfaus, J. G., and Phillips, A. G. 1992. Dopamine functions in appetitive and defensive behaviours. Prog. Neurobiol. 39, 247–279.

Brandes, J. S. and Johnson, A. K. 1978. Recovery of feeding in rats following frontal neocortical ablations. Physiol. Behav. 20, 763–770.

Breiter, H. C., Gollub, R. L., Weisskoff, R. M., Kennedy, D. N., Makris, N., Berke, J. D., Goodman, J. M., Kantor, H. L., Gastfriend, D. R., Riorden, J. P., Mathew, R. T., Rosen, B. R., and Hyman, S. E. 1997. Acute effects of cocaine on human brain activity and emotion. Neuron 19, 591–611.

Brog, J. S., Salyapongse, A., Deutch, A. Y., and Zahm, D. S. 1993. The patterns of afferent innervation of the core and shell in the ''accumbens'' part of the rat ventral striatum: immunohistochemical detection of retrogradely transported fluoro-gold. J. Comp. Neurol. 338, 255–278.

Brown, D. R. and Holtzman, S. G. 1979. Suppression of deprivation-induced food and water intake in rats and mice by naloxone. Pharmacol. Biochem. Behav. 11, 567–573.

Bures, J., Bermúdez-Rattoni, F., and Yamamoto, T. 1998. Conditioned Taste Aversion: Memory of a Special Kind, pp. 1–178. Oxford University Press.

Chauncey, H. H. and Feller, R. P. 1967. Measurement of Human Gustatory Perception Using the Parotid Gland Secretion Rate. In: Olfaction and Taste (*ed*. T. Hayashi), Vol. II, pp. 265–280. Pergamon.

Cole, S. O. 1983. Combined effects of chlordiazepoxide treatment and food deprivation on concurrent measures of feeding and activity. Pharmacol. Biochem. Behav. 18, 369–372.

Cooper, S. J. 1983. Effects of opiate agonists and antagonists on fluid intake and saccharin choice in the rat. Neuropharmacology 22, 323–328.

Cooper, S. J. 1987. Chlordiazepoxide-induced selection of saccharin-flavoured food in the food-deprived rat. Physiol. Behav. 41, 539–542.

Cooper, S. J. 2004. Endocannabinoids and food consumption: comparisons with benzodiazepine and opioid palatability-dependent appetite. Eur. J. Pharmacol. 500, 37–49.

Cooper, S. J. and Estall, L. B. 1985. Behavioural pharmacology of food, water and salt intake in relation to drug actions at benzodiazepine receptors. Neurosci. Biobehav. Rev. 9, 5–19.

Cooper, S. J. and Green, A. E. 1993. The benzodiazepine receptor partial agonists, bretazenil (Ro 16-6028) and Ro 17-1812, affect saccharin preference and quinine aversion in the rat. Behav. Pharmacol. 4, 81–85.

Cooper, S. J. and Kirkham, T. C. 1993. Opioid Mechanisms in the Control of Food Consumption and Taste Preferences. In: Handbook of Experimental Pharmacology. Opioids II, Vol. 104/II (*ed*. A. Herz), pp. 239–262. Springer-Verlag.

Cooper, S. J. and McClelland, A. 1980. Effects of chlordiazepoxide, food familiarization, and prior shock experience on food choice in rats. Pharmacol. Biochem. Behav. 12, 23–28.

Cooper, S. J. and Yerbury, R. E. 1986. Benzodiazepine-induced hyperphagia: stereospecificity and antagonism by pyrazoloquinolines, CGS 9895 and CGS 9896. Psychopharmacology (Berlin) 89, 462–466.

Cooper, S. J. and Yerbury, R. E. 1988. Clonazepam selectively increases saccharin ingestion in a two-choice test. Brain Res. 456, 173–176.

Cooper, S. J., van der Hoek, G., and Kirkham, T. C. 1988. Bi-directional changes in sham feeding in the rat produced by benzodiazepine receptor ligands. Physiol. Behav. 42, 211–216.

Devane, W. A., Hanus, L., Breuer, A., Pertwee, R. G., Stevenson, L. A., Griffin, G., Gibson, D., Mandelbaum, A., Etinger, A., and Mechoulam, R. 1992. Isolation and structure of a brain constituent that binds to the cannabinoid receptor. Science 258, 1946–1949.

DiNardo, L. A. and Travers, J. B. 1994. Hypoglossal neural activity during ingestion and rejection in the awake rat. J. Neurophysiol. 72, 1181–1191.

Divac, I., Kosmal, A., Bjorklund, A., and Lindvall, O. 1978. Subcortical projections to the prefrontal cortex in the rat as revealed by the horseradish peroxidase technique. Neuroscience 3, 785–796.

Domjan, M. 1976. Determinants of the enhancement of flavored-water intake by prior exposure. J. Exp. Psychol. Anim. Behav. Process 2, 17–27.

Doyle, T. G., Berridge, K. C., and Gosnell, B. A. 1993. Morphine enhances hedonic taste palatability in rats. Pharmacol. Biochem. Behav. 46, 745–749.

Drewnowski, A., Krahn, D. D., Demitrack, M. A., Nairn, K., and Gosnell, B. A. 1992. Taste responses and preferences for sweet high-fat foods: evidence for opioid involvement. Physiol. Behav. 51, 371–379.

Elizalde, G. and Sclafani, A. 1990. Flavor preferences conditioned by intragastric Polycose infusions: a detailed analysis using an electronic esophagus preparation. Physiol. Behav. 47, 63–77.

Emmelin, N. and Holmberg. J. 1967. Impulse frequency in secretory nerves of salivary glands. J. Physiol. Lond. 191, 205–214.

Fanselow, G. and Birk, J. 1982. Flavor–flavor associations induce hedonic shifts in taste preference. Anim. Learn. Behav. 10, 223–228.

Fantino, M., Hosotte, J., and Apfelbaum, M. 1986. An opioid antagonist, naltrexone, reduces preference for sucrose in humans. Am. J. Physiol. 251, R91–R96.

Faurion, A., Cerf, B., Van De Moortele, P. F., Lobel, E., Mac Leod, P., and Le Bihan, D. 1999. Human taste cortical areas studied with functional magnetic resonance imaging: evidence of functional lateralization related to handedness. Neurosci. Lett. 277, 189–192.

Feller, R. P., Sharon, I. M., Chauncey, H. H., and Shannon, I. L. 1965. Gustatory perception of sour, sweet, and salt mixtures using parotid gland flow rate. J. Appl. Physiol. 20, 1341–1344.

Fischer, U., Hommel, H., Ziegler, M., and Michael, R. 1972. The mechanism of secretion after oral glucose administration. I. Multiphasic course of insulin mobilization after oral administration of glucose in conscious dogs. Diabetologia 8, 104–110.

Flowers, S. H., Dunham, E. S., and Barbour, H. G. 1929. Addiction edema, and withdrawal edema in morphinized rats. Proc. Soc. Exp. Biol. Med. 26, 572–574.

Foltin, R. W., Brady, J. V., and Fischman, M. V. 1986. Behavioral analysis of marijuana effects on food intake in humans. Pharmacol. Biochem. Behav. 25, 577–582.

Foltin, R. W., Ellis, S., and Schuster, C. R. 1985. Specific antagonism by Ro15-1788 of benzodiazepine-induced increases in food intake in rhesus monkeys. Pharmacol. Biochem. Behav. 23, 249–252.

Foltin, R. W., Fischman, M. W., and Byrne, M. F. 1989. Food intake in baboons: effects of diazepam. Psychopharmacology (Berl.) 97, 443–447.

Funakoshi, M. and Kawamura, Y. 1967. Relations Between Taste Qualities and Parotid Gland Secretion Rate. In: Olfaction and Taste II (*ed*. T. Hayashi), pp. 281–287. Pergamon Press.

Funakoshi, M., Kasahara, Y., Yamamoto, T., and Kawamura, Y. 1972. Taste Coding and Central Perception. In: Olfaction and Taste IV (*ed*. D. Schneider), pp. 336–342. Wissenschaftlich Verlagsgesellschaft MBH.

Furudono, Y., Ando, C., Yamamoto, C., Kobashi, M., and Yamamoto, T. 2006. Involvement of specific orexigenic neuropeptides in sweetener-induced overconsumption in rats. Behav. Brain Res. 175, 241–248.

Ganchrow, J. R., Oppenheimer, M., and Steiner, J. E. 1979. Behavioral displays to gustatory stimuli in newborn rabbit pups. Chem. Senses Flavor 4, 49–61.

Gantt, W. H. 1973. The nervous secretion of saliva. Quantitative studies in the natural unconditioned reflex secretion of parotid saliva. Am. J. Physiol. 119, 493–507.

Geary, N. and Smith, G. P. 1985. Pimozide decreases the positive reinforcing effect of sham fed sucrose in the rat. Pharmacol. Biochem. Behav. 22, 787–790.

Giza, B. K., Ackroff, K., McCaughey, S. A., Sclafani, A., and Scott, T. R. 1997. Preference conditioning alters taste responses in the nucleus of the solitary tract of the rat. Am. J. Physiol. 273, R1230–R1240.

Gjorstrup, P. 1980. Taste and chewing as stimuli for the secretion of amylase from the parotid gland of the rabbit. Acta. Physiol. Scand. 110, 295–301.

Glass, M. J., Billington, C. J., and Levine, A. S. 1999. Opioids and food intake: distributed functional neural pathway? Neuropeptides 33, 360–368.

Gosnell, B. A. 1987. Central structures involved in opioid-induced feeding. Fed. Proc. 46, 163–167.

Grandison, L. and Guidotti, A. 1977. Stimulation of food intake by muscimol and β-endorphin. Neuropharmacology 16, 533–536.

Gray, R. W. and Cooper, S. J. 1995. Benzodiazepines and palatability: taste reactivity in normal ingestion. Physiol. Behav. 58, 853–859.

Grill, H. J. and Norgren, R. 1978a. The taste reactivity test. I. Mimetic responses to gustatory stimuli in neurologically normal rats. Brain Res. 143, 263–279.

Grill, H. J. and Norgren, R. 1978b. The taste reactivity test. II. Mimetic responses to gustatory stimuli in chronic thalamic and chronic decerebrate rats. Brain Res. 143, 281–297.

Groenewegen, H. J., Berendse, H. W., and Haber, S. N. 1993. Organization of the output the ventral striatopallidal system in the rat: ventral pallidal efferents. Neuroscience 57, 113–142.

Gutiérrez, R., Téllez, L. A., and Bermúdez-Rattoni, F. 2003. Blockade of cortical muscarinic but not NMDA receptors prevents a novel taste from becoming familiar. Eur. J. Neurosci. 17, 1556–1562.

Hajnal, A., Smith, G. P., and Norgren, R. 2004. Oral sucrose stimulation increases accumbens dopamine in the rat. Am. J. Physiol. Regul. Integr. Comp. Physiol. 286, R31–R37.

Halsell, C. B., Travers, S. P., and Travers, J. B. 1996. Ascending and descending projections from the rostral nucleus of the solitary tract originate from separate neuronal populations. Neuroscience 72, 185–197.

Hanamori, T., Kunitake, T., Kato, K., and Kannan, H. 1998. Responses of neurons in the insular cortex to gustatory, visceral, and nociceptive stimuli in rats. J. Neurophysiol. 79, 2535–2545.

Haney, M., Comer, S. D., Fischman, M. W., and Foltin, R. W. 1997. Alprazolam increases food intake in humans. Psychopharmacology (Berl.) 132, 311–314.

Heimer, L., Zahm, D. S., Churchill, L., Kalivas, P. W., and Wohltmann, C. 1991. Specificity in the projection patterns of accumbal core and shell in the rat. Neuroscience 41, 89–125.

Herbert, H., Moga, M. M., and Saper, C. B. 1990. Connections of the parabrachial nucleus with the nucleus of the solitary tract and the medullary reticular formation in the rat. J. Comp. Neurol. 293, 540–580.

Hernádi, I., Karádi, Z., Vígh, J., Petykó, Z., Egyed, R., Berta, B., and Lénárd, L. 2000. Alterations of conditioned taste aversion after microiontophoretically applied neurotoxins in the medial prefrontal cortex of the rat. Brain Res. Bull. 53, 751–758.

Higgs, S. and Cooper, S. J. 1996a. Increased food intake following injection of the benzodiazepine receptor agonist midazolam into the IVth ventricle. Pharmacol. Biochem. Behav. 55, 81–86.

Higgs, S. and Cooper, S. J. 1996b. Hyperphagia induced by direct administration of midazolam into the parabrachial nucleus of the rat. Eur. J. Pharmacol. 313, 1–9.

Higgs, S. and Cooper, S. J. 1997. Midazolam-induced rapid changes in licking behaviour: evidence for involvement of endogenous opioid peptides. Psychopharmacology (Berl.) 131, 278–286.

Higgs, S. and Cooper, S. J. 1998a. Effects of benzodiazepine receptor ligands on the ingestion of sucrose, Intralipid, and maltodextrin: an investigation using a microstructural analysis of licking behavior in a brief contact test. Behav. Neurosci. 112, 447–457.

Higgs, S. and Cooper, S. J. 1998b. Evidence for early opioid modulation of licking responses to sucrose and Intralipid: a microstructural analysis in the rat. Psychopharmacology (Berl.) 139, 342–355.

Higgs, S., Williams, C. M., and Kirkham, T. C. 2003. Cannabinoid influences on palatability: microstructural analysis of sucrose drinking after Δ9-tetrahydrocannabinol, anandamide, 2-arachidonoyl glycerol and SR141716. Psychopharmacology (Berlin) 165, 370–377.

Holtzman, S. G. 1974. Behavioral effects of separate and combined administration of naloxone and d-amphetamine. J. Pharmacol. Exp. Ther. 189, 51–60.

Hyman, S. E. 1988. Neurobiology: a new image for fear and emotion. Nature 393, 417–418.

Inui, A. 2000. Transgenic approach to the study of body weight regulation. Pharmacol. Rev. 52, 35–62.

Jacobs, K. M., Mark, G. P., and Scott, T. R. 1988. Taste responses in the nucleus tractus solitarius of sodium-deprived rats. J. Physiol. (Lond.) 406, 393–410.

Janowitz, H. D., Hollander, F., Orringer, P., Levy, M. H., Winkelstein, A., Kaufman, M. R., and Margolin, S. G. 1950. A quantitative study of the gastric secretory response to sham feeding in a human subject. Gastroenterology 16, 104–116.

Karádi, Z., Lukáts, B., Papp, S.z., Egyed, R., Lénárd, L., and Takács, G. 2005. Involvement of forebrain glucose-monitoring neurons in taste information processing: electrophysiological and behavioral studies. Chem. Senses 30, i168–i169.

Karimnamazi, H. and Travers, J. B. 1998. Differential projections from gustatory responsive regions of the parabrachial nucleus to the medulla and forebrain. Brain Res. 813, 283–302.

Katz, D. B., Simon, S. A., and Nicolelis, M. A. L. 2001. Dynamic and multimodal responses of gustatory cortical neurons in awake rats. J. Neurosci. 21, 4478–4489.

Kawamura, Y. and Yamamoto, T. 1978. Studies on neural mechanisms of the gustatory-salivary reflex in rabbits. J. Physiol. (Lond.) 285, 35–47.

Kelley, A. E., Bakshi, V. P., Haber, S. N., Steininger, T. L., Will, M. J., and Zhang, M. 2002. Opioid modulation of taste hedonics within the ventral striatum. Physiol. Behav. 76, 365–377.

Kephalas, T. A., Kiburis, J., Michael, C. M., Miras, C. J., and Papadakis, D. P. 1976. Some Aspects of Cannabis Smoke Chemistry. In: Marihuana: Chemistry, Biochemistry, and Cellular Affects (*ed*. G. G. Nahas), pp. 39–49. Springer-Verlag.

Kerr, A. C. 1961. The Physiological Regulation of Salivary Secretions in Man, Pergamon Press.

Kinomura, S., Kawashima, R., Yamada, K., Ono, S., Itoh, M., Yoshioka, S., Yamaguchi, T., Matsui, H., Miyazawa, H., Itoh, H., Goto, R., Fujiwara, T., Satoh, K., and Fukuda, H. 1994. Functional anatomy of taste perception in the human brain studied with positron emission tomography. Brain Res. 659, 263–266.

Kirkham, T. C. and Cooper, S. J. 1988. Attenuation of sham feeding by naloxone is stereospecific: evidence for opioid mediation of orosensory reward. Physiol. Behav. 43, 845–847.

Kirkham, T. C., Williams, C. M., Fezza, F., and Di Marzo, V. 2002. Endocannabinoid levels in rat limbic forebrain and hypothalamus in relation to fasting, feeding and satiation: stimulation of eating by 2-arachidonoyl glycerol. Br. J. Pharmacol. 136, 550–557.

Kita, H. and Oomura, Y. 1981. Reciprocal connections between the lateral hypothalamus and the frontal cortex in the rat: Electrophysiological and anatomical observations. Brain Res. 213, 1–16.

Kobashi, M. and Bradley, R. M. 1998. Effects of GABA on neurons of the gustatory and visceral zones of the parabrachial nucleus in rats. Brain Res. 799, 323–328.

Kobashi, M., Furudono, Y., Matsuo, R., and Yamamoto, T. 2003. Central orexin facilitates gastric relaxation and contractility in rats. Neurosci. Lett. 332, 171–174.

Kobashi, M., Mizutani, M., and Matsuo, R. 2000. Water stimulation of the posterior oral cavity induces inhibition of gastric motility. Am. J. Physiol. 279, R778–R785.

Kobayakawa, T., Endo, H., Ayabe-Kanamura, S., Kumagai, T., Yamaguchi, Y., Kikuchi, Y., Takeda, T., Saito, S., and Ogawa, H. 1996. The primary gustatory area in human cerebral cortex studied by magnetoencephalography. Neurosci. Lett. 212, 155–158.

Kobayashi, M., Takeda, M., Hattori, N., Fukunaga, M., Sasabe, T., Inoue, N., Nagai, Y., Sawada, T., Sadato, N., and Watanabe, Y. 2004. Functional imaging of gustatory perception and imagery: top-down processing of gustatory signals. Neuroimage 23, 1271–1282.

Kolb, B. and Nonneman, A. J. 1975. Prefrontal cortex and the regulation of food intake in the rat. J. Comp. Physiol. Psychol. 88, 806–815.

Kosobud, A. E., Harris, G. C., and Chapin, J. K. 1994. Behavioral associations of neuronal activity in the ventral tegmental area of the rat. J. Neurosci. 14, 7117–7129.

Kotz, C. M., Billington, C. J., and Levine, A. S. 1997. Opioids in the nucleus of the solitary tract are involved in feeding in the rat. Am. J. Physiol. 272, R1028–R1032.

Le Magnen, J., Marfaing-Jallat, P., Miceli, D., and Devos, M. 1980. Pain modulating and reward systems: a single brain mechanism? Pharmacol. Biochem. Behav. 12, 729–733.

Li, C. S., Davis, B. J., and Smith, D. V. 2003. Opioid modulation of taste responses in the NTS. Brain Res. 965, 21–34.

Ljungberg, T., Apicella, P., and Schultz, W. 1992. Responses of monkey dopamine neurons during learning of behavioral reactions. J. Neurophysiol. 67, 145–163.

Lukáts, B., Papp, S.z., Szalay, C.s., Gode, J., Lénárd, L., and Karádi, Z. 2002. Gustatory neurons in the nucleus accumbens and the mediodorsal prefrontal cortex of the rat. Acta Physiol. Hung. 89, 250.

Maldonado-Irizarry, C. S., Swanson, C. J., and Kelley, A. E. 1995. Glutamate receptors in the nucleus accumbens shell control feeding behavior via the lateral hypothalamus. J. Neurosci. 15, 6779–6788.

Manabe, Y., Kuroda, K., Imaizumi, M., Inoue, K., Sako, N., Yamamoto, T., Fushiki, T., and Hanai, K. 2000. Diazepam-binding inhibitor-like activity in rat cerebrospinal fluid after stimulation by an aversive quinine taste. Chem. Senses 25, 739–746.

Manabe, Y., Toyoda, T., Kuroda, K., Imaizumi, M., Yamamoto, T., and Fushiki, T. 2001. Effect of diazepam binding inhibitor (DBI) on the fluid intake, preference and the taste reactivity in mice. Behav. Brain Res. 126, 197–204.

Mansour, A., Khachaturian, H., Lewis, M. E., Akil, H., and Watson, S. J. 1987. Autoradiographic differentiation of mu, delta, and kappa opioid receptors in the rat forebrain and midbrain. J. Neurosci. 7, 2445–2464.

Maren, S. and Fanselow, M. S. 1996. The amygdala and fear conditioning: has the nut been cracked? Neuron 16, 237–240.

Margules, D. L. and Stein, L. 1967. Neuroleptics vs. Tranquilizers: Evidence from Animals of Mode and Site of Action. In: *Neuropsychopharmacology (ed*. H. Brill), pp. 74–80. Excerpta Medica Foundation.

Martin, W. R., Wikler, A., Eades, C. G., and Persor, F. T. 1963. Tolerance to and physical dependence on morphine in rats. Psychopharmacologia 4, 247–260.

Matsuo, R. and Yamamoto, T. 1989. Gustatory-salivary reflex: neural activity of sympathetic and parasymathetic fibers innervating the submandibular gland of the hamster. J. Auton. Nerv. Syst. 26, 187–197.

Matsuo, R., Yamamoto, T., Yoshitaka, K., and Morimoto, T. 1989. Neural substrates for reflex salivation induced by taste, mechanical, and thermal stimulation of the oral region in decerebrate rats. Jpn. J. Physiol. 39, 349–357.

Matsuo, R., Yamauchi, Y., Kobashi, M., Funahashi, M., Mitoh, Y., and Adachi, A. 2001. Role of parabrachial nucleus in submandibular salivary secretion induced by bitter taste stimulation in rats. Auton. Neurosci. 88, 61–73.

McDonald, A. J. and Jackson, T. R. 1987. Amygdaloid connections with posterior insular and temporal cortical areas in the rat. J. Comp. Neurol. 262, 59–77.

McDonald, A. J., Shammah-Lagnado, S. J., Shi, C., and Davis, M. 1999. Cortical afferents to the extended amygdala. Ann. N. Y. Acad. Sci. 877, 309–338.

McLaughlin, C. L. and Baile, C. A. 1979. Cholecystokinin, amphetamine and diazepam and feeding in lean and obese Zucker rats. Pharmacol. Biochem. Behav. 10, 87–93.

McLean, S. and Hoebel, B. G. 1983. Feeding induced by opiates injected into the paraventricular hypothalamus. Peptides 4, 287–292.

Meredith, G. E., Pennartz, C. M., and Groenewegen, H. J. 1993. The cellular framework for chemical signaling in the nucleus accumbens. Prog. Brain Res. 99, 3–24.

Miller, C. C., Murray, T. F., Freeman, K. G., and Edwards, G. L. 2004. Cannabinoid agonist, CP 55,940, facilitates intake of palatable foods when injected into the hindbrain. Physiol. Behav. 80, 611–616.

Miller, F. R. and Sherrington, C. R. 1916. Some observations on the buccopharygeal stage of reflex deglutition the cat. Q. J. Exp. Physiol. 9, 147–186.

Mogenson, G. J., Jones, D. L., and Yim, C. Y. 1980. From motivation to action: functional interface between limbic system and the motor system. Prog. Neurobiol. 14, 69–97.

Morris, J. S., Frith, C. D., Perrett, D. I., Rowland, D., Young, A. W., Calder, A. J., and Dolan, R. J. 1996. A differential neural response in the human amygdala to fearful and happy facial expressions. Nature 383, 812–815.

Mucha, R. F. and Herz, A. 1986. Preference conditioning produced by opioid active and inactive isomers of levorphanol and morphine in rat. Life Sci. 38, 241–249.

Nachman, M. and Jones, D. R. 1974. Learned taste aversions over long delays in rats: the role of learned safety. J. Comp. Physiol. Psychol. 86, 949–956.

Nakamura, K. and Norgren, R. 1995. Sodium-deficient diet reduces gustatory activity in the nucleus of the solitary tract of behaving rats. Am. J. Physiol. 269: R647–R661.

Newbrun, E. 1962. Observations on the amylase content and flow rate of human saliva following gustatory stimulation. J. Dent. Res. 41, 459–465.

Nicolaidis, S. 1977. Sensory-Neuroendocrine Reflexes and Their Anticipatory and Optimizing Role on Metabolism. In: The Chemical Senses and Nutrition (*eds*. M. R. Kare and O. Maller), pp. 123–140. Academic Press.

Niijima, A. 1991. Effects of oral and intestinal stimulation with umami substance on gastric vagus activity. Physiol. Behav. 49, 1025–1028.

Niijima, A., Togiyama, T., and Adachi, A. 1990. Cephalic-phase insulin release induced by taste stimulus of monosodium glutamate (umami taste). Physiol. Behav. 48, 905–908.

Nishijo, H., Ono, T., and Nishino, H. 1988a. Topographic distribution of modality-specific amygdalar neuron in alert monkey. J. Neurosci. 8, 3556–3569.

Nishijo, H., Ono, T., and Nishino, H. 1988b. Single neuron responses in amygdala of alert monkey during complex sensory stimulation with affective significance. J. Neurosci. 8, 3570–3583.

Nishijo, H., Uwano, T., Tamura, R., and Ono, T. 1998c. Gustatory and multimodal neuronal responses in the amygdala during licking and discrimination of sensory stimuli in awake rats. J. Neurophysiol. 79, 21–36.

Norgren, R. 1995. Gustatory System. In: *The Rat Nervous System (ed*. G. Paxinos), pp. 751–771. Academic Press.

Novis, B. H., Bank, S., and Marks, I. N. 1971. The cephalic phase of pancreatic secretion in man. Scand. J. Gastroenterol. 6, 417–421.

Nowlis, G. H. 1973. Taste-Elicited Tongue Movements in Human Newborn Infants: An Approach to Palatability. In: 4th Symposium on Oral Sensation and Perception (*ed*. J. F. Bosma), pp. 292–303. US Government Printing Office.

O′Doherty, J., Rolls, E. T., Francis, S., Bowtell, R., and McGlone, F. 2001. Representation of pleasant and aversive taste in the human brain. J. Neurophysiol. 85, 1315–1321.

Ohara, I., Naruse, M. M., and Itokawa, Y. 1996. The effect of palatability and feeding conditions on digestive functions in rats. J. Am. Coll. Nutr. 15, 186–191.

Ohara, I., Otsuka, S., and Yugari, Y. 1988. Cephalic phase response of pancreatic exocrine secretion in conscious dogs. Am. J. Physiol. 254, G416–G423.

Olds, J. and Milner, P. M. 1954. Positive reinforcement produced by electrical stimulation of septal area and other regions of rat brain. J. Comp. Physiol. Psychol. 47, 419–427.

Parker, L. A. 1991. Chlordiazepoxide nonspecifically enhances consumption of saccharin solution. Pharmacol. Biochem. Behav. 38, 375–377.

Pavlov, I. P. 1902. The Work of the Digestive Glands. Charles Griffin.
Peciña, S. and Berridge, K. C. 1995. Central enhancement of taste pleasure by intraventricular morphine. Neurobiology Bp 3, 269–280.
Peciña, S. and Berridge, K. C. 1996. Brainstem mediates diazepam enhancement of palatability and feeding: microinjections into forth ventricle versus lateral ventricle. Brain Res. 727, 22–30.
Peciña, S. and Berridge, K. C. 2000. Opioid site in nucleus accumbens shell mediates eating and hedonic 'liking' for food: map based on microinjection Fos plumes. Brain Res. 863, 71–86.
Peciña, S., Cagniard, B., Berridge, K. C., Aldridge, J. W., and Zhuang, X. 2003. Hyperdopaminergic mutant mice have higher ''wanting'' but not 'liking' for sweet rewards. J. Neurosci. 23, 9395–9402.
Pérez-Jaranay, J. M. and Vives, F. 1991. Electrophysiological study of the response of medial prefrontal cortex neurons to stimulation of the basolateral nucleus of the amygdala in the rat. Brain Res. 564, 97–101.
Poschel, B. P. H. 1971. A simple and specific screen for benzodiazepine-like drugs. Psychopharmacologia 19, 193–198.
Ricardo, J. A. and Koh, E. T. 1978. Anatomical evidence of direct projections from the nucleus of the solitary tract to the hypothalamus, amygdala, and other forebrain structures in the rat. Brain Res. 153, 1–26.
Richards, J. G. and Mohler, H. 1984. Benzodiazepine receptors. Neuropharmacology 23, 233–242.
Robinson, T. G. and Beart, P. M. 1988. Excitant amino acid projections from rat amygdala and thalamus to nucleus accumbens. Brain Res. Bull. 20, 467–471.
Rolls, E. T. 2004. The functions of the orbitofrontal cortex. Brain Cogn. 55, 11–29.
Rolls, E. T. and Baylis, L. L. 1994. Gustatory, olfactory, and visual convergence within the primate orbitofrontal cortex. J. Neurosci. 14, 5437–5452.
Rolls, E. T., Critchley, H. D., Browning, A. S., Hernadi, I., and Lenard, L. 1999. Responses to the sensory properties of fat of neurons in the primate orbitofrontal cortex. J. Neurosci. 19, 1532–1540.
Rolls, E. T., Verhagen, J. V., and Kadohisa, M. 2003. Representations of the texture of food in the primate orbitofrontal cortex: neurons responding to viscosity, grittiness, and capsaicin. J. Neurophysiol. 90, 3711–3724.
Saper, C. B. 1982. Convergence of autonomic and limbic connections in the insular cortex of the rat. J. Comp. Neurol. 210, 163–173.
Schoenfeld, M. A., Neuer, G., Tempelmann, C., Schüßler, K., Noesselt, T., Hopf, J. M., and Heinze, H. J. 2004. Functional magnetic resonance tomography correlates of taste perception in the human primary taste cortex. Neuroscience 127, 347–353.
Schultz, W. and Romo, R. 1990. Dopamine neurons of the monkey midbrain: contingencies of responses to stimuli eliciting immediate behavioral reactions. J. Neurophysiol. 63, 607–624.
Schwartz, M. W., Woods, S. C., Porte, D., Jr., Sleeley, R. J., and Baskin, D. G. 2000. Central nervous system control of food intake. Nature 404, 661–671.
Sclafani, A. 2004. Oral and postoral determinants of food reward. Physiol. Behav. 81, 773–779.
Sclafani, A., Azzara, A. V., Touzani, K., Grigson, P. S., and Norgren, R. 2001. Parabrachial nucleus lesions block taste and attenuate flavor preference and aversion conditioning in rats. Behav. Neurosci. 115, 920–933.
Scott, T. R. and Plata-Salaman, C. R. 1999. Taste in the monkey cortex. Physiol. Behav. 67, 489–511.
Scott, T. R., Yaxley, S., Siekiewicz, Z. J., and Rolls, E. T. 1986. Gustatory responses in the frontal opercular cortex of the alert cynomolgus monkey. J. Neurophysiol. 56, 876–890.
Sewards, T. V. 2004. Dual separate pathways for sensory and hedonic aspects of taste. Brain Res. Bull. 62, 271–283.
Shammah-Lagnado, S. J., Costa, M. S. M. O., and Ricardo, J. A. 1992. Afferent connections of the parvocellular reticular formation: a horseradish peroxidase study in the rat. Neuroscience 50, 403–425.
Shi, C.-J. and Cassell, M. D. 1998. Cortical, thalamic, and amygdaloid connections of the anterior and posterior insular cortices. J. Comp. Neurol. 399, 440–468.
Shimura, T., Imaoka, H., Okazaki, Y., Kanamori, Y., Fushiki, T., and Yamamoto, T. 2005. Involvement of the mesolimbic system in palatability-induced ingestion. Chem. Senses 30, i188–i189.
Shimura, T., Imaoka, H., and Yamamoto, T. 2006. Neurochemical modulation of ingestive behavior in the ventral pallidum. Eur. J. Neurosci. 23, 1596–1604.
Shimura, T., Kamada, Y., and Yamamoto, T. 2002a. Ventral tegmental lesions reduce overconsumption of normally preferred taste fluid in rats. Behav. Brain Res. 134, 123–130.
Shimura, T., Komori, M., and Yamamoto, T. 1997a. Acute sodium deficiency reduces gustatory responsiveness to NaCl in the parabrachial nucleus of rats. Neurosci. Lett. 236, 33–36.
Shimura, T., Tanaka, H., and Yamamoto, T. 1997b. Salient responsiveness of parabrachial neurons to the conditioned stimulus after the acquisition of taste aversion learning in rats. Neuroscience 81, 239–247.
Shimura, T., Tokita, K., and Yamamoto, T. 2002b. Parabrachial unit activities after the acquisition of conditioned taste aversion to a nonpreferred HCl solution in rats. Chem. Senses 27, 153–158.
Shimura, T., Watanabe, U., Yanagawa, Y., and Yamamoto, T. 2004. Altered taste function in mice deficient in the 65-kDa isoform of glutamate decarboxylase. Neurosci. Lett. 356, 171–174.
Shipley, M. T. and Geinisman, Y. 1984. Anatomical evidence for convergence of olfactory, gustatory, and visceral afferent pathways in mouse cerebral cortex. Brain Res. Bull. 12, 221–226.
Small, D. M., Jones-Gotman, M., Zatorre, R. J., Petrides, M., and Evance, A. C. 1997. Flavor processing: more than the sum of its part. Neuroreport 8, 3913–3917.
Small, D. M., Voss, J., Mak, Y. E., Simmons, K. B., Parrish, T., and Gitelman, D. 2004. Experience-dependent neural integration of taste and smell in the human brain. J. Neurophysiol. 92, 1892–1903.
Small, D. M., Zald, D. H., Jones-Gotman, M., Zatorre, R. J., Pardo, J. V., Stephen, F., and Petrides, M. 1999. Human cortical gustatory areas: a review of functional neuroimaging data. Neuroreport 10, 7–14.
Small, D. M., Zatorre, R. J., Dagher, A., Evans, A. C., and Jones-Gotman, M. 2001. Changes in brain activity related to eating chocolate: from pleasure to aversion. Brain 124, 1720–1733.
Söderpalm, A. H. and Berridge, K. C. 2000. The hedonic impact and intake of food are increased by midazolam microinjection in the parabrachial nucleus. Brain Res. 877, 288–297.
Söderpalm, A. H. and Hansen, S. 1998. Benzodiazepines enhance the consumption and palatability of alcohol in the rat. Psychopharmacology (Berl.) 137, 215–222.
Steffens, A. B. 1976. Influence of the oral cavity on insulin release in the rat. Am. J. Physiol. 230, 1411–1415.
Steiner, J. E. 1973. The Gustofacial Response: Observation on Normal and Anencephalic Newborn Infants. In: 4th Symposium

on Oral Sensation and Perception (*ed*. J. F. Bosma), pp. 254–278. US Government Printing Office.
Stratford, T. R. and Kelley, A. E. 1997. GABA in the nucleus accumbens shell participates in the central regulation of feeding behavior. J. Neurosci. 17, 4434–4440.
Stratford, T. R. and Kelley, A. E. 1999. Evidence of a functional relationship between the nucleus accumbens shell and lateral hypothalamus subserving the control of feeding behavior. J. Neurosci. 19, 11040–11048.
Stratford, T. R., Kelley, A. E., and Simansky, K. J. 1999. Blockade of GABAA receptors in the medial ventral pallidum elicits feeding in satiated rats. Brain Res. 825, 199–203.
Stratford, T. R., Swanson, C. J., and Kelley, A. 1998. Specific changes in food intake elicited by blockade or activation of glutamate receptors in the nucleus accumbens shell. Behav. Brain Res. 93, 43–50.
Tabuchi, E., Ono, T., Nishijo, H., and Torii, K. 1991. Amino acid and NaCl appetite, and LHA neuron responses of lysine-deficient rat. Physiol. Behav. 49, 951–964.
Tokita, K., Karádi, Z., Shimura, T., and Yamamoto, T. 2004. Centrifugal inputs modulate taste aversion learning associated parabrachial neuronal activities. J. Neurophysiol. 92, 265–279.
Touzani, K. and Sclafani, A. 2001. Conditioned flavor preference and aversion: role of the lateral hypothalamus. Behav. Neurosci. 115, 84–93.
Travers, J. B., Urbanek, K., and Grill, H. J. 1999. Fos-like immunoreactivity in the brain stem following oral quinine stimulation in decerebrate rats. Am. J. Physiol. 277, R384–R394.
Treesukosol, Y., Ishizuka, T., Yamamoto, C., Senda, K., Tsutsumi, S., Yamatodani, A., and Yamamoto, T. 2005. Hypothalamic histamine release by taste stimuli in freely moving rats: possible implication of palatability. Behav. Brain Res. 164, 67–72.
Treit, D., Berridge, K. C., and Schultz, C. E. 1987. The direct enhancement of positive palatability by chlordiazepoxide is antagonized by Ro 15-1788 and CGS 8216. Pharmacol. Biochem. Behav. 26, 709–714.
Weiffenbach, J. M. and Thach, B. T. 1973. Elicited Tongue Movements: Touch and Taste in the Mouth of the Neonate. In: 4th Symposium on Oral Sensation and Perception (*ed*. J. F. Bosma), pp. 232–243. US Government Printing Office.
Williams, C. M. and Kirkham, T. C. 2002. Observational analysis of feeding induced by Δ9-THC and anandamide. Physiol. Behav. 76, 241–250.
Wilson, J. D., Nicklous, D. M., Aloyo, V. J., and Simansky, K. J. 2003. An orexigenic role for mu-opioid receptors in the lateral parabrachial nucleus. Am. J. Physiol. Regul. Integr. Comp. Physiol. 285, R1055–R1065.
Wise, R. A. 1982. Neuroleptics and operant behavior: the anhedonia hypothesis. Behav. Brain Sci. 5, 39–87.
Wise, R. A. 2002. Brain reward circuitry: insights from unsensed incentives. Neuron 36, 229–240.
Wise, R. A. and Dawson, V. 1974. Diazepam-induced eating and lever pressing for food in sated rats. J. Comp. Physiol. Psychol. 86, 930–941.
Wise, R. A., Spindler, J., deWit, H., and Gerber, G. J. 1978. Neuroleptic-induced ''anhedonia'' in rats: pimozide blocks reward quality of food. Science 201, 262–264.
Woods, J. S. and Leibowitz, S. F. 1985. Hypothalamic sites sensitive to morphine and naloxone: effects on feeding behavior. Pharmacol. Biochem. Behav. 23, 431–438.
Xenakis, S. and Sclafani, A. 1981. The effects of pimozide on the consumption of a palatable saccharin-glucose solution in the rat. Pharmacol. Biochem. Behav. 15, 435–442.
Yamamoto, C., Nagai, H., Takahashi, K., Nakagawa, S., Yamaguchi, M., Tonoike, M., and Yamamoto, T. 2006. Cortical representation of taste modifying action of miracle fruit in humans. Neuroimage 33, 1145–1151.
Yamamoto, C., Takehara, S., Morikawa, K., Nakagawa, S., Yamaguchi, M., Iwaki, S., Tonoike, M., and Yamamoto, T. 2003. Magenetoencephalographic study of cortical activity evoked by electrogustatory stimuli. Chem. Senses 28, 245–251.
Yamamoto, T. 2007. Brain regions responsible for the expression of conditioned taste aversion in rats. Chem. Senses 32, 105–109.
Yamamoto, T. and Kawamura, Y. 1977. Responses of the submandibular secretory nerve to taste stimuli. Brain Res. 130, 152–155.
Yamamoto, T., Fujimoto, Y., Shimura, T., and Sakai, N. 1995. Conditioned taste aversion in rats with excitotoxic brain lesions. Neurosci. Res. 22, 31–49.
Yamamoto, T., Matsuo, R., Ichikawa, H., Wakisaka, S., Akai, M., Imai, Y., Yonehara, N., and Inoki, R. 1990. Aversive taste stimuli increase CGRP levels in the gustatory insular cortex of the rat. Neurosci. Lett. 112, 167–172.
Yamamoto, T., Matsuo, R., Kiyomitsu, Y., and Kitamura, R. 1988. Sensory inputs from the oral region to the cerebral cortex in behaving rats: An analysis of unit responses in cortical somatosensory and taste areas during ingestive behavior. J. Neurophysiol. 60, 1303–1321.
Yamamoto, T., Matsuo, R., Kiyomitsu, Y., and Kitamura, R. 1989a. Taste responses of cortical neurons in freely ingesting rats. J. Neurophysiol. 61, 1244–1258.
Yamamoto, T., Matsuo, R., Kiyomitsu, Y., and Kitamura, R. 1989b. Response properties of lateral hypothalamic neurons during ingestive behavior with special reference to licking of various taste solutions. Brain Res. 481, 286–297.
Yamamoto, T., Nagai, T., Shimura, T., and Yasoshima, Y. 1998. Roles of chemical mediators in the taste system. Jpn. J. Pharmacol. 76, 325–348.
Yamamoto, T., Sako, N., and Maeda, S. 2000. Effects of taste stimulation on β-endorphin levels in rat cerebrospinal fluid and plasma. Physiol. Behav. 69, 345–350.
Yamamoto, T., Shimura, T., Sakai, N., and Ozaki, N. 1994a. Representation of hedonics and quality of taste stimuli in the parabrachial nucleus of the rat. Physiol. Behav. 56, 1197–1202.
Yamamoto, T., Shimura, T., Sako, N., Yasoshima, Y., and Sakai, N. 1994b. Neural substrates for conditioned taste aversion in the rat. Behav. Brain Res. 65, 123–137.
Yamamoto, T., Yuyama, N., Kato, T., and Kawamura, Y. 1985a. Gustatory responses of cortical neurons in rats. II. Information processing of taste quality. J. Neurophysiol. 53, 1356–1369.
Yamamoto, T., Yuyama, N., Kato, T., and Kawamura, Y. 1985b. Gustatory responses of cortical neurons in rats. III. Neural and behavioral measures compared. J. Neurophysiol. 53, 1370–1386.
Yasoshima, Y. and Yamamoto, T. 1998. Short-term and long-term excitability changes of the insular cortical neurons after the acquisition of taste aversion learning in behaving rats. Neuroscience 284, 1–5.
Yasoshima, Y., Scott, T. R., and Yamamoto, T. 2006. Memory-dependent c-Fos expression in the nucleus accumbens and extended amygdala following the expression of a conditioned taste aversive in the rat. Neuroscience 141, 35–45.
Yoshimura, H., Sugai, T., Segami, N., and Onoda, N. 2005. Chemotopic arrangement for taste quality discrimination in the cortical taste area. Chem. Senses 30, i164–i165.
Zald, D. H. and Pardo, J. V. 1997. Emotion, olfaction, and the human amygdala: Amygdala activation during aversive olfactory stimulation. Proc. Natl. Acad. Sci. U. S. A. 94, 4119–4124.
Zald, D. H., Hagen, M. C., and Pardo, J. V. 2002. Neural correlates of tasting concentrated quinine and sugar solutions. J. Neurophysiol. 87, 1068–1075.

Zald, D. H., Lee, J. T., Fluegel, K. W., and Pardo, J. V. 1998. Aversive gustatory stimulation activates limbic circuits in humans. Brain 121, 1143–1154.
Zhang, M. and Kelley, A. E. 1997. Opiate agonists microinjected into the nucleus accumbens enhance sucrose drinking in rats. Psychopharmacology (Berl.) 132, 350–360.
Zhang, M. and Kelley, A. E. 2000. Enhanced intake of high-fat food following striatal mu-opioid stimulation: microinjection mapping and fos expression. Neuroscience 99, 267–277.
Zhang, M. and Kelley, A. E. 2002. Intake of saccharin, salt, and ethanol solutions is increased by infusion of a mu opioid agonist into the nucleus accumbens. Psychopharmacology (Berl.) 159, 415–423.
Zhang, M., Gosnell, B. A., and Kelley, A. E. 1998. Intake of high-fat food is selectively enhanced by mu opioid receptor stimulation within the nucleus accumbens. J. Pharmacol. Exp. Ther. 285, 908–914.

Further Reading

Ikuno, H. and Sakaguchi, T. 1990. Gastric vagal functional distribution in the secretion of gastric acid produced by sweet taste. Brain Res. Bull. 25, 429–431.
Yamamoto, T. 1994. A Neural Model for Taste Aversion Learning. In: Olfaction and Taste XI (*eds*. K. Kurihara, N. Suzuki, and H, Ogawa), pp. 471–474. Springer.

Relevant Website

http://www.ctalearning.com – A. L. Riley and K. B. Freeman. Conditioned Taste Aversion: An Annotated Bibliography.

4.25 Dopamine Release by Sucrose

A Hajnal and R Norgren, Milton S. Hershey Medical Center, Hershey, PA, USA

© 2008 Elsevier Inc. All rights reserved.

4.25.1	Ingestive Behavior and Reward	459
4.25.2	Dopamine and Reward	459
4.25.3	Dopamine and Sucrose Preference	460
4.25.4	Central Pathways of Sucrose Reward	462
4.25.5	Chronic Effects of Sucrose Ingestion	463
4.25.6	Sucrose Reward without Dopamine	463
4.25.7	Summary	464
References		464

4.25.1 Ingestive Behavior and Reward

Sucrose is a prototypical reward in animal behavior studies. It is a simple compound, can be delivered easily in water, and sustains reliable performance without food or water restriction. Under ordinary circumstances, humans report sucrose as sweet and pleasurable. The generality of this experience allows scientists to infer that similar subjective events occur in other animals. In behavioral terms, reward is defined operationally as an event – a stimulus – that increases the probability of a contiguous response being emitted again (Thorndike, E., 1911). When studying the neural bases for reward, however, operational definitions are less satisfactory because the goal is to understand the so-called intervening variable, that is, what humans term pleasure.

The normal behavioral response to sucrose is ingestion. It is organized in the caudal brainstem because the entire sequence appears in anencephalic infants and chronically decerebrate rats neither of which have functional forebrains (Steiner, J. E., 1973; Grill, H. J. and Norgren, R., 1978a). In decerebrate rats, ingestion and rejection are near normal but largely stimulus bound (Grill, H. J. and Norgren, R., 1978b). Although short-term plasticity can occur, behavior in decerebrates cannot be altered permanently by experience (Grigson, P. S. *et al.*, 1997). The forebrain is necessary for learning and memory to influence consummatory behavior. This influence can be manifested in the consummatory behavior itself, such as with a learned preference or aversion (Sclafani, A., 1997). More frequently, the influence of learning appears in the appetitive phase, as when a deprived animal returns to a place where it had previously encountered food (Craig, W., 1918). Thus, the forebrain is necessary for the full expression of the motivation and reward systems that activate and direct the appetitive behavior needed to bring the animal into contact with the consummatory stimuli (Norgren, R. *et al.*, 2003).

In short, the neural circuits needed for discriminative ingestion and rejection behavior are complete in the brainstem. The systems that animate adaptive behavior in the real world – learning, memory, motivation, and reward – require the forebrain. Therefore, in order to investigate the neural basis for sucrose reward, we must identify an index for this function that depends on the forebrain and is not directly related to behavior. Although far from perfect, the best candidate available is dopamine release, specifically in the nucleus accumbens (NAcc; Ikemoto, S. and Panksepp, J., 1999; Wise, R. A., 2005).

4.25.2 Dopamine and Reward

The neural substrate for reward remains a challenge because the concept itself is illusive. Despite this limitation, extensive research has been devoted to the neural bases of reward. As a result, a network of nuclei and neurotransmitters has been identified that influence reward functions, even if the nature of that influence is far from settled. Among the most studied of these putative reward substrates is the mesolimbic or mesoaccumbens dopamine system. Experimental manipulations of this system disrupt behavior guided by both natural and non-natural rewards (Smith, G. P., 1995; Wise, R. A., 2002). Conversely, both natural and drug rewards activate this pathway (Smith, G. P., 1995; Wise, R. A., 2002; 2005) which originates from the

ventral tegmental area (VTA) of the brainstem (Oades, R. D. and Halliday, G. M., 1987). Although its role in reward is debated (Berridge, K. C. and Robinson, T. E., 1998; Cannon, C. M. and Palmiter, R. D., 2003), no one denies that dopamine release occurs in the mesoaccumbens dopamine system when normally preferred stimuli are presented to an animal. The contention arises over interpreting the significance of the release. Does it signify a broader phenomenon, such as arousal, attention, learning, or reward, or a more restricted category, such as uncertainty, novelty, expected value, or incentive (Di Chiara, G., 1998; Ikemoto, S. and Panksepp, J., 1999; Salamone, J. D. *et al.*, 2003; Schultz, W., 2005; Wise, R. A., 2005)? In what follows, and particularly in our own work, we assume only that dopamine release tracks the incentive valence of reward, that it provides a forebrain index of sensory events that the animal will work to obtain.

The presentation or even the anticipation of food stimulates dopamine neurons in the VTA and dopamine release preferentially in the shell of the NAcc (Church, W. H. *et al.*, 1987; Hernandez, L. and Hoebel, B. G., 1988a; 1988b; Radhakishun, F. S. *et al.*, 1988; Yoshida, M. *et al.*, 1992; Inoue, K. *et al.*, 1993; Westerink, B. H. *et al.*, 1994; Wilson, C. *et al.*, 1995). In addition to the NAcc, food intake results in dopamine release in other terminal regions of the VTA projections such in the prefrontal cortex (Hernandez, L. and Hoebel, B. G., 1990; Feenstra, M. G. and Botterblom, M. H., 1996) and the central nucleus of the amygdala (Hajnal, A. and Lenard, L., 1997). Although imaging methods have been useful, primarily in human studies (Wang, G. J. *et al.*, 2002; McClure, S. M. *et al.*, 2004; Rolls, E. T., 2005), the majority of available data derive from *in vivo* microdialysis studies, a method that permits direct measurement of central dopamine release and metabolism during behavior (Hoebel, B. G. *et al.*, 1989; Westerink, B. H., 1995). Dialysis typically requires 5–20 min samples to detect significant changes in dopamine flux. Advances in voltammetry have decreased the detection threshold during ingestive behavior into the millisecond range (Kiyatkin, E. A. and Gratton, A., 1994; Roitman, M. F. *et al.*, 2004).

4.25.3 Dopamine and Sucrose Preference

During ingestion dopamine release in the NAcc is a function of the oral stimulus, previous experience, and motivational state (Bassareo, V. and Di Chiara, G., 1997; 1999; Norgren, R. *et al.*, 2003; Smith, G. P., 2004). Most relevant feeding experiments were performed under deprivation condition that by itself augments the incentive value of external stimuli (Carr, K. D., 1996; Pothos, E. N., 2001). Deprivation also prevents habituation of accumbens dopamine release (i.e., latent inhibition) after repeated exposure to ingestive stimuli (Bassareo, V. and Di Chiara, G., 1999). Nevertheless, rats fed *ad libitum* on standard food still exhibit an increase of NAcc dopamine when given a more preferred diet (Ahn, S. and Phillips, A. G., 1999; Cenci, M. A. *et al.*, 1992; Mitchell, J. B. and Gratton, A., 1992; Wilson, C. *et al.*, 1995). In fact, highly preferred food itself reliably elicits an increase in the extracellular dopamine in the NAcc (Mark, G. P. *et al.*, 1991; Mitchell, J. B. and Gratton, A., 1992; Hajnal, A. and Norgren, R., 2001) and also increases somatodendritic dopamine release in the VTA, where the mesoaccumbens pathway originates (Zhang, H. *et al.*, 1994). Moreover, repeated access to palatable sucrose solution consistently results in dopamine release in the NAcc over several days (Hajnal, A. and Norgren, R., 2001; 2002; Rada, P. *et al.*, 2005), an effect that can be reproduced even when the postabsorptive effects are eliminated using sham feeding preparation (Hajnal, A. *et al.*, 2004a). This observation supports the notion that dopamine tracks the hedonic value of an (oro)sensory stimulus.

Another indication that dopamine influences feeding behavior in general and sucrose preference in particular comes from studies that interfere with the postsynaptic receptors for this neurotransmitter. Systemic injection of D1 and D2 dopamine receptor antagonists reduced both real and sham feeding of sucrose (Geary, N. and Smith, G. P., 1985; Smith, G. P. and Schneider, L. H., 1988; Schneider, L. H., 1989; Cooper, S. J. *et al.*, 1993; Duong, A. and Weingarten, H. P., 1993; Hsiao, S. and Smith, G. P., 1995). Learned preference for sucrose also is decreased with administration of dopamine receptor antagonists (Yu, W. Z. *et al.*, 2000a; 2000b). Furthermore, dopamine-deficient (DD) mice can eat but are not motivated to do so (Szczypka, M. S. *et al.*, 1999b), suggesting that DD mice are unable to integrate and process the neuronal signals necessary to stimulate and maintain feeding. In fact, dopamine replacement re-establishes preference for sucrose in DD mice (Szczypka, M. S. *et al.*, 1999a). Lesions to the VTA also have been shown to reduce sucrose preference (Shimura, T. *et al.*, 2002). These studies demonstrate that dopamine and its receptors are important for initiating and maintaining sucrose

ingestion, but they do not reveal where in the brain (or the body) these actions take place.

The opposite relationship, that is, that sucrose intake can be increased by pharmacological manipulation, provides more specific information. In this case, nomifensine, a blocker of dopamine uptake, infused into the accumbens by reverse microdialysis increased dopamine in the accumbens and increased sucrose intake (Hajnal, A. and Norgren, R., 2001). Although nomifensine also affects other monoamine transporters, low doses of the dopamine receptor antagonists SCH 23390 and sulpiride dialyzed together with the reuptake blocker into the accumbens abolished both the increased dopamine and the increased sucrose licking (Hajnal, A. and Norgren, R., 2001).

Less specific evidence for accumbens dopamine modulating reward arises from the cross-sensitization effects of sucrose and the indirect dopamine agonist amphetamine. Compared with NaCl-treated controls, rats previously sensitized to amphetamine increased their locomotor activity after brief access to sucrose (Avena, N. M. and Hoebel, B. G., 2003a). Similarly, rats receiving restricted sucrose access exhibited higher locomotor activity when subsequently injected with amphetamine (Avena, N. M. and Hoebel, B. G., 2003b; Hajnal, A. *et al.*, 2004b). In addition, rats that spontaneously ingested more sucrose showed increased amphetamine-induced dopamine overflow in the caudal NAcc relative to those that licked less sucrose (Sills, T. L. and Vaccarino, F. J., 1996). These studies imply a reciprocal relationship between dopamine flux and ingestion of sucrose. Dopamine tracks sucrose intake even if the causal direction is less obvious.

Direct measures of accumbens dopamine during sucrose ingestion are surprisingly scarce. Oddly, indirect measures are the norm. In these experiments, accumbens dopamine is more often measured using a conditioned stimulus that was paired with sucrose or some other normally preferred chemical such as saccharin. In naive rats licking a saccharin solution causes an increase in accumbens dopamine, measured with microdialysis (Mark, G. P. *et al.*, 1991; Grigson, P. S. *et al.*, 2004). Fructose has similar effects in rats (Hajnal, A., personal communication). Both saccharin and fructose taste sweet to humans, are preferred by rats (Sclafani, A. and Nissenbaum, J. W., 1985; Sclafani, A. and Mann, S., 1987; Sclafani, A. *et al.*, 1998), and exert reinforcing effects when used as conditioned stimuli (Sclafani, A. and Ackroff, K., 1994). Microdialysis experiments with unconditioned sucrose, however, have been done only recently in our laboratory.

In the first experiment, we established the effect of sucrose ingestion on dopamine in the NAcc. Rats were placed on a 16 h water deprivation schedule and trained to lick either water or 0.3 M sucrose for 20 min each morning for about 1 week. Then the microdialysis probes were inserted into the caudomedial NAcc and left in place for 3 days. The fluid access schedule was continued as before, that is, each rat had access to water and sucrose at least once. Although deprived overnight (~18 h), ingesting water failed to alter dopamine levels. Licking 0.3 M sucrose for 20 min, however, produced a 300% increase in dopamine overflow in the NAcc (Hajnal, A. and Norgren, R., 2001). The effect was impressive, but linking it directly to the reward value of sucrose was not that straightforward. The rats ingested considerably more sucrose solution than water and, even in 20 min, the sucrose would have produced metabolic feedback to which the brain was sensible. To control for these possibly confounding effects, we did two further experiments using essentially the same paradigm.

First, we trained rats to sham feed sucrose – the rats lick normally from a spout, but the fluid drains from a chronic gastric fistula. Then they were allowed to sham lick three different concentrations of sucrose, while accumbens dopamine release was assessed by microdialysis. Even without significant metabolic consequences, accumbens dopamine increased as a function of sucrose concentration. In a third set of rats, we again varied concentration, but clamped total intake during the 20 min sampling period to 75% of what each rat normally ingested of the weakest solution. Even with ingested volume controlled, accumbens dopamine release rose as a function of increasing sucrose concentration (Hajnal, A. *et al.*, 2004a). If we operationally define hedonic value by relative preference, then sucrose reward varies directly with its concentration because, in brief access tests, rats prefer stronger solutions to weaker ones (Davis, J. D., 1973; Spector, A. C. *et al.*, 1993; Contreras, R. J. *et al.*, 1995). Because accumbens dopamine release also varies directly with sucrose concentration, we can take these values as a forebrain index of gustatory reward. Although the exact relationship between dopamine and reward remains undetermined, this effect is sufficient to propose NAcc dopamine as a tool to track capacity of taste stimuli to engage motivational systems.

4.25.4 Central Pathways of Sucrose Reward

Intraoral intake of sucrose increases dopamine in the nucleus of the solitary tract (Bednar, I. *et al.*, 1994), the first central relay of the gustatory system (Lundy, R. F., Jr. and Norgren, R., 2004b). The NAcc receives axonal projections from the caudal part of the nucleus of the solitary tract, but the taste neurons are in the rostral half of the nucleus (Zagon, A. *et al.*, 1994). The accumbens also sends reciprocal projections to the nucleus of the solitary tract (Brog, J. S. *et al.*, 1993; Stratford, T. R. and Kelley, A. E., 1999) via a circuit that includes the parabrachial nucleus (PBN; Usuda, I. *et al.*, 1998). Given its distribution, the involvement of this direct loop in gustatory functions is conceivable, but unlikely. In rodents, the major rostral projection of gustatory neurons is from the anterior aspect of the nucleus of the solitary tract to the caudomedial PBN. From the PBN, the central gustatory system bifurcates, one arm forming a standard thalamocortical axis, the other distributing widely in the limbic forebrain (Lundy, R. F., Jr. and Norgren, R., 2004a). The PBN, which includes the second central gustatory relay, projects densely to the central nucleus of the amygdala, the lateral hypothalamus, and the bed nucleus of the stria terminalis (Norgren, R., 1976; 1978), all of which send axons to the NAcc shell (Kirouac, G. J. and Ganguly, P. K., 1995). The thalamocortical gustatory system can also reach NAcc via substantial connections to the central nucleus of the amygdala, lateral hypothalamus, and the prefrontal cortex (Kosar, E. *et al.*, 1986; Shi, C. J. and Cassell, M. D., 1998; Lundy, R. F., Jr. and Norgren, R., 2004b).

Because all these areas figure prominently in theories of motivation and reward, we decided to determine which forebrain taste pathway supported the release of dopamine in the NAcc during sucrose licking (Pfaffmann, C. *et al.*, 1977). After bilateral lesions of the thalamic taste relay, the accumbens dopamine response during sucrose ingestion was identical to that of sham-operated controls. After similar damage in the PBN, sucrose licking elicited less than one-third of the NAcc dopamine as the controls (Figure 1; Hajnal, A. and Norgren, R., 2005).

We performed another, similar experiment using immunohistochemical staining of Fos, the nuclear phosphoprotein product of the early-immediate gene c-Fos (Mungardee, S. S. *et al.*, 2004). After having similar, bilateral lesions the PBN or the thalamic

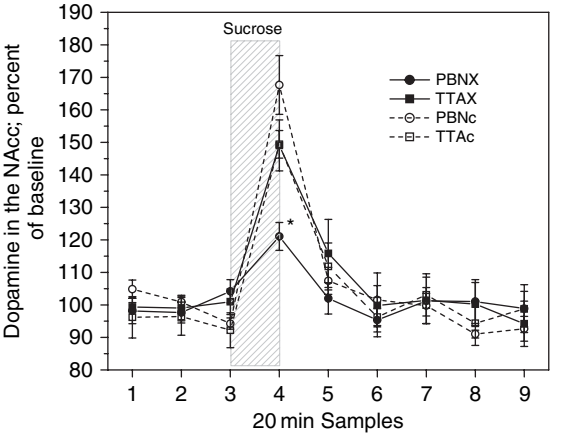

Figure 1 Extracellular levels of dopamine in the nucleus accumbens (NAcc), expressed as a percentage of mean baseline (± standard error of the mean) before, during, and after a 20 min presentation of 0.3 M sucrose (bracket). The rats received ibotenic-acid microlesions in the parabrachial nucleus PBN (PBNX), the thalamic taste area (TTAX), or control surgeries using physiological NaCl injections to the same areas (PBNc, TTAc). Asterisk denotes statistically significant difference based on *post hoc* comparisons between groups ($^{*}P < 0.01$). Adapted from Hajnal, A. and Norgren, R. (2005) Taste pathways that mediate accumbens dopamine release by sapid sucrose. Physiol. Behav. 84, 363–369, with permission from Elsevier.

taste relay, rats were allowed to sham-feed sucrose or water for 1 h. Their brains were then cut and stained for the Fos protein. In the controls and the rats that received thalamic lesions (Figure 2), sham-licking sucrose produced more Fos in the shell of the NAcc than did ingestion of water. In contrast, lesions of the gustatory PBN reduced the overall level of Fos staining and eliminated the differential effect of licking sucrose (Figure 2). These complimentary data represent the first demonstration that the affective character of a sensory stimulus might separate from the thalamocortical stream as early as the second central synapse.

Knowing the pathways through which a normally preferred taste influences a forebrain index of reward says little about the sensory signal that elicits the effect. Sucrose appears to be inherently rewarding. Nevertheless, a full gastrointestinal tract can reduce sugar intake to near zero, implying that the sensory signal no longer is preferred. Conversely, during a negative sodium balance, a normally rejected 0.5 M NaCl solution is avidly consumed. In fact, for most stimuli, reward value is imposed either through learning or through the physiological state of the animal. This could be accomplished by altering the

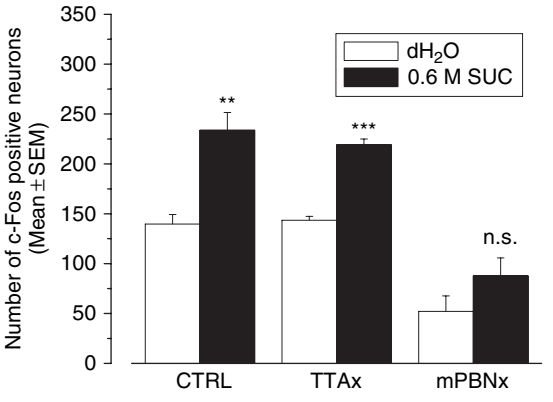

Figure 2 Number of c-Fos positive neurons in the shell of the nucleus accumbens after ibotenic acid microlesions to the thalamic taste area (TTAx) or the medial PBN (mPBNx) in rats exposed to sham drinking of 0.6 M sucrose (SUC) or water (dH_2O). Asterisks denote results from *post hoc* analysis (**, $P < 0.01$; ***, $P < 0.001$; n.s., not significant; SEM, standard error of the mean).

sensory message itself, before it engages the motivation and reward systems, by gating the message within those systems, or both.

We have examined the former proposition because the convergence of visceral afferent, gustatory, and forebrain centrifugal systems in the brainstem relays provides the anatomical framework for such an interaction. Alterations in the response properties of taste neurons in the nucleus of the solitary tract and in the PBN are coincident with behavioral changes in hedonic value (Norgren, R. *et al.*, 2003). For instance, intraduodenal lipid infusions, which reduces intake of sucrose (Foster, L. A. *et al.*, 1996), also decreased the response of PBN sucrose-best cells to sucrose by 55%, but was without effect on sucrose-evoked responses in other cell types (Hajnal, A. *et al.*, 1999). Similar if less specific modulation of taste processing also can be produced by inducing a negative sodium balance or by activating descending projections from reciprocally connected forebrain regions such as the lateral hypothalamus, central amygdala, and the gustatory cortex (Contreras, R. J., 1977; Nakamura, K. and Norgren, R., 1995; Lundy, R. F., Jr. and Norgren, R., 2001; Cho, Y. K. *et al.*, 2002; 2003; Tamura, R. and Norgren, R., 2003; Lundy, R. F., Jr. and Norgren, R., 2004a; Li, C. S. *et al.*, 2005). These observations demonstrate that both physiological and forebrain modulation occur before gustatory neural gustatory activity reaches the mesoaccumbens dopamine system. Whether or not this modulation influences the capacity of tastes to release dopamine, much less their hedonic tone, remains to be determined.

4.25.5 Chronic Effects of Sucrose Ingestion

So far we have discussed only the acute effects of oral sucrose stimulation. In addition to short-term dopamine activation, ingestion of preferred foods, such as glucose or sucrose may result in a lasting neuroadaptation within the mesoaccumbens dopamine system (Colantuoni, C. *et al.*, 2001; Avena, N. M. and Hoebel, B. G., 2003b). We observed that, after as few as 6 days, scheduled, daily, 20 min access to 0.3 M sucrose results in upregulation of the dopamine membrane transporter and downregulation of the D2 dopamine receptors (Bello, N. T. *et al.*, 2002; 2003). Although the function of this neuroadaptation is not clear, accumulating evidence supports the hypothesis that dopamine plays an important role metabolic regulation and energy balance, including in human obesity (Figlewicz, D. P. *et al.*, 1994; 1996; 1998; Patterson, T. A. *et al.*, 1998; Wang, J. *et al.*, 2001; Wang, G. J. *et al.*, 2002; Wang, J. *et al.*, 2002). Chronic food restriction reduces basal dopamine levels in rats and increases consummatory responses to both food and drug rewards (Pothos, E. N. *et al.*, 1995). Similar manipulations also increase bingeing on palatable meals (Hagan, M. M. and Moss, D. E., 1997). Finally, we demonstrated that blocking dopamine reuptake in NAcc of deprived rats accentuates sucrose intake (Hajnal, A. and Norgren, R., 2001). Taken together, these data indicate that dopamine and the NAcc contribute to the control of feeding behavior in part through influencing preference.

4.25.6 Sucrose Reward without Dopamine

It is important to remember that we use accumbens dopamine flux as an index of reward, not as its equivalent. The most dramatic proof of this distinction comes from genetically engineered mice that never produce dopamine, but exhibit near normal sucrose preferences (Cannon, C. M. and Palmiter, R. D., 2003). Opioids are clearly involved with affective responses and, within the NAcc, they may be responsible for the hedonic modulation of taste information (Kelley, A. E. *et al.*, 2002). Opioid antagonists reduce intake of palatable foods in real (Cooper, S. J.,

1982; 1983; Cooper, S. J. *et al.*, 1985; Lynch, W. C., 1986) and sham feeding (Kirkham, T. C. and Cooper, S. J., 1988; Kirkham, T. C., 1990). They also decrease oral motor responses to sucrose in the taste reactivity test (Parker, L. A. *et al.*, 1992). Conversely, when given intermittent access to sugar solutions, rats exhibit increased binding of μ-1 opioid receptors in the NAcc (Colantuoni, C. *et al.*, 2001). Similar evidence exists for serotonin, neuropeptide Y, cholecystokinin, leptin, and acetylcholine, among others (Waldbillig, R. J. and Bartness, T. J., 1982; Gosnell, B. A. and Hsiao, S., 1984; Montgomery, A. M. and Burton, M. J., 1986; Leibowitz, S. F. *et al.*, 1992; Eckel, L. A. and Ossenkopp, K. P., 1994; De Jonghe, B. C. *et al.*, 2005; Hajnal, A. *et al.*, 2005; Kelley, A. E. *et al.*, 2005). All of these factors ultimately may affect the activation of the mesoaccumbens dopamine system, but the relationships are not simple.

Even if the final common path for all these other neurotransmitters does include dopamine, many of them also influence the code for gustatory afferent activity more directly, even at the level of the taste buds. Specifically, neuropeptide Y, cholecystokinin, acetylcholine, and serotonin receptors all have been identified on taste receptor cells (Herness, S. and Chen, Y., 1997; Herness, S. *et al.*, 2002; Huang, Y. J. *et al.*, 2005; Ogura, T. and Lin, W., 2005; Zhao, F. L. *et al.*, 2005). Insulin and leptin receptors also occur on taste receptor cells (Shigemura, N. *et al.*, 2003; Suzuki, Y. *et al.*, 2005). In fact, leptin receptors occur exclusively on sweet taste receptor cells. The exaggerated sweet preference seen in some obese animal models might be related to a malfunction in these leptin receptors (Kawai, K. *et al.*, 2000; Ninomiya, Y. *et al.*, 2002; Shigemura, N. *et al.*, 2004). In normal mice, administration of leptin suppresses single fiber responses in the chorda tympani and glossopharyngeal nerves to sucrose and saccharin but not to other stimuli (Kawai, K. *et al.*, 2000). These direct peripheral effects on the taste system illustrate the multiple systems that can influence gustatory coding. All of these neurotransmitters and peptides play important parts in the control of ingestive behavior and energy balance. Thus, they are obvious candidates for mediating the hedonic tone of taste whose biologic role is to arbitrate ingestion and rejection behavior.

4.25.7 Summary

Sucrose ingestion releases dopamine within the NAcc. This response is concentration dependent, but does not require gastrointestinal or metabolic feedback. This central response arises from the oral gustatory properties of sucrose. Specifically, the accumbens response appears to reflect the hedonic character of sweet stimuli in general. When saccharin is made aversive by association with visceral malaise, this stimulus switches from increasing extracellular dopamine to inhibiting its release (Mark, G. P. *et al.*, 1991). While sucrose licking does increase dopamine release, the obverse also is true. Increasing dopamine availability in the NAcc increases intake of sucrose solutions and blocking D1 dopamine receptors inhibits it (Hajnal, A. and Norgren, R., 2001).

Despite these close relationships, a direct causal link between taste and reward in the accumbens is unlikely. Sucrose intake is not compromised by dopaminergic lesions and is near normal in dopamine knockout mice. Thus, dopamine activation is related to the orosensory properties of sucrose and probably to its hedonic value, but that increase is not the equivalent of sucrose reward. In fact, accumbens dopamine may not be necessary for the expression of sucrose preference, but it does track the hedonic value underlying the behavior. If true, this assertion does not apply just to sucrose or even to gustatory stimuli but probably to rewards in general (Wightman, R. M. and Robinson, D. L., 2002). Normal biological rewards are elicited by external events, consummatory stimuli, of which sucrose is a prime exemplar (Craig, W., 1918). The reward value, however, is not determined by the stimulus, but depends on the immediate and remembered circumstances of the animal. The hedonic valence is then added to the afferent sensory neural activity resulting from the stimulus somewhere between the peripheral receptors and behavior. Determining how this comes about remains a central goal of neuroscience.

References

Ahn, S. and Phillips, A. G. 1999. Dopaminergic correlates of sensory-specific satiety in the medial prefrontal cortex and nucleus accumbens of the rat. J. Neurosci. 19, RC29.

Avena, N. M. and Hoebel, B. G. 2003a. A diet promoting sugar dependency causes behavioral cross-sensitization to a low dose of amphetamine. Neuroscience 122, 17–20.

Avena, N. M. and Hoebel, B. G. 2003b. Amphetamine-sensitized rats show sugar-induced hyperactivity (cross-sensitization) and sugar hyperphagia. Pharmacol. Biochem. Behav. 74, 635–639.

Bassareo, V. and Di Chiara, G. 1997. Differential influence of associative and nonassociative learning mechanisms on the responsiveness of prefrontal and accumbal dopamine

transmission to food stimuli in rats fed *ad libitum*. J. Neurosci. 17, 851–861.
Bassareo, V. and Di Chiara, G. 1999. Modulation of feeding-induced activation of mesolimbic dopamine transmission by appetitive stimuli and its relation to motivational state. Eur. J. Neurosci. 11, 4389–4397.
Bednar, I., Qian, M., Qureshi, G. A., Kallstrom, L., Johnson, A. E., Carrer, H., and Sodersten, P. 1994. Glutamate inhibits ingestive behaviour. J. Neuroendocrinol. 6, 403–408.
Bello, N. T., Lucas, L. R., and Hajnal, A. 2002. Repeated sucrose access influences dopamine D2 receptor density in the striatum. Neuroreport 13, 1575–1578.
Bello, N. T., Sweigart, K. L., Lakoski, J. M., Norgren, R., and Hajnal, A. 2003. Restricted feeding with scheduled sucrose access results in an upregulation of the rat dopamine transporter. Am. J. Physiol. Regul. Integr. Comp. Physiol. 284, R1260–R1268.
Berridge, K. C. and Robinson, T. E. 1998. What is the role of dopamine in reward: hedonic impact, reward learning, or incentive salience? Brain Res. Brain Res. Rev. 28, 309–369.
Brog, J. S., Salyapongse, A., Deutch, A. Y., and Zahm, D. S. 1993. The patterns of afferent innervation of the core and shell in the ''accumbens'' part of the rat ventral striatum: immunohistochemical detection of retrogradely transported fluoro-gold. J. Comp. Neurol. 338, 255–278.
Cannon, C. M. and Palmiter, R. D. 2003. Reward without dopamine. J. Neurosci. 23, 10827–10831.
Carr, K. D. 1996. Feeding, drug abuse, and the sensitization of reward by metabolic need. Neurochem. Res. 21, 1455–1467.
Cenci, M. A., Kalen, P., Mandel, R. J., and Bjorklund, A. 1992. Regional differences in the regulation of dopamine and noradrenaline release in medial frontal cortex, nucleus accumbens and caudate-putamen: a microdialysis study in the rat. Brain Res. 581, 217–228.
Cho, Y. K., Li, C. S., and Smith, D. V. 2002. Taste responses of neurons of the hamster solitary nucleus are enhanced by lateral hypothalamic stimulation. J. Neurophysiol. 87, 1981–1992.
Cho, Y. K., Li, C. S., and Smith, D. V. 2003. Descending influences from the lateral hypothalamus and amygdala converge onto medullary taste neurons. Chem. Senses 28, 155–171.
Church, W. H., Justice, J. B., Jr., and Neill, D. B. 1987. Detecting behaviorally relevant changes in extracellular dopamine with microdialysis. Brain Res. 412, 397–399.
Colantuoni, C., Schwenker, J., McCarthy, J., Rada, P., Ladenheim, B., Cadet, J. L., Schwartz, G. J., Moran, T. H., and Hoebel, B. G. 2001. Excessive sugar intake alters binding to dopamine and mu-opioid receptors in the brain. Neuroreport 12, 3549–3552.
Contreras, R. J. 1977. Changes in gustatory nerve discharges with sodium deficiency: a single unit analysis. Brain Res. 121, 373–378.
Contreras, R. J., Carson, C. A., and Pierce, C. E. 1995. A novel psychophysical procedure for bitter taste assessment in rats. Chem. Senses 20, 305–312.
Cooper, S. J. 1982. Palatability-induced drinking after administration of morphine, naltrexone and diazepam in the non-deprived rat. Subst. Alcohol Actions Misuse 3, 259–266.
Cooper, S. J. 1983. Effects of opiate agonists and antagonists on fluid intake and saccharin choice in the rat. Neuropharmacology 22, 323–328.
Cooper, S. J., Francis, J., and Barber, D. J. 1993. Selective dopamine D-1 receptor agonists, SK&F 38393 and CY 208-243 reduce sucrose sham-feeding in the rat. Neuropharmacology 32, 101–102.
Cooper, S. J., Jackson, A., Morgan, R., and Carter, R. 1985. Evidence for opiate receptor involvement in the consumption of a high palatability diet in nondeprived rats. Neuropeptides 5, 345–348.
Craig, W. 1918. Appetites and aversions as constituents of instincts. Biol. Bull. 91–107.
Davis, J. D. 1973. The effectiveness of some sugars in stimulating licking behavior in the rat. Physiol. Behav. 11, 39–45.
De Jonghe, B. C., Hajnal, A., and Covasa, M. 2005. Increased oral and decreased intestinal sensitivity to sucrose in obese, prediabetic CCK-A receptor-deficient OLETF rats. Am. J. Physiol. Regul. Integr. Comp. Physiol. 288, R292–R300.
Di Chiara, G. 1998. A motivational learning hypothesis of the role of mesolimbic dopamine in compulsive drug use. J. Psychopharmacol. 12, 54–67.
Duong, A. and Weingarten, H. P. 1993. Dopamine antagonists act on central, but not peripheral, receptors to inhibit sham and real feeding. Physiol. Behav. 54, 449–454.
Eckel, L. A. and Ossenkopp, K. P. 1994. Cholecystokinin reduces sucrose palatability in rats: evidence in support of a satiety effect. Am. J. Physiol. 267, R1496–R1502.
Feenstra, M. G. and Botterblom, M. H. 1996. Rapid sampling of extracellular dopamine in the rat prefrontal cortex during food consumption, handling and exposure to novelty. Brain Res. 742, 17–24.
Figlewicz, D. P., Brot, M. D., McCall, A. L., and Szot, P. 1996. Diabetes causes differential changes in CNS noradrenergic and dopaminergic neurons in the rat: a molecular study. Brain Res. 736, 54–60.
Figlewicz, D. P., Patterson, T. A., Johnson, L. B., Zavosh, A., Israel, P. A., and Szot, P. 1998. Dopamine transporter mRNA is increased in the CNS of Zucker fatty (fa/fa) rats. Brain Res. Bull. 46, 199–202.
Figlewicz, D. P., Szot, P., Chavez, M., Woods, S. C., and Veith, R. C. 1994. Intraventricular insulin increases dopamine transporter mRNA in rat VTA/substantia nigra. Brain Res. 644, 331–334.
Foster, L. A., Nakamura, K., Greenberg, D., and Norgren, R. 1996. Intestinal fat differentially suppresses sham feeding of different gustatory stimuli. Am. J. Physiol. 270, R1122–R1125.
Geary, N. and Smith, G. P. 1985. Pimozide decreases the positive reinforcing effect of sham fed sucrose in the rat. Pharmacol. Biochem. Behav. 22, 787–790.
Gosnell, B. A. and Hsiao, S. 1984. Effects of cholecystokinin on taste preference and sensitivity in rats. Behav. Neurosci. 98, 452–460.
Grigson, P. S., Acharya, N. K., and Hajnal, A. 2004. A single saccharin-morphine pairings leads to a conditioned reduction in CS intake and accumbens dopamine. Program No. 119.17, 2004 Abstract Viewer/Itinerary Planner. Society for Neuroscience (online).
Grigson, P. S., Kaplan, J. M., Roitman, M. F., Norgren, R., and Grill, H. J. 1997. Reward comparison in chronic decerebrate rats. Am. J. Physiol. 273, R479–R486.
Grill, H. J. and Norgren, R. 1978a. The taste reactivity test. II. Mimetic responses to gustatory stimuli in chronic thalamic and chronic decerebrate rats. Brain Res. 143, 281–297.
Grill, H. J. and Norgren, R. 1978b. Chronically decerebrate rats demonstrate satiation but not bait shyness. Science 201, 267–269.
Hagan, M. M. and Moss, D. E. 1997. Persistence of binge-eating patterns after a history of restriction with intermittent bouts of refeeding on palatable food in rats: implications for bulimia nervosa. Int. J. Eat. Disord. 22, 411–420.
Hajnal, A. and Lenard, L. 1997. Feeding-related dopamine in the amygdala of freely moving rats. Neuroreport 8, 2817–2820.
Hajnal, A. and Norgren, R. 2001. Accumbens dopamine mechanisms in sucrose intake. Brain Res. 904, 76–84.

Hajnal, A. and Norgren, R. 2002. Repeated access to sucrose augments dopamine turnover in the nucleus accumbens. Neuroreport 13, 2213–2216.

Hajnal, A. and Norgren, R. 2005. Taste pathways that mediate accumbens dopamine release by sapid sucrose. Physiol. Behav. 84, 363–369.

Hajnal, A., Covasa, M., Acharya, N. K., and Bello, N. T. 2004b. Altered dopamine functions in obese CCK-A receptor deficient (OLETF) rats: reduced motor activity and responsiveness to amphetamine and chronic sucrose feeding, lower dopamine transporter binding. Program No. 75.19, 2004 Abstract Viewer/Itinerary Planner. Society for Neuroscience (online).

Hajnal, A., Covasa, M., and Bello, N. T. 2005. Altered taste sensitivity in obese, pre-diabetic OLETF rats lacking CCK-1 receptors. Am. J. Physiol. Regul. Integr. Comp. Physiol. 289, R1675–R1686.

Hajnal, A., Smith, G. P., and Norgren, R. 2004a. Oral sucrose stimulation increases accumbens dopamine in the rat. Am. J. Physiol. Regul. Integr. Comp. Physiol. 286, R31–R37.

Hajnal, A., Takenouchi, K., and Norgren, R. 1999. Effect of intraduodenal lipid on parabrachial gustatory coding in awake rats. J. Neurosci. 19, 7182–7190.

Hernandez, L. and Hoebel, B. G. 1988a. Feeding and hypothalamic stimulation increase dopamine turnover in the accumbens. Physiol. Behav. 44, 599–606.

Hernandez, L. and Hoebel, B. G. 1988b. Food reward and cocaine increase extracellular dopamine in the nucleus accumbens as measured by microdialysis. Life Sci. 42, 1705–1712.

Hernandez, L. and Hoebel, B. G. 1990. Feeding can enhance dopamine turnover in the prefrontal cortex. Brain Res. Bull. 25, 975–979.

Herness, S. and Chen, Y. 1997. Serotonin inhibits calcium-activated K^+ current in rat taste receptor cells. Neuroreport 8, 3257–3261.

Herness, S., Zhao, F. L., Lu, S. G., Kaya, N., and Shen, T. 2002. Expression and physiological actions of cholecystokinin in rat taste receptor cells. J. Neurosci. 22, 10018–10029.

Hoebel, B. G., Hernandez, L., Schwartz, D. H., Mark, G. P., and Hunter, G. A. 1989. Microdialysis studies of brain norepinephrine, serotonin, and dopamine release during ingestive behavior. Theoretical and clinical implications. Ann. N. Y. Acad. Sci. 575, 171–191; discussion 192–173.

Hsiao, S. and Smith, G. P. 1995. Raclopride reduces sucrose preference in rats. Pharmacol. Biochem. Behav. 50, 121–125.

Huang, Y. J., Maruyama, Y., Lu, K. S., Pereira, E., Plonsky, I., Baur, J. E., Wu, D., and Roper, S. D. 2005. Mouse taste buds use serotonin as a neurotransmitter. J. Neurosci. 25, 843–847.

Ikemoto, S. and Panksepp, J. 1999. The role of nucleus accumbens dopamine in motivated behavior: a unifying interpretation with special reference to reward-seeking. Brain Res. Brain Res. Rev. 31, 6–41.

Inoue, K., Kiriike, N., Okuno, M., Ito, H., Fujisaki, Y., Matsui, T., and Kawakita, Y. 1993. Scheduled feeding caused activation of dopamine metabolism in the striatum of rats. Physiol. Behav. 53, 177–181.

Kawai, K., Sugimoto, K., Nakashima, K., Miura, H., and Ninomiya, Y. 2000. Leptin as a modulator of sweet taste sensitivities in mice. Proc. Natl. Acad. Sci. U. S. A. 97, 11044–11049.

Kelley, A. E., Baldo, B. A., Pratt, W. E., and Will, M. J. 2005. Corticostriatal-hypothalamic circuitry and food motivation: integration of energy, action and reward. Physiol. Behav. 86, 773–795.

Kelley, A. E., Bakshi, V. P., Haber, S. N., Steininger, T. L., Will, M. J., and Zhang, M. 2002. Opioid modulation of taste hedonics within the ventral striatum. Physiol. Behav. 76, 365–377.

Kirkham, T. C. 1990. Enhanced anorectic potency of naloxone in rats sham feeding 30% sucrose: reversal by repeated naloxone administration. Physiol. Behav. 47, 419–426.

Kirkham, T. C. and Cooper, S. J. 1988. Attenuation of sham feeding by naloxone is stereospecific: evidence for opioid mediation of orosensory reward. Physiol. Behav. 43, 845–847.

Kirouac, G. J. and Ganguly, P. K. 1995. Topographical organization in the nucleus accumbens of afferents from the basolateral amygdala and efferents to the lateral hypothalamus. Neuroscience 67, 625–630.

Kiyatkin, E. A. and Gratton, A. 1994. Electrochemical monitoring of extracellular dopamine in nucleus accumbens of rats lever-pressing for food. Brain Res. 652, 225–234.

Kosar, E., Grill, H. J., and Norgren, R. 1986. Gustatory cortex in the rat. II. Thalamocortical projections. Brain Res. 379, 342–352.

Leibowitz, S. F., Xuereb, M., and Kim, T. 1992. Blockade of natural and neuropeptide Y-induced carbohydrate feeding by a receptor antagonist PYX-2. Neuroreport 3, 1023–1026.

Li, C. S., Cho, Y. K., and Smith, D. V. 2005. Modulation of parabrachial taste neurons by electrical and chemical stimulation of the lateral hypothalamus and amygdala. J. Neurophysiol. 93, 1183–1196.

Lundy, R. F., Jr. and Norgren, R. 2001. Pontine gustatory activity is altered by electrical stimulation in the central nucleus of the amygdala. J. Neurophysiol. 85, 770–783.

Lundy, R. F., Jr. and Norgren, R. 2004a. Activity in the hypothalamus, amygdala, and cortex generates bilateral and convergent modulation of pontine gustatory neurons. J. Neurophysiol. 91, 1143–1157.

Lundy, R. F., Jr. and Norgren, R. 2004b. Gustatory System. In: The Rat Nervous System (*ed*. G. Paxinos), pp. 891–921. Elsevier.

Lynch, W. C. 1986. Opiate blockade inhibits saccharin intake and blocks normal preference acquisition. Pharmacol. Biochem. Behav. 24, 833–836.

Mark, G. P., Blander, D. S., and Hoebel, B. G. 1991. A conditioned stimulus decreases extracellular dopamine in the nucleus accumbens after the development of a learned taste aversion. Brain Res. 551, 308–310.

McClure, S. M., York, M. K., and Montague, P. R. 2004. The neural substrates of reward processing in humans: the modern role of fMRI. Neuroscientist 10, 260–268.

Mitchell, J. B. and Gratton, A. 1992. Partial dopamine depletion of the prefrontal cortex leads to enhanced mesolimbic dopamine release elicited by repeated exposure to naturally reinforcing stimuli. J. Neurosci. 12, 3609–3618.

Montgomery, A. M. and Burton, M. J. 1986. Effects of peripheral 5-HT on consumption of flavoured solutions. Psychopharmacology (Berl.) 88, 262–266.

Mungardee, S. S., Lundy, R. F., Jr., Caloiero, V. G., and Norgren, R. 2004. Forebrain c-Fos expression following sham exposure to sucrose after central gustatory lesions: a quantitative study, Society for Neuroscience. Abstract Viewer/Itenary Planner. Washington, DC.

Nakamura, K. and Norgren, R. 1995. Sodium-deficient diet reduces gustatory activity in the nucleus of the solitary tract of behaving rats. Am. J. Physiol. 269, R647–R661.

Ninomiya, Y., Shigemura, N., Yasumatsu, K., Ohta, R., Sugimoto, K., Nakashima, K., and Lindemann, B. 2002. Leptin and sweet taste. Vitam. Horm. 64, 221–248.

Norgren, R. 1976. Taste pathways to hypothalamus and amygdala. J. Comp. Neurol. 166, 17–30.

Norgren, R. 1978. Projections from the nucleus of the solitary tract in the rat. Neuroscience 3, 207–218.

Norgren, R., Grigson, P. S., Hajnal, A., and Lundy, R. F., Jr. 2003. Motivational Modulation of Taste. In: Cognition and Emotion in the Brain (*eds*. T. Ono, G. Matsumoto, R. R. Llinas, A. Berthoz, R. Norgren, H. Nishijo, and R. Tamura), pp. 319–334. Elsevier.

Oades, R. D. and Halliday, G. M. 1987. Ventral tegmental (A10) system: neurobiology. 1. Anatomy and connectivity. Brain Res. 434, 117–154.

Ogura, T. and Lin, W. 2005. Acetylcholine and acetylcholine receptors in taste receptor cells. Chem. Senses 30 Suppl 1, i41.

Parker, L. A., Maier, S., Rennie, M., and Crebolder, J. 1992. Morphine- and naltrexone-induced modification of palatability: analysis by the taste reactivity test. Behav. Neurosci. 106, 999–1010.

Patterson, T. A., Brot, M. D., Zavosh, A., Schenk, J. O., Szot, P., and Figlewicz, D. P. 1998. Food deprivation decreases mRNA and activity of the rat dopamine transporter. Neuroendocrinology 68, 11–20.

Pfaffmann, C., Norgren, R., and Grill, H. J. 1977. Sensory affect and motivation. Ann. N. Y. Acad. Sci. 290, 18–34.

Pothos, E. N. 2001. The effects of extreme nutritional conditions on the neurochemistry of reward and addiction. Acta Astronaut. 49, 391–397.

Pothos, E. N., Creese, I., and Hoebel, B. G. 1995. Restricted eating with weight loss selectively decreases extracellular dopamine in the nucleus accumbens and alters dopamine response to amphetamine, morphine, and food intake. J. Neurosci. 15, 6640–6650.

Rada, P., Avena, N. M., and Hoebel, B. G. 2005. Daily bingeing on sugar repeatedly releases dopamine in the accumbens shell. Neuroscience 134, 737–744.

Radhakishun, F. S., van Ree, J. M., and Westerink, B. H. 1988. Scheduled eating increases dopamine release in the nucleus accumbens of food-deprived rats as assessed with on-line brain dialysis. Neurosci. Lett. 85, 351–356.

Roitman, M. F., Stuber, G. D., Phillips, P. E., Wightman, R. M., and Carelli, R. M. 2004. Dopamine operates as a subsecond modulator of food seeking. J. Neurosci. 24, 1265–1271.

Rolls, E. T. 2005. Taste, olfactory, and food texture processing in the brain, and the control of food intake. Physiol. Behav. 85, 45–56.

Salamone, J. D., Correa, M., Mingote, S., and Weber, S. M. 2003. Nucleus accumbens dopamine and the regulation of effort in food-seeking behavior: implications for studies of natural motivation, psychiatry, and drug abuse. J. Pharmacol. Exp. Ther. 305, 1–8.

Schneider, L. H. 1989. Orosensory self-stimulation by sucrose involves brain dopaminergic mechanisms. Ann. N. Y. Acad. Sci. 575, 307–319.

Schultz, W. 2006. Behavioral theories and the neurophysiology of reward. Annu. Rev. Psychol. 57, 87–115.

Sclafani, A. 1997. Learned controls of ingestive behaviour. Appetite 29, 153–158.

Sclafani, A. and Ackroff, K. 1994. Glucose- and fructose-conditioned flavor preferences in rats: taste versus postingestive conditioning. Physiol. Behav. 56, 399–405.

Sclafani, A. and Mann, S. 1987. Carbohydrate taste preferences in rats: glucose, sucrose, maltose, fructose and polycose compared. Physiol. Behav. 40, 563–568.

Sclafani, A. and Nissenbaum, J. W. 1985. On the role of the mouth and gut in the control of saccharin and sugar intake: a reexamination of the sham-feeding preparation. Brain Res. Bull. 14, 569–576.

Sclafani, A., Thompson, B., and Smith, J. C. 1998. The rat's acceptance and preference for sucrose, maltodextrin, and saccharin solutions and mixtures. Physiol. Behav. 63, 499–503.

Shi, C. J. and Cassell, M. D. 1998. Cortical, thalamic, and amygdaloid connections of the anterior and posterior insular cortices. J. Comp. Neurol. 399, 440–468.

Shigemura, N., Miura, H., Kusakabe, Y., Hino, A., and Ninomiya, Y. 2003. Expression of leptin receptor (Ob-R) isoforms and signal transducers and activators of transcription (STATs) mRNAs in the mouse taste buds. Arch. Histol. Cytol. 66, 253–260.

Shigemura, N., Ohta, R., Kusakabe, Y., Miura, H., Hino, A., Koyano, K., Nakashima, K., and Ninomiya, Y. 2004. Leptin modulates behavioral responses to sweet substances by influencing peripheral taste structures. Endocrinology 145, 839–847.

Shimura, T., Kamada, Y., and Yamamoto, T. 2002. Ventral tegmental lesions reduce overconsumption of normally preferred taste fluid in rats. Behav. Brain Res. 134, 123–130.

Sills, T. L. and Vaccarino, F. J. 1996. Individual differences in sugar consumption following systemic or intraaccumbens administration of low doses of amphetamine in nondeprived rats. Pharmacol. Biochem. Behav. 54, 665–670.

Smith, G. P. 1995. Dopamine and Food Reward. In: Progress in Psychobiology and Physiological Psychology (*eds*. S. Fluharty, A. Morrion, J. Sprague, and E. Stellar), pp. 83–144. Academic Press.

Smith, G. P. 2004. Accumbens dopamine mediates the rewarding effect of orosensory stimulation by sucrose. Appetite 43, 11–13.

Smith, G. P. and Schneider, L. H. 1988. Relationships between mesolimbic dopamine function and eating behavior. Ann. N. Y. Acad. Sci. 537, 254–261.

Spector, A. C., Grill, H. J., and Norgren, R. 1993. Concentration-dependent licking of sucrose and sodium chloride in rats with parabrachial gustatory lesions. Physiol. Behav. 53, 277–283.

Steiner, J. E. 1973. The gustofacial response: observation on normal and anencephalic newborn infants. Symp. Oral Sens. Percept. 254–278.

Stratford, T. R. and Kelley, A. E. 1999. Evidence of a functional relationship between the nucleus accumbens shell and lateral hypothalamus subserving the control of feeding behavior. J. Neurosci. 19, 11040–11048.

Suzuki, Y., Takeda, M., Sakakura, Y., and Suzuki, N. 2005. Distinct expression pattern of insulin-like growth factor family in rodent taste buds. J. Comp. Neurol. 482, 74–84.

Szczypka, M. S., Mandel, R. J., Donahue, B. A., Snyder, R. O., Leff, S. E., and Palmiter, R. D. 1999a. Viral gene delivery selectively restores feeding and prevents lethality of dopamine-deficient mice. Neuron 22, 167–178.

Szczypka, M. S., Rainey, M. A., Kim, D. S., Alaynick, W. A., Marck, B. T., Matsumoto, A. M., and Palmiter, R. D. 1999b. Feeding behavior in dopamine-deficient mice. Proc. Natl. Acad. Sci. U. S. A. 96, 12138–12143.

Tamura, R. and Norgren, R. 2003. Intracranial renin alters gustatory neural responses in the nucleus of the solitary tract of rats. Am. J. Physiol. Regul. Integr. Comp. Physiol. 284, R1108–R1118.

Thorndike, E. 1911. Animal Intelligence: Experimental Studies. MacMillan.

Usuda, I., Tanaka, K., and Chiba, T. 1998. Efferent projections of the nucleus accumbens in the rat with special reference to subdivision of the nucleus: biotinylated dextran amine study. Brain Res. 797, 73–93.

Waldbillig, R. J. and Bartness, T. J. 1982. The suppression of sucrose intake by cholecystokinin is scaled according to the magnitude of the orosensory control over feeding. Physiol. Behav. 28, 591–595.

Wang, G. J., Volkow, N. D., and Fowler, J. S. 2002. The role of dopamine in motivation for food in humans: implications for obesity. Expert Opin. Ther. Targets 6, 601–609.

Wang, J., Liu, Z. L., and Chen, B. 2001. Association study of dopamine D2, D3 receptor gene polymorphisms with motor fluctuations in PD. Neurology 56, 1757–1759.

Westerink, B. H. 1995. Brain microdialysis and its application for the study of animal behaviour. Behav. Brain Res. 70, 103–124.

Westerink, B. H., Teisman, A., and de Vries, J. B. 1994. Increase in dopamine release from the nucleus accumbens in response to feeding: a model to study interactions between drugs and naturally activated dopaminergic neurons in the rat brain. Naunyn Schmiedebergs Arch. Pharmacol. 349, 230–235.

Wightman, R. M. and Robinson, D. L. 2002. Transient changes in mesolimbic dopamine and their association with 'reward'. J. Neurochem. 82, 721–735.

Wilson, C., Nomikos, G. G., Collu, M., and Fibiger, H. C. 1995. Dopaminergic correlates of motivated behavior: importance of drive. J. Neurosci. 15, 5169–5178.

Wise, R. A. 2002. Brain reward circuitry: insights from unsensed incentives. Neuron 36, 229–240.

Wise, R. A. 2005. Forebrain substrates of reward and motivation. J. Comp. Neurol. 493, 115–121.

Yoshida, M., Yokoo, H., Mizoguchi, K., Kawahara, H., Tsuda, A., Nishikawa, T., and Tanaka, M. 1992. Eating and drinking cause increased dopamine release in the nucleus accumbens and ventral tegmental area in the rat: measurement by *in vivo* microdialysis. Neurosci. Lett. 139, 73–76.

Yu, W. Z., Silva, R. M., Sclafani, A., Delamater, A. R., and Bodnar, R. J. 2000a. Role of D(1) and D(2) dopamine receptors in the acquisition and expression of flavor-preference conditioning in sham-feeding rats. Pharmacol. Biochem. Behav. 67, 537–544.

Yu, W. Z., Silva, R. M., Sclafani, A., Delamater, A. R., and Bodnar, R. J. 2000b. Pharmacology of flavor preference conditioning in sham-feeding rats: effects of dopamine receptor antagonists. Pharmacol. Biochem. Behav. 65, 635–647.

Zagon, A., Totterdell, S., and Jones, R. S. 1994. Direct projections from the ventrolateral medulla oblongata to the limbic forebrain: anterograde and retrograde tract-tracing studies in the rat. J. Comp. Neurol. 340, 445–468.

Zhang, H., Kiyatkin, E. A., and Stein, E. A. 1994. Behavioral and Pharmacological modulation of ventral tegmental dendritic dopamine release. Brain Res. 656, 59–70.

Zhao, F. L., Shen, T., Kaya, N., Lu, S. G., Cao, Y., and Herness, S. 2005. Expression, physiological action, and coexpression patterns of neuropeptide Y in rat taste-bud cells. Proc. Natl. Acad. Sci. U. S. A. 102, 11100–11105.

4.26 The Representation of Flavor in the Brain

E T Rolls, University of Oxford, Oxford, UK

© 2008 Elsevier Inc. All rights reserved.

4.26.1	Taste Processing in the Primate Cortex	469
4.26.1.1	Pathways	469
4.26.1.2	The Primary and Secondary Taste Cortex	469
4.26.1.3	Five Prototypical Tastes, Including Umami	470
4.26.2	The Pleasantness of the Taste of Food	470
4.26.3	The Representation of Flavor: Convergence of Olfactory and Taste Inputs	470
4.26.4	The Rules Underlying the Formation of Flavor Representations in the Primate Cortex	471
4.26.5	The Responses of Orbitofrontal Cortex Taste and Olfactory Neurons to the Texture, and Temperature of Food	472
4.26.6	The Representation of the Pleasantness of Flavor in the Brain: Olfactory and Visual Sensory-Specific Satiety, and Their Representation in the Primate Orbitofrontal Cortex	473
4.26.7	Functional Neuroimaging Studies in Humans	473
4.26.7.1	Taste	473
4.26.7.2	Odor	474
4.26.7.3	Olfactory-Taste Convergence to Represent Flavor	474
4.26.7.4	Cognitive Influences on Olfactory and Flavor Processing	476
References		477

Glossary

flavor A sensation produced by the combination of the taste, smell, and texture of food. *reward* A stimulus such as food for which an animal will work (see Rolls, E. T., 2005a).

sensory-specific satiety A reduction in the pleasantness of and appetite for a food that has been eaten to satiety in a meal which is partly specific to the food eaten in a meal.

umami The fifth taste, produced by the stimuli monosodium glutamate and 5′-ribonucleotides such as inosine monophosphate and guanosine monophosphate.

4.26.1 Taste Processing in the Primate Cortex

4.26.1.1 Pathways

A diagram of the taste and related olfactory, somatosensory, and visual pathways in primates is shown in Figure 1. Of particular interest is that in primates there is a direct projection from the rostral part of the nucleus of the solitary tract (NTS) to the taste thalamus and thus to the primary taste cortex in the frontal operculum and adjoining insula, with no pontine taste area and associated subcortical projections as in rodents (Norgren, R., 1984; Pritchard, T. C. *et al.*, 1986).This emphasis on cortical processing of taste in primates may be related to the great development of the cerebral cortex in primates, and the advantage of using extensive and similar cortical analysis of inputs from every sensory modality before the analyzed representations from each modality are brought together in multimodal regions to form representations of flavor.

4.26.1.2 The Primary and Secondary Taste Cortex

The primary taste cortex is in the rostral insula and adjacent frontal operculum (Pritchard, T. C. *et al.*, 1986). A secondary cortical taste area in primates was discovered by Rolls E. T. *et al.* (1990) in the caudolateral orbitofrontal cortex, extending several millimeters in front of the primary taste cortex, and also extending to more medial parts of the orbitofrontal cortex (Rolls, E. T. and Baylis, L. L., 1994).

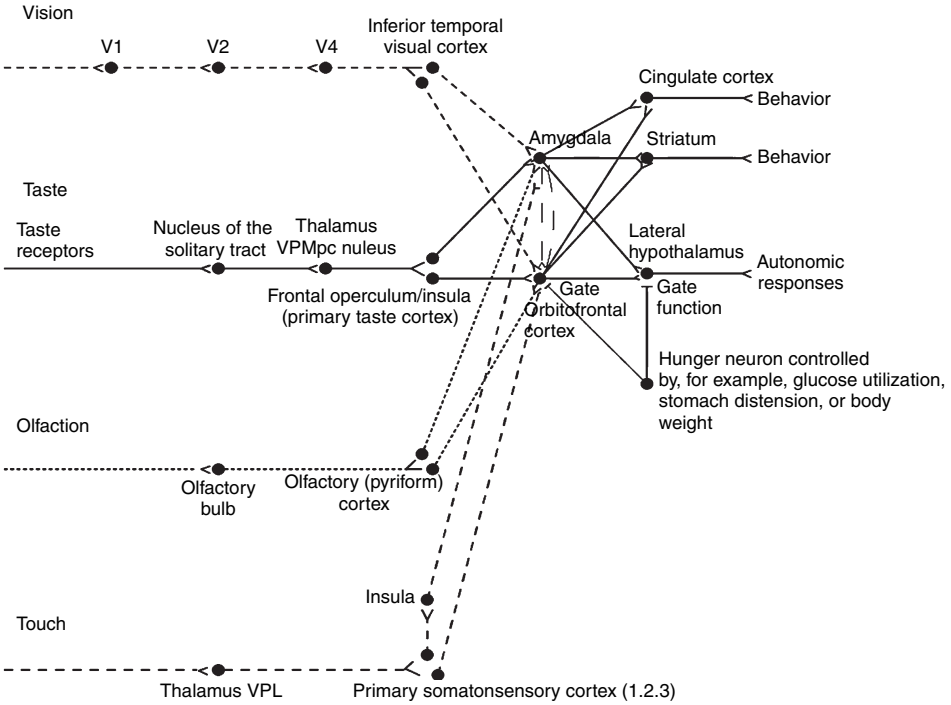

Figure 1 Schematic diagram of the taste and olfactory pathways in primates showing how they converge with each other and with visual pathways. The gate functions shown refer to the finding that the responses of taste neurons in the orbitofrontal cortex and the lateral hypothalamus are modulated by hunger. VPMpc, ventralposteromedial thalamic nucleus; V1, V2, V4, visual cortical areas.

4.26.1.3 Five Prototypical Tastes, Including Umami

In the primary and secondary taste cortex, there are many neurons that respond best to each of the four classical prototypical tastes sweet, salt, bitter and sour (Scott, T. R. *et al.*, 1986; Yaxley, S. *et al.*, 1988; Rolls, E. T. *et al.*, 1990; Rolls, E. T., 1997; Rolls, E. T. and Scott, T. R., 2003), but also there are many neurons that respond best to umami tastants such as glutamate (which is present in many natural foods such as tomatoes, mushrooms and milk; Baylis, L. L. and Rolls, E. T., 1991) and inosine monophosphate (which is present in meat and some fish such as tuna; Rolls, E. T. *et al.*, 1996a).

4.26.2 The Pleasantness of the Taste of Food

The modulation of the reward value of a sensory stimulus such as the taste of food by motivational state, for example hunger, is one important way in which motivational behavior is controlled (Rolls, E. T., 2005a). The subjective correlate of this modulation is that food tastes pleasant when hungry, and tastes hedonically neutral when it has been eaten to satiety. We have found that the modulation of taste-evoked signals by motivation is not a property found in early stages of the primate gustatory system including the nucleus of the solitary tract (Yaxley, S. *et al.*, 1985) and the primary taste cortex (frontal opercular, Rolls, E. T. *et al.*, 1988; insular, Yaxley, S. *et al.*, 1988). In contrast, in the secondary taste cortex, in the caudolateral part of the orbitofrontal cortex, the responses of neurons to the taste of glucose decreases to zero while the monkey is fed glucose to satiety (Rolls, E. T. *et al.*, 1989). It is an important principle that the identity of a taste, and its intensity, are represented separately (in the primary taste cortex) from its pleasantness (in the secondary taste cortex) (Rolls, E. T., 2005a). Thus it is possible to represent what a taste is, and to learn about it, even when we are not hungry.

4.26.3 The Representation of Flavor: Convergence of Olfactory and Taste Inputs

Neuronal responses in the primate primary taste cortex are not driven by olfactory inputs during normal taste/smell tests (Verhagen, J. V. *et al.*, 2004).

However, we found (Rolls, E. T. and Baylis, L. L., 1994) that in the orbitofrontal cortex taste areas, of 112 single neurons which responded to any of these modalities, many were unimodal (taste 34%, olfactory 13%, visual 21%), but were found in close proximity to each other. Some single neurons showed convergence, responding for example to taste and visual inputs (13%), taste and olfactory inputs (13%), and olfactory and visual inputs (5%). Some of these multimodal single neurons had corresponding sensitivities in the two modalities, in that they responded best to sweet tastes (e.g., 1M glucose), and responded more in a visual discrimination task to the visual stimulus which signified sweet fruit juice than to that which signified saline; or responded to sweet taste, and in an olfactory discrimination task to fruit odor (see Figure 2). The different types of neurons (unimodal in different modalities, and multimodal) were frequently found close to one another in tracks made into this region, consistent with the hypothesis that the multimodal representations are actually being formed from unimodal inputs to this region.

It thus appears to be in these orbitofrontal cortex areas that flavor representations are built, where flavor is taken to mean a representation which is evoked best by a combination of gustatory and olfactory input.

The primate amygdala has neurons that combine representations of taste and oral texture (Kadohisa, M. *et al.*, 2005b), and visual stimuli (Wilson, F. A. W. and Rolls, E. T., 2005), and olfactory inputs also reach the amygdala, but less is known about olfactory-taste association learning in the primate amygdala.

4.26.4 The Rules Underlying the Formation of Flavor Representations in the Primate Cortex

Critchley H. D. and Rolls E. T. (1996c) showed that 35% of orbitofrontal cortex olfactory neurons categorized odors based on their taste association in an olfactory-to-taste discrimination task. Rolls E. T. *et al.* (1996a) found that 68% of orbitofrontal cortex odor-responsive neurons modified their responses in some way following changes in the taste reward associations of the odorants during olfactory-taste discrimination learning and its reversal. (In an olfactory discrimination experiment, if a lick response to one odor, the S+, is made a drop of glucose taste reward is obtained; if incorrectly a lick response is made to another odor, the S−, a drop of aversive saline is obtained. At some time in the experiment, the contingency between the odor and the taste is reversed, and when the meaning of the two odors alters, so does the behavior. It is of interest to investigate in which parts of the olfactory system the neurons show reversal, for where they do, it can be concluded that the neuronal response to the odor depends on the taste with which it is associated, and does not depend primarily on the physicochemical structure of the odor). An example of a neuron showing olfactory-to-taste reversal is shown in Figure 3. These findings demonstrate directly a coding principle in primate olfaction whereby the responses of some orbitofrontal cortex olfactory neurons are modified by and depend upon the taste with which the

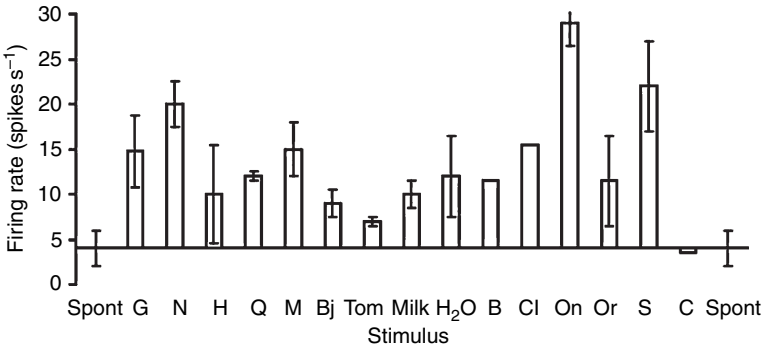

Figure 2 Olfactory to taste convergence on to a single neuron in the macaque orbitofrontal cortex. Spont, spontaneous; G, 1 M glucose; N, 0.1 M NaCl; H, 0.01 M hycrochloride; Q, 0.001 M quinine hycrochloride; M, 0.1 M monosodium glutamate; Bj, 20% blackcurrant juice; Tom, tomato juice; B, banana odor; Cl, clove oil odor; On, onion odor; Or, orange odor; S, salmon odor; C, control no-odor presentation. The mean responses ± standard error of the means are shown. The neuron responded best to the savory tastes of NaCl and monosodium glutamate and to the consonant odors of onion and salmon. Adapted from Rolls, E. T. and Baylis, L. L. 1994. Gustatory, olfactory, and visual convergence within the primate orbitofrontal cortex. J. Neurosci. 14, 5437–5452.

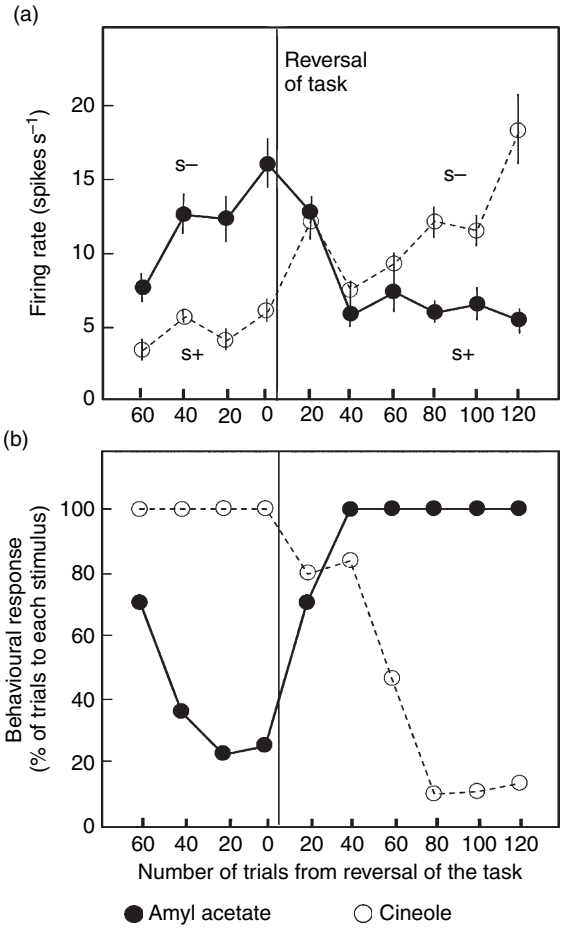

Figure 3 Flavor learning: olfactory to taste association reversal by an orbitofrontal cortex neuron. (a) The activity of a single orbitofrontal olfactory neuron during the performance of a two-odor olfactory discrimination task and its reversal is shown. Each point represents the mean poststimulus activity of the neuron in a 500 ms period on approximately 10 trials of the different odorants. The standard errors of these responses are shown. The odorants were amyl acetate (closed circle; initially s–) and cineole (open circles; initially s+). After 80 trials of the task the reward associations of the stimuli were reversed. This neuron reversed its responses to the odorants following the task reversal. (b) The behavioral responses of the monkey during the performance of the olfactory discrimination task. The number of lick responses to each odorant is plotted as a percentage of the number of trials to that odorant in a block of 20 trials of the task. Adapted from Rolls, E. T., Critchley, H., Mason, R., and Wakeman, E. A. 1996. Orbitofrontal cortex neurons: role in olfactory and visual association learning. J. Neurophysiol. 75, 1970–1981.

odor is associated (Rolls, E. T., 2001; 2002a; 2002b; Deco, G. and Rolls, E. T., 2005b).

Some neurons in the same orbitofrontal cortex region are influenced by the sight as well as by the taste of food, and this is a learned convergence (Thorpe, S. J. *et al.*, 1983; Rolls, E. T. *et al.*, 1996b). As a result of this learning, food choice based on the visual–taste association can be made, and potentially the sight of food can influence its perceived taste. It is of interest that the olfactory-taste association learning is less complete, and much slower, than the modifications found for orbitofrontal visual neurons during visual–taste learning and its reversal (Rolls, E. T. *et al.*, 1996b). This relative inflexibility of olfactory responses is consistent with the need for some stability in odor–taste associations to facilitate the formation and perception of flavors.

Some orbitofrontal cortex olfactory neurons do not code in relation to the taste with which the odor is associated (Critchley, H. D. and Rolls, E. T., 1996c) so that there is also a taste-independent representation of odor in this region.

4.26.5 The Responses of Orbitofrontal Cortex Taste and Olfactory Neurons to the Texture, and Temperature of Food

The texture of food may be considered as a component of the flavor of food. The texture of food, including its viscosity, influences some neurons in the primary taste cortex that have taste responses (Verhagen, J. V. *et al.*, 2004). These texture inputs also thereby influence neurons in the primate orbitofrontal cortex (Rolls, E. T. *et al.*, 2003b), which thus becomes a region where flavor representations can be influenced by the taste, smell, sight and texture of food. Some of the orbitofrontal cortex neurons with texture-related responses encode parametrically the viscosity of food in the mouth (shown using a methyl cellulose series in the range 1–10 000 centiPoise) (see Figure 3), and others independently encode the particulate quality of food in the mouth, produced quantitatively for example by adding 20–100 μm microspheres to methyl cellulose (Rolls, E. T. *et al.*, 2003b). Other neurons respond to water, and others to the somatosensory stimuli astringency as exemplified by tannic acid (Critchley, H. D. and Rolls, E. T., 1996a), and to capsaicin (Rolls, E. T. *et al.*, 2003b; Kadohisa, M. *et al.*, 2004; 2005a).

Texture in the mouth is an important indicator of whether fat is present in a food, which is important not only as a high value energy source, but also as a potential source of essential fatty acids. In the orbitofrontal cortex, Rolls E. T. *et al.* (1999) have found a

population of neurons that responds when fat is in the mouth. The fat-related responses of these neurons are produced at least in part by the texture of the food rather than by chemical receptors sensitive to certain chemicals, in that such neurons typically respond not only to foods such as cream and milk containing fat, but also to paraffin oil (which is a pure hydrocarbon) and to silicone oil ($Si(CH_3)O_2)_n$). Moreover, the texture channel through which these fat-sensitive neurons are activated are separate from viscosity sensitive channels, in that the responses of these neurons cannot be predicted by the viscosity of the oral stimuli (Verhagen, J. V. *et al.*, 2003). Some of the fat-related neurons do though have convergent inputs from the chemical senses, in that in addition to taste inputs, some of these neurons respond to the odor associated with a fat, such as the odor of cream (Rolls, E. T. *et al.*, 1999). Feeding to satiety with fat (e.g., cream) decreases the responses of these neurons to zero on the food eaten to satiety, but if the neuron receives a taste input from for example glucose taste, that is not decreased by feeding to satiety with cream. Thus there is a representation of the macronutrient fat in this brain area, and the activation produced by fat is reduced by eating fat to satiety.

In addition, we have shown recently (Kadohisa, M. *et al.*, 2004; 2005a) that some neurons in the orbitofrontal cortex reflect the temperature of substances in the mouth, and that this temperature information is represented independently of other sensory inputs by some neurons, and in combination with taste or texture by other neurons.

4.26.6 The Representation of the Pleasantness of Flavor in the Brain: Olfactory and Visual Sensory-Specific Satiety, and Their Representation in the Primate Orbitofrontal Cortex

In the orbitofrontal cortex, it is found that the decreases in the responsiveness of the neurons are relatively specific to the food with which the monkey has been fed to satiety. For example, in seven experiments in which the monkey was fed glucose solution, neuronal responsiveness decreased to the taste of the glucose but not to the taste of blackcurrant juice. Conversely, in two experiments in which the monkey was fed to satiety with fruit juice, the responses of the neurons decreased to fruit juice but not to glucose (Rolls, E. T. *et al.*, 1989).

It has also been possible to investigate whether the olfactory representation in the orbitofrontal cortex is affected by hunger, and thus whether the pleasantness of odor is represented in the orbitofrontal cortex. In satiety experiments, Critchley H. D. and Rolls E. T. (1996b) showed that the responses of some olfactory neurons to a food odor are decreased during feeding to satiety with a food (e.g., fruit juice) containing that odor. In particular, seven of nine olfactory neurons that were responsive to the odors of foods, such as blackcurrant juice, were found to decrease their responses to the odor of the satiating food. The decrease was typically at least partly specific to the odor of the food that had been eaten to satiety, potentially providing part of the basis for sensory-specific satiety. It was also found for eight of nine neurons that had selective responses to the sight of food that they demonstrated a sensory-specific reduction in their visual responses to foods following satiation. These findings show that the olfactory and visual representations of food, as well as the taste representation of food, in the primate orbitofrontal cortex are modulated by hunger. Usually a component related to sensory-specific satiety can be demonstrated. It is thus the orbitofrontal cortex which computes sensory-specific satiety, and it is in areas such as this and the areas that receive from it that neuronal activity may be related to whether a food tastes pleasant, and to whether the food should be eaten (see Scott, T. R. *et al.*, 1995; Critchley, H. D. and Rolls, E. T., 1996c; Rolls, E. T. and Rolls, J. H., 1997; Rolls, E. T., 1999; 2000a; 2000b; Rolls, E. T. and Scott, T. R., 2003; Rolls, E. T., 2005a; 2005b; 2006).

The enhanced eating when a variety of foods is available, as a result of the operation of sensory-specific satiety, may have been advantageous in evolution in ensuring that different foods with important different nutrients were consumed, but today in humans, when a wide variety of foods is readily available, it may be a factor that can lead to overeating and obesity (Rolls, E. T., 2005a).

4.26.7 Functional Neuroimaging Studies in Humans

4.26.7.1 Taste

In humans it has been shown in neuroimaging studies using functional magnetic resonance imaging (fMRI) that taste activates an area of the anterior insula/frontal operculum, which is probably the primary

taste cortex, and part of the orbitofrontal cortex, which is probably the secondary taste cortex (Francis, S. *et al.*, 1999; Small, D. M. *et al.*, 1999; O'Doherty, J. *et al.*, 2001; de Araujo, I. E. T. *et al.*, 2003b; Faurion, A. *et al.*, 2005). Another study has recently shown that umami taste stimuli, including monosodium glutamate, activate similar cortical regions of the human taste system to those activated by a prototypical taste stimulus, glucose (de Araujo, I. E. T. *et al.*, 2003a). A part of the rostral anterior cingulate cortex (ACC) was also activated in this study, as it is in many studies by taste, odor, flavor, and oral texture (Rolls, E. T., 2007). O'Doherty J. *et al.* (2001) showed that the human amygdala was as much activated by the affectively pleasant taste of glucose as by the affectively negative taste of NaCl, and thus provided evidence that the human amygdala is not especially involved in processing aversive as compared to rewarding stimuli.

4.26.7.2 Odor

In humans, in addition to activation of the pyriform (olfactory) cortex (Zald, D. H. and Pardo, J. V., 1997; Sobel, N. *et al.*, 2000; Poellinger, A. *et al.*, 2001), there is strong and consistent activation of the orbitofrontal cortex by olfactory stimuli (Zatorre, R. J. *et al.*, 1992; Francis, S. *et al.*, 1999). In an investigation of where the pleasantness of olfactory stimuli might be represented in humans, O'Doherty J. *et al* (2000) showed that the activation of an area of the orbitofrontal cortex to banana odor was decreased (relative to a control vanilla odor) after bananas were eaten to satiety. Thus activity in a part of the human orbitofrontal cortex olfactory area is related to sensory-specific satiety, and this is one brain region where the pleasantness of odor is represented. Flavor sensory-specific satiety is also represented in the human orbitofrontal cortex, in that when a whole food (either chocolate milk, or tomato juice) is eaten to satiety activation to the flavor of the food eaten to satiety, but not to the other flavor, decreases in the orbitofrontal cortex but not in the primary taste cortex (Kringelbach, M. L. *et al.*, 2003; see Figure 4).

An important issue is whether there are separate regions of the brain discriminable with fMRI that represent pleasant and unpleasant odors. To investigate this, we measured the brain activations produced by three pleasant and three unpleasant odors. The pleasant odors chosen were linalyl acetate (floral, sweet), geranyl acetate (floral), and alpha-ionone (woody, slightly food-related). (Chiral substances were used as racemates.) The unpleasant odors chosen were hexanoic acid, octanol, and isovaleric acid. We found that they activated dissociable parts of the human brain (Rolls, E. T. *et al.*, 2003a). Pleasant but not unpleasant odors were found to activate a medial region of the rostral orbitofrontal cortex. Further, there was a correlation between the subjective pleasantness ratings of the six odors given during the investigation with activation of a medial region of the rostral orbitofrontal cortex. In contrast, a correlation between the subjective unpleasantness ratings of the six odors was found in regions of the left and more lateral orbitofrontal cortex. Activation was also found in the ACC, with a middle part of the anterior cingulate activated by both pleasant and unpleasant odors, and a more anterior part of the ACC showing a correlation with the subjective pleasantness ratings of the odors. Activation in primary olfactory cortical areas was not correlated with the pleasantness of the odor, but was correlated with the intensity (Rolls, E. T. *et al.*, 2003a).

4.26.7.3 Olfactory-Taste Convergence to Represent Flavor

To investigate where in the human brain interactions between taste and odor stimuli may be realized to implement flavor, we performed an event-related fMRI study with sucrose and monosodium glutamate taste, and strawberry and methional (chicken) odors, delivered unimodally or in different combinations (de Araujo, I. E. T. *et al.*, 2003c). The brain regions that were activated by both taste and smell included parts of the caudal orbitofrontal cortex, amygdala, insular cortex and adjoining areas, and ACC. It was shown that a small part of the anterior (putatively agranular) insula responds to unimodal taste and to unimodal olfactory stimuli; and that a part of the anterior frontal operculum is a unimodal taste area (putatively primary taste cortex) not activated by olfactory stimuli. Activations to combined olfactory and taste stimuli where there was little or no activation to either alone (providing positive evidence for interactions between the olfactory and taste inputs) were found in a lateral anterior part of the orbitofrontal cortex. Correlations with consonance ratings for the smell and taste combinations, and for their pleasantness, were found in a medial anterior part of the orbitofrontal cortex (see Figure 5). These results provide evidence on the neural substrate for the convergence of taste and olfactory stimuli to produce flavor in humans, and where the pleasantness of flavor is represented in the human brain (de Araujo, I. E. T. *et al.*, 2003c).

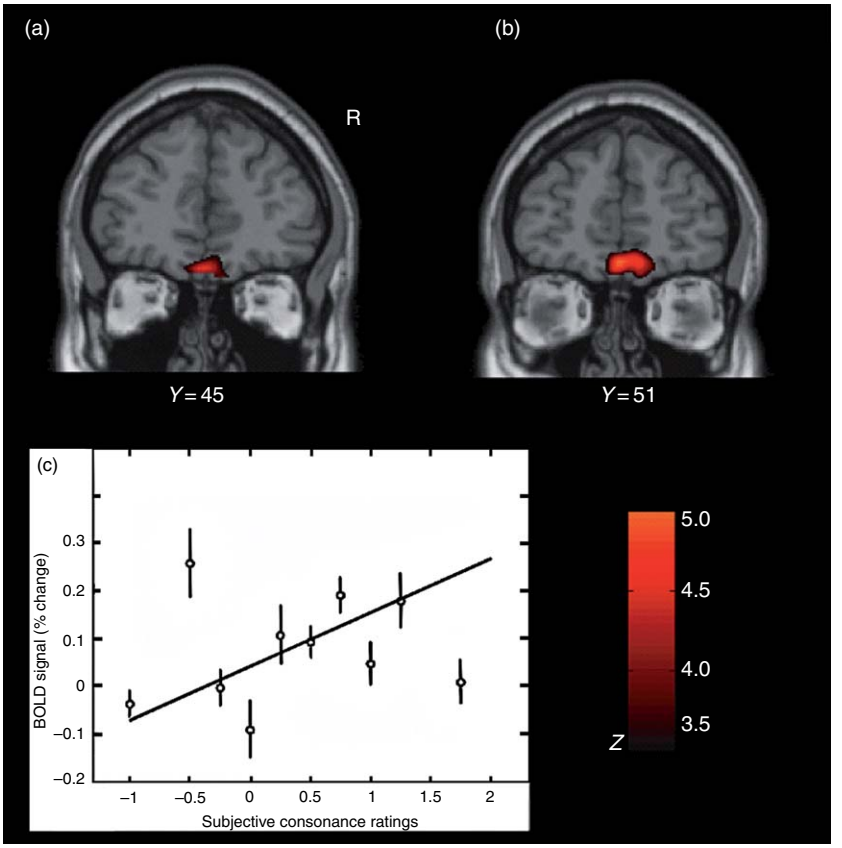

Figure 4 Flavor formation in the human brain, shown by cross-modal olfactory–taste convergence. Brain areas where activations were correlated with the subjective ratings for stimulus (taste–odor) consonance and pleasantness. (a) A second-level, random effects analysis based on individual contrasts (the consonance ratings being the only effect of interest) revealed a significant activation in a medial part of the anterior orbitofrontal cortex. (b) Random effects analysis based on the pleasantness ratings showed a significant cluster of activation located in a (nearby) medial part of the anterior orbitofrontal cortex. The images were thresholded at $P < 0.0001$ for illustration. (c) The relation between the blood oxygen level-dependent (BOLD) signal from the cluster of voxels in the medial orbitofrontal cortex shown in (a) and the subjective consonance ratings. The analyses shown included all the stimuli included in this investigation. The means and standard errors of the mean across subjects are shown, together with the regression line, for which $r = 0.52$. Adapted from de Araujo, I. E. T., Rolls, E. T., Kringelbach, M. L., McGlone, F., and Phillips, N. 2003c. Taste-olfactory convergence, and the representation of the pleasantness of flavour, in the human brain. Eur. J. Neurosci. 18, 2374–2390.

We have also investigated how the flavor of savory foods is produced. Umami taste is produced by glutamate acting on a fifth taste system. However, glutamate presented alone as a taste stimulus is not highly pleasant, and does not act synergistically with other tastes (sweet, salt, bitter and sour). McCabe C. and Rolls E. T. (2007) showed that when glutamate is given in combination with a consonant, savory, odor (vegetable), the resulting flavor can be much more pleasant. Moreover, we showed using functional brain imaging with fMRI that the glutamate and savory odor combination produced much greater activation of the medial orbitofrontal cortex and pregenual cingulate cortex than the sum of the activations by the taste and olfactory components presented separately. Supralinear effects were much less (and significantly less) evident for sodium chloride and vegetable odor. Further, activations in these brain regions were correlated with the pleasantness, consonance of the taste and olfactory components, and the fullness of the flavor, of the stimuli. We thus proposed that glutamate acts by the nonlinear effects it can produce when combined with a consonant odor (McCabe, C. and Rolls, E. T., 2007). I therefore propose the concept that umami can be thought of as a rich and delicious flavor that is produced by a combination of glutamate taste and a consonant savory odor. Glutamate is thus a flavor enhancer because of the way that it can combine supralinearly with consonant odors.

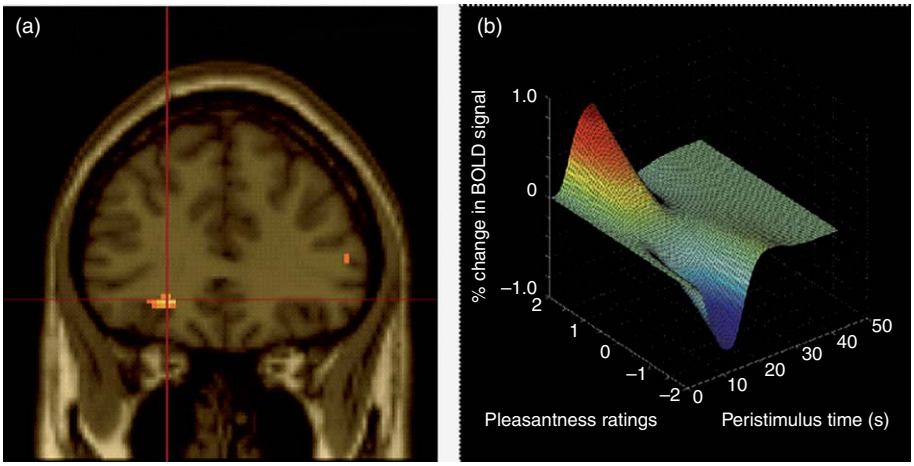

Figure 5 Areas of the human orbitofrontal cortex with activations correlating with pleasantness ratings for flavor in a sensory-specific satiety design. (a) Coronal section through the region of the orbitofrontal cortex from the random effects group analysis showing the peak in the left orbitofrontal cortex (Talairach co-ordinates *X, Y, Z* = −22, 34, −8, z-score = 4.06), in which the blood oxygen level-dependent (BOLD) signal in the voxels shown in yellow was significantly correlated with the subjects' subjective pleasantness ratings of the foods throughout an experiment in which the subjects were hungry and found the food pleasant, and were then fed to satiety with the food, after which the pleasantness of the food decreased to neutral or slightly unpleasant. The design was a sensory-specific satiety design, and the pleasantness of the food not eaten in the meal, and the BOLD activation in the orbitofrontal cortex, were not altered by eating the other food to satiety. The two foods were tomato juice and chocolate milk. (b) Plot of the magnitude of the fitted hemodynamic response from a representative single subject against the subjective pleasantness ratings (on a scale from −2 to +2) and peristimulus time in seconds. Adapted from Kringelbach, M. L., O'Doherty, J., Rolls, E. T., and Andrews, C. 2003. Activation of the human orbitofrontal cortex to a liquid food stimulus is correlated with its subjective pleasantness. Cereb. Cortex 13, 1064–1071.

4.26.7.4 Cognitive Influences on Olfactory and Flavor Processing

In line with the neuronal convergence of visual and taste inputs on to single neurons in the orbitofrontal cortex (see above), it is found that the sight of food can influence its perceived flavor, and an fMRI correlate of this has been reported (Osterbauer, R. A. *et al.*, 2005). An example of this interaction is that if a white wine is colored red, then adjectives used to describe the flavor of red wine are used to describe the flavor of the white wine.

To investigate how cognitive this influence could be, de Araujo I. E. T. *et al.* (2005) delivered a standard test odor (isovaleric acid with added cheese flavor), but paired it on some trials with a (visually presented) word label Cheddar cheese, and on other trials with the word label body odor. It was found that the word label produced a large modulation of the olfactory activation in the secondary olfactory cortex in the orbitofrontal cortex (with also some modulation in the amygdala). Moreover, the activations in the orbitofrontal cortex were correlated with the pleasantness ratings given by the subjects of the test odor, which were influenced by the word label. In a control with clean air from the olfactometer, the word labels had much less influence, so that their effect was in particular to modulate the activations being produced in the secondary olfactory cortex by an olfactory stimulus. Thus cognitive influences from the linguistic level, the level of words, can reach down into the secondary olfactory cortex in the orbitofrontal cortex, and modulate their representation of olfactory stimuli (de Araujo, I. E. T. *et al.*, 2005). The mechanism is probably similar to the way in which top-down attentional processes operate, that is by a biased competition mechanism (Rolls, E. T. and Deco, G., 2002; Deco, G. and Rolls, E. T., 2003; 2004; 2005a; 2005c).

It is thus becoming possible to start to understand not only where flavor is represented in the brain, but also how the affective value of smell, taste and flavor are represented, how these representations are influenced by visual stimuli and cognitive states, and how these representations fit into a wider picture of the brain processes underlying the affective or hedonic value of stimuli. This in turn helps to advance understanding of the neural basis of appetite, the control of food intake, and emotion, and their disorders (Rolls, E. T., 2005a).

Acknowledgments

Some of the research from the author's laboratory was supported by the Medical Research Council.

References

Baylis, L. L. and Rolls, E. T. 1991. Responses of neurons in the primate taste cortex to glutamate. Physiol. Behav. 49, 973–979.

Critchley, H. D. and Rolls, E. T. 1996a. Hunger and satiety modify the responses of olfactory and visual neurons in the primate orbitofrontal cortex. J. Neurophysiol. 75, 1673–1686.

Critchley, H. D. and Rolls, E. T. 1996b. Responses of primate taste cortex neurons to the astringent tastant tannic acid. Chem. Senses 21, 135–145.

Critchley, H. D. and Rolls, E. T. 1996c. Olfactory neuronal responses in the primate orbitofrontal cortex: analysis in an olfactory discrimination task. J. Neurophysiol. 75, 1659–1672.

de Araujo, I. E. T., Kringelbach, M. L., and Rolls, E. T. 2003a. Taste-olfactory convergence, and the representation of the pleasantness of flavour, in the human brain. Eur. J. Neurosci. 18, 2374–2390.

de Araujo, I. E. T., Kringelbach, M. L., Rolls, E. T., and Hobden, P. 2003b. The representation of umami taste in the human brain. J. Neurophysiol. 90, 313–319.

de Araujo, I. E. T., Kringelbach, M. L., Rolls, E. T., and McGlone, F. 2003c. Human cortical responses to water in the mouth, and the effects of thirst. J. Neurophysiol. 90, 1865–1876.

de Araujo, I. E. T., Rolls, E. T., Kringelbach, M. L., McGlone, F., and Phillips, N. 2003c. Taste-olfactory convergence, and the representation of the pleasantness of flavour, in the human brain. Eur. J. Neurosci. 18, 2374–2390.

de Araujo, I. E. T., Rolls, E. T., Velazco, M. I., Margot, C., and Cayeux, I. 2005. Cognitive modulation of olfactory processing. Neuron 46, 671–679.

Deco, G. and Rolls, E. T. 2003. Attention and working memory: a dynamical model of neuronal activity in the prefrontal cortex. Eur. J. Neurosci. 18, 2374–2390.

Deco, G. and Rolls, E. T. 2004. A neurodynamical cortical model of visual attention and invariant object recognition. Vision Res. 44, 621–644.

Deco, G. and Rolls, E. T. 2005a. Attention, short-term memory, and action selection: a unifying theory. Prog. Neurobiol. 76, 236–256.

Deco, G. and Rolls, E. T. 2005b. Synaptic and spiking dynamics underlying reward reversal in orbitofrontal cortex. Cerebral Cortex 15, 15–30.

Deco, G. and Rolls, E. T. 2005c. Neurodynamics of biased competition and co-operation for attention: a model with spiking neurons. J. Neurophysiol. 94, 295–313.

Faurion, A., Kobayakawa, T., and Cerf-Ducastel, B. 2005. Cerebral imaging in taste. Chem. Senses 30, i230–i231.

Francis, S., Rolls, E. T., Bowtell, R., McGlone, F., O'Doherty, J., Browning, A., Clare, S., and Smith, E. 1999. The representation of pleasant touch in the brain and its relationship with taste and olfactory areas. Neuroreport 10, 453–459.

Kadohisa, M., Rolls, E. T., and Verhagen, J. V. 2004. Orbitofrontal cortex neuronal representation of temperature and capsaicin in the mouth. Neuroscience 127, 207–221.

Kadohisa, M., Rolls, E. T., and Verhagen, J. V. 2005a. Neuronal representations of stimuli in the mouth: the primate insular taste cortex, orbitofrontal cortex, and amygdala. Chem. Senses 30, 401–409.

Kadohisa, M., Rolls, E. T., and Verhagen, J. V. 2005b. The primate amygdala: neuronal representations of the viscosity, fat texture, grittiness and taste of foods. Neuroscience 132, 33–48.

Kringelbach, M. L., O'Doherty, J., Rolls, E. T., and Andrews, C. 2003. Activation of the human orbitofrontal cortex to a liquid food stimulus is correlated with its subjective pleasantness. Cereb. Cortex 13, 1064–1071.

McCabe, C. and Rolls, E. T. 2007. Umami: a delicious flavor formed by convergence of taste and olfactory pathways in the human brain. Eur. J. Neurosci. 25, 1855–1864.

Norgren, R. 1984. Central Neural Mechanisms of Taste. In: Handbook of Physiology – The Nervous System III Sensory Processes 1 (*ed*. I. Darien-Smith), pp. 1087–1128. American Physiological Society.

O'Doherty, J., Rolls, E. T., Francis, S., Bowtell, R., McGlone, F., Kobal, G., Renner, B., and Ahne, G. 2000. Sensory-specific satiety related olfactory activation of the human orbitofrontal cortex. Neuroreport 11, 893–897.

O'Doherty, J., Rolls, E. T., Francis, S., Bowtell, R., and McGlone, F. 2001. The representation of pleasant and aversive taste in the human brain. J. Neurophysiol. 85, 1315–1321.

Osterbauer, R. A., Matthews, P. M., Jenkinson, M., Beckmann, C. F., Hansen, P. C., and Calvert, G. A. 2005. The color of scents: chromatic stimuli modulate odor responses in the human brain. J. Neurophysiol. 93, 3434–3441.

Poellinger, A., Thomas, R., Lio, P., Lee, A., Makris, N., Rosen, B. R., and Kwong, K. K. 2001. Activation and habituation in olfaction – an fMRI study. Neuroimage 13, 547–560.

Pritchard, T. C., Hamilton, R. B., Morse, J. R., and Norgren, R. 1986. Projections of thalamic gustatory and lingual areas in the monkey, *Macaca fascicularis*. J. Comp. Neurol. 244, 213–228.

Rolls, E. T. 1997. Taste and olfactory processing in the brain and its relation to the control of eating. Crit. Rev. Neurobiol. 11, 263–287.

Rolls, E. T. 1999. The Brain and Emotion. Oxford University Press.

Rolls, E. T. 2000a. The orbitofrontal cortex and reward. Cereb. Cortex 10, 284–294.

Rolls, E. T. 2000b. Taste, Olfactory, Visual and Somatosensory Representations of the Sensory Properties of Foods in the Brain, and their Relation to the Control of Food Intake. In: Neural and Metabolic Control of Macronutrient Intake (*eds*. H. R. Berthoud and R. J. Seeley), pp. 247–262. CRC Press.

Rolls, E. T. 2001. The rules of formation of the olfactory representations found in the orbitofrontal cortex olfactory areas in primates. Chem. Senses 26, 595–604.

Rolls, E. T. 2002a. The Cortical Representation of Taste and Smell. In: Olfaction, Taste and Cognition (*eds*. G. Rouby, B. Schaal, D. Dubois, R. Gervais, and A. Holley), pp. 367–388. Cambridge University Press.

Rolls, E. T. 2002b. The Functions of the Orbitofrontal Cortex. In: Principles of Frontal Lobe Function (*eds*. D. T. Stuss and R. T. Knight), pp. 354–375. Oxford University Press.

Rolls, E. T. 2005a. Emotion Explained. Oxford University Press.

Rolls, E. T. 2005b. Taste, olfactory, and food texture processing in the brain, and the control of food intake. Physiol. Behav. 85, 45–56.

Rolls, E. T. 2006. Brain mechanisms underlying flavour and appetite. Philos. Trans. R. Soc. B 361, 1123–1136.

Rolls, E. T. 2007. The Anterior and Midcingulate Cortices and Reward. In: Cingulate Neurobiology and Disease, Vol. 1,

Infrastructure, Diagnosis and Treatment (*ed*. B. Vogt), Chapter 8. Oxford University Press.
Rolls, E. T. and Baylis, L. L. 1994. Gustatory, olfactory, and visual convergence within the primate orbitofrontal cortex. J. Neurosci. 14, 5437–5452.
Rolls, E. T. and Deco, G. 2002. Computational Neuroscience of Vision. Oxford University Press.
Rolls, E. T. and Rolls, J. H. 1997. Olfactory sensory-specific satiety in humans. Physiol. Behav. 61, 461–473.
Rolls, E. T. and Scott, T. R. 2003. Central Taste Anatomy and Neurophysiology. In: Handbook of Olfaction and Gustation, 2nd edn. (*ed*. R. L. Doty), pp. 679–705. Dekker.
Rolls, E. T., Critchley, H. D., and Treves, A. 1996b. The representation of olfactory information in the primate orbitofrontal cortex. J. Neurophysiol. 75, 1982–1996.
Rolls, E. T., Critchley, H. D., Browning, A. S., Hernadi, A., and Lenard, L. 1999. Responses to the sensory properties of fat of neurons in the primate orbitofrontal cortex. J. Neurosci. 19, 1532–1540.
Rolls, E. T., Critchley, H., Wakeman, E. A., and Mason, R. 1996a. Responses of neurons in the primate taste cortex to the glutamate ion and to inosine 5′-monophosphate. Physiol. Behav. 59, 991–1000.
Rolls, E. T., Kringelbach, M. L., and de Araujo, I. E. T. 2003a. Different representations of pleasant and unpleasant odors in the human brain. Eur. J. Neurosci. 18, 695–703.
Rolls, E. T., Scott, T. R., Sienkiewicz, Z. J., and Yaxley, S. 1988. The responsiveness of neurones in the frontal opercular gustatory cortex of the macaque monkey is independent of hunger. J. Physiol. 397, 1–12.
Rolls, E. T., Sienkiewicz, Z. J., and Yaxley, S. 1989. Hunger modulates the responses to gustatory stimuli of single neurons in the caudolateral orbitofrontal cortex of the macaque monkey. Eur. J. Neurosci. 1, 53–60.
Rolls, E. T., Verhagen, J. V., and Kadohisa, M. 2003b. Representations of the texture of food in the primate orbitofrontal cortex: neurons responding to viscosity, grittiness and capsaicin. J. Neurophysiol. 90, 3711–3724.
Rolls, E. T., Yaxley, S., and Sienkiewicz, Z. J. 1990. Gustatory responses of single neurons in the caudolateral orbitofrontal cortex of the macaque monkey. J. Neurophysiol. 64, 1055–1066.
Scott, T. R., Yan, J., and Rolls, E. T. 1995. Brain mechanisms of satiety and taste in macaques. Neurobiology 3, 281–292.
Scott, T. R., Yaxley, S., Sienkiewicz, Z. J., and Rolls, E. T. 1986. Gustatory responses in the frontal opercular cortex of the alert cynomolgus monkey. J. Neurophysiol. 56, 876–890.
Small, D. M., Zald, D. H., Jones-Gotman, M., Zatorre, R. J., Pardo, J. V., Frey, S., and Petrides, M. 1999. Human cortical gustatory areas: a review of functional neuroimaging data. Neuroreport 10, 7–14.
Sobel, N., Prabkakaran, V., Zhao, Z., Desmond, J. E., Glover, G. H., Sullivan, E. V., and Gabrieli, J. D. E. 2000. Time course of odorant-induced activation in the human primary olfactory cortex. J. Neurophysiol. 83, 537–551.
Thorpe, S. J., Rolls, E. T., and Maddison, S. 1983. Neuronal activity in the orbitofrontal cortex of the behaving monkey. Exp. Brain Res. 49, 93–115.
Verhagen, J. V., Kadohisa, M., and Rolls, E. T. 2004. The primate insular/opercular taste cortex: neuronal representations of the viscosity, fat texture, grittiness and taste of foods in the mouth. J. Neurophysiol. 92, 1685–1699.
Verhagen, J. V., Rolls, E. T., and Kadohisa, M. 2003. Neurons in the primate orbitofrontal cortex respond to fat texture independently of viscosity. J. Neurophysiol. 90, 1514–1525.
Wilson, F. A. W. and Rolls, E. T. 2005. The primate amygdala and reinforcement: a dissociation between rule-based and associatively-mediated memory revealed in amygdala neuronal activity. Neuroscience 133, 1061–1072.
Yaxley, S., Rolls, E. T., and Sienkiewicz, Z. J. 1988. The responsiveness of neurons in the insular gustatory cortex of the macaque monkey is independent of hunger. Physiol. Behav. 42, 223–229.
Yaxley, S., Rolls, E. T., Sienkiewicz, Z. J., and Scott, T. R. 1985. Satiety does not affect gustatory activity in the nucleus of the solitary tract of the alert monkey. Brain Res. 347, 85–93.
Zald, D. H. and Pardo, J. V. 1997. Emotion, olfaction, and the human amygdala: amygdala activation during aversive olfactory stimulation. Proc. Natl. Acad. Sci. U. S. A. 94, 4119–4124.
Zatorre, R. J., Jones-Gotman, M., Evans, A. C., and Meyer, E. 1992. Functional localization of human olfactory cortex. Nature 360, 339–340.

Further Reading

Aggleton, J. P. (*ed*). 2000. The Amygdala 2nd. Edn., Oxford University Press.
Zald, D. H. and Rauch, S. L. (*eds*.) 2006. The Orbitofrontal Cortex. Oxford University Press.

4.27 The Aging Gustatory System

S S Schiffman, Duke University Medical Center, Durham, NC, USA

© 2008 Elsevier Inc. All rights reserved.

4.27.1	**Introduction**	479
4.27.2	**Changes of Taste at Threshold Levels**	480
4.27.2.1	Taste Thresholds in a General Elderly Population	480
4.27.2.1.1	Sodium salts	482
4.27.2.1.2	Bitter compounds	483
4.27.2.1.3	Sweet compounds	483
4.27.2.1.4	Acids	484
4.27.2.1.5	Astringent compounds	484
4.27.2.1.6	Amino acids	485
4.27.2.1.7	Glutamate salts	485
4.27.2.1.8	Fats (emulsified oils)	485
4.27.2.1.9	Complex polysaccharides/gums	485
4.27.2.1.10	Electric taste	485
4.27.2.2	Nonuniformity of Taste Loss	485
4.27.2.3	Taste Thresholds and Nutritional Value	486
4.27.3	**Suprathreshold Taste Recognition and Identification**	486
4.27.3.1	Magnitude Estimation	486
4.27.3.2	Difference Thresholds	487
4.27.3.3	Qualitative Perception in the Elderly	487
4.27.3.4	Other Suprathreshold Findings in the Elderly	488
4.27.4	**Medications Associated with Taste Alterations**	488
4.27.5	**Medical Conditions Associated with Taste Complaints**	491
4.27.6	**Cause of Taste Losses in the Absence of Drugs and Disease**	492
4.27.7	**Final Comment**	494
References		495

4.27.1 Introduction

Demographic shifts in the global population are occurring rapidly with escalation in both the number and the percentage of elderly persons (Cohen, J. E., 2003; Administration on Aging, 2004). Over 400 million people worldwide are currently 65 years of age or greater (Davies, A. M., 1989; Cohen, J. E., 2003), and this number is expected to exceed 1.5 billion by 2050 (Cohen, J. E., 2003). A significant proportion of this population will have taste impairments that can potentially alter the health and well-being of the elderly. While disorders of taste can occur throughout the lifespan, they are far more prevalent in an older population. Diagnostic terms for taste disorders include ageusia (absence of taste), hypogeusia (diminished sensitivity of taste), and dysgeusia (distortion of normal taste). Research studies and clinical reports indicate that hypogeusia and dysgeusia commonly occur in older individuals (Schiffman, S. S., 1993; 1997) while ageusia is relatively rare (Pribitkin, E. *et al*., 2003). The aim of this chapter is to provide an overview of gustatory perception in older individuals. Topics to be covered include changes of taste perception at thresholds levels, changes of taste perception at suprathreshold levels, medications and medical conditions associated with taste alterations, as well as taste losses in the absence of drugs and disease.

An intact sense of taste is vital for persons of all ages. Taste is a phylogenetically primitive sense that serves both as a precautionary mechanism and as the initial internal analyzer for materials ingested into the oral cavity. It enables us to distinguish between nutritive chemicals (such as sugars) and potentially harmful compounds (such as bitter toxic alkaloids).

Failure to detect the bitter taste warning from alkaloid poisons at the gateway to the stomach and intestines can have deadly consequences. Overall, taste sensations serve as a quality check for the identity and safety of food in the mouth (i.e., should we swallow the contents in our mouths or spit them out?). In addition to their role in identity and safety, taste sensations (along with smell and trigeminal sensations) contribute to the digestion of food by triggering salivary, gastric, pancreatic, and intestinal secretions that prepare the body for the absorption of nutrients (Giduck, S. A. *et al.*, 1987; Schiffman, S. S., and Warwick, Z. S., 1992; Teff, K. L. and Engelman, K., 1996). Gustatory signals additionally serve as indicators of the nutritional value of a food from a learned association of the food's taste with its postingestive effects (Warwick, Z. S. and Schiffman, S. S., 1991; Drewnowski, A. *et al.*, 1995; Stubbs, R. J. and Whybrow, S., 2004). This learned association of taste signals with metabolic consequences enables food intake and meal size to be modulated in anticipation of nutritional needs. Thus, alterations in the ability to taste are not merely an inconvenience but rather can impact survival, general health, and quality of life.

The qualitative range of taste has not been fully established. Traditionally, much taste research has presumed the existence of only four (or possibly five) independent taste qualities, the four so-called basic or primary tastes (sweet, sour, salty, and bitter) and a fifth quality, the taste of glutamate salts called umami. However, data are accumulating that suggest other sensory qualities such as fatty (Gilbertson, T. A. *et al.*, 1997), metallic (Schiffman, S. S., 2000), starchy/polysaccharide (Sclafani, A., 2004), chalky (Schiffman, S. S., and Erickson, R. P., 1993), and astringent (Schiffman, S. S., *et al.*, 1992) are carried by taste nerves. Thus, while the terms sweet, sour, salty, and bitter may be familiar and have linguistic relevance, they do not describe the entire range of tastes perceived by humans and other animals.

The ability to perceive the taste signals of specific sensory qualities (such as salty or sweet) are especially important for subgroups of the elderly population such as those with hypertension who must comply with salt-restricted diets or those with diabetes who must reduce their consumption of sugar (Schiffman, S. S., 1997). Reduced sensitivity to the oral component of fats in the elderly can increase their risk of cardiovascular disease, diabetes, hypertension, and other conditions in which high fat intake is contraindicated. Taste losses along with other physiological and psychological factors also contribute to the observed decline in food intake in many older persons (Morley, J. E., 2001). Overall, taste disorders that impair or distort the taste of palatable as well as unpalatable substances can increase the risk of numerous adverse safety and health-related issues for an elderly population.

4.27.2 Changes of Taste at Threshold Levels

4.27.2.1 Taste Thresholds in a General Elderly Population

An overview of research studies indicates that the detection threshold (DT) and recognition threshold (RT) for simple basic tastes (sweet, sour, salty, and bitter) are moderately elevated in older persons compared to a younger cohort (e.g., Richter, C. P. and Campbell, K. H., 1940; Harris, H. and Kalmus, H., 1949; Bourlière, F. *et al.*, 1958; Hinchcliff, R. 1958; Cooper, R. M. *et al.*, 1959; Kalmus, H. and Trotter, W. R., 1962; Glanville, E. V. *et al.*, 1964; Smith, S. E. and Davies, P. D., 1973; Grzegorczyk, P. B. *et al.*, 1979; Murphy, C., 1979; Schiffman, S.S. *et al.*, 1979; Dye, C. J. and Koziatek, D. A., 1981; Schiffman, S. S. *et al.*, 1981; Moore, L. M. *et al.*, 1982; Weiffenbach, J. M. *et al.*, 1982; Schiffman, S. S. *et al.*, 1990; 1991; Schiffman, S. S., 1993; Schiffman, S. S. *et al.*, 1994; Stevens, J. C. *et al.*, 1995; Stevens, J. C., 1996; Stevens J. C. and Traverzo, A., 1997; Schiffman, S. S. *et al.*, 1998; Mojet, J. *et al.*, 2001; Yamauchi, Y. *et al.*, 2002; Fukunaga, A. *et al.*, 2005). An elevated DT indicates that the elderly require the presence of more molecules (or ions) for a sensation to be perceived compared to younger persons – that is, the elderly have reduced absolute sensitivity. An elevated RT signifies that a greater concentration of a tastant is required before it can be correctly identified. Furthermore, thresholds are higher for a compound in a mixture than in a simple aqueous solution (Stevens, J. C. and Traverzo, A., 1997), that is, other ingredients in a mixture can mask significant food components such as NaCl, making it harder to detect and recognize salt in food than alone in a simple aqueous solution.

Tables 1–9 show the results of studies that compare mean thresholds for the elderly with those of the young for a range of compounds including sodium salts with different anions (Schiffman, S. S. *et al.*, 1990), bitter compounds (Schiffman, S. S. *et al.*, 1994), sweeteners (Schiffman, S. S. *et al.*, 1981), acids

Table 1 Mean detection and recognition thresholds for elderly and young subjects for sodium salts with different anions

	Detection thresholds			*Recognition thresholds for saltiness*		
	Elderly, E (M)	*Young, Y (M)*	*E/Y*	*Elderly, E (M)*	*Young, Y (M)*	*E/Y*
MSG (monosodium glutamate, $\lambda = 26.0$)[a]	0.00638	0.00126	5.06	0.0091	0.00207	4.41
Na acetate ($\lambda = 40.9$)	0.0190	0.00242	7.84	0.0229	0.00952	2.41
Na ascorbate ($\lambda = 39.7$)	0.0250	0.00404	6.19	0.0265	0.00809	3.28
Na carbonate ($\lambda = 44.5$)	0.00829	0.00218	3.79	0.0234	0.00425	5.51
Na chloride ($\lambda = 76.3$)	0.01850	0.00238	7.76	0.0227	0.00815	2.79
Na citrate ($\lambda = 210.6$)	0.0130	0.000531	24.5	0.0187	0.00190	9.84
Na phosphate monobasic ($\lambda = 33.0$)	0.0160	0.00307	5.21	0.0253	0.01140	2.22
Na succinate ($\lambda = 117.6$)	0.0138	0.000854	16.2	0.0167	0.00217	7.71
Na sulfate ($\lambda = 160.0$)	0.0283	0.000981	28.8	0.0349	0.00322	10.86
Na tartrate ($\lambda = 119.2$)	0.0159	0.00151	10.5	0.0277	0.00295	9.39

[a] λ is the molar conductivity of the anion at infinite dilution, 25 °C, $ohm^{-1}\,cm^2\,mol^{-1}$.
Data are from Schiffman, S. S., Crumbliss, A. L., Warwick, Z. S., and Graham, B. G. 1990. Thresholds for sodium salts in young and elderly subjects: correlation with molar conductivity of anion. Chem. Senses 15, 671–678.

Table 2 Mean detection and recognition thresholds for bitter compounds in elderly and young subjects

	Detection thresholds			*Recognition thresholds*		
	Elderly (E)	*Young (Y)*	*E/Y*	*Elderly (E)*	*Young (Y)*	*E/Y*
Caffeine ($\log P = -0.097$)[a]	1.99 mM	1.30 mM	1.53	6.74 mM	1.87 mM	3.60
Denatonium benzoate ($\log P = -0.088$)	0.0323 μM	0.0115 μM	2.81	0.0387 μM	0.0123 μM	3.14
KNO_3 ($\log P = -4.0$)	32.7 mM	1.91 mM	17.1	271 mM	5.97 mM	45.4
$MgCl_2$ ($\log P = -3.026$)	5.20 mM	1.02 mM	5.10	21.8 mM	20.3 mM	1.07
$MgNO_3$ ($\log P = -4.0$)	33.3 mM	1.40 mM	23.8	191 mM	14.8 mM	12.9
$MgSO_4$ ($\log P = -4.0$)	6.08 mM	0.323 mM	18.8	14.8 mM	2.59 mM	5.71
Naringin ($\log P = -0.114$)	0.138 mM	0.0427 mM	3.23	0.195 mM	0.0561 mM	3.48
Phenylthiocarbamide ($\log P = +0.743$)	1.26 mM	0.591 mM	2.13	1.74 mM	1.21 mM	1.44
Quinine HCl ($\log P = +1.082$)	8.07 μM	3.99 μM	2.02	12.3 μM	4.75 μM	2.59
Quinine sulfate ($\log P = +1.036$)	8.75 μM	2.04 μM	4.29	12.3 μM	2.53 μM	4.86
Sucrose octaacetate ($\log P = +1.010$)	5.32 μM	3.89 μM	1.37	22.8 μM	5.30 μM	4.30
Urea ($\log P = -2.190$)	0.116 M	0.103 M	1.12	0.245 M	0.134 M	1.83

[a] Logarithm of the 1-octanol/water partition coefficient.
Data are from Schiffman, S. S., Gatlin, L. A., Frey, A. E., Heiman, S. A., Stagner, W. C., and Cooper, D. C. 1994. Taste perception of bitter compounds in young and elderly persons: relation to lipophilicity of bitter compounds. Neurobiol. Aging 15, 743–750.

(Schiffman, S. S., 1993), astringent compounds (Schiffman, S. S. *et al.*, 1989), amino acids (Schiffman, S. S. *et al.*, 1979) including glutamate salts (Schiffman, S. S. *et al.*, 1991), fats (Schiffman, S. S., *et al.*, 1998), and gums (Schiffman, S. S. *et al.*, 1989). The subjects in these studies were elderly individuals who took an average of 3.4 medications but who otherwise led active, normal lives. For DTs, the ratio of DT (elderly)/DT (young) revealed that DTs in the elderly were higher by the following amounts: 11.6 times higher for sodium salts; 2.7 times higher for sweeteners; 4.3 times higher for acids; 2.8 for astringent compounds; 7.0 times higher for bitter compounds; 2.5 times higher for amino acids; 5.0 times higher for glutamate salts; 3.1 times higher for fats/oils; and 3.7 times higher for polysaccharides/gums. The average loss in detection across this qualitative range of compounds is 4.74. However, the degree of loss within a group (such as sodium salts) was not uniform but rather varied with the chemical structure of the compounds tested. For RTs, the ratio of RT (elderly)/RT (young) revealed that RTs in the elderly were higher by the following amounts: 5.8 times higher for sodium salts; 2.1 times higher for sweeteners; 6.8 times higher for acids with sour tastes; 3.0 for astringent compounds; 7.5 times higher for bitter compounds; and 3.0 times higher for polysaccharides/gums. The average loss in recognition across these taste qualities is 4.7.

Table 3 Mean detection and recognition thresholds for sweeteners in elderly and young subjects

	Detection thresholds			*Recognition thresholds*		
	Elderly (E)	***Young (Y)***	***E/Y***	***Elderly (E)***	***Young (Y)***	***E/Y***
Acesulfame-K	74.7 μM	44.4 μM	1.68	239 μM	161 μM	1.48
Aspartame	91.3 μM	22.4 μM	4.07	124 μM	44.9 μM	2.76
Calcium cyclamate	0.412 mM	0.266 mM	1.55	1.69 mM	1.33 mM	1.27
Fructose	10.1 mM	4.39 mM	2.30	26.4 mM	16.6 mM	1.59
Monellin	0.0913 μM	0.0195 μM	4.67		0.0676 μM	
Neohesperidin dihydrochalcone	4.60 μM	2.20 μM	2.09		5.28 μM	
Rebaudioside	13.0 μM	4.61 μM	2.82		13.6 μM	
Sodium saccharin	42.4 μM	14.7 μM	2.88	137 μM	49.7 μM	2.76
Stevioside	16.0 μM	5.31 μM	3.02		23.7 μM	
Thaumatin	0.133 μM	0.0716 μM	1.86		0.201 μM	
D-Tryptophan	0.322 mM	0.109 mM	2.95	1.45 mM	0.546 mM	2.66

Data are from Schiffman, S. S., Lindley, M. G., Clark, T. B., and Makino, C. 1981. Molecular mechanism of sweet taste: relationship of hydrogen bonding to taste sensitivity for both young and elderly. Neurobiol. Aging 2, 173–185.

Table 4 Mean detection and recognition thresholds for acids in elderly and young subjects

	Detection thresholds			*Recognition thresholds for sourness*		
Stimulus	***Elderly, E (mM)***	***Young, Y (mM)***	***E/Y***	***Elderly, E (mM)***	***Young, Y (mM)***	***E/Y***
Acetic acid	0.273	0.106	2.58	0.819	0.294	2.79
Ascorbic acid	0.725	0.281	2.58	2.190	0.396	5.53
Citric acid	0.375	0.0498	7.53	0.816	0.131	6.23
Glutamic acid	0.463	0.0920	5.03	1.500	0.309	4.85
Hydrochloric acid	0.200	0.0179	11.17	0.477	0.0226	21.11
Succinic acid	0.188	0.132	1.42	1.330	0.174	7.64
Sulfuric acid	0.100	0.0468	2.14	0.170	0.0468	3.63
Tartaric acid	0.163	0.0864	1.89	0.297	0.131	2.27

Data are from Schiffman, S. S. 1993. Perception of taste and smell in elderly persons. Crit. Rev. Food Sci. Nutr. 33, 17–26.

Table 5 Mean detection and recognition thresholds for acidic/astringent compounds in elderly and young subjects

	Detection thresholds			*Recognition thresholds for astringency*		
Stimulus	***Elderly, E (mM)***	***Young, Y (mM)***	***E/Y***	***Elderly, E (mM)***	***Young, Y (mM)***	***E/Y***
Gallic acid	0.780	0.250	3.12	2.07	1.10	1.88
Tartaric acid	0.220	0.0549	4.01	0.324	0.0689	4.70
Tannic acid	0.072	0.0271	2.66	0.295	0.0528	5.59
Catechin	1.48	1.18	1.25	2.500	1.56	1.60
Ammonium alum	0.172	0.0780	2.21	0.487	0.244	2.00
Potassium alum	0.454	0.120	3.78	1.380	0.723	1.91

4.27.2.1.1 Sodium salts

Table 1 compares the taste DTs and RTs for 10 sodium salts in young and elderly persons (see Schiffman, S. S. *et al.*, 1990). The DTs of these salts were highly correlated with the molar conductivity of the anion. Molar conductivity (λ) is a measure of the electrical charge carried by the anion per unit time. Furthermore, age-related decrements as determined by the ratio DT (elderly)/DT (young) were greatest for anions with the largest molar conductivity (Na sulfate, Na tartrate, Na citrate, and Na succinate). That is, age-related losses in sensitivity

to sodium salts were greatest for anions with the highest charge mobility. RTs are also given in Table 1 for those subjects who did perceive saltiness; however, some subjects did not recognize a salty component for some of these sodium salts at concentrations 64 times higher than the DT.

Table 6 Mean detection thresholds for amino acids in elderly and young subjects

Stimulus	*Elderly (E)*	*Young (Y)*	*E/Y*
L-Alanine	19.5 mM	16.2 mM	1.20
L-Arginine	1.12 mM	1.20 mM	0.93
L-Arginine HCl	2.39 mM	1.23 mM	1.94
L-Asparagine	9.33 mM	1.62 mM	5.75
L-Aspartic acid	0.501 mM	0.182 mM	2.75
L-Cysteine	0.390 mM	0.0630 mM	6.19
L-Cysteine HCl	20.0 μM	16.0 μM	1.25
L-Glutamic acid	0.100 mM	0.0630 mM	1.59
L-Glutamine	26.9 mM	9.77 mM	2.75
L-Glycine	0.0617 M	0.0309 M	2.00
L-Histidine	6.45 mM	1.23 mM	5.24
L-Histidine HCl	0.389 mM	0.0794 mM	4.90
L-Isoleucine	12.0 mM	7.41 mM	1.62
L-Leucine	12.9 mM	6.45 mM	2.00
L-Lysine	2.24 mM	0.708 mM	3.16
L-Lysine HCl	2.09 mM	0.447 mM	4.68
L-Methionine	2.63 mM	3.72 mM	0.71
L-Phenylalanine	19.1 mM	6.61 mM	2.89
L-Proline	0.0372 M	0.0151 M	2.46
L-Serine	0.0263 M	0.0209 M	1.26
L-Threonine	0.020 M	0.0257 M	0.78
L-Tryptophan	2.88 mM	2.29 mM	1.26
L-Valine	0.0115 M	0.00416 M	2.76

Data are from Schiffman, S. S., Hornack, K., and Reilly, D. 1979. Increased taste thresholds of amino acids with age. Am. J. Clin. Nutr. 32, 1622–1627.

4.27.2.1.2 Bitter compounds

Table 2 compares the DTs and RTs for 12 bitter compounds in young and elderly subjects (see Schiffman, S. S. *et al.*, 1994). Subjects included both tasters and nontasters of the bitter compound phenylthiocarbamide (PTC). A strong relationship between bitter threshold values and the logarithm of the octanol/water partition coefficient ($\log P$) was found for both young and elderly subjects. The logarithm of the 1-octanol/water partition coefficient ($\log P$) is a measure of the lipophilicity of the bitter compound. The greatest losses at the threshold level for the elderly were for the least lipophilic compounds, that is, $MgNO_3$, $MgSO_4$, and KNO_3. There were no differences in DTs or RTs for tasters and nontasters of PTC with the exception of PTC itself.

4.27.2.1.3 Sweet compounds

Table 3 compares the taste DTs and RTs for 11 sweeteners in young and elderly persons. Sweeteners with the highest DTs are natural sugars for both age groups (see Schiffman, S. S. *et al.*, 1981). The fact that high concentrations are needed for the detection of sugars may have had survival value for past generations who needed to choose only the most caloric foods in a natural environment. Sweeteners with the lowest DTs (i.e., low concentrations are

Table 7 Mean detection thresholds for glutamate salts with and without the taste enhancer inosine 5′-monophosphate (IMP) in elderly and young subjects

Stimulus	*Elderly (E)*	*Young (Y)*	*E/Y*
Sodium glutamate	2.83 mM	0.902 mM	3.14
Sodium glutamate with 0.1 mM IMP	0.888 mM	0.113 mM	7.86
Sodium glutamate with 1 mM IMP	0.145 mM	0.0480 mM	3.02
Potassium glutamate	7.69 mM	0.902 mM	8.53
Potassium glutamate with 0.1 mM IMP	0.549 mM	0.106 mM	5.18
Potassium glutamate with 1 mM IMP	0.0928 mM	0.0108 mM	8.59
Ammonium glutamate	4.26 mM	1.08 mM	3.94
Ammonium Glutamate with 0.1 mM IMP	0.458 mM	0.139 mM	3.29
Ammonium glutamate with 1 mM IMP	0.129 mM	0.0343 mM	3.76
Calcium diglutamate	1.09 mM	0.292 mM	3.73
Calcium diglutamate with 0.1 mM IMP	0.327 mM	0.0606 mM	5.40
Calcium diglutamate with 1 mM IMP	0.0692 mM	0.0190 mM	3.64
Magnesium diglutamate	1.86 mM	0.253 mM	7.35
Magnesium diglutamate with 0.1 mM IMP	0.289 mM	0.0421 mM	6.86
Magnesium diglutamate with 1 mM IMP	0.0452 mM	0.0257 mM	1.76
IMP	1.99 mM	0.430 mM	4.63

Data are from Schiffman, S. S., Frey, A. E., Luboski, J. A., Foster, M. A., and Erickson, R. P. 1991. Taste of glutamate salts in young and elderly subjects: role of inosine 5′-monophosphate and ions. Physiol. Behav. 49, 843–854.

Table 8 Mean detection thresholds (%) for three oils (MCT, soybean, and mineral) in four emulsifiers (acacia gum, Emplex, Tween 80, and Na caseinate) in oil-in-water emulsion

Oil	*Emulsifier*	*Elderly subjects (%)*	*Young subjects (%)*	*Ratio, E/Y*
MCT[a]	Acacia	10.1	2.85	3.54
Soybean	Acacia	12.9	4.02	3.20
Mineral	Acacia	9.77	4.43	2.20
MCT	Emplex	25.0	3.93	6.37
Soybean	Emplex	14.9	6.52	2.28
Mineral	Emplex	20.0	8.85	2.26
MCT	Tween 80	19.3	5.35	3.60
Soybean	Tween 80	17.7	5.85	3.02
Mineral	Tween 80	19.9	5.77	3.44
MCT	Na caseinate	13.6	6.18	2.20
Soybean	Na caseinate	13.0	5.35	2.43
Mineral	Na caseinate	13.4	4.27	3.13

[a]Medium-chain triglycerides.
Data are from Schiffman, S. S., Graham, B. G., Sattely-Miller, E. A., and Warwick, Z. S. 1998. Orosensory perception of dietary fat. Curr. Dir. Psychol. Sci. 7, 137–143.

Table 9 Mean detection and recognition thresholds for five polysaccharides/gums

	Detection thresholds			*Recognition thresholds for thickness*		
Stimulus	*Elderly, E (%)*	*Young, Y (%)*	*E/Y*	*Elderly, E (%)*	*Young, Y (%)*	*E/Y*
Acacia gum	1.02	0.644	1.58	3.12	1.44	2.17
Guar gum	0.116	0.057	2.04	0.42	0.22	1.91
Locust bean gum	0.43	0.061	7.05	0.74	0.22	3.36
Xanthan gum	0.238	0.0396	6.01	0.41	0.071	5.77
Algin	0.115	0.0605	1.90	0.26	0.15	1.73

Data from Schiffman, S. S., Rascoe, D., and Garcia, R. A. 1989. The effects of age and race on thresholds and magnitude estimates of edible gums. Chem. Senses 14, 743.

detected) for both age groups were those compounds with the greatest possible sites capable of intermolecular hydrogen bonding with the sweetener taste receptor. The RTs for the large sweetener molecules such as monellin and thaumatin were extremely variable in the elderly, so means are not given.

4.27.2.1.4 Acids

Table 4 compares the DTs and RTs for eight acids with sour tastes in young and elderly persons (Schiffman, S. S., 1993). The loss in sensitivity with age for HCl, the acid with the lowest molecular weight, was significantly greater than losses for the organic acids.

4.27.2.1.5 Astringent compounds

DTs and RTs for six astringent compounds are given in Table 5. DTs for astringent compounds are in the same general range as that for the acids in Table 4. This is most likely due to the fact that all of these astringent compounds have pH values below 3.5 at the concentrations tested. RTs for astringency were up to six times higher than the DTs for astringent compounds in young subjects and four times higher for elderly subjects. Each of these astringent compounds was reported to have sour and bitter tastes that emerged at concentrations intermediate between the DT and RT for astringency. Astringent compounds are found in natural food products and are important sensory components of many beverages such as wine, tea, and fruit juices (Bate-Smith, E. C., 1954; Robichaud, J. L. and Noble, A. C., 1990). Astringency is associated with a drying or a puckering sensation on the tongue and in the oral cavity. A portion of this sensation appears to be transmitted through gustatory nerves because patients with severed trigeminal nerves report drying or puckering sensations on the tongue (the trigeminal nerve innervates the buccal cavity of the mouth and the first 2/3 of the tongue) (Schiffman, S. S., unpublished clinical tests).

4.27.2.1.6 Amino acids

Table 6 compares the taste DTs for 19 L-amino acids and 4 monohydrochloride derivatives in young and elderly persons (see Schiffman, S. S. *et al.*, 1979). The ratio DT (elderly)/DT (young) for 20 of the 23 amino acid compounds was >1, which was highly statistically significant. There were no major differences in the degree of loss with compound type although age-related losses tended to be higher for two amino acids with side chains containing basic groups (L-histidine and L-lysine) and their monohydrochloride derivatives.

4.27.2.1.7 Glutamate salts

Table 7 compares the DTs for five glutamate salts (sodium glutamate, potassium glutamate, ammonium glutamate, calcium diglutamate, and magnesium diglutamate) in young and elderly persons (see Schiffman, S. S. *et al.*, 1991). The effect of inosine 5′-monophosphate (IMP), a taste enhancer, on taste thresholds of glutamate compounds at two concentrations (0.1 and 1.0 mM IMP) was also investigated. While 0.1 mM IMP lowered thresholds for all the five salts in young but not older subjects, 1 mM IMP lowered thresholds in both young and elderly groups.

4.27.2.1.8 Fats (emulsified oils)

Recent data suggest that fats and oils have taste components because sensations from these stimuli can be detected on the lateral posterior sides of the tongue without tongue movement (Schiffman, S. S. *et al.*, 1998), and electrophysiological data indicate that fatty acids activate taste nerves (Gilbertson, T. A. *et al.*, 1997). Table 8 compares the mean DTs for three different oils in four different emulsifiers in young and elderly subjects. The oils were refined, bleached, deodorized soybean oil (long-chain triglyceride, LCT); medium-chain triglyceride (MCT) oil; and light mineral oil. These fats are LCTs, MCTs, and a mixture of liquid hydrocarbons from petroleum, respectively. Oil-in-water emulsions were made with each oil using one of the four different emulsifiers: Polysorbate 80 (Tween® 80), sodium stearoyl lactylate (Emplex), sodium caseinate, and acacia gum. Statistical analysis revealed significant main effects for age (elderly had higher thresholds) and emulsifier. The low DTs of the oils emulsified in acacia gum (which suspends fat globules in a matrix rather than acting as a surfactant) accounted for the main effect of emulsifier. There were no significant differences in the thresholds with or without nose clips. The mean DT of the oils across all conditions for young subjects was 5.30% oil (v/v) while mean DTs for the elderly was 15.8% oil (v/v). The lowest mean DT was obtained for MCT oil in acacia gum for young subjects (2.85%). The highest mean DT was obtained for MCT oil in Emplex for elderly subjects (25.0%).

4.27.2.1.9 Complex polysaccharides/gums

Gums are complex polysaccharides used as thickening and gelling agents in many foods such as mayonnaise, ice cream, syrups, cheese, and dietetic foods (Klose, R. E. and Glicksman, M., 1972). A portion of the oral sensation from polysaccharides in humans is transmitted through gustatory nerves because patients with severed trigeminal nerves can differentiate between water alone and gums in water when dropped on the tongue (Schiffman, S. S., unpublished clinical tests). Animal data also suggest that polysaccharides may have a taste (Sclafani, A. 2004). DTs and RTs for gums commonly added to foods are given in Table 9 (from Schiffman, S. S. *et al.* 1989). The ratio of DT (elderly)/DT (young) varied with the gum structure from 1.58 for acacia gum to 7.05 for locust bean gum. On the descriptor scales, subjects not only commented on the thickness but also used adjectives such as starchy.

4.27.2.1.10 Electric taste

Taste thresholds for electric stimulation of the tongue have also been compared in young and elderly subjects. Like thresholds for chemicals, these thresholds tend to be elevated with increasing age (Krarup, B. 1958; Hughes, G. 1969; Nakazato, M. *et al.*, 2002; Terada, T. *et al.*, 2004; Kettaneh, A. *et al.* 2005).

4.27.2.2 Nonuniformity of Taste Loss

It can be seen from the above studies that different stimuli have varying degrees of loss depending upon their chemical structure. This fact is reemphasized by a study of 65 elderly (aged 65–85 years) who were taking no medications other than vitamins. Correlations of taste DTs and RTs for NaCl, quinine HCl (QHCl), and sucrose with one another for unmedicated elderly are given in Table 10. DTs and RTs for a specific tastant were highly correlated with one another: QHCl DT–QHCl RT ($r = 0.69$), NaCl DT–NaCl RT ($r = 0.64$), and sucrose DT–sucrose RT ($r = 0.5$). RTs for NaCl, sucrose, and QHCl were also significantly correlated with one

Table 10 Correlation between thresholds with the same and different taste qualities

	NaCl DT	*NaCl RT*	*Sucrose DT*	*Sucrose RT*	*QHCl DT*	*QHCl RT*
NaCl DT	1.00	0.64, $p < 0.0001$	0.12, $p = 0.1886$	0.19, $p = 0.0304$	0.14, $p = 0.1228$	0.15, $p = 0.0861$
NaCl RT		1.00	0.13, $p = 0.1569$	0.30, $p = 0.0006$	0.17, $p = 0.0616$	0.27, $p = 0.0023$
Sucrose DT			1.00	0.50, $p < 0.0001$	0.08, $p = 0.3920$	0.06, $p = 0.5056$
Sucrose RT				1.00	0.19, $p = 0.0352$	0.26, $p = 0.0029$
QHCl DT					1.00	0.69, $p < 0.0001$
QHCl RT						1.00

another but to a lesser degree than the DTs and RTs for a specific tastant: NaCl RT–sucrose RT ($r = 0.30$), NaCl RT–QHCl RT ($r = 0.27$), and sucrose RT–QHCl RT ($r = 0.26$). All other taste intercorrelations among taste measures in Table 10 were 0.19 or less. Thus, if a person has a loss for the salty taste of NaCl, this does not necessarily mean that the person has a loss for other compounds.

4.27.2.3 Taste Thresholds and Nutritional Value

An interesting trend in threshold concentration levels in Tables 1–9 for both young and elderly is that compounds with high caloric or nutritional value such as sugars, fats, and amino acids tend to have higher DTs than certain noxious bitter compounds that can be detected in minute amounts. One possible explanation for the higher DTs for sugars, amino acids, and fats is that this allows only the high-caloric foods to be perceived in a natural setting rather than foods with low nutritional value. That is, too much taste at low concentrations could inhibit the intake of adequate calories.

4.27.3 Suprathreshold Taste Recognition and Identification

4.27.3.1 Magnitude Estimation

Suprathreshold taste studies using magnitude estimation (which relates the perceived intensity to concentration) show decrements in perceived intensity in the elderly (see Schiffman, S. S., 1997, for review). The slope of the psychophysical function that relates perceived intensity and concentration declines with age for a broad range of stimuli (Schiffman, S. S. and Clark, T. B. 1980; Schiffman, S. S., *et al.*, 1981; Cowart, B. J., 1983; Schiffman, S. S., *et al.*, 1994; Mojet, J. *et al.*, 2003). Cowart B. J. (1983) found that the ratios of slope (young)/slope (elderly) for basic tastes were as follows: sucrose, 1.39; citric acid, 1.30; NaCl, 1.25, and quinine sulfate, 1.73. Schiffman S. S. and Clark T. B. (1980) reported that the slopes of the perceived intensity/concentration curves for 23 amino acids for elderly subjects were always flatter than the slopes for young subjects. The mean ratio of slope (young)/slope (elderly) for all the 23 amino acids was 2.55. However, the ratio of the slopes varied greatly with the amino acids. The ratios for two amino acids with side chain containing acidic groups, L-aspartic acid and L-glutamic acid, were 10.9 and 4.5, respectively, while the ratios for L-lysine and L-proline were only 1.10 and 1.28, respectively.

Schiffman S. S. *et al.* (1981) reported that the mean ratio of slope (young)/slope (elderly) for ten sweeteners (all of those in Table 3 except monellin) was 2.06 with ratios greater than 1.0 for all sweeteners. Although the variability in the slopes for sweeteners was not as great as for amino acids, there was nonuniformity in the flattening of the slopes, which suggests that receptor site compositions for sweeteners can be altered by the aging process. The greatest depression in slope with age was found for thaumatin, rebaudioside, and neohesperidin dihydrochalcone, which are relatively large sweetener molecules with more possible sites for hydrogen bonding with the receptor. Schiffman S. S. *et al.* (1994) also used magnitude estimation to compare slopes for a set of bitter compounds (caffeine, denatonium benzoate, $MgCl_2$, $MgNO_3$, quinine HCl, quinine sulfate, and sucrose octa-acetate) in young and elderly subjects. Both tasters and nontasters of the bitter compound PTC were included as subjects in the study. The mean ratio of slope (young)/slope (elderly) for tasters was 1.76 and the mean ratio of slope (young)/slope (elderly) for nontasters was 1.19. This suggests that suprathreshold loss can be slightly greater for tasters than for nontasters. Mojet J. *et al.* (2003) also reported that the slopes of the psychophysical functions for the sweet, bitter, and umami

tastants in water were flatter in the elderly than in the young. As a group these studies indicate that suprathreshold taste intensity is reduced in elderly persons, and there is evidence for a differential decline based on the chemical structure. The relative contribution of normal aging and other health factors to this decline is not known, however, because medications were not controlled in these studies.

4.27.3.2 Difference Thresholds

Losses also occur in the ability to discriminate between different suprathreshold intensities of the same stimulus. Gilmore M. M. and Murphy C. (1989) found that while young subjects generally needed a 34% difference in concentration to perceive a perceptible difference in the bitterness of caffeine, the elderly required an increment of 74% increase. Schiffman S. S. (1993) reported that while young subjects generally needed only a 6–12% difference in a moderately intense concentration of NaCl to perceive a change, the elderly required an increment of 25% to distinguish a difference in saltiness. Nordin S. *et al.* (2003) also found that difference thresholds for citric acid and NaCl were larger in older individuals.

4.27.3.3 Qualitative Perception in the Elderly

In order to determine if there are any age-related differences in the qualitative taste perception, young and elderly subjects were asked to rate 20 tastants. Each tastant was evaluated on five different adjectives (sweet, sour, salty, bitter, and other) for a total of ten points distributed among the five qualities (Schiffman, S. S., 2000). Subjects were also asked to judge whether each stimulus gave the impression of a single taste (singular) or gave the impression that it existed in the form of two or more component tastes (nonsingular). The mean ratings for sweet, salty, sour, bitter, and other for each tastant in young and elderly subjects along with the percentage of subjects who perceived the tastant as singular are given in Table 11. Several findings emerged from the study. First, neither young nor elderly categorized tastants into four discrete groups; rather the majority of tastes were found to have an other component. That is,

Table 11 Mean quality and singularity ratings of 20 tastants by 12 young and 12 elderly subjects[a]

	Sweet		*Salty*		*Sour*		*Bitter*		*Other*		*Singular (%)*	
	Y	*E*	*Y*	*E*	*Y*	*E*	*Y*	*E*	*Y*	*E*	*Y*	*E*
Acetic acid (0.1 M)	0.8	1.7	1.1	0.8	4.8	6.2	3.1	0.2	0.2	1.1	58.3	25.0
L-Arginine (0.5 M)	1.0	0	0.2	0.8	1.3	0	2.4	0.9	5.1	8.3	66.7	58.3
Citric acid (0.01 M)	0.2	0	0.8	0.5	4.8	5.1	3.2	3.1	1.0	1.3	58.3	25.0
L-Cysteine HCl (0.005 M)	0.9	0	0.9	0.8	4.0	3.2	0.9	2.3	3.3	3.7	25.0	41.7
Fructose (0.8 M)	9.3	8.9	0.1	0	0	0	0.1	0	0.5	1.1	83.3	83.3
Glycine (0.5 M)	5.4	7.7	0.5	0.1	0.3	0.3	0.3	1.4	3.5	0.5	58.3	50.0
HCl (0.01 M)	0.1	0.3	1.7	0.4	5.5	5.7	2.4	1.2	0.3	2.4	33.3	58.3
KCl (0.3 M)	0	0.4	5.5	6.1	2.0	0.8	1.4	2.7	1.1	0	25	25.0
K_2SO_4 (0.3 M)	0.3	1.8	1.4	0.5	2.3	0.5	3.1	2.8	2.9	4.4	25	8.3
$MgCl_2$ (0.1 M)	0.8	1	1.7	0.8	1.3	0	4.8	2.6	1.4	5.6	16.7	50.0
Na glutamate (0.05 M)	0.7	1.1	1.1	0.5	0.6	0	1.0	0.7	6.6	7.7	50	66.7
Na acetate (0.85 M)	0.3	0	6.3	3.6	1.1	3.5	1.1	0.4	1.2	2.5	16.7	50.0
NaCl (0.2 M)	0.3	0.1	7.8	6.8	0.9	1.5	0.8	1.1	0.2	0.5	58.3	50.0
Na_2CO_3 (0.1 M)	0.2	0	0.7	1.5	1.2	1.3	5.5	3.3	2.4	3.9	25	33.3
Na saccharin (0.0025 M)	7.4	8.2	0.1	0.4	0.8	0	0.7	0.4	1.0	1.0	33.3	50.0
NH_4Cl (0.1 M)	0	0	3.6	3.3	1.6	1.2	4.5	5.0	0.3	0.5	8.3	41.7
Quinine HCl (0.001 M)	0	0	0	0	0.4	0	9.3	9.1	0.3	0.9	91.7	16.7
Succinic acid (0.01 M)	0.3	0.8	0.8	2.8	5.5	4.0	1.6	1.1	1.8	1.3	41.7	33.3
Sucrose (0.8 M)	8.9	9.0	0	0	0	0.8	0	0	1.1	0.2	75.0	91.7
Urea (1.0 M)	0.3	0	0.8	0.3	0.4	0	6.2	4.8	2.3	4.9	58.3	75.0
Totals	37.2	41.0	35.1	30.0	38.8	34.1	52.4	43.1	36.5	51.8	908.2	933.3

[a]Subjects rated the taste of each compound on five different scales (sweet, sour, salty, bitter, and other) for a total of 10 points distributed in any way among the five categories. Subjects also judged whether each stimulus was singular (gave the impression of a single taste) or nonsingular (gave the impression that it existed in the form of two or more component tastes).

neither young nor elderly subjects, while wearing nose plugs, limited their ratings of the 20 tastants to sweet, sour, salty, and bitter alone. Second, the magnitude of the total (sum) ratings on other for elderly subjects was greater than for any of the four so-called primary tastes, that is, these stimuli clearly had qualities other than sweet, salty, sour, or bitter. The higher number of off-tastes perceived by the elderly were most likely the result of medications and medical conditions (see Schiffman, S. S., 2007). Third, stimuli that are considered to be primary or basic tastes such as NaCl (salty), urea (bitter), and citric acid (sour) were not found to be any more singular (which one should expect if a taste is basic or unique) than other stimuli for both age groups although the degree of singularity depended on the stimulus.

4.27.3.4 Other Suprathreshold Findings in the Elderly

Murphy C. (1986) found that the elderly tend to find salt and sugar more pleasant at higher concentrations that do younger subjects, which is consistent with the loss of sensitivity. Warwick Z. S. and Schiffman S. S. (1990) found that the fat content in sugar/fat and salt/fat mixtures was unrelated to pleasantness ratings for elderly subjects, which is consistent with the fact that elderly have elevated thresholds for oils. Byrd E. and Gertman S. (1959) found no significant age-related decreases in the ability to identify suprathreshold concentrations of sweet (sucrose), sour (citric acid), salty (NaCl), and bitter (quinine HCl) in water but there was a consistent trend toward diminished positive identification with age. However, the elderly were clearly less able to discriminate between the taste qualities in real food products (Mojet, J. *et al.*, 2004). Schiffman S. (1979) also found that the elderly (while blindfolded) have reduced ability to identify blended foods on the basis of taste (and smell).

4.27.4 Medications Associated with Taste Alterations

Medications can play a major role in taste losses and distortions (Schiffman, S. S. *et al.*, 2002; Schiffman, S. S., 2007) but the majority of taste changes attributed to specific drugs are based on clinical reports rather than on experimental studies. Oral sensory complaints including taste problems are more prevalent in elderly who use medications (Schiffman, S. S., 1997; Schiffman, S. S., and Zervakis, J., 2002; Nagler, R. M. and Hershkovich, O., 2005). Table 12 lists hundreds of medications that have been clinically associated with complaints such as loss of taste, altered taste, and metallic taste. Most major drug classes have been implicated in taste disturbances. However, because quantitative assessments of large populations taking specific medications have not been performed, it is not yet known whether clinically reported taste complaints (e.g., case reports) are indeed gustatory or olfactory in nature, or if they are actually caused by medications or the medical conditions they are designed to treat. Furthermore, according to the Physicians' Desk Reference (2000–2005), adverse taste complaints from medications afflict only a minority of patients taking a drug but the actual prevalence of medication-induced losses awaits determination by experimental testing procedures.

Table 12 Medications associated clinically and experimentally with taste loss

AIDS- and HIV-related therapeutic drugs
Didanosine
Indinavir
Lamivudine
Nelfinavir
Nevirapine
Pyrimethamine
Ritonavir
Saquinavir
Stavudine
Zalcitabine
Zidovudine
Amebicides and anthelmintics
Metronidazole
Niclosamide
Niridazole
Anesthetics
Benzocaine (ethyl aminobenzoate)
Dibucaine hydrochloride
Euprocin
Lidocaine
Procaine hydrochloride
Propofol
Tropacocaine
Anticholesteremics and antilipidemics
Atorvastatin calcium
Cholestyramine
Clofibrate

(*Continued*)

Table 12 (Continued)

Fluvastatin sodium
Gemfibrozil
Lovastatin
Pravastatin sodium
Probucol
Simvastatin

Anticoagulants
Phenindione
Warfarin sodium

Antihistamines
Chlorpheniramine maleate
Loratadine
Terfenadine and pseudoephedrine

Antimicrobials
Amphotericin B
Ampicillin
Atovaquone
Aztreonam
Bleomycin
Carbenicillin indanyl sodium
Cefamandole
Cefpodoxime proxetil
Ceftriaxone sodium
Cefuroxime axetil
Cinoxacin
Ciprofloxacin
Clarithromycin
Clindamycin phosphate
Clofazimine
Dapsone
Enoxacin
Ethambutol hydrochloride
Griseofulvin
Imipenem–cilastatin sodium
Lincomycin HCl
Lomefloxacin HCl
Mezlocillin sodium
Norfloxacin
Ofloxacin
Pentamidine isethionate
Piperacillin and tazobactam sodium
Pyrimenthamine
Rifabutin
Sulfamethoxazole
Trimethoprim
Tetracyclines
Ticarcillin disodium and clavulanate potassium
Tyrothricin

Antiproliferative, including immunosuppressive agents
Aldesleukin
Azathioprine
Carmustine
Cisplatin
Carboplatin
Doxorubicin and methotrexate
Fluorouracil
Interferon α-2a (recombinant)
Interferon α-2b (recombinant)
Vincristine sulfate

Antirheumatic, antiarthritic, analgesic, antipyretic, and anti-inflammatory
Auranofin
Aurothioglucose
Benoxaprofen
Butorphanol tartrate
Choline magnesium trisalicylate
Colchicine
Dexamethasone
Diclofenac potassium/diclofenac sodium
Dimethyl sulfoxide
Etodolac
Fenoprofen calcium
Flurbiprofen
Gold,
Gold sodium thiomalate
Hydrocortisone
Hydromorphone HCl
Ibuprofen
Ketoprofen
Ketorolac tromethamine
Morphine sulfate
Nabumetone
Nalbuphine HCl
Oxaprozin
D-Penicillamine and penicillamine
Pentazocine lactate
Phenylbutazone
Piroxicam
Salicylates
Sulindac
Sumatriptan succinate
5-Thiopyridoxine

Antispasmodics, irritable bowel syndrome
Dicylomine HCl
Oxybutynin chloride
Phenobarbital + hyoscyamine SO4 + atropine SO4 + scopolamine hydrobromide

Antithyroid agents
Carbimazole
Methimazole
Methylthiouracil
Propylthiouracil
Thiouracil

Antiulcerative
Clidinium bromide
Famotidine
Glycopyrrolate
Hyoscyamine sulfate
Mesalamine
Misoprostol
Omeprazole
Propantheline bromide
Sulfasalazine

(*Continued*)

Table 12 (Continued)

Antiviral
Acyclovir
Foscarnet sodium
Idoxuridine
Interferon α-n3
Interferon β-1b
Rimantadine HCl

Agents for dental hygiene
Sodium fluoride
Sodium lauryl sulfate
Chlorhexidine digluconate mouthrinses

Bronchodilators and antiasthmatic drugs
Albuterol sulfate
Beclomethasone dipropionate
Bitolterol mesylate
Cromolyn sodium
Ephedrine HCl + phenobarbitol + potassium iodide + theophylline calcium salicylate
Flunisolide
Metaproterenol sulfate
Nedocromil
Pirbuterol acetate inhalation aerosol
Terbutaline sulfate

Cardiovascular medications including diuretics, antiarrhythmic, antihypertensive, and antifibrillatory agents
Acetazolamide
Adenosine
Amiodarone HCl
Amiloride and its analogs
Amlodipine besylate
Benazepril HCl + hydrochlorothiazide
Bepridil HCl
Betaxolol HCl
Bisoprolol fumarate and bisoprolol fumarate with hydrochlorothiazide
Captopril and captopril/hydrochlorothiazide
Clonidine
Diazoxide
Diltiazem
Doxazosin mesylate
Enalapril and derivatives
Esmolol HCl
Ethacrynic acid
Flecainide acetate
Fosinopril sodium
Guanfacine HCl
Hydrochlorothiazide
Labetalol HCl
Metolazone
Mexiletine HCl
Moricizine HCl
Nifedipine
Procainamide HCl
Propafenone HCl
Propranolol HCl
Ramipril
Spironolactone
Tocainide HCl

Hyper- and hypoglycemic drugs
Diazoxide
Glipizide
Phenformin and derivatives

Hypnotics and sedatives
Estazolam
Flurazepam HCl
Midazolam HCl
Prochlorperazine
Promethazine HCl
Quazepam
Triazolam
Zolpidem tartrate
Zoplicone

Muscle relaxants and drugs for treatment of Parkinson's disease
Baclofen
Chlormezanone
Cyclobenzaprine HCl
Dantrolene sodium
Levodopa
Methocarbamol
Pergolide mesylate
Selegiline HCl

Psychopharmacologic including antiepileptic
Alprazolam
Amitriptyline HCl
Amoxapine
Buspirone HCl
Carbamazepine
Chlordiazepoxide + amitriptyline HCl
Clomipramine HCl
Clozapine
Desipramine HCl
Doxepin HCl
Felbamate
Fluoxetine HCl
Imipramine HCl and imipramine pamoate
Lithium carbonate
Maprotiline HCl
Nortriptyline HCl
Paroxetine HCl
Perphenazine–amitriptyline HCl
Phenytoin
Pimozide
Protriptyline HCl
Psilocybin
Risperidone
Sertraline HCl
Trazodone HCl
Trifluoperazine HCl
Trimipramine maleate
Venlafaxine HCl

Sympathomemetic drugs
Amphetamine
Benzphetamine HCl
Dextroamphetamine sulfate
Fenfluramine HCl
Mazindol

(*Continued*)

Table 12 (Continued)

Methamphetamine HCl
Phendimetrazine tartrate
Phentermine resin and phentermine HCl

Vasodilators
Bamifylline hydrochloride
Diltiazem
Dipyridamole
Isosorbide mononitrate
Nitroglycerin patch
Oxyfedrine

Others (indication)
Allopurinol (reduces serum and urinary uric acid)
Antihemophilic factor (recombinant) (clotting factor – hemophilia)
Antithrombin III (human) (antithrombin III deficiency)
Calcitonin (Paget's disease, hypercalcemia, osteoporosis)
Cyclosporine (prevent rejection of liver, heart, and kidney transplants)
Etidronate (hypercalcemia, antipsoriatic)
Etretinate (antipsoriatic)
Germine monoacetate (Eaton–Lambert syndrome)
Granisetron HCl (antiemetic/antinauseant)
Histamine phosphate (control for allergic skin testing)
Iohexol (diagnostic imaging product)
Iron sorbitex (hematinic)
Leuprolide acetate (inhibits gonadotropin secretion/ prostatic cancer)
Levamisole HCl (immunomodulator – restores depressed immune function)
Mesna (detoxifying agent)
Methazolamide (carbonic anhydrase inhibitor)
Methylergonovine maleate (prevents postpartum hemorrhage)
Midodrine (hypotension)
Nicotine (smoking cessation)
Nicotine polacrilex (smoking cessation)
Oxycodone HCl (pain)
Pentoxifylline (blood viscosity modulator)
Potassium iodide (expectorant)
Sermorelin acetate (diagnostic)
Succimer (lead poisoning)
Terbinafine
Ursodiol (gall stone dissolution)
Vitamin D/calcitriol (hypocalcemia)
Vitamin K1/phytonadione (coagulation disorders)

See Schiffman S. S. and Zervakis J. (2002) for more details.

Currently, little is known about the sites of action or cascade of cellular events by which medications induce taste complaints. However, medications can impact taste perception at several levels of the nervous system including the peripheral receptors, chemosensory neural pathways, and/or the brainstem and brain. Medications can induce a taste at receptor sites that are localized on either the apical or the basolateral membranes of taste cells. The plasma concentrations of some drugs (e.g., saquinavir) are greater than the taste thresholds and thus can activate receptors on the blood side of taste cells (Schiffman, S. S. *et al*., 1999). For most drugs, however, the salivary or plasma concentrations of drugs tend to be lower than the taste threshold values (see Schiffman, S. S. *et al*., 2002). Yet, drugs or their metabolites can accumulate in taste buds over time to reach concentrations that are greater than taste DTs. Drugs can also alter taste transduction mechanisms or can permeate the blood–brain barrier to interfere with taste signaling at the neural levels.

4.27.5 Medical Conditions Associated with Taste Complaints

A vast range of medical conditions has been reported to affect the sense of taste (Table 13), and clinical studies of wasting patients indicate that taste losses are especially severe (Schiffman, S. S., 1983; Schiffman, S. S., and Wedral, E., 1996). However, in most of these studies, patients who were evaluated for taste perception were also being treated with medications for their medical condition, so it is impossible to determine the relative contribution of disease states and medications to taste losses. Cancer is an example of a chronic medical condition in which patients are especially vulnerable to taste disorders (Schiffman, S. S. and Graham, B. G., 2000). Taste changes occur both in untreated cancer patients (Brewin, T. B., 1980; Ovesen, L. *et al*., 1991) and those treated with chemotherapy (Nielsen, S. S. *et al*., 1980; Fetting, J. *et al*., 1985; Lindley, C. *et al*., 1996) and radiation (Conger, A. D., 1973).

Cancer disproportionately impacts the elderly (Cohen, H. J., 1998) with 60% of all malignant tumors diagnosed in persons aged 65 years and above. Furthermore, 69% of all cancer deaths occur in this age group. Table 14 gives an overview of the taste changes that have been measured in cancer patients using various psychophysical testing techniques. The data suggest that cancer and its treatment impair the ability to detect the presence of basic tastes, reduce the perceived intensity of suprathreshold concentrations of tastants, and interfere with the ability to discriminate and identify tastes and smells. Threshold losses have also been detected using electrogustometry (Berteretche, M. V. *et al*., 2004). Table 15 gives an overview of the food aversions, complaints, and altered preferences reported by cancer patients.

Table 13 Medical conditions associated clinically and experimentally with taste loss

Nervous system disorders
Alzheimer's disease
Bell's palsy
Damage to chorda tympani
Guillain–Barre syndrome
Familial dysautonomia
Head trauma
Multiple sclerosis
Raeder's paratrigeminal syndrome
Tumors and lesions
Nutritional disorders
Cancer
Chronic renal failure
Liver disease including cirrhosis
Niacin (vitamin B_3) deficiency
Thermal burn
Zinc deficiency
Endocrine disorders
Adrenal cortical insufficiency
Congenital adrenal hyperplasia
Cretinism
Cushing's syndrome
Panhypopituitarism
Hypothyroidism
Diabetes mellitus
Gonadal dysgenesis (Turner's syndrome)
Pseudohypoparathyroidism
Local disorders
Facial hypoplasia
Glossitis and other oral disorders
Leprosy
Oral Crohn's disease
Radiation therapy
Sjögren's syndrome
Other
Amyloidosis and sarcoidosis
Cystic fibrosis
High altitude
Hypertension
Influenza-like infections
Laryngectomy
Major depressive disorder

See Schiffman S. S. and Zervakis J. (2002) for more details.

These data suggest that at least half of the cancer patients may have impaired taste functioning at some point during the course of their disease and treatment (e.g., DeWys, W. D. and Walters, K., 1975). The duration of losses can last from several weeks to 6 months or more (Conger, A. D., 1973; Mossman, K. *et al.*, 1982; Ophir, D. *et al.*, 1988; Maes, A. *et al.*, 2002).

The causes of altered taste perception in cancer are not well understood but metabolic changes induced by the presence of a neoplasm as well as damage to the sensory receptors by radio- and chemotherapies are likely involved. Radiation therapy and chemotherapy not only affect the turnover of taste and smell receptors but can also alter the anatomical integrity of the taste bud. Oral complications of cancer such as infections (fungal, viral, bacterial), ulcers, drug-induced stomatitis, and dry mouth may also play a role. In a recent study, tasting of the bitterness of 6-*n*-propylthiouracil (PROP) bitterness was also associated with the development of colonic neoplasms (Basson, M. D., *et al.*, 2005). The ability to taste the bitterness of PROP is genetically determined. The presumed reason for this association was that persons who perceive the bitter taste PROP would be more likely to avoid foods such as vegetables that are high in antioxidants.

4.27.6 Cause of Taste Losses in the Absence of Drugs and Disease

The cause of taste changes in the elderly in the absence of medications and disease is not fully understood. Early studies with large sample sizes suggested that losses in the number of papillae and/or taste buds occurred in the elderly (Arey, L. B. *et al.*, 1935; Mochizuki, Y., 1937; 1939; Moses, S. W. *et al.*, 1967). However, later studies in a smaller number of older individuals suggested that such losses with age are minimal (Arvidson, A., 1979; Miller, I. J., Jr., 1986; Bradley, R. M., 1988; Miller, I. J., Jr., 1988). These later studies are difficult to reconcile with earlier studies and with more recent psychophysical studies that show striking localized deficits (i.e., regional losses) in taste perception over different areas of the tongue in older individuals (Bartoshuk, L. M. *et al.*, 1987; Matsuda, T. and Doty, R. L., 1995). Furthermore, studies of the lingual surface have found entirely flat areas on the surface of the tongue without papillae in old age (Kobayashi, K. *et al.*, 2001).

Reduced renewal of taste cells may account for some age-related losses. While taste cells normally replicate every 10–10.5 days (Beidler, L. M. and Smallman, R. L., 1965), delayed cell renewal and highly vacuolated cytoplasm have been reported to occur in taste buds of aged mice (Fukunaga, A., 2005). Decreased levels of estrogen and testosterone in the elderly may play a role in reduced cell renewal in taste buds since animal models indicate that estrogen and testosterone increase mitotic activity (Eartly, H. *et al.*, 1951; Zhang, Z. *et al.*, 1998). Endocrine factors

Table 14 Alterations of taste performance in cancer patients

Taste loss	*Type of cancer*	*Effect of therapy*	*Reference*
Elevated detection and recognition thresholds for NaCl (salt), sucrose (sweet), HCl (sour), and urea (bitter) prior to radiotherapy; salty, sweet, and bitter further impaired by radiotherapy	Various malignant neoplasms	Radiotherapy further impaired taste loss	Bolze M. S. *et al.* (1982)
Elevated recognition thresholds for sucrose (sweet), HCl (sour), quinine HCl (bitter) during radiotherapy; recovery by 120 days	Oropharyngeal cancers	Radiotherapy	Conger A. D. (1973)
Elevated detection and recognition thresholds, especially for bitter and salt thresholds during radiotherapy	Head and neck	Radiotherapy	Mossman K. L. and Henkin R. I. (1978)
Elevated NaCl (salty) recognition thresholds	Breast and colon	Prior to treatment	Carson J. A. and Gormican A. (1977)
Elevated recognition threshold for hydrochloric acid (sour); individual differences in bitter and sweet threshold changes	Lung	Prior to therapy	Williams L. R. and Cohen M. H. (1978)
Elevated taste recognition thresholds for NaCl, sucrose, quinine sulfate, picric acid; thresholds returned to normal 6 weeks post-treatment	Oropharyngeal	During and after radiotherapy	Kalmus H. and Farnsworth D. (1959)
Thresholds for NaCl (salt), tartaric acid (sour), sucrose (sweet), and quinine (bitter) elevated by radiation and chemotherapy; recovery was not complete by 1 year	Oral squamous cell carcinoma	Radiation and chemotherapy	Tomita Y. and Osaki T. (1990)
Elevated glucose recognition threshold	Various malignant neoplasms	During chemotherapy	Bruera E. *et al.* (1984)
Significant increase in electrical taste detection threshold; no change in smell threshold	Lung, ovary, and breast	Increase in untreated patients; thresholds decreased only in patients who responded to chemotherapy (after 2 to 3 months)	Ovesen L. *et al.* (1991)
Significant decrease in recognition threshold for urea (bitter)	Gastrointestinal		Hall J. C. *et al.* (1980)
Loss of ability to discriminate between different concentrations of salt, sweet, sour, and bitter	Melanoma	During nine courses of chemotherapy	Mulder N. H. *et al.* (1983)
Significant reduction in smell identification in patients with estrogen receptor; positive breast cancer	Breast cancer	Mixed sample (treated and untreated)	Lehrer S. *et al.* (1985)

including castration and thyroidectomy have long been known to depress cell proliferation in other tissues such as small-bowel epithelium (Hopper, A. F. *et al.*, 1972; Williamson, R. C., 1978). There may be some shrinkage of taste projection areas in the brainstem because images of the cross section of the upper part of the medulla oblongata suggest slight reductions in size with age and tooth loss in some individuals (Yamamoto, T. *et al.*, 2005). Decreased performance on psychophysical taste tests in the elderly can also be related to structural changes in the hippocampus and amygdala (Scheibel, M. E. and Scheibel, A. B., 1975; Tomlinson, B. E. and Henderson, G., 1976). Damage to the amygdala and the hippocampus has been shown to interfere with registering and valuing behavior (Pribram, K. H. 1971). Environmental pollutants can also impact taste receptors and/or projections to the central nervous system (Schiffman, S. S. and Nagle, H. T., 1992). Hyposalivation and low perceived salivary flow have also been reported to lower satisfaction with tasting foods (Ikebe, K. *et al.*, 2002).

Table 15 Taste complaints and altered food preferences in cancer patients

Sensory loss	*Type of cancer*	*Effect of therapy*	*Reference*
Food aversions and cravings	Various malignant neoplasms	Radiotherapy	Brewin T. B. (1982)
Reduced palatability of high-protein foods, cereals, and sweets in patients with taste aversions	Various	Treated and untreated	Vickers Z. M. *et al.* (1981)
All food tasted nauseating, greasy or rancid; wine tasted metallic; water tasted salty	Oropharyngeal	Developed during first two weeks of radiotherapy	Kalmus H. and Farnsworth D. (1959)
Patients developed aversions to sweets, meats, caffeinated beverages, high fat and greasy foods during therapy	Breast and lung	Prior to and during chemotherapy	Mattes R. D. *et al.* (1987)
Symptom of reduced appetite correlates with elevated recognition threshold for sucrose (sweet); meat aversion correlates with lowered thresholds for urea (bitter)	Various		DeWys W. D. and Walters K. (1975)
Highly varied hedonic responses to beverages containing five suprathreshold concentrations of citric acid (in lemonade), NaCl (in unsalted tomato juice), urea (in tonic water), and sucrose (in cherry drink); anorectics preferred lower sweetness levels than nonanorectics; yet sweet foods constituted a greater percentage of their daily caloric intake	Upper gastrointestinal and lung	Patients on chemotherapy had less distinct preference for any of the five concentrations of sucrose, particularly high levels	Trant A. S. *et al.* (1982)
Percentage of patients reporting taste problems increased from 18% prior to radiation to over 80% during the 5th week of radiation; foods with abnormal taste included high-protein foods (meat, eggs, dairy), fruits, vegetables, sweet, breads, cereal, coffee, and tea	Head and neck cancer	During radiotherapy	Chencharick J. D. and Mossman K. L. (1983)
Complaints of metallic, bitter, or decreased taste; distorted sweet taste	Breast and lung	Chemotherapy – cisplatin	Rhodes V. A. *et al.* (1994)

The mechanism for some taste losses may also involve neurodegeneration that can accompany cytokine-mediated inflammatory processes (see Viviani, B. *et al.*, 2004, for description). Inflammatory processes involving cytokines and inflammation mediators with subsequent cell death have been implicated in age-related losses in olfaction (Ge, Y. *et al.*, 2002; Conley, D. B. *et al.*, 2003; Kern, R. C. *et al.*, 2004; Raviv, J. R. and Kern, R. C., 2004). Similarly, taste alterations subsequent to infection as well as losses in normal aging may also be caused by the neurotoxic effects of cytokines and mediators. It is noteworthy that impairments in taste perception are associated with the presence of *Candida albicans* in the oral cavity (Sakashita, S. *et al.*, 2004). A general decline in immune functioning, including cytokine dysregulation, is a hallmark of aging (Wilson, C. J. *et al.*, 2002). Thus, inflammatory processes that induce neural damage and apoptosis in the taste system may account for reduced sensitivity from normal aging as well as from infections. Environmental pollutants may play a role in the inflammatory processes (see Schiffman, S. S. and Nagle, H. T., 1992).

4.27.7 Final Comment

Losses in taste perception occur in the elderly with elevated DTs and RTs as well as decrements in perceived suprathreshold intensity. While loss in taste sensitivity occurs during normal aging in the absence of disease or medications, losses can be significantly exacerbated by medical conditions and drugs. Dysgeusia increases in persons taking

medications (e.g., cardiac medications), but the relative contribution of medications and medical conditions to these taste distortions is not fully understood.

Acknowledgments

This research was supported by a grant to Dr. Susan Schiffman and Duke University from the National Institute on Aging AG00443.

References

Administration on Aging AoA 2004. A Profile of Older Americans: 2004, pp. 1–18. U.S. Department of Health and Human Services, http://www.aoa.gov/prof/Statistics/profile/2004/2004profile.pdf, accessed 21 December 2005.

Arey, L. B., Tremaine, M. J., and Monzingo, F. L. 1935. The numerical and topographical relations of taste buds to human circumvallate papillae throughout the life span. Anat. Rec. 64, 9–25.

Arvidson, K. 1979. Location and variation in number of taste buds in human fungiform papillae. Scand. J. Dent. Res. 87, 435–442.

Bartoshuk, L. M., Desnoyers, S., Hudson, C., Marks, L., O'Brien, M., Catalanotto, F., Gent, J., Williams, D., and Ostrum, K. M. 1987. Tasting on localized areas. Ann. N. Y. Acad. Sci. 510, 166–168.

Basson, M. D., Bartoshuk, L. M., Dichello, S. Z., Panzini, L., Weiffenbach, J. M., and Duffy, V. B. 2005. Association between 6-*n*-propylthiouracil (PROP) bitterness and colonic neoplasms. Dig. Dis. Sci. 50(3), 483–489.

Bate-Smith, E. C. 1954. Astringency in foods. Food 23, 124–135.

Beidler, L. M. and Smallman, R. L. 1965. Renewal of cells within taste buds. J. Cell Biol. 27, 263–272.

Berteretche, M. V., Dalix, A. M., d'Ornano, A. M., Bellisle, F., Khayat, D., and Faurion, A. 2004. Decreased taste sensitivity in cancer patients under chemotherapy. Support Care Cancer 12(8), 571–576.

Bolze, M. S., Fosmire, G. J., Stryker, J. A., Chung, C. K., and Flipse, B. G. 1982. Taste acuity, plasma zinc levels, and weight loss during radiotherapy: a study of relationships. Radiology 144, 163–169.

Bourlière, F., Cendron, H., and Rapaport, A. 1958. Modification avec l'age des seuils gustatifs de perception et de reconnaissance aux saveurs salée et sucrée, chez l'homme. Gerontologia 2, 104–112.

Bradley, R. M. 1988. Effects of aging on the anatomy and neurophysiology of taste. Gerodontics 4, 244–248.

Brewin, T. B. 1980. Can a tumour cause the same appetite perversion or taste change as a pregnancy? Lancet 2, 907–908.

Brewin, T. B. 1982. Appetite perversions and taste changes triggered or abolished by radiotherapy. Clin. Radiol. 33, 471–475.

Bruera, E., Carraro, S., Roca, E., Cedaro, L., and Chacon, R. 1984. Association between malnutrition and caloric intake, emesis, psychological depression, glucose taste, and tumor mass. Cancer Treat. Rep. 68, 873–876.

Byrd, E. and Gertman, S. 1959. Taste sensitivity in ageing persons. Geriatrics 14, 381–384.

Carson, J. A. and Gormican, A. 1977. Taste acuity and food attitudes of selected patients with cancer. J. Am. Diet Assoc. 70, 361–365.

Chencharick, J. D. and Mossman, K. L. 1983. Nutritional consequences of the radiotherapy of head and neck cancer. Cancer 51, 811–815.

Cohen, H. J. 1998. Cancer and Aging: Overview. In: American Society of Clinical Oncology Education Book (*ed*. M. C. Perry), pp. 223–226. American Society of Clinical Oncology.

Cohen, J. E. 2003. Human population: the next half century. Science 302, 1172–1175.

Conger, A. D. 1973. Loss and recovery of taste acuity in patients irradiated to the oral cavity. Radiat. Res. 53, 338–347.

Conley, D. B., Robinson, A. M., Shinners, M. J., and Kern, R. C. 2003. Age-related olfactory dysfunction: cellular and molecular characterization in the rat. Am. J. Rhinol. 17(3), 169–175.

Cooper, R. M., Bilash, I., and Zubek, J. P. 1959. The effect of age on taste sensitivity. J. Gerontol. 14, 56–58.

Cowart, B. J. 1983. Direct scaling of the intensity of basic tastes: a life span study. *Paper presented at the Annual Meeting of the Association of Chemoreception Sciences*, Sarasota, FL.

Davies, A. M. 1989. Older populations, aging individuals and health for all. World Health Forum 10, 299–306; discussion 306–321.

DeWys, W. D. and Walters, K. 1975. Abnormalities of taste sensation in cancer patients. Cancer 36, 1888–1896.

Drewnowski, A., Krahn, D. D., Demitrack, M. A., Nairn, K., and Gosnell, B. A. 1995. Naloxone, an opiate blocker, reduces the consumption of sweet high-fat foods in obese and lean female binge eaters. Am. J. Clin. Nutr. 61, 1206–1212.

Dye, C. J. and Koziatek, D. A. 1981. Age and diabetes effects on threshold and hedonic perception of sucrose solutions. J. Gerontol. 36, 310–315.

Eartly, H., Grad, B., and Leblond, C. P. 1951. The antagonistic relationship between testosterone and thyroxine in maintaining the epidermis of the male rat. Endocrinology 49(6), 677–686.

Fetting, J., Wilcox, P. M., Sheidler, V. R., Enterline, J. P., Donehower, R. C., and Grochow, L. B. 1985. Tastes associated with parenteral chemotherapy for breast cancer. Cancer Treat. Rep. 69, 1249–1251.

Fukunaga, A. 2005. Age-related changes in renewal of taste bud cells and expression of taste cell-specific proteins in mice. Kokubyo Gakkai Zasshi, Japan 72, 84–89.

Fukunaga, A., Uematsu, H., and Sugimoto, K. 2005. Influences of aging on taste perception and oral somatic sensation. J. Gerontol. A Biol. Sci. Med. Sci. 60(1), 109–113.

Ge, Y., Tsukatani, T., Nishimura, T., Furukawa, M., and Miwa, T. 2002. Cell death of olfactory receptor neurons in a rat with nasosinusitis infected artificially with Staphylococcus. Chem. Senses 27(6), 521–527.

Giduck, S. A., Threatte, R. M., and Kare, M. R. 1987. Cephalic reflexes: their role in digestion and possible roles in absorption and metabolism. J. Nutr. 117, 1191–1196.

Gilbertson, T. A., Fontenot, D. T., Liu, L., Zhang, H., and Monroe, W. T. 1997. Fatty acid modulation of K^+ channels in taste receptor cells: gustatory cues for dietary fat. Am. J. Physiol. 272, C1203–C1210.

Gilmore, M. M. and Murphy, C. 1989. Aging is associated with increased Weber ratios for caffeine, but not for sucrose. Percept. Psychophys. 46(6), 555–559.

Glanville, E. V., Kaplan, A. R., and Fischer, R. 1964. Age, sex, and taste sensitivity. J. Gerontol. 19, 474–478.

Grzegorczyk, P. B., Jones, S. W., and Mistretta, C. M. 1979. Age-related differences in salt taste acuity. J. Gerontol. 34, 834–840.

Hall, J. C., Staniland, J. R., and Giles, G. R. 1980. Altered taste thresholds in gastro-intestinal cancer. Clin. Oncol. 6, 137–142.

Harris, H. and Kalmus, H. 1949. The measurement of taste sensitivity to phenylthiourea (P.T.C.). Ann. Eugen. 15, 24–31.

Hinchcliff, R. 1958. Clinical quantitative gustometry. Acta Otolaryngol. 49, 453–466.

Hopper, A. F., Rose, P. M., and Wannemacher, R. W., Jr. 1972. Cell population changes in the intestinal mucosa of protein-depleted or starved rats. II. Changes in cellular migration rates. J. Cell Biol. 53(1), 225–230.

Hughes, G. 1969. Changes in taste sensitivity with advancing age. Gerontol. Clin. 11, 224–230.

Ikebe, K., Sajima, H., Kobayashi, S., Hata, K., Morii, K., Nokubi, T., and Ettinger, R. L. 2002. Association of salivary flow rate with oral function in a sample of community-dwelling older adults in Japan. Oral Surg. Oral Med. Oral Pathol. 94(2), 184–190.

Kalmus, H. and Farnsworth, D. 1959. Impairment and recovery of taste following irradiation of the oropharynx. J. Laryngol. Otol. 73, 180–182.

Kalmus, H. and Trotter, W. R. 1962. Direct assessment of the effect of age on P.T.C. sensitivity. Ann. Hum. Genet. 26, 145–149.

Kern, R. C., Conley, D. B., Haines, G. K., 3rd, and Robinson, A. M. 2004. Treatment of olfactory dysfunction. II. Studies with minocycline. Laryngoscope 114(12), 2200–2204.

Kettaneh, A., Paries, J., Stirnemann, J., Steichen, O., Eclache, V., Fain, O., and Thomas, M. 2005. Clinical and biological features associated with taste loss in internal medicine patients. A cross-sectional study of 100 cases.Appetite 44(2), 163–169.

Klose, R. E. and Glicksman, M. 1972. Gums. In: Handbook of Food Additives, 2nd edn. (*ed*. T. E. Furia), pp. 295–359. The Chemical Rubber.

Kobayashi, K., Kumakura, M., Yoshimura, K., and Shindo, J. 2001. Stereo-structural study of the lingual papillae and their connective tissue cores in relation to ageing changes in the human tongue. Ital. J. Anat. Embryol. 106(2 Suppl. 1), 305–311.

Krarup, B. 1958. Electro-gustometry: a method for clinical taste examinations. Acta Otolaryngol. (Stockh.) 49, 294–305.

Lehrer, S., Levine, E., and Bloomer, W. D. 1985. Abnormally diminished sense of smell in women with oestrogen receptor positive breast cancer. Lancet 2, 333.

Lindley, C., Lowder, D., Sauls, A., McCune, J., Sawyer, W., and Eatmon, T. 1996. Patient perception of the impact and magnitude of the side-effects of chemotherapy: the Coates study revisited (Meeting abstract). Proc. Annu. Meet. Am. Soc. Clin. Oncol 15, A1652.

Maes, A., Huygh, I., Weltens, C., Vandevelde, G., Delaere, P., Evers, G., and Van den Bogaert, W. 2002. De Gustibus: time scale of loss and recovery of tastes caused by radiotherapy. Radiother. Oncol. 63(2), 195–201.

Matsuda, T. and Doty, R. L. 1995. Regional taste sensitivity to NaCl: relationship to subject age, tongue locus and area of stimulation. Chem. Senses 20(3), 283–290.

Mattes, R. D., Arnold, C., and Boraas, M. 1987. Management of learned food aversions in cancer patients receiving chemotherapy. Cancer Treat. Rep. 71, 1071–1078.

Miller, I. J., Jr. 1986. Variation in human fungiform taste bud densities among regions and subjects. Anat. Rec. 216(4), 474–482.

Miller, I. J., Jr. 1988. Human taste bud density across adult age groups. J. Gerontol. 43(1), B26–B30.

Mochizuki, Y. 1937. An observation on the numerical and topographical relations of the taste buds to circumvallate papillae of Japanese. Okajimas Folia Anat. Jpn 15, 595–608.

Mochizuki, Y. 1939. Studies on the papillae foliata of Japanese. II. The number of taste buds.Okajimas Folia Anat. Jpn 18, 355–369.

Mojet, J., Christ-Hazelhof, E., and Heidema, J. 2001. Taste perception with age: generic or specific losses in threshold sensitivity to the five basic tastes? Chem. Senses 26(7), 845–860.

Mojet, J., Heidema, J., and Christ-Hazelhof, E. 2003. Taste perception with age: generic or specific losses in supra-threshold intensities of five taste qualities? Chem. Senses 28(5), 397–413.

Mojet, J., Heidema, J., and Christ-Hazelhof, E. 2004. Effect of concentration on taste–taste interactions in foods for elderly and young subjects. Chem. Senses 29(8), 671–681.

Moore, L. M., Nielsen, C. R., and Mistretta, C. M. 1982. Sucrose taste thresholds: age-related differences. J. Gerontol. 37, 64–69.

Morley, J. E. 2001. Decreased food intake with aging. J. Gerontol. A Biol. Sci. Med. Sci. 56 Spec. No. 2, 81–88.

Moses, S. W., Rotem, Y., Jagoda, N., Talmor, N., Eichhorn, F., and Levin, S. 1967. A clinical, genetic and biochemical study of familial dysautonomia in Israel. Isr. J. Med. Sci. 3, 358–371.

Mossman, K. L. and Henkin, R. I. 1978. Radiation-induced changes in taste acuity in cancer patients. Int. J. Radiat. Oncol. Biol. Phys. 4, 663–670.

Mossman, K., Shatzman, A., and Chencharick, J. 1982. Long-term effects of radiotherapy on taste and salivary function in man. Int. J. Radiat. Oncol. Biol. Phys. 8, 991–997.

Mulder, N. H., Smit, J. M., Kreumer, W. M., Bouman, J., Sleijfer, D. T., Veeger, W., and Schraffordt Koops, H. 1983. Effect of chemotherapy on taste sensation in patients with disseminated malignant melanoma. Oncology 40, 36–38.

Murphy, C. 1979. The Effect of Age on Taste Sensitivity. In: Special Senses in Aging: A Current Biological Assessment (*eds*. S. S. Han and D. H. Coons), pp. 21–33. University of Michigan Institute of Gerontology.

Murphy, C. 1986. Taste and Smell in the Elderly. In: Clinical Measurement of Taste and Smell (*eds*. H. L. Meiselman and R. S. Rivlin), pp. 343–372. MacMillan Publishing.

Nagler, R. M. and Hershkovich, O. 2005. Relationships between age, drugs, oral sensorial complaints and salivary profile. Arch. Oral Biol. 50(1), 7–16.

Nakazato, M., Endo, S., Yoshimura, I., and Tomita, H. 2002. Influence of aging on electrogustometry thresholds. Acta Otolaryngol. Suppl. 546, 16–26.

Nielsen, S. S., Theologides, A., and Vickers, Z. M. 1980. Influence of food odors on food aversions and preferences in patients with cancer. Am. J. Clin. Nutr. 33, 2253–2261.

Nordin, S., Razani, L. J., Markison, S., and Murphy, C. 2003. Age-associated increases in intensity discrimination for taste. Exp. Aging Res. 29(3), 371–381.

Ophir, D., Guterman, A., and Gross-Isseroff, R. 1988. Changes in smell acuity induced by radiation exposure of the olfactory mucosa. Arch. Otolaryngol. Head Neck Surg. 114, 853–855.

Ovesen, L., Srensen, M., Hannibal, J., and Allingstrup, L. 1991. Electrical taste detection thresholds and chemical smell detection thresholds in patients with cancer. Cancer 68, 2260–2265.

Pribitkin, E., Rosenthal, M. D., and Cowart, B. J. 2003. Prevalence and causes of severe taste loss in a chemosensory clinic population. Ann. Otol. Rhinol. Laryngol. 112(11), 971–978.

Pribram, K. H. 1971. Languages of the Brain, p. 345. Prentice-Hall.

Raviv, J. R. and Kern, R. C. 2004. Chronic sinusitis and olfactory dysfunction. Otolaryngol. Clin. North Am. 37(6), 1143–1157, v–vi.

Rhodes, V. A., McDaniel, R. W., Hanson, B., Markway, E., and Johnson, M. 1994. Sensory perception of patients on

selected antineoplastic chemotherapy protocols. Cancer Nurs. 17, 45–51.
Richter, C. P. and Campbell, K. H. 1940. Sucrose taste thresholds of rats and humans. Am. J. Physiol. 128, 291–297.
Robichaud, J. L. and Noble, A. C. 1990. Astringency and bitterness of selected phenolics in wine. J. Sci. Food Agric. 53, 343–353.
Sakashita, S., Takayama, K., Nishioka, K., and Katoh, T. 2004. Taste disorders in healthy ''carriers'' and ''non-carriers'' of *Candida albicans* and in patients with candidosis of the tongue. J. Dermatol. 31(11), 890–897.
Scheibel, M. E. and Scheibel, A. B. 1975. Structural Changes in the Aging Brain. In: Aging: Clinical, Morphological, and Neurochemical Aspects in the Aging Central Nervous System (*eds*. H. Brody, D. Harman, and J. Ordy), Vol. 1, pp. 11–37. Raven Press.
Schiffman, S. 1979. Changes in Taste and Smell with Age: Psychophysical Aspects. In: Sensory Systems and Communication in the Elderly, Vol. 10, Aging (*eds*. J. M. Ordy and K. Brizzee), pp. 227–246. Raven Press
Schiffman, S. S. 1983. Taste and smell in disease. N. Engl. J. Med. 308, 1275–1279, 1337–1343.
Schiffman, S. S. 1993. Perception of taste and smell in elderly persons. Crit. Rev. Food Sci. Nutr. 33, 17–26.
Schiffman, S. S. 1997. Taste and smell losses in normal aging and disease. JAMA 278, 1357–1362.
Schiffman, S. S. 2000. Taste quality and neural coding: implications from psychophysics and neurophysiology. Physiol. Behav. 69, 147–159.
Schiffman, S. S. 2007. Critical illness and changes in sensory perception. Proc. Nutr. Soc. (in press).
Schiffman, S. S. and Clark, T. B. 1980. Magnitude estimates of amino acids for young and elderly subjects. Neurobiol. Aging 1, 81–91.
Schiffman, S. S. and Erickson, R. P. 1993. Psychophysics: Insights into Transduction Mechanisms and Neural Coding. In: Mechanisms of Taste Transduction (*eds*. S. A. Simon and S. D. Roper), pp. 395–424. CRC Press.
Schiffman, S. S. and Graham, B. G. 2000. Taste and smell perception affect appetite and immunity in the elderly. Eur. J. Clin. Nutr. 54(Suppl. 3), S54–S63.
Schiffman, S. S. and Nagle, H. T. 1992. Effect of environmental pollutants on taste and smell. Otolaryngol. Head Neck Surg. 106, 693–700.
Schiffman, S. S. and Warwick, Z. S. 1992. The Biology of Taste and Food Intake. In: The Science of Food Regulation: Food Intake, Taste, Nutrient Partitioning, and Energy Expenditure (*eds*. G. A. Bray and D. H. Ryan), Vol. 2, pp. 293–312. Pennington Center Nutrition Series Louisiana State University Press.
Schiffman, S. S. and Wedral, E. 1996. Contribution of taste and smell losses to the wasting syndrome. Age Nutr. 7, 106–120.
Schiffman, S. S. and Zervakis, J. 2002. Taste and smell perception in the elderly: effect of medications and disease. Adv. Food Nutr. Res. 44, 248–346.
Schiffman, S. S., Crumbliss, A. L., Warwick, Z. S., and Graham, B. G. 1990. Thresholds for sodium salts in young and elderly subjects: correlation with molar conductivity of anion. Chem. Senses 15, 671–678.
Schiffman, S. S., Frey, A. E., Luboski, J. A., Foster, M. A., and Erickson, R. P. 1991. Taste of glutamate salts in young and elderly subjects: role of inosine 5′-monophosphate and ions. Physiol. Behav. 49, 843–854.
Schiffman, S. S., Gatlin, L. A., Frey, A. E., Heiman, S. A., Stagner, W. C., and Cooper, D. C. 1994. Taste perception of bitter compounds in young and elderly persons: relation to lipophilicity of bitter compounds. Neurobiol. Aging 15, 743–750.
Schiffman, S. S., Graham, B. G., Sattely-Miller, E. A., and Warwick, Z. S. 1998. Orosensory perception of dietary fat. Curr. Dir. Psychol. Sci. 7, 137–143.
Schiffman, S. S., Hornack, K., and Reilly, D. 1979. Increased taste thresholds of amino acids with age. Am. J. Clin. Nutr. 32, 1622–1627.
Schiffman, S. S., Lindley, M. G., Clark, T. B., and Makino, C. 1981. Molecular mechanism of sweet taste: relationship of hydrogen bonding to taste sensitivity for both young and elderly. Neurobiol. Aging 2, 173–185.
Schiffman, S. S., Rascoe, D., and Garcia, R. A. 1989. The effects of age and race on thresholds and magnitude estimates of edible gums. Chem. Senses 14, 743.
Schiffman, S. S., Suggs, M. S., Sostman, A. L., and Simon, S. A. 1992. Chorda tympani and lingual nerve responses to astringent compounds in rodents. Physiol. Behav. 51, 55–63.
Schiffman, S. S., Zervakis, J., Graham, B. G., and Westhall, H. L. 2002. Age-Related Chemosensory Losses: Effect of Medications. In: Chemistry of Taste (*eds*. P. Givens and D. Paredes), pp. 94–108. American Chemical Society.
Schiffman, S. S., Zervakis, J., Heffron, S., and Heald, A. E. 1999. Effect of protease inhibitors on the sense of taste. Nutrition 15, 767–772.
Sclafani, A. 2004. The sixth taste? Appetite 43, 1–3.
Smith, S. E. and Davies, P. D. 1973. Quinine taste thresholds: a family study and a twin study. Ann. Hum. Genet. 37, 227–232.
Sternlieb, I. and Scheinberg, I. H. 1964. Penicillamine therapy for hepatolenticular degeneration. JAMA 189, 748–754.
Stevens, J. C. 1996. Detection of tastes in mixture with other tastes: issues of masking and aging. Chem. Senses 21(2), 211–221.
Stevens, J. C. and Traverzo, A. 1997. Detection of a target taste in a complex masker. Chem. Senses 22(5), 529–534.
Stevens, J. C., Cruz, L. A., Hoffman, J. M., and Patterson, M. Q. 1995. Taste sensitivity and aging: high incidence of decline revealed by repeated threshold measures. Chem. Senses 20(4), 451–459.
Stubbs, R. J. and Whybrow, S. 2004. Energy density, diet composition and palatability: influences on overall food energy intake in humans. Physiol. Behav. 81(5), 755–764.
Teff, K. L. and Engelman, K. 1996. Palatability and dietary restraint: effect on cephalic phase insulin release in women. Physiol. Behav. 60, 567–573.
Terada, T., Sone, M., Tsuji, K., Mishiro, Y., and Sakagami, M. 2004. Taste function in elderly patients with unilateral middle ear disease. Acta Otolaryngol. Suppl. 553, 113–116.
Tomita, Y. and Osaki, T. 1990. Gustatory impairment and salivary gland pathophysiology in relation to oral cancer treatment. Int. J. Oral Maxillofac. Surg. 19, 299–304.
Tomlinson, B. E. and Henderson, G. 1976. Some Quantitative Cerebral Findings in Normal and Demented Old People. In: Neurobiology of Aging (*eds*. R. D. Terry and S. Gershon), Vol. 3 , pp. 183–204. Raven Press.
Trant, A. S., Serin, J., and Douglass, H. O. 1982. Is taste related to anorexia in cancer patients? Am. J. Clin. Nutr. 36, 45–58.
Vickers, Z. M., Nielsen, S. S., and Theologides, A. 1981. Food preferences of patients with cancer. J. Am. Diet. Assoc. 79, 441–445.
Viviani, B., Bartesaghi, S., Corsini, E., Galli, C. L., and Marinovich, M. 2004. Cytokines role in neurodegenerative events. Toxicol. Lett 149(1–3), 85–89.
Warwick, Z. S. and Schiffman, S. S. 1990. Sensory evaluations of fat-sucrose and fat-salt mixtures: relationship to age and weight status. Physiol. Behav. 48, 633–636.
Warwick, Z. S. and Schiffman, S. S. 1991. Flavor–calorie relationships: effect on weight gain in rats. Physiol. Behav. 50, 465–470.
Weiffenbach, J. M., Baum, B. J., and Burghauser, R. 1982. Taste thresholds: quality specific variation with human aging. J. Gerontol. 37, 372–377.
Williams, L. R. and Cohen, M. H. 1978. Altered taste thresholds in lung cancer. Am. J. Clin. Nutr. 31, 122–125.

Williamson, R. C. 1978. Intestinal adaptation. Mechanisms of control. N. Engl. J. Med. 298(26), 1444–1450.
Wilson, C. J., Finch, C. E., and Cohen, H. J. 2002. Cytokines and cognition – the case for a head-to-toe inflammatory paradigm. J. Am. Geriatr. Soc. 50(12), 2041–2056.
Yamamoto, T., Shibata, M., Goto, N., Ezure, H., Ito, J., and Suzuki, M. 2005. Morphometric evaluation of the human tractus solitarius. Okajimas Folia Anat. Jpn 82(1), 5–8.
Yamauchi, Y., Endo, S., and Yoshimura, I. 2002. A new whole-mouth gustatory test procedure. II. Effects of aging, gender and smoking. Acta Otolaryngol. Suppl. 546, 49–59.
Zhang, Z., Laping, J., Glasser, S., Day, P., and Mulholland, J. 1998. Mediators of estradiol-stimulated mitosis in the rat uterine luminal epithelium. Endocrinology 139(3), 961–966.

4.28 Signal Transduction in the Olfactory Receptor Cell

H Takeuchi and T Kurahashi, Osaka University, Osaka, Japan

© 2008 Elsevier Inc. All rights reserved.

4.28.1	Outline of the Olfactory Signal Transduction	499
4.28.2	Receptor Potential as an Initial Membrane Excitation	499
4.28.3	Differences of Single Olfactory Receptor Cells in Functional Ligand Affinities	501
4.28.4	Can Olfactory Receptor Cells Detect a Single Odorant Molecule?	501
4.28.5	Enzyme – Second Messenger: cyclic AMP and $InsP_3$	502
4.28.6	Cyclic Nucleotide-Gated Channel	503
4.28.7	Ca^{2+}-Activated Cl^- Channel	504
4.28.8	Ca^{2+}-Activated K^+ Channel (Possibility for the Inhibitory Response)	504
4.28.9	Signal Amplification: Comparison with the Phototransduction	504
4.28.10	Adaptation	506
4.28.11	Functional Roles of Molecular Elements in the Olfactory Cilia	507
4.28.12	Resting Membrane Potential and Spike Discharges	508
4.28.13	Modulation of Membrane Excitability of the Olfactory Receptor Cell	509
References		509

4.28.1 Outline of the Olfactory Signal Transduction

During the past decades, a huge amount of knowledge has been accumulated in the research filed regarding the molecular mechanisms mediating olfactory energy conversion. The outline of this signal transduction is summarized as follows (see Figures 2(a) and 6). In the genomic DNA, the olfactory receptor cells (ORCs) prepare multiple types of genes encoding seven-transmembrane-domain receptors. Individual receptor cells select only one type of receptor protein gene for the functional expression on their ciliary surface. The receptor proteins are coupled to the olfaction-specific G protein (termed G_{olf}) that activates type-III adenylyl cyclase (AC). This enzyme converts cytoplasmic ATP to cyclic AMP (cAMP). These sequential chemical reactions finally lead to the openings of ion channels that underlie cell excitation (transduction channel). Although the natural ligands for olfaction have large diversity exceeding 100 000 varieties, the signal thus converges into only one type of second messenger, cAMP, through the enzymatic cascade equipped in the sensory cilia. Another parallel pathway utilizing phospholipase C (PLC) – $InsP_3$ – may coexist for the chemical sensation for particular species of animals and/or odorants.

4.28.2 Receptor Potential as an Initial Membrane Excitation

As in the general neurons, excitation of the ORCs is the change in the electrical potential across the plasma membrane. The resting membrane potential is set at −50 to −70 mV. Odorant stimulation induces depolarization (change in the membrane potential to the positive direction; Figure 1).

The key molecular element that converts the chemical energy into the biological signal is the transduction channel located in the ciliary membrane. Openings of transduction channels cause a change in the membrane potential depending on the input resistance of the ORC membrane. Usually, the input resistance of the ORC is >5 GΩ, and therefore, only 1 pA of current can induce >5 mV of change in the membrane potential. This initial depolarization is called the receptor potential. The time course of the receptor potential is roughly the same as the time course of opening and closing of the transduction channel. This potential change is characterized by its graded property; information about the strength of the stimulants is represented as a magnitude of the depolarization (Figure 1). Since this potential is slow and graded, it cannot conduct to the brain along the thin and long axon; its amplitude is exponentially reduced with the longitudinal

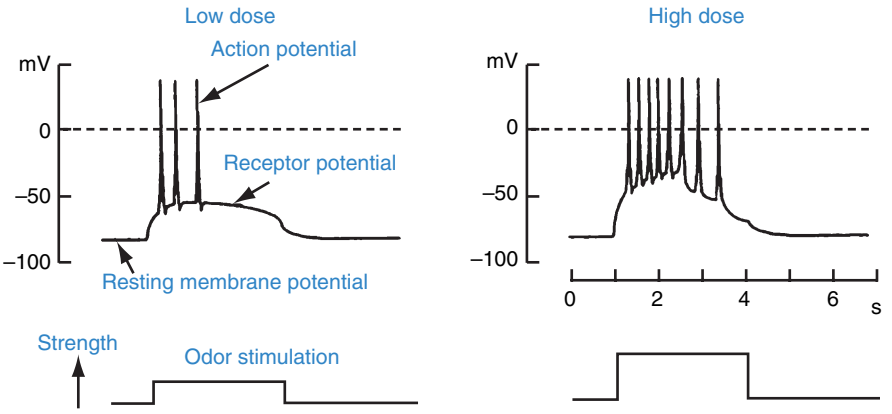

Figure 1 Membrane excitation of the single ORC to low and high doses of odorant stimuli.

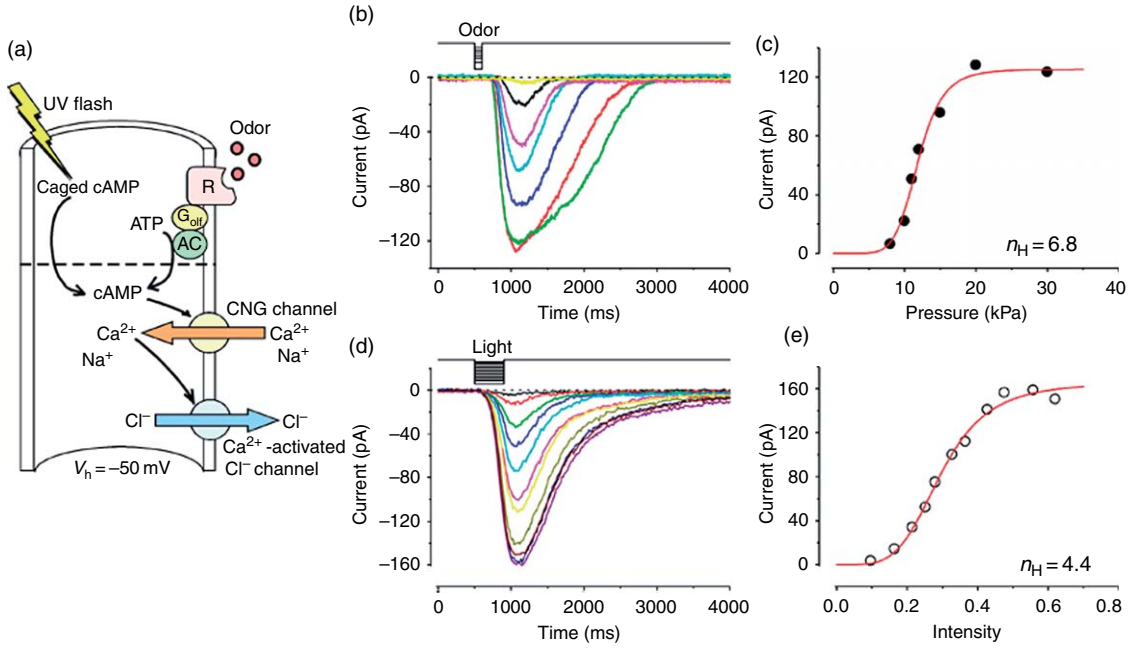

Figure 2 Dose–response relation of single ORCs. (a) Olfactory cilia were stimulated both by odorant and cytoplasmic cAMP emitted by the photolysis of caged cAMP. (b) Odorant-induced response. (c) Dose–response relation. (d) cAMP-induced response. Different cell from (b). (e) Intensity–response relation. Adapted from Takeuchi, H. and Kurahashi, T. 2005. Mechanism of signal amplification in the olfactory sensory cilia. J. Neurosci. 25(48), 11084–11091.

distance from the generation site (cilia). In order to transmit the odorant information to the brain, ORCs induce self-regenerating action potentials (spikes) that do not show signal decay during its conduction. In the action potentials, firing frequencies represent the information about the strength of the stimulants.

The transduction current is unique, in that the magnitude of the excitation shows a very high cooperativity; a small change in the odorant dose is reflected to a big change in the response amplitude. When the inward current responses recorded under the whole-cell voltage-clamp condition are plotted versus stimulus strength, the relation is fitted by the Hill equation (eqn [1]) with very high Hill coefficient (n_H),

$$I = I_{max} \frac{C^{n_H}}{C^{n_H} + K_{1/2}^{n_H}} \quad [1]$$

where I is the current, C is the dose of the ligand, and $K_{1/2}$ is the half-maximum dose. Hill coefficient is an index to express cooperativity and is about 5–6 (Figure 2). If there is no cooperativity, this number becomes 1. Since the same n_H value can be obtained when the cytoplasmic cAMP concentration ($[cAMP]_i$) is increased by the photolysis of caged

cAMP, the high cooperativity is concluded to be achieved after the cAMP production (see below for the detailed mechanisms).

4.28.3 Differences of Single Olfactory Receptor Cells in Functional Ligand Affinities

As described in earlier chapters, genomic DNA contains a large family of genes encoding the odorant receptors, and individual ORCs choose only one type of gene for functional expression. Therefore, investigating the spectrum of single ORCs is equivalent to the survey of the functional spectrum of single odorant receptor in native cells. Since the number of ligand is over 100 000 and since the number of the odorant receptor is 100–1000, it is obvious that the binding of odorants to the odorant receptor is one to many.

When single ORCs were stimulated by two different species of odorants, ORCs show a variety of responsiveness, including cells responding to either types of odorants, cells responding to both, and cells responding to neither (Figure 3). The presence of cells responding to different types of odorants indicates that the single odorant receptor can bind to many different odorants. One may think that the ligand–receptor interaction is an independent event (i.e., random bindings of ligands into the receptors). It seems likely, however, that in the ORCs, the odorant receptors have preferential recognition for certain spectrum of odorants. When the responsiveness to both cineole and lilial stimuli are examined in single receptor cells, there is a positive dependence in the conditional probabilities (therefore the positive correlations, Figure 3(c)); cells responding to cineole are observed in cells responding to lilial more frequently than in cells insensitive to lilial, vice versa cells responding to lilial are observed in cells responding to cineole more frequently than in cells insensitive to cineole (Figure 3(d)). There may be some correlation between the preference of the odorant receptor and the quality of the smell. At this point, unfortunately, there is no systematic study in the receptor preference of ligands and needs to be clarified in future.

4.28.4 Can Olfactory Receptor Cells Detect a Single Odorant Molecule?

In vision, the rod photoreceptor cell can detect a signal from the quantum unit of light, a single photon. Following this knowledge, scientists have been looking for the unitary events in the olfactory response; namely, a response induced by a single odorant molecule. In 1995, Menini and co-workers reported that the response of single ORCs to a low concentration of odorant (*c.* 1 μM, detecting-threshold dose) was very noisy. The noise component was observed as bump-like events, and they suggested that these bump responses may express unitary events caused by the hitting of single odorant molecules to the single olfactory receptor proteins. The amplitude of the events was approximately 1 pA. Immediately after their observations, however, Lowe and Gold showed that application of cAMP into the cytoplasm of the ORCs causes responses with very similar profile as odorant responses that have bump-like current

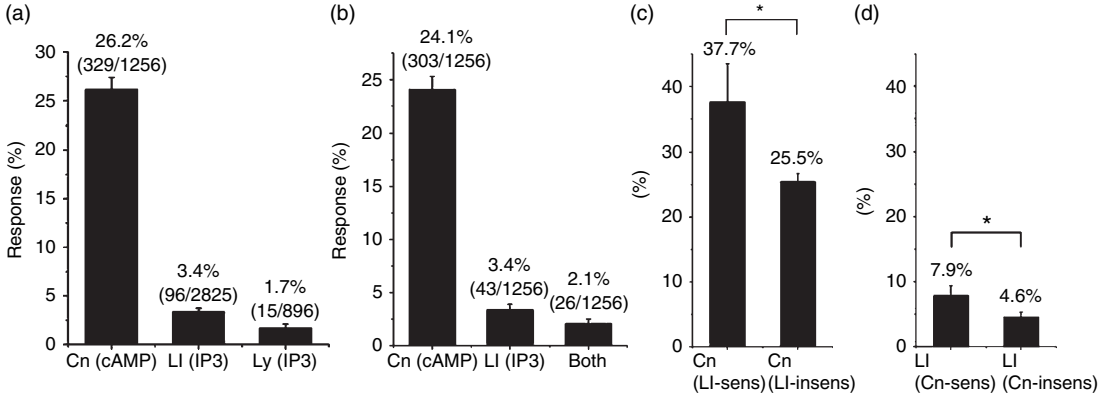

Figure 3 Responsiveness of single ORCs to odorants. (a) Responsiveness to cineole (Cn), lilial (LI), and lyral (Ly). (b) Responsiveness of single ORCs when cells were stimulated by both Cn and LI. (c and d) Conditional probabilities derived from the experiment of (b) Adapted from Takeuchi, H., Imanaka, Y., Hirono, J., and Kurahashi, T. 2003. Cross-adaptation between olfactory responses induced by two subgroups of odorant molecules. J. Gen. Physiol. 122, 255–264.

fluctuations. Since there is no odorants in the experiments that employed the cAMP introduction, bump-like current responses are not attributable to the odorant bindings to the receptors. Their interpretation for the bump response is that the olfactory signal transduction is intrinsically noisy and that the basal noise is clipped off by a strong nonlinear amplification established by the sequential openings of two types of ionic channels: cyclic nucleotide-gated (CNG) and Cl^- channels (see Section 4.28.9).

Just very recently, Bhandawat and co-workers showed that unitary events for olfactory transduction were observed only when the Ca ions were removed from the surrounding media. In this specific condition, the amplitude of the unitary events was 0.9 pA. At the physiological condition containing Ca^{2+}, however, unitary events became undetectable and could be estimated only with a noise analysis by variance/mean–mean relationship and were estimated to be 0.01 pA. This value is very small; even smaller than the basal fluctuations by the intrinsic noise. It thus seems unlikely that the unitary events for the single odorant detection are observed as an olfactory response. One may feel this feature in the ORC quite puzzling, in that rod photoreceptors can detect single photon. However, even among the photoreceptor cell, cone-type photoreceptor cells are not able to detect single photon. In this sense, it is rather appropriate to consider that the rod photoreceptor cell is specifically adapted to have a unique and strong amplification system. As for the signal amplification in the ORC, a recent work by Takeuchi and Kurahashi has directly shown that the enzymatic processes of olfactory sensory cilia have low amplification (see Section 4.28.9).

4.28.5 Enzyme – Second Messenger: cyclic AMP and $InsP_3$

For a long period of time, it has been believed that two independent pathways utilizing either AC-cAMP system or the PLC-InsP3 system mediate the olfactory signal transduction. In other words, odorant species are divided into two subgroups: one is called the cAMP odorant and another $InsP_3$ odorant (for history and evidence, see Schild, D. and Restrepo, D., 1998). There have been several approaches that have tried to identify the second messenger mediating olfactory transduction. Gold and his collaborators used gene-targeting methods to find out if electro-olfactogram (EOG) responses are affected in mice that lacks molecular elements constituting the cAMP pathway (CNG channels; G_{olf}; AC type III). EOG responses to $InsP_3$ odorants were abolished or reduced in animals that lacked any of those elemental proteins. In addition, Zufall's group showed that the inhibitor of AC reduced the response induced by $InsP_3$ odorants. In a recent work by Takeuchi and co-workers, the effects of cytoplasmic cNMPs in sensory cilia were directly examined in cells that retained their response abilities to odorants (including $InsP_3$ odorants). They showed that responses induced by both cAMP and $InsP_3$ odorants resemble each other and show almost perfect symmetrical cross-adaptation. The degree of cross-adaptation between the cAMP odorant and the $InsP_3$ odorant matched perfectly, which cannot be explained simply by coincidences in parallel systems. Furthermore, they showed that the response induced by the cytoplasmic cAMP is changed depending on the dose of $InsP_3$ odorants (Figure 4). The additive

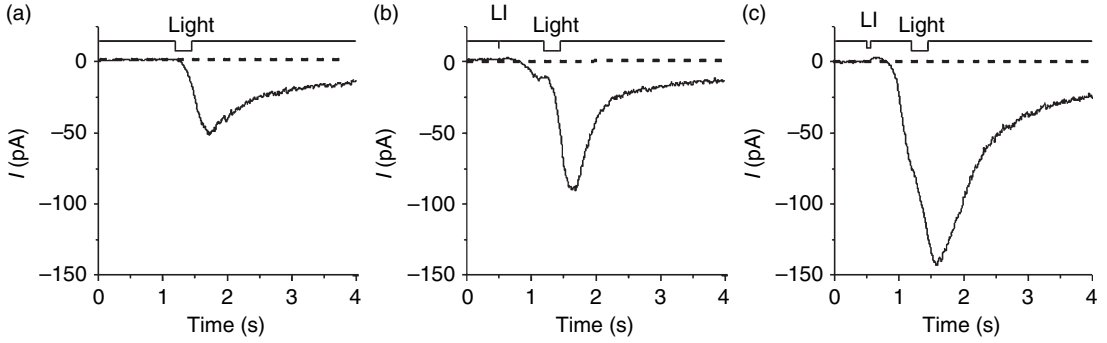

Figure 4 Summation of cAMP-induced current on the lilial (LI)-induced current in the single ORC. Cytoplasmic cAMP was jumped by a flash photolysis of caged cAMP. Lilial stimuli were applied from the puffer pipette to the cilia. Note that the amplitude of cAMP response (light) is affected by the presence of the lilial. Takeuchi, H. and Kurahashi, T. 2003. Identification of second messenger mediating signal transduction in the olfactory receptor cell. J. Gen. Physiol. 122(5), 557–567.

effects could be explained by assuming that $InsP_3$ odorants do increase the cytoplasmic cAMP. All together, it is highly likely that the main stream of olfactory signal transduction is uniformly mediated by cAMP for a wide variety of odorants through a universal second messenger.

Just very recently, however, Restrepo's group showed that mice lacking their CNG channels could still have abilities of responding to particular types of odorants. This result indicates that there is a pathway that is independent from the cAMP-mediated pathway. However, EOG responses in mutant mice were all reduced in comparison to those observed in the wild type. Nonlinear summation observed in the $InsP_3$ odorant response (see Figure 4) does indicate the increase of cAMP, but does not completely rule out the possibilities for the some fractions responses to be evoked in the $InsP_3$-mediated pathway. Coupled with the fact that ORCs in some particular animals (e.g., lobster) use $InsP_3$ as a second messenger, certain fraction of the responses may be mediated by the $InsP_3$-dependent pathway.

4.28.6 Cyclic Nucleotide-Gated Channel

The discovery of cationic channel that is directly gated by cytoplasmic cyclic nucleotide was first made on a work applied to the rod photoreceptor cell. This finding actually ended the long-standing question of what kind of substance (second messenger) transmits the information from the disk membrane (where photopigments are located) to the plasma membrane (where ionic channels mediating cell excitation are present). This historical finding provided a big impact not only on the research on the photoreceptor cell, but also for the research on other sensory and neuronal signal transduction system. Nakamura T. and Gold G.H. (1987) applied the inside-out patch clamp method onto the ciliary membrane of the toad ORC and confirmed electrophysiologically the presence of homologous channel in the ORC. Following the electrophysiological evidence, the gene that encodes the CNG channel was identified. The amino acid sequences of the cloned CNG channels have high identity between rod and ORCs. Both express six membrane-spanning domains and one pore region (Figure 5). The ionic channel is cation-selective, and this is well consistent with the fact that the odorant-activated channels are cation-selective when measured under the Ca^{2+}-free condition (therefore no involvements of Cl^- component).

It is speculated now that the native olfactory channel consists of tetramer using three alpha subunits (CNGA2 and CNGA4) and one beta subunit CNGB1b (stoichiometry 2:1:1 CNGA2:CNGA4:CNGB1b). Among them, CNGA4 subunit seems to be essential to establish Ca^{2+}-calmodulin (Ca-CAM) effect that regulates the olfactory adaptation (see Section 4.28.10).

In the amphibian, CNG channels express a strong localization to the ciliary membrane where olfactory transduction takes place. The density of the channels are as high as 1000 μm^{-2}. In the rodents, however, the distribution of the CNG channels seems to be relatively spread. At this point, there is no physiological explanation why CNG channels are strongly polarized in the amphibian and why they are spread over the cell in the rodent.

Single events for the CNG current can be directly observed when the divalent cations were

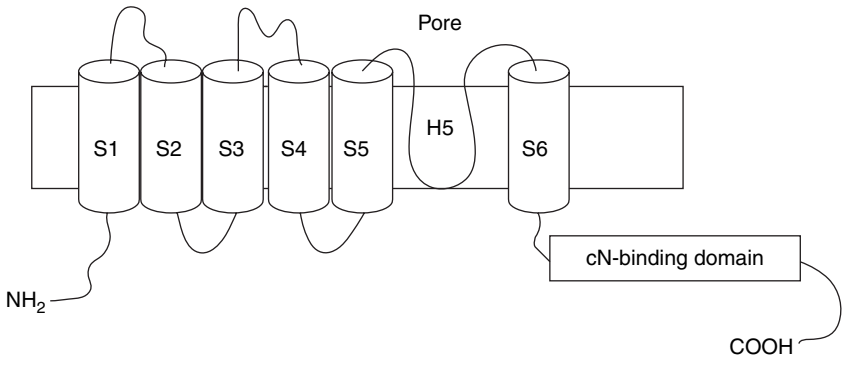

Figure 5 Structure of the subunit of the CNG channel. Both N- and C-terminals are located in the cytoplasmic side. There are six transmembrane domains (S1–S6) and one loop region (H5).

removed from the media. The size of unitary current is about 1 pA when the membrane potential is held at +50 mV. Open–close transition is about the order of 100 ms. In the presence of physiological Ca^{2+} and Mg^{2+}, however, such unitary conductance cannot be observed, because of a flickering-block of channels by divalent cations. This makes the channel event extremely small. Furthermore, the channel density is extremely high. These features allow the summed transduction current to express very high S/N ratio.

4.28.7 Ca^{2+}-Activated Cl^- Channel

Kleene S. and Gesteland R. C. (1991) first reported that olfactory sensory cilia contained Cl^- channels that were sensitive to cytoplasmic Ca^{2+}. Since CNG channels have a very high permeability to Ca^{2+} ($P_{Ca}/P_{Na} = 6.5$), opening of the CNG channel allows Ca^{2+} to enter into the ciliary cytoplasm during the odorant response, which leads to the activation of Ca^{2+}-activated Cl^- channels located in the cilia. Initially, the real function of the Cl^- channel was not identified, and a likely possibility assumed at that point was that Cl^- channel may be responsible for the hyperpolarization of the cell; generally, in neurons, Cl^- channels are functional for generating inhibitory responses. Kurahashi T. and Yau K. W. (1993) demonstrated, however, that in the newt ORCs, the transduction inward current actually consists of two ionic components, cationic and anionic currents. Surprisingly, the Cl^- current was inward, which causes a membrane depolarization. In 1995, Ache's group showed that cytoplasmic Cl^- concentration in the ORC was high enough to induce depolarizing response. Recent works revealed that Cl ions are up-taken into the cell with an Na^+–K^+–$2Cl^-$ co-transporter called NKCC1.

As for the physiological roles of this unusual Cl^- channel, there are two possible molecular functions proposed for the ORC. First, asymmetrical ion flow achieved by the both cations and anions may serve a stability of the inward current under unstable ionic conditions which seems to be caused quite frequently in the olfactory organ that is directly exposed to the external environment. Second, addition of the sequential ion channel causes a boosting of the total current, providing a signal amplification. Especially with both CNG and Cl^- currents having high cooperativities (Hill coefficient of about 2 for each), the final current expresses extremely high nonlinear amplification (cooperativity of 5–6; see Figure 1).

Ca^{2+}-activated Cl^- channel has a unitary conductance of 0.8 pS and the density 70 channels μm^{-2}, when measured with the noise analysis method (by Kleene). Similar to the CNG channels, this channel has small unitary event and the high density. Again these features establish a signal transduction with high S/N ratio. At this point, unfortunately, the molecular structure of this Cl^- channel is not yet identified.

4.28.8 Ca^{2+}-Activated K^+ Channel (Possibility for the Inhibitory Response)

Potassium channel that is directly gated by cytoplasmic Ca^{2+} is commonly distributed to the neuronal system including the ORC. Bacigalupo's group has shown that the olfactory sensory cilia contain this type of channel with inside-out preparation and the immuno-cyto-chemistry. With the same mechanism as the Ca^{2+}-activated Cl^- channel, it is very likely that this K^+ channel is open when the CNG channel allows Ca^{2+} to enter the ciliary cytoplasm.

However, the physiological role of this K^+ channel is still under speculation. One of the most intriguing possibilities is that the opening of K^+ channel may induce cell hyperpolarization and therefore cause inhibitory responses in the ORC activities. Although the actual equilibrium potential for K^+ at the sensory cilia is not identified in the ORC, common sense of the neuronal system is that K^+ channel is inhibitory. Since very early stage of electrophysiological works on ORCs, it has been reported that certain types of odorants and ORCs express inhibitory responses. These cells may express a large number of K^+ channels on their ciliary plasma membrane.

4.28.9 Signal Amplification: Comparison with the Phototransduction

For a long period of time, researches on olfactory transduction system have been limited on rather qualitative descriptions because of experimental difficulties accompanying the use of diverse ligands, multiple receptors, and the fine structure of the sensory cilia. By overcoming those experimental

difficulties, a recent work by Takeuchi and Kurahashi was conducted to understand the mechanism of signal amplification in the olfactory transduction system. cAMP dynamics was inversely estimated from the activities of CNG channels. As a result, cAMP-production rate was in an order of 2×10^4 s^{-1} per cilium at the maximum odorant stimulus. The cAMP molecules must be produced from many odorant receptors on the ciliary surface (immunostaining against the receptor protein generally shows their presences to be homogeneous, spanning the entire cilia). It is therefore suggested that the odorant receptor triggers very small activities of enzymatic reaction.

It has been pointed out that the olfactory transduction system is very homologous as the phototransduction system, in that both systems are mediated by receptor – G protein – effecter enzyme and the CNG channel. In the rod photoreceptor cell, light-activated protein reactions have been fairly well described. Activation of single rhodopsin by a single photon triggers 10^2–10^3 molecular changes in transducin–phosphodiesterase (PDE) cascade, which leads to the breakdown of 10^4–10^5 cGMP molecules in a second (Figure 6). This number is much bigger than that observed in the ORC, as is obvious in a comparison between extreme opposite situations, maximum versus unitary rates.

As described before, Bhandawat *et al.* showed that the olfactory unitary event, presumably evoked by a single odorant molecule, could be very small. They considered that such small unitary event was attributable to that the lifetime of individual odorant receptor molecules was very short (i.e., 1 ms). As comparison, in rods, a single photon switches the status of single rhodopsin molecule into an active form that lasts for >1 s. During its long lifetime, many transducin–PDE molecules are activated, which leads to the generation of the single photon response. Since the excitation of the single rhodopsin by a single photon is by chance and very instantaneous, rods may have to acquire a high amplification at the receptor–enzyme level. In case of chemical sensations, however, stimulants can be staying around until they are removed.

Nevertheless, it may be still puzzling that the olfactory enzymes use very low signal amplification. In olfaction, however, activation of G-protein-coupled receptor (GPCR) produces cAMP, instead of the breakdown of cGMP in the rod. Therefore, the low amplification in olfactory enzymes would be an efficient way to avoid loss of ATP. Apparently, signal transduction with a small number of molecules is achieved by the fine ciliary structure that has high surface–volume ratio in which even a small change in the absolute number of molecules is reflected as a big change in the concentration. In addition, the ORC has a unique and strong nonlinear amplification detecting a slight change in the odorant dose, which is regulated by Ca^{2+} that flows through the CNG channel; cytoplasmic increase of Ca^{2+} in turn activates excitatory Cl^- current to boost the net

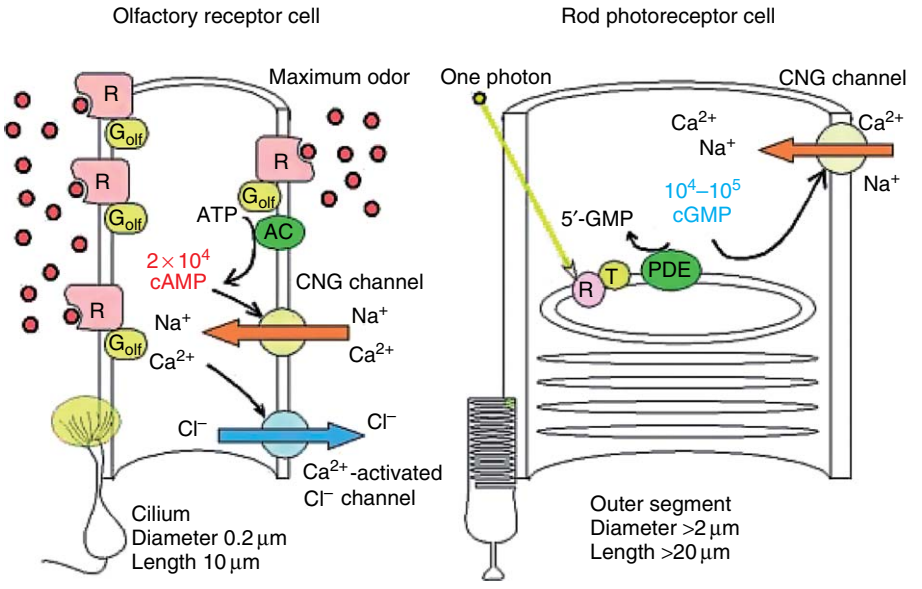

Figure 6 Mechanisms of olfactory transduction and phototransduction.

transduction current. Thus, the sequential openings of two ion channels establish a high nonlinear amplification in olfaction, utilizing Ca^{2+} as a third messenger that is not present in the phototransduction system.

4.28.10 Adaptation

It has been known that the olfactory sensation becomes gradually smaller during the long exposure to the odorant environment (Figure 7(a)). Also, when the odorant pulses are delivered twice, the secondary response becomes smaller than the initial response. The reduced response becomes recovered as the inter-interval is prolonged (Figure 8).

These phenomena are generally called as fatigue, desensitization, or adaptation. One may use these words to the same concept when the response amplitude is gradually reduced as time processed. However, the fundamental concepts are thought to be different.

Among them, the word adaptation is used especially when the dose–response relation is shifted to

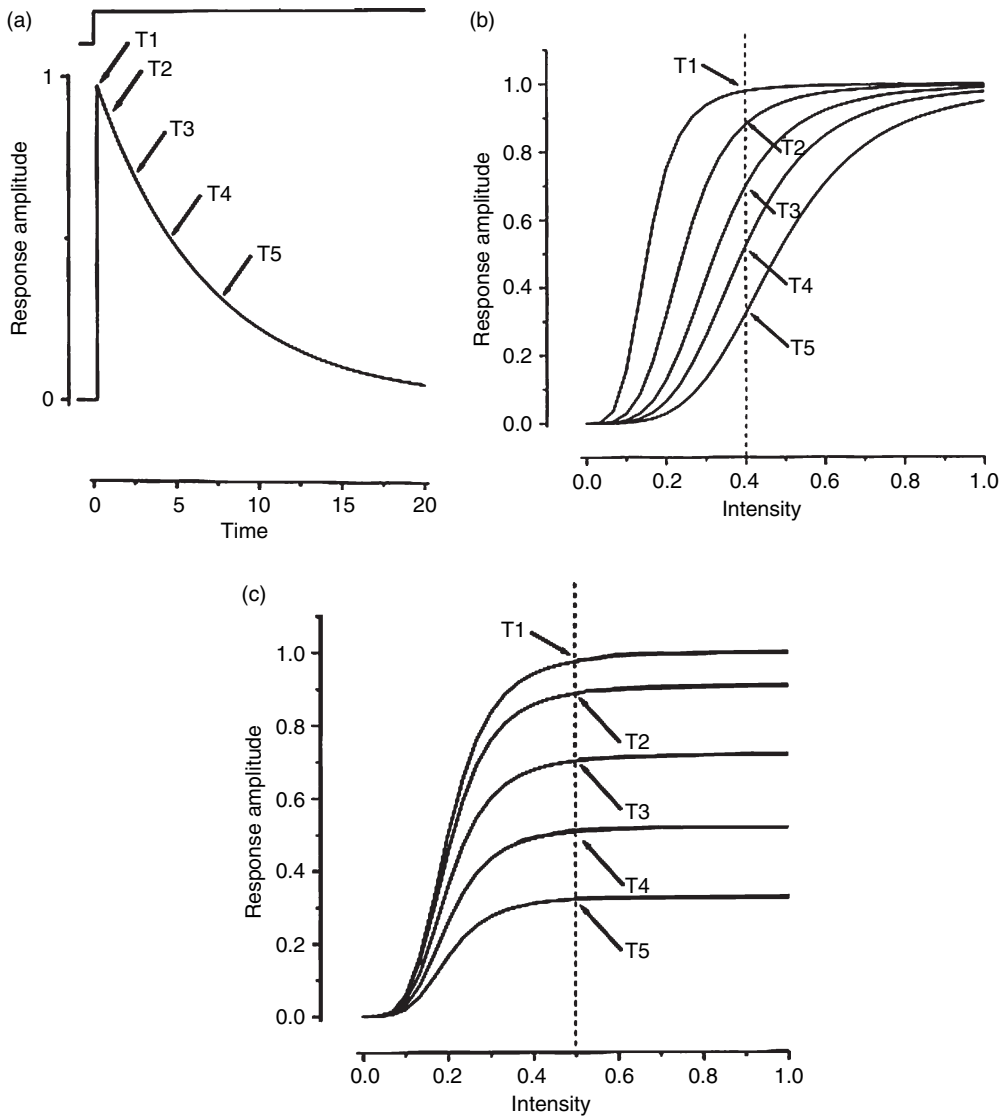

Figure 7 Response decay explained by either the change in $K_{1/2}$ (b) or change in I_{max} (c). (a) Time course of the odorant-induced current. (b) Gradual change of the dose–response relation accompanying the increase of $K_{1/2}$. (c) Gradual change of the dose–response relation accompanying the reduction of I_{max}.

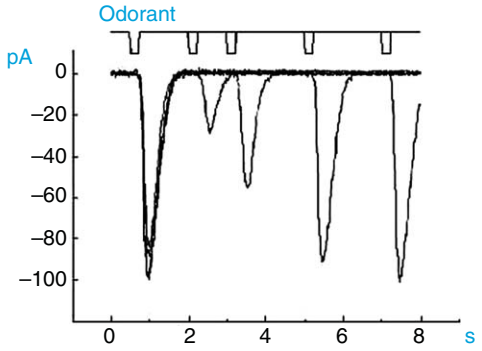

Figure 8 Adaptation and recovery of single ORC responses. Note that the amplitude of the secondary responses is reduced in size. This current reduction is attributable to the change in the dose–response relation as in Figure 9. As the inter-interval is increased, the current amplitude returns to the initial level. Complete recovery is observed after *c*. 10 s.

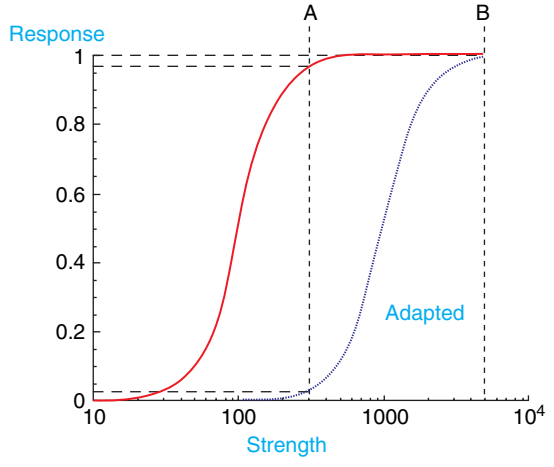

Figure 9 Contribution of sensory adaptation on establishing a wide dynamic range. Dose–response relation is shifted in order to expand the dynamic range. Under the standard condition (red curve), the ORC cannot discriminate the change in the stimulus strength between A and B. In the adapted state (blue, dashed line), A and B can be discriminated as a difference in the response amplitude.

cover a wider range for the stimulus strength. As illustrated in Figure 9, shift of the dose–response curve (change in $K_{1/2}$) can establish two competitive functions; signal amplification and wide dynamic range. In contrast, desensitization or fatigue during a long step includes all decaying phenomena. For instance, change in the I_{max} can also express the same phenomenon, but in this case, the dynamic range is not changed (Figures 7(b) and 7(c)).

The ORC itself has an ability of adaptation. This sensory adaptation is achieved in the ciliary molecular circuit that utilizes the Ca^{2+} movement through the CNG channel. Influx of Ca^{2+} causes an increase in the cytoplasmic Ca^{2+} concentration. Cytoplasmic Ca^{2+} binds to the CAM that has already attached to the CAM-binging domain locating N-terminal cytoplasmic chain of the CNG channel. This causes reduction of the ligand affinity leading to the change of the total sensitivity. In contrast, mechanisms causing olfactory fatigue are still not yet well identified.

Ca ions that flowed through the CNG channels play crucial roles in the ORCs as described (activation of Cl^- and K^+ channel, regulation for adaptation). This Ca^{2+} must be excluded from the cilia. Unfortunately, at this moment, there is little information about the Ca^{2+} extrusion system. Electrophysiological data show that Ca^{2+} extrusion mechanism in the olfactory sensory cilia is dependent on the presence of external Na^+. As a homologous biological system, photoreceptor outer segment is equipped with Na/Ca/K exchanger that regulates cytoplasmic Ca^{2+} level. There is a possibility that the same molecular element is present in the olfactory sensory cilia (for detail, see Matthews, H. R. and Reisert, J., 2003).

4.28.11 Functional Roles of Molecular Elements in the Olfactory Cilia

As described, the molecular network within the sensory cilia establishes an elegant and sophisticated signal processing. Active time courses of the molecular elements were investigated by the series of works done by Takeuchi H. and Kurahashi T. (2002; 2003; 2005), in which odorant-induced response and cAMP-induced response were directly compared in the living olfactory cilia (Figure 10).

Very short lifetime of the active odorant receptor is extended while the signal is transmitted to G_{olf} and AC (Figure 11). cAMP molecules survives longer than the active time of AC, until they are hydrolyzed by the activity of PDE. In addition, cytoplasmic Ca^{2+} may be kept for some period of time, until Ca^{2+}-binding proteins trap them or until they are excluded. These time courses of cytoplasmic factors will further extend the active time for the signals.

During the active lifetime of cAMP, CNG channels are kept open, which allows Ca^{2+} to enter into the cytoplasm. This Ca^{2+} opens Ca^{2+}-activated Cl^- channels. At this stage, the signal amplitude is boosted in a nonlinear manner. A long step of odorant

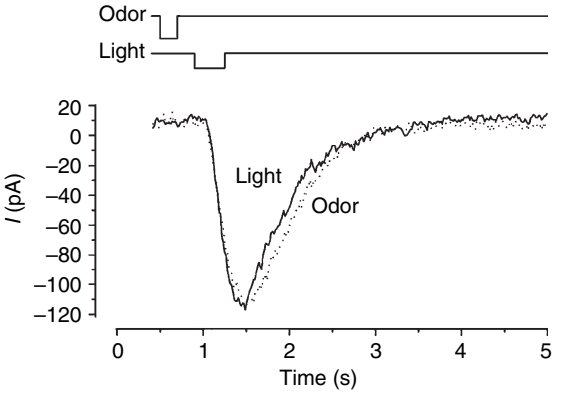

Figure 10 Estimation of odor-activated AC activity by a response-clamp experiment. Cytoplasmic cyclic nucleotide (cGMP having the same effect as cAMP) was increased by photolysis of cytoplasmic caged cGMP. The light condition was adjusted to induce an identical waveform of response as the odorant response. In this experimental condition, the period of light exposure is comparable to the activation of odorant-induced AC activity. Note that the light exposure is delayed from the odorant stimulation and that the period is longer. Also, the current response lasts longer than the light exposure. This indicates that cytoplasmic elements (cAMP and/or Ca^{2+}) remain longer than the AC activity. From Takeuchi, H. and Kurahashi, T. 2002. Photolysis of caged cyclic AMP in the ciliary cytoplasm of the newt olfactory receptor cell. J. Physiol. (Lond.) 541(Pt 3), 825–833.

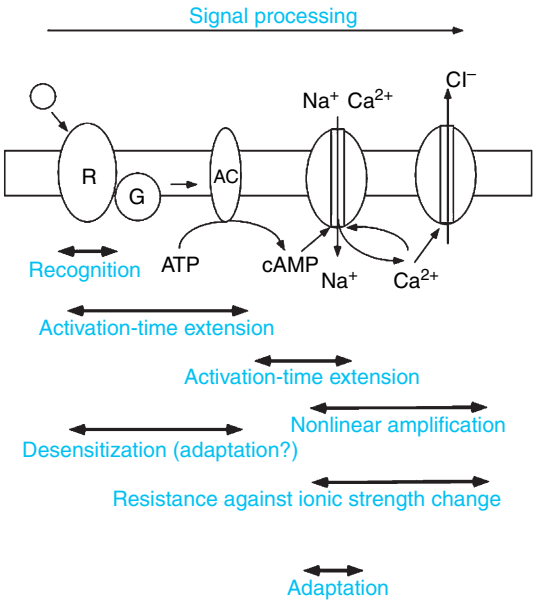

Figure 11 Functional roles of olfactory molecular elements.

stimulation causes gradual increase of cAMP production rate, and $[cAMP]_i$ increases superlinearly with time for over a second. Therefore, the rising phase of the response becomes very rapid and instantaneous.

The combination of cation and anion components is also important for the resistance against the change in the external ionic strength. Having both ion channels together, any change in the cationic current accompanied with the change in the NaCl concentration can be compensated by the inverse stream of the anions.

Adaptation is regulated by the Ca^{2+}-feedback to the CNG channel where very high nonlinear amplification is established. In addition, there is a possibility that desensitization is also regulated at the upstream point from the AC. These molecular roles are summarized in Figure 11.

4.28.12 Resting Membrane Potential and Spike Discharges

As has been generally known for neurons, the olfactory cell is equipped with an excitatory membrane having several types of voltage-gated ion channel. Most of them are distributed in the interstitial area (dendrosomatic regions) of the ORC. As described, the resting potential of the ORC is about −50 to −70 mV. This value is close to the equilibrium potential for the K ions, and it is therefore likely that the resting potential is determined by the K-dominant component. In case of rodents, an ionic channel that is activated by the hyperpolarization (I_h channel) seems to be involved in the determination of the resting potential. Since I_h channels have permeability to both Na^+ and K^+, the resting potential of these cells may be a bit depolarized. This may provide an important function that the resting potential is closed to the spike-firing threshold. However, such I_h channels are not observed in amphibian. Because of this, amphibian ORCs have very high input resistance (>5 GΩ). Such high input resistance would be remarkable especially at the hyperpolarizing voltage region. It may be possible to think that inhibitory responses (presumably evoked by the Ca^{2+}-activated K^+ channels) are dominant for the amphibian.

For the spike discharges, voltage-dependent Na^+ and Ca^{2+} channels have been shown to be involved in their generations. Essentially, Na^+ channel is a major element that is needed for the spike generation, and Ca^{2+} channel (especially T-type) has an ability of lowering the threshold. The falling phase is shaped by the action of K^+ channel (delayed rectifier and transient K^+ channels) (Table 1).

Table 1 Ionic channels equipped in the olfactory receptor cell

	Functions
Transduction channels	
CNG channel	Initiation of membrane excitation
Ca^{2+}-activated Cl^- channel	Boosting the transduction current
Ca^{2+}-activated K^+ channel	Inhibitory response (?)
$InsP_3$-gated channel	Parallel transduction pathway (?)
Voltage-dependent channels	
Na^+ channel	Initiation of spikes
L-type Ca^{2+} channel	Ca^{2+} uptake, generation of spike
T-type Ca^{2+} channel	Lowering the spike threshold
Delayed K^+ channel	Sharpen the spike falling phase
Transient K^+ channel (A channel)	Sharpen the spike falling phase Repetitive spikes (re-activation of Na)
Ca^{2+}-activated K^+ channel	Resting membrane potential Spike falling phase
Hyperpolarization-activated cation (h) channel (rodents)	Resting membrane potential

4.28.13 Modulation of Membrane Excitability of the Olfactory Receptor Cell

As described, the ORC is the entrance for the olfactory sensation. It is likely that this step is controlled by a number of endocrine factors. First observation was that adrenalin changed spike initiation patterns by modulating activities of voltage-gated Na^+ and Ca^{2+} channels via an ATP-dependent protein kinase. Besides, dopamine, Ach, serotonin, and LHRH have been shown to modulate the activities of ORCs (for details; see bibliography by Narusuye, K. *et al.*, 2003 and related articles). These findings raise a possibility that the olfactory input is changed depending on the physical and emotional status. In the psychological works, there are cumulative data showing that the olfactory sensation is strongly influenced by the body condition. It is highly expected that in near future the modulatory effects by endocrine factors on ORCs are correlated with the human olfactory sensations.

References

Kleene, S. and Gesteland, R. C. 1991. Calcium-activated chloride conductance in frog olfactory cilia. J. Neurosci. 11, 3624–3629.

Kurahashi, T. and Yau, K. W. 1993. Co-existence of cationic and chloride components in odorant-induced current of vertebrate olfactory receptor cells. Nature 363, 71–74.

Matthews, H. R. and Reisert, J. 2003. Calcium, the two-faced messenger of olfactory transduction and adaptation. Curr. Opin. Neurobiol. 13(4), 469–475.

Nakamura, T. and Gold, G. H. 1987. A cyclic nucleotide-gated conductance in olfactory receptor cilia. Nature 325, 442–444.

Narusuye, K., Kawai, F., and Miyachi, E. 2003. Spike encoding of olfactory receptor cells. Neurosci. Res. 46(4), 407–413.

Schild, D. and Restrepo, D. 1998. Transduction mechanisms in vertebrate olfactory receptor cells. Physiol. Rev. 78(2), 429–466.

Takeuchi, H. and Kurahashi, T. 2002. Photolysis of caged cyclic AMP in the ciliary cytoplasm of the newt olfactory receptor cell. J Physiol. 541(Pt 3), 825–833.

Takeuchi, H. and Kurahashi, T. 2003. Identification of second messenger mediating signal transduction in the olfactory receptor cell. J. Gen. Physiol. 122(5), 557–567.

Takeuchi, H. and Kurahashi, T. 2005. Mechanism of signal amplification in the olfactory sensory cilia. J. Neurosci. 25(48), 11084–11091.

Takeuchi, H., Imanaka, Y., Hirono, J., and Kurahashi, T. 2003. Cross-adaptation between olfactory responses induced by two subgroups of odorant molecules. J. Gen. Physiol. 122, 255–264.

Further Reading

Bhandawat, V., Reisert, J., and Yau, K. W. 2005. Elementary response of olfactory receptor neurons to odorants. Science 308, 1931–1934.

Buck, L. and Axel, R. 1991. A novel multigene family may encode odorant receptors: a molecular basis for odor recognition. Cell 65, 175–187.

Delgado, R., Saavedra, M. V., Schmachtenberg, O., Sierralta, J., and Bacigalupo, J. 2003. Presence of Ca^{2+}-dependent K^+ channels in chemosensory cilia support a role in odor transduction. J. Neurophysiol. 90, 2022–2028.

Kurahashi, T. and Menini, A. 1997. Mechanism of odorant adaptation in the olfactory receptor cell. Nature 385, 725–729.

Zhainazarov, A. B. and Ache, B. W. 1995. Odor-induced currents in Xenopus olfactory receptor cells measured with perforated-patch recording. J. Neurosci. 74, 479–483.

4.29 Olfactory Cyclic Nucleotide-Gated Ion Channels

M-C Broillet, University of Lausanne, Lausanne, Switzerland

© 2008 Elsevier Inc. All rights reserved.

4.29.1	Introduction	511
4.29.2	Phylogeny	511
4.29.3	Structure	513
4.29.3.1	Pore	514
4.29.3.2	Cyclic Nucleotide-Binding Domain	515
4.29.3.3	C-Linker region	516
4.29.3.4	Amino-Terminal Domain	517
4.29.4	Physiology	518
4.29.5	Modulation	520
4.29.6	Pharmacology	521
4.29.7	Conclusion	521
References		522

4.29.1 Introduction

Nakamura T. and Gold G. H. (1987) using excised patches of cilia membrane from olfactory neurons recorded macroscopic ionic currents directly activated by cAMP. The ion channel responsible for this conductance has since then been cloned and identified in several species (Kaupp, U. B. and Seifert, R., 2002). Cyclic nucleotide-gated (CNG) channels form a family of ion channels that are structurally related to voltage-gated channels (Figure 1). They require the binding of at least two cyclic nucleotide molecules for activation (Zufall, F. *et al.*, 1991; Biskup, C. *et al.*, 2007). Although they have recently been identified in an assortment of cell types and tissues, they are most prevalent in the peripheral sensory receptor cells of the visual and olfactory systems (Kaupp, U. B. and Seifert, R., 2002; Pifferi, S. *et al.*, 2006). In olfactory neurons, these channels can be activated by either cAMP ($K_d = 20\,\mu M$) or cGMP ($K_d = 5\,\mu M$), although it is generally believed that under normal physiological conditions it is a rise in intracellular cAMP that is responsible for channel activation (Firestein, S. and Zufall, F., 1994; Shepherd, G. M., 1994). A high density of CNG channels is present on the ciliary membrane of olfactory neurons. These channels are selective for cations, and their activation leads to cell membrane depolarization. Native CNG channels are known to be permeable to Ca^{2+} ions, but because the Ca^{2+} ions bind to sites on their way through the pore they also act to block monovalent currents (Frings, S. *et al.*, 1995; Zagotta, W. N. and Siegelbaum, S. A., 1996).

4.29.2 Phylogeny

In vertebrates, six members of the CNG channel gene family have been identified. These genes are grouped according to sequence similarity into two subtypes, CNGA and CNGB (Bradley, J. *et al.*, 2001a). Additional genes coding for CNG channels have been cloned from *Drosophila melanogaster* and *Caenorhabditis elegans*. The phylogenetic relationship of these channels is shown in Figure 2.

The first cDNA clone for a subunit of a CNG channel, CNGA1 (previously called α1, CNG1 or RCNC1) has been isolated from bovine retina (Kaupp, U. B. *et al.*, 1989). CNGA1 is expressed in rod photoreceptors and produces functional channels that are gated by cGMP when expressed exogenously either in *Xenopus* oocytes or in a human embryonic kidney cell line (HEK293). Mutations in CNGA1 in humans cause an autosomal recessive form of retinitis pigmentosa, a degenerative form of blindness (Dryja, T. P. *et al.*, 1995). Later, the second subunit of the rod channel, CNGB1 (previously called β_1 CNG4 or RCNC2), has been isolated and cloned (Chen, T.-Y. *et al.*, 1993; Korschen, H. G. *et al.*, 1995). CNGB1 subunits expressed alone do not produce functional CNG channels, but coexpression of CNGA1 and CNGB1 subunits yields heteromeric channels with permeation, modulation, pharmacology, and cyclic-nucleotide specificity similar to that of native channels (Chen, T.-Y. *et al.*, 1993; Korschen, H. G. *et al.*, 1995). CNG channels form tetrameric

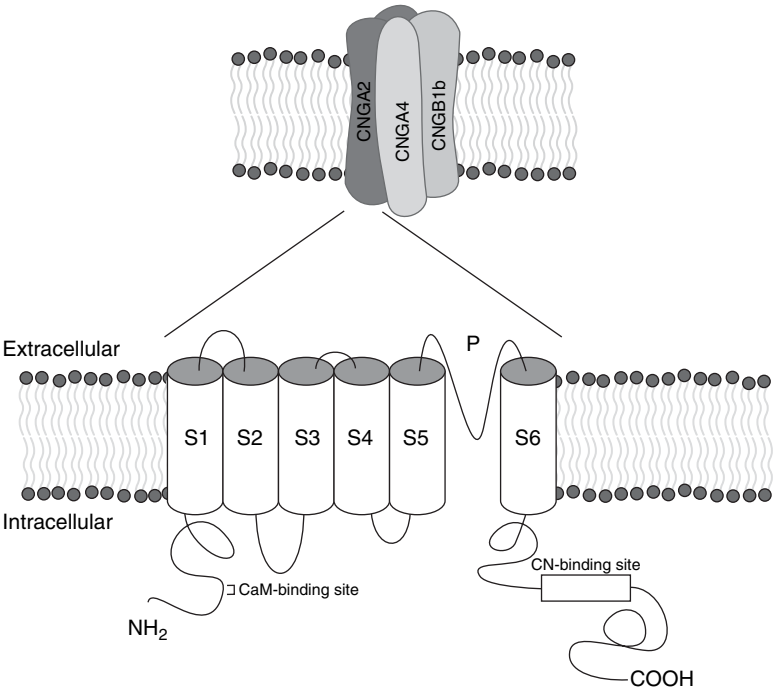

Figure 1 Tetrameric model of an olfactory CNG channel comprising two CNGA2, one CNGA4, and one CNGB1b subunits. A schematic representation of the two-dimensional architecture of one CNG channel subunit is also shown. S1–S6 are the putative transmembrane domains and P is the putative pore region. The cyclic nucleotide (CN)-binding site is defined by homology to the sequences of cAMP and cGMP binding proteins. The position of the Ca^{2+}-calmodulin (CaM) binding site is indicated for an olfactory CNGA2 subunit.

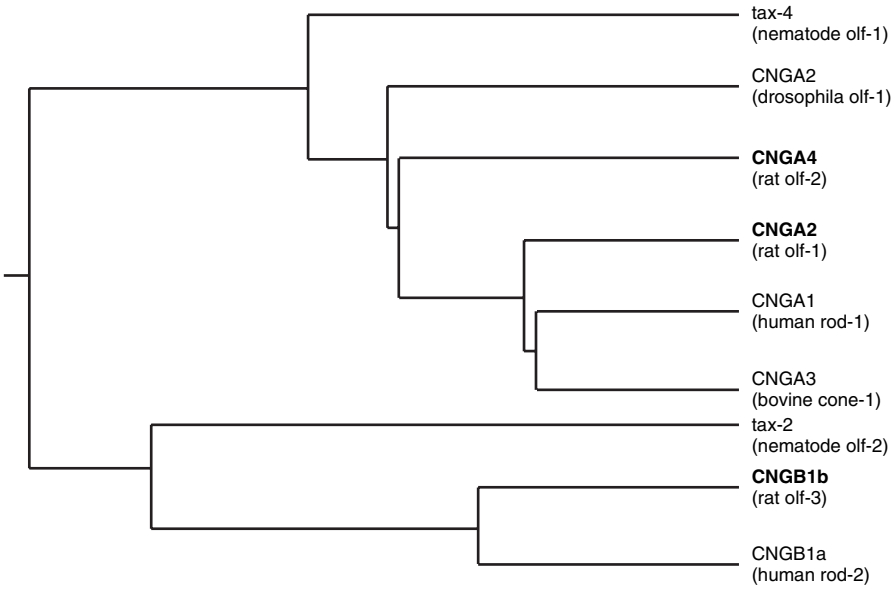

Figure 2 Phylogenetic tree of the olfactory and retinal CNG channels subunits. The tree was calculated on the basis of the sequence alignments with the transmembrane domains and the cyclic nucleotide binding site of the respective subunits.

molecules (Varnum, M. D. *et al.*, 1995; Gordon, S. E. and Zagotta, W. N., 1995b; Liu, D. T. *et al.*, 1996) with a stoichiometry of three CNGA1 subunits and one CNGB1 subunit (Weitz, D. *et al.*, 2002; Zheng, J. *et al.*, 2002; Zhong, H. *et al.*, 2002).

The CNG channels from cone photoreceptors are composed of two other types of subunits, CNGA3 (previously called $\alpha 2$, CNG3 or CCNC1) and CNGB3 (previously called $\beta 2$, CNG6 or CCNC2) (Bonigk, W. *et al.*, 1993; Gerstner, A. *et al.*, 2000) with a stoichiometry of two CNGA3 and two CNGB3 (Peng, C. *et al.*, 2004). CNGA3 subunits, but not CNGB3 subunits, form functional channels when expressed in heterologous systems. Mutations in human CNGA3 and CNGB3 have been linked to complete achromatopsia (also referred to as rod monochromacy or total color blindness), a rare, autosomal recessive inherited and congenital disorder characterized by the complete inability to discriminate between colors (Kohl, S. *et al.*, 1998; Sundin, O. H. *et al.*, 2000; Wissinger, B. *et al.*, 2001).

Native olfactory CNG channels are constructed from three different but highly homologous subunits (Figure 1), the CNGA2 (previously called $\alpha 3$, CNG2 or OCNC1) (Dhallan, R. S. *et al.*, 1990), the CNGA4 (previously called $\alpha 4$, CNG5 or OCNC2) (Bradley, J. *et al.*, 1994; Liman, E. R. and Buck, L. B., 1994), and the CNGB1b (previously called $\beta 1$, CNG4.3 or RCNC2) (Sautter, A. *et al.*, 1998; Bonigk, W. *et al.*, 1999) subunits. The stoichiometry of olfactory CNG channels has been identified using fluorescently tagged subunits and fluorescence resonance energy transfer (Zheng, J. and Zagotta, W. N., 2004). They are tetrameric molecules composed of two CNGA2, one CNGA4 and one CNGB1b subunits. The CNGA2 subunits form cAMP-activated channels when heterologously expressed in mammalian cells (Dhallan, R. S. *et al.*, 1990). This conductance is less sensitive to cAMP than the native rat channel and shows very little rectification in the absence of divalent cations, whereas the native CNG conductance is outward rectifying in the presence of physiological calcium concentration (Frings, S. *et al.*, 1992; Bonigk, W. *et al.*, 1999). The second olfactory subunit cloned (CNGA4) is 52% identical to the CNGA2 (Bradley, J. *et al.*, 1994; Liman, E. R. and Buck, L. B., 1994). The expression of CNGA4 alone in *Xenopus* oocytes or its transfection into HEK293 cells shows no activation by cyclic nucleotides (Bradley, J. *et al.*, 1994; Liman, E. R. and Buck, L. B., 1994). When the CNGA2 and the CNGA4 are coexpressed in mammalian cells (Bradley, J. *et al.*, 1994) or *Xenopus* oocytes (Liman, E. R. and Buck, L. B., 1994), an outward rectifying cation conductance exhibiting a cAMP sensitivity closer to the native CNG channel is observed. The third subunit of the olfactory CNG channel, the CNGB1b (Sautter, A. *et al.*, 1998; Bonigk, W. *et al.*, 1999), is a spliced form of the rod photoreceptor CNGB1a subunit. When this subunit is coexpressed with the CNGA2 and CNGA4 subunit in HEK293 cells, it creates channels with sensitivity for cAMP, discrimination between Na^+ and K^+, single-channel conductance, kinetics of open–closed transitions and the presence of subconductance states similar to the native olfactory channel.

Two extra CNG channel subunits have been identified in *D. melanogaster*. The first one is expressed in the antennae and in the visual system, suggesting that CNG channels may be involved in the transduction of light in invertebrates (Baumann, A. *et al.*, 1994) and the second, a putative CNG-like channel subunit, is expressed in the brain (Miyazu, M. *et al.*, 2000). Two CNG channel subunits, Tax-2 and Tax-4, have also been cloned in *C. elegans* (Coburn, C. M. and Bargmann, C. I., 1996; Komatsu, H. *et al.*, 1996); they are required for chemosensation, thermosensation, and normal axon outgrowth of sensory neurons.

4.29.3 Structure

CNG channels are composed of four subunits around a centrally located pore (Gordon, S. E. and Zagotta, W. N., 1995b; Liu, D. T. *et al.*, 1996; Varnum, M. D. and Zagotta, W. N., 1996). Each subunit contains six transmembrane segments, a reentrant P-loop and intracellular amino- and carboxy-terminal regions (Figure 1) (Kaupp, U. B. *et al.*, 1989; Molday, R. S. *et al.*, 1991; Wohlfart, P. *et al.*, 1992; Liu, D. T. *et al.*, 1996). The P-loop and the S6 segment line the ion-conducting pore. The carboxy-terminal region contains a cyclic nucleotide (CN)-binding site and a region connecting it to the S6 segment (the C-linker region). The amino-terminal region and the region following the CN-binding domain have specialized functions for each of the CNG channel subtypes. A series of elegant experiments with cloned channels and chimeric constructs have identified several regions as well as specific residues distributed, in particular, throughout the approximately 500 amino acids of the CNGA1 (retinal) or the CNGA2 (olfactory) subunit proteins that play a key role in channel regulation (Matulef, K. and Zagotta, W. N., 2003). The characteristics of these regions will be discussed below.

4.29.3.1 Pore

The pore region of the channel controls both the single-channel conductance and the pore diameter of the channel (Goulding, E. H. *et al.*, 1993). The determination of how ions permeate the channel and how the ionic selectivity occurs is of great physiological importance because ion permeation is responsible for generating membrane depolarization which is critical for electrical signaling, but also the CNG channels are permeable to Ca^{2+} which is an important element in the activation of intracellular targets. Balasubramanian S. *et al.* (1997) have demonstrated that the permeation properties of the olfactory CNG channels are significantly different from those of photoreceptor CNG channels. Their results further indicate that Na^{+} currents through these channels do not obey the independence principle and show saturation kinetics with K(m)s in the range of 100–150 mM. They also display a lack of voltage dependence of conductance in asymmetric solutions that suggests that ion-binding sites are situated midway along the channel pore.

Wells G. B. and Tanaka J. C. (1997) have developed a two-site, Eyring rate theory model of ionic permeation for CNG channels. The parameters of the model are optimized by simultaneously fitting current–voltage data sets from excised photoreceptor patches in electrolyte solutions containing one or more of the following ions: Na^{+}, Ca^{2+}, Mg^{2+}, and K^{+}. The model accounts well for the shape of the IV relations, the binding affinity for Na^{+}, the reversal potential values with single-sided additions of calcium or magnesium and biionic KCl, and the $K_{1/2}$ and voltage dependence for divalent block from the cytoplasmic side of the channel. The differences between the predicted $K_{1/2}$s for extracellular block by Ca^{2+} and Mg^{2+} and the values obtained from heterologous expression of only the CNGA1 subunit of the channel suggest that the CNGB1 subunit or a cell-specific factor affects the interaction of divalent cations at the external but not the internal face of the channel. The model predicts concentration-dependent permeability ratios with single-sided addition of calcium and magnesium and anomalous mole fraction effects under a limited set of conditions for both monovalent and divalent cations. Calcium and magnesium are predicted to carry 21 and 10%, respectively, of the total current in the retinal rod cell at −60 mV.

In addition to permeating the CNG channel, Ca^{2+} also profoundly blocks the current flow carried by monovalent cations through the channels (Zagotta, W. N. and Siegelbaum, S. A., 1996) similar to the behavior observed in voltage-activated Ca^{2+}-channels (Almers, W. and McCleskey, E. W., 1984). Supposedly, this behavior implies the high-affinity binding of Ca^{2+} to a single acidic amino acid residue located in the pore of the channel (E363 for the rod CNG channel and E333 for the catfish olfactory CNG channel) (Root, M. J. and MacKinnon, R., 1993). These authors have also implicated this particular glutamate residue as being important in the external rapid proton block of CNG channels, another characteristic that the CNG channels share with Ca^{2+} channels. Gavazzo P. *et al.* (1997) have examined the modulation by internal protons of the bovine CNGA1 and CNGA2 subunits. Increasing internal proton concentrations causes a partial blockage of the single-channel current, consistent with protonation of a single acidic site with a pK1 of 4.5–4.7, both in rod and in olfactory CNG channels. Channel gating properties are also affected by internal protons. The open probability at low cyclic nucleotide concentrations is greatly increased by lowering pH_i, and the increase is larger when channels are activated by cAMP than by cGMP. Therefore, internal protons affect both channel permeation and gating properties, causing a reduction in single-channel current and an increase in open probability. These effects are likely to be caused by different titratable groups on the channel.

Amino acid conservation among a wide range of P-loop-containing channels suggests that the structures of the KcsA, a bacterial potassium channel (Doyle, D. A. *et al.*, 1998), and of the MthK, another channel (Jiang, Y. *et al.*, 2002a; 2002b), may serve as general models for the closed and open state conformations of CNG channels. Experimental evidence using cysteine mutations suggests that the cytoplasmic opening of the CNG channel pore is narrow when channels are closed and widens when channels open (Flynn, G. E. and Zagotta, W. N., 2001). Cysteine-scanning mutagenesis studies suggest that the pore helix, near the selectivity filter, undergoes a conformational change during channel activation (Becchetti, A. *et al.*, 1999; Liu, J. and Siegelbaum, S. A., 2000). Recently, site-directed mutagenesis and inside-out patch-clamp recordings (Qu, W. *et al.*, 2006) have been used to investigate ion permeation and selectivity of the rat CNGA2 channels expressed in HEK293 cells. A single point mutation of the negatively charged P-loop glutamate (E342) to either a positively charged lysine or

arginine has resulted in functional channels, which consistently respond to cGMP, although the currents are generally extremely small. These results show that it is predominantly the charge of the E342 residue in the P-loop that controls the cation–anion selectivity of this channel. These results also have potential implications for the determinants of anion–cation selectivity in the large family of P-loop-containing channels.

4.29.3.2 Cyclic Nucleotide-Binding Domain

Since the demonstration by Fesenko E. E. *et al.* (1985) and Nakamura T. and Gold G. H. *et al.* (1987) that CNG channels could be directly activated by intracellular cyclic nucleotides, a highly conserved stretch of approximately 120 amino acids homologous to the CN-binding domains of other proteins like the cAMP or cGMP protein kinases has been identified. It consists of a short amino-terminal α helix preceding an eight-stranded anti-parallel β roll that is followed by two α helices (Zagotta, W. N. and Siegelbaum, S. A., 1996). A structural model of the retinal CNG channel CN-binding site has also been constructed (Kumar, V. D. and Weber, I. T., 1992).

The retinal and olfactory CNG channels share a high degree of sequence similarity (over 80% amino acids identity) in the CN-binding sites, but they have very different cyclic nucleotide selectivities. cGMP is a more potent and effective agonist of the retinal channel (Fesenko, E. E. *et al.*, 1985) while cAMP and cGMP have very similar effects on the olfactory channel (Zufall, F. *et al.*, 1994). Varnum M. D. *et al.* (1995) have investigated the molecular mechanism for ligand discrimination of CNG channels. They have found that the retinal photoreceptors and olfactory neurons CNG channels are differentially activated by ligands that varied only in their purine ring structure. The nucleotide selectivity of the retinal bovine CNG channel (cGMP > cIMP $\gg$ cAMP) is significantly altered by neutralization of a single aspartic acid residue (D604) in the CN-binding site (cGMP $\geq$ cAMP > cIMP). Substitution by a nonpolar residue at this position inverts agonist selectivity (cAMP $\gg$ cIMP $\geq$ cGMP). These effects result from an alteration in the relative ability of the agonists to promote the allosteric conformational change associated with channel activation, not from a modification in their initial binding affinity. These authors propose a general mechanism for guanine nucleotide discrimination, in common with that observed in high-affinity GTP-binding proteins, involving the formation of a pair of hydrogen bonds between the aspartic acid side chain and N1 and N2 of the guanine ring. This amino acid residue (D604) appears to play a critical role in the selective activation of the retinal CNG channel by cGMP. The presence of a methionine at this position in CNGA4 is sufficient to explain the altered ligand specificity of the native olfactory channel (Shapiro, M. S. and Zagotta, W. N., 2000).

The functional effects of each ligand-binding event have always been difficult to assess because ligands continuously bind and unbind at each site. Furthermore, in retinal rod photoreceptors, the low cytoplasmic concentration of cyclic GMP means that CNG channels exist primarily in partially liganded states. Ruiz M. L. and Karpen J. W. (1997) have studied single CNG channel behavior with the use of a photoaffinity analogue of cGMP that tethered cGMP moieties covalently to their binding sites to show that single retinal CNG channels could be effectively locked in four distinct ligand-bound states. Their results indicate that CNG channels open more than they would spontaneously when two ligands are bound (approximately 1% of the maximum current), significantly more with three ligands bound (approximately 33%), and open maximally with four ligands bound. In each ligand-bound state, channels open to two or three different conductance states. These findings place strong constraints on the activation mechanism of CNG channels.

This issue has been investigated further by Liu D. T. *et al.* (1998). These authors observe the effects of individual binding events on channel activation by studying CNG channels containing one, two, three, or four functional CN-binding sites. They find that the binding of a single ligand significantly increases channel opening, although four ligands are required for full channel activation. Their data are inconsistent with models in which the four subunits activate in a single concerted step (Monod-Wyman-Changeux model) or in four independent steps (Hodgkin-Huxley model). Instead, the four subunits of the channel may associate and activate as two independent channel dimers.

A molecular mechanism for the conformational changes that occur in the ligand-binding domain during channel activation has been proposed (Varnum, M. D. *et al.*, 1995). In this mechanism, the CN initially binds to the closed channel primarily by interactions between the β roll and the ribose and cyclic phosphate of the CN. CN binding is followed by a conformational change in the CN-

binding site that is coupled to the opening of the pore. This conformational change in the CN-binding site is proposed to involve a relative movement of the C-helices toward the β rolls of each subunit, allowing the D604 residues to interact with the purine rings of the bound CN. This interaction could provide a significant portion of the energy required to drive an otherwise unfavorable opening conformational change. This mechanism is supported by additional experiments. Mutation in the β roll of R559, the residue that forms the primary salt bridge with the phosphate of the CN, dramatically inhibits the initial binding of ligand, decreasing the apparent affinity of the channel for cAMP and cGMP (Tibbs, G. R. *et al.*, 1998). Furthermore, cysteine modification of C505 in the β roll primarily affects the initial binding of cGMP, whereas modification of an introduced cysteine in the C-helix, G597C, primarily affects the agonist potency (Matulef, K. *et al.*, 1999). It has been shown that cysteine residues in the C-helix produce an intersubunit disulfide bond primarily when the channel is closed (Matulef, K. and Zagotta, W., 2002; Mazzolini, M. *et al.*, 2002), suggesting that the C-helices might be nearer to each other or more flexible in the closed state of the channel and separate upon opening. It is still not known how the binding of the ligands to the channel subunits is translated into channel opening. The activation of olfactory CNG channels has been studied further by photolysis-induced jumps of cGMP or cAMP (Nache, V. *et al.*, 2005) and found to be highly cooperative. A model containing three highly cooperative binding sites with a ligand affinity high–low–high described their experimental data most adequately. Recently, Biskup C. *et al.* (2007) have studied homomeric CNGA2 channels in inside-out membrane patches by simultaneously determining channel activation and ligand binding, using the fluorescent cGMP analogue 8-DY547-cGMP as the ligand. They have shown that four ligands bind to the channels and that there is significant interaction between the binding sites. Among the binding steps, the second is most critical for channel opening: its association constant is three orders of magnitude smaller than the others and it triggers a switch from a mostly closed to a maximally open state. These results contribute to unraveling the role of the subunits in the cooperative mechanism of CNGA2 channel activation and could be of general relevance for the activation of other ion channels and receptors.

4.29.3.3 C-Linker region

The CN-binding site is connected to the last transmembrane segment of the channel by a chain of approximately 90 amino acids known as the C-linker region. Experimental evidences suggest that the N-terminal region of the channel and the C-linker region influence the apparent agonist affinity and efficacy with which the cyclic nucleotides open the channel. The C-linker region has been implicated by several studies as being critical in the gating reaction that leads to channel activation subsequent to CN binding.

As a first attempt toward understanding the channel-gating process, Gordon S. E. and Zagotta W. N. (1995a) have studied the mechanism of potentiation of expressed rod CNG channels by Ni^{2+}. They have found that coordination binding of Ni^{2+} between histidine residues (H420) on adjacent channel subunits occurs when the channels are open. Mutation of H420 to lysine completely eliminates the potentiation by Ni^{2+} but does not markedly alter the apparent cGMP affinity of the channel, indicating that the introduction of positive charge at the Ni^{2+}-binding site is not sufficient to produce potentiation. Deletion or mutation of most of the other histidines present in the channel do not diminish Ni^{2+} potentiation. These authors have also examined the role of subunit interactions in Ni^{2+} potentiation by generating heteromultimeric channels using dimers of the rod CNG channel. Injection of single heterodimers (wt/H420Q or H420Q/wt) in which one subunit contains H420 and the other does not resulted in channels that are not potentiated by Ni^{2+}. However, coinjection of both heterodimers into *Xenopus* oocytes results in channels that exhibit potentiation. The H420 residues probably occurs predominantly in nonadjacent subunits when each heterodimer is injected individually, but when the two heterodimers are coinjected, the H420 residues could occur in adjacent subunits as well. Their results suggest that the mechanism of Ni^{2+} potentiation involves intersubunit coordination of Ni^{2+} by H420. Based on the preferential binding of Ni^{2+} to open channels, they suggest that alignment of H420 residues of neighboring subunits into the Ni^{2+}-coordinating position may be associated with channel opening. These authors have also identified the corresponding histidine residue on olfactory CNGA2 subunits (H396) to have an opposite effect, an inhibition, on Ni^{2+} binding (Gordon, S. E. and Zagotta, W. N., 1995c). Thus, this particular C-linker

region of the channel probably undergoes a movement during the opening transition (Gordon, S. E. and Zagotta, W. N., 1995a; 1995b). Indeed, a histidine scan of the region just below the S6 in CNGA1 channels has found that histidines introduced at positions 416 and 420 caused Ni^{2+} to stabilize the open state (Johnson, J. P., Jr. and Zagotta, W. N., 2001). The state dependence of Ni^{2+} coordination suggests a model in which a translation and clockwise rotation of this region relative to the central axis of the pore are involved in channel activation.

The cone and olfactory CNG channels also differ considerably in cyclic nucleotide affinity and efficacy. Zong X. *et al.* (1998) have found that three amino acids in the C-linker region are major determinants of gating in these CNG channels. Indeed, the replacement of three amino acids in the cone C-linker by the corresponding amino acids of the olfactory channel (I439V, D481A, and D494S) profoundly enhances the cAMP efficacy and increases the affinities for cAMP and cGMP. Unlike the wild-type cone channel, the mutated channel exhibits similar (olfactory) single-channel kinetics for both cGMP and cAMP, explaining the increase in cAMP efficacy. Therefore, the identified amino acids appear to be major determinants of CNG channel gating.

Among the other key amino acid residues of the C-terminal end of the channel are a series of intracellularly located cysteine residues in or near the CN-binding site (Biel, M. *et al.*, 1996). These residues are thought to affect the gating reaction either through subunit–subunit interactions or within single subunits (Varnum, M. D. and Zagotta, W. N., 1996; Gordon, S. E. *et al.*, 1997). At least one of those cysteines has been proposed as a site which undergoes redox modulation by reactive nitrogen species *via* S-nitrosylation. Indeed, biochemical experiments allowed Broillet M.-C. and Firestein S. (1996) to find that the cysteine in position C460 in the CNGA2 subunit of the rat is the critical residue in the reaction that leads to channel activation by nitric oxide (NO). This particular cysteine residue is located within the C-linker region just N-terminal to the CN-binding site.

Brown L. A. *et al.* (1998) have probed the structural changes that occur during channel activation by CN using SH-modifying reagents on the bovine CNGA1 subunit. Treatment with these reagents dramatically potentiates the channel's response to both cAMP and cGMP. This potentiation is abolished by conversion of the cysteine residue C481 to a nonreactive alanine residue. Potentiation occurs more rapidly in the presence of saturating cGMP, indicating that this region of the channel is more accessible when the channel is open. C481 is located in the C-linker region between the S6 transmembrane domain and CN-binding site and corresponds to the C460 residue of the olfactory channel which is the NO target site. These results suggest that this region of the channel undergoes significant movement during the activation process and is critical for coupling ligand binding to pore opening. Brown L. A. *et al.* (1998) also claim that potentiation, however, is not mediated by the recently reported interaction between the amino- and carboxy-terminal regions of the CNGA1 subunit because deletion of the entire amino-terminal domain had little effect on potentiation by SH-modifying reagents.

Other parts of the C-linker have also been found to affect the allosteric opening transition. The *C. elegans* TAX-4 channel has a much higher cyclic nucleotide efficacy and sensitivity than the bovine CNGA1 channel (Komatsu, H. *et al.*, 1996; Paoletti, P. *et al.*, 1999). These differences are largely due to three residues in the C-linker, R460, I465, and N466 (numbers correspond to CNGA1 channels) (Paoletti, P. *et al.*, 1999). In addition, differences between gating of CNGA3 and CNGA2 channels have been attributed to three amino acids in the C-linker (I415, D457, and D470) (Zong, X. *et al.*, 1998). Also, protons bind to H468 in CNGA1 channels, causing a potentiation similar to that caused by Ni^{2+} (Gordon, S. E. *et al.*, 1996). Another residue in the C-linker near the beginning of the CNBD, C481, undergoes state-dependent modification by the cysteine-modifying reagents *N*-ethylmaleimide and methanethiosulfonate-ethyltrimethylammonium (Gordon, S. E. *et al.*, 1997; Brown, L. A. *et al.*, 1998). A fluorophore attached to this site has also been shown to undergo state-dependent quenching (Zheng, J. and Zagotta, W. N., 2000). These studies suggest that the entire C-linker region may be involved in the allosteric opening transition.

4.29.3.4 Amino-Terminal Domain

The amino-terminal region of some CNG channels has been found to affect the allosteric opening transition. CNGA2 channels have a lower free energy of opening compared with that of CNGA1 channels (Goulding, E. H. *et al.*, 1994; Liu, M. *et al.*, 1994; Gordon, S. E. *et al.*, 1995b; Fodor, A. A. *et al.*, 1997). Replacing the amino-terminal domain of CNGA1 with that of CNGA2 decreases the free energy of opening, whereas replacing the amino-terminal domain of CNGA2 with that of CNGA1 increases the free energy

of opening (Goulding, E. H. *et al.*, 1994; Gordon, S. E. *et al.*, 1995b). Single-channel analysis shows that the CNGA2 amino terminus stabilizes the open state, causing a dramatic increase in the open probability for partial agonists such as cAMP (Sunderman, E. R. and Zagotta, W. N., 1999). Deleting part of the CNGA2 amino-terminal region decreases the open probability for cAMP and the apparent affinity for cGMP, suggesting that this region has an autoexcitatory effect on channel gating (Liu, M. *et al.*, 1994).

Using polypeptides expressed in bacteria, the amino- and carboxy-terminal regions of CNGA2 have been found to interact directly (Varnum, M. D. and Zagotta, W. N., 1997). Furthermore, this interaction can be blocked by the addition of Ca^{2+}-calmodulin, not by the addition of either Ca^{2+} or calmodulin alone (Varnum, M. D. and Zagotta, W. N., 1997) leading to a proposed mechanism for Ca^{2+}-calmodulin modulation in which the CNGA2 amino-terminal domain has an autoexcitatory effect by interacting with the CNGA2 carboxy-terminal domain, and Ca^{2+}-calmodulin inhibits CNGA2 channels by preventing this interaction.

4.29.4 Physiology

One important model system to study the different functions of CNG channels is the olfactory system (Firestein, S. and Zufall, F., 1994). The remarkable capacity to discriminate among a wide range of odor molecules begins at the level of the olfactory sensory neurons (OSNs). These particular neurons perform the complex task of converting the chemical information contained in the odor molecules into changes in membrane potential (Shepherd, G. M., 1994). The different steps of the transduction cascade (Figure 3) can be summarized as follows: when a receptor molecule is occupied by an odorant, it activates a specific GTP-binding protein (G_{olf}), which modulates the activity of an adenylyl cyclase (AC type III), an enzyme producing the second messenger cAMP. cAMP directly activates a CNG channel representing the first step in the generation of the electrical response. Ca^{2+} entering *via* the CNG channel gates a Ca^{2+}-activated Cl^- channel that contributes substantially to the sensory response. Ca^{2+} also binds to calmodulin lowering the ligand sensitivity of the CNG channels. Ca^{2+}-calmodulin also stimulates the activity of a phosphodiesterase reducing the concentration of cAMP. Ca^{2+} is finally extruded by an Na^+/Ca^{2+} exchanger. This cascade of events results in the cell membrane shifting its resting potential from −65 to −45 mV. This depolarization spreads by passive current flow through the dendrite to the soma where it activates voltage-gated Na^+ channels, initiating impulse generation. The combination of Na^+ current with voltage-dependent K^+ currents and with a small

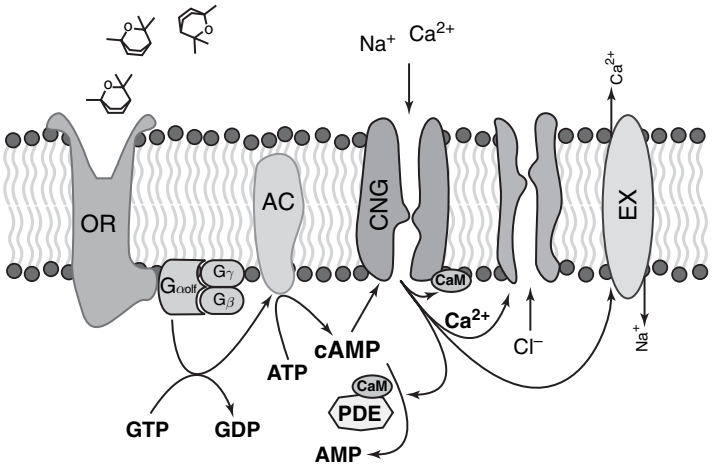

Figure 3 The olfactory transduction cascade. The binding of an odorant molecule (cineole is represented here) to the odorant receptor (OR) leads to the interaction of the receptor to a GTP-binding protein (G_{olf}). This interaction in turn leads to the release of the GTP-coupled alpha subunit of the G protein, which then stimulates the adenylyl cyclase (AC) to produce elevated levels of cAMP. The increase of cAMP opens cyclic nucleotide-gated channels (CNG) causing an odorant-induced inward current carried by Na^+ and Ca^{2+} ions and an alteration of the membrane potential. Ca^{2+} entering *via* the CNG channel gates a Ca^{2+}-activated Cl^- channel that contributes substantially to the sensory response. Ca^{2+} also binds to calmodulin (CaM) lowering the ligand sensitivity of the CNG channels. Ca^{2+}-calmodulin also stimulates the activity of a phosphodiesterase (PDE) reducing the concentration of cAMP. Ca^{2+} is finally extruded by a Na^+/Ca^{2+} exchanger (EX).

Ca^{2+} current acts to produce one or more action potentials that can propagate *via* the axon to the olfactory bulb of the brain.

In OSNs, odors do not only trigger the signaling cascade but also generate various mechanisms to fine-tune the odor-induced current, including a low-selective odor inhibition of the olfactory signal. This wide-range olfactory inhibition is taking place at the level of the CNG channels (Delay, R. and Restrepo, D., 2004; Chen, T. Y. *et al.*, 2006). Interestingly, the inhibitory effect is small in the homomeric CNGA2 channels but larger in channels consisting all olfactory native subunits. The potency of the suppression on the cloned CNG channel appears to be smaller than that previously shown in native olfactory neurons, suggesting that CNG channels switch on and off the olfactory signaling pathway and that the on and off signals may both be amplified by the subsequent olfactory signaling steps.

Nonmotile cilia on OSNs compartmentalize signaling molecules, including odorant receptors and CNG channels, allowing for efficient, spatially confined responses to sensory stimuli. Indeed, CNG channels have been found to have a particular spatial distribution along the ciliary length of OSNs (Flannery, R. J. *et al.*, 2006). The proximal cilia segment, which (in frog) is the first 20% of the cilium, appears to express a small fraction of the CNG channels, whereas the distal segment contains the majority, mostly clustered in one region. Movement of proteins within the cilia is governed by intraflagellar transport, a process that facilitates bidirectional movement along microtubules. Work in *C. elegans* has established that heterotrimeric and homodimeric kinesin-2 family members play a critical role in anterograde transport. Recently, it has been shown that the ciliary targeting of olfactory CNG channels requires the presence of both the CNGB1b channel subunit and the kinesin-2 motor protein, KIF17 (Flannery, R. J. *et al.*, 2006). A critical carboxy-terminal motif (RVxP) on CNGB1b is required for ciliary trafficking of olfactory CNG channels. These results have been further confirmed by the invalidation of the CNGB1 protein leading to olfactory dysfunction and subciliary CNG channel trapping (Michalakis, S. *et al.*, 2006). Indeed, in CNGB1-/- mice, the CNGA2/CNGA4 channels are targeted to the plasma membrane of olfactory knobs but fail to be trafficked into olfactory cilia. Interestingly, a similar trafficking defect can be observed in mice deficient for the CNGA4 subunit. These results demonstrate that CNGB1 has a dual function *in vivo*. First, it gives the olfactory CNG channel a variety of modulatory and biophysical properties tailored to the specific requirements of olfactory transduction. Second, together with the CNGA4 subunit, CNGB1 is needed for ciliary targeting of the olfactory CNG channel.

Olfactory axons are able to elongate and establish synaptic contacts with target neurons in the olfactory bulb throughout adulthood. Axonal pathfinding and target recognition are critical steps in the formation of specific axonal connections in the developing nervous system. These processes could be controlled by local cues, either molecular or structural, that develop in the region of the axon tract. Recently, cyclic nucleotides have been receiving much attention as important regulators in determining whether environmental cues are functioning as attractive or repulsive for growth cone behavior (Song, H. J. *et al.*, 1997; Hopker, V. H. *et al.*, 1999; Song, H. J. and Poo, M. M., 1999). The effects of cyclic nucleotides on growth cone behavior may be partially mediated by CNG channels. CNG channel subunits have been identified in chemosensory neurons in *C. elegans* and shown to be important in the growth and targeting of axons (Coburn, C. M. and Bargmann, C. I., 1996). Active growth cones have been shown to exhibit Ca^{2+} waves which may spread into the neurite (Gu, X. and Spitzer, N. C., 1995; Spitzer, N. C. *et al.*, 1995). These effects are dependent on extracellular calcium, but none of the voltage-gated Ca^{2+} calcium channels expressed in growth cones seem to be involved (Gomez, T. M. *et al.*, 1995; Gottmann, K. and Lux, H. D., 1995). It is possible that CNG channels play an important function in the regulation of Ca^{2+} in the growth cone. Besides the effects of cyclic nucleotides on growth cone behavior, NO has also been shown to significantly affect growth cone behavior. Cheung W. S. *et al.* (2000) showed that NO can stabilize growth cone filopodia, similar to previous findings with 8-Br-cAMP. Van Wagenen S. and Rehder V. (1999) have extended these findings by showing that the response of the growth cone to NO is mediated via a cascade implying cGMP and entry of external Ca^{2+}. These effects of NO on growth cone behavior may also be mediated by CNG channels. Thus, Kafitz K. W. *et al.* (2000) have shown that cyclic nucleotides and NO activate a calcium entry mechanism in olfactory receptor growth cones with properties similar to the CNG channels. Since CNG channels, especially the NO-gated homomeric CNGA4 channels, are highly permeable to Ca^{2+} (Broillet, M.-C. and Firestein, S., 1997) this may

provide a direct mechanism through which NO can regulate calcium levels and behavior of growth cones. In summary, CNG channels present at the membrane of the olfactory growth cones might play a key role in OSNs development and turnover.

4.29.5 Modulation

CNG channels are modulated by cellular factors, including phosphorylation enzymes (Gordon, S. E. *et al.*, 1992; Molokanova, E. *et al.*, 1997; Muller, F. *et al.*, 1998), transition metal divalent cations (Ildefonse, M. *et al.*, 1992; Karpen, J. W. *et al.*, 1993; Gordon, S. E. and Zagotta, W. N., 1995a), lipids such as diacylglycerol (Gordon, S. E. *et al.*, 1995a; Crary, J. I. *et al.*, 2000a; 2000b), endogenous Ca^{2+}-binding proteins (Gordon, S. E. and Zagotta, W. N., 1995b) (Balasubramanian, S. *et al.*, 1996; Rebrik, T. I. and Korenbrot, J. I., 1998) and, in particular, Ca^{2+}-calmodulin (Hsu, Y.-T. and Molday, R. S., 1993; Chen, T.-Y. and Yau, K.-W. 1994; Gordon, S. E. and Zagotta, W. N., 1995b).

When exposed to short repetitive pulses of odors, OSNs rapidly adapt to the stimulus by decreasing their responsiveness in a Ca^{2+}-dependent manner (Kurahashi, T. and Shibuya, T., 1990). Kurahashi T. and Menini A. (1997) have investigated the localization of the principal molecular mechanism for adaptation in the olfactory transduction process and have shown that both the cAMP- and the odor-induced responses have similar adaptation properties, indicating that the entire adaptation process takes place after the production of cAMP and may be mediated by Ca^{2+}-calmodulin-dependent inhibition of the olfactory CNG channel. Experiments on olfactory adaptation performed in knockout mice of the CNGA4 subunit have confirmed that the molecular mechanism for adaptation is localized at the channel level, most likely through CNG channel inhibition by Ca^{2+}-calmodulin (Munger, S. D. *et al.*, 2001). Moreover, comparing properties of native channels with heterologously expressed heteromeric channels, the modulatory subunits CNGA4 and CNGB1b have been shown to be responsible for the physiological modulation of the olfactory CNG channel by Ca^{2+}-calmodulin. Bradley J. *et al.* (2001a; 2001b; 2004) and Munger S. D. *et al.* (2001) measured, in excised patches containing native heteromeric olfactory CNG channels, a fast current inhibition upon addition of Ca^{2+}-calmodulin that persisted for several seconds also after calmodulin was removed in Ca^{2+}-free solution. CNGA4 indeed has calmodulin binding sites. CNGA4 has a IQ-type calmodulin binding site located at the C-terminal region, while CNGB1b has a similar IQ-type site located at the N-terminal region and a basic amphiphilic α-helix (Baa) motif in the C-terminal region. It has been shown that the IQ-type sites are necessary and sufficient for Ca^{2+}-calmodulin channel inhibition, whereas the Baa-type site is not necessary (Bradley, J. *et al.*, 2004; 2005). However, the molecular mechanism by which the binding of Ca^{2+}-calmodulin decreases the ligand sensitivity of the olfactory channel is not yet understood.

Multiple studies of native CNG channels have shown that the addition of micromolar concentrations of intracellular Ca^{2+} is able to decrease the channel sensitivity to cGMP or cAMP, probably by activating a Ca^{2+}-responsive endogenous factor already pre-associated with the channel (Kramer, R. H. and Siegelbaum, S. A., 1992; Lynch, J. W. and Lindemann, B., 1994; Gordon, S. E. *et al.*, 1995b; Balasubramanian, S. *et al.*, 1996; Rebrik, T. I. and Korenbrot, J. I. 1998; Kleene, S. J., 1999; Bradley, J. *et al.*, 2004). Bradley J. *et al.* (2004) have shown that Ca^{2+}-free calmodulin, called apocalmodulin, is able to bind to the heterologously expressed heteromeric olfactory CNG channels even in the absence of Ca^{2+}. Moreover, when Ca^{2+} concentration rises above 100 nM, Ca^{2+} can rapidly modulate the CNG channel sensitivity by directly binding to the pre-associated calmodulin. Furthermore, it has been suggested (Bradley, J. *et al.*, 2004) that, in native channels also, the pre-associated endogenous factor can be apocalmodulin, although a demonstration is still missing. Since Ca^{2+} enters into the olfactory cilia through the CNG channel itself, the pre-associated Ca^{2+}-responsive factor can provide a very fast feedback modulation at the channel level. It has been further verified that the CNGA4 channel subunit plays a central role in Ca^{2+}-calmodulin-dependent odor adaptation (Bradley, J. *et al.*, 2001b; Kelliher, K. R. *et al.*, 2003). Recently, phosphatidylinositol-3,4,5-trisphosphate (PIP3) has been shown to inhibit the activation of the olfactory CNG channels binding to the amino-terminal region of the channel occluding the action of Ca^{2+}-calmodulin (Brady, J. D. *et al.*, 2006).

In addition to their activation by cyclic nucleotides, NO-generating compounds can directly open the olfactory CNG channels through a redox reaction that results in the S-nitrosylation of a free SH group on a cysteine residue (Broillet, M.-C. and

Firestein, S., 1996). This posttranslational modification, comparable to phosphorylation, can modulate the activity of different proteins such as the NMDA receptor, caspases, and others. The NO target site on the CNG channel has been identified by mutating the four candidate intracellular cysteine residues Cys-460, Cys-484, Cys-520, and Cys-552 of the rat CNGA2 subunit into serine residues. All mutant channels continue to be activated by cyclic nucleotides, but only one of them, the C460S mutant channel, exhibits a total loss of NO sensitivity (Broillet, M.-C., 2000). This result is further supported by a similar lack of NO sensitivity that is found for a natural mutant of this precise cysteine residue, the *D. melanogaster* CNG channel. Cys-460 is located in the C-linker region of the channel known to be important in channel gating. Kinetic analyses suggest that at least two of these Cys-460 residues on different channel subunits are involved in the activation by NO. These results show that one single cysteine residue is responsible for NO sensitivity but that several channel subunits need to be activated for channel opening by NO. The corresponding cysteine on the CNGA4 subunit is the cysteine 352. This subunit cannot form homomeric channels that can be activated by cyclic nucleotides, but they can be activated by NO. The properties of these NO-gated channels reveal striking differences with those of either the native rat olfactory CNG channels or the homomeric CNGA2 channels such as the presence of open channel noise and a very different calcium permeability (Broillet, M.-C. and Firestein, S., 1997). These homomeric CNGA4 channels may be expressed at different cellular locations such as the immature olfactory neurons or the vomeronasal neurons and fulfill different physiological roles than the heteromeric CNG channels.

Recently, patch-clamp experiments have revealed that many OSNs respond not only to odors, but also to mechanical stimuli delivered by pressure ejections of odor-free Ringer solution (Grosmaitre, X. *et al.*, 2007). The mechanical responses correlate directly with the pressure intensity and show several properties similar to those induced by odors, including onset latency, reversal potential and adaptation to repeated stimulation. Blocking adenylyl cyclase III or knocking out the CNGA2 subunit eliminates both the odor and the mechanical responses, suggesting that both are mediated by a shared cAMP/CNG channel cascade. This mechanosensitivity enhances the firing frequency of individual neurons when they are weakly stimulated by odors and most likely drives the rhythmic activity (theta oscillation) in the olfactory bulb to synchronize with respiration.

4.29.6 Pharmacology

Although there is a formidable array of specific blockers for sodium, calcium, and potassium channels, specific blockers for CNG channels are scarce. A number of pharmacological agents including L-*cis*-diltiazem (Haynes, L. W., 1992), tetracaine (Fodor, A. A. *et al.*, 1997), pimozide (Nicol, G. D., 1993), and LY-58558 (Leinders-Zufall, T. and Zufall, F., 1995) have been reported to block the current through CNG channels, but these agents have significant drawbacks. First, they exert their effect on the cytoplasmic face of the channel, making their utility questionable in more intact preparations. Second, these blockers have multiple targets, making results difficult to interpret. Recently, Brown R. L. *et al.* (1999) have found a peptide toxin purified from the venom of the Australian King Brown snake, which they have named pseudechetoxin (PsTx). When applied to the extracellular face of membrane patches containing rat CNGA2 channels, PsTx blocks the cGMP-dependent current with a K_i of 5 nM. The block is independent of voltage and requires only a single molecule of toxin. PsTx also blocks CNG channels composed of bovine CNGA1 subunits with high affinity (100 nM), but it is less effective on the heteromeric version of the rod channel (K_i approximately 3 μM). PsTs acts as a pore blocker occluding the entrance to the channel by forming high-affinity contacts with the pore turret (Brown, R. L. *et al.*, 1999). This toxin is structurally classified as a cysteine-rich secretory protein and exhibits structural features that are quite distinct from those of other known small peptidic channel blockers (Yamazaki, Y. *et al.*, 2002). It has now been crystallized and analyzed using X-ray diffraction. PsTx could to be a valuable pharmacological tool for studies on the structure and physiology of CNG channels.

4.29.7 Conclusion

The activation of CNG channels is a complex process comprising the initial ligand binding and a consecutive allosteric transition from a closed to an open configuration. The recent studies on CNG channels have demonstrated the importance of different regions of the protein in activation and modulation of this class of ion channels.

The direct activation by cyclic nucleotides is not only controlled at the CN-binding site where cyclic nucleotide recognition and channel activation take place but particular amino acid residues located elsewhere on the protein also modulate the affinity and efficacy of cAMP or cGMP. Allosteric changes in the CN-binding site, movement of certain regions of the channel molecule, like the C-linker region, seem to be of fundamental importance in the control of the gating mechanisms of the channel. The pore region is responsible for ionic selectivity and for the control of physiological Ca^{2+} permeation, whereas the amino-terminal and the carboxy-terminal regions of the channel take part in channel modulation.

CNG channels first identified in rods and olfactory receptors are now distributed throughout the different cells of the body and may have important roles such as cell motility, secretion, development, and neural plasticity. Indeed, CNG channels have been found in the central nervous system (Kingston, P. A. *et al.*, 1996; Bradley, J. *et al.*, 1997; Wei, J. Y. *et al.*, 1998) and have been implicated in processes as diverse as synaptic modulation, central communication, plasticity, and axon outgrowth in animals ranging from the nematode to mammals (Coburn, C. M. and Bargmann, C. I., 1996; Zufall, F. *et al.*, 1997). CNG channel subunits, in particular the olfactory CNG channel subunits have been identified in the brain (Bradley, J. *et al.*, 1997; Kingston, P. A. *et al.*, 1999; Podda, M. V. *et al.*, 2005; Tetreault, M. L. *et al.*, 2006). Specific subsets of neurons such as the CA1 and CA3 neurons of the hippocampus express CNG channel subunits (Kuzmiski, J. B. and MacVicar, B. A., 2001) suggesting that these channels have a particular function in the central nervous system that is related specifically to certain cell types, rather than being of a general housekeeping nature (Zufall, F. *et al.*, 1997; Wei, J. Y. *et al.*, 1998). Ca^{2+} imaging studies have found that a rise in intracellular Ca^{2+} in hippocampal neurons could result from elevated intracellular cyclic nucleotide concentrations, suggesting that CNG channels play a role in the synaptic plasticity underlying learning and memory (Leinders-Zufall, T. *et al.*, 1995; Bradley, J. *et al.*, 1997; Kingston, P. A. *et al.*, 1999). Indeed, long-term potentiation is attenuated in mutant mice lacking CNGA2 (Parent, A. *et al.*, 1998).

A CNG channel, similar to the olfactory CNGA2, is also expressed throughout the heart of the mouse, but its function remains unclear (Ruiz, M. L. *et al.*, 1996). As sensors of cyclic nucleotide concentrations and conduits for Ca^{2+} entry, CNG channels may play a role in regulating the heart rate and contraction. The cloning and first functional characterization of a plant CNG channel occurred from the *Arabidopsis* cDNA (Leng, Q. *et al.*, 1999). This channel could, like its animal counterparts, translate stimulus-induced changes in cytosolic cyclic nucleotides into altered cell membrane potential and/or cation flux as part of signal cascade pathway(s) that remain to be identified. Future work will reveal new functions for CNG channels as well as more information about their structure–functions and modulation.

Acknowledgments

I gratefully thank Olivier Randin for assistance in producing the figures. M.-C. B. is supported by grants from the Fonds National Suisse de la Recherche and the Leenaards Foundation.

References

Almers, W. and McCleskey, E. W. 1984. Non-selective conductance in calcium channels of frog muscle: calcium selectivity in a single-file pore. J. Physiol. 353, 585–608.

Balasubramanian, S., Lynch, J. W., and Barry, P. H. 1996. Calcium-dependent modulation of the agonist affinity of the mammalian olfactory cyclic nucleotide-gated channel by calmodulin and a novel endogenous factor. Membr. Biol. 152, 13–23.

Balasubramanian, S., Lynch, J. W., and Barry, P. H. 1997. Concentration dependence of sodium permeation and sodium ion interactions in the cyclic AMP-gated channels of mammalian olfactory receptor neurons. J. Membr. Biol. 159(1), 41–52.

Baumann, A., Frings, S., Godde, M., Seifert, R., and Kaupp, U. B. 1994. Primary structure and functional expression of a *Drosophila* cyclic nucleotide-gated channel present in eyes and antennae. EMBO J. 13, 5040–5050.

Becchetti, A., Gamel, K., and Torre, V. 1999. Cyclic nucleotide-gated channels. Pore topology studied through the accessibility of reporter cysteines. J. Gen. Physiol. 114, 377–392.

Biel, M., Zong, X., and Hofmann, F. 1996. Cyclic nucleotide-gated cation channels: molecular diversity, structure and cellular functions. Trends Cardiovasc. Med. 6, 274–280.

Biskup, C., Kusch, J., Schulz, E., Nache, V., Schwede, F., Lehmann, F., Hagen, V., and Benndorf, K. 2007. Relating ligand binding to activation gating in CNGA2 channels. Nature 446, 440–443.

Bonigk, W., Altenhofen, W., Muller, F., Dose, A., Illing, M., Molday, R. S., and Kaupp, U. B. 1993. Rod and cone photoreceptor cells express distinct genes for cGMP-gated channels. Neuron 10, 865–877.

Bonigk, W., Bradley, J., Muller, F., Sesti, F., Boekhoff, I., Ronnett, G. V., Kaupp, U. B., and Frings, S. 1999. The native rat olfactory cyclic nucleotide-gated channel is composed of three distinct subunits. J. Neurosci. 19, 5332–5347.

Bradley, J., Bonigk, W., Yau, K. W., and Frings, S. 2004. Calmodulin permanently associates with rat olfactory CNG

channels under native conditions. Nat. Neurosci. 7, 705–710.
Bradley, J., Frings, S., Yau, K. W., and Reed, R. 2001a. Nomenclature for ion channel subunits. Science 294, 2095–2096.
Bradley, J., Li, J., Davidson, N., Lester, H. A., and Zinn, K. 1994. Heteromeric olfactory cyclic nucleotide-gated channels: a subunit that confers increased sensitivity to cAMP. Proc. Natl. Acad. Sci. U. S. A. 91, 8890–8894.
Bradley, J., Reisert, J., and Frings, S. 2005. Regulation of cyclic nucleotide-gated channels. Curr. Opin. Neurobiol. 15, 343–349.
Bradley, J., Reuter, D., and Frings, S. 2001b. Facilitation of calmodulin-mediated odor adaptation by cAMP-gated channel subunits. Science 294, 2176–2178.
Bradley, J., Zhang, Y., Bakin, R., Lester, H. A., Ronnett, G. V., and Zinn, K. 1997. Functional expression of the heteromeric ''olfactory'' cyclic nucleotide-gated channel in the hippocampus: a potential effector of synaptic plasticity in brain neurons. J. Neurosci. 17, 1993–2005.
Brady, J. D., Rich, E. D., Martens, J. R., Karpen, J. W., Varnum, M. D., and Brown, R. L. 2006. Interplay between PIP3 and calmodulin regulation of olfactory cyclic nucleotide-gated channels. Proc. Natl. Acad. Sci. U. S. A. 103, 15635–15640.
Broillet, M.-C. 2000. A single intracellular cysteine residue is responsible for the activation of the olfactory cyclic nucleotide-gated channel by NO. J. Biol. Chem. 275, 15135–15141.
Broillet, M.-C. and Firestein, S. 1996. Direct activation of the olfactory cyclic nucleotide-gated channel through modification of sulfhydryl groups by NO compounds. Neuron 16, 377–385.
Broillet, M.-C. and Firestein, S. 1997. Beta-subunits of the olfactory cyclic nucleotide-gated channel form a nitric oxide activated Ca^{2+} channel. Neuron. 18, 951–958.
Brown, L. A., Snow, S. D., and Haley, T. L. 1998. Movement of gating machinery during the activation of rod cyclic nucleotide-gated channels. Biophys. J. 75, 825–833.
Brown, R. L., Haley, T. L., West, K. A., and Crabb, J. W. 1999. Pseudechetoxin: a peptide blocker of cyclic nucleotide-gated ion channels. Proc. Natl. Acad. Sci. U. S. A. 96, 754–759.
Chen, T.-Y. and Yau, K.-W. 1994. Direct modulation by Ca^{2+}-calmodulin of cyclic nucleotide-activated channel of rat olfactory receptor neurons. Nature 368, 545–548.
Chen, T.-Y., Peng, Y.-W., Dhallan, R. S., Ahamed, B., Reed, R. R., and Yau, K.-W. 1993. A new subunit of the cyclic nucleotide-gated cation channel in retinal rods. Nature 362, 764–767.
Chen, T. Y., Takeuchi, H., and Kurahashi, T. 2006. Odorant inhibition of the olfactory cyclic nucleotide-gated channel with a native molecular assembly. J. Gen. Physiol. 128, 365–371.
Cheung, W. S., Bhan, I., and Lipton, S. A. 2000. Nitric oxide (NO) stabilizes whereas nitrosonium ($NO+$) enhances filopodial outgrowth by rat retinal ganglion cells *in vitro*. Brain Res. 868, 1–13.
Coburn, C. M. and Bargmann, C. I. 1996. A putative cyclic nucleotide-gated channel is required for sensory development and function in *C. elegans*. Neuron 17, 695–706.
Crary, J. I., Dean, D. M., Maroof, F., and Zimmerman, A. L. 2000a. Mutation of a single residue in the S2–S3 loop of CNG channels alters the gating properties and sensitivity to inhibitors. J. Gen. Physiol. 116, 769–780.
Crary, J. I., Dean, D. M., Nguitragool, W., Kurshan, P. T., and Zimmerman, A. L. 2000b. Mechanism of inhibition of cyclic nucleotide-gated ion channels by diacylglycerol. J. Gen. Physiol. 116, 755–768.
Delay, R. and Restrepo, D. 2004. Odorant responses of dual polarity are mediated by cAMP in mouse olfactory sensory neurons. J. Neurophysiol. 92, 1312–1319.
Dhallan, R. S., Yau, K. W., Schrader, K. A., and Reed, R. R. 1990. Primary structure and functional expression of a cyclic nucleotide-activated channel from olfactory neurons. Nature 347, 184–187.
Doyle, D. A., Morais Cabral, J., Pfuetzner, R. A., Kuo, A., Gulbis, J. M., Cohen, S. L., Chait, B. T., and MacKinnon, R. 1998. The structure of the potassium channel: molecular basis of K^+ conduction and selectivity. Science 280, 69–77.
Dryja, T. P., Finn, J. T., Peng, Y. W., McGee, T. L., Berson, E. L., and Yau, K. W. 1995. Mutations in the gene encoding the alpha subunit of the rod cGMP-gated channel in autosomal recessive retinitis pigmentosa. Proc. Natl. Acad. Sci. U. S. A. 92, 10177–10181.
Fesenko, E. E., Kolesnikov, S. S., and Lyubarsky, A. L. 1985. Induction by cyclic GMP of cationic conductance in plasma membrane of retinal rod outer segment. Nature 313, 310–313.
Firestein, S. and Zufall, F. 1994. The cyclic nucleotide-gated channel of olfactory receptor neurons. Semin. Cell Biol. 5, 39–46.
Flannery, R. J., French, D. A., and Kleene, S. J. 2006. Clustering of cyclic nucleotide-gated channels in olfactory cilia. Biophys. J. 91, 179–188.
Flynn, G. E. and Zagotta, W. N. 2001. Conformational changes in S6 coupled to the opening of cyclic nucleotide-gated channels. Neuron 30, 689–698.
Fodor, A. A., Black, K. D., and Zagotta, W. N. 1997. Tetracaine reports a conformational change in the pore of cyclic nucleotide-gated channels. J. Gen. Physiol. 110, 591–600.
Frings, S., Lynch, J. W., and Lindemann, B. 1992. Properties of cyclic nucleotide-gated channels mediating olfactory transduction. J. Gen. Physiol. 100, 45–67.
Frings, S., Seifert, R., Godde, M., and Kaupp, U. B. 1995. Profoundly different calcium permeation and blockage determine the specific function of distinct cyclic nucleotide-gated channels. Neuron 15, 169–179.
Gavazzo, P., Picco, C., and Menini, A. 1997. Mechanism of modulation by internal protons of cyclic nucleotide-gated channels cloned from sensory cells. Proc. R. Soc. Lond. B. Biol. Sci. 264(1385), 1157–1165.
Gerstner, A., Zong, X., Hofmann, F., and Biel, M. 2000. Molecular cloning and functional characterization of a new modulatory cyclic nucleotide-gated subunit from mouse retina. J. Neurosci. 20, 1324–1332.
Gomez, T. M., Snow, D. M., and Letourneau, P. C. 1995. Characterization of spontaneous calcium transients in nerve growth cones and their effect on growth cone migration. Neuron 14, 1233–1246.
Gordon, S. E., Brautigan, D. L., and Zimmerman, A. L. 1992. Protein phosphatases modulate the apparent agonist affinity of the light-regulated ion channel in retinal rods. Neuron 9, 739–748.
Gordon, S. E., Downing-Park, J., Tam, B., and Zimmerman, A. L. 1995a. Diacylglycerol analogs inhibit the rod cGMP-gated channel by a phosphorylation-independent mechanism. Biophys. J. 69, 409–417.
Gordon, S. E., Downing-Park, J., and Zimmerman, A. L. 1995b. Modulation of the cGMP-gated ion channel in frog rods by calmodulin and an endogenous inhibitory factor. J. Physiol. 486(Pt 3), 533–546.
Gordon, S. E., Oakley, J. C., Varnum, M. D., and Zagotta, W. N. 1996. Altered ligand specificity by protonation in the ligand binding domain of cyclic nucleotide-gated channels. Biochemistry 35, 3994–4001.

Gordon, S. E., Varnum, M. D., and Zagotta, W. N. 1997. Direct interaction between amino- and carboxyl-terminal domains of cyclic nucleotide-gated channels. Neuron 19, 431–441.

Gordon, S. E. and Zagotta, W. N. 1995a. A histidine residue associated with the gate of the cyclic nucleotide-activated channels in rod photoreceptors. Neuron 14, 177–183.

Gordon, S. E. and Zagotta, W. N. 1995b. Localization of regions affecting an allosteric transition in cyclic nucleotide-activated channels. Neuron 14, 857–864.

Gordon, S. E. and Zagotta, W. N. 1995c. Subunit interactions in coordination of Ni^{2+} in cyclic nucleotide-gated channels. Proc. Natl. Acad. Sci. U. S. A. 92, 10222–10226.

Gottmann, K. and Lux, H. D. 1995. Growth cone calcium ion channels: properties, clustering, and functional roles. Perspect. Dev. Neurobiol. 2, 371–377.

Goulding, E. H., Tibbs, G. R., Liu, D., and Siegelbaum, S. A. 1993. Role of H5 domain in determining pore diameter and ion permeation through cyclic nucleotide-gated channels. Nature 61–64.

Goulding, E. H., Tibbs, G. R., and Siegelbaum, S. A. 1994. Molecular mechanism of cyclic nucleotide-gated channel activation. Nature 372, 369–374.

Grosmaitre, X., Santarelli, L. C., Tan, J., Luo, M., and Ma, M. 2007. Dual functions of mammalian olfactory sensory neurons as odor detectors and mechanical sensors. Nat. Neurosci. 10, 348–354.

Gu, X. and Spitzer, N. C. 1995. Distinct aspects of neuronal differentiation encoded by frequency of spontaneous Ca^{2+} transients. Nature 375, 784–787.

Haynes, L. W. 1992. Block of the cyclic GMP-gated channel of vertebrate rod and cone photoreceptors by *l-cis*-diltiazem. J. Gen. Physiol. 100, 783–801.

Hopker, V. H., Shewan, D., Tessier-Lavigne, M., Poo, M., and Holt, C. 1999. Growth-cone attraction to netrin-1 is converted to repulsion by laminin-1. Nature 401, 69–73.

Hsu, Y.-T. and Molday, R. S. 1993. Modulation of the cGMP-gated channel of rod photoreceptor cells by calmodulin. Nature 361, 76–79.

Ildefonse, M., Crouzy, S., and Bennett, N. 1992. Gating of retinal rod cation channel by different nucleotides: comparative study of unitary currents. J. Membr. Biol. 130, 91–104.

Jiang, Y., Lee, A., Chen, J., Cadene, M., Chait, B. T., and MacKinnon, R. 2002a. Crystal structure and mechanism of a calcium-gated potassium channel. Nature 417, 515–522.

Jiang, Y., Lee, A., Chen, J., Cadene, M., Chait, B. T., and MacKinnon, R. 2002b. The open pore conformation of potassium channels. Nature 417, 523–526.

Johnson, J. P., Jr. and Zagotta, W. N. 2001. Rotational movement during cyclic nucleotide-gated channel opening. Nature 412, 917–921.

Kafitz, K. W., Leinders-Zufall, T., Zufall, F., and Greer, C. A. 2000. Cyclic GMP evoked calcium transients in olfactory receptor cell growth cones. Neuroreport 11, 677–681.

Karpen, J. W., Brown, R. L., Stryer, L., and Baylor, D. A. 1993. Interactions between divalent cations and the gating machinery of cyclic GMP-activated channels in salamander retinal rods. J. Gen. Physiol. 101, 1–25.

Kaupp, U. B. and Seifert, R. 2002. Cyclic nucleotide-gated ion channels. Physiol. Rev. 82, 769–824.

Kaupp, U. B., Niidome, T., Tanabe, T., Terada, S., Bonigk, W., Stuhmer, W., Cook, N. J., Kangawa, K., Matsuo, H., Hirose, T., Miyata, T., and Numa, S. 1989. Primary structure and functional expression from complementary DNA of the rod photoreceptor cyclic GMP-gated channel. Nature 342, 762–766.

Kelliher, K. R., Ziesmann, J., Munger, S. D., Reed, R. R., and Zufall, F. 2003. Importance of the CNGA4 channel gene for odor discrimination and adaptation in behaving mice. Proc. Natl. Acad. Sci. U. S. A. 100, 4299–4304.

Kingston, P. A., Zufall, F., and Barnstable, C. J. 1996. Rat hippocampal neurons express genes for both rod retinal and olfactory cyclic nucleotide-gated channels: novel targets for cAMP/cGMP function. Proc. Natl. Acad. Sci. U. S. A. 93, 10440–10445.

Kingston, P. A., Zufall, F., and Barnstable, C. J. 1999. Widespread expression of olfactory cyclic nucleotide-gated channel genes in rat brain: implications for neuronal signalling. Synapse 32, 1–12.

Kleene, S. J. 1999. Both external and internal calcium reduce the sensitivity of the olfactory cyclic-nucleotide-gated channel to CAMP. J. Neurophysiol. 81, 2675–2682.

Kohl, S., Marx, T., Giddings, I., Jagle, H., Jacobson, S. G., Apfelstedt-Sylla, E., Zrenner, E., Sharpe, L. T., and Wissinger, B. 1998. Total colourblindness is caused by mutations in the gene encoding the alpha-subunit of the cone photoreceptor cGMP-gated cation channel. Nat. Genet. 19, 257–259.

Komatsu, H., Mori, I., Rhee, J.-S., Akaike, N., and Ohshima, Y. 1996. Mutations in a cyclic nucleotide-gated channel lead to abnormal thermosensation and chemosensation in *C. elegans*. Neuron 17, 707–718.

Korschen, H. G., Illing, M., Seifert, R., Sesti, F., Williams, A., Gotzes, S., Colville, C., Muller, F., Dose, A., Godde, M., *et al.* 1995. A 240 kDa protein represents the complete beta subunit of the cyclic nucleotide-gated channel from rod photoreceptor. Neuron 15, 627–636.

Kramer, R. H. and Siegelbaum, S. A. 1992. Intracellular Ca^{2+} regulates the sensitivity of cyclic nucleotide-gated channels in olfactory receptor neurons. Neuron 9, 897–906.

Kumar, V. D. and Weber, I. T. 1992. Molecular model of the cyclic GMP-binding domain of the cyclic GMP-gated ion channel. Biochemistry 31, 4643–4649.

Kurahashi, T. and Menini, A. 1997. Mechanism of odorant adaptation in the olfactory receptor cell. Nature 385, 725–729.

Kurahashi, T. and Shibuya, T. 1990. Ca^{2+}-dependent adaptive properties in the solitary olfactory receptor cells of the newt. Br. Res. 515, 261–268.

Kuzmiski, J. B. and MacVicar, B. A. 2001. Cyclic nucleotide-gated channels contribute to the cholinergic plateau potential in hippocampal CA1 pyramidal neurons. J. Neurosci. 21, 8707–8714.

Leinders-Zufall, T. and Zufall, F. 1995. Block of cyclic nucleotide-gated channels in salamander olfactory receptor neurons by the guanylyl cyclase inhibitor LY83583. J. Neurophysiol. 74, 2759–2762.

Leinders-Zufall, T., Rosenboom, H., Barnstable, C. J., Shepherd, G. M., and Zufall, F. 1995. A calcium-permeable cGMP-activated cation conductance in hippocampal neurons. Neuroreport 6, 45–49.

Leng, Q., Mercier, R. W., Yao, W., and Berkowitz, G. A. 1999. Cloning and first functional characterization of a plant cyclic nucleotide-gated cation channel. Plant Physiol. 121, 753–761.

Liman, E. R. and Buck, L. B. 1994. A second subunit of the olfactory cyclic nucleotide-gated channel confers high sensitivity to cAMP. Neuron 13, 611–621.

Liu, J. and Siegelbaum, S. A. 2000. Change of pore helix conformational state upon opening of cyclic nucleotide-gated channels. Neuron 28, 899–909.

Liu, D. T., Tibbs, G. R., Paoletti, P., and Siegelbaum, S. A. 1998. Constraining ligand-binding site stoichiometry suggests that a cyclic nucleotide-gated channel is composed of two functional dimers. Neuron 21, 235–248.

Liu, D. T., Tibbs, G. R., and Siegelbaum, S. A. 1996. Subunit stoichiometry of cyclic nucleotide-gated channels and effects of subunit order on channel function. Neuron 16, 983–990.

Liu, M., Chen, T., Ahamed, B., Li, J., and Yau, K. W. 1994. Calcium-calmodulin modulation of the olfactory cyclic nucleotide-gated cation channel. Science 266, 1348–1354.

Lynch, J. W. and Lindemann, B. 1994. Cyclic nucleotide-gated channels of rat olfactory receptor cells: divalent cations control the sensitivity to cAMP. J. Gen. Physiol. 103, 87–106.

Matulef, K. and Zagotta, W. 2002. Multimerization of the ligand binding domains of cyclic nucleotide-gated channels. Neuron 36, 93–103.

Matulef, K. and Zagotta, W. N. 2003. Cyclic nucleotide-gated ion channels. Annu. Rev. Cell Dev. Biol. 19, 23–44.

Matulef, K., Flynn, G. E., and Zagotta, W. N. 1999. Molecular rearrangements in the ligand-binding domain of cyclic nucleotide-gated channels. Neuron 24, 443–452.

Mazzolini, M., Punta, M., and Torre, V. 2002. Movement of the C-helix during the gating of cyclic nucleotide-gated channels. Biophys. J. 83, 3283–3295.

Michalakis, S., Reisert, J., Geiger, H., Wetzel, C., Zong, X., Bradley, J., Spehr, M., Huttl, S., Gerstner, A., Pfeifer, A., Hatt, H., Yau, K. W., and Biel, M. 2006. Loss of CNGB1 protein leads to olfactory dysfunction and subciliary cyclic nucleotide-gated channel trapping. J. Biol. Chem. 281, 35156–35166.

Miyazu, M., Tanimura, T., and Sokabe, M. 2000. Molecular cloning and characterization of a putative cyclic nucleotide-gated channel from *Drosophila melanogaster*. Insect Mol. Biol. 9, 283–292.

Molday, R. S., Molday, L. L., Dose, A., Clark-Lewis, I., Illing, M., Cook, N. J., Eismann, E., and Kaupp, U. B. 1991. The cGMP-gated channel of the rod photoreceptor cell characterization and orientation of the amino terminus. J. Biol. Chem. 266, 21917–21922.

Molokanova, E., Trivedi, B., Savchenko, A., and Kramer, R. H. 1997. Modulation of rod photoreceptor cyclic nucleotide-gated channels by tyrosine phosphorylation. J. Neurosci. 17, 9068–9076.

Muller, F., Bonigk, W., Sesti, F., and Frings, S. 1998. Phosphorylation of mammalian olfactory cyclic nucleotide-gated channels increases ligand sensitivity. J. Neurosci. 18(1), 164–173.

Munger, S. D., Lane, A. P., Zhong, H., Leinders-Zufall, T., Yau, K. W., Zufall, F., and Reed, R. R. 2001. Central role of the CNGA4 channel subunit in Ca^{2+}-calmodulin-dependent odor adaptation. Science 294, 2172–2175.

Nache, V., Schulz, E., Zimmer, T., Kusch, J., Biskup, C., Koopmann, R., Hagen, V., and Benndorf, K. 2005. Activation of olfactory-type cyclic nucleotide-gated channels is highly cooperative. J. Physiol. 569, 91–102.

Nakamura, T. and Gold, G. H. 1987. A cyclic nucleotide-gated conductance in olfactory receptor cilia. Nature 325, 442–444.

Nicol, G. D. 1993. The calcium channel antagonist, pimozide, blocks the cyclic GMP-activated current in rod photoreceptors. J. Pharmacol. Exp. Ther. 265, 626–632.

Paoletti, P., Young, E. C., and Siegelbaum, S. A. 1999. C-Linker of cyclic nucleotide-gated channels controls coupling of ligand binding to channel gating. J. Gen. Physiol. 113, 17–33.

Parent, A., Schrader, K., Munger, S. D., Reed, R. R., Linden, D. J., and Ronnett, G. V. 1998. Synaptic transmission and hippocampal long-term potentiation in olfactory cyclic nucleotide-gated channel type 1 null mouse. Am. Physiol. Soc. 79, 3295–3301.

Peng, C., Rich, E. D., and Varnum, M. D. 2004. Subunit configuration of heteromeric cone cyclic nucleotide-gated channels. Neuron 42, 401–410.

Pifferi, S., Boccaccio, A., and Menini, A. 2006. Cyclic nucleotide-gated ion channels in sensory transduction. FEBS Lett. 580, 2853–2859.

Podda, M. V., Marcocci, M. E., Del Carlo, B., Palamara, A. T., Azzena, G. B., and Grassi, C. 2005. Expression of cyclic nucleotide-gated channels in the rat medial vestibular nucleus. Neuroreport 16, 1939–1943.

Qu, W., Moorhouse, A. J., Chandra, M., Pierce, K. D., Lewis, T. M., and Barry, P. H. 2006. A single P-loop glutamate point mutation to either lysine or arginine switches the cation–anion selectivity of the CNGA2 channel. J. Gen. Physiol. 127, 375–389.

Rebrik, T. I. and Korenbrot, J. I. 1998. In intact cone photoreceptors, a Ca^{2+}-dependent, diffusible factor modulates the cGMP-gated ion channels differently than in rods. J. Gen. Physiol. 112, 537–548.

Root, M. J. and MacKinnon, R. 1993. Identification of an external divalent cation-binding site in the pore of a cGMP-activated channel. Neuron 11, 459–466.

Ruiz, M. L. and Karpen, J. W. 1997. Single cyclic nucleotide-gated channels locked in different ligand-bound states. Nature 389, 389–392.

Ruiz, M. L., London, B., and Nadal-Ginard, B. 1996. Cloning and characterization of an olfactory cyclic nucleotide-gated channel expressed in mouse heart. J. Mol. Cell Cardiol. 28, 1453–1461.

Sautter, A., Zong, X., Hofmann, F., and Biel, M. 1998. An isoform of the rod photoreceptor cyclic nucleotide-gated channel b subunit expressed in olfactory neurons. Proc. Natl. Acad. Sci. U. S. A. 95, 4696–4701.

Shapiro, M. S. and Zagotta, W. N. 2000. Structural basis for ligand selectivity of heteromeric olfactory cyclic nucleotide-gated channels. Biophys. J. 78, 2307–2320.

Shepherd, G. M. 1994. Discrimination of molecular signals by the olfactory receptor neuron. Neuron 13, 771–790.

Song, H. J. and Poo, M. M. 1999. Signal transduction underlying growth cone guidance by diffusible factors. Curr. Opin. Neurobiol. 9, 355–363.

Song, H. J., Ming, G. L., and Poo, M. M. 1997. cAMP-induced switching in turning direction of nerve growth cones. Nature 388, 275–279.

Spitzer, N. C., Olson, E., and Gu, X. 1995. Spontaneous calcium transients regulate neuronal plasticity in developing neurons. J. Neurobiol. 26, 316–324.

Sunderman, E. R. and Zagotta, W. N. 1999. Sequence of events underlying the allosteric transition of rod cyclic nucleotide-gated channels. J. Gen. Physiol. 113, 621–640.

Sundin, O. H., Yang, J. M., Li, Y., Zhu, D., Hurd, J. N., Mitchell, T. N., Silva, E. D., and Maumenee, I. H. 2000. Genetic basis of total colourblindness among the Pingelapese islanders. Nat. Genet. 25, 289–293.

Tetreault, M. L., Henry, D., Horrigan, D. M., Matthews, G., and Zimmerman, A. L. 2006. Characterization of a novel cyclic nucleotide-gated channel from zebrafish brain. Biochem. Biophys. Res. Commun. 348, 441–449.

Tibbs, G. R., Liu, D. T., Leypold, B. G., and Siegelbaum, S. A. 1998. A state-independent interaction between ligand and a conserved arginine residue in cyclic nucleotide-gated channels reveals a functional polarity of the cyclic nucleotide binding site. J. Biol. Chem. 273, 4497–4505.

Van Wagenen, S. and Rehder, V. 1999. Regulation of neuronal growth cone filopodia by nitric oxide. J. Neurobiol. 39, 168–185.

Varnum, M. D. and Zagotta, W. N. 1996. Subunit interactions in the activation of cyclic nucleotide-gated ion channels. Biophys. J. 70, 2667–2679.

Varnum, M. D. and Zagotta, W. N. 1997. Interdomain interactions underlying activation of cyclic nucleotide-gated channels. Science 278, 110–113.

Varnum, M. D., Black, K. D., and Zagotta, W. N. 1995. Molecular mechanism for ligand discrimination of cyclic nucleotide-gated channels. Neuron. 15, 619–625.

Wei, J. Y., Roy, D. S., Leconte, L., and Barnstable, C. J. 1998. Molecular and pharmacological analysis of cyclic nucleotide-gated channel function in the central nervous system. Prog. Neurobiol. 56, 37–64.

Weitz, D., Ficek, N., Kremmer, E., Bauer, P. J., and Kaupp, U. B. 2002. Subunit stoichiometry of the CNG channel of rod photoreceptors. Neuron 36, 881–889.

Wells, G. B. and Tanaka, J. C. 1997. Ion selectivity predictions from a two-site permeation model for the cyclic nucleotide-gated channel of retinal rod cells. Biophys. J. 72(1), 127–140.

Wissinger, B., Gamer, D., Jagle, H., Giorda, R., Marx, T., Mayer, S., Tippmann, S., Broghammer, M., Jurklies, B., Rosenberg, T., Jacobson, S. G., Sener, E. C., Tatlipinar, S., Hoyng, C. B., Castellan, C., Bitoun, P., Andreasson, S., Rudolph, G., Kellner, U., Lorenz, B., Wolff, G., Verellen-Dumoulin, C., Schwartz, M., Cremers, F. P., Apfelstedt-Sylla, E., Zrenner, E., Salati, R., Sharpe, L. T., and Kohl, S. 2001. CNGA3 mutations in hereditary cone photoreceptor disorders. Am. J. Hum. Genet. 69, 722–737.

Wohlfart, P., Haase, W., Molday, R. S., and Cook, N. J. 1992. Antibodies against synthetic peptides used to determine the topology and site of glycosylation of the cGMP-gated channel from bovine rod photoreceptors. J. Biol. Chem. 267, 644–648.

Yamazaki, Y., Brown, R. L., and Morita, T. 2002. Purification and cloning of toxins from elapid venoms that target cyclic nucleotide-gated ion channels. Biochemistry 41, 11331–11337.

Zagotta, W. N. and Siegelbaum, S. A. 1996. Structure and function of cyclic nucleotide-gated channels. Annu. Rev. Neurosci. 19, 235–263.

Zheng, J. and Zagotta, W. N. 2000. Gating rearrangements in cyclic nucleotide-gated channels revealed by patch-clamp fluorometry. Neuron 28, 369–374.

Zheng, J. and Zagotta, W. N. 2004. Stoichiometry and assembly of olfactory cyclic nucleotide-gated channels. Neuron 42, 411–421.

Zheng, J., Trudeau, M. C., and Zagotta, W. N. 2002. Rod cyclic nucleotide-gated channels have a stoichiometry of three CNGA1 subunits and one CNGB1 subunit. Neuron 36, 891–896.

Zhong, H., Molday, L. L., Molday, R. S., and Yau, K. W. 2002. The heteromeric cyclic nucleotide-gated channel adopts a 3A:1B stoichiometry. Nature 420, 193–198.

Zong, X., Zucker, H., Hofmann, F., and Biel, M. 1998. Three amino acids in the C-linker are major determinants of gating in cyclic nucleotide-gated channels. EMBO J. 17, 353–362.

Zufall, F., Firestein, S., and Shepherd, G. M. 1991. Analysis of single cyclic-nucleotide gated channels in olfactory receptor cells. J. Neurosci. 11, 3573–3580.

Zufall, F., Firestein, S., and Shepherd, G. M. 1994. Cyclic nucleotide-gated ion channels and sensory transduction in olfactory receptor neurons. Annu. Rev. Biophys. Biomol. Struct. 23, 577–607.

Zufall, F., Shepherd, G. M., and Barnstable, C. J. 1997. Cyclic nucleotide-gated channels as regulators of CNS development and plasticity. Curr. Opin. Neurobiol. 7, 404–412.

4.30 Structure, Expression, and Function of Olfactory Receptors

K Touhara, The University of Tokyo, Chiba, Japan

© 2008 Elsevier Inc. All rights reserved.

4.30.1	**Introduction**	527
4.30.2	**Structure**	528
4.30.2.1	Protein Structure	528
4.30.2.2	Olfactory Receptor Genes	529
4.30.2.3	Olfactory Receptor Pseudogenes	530
4.30.2.4	Genomic Structure	530
4.30.3	**Expression**	530
4.30.3.1	Single-Receptor Gene Choice	530
4.30.3.2	Spatial Expression Pattern	531
4.30.3.3	Temporal Expression Pattern	532
4.30.3.4	Ectopic Expression	532
4.30.4	**Function I: An Odorant Sensor**	533
4.30.4.1	General Considerations for Functional Expression	533
4.30.4.2	Odorant Response Assays	534
4.30.4.3	Olfactory Receptor Pharmacology	534
4.30.4.4	Odorant-Binding Site	536
4.30.4.5	Odorant Sensitivity and Specificity	537
4.30.5	**Function II: Others**	538
4.30.5.1	Axon Guidance	538
4.30.5.2	Chemosensor	539
4.30.5.3	Pheromone Detector	539
4.30.6	**Remaining Problems**	540
References		540

4.30.1 Introduction

Titus Lucretius Carus, a Roman poet and philosopher, proposed in his book *On the Nature of Things* (50 BC) that a variety of odors exist because each odorant possesses a unique structure (Lucretius, T., 1995). In the mid-twentieth century, this concept was established as the stereospecific receptor theory, which provides an explanation for the molecular mechanisms underlying the remarkable olfactory sensing system (Amoore, J. E., 1963). The receptor theory postulates that there are receptor sites for odorants and that odor perception occurs only when the structure of an odorant molecule and the binding site match. Other theories including vibrational theory, puncturing theory, radiational theory, and absorption theory have been proposed to explain odor perception, but they remain unproven.

Based on the evidence for the involvement of G protein-mediated signaling and ion channels in olfactory signal transduction (Pace, U. *et al.*, 1985; Sklar, P. B. *et al.*, 1986; Nakamura, T. and Gold, G. H., 1987; Breer, H. *et al.*, 1990; Dhallan, R. S. *et al.*, 1990), Buck and Axel hypothesized that receptor proteins for odorants must be expressed in the olfactory epithelium and must belong to a family of seven-transmembrane G-protein-coupled receptors (GPCRs) (Buck, L. B., 2004). State-of-the-art molecular biology techniques allowed them to identify a multigene family that appears to encode receptors for odorants (Buck, L. and Axel, R., 1991). The proteins were named olfactory or odorant receptors (ORs). The former name was given because the proteins are expressed in olfactory neurons and play a crucial role in olfaction, and the latter because the proteins bind odorant molecules; however, strictly saying, neither terminology is correct because ORs

have since been found in tissues other than the olfactory epithelium and because ORs have functions in addition to acting as odorant sensors (Spehr, M. *et al.*, 2006a). Nonetheless, the main role of the OR family is to provide a molecular basis for recognition and discrimination of thousands of odorant molecules in the olfactory sensory system.

4.30.2 Structure

4.30.2.1 Protein Structure

OR proteins are classified as members of the GPCR superfamily because of the presence of structural features common to GPCRs (Buck, L. and Axel, R., 1991; Strader, C. D. *et al.*, 1994) and because they couple to and activate heterotrimeric G proteins (Krautwurst, D. *et al.*, 1998; Kajiya, K. *et al.*, 2001). ORs possess seven hydrophobic transmembrane domains, a disulfide bond between the conserved cysteines in the extracellular loops, a conserved glycosylation site in the N-terminal region (Katada, S. *et al.*, 2004), and several amino acid sequences that are conserved in the OR family (Zozulya, S. *et al.*, 2001; Zhang, X. and Firestein, S., 2002) (Figure 1). The OR consensus sequences reside within the cytoplasmic side of each transmembrane regions and include PMYFFL (transmembrane domain [TM]2), MAYDRYVAIC (TM3), KAFSTC (TM6), and PMLNPXXY (TM7). Although these consensus sequences vary somewhat between species, they have been widely used to retrieve OR genes from genome. In addition, extensive motif analysis has revealed more than 80 specific short motifs, some of which constitute signature sequences for the OR subfamily of a certain species or have implications for the function and evolution the ORs (Liu, A. H. *et al.*, 2003). These conserved motifs likely contribute to the proper folding of ORs in the plasma membrane so that ORs can bind odorants and couple to appropriate G proteins. The transmembrane regions, on the other hand, help form the odorant-binding pocket (Figure 1). The sequences in the binding pocket are relatively variable, allowing ORs to bind a wide spectrum of odorant molecules (Singer, M. S. *et al.*, 1996; Pilpel, Y. and Lancet, D., 1999; Floriano, W. B. *et al.*, 2000; Singer, M. S., 2000; Floriano, W. B. *et al.*, 2004; Man, O. *et al.*, 2004; Katada, S. *et al.*, 2005). Overall, the three-dimensional structure of the OR is probably similar to that of rhodopsin, which has been determined by a combination of computer modeling, site-directed mutation, and

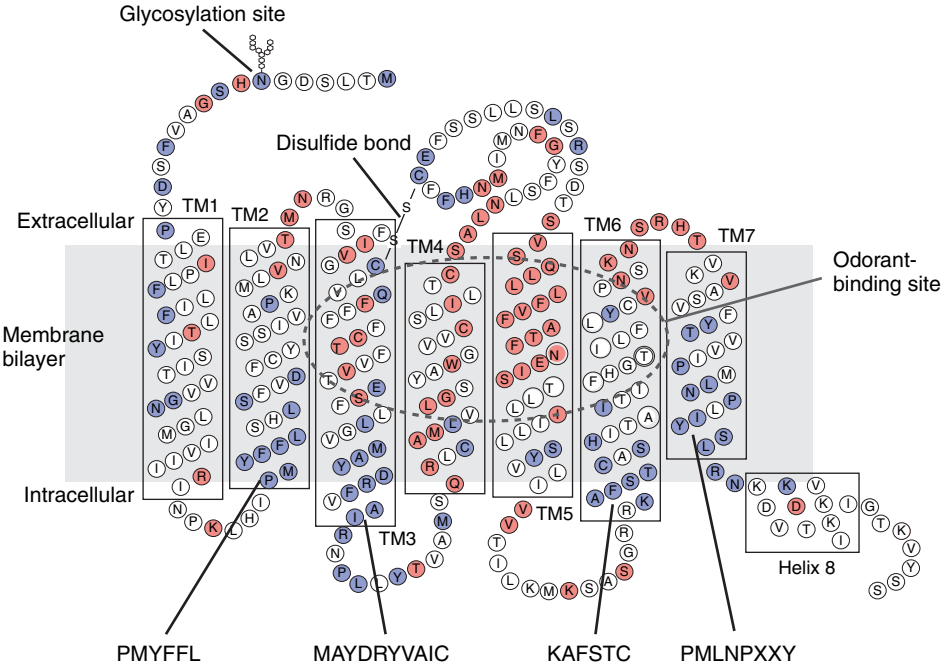

Figure 1 Structure and topology of an olfactory receptor (OR) protein. Conserved sequence motifs, glycosylation site, and disulfide bond in the OR family are shown. The odorant-binding site is in the space formed by TM3-6 (dotted circle). Red, variable amino acids in the OR family; blue, conserved amino acids in the OR family. TM, transmembrane domain.

X-ray crystallography and which is the only GPCR structure that has been solved so far (see Odorant-Binding Site) (Katada, S. *et al.*, 2005).

4.30.2.2 Olfactory Receptor Genes

It has been estimated that the OR family includes at least several hundred members in the rat (Buck, L. and Axel, R., 1991). In the last decade or so, the genome sequence projects have enabled the comprehensive analysis of the OR gene family and have revealed the genomic structure and distribution of the OR genes from various organisms (Mombaerts, P., 2004). The most recent data for vertebrate ORs are shown in Table 1. In mammals, the OR repertoire comprises 800–1500 members, whereas in fish, the OR family has only approximately 100 members (Niimura, Y. and Nei, M., 2005c). Thus, expansion of the OR gene family occurred when animals shifted their living space from an aquatic to a terrestrial environment.

Based on phylogenetic analysis, the mammalian OR genes can be classified into two different groups: class I and class II (Glusman, G. *et al.*, 2001; Zozulya, S. *et al.*, 2001; Zhang, X. and Firestein, S., 2002) (Figure 2). This classification is based on the finding that frog (*Xenopus laevis*) has two different classes of OR genes: one (class I) that is similar to fish OR genes and a second (class II) that is similar to mammalian OR genes (Freitag, J. *et al.*, 1995). For example, the numbers of intact class I OR genes in human and mouse are 57 and 115 of 388 and 1037 total intact OR genes, respectively (Niimura, Y. and Nei, M., 2005c). Later studies revealed, however, that mammalian class I genes formed a distinct clade from fish OR genes that can be further divided into nine subgroups (Niimura, Y. and Nei, M., 2005c) (Figure 2). The amphibian OR repertoire turns out to be similar to both fish and mammal ORs,

Table 1 Functional and nonfunctional OR genes in various vertebrate species

	Organism	*Total genes*	*Intact genes*	*Pseudogene* (%)	*Reference*[a]
Mammal	Human	802	388	52	Niimura Y. and Nei M. (2005a; 2005b; 2005c)
	Mouse	1391	1037	25	Niimura Y. and Nei M. (2005a; 2005b; 2005c)
	Rat	1493	1202	20	Quignon P. *et al.* (2005)
	Dog	1094	872	20	Quignon P. *et al.* (2005)
Bird	Chicken[b]	554	78	86	Niimura Y. and Nei M. (2005a; 2005b; 2005c)
Amphibian	*X. tropicalis*	888	410	54	Niimura Y. and Nei M. (2005a; 2005b; 2005c)
Fish	Zebrafish	133	98	26	Niimura Y. and Nei M. (2005a; 2005b; 2005c)
	Puffer fish	94	40	57	Niimura Y. and Nei M. (2005a; 2005b; 2005c)

[a]Note that there have been many reports on the estimates of the numbers of olfactory receptor (OR) genes, but the most recent ones are shown here. The numbers will be subject to change slightly with time in the future.
[b]The actual number of chicken ORs appears to be much larger due to numerous short contings in the draft genome.

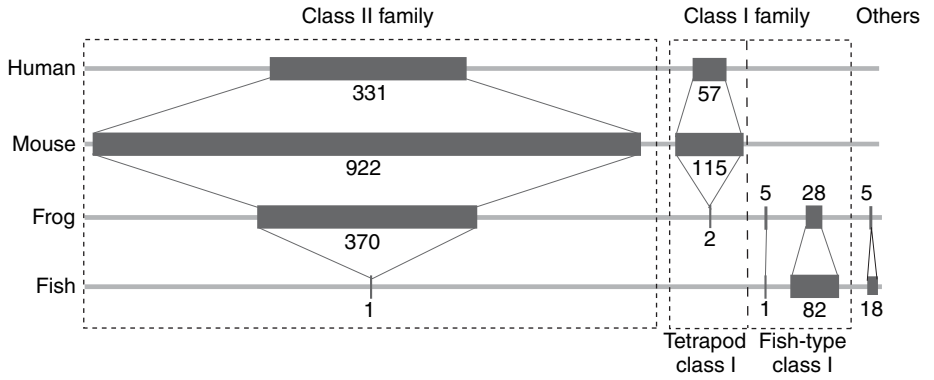

Figure 2 Numbers of functional olfactory receptor (OR) genes belonging to different groups in four species. The class II family has originated from one ancestral gene in fish. The class I family can be divided into two classes; tetrapod class I and fish-type class I.

suggesting that there are at least three evolutional lineages (i.e., fish, amphibian, and mammal) in the vertebrate OR gene family (Niimura, Y. and Nei, M., 2005c).

Relatively few OR genes have been found in insects. For example, there are 62 OR genes expressed in the antenna and the maxillary palps in *Drosophila melanogaster* (Clyne, P. J. *et al.*, 1999; Gao, Q. and Chess, A., 1999; Vosshall, L. B. *et al.*, 1999). Similar numbers of OR genes have been found in the genome of the malaria mosquito (Fox, A. N. *et al.*, 2002; Hill, C. A. *et al.*, 2002) and from several moths (Krieger, J. *et al.*, 2002; 2003; Nakagawa, T. *et al.*, 2005). The insect ORs have the following unique features: (1) they lack obvious homology with vertebrate ORs or other GPCRs (Robertson, H. M. *et al.*, 2003); (2) there do not appear to be pseudogenes (Robertson, H. M. *et al.*, 2003); (3) they are coexpressed and heterodimerize with the unique OR, which is highly conserved across diverse insect species, also known as the Or83b family (Larsson, M. C. *et al.*, 2004; Nakagawa, T. *et al.*, 2005; Neuhaus, E. M. *et al.*, 2005); and (4) their membrane topology is distinct from conventional GPCRs so that their N-termini are located intracellularly (Benton, R. *et al.*, 2006).

4.30.2.3 Olfactory Receptor Pseudogenes

A significant portion of the OR gene family has been pseudogenized in vertebrates. Hominoids possess a high pseudogene content (~50%), whereas only ~20% of OR genes are pseudogenes in mouse and dog and 25–35% are pseudogenes in primates (Gilad, Y. *et al.*, 2004; Niimura, Y. and Nei, Y., 2005c; Quignon, P. *et al.*, 2005) (Table 1). The ORs are the most changeable gene family and still undergo rapid molecular evolution by tandem gene duplication and pseudogenization in the lineage of each animal species. For example, the mouse lineage acquired a few hundred new OR genes after the human–mouse divergence, indicating that both gene expansion in the mouse lineage and gene loss in the human lineage contribute to the differences in the numbers of functional ORs (Niimura, Y. and Nei, M., 2005b). The OR gene dynamics could also be pressured by the state of the environment and the type of sense that is utilized for social and sexual behavior. The fraction of pseudogenes in the OR family has increased during evolution in the order of rodents, monkeys, and humans, suggesting that the reduced sense of smell correlates with the loss of functional OR genes. Indeed, in whale and dolphin, in which the auditory system is dominant, 70–80% of OR genes appear to be pseudogenes (Y. Go, personal communication).

4.30.2.4 Genomic Structure

The OR genes are encoded by an exon that contains an intronless coding region of ~1 kb along with one to four upstream exons (Lane, R. P. *et al.*, 2001; Young, J. M. and Trask, B. J., 2002). The OR genes form genomic clusters and are distributed widely in chromosomes; however, the distribution is not even, and almost half of the mouse OR genes are located on chromosomes 2 and 7, which have orthologous relationships with chromosome 11 in human (Niimura, Y. and Nei, M., 2005a). The majority of the OR gene family has multiple transcriptional isoforms (Asai, H. *et al.*, 1996; Lane, R. P. *et al.*, 2001; Volz, A. *et al.*, 2003; Fukuda, N. and Touhara, K., 2006). Further, OR genes are highly polymorphic as suggested for human leukocyte antigen-linked OR genes (Ehlers, A. *et al.*, 2000; Eklund, A. C. *et al.*, 2000) and dog OR genes (Tacher, S. *et al.*, 2005), which may account for individual differences in the ability to perceive odor and may sometimes cause specific anosmia.

4.30.3 Expression

4.30.3.1 Single-Receptor Gene Choice

Each olfactory sensory neuron expresses just one of the 1000 ORs (Serizawa, S. *et al.*, 2004; Shykind, B. M., 2005). The one-neuron one-receptor rule has been confirmed by a variety of techniques, namely, *in situ* hybridization (Ngai, J. *et al.*, 1993; Ressler, K. J. *et al.*, 1993; Vassar, R. *et al.*, 1993), single-cell reverse transcriptase-polymerase chanin reaction (RT-PCR) analysis (Malnic, B. *et al.*, 1999; Touhara, K. *et al.*, 1999), and transgenic experiments (Qasba, P. and Reed, R. R., 1998; Serizawa, S. *et al.*, 2000; Vassalli, A. *et al.*, 2002; Serizawa, S. *et al.*, 2003). Further, the selected OR appears to be transcribed from only one of two alleles, either the maternal or paternal allele (Chess, A. *et al.*, 1994; Ishii, T. *et al.*, 2001). This mutually exclusive expression pattern is preserved even between transgenes and endogenous copies, supporting the stochastic model (Qasba, P. and Reed, R. R., 1998; Serizawa, S. *et al.*, 2000; Vassalli, A. *et al.*, 2002; Serizawa, S. *et al.*, 2003). Indeed, the single OR choice is observed from a minigene that contains

a few kilobases upstream of the transcription start site, implicating the involvement of cis-regulatory elements (Qasba, P. and Reed, R. R., 1998; Vassalli, A. *et al.*, 2002; Oka, Y. *et al.*, 2006).

The expression of one cluster of OR genes including MOR28 in transgenic mice requires a long upstream region of ~100 kb containing an enhancer element called the H-region (Serizawa, S. *et al.*, 2000; 2003). This locus control region, H, appears to associate with multiple OR promoters and act as a cis-acting enhancer element (Lomvardas, S. *et al.*, 2006) (Figure 3). In olfactory neurons, one of the two H-region alleles is methylated, suggesting that the H-enhancer is functionally monoallelic, therefore ensuring selection of a single receptor (Lomvardas, S. *et al.*, 2006).

In addition to positive regulation of OR gene expression by cis-regulatory elements, negative feedback regulation must occur to suppress the expression of additional receptors (Serizawa, S. *et al.*, 2003; Lewcock, J. W. and Reed, R. R., 2004; Shykind, B. M. *et al.*, 2004). It appears that functional OR proteins but not mRNA play an inhibitory role in preventing further activation of other OR genes, although the molecular mechanism remains to be elucidated (Figure 3).

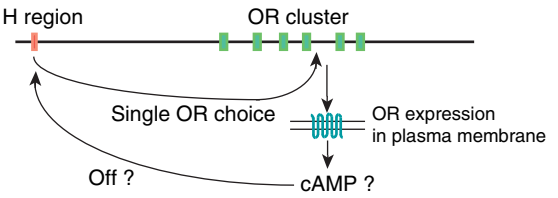

Figure 3 A model for olfactory receptor (OR) gene expression. The H-region containing an enhancer element associates with multiple OR promoters on different chromosomes to activate OR gene expression. The expressed functional OR proteins transmit inhibitory signals to block the action of the H-enhancer, resulting in the expression of only one functional OR in a sensory neuron.

4.30.3.2 Spatial Expression Pattern

In mouse and rat, *in situ* hybridization experiments using different OR probes have suggested that each OR gene is expressed only in a certain region of the olfactory epithelium (Nef, P. *et al.*, 1992; Strotmann, J. *et al.*, 1992; Ressler, K. J. *et al.*, 1993; Vassar, R. *et al.*, 1993; Strotmann, J. *et al.*, 1994). Thus, the epithelium can be divided into at least four spatial zones expressing different sets of OR genes (Sullivan, S. L. *et al.*, 1996) (Figure 4). The distinct spatial expression pattern appears to be conserved among the vertebrate species, although the expression of fish ORs is not as clearly segregated as that of mammalian ORs (Ngai, J. *et al.*, 1993; Weth, F. *et al.*, 1996). Initially, the

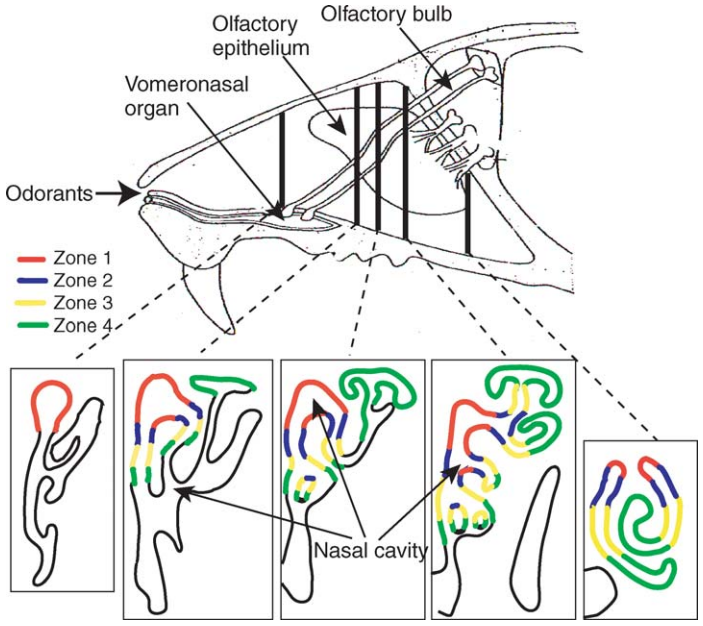

Figure 4 Anatomic structure of nasal cavity and olfactory receptor (OR) expression zones in the olfactory epithelium. The spatial expression zones are depicted in four different colors for clarity, but OR genes are expressed in a unique and distinct zone in a continuous and overlapping manner.

spatial zones observed in rodents were thought to be sharply segregated, but careful *in situ* hybridization studies revealed that each OR gene is expressed in a unique and distinct zone in a continuous and overlapping manner (Norlin, E. M. *et al.*, 2001; Iwema, C. L. *et al.*, 2004; Miyamichi, K. *et al.*, 2005). Therefore, multiple overlapping bands are formed along the dorsomedial/ventrolateral axis, although the boundary of the most dorsal region corresponding to the olfactory cell adhesion molecule (OCAM)-negative neuronal layer was maintained.

There are some exceptions to the zonal expression rule. First, some OR genes are expressed in the septal organ, which is an isolated island of olfactory sensory neurons located on the nasal septum near the entrance of the nasopharynx (Kaluza, J. F. *et al.*, 2004; Tian, H. and Ma, M., 2004). Second, the OR37 subfamily shows a patch-like distribution in clustered populations of neurons in central turbinates (Strotmann, J. *et al.*, 1999). Although there are some promoter motifs that might control the expression domain in the nasal cavity, the regulatory factors that determine the positional information remain to be identified.

4.30.3.3 Temporal Expression Pattern

In rodents, OR genes start to be expressed during the embryonic stages. The onset of expression in mice is at embryonic day (E) 12–14 as determined by *in situ* hybridization for several ORs (Strotmann, J. *et al.*, 1995; Sullivan, S. L. *et al.*, 1995). Microarray analysis of the developmental course of OR gene expression revealed that the number of transcribed OR genes remains at a relatively low level until birth (100–200 ORs), and a large number of OR genes are detectable only after birth (Zhang, X. *et al.*, 2004). At 2–3 weeks after birth, the number of detected OR genes reached a peak (~500 ORs) (Zhang, X. *et al.*, 2004). Recently, specific antibodies against ORs have become available (Barnea, G. *et al.*, 2004; Strotmann, J. *et al.*, 2004), and they have revealed that OR proteins are present in dendritic knobs of olfactory sensory neurons as early as E12 and before the initiation of ciliogenesis (Schwarzenbacher, K. *et al.*, 2005). Because the olfactory cilia are formed at E13, the OR proteins appear to migrate into developing cilia, and strong labeling by the antibody is observed in the expanded tips of the cilia. Up to E18, the number of cilia per neuron continues to increase, during which OR immunostaining is clearly visible.

4.30.3.4 Ectopic Expression

OR expression is not restricted to olfactory sensory neurons. Expression of ORs in nonolfactory tissues was first observed in the male germ line (Parmentier, M. *et al.*, 1992). Since then, ectopic OR transcripts have been found in a variety of tissues including the spleen and insulin-secreting cells (Blache, P. *et al.*, 1998), lingual epithelial cells of the tongue (Durzynski, L. *et al.*, 2005; Gaudin, J. C. *et al.*, 2006), ganglia of the autonomic nervous system (Weber, M. *et al.*, 2002), pyramidal neurons in the cerebral cortex of the brain (Otaki, J. M. *et al.*, 2004), the colon (Yuan, T. T. *et al.*, 2001), myocardial cells in developing heart (Drutel, G. *et al.*, 1995; Ferrand, N. *et al.*, 1999), the prostate gland (Yuan, T. T. *et al.*, 2001), and erythroid cells (Feingold, E. A. *et al.*, 1999). Polyclonal antibodies against an OR expressed in dog sperm bind specifically to the midpiece of the flagellum of mature sperm (Vanderhaeghen, P. *et al.*, 1993; Walensky, L. D. *et al.*, 1995). In other cases, the transcripts have been detected mainly by RT-PCR, and therefore, the expression level might be too low to be considered functional. Indeed, an RNase protection assay and microarray analysis estimated that a total of 50–70 OR genes are expressed in mouse testis (Vanderhaeghen, P. *et al.*, 1997a; 1997b; Zhang, X. *et al.*, 2004), whereas a careful *in situ* hybridization study revealed that only up to 10–20 OR genes were actually detected at a significant level (Fukuda, N. and Touhara, K., 2006) (Figure 5(a)). The testicular ORs are expressed in a subset of the seminiferous

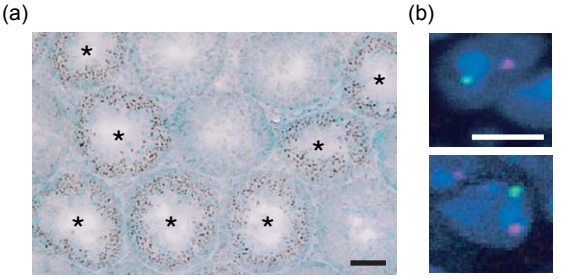

Figure 5 Expression of olfactory receptor (OR) genes in mouse testis. (a) *In situ* hybridization showing expression of an OR in a subset of the seminiferous tubules (asterisks). Scale bar = 0.1 mm. (b) Double-*in situ* hybridization of ORs showing two signals derived from two ORs in nuclei of round spermatids. Scale bar = 10 μm. Adapted from Fukuda, N. and Touhara, K. 2006. Developmental expression patterns of testicular olfactory receptor genes during mouse spermatogenesis. Genes Cells 11, 71–81, with permission from Blackwell Publishing.

tubules, suggesting that they are expressed at specific stages during spermatogenesis (Fukuda, N. and Touhara, K., 2006). Phylogenetic analysis suggests that there is no unique characteristic sequence similarity among the testicular OR genes (Vanderhaeghen, P. *et al.*, 1997b; Zhang, X. *et al.*, 2004; Fukuda, N. and Touhara, K., 2006). Double-*in situ* hybridization experiments showed that, in contrast to olfactory neurons, more than one OR could be expressed in a single spermatogenic cell, indicating that the transcriptional regulation of OR genes in testis is distinct from that in the olfactory system (Fukuda, N. and Touhara, K., 2006) (Figure 5(b)).

4.30.4 Function I: An Odorant Sensor

4.30.4.1 General Considerations for Functional Expression

Understanding of OR function has progressed slowly due to a lack of appropriate heterologous systems for expressing and assaying odorant responses (McClintock, T. S. and Sammeta, N., 2003). Therefore, olfactory neurons themselves were first targeted as an OR expression system (Zhao, H. *et al.*, 1998) because they should possess the appropriate cellular machinery for expressing ORs and transmitting odorant signals. Adenovirus-mediated gene transfer was used to overexpress ectopic ORs in the olfactory epithelium, and the ligand responses were measured either by electro-olfactography (Zhao, H. *et al.*, 1998) or by Ca^{2+} imaging of infected neurons (Touhara, K. *et al.*, 1999) (Figure 6(a)). In addition, a gene-targeting approach was utilized to tag defined OR-expressing olfactory neurons with green fluorescent proteins, after which the responses of the fluorescent cells to the cognate odorants were recorded (Bozza, T. *et al.*, 2002; Grosmaitre, X. *et al.*, 2006). Although this homologous *in vivo* expression system gives reliable odorant responses, high-throughput ligand screening necessitates establishment of heterologous expression systems.

Several attempts have been made to achieve functional expression of ORs on the cell surface in heterologous systems. In some cases, adding an N-terminal leader sequence from another GPCR resulted in a limited expression of functional ORs in the plasma membrane and in a successful odorant response in a heterologous system such as HEK293 cells (Krautwurst, D. *et al.*, 1998; Wetzel, C. H. *et al.*, 1999; Kajiya, K. *et al.*, 2001). Additional studies have shown that glycosylation of the N-terminus of ORs is required for proper translocation to the plasma membrane (Katada, S. *et al.*, 2004). In addition, the one-transmembrane protein RTP1, which has been referred to as an OR chaperone, appears to enhance cell-surface expression of ORs, and many ORs have been deorphanized by coexpressing them with RTP1 (Saito, H. *et al.*, 2004). In addition, Ric8B, a putative guanine nucleotide exchange factor for Gαolf, promotes efficient signal transduction of ORs (Von Dannecker, L. E. *et al.*, 2006). Thus, introduction of all the factors required for OR expression present in olfactory neurons is expected to solve the problems of heterologous expression. In addition, a method for maintaining cell-surface localization is needed because the ORs undergo continuous internalization and recycling in heterologous cells (Jacquier, V. *et al.*, 2006). Thus, the level of surface expression appears

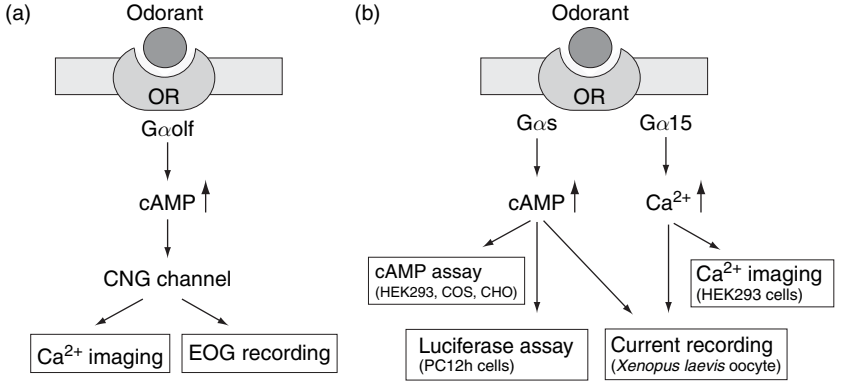

Figure 6 Odorant response assays for an olfactory receptor (OR). (a) Homologous expression of an OR in olfactory neurons. Odorant responses are monitored by Ca^{2+} imaging or electro-olfactogram (EOG). CNG, cyclic nucleotide gated. (b) Heterologous expression of an OR in mammalian cell lines or *Xenopus laevis* oocytes. Odorant responses are measured by Gαs-cAMP or Gα15-Ca^{2+} signaling.

to be critical for OR assays. Finally, it should be noted that there are dramatic differences even between HEK293 cells from different laboratories.

4.30.4.2 Odorant Response Assays

Ca^{2+} imaging has been one of the most common and reliable methods for detecting activation of orphan GPCRs in high-throughput ligand screening. The Ca^{2+} imaging assay, however, is limited to GPCRs that couple to Gαq-type G-proteins. For GPCRs that couple to unknown G proteins, the G-protein α subunit, Gα15, is often used to force the signaling to an inositol phosphate-mediated cascade because of its promiscuity for GPCRs. This strategy has been successfully applied to ORs that couple to the olfactory Gαs-type G-protein, Gαolf, which mediates increases in cAMP in olfactory neurons. Thus, in HEK293 cells coexpressing Gα15 and ORs, Ca^{2+} responses are observed when the cells are stimulated with their ligands (Krautwurst, D. *et al.*, 1998; Kajiya, K. *et al.*, 2001; Touhara, K. *et al.*, 2006) (Figures 6(b) and 7).

Without coexpression of Gα15, ORs activate endogenous Gαs upon ligand stimulation in various mammalian cell lines (e.g., HEK293, COS-7, and CHO-K1 cells) (Kajiya, K. *et al.*, 2001; Katada, S. *et al.*, 2003). Odorant-induced cAMP increases have been measured using an enzyme-linked immunoassay (Touhara, K. *et al.*, 2006) (Figure 6(b)). Alternatively, a luciferase-reporter assay system using the zif268 promoter allows luminescent detection of cAMP increases upon stimulation with an odorant (Katada, S. *et al.*, 2003). For example, in PC12h cells cotransfected with an OR and the luciferase-reporter construct, odorant stimulation produces dose-dependent increases in luciferase activity (Katada, S. *et al.*, 2003).

The *X. laevis* oocyte is another good heterologous expression system for ORs (Figure 6(b)). Ca^{2+} increases via an endogenous Ca^{2+}-dependent Cl^- channel can be electrophysiologically detected by coexpressing Gα15, and Gαs-mediated cAMP increases can be detected by coexpressing a cAMP-dependent Cl^- channel, CFTR (Katada, S. *et al.*, 2003; Abaffy, T. *et al.*, 2006; Touhara, K. *et al.*, 2006). The whole-cell voltage-clamp method allows for measurement of whole-cell ion currents flowing through the membrane via these ion channels. The current induced by an odorant stimulus can be further amplified by measuring the conductance at +60 mV with depolarization step pulses (Touhara, K. *et al.*, 2006).

To elucidate the structural features of an OR at the atomic level, it is necessary to develop a system for overexpressing and crystallizing the OR. This is a problem not only for ORs but also other GPCRs because of the difficulty in handling seven-transmembrane proteins. In this regard, yeast has been proposed as a good overexpression system for future structural analyses of ORs (Pajot-Augy, E. *et al.*, 2003).

4.30.4.3 Olfactory Receptor Pharmacology

The best characterized OR is a mouse OR, mOR-EG (MOR174-9), which was originally isolated from a single eugenol-responsive neuron by Ca^{2+} imaging

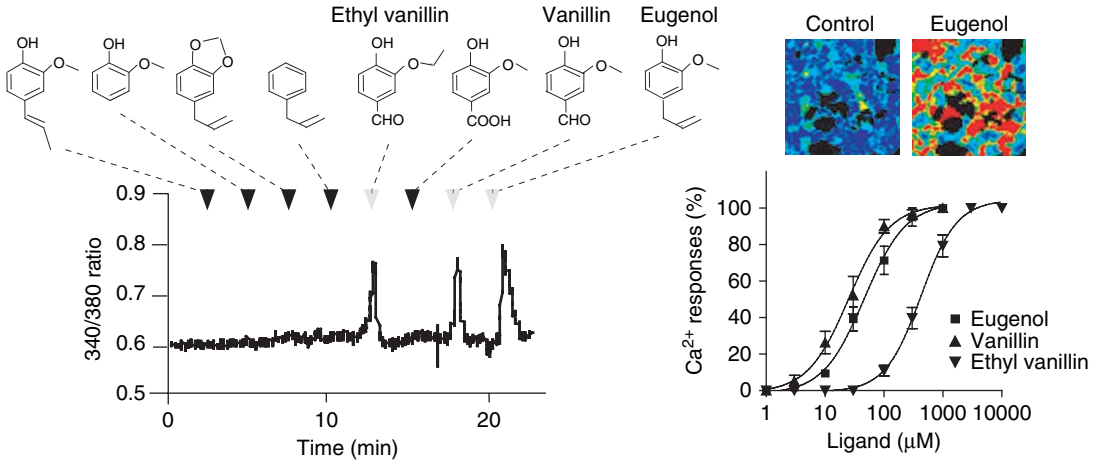

Figure 7 Ca^{2+} responses and dose–response profiles for various ligands in HEK293 cells expressing mOR-EG and Gα15. mOR-EG responds to eugenol, vanillin, and ethyl vanillin with different EC_{50} values. Red cells indicate high levels of intracellular Ca^{2+} and blue cells represent the basal levels in pseudocolored images.

and single-cell RT-PCR techniques (Kajiya, K. *et al.*, 2001). The mOR-EG recognizes 22 odorants that share certain molecular determinants, with EC_{50} values ranging from a few to several hundred micromolar (Katada, S. *et al.*, 2005) (Figures 7 and 8). The structure–activity relationship studies for mOR-EG suggested that ORs have a broad but selective molecular receptive range, and the selectivity is determined by shape, size, functional group, and length of a ligand. This pharmacological concept is generally common to many ORs as has been shown by studies on rat I7 (Araneda, R. C. *et al.*, 2000) and other deorphanized ORs (Wetzel, C. H. *et al.*, 1999; Bozza, T. *et al.*, 2002; Gaillard, I. *et al.*, 2002; Levasseur, G. *et al.*, 2003; Spehr, M. *et al.*, 2003; Matarazzo, V. *et al.*, 2005; Shirokova, E. *et al.*, 2005); however, there seem to be some ORs whose ligand spectra are relatively narrow. The ligand specificity appears to be determined by the environment of the binding site in each OR. Considering that there are a thousand ORs, each of which has a unique ligand spectrum, and that each odorant is recognized by multiple ORs, it is reasonable to conclude that odorant information is coded by a combination of ORs activated by the odorant (Malnic, B. *et al.*, 1999; Kajiya, K. *et al.*, 2001; Touhara, K., 2002) (Figure 9).

As is the case of ligands for other GPCRs, odorants function not only as agonists for some ORs but also as antagonists for others, suggesting that the interaction between ORs and odorants in the mixture can be more complex than expected (Figure 10). For example, the eugenol response to mOR-EG was potently blocked by some structurally related odorants such as methyl isoeugenol and isosafrol (Oka, Y. *et al.*, 2004a; 2004b). The antagonism was observed in mOR-EG-expressing olfactory neurons using an intact olfactory epithelium slice (Omura, M. *et al.*, 2003; Oka, Y. *et al.*, 2004b). Furthermore, rat I7 has been shown to be antagonized by citral (Araneda, R. C. *et al.*, 2000), and undecanal was found to be an inhibitor of hOR17-4 (Spehr, M. *et al.*, 2003). Thus, the antagonism between odorants may contribute significantly to the formation of the receptor code for an odorant mixture in the olfactory system. In reality, however, this type of interaction may be rare because few odorants act as antagonists. Indeed, optical recording in the olfactory bulb shows that a receptor code for a natural odor such as coffee or cumin is basically the sum of the responses to its individual components (Lin da, Y. *et al.*, 2006). Quantitative recording using a Ca^{2+} imaging technique, however, demonstrated that a partial inhibition of the response by antagonists occurs in the OR-defined glomerulus, which may contribute to a change in odor perception (Y. Oka and K. Touhara, unpublished observation).

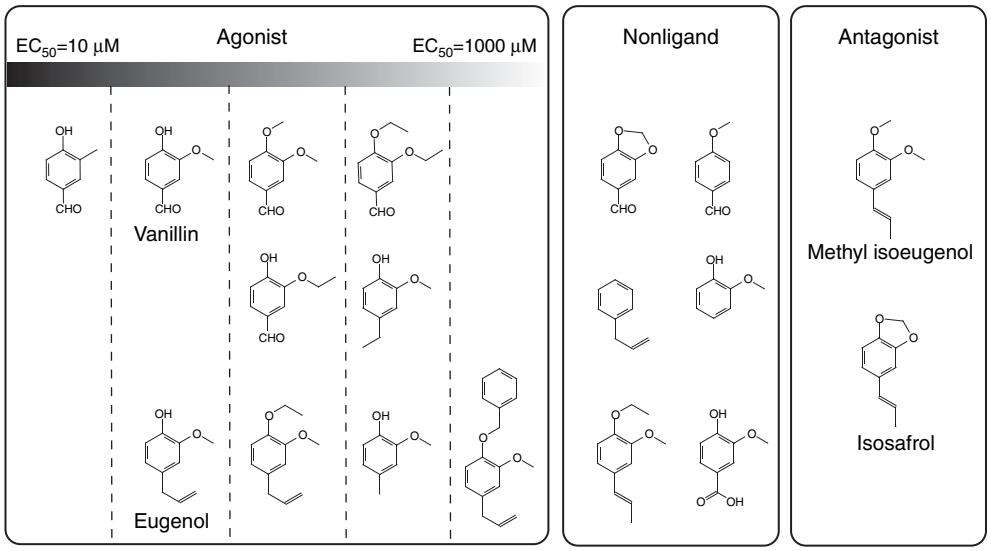

Figure 8 Structure of agonists and antagonists of mOR-EG. The compounds on the left-most side exhibit the lowest EC_{50} values. Adapted from Touhara, K., Katada, S., Nakagawa, T., and Oka, Y. 2006. Ligand screening of olfactory receptors. In: *G Protein-Coupled Receptors: Structure, Function, and Ligand Screening* (eds. T. Haga and S. Takeda), pp. 85–109. CRC press.

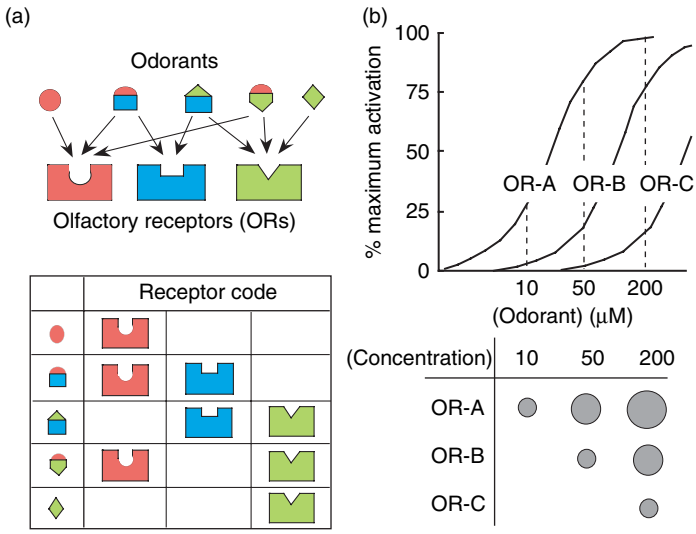

Figure 9 A combinatorial receptor code for an odorant. (a) A receptor code for an odorant is determined by a combination of activated olfactory receptors (ORs). (b) An odorant is recognized by a subset of ORs that have different affinities, thereby resulting in different receptor codes with increasing odorant concentrations.

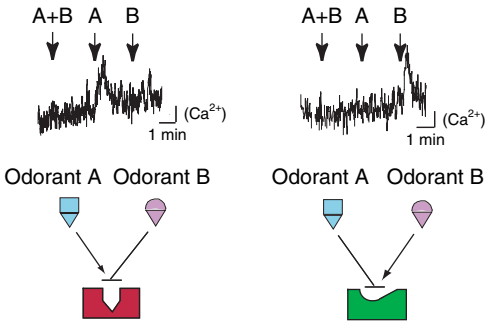

Figure 10 Olfactory receptor antagonism between odorants. Ca^{2+} response profiles of olfactory neurons that respond to odorant A or B that is inhibited by odorant B or A, respectively (see Oka, Y. *et al.*, 2004 for more detail).

4.30.4.4 Odorant-Binding Site

Multiple alignment analysis of the OR superfamily identified highly conserved and variable regions that are probably involved in structural organization and in ligand recognition, respectively (Buck, L. and Axel, R., 1991; Zhang, X. and Firestein, S., 2002). Some of the earlier attempts such as correlated mutation analysis (Singer, M. S. *et al.*, 1996) and Fourier analysis of multiple OR sequences (Pilpel, Y. and Lancet, D., 1999; Man, O. *et al.*, 2004) further supported the hypothesis that variable residues are responsible for odorant binding. Alternatively, when cognate ligands for ORs are known, odorant-sensing residues have been predicted using a combination of computer modeling and docking simulation. A total of 10–20 residues in TM3, 4, 5, and 6 are predicted to be involved in ligand recognition and responsible for odorant specificity of ORs based on the coordinates of bacteriorhodopsin, a non-GPCR seven-transmembrane helix protein (Singer, M. S. and Shepherd, G. M., 1994), a later rhodopsin X-ray structure (Floriano, W. B. *et al.*, 2000; Singer, M. S., 2000), a recent computationally determined three-dimensional structure predicted using only the primary sequence (Vaidehi, N. *et al.*, 2002; Floriano, W. B. *et al.*, 2004; Hall, S. E. *et al.*, 2004; Hummel, P. *et al.*, 2005), and computer modeling and calculation of the lowest ligand-binding energy for several ORs.

A systematic experimental approach to identify the odorant-binding site was taken for mOR-EG (Katada, S. *et al.*, 2005). To define the odorant-binding environment, functional analysis was carried out on a series of site-directed mutants along with parallel ligand docking simulations. Most of the critical residues involved in odorant recognition, and therefore sensitive to mutation, were hydrophobic, and the binding pocket was formed by TM3, TM5, and TM6 (Katada, S. *et al.*, 2005) (Figure 11). The spatial location of the binding pocket is similar to that for other biogenic GPCRs, but unlike other GPCRs, which tend to form multiple electrostatic interactions with their ligands, hydrophobic amino acids appear to play critical roles in odorant recognition by ORs. The accuracy of the binding model was confirmed by

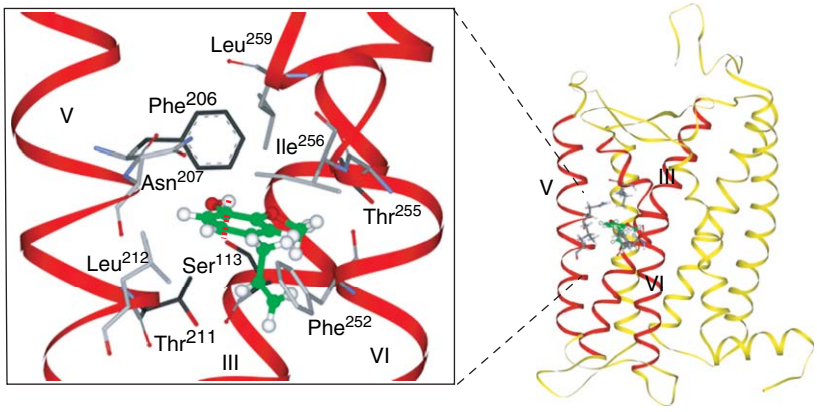

Figure 11 A model for binding of eugenol to mOR-EG and the orientation of amino acids in the binding site. Eugenol is shown in green, and TMIII, V, and VI are shown as red ribbons. Adapted from Katada, S., Hirokawa, T., Oka, Y., Suwa, M., and Touhara, K. 2005. Structural basis for a broad but selective ligand spectrum of a mouse olfactory receptor: mapping the odorant-binding site. J. Neurosci. 25, 1806–1815, Copyright 2005 by the Society of Neuroscience, with permission.

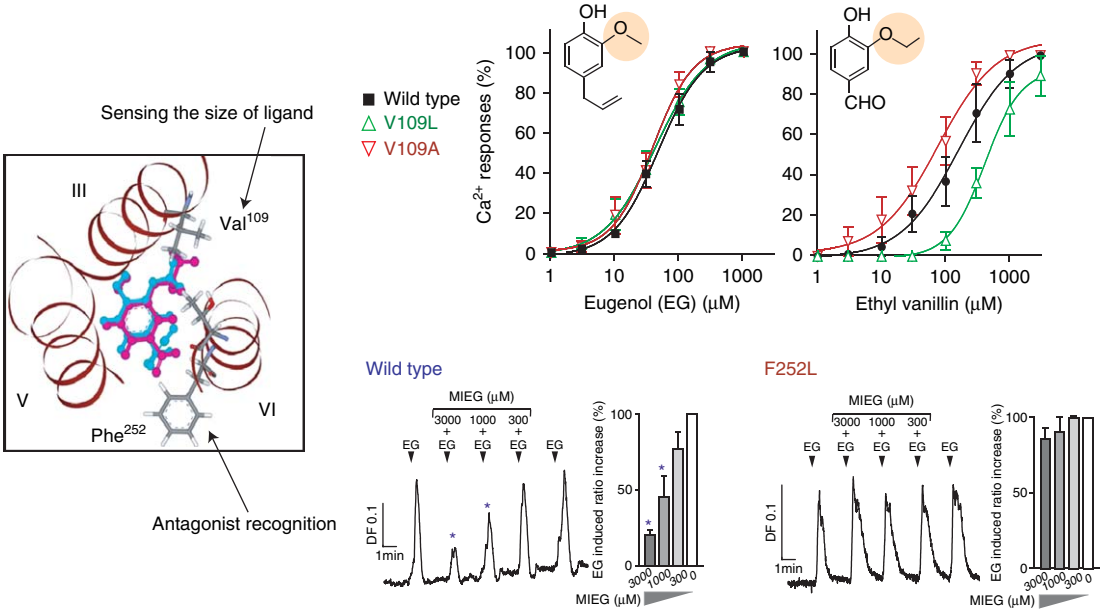

Figure 12 Roles of Val109 and Phe252 in the binding pocket of mOR-EG. Eugenol and ethyl vanillin are shown in blue and pink, respectively, in top view of the bound mOR-EG structures. The mutational analyses show that Val109 senses the size of the ligand, while Phe252 is involved in antagonist recognition (see Katada, S. *et al.*, 2005 for more detail). Adapted from Katada, S., Hirokawa, T., Oka, Y., Suwa, M., and Touhara, K. 2005. Structural basis for a broad but selective ligand spectrum of a mouse olfactory receptor: mapping the odorant-binding site. J. Neurosci. 25, 1806–1815, Copyright 2005 by the Society of Neuroscience, with permission.

the fact that single amino acid changes caused predictable changes in agonist and antagonist specificity (Katada, S. *et al.*, 2005) (Figure 12). Thus, the stereospecific receptor theory was proven by the functional identification of the odorant-binding site, and it appears that ligand information is transduced by the three-dimensional configuration of the binding pocket and its specific odorant ligand.

4.30.4.5 Odorant Sensitivity and Specificity

The sensitivity of ORs to odorants in heterologous expression systems is relatively high compared to that in the olfactory system; specifically, the threshold concentrations for the best ligand in each OR range from a few to several hundred micromolar (Mombaerts, P., 2004). This is not simply due to problems of the

heterologous expression system because the sensitivity of olfactory sensory neurons expressing the same OR is similar (Oka, Y. *et al.*, 2004b; 2006) (Figure 13(a)). The odorant sensitivity of glomeruli innervated by olfactory neurons expressing a defined OR, however, is approximately 1000-fold higher than that of peripheral neurons (Oka, Y. *et al.*, 2006) (Figure 13(a)). In addition, the specificity of the in vivo odorant response in an OR-defined glomerulus is different from that suggested by the *in vitro* pharmacology in a heterologous system (Oka, Y. *et al.*, 2006) (Figure 13(b)). The higher apparent sensitivity and specificity to odorants *in vivo* seems to be due to a contribution of the olfactory mucosa, which provides a site for efficiently concentrating odorants and carrying them to the receptor site. An important caveat to this is that the ligand specificity of ORs in heterologous OR expression systems may not always reflect the specificity observed in the olfactory bulb *in vivo*.

4.30.5 Function II: Others

4.30.5.1 Axon Guidance

Olfactory sensory neurons expressing a given OR project their axons to defined glomeruli in the olfactory bulb (Ressler, K. J. *et al.*, 1994; Vassar, R. *et al.*, 1994; Mombaerts, P. *et al.*, 1996) (Figure 14). Receptor deletion or swapping experiments suggest that the OR protein itself is instructive for the guidance of olfactory neuron axons (Wang, F. *et al.*, 1998). Indeed, the OR proteins are present in olfactory axonal terminals (Barnea, G. *et al.*, 2004; Strotmann, J. *et al.*, 2004) as well as in cells of the cribriform mesenchyme, which are involved in fasciculation and sorting of outgrowing axons (Schwarzenbacher, K. *et al.*, 2006). A point mutation in the OR protein results in the formation of novel glomeruli, indicating that the OR amino acid sequence encodes information about axonal identity (Feinstein, P. and Mombaerts, P., 2004). The OR, however, is not

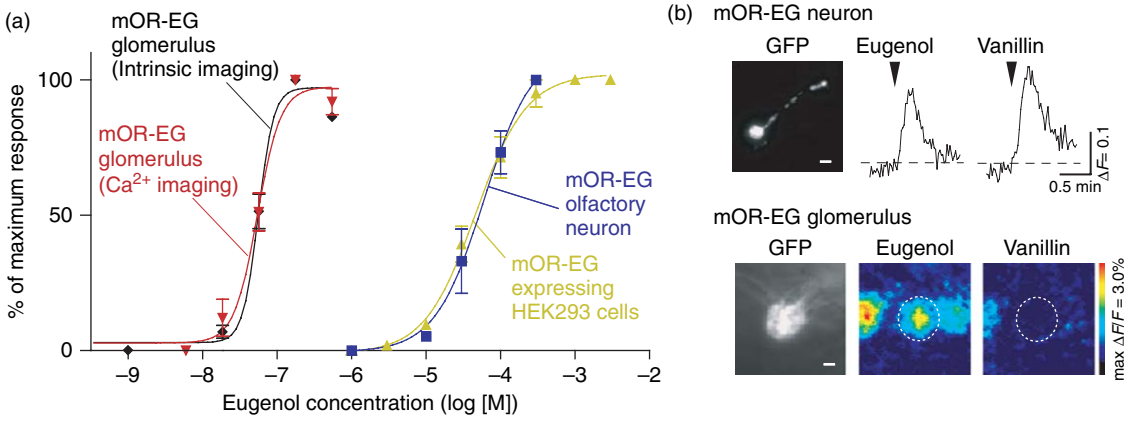

Figure 13 Different odorant sensitivity and specificity between olfactory neurons expressing mOR-EG and the corresponding mOR-EG glomerulus. (a) Dose–response analysis of mOR-EG *in vivo* and *in vitro*. The mOR-EG glomerulus exhibits higher sensitivity compared to the response properties determined in HEK293 cells or in mOR-EG-expressing neurons. (b) Odorant responses in mOR-EG-expressing olfactory neurons (upper panel) and in mOR-EG glomerulus (lower panel). The mOR-EG-expressing neurons showed responses to vanillin, whereas the mOR-EG glomerulus did not respond to vanillin (see Oka, Y. *et al.*, 2006 for more detail).

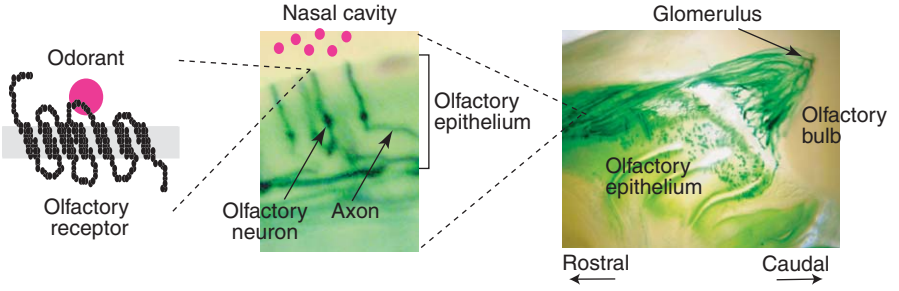

Figure 14 Fluorescent images of the olfactory epithelium and the olfactory bulb of gene-targeted mice expressing LacZ in mOR-EG-expressing olfactory neurons.

the only player in axonal convergence; membrane receptors such as the ephrin receptor and the neuropilin may be coordinately involved in determining the sensory map in the olfactory bulb (Pasterkamp, R. J. *et al.*, 1999; Cutforth, T. *et al.*, 2003). In addition, the instructive role in axon guidance is not restricted to an OR. Also, β2-adrenergic receptor can substitute for an OR in glomerular formation, suggesting that GPCRs have common functions (Feinstein, P. *et al.*, 2004). Both ORs and the β2-adrenergic receptor couple to the stimulatory G proteins, Gαs, which may account for the common functions of these receptors. In agreement with this, OR-mediated Gαs signaling has been shown to be one of the positional determinants (Imai, T. *et al.*, 2006). Thus, the OR proteins expressed on the olfactory neuronal cilia and dendrites recognize odorants from the external environment, whereas the same OR proteins localized on axon termini appear to function as key mediators of proper axon guidance.

4.30.5.2 Chemosensor

Analogous to axon guidance, wherein olfactory neurons are attracted and directed to a defined glomerulus by the ORs, testicular ORs are likely involved in proper navigation of sperm toward the egg in mammals (Spehr, M. *et al.*, 2006a). In sperm, human OR17-4 recognizes bourgeonal, a floral aldehyde odorant, resulting in induction of chemotaxis and chemokinesis (Spehr, M. *et al.*, 2003). Similarly, MOR23 expressed in mouse sperm recognizes the floral aldehyde odorant lyral, which regulates sperm motility (Fukuda, N. *et al.*, 2004) (Figure 15). Since both bourgeonal and lyral are synthetic fragrances, identification of the endogenous ligands for these ORs is necessary to demonstrate the biological relevance of sperm ORs. Multiple testicular ORs are expressed by various types of spermatids and spermatocytes in different developmental stages in mice, suggesting that some ORs are involved in spermatogenesis rather than in sperm physiology (Fukuda, N. and Touhara, K., 2006) (Figure 5). In any event, ORs may function as chemosensors in nonolfactory tissues.

4.30.5.3 Pheromone Detector

Pheromones are substances that are utilized for intraspecies communication (Karlson, P. and Luscher, M., 1959; Stowers, L. and Marton, T. F., 2005; Touhara, K., in press). In mice, pheromones are detected by two olfactory systems: the main olfactory system and the vomeronasal system (Halpern, M. and Martinez-Marcos, A., 2003; Baxi, K. N. *et al.*, 2006; Spehr, M. *et al.*, 2006b). Thus, the ORs in the main olfactory system recognize both odorants and volatile pheromones. In fish, ORs seem to play a role in recognizing putative pheromones such as bile acid, prostaglandin, and steroid derivatives (Friedrich, R. W. and Korsching, S. I., 1998; Sorensen, P. W. and Caprio, J., 1998; Luu, P. *et al.*, 2004). Similarly, some insect ORs are utilized as sex pheromone receptors (Nakagawa, T. *et al.*, 2005). In contrast to mammalian ORs, which function as monomers, formation of heterodimers is required for the function of ORs as pheromone sensors in insects (Nakagawa, T. *et al.*, 2005) (Figure 16). During evolution, each species

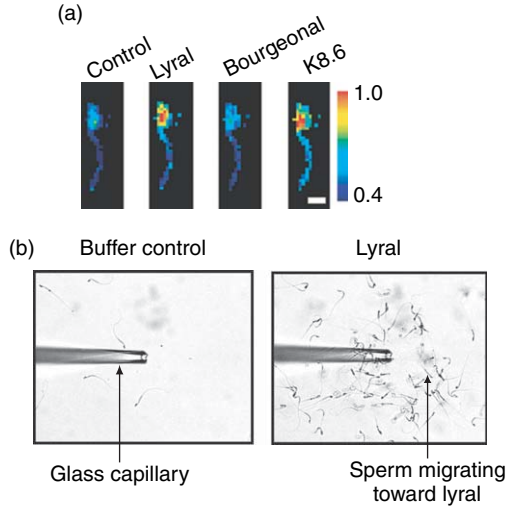

Figure 15 Responses of mouse sperm to lyral, a ligand for MOR23. (a) Pseudocolored image of Ca^{2+} levels in mature mouse sperm responding to lyral and K8.6. (b) Images of mouse sperm that show accumulation around the tip of a glass microcapillary containing lyral. Adapted from Fukuda, N., Yomogida, K., Okabe, M., and Touhara, K. 2004. Functional characterization of a mouse testicular olfactory receptor and its role in chemosensing and in regulation of sperm motility. J. Cell. Sci. 117, 5835–5845.

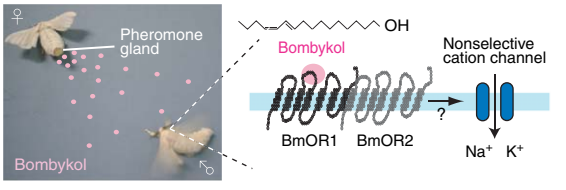

Figure 16 Responses of male silk moths to sex pheromone, bombykol, produced by female moths. Bombykol is recognized by a hetrodimeric complex of two olfactory receptors (ORs), BmOR1 and BmOR2, and elicits nonselective cation channel activity (see Nakagawa, T. *et al.*, 2005 for more detail).

selected an appropriate OR as a pheromone sensor, and the sensor has acquired unique signal transduction mechanisms, which provide high sensitivity and specificity for the target pheromone.

4.30.6 Remaining Problems

The discovery of the OR superfamily and subsequent experimental evidence validated the stereospecific receptor theory, which states that each functional group of an odorant is a molecular determinant for the odorant's interaction with an OR. The fact that the olfactory neuronal circuits follow the one-neuron one-receptor rule and OR-instructed axonal convergence suggests that a combinatorial receptor code for each odorant is transmitted to the olfactory bulb without the information being mixed.

Several questions remain to be answered. For example, how are OR proteins transported to the cilia? What is the mechanism mediating the negative feedback of OR expression? How is the zonal expression pattern formed? Is the presence of olfactory mucus crucial for the olfactory sensitivity and specificity? Is there an endogenous ligand for ORs expressed in nonolfactory tissues? Is the vibrational theory completely dead? How are small molecules such as CO_2 and H_2S recognized? What is the three-dimensional structure of an OR? What are the molecular dynamics of an OR upon ligand binding? Is there a relationship between OR polymorphism and anosmia? What are the differences in neuronal circuits between odorants with physiological effects and those without? Some of these questions will have been explored by the time that this review is in press, but there are always remaining questions because olfaction is the most mysterious of the senses.

Acknowledgments

I would like to thank the members of Touhara laboratory for providing data. This work was supported in part by grants from the Ministry of Education, Science, Sports, and Culture (MEXT), the Japan Society for the Promotion of Science (JSPS), and the Program for Promotion of Basic Research Activities for Innovative Biosciences (PROBRAIN) in Japan.

References

Abaffy, T., Matsunami, H., and Luetje, C. W. 2006. Functional analysis of a mammalian odorant receptor subfamily. J. Neurochem. 97, 1506–1518.

Amoore, J. E. 1963. Stereochemical theory of olfaction. Nature 198, 271–272.

Araneda, R. C., Kini, A. D., and Firestein, S. 2000. The molecular receptive range of an odorant receptor. Nat. Neurosci. 3, 1248–1255.

Asai, H., Kasai, H., Matsuda, Y., Yamazaki, N., Nagawa, F., Sakano, H., and Tsuboi, A. 1996. Genomic structure and transcription of a murine odorant receptor gene: differential initiation of transcription in the olfactory and testicular cells. Biochem. Biophys. Res. Commun. 221, 240–247.

Barnea, G., O'Donnell, S., Mancia, F., Sun, X., Nemes, A., Mendelsohn, M., and Axel, R. 2004. Odorant receptors on axon termini in the brain. Science 304, 1468.

Baxi, K. N., Dorries, K. M., and Eisthen, H. L. 2006. Is the vomeronasal system really specialized for detecting pheromones? Trends Neurosci. 29, 1–7.

Benton, R., Sachse, S., Michnick, S. W., and Vosshall, L. B. 2006. Atypical membrane topology and heteromeric function of Drosophila odorant receptors in vivo. PLoS Biol. 4, e20.

Blache, P., Gros, L., Salazar, G., and Bataille, D. 1998. Cloning and tissue distribution of a new rat olfactory receptor-like (OL2). Biochem. Biophys. Res. Commun. 242, 669–672.

Bozza, T., Feinstein, P., Zheng, C., and Mombaerts, P. 2002. Odorant receptor expression defines functional units in the mouse olfactory system. J. Neurosci. 22, 3033–3043.

Breer, H., Boekhoff, I., and Tareilus, E. 1990. Rapid kinetics of second messenger formation in olfactory transduction. Nature 345, 65–68.

Buck, L. B. 2004. The search for odorant receptors. Cell 116, S117–S119, 111 p following S119.

Buck, L. and Axel, R. 1991. A novel multigene family may encode odorant receptors: a molecular basis for odor recognition. Cell 65, 175–187.

Chess, A., Simon, I., Cedar, H., and Axel, R. 1994. Allelic inactivation regulates olfactory receptor gene expression. Cell 78, 823–834.

Clyne, P. J., Warr, C. G., Freeman, M. R., Lessing, D., Kim, J., and Carlson, J. R. 1999. A novel family of divergent seven-transmembrane proteins: candidate odorant receptors in Drosophila. Neuron 22, 327–338.

Cutforth, T., Moring, L., Mendelsohn, M., Nemes, A., Shah, N. M., Kim, M. M., Frisen, J., and Axel, R. 2003. Axonal ephrin-As and odorant receptors: coordinate determination of the olfactory sensory map. Cell 114, 311–322.

Dhallan, R. S., Yau, K. W., Schrader, K. A., and Reed, R. R. 1990. Primary structure and functional expression of a cyclic nucleotide-activated channel from olfactory neurons. Nature 347, 184–187.

Drutel, G., Arrang, J. M., Diaz, J., Wisnewsky, C., Schwartz, K., and Schwartz, J. C. 1995. Cloning of OL1, a putative olfactory receptor and its expression in the developing rat heart. Receptors Channels 3, 33–40.

Durzynski, L., Gaudin, J. C., Myga, M., Szydlowski, J., Gozdzicka-Jozefiak, A., and Haertle, T. 2005. Olfactory-like receptor cDNAs are present in human lingual cDNA libraries. Biochem. Biophys. Res. Commun. 333, 264–272.

Ehlers, A., Beck, S., Forbes, S. A., Trowsdale, J., Volz, A., Younger, R., and Ziegler, A. 2000. MHC-linked olfactory receptor loci exhibit polymorphism and contribute to extended HLA/OR-haplotypes. Genome Res. 10, 1968–1978.

Eklund, A. C., Belchak, M. M., Lapidos, K., Raha-Chowdhury, R., and Ober, C. 2000. Polymorphisms in the

HLA-linked olfactory receptor genes in the Hutterites. Hum. Immunol. 61, 711–717.
Feingold, E. A., Penny, L. A., Nienhuis, A. W., and Forget, B. G. 1999. An olfactory receptor gene is located in the extended human beta-globin gene cluster and is expressed in erythroid cells. Genomics 61, 15–23.
Feinstein, P. and Mombaerts, P. 2004. A contextual model for axonal sorting into glomeruli in the mouse olfactory system. Cell 117, 817–831.
Feinstein, P., Bozza, T., Rodriguez, I., Vassalli, A., and Mombaerts, P. 2004. Axon guidance of mouse olfactory sensory neurons by odorant receptors and the beta2 adrenergic receptor. Cell 117, 833–846.
Ferrand, N., Pessah, M., Frayon, S., Marais, J., and Garel, J. M. 1999. Olfactory receptors, Golf alpha and adenylyl cyclase mRNA expressions in the rat heart during ontogenic development. J. Mol. Cell. Cardiol. 31, 1137–1142.
Floriano, W. B., Vaidehi, N., and Goddard, W. A., III. 2004. Making sense of olfaction through predictions of the 3-D structure and function of olfactory receptors. Chem. Senses 29, 269–290.
Floriano, W. B., Vaidehi, N., Goddard, W. A., III. Singer, M. S., and Shepherd, G. M. 2000. Molecular mechanisms underlying differential odor responses of a mouse olfactory receptor. Proc. Natl. Acad. Sci. U.S.A. 97, 10712–10716.
Fox, A. N., Pitts, R. J., and Zwiebel, L. J. 2002. A cluster of candidate odorant receptors from the malaria vector mosquito, *Anopheles gambiae*. Chem. Senses 27, 453–459.
Freitag, J., Krieger, J., Strotmann, J., and Breer, H. 1995. Two classes of olfactory receptors in *Xenopus laevis*. Neuron 15, 1383–1392.
Friedrich, R. W. and Korsching, S. I. 1998. Chemotopic, combinatorial, and noncombinatorial odorant representations in the olfactory bulb revealed using a voltage-sensitive axon tracer. J. Neurosci. 18, 9977–9988.
Fukuda, N. and Touhara, K. 2006. Developmental expression patterns of testicular olfactory receptor genes during mouse spermatogenesis. Genes Cells 11, 71–81.
Fukuda, N., Yomogida, K., Okabe, M., and Touhara, K. 2004. Functional characterization of a mouse testicular olfactory receptor and its role in chemosensing and in regulation of sperm motility. J. Cell. Sci. 117, 5835–5845.
Gaillard, I., Rouquier, S., Pin, J. P., Mollard, P., Richard, S., Barnabe, C., Demaille, J., and Giorgi, D. 2002. A single olfactory receptor specifically binds a set of odorant molecules. Eur. J. Neurosci. 15, 409–418.
Gao, Q. and Chess, A. 1999. Identification of candidate Drosophila olfactory receptors from genomic DNA sequence. Genomics 60, 31–39.
Gaudin, J. C., Breuils, L., and Haertle, T. 2006. Mouse orthologs of human olfactory-like receptors expressed in the tongue. Gene 381, 42–48.
Gilad, Y., Wiebe, V., Przeworski, M., Lancet, D., and Paabo, S. 2004. Loss of olfactory receptor genes coincides with the acquisition of full trichromatic vision in primates. PLoS Biol. 2, E5.
Glusman, G., Yanai, I., Rubin, I., and Lancet, D. 2001. The complete human olfactory subgenome. Genome Res. 11, 685–702.
Grosmaitre, X., Vassalli, A., Mombaerts, P., Shepherd, G. M., and Ma, M. 2006. Odorant responses of olfactory sensory neurons expressing the odorant receptor MOR23: a patch clamp analysis in gene-targeted mice. Proc. Natl. Acad. Sci. U. S. A. 103, 1970–1975.
Hall, S. E., Floriano, W. B., Vaidehi, N., and Goddard, W. A., III. 2004. Predicted 3-D structures for mouse I7 and rat I7 olfactory receptors and comparison of predicted odor recognition profiles with experiment. Chem. Senses 29, 595–616.
Halpern, M. and Martinez-Marcos, A. 2003. Structure and function of the vomeronasal system: an update. Prog. Neurobiol. 70, 245–318.
Hill, C. A., Fox, A. N., Pitts, R. J., Kent, L. B., Tan, P. L., Chrystal, M. A., Cravchik, A., Collins, F. H., Robertson, H. M., and Zwiebel, L. J. 2002. G protein-coupled receptors in *Anopheles gambiae*. Science 298, 176–178.
Hummel, P., Vaidehi, N., Floriano, W. B., Hall, S. E., and Goddard, W. A., III. 2005. Test of the binding threshold hypothesis for olfactory receptors: explanation of the differential binding of ketones to the mouse and human orthologs of olfactory receptor 912-93. Protein Sci. 14, 703–710.
Imai, T., Suzuki, M., and Sakano, H. 2006. Roles of G protein-mediated cAMP signals in positioning glomeruli in the mouse olfactory bulb. Science 314, 657–6661.
Ishii, T., Serizawa, S., Kohda, A., Nakatani, H., Shiroishi, T., Okumura, K., Iwakura, Y., Nagawa, F., Tsuboi, A., and Sakano, H. 2001. Monoallelic expression of the odourant receptor gene and axonal projection of olfactory sensory neurones. Genes Cells 6, 71–78.
Iwema, C. L., Fang, H., Kurtz, D. B., Youngentob, S. L., and Schwob, J. E. 2004. Odorant receptor expression patterns are restored in lesion-recovered rat olfactory epithelium. J. Neurosci. 24, 356–369.
Jacquier, V., Prummer, M., Segura, J. M., Pick, H., and Vogel, H. 2006. Visualizing odorant receptor trafficking in living cells down to the single-molecule level. Proc. Natl. Acad. Sci. U.S.A.
Kajiya, K., Inaki, K., Tanaka, M., Haga, T., Kataoka, H., and Touhara, K. 2001. Molecular bases of odor discrimination: Reconstitution of olfactory receptors that recognize overlapping sets of odorants. J. Neurosci. 21, 6018–6025.
Kaluza, J. F., Gussing, F., Bohm, S., Breer, H., and Strotmann, J. 2004. Olfactory receptors in the mouse septal organ. J. Neurosci. Res. 76, 442–452.
Karlson, P. and Luscher, M. 1959. Pheromones: a new term for a class of biologically active substances. Nature 183, 55–56.
Katada, S., Hirokawa, T., Oka, Y., Suwa, M., and Touhara, K. 2005. Structural basis for a broad but selective ligand spectrum of a mouse olfactory receptor: mapping the odorant-binding site. J. Neurosci. 25, 1806–1815.
Katada, S., Nakagawa, T., Kataoka, H., and Touhara, K. 2003. Odorant response assays for a heterologously expressed olfactory receptor. Biochem. Biophys. Res. Commun. 305, 964–969.
Katada, S., Tanaka, M., and Touhara, K. 2004. Structural determinants for membrane trafficking and G protein selectivity of a mouse olfactory receptor. J. Neurochem. 90, 1453–1463.
Krautwurst, D., Yau, K. W., and Reed, R. R. 1998. Identification of ligands for olfactory receptors by functional expression of a receptor library. Cell 95, 917–926.
Krieger, J., Klink, O., Mohl, C., Raming, K., and Breer, H. 2003. A candidate olfactory receptor subtype highly conserved across different insect orders. J. Comp. Physiol. A Neuroethol. Sens. Neural Behav. Physiol. 189, 519–526.
Krieger, J., Raming, K., Dewer, Y. M., Bette, S., Conzelmann, S., and Breer, H. 2002. A divergent gene family encoding candidate olfactory receptors of the moth *Heliothis virescens*. Eur. J. Neurosci. 16, 619–628.
Lane, R. P., Cutforth, T., Young, J., Athanasiou, M., Friedman, C., Rowen, L., Evans, G., Axel, R., Hood, L., and Trask, B. J. 2001. Genomic analysis of orthologous mouse and human olfactory receptor loci. Proc. Natl. Acad. Sci. U.S.A. 98, 7390–7395.
Larsson, M. C., Domingos, A. I., Jones, W. D., Chiappe, M. E., Amrein, H., and Vosshall, L. B. 2004. Or83b encodes a

broadly expressed odorant receptor essential for Drosophila olfaction. Neuron 43, 703–714.
Levasseur, G., Persuy, M. A., Grebert, D., Remy, J. J., Salesse, R., and Pajot-Augy, E. 2003. Ligand-specific dose-response of heterologously expressed olfactory receptors. Eur. J. Biochem. 270, 2905–2912.
Lewcock, J. W. and Reed, R. R. 2004. A feedback mechanism regulates monoallelic odorant receptor expression. Proc. Natl. Acad. Sci. U.S.A. 101, 1069–1074.
Lin da, Y., Shea, S. D., and Katz, L. C. 2006. Representation of natural stimuli in the rodent main olfactory bulb. Neuron 50, 937–949.
Liu, A. H., Zhang, X., Stolovitzky, G. A., Califano, A., and Firestein, S. J. 2003. Motif-based construction of a functional map for mammalian olfactory receptors. Genomics 81, 443–456.
Lomvardas, S., Barnea, G., Pisapia, D. J., Mendelsohn, M., Kirkland, J., and Axel, R. 2006. Interchromosomal interactions and olfactory receptor choice. Cell 126, 403–413.
Lucretius, L. 1995. *On the Nature of Things: De rerum natura*. The Johns Hopkins Univ. Pr., Anthony M. Esolen, transl. Baltimore.
Luu, P., Acher, F., Bertrand, H. O., Fan, J., and Ngai, J. 2004. Molecular determinants of ligand selectivity in a vertebrate odorant receptor. J. Neurosci. 24, 10128–10137.
Malnic, B., Hirono, J., Sato, T., and Buck, L. B. 1999. Combinatorial receptor codes for odors. Cell 96, 713–723.
Man, O., Gilad, Y., and Lancet, D. 2004. Prediction of the odorant binding site of olfactory receptor proteins by human-mouse comparisons. Protein Sci. 13, 240–254.
Matarazzo, V., Clot-Faybesse, O., Marcet, B., Guiraudie-Capraz, G., Atanasova, B., Devauchelle, G., Cerutti, M., Etievant, P., and Ronin, C. 2005. Functional characterization of two human olfactory receptors expressed in the baculovirus Sf9 insect cell system. Chem. Senses 30, 195–207.
McClintock, T. S. and Sammeta, N. 2003. Trafficking prerogatives of olfactory receptors. Neuroreport 14, 1547–1552.
Miyamichi, K., Serizawa, S., Kimura, H. M., and Sakano, H. 2005. Continuous and overlapping expression domains of odorant receptor genes in the olfactory epithelium determine the dorsal/ventral positioning of glomeruli in the olfactory bulb. J. Neurosci. 25, 3586–3592.
Mombaerts, P. 2004. Genes and ligands for odorant, vomeronasal and taste receptors. Nat. Rev. Neurosci. 5, 263–278.
Mombaerts, P., Wang, F., Dulac, C., Chao, S. K., Nemes, A., Mendelsohn, M., Edmondson, J., and Axel, R. 1996. Visualizing an olfactory sensory map. Cell 87, 675–686.
Nakagawa, T., Sakurai, T., Nishioka, T., and Touhara, K. 2005. Insect sex-pheromone signals mediated by specific combinations of olfactory receptors. Science 307, 1638–1642.
Nakamura, T. and Gold, G. H. 1987. A cyclic nucleotide-gated conductance in olfactory receptor cilia. Nature 325, 442–444.
Nef, P., Hermans-Borgmeyer, I., Artieres-Pin, H., Beasley, L., Dionne, V. E., and Heinemann, S. F. 1992. Spatial pattern of receptor expression in the olfactory epithelium. Proc. Natl. Acad. Sci. U. S. A. 89, 8948–8952.
Neuhaus, E. M., Gisselmann, G., Zhang, W., Dooley, R., Stortkuhl, K., and Hatt, H. 2005. Odorant receptor heterodimerization in the olfactory system of *Drosophila melanogaster*. Nat. Neurosci. 8, 15–17.
Ngai, J., Chess, A., Dowling, M. M., Necles, N., Macagno, E. R., and Axel, R. 1993. Coding of olfactory information: topography of odorant receptor expression in the catfish olfactory epithelium. Cell 72, 667–680.
Niimura, Y. and Nei, M. 2005a. Comparative evolutionary analysis of olfactory receptor gene clusters between humans and mice. Gene 346, 13–21.
Niimura, Y. and Nei, M. 2005b. Evolutionary changes of the number of olfactory receptor genes in the human and mouse lineages. Gene 346, 23–28.
Niimura, Y. and Nei, M. 2005c. Evolutionary dynamics of olfactory receptor genes in fishes and tetrapods. Proc. Natl. Acad. Sci. U.S.A. 102, 6039–6044.
Norlin, E. M., Alenius, M., Gussing, F., Hagglund, M., Vedin, V., and Bohm, S. 2001. Evidence for gradients of gene expression correlating with zonal topography of the olfactory sensory map. Mol. Cell. Neurosci. 18, 283–295.
Oka, Y., Katada, S., Omura, M., Suwa, M., Yoshihara, Y., and Touhara, K. 2006. Functional odorant-receptor map in the mouse olfactory bulb: in vivo sensitivity and specificity. Neuron 52, 857–869.
Oka, Y., Nakamura, A., Watanabe, H., and Touhara, K. 2004a. An odorant derivative as an antagonist for an olfactory receptor. Chem Senses 29, 815–822.
Oka, Y., Omura, M., Kataoka, H., and Touhara, K. 2004b. Olfactory receptor antagonism between odorants. EMBO J. 23, 120–126.
Omura, M., Sekine, H., Shimizu, T., Kataoka, H., and Touhara, K. 2003. In situ Ca^{2+} imaging of odor responses in a coronal olfactory epithelium slice. Neuroreport 14, 1123–1127.
Otaki, J. M., Yamamoto, H., and Firestein, S. 2004. Odorant receptor expression in the mouse cerebral cortex. J. Neurobiol 58, 315–327.
Pace, U., Hanski, E., Salomon, Y., and Lancet, D. 1985. Odorant-sensitive adenylate cyclase may mediate olfactory reception. Nature 316, 255–258.
Pajot-Augy, E., Crowe, M., Levasseur, G., Salesse, R., and Connerton, I. 2003. Engineered yeasts as reporter systems for odorant detection. J. Recept. Signal Transduct. Res. 23, 155–171.
Parmentier, M., Libert, F., Schurmans, S., Schiffmann, S., Lefort, A., Eggerickx, D., Ledent, C., Mollereau, C., Gerard, C., Perret, J. *et al.* 1992. Expression of members of the putative olfactory receptor gene family in mammalian germ cells. Nature 355, 453–455.
Pasterkamp, R. J., Ruitenberg, M. J., and Verhaagen, J. 1999. Semaphorins and their receptors in olfactory axon guidance. Cell. Mol. Biol. (Noisy-le-grand) 45, 763–779.
Pilpel, Y. and Lancet, D. 1999. The variable and conserved interfaces of modeled olfactory receptor proteins. Protein Sci. 8, 969–977.
Qasba, P. and Reed, R. R. 1998. Tissue and zonal-specific expression of an olfactory receptor transgene. J. Neurosci. 18, 227–236.
Quignon, P., Giraud, M., Rimbault, M., Lavigne, P., Tacher, S., Morin, E., Retout, E., Valin, A. S., Lindblad-Toh, K., Nicolas, J., and Galibert, F. 2005. The dog and rat olfactory receptor repertoires. Genome Biol. 6, R83.
Ressler, K. J., Sullivan, S. L., and Buck, L. B. 1993. A zonal organization of odorant receptor gene expression in the olfactory epithelium. Cell 73, 597–609.
Ressler, K. J., Sullivan, S. L., and Buck, L. B. 1994. Information coding in the olfactory system: evidence for a stereotyped and highly organized epitope map in the olfactory bulb. Cell 79, 1245–1255.
Robertson, H. M., Warr, C. G., and Carlson, J. R. 2003. Molecular evolution of the insect chemoreceptor gene superfamily in *Drosophila melanogaster*. Proc. Natl. Acad. Sci. U. S. A. 100 (Suppl. 2), 14537–14542.
Saito, H., Kubota, M., Roberts, R. W., Chi, Q., and Matsunami, H. 2004. RTP family members induce functional expression of mammalian odorant receptors. Cell 119, 679–691.

Schwarzenbacher, K., Fleischer, J., and Breer, H. 2005. Formation and maturation of olfactory cilia monitored by odorant receptor-specific antibodies. Histochem. Cell Biol. 123, 419–428.

Schwarzenbacher, K., Fleischer, J., and Breer, H. 2006. Odorant receptor proteins in olfactory axons and in cells of the cribriform mesenchyme may contribute to fasciculation and sorting of nerve fibers. Cell Tissue Res. 323, 211–219.

Serizawa, S., Ishii, T., Nakatani, H., Tsuboi, A., Nagawa, F., Asano, M., Sudo, K., Sakagami, J., Sakano, H., Ijiri, T., Matsuda, Y., Suzuki, M., Yamamori, T., and Iwakura, Y. 2000. Mutually exclusive expression of odorant receptor transgenes. Nat. Neurosci. 3, 687–693.

Serizawa, S., Miyamichi, K., Nakatani, H., Suzuki, M., Saito, M., Yoshihara, Y., and Sakano, H. 2003. Negative feedback regulation ensures the one receptor–one olfactory neuron rule in mouse. Science 302, 2088–2094.

Serizawa, S., Miyamichi, K., and Sakano, H. 2004. One neuron–one receptor rule in the mouse olfactory system. Trends Genet. 20, 648–653.

Shirokova, E., Schmiedeberg, K., Bedner, P., Niessen, H., Willecke, K., Raguse, J. D., Meyerhof, W., and Krautwurst, D. 2005. Identification of specific ligands for orphan olfactory receptors. G protein-dependent agonism and antagonism of odorants. J. Biol. Chem. 280, 11807–11815.

Shykind, B. M. 2005. Regulation of odorant receptors: one allele at a time. Hum. Mol. Genet. 14 (Spec No. 1), R33–R39.

Shykind, B. M., Rohani, S. C., O'Donnell, S., Nemes, A., Mendelsohn, M., Sun, Y., Axel, R., and Barnea, G. 2004. Gene switching and the stability of odorant receptor gene choice. Cell 117, 801–815.

Singer, M. S. 2000. Analysis of the molecular basis for octanal interactions in the expressed rat 17 olfactory receptor. Chem. Senses 25, 155–165.

Singer, M. S. and Shepherd, G. M. 1994. Molecular modeling of ligand–receptor interactions in the OR5 olfactory receptor. Neuroreport 5, 1297–1300.

Singer, M. S., Weisinger-Lewin, Y., Lancet, D., and Shepherd, G. M. 1996. Positive selection moments identify potential functional residues in human olfactory receptors. Receptors Channels 4, 141–147.

Sklar, P. B., Anholt, R. R., and Snyder, S. H. 1986. The odorant-sensitive adenylate cyclase of olfactory receptor cells. Differential stimulation by distinct classes of odorants. J. Biol. Chem. 261, 15538–15543.

Sorensen, P. W. and Caprio, J. 1998. Chemoreception. In: *The Physiology of Fishes* (*ed*. D. H. Evans), pp. 375–405. CRC Press.

Spehr, M., Gisselmann, G., Poplawski, A., Riffell, J. A., Wetzel, C. H., Zimmer, R. K., and Hatt, H. 2003. Identification of a testicular odorant receptor mediating human sperm chemotaxis. Science 299, 2054–2058.

Spehr, M., Schwane, K., Riffell, J. A., Zimmer, R. K., and Hatt, H. 2006a. Odorant receptors and olfactory-like signaling mechanisms in mammalian sperm. Mol. Cell. Endocrinol. 250, 128–136.

Spehr, M., Spehr, J., Ukhanov, K., Kelliher, K. R., Leinders-Zufall, T., and Zufall, F. 2006b. Parallel processing of social signals by the mammalian main and accessory olfactory systems. Cell. Mol. Life Sci. 63, 1476–1484.

Stowers, L. and Marton, T. F. 2005. What is a pheromone? Mammalian pheromones reconsidered. Neuron 46, 699–702.

Strader, C. D., Fong, T. M., Tota, M. R., and Underwood, D. 1994. Structure and function of G protein-coupled receptors. Annu. Rev. Biochem. 63, 101–132.

Strotmann, J., Hoppe, R., Conzelmann, S., Feinstein, P., Mombaerts, P., and Breer, H. 1999. Small subfamily of olfactory receptor genes: structural features, expression pattern and genomic organization. Gene 236, 281–291.

Strotmann, J., Levai, O., Fleischer, J., Schwarzenbacher, K., and Breer, H. 2004. Olfactory receptor proteins in axonal processes of chemosensory neurons. J. Neurosci. 24, 7754–7761.

Strotmann, J., Wanner, I., Helfrich, T., Beck, A., and Breer, H. 1994. Rostro-caudal patterning of receptor-expressing olfactory neurones in the rat nasal cavity. Cell Tissue Res. 278, 11–20.

Strotmann, J., Wanner, I., Helfrich, T., and Breer, H. 1995. Receptor expression in olfactory neurons during rat development: in situ hybridization studies. Eur. J. Neurosci. 7, 492–500.

Strotmann, J., Wanner, I., Krieger, J., Raming, K., and Breer, H. 1992. Expression of odorant receptors in spatially restricted subsets of chemosensory neurones. Neuroreport 3, 1053–1056.

Sullivan, S. L., Adamson, M. C., Ressler, K. J., Kozak, C. A., and Buck, L. B. 1996. The chromosomal distribution of mouse odorant receptor genes. Proc. Natl. Acad. Sci. U.S.A. 93, 884–888.

Sullivan, S. L., Bohm, S., Ressler, K. J., Horowitz, L. F., and Buck, L. B. 1995. Target-independent pattern specification in the olfactory epithelium. Neuron 15, 779–789.

Tacher, S., Quignon, P., Rimbault, M., Dreano, S., Andre, C., and Galibert, F. 2005. Olfactory receptor sequence polymorphism within and between breeds of dogs. J. Hered. 96, 812–816.

Tian, H. and Ma, M. 2004. Molecular organization of the olfactory septal organ. J. Neurosci. 24, 8383–8390.

Touhara, K. 2002. Odor discrimination by G protein-coupled olfactory receptors. Microsc. Res. Tech. 58, 135–141.

Touhara, K. Molecular biology of peptide pheromone production and reception in mice. Adv. Genet. (in press).

Touhara, K., Katada, S., Nakagawa, T., and Oka, Y. 2006. Ligand screening of olfactory receptors. In: *G Protein-Coupled Receptors: Structure, Function, and Ligand Screening* (*eds*. T. Haga and S. Takeda), pp. 85–109. CRC press.

Touhara, K., Sengoku, S., Inaki, K., Tsuboi, A., Hirono, J., Sato, T., Sakano, H., and Haga, T. 1999. Functional identification and reconstitution of an odorant receptor in single olfactory neurons. Proc. Natl. Acad. Sci. U. S. A. 96, 4040–4045.

Vaidehi, N., Floriano, W. B., Trabanino, R., Hall, S. E., Freddolino, P., Choi, E. J., Zamanakos, G., and Goddard, W. A., III. 2002. Prediction of structure and function of G protein-coupled receptors. Proc. Natl. Acad. Sci. U. S. A. 99, 12622–12627.

Vanderhaeghen, P., Schurmans, S., Vassart, G., and Parmentier, M. 1993. Olfactory receptors are displayed on dog mature sperm cells. J. Cell Biol. 123, 1441–1452.

Vanderhaeghen, P., Schurmans, S., Vassart, G., and Parmentier, M. 1997a. Molecular cloning and chromosomal mapping of olfactory receptor genes expressed in the male germ line: evidence for their wide distribution in the human genome. Biochem. Biophys. Res. Commun. 237, 283–287.

Vanderhaeghen, P., Schurmans, S., Vassart, G., and Parmentier, M. 1997b. Specific repertoire of olfactory receptor genes in the male germ cells of several mammalian species. Genomics 39, 239–246.

Vassalli, A., Rothman, A., Feinstein, P., Zapotocky, M., and Mombaerts, P. 2002. Minigenes impart odorant receptor-specific axon guidance in the olfactory bulb. Neuron 35, 681–696.

Vassar, R., Chao, S. K., Sitcheran, R., Nunez, J. M., Vosshall, L. B., and Axel, R. 1994. Topographic organization of sensory projections to the olfactory bulb. Cell 79, 981–991.

Vassar, R., Ngai, J., and Axel, R. 1993. Spatial segregation of odorant receptor expression in the mammalian olfactory epithelium. Cell 74, 309–318.

Volz, A., Ehlers, A., Younger, R., Forbes, S., Trowsdale, J., Schnorr, D., Beck, S., and Ziegler, A. 2003. Complex

transcription and splicing of odorant receptor genes. J. Biol. Chem. 278, 19691–19701.
Von Dannecker, L. E., Mercadante, A. F., and Malnic, B. 2006. Ric-8B promotes functional expression of odorant receptors. Proc. Natl. Acad. Sci. U. S. A. 103, 9310–9314.
Vosshall, L. B., Amrein, H., Morozov, P. S., Rzhetsky, A., and Axel, R. 1999. A spatial map of olfactory receptor expression in the Drosophila antenna. Cell 96, 725–736.
Walensky, L. D., Roskams, A. J., Lefkowitz, R. J., Snyder, S. H., and Ronnett, G. V. 1995. Odorant receptors and desensitization proteins colocalize in mammalian sperm. Mol. Med. 1, 130–141.
Wang, F., Nemes, A., Mendelsohn, M., and Axel, R. 1998. Odorant receptors govern the formation of a precise topographic map. Cell 93, 47–60.
Weber, M., Pehl, U., Breer, H., and Strotmann, J. 2002. Olfactory receptor expressed in ganglia of the autonomic nervous system. J. Neurosci. Res. 68, 176–184.
Weth, F., Nadler, W., and Korsching, S. 1996. Nested expression domains for odorant receptors in zebrafish olfactory epithelium. Proc. Natl. Acad. Sci. U. S. A. 93, 13321–13326.
Wetzel, C. H., Oles, M., Wellerdieck, C., Kuczkowiak, M., Gisselmann, G., and Hatt, H. 1999. Specificity and sensitivity of a human olfactory receptor functionally expressed in human embryonic kidney 293 cells and *Xenopus laevis* oocytes. J. Neurosci. 19, 7426–7433.
Young, J. M. and Trask, B. J. 2002. The sense of smell: genomics of vertebrate odorant receptors. Hum. Mol. Genet. 11, 1153–1160.
Young, J. M., Shykind, B. M., Lane, R. P., Tonnes-Priddy, L., Ross, J. A., Walker, M., Williams, E. M., and Trask, B. J. 2003. Odorant receptor expressed sequence tags demonstrate olfactory expression of over 400 genes, extensive alternate splicing and unequal expression levels. Genome Biol. 4, R71.
Yuan, T. T., Toy, P., McClary, J. A., Lin, R. J., Miyamoto, N. G., and Kretschmer, P. J. 2001. Cloning and genetic characterization of an evolutionarily conserved human olfactory receptor that is differentially expressed across species. Gene 278, 41–51.
Zhang, X. and Firestein, S. 2002. The olfactory receptor gene superfamily of the mouse. Nat. Neurosci. 5, 124–133.
Zhang, X., Rogers, M., Tian, H., Zou, D. J., Liu, J., Ma, M., Shepherd, G. M., and Firestein, S. J. 2004. High-throughput microarray detection of olfactory receptor gene expression in the mouse. Proc. Natl. Acad. Sci. U.S.A. 101, 14168–14173.
Zhao, H., Ivic, L., Otaki, J. M., Hashimoto, M., Mikoshiba, K., and Firestein, S. 1998. Functional expression of a mammalian odorant receptor. Science 279, 237–242.
Zozulya, S., Echeverri, F., and Nguyen, T. 2001. The human olfactory receptor repertoire. Genome Biol. 2, RESEARCH0018.

4.31 Regulation of Expression of Odorant Receptor Genes

A Tsuboi and H Sakano, University of Tokyo, Tokyo, Japan

© 2008 Elsevier Inc. All rights reserved.

4.31.1	**Organization and Structure of the Odorant Receptor Genes**	545
4.31.2	**Zone-Specific Expression of Odorant Receptor Genes in the Olfactory Epithelium**	546
4.31.2.1	Class I Odorant Receptors	546
4.31.2.2	Class II Odorant Receptors	546
4.31.3	**Single Odorant Receptor Expression in Each Olfactory Sensory Neuron**	546
4.31.4	**Allelic Exclusion of Odorant Receptor Genes**	547
4.31.5	**Single Odorant Receptor Gene Expression**	547
4.31.5.1	Positive Regulation	547
4.31.5.2	Negative Regulation	548
4.31.6	***Cis*-Elements and *Trans*-Factors for Odorant Receptor Gene Expression**	550
4.31.7	**Conclusion**	550
References		550

Glossary

ISH *In situ* hybridization
LCR Locus control region
OB Olfactory bulb
OE Olfactory epithelium
OR Odorant receptor
OSN Olfactory sensory neuron

4.31.1 Organization and Structure of the Odorant Receptor Genes

A multigene family encoding odorant receptor (OR) molecules was first identified in rat, which consists of hundreds of related OR genes (Buck, L. and Axel, R., 1991). In humans, only ~350 of the 800 OR genes have an intact open reading frame and are assumed to be functional (Glusman, G. *et al.*, 2001; Malnic, B. *et al.*, 2004). In the mouse, of ~1400 OR sequences, some 20% are pseudogenes (Young, J. M. *et al.*, 2002; Zhang, X. and Firestein, S., 2002; Godfrey, P. A. *et al.*, 2004; Zhang, X. *et al.*, 2004a). The mouse repertoire of ~1100 functional OR genes is the largest multigene family that encompasses ~5% of all genes. Mouse ORs are grouped into ~230 subfamilies, based on the amino acid identities of >40% (Zhang, X. and Firestein, S., 2002). Vertebrate OR genes are divided phylogenetically into two different classes, I and II. The class I genes resemble the fish OR genes, while the class II genes are unique to terrestrial vertebrates. The mouse OR genes are clustered at ~50 different loci spread over almost all chromosomes. Each cluster contains 1–189 OR genes, with an average intergenic distance of ~25 kb. Most OR genes are composed of two to five exons, where usually one exon encodes the entire protein. At least two-thirds of OR genes exhibit multiple transcriptional variants with alternative isoforms of noncoding exons (Young, J. M. *et al.*, 2003). Comparative analysis of the mouse and human OR genes revealed that coding homologies within the clusters are accounted for by recent gene duplication as well as gene conversion among the coding sequences (Nagawa, F. *et al.*, 2002). To maintain the integrity of the domain structure of the olfactory sensory map, gene conversion may have played an active role in maintaining the sequence similarities between the paralogs of the OR genes.

4.31.2 Zone-Specific Expression of Odorant Receptor Genes in the Olfactory Epithelium

In rodents, the olfactory epithelium (OE) can be divided into at least four distinct zones, based on the expression patterns of OR genes (Ressler, K. J. *et al.*, 1993; Vassar, R. *et al.*, 1993; Strotmann, J. *et al.*, 1994a; 1994b). The most dorsomedial zone of the OE is defined as zone 1, according to the nomenclature of Sullivan S. L. *et al.* (1996). Zone 1 olfactory sensory neurons (OSNs) are positive for olfactory medium-chain acyl-CoA synthetase (O-MACS) (Oka, Y. *et al.*, 2003), but negative for olfactory cell adhesion molecule (OCAM) (Yoshihara, Y. *et al.*, 1997). Conversely, nonzone 1 OSNs are negative for O-MACS, but positive for OCAM.

4.31.2.1 Class I Odorant Receptors

The class I ORs were first identified in fishes (Ngai, J. *et al.*, 1993) and later found in amphibians (Freitag, J. *et al.*, 1995). They are assumed to recognize water-soluble odorous ligands. Class I ORs are also found in mammals, including human (Glusman, G. *et al.*, 2001; Malnic, B. *et al.*, 2004) and mouse (Zhang, X. and Firestein, S., 2002; Young, J. M. *et al.*, 2002; Zhang, X. *et al.*, 2004a; Godfrey, P. A. *et al.*, 2004). In the mouse, there are over 150 class I OR genes, classified into 42 subfamilies (Zhang, X. and Firestein, S., 2002; Zhang, X. *et al.*, 2004a). They are all clustered at a single locus on the mouse chromosome 7. A high-throughput microarray and *in situ* hybridization analyses revealed that almost all class I OR genes are expressed in zone 1 (Zhang, X. *et al.*, 2004b; Tsuboi, A. *et al.* 2006). It is possible that they are coordinately regulated by a common locus control region (LCR) and/or promoter sequences.

4.31.2.2 Class II Odorant Receptors

In contrast to class I, class II OR genes account for a large share of the mammalian OR repertoire. ISH analyses with various OR gene probes demonstrated that each OR gene is expressed in a restricted area in the OE. It has been reported that OSNs expressing a given OR gene are confined to one of the four OE zones but are randomly distributed within the zone (Ressler, K. J. *et al.*, 1993; Vassar, R. *et al.*, 1993; Strotmann, J. *et al.*, 1994a; 1994b). This appears to be true for zone 1-specific class I genes (Tsuboi, A. *et al.*, 2006). However, for most class II OR gene, the expression area is not always confined to one of the four conventional zones (Norlin, E. M. *et al.*, 2001; Iwema, C. L. *et al.*, 2004; Miyamichi, K. *et al.*, 2005). Expression areas appear to be specific to each OR gene and are arranged in an overlapping and continuous manner in the OE. It was demonstrated by DiI retrograde staining experiments that the dorsal/ventral arrangement of glomeruli in the olfactory bulb (OB) is well correlated with the expression areas of corresponding ORs along the dorsomedial/ventrolateral (DM/VL) axis in the OE (Miyamichi, K. *et al.*, 2005). How is the area-specific expression regulated for the OR genes? It has been assumed that zone-specific transcription factors for the OR genes are responsible for the regulation. However, if the expression areas of various ORs are arranged in a continuous and overlapping manner, we may have to consider an alternative mechanism, one that detects a gradient or the relative location in the OE for each OR gene along the DM/VL axis. If this is the case, the choice of the OR genes may be more restricted by the location of the OSN in the OE than what has been thought.

4.31.3 Single Odorant Receptor Expression in Each Olfactory Sensory Neuron

OSN axons expressing the same OR converge to a specific set of glomeruli in the OB. In the mammalian olfactory system, single OR gene choice and OR-instructed axonal projection are fundamental to the conversion of olfactory signals to a topographic map in the OB. Quantitative analysis of ISH led to the suggestion that each OSN expresses a limited member of OR gene, possibly one (Ngai, J. *et al.*, 1993; Ressler, K. J. *et al.*, 1993; Vassar, R. *et al.*, 1993). Subsequent cDNA analyses of a single OSN revealed that only one OR is expressed in each cell (Malnic, B. *et al.*, 1999). The first evidence for the one glomerulus–one receptor rule came from ISH of OB slices detecting OR mRNA at the axon termini within a glomerulus (Ressler, K. J. *et al.*, 1994; Vassar, R. *et al.*, 1994; Tsuboi, A. *et al.*, 1999; 2006). Each OR probe detected a pair of glomeruli, one glomerulus on the lateral and the other on the medial side of the OB. Subsequent studies using the marker-tagged OR gene allowed visualization of individual axons (Mombaerts, P. *et al.*, 1996; Wang, F. *et al.*, 1998). In such animals, all OSN axons expressing a given OR converge on a

specific set of glomeruli. Thus, odorant stimuli that have activated OSNs in the OE are converted to a topographic map of activated glomeruli, that is, an odor map in the OB (Uchida, N. *et al.*, 2000).

4.31.4 Allelic Exclusion of Odorant Receptor Genes

Autosomal genes come in two alleles, the paternal and maternal, and most of them are expressed biallelically. However, some are expressed monoallelically, for example, the antigen receptor genes and a few interleukin genes. Allelic exclusion was also observed in the OR gene system by using PCR to detect the polymorphisms in the transcripts from the paternal and maternal alleles of a particular OR gene (Chess, A. *et al.*, 1994). Gene-targeted mice, in which both alleles were differently tagged, have demonstrated the monoallelic expression of the OR gene (Strotmann, J. *et al.*, 2000): among thousands of cells examined, no OSN expressed both markers, simultaneously. Furthermore, the nuclei of OSNs were analyzed by fluorescent *in situ* hybridization (FISH) using OR gene probes (Ishii, T. *et al.*, 2001). RNA- and DNA-FISH were performed to detect the transcriptionally active site and the chromosomal location of the genomic sequence, respectively. In this experiment, DNA-FISH detected two genomic loci in the nuclei, one for the paternal and the other for the maternal allele, while RNA-FISH detected the primary transcripts at only one of the two genomic sites. Together, these results confirmed the monoallelic expression of the OR gene. Monoallelic expression of OR molecules appears to be quite important, not only in recognizing the ligand, but also in projecting axons to a specific site in the OB. If two different OR molecules were expressed from both alleles, this would cause confusion in the bundling and pathfinding of OSN axons.

Exclusion has also been found between the endogenous and the transgenic OR gene alleles, and even among the tandemly linked transgenic alleles with the same coding and promoter sequences (Serizawa, S. *et al.*, 2000). These studies demonstrate that under any circumstance, no more than one OR allele can be expressed in each neuron. Such an unusual mode of gene expression, monoallelic and mutually exclusive, has previously been shown only for the antigen receptor genes of the immune system.

4.31.5 Single Odorant Receptor Gene Expression

4.31.5.1 Positive Regulation

What kind of mechanisms would be possible to maintain the expression of only a single OR gene in each OSN? On the basis of previous studies on other multigene families, three activation mechanisms have been considered for the choice and activation of OR genes (Kratz, E. *et al.*, 2002):

1. DNA recombination, which brings a promoter and the enhancer region into close proximity;
2. gene conversion, which transfers a copy of the gene into the expression cassette; and
3. LCR, which interacts with only one promoter site.

Irreversible DNA changes, that is, recombination and gene conversion, have been attractive explanations for single OR gene expression because of the many parallels between the immune and the olfactory systems. However, two groups have independently cloned mice from postmitotic OSN nuclei, and found that the mice showed no irreversible DNA changes in the OR genes (Eggan, K. *et al.*, 2004; Li, J. *et al.*, 2004). Furthermore, these mice did not exhibit monoclonal expression of the OR in the donor OSN. Thus, the DNA rearrangement models for OR gene activation were finally excluded. Because the gene translocation models appeared unlikely, the third possibility was explored, a *cis*-acting DNA region, for example, LCR, that might regulate the expression of the OR genes. Sequence comparison of the mouse and human genomes revealed a 2 kb homology (H) region far upstream of the *MOR28* cluster (Figure 1) (Nagawa, F. *et al.*, 2002). Deletion of the H region abolished the expression of all OR gene members in the cluster on a yeast artificial chromosome (YAC) transgene (Serizawa, S. *et al.*, 2003). Furthermore, attachment of the H region to the truncated transgenic constructs lacking the upstream sequence restored the expression of the OR gene cluster (Serizawa, S. *et al.*, 2003). Interestingly, when the H region was relocated closer to the cluster, the number of OSNs expressing the proximal OR gene was greatly increased. This probably explains why the H region is located far from the OR gene cluster in the chromosome. If the H region were located too close to the cluster, the proximal OR gene would be activated frequently and the downstream genes would rarely be chosen. These results indicate that the H region is a *cis*-acting LCR that activates the *MOR28* cluster, although it is yet to be studied whether the LCR is commonly

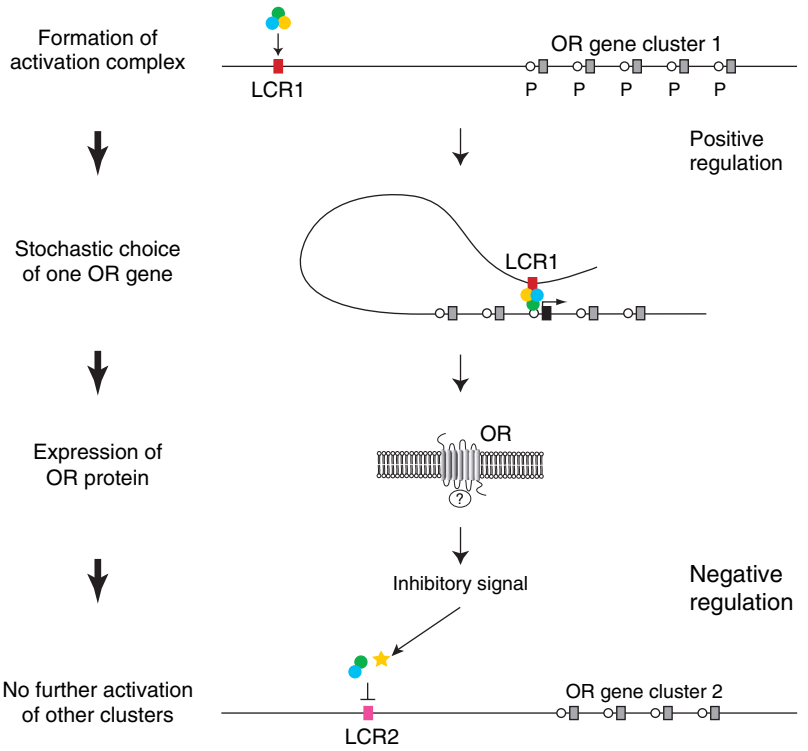

Figure 1 A model for the single odorant receptor (OR) gene expression. It is assumed that the activation complex formed in the locus control region (LCR) stochastically chooses one promoter (P) site by random collision, activating one particular OR gene member within the cluster (positive regulation). Once a functional gene is expressed, the OR molecules may transmit inhibitory signals to block the further activation of additional OR genes or clusters (negative regulation). Stochastic activation of an OR gene and negative feedback regulation by the OR gene product, together, can ensure the maintenance of the one receptor–one neuron rule in the mammalian olfactory system.

found in other OR gene clusters. In some transgenic experiments, a short stretch of DNA containing only the exons of the OR gene and its promoter are sufficient for the transgene to be expressed (Qasba, P. and Reed, R. R., 1998; Vassalli, A. *et al.*, 2002; Lewcock, J. W. and Reed, R. R., 2004). How does this happen? It is possible that these short DNA segments contain an enhancer or have integrated into a transcriptionally active region of chromatin, nearby another enhancer or LCR. It appears that two regulatory regions, LCR and promoter, cooperate in expressing the OR genes. It is possible that the chromatin-remodeling complex formed in the LCR activates the OR gene cluster, and that the LCR–promoter association initiates the transcription of the targeted OR gene (Figure 1).

4.31.5.2 Negative Regulation

It is important to ask how the expression of one particular OR gene is maintained. It appears that the activation complex formed in the LCR interacts with only one promoter site in the OR gene cluster (Figure 1), as has been reported for other gene systems, for example, the human visual pigment genes (Wang, Y. *et al.*, 1999; Smallwood, P. M. *et al.*, 2002) and globin genes (Li, Q. *et al.*, 1999). However, this would not preclude the activation of a second OR from the other allele or other OR gene clusters. To achieve mutually exclusive expression, negative feedback regulation may be needed to prohibit the further activation of other OR genes or OR gene clusters. It is known that a substantial number of pseudogenes are present in the mammalian OR gene families; ~20% of total OR genes in mouse (Young, J. M. *et al.*, 2002; Zhang, X. and Firestein, S., 2002; Godfrey, P. A. *et al.*, 2004; Zhang, X. *et al.*, 2004a) and ~60% in human are nonfunctional (Glusman, G. *et al.*, 2001; Malnic, B. *et al.*, 2004). In the scenario where the activated LCR has committed to a pseudogene, another LCR must undergo a similar process to ensure the activation of an intact OR gene. Once a functional OR gene has been chosen

and expressed, this trial must be halted. It has been proposed that the functional OR proteins may prevent further activation of other OR genes in the cell (Figure 2). Coexpression analysis of OSNs with the naturally occurring frameshift mutants supported the feedback mechanism (Serizawa, S. *et al.*, 2003) (Figure 2). Activation of secondary OR genes was also seen with transgenic OR genes lacking either the entire coding region (Serizawa, S. *et al.*, 2003; Feinstein, P. *et al.*, 2004; Lewcock, J. W. and Reed, R. R., 2004; Shykind, B. M. *et al.*, 2004) or the start codon (Lewcock, J. W. and Reed, R. R., 2004) (Figure 2). These observations suggest that the OR gene product – not mRNA but protein – has a regulatory role in preventing the secondary activation of other OR genes (Figure 2). How is this negative regulation achieved? In the antigen receptor genes, further V(D)J joining ceases as soon as a functional gene is generated, whereas rearrangement continues when the joining is unsuccessful (i.e., out-of-frame). For the Ig heavy-chain genes, the pre-B-cell receptor provides an inhibitory signal via spleen tyrosine kinase (Syk) (Schweighoffer, E. *et al.*, 2003) to preclude further rearrangement in the heavy-chain locus, possibly by changes in chromatin structure (Karasuyama, H. *et al.*, 1996; Chowdhury, D. and Sen, R., 2004; Goldmit, M. and Bergman, Y., 2004; Mostoslavsky, R. *et al.*, 2004). An analogous feedback regulation is postulated for OR gene expression; however, the exact nature of inhibitory signals and target molecules is yet to be discovered. In the feedback model, attempts to activate functional OR genes can continue in two classes of OSNs: those that have not yet activated any OR gene and those that have activated OR pseudogenes. This prevents a large fraction of developing OSNs from becoming receptorless. Other possible mechanisms have been proposed to ensure the monogenic expression of the OR gene. Among them, the oligogenic model assumes that the OR gene activation occurs stochastically in each OSN according to a Poisson distribution (Mombaerts, P., 2004). In this model, it is assumed that OSNs that do not express an OR cannot survive, and that those expressing two or more OR genes are actively eliminated (negative selection), possibly because of the confusion in bundling and pathfinding.

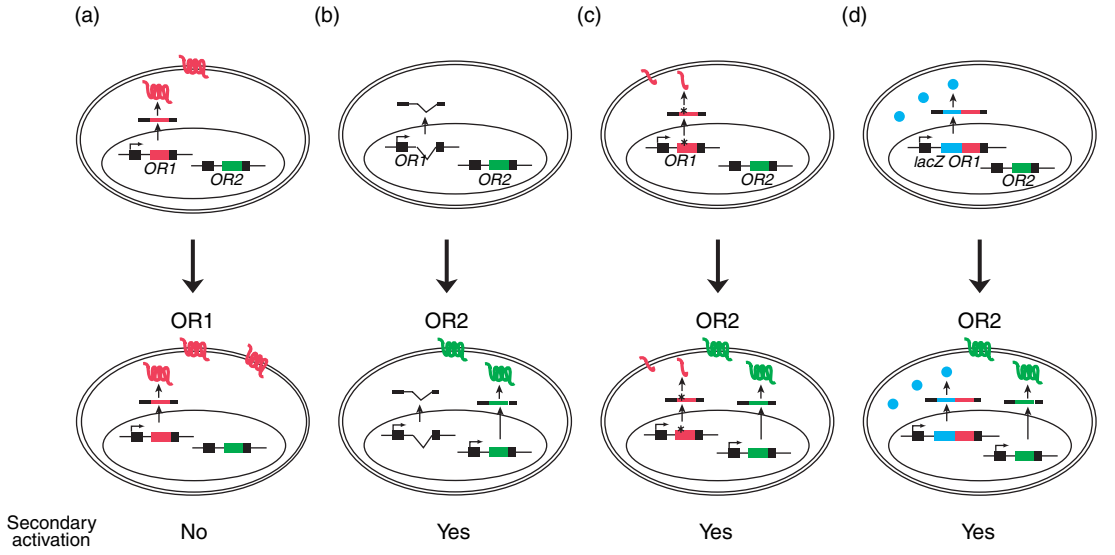

Figure 2 Inhibition of secondary odorant receptor (OR) gene activation by functional OR proteins. (a) Functional OR. When the activated OR gene (*OR1*) expresses functional OR proteins, activation of other OR genes (*OR2*) is inhibited. (b) Coding deletion (no OR). When the entire coding region is deleted, the activated mutant gene (*OR1*) cannot suppress the secondary activation of other OR genes (*OR2*). (c) Frameshift OR (short peptide). From the frameshifted pseudogenes, the full-length mRNA is synthesized. However, such pseudogenes express only short abnormal peptides because of premature stop codons created by frameshift mutations, and permit secondary activation of other OR genes (*OR2*). (d) The mRNA-alone construct (no OR). From this *lacZ–OR1* fusion gene, bicistronic mRNA is synthesized. Owing to the absence of the initiation codon in *OR1*, this mRNA produces only β-galactosidase (β-Gal). Because no OR1 protein is expressed, the secondary activation of other OR genes (*OR2*) is permitted.

4.31.6 *Cis*-Elements and *Trans*-Factors for Odorant Receptor Gene Expression

What kind of regulatory sequences and protein factors are needed for the single OR gene choice and zone-specific expression? Using full-length cDNA and 5′-RACE (rapid amplification of cDNA ends) analyses, conserved promoter sequences have been searched for in the OR gene system. However, no common promoter motifs were found for the 18 OR genes belonging to the *P2* cluster (Lane, R. P. *et al.*, 2001). Recently, based on the expression of transgenic minigenes, putative homeodomain, and Olf-1/EBF (O/E)-like binding sequences were identified in the immediately upstream regions of mouse, rat, and human OR genes including *MOR23*, *M71* (Vassalli, A. *et al.*, 2002), and *mOR37* (Hoppe, P. *et al.*, 2003). The homeodomain sequence was found to interact with a LIM-homeodomain protein, Lhx2 (Hoppe, P. *et al.*, 2003; Hirota, J. and Mombaerts, P., 2004), whereas the O/E-like motif is known to be recognized by O/E-1, -2, -3, and -4 helix–loop–helix transcription factors (Wang, S. S. *et al.*, 1997; 2002). Furthermore, the minimal promoter region for the *M71* gene expression has been defined with the transgenic minigene containing the homeodomain and O/E-like binding sequences (Rothman, A. *et al.*, 2005). Double mutations in both sites abolished the transgene expression. It has been proposed that the homeodomain and O/E sequences regulate the probability of *M71* gene choice differentially across the OE.

Recently, two competing gene loci in naive T helper (Th) cells, one for interleukin (IL)-4 on chromosome 11 and the other for γ interferon on chromosome 10, associate with each other via LCR in the IL-4 locus (Spilianakis, C. G. *et al.*, 2005). Such interchromosomal associations may not be restricted to the Th lymphokine system, but may instead underlie the general phenomenon of alternative gene regulation of multiple genetic loci, for example, the OR gene system. Because there are more than 50 different OR gene clusters scattered on many different chromosomes, the system needs to limit the number of activated clusters, ideally to one, to reduce the likelihood of the simultaneous activation of multiple OR genes. If the OR gene LCR can act interchromosomally like the IL-4 LCR, it would eliminate the need for every OR gene cluster to carry its own LCR (Lomvardas, S. *et al.*, 2006). Although it is yet to be clarified how many LCRs are present in the OR gene system, *trans*-acting LCR can contribute to the mutually exclusive activation of OR gene clusters scattered on many different chromosomes. Spatial organization of active chromatin structures and their cross talk within the nucleus may play key roles in regulating the coordinate expression of competing gene loci on different chromosomes.

4.31.7 Conclusion

In the mammalian olfactory system, each OSN activates only one functional OR gene in a monoallelic and mutually exclusive manner. Such unique expression forms the genetic basis for the OR-instructed axonal projection of OSNs to the OB (Imai, T. *et al.*, 2006; Serizawa, S. *et al.*, 2006). Thus, the one neuron–one receptor rule is essential for the conversion of olfactory signals received in the OE into a topographical map in the OB. One example of LCR has been reported for the mouse OR gene cluster which contains *MOR28*. Like the LCR in other gene systems, physical interaction between the LCR and the promoter probably enables the expression of only one OR gene within the cluster. This model is attractive because it reduces the likelihood of the simultaneous activation of two different OR genes, from a probability among ~1400 genes to that among ~50 loci. Recent transgenic experiments demonstrated that the mutant OR genes lacking either the entire coding sequence or the start codon can permit a second OR gene to be expressed. An inhibitory role has been postulated for the functional OR proteins to prevent the further activation of other OR genes, although the exact mechanism has yet to be elucidated. Stochastic activation of an OR gene by LCR and negative feedback regulation by the OR gene product, together, might ensure the maintenance of the one neuron–one receptor rule in the mammalian olfactory system.

References

Buck, L. and Axel, R. 1991. A novel multigene family may encode odorant receptors: a molecular basis for odor recognition. Cell 65, 175–187.

Chess, A. *et al.* 1994. Allelic inactivation regulates olfactory receptor gene expression. Cell 78, 823–834.

Chowdhury, D. and Sen, R. 2004. Mechanisms for feedback inhibition of the immunoglobulin heavy chain locus. Curr. Opin. Immunol. 16, 235–240.

Eggan, K. *et al.* 2004. Mice cloned from olfactory sensory neurons. Nature 428, 44–49.
Feinstein, P. *et al.* 2004. Axon guidance of mouse olfactory sensory neurons by odorant receptors and the beta2 adrenergic receptor. Cell 117, 833–846.
Freitag, J. *et al.* 1995. Two classes of olfactory receptors in *Xenopus laevis*. Neuron 15, 1383–1392.
Glusman, G. *et al.* 2001. The complete human olfactory subgenome. Genome Res. 11, 685–702.
Godfrey, P. A. *et al.* 2004. The mouse olfactory receptor gene family. Proc. Natl. Acad. Sci. U. S. A. 101, 2156–2161.
Goldmit, M. and Bergman, Y. 2004. Monoallelic gene expression: a repertoire of recurrent themes. Immunol. Rev. 200, 197–214.
Hirota, J. and Mombaerts, P. 2004. The LIM-homeodomain protein Lhx2 is required for complete development of mouse olfactory sensory neurons. Proc. Natl. Acad. Sci. U. S. A. 101, 8751–8755.
Hoppe, P. *et al.* 2003. The clustered olfactory receptor gene family 262: genomic organization, promotor elements, and interacting transcription factors. Genome Res. 13, 2674–2685.
Imai, T. *et al.* 2006. Odorant receptor-derived cAMP signals direct axonal targeting. Science 314, 657–661.
Ishii, T. *et al.* 2001. Monoallelic expression of the odourant receptor gene and axonal projection of olfactory sensory neurones. Genes Cells 6, 71–78.
Iwema, C. L. *et al.* 2004. Odorant receptor expression patterns are restored in lesion-recovered rat olfactory epithelium. J. Neurosci. 24, 356–369.
Karasuyama, H. *et al.* 1996. Surrogate light chain in B cell development. Adv. Immunol. 63, 1–41.
Kratz, E. *et al.* 2002. Odorant receptor gene regulation: implications from genomic organization. Trends Genet. 18, 29–34.
Lane, R. P. *et al.* 2001. Genomic analysis of orthologous mouse and human olfactory receptor loci. Proc. Natl. Acad. Sci. U. S. A. 98, 7390–7395.
Lewcock, J. W. and Reed, R. R. 2004. A feedback mechanism regulates monoallelic odorant receptor expression. Proc. Natl. Acad. Sci. U. S. A. 101, 1069–1074.
Li, Q. *et al.* 1999. Locus control regions: coming of age at a decade plus. Trends Genet. 15, 403–408.
Li, J. *et al.* 2004. Odorant receptor gene choice is reset by nuclear transfer from mouse olfactory sensory. Nature 428, 393–399.
Lomvardas, S. *et al.* 2006. Interchromosomal interactions and olfactory recepter choice. Cell 126, 403–413.
Malnic, B. *et al.* 1999. Combinatorial receptor codes for odors. Cell 96, 713–723.
Malnic, B. *et al.* 2004. The human olfactory receptor gene family. Proc. Natl. Acad. Sci. U. S. A. 101, 2584–2589.
Miyamichi, K. *et al.* 2005. Continuous and overlapping expression domains of odorant receptor genes in the olfactory epithelium determine the dorsal/ventral positioning of glomeruli in the olfactory bulb. J. Neurosci. 25, 3586–3592.
Mombaerts, P. 2004. Odorant receptor gene choice in olfactory sensory neurons: the one receptor–one neuron hypothesis revisited. Curr. Opin. Neurobiol. 14, 31–36.
Mombaerts, P. *et al.* 1996. Visualizing an olfactory sensory map. Cell 87, 675–686.
Mostoslavsky, R. *et al.* 2004. The lingering enigma of the allelic exclusion mechanism. Cell 118, 539–544.
Nagawa, F. *et al.* 2002. Genomic analysis of the murine odorant receptor MOR28 cluster: a possible role of gene conversion in maintaining the olfactory map. Gene 292, 73–80.
Ngai, J. *et al.* 1993. The family of genes encoding odorant receptors in the channel catfish. Cell 72, 657–666.
Norlin, E. M. *et al.* 2001. Evidence for gradients of gene expression correlating with zonal topography of the olfactory sensory map. Mol. Cell. Neurosci. 18, 283–295.
Oka, Y. *et al.* 2003. O-MACS, a novel member of the medium-chain acyl-CoA synthetase family, specifically expressed in the olfactory epithelium in a zone-specific manner. Eur. J. Biochem. 270, 1995–2004.
Qasba, P. and Reed, R. R. 1998. Tissue and zonal-specific expression of an olfactory receptor transgene. J. Neurosci. 18, 227–236.
Ressler, K. J. *et al.* 1993. A zonal organization of odorant receptor gene expression in the olfactory epithelium. Cell 73, 597–609.
Ressler, K. J. *et al.* 1994. Information coding in the olfactory system: evidence for a stereotyped and highly organized epitope map in the olfactory bulb. Cell 79, 1245–1255.
Rothman, A. *et al.* 2005. The promoter of the mouse odorant receptor gene *M71*. Mol. Cell. Neurosci. 28, 535–546.
Schweighoffer, E. *et al.* 2003. Unexpected requirement for ZAP-70 in pre-B cell development and allelic exclusion. Immunity 18, 523–533.
Serizawa, S. *et al.* 2000. Mutually exclusive expression of odorant receptor transgenes. Nat. Neurosci. 3, 687–693.
Serizawa, S. *et al.* 2003. Negative feedback regulation ensures the one receptor–one olfactory neuron rule in mouse. Science 302, 2088–2094.
Serizawa, S. *et al.* 2006. A neuronal identity code for the odorant receptor specific and activity dependent axon sorting. Cell 127, 1057–1069.
Shykind, B. M. *et al.* 2004. Gene switching and the stability of odorant receptor gene choice. Cell 117, 801–815.
Smallwood, P. M. *et al.* 2002. Role of a locus control region in the mutually exclusive expression of human red and green cone pigment genes. Proc. Natl. Acad. Sci. U. S. A. 99, 1008–1011.
Spilianakis, C. G. *et al.* 2005. Interchromosomal associations between alternatively expressed loci. Nature 435, 637–645.
Strotmann, J. *et al.* 1994a. Rostrocaudal patterning of receptor-expressing olfactory neurones in the rat nasal cavity. Cell Tissue Res. 278, 11–20.
Strotmann, J. *et al.* 1994b. Olfactory neurons expressing distinct odorant receptor subtypes are spatially segregated in the nasal epithelium. Cell Tissue Res. 276, 429–438.
Strotmann, J. *et al.* 2000. Local permutations in the glomerular array of the mouse olfactory bulb. J. Neurosci. 20, 6927–6938.
Sullivan, S. L. *et al.* 1996. The chromosomal distribution of mouse odorant receptor genes. Proc. Natl. Acad. Sci. U. S. A. 93, 884–888.
Tsuboi, A. *et al.* 1999. Olfactory neurons expressing closely linked and homologous odorant receptor genes tend to project their axons to neighboring glomeruli on the olfactory bulb. J. Neurosci. 19, 8409–8418.
Tsuboi, A. *et al.* 2006. Olfactory sensory neurons expressing class I odorant receptors converge their axons on an anotero-dorsal domain of the olfactory bulb in the mouse. Eur. J. Neurosci. 23, 1436–1444.
Uchida, N. *et al.* 2000. Odor mps in the mammalian olfactory bulb: domain organization and odorant structural features. Nat. Neurosci. 3, 1035–1043.
Vassalli, A. *et al.* 2002. Minigenes impart odorant receptor-specific axon guidance in the olfactory bulb. Neuron 35, 681–696.
Vassar, R. *et al.* 1993. Spatial segregation of odorant receptor expression in the mammalian olfactory epithelium. Cell 74, 309–318.
Vassar, R. *et al.* 1994. Topographic organization of sensory projections to the olfactory bulb. Cell 79, 981–991.
Wang, S. S. *et al.* 1997. The characterization of the Olf-1/EBF-like HLH transcription factor family: implications in olfactory

gene regulation and neuronal development. J. Neurosci. 17, 4149–4158.
Wang, F. *et al.* 1998. Odorant receptors govern the formation of a precise topographic map. Cell 93, 47–60.
Wang, Y. *et al.* 1999. Mutually exclusive expression of human red and green visual pigment-reporter transgenes occurs at high frequency in murine cone photoreceptors. Proc. Natl. Acad. Sci. U. S. A. 96, 5251–5256.
Wang, S. S. *et al.* 2002. Cloning of a novel Olf-1/EBF-like gene, O/E-4, by degenerate oligo-based direct selection. Mol. Cell. Neurosci. 20, 404–414.
Yoshihara, Y. *et al.* 1997. OCAM: A new member of the neural cell adhesion molecule family related to zone-to-zone projection of olfactory and vomeronasal axons. J. Neurosci. 17, 5830–5842.
Young, J. M. *et al.* 2002. Different evolutionary processes shaped the mouse and human olfactory receptor gene families. Hum. Mol. Genet. 11, 535–546.
Young, J. M. *et al.* 2003. Odorant receptor expressed sequence tags demonstrate olfactory expression of over 400 genes, extensive alternative splicing and unequal expression levels. Genome Biol. 4, R71.
Zhang, X. and Firestein, S. 2002. The olfactory receptor gene superfamily of the mouse. Nat. Neurosci. 5, 124–133.
Zhang, X. *et al.* 2004a. Odorant and vomeronasal receptor genes in two mouse genome assemblies. Genomics 83, 802–811.
Zhang, X. *et al.* 2004b. High-throughput microarray detection of olfactory receptor gene expression in the mouse. Proc. Natl. Acad. Sci. U. S. A. 101, 14168–14173.

4.32 Genomics of Odor Receptors in Zebrafish

J Ngai and T S Alioto, University of California, Berkeley, CA, USA

© 2008 Elsevier Inc. All rights reserved.

4.32.1	Introduction	553
4.32.2	The Zebrafish OR Repertoire	553
4.32.3	Genomic Distribution of Zebrafish OR Genes	554
4.32.4	Phylogeny of Zebrafish OR Genes	554
4.32.5	Comparison of the Zebrafish, Mouse, and Pufferfish OR Repertoires	554
4.32.6	Conserved Motifs in Predicted OR Protein Sequences	557
4.32.7	Evolution of the Vertebrate OR Gene Repertoire	559
References		560

4.32.1 Introduction

The *OR* gene superfamily is the largest multigene superfamily described in mammalian genomes. Surveys of the completed mouse genome sequence have indicated the existence of about 1068 potential intact *OR* genes (comprising at least 228 subfamilies) and 334 pseudogenes (Zhang, X. and Firestein, S., 2002; Zhang, X. *et al.*, 2004). In humans, there are ~350 intact *OR* genes and ~400 pseudogenes (Glusman, G. *et al.*, 2001; Zozulya, S. *et al.*, 2001; Niimura, Y. and Nei, M., 2003; Malnic, B. *et al.*, 2004). By way of contrast, molecular cloning and genomic DNA blot hybridizations in fish species suggest an *OR* repertoire size approximately five- to tenfold smaller than that of mammalian species (Ngai, J. *et al.*, 1993; Barth, A. L. *et al.*, 1997).

An understanding of how vertebrate olfactory receptor repertoires evolved can be gained from comparing the properties and organization of genes from divergent vertebrate species. In this regard, the zebrafish, *Danio rerio*, provides a useful model for comparative genomics studies, owing to intensive efforts to sequence this species' genome as well as a large research community using the zebrafish as a model experimental organism. In early studies, approximately 30 zebrafish *OR* sequences were identified previously using polymerase chain reaction (PCR) and homology-based techniques (Barth, A. L. *et al.*, 1996; Byrd, C. A. *et al.*, 1996; Weth, F. *et al.*, 1996; Barth, A. L. *et al.*, 1997; Vogt, R. G. *et al.*, 1997; Dugas, J. C. and Ngai, J., 2001). Although a number of phylogenetic reconstructions have been made (Freitag, J. *et al.*, 1995; 1998; 1999; Glusman, G. *et al.*, 2000; Dugas, J. C. and Ngai, J., 2001; Aparicio, S. *et al.*, 2002; Zhang, X. and Firestein, S., 2002; Irie-Kushiyama, S. *et al.*, 2004; Zhang, X. *et al.*, 2004), a more accurate view of the OR superfamily's evolutionary history would be facilitated by comparisons between genomic datasets that include a more complete representation of member genes from each species. To this end, genome database mining on the zebrafish genome sequence provided by the Sanger Institute *D. rerio* Sequencing Project has allowed a description of the complete *OR* gene repertoire in this species (Alioto, T. S. and Ngai, J., 2005; Niimura, Y. and Nei, M., 2005). An analysis of these receptor sequences and comparison with other vertebrate OR repertoires provide insights into the evolution of this chemosensory receptor superfamily in vertebrates.

4.32.2 The Zebrafish OR Repertoire

Iterative BLAST searches of the third (Zv3) and fourth (Zv4) draft zebrafish genome assemblies were conducted using previously identified ORs as query sequences (Alioto, T. S. and Ngai, J., 2005) (see also Niimura, Y. and Nei, M., 2005). This search identified 143 intact *OR* genes (136 with no disruptions), 7 partial genes, 10 pseudogenes greater than 700 bp in length, and 15 gene fragments shorter than 700 bp (Table 1). The total *OR* gene count is a conservative estimate of the true size of the OR repertoire, with between 78% (136/175) and 86% ([143 + 7]/175) of identifiable OR sequences consisting of potentially functional *OR* genes.

OR families are typically defined as monophyletic groups, with members that share greater than 40% amino acid identity, whereas subfamily members share greater than 60% amino acid identity (Lancet, D. and Ben-Arie, N., 1993). Using these operational

Table 1 Summary of identified teleost OR genes

	Zebrafish	*Fugu*	*Tetraodon*
Intact genes[a]	143 (7)	44 (3)	42 (6)
Partial genes[b]	7	9	4
Pseudogenes[c]	10	4	11
Total	160	57	57

[a]A gene is operationally defined as intact if it possesses a full-length OR protein coding sequence with no more than one disruption. For each species, the number of genes with a single disruption is listed in parentheses; the remainder contain no disruptions.
[b]A sequence encoding ≤275 contiguous amino acids, missing specific features characteristic of ORs (see the text for details), or missing start or stop codons is classified as a partial gene.
[c]A sequence is defined as a pseudogene if it is a partial gene with one or more disruption or a full-length gene with two or more disruptions.
From Alioto, T.S. and Ngai, J. 2005. The odorant receptor repertoire of teleost fish. BMC Genomics 6–173.

definitions, zebrafish *OR* genes were classified into families and subfamilies by reconstructing their phylogeny using neighbor-joining and maximum likelihood algorithms (Alioto, T. S. and Ngai, J., 2005). Clades of *OR* genes with less than ∼40% and less than ∼60% interbranch amino acid identity were used to group genes into distinct families and subfamilies, respectively. The average percent identity between families is approximately 25%, while the maximum observed percent identity between any two ORs of different families is 39% (Alioto, T. S. and Ngai, J., 2005).

4.32.3 Genomic Distribution of Zebrafish OR Genes

Previous studies have demonstrated that *OR* genes are clustered in vertebrate genomes (Ben-Arie, N. *et al.*, 1994; Dugas, J. C. and Ngai, J., 2001; Young, J. M. *et al.*, 2002; Zhang, X. and Firestein, S., 2002; Zhang, X. *et al.*, 2004). In mammalian genomes, *OR* genes are distributed widely, residing on 18 chromosomes in the mouse (Zhang, X. and Firestein, S., 2002) and 21 chromosomes in humans (Glusman, G. *et al.*, 2001; Malnic, B. *et al.*, 2004). From the zebrafish Zv3 and Zv4 assemblies, 119 of the identified zebrafish *OR* genes are distributed in five major clusters containing between 14 and 31 genes each (Alioto, T. S. and Ngai, J., 2005). There are two clusters on chromosome 15, two on chromosome 21, one on chromosome 10, several small clusters on chromosomes 8, 14, and 17, and in a few cases, genes exist as singletons (Figure 1). Genomic locations were assignable for ∼80% of the *OR* genes identified, with 29 remaining unassigned (Alioto, T. S. and Ngai, J., 2005). Subfamilies are largely contiguous, and subfamily members usually share the same transcriptional orientation, suggesting tandem duplication as a mechanism of expansion within a subfamily (Dugas, J. C. and Ngai, J., 2001; Kratz, E. *et al.*, 2002). The tight clustering of subfamily members in the zebrafish genome differs from the organization seen in mammalian genomes, which exhibit a higher degree of dispersion of related *OR* genes (Ben-Arie, N. *et al.*, 1994; Dugas, J. C. and Ngai, J., 2001; Young, J. M. *et al.*, 2002; Zhang, X. and Firestein, S., 2002; Zhang, X. *et al.*, 2004).

4.32.4 Phylogeny of Zebrafish OR Genes

A phylogenetic tree of the 143 intact *OR* genes and four full-length pseudogenes was constructed using a neighbor joining algorithm (Figure 2(a); Alioto, T. S. and Ngai, J., 2005). From this information, it is possible to discern the relationships between the OR genes and infer their evolutionary origins. Based on this analysis, zebrafish ORs could be classified into eight families (≥40% intrafamily sequence identity) and 40 subfamilies (≥60% intrasubfamily sequence identity). Most of the gene families contain between 12 and 40 genes each; the two smallest families, family A and family B, contain six genes and one gene each, respectively. The intrasubfamily identity threshold was lowered for three subfamilies, OR102, OR115, and OR125, to generate monophyletic clades. High bootstrap support (Figure 2(a)) justifies these classifications, with all subfamilies exhibiting bootstrap scores of 100%. In addition, the topology of the phylogenetic tree shown in Figure 2 is supported by an independent phylogenetic reconstruction using a maximum likelihood algorithm (Alioto, T. S. and Ngai, J., 2005).

4.32.5 Comparison of the Zebrafish, Mouse, and Pufferfish OR Repertoires

To gain additional insight into how the *OR* gene superfamily evolved in vertebrates, the zebrafish ORs were aligned to the set of OR sequences identified in the mouse genome (Alioto, T. S. and Ngai, J., 2005). Mouse ORs can be classified into two groups, class I and class II, each showing on average greater than 40% intragroup sequence identity (Zhang, X. and Firestein, S., 2002). Based on their greater similarity to the limited number of fish *OR* genes previously identified, class I genes from amphibians and mammals have been

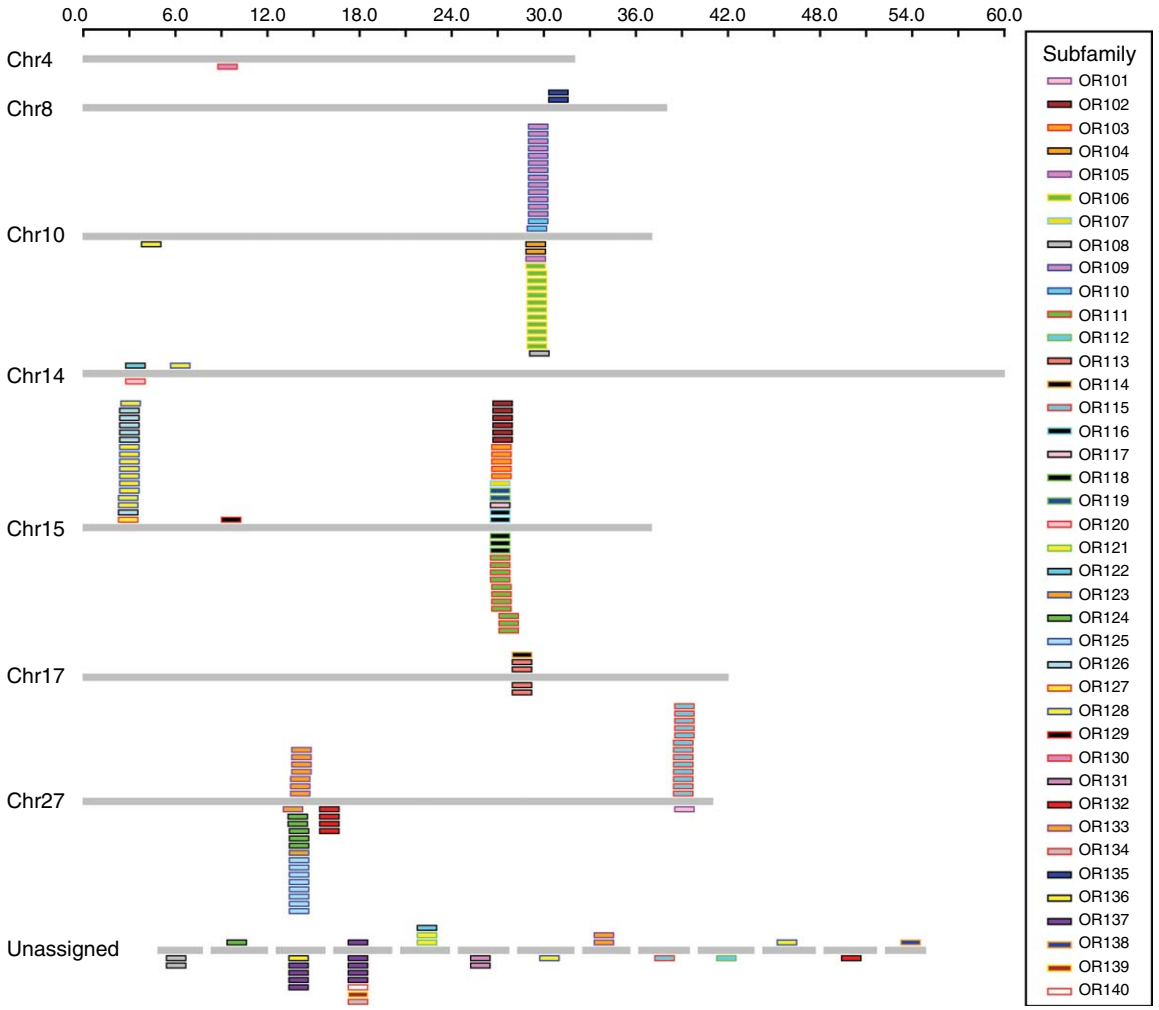

Figure 1 Chromosomal distribution of zebrafish *OR* genes. The majority of OR genes are organized in large clusters at only a few loci in the zebrafish genome. OR genes are depicted as boxes above (plus strand) or below (minus strand) a line representing each chromosome that encodes ORs. Genes are color coded according to subfamily. From Alioto, T.S. and Ngai, J. 2005. The odorant receptor repertoire of teleost fish. BMC Genomics 6, 173.

referred to as fish-like (Freitag, J. *et al.*, 1995; Glusman, G. *et al.*, 2001; Zhang, X. and Firestein, S., 2002). However, an analysis of the complete set of zebrafish *OR* genes indicates that this view cannot be generalized to the entire fish OR repertoire (Alioto, T. S. and Ngai, J., 2005). Mammalian class I and class II genes can in fact be grouped more closely with only two of eight approximately equidistantly related zebrafish families; class I genes show close similarity to only a small subset of zebrafish *OR* genes (*OR112-1*, *OR113-1*, *OR113-2*, and *OR114-1*, which together comprise family A), and one zebrafish gene (*OR101-1*, comprising the single member family B) clusters together with mammalian class II genes (Figure 2(b)). Overall, mouse class I exhibits similar average pairwise identity to the zebrafish families ($27.3 \pm 4.8\%$ identity (mean $\pm$ standard deviation); range: 17–32%) as mouse class II ($27.7 \pm 5.5\%$; range: 18–38%); the difference in mean values is not significant in a two-tailed *t*-test ($p = 0.89$).

A comparison with other teleost *OR* genes further reveals that six of the eight zebrafish OR families overlap with families from two pufferfish species, fugu (*Takifugu rubripes*) and tetraodon (*Tetraodon nigroviridis*) (Table 1 and Figure 2(c); Alioto, T. S. and Ngai, J., 2005). Families B and G do not appear to be present in the two pufferfish genomes. Interestingly, family H is clearly the most divergent family of teleost ORs (Figure 2(c); Alioto, T. S. and Ngai, J., 2005). The location of the outgroup melanocortin receptor between family H and the other families supports the

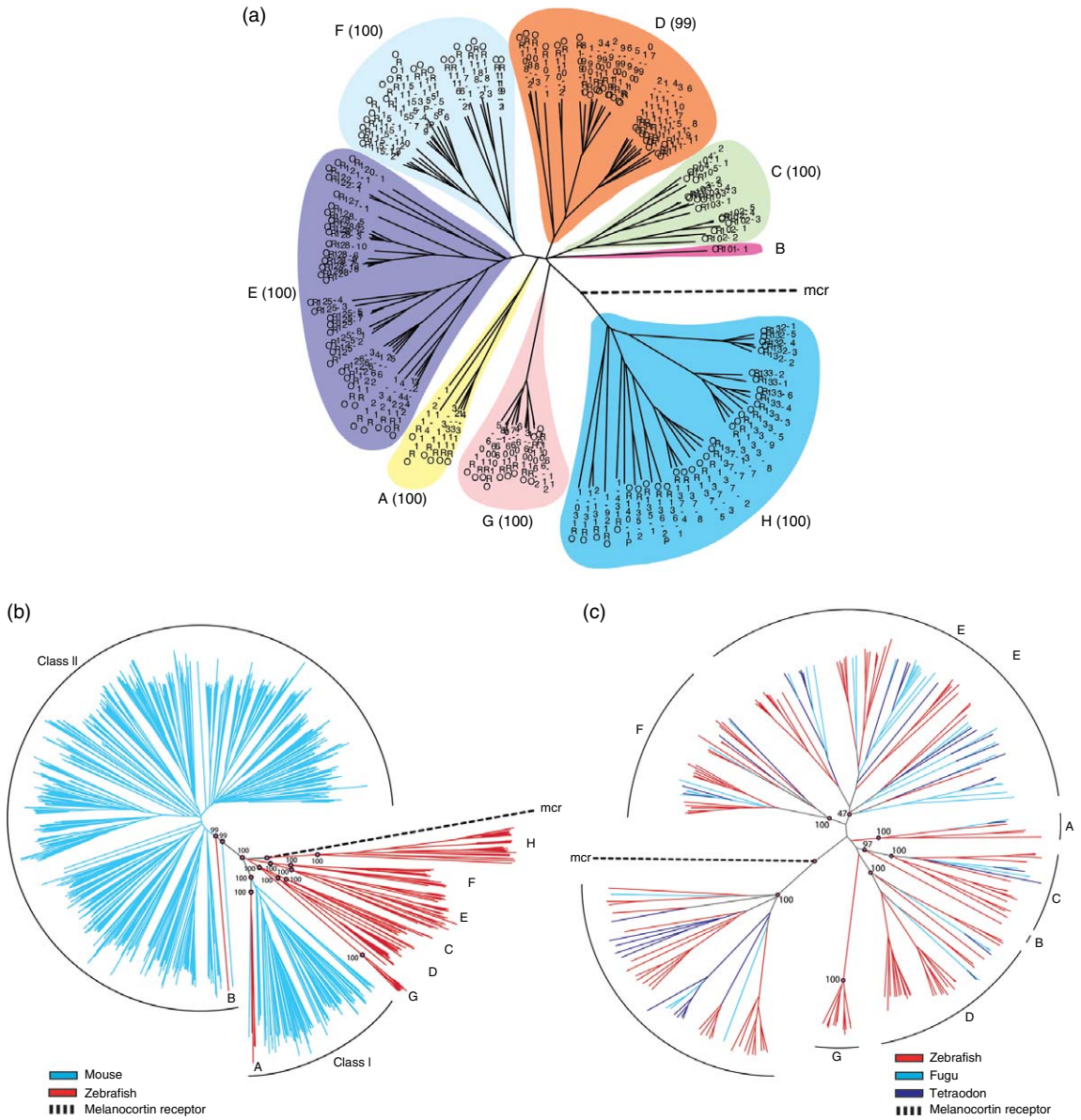

Figure 2 Phylogeny of zebrafish and other vertebrate OR families. (a) Phylogeny of zebrafish receptors. A neighbor-joining tree was constructed based on an alignment of the predicted amino acid sequences of 143 intact genes and four full-length pseudogenes identified from the zebrafish genome. *OR* genes are named by subfamily and colored by family. The eight gene families are labeled A–H. The zebrafish melanocortin receptor branch (dotted line labeled mcr) indicates the root of the tree. Bootstrap scores for each family are indicated in parentheses. (b) Phylogenetic relationship among zebrafish and mouse odorant receptors. The following sets of genes were aligned and used to construct a tree by neighbor joining: the mouse odorant receptors, mORs; the subset of 136 intact zebrafish ORs with no disruptions (highlighted in red); and mouse melanocortin receptors (mcr). Note the presence of *OR* gene subfamilies *OR112*, *OR113*, and *OR114* (family A) within the class I clade and zebrafish *OR101-1* (family B) within the Class II clade. Bootstrap scores corresponding to selected nodes are indicated. (c) Phylogeny of the complete OR repertoires of zebrafish, fugu and tetraodon. One hundred thirty-six nondisrupted genes from zebrafish, 42 nondisrupted genes from fugu, and 42 nondisrupted genes from tetraodon were used in this neighbor-joining analysis. Families are labeled A–H and correspond to the zebrafish families shown in panel (a). Bootstrap scores corresponding to selected nodes are indicated. From Alioto, T.S. and Ngai, J. 2005. The odorant receptor repertoire of teleost fish. BMC Genomics 6, 173.

conclusion that this family is the result of a very ancient gene duplication event. Based on the degree of divergence from other *OR* gene families, it is possible that the genes comprising family H may not in fact encode bona fide odorant receptors. However, family H forms a cluster distinct from non-OR G-protein-coupled receptors (GPCRs) in a phylogenetic tree comprising mouse and zebrafish ORs together with a set of 199 non-OR type I (rhodopsin class) mouse GPCRs (Figure 3). Thus, we consider the family H sequences operationally as *OR* genes. More generally, this phylogenetic reconstruction based on OR and non-OR GPCRs reveals that the ORs as a group are distinct from the other type I GPCRs.

4.32.6 Conserved Motifs in Predicted OR Protein Sequences

Previous studies of vertebrate ORs have identified a number of conserved sequence motifs characteristic of these receptors (Pilpel, Y. and Lancet, D., 1999;

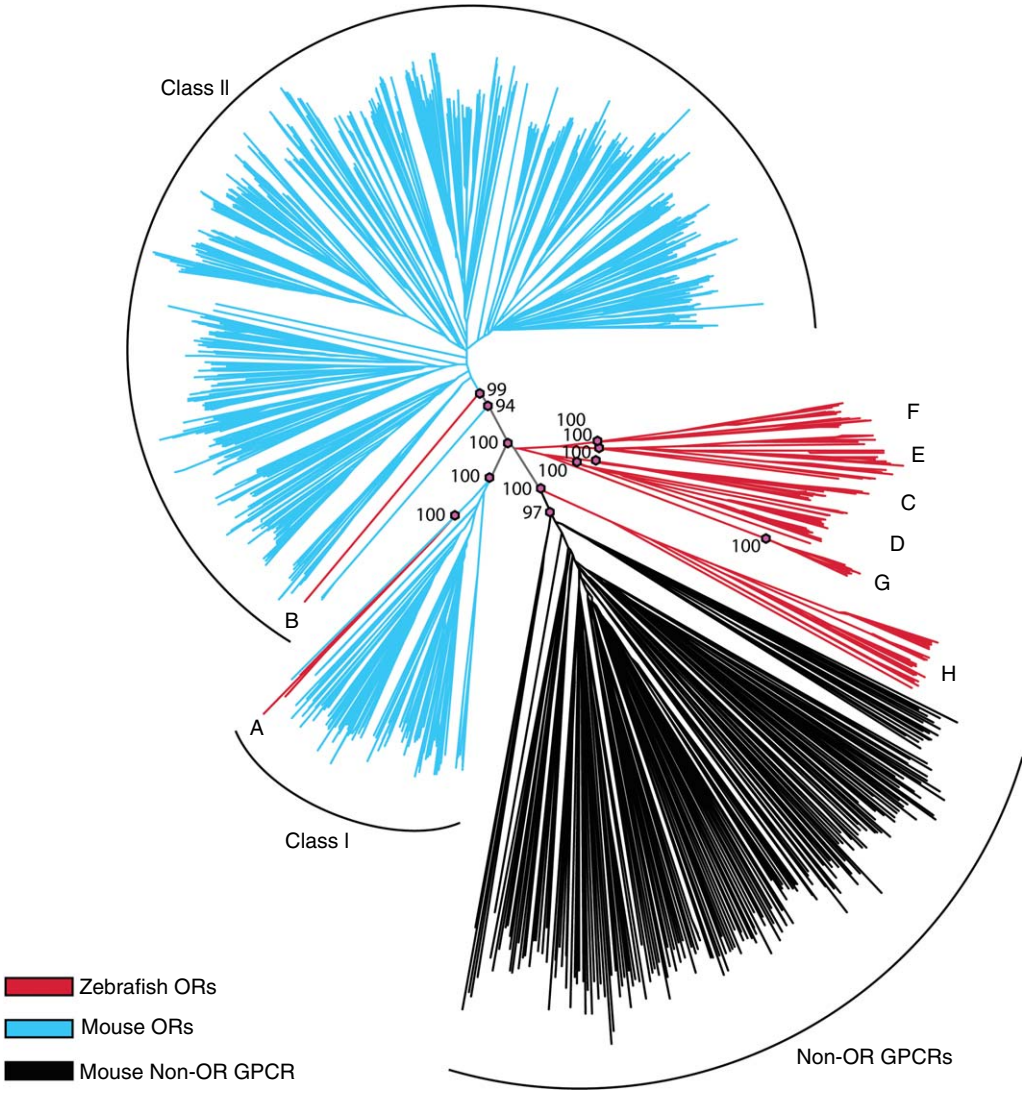

Figure 3 Phylogeny of zebrafish and mouse ORs rooted by mouse non-OR GPCRs. The following sets of genes were aligned: the mouse odorant receptors, mORs; the subset of 136 intact zebrafish ORs with no disruptions; and 199 mouse non-odorant rhodopsin-like GPCRs downloaded from GPCRDB (G-protein-coupled receptor database). A phylogenetic tree was then generated by neighbor joining. The expanded representation of non-OR GPCRs in this phylogeny more clearly demonstrates the segregation of OR and non-OR GPCRs as well as the approximately equal distance of zebrafish families C–H from the mouse class I and class II OR genes. From Alioto, T.S. and Ngai, J. 2005. The odorant receptor repertoire of teleost fish. BMC Genomics 6, 173.

Zozulya, S. *et al.*, 2001; Zhang, X. and Firestein, S., 2002). These include the following: an N-linked glycosylation site NX[TS]X in the N-terminal domain; the motif MA[FY][DE]RYVAIC located at the third transmembrane domain (TM3)/second intracellular loop (IC2) junction which is thought to interact with G-proteins (specifically G_{olf}); three conserved cysteine residues in the second extracellular loop (EC2) thought to partake in disulfide bonding; and the motif KAFSTCXSH in IC3 containing an intracellular cysteine conserved in GPCRs and potential phosphorylation sites. These motifs are conserved in all the zebrafish *OR* families, with the exception of Family H, in which only the MAYDRYVAIC motif is conserved. This sequence conservation is illustrated by a sequence logo generated from the alignment of predicted full-length zebrafish OR coding sequences (Figure 4(a); Alioto, T. S. and Ngai, J., 2005). In this representation, the relative frequency with which an amino acid appears at a given position is reflected by the height of its one-letter amino acid code in the logo, with the total height at a given position proportional to the level of sequence conservation. Interestingly, when compared to the sequence logo representing the alignment of mouse class I and class II ORs (Figure 4(b)), the zebrafish OR logo shows lower conservation

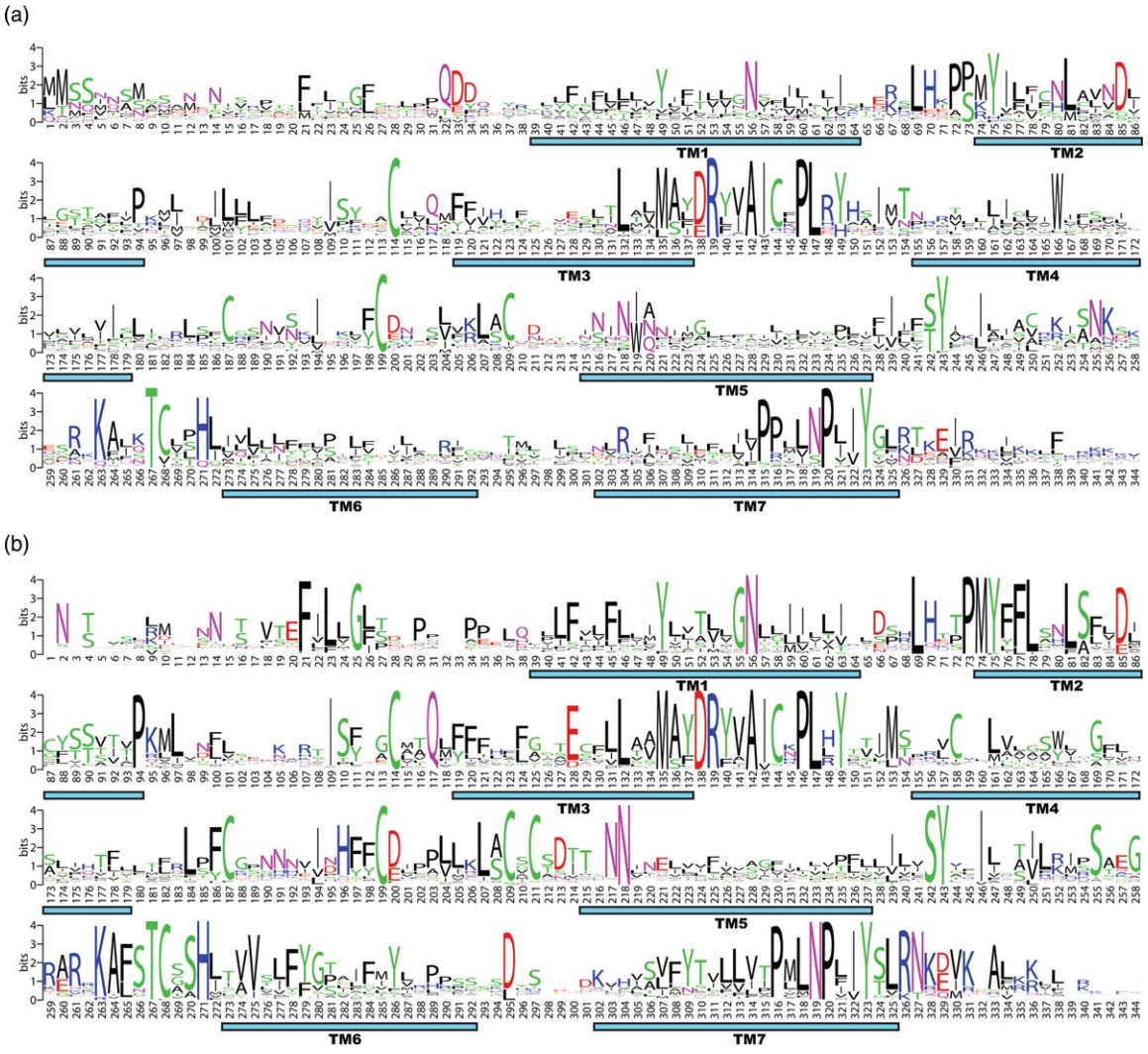

Figure 4 Sequence logos of zebrafish and mouse OR families. Conservation of predicted amino acid sequence for the zebrafish (a) and mouse (b) OR repertoires is shown graphically (see the text). *Y*-axis, information content. *X*-axis, residue position. For this analysis, positions with gaps in more than 95% of sequences, as well as poorly aligned N- and C-terminal sequences, were removed. Positions in the species-specific logos are identical according to this alignment. From Alioto, T.S. and Ngai, J. 2005. The odorant receptor repertoire of teleost fish. BMC Genomics 6, 173.

amongst the predicted zebrafish receptor sequences (reflected by the more numerous and shorter letters at individual positions in the logo), revealing the greater diversity within the zebrafish versus mouse OR superfamily (Alioto, T. S. and Ngai, J., 2005).

4.32.7 Evolution of the Vertebrate OR Gene Repertoire

The characterization of the complete *OR* repertoires from both fish and mammalian species allows an informed analysis of *OR* gene evolution in the vertebrate lineage. From the comparative analysis of mammalian and teleost OR sequences, a model for OR gene evolution in vertebrates can be proposed (Alioto, T. S. and Ngai, J., 2005): *OR* genes in present-day vertebrates likely descended from eight ancestral *OR* genes (or gene families) that existed at the time of the split between ray-finned and lobe-finned fish (the ancestors of teleosts and tetrapods, respectively) approximately 450 million years ago (Hedges, S. B., 2002). A phylogenetic reconstruction based on mouse and zebrafish ORs and 199 mouse non-OR GPCRs (Figure 3) indicates that the ORs form a group distinct from all other type I GPCRs, possibly reflecting a very ancient duplication event(s) and/or rapid divergence of the ORs in the evolution of type I GPCRs. The estimate of ancestral *OR* gene number is based on the identification of eight *OR* gene families in teleosts, two of which show somewhat higher similarity to the two *OR* gene families in mammals. The grouping of zebrafish and pufferfish *OR* genes into common families indicates that the gene duplication events that gave rise to the major OR families probably occurred prior to the speciation of teleosts. In addition, the greater similarities between zebrafish family A and mouse class I, and between zebrafish family B and mouse class II, infer that the ancestral genes for these families existed before the tetrapodon/teleost split. Our model therefore suggests a history during which ancestral genes or gene families were selectively lost during the evolution of the different vertebrate lineages (Figure 5). Of the ancestral families, zebrafish retained eight families, fugu and tetraodon retained six families, and mammals retained two families.

It is also possible that the four to six gene families unique to teleosts descended from family A/class I and/or family B/class II ancestral genes, after the tetrapodon/teleost split. Such a scenario seems unlikely, however, considering the roughly equivalent

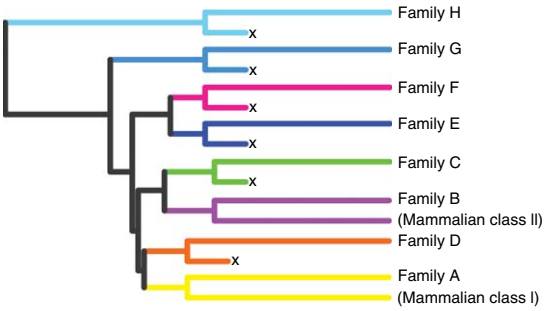

Figure 5 Model for vertebrate *OR* gene family evolution. We hypothesize the existence of a minimum of eight ancestral *OR* genes or gene families at the time of the last common ancestor between the tetrapodon and fish lineages. The phylogeny of OR families can be explained by differential family and subfamily expansion and gene death (X's on mouse lineages). Mammalian class I and class II represent a large expansion of two of these major OR families, each of which also encompasses zebrafish *OR* genes. Branch lengths not drawn to scale.

degree of divergence exhibited between seven of the eight teleost gene families (including family A and family B). Moreover, amphibian and avian OR genes can be grouped into six of the eight identified OR families (family A/class I, family B/class II, family C, family E, family F, and family H), further implicating the presence of common ancestral genes for these families prior to the tetrapodon/teleost split (Niimura, Y. and Nei, M., 2005).

Mechanisms of gene or family loss in a particular vertebrate lineage may have involved a number of processes, for example, gene conversion, pseudogenization of all genes in a family, unequal crossover recombination events during meiosis, or larger chromosomal rearrangements. From the available data, it is not possible to infer the precise order and rate of *OR* gene family expansion and contraction, or speciation events. Nonetheless, six of the retained *OR* gene families were subject to a substantial net expansion and diversification in zebrafish (and to a lesser degree in the pufferfish), while the other two ancestors gave rise to the present-day mammalian class I and class II ORs as well as to a small number of zebrafish genes. We hypothesize that relaxed selective pressure on a subset of the ancestral tetrapodon OR repertoire led to the loss of major *OR* gene families in the mammalian lineage. The expansion within the two remaining gene families was likely driven by the adaptation to the terrestrial odorous environment. Thus, different selective pressures found in the aquatic and terrestrial environments led to different sizes and shapes of the OR repertoires of fish and mammals.

It is generally thought that the diversity of OR sequences – as represented in the number of receptor families – underlies the diversity of chemical structures or odor space that can be detected by an organism's olfactory system. Thus, with approximately six to eight *OR* gene families retained over evolutionary time (vs. two in mammals), fish may be capable of detecting a larger diversity of chemical structures than mammals. However, the larger total number of OR sequences in mammals (~1000 vs. ~100 in fish) presumably allows a finer discrimination amongst the compounds that are detected by the mammalian olfactory system.

References

Alioto, T. S. and Ngai, J. 2005. The odorant receptor repertoire of teleost fish. BMC Genomics 6, 173.

Aparicio, S., Chapman, J., Stupka, E., Putnam, N., Chia, J. M., Dehal, P., Christoffels, A., Rash, S., Hoon, S., Smit, A., *et al.* 2002. Whole-genome shotgun assembly and analysis of the genome of *Fugu rubripes*. Science 297, 1301–1310.

Barth, A. L., Dugas, J. C., and Ngai, J. 1997. Noncoordinate expression of odorant receptor genes tightly linked in the zebrafish genome. Neuron 19, 359–369.

Barth, A. L., Justice, N. J., and Ngai, J. 1996. Asynchronous onset of odorant receptor expression in the developing zebrafish olfactory system. Neuron 16, 23–34.

Ben-Arie, N., Lancet, D., Taylor, C., Khen, M., Walker, N., Ledbetter, D. H., Carrozzo, R., Patel, K., Sheer, D., Lehrach, H., and North, M. A. 1994. Olfactory receptor gene cluster on human chromosome 17: possible duplication of an ancestral receptor repertoire. Hum. Mol. Genet. 3, 229–235.

Byrd, C. A., Jones, J. T., Quattro, J. M., Rogers, M. E., Brunjes, P. C., and Vogt, R. G. 1996. Ontogeny of odorant receptor gene expression in zebrafish, *Danio rerio*. J. Neurobiol. 29, 445–458.

Dugas, J. C. and Ngai, J. 2001. Analysis and characterization of an odorant receptor gene cluster in the zebrafish genome. Genomics 71, 53–65.

Freitag, J., Beck, A., Ludwig, G., von Buchholtz, L., and Breer, H. 1999. On the origin of the olfactory receptor family: receptor genes of the jawless fish (*Lampetra fluviatilis*). Gene 226, 165–174.

Freitag, J., Krieger, J., Strotmann, J., and Breer, H. 1995. Two classes of olfactory receptors in *Xenopus laevis*. Neuron 15, 1383–1392.

Freitag, J., Ludwig, G., Andreini, I., Rossler, P., and Breer, H. 1998. Olfactory receptors in aquatic and terrestrial vertebrates. J. Comp. Physiol. [A] 183, 635–650.

Glusman, G., Sosinsky, A., Ben-Asher, E., Avidan, N., Sonkin, D., Bahar, A., Rosenthal, A., Clifton, S., Roe, B., Ferraz, C., *et al.* 2000. Sequence, structure, and evolution of a complete human olfactory receptor gene cluster. Genomics 63, 227–245.

Glusman, G., Yanai, I., Rubin, I., and Lancet, D. 2001. The complete human olfactory subgenome. Genome Res. 11, 685–702.

Hedges, S. B. 2002. The origin and evolution of model organisms. Nat. Rev. Genet. 3, 838–849.

Irie-Kushiyama, S., Asano-Miyoshi, M., Suda, T., Abe, K., and Emori, Y. 2004. Identification of 24 genes and two pseudogenes coding for olfactory receptors in Japanese loach, classified into four subfamilies: a putative evolutionary process for fish olfactory receptor genes by comprehensive phylogenetic analysis. Gene 325, 123–135.

Kratz, E., Dugas, J. C., and Ngai, J. 2002. Odorant receptor gene regulation: implications from genomic organization. Trends Genet. 18, 29–34.

Lancet, D. and Ben-Arie, N. 1993. Olfactory receptors. Curr. Biol. 3, 668–674.

Malnic, B., Godfrey, P. A., and Buck, L. B. 2004. The human olfactory receptor gene family. Proc. Natl. Acad. Sci. U. S. A. 101, 2584–2589.

Ngai, J., Dowling, M. M., Buck, L., Axel, R., and Chess, A. 1993. The family of genes encoding odorant receptors in the channel catfish. Cell 72, 657–666.

Niimura, Y. and Nei, M. 2003. Evolution of olfactory receptor genes in the human genome. Proc. Natl. Acad. Sci. U. S. A. 100, 12235–12240.

Niimura, Y. and Nei, M. 2005. Evolutionary dynamics of olfactory receptor genes in fishes and tetrapods. Proc. Natl. Acad. Sci. U. S. A. 102, 6039–6044.

Pilpel, Y. and Lancet, D. 1999. The variable and conserved interfaces of modeled olfactory receptor proteins. Protein Sci. 8, 969–977.

Vogt, R. G., Lindsay, S. M., Byrd, C. A., and Sun, M. 1997. Spatial patterns of olfactory neurons expressing specific odor receptor genes in 48-hour-old embryos of zebrafish *Danio rerio*. J. Exp. Biol. 200 (Pt 3), 433–443.

Weth, F., Nadler, W., and Korsching, S. 1996. Nested expression domains for odorant receptors in zebrafish olfactory epithelium. Proc. Natl. Acad. Sci. U. S. A. 93, 13,321–13,326.

Young, J. M., Friedman, C., Williams, E. M., Ross, J. A., Tonnes-Priddy, L., and Trask, B. J. 2002. Different evolutionary processes shaped the mouse and human olfactory receptor gene families. Hum. Mol. Genet. 11, 535–546.

Zhang, X. and Firestein, S. 2002. The olfactory receptor gene superfamily of the mouse. Nat. Neurosci. 5, 124–133.

Zhang, X., Rodriguez, I., Mombaerts, P., and Firestein, S. 2004. Odorant and vomeronasal receptor genes in two mouse genome assemblies. Genomics 83, 802–811.

Zozulya, S., Echeverri, F., and Nguyen, T. 2001. The human olfactory receptor repertoire. Genome Biol. 2, RESEARCH0018.

Relevant Website

http://www.gpcr.org/7tm – G-protein-coupled receptor database.

4.33 Genomics of Invertebrate Olfaction

J D Bohbot, R J Pitts, and L J Zwiebel, Vanderbilt University, Nashville, TN, USA

© 2008 Elsevier Inc. All rights reserved.

4.33.1	Introduction	562
4.33.2	An Overview of Invertebrate Chemosensory Organs and Their Molecular Components	563
4.33.3	Odor Recognition	566
4.33.3.1	Insect Odorant-Binding Proteins	566
4.33.3.1.1	Comparative evolutionary genomics	566
4.33.3.1.2	Functional genomics of Obps	570
4.33.3.2	Insect Chemosensory Proteins	571
4.33.3.2.1	Genomic organization and gene structure of Csps	572
4.33.3.2.2	Functional genomics of Csps	572
4.33.3.3	Odorant Receptors	573
4.33.3.3.1	Insect odorant receptors	574
4.33.3.3.2	Caenorhabditis elegans chemoreceptors	578
4.33.4	Signaling Cascade	579
4.33.4.1	Guanine Nucleotide-Binding Proteins and Effector Genes	580
4.33.4.1.1	Insects	580
4.33.4.1.2	Caenorhabditis elegans	581
4.33.4.2	Ion Channels	581
4.33.5	Regulators of Signaling	582
4.33.5.1	Arrestins and G-Protein-Coupled Receptor Kinases	582
4.33.5.2	The Caenorhabditis elegans Calcineurin TAX-6	582
4.33.5.3	Other Protein Kinases	583
4.33.6	Conclusion and Perspectives	583
References		584

Glossary

gene A segment of DNA that represents a fundamental unit of heredity.

gene cluster Set of two or more related genes physically located nearby in the genome and encoding similar proteins.

genome The complete genetic content of an organism.

G-protein-coupled receptor (GPCR) Superfamily of seven transmembrane proteins functioning in signal transduction cascades including odorant/taste receptors, photoreceptors, dopamine receptors, acetylcholine receptors, and opioid receptors.

insect Arthropods with three pairs of legs and three body parts.

invertebrate Heterogenous cluster of animals based on their lack of internal skeleton including protozoa, annelids, echinoderms, mollusks, and arthropods.

locus Specific chromosomal location of a gene in the genome.

nematode Commonly known as roundworms based on their worm-like appearance.

odorant Chemical compound stimulating the olfactory system.

odorant-binding protein Small water-soluble proteins thought to bind odorants.

odorant receptor Subclass of membrane proteins belonging to the GPCR superfamily displaying affinity to various odorants.

olfaction Sense of smell.

ortholog Two genes in two separate species that derived from a common ancestral gene by speciation.

sensillum Morphological unit consisting of sensory neurons and accessory cells located on the surface of sensory tissues.

signal transduction Cellular process consisting of converting a signal into another. It is supported by a cascade of molecular components including receptors, enzymes, and ion channels.

synteny Describes the conserved arrangement of genes between related species.

4.33.1 Introduction

The diversity of the animal lineages and their adaptations to various environments are a testament to the formidable natural creativity of life. Within the context of the requirement for mobility, constraints such as gravity have been addressed differently across phyla: while some organisms escape immobility through the use of 2, 4, or 1000 legs, others choose to fly or crawl. In a similar context we may ask the question: how have the challenges of olfaction been answered in phylogenetically diverse phyla?

Olfaction is of fundamental importance in the life cycle and life histories of invertebrates such as insects, crustaceans, or round worms and has been described as the chemosensory modality dedicated to the detection of small airborne chemicals called odorants. Several observations challenge this definition. Aquatic animals use anatomically and molecularly similar chemosensory systems to detect low molecular weight, water-soluble compounds, blurring the distinction between olfaction and gustation. More compelling is the fact that, in general terms, the biochemistry of chemical recognition (chemosensation), that is, the initial physical interactions between the organism olfactory machinery and the environmental stimulus, occurs in a uniformly water-soluble medium. Accordingly, although the distinctive characteristics of gustatory and olfactory processes remain to be determined, the olfactory system must achieve four fundamental requirements that may best be summarized as: speed, tuning breadth, discrimination, and sensitivity. These elements represent the fact that within a few milliseconds, the organism must recognize and discriminate low-concentration odorants amongst a potentially unlimited set of qualitatively different chemical stimuli.

These requirements are even more salient among invertebrates that typically rely on olfaction as their main sensory modality. Experimental expediency and the relative simplicity of invertebrates compared to vertebrates have fostered the study of model organisms such as insects, crustaceans, and nematodes to advance our understanding of the underlying molecular and cellular mechanisms of olfaction. On the surface, the organization and the physiology of the chemosensory systems of arthropods and nematodes vary widely. Are these differences solely a reflection of genetic variability or do they derive from conserved principles? From the early 1980s to late 1990s, several olfactory components had been identified by biochemical and genetic extraction methods. However, the bulk of olfactory genes remained largely uncharacterized especially in the case of highly divergent gene families for which a homology-based approach proved inadequate. The availability of whole genome sequence of *Caenorhabditis elegans* and *Drosophila melanogaster* would change the equation forever (Consortium, C. E. S., 1998; Adams, M. D. *et al.*, 2000) to allow the analysis of large amounts of data and to facilitate the identification of olfactory gene families (Table 1). Importantly, many candidate olfactory genes are still to be functionally validated while others with unknown function remain unidentified. In this context, it is noteworthy that much of the work on invertebrate olfaction has been driven by visual and olfactory system studies in mammals.

What are olfactory genes and how many are there in any given organism? What are their functions? How and when do these gene families interact to generate complex phenotypes? The genomic era is still in its infancy, but it has already opened tremendous opportunities to study these questions. As more genomes become available, comparative genomics will likely reveal how chromosomal organization and rearrangements affect the nascent divergence of phylogenetically related species. Of particular interest is the analysis of orthologous genes across diverse taxa. Although at present, the olfactory genomics of invertebrates is limited to a handful of phylogenetically distant organisms, entire orthologous gene families have nevertheless been identified facilitating the elucidation of function using reverse genetic tools or by functional inference in several instances.

Table 1 Known gene families implicated in olfactory primary coding in *Anopheles gambiae*, *Drosophila melanogaster*, and *Caenorhabditis elegans*

		D. melanogaster	*An. gambiae*	*C. elegans*	*References*
Receptor genes	*Obp*	33/1	29	ND	a, b
	Csp	4/1*	6	ND	c, d
	Or/Cr	62/37	79/2	1699/1	e, f, g, h, i, j
$G\alpha$ subunit genes		6/1	6/1	21/5	k, l, m, n, o
Effector genes	*Tm-Gc*	12	ND	28/2	p, q, r
	Tm-Ac	6/1	ND	4	s, t
	Plc	3/1	ND	1/1*	u, v
	Pde	2/1	ND	ND	w, x
Ion channel genes	*Cng*	4/1	ND	6/2	y, z, a′, b′
	K channels (eag)	2/1	ND	2	c′
	Trp	4	ND	11/2	d′, e′, f′
RGS genes	*Arr*	4/2	4/2	2/1	g′, h′
	Grk	2	2	2/1	i′, j′
	Ip3k	2/1	ND	ND	v
	Itpr	1/1	ND	ND	k′
	nPkc	1	ND	2/2	l′
	Calcineurin	ND	ND	1/1	m′
	Pkg	ND	ND	2/1	n′
	Dgk	ND	ND	5/2	o′
	RdgB	1/1	ND	ND	p′

[a]Hekmat-Scafe D. S. *et al.* (2002); [b]Xu, P. X. *et al.* (2003); Xu, P. *et al.* (2005); [c]Wanner K. W. *et al.* (2004); [d]McKenna M. P. *et al.* (1994); [e]Hill C. A. *et al.* (2002); [f]Vosshall L. B. *et al.* (2000); [g]Hallem E. A. and Carlson J. R. (2006); [h]Robertson H. M. and Thomas J. H. (2006); [i]Sengupta P. *et al.* (1996); [j]Hallem E. A. *et al.* (2004b); [k]Jansen G. *et al.* (1999); [l]Lans H. *et al.* (2004); [m]Zwaal R. R. *et al.* (1997); [n]Rutzler M. R. *et al.* (2006); [o]Roayaie K. *et al.* (1998); [p]Fitzpatrick D. A. *et al.* (2006); [q]L'etoile N. D. and Bargmann C. I. (2000); [r]Birnby D. A. *et al.* (2000); [s]Martin F. *et al.* (2001); [t]Korswagen H. C. *et al.* (1998); [u]Riesgo-Escovar J. *et al.* (1995); [v]Gomez-Diaz C. *et al.* (2006); [w]Gomez-Diaz C. *et al.* (2004); [x]Martin F. *et al.* (2001); [y]Baumann A. *et al.* (1994); [z]Komatsu H. *et al.* (1999); [a′]Coburn C. M. and Bargmann, (1996); [b′]Kaupp U. P. and Seifert R. (2002); [c′]Dubin A. E. *et al.* (1998); [d′]Stortkuhl K. F. *et al.* (1999); [e′]Tobin D. *et al.* (2002); [f′]Colbert H. A. and Bargmann C. I. (1995); [g′]Palmitessa A. *et al.* (2005); [h′]Merrill C. E. *et al.* (2003; 2005); [i′]Cassil J. A. *et al.* (1991); [j′]Fukuto H. S. *et al.* (2004); [k′]Deshpande M. *et al.* (2000); [l′]Okochi Y. *et al.* (2005); [m′]Kuhara A. *et al.* (2002); [n′]L'etoile N. D. *et al.* (2002); [o′]Matsuki M. *et al.* (2006); [p′]Riesgo-Escovar J. R. *et al.* (1994).

Numbers on the left indicate genes with putative olfactory functions and numbers on the right indicate functionally characterized genes. Genes with putative olfactory function are indicated by an asterisk* and unidentified family are indicated by ND (nondetermined). RGS, regulator of G protein signaling; Tm, transmembrane.

This chapter will discuss the current state of knowledge of gene families involved in odor reception, olfactory transduction, and adaptation. It will mainly draw from the study of three best-described invertebrate genomes: *D. melanogaster*, *Anopheles gambiae*, and *C. elegans*. We have included a brief comparative description of the cellular and the molecular participants in the invertebrate olfactory organs. A more detailed discussion of invertebrate olfactory systems is described in chapter 22. We structured our discussion to mimic the successive stages of primary olfactory sensing and adaptation, beginning with odor recognition, olfactory transduction and ending with regulation of primary sensory processing, as we review the organization, structure, regulation, and function of olfactory genes in insects and nematodes.

4.33.2 An Overview of Invertebrate Chemosensory Organs and Their Molecular Components

In insects, olfaction is mediated by thousands of primary olfactory receptor neurons (ORNs) segregated by groups of two or more in small olfactory organs called sensilla (Figure 1). The dendrites of these neurons project in perforated hollow cuticular structures of various morphological types and are mainly arrayed on the antennal surface. In *C. elegans*, volatile chemicals are detected by five pairs (AWA, AWB, AWC, ASH, and ADL) of chemoreceptor neurons (CRNs) located in the main sensory organs known as the amphid sensilla (Bargmann, C. I. *et al.*, 1993). These organs sit on each side of the buccal cavity and communicate with the external environment via a

prominent pore. Each CRN responds to many different compounds (Bargmann, C. I. and Horvitz, H. R., 1991). Despite overall morphological similarity, it is becoming more and more apparent that morphological differences result from ecological adaptations rather than based on olfactory-related requirements. In the case of the terrestrial giant robber crab, olfactory receptors (aesthetascs) display morphological and

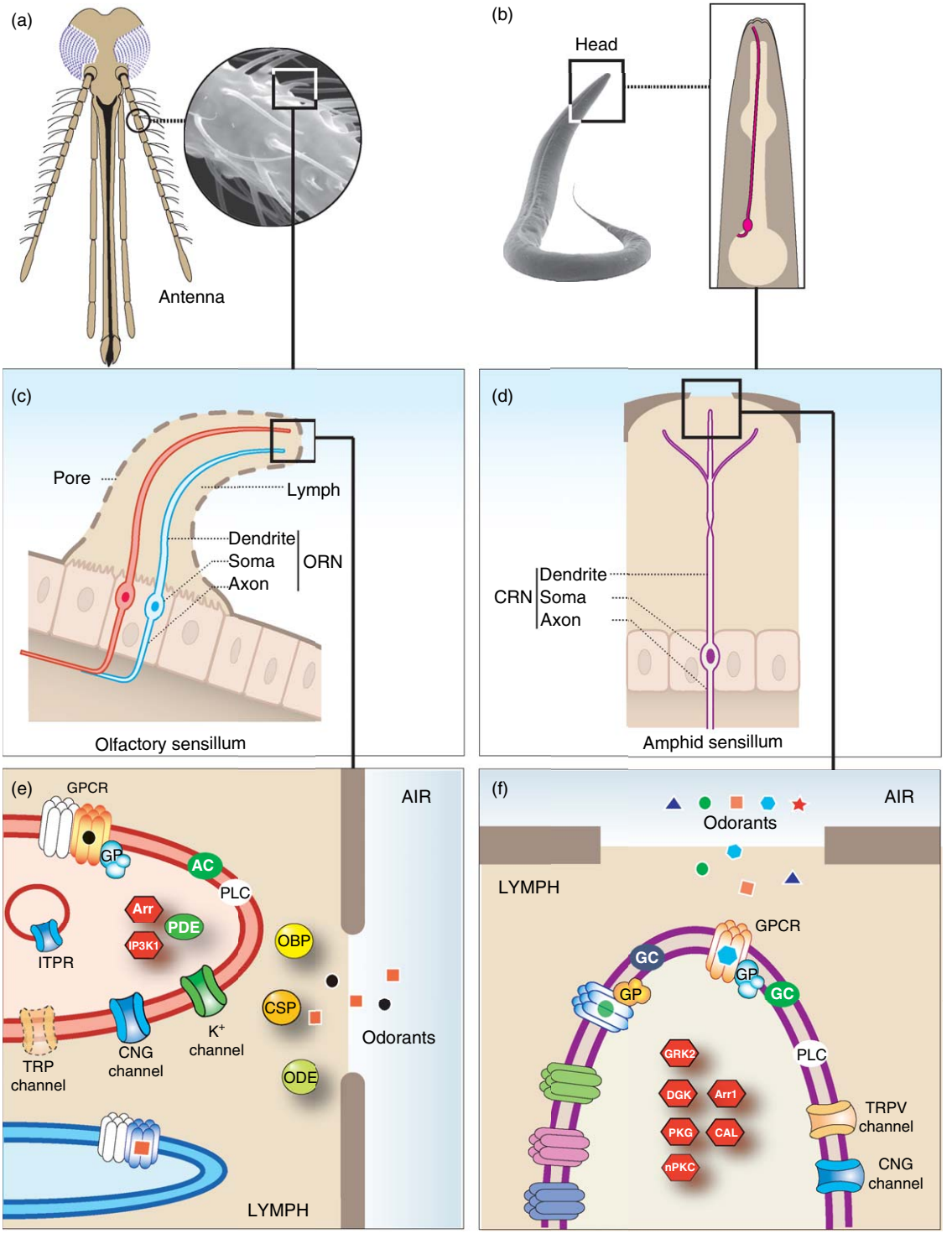

physiological attributes intermediate between marine crustaceans and insects (Stensmyr, M. C. *et al.*, 2005). Drosophila olfactory sensilla exhibit over a dozen morphological subtypes, which do not seemingly relate to olfactory function (Shanbhag, S. R. *et al.*, 1999; Stocker, R. F., 2001).

Despite the diverse morphologies, the partitioned nature of these structures remains invariant between insects, crustaceans, and nematodes and represents a defining hallmark of invertebrates. Thus, it is not surprising that similar adaptive features are reflected by common cellular and molecular strategies. Olfactory sensilla are highly specialized cell clusters encased in the olfactory epithelium such that the ORNs are separated and protected from the environment by an aqueous fluid on its apical side and physiologically supported by accessory cells on its basal side. The physical and biochemical demands imposed by this system require an odorant to cross the extracellular sensillum lymph to reach the molecular receptor located on the surface of the dendritic membrane in order to activate the intracellular transduction machinery. Furthermore, another defining specificity is that insect odorant receptors (ORs) almost certainly require the association with a heterodimer partner homolog (Benton, R. *et al.*, 2006) for proper activation of intracellular downstream effectors such as a heterotrimeric G protein (GP) (Laue, M. *et al.*, 1997) and a cyclic nucleotide-gated (CNG) ion channel (Baumann, A. *et al.*, 1994; Dubin, A. E. and Harris, G. L., 1997).

Studies in cockroach, Drosophila, and lobsters implicate both a GP-coupled adenylyl cyclase (AC) and a GP-coupled phospholipase C (PLC) transduction cascades in olfactory reception (Boekhoff, I. *et al.*, 1990a; 1990b; Boekhoff, I. *et al.*, 1994; Riesgo-Escovar, J. *et al.*, 1995; Deshpande, M. *et al.*, 2000; Martin, F. *et al.*, 2001). Putative targets of these effector genes include a CNG channel and a cyclic nucleotide-modulated K^+ channel (Baumann, A. *et al.*, 1994; Dubin, A. E. *et al.*, 1998). Signal termination appears to be mediated by several enzymes including a cyclic adenosine monophosphate (cAMP)-phosphodiesterase (cAMP-PDE), an inositol 1,4,5-triphosphate kinase 1 (IP3K1), and two sensory arrestins (ARRs) (Martin, F. *et al.*, 2001; Merrill, C. E. *et al.*, 2002; 2003; Gomez-Diaz, C. *et al.*, 2004; Merrill, C. E. *et al.*, 2005; Gomez-Diaz, C. *et al.*, 2006). Regulation of GP signaling requires a transient receptor potential (TRP) Ca^{2+} channel (Bergamasco, C. and Bazzicalupo, P., 2006) and an inositol 1,4,5-triphosphate receptor (ITPR).

Rapid ORN activation depends on cellular and molecular mechanisms that facilitate the transport and the clearance of biologically active/toxic compounds. Although G-protein-coupled receptors (GPCRs), also known as seven-transmembrane receptors, and their GP partners are invariably used as ORs across diverse phyla, there is significant variation as to how these receptors interact with their molecular environment. Within invertebrate lineages, the main difference between arthropods and nematodes consists of divergent molecular strategies upstream of the GPCRs within the fluid compartment of the sensillum. Insect ORs interact with an extracellular perireceptor pathway that potentially includes various odorant-binding protein (OBP) members, possibly chemosensory proteins (CSPs) and odorant-degrading enzymes (ODEs).

ODEs comprise members of the cytochrome P450s, gluthatione-*S*-transferase and carboxylesterases supergene families that have often been implicated in olfactory signaling based on inferential expression patterns. In particular, in mosquitoes and other insects, ODEs play an important role in insecticide metabolism/resistance (Ranson, H. *et al.*, 2002), and several reports have suggested a possible

Figure 1 Comparison of the olfactory systems of arthropods and nematodes. (a)The antenna of a mosquito and (b) the head of *Caenorhabditis elegans* are magnified in (c) and (d), respectively, to show the cellular organization of insect olfactory sensillum and amphid sensillum. Two odorant receptor neurons (ORNs) and only one of the chemoreceptor neuron (CRN) are shown for clarity purposes. Close up of the dendritic termini are shown in (e) and (f) to show the various molecular components involved in olfactory sensing in both invertebrate systems. The molecular components of odor reception include the bona fide odorant-activated G-protein-coupled receptors (GPCRs). An additional role in odor coding has been proposed for the insect odorant binding proteins (OBPs) and chemosensory proteins (CSPs). Heterotrimeric G proteins (GPs) activate a variety of intracellular signal transduction pathways. Two main intracellular signaling routes are mediated by a phospholipase C (PLC) and adenylyl/guanylyl cyclase (AC and GC). These effector proteins target various receptors and ion channels such as an inositol triphosphate receptor (ITPR) and transient receptor potential (TRP), cyclic nucleotide-gated (CNG) potassium (K^+) channels. Regulation of GP/GPCR signaling is mediated by arrestins (ARR) and G protein-coupled receptor kinases (GRK). Calcineurin (CAL), protein kinases G and C (PKG, nPKC), and diacyl glycerol kinases (DGKs) modulate primary sensing by targeting various components of the transductory cascade. Picture of the *C. elegans* was kindly provided by Z. Altun and D. Hall.

role for ODEs in xenobiotic/odorant clearance based solely on their expression in olfactory tissues (Hovemann, B. T. *et al.*, 1997; Rogers, M. E. *et al.*, 1999; Maibeche-Coisne, M. *et al.*, 2005; Lycett, G. J. *et al.*, 2006). Owing to this paucity of specific data tying these genes to olfactory signaling, an in-depth analysis of ODEs superfamilies has not been included in this chapter. A review of ODEs is available from Vogt R. G. (2003).

For expediency we will focus on the chemosensory gene families in *C. elegans* restricted to the AWA, AWB and AWC neurons, which together mediate chemotaxis to a range of volatile attractants. A detailed review of the full chemical sensitivity in *C. elegans* is available from Bergamasco C. and Bazzicalupo P. (2006). Interestingly, no OBPs, CSPs, or ODEs have been described in nematodes (Rubin, G. M. *et al.*, 2000). The transduction pathways of *C. elegans* and insects are generally similar as they both use GPCRs and GPs (Zwaal, R. R. *et al.*, 1997; Roayaie, K. *et al.*, 1998; Lans, H. *et al.*, 2004) to target, in some cases, homologous ion channels (Colbert, H. A. and Bargmann, C. I., 1995; Tobin, D. *et al.*, 2002). However, *C. elegans* seems to favor cyclic guanosine monophosphate (cGMP) over cAMP as a second messenger (Birnby, D. A. *et al.*, 2000; L'etoile, N. D. and Bargmann, C. I., 2000). Moreover, the regulation of GP signaling in *C. elegans* involves several protein kinases (L'etoile, N. D. *et al.*, 2002; Fukuto, H. S. *et al.*, 2004; Okochi, Y. *et al.*, 2005; Matsuki, M. *et al.*, 2006), a single ARR and calcineurin (Kuhara, A. *et al.*, 2002; Palmitessa, A. *et al.*, 2005).

4.33.3 Odor Recognition

Upon entering the sensillum, an odorant is presumed to transverse the sensillum lymph in order to activate the OR. While this process is the initial component of odor recognition in arthropods and worms, the precise mechanisms and functional roles of molecular players such as OBPs and CSPs remain unclear. Nevertheless, these gene families have been proposed to play significant roles in the general process of perireception, that is, interaction of an odorant with molecular components preceding OR activation. Indeed, *Ors*, *Obps*, and *Csps* are ancient and diverse gene families, which are likely a reflection of their evolutionary value in olfactory signal transduction.

4.33.3.1 Insect Odorant-Binding Proteins

The OBP designation derives from their initial discovery in the silk moth *Antheraea polyphemus* where the first pheromone-binding protein (*Apol*PBP) was shown to bind *in vitro* one of the female sex pheromone component in the aqueous lymph bathing the pheromone-sensitive neuron (Vogt, R. G. and Riddiford, L. M., 1981). Membership in this gene family is contingent on the following four requirements: antennal-specific expression, putative odor-binding capability, overall size of approximately 14 kDa and the presence of six conserved cysteine residues at characteristic positions (six-cysteine motif). OBPs of the lipocalin family have also been described in higher vertebrates but despite their common name with their insect counterparts, both families do not share any similarity at the sequence and at the structural levels suggesting convergent evolution in both lineages (Pelosi, P., 1994; Tegoni, M. *et al.*, 2000). With the growing number of OBP reports in other insect orders, it became apparent that all criteria could not always be met and OBP membership relied primarily on circumstantial functional evidences in the face of relaxed sequence homology. The identification of multiple OBPs in several insect species and the description of a new subfamily of OBPs called general odorant-binding proteins (GOBPs) in Lepidoptera provided good support that OBPs were part of a multigene family with an intrinsic role in perireception (Vogt, R. G. *et al.*, 1989; 1991; Robertson, H. M. *et al.*, 1999). This notion would be strengthened by the identification of *Obp* genes in a wide range of insect species including Coleoptera (Nikonov, A. A. *et al.*, 2002), Hymenoptera (Briand, L. *et al.*, 2001), Diptera (Kim, M. S. *et al.*, 1998), Orthoptera (Picone, D. *et al.*, 2001), Dictyoptera (Riviere, S. *et al.*, 2003), and Heteroptera (Vogt, R. G. *et al.*, 1999). Approximately 20 years after the initial *Apol*PBP characterization, the availability of *D. melanogaster* and *An. gambiae* genomes resulted in an explosion of putative *Obps* when over 50 genes were described based on similar structural features but not necessarily based on similar functional properties (Hekmat-Scafe, D. S. *et al.*, 2002; Xu, P. X. *et al.*, 2003).

4.33.3.1.1 Comparative evolutionary genomics

The genomes of *D. melanogaster* and *An. gambiae* contain 49 and 57 potential *Obp* genes, respectively (Hekmat-Scafe, D. S. *et al.*, 2002; Xu, P. X. *et al.*, 2003).

Within this classification, the six-cysteine motif, as a structural standard, has not always been completely adhered to, and *Obp* classification has relied on more broadly based sequence homology strategies using different variations of the BLAST algorithm (Altschul, S. F. *et al.*, 1990). Alignment of deduced OBP sequences indicates a diverse family of proteins with low-average amino acid identity within a given species of approximately 15–20% range (from 5% to 100% and from 9.2% to 62.6% range in *An. gambiae* and *D. melanogaster*, respectively) (Galindo, K. and Smith, D. P., 2001). OBP protein size typically ranges from 14 to 35 kDa and most have a potential peptide signal at their N-terminus. Moreover, this heterogeneous group encompasses several variations of the typical *Obp* gene group. In *D. melanogaster*, the *Obp* gene family includes 29 classic, 14 plus-C, and 6 minus-C genes. In *An. gambiae*, there are 29 typical, 12 plus-C, and 16 atypical *Obp* genes (see description below). The classic *Obp* genes are predicted to encode short 14 kDa proteins with six stereotypically placed cysteine residues and represent the archetype to which all other *Obp* types are compared. Most *Obp* genes include up to three introns that are distributed between the nine conserved positions shown in Figure 2. Generally, the first intron is located immediately downstream of the DNA encoding the putative peptide signal, which is presumably necessary for the extracellular expression of the mature protein. In the majority of cases (>80%), these introns occur between codons (phase 0) (Hekmat-Scafe, D. S. *et al.*, 2002). Classical *Obps* are predicted to encode six α-helical proteins and to form a globular compact structure reinforced by the presence of three disulfide bridges as shown by the structural studies on the pheromone-binding protein (PBP) of *Bombyx mori* (*Bmor*PBP) (Sandler, B. H. *et al.*, 2000).

Although these genes are distributed throughout the genome, most of them are cytogenetically clustered (Figure 3). In the case of *D. melanogaster*, more than half of the *Obp* genes (57%) are located on chromosome *2R*, where 14 *Obp* genes are clustered within a 825-kb stretch that also encompasses OR gene *Or56a* (Galindo, K. and Smith, D. P., 2001; Graham, L. A. and Davies, P. L., 2002; Hekmat-Scafe, D. S. *et al.*, 2002). In contrast, chromosome 2L of *D. melanogaster* carries only one *Obp* gene. *An. gambiae Obp* gene clusters are more dispersed and characteristically smaller. In both species these gene clusters tend to be localized at the tips of chromosome and rather than being organized in tandem arrays, typically occur in forward and backward orientations, suggesting that this family is rapidly evolving via multiple duplication and rearrangement events.

Many sequence analyses have been done on OBPs mainly to understand the structural relationships between members of this highly divergent gene family. All OBPs described to date have been restricted to insects within the Neoptera superorder. They include Lepidoptera, Diptera, Hymenoptera, Coleoptera (holometabolous insects), and one Hemiptera (hemimetabolous insects). Phylogenetic analyses have shown that three subfamilies seem to be monophyletic (i.e., subgroups of OBPs belonging to one insect lineage). The PBP/GOBP subfamily is restricted to the Lepidoptera (Figure 4). Their

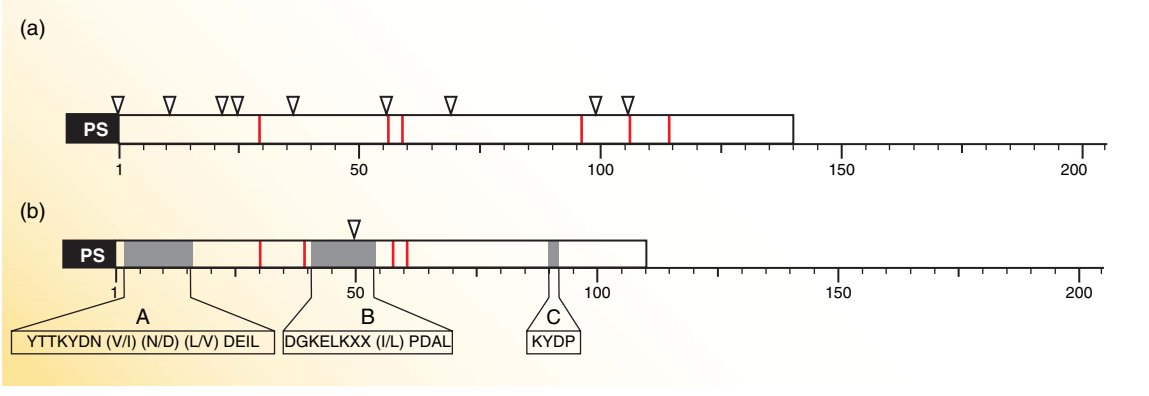

Figure 2 Gene structure and protein motifs of the *Obp* and *Csp* gene families. (a) Odorant-binding protein (OBP): The intron locations (arrowheads) and cysteine residues (vertical red bars) are shown relative to a scale of the average protein size in amino acids. Data from Hekmat-Scafe, D. S., Scafe, C. R., Mckinney, A. J., and Tanouye, M. A. 2002. Genome-wide analysis of the odorant-binding protein gene family in *Drosophila melanogaster*. Genome Res. 12, 1357–1369. (b) Chemosensory protein (CSP): Conserved amino acid motifs A, B, and C are shaded in gray. Data from Wanner, K. W., Willis, L. G., Theilmann, D. A., Isman, M. B., Feng, Q., and Plettner, E. 2004. Analysis of the insect os-d-like gene family. J. Chem. Ecol. 30, 889–911.

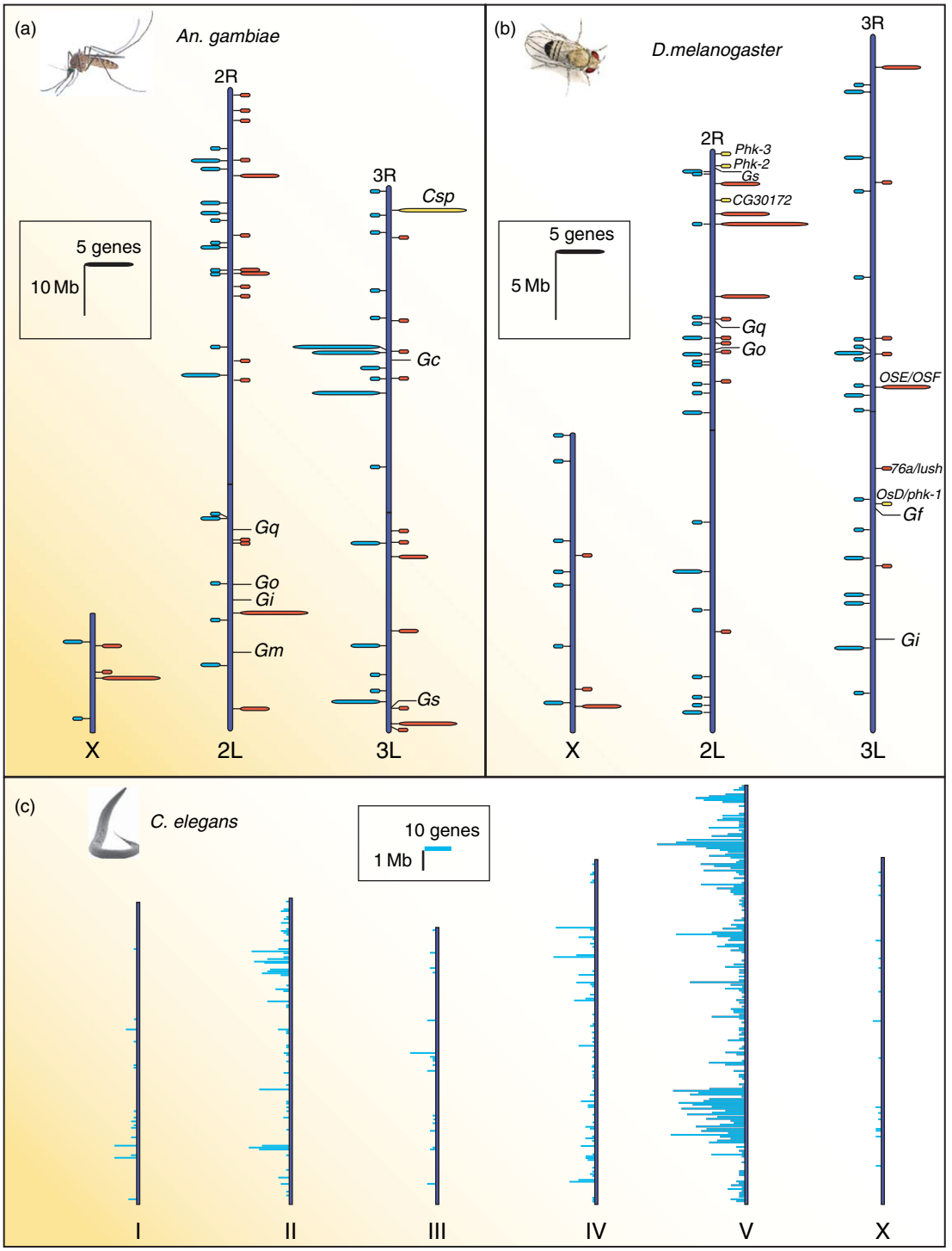

Figure 3 Physical map of *Or*, *Obp*, and *Cr* genes in *Anopheles gambiae*, *Drosophila melanogaster,* and *Caenorhabditis elegans*. Genomic locations of *Or* (blue), *Csps* (yellow), and *Obps* (red) are listed on each chromosome of (a) *An. gambiae* and (b) *D. melanogaster* (data from Hill, C. A. *et al.*, 2002; Robertson, H. M. *et al.*, 2003; Xu, P. X. *et al.*, 2003; Hekmat-Scafe, D. S. *et al.*, 2002; Galindo, K. and Smith, D. P., 2001; Zhou, J. J. *et al.*, 2004; Biessmann, H. *et al.*, 2005; Wanner, K. W. *et al.*, 2004). (c) Positions in the entire *C. elegans* genome of all analyzed members of chemoreceptor (*Cr*) families. Adapted from Robertson, H. M. and Thomas, J. H. The putative chemoreceptor families of *C. elegans* (January 6, 2006), WormBook, ed. The *C. elegans* Research Community, WormBook, doi/10.1895/wormbook.1.66.1, http://www.wormbook.org. Picture of the *C. elegans* was kindly provided by Z. Altun and D. Hall.

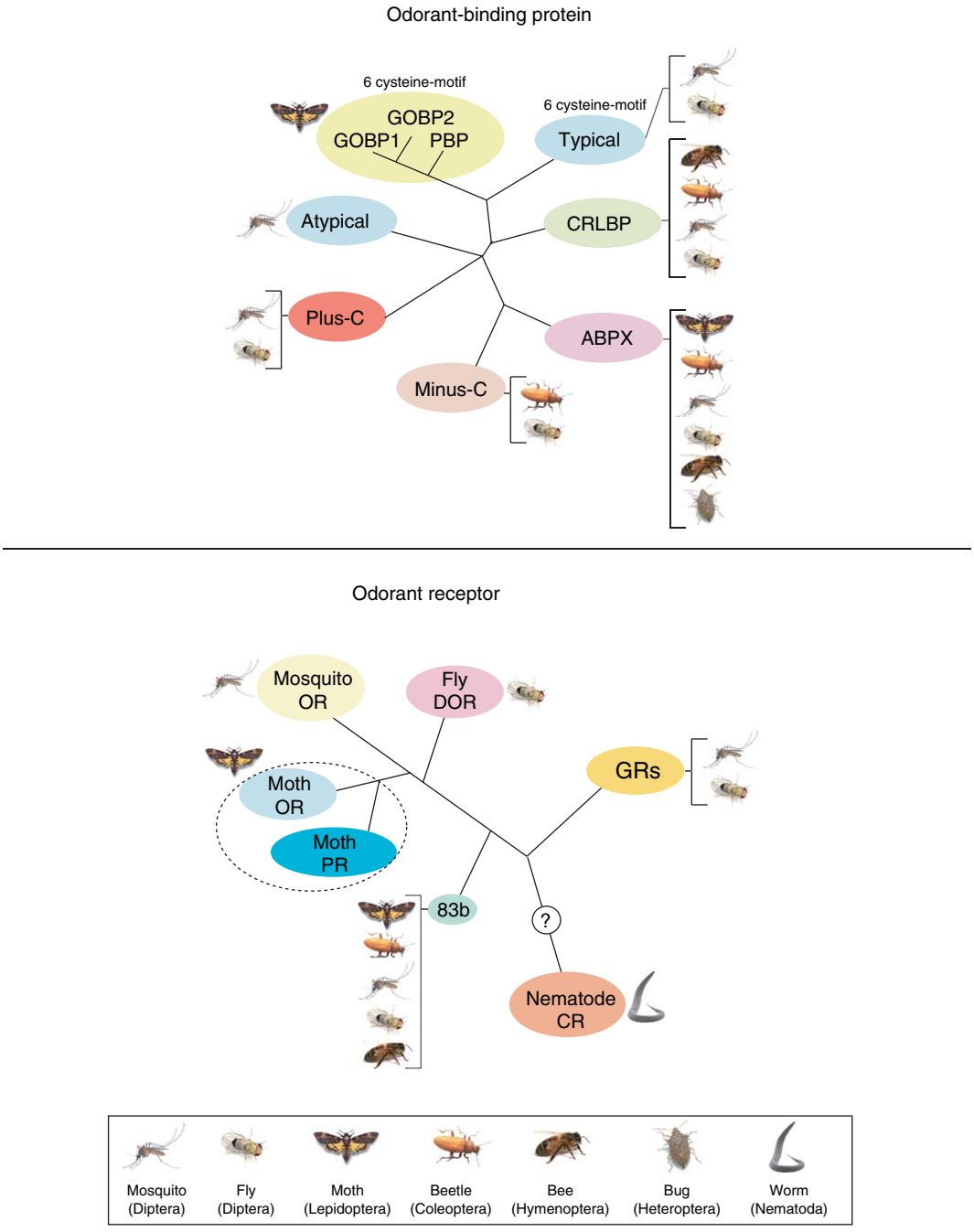

Figure 4 Stylized representation of the phylogenetic relationships of the insect *Obp* and invertebrate *Or* gene families. While the phylogenetic trees of odorant-binding proteins (OBPs) and odorant receptors (ORs) proteins are meant to display the various subfamilies (colored ovals), the phylogenetic relationships represented here do not represent true phylogenetic distances.

absence from other insect lineages suggests that this family arose within the Lepidoptera. This subfamily is subdivided into three subgroups based on sequence homology: PBP, GOBP1, and GOBP2 groups. PBPs are highly divergent (20–95% amino acid identity) while within one GOBP group the percentage of amino acid increases to 90%. In the case of the *Manduca sexta* PBP1–GOBP2 cluster, gene duplication

is one of the mechanisms that is likely to be responsible for generating molecular diversity (Vogt, R. G. *et al.*, 2002). Here, it was shown that both genes are approximately 2 kb apart, share identical exon-intron boundaries and are oriented in the same direction. As in the case of *D. melanogaster*, evolutionarily related genes seemingly share similar genomic features such as close cytogenetic position (gene clustering) and identical exon–intron boundaries. Although, it is important to know that these common features do not necessarily mean similar expression pattern and/or functional relationships.

Plus-C *Obps* have been identified only in Dipterans and thus must have arisen prior to the mosquito/fly divergence ~250 million years ago (mya). In Diptera, there are approximately a dozen Plus-C subfamily members per genome that are distributed in a few clusters (Zhou, J. J. *et al.*, 2004). The Plus-C group contains several divergent features from the classical *Obps*. Most notably a unique exon/intron usage not present in other *Obp* subgroups. In addition, Plus-C proteins average length 250 AA in length including 12 cysteine residues. Eleven Plus-C *Obps* have been described in *Drosophila pseudoobscura* (Zhou, J. J. *et al.*, 2004) and each of them has a strong counterpart in *D. melanogaster* as suggested by phylogenetic analysis. Significantly, the clustering pattern and synteny between these two Drosophilids is also extremely conserved for animals that diverged approximately 25–55 mya (Richards, S. *et al.*, 2005), and this may be indicative of similar function across all Drosophilids. This genomic organization suggests that many of these genes arose via duplication and evolved rapidly. There is only partial sequence similarity between Plus-C OBPs in these two species (overall 20%), and the majority has been shown to be expressed in the antenna and possess a peptide signal (Zhou, J. J. *et al.*, 2004; Biessmann, H. *et al.*, 2005).

Minus-C *Obp* genes have also been identified in several insect orders including Diptera and Coleoptera (Figure 4). Most *D. melanogaster* Minus-C genes (four out of six) are clustered at the tip of chromosome 3R, exhibit very low sequence similarity (~20% amino acid identity), and lack two of the six canonical cysteine residues, usually C2 and C5. Interestingly, non-Diptera Minus-C *Obps* also lack cysteines C2 and C5. Among them, *Tenebrio molitor* B1, B2, and Thp12 are hemolymph proteins (Paesen, G. C. and Happ, G. M., 1995; Rothemund, S. *et al.*, 1999; Graham, L. A. and Davies, P. L., 2002) suggesting that their *Drosophila* homologs may also have nonolfactory functions. However, the other two *Drosophila* Minus-C proteins each contain all six cysteine residues, are expressed in the antennae (Galindo, K. and Smith, D. P., 2001) raising the possibility that olfactory function may be dependent upon the retention of a set of particular structural motifs.

Atypical *Obps* are more similar to the classic *Obp* genes but distinct from the plus-C class, and thus far have been found only in *An. gambiae* where 16 genes are predicted, and it is likely that this subfamily arose after the fly/mosquito divergence (Xu, P. X. *et al.*, 2003). Indeed homology searches have failed to identify atypical *Obps* in *Drosophila*. While atypical *Obps* display the six-cysteine hallmark of classic *Obps*, they display a characteristically elongated C-terminus containing up to seven additional cysteine residues located downstream of the six-cysteine motif. Furthermore, atypical *Obp* genes lack introns in their predicted coding regions. Two clusters of seven and three genes are located on chromosome X and 3L, respectively, with the remaining genes being scattered throughout the genome. As is typical for other *Obp* classes these genes share a low 20.2% amino acid identity (Hekmat-Scafe, D. S. *et al.*, 2002).

The antennal-binding protein family (ABPX) (Krieger, J. *et al.*, 1996) encompasses *Obps* from several insect orders (Figure 4). They were first identified in *B. mori* where they displayed little homology to the PBP/GOBP subfamily. To date, this subfamily includes several Drosophila and mosquito genes including olfactory-specific proteins E and F (*OS-E*, *OS-F*), *Ag-Obp1*, *Ag-Obp2*, *Ag-Obp3*, and *Ag-Obp17*, the *Lygus* antennal protein (LAP) (Vogt, R. G. *et al.*, 1999), several beetle *Obps* (Wojtasek, H. and Leal, W. S., 1999), and a single queen bee *Obp* (Danty, E. *et al.*, 1999). Lastly, a separate but related class of OBP-like proteins known as the chemical sense-related lipophilic ligand-binding proteins (CRLBP) were first identified in the contact chemoreceptor sensilla of the blowfly *Phormia regina* (Ozaki, M. *et al.*, 1995; Tsuchihara, K. *et al.*, 2005). Other CRLBP members have been identified in Coleoptera (Wojtasek, H. and Leal, W. S., 1999), Diptera, and in the honeybee *Apis mellifera* (Danty, E. *et al.*, 1999).

4.33.3.1.2 Functional genomics of Obps

Obps or *Obp*-like genes have been identified in vertebrates and insects. Although both OBP families are phylogenetically unrelated, both taxa have developed similar mechanisms at the perireceptor level to facilitate or to modulate the interaction between ORs and their ligands. It is therefore striking that no OBPs have been described in *C. elegans* suggesting that the nematode chemosensory system has evolved

without the requirement of *Obps* for its signal transduction pathway. This raises the possibility as to whether OBPs are required for olfactory functions in all cases. What is the evidence supporting such function for this gene family? And, do these proteins possess *bone fide* odorant-binding capabilities?

The assumption of their olfactory involvement was for more than 20 years circumstantial and relied on *in vitro* experiments that were rather difficult to interpret. Evidences largely drew from the differential pattern of *Obp* expression that was distinguished by high levels of antennal transcripts. Indeed, the central dogma of OBP expression studies consistently maintained that moth PBPs were preferentially expressed in male pheromone-sensitive trichoid sensilla whereas GOBPs were expressed in the general plant-volatile-sensitive basiconic sensilla of both sexes (Vogt, R. G. *et al.*, 1991). This situation changed when the expression of PBPs and GOBPs was reported in male and female adult moths and of GOBPs in larvae albeit with different expression patterns (Vogt, R. G. *et al.*, 2002). Furthermore, immunocytochemistry experiments were able to localize their exact expression to the sensillum lymph bathing the ORN (Steinbrecht, R. A., 1998).

The crystal structure of *B. mori* PBP and its natural bound ligand, bombykol, provided a structural model to investigate the nature of this molecular relationship and the potential consequences on OR activation by such a complex (Sandler, B. H. *et al.*, 2000). Five additional OBP structures have been resolved from different insect orders including *Dmel*-LUSH (Kruse, S. W. *et al.*, 2003), cockroach *Leucophaea maderae* PBP (Lartigue, A. *et al.*, 2003), the honeybee *A. mellifera* ASP1 (Lartigue, A. *et al.*, 2004), *A. polyphemus* PBP (Mohanty, S. *et al.*, 2004), and *An. gambiae* OBP1 (Wogulis, M. *et al.*, 2006). In all cases a similar potential of hydrogen (PH)-dependent mechanism seems likely to be responsible for the release of the ligand.

Definitive evidence for olfactory function was provided by the characterization of the only mutant defective for OBP expression: the *Drosophila OBP76a* mutant, also referred to as *lush* (Figure 5). *Lush* mutants display an abnormal attraction to toxic levels of ethanol (Kim, M. S. *et al.*, 1998) and a loss of sensitivity to the aggregation of pheromone 11-*cis*-vaccenyl acetate (VA) (Xu, P. *et al.*, 2005). These two compounds are detected by two different subsets of trichoid sensilla also corresponding to *lush* expression. Transgenic rescue and the introduction of LUSH protein into the recording pipette of VA-sensitive neuron in mutant flies were shown to restore the electrophysiological response to this compound. More importantly, using alternative putative carrier such as DmelOBP83a (OSF) or bovine serum albumin (BSA) did not restore the wild-type phenotype demonstrating that *lush* is specifically required for the transduction pathway of VA.

If *Obp* expression in olfactory sensilla can be used to infer olfactory function, then their expression in nonolfactory tissues requires the assumption of alternative functions. In *Drosophila*, where Galindo K. and Smith D. P. (2001) studied the expression pattern of over 30 *Obps* by LacZ promoter fusions, four classes were distinguished based on their expression pattern: olfactory, taste, olfactory and taste, and nonchemosensory. The last class includes the Drosophila *Obp19d* (*pbprp2*) whose expression is quite ubiquitous and is expressed in olfactory sensilla coeloconic, in various taste organs, and in the epidermis (Park, S. K. *et al.*, 2000; Galindo, K. and Smith, D. P., 2001; Shanbhag, S. R. *et al.*, 2001). Accordingly, a scavenger function has been proposed for this class of *Obps* (Park, S. K. *et al.*, 2000; Shanbhag, S. R. *et al.*, 2001).

4.33.3.2 Insect Chemosensory Proteins

The *Csp* gene family also encodes a group of small, water-soluble proteins presumed to act as carriers for small hydrophobic compounds. CSPs are smaller (~110 AA) than OBPs and have four cysteine residues whose positions are also strictly conserved. The crystal structure of the noctuid *Mamestra brassicae* CSP-A6 has six α-helices surrounding a hydrophobic binding pocket and two disulfide bridges in a folding pattern different from that of OBPs (Lartigue, A. *et al.*, 2002). The first member of this family (A10) was identified in *D. melanogaster* and due to its antennal expression was denoted as olfactory-specific D or OS-D (McKenna, M. P. *et al.*, 1994). Subsequent members of this family were referred as OS-D like, pherokine (Phk), or sensory appendage protein (SAP) based on their expression in various sensory structures. CSPs have been identified in many insect orders including Hymenoptera, Diptera, Lepidoptera, Dictyoptera, Orthoptera, Hemiptera, and Phasmatodea. The hallmark of the encoded protein family includes four invariant cysteine residues at conserved positions $CX_6CX_{18}CX_2$. There are two classes of CSPs. The first class contains three conserved amino acid motifs: an N-terminal motif A [YTTKYDN(V/I)(N/D)(L/V)DEIL], a central motif B [DGKELKXX(I/L)PDAL], and a C-terminal motif C [KYDP] (Figure 2). Proteins that diverge from this pattern belong

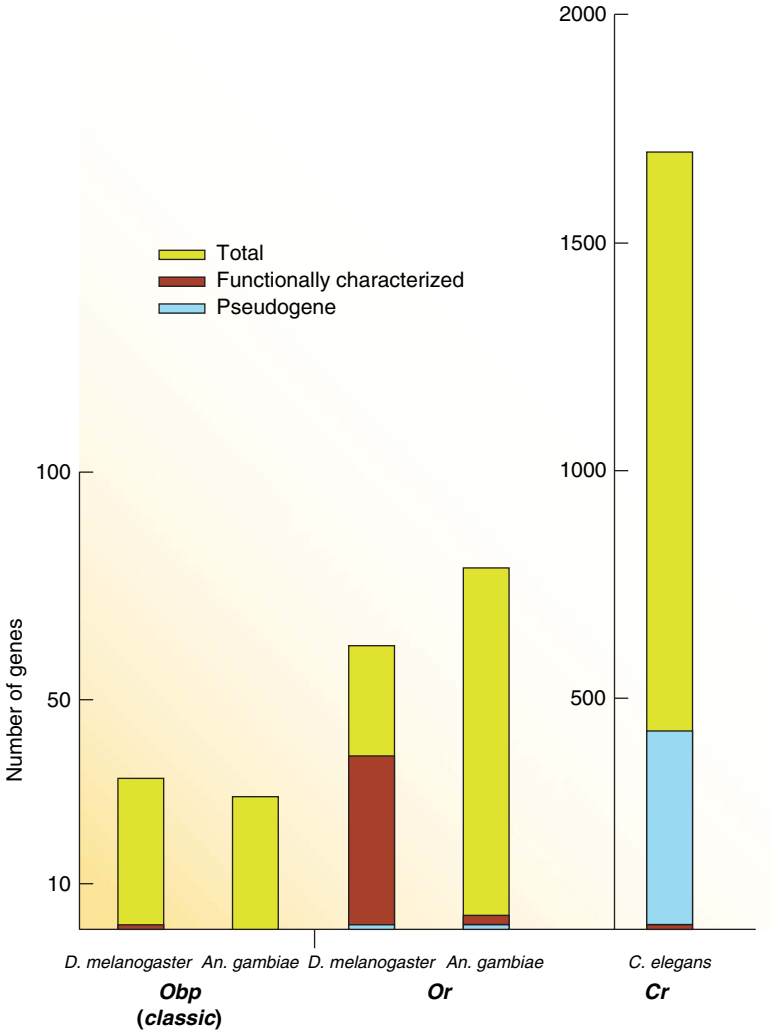

Figure 5 Known gene families in insects and nematodes. (a) *Or* and *Obp* gene repertoires in *Anopheles gambiae*, *Drosophila melanogaster*, and *Caenorhabditis elegans*. Green, total number of genes; blue, number of pseudogenes; and brown, functionally characterized genes.

to a second class. The conservation of sequence, structural motifs, intron site, and genomic clustering in the insect Neoptera infraclass (insect with wing folding) suggest an ancient origin predating the Neoptera–Paleoptera divergence. See Wanner K. W. *et al.* (2004) for a detailed review.

4.33.3.2.1 Genomic organization and gene structure of Csps

How do *Csp* repertoires compare to *Obp* repertoires? The genome of *D. melanogaster*, *D. pseudoobscura*, *A. mellifera*, and *An. gambiae* have 4, 4, 6, and 6 *Csp* genes, respectively (Wanner, K. W. *et al.*, 2004). Generally, CSPs are more conserved than OBPs with an average of 50% amino acid identity within and between species and typically have 0 or 1 introns (Figure 2). When present, the intron splice site is strictly conserved one nucleotide past an invariant lysine residue (phase 1 intron). All *An. gambiae Csp* genes are clustered within a 120 kb stretch on chromosome 3R, while in *Drosophila*, Os-D is isolated on chromosome 3L and three other *Csps* are located within ~1 Mb of each other on chromosome 2R. Synteny is highly conserved between *D. melanogaster* and *D. pseudoobscura*.

4.33.3.2.2 Functional genomics of Csps

The function of the *Csp* genes has been inferred exclusively based on indirect evidence such as expression patterns and structural studies. Contrary to *Obps*, *Csps*

are, for the most part, expressed in several chemosensory and nonchemosensory tissues. *In situ* hybridization and *in vitro* binding studies of the moth *M. brassicae Csp* (*MbraCsp*) genes and their encoded proteins correlate their expression to the antenna and proboscis tissues. CSPs were also found in the pheromone gland, which is lacking olfactory organs (Nagnan-Le Meillour, P. *et al.*, 2000; Jacquin-Joly, E. *et al.*, 2001). In locusts different subclasses of *Csps* are associated with different tissues including the gustatory sensilla chaetica, which are distributed throughout the body and in the subcuticular space between the antennal epithelium and the cuticle (Angeli, S. *et al.*, 1999; Jin, X. *et al.*, 2005). Interestingly, in locust sensilla chaetica, CSPs are restricted to the noninnervated sensillum lymph compartment suggesting that they act outside of chemosensory processes.

The Drosophila genome (Figure 3) contains four *Csp* genes and encapsulates the multifunctional reality of the *Csp* gene family. *DmelOS-D/pherokine-1* expression is associated with the coeloconic sensilla on the antenna. Pherokine-2 (Phk-2 also known as ejaculatory bulb protein III PEBIII) is expressed solely in male ejaculatory bulbs, which contains VA. During copulation, VA is transferred to the female and has an antiaphrodisiac effect on male courtship (Brieger, G. and Butterworth, F. M., 1970). Interestingly, Phk-2 shares 50% identity with *M. brassicae* CSP (MbraOBP2) that binds VA *in vitro* (Bohbot, J. *et al.*, 1998). Phk-2 is also 53% identical to the *Periplaneta americana* protein p10, whose expression is significantly enhanced during leg regeneration of juvenile cockroaches and is also expressed in other tissues of juveniles and adults (antenna and head) (Kitabayashi, A. N. *et al.*, 1998). Both Phk-2 and Phk-3 expression are enhanced following viral and bacterial infection, respectively (Sabatier, L. *et al.*, 2003). The authors suggested that pherokines, including OSD, present a defense mechanism against microorganism entry regions such as the sensillum where the lymph and the environment are in contact.

In conclusion, the ubiquitous expression pattern of CSPs, their specific mode of regulation, and broad ligand recognition capabilities (Nagnan-Le Meillour, P. *et al.*, 2000; Jacquin-Joly, E. *et al.*, 2001; Lartigue, A. *et al.*, 2002) are consistent with the suggestion that this gene family is involved in the transport of hydrophobic ligands in various physiological pathways.

4.33.3.3 Odorant Receptors

The most numerous and well-studied chemosensory genes are the ORs, followed distantly by the gustatory receptors (GRs). While the ORs are a clear subclass of chemoreceptors in insects (Figure 4) (Hill, C. A. *et al.*, 2002; Robertson, H. M. *et al.*, 2003; Bohbot, J., *et al.*, 2007; Nene, V., *et al.*, 2007) the distinction between olfaction and gustation, and thus ORs and GRs, is less clear in the nematode *C. elegans* (Bergamasco, C. and Bazzicalupo, P., 2006). For the purpose of this chapter, the *C. elegans* chemosensory receptors will be considered as olfactory genes, although their relationship to insect ORs is ambiguous at best (Figure 4). As a class, ORs dominate the invertebrate GPCR landscape, accounting for one-quarter to one-half of all GPCRs in insect genomes (Hill, C. A. *et al.*, 2002; Bohbot *et al.*, in preparation) and perhaps more than half of all GPCRs in *C. elegans* (Ono, Y. *et al.*, 2005; Robertson, H. M. and Thomas, J. H., 2006).

As a whole, the invertebrate ORs are an extremely divergent family of genes, often displaying very low similarity among members within the same species and with few apparent orthologues between species (Robertson, H. M. *et al.*, 2003; Ache, B. W. and Young, J. W., 2005; Robertson, H. M. and Thomas, J. H., 2006). While the vertebrate ORs are also characteristically divergent they show much more similarity than their invertebrate counterparts (Mombaerts, P., 2004). Furthermore, vertebrate ORs lack introns while the invertebrate *Or* genes contain introns, making their annotations considerably less straightforward. Intron gain and loss in invertebrate ORs is evident and has been used as one indicator of their phylogenetic relationships (Robertson, H. M., 1998; 2000; Robertson, H. M. *et al.*, 2003). As is the case for vertebrate *Or* genes, invertebrate OR loci are often clustered, ranging from just a few tandem genes in *D. melanogaster* (Robertson, H. M. *et al.*, 2003) to an enormous proliferation of loci on *C. elegans* chromosome V (Figure 3) (Robertson, H. M. and Thomas, J. H., 2006). In many cases, tandem or clustered groups of genes are paralogous, representing recent duplications of receptors. Another distinction between the vertebrate and invertebrate OR families is in the number of apparent pseudogenes. Vertebrate genomes contain as many as 50% *Or* pseudogenes (Mombaerts, P., 2004; Ache, B. W. and Young, J. M., 2005), and as many as one-third of the chemoreceptors have been reported as pseudogenes in the N2 strain of *C. elegans* (Robertson, H. M., 1998; 2000; Robertson, H. M. and Thomas, J. H., 2006). In contrast, insects families retain very few *Or* pseudogenes (Hill, C. A. *et al.*, 2002; Robertson, H. M. *et al.*, 2003; Ache, B. W. and Young, J. M., 2005; Bohbot *et al.*, in preparation). Together with the widespread occurrence of single nucleotide polymorphisms in the

insect and the nematode ORs (Hill, C. A. *et al.*, 2002; Robertson, H. M. and Thomas, J. H., 2006; Bohbot *et al.*, in preparation), their overall divergence, intron flux, and duplications suggest that the invertebrate ORs are very rapidly evolving gene families. This rapid evolution may have arisen out of the need for adapting to changing environments, mating specificity, and otherwise differing life histories of divergent species (Robertson, H. M. *et al.*, 2003; Robertson, H. M. and Thomas, J. H., 2006).

4.33.3.3.1 Insect odorant receptors

The identification of the first vertebrate ORs (Buck, L. and Axel, R., 1991) led to a major effort by several groups interested in identifying insect ORs. Nearly a decade later, the release of the *D. melanogaster* genome facilitated the identification of a family of ORs from *D. melanogaster* (Clyne, P. J. *et al.*, 1999; Gao, Q. and Chess, A., 1999; Vosshall, L. B. *et al.*, 1999). Since then a significant body of work has been put forth describing insect *Or* genes, their patterns of expression, functions, and implications for odor coding (Robertson, H. M. *et al.*, 2003; Hallem, E. *et al.*, 2004a; Hallem, E. A. *et al.*, 2004b; Jacquin-Joly, E. and Merlin, C., 2004; Ache, B. W. and Young, J. M., 2005; Dahanukar, A. *et al.*, 2005; Jefferis, G. S. X. E., 2005; Rutzler, M. and Zwiebel, L., 2005). The completion of the genome of the malaria mosquito, *An. gambiae* (Holt, R. A. *et al.*, 2002), led to the description of a second complete insect OR gene family and to the comparison of *An. gambiae* and *D. melanogaster* OR repertoires (Fox, A. N. *et al.*, 2001; Hill, C. A. *et al.*, 2002). Multiple ORs have now been identified in species from at least four other insect orders including Diptera, Lepidoptera, Hymenoptera (Krieger, J. *et al.*, 2003), and Coleoptera (reviewed in Hallem, E. A. *et al.*, 2006). Furthermore, a single OR is highly conserved across insect orders, widely coexpressed with other ORs, and required for their function (Krieger, J. *et al.*, 2003; Larsson, M. C. *et al.*, 2004; Pitts, R. J. *et al.*, 2004; Jones, W. D. *et al.*, 2005; Xia, Y. and Zwiebel, L. J., 2006) (Figure 4). It is apparent that with several insect genome projects nearly completed or about to be initiated, the future of comparative genomics is certain to yield new and exciting information.

4.33.3.3.1.(i) Drosophila odorant receptors When homology-based cloning efforts repeatedly failed, the first wave of insect OR identification was the direct result of a novel approach for bioinformatics-based searches of the *D. melanogaster* genome project (Clyne, P. J. *et al.*, 1999). The complete set of *D. melanogaster* 60 *Or* genes (*DOrs*) encoding 62 Drosophila olfactory receptor (DOR) peptides in the Drosophila genome (Robertson, H. M. *et al.*, 2003) followed soon after (Vosshall, L. B. *et al.*, 1999; Vosshall, L. B., 2000), launching a revolution in insect olfactory research, most of which will be reviewed in other chapters in this volume. DORs are a very divergent family, most sharing less than 20% identity, with limited subfamilies having >40% identity (Vosshall, L. B., 2000). In contrast, their vertebrate counterparts generally display a much higher level of similarity of at least 40% among mouse ORs, for example (Zhang, X. and Firestein, S., 2002).

DOrs display interesting gene structures, some of which are conserved among animal ORs. For example, *DOrs* are dispersed as single genes throughout the Drosophila genome (Figure 3) (Robertson, H. M. *et al.*, 2003). Those genes that are grouped occur as doublets or triplets and generally are most similar to one another, suggesting that they represent gene duplication events (Robertson, H. M. *et al.*, 2003). The *DOr19a* and *DOr19b* genes, which are tightly linked, inverted relative to one another, and whose peptide translations are >90% identical, are an example of one such recent duplication (Robertson, H. M. *et al.*, 2003). In contrast to the widely dispersed locations of *DOrs*, *Ors* from other insects and *C. elegans* are often found in moderate to large clusters (Figure 3) (Hill, C. A. *et al.*, 2002; Robertson, H. M. and Thomas, J. H., 2006), and significant clustering is also common for vertebrate *Or* genes (Mombaerts, P., 2004). Two *DOrs* apparently produce multiple proteins by alternate splicing (Robertson, H. M. *et al.*, 2003). *DOr46a* and *DOr69a* each produce a second 'b' peptide, *DOr46a* by the splicing of a single C-terminal exon encoding the seventh transmembrane (TM) and *DOr69a* by the splicing of two C-terminal exons encoding the sixth and seventh TMs, to unique N-terminal exons (Robertson, H. M. *et al.*, 2003). Alternative splicing is a feature common to insect GRs (Clyne, P. J. *et al.*, 2000; Hill, C. A. *et al.*, 2002) and has been documented at low frequency in vertebrate ORs (Young, J. *et al.*, 2003), which lack introns (Mombaerts, P., 2004). In contrast, *DOrs* contain between one and nine introns with typically four of the C-terminal introns likely to be ancestral in the *DOr* lineage, two of which are shared with *DGrs*, reflecting their common derivation (Figure 6) (Robertson, H. M. *et al.*, 2003).

DOrs are expressed in adult antennae, maxillary palps, and in the dorsal organ of larvae (Clyne, P. J. *et al.*, 1999; Gao, Q. and Chess, A., 1999; Vosshall, L. B.

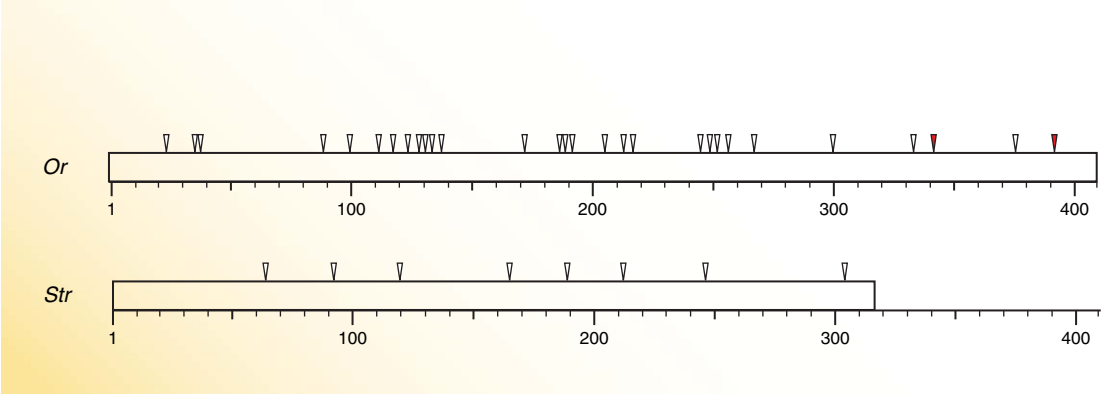

Figure 6 Locations of introns in the *Or*/*Str* genes in *Drosophila* and *Caenorhabditis elegans*. The intron locations (arrowheads) are shown relative to a scale of the average receptor size in amino acids. Red introns indicate ancient introns. Data from Robertson H. M. *et al.* (2003) and Robertson H. M. (1998).

et al., 1999; Vosshall, L. B. *et al.*, 2000). Their expression is limited to specific sensillar types in stereotypic regions of the antennae, and their patterns and projections are conserved from individual to individual (Vosshall, L. B. *et al.*, 2000). While generally little is known about the regulation of *DOr* expression, one important example stands out. The *D. melanogaster* mutant, *abnormal chemosensory jump 6* (*acj6*), was isolated based on its reduced jumping response to odor stimuli (McKenna, M. P. *et al.*, 1989), as well as defects of olfactory physiology (Ayer, R. K. and Carlson, J., 1991). A*cj6* encodes a Pitl Octl Unc-86 (POU) domain transcription factor that is expressed in ORNs and directly effects the expression of several *DOrs* (Clyne, P. J. *et al.*, 1999). The regulation of *Or* expression level and location is likely to play a significant role in establishing olfactory sensitivity. Future studies will undoubtedly reveal the *cis*-acting DNA elements and *trans*-acting protein factors that are involved in *Or* gene regulation and that whether these elements are conserved among invertebrates.

Functional studies of invertebrate ORs will be more thoroughly discussed in other chapters in this volume. But as they relate to receptor gene similarities the following points are worth mentioning. More than half of the *DOrs* have been functionally characterized (Figure 5) (Dobritsa, A. A. *et al.*, 2003; Hallem, E. *et al.*, 2004a; Goldman, A. L. *et al.*, 2005; Kreher, S. A. *et al.*, 2005) and most receptors appear broadly tuned to many different odors across different molecular classes (Hallem, E. *et al.*, 2004a). Surprisingly, phylogenetically related receptors are not necessarily tuned to related compounds (Hallem, E. *et al.*, 2004a). For example, DOR9a and DOR47a, while forming a monophyletic clade in a phylogenetic analysis, are tuned to multiple, nonoverlapping odorants (Hallem, E. *et al.*, 2004a). It is too early to comment as to whether this complex relationship between ligand specificity and OR homology may prove to be a general trend for invertebrate ORs.

4.33.3.3.1.(ii) Anopheles odorant receptors Soon after the identification of *DOrs*, candidate *Or* genes were identified with homology-based approaches from *An. gambiae* (*AgGPRors*) (Fox, A. N. *et al.*, 2001; 2002). The completion of the *An. gambiae* genome sequence (Holt, R. A. *et al.*, 2002) facilitated the characterization of 79 *AgGPRors*, representing the second complete set of insect *Ors*. Like their *DOr* counterparts, the *AgGPRors* are a very diverse group of genes, the vast majority share less than 20% identity at the amino acid level, although 28 pairwise identities are higher than 70% (Fox, A. N. *et al.*, 2001; Fox, A. N. *et al.*, 2002; Hill, C. A. *et al.*, 2002). Indeed, several AgGPRors are so similar (>90% identity for proteins encoded by *AgGPRors75,76,78* and *AgGPRors77,79*) as to suggest that they are either very recent duplications or alternatively alleles of the same gene that has been erroneously ascribed separate loci in the annotation of a mixed haplotype genome.

Phylogenetic comparison of the *DmOrs* and *AgGPRors* illustrates the extreme divergence between insect OR that has become the hallmark of these gene families. Most groupings with high bootstrap support are made up of receptors from the same species while only a few highly divergent ORs from both species are grouped together (Hill, C. A. *et al.*, 2002).

AgGPROR7 is the sequence as well as the functional orthologue of DOR83b and represents a unique OR subfamily (see below), the two sharing a remarkable 78% identity and ~90% similarity (Pitts, R. J. *et al.*, 2004). The next best examples are AgGPRor2 and DmOr43a, which share just 36% identity and ~70% similarity (Fox, A. N. *et al.*, 2001; Hill, C. A. *et al.*, 2002). Interestingly, AgGPRor2 and DmOr43a do not appear to share odorant ligand specificity (Storkuhl, K. F. and Kettler, R., 2001; Wetzel, C. H. *et al.*, 2001; Hallem, E. *et al.*, 2004a; Hallem, E. A. *et al.*, 2004b).

The *AgGPRors* are dispersed on all three chromosomes, although there are several tightly linked loci with as many as nine genes (Figure 3) (Hill, C. A. *et al.*, 2002). In each case the clustered genes are very similar to one another and are generally transcribed in the same direction, indicating that they have likely arisen as a result of multiple duplication events (Hill, C. A. *et al.*, 2002). Like the *DOrs*, all *AgGPRors* contain introns (Fox, A. N. *et al.*, 2001; 2002; Hill, C. A. *et al.*, 2002; Pitts, R. J. *et al.*, 2004), and many *AgGPRors* share one or more 3′ ancestral introns of *DOrs*, supporting a common, distant derivation (Pitts, R. J. *et al.*, 2004; Zwiebel lab, unpublished data).

To date, two *AgGPRors* have been functionally characterized (Hallem, E. A. *et al.*, 2004b). One of those genes, *AgGPRor1*, displays enhanced female expression that is downregulated after blood feeding (Fox, A. N. *et al.*, 2001) and is sensitive to a component of human sweat (Hallem, E. A. *et al.*, 2004b). This is an intriguing finding and may ultimately lead to the design of strategies to interfere in Anopheles, if not mosquito-specific, in the olfactory-driven behaviors, such as host-seeking, in these disease vectors.

4.33.3.3.1.(iii) Lepidopteran odorant receptors

The first Lepidopteran candidate *Ors* (*HR1–HR9*) was identified and cloned from the tobacco budworm moth, *Heliothis virescens*, as a result of screening a proprietary genome project (Krieger, J. *et al.*, 2002). Twelve more *Ors* were subsequently identified, many of which have been classified as candidate pheromone receptors (PRs) and are discussed below (Krieger, J. *et al.*, 2004). While this analysis is presumed to represent only a subset of the OR repertoire from *H. virescens*, we can make several inferences albeit limited in their scope from this work. As noted for other insect ORs, the putative HRs have a canonical seven-TM structure, but are nevertheless a very divergent group of genes whose conceptual translations share very low sequence identity with *D. melanogaster* ORs and GRs (Krieger, J. *et al.*, 2002). Intraspecifically, HRs share low identity among the nonpheromone receptor candidates, generally 8–15%, the highest identities being 52% and 34% between HR7 and HR9 (Krieger, J. *et al.*, 2002) and HR7 and HR12, respectively (Krieger, J. *et al.*, 2004). Although genomic DNA fragments were identified from the *H. virescens* genome, no data regarding introns or map positions were presented (Krieger, J. *et al.*, 2002), and the fact that the *H. virescens* genome is a nonpublic resource has made genomics comparisons with other insect ORs impossible at present. All candidate receptors examined by RT-PCR were expressed in antennae with a subset expressed in other chemosensory tissues (Krieger, J. *et al.*, 2002; 2004). *In situ* hybridization revealed that two receptors, *HR6* and *HR8*, are expressed in distinct groups of antennal neurons (Krieger, J. *et al.*, 2002). Interestingly, it has been suggested that a subset of the identified *H. virescens ORs* might, in fact, encode functional GRs. Specifically, HRs1, 4, and 5 are expressed in tissues with potential gustatory function (Krieger, J. *et al.*, 2002) and form a monophyletic clade distinct from other HRs that shares their most significant cross-species similarity with *D. melanogaster* GRs (Krieger, J. *et al.*, 2004).

Eleven candidate PRs have now been identified from two moth species: six from *H. virescens* (Krieger, J. *et al.*, 2004; 2005) and five from the silkmoth, *B. mori* (Sakurai, T. *et al.*, 2004; Krieger, J. *et al.*, 2005; Nakagawa, T. *et al.*, 2005). Currently little is known about the genomics of these receptors beyond their coding sequences, peptide alignments, and phylogenies; accordingly, any speculation as to potential paralogy and orthology among these receptors must therefore await the completion of a more extended set of characterizations. Only the genomic structure of *BmOr-1* has been presented (Sakurai, T. *et al.*, 2004). The PR conceptual translations have low sequence similarity to ORs from other insect species and they form their own monophyletic clade within the limited moth receptor family (Krieger, J. *et al.*, 2004; Sakurai, T. *et al.*, 2004; Krieger, J. *et al.*, 2005). Their similarity to one another ranges from 35% to 70% identity within a species to greater than 40% identity between BmOR-3 and HRs 4, 11, 14, 15, and 16 (Krieger, J. *et al.*, 2005). The PRs are also longer, on average, than other insect ORs averaging 430 AA in *H. virescens* and 425 AA in *B. mori* (Krieger, J. *et al.*, 2005) as compared to an average of ~400 AA for *D. melanogaster* and *An. gambiae* ORs, respectively (Hill, C. A. *et al.*, 2002; Robertson, H. M. *et al.*, 2003).

A limited set of expression analyses and functional characterizations have been carried out for PRs. The expression of five of the six candidate *H. virescens* PRs and four of the five candidate *B. mori* PRs are either enhanced in or specific to male antennae, which is consistent with a putative role in pheromone sensing (Krieger, J. *et al.*, 2004; Sakurai, T. *et al.*, 2004; Krieger, *et al.*, 2005; Nakagawa, T. *et al.*, 2005; Gohl, T. and Krieger, J. R., 2006). Furthermore, an antibody against HR13 labels dendrites in the sensilla trichodea type 1, which are found only on male antennae and most of which are sensitive to the major component of the *H. virescens* female pheromone (Gohl, T. and Krieger, J. R., 2006). The silkmoth receptor BmOR-1 detects bombykol, the sole female sex pheromone, as shown by ectopic expression in female antennae, as well as heterologous expression in *Xenopus laevis* oocytes (Sakurai, T. *et al.*, 2004; Nakagawa, T. *et al.*, 2005). In these latter studies, while BmOR-1 alone induced a significant response to bombykol in oocytes, coexpression of the 83b subfamily member BmOR-2 greatly increased both the fraction of responsive oocytes and the magnitude of the individual responses (Nakagawa, T. *et al.*, 2005) leading to the suggestion, subsequently verified by *in situ* hybridization, that *BmOr-1* and *BmOr-3* neurons coexpress *BmOr2* (Nakagawa, T. *et al.*, 2005). In contrast, another study also used *in situ* hybridization to localize these receptors and drew the opposite conclusion, stating that neither *BmOr-1* nor *BmOr-3* colocalize with *BmOr-2* (Krieger, J. *et al.*, 2005). This striking paradox must await further investigation for its resolution and will undoubtedly be important, given the implication that 83b subfamily members may not be required for pheromone sensing in insects, but instead function only in general odorant perception.

4.33.3.3.1.(iv) DOr83b family From its initial identification and subsequent expression analysis, *DOr83b* gene was singled out as a potentially extraordinary OR (Vosshall, L. B. *et al.*, 2000). It is much longer than the average DOR, having an extended loop between the fourth and fifth putative transmembrane regions and, more strikingly, is expressed in nearly all antennae and maxillary palp neurons in *D. melanogaster* (Vosshall, L. B. *et al.*, 2000). The subsequent identification of *AgGPRor7* in *An. gambiae*, *AaGPRor7* in *Ae. Aegypti*, and *HR2* in *H. virescens* demonstrated that *DOr83b* is also extremely well conserved in other insects and represents an important receptor subfamily (Krieger, J. *et al.*, 2002; Melo, A. C. *et al.*, 2004; Pitts, R. J. *et al.*, 2004). In addition, conserved intron position between *DOr83b* and *AgGPRor7* as well as microsynteny with respect to neighboring genome regions also suggested true orthology, the first of its kind among insect ORs (Hill, C. A. *et al.*, 2002). Krieger J. *et al.* (2003) identified member genes from species representing multiple insect orders including Lepidoptera (*B. mori* and *Antheraea pernyi*), Diptera (*Calliphora erythrocephala*), Hymenoptera (*A. mellifera*) and Coleoptera (*T. molitor*), demonstrating the broad conservation of the 83b family.

The *DOr83b* subgroup is unique to insects and forms an ancestral monophyletic clade within the larger insect OR family, which interestingly is more similar than other ORs to GRs (Figure 4) (Robertson, H. M. *et al.*, 2003). The exceptional degree of sequence conservation and expression characteristics raised the obvious hypothesis that the *DOr83b* family might represent a nonconventional OR subfamily that is crucial to insect olfactory signal transduction (Vosshall, L. B., 2000). Indeed, several studies have since demonstrated its functional significance in olfaction. Initially, *DOr83b* knockdowns carried out in *D. melanogaster* using either reverse genetics or RNA interference (Larsson, M. C. *et al.*, 2004; Neuhaus, E. M. *et al.*, 2005) revealed an absolute requirement for *DOr83b* in normal olfactory responses. Furthermore, DOR83b was shown necessary and sufficient for the proper localization and retention of other conventional DOrs to the dendritic membrane (Larsson, M. C. *et al.*, 2004; Benton, R. *et al.*, 2006). Testing this hypothesis even further, transgenic expression of *DOr83b* orthologues from three different insect species in the antennae of *DOr83b*-mutant flies restored odorant sensitivity as well as the correct localization of conventional *DOrs* to ORN dendrites, providing direct evidence of their functional conservation (Jones, W. D. *et al.*, 2005). While heterologous expression studies revealed that members of the DOr83b family dimerize with conventional ORs and thereby enhance odorant response sensitivity (Wetzel, C. H. *et al.*, 2001; Sakurai, T. *et al.*, 2004; Neuhaus, E. M. *et al.*, 2005), DOR83b does not independently confer odorant sensitivity (Dobritsa, A. A. *et al.*, 2003; Benton, R. *et al.*, 2006). Lastly, recent studies suggest that DOr83b and other DOrs may have an unexpectedly inverted conformation in the dendritic membrane, with their N-termini located intracellularly and their C-termini located extracellularly (Benton, R. *et al.*, 2006). This potentially unique conformation, along with the apparent lack

of an 83b subfamily member of nonconventional ORs, further distinguishes the molecular components of insect olfactory signal transduction from its counterparts in both vertebrate and *C. elegans*. It will now be interesting to determine how far back in the hexapod lineage this receptor can be identified. We may indeed find that the principles of olfaction elucidated in insect model systems are conserved in older hexapods and even in other arthropod lineages, giving us insight into the evolution of olfaction in general, and potentially providing opportunities for broad-based control strategies that rely on olfaction for their implementation.

4.33.3.3.2 *Caenorhabditis elegans chemoreceptors*

Four years after the identification of vertebrate ORs (Buck, L. and Axel, R., 1991), the first candidate invertebrate chemoreceptors (*CeCrs*) were identified through bioinformatic methods in the soil nematode, *C. elegans* (Troemel, E. R. *et al.*, 1995). The expression of a subset of *CeCrs* was observed in chemosensitive neurons, consistent with the proposed chemoreceptor functions (Troemel, E. R. *et al.*, 1995). Since then, more than 20 gene families composed of nearly 1300 intact genes, and over 400 apparent pseudogenes, accounting for roughly 7% of all *C. elegans* genes, have been described (Robertson, H. M. and Thomas, J. H., 2006). By convention, *CeCr* gene family names usually begin with the initials *sr* for serpentine receptor, the exception being the *str* family, which stands for seven-transmembrane domain (Troemel, E. R. *et al.*, 1997).

The *CeCr* genes share many of the characteristics common to insect ORs inasmuch as they are very divergent, both within and between families (Robertson, H. M. and Thomas, J. H., 2006). While their topology places them squarely within the GPCR superfamily, their phylogenetic relationships to insect ORs have not been fully explored, making it difficult to address whether they share a common chemoreceptor lineage or were derived independently (Figure 4). What is clear is that the *CeCrs* cluster on a massive scale in the *C. elegans* genome (Figure 3). As a rule, closely related genes tend to be located near each other (Robertson, H. M., 2000; 2001; Chen, N. *et al.*, 2005). Similar to other invertebrate *Ors*, *CeCrs* contain small introns (Robertson, H. M., 1998; 2000). One distinguishing overall characteristic of the *CeCr* gene products is their small size (Figure 6). As we have already noted above, insect ORs have an average length of about 400 AA. However, the *CeCr* peptides are generally predicted to have lengths of 350 AA or less, resulting in smaller loop regions between predicted transmembrane domains (Troemel, E. R. *et al.*, 1995; Robertson, H. M., 1998; Robertson, H. M., 2000; Chen, N. *et al.*, 2005; Robertson, H. M. and Thomas, J. H., 2006 #3625). Finally, the small number of chemosensory neurons (<40) relative to the large number of *CeCrs* implies that multiple chemoreceptor proteins must be expressed in single sensory neurons (Figure 1) (Bergamasco, C. and Bazzicalupo, P., 2006), a feature that is not shared with insect ORs that are thought to express a single conventional *Or* (Ache, B. W. and Young, J. M., 2005).

Although not all *CeCrs* are expected to act as traditional ORs, sensitive to volatile odorants, we will consider them together as one large superfamily with the understanding that future studies will begin to elucidate the spectrum of *CeCr* functions. A recent review summarizes the size and the diversity of the *CeCr* superfamily in this way, "This large genetic investment might result from an extreme dependence on chemosensory abilities in the absence of visual and auditory systems. On the basis of genetic complexity, this system probably constitutes the bulk of signal transduction that occurs in *C. elegans*" (Robertson, H. M. and Thomas, J. H., 2006). Furthermore, the completion of the *Caenorhabditis briggsae* genome allowed comparative studies of candidate chemoreceptors between *C. elegans* and *C. briggsae*, species that have diverged 80–110 mya (Stein, L. D. *et al.*, 2003) and revealed extreme divergence between the two *Cr* repertoires resulting from frequent amplifications of *CeCrs* relative to their *C. briggsae* counterparts (Robertson, H. M. and Thomas, J. H., 2006).

4.33.3.3.2.(i) Str/srh gene families The phylogenetically related *str* and *srh* genes are the largest individual *CeCr* families together comprising about 600 genes (Robertson, H. M. and Thomas, J. H., 2006). Phylogenetic studies of *str*/*srh* genes within *C. elegans* and between C. *elegans* and *C. briggsae* suggest that these receptors are in a constant state of change driven by the processes of gene duplication, deletion, intron gain and loss, and movement within the respective genome (Robertson, H. M., 1998; 2000; 2001). Interestingly, many of the nearly 200 apparent *str* and *srh* pseudogenes in the N2 strain encode full-length *CeCr* proteins in other nematode strains (Stewart, M. K. *et al.*, 2005). This finding and the discovery of several other nucleotide polymorphisms indicate extensive gene diversity in wild *C. elegans* populations

(Stewart, M. K. *et al.*, 2005). Incredibly, more than 80% of the *str* and *srh* genes are concentrated on chromosome V (Robertson, H. M., 1998; 2000; 2001; Robertson, H. M. and Thomas, J. H., 2006). This intriguing theme is repeated for most other *CeCr* loci (Figure 3) (Ono, Y. *et al.*, 2005; Robertson, H. M. and Thomas, J. H., 2006).

4.33.3.3.2.(ii) Sra/srab gene families The *sra* and *srab* are two of the smaller *CeCr* families, but important in the amount of attention they have received. The *sra* genes were among the first candidate *CeCrs* identified (Troemel, E. R. *et al.*, 1995). This *sra* family is composed of 32 genes and 7 pseudogenes (Robertson, H. M. and Thomas, J. H., 2006). Twenty-two *srab* genes and five pseudogenes were recently identified based on their similarity to the *sra* genes (Chen, N. *et al.*, 2005). Both *sra* and *srab* families have an average translation of about 330 AA (Robertson, H. M. and Thomas, J. H., 2006). *Sra* genes are concentrated on chromosomes I and II, while the *srab* genes are almost all located on chromosome V and nearly all *srab* family members lack an *sra*-defining protein motif, and phylogenetic analysis clearly segregates them into a distinct subfamily (Chen, N. *et al.*, 2005). There are small numbers of orthologues between *sra* and *srab* genes in *C. elegans* and *C. briggsae* based on sequence alignments and genome synteny (Chen, N. *et al.*, 2005). Those *C. elegans*/*C. briggsae* gene pairs that are existent are substantially diverged and are not considered to be true orthologues (Robertson, H. M. and Thomas, J. H., 2006). Furthermore, the *sra* and *srab* gene families are significantly expanded in *C. elegans* relative to *C. briggsae* due to apparent duplication events in *C. elegans* (Chen, N. *et al.*, 2005).

4.33.3.3.2.(iii) CeCr function Genetic studies have supported a chemoreceptive role for selective *CeCr* genes. Certainly, the most compelling example of this is the characterization of *odr-10*, an *str* family member that encodes a receptor mediating the olfactory response to diacetyl (Sengupta, P. *et al.*, 1996). *Odr-10* remains the sole *CeCr* with an identified ligand (Figure 5).

In the absence of additional functional studies, numerous investigations have examined *CeCr* expression patterns as a means of supporting their classification as chemoreceptors. For example, four *sra* genes were expressed in chemosensitive amphid neurons in the head (Troemel, E. R. *et al.*, 1995) while expression of three *srab* genes was observed in tail chemosensitive neurons, two of those also showing expression in head chemosensory neurons (Chen, N. *et al.*, 2005). *Str-2* is expressed only in AWC neurons (Colosimo, M. E. *et al.*, 2003) and *odr-10* is expressed in AWA neurons (Sengupta, P. *et al.*, 1996). Furthermore, while a summary of the data from several promoter: Green Fluorescent Protein (GFP) expression studies illustrates that most *CeCrs* (48/63) are expressed in sensory tissues while many others (15/63) are not (Robertson, H. M. and Thomas, J. H., 2006). Another study identified a promoter element, common to numerous *srh* and *sri* genes, that is capable of ectopically driving *odr-10* expression in the ADL neuron (McCarroll, S. A. *et al.*, 2005). Finally, a microarray-based study determined that five *CeCrs* were among the most prevalent genes expressed in the RNA derived from the AWB neuron, a result confirmed by promoter:GFP experiments (Colosimo, M. E. *et al.*, 2004).

While many of the experiments described above support a chemoreceptive function for *CeCrs*, the supposition that all *CeCr* gene products act either as volatile ORs or soluble tastant receptors remains tenuous at best. Multiple *CeCrs* from different families, as suggested either by their similarities to other genes with known function, expression patterns, or mutant phenotypes, might well have other functions. For example, the *srw* family shares its origins with FMRFamide and other peptide receptors (Robertson, H. M. and Thomas, J. H., 2006). Although a proposed role for the *srw* gene as environmental peptide receptors has merit, some of these 145 genes may operate in other capacities, perhaps as cell–cell communication receptors. In fact, at least one *CeCr* does not seem to function as a chemoreceptor at all. *sra-11* is expressed in interneurons downstream of sensory neurons and an *sra-11* null mutation disrupts olfactory imprinting, a specific type of olfactory-driven memory (Remy, J.-J. and Hobert, O., 2005) for at least two different odorants suggesting that *sra-11* has a general role in the process. While it seems likely that the majority of *CeCrs* do indeed act as receptors of environmental stimuli, much more study is required to fully appreciate the multiplicity of receptive roles, both external and internal, that this large superfamily may or may not carry out.

4.33.4 Signaling Cascade

For better or worse, the identification of genes involved in olfactory transduction in invertebrates has historically been restricted to the molecular

context derived from the knowledge acquired in the vertebrate visual and olfactory systems. These pathways have been elegantly studied and extensively reviewed elsewhere (Hildebrand, J. G. and Shepherd, G. M., 1997), and molecular, cellular, and genetic studies indicate that, for the most part, similar gene families are required in invertebrate olfactory transduction. Even so, it is essential to appreciate that several studies elaborated in this chapter have pointedly demonstrated that insect olfactory systems display several unique characteristics that argue against a wholesale acceptance of vertebrate signal transduction paradigms. Indeed, the novel function and conformation of both nonconventional and conventional ORs in Drosophila has fostered the suggestion that insect chemosensory transduction processes may in fact involve non-GPCR mechanisms (Benton, R. *et al.*, 2006).

4.33.4.1 Guanine Nucleotide-Binding Proteins and Effector Genes

4.33.4.1.1 Insects

GPs are a heterotrimeric assemblage of an alpha (α), beta (β) and gamma (γ) subunits as ancient as the eukaryote divergence (Jones, A. M. and Assmann, S. M., 2004). GPs may best be considered as molecular switches: located in the cell membrane, they modulate the activity of a variety of intracellular effector molecules once activated by GPCRs. Although the exact mechanism of GPs activation remains ambiguous, odorant-induced conformational change of the GPCR is likely to be required. The Gα subunit in particular seems to be interacting directly with the OR since both visual and olfactory systems rely on GPCRs (Grobner, G. *et al.*, 2000; Vogt, R. G., 2006).

Six Gα genes have been identified in the genomes of *D. melanogaster* and *An. gambiae* (Figure 3). *An. gambiae* $G_q\alpha$ (*agq*), *ago*, *agi*, and *agm* are located within a large 24-Mb segment on chromosome 2L while *ags* and *agc* are located on 3L and 3R, respectively. Phylogenetic analysis supports that *ago* and *agi* derive from a common ancestor as suggested by their relative genomic proximity (~3 Mb) (Rutzler, M. R. *et al.*, 2006). Drosophila Gα genes (*dg*) are located ~2 Mb apart on 2R and 3L with *dgo* and *dgq*. Importantly, splice variants of $G_q\alpha$ are components of the phototransduction pathway and are also expressed in chemosensory cells (Scott, K. *et al.*, 1995; Talluri, S. *et al.*, 1995). According to immunolocalization studies, $G_q\alpha$ protein is associated to the dendrite of *B. mori* and *An. gambiae* ORN (Laue, M. *et al.*, 1997; Rutzler, M. R. *et al.*, 2006), and functional evidence for $G_q\alpha$ requirement in olfactory transduction has been provided by RNAi mediated silencing experiments in the Drosophila antenna (Kalidas, S. and Smith, D. P., 2002). In these studies, altered olfactory responses were odor-dependent suggesting that there are more than one type of olfactory GP or, indeed, that alternative transduction mechanisms coexist.

In fact, molecular and electrophysiological approaches provide support for the hypothesis that two transduction pathways may be active in invertebrate olfactory transduction. One depends on the second messenger 1,4,5 inositol triphosphate (IP3) and the other depends on cAMP. In the lobster *Panulirus argus*, both cAMP and IP3 pathways are activated in response to stimulation with complex odor mixtures suggesting that both an AC and a PLC are targeted (Boekhoff, I. *et al.*, 1994).

A PLCβ is almost certainly involved in the olfactory transduction pathway of insects. In Drosophila, olfactory and visual physiology is dependent on the activity of the *norpA* PLC gene, which acts downstream of GPs (Riesgo-Escovar, J. *et al.*, 1995) although *norpA* activity in olfactory tissues is thus far restricted to the maxillary palp. The transient increase of IP3, a breakdown product of PIP2 by PLC, following exposure to odorants also supports a GP-mediated transduction pathway in insects (Breer, H. *et al.*, 1990). In Drosophila, recovery from olfactory adaptation is mediated by a phosphatidylinositol transfer protein gene dubbed *retinal degeneration B* (*Rdgb*), (Riesgo-Escovar, J. R. *et al.*, 1994). *Rdgb* mutants display delayed return to the resting potential following exposure to odorants. *Rdgb* encodes a six-transmembrane domain protein, which contains Ca^{+} binding domains involved in IP3 formation. In addition to being expressed in the eye, this gene is present in the antenna, labellum, and maxillary palp where it is thought to play a role in membrane metabolism.

Mutations of the Drosophila rutabaga (*rut*) and dunce (*Dun*) genes affect the cAMP transduction pathway (Martin, F. *et al.*, 2001; Gomez-Diaz, C. *et al.*, 2004). *Rut* and *Dun* encode an AC and a cAMP-PDE, respectively. Both genes express in the antenna, and the mutants exhibit defective electrophysiological and behavioral olfactory responses coherent with the initial stage of odorant transduction. Both genes are members of small families: six ACs and two cAMP-PDE have been identified in the fly genome.

4.33.4.1.2 *Caenorhabditis elegans*

Twenty-one $G\alpha$ genes are in the genome of *C. elegans* (Jansen, G. *et al.*, 1999; Bergamasco, C. and Bazzicalupo, P., 2006). Two clusters of five and nine genes are located on chromosomes I and V, respectively. Phylogenetic analysis shows that there is one orthologue for each of the four vertebrate $G\alpha$ subunits ($G\alpha_{o/i}$, $G\alpha_s$, $G\alpha_q$, and $G\alpha_{12}$) sharing over 68% amino acid identity (Roayaie, K. *et al.*, 1998). *C. elegans* GPs are widely expressed in the nervous system but six $G\alpha$ subunits are expressed in the two pairs of AWA and AWC neurons that mediate odorant attraction (Bargmann, C. I. *et al.*, 1993; Troemel, E. R. *et al.*, 1995; 1997; Jansen, G. *et al.*, 1999). Based on GFP fusion constructs and immunocytological studies, five $G\alpha$ proteins (GPA-2, GPA-3, GPA-5, GPA-13, and ODR-3) are localized to the ciliated dendrites suggesting that they presumably interact with GPCRs in a complex signaling network (Jansen, G. *et al.*, 1999; Lans, H. *et al.*, 2004).

In *C. elegans*, GP targets are likely to include AC and guanylyl cyclase (GC), cGMP-PDE and phospholipases. While in vertebrate, olfaction CNG channels activation is mediated by an AC/cAMP pathway, this role is performed in *C. elegans* by GCs. Two transmembrane GP-sensitive GCs (tGCs) are clearly required for chemosensory transduction in *C. elegans*. Both ODR-1 and DAF-11 (abnormal *da*uer *f*ormation) are located in the cilia of various chemosensory neurons including the olfactory neuron AWC (Birnby, D. A. *et al.*, 2000; L'etoile, N. D. and Bargmann, C. I., 2000). At least 26 additional transmembrane and 7 soluble GC genes have been identified in the *C. elegans* genome, suggesting that this organism favors cGMP over cAMP second messengers to activate downstream ion channels. Phylogenetic analyses show that 21 of the tGCs form a lineage-specific expansion that correlates with the proximity of these genes on the chromosomes (Fitzpatrick, D. A. *et al.*, 2006).

4.33.4.2 Ion Channels

CNG and TRP ion channels function in many vertebrate sensory transduction pathways. *Drosophila* and *C. elegans* each have four and six CNG channel genes, respectively, and at least two reports suggest that ion channel genes are active in Drosophila olfaction. One gene encodes an apparent vertebrate CNG Ca^+ channel homolog (*Dmel*CNG) and the gene *ether a go-go* (*eag*) encodes a putative cyclic nucleotide-modulated K^+ channel (Baumann, A. *et al.*, 1994; Dubin, A. E. *et al.*, 1998). *Dmel*CNG is expressed in the antennal and eye tissues and physiological studies suggest that this is a Ca^+ channel modulated by cGMP (Baumann, A. *et al.*, 1994). Mutant *eag* flies exhibit defective olfactory phenotype in a subset of olfactory sensilla (Dubin, A. E. *et al.*, 1998). Although not related to *Dmel*CNG, the *eag* gene also requires cyclic nucleotides for activity and contains a consensus cyclic nucleotide-binding site. No other ion channels have been identified as possible downstream target of effector genes in primary olfactory sensing. However, there is one report suggesting that a TRP channel is involved in olfactory adaptation in the developing Drosophila antenna (Stortkuhl, K. F. *et al.*, 1999), but this gene could not be detected in mature adult antenna. Lastly, an ITPR is expressed strongly in this tissue and is required for the maintenance of olfactory adaptation (Deshpande, M. *et al.*, 2000).

The *C. elegans* CNG consists of the α-subunit TAX-2 (abnormal chemo*tax*is) and the β-subunit TAX-4 involved in thermosensation and chemosensation (Coburn, C. M. and Bargmann, C. I., 1996). TAX-2 and TAX-4 are most similar to the vertebrate α and β subunits of the rod photoreceptors. Heterologous expression of TAX-2/TAX-4 has shown that this CNG channel is preferably activated by cGMP over cAMP and following its activation opens to Ca^+ currents (Komatsu, H. *et al.*, 1999) and loss of function mutants in either gene-display-defective chemotaxis to a subset of volatile compounds in the AWC and AWB neurons (Coburn, C. M. and Bargmann, C. I., 1996).

In contrast to the TAX-2/TAX-4 CNG channel that is active in AWB and AWC neurons, most chemosensory neurons in *C. elegans* use a TRP (vanilloid-related subfamily)-related ion channel for primary sensation and adaptation (Colbert, H. A. and Bargmann, C. I., 1995) whose closest vertebrate homologue is the nociceptive capsaicin receptor (Minke, B. and Cook, B., 2002). The *C. elegans* genome harbors five *trp* genes including *osm-9* (abnormal *osm*otic avoidance) and four *ocr* genes (*osm-9*/*c*apsaicin *r*eceptor-related). Combinations of OSM-9 and OCR subunits determine the function of the resulting TRP channels (Tobin, D. *et al.*, 2002). *Osm-9 lf* mutants in the AWA and ASH neurons exhibit strong chemosensory defects caused by the suppression of calcium currents after stimulation with a wide range of odorants. This suggests that most, if not all, transductory signaling converges on this ion channel. In the AWA and ASH neurons, OSM-9 requires OCR-2 for signal transduction and both are located

on the ciliated end of the dendrite (for review, see Bergamasco, C. and Bazzicalupo, P., 2006). In the AWC neuron, OSM-9 alone is involved in olfactory adaptation, negatively modulating olfactory responses to prolonged odor exposure (Colbert, H. A. and Bargmann, C. I., 1995).

4.33.5 Regulators of Signaling

4.33.5.1 Arrestins and G-Protein-Coupled Receptor Kinases

In mammalian systems, signal termination is mediated by two small gene families: GPCR kinases (GRKs) and ARRs. GRKs phosphorylate activated GPCRs, which are in turn targeted by ARRs, which disrupts the GPCR–GP complex (Krupnick, J. G. *et al.*, 1997). This promotes several events including clathrin-mediated receptor internalization/degradation and other downstream pathways (for reviews, see Lefkowitz, R. J. and Shenoy, S. K., 2005; Reiter, E. and Lefkowitz, R. J., 2006).

Thus far, two putative Drosophila (*DmGrk1* and *DmGrk2*) and two *C. elegans* GRKs (*Ce-Grk-1* and *Ce-Grk-2*) have been identified (Cassill, J. A. *et al.*, 1991; Fukuto, H. S. *et al.*, 2004; Reiter, E. and Lefkowitz, R. J., 2006). Not surprisingly, invertebrate *Grk* genes share considerable homology with their vertebrate counterparts. *Ce*-GRK1 and *Ce*-GRK-2 are 56% and 66% identical with human GRK5 and GRK3, respectively. *DmGrk1/2* and *Ce-Grk2* are broadly expressed throughout development and in various tissues including the CNS suggesting that they may function in multiple developmental and neuronal pathways. While the function of *Grk* genes in Drosophila olfaction has not been established, *Ce-grk2* (*lf*) mutants exhibit a significant chemosensory defect consisting of a loss of response to octanol (Fukuto, H. S. *et al.*, 2004).

As is the case for vertebrates, four *arrestin* genes have been identified in the genome of *D. melanogaster* and *An. gambiae* (*DmArr1-4* and *AgArr1-4*, respectively). *DmArr1* and *DmArr2* are expressed in photoreceptors and ORNs (Merrill, C. E. *et al.*, 2002). Consistent with a role in olfactory signal transduction, hypomorphic alleles of both *DmArr1* and *DmArr2* display significant reductions in olfactory responses to various odorants, and *DmArr1* larvae show defective chemotaxis in behavioral experiments (Merrill, C. E. *et al.*, 2005). Interestingly, these phenotypes are variable depending on odorants stimuli suggesting that in insect ORNs, *Arr1* and *Arr2* may participate in two independent desensitization pathways.

There are four subclasses of insect ARRs based on sequence similarity. Insects *Arr1* and *Arr2* encode approximately 400 AA proteins. They are referred to as sensory ARRs because of their broad expression in the olfactory and visual tissues. However, while the ARR1 primary amino acid sequence contains all the conserved domains of vertebrate ARRs, ARR2 lacks the C-terminal clathrin binding domain (Merrill, C. E. *et al.*, 2002; 2003). *Arr3* genes on the other hand encode considerably larger proteins and include the *D. melanogaster Kurtz* (*DmKrz*), a gene expressed throughout development in a multitude of tissues including the nervous system (Roman, G. *et al.*, 2000) and mutations in which larval are lethal. *Arr3* genes exhibit most of the canonical motifs found in vertebrate nonvisual ARRs. The fourth subclass of ARR genes (*Arr4* alleles) is significantly different from the other types, hence their annotation as atypical.

In contrast, the *C. elegans* genome apparently encodes a single ARR (*Ce-Arr1*) gene, which shares significant sequence homology to vertebrate nonvisual ARRs (65% similarity) and is most similar to the nonsensory ARR3/KURTZ ARR subtypes with 70% amino acid similarity, including well-characterized motifs known to interact with various molecular partners (Palmitessa, A. *et al.*, 2005). However, in contrast to *Kurtz*, *Ce-Arr1* mutants in *C. elegans* are viable and develop normally. Interestingly, while null mutants fail to adapt the following odorant stimulation, adaptation is restored in the C-terminal-truncated *Ce-Arr1* rescue mutant albeit with reduced recovery from adaptation capabilities demonstrating a dual role for *Ce-Arr1* in adaptation and recovery from adaptation in the AWC neuron. Although expressed broadly throughout the nervous system, *Ce-Arr1* is more highly expressed within the AWA, AWB, AWC, ASH, and ADL chemosensory neurons, where it overlaps with the expression of sensory GPs as described above. Palmitessa A. *et al.* (2005) determined that desensitization and adaptation require the N-terminal region to prevent the phosphorylated GPCR from interacting with the GP, while recovery from adaptation depends on the various components of the endocytic machinery and is mediated by the C-terminal domain.

4.33.5.2 The Caenorhabditis elegans Calcineurin TAX-6

The vertebrate calcineurin is a Ca^{+}/calmodulin (CaM)-dependent protein phophatase that acts as a positive regulator of calcium-dependent signals in

various biological pathways. The CaM and the B-subunit are required to activate the catalytic activity of the A-subunit. Ce-TAX-6 is 77% identical to the A-subunit (Kuhara, A. *et al.*, 2002). A putative homolog of the B-subunit has been identified in the worm genome and share 80% amino acid identity with its vertebrate counterpart. *Tax-6* mutants display several phenotypes indicating the pleiotropic nature of this gene. In the AWC neuron, *tax-6* mutants display diminished olfactory responsiveness reflected by enhanced adaptation when exposed to various odorants. The mechanism underlying this chemosensory is unknown but it requires the presence of a functional TRPV OSM-9 channel.

4.33.5.3 Other Protein Kinases

In addition to the core components of olfactory signal transduction thus far discussed, there is good evidence that implicates an ever increasing set of protein kinase-associated pathways in invertebrate chemosensory processes. Indeed, in further support of IP3-based second messenger pathways in insect olfactory transduction cascades is the identification of the Drosophila *IP3 kinase1* gene (*IP3K1*) (Gomez-Diaz, C. *et al.*, 2006). IP3K1 mediates IP3 degradation and is expressed in multiple locations including the olfactory appendages and the head. Importantly, gain-of-function *IP3K* Drosophila mutants exhibit diminished olfactory sensitivity due to increased recovery times (Gomez-Diaz, C. *et al.*, 2006).

In *C. elegans*, the signal termination in the AWC olfactory neuron is characterized by short- and long-term adaptation components that are mediated by a cGMP-dependent kinase (EGL-4) (L'etoile, N. D. *et al.*, 2002). EGL-4 and mammal protein kinase G (PKG) share similar functional domains including cGMP-binding motifs and a serine/threonine kinase domain (L'etoile, N. D. *et al.*, 2002). The latter domain has been shown to regulate the TAX-2/TAX-4 CNG channel by targeting a specific phosphorylation site on the TAX-2 subunit. A longer adaptation mechanism seems to be mediated by EGL-4 nuclear translocation and by regulation of gene expression. This mechanism is present in mammalian systems and is assumed by PKG (Gudi, T. *et al.*, 1997).

Expression and mutant analyses show that the protein kinase C (PKC) genes *ttx-4* and *tpa-1* are involved in multiple sensory pathways including olfaction (Okochi, Y. *et al.*, 2005). These genes encode protein homologs to the human novel PKC (over 50% amino acid identity) and Drosophila PKC (60% amino acid identity), and both have Di Acyl Glycerol-binding domains. The chemotaxis defects observed in *ttx-4* and *tpa-1 lf* mutants are rescued by an exogenous DAG analog implicating these two genes in the regulation of the second messenger pathway pertaining to olfactory sensation.

Lastly, five DAG kinase genes (*dgk*) have been identified in the *C. elegans* genome of which *dgk-1* and *dgk-3* act redundantly to reduce DAG levels and have been shown to participate in olfactory adaptation (Matsuki, M. *et al.*, 2006). The effects of DAG and other genes known to participate in DAG-mediated pathways provide strong support that phospholipase-based effectors are active in this complex regulatory network. Still, the jury is out as to the precise mechanisms underlying olfactory signaling within the invertebrate systems under study. At this point there is a growing body of circumstantial evidence but, if we may take the courtroom analogy one step further, no smoking gun to provide hard proof implicating any specific pathway(s).

4.33.6 Conclusion and Perspectives

The study of the olfactory subgenomes of insects and worms indicate that olfactory organs use similar gene families for the detection and conversion of chemical signals. Whether these shared molecular strategies are the result of evolutionary convergence as a response to a common chemical environment and/or a reflection of shared ancestry is difficult to discern. The large *Obp*/*Or* gene families described in this chapter display elements of similar genomic dynamics. For example, the majority of genes in a given family within a given genome occur in clusters and their phylogenetic relations surely reflect sequence homology that often correlates with cytogenetic position implying that local gene expansion has resulted from intrachromosomal gene duplications. It can also be reasonably argued that sequence homology between vertebrate and invertebrate gene families, in particular in the components of signal transduction, provides strong support for shared ancestry. Although important, this maxim is not so evident in the case of the chemosensory GPCRs and OBPs, which may represent two genetic interfaces between the ORN and the odors. The repertoires of these gene families are highly divergent even within species with only few orthologues shared between species. This type of comparison clearly indicates that this family displays lineage-specific expansions and reductions indicating ongoing genetic turn over and rapid evolution.

All GPCRs are presumed to have seven-transmembrane domains and interact with highly conserved or analogous transductory elements. The identification of which is the result of both directed research based on the mammalian olfactory and visual systems and also through discovery-based approaches epitomized by the use of forward genetic screens. Whereas both worms and insects use GPCRs as the initial recognition step, insects have developed a singular mechanism requiring the combination of a generic nonconventional GPCR and an odorant-specific conventional OR. While it appears likely that this unique adaptation is profound and may be specific to arthropods, the functional implications of this mechanism within these taxa remain unknown. In addition, the proposed reverse topology of insect ORs potentially makes this system truly novel as it adds a level a complexity in the molecular architecture of olfactory transduction. Interestingly, despite all these structural differences and sequence divergence, GPCRs of vertebrate and invertebrate interact with conserved GPs.

An equally striking difference between insects and worms resides in the divergent molecular strategies observed upstream of the chemosensory GPCRs. While insects have a moderate number of *Ors* and *Obps*, worms do not have *Obps* but have a much larger *Or* repertoire. It has been proposed that OBPs contribute to the odor coding by interacting with the ORs. But as we pointed earlier, there are very few reports suggesting a strict requirement of these proteins for proper olfactory function. Also, the number of authentic *C. elegans* chemoreceptors are probably smaller as indicated by a recent research.

Overall, it is certain that the number of genes involved in olfactory pathways will increase as more genetic screens and reverse genetic tools are applied to invertebrate systems. The most challenging task lays ahead in forging an understanding of the regulation and the network of epistatic interactions among olfactory genes that serve to provide the basis for the downstream processing of olfactory information that ultimately results in learning, memory, and which form the basis for critical behavioral decisions.

References

Ache, B. W. and Young, J. M. 2005. Olfaction: diverse species, conserved principles. Neuron 48, 417–430.

Adams, M. D., Celniker, S. E., Holt, R. A., Evans, C. A., Gocayne, J. D., Amanatides, P. G., Scherer, S. E., Li, P. W., Hoskins, R. A., Galle, R. F., George, R. A., Lewis, S. E., Richards, S., Ashburner, M., Henderson, S. N., Sutton, G. G., Wortman, J. R., Yandell, M. D., Zhang, Q., Chen, L. X., Brandon, R. C., Rogers, Y. H., Blazej, R. G., Champe, M., Pfeiffer, B. D., Wan, K. H., Doyle, C., Baxter, E. G., Helt, G., Nelson, C. R., Gabor, G. L., Abril, J. F., Agbayani, A., An, H. J., Andrews-Pfannkoch, C., Baldwin, D., Ballew, R. M., Basu, A., Baxendale, J., Bayraktaroglu, L., Beasley, E. M., Beeson, K. Y., Benos, P. V., Berman, B. P., Bhandari, D., Bolshakov, S., Borkova, D., Botchan, M. R., Bouck, J., Brokstein, P., Brottier, P., Burtis, K. C., Busam, D. A., Butler, H., Cadieu, E., Center, A., Chandra, I., Cherry, J. M., Cawley, S., Dahlke, C., Davenport, L. B., Davies, P., De Pablos, B., Delcher, A., Deng, Z., Mays, A. D., Dew, I., Dietz, S. M., Dodson, K., Doup, L. E., Downes, M., Dugan-Rocha, S., Dunkov, B. C., Dunn, P., Durbin, K. J., Evangelista, C. C., Ferraz, C., Ferriera, S., Fleischmann, W., Fosler, C., Gabrielian, A. E., Garg, N. S., Gelbart, W. M., Glasser, K., Glodek, A., Gong, F., Gorrell, J. H., Gu, Z., Guan, P., Harris, M., Harris, N. L., Harvey, D., Heiman, T. J., Hernandez, J. R., Houck, J., Hostin, D., Houston, K. A., Howland, T. J., Wei, M. H., Ibegwam, C., *et al.* 2000. The genome sequence of *Drosophila melanogaster*. Science 287, 2185–2195.

Altschul, S. F., Gish, W., Miller, W., Myers, E. W., and Lipman, D. J. 1990. Basic local alignment search tool. J. Mol. Biol. 215, 403–410.

Angeli, S., Ceron, F., Scaloni, A., Monti, M., Monteforti, G., Minnocci, A., Petacchi, R., and Pelosi, P. 1999. Purification, structural characterization, cloning and immunocytochemical localization of chemoreception proteins from *Schistocerca gregaria*. Eur. J. Biochem. 262, 745–754.

Ayer, R. K., Jr. and Carlson, J. 1991. Acj6: a gene affecting olfactory physiology and behavior in *Drosophila*. PNAS 88, 5467–5471.

Bargmann, C. I. and Horvitz, H. R. 1991. Chemosensory neurons with overlapping functions direct chemotaxis to multiple chemicals in *C. elegans*. Neuron 7, 729–742.

Bargmann, C. I., Hartwieg, E., and Horvitz, H. R. 1993. Odorant-selective genes and neurons mediate olfaction in *C. elegans*. Cell 74, 515–527.

Baumann, A., Frings, S., Godde, M., Seifert, R., and Kaupp, U. B. 1994. Primary structure and functional expression of a *Drosophila* cyclic nucleotide-gated channel present in eyes and antennae. Embo J. 13, 5040–5050.

Benton, R., Sachse, S., Michnick, S. W., and Vosshall, L. B. 2006. Atypical membrane topology and heteromeric function of *Drosophila* odorant receptors *in vivo*. PLoS Biol. 4, e20.

Bergamasco, C. and Bazzicalupo, P. 2006. Signaling in the chemosensory systems: chemical sensitivity in *Caenorhabditis elegans*. Cell Mol. Life Sci. 63, 1510–1522.

Biessmann, H., Nguyen, Q. K., Le, D., and Walter, M. F. 2005. Microarray-based survey of a subset of putative olfactory genes in the mosquito *Anopheles gambiae*. Insect Mol. Biol. 14, 575–589.

Birnby, D. A., Link, E. M., Vowels, J. J., Tian, H., Colacurcio, P. L., and Thomas, J. H. 2000. A transmembrane guanylyl cyclase (daf-11) and hsp90 (daf-21) regulate a common set of chemosensory behaviors in *Caenorhabditis elegans*. Genetics 155, 85–104.

Boekhoff, I., Michel, W. C., Breer, H., and Ache, B. W. 1994. Single odors differentially stimulate dual second messenger pathways in lobster olfactory receptor cells. J. Neurosci. 14, 3304–3309.

Boekhoff, I., Raming, K., and Breer, H. 1990a. Pheromone-induced stimulation of inositol-trisphosphate formation in insect antennae is mediated by G-proteins. J. Comp. Physiol. B 160, 99–103.

Boekhoff, I., Strotmann, J., Raming, K., Tareilus, E., and Breer, H. 1990b. Odorant-sensitive phospholipase C in insect antennae. Cell Signal 2, 49–56.

Bohbot, J., Pitts, R. J., Kwon, H.-W. and Rützler, M. 2007. Molecular characterization of the *Aedes aegypti* odorant receptor gene family. Insect Mol. Biol. (accepted).

Bohbot, J., Sobrio, F., Lucas, P., and Nagnan-Le Meillour, P. 1998. Functional characterization of a new class of odorant-binding proteins in the moth *Mamestra brassicae*. Biochem. Biophys. Res. Commun. 253, 489–494.

Breer, H., Boekhoff, I., and Tareilus, E. 1990. Rapid kinetics of second messenger formation in olfactory transduction. Nature 345, 65–68.

Briand, L., Nespoulous, C., Huet, J. C., Takahashi, M., and Pernollet, J. C. 2001. Ligand binding and physico-chemical properties of asp2, a recombinant odorant-binding protein from honeybee (*Apis mellifera* l.). Eur. J. Biochem. 268, 752–760.

Brieger, G. and Butterworth, F. M. 1970. *Drosophila melanogaster*: identity of male lipid in reproductive system. Science 167, 1262.

Buck, L. and Axel, R. 1991. A novel mulitgene family may encode odorant receptors: a molecular basis for odor recognition. Cell 65, 175–187.

Cassill, J. A., Whitney, M., Joazeiro, C. A., Becker, A., and Zuker, C. S. 1991. Isolation of *Drosophila* genes encoding G protein-coupled receptor kinases. Proc. Natl. Acad. Sci. U. S. A. 88, 11067–11070.

Chen, N., Pai, S., Zhao, Z., Mah, A., Newbury, R., Johnsen, R. C., Altun, Z., Moerman, D. G., Baillie, D. L., and Stein, L. D. 2005. Identification of a nematode chemosensory gene family. PNAS 102, 146–151.

Clyne, P. J., Warr, C. G., and Carlson, J. R. 2000. Candidate taste receptors in *Drosophila*. Science 287, 1830–1834.

Clyne, P. J., Warr, C. G., Freeman, M. R., Lessing, D., Kim, J., and Carlson, J. R. 1999. A novel family of divergent seven-transmembrane proteins: candidate odorant receptors in *Drosophila*. Neuron 22, 327–338.

Coburn, C. M. and Bargmann, C. I. 1996. A putative cyclic nucleotide-gated channel is required for sensory development and function in *C. elegans*. Neuron 17, 695–706.

Colbert, H. A. and Bargmann, C. I. 1995. Odorant-specific adaptation pathways generate olfactory plasticity in *C. elegans*. Neuron 14, 803–812.

Colosimo, M. E., Brown, A., Mukhopadhyay, S., Gabel, C., Lanjuin, A. E., Samuel, A. D. T., and Sengupta, P. 2004. Identification of thermosensory and olfactory neuron-specific genes via expression profiling of single neuron types. Curr. Biol. 14, 2245–2251.

Colosimo, M. E., Tran, S., and Sengupta, P. 2003. The divergent orphan nuclear receptor odr-7 regulates olfactory neuron gene expression via multiple mechanisms in *C. elegans*. Genetics 165, 1779–1791.

Consortium, C. E. S. 1998. Genome sequence of the nematode *C. elegans*: a platform for investigating biology. Science 282, 2012–2018.

Dahanukar, A., Hallem, E. A., and Carlson, J. R. 2005. Insect chemoreception. Curr. Opin. Neurobiol. 15, 423–430.

Danty, E., Briand, L., Michard-Vanhee, C., Perez, V., Arnold, G., Gaudemer, O., Huet, D., Huet, J. C., Ouali, C., Masson, C., and Pernollet, J. C. 1999. Cloning and expression of a queen pheromone-binding protein in the honeybee: an olfactory-specific, developmentally regulated protein. J. Neurosci. 19, 7468–7475.

Deshpande, M., Venkatesh, K., Rodrigues, V., and Hasan, G. 2000. The inositol 1,4,5-trisphosphate receptor is required for maintenance of olfactory adaptation in *Drosophila* antennae. J. Neurobiol. 43, 282–288.

Dobritsa, A. A., Van Der Goes Van Naters, W., Warr, C. G., Steinbrecht, R. A., and Carlson, J. R. 2003. Integrating the molecular and cellular basis of odor coding in the *Drosophila* antenna. Neuron 37, 827–841.

Dubin, A. E. and Harris, G. L. 1997. Voltage-activated and odor-modulated conductances in olfactory neurons of *Drosophila melanogaster*. J. Neurobiol. 32, 123–137.

Dubin, A. E., Liles, M. M., and Harris, G. L. 1998. The K^+ channel gene ether a go–go is required for the transduction of a subset of odorants in adult *Drosophila melanogaster*. J. Neurosci. 18, 5603–5613.

Fitzpatrick, D. A., O'halloran, D. M., and Burnell, A. M. 2006. Multiple lineage specific expansions within the guanylyl cyclase gene family. BMC Evol. Biol. 6, 26.

Fox, A. N., Pitts, R. J., Robertson, H. M., Carlson, J. R., and Zwiebel, L. J. 2001. Candidate odorant receptors from the malaria vector mosquito *Anopheles gambiae* and evidence of down-regulation in response to blood feeding. Proc. Natl. Acad. Sci. U. S. A. 98, 14693–14697.

Fox, A. N., Pitts, R. J., and Zwiebel, L. J. 2002. A cluster of candidate odorant receptors from the malaria vector mosquito, *Anopheles gambia*e. Chem. Senses 27, 453–459.

Fukuto, H. S., Ferkey, D. M., Apicella, A. J., Lans, H., Sharmeen, T., Chen, W., Lefkowitz, R. J., Jansen, G., Schafer, W. R., and Hart, A. C. 2004. G protein-coupled receptor kinase function is essential for chemosensation in *C. elegans*. Neuron 42, 581–593.

Galindo, K. and Smith, D. P. 2001. A large family of divergent *Drosophila* odorant-binding proteins expressed in gustatory and olfactory sensilla. Genetics 159, 1059–1072.

Gao, Q. and Chess, A. 1999. Identification of candidate *Drosophila* olfactory receptors from genomic DNA sequence. Genomics 60, 31–39.

Gohl, T. and Krieger, J. R. 2006. Immunolocalization of a candidate pheromone receptor in the antenna of the male moth, *Heliothis virescens*. Invertebr. Neurosci. 6, 13–21.

Goldman, A. L., Van Der Goes Van Naters, W., Lessing, D., Warr, C. G., and Carlson, J. R. 2005. Coexpression of two functional odor receptors in one neuron. Neuron 45, 661–666.

Gomez-Diaz, C., Martin, F., and Alcorta, E. 2004. The camp transduction cascade mediates olfactory reception in *Drosophila melanogaster*. Behav. Genet. 34, 395–406.

Gomez-Diaz, C., Martin, F., and Alcorta, E. 2006. The inositol 1,4,5-triphosphate kinase1 gene affects olfactory reception in *Drosophila melanogaster*. Behav. Genet. 36, 309–321.

Graham, L. A. and Davies, P. L. 2002. The odorant-binding proteins of *Drosophila melanogaster*: annotation and characterization of a divergent gene family. Gene 292, 43–55.

Grobner, G., Burnett, I. J., Glaubitz, C., Choi, G., Mason, A. J., and Watts, A. 2000. Observations of light-induced structural changes of retinal within rhodopsin. Nature 405, 810–813.

Gudi, T., Lohmann, S. M., and Pilz, R. B. 1997. Regulation of gene expression by cyclic GMP-dependent protein kinase requires nuclear translocation of the kinase: identification of a nuclear localization signal. Mol. Cell Biol. 17, 5244–5254.

Hallem, E., Ho, M. G., and Carlson, J. R. 2004a. The molecular basis of odor coding in the *Drosophila* antenna. Cell 117, 965–979.

Hallem, E. A. and Carlson, J. R. 2006. Coding of odors by a receptor repertoire. Cell 125, 143–160.

Hallem, E. A., Dahanukar, A., and Carlson, J. R. 2006. Insect odor and taste receptors. Annu. Rev. Entomol. 51, 113–135.

Hallem, E. A., Nicole Fox, A., Zwiebel, L. J., and Carlson, J. R. 2004b. Olfaction: mosquito receptor for human-sweat odorant. Nature 427, 212–213.

Hekmat-Scafe, D. S., Scafe, C. R., Mckinney, A. J., and Tanouye, M. A. 2002. Genome-wide analysis of the odorant-binding protein gene family in *Drosophila melanogaster*. Genome Res. 12, 1357–1369.

Hildebrand, J. G. and Shepherd, G. M. 1997. Mechanisms of olfactory discrimination: converging evidence for common principles across phyla. Annu. Rev. Neurosci. 20, 595–631.

Hill, C. A., Fox, A. N., Pitts, R. J., Kent, L. B., Tan, P. L., Chrystal, M. A., Cravchik, A., Collins, F. H., Robertson, H. M., and Zwiebel, L. J. 2002. G protein-coupled receptors in *Anopheles gambiae*. Science 298, 176–178.

Holt, R. A., Subramanian, G. M., Halpern, A., Sutton, G. G., Charlab, R., Nusskern, D. R., Wincker, P., Clark, A. G., Ribeiro, J. M., Wides, R., Salzberg, S. L., Loftus, B., Yandell, M., Majoros, W. H., Rusch, D. B., Lai, Z., Kraft, C. L., Abril, J. F., Anthouard, V., Arensburger, P., Atkinson, P. W., Baden, H., De Berardinis, V., Baldwin, D., Benes, V., Biedler, J., Blass, C., Bolanos, R., Boscus, D., Barnstead, M., Cai, S., Center, A., Chatuverdi, K., Christophides, G. K., Chrystal, M. A., Clamp, M., Cravchik, A., Curwen, V., Dana, A., Delcher, A., Dew, I., Evans, C. A., Flanigan, M., Grundschober-Freimoser, A., Friedli, L., Gu, Z., Guan, P., Guigo, R., Hillenmeyer, M. E., Hladun, S. L., Hogan, J. R., Hong, Y. S., Hoover, J., Jaillon, O., Ke, Z., Kodira, C., Kokoza, E., Koutsos, A., Letunic, I., Levitsky, A., Liang, Y., Lin, J. J., Lobo, N. F., Lopez, J. R., Malek, J. A., Mcintosh, T. C., Meister, S., Miller, J., Mobarry, C., Mongin, E., Murphy, S. D., O'brochta, D. A., Pfannkoch, C., Qi, R., Regier, M. A., Remington, K., Shao, H., Sharakhova, M. V., Sitter, C. D., Shetty, J., Smith, T. J., Strong, R., Sun, J., Thomasova, D., Ton, L. Q., Topalis, P., Tu, Z., Unger, M. F., Walenz, B., Wang, A., Wang, J., Wang, M., Wang, X., Woodford, K. J., Wortman, J. R., Wu, M., Yao, A., Zdobnov, E. M., Zhang, H., Zhao, Q., *et al.* 2002. The genome sequence of the malaria mosquito *Anopheles gambiae*. Science 298, 129–149.

Hovemann, B. T., Sehlmeyer, F., and Malz, J. 1997. *Drosophila melanogaster* NADPH-cytochrome p450 oxidoreductase: pronounced expression in antennae may be related to odorant clearance. Gene 189, 213–219.

Jacquin-Joly, E. and Merlin, C. 2004. Insect olfactory receptors: contributions of molecular biology to chemical ecology. J. Chem. Ecol. 30, 2359–2397.

Jacquin-Joly, E., Vogt, R. G., Francois, M. C., and Nagnan-Le Meillour, P. 2001. Functional and expression pattern analysis of chemosensory proteins expressed in antennae and pheromonal gland of *Mamestra brassicae*. Chem. Senses 26, 833–844.

Jansen, G., Thijssen, K. L., Werner, P., Van Der Horst, M., Hazendonk, E., and Plasterk, R. H. 1999. The complete family of genes encoding g proteins of *Caenorhabditis elegans*. Nat. Genet. 21, 414–419.

Jefferis, G. S. X. E. 2005. Insect olfaction: a map of smell in the brain. Curr. Biol. 15, R668–R670.

Jin, X., Brandazza, A., Navarrini, A., Ban, L., Zhang, S., Steinbrecht, R. A., Zhang, L., and Pelosi, P. 2005. Expression and immunolocalisation of odorant-binding and chemosensory proteins in locusts. Cell Mol. Life Sci. 62, 1156–1166.

Jones, A. M. and Assmann, S. M. 2004. Plants: the latest model system for G-protein research. EMBO Rep. 5, 572–578.

Jones, W. D., Nguyen, T. A., Kloss, B., Lee, K. J., and Vosshall, L. B. 2005. Functional conservation of an insect odorant receptor gene across 250 million years of evolution. Curr. Biol. 15, R119–R121.

Kalidas, S. and Smith, D. P. 2002. Novel genomic cdna hybrids produce effective RNA interference in adult *Drosophila*. Neuron 33, 177–184.

Kaupp, U. B. and Seifert, R. 2002. Cyclic nucleotide-gated ion channels. Physiol. Rev. 82, 769–824.

Kim, M. S., Repp, A., and Smith, D. P. 1998. Lush odorant-binding protein mediates chemosensory responses to alcohols in *Drosophila melanogaster*. Genetics 150, 711–721.

Kitabayashi, A. N., Arai, T., Kubo, T., and Natori, S. 1998. Molecular cloning of cdna for p10, a novel protein that increases in the regenerating legs of *Periplaneta americana* (American cockroach). Insect Biochem. Mol. Biol. 28, 785–790.

Komatsu, H., Jin, Y. H., L'etoile, N., Mori, I., Bargmann, C. I., Akaike, N., and Ohshima, Y. 1999. Functional reconstitution of a heteromeric cyclic nucleotide-gated channel of *Caenorhabditis elegans* in cultured cells. Brain Res. 821, 160–168.

Korswagen, H. C., van der Linden, A. M., and Plasterk, R. H. 1998. G protein hyperactivation of the *Caenorhabditis elegans* adenylyl cyclase SGS-1 induces neuronal degeneration. EMBO J. 17, 5059–5065.

Kreher, S. A., Kwon, J. Y., and Carlson, J. R. 2005. The molecular basis of odor coding in the *Drosophila* larva. Neuron 46, 445–456.

Krieger, J., Große-Wilde, E., Gohl, T., and Breer, H. 2005. Candidate pheromone receptors of the silkmoth *Bombyx mori*. Eur. J. Neurosci. 21, 2167–2176.

Krieger, J., Grosse-Wilde, E., Gohl, T., Dewer, Y. M., Raming, K., and Breer, H. 2004. Genes encoding candidate pheromone receptors in a moth (*Heliothis virescens)*. Proc. Natl. Acad. Sci. U. S. A. 101, 11845–11850.

Krieger, J., Klink, O., Mohl, C., Raming, K., and Breer, H. 2003. A candidate olfactory receptor subtype highly conserved across different insect orders. J. Comp. Physiol. A Neuroethol. Sens. Neural Behav. Physiol. 189, 519–526.

Krieger, J., Raming, K., Dewer, Y. M., Bette, S., Conzelmann, S., and Breer, H. 2002. A divergent gene family encoding candidate olfactory receptors of the moth *Heliothis virescens*. Eur. J. Neurosci. 16, 619–628.

Krieger, J., Von Nickisch-Rosenegk, E., Mameli, M., Pelosi, P., and Breer, H. 1996. Binding proteins from the antennae of *Bombyx mori*. Insect Biochem. Mol. Biol. 26, 297–307.

Krupnick, J. G., Gurevich, V. V., and Benovic, J. L. 1997. Mechanism of quenching of phototransduction. Binding competition between arrestin and transducin for phosphorhodopsin. J. Biol. Chem. 272, 18125–18131.

Kruse, S. W., Zhao, R., Smith, D. P., and Jones, D. N. 2003. Structure of a specific alcohol-binding site defined by the odorant binding protein lush from *Drosophila melanogaster*. Nat. Struct. Biol. 10, 694–700.

Kuhara, A., Inada, H., Katsura, I., and Mori, I. 2002. Negative regulation and gain control of sensory neurons by the *C. elegans* calcineurin tax-6. Neuron 33, 751–763.

L'etoile, N. D. and Bargmann, C. I. 2000. Olfaction and odor discrimination are mediated by the *C. elegans* guanylyl cyclase odr-1. Neuron 25, 575–586.

L'etoile, N. D., Coburn, C. M., Eastham, J., Kistler, A., Gallegos, G., and Bargmann, C. I. 2002. The cyclic GMP-dependent protein kinase EGL-4 regulates olfactory adaptation in *C. elegans*. Neuron 36, 1079–1089.

Lans, H., Rademakers, S., and Jansen, G. 2004. A network of stimulatory and inhibitory Galpha-subunits regulates olfaction in *Caenorhabditis elegans*. Genetics 167, 1677–1687.

Larsson, M. C., Domingos, A. I., Jones, W. D., Chiappe, M. E., Amrein, H., and Vosshall, L. B. 2004. Or83b encodes a broadly expressed odorant receptor essential for *Drosophila* olfaction. Neuron 43, 703–714.

Lartigue, A., Campanacci, V., Roussel, A., Larsson, A. M., Jones, T. A., Tegoni, M., and Cambillau, C. 2002. X-ray

structure and ligand binding study of a moth chemosensory protein. J. Biol. Chem. 277, 32094–32098.
Lartigue, A., Gruez, A., Briand, L., Blon, F., Bezirard, V., Walsh, M., Pernollet, J. C., Tegoni, M., and Cambillau, C. 2004. Sulfur single-wavelength anomalous diffraction crystal structure of a pheromone-binding protein from the honeybee *Apis mellifera* l. J. Biol. Chem. 279, 4459–4464.
Lartigue, A., Gruez, A., Spinelli, S., Riviere, S., Brossut, R., Tegoni, M., and Cambillau, C. 2003. The crystal structure of a cockroach pheromone-binding protein suggests a new ligand binding and release mechanism. J. Biol. Chem. 278, 30213–30218.
Laue, M., Maida, R., and Redkozubov, A. 1997. G-protein activation, identification and immunolocalization in pheromone-sensitive sensilla trichodea of moths. Cell Tissue Res. 288, 149–158.
Lefkowitz, R. J. and Shenoy, S. K. 2005. Transduction of receptor signals by beta-arrestins. Science 308, 512–517.
Lycett, G. J., Mclaughlin, L. A., Ranson, H., Hemingway, J., Kafatos, F. C., Loukeris, T. G., and Paine, M. J. 2006. *Anopheles gambiae* p450 reductase is highly expressed in oenocytes and *in vivo* knockdown increases permethrin susceptibility. Insect Mol. Biol. 15, 321–327.
Maibeche-Coisne, M., Merlin, C., Francois, M. C., Porcheron, P., and Jacquin-Joly, E. 2005. P450 and p450 reductase cdnas from the moth *Mamestra brassicae*: cloning and expression patterns in male antennae. Gene 346, 195–203.
Martin, F., Charro, M. J., and Alcorta, E. 2001. Mutations affecting the camp transduction pathway modify olfaction in *Drosophila*. J. Comp. Physiol. A 187, 359–370.
Matsuki, M., Kunitomo, H., and Iino, Y. 2006. Goalpha regulates olfactory adaptation by antagonizing Gqalpha-DAG signaling in *Caenorhabditis elegans*. Proc. Natl. Acad. Sci. U. S. A. 103, 1112–1117.
Mccarroll, S. A., Li, H., and Bargmann, C. I. 2005. Identification of transcriptional regulatory elements in chemosensory receptor genes by probabilistic segmentation. Curr. Biol. 15, 347–352.
Mckenna, M. P., Hekmat Scafe, D. S., Gaines, P., and Carlson, J. R. 1994. Putative *Drosophila* pheromone-binding proteins expressed in a subregion of the olfactory system. J. Biol. Chem. 269, 16340–16347.
Mckenna, M., Monte, P., Helfand, S. L., Woodard, C., and Carlson, J. 1989. A simple chemosensory response in *Drosophila* and the isolation of acj mutants in which it is affected. PNAS 86, 8118–8122.
Melo, A. C., Rutzler, M., Pitts, R. J., and Zwiebel, L. J. 2004. Identification of a chemosensory receptor from the yellow fever mosquito, *Aedes aegypti*, that is highly conserved and expressed in olfactory and gustatory organs. Chem. Senses 29, 403–410.
Merrill, C. E., Pitts, R. J., and Zwiebel, L. J. 2003. Molecular characterization of arrestin family members in the malaria vector mosquito, *Anopheles gambiae*. Insect Mol. Biol. 12, 641–650.
Merrill, C. E., Riesgo-Escovar, J., Pitts, R. J., Kafatos, F. C., Carlson, J. R., and Zwiebel, L. J. 2002. Visual arrestins in olfactory pathways of *Drosophila* and the malaria vector mosquito *Anopheles gambiae*. Proc. Natl. Acad. Sci. U. S. A. 99, 1633–1638.
Merrill, C. E., Sherertz, T. M., Walker, W. B., and Zwiebel, L. J. 2005. Odorant-specific requirements for arrestin function in *Drosophila* olfaction. J. Neurobiol. 63, 15–28.
Minke, B. and Cook, B. 2002. Trp channel proteins and signal transduction. Physiol. Rev. 82, 429–472.
Mohanty, S., Zubkov, S., and Gronenborn, A. M. 2004. The solution NMR structure of *Antheraea polyphemus* PBP provides new insight into pheromone recognition by pheromone-binding proteins. J. Mol. Biol. 337, 443–451.
Mombaerts, P. 2004. Genes and ligands for odorant, vomeronasal and taste receptors. Nat. Rev. Neurosci. 5, 263–278.
Nagnan-Le Meillour, P., Cain, A. H., Jacquin-Joly, E., Francois, M. C., Ramachandran, S., Maida, R., and Steinbrecht, R. A. 2000. Chemosensory proteins from the proboscis of *Mamestra brassicae*. Chem. Senses 25, 541–553.
Nakagawa, T., Sakurai, T., Nishioka, T., and Touhara, K. 2005. Insect sex-pheromone signals mediated by specific combinations of olfactory receptors. Science 307, 1638–1642.
Nene, V., Wortman, J. R., Lawson, D., Haas, B., Kodira, C., Tu, Z. J., Loftus, B., Xi, Z., Megy, K., Grabherr, M., Ren, Q., Zdobnov, E. M., Lobo, N. F., Campbell, K. S., Brown, S. E., Bonaldo, M. F., Zhu, J., Sinkins, S. P., Hogenkamp, D. G., Amedeo, P., Arensburger, P., Atkinson, P. W., Bidwell, S., Biedler, J., Birney, E., Bruggner, R. V., Costas, J., Coy, M. R., Crabtree, J., Crawford, M., Debruyn, B., Decaprio, D., Eiglmeier, K., Eisenstadt, E., El-Dorry, H., Gelbart, WM., Gomes, S. L., Hammond, M., Hannick, L. I., Hogan, J. R., Holmes, M. H., Jaffe, D., Johnston, J. S., Kennedy, R. C., Koo, H., Kravitz, S., Kriventseva, E. V., Kulp, D., Labutti, K., Lee, E., Li, S., Lovin, D. D., Mao, C., Mauceli, E., Menck, C. F., Miller, J. R., Montgomery, P., Mori, A., Nascimento, A. L., Naveira, H. F., Nusbaum, C., O'leary, S., Orvis, J., Pertea, M., Quesneville, H., Reidenbach, K. R., Rogers, Y. H., Roth, C. W., Schneider, J. R., Schatz, M., Shumway, M., Stanke, M., Stinson, E. O., Tubio, J. M., Vanzee, J. P., Verjovski-Almeida, S., Werner, D., White, O., Wyder, S., Zeng, Q., Zhao, Q., Zhao, Y., Hill, C. A., Raikhel, A. S., Soares, M. B., Knudson, D. L., Lee, N. H., Galagan, J., Salzberg, S. L., Paulsen, I. T., Dimopoulos, G., Collins, F. H., Birren, B., Fraser-Liggett, C. M., and Severson, D. W. 2007. Science 316, 1718–1723.
Neuhaus, E. M., Gisselmann, G., Zhang, W., Dooley, R., Stortkuhl, K., and Hatt, H. 2005. Odorant receptor heterodimerization in the olfactory system of *Drosophila melanogaster*. Nat. Neurosci. 8, 15–17.
Nikonov, A. A., Peng, G., Tsurupa, G., and Leal, W. S. 2002. Unisex pheromone detectors and pheromone-binding proteins in scarab beetles. Chem. Senses 27, 495–504.
Okochi, Y., Kimura, K. D., Ohta, A., and Mori, I. 2005. Diverse regulation of sensory signaling by *C. elegans* nPKC-epsilon/eta TTX-4. Embo J. 24, 2127–2137.
Ono, Y., Fujibuchi, W., and Suwa, M. 2005. Automatic gene collection system for genome-scale overview of G-protein coupled receptors in eukaryotes. Gene 364, 63–73.
Ozaki, M., Morisaki, K., Idei, W., Ozaki, K., and Tokunaga, F. 1995. A putative lipophilic stimulant carrier protein commonly found in the taste and olfactory systems. A unique member of the pheromone-binding protein superfamily. Eur. J. Biochem. 230, 298–308.
Paesen, G. C. and Happ, G. M. 1995. The B proteins secreted by the tubular accessory sex glands of the male mealworm beetle, *Tenebrio molitor*, have sequence similarity to moth pheromone-binding proteins. Insect Biochem. Mol. Biol. 25, 401–408.
Palmitessa, A., Hess, H. A., Bany, I. A., Kim, Y. M., Koelle, M. R., and Benovic, J. L. 2005. *Caenorhabditus elegans* arrestin regulates neural G protein signaling and olfactory adaptation and recovery. J. Biol. Chem. 280, 24649–24662.
Park, S. K., Shanbhag, S. R., Wang, Q., Hasan, G., Steinbrecht, R. A., and Pikielny, C. W. 2000. Expression patterns of two putative odorant-binding proteins in the olfactory organs of *Drosophila melanogaster* have different implications for their functions. Cell Tissue Res. 300, 181–192.
Pelosi, P. 1994. Odorant-binding proteins. Crit. Rev. Biochem. Mol. Biol. 29, 199–228.

Picone, D., Crescenzi, O., Angeli, S., Marchese, S., Brandazza, A., Ferrara, L., Pelosi, P., and Scaloni, A. 2001. Bacterial expression and conformational analysis of a chemosensory protein from *Schistocerca gregaria*. Eur. J. Biochem. 268, 4794–4801.

Pitts, R. J., Fox, A. N., and Zwiebel, L. J. 2004. A highly conserved candidate chemoreceptor expressed in both olfactory and gustatory tissues in the malaria vector, *Anopheles gambiae*. Proc. Natl. Acad. Sci. U. S. A. 101, 5058–5063.

Ranson, H., Claudianos, C., Ortelli, F., Abgrall, C., Hemingway, J., Sharakhova, M. V., Unger, M. F., Collins, F. H., and Feyereisen, R. 2002. Evolution of supergene families associated with insecticide resistance. Sci. 298, 179–181.

Reiter, E. and Lefkowitz, R. J. 2006. GRKs and beta-arrestins: roles in receptor silencing, trafficking and signaling. Trends Endocrinol. Metab. 17, 159–165.

Remy, J.-J. and Hobert, O. 2005. An interneuronal chemoreceptor required for olfactory imprinting in *C. elegans*. Science 309, 787–790.

Richards, S., Liu, Y., Bettencourt, B. R., Hradecky, P., Letovsky, S., Nielsen, R., Thornton, K., Hubisz, M. J., Chen, R., Meisel, R. P., Couronne, O., Hua, S., Smith, M. A., Zhang, P., Liu, J., Bussemaker, H. J., Van Batenburg, M. F., Howells, S. L., Scherer, S. E., Sodergren, E., Matthews, B. B., Crosby, M. A., Schroeder, A. J., Ortiz-Barrientos, D., Rives, C. M., Metzker, M. L., Muzny, D. M., Scott, G., Steffen, D., Wheeler, D. A., Worley, K. C., Havlak, P., Durbin, K. J., Egan, A., Gill, R., Hume, J., Morgan, M. B., Miner, G., Hamilton, C., Huang, Y., Waldron, L., Verduzco, D., Clerc-Blankenburg, K. P., Dubchak, I., Noor, M. A., Anderson, W., White, K. P., Clark, A. G., Schaeffer, S. W., Gelbart, W., Weinstock, G. M., and Gibbs, R. A. 2005. Comparative genome sequencing of *Drosophila pseudoobscura*: chromosomal, gene, and *cis*-element evolution. Genome Res. 15, 1–18.

Riesgo-Escovar, J., Raha, D., and Carlson, J. R. 1995. Requirement for a phospholipase C in odor response: overlap between olfaction and vision in *Drosophila*. Proc. Natl. Acad. Sci. U. S. A. 92, 2864–2868.

Riesgo-Escovar, J. R., Woodard, C., and Carlson, J. R. 1994. Olfactory physiology in the *Drosophila* maxillary palp requires the visual system gene *rdgB*. J. Comp. Physiol. A 175, 687–693.

Riviere, S., Lartigue, A., Quennedey, B., Campanacci, V., Farine, J. P., Tegoni, M., Cambillau, C., and Brossut, R. 2003. A pheromone-binding protein from the cockroach *Leucophaea maderae*: cloning, expression and pheromone binding. Biochem. J. 371, 573–579.

Roayaie, K., Crump, J. G., Sagasti, A., and Bargmann, C. I. 1998. The G alpha protein ODR-3 mediates olfactory and nociceptive function and controls cilium morphogenesis in *C. elegans* olfactory neurons. Neuron 20, 55–67.

Robertson, H. M. 1998. Two large families of chemoreceptor genes in the nematodes *Caenorhabditis elegans* and *Caenorhabditis briggsae* reveal extensive gene duplication, diversification, movement, and intron loss. Genome Res. 8, 449–463.

Robertson, H. M. 2000. The large srh family of chemoreceptor genes in *Caenorhabditis* nematodes reveals processes of genome evolution involving large duplications and deletions and intron gains and losses. Genome Res. 10, 192–203.

Robertson, H. M. 2001. Updating the str and srj (stl) families of chemoreceptors in *Caenorhabditis* nematodes reveals frequent gene movement within and between chromosomes. Chem. Senses 26, 151–159.

Robertson, H. M. and Thomas, J. H. 2006. The putative chemoreceptor families of *C. elegans*, http://www.wormbook.org, doi/10.1895/wormbook.1.66.1.

Robertson, H. M., Martos, R., Sears, C. R., Todres, E. Z., Walden, K. K., and Nardi, J. B. 1999. Diversity of odourant binding proteins revealed by an expressed sequence tag project on male *Manduca sexta* moth antennae. Insect Mol. Biol. 8, 501–518.

Robertson, H. M., Warr, C. G., and Carlson, J. R. 2003. Molecular evolution of the insect chemoreceptor gene superfamily in *Drosophila melanogaster*. Proc. Natl. Acad. Sci. U. S. A. 100(Suppl. 2), 14537–14542.

Rogers, M. E., Jani, M. K., and Vogt, R. G. 1999. An olfactory-specific glutathione-*S*-transferase in the sphinx moth *Manduca sexta*. J. Exp. Biol. 202, 1625–1637.

Roman, G., He, J., and Davis, R. L. 2000. Kurtz, a novel nonvisual arrestin, is an essential neural gene in *Drosophila*. Genetics 155, 1281–1295.

Rothemund, S., Liou, Y. C., Davies, P. L., Krause, E., and Sonnichsen, F. D. 1999. A new class of hexahelical insect proteins revealed as putative carriers of small hydrophobic ligands. Structure 7, 1325–1332.

Rubin, G. M., Yandell, M. D., Wortman, J. R., Gabor Miklos, G. L., Nelson, C. R., Hariharan, I. K., Fortini, M. E., Li, P. W., Apweiler, R., Fleischmann, W., Cherry, J. M., Henikoff, S., Skupski, M. P., Misra, S., Ashburner, M., Birney, E., Boguski, M. S., Brody, T., Brokstein, P., Celniker, S. E., Chervitz, S. A., Coates, D., Cravchik, A., Gabrielian, A., Galle, R. F., Gelbart, W. M., George, R. A., Goldstein, L. S., Gong, F., Guan, P., Harris, N. L., Hay, B. A., Hoskins, R. A., Li, J., Li, Z., Hynes, R. O., Jones, S. J., Kuehl, P. M., Lemaitre, B., Littleton, J. T., Morrison, D. K., Mungall, C., O'farrell, P. H., Pickeral, O. K., Shue, C., Vosshall, L. B., Zhang, J., Zhao, Q., Zheng, X. H., and Lewis, S. 2000. Comparative genomics of the eukaryotes. Science 287, 2204–2215.

Rutzler, M. and Zwiebel, L. 2005. Molecular biology of insect olfaction: recent progress and conceptual models. J. Comp. Physiol. A Neuroethol. Sens. Neural Behav. Physiol., 1–14.

Rutzler, M. R., Lu, T., and Zwiebel, L. J. 2006. The ga encoding gene family of the malaria vector mosquito *Anopheles gambiae*: expression analysis and immunolocalization of agaq and agao in female antennae. J. Comp. Neurol., 499, 533–545.

Sabatier, L., Jouanguy, E., Dostert, C., Zachary, D., Dimarcq, J. L., Bulet, P., and Imler, J. L. 2003. Pherokine-2 and -3. Eur. J. Biochem. 270, 3398–3407.

Sakurai, T., Nakagawa, T., Mitsuno, H., Mori, H., Endo, Y., Tanoue, S., Yasukochi, Y., Touhara, K., and Nishioka, T. 2004. Identification and functional characterization of a sex pheromone receptor in the silkmoth *Bombyx mori*. Proc. Natl. Acad. Sci. U. S. A. 101, 16653–16658.

Sandler, B. H., Nikonova, L., Leal, W. S., and Clardy, J. 2000. Sexual attraction in the silkworm moth: structure of the pheromone-binding-protein-bombykol complex. Chem. Biol. 7, 143–151.

Scott, K., Becker, A., Sun, Y., Hardy, R., and Zuker, C. 1995. Gq alpha protein function *in vivo*: genetic dissection of its role in photoreceptor cell physiology. Neuron 15, 919–927.

Sengupta, P., Chou, J. H., and Bargmann, C. I. 1996. Odr-10 encodes a seven transmembrane domain olfactory receptor required for responses to the odorant diacetyl. Cell 84, 899–909.

Shanbhag, S. R., Hekmat-Scafe, D., Kim, M. S., Park, S. K., Carlson, J. R., Pikielny, C., Smith, D. P., and Steinbrecht, R. A. 2001. Expression mosaic of odorant-binding proteins in *Drosophila* olfactory organs. Microsc. Res. Tech. 55, 297–306.

Shanbhag, S. R., Müller, B., and Steinbrech, R. A. 1999. Atlas of olfactory organs of *Drosophila melanogaster.* 1.Types, external organization, innervation and distribution of olfactory sensilla. Int. J. Insect Morphol. Embryol. 28, 377–397.

Stein, L. D., Bao, Z., Blasiar, D., Blumenthal, T., Brent, M. R., Chen, N., Chinwalla, A., Clarke, L., Clee, C., Coghlan, A., Coulson, A., Eustachio, P., Fitch, D. H. A., Fulton, L. A., Fulton, R. E., Griffiths-Jones, S., Harris, T. W., Hillier, L. W., Kamath, R., Kuwabara, P. E., Mardis, E. R., Marra, M. A., Miner, T. L., Minx, P., Mullikin, J. C., Plumb, R. W., Rogers, J., Schein, J. E., Sohrmann, M., Spieth, J., Stajich, J. E., Wei, C., Willey, D., Wilson, R. K., Durbin, R., and Waterston, R. H. 2003. The genome sequence of *Caenorhabditis briggsae*: a platform for comparative genomics. PLoS Biol. 1, e45.

Steinbrecht, R. A. 1998. Odorant-binding proteins: expression and function. Ann. N. Y. Acad. Sci. 855, 323–332.

Stensmyr, M. C., Erland, S., Hallberg, E., Wallen, R., Greenaway, P., and Hansson, B. S. 2005. Insect-like olfactory adaptations in the terrestrial giant robber crab. Curr. Biol. 15, 116–121.

Stewart, M. K., Clark, N. L., Merrihew, G., Galloway, E. M., and Thomas, J. H. 2005. High genetic diversity in the chemoreceptor superfamily of *Caenorhabditis elegans*. Genetics 169, 1985–1996.

Stocker, R. F. 2001. *Drosophila* as a focus in olfactory research: mapping of olfactory sensilla by fine structure, odor specificity, odorant receptor expression, and central connectivity. Microsc. Res. Tech. 55, 284–296.

Storkuhl, K. F. and Kettler, R. 2001. Functional analysis of an olfactory receptor in *Drosophila melanogaster*. PNAS 98, 9381–9385.

Stortkuhl, K. F., Hovemann, B. T., and Carlson, J. R. 1999. Olfactory adaptation depends on the trp Ca^{2+} channel in *Drosophila*. J. Neurosci. 19, 4839–4846.

Talluri, S., Bhatt, A., and Smith, D. P. 1995. Identification of a *Drosophila* G protein alpha subunit (dGq alpha-3) expressed in chemosensory cells and central neurons. Proc. Natl. Acad. Sci. U. S. A. 92, 11475–11479.

Tegoni, M., Pelosi, P., Vincent, F., Spinelli, S., Campanacci, V., Grolli, S., Ramoni, R., and Cambillau, C. 2000. Mammalian odorant binding proteins. Biochim. Biophys. Acta 1482, 229–240.

Tobin, D., Madsen, D., Kahn-Kirby, A., Peckol, E., Moulder, G., Barstead, R., Maricq, A., and Bargmann, C. 2002. Combinatorial expression of TRPV channel proteins defines their sensory functions and subcellular localization in *C. elegans* neurons. Neuron 35, 307–318.

Troemel, E. R., Chou, J. H., Dwyer, N. D., Colbert, H. A., and Bargmann, C. I. 1995. Divergent seven transmembrane receptors are candidate chemosensory receptors in *C. elegans*. Cell 83, 207–218.

Troemel, E. R., Kimmel, B. E., and Bargmann, C. I. 1997. Reprogramming chemotaxis responses: sensory neurons define olfactory preferences in *C. elegans*. Cell 91, 161–169.

Tsuchihara, K., Fujikawa, K., Ishiguro, M., Yamada, T., Tada, C., Ozaki, K., and Ozaki, M. 2005. An odorant-binding protein facilitates odorant transfer from air to hydrophilic surroundings in the blowfly. Chem. Senses 30, 559–564.

Vogt, R. G. 2003. Insect Pheromone Biochemistry and Molecular Biology. Elsevier Academic Press.

Vogt, R. G. 2006. How sensitive is a nose? Sci. STKE, pe8.

Vogt, R. G. and Riddiford, L. M. 1981. Pheremone binding and inactivation by moth antennae. Nature 293, 161–163.

Vogt, R. G., Callahan, F. E., Rogers, M. E., and Dickens, J. C. 1999. Odorant binding protein diversity and distribution among the insect orders, as indicated by LAP, an OBP-related protein of the true bug *Lygus lineolaris* (Hemiptera, Heteroptera). Chem. Senses 24, 481–495.

Vogt, R. G., Kohne, A. C., Dubnau, J. T., and Prestwich, G. D. 1989. Expression of pheromone binding proteins during antennal development in the gypsy moth *Lymantria dispar*. J. Neurosci. 9, 3332–3346.

Vogt, R. G., Prestwich, G. D., and Lerner, M. R. 1991. Odorant-binding-protein subfamilies associate with distinct classes of olfactory receptor neurons in insects. J. Neurobiol. 22, 74–84.

Vogt, R. G., Rogers, M. E., Franco, M. D., and Sun, M. 2002. A comparative study of odorant binding protein genes: differential expression of the PBP1–GOBP2 gene cluster in *Manduca sexta* (Lepidoptera) and the organization of OBP genes in *Drosophila melanogaster* (Diptera). J. Exp. Biol. 205, 719–744.

Vosshall, L. B. 2000. Olfaction in *Drosophila*. Curr. Opin. Neurobiol. 10, 498–503.

Vosshall, L. B., Amrein, H., Morozov, P. S., Rzhetsky, A., and Axel, R. 1999. A spatial map of olfactory receptor expression in the *Drosophila* antenna. Cell 96, 725–736.

Vosshall, L. B., Wong, A. M., and Axel, R. 2000. An olfactory sensory map in the fly brain. Cell 102, 147–159.

Wanner, K. W., Willis, L. G., Theilmann, D. A., Isman, M. B., Feng, Q., and Plettner, E. 2004. Analysis of the insect os-d-like gene family. J. Chem. Ecol. 30, 889–911.

Wetzel, C. H., Behrendt, H., Gisselmann, G., Storkuhl, K. F., Hovemann, B., and Hatt, H. 2001. Functional expression and characterization of a *Drosophila* odorant receptor in a heterologous cell system. PNAS 98, 9377–9380.

Wogulis, M., Morgan, T., Ishida, Y., Leal, W. S., and Wilson, D. K. 2006. The crystal structure of an odorant binding protein from *Anopheles gambiae*: evidence for a common ligand release mechanism. Biochem. Biophys. Res. Commun. 339, 157–164.

Wojtasek, H. and Leal, W. S. 1999. Degradation of an alkaloid pheromone from the pale-brown chafer, *Phyllopertha diversa* (Coleoptera: Scarabaeidae), by an insect olfactory cytochrome p450. FEBS Lett. 458, 333–336.

Xia, Y. and Zwiebel, L. J. 2006. Identification and characterization of an odorant receptor from the West Nile Virus mosquito, *Culex quinquefasciatus*. Insect Biochem. Mol. Biol. 36, 169–176.

Xu, P., Atkinson, R., Jones, D. N., and Smith, D. P. 2005. *Drosophila* OBP LUSH is required for activity of pheromone-sensitive neurons. Neuron 45, 193–200.

Xu, P. X., Zwiebel, L. J., and Smith, D. P. 2003. Identification of a distinct family of genes encoding atypical odorant-binding proteins in the malaria vector mosquito, *Anopheles gambiae*. Insect Mol. Biol. 12, 549–560.

Young, J., Shykind, B., Lane, R., Tonnes-Priddy, L., Ross, J., Walker, M., Williams, E., and Trask, B. 2003. Odorant receptor expressed sequence tags demonstrate olfactory expression of over 400 genes, extensive alternate splicing and unequal expression levels, http://genomebiology.Com/2003/4/11/r71. Genome Biol. 4, R71.

Zhang, X. and Firestein, S. 2002. The olfactory receptor gene superfamily of the mouse. Nat. Neurosci. 5, 124–133.

Zhou, J. J., Huang, W., Zhang, G. A., Pickett, J. A., and Field, L. M. 2004. ''Plus-c'' odorant-binding protein genes in two *Drosophila* species and the malaria mosquito *Anopheles gambiae*. Gene 327, 117–129.

Zwaal, R. R., Mendel, J. E., Sternberg, P. W., and Plasterk, R. H. 1997. Two neuronal G proteins are involved in chemosensation of the *Caenorhabditis elegans* Dauer-inducing pheromone. Genetics 145, 715–727.

4.34 Regeneration of the Olfactory Epithelium

J E Schwob, Tufts University School of Medicine, Boston, MA, USA

R M Costanzo, Virginia Commonwealth University, Richmond, VA, USA

© 2008 Elsevier Inc. All rights reserved.

4.34.1	**Introduction and Early Literature**	592
4.34.2	**Structure of the Olfactory Mucosa: Layers and Compartments**	592
4.34.2.1	Sensory Neurons	592
4.34.2.2	Supporting Cells	594
4.34.2.3	Basal Cells	594
4.34.2.4	Bowman's Glands/Ducts	595
4.34.2.5	Cells of the Lamina Propria	595
4.34.2.6	Fascicles of the Olfactory Nerve	595
4.34.3	**Ongoing Olfactory Neurogenesis**	595
4.34.4	**Response to Injury – Reconstitution of the Epithelium**	597
4.34.4.1	Toxic Injury to the Olfactory Epithelium	597
4.34.4.2	Epithelial Response to Nerve Transection or Olfactory Bulb Ablation	598
4.34.4.3	Effects of Viral Infection on the Olfactory Epithelium	598
4.34.5	**Stem and Progenitor Cells of the Adult Olfactory Epithelium**	599
4.34.5.1	Some Global Basal Cells Are Multipotent Progenitors	599
4.34.5.2	Globose Basal Cells Are the Only Population for Which Functional Heterogeneity Has Been Demonstrated	599
4.34.5.3	Quiescent Globose Basal Cells	601
4.34.5.4	Are Some Cells Among the Globose Basal Cells Tissue Stem Cells of the Olfactory Epithelium?	601
4.34.5.5	Progenitor Capacity of Other Epithelial Cell Types	602
4.34.6	**Reinervation of the Olfactory Bulb**	602
4.34.6.1	Normal Organization of the Axonal Projection from the Olfactory Epithelium onto the Olfactory Bulb	602
4.34.6.2	Organization of the Projection Following Recovery from Injury to the Periphery	604
4.34.6.3	Disorganization of the Projection Following Olfactory Nerve Transection	605
4.34.6.4	Functional Recovery Following Epithelial Lesion or Nerve Transection	605
4.34.6.5	Summary	606
4.34.7	**Conclusions and Unanswered Questions**	606
4.34.8	**Note Added in Proof**	607
References		607

Glossary

BHLH Basic helix–loop–helix transcription factor family.
CDKI Cyclin-dependent kinase inhibitor.
FACS Fluorescence-activated cell sorter.
GBC Globose basal cell.
HBC Horizontal basal cell.
MeBr Methyl bromide.
OB Olfactory bulb.
OE Olfactory epithelium.
ON Olfactory nerve.
OR Odorant receptor.

4.34.1 Introduction and Early Literature

The capacity of the olfactory epithelium (OE), especially its population of sensory neurons, to recover after injury, reconnect with the central nervous system (CNS), and reestablish function has been known from the first half of the twentieth century (Nagahara, Y., 1940). In addition to experimental studies on the consequences of transection of the olfactory nerve (ON) along its course from the OE to the olfactory bulb (OB), an extensive literature documents sensory recovery in humans in the large cohort of children and young adults who were treated by irrigation with zinc sulfate as a means of polio prophylaxis. Subsequent experimental investigations demonstrated anatomical reconstitution of the epithelium following zinc sulfate treatment in a variety of experimental species, including primates (Schultz, E. W., 1941; Schultz, E. W. and Gebhardt, S. P., 1942; Schultz, E. W., 1960; Mulvaney, B. D. and Heist, H. E., 1971; Matulionis, D. H., 1975; 1976). Studies performed by Graziadei, Moulton, and colleagues in the 1960s and 1970s demonstrated that the epithelium of laboratory animals harbored a population of rapidly proliferating cells that functioned as neuronal progenitors and gave rise to neurons (Moulton, D. G. *et al.*, 1970; Graziadei, P. P. and Metcalf, J. F., 1971; Graziadei, P. P., 1973; Moulton, D. G., 1974; Graziadei, P. P. C. and Monti Graziadei, G. A., 1978; Graziadei, P. P. and Monti Graziadei, G. A., 1979). This remarkable and seminal discovery invigorated the cellular and molecular investigations of olfactory neurogenesis, which have carried on to this day.

From a teleological perspective, the persistence of neurogenesis in the normal adult OE and the anatomical and functional recovery following injury to the epithelium or the nerve are highly adaptive. The epithelium is particularly vulnerable to any number of toxins, infectious agents, or other forms of insult, given the direct contact of the neural elements with the ambient, airborne environment. Moreover, the neurons and their axons form a direct conduit from the outer world into the CNS that may be used as a route of entry to the brain by pathogens, such as neurotropic viruses (Twomey, J. A. *et al.*, 1979; Monath, T. P. *et al.*, 1983; Stroop, W. G. *et al.*, 1984; Barnett, E. M. *et al.*, 1993; Barnett, E. M. and Perlman, S., 1993). Thus, a propensity for the neurons to die with little provocation may provide a survival advantage in the short term for the organism by preventing the transmission of pathogens, but requires some capacity for compensatory reconstitution of the system after the exposure period has passed.

The intent of this review is to summarize the current state of our knowledge regarding cellular renewal in the normal OE, the enhanced production of neurons and nonneural cell types after injury, reinnervation of the bulb following epithelial reconstitution, and restoration of sensory function subsequent to anatomical recovery. We will not consider the vomeronasal system.

For heuristic purposes, our discussion will focus first on the epithelium and its capacity for reconstitution and then turn to the ON and its innervation of the bulb.

4.34.2 Structure of the Olfactory Mucosa: Layers and Compartments

The olfactory mucosa forms a continuous sheet lining the posterodorsal part of the nasal septum, the tips of the opposing nasal turbinates, and much of the turbinate shafts and cul-de-sacs at the same level (Moulton, D. G. and Beidler, L. M., 1967; Grazaiadei, P. P. C., 1971). In addition, a small patch of olfactory mucosa, termed the nasal septal organ (NSO) (of Masera), detaches from this sheet at an early embryological stage and comes to reside just dorsal to the opening of the nasopharyngeal duct (Bojsen-Moller, F., 1975; Weiler, E. and Farbman, A. I., 2003); the NSO is, for all intents and purposes, identical to the main OE in morphology, molecular phenotype, and function, and will not be considered separately (Taniguchi, K. *et al.*, 1993).

The olfactory mucosa consists of a pseudostratified epithelium and a lamina propria that rests directly on the bony and cartilagenous skeleton of the nose (de Lorenzo, A. J., 1957; Andres, K. H., 1966; Moulton, D. G. and Beidler, L. M., 1967; Grazaiadei, P. P. C., 1971; Graziadei, P. P. and Monti Graziadei, G. A., 1979). The epithelium contains a handful of cell types: neurons, supporting cells and basal cells (Figure 1(a)). Each of these categories may be further subdivided.

4.34.2.1 Sensory Neurons

The population of neurons consists of both mature, ciliated, olfactory marker protein (OMP)-expressing and immature, GAP-43 (+) cells that have yet to

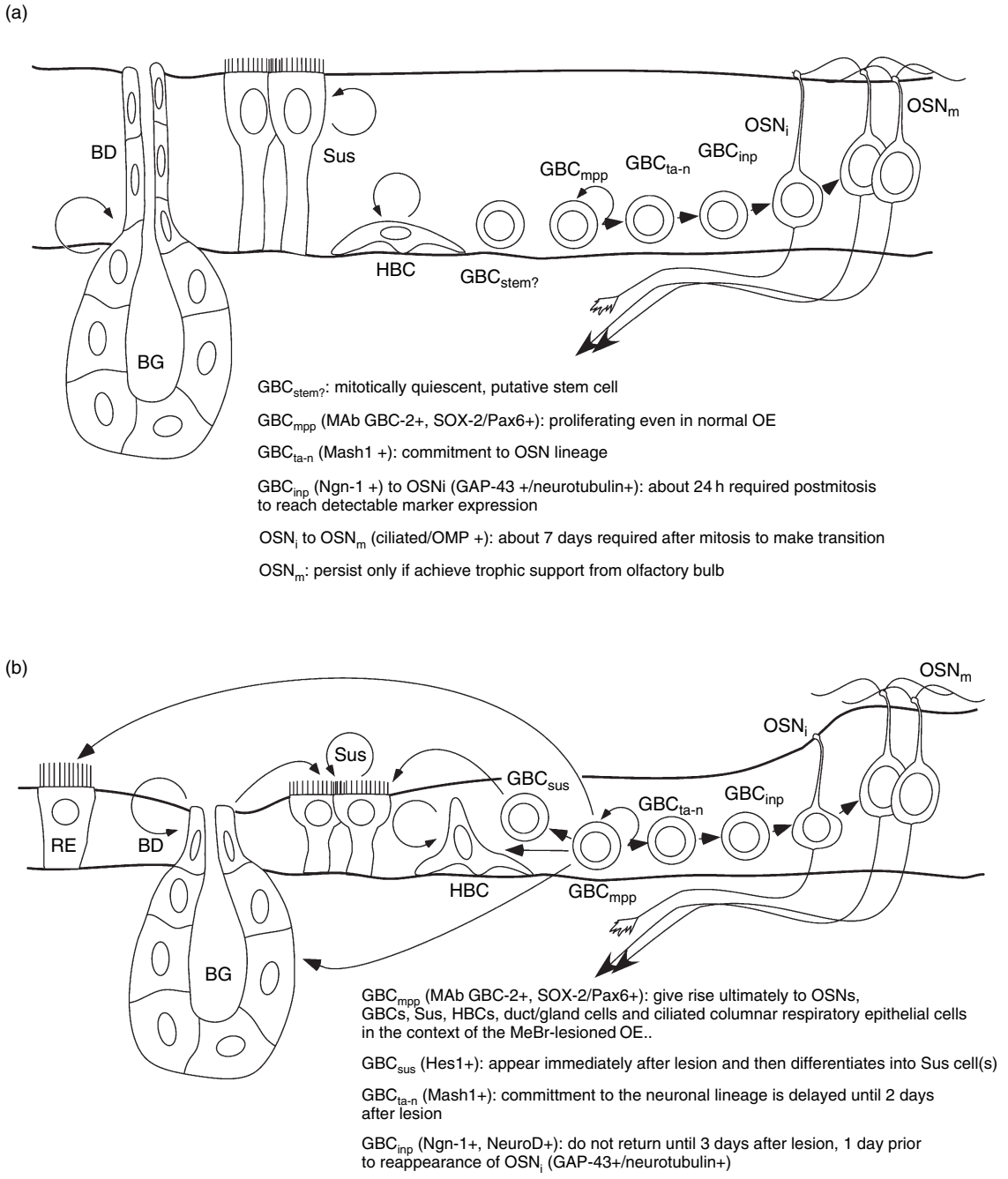

Figure 1 The processes of cellular renewal differ between normal and lesioned olfactory epithelium. (a) In normal epithelium or in epithelium in which the population of neurons has been depleted as a consequence of acute damage to olfactory nerve or bulb or where neuronal turnover is accelerated for neurons born following bulb ablation, the various cell types arise via self-replacement or, in the case of the sensory neurons, from the mitosis of globose basal cells (GBC). (b) In contrast to the foregoing, following methyl bromide exposure, more promiscuous lineage relationships emerge: GBCs will give rise to neurons and themselves (a form of self-renewal), of course, but also to horizontal basal cells (HBCs), sustentacular (Sus) cells, Bowman gland (BG), and duct (BD) cells, and even respiratory epithelial (RE) cells. In essence, GBCs are demonstrably as potent in the context of the nasal epithelium as the cells of the olfactory placode. BD cells also evince a greater than normal potency and contribute to the replacement of the Sus cell population. The GBC population is heterogeneous with respect to functional phenotype, and the various kinds can be distinguished on the basis of their expression of member of various transcription factor families.

elaborate cilia (Verhaagen, J. *et al.*, 1989; Meiri, K. F. *et al.*, 1991). The population of typical olfactory neurons can be subdivided further on the basis of which single odorant receptor (OR) is expressed from among the family of about 1300 OR genes (Buck, L. and Axel, R., 1991; Zhang, X. and Firestein, S., 2002). That choice is constrained by a neuron's position along the dorsomedial-to-ventrolateral axis of the epithelium. Along that axis, each OR is limited to a narrow band that reaches through the anteroposterior extent of the OE (Ressler, K. J. *et al.*, 1993; Vassar, R. *et al.*, 1993). Although the spatial organization has been described as sharply bounded and zonal, more recent studies suggest that each OR-defined band overlaps partially with a number of other ones (Iwema, C. L. *et al.*, 2004; Miyamichi, K. *et al.*, 2005). As a consequence, the organization of OR expression across epithelial space is better described as a very large number of bands that gradually shift in position along that dorsomedial-to-ventrolateral axis, rather than a very small number of zones. From a developmental perspective, the organization in shifting, sharply bounded bands is as easily explained as the four-zone model; for example, a cell's response to a gradient of a signaling molecule can generate shifting bands as easily as a discrete number of stripes (Wolpert, L., 1989). Other features of the neuronal phenotype are also position-dependent including connectivity and expression of certain cell-surface markers, and may also be sharply bounded (Mori, K. *et al.*, 1985; Schwob, J. E. and Gottlieb, D. I., 1986; 1988, Schwarting, G. A. and Crandall, J. E., 1991; Schwarting, G. A. *et al.*, 1992; Yoshihara, Y. *et al.*, 1997).

In addition to the foregoing, atypical olfactory neurons are concentrated in (but not limited to) the epithelium lining the cul-de-sacs of the posterior nasal cavity, which differ from the majority. The sensory transduction apparatus is based on guanylyl cyclase expression rather than adenylyl cyclase; they lack OMP; finally, they project to the necklace glomeruli at the posterior edge of the glomerular sheet (Shinoda, K. *et al.*, 1989; 1993, Juilfs, D. M. *et al.*, 1997; Ring, G. *et al.*, 1997). The neurons elaborate thin unmyelinated axons that gather at the basal lamina under the arch-like process of the horizontal basal cells (HBCs) where the axons first come into contact with the glia of the ON.

4.34.2.2 Supporting Cells

The microvillar-capped supporting cells whose nuclei reside at the apex of the epithelium can be subdivided into sustentacular (Sus) and microvillar cells. Sus cells contain abundant smooth endoplasmic reticulum, while microvillar cells do not. Both express cytokeratins 8 and 18, but otherwise have different biochemical profiles: Sus cells stain with MAbs SUS-1 and SUS-4, while microvillar cells label with the MAb 1A-6, the lectin Iβ-4 from *Bandeiraea simplicifolia* (BS-I), and express ankyrin. Furthermore, other characteristics can be used to differentiate the two types of microvillar cells (Hempstead, J. L. and Morgan, J. I., 1985a; Goldstein, B. J. and Schwob, J. E., 1996; Asan, E. and Drenckhahn, D., 2005).

4.34.2.3 Basal Cells

The population of basal cells can be subdivided on the basis of their relationship to the basal lamina. Horizontal (or dark) basal cells (HBCs) attach directly to the basal lamina via desmosomes, express cytokeratins 5 and 14, the epidermal growth factor-receptor (EGF-R), intercellular adhesion molecule (ICAM), integrins, and a carbohydrate moiety recognized by the lectin BS-I (Graziadei, P. P. and Monti Graziadei, G. A., 1979; Holbrook, E. H. *et al.*, 1995; Carter, L. A. *et al.*, 2004).

Globose (or light) basal cells (GBCs) are situated at a remove from the basal lamina, and are distributed nonuniformly across the tangential extent of the epithelium (Graziadei, P. P. and Monti Graziadei, G. A., 1979; Holbrook, E. H. *et al.*, 1995; Loo, A. T. *et al.*, 1996). Conventionally, GBCs have been identified and defined on exclusionary grounds; cells have been classified as GBCs if morphologic simplicity and molecular phenotype indicate that they are not HBCs, not neurons, and not duct cells. A few positive markers have been generated, which are not strictly limited to the GBC population (Goldstein, B. J. and Schwob, J .E., 1996; Goldstein, B. J. *et al.*, 1997; Jang, W. *et al.*, 2003). For example, several monoclonal antibodies (MAbs) label GBCs along with neurons in normal epithelium, but not the other cell types. One of these MAbs – GBC-3 – binds to the 34 kDa, that is, immature, form of the laminin-receptor protein (iLRP) (Jang, W. *et al.*, 2007).

In addition, subsets of GBCs are labeled by a variety of TFs of the basic helix–loop–helix (bHLH), LHX, Msx, Pax, and SOX families, as well as others (Cau, E. *et al.*, 1997; 2000, Norlin, E. M. *et al.*, 2001; Cau, E. *et al.*, 2002; Suzuki, Y. *et al.*, 2003; Hirota, J. and Mombaerts, P., 2004; Kolterud, A. *et al.*, 2004; Guo, Z. *et al.*, 2005b). Thus, it appears that the

population of GBCs is markedly heterogeneous on biochemical grounds that likely correspond with differences in their capacities as progenitor cells.

A third type of basal cell has also been noted on ultrastructural grounds; it extends a foot process, contacts the basal lamina via an adherens junction, and is more irregularly shaped than most other GBCs (Graziadei, P. P. and Monti Graziadei, G. A., 1979; Holbrook, E. H. *et al.*, 1995). Some authors have considered these cells as a transition stage between HBCs and GBCs (or vice versa) (Graziadei, P. P. and Monti Graziadei, G. A., 1979), but no evidence other than morphological can be adduced for this notion. Because, in fact, the third type cells attach by adherens and not desmosomal junctions, there are really no data, morphologic or otherwise, to indicate intermediacy of this third type of basal cell or to draw a lineage relationship between GBCs and HBCs. However, little else is known about this type.

4.34.2.4 Bowman's Glands/Ducts

The final elements in the epithelium are Bowman's ducts, which extend from the Bowman's glands in the lamina propria to the apical surface where the mucus formed by the glands is discharged. The glands themselves are found within the lamina propria. The ducts and gland cells share some phenotypic characteristics with Sus cells, including a common reactivity with several MAbs and high expression of cytochrome P450s (Hempstead, J. L. and Morgan, J. I., 1985a; 1985b; Chen, Y. *et al.*, 1992; Huard, J. M. *et al.*, 1998).

4.34.2.5 Cells of the Lamina Propria

Other elements in the lamina propria include fibroblasts, migrating lymphocytes, and tissue macrophages. There may be other cell types within the lamina propria; for example, cells express retinoic acid (RA)-synthesizing enzymes at differential levels as a function of position along a dorsomedial-to-ventrolateral axis have not yet been fully characterized as to type. Whether fibroblastic or not, they may be critical for the reassembly of the system after lesion.

4.34.2.6 Fascicles of the Olfactory Nerve

The fascicles of the olfactory and vomeronasal nerve also course through the lamina propria. At a macroscopic level, the nerve begins as small bundles of axons that are evident where the basal lamina is breached. During their course posteriorward, the bundles gradually sink more deeply into the lamina propria where they obliquely contact, fuse with, and form larger fascicles of the nerve. The microscopic organization of the fascicles differs markedly from that of other peripheral nerves. The glia of the ON fascicles, termed olfactory ensheathing cells (OECs), are found within the perineurial sheath, which is formed by what have been termed ON fibroblasts (de Lorenzo, A. J., 1957; Andres, K. H., 1966; Barber, P. C. and Lindsay, R. M., 1982; Field, P. *et al.*, 2003; Li, Y. *et al.*, 2005). The perikarya of the OECs are found plastered against the edge of the nerve or of the endoneurial septae that subdivide the larger fascicles, while their processes interdigitate among the olfactory axons. In contrast to the mature spinal nerve in which single unmyelinated axons are segregated each within its own individual trough (Peters, A. *et al.*, 1991), collections of olfactory axons are in intimate contact with each other and isolated from the environment by the sheet-like processes of the OECs (de Lorenzo, A. J., 1957; Andres, K. H., 1966; Barber, P. C. and Lindsay, R. M., 1982; Field, P. *et al.*, 2003; Li, Y. *et al.*, 2005). In that respect, the relationship of bundles of olfactory axons and OEC glia in the adult is like that of the Schwann cell and axons of growing spinal nerves in the embryo, only writ large (Peters, A. *et al.*, 1991). The unique relationship between olfactory axons and glia begins within the pocket formed between the overarching processes of the HBCs and the basal lamina where the axons exit the epithelium and is maintained up to the entry of the axons into the neuropil of the olfactory glomeruli (Holbrook, E. H. *et al.*, 1995; Li, Y. *et al.*, 2005).

4.34.3 Ongoing Olfactory Neurogenesis

The intrinsic capacity of the OE to produce neurons throughout life was implicit in the demonstrations of structural and functional recovery by the olfactory system following experimental injury. However, a more direct understanding of the basis for ongoing neurogenesis came from the discoveries of the 1960s and 1970s by Graziadei, Moulton, and their respective colleagues that cells near the base of the OE in adult rodents incorporate labeled analogues of thymidine after pulse administration and that the thymidine-labeled cells can be chased with time and watched as they differentiate into neurons and then eventually disappear (Figure 1(a)) (Moulton, D. G. *et al.*, 1970; Graziadei, P. P. and Metcalf, J. F.,

1971; Graziadei, P. P., 1973; Moulton, D. G., 1974; Graziadei, P. P.C. and Monti Graziadei, G. A., 1978; Graziadei, P. P. and Monti Graziadei, G. A., 1979). During their cellular differentiation, the newborn neurons first extend a dendrite and express the axonal growth protein GAP-43 (Verhaagen, J. *et al.*, 1989; Meiri, K. F. *et al.*, 1991; Schwob, J. E. *et al.*, 1995). Within about a week of their birth the neurons have elaborated cilia, turned off GAP-43, and turned on OMP (Miragall, F. and Monti Graziadei, G. A., 1982; Schwob, J. E. *et al.*, 1995). OR expression lags the onset of neuronal differentiation by a few days, but is seen before OMP is expressed (Iwema, C. L. and Schwob, J. E., 2003).

Of the two cell types in the basal zone of the OE, tracing of cell lineage by use of a replication-incompetent, retrovirally derived vector (RRVV) or by dye injection into basal cells both show that neurons derive from GBCs (Schwartz Levey, M. *et al.*, 1992; Caggiano, M. *et al.*, 1994; Schwob, J. E. *et al.*, 1994a). The lineage analyses correspond with the demonstration that there is a parallel increase in GBC proliferation and neuronal production occasioned by damage to the ON and OB (Schwartz Levey, M. *et al.*, 1991). Subsequent analyses of the sequential expression of TFs that activate neurogenesis (i.e., Mash1, Ngn1, and NeuroD1) by GBCs during development and after lesion, provide a further indication that GBCs are the proximate precursors of neurons in the OE (Guillemot, F. *et al.*, 1993; Gordon, M. K. *et al.*, 1995; Cau, E. *et al.*, 1997; 2002; Manglapus, G. L. *et al.*, 2004).

Does GBC proliferation and neuron production persist throughout life? In most humans and experimental animals, the answer is yes. However, in humans, biopsies do show areas of epithelium that remain olfactory in character (i.e., containing microvillar-capped Sus cells) but are aneuronal, suggesting that the neurogenic capacity of the olfactory stem and progenitor cells can be exhausted (Holbrook, E. L. *et al.*, 2005). Interestingly, the same neurogenic exhaustion is observed in rodents in which an oncogene is expressed under the control of the OMP promoter (Largent, B. L. *et al.*, 1993); as the expression of an oncogene in a terminally differentiated cell often initiates programmed cell death (Al-Ubaidi, M. R. *et al.*, 1997; Feddersen, R. M. *et al.*, 1997), neuronal turnover may be grossly accelerated, and from an early stage, in these transgenic mice.

At the time the original data were obtained indicating adult neurogenesis, only the olfactory neurons were believed to be subject to replacement. Subsequently, the birth of other neuronal populations in adults, including the interneurons of the OB, was demonstrated elsewhere in the adult nervous system (Kaplan, M. S. and Hinds, J. W., 1977; Kaplan, M. S. *et al.*, 1985; Lois, C. and Alvarez-Buylla, A., 1993; 1994; Menezes, J. R. *et al.*, 1995). Nonetheless, the rate of production as a percentage of the established population appears higher in the OE than anywhere else, and more subject to regulation on the basis of need.

The original observations on basal cell proliferation were interpreted as an indication that sensory neurons within the OE had a fixed, finite lifespan, like epithelial cells of gut or skin (Moulton, D. G. *et al.*, 1970; Graziadei, P. P. and Metcalf, J. F., 1971; Graziadei, P. P., 1973; Moulton, D. G., 1974; 1975; Graziadei, P. P. C. and Monti Graziadei, G. A., 1978; Graziadei, P. P. and Monti Graziadei, G. A., 1979). Moreover, the rate of proliferation was used as a means of estimating that the neurons lived for about a month, on average. However, the pulse–chase data cannot be interpreted as providing evidence for the notion that the turnover of mature, synaptically connected olfactory sensory neurons (OSNs) occurs automatically at the end of a fixed (relatively) brief lifespan. Neither the original nor subsequent data preclude the notion that turnover might take place within a reserve population of unconnected, relatively immature neurons. In fact, neurons undergoing programmed cell death or apoptosis are found within both the immature and OMP-positive population in the normal adult OE (Holcomb, J. D. *et al.*, 1995; Deckner, M. L. *et al.*, 1997); in that vein it is also important to note that the onset of OMP expression is NOT by itself an indication of synaptic connectivity. Subsequent demonstrations have also weakened the association between ongoing neurogenesis and any prescribed replacement of mature neurons in the protected environment experienced by laboratory-housed animals. For example, the lifespan of newly born OSNs from animals that are in a pathogen-free, filtered air environment may be as long as a year (Hinds, J. W. *et al.*, 1984). Moreover, when the preexisting neurons are tagged by retrograde transport of a stable marker from the bulb, the labeled OSNs persist for a period of time that is substantially longer than a month (Mackay-Sim, A. and Kittel, P. W., 1991b); unfortunately, these data do not permit a determination of whether lifespan is indefinite once a neuron becomes established. Finally, a mechanism exists that allows the system to regulate survival of newly generated neurons on the basis of their connectivity status, which would be required if lifespan is not inherently limited. In more specific

terms, OSNs exhibit a trophic dependency on the OB for their prolonged survival, such that lifespan is abbreviated for neurons born in the absence of the bulb (Monti Graziadei, G. A., 1983; Biffo, S. *et al.*, 1992; Schwob, J. E. *et al.*, 1992; Carr, V. M. and Farbman, A. I., 1993; Mackay-Sim, A. and Chuah, M. L., 2000). Trophic dependency is a means by which the system might eliminate those newly born neurons that fail to make any or the appropriate synaptic connections (Purves, D., 1988). Thereby the size of the sensory population may be regulated in accordance with the status of the target, which might, itself, be modified by sensory activity and odorant saliency, among other influences. Given these provisos, it is fair to say that the definitive experiments have not yet been done that would allow us to determine the lifespan of preexisting sensory neurons in the laboratory environment or any other milieu.

4.34.4 Response to Injury – Reconstitution of the Epithelium

The primary olfactory system has been subjected to three general forms of experimental injury: direct toxic injury to the OE; traumatic injury to the ON, OB, or both; and viral infection following intranasal inoculation.

4.34.4.1 Toxic Injury to the Olfactory Epithelium

Damage to the OE ensues in some cases by direct contact of a toxin with the epithelium; the two most widely used of these are zinc-containing salts, in particular zinc sulfate, delivered by intranasal infusion (Smith, C. G., 1938; Schultz, E. W., 1960; Matulionis, D. H., 1975; 1976; Harding, J. W. *et al.*, 1978; Cancalon, P., 1982; Burd, G. D., 1993), and MeBr, for which passive inhalation is the route of exposure (Hurtt, M. E. *et al.*, 1987; 1988; Schwob, J. E. *et al.*, 1995). In other cases, some toxins damage or destroy the OE after systemic administration; among these are 3-methyl indole (skatol), dichlobenil, and methimazole (Schwob, J. E. *et al.*, 1994b; Brittebo, E. B., 1995; Genter, M. B. *et al.*, 1995; 1996; Slotnick, B. *et al.*, 2001). The mechanism by which zinc sulfate causes relatively selective damage to the OE after intranasal administration is not known in any detail, although speculation has centered on the protein-coagulative properties of the salt (Schultz, E. W. and Gebhardt, S. P., 1942). MeBr, which effect is absolutely selective for damage to the OE within the nose, is apparently converted to an active free radical toxin via biotransformation enzymes in the epithelium, most likely one or more members of the cytochrome P450 family (Reed, C. J. *et al.*, 1995). Other features of the olfactory toxicity of MeBr that reflect the need for activation include the relative insensitivity of younger animals, the strain dependence of efficacy in mice, and the absolute refractoriness to lesion under circumstances when the biotransformation systems are substantially diminished relative to normal (e.g., the OE cannot be lesioned again by a subsequent exposure to toxin during the immediate post-MeBr lesion period when cytochrome P450 enzymes are far below normal levels) (Schwob, J. E., unpublished results). Other systemically acting toxins, for example, skatol, may also exert their effect after enzymatic activation by that system.

The immediate effects of lesion have been studied in some detail for both zinc sulfate and MeBr. However, much of the zinc literature predates the availability and use of cell-type-specific reagents to study reconstitution of the OE. Accordingly, the timing and events of epithelial recovery is better known from the studies of MeBr lesions published more recently (Figure 1(b)). In virtually all cases where a direct comparison can be made, the findings with MeBr are highly analogous to those seen following zinc sulfate.

Inhalation of the toxin in MeBr-sensitive animals leads to a rapid loss (sloughing) of all neurons and supporting cells in over 95% of the OE within 24 h, and damage to those populations in the remainder of the tissue (Schwob, J. E. *et al.*, 1995). In addition, the Bowman's glands in the lamina propria are damaged but incompletely. The GBC, HBC, and duct cell populations also sustain some loss. In particular, HBCs disappear from the ventral OE in lesioned rats (but not mice) by the third day after exposure. In contrast, agents like methimazole take several days to produce maximal damage, which makes study of the initial events during epithelial regeneration difficult due to the concurrence of cell loss and replacement (Brittebo, E. B., 1995; Genter, M. B. *et al.*, 1995; Bergstrom, U. *et al.*, 2003). Within 2 days after MeBr, the remaining cells undergo a quick upsurge in proliferation. The first neurons to reappear do so at about 4 days after lesion, and then mature, that is, express OMP, around the middle of the second week after lesion, at roughly the same time as the first returning axons reinnervate glomeruli in the bulb. Likewise, the Sus cells begin to reappear within a few days, and reform a distinct

layer at the apex of the epithelium by 10 days after lesion. By 6–8 weeks after MeBr, the majority of the OE has stabilized to a state that is indistinguishable from normal, as judged by the rate of GBC proliferation, the relative proportion of immature-to-mature OSNs, and the restoration of normal or near-normal levels of expression of cytochrome P450 enzymes (Schwob, J. E. *et al.*, 1995).

Depending on its severity, the initial lesion may preclude the recovery of the lesioned epithelium as olfactory, and the events underlying failure may model the pathophysiology of some forms of human olfactory dysfunction (Schwob, J. E. *et al.*, 1994b; Jang, W. *et al.*, 2003). For example, MeBr lesion can be enhanced such that all GBCs are eliminated from patches of the OE; the GBC-depleted areas reconstitute as respiratory epithelium (a form of metaplasia) (Jang, W. *et al.*, 2003). The same kind of metaplasia, is observed following zinc sulfate infusion or a combination of skatol injection and MeBr inhalation, and is often more extensive than with MeBr (Smith, C. G., 1938; Burd, G. D., 1993; Schwob, J. E. *et al.*, 1994b).

4.34.4.2 Epithelial Response to Nerve Transection or Olfactory Bulb Ablation

In contrast to the effects of and response to directly acting toxins, cell loss following nerve or bulb injury is limited to the OSNs. Nerve transection or bulb ablation causes retrograde degeneration of the neurons via a caspase-mediated process of programmed cell death (or apoptosis) within the space of a few days (Harding, J. *et al.*, 1977; Monti Graziadei, G. A. and Graziadei, P. P., 1979; Simmons, P. A. *et al.*, 1981; Costanzo, R. M. and Graziadei, P. P., 1983; Monti Graziadei, G. A., 1983; Verhaagen, J. *et al.*, 1990; Schwartz Levey, M. *et al.*, 1991; Carr, V. M. and Farbman, A. I., 1992; Gordon, M. K. *et al.*, 1995; Holcomb, J. D. *et al.*, 1995; Calof, A. L. *et al.*, 1998; Cowan, C. M. *et al.*, 2001; Cowan, C. M. and Roskams, A. J., 2002). Neuronal loss causes the upregulation of GBC proliferation only; the feedback inhibition from OSNs onto the mitotic activity of GBCs in the normal OE, which is apparently mediated by bone morphogenetic proteins (BMPs) 4 and 7 and by growth differentiation factor (GDF)11, is released (Gordon, M. K. *et al.*, 1995; Shou, J. *et al.*, 1999; 2000; Wu, H. H. *et al.*, 2003). Moreover, cytokines, including leukemia inhibitory factor (LIF), that are released by infiltrating macrophages may also play a role in the activation of GBCs in response to neuronal degeneration (Nan, B. *et al.*, 2001; Bauer, S. *et al.*, 2003). As a consequence, expansive proliferation occurs within the GBC population, followed by an increased rate of neuronal production (Figure 1(a)) (Monti Graziadei, G. A. and Graziadei, P. P., 1979; Schwartz Levey, M. *et al.*, 1991). Basal cell proliferation and neuron production remains elevated over the long term in bulb-ablated animals, and perhaps nerve transected ones as well (Schwob, J. E. *et al.*, 1992). Following ablation, the abbreviated lifespan caused by the loss of trophic support from the bulb is such that the neuronal population is dominated by immature OSNs, instead of mature ones, while the size of the population always remains less than that of normal OE, despite accelerated neurogenesis (Verhaagen, J. *et al.*, 1990; Biffo, S. *et al.*, 1992; Schwob, J. E. *et al.*, 1992; Konzelmann, S. *et al.*, 1998). In contrast, nerve transection permits substantial though incomplete reinnervation of the bulb as well as some mistargeting; as a consequence, the population of OSNs recovers more fully toward normal than after bulb ablation (Monti Graziadei, G. A. and Graziadei, P. P., 1979; Graziadei, P. P. and Monti Graziadei, G. A., 1980; Costanzo, R. M., 1984; 1985; Koster, N. L. and Costanzo, R. M., 1996; Yee, K. K. and Costanzo, R. M., 1998; Costanzo, R. M., 2000; Christensen, M. D. *et al.*, 2001; Costanzo, R. M., 2005).

Other cell populations in the OE show a response to the lesion, although it is not mitotic. For example, the levels of cytochrome P450 enzymes decrease in Sus cells (Walters, E. *et al.*, 1992). In addition, Sus cells become active phagocytes (Suzuki, Y. *et al.*, 1995; 1996).

4.34.4.3 Effects of Viral Infection on the Olfactory Epithelium

The damage to the epithelium caused by viral infection is a much more frequent antecedent of olfactory dysfunction in humans than either toxin exposure or head trauma (for which nerve transection and/or bulb ablation is generally held to be analogous) (Doty, R. L., 1979; Moran, D. T. *et al.* 1992; Seiden, A. M., 2004; Holbrook, E. H. and Leopold, D. A., 2006). Biopsies of the human mucosa and specimens taken at autopsy indicate that the replacement of olfactory by respiratory epithelium is not a rare event in the human mucosa (Nakashima, T. *et al.*, 1984; Nakashima, T. *et al.*, 1985). Indeed, loss of neurogenic capacity due to respiratory metaplasia or stem cell exhaustion can become complete, leading to anaxonic, fibrotic ON fascicles (Holbrook, E. H. *et al.*, 2005). (Collagen

deposition and fibrosis of ON fascicles is also observed in Macaque, but not in rodents (Graziadei, P. P. *et al.*, 1980).) Experimental models that duplicate the changes observed following viral infections in humans are rare and mechanistically obscure. However, it is worth noting that certain neurotropic viruses can gain entry to the CNS by infection of OSNs and anterograde transport to, and release from, the terminals of the ON, without killing the infected sensory neurons (Barthold, S. W., 1988; Schwob, J. E. *et al.*, 2001). To the extent that they cause downstream damage to the OB, the OE can come to resemble that which is harvested from bulbectomized animals.

4.34.5 Stem and Progenitor Cells of the Adult Olfactory Epithelium

The unique capacity of the OE to reconstitute after injury, for example, following inhalation of MeBr, reflects and requires the persistence of one or more types of neurocompetent stem cells, from which spring the downstream progenitors that eventually give rise to the various missing cell types. Of necessity, neurocompetent stem cells must be found within one or more of the three cell types that are spared following MeBr lesion: GBCs, HBCs, or duct cells. Of equal necessity, candidate olfactory stems must satisfy a certain operational definition that emerged from studies of cellular renewal in tissues like skin and gut, as follows. Tissue stem cells are totipotent (with respect to the tissue in question), infinitely self-renewing, and mitotically quiescent when the tissue is undamaged (Hall, P. A. and Watt, F. M., 1989; Rao, M. S., 1999; Watt, F. M., 2001; Alonso, L. and Fuchs, E., 2003; Pevny, L. and Rao, M. S., 2003). In the conventional model, progenitors of progressively more limited differentiative potency or capacity for self-renewal or both arise from and are downstream of the stems. Most investigators identify a kind of lineage-restricted progenitor that retains a capacity for expansive proliferation and call it a transit-amplifying (TA) cell (Potten, C. S. and Loeffler, M., 1990; Potten, C. S., 1998; Watt, F. M., 2001; Alonso, L. and Fuchs, E., 2003). Further downstream are the cells that are charged with giving rise to the differentiated tissue elements, and are called immediate precursors, for example, immediate neuronal precursors (INPs) in the OE.

4.34.5.1 Some Global Basal Cells Are Multipotent Progenitors

Our current understanding of the players and processes underlying cellular renewal in the olfactory system is based on RRVV lineage tracing experiments (Huard, J. M. *et al.*, 1998), *in vivo* transplantation studies using purified populations of cells (Goldstein, B. J. *et al.*, 1998; Chen, X. *et al.*, 2004), on gene expression analysis following lesion or in the embryonic placode (Manglapus, G. L. *et al.*, 2004), on the consequences of gene mutation (Cau, E. *et al.*, 1997; Fisher, A. and Caudy, M., 1998; Cau, E. *et al.*, 2000; 2002; Murray, R. C. *et al.*, 2003), and on *in vitro* studies (Shou, J. *et al.*, 1999; Satoh, M. and Yoshida, T., 2000; Carter, L. A. *et al.*, 2004). All of these data indicate that some cells within the population of GBCs are capable of a broad multipotency in the context of the MeBr-lesioned OE; hence, the GBCs may ultimately be responsible for the reconstitution of much of the OE after lesion and not merely the neuronal population (Figures 1(b) and 2). In aggregate, GBCs give rise to GBCs (a form of self-renewal), neurons, Sus cells, microvillar cells, HBCs, duct and gland cells, and even respiratory epithelial cells. Not all cell types are found in all clones – individual clones from transplanted GBCs or from RRVV-labeled progenitors may contain multiple cell types, or may consist of neurons or Sus cells alone – but there is a rough correlation between large clones, a greater number of cell types, and the presence of GBCs (i.e., a form of self-renewal). Hence, the differentiative potency of GBCs in the MeBr-lesioned OE seems to be as broad as that of the olfactory placodal cells, which are the embryonic precursors for all of the nasal lining. It is important to note that some multipotent cells present in the normal epithelium are active in the mitotic cycle as shown by infectability with RRVV *ex vivo* prior to transplantation into a host. Thus, the decision between neuropotency and multipotency is one that is made on a continuous basis in the normal OE.

4.34.5.2 Globose Basal Cells Are the Only Population for Which Functional Heterogeneity Has Been Demonstrated

Among the GBC population of both embryonic and adult OE are subsets that can be distinguished one from the next on the basis of their expression of TFs of the bHLH family of TFs, which in turn appear to correlate with difference in their potency as precursors (Cau, E. *et al.*, 1997; 2000; 2002; Manglapus, G. L. *et al.*, 2004). In particular, observations on mice

bearing engineered mutations of the bHLH family members as well as analyses of TF expression in developing and regenerating OE have lead to a conceptualization of flow through the GBC population that acknowledges the diversity of precursor types (Figure 2). At the origin are the stem cells and broadly multipotent GBCs ($GBCs_{MPP}$) capable of giving rise to all cell types present in the OE as well as the respiratory epithelial cells normally found elsewhere in the nasal lining; it is likely that some, possibly most, broadly potent GBCs are not stems. Downstream of them are cells en route to terminally differentiated neurons only; among the downstream elements committed to neurogenesis are transit-amplifying GBCs ($GBCs_{TA}$) and INPs. Based on a comparison with TF markers, GBCs of all three functional types – MPPs, TAs, and INPs – are actively proliferating in the normal OE. In the usual formulation, the cellular flow in this model is depicted as unidirectional, and from less committed to more (Figure 2). However, as a greater appreciation for the plasticity of stems and progenitors has emerged, a case can be made for reevaluating the conventional notion of unidirectional flow.

Some of the molecular correlates of multipotency among the GBCs can be adduced (Figure 2). $GBCs_{MPP}$ express antigens that are recognized by MAbs GBC-1, GBC-2, and GBC-3 (the latter recognizing a carbohydrate moiety on iLRP) based on the comparison of timing of expression after MeBr lesion, the outcome of RRVV infection, and the use of these antibodies for fluorescence-activated cell sorter (FACS) (Goldstein, B. J. and Schwob, J. E., 1996; Goldstein, B. J. *et al.*, 1997; Huard, J. M. *et al.*, 1998; Jang, W. *et al.*, 2003; Chen, X. *et al.*, 2004; Jang, W. *et al.*, 2007). However, none of the three differentiates GBC_{MPP} from GBCs committed to making neurons selectively.

The timing of bHLH TF expression relative to recovery of the OE after MeBr lesion (Manglapus, G. L. *et al.*, 2004) and the pattern of gene expression and epithelial composition in Mash1 (−/−) mutant animals, (Guillemot, F. *et al.*, 1993; Cau, E. *et al.*, 1997) help narrow and contrast the molecular profile of the MPPs and other progenitors. These data suggest that the $GBCs_{MPP}$ do not express Mash1, nor the TFs NeuroD and Ngn1, which are expressed after Mash1 in the embryonic and in the regenerating OE. $GBCs_{TA}$ that are downstream of the $GBCs_{MPP}$ and

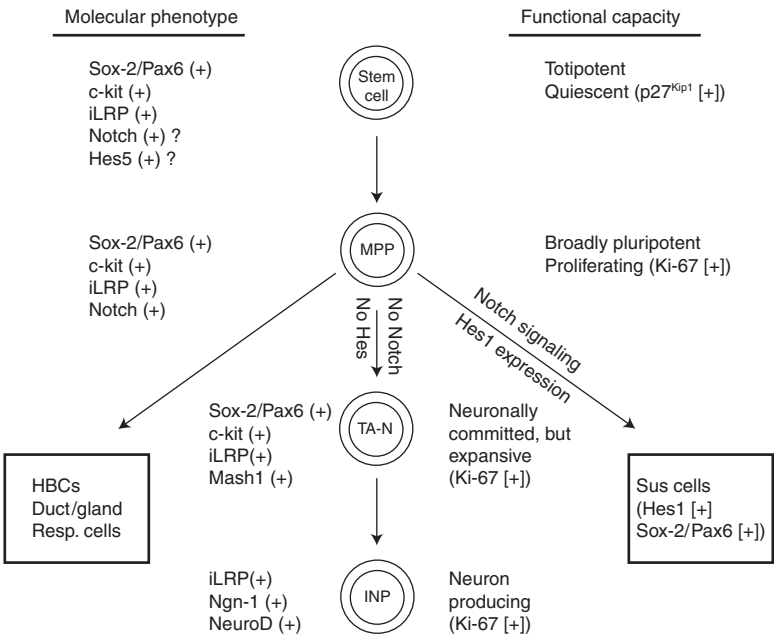

Figure 2 Functional classification and categorization of globose basal cells (GBCs) correlates with molecular phenotype. Central to differences in progenitor capacity seem to be members of the basic helix–loop–helix family of transcription factors (Hes, Mash, Ngn, and NeuroD) as well as the transcription factors Sox-2 and Pax6. For the latter factors, the pattern of expression in normal epithelium and during recovery from methyl bromide (MeBr) lesion suggests that they repress neuronal differentiation, which they do in other parts of the nervous system, a function which is required up to the final progenitor cell stage in the epithelium.

committed to a neuronal fate express Mash1, based on an analysis of Mash1 mutant mice and of the timing of its expression relative to lesion and embryonic development. Other GBCS that are further downstream and act as immediate neuronal precursors or producers ($GBCs_{INP}$) express NeuroD and/or Ngn1. All three functional types are present and mitotically active in the normal OE.

The same kind of analysis eliminates the bHLH TF Hes1 as a marker for, or critical to, the function of $GBCs_{MPP}$. Although *Hes1* expression appears in a substantial number of GBCs within 1 day of MeBr lesion, quickly thereafter the *Hes1* (+) cells shift apicalward and differentiate into Sus cells (Manglapus, G. L. *et al.*, 2004). The differentiation of *Hes1* (+) GBCs ($GBCs_{Sus}$) into Sus cells fits with the specific expression of Hes1 by Sus cells in OE of normal or bulbectomized animals; in these settings the GBC population makes only neurons. Thus, *Hes1* expression by GBCs does not indicate multipotency *per se* but seems to convey commitment to a Sus cell lineage. Parenthetically, *Hes1* is not needed to make Sus cells when expression of the *Mash1* gene is eliminated by genetic recombination, as supporting cells of the *Mash1* mutant mice do not express *Hes1* (Cau, E. *et al.*, 2000). These data fit with a demonstrated role for Hes1 protein, namely the suppression of *Mash1* expression; in the absence of *Mash1*, no such repression is needed.

However, the expression patterns of the TFs SOX-2 and Pax6 – high-mobility group (HMG) and paired domain TFs, respectively, that frequently cooperate in regulating gene transcription – indicate that $GBCs_{MPP}$ can be identified as GBCs that express these two TFs, and are not marked by expression of Mash1, or HBC, or Sus cell markers (cell types which also express the two TFs). In more specific terms, all GBCs in the OE from the immediate postlesion period express SOX-2 and Pax6 (Guo, Z. *et al.*, 2005a; 2005b); at this time the vast majority of GBCs are proliferating and either multipotent or making Sus cells. In their joint expression of SOX-2 and Pax6, $GBCs_{MPP}$ resemble the cells of the olfactory placode/pit (Grindley, J. C. *et al.*, 1995), which are the embryonic founders for the OE (as well as all other parts of the lining of the nasal cavity). Furthermore, stem cells of the embryonic CNS also seem to express both SOX-2 and Pax6 (Gotz, M. *et al.*, 1998; Marquardt, T. *et al.*, 2001; Chi, N. and Epstein, J. A., 2002; Avilion, A. A. *et al.*, 2003; Graham, V. *et al.*, 2003; Ellis, P. *et al.*, 2004; Brazel, C. Y. *et al.*, 2005; Englund, C. *et al.*, 2005).

In the final analysis, despite satisfying the multipotency criterion, it is unlikely that the actively proliferating $GBCs_{MPP}$ are stems, but rather they are most likely downstream of the bona fide stem cells.

4.34.5.3 Quiescent Globose Basal Cells

Among the GBC population are ones that express another characteristic of stem cells, namely prolonged mitotic quiescence. Hinds (Hinds, J. W. *et al.*, 1984) and then MacKay-Sim (Mackay-Sim, A. and Kittel, P., 1991a) recognized a population of basal cells that retained thymidine label for a prolonged period of time, but did not determine whether the label-retaining basal cells were HBCs or GBCs or both. Recent work extends the earlier observations and shows that some GBCs in normal OE express the cyclin-dependent kinase inhibitor (CDKI) $p27^{Kip1}$, and some retain BrdU label for periods of a month or more (Chen, X., 2003). MeBr lesion causes them to reenter the mitotic cycle with the consequence that p27 (+) cells disappear during the ramping up of proliferation during the acute postlesion period. Beginning 4 days after lesion, some GBCs return to quiescence; p27 (+) GBCs reappear and BrdU label begins to be retained by some GBCs. The kinetic characteristics of this population are like those of stems in other tissues, for example, the cornea.

4.34.5.4 Are Some Cells Among the Globose Basal Cells Tissue Stem Cells of the Olfactory Epithelium?

Of the characteristics of stem cells, some GBCs satisfy the totipotency criterion (with regard to the OE), including regeneration of GBCs, which implies at least a limited capacity for self-renewal. The data also show that some GBCs are quiescent for a long period of time. Finally, loss of GBCs results in a failure of neurogenesis and respiratory metaplasia. All of these are necessary characteristics for identifying stem cells, but are not sufficient. Unfortunately, we do not yet have the kinds of assays that allow us to define extensive self-renewal, as has been done for CNS stem cells, among others. Nonetheless, the findings gathered to date are highly suggestive that mitotically quiescent, SOX-2/Pax6 (+) GBCs are true tissue stem cells.

4.34.5.5 Progenitor Capacity of Other Epithelial Cell Types

The other stem cell candidates in the OE are the HBCs and duct/gland cells (Mulvaney, B. D. and Heist, H. E., 1971; Graziadei, P. P. and Monti Graziadei, G. A., 1979). The duct/gland cells do not seem to have any degree of neuropotency. When MeBr exposure is adjusted to cause a more severe lesion of the OE destroying all of the HBCs and GBCs in an area, the damaged OE is replaced by respiratory epithelium, even though gland cells proliferate and erupt superficial to the basal lamina (Jang, W. *et al.*, 2003). Nor do transplanted duct cells do anything other than give rise to Sus/duct cells (Chen, X. *et al.*, 2004). Although there is some evidence for expression of neuronal markers by HBCs *in vitro* (Satoh, M. and Yoshida, T., 2000; Carter, L. A. *et al.*, 2004), transplantation is not effective in generating other cell types. In the lesioned OE of mice, the HBCs do not engraft (perhaps because they are preserved and proliferate throughout OE in contrast to their disappearance from ventral OE as a consequence of toxin exposure in rats) (Chen, X. *et al.*, 2004). In MeBr-lesioned rats, HBCs labeled by the uptake of fluorescent latex microspheres (beads) do engraft but do not seem to do anything except make other HBCs. However, morphological analysis, and rare RRVV-labeled clones suggest that the HBCs can generate Sus cells as well as themselves in the context of the MeBr-lesioned OE. By no means can the extant *in vivo* data be considered definitive. Thus, we cannot yet discard the hypothesis that neurocompetent stem cells might also be found among the HBCs.

4.34.6 Reinervation of the Olfactory Bulb

Anecdotal reports of functional recovery in humans following either epithelial lesion or nerve transection imply some degree of reinnervation of the bulb by the newly born neurons of the reconstituted epithelium. In the context of the piecemeal turnover of the OSN population during normal life, that nascent innervation of the bulb by newly born neurons is remarkably precise as shown intuitively by the perceptual stability of olfaction in humans and the maintenance of precise connectivity in lab animals, both of which are the norm in adult life (Figure 3(a)). What then of the wholesale loss and reformation of the axonal projection onto the bulb following peripheral lesion? What do axon growth and synaptogenesis in that setting tell us of mechanisms regulating innervation of the bulb and their action following lesion?

4.34.6.1 Normal Organization of the Axonal Projection from the Olfactory Epithelium onto the Olfactory Bulb

The projection of the OE onto the OB is organized at three levels: At its coarsest, the organization of the projection is rhinotopic, in which there is a rough correspondence between regions of the OE and the part of the glomerular layer that they target: dorsal OE to dorsomedial OB, lateral OE to lateral and dorsolateral OB, etc. (Astic, L. and Saucier, D., 1986; Saucier, D. and Astic, L., 1986; Astic, L. *et al.*, 1987; Schoenfeld, T. A. *et al.*, 1994). The boundaries between one target region in the bulb and the next are probably not sharp. The graded, shifting projection at the boundary is demonstrated by the distribution of axons from biochemically distinct populations of neurons, that is, ventrolateral, OCAM/mamFasII (+) versus dorsomedial, OCAM/mamFasII (−), which are sharply delimited in the OE but whose axons intermingle in selected glomeruli at the margins between groups of wholly positive or wholly negative glomeruli (Mori, K. *et al.*, 1985; Schwob, J. E. and Gottlieb, D. I., 1986). As a consequence, the axon terminal field of the neuropil of some of these border glomeruli exhibit intermediate levels of immunohistochemical staining with the anti-OCAM/mamFasII MAb RB-8.

The next more precise level of the projection – that is, onto groups of glomeruli – reflects the identity of the OR expressed by the neurons in question. Thus, neurons in the unlesioned adult OE expressing a particular OR, for example, as shown for P2, OR37A, and OR37C, will target one or two glomeruli within a roughly 250 μm-diameter patch consisting of about 30 or so potential target glomeruli (Strotmann, J. *et al.*, 2000; Schaefer, M. L. *et al.*, 2001). The target patch is found in a consistent location from animal to animal relative to defined landmarks of the bulb. For convenience, that level of specificity can be termed receptotopic. Within that patch, location is inconsistent; for example, the glomerulus innervated by OR37A is found in all possible relations to the one innervated by OR37C in the same patch: anterior, posterior, medial, or lateral to the OR37C glomerulus. Thus, a patch is shared as a target by multiple different kinds of OR-defined sensory neurons.

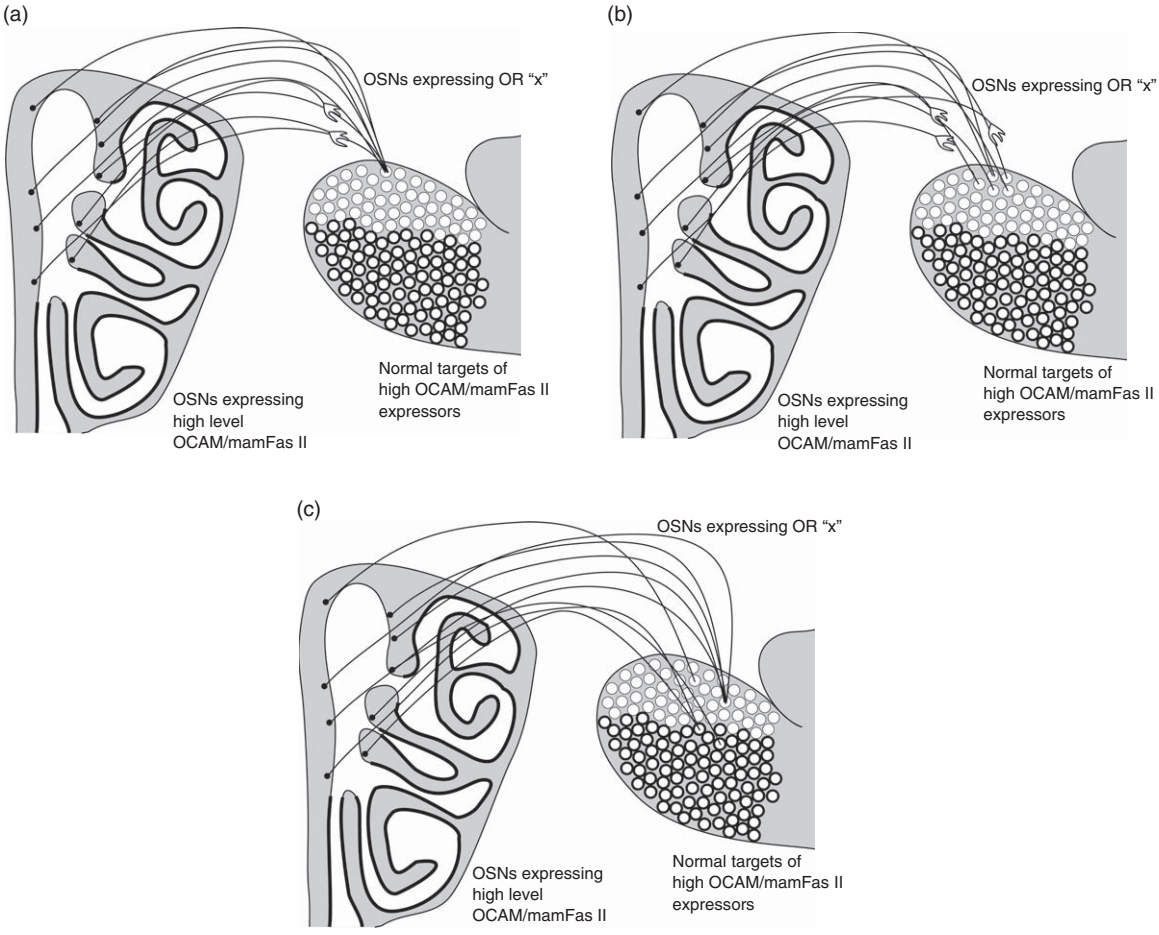

Figure 3 The accuracy of reinnervation of the olfactory bulb by newly born sensory neurons depends on the extent of neuron loss, and on the occurrence of damage to the olfactory nerve. (a) Glomerular targeting in the peripheral olfactory projection of normal animals, i.e., during piecemeal turnover of the neuronal population is highly accurate, and maintains preexisting glomerulotopy. The same outcome is observed when one odorant receptor (OR)-defined group of sensory neurons is ablated and then regenerated. The thick dark line in the cartoon of the nose on the right indicates the part of the olfactory epithelium in which neurons (OSNs) express OCAM/mamFas II at a high level. The glomeruli outlined with the thick dark line represent the normal targets for the high OCAM/mamFas II-expressing neurons. (b) Like the normal, following wholesale neuronal turnover caused by exposure to methyl bromide (MeBr), rhinotopy is restored, and the newly born neurons target approximately the same area within the glomerular sheet, reestablishing receptotopy. However, in contrast with normal, no longer do all of the group of OR-defined neurons converge onto a single glomerulus. (c) Following transection of the olfactory nerve, rhinotopy is distorted – as indicated by the low OCAM/mamFas II-expressing OSNs that innervate what are normally targets for high expressors – and neither targeting to the usual region of the glomerular layer nor convergence onto a single glomerulus is restored.

At its most precise, the projection onto the normal OB is characterized by the convergence of like fibers, that is, those expressing the same OR, most often onto a single glomerulus within the patch, which they seem to fill homogeneously and from which other OR-defined axonal types are apparently excluded (Mombaerts, P. *et al.*, 1996; Wang, F. *et al.*, 1998; Potter, S. M. *et al.*, 2001; Treloar, H. B. *et al.*, 2002; Feinstein, P. and Mombaerts, P., 2004; Feinstein, P. *et al.*, 2004). Studies during the normal development of the projection suggest that unlike fibers intermingle initially within the common patch, but then the active coalescence of like fibers and their progressive segregation from unlike fibers comes to account for both the remarkable convergence of like fibers and the final position of the target glomerulus within the patch (Conzelmann, S. *et al.*, 2001). For convenience, the level of specificity implied by the convergence of like fibers onto a single glomerulus can be termed glomerulotopic.

4.34.6.2 Organization of the Projection Following Recovery from Injury to the Periphery

To what extent are the three levels of specificity that characterize the projection from OE onto OB in normal animals restored following reconstitution of the periphery and reinnervation of the bulb? Two settings may be contrasted: one in which the sensory neuron population undergoes wholesale turnover, for example, the cycle of destruction and reconstitution initiated by a general olfactotoxic agent (Schwob, J. E. *et al.*, 1999; Iwema, C. L. and Schwob, J. E., 2001; St John, J. A. and Key, B., 2003; Carr, V. M. *et al.*, 2004); the second, in which a specific OR-defined set of neurons has been eliminated through genetic means, for example, selective killing of P2 neurons via P2- and tetracycline-regulated expression of diptheria toxin (Gogos, J. A. *et al.*, 2000). In the case of MeBr lesion, the newly born neurons begin to fill the glomerular layer by 7 days after lesion, begin to reenter glomeruli near the end of the second week, fill them by the end of the third week and have stabilized by the end of the eighth week after lesion (Schwob, J. E. *et al.*, 1999).

The first issue that must be addressed following wholesale turnover of the sensory neuronal population is the fidelity with which the number and distribution of the various OR-defined classes of OSNs is restored across the epithelial sheet. Recent experiments utilized unilateral naris closure during the period of MeBr exposure (which has the effect of protecting the closed side from the effects of the gas almost completely), long postlesion survivals, and *in situ* hybridization (ISH) using multiple OR probes to compare lesioned-recovered and unlesioned OE (Iwema, C. L. *et al.*, 2004). Remarkably, the spatial patterning of OR expression was equivalent on the two sides, and the numbers of neurons labeled with the probe were also very similar in the lesioned-recovered epithelium as compared to the unlesioned. The extent of recovery is all the more striking given the partial depletion of the GBC population by the lesion and the degree of respiratory metaplasia in the ventrolateral areas of the epithelium. *A priori*, one can imagine two mechanisms by which position across the epithelial sheet comes to constrain OR expression: either the stem cells have a memory of place which is responsible for spatially imposed restrictions as the neurons are regenerated, or environmental cues derived from the lamina propria drive OR selection, at least after lesion from which effects the lamina cells would be protected. Of the two, the damage to the GBC population, which almost certainly must vary from animal to animal with respect to the OR-defined boundaries, suggests that cues external to the stem–progenitor-differentiating neuron hold sway and drive OR choice.

Despite the impressive degree to which the periphery is restored, a severe epithelial lesion is accompanied by targeting errors during reinnervation of the bulb. Projection errors can be detected at a very gross level as a reduction in the overall extent of reinnervation. Thus, when the severity of the initial lesion is enhanced, such that the recovery of the lesioned epithelium is incomplete and reduced to about four-fifths of its normal surface area, glomeruli at and near the posterior margins of the glomerular sheet remain denervated permanently (Schwob, J. E. *et al.*, 1999). Given that the reduction in the innervating population is not selective to a particular OR-defined type, the failure to reinnervate the posterior bulb indicates errors in receptotopic targeting. Interestingly, that failure in the anteroposterior dimension does not seem to interfere with the establishment of rhinotopic territories. Retrograde tract tracing experiments following selective labeling of the dorsomedial versus ventrolateral glomerular layer suggest little or no breakdown in the gross rhinotopic targeting onto the bulb (Schwob and Hamlin, unpublished results). That return to normalcy is confirmed by using the OCAM/mamFasII-specific MAb RB-8 to define the respective projections of the corresponding epithelial territories onto the bulb of rats following recovery from unilateral epithelial lesion.

The analyses of reinnervation by specific types of OSNs confirm that interpretation. Following peripheral lesion of P2-IRES-tauLacZ strain of transgenic mice with MeBr or with dichlobenil, the P2 fibers no longer converge to a single glomerulus on each surface of the bulb (Figure 3(b)) (Iwema, C. L. and Schwob, J. E., 2001; St. John, J. A. and Key, B., 2003). Instead, multiple glomeruli in the vicinity of the original one become innervated, but the P2 fibers in them are now only one part of a mix of axons of different types, in other words, the P2 fibers are only some of the OMP (+) axons innervating those glomeruli. Indeed, the P2 fibers tend to be plastered at the edges of the glomerular neuropil where they are more densely clustered than usual. The projection of other neuron types onto the bulb is also degraded relative to the unlesioned projection; like P2 neurons they come to innervate more than the normal number of glomeruli (Carr, V. M. *et al.*, 2004). Thus, the

capacity to target a specific region or target patch within the glomerular layer is maintained, at least at anterior levels of the bulb, but no longer do the fibers converge properly and selectively.

In contrast, the projection to the P2 glomeruli is restored to its normal uniglomerular pattern following selective ablation by genetic means of all but a very small percentage of the extant P2 neurons, and their subsequent regeneration (Gogos, J. A. *et al.*, 2000). However, the environment experienced by the nascent P2 axons is quite different between global lesions and the selective ablation of one and only one population in two respects. First, following selective ablation the new P2 axons grow through ON fascicles that are very like normal having lost only about 0.1% of their fibers (less than the number that degenerate due to neuronal turnover – whether immature or not). The status of the ON itself seems to play some role during reinnervation judging by the loss of regional targeting during recovery from nerve transection. Second, the capacity to return to a specific region within the glomerular layer (true of the reinnervating axons with either selective or global destruction of the neurons) may reflect the fasciculation of like axons – not the P2 axons in this case, but all of the other types of axons that are targeting the area. In this interpretation, newly born, non-P2 neurons that target adjacent glomeruli may track or fasciculate along preexisting like axons to their proper target, that is, being actively directed away from the unoccupied P2 glomerulus. In contrast, the P2 neurons are not directed away from the P2 glomerulus, and would, therefore, have an advantage over unlike fibers in targeting it during their regeneration. In the free-for-all that would occur in the glomerular layer when preexisting axons are eliminated and a coherent wave of nascent fibers reach the bulb, it is only too easy to imagine that P2 or other axons would innervate multiple glomeruli and become stably ensconced in them. Some experimental evidence can be adduced for the importance of the preexisting fibers and the specificity of reinnervation. Neurons innervating atypical, necklace glomeruli at the posterior margin of the bulb are relatively less severely affected by MeBr lesion than the vast majority innervating the typical glomeruli, as a consequence of their concentration at the cribriform plate in areas relatively lacking cytochrome P450-expressing supporting cells. Thus, one can adjust the lesion conditions to spare about 50% of the preexisting neurons; in this case, the regenerated axons that target the necklace glomeruli end up reinnervating their original ones (which can be identified on the basis of position at the margin of the glomerular layer) (Ring, G. *et al.*, 1997). In contrast, lesions that destroy upward of 80% of the preexisting necklace neurons lead to mistargeting of necklace neurons into nonnecklace glomeruli.

4.34.6.3 Disorganization of the Projection Following Olfactory Nerve Transection

Although the projection of epithelium onto bulb is restored at the level of rhinotopy and receptotopy following MeBr lesion or other injuries to the periphery, ON transection results in significant changes to the ON projection patterns (Figure 3(c)). Following a complete transection of the ON, reinnervation of the bulb does not restore the normal topographical mapping of projections onto the OB (Christensen, M. D. *et al.*, 2001). The physical disruption of these nerves fibers and their perineural sheaths presents a challenge to regenerating nerve fibers as they grow back and reestablish connections in the bulb. The absence of guidance molecules present during early development as well as other factors may leave the regenerating axons with little or no cues to find their normal targets. ON transection experiments with P2-ITL mice show that regenerating axons often project widely across the OB during recovery, losing receptotopic specificity as shown by their innervation of multiple glomerular patches and losing rhinotopic specificity to a minor degree (Figure 3(c)) (Costanzo, R. M., 2000; 2005). Some of the regenerated axons projected diffusely while others innervated only a single locus in the bulb. In addition, while P2 nerve fibers continue to converge onto individual glomeruli, these glomeruli often received a mixed innervation that includes additional OR types. These results demonstrate that normal mapping of OR information onto the bulb is more substantially disrupted following recovery from nerve transection than after peripheral lesion. The remapping of odorant projections in the OB elicited by nerve transection potentially explains why animals must relearn how to perform odor discrimination tasks after recovery. Nonetheless, the rewired OB apparently provides sufficient spatial resolution of OR mapping to restore odor discrimination function.

4.34.6.4 Functional Recovery Following Epithelial Lesion or Nerve Transection

Despite the degradation in mapping of the OE onto the bulb after recovery from either peripheral injury or nerve lesion, there is a surprising degree of recovery in sensory function following the reconstitution of the epithelium and reinnervation of the bulb. In

the case of MeBr lesion, rats trained on a five-odorant identification task – a task on which they normally perform at 90% correct or better – show a rapid return to criterion performance when retesting begins at 2 months postlesion when the regenerated projection has stabilized (Youngentob, S. L. and Schwob, J. E., 1997). However, multidimensional scaling analysis of the patterns in the stimulus–response matrix across the animals indicates that the lesioned-recovered animals do perceive and process the test odorants differently than unlesioned animals tested after equivalent rest periods. In other words, the lesioned-recovered animals make different kinds of mistakes, that is, confusions, when performing the task.

Restoration of odor-mediated behavior following recovery from ON transection has been reported in a variety of species including the pigeon (Oley, N. *et al.*, 1975; Walker, J. C. *et al.*, 1981), goldfish (von Rekowski, C. and Zippel, H. P., 1993), mouse (Harding, J. W. and Wright, J. W., 1979), and hamster (Yee, K. K. and Costanzo, R. M., 1995). There is a direct correlation between the time course of OB reinnervation and recovery of odor detection and discrimination function. These studies raise an important question; does the perception of an odor change after recovery from nerve transection, when normal receptotopic specificity is lost? To address this question Yee K. K. and Costanzo R. M. (1998) studied performance on an odor discrimination tasks before and 40 days after ON transection in hamster. Animals were trained to discriminate between two unfamiliar odors, strawberry, and cinnamon, before surgery and then retested after 40 days of recovery. At this time point, the OB is reinnervated by a large number of newly regenerated ON fibers. Animals receiving a sham surgical procedure that leaves the ONs intact were able to perform the odor discrimination task 40 days after sham surgery, without food reinforcement. Those animals that received the nerve transection procedure performed at chance levels. However, if food reinforcement was given when the correct odorant was selected, recovery animals were able to relearn the odor discrimination task within a few days. When animals were tested on day 40 with completely new odors, baby powder, and coffee, both the sham and the reinnervated animals were able to learn the odor discrimination task within a few days. These results suggest that although there are likely to be alterations in the way nerve fibers reconnect to the OB following nerve transaction, after recovery these animals are capable of making odor discriminations but they must relearn the task. It is likely that the original perception of the odors as cinnamon and strawberry changed and that the animals must learn how to reinterpret these odors using the new mapping of ORs onto the bulb. Remarkably, the olfactory system has the capacity to restore its connections to the OB after injury, and even when significant changes occur to the OR mapping the animal can learn to use the new maps and recover olfactory function.

4.34.6.5 Summary

Aberrant connections are formed in the peripheral olfactory system following recovery from peripheral lesion or nerve transection. Rhinotopy and receptotopy – but not glomerultopy – are restored following epithelial lesion. In contrast, rhinotopy is somewhat compromised while receptotopy and glomerulotopy are severely disrupted following nerve transection. Nonetheless, neither form of lesion precludes sensory function following reconstitution of the epithelium and reinnervation of the bulb. However, the errors – which are of greater magnitude following nerve lesion – do change the encoding of odorants by the OB. Despite the reinnervation of the bulb, for these lesioned animals, as for humans presenting with olfactory dysfunction, a rose may no longer smell the same as a rose.

4.34.7 Conclusions and Unanswered Questions

The foregoing provides a summary of what we know of the recovery of the peripheral olfactory apparatus – the epithelium and its projection onto the bulb – following either reversible destruction of the epithelium or transection of the ON. From the phenomenological perspective, we now know the events that occur during epithelial reconstitution in substantial detail and those underlying reinnervation of the bulb somewhat less. However, our knowledge of cellular and molecular mechanism is still very far from complete. An integrated picture of the signals and transduction cascades that combine to regulate the choice point faced by the multipotent stem/progenitors is lacking and will remain obscure until certain conditions are met. Among them we need reagents and protocols that can be used to identify, isolate and characterize olfactory stem cells, and have them recapitulate the differentiation *in vitro* that they accomplish so effortlessly *in vivo*.

Once the stem cells are in hand, subsidiary questions of their therapeutic usefulness in the OE; for example, in replacing stem cells whose destruction or exhaustion underlies olfactory dysfunction, or in other settings, including their differentiation into OECs and implantation into injured spinal cord (Li, Y. *et al*., 1997), can be more profitably addressed. Likewise, we have little in-depth understanding of the mechanisms for maintaining the precision of axon targeting in the adult, which goes somewhat awry following epithelial lesion and is substantially disordered by injury to theON. If the sparing of preexisting fibers does promote accurate reinnervation, how are like-axons recognized and how do they form a substrate for growth? The recovery of olfactory function despite the scrambling of connections raises the specter of reorganization in central olfactory processing and leads to questions of whether sensory activity during the reinnervation process might impact that recovery. As our understanding of basic mechanism deepens it is reasonable to expect that useful therapies will begin to emerge.

4.34.8 Note Added in Proof

Subsequent to the preparation of this chapter a paper was published describing the contributions of HBCs to the repair of the OE following injury by MeBr or another direct acting toxin (Leung, C. T. *et al*., 2007). Their data report the use of a genetic lineage tracing technique in which cells that derive from HBCs are marked by the expression of LacZ due to the activation of Cre recombinase selectively in cells that make cytokeratin 5. In the epithelium of normal or bulbectomized mice, HBCs give rise only to HBCs throughout the life of the animal. However, after direct epithelial injury HBCs contribute to the roughly the same cell types as GBCs after transplantation, namely HBCs and GBCs themselves, neurons, sustentacular cells, and duct/gland cells; GBCs can give rise to respiratory epithelial cells, but HBCs have not yet been shown to give rise to them. Thus, it would appear that the HBCs, despite their relatively late emergence during the perinatal period in the development of the OE, serve as an additional reserve population with extensive multipotency *in vivo* and *in vitro* that is called upon when GBCs have been destroyed (a characteristic of the MeBr-lesioned mouse to a much greater extent than in lesioned rats). The persistence of two cell populations with the multipotency that is characteristic of tissue stem cells is reminiscent of other neurogenic populations, including that of the subventricular zone in the adult forebrain in which both type B and type C cells have the characteristics of neural stem cells. Furthermore, the situation in the olfactory epithelium may be a reflection of a more primitive character than that of the differentiated CNS. The GBCs share characteristics of the cells that compose the olfactory placode and the early stages of its invagination, including the expression of Pax6, Sox2, and, somewhat later, Mash1, before the HBCs emerge around the time of birth. The sequence may be conceptualized as if the primitive neuroepithelial cells of the neural plate and early tube are retained even after radial glia and subsequent glial forms of the subventricular zone emerge to serve as neurocompetent stem cells.

References

Alonso, L. and Fuchs, E. 2003. Stem cells of the skin epithelium. Proc. Natl. Acad. Sci. U. S. A. 100(Suppl. 1), 11830–11835.

Andres, K. H. 1966. The fine structure of the olfactory region of macrosmatic animals. Z. Zellforsch. Mikrosk. Anat. 69, 140–154.

Asan, E. and Drenckhahn, D. 2005. Immunocytochemical characterization of two types of microvillar cells in rodent olfactory epithelium. Histochem. Cell Biol. 123, 157–168.

Astic, L. and Saucier, D. 1986. Anatomical mapping of the neuroepithelial projection to the olfactory bulb in the rat. Brain Res. Bull. 16, 445–454.

Astic, L., Saucier, D., and Holley, A. 1987. Topographical relationships between olfactory receptor cells and glomerular foci in the rat olfactory bulb. Brain Res. 424, 144–152.

Avilion, A. A., Nicolis, S. K., Pevny, L. H., Perez, L., Vivian, N., and Lovell-Badge, R. 2003. Multipotent cell lineages in early mouse development depend on SOX2 function. Genes Dev. 17, 126–140.

Barber, P. C. and Lindsay, R. M. 1982. Schwann cells of the olfactory nerves contain glial fibrillary acidic protein and resemble astrocytes. Neuroscience 7, 3077–3090.

Barnett, E. M. and Perlman, S. 1993. The olfactory nerve and not the trigeminal nerve is the major site of CNS entry for mouse hepatitis virus, strain JHM. Virology 194, 185–191.

Barnett, E. M., Cassell, M. D., and Perlman, S. 1993. Two neurotropic viruses, herpes simplex virus type 1 and mouse hepatitis virus, spread along different neural pathways from the main olfactory bulb. Neuroscience 57, 1007–1025.

Barthold, S. W. 1988. Olfactory neural pathway in mouse hepatitis virus nasoencephalitis. Acta Neuropathol. (Berl.) 76, 502–506.

Bauer, S., Rasika, S., Han, J., Mauduit, C., Raccurt, M., Morel, G., Jourdan, F., Benahmed, M., Moyse, E., and Patterson, P. H. 2003. Leukemia inhibitory factor is a key signal for injury-induced neurogenesis in the adult mouse olfactory epithelium. J. Neurosci. 23, 1792–1803.

Bergstrom, U., Giovanetti, A., Piras, E., and Brittebo, E. B. 2003. Methimazole-induced damage in the olfactory mucosa: effects on ultrastructure and glutathione levels. Toxicol. Pathol. 31, 379–387.

Biffo, S., Pognetto, M. S., Di Cantogno, L. V., Perroteau, I., and Fasolo, A. 1992. Bulbectomy enhances neurogenesis and cell turnover of primary olfactory neurons but does not abolish carnosine expression. Eur. J. Neurosci. 4, 1398–1406.

Bojsen-Moller, F. 1975. Demonstration of terminalis, olfactory, trigeminal and perivascular nerves in the rat nasal septum. J. Comp. Neurol. 159, 245–256.

Brazel, C. Y., Limke, T. L., Osborne, J. K., Miura, T., Cai, J., Pevny, L., and Rao, M. S. 2005. Sox2 expression defines a heterogeneous population of neurosphere-forming cells in the adult murine brain. Aging Cell 4, 197–207.

Brittebo, E. B. 1995. Metabolism-dependent toxicity of methimazole in the olfactory nasal mucosa. Pharmacol. Toxicol. 76, 76–79.

Buck, L. and Axel, R. 1991. A novel multigene family may encode odorant receptors: a molecular basis for odor recognition. Cell 65, 175–187.

Burd, G. D. 1993. Morphological study of the effects of intranasal zinc sulfate irrigation on the mouse olfactory epithelium and olfactory bulb. Microsc. Res. Tech. 24, 195–213.

Caggiano, M., Kauer, J. S., and Hunter, D. D. 1994. Globose basal cells are neuronal progenitors in the olfactory epithelium: a lineage analysis using a replication-incompetent retrovirus. Neuron 13, 339–352.

Calof, A. L., Rim, P. C., Askins, K. J., Mumm, J. S., Gordon, M. K., Iannuzzelli, P., and Shou, J. 1998. Factors regulating neurogenesis and programmed cell death in mouse olfactory epithelium. Ann. N. Y. Acad. Sci. 855, 226–229.

Cancalon, P. 1982. Degeneration and regeneration of olfactory cells induced by $ZnSO_4$ and other chemicals. Tissue Cell 14, 717–733.

Carr, V. M. and Farbman, A. I. 1992. Ablation of the olfactory bulb up-regulates the rate of neurogenesis and induces precocious cell death in olfactory epithelium. Exp. Neurol. 115, 55–59.

Carr, V. M. and Farbman, A. I. 1993. The dynamics of cell death in the olfactory epithelium. Exp. Neurol. 124, 308–314.

Carr, V. M., Ring, G., Youngentob, S. L., Schwob, J. E., and Farbman, A. I. 2004. Altered epithelial density and expansion of bulbar projections of a discrete HSP70 immunoreactive subpopulation of rat olfactory receptor neurons in reconstituting olfactory epithelium following exposure to methyl bromide. J. Comp. Neurol. 469, 475–493.

Carter, L. A., MacDonald, J. L., and Roskams, A. J. 2004. Olfactory horizontal basal cells demonstrate a conserved multipotent progenitor phenotype. J. Neurosci. 24, 5670–5683.

Cau, E., Casarosa, S., and Guillemot, F. 2002. Mash1 and Ngn1 control distinct steps of determination and differentiation in the olfactory sensory neuron lineage. Development 129, 1871–1880.

Cau, E., Gradwohl, G., Casarosa, S., Kageyama, R., and Guillemot, F. 2000. Hes genes regulate sequential stages of neurogenesis in the olfactory epithelium. Development 127, 2323–2332.

Cau, E., Gradwohl, G., Fode, C., and Guillemot, F. 1997. Mash1 activates a cascade of bHLH regulators in olfactory neuron progenitors. Development 124, 1611–1621.

Chen, X. 2003. Functional Capacity of Progenitor Cells in the Olfactory Epithelium. PhD thesis, Program in Cell, Molecular, and Developmental Biology. Tufts University

Chen, X., Fang, H., and Schwob, J. E. 2004. Multipotency of purified, transplanted globose basal cells in olfactory epithelium. J. Comp. Neurol. 469, 457–474.

Chen, Y., Getchell, M. L., Ding, X., and Getchell, T. V. 1992. Immunolocalization of two cytochrome P450 isozymes in rat nasal chemosensory tissue. Neuroreport 3, 749–752.

Chi, N. and Epstein, J. A. 2002. Getting your Pax straight: pax proteins in development and disease. Trends Genet. 18, 41–47.

Christensen, M. D., Holbrook, E. H., Costanzo, R. M., and Schwob, J. E. 2001. Rhinotopy is disrupted during the re-innervation of the olfactory bulb that follows transection of the olfactory nerve. Chem. Senses 26, 359–369.

Conzelmann, S., Malun, D., Breer, H., and Strotmann, J. 2001. Brain targeting and glomerulus formation of two olfactory neuron populations expressing related receptor types. Eur. J. Neurosci. 14, 1623–1632.

Costanzo, R. M. 1984. Comparison of neurogenesis and cell replacement in the hamster olfactory system with and without a target (olfactory bulb). Brain Res. 307, 295–301.

Costanzo, R. M. 1985. Neural regeneration and functional reconnection following olfactory nerve transection in hamster. Brain Res. 361, 258–266.

Costanzo, R. M. 2000. Rewiring the olfactory bulb: changes in odor maps following recovery from nerve transection. Chem. Senses 25, 199–205.

Costanzo, R. M. 2005. Regeneration and rewiring the olfactory bulb. Chem. Senses 30(Suppl. 1), 133–134.

Costanzo, R. M. and Graziadei, P. P. 1983. A quantitative analysis of changes in the olfactory epithelium following bulbectomy in hamster. J. Comp. Neurol. 215, 370–381.

Cowan, C. M. and Roskams, A. J. 2002. Apoptosis in the mature and developing olfactory neuroepithelium. Microsc. Res. Tech. 58, 204–215.

Cowan, C. M., Thai, J., Krajewski, S., Reed, J. C., Nicholson, D. W., Kaufmann, S. H., and Roskams, A. J. 2001. Caspases 3 and 9 send a pro-apoptotic signal from synapse to cell body in olfactory receptor neurons. J. Neurosci. 21, 7099–7109.

Deckner, M. L., Risling, M., and Frisen, J. 1997. Apoptotic death of olfactory sensory neurons in the adult rat. Exp. Neurol. 143, 132–140.

Doty, R. L. 1979. A review of olfactory dysfunctions in man. Am. J. Otolaryngol. 1, 57–79.

Ellis, P., Fagan, B. M., Magness, S. T., Hutton, S., Taranova, O., Hayashi, S., McMahon, A., Rao, M., and Pevny, L. 2004. SOX2, a persistent marker for multipotential neural stem cells derived from embryonic stem cells, the embryo or the adult. Dev. Neurosci. 26, 148–165.

Englund, C., Fink, A., Lau, C., Pham, D., Daza, R. A., Bulfone, A., Kowalczyk, T., and Hevner, R. F. 2005. Pax6, Tbr2, and Tbr1 are expressed sequentially by radial glia, intermediate progenitor cells, and postmitotic neurons in developing neocortex. J. Neurosci. 25, 247–251.

Feddersen, R. M., Yunis, W. S., O'Donnell, M. A., Ebner, T. J., Shen, L., Iadecola, C., Orr, H. T., and Clark, H. B. 1997. Susceptibility to cell death induced by mutant SV40 T-antigen correlates with Purkinje neuron functional development. Mol. Cell. Neurosci. 9, 42–62.

Feinstein, P. and Mombaerts, P. 2004. A contextual model for axonal sorting into glomeruli in the mouse olfactory system. Cell 117, 817–831.

Feinstein, P., Bozza, T., Rodriguez, I., Vassalli, A., and Mombaerts, P. 2004. Axon guidance of mouse olfactory sensory neurons by odorant receptors and the beta2 adrenergic receptor. Cell 117, 833–846.

Field, P., Li, Y., and Raisman, G. 2003. Ensheathment of the olfactory nerves in the adult rat. J. Neurocytol. 32, 317–324.

Fisher, A. and Caudy, M. 1998. The function of hairy-related bHLH repressor proteins in cell fate decisions. BioEssays 20, 298–306.

Genter, M. B., Deamer, N. J., Blake, B. L., Wesley, D. S., and Levi, P. E. 1995. Olfactory toxicity of methimazole: dose–response and structure–activity studies and characterization

of flavin-containing monooxygenase activity in the Long–Evans rat olfactory mucosa. Toxicol. Pathol. 23, 477–486.

Genter, M. B., Owens, D. M., Carlone, H. B., and Crofton, K. M. 1996. Characterization of olfactory deficits in the rat following administration of 2,6-dichlorobenzonitrile (dichlobenil), 3,3′-iminodipropionitrile, or methimazole. Fundam. Appl. Toxicol. 29, 71–77.

Gogos, J. A., Osborne, J., Nemes, A., Mendelsohn, M., and Axel, R. 2000. Genetic ablation and restoration of the olfactory topographic map. Cell 103, 609–620.

Goldstein, B. J. and Schwob, J. E. 1996. Analysis of the globose basal cell compartment in rat olfactory epithelium using GBC-1, a new monoclonal antibody against globose basal cells. J. Neurosci. 16, 4005–4016.

Goldstein, B. J., Fang, H., Youngentob, S. L., and Schwob, J. E. 1998. Transplantation of multipotent progenitors from the adult olfactory epithelium. Neuroreport 9, 1611–1617.

Goldstein, B. J., Wolozin, B. L., and Schwob, J. E. 1997. FGF2 suppresses neuronogenesis of a cell line derived from rat olfactory epithelium. J. Neurobiol. 33, 411–428.

Gordon, M. K., Mumm, J. S., Davis, R. A., Holcomb, J. D., and Calof, A. L. 1995. Dynamics of MASH1 expression *in vitro* and *in vivo* suggest a non-stem cell site of MASH1 action in the olfactory receptor neuron lineage. Mol. Cell Neurosci. 6, 363–379.

Gotz, M., Stoykova, A., and Gruss, P. 1998. Pax6 controls radial glia differentiation in the cerebral cortex. Neuron 21, 1031–1044.

Graham, V., Khudyakov, J., Ellis, P., and Pevny, L. 2003. SOX2 functions to maintain neural progenitor identity. Neuron 39, 749–765.

Grazaiadei, P. P. C. 1971. The Olfactory Mucosa of Vertebrates. In: Chemical Senses. Part I Olfaction (*ed*. L. M. Beidler), pp. 27–58. Springer-Verlag.

Graziadei, P. P. 1973. Cell dynamics in the olfactory mucosa. Tissue Cell 5, 113–131.

Graziadei, P. P. and Metcalf, J. F. 1971. Autoradiographic and ultrastructural observations on the frog's olfactory mucosa. Z. Zellforsch. Mikrosk. Anat. 116, 305–318.

Graziadei, P. P. C. and Monti Graziadei, G. A. 1978. Continuous Nerve Cell Renewal in the Olfactory System. In: Handbook of Sensory Physiology (*ed*. M. Jacobson), Vol. IX, pp. 55–82. Springer.

Graziadei, P. P. and Monti Graziadei, G. A. 1979. Neurogenesis and neuron regeneration in the olfactory system of mammals. I. Morphological aspects of differentiation and structural organization of the olfactory sensory neurons. J. Neurocytol. 8, 1–18.

Graziadei, P. P. and Monti Graziadei, G. A. 1980. Neurogenesis and neuron regeneration in the olfactory system of mammals. III. Deafferentation and reinnervation of the olfactory bulb following section of the fila olfactoria in rat. J. Neurocytol. 9, 145–162.

Graziadei, P. P., Karlan, M. S., Graziadei, G. A., and Bernstein, J. J. 1980. Neurogenesis of sensory neurons in the primate olfactory system after section of the fila olfactoria. Brain Res. 186, 289–300.

Grindley, J. C., Davidson, D. R., and Hill, R. E. 1995. The role of Pax-6 in eye and nasal development. Development 121, 1433–1442.

Guillemot, F., Lo, L. C., Johnson, J. E., Auerbach, A., Anderson, D. J., and Joyner, A. L. 1993. Mammalian achaete-scute homolog 1 is required for the early development of olfactory and autonomic neurons. Cell 75, 463–476.

Guo, Z., Manglapus, G. L., Harris, M. E., and Schwob, J. E. 2005a. Expression of Pax6 in olfactory epithelium. Chem. Senses 30, A186.

Guo, Z., Manglapus, G. L., and Schwob, J. E. 2005b. Characterization of Sox2 expression in olfactory epithelium. Soc. Neurosci. Abstr. 31, Program No. 478.477.

Hall, P. A. and Watt, F. M. 1989. Stem cells: the generation and maintenance of cellular diversity. Development 106, 619–633.

Harding, J. W. and Wright, J. W. 1979. Reversible effects of olfactory nerve section on behavior and biochemistry in mice. Brain Res. Bull. 4, 17–22.

Harding, J. W., Getchell, T. V., and Margolis, F. L. 1978. Denervation of the primary olfactory pathway in mice. V. Long-term effect of intranasal $ZnSO_4$ irrigation on behavior, biochemistry and morphology. Brain Res. 140, 271–285.

Harding, J., Graziadei, P. P., Monti Graziadei, G. A., and Margolis, F. L. 1977. Denervation in the primary olfactory pathway of mice. IV. Biochemical and morphological evidence for neuronal replacement following nerve section. Brain Res. 132, 11–28.

Hempstead, J. L. and Morgan, J. I. 1985a. A panel of monoclonal antibodies to the rat olfactory epithelium. J. Neurosci. 5, 438–449.

Hempstead, J. L. and Morgan, J. I. 1985b. Monoclonal antibodies reveal novel aspects of the biochemistry and organization of olfactory neurons following unilateral olfactory bulbectomy. J. Neurosci. 5, 2382–2387.

Hinds, J. W., Hinds, P. L., and McNelly, N. A. 1984. An autoradiographic study of the mouse olfactory epithelium: evidence for long-lived receptors. Anat. Rec. 210, 375–383.

Hirota, J. and Mombaerts, P. 2004. The LIM-homeodomain protein Lhx2 is required for complete development of mouse olfactory sensory neurons. Proc. Natl. Acad. Sci. U. S. A. 101, 8751–8755.

Holbrook, E. H. and Leopold, D. A. 2006. An updated review of clinical olfaction. Curr. Opin. Otolaryngol. Head. Neck. Surg. 14, 23–28.

Holbrook, E. H., Leopold, D. A., and Schwob, J. E. 2005. Abnormalities of axon growth in human olfactory mucosa. Laryngoscope 115, 2144–2154.

Holbrook, E. H., Szumowski, K. E., and Schwob, J. E. 1995. An immunochemical, ultrastructural, and developmental characterization of the horizontal basal cells of rat olfactory epithelium. J. Comp. Neurol. 363, 129–146.

Holcomb, J. D., Mumm, J. S., and Calof, A. L. 1995. Apoptosis in the neuronal lineage of the mouse olfactory epithelium: regulation *in vivo* and *in vitro*. Dev. Biol. 172, 307–323.

Huard, J. M., Youngentob, S. L., Goldstein, B. J., Luskin, M. B., and Schwob, J. E. 1998. Adult olfactory epithelium contains multipotent progenitors that give rise to neurons and non-neural cells. J. Comp. Neurol. 400, 469–486.

Hurtt, M. E., Morgan, K. T., and Working, P. K. 1987. Histopathology of acute toxic responses in selected tissues from rats exposed by inhalation to methyl bromide. Fundam. Appl. Toxicol. 9, 352–365.

Hurtt, M. E., Thomas, D. A., Working, P. K., Monticello, T. M., and Morgan, K. T. 1988. Degeneration and regeneration of the olfactory epithelium following inhalation exposure to methyl bromide: pathology, cell kinetics, and olfactory function. Toxicol. Appl. Pharmacol. 94, 311–328.

Iwema, C. L. and Schwob, J. E. 2001. P2 olfactory sensory neurons do not converge appropriately in the olfactory bulb following peripheral lesion. Soc. Neurosci. Abstr. 27, in press.

Iwema, C. L. and Schwob, J. E. 2003. Odorant receptor expression as a function of neuronal maturity in the adult rodent olfactory system. J. Comp. Neurol. 459, 209–222.

Iwema, C. L., Fang, H., Kurtz, D. B., Youngentob, S. L., and Schwob, J. E. 2004. Odorant receptor expression patterns are restored in lesion-recovered rat olfactory epithelium. J. Neurosci. 24, 356–369.

Jang, W., Kim, K. P., and Schwob, J. E. 2007. Non-integrin laminin receptor precursor protein is expressed on olfactory stem and progenitor cells. J. Comp. Neurol. 502, 367–381.

Jang, W., Youngentob, S. L., and Schwob, J. E. 2003. Globose basal cells are required for reconstitution of olfactory epithelium after methyl bromide lesion. J. Comp. Neurol. 460, 123–140.

Juilfs, D. M., Fulle, H. J., Zhao, A. Z., Houslay, M. D., Garbers, D. L., and Beavo, J. A. 1997. A subset of olfactory neurons that selectively express cGMP-stimulated phosphodiesterase (PDE2) and guanylyl cyclase-D define a unique olfactory signal transduction pathway. Proc. Natl. Acad. Sci. U. S. A. 94, 3388–3395.

Kaplan, M. S. and Hinds, J. W. 1977. Neurogenesis in the adult rat: electron microscopic analysis of light radioautographs. Science 197, 1092–1094.

Kaplan, M. S., McNelly, N. A., and Hinds, J. W. 1985. Population dynamics of adult-formed granule neurons of the rat olfactory bulb. J. Comp. Neurol. 239, 117–125.

Kolterud, A., Alenius, M., Carlsson, L., and Bohm, S. 2004. The Lim homeobox gene Lhx2 is required for olfactory sensory neuron identity. Development 131, 5319–5326.

Konzelmann, S., Saucier, D., Strotmann, J., Breer, H., and Astic, L. 1998. Decline and recovery of olfactory receptor expression following unilateral bulbectomy. Cell Tissue Res. 294, 421–430.

Koster, N. L. and Costanzo, R. M. 1996. Electrophysiological characterization of the olfactory bulb during recovery from sensory deafferentation. Brain Res. 724, 117–120.

Largent, B. L., Sosnowski, R. G., and Reed, R. R. 1993. Directed expression of an oncogene to the olfactory neuronal lineage in transgenic mice. J. Neurosci. 13, 300–312.

Leung, C. T., Coulombe, P. A., and Reed, R. R. 2007. Contribution of olfactory neural stem cells to tissue maintenance and regeneration. Nat. Neurosci. 10, 720–726.

Li, Y., Field, P. M., and Raisman, G. 1997. Repair of adult rat corticospinal tract by transplants of olfactory ensheathing cells. Science 277, 2000–2002.

Li, Y., Field, P. M., and Raisman, G. 2005. Olfactory ensheathing cells and olfactory nerve fibroblasts maintain continuous open channels for regrowth of olfactory nerve fibres. Glia 52, 245–251.

Lois, C. and Alvarez-Buylla, A. 1993. Proliferating subventricular zone cells in the adult mammalian forebrain can differentiate into neurons and glia. Proc. Natl. Acad. Sci. U. S. A. 90, 2074–2077.

Lois, C. and Alvarez-Buylla, A. 1994. Long-distance neuronal migration in the adult mammalian brain. Science 264, 1145–1148.

Loo, A. T., Youngentob, S. L., Kent, P. F., and Schwob, J. E. 1996. The aging olfactory epithelium: neurogenesis, response to damage, and odorant-induced activity. Int. J. Dev. Neurosci. 14, 881–900.

de Lorenzo, A. J. 1957. Electron microscopic observations of the olfactory mucosa and olfactory nerve. J. Biophys. Biochem. Cytol. 3, 839–850.

Mackay-Sim, A. and Chuah, M. I. 2000. Neurotrophic factors in the primary olfactory pathway. Prog. Neurobiol. 62, 527–559.

Mackay-Sim, A. and Kittel, P. 1991a. Cell dynamics in the adult mouse olfactory epithelium: a quantitative autoradiographic study. J. Neurosci. 11, 979–984.

Mackay-Sim, A. and Kittel, P. W. 1991b. On the life span of olfactory receptor neurons. Eur. J. Neurosci. 3, 209–215.

Manglapus, G. L., Youngentob, S. L., and Schwob, J. E. 2004. Expression patterns of basic helix–loop–helix transcription factors define subsets of olfactory progenitor cells. J. Comp. Neurol. 479, 216–233.

Marquardt, T., Ashery-Padan, R., Andrejewski, N., Scardigli, R., Guillemot, F., and Gruss, P. 2001. Pax6 is required for the multipotent state of retinal progenitor cells. Cell 105, 43–55.

Matulionis, D. H. 1975. Ultrastructural study of mouse olfactory epithelium following destruction by $ZnSO_4$ and its subsequent regeneration. Am. J. Anat. 142, 67–89.

Matulionis, D. H. 1976. Light and electron microscopic study of the degeneration and early regeneration of olfactory epithelium in the mouse. Am. J. Anat. 145, 79–99.

Meiri, K. F., Bickerstaff, L. E., and Schwob, J. E. 1991. Monoclonal antibodies show that kinase C phosphorylation of GAP-43 during axonogenesis is both spatially and temporally restricted *in vivo*. J. Cell Biol. 112, 991–1005.

Menezes, J. R., Smith, C. M., Nelson, K. C., and Luskin, M. B. 1995. The division of neuronal progenitor cells during migration in the neonatal mammalian forebrain. Mol. Cell Neurosci. 6, 496–508.

Miragall, F. and Monti Graziadei, G. A. 1982. Experimental studies on the olfactory marker protein. II. Appearance of the olfactory marker protein during differentiation of the olfactory sensory neurons of mouse: an immunohistochemical and autoradiographic study. Brain Res. 239, 245–250.

Miyamichi, K., Serizawa, S., Kimura, H. M., and Sakano, H. 2005. Continuous and overlapping expression domains of odorant receptor genes in the olfactory epithelium determine the dorsal/ventral positioning of glomeruli in the olfactory bulb. J. Neurosci. 25, 3586–3592.

Mombaerts, P., Wang, F., Dulac, C., Chao, S. K., Nemes, A., Mendelsohn, M., Edmondson, J., and Axel, R. 1996. Visualizing an olfactory sensory map. Cell 87, 675–686.

Monath, T. P., Cropp, C. B., and Harrison, A. K. 1983. Mode of entry of a neurotropic arbovirus into the central nervous system. Reinvestigation of an old controversy. Lab. Invest. 48, 399–410.

Monti Graziadei, G. A. 1983. Experimental studies on the olfactory marker protein. III. The olfactory marker protein in the olfactory neuroepithelium lacking connections with the forebrain. Brain Res. 262, 303–308.

Monti Graziadei, G. A. and Graziadei, P. P. 1979. Neurogenesis and neuron regeneration in the olfactory system of mammals. II. Degeneration and reconstitution of the olfactory sensory neurons after axotomy. J. Neurocytol. 8, 197–213.

Moran, D. T., Jafek, B. W., Eller, P. M., and Rowley, J. C., III. 1992. Ultrastructural histopathology of human olfactory dysfunction. Microsc. Res. Tech. 23, 103–110.

Mori, K., Fujita, S. C., Imamura, K., and Obata, K. 1985. Immunohistochemical study of subclasses of olfactory nerve fibers and their projections to the olfactory bulb in the rabbit. J. Comp. Neurol. 242, 214–229.

Moulton, D. G. 1974. Dynamics of cell populations in the olfactory epithelium. Ann. N. Y. Acad. Sci. 237, 52–61.

Moulton, D. G. 1975. Cell Renewal in The Olfactory Epithelium. In: Olfaction and Taste, V (*eds*. D. A. Denton and J. P. Coghlan), pp. 111–114. Academic Press.

Moulton, D. G. and Beidler, L. M. 1967. Structure and function in the peripheral olfactory system. Physiol. Rev. 47, 1–52.

Moulton, D. G., Celebi, G., and Fink, R. P. 1970. Olfaction in Mammals – Two Aspects: Proliferation of Cells in The Olfactory Epithelium and Sensitivity to Odours. In: Ciba Foundation Symposium on Taste and Smell in Vertebrates (*eds*. G. E. W. Wolstenholme and J. Knight), pp. 227–250. Churchill.

Mulvaney, B. D. and Heist, H. E. 1971. Regeneration of rabbit olfactory epithelium. Am. J. Anat. 131, 241–252.

Murray, R. C., Navi, D., Fesenko, J., Lander, A. D., and Calof, A. L. 2003. Widespread defects in the primary olfactory pathway caused by loss of Mash1 function. J. Neurosci. 23, 1769–1780.

Nagahara, Y. 1940. Experimentelle Studien uber die histologiischen Veranderungen des Geruchsorgan nach der Olfactoriusdurschneidung. Beitrage zur Kenntnis des feineren Baus des Geruchsorgans. Jpn. J. Med. Sci. V. Pathol. 5, 165–169.

Nakashima, T., Kimmelman, C. P., Snow, J. B., and Jr 1984. Structure of human fetal and adult olfactory neuroepithelium. Arch. Otolaryngol. 110, 641–646.

Nakashima, T., Kimmelman, C. P., Snow, J. B., and Jr 1985. Olfactory marker protein in the human olfactory pathway. Arch. Otolaryngol. 111, 294–297.

Nan, B., Getchell, M. L., Partin, J. V., and Getchell, T. V. 2001. Leukemia inhibitory factor, interleukin-6, and their receptors are expressed transiently in the olfactory mucosa after target ablation. J. Comp. Neurol. 435, 60–77.

Norlin, E. M., Alenius, M., Gussing, F., Hagglund, M., Vedin, V., and Bohm, S. 2001. Evidence for gradients of gene expression correlating with zonal topography of the olfactory sensory map. Mol. Cell Neurosci. 18, 283–295.

Oley, N., DeHan, R. S., Tucker, D., Smith, J. C., and Graziadei, P. P. 1975. Recovery of structure and function following transection of the primary olfactory nerves in pigeons. J. Comp. Physiol. Psychol. 88, 477–495.

Peters, A., Palay, S. L., and Webster, H. D. 1991. The Fine Structure of the Nervous System: Neurons and Their Supporting Cells. Oxford University Press.

Pevny, L. and Rao, M. S. 2003. The stem-cell menagerie. Trends Neurosci. 26, 351–359.

Potten, C. S. 1998. Stem cells in gastrointestinal epithelium: numbers, characteristics and death. Philos. Trans. R. Soc. Lond. B Biol. Sci. 353, 821–830.

Potten, C. S. and Loeffler, M. 1990. Stem cells: attributes, cycles, spirals, pitfalls and uncertainties. Lessons for and from the crypt. Development 110, 1001–1020.

Potter, S. M., Zheng, C., Koos, D. S., Feinstein, P., Fraser, S. E., and Mombaerts, P. 2001. Structure and emergence of specific olfactory glomeruli in the mouse. J. Neurosci. 21, 9713–9723.

Purves, D. 1988. Body and Brain. A Trophic Theory of Neural Connections. Harvard University Press.

Rao, M. S. 1999. Multipotent and restricted precursors in the central nervous system. Anat. Rec. (New Anat.) 257, 137–148.

Reed, C. J., Gaskell, B. A., Banger, K. K., and Lock, E. A. 1995. Olfactory toxicity of methyl iodide in the rat. Arch. Toxicol. 70, 51–56.

von Rekowski, C. and Zippel, H. P. 1993. In goldfish the qualitative discriminative ability for odors rapidly returns after bilateral nerve axotomy and lateral olfactory tract transection. Brain Res. 618, 338–340.

Ressler, K. J., Sullivan, S. L., and Buck, L. B. 1993. A zonal organization of odorant receptor gene expression in the olfactory epithelium. Cell 73, 597–609.

Ring, G., Mezza, R. C., and Schwob, J. E. 1997. Immunohistochemical identification of discrete subsets of rat olfactory neurons and the glomeruli that they innervate. J. Comp. Neurol. 388, 415–434.

Satoh, M. and Yoshida, T. 2000. Expression of neural properties in olfactory cytokeratin-positive basal cell line. Brain Res. Dev. Brain Res. 121, 219–222.

Saucier, D. and Astic, L. 1986. Analysis of the topographical organization of olfactory epithelium projections in the rat. Brain Res. Bull. 16, 455–462.

Schaefer, M. L., Finger, T. E., and Restrepo, D. 2001. Variability of position of the P2 glomerulus within a map of the mouse olfactory bulb. J. Comp. Neurol. 436, 351–362.

Schoenfeld, T. A., Clancy, A. N., Forbes, W. B., and Macrides, F. 1994. The spatial organization of the peripheral olfactory system of the hamster. Part I: Receptor neuron projections to the main olfactory bulb. Brain Res. Bull. 34, 183–210.

Schultz, E. W. 1941. Regeneration of olfactory cells. Proc. Soc. Exp. Biol. Med. 46, 41–43.

Schultz, E. W. 1960. Repair of the olfactory mucosa with special reference to regeneration of olfactory cells (sensory neurons). Am. J. Pathol. 37, 1–19.

Schultz, E. W. and Gebhardt, S. P. 1942. Studies on chemical prophylaxis of experimental poliomyelitis. J. Infect. Dis. 70, 7–50.

Schwarting, G. A. and Crandall, J. E. 1991. Subsets of olfactory and vomeronasal sensory epithelial cells and axons revealed by monoclonal antibodies to carbohydrate antigens. Brain Res. 547, 239–248.

Schwarting, G. A., Deutsch, G., Gattey, D. M., and Crandall, J. E. 1992. Glycoconjugates are stage- and position-specific cell surface molecules in the developing olfactory system. 1. The CC1 immunoreactive glycolipid defines a rostrocaudal gradient in the rat vomeronasal system. J. Neurobiol. 23, 120–129.

Schwartz Levey, M., Chikaraishi, D. M., and Kauer, J. S. 1991. Characterization of potential precursor populations in the mouse olfactory epithelium using immunocytochemistry and autoradiography. J. Neurosci. 11, 3556–3564.

Schwartz Levey, M., Cinelli, A. R., and Kauer, J. S. 1992. Intracellular injection of vital dyes into single cells in the salamander olfactory epithelium. Neurosci. Lett. 140, 265–269.

Schwob, J. E. and Gottlieb, D. I. 1986. The primary olfactory projection has two chemically distinct zones. J. Neurosci. 6, 3393–3404.

Schwob, J. E. and Gottlieb, D. I. 1988. Purification and characterization of an antigen that is spatially segregated in the primary olfactory projection. J. Neurosci. 8, 3470–3480.

Schwob, J. E., Huard, J. M., Luskin, M. B., and Youngentob, S. L. 1994a. Retroviral lineage studies of the rat olfactory epithelium. Chem. Senses 19, 671–682.

Schwob, J. E., Saha, S., Youngentob, S. L., and Jubelt, B. 2001. Intranasal inoculation with the olfactory bulb line variant of mouse hepatitis virus causes extensive destruction of the olfactory bulb and accelerated turnover of neurons in the olfactory epithelium of mice. Chem. Senses 26, 937–952.

Schwob, J. E., Szumowski, K. E., and Stasky, A. A. 1992. Olfactory sensory neurons are trophically dependent on the olfactory bulb for their prolonged survival. J. Neurosci. 12, 3896–3919.

Schwob, J. E., Youngentob, S. L., and Meiri, K. F. 1994b. On the formation of neuromata in the primary olfactory projection. J. Comp. Neurol. 340, 361–380.

Schwob, J. E., Youngentob, S. L., and Mezza, R. C. 1995. Reconstitution of the rat olfactory epithelium after methyl bromide-induced lesion. J. Comp. Neurol. 359, 15–37.

Schwob, J. E., Youngentob, S. L., Ring, G., Iwema, C. L., and Mezza, R. C. 1999. Reinnervation of the rat olfactory bulb after methyl bromide-induced lesion: timing and extent of reinnervation. J. Comp. Neurol. 412, 439–457.

Seiden, A. M. 2004. Postviral olfactory loss. Otolaryngol. Clin. North. Am. 37, 1159–1166.

Shinoda, K., Ohtsuki, T., Nagano, M., and Okumura, T. 1993. A possible functional necklace formed by placental antigen X-P2-immunoreactive and intensely acetylcholinesterase-reactive (PAX/IAE) glomerular complexes in the rat olfactory bulb. Brain Res. 618, 160–166.

Shinoda, K., Shiotani, Y., and Osawa, Y. 1989. Necklace olfactory glomeruli form unique components of the rat primary olfactory system. J. Comp. Neurol. 284, 362–373.

Shou, J., Murray, R. C., Rim, P. C., and Calof, A. L. 2000. Opposing effects of bone morphogenetic proteins on neuron production and survival in the olfactory receptor neuron lineage. Development 127, 5403–5413.

Shou, J., Rim, P. C., and Calof, A. L. 1999. BMPs inhibit neurogenesis by a mechanism involving degradation of a transcription factor. Nat. Neurosci. 2, 339–345.

Simmons, P. A., Rafols, J. A., and Getchell, T. V. 1981. Ultrastructural changes in olfactory receptor neurons following olfactory nerve section. J. Comp. Neurol. 197, 237–257.

Slotnick, B., Bodyak, N., and Davis, B. J. 2001. Olfactory marker protein immunohistochemistry and the anterograde transport of horseradish peroxidase as indices of damage to the olfactory epithelium. Chem. Senses 26, 605–610.

Smith, C. G. 1938. Changes in the olfactory mucosa and the olfactory nerves following intranasal treatment with one per cent zinc sulphate. Can. Med. Assoc. J. 39, 138–140.

St John, J. A. and Key, B. 2003. Axon mis-targeting in the olfactory bulb during regeneration of olfactory neuroepithelium. Chem. Senses 28, 773–779.

Stroop, W. G., Rock, D. L., and Fraser, N. W. 1984. Localization of herpes simplex virus in the trigeminal and olfactory systems of the mouse central nervous system during acute and latent infections by *in situ* hybridization. Lab. Invest. 51, 27–38.

Strotmann, J., Conzelmann, S., Beck, A., Feinstein, P., Breer, H., and Mombaerts, P. 2000. Local permutations in the glomerular array of the mouse olfactory bulb. J. Neurosci. 20, 6927–6938.

Suzuki, Y., Mizoguchi, I., Nishiyama, H., Takeda, M., and Obara, N. 2003. Expression of Hes6 and NeuroD in the olfactory epithelium, vomeronasal organ and non-sensory patches. Chem. Senses 28, 197–205.

Suzuki, Y., Schafer, J., and Farbman, A. I. 1995. Phagocytic cells in the rat olfactory epithelium after bulbectomy. Exp. Neurol. 136, 225–233.

Suzuki, Y., Takeda, M., and Farbman, A. I. 1996. Supporting cells as phagocytes in the olfactory epithelium after bulbectomy. J. Comp. Neurol. 376, 509–517.

Taniguchi, K., Arai, T., and Ogawa, K. 1993. Fine structure of the septal olfactory organ of Masera and its associated gland in the golden hamster. J. Vet. Med. Sci. 55, 107–116.

Treloar, H. B., Feinstein, P., Mombaerts, P., and Greer, C. A. 2002. Specificity of glomerular targeting by olfactory sensory axons. J. Neurosci. 22, 2469–2477.

Twomey, J. A., Barker, C. M., Robinson, G., and Howell, D. A. 1979. Olfactory mucosa in herpes simplex encephalitis. J. Neurol. Neurosurg. Psychiatr. 42, 983–987.

Vassar, R., Ngai, J., and Axel, R. 1993. Spatial segregation of odorant receptor expression in the mammalian olfactory epithelium. Cell 74, 309–318.

Verhaagen, J., Oestreicher, A. B., Gispen, W. H., and Margolis, F. L. 1989. The expression of the growth associated protein B50/GAP43 in the olfactory system of neonatal and adult rats. J. Neurosci. 9, 683–691.

Verhaagen, J., Oestreicher, A. B., Grillo, M., Khew-Goodall, Y. S., Gispen, W. H., and Margolis, F. L. 1990. Neuroplasticity in the olfactory system: differential effects of central and peripheral lesions of the primary olfactory pathway on the expression of B-50/GAP43 and the olfactory marker protein. J. Neurosci. Res. 26, 31–44.

Walker, J. C., Smith, J. C., Rashotte, M. E., and Switzer, R. C. 1981. Behavioral and Anatomical Study of Olfactory Nerve Reconstitution in Pigeons. In: Olfaction and Taste VII (*ed*. H. Van der Starre), p. 409. Information Retrieval Ltd.

Walters, E., Buchheit, K., and Maruniak, J. A. 1992. Receptor neuron losses result in decreased cytochrome P-450 immunoreactivity in associated non-neuronal cells of mouse olfactory mucosa. J. Neurosci. Res. 33, 103–111.

Wang, F., Nemes, A., Mendelsohn, M., and Axel, R. 1998. Odorant receptors govern the formation of a precise topographic map. Cell 93, 47–60.

Watt, F. M. 2001. Stem cell fate and patterning in mammalian epidermis. Curr. Opin. Genet. Dev. 11, 410–417.

Weiler, E. and Farbman, A. I. 2003. The septal organ of the rat during postnatal development. Chem. Senses 28, 581–593.

Wolpert, L. 1989. Positional information revisited. Development 107(Suppl.), 3–12.

Wu, H. H., Ivkovic, S., Murray, R. C., Jaramillo, S., Lyons, K. M., Johnson, J. E., and Calof, A. L. 2003. Autoregulation of Neurogenesis by GDF11. Neuron 37, 197–207.

Yee, K. K. and Costanzo, R. M. 1995. Restoration of olfactory mediated behavior after olfactory bulb deafferentation. Physiol. Behav. 58, 959–968.

Yee, K. K. and Costanzo, R. M. 1998. Changes in odor quality discrimination following recovery from olfactory nerve transection. Chem. Senses 23, 513–519.

Yoshihara, Y., Kawasaki, M., Tamada, A., Fujita, H., Hayashi, H., Kagamiyama, H., and Mori, K. 1997. OCAM: A new member of the neural cell adhesion molecule family related to zone-to-zone projection of olfactory and vomeronasal axons. J. Neurosci. 17, 5830–5842.

Youngentob, S. L. and Schwob, J. E. 1997. Changes in odorant quality perception following methyl bromide induced lesions of the olfactory epithelium. Chem. Senses 22, 830–831.

Zhang, X. and Firestein, S. 2002. The olfactory receptor gene superfamily of the mouse. Nat. Neurosci. 5, 124–133.

4.35 Regeneration in the Olfactory Bulb

P-M Lledo, Pasteur Institute, Paris, France

© 2008 Elsevier Inc. All rights reserved.

4.35.1	Introduction	614
4.35.2	The Mammalian Olfactory Bulb Network	614
4.35.3	Building Neuronal Networks during Adulthood	615
4.35.3.1	Producing New Neurons	616
4.35.3.2	Maturation and Functional Integration	616
4.35.4	Functions of Newly Formed Interneurons in the Olfactory Bulb	617
4.35.5	Properties Conferred by Neurons Generated in Adulthood	618
4.35.6	Adult Neurogenesis: A Neural Basis for Experience-Induced Plasticity	619
4.35.7	Ethological Relevance of Adult Neurogenesis	619
4.35.8	Concluding Remarks	620
References		621

Glossary

adult neurogenesis The entire set of events leading to the production of new neurons in the adult brain, from precursor cell division to functionally integrated survival.

commitment Engaging in a program leading to differentiation. For a stem cell, this means exit from self-renewal.

green fluorescent protein (GFP) An autofluorescent protein that was originally isolated from the jellyfish *Aequorea victoria*. It can be genetically conjugated with proteins to make them fluorescent. The most widely used mutant, enhanced GFP (eGFP), has an emission maximum at 510 nm.

lentivirus vector A retrovirus vector derived from human immunodeficiency virus (HIV), which infects both dividing and nondividing cells.

multipotent Can form multiple lineages that constitute an entire tissue or tissues. Example: hematopoietic stem cells.

neurogenic niche Cellular microenvironment providing support and stimuli necessary to sustain self-renewal.

oligopotent Able to form two or more lineages within a tissue. Example: a neural stem cell that can create a subset of neurons in the brain.

pluripotent Able to form all the body's cell lineages, including germ cells, and some or even all extraembryonic cell types. Example: embryonic stem cells.

potency The range of commitment options available to a cell.

precursor CNS stem cells and all progenitors are generally referred to as precursor cells.

progenitor A mitotic cell with a fast dividing cell cycle that retains the ability to proliferate and to give rise to terminally differentiated cells, but is not capable of indefinite self-renewal.

stem cell A cell that can continuously produce unaltered daughters and also has the ability to produce daughter cells that have different, more restricted properties.

stem cells plasticity Unproven notion that tissue stem cells may broaden potency in response to physiological demands or insults.

totipotent Sufficient to form entire organism. Totipotency is seen in zygote and plant meristem cells; not demonstrated for any vertebrate stem cell.

transit-amplifying cell Proliferative stem cell progeny fated for differentiation. Initially may not be committed and may retain self-renewal.

two-photon microscopy Microscopy in which fluorochromes are stimulated, not by a single high-energy photon, but quasi-simultaneously by two photons of low energy, greatly reducing both light scattering and photodynamic sample damage.

unipotent Forms a single lineage. Example: spermatogonial stem cells.

4.35.1 Introduction

Modern neurobiology has shown that complex biological systems, such as the vertebrate brain, are constructed from similar, repeated units. In the central nervous system (CNS), these units, or modules, are composed of networks with opposite effects – excitation and inhibition. Excitation was initially assumed to play the dominant role in information processing, whereas inhibition was thought to prevent excessive activity. Local inhibitory neurons appeared to be simple elements that regulated excitatory neuronal activity. Thus, as in the Chinese Yin and Yang philosophy, the activity of a large network of principal excitatory (glutamatergic) neurons was thought to be purposefully balanced by local circuit inhibitory neurons.

The γ-aminobutyric acid (GABA)-releasing neuron, also referred to as the local circuit inhibitory interneuron, is one of the most studied types of interneuron. Recent investigations have indicated that the initial concept of interneuron is an oversimplification, requiring readjustment to accommodate cell types and functions that would not strictly fit the definition cited above. For instance, combined anatomical, electrophysiological, and pharmacological approaches have recently provided new insight into the roles of interneurons at several levels. At the cellular level, these cells govern action potential generation, firing pattern, precise timing of the discharge of individual principal cells in relation to the emergent behavior of the entire cell assembly, membrane potential oscillations, and dendritic calcium spikes. At the network level, inhibitory interneurons are considered to play an important role in controlling synaptic strength and plasticity and the generation of large-scale synchronous oscillatory activity.

Interneurons have generated considerable research interest, but studies of their function are limited by their tremendous heterogeneity in morphology and connectivity, the principal neurons being much more uniform in their appearance. This limitation has tended to push attempts to characterize interneuron subtypes into the domain of neurochemical content, based on calcium-binding proteins or neuromodulators. However, neurochemically identical cells may have surprisingly different functional properties, further complicating classification. Furthermore, as inhibitory interneurons exert pleiotropic effects on brain microcircuits, any characterization based solely on function is almost certain to prove problematic. Thus, a classification of interneurons can only be considered valid if it takes into account morphological, biochemical, and physiological characteristics. This criterion is satisfied for the first central relay of sensory information about odor, the olfactory bulb. This chapter provides an overview of the constitution of the bulbar interneuron population, current knowledge concerning the functions of these cells, their replacement and the possible role of adult neurogenesis in perception and memory. Due to space constraints, this review focuses exclusively on the mammalian olfactory bulb.

4.35.2 The Mammalian Olfactory Bulb Network

The main projection neurons of the bulb, the mitral cells, are located in a single lamina, the mitral cell layer (Figure 1). The primary dendrite of the mitral cell, extending vertically from the soma, contacts a single glomerulus, at which massive interactions with periglomerular interneurons and olfactory nerve terminals occur. Periglomerular interneurons are heterogeneous, including both GABAergic and dopaminergic subtypes. In contrast, mitral cell secondary dendrites radiate horizontally, for up to 1 μm, almost entirely spanning the olfactory bulb (Mori, K. *et al.*, 1983). In the external plexiform layer, they interact with inhibitory axonless interneurons – the granule cells – which constitute the largest cellular population within the bulb. The projection neurons engage with this extensive local circuit through dendrodendritic synaptic contacts. This reciprocal circuit provides the basis for the reliable, spatially localized, recurrent inhibition of mitral cells (Rall, W. *et al.*, 1966). The synaptic depolarization of mitral cells, driven by persistent excitatory input from the sensory neurons, triggers glutamate release from the dendrites of these cells, resulting in the depolarization of interneuron dendrites and spines. This, in turn, elicits the direct release of GABA into the mitral cell. Thus, in the olfactory bulb, the quality of the odor stimulus is initially encoded by a specific combination of activated mitral cells, as a function of GABAergic inhibition. As a single granule cell is believed to contact a number of output neurons (Shepherd, G. M. *et al.*, 2004), the reciprocal inhibitory synaptic connection helps to synchronize mitral cell activity (Lagier, S. *et al.*, 2004).

Following activation of the glomeruli, the network of output neurons and local interneurons adds a second

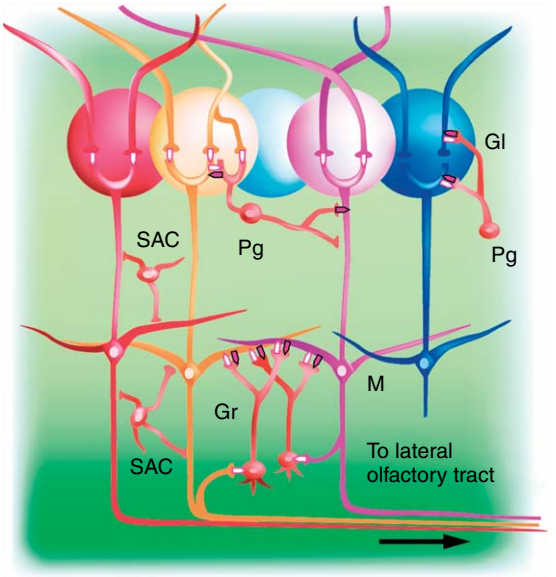

Figure 1 Wiring of the olfactory bulb. Each sensory neuron expresses only one of the 1000 odorant receptor genes and the axons from all cells expressing that particular receptor converge onto one or a few glomeruli (Gl) in the olfactory bulb. The nearly 2000 glomeruli in the rat olfactory bulb are spherical knots of neuropil, about 50–100 μm in diameter, which contain the incoming axons of sensory neurons and the apical dendrites of the projection neuron of the olfactory bulb, the mitral cell (M). Mitral axons leaving the olfactory bulb project widely to higher brain structures including the piriform cortex, hippocampus, and amygdala. Processing of the olfactory message into the bulb occurs through three populations of interneurons: periglomerular cells (Pg), granule cells (Gr), and short axon cells (SAC).

combinatorial layer to the representation of olfactory information. Contacts mediated by bulbar output neurons and local interneurons may contribute to the global reformatting of odor representations, in the form of a stimulus-dependent, temporal redistribution of activity across the olfactory bulb. In this context, lateral inhibition can be seen as a means of sharpening odor representation by a neuronal population (see below). Inhibitory circuits with different topologies are likely to form, depending on the sensory neuron afferents stimulated and the local interneuron connections activated following stimulation. Two combinatorial encoders therefore seem to be involved in information processing (Lledo, P.-M. *et al.*, 2005). The first is the olfactory receptor repertoire expressed by the ensemble of sensory neurons, which transduces receptor activation patterns into a glomerular odor image (Korsching, S., 2002). The secondary encoder is the intricate interneuron network, which extracts higher-order features from the odor images, converting them into timing relationships across the firing output neurons (Laurent, G., 2002). Three assumptions can be made, based on the combination of these two encoders of the olfactory bulb. First, the neural synchronization of glomerular outputs may enhance the representation of a complex olfactory stimulus by integrating the different signal streams activated by the odor into a unified olfactory image in the sensory cortex. Second, the activation of neuronal assemblies in the bulb modulates groups of neurons in the forebrain, bringing into play an olfactory signal-decoding mechanism. It has been suggested that the olfactory forebrain uses coincidence detector neurons to identify the various patterns of activity in the bulb (Mori, K. *et al.*, 1999). In this model, synchronized oscillations are seen as a means by which signals from different olfactory neurons are temporally connected for detection. Finally, the neurons in the olfactory bulb that relay activity to the rest of the brain interact extensively with each other, both directly and through a network of coupled interneurons. The relay neurons can engage in highly synchronous oscillatory activity, thereby forming assemblies that conveying information about a particular odor blend. As described below, the continuous turnover of interneurons plays an important role in adjusting the spatiotemporal processes of the olfactory bulb to the level of complexity and novelty of odors encountered by the animal.

4.35.3 Building Neuronal Networks during Adulthood

Postdevelopmental neurogenesis is conserved across evolutionary boundaries, from crustaceans to higher vertebrates, such as birds, rodents, and primates, including humans. The extent of postnatal neurogenesis decreases with increasing brain complexity, with adult neurogenesis in lower vertebrates, such as lizards, providing a massive additional supply of neurons capable of regenerating entire areas of the brain, whereas mammalian neurogenesis is restricted to only a few regions of the brain and to the replacement of newborn neurons. The degree of postdevelopmental neurogenesis in a given species may depend on a trade-off between the benefits accruing from the creation of new neurons and the problems generated by these neurons in terms of their integration into the network circuitry. In more complex brains such as those of mammals, the problems of newborn neuron integration seem to outweigh the potential benefits and adult

neurogenesis in normal conditions is probably confined to just two regions: the subgranular zone of the hippocampal dentate gyrus and the subventricular zone (SVZ), which contributes interneurons to the olfactory bulb (Alvarez-Buylla, A. and Garcia-Verdugo, J. M., 2002). There is some evidence to suggest that constitutive neurogenesis occurs in other regions of the adult brain, but this remains to be demonstrated (Rakic, P., 2002).

4.35.3.1 Producing New Neurons

Astrocytes in the adult SVZ, which lines the border between the striatum and the lateral ventricle to form a neurogenic niche, act as slow-dividing adult neural stem cells with high potency, generating transit-amplifying cells before transforming into neuroblast precursors (Doetsch, F., 2003) (Figure 2). These neuroblasts proceed toward the olfactory bulb along an intricate path of migration known as the rostral migratory stream (RMS). More than 30 000 neuroblasts leave the rodent SVZ and enter the RMS each day (Alvarez-Buylla, A. and Lim, D. A., 2004). In the RMS, they are not guided by radial glia, but instead migrate tangentially in chains through tubular structures formed by specialized astrocytes. These newborn cells then detach from the chains and migrate radially into the olfactory bulb, where they mature into olfactory inhibitory interneurons of two main types – granule cells and periglomerular cells – and integrate into networks. Both these cell types make only local contacts, directly or indirectly modulating the processing of sensory information by the mitral cells.

4.35.3.2 Maturation and Functional Integration

The use of replication-incompetent lentiviruses to transduce stem cells in the SVZ and label them with enhanced green fluorescent protein (eGFP) has made it possible to characterize the commitment of adult stem cells. The presence of GFP has made possible both morphological and electrophysiological characterization of the newly formed olfactory bulb neurons during their migration and differentiation (Belluzzi, O. *et al.*, 2003; Carleton, A. *et al.*, 2003). The morphology of newly generated cells becomes more complex in the first few weeks after their generation. Granule cells form more elaborate dendrites extending into the external plexiform layer of the bulb, and become fully mature morphologically within about 2 weeks. In contrast, periglomerular cells may take about 4 weeks to develop their full dendritic and axonal morphology (Belluzzi, O. *et al.*, 2003); a period of time similar to that required for the maturation of hippocampal cells generated during adulthood (Figure 3). During this maturation, immature bulbar interneurons express transient marker proteins, including TUJ1 and TUC4 (Lledo, P.-M. *et al.*, 2006). Functionally, as in the adult hippocampus, the first synapses made with new cells are GABAergic, and these contacts are followed by glutamatergic inputs several days later. The developmental sequence of voltage-dependent currents and synaptic connections differentiates between newly formed periglomerular and granule cells (and between bulbar and hippocampal granule cells). In periglomerular cells, maturation of the voltage-dependent sodium current, and consequently the capacity of the newly generated cells to fire action

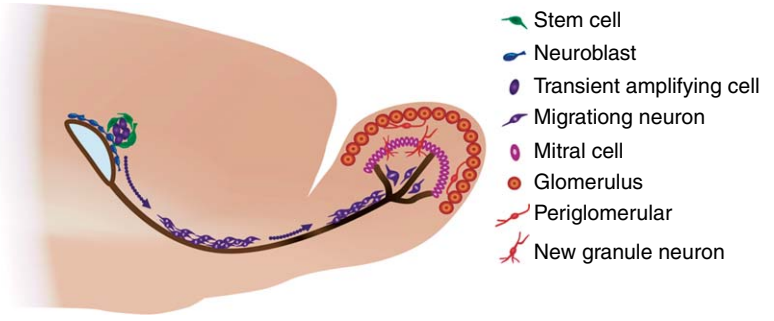

Figure 2 The subventricular zone (SVZ)–olfactory bulb pathway constitutes one of the two neurogenic niches in the adult forebrain. Mauve arrows indicate the tangential migration of neuroblasts from the lateral ventricle (filled in blue) toward the olfactory bulb. Neurogenesis refers to the replacement of bulbar local interneurons in the olfactory bulb.

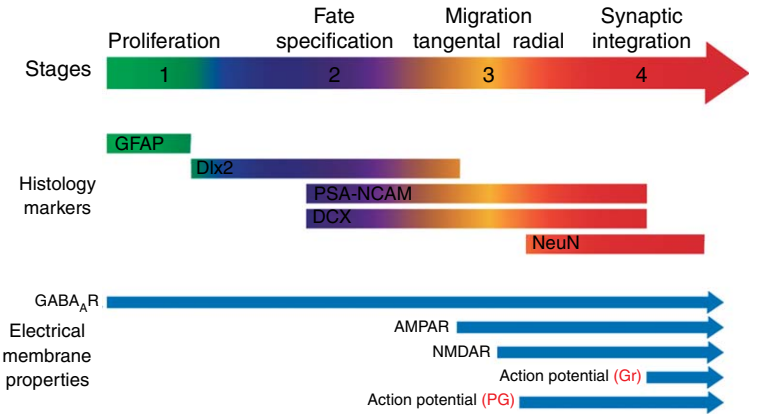

Figure 3 Postmitotic maturation of newborn neurons in the adult forebrain. The schema shows the functional stages through which adult-born neuron progress before becoming fully mature. This simplified state of affairs comes with a number of caveats, since the maturation of individual adult-born neurons has yet to be followed, maturation stages are likely to reflect a continuum rather than discrete steps, and maturation time points are likely to vary considerably from cell to cell. For this last reason, ages here represent the earliest age at which particular properties have been observed in a given cell type. Note also that maturation certainly does not stop at stage 4: arbor complexity and spine density can increase up to 4 months after the birth of a newborn neuron. It is noteworthy that receptor expression precedes synaptic activation, and γ-aminobutyric acid (GABA)-mediated input precedes glutamatergic input. Olfactory bulb granule cells show atypical maturation in that they only fire sodium-based action potentials after they have begun to receive synaptic input.

potentials, seems to precede the appearance of synaptic contacts, whereas the opposite pattern is observed in granule cells (Belluzzi, O. *et al.*, 2003; Carleton, A. *et al.*, 2003). The later maturation of granule cell excitability may prevent the preexisting circuitry in the adult from being disrupted during the insertion of newly formed cells. Alternatively, as even mature granule cells lack an axon, it may result purely from morphological differences between granule and periglomerular neurons. Further studies are required to determine whether newly generated neurons form functional synapses with their downstream target neurons and release appropriate neurotransmitters, which would unequivocally demonstrate their integration into adult networks.

Below, I summarize the contributions of early work in the field to the current framework for understanding the role of newborn interneurons in the adult olfactory bulb network. I will also review the more recent findings that have dramatically reshaped our view of the integration of newly formed neurons into adult networks. At first glance, this neurogenesis may be seen as a putative response to the death and turnover of the primary olfactory receptor neurons that occurs throughout the life of the animal. However, as we will see below, adult neurogenesis also endows the bulb with unique properties.

4.35.4 Functions of Newly Formed Interneurons in the Olfactory Bulb

Ongoing neurogenesis and migration in adults have been extensively documented, but their functional consequences remain unclear. As the largest neuronal population in the olfactory bulb consists of granule cells, which outnumber the projection neurons by at least 100:1 (Shepherd, G. M. *et al.*, 2004), and one granule cell contacts several mitral cells, with each mitral cell, in turn, contacting a large number of pyramidal cells from the pyriform cortex, the integration of transient newly formed neurons into an upstream position in the olfactory bulb is ideal for amplifying the effects of neurogenesis throughout the olfactory pathway. If the continuous generation of interneurons throughout the animal's life is necessary for olfaction, then changes in migration processes – resulting in changes in the recruitment of new interneurons – should affect olfactory processing. Studies of transgenic mice with low levels of adult neurogenesis have been carried out to test this hypothesis. For example, NCAM-mutant mice have been studied as these mice display lower than normal levels of neuroblast migration. The quantification of bulbar neurogenesis revealed 40% fewer newly formed interneurons in adult knockout mice than in the wild type.

This impairment of neurogenesis was accompanied by changes in odor discrimination (Gheusi, G. *et al.*, 2000), revealing a specific role for newly formed interneurons in the downstream coding of olfactory information. This observation was supported by observations in another transgenic line with impaired $GABA_A$ receptor-mediated synaptic inhibition (Nusser, Z. *et al.*, 2001) and by theoretical analyses (Cecchi, G. A. *et al.*, 2001). Based on these data, it appears that a critical level of inhibition, mediated by the activation of $GABA_A$ receptors located on the secondary dendrites of bulbar projection neurons, is required for olfactory processing. In addition, as the olfactory bulb is also involved in consolidating processes associated with long-term odor memory, changes in the number of GABAergic interneurons may regulate both olfactory perception and memory.

This issue has been investigated, by studies aiming to determine whether a change in the number of newly formed bulbar interneurons alters olfactory memory. In these experiments, animals were reared in a complex olfactory environment. Exposure to enriched sensory surroundings has many positive effects on brain structure and function, increasing the number of dendritic branches and spines, enlarging synapses, increasing the number of glial cells and improving performance in tests of spatial memory (Rosenzweig, M. R. and Bennett, E. L., 1996). Mice reared in enriched olfactory environments produce twice as many new interneurons as other mice. This increase is specific to the olfactory bulb, with no changes observed in the other neurogenic zone, the dentate gyrus of the adult hippocampus. Animals with higher levels of neurogenesis retain learned olfactory information for longer periods of time than controls (Rochefort, C. *et al.*, 2002). In particular, animals reared in enriched olfactory environments recognize familiar odors in more readily and in a more sustained manner than animals reared in standard conditions. Although the potential consequences of an enriched environment for synaptic efficacy and/or mitral cell activity were not specifically explored, these results are consistent with the existence of a correlation between the size of the newly formed interneuron population and odor memory.

4.35.5 Properties Conferred by Neurons Generated in Adulthood

Although recent estimates suggest that many more neurons are produced during adulthood than was initially thought, the estimated rate of neuron production in adulthood remains lower than that during development. Consequently, if the neurons generated during adulthood have similar functional properties to those generated in early life, then adult neurogenesis probably has an insignificant impact. In contrast, if adult-generated neurons have unique properties, giving them a greater impact than more mature neurons, then their continual integration into the functional circuitry would be expected to have major effects. Recent observations of both the hippocampus and the olfactory bulb are consistent with this second hypothesis. Indeed, newly formed neurons seem to display robust plasticity that cannot be inhibited by GABA, which is not the case for mature neurons. As new neurons are structurally plastic (Figure 4), they may well be very sensitive to changes in the animal's environment and life experiences. This suggests that adult neurogenesis is functionally important, as it results in a continual influx of neurons that are, at least temporarily, immature, with unique physiological properties.

As described above, bulbar interneurons play an essential role in shaping the olfactory information that reaches the olfactory cortex. As the cells generated in the adult SVZ differentiate exclusively into bulbar interneurons, they probably contribute to essential aspects of olfactory processing. Experimental studies and modeling have provided evidence that newly formed granule cells play a role in olfactory discrimination, but the more general functions of these cells remain to be characterized. Adult neurogenesis is unlikely to be of immediate functional

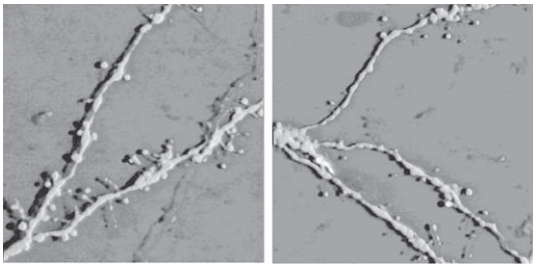

Figure 4 The adult neurogenesis brings plastic elements to preexisting neuronal networks. Images of green fluorescent protein (GFP)-labeled newborn interneurons taken with a two-photon microscope. The newborn interneurons developed in active (left panel) or inoperative (right panel) olfactory bulb networks. Note reduced spine density for newborn interneurons maturing in the quiescent olfactory bulb.

benefit, because it takes several days to generate a new, functionally integrated interneuron (Figure 3). Cells generated during adulthood develop neurites within a few weeks. It is clear that the new connections cannot constitute a response to the particular functional event triggering neurogenesis, because these connections may well not form until after the trigger event has ended. Olfactory bulb neurogenesis should therefore be considered a long-term, as opposed to a short-term adjustment of the bulbar circuitry to a higher level of experience governed by olfaction.

4.35.6 Adult Neurogenesis: A Neural Basis for Experience-Induced Plasticity

It seems reasonable to assume that the mind and brain benefit from active living; this hypothesis is supported by several observations, including the results of epidemiological studies. It has also been clearly established that both physical and intellectual activities have a positive influence on the incidence of neurodegenerative disorders and cognitive decline. The continuous neurogenesis observed in the olfactory region of adult animals provides us with a unique model for studying the effects of sensory-driven activity and its benefits. In the olfactory bulb, the role of environment-induced activity can be explored not only during the neonatal period, when the developing structures are refined and stabilized, but also in adulthood, when more delicate regulation occurs. Several studies have demonstrated that changes in the level of sensory activity do not affect the proliferation and tangential migration of neuroblasts. Instead, they seem to regulate the number of newly generated neurons reaching the olfactory bulb and the level of cell death. Thus, sensory-driven activity may play an important role in several steps of adult neurogenesis (Figure 5). This, in turn, would greatly modify the number of new interneurons, thereby altering the inhibitory–excitatory balance in the bulbar neuronal networks. There is clear evidence that adult neurogenesis can be regulated, but most of the data on adult mammalian neurogenesis have been obtained from laboratory animals, kept under artificial conditions very different from their natural habitat. Even the odor-enriched environments used in experiments are arguably much poorer in terms of sensory stimulation than conditions in the wild.

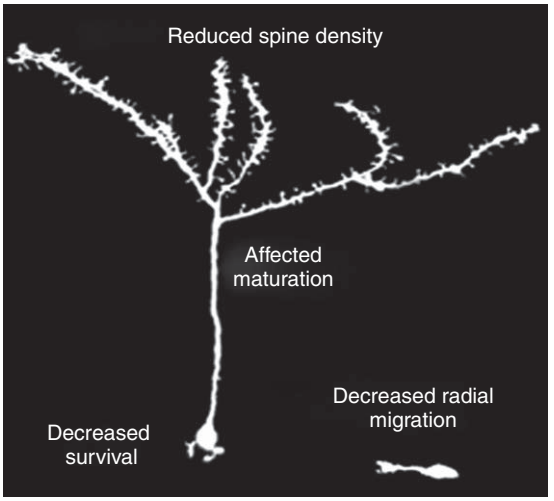

Figure 5 Role of sensory activity in shaping the adult neurogenesis. Using sensory deprivation paradigm, it has been demonstrated that odor-induced activity is required for normal radial migration of neuroblasts, their survival and maturation and the maintenance of spine density.

4.35.7 Ethological Relevance of Adult Neurogenesis

Although it is clear that the adult olfactory bulb integrates neurons throughout life, the reason for this remains unclear. What are the new neurons used for and how can an existing functional neural network integrate and even actively recruit new neurons? Current theories concerning cognition are based on the assumption that the adult brain is a stable network in terms of the number of neurons. According to this scheme, structural neural plasticity occurs only at the level of synapses, dendrites, and neurites. The demonstration of adult bulbar neurogenesis – the generation of new interneurons from resident neuronal stem cells and their integration into the bulbar circuit – has called this assumption into question. In light of results on the activity-dependent regulation of adult bulbar neurogenesis, some conclusions concerning why and how new neurons contribute to bulbar function can be made. I suggest that neurogenesis does not simply add neurons to enhance memory, but that it also strategically inserts new cells with unique properties (Figure 3). The multiple stages in the maturation of new neurons might provide a more extended substrate for plasticity. The newly formed neurons may provide the olfactory bulb with a large repository of plastic cells, enabling it to respond more effectively to

changes in the environment and to life experiences (Figure 5). For instance, new neurons may respond preferentially to hormones, learning, and other forms of experience-induced activity. These aspects have been well documented in various biologically relevant models described briefly below.

Female mice form a memory of the pheromones of the male they mate with, a phenomenon known as the Bruce effect. This memory leads to disruption of the pregnancy when the female is exposed to the pheromones of other males (Bruce, H. M., 1959). It is formed during mating and requires a period of about 3–4 h of exposure to the male's pheromones. Brennan P. A. *et al.* (1995) used a microdialysis approach to explore changes in a range of neurotransmitters that occur when female mice form a memory of their stud male. The main change in the accessory olfactory bulb is a decrease in glutamate/GABA ratio following memory formation in response to the mating male's pheromones. The increase in GABA release reflects a higher inhibitory tone at the reciprocal synapses. Brennan P. A. *et al.* (1995) interpreted this mechanism as a way of reducing excitation from mitral cells, which mediate the input from the mating male's pheromones, prevent the blockage of pregnancy. In contrast, exposure to a different male would activate a different subpopulation of mitral cells, not previously subjected to an increase in inhibitory control, thereby eliciting central pregnancy-blocking mechanisms. These processes are not restricted to the formation of a memory of the mating male's pheromones. Similar events have been observed in the olfactory bulb of ewes during the development of a specific ability to recognize their own lambs, enabling them to reject other lambs that attempt to suckle. After parturition, an increase in glutamate and GABA release occurs in the ewe's olfactory bulb in response to odors from her own lamb, but not to odors from other lambs (Kendrick, K. M. *et al.*, 1992). Once the ewe has established a selective bond with its lamb, the ratio of glutamate to GABA decreases in response to the lamb's odor, suggesting, once again, the existence of changes in the gain of reciprocal synapses between mitral and granule cells.

These examples illustrate changes in the excitatory–inhibitory balance in the olfactory bulb occurring during the establishment of specific social preferences. Similar changes have recently been shown to occur in circumstances involving olfactory learning in a broader context. For instance, the use of a conditioning procedure in which adult mice were trained, using odor, to dig through wood shavings to obtain a buried piece of sugar, has produced interesting findings. Following conditioning, the presentation of the odor previously associated with the reward induces an increase in both glutamate and GABA levels in the olfactory bulb and a decrease in the balance between excitatory and inhibitory transmitters. In contrast, no change is observed if animals are exposed to a nonconditioning odor, indicating that the increase in inhibition occurs only for relevant odors. These findings highlight the significance of the changes in the excitatory–inhibitory ratio that occur in the olfactory bulb following learning. The neurochemistry of inhibition enhancement is reminiscent of the upregulation of the permanent supply of bulbar interneurons correlated with a stronger memory in odor-enriched mice. Together, these findings indicate that adult bulbar neurogenesis may be involved in many natural types of behavior yet to be explored.

4.35.8 Concluding Remarks

We still do not know why there are new neurons in the adult brain, but research into the regulation of adult neurogenesis, and an increasing number of studies investigating the function of the new cells, have led to two conclusions. First, bulbar neurogenesis is affected by relevant behavior, including behavior specifically related to bulbar function, in particular. Second, changes in the rate or extent of neurogenesis have an effect on subsequent behavior. Thus, behavior may change the structure of the olfactory bulb, and changes in structure can subsequently modify, or at least affect, subsequent behavior. The correlation between activity and adult neurogenesis suggests that new neurons are involved general aspects of bulbar function, probably sustaining the ability of the adult network to adapt information processing to relevant ethological needs.

The sense of smell has played an essential role in mammalian evolution. Odor representation is dynamic and highly complex, and may require unique plasticity mechanisms. Neurogenesis, migration, and the replacement of new neurons in the olfactory bulb are probably involved in this adaptive mechanism. As it takes time for new neurons to mature and become integrated into synapses, adult neurogenesis probably contributes to slow, long-term adjustments of the bulbar circuitry, rather than to fast and acute plastic changes. However, new neurons

may also be involved in faster mechanisms. Several new bulbar interneurons die within a month of maturation. Recent results show that newly formed granule cells maintain synaptic contacts during this period of rapid cell death. The selective elimination of neurons may make it possible to modify the circuitry more rapidly. The ability to mold the integration of new neurons and to eliminate older cells continually, without depleting the neuronal population, may provide neuronal networks with adaptive potential unequalled by synaptic plasticity alone.

In this brief review, I have tackled two of the main problems relating to the existence of newborn neurons in the adult olfactory bulb. Both are fundamental issues. First, I have discussed the role of adult neurogenesis in the context of bulbar function. Assuming that the bulb processes odor information before relaying it to the olfactory cortex, I hypothesize that adult neurogenesis allows the olfactory bulb to adjust the degree of processing appropriately. Second, the existence of a pool of juvenile neurons, enabling the system to adapt to future similar situations, raises the possibility that adult neurogenesis acts *post hoc* to provide a structural basis for brain plasticity. Research on adult neurogenesis in the olfactory bulb is thus not only interesting in itself, but also provides new avenues of exploration to increase our understanding of adult brain plasticity.

Acknowledgments

I thank Cecile Moreau for help with illustrations. This work was supported by the Fédération pour la Recherche sur le Cerveau, the Fondation pour la Recherche Médicale and the Agence Nationale de la Recherche (ANR-05-Neur-028-01).

References

Alvarez-Buylla, A. and Garcia-Verdugo, J. M. 2002. Neurogenesis in adult subventricular zone. J. Neurosci. 22, 629–634.

Alvarez-Buylla, A. and Lim, D. A. 2004. For the long run: maintaining germinal niches in the adult brain. Neuron 41, 683–686.

Belluzzi, O., Benedusi, M., Ackman, J., and LoTurco, J. J. 2003. Electrophysiological differentiation of new neurons in the olfactory bulb. J. Neurosci. 23, 10411–10418.

Brennan, P. A., Kendrick, K. M., and Keverne, K. B. 1995. Neurotransmitter release in the accessory olfactory bulb during and after the formation of an olfactory memory in mice. Neuroscience 69, 1075–1086.

Bruce, H. M. 1959. An exteroceptive block to pregnancy in the mouse. Nature 184, 105.

Carleton, A., Petreanu, L. T., Lansford, R., Alvarez-Buylla, A., and Lledo, P. M. 2003. Becoming a new neuron in the adult olfactory bulb. Nat. Neurosci. 6, 507–518.

Cecchi, G. A., Petreanu, L. T., Alvarez-Buylla, A., and Magnasco, M. O. 2001. Unsupervised learning in a model of adult neurogenesis. J. Comp. Neurosci. 11, 175–182.

Doetsch, F. 2003. The glial identity of neural stem cells. Nat. Neurosci. 6, 1127–1134.

Gheusi, G., Cremer, H., McLean, H., Chazal, G., Vincent, J. D., and Lledo, P. M. 2000. Importance of newly generated neurons in the adult olfactory bulb for odor discrimination. Proc. Natl. Acad. Sci. U. S. A. 97, 1823–1828.

Kendrick, K. M., Levy, F., and Keverne, E. B. 1992. Changes in the sensory processing of olfactory signals induced by birth in sheep. Science 256, 833–836.

Korsching, S. 2002. Olfactory maps and odor images. Curr. Opin. Neurobiol. 12, 387–392.

Lagier, S., Carleton, A., and Lledo, P. M. 2004. Interplay between local GABAergic interneurons and relay neurons generates gamma oscillations in the rat olfactory bulb. J. Neurosci. 24, 4382–4392.

Laurent, G. 2002. Olfactory network dynamics and the coding of multidimensional signals. Nat. Rev. Neurosci. 3, 884–895.

Lledo, P.-M., Gheusi, G., and Vincent, J. D. 2005. Information processing in the mammalian olfactory system. Physiol. Rev. 85, 281–317.

Lledo, P.-M., Grubb, M., and Alonso, M. 2006. Adult neurogenesis and functional plasticity in neuronal circuits. Nat. Neurosci. Rev. 7, 179–193.

Mori, K., Kishi, K., and Ojima, H. 1983. Distribution of dendrites of mitral, displaced mitral, tufted, and granule cells in the rabbit olfactory bulb. J. Comp. Neurol. 219, 339–355.

Mori, K., Nagao, H., and Yoshihara, Y. 1999. The olfactory bulb: coding and processing of odor molecule information. Science 286, 711–715.

Nusser, Z., Kay, L. M., Laurent, G., Homanics, G. E., and Mody, I. 2001. Disruption of GABAA receptors on GABAergic interneurons leads to increased oscillatory power in the olfactory bulb network. J. Neurophysiol. 86, 2823–2833.

Rakic, P. 2002. Adult neurogenesis in mammals: an identity crisis. J. Neurosci. 22, 614–618.

Rall, W., Shepherd, G. M., Reese, T. S., and Brightman, M. W. 1966. Dendrodendritic synaptic pathway for inhibition in the olfactory bulb. Exp. Neurol. 14, 44–56.

Rochefort, C., Gheusi, G., Vincent, J. D., and Lledo, P. M. 2002. Enriched odor exposure increases the number of newborn neurons in the adult olfactory bulb and improves odor memory. J. Neurosci. 22, 2679–2689.

Rosenzweig, M. R. and Bennett, E. L. 1996. Psychobiology of plasticity: effects of training and experience on brain and behavior. Behav. Brain Res. 78, 57–65.

Shepherd, G. M., Chen, W. R., and Greer, C. A. 2004. Olfactory Bulb. In: The Synaptic Organization of the Brain, 5th edn. (*ed*. G. M. Shepherd), pp. 165–216. Oxford University Press.

Further Reading

Kashiwadani, H., Sasaki, Y. F., Uchida, N., and Mori, K. 1999. Synchronized oscillatory discharges of mitral/tufted cells with different molecular receptive ranges in the rabbit olfactory bulb. J. Neurophysiol. 82, 1786–1792.

Petreanu, L. and Alvarez-Buylla, A. 2002. Maturation and death of adult-born olfactory bulb granule neurons: role of olfaction. J. Neurosci. 22, 6106–6113.

Rall, W. and Shepherd, G. M. 1968. Theoretical reconstruction of field potentials and dendrodendritic synaptic interactions in olfactory bulb. J. Neurophysiol. 31, 884–915.

Relevant Websites

http://www.apuche.org – Olfactory Image Archive at University of Maryland, Baltimore (USA).

http://leonserver.bio.uci.edu – Olfactory maps at University of California, Irvine (USA).

http://www.pasteur.fr – Perception and Memory Laboratory at Pasteur Institute (France).

http://www.uchsc.edu – Restrepo Laboratory at the University of Colorado Health Center (USA).

http://senselab.med.yale.edu – The SenseLab Project at Yale University (USA).

4.36 Architecture of the Olfactory Bulb

C A Greer, M C Whitman, L Rela, F Imamura, and D Rodriguez Gil, Yale University School of Medicine, New Haven, CT, USA

© 2008 Elsevier Inc. All rights reserved.

4.36.1	**Introduction**	625
4.36.2	**Nasal Cavity**	625
4.36.2.1	Olfactory Epithelium	625
4.36.3	**Olfactory Bulb – Laminar Organization**	626
4.36.3.1	Olfactory Nerve Layer	626
4.36.3.2	Glomerular Layer	627
4.36.3.3	External Plexiform Layer	628
4.36.3.4	Mitral Cell Layer	628
4.36.3.5	Internal Plexiform Layer	628
4.36.3.6	Granule Cell Layer	628
4.36.3.7	Subependymal Zone – Rostral Migratory Stream	628
4.36.4	**Olfactory Bulb – Cell Populations**	629
4.36.4.1	Projection Neurons	629
4.36.4.1.1	Mitral cells	629
4.36.4.1.2	Tufted cells	629
4.36.4.2	Interneurons	630
4.36.4.2.1	Periglomerular cells	630
4.36.4.2.2	External tufted cells	630
4.36.4.2.3	Short axon cells	630
4.36.4.2.4	Van Gehuchten cells	630
4.36.4.2.5	Blanes cells	630
4.36.4.2.6	Granule cells	631
4.36.4.3	Glia	631
4.36.5	**Olfactory Bulb – Synaptic Organization**	632
4.36.5.1	Glomerular Layer	632
4.36.5.2	External Plexiform Layer	633
4.36.5.3	Mitral Cell Layer	635
4.36.5.4	Internal Plexiform Layer	635
4.36.5.5	Granule Cell Layer	635
4.36.5.6	Electrical Synapses in the Olfactory Bulb	635
4.36.6	**Lateral Olfactory Tract and Olfactory Cortex**	635
4.36.7	**Adult Neurogenesis and the Olfactory Bulb**	636
4.36.8	**Summary**	636
References		637

Glossary

cilia Nonmotile extensions of the olfactory sensory neurons within the lumen of the nasal cavity. The cilia are suspended in a layer of mucous, express odor receptors on their surface, and increase significantly the surface area of the olfactory sensory neurons.

dendrodendritic synapse Synapses occurring between two dendrites or between a dendrite and a dendritic spine. In the olfactory bulb dendrodendritic synapses form between mitral/tufted cells and granule cells in the external plexiform layer and between mitral/tufted cells and peri/juxtaglomerular cells in the glomerular layer.

gap junctions Intercellular channels that allow the diffusion of ions and metabolites and constitute the structural basis of electrical synapses. They may be

homotypic, composed of identical hemichannels (or connexons) provided by each of the connected cells, or heterotypic, composed of different connexons. In vertebrates, each connexon is normally a hexamer of connexins.

glomerulus Spherical area of neuropil where olfactory sensory neuron axons terminate and make synaptic contact with mitral, tufted, and periglomerular cells. Glomeruli are molecularly homogeneous in that all of the sensory axons terminating in one glomerulus arise from sensory neurons expressing the same odor receptor.

granule cell A major interneuron in the olfactory bulb. Granule cells are anaxonic, they lack axons, and both input and output synapses occur through specialized dendritic spines found on their apical dendrites within the external plexiform layer. Granule cells establish these dendrodendritic synapses with the secondary dendrites of mitral and tufted cells. Input synapses, from centrifugal fibers and axon collaterals of mitral and tufted cells, also occur at the cell bodies and basal dendrites in the granule cell layer. New granule cells continue to be generated in the adult and migrate into the olfactory bulb via the rostral migratory stream.

lateral olfactory tract A myelinated tract of axons from mitral and tufted cells extending from the olfactory bulb to the cortex. As axons exit the lateral olfactory tract they terminate in layer Ia of cortex, where they synapse on the apical dendrites of cortical pyramidal neurons.

mitral cell Major projection neuron from olfactory bulb to cortex. The cell bodies comprise a monolayer in the adult olfactory bulb. The apical dendrite arborizes in a single glomerulus while the lateral dendrites extend out in the external plexiform layer perpendicular to the radial axis of the olfactory bulb. The mitral cell axons distribute broadly in piriform cortex.

olfactory ensheathing cells Glia that encompass fascicles of olfactory sensory neuron axons in the olfactory nerve and in the olfactory nerve layer of the olfactory bulb. The ensheathing cells are important in the ongoing growth of new axons from the epithelium to the olfactory bulb. Due to their ability to support axon outgrowth in the olfactory system, the ensheathing cells have also found application in spinal cord injury where transplants of the ensheathing cells can improve axon regeneration.

olfactory nerve A collection of olfactory sensory neuron axon fascicles, surrounded by the processes of olfactory ensheathing cells, that extends from the olfactory epithelium to the olfactory bulb. As the nerve merges with the olfactory bulb, it becomes the olfactory nerve layer.

olfactory sensory neuron A specialized receptor found in the olfactory epithelium. The apical dendrite extends in the lumen of the nasal cavity where multiple cilia extend. The olfactory sensory neurons each express only 1 of 1000 different odor receptors in rodents. The olfactory sensory neurons are derived from a population of basal cells that appear to provide for ongoing replacement of the sensory neurons throughout life.

peri/juxtaglomerular cells These surround the glomeruli of the olfactory bulb and extend dendritic processes into the glomeruli where some receive input from the olfactory sensory neuron axons and most participate in dendrodendritic synapses with the apical dendrites of mitral and tufted cells. Axons from the peri/juxtaglomerular cells can extend considerable distances in the glomerular layer to mediate interactions with distant glomeruli. Peri/juxtaglomerular cells can be further divided into multiple subpopulations based on their molecular phenotype including the expression of neurotransmitters and calcium-binding proteins. Like granule cells, peri/juxtaglomerular cells continue to be generated in the adult.

rostral migratory stream A well-defined glial lined tract via which neuroblasts from the subventricular zone migrate into the olfactory bulb.

sustentacular cells Nonsensory supporting cells that surround the olfactory sensory neurons in the olfactory epithelium. The sustentacular cells may contribute to the removal of odorants or other molecules from the nasal cavity.

tufted cell Includes three subpopulations of olfactory bulb neurons. Deep and middle tufted cells, named for the positions of the cell bodies in the external plexiform layer, are organized and project to higher regions in a manner similar to that of mitral cells. External tufted cells are proximal to the glomeruli and mediate intrabulbar connections.

4.36.1 Introduction

The olfactory bulb is the first relay in the processing of volatile odor information in the central nervous system. Odor processing begins in the olfactory epithelium (OE), where the sensory neurons are located, and then proceeds in a hierarchical manner into the olfactory bulb, followed by primary olfactory (piriform) cortex. Tertiary cortical projections are widespread throughout the neuroaxis. As has been noted previously, the fundamental principles of organization and information flow in the olfactory system are broadly conserved across species as well as phyla.

The volatile signals processed by the olfactory system are used widely in regulating feeding behavior and preferences, avoidance, territorial marking, recognition of self versus nonself, emotional states, among others. A comprehensive review of the behavioral significance of the olfactory system is beyond the scope of this chapter, as is a fully integrated description of hierarchical organization of the pathway. The focus here will be on the structural and synaptic organization of the olfactory bulb, with reference to the OE and primary olfactory cortex as needed to help interpret general architectural principles found in the olfactory bulb. Because the organization of olfactory systems, and the olfactory bulb in particular, is widely conserved, much of the information presented here will be based on studies carried out in rodents. As will be reviewed below, the olfactory bulb is laminated, like an onion, and includes a minimum of seven primary layers: (1) the olfactory nerve layer (ONL); (2) the glomerular layer; (3) the external plexiform layer (EPL); (4) the mitral cell layer; (5) the internal plexiform layer (IPL); (6) the granule cell layer; and (7) the subependymal layer or rostral migratory stream. Each of the layers is distinguished by its cellular composition and/or synaptic organization. We will begin with a brief review of the OE because it gives rise to the axons that will constitute the outermost layer of the olfactory bulb.

We apologize to those whose work has not received appropriate attention in this chapter due to space limitations. For further details on aspects of the organization of the olfactory bulb discussed here, readers are referred to several recent excellent and comprehensive reviews (Shepherd, G. M. *et al.*, 2004; Lledo, P. M. *et al.*, 2006; Wachowiak, M. and Shipley, M. T., 2006).

4.36.2 Nasal Cavity

4.36.2.1 Olfactory Epithelium

Odor processing begins in the OE where odorants, ligands, bind with subpopulations of olfactory sensory neurons (OSNs). The epithelium is pseudostratified and includes three primary populations of cells: the OSNs, sustentacular or supporting cells, and a basal cell population that generates new sensory neurons throughout life (Graziadei, P. P. C. and Monti-Graziadei, G. A., 1978; Newman, M. P. *et al.*, 2000). The sensory neurons are highly polarized, with an apical dendrite extending to the epithelial surface where it enlarges to include multiple cilia and a thin axon (~0.2 μm in diameter) extending from the basal pole (Cuschieri, A. and Bannister, L. H., 1975). Deep to the basal lamina, the axons coalesce into fascicles that ascend and become the olfactory nerve. As the axons exit the epithelium, they are accompanied by a specialized glia cell, the olfactory ensheathing cell/glia (OEC) (Doucette, J. R., 1984). While the axons remain unmyelinated, processes from the OECs do surround the fascicles of the olfactory nerve and interdigitate among the axons. Diverse lines of evidence suggest that the OECs play an important role in the ability of the olfactory nerve to sustain continued axon growth as new sensory neurons are generated (Kafitz, K. W. and Greer, C. A., 1999).

Since the identification in 1991 (Buck, L. and Axel, R., 1991) of the large family of genes (~1000 in rodents) coding for odor receptors (ORs), the tools of molecular biology have provided for unique insights into the organization of the OE and nerve. The OSNs are believed to express only one functional OR (Chess, A. *et al.*, 1994; Serizawa, S. *et al.*, 2003), and the application of embryonic stem cell engineering has allowed the introduction of markers, either LacZ or GFP, downstream from the promoters of specific ORs (Mombaerts, P. *et al.*, 1996). Thus, the full repertoire of sensory neurons expressing a specific OR can be visualized in their entirety, from their cell bodies in the OE to the terminal portions of their axons in the olfactory bulb. Although axons of the OSNs expressing the same OR coalesce onto one or two glomeruli in the olfactory bulb (typically one glomerulus on each side of the olfactory bulb), the cell bodies are stochastically distributed within a limited region/zone of the OE (Ressler, K. J. *et al.*, 1993; Vassar, R. *et al.*, 1993; Miyamichi, K. *et al.*, 2005) where they neighbor with OSNs expressing different ORs. Initially, it was thought that the OE was delimited into four distinct

zones, each of which contained a specific subset of ORs (Ressler, K. J. *et al.*, 1993; Vassar, R. *et al.*, 1993). The most recent evidence, however, is that while each OR has a very limited band of expression within the OE, these are contiguous and overlapping (Iwema, C. L. *et al.*, 2004; Miyamichi, K. *et al.*, 2005). The heterogeneous mixture of molecularly defined OSNs continues as their axons exit the OE; axon fascicles within the OE but deep to the basal lamina are initially composed of heterogeneous populations of axons and show no evidence of topographical sorting.

The olfactory nerve exits the OE as the fascicles begin to enter the cranial cavity via a series of small foramen in the cribiform plate of the ethmoid bone. As the nerve contacts the rostral and rostral–ventral quadrants of the olfactory bulb, a complex process of defasciculation begins and the outermost layer of the olfactory bulb, the ONL, is formed (Au, W. W. *et al.*, 2002) (Figure 1).

4.36.3 Olfactory Bulb – Laminar Organization

4.36.3.1 Olfactory Nerve Layer

The OECs that were associated with the OSN axons as they exited the OE continue to define the organization of fascicles in the ONL. The OECs in the outermost olfactory nerve layer (ONLo) express the low-affinity nerve growth factor receptor p75 (Au, W. W. *et al.*,

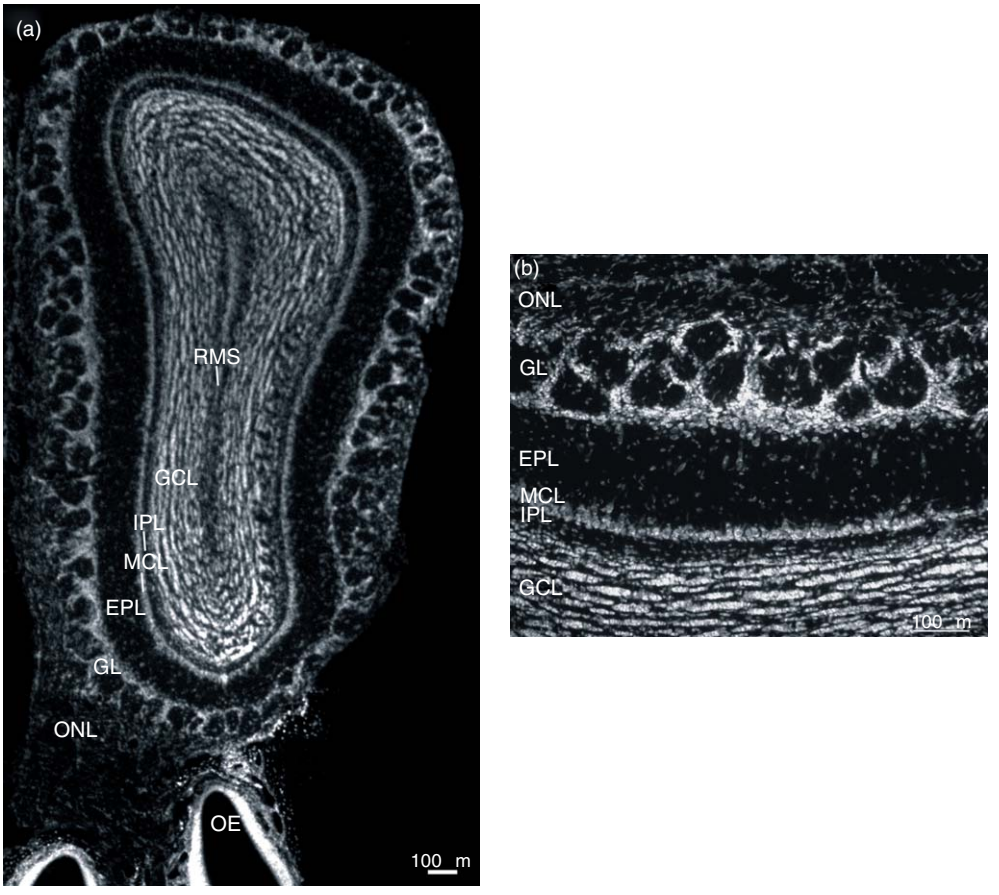

Figure 1 (a) Nissl-stained transverse section of the mouse olfactory bulb showing the laminar organization. The dorsal recess of the nasal cavity and olfactory epithelium are seen below. The spherical glomeruli delineated by periglomerular cells, the paucity of cells within the external plexiform layer, and the well-defined mitral cell layer and deeper granule cell layer are distinctive features of the olfactory bulb. Note that at this level, the laminae are continuous around the circumference of the olfactory bulb. (b) Higher magnification image of the Nissl-stained olfactory bulb. Note the differences in the sizes of the cells surrounding the glomeruli, periglomerular versus juxtaglomerular, and the large cell bodies in the mitral cell layer. The granule cells are distributed in clusters, islets, between which axons from both mitral/tufted cells and centrifugal axons travel. ONL, olfactory nerve layer; GL, glomerular layer; EPL, external plexiform layer; MCL, mitral cell layer; IPL, inner plexiform layer; GR, granule cell layer; RMS, rostral migratory stream; OE, olfactory epithelium. Calibration bars, 100 μm.

2002), while those in the inner nerve layer (ONLi) express the transcription factor TROY (Hisaoka, T. *et al.*, 2004). In parallel, the organization of fascicles differs in the ONLo and ONLi (Au, W. W. *et al.*, 2002). In the former, fascicles defined by the processes of the OECs are small, well defined, and tend to have axons with aligned trajectories. In the ONLi, the fascicles are larger and the trajectories of axons are often mixed. This has led to the suggestion that axons in the ONLo are *en route* while those in the ONLi are reorganizing into molecularly homogeneous fascicles that will coalesce into the same glomerulus. Throughout their length, the OSN axons remain fairly stable with a diameter of ~0.2 μm, but as they enter the ONLi and draw proximal to the glomerular layer, they increase somewhat in diameter to ~0.3 μm. Similar increases are seen elsewhere in the nervous system as axons begin to approach a target region of arborization and synapse formation. OSN axons do not branch within the ONL; arborization of the axons occurs after they enter a glomerulus (Klenoff, J. R. and Greer, C. A., 1998) (Figure 2).

4.36.3.2 Glomerular Layer

The glomeruli of the olfactory bulb, like glomeruli elsewhere in the nervous system, are compact areas of neuropil and contain the first synapses from the OSN axons. The glomeruli are encapsulated by glia cells, some of which extend processes into the neuropil (Kasowski, H. J. *et al.*, 1999; Wachowiak, M. and Shipley, M. T., 2006 for detailed review). In addition, glomeruli are delineated by a large population of peri- and juxtaglomerular cells.

The OSN axons penetrate a glomerulus at the top, predominately from the ONLi, although many examples are found of single axons or very small fascicles of two to five axons that enter from a variety of tangents (Treloar, H. B. *et al.*, 2002) including the EPL (see below). Within the glomerulus, each axon arborizes to generate 10–12 branches, each of which ends in a terminal bouton (Klenoff, J. R. and Greer, C. A., 1998). The OSN axons within the glomerulus also characteristically have varicosities along their length. Both the varicosities and terminal boutons establish synapses with the dendrites of the projection neurons, mitral and tufted cells, and interneurons, the peri/juxtaglomerular cells (Kasowski, H. J. *et al.*, 1999).

A hallmark of glomerular organization is the specificity with which a subset of axons coalesce within a specific glomerulus. As noted above, while all of the OSNs expressing a specific OR are broadly distributed across a restricted zone in the epithelium, after their axons reach the olfactory bulb, they defasciculate and reorganize into fascicles targeted for a specific region of the bulb (i.e., caudal–medial). The refinement of fascicles into more homogeneous collections of axons that express the same OR occurs when the axons are proximal to the glomerulus, predominately within the ONLi. While early in development there is evidence

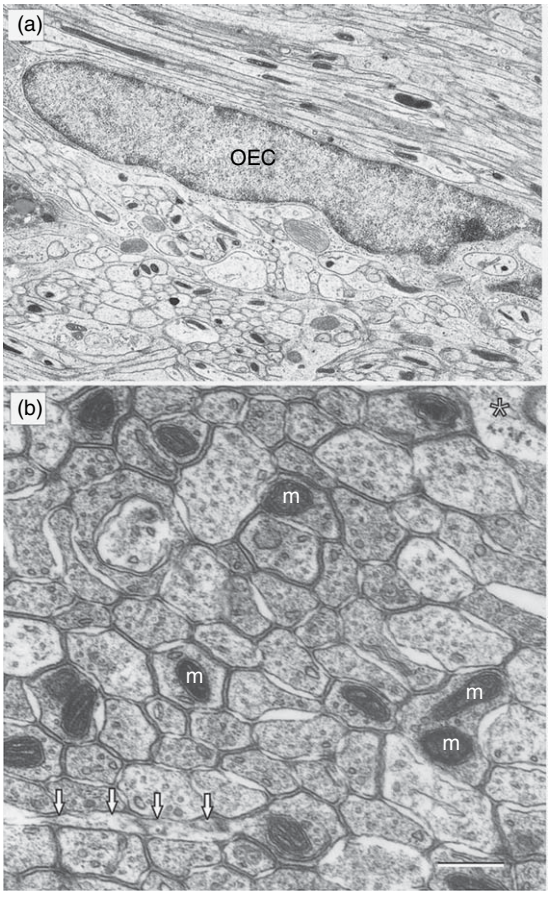

Figure 2 Electron micrographs from the olfactory nerve layer of the olfactory bulb. (a) Low magnification showing both longitudinally and transversely sectioned olfactory sensory neuron axons in the nerve layer. The nucleus (OEC) and some of the surrounding cytoplasm of an olfactory ensheathing cell is in the center of the image. Note that processes extending from the ensheathing cells surround bundles of the axons to form fascicles. (b) Higher magnification of a subset of olfactory sensory neuron axons. Ensheathing cell process (* and arrows) distribute among the axons. The fine structure of the axons includes mitochondria (m) as well as micro- and neurotubules. There is some variability in cross-sectional diameter, but the mean diameter of the olfactory sensory axons approximates 0.2 μm. OEC, olfactory ensheathing cell; m, mitochondria. Calibration bar (shown in b), 1.5 μm in (a) and 0.2 μm in (b).

of heterogeneous OSN axons terminating in the same glomerulus (Zou, D. J. *et al.*, 2004), in the adult all of the axons synapsing within a glomerulus express the same OR (Treloar, H. B. *et al.*, 2002). The specificity and potential mechanisms that influence the coalescence of molecularly homogeneous OSN axons are discussed elsewhere in this volume but may include functional activity as well as adhesion mediated via the expression of ORs in both the axon and growth cone (Feinstein, P. and Mombaerts, P., 2004; Imai, T. *et al.*, 2006; Serizawa, S. *et al.*, 2006).

The interior of the glomerulus contains three primary elements: (1) the arborized axons of the OSNs; (2) the arborized dendritic processes of the projection neurons and glomerular layer neurons; and (3) the processes of glia cells. The interior of the glomerulus is free of cell bodies; rather, both the glia cell and peri/juxtaglomerular cell bodies help to define the perimeter of the glomerulus. At the ultrastructural level, two primary compartments can be identified within the glomerulus (Kasowski, H. J. *et al.*, 1999; Schoppa, N. E. and Westbrook, G. L., 2001). The first contains bundles of dendrites with no or few axons. The second contains numerous axonal boutons and scattered dendritic processes. As will be noted below, local circuit dendrodendritic synapses occur predominately within the dendritic compartment of the glomerulus, while the axodendritic synapses from the OSNs are found predominately within the axonal compartment. Between the intraglomerular compartments, the thin processes of glia cells contribute to segregation and isolation of synaptic circuits. The organization of synapses within the glomerulus will be discussed further below.

4.36.3.3 External Plexiform Layer

The EPL contains scattered populations of cell bodies, including tufted cells and short axon cells, but it is predominately an area of complex neuropil. The apical dendritic processes of projection neurons extend unbranched through the EPL as they target glomeruli where they arborize. In contrast, the secondary dendritic process of the projection neurons extend laterally very broadly in the EPL, in some cases through two-third of the circumference of the olfactory bulb (Mori, K. *et al.*, 1981). The secondary dendrites exhibit some branching, but it appears limited to no more than third or fourth order (Macrides, F. and Schneider, S. P., 1982; Mori, K. *et al.*, 1983; Orona, E. *et al.*, 1984). Also arborizing here are the dendritic processes of the main population of interneurons in the olfactory bulb, the granule cells. The spiny dendrites of these interneurons establish reciprocal dendrodendritic synapses with the secondary dendrites of the projection neurons.

4.36.3.4 Mitral Cell Layer

The mitral cell layer includes the somata of the primary population of projection neurons in the olfactory bulb, the mitral cells. The mitral cells constitute a monolayer in the olfactory bulb, or a sheet that is roughly the thickness of a single mitral cell soma. Additionally, scattered throughout the mitral cell layer are the somata of numerous granule cells. In fact, granule cells make up the majority of cells with somata in the mitral cell layer (Frazier, L. L. and Brunjes, P. C., 1988; Imamura, F. *et al.*, 2006).

4.36.3.5 Internal Plexiform Layer

The IPL includes the axons of projection neurons that will later coalesce to form the lateral olfactory tract, projecting to olfactory cortical targets. The IPL also includes the axons of intrabulbar cells from the juxtaglomerular region that appear to contact homotypic regions on the opposite side of the olfactory bulb (Liu, W. L. and Shipley, M. T., 1994; Belluscio, L. *et al.*, 2002).

4.36.3.6 Granule Cell Layer

The granule cell layer includes organized islets of granule cell somata whose dendrites project into the EPL. Coursing between the islets of granule cells are the axons from the projection neurons that are moving toward the caudal–ventral–lateral aspect of the olfactory bulb where they join to form the lateral olfactory tract. As will be discussed further below, the granule cell layer can be divided into superficial, deep, and intermediate granule cell populations.

4.36.3.7 Subependymal Zone – Rostral Migratory Stream

The innermost region of the olfactory bulb is alternatively identified as a residual of the ventricular extension present during early development, the subependymal zone, or as the terminal region of the rostral migratory stream, the path of migrating neuroblasts, which form new olfactory bulb interneurons in the adult. The rostral migratory stream appears well defined and compact at the caudal pole of the olfactory bulb, as it extends from the olfactory

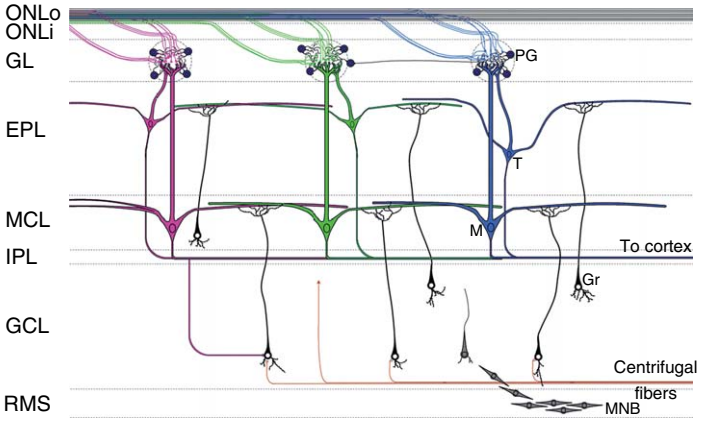

Figure 3 Schematic of the primary cellular organization of the olfactory bulb. Subpopulations of axons, shown in magenta, green, and blue, innervate specific glomeruli based on odor receptor expression. The apical dendritic processes of the projection neurons, mitral, and tufted cells arborize within the glomerulus, as do the dendritic processes of the periglomerular cells. The other primary population of interneurons, granule cells, have their somata located in the granule cell layer and an apical spiny dendrite that arborizes in the external plexiform layer. Axons of periglomerular cells mediate interglomerular actions, while centrifugal axons distribute across the olfactory bulb laminae. ONLo, outer olfactory nerve layer; ONLi, inner olfactory nerve layer; GL, glomerular layer; EPL, external plexiform layer; MCL, mitral cell layer; IPL, internal plexiform layer; GCL, granule cell layer; RMS, rostral migratory stream; PG, periglomerular cell; T, tufted cell; M, mitral cell, Gr, granule cell; MNB, migrating neuroblast.

peduncle, but becomes widely dispersed and indistinct in the rostral pole of the olfactory bulb (Figure 3).

4.36.4 Olfactory Bulb – Cell Populations

4.36.4.1 Projection Neurons

4.36.4.1.1 Mitral cells

Mitral cells are the most prominent population of projection neurons. Their cell bodies, 20–25 μm in diameter, are located in a monolayer, the mitral cell layer. A single apical dendrite (there are some exceptions to this rule) extends from the mitral cell to a single glomerulus where it arborizes extensively including fifth- and sixth-order branches (Price, J. L. and Powell, T. P., 1970c). The numbers are somewhat variable, but approximately 25 mitral cells terminate in each of the 2000 glomeruli found in the mouse olfactory bulb (Royet, J. P. *et al.*, 1998). Also extending from the mitral cell are secondary dendrites that remain restricted to the EPL and can continue for up to two-third of the circumference of the olfactory bulb (Mori, K. *et al.*, 1981). Of interest, the secondary dendrites of mitral cells appear to remain restricted to the deepest portion of the EPL, proximal to the mitral cell layer (Mori, K. *et al.*, 1983; Orona, E. *et al.*, 1984). An axon extends from the basal pole of the mitral cell and joins other axons in the deeper IPL. Myelination occurs quickly, most likely within the IPL. Collateral branches of mitral cell axons appear to extend up into the EPL (Ramon, Y. and Cajal, S., 1911), though the evidence for this is sometimes conflicting (Kishi, K. *et al.*, 1984; Orona, E. *et al.*, 1984). The major axon branches continue on toward the caudal–ventral–lateral aspect of the olfactory bulb where they form the lateral olfactory tract. The axons of the mitral cells distribute broadly throughout olfactory cortical structures.

4.36.4.1.2 Tufted cells

The second population of projection neurons are tufted cells whose diameter is only slightly less than that of mitral cells, approximately 20 μm. Tufted cells are located both proximal to the mitral cell layer (deep tufted cells) and midway in the EPL (middle tufted cells). There is also a population of external tufted cells that are included in the juxtaglomerular population of cells (Pinching, A. J. and Powell, T. P., 1971c), but these appear to have their axons restricted to intrabulbar circuits (Liu, W. L. and Shipley, M. T., 1994; Belluscio, L. *et al.*, 2002). The apical dendrites of the middle and deep tufted cells behave similarly to those of mitral cells – extensive arborization within a single glomerulus. The secondary dendrites, however, differ in that they remain restricted to the most superficial portion of

the EPL, proximal to the glomerular layer (Macrides, F. and Schneider, S. P., 1982; Mori, K. *et al.*, 1983; Orona, E. *et al.*, 1984). The differential distribution of the secondary dendrites of mitral and tufted cells, in the deep and superficial EPL, respectively, coupled with subpopulations of granule cells discussed below, lends credibility to the notion that the mitral and tufted cells may mediate parallel circuits for processing odor information. The axons of the middle and deep tufted cells, like those of the mitral cells, are myelinated, collect initially in the IPL, and then coalesce with the formation of the lateral olfactory tract. Their cortical targets appear to differ from those of mitral cells, with the tufted cells restricted to the most rostral regions of olfactory cortex and the more medial olfactory tubercle (Haberly, L. B. and Price, J. L., 1977).

4.36.4.2 Interneurons

As has been reviewed by a number of authors, there is an almost bewildering array of interneurons found in the olfactory bulb (Schneider, S. P. and Macrides, F., 1978; Shipley, M. T. and Ennis, M., 1996; Shepherd, G. M. *et al.*, 2004; Wachowiak, M. and Shipley, M. T., 2006). Those discussed below represent the major populations whose connectivity and functional properties are best understood.

4.36.4.2.1 Periglomerular cells

The largest population of glomerular layer interneurons are the periglomerular cells. As suggested by their name, the cell bodies, 6–8 μm in diameter, surround and define individual glomeruli. They have brushy and highly branched dendritic processes, often including spine-like extensions. The dendritic process typically arborizes in a single glomerulus, although exceptions in which two or more glomeruli are innervated by separate arbors from a single cell are sometimes seen (Pinching, A. J. and Powell, T. P., 1971c). The axons of periglomerular cells can extend for three to six glomeruli distant from the somata and often branch (Pinching, A. J. and Powell, T. P., 1972; Wachowiak, M. and Shipley, M. T., 2006 for review). The target regions of the periglomerular axons are not always evident, but appear to include extraglomerular apical trunks of projection neurons as well as other periglomerular cells (Pinching, A. J. and Powell, T. P., 1971b). In recent years, it has become increasingly clear that the periglomerular cells may be further subdivided into several subpopulations based on their molecular phenotype and synaptic connections (Kosaka, K. and Kosaka, T., 2005a; Whitman , M. C. and Greer, C. A., 2007).

4.36.4.2.2 External tufted cells

External tufted cells, found predominately at the glomerular layer, EPL border, are slightly larger than the periglomerular cells, approximately 12–15 μm in diameter, with a cell body that is generally elliptical. An apical dendritic process runs parallel to the glomerular layer until it enters and arborizes in a single glomerulus. A secondary dendrite, much shorter than those encountered in mitral or the deep and middle tufted cells (Macrides, F. and Schneider, S. P., 1982), runs parallel and proximal to the glomerular layer. The axons of the external tufted cells extend through the EPL and into the IPL where they travel to a homotypic site on the opposite side of the olfactory bulb (Liu, W. L. and Shipley, M. T., 1994). The external tufted cells may provide a functional link between the two complementary regions in each half of the olfactory bulb that receive the same odor information (Belluscio, L. *et al.*, 2002).

4.36.4.2.3 Short axon cells

Short axon cells in the glomerular layer, located proximal to the nerve layer, are the rarest glomerular layer interneurons. They are slightly larger than periglomerular cells, 8–12 μm in diameter, and have a dendritic arbor that appears to surround the glomeruli, rather than densely innervating them as is seen with the periglomerular cells. Their axons, like those of the periglomerular cells, remain restricted to the juxtaglomerular region. Recent evidence suggests that this may contribute to circuits that include the external tufted cells and periglomerular cells of distant glomeruli.

4.36.4.2.4 Van Gehuchten cells

Short axon cells, Van Gehuchten cells (Schneider, S. P. and Macrides, F., 1978), are the predominate interneurons found in the EPL, and even these are relatively rare. They have a limited dendritic arbor within the EPL and axonal branches that distribute within both the EPL and mitral cell layer where they are thought to contact tufted and mitral cells, respectively.

4.36.4.2.5 Blanes cells

Blanes cells, first described at the end of the nineteenth century (Blanes, T., 1898), have remained largely unknown until recent data suggested they

may interact with olfactory bulb granule cells (Pressler, R. T. and Strowbridge, B. W., 2006). Blanes cells are found throughout the granule cell layer of the olfactory bulb. They have an extensive arborization of spiny dendrites that remain restricted to the granule cell layer. Blanes cell axons remain local with the granule cell layer and are believed to contact the basal dendrites or somata of granule cells. With a cell diameter of approximately 15 μm, Blanes cells are easily distinguished from granule cells.

4.36.4.2.6 Granule cells

The granule cell layer is distinctive due to the arrangement of granule cell somata into rows or islets. Granule cells are small, 8–10 μm in diameter. They have a well-developed apical dendrite that extends into the EPL where it arborizes and becomes heavily invested with dendritic spines. A smaller less arborized basal dendrite is also present that remains restricted to the granule cell layer. Of perhaps greatest interest, the olfactory bulb granule cells are anaxonic; they do not develop an axon (Price, J. L. and Powell, T. P., 1970a). All of the synaptic input and output functions occur via the dendrites. The dendritic spines, also known as gemmules, of the granule cell are somewhat unusual in both receiving and making synapses. Contiguous compartments within the spine are specialized for efferent or afferent function (Rall, W. *et al.*, 1966; Price, J. L. and Powell, T. P., 1970b). In addition, the spine necks are often quite long (>5 μm), and the major axes of the spine head can exceed 2 μm × 5 μm (Woolf, T. B. *et al.*, 1991a; 1991b). The distribution/density of spines is highest throughout the arbor in the EPL, with only an occasional spine seen in the ascending apical dendritic trunk (Price, J. L. and Powell, T. P., 1970a). Granule cells can be divided into at least three subpopulations: (1) those whose cell bodies are located deep within the granule cell layer and whose apical dendritic arbor is limited to the deep EPL, proximal to the mitral cell layer; (2) those whose cell bodies are located more superficially in the granule cell layer and whose dendrites extend unbranched through the deep EPL until they reach the superficial EPL where they arborize extensively; and (3) those whose apical dendrites arborize within both the superficial and deep EPL (Mori, K. *et al.*, 1983; Orona, E. *et al.*, 1983; Greer, C. A., 1987; Imamura, F. *et al.*, 2006). Recalling the differential distribution of the secondary dendrites of mitral and tufted cells (Mori, K. *et al.*, 1983), the organization of the granule cell dendrites suggest that deep granule cells may interact preferentially with mitral cell dendrites while the superficial granule cells interact preferentially with tufted cell dendrites. Other populations of interneurons, such as Blanes cells, Henson's cells and short axon Golgi cells are also found in the granule cell layer but occur at a low frequency and are not as well characterized (Price, J. L. and Powell, T. P., 1970c; Schneider, S. P. and Macrides, F., 1978).

4.36.4.3 Glia

Beginning in the nerve layer, a distinct population of glia are identified, the OEC/glia. These have thin processes that wrap fascicles of OSN axons, beginning deep to the basal lamina in the OE and continuing up to the olfactory bulb glomeruli (Doucette, R., 1991; 1993; Au, W. W. *et al.*, 2002). Several lines of evidence suggest that the olfactory ensheathing glia may contribute to the ability of the OSN axons to successfully extend and innervate glomeruli throughout life (Doucette, R., 1990). Of further interest, the olfactory ensheathing glia have captured the interest of laboratories working on problems such as spinal cord injury where transplants of glia purified from the olfactory nerve appear to promote and improve recovery following injury (Ramon-Cueto, A. *et al.*, 1998; Bartolomei, J. C. and Greer, C. A., 2000).

The shells of the glomeruli are formed, in part, by astrocytes that surround and delineate the surface (Bailey, M. S. and Shipley, M. T., 1993; Chang, C. Y. *et al.*, 2003). Processes extending from their cell bodies distribute within the glomeruli and contribute to the segregation of the axonal and dendritic synaptic compartments (Chao, T. I. *et al.*, 1997).

The EPL, mitral cell layer, and granule cell layer have small populations of astrocytes. It is of interest to point out that many of the synapses within the EPL lack the tight glia wrapping seen elsewhere in the nervous system (Bailey, M. S. and Shipley, M. T., 1993). The rostral migratory stream, however, particularly at the more caudal pole of the olfactory bulb, is defined in part by a compact population of astrocytes that surround and closely interdigitate with the migrating neuroblasts. Much remains to be learned about the properties of this population of glia, but they do appear to contribute to both the migratory dynamics of the neuroblasts and their topographically restricted path (Lois, C. *et al.*, 1996) (Figure 4).

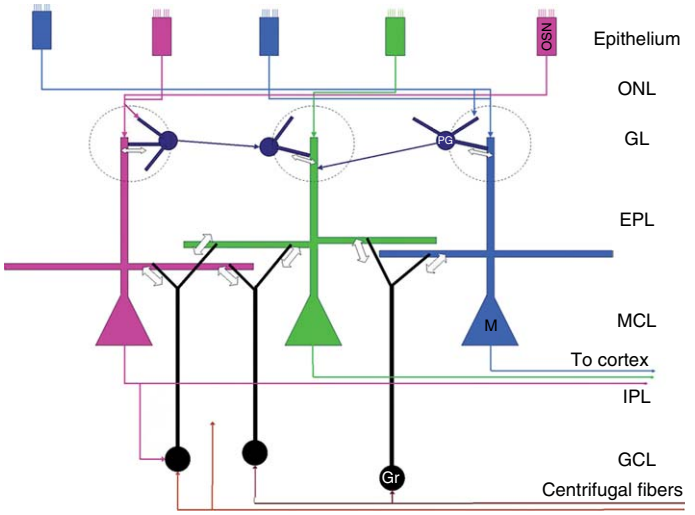

Figure 4 Schematic illustrating primary synaptic interactions in the olfactory bulb. After sorting into specific glomeruli, the axons of the olfactory sensory neurons make excitatory synapses onto the apical dendrites of the projection neurons, mitral, and tufted cells, as well as onto the periglomerular cell dendrites. Intraglomerular circuits also include reciprocal dendrodendritic synapses between the mitral/tufted cell dendrites and the periglomerular cell dendrites. Periglomerular cells can also influence activity in neighboring glomeruli by axodendritic synapses onto mitral/tufted cells and other periglomerular cells. In the external plexiform layer, spiny granule cell dendrites establish reciprocal dendrodendritic synapses with the secondary or lateral dendrites of mitral/tufted cells. Centrifugal axons terminate heavily in the granule cell layer as well as in the external plexiform and glomerular layers of the olfactory bulb. OSN, olfactory sensory neuron; PG, periglomerular cell, M, mitral cell; Gr, granule cell. Arrows indicate the polarity of the synapses – unidirectional or bidirectional.

4.36.5 Olfactory Bulb – Synaptic Organization

4.36.5.1 Glomerular Layer

Our models of synaptic organization in the glomerular layer are becoming increasingly complex as new tools are applied that distinguish between subpopulations of juxtaglomerular neurons and the distribution of their axons and dendritic processes (Chen, W. R. and Shepherd, G. M., 2006; Wachowiak, M. and Shipley, M. T., 2006). Many questions regarding the specificity of synapses within and between glomeruli remain unanswered. The synaptic organization discussed below reflects our current understanding of the basic model for which most information has been compiled.

As was noted earlier, the neuropil of the glomeruli can be divided into two distinct compartments: (1) the axonal compartment which contains the terminal boutons of the OSN axons and scattered dendritic processes; and (2) the dendritic compartment which contains bundles of closely apposed dendrites. This segregation is the foundation for the isolation of primary afferent versus local circuit synapses in the glomerulus (Schild, D. and Riedel, H., 1992; Kasowski, H. J. *et al.*, 1999) (Figure 5).

The axons of the OSNs do not branch until they innervate a glomerulus. As they enter the glomerulus, primarily at the boundary of the ONL and glomerular layer, the axons are tightly bundled but within the glomerular neuropil they separate and arborize (Pinching, A. J. and Powell, T. P., 1971a). Each axon establishes only a limited number of synapses; usually no more than 10–15 Gray Type I asymmetrical synapses with the dendrites of projection neurons or interneurons. The OSN axon specializations include both *en passant* varicosities and terminal boutons. Both specializations are filled with many small spherical vesicles, characteristic of glutamate, and often appear quite electron dense. Single dendritic processes are often seen surrounded by multiple OSN axon boutons, each of which is making a synapse. Although the distribution of the terminal boutons and *en passant* specialization of the axons is spatially restricted within the glomerulus, it is not known if their synapses converge onto the dendrites of the same cell or diverge and broadly synapse with the dendrites of many cells. Of interest, the axodendritic synapses from the OSN axons are found predominately toward the thinner tips/branches of the dendrites within the glomerulus (Pinching, A. J. and Powell, T. P., 1971a; Shepherd, G. M., 1972).

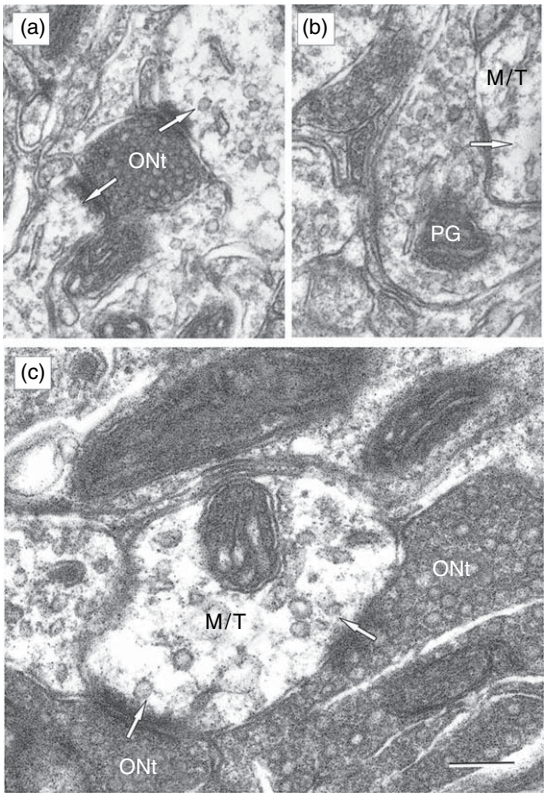

Figure 5 Electron micrographs of the primary synaptic appositions in the glomeruli of the olfactory bulb. In (a) and (c) olfactory sensory axon terminal boutons (ONt) are seen making asymmetrical synapses onto pale dendrites tentatively identified as mitral/tufted (M/T). The ONt is characterized by its electron dense appearance and clustering many small spherical vesicles adjacent to the presynaptic membrane. The target dendrite is recognized by the asymmetrical thickening of the postsynaptic membrane. In (b) a periglomerular cell (PG) is seen making a symmetrical synapse on an M/T dendrite. The PG dendrite has slightly elliptically shaped vesicles, and the pre- and postsynaptic membrane are symmetrical. Arrows indicate the polarity of the synapses. ONt, olfactory sensory axon terminal bouton; PG, periglomerular cell dendrite; M/T, mitral/tufted cell dendrite. Calibration bar (shown in c), 160 nm in (a) and 200 nm in (b) and (c).

Within the dendritic compartment of the glomerulus, the tightly bundled dendrites of the projection neurons and periglomerular cells establish reciprocal dendrodendritic synapses. The excitatory Gray Type I dendritic synapse is characterized by a small collection of spherical vesicles closely apposed to the dendritic membrane of a mitral or tufted cell. The apposed process, a periglomerular cell dendrite, has a thick postsynaptic specialization. Although the reciprocal synapse from the periglomerular cell to the mitral/tufted cell is occasionally seen in the same plane of section, it is much more common for them to be separated and recognized as reciprocal connections only following serial sectioning and reconstruction. The periglomerular synapse can be found in both spine-like processes or in the shafts of periglomerular cell dendrites. The inhibitory Gray Type II synapse from the periglomerular cell dendrite to the mitral/tufted cell dendrite includes a collection of vesicles, often elliptical in shape and adjacent to the presynaptic membrane. The specialization on the postsynaptic membrane is a thickening symmetrical to that seen on the presynaptic membrane. In contrast to the location of the primary afferent axodendritic synapses on the finer terminal branches of the dendrites, the Gray Type II synapses are most often found on larger trunks and at branch points (Pinching, A. J. and Powell, T. P., 1971a; Shepherd, G. M., 1972). This is consistent with the spatial distribution of excitatory and inhibitory synapses described in cortex and suggests that the inhibitory synapse can function as a gatekeeper that modulates excitatory inputs.

Recent evidence suggests that external tufted cells and glomerular layer short axon cells may also contribute to dynamic regulation of center-surround inhibition among glomeruli (Aungst, J. L. *et al.*, 2003). The short axon cells are believed to influence glomeruli up to 500 µm distant. Activation of the short axon cells occurs via a direct input of the OSN axons onto external tufted cells which, in turn, excite the short axon cells. While the full details of this and other glomerular circuits remain to be established, it is clear that the glomerular layer includes the circuitry for complex processing and integration of odor stimuli.

The terminals of centrifugal axons are also found in both the glomerular neuropil and juxtaglomerular space. These arise from several sources including the anterior olfactory nucleus, horizontal limb of the diagonal band, the raphe nucleus, and the locus coeruleus. While it is evident that these circuits help to modify intraglomerular information processing, their full nature has yet to be resolved (e.g., Wachowiak, M. and Shipley, M. T., 2006).

4.36.5.2 External Plexiform Layer

The EPL is the site of the most well-studied reciprocal dendrodendritic synapse in the mammalian nervous system: the mitral/tufted granule cell dendritic spine synapse (Hirata, Y., 1964; Andres, K. H., 1965; Rall, W. *et al.*, 1966; Landis, D. M. *et al.*, 1974;

Jackowski, A. *et al*., 1978). The basic features are similar to those described about for the glomerular local circuits but, in the EPL the reciprocal synapse can often be seen in a single plane since the specialization is restricted to the granule cell spine (gemmule). The secondary dendrites of mitral/tufted cells can be quite large (>4 μm in cross section), and the clusters of spherical vesicles associated with the presynaptic specialization of the Gray Type I synapse often appear quite isolated. At the level of the electron microscope, there are no obvious structural determinants that regulate the clustering of vesicles, although recent evidence shows that vesicle-associated proteins regulating clustering, mobilization, and recycling are present in these presynaptic dendrites (Greer laboratory, unpublished observations). The apposed granule cell spine has an asymmetric thickening immediately opposite the clustering of vesicles within the mitral/tufted cell dendrite (Figure 6).

The granule cell spine, in addition to the asymmetric postsynaptic membrane specialization, appears somewhat unique. It is filled with a large cluster of elliptical vesicles that are closely apposed to the symmetrical membrane thickenings characteristic of the Gray Type II synapse. Often the transition in the structure of the membrane between the asymmetrical postsynaptic thickening and the presynaptic symmetrical thickening is abrupt; the two specializations do not always appear to be separated by nonspecialized membrane leading to speculation about the independence of these two synapses. The granule cell dendritic spine, as was noted earlier, often has a very thin and long neck. Nevertheless, mitochondria can be

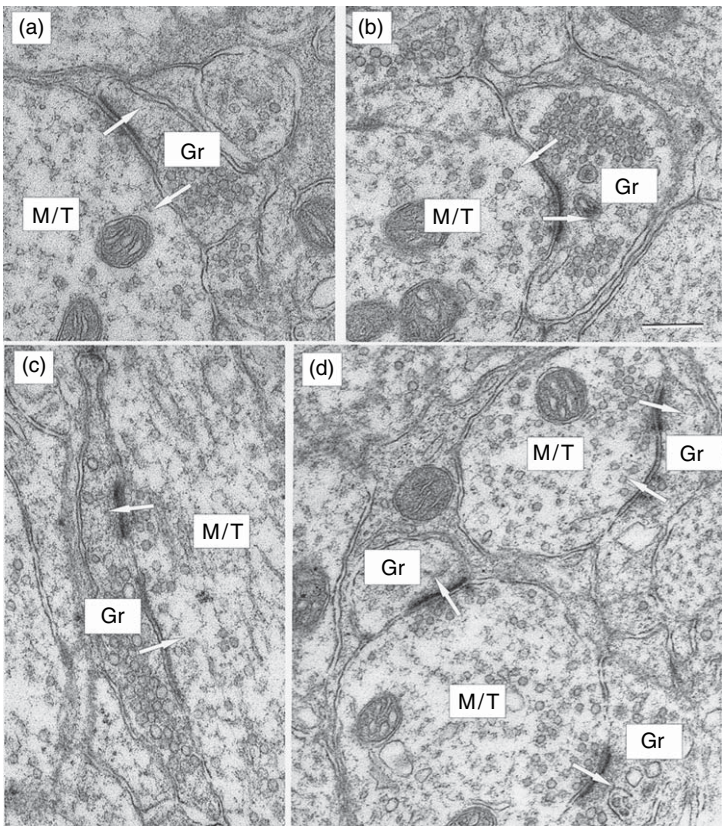

Figure 6 Electron micrographs of the reciprocal dendrodendritic synapses in the external plexiform layer of the olfactory bulb. In (a)–(d), examples of reciprocal dendrodendritic synapses between mitral/tufted (M/T) dendrites and granule cell spines (Gr) are shown. The asymmetrical synapse from the M/T to the Gr is characterized by a smaller collection of vesicles adjacent to the presynaptic membrane of the M/T dendrite and an asymmetrical thick postsynaptic specialization on the Gr membrane. The reciprocal symmetrical synapse is characterized by a larger collection of elliptical or heterogeneous vesicles and a symmetrical thickening of the pre- and postsynaptic membranes. Arrows indicate the polarity of the synapses. M/T, mitral/tufted cell dendrite; Gr, granule cell spine. Calibration bar (shown in b), 200 nm.

found extending from the parent dendrite into the spine head, as does smooth endoplasmic reticulum (Cameron, H. A. *et al.*, 1991; Woolf, T. B. *et al.*, 1991a). Reports of free and polyribosome clusters are also common. As was found for the mitral/tufted cell dendrites, the granule cell spines exhibit an array of vesicle-associated proteins consistent with the role as a presynaptic compartment. Given the immediate proximity of the reciprocal synapses found in the EPL, one can argue that this is the smallest microcircuit found in the nervous system.

4.36.5.3 Mitral Cell Layer

The ascending dendrites of granule cells also establish somatodendritic synapses with mitral cell bodies in the mitral cell layer. The features of these appear indistinguishable from those described above for the dendrodendritic synapses. Although it seems reasonable that tufted cell bodies may also be involved in somatodendritic synapses with granule cells in the EPL, none have been described.

4.36.5.4 Internal Plexiform Layer

Immunohistochemical and electron microscopy studies suggest that the collaterals of external tufted cells make synapses onto the ascending dendrites of granule cells within the IPL (Liu, W. L. and Shipley, M. T., 1994). More recent studies suggest that these connections are topographically organized so that the glomeruli on the opposite sides of the olfactory bulb that receive input from the same OR are synaptically linked via the external tufted cell circuit (Belluscio, L. *et al.*, 2002; Lodovichi, C. *et al.*, 2003; Marks, C. A. *et al.*, 2006).

4.36.5.5 Granule Cell Layer

The basal dendrites of the granule cells in the granule cell layer receive synaptic input from a variety of sources (Price, J. L. and Powell, T. P., 1970a). Axon collaterals from mitral and tufted cells form asymmetric synapses on granule cell basal dendrites as do axons from the anterior olfactory nucleus, anterior commissure, olfactory cortex, horizontal limb of the diagonal band (Carson, K. A., 1984; Shipley, M. T. and Adamek, G. D., 1984), the locus coeruleus (McLean, J. H. *et al.*, 1989; McLean, J. H. and Shipley, M. T., 1991), and the raphe nucleus (McLean, J. H. and Shipley, M. T., 1987). While their specific functions and role in modulating information processing in the olfactory bulb are not entirely clear, it is evident that the synaptic actions of these circuits will activate the granule cells and, in turn, their dendrodendritic circuits within the EPL. Thus, as is typical of most sensory systems, centrifugal and feedback circuits contribute to the flow of information through the olfactory bulb.

4.36.5.6 Electrical Synapses in the Olfactory Bulb

Gap junctions were long known to be the structural correlates of electrical coupling between cells (Rash, J. E. *et al.*, 1998); however, accumulating evidence that electrical coupling can confer unique properties to neural circuits has lately increased the interest in their distribution and properties (Rela, L. and Szczupak, L., 2004). As in other regions of the brain, gap junctions have been found in the olfactory bulb. In the ONL, gap junctions are abundant in the olfactory ensheathing glia, but seem to be absent from OSN axons (Rash, J. E. *et al.*, 2005). Within glomeruli, gap junctions are found between mitral/tufted dendrites, as well as between mitral/tufted cell dendrites and periglomerular cell dendrites, perhaps complementing the reciprocal dendrodendritic synapses (Pinching, A. J. and Powell, T. P., 1971b; Christie, J. M. *et al.*, 2005; Kosaka, T. and Kosaka, K., 2005b; Rash, J. E. *et al.*, 2005). Consistent with an interaction between chemical and electrical synapses, in the EPL examples of mixed synapses that include both gap junctions and conventional dendrodendritic synapses are reported between mitral/tufted cell secondary dendrites and granule cell spines. In the mitral cell layer, somatodendritic synapses between mitral and granule cells may also involve a combination of chemical and electrical components, as suggested by the identification of structures compatible with gap junctions in mitral/tufted cell perikarya (Miragall, F. *et al.*, 1996). Finally, gap junction coupling between granule cell bodies represents a plausible mechanism to synchronize the activity of clusters of these inhibitory interneurons (Reyher, C. K. *et al.*, 1991; Gibson, J. R. *et al.*, 1999; Galarreta, M. and Hestrin, S., 2001).

4.36.6 Lateral Olfactory Tract and Olfactory Cortex

The lateral olfactory tract forms at the caudal–lateral–ventral aspect of the olfactory bulb with the

coalescence of mitral and tufted cell axons following their passage through the IPL and islets of granule cells. Because the axons are myelinated, in gross dissection the tract appears white. As the tract proceeds caudally, it moves to a more ventral position. Within the tract, the myelinated profiles of the projection neuron axons have a bimodal distribution for cross-sectional diameter. The larger profiles (~1.42 μm) are believed to arise from mitral cells while the smaller profiles (~1.14 μm) are axons from the middle and deep tufted cells (Price, J. L. and Sprich, W. W., 1975; Bartolomei, J. C. and Greer, C. A., 2000). In cortex, the axons exit the lateral olfactory tract and enter layer Ia where they make Gray Type I excitatory synapses with the spiny apical dendrites of both layer II and layer III pyramidal cells (Westrum, L. E., 1975; Wouterlood, F. G. and Nederlof, J., 1983; Schwob, J. E. and Price, J. L., 1984). In cortex, the distribution of the projection neuron axons is complex and remains somewhat controversial (Wilson, D. A. *et al.*, 2006). One line of evidence from functional studies suggest that the axons have terminal fields that maintain the molecular specificity of OR input first established at the level of the glomerulus (Zou, Z. *et al.*, 2001; 2005). This is also consistent with recent analyses using pseudorabies virus to characterize olfactory bulb – cortical topography (Willhite, D. C. *et al.*, 2006). Earlier retrograde tracing, however, suggested that axon collaterals of single mitral cells diverged broadly throughout the rostral–caudal extent of cortex (Haberly, L. B. and Price, J. L., 1977; Scott, J. W. *et al.*, 1980; Luskin, M. B. and Price, J. L., 1982; Zou, Z. *et al.*, 2001; Fukushima, N. *et al.*, 2002). Further discussion of the synaptic organization of piriform cortex is beyond the scope of this chapter other than to comment that it is complex and includes feedback circuits both within cortex as well as centrifugals to the ipsilateral olfactory bulb and to the contralateral olfactory pathway via the anterior commissure (de Olmos, J. *et al.*, 1978; Haberly, L. B. and Price, J. L., 1978a; 1978b; Luskin, M. B. and Price, J. L., 1983a; 1983b). New studies will help to clarify the complex relationship between the olfactory bulb and cortex including the organization of the cortically derived centrifugal axons that return to the bulb.

4.36.7 Adult Neurogenesis and the Olfactory Bulb

While it has been recognized for some time that the OSNs turn over and are replaced by a population of basal cells in the OE, the magnitude of adult neurogenesis of olfactory bulb neurons has been recognized relatively recently (Altman, J., 1969; Kaplan, M. S. and Hinds, J. W., 1977; Lois, C. and Alvarez-Buylla, A., 1994). Several excellent reviews are available that summarize our current understanding of neurogenesis within the subventricular zone, the migration of neuroblasts via the rostral migratory stream into the olfactory bulb, and the ensuing differentiation of the migrating cells into granule and periglomerular cells (Alvarez-Buylla, A. and Garcia-Verdugo, J. M., 2002; Lennington, J. B. *et al.*, 2003; Doetsch, F. and Hen, R., 2005; Lledo, P. M. and Saghatelyan, A., 2005; Lledo, P. M. *et al.*, 2006). In the context of the plasticity of olfactory bulb synaptic circuits, many questions remain about the mechanisms influencing cellular loss and replacement among these populations of interneurons and the determinants of newly established synapses (Whitman, M. C. and Greer, C. A., 2007). It may be that the ongoing turnover of these populations of interneurons is a solution to the dynamic and transient nature of odor stimuli – an approach to nervous system plasticity that may function in concert with other mechanisms of synaptic plasticity including long-term potentiation and long-term depression (Figure 7).

4.36.8 Summary

The molecular, cellular, and synaptic organization of the olfactory bulb continue to pose significant challenges in understanding the dynamic nature of this structure and how the organization of the system may contribute to odor coding/processing. The advent of powerful molecular tools toward the end of the twentieth century has resulted in significant new insights into the complex wiring of the olfactory bulb, but many questions remain unanswered. Among the challenges that remain are understanding the developmental events that underlie the specificity of afferent axon convergence as well as the extraordinary precision of local synaptic circuits in the olfactory bulb and their ongoing remodeling.

Acknowledgments

Work from the author's laboratory has been generously supported by grants from NIH-NIDCD and NIH-NIA. The authors express the appreciation to other members of the laboratory for helpful discussions.

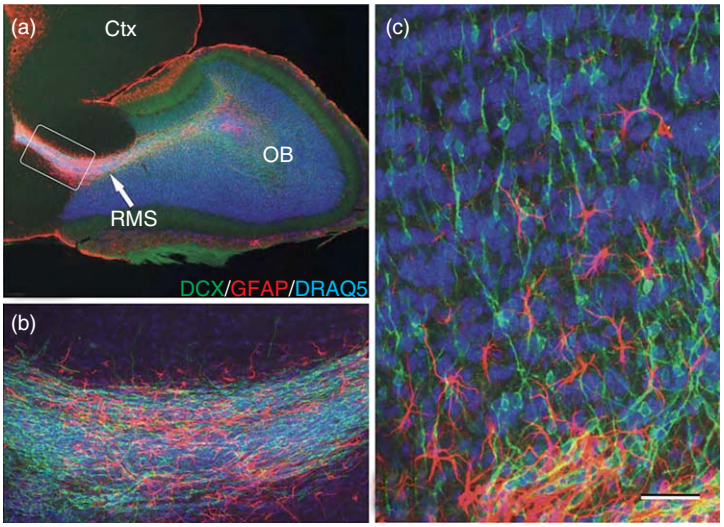

Figure 7 The rostral migratory stream and migrating neurons in the olfactory bulb. In (a), a sagittal section of the rostral brain and olfactory bulb shows the rostral migratory stream (RMS) as it travels from the subventricular zone, through the olfactory peduncle, and into the olfactory bulb. Doublecortin (DCX) staining shows the migrating neuroblasts while staining for glial fibrillary acitic protein (GFAP) shows the glial cells that surround the RMS. DRAQ5 identifies nuclei. In (b), the boxed area in (a) is shown at higher magnification. The density of GFAP-positive glia surrounding the chains of DCX-positive migrating neuroblasts is more apparent. In (c), the DCX-positive cells are exiting the RMS (bottom of image) and beginning to either differentiate as granule cells or migrate to the glomerular layer and differentiate into periglomerular cells. Ctx, cortex; RMS, rostral migratory stream; OB, olfactory bulb. Calibration bar (shown in c), 300 μm in (a); 100 μm in (b); and 40 μm in (c).

References

Altman, J. 1969. Autoradiographic and histological studies of postnatal neurogenesis. IV. Cell proliferation and migration in the anterior forebrain, with special reference to persisting neurogenesis in the olfactory bulb. J. Comp. Neurol. 137, 433–457.

Alvarez-Buylla, A. and Garcia-Verdugo, J. M. 2002. Neurogenesis in adult subventricular zone. J. Neurosci. 22, 629–634.

Andres, K. H. 1965. The fine structure of the olfactory bulb in rats with special reference to the synaptic connections. Z. Zellforsch. Mikrosk. Anat. 65, 530–561.

Au, W. W., Treloar, H. B., and Greer, C. A. 2002. Sublaminar organization of the mouse olfactory bulb nerve layer. J. Comp. Neurol. 446, 68–80.

Aungst, J. L., Heyward, P. M., Puche, A. C., Karnup, S. V., Hayar, A., Szabo, G., and Shipley, M. T. 2003. Centre-surround inhibition among olfactory bulb glomeruli. Nature 426, 623–629.

Bailey, M. S. and Shipley, M. T. 1993. Astrocyte subtypes in the rat olfactory bulb: morphological heterogeneity and differential laminar distribution. J. Comp. Neurol. 328, 501–526.

Bartolomei, J. C. and Greer, C. A. 2000. Olfactory ensheathing cells: bridging the gap in spinal cord injury. Neurosurgery 47, 1057–1069.

Belluscio, L., Lodovichi, C., Feinstein, P., Mombaerts, P., and Katz, L. C. 2002. Odorant receptors instruct functional circuitry in the mouse olfactory bulb. Nature 419, 296–300.

Blanes, T. 1898. Sobre algunos puntos dudoses de la estructuradel bulbo olfatorio. Revta Trimest. Microgr. 3, 99–127.

Buck, L. and Axel, R. 1991. A novel multigene family may encode odorant receptors: a molecular basis for odor recognition. Cell 65, 175–187.

Cameron, H. A., Kaliszewski, C. K., and Greer, C. A. 1991. Organization of mitochondria in olfactory bulb granule cell dendritic spines. Synapse 8, 107–118.

Carson, K. A. 1984. Quantitative localization of neurons projecting to the mouse main olfactory bulb. Brain Res. Bull. 12, 629–634.

Chang, C. Y., Chien, H. F., Jiangshieh, Y. F., and Wu, C. H. 2003. Microglia in the olfactory bulb of rats during postnatal development and olfactory nerve injury with zinc sulfate: a lectin labeling and ultrastrucutural study. Neurosci. Res. 45, 325–333.

Chao, T. I., Kasa, P., and Wolff, J. R. 1997. Distribution of astroglia in glomeruli of the rat main olfactory bulb: exclusion from the sensory subcompartment of neuropil. J. Comp. Neurol. 388, 191–210.

Chen, W. R. and Shepherd, G. M. 2006. The olfactory glomerulus: a cortical module with specific functions. J. Neurocytol. 34, 353–360.

Chess, A., Simon, I., Cedar, H., and Axel, R. 1994. Allelic inactivation regulates olfactory receptor gene expression. Cell 78, 823–834.

Christie, J. M., Bark, C., Hormuzdi, S. G., Helbig, I., Monyer, H., and Westbrook, G. L. 2005. Connexin36 mediates spike synchrony in olfactory bulb glomeruli. Neuron 46, 761–772.

Cuschieri, A. and Bannister, L. H. 1975. The development of the olfactory mucosa in the mouse: electron microscopy. J. Anat. 119, 471–498.

de Olmos, J., Hardy, H., and Heimer, L. 1978. The afferent connections of the main and the accessory olfactory bulb formations in the rat: an experimental HRP-study. J. Comp. Neurol. 181, 213–244.

Doetsch, F. and Hen, R. 2005. Young and excitable: the function of new neurons in the adult mammalian brain. Curr. Opin. Neurobiol. 15, 121–128.

Doucette, J. R. 1984. The glial cells in the nerve fiber layer of the rat olfactory bulb. Anat. Rec. 210, 385–391.

Doucette, R. 1990. Glial influences on axonal growth in the primary olfactory system. Glia 3, 433–449.
Doucette, R. 1991. PNS-CNS transitional zone of the first cranial nerve. J. Comp. Neurol. 312, 451–466.
Doucette, R. 1993. Glial cells in the nerve fiber layer of the main olfactory bulb of embryonic and adult mammals. Microsc. Res. Tech. 24, 113–130.
Feinstein, P. and Mombaerts, P. 2004. A contextual model for axonal sorting into glomeruli in the mouse olfactory system. Cell 117, 817–831.
Frazier, L. L. and Brunjes, P. C. 1988. Unilateral odor deprivation: early postnatal changes in olfactory bulb cell density and number. J. Comp. Neurol. 269, 355–370.
Fukushima, N., Oikawa, S., Yokouchi, K., Kawagishi, K., and Moriizumi, T. 2002. The minimum number of neurons in the central olfactory pathway in relation to its function: a retrograde fiber tracing study. Chem. Senses 27, 1–6.
Galarreta, M. and Hestrin, S. 2001. Electrical synapses between GABA-releasing interneurons. Nat. Rev. Neurosci. 2, 425–433.
Gibson, J. R., Beierlein, M., and Connors, B. W. 1999. Two networks of electrically coupled inhibitory neurons in neocortex. Nature 402, 75–79.
Graziadei, P. P. C. and Monti-Graziadei, G. A. 1978. Continuous Nerve Cell Renewal in the Olfactory System. In: Handbook Sensory Physiology. Development of Sensory Systems (*ed*. M. Jacobson), Vol. IX, pp. 55–83. Springer.
Greer, C. A. 1987. Golgi analyses of dendritic organization among denervated olfactory bulb granule cells. J. Comp. Neurol. 257, 442–452.
Haberly, L. B. and Price, J. L. 1977. The axonal projection patterns of the mitral and tufted cells of the olfactory bulb in the rat. Brain Res. 129, 152–157.
Haberly, L. B. and Price, J. L. 1978a. Association and commissural fiber systems of the olfactory cortex of the rat. II. Systems originating in the olfactory peduncle. J. Comp. Neurol. 181, 781–807.
Haberly, L. B. and Price, J. L. 1978b. Association and commissural fiber systems of the olfactory cortex of the rat. J. Comp. Neurol. 178, 711–740.
Hirata, Y. 1964. Some observations on the fine structure of the synapses in the olfactory bulb of the mouse, with particular reference to the atypical synaptic configurations. Arch. Histol. Jpn. 24, 293–302.
Hisaoka, T., Morikawa, Y., Kitamura, T., and Senba, E. 2004. Expression of a member of tumor necrosis factor receptor superfamily, TROY, in the developing olfactory system. Glia 45, 313–324.
Imai, T., Suzuki, M., and Sakano, H. 2006. Odorant receptor-derived cAMP signals direct axonal targeting. Science 314, 657–661.
Imamura, F., Nagao, H., Naritsuka, H., Murata, Y., Taniguchi, H., and Mori, K. 2006. A leucine-rich repeat membrane protein, 5T4, is expressed by a subtype of granule cells with dendritic arbors in specific strata of the mouse olfactory bulb. J. Comp. Neurol. 495, 754–768.
Iwema, C. L., Fang, H., Kurtz, D. B., Youngentob, S. L., and Schwob, J. E. 2004. Odorant receptor expression patterns are restored in lesion-recovered rat olfactory epithelium. J. Neurosci. 24, 356–369.
Jackowski, A., Parnavelas, J. G., and Lieberman, A. R. 1978. The reciprocal synapse in the external plexiform layer of the mammalian olfactory bulb. Brain Res. 159, 17–28.
Kafitz, K. W. and Greer, C. A. 1999. Olfactory ensheathing cells promote neurite extension from embryonic olfactory receptor cells *in vitro*. Glia 25, 99–110.
Kaplan, M. S. and Hinds, J. W. 1977. Neurogenesis in the adult rat: electron microscopic analysis of light radioautographs. Science 197, 1092–1094.
Kasowski, H. J., Kim, H., and Greer, C. A. 1999. Compartmental organization of the olfactory bulb glomerulus. J. Comp. Neurol. 407, 261–274.
Kishi, K., Mori, K., and Ojima, H. 1984. Distribution of local axon collaterals of mitral, displaced mitral, and tufted cells in the rabbit olfactory bulb. J. Comp. Neurol. 225, 511–526.
Klenoff, J. R. and Greer, C. A. 1998. Postnatal development of olfactory receptor cell axonal arbors. J. Comp. Neurol. 390, 256–267.
Kosaka, K. and Kosaka, T. 2005a. Synaptic organization of the glomerulus in the main olfactory bulb: compartments of the glomerulus and heterogeneity of the periglomerular cells. Anat. Sci. Int. 80, 80–90.
Kosaka, T. and Kosaka, K. 2005b. Intraglomerular dendritic link connected by gap junctions and chemical synapses in the mouse main olfactory bulb: electron microscopic serial section analyses. Neuroscience 131, 611–625.
Landis, D. M., Reese, T. S., and Raviola, E. 1974. Differences in membrane structure between excitatory and inhibitory components of the reciprocal synapse in the olfactory bulb. J. Comp. Neurol. 155, 67–91.
Lennington, J. B., Yang, Z., and Conover, J. C. 2003. Neural stem cells and the regulation of adult neurogenesis. Reprod. Biol. Endocrinol. 1, 99.
Liu, W. L. and Shipley, M. T. 1994. Intrabulbar associational system in the rat olfactory bulb comprises cholecystokinin-containing tufted cells that synapse onto the dendrites of GABAergic granule cells. J. Comp. Neurol. 346, 541–558.
Lledo, P. M. and Saghatelyan, A. 2005. Integrating new neurons into the adult olfactory bulb: joining the network, life–death decisions, and the effects of sensory experience. Trends Neurosci. 28, 248–254.
Lledo, P. M., Alonso, M., and Grubb, M. S. 2006. Adult neurogenesis and functional plasticity in neuronal circuits. Nat. Rev. Neurosci. 7, 179–193.
Lodovichi, C., Belluscio, L., and Katz, L. C. 2003. Functional topography of connections linking mirror-symmetric maps in the mouse olfactory bulb. Neuron 38, 265–276.
Lois, C. and Alvarez-Buylla, A. 1994. Long-distance neuronal migration in the adult mammalian brain. Science 264, 1145–1148.
Lois, C., Garcia-Verdugo, J. M., and Alvarez-Buylla, A. 1996. Chain migration of neuronal precursors. Science 271, 978–981.
Luskin, M. B. and Price, J. L. 1982. The distribution of axon collaterals from the olfactory bulb and the nucleus of the horizontal limb of the diagonal band to the olfactory cortex, demonstrated by double retrograde labeling techniques. J. Comp. Neurol. 209, 249–263.
Luskin, M. B. and Price, J. L. 1983a. The topographic organization of associational fibers of the olfactory system in the rat, including centrifugal fibers to the olfactory bulb. J. Comp. Neurol. 216, 264–291.
Luskin, M. B. and Price, J. L. 1983b. The laminar distribution of intracortical fibers originating in the olfactory cortex of the rat. J. Comp. Neurol. 216, 292–302.
Macrides, F. and Schneider, S. P. 1982. Laminar organization of mitral and tufted cells in the main olfactory bulb of the adult hamster. J. Comp. Neurol. 208, 419–430.
Marks, C. A., Cheng, K., Cummings, D. M., and Belluscio, L. 2006. Activity-dependent plasticity in the olfactory intrabulbar map. J. Neurosci. 26, 11257–11266.
McLean, J. H. and Shipley, M. T. 1987. Serotonergic afferents to the rat olfactory bulb. I. Origins and laminar specificity of serotonergic inputs in the adult rat. J. Neurosci. 7, 3016–3028.
McLean, J. H. and Shipley, M. T. 1991. Postnatal development of the noradrenergic projection from locus coeruleus to the olfactory bulb in the rat. J. Comp. Neurol. 304, 467–477.

McLean, J. H., Shipley, M. T., Nickell, W. T., Aston-Jones, G., and Reyher, C. K. 1989. Chemoanatomical organization of the noradrenergic input from locus coeruleus to the olfactory bulb of the adult rat. J. Comp. Neurol. 285, 339–349.

Miragall, F., Simburger, E., and Dermietzel, R. 1996. Mitral and tufted cells of the mouse olfactory bulb possess gap junctions and express connexin43 mRNA. Neurosci. Lett. 216, 199–202.

Miyamichi, K., Serizawa, S., Kimura, H. M., and Sakano, H. 2005. Continuous and overlapping expression domains of odorant receptor genes in the olfactory epithelium determine the dorsal/ventral positioning of glomeruli in the olfactory bulb. J. Neurosci. 25, 3586–3592.

Mombaerts, P., Wang, F., Dulac, C., Chao, S. K., Nemes, A., Mendelsohn, M., Edmondson, J., and Axel, R. 1996. Visualizing an olfactory sensory map. Cell 87, 675–686.

Mori, K., Kishi, K., and Ojima, H. 1983. Distribution of dendrites of mitral, displaced mitral, tufted, and granule cells in the rabbit olfactory bulb. J. Comp. Neurol. 219, 339–355.

Mori, K., Nowycky, M. C., and Shepherd, G. M. 1981. Electrophysiological analysis of mitral cells in the isolated turtle olfactory bulb. J. Physiol. 314, 281–294.

Newman, M. P., Feron, F., and Mackay-Sim, A. 2000. Growth factor regulation of neurogenesis in adult olfactory epithelium. Neuroscience 99, 343–350.

Orona, E., Rainer, E. C., and Scott, J. W. 1984. Dendritic and axonal organization of mitral and tufted cells in the rat olfactory bulb. J. Comp. Neurol. 226, 346–356.

Orona, E., Scott, J. W., and Rainer, E. C. 1983. Different granule cell populations innervate superficial and deep regions of the external plexiform layer in rat olfactory bulb. J. Comp. Neurol. 217, 227–237.

Pinching, A. J. and Powell, T. P. 1971a. The neuropil of the glomeruli of the olfactory bulb. J. Cell. Sci. 9, 347–377.

Pinching, A. J. and Powell, T. P. 1971b. The neuropil of the periglomerular region of the olfactory bulb. J. Cell. Sci. 9, 379–409.

Pinching, A. J. and Powell, T. P. 1971c. The neuron types of the glomerular layer of the olfactory bulb. J. Cell. Sci. 9, 305–345.

Pinching, A. J. and Powell, T. P. 1972. Experimental studies on the axons intrinsic to the glomerular layer of the olfactory bulb. J. Cell. Sci. 10, 637–655.

Pressler, R. T. and Strowbridge, B. W. 2006. Blanes cells mediate persistent feedforward inhibition onto granule cells in the olfactory bulb. Neuron 49, 889–904.

Price, J. L. and Powell, T. P. 1970a. The morphology of the granule cells of the olfactory bulb. J. Cell Sci. 7, 91–123.

Price, J. L. and Powell, T. P. 1970b. The synaptology of the granule cells of the olfactory bulb. J. Cell Sci. 7, 125–155.

Price, J. L. and Powell, T. P. 1970c. The mitral and short axon cells of the olfactory bulb. J. Cell Sci. 7, 631–651.

Price, J. L. and Sprich, W. W. 1975. Observations on the lateral olfactory tract of the rat. J. Comp. Neurol. 162, 321–336.

Rall, W., Shepherd, G. M., Reese, T. S., and Brightman, M. W. 1966. Dendrodendritic synaptic pathway for inhibition in the olfactory bulb. Exp. Neurol. 14, 44–56.

Ramon-Cueto, A., Plant, G. W., Avila, J., and Bunge, M. B. 1998. Long-distance axonal regeneration in the transected adult rat spinal cord is promoted by olfactory ensheathing glia transplants. J. Neurosci. 18, 3803–3815.

Ramón y Cajal, S. 1911. Histologie du Système Nerveux de l'Homme et des Vertébrés. Paris, Maloine.

Rash, J. E., Davidson, K. G., Kamasawa, N., Yasumura, T., Kamasawa, M., Zhang, C., Michaels, R., Restrepo, D., Ottersen, O. P., Olson, C. O., and Nagy, J. I. 2005. Ultrastructural localization of connexins (Cx36, Cx43, Cx45), glutamate receptors and aquaporin-4 in rodent olfactory mucosa, olfactory nerve and olfactory bulb. J. Neurocytol. 34, 307–341.

Rash, J. E., Yasumura, T., and Dudek, F. E. 1998. Ultrastructure, histological distribution, and freeze-fracture immunocytochemistry of gap junctions in rat brain and spinal cord. Cell Biol. Int. 22, 731–749.

Reyher, C. K., Lubke, J., Larsen, W. J., Hendrix, G. M., Shipley, M. T., and Baumgarten, H. G. 1991. Olfactory bulb granule cell aggregates: morphological evidence for interperikaryal electrotonic coupling via gap junctions. J. Neurosci. 11, 1485–1495.

Rela, L. and Szczupak, L. 2004. Gap junctions: their importance for the dynamics of neural circuits. Mol. Neurobiol. 30, 341–357.

Ressler, K. J., Sullivan, S. L., and Buck, L. B. 1993. A zonal organization of odorant receptor gene expression in the olfactory epithelium. Cell 73, 597–609.

Royet, J. P., Distel, H., Hudson, R., and Gervais, R. 1998. A re-estimation of the number of glomeruli and mitral cells in the olfactory bulb of rabbit. Brain Res. 788, 35–42.

Schild, D. and Riedel, H. 1992. Significance of glomerular compartmentalization for olfactory coding. Biophys. J. 61, 704–715.

Schneider, S. P. and Macrides, F. 1978. Laminar distributions of internuerons in the main olfactory bulb of the adult hamster. Brain Res. Bull. 3, 73–82.

Schoppa, N. E. and Westbrook, G. L. 2001. Glomerulus-specific synchronization of mitral cells in the olfactory bulb. Neuron 31, 639–651.

Schwob, J. E. and Price, J. L. 1984. The development of lamination of afferent fibers to the olfactory cortex in rats, with additional observations in the adult. J. Comp. Neurol. 223, 203–222.

Scott, J. W., McBride, R. L., and Schneider, S. P. 1980. The organization of projections from the olfactory bulb to the piriform cortex and olfactory tubercle in the rat. J. Comp. Neurol. 194, 519–534.

Serizawa, S., Miyamichi, K., Nakatani, H., Suzuki, M., Saito, M., Yoshihara, Y., and Sakano, H. 2003. Negative feedback regulation ensures the one receptor-one olfactory neuron rule in mouse. Science 302, 2088–2094.

Serizawa, S., Miyamichi, K., Takeuchi, H., Yamagishi, Y., Suzuki, M., and Sakano, H. 2006. A neuronal identity code for the odorant receptor-specific and activity-dependent axon sorting. Cell 127, 1057–1069.

Shepherd, G. M. 1972. Synaptic organization of the mammalian olfactory bulb. Physiol. Rev. 52, 864–917.

Shepherd, G. M., Chen, W., and Greer, C. A. 2004. Olfactory Bulb. In: Synaptic Organization of the Brain (*ed*. G. M. Sherpherd), pp. 165–216. Oxford University Press.

Shipley, M. T. and Adamek, G. D. 1984. The connections of the mouse olfactory bulb: a study using orthograde and retrograde transport of wheat germ agglutinin conjugated to horseradish peroxidase. Brain Res. Bull. 12, 669–688.

Shipley, M. T. and Ennis, M. 1996. Functional organization of olfactory system. J. Neurobiol. 30, 123–176.

Treloar, H. B., Feinstein, P., Mombaerts, P., and Greer, C. A. 2002. Specificity of glomerular targeting by olfactory sensory axons. J. Neurosci. 22, 2469–2477.

Vassar, R., Ngai, J., and Axel, R. 1993. Spatial segregation of odorant receptor expression in the mammalian olfactory epithelium. Cell 74, 309–318.

Wachowiak, M. and Shipley, M. T. 2006. Coding and synaptic processing of sensory information in the glomerular layer of the olfactory bulb. Semin. Cell Dev. Biol. 17, 411–423.

Westrum, L. E. 1975. Electron microscopy of synaptic structures in olfactory cortex of early postnatal rats. J. Neurocytol. 4, 713–732.

Whitman, M. C. and Greer, C. A. 2007. Adult-generated neurons exhibit diverse developmental fates. Dev. Neurobiol. 67, 1079–1093.

Willhite, D. C., Nguyen, K. T., Masurkar, A. V., Greer, C. A., Shepherd, G. M., and Chen, W. R. 2006. Viral tracing identifies distributed columnar organization in the olfactory bulb. Proc. Natl. Acad. Sci. U. S. A. 103, 12592–12597.

Wilson, D. A., Kadohisa, M., and Fletcher, M. L. 2006. Cortical contributions to olfaction: plasticity and perception. Semin. Cell Dev. Biol. 17, 462–470.

Woolf, T. B., Shepherd, G. M., and Greer, C. A. 1991a. Serial reconstructions of granule cell spines in the mammalian olfactory bulb. Synapse 7, 181–192.

Woolf, T. B., Shepherd, G. M., and Greer, C. A. 1991b. Local information processing in dendritic trees: subsets of spines in granule cells of the mammalian olfactory bulb. J. Neurosci. 11, 1837–1854.

Wouterlood, F. G. and Nederlof, J. 1983. Terminations of olfactory afferents on layer II and III neurons in the entorhinal area: degeneration-Golgi-electron microscopic study in the rat. Neurosci. Lett. 36, 105–110.

Zou, D. J., Feinstein, P., Rivers, A. L., Mathews, G. A., Kim, A., Greer, C. A., Mombaerts, P., and Firestein, S. 2004. Postnatal refinement of peripheral olfactory projections. Science 304, 1976–1979.

Zou, Z., Li, F., and Buck, L. B. 2005. Odor maps in the olfactory cortex. Proc. Natl. Acad. Sci. U. S. A. 102, 7724–7729.

Zou, Z., Horowitz, L. F., Montmayeur, J. P., Snapper, S., and Buck, L. B. 2001. Genetic tracing reveals a stereotyped sensory map in the olfactory cortex. Nature 414, 173–179.

4.37 Physiology of the Main Olfactory Bulb

M Ennis, University of Tennessee Health Science Center, Memphis, TN, USA

A Hayar, University of Arkansas for Medical Sciences, Little Rock, AR, USA

© 2008 Elsevier Inc. All rights reserved.

4.37.1 Overview of Main Olfactory Bulb Circuitry 642
4.37.1.1 Projections of Olfactory Receptor Neurons to Main Olfactory Bulb 642
4.37.1.2 MOB Circuitry 643
4.37.2 Neurophysiology of the Glomerular Layer 643
4.37.2.1 Neurophysiological Properties of Glomerular Layer Neurons 643
4.37.2.1.1 ET cells 644
4.37.2.1.2 PG cells 647
4.37.2.1.3 SA cells 648
4.37.2.2 Electrophysiology of Intraglomerular Circuitry 648
4.37.2.2.1 Excitatory systems in the GL 648
4.37.2.2.2 Inhibitory systems in the GL 653
4.37.2.3 Electrophysiology of Interglomerular Circuitry 659
4.37.3 Neurophysiology of External Plexiform Layer 659
4.37.3.1 Tufted Cells 659
4.37.3.2 EPL Interneurons 660
4.37.4 Neurophysiology of Mitral Cells 660
4.37.4.1 Anatomical Features 660
4.37.4.2 Spontaneous Discharge and Intrinsic Membrane Properties 660
4.37.4.3 Dendritic Spike Propagation 662
4.37.4.4 Modulation by mGluRs and DA 663
4.37.5 Neurophysiology of Neurons in the Granule Cell Layer 663
4.37.5.1 Neuron Types of the GCL 663
4.37.5.2 Neurophysiology of GCs 664
4.37.5.3 Neurophysiology of Blanes Cells 665
4.37.6 Dendrodendritic Transmission Between Mitral/Tufted Cells and Granule Cells 666
4.37.6.1 Overview of Mitral/Tufted Cell–GC Dendrodendritic Interactions 666
4.37.6.2 Excitatory Transmission from Mitral/Tufted Cells to GCs 666
4.37.6.3 Inhibitory Transmission from GCs to Mitral/Tufted Cells 666
4.37.6.4 Dendrodendritic Inhibition 666
4.37.6.4.1 Self-inhibition 666
4.37.6.4.2 Lateral inhibition 667
4.37.6.4.3 Role of Ca^{2+} influx through *N*-methyl D-aspartate receptors and voltage-dependent Ca^{2+} channels 667
4.37.6.4.4 Local vs. global modes of dendrodendritic inhibition 668
4.37.6.4.5 Temporal modulation of dendrodendritic inhibition 668
4.37.7 Neurophysiology of New, Adult-Born Neurons 668
4.37.8 Neurophysiology of Primary Olfactory Cortical Inputs to Main Olfactory Bulb 668
4.37.9 Oscillations and Synchrony in Main Olfactory Bulb 669
4.37.9.1 Oscillations 669
4.37.9.1.1 Theta rhythm 669
4.37.9.1.2 Gamma rhythm 670
4.37.9.2 Synchrony 670
4.37.9.2.1 Synchrony among JG cells 670
4.37.9.2.2 Synchrony among mitral cells 671
4.37.9.3 Oscillations, Synchrony and Odor Coding 672

4.37.10	**Neurophysiology of Neuromodulatory Inputs to Main Olfactory Bulb**	673
4.37.10.1	Cholinergic Inputs to MOB	673
4.37.10.2	Noradrenergic Input to MOB	674
4.37.10.3	Serotonergic (5-HT) Input to MOB	675
References		676

Glossary

apamin A blocker of SK-type potassium channels.
AP5 An NMDA receptor antagonist.
CNQX An AMPA receptor antagonist.
field potentials Extracellularly recorded voltages representing summed currents from a population of neurons.
gabazine A $GABA_A$ receptor antagonist.
ZD 7288 A blocker of Ih channels.
4-AP A blocker of A-type potassium channels (I_A).

4.37.1 Overview of Main Olfactory Bulb Circuitry

4.37.1.1 Projections of Olfactory Receptor Neurons to Main Olfactory Bulb

As discussed elsewhere (Chapter Signal Transduction in the Olfactory Receptor Cell), odors are transduced by olfactory receptor neurons (ORNs), giving rise to action potentials. The action potentials propagate along the axons of ORNs – the olfactory nerve (ON) fibers. These fibers form bundles which then collect as groups of fascicles, pass through the cribriform plate, and synapse in the main olfactory bulb (MOB). Within the MOB, ON axons terminate and synapse with neural elements in the glomerular layer (GL). Based on anatomical considerations (high packing density of unmyelinated axons), it has been speculated that ephaptic interactions (current spread through the extracellular space) might synchronize ON fibers. Computational modeling studies (Bokil, H. *et al.*, 2001) suggest that spikes in a single ON axon evoke spikes in adjacent axons, thus leading to synchronous firing of a large number of axons. These findings suggest that ephaptic interactions among neighboring axons may synchronize spikes among ON fibers converging on the same glomerulus.

ORNs expressing the same odorant receptor project to one or two glomeruli located on the medial and/or lateral side of each MOB (Figure 1; Ressler, K. J. *et al.*, 1993; 1994; Vassar, R. *et al.*, 1994; Mombaerts, P. *et al.*, 1996; Wang, F. *et al.*, 1998; Potter, S. M. *et al.*, 2001; Treloar, H. B. *et al.*, 2002). Studies in transgenic animals showed that this projection pattern is topographically fixed across animals. That is, the same glomeruli identified in different mice receive inputs from the same restricted population of ORNs bearing the same receptor (Mombaerts, P. *et al.*, 1996; Wang, F. *et al.*, 1998; Potter, S. M. *et al.*, 2001; Treloar, H. B. *et al.*, 2002). Rough calculations confirm an approximately 1:2 ratio between the number of different types of receptors (~1000) and the total number of glomeruli (~1800) in mice.

ORNs utilize glutamate as their primary neurotransmitter (Sassoe-Pognetto, M. *et al.*, 1993). Carnosine, a soluble dipeptide, is uniquely expressed in high concentrations in mammalian ORNs, and it is present in ON axon terminals in the GL (Ferriero, D. and Margolis, F. L., 1975; Margolis, F. L., 1980; Biffo, S. *et al.*, 1990). Carnosine colocalizes with glutamate in the ON axon terminals (Sassoe-Pognetto, M. *et al.*, 1993), and it satisfies criteria for neurotransmitter candidacy, including (1) carnosine synthetic and degradative enzymes are present in ORNs; (2) the peptide is released by depolarization in a Ca^{2+}-dependent manner in ON synaptosomes; (3) high-affinity binding sites for carnosine are present in the GL (Ferriero, D. and Margolis, F. L., 1975; Margolis, F. L., 1980; Burd, G. D. *et al.*, 1982; Rochel, S. and Margolis, F. L., 1982; Margolis, F. L. *et al.*, 1983; Margolis, F. L. and Grillo, M., 1984; Margolis, F. L. *et al.*, 1985; 1987; Biffo, S. *et al.*, 1990). Zinc and copper are also present in high concentrations in ON axon terminals (Biffo, S. *et al.*, 1990). The potential neuromodulatory roles of carnosine, zinc, and copper are discussed below.

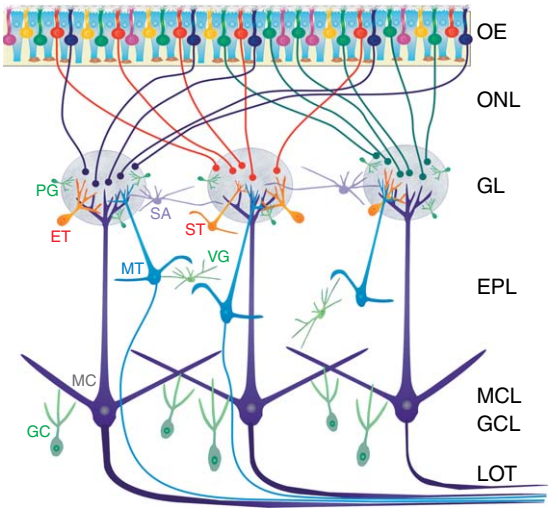

Figure 1 Schematic illustration of the basic circuitry of the main olfactory bulb (MOB) including the projections of olfactory receptor neurons (ORNs) from the olfactory epithelium (OE) to the glomerular layer (GL). Note that ORNs expressing different odorant receptor genes (shown as blue, red, or green cells) are interspersed and widely distributed, yet the axons of ORNs expressing the same odorant receptor gene converge onto the same glomerulus (or pairs of medial and lateral glomeruli) in the GL. Axons of ORNs travel in the olfactory nerve layer (ONL) and synapse in the GL on the dendrites of mitral cells (MC), tufted cells (external tufted cell, ET; middle tufted cell, MT), and generic juxtaglomerular (JG) neurons, which include periglomerular (PG) cells, ET cells, and short axon (SA) cells. SA cells interconnect different glomeruli. There are serial and reciprocal synapses between the apical dendrites of mitral/tufted cells and the processes of JG neurons. Superficial tufted (ST) cells are located in the superficial EPL or at the GL–EPL border. The lateral dendrites of mitral/tufted cells form serial and reciprocal synapses with the apical dendrites of granule cells (GC) in the EPL. The majority of GCs are concentrated in the GC layer (GCL) but many lie within the MCL. The axons of mitral/tufted cells project locally to GCs (not shown) and also to primary olfactory cortex via the lateral olfactory tract (LOT). The bulb also contains other populations of interneurons neurons, including the Van Gehuchten (VG) cells within the EPL.

4.37.1.2 MOB Circuitry

The MOB in rodents is situated at the rostral pole of the cranial cavity, and it is connected to the frontal cortex by a slender peduncle. The bulb can be thought of as a cylinder composed of distinct layers or laminae that are concentrically organized. These layers, from superficial to deep, are the ON layer (ONL), GL, external plexiform layer (EPL), mitral cell layer (MCL), internal plexiform layer (IPL), granule cell layer (GCL), and the ependymal layer (Figure 1). The ONL consists of ON axons and glial cells (Cajal, R. S. Y., 1911a; 1911b; Pinching, A. J. and Powell, T. P., 1971b; Doucette, R., 1989). Deep to the ONL, the GL is comprised of neutropil-rich ovoid structures – the glomeruli – each of which is surrounded by a shell of small neurons and glia. Within the glomeruli, ON axons form synapses with mitral and tufted cells, as well as with the intrinsic neurons of the GL – the juxtaglomerular (JG) cells. Adjacent glomeruli are somewhat isolated from each other by astrocytes residing in the glomerular shell (Bailey, M. S. and Shipley, M. T., 1993). The EPL lies beneath or deep to the glomeruli, and it primarily consists of dense neuropil formed by the dendrites of mitral cells and GCs that ascend from the MCL and GCL, respectively. The EPL also contains several subtypes of tufted cells and intrinsic interneurons. The dominant feature of the EPL is nevertheless the extensive dendrodendritic synapses between mitral/tufted cells and GCs. Deep to the EPL, the MCL is a thin layer that contains the somata of mitral cells, as well as numerous GCs (Cajal, R. S. Y., 1911a; 1911b). Together with tufted cells, mitral cells are the major class of output cells of the bulb. They extend a single apical dendrite into the GL, where it arborizes extensively throughout much of a single glomerulus (Figure 1). The apical dendrites are synaptically contacted by ON terminals (Price, J. L. and Powell, T. P. S., 1970a; Shepherd, G. M., 1972). The secondary or lateral dendrites of mitral cells ramify in the EPL where they form dendrodendritic synapses with dendrites of GCs. Mitral/tufted cell axons terminate within the bulb in the IPL and GCL (Mori, K. *et al.*, 1983; Price, J. L. and Powell, T. P. S., 1970c), or exit the MOB and innervate a number of olfactory-related brain regions collectively known as the primary olfactory cortex (POC). Deep to the MCL, the IPL is the relatively thin layer with a low density of cells. The GCL is the deepest neuronal layer in the bulb, and it contains the largest number of cells. Most of the neurons of the GCL are the GCs, but there are also small numbers of Golgi cells, Cajal cells, and Blanes cells. The GCs are inhibitory GABAergic cells that form dendrodendritic synapses with mitral/tufted cells in the EPL.

4.37.2 Neurophysiology of the Glomerular Layer

4.37.2.1 Neurophysiological Properties of Glomerular Layer Neurons

The neurons of the GL are classified into three cell types, which include: (1) periglomerular (PG) cells,

(2) external tufted (ET) cells, and (3) short axon (SA) cells (Golgi, C. 1875; Van Gehuchten, L. E. and Martin, A., 1891; Blanes, T., 1898; Cajal, R. S. Y., 1911a; 1911b; Pinching, A. J. and Powell, T. P., 1971a; 1971b; 1971c; 1972b; 1972c). Collectively, the intrinsic neurons of the GL are referred to as JG cells. The term JG is also used here with regard to cited studies in which the subtype of glomerular neuron was not specified. The morphology and features of these cells are only briefly reviewed here as more detailed descriptions are available (Hayar, A. *et al.*, 2004a; 2004b).

4.37.2.1.1 ET cells

These are relatively large (10–15 μm) cells that are dispersed in the JG regions surrounding/deep to the glomeruli (Figures 1 and 2). Most have one apical dendrite that arborizes extensively throughout one glomerulus (Pinching, A. J. and Powell, T. P., 1971a; Hayar, A. *et al.*, 2004a; 2004b). Rarely, ET cells have two or three apical dendrites that ramify in different glomeruli. Most ET cells have secondary or lateral dendrites that extend in the superficial EPL. Some ET cells have axons that appear to synapse with PG cells or SA cells, or more infrequently project out of MOB (Pinching, A. J. and Powell, T. P., 1971a). ET cells are somewhat similar to tufted cells of the EPL and to mitral cells, but growing evidence suggests that all tufted cell subtypes exhibit distinct anatomical and physiological properties.

The most distinctive physiological feature of ET cells *in vitro* is their spontaneous rhythmical bursting (Hayar, A. *et al.*, 2004a; 2004b; 2005) (Figure 2). JG cells with burst characteristics have been reported *in vivo* (Getchell, T. V. and Shepherd, G. M., 1975; Wellis, D. P. and Scott, J. W., 1990). However, because of the difficulty of recording small JG neurons *in vivo*, the identity of these cells and the basis of their bursting behavior remained unknown. The rhythmical burst-firing mode was characteristic of morphologically confirmed ET neurons (Hayar, A. *et al.*, 2004a). By contrast, PG and SA cells do not spontaneously generate spike bursts nor can they be induced to do so by intracellular current injections (Figure 2). Each ET cell bursts at its own characteristic frequency. As a population, ET cell burst frequencies range from ~1 to 8 Hz, with a mean of 3.3 ± 0.18 bursts/s. This range overlaps with the theta frequency range (2–12 Hz) prominent in oscillatory neural activity in the rodent olfactory network (see Oscillations and Synchrony in Main Olfactory Bulb); the theta range includes components related to low frequency (1–3 Hz) passive sniffing as well as a higher frequency component (5–10 Hz) characteristic of active investigative sniffing (Adrian, E. D., 1950; Welker, W. I., 1964; Macrides, F. *et al.*, 1982; Eeckman, F. H. and Freeman, W. J., 1990; Kay, L. M. and Laurent, G., 1999; Kay, L. M., 2003). ET cells also receive spontaneous bursts of inhibitory postsynaptic currents (IPSCs) from PG cells (Hayar, A. *et al.*, 2005). ON stimulation evokes an excitatory postsynaptic current (EPSC) in ET cells that is followed by IPSC bursts (Hayar, A. *et al.*, 2005). Both the spontaneous and ON-evoked IPSCs in ET cells are driven primarily by activation of AMPA receptors.

Several lines of evidence indicate that bursting is an intrinsic property of ET cells. First, bursting deteriorates rapidly after establishment of whole-cell recording mode. This pronounced rundown of bursting may explain the low reported incidence of spontaneous bursting in JG cells in some whole-cell recording studies (Bardoni, R. *et al.*, 1995; Puopolo, M. and Belluzzi, O. 1996; McQuiston, A. R. and Katz, L. C., 2001). The rundown of bursting could be due to intracellular dialysis of an intracellular messenger important to maintain spontaneous activity (Alreja, M. and Aghajanian, G. K., 1995). Additional evidence in support of the intrinsic mechanism for bursting are the findings that: (1) burst frequency is voltage dependent and (2) bursting persists in blockers of glutamate and $GABA_A$ receptors. This eliminates the possibility that bursting is driven by glutamatergic input from the ON, glutamatergic dendrodendritic interactions among ET cells and/or mitral cells, or by disinhibition (Aroniadou-Anderjaska, V. *et al.*, 1999b; Isaacson, J. S., 1999; Carlson, G. C. *et al.*, 2000; Friedman, D. and Strowbridge, B. W., 2000; Salin, P. A. *et al.*, 2001; Schoppa, N. E. and Westbrook, G. L., 2001). Moreover, spontaneous bursting was not blocked by Cd^{2+}, which suppresses Ca^{2+}-dependent neurotransmitter release, ruling out the potential involvement of other neurotransmitters. Depolarizing current injections evoke in ET cells a low-threshold Ca^{2+} spike (LTS) that was eliminated by the Ca^{2+} channel blockers, Cd^{2+} and Ni^{2+} (McQuiston, A. R. and Katz, L. C., 2001; Hayar, A. *et al.*, 2004a). This suggested that the LTS might generate ET cell bursting. However, this is unlikely for several reasons. First, bursting in ET cells persisted after the LTS was blocked. Second, ET cell bursting was abolished by extracellular TTX or by intracellular QX-314, whereas the LTS persisted. Third, the activation threshold of the LTS (−38 mV) was approximately 15 mV more depolarized than the membrane potential from which bursting arises, on average −53 mV. Ca^{2+} may modulate bursting as

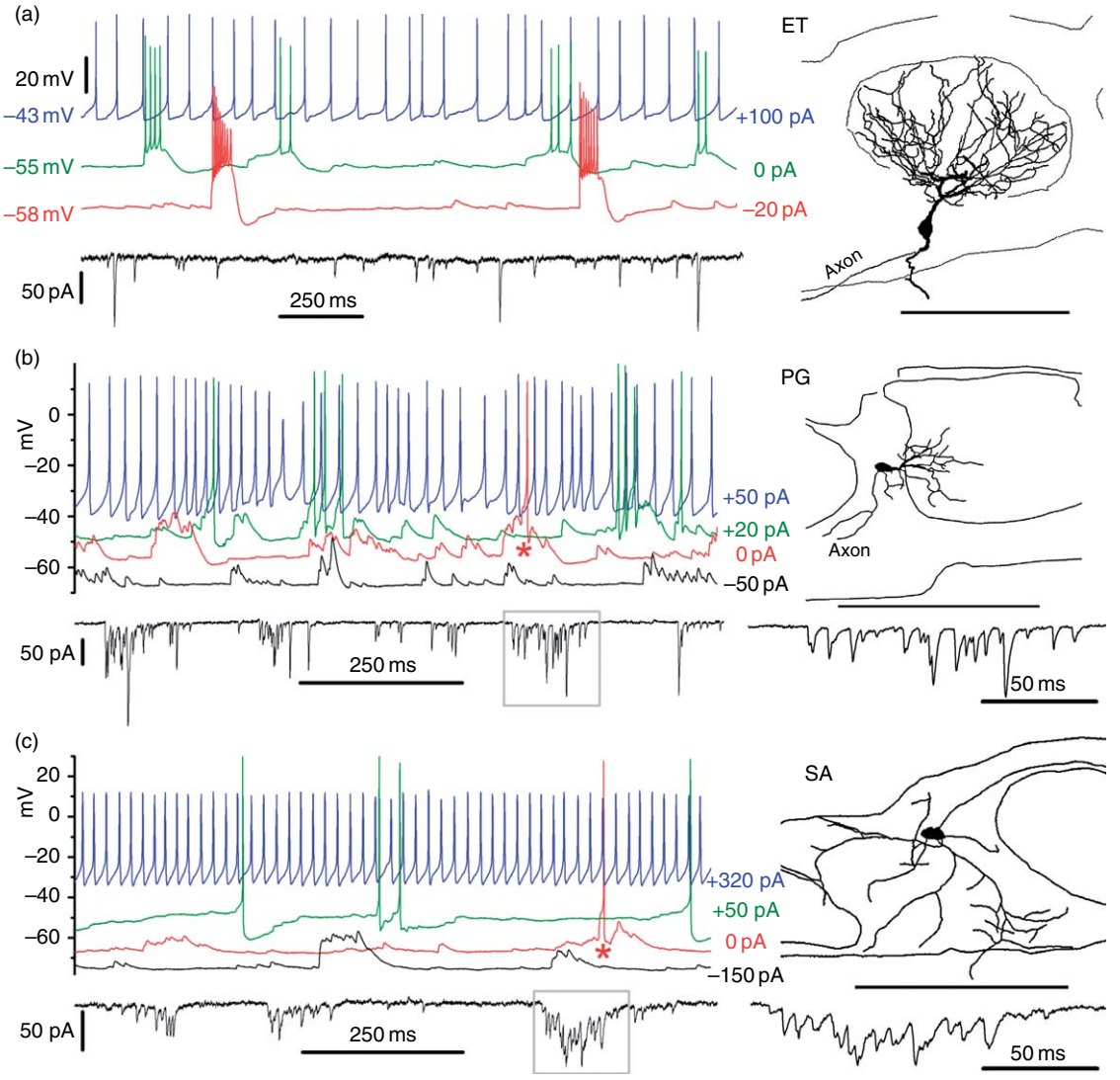

Figure 2 External tufted (ET) cells spontaneously generate rhythmic spike bursts, whereas periglomerular (PG) and short axon (SA) cells receive spontaneous bursts of excitatory synaptic input. Panels (a), (b), and (c) show the typical electrophysiological and morphological features of an ET, a PG, and a SA cell, respectively. The ET cell has highly branched tufted dendrites that ramify throughout a single glomerulus. The PG cell has relatively small soma and one to three relatively thick primary dendritic shafts that give rise to thinner branches ramifying within a subregion of a single glomerulus. The SA cell has several poorly branched dendrites that extended into or between two and four glomeruli. Scale bars below drawings, 100 μm. Current clamp recordings show resting spontaneous activity and effects of current injections. At rest (0 pA), the ET cell generates spontaneous bursts of spikes, whereas the PG and SA cells receive spontaneous bursts of EPSPs and generates spikes infrequently (asterisks). Bottom traces in a, b, and c show voltage-clamp recordings (holding potential = −60 mV) of spontaneous EPSCs in the same cells; regions enclosed in the box in b and c are shown at faster timescale at right. Note the bursting pattern of EPSCs in the PG and SA cells. Adapted from Hayar, A., Karnup, S., Ennis, M., and Shipley, M. T. 2004b. External tufted cells: a major excitatory element that coordinates glomerular activity. J. Neurosci. 24, 6676–6685, with permission from The Society for Neuroscience.

Ca^{2+} channel blockers prolonged burst duration (Hayar, A. *et al.*, 2004a). Ca^{2+} channel blockers also increased the interburst interval, but this could be due to a charge screening effect. Moreover, ET cells have a hyperpolarization-activated cation conductance (Ih) that is prominent at resting membrane potential (Figure 3). Ih current was found in all JG cells (Cadetti, L. and Belluzzi, O., 2001). However, other results (Hayar, A., unpublished observations) indicate that Ih is very strong in ET cells compared to PG and

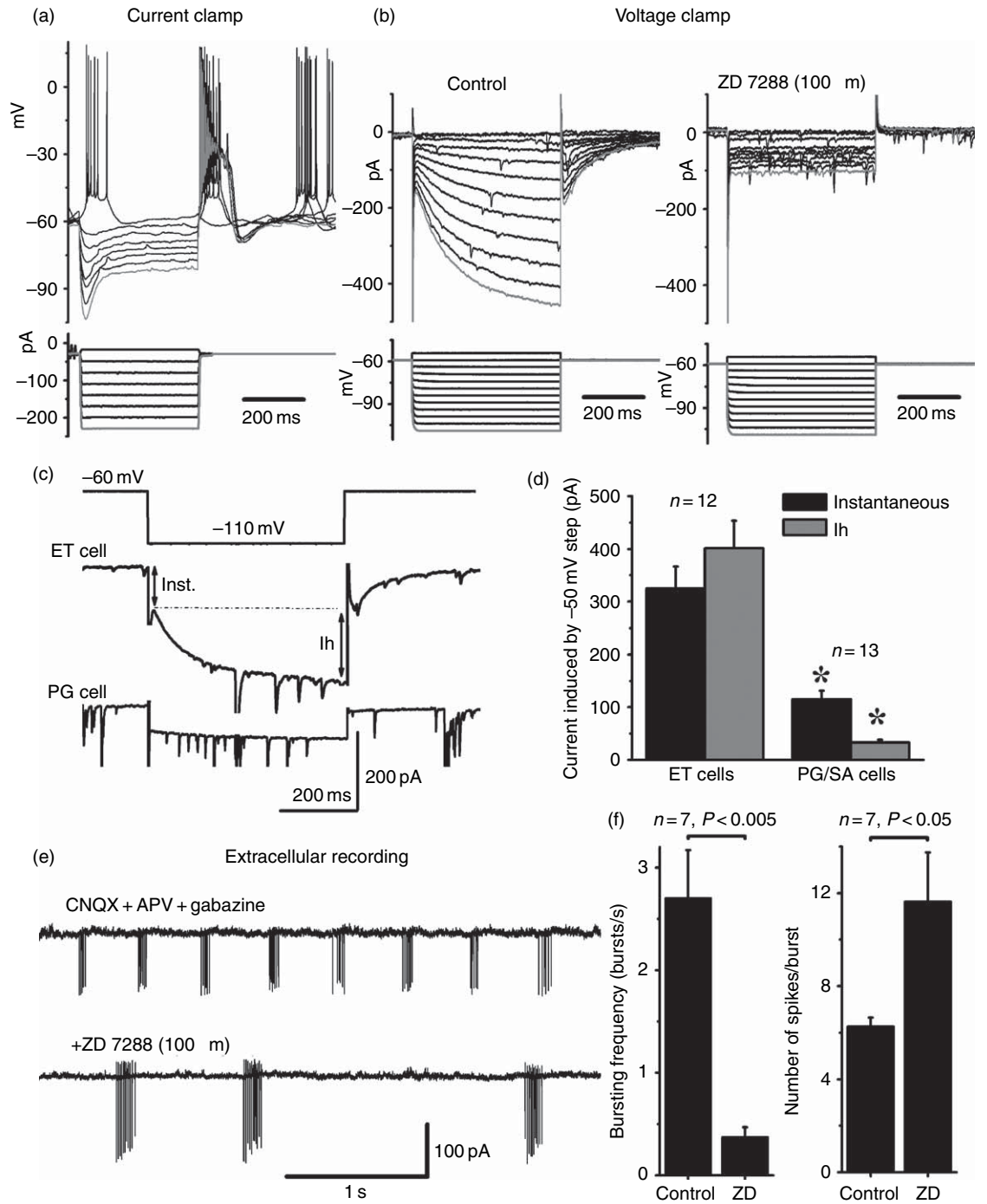

Figure 3 External tufted (ET) cells have a prominent Ih current. (a) Responses of an ET to hyperpolarizing and depolarizing current steps (bottom) in current clamp mode. Note the sag induced by membrane hyperpolarization, indicative of the presence of Ih current. After releasing the cell from the hyperpolarizing current, a rebound burst of spikes occurred. (b) Response of the same cell to membrane voltage steps (bottom) in voltage-clamp mode. A time-dependent inward current (Ih) was produced with hyperpolarizing voltage steps (<− 70 mV) followed by a rebound smaller inward current, which were blocked by the selective Ih current blocker, ZD 7288. (c) A periglomerular (PG) cell exhibits a much smaller Ih current (in response to a hyperpolarizing step from −60 to −110 mV, voltage-clamp mode) than an ET cell. (d) Group data show that ET cells have significantly larger Ih current than PG and short axon (SA) cells. The instantaneous current (Inst) reflects the membrane conductance which is larger in ET cells, indicating that PG/SA cells have on average a relative much higher input resistance. (e) The bursting frequency of an extracellularly recorded spontaneously bursting ET cell (in the presence of CNQX, AP5, and gabazine) decreased in response to application of the Ih blocker ZD 7288. However, the number of spikes/burst increased as shown in the grouped data in (f).

SA cells and that it contributes to tonic depolarization of ET cells because the specific Ih blocker, ZD 7288, significantly reduced the bursting frequency (Figure 3). Ih participates in burst timing and rhythmicity in other brain structures (DiFrancesco, D. 1993; Lüthi, A. and McCormick, D. A. 1998; Pape, H. C. 1996) and is modulated by Ca^{2+}. Thus, Ih and Ca^{2+} may play a role in burst termination and/or setting the interburst interval.

Rhythmic bursting, but not the LTS, was blocked by extracellular TTX and by intracellular dialysis with QX-314. These results suggest that, as for many neocortical neurons (Brumberg, J. C. *et al.*, 2000), burst generation in ET cells requires slowly inactivating Na^+ channels, that is, a persistent Na^+ current. Indeed, all ET cells tested had a prominent TTX-sensitive, persistent Na^+ current. The characteristics of this current are well suited to trigger spontaneous bursting in ET cells. The inward current activates near −60 mV, slightly hyperpolarized to the mean ET cell resting potential (−52 mV). Thus, it is reasonable to conjecture that as this persistent Na^+ current slowly depolarizes the ET cell membrane, additional Na^+ channels are activated further depolarizing the membrane to the threshold for action potential generation. This current maintains a level of depolarization sufficient to generate additional action potentials until another mechanism(s), possibly involving Ca^{2+} (see above), terminates the burst by transiently hyperpolarizing the membrane below the activation threshold for the persistent Na^+ current. As the membrane repolarizes, the persistent Na^+ current is re-engaged, and the burst cycle is repeated.

4.37.2.1.2 PG cells

These cells are the most numerous cells in the GL, and they are thought to be inhibitory in nature. They are small (5–8 μm), spherical or ovoid, and they are distributed in the PG regions surrounding the glomeruli (Figures 1 and 2). Their dendrites are typically restricted to a small subregion of a glomerulus (Pinching, A. J. and Powell, T. P., 1971a; Hayar, A. *et al.*, 2004a; 2004b). Their dendrites receive asymmetrical (morphologically excitatory) synapses from ET and mitral/tufted cell dendrites; only a relatively small subpopulation of PG cells receives synapses from ON terminals. Some of the mitral/tufted cell to PG cell synapses are paired with reciprocal symmetrical (morphologically inhibitory) synapses from PG cells back onto the parent mitral/tufted cell dendrites (Pinching, A. J. and Powell, T. P., 1971b; Toida, K. *et al.*, 1998; Kasowski, H. J. *et al.*, 1999; Toida, K. *et al.*, 2000). Physiological recordings indicate that PG cells also receive monosynaptic dendrodendritic excitatory input from ET cells (Hayar, A. *et al.*, 2004b). Axons of PG cells are rare but have been reported to extend over distances equivalent to four to five glomeruli (Blanes, T., 1898; Pinching, A. J. and Powell, T. P., 1971a; Hayar, A. *et al.*, 2004a). They appear to form symmetrical (morphologically inhibitory) synapses onto mitral/tufted cell dendrites and onto ET cells and other JG cells (Pinching, A. J. and Powell, T. P., 1971c). Most PG cells are GABAergic (Ribak, C. E. *et al.*, 1977; Mugnaini, E. *et al.*, 1984; Kosaka, T. *et al.*, 1985; 1987a; 1987b; 1987c; Kosaka, K. *et al.*, 1987; 1988). The GL also contains the largest population of dopamine (DA)-containing cells in the brain. The majority of DA-containing cells are PG cells, but some ET cells are also dopaminergic (Halász, N. *et al.*, 1977; Davis, B. J. and Macrides, F., 1983; Halász, N. *et al.*, 1985; Gall, C. *et al.*, 1986; McLean, J. H. and Shipley, M. T., 1988). About 80% of the DA cells contain GABA, which corresponds to about 50% of GABAergic cells (Kosaka, T. *et al.*, 1985; Gall, C. M. *et al.*, 1987; Kosaka, T. *et al.*, 1987b; Kosaka, K. *et al.*, 1987; 1988; 1995). Therefore, the DA PG neurons are regarded as a subpopulation of GABAergic neurons. Some PG cell subtypes also stain for thyrotropin-releasing hormone (TRH), enkephalin, nicotinamide adenine dinucleotide phosphate (NADPH)-diaphorase, neuropeptide-Y (NPY), somatostatin, and vasoactive intestinal polypeptide (VIP) (Bogan, N. *et al.*, 1982; Davis, B. J. *et al.*, 1982; Gall, C. *et al.*, 1986; Scott, J. W. *et al.*, 1987; Merchenthaler, I. *et al.*, 1988; Tsuruo, Y. *et al.*, 1988; Sanides-Kohlrausch, C. and Wahle, P., 1990a; Davis, B. J., 1991; Alonso, J. R. *et al.*, 1993; Kosaka, K. *et al.*, 1995; 1998; Kosaka, T. *et al.*, 1987c).

The spontaneous activity patterns of PG and SA cells differ markedly from ET cells. PG and SA cells *in vitro* have relatively low levels of spontaneous spike activity and lack the capacity to generate spike bursts in response to depolarizing currents (Figure 2) (Hayar, A. *et al.*, 2004a; 2004b). In slices, spikes in PG cells are driven primarily by spontaneous glutamatergic excitatory postsynaptic potentials (EPSPs). However, because of their heterogeneous neurochemical characteristics, PG cells are also likely to be functionally heterogeneous. For example, some studies have reported that different PG cell subtypes appear to exhibit different K^+

conductances (Puopolo, M. and Belluzzi, O. 1998) as well as different firing behaviors (McQuiston, A. R. and Katz, L. C., 2001). An estimated 10% of PG neurons in adulthood are positive for tyrosine hydroxylase (TH) (McLean, J. H. and Shipley, M. T., 1988; Kratskin, I. and Belluzzi, O., 2003), the rate-limiting enzyme for DA synthesis. Dopaminergic neurons have been recently identified *in vitro* using a transgenic mouse strain harboring an eGFP (enhanced green fluorescent protein) reporter construct under the promoter of TH. The most prominent feature of these cells when recorded in acutely dissociated cell culture preparations was the presence of regular spontaneous spiking at ~8 Hz. In these cells, five main voltage-dependent conductances were identified (Pignatelli, A. *et al.*, 2005): the two having largest amplitude were a fast transient Na^+ current and a delayed rectifier K^+ current. In addition, they have three smaller inward currents, sustained by Na^+ ions (persistent type) and by Ca^{2+} ions (low-voltage-activated (LVA) and high-voltage-activated (HVA)). The pacemaking activity was shown to be supported by the interplay of the persistent Na^+ current and of a T-type Ca^{2+} current. Transgenic mice in which catecholaminergic neurons expressed human placental alkaline phosphatase (PLAP) on the outer surface of the plasma membrane were also used to identify dissociated dopaminergic PG neurons (Puopolo, M. *et al.*, 2005). Dopaminergic PG cells spontaneously generated action potentials in a rhythmic fashion with an average frequency of 8 Hz. It was found that substantial Ca^{2+} current and TTX-sensitive Na^+ current flow during the interspike depolarization. These results show that dopaminergic PG cells have intrinsic pacemaking activity, supporting the possibility that they can maintain a tonic release of DA to modulate the sensitivity of the olfactory system during odor detection.

4.37.2.1.3 SA cells

These cells are roughly the same size (8–12 μm) as ET cells. They are distinguished by multiple dendrites that seem to harvest information from multiple glomeruli (Figures 1 and 2) (Hayar, A. *et al.*, 2004b). The dendrites may receive synaptic inputs from ET and mitral/tufted cell dendrites (Hayar, A. *et al.*, 2004b), tufted cell axon collaterals, or other SA cells. SA cells have axons that can extend up to 1–2 mm within the GL (Aungst, J. L. *et al.*, 2003). The axons appear to synapse primarily onto the dendrites of PG cells (Pinching, A. J. and Powell, T. P., 1971a). They do not receive direct ON input (Pinching, A. J. and Powell, T. P., 1971c; Hayar, A. *et al.*, 2004b). Their resting spontaneous activity patterns in MOB slices appear to be very similar to that of PG cells (Hayar, A. *et al.*, 2004b).

4.37.2.2 Electrophysiology of Intraglomerular Circuitry

4.37.2.2.1 Excitatory systems in the GL

4.37.2.2.1.(i) ON glutamatergic synaptic input to JG and mitral/tufted cells All studies to date have identified glutamate as the major transmitter at ON synapses onto the dendrites of JG neurons, as well as those of mitral/tufted cells in the GL. Release of glutamate from ON terminals is controlled by N- and P/Q-type Ca^{2+} channels (Isaacson, J. S. and Strowbridge, B. W., 1998; Murphy, G. J. *et al.*, 2004). Each glomerulus contains the apical dendritic tufts of about 20 mitral cells, 200 tufted cells, and 1500–2000 JG cells (reviewed in Ennis, M. *et al.*, 2007). A variety of studies demonstrated that sensory transmission from ON axon terminals to these dendrites is mediated by glutamate acting primarily at alpha-amino-3-hydroxy-5-methyl-4-isoxazole propionic acid (AMPA) and *N*-methyl D-aspartate (NMDA) ionotropic glutamate receptor subtypes (Bardoni, R. *et al.*, 1996; Ennis, M. *et al.*, 1996; Aroniadou-Anderjaska, V. *et al.*, 1997; Chen, W. R. and Shepherd, G. M., 1997; Keller, A. *et al.*, 1998; Aroniadou-Anderjaska, V. *et al.*, 1999a; Ennis, M. *et al.*, 2001). Thus, JG and mitral/tufted cell responses to ON input are excitatory (Figures 4 and 5). In addition, metabotropic glutamate receptors (mGluRs) are expressed by nearly all MOB neurons (see Ennis, M. *et al.*, 2007 for review). Comparatively less is known about the role of mGluRs at ON synapses. Electrophysiological and Ca^{2+}-imaging studies have reported that ON stimulation evokes an mGluR1-sensitive synaptic component in ~40% of mitral cells in normal physiological conditions in the slice (De Saint Jan, D. and Westbrook, G. L., 2005; Ennis, M. *et al.*, 2006; Yuan, Q. and Knopfel, T., 2006). In the presence of ionotropic glutamate receptor antagonists, ON-evoked, mGluR1-mediated synaptic responses were markedly enhanced by inhibition of glutamate transporters (e.g., TBOA) (Figure 5). Thus, activation of mGluR1 is tightly regulated by glutamate uptake mechanisms. mGluR1-mediated responses were maximal with bursts of 50–100 Hz ON spikes, similar to frequencies of odor-induced spikes in ORNs *in vivo* (Duchamp-Viret, P. *et al.* 1999). Activation of mGluRs has also been suggested

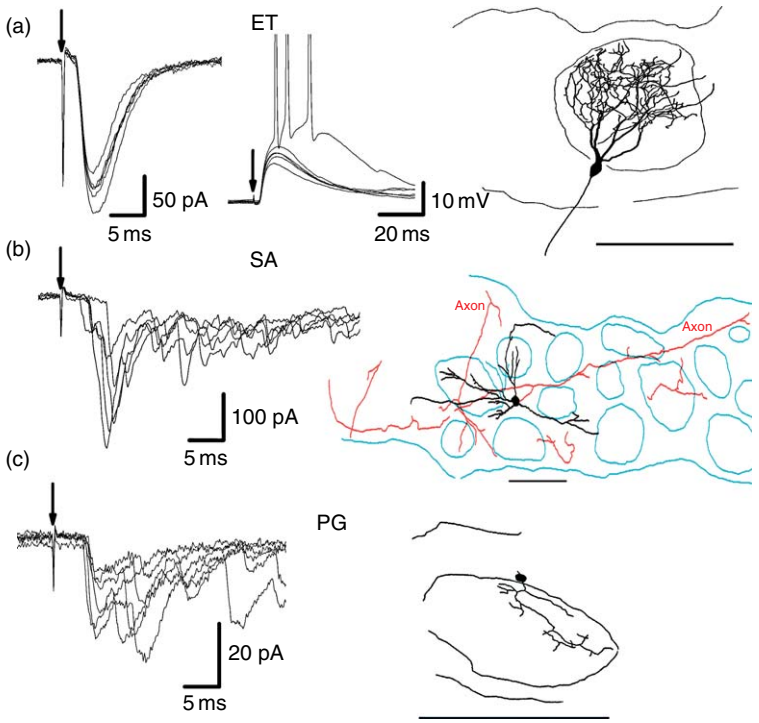

Figure 4 Olfactory nerve (ON)-evoked synaptic responses in juxtaglomerular (JG) cell subtypes. Panels a–c show six superimposed voltage-clamp traces (holding potential = −60 mV in this and subsequent panels) of ON-evoked EPSCs in external tufted (ET), short axon (SA), and periglomerular (PG) cells, respectively. Arrows indicate time of stimulation. Cell morphology is shown at right. Scale bars, 100 μm. ON stimulation produced short, constant latency EPSCs in the ET cell (a, left panel), indicative of monosynaptic input. In current clamp, ON stimulation evoked a constant, short latency EPSPs of variable amplitude (a, middle panel). The largest EPSPs triggered the generation of a burst of action potentials (truncated for clarity). Panels b and c show that ON stimulation evoked longer, variable latency EPSCs bursts in SA (b) and PG (c) cells, indicative of di- or polysynaptic responses. Adapted from Hayar, A. *et al.*, 2004, J. Neurosci. 24, 6676–6685., with permission from The Society for Neuroscience.

to produce long-term depression at ON to mitral cell synapses (Mutoh, H. *et al.*, 2005).

All ET cells receive monosynaptic ON input, which appears to be primarily mediated by AMPA and NMDA receptors in normal physiological conditions *in vitro* (Figure 4) (Hayar, A. *et al.*, 2004a; 2004b; 2005). If the amplitude of an ON-evoked EPSP reaches threshold for spike generation, a spike burst is always triggered in ET cells (Hayar, A. *et al*, 2004a). Further increases in ON stimulation strength produce the same all-or-none burst. Thus, ET cells receive monosynaptic ON input that is converted into an all-or-none spike burst. Accordingly, ET cells amplify suprathreshold sensory input at the first stage of synaptic transfer in the olfactory system. ET cells also readily entrain to rhythmic ON input delivered at theta frequencies (5–10 Hz) characteristic of investigative sniffing in rodents. As noted above, the intrinsic spontaneous bursting rate of ET cells ranges from 1 to 8 bursts/s. This might suggest that ET cells with different spontaneous bursting rates may be preferentially entrained by repetitive sensory input at or near their intrinsic bursting frequency. This turns out not to be the case as ET cells, irrespective of their intrinsic spontaneous bursting frequencies, can be entrained by repetitive, 5–10 Hz ON input (Hayar, A. *et al.*, 2004a).

The majority of PG cells exhibit longer latency, prolonged bursts of EPSP/Cs in response to ON stimulation than ET cells (Figure 4). The long, variable latency of these responses is indicative of di- or polysynaptic ON input. Thus, most SA and PG cells do not appear to receive direct ON input, perhaps because their dendrites ramify in glomerular compartments devoid of ON terminals. Only 20% of PG cells had short, relatively constant latency EPSCs following ON stimulation, and in some of these cells, the short latency synaptic response was followed by a delayed burst of EPSP/Cs. SA cells also

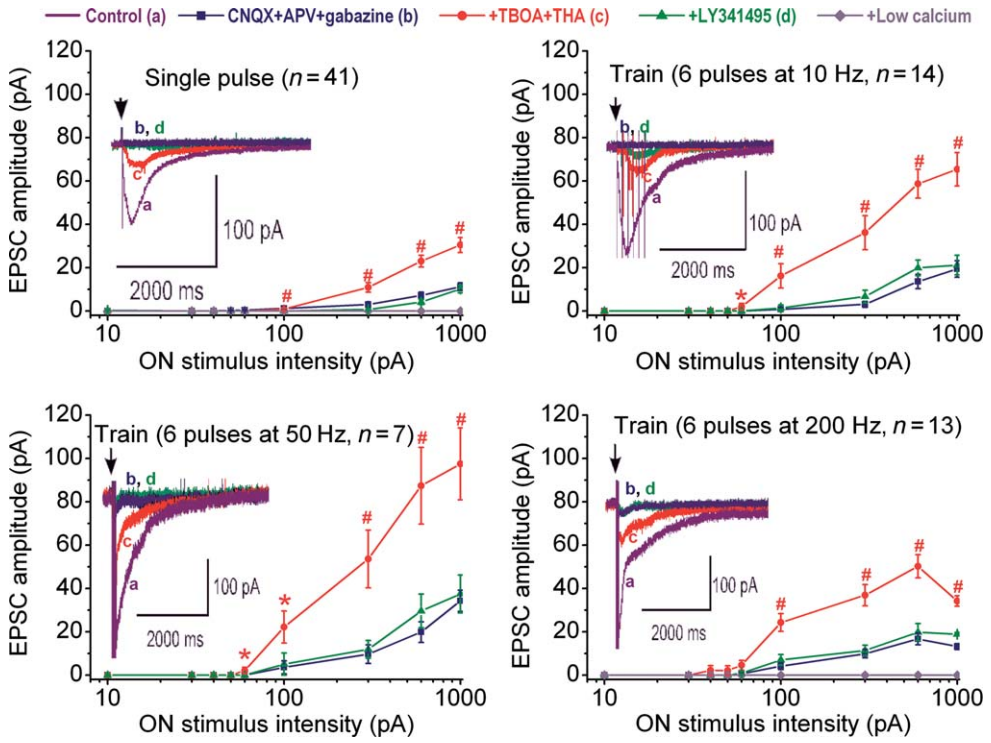

Figure 5 Olfactory nerve (ON)-evoked EPSCs elicited in the presence of glutamate uptake inhibitors (TBOA and THA) are dependent on stimulation intensity and frequency. The four panels show plots of the peak amplitude of ON-evoked EPSCs as a function of ON stimulation intensity (10–1000 μA); each panel shows data for a different ON stimulation frequency. Insets in each graph show traces of ON-evoked EPSCs in different pharmacological conditions; traces are averages of five ON-evoked EPSCs. Colored lines correspond to the pharmacological conditions indicated at the top; note that control data are not plotted on the line graphs. TBOA–THA significantly increases the ON-evoked EPSCs at a threshold intensity of 60–100 μA for all frequencies. Residual responses remaining in the presence of LY341495 and CNQX, APV, and gabazine were abolished by low Ca^{2+}-ACSF, as shown for the single-pulse and 200 Hz stimulation frequencies. $^{*}P < 0.05$, $\#P < 0.001$ vs. CNQX, APV, and gabazine. Adapted from Ennis, M., Zhu, M., Heinbockel, T., and Hayar, A. 2006. Olfactory nerve-evoked metabotropic glutamate receptor-mediated responses in olfactory bulb mitral cells. J. Neurophysiol. 95, 2233–2241, with permission from The American Physiological Society.

responded to ON stimulation with long, variable latency, prolonged bursts of EPSP/Cs and never exhibited responses consistent with monosynaptic ON input (Figure 4). These findings indicate that (1) SA cells and most PG cells lack direct ON input and (2) ET cells along with mitral/tufted cells are the major postsynaptic targets of ON inputs.

Since most (~80%) PG cells, and all SA cells, lack monosynaptic ON input, this suggests that most PG cells are functionally associated with glomerular compartments lacking ON terminals. Anatomical studies have revealed that the glomeruli have a bicompartmental organization. Each glomerulus has several interdigitating compartments, one of which is rich in ON terminals and the second of which is devoid of ON input (Kosaka, K. *et al.*, 1997; Kasowski, H. J. *et al.*, 1999). Calbindin-positive JG neurons extend their dendrites only into glomerular compartments devoid of ON terminals, suggesting that they do not receive direct sensory innervation (Toida, K. *et al.*, 1998; 2000). It is reasonable to speculate, therefore, that the SA and PG cells that do not receive direct input (Hayar, A. *et al.*, 2004b) may correspond to these calbindin-positive JG neurons. These PG cells might provide localized inhibition to mitral/tufted cell dendrites, or other nearby JG cells. Dopaminergic and GABAergic PG cells presynaptically inhibit ON terminals (Hsia, A. Y. *et al.*, 1999; Wachowiak, M. and Cohen, L. B., 1999; Aroniadou-Anderjaska, V. *et al.*, 2000; Berkowicz, D. A. and Trombley, P. Q., 2000; Ennis, M. *et al.*, 2001; Murphy, G. J. *et al.*, 2005; Wachowiak, M. *et al.*, 2005). Since at least 20% of PG cells receive monosynaptic ON input, it is possible that these cells primarily mediate this presynaptic inhibition of the ON. In contrast

to PG cells, SA cells extend dendrites and axons across multiple glomeruli and are thought to be involved in interglomerular functions, such as center-surround inhibition of neighboring glomeruli (Aungst, J. L. *et al.*, 2003).

4.37.2.2.1.(ii) Spillover of dendritically released glutamate As noted above, the apical dendrites of ET and mitral/tufted cells that ramify in the glomeruli release glutamate. Although the dendrites of these cell types do not form synapses with each other, the release of glutamate from the apical dendrites has been reported to produce nonsynaptically mediated excitation (i.e., glutamate spillover) of the parent cell releasing glutamate (self- or autoexcitation) or neighboring cells (Figure 6). Such excitation is facilitated by removal of Mg^{2+} from the extracellular media, which enhances the activation of NMDA receptors. Alternatively, spillover-mediated excitatory responses can be facilitated in the presence of physiological levels of extracellular Mg^{2+} by blockade of $GABA_A$ receptors (Salin, P. A. *et al.*, 2001; Friedman, D. and Strowbridge, B. W., 2000). Under such conditions, intracellular depolarization of individual mitral cells produces long-duration, NMDA receptor-dependent excitation of the same cell or adjacent mitral cells (Aroniadou-Anderjaska, V. *et al.*, 1999b; Isaacson, J. S., 1999; Friedman, D. and Strowbridge, B. W., 2000; Salin, P. A. *et al.*, 2001; Christie, J. M. and Westbrook, G. L., 2006). ET cells have also been reported to exhibit such self-excitation (Murphy, G. J. *et al.*, 2005). The mitral cell self-excitation can be blocked by intracellular Ca^{2+} chelation or blockade of voltage-gated Ca^{2+} channels (Friedman, D. and Strowbridge, B. W., 2000; Salin, P. A. *et al.*, 2001). The self-excitation responses are graded and increase with the number of spikes or depolarizing pulses applied to the mitral cell (Friedman, D. and Strowbridge, B. W., 2000; Salin, P. A. *et al.*, 2001). It has been suggested that the NMDA autoreceptors may serve to increase the firing frequency of mitral cells during prolonged discharges (Friedman, D. and Strowbridge, B. W., 2000). Such excitation can also be evoked by antidromic activation of mitral cells (Figure 6) (Chen, W. R. and Shepherd, G. M., 1997; Aroniadou-Anderjaska, V. *et al.*, 1999b). This glutamate spillover-mediated, NMDA receptor-dependent excitation appears to occur chiefly among the lateral dendrites of mitral cells, while an AMPA receptor-dependent spillover occurs among the apical dendrites of mitral/tufted cells (Aroniadou-Anderjaska, V. *et al.*, 1999b; Salin, P. A. *et al.*, 2001; Schoppa, N. E. and Westbrook, G. L., 2001; 2002; Christie, J. M. and Westbrook, G. L., 2006). Electrotonic coupling among mitral cell dendrites in the same glomerulus facilitates spillover responses mediated by AMPA receptors (Schoppa, N. E. and Westbrook, G. L., 2002; Christie, J. M., and Westbrook, G. L., 2006).

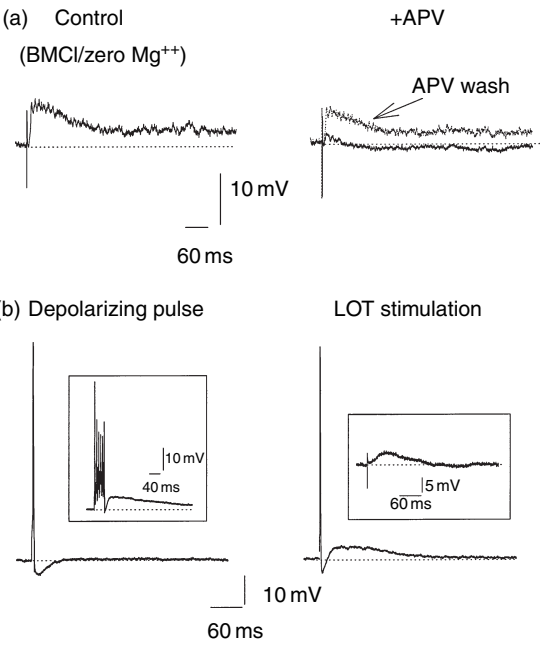

Figure 6 Mitral cells generate an NMDA receptor-dependent EPSP in response to antidromic stimulation of neighboring mitral/tufted cells. Panels a and b show recordings from two different cells in Mg^{2+}-free medium and bicuculline (10 μM). (a) Antidromic activation of mitral/tufted cells by lateral olfactory tract (LOT) stimulation, subthreshold for the recorded neuron, evoked an EPSP that was reversibly blocked by bath-applied APV (50 μM). (b) Mitral cell shown did not produce a prolonged depolarization in response to a 5 ms intracellular current pulse. However, a prolonged depolarization was evoked by longer current pulses (40 ms, shown in inset) or LOT stimulation with or without (inset) an antidromic spike. Traces are averages of five to ten sweeps. Reprinted from V. Aroniadou-Anderjaska, V., Ennis, M., and Shipley, M. T. 1999b. Dendrodendritic recurrent excitation in mitral cells of the rat olfactory bulb. J. Neurophysiol. 82, 489–494, with permission from The American Physiological Society.

Other glomerulus-specific glutamate-mediated excitatory interactions among mitral cells have been reported. Reciprocal glutamate-mediated excitation was reported between closely adjacent mitral cells whose apical dendrites extended into the same glomerulus (Urban, N. N. and Sakmann, B., 2002). The latency for the mitral to mitral cell EPSPs was surprisingly short, in line with monosynaptic mediation,

despite the fact that mitral cells do not form anatomical synapses with each other. The EPSP was primarily mediated by AMPA receptors and originated within the GL, suggesting that they are generated in the apical dendrites of mitral cells. In contrast to the preceding studies, Carlson G. C. *et al.* (2000) reported that ON stimulation and antidromic activation of multiple mitral/tufted cells, but never activation of single mitral cells, elicited long-lasting depolarizations (LLDs) in mitral cells. The LLDs were all-or-none in nature, required activation of AMPA receptors, and originated in the glomeruli. Further, spontaneous LLDs were synchronous among mitral cells associated with the same, but not different glomeruli. The LLDs appear to be a network phenomenon, presumably reflecting recurrent, intraglomerular glutamate release from an ensemble of mitral/tufted cell apical dendrites. Recently, Karnup S. V. *et al.* (2006) described field potentials that are generated spontaneously in the GL in olfactory bulb slices (Figure 7). These spontaneous glomerular local field potentials (sGLFPs) had variable shape and amplitude and occurred at irregular intervals. They are similar to LLDs in mitral cells (Carlson, G. C. *et al.*, 2000) in that they are mediated mostly by AMPA/kainate receptors and are enhanced during blockade of $GABA_A$ receptors. They persisted after the removal of the MCL, indicating that they are predominantly generated from by GL neurons. Nevertheless, they were correlated with mitral cell postsynaptic LLDs, suggesting the existence of a common generator (Figure 7). The observation that sGLFPs precede LLDs in mitral cells suggests that mitral cells are followers rather than initiators of population events. The most likely scenario is that mitral cells are activated when a critical number of glutamate-releasing JG neurons (presumably ET cells) are activated. Such a triggering mechanism may be produced by synchronous spike bursts in ET cells of the same glomerulus (Hayar, A. *et al.*, 2004a; 2004b). The role of spillover-mediated excitation among mitral/tufted cells is discussed below in Synchrony.

4.37.2.2.1.(iii) ET and mitral/tufted cell dendrodendritic input to PG and SA cells ET and mitral/tufted cells form glutamatergic dendrodendritic synapses with PG and SA cells. This topic is

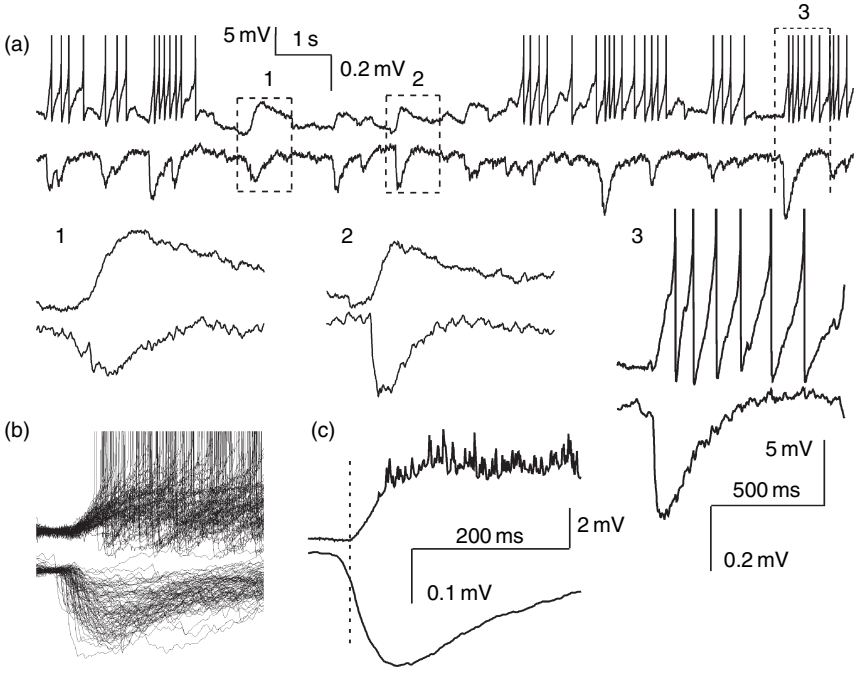

Figure 7 Glomerular and mitral cell long-lasting depolarizations (LLDs). Simultaneous recordings of spontaneous LLDs (sLLDs) in a mitral cell and spontaneous glomerular layer field potentials (sGLFPs) from the glomerulus containing the mitral cell tuft. (a) Dual sweep of intracellular (upper trace) and field activity (lower trace). Spikes of the mitral cell are truncated. Insets with an expanded timescale demonstrate variability of sGLFP locked to sLLD and different kinetics of sGLFP as compared with sLLD. (b) Overlapping sweeps with sLLD/sGLFP pairs ($n = 80$). Note 10-fold difference between smallest and biggest sGLFP indicating different amount of cells involved in successive sGLFP in a given glomerulus. (c) Averaged sLLD and sGLFP ($n = 80$) with the reference point set at the sLLD onset show 9.8 ms delay of sLLD upon initiation of sGLFP.

discussed below in *ET and mitral/tufted cell dendrodendritic interactions with PG and SA cells*.

4.37.2.2.2 Inhibitory systems in the GL

4.37.2.2.2.(i) Presynaptic inhibition of ON terminals

4.37.2.2.2.(i).(a) DA and D2 receptors The GL contains several hundred thousand DA neurons – PG neurons – but the MOB receives no known extrinsic DA input. In mammals, D1 receptor mRNA is expressed in the GL and GCL (Coronas, V. *et al.*, 1997), while immunocytochemical localization of D1 receptors is faint and primarily in the GCL (Levey, A. I. *et al.*, 1993). By contrast, D1-like binding is present at very low levels in all layers of the MOB with the exception of the ONL (Mansour, A. *et al.*, 1990; Nickell, W. T. *et al.*, 1991; Coronas, V. *et al.*, 1997). The functional significance of D1 receptors in MOB remains unclear. By contrast, only the ONL and GL have high densities of D2 receptors in rats and mice (Mansour, A. *et al.*, 1990; Nickell, W. T. *et al.*, 1991; Levey, A. I. *et al.*, 1993; Coronas, V. *et al.*, 1997; Koster, N. L. *et al.*, 1999) and to a lesser extent in guinea pigs, but not in cats or monkeys (Camps, M. *et al.*, 1990). In the GL, the JG neurons express D2 receptors (Mansour, A. *et al.*, 1990). Some immunocytochemical labeling for D2 receptors, as well as *in situ* hybridization, has been reported in the GCL and EPL; however D2-binding sites are consistently restricted to the ONL and GL (Mansour, A. *et al.*, 1990; Levey, A. I. *et al.*, 1993; Coronas, V. *et al.*, 1997). Other anatomical evidence indicates that most, if not all, of the D2 receptors in the GL occur on ON axon terminals. ORNs express D2 receptors and bulbectomy, a manipulation that causes retrograde degeneration of ORNs, eliminates D2 receptor mRNA in the olfactory epithelium (Koster, N. L. *et al.*, 1999). Taken together, these findings indicate that DA released from JG neurons may presynaptically modulate ON terminals via activation of D2 receptors.

In agreement with this, DA and D2 receptor agonists reduced spontaneous and ON-evoked activity in mitral and JC cells (Figure 8), as well as odor-evoked activity in the GL and odor detection performance, in a variety of species (Nowycky, M. C. *et al.*, 1983; Doty, R. L. and Risser, J. M., 1989; Sallaz, M. and Jourdan, F., 1992; Hsia, A. Y. *et al.*, 1999; Wachowiak, M. and Cohen, L. B., 1999; Berkowicz, D. A. and Trombley, P. Q., 2000; Ennis, M. *et al.*, 2001). These effects are mediated by presynaptic suppression of glutamate release from ON terminals via inhibition of Ca^{2+} influx (Wachowiak, M. and Cohen, L. B., 1999). In a similar manner, DA and D2 receptor agonists suppressed spontaneous and ON-evoked activity in JG cells but had no effect on mitral to JG cell transmission (Ennis, M. *et al.*, 2001). The inhibitory effects of DA were abolished in D2 receptor-knockout mice (Ennis, M. *et al.*, 2001). Presynaptic inhibition of ON terminals by DA (and GABA, see below) provides a mechanism for increasing the range of concentrations that can be processed by MOB neurons: as activity increases in ON terminals, DA JG cells are more strongly excited. This, in turn, provides negative feedback onto ON terminals, reducing the release of glutamate. Such a scheme would effectively increase the dynamic range of information transfer from ORNs to MOB neurons. Interestingly, systemic administration of D2 receptor agonists has been reported to prevent odorant-specific 2-dexyglucose patterns in MOB and to reduce odorant detectability (Doty, R. L. and Risser, J. M., 1989; Sallaz, M. and Jourdan, F., 1992). Related to this question of how DA participates in odor processing is the degree to which these receptors are tonically active *in vivo*? If, for example, ON terminals are tonically inhibited by DA via D2 receptors, this might serve to filter out weak signals (noise). This might sharpen the spatial pattern of active glomeruli and facilitate detection of predominant odors. There is experimental support for this possibility. Blockade of D2-like receptors by systemic administration of spiperone increased the number of mitral cells that responded to single or multiple odorants (Wilson, D. A. and Sullivan, R. M., 1995). One interpretation of this study is that reduced D2 presynaptic inhibition of ON terminals increases the odor responsiveness of mitral cells but does so at the cost of reduced odorant discrimination.

4.37.2.2.2.(i).(b) GABA and $GABA_B$ receptors $GABA_B$ receptors play a presynaptic inhibitory role similar to that just described for D2 receptors. As noted above, GABAergic PG cells represent a large population of GL interneurons. In the rat MOB, the glomeruli have the highest concentration of $GABA_B$ receptors as determined by radioligand binding (Bowery, N. G. *et al.*, 1987; Chu, D. C. M. *et al.*, 1990) and by immunohistochemical localization of $GABA_B$ receptor subunits (Margeta-Mitrovic, M. *et al.*, 1999). EM immunohistochemistry revealed that the dense labeling in the GL is due to the presence of $GABA_B$ receptors on ON terminals and on the somata of PG cells (Bonino, M. *et al.*, 1999). A variety of imaging

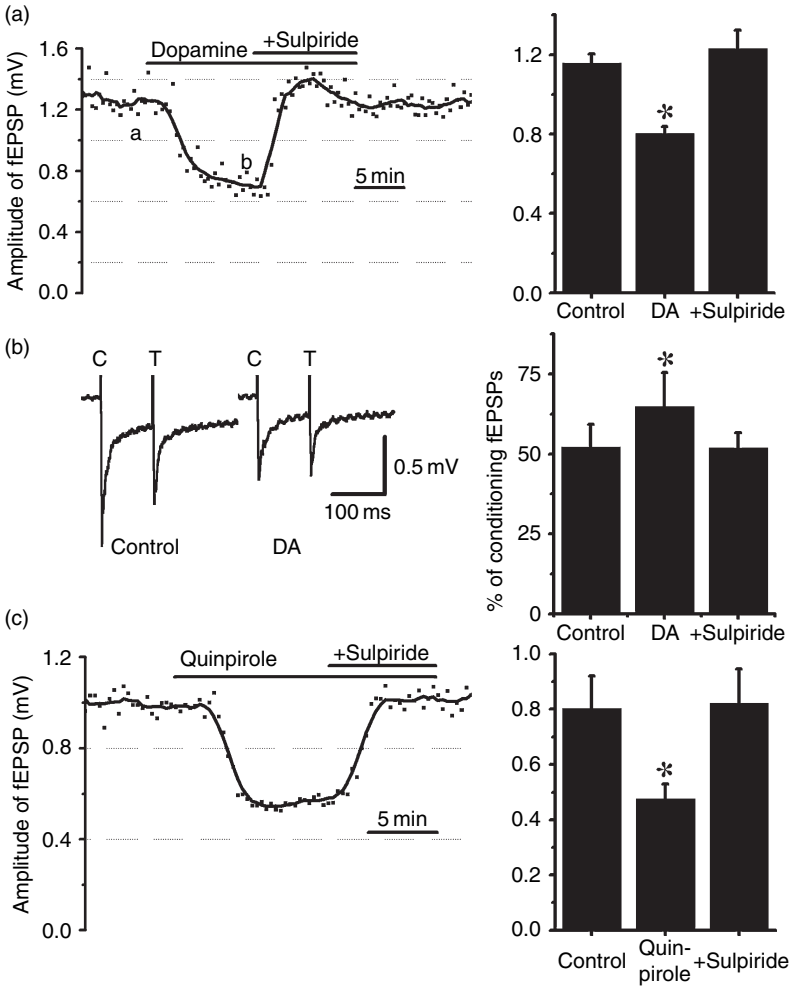

Figure 8 Dopamine (DA) suppresses the olfactory nerve (ON)-evoked field excitatory postsynaptic potential (fEPSP) recorded in the rat glomerular layer (GL). (a) Line graph from a typical experiment showing the suppression of the GL fEPSP by bath application of DA (40 μM). Values represent the peak amplitude ± SE of the fEPSP. DA-induced suppression (30.7%) was fully reversed by the D2 antagonist sulpiride (100 μM). Group data at the right from similar experiments show that DA significantly suppresses ($n = 5$, $^*P = 0.005$) the ON-evoked fEPSP, an effect fully reversed by sulpiride ($n = 4$). (b) Records show responses to paired-pulse stimulation of the ON (100-ms interstimulus intervals) before (Control) and during application of DA (DA); control and DA records correspond to time points a and b indicated in panel a. In control artificial cerebrospinal fluid (ACSF), paired ON shocks produced pronounced paired-pulse depression of the test fEPSP. DA preferentially suppressed the conditioning shock fEPSP and decreased paired-pulse depression. Traces are averages of five sweeps. Bar graph of group data showing the change in paired-pulse responses to ON stimulation; data are expressed as the amplitude of the test fEPSP as a percentage of the conditioning fEPSP. Note that DA significantly reduced paired-pulse depression ($n = 4$, $^*P = 0.01$). (c) Line graph showing the suppression of the GL fEPSP by bath application of quinpirole (100 μM). Sulpiride (100 μM) fully reversed the quinpirole-induced suppression. Group data for similar experiments are shown in the bar graphs to the right ($n = 10$, $^*P < 0.0001$). Reprinted from Ennis, M., Zhou, F. M., Ciombor, K. J., Aroniadou-Anderjaska, V., Hayar, A., Borrelli, E., Zimmer, L. A., Margolis, F., and Shipley, M. T. 2001. Dopamine D2 receptor-mediated presynaptic inhibition of olfactory nerve terminals. J. Neurophysiol. 86, 2986–2997, with permission from The American Physiological Society.

and electrophysiological studies have provided solid evidence that GABA released from PG neurons presynaptically inhibits glutamate release from ON terminals via activation of these $GABA_B$ receptors (Figure 9) (Keller, A. *et al.*, 1998; Wachowiak, M. and Cohen, L. B., 1999; Aroniadou-Anderjaska, V. *et al.*, 2000; Palouzier-Paulignan, B. *et al.*, 2002; Murphy, G. J. *et al.*, 2005). The presynaptic inhibition of glutamate release is mediated by the suppression of Ca^{2+} influx into ON terminals (Wachowiak, M. *et al.*,

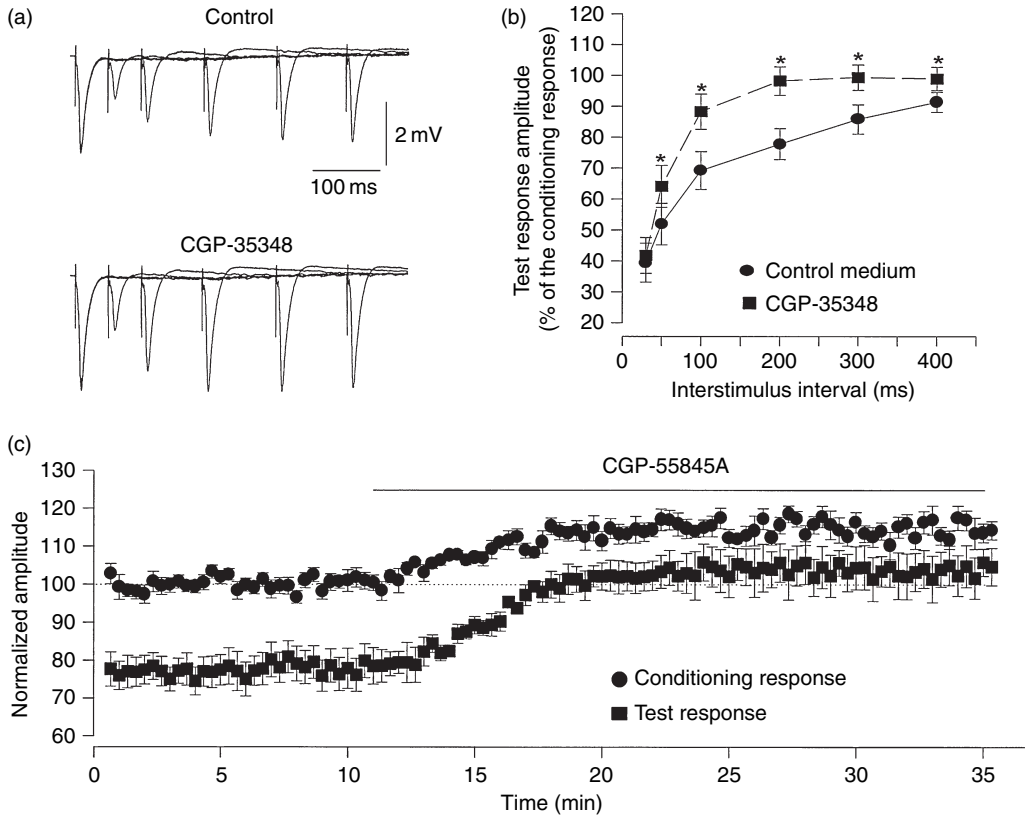

Figure 9 $GABA_B$ receptors on olfactory nerve (ON)terminals are activated both tonically and in response to ON stimulation. $GABA_B$ antagonists increase both conditioning and test responses of mitral/tufted cells to paired-pulse stimulation of the ON, while reducing paired-pulse depression (PPD) of test responses. In all experiments, AP5 is included in the medium. (a) Responses to paired-pulse stimulation of the ON (interstimulus intervals 50, 100, 200, 300, and 400 ms) before and after application of the $GABA_B$ antagonist CGP-35348 (1 mM). The $GABA_B$ antagonist increased the amplitude of the conditioning response and reduced or blocked PPD. Each trace is an average of five sweeps, and five traces are superimposed. (b) Group data ($n = 10$) of the effects of CGP-35348 (500 μM to 1 mM) on PPD of the ON-evoked glomerular field EPSP. The reduction of PPD was statistically significant ($^*P < 0.05$) at interstimulus intervals from 50 to 400 ms. (c) Time course of the effects of CGP-55845A (10 μM) on conditioning and test responses (interstimulus interval 100 ms). Group data from six slices. Reprinted from Aroniadou-Anderjaska, V., Zhou, F. M., Priest, C. A., Ennis, M., and Shipley, M. T. 2000. Tonic and synaptically evoked presynaptic inhibition of sensory input to the rat olfactory bulb via GABA(B) heteroreceptors. J. Neurophysiol. 84, 1194–1203, with permission from The American Physiological Society.

2005). Stimulation of individual PG cells has been reported to inhibit, via $GABA_B$ receptors, ON input onto the stimulated cell (Murphy, G. J. *et al.*, 2005). The MOB also contains the highest levels of the putative inhibitory transmitter taurine, exceeding concentrations of GABA and glutamate (Collins, G. G., 1974; Margolis, F. L., 1974; Banay-Schwartz, M. *et al.*, 1989a; 1989b; Ross, C. D. *et al.*, 1995; Kamisaki, Y. *et al.*, 1996). Taurine is found in ON axons, in various neurons, and in astrocytes (Kratskin, I. L. *et al.*, 2000; Kratskin, I. and Belluzzi, O., 2002; Pow, D. V. *et al.*, 2002). In the ON terminals and some postsynaptic dendrites, taurine is colocalized with glutamate (Didier, A. *et al.*, 1994). Observation of spontaneous taurine release from MOB synaptosomes suggests that taurine may be abundantly released (Kamisaki, Y. *et al.*, 1996). In electrophysiological recordings, taurine directly activated presynaptic $GABA_B$ receptors and inhibited ON terminals, and it also induced Cl^- currents in mitral/tufted cells. Surprisingly, taurine had no direct effect on PG cells (Belluzzi, O. *et al.*, 2004).

4.37.2.2.2.(i).(c) ET and mitral/tufted cell dendrodendritic interactions with PG and SA cells As noted above, ET and mitral/tufted cells form excitatory glutamatergic dendrodendritic synapses with PG and SA cells in the glomeruli. PG cells, and

perhaps SA cells, in turn, form inhibitory GABAergic dendrodendritic synapses with ET and mitral/tufted cells. Although the ET and mitral/tufted cell input is excitatory, this topic is considered here for simplicity. Compared to the dendrodendritic synapses between mitral/tufted and GCs in the EPL, far less is known about the properties of the dendrodendritic synapses in the GL. PG and SA cells were reported to receive spontaneous bursts of glutamatergic EPSCs (Hayar, A. *et al.*, 2004b). Since SA cells and most PG cells do not receive direct ON input, this input must arise from other excitatory elements within the glomeruli. Prime candidates include the apical dendrites of ET cells and mitral tufted cells. Consistent with this, stimulation of the MCL or lateral olfactory tract (LOT) has been used to produce antidromic spikes which propagate into, and trigger glutamate release from, mitral/tufted cell apical dendrites. Such stimulation was reported to excite JG cells in the GL (Ennis, M. *et al.*, 2001). More recently, spontaneous spike bursts or direct depolarization of individual ET cells to elicit spike bursts were reported to trigger EPSC bursts in PG and SA cells mediated by activation of AMPA receptors (Figure 10) (Hayar, A. *et al.*, 2004b). The latency of the evoked EPSCs (0.85 ms) was indicative of monosynaptic input to PG cells from ET cells. Additional studies demonstrated that this ET cell to PG/SA cell excitatory transmission is intraglomerular as it was only observed between cells associated with the same glomerulus. Stimulation of an individual ET cell was reported to produce large EPSCs and Ca^{2+} spikes in PG cells (Murphy, G. J. *et al.*, 2005). The NMDA receptor antagonist 2-amino-5-phosphono-valeric acid (APV) had minimal effects on the EPSP but abolished the Ca^{2+} spike. The same study reported that stimulation of a single ET cell excites two to seven unidentified JG cells within the same glomerulus, suggesting that individual ET cells synapse with multiple PG cells.

Single spikes in ET cells are relatively ineffective in triggering GABA release from PG cells (Murphy, G. J. *et al.*, 2005). Multiple spikes, leading to LVA Ca^{2+} currents, are much more effective in releasing GABA from PG cells (Murphy, G. J. *et al.*, 2005). These findings suggest that GABA release from PG cells may be preferentially triggered when these cells receive strong synaptic input. ET cells, individually and collectively, provide strong input to PG cells. Spike bursts in individual ET cells robustly activate PG cells. Additionally, individual ET cells appear to activate, on average, five PG cells (Murphy, G. J. *et al.*, 2005). Since ET cells spontaneously generate synchronous spike bursts and provide convergent input to a multiple PG cells, they are likely to drive tonic release of GABA from PG cells. By contrast, dendrodendritic input from mitral cells, which do not spontaneously burst *in vitro*, may play a larger role in driving GABA release following sensory input.

PG cells contain GABA, and thus activation of these cells will cause dendrodendritic inhibition of ET and mitral/tufted cell dendrites in the glomeruli. PG cell axons also form symmetrical synapses onto the mitral/tufted cell dendrites and onto PG and SA cells (Pinching, A. J. and Powell, T. P., 1971c). Physiological studies support the notion that PG cells receive excitatory input from mitral/tufted cells and ET cells, and in return, make feedforward and feedback inhibitory GABAergic synapses onto these cells (Shepherd, G. M. and Greer, C. A., 1998; Hayar, A. *et al.*, 2004b). Such inhibition is thought to be primarily mediated by $GABA_A$ receptors. ET cells exhibit spontaneous bursts of IPSCs, indicating that these are tonically inhibited by GABAergic inputs (Figure 11) (Hayar, A. *et al.*, 2005). Spontaneous or ON-evoked EPSCs in ET cells are followed by bursts of IPSCs that are synchronous among ET cells of the same glomerulus. Thus, inhibitory GABAergic input from PG cells may coordinate the activity of ET cells associated with the same glomerulus. Intracellular depolarization of ET cells leads to GABAergic inhibition due to activation of dendrodendritic synapses with PG cells (Murphy, G. J. *et al.*, 2005). Using this paradigm, the feedback inhibition produced by ET cell depolarization was reduced by nimodopine, a blocker of L-type Ca^{2+} channels; nimodipine, however, did not reduce GABA release from PG cells. Subsequent experiments, using paired recordings of PG cells, suggested that GABA exocytosis from these cells is governed primarily by activation of HVA, P/Q-type Ca^{2+} channels. The L-type antagonist nimodipine did not directly alter GABA exocytosis from PG cells, leading to the conclusion that activation of LVA currents can facilitate GABA release from PG cells, but these channels are not directly coupled to GABA exocytosis. These studies and others (Smith, T. C. and Jahr, C. E., 2002) also indicate that PG cells, under certain circumstances, can release GABA onto themselves, and perhaps neighboring PG cells. GABA has been reported to depolarize PG cells at their resting potential, probably due to elevated intracellular chloride concentrations (Siklos, L. *et al.*, 1995; Smith, T. C. and Jahr, C. E., 2002). It was suggested

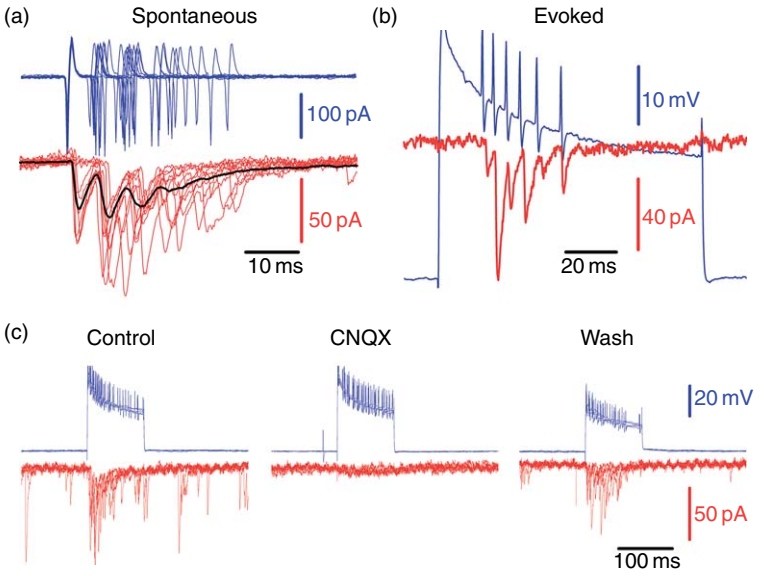

Figure 10 External tufted (ET) cells provide monoexcitatory synaptic input to periglomerular (PG) and short axon (SA) cells. (a) Dual recordings from an ET cell in cell-attached mode (blue traces) and a PG/SA cell in whole-cell voltage-clamp mode (red traces). Left panel (Spontaneous) shows 10 superimposed spontaneous spike burst-triggered traces (triggered on the first spike in the burst); black line is the average of 135 similar traces. Note that spontaneous action currents (blue trace) are accompanied by phase-locked busts of EPSCs (red trace). (b) (Evoked) shows an example of a burst of EPSCs (red trace) evoked by a burst of spikes elicited by extracellular injection of a positive current pulse (700 pA, 100 ms). Note close correspondence between evoked spikes in the ET cell and EPSCs in the SA/PG cell. (d) Recordings from the same two cells shown in panels a and b before (Control), during, and after (Wash) application of CNQX (10 μM). Note that bursts of EPSCs (red traces) in the SA/PG cell elicited by current injection-evoked spikes (blue traces) in the ET cell are completely blocked by CNQX (middle) in a reversible manner (right). CNQX also reversibly abolished spontaneous EPSCs. All panels show five superimposed sweeps. Adapted from Hayar, A., Karnup, S., Ennis, M., and Shipley, M. T. 2004b. External tufted cells: a major excitatory element that coordinates glomerular activity. J. Neurosci. 24, 6676–6685, with permission from The Society for Neuroscience.

that GABA inhibits PG cells by activating a chloride conductance that reduces the neuronal input resistance and shunts excitatory inputs. GABA released from PG cells was recently shown to inhibit other PG cells in the same glomerulus via $GABA_A$ receptors (Murphy, G. J. *et al.*, 2005). Because PG cell dendrites ramify within a restricted portion of a glomerulus, their functional interactions are presumably localized to microdomains of the extensive mitral/tufted cell dendritic arbors, or to nearby JG cells (Kasowski, H. J. *et al.*, 1999).

4.37.2.2.2.(ii) Neuromodulation in the GL

Neuromodulatory systems in the GL include carnosine and certain heavy metals (copper and zinc), and neuromodulatory inputs from centrifugal afferents. Centrifugal inputs are discussed below (see Neurophysiology of Neuromodulatory Inputs to Main Olfactory Bulb). Carnosine, a dipeptide synthesized by ORNs, is localized in ON terminals in the GL and fulfills many criteria for neurotransmitter candidacy. However, no direct postsynaptic actions of carnosine have been revealed to date (MacLeod, N. K. and Straughan, D. W., 1979; Nicoll, R. A. and Alger, B. E., 1980; Frosch, M. P. and Dichter, M. A., 1982; Trombley, P. Q. *et al.*, 1998). Carnosine did not affect currents evoked by glutamate, GABA, or glycine in cultured MOB neurons (Trombley, P. Q. *et al.*, 1998). Because carnosine is a chelator of both zinc and copper, it has been suggested that it might modulate transmission at ON synapses by regulating zinc and copper. Depending on the concentration, both zinc and copper can augment or block responses mediated by NMDA and GABA receptors. Both zinc and copper inhibit *N*-methyl D-aspartate (NMDA) and gamma-aminobutyric acid (GABA) receptor-mediated currents and synaptic transmission in MOB neurons (Trombley, P. Q. and Shepherd, G. M., 1996; Trombley, P. Q. *et al.*, 1998). Carnosine prevented the actions of copper and reduced the effects of zinc. These results suggest that carnosine may indirectly influence glutamate actions on MOB

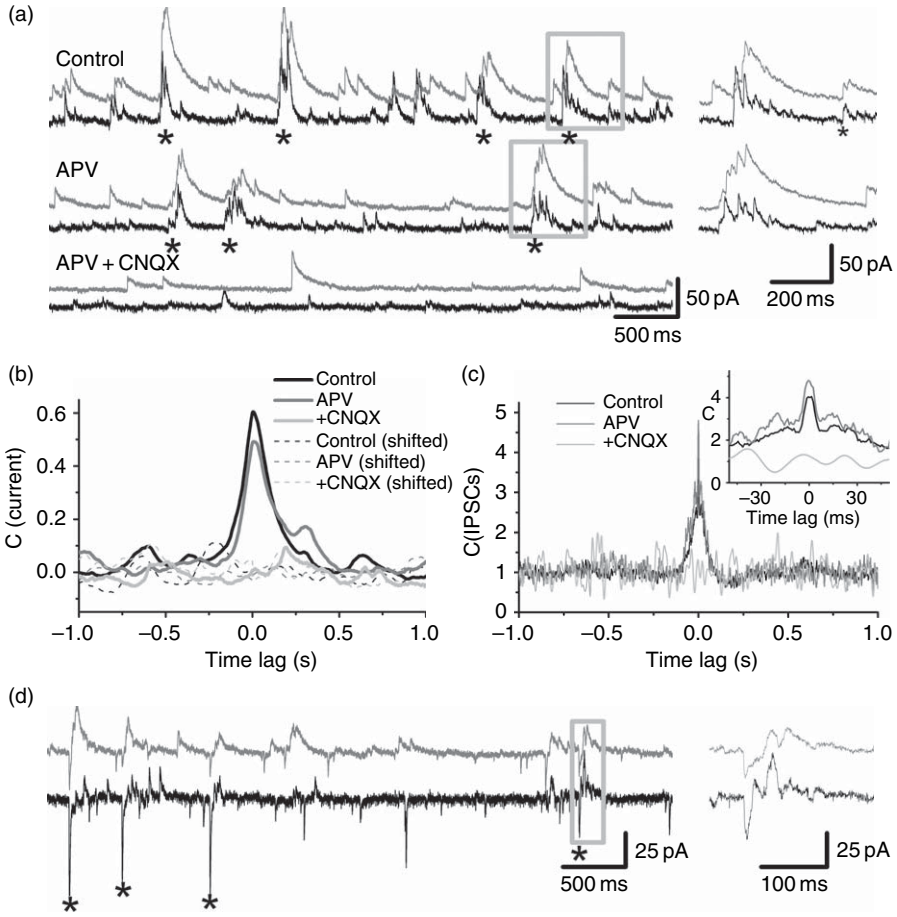

Figure 11 Synchronous bursts of IPSCs in external tufted (ET) cell pairs. All data in this figure were obtained from the same ET cell pair. (a) Simultaneous whole-cell voltage-clamp recordings (holding potential = 0 mV) from two ET cells (gray and black traces, respectively) show synchronous IPSC bursts (asterisks) before and during application of AP5 (50 μM). Note that although AP5 reduced burst frequency, bursts remained synchronous in the two cells. Additional application of CNQX eliminated the IPSC burst synchrony. Areas highlighted in rectangles are shown at faster timescale at right. (b) Membrane current cross-correlograms (50 s recording samples, 2 ms bins) in control, APV, and after additional application of CNQX. Note the significant peak at zero lag time in control and APV. There was no significant correlation after application of CNQX. The 99.73% confidence limit was determined by cross-correlating traces shifted by 5 s (dashed traces). (c) Cross-correlogram of the IPSC trains (5 min recording samples, 1 ms bins) show a significant narrow peak (see inset) at zero time lag, indicating synchronous IPSCs in the two recorded cells. The narrow peak was superimposed on a broader peak corresponding to the longer duration correlated IPSC bursts. CNQX abolished correlation and synchrony of IPSCs. (d) Simultaneous whole-cell voltage-clamp recordings (holding potential = – 30 mV) from the same two ET cells showing synchronous EPSCs followed by IPSC bursts; recording highlighted in rectangle is shown at faster timescale at right. Recordings obtained before the application of synaptic blockers (CNQX, AP5, gabazine) in (a). Adapted from Hayar, A., Shipley, M. T., and Ennis, M. 2005. Olfactory bulb external tufted cells are synchronized by multiple intraglomerular mechanisms. J. Neurosci. 25, 8197–8208, with permission from The Society for Neuroscience.

neurons by modulating the effects of synaptically released zinc and copper. What roles might carnosine, zinc, and copper play in olfactory processing? At present, there are no clear answers to this question. Is carnosine, like other peptide transmitters, preferentially released by high frequencies of ON activity? If so, carnosine may be preferentially released during intense odor stimulation. Zinc is known to be preferentially released during high-frequency neural activity. There are neurotoxic effects of zinc and copper, and Trombley (Horning, M. S. *et al.*, 2000) has speculated that carnosine, by preventing the actions of these metals, may serve an important neuroprotective function, perhaps to protect MOB neurons during intense or high-frequency activity.

4.37.2.3 Electrophysiology of Interglomerular Circuitry

Interglomerular interactions are poorly understood. As noted above, SA cells frequently have multiple dendrites (three to five) that extend over several (two to four) glomeruli (Aungst, J. L. *et al.*, 2003). Thus, these cells may receive odor information from multiple glomeruli. These cells do not receive direct ON input, but instead appear to receive olfactory input indirectly from ET and mitral/tufted cells (Hayar, A. *et al.*, 2004b). In turn, SA cells give rise to an axon that extends for considerable distances (~0.85 mm) in the GL (Aungst, J. L. *et al.*, 2003). Imaging studies suggest that the SA cells may be involved in lateral inhibition between glomeruli. Stimulation of the GL was reported to produce monosynaptic excitation of most ET and PG cells neurons in neighboring glomeruli mediated by activation of ionotropic glutamate receptors (Aungst, J. L. *et al.*, 2003). This suggests the intriguing possibility that SA cells are excitatory. Further, a prepulse to one glomerulus inhibited ON-evoked excitation of mitral cells in another glomerulus. It was concluded that the net functional effect of SA cell activation is to excite PG cells in other glomeruli, causing the release of GABA and inhibition of mitral cell responses to ON input. Taken together, these findings suggest that SA cells represent a major neural element for interglomerular interactions and that these cells may provide a substrate for center-surround inhibition – a common mechanism to enhance stimulus contrast in sensory circuits.

4.37.3 Neurophysiology of External Plexiform Layer

4.37.3.1 Tufted Cells

Tufted cells are the most numerous cells of the EPL. Three subclasses of tufted cells are recognized based on location in the EPL: superficial, middle, and deep tufted cells (Cajal, R. S. Y., 1890; Pinching, A. J. and Powell, T. P., 1971a; Macrides, F. and Schneider, S. P., 1982; Orona, E. *et al.*, 1984). Like ET cells and mitral cells, tufted cells of the mammalian EPL have one (or rarely several) apical dendrite(s) ending in a glomerular tuft (Cajal, R. S. Y., 1890). Like mitral cells, their apical dendrites receive ON input, and they form reciprocal dendrodendritic synapses with the dendrites of PG and SA cells. Their lateral dendrites ramify in the EPL and form dendrodendritic synapses with GCs and other inhibitory interneurons within the EPL. The neurophysiology of dendrodendritic interactions between mitral/tufted cells and GCs in the EPL is discussed below. Axonal projections of middle and deep tufted cells are similar, but not identical, to those of mitral cells (Schoenfeld, T. A. and Macrides, F., 1984; Schoenfeld, T. A. *et al.*, 1985). The local axon collaterals of tufted cells course mainly in the IPL. The projections of tufted cells beyond the MOB terminate densely in the anterior olfactory nucleus and, to a lesser extent, in other rostral olfactory cortical structures (Schoenfeld, T. A. *et al.*, 1985; Scott, J. W., 1986). Few tufted cell axons project into more caudal POC regions.

Tufted cells utilize glutamate as their principle transmitter (Liu, C. J. *et al.*, 1989; Christie, J. M. *et al.*, 2001), but they also stain for a number of other substances, including cholecystokinin (CCK). *In vivo* electrophysiological recordings have shown that the sensitivity of tufted cell subtypes to ON stimulation is correlated with the depth of the lateral dendrites within the EPL. The more superficial tufted cells are more easily excited by ON stimulation than the deeper tufted cells (Schneider, S. P. and Scott, J. W., 1983; Wellis, D. P. *et al.*, 1989; Ezeh, P. I. *et al.*, 1993). In response to odor stimulation, superficially located tufted cells also exhibit more prolonged excitation than mitral cells (Luo, M. and Katz, L., 2001). More recent studies have reported that tufted cells can be excited for up to several minutes following odorant presentation (Luo, M. and Katz, L., 2001). Thus, anatomically distinct tufted cell subtypes appear to be functionally distinct. In slices, tufted cells have been observed to exhibit spontaneous and ON-evoked bursting activity somewhat similar to that of ET cells (Hamilton, K. A. *et al.*, 2005). The extent to which such bursting varies among different tufted cell subtypes, as well as the mechanisms generating bursting, is unknown.

Many superficial tufted cells contain CCK (Seroogy, K. B. *et al.*, 1985), and their axons give rise to a reciprocal network, the intrabulbar association system (IAS) that connects lateral and medial regions of each MOB (Schoenfeld, T. A. *et al.*, 1985). The axons of the IAS travel to the opposite side of the bulb and terminate on the apical dendrites of GCs coursing through the IPL en route to the EPL (Liu, W. L. and Shipley, M. T., 1994). The IAS projection exhibits a high degree of point-to-point specificity. The IAS projections from tufted cells associated with a single glomerulus preferentially target the IPL deep to the second glomerulus on the other side of MOB

(Belluscio, L. *et al.*, 2002; Lodovichi, C. *et al.*, 2003). Thus, the IAS appears to modulate the activities of subsets of MOB neurons receiving input from ORNs expressing the same receptor, on opposite sides of the MOB. CCK typically is excitatory, and therefore the IAS may depolarize GCs.

4.37.3.2 EPL Interneurons

The EPL contains anatomically and neurochemically heterogeneous subtypes of intrinsic interneurons (for review, see Ennis, M. *et al.*, 2007). Many EPL interneurons stain for GABA and are therefore presumed to be inhibitory (Mugnaini, E. *et al.*, 1984; Gall, C. M. *et al.*, 1987; Kosaka, T. *et al.*, 1987c; Ohm, T. G. *et al.*, 1990). EPL interneuron subtypes are neurochemically diverse and stain for a number of neurotransmitter markers, including NADPH diaphorase (Scott, J. W. *et al.*, 1987; Villalba, R. M. *et al.*, 1989; Alonso, J. R. *et al.*, 1995), substance P (Baker, H., 1986; Wahle, P. *et al.*, 1990), enkephalin (Bogan, N. *et al.*, 1982; Davis, B. J. *et al.*, 1982), NPY (Gall, C. *et al.*, 1986; Scott, J. W. *et al.*, 1987; Sanides-Kohlrausch, C. and Wahle, P., 1990a), neurotensin and somatostatin (Matsutani, S. *et al.*, 1988), and VIP (Gall, C. *et al.*, 1986; López-Mascaraque, L. *et al.*, 1989; Sanides-Kohlrausch, C. and Wahle, P., 1990b; Nakajima, T. *et al.*, 1996). The role of these transmitters in the function of EPL interneurons is not known. EPL interneurons are thought to interact chiefly with mitral/tufted cell dendrites (López-Mascaraque, L. *et al.*, 1990; Nagayama, S. *et al.*, 2004) and possibly GC dendrites (Schneider, S. P. and Macrides, F., 1978). Combined morphological and electrophysiological analyses showed that GABAergic EPL interneurons with highly varicose dendrites are excited polysynaptically by ON stimulation, most likely via input from nearby mitral/tufted cells (Hamilton, K. A. *et al.*, 2005). The interneurons exhibit high levels of spontaneous glutamatergic synaptic activity mediated by AMPA/kainate receptors, consistent with GluR1 AMPA receptor subunit staining in these cells (Petralia, R. S. and Wenthold, R. J., 1992; Giustetto, M. *et al.*, 1997; Montague, A. A. and Greer, C. A., 1999; Hamilton, K. A. and Coppola, D. M., 2003). Many EPL interneurons have dendrites that spanned several adjacent glomeruli, suggesting that they may provide localized inhibition of mitral/tufted cells that are topographically related to overlying glomeruli (Hamilton, K. A. *et al.*, 2005).

4.37.4 Neurophysiology of Mitral Cells

4.37.4.1 Anatomical Features

Deep to the EPL is the MCL, a thin layer that contains the somata of mitral cells as well as numerous GCs (Cajal, R. S. Y., 1911a; 1911b). In fact, there are ~40,000 mitral cells (Meisami, E., 1989) and ~100,000 GCs in the MCL (Frazier, L. L. and Brunjes, P. C., 1988). Thus, mitral cells comprise less than one-half of the cells in the MCL. Together with tufted cells, mitral cells are the major class of output cells of the bulb. As noted above, mitral cells extend a single apical dendrite into one glomerulus. There are about 25 mitral cells (and 50 tufted cells) associated with a single glomerulus (Cajal, R. S. Y., 1911a; 1911b; Allison, A., 1953). The apical dendrites are synaptically contacted by ON terminals (Price, J. L. and Powell, T. P. S., 1970a; Shepherd, G. M., 1972). The secondary or lateral dendrites of mitral cells ramify in the EPL where they may extend up to 1–2 mm. These lateral dendrites participate in dendrodendritic synapses with dendrites of GCs, as reviewed below (see Dendrodendritic Transmission Between Mitral/Tufted Cells and Granule Cells). Mitral cells have been subdivided into two classes, Type I and Type II, based on extension of dendrites into the deep or superficial parts of the EPL, respectively (Orona, E. *et al.*, 1984). Type II mitral cells are more easily excited by ON stimulation than Type I mitral cells (Schneider, S. P. and Scott, J. W., 1983; Wellis, D. P. *et al.*, 1989; Ezeh, P. I. *et al.*, 1993). Mitral cell lateral dendrites receive centrifugal axon inputs and inputs from EPL interneurons (Jackowski, A. *et al.*, 1978; Toida, K. *et al.*, 1996). Mitral cells give off axon collaterals, which terminate within the bulb, in the IPL and GCL (Price, J. L. and Powell, T. P. S., 1970c; Mori, K. *et al.*, 1983), or exit the MOB and innervate a number of olfactory-related brain regions collectively known as the POC. Mitral (and tufted) cells are glutamatergic, and the neuropeptide corticotropin-releasing factor (CRF) has been demonstrated in mitral and some tufted cells. Substance P has been detected in approximately one-half of mitral cells by in situ hybridization (Warden, M. K. and Young, W. S., 1988), but they do not stain for substance P immunocytochemistry (Inagaki, S. *et al.*, 1982; Shults, C. W. *et al.*, 1984; Baker, H., 1986).

4.37.4.2 Spontaneous Discharge and Intrinsic Membrane Properties

In vivo extracellular recording studies in anesthetized animals indicate that most mitral cells fire at fairly

high spontaneous rates (6–30 Hz; mean rate, ~18 Hz) (Chaput, M. and Holley, A., 1979; Chaput, M., 1983; Yu, G.-Z. *et al.*, 1993; Jiang, M. R. *et al.*, 1996). They also exhibit periodic, long-duration (several minutes) tonic increases and decreases in firing rates that may be related to anesthesia (Yu, G.-Z. *et al.*, 1993; Jiang, M. R. *et al.*, 1996); mitral cells are less responsive to ON during the periods of reduced spontaneous activity. In awake rats, mitral cells firing rates range from 1 to 33 Hz with a mean rate of 12 Hz (Kay, L. M. and Laurent, G., 1999). A detailed consideration of mitral cell odor responses, receptive fields, and plasticity is beyond the scope of this chapter, and readers are referred to recent work in this area (Kashiwadani, H. *et al.*, 1999; Kay, L. M. and Laurent, G., 1999; Luo, M. and Katz, L., 2001; Fletcher, M. L. and Wilson, D. A., 2003; Nagayama, S. *et al.*, 2004; Mori, K. *et al.*, 2006).

Mitral cell spontaneous firing patterns and odor responses *in vivo* are modulated as a function of the respiratory cycle. Recent patch clamping studies in anesthetized rodents has provided new information on properties of mitral spontaneous and odor-evoked discharge. Mitral cells exhibit subthreshold membrane potential oscillations or action potentials synchronized to or modulated by respiration, which occurs in the theta frequency range, 1–12 Hz (Philpot, B. D. *et al.*, 1997; Chalansonnet, M. and Chaput, M. A., 1998; Kay, L. M. and Laurent, G., 1999; Charpak, S. *et al.*, 2001; Luo, M. and Katz, L., 2001; Debarbieux, F. *et al.*, 2003; Margrie, T. W. and Schaefer, A. T., 2003). The peak depolarization of the membrane potential oscillation coincides with the peak of the inhalation phase (Margrie, T. W. and Schaefer, A. T., 2003). The rhythmic membrane potential oscillations are blocked by glutamate receptor antagonists, demonstrating that they are synaptically mediated (Margrie, T. W. and Schaefer, A. T., 2003). Combined intrinsic imaging of glomerular odor responses and intracellular recordings from mitral cells suggest that mitral cells recorded below odor responsive glomeruli are excited by the odor, whereas those cells distant from the activated glomeruli show no response or are inhibited (Luo, M. and Katz, L., 2001). In responses to excitatory odors, mitral cells typically generate EPSPs and spikes that are synchronized to the inspiratory phase of respiration which occurs in the theta frequency range (Charpak, S. *et al.*, 2001; Margrie, T. W. *et al.*, 2001; Cang, J. and Isaacson, J. S., 2003; Debarbieux, F. *et al.*, 2003; Margrie, T. W. and Schaefer, A. T., 2003). EPSP amplitudes vary proportionately with the strength of the odor stimulus, and spikes are often launched from the rising phase of odor-evoked EPSPs (Cang, J. and Isaacson, J. S., 2003; Margrie, T. W. and Schaefer, A. T., 2003). The latency of the first spike following odor stimuli is inversely proportional to the number of spikes per respiratory cycle such that shorter latencies are observed when spike bursts are elicited (Cang, J. and Isaacson, J. S., 2003; Margrie, T. W. and Schaefer, A. T., 2003). This suggests that the initial spike latency may provide information about the strength of sensory input; that is, the concentration of odors. Sufficiently strong odor stimulation triggers a spike burst, with spikes in the burst occurring within the β–γ frequency range (20–60 Hz) (Debarbieux, F. *et al.*, 2003). The interburst spike frequency is constant across bursts that vary in the number of spikes (Margrie, T. W. and Schaefer, A. T., 2003). This suggests that the instantaneous spike frequency probably is not modulated by network-driven factors. Mitral cells also exhibit inhibitory responses to odors (Luo, M. and Katz, L., 2001; Margrie, T. W. *et al.*, 2001; Cang, J. and Isaacson, J. S., 2003). The strength of odor-evoked inhibitory postsynaptic potentials (IPSPs) does not vary with the concentration of the odor stimulus (Cang, J. and Isaacson, J. S., 2003). However, the IPSP amplitudes are larger during the initial respiratory cycle compared to subsequent cycles in the presence of an odorant.

In slices, mitral cell spontaneous discharge is more modest (1–6 Hz, mean, 3 Hz), presumably because tonic sensory input is absent (Ennis, M. *et al.*, 1996, Ciombor, K. J. *et al.*, 1999; Heyward, P. M. *et al.*, 2001). Mitral cell spontaneous firing is intrinsically generated and persists in the presence of blockers of ionotropic glutamate and GABA receptors (Ennis, M. *et al.*, 1996; Heyward, P. M. *et al.*, 2001). Patch clamp recordings have revealed that mitral cells exhibit intrinsic membrane bistability (Heyward, P. M. *et al.*, 2001; Heinbockel, T. *et al.*, 2004). They spontaneously alternate between a perithreshold upstate membrane potential and a more hyperpolarized (approximately −10 mV) downstate membrane potential (Figure 13). Bistability is typically encountered in mitral cells recorded in the depth of the slice (>70 μm from the surface) and may be absent in superficially located cells. Spontaneous or ON-evoked spikes are readily launched from the upstate, and a spike afterhyperpolarization or a hyperpolarization induced by an IPSP or current injection of sufficient amplitude resets the cell to the downstate.

In the downstate, more robust ON input is necessary to trigger spikes. The upstate is also characterized by high-frequency (10–50 Hz) subthreshold membrane potential oscillations that appear to be mediated by a balance between opposing K^+ currents and TTX-sensitive Na^+ currents (Desmaisons, D. *et al.*, 1999; Heyward, P. M. *et al.*, 2001; Balu, R. *et al.*, 2004). Inhibitory synaptic input (e.g., IPSPs) can reset the phase of the oscillations and the timing of mitral cell spikes (Desmaisons, D. *et al.*, 1999). The downstate appears to be maintained by slowly inactivating outward currents (e.g., K^+ currents), and the transition from the downstate to the upstate is due to inactivation of the outward currents and activation of regenerative voltage-dependent inward currents (e.g., TTX-sensitive, persistent Na^+ currents). The transition from the upstate to the downstate may reflect voltage-dependent inactivation of inward currents and activation of outward currents initiated by action potentials. Other aspects of mitral cell spontaneous activity are discussed below in Oscillations and Synchrony in Main Olfactory Bulb.

Further studies indicated that mitral cell-evoked activity is regulated by interactions between subthreshold TTX-sensitive Na^+ currents and by 4-amonipyridine (4-AP)-sensitive K^+ currents, such as transient outward or I_D currents (Balu, R. *et al.*, 2004). In response to sustained depolarization pulses, mitral cells generate intermittent spike clusters at 20–40 Hz, with clusters occurring with variable timing at theta frequencies (1–5 Hz). Brief repolarizations to recover inactivated Na^+ currents during sustained depolarizing pulses eliminated spike variability. Brief depolarizing pulses or simulated EPSPs mimicking rhythmic ON input during sniffing elicited highly precise spike clusters. The first EPSP frequently failed to elicit spikes, but decreased the spike threshold for subsequent EPSPs. 4-AP caused spikes to be triggered by the first EPSP but impaired precise spike timing to subsequent EPSPs. 4-AP also abolished intermittent or clustered firing during sustained depolarizations. Taken together, these findings suggest that intrinsic properties of mitral cells yield variable spiking responses to sustained depolarizations but allow temporally precise or phase-locked spiking responses to brief phasic input. Based on this, it has been suggested that mitral cells may be functionally analogous to high-pass filters, preferentially responding to phasic events that occur at theta frequencies (Balu, R. *et al.*, 2004).

Mitral cells also exhibit afterhyperpolarizations mediated by Ca^{2+}-dependent K^+ conductances (Maher, B. J. and Westbrook, G. L., 2005). Step depolarization of mitral cells to +10 mV elicits outward currents that are attenuated by Cd^{2+} or the SK K^+ channel antagonist apamin. This current was reported to be absent in GCs. The SK current could be activated by Ca^{2+} influx via NMDA receptors or voltage-dependent Ca^{2+} channels. Apamin application increased the depolarization-evoked firing frequency of mitral cells. Other studies indicate that mitral cells lack, or have very weak, H-type currents (Djurisic, M. *et al.*, 2004). Mitral cells also express Kv1.3, a rapidly activating, moderately slow inactivating type of voltage-gated K^+ channels (Fadool, D. A. *et al.*, 2004). Mitral cells from Kv1.3-knockout mice have more depolarized resting potentials and smaller, broader spikes in comparison with those from wildtype mice.

4.37.4.3 Dendritic Spike Propagation

In vivo, odors have been reported to elicit fast prepotentials in mitral cells thought to represent truncated spikes generated in the apical dendrites (see Mori, K., 1987 for review). Similar fast prepotentials have been observed in slices (Chen, W. R. and Shepherd, G. M., 1997). More recent findings in MOB slices demonstrate that both the apical and lateral dendrites of mitral cells actively propagate action potentials. Spike elicited at the soma backpropagate nondecrementally along the apical dendrite and vice versa (Bischofberger, J. and Jonas, P., 1997; Chen, W. R. *et al.*, 1997; Isaacson, J. S. and Strowbridge, B. W., 1998; Debarbieux, F. *et al.*, 2003). The ability of the apical dendrite to generate spikes is due to the presence of TTX-sensitive Na^+ channels (Bischofberger, J. and Jonas, P., 1997). These studies suggest that with sufficiently strong ON input, spikes can be initiated in the apical dendrite and conducted to the soma without decrement. However, the site of spike initiation can be controlled by inhibitory inputs to the soma. With leak levels of ON stimulation, spikes are preferentially triggered at the soma, but this can be blocked by IPSPs at the soma or proximal segments of the lateral dendrite (Chen, W. R. *et al.*, 1997; Djurisic, M. *et al.*, 2004). With stronger levels of ON input, inhibitory inputs to the soma shifted the spike initiation site to the apical dendrite. ON-evoked EPSPs by contrast are decremental, and they decrease in amplitude by ~30% over a 300-μm distance in the apical dendrite (Djurisic, M. *et al.*, 2004).

Similar studies demonstrate actively propagating Na^+ spikes in mitral cell lateral dendrites

(Margrie, T. W. *et al.*, 2001; Xiong, W. and Chen, W. R., 2002). This suggests that spikes in single mitral cells, via activation of mitral to granule synapses, could conceivably inhibit mitral cells at considerable distances throughout the MOB. However, whether the spike propagation is nondecremental along the full length of the lateral dendrite is unclear as propagation has been reported to be attenuating (Margrie, T. W. *et al.*, 2001; Lowe, G., 2002; Christie, J. M. and Westbrook, G. L., 2003) or nonattenuating (Margrie, T. W. *et al.*, 2001; Xiong, W. and Chen, W. R., 2002; Debarbieux, F. *et al.*, 2003). Spike attenuation was reported to be caused by activation of A-type K^+ channels in the lateral dendrites (Christie, J. M. and Westbrook, G. L., 2003). Regenerative Ca^{2+} currents do not appear to play a role in dendritic spikes (Charpak, S. *et al.*, 2001; Margrie, T. W. *et al.*, 2001; Xiong, W. and Chen, W. R., 2002; Christie, J. M. and Westbrook, G. L., 2003). Local synaptic inhibitory input (GABAergic IPSPs) can block propagation of spikes in the lateral dendrite (Margrie, T. W. *et al.*, 2001; Lowe, G., 2002; Xiong, W. and Chen, W. R., 2002). Such inhibition is more influential when it occurs at the soma and/or proximal dendrites. Thus, inhibitory input to the soma and lateral dendrites may spatially constrain the range and magnitude of lateral inhibition (see also Dendrodendritic Inhibition).

4.37.4.4 Modulation by mGluRs and DA

In dissociated cultured rat and frog MOB neuronal preparations, Group I mGluRs increased Ca^{2+} release from internal stores in mitral/tufted cells as well as in MOB interneurons (Geiling, H. and Schild, D., 1996; Carlson, G. C. *et al.*, 1997), or it depolarized and increased the frequency of miniature excitatory postsynaptic currents in mitral cells (Schoppa, N. E. and Westbrook, G. L., 1997). Other studies indicate that activation of Group III mGluRs with AP4 inhibits Ca^{2+} currents in mitral cells and presynaptically decreases mitral cell to GC synaptic transmission (Trombley, P. Q. and Westbrook, G. L., 1992). More recent studies in rat and mouse MOB slices demonstrate that activation of mGluR1 directly depolarizes and increases the firing of MCs and that these effects persist in the presence of blockers of fast synaptic transmission (Figure 12) (Heinbockel, T. *et al.*, 2004). The same study showed that mGluR1 induces a voltage-dependent inward current consisting of multiple components. mGluR1 antagonists also altered mitral cell membrane potential bistability, increasing the duration of the upstates and downstates, and substantially attenuated ON-evoked spikes (Figure 13). These findings suggest that endogenous glutamate tonically modulates MC excitability and responsiveness to ON input via activation of mGluR1. Although DA has no direct effect on resting membrane properties of mitral cells, pharmacological activation of D2 receptors was found to reduce glutamate release from mitral cells onto olfactory bulb interneurons in culture via inhibition of N and/or P/Q HVA Ca^{2+} channels (Davila, N. G. *et al.*, 2003).

4.37.5 Neurophysiology of Neurons in the Granule Cell Layer

4.37.5.1 Neuron Types of the GCL

GCs are axon-less cells with small cell bodies that are mostly tightly packed into row-like aggregates of three to nine somata in the GCL (Reyher, C. K. *et al.*, 1991). More superficially located GCs are also found mixed with mitral cell bodies within the MCL. Most GCs have an apical dendrite that ramifies within the EPL and shorter basal dendrites that ramify within the GCL. A differential sublaminar distribution has been observed for the dendrites of superficial and deep GCs. The apical dendrites of superficial GCs have very dense spines, and they terminate within both the superficial and deep portions of the EPL. By contrast, the apical dendrites of deeper GCs terminate preferentially within the deep EPL (Orona, E. *et al.*, 1983; Greer, C. A., 1987). Most GCs contain GABA (Ribak, C. E. *et al.*, 1977), but some contain enkephalin (Bogan, N. *et al.*, 1982; Davis, B. J. *et al.*, 1982). GC apical dendrites receive asymmetrical synapses from, and make symmetrical synapses onto, mitral/tufted cells. GCs also receive asymmetrical synapses from a variety of centrifugal afferents, including inputs from neuromodulatory transmitter systems (see Neurophysiology of Neuromodulatory Inputs to Main Olfactory Bulb) and POC (see Neurophysiology of Primary Olfactory Cortical Inputs to Main Olfactory Bulb) (Price, J. L. and Powell, T. P. S., 1970c). Centrifugal fibers arise from neurons in POC (e.g., piriform cortex (PC) and anterior olfactory nucleus) and comprise the bulk of synaptic contacts onto GC somata and proximal dendrites within the GCL (Price, J. L. and Powell, T. P. S., 1970c). GCs also receive synapses from the collateral branches of mitral and tufted cell axons, as well as inputs from

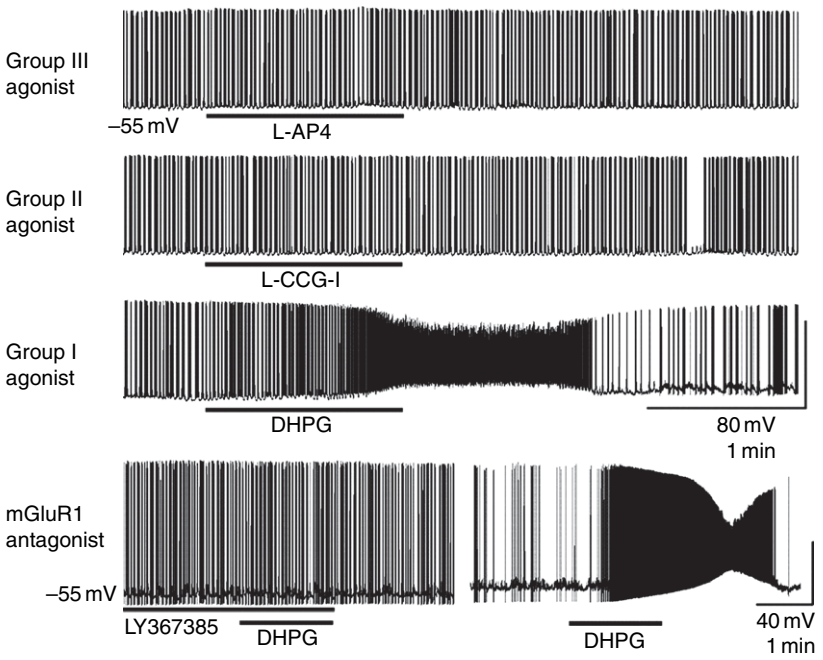

Figure 12 The group I mGluR agonist (RS)-3,5-dihydroxyphenylglycine (DHPG) depolarizes and increases the firing of mitral cells. Mitral cells were activated by group I, but not group II or III, mGluR agonists. Bath application of the group III mGluR agonist L(+)-2-amino-4-phosphonobutyric acid (AP4; 100 μM) or the group II mGluR agonist (2S,3S,4S)-CCG/(2S,1'S,2'S)-2-(carboxycyclopropyl)glycine (L-CCG-I; 20 μM) did not alter the membrane potential or firing rate of this mouse mitral cell (MC) in current clamp recordings. The same cell was activated by the selective group I agonist DHPG. The selective mGluR1 antagonist ({alpha}S)-{alpha}-amino-{alpha}-[(1S,2S)-2-carboxycyclopropyl]-9H-xanthine-9-propanoic acid (LY367385, 100 μM) blocked the actions of the group I mGluR agonist DHPG (50 μM) in another mouse MC. After washout (>15 min), reapplication of DHPG robustly depolarized and increased MC spontaneous discharge. All experiments were performed in the presence of blockers of fast synaptic transmission: CNQX (10 μM), APV (50 μM), and gabazine (5 μM). Reprinted from Heinbockel, T., Heyward, P., Conquet, F., and Ennis, M. 2004. Regulation of main olfactory bulb mitral cell excitability by metabotropic glutamate receptor mGluR1. J. Neurophysiol. 92, 3085–3096, with permission from The American Physiological Society.

Golgi, Cajal, and Blanes cells (Price, J. L. and Powell, T. P. S., 1970c).

The IPL and GCL also contain several interneuron subtypes (short-axon cells; Golgi, Cajal, and Blanes cells) that have dendrites and axons that ramify within the EPL, MCL, and GCL (Price, J. L. and Powell, T. P. S., 1970b; Schneider, S. P. and Macrides, F., 1978; Cajal, R. S. Y., 1890; Van Gehuchten, L. E. and Martin, A., 1891; Blanes, T., 1898; López-Mascaraque, L. *et al.*, 1990). These cells stain for a number of transmitters, including GABA, VIP, NPY, enkephalin, and somatostatin (see Ennis, M. *et al.*, 2007 for review). With the exception of Blanes cells, very little is known about the functions of the deep interneurons, but all are presumed to be inhibitory. Blanes cells have numerous dendrites emerging from all sides of the soma. The axons from these cells can extend considerable distances, but they typically remain within the GCL (Cajal, R. S. Y., 1911a; 1911b; Pressler, R. T. and Strowbridge, B. W., 2006). The anatomical features of other interneurons in the IPL/GCL are reviewed elsewhere (Ennis, M. *et al.*, 2007).

4.37.5.2 Neurophysiology of GCs

In vivo and in slice preparations, GCs spontaneous spiking is relatively infrequent, probably due to their relatively hyperpolarized resting potential (−65 to −75 mV) and appears to be driven primarily by spontaneous glutamatergic input (Wellis, D. P. and Scott, J. W., 1990; Cang, J. and Isaacson, J. S., 2003; Zelles, T. *et al.*, 2006; Heinbockel, T. *et al.*, 2007). Synaptic input or direct depolarization can elicit Na^+ and Ca^{2+} spikes in GCs (Halabisky, B. *et al.*, 2000; Pinato, G. and Midtgaard, J., 2003; 2005; Egger, V. *et al.*, 2005). By contrast to mitral cells, odor-evoked responses in GCs attenuate rapidly after the first respiratory cycle (Cang, J. and Isaacson, J. S., 2003).

GCs express Ca^{2+} currents which activate at approximately −60 mV and peak at 0–5 mV (Chen, W. R.

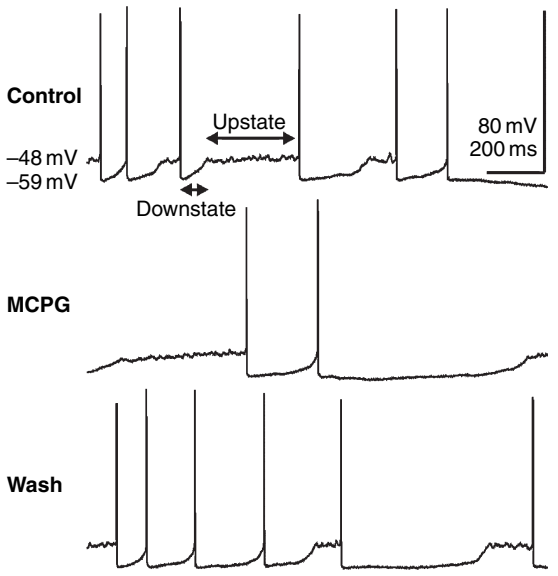

Figure 13 Activation and blockade of mGluRs modulates mitral cell (MC) spontaneous activity and membrane bistability. Upper trace: Current clamp recording showing membrane bistability in a rat MC. Middle trace: Bath application of MCPG (500 μM) reduced the firing frequency of the MC and prolonged the upstates and downstates. Bottom trace: the effects of MCPG were reversible on washout. Reprinted from Heinbockel, T., Heyward, P., Conquet, F., and Ennis, M. 2004. Regulation of main olfactory bulb mitral cell excitability by metabotropic glutamate receptor mGluR1. J. Neurophysiol. 92, 3085–3096, with permission from The American Physiological Society.

et al., 2000; Isaacson, J. S. and Vitten, H., 2003). These currents involve both LVA T-type Ca^{2+} currents and HVA Ca^{2+} currents (Isaacson, J. S. and Vitten, H., 2003). T-type currents can be activated by depolarization subthreshold for spike initiation and have been linked to GABA release from GCs (Egger, V. *et al.*, 2003). Small subthreshold EPSPs seem to produce Ca^{2+} transients restricted to dendritic spines (Egger, V. *et al.*, 2005). These Ca^{2+} transients appear to involve several sources, including LVA and HVA Ca^{2+} channels, NMDA receptors, and Ca^{2+}-induced Ca^{2+} release (Egger, V. *et al*, 2005). Sufficiently large EPSPs can trigger an all-or-none LTS that propagates throughout the GC dendrites (Egger, V. *et al.*, 2005). LTSs in GC soma have been described in amphibians (Pinato, G. and Midtgaard, J., 2003; 2005).

GC activity is strongly regulated by several K^+ conductances. They have a strong transient A-type K^+ current, I_A (Schoppa, N. E. and Westbrook, G. L., 1999). I_A in these cells activates at approximately −44 mV, at or near the threshold for spike generation (−47 mV). Many I_A channels are only half-inactivated at GC resting membrane potential, and thus are available to affect depolarizing inputs (Schoppa, N. E. and Westbrook, G. L., 1999). Blockade of I_A with 4-AP decreases the lag or delay for evoked spikes. The I_A channels are expressed in the distal dendrites of GCs where they tend to counter brief depolarizing synaptic inputs. BK-type or high-conductance Ca^{2+}-activated K^+ currents involved in spike repolarization of afterhyperpolarization are engaged in GCs by strong depolarization or activation of NMDA receptors (Isaacson, J. S. and Murphy, G. J. 2001). Anatomically, gap junctions have been reported among GCs (Reyher, C. K. *et al.*, 1991), although electrophysiological studies found no evidence for electrotonic coupling (Schoppa, N. E., 2006). GCs in the GCL are potently activated by mGluR1 agonists, which depolarize and increase the firing rate of these cells (Heinbockel, T. *et al.*, 2007). By contrast, mGluR1 antagonists reduce mitral/tufted cell-evoked excitation of GCs.

4.37.5.3 Neurophysiology of Blanes Cells

Blanes cells are neurophysiologically distinct from GCs (Pressler, R. T. and Strowbridge, B. W., 2006). They have lower input resistance, more depolarized resting potential, and more hyperpolarized spike threshold than GCs. Stimulation of Blanes cells elicits monosynaptic GABAergic IPSPs in GCs, but Blanes cells do not receive reciprocal input from GCs. These cells generate prominent afterdepolarizations (ADPs) after action potentials that are triggered by Ca^{2+} influx through non-L-type channels. ADPs were suppressed by flufenamic acid, a blocker of nonspecific cation currents (I_{CAN}). Taken together, these findings suggest that the ADP is mediated by a Ca^{2+}-dependent I_{CAN}. Brief depolarization triggers unusually prolonged (up to 44 min) persistent spiking in Blanes cells. Persistent firing could also be triggered by excitatory synaptic input elicited by stimulation in the GCL or the GL. Stimuli that evoked persistent firing in Blanes cells also produced prolonged barrages of IPSCs in GCs. These findings indicate that Blanes cells play a major role in prolonged modulation of the excitability state of GCs, which in turn would impact on the activity of mitral/tufted output neurons. Blanes cells preferentially target the basal dendrites and somata of GCs, and like GCs, Blanes cells may receive centrifugal feedback projections from POC. If so, then direct

activation of GCs by POC inputs may be followed by prolonged Blanes cell-mediated inhibition of GCs. Thus, the activity state of Blanes cells may provide a gate on excitatory feedback projections from POC to GCs, which in turn, would modulate GC inhibition of mitral/tufted cells.

4.37.6 Dendrodendritic Transmission Between Mitral/Tufted Cells and Granule Cells

4.37.6.1 Overview of Mitral/Tufted Cell–GC Dendrodendritic Interactions

The majority of synapses of the EPL are between the lateral dendrites of mitral/tufted cells and the dendrites of GCs. Most of the synapses are: (1) asymmetrical synapses from the mitral/tufted cell lateral dendrites onto GC dendrites, and (2) symmetrical synapses from the spines (gemmules) of GC dendrites onto the mitral/tufted cell lateral dendrites (Price, J. L. and Powell, T. P. S., 1970b; 1970c; 1970d). These synapses are mostly reciprocal (Hirata, Y., 1964; Rall, W. *et al*., 1966; Price, J. L. and Powell, T. P. S., 1970d; Woolf, T. B. *et al*., 1991) and therefore occur in roughly equal proportion (Jackowski, A. *et al*., 1978). One mitral/tufted cell can therefore receive feedback inhibition as well as lateral inhibition from GCs that are excited by other mitral/tufted cells.

4.37.6.2 Excitatory Transmission from Mitral/Tufted Cells to GCs

Spike-evoked Ca^{2+} transients in mitral cells, and presumably glutamate release, is abolished by Cd^{2+} but not Ni^{2+}, indicating that it requires activation of HVA Ca^{2+} channels (Isaacson, J. S. and Strowbridge, B. W., 1998). Intracellular Ca^{2+} buffering in mitral cells indicates that the Ca^{2+} channels that trigger dendritic glutamate release are located nearby active release sites (Isaacson, J. S. and Strowbridge, B. W., 1998). In normal or Mg^{2+}-free extracellular media, stimulation of mitral/tufted cells evokes dual-component EPSCs in GCs, consisting of a fast AMPA receptor component and a slow NMDA receptor component (Isaacson, J. S. and Strowbridge, B. W., 1998; Schoppa, N. E. *et al*., 1998; Aroniadou-Anderjaska, V. *et al*., 1999a; Chen, W. R. *et al*., 2000; Isaacson, J. S., 2001). AMPA receptors in cultured GCs desensitize rapidly and have little or no Ca^{2+} permeability (Blakemore, L. J. and Trombley, P. Q., 2003), suggesting that GC AMPA receptors must include GluR2 subunits, which regulate Ca^{2+} permeability (Jardemark, K. *et al*., 1997). The AMPA receptor synaptic component evoked by mitral/tufted cell input is less effective than the NMDA receptor component in evoking spikes in GCs, especially in Mg^{2+}-free conditions (Schoppa, N. E. *et al*., 1998). As noted above, block of I_A enhances the ability of the AMPA receptor component to trigger spikes in GCs (Schoppa, N. E. and Westbrook, G. L., 1999). Paired-pulse stimulation of mitral cells can produce either facilitation or depression of the GC excitatory response to the second pulse, but on average leads to paired-pulse facilitation (Dietz, S. B. and Murthy, V. N., 2005). With repetitive stimulation trains, mitral to GC responses were suppressed less than GC to mitral cell inhibitory responses. Mitral/tufted cell to GC transmission may be modulated by mGluRs and monoaminergic transmitters (see Section Neurophysiology of Neuromodulatory Inputs to Main Olfactory Bulb). Activation of Group III mGluR was reported presynaptically to decrease mitral cell to GC synaptic transmission (Trombley, P. Q. and Westbrook, G. L., 1992).

4.37.6.3 Inhibitory Transmission from GCs to Mitral/Tufted Cells

Activation of GCs evokes IPSPs/IPSCs in mitral cells mediated by activation of $GABA_A$ receptors (Chen, W. R. *et al*., 2000; Isaacson, J. S. and Vitten, H., 2003; Dietz, S. B. and Murthy, V. N., 2005). Paired-pulse or repetitive activation of GCs typically produces paired-pulse inhibition of mitral cell synaptic responses; that is, the response to the second or subsequent pulses are smaller than that to the first (Isaacson, J. S. and Vitten, H., 2003; Dietz, S. B. and Murthy, V. N., 2005). Pharmacological activation of $GABA_B$ receptors on GCs has been reported to reduce GABA release from these cells via inhibition of HVA Ca^{2+} currents (Isaacson, J. S. and Vitten, H., 2003).

4.37.6.4 Dendrodendritic Inhibition

4.37.6.4.1 Self-inhibition

Intracellular stimulation of single mitral cells in the presence or absence of TTX results in a dendrodendritically mediated feedback IPSPs/IPSCs, that is, self-inhibition or feedback inhibition (Isaacson, J. S. and Strowbridge, B. W., 1998; Schoppa, N. E. *et al*., 1998; Chen, W. R. *et al*., 2000; Halabisky, B. *et al*., 2000; Dietz, S. B. and Murthy, V. N., 2005). Subsequent studies demonstrated that TTX has opposite effects

on self-inhibition that depend upon the strength of the mitral cell depolarizing pulse; that is, the amount of glutamate released by the mitral cell (Halabisky, B. *et al.*, 2000). Short-pulse (2–3 ms) self-inhibition is reduced, whereas long-pulse (>25 ms) inhibition is enhanced, by TTX. The feedback inhibition is of long duration (1–2 s) and consists of a flurry of individual IPSPs/IPSCs. The slow kinetics suggest that the feedback IPSPs/IPSCs is mediated by asynchronous GABA release from multiple GCs (Schoppa, N. E. *et al.*, 1998). In normal extracellular levels of Mg^{2+}, the self-inhibition is reduced to similar levels by AMPA or NMDA receptor antagonism and is abolished when antagonists to both receptors are applied (Isaacson, J. S. and Strowbridge, B. W., 1998). Mg^{2+}-free conditions enhance self-inhibition and cause it to be dominated by activation of NMDA receptors; under these conditions, AMPA receptors have only a minor effect of the magnitude of self-inhibition (Isaacson, J. S. and Strowbridge, B. W., 1998; Schoppa, N. E. *et al.*, 1998; Chen, W. R. *et al.*, 2000; Isaacson, J. S., 2001; Halabisky, B. and Strowbridge, B. W., 2003). Similar findings were obtained for tufted cell self-inhibition (Christie, J. M. *et al.*, 2001). As will be discussed below, lateral inhibition has been reported to be strongly regulated by the I_A current in GCs. Self-inhibition has been reported to be unaffected (Halabisky, B. *et al.*, 2000) or enhanced (Schoppa, N. E. and Westbrook, G. L., 1999; Isaacson, J. S., 2001) by blockers of I_A. Self-inhibition is unaffected by the L-type Ca^{2+} channel antagonist (nifedipine) or T- or R-type Ca^{2+} channel antagonists (50 μM Cd^{2+}) but is markedly attenuated by the P/Q- and N-type antagonist ω-conotoxin MVIIC (Isaacson, J. S. and Strowbridge, B. W., 1998). Self-inhibition is reduced by $GABA_B$ receptor agonists, presumably by reducing HVA currents in GCs (Isaacson, J. S. and Vitten, H., 2003). It is also reduced by mGluR antagonists (Heinbockel, T. *et al.*, 2007).

4.37.6.4.2 Lateral inhibition

Stimulation of one mitral cell in the presence of TTX results in a dendrodendritically mediated mitral-granule-mitral cell IPSPs/IPSCs, that is, feedforward or lateral inhibition (Isaacson, J. S. and Strowbridge, B. W., 1998; Urban, N. N. and Sakmann, B., 2002). Like self-inhibition, lateral inhibition in Mg^{2+}-free conditions is completely abolished by NMDA receptor antagonists; in normal extracellular media, AMPA receptors seem to play a more important role when the lateral inhibition is evoked by weaker stimulation (Isaacson, J. S. and Strowbridge, B. W., 1998; Schoppa, N. E. *et al.*, 1998). The spatial extent of lateral inhibition among mitral cells has been reported to be greater than that for tufted cells. Tufted cell lateral inhibition is limited to several glomerular widths (<400 μm) as opposed to 750 μm for mitral cells (Christie, J. M. *et al.*, 2001). The weaker lateral inhibition of tufted cells could merely be due to the fact that their lateral dendrites are relatively short (Mori, K. *et al.*, 1983; Orona, E. *et al.*, 1984). The I_A current strongly regulates the duration of lateral inhibition and the role of AMPA receptors. 4-AP reduces the duration of lateral inhibition and increases the contribution of AMPA receptors. As noted above, 4-AP blocks I_A, which normally occludes or counters the brief AMPA receptor-mediated depolarization and spiking in GCs. I_A blockade disinhibits the AMPA receptor-mediated synaptic component, reduces the latency of evoked spikes, and therefore leads to more rapid and synchronous GABA release from GCs (Schoppa, N. E. and Westbrook, G. L., 1999). Consequently, 4-AP reduces the contribution of the slow kinetics of the NMDA receptor-mediated synaptic component to GC GABA release. The results were somewhat different for self-inhibition, in which the amplitude of early IPSC component was markedly increased, as was the total duration of the IPSC. Blockade of SK currents in mitral cells enhances lateral inhibition (Maher, B. J. and Westbrook, G. L., 2005).

4.37.6.4.3 Role of Ca^{2+} influx through *N*-methyl D-aspartate receptors and voltage-dependent Ca^{2+} channels

Later studies demonstrated that Ca^{2+} influx through the NMDA receptor can directly trigger GABA release from GCs (Halabisky, B. *et al.*, 2000; Chen, W. R. *et al.*, 2000; Isaacson, J. S., 2001). Thus, NMDA applied focally into the EPL in the presence of the HVA Ca^{2+} channel blocker, Cd^{2+}, elicited IPSCs in mitral cells. Similar results were obtained in Mg^{2+}-free conditions when flash photolysis was used to increase intracellular Ca^{2+} in the mitral cell (Chen, W. R. *et al.*, 2000; Isaacson, J. S., 2001); the photolysis-induced IPSC could be blocked by NMDA receptor antagonists or Cd^{2+} (Chen, W. R. *et al.*, 2000; Isaacson, J. S., 2001). The NMDA-evoked IPSC did not depend on Ca^{2+} release from internal stores as it was unaffected by thapsigargin (Halabisky, B. *et al.*, 2000; Chen, W. R. *et al.*, 2000). However, IPSCs elicited by NMDA or KCl

application in the GCL were blocked by Cd^{2+} (Halabisky, B. *et al.*, 2000). These findings suggest that Ca^{2+} influx via NMDA receptors near dendrodendritic synapses, presumably on GC spines, is directly coupled to GABA release. However, depolarization at more remote sites (GC somata/proximal dendrites) induces Ca^{2+} influx via HVA Ca^{2+} channels.

4.37.6.4.4 Local vs. global modes of dendrodendritic inhibition

Current views are that weak stimulation producing small synaptic responses in GCs, and thus Ca^{2+} influx into isolated GCs spines, triggers GABA release and inhibition of mitral cell dendrites that are synaptically coupled to those spines. Such inhibition would tend to be spatially localized. Both NMDA receptors and voltage-dependent Ca^{2+} channels can provide the Ca^{2+} influx necessary for GABA release from spines. By contrast, stronger levels of mitral/tufted cell input that generate actively propagating Na^{+} spikes would produce more global or widespread inhibition of mitral/tufted cells (Chen, W. R. *et al.*, 2000; Egger, V. *et al.*, 2003). As noted above, sufficiently large EPSPs subthreshold for Na^{+} spikes can trigger an all-or-none LTS that propagates throughout the GC dendrites (Egger, V. *et al.*, 2005). Thus, the LTS is an additional candidate for global lateral inhibition.

4.37.6.4.5 Temporal modulation of dendrodendritic inhibition

In slices, paired-pulse mitral cell stimulation experiments show that self-inhibition elicited by the second pulse was markedly reduced and recovered with a time constant of ~6 s (Dietz, S. B. and Murthy, V. N., 2005). This finding may, in part, account for the decrement in GABAergic synaptic input to mitral cells across respiratory cycles during odor stimulation (Cang, J. and Isaacson, J. S., 2003). The observation that GC odor responses subside across sniffs may also lead to reduced dendrodendritic inhibition during respiration. Thus, the strength of dendrodendritic inhibition is likely to be temporally modulated with respect to respiration. Other studies indicate that higher frequency local γ-oscillatory activity generated by mitral cell–GC interactions may also modulate GABAergic inhibition. Local γ-frequency stimulation in the GCL or ELP can facilitate mitral cell feedback and lateral inhibition by relieving the Mg^{2+} block of NMDA receptors on GCs (Halabisky, B. and Strowbridge, B. W., 2003).

4.37.7 Neurophysiology of New, Adult-Born Neurons

The deepest layer in the MOB is the subependymal layer (also called subventricular zone), which is a cell-poor region lining the ventricle (if present) in adults. Most MOB interneurons originate postnatally from progenitor cells within this layer (Hinds, J. W., 1968; Altman, J., 1969; Bayer, S. A., 1983). In adults, interneurons (primarily GCs and PG cells) are continually generated from these progenitor cells, and their offspring generated en route migrates to the MOB within the rostral migratory stream (RMS; Luskin, M. B., 1993; Lois, C. and Alvarez-Buylla, A., 1994; Smith, C. and Lushkin, M. B., 1998; Wichterle, H. *et al.*, 2001). Two subsets of new interneurons have been identified, which express either TH, which is required for DA synthesis, or Ca^{2+} calmodulin-dependent protein kinase IV during migration (Baker, H. *et al.*, 2001). Both the progenitors and new interneurons express functional $GABA_A$ receptors. Electrophysiological studies indicate that the new interneurons subsequently express functional AMPA receptors, then NMDA receptors, before they exhibit spiking activity, responses to ON stimulation, and spontaneous glutamatergic EPSCs (Belluzzi, O. *et al.*, 2003; Carleton, A. *et al.*, 2003). These electrophysiological studies provide evidence that the new interneurons become functionally integrated into the MOB circuitry. Neural cell-adhesion protein-deficient mice, which exhibit defective migration of new interneurons into the GCL and a reduced MOB size, have been shown to exhibit impaired odor discrimination (Gheusi, G. *et al.*, 2000). Although threshold detection and short-term odor memory were normal in these mice, in normal mice both olfactory memory and survival of the new interneurons were improved following rearing in an odor-enriched environment (Rochefort, C. *et al.*, 2002). Thus, the neurons of the subependymal layer and RMS appear to be important both to MOB development and to certain olfactory functions during adulthood.

4.37.8 Neurophysiology of Primary Olfactory Cortical Inputs to Main Olfactory Bulb

Extrinsic afferent input to MOB, also referred to as centrifugal fibers, can be subdivided into two

classes: (1) inputs arising from nonolfactory, so-called neuromodulatory transmitter systems including ACh, norepinephrine (NE), and 5-HT (these neuromodulatory inputs are discussed below in Neurophysiology of Neuromodulatory Inputs to Main Olfactory Bulb), and (2) feedback inputs arising from olfactory-related structures, in particular those arising from POC. Feedback projections to MOB from POC arises predominantly from glutamatergic, pyramidal neurons in layers II and III of piriform cortex, as well as other POC structures (for review, see Ennis, M. *et al.*, 2007). These projections massively target GCs, where they form asymmetrical synapses on the cell bodies, basal dendrites, and spines of GCs (Price, J. L. and Powell, T. P. S., 1970a). Activation of these feedback projections produces a negative field potential recorded in the GCL (Walsh, R. R., 1959; Nakashima, M. *et al.*, 1978), as expected if excitatory currents are flowing into GCs. Similar stimulation elicits IPSPs in mitral cells (Yamamoto, C. *et al.*, 1963; Nicoll, R. A., 1971; Mori, K. and Takagi, S. F., 1978), due to excitation of GCs, followed by GABA release onto mitral cells, that is, dendrodendritic inhibition (Halász, N. and Shepherd, G. M., 1983). The transmitter of these feedback projections to GCs is glutamate. Activation of POC input to MOB excites GCs as measured by voltage-sensitive dye and field potential recordings *in vitro*. This excitation is mediated by glutamate acting at both AMPA and NMDA receptors (Laaris, N. *et al.*, 2007). A major function of these projections is to provide an inhibitory regulation of the firing rate and excitability state of mitral/tufted cells. Activation of these inputs modifies (inhibits) odor responses in MOB (Kerr, D. I. B. and Hagbarth, K. E., 1955).

4.37.9 Oscillations and Synchrony in Main Olfactory Bulb

4.37.9.1 Oscillations

Oscillations and synchronous activity are characteristic features of spontaneous and odor-driven activity in the MOB and other olfactory structures. A detailed consideration of oscillations in the MOB is beyond the scope of the present review and has recently been reviewed elsewhere (Lledo, P. M. *et al.*, 2005; Gelperin, A., 2006; Kepecs, A. *et al.*, 2006). Prominent oscillatory activity is present in MOB field potentials, which primarily reflect synchronized subthreshold membrane potentials arising from large neuronal populations, or in membrane potential or spike activity of individual MOB neurons. Sensory input to the olfactory system occurs as a result of respiration which by its very nature is cyclical or rhythmical. Relatively low-frequency oscillations synchronized to respiration, in the presence and absence of odors, occur in the theta band (2–12 Hz). Higher frequency oscillations, superimposed on the theta, occur in the beta (15–40 Hz) and gamma (30–80 Hz) bands. Beta frequency oscillations are relatively poorly understood, but have recently been discussed elsewhere (Neville, K. R. and Haberly, L. B., 2003; Martin, C. *et al.*, 2004; Fletcher, M. L. *et al.*, 2005). Lower frequency oscillatory (0.1–0.03 Hz) and synchronous activity has been observed in MOB slices under certain conditions (Puopolo, M. and Belluzzi, O., 2001).

4.37.9.1.1 Theta rhythm

In the MOB, 2 to 12 Hz oscillations are referred to as theta principally because they occupy a highly overlapping frequency band with hippocampal theta oscillations (Kay, L. M. and Laurent, G., 1999; Kay, L. M., 2003; 2005). As noted above, theta frequency oscillations are driven by, and thus synchronized or phase-locked with, respiration. Therefore, the specific theta frequency varies with the sniffing frequency (i.e., the pattern of airflow across the nasal epithelium) and includes components related to low-frequency (1–3 Hz) passive sniffing as well as a higher frequency component (5–12 Hz) characteristic of active investigative sniffing (Adrian, E. D., 1950; Welker, W. I., 1964; Macrides, F. *et al.*, 1982; Eeckman, F. H. and Freeman, W. J., 1990; Kay, L. M. and Laurent, G., 1999; Kay, L. M., 2003). As noted earlier, mitral cell subthreshold membrane potential oscillations and/or spike activity is synchronized with certain phases of the respiratory cycle. Manipulations that impair or disrupt respiratory-driven input to the MOB disrupts mitral cell activity and decouples it from the respiratory cycle (Philpot, B. D. *et al.*, 1997). Thus, theta oscillations appear to be driven by the pattern of respiratory-driven input to MOB. However, intrinsic membrane and synaptic properties enhance the ability of some MOB neurons to entrain or synchronize with rhythmical respiratory-driven activity. For example, ET cells in MOB slices intrinsically generate spike bursts at frequencies ranging from ~1 to 8 Hz, and readily entrain to patterned sensory input over this same range. Thus, the properties of these

cells may allow them to discharge in synchrony with the respiratory cycle.

4.37.9.1.2 Gamma rhythm

Gamma oscillations arise during odorant or direct ON stimulation and appear to be generated intrinsically in the MOB. Thus, they persist when centrifugal input to the bulb is severed or impaired (Gray, C. M. and Skinner, J. E., 1988; Neville, K. R. and Haberly, L. B., 2003). As with theta oscillations, odor- or ON-evoked gamma oscillations are apparent in the EEG, MOB field potentials, and subthreshold membrane potential and spiking activity of mitral cells (Adrian, E. D., 1950; Eeckman, F. H. and Freeman, W. J., 1990; Kay, L. M. and Freeman, W. J., 1998; Kashiwadani, H. *et al.*, 1999; Debarbieux, F. *et al.*, 2003; Friedman, D. and Strowbridge, B. W., 2003; Neville, K. R. and Haberly, L. B., 2003; Lagier, S. *et al.*, 2004; Martin, C. *et al.*, 2004; Fletcher, M. L. *et al.*, 2005). Current source-density analyses indicate that the gamma oscillations in MOB field potentials primarily reflect synaptic currents flowing in GCs (Neville, K. R. and Haberly, L. B., 2003). Multisite recordings demonstrated that the phase of gamma oscillation may vary in different parts of the MOB, especially at low odor concentrations. Gamma oscillations are thought to arise primarily as a result of rhythmic or reverbatory interactions between mitral/tufted cells and inhibitory interneurons, chiefly GCs (Friedman, D. and Strowbridge, B. W., 2003; Neville, K. R. and Haberly, L. B., 2003; Lagier, S. *et al.*, 2004). Mitral cell activity is synchronized with γ-frequency MOB field potentials and also with GABAergic synaptic input (Lagier, S. *et al.*, 2004). The duration of mitral cell to GC synaptic input occurs over a time course of approximately one-half cycle of the gamma oscillation. Gamma oscillatory activity in mitral cells is suppressed or attenuated by glutamate receptor antagonists (decreasing mitral/tufted cell excitation of GCs) or by $GABA_A$ receptor antagonists (blocking GC-mediated inhibition of mitral/tufted cells) (Friedman, D. and Strowbridge, B. W., 2003; Lagier, S. *et al.*, 2004). In $GABA_A$ $\beta 3$ receptor subunit-deficient mice, functional expression of GC $GABA_A$ receptors was almost eliminated (Nusser *et al.*, 2001). In these mice amplitudes of mitral/tufted cell miniature IPSPs, theta-frequency oscillations, and γ-frequency oscillations were increased, and discrimination of closely related mixtures of alcohols after training was poor relative to normal mice. Gamma oscillations also appear to involve electrical synapses as they are suppressed by gap junction inhibitors (Friedman, D. and Strowbridge, B. W., 2003). Consistent with this, gamma oscillations are disrupted in connexin36-knockout mice (Hormuzdi, S. G. *et al.*, 2001). Intrinsic membrane properties of mitral cells may facilitate gamma oscillatory activity and spiking. When near spike threshold, mitral cells exhibit intrinsically generated subthreshold membrane potential oscillations in the γ-frequency range (Chen, W. R. and Shepherd, G. M., 1997; Desmaisons, D. *et al.*, 1999).

4.37.9.2 Synchrony

Synchrony can be defined as a temporal coincidence between two or more events that have a low probability of occurring by random or chance. Neurons involved in the detection and processing of odors show temporally correlated or synchronized activity, a feature that is expected to have functional relevance for understanding the population code in the olfactory system (Laurent, G., 2002).

4.37.9.2.1 Synchrony among JG cells

JG neurons associated with the same glomerulus exhibit highly synchronous spontaneous activity. Simultaneous recordings of ET–PG or ET–SA cell pairs demonstrated that spikes in ET cells drive synchronous activity in PG and SA cells, but only if the dendrites of both cells ramified in the same glomerulus (Figure 14) (Hayar, A. *et al.*, 2004b). This intraglomerular synchronous activity is driven by glutamatergic input from ET cells to PG/SA cells and is abolished by AMPA receptor antagonists. Similar studies revealed that spontaneous spikes and subthreshold membrane potential activity (i.e., EPSPs, IPSPs) among ET cells of the same glomerulus is highly synchronous (Figure 14) (Hayar, A. *et al.*, 2004b; 2005). Interestingly, the frequency of spontaneous inhibitory input to ET cells, which primarily originates from PG cells, occurs around 50 Hz (γ frequency) and is similar to the frequency of ON-evoked γ-oscillations in mitral cells (mean 45 Hz, Lagier, S. *et al.*, 2004). Although spontaneous synaptic input can synchronize ET cells, synchrony among these cells persists when ionotropic glutamate and GABA receptors are blocked (Hayar, A. *et al.*, 2004b; 2005). Additional electrophysiological results demonstrated that ET cells of the same glomerulus are electrotonically coupled via gap junctions with a relatively small conductance (0.1 nS). Spontaneous synchrony among ET cells is

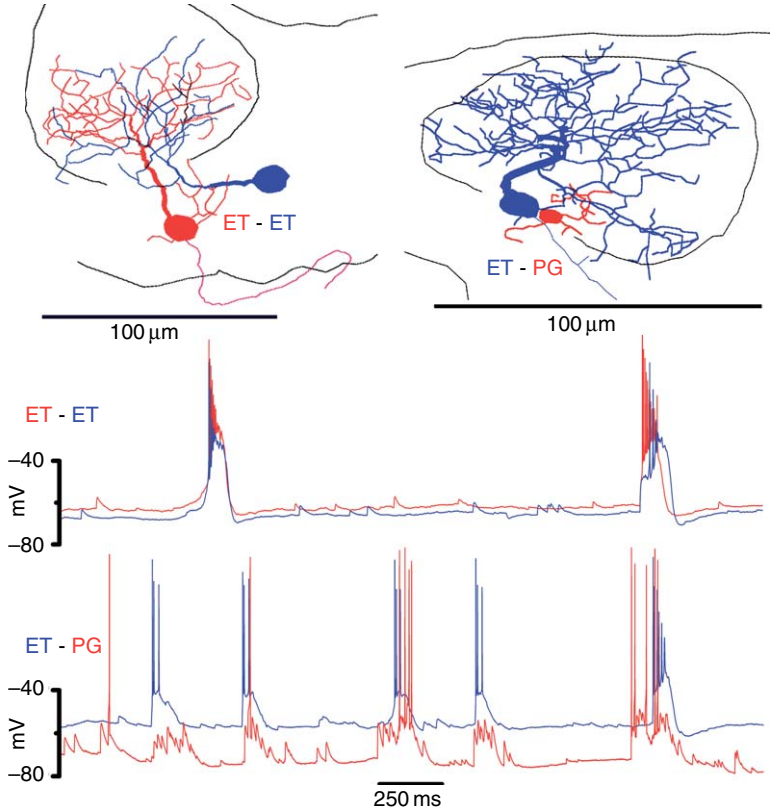

Figure 14 Synchronous activity among juxtaglomerular (JG) cells associated with the same glomerulus. Upper panel shows reconstructions of the recorded cells (left, two external tufted (ET) cells; right, an ET cell and a periglomerular (PG) cell). Middle panel: Dual whole-cell current clamp recording from two ET cells (red and blue traces, respectively) showing correlation of spike bursts and membrane potentials. Lower panel: Dual whole-cell current clamp recordings show that EPSP bursts and spikes in a PG cell (red trace) are synchronous with spike bursts in an ET cell (blue trace).

abolished by the gap junction blocker carbenoxolone (Hayar, A. *et al.*, 2005). These results are consistent with anatomical evidence for gap junctions between mitral/tufted cell apical dendrites (See Section 4.37.9.2.2). Unlike mitral cells, which exhibit a narrow window of spike-to-spike correlation (see below; Schoppa, N. E. and Westbrook, G. L., 2002), ET cells exhibit a broader window of burst-to-burst correlation. The narrow window of correlation among mitral cells is due to the fact that mitral cell spikes induced fast EPSPs in other mitral cells (Schoppa, N. E. and Westbrook, G. L., 2002). In contrast, ET cells seem to communicate mainly via slow inward currents produced by gap junctions with relatively low conductance. Therefore, one potential function of gap junctions in ET cells is to filter fast spiking activity and propagate slow membrane potential oscillations, which are driven mainly by persistent Na^+ current (Hayar, A. *et al.*, 2004a).

4.37.9.2.2 Synchrony among mitral cells

Synchronous activity in the mammalian MOB occurs among mitral cells that send an apical dendrite to receive input from a single glomerulus. By using simultaneous recordings from pairs of mitral cells, it has been shown that pairs with apical dendrites in the same glomerulus display highly synchronized synaptic and/or spike activity, whereas pairs associated with different glomeruli do not. As reviewed earlier, mitral cells associated with the same glomerulus exhibit synchronous AMPA receptor-mediated LLDs that spontaneously occur at a frequency of ~1 Hz (Carlson, G. C. *et al.*, 2000). LLDs (Figure 7) are generated by network activity in the glomeruli and could be elicited by ON or antidromic stimulation, but never by depolarization of single mitral cells. Subsequent studies demonstrated that slow (2 Hz) oscillations and spikes elicited by single ON shocks or NMDA application were synchronous among mitral cells of the same glomerulus; cells

associated with distant glomeruli did not exhibit synchrony, while those associated with adjacent glomeruli exhibited temporally correlated but not synchronous oscillations (Schoppa, N. E. and Westbrook, G. L., 2001; 2002). The synchronous activity among mitral cells was abolished by AMPA receptor antagonists and dampened by mGluR antagonists (Schoppa, N. E. and Westbrook, G. L., 2001; 2002). These and later studies indicated that mitral cell apical dendrites in the same glomerulus exhibit electrotonic coupling (Schoppa, N. E. and Westbrook, G. L., 2002; Christie, J. M. *et al.*, 2005). In mouse MOB slices, current injections into one cell elicited correlated spikes in a second mitral cell if the dendrites extended into the same glomerulus. Such synchrony, however, was absent in slices from connexin36-knockout mice (Christie, J. M. *et al.*, 2005). Connexins are a member of gap junction proteins involved in electrical signaling between cells. The preceding finding is consistent with the presence of high levels of connexin36 in MOB neurons, and specifically in mitral/tufted dendrites (Condorelli, D. F. *et al.*, 1998; 2000; Belluardo, N. *et al.*, 2000; Rash, J. E. *et al.*, 2000; Teubner, B. *et al.*, 2000; Zhang, C. and Restrepo, D., 2003; Christie, J. M. *et al.*, 2005). Other studies have also reported gap junctions in, or between, mitral/tufted cell dendrites (Paternostro, M. A. *et al.*, 1995; Miragall, F. *et al.*, 1996; Kosaka, T. and Kosaka, K., 2003; 2004). In slices from wildtype, but not connexin36-knockout mice, a spike elicited in one mitral cell evoked an AMPA receptor-mediated potential (D_{AMPA}) in the second mitral cell (Christie, J. M. *et al.*, 2005). Correlated spiking in connexin36-knockout mice could be reinstated by boosting glutamate levels with uptake inhibitors. Taken together, these findings indicate that electrical coupling is necessary to drive D_{AMPA}, which in turn, drives correlated spiking among mitral cells. Thus, the apical dendrites of mitral cells generate a unique form of electrochemical transmission. The dependence of correlated spiking on AMPA receptors is a distinct feature of mitral–mitral cell synchrony.

GABAergic inhibition is also thought to play an important role in synchronizing mitral cell activity. As noted earlier, γ-frequency oscillation and spiking is a prominent feature of mitral cell odor-evoked activity. Spontaneous synchronous IPSPs can reset the phase of subthreshold membrane oscillations and synchronize the firing of multiple mitral cells (Desmaisons, D. *et al.*, 1999). Correlated IPSPs might also contribute to the odor-elicited high-frequency oscillations in the olfactory bulb of adult rats (Fletcher, M. L. *et al.*, 2005). The frequency of ON-evoked local field potential oscillations (mean 45 Hz, Lagier, S. *et al.*, 2004) recorded in the MCL is attributed to rhythmic dendrodendritic granule to mitral cell inhibition. Unlike glomerular mechanisms, GABAergic inhibition appears to synchronize mitral cells associated with different glomeruli. Mitral cell associated with different glomeruli can be synchronized by rhythmic stimulation of the ON at theta frequencies (Schoppa, N. E., 2006). Such synchrony does not depend upon electrotonic coupling, but appears to be driven by synchronous IPSPs from GCs, such that synchronous spikes in mitral cells occur during the recovery from the synchronous IPSP. One possible function of spike synchrony among mitral cells of different odorant receptor specificities is to provide a mechanism for downstream cortical neurons to decode information about different odorant receptors (Schoppa, N. E., 2006). As would be required by such a mechanism, labeling studies suggest that each pyramidal cell in the anterior piriform cortex receives anatomical connections from mitral cells with different odorant receptor specificities (Zou, Z. *et al.*, 2001). Assuming that pyramidal cells in the olfactory cortex have synaptic integration windows comparable to other pyramidal neurons (e.g., $\sim$7 ms), synchrony among mitral cells would promote the summation of EPSPs and the likelihood that cortical neurons fire action potentials in response to input from activated mitral cells of different odorant receptor specificities.

4.37.9.3 Oscillations, Synchrony and Odor Coding

Temporal firing patterns, including rhythmic oscillations and neuronal synchronization, are thought to be important in sensory information processing (Alonso, J. M. *et al.*, 1996; Konig, P. *et al.*, 1996; Roy, S. A. and Alloway, K. D., 2001) including odor coding (for review, see Friedrich, R. W., 2002). Rhythmic activity and synchrony are thought to coordinate intra- and interstructural communication. Olfactory information is thought to be encoded, at least in part, by network oscillations (Wehr, M. and Laurent, G., 1996; Kauer, J. S., 1998; Kay, L. M. and Laurent, G., 1999). In the first stage of olfactory processing, network interactions within each glomerulus act to synchronize the discharge of mitral cells associated with that glomerulus to the theta pattern of rhythmical sensory input. By temporally binding the discharge of mitral cells, such

synchrony would maximize the transfer of sensory input onto the output neurons. This, in turn, would facilitate faithful transfer of glomerular sensory input to higher order olfactory structures (i.e., POC). In other words, temporal summation of EPSPs produced by synchronous spikes from the glomerular ensemble of mitral/tufted cells would increase the likelihood of spike initiation in postsynaptic POC neurons. Glomerular synchrony may be a particularly important amplification mechanism when odor concentrations are insufficient to activate all mitral cells of a particular glomerulus. Odors typically activate multiple glomeruli, but the mechanism that drives the sensory input (respiration) is common to all glomeruli. Does this imply that oscillations and synchrony should be phase-locked across responsive glomeruli? This does not seem to be the case as the widespread distribution of ORNs and their odorant response kinetics produce temporal variations in odor response properties in different glomeruli. Thus, different glomeruli activated by the same odorant exhibit temporally distinct response profiles (Spors, H. *et al.*, 2006). It is likely, therefore, that at least initially there will be temporal differences in the phase of oscillatory neuronal activity and synchrony among neurons in different responsive glomeruli. In addition, both glomerular odor activity patterns and discharge of mitral cells change within and across sniffs (Friedrich, R. W., 2002; Spors, H. *et al.*, 2006), and as noted above, the phase of gamma oscillations may not always be uniform throughout the MOB. Neurons in POC appear to receive convergent input from multiple glomeruli (Zou, Z. *et al.*, 2001; Illig, K. R. and Haberly, L. B., 2003). Temporal variations in activity patterns from different glomeruli, via mitral/tufted cells, may be an important element in odor recognition and discrimination.

4.37.10 Neurophysiology of Neuromodulatory Inputs to Main Olfactory Bulb

MOB receives extrinsic inputs from cholinergic, noradrenergic, and serotonergic groups in the basal forebrain and brainstem. As these inputs innervate neurons in multiple layers of MOB, and therefore modulate multiple neuronal subtypes, their physiological effects are collectively reviewed here.

4.37.10.1 Cholinergic Inputs to MOB

In the mouse, about 3.5% of all neurons that project to the bulb originate in the nucleus of the horizontal limb of the diagonal band (NDB); far fewer originate in the vertical limb of DB (Carson, K. A., 1984; Shipley, M. T., and Adamek, G. D., 1984). At least two distinct transmitter-specific populations of NDB neurons project to the MOB (Zaborszky, L., *et al.*, 1986). About 20% of the NDB neurons that project to the bulb are cholinergic; most of these cells are concentrated in the rostromedial portion of the horizontal limb of NDB. Many NDB–MOB projection neurons are GABAergic and occur mainly in the caudo-lateral aspect of NDB (Zaborszky, L., *et al.*, 1986). Choline acetyltransferase, the biosynthetic enzyme for ACh synthesis, is located in axons distributed across most layers of the MOB, except the ONL; cholinergic fibers are especially heavy in the GL and IPL (Ennis, M. *et al.*, 2007). As reviewed elsewhere, muscarinic and nicotinic receptors are found in most layers of MOB (Ennis, M. *et al.*, 2007).

Electrical activation of NBD has been reported to depress (Nickell, W. T. and Shipley, M. T., 1988) or to increase (Kunze, W. A. A. *et al.*, 1991; 1992) mitral cell activity indirectly via primary effects on GABAergic GCs. NDB stimulation also reduced the field potential in the MOB caused by stimulation of the anterior commissure (Nickell, W. T. and Shipley, M. T., 1993), an effect mediated by presynaptic inhibition of anterior commissure terminals via muscarinic receptors. One interpretation of these results is that cholinergic input to MOB may function to modulate interhemispheric transmission of olfactory information. In this regard, it is noteworthy that anterior commissural fibers are required for access and recall of olfactory memories between the two hemispheres. Infusion of ACh into MOB was reported to reduce paired-pulse depression of LOT-evoked field potentials recorded in the GCL. This effect was attributed to muscarinic receptor-mediated inhibition of GABA release from GCs (Elaagouby, A. *et al.*, 1991). In slice preparations, nicotinic but not muscarinic receptor agonists directly excited mitral cells, and this effect appeared to be due to an inward current with a reversal potential of -5 to $+10$ mV (Castillo, P. E. *et al.*, 1999). In slices, muscarinic receptor agonists inhibited GCs (Castillo, P. E. *et al.*, 1999), and paradoxically, also appeared to increase GABA release from these cells. The same study reported that in the GL only bipolar PG cells were sensitive to nicotine (Castillo, P. E.

et al., 1999). The morphological identity of these cells is unclear. Behaviorally, muscarinic receptor antagonists impair discrimination among closely related odors (Fletcher, M. L. and Wilson, D. A., 2002).

4.37.10.2 Noradrenergic Input to MOB

A significant modulatory input to the bulb is from the pontine nucleus locus coeruleus (LC). In the rat, all LC neurons contain the neurotransmitter, NE; LC contains the largest population of NE neurons in the brain. It has been estimated that up to 40% of LC neurons (400–600 of a total of 1600 LC neurons) project to the bulb in the rat (Shipley, M. T. *et al.*, 1985). A subset of LC neurons projecting to MOB contain NPY (Bouna, S. *et al.*, 1994). LC axons project mainly to the subglomerular layers of the bulb, particularly in the IPL and GCL (McLean, J. H., *et al.*, 1989). The EPL and MCL are moderately innervated, while the GL is nearly devoid of NE input. NE receptors occur in multiple layers of the MOB and are expressed by multiple cell types, in general consistent with the pattern of NE fiber innervation (for review, see Ennis, M. *et al.*, 2007).

While NE clearly plays significant roles in olfactory function, the effects of NE at the cellular and network levels are somewhat discrepant. For example, LC stimulation was reported to have no effect on LOT-evoked field potentials recorded in the GCL (Perez, H. *et al.*, 1987). A subsequent study reported that LC stimulation initially decreased and then subsequently increased paired-pulse depression of GC field potential responses to LOT stimulation (Okutani, F. *et al.*, 1998). These effects were attributed to activation of β receptors. Another field potential study reported that NE infusion into MOB, acting at $\alpha 1$ receptors, increased the depolarization of GC dendrites elicited by LOT stimulation. Mitral cell responses to antidromic shocks were not affected, suggesting that NE excites GCs (Mouly, A. M. *et al.*, 1995). In neonatal animals, β receptor stimulation in MOB decreased LOT-evoked, paired-pulse inhibition of GC field potentials (Wilson, D. A. and Leon, M. 1988). It is unclear if this was mediated by presynaptic inhibition of transmitter release from MCs and/or increased excitability of GCs.

Cellular recording studies are also somewhat discrepant. In the rabbit and cat, Salmoiraghi *et al.* (1964) and McLennan (1971) found that iontophoretically applied NE inhibited mitral cells. This effect was blocked by the $GABA_A$ receptor antagonist, bicuculline. In the isolated turtle bulb (Jahr and Nicoll, 1982), mitral cell spike rate increased and IPSPs decreased following both application of NE. In dissociated MOB cultures, NE decreased mitral to granule dendrodendritic synaptic transmission by acting presynaptically at $\alpha 2$ receptors to decrease Ca^{2+} currents in both granule and mitral cells (Trombley, P. Q., 1992; Trombley, P. Q. and Shepherd, G. M., 1992).

NE release or NE agonists have more consistent effects on ON-evoked responses in mitral cells. NE release, evoked by selective chemical activation of LC *in vivo*, enhanced the response of mitral cells in response to weak (i.e. perithreshold) but not strong (i.e. suprathreshold) stimulation of the olfactory epithelium (Jiang, M. R. *et al.*, 1996). Interestingly, NE release from LC axon terminals is facilitated and suppressed by activation of presynaptic nicotinic and muscarinic cholinergic receptors, respectively (El-Etri, M. M. *et al.*, 1999). Consistent with these *in vivo* findings, application of NE or $\alpha 1$ receptor agonists, but not $\alpha 2$ or β-receptor agonists, selectively increased mitral cell responses to perithreshold intensity ON stimulation in rat MOB slices (Figure 15) (Ciombor, K. J. *et al.*, 1999). Noradrenergic agonists were without effect on ON-evoked field potentials recorded in the GL, or on ON-evoked postsynaptic currents in mitral cells (Hayar, A. *et al.*, 2001). This suggests that NE-evoked modulation of ON-evoked mitral cell spiking is mediated by postsynaptic actions on bulb neurons. In voltage-clamp recordings, NE or $\alpha 1$ agonists directly evoked an inward current in mitral cells that appeared to be due to closure of K^+ channels (Figure 16). In current clamp recordings from bistable mitral cells, $\alpha 1$ agonists shifted the membrane potential from the downstate (-52 mV) toward the upstate (-40 mV) and significantly increased spike generation in response to perithreshold ON input. Taken together, these findings suggest that NE release directly alters mitral cell excitability in a manner that could increase their sensitivity to weak ON input, perhaps to improve the detection of weak odorants.

NE inputs to the bulb are critical to olfactory function. Olfactory cues increase the discharge of LC neurons in behaving animals (Aston-Jones, G. and Bloom, F. E., 1981) and trigger rapid increases in NE levels in the MOB (Chanse, N. T. and Kopin, I. J., 1968; Rosser, A. E. and Keverne, E. B., 1985; Brennan, P. *et al.*, 1990). LC projections to the main and accessory olfactory bulb are pivotal to the formation of specific olfactory memories, pheromonal

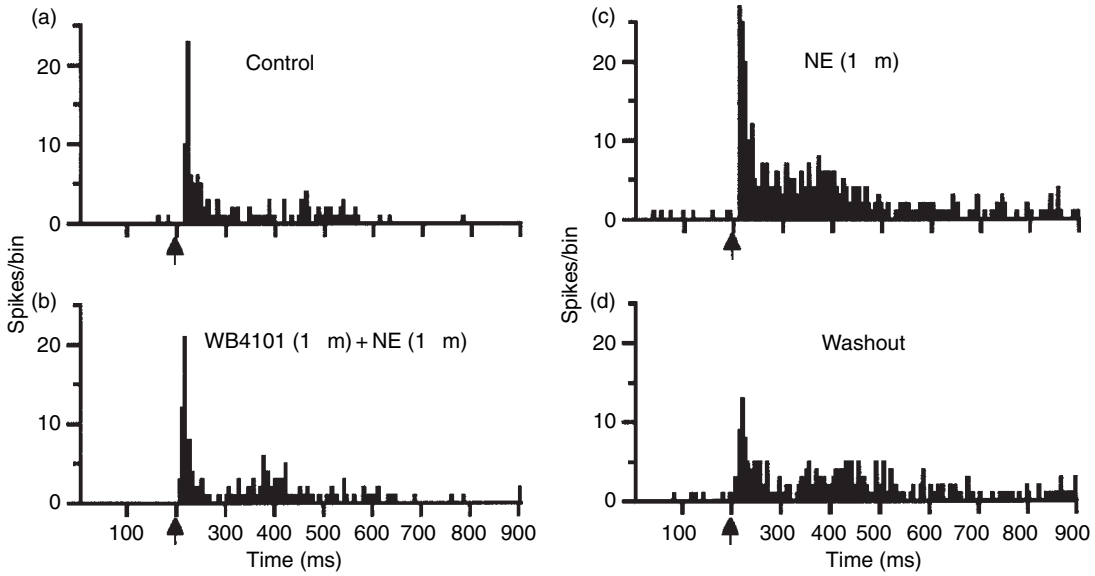

Figure 15 The α1 receptor antagonist WB-4101 prevents norepinephrine (NE)-induced facilitation of mitral cell excitatory responses to perithreshold intensity olfactory nerve (ON) stimulation. (a–d) Peri-stimulus time histograms (PSTHs) showing responses of a mitral cell to perithreshold intensity ON shocks (12 μA, at arrows). (a and b) In the presence of WB-4101 (1 μM), superfusion of NE (1 μM) did not alter (103% of control) the early excitation elicited by ON stimulation. (c) After washout of WB-4101, NE substantially increased (184% of control) the early excitatory response component. (d) The facilitation of the early excitation recovered by 53 min after washout of NE. All PSTHs were generated for 50 consecutive ON shocks. Reprinted from Ciombor, K. J., Ennis, M., and Shipley, M. T. 1999. Norepinephrine increases rat mitral cell excitatory responses to weak olfactory nerve input via alpha-1 receptors *in vitro*. Neuroscience 90, 595–606, with permission from Elsevier, Ltd.

regulation of pregnancy and post-partum maternal behavior (Kaba, H. and Keverne, E. B., 1988; Brennan, P. *et al.*, 1990; Kendrick, K. M. *et al.*, 1992). NE plays an important role in the so-called Bruce effect in mice: when impregnated female mice are exposed to the odor of a strange male, they abort; if exposed to the odor of the impregnating male, they do not abort (Kaba, H. and Keverne, E. B., 1989). Systemic administration of adrenergic receptor antagonists or 6-OHDA lesions, selectively destroying only the NE inputs to the MOB, causes the female to abort when presented with the odor of the impregnating male (Rosser, A. E. and Keverne, E. B., 1985; Kaba, H. and Keverne, E. B., 1988; Brennan, P. *et al.*, 1990). Finally, NE has been shown to play a critical role in olfactory learning in young animals. In neonatal rats, NE release via tactile stimulation leads to a preference for an odor associatively paired with this stimulation (Sullivan, R. M. *et al.*, 1989). The conditioned preference is associated with odor-specific metabolic changes in the bulb (Coopersmith, R. and Leon, M., 1984). Following the conditioning, there is an increased inhibition of mitral cells by the odor (Sullivan, R. M. *et al.*, 1989). Such conditioning is abolished by eliminating NE input to the bulb or via β-receptor antagonists (Sullivan, R. M. *et al.*, 1989; Wilson, D. A. and Sullivan, R. M., 1991; Sullivan, R. M. *et al.*, 1992; 2000; Moriceau, S. and Sullivan, R. M., 2004). Recent studies from McLean's laboratory demonstrate that this β-receptor-dependent neonatal learning involves activation of intracellular cAMP and cAMP-response element-binding protein (CREP) pathways (Yuan, Q. *et al.*, 2003; McLean, J. H. and Harley, C. W., 2004).

4.37.10.3 Serotonergic (5-HT) Input to MOB

The midbrain dorsal and median raphe provides strong serotonergic inputs to the MOB. In the rat, about 1000 dorsal and 300 median raphe neurons project to the bulb (McLean, J. H. and Shipley, M. T., 1987a; 1987b). 5-HT fibers are present in all layers of MOB, but with varying densities. Input to the GL is especially dense, while the EPL contains very low density. The MCL, IPL, and GCL have a fairly heavy and uniform innervation, but not as dense as that of the GL. Thick serotonergic fibers preferentially innervate the glomeruli of MOB, while

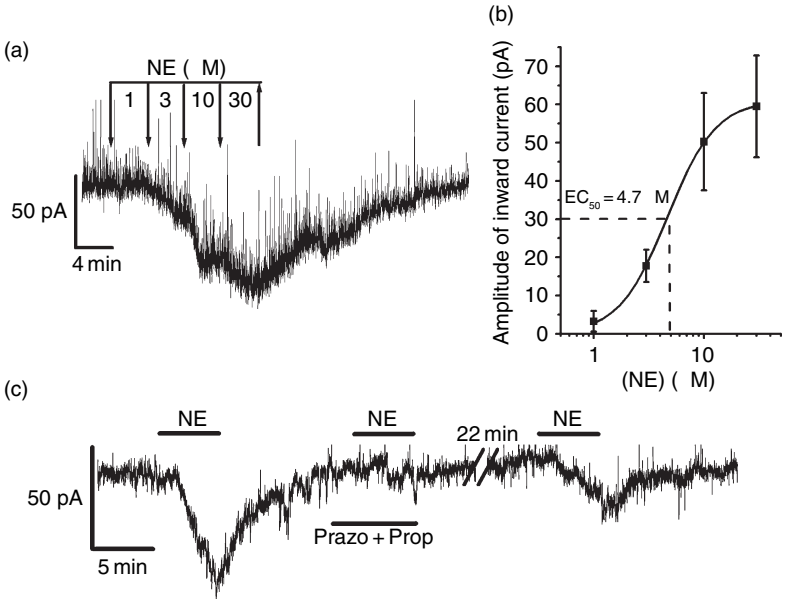

Figure 16 Effect of norepinephrine (NE) in voltage-clamp recordings from mitral cells. (a) Inward currents evoked by NE at different concentrations (1, 3, 10, and 30 μM added cumulatively, 4 min at each concentration). (b) A sigmoidal curve was fitted to the NE concentration–response data obtained from four cells. The holding potential was −60 mV. (c) The response to a second application of NE (30 μM) was blocked in the presence of the alpha 1 receptor antagonist prazosin (Prazo; 1 μM) and the beta receptor antagonist propranolol (Prop; 10 μM). The NE-induced inward current recovered partially after washout of the antagonists (about 30 min). Reprinted from Hayar, A., Heyward, P. M., Heinbockel, T., Shipley, M. T., and Ennis, M. 2001. Direct excitation of mitral cells via activation of alpha1-noradrenergic receptors in rat olfactory bulb slices. J. Neurophysiol. 86, 2173–2182, with permission from The American Physiological Society.

thinner serotonergic axons preferentially innervate inframitral layers (McLean, J. H. and Shipley, M. T., 1987a; 1987b). In neocortex, thick axons arise from the median raphe and thin axons arise from dorsal raphe (McLean, J. H. and Shipley, M. T., 1987a; 1987b), and the same segregation occurs in MOB. In agreement with the 5-HT fiber distribution, 5-HT receptors are localized in most layers of the MOB (for review, see Ennis, M. *et al.*, 2007).

In the GL, it was recently reported that 5-HT depolarized 34% of JG cells *in vitro* via activation of $5HT_{2C}$ receptors (Hardy, A. *et al.*, 2005). The 5-HT-induced depolarization was due to activation of a nonselective cation current with a reversal potential of −44 mV. The heterogeneous electrophysiological properties of 5-HT-responsive JG cells suggested that several types of JG cells could be targeted by 5-HT centrifugal fibers. A subset of mitral cells was also depolarized by 5-HT acting at $5\text{-}HT_{2A}$ receptors. By contrast with these results, another subset of mitral cells was hyperpolarized by 5-HT, an action that was indirectly mediated by GCs as it was blocked by $GABA_A$ receptor antagonists (Hardy, A. *et al.*, 2005). This effect of 5-HT was also thought to be mediated by $5\text{-}HT_{2A}$ receptors. Behavioral studies indicate that lesion of serotonergic fibers reversed conditioned olfactory learning (Morizumi, T. *et al.*, 1994) and also induced glomerular atrophy. Behavioral work on neonates by McLean (McLean, J. H. *et al.*, 1996) showed that 5-HT depletion or $5\text{-}HT_2$ receptor antagonism compromised olfactory learning and that 5-HT release or $5\text{-}HT_2$ receptor activation promoted odor conditioning. 5-HT release also appears to facilitate β receptor-mediated, NE-induced olfactory learning by facilitating cAMP-mediated mechanisms (McLean, J. H. and Harley, C. W., 2004).

Acknowledgments

We acknowledge the grant support for portions of this chapter that refer to research of the authors: PHS Grants DC03195, DC06356, DC07123, and RR020146.

References

Adrian, E. D. 1950. The electrical activity of the olfactory bulb. Electroencephalogr. Clin. Neurophysiol. 2, 377–388.

Allison, A. 1953. The morphology of the olfactory system in the vertebrates. Biol. Rev. Camb. Philos. Soc. 28, 195–244.

Alonso, J. M., Usrey, W. M., and Reid, R. C. 1996. Precisely correlated firing in cells of the lateral geniculate nucleus. Nature 383, 815–819.

Alonso, J. R., Arévalo, R., Garcia-Ojeda, E., Porteros, A., Briñón, J. G., and Aijón, J. 1995. NADPH-diaphorase active and calbindin D-28k-immunoreactive neurons and fibers in the olfactory bulb of the hedgehog (*Erinaceus europaeus*). J. Comp. Neurol. 351, 307–327.

Alonso, J. R., Arévalo, R., Porteros, A., Briñón, J. G., Lara, J., and Aijón, J. 1993. Calbindin D-28K and NADPH-diaphorase activity are localized in different populations of periglomerular cells in the rat olfactory bulb. J. Chem. Neuroanat. 6, 1–6.

Alreja, M. and Aghajanian, G. K. 1995. Use of the whole-cell patch-clamp method in studies on the role of cAMP in regulating the spontaneous firing of locus coeruleus neurons. J. Neurosci. Methods 59, 67–75.

Altman, J. 1969. Autoradiographic and histological studies of postnatal neurogenesis. IV. Cell proliferation and migration in the anterior forebrain, with special reference to persisting neurogenesis in the olfactory bulb. J. Comp. Neurol. 137, 433–457.

Aroniadou-Anderjaska, V., Ennis, M., and Shipley, M. T. 1997. Glomerular synaptic responses to olfactory nerve input in rat olfactory bulb slices. Neuroscience 79, 425–434.

Aroniadou-Anderjaska, V., Ennis, M., and Shipley, M. T. 1999a. Current-source density analysis in the rat olfactory bulb: laminar distribution of kainate/AMPA and NMDA receptor-mediated currents. J. Neurophysiol. 81, 15–28.

Aroniadou-Anderjaska, V., Ennis, M., and Shipley, M. T. 1999b. Dendrodendritic recurrent excitation in mitral cells of the rat olfactory bulb. J. Neurophysiol. 82, 489–494.

Aroniadou-Anderjaska, V., Zhou, F. M., Priest, C. A., Ennis, M., and Shipley, M. T. 2000. Tonic and synaptically evoked presynaptic inhibition of sensory input to the rat olfactory bulb via GABA(B) heteroreceptors. J. Neurophysiol. 84, 1194–1203.

Aston-Jones, G. and Bloom, F. E. 1981. Norepinephrine-containing locus coeruleus neurons in behaving rats exhibit pronounced responses to non-noxious environmental stimuli. J. Neurosci. 1, 887–900.

Aungst, J. L., Heyward, P. M., Puche, A. C., Karnup, S. V., Hayar, A., Szabo, G., and Shipley, M. T. 2003. Center-surround inhibition among olfactory bulb glomeruli. Nature 426, 623–629.

Bailey, M. S. and Shipley, M. T. 1993. Astrocyte subtypes in the rat olfactory bulb: morphological heterogeneity and differential laminar distribution. J. Comp. Neurol. 328, 501–526.

Baker, H. 1986. Species differences in the distribution of substance P and tyrosine hydroxylase immunoreactivity in the olfactory bulb. J. Comp. Neurol. 252, 206–226.

Baker, H., Liu, N., Chun, H. S., Saino, S., Berlin, R., Volpe, B., and Son, J. H. 2001. Phenotypic differentiation during migration of dopaminergic progenitor cells to the olfactory bulb. J. Neurosci. 21, 8505–8513.

Balu, R., Larimer, P., and Strowbridge, B. W. 2004. Phasic stimuli evoke precisely timed spikes in intermittently discharging mitral cells. J. Neurophysiol. 92, 743–753.

Banay-Schwartz, M., Lajtha, A., and Palkovits, M. 1989a. Changes with aging in the levels of amino acids in rat CNS structural elements: I glutamate and related amino acids. Neurochem. Res. 14, 555–562.

Banay-Schwartz, M., Lajtha, A., and Palkovits, M. 1989b. Changes with aging in the levels of amino acids in rat CNS structural elements: II. Taurine and small neutral amino acids. Neurochem. Res. 14, 563–570.

Bardoni, R., Magherini, P. C., and Belluzzi, O. 1995. Sodium current in periglomerular cells of frog olfactory bulb *in vitro*. Brain Res. 703, 19–25.

Bardoni, R., Magherini, P. C., and Belluzzi, O. 1996. Excitatory synapses in the glomerular triad of frog olfactory bulb *in vitro*. Neuroreport 7, 1851–1855.

Bayer, S. A. 1983. 3H-Thymidine-radiographic studies of neurogenesis in the rat olfactory bulb. Exp. Brain Res. 50, 329–340.

Belluardo, N., Mudò, G., Trovato-Salinaro, A., Le Gurun, S., Charollais, A., Serre-Beinier, V., Amato, G., Haefliger, J.-A., Meda, P., and Condorelli, D. F. 2000. Expression of connexin36 in the adult and developing rat brain. Brain Res. 865, 121–138.

Belluscio, L., Lodovichi, C., Feinstein, P., Mombaerts, P., and Katz, L. C. 2002. Odorant receptors instruct functional circuitry in the mouse olfactory bulb. Nature 419, 296–300.

Belluzzi, O., Benedusi, M., Ackman, J., and LoTurco, J. 2003. Electrophysiological identification of new neurons in the olfactory bulb. J. Neurosci. 23, 10411–10418.

Belluzzi, O., Puopolo, M., Benedusi, M., and Kratskin, I. 2004. Selective neuroinhibitory effects of taurine in slices of rat main olfactory bulb. Neuroscience 124, 929–944.

Berkowicz, D. A. and Trombley, P. Q. 2000. Dopaminergic modulation at the olfactory nerve synapse. Brain Res. 855, 90–99.

Biffo, S., Grillo, M., and Margolis, F. L. 1990. Cellular localization of carnosine-like and anserine-like immunoreactivities in rodent and avian central nervous system. Neuroscience 35, 637–651.

Bischofberger, J. and Jonas, P. 1997. Action potential propagation into the presynaptic dendrites of rat mitral cells. J. Physiol. 504, 359–365.

Blakemore, L. J. and Trombley, P. Q. 2003. Kinetic variability of AMPA receptors among olfactory bulb neurons in culture. Neuroreport 14, 965–970.

Blanes, T. 1898. Sobre algunos puntos dudosos de la estructura del bulbo olfactorio. Revista Trimestral microgafica 3, 99–127.

Bogan, N., Brecha, N., Gall, C., and Karten, H. J. 1982. Distribution of enkephalin-like immunoreactivity in the rat main olfactory bulb. Neuroscience 7, 895–906.

Bokil, H., Laaris, N., Ennis, M., and Keller, A. 2001. Ephaptic interactions in the mammalian olfactory system. J. Neurosci. 21, RC173.

Bonino, M., Cantino, D., and Sassoe-Pognetto, M. 1999. Cellular and subcellular localization of gamma-aminobutyric acid B receptors in the rat olfactory bulb. Neurosci. Lett. 274, 195–198.

Bouna, S., Gysling, K., Calas, A., and Araneda, S. 1994. Some noradrenergic neurons of locus ceruleus-olfactory pathways contain neuropeptide-Y. Brain Res. Bull. 34, 413–417.

Bowery, N. G., Hudson, A. L., and Price, G. W. 1987. GABAA and GABAB receptor site distribution in the rat central nervous system. Neuroscience 20, 365–383.

Brennan, P., Kaba, H., and Keverne, E. B. 1990. Olfactory recognition: a simple memory system. Science 250, 1223–1226.

Brumberg, J. C., Nowak, L. G., and McCormick, D. A. 2000. Ionic mechanisms underlying repetitive high-frequency burst firing in supragranular cortical neurons. J. Neurosci. 20, 4829–4843.

Burd, G. D., Davis, B. J., Macrides, F., Grillo, M., and Margolis, F. 1982. Carnosine in primary afferents of the olfactory system: an autoradiographic and biochemical study. J. Neurosci. 2, 244–255.

Cadetti, L. and Belluzzi, O. 2001. Hyperpolarisation-activated current in glomerular cells of the rat olfactory bulb. Neuroreport 12, 3117–3120.

Cajal, S. R. Y. 1890. The origins and terminations of the olfactory, optic, and acoustic nerves in vertebrates. In: *Studies on the Cerebral Cortex [Limbic Structures]*. (Translated by L.M. Kraft (1955)), pp. 1–27 The Year Book Publishers.

Cajal, S. R. Y. 1911a. Olfactory apparatus: olfactory mucosa and olfactory bulb or first-order olfactory center, In: Histology of the Nervous System, Vol. II. (Translated by N. Swanson and L. Swanson (1995)), pp. 532–554. Oxford University Press.

Cajal, R. S. Y. 1911b. *Histologie du Systeme Nerveux de l'Hommes et des Vertebres*. Paris: Maloine.

Camps, M., Kelly, P. H., and Palacios, J. M. 1990. Autoradiographic localization of D1 and D2 receptors in the brain of several mammalian species. J. Neural Transm. 80, 105–127.

Cang, J. and Isaacson, J. S. 2003. *In vivo* whole-cell recording of odor-evoked synaptic transmission in the rat olfactory bulb. J. Neurosci. 23, 4108–4116.

Carleton, A., Petreanu, L. T., Lansford, R., Alvarez-Buylla, A., and Lledo, P.-M. 2003. Becoming a new neuron in the adult olfactory bulb. Nat. Neurosci. 6, 507–518.

Carlson, G. C., Shipley, M. T., and Keller, A. 2000. Long-lasting depolarizations in mitral cells of the rat olfactory bulb. J. Neurosci. 20, 2011–2021.

Carlson, G. C., Slawecki, M. L., Lancaster, E., and Keller, A. 1997. Distribution and activation of intracellular Ca^{2+} stores in cultured olfactory bulb neurons. J. Neurophysiol. 78, 2176–2185.

Carson, K. A. 1984. Quantitative localization of neurons projecting to the mouse main olfactory bulb. Brain Res. Bull. 12, 629–634.

Castillo, P. E., Carleton, A., Vincent, J. D., and Lledo, P. M. 1999. Multiple and opposing roles of cholinergic transmission in the main olfactory bulb. J. Neurosci. 19, 9180–9191.

Chalansonnet, M. and Chaput, M. A. 1998. Olfactory bulb output cell temporal response patterns to increasing odor concentrations in freely breathing rats. Chem. Senses 23, 1–9.

Chanse, N. T. and Kopin, I. J. 1968. Stimulus-induced release of substances from olfactory bulb using the push–pull cannula. Nature 217, 466–498.

Chaput, M. 1983. Effects of olfactory peduncle sectioning on the single unit responses of olfactory bulb neurons to odor presentation in awake rabbits. Chem. Senses 8, 161–177.

Chaput, M. and Holley, A. 1979. Spontaneous activity of olfactory bulb neurons in awake rabbits, with some observations on the effects of pentobarbital anaesthesia. J. Physiol. (Paris) 75, 939–948.

Charpak, S., Mertz, J., Beaurepaire, E., Moreaux, L., and Delaney, K. 2001. Odor-evoked calcium signals in dendrites of rat mitral cells. Proc. Natl. Acad. Sci. U. S. A. 98, 1230–1234.

Chen, W. R. and Shepherd, G. M. 1997. Membrane and synaptic properties of mitral cells in slices of rat olfactory bulb. Brain Res. 745, 189–196.

Chen, W. R., Midtgaard, J., and Shepherd, G. M. 1997. Forward and backward propagation of dendritic impulses and their synaptic control in mitral cells. Science 278, 463–467.

Chen, W. R., Xiong, W., and Shepherd, G. M. 2000. Analysis of relations between NMDA receptors and GABA release at olfactory bulb reciprocal synapses. Neuron 25, 625–633.

Christie, J. M. and Westbrook, G. L. 2003. Regulation of backpropagating action potential in mitral cell lateral dendrites by A-type potassium currents. J. Neurophysiol. 89, 2466–2472.

Christie, J. M. and Westbrook, G. L. 2006. Lateral excitation within the olfactory bulb. J. Neurosci. 26, 2269–2277.

Christie, J. M., Bark, C., Hormuzdi, S. G., Helbig, I., Monyer, H., and Westbrook, G. L. 2005. Connexin36 mediates spike synchrony in olfactory bulb glomeruli. Neuron 46, 761–772.

Christie, J. M., Schoppa, N. E., and Westbrook, G. L. 2001. Tufted cell dendrodendritic inhibition in the olfactory bulb is dependent on NMDA receptor activity. J. Neurophysiol. 85, 169–173.

Chu, D. C. M., Albin, R. L., Young, A. B., and Penney, J. B. 1990. Distribution and kinetics of GABAB binding sites in rat central nervous system: a quantitative autoradiographic study. Neuroscience 34, 341–357.

Ciombor, K. J., Ennis, M., and Shipley, M. T. 1999. Norepinephrine increases rat mitral cell excitatory responses to weak olfactory nerve input via alpha-1 receptors *in vitro*. Neuroscience 90, 595–606.

Collins, G. G. 1974. The rates of synthesis, uptake and disappearance of [14C]-taurine in eight areas of the rat central nervous system. Brain Res. 76, 447–459.

Condorelli, D. F., Belluardo, N., Trovato-Salimaro, A., and Mudò 2000. Expression of Cx36 in mammalian neurons. Brain Res. Rev. 32, 72–85.

Condorelli, D. F., Parenti, R., Spinella, F., Salinaro, A. T., Belluardo, N., Cardile, V., and Cicirata, F. 1998. Cloning of a new gap junction gene (Cx36) highly expressed in mammalian neurons. Eur. J. Neurosci. 10, 1202–1208.

Coopersmith, R. and Leon, M. 1984. Enhanced neural response to familiar olfactory cues. Science 225, 849–851.

Coronas, V., Srivastava, L. K., Liang, J. J., Jourdan, F., and Moyse, E. 1997. Identification and localization of dopamine receptor subtypes in rat olfactory mucosa and bulb: a combined in situ hybridization and ligand binding radioautographic approach. J. Chem. Neuroanat. 12, 243–257.

Davila, N. G., Blakemore, L. J., and Trombley, P. Q. 2003. Dopamine modulates synaptic transmission between rat olfactory bulb neurons in culture. J. Neurophysiol. 90, 395–404.

Davis, B. J. 1991. NADPH-diaphorase activity in the olfactory system of the hamster and rat. J. Comp. Neurol. 314, 493–511.

Davis, B. J. and Macrides, F. 1983. Tyrosine hydroxylase immunoreactive neurons and fibers in the olfactory system of the hamster. J. Comp. Neurol. 214, 427–440.

Davis, B. J., Burd, G. D., and Macrides, F. 1982. Localization of methionine-enkephalin, substance P, and somatostatin immunoreactivities in the main olfactory bulb of the hamster. J. Comp. Neurol. 204, 377–383.

Debarbieux, F., Audinat, E., and Charpak, S. 2003. Action potential propagation in dendrites of rat mitral cells *in vivo*. J. Neurosci. 23, 5553–5560.

Desmaisons, D., Vincent, J-D., and Lledo, P-M. 1999. Control of action potential timing by intrinsic subthreshold oscillations in olfactory bulb neurons. J. Neurosci. 19, 10727–10737.

De Saint Jan, D. and Westbrook, G. L. 2005. Detecting activity in olfactory bulb glomeruli with astrocyte recording. J. Neurosci. 25, 2917–2924.

Didier, A., Ottersen, O. P., and Storm-Mathisen, J. 1994. Differential subcellular distribution of glutamate and taurine in primary olfactory neurons. Neuroreport 6, 145–148.

Dietz, S. B. and Murthy, V. N. 2005. Contrasting short-term plasticity at two sides of the mitral-granule reciprocal synapse in the mammalian olfactory bulb. J. Physiol. 569, 475–488.

DiFrancesco, D. 1993. Pacemaker mechanisms in cardiac tissue. Annu. Rev. Physiol. 55, 455–472.

Djurisic, M., Antic, S., Chen, W. R., and Zecevic, D. 2004. Voltage imaging from dendrites of mitral cells: EPSP attenuation and spike trigger zones. J. Neurosci. 24, 6703–6714.

Doty, R. L. and Risser, J. M. 1989. Influence of the D-2 dopamine receptor agonist quinpirole on the odor detection performance of rats before and after spiperone administration. Psychopharmacology 98, 310–315.

Doucette, R. 1989. Development of the nerve fiber layer in the olfactory bulb of mouse embryos. J. Comp. Neurol. 285, 514–527.

Duchamp-Viret, P., Chaput, M. A., and Duchamp, A. 1999. Odor response properties of rat olfactory receptor neurons. Science 284, 2171–2174.

Eeckman, F. H. and Freeman, W. J. 1990. Correlations between unit firing and EEG in the rat olfactory system. Brain Res. 528, 238–244.

Egger, V., Svoboda, K., and Mainen, Z. F. 2003. Mechanisms of lateral inhibition in the olfactory bulb: efficiency and modulation of spike-evoked calcium influx into granule cells. J. Neurosci. 23, 7551–7558.

Egger, V., Svoboda, K., and Mainen, Z. F. 2005. Dendrodendritic synaptic signals in olfactory bulb granule cells: local spine boost and global low-threshold spike. J. Neurosci. 25, 3521–3530.

Elaagouby, A., Ravel, N., and Gervais, R. 1991. Cholinergic modulation of excitability in the rat olfactory bulb: effect of local application of cholinergic agents on evoked field potentials. Neuroscience 45, 653–662.

El-Etri, M. M., Griff, E. R., Ennis, M., and Shipley, M. T. 1999. Evidence for cholinergic regulation of basal norepinephrine in the rat olfactory bulb. Neuroscience 93, 611–617.

Ennis, M., Hamilton, K. A., and Hayar, A. 2007. Neurochemistry of the main olfactory system. In: Sensory Neurochemistry In: Handbook of Neurochemistry and Molecular Neurobiology 3rd Edition (*ed*. A. Lajtha), Vol. 20, Sensory Neurochemistry (*ed* D. A. Johnson) pp. 137–204. Spinger.

Ennis, M., Zhou, F. M., Ciombor, K. J., Aroniadou-Anderjaska, V., Hayar, A., Borrelli, E., Zimmer, L. A., Margolis, F., and Shipley, M. T. 2001. Dopamine D2 receptor-mediated presynaptic inhibition of olfactory nerve terminals. J. Neurophysiol. 86, 2986–2997.

Ennis, M., Zhu, M., Heinbockel, T., and Hayar, A. 2006. Olfactory nerve-evoked metabotropic glutamate receptor-mediated responses in olfactory bulb mitral cells. J. Neurophysiol. 95, 2233–2241.

Ennis, M., Zimmer, L. A., and Shipley, M. T. 1996. Olfactory nerve stimulation activates rat mitral cells via NMDA and non- NMDA receptors *in vitro*. Neuroreport 7, 989–992.

Ezeh, P. I., Wellis, D. P., and Scott, J. W. 1993. Organization of inhibition in the rat olfactory bulb external plexiform layer. J. Neurophysiol. 70, 263–274.

Fadool, D. A., Tucker, K., Perkins, R., Fasciani, G., Thompson, R. N., Parsons, A. D., Overton, J. M., Koni, P. A., Flavell, R. A., and Kaczmarek, L. K. 2004. Kv1.3 channel gene-targeted deletion produces ''Super-Smeller Mice'' with altered glomeruli, interacting scaffolding proteins, and biophysics. Neuron 41, 389–404.

Ferriero, D. and Margolis, F. L. 1975. Denervation in the primary olfactory pathway of mice. II. Effects on carnosine and other amine compounds. Brain Res. 94, 75–86.

Fletcher, M. L. and Wilson, D. A. 2002. Experience modifies olfactory acuity: acetylcholine-dependent learning decreases behavioral generalization between similar odorants. J. Neurosci. 22, RC201.

Fletcher, M. L. and Wilson, D. A. 2003. Olfactory bulb mitral-tufted cell plasticity: odorant-specific tuning reflects previous odorant exposure. J. Neurosci. 23, 6946–6955.

Fletcher, M. L., Smith, A. M., Best, A. R., and Wilson, D. A. 2005. High-frequency oscillations are not necessary for simple olfactory discriminations in young rats. J. Neurosci. 25, 792–798.

Frazier, L. L. and Brunjes, P. C. 1988. Unilateral odor deprivation: early postnatal changes in olfactory bulb cell density and number. J. Comp. Neurol. 269, 355–370.

Friedman, D. and Strowbridge, B. W. 2000. Functional role of NMDA autoreceptors in olfactory mitral cells. J. Neurophysiol. 84, 39–50.

Friedman, D. and Strowbridge, B. W. 2003. Both electrical and chemical synapses mediate fast network oscillations in the olfactory bulb. J. Neurophysiol. 89, 2601–2610.

Friedrich, R. W. 2002. Real time odor representations. Trends Neurosci. 25, 487–489.

Frosch, M. P. and Dichter, M. A. 1982. Physiology and pharmacology of olfactory bulb neurons in dissociated cell culture. Brain Res. 290, 321–332.

Gall, C., Seroogy, K. B., and Brecha, N. 1986. Distribution of VIP- and NPY-like immunoreactivities in rat main olfactory bulb. Brain Res. 374, 389–394.

Gall, C. M., Hendry, S. H. C., Seroogy, K. B., Jones, E. G., and Haycock, J. W. 1987. Evidence for coexistence of GABA and dopamine in neurons of the rat olfactory bulb. J. Comp. Neurol. 266, 307–318.

Geiling, H. and Schild, D. 1996. Glutamate-mediated release of Ca^{2+} in mitral cells of the olfactory bulb. J. Neurophysiol. 76, 563–570.

Gelperin, A. 2006. Olfactory computations and network oscillation. J. Neurosci. 26, 1663–1668.

Getchell, T. V. and Shepherd, G. M. 1975. Synaptic actions on mitral and tufted cells elicited by olfactory nerve volleys in the rabbit. J. Physiol. 251, 497–522.

Gheusi, G., Cremer, H., McLean, H., Chazal, G., Vincent, J.-D., and Lledo, P.-M. 2000. Importance of newly generated neurons in the adult olfactory bulb for odor discrimination. Proc. Natl. Acad. Sci. U. S. A. 97, 1823–1828.

Giustetto, M., Bovolin, P., Fasolo, A., Bonino, M., Cantino, D., and Sassoe-Pognetto, M. 1997. Glutamate receptors in the olfactory bulb synaptic circuitry: heterogeneity and synaptic localization of *N*-methyl-D-aspartate receptor subunit 1 and AMPA receptor subunit 1. Neuroscience 76, 787–798.

Golgi, C. 1875. Sulla Fina Structrura del Bulbi Olfattori. Rev Sper Feniatr 1, 405–425.

Gray, C. M. and Skinner, J. E. 1988. Centrifugal regulation of olfactory bulb of the waking rabbit as revealed by reversible cryogenic blockade. Exp. Brain Res. 69, 378–386.

Greer, C. A. 1987. Golgi analyses of dendritic organization among denervated olfactory bulb granule cells. J. Comp. Neurol. 256, 442–452.

Halabisky, B. and Strowbridge, B. W. 2003. γ-Frequency excitatory input to granule cells facilitates dendrodendritic inhibition in the rat olfactory bulb. J. Neurophysiol. 90, 644–654.

Halabisky, B., Friedman, D., Radojicic, M., and Strowbridge, B. W. 2000. Calcium influx through NMDA receptors directly evokes GABA release in olfactory bulb granule cells. J. Neurosci. 20, 5124–5134.

Halász, N. and Shepherd, G. M. 1983. Neurochemistry of the vertebrate olfactory bulb. Neuroscience 10, 579–619.

Halász, N., Hokfelt, T., Norman, A. W., and Goldstein, M. 1985. Tyrosine hydroxylase and 28K-vitamin D-dependent calcium binding protein are localized in different subpopulations of periglomerular cells of the rat olfactory bulb. Neurosci. Lett. 61, 103–107.

Halász, N., Ljungdahl, A., Hokfelt, T., Johansson, O., Goldstein, M., Park, D., and Biberfeld, P. 1977. Transmitter histochemistry of the rat olfactory bulb. I. Immunohistochemical localization of monoamine synthesizing enzymes. Support for intrabulbar, peri-glomerular dopamine neurons. Brain Res. 126, 455–474.

Hamilton, K. A. and Coppola, D. M. 2003. Distribution of GluR1 is altered in the olfactory bulb following neonatal naris occlusion. J. Neurobiol. 54, 326–336.

Hamilton, K. A., Heinbockel, T., Ennis, M., Szabó, G., Erdélyi, F., and Hayar, A. 2005. Properties of external plexiform layer interneurons in mouse olfactory bulb slices. Neuroscience 133, 819–829.

Hardy, A., Palouzier-Paulignan, B., Duchamp, A., Royet, J. P., and Duchamp-Viret, P. 2005. 5-hydroxytryptamine action in the rat olfactory bulb: *In vitro* electrophysiological patch-clamp recordings of juxtaglomerular and mitral cells. Neuroscience 131, 717–731.

Hayar, A., Heyward, P. M., Heinbockel, T., Shipley, M. T., and Ennis, M. 2001. Direct excitation of mitral cells via activation of alpha1-noradrenergic receptors in rat olfactory bulb slices. J. Neurophysiol. 86, 2173–2182.

Hayar, A., Karnup, S., Ennis, M., and Shipley, M. T. 2004b. External tufted cells: a major excitatory element that coordinates glomerular activity. J. Neurosci. 24, 6676–6685.

Hayar, A., Karnup, S., Shipley, M. T., and Ennis, M. 2004a. Olfactory bulb glomeruli: external tufted cells intrinsically burst at theta frequency and are entrained by patterned olfactory input. J. Neurosci. 24, 1190–1199.

Hayar, A., Shipley, M. T., and Ennis, M. 2005. Olfactory bulb external tufted cells are synchronized by multiple intraglomerular mechanisms. J. Neurosci. 25, 8197–8208.

Heinbockel, T., Heyward, P., Conquet, F., and Ennis, M. 2004. Regulation of main olfactory bulb mitral cell excitability by metabotropic glutamate receptor mGluR1. J. Neurophysiol. 92, 3085–3096.

Heinbockel, T., Laaris, N., and Ennis, M. 2007. Metabotropic glutamate receptors in the main olfactory bulb drive granule cell-mediated inhibition. J. Neurophysiol. 97, 858–870.

Heyward, P. M., Ennis, M., Keller, A., and Shipley, M. T. 2001. Membrane bistability in olfactory bulb mitral cells. J. Neurosci. 21, 5311–5320.

Hinds, J. W. 1968. Autoradiographic study of histogenesis in the mouse olfactory bulb. I. Time of origin of neurons and neuroglia. J. Comp. Neurol. 134, 287–304.

Hirata, Y. 1964. Some observations on the fine structure of the synapses in the olfactory bulb of the mouse, with particular reference to the atypical synaptic configurations. Arch. Histol. Jpn. 24, 293–302.

Hormuzdi, S. G., Pais, I., LeBleu, F. E. N., Towers, S. K., Rozoz, A., Buhl, E. H., Whittington, M. A., and Monyer, H. 2001. Impaired electrical signaling disrupts gamma frequency oscillations in connexin 36-deficient mice. Neuron 31, 487–495.

Horning, M. S., Blakemore, L. J., and Trombley, P. Q. 2000. Endogenous mechanisms of neuroprotection: role of zinc, copper, and carnosine. Brain Res. 852, 56–61.

Hsia, A. Y., Vincent, J. D., and Lledo, P. M. 1999. Dopamine depresses synaptic inputs into the olfactory bulb. J. Neurophysiol. 82, 1082–1085.

Illig, K. R. and Haberly, L. B. 2003. Odor-evoked activity is spatially distributed in piriform cortex. J. Comp. Neurol. 457, 361–373.

Inagaki, S., Sakanaka, M., Shiosaka, S., Senba, E., Takatsuki, K., Takagi, H., Kawai, Y., Minagawa, H., and Tohyama, M. 1982. Ontogeny of substance P-containing neuron system of the rat: immunohistochemical analysis – I. Forebrain and upper brain stem. Neuroscience 7, 251–277.

Isaacson, J. S. 1999. Glutamate spillover mediates excitatory transmission in the rat olfactory bulb. Neuron 23, 377–384.

Isaacson, J. S. 2001. Mechanisms governing dendritic gamma-aminobutyric acid (GABA) release in the rat olfactory bulb. Proc. Natl. Acad. Sci. U.S. A. 98, 337–342.

Isaacson, J. S. and Murphy, G. J. 2001. Glutamate-mediated extrasynaptic inhibition: direct coupling of NMDA receptors to Ca^{2+}-activated K^{+} channels. Neuron 31, 1027–1034.

Isaacson, J. S. and Strowbridge, B. W. 1998. Olfactory reciprocal synapses: dendritic signaling in the CNS. Neuron 20, 749–761.

Isaacson, J. S. and Vitten, H. 2003. GABAB receptors inhibit dendrodendritic transmission in the rat olfactory bulb. J. Neurosci. 23, 2032–2039.

Jackowski, A., Parnavelas, J. G., and Lieberman, A. R. 1978. The reciprocal synapse in the external plexiform layer of the mammalian olfactory bulb. Brain Res. 159, 17–28.

Jahr, C. E. and Nicoll, R. A. 1982. Noradrenergic modulation of dendrodendritic inhibition in the olfactory bulb. Nature 297, 227–229.

Jardemark, K., Nilsson, M., Muyderman, H., and Jacobson, I. 1997. Ca2+ ion permeability properties of (RS)α-amino-3-hydroxy-5-methyl-4-isoxazolepropionate (AMPA) receptors in isolated interneurons from the olfactory bulb of the rat. J. Neurophysiol. 77, 702–708.

Jiang, M. R., Griff, E. R., Ennis, M., Zimmer, L. A., and Shipley, M. T. 1996. Activation of locus coeruleus enhances the responses of olfactory bulb mitral cells to weak olfactory nerve input. J. Neurosci. 16, 6319–6329.

Kaba, H. and Keverne, E. B. 1988. The effect of microinfusions of drugs into the accessory olfactory block to pregnancy. Neuroscience 25, 1007–1011.

Kamisaki, Y., Wada, K., Nakamoto, K., and Itoh, T. 1996. Effects of taurine on GABA release from synaptosomes of rat olfactory bulb. Amino Acids 10, 49–57.

Karnup, S. V., Hayar, A., Shipley, M. T., and Kurnikova, M. G. 2006. Spontaneous field potentials in the glomeruli of the olfactory bulb: the leading role of juxtaglomerular cells. Neuroscience 142, 203–221.

Kashiwadani, H., Sasaki, Y. F., Uchida, N., and Mori, K. 1999. Synchronized oscillatory discharges of mitral/tufted cells with different molecular receptive ranges in the rabbit olfactory bulb. J. Neurophysiol. 182, 1786–1792.

Kasowski, H. J., Kim, H., and Greer, C. A. 1999. Compartmental organization of the olfactory bulb glomerulus. J. Comp. Neurol. 407, 261–274.

Kauer, J. S. 1998. Olfactory processing: a time and place for everything. Curr. Biol. 8, R282–R283.

Kay, L. M. 2003. A challenge to chaotic intinerancy from brain dynamics. Chaos 13, 1057–1066.

Kay, L. M. 2005. Theta oscillations and sensorimotor performance. Proc. Natl. Acad. Sci. U. S. A. 102, 3863–3868.

Kay, L. M. and Freeman, W. J. 1998. Bidirectional processing in the olfactory-limbic axis during olfactory behavior. Behav. Neurosci. 112, 541–553.

Kay, L. M. and Laurent, G. 1999. Odor- and context-dependent modulation of mitral cell activity in behaving rats. Nat. Neurosci. 2, 1003–1009.

Keller, A., Yagodin, S., Aroniadou-Anderjaska, V., Zimmer, L. A., Ennis, M., Sheppard, N. F., Jr, and Shipley, M. T. 1998. Functional organization of rat olfactory bulb glomeruli revealed by optical imaging. J. Neurosci. 18, 2602–2612.

Kendrick, K. M., Levy, F., and Keverne, E. B. 1992. Changes in the sensory processing of olfactory signals induced by birth in sheep. Science 256, 833–836.

Kepecs, A., Uchida, N., and Mainen, Z. F. 2006. The sniff as a unit of olfactory processing. Chem. Senses 31, 167–179.

Kerr, D. I. B. and Hagbarth, K. E. 1955. An investigation of the olfactory centrifugal system. J. Neurophysiol. 18, 362–374.

Konig, P., Engel, A. K., and Singer, W. 1996. Integrator or coincidence detector? The role of the cortical neuron revisited. Trends Neurosci. 19, 130–137.

Kosaka, K., Aika, Y., Toida, K., Heizmann, C. W., Hunziker, W., Jacobowitz, D. M., Nagatsu, I., Streit, P., Visser, T. J., and Kosaka, T. 1995. Chemically defined neuron groups and their subpopulations in the glomerular layer of the rat main olfactory bulb. Neurosci. Res. 23, 73–88.

Kosaka, K., Hama, K., Nagatsu, I., Wu, J. Y., and Kosaka, T. 1988. Possible coexistence of amino acid (gamma-aminobutyric acid), amine (dopamine) and peptide (substance P); neurons containing immunoreactivities for glutamic acid decarboxylase, tyrosine hydroxylase and substance P in the hamster main olfactory bulb. Exp. Brain Res. 71, 633–642.

Kosaka, K., Hama, K., Nagatsu, I., Wu, J. Y., Ottersen, O. P., Storm-Mathisen, J., and Kosaka, T. 1987. Postnatal development of neurons containing both catecholaminergic and GABAergic traits in the rat main olfactory bulb. Brain Res. 403, 355–360.

Kosaka, K., Toida, K., Aika, Y., and Kosaka, T. 1998. How simple is the organization of the olfactory glomerulus?: the heterogeneity of so-called periglomerular cells. Neurosci. Res. 30, 101–110.

Kosaka, K., Toida, K., Margolis, F. L., and Kosaka, T. 1997. Chemically defined neuron groups and their subpopulations in the glomerular layer of the rat main olfactory bulb – II. Prominent differences in the intraglomerular dendritic arborization and their relationship to olfactory nerve terminals. Neuroscience 76, 775–786.

Kosaka, T. and Kosaka, K. 2003. Neuronal gap junctions in the rat main olfactory bulb, with special reference to intraglomerular gap junction. Neurosci. Res. 45, 189–209.

Kosaka, T. and Kosaka, K. 2004. Neuronal gap junctions between intraglomerular mitral/tufted cell dendrites in the mouse main olfactory bulb. Neurosci. Res. 49, 373–378.

Kosaka, T., Hataguchi, Y., Hama, K., Nagatsu, I., and Wu, J. Y. 1985. Coexistence of immunoreactivities for glutamate decarboxylase and tyrosine hydroxylase in some neurons in the periglomerular region of the rat main olfactory bulb: possible coexistence of gamma-aminobutyric acid (GABA) and dopamine. Brain Res. 343, 166–171.

Kosaka, T., Kosaka, K., Hama, K., Wu, J.-Y., and Nagatsy, I. 1987a. Differential effect of functional olfactory deprivation on the GABAergic and catecholaminergic traits in the rat main olfactory bulb. Brain Res. 413, 197–203.

Kosaka, T., Kosaka, K., Hataguchi, Y., Nagatsu, I., Wu, J. Y., Ottersen, O. P., Storm-Mathisen, J., and Hama, K. 1987b. Catecholaminergic neurons containing GABA-like and/or glutamic acid decarboxylase-like immunoreactivities in various brain regions of the rat. Exp. Brain Res. 66, 191–210.

Kosaka, T., Kosaka, K., Heizmann, C. W., Nagatsu, I., Wu, J. Y., Yanaihara, N., and Hama, K. 1987c. An aspect of the organization of the GABAergic system in the rat main olfactory bulb: laminar distribution of immunohistochemically defined subpopulations of GABAergic neurons. Brain Res. 411, 373–378.

Koster, N. L., Norman, A. B., Richtand, N. M., Nickell, W. T., Puche, A. C., Pixley, S. K., and Shipley, M. T. 1999. Olfactory receptor neurons express D2 dopamine receptors. J. Comp. Neurol. 411, 666–673.

Kratskin, I. and Belluzzi, O. 2002. Immunohistochemical localization of the taurine-synthesizing enzyme in the rat olfactory bulb. Chem. Senses 27, 46.

Kratskin, I. and Belluzzi, O. 2003. Anatomy and neurochemistry of the olfactory bulb. In: *Handbook of Olfaction and Gustation,* 2nd Edition (*ed*. R. L. Doty), pp. 139–164. Marcel Dekker.

Kratskin, I. L., Rio, J. P., Kenigfest, N. B., Doty, R. L., and Repérant, J. 2000. A light and electron microscopic study of taurine-like immunoreactivity in the main olfactory bulb of frogs. J. Chem. Neuroanat. 18, 87–101.

Kunze, W. A. A., Shafton, A. D., Kemm, R. E., and McKenzie, J. S. 1991. Effect of stimulating the nucleus of the horizontal limb of the diagonal band on single unit activity in the olfactory bulb. Neuroscience 40, 21–27.

Kunze, W. A. A., Shafton, A. D., Kemm, R. E., and McKenzie, J. S. 1992. Intracellular responses of olfactory bulb granule cells to stimulating the horizontal diagonal band nucleus. Neuroscience 48, 363–369.

Laaris, N., Heinbockel, T., and Ennis, M. 2007. Complementary Postsynaptic activity patterns elicited in olfactory bulb by stimulation mitral/tufted an centrifugal fiber inputs to granule cells. J. Neurophysiol. 97, 296–306.

Lagier, S., Carleton, A., and Lledo, P. M. 2004. Interplay between local GABAergic interneurons and relay neurons generates gamma oscillations in the rat olfactory bulb. J. Neurosci. 24, 4382–4392.

Laurent, G. 2002. Olfactory network dynamics and the coding of multidimensional signals. Nat. Rev. Neurosci. 3, 884–895.

Levey, A. I., Hersch, S. M., Rye, D. B., Sunahara, R. K., Niznik, H. B., Kitt, C. A., Price, D. L., Maggio, R., Brann, M. R., and Ciliax, B. J. 1993. Localization of D1 and D2 dopamine receptors in brain with subtype-specific antibodies. Proc. Natl. Acad. Sci. U. S. A. 90, 8861–8865.

Liu, C. J., Grandes, P., Matute, C., Cuenod, M., and Streit, P. 1989. Glutamate-like immunoreactivity revealed in rat olfactory bulb, hippocampus and cerebellum by monoclonal antibody and sensitive staining method. Histochemistry 90, 427–445.

Liu, W. L. and Shipley, M. T. 1994. Intrabulbar associational system in the rat olfactory bulb comprises cholecystokinin-containing tufted cells that synapse onto the dendrites of GABAergic granule cells. J. Comp. Neurol. 346, 541–558.

Lledo, P. M., Gheusi, G., and Vincent, J. D. 2005. Information processing in the mammalian olfactory system. Physiol. Rev. 85, 281–317.

Lodovichi, C., Belluscio, L., and Katz, L. C. 2003. Functional topography of connections linking mirror-symmetric maps in the mouse olfactory bulb. Neuron 38, 265–276.

Lois, C. and Alvarez-Buylla, A. 1994. Long-distance neuronal migration in the adult mammalian brain. Science 264, 1145–1148.

López-Mascaraque, L., de Carlos, J. A., and Valverde, F. 1990. Structure of the olfactory bulb of the hedgehog (*Erinaceus europaeus*): a Golgi study of the intrinsic organization of the superficial layers. J. Comp. Neurol. 301, 243–261.

López-Mascaraque, L., Villalba, R. M., and de Carlos, J. A. 1989. Vasoactive intestinal polypeptide-immunoreactive neurons in the main olfactory bulb of the hedgehog (*Erinaceus europaeus*). Neurosci. Lett. 98, 19–21.

Lowe, G. 2002. Inhibition of backpropagating action potentials in mitral cell secondary dendrites. J. Neurophysiol. 88, 64–85.

Luo, M. and Katz, L. 2001. Response correlation maps of neurons in the mammalian olfactory bulb. Neuron 32, 1165–1179.

Luskin, M. B. 1993. Restricted proliferation and migration of postnatally generated neurons derived from the forebrain subventricular zone. Neuron 11, 173–189.

Lüthi, A. and McCormick, D. A. 1998. H-current: properties of a neuronal and network pacemaker. Neuron 21, 9–12.

MacLeod, N. K. and Straughan, D. W. 1979. Responses of olfactory bulb neurones to the dipeptide carnosine. Exp. Brain Res. 34, 183–188.

Macrides, F. and Schneider, S. P. 1982. Laminar organization of mitral and tufted cells in the main olfactory bulb of the adult hamster. J. Comp. Neurol. 208, 419–430.

Macrides, F., Eichenbaum, H. B., and Forbes, W. B. 1982. Temporal relationship between sniffing and the limbic theta rhythm during odor discrimination and reversal learning. J. Neurosci. 2, 1705–1717.

Maher, B. J. and Westbrook, G. L. 2005. SK channel regulation of dendritic excitability and dendrodendritic inhibition in the olfactory bulb. J. Neurophysiol. 94, 3743–3750.

Mansour, A., Meador-Woodruff, J. H., Bunzow, J. R., Civelli, O., Akil, H., and Watson, S. J. 1990. Localization of dopamine D2 receptor mRNA and D1 and D2 receptor binding in the rat brain and pituitary: an in situ hybridization-receptor autoradiographic analysis. J. Neurosci. 10, 2587–2600.

Margeta-Mitrovic, M., Mitrovic, I., Riley, R. C., Jan, L. Y., and Basbaum, A. I. 1999. Immunohistochemical localization of GABA(B) receptors in the rat central nervous system. J. Comp. Neurol. 405, 299–321.

Margolis, F. L. 1974. Carnosine in the primary olfactory pathway. Science 184, 909–911.

Margolis, F. L. 1980. Carnosine: an olfactory neuropeptide. In: *The Role of Peptides in Neuronal Function* (*eds*. J. L. Barker and T. G. J. Smith), pp. 545–572. Dekker.

Margolis, F. L. and Grillo, M. 1984. Carnosine, homocarnosine and anserine in vertebrate retinas. Neurochem. Int. 6, 207–209.

Margolis, F. L., Grillo, M., Grannot-Reisfeld, N., and Farbman, A. I. 1983. Purification, characterization and immunocytochemical localization of mouse kidney carnosinase. Biochim. Biophys. Acta 744, 237–248.

Margolis, F. L, Grillo, M., Hempstead, J., and Morgan, J. I. 1987. Monoclonal antibodies to mammalian carnosine synthetase. J. Neurochem. 48, 593–600.

Margolis, F. L, Grillo, M., Kawano, T., and Farbman, A. I. 1985. Carnosine synthesis in olfactory tissue during ontogeny: Effect of exogenous b-alanine. J. Neurochem. 44, 1459–1464.

Margrie, T. W. and Schaefer, A. T. 2003. Theta oscillation coupled spike latencies yield computational vigour in a mammalian sensory system. J. Physiol. 546, 363–374.

Margrie, T. W., Sakmann, B., and Urban, N. N. 2001. Action potential propagation in mitral cell lateral dendrites is decremental and controls recurrent and lateral inhibition in the mammalian olfactory bulb. Proc. Natl. Acad. Sci. U. S. A. 98, 319–324.

Martin, C., Gervais, R., Hugues, E., Messaoudi, B., and Ravel, N. 2004. Learning modulation of odor-induced oscillatory responses in the rat olfactory bulb: a correlate of odor recognition? Neurosci. 24, 389–397.

Matsutani, S., Senba, E., and Tohyama, M. 1988. Neuropeptide- and neurotransmitter-related immunoreactivities in the developing rat olfactory bulb. J. Comp. Neurol. 272, 331–342.

McLean, J. H. and Harley, C. W. 2004. Olfactory learning in the rat pup: a model that may permit visualization of a mammalian memory trace. Neuroreport 15, 1691–1697.

McLean, J. H. and Shipley, M. T. 1987a. Serotonergic afferents to the rat olfactory bulb: I Origins and laminar specificity of serotonergic inputs in the adult rat. J. Neurosci. 7, 3016–3028.

McLean, J. H. and Shipley, M. T. 1987b. Serotonergic afferents to the rat olfactory bulb: II Changes in fiber distribution during development. J. Neurosci. 7, 3029–3039.

McLean, J. H. and Shipley, M. T. 1988. Postmitotic, postmigrational expression of tyrosine hydroxylase in olfactory bulb dopaminergic neurons. J. Neurosci. 8, 3658–3669.

McLean, J. H., Darby-King, A., and Hodge, E. 1996. 5-HT2 receptor involvement in conditioned olfactory learning in the neonatal rat pup. Behav. Neurosci. 110, 1426–1434.

McLean, J. H., Shipley, M. T., Nickell, W. T., Aston-Jones, G., and Reyher, C. K. 1989. Chemoanatomical organization of the noradrenergic input from locus coeruleus to the olfactory bulb of the adult rat. J. Comp. Neurol. 285, 339–349.

McLennan, H. 1971. The Pharmacology of inhibition of mitral cells in the olfactory bulb. Brain. Res. 29, 177–184.

McQuiston, A. R. and Katz, L. C. 2001. Electrophysiology of interneurons in the glomerular layer of the rat olfactory bulb. J. Neurophysiol. 86, 1899–1907.

Meisami, E. 1989. A proposed relationship between increases in the number of olfactory receptor neurons, convergence ratio and sensitivity in the developing rat. Brain Res. Dev. Brain. Res. 46, 9–19.

Merchenthaler, I., Csernus, V., Csontos, C., Petrusz, P., and Mess, B. 1988. New data on the immunocytochemical localization of thyrotropin-releasing hormone in the rat central nervous system. Am. J. Anat. 181, 359–376.

Miragall, F., Simburger, E., and Dermietzel, R. 1996. Mitral and tufted cells of the mouse olfactory bulb possess gap junctions and express connecin43 mRNA. Neurosci. Lett. 216, 199–202.

Mombaerts, P., Wang, F., Dulac, C., Chao, S. K., Nemes, A., Mendelsohn, M., Edmondson, J., and Axel, R. 1996. Visualizing an olfactory sensory map. Cell 87, 675–686.

Montague, A. A. and Greer, C. A. 1999. Differential distribution of ionotropic glutamate receptor subunits in the rat olfactory bulb. J. Comp. Neurol. 405, 233–246.

Mori, K. 1987. Membrane and synaptic properties of identified neurons in the olfactory bulb. Prog. Neurobiol. 29, 275–320.

Mori, K. and Takagi, S. F. 1978. Activation and inhibition of olfactory bulb neurones by anterior commissure volleys in the rabbit. J. Physiol. (Lond.) 279, 589–604.

Mori, K., Kishi, K., and Ojima, H. 1983. Distribution of dendrites of mitral, displaced mitral, tufted, and granule cells in the rabbit olfactory bulb. J. Comp. Neurol. 219, 339–355.

Mori, K., Takahashi, Y. K., Igarashi, K. M., and Yamaguchi, M. 2006. Maps of odorant molecular features in the mammalian olfactory bulb. Physiol. Rev. 86, 409–433.

Moriceau, S. and Sullivan, R. M. 2004. Unique neural circuitry for neonatal olfactory learning. J. Neurosci. 24, 1182–1189.

Morizumi, T., Tsukatani, H., and Miwa, T. 1994. Olfactory disturbance induced by deafferentation of serotonergic fibers in the olfactory bulb. Neuroscience 61, 733–738.

Mouly, A. M., Elaagouby, A., and Ravel, N. 1995. A study of the effects of noradrenaline in the rat olfactory bulb using evoked field potential response. Brain Res. 681, 47–57.

Mugnaini, E., Oertel, W. H., and Wouterlood, F. F. 1984. Immunocytochemical localization of GABA neurons and dopamine neurons in the rat main and accessory olfactory bulbs. Neurosci. Lett. 47, 221–226.

Murphy, G. J., Darcy, D. P., and Isaacson, J. S. 2005. Intraglomerular inhibition: signaling mechanisms of an olfactory microcircuit. Nat. Neurosci. 8, 354–364.

Murphy, G. J., Glickfeld, L. L., Balsen, Z., and Isaacson, J. S. 2004. Sensory neuron signaling to the brain: properties of transmitter release from olfactory nerve terminals. J. Neurosci. 24, 3023–3030.

Mutoh, H., Yuan, Q., and Knöpfel, T. 2005. Long-term depression at olfactory nerve synapses. J. Neurosci. 25, 4252–4259.

Nagayama, S., Takahashi, Y. K., Yoshihara, Y., and Mori, K. 2004. Mitral and tufted cells differ in the decoding manner of odor maps in the rat olfactory bulb. J. Neurophysiol. 91, 2532–2540.

Nakajima, T., Okamura, M., Ogawa, K., and Taniguchi, K. 1996. Immunohistochemical and enzyme histochemical characteristics of short axon cells in the olfactory bulb of the golden hamster. J. Vet. Med. Sci. 58, 903–908.

Nakashima, M., Mori, K., and Takagi, S. F. 1978. Centrifugal influence on olfactory bulb activity in the rabbit. Brain Res. 154, 301–316.

Neville, K. R. and Haberly, L. B. 2003. Beta and gamma oscillations in the olfactory system of the urethane-anesthetized rat. J. Neurophysiol. 90, 3921–3930.

Nickell, W. T. and Shipley, M. T. 1988. Neurophysiology of magnocellular forebrain inputs to the olfactory bulb in the rat: frequency potentiation of field potentials and inhibition of output neurons. J. Neurosci. 8, 4492–4502.

Nickell, W. T. and Shipley, M. T. 1992. Neurophysiology of the olfactory bulb. In: *Science of Olfaction* (*eds*. M. J. Serby and K. L. Chobor), pp. 172–212. Springer.

Nickell, W. T. and Shipley, M. T. 1993. Evidence for presynaptic inhibition of the olfactory commissural pathway by cholinergic agonists and stimulation of the nucleus of the diagonal band. J. Neurosci. 13, 650–659.
Nickell, W. T., Norman, A. B., Wyatt, L. M., and Shipley, M. T. 1991. Olfactory bulb DA receptors may be located on terminals of the olfactory nerve. Neuroreport 2, 9–12.
Nicoll, R. A. 1971. Pharmacological evidence for GABA as the transmitter in granule cell inhibition in the olfactory bulb. Brain Res. 35, 137–149.
Nicoll, R. A. and Alger, B. E. 1980. Peptides as putative excitatory neurotransmitters: carnosine, enkephalin, substance P and TRH. Proc. R. Soc. Lond. 210, 133–149.
Nowycky, M. C., Halasz, N., and Shepherd, G. M. 1983. Evoked field potential analysis of dopaminergic mechanisms in the isolated turtle olfactory bulb. Neuroscience 8, 717–722.
Nusser, Z., Kay, L. M., Laurent, G., Homanics, G. E., and Mody, I. 2001. Disruption of GABAA receptors on GABAergic interneurons leads to increased oscillatory power in the olfactory bulb network. J. Neurophysiol. 86, 2823–2833.
Ohm, T. G., Müller, H., Ulfig, N., and Braak, E. 1990. Glutamic-acid-decarboxylase- and parvalbumin-like-immunoreactive structures in the olfactory bulb of the human adult. J. Comp. Neurol. 291, 1–8.
Okutani, F., Kaba, H., Takahashi, S., and Seto, K. 1998. The biphasic effect of locus coeruleus noradrenergic activation on dendrodendritic inhibition in the rat olfactory bulb. Brain Res. 783, 272–279.
Orona, E., Rainer, E. C., and Scott, J. W. 1984. Dendritic and axonal organization of mitral and tufted cells in the rat olfactory bulb. J. Comp. Neurol. 226, 346–356.
Orona, E., Scott, J. W., and Rainer, E. C. 1983. Different granule cell populations innervate superficial and deep regions of the external plexiform layer in rat olfactory bulb. J. Comp. Neurol. 217, 227–237.
Palouzier-Paulignan, B., Duchamp-Viret, P., Hardy, A. B., and Duchamp, A. 2002. GABA(B) receptor-mediated inhibition of mitral/tufted cell activity in the rat olfactory bulb: a whole-cell patch-clamp study *in vitro*. Neuroscience 111, 241–250.
Pape, H. C. 1996. Queer current and pacemaker: the hyperpolarization-activated cation current in neurons. Annu. Rev. Physiol. 58, 299–327.
Paternostro, M. A., Reyher, C. K. H., and Brunjes, P. C. 1995. Intracellular injections of Lucifer Yellow into lightly fixed mitral cells reveal neuronal dye-coupling in the developing rat olfactory bulb. Dev. Brain Res. 84, 1–10.
Perez, H., Hernandez, A., and Almli, C. R. 1987. Locus coeruleus stimulation modulates olfactory bulb evoked potentials. Brain Res. Bull. 18, 767–770.
Petralia, R. S. and Wenthold, R. J. 1992. Light and electron immunocytochemical localization of AMPA-selective glutamate receptors in the rat brain. J. Comp. Neurol. 318, 329–354.
Philpot, B. D., Foster, T. C., and Brunjes, P. C. 1997. Mitral/tufted cell activity is attenuated and becomes uncoupled from respiration following naris closure. J. Neurobiol. 33, 374–386.
Pignatelli, A., Kobayashi, K., Okano, H., and Belluzzi, O. 2005. Functional properties of dopaminergic neurones in the mouse olfactory bulb. J. Physiol. 564, 501–514.
Pinato, G. and Midtgaard, J. 2003. Regulation of granule cell excitability by a low-threshold calcium spike in turtle olfactory bulb. J. Neurophysiol. 90, 3341–3351.
Pinato, G. and Midtgaard, J. 2005. Dendritic sodium spikelets and low-threshold calcium spikes in turtle olfactory bulb granule cells. J. Neurophysiol. 93, 1285–1294.
Pinching, A. J. and Powell, T. P. 1971a. The neuron types of the glomerular layer of the olfactory bulb. J. Cell Sci. 9, 305–345.
Pinching, A. J. and Powell, T. P. 1971b. The neuropil of the glomeruli of the olfactory bulb. J. Cell Sci. 9, 347–377.
Pinching, A. J. and Powell, T. P. 1971c. The neuropil of the periglomerular region of the olfactory bulb. J. Cell Sci. 9, 379–409.
Pinching, A. J. and Powell, T. P. 1972b. Experimental studies on the axons intrinsic to the glomerular layer of the olfactory bulb. J. Cell Sci. 10, 637–655.
Pinching, A. J. and Powell, T. P. 1972c. The termination of centrifugal fibres in the glomerular layer of the olfactory bulb. J. Cell Sci. 10, 621–635.
Potter, S. M., Zheng, C., Koos, D. S., Feinstein, P., Fraser, S. E., and Mombaerts, P. 2001. Structure and emergence of specific olfactory glomeruli in the mouse. J. Neurosci. 21, 9713–9723.
Pow, D. V., Sullivan, R., Reye, P., and Hermanussen, S. 2002. Localization of taurine transporters, taurine, and 3H taurine accumulation in the rat retina, pituitary, and brain. Glia 37, 153–168.
Pressler, R. T. and Strowbridge, B. W. 2006. Blanes cells mediate persistent feedforward inhibition onto granule cells in the olfactory bulb. Neuron 49, 889–904.
Price, J. L. and Powell, T. P. S. 1970a. An electron-microscopic study of the termination of the afferent fibres to the olfactory bulb from the cerebral hemisphere. J. Cell Sci. 7, 157–187.
Price, J. L. and Powell, T. P. S. 1970b. The mitral and short axon cells of the olfactory bulb. J. Cell Sci. 7, 631–651.
Price, J. L. and Powell, T. P. S. 1970c. The morphology of the granule cells of the olfactory bulb. J. Cell Sci. 9, 91–123.
Price, J. L. and Powell, T. P. S. 1970d. The synaptology of the granule cells of the olfactory bulb. J. Cell Sci. 7, 125–155.
Puopolo, M. and Belluzzi, O. 1996. Sodium current in periglomerular cells of rat olfactory bulb *in vitro*. Neuroreport 7, 1846–1850.
Puopolo, M. and Belluzzi, O. 1998. Functional heterogeneity of periglomerular cells in the rat olfactory bulb. Eur. J. Neurosci. 10, 1073–1083.
Puopolo, M. and Belluzzi, O. 2001. NMDA-dependent, network-driven oscillatory activity induced by bicuculline or removal of Mg2+ in rat olfactory bulb neurons. Eur. J. Neurosci. 13, 92–102.
Puopolo, M., Bean, B. P., and Raviola, E. 2005. Spontaneous activity of isolated dopaminergic periglomerular cells of the main olfactory bulb. J. Neurophysiol. 94, 3618–3627.
Rall, W., Shepherd, G. M., Reese, T. S., and Brightman, M. W. 1966. Dendrodendritic synaptic pathway for inhibition in the olfactory bulb. Exp. Neurol. 14, 44–56.
Rash, J. E., Staines, W. A., Yasmura, T., Patel, D., Furman, D. S., Stelmack, G. L., and Nagy, J. I. 2000. Immunogold evidence that the neuronal gap junctions in adult rat brain and spinal cord contain connexin-36 but not connexin-32 or connexin-43. Proc. Natl. Acad. Sci. U. S. A. 97, 7573–7578.
Ressler, K. J., Sullivan, S. L., and Buck, L. B. 1993. A zonal organization of odorant receptor gene expression in the olfactory epithelium. Cell 73, 597–609.
Ressler, K. J., Sullivan, S. L., and Buck, L. B. 1994. Information coding in the olfactory system: evidence for a stereotyped and highly organized epitope map in the olfactory bulb. Cell 79, 1245–1255.
Reyher, C. K., Lubke, J., Larsen, W. J., Hendrix, G. M., Shipley, M. T., and Baumgarten, H. G. 1991. Olfactory bulb granule cell aggregates: morphological evidence for interperikaryal electrotonic coupling via gap junctions. J. Neurosci. 11, 1485–1495.
Ribak, C. E., Vaughn, J. E., Saito, K., Barber, R., and Roberts, E. 1977. Glutamate decarboxylase localization in neurons of the olfactory bulb. Brain Res. 126, 1–18.

Rochefort, C., Gheusi, G., Vincent, J.-D., and Lledo, P.-M. 2002. Enriched odor exposure increases the number of newborn neurons in the adult olfactory bulb and improves odor memory. J. Neurosci. 22, 2679–2689.

Rochel, S. and Margolis, F. L. 1982. Carnosine release from olfactory bulb synaptosomes is calcium-dependent and depolarization-stimulated. J. Neurochem. 38, 505–1514.

Ross, C. D., Godfrey, D. A., and Parli, J. A. 1995. Amino acid concentrations and selected enzyme activities in rat auditory, olfactory, and visual systems. Neurochem. Res. 20, 1483–1490.

Rosser, A. E. and Keverne, E. B. 1985. The importance of central noradrenergic neurones in the formation of an olfactory memory in the prevention of pregnancy block. Neuroscience 15, 1141–1147.

Roy, S. A. and Alloway, K. D. 2001. Coincidence detection or temporal integration? What the neurons in somatosensory cortex are doing. J. Neurosci. 21, 2462–2473.

Salin, P. A., Lledo, P. M., Vincent, J. D., and Charpak, S. 2001. Dendritic glutamate autoreceptors modulate signal processing in rat mitral cells. J. Neurophysiol. 85, 1275–1282.

Sallaz, M. and Jourdan, F. 1992. Apomorphine disrupts odour-induced patterns of glomerular activation in the olfactory bulb. Neuroreport 3, 833–836.

Salmoiraghi, G. C., Bloom, F. E., and Costa, E. 1964. Aderenergic mechanisms in rabbit olfactory bulb. Am. J. Physiol. 207, 1417–1424.

Sanides-Kohlrausch, C. and Wahle, P. 1990a. Morphology of neuropeptide Y-immunoreactive neurons in the cat olfactory bulb and olfactory peduncle: postnatal development and species comparison. J. Comp. Neurol. 291, 468–489.

Sanides-Kohlrausch, C. and Wahle, P. 1990b. VIP- and PHI-immunoreactivity in olfactory centers of the adult cat. J. Comp. Neurol. 294, 325–339.

Sassoe-Pognetto, M., Cantino, D., and Panzanelli, P. 1993. Presynaptic co-localization of carnosine and glutamate in olfactory neurons. Neuroreport 5, 7–10.

Schneider, S. P. and Macrides, F. 1978. Laminar distributions of interneurons in the main olfactory bulb of the adult hamster. Brain Res. Bull. 3, 73–82.

Schneider, S. P. and Scott, J. W. 1983. Orthodromic response properties of rat olfactory mitral and tufted cells correlate with their projection patterns. J. Neurophysiol. 50, 358–378.

Schoenfeld, T. A. and Macrides, F. 1984. Topographic organization of connections between the main olfactory bulb and pars externa of the anterior olfactory nucleus in the hamster. J. Comp. Neurol. 227, 121–135.

Schoenfeld, T. A., Marchand, J. E., and Macrides, F. 1985. Topographic organization of tufted cell axonal projections in the hamster main olfactory bulb: an intrabulbar associational system. J. Comp. Neurol. 235, 503–518.

Schoppa, N. E. 2006. Synchronization of olfactory bulb mitral cells by precisely timed inhibitory inputs. Neuron 49, 271–283.

Schoppa, N. E. and Westbrook, G. L. 1997. Modulation of mEPSCs in olfactory bulb mitral cells by metabotropic glutamate receptors. J. Neurophysiol. 78, 1468–1475.

Schoppa, N. E. and Westbrook, G. L. 1999. Regulation of synaptic timing in the olfactory bulb by an A-type potassium current. Nat. Neurosci. 2, 1106–1113.

Schoppa, N. E. and Westbrook, G. L. 2001. Glomerulus-specific synchronization of mitral cells in the olfactory bulb. Neuron 31, 639–651.

Schoppa, N. E. and Westbrook, G. L. 2002. AMPA receptors drive correlated spiking in olfactory bulb glomeruli. Nat. Neurosci. 5, 1194–1202.

Schoppa, N. E., Kinzie, J. M., Sahara, Y., Segerson, T. P., and Westbrook, G. L. 1998. Dendrodendritic inhibition in the olfactory bulb is driven by NMDA receptors. J. Neurosci. 18, 6790–6802.

Scott, J. W. 1986. The olfactory bulb and central pathways. Experientia 42, 223–232.

Scott, J. W., McDonald, J. K., and Pemberton, J. L. 1987. Short axon cells of the rat olfactory bulb display NADPH-diaphorase activity, neuropeptide Y-like immunoreactivity, and somatostatin-like immunoreactivity. J. Comp. Neurol. 260, 378–391.

Seroogy, K. B., Brecha, N., and Gall, C. 1985. Distribution of cholecystokinin-like immunoreactivity in the rat main olfactory bulb. J Comp. Neurol. 239, 373–383.

Shepherd, G. M. 1972. Synaptic organization of the mammalian olfactory bulb. Physiol. Rev. 52, 864–917.

Shepherd, G. M. and Greer, C. A. 1998. The olfactory bulb. In: *The Synaptic Organization of the Brain* (*ed*. G. M. Shepherd), pp. 159–203. Oxford University Press.

Shipley, M. T. and Adamek, G. D. 1984. The connections of the mouse olfactory bulb: a study using orthograde and retrograde transport of wheat germ agglutinin conjugated to horseradish peroxidase. Brain Res. Bull. 12, 669–688.

Shipley, M. T., Halloran, F. J., and de la Torre, J. 1985. Surprisingly rich projection from locus coeruleus to the olfactory bulb in the rat. Brain Res. 329, 294–299.

Shults, C. W., Quirion, R., Chronwall, B., Chase, T. N., and O'Donohue, T. L. 1984. A comparison of the anatomical distribution of substance P and substance P receptors in the rat central nervous system. Peptides 5, 1097–1128.

Siklos, L., Rickmann, M., Joo, F., Freeman, W. J., and Wolff, J. R. 1995. Chloride is preferentially accumulated in a subpopulation of dendrites and periglomerular cells of the main olfactory bulb in adult rats. Neuroscience 64, 165–172.

Smith, C. and Lushkin, M. B. 1998. Cell cycle length of olfactory bulb neuronal progenitors in the rostral migratory stream. Dev Dyn. 213, 220–227.

Smith, T..C. and Jahr, C. E. 2002. Self-inhibition of olfactory bulb neurons. Nat. Neurosci. 5, 760–766.

Spors, H., Wachowiak, M., Cohen, L. B., and Friedrich, R. W. 2006. Temporal dynamics and latency patterns of receptor neuron input to the olfactory bulb. J. Neurosci. 26, 1247–1259.

Sullivan, R. M., Stackenwalt, G., Nasr, F., Lemon, C., and Wilson, D. A. 2000. Association of an odor with activation of olfactory bulb noradrenergic beta-receptors or locus coeruleus stimulation is sufficient to produce learned approach responses to that odor in neonatal rats. Behav. Neurosci. 114, 957–962.

Sullivan, R. M., Wilson, D. A., and Leon, M. 1989. Norepinephrine and learning-induced plasticity in infant rat olfactory system. J. Neurosci. 9, 3998–4006.

Sullivan, R. M., Zyzak, D. R., Skierkowski, P., and Wilson, D. A. 1992. The role of olfactory bulb norepinephrine in early olfactory learning. Brain Res. Dev. 70, 279–282.

Teubner, B., Degen, J., Söhl, G., Güldenagel, M., Bukauskas, F. F., Trexler, E. B., Verselis, V. K., De Zeeuw, C. I., Lee, C. G., Kozak, C. A., Petrasch-Parwez, E., Dermietzel, R., and Willecke, K. 2000. Functional expression of the murine connexin 36 gene coding for a neuron-specific gap junctional protein. J. Membr. Biol. 176, 249–263.

Toida, K., Kosaka, K., Aika, Y., and Kosaka, T. 2000. Chemically defined neuron groups and their subpopulations in the glomerular layer of the rat main olfactory bulb – IV. Intraglomerular synapses of tyrosine hydroxylase-immunoreactive neurons. Neuroscience 101, 11–17.

Toida, K., Kosaka, K., Heizmann, C. W., and Kosaka, T. 1996. Electron microscopic serial-sectioning/reconstruction study of parvalbumin-containing neurons in the external plexiform layer of the rat olfactory bulb. Neuroscience 72, 449–466.

Toida, K., Kosaka, K., Heizmann, C. W., and Kosaka, T. 1998. Chemically defined neuron groups and their subpopulations in the glomerular layer of the rat main olfactory bulb: III Structural features of calbindin D28K-immunoreactive neurons. J. Comp. Neurol. 392, 179–198.
Treloar, H. B., Feinstein, P., Mombaerts, P., and Greer, C. A. 2002. Specificity of glomerular targeting by olfactory sensory axons. J. Neurosci. 22, 2469–2477.
Trombley, P. Q. 1992. Norepinephrine inhibits calcium currents and EPSPs via a G-protein-coupled mechanism in olfactory bulb neurons. J. Neurosci. 12, 3992–3998.
Trombley, P. Q. and Shepherd, G. M. 1992. Noradrenergic inhibition of synaptic transmission between mitral and granule cells in mammalian olfactory bulb cultures. J. Neurosci. 12, 3985–3991.
Trombley, P. Q. and Shepherd, G. M. 1996. Differential modulation zinc and copper of amino acid receptors from rat olfactory bulb neurons. J. Neurophysiol. 76, 2536–2546.
Trombley, P. Q. and Westbrook, G. L. 1992. L-AP4 inhibits calcium currents and synaptic transmission via a G-protein-coupled glutamate receptor. J. Neurosci. 12, 2043–2050.
Trombley, P. Q., Horning, M. S., and Blakemore, L. J. 1998. Carnosine modulates zinc and copper effects on amino acid receptors and synaptic transmission. Neuroreport 9, 3503–3507.
Tsuruo, Y., Hokfelt, T., and Visser, T. J. 1988. Thyrotropin-releasing hormone (TRH)-immunoreactive neuron populations in the rat olfactory bulb. Brain Res. 447, 183–187.
Urban, N. N. and Sakmann, B. 2002. Reciprocal intraglomerular excitation and intra- and interglomerular lateral inhibition between mouse olfactory bulb mitral cells. J. Physiol. (Lond.) 542, 355–367.
Van Gehuchten, L. E. and Martin, A. 1891. Le bulbe olfactif chez quelques mammiferes. Cellule 205–237.
Vassar, R., Chao, S. K., Sitcheran, R., Nunez, J. M., Vosshall, L. B., and Axel, R. 1994. Topographic organization of sensory projections to the olfactory bulb. Cell 79, 981–991.
Villalba, R. M., Rodrigo, J., Alvarez, F. J., Achaval, M., and Martinez-Murillo, R. 1989. Localization of C-PON immunoreactivity in the rat main olfactory bulb. Demonstration that the population of neurons containing endogenous C-PON display NADPH-diaphorase activity. Neuroscience 33, 373–382.
Wachowiak, M. and Cohen, L. B. 1999. Presynaptic inhibition of primary olfactory afferents mediated by different mechanisms in lobster and turtle. J. Neurosci. 19, 8808–8817.
Wachowiak, M., McGann, J. P., Heyward, P. M., Shao, Z., Puche, A. C., and Shipley, M. T. 2005. Inhibition [corrected] of olfactory receptor neuron input to olfactory bulb glomeruli mediated by suppression of presynaptic calcium influx. J. Neurophysiol. 94, 2700–2712.
Wahle, P., Sanides-Kohlrausch, S., Meyer, G., and Lubke, J. 1990. Substance P- and opioid immunoreactive structures in olfactory centers of the cat: adult pattern and postnatal development. J. Comp. Neurol. 302, 349–369.
Walsh, R. R. 1959. Olfactory bulb potentials evoked by electrical stimulation of the contralateral bulb. Am. J. Physiol. 196, 327–329.
Wang, F., Nemes, A., Mendelsohn, M., and Axel, R. 1998. Odorant receptors govern the formation of a precise topographic map. Cell 93, 47–60.
Warden, M. K. and Young, W. S. 1988. Distribution of cells containing mRNAs encoding substance P and neurokinin B in the rat central nervous system. J. Comp. Neurol. 272, 90–113.
Wehr, M. and Laurent, G. 1996. Odour encoding by temporal sequences of firing in oscillating neural assemblies. Nature 384, 162–166.
Welker, W. I. 1964. Analysis of sniffing of the albino rat. Behavior 22, 223–244.
Wellis, D. P. and Scott, J. W. 1990. Intracellular responses of identified rat olfactory bulb interneurons to electrical and odor stimulation. J. Neurophysiol. 64, 932–947.
Wellis, D. P., Scott, J. W., and Harrison, T. A. 1989. Discrimination among odorants by single neurons of the rat olfactory bulb. J. Neurophysiol. 61, 1161–1177.
Wichterle, H., Turnbull, D. H., Nery, S., Fishell, G., and Alvareq-Buylla, A. 2001. In utero fate mapping reveals distinct migratory pathways and fates of neurons born in the mammalian basal forebrain. Development 128, 3759–3771.
Wilson, D. A. and Leon, M. 1988. Noradrenergic modulation of olfactory bulb excitability in the postnatal rat. Dev. Brain Res. 42, 69–75.
Wilson, D. A. and Sullivan, R. M. 1991. Olfactory associative conditioning in infant rats with brain stimulation as reward: II. Norepinephrine mediates a specific component of the bulb response to reward. Behav. Neurosci. 105, 843–849.
Wilson, D. A. and Sullivan, R. M. 1995. The D2 antagonist spiperone mimics the effects of olfactory deprivation on mitral/tufted cell odor response patterns. J. Neurosci. 15, 5574–5581.
Woolf, T. B., Shepherd, G. M., and Greer, C. A. 1991. Serial reconstruction of granule cell spines in the mammalian olfactory bulb. Synapse 7, 181–191.
Xiong, W. and Chen, W. R. 2002. Dynamic gating of spike propagation in the mitral cell lateral dendrites. Neuron 34, 115–126.
Yamamoto, C., Yamamoto, T., and Iwama, K. 1963. The inhibitory systems in the olfactory bulb studied by intracellular recording. J. Neurophysiol. 26, 403–415.
Yu, G.-Z., Kaba, H., Saito, H., and Seto, K. 1993. Heterogeneous characteristics of mitral cells in the rat olfactory bulb. Brain Res. Bull. 31, 701–706.
Yuan, Q. and Knopfel, T. 2006. Olfactory nerve stimulation-evoked mGluR1 slow potentials, oscillations and calcium signaling in mouse olfactory bulb mitral cells. J. Neurophysiol. 95, 3097–3104.
Yuan, Q., Harley, C. W., and McLean, J. H. 2003. Mitral cell α1 and 5-HT2A receptor colocalization and cAMP coregulation: a new model of norepinephrine-induced learning in the olfactory bulb. Learn Mem. 10, 5–15.
Zaborszky, L., Carlsen, J., Brashear, H. R., and Heimer, L. 1986. Cholinergic and GABAergic afferents to the olfactory bulb in the rat with special emphasis on the projection neurons in the nucleus of the horizontal limb of the diagonal band. J. Comp. Neurol. 243, 488–509.
Zelles, T., Boyd, J. D., Hardy, A. B., and Delaney, K. R. 2006. Branch-specific Ca2+ influx from Na+-dependent dendritic spikes in olfactory granule cells. J. Neurosci. 26, 30–40.
Zhang, C. and Restrepo, D. 2003. Heterogeneous expression of connexin 36 in the olfactory epithelium and glomerular layer of the olfactory bulb. J. Comp. Neurol. 459, 426–439.
Zou, Z., Horowitz, L. F., Montmayeur, J. P., Snapper, S., and Buck, L. B. 2001. Genetic tracing reveals a stereotyped sensory map in the olfactory cortex. Nature 414, 173–179.

Further Reading

Duchamp-Viret, P., Coronas, V., Delaleu, J.-C., Moyse, E., and Duchamp, A. 1997. Dopaminergic modulation of mitral cell activity in the frog olfactory bulb: a combined radioligand binding-electrophysiological study. Neuroscience 79, 203–216.

Duchamp-Viret, P., Delaleu, J. C., and Duchamp, A. 2000. $GABA_B$-mediated action in the frog olfactory bulb makes odor responses more salient. Neuroscience 97, 771–777.

Kaba, H., Rosser, A., and Keverne, B. 1989. Neural basis of olfactory memory in the context of pregnancy block. Neuroscience 32, 657–662.

Persohn, E., Malherbe, P., and Richards, J. G. 1992. Comparative molecular neuroanatomy of cloned GABAA receptor subunits in the rat CNS. J. Comp. Neurol. 326, 193–216.

Pinching, A. J. and Powell, T. P. 1972a. A study of terminal degeneration in the olfactory bulb of the rat. J. Cell Sci. 10, 585–619.

4.38 Olfactory Cortex

D A Wilson, University of Oklahoma, Norman, OK, USA

© 2008 Elsevier Inc. All rights reserved.

4.38.1	**Introduction**	687
4.38.1.1	Functions of Sensory Cortex	688
4.38.2	**Cortical Neurocircuitry**	689
4.38.2.1	Cortical–Cortical Connectivity	690
4.38.2.2	Piriform Cortex Synaptic Physiology	692
4.38.2.3	Olfactory Thalamocortical Pathway Functional Anatomy	693
4.38.3	**Cortical Sensory Physiology**	693
4.38.3.1	Odorant Intensity	693
4.38.3.2	Odorant Quality	694
4.38.3.3	Sensory Gating	699
4.38.3.4	Odorant Familiarity and Meaning	701
4.38.3.5	Nonolfactory Context	703
4.38.4	**Summary of Olfactory Cortical Information Processing and Unresolved Issues**	703
4.38.4.1	Odor Discrimination	703
4.38.4.2	Sensory Gating	704
4.38.4.3	Background Segmentation	704
4.38.4.4	Corticobulbar Feedback and Laterality	705
References		705

Glossary

odorant The physical stimulus that gives rise to the perception of an odor. The same odorant may give rise to different odor percepts, depending on context, expectation, and past experience.

paleocortex An evolutionarily old cortical structure with generally three lamina, as opposed to the six-layered evolutionarily more recent neocortex. Piriform cortex is an example of paleocortex.

perceptual learning An enhancement in fine sensory discrimination based on past experience. Perceptual learning has been demonstrated in most sensory modalities including vision, audition, somatosensation, and olfaction.

thalamocortical system An organization typical of most sensory systems, wherein a thalamic nucleus receives input from the sensory peripheral circuits and transmits this information to the sensory neocortex, Olfaction includes both a nonthalamocortical system of olfactory bulb projections directly to the piriform cortex, and also a thalamocortical system of mediodorsal thalamic nucleus input to the orbitofrontal cortex.

4.38.1 Introduction

Sensory receptors are generally highly analytical. Your retina and photoreceptors pixilate this printed page into tiny points of light within a relatively narrow range of wavelengths. The tips of your fingers have separate receptor populations for rough surfaces and smooth surfaces, and for hot and cold. As noted in earlier chapters, your nose contains several hundred different olfactory receptors responsive to different submolecular features of volatile compounds, huge subsets of which are activated when inhaling chemically rich everyday odors such as cheese or wine. In contrast, sensory cortex is often the epitome of synthetic. In visual sensory cortex, pixilated images get combined with past experience to allow to one see and recognize objects. In somatosensory cortex, smooth gets put together with cold when we run

our finger tips over an ice cube. And in the olfactory sensory cortex, the 655 different volatiles rising over a cup of coffee, so carefully dissected by the olfactory periphery, get merged into the only stimulus capable of getting me out of bed this morning – the single percept, coffee.

This chapter will review our current understanding of the structure and function of olfactory sensory cortex. Olfaction is unique among mammalian sensory systems in that second-order neurons project directly to the primary sensory cortex, without an intervening thalamic relay. However, there is also a thalamocortical olfactory pathway, highly interconnected with primary olfactory cortex and only just beginning to be fully explored. While our understanding of peripheral mechanisms of olfactory coding has grown exponentially in the past decade or two, it is increasingly apparent that to understand olfactory perception we must understand what olfactory sensory cortex does. For example, knowing that there are different opsin proteins in the cones of your retina differentially sensitive to light wavelength is not sufficient to explain the visual perception of a rainbow or an orchid. Similarly, our perception of, and ability to discriminate between, odors depends not only on events happening at the receptor, but very critically on events within sensory cortex. The experience- and context-dependent nature of olfactory perception, in fact, make very clear that knowing which receptors and olfactory bulb glomeruli are activated by a particular stimulus is insufficient to predict the resulting percept. We will review what we currently understand about the contribution of olfactory cortex to odor coding and the mechanisms underlying these contributions.

4.38.1.1 Functions of Sensory Cortex

Sensory cortical circuits have at least three primary functions (see Figure 1). The first is to elaborate upon the representation of afferent input begun by more peripheral structures. This cortical elaboration may occur through processes such as decorrelation of patterned afferent activity to enhance discrimination of similar patterns, convergence and synthesis of diverse inputs to promote emergence of wholistic

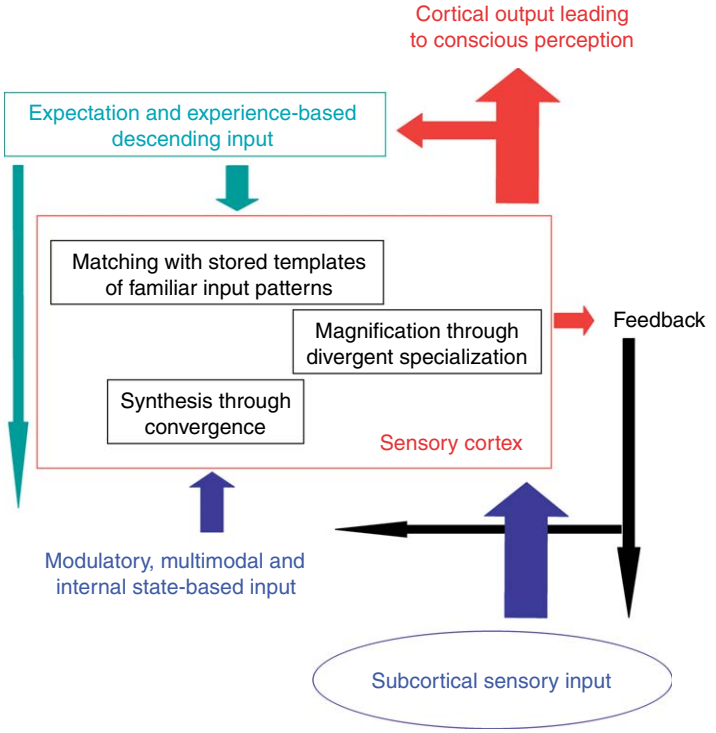

Figure 1 A schematic representation of some of the basic functions ascribed to primary and earlier higher-order sensory cortices. In thalamocortical sensory systems, sensory cortex plays a central role in constructing sensory images from the feature analyzed input it receives, which are ultimately important for conscious perception. Sensory cortex also plays an important role in feedback processes, underlying attention and expectation-induced changes in sensory processing.

percepts, and comparison of afferent activity patterns with stored templates to promote recognition. Furthermore, sensory cortices often embellish this emerging representation with information from other sensory modalities, memory, and emotional and internal state. The second function of sensory cortices is to use the information obtained through these convergent processes to provide feedback to peripheral stages in order to selectively modify gain or acuity, just as sensory cortex itself is under the influence of higher-order cortices. Finally, sensory cortical efferents provide downstream structures with highly processed representations of sensory stimuli and their associated external and internal context to drive behavioral and cognitive outcomes. In effect, sensory cortex can be the first stage of conscious perception.

In performing these functions, sensory cortices utilize at least three basic tools. The first tool is convergence. Stimulus features extracted by peripheral circuits begin to be merged through anatomical convergence in the sensory cortex. Hierarchical processing in the visual system is a classic example, wherein spots of light extracted by center-surround receptive fields in the retina and visual thalamus are merged through anatomical convergence into bars and contrast edges driving visual cortex neurons. Convergence can occur both within a sensory modality, such as the hierarchical visual processing just mentioned, and on a wider scale including disparate regions of sensory cortex as well as potentially including multimodal interactions.

The second tool used by sensory cortices, and directly related to convergence, is synaptic plasticity. Experience-dependent synaptic plasticity is critical for both developmental emergence of local cortical circuits and fine-tuning of those circuits throughout life. This plasticity can allow increased processing power to be devoted to familiar or learned important stimuli by adjusting receptive fields and cortical maps. It can also help to associate stimuli and stimulus features which frequently co-occur to form templates or internal representations of perceptual objects. An advantage of object representation is an increased ability to recognize familiar objects despite degraded inputs or background interference. Finally, synaptic plasticity can allow on-line adjustment of stimulus processing through experience-dependent short-term modulation of synaptic strength.

A third sensory cortical tool is magnification. In nearly all thalamocortical sensory systems, pathways display anatomical organizations laid out as functional sensory maps. Retinotopic, tonotopic, and somatotopic maps are all examples of sensory maps which are expressed within the corresponding sensory cortex. Within each of these cortical maps, cortical space is not divided evenly across sensory space, but rather there are regions of disproportionate investment in specific areas of sensory space. The fovea, which covers a physically very small region of the retina, commands a relatively huge physical proportion of the visual cortex. Similarly, the small range of auditory frequencies corresponding to biologically important sounds (e.g., human voice in humans, echolocating sounds in bats) dominate cortical space within audition. Furthermore, the somatosensory cortex devotes a large region to inputs from the fingers, which account for a relatively small proportion of the human body surface. Thus, cortical processing power, as indexed by cortical volume, is differentially devoted to some regions of sensory world over others, in effect magnifying those stimuli which fall on those receptors. Beyond this magnification in cortical maps, additional cortical space can also be specialized for important stimuli, outside the primary sensory pathway. For example, the fusiform face region in the primate visual system is largely devoted to processing biologically important face stimuli. Similar specializations are seen in other systems, for example the Doppler-shift compensation area in bat echolocating auditory cortex which allows calculation of relative speed of approach toward prey targets.

As we review the structure and physiology of olfactory cortex, the functions and tools used by other sensory systems will be used as guideposts to determine how different (or similar) olfaction is to the other senses. In the following section, we will review the anatomical organization of olfactory cortex, local circuit connectivity, and afferent and efferent connections. We will then review current synaptic and sensory physiological data, followed by an abstraction of general principles of olfactory cortical function.

4.38.2 Cortical Neurocircuitry

The olfactory cortex consists of a collection of laminar structures arranged along the ventrolateral surface of the mammalian brain which receive direct input from olfactory bulb mitral and/or tufted cells (see Figure 2). These target structures include the anterior olfactory cortex, piriform cortex, olfactory

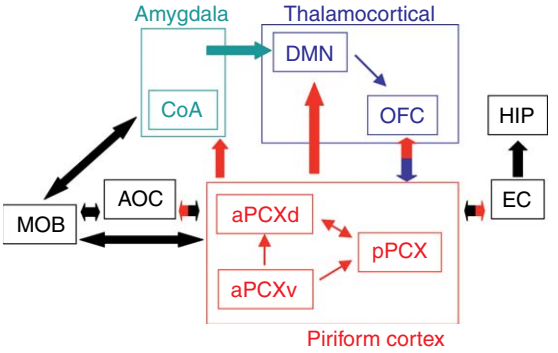

Figure 2 A schematic representation of the major olfactory cortical areas and their interrelationships. Additional details can be found in Cleland T. A. and Linster C. (2003) and Neville K. R. and Haberly L. (2004). This review focuses on the piriform and orbitofrontal cortices. Almost nothing is known regarding the sensory physiology of the anterior olfactory cortex (AOC). MOB, main olfactory bulb; AOC, anterior olfactory cortex; aPXDd, dorsal anterior piriform cortex; aPCXv, ventral anterior piriform cortex; pPCX, posterior piriform cortex; CoA, cortical nucleus of the amygdala; DMN, dorsomedial nucleus of the thalamus; OFC, orbitofrontal cortex; EC, entorhinal cortex; HIP, hippocampus.

tubercle, and the cortical nucleus of the amygdala (Haberly, L. B., 2001). Each of these structures is trilaminar paleocortex, with olfactory bulb afferent input terminating in superficial layer I, a pyramidal cell dense layer II, and a layer III composed of association fiber axons, deep pyramidal cell somata, and interneurons. The olfactory cortex does not express a columnar organization, but rather receives afferent input as a wave of activity spreading caudally through its arrayed dendritic trees. Each of the olfactory cortical structures is interconnected and also project back to the olfactory bulb.

In addition to the paleocortical areas, the olfactory system also includes a thalamocortical pathway, with a projection from the piriform cortex to the dorsomedial nucleus of the thalamus, which in turn projects to the orbitofrontal cortex. The dorsomedial nucleus of the thalamus also receives input from the amygdala and other limbic areas. There are also direct, reciprocal connections between the orbitofrontal cortex and the piriform cortex (Neville, K. R. and Haberly, L., 2004). Orbitofrontal cortex is located anterior in the mammalian brain and juxtaposes piriform cortex along the rhinal fissure in rodents. The orbitofrontal cortex is neocortical in structure and thus displays a six-layer, presumably columnar organization.

While the anatomy of all of these cortical areas dealing with olfaction has been described to some extent in the literature, the piriform cortex has received the most attention. Thus, this review will emphasize piriform cortical structure and function. This emphasis is not meant to imply dominance of the piriform cortex in olfactory processing and perception, but rather, unfortunately, reflects a search where the light is currently brightest. That is, while the piriform cortex, and increasingly orbitofrontal cortex, appear to perform computations of critical importance for the rich experience that is olfactory perception, we simply do not have sufficient data at present to state definitively how areas such as the anterior olfactory cortex and olfactory tubercle contribute.

4.38.2.1 Cortical–Cortical Connectivity

The piriform cortex can be cytoarchitecturally divided into at least four major subregions. In rodents, the anterior piriform cortex is defined as extending caudally from the anterior olfactory cortex to the caudal end of the lateral olfactory tract. Immediately caudal to the anterior piriform cortex lies the posterior piriform cortex. Mitral cell axons no longer lie in a dense tract, but instead diffusely spread in a thin layer across the posterior piriform cortical surface. In addition to this anterior–posterior division, the anterior piriform can be further subdivided into a dorsal and ventral component. Each of these four subdivisions expresses differences in cortical–cortical connectivity and, as more research is performed, increasingly demonstrates differences in sensory physiology (see Section 4.38.3).

The piriform cortex receives direct input from the olfactory bulb, as do all other olfactory cortical structures (see Figure 3). Single mitral/tufted cell axons terminate in small patches in piriform cortex. Mitral cells conveying input from specific olfactory receptor types terminate in overlapping patches in anterior piriform cortex, and even more broadly in posterior piriform (Zou, Z. *et al.*, 2001). The primary target of olfactory bulb input to cortical areas is pyramidal cell apical dendrites.

Pyramidal cells within the piriform cortex can be divided into at least three subgroups, deep pyramidal cells with somata in layer III, pyramidal cells with somata in layer II, and semilunar pyramidal cells with somata in superficial layer II (layer IIa). Each of these neuron classes has spiny apical dendrites extending into superficial layer I. Mitral/tufted cell afferent

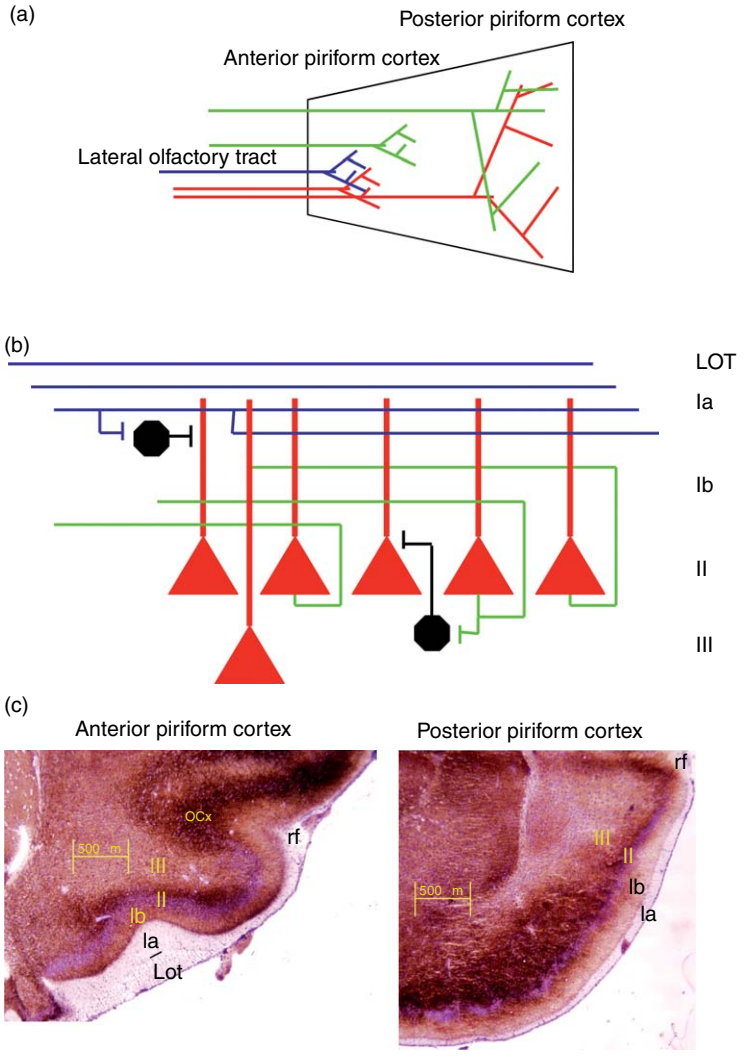

Figure 3 Piriform cortical circuitry. (a) Mitral cells conveying input from olfactory receptor neuron expressing specific olfactory receptor genes terminate in patches in the anterior piriform cortex that overlap with termination zones of mitral cells conveying information from other receptors. Mitral cell termination in the posterior piriform is much more diffuse with information from different receptors broadly overlapping. (b) A schematic representation of piriform circuitry emphasizing lamination of afferent (blue) and association (green) fiber input into trilaminar cortical sheet. Black cells represent local feedforward and feedback inhibitory interneurons. (c) Coronal sections through the anterior and posterior piriform cortex stained with Timm stain for heavy metals which selectively stain intracortical association fiber axons brown and counterstained with cresyl violet. Notice the proportional differences in association fiber input to neurons in dorsal anterior piriform and posterior piriform cortex relative to ventral anterior piriform cortex. rf, rhinal fissure; Ocx, orbital cortex; LOT, lateral olfactory tract.

input to the piriform terminates on the distal most regions of the apical dendrites in cortical layer Ia. Semilunar pyramidal cells may receive largely exclusive excitatory input from mitral/tufted cells, as semilunar cells possess large dendritic spines within layer Ia, but not within layer Ib. Axons of pyramidal cells form the intracortical association fiber system, generally synapsing on spines of both the apical and basal dendrites of other piriform cortical neurons. Individual pyramidal cells have diffuse projections throughout the ipsilateral piriform cortex, and extending into the orbitofrontal cortex and other olfactory cortical areas, the cortical nucleus of the amygdala, as well as the ipsilateral olfactory bulb. Other ipsilateral projects include the dorsomedial nucleus of the thalamus, the hypothalamus, and

entorhinal cortex. These neurons also send axons to the contralateral piriform via the anterior commissure. Semilunar cells also project widely throughout the piriform cortex but do not send feedback to the olfactory bulb. The piriform cortex receives input from a number of areas other than the olfactory bulb, including the entorhinal cortex, orbitofrontal cortex, and amygdala. More complete recent descriptions of local and extrinsic circuitry can be found in Cleland T. A. and Linster C. (2003) and Neville K. R. and Haberly L. (2004).

Olfactory areas also receive input from a variety of modulatory systems, including the noradrenergic nucleus locus coeruleus, the cholinergic horizontal limb of the diagonal band, and serotonergic raphe nucleus. These systems have been shown to play important roles in olfactory cortical function and plasticity (see Section 4.38.3).

In addition to pyramidal cells, there are a variety of classes of inhibitory interneurons. Interneurons in layer I appear to receive input from the lateral olfactory tract and in turn synapse onto apical dendritic shafts of piriform cortical pyramidal cells in a feedforward inhibitory circuit. Interneurons with somata in layer III receive input from pyramidal cell axon collaterals and feedback onto neighboring pyramidal cell somata and basal dendritic shafts. However, extensive variations from these canonical patterns exist (Neville, K. R. and Haberly, L., 2004).

4.38.2.2 Piriform Cortex Synaptic Physiology

Mitral/tufted cell axons terminating on distal apical dendrites of piriform cortical pyramidal neurons release glutamate as a neurotransmitter (Jung, M. W. *et al*., 1990). Both AMPA and NMDA receptors are located postsynaptically on pyramidal cell apical dendrites. Mitral/tufted cell presynaptic terminals express metabotropic glutamate receptors, as well as receptors for modulatory inputs such as norepinephrine. Activation of NMDA receptors appears to be regulated in part by apical dendritic inhibition mediated by layer I gamma-aminobutyric acid (GABA)ergic interneurons. Layer III GABAergic interneurons synapse heavily on pyramidal cell somata and induce current shunting inhibition. Thus, these two forms of inhibition can be both anatomically and functionally distinct.

Activation of the lateral olfactory tract evokes an excitatory postsynaptic potential (EPSP) in the distal half of the pyramidal cell which, due to the electrotonic distance, can be reduced by 75% at the cell body (Ketchum, K. L. and Haberly, L. B., 1993). Depolarization of pyramidal cells to spike threshold activates the glutamatergic association fiber system, and thus within approximately 5 m, the afferent-evoked EPSP is followed by an association fiber-evoked EPSP. These EPSPs are due to activation of synapses in the proximal half of the apical dendrite; thus, they decay much less than lateral olfactory tract-evoked EPSPs. The association synapse-mediated EPSPs, however, coincide with feedback inhibitory portrynaptic potentials (IPSPs). Following this initial rapid sequence of synaptic events, a later, prolonged K^+-mediated IPSP is apparent. This sequence of events can initiate oscillatory (gamma frequency) activity within the piriform following a single afferent volley as association fiber activity circulates throughout the piriform. Single-unit activity in the piriform has been shown to occur in phase with the gamma frequency oscillation, as would be expected given its generation mechanism (Eeckman, F. H. and Freeman, W. J., 1990).

Modulatory inputs to the piriform cortex appear to have differential effects on the afferent and intrinsic fiber pathways. Both acetylcholine and norepinephrine have direct effects on piriform cortical neurons, but interestingly they also have presynaptic effects on synaptic transmission. Both acetylcholine and norepinephrine preferentially depress association fiber excitatory synapses, while having minimal impact on lateral olfactory tract afferent input (Hasselmo, M. E. *et al*., 1990; Hasselmo, M. E. and Bower, J. M., 1992).

Both lateral olfactory tract and association fiber synapses express use-dependent plasticity that may be involved in piriform cortical odor information processing. As described below, lateral olfactory tract synapses express a short-term depression following intense electrical or odor-evoked activation that recovers within 2 min (Best, A. R. and Wilson, D. A., 2004). This depression is composed of two phases, a short (<15 s) phase that is consistent with neurotransmitter depletion and a longer phase (<2 min) that can be blocked by antagonists of presynaptic group III metabotropic glutamate receptors (Best, A. R. and Wilson, D. A., 2004).

Lateral olfactory tract and the association fiber synapses also express long-term potentiation, though potentiation of the lateral olfactory tract synapses appear minimal at best (Neville, K. R. and Haberly, L., 2004). The association fiber synapses display

robust (20–30%), NMDA receptor-dependent, long-term potentiation. Theta burst stimulation paradigms, which involve short gamma (40–100 Hz) frequency bursts of pulses with the burst delivered at theta (5–10 Hz) frequency appear most effective at inducing long-term potentiation in association fiber synapses. These stimulation parameters roughly match what would occur during active sniffing at theta frequency.

This physiology and pharmacology suggests a particularly important role for association fibers in piriform cortical function and plasticity. Association fibers are electrotonically closer to the somata, are more plastic, and more strongly influenced by modulatory inputs than is the primary cortical afferent. The differential roles of these two excitatory cortical pathways in information processing by olfactory cortex are discussed below.

4.38.2.3 Olfactory Thalamocortical Pathway Functional Anatomy

In addition to the direct olfactory bulb input to the primary olfactory cortical areas, the olfactory pathway also includes a thalamic representation and a thalamocortical projection. The piriform cortex projects to the mediodorsal thalamic nucleus which in turn projects to the orbitofrontal cortex (and other prefrontal regions). The mediodorsal thalamus also receives input from the cortical and basal nuclei of the amygdala, potentially enriching the olfactory input to orbitofrontal cortex with emotional context (Schoenbaum, G. *et al*., 2003a). The orbitofrontal cortex also receives direct input from piriform cortex, in addition to its thalamic input, leading to a convergent triangulation between piriform, mediodorsal thalamus, and orbitofrontal cortex. As in the piriform cortex, orbitofrontal neurons respond not only to specific odors, but also to odor-contextual cues (Schoenbaum, G. and Eichenbaum, H., 1995; Rolls, E. T., 2004). Orbitofrontal cortex neurons also respond to specific odor-taste compounds, potentially contributing to taste and odor hedonics.

The specific functions of thalamocortical olfactory pathways in odor perception are not known. Lesions of the dorsomedial thalamus in rats impair learning and memory of discriminative odor cues, although this impairment appears to not be related to odor discrimination per se, but rather may represent a memory disruption (Zhang, Y. *et al*., 1998).

Single neurons in the orbitofrontal cortex of both rodents and primates encode both odor quality and odor associations. In primates, both the identity of an odor being inhaled and its reinforcement value and taste associations can be extracted from orbitofrontal cortex neuron spike trains (Rolls, E. T., 2004). Odor quality is encoded very sparsely in orbitofrontal cortex, and there is diversity in responses with, for example, some neurons encoding odor quality independently of reinforcement associations and some encoding the reinforcement associations. Similar results have been seen in rat orbitofrontal cortex and have led to the suggestion that the orbitofrontal cortex integrates sensory representations with associated reward value to help guide motivated behavior – a conclusion supported by lesion studies (Schoenbaum, G. *et al*., 2003b). Given the interconnectivity between the orbitofrontal and piriform cortices, however, the specific role of thalamocortical inputs versus cortical–cortical inputs to orbitofrontal cortex in this higher-order sensory representation is unknown. It is interesting to speculate that the orbitofrontal cortex may serve in part in a magnification role as discussed above, providing dedicated additional processing support for hedonically important odors beyond that performed in the piriform cortex.

4.38.3 Cortical Sensory Physiology

Despite the wealth of information regarding olfactory cortical circuitry and synaptic physiology, our understanding of olfactory cortical sensory physiology lags far behind most other sensory systems. As more knowledge is gained as to the nature of sensory information being fed into the cortex, and as more people turn centrally to understand how the outcome of peripheral coding is acted upon by cortical circuits, this lag should be rapidly reduced. This section will review our current state of understanding regarding cortical coding of odor intensity, quality, familiarity, and context. Sensory physiological and computational work suggests that the piriform cortex is critically involved in synthetic coding of complex odorants and in some cases their nonolfactory contexts, gating olfactory information flow relative to experience and behavioral state, and creating templates of familiar and learned odorants which facilitates recognition and discrimination.

4.38.3.1 Odorant Intensity

Piriform cortical representation of odor intensity has been sorely understudied. Intensity codes in other

systems include a variety of options. Firing rate of individual neurons can be correlated with stimulus intensity. Similarly, the number or type of activated neurons can change with intensity. For example, there may be neurons with differing thresholds that are preferentially activated by high or low intensities. Finally, temporal patterning of individual or ensemble activity may be correlated with stimulus intensity.

Recently, Sugai and colleagues have examined the spatial extent of piriform cortical activation by odors of varying intensity (Sugai, T. *et al.*, 2005). Using a combination of intrinsic signal imaging and single-unit recording in the dorsal anterior piriform cortex, these authors report a rostral to caudal spread of activity as odor concentration increases. Thus, single units in caudal regions of the dorsal anterior piriform cortex had higher-odor thresholds than more rostral cells. Interestingly, these results correspond with findings that superficial tufted cells in the olfactory bulb project more heavily to rostral portions of the piriform cortex and are more responsive to olfactory nerve input compared to internal tufted or mitral cells which have higher thresholds and project more caudally. Thus, the differential sensitivity and projection patterns of cortical afferents could produce a rostral to caudal gradient of odor sensitivity across the piriform cortex.

It should also be noted that that there is a rostral to caudal gradient of cortical feedback to the olfactory bulb, wherein more caudal olfactory cortical neurons terminate on deep granule cells and more rostral cortical neurons terminate on more superficial granule cells. Deep granule cells are believed to synapse preferentially with mitral and internal tufted cells, while superficial granule cells may preferentially synapse with middle or external tufted cells. Thus, the rostral to caudal sensitivity gradient in cortex could be a part of a closed feedback loop to specific populations of olfactory bulb output neurons. Tufted and mitral cells also display differential phase locking to the respiratory cycle, with tufted cells firing earlier in the respiratory cycle than mitral cells, potentially creating rostral–caudal temporal gradients in cortical activity relative to intensity as well.

One important issue that the olfactory cortex must deal with, however, is that the afferent input to the cortex may change with stimulus intensity. Olfactory receptors, olfactory glomerular layer spatial patterns, and mitral/tufted output are all modified by changes in stimulus intensity. Some odorants change in perceptual quality as stimulus intensity increases; however, most odorants are qualitatively stable over many orders of magnitude of concentration (Laing, D. G. *et al.*, 2003). Therefore, cortical circuits described below may be particularly important for maintaining odorant-specific patterns of cortical output across concentration range, thus maintaining perceptual quality despite intensity-induced changes in afferent input.

4.38.3.2 Odorant Quality

Cortical coding of odorant quality ultimately involves two levels of information. At one level, cortical odorant quality encoding may reflect the structural make-up of the inhaled stimulus – essentially a reflection of the sum of the odorant features extracted by more peripheral circuits. However, odor perception must involve coding beyond a simple reflection of convergent input. For example, structurally similar molecules (similar collections of features) can smell quite different, and similar smells may derive from structurally dissimilar molecules. Furthermore, the perceived smell of a banana is relatively stable, regardless of the background odorants inhaled at the same time whose components should mix with those of the banana at the receptor sheet. Finally, the integral hedonic quality of that banana smell perception is dependent on current internal state (e.g., hunger vs. nausea) and expectations. Thus, a full account of cortical odorant quality coding (and ultimately odor perception) must go beyond simple description of responses to isolated monomolecular stimuli and begin to describe such higher-order perceptual quality phenomenon as mixture synthesis, sensory gating, figure-ground separation, and the effects of expectation.

In fact, an examination of odorant receptive fields of piriform cortical neurons (see Figure 4) suggests superficial similarity to those of olfactory bulb mitral/tufted cells. Individual cortical neurons respond to multiple odorants (Wilson, D. A., 1998; 2000; Litaudon, P. *et al.*, 2003) and demonstrate differential responsiveness to odorant features such as carbon chain length (Wilson, D. A. and Stevenson, R. J., 2003). Selectivity for simple odorants is increased in neurons in posterior piriform compared to anterior piriform cortex (Litaudon, P. *et al.*, 2003), and in fact appears to increase as one moves from piriform to orbitofrontal cortex (Tanabe, T. *et al.*, 1975), suggesting a possible refinement of odorant identity coding in a hierarchical manner.

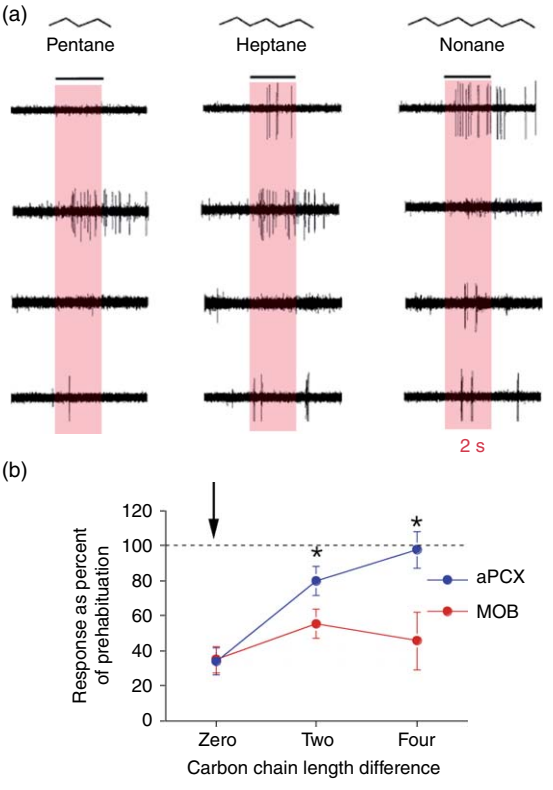

Figure 4 Examples of anterior piriform cortex single-unit responses to odorant stimuli. (a) Responses of four different anterior piriform cortical neurons to second stimuli presented during the red-shaded region. Note that, similar to reports of olfactory receptor neurons and mitral/tufted cells, piriform cortical neurons respond differentially to odorants varying along a specific dimension such as carbon chain length. (b) However, using a cross-adaptation procedure to determine odorant discrimination abilities of these neurons revealed that cortical neurons were significantly better at discriminating between odorants within their receptive fields than mitral/tufted cells of the main olfactory bulb (MOB). aPCX, anterior piriform cortex.

In contrast to a possible intensity-dependent spatial activation of the piriform cortex described above, initial attempts to describe odorant quality-dependent spatial patterns of piriform cortical activation were largely unsuccessful. Studies utilizing 2-deoxyglucose metabolic activity imaging, intrinsic signal imaging, voltage sensitive dye imaging, and immediate early gene immunohistochemistry (Litaudon, P. *et al.*, 1997; Illig, K. R. and Haberly, L. B., 2003; Sugai, T. *et al.*, 2005) have all failed to detect precise monomolecular odorant quality-specific patterns of piriform cortex activation comparable to those seen in the olfactory bulb.

Illig K. R. and Haberly L. B. (2003) reported (see Figure 5) that monomolecular odorant stimulation evoked rostrocaudal bands of c-fos labeling of pyramidal cells in anterior piriform cortex. However, these bands appeared to correspond primarily with the anatomical subdivisions of the anterior piriform more than demonstrate an odorant-specific pattern. Thus for example, most odorants more strongly activated the dorsal anterior piriform and a narrow band of ventrally located cells than the intermediate regions of the anterior piriform cortex. The authors suggested that there may be subtle variations in c-fos labeling that could be odor specific, but that there were no clear odorant-specific patches evident.

Recent work by the Buck laboratory using a more diverse odorant set and more quantitative analyses of odorant-evoked Fos-staining patterns suggests there may in fact be regional specificity in response to odorants within the anterior piriform cortex (Zou, Z. *et al.*, 2005). Structurally similar odorants evoke odorant-specific spatial patterns of neural activation within the anterior piriform cortex. Activated neurons are dispersed within activated regions; thus individual neighboring neurons do not necessarily have similar response properties. Similarly, mapping of single-unit odorant responses and cell locations shows no strong spatial clustering of neurons responsive to molecularly and perceptually dissimilar odorants in anterior piriform cortex (Kadohisa, M. and Wilson, D. A., 2006), though this has not yet been thoroughly investigated.

If the piriform cortex processes odors as synthetic objects built through experience as discussed elsewhere, then perhaps strong spatial clustering or mapping of activity evoked by particular odorants would not be expected. For example, although inferotemporal visual cortical neurons responding to a particular visual object lie within a particular cortical column, neighboring columns may contain neurons responding to completely different visual objects (Tanaka, K., 2000; see Figure 6). As experience throughout life shapes the tuning properties of these cortical neurons, objects become encoded by randomly scattered cortical neurons, with neurons maximal responsive to ball objects, located next to neurons responsive to tree objects and star-shaped objects. Similarly, we predict that the location of piriform cortical neurons responding to odor objects will not conform to a consistent organized map, but rather show discontinuities. This effect may be more pronounced in posterior piriform than in anterior

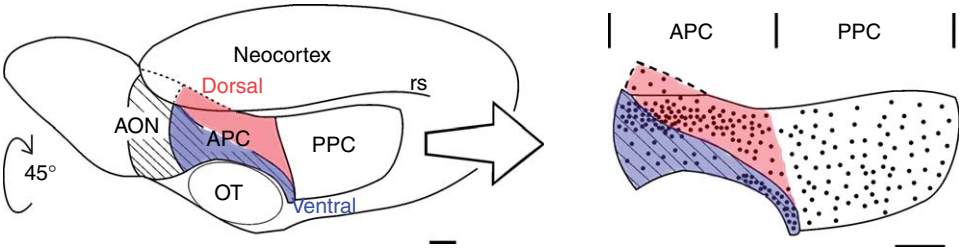

Figure 5 Odorant-evoked neural activity in the piriform cortex as revealed by c-fos immunohistochemistry (Illig, K. R. and Haberly, L. B., 2003). (Left) Image of the rat brain viewed from the side with the subregions of the piriform cortex displayed. (Right) Patterning of activated neurons in response to odorant stimulation. No distinct odorant-specific differences were noticed in activation patterns in piriform, although distinct subregion differences in odorant responsiveness were noted. Recent work by Zou Z. *et al.* (2005), using similar techniques, suggests that odorant-specific patterning may be present in the anterior piriform. Both studies clearly demonstrate that odorant-evoked activity is dispersed, with individual neighboring neurons responsive to different odorants. It must be noted, however, that the techniques used would not reveal neurons with rapidly adapting responses (Wilson, D. A., 1998). APC, anterior piriform cortex; PPC, posterior piriform cortex. Image adapted from original image provided by Kurt Illig.

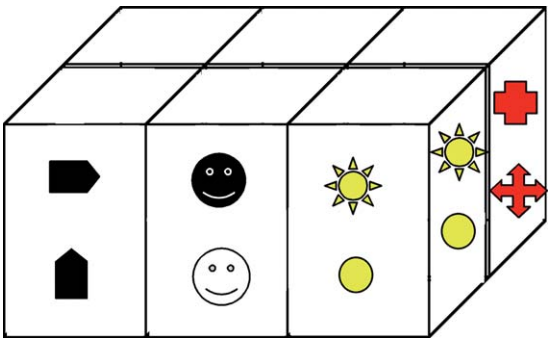

Figure 6 Schematic representation of the spatial organization of visual object encoding in the primate visual inferotemporal cortex. Although primary visual cortex is highly and predictably organized, in inferotemporal cortex where neurons have receptive fields for visual objects, the organization is less predictable. Neurons within a single column may have receptive fields for similar objects, perhaps at different views or angles, but neurons in neighboring columns may have receptive fields for completely different objects. Such a dispersed organization may also be expected to occur in piriform cortex for odor objects. Adapted from Tanaka, K. 2000. Mechanisms of visual object recognition studied in monkeys. Spat. Vis. 13, 147–163.

piriform as association fibers come to dominate excitatory control.

While much of sensory physiology in the olfactory system has focused on monomolecular odorants, most odorants experienced in nature are complex mixtures. However, as noted above, while composed of often hundreds of different components, these natural mixtures are perceived as individual, indivisible odor objects. For at least 20 years, the piriform cortex has been seen as a possible site of synthetic odor quality processing in olfaction. Mitral/tufted cells, conveying information about specific odorant features (Fletcher, M. L. and Wilson, D. A., 2003; Lin da, Y. *et al.*, 2005), converge onto individual piriform cortical pyramidal cells through overlapping, patchy axonal termination zones (Zou, Z. *et al.*, 2001). Thus, through simple coincidence detection, single cortical neurons could transmit information concerning the occurrence of specific combinations of odorant features. However, simple coincidence detection is insufficient to account for complex odor processing such as occurs in odorant figure-ground separation (Kadohisa, M. and Wilson, D. A., 2006) (see Section 4.38.4.3). In the situation where odorants are experienced against a background (nearly all situations), those odorants would be merged with the background based on their coincident inhalation resulting in context-variant odor perception of stable objects. This does not generally occur, and thus a separate mechanism, beyond simple afferent coincidence detection, must be invoked.

Intracortical association fibers and synaptic plasticity may solve the problem of stable odor representations regardless of background, and often regardless of variations in stimulus make-up or intensity. As noted above, single piriform cortical neurons have axon collaterals broadly dispersed throughout the piriform cortex (Johnson, D. M. *et al.*, 2000). Unique combinations of mitral cell-mediated odorant feature input should activate a unique ensemble of piriform cortical pyramidal neurons, based on termination patterns of those mitral cell axons. In some cases, individual cortical neurons will receive convergent input from mitral cells

conveying information regarding two or more odorant features, and in other cases a cortical neuron may receive input regarding a single odorant feature, depending on the pattern of mitral cell–cortical connectivity. Cortical pyramidal cells sufficiently activated by this input in turn activate additional cortical neurons via the intracortical association fibers, thus greatly expanding the combinatorial activation of single cortical neurons.

Specifically, imagine an odorant composed of features A, B, and C. Each of these features is recognized by individual mitral cells which convey processed feature information to the cortex. Through simple anatomical convergence and coincidence detection, individual cortical neurons receive partial combinatorial information (AB, AC, and BC), depending on the initial state of afferent connectivity for each cortical neuron (it should be noted that odor experience early in development can modify overall mitral cell termination patterns in piriform cortex) (Wilson, D. A. *et al*., 2000).

Pyramidal neurons activated by these partial combinations can then, via intracortical association fibers, create more complete combinations on other cortical neurons, resulting in an ensemble of neurons driven by the complete ABC mixture. This process can occur passively on each new presentation of ABC through coincidence detection. However, given the subtle variations inherent in naturally occurring complex mixtures (with exceptions for tightly controlled pheromonal mixtures), including variation in mixture component ratios, variation in overall intensity, occasional missing or extra components, each new presentation of that mixture may evoke a different ensemble of cortical neuron activation, and in turn a different percept. Plasticity of intracortical association fiber synapses, and creation of stored templates of previously experienced patterns of input, could allow perceptual stability of complex mixtures over time.

In effect, the piriform cortex has been hypothesized to function as a form of auto-associative, content-addressable memory. Circuits using content-addressable memory allow an input pattern to be entered, and then the entire memory array circuit is searched to determine whether that pattern exists in the stored memory, and in some cases identifies other items associated with that pattern. This process is distinct from common computer random access memory wherein the input is an address or storage site and the output is the contents of that site. Thus, content-addressable memory allows familiar input patterns to be recognized, completed and elaborated upon, even in the face of degraded input. As input patterns become more divergent, they activate different memory templates, and thus different odorant representations. In contrast, two well-learned representations can involve very similar inputs and yet evoke distinctly separate stored representation.

Cortical content-addressable memory can rely on associative synaptic plasticity such as long-term potentiation described above. As combinations of odorant features co-occur, association fibers conveying information about these features and their combinations are strengthened through associative plasticity (Haberly, L. B., 2001). On subsequent presentation of the experienced, familiar pattern, circuits containing these now strengthened synapses are more easily activated – signaling a matched template. If the input pattern is degraded or slightly modified, the template pattern can be completed because of the enhanced synaptic strength (Hasselmo, M. E. and Barkai, E., 1995). In fact, with experience, anterior piriform cortical neurons learn to distinguish binary mixtures from their components (Wilson, D. A., 2003). Through this process, odor experience and familiarization come to have strong effects on odor discrimination and perceptual stability (Wilson, D. A. and Stevenson, R. J., 2003). In fact, pharmacological disruption of normal synaptic plasticity within the piriform cortex can disrupt experience-induced enhancement in cortical odorant discrimination. Furthermore, when content-addressable memory is combined with selective cortical afferent adaptation, the piriform can begin to perform more complex functions such as figure-ground separation (see below).

There is a distinct difference in the relative contribution of the afferent lateral olfactory tract and the intrinsic association fiber system to the anterior and posterior regions of the piriform cortex. The anterior piriform cortex is dominated by excitatory input from the lateral olfactory tract, as evidenced both anatomically (see Figure 3) and physiologically. In contrast, the posterior piriform cortex is dominated by association fiber excitatory activity from both within the piriform cortex and from other cortical areas. For example, local field potential oscillations recorded in the anterior piriform cortex are similar in frequency characteristics and strongly coherent with the olfactory bulb, while the oscillations in the posterior piriform are more similar to, and strongly coherent with, the entorhinal cortex. In light of the association fiber plasticity described above, this

difference suggests that odor quality representations by ensembles of neurons within these two areas may also differ substantially.

In the only comparison of anterior and posterior piriform single-unit activity, Litaudon and colleagues reported that cells in posterior piriform showed less spontaneous activity and responded to fewer odors than cells in the anterior piriform cortex (Litaudon, P. *et al.*, 2003). Posterior cortical cells were more diverse in their activity phase relationship to the respiratory cycle than were anterior cells, again suggesting a reduced reliance on lateral olfactory tract-driven activity and more on association fiber activity. Precise comparisons of odorant receptive fields or responses to complex odor mixtures and learned odor objects were not made, although the reduced odor responsiveness in the posterior hints at a more narrow tuning.

We are currently examining the effects of familiarity with odorant mixtures on responses to mixtures and their components in the anterior and posterior piriform cortex, with the hypothesis that posterior neurons may become highly selective for familiar mixtures. In fact, in several studies of piriform cortical responses to novel binary mixtures, cells responding selectively to the mixture, without also responding to one or both of the components, are extremely rare (Kadohisa, M. and Wilson, D. A., 2006). It is hypothesized that as odor mixtures become more familiar, piriform cortical neurons, perhaps especially posterior cortical neurons, will enhance their responsiveness to the familiar mixtures independent of their existing responsiveness to the components alone. This could result in stimulus response patterns similar to that observed in visual inferotemporal cortex, wherein single units may respond vigorously to a visual object (e.g., a face) yet not to components of the object if presented in isolation (Figure 7).

The preceding discussion of odorant quality coding has focused on the structural aspects of odorant molecules as the discriminant variable. Ultimately, of course, odor quality encoding moves away from molecular structure toward perceptual objects, where similar molecular structures may have distinctly different odor qualities, and different molecular structures can evoke similar odor qualities. Recent human cortical fMRI imaging works confirms that perceptual odor quality is a cortical phenomenon. Using a creative cross-habituation paradigm, Gottfried and colleagues suggest that the human anterior piriform cortex encodes information about the structural conformation of odorants (e.g., aldehydes cross-adapt with aldehydes regardless of their perceptual quality), while the posterior piriform cortex encodes the perceptual conformation of odors (e.g., fruity odors cross-adapt with fruity odors

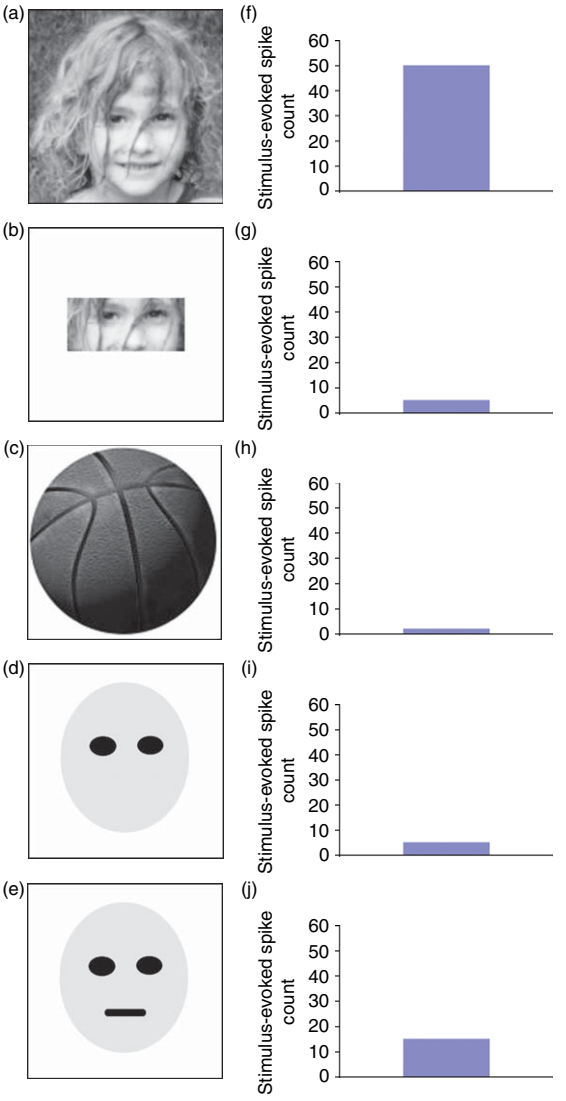

Figure 7 Representation of single-unit response properties in primate visual inferotemporal cortex. Individual inferotemporal neurons have receptive fields for visual objects and are often much less responsive or nonresponsive to individual features of those objects. These receptive fields emerge with experience and are believed to be dependent on plasticity of intracortical association fiber synapses. Similar response properties are predicted for familiar complex odor objects and their components in piriform cortex. Adapted from Tanaka, K. 2000. Mechanisms of visual object recognition studied in monkeys. Spat. Vis. 13, 147–163.

regardless of their structural make-up). These data, if confirmed, are an excellent example of the emergence of odor quality through synthesis within the piriform cortex. Similarly, presentation of the odorant isovaleric acid can produce the perception either of cheese or of an unpleasant percept of vomit or body odor. When subjects were informed they were smelling cheese, the orbitofrontal cortex was activated. However, when the same molecular stimulus was labeled as body odor, the orbitofrontal cortex was not activated (DeAraujo, I. E. *et al.*, 2005). This strongly suggests that perceptual odor quality is an emergent property of the cortical synthesis of odorant input with multimodal, internal state, and expectation information to create a unique perceptual object.

A final point regarding encoding of odor quality in the piriform cortex involves multimodal, hedonic, and context-dependent components of the representation. As discussed in more detail below, cortical odor representations – similar to their perceptual outcome – can be multifaceted. The smell of an orange can include taste components (e.g., sweet), hedonic components (which may vary depending on recent experience, e.g., sensory specific satiety), and even visual imagery components (e.g., visual imagery of the color or of the fruit). Olfactory cortical areas, including both the piriform cortex and the orbitofrontal cortex, can serve as sites of multimodal and hedonic convergence (Schoenbaum, G. and Eichenbaum, H., 1995; Rolls, E. T., 2004), which may allow for the richness of odor quality perception.

In summary, cortical coding of odor quality appears to go far beyond a simple read-out of peripheral odorant feature extraction, allowing for a synthetic process wherein cortical odor coding and odor perception are shaped by past experience. Experience-dependent cortical synthetic processing enhances discriminability and perceptual constancy of familiar odors and adds multimodal complexity to odor quality representations. The cortical circuitry underlying these phenomena is characteristic of an auto-associative, content-addressable memory system, relying on synaptic plasticity of the intrinsic association fiber system to store templates of familiar patterns of afferent input. In accord with this view, disruption of cortical synaptic plasticity disrupts experience-dependent cortical odorant quality discrimination. Given this view of cortical odor representation, it is hypothesized, and generally supported by the data, that odor quality will be encoded by dispersed ensembles of cortical neurons, with minimal clustering of cells sharing similar tuning characteristics. It must also be emphasized that quality discrimination of familiar odorants occurs very rapidly in both freely breathing animals and humans, general within a single sniff. The memory-based process described here could facilitate this rapid processing.

4.38.3.3 Sensory Gating

In addition to serving as the primary site of synthesis and recognition of perceptual objects, sensory cortex is also a critical component of the circuitry underlying attention and sensory gating. Cortical processing resources can be differentially allocated over perceptual space and time depending on internal state and arousal, recent stimulation history, and cognitively directed attention. In olfaction, evidence has been obtained for a direct role of the anterior piriform cortex in sensory gating related to both internal state and recent stimulation history.

In thalamocortical sensory systems, the sensory-evoked activity of thalamic neurons is modulated by arousal and the sleep–wake cycle. For example, in the auditory system of restrained, unanesthetized guinea pigs, tone-evoked responses of auditory thalamic neurons decrease in magnitude and become more selective during slow-wave sleep compared to waking (Edeline, J. M. *et al.*, 2000). These changes appear to occur within the thalamus, as subthalamic activity is either not modulated or variably modulated by sleep–wake cycles. The decrease in thalamic excitability appears to be mediated by a membrane hyperpolarization during slow-wave sleep, presumably driven by changes in modulatory input. The decreased thalamic response during slow-wave sleep still allows accurate throughput of frequency-specific information to the cortex, however at a much reduced level (Edeline, J. M. *et al.*, 2000).

In the olfactory system, a similar state-dependent modulation of information transfer occurs, though it appears in the anterior piriform cortex. In urethane anesthetized rats, which display electrographic evidence of spontaneous slow-wave and fast-wave neocortical EEG transitions, anterior piriform cortical neurons decrease their responsiveness to odor input during the slow-wave state (comparable to slow-wave sleep) relative to responsiveness during the fast-wave state (perhaps comparable to awake or fast-wave sleep states) (Murakami, M. *et al.*, 2005). Electrical stimulation of the brainstem which shifts activity between these two states similarly modifies

cortical odorant responsiveness. Olfactory bulb evoked activity is not reliably modified in a state-dependent manner, suggesting a piriform cortical origin for these changes. In fact, similar to the mechanism of thalamic modulation, anterior piriform cortical neurons show a hyperpolarization during the slow-wave state that can account for the reduced sensory responsiveness (Murakami, M. *et al.*, 2005). Whether similar changes occur in olfactory thalamus is not known.

A second form of sensory gating is based on recent stimulation history and is commonly associated with adaptation or habituation to background or currently nonsignificant stimuli. In thalamocortical systems, precise mechanisms of sensory habituation have not been determined. In general, however, adaptation to prolonged or repeated stimuli tends to be most pronounced in the sensory cortex compared to subcortical areas. Two specific mechanisms for cortical adaptation have been suggested. First, similar to the state-dependent gating mechanism described above, in the visual system, there is evidence for a sensory-dependent hyperpolarization in visual cortical neurons following prolonged stimulation (Carandini, M. and Ferster, D., 1997). As with state-dependent gating, this hyperpolarization could reduce excitability and sensory-evoked responses in cortical neurons. A second proposed mechanism in thalamocortical systems is a stimulation-dependent synaptic depression of thalamic inputs to visual sensory cortex (Chung, S. *et al.*, 2002). Synaptic depression has also been proposed as a mechanism of adaptation of brainstem-mediated acoustic startle reflexes.

In the olfactory system, neurons in the anterior piriform cortex express significantly more rapid and complete adaptation to prolonged or repeated odor stimulation than their subcortical afferents, mitral/tufted cells in the olfactory bulb (Wilson, D. A., 1998). In awake animals performing a simple odor task, piriform neurons rapidly reduce their odor responses to a short burst of a few spikes (McCollum, J. *et al.*, 1991). In anesthetized animals, the adaptation is odorant specific, expressed in both evoked firing and subthreshold postsynaptic potentials, and recovers within 2 min following a 50 s odorant exposure. There is no corresponding hyperpolarization to account for the decreased odor responsiveness (Wilson, D. A., 1998). However, intracellularly recorded postsynaptic potentials in response to both odorant stimulation and electrical stimulation of the lateral olfactory tract are transiently depressed during and after prolonged odorant exposure (Wilson, D. A., 1998). These results suggest that synaptic depression of cortical afferents may underlie short-term cortical odorant adaptation.

To test this hypothesis, the synaptic depression evoked by odorant exposure was modeled in vitro using patterned electrical stimulation of the lateral olfactory tract in slices of anterior piriform cortex. Electrical stimulation of the lateral olfactory tract in vitro, in a manner meant to mimic odorant-evoked mitral cell activity, induced a short-term synaptic depression, with a magnitude and duration similar to that of odorant exposure-induced cortical odor adaptation (Best, A. R. and Wilson, D. A., 2004). This synaptic depression could be blocked by the metabotropic glutamate receptor group II/III (mGluRIII) antagonist CPPG. mGluRIII receptors are expressed on the presynaptic terminals of mitral cell axons, and when activated, reduce neurotransmitter release. *In vivo*, bilateral infusion of CPPG into the anterior piriform cortex prevents adaptation of both cortical and simple behavioral responses to odorants (Best, A. R. and Wilson, D. A., 2004; Best, A. R. *et al.*, 2005). These studies are the most complete mechanistic description of sensory adaptation in any mammalian sensory system and demonstrate the power of taking advantage of the relatively simple structure of the olfactory system to address questions of this nature.

Rapid cortical adaptation in the olfactory system may not only be important for reducing responses to persistent stimuli, but also may play an important role in olfactory figure-ground separation. The piriform cortex can function as a high-pass filter, responding most strongly to new stimuli and much less so to stable stimuli. As odorants are encountered against a background, the piriform cortex can respond as if these new odorants were in isolation. In contrast, under similar conditions, mitral/tufted cells respond to the actual inhaled stimulus – a mixture of background and new additive. Rapid cortical adaptation thus can allow the piriform cortex to selective read olfactory bulb output, ignoring temporally stable components (background) while remaining responsive to novel stimuli occurring against this background (Kadohisa, M. and Wilson, D. A., 2006).

Cortical adaptation may also play a role in modulation of cortical responsiveness to food stimuli based on recent feeding patterns. Sensory-specific satiety is a decrease in behavioral responsiveness to a particular food stimulus (e.g., banana's) following

prolonged feeding with that stimulus. The behavioral satiety can be highly stimulus specific (Rolls, E. T., 2004). In primates, behavioral sensory-specific satiety is associated with a corresponding decrease in responsiveness of orbitofrontal cortex neurons to that stimulus.

Together, these descriptions of state-dependent and experience-dependent sensory gating suggest a role for anterior piriform cortex that combines both thalamic and cortical components of sensory gating in thalamocortical systems. The state-dependent process and mechanism mediated by thalamic neurons in other sensory systems is expressed in anterior piriform cortical neurons in olfaction. Similarly, the experience-dependent adaptation mediated by cortical neurons in other sensory systems is expressed in anterior piriform cortical neurons in olfaction. The separation of these two function in thalamocortical systems may be in response to differences in the nature of the stimulus representation or other information processing demands in these nonolfactory sensory systems.

A third form of sensory gating – cognitively directed attention – has not been explored to any major extent in olfaction. Attention has been likened to a searchlight, wherein differential processing power can be devoted to some portions of a sensory scene compared to other portions of the same scene (Crick, F., 1984). This may be most easily imagined as occurring in the visual or auditory systems. An example might include switching auditory attention between different, simultaneously occurring conversations. It is not clear whether a similar phenomenon exists in olfaction, although it is anecdotally possible to adapt to a background odor and then redirect attention toward that odor and begin to perceive it again.

In thalamocortical sensory systems, the thalamic reticular nucleus may play an important role in the attentional search light. The thalamic reticular nucleus is a thin lamina of neurons along the superficial edge of the thalamus and is organized both topographically and according to modality. For example, a subset of reticular thalamic neurons receive input from visual cortex and project to visual lateral geniculate nucleus neurons in a retinotopic manner. The reticular thalamus receives excitatory input from both sensory thalamus and sensory cortex, and projects back to sensory thalamus. Importantly, this feedback to sensory thalamus is inhibitory. Thus, the reticular thalamus is a group of inhibitory neurons, receiving cortical feedback (as well as state-dependent modulatory inputs) and capable of gating the flow of thalamic information to the sensory cortex. The reticular thalamus thus could play a role in attentional changes in sensory coding, through enhancing processing of important information while suppressing processing of unimportant or unexpected information.

Although data on olfactory-directed attention and scene analysis are limited at best, it is interesting to note a potential olfactory circuit analogy to the reticular thalamic circuit described above. Olfactory bulb granule cells monitor mitral cell output via dendrodendritic synapses and receive axosomatic and axodendritic synapses from cortical feedback fibers. While several hypotheses exist regarding the role of mitral–granule cell reciprocal connections in lateral and feedback inhibition, these hypotheses largely overlook the impact of huge excitatory input to granule cells from olfactory cortical areas. Olfactory cortical feedback to the bulb could provide a higher-order modulation of granule cell excitability, resulting in top-down control of olfactory processing of sensory afferent activity. This cortical modulation of granule cell excitability could be evidenced by changes in gamma frequency local field potential oscillations during periods of strong descending input to the bulb, just as has been found in freely behaving animals performing well-learned olfactory behaviors, as described above. Thus, the olfactory cortex, through descending control based on attention and expectancy, could modulate how the olfactory bulb processes odors (Kay, L. M. and Laurent, G., 1999).

4.38.3.4 Odorant Familiarity and Meaning

In thalamocortical sensory systems, individual neuron receptive fields and cortical maps are shaped by experience. Familiar or learned, important stimuli have enhanced representations at the single cell and circuit level, while less familiar or unimportant stimuli have reduced representations. Where it has been examined, these learned changes in cortical sensory representations involve modifications of intracortical association fiber connectivity, potentially including both excitatory and inhibitory synapses, and are mediated by phenomena such as long-term potentiation and long-term depression. The synaptic and local circuit plasticity induced by experience can lead to changes in sensory acuity (perceptual learning) as well as memory of the learned stimuli (associative learning). Experience

also appears to be important in creating synthetic receptive fields, for example in higher-order inferotemporal visual cortex.

Experience also shapes olfactory cortical circuit function (Wilson, D. A. *et al.*, 2004). As noted above, simple odor exposure can result in cortical afferent synaptic depression and cortical odor adaptation. However, several forms of experience-dependent plasticity contributing to odor discrimination and odor memory have also been described in the piriform cortex. This plasticity includes synaptic and circuit changes necessary to synthesize multiple odor features into unique objects distinct from those components as a process of perceptual learning, as well as circuit and membrane biophysical changes important for associative memory of learned odors and the rules involved in learning new odors.

As noted above, familiar odors are more easily identified and discriminated from similar odors than are novel odors (Wilson, D. A. and Stevenson, R. J., 2003). This experience-induced increase in olfactory acuity may be due in part to changes in feature encoding by olfactory bulb circuitry (Fletcher, M. L. and Wilson, D. A., 2003), but also appears to be critically dependent on changes within olfactory cortex. For example, single units in the anterior piriform cortex are unable to discriminate between single odorants and binary mixtures made of those components as determined with a simple habituation/cross-habituation paradigm. Thus, exposure to a novel binary mixture for 10 s is sufficient to cause adaptation of anterior piriform cortical neuron responses to that mixture and causes cross-adaptation to the components of that mixture (Wilson, D. A., 2003). This suggests that these neurons do not discriminate between this novel (never smelled by the animal before) mixture and its components. However, simply extending the duration of exposure to the mixture to 50 s is sufficient to reduce cross-adaptation between the mixture and its components, suggesting that as the mixture becomes more familiar, it becomes more distinctive from similar odors. Olfactory bulb mitral/tufted cells do not appear to be capable of discriminating mixtures from their components in similar conditions. This supports the hypothesis that mitral/tufted cells encode for odorant features, rather than odors as a whole. These cells will respond to any odorant containing a particular feature, and adaptation to that feature will reduce responsiveness to all odors sharing it.

The familiarization effect on cortical odorant discrimination appears to involve plasticity within cortical circuits as noted above in the discussion of content-addressable memory. Application of the muscarinic acetylcholine receptor antagonist scopolamine directly onto the anterior piriform cortex during initial odorant exposure prevents experience-dependent enhancement in cortical odor discrimination (Wilson, D. A. and Stevenson, R. J., 2003). Cholinergic input to the piriform cortex comes primarily from the horizontal limb of the diagonal band and has been shown to modulate both synaptic transmission of piriform cortical associative fiber synapses and plasticity of those synapses. This selective modulation of association fiber pathways might be expected to strongly influence the content-addressable memory function hypothesized to be involved in odor representations, thus impairing odor recognition and discrimination (Hasselmo, M. E. and Barkai, E., 1995).

In addition to perceptual learning, odor experience can also result in associative memories wherein odors acquire predictive value or meaning. Associative olfactory conditioning modifies c-fos expression and 2-deoxyglucose uptake in piriform cortex in response to the conditioned odor, with differential effects on anterior and posterior regions (Datiche, F. *et al.*, 2001; Roth, T. L. and Sullivan, R. M., 2005). Associative conditioning also modifies the effectiveness of olfactory bulb electrically evoked responses in the piriform cortex, again most prominently in the posterior regions. Using high-speed voltage-sensitive dye imaging across a wide region of the piriform cortex, Litaudon P. *et al* (1997) reported that the most significant changes in piriform cortical responsiveness to olfactory bulb input following conditioning were in the longer-latency components of the evoked response, suggesting a primary effect on association fiber synapses. These results further argue that cortical representations of familiar odorants, stored by changes in association connections, may include nonolfactory components.

In fact, activity of neurons in both the piriform cortex and orbitofrontal cortex is influenced by a variety of nonolfactory stimuli in awake animals, including visuospatial or expectancy cues in a well-learned odor discrimination task. Schoenbaum and colleagues (Schoenbaum, G. and Eichenbaum, H., 1995) found no significant difference between piriform cortical neuron single-unit activity and orbitofrontal cortical neuron activity in an odor learning task, with cells in both areas responding to such apparently nonolfactory phases of the task as approach to the odor sampling port and water reward consumption.

In a series of well-designed experiments, Barkai and colleagues have found that the piriform cortex is also modified by odor rule learning in a form of metaplasticity (Saar, D. and Barkai, E., 2003). Rats trained in a series of simple odor discrimination tasks (go, no-go discrimination) dramatically improve their acquisition over repeated odor pairs. For example, if training on an odor A versus odor B task is followed by similar C versus D and then E versus F discriminations, acquisition on the E versus F or subsequent pairings can often occur on a single trial. This has been described as odor set learning, odor rule learning, or learning to learn. Barkai has found that such odor rule learning is associated with heightened excitability of piriform cortical (Saar, D. and Barkai, E., 2003) and hippocampal neurons, as well as changes in dendritic spine number on piriform cortical pyramidal cell dendrites. The membrane excitability changes in piriform cortex are acetylcholine dependent and work through cholinergic reduction of a K-mediated after-hyperpolarization (Saar, D. and Barkai, E., 2003). This enhanced excitability and connectivity may facilitate learning of subsequent odor pairs, as the change would be expected to be a whole-cell phenomenon and thus not odor specific.

4.38.3.5 Nonolfactory Context

As noted above, activity of olfactory cortical neurons is modulated by a variety of nonolfactory stimuli. This modulation could reflect a direct multisensory input to olfactory cortex. For example, the orbitofrontal cortex receives strong input from gustatory and orosensory areas (Rolls, E. T., 2004), and the piriform cortex receives strong input from the multisensory entorhinal cortex (Neville, K. R. and Haberly, L., 2004). The orbitofrontal and piriform cortices are also reciprocally interconnected; thus, there are multiple opportunities for multisensory convergence in either structure. In addition, nonolfactory modulation of olfactory cortical activity could reflect input from nonsensory-specific areas responsive to changes in arousal or behavioral state. For example, the olfactory system is richly innervated by noradrenergic fibers from the nucleus locus coeruleus. Activation of the locus coeruleus can modify piriform cortical single-unit excitability and activity phase relationship to the respiratory cycle (Bouret, S. and Sara, S. J., 2002), either through direct modulation of cortical synaptic physiology or through modulation of olfactory bulb afferent activity (Jiang, M. *et al.*, 1996). Similarly, cholinergic input to the olfactory cortex can modulate piriform cortical synaptic physiology. Both of these systems have direct effects on cortical pyramidal cells, as well as modulatory effects on association fiber synaptic function. They can also both modulate synaptic plasticity in the piriform cortex as noted above, as well as olfactory bulb local circuits (Sullivan, R. M. and Wilson, D. A., 1994).

Modulatory inputs such as from the locus coeruleus and horizontal limb of the diagonal band can signal changes in arousal and internal behavioral state. In doing so, they can differentially influence response properties of olfactory cortical circuits depending on context and expectations. For example, the response seen in the olfactory bulb and piriform cortex as an animal performs a well-learned task of approaching an odor port may reflect either a nonspecific change in cortical arousal and attention signaled by the locus coeruleus or cholinergic inputs. Alternatively, it may reflect other, more specific top-down activation, for example from the entorhinal and higher cortex (Kay, L. M. *et al.*, 1996). Dissecting the differential roles of these two forces will be an important future avenue of research for understanding the effects of context and expectancy in cortical odor processing.

4.38.4 Summary of Olfactory Cortical Information Processing and Unresolved Issues

4.38.4.1 Odor Discrimination

There is increasing evidence that odor discrimination, identification, and adaptation all require olfactory cortical involvement. In humans, lesions of temporal lobe structures that include olfactory cortex, diseases that affect temporal lobe cortical memory areas, and some developmental disorders have all been shown to impair odor identification and discrimination in the absence of impairment of odor detection thresholds (Wilson, D. A. and Stevenson, R. J., 2003). The thesis presented here and elsewhere (Haberly, L. B., 2001; Wilson, D. A. and Stevenson, R. J., 2003) is that olfactory cortex synthesizes odorant features extracted at the periphery and refined by the olfactory bulb into unique perceptual odor objects. This synthesis is an active process involving synaptic plasticity and memory of familiar input patterns. Experience with complex odors results in plasticity of intracortical association fiber synapses within the olfactory cortex, leading to the formation of a content-addressable memory for that odor amongst an ensemble of activated cortical neurons. Subsequent

activation of the cortical circuit with the same, or similar input, reactivates the complete ensemble, leading to odor recognition. As two similar inputs are repeatedly, separately activated, they may come to diverge, enhancing odor discrimination. Thus, experience with odors and the resulting cortical plasticity enhances odor perceptual acuity (olfactory perceptual learning). These general mechanisms are hypothesized to be similar to those involved in visual object recognition and the emergence of visual object receptive fields in inferotemporal cortex. Further examination of odor quality coding in the olfactory cortex, using multiple single-unit ensemble recording, is clearly warranted. In addition, it is now clear that odor quality discriminations can be made within a single sniff in both humans and rodents. A closer analysis of the temporal dimensions of odor quality coding in olfactory cortex should also prove fruitful.

Odor objects may be multimodal, including for example gustatory or other integral components. The influence of stimulus color on odor perception (Gottfried, J. A. and Dolan, R. J., 2003) and the inclusion of gustatory descriptors for purely olfactory stimuli (Stevenson, R. J. *et al.*, 1995) are good examples of this process. The multimodal inputs to olfactory cortex, combined with the synthetic processing just summarized, could easily contribute to this multimodal perception. In fact, associative experience with odors and tastes can facilitate the merger of their perceptual properties.

As in other sensory systems, olfaction may include specialist subregions for specific classes of odorants or odor functions. The orbitofrontal cortex, for example, while heavily interconnected with the piriform cortex, may be particularly important for food odors and other hedonically charged odorants. The different subregions of the piriform cortex may also have specialized roles in olfaction, with for example the posterior piriform more involved in higher-order or multimodal odor representations, though this is a topic in need of further research. In fact, the sensory physiology of large regions of olfactory cortex have not been examined at all.

Finally, it must be emphasized that odorant molecular structure is not synonymous with odor quality percept. Expectations, past experience, internal state, and stimulus intensity can all affect how a given inhaled molecular stimulus is perceived. A major point of this review, and new human imaging evidence (DeAraujo, I. E. *et al.*, 2005), suggests that the transform from molecular features to perceptual object is a cortical event.

4.38.4.2 Sensory Gating

Sensory gating takes several forms including modulation of sensation and perception due to changes in arousal, recent stimulus exposure, and selective attention. Olfactory cortex appears to play a major role in the first two sensory gating phenomena, and may be expected to also be involved in the latter. Spontaneous alternation between fast-wave and slow-wave cortical states, roughly comparable to alert and sleep states respectively, produces corresponding shifts in the state of piriform cortical membrane depolarization. Fast-wave cortical states are associated with depolarized piriform cortical neurons and robust responsiveness to odorant stimulation, while slow-wave states are associated with membrane hyperpolarization and reduced sensory responsiveness (Murakami, M. *et al.*, 2005). In this way, the piriform cortex can gate sensory throughput to higher cortical areas based on arousal level. Similarly, the piriform cortex is a critical component of odor habituation. Activity-dependent presynaptic depression of cortical afferents can account for both cortical and simple behavioral adaptation to odors (Best, A. R. and Wilson, D. A., 2004; Best, A. R. *et al.*, 2005). Prevention of cortical short-term adaptation prevents adaptation of simple behavioral responses, demonstrating that adaptation of receptors in the nose cannot account for short-term behavioral habituation.

Cortical mechanisms of selective attention in olfaction have not been examined. A hypothesis is proposed that olfactory cortical feedback to the olfactory bulb granule cell layer may play a role similar to cortical input to the reticular thalamus in other sensory systems (Crick, F., 1984). Another possibility is that short-term cortical adaptation may be reversible, for example through noradrenergic input (Best, A. R. and Wilson, D. A., 2004), thus allowing an arousal or attentional shift to enhance cortical responsiveness to previously adapted odors. This area requires further attention.

4.38.4.3 Background Segmentation

A cortical and perceptual function that merges odor discrimination and sensory gating is figure-ground separation. In the natural world, odorants are invariable experienced against backgrounds, yet the perceived quality of the foreground odorants can remain constant despite background changes. If odor discrimination and identity were dependent solely on identification of

inhaled features, then odorants experienced against backgrounds would change in quality dependent on the identity of the background. Formation of odorant objects in cortical memory, combined with odor-specific cortical adaptation to background odorants, solves the problem of olfactory figure-ground separation. In fact, recent evidence suggests that piriform cortical neurons respond to odorants against a preexisting background odorant as if the background were not present (Kadohisa, M. and Wilson, D. A., 2006). Olfactory bulb mitral/tufted cells, in contrast, respond to the same situation as if a binary mixture of the background and foreground odorants were present (as they are). Thus, cortical plasticity may be critical for this important ability of the olfactory system to deal with variation in stimulus complexity and analysis of olfactory scenes.

4.38.4.4 Corticobulbar Feedback and Laterality

As in all sensory systems, the olfactory system includes a rich feedback circuitry. In thalamocortical sensory systems, cortical feedback plays an important role in experience and expectation modulation of sensory acuity and sensitivity, as well as selective attention. In olfaction, the olfactory bulb receives strong input from all olfactory cortical structures, and olfactory cortical structures are strongly interconnected and receive descending input from higher-order cortex (Neville, K. R. and Haberly, L. B., 2003). These feedback pathways are activated by past experience and expectancy and may shape odor sensitivity and acuity. This is another area in need of future research.

Similarly, many sensory and higher-order systems express some lateralization of function. The olfactory cortex includes extensive commissural connectivity, and piriform cortical neurons are differentially sensitive to unilateral and bilateral odorant stimulation. Human imaging work suggests there may be some lateralization of function in olfaction (Zatorre, R. J. *et al*., 1992), though this needs to be further examined. The causes and consequences of lateralized cortical function in olfaction should be examined.

In summary, as in all other sensory systems, olfactory cortical structures underlie the critical transition from peripheral analytical processing to synthetic, global processing that leads to the rich perceptual experience that defines the sense of smell. The unique nature of the stimulus in olfaction, however, creates unique problems for processing this information. Though substantial progress has been made in the past 10 years toward understanding the role of olfactory cortex in smell, the field is poised to make major strides by the time this volume is revised.

References

Best, A. R. and Wilson, D. A. 2004. Coordinate synaptic mechanisms contributing to olfactory cortical adaptation. J. Neurosci. 24, 652–660.

Best, A. R., Thompson, J. V., Fletcher, M. L., and Wilson, D. A. 2005. Cortical metabotropic glutamate receptors contribute to habituation of a simple odor-evoked behavior. J. Neurosci. 25, 2513–2517.

Bouret, S and Sara, S. J. 2002. Locus coeruleus activation modulates firing rate and temporal organization of odour-induced single-cell responses in rat piriform cortex. Eur. J. Neurosci. 16, 2371–2382.

Carandini, M. and Ferster, D. 1997. A tonic hyperpolarization underlying contrast adaptation in cat visual cortex. Science 276, 949–952.

Chung, S., Li, X., and Nelson, S. B. 2002. Short-term depression at thalamocortical synapses contributes to rapid adaptation of cortical sensory responses in vivo. Neuron 34, 437–446.

Cleland, T. A. and Linster, C. 2003. Central Olfactory Structures. In: Handbook of Olfaction and Gustation, 2nd edn. (*ed*. R. L. Doty), pp. 165–180. Dekker.

Crick, F. 1984. Function of the thalamic reticular complex: the searchlight hypothesis. Proc. Natl. Acad. Sci. U. S. A. 81, 4586–4590.

Datiche, F., Roullet, F., and Cattarelli, M. 2001. Expression of Fos in the piriform cortex after acquisition of olfactory learning: an immunohistochemical study in the rat. Brain Res. Bull. 55, 95–99.

DeAraujo, I. E., Rolls, E. T., Velazco, M. I., Margot, C., and Cayeux, I. 2005. Cognitive modulation of olfactory processing. Neuron 46, 671–679.

Edeline, J. M., Manunta, Y., and Hennevin, E. 2000. Auditory thalamus neurons during sleep: changes in frequency selectivity, threshold, and receptive field size. J. Neurophysiol. 84, 934–952.

Eeckman, F. H. and Freeman, W. J. 1990. Correlations between unit firing and EEG in the rat olfactory system. Brain Res. 528, 238–244.

Fletcher, M. L. and Wilson, D. A. 2003. Olfactory bulb mitral-tufted cell plasticity: odorant-specific tuning reflects previous odorant exposure. J. Neurosci. 23, 6946–6955.

Gottfried, J. A. and Dolan, R. J. 2003. The nose smells what the eye sees: crossmodal visual facilitation of human olfactory perception. Neuron 39, 375–386.

Haberly, L. B. 2001. Parallel-distributed processing in olfactory cortex: new insights from morphological and physiological analysis of neuronal circuitry. Chem. Senses 26, 551–576.

Hasselmo, M. E. and Barkai, E. 1995. Cholinergic modulation of activity-dependent synaptic plasticity in the piriform cortex and associative memory function in a network biophysical simulation. J. Neurosci. 15, 6592–6604.

Hasselmo, M. E. and Bower, J. M. 1992. Cholinergic suppression specific to intrinsic not afferent fiber synapses in rat piriform (olfactory) cortex. J. Neurophysiol. 67, 1222–1229.

Hasselmo, M. E., Wilson, M. A., Anderson, B. P., and Bower, J. M. 1990. Associative memory function in piriform (olfactory) cortex: computational modeling and neuropharmacology. Cold Spring Harb. Symp. Quant. Biol. 55, 599–610.

Illig, K. R. and Haberly, L. B. 2003. Odor-evoked activity is spatially distributed in piriform cortex. J. Comp. Neurol. 457, 361–373.

Jiang, M., Griff, E. R., Ennis, M., Zimmer, L. A., and Shipley, M. T. 1996. Activation of locus coeruleus enhances the responses of olfactory bulb mitral cells to weak olfactory nerve input. J. Neurosci. 16, 6319–6329.

Johnson, D. M., Illig, K. R., Behan, M., and Haberly, L. B. 2000. New features of connectivity in piriform cortex visualized by intracellular injection of pyramidal cells suggest that ''primary'' olfactory cortex functions like ''association'' cortex in other sensory systems. J. Neurosci. 20, 6974–6982.

Jung, M. W., Larson, J., and Lynch, G. 1990. Role of NMDA and non-NMDA receptors in synaptic transmission in rat piriform cortex. Exp. Brain. Res. 82, 451–455.

Kadohisa, M. and Wilson, D. A. 2006. Olfactory cortical adaptation facilities detection of odors against background. J. Neurophysiol. 95, 1888–1896.

Kay, L. M. and Laurent, G. 1999. Odor- and context-dependent modulation of mitral cell activity in behaving rats. Nat. Neurosci. 2, 1003–1009.

Kay, L. M., Lancaster, L. R., and Freeman, W. J. 1996. Reafference and attractors in the olfactory system during odor recognition. Int. J. Neural Syst. 7, 489–495.

Ketchum, K. L. and Haberly, L. B. 1993. Membrane currents evoked by afferent fiber stimulation in rat piriform cortex. I. Current source-density analysis. J. Neurophysiol. 69, 248–260.

Laing, D. G., Legha, P. K., Jinks, A. L., and Hutchinson, I. 2003. Relationship between molecular structure, concentration and odor qualities of oxygenated aliphatic molecules. Chem. Senses 28, 57–69.

Lin da, Y., Zhang, S. Z., Block, E., and Katz, L. C. 2005. Encoding social signals in the mouse main olfactory bulb. Nature 434, 470–477.

Litaudon, P., Amat, C., Bertrand, B., Vigouroux, M., and Buonviso, N. 2003. Piriform cortex functional heterogeneity revealed by cellular responses to odours. Eur. J. Neurosci. 17, 2457–2461.

Litaudon, P., Mouly, A. M., Sullivan, R., Gervais, R., and Cattarelli, M. 1997. Learning-induced changes in rat piriform cortex activity mapped using multisite recording with voltage sensitive dye. Eur. J. Neurosci. 9, 1593–1602.

McCollum, J., Larson, J., Otto, T., Schottler, F., Granger, R., and Lynch, G. 1991. Short-latency single-unit processing in olfactory cortex. J. Cogn. Neurosci. 3, 293–299.

Murakami, M., Kashiwadani, H., Kirino, Y., and Mori, K. 2005. State-dependent sensory gating in olfactory cortex. Neuron 46, 285–296.

Neville, K. R. and Haberly, L. B. 2003. Beta and gamma oscillations in the olfactory system of the urethane-anesthetized rat. J. Neurophysiol. 90, 3921–3930.

Neville, K. R. and Haberly, L. 2004. Olfactory Cortex. In: The Synaptic Organization of the Brain, 5th edn. (*ed*. G. M. Shepherd), pp. 415–454. Oxford University Press.

Rolls, E. T. 2004. The functions of the orbitofrontal cortex. Brain Cogn. 55, 11–29.

Roth, T. L. and Sullivan, R. M. 2005. Memory of early maltreatment: neonatal behavioral and neural correlates of maternal maltreatment within the context of classical conditioning. Biol. Psychiatry 57, 823–831.

Saar, D. and Barkai, E. 2003. Long-term modifications in intrinsic neuronal properties and rule learning in rats. Eur. J. Neurosci. 17, 2727–2734.

Schoenbaum, G. and Eichenbaum, H. 1995. Information coding in the rodent prefrontal cortex. I. Single-neuron activity in orbitofrontal cortex compared with that in pyriform cortex. J. Neurophysiol. 74, 733–750.

Schoenbaum, G., Setlow, B., and Ramus, S. J. 2003a. A systems approach to orbitofrontal cortex function: recordings in rat orbitofrontal cortex reveal interactions with different learning systems. Behav. Brain Res. 146, 19–29.

Schoenbaum, G., Setlow, B., Saddoris, M. P., and Gallagher, M. 2003b. Encoding predicted outcome and acquired value in orbitofrontal cortex during cue sampling depends upon input from basolateral amygdala. Neuron 39, 855–867.

Stevenson, R. J., Prescott, J., and Boakes, R. A. 1995. The acquisition of taste properties by odors. Learn. Motiv. 26, 433–455.

Sugai, T., Miyazawa, T., Fukuda, M., Yoshimura, H., and Onoda, N. 2005. Odor-concentration coding in the guinea-pig piriform cortex. Neuroscience 130, 769–781.

Sullivan, R. M. and Wilson, D. A. 1994. The locus coeruleus, norepinephrine, and memory in newborns. Brain Res. Bull. 35, 467–472.

Tanabe, T., Iino, M., and Takagi, S. F. 1975. Discrimination of odors in olfactory bulb, pyriform-amygdaloid areas, and orbitofrontal cortex of the monkey. J. Neurophysiol. 38, 1284–1296.

Tanaka, K. 2000. Mechanisms of visual object recognition studied in monkeys. Spat. Vis. 13, 147–163.

Wilson, D. A. 1998. Habituation of odor responses in the rat anterior piriform cortex. J. Neurophysiol. 79, 1425–1440.

Wilson, D. A. 2000. Comparison of odor receptive field plasticity in the rat olfactory bulb and anterior piriform cortex. J. Neurophysiol. 84, 3036–3042.

Wilson, D. A. 2003. Rapid, experience-induced enhancement in odorant discrimination by anterior piriform cortex neurons. J. Neurophysiol. 90, 65–72.

Wilson, D. A. and Stevenson, R. J. 2003. Olfactory perceptual learning: the critical role of memory in odor discrimination. Neurosci. Biobehav. Rev. 27, 307–328.

Wilson, D. A., Best, A. R., and Brunjes, P. C. 2000. Trans-neuronal modification of anterior piriform cortical circuitry in the rat. Brain Res. 853, 317–322.

Wilson, D. A., Best, A. R., and Sullivan, R. M. 2004. Plasticity in the olfactory system: lessons for the neurobiology of memory. Neuroscientist 10, 513–524.

Zatorre, R. J., Jones-Gotman, M., Evans, A. C., and Meyer, E. 1992. Functional localization and lateralization of human olfactory cortex. Nature 360, 339–340.

Zhang, Y., Burk, J. A., Glode, B. M., and Mair, R. G. 1998. Effects of thalamic and olfactory cortical lesions on continuous olfactory delayed nonmatching-to-sample and olfactory discrimination in rats (*Rattus norvegicus*). Behav. Neurosci. 112, 39–53.

Zou, Z., Fusheng, L., and Buck, L. B. 2005. Odor maps in the olfactory cortex. Proc. Natl. Acad. Sci. U. S. A. 102, 7724–7729.

Zou, Z., Horowitz, L. F., Montmayeur, J. P., Snapper, S., and Buck, L. B. 2001. Genetic tracing reveals a stereotyped sensory map in the olfactory cortex. Nature 414, 173–179.

4.39 Modeling of Olfactory Processing

C Linster and T A Cleland, Cornell University, Ithaca, NY, USA

© 2008 Elsevier Inc. All rights reserved.

4.39.1	Introduction	707
4.39.2	Filtering and Contrast Enhancement	708
4.39.3	Mechanisms Underlying Oscillations and Spike Synchronization	712
4.39.4	Odor Segmentation and Associative Memory Function	713
4.39.5	Detailed Biophysical Models of OB Neurons	713
4.39.6	Conclusions	714
References		715

Glossary

associative memory In this context, the term refers to a type of neural network in which associations between different elements of a stimulus are stored by strengthening connections between these elements. The most important feature of an associative memory is that it will restore a previously stored pattern when presented with an incomplete or distorted version of this pattern.

attractor In dynamical systems analysis, an attractor is any state of a system in which it will remain if otherwise undisturbed. The attractor of a simple pendulum is the vertical position; adding magnets or other disturbances to the system may move the attractor to a new position, or generate additional attractors. Attractors need not be single points; cyclic attractors are common.

Hebbian learning A type of plasticity (learning) rule in which interactions between simultaneously active elements, such as neurons, are strengthened incrementally.

molecular receptive range Equivalent to receptive field for different chemical ligands. In the olfactory system, a neuron's molecular receptive range describes the ensemble of chemicals to which it is responsive.

olfactory bulb Cortical telencephalic structure receiving direct afferent input from olfactory sensory neurons located in the nasal cavity, as well as efferent input from multiple regions of the brain.

signal-to-noise ratio Engineering term quantifying the proportion of the signal of interest (signal) in the total information stream that is transmitted (signal + noise). Low signal-to-noise ratios render it difficult to detect or interpret the signal, as it is buried in noise.

4.39.1 Introduction

In natural environments, airborne chemical stimuli are distributed unpredictably in time and space, and odorants from innumerable sources intermix freely. The olfactory system must be able to detect potential signals of interest within these chemically noisy environments, correctly extract these signals from a complex and changing odor background to form stimulus representations, compare these constructed representations to those of previously experienced odors, differentiate relevant from irrelevant stimuli, and cue an appropriate response. Many of the neural circuit elements comprising the olfactory system have been proposed to contribute to these processes in particular ways; in particular, multiple feedback and feed-forward interactions among olfactory structures, as well as between olfactory and nonolfactory areas, are thought to contribute to the filtering and construction of olfactory representations. Computational models of olfactory processing have been increasingly utilized to describe and interpret these complex and interrelated phenomena.

Primary olfactory sensory neurons (OSNs) number in the millions in rodents. Their axons are highly convergent, targeting specific, discrete neuropilar

synaptic regions within the input layer of the olfactory bulb called glomeruli. In hamsters, for example, between 1300 and 4700 OSNs presumably expressing the same odorant receptor complement converge upon each glomerulus (Schoenfeld, T. A. and Knott, T. K., 2004). These large populations of redundant OSNs and their correspondingly high convergence ratios have been proposed to yield advantages such as improved stimulus sensitivity, an improved signal-to-noise ratio, and an increased range of tuning to different odorant concentrations (van Drongelen, W. *et al*., 1978; Duchamp-Viret, P. *et al*, 1989; Meisami, E., 1989; Cleland, T. A. and Linster, C., 1999). The molecular receptive ranges, or chemical receptive fields, of these odorant receptors overlap substantially, such that the identity of odorants is not associated with the activation of a specific receptor, but rather is represented by a distributed, combinatorial code (Adrian, E. D., 1953; Moulton, D. G., 1967; Stewart, W. B. *et al*., 1979; Kauer, J. S., 1991), now recognized as a pattern of activation across many receptors. Owing to the specific convergence of OSN axons, these odor-specific activity patterns can be most clearly observed in imaging studies of olfactory bulb glomeruli (Friedrich, R. W. and Korsching, S. I., 1997; Rubin, B. D. and Katz, L. C., 1999; Meister, M. and Bonhoeffer, T., 2001; Wachowiak, M. *et al*., 2002). These overlapping representations underlie two critical properties of the olfactory system that a labeled-line solution would not. First, the number of unique odor representations is not limited to the number of different receptor types (roughly 1000 in mice) (Mombaerts, P., 1996), but can be estimated as m^n, where n denotes the number of receptor types and m denotes the number of recognizable states that each sensor can assume, ultimately limited by the signal-to-noise ratio of the system. Even if only two receptor states, active and inactive, are recognized, this enables roughly 2^{1000} potential odor stimuli to be discriminated in mice. Second, the fact that structurally and perceptually similar odorant molecules will activate correspondingly overlapping sets of olfactory receptors (Linster, C. *et al*., 2001; Cleland, T. A., *et al*., 2002; Linster, C. *et al*., 2002) establishes a basis for the recognition of stimulus similarity in the olfactory system. This is a prerequisite for basic postsensory cognitive processes such as generalization (Shepard, R. N. and Chang, J. J., 1963; Shepard, R. N., 1987; Cleland, T. A. *et al*., 2002) and a tolerance for variance among repeated stimulus samples that a labeled-line system would have no clear means of generating.

Distributed patterns of activity in response to chemical stimuli are transmitted to the olfactory bulb via OSN axons that terminate in the glomeruli of its input layer. The olfactory bulb is believed to filter and transform these incoming sensory data, performing normalization, contrast enhancement, and similar operations before conveying the processed olfactory information to several different secondary olfactory structures via mitral cell axon collaterals (Cleland, T. A. and Linster, C., 2003). Notably, the bulb constitutes the last common stage at which olfactory sensory representations can be processed before the signal diverges dramatically into these multiple secondary structures. It is clear from recent investigations that the perceptual qualities of odorants can be predicted, to a limited degree, from the patterns of activation that they evoke at the olfactory bulb input layer (Linster, C. and Hasselmo, M. E., 1999; Linster, C. *et al*., 2001; Cleland, T. A. *et al*., 2002; Linster, C. *et al*., 2002). However, several aspects of odor perception, for example, changes in perception and discrimination capacity due to odor intensity or prior experience, cannot be predicted solely by this first-order representation as reflected in glomerular activation patterns. Furthermore, the olfactory bulb receives substantial centrifugal projections from both cortical and neuromodulatory centers, and its activity is strongly regulated by learning and experience. It is therefore safe to assume that the olfactory bulb plays an important role in processing incoming sensory information. Indeed, many models of olfactory bulb signal processing have been developed, which are grouped here into studies of (1) filtering and contrast enhancement, (2) mechanisms underlying oscillations and spike synchronization, and (3) odor segmentation and associative memory function. In addition, a number of detailed biophysical models of bulbar neurons have been constructed, in many cases, to address how their intrinsic properties underlie and interact with network properties.

4.39.2 Filtering and Contrast Enhancement

The high convergence ratio between OSNs expressing a particular odorant receptor and their target glomeruli in the olfactory bulb (Figure 1(a)) is believed to improve the signal-to-noise ratio during odorant detection (van Drongelen, W. *et al*., 1978), potentially overcoming the limiting noise inherent in

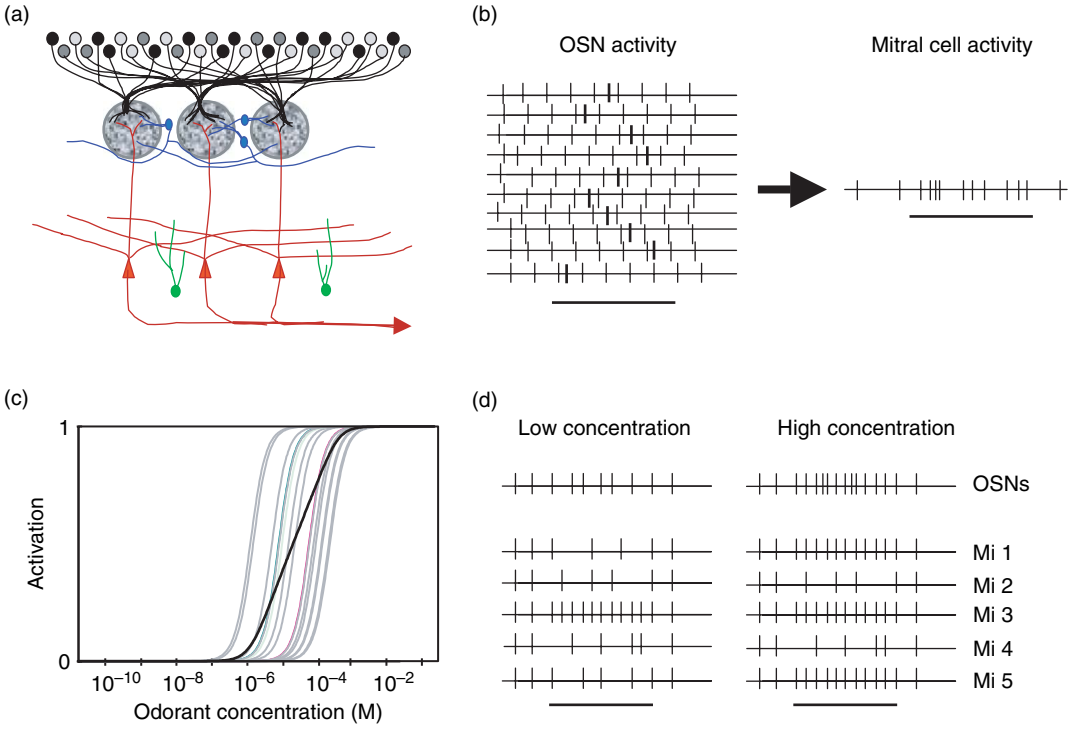

Figure 1 Glomerular computations and convergence. (a) Simplified structure of the olfactory bulb as represented in most computational models. Large populations of olfactory sensory neurons (OSNs) expressing the same receptor (particular shades of gray) converge onto common glomeruli in the olfactory bulb, within which they synapse onto the dendrites of periglomerular (blue) and mitral (red) cells. Mitral cells also excite granule cells (green) via their lateral dendrites, and granule cells in turn inhibit mitral cells; functionally, this mediates lateral inhibition between mitral cells. Periglomerular cells are primarily associated with one or a small number of glomeruli and project axons to a few other glomeruli; these have also been suggested to mediate lateral inhibition between mitral cells. A number of other cell types have also been characterized in the bulb, such as short-axon and tufted cells that are rarely included in computational models; furthermore, established heterogeneity within the cell types modeled has usually been neglected. (b) The high convergence of OSN axons onto mitral cells within each glomerulus significantly improves the signal-to-noise ratio in mitral cells as compared with OSNs. Even if a weak odorant stimulus were to evoke only a single additional spike in each OSN above its basal rate of spiking (OSN activity; bold lines), this high convergence ratio can generate a robust odor responses in a postsynaptic mitral cell (Mitral cell activity), hence enabling mitral cells to reliably represent odor stimuli at lower concentrations than can OSNs (van Drongelen, W. *et al.*, 1978). Horizontal bars depict the time of odorant presentation. (c) While OSN concentration–activation curves are steep, enabling accurate representations of ligand–receptor binding over a range of roughly one log unit concentration, the considerably broader curves observed in glomeruli can be explained if the convergent OSN population is nonuniform in spare receptor capacity or other determinants of intracellular gain (Cleland, T. A. and Linster, C., 1999). If OSNs with identical odorant selectivity but exhibiting different functional spare receptor capacities (gray sigmoids) project onto a single glomerulus, the summed concentration–activation curve of that glomerulus can span several log units of concentration (black sigmoid). (d) Frequency-to-spatial transformation by local glomerular circuits would activate different populations of mitral cells within each glomerulus as a function of the average firing rate of the convergent OSNs (Anton, P. S. *et al.*, 1991). Low concentration odorants (left panel) evoke weak activity in a given receptor-specific OSN subpopulation, generating increased activity in only one mitral cell. In contrast, a high concentration odor stimulus (right panel) evokes greater activity in the OSN population and hence generates measurable excitatory responses in three mitral cells. Horizontal bars depict the time of odorant presentation.

the transduction mechanisms of individual OSNs (Lowe, G. and Gold, G. H., 1995). In principle, this property improves the coding capacity of the olfactory system, increasing the number of different odor-specific patterns that can be discriminated, as well as improving the maximum reliable sensitivity of the system (Figure 1(b)). Another modeling study has suggested that this same property can be employed to increase the range of odor ligand concentrations that can be represented by olfactory bulb glomeruli without saturation (Figure 1(c)) (Cleland, T. A. and Linster, C., 1999). This hypothesis provides a possible

answer to the conundrum of how collective concentration–response curves measured by glomerular imaging can be substantially broader than those measured in individual OSN recordings (Friedrich, R. W. and Korsching, S. I., 1997; Bozza, T. *et al.*, 2002), enabling preservation of the ratios of activation levels among glomeruli across broader concentration ranges and hence potentially facilitating the recognition of odor quality across changes in concentration. Another approach has been suggested by Anton P. S. *et al.* (1991). Noting that the activity of each glomerulus is sampled and conveyed centrally by a number of mitral cells (on the order of 50 in hamsters) (Schoenfeld, T. A. and Knott, T. K., 2004), and that mitral cell firing frequencies do not scale monotonically with concentration as do those of OSNs, these authors proposed that the synaptic circuitry within each glomerulus could compute a frequency-to-spatial transformation on the incoming information. That is, the number of responding mitral cells within a glomerulus, but not their firing rate, would depend on the firing rates of the sensory neurons projecting to that glomerulus in response to odor stimulation (Figure 1(d)).

Contrast enhancement is a common property of sensory systems that narrows, or sharpens, sensory representations by specifically inhibiting neurons on the periphery of the representation, hence enhancing the contrast between signal and background. A number of computational models have investigated the contrast enhancement potential of olfactory bulb circuitry (Figure 2(a)), most of which, by analogy with the retina, have investigated the potential role of lateral inhibitory projections. Classically, bulb models have emphasized lateral inhibition mediated by mitral cell lateral dendrites (Rall, W. and Shepherd, G. M., 1968; Shepherd, G. M. and Brayton, R. K., 1979; Schild, D., 1988; Urban, N. N., 2002; Davison, A. P. *et al.*, 2003). These lateral dendrites form reciprocal synapses with inhibitory granule cell spines in the external plexiform layer of the bulb, forming a network through which mitral cells inhibit one another as well as themselves (Isaacson, J. S. and Strowbridge, B. W., 1998), although the region receiving this inhibition is not clearly localized (Luo, M. and Katz, L. C., 2001; Debarbieux, F. *et al.*, 2003; Djurisic, M. *et al.*, 2004). Subsequent models proposed that contrast enhancement was instead mediated by lateral inhibition mediated by the relatively superficial periglomerular (PG) cells (Linster, C. and Gervais, R., 1996; Linster, C. and Hasselmo, M., 1997) (Figures 1(a) and 2(b)). This hypothesis offered the substantial advantage that lateral inhibition could be delivered onto mitral cells in the glomerular region of their apical dendrites, a location better capable of preventing spike initiation in these cells. In a model based on this hypothesis, Linster C. and Hasselmo M. (1997) further showed that if the activation of PG cells is modulated by cholinergic inputs from the horizontal limb of the diagonal band, a relatively stable number of active mitral cells can be maintained independent of the intensity of olfactory input or the set of OSNs activated by the odorant. In this model, granule cells served instead to modulate the gain of mitral cell activity and were necessary in order to obtain stable average firing rates. Indeed, subsequent studies have shown that PG cells are appropriately modulated by acetylcholine (Castillo, P. E. *et al.*, 1999), and some of the behavioral predictions from these models have been tested in rats (Linster, C. and Cleland, T. A., 2002; Linster, C. *et al.*, 2003; Mandairon, N. *et al.*, 2006).

Contrast enhancement, the effects of which have been observed in the olfactory bulb (Yokoi, M. *et al.*, 1995), can be functionally defined as a process of competition between neurons proportional to the similarity of the information that they mediate. Simplified models of the olfactory system, based on one-dimensional odor subspaces, have been able to implement contrast enhancement using lateral inhibition (Linster, C. and Gervais, R., 1996; Linster, C. and Hasselmo, M., 1997; Linster, C. and Smith, B. H., 1997; Linster, C. and Hasselmo, M., 1999; Linster, C. and Cleland, T. A., 2001; Cleland, T. A. and Linster, C., 2002) and have been effective at interpreting behavioral and physiological data derived from single monotonically varying odorant series (Yokoi, M. *et al.*, 1995; Linster, C. and Hasselmo, M. E., 1999; Cleland, T. A. *et al.*, 2002; Cleland, T. A. and Narla, V. A., 2003). However, to escape this limitation and model more realistic, high-dimensional odor spaces (Hudson, R., 1999; Korsching, S. I., 2001; Alkasab, T. K. *et al.*, 2002), subsequent models have relied upon networks constructed so that the strength of PG-mediated inhibition is effectively proportional to receptive field similarity rather than the physical proximity of glomeruli. Networks based on this assumption have been shown to best reproduce calcium imaging data obtained from honeybee OSNs and projection neurons (analogous to mitral cells), while networks based on decremental lateral inhibition performed comparably to networks based on random inhibitory projections (Linster, C. *et al.*, 2005). Another such model has successfully reproduced mixture processing properties

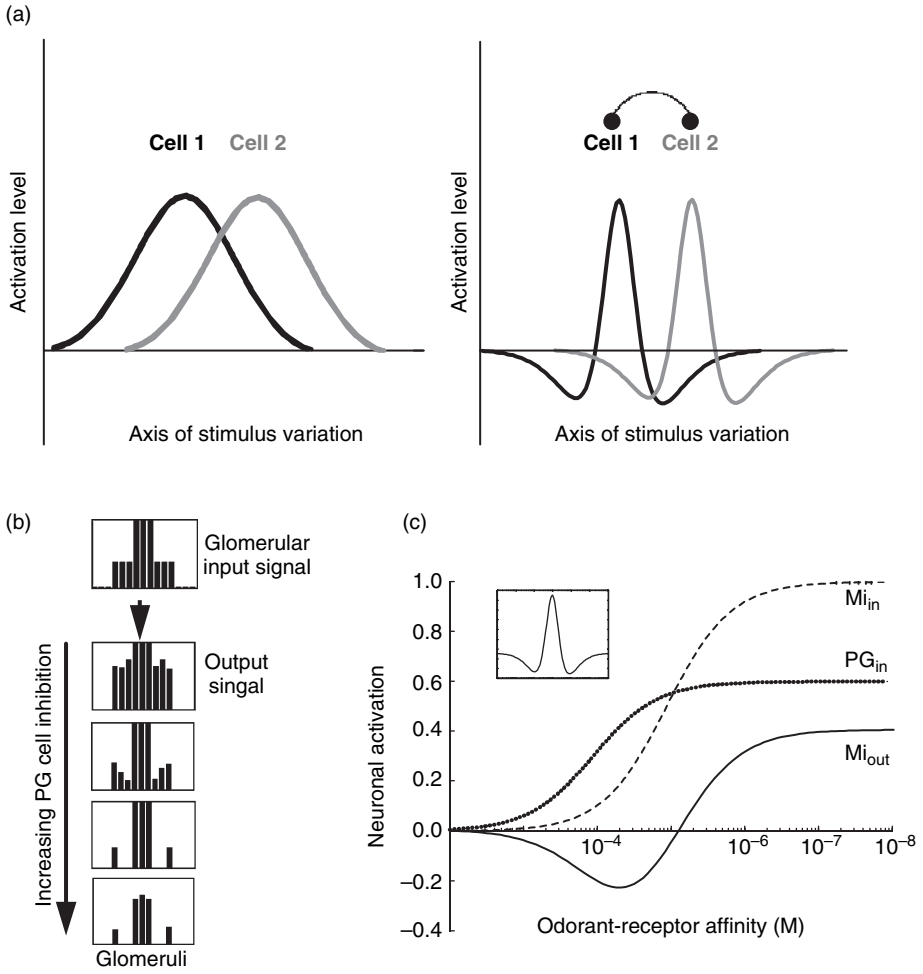

Figure 2 Contrast enhancement. (a) Contrast enhancement is a phenomenon observed in most sensory systems by which marginally activated neurons are excluded from a stimulus-specific ensemble by inhibition, hence sharpening the sensory representation and differentiating it from other, similar representations. In the absence of contrast enhancement, the tuning curves of cells 1 and 2 substantially overlap (left panel). If contrast enhancement is enabled, e.g., by the addition of lateral inhibition such that each cell inhibits the other, the two cells both become more narrowly tuned, and their receptive fields may no longer overlap (right panel). (b) Computational models of the olfactory bulb have proposed that inhibitory periglomerular (PG) cells could mediate contrast enhancement in the glomerular layer of the olfactory bulb. In these models, PG cells receive direct sensory input within a given glomerulus and inhibit mitral cells in neighboring glomeruli via axonal projections (Figure 1(a)). If an odor stimulus activates a range of neighboring glomeruli (Glomerular input signal), increasing the level of PG cell-mediated inhibition would lead to concomitantly sharpened representations among mitral cells, the output layer of the olfactory bulb. With strong contrast enhancement, only the most strongly activated mitral cells are activated, while weakly activated mitral cells are inhibited (Linster, C. and Gervais, R., 1996; Linster, C. and Hasselmo, M. E., 1997). (c) Nontopographical contrast enhancement based on local glomerular computations. In this model, contrast enhancement is generated within the stimulus–response profile of each individual glomerulus, resulting in sharpening of the odor-evoked representation across the glomerular layer. Within each glomerulus, mitral (Mi_{in}) and periglomerular (PG_{in}) cells have the same tuning curves but different response properties, and both receive parallel input from olfactory sensory neurons (OSNs). Mitral cell output (Mi_{out}) is additionally shaped by PG-mediated dendrodendritic inhibition, such that only the most strongly excited mitral cells are activated, while more weakly excited mitral cells exhibit net inhibitory responses (Cleland, T. A. and Sethupathy, P., 2006). The shape of the Mi_{out} curve generates the familiar on-center/inhibitory-surround function of contrast enhancement (inset).
(b) Reproduced from Linster, C. and Gervais, R. 1996. Investigation of the role of interneurons and their modulation by centrifugal fibers in a neural model of the olfactory bulb. J. Comput. Neurosci. 3(3), 225–246, with permission from springer.

measured in rats (Wiltrout, C. *et al.*, 2003; Linster, C. and Cleland, T. A., 2004). Finally, nontopographical models take an entirely different approach to olfactory contrast enhancement, relying solely on intraglomerular computations and broad feedback inhibition to effect contrast enhancement via a 'winner-take-most' algorithm (Figure 2(c)) (Cleland, T. A. and Sethupathy, P., 2006; Cleland, T. A. *et al.*, 2007). This approach does not rely on odorant feature similarities being embedded into bulbar odor maps *a priori*, as it is independent of the physical location of glomeruli and of specific lateral inhibitory projections. Rather, the maps of stimulus feature similarity that underlie contrast enhancement are naturally inherited from the cross-activation patterns of OSNs by odorants.

4.39.3 Mechanisms Underlying Oscillations and Spike Synchronization

While recent models have begun to favor glomerular layer mechanisms for contrast enhancement, granule cell activity also clearly shapes mitral cell response patterns, and hence the presumptive odor representations that emerge from the olfactory bulb. Specifically, several computational models of the olfactory bulb have suggested that the temporal pattern of spiking among mitral cells may play a role in odor representation (Schild, D., 1988; Meredith, M., 1992; White, J. *et al.*, 1992; 1998; White, J. and Kauer, J. S., 2001). While it is clear that temporal response patterns in mitral cells do change as a function of odor identity (Figure 3(a)), there is as yet no broadly accepted theory of how these response patterns may contribute to the representation of odorant stimuli.

One of the most widely studied features of olfactory bulb processing has been the dynamic oscillatory activity patterns observed in the bulb in response to odor stimulation. Models of these phenomena have traditionally studied these responses as coupled oscillators, attributing the dynamics to reciprocal feedback interactions between mitral cell secondary dendrites and granule cells (Figure 3(b)) (Freeman, W. J., 1979; 1987; Li, Z. and Hopfield, J. J., 1989; Grobler, T. and Erdi, P., 1991; Erdi, P. *et al.*, 1993; Freeman, W. J., 1994; Ermentrout, G. B. and Kleinfeld, D., 2001). Some researchers have proposed that odor quality may be represented in dynamic attractors formed in the olfactory bulb (Freeman, W. J., 1979; 1987; Li, Z. and Hopfield, J. J., 1989; Erdi, P. *et al.*, 1993; Freeman, W. J., 1994; Fukai, T., 1996; Hoshino, O.

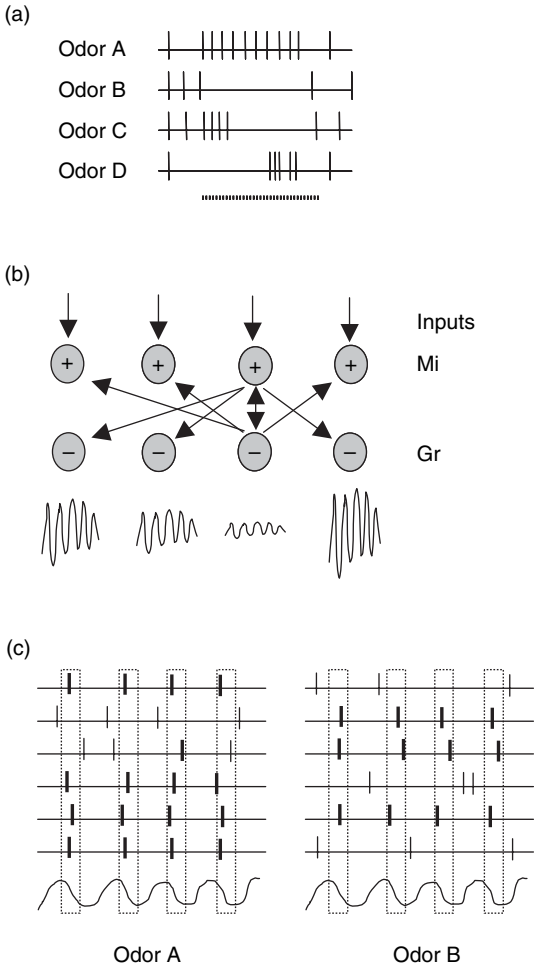

Figure 3 Oscillations and synchrony. (a) Any given mitral cell in the olfactory bulb may respond to different odorant stimuli (A, B, C, and D) with a variety of temporally complex spike patterns including interwoven excitatory and inhibitory phases. It has been proposed that these temporal patterns may contribute to odor representations in the vertebrate olfactory bulb and the analogous insect antennal lobe (Laurent, G., 1999; Laurent, G. *et al.*, 2001). Horizontal bar depicts the time of odorant presentation. (b) The reciprocal synaptic interactions between mitral (Mi) and granule (Gr) cells have often been simulated as a system of coupled oscillators driven by external inputs. In such models, variance of stimulus amplitudes across these inputs generates a map of field oscillations with variable amplitudes and fixed phase lags across the olfactory bulb. For clarity, the output from only a single column is depicted. (c) Field oscillatory dynamics are believed to reflect and/or influence spike timing in mitral cells, potentially resulting in odor-specific populations of mitral cells based on spike synchrony rather than overall activity. While the overall activity patterns evoked by odors A and B are very similar, selection for spikes relatively synchronized with one another and with the oscillatory field potential reveals two clearly odor-specific subpopulations (bold spikes within dotted boxes).

et al., 1998; Breakspear, M., 2001). However, it is increasingly clear that the dynamics of the olfactory bulb are tightly coupled with those of the piriform cortex, and that both depend on mutual feedback between the two structures (Gray, C. M. and Skinner, J. E., 1988; Neville, K. R. and Haberly, L. B., 2003; Martin, C. *et al.*, 2004); combined bulb–cortex models have suggested possible roles for these interactions (Fukai, T., 1996; Li, Z. and Hertz, J., 2000). Other aspects of piriform cortical dynamics have also been modeled (Wilson, M. and Bower, J. M., 1992; Liljenstrom, H. and Hasselmo, M. E., 1995; Claverol, E. T. *et al.*, 2002; Xu, D. and Principe, J. C., 2004), albeit with less focus on their functional role (but see Granger, R. and Lynch, G., 1991).

Recently, models of these field oscillatory properties have begun to emphasize their relationship to the regulation of spike timing in mitral cells (Davison, A. P. *et al.*, 2003; Margrie, T. W. and Schaefer, A. T., 2003), suggesting that patterns of spike synchronization among mitral cells responding to the same sensory input are important contributors to the odorant representation at this level (Figure 3(c)). This phenomenon has been extensively modeled in the insect antennal lobe, a functionally comparable analog of the olfactory bulb. In these models, the regulation of spike synchronization among secondary neurons can mediate stimulus salience and contrast enhancement between similar odorants (Linster, C. and Cleland, T. A., 2001; Cleland, T. A. and Linster, C., 2002) and can dramatically influence the readout of information at the next level of processing (Sivan, E. and Kopell, N., 2004).

4.39.4 Odor Segmentation and Associative Memory Function

Odor segmentation is the general term for the problem of how the olfactory system is able to segregate and identify different odorants that are encountered simultaneously. As most odors comprise multiple separate odorant molecules, it is far from clear how the olfactory system can parse the multitude of odorant stimuli present at any given time and attribute each to appropriately separate sources. One approach has been to hypothesize that odors emitted from different sources can be segregated by OB circuitry based on their differential fluctuations in time (Fort, J. C. and Rospars, J. P., 1992; Hendin, O. *et al.*, 1998; Hopfield, J. J., 1999). Odor segmentation could thereafter be performed in the OB using source-separation algorithms dependent upon associative memory function. Generally, such models hypothesize that associative memories for patterns of olfactory bulb activity evoked by known odorants become embedded in bulbar circuitry and can then be used to recognize these patterns when they recur, even in degraded form. Specifically, a model by Hendin O. *et al.* (1998) illustrates how, if the glomerular layer feeds into a mitral–granule cell layer for which appropriate dynamics for an associative memory function have been implemented, each odor can be separately represented in successive inhalation cycles when multiple (known) odors are presented at the same time.

Olfactory associative memory functions have been more commonly attributed to the piriform cortex, one of the targets of mitral cell axons projecting from the olfactory bulb (Figure 4). Specifically, the piriform cortex has been proposed to mediate the associative memory functions necessary for odor-context learning (Haberly, L. B. and Bower, J. M., 1989; Hasselmo, M. E. *et al.*, 1990; Haberly, L. B., 2001) and hierarchical clustering (Ambros-Ingerson, J. *et al.*, 1990). Indeed, the extensive intrinsic feedback network in this cortex and its integration with afferent inputs closely resembles the structure of traditional theoretical associative memory networks as first described by Marr D. (1971). Several laboratories have constructed models of piriform cortex implementing these associative memory functions (Haberly, L. B. and Bower, J. M., 1989; Ambros-Ingerson, J. *et al.*, 1990; Hasselmo *et al.*, 1990; Barkai, E. and Hasselmo, M. E., 1994; Hasselmo, M. E. *et al.*, 1997) as well as exploring the role of cholinergic modulation in their regulation (Hasselmo, M. E. *et al.*, 1990; 1997; Patil, M. M. and Hasselmo, M. E., 1999; Linster, C. and Hasselmo, M. E., 2001; Linster, C. *et al.*, 2003).

4.39.5 Detailed Biophysical Models of OB Neurons

Most models of the olfactory system to date have emphasized network-level interactions and the properties of olfactory bulb and piriform cortical circuitry, using simplified cell models conducive to these larger-scale simulations. However, several relatively detailed biophysical models of olfactory neurons – particularly OSNs and mitral cells – have also been constructed. Several detailed OSN models have illustrated how ligand–receptor binding and nonlinear transduction processes can underlie several experimentally observed response properties of these cells (Malaka, R. *et al.*, 1995; Rospars, J. P. *et al.*, 1996;

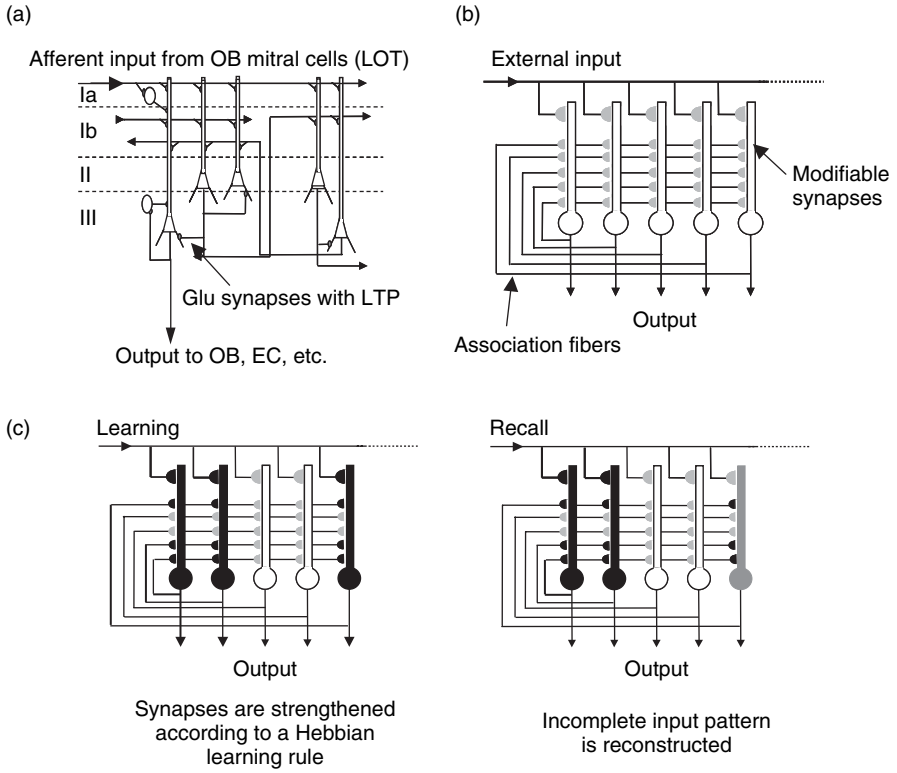

Figure 4 Associative memory function in olfactory cortex. (a) Piriform cortex (PC) exhibits the fundamental anatomical features necessary for the implementation of associative memory: extrinsic input from the olfactory bulb (OB) to each pyramidal cell via the lateral olfactory tract (LOT) and extensive intrinsic excitatory connections among pyramidal cells. These intrinsic associative connections are subject to synaptic plasticity, also crucial for associative memory function, and exhibit long-term potentiation (LTP). Additionally, several classes of local inhibitory interneurons have been described in the piriform cortex. Piriform pyramidal neurons project back to the OB, as well as to other structures such as the entorhinal cortex (EC). (b) Schematic representation of an associative memory network. The critical features are (1) external inputs to associative neurons, (2) all-to-all excitatory connections among these neurons, and (3) a learning rule that modifies the strengths of these connections when external inputs are being learned by the network. (c) Learning and recall in an associative memory network. Learning (left panel): An olfactory stimulus activates a subset of pyramidal cells (three dark cells) via distributed afferent projections from the OB to the PC. During learning, excitatory synaptic connections between pyramidal cells activated by that odorant are strengthened via a Hebbian plasticity rule (dark semicircles denote strengthened synapses). Recall (right panel): After learning of a pattern, if a noisy or degraded example of that pattern is presented to the system, the stored odorant pattern can be reconstructed due to the previously strengthened connections. Dark semicircles denote strengthened synapses. Owing to the previously strengthened synapses, activation of the two dark cells secondarily activates a third cell (gray), reconstructing the previously learned pattern.

Vermeulen, A. *et al.*, 1996; 1997; Kaissling, K. E., 1998; Lansky, P. and Rospars, J. P., 1998; Vermeulen, A. and Rospars, J. P., 1998; Cleland, T. A. and Linster, C., 1999; Rospars, J. P. *et al.*, 2000; Kaissling, K. E., 2001; Kaissling, K. E. and Rospars, J. P., 2004). Compartmental models of mitral cells have been used to elucidate intrinsic cellular phenomena, such as the localization of spike initiation in mitral cells (Shen, G. Y. *et al.*, 1999; Chen, W. R. *et al.*, 2002), or long-term potentiation at the OSN-mitral synapse (Ennis, M. *et al.*, 1998). Other compartmental models have focused on bridging the gap between cellular and systems properties in both vertebrate and insect systems (Bhalla, U. S. and Bower, J. M., 1993; Davison, A. P. *et al.*, 2000; Bazhenov, M. *et al.*, 2001; Davison, A. P. *et al.*, 2003; Cleland, T. A. and Sethupathy, P., 2006; Rubin, D. B. and Cleland, T. A., 2006; Cleland, T. A. *et al.*, 2007).

4.39.6 Conclusions

Computational models have an established and growing role within systems neuroscience. As our

understanding of neural processing and interactions becomes more sophisticated, computer models of these systems are increasingly necessary in order to understand and interpret experimental results. Models serve as proofs of concept, tests of sufficiency, and as quantitative embodiments of working hypotheses. In the olfactory system in particular, computational modeling will no doubt be essential to understanding the integration of the many factors influencing the construction and transformation of odor representations.

References

Adrian, E. D. 1953. Sensory messages and sensation; the response of the olfactory organ to different smells. Acta Physiol. Scand. 29(1), 5–14.

Alkasab, T. K., White, J., and Kauer, J. S. 2002. A computational system for simulating and analyzing arrays of biological and artificial chemical sensors. Chem. Senses 27(3), 261–275.

Ambros-Ingerson, J., Granger, R., and Lynch, G. 1990. Simulation of paleocortex performs hierarchical clustering. Science 247(4948), 1344–1348.

Anton, P. S., Lynch, G., and Granger, R. 1991. Computation of frequency-to-spatial transform by olfactory bulb glomeruli. Biol. Cybern. 65(5), 407–414.

Barkai, E. and Hasselmo, M. E. 1994. Modulation of the input/output function of rat piriform cortex pyramidal cells. J. Neurophysiol. 72(2), 644–658.

Bazhenov, M., Stopfer, M., Rabinovich, M., Abarbanel, H. D., Sejnowski, T. J., and Laurent, G. 2001. Model of cellular and network mechanisms for odor-evoked temporal patterning in the locust antennal lobe. Neuron 30(2), 569–581.

Bhalla, U. S. and Bower, J. M. 1993. Exploring parameter space in detailed single neuron models: simulations of the mitral and granule cells of the olfactory bulb. J. Neurophysiol. 69(6), 1948–1965.

Bozza, T., Feinstein, P., Zheng, C., and Mombaerts, P. 2002. Odorant receptor expression defines functional units in the mouse olfactory system. J. Neurosci. 22(8), 3033–3043.

Breakspear, M. 2001. Perception of odors by a nonlinear model of the olfactory bulb. Int. J. Neural Syst. 11(2), 101–124.

Castillo, P. E., Carleton, A., Vincent, J. D., and Lledo, P. M. 1999. Multiple and opposing roles of cholinergic transmission in the main olfactory bulb. J. Neurosci. 19(21), 9180–9191.

Chen, W. R., Shen, G. Y., Shepherd, G. M., Hines, M. L., and Midtgaard, J. 2002. Multiple modes of action potential initiation and propagation in mitral cell primary dendrite. J. Neurophysiol. 88(5), 2755–2764.

Claverol, E. T., Brown, A. D., and Chad, J. E. 2002. A large-scale simulation of the piriform cortex by a cell automaton-based network model. IEEE Trans. Biomed. Eng. 49(9), 921–935.

Cleland, T. A. and Linster, C. 1999. Concentration tuning mediated by spare receptor capacity in olfactory sensory neurons: a theoretical study. Neural Comput. 11(7), 1673–1690.

Cleland, T. A. and Linster, C. 2002. How synchronization properties among second-order sensory neurons can mediate stimulus salience. Behav. Neurosci. 116(2), 212–221.

Cleland, T. A. and Linster, C. 2003. Central Olfactory Processing. In: Handbook of Olfaction and Gustation, 2nd Edn, (*ed*. R. L. Doty), pp. 165–180. Dekker.

Cleland, T. A. and Narla, V. A. 2003. Intensity modulation of olfactory acuity. Behav. Neurosci. 117(6), 1434–1440.

Cleland, T. A. and Sethupathy, P. 2006. Non-topographical contrast enhancement in the olfactory bulb BMC Neurosci. 7, 7.

Cleland, T. A, Johnson, B. A., Leon, M., and Linster, C. 2007. Relational representation in the olfactory system. Proc. Natl. Acad. Sci. U.S.A. 104(6), 1953–1958.

Cleland, T. A., Morse, A., Yue, E. L., and Linster, C. 2002. Behavioral models of odor similarity. Behav. Neurosci. 116(2), 222–231.

Davison, A. P., Feng, J., and Brown, D. 2000. A reduced compartmental model of the mitral cell for use in network models of the olfactory bulb. Brain Res. Bull. 51(5), 393–399.

Davison, A. P., Feng, J., and Brown, D. 2003. Dendrodendritic inhibition and simulated odor responses in a detailed olfactory bulb network model. J. Neurophysiol. 90(3), 1921–1935.

Debarbieux, F., Audinat, E., and Charpak, S. 2003. Action potential propagation in dendrites of rat mitral cells *in vivo*. J. Neurosci. 23(13), 5553–5560.

Djurisic, M., Antic, S., Chen, W. R., and Zecevic, D. 2004. Voltage imaging from dendrites of mitral cells: EPSP attenuation and spike trigger zones. J. Neurosci. 24(30), 6703–6714.

van Drongelen, W., Holley, A., and Doving, K. B. 1978. Convergence in the olfactory system: quantitative aspects of odour sensitivity. J. Theor. Biol. 71(1), 39–48.

Duchamp-Viret, P., Duchamp, A., and Vigouroux, M. 1989. Amplifying role of convergence in olfactory system a comparative study of receptor cell and second-order neuron sensitivities. J. Neurophysiol. 61(5), 1085–1094.

Ennis, M., Linster, C., Aroniadou-Anderjaska, V., Ciombor, K., and Shipley, M. T. 1998. Glutamate and synaptic plasticity at mammalian primary olfactory synapses. Ann. N. Y. Acad. Sci. 855, 457–466.

Erdi, P., Grobler, T., Barna, G., and Kaski, K. 1993. Dynamics of the olfactory bulb: bifurcations, learning, and memory. Biol. Cybern. 69(1), 57–66.

Ermentrout, G. B. and Kleinfeld, D. 2001. Traveling electrical waves in cortex: insights from phase dynamics and speculation on a computational role. Neuron 29(1), 33–44.

Fort, J. C. and Rospars, J. P. 1992. Modelling of the qualitative discrimination of odours in the first two layers of olfactory system by Jutten and Herault algorithm. C. R. Acad. Sci. III 315(9), 331–336.

Freeman, W. J. 1979. Nonlinear dynamics of paleocortex manifested in the olfactory EEG. Biol. Cybern. 35(1), 21–37.

Freeman, W. J. 1987. Simulation of chaotic EEG patterns with a dynamic model of the olfactory system. Biol. Cybern. 56(2–3), 139–150.

Freeman, W. J. 1994. Characterization of state transitions in spatially distributed, chaotic, nonlinear, dynamical systems in cerebral cortex. Integr. Physiol. Behav. Sci. 29(3), 294–306.

Friedrich, R. W. and Korsching, S. I. 1997. Combinatorial and chemotopic odorant coding in the zebrafish olfactory bulb visualized by optical imaging. Neuron 18(5), 737–752.

Fukai, T. 1996. Bulbocortical interplay in olfactory information processing via synchronous oscillations. Biol. Cybern. 74(4), 309–317.

Granger, R. and Lynch, G. 1991. Higher olfactory processes: perceptual learning and memory. Curr. Opin. Neurobiol. 1(2), 209–214.

Gray, C. M. and Skinner, J. E. 1988. Centrifugal regulation of neuronal activity in the olfactory bulb of the waking rabbit as

revealed by reversible cryogenic blockade. Exp. Brain Res. 69(2), 378–386.
Grobler, T. and Erdi, P. 1991. Dynamic phenomena in the olfactory bulb. Acta Biochim. Biophys. Hung. 26(1–4), 61–65.
Haberly, L. B. 2001. Parallel-distributed processing in olfactory cortex: new insights from morphological and physiological analysis of neuronal circuitry. Chem. Senses 26(5), 551–576.
Haberly, L. B. and Bower, J. M. 1989. Olfactory cortex: model circuit for study of associative memory? Trends Neurosci. 12(7), 258–264.
Hasselmo, M. E., Linster, C., Patil, M., Ma, D., and Cekic, M. 1997. Noradrenergic suppression of synaptic transmission may influence cortical signal-to-noise ratio. J. Neurophysiol. 77(6), 3326–3339.
Hasselmo, M. E., Wilson, M. A., Anderson, B. P., and Bower, J. M. 1990. Associative memory function in piriform (olfactory) cortex: computational modeling and neuropharmacology. Cold Spring Harb. Symp. Quant. Biol. 55, 599–610.
Hendin, O., Horn, D., and Tsodyks, M. V. 1998. Associative memory and segmentation in an oscillatory neural model of the olfactory bulb. J. Comput. Neurosci. 5(2), 157–169.
Hopfield, J. J. 1999. Odor space and olfactory processing: collective algorithms and neural implementation. Proc. Natl. Acad. Sci. U. S. A. 96(22), 12506–12511.
Hoshino, O., Kashimori, Y., and Kambara, T. 1998. An olfactory recognition model based on spatio-temporal encoding of odor quality in the olfactory bulb. Biol. Cybern. 79(2), 109–120.
Hudson, R. 1999. From molecule to mind: the role of experience in shaping olfactory function. J. Comp. Physiol. [A], 185(4), 297–304.
Isaacson, J. S. and Strowbridge, B. W. 1998. Olfactory reciprocal synapses: dendritic signaling in the CNS. Neuron 20(4), 749–761.
Kaissling, K. E. 1998. A quantitative model of odor deactivation based on the redox shift of the pheromone-binding protein in moth antennae. Ann. N.Y. Acad. Sci. 855, 320–322.
Kaissling, K. E. 2001. Olfactory perireceptor and receptor events in moths: a kinetic model. Chem. Senses 26(2), 125–150.
Kaissling, K. E. and Rospars, J. P. 2004. Dose–response relationships in an olfactory flux detector model revisited. Chem. Senses 29(6), 529–531.
Kauer, J. S. 1991. Contributions of topography and parallel processing to odor coding in the vertebrate olfactory pathway. Trends Neurosci. 14(2), 79–85.
Korsching, S. I. 2001. Odor maps in the brain: spatial aspects of odor representation in sensory surface and olfactory bulb. Cell. Mol. Life Sci. 58(4), 520–530.
Lansky, P. and Rospars, J. P. 1998. Odorant concentration and receptor potential in olfactory sensory neurons. Biosystems 48(1–3), 131–138.
Laurent, G. 1999. A systems perspective on early olfactory coding. Science 286(5440), 723–728.
Laurent, G., Stopfer, M., Friedrich, R. W., Rabinovich, M. I., Volkovskii, A., and Abarbanel, H. D. 2001. Odor encoding as an active, dynamical process: experiments, computation, and theory. Annu. Rev. Neurosci. 24, 263–297.
Li, Z. and Hertz, J. 2000. Odour recognition and segmentation by a model olfactory bulb and cortex. Network 11(1), 83–102.
Li, Z. and Hopfield, J. J. 1989. Modeling the olfactory bulb and its neural oscillatory processings. Biol. Cybern. 61(5), 379–392.
Liljenstrom, H. and Hasselmo, M. E. 1995. Cholinergic modulation of cortical oscillatory dynamics. J. Neurophysiol. 74(1), 288–297.
Linster, C. and Cleland, T. A. 2001. How spike synchronization among olfactory neurons can contribute to sensory discrimination. J. Comput. Neurosci. 10(2), 187–193.
Linster, C. and Cleland, T. A. 2002. Cholinergic modulation of sensory representations in the olfactory bulb. Neural Netw. 15(4–6), 709–717.
Linster, C. and Cleland, T. A. 2004. Configurational and elemental odor mixture perception can arise from local inhibition. J. Comput. Neurosci. 16(1), 39–47.
Linster, C. and Gervais, R. 1996. Investigation of the role of interneurons and their modulation by centrifugal fibers in a neural model of the olfactory bulb. J. Comput. Neurosci. 3(3), 225–246.
Linster, C. and Hasselmo, M. 1997. Modulation of inhibition in a model of olfactory bulb reduces overlap in the neural representation of olfactory stimuli. Behav. Brain Res. 84(1–2), 117–127.
Linster, C. and Hasselmo, M. E. 1999. Behavioral responses to aliphatic aldehydes can be predicted from known electrophysiological responses of mitral cells in the olfactory bulb. Physiol. Behav. 66(3), 497–502.
Linster, C. and Hasselmo, M. E. 2001. Neuromodulation and the functional dynamics of piriform cortex. Chem Senses 26(5), 585–594.
Linster, C. and Smith, B. H. 1997. A computational model of the response of honey bee antennal lobe circuitry to odor mixtures: overshadowing, blocking and unblocking can arise from lateral inhibition. Behav. Brain Res. 87(1), 1–14.
Linster, C., Johnson, B. A., Morse, A., Yue, E., and Leon, M. 2002. Spontaneous versus reinforced olfactory discriminations. J. Neurosci. 22(16), 6842–6845.
Linster, C., Johnson, B. A., Yue, E., Morse, A., Xu, Z., Hingco, E. E., Choi, Y., Choi, M., Messiha, A., and Leon, M. 2001. Perceptual correlates of neural representations evoked by odorant enantiomers. J. Neurosci. 21(24), 9837–9843.
Linster, C., Maloney, M., Patil, M., and Hasselmo, M. E. 2003. Enhanced cholinergic suppression of previously strengthened synapses enables the formation of self-organized representations in olfactory cortex. Neurobiol. Learn. Mem. 80(3), 302–314.
Linster, C., Sachse, S., and Galizia, G. 2005. Computational modeling suggests that response properties rather than spatial position determine connectivity between olfactory glomeruli. J. Neurophysiol. 93(6), 3410–3417.
Lowe, G. and Gold, G. H. 1995. Olfactory transduction is intrinsically noisy. Proc. Natl. Acad. Sci. U.S.A. 92(17), 7864–7868.
Luo, M. and Katz, L. C. 2001. Response correlation maps of neurons in the mammalian olfactory bulb. Neuron 32(6), 1165–1179.
Malaka, R., Ragg, T., and Hammer, M. 1995. Kinetic models of odor transduction implemented as artificial neural networks. Simulations of complex response properties of honeybee olfactory neurons. Biol. Cybern. 73(3), 195–207.
Mandairon, N., Ferretti, C. J., Stack, C. M., Rubin, D. B., Cleland, T. A., and Linster, C. 2006. Cholinergic modulation in the olfactory bulb influences spontaneous olfactory discrimination in adult rats. Eur. J. Neurosci. 24(11), 3234–3244.
Margrie, T. W. and Schaefer, A. T. 2003. Theta oscillation coupled spike latencies yield computational vigour in a mammalian sensory system. J. Physiol. 546(Pt 2), 363–374.
Marr, D. 1971. Simple memory: a theory for archicortex. Philos. Trans. R. Soc. Lond. B Biol. Sci. 262(841), 23–81.
Martin, C., Gervais, R., Hugues, E., Messaoudi, B., and Ravel, N. 2004. Learning modulation of odor-induced oscillatory responses in the rat olfactory bulb: a correlate of odor recognition? J. Neurosci. 24(2), 389–397.
Meisami, E. 1989. A proposed relationship between increases in the number of olfactory receptor neurons, convergence

ratio and sensitivity in the developing rat. Brain Res. Dev. Brain Res. 46(1), 9–19.
Meister, M. and Bonhoeffer, T. 2001. Tuning and topography in an odor map on the rat olfactory bulb. J. Neurosci. 21(4), 1351–1360.
Meredith, M. 1992. Neural circuit computation: complex patterns in the olfactory bulb. Brain Res. Bull. 29(1), 111–117.
Mombaerts, P. 1996. Targeting olfaction. Curr. Opin. Neurobiol. 6(4), 481–486.
Moulton, D. G. 1967. Spatio-temporal patterning of response in the olfactory system. In: Olfaction and Taste II (*ed*. T. Hayashi), pp. 109–116. Pergamon.
Neville, K. R. and Haberly, L. B. 2003. Beta and gamma oscillations in the olfactory system of the urethane-anesthetized rat. J. Neurophysiol. 90(6), 3921–3930.
Patil, M. M. and Hasselmo, M. E. 1999. Modulation of inhibitory synaptic potentials in the piriform cortex. J. Neurophysiol. 81(5), 2103–2118.
Rall, W. and Shepherd, G. M. 1968. Theoretical reconstruction of field potentials and dendrodendritic synaptic interactions in olfactory bulb. J. Neurophysiol. 31(6), 884–915.
Rospars, J. P., Lansky, P., Duchamp-Viret, P., and Duchamp, A. 2000. Spiking frequency versus odorant concentration in olfactory receptor neurons. Biosystems 58(1–3), 133–141.
Rospars, J. P., Lansky, P., Tuckwell, H. C., and Vermeulen, A. 1996. Coding of odor intensity in a steady-state deterministic model of an olfactory receptor neuron. J. Comput. Neurosci. 3(1), 51–72.
Rubin, D. B. and Cleland, T. A. 2006. Dynamical mechanisms of odor processing in olfactory bulb mitral cells. J. Neurophysiol. 96(2), 555–568.
Rubin, B. D. and Katz, L. C. 1999. Optical imaging of odorant representations in the mammalian olfactory bulb. Neuron 23(3), 499–511.
Schild, D. 1988. Principles of odor coding and a neural network for odor discrimination. Biophys. J. 54(6), 1001–1011.
Schoenfeld, T. A. and Knott, T. K. 2004. Evidence for the disproportionate mapping of olfactory airspace onto the main olfactory bulb of the hamster. J. Comp. Neurol. 476(2), 186–201.
Shen, G. Y., Chen, W. R., Midtgaard, J., Shepherd, G. M., and Hines, M. L. 1999. Computational analysis of action potential initiation in mitral cell soma and dendrites based on dual patch recordings. J. Neurophysiol. 82(6), 3006–3020.
Shepard, R. N. 1987. Toward a universal law of generalization for psychological science. Science 237(4820), 1317–1323.
Shepard, R. N. and Chang, J. J. 1963. Stimulus generalization in the learning of classifications. J. Exp. Psychol. 65, 94–102.
Shepherd, G. M. and Brayton, R. K. 1979. Computer simulation of a dendrodendritic synaptic circuit for self- and lateral-inhibition in the olfactory bulb. Brain Res. 175(2), 377–382.
Sivan, E. and Kopell, N. 2004. Mechanism and circuitry for clustering and fine discrimination of odors in insects. Proc. Natl. Acad. Sci. U. S. A. 101(51), 17861–17866.
Stewart, W. B., Kauer, J. S., and Shepherd, G. M. 1979. Functional organization of rat olfactory bulb analysed by the 2-deoxyglucose method. J. Comp. Neurol. 185(4), 715–734.
Urban, N. N. 2002. Lateral inhibition in the olfactory bulb and in olfaction. Physiol. Behav. 77(4–5), 607–612.
Vermeulen, A. and Rospars, J. P. 1998. Dendritic integration in olfactory sensory neurons: a steady-state analysis of how the neuron structure and neuron environment influence the coding of odor intensity. J. Comput. Neurosci. 5(3), 243–266.
Vermeulen, A., Lansky, P., Tuckwell, H., and Rospars, J. P. 1997. Coding of odour intensity in a sensory neuron. Biosystems 40(1–2), 203–210.
Vermeulen, A., Rospars, J. P., Lansky, P., and Tuckwell, H. C. 1996. Coding of stimulus intensity in an olfactory receptor neuron: role of neuron spatial extent and passive dendritic backpropagation of action potentials. Bull. Math. Biol. 58(3), 493–512.
Wachowiak, M., Cohen, L. B., and Zochowski, M. R. 2002. Distributed and concentration-invariant spatial representations of odorants by receptor neuron input to the turtle olfactory bulb. J. Neurophysiol. 87(2), 1035–1045.
White, J. and Kauer, J. S. 2001. Exploring olfactory population coding using an artificial olfactory system. Prog. Brain Res. 130, 191–203.
White, J., Dickinson, T. A., Walt, D. R., and Kauer, J. S. 1998. An olfactory neuronal network for vapor recognition in an artificial nose. Biol. Cybern. 78(4), 245–251.
White, J., Hamilton, K. A., Neff, S. R., and Kauer, J. S. 1992. Emergent properties of odor information coding in a representational model of the salamander olfactory bulb. J. Neurosci. 12(5), 1772–1780.
Wilson, M. and Bower, J. M. 1992. Cortical oscillations and temporal interactions in a computer simulation of piriform cortex. J. Neurophysiol. 67(4), 981–995.
Wiltrout, C., Dogra, S., and Linster, C. 2003. Configurational and nonconfigurational interactions between odorants in binary mixtures. Behav. Neurosci. 117(2), 236–245.
Xu, D. and Principe, J. C. 2004. Dynamical analysis of neural oscillators in an olfactory cortex model. IEEE Trans. Neural Netw. 15(5), 1053–1062.
Yokoi, M., Mori, K., and Nakanishi, S. 1995. Refinement of odor molecule tuning by dendrodendritic synaptic inhibition in the olfactory bulb. Proc. Natl. Acad. Sci. U. S. A. 92(8), 3371–3375.

4.40 Understanding Olfactory Coding via an Analysis of Odorant-Evoked Glomerular Response Maps

B A Johnson and M Leon, University of California, Irvine, CA, USA

© 2008 Elsevier Inc. All rights reserved.

4.40.1	Introduction	719
4.40.2	Combinatorial Coding	719
4.40.3	Molecular Feature Detection	720
4.40.4	Chemotopic Progressions	720
4.40.5	Predictive Value of Activity Maps	721
4.40.6	Summary	722
References		722

Glossary

glomeruli Ball-like regions in which homologous olfactory receptor neurons synapse with second-order neurons in the olfactory bulb.
neuropil A dense network of neural and glial processes.
combinatorial coding The sensory processing of odorant chemicals by the binding of their multiple chemical features to multiple odorant receptors.
2-deoxyglucose A glucose analog that is incompletely metabolized in cells and that can be used for mapping neural activity.
hydrophobic A property that describes the degree of resistance of a molecule to mix with water.
tuning Describes the relationship between systematic changes in the physical properties of sensory stimuli and the level of neural response in a sensory system.
aliphatic Possessing a nonaromatic hydrocarbon structure.
enantiomers Molecules that are non-superimposable mirror images of one another.

4.40.1 Introduction

Buck L. B. and Axel R. (1991) reported the discovery of rat odorant receptor genes and began a series of studies that clarified the foundation of odor perception. Most olfactory sensory neurons in the nose appear to express only one of these genes, and while homologous sensory neurons expressing the same odorant receptor gene are distributed in fairly broad zones stretching from anterior to posterior within the main olfactory epithelium (Ressler, K. J. *et al.*, 1993), they converge in their projections to the brain and connect to a small number of glomeruli in the main olfactory bulb (Vassar, R. *et al.*, 1994). Glomeruli are roughly spherical masses of neuropil that contain synapses between sensory neuron axons and dendrites of projection neurons and interneurons. The typical projection from homologous sensory neurons involves one glomerulus or small grouping of glomeruli on the lateral aspect and a similar projection on the medial aspect of the bulb (Mombaerts, P. *et al.*, 1996). All sensory neuron synapses in a glomerulus appear to be from cells expressing the same receptor (Treloar, H. B. *et al.*, 2002).

This orderly projection pattern, which is consistent across different animals, suggests that one can get a read-out of odorant receptor activation from the pattern of odorant-evoked activity in the glomerular layer. This prediction now has been tested using a variety of activity-mapping methods. In our own work, we use the uptake of radiolabeled 2-deoxyglucose (2DG) as a metabolic marker, as this is the only method currently able to give a quantitative measure of relative activity throughout the entire structure at a spatial resolution sufficient to detect activity in a single glomerulus.

4.40.2 Combinatorial Coding

Even pure, simple odorant molecules tend to activate multiple locations in the olfactory bulb, and each area

of activation tends to encompass many glomeruli (Johnson, B. A. *et al.*, 1998; 1999). These findings suggest that odor perception probably arises from a combination of activated odorant receptors. Similar conclusions have come from the study of sensory neurons expressing distinct receptor genes (Malnic, B. *et al.*, 1999), from the study of glomerular responses using other methods (Uchida, N. *et al.*, 2000; Wachowiak, M. and Cohen, L. B., 2001), and from the study of action potentials in mitral cells (Imamura, K. *et al.*, 1992). Indeed, there are far more unique odor perceptions than there are odorant receptors, a situation that logically necessitates a combinatorial code.

4.40.3 Molecular Feature Detection

Most receptors appear not to interact with the entirety of their ligand molecules. Rather, parts of the ligand molecule can be modified with minimal impact on receptor binding and activation, while other parts of the ligand molecule are more critical. Indeed, one can think of receptors as detectors of these critical molecular features. We have designed a large number of experiments using sets of odorants differing systematically in chemical structure to explore the detection of molecular features by odorant receptors. In one experiment, each of two ethyl esters stimulated 2DG uptake in a part of the bulb that was not activated by either of two isoamyl esters (Johnson, B. A. *et al.*, 1998). Conversely, both isoamyl esters activated a location not stimulated by either ethyl ester. The activity patterns were consistent with the recognition of the ethyl and isoamyl groups as distinct features by different glomerular modules in the bulb. All four esters stimulated a distinct, overlapping module, consistent with the overall similarity in their core structure.

We tested a set of five odorants sharing a straight-chained hydrocarbon structure but differing in oxygen-containing functional groups to determine whether functional groups would be recognized as distinct molecular features (Johnson, B. A. and Leon, M., 2000a). While all of these odorants stimulated a cluster of glomeruli in the posterior bulb, consistent with their shared hydrocarbon structure, they activated distinct anterior modules, consistent with the recognition of functional groups as distinct features. When we used carboxylic acid odorants that differed greatly in hydrocarbon structure, anterior clusters of activated glomeruli overlapped, consistent with the shared acid functional group, but the posterior patterns differed greatly, consistent with the recognition of different hydrocarbon structures as distinct features (Johnson, B. A. and Leon, M., 2000b). As we increased our sample of the odorant world to include more and more complex molecules, the data showed that the recognition of functional groups as molecular features is not entirely independent of hydrocarbon structure, but rather, that the two types of features interact to determine which glomeruli are activated (Johnson, B. A. *et al.*, 2005a; 2005b).

4.40.4 Chemotopic Progressions

Chemotopy refers to any systematic spatial representation of odorant chemistry. We have been particularly interested in determining whether the olfactory system uses this kind of spatial organization in odor coding. Indeed, glomeruli of related specificity are arrayed systematically within response modules. Uptake of 2DG in a medial, acid-sensitive glomerular module shifted ventrally with increasing carbon number in a series of straight-chained carboxylic acids (Johnson, B. A. *et al.*, 1999). In the corresponding lateral module, uptake shifted both rostrally and ventrally. Separate responses in the posterior, lateral, and the medial bulb also shifted ventrally with increasing carbon number. By using a series of carboxylic acids of the same carbon number, but with different hydrocarbon structures, we found that the ventral shift in the medial acid-responsive module appeared to be due specifically to changes in molecular length (Johnson, B. A. and Leon, M., 2000b). More recently, we found ventral progressions of activity with increasing odorant carbon number using aldehydes, esters, acetates, primary and secondary alcohols, ketones, and alkanes in a number of different glomerular regions, suggesting that such chemotopic progressions represent a fundamental organizational principle in the olfactory system (Johnson, B. A. *et al.*, 2004; Ho *et al.*, 2006) (Figure 1).

Why are the chemotopic progressions with increasing carbon number always in the ventral direction? One possibility is that the chemotopic progressions are related to the spatial distributions of the odorants themselves across the olfactory epithelium. Mozell and co-workers have shown that odorants partition across the epithelium chromatographically (Mozell, M. M., 1964; Hornung, D. E. and Mozell, M. M., 1977; Mozell, M. M. *et al.*, 1987). Molecules that are more water soluble (hydrophilic)

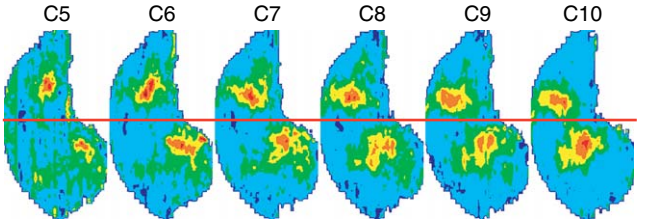

Figure 1 Chemotopic progression of glomerular responses in the ventral and rostral direction with increasing carbon number in straight-chained aldehydes. The maps are in a ventral-centered orientation such that the red line indicates the ventral extremity of the bulb. In each map, rostral is to the left. Warmer colors indicate higher uptake of the metabolic marker, 2-deoxyglucose.

absorb more readily into the olfactory mucosa, which would prevent them from reaching the more peripheral and ventral parts of the rat epithelium (Schoenfeld, T. A. and Knott, T. K., 2004). The less water-soluble (more hydrophobic) odorant molecules would be freer to distribute across the epithelium to reach the more peripheral and ventral zones. Longer odorants within any homologous series of straight-chained chemicals would be more hydrophobic and therefore would be expected to reach the peripheral and ventral epithelium. Because the more peripheral and ventral regions of the epithelium project to more ventral bulbar targets (Schoenfeld, T. A. *et al.*, 1994), this topography could explain the ventral chemotopic progressions within many glomerular modules in the olfactory bulb (Johnson, B. A. *et al.*, 2004).

Local bulbar anatomy suggests that chemotopic progressions in the glomerular layer might have important functional consequences. Reciprocal synapses between mitral cell projection neurons and inhibitory interneurons in the glomerular layer and in the external plexiform layer are expected to create local lateral inhibitory networks. Strong activity in mitral cells associated with a given glomerulus would likely suppress activity in less strongly stimulated mitral cells associated with neighboring glomeruli (Mori, K. and Shepherd, G. M., 1994; Aungst, J. L. *et al.*, 2003). This pattern of activity would be predicted to tune individual mitral cells to a more narrow range of molecules than would excite individual sensory neurons. Indeed, pharmacological blockade of inhibition in the bulb widens the molecular receptive range of mitral cells (Yokoi, M. *et al.*, 1995). Chemotopic progressions ensure that the glomeruli that are nearest neighbors within a module would have the most similar specificity within a homologous series, thereby ensuring that tuning involves the most similar odorant molecules.

4.40.5 Predictive Value of Activity Maps

The value of any scientific observation is perhaps best judged by whether it allows one to predict the outcome of future experiments. Maps of odorant-evoked 2DG uptake across the glomerular layer of the olfactory bulb have been predictive in two senses: they have predicted aspects of the patterns that would be evoked by previously untested odorants, and they have predicted relative similarities in odors perceived by rats. The original associations between functional group-related molecular features and activity in particular anterior glomerular modules (Johnson, B. A. and Leon, M., 2000a) successfully predicted that other simple aliphatic odorant chemicals possessing the same features would also stimulate those modules (Johnson, B. A. *et al.*, 2002; 2004). Aspects of glomerular activity patterns related to hydrocarbon structure also have had predictive value (Johnson, B. A. *et al.*, 2002). The ventral shifts in activity that we observed with increasing carbon number for aliphatic, oxygen-containing odorants (Johnson, B. A. *et al.*, 1999; 2004) led us to predict that even larger straight-chained molecules might stimulate an extremely ventral portion of the bulb that we had not seen activated previously. We tested this prediction using very long alkanes such as pentadecane, which indeed activated the extreme ventral aspect (Ho *et al.*, 2006).

As part of our exploration of the relationships between odorant chemistry and bulbar activity patterns, we mapped responses to three pairs of odorant enantiomers: carvone, limonene, and terpinen-4-ol. The patterns evoked by the two carvones were more distinct than those for the other two enantiomer pairs (Linster, C. *et al.*, 2001). We therefore predicted that the odors of the carvone enantiomers might be more readily distinguished than those of the limonenes and

terpinen-4-ols. Indeed, a cross-habituation assay revealed that rats spontaneously distinguished the carvones, but treated limonene and terpinen-4-ol enantiomers as being similar in odor (Linster, C. *et al.*, 2001). The quantitative differences in activity patterns across homologous series of acids and alkanes also correlated well with behavioral measures of odor discrimination (Cleland, T. A. *et al.*, 2002; Ho *et al.*, 2006).

4.40.6 Summary

As predicted from the projection patterns of olfactory sensory neurons expressing distinct odorant receptor genes, different odorants generate different spatial activity patterns in the olfactory bulb. Mapping activity patterns in response to odorants differing systematically in structure has shown that receptors likely extract information about odorant chemistry, especially regarding functional groups and hydrocarbon structure. The bulb responses are organized in space according to the relative specificity of the input, such that increasingly long straight-chained odorants optimally stimulate increasingly ventral glomeruli. Finally, the overall pattern of glomerular activation is related to the odor perceived by rats.

Acknowledgments

This work has been supported by grants DC6516, DC3545, and DC6391from NIDCD.

References

Aungst, J. L., Heyward, P. M., Puche, A. C., Karnup, S. V., Hayar, A., Szabo, G., and Shipley, M. T. 2003. Centre-surround inhibition among olfactory bulb glomeruli. Nature 426, 623–629.

Buck, L. B. and Axel, R. 1991. A novel multigene family may encode odorant receptors: a molecular basis for odor recognition. Cell 65, 175–187.

Cleland, T. A., Morse, A., Yue, E. L., and Linster, C. 2002. Behavioral models of odor similarity. Behav. Neurosci. 116, 222–231.

Ho, S. L., Johnson, B. A., and Leon, M. 2006. Long hydrocarbon chains serve as unique molecular features recognized by ventral glomeruli of the rat olfactory bulb. J. Comp. Neurol. 498, 16–30.

Hornung, D. E. and Mozell, M. M. 1977. Factors influencing the differential sorption of odorant molecules across the olfactory mucosa. J. Gen. Physiol. 69, 343–361.

Imamura, K., Mataga, N., and Mori, K. 1992. Coding of odor molecules by mitral/tufted cells in rabbit olfactory bulb. I. Aliphatic compounds. J. Neurophysiol. 68, 1986–2002.

Johnson, B. A. and Leon, M. 2000a. Modular representations of odorants in the glomerular layer of the rat olfactory bulb and the effects of stimulus concentration. J. Comp. Neurol. 422, 496–509.

Johnson, B. A. and Leon, M. 2000b. Odorant molecular length: one aspect of the olfactory code. J. Comp. Neurol. 426, 330–338.

Johnson, B. A., Farahbod, H., and Leon, M. 2005b. Interactions between odorant functional group and hydrocarbon structure influence activity in glomerular response modules in the rat olfactory bulb. J. Comp. Neurol. 483, 205–216.

Johnson, B. A., Farahbod, H., Saber, S., and Leon, M. 2005a. Effects of functional group position on spatial representations of aliphatic odorants in the rat olfactory bulb. J. Comp. Neurol. 483, 192–204.

Johnson, B. A., Farahbod, H., Xu, Z., Saber, S., and Leon, M. 2004. Local and global chemotopic organization: general features of the glomerular representations of aliphatic odorants differing in carbon number. J. Comp. Neurol. 480, 234–249.

Johnson, B. A., Ho, S. L., Xu, Z., Yihan, J. S., Yip, S., Hingco, E. E., and Leon, M. 2002. Functional mapping of the rat olfactory bulb using diverse odorants reveals modular responses to functional groups and hydrocarbon structural features. J. Comp. Neurol. 449, 180–194.

Johnson, B. A., Woo, C. C., Hingco, E. E., Pham, K. L., and Leon, M. 1999. Multidimensional chemotopic responses to n-aliphatic acid odorants in the rat olfactory bulb. J. Comp. Neurol. 409, 529–548.

Johnson, B. A., Woo, C. C., and Leon, M. 1998. Spatial coding of odorant features in the glomerular layer of the rat olfactory bulb. J. Comp. Neurol. 393, 457–471.

Linster, C., Johnson, B. A., Yue, E., Morse, A., Xu, Z., Hingco, E., Choi, Y., Choi, M., Messiha, A., and Leon, M. 2001. Perceptual correlates of neural representations evoked by odorant enantiomers. J. Neurosci. 21, 9837–9843.

Malnic, B., Hirono, J., Sato, T., and Buck, L. B. 1999. Combinatorial receptor codes for odors. Cell 96, 713–723.

Mombaerts, P., Wang, F., Dulac, C., Chao, S. K., Nemes, A., Mendelsohn, M., Edmonson, J., and Axel, R. 1996. Visualizing an olfactory sensory map. Cell 87, 675–686.

Mori, K. and Shepherd, G. M. 1994. Emerging principles of molecular signal processing by mitral/tufted cells in the olfactory bulb. Semin. Cell Biol. 5, 65–74.

Mozell, M. M. 1964. Evidence for sorption as a mechanism of the olfactory analysis of vapors. Nature 203, 1181–1182.

Mozell, M. M., Sheehe, P. R., Hornung, D. E., Kent, P. F., Youngentob, S. L., and Murphy, S. J. 1987. ''Imposed'' and ''inherent'' mucosal activity patterns. J. Gen. Physiol. 90, 625–650.

Ressler, K. J., Sullivan, S. L., and Buck, L. B. 1993. A zonal organization of odorant receptor gene expression in the olfactory epithelium. Cell 73, 597–609.

Schoenfeld, T. A. and Knott, T. K. 2004. Evidence for the disproportionate mapping of olfactory airspace onto the main olfactory bulb of the hamster. J. Comp. Neurol. 476, 186–201.

Schoenfeld, T. A., Clancy, A. N., Forbes, W. B., and Macrides, F. 1994. The spatial organization of the peripheral olfactory system of the hamster. I. Receptor neuron projections to the main olfactory bulb. Brain Res. Bull. 34, 183–210.

Treloar, H. B., Feinstein, P., Mombaerts, P., and Greer, C. A. 2002. Specificity of glomerular targeting by olfactory sensory axons. J. Neurosci. 22, 2469–2477.

Uchida, N., Takahashi, Y. K., Tanifuji, M., and Mori, K. 2000. Odor maps in the mammalian olfactory bulb: domain

organization and odorant structural features. Nat. Neurosci. 3, 1035–1043.
Vassar, R., Chao, S. K., Sitcheran, R., Nuñez, J. M., Vosshall, L. B., and Axel, R. 1994. Topographic organization of sensory projections to the olfactory bulb. Cell 79, 981–991.
Wachowiak, M. and Cohen, L. B. 2001. Representation of odorants by receptor neuron input to the mouse olfactory bulb. Neuron 32, 723–735.
Yokoi, M., Mori, K., and Nakanishi, S. 1995. Refinement of odor molecule tuning by dendrodendritic synaptic inhibition in the olfactory bulb. Proc. Natl. Acad. Sci. U. S. A. 92, 3371–3375.

Further Reading

Arctander, S. 1994. Perfume and Flavor Chemicals (Aroma Chemicals). Allured Publishing Company.
Dravnieks, A. 1985. Atlas of Odor Character Profiles. ASTM Data Series DS 61.
Johnson, B. A. and Leon, M. 2007. Chemotopic odorant coding in a mammalian olfactory system. J. Comp. Neurol. 503, 1–34.
Takahashi, Y. K., Kurosaki, M., Hirono, S., and Mori, K. 2004. Topographic representation of odorant molecular features in the rat olfactory bulb. J. Neurophysiol. 92, 2413–2427.

4.41 Insect Olfaction

G Galizia, Universität Konstanz, Konstanz, Germany

© 2008 Elsevier Inc. All rights reserved.

4.41.1	**Introduction**	729
4.41.2	**Cellular Organization of the Antennal Lobe**	730
4.41.2.1	Antennal Lobe Glomeruli	730
4.41.2.2	Glomerular Atlas of the Antennal Lobe	731
4.41.2.3	Sensory Neuron Axons	732
4.41.2.3.1	Antennal nerves	732
4.41.2.3.2	Olfactory sensory neuron numbers	732
4.41.2.3.3	Projection of olfactory sensory neurons into the antennal lobe	732
4.41.2.3.4	Targeting mechanisms of olfactory sensory neurons	733
4.41.2.3.5	Olfactory sensory neuron odor responses	733
4.41.2.3.6	Olfactory sensory neuron transmitters	734
4.41.2.4	Local Neurons	735
4.41.2.4.1	Morphology of local neurons	735
4.41.2.4.2	Local neuron numbers	736
4.41.2.4.3	Transmitters used by local neurons	736
4.41.2.4.4	Physiology of local neurons	736
4.41.2.5	Projection Neurons	737
4.41.2.5.1	Projection neuron morphology and tracts	737
4.41.2.5.2	Projection neuron numbers	738
4.41.2.5.3	Projection neuron transmitters	739
4.41.2.5.4	Projection neuron physiology	739
4.41.2.6	Feedback Neurons and Biogenic Amines	739
4.41.2.7	Glial Cells	741
4.41.2.8	Cellular Organization and Number Relationships	741
4.41.3	**Functional Organization in the Antennal Lobe**	741
4.41.3.1	Odor-Evoked Activity Across Glomeruli	742
4.41.3.2	Processing in the Antennal Lobe	743
4.41.3.2.1	Contrast enhancement in the antennal lobe	743
4.41.3.2.2	Sensitivity optimization in the antennal lobe	744
4.41.3.2.3	Temporal activity structures	744
4.41.3.3	Combinatorial Odor Codes	745
4.41.3.4	Coding Odor Concentration and Odor Mixtures	745
4.41.3.5	Coding of Special Odors	746
4.41.3.5.1	Sexual pheromones	746
4.41.3.5.2	Nonsexual pheromones	747
4.41.3.5.3	Carbon dioxide	747
4.41.3.5.4	Humidity	748
4.41.3.5.5	Other special odors	748
4.41.3.6	Effects of Memory	748
4.41.4	**Cellular Organization of the Mushroom Bodies**	749
4.41.4.1	Kenyon Cells	749
4.41.4.2	Projection Neuron Input	750
4.41.4.3	Local Inhibitory and Modulatory Neurons; Mushroom Body Glomeruli	751
4.41.4.4	Output Lobe Circuitry	751
4.41.5	**Functional Organization of the Mushroom Bodies**	751
4.41.5.1	Odor-Evoked Activity and Processing	751

4.41.5.2	Olfactory Coding	752
4.41.5.3	Effects of Memory	752
4.41.6	**Cellular and Functional Organization of the Lateral Protocerebrum**	753
4.41.7	**The Larval System**	754
4.41.8	**Olfactory Behavior**	754
4.41.8.1	Odor Learning	754
4.41.8.2	Attractive and Repulsive Odors	755
4.41.8.3	Social Communication – Pheromones	755
4.41.8.4	Sexual Communication – Pheromones	756
4.41.8.5	Navigation – Innate Odors	756
4.41.8.6	Navigation – Learned Odors	757
4.41.9	**Limitations and Potential of Using Insects to Study Olfactory Coding**	757
References		758

Glossary

2-DG labeling A technique used to label active cells. Radioactive 2-DG ([^{14}C]2-deoxyglucose) is injected into the animal. Physiologically active cells accumulate 2-DG because it is taken up as a glucose analogue but accumulates because it cannot be metabolized. Cells that are particularly active accumulate more 2-DG and are therefore apparent in an autoradiograph. For each activity map, a single animal has to be killed.

acetylcholine (ACh) A neurotransmitter. In the insect brain, ACh is the major excitatory transmitter between neurons. The major excitatory neurotransmitter at the insect neuromuscular junction is glutamate.

antennal lobe (AL) The first neuropil in the insect brain to receive olfactory information, comparable to the mammalian olfactory bulb. It is located in the deutocerebrum.

antennal mechanosensory and motor center (AMMC) Neuropil situated in the deutocerebrum dorsally to the insect's AL (also called dorsal lobe). Among others, it receives the axonal terminals of mechanoreceptor cells on the antenna and contains the somata of antennal motor neurons.

antennocerebralis tract (ACT) Axonal tract between the AL and the protocerebrum. There are several ACTs in each brain, traveling in different routes.

arista Feather-like appendix on the *Drosophila* antenna involved in forming a recipient structure for vibrations. Sensory sensilla are also located on the arista.

associative memory See *Pavlovian conditioning*.

biogenic amines Neurotransmitters that have an amine group, comprising catecholamines (epinephrine, dopamine, and norepinephrine = noradrenalin) and indoles (tryptophan and serotonin). Many of them are involved in modulatory functions in the insect brain.

blocking Term from learning psychology. Assume that an association of a stimulus A with a reward is learned, and subsequently stimulus A is trained together with a stimulus B (i.e., AB). When learning about B is reduced (even though B was trained as a compound in AB), then A has blocked B. Blocking is generally explained using cognitive concepts of attention or expectation.

boutons Presynaptic structures in neurons.

calcium-sensitive dye A dye that changes its light properties as a function of calcium concentration. Most are fluorescent substances. These dyes are often used as reporter molecules for neural activity. Examples are calcium green, FURA, and fluo-3.

calyx, calyces See *mushroom body*.

cameleon See *G-CaMP*.

classical conditioning See *Pavlovian conditioning*.

combinatorial code A coding logic whereby information is not stored in a single channel (see *labeled line*), but rather across several channels. Different combinations of active channels indicate different information. Take, for example, 10 channels: simultaneous activity in channels 1, 3, and 5 constitutes a different combination (and thus coded information) than activity in channels 1, 3, and 6. A combinatorial code greatly amplifies the coding capacity of a given number of channels.

conditioned stimulus (CS) See *Pavlovian conditioning*.

deutocerebrum See *supraesophageal ganglia*.

differential training In Pavlovian conditioning, when two stimuli are used as CS, with one being rewarded and the other not, or one being punished and the other not.

dorsal lobe (DL) Neuropil in the deutocerebrum located dorsally to the AL. Contains the AMMC.

G-CaMP A genetically engineered fluorescent protein that changes its fluorescent properties with changing Ca^{2+} concentration. G-CaMP can be used to monitor cell activity when it is expressed in a cell. Another such reporter protein is cameleon. The two differ in spectral properties, Ca^{2+} affinity, and binding kinetics.

gamma-aminobutyric acid (GABA) Neurotransmitter that in most cases binds to receptors that have an inhibitory effect on the recipient cell. GABA is the most important inhibitory transmitter in the brain.

glomerulus Named after the spherical arrangement of dense neuropil in the AL which is apparent in microscopic sections, the glomeruli form the functional units within the AL. Generally, they collect all input from a particular type of olfactory sensory neurons (OSNs).

habituation A term from learning psychology. An animal habituates to a repeatedly presented stimulus and ignores its presence. Habituation is different from sensory adaptation or fatigue. Habituation is a nonassociative learning phenomenon: a strong stimulus of a different or even the same modality can instantly dishabituate an animal, showing that sensory information about the stimulus is not reduced.

hemimetabolous insects Insects that go through several developmental stages (instar larvae) that resemble the adult stage. Metamorphosis is gradual, without a pupal stage. For example, cockroaches and locusts. See also *holometabolous insects*.

heterogeneous local neuron (heteroLN) In this chapter, local neurons in the AL that branch in many glomeruli but have a clear polarity in that one or at most a few glomeruli are densely innervated, while most glomeruli are innervated only sparsely.

holometabolous insects Insects that undergo complete developmental metamorphosis, with a larval stage, followed by a pupal stage, followed by the adult. The larva is very different from the adult and generally occupies a different ecological niche. The best-known example is the butterfly, with the caterpillar larva. Bees, flies, and moths are holometabolous.

homogeneous LN In this chapter, local neurons in the AL that branch in many glomeruli without a clear polarity.

ionotropic receptor Ligand-gated ion channels that mediate fast excitatory or inhibitory neurotransmission.

Kenyon cell (KC) Intrinsic cell of the mushroom body in insects, first described by Kenyon F. C. in 1896.

labeled line Coding principle whereby a single channel carries information independently from the activity status of other channels, as opposed to a combinatorial code. In a binary system, four channels can carry 4 bits of information in a labeled line system, while four channels can carry 16 bits of information in a combinatorial code.

latent inhibition Term from learning psychology, which refers to the effect of unreinforced preexposure with a CS that leads to a reduced learning.

local neuron (LN) In this chapter used for neurons that are local to the AL, i.e., their entire branching arbors are confined within the AL.

mating disruption A technique in pest control aimed at modifying pest behavior with semiochemicals. For example, when large quantities of female pheromone are released in the environment, males are less efficient in finding their females, and thus natural mating patterns are disrupted.

metabotropic receptor A type of neurotransmitter receptor that, upon binding with a neurotransmitter, activates an intracellular second messenger cascade (e.g., involving cAMP), as opposed to opening an ion channel.

***molecular receptive range* (MRR)** The chemosensory response properties of a chemoreceptor or of a chemosensory neuron, i.e., the range of molecules for which the receptor is receptive.

multielectrode array A technique to measure many neurons at the same time with multiple electrodes that penetrate the brain. Each electrode can record extracellular activity from one or a few cells in its vicinity. Different cells are sorted by the spike shapes that they produce. Some multielectrode arrays are made of silicon and others of isolated wires.

mushroom body (MB) A structure in the insect protocerebrum. The intrinsic cells of the MBs are the KCs. Their somata and dendrites form the calyx, and their axons form the α-lobe, β-lobe, and

γ-lobe. The name comes from the shape of this structure, reminiscent of a mushroom.

negative patterning Term from learning psychology. In negative patterning, two single stimuli are reinforced, but their compound is not (i.e., A^+, B^+, AB^-). Therefore, while A and B each have predictive power for the reward, their mixture has not. Solving a negative patterning problem requires configural association and cannot be solved with elemental learning alone (see also *positive patterning*).

neuropeptides Short-chain peptides in the brain, e.g., enkephalins and endorphins, that function as intercellular messengers. There is a large variety of peptides, which are often species-specific and have dedicated receptors in the recipient cells. Peptides are often released as cotransmitters and modulate the affect of a transmitter at the recipient cell.

neuropil A dense feltwork of neural processes (dendrites, axons, and neurites) and glial processes. Generally, in insects, the cell bodies of the brain are arranged peripherally and the neuropil areas contain only very few cell bodies.

nitric oxide (NO) A gas that is also produced by cells and functions as a messenger between cells.

olfactory binding protein (OBP) A protein in the sensillar lymph of olfactory sensilla that participates in the olfactory process. Its function is as yet unclear. Among the current hypotheses for its function are that it might help dissolve the odors in the aqueous lymph or that might remove odor from the receptor after it has interacted.

olfactory bulb (OB) The vertebrate counterpart to the insect AL.

olfactory receptor (OR) A seven-transmembrane protein in OSNs that interacts with the odorant molecules and initiates the intracellular transduction cascade.

olfactory sensilla In insects, ORs are housed in sensilla, which are cuticular structures with pores on the insect's surface. Sensilla vary greatly in shape and size, including hair-like protrusions, flat plates, or funnel-like indentations.

olfactory sensory neuron (OSN) The primary olfactory neurons. OSNs express ORs on their dendrites and express the transduction cascade. Upon contact with the appropriate stimulus, they send action potentials (APs) along their axons into the ALs in the brain. Often referred to as OR neurons, or sometimes even receptors. The latter term is now avoided in order to prevent confusion with the OR proteins.

Pavlovian conditioning Also called classical conditioning. A neutral stimulus (the CS) is repeatedly presented immediately before a reward (or punishment, the unconditioned stimulus, US), so that the CS has predictive value for the US. The animal learns the coincidence of the two events forming an associative memory. Before learning, only the US leads to a response (the unconditioned response, UR). After learning, also the CS leads to a response (the conditioned response, CR). In Pavlov's famous dog experiment, the bell is the CS, the food is the US, and salivation is the UR and the CR. In bee PER (proboscis extension reflex) conditioning, the CS is an odor stimulus, the US is nectar (or sugar water), and the CR is the extension of the bee's proboscis (PER).

pheromone Chemical substance used for communication within a species. Sexual pheromones are used for sexual attraction and/or arousal. Other pheromones include alarm pheromones and trail pheromones in ants. The first pheromone to be isolated biochemically was Bombycol, the sexual pheromone of the moth *Bombix mori*, found by Butenand A. in the 1950s. Chemical messengers are also used between species: those advantageous for the receiver are called kairomones, those advantageous for the emitter are called allomones, and those that benefit both are called synomones.

Picrotoxin A pharmacological substance that blocks many ionotropic chloride channels. Generally, these channels are GABAergic receptors, and Picrotoxin is used to block these receptors.

positive patterning Term from learning psychology. In positive patterning, two single stimuli are not reinforced, but their compound is (i.e., A^-, B^-, AB^+). Therefore, neither A alone nor B alone has predictive power for the reward, but only their mixture. Unlike negative patterning, positive patterning can be solved with elemental learning mechanisms, without the need of configural association.

proboscis extension reflex (PER) The response to an appetitive stimulus. For example, when a honeybee is presented a drop of sugar water, it reflexively extends its proboscis.

projection neuron (PN) In this chapter, a neuron that projects out from the AL.

protocerebrum See *supraesophageal ganglia*.

subesophageal ganglia (SEG) The insect brain consists of the supraesophageal ganglia, which are

joined to the SEG by two connectives. Together, these structures form a ring around the esophagus. The SEG consists of a fusion of several pairs of ganglia. Often referred to as SOG (based on British spelling: suboesophageal ganglia).

supraesophageal ganglia The insect brain consists of a fusion of several ganglia arranged above the esophagus. The anterior part is the protocerebrum, which contains the MBs, the central complex, and the optic lobes. The posterior part contains the deutocerebrum (AL and DL) and the smaller tritocerebrum.

synaptopHluorin An artificially created fluorescent protein that changes its fluorescent properties with changing pH value and is localized in synaptic vesicles. synaptopHluorin can be used to monitor synaptic transmitter release when it is expressed in a cell.

tritocerebrum See *supraesophageal ganglia*.

unconditioned stimulus (US) See *Pavlovian conditioning*.

voltage-sensitive dye (VSD) A dye that intercalates into cell membranes and changes its light properties with the membrane potential. VSDs can be used to measure membrane potentials of cells with light.

α-lobe See *mushroom body*.

γ-lobe See *mushroom body*.

4.41.1 Introduction

In order to understand how the insect brain processes information, it is necessary to understand the anatomy and physiology of the neurons involved in this task. In a very simplified picture, information by olfactory sensory neurons (OSNs) is processed first in the antennal lobes (ALs), and then in the mushroom bodies (MBs) and the lateral protocerebrums (LPs). In this chapter, these three areas are treated sequentially, and information about morphology, physiology, and function is collected for each. At the end, olfactory behavior in insects is discussed.

It is useful to separate at least three transformation steps involved in olfactory coding, which correspond to transformations between four multidimensional spaces. First is the external multidimensional space, that is, the odor world, which has dimensionality and axes defined by the chemical and physical properties of the odorant molecules. Some of these axes are easy to define, like carbon chain length for simple hydrocarbons or electronegativity for functional group residues. Molecular resonance frequencies, which are exploited in spectroscopic techniques, also define a classification system (Turin, L., 1996). However, any arrangement of molecules in such a multidimensional space is a matter of definition, rather than reflecting a naturally dictated order. The second one is a biologically defined multidimensional space, where each dimension is given by the response properties of OSNs. The mapping of the physical–chemical space onto the receptive space is the first step in olfactory coding. It consists of interactions with olfactory binding proteins (OBPs) and other extracellular proteins, the olfactory receptor proteins (ORs), and intracellular second messenger pathways. The third multidimensional space consists of activity patterns across neurons in the AL and its several additional transformations along processing steps within the brain, which are mediated by the neural networks within the AL or the MBs. These steps enhance information that is relevant to the animal and filter less-relevant content, increase signal over noise, optimize sensitivity, and/or reformat the coding scheme in a way that makes it easier and more reliable to decode, so that information is better stored and/or extracted. This information consists of any combination of (1) the identity of an odor stimulus (an identification task), (2) its concentration (a measurement along a continuous variable), (3) the identity of odor components in a mixture (an analytical task), (4) the identity of a combination of odor components in a mixture (a synthetic task), and (5) the analysis of odor plume sequences (a temporal task). Finally, the last and biologically most relevant olfactory space is the perceptual space, which results in behavioral decisions. Thus, the first, physical odor space (of unknown order and dimensionality) is mapped onto a primary, receptive odor space (with a clearly defined dimensionality dictated by the number of ORs), then transformed into several physiological spaces (which might work sequentially, in parallel, or both), which in turn is the basis for the perceptual odor space.

4.41.2 Cellular Organization of the Antennal Lobe

The AL is the first neuropil in the insect brain that processes olfactory information. It is evolutionarily shared within the protostome clade and present in all insects, with the exception of some anosmic species where it was secondarily lost (Strausfeld, N. J. and Hildebrand, J. G., 1999). Both in its structure and in its function, it is remarkably similar and analogous to the vertebrate OB, although it evolved independently (Strausfeld, N. J. and Hildebrand, J. G., 1999). There is one major difference in design, which reflects a structural difference between the nervous tissue in insects and that in vertebrates: In the insect brain, most neuronal cell bodies lie at the periphery of the brain, and they extend neurites that branch within the brain, forming axons and dendrites. In the AL, neurons have their somata in cell clusters around the AL itself and branch in olfactory glomeruli, which are the interaction sites of OSNs, local neurons (LNs), projection neurons (PNs), and others. Very few synapses are found outside the glomerulus (Gascuel, J. and Masson, C., 1991; Boeckh, J. and Tolbert, L. P., 1993). In vertebrates, the bulb is organized in a more columnar fashion, with cellular interactions within several layers beneath the olfactory glomeruli, and LN networks separated in these layers. To a first approximation, therefore, the insect glomerulus is functionally comparable to a vertebrate glomerular column, rather than to the glomerulus alone. However, this analogy remains an approximation, because the OB is not columnar beneath the glomerulus. For example, mitral cell somata can be displaced laterally with respect to the glomerulus innervated by their dendritic tuft (Shepherd, G. M. and Greer, C. A., 1998).

The considerable similarity to vertebrates should not prevent us to recognize that within insects the diversity of AL organization is large (Schachtner, J. *et al.*, 2005). Insects have an evolutionary history of over 400 000 000 years, and most modern insect orders were already present since 250 000 000 years, which allows for considerable divergent evolution (Grimaldi, D. A. and Engel, M. S., 2004). As a minor example, cell somata are arranged in distinct clusters around the AL in most insects, but the distribution of cell bodies for functionally different neurons (e.g., LNs vs. PNs) is not conserved among species. In the following, I will mention the different organizational principles found in those species that have been studied in more detail than others. For hemimetabolous insects, most results are from locusts, among which *Locusta migratoria* (Orthoptera), and cockroaches, notably *Periplaneta americana* (Blattodea). In holometabolous insects, the best studied are the fruit fly, *Drosophila melanogaster* (Diptera), a variety of moths, in particular *Manduca sexta* (Lepidoptera), and the honeybee, *Apis mellifera* (Hymenoptera). Where useful, I will follow the sequence bee, moth, fly, cockroach, and locust for clarity.

4.41.2.1 Antennal Lobe Glomeruli

A striking similarity across animal phyla is the glomerular organization of the primary neuropil of the olfactory system, be it the OB of vertebrates or the AL in insects (Hildebrand, J. G. and Shepherd, G. M., 1997). This unique structural principle might reflect a basic property of olfactory coding, possibly because there is no physical property common to all odors that can be mapped in a small number of dimensions. Such an oligodimensional representation is possible for spatial position of light stimuli, or frequency coding for sounds. Color coding, however, does not make use of the unidimensional property of photon wavelength but rather creates artificial dimensions with different color-sensitive photoreceptors and subsequent color-opponency channels, which can be very few (two such channels in humans and honeybees). Olfaction is intrinsically multidimensional, and a glomerular morphology may be a structural organization that helps convert a multidimensional set of inputs into a topological map. The resulting glomerular organizing principle would be functionally dictated. Alternatively, a glomerular organization may just be the most parsimonious organization of many coalescing axons with equal response properties, resulting from the convergence of OSNs onto one point in the central nervous system.

In insects, the number, shape, and arrangement of glomeruli vary greatly among species: an adult *Drosophila* fruit fly has less than 50 glomeruli (Stocker, R. F., 1994; Laissue, P. P. *et al.*, 1999), a moth (*Manduca*) has ~60 (Sanes, J. R. and Hildebrand, J. G., 1976b; Rospars, J. P. and Hildebrand, J. G., 1992), a cockroach has ~125 (Ernst, K. D. *et al.*, 1977), a worker honeybee has ~160 (Flanagan, D. and Mercer, A. R., 1989a; Galizia, C. G. *et al.*, 1999b), and some ant species have over 200 (Rospars, J. P., 1988) or even 400 glomeruli (Ozaki, M., personal communication). In many species, glomeruli are arranged around a central area of the AL, the coarse neuropil, while in

others, generally smaller animals, glomeruli are more densely packed, filling most of the AL. Glomeruli are the functional units within the AL, but nevertheless, there is a substructure within them. In bees the outer cap and the core of each glomerulus receive input from different neuron types: OSNs innervate the outer cap, and within this cap, the antenna is topologically arranged. Many LNs innervate only the core of those glomeruli that they sparsely innervate. In honeybees, serotonergic neurons innervate only the cap and dopaminergic neurons only the core. Consequently, each glomerulus is concentrically organized, and the cap may serve a function different from the core. Furthermore, in immunostainings for protein kinase C (PKC), small circular regions of dense staining are visible within honeybee glomeruli (Müller, U., personal communication; see also Grünbaum, L. and Müller, U., 1998). In mass-fills of OSNs similar dense knots can be seen (own observations). Whether these two substructures coincide is not known, and their functional significance, if any, also remains obscure. A subcompartmentalization of glomeruli has been shown for *Drosophila* (Laissue, P. P. *et al.*, 1999) and is also known from vertebrates (Kasowski, H. J. *et al.*, 1999). Morphologically and most likely functionally, there is an inner life to a glomerulus that remains to be elucidated: possibly, glomeruli are not the smallest unit of the olfactory code.

The term glomeruli is also used in locusts, even though their arrangement differs from that in most other species (Ignell, R. *et al.*, 2001). There are about 1000 glomeruli, with each receptor neuron axon innervating several of them, and each projection neuron branching in many of them (Ernst, K. D. *et al.*, 1977; Anton, S. and Hansson, B. S., 1996). It is clear that there is no morphological homology between the locust glomeruli and those of other insects. Nevertheless, anatomically they are dense knots of neuropil and therefore referred to as glomeruli. Furthermore, even if the AL is structured differently, basic mechanisms of olfactory coding may still be the same in locusts and other insects. For example, application of the chloride channel blocker Picrotoxin has similar effects on the temporal response structure in PNs in bees (Stopfer, M. *et al.*, 1997) and in locusts (MacLeod, K. and Laurent, G., 1996). Therefore, a comparative approach, and a thorough comparison of results from all species, is needed.

The most complete ultrastructural analysis of synaptic connections between neurons in the AL has been done in cockroaches. Briefly, almost any possible synaptic contact is realized (Malun, D. 1991a; 1991b; Distler, P. G. and Boeckh, J., 1996; 1997a; Distler, P. G. *et al.*, 1998b). That is, OSNs synapse onto LNs and onto PNs, and their presynaptic terminals themselves receive input from AL neurons. LNs synapse onto OSN terminals, other LNs, and PNs. PNs get input from OSNs and LNs, and they synapse onto other cells in the AL. No synapses from PNs onto OSNs have been found. The presence of LN input to OSNs indicates that the AL network already controls magnitude and maybe timing of afferent input activity, as shown in crustaceans and vertebrates (Wachowiak, M. *et al.*, 2002).

4.41.2.2 Glomerular Atlas of the Antennal Lobe

The low numbers of glomeruli in insects, and their characteristic arrangements and sizes, have allowed mapping them, and creating 3D-Atlases (Rospars, J. P., 1988). Initially, these were morphological descriptions based on serial sections, but in recent years confocal reconstructions of whole ALs have been used. Computer-based atlases are increasingly available over the Internet and can be used for relating findings to identified glomeruli, thus greatly enhancing the comparability of results among research groups. Unfortunately, the electronic format used by different laboratories and for different species still needs unification. The quest for electronic brain atlases in general (Toga, A. W. and Thompson, P. M., 2001) will soon lead to more uniform standards among insect researches, not only for the AL, but also for the entire brain (Rein, K. *et al.*, 2002; Brandt, R. *et al.*, 2005).

The honeybee AL has been mapped, and glomeruli were named according to the antennal tract that innervates them (T1–T4) and a number (i.e., T1-1, T1-2, or T3-33) (Flanagan, D. and Mercer, A. R., 1989a). An electronic version based on confocal sections was published later (Galizia, C. G. *et al.*, 1999b) and is available for download over the Internet (see Relevant Websites section).

Atlases are also available for different moth species (Rospars, J. P. and Hildebrand, J. G., 1992; Berg, B. G. *et al.*, 2002; Huetteroth, W. and Schachtner, J., 2005; Ignell, R. *et al.*, 2005; Masante-Roca, I. *et al.*, 2005; Skiri, H. T. *et al.*, 2005).

The *Drosophila* AL was first mapped based on serial sections (Stocker, R. F. *et al.*, 1990) and later based on confocal sections (Laissue, P. P. *et al.*, 1999). Each of the 43 glomeruli mapped so far is named with a letter or

two indicating the AL area and a number, e.g., DM2 for dorsomedial-2. This atlas is also freely available for downloading (see Relevant Websites section). Glomeruli that are identified later can be easily included into this nomenclature (Couto, A. *et al.*, 2005).

Currently, there is no glomerular atlas for cockroaches. It is unlikely that there will ever be an atlas for locusts, given the ambiguity of glomerular borders and the high number of glomeruli.

4.41.2.3 Sensory Neuron Axons

4.41.2.3.1 Antennal nerves

Chemosensory neurons are present on the surface of many areas of the insect body, including legs, wings, genitalia, and head appendices. All (nonanosmic) insects have olfactory sensilla that contain OSNs on their antennae, and some, notably dipterans, also on the maxillary palps. Structure and function of OSNs and the diversity of olfactory sensilla are treated in other chapters. OSN axons project to the AL via the antennal tract(s). In many species, there is more than one antennal tract. In honeybees, there are four tracts, T1–T4, that innervate different glomeruli (Suzuki, H., 1975). The honeybee T1 and T3 innervate ~70 glomeruli each, and T2 and T4 innervate seven glomeruli each (Arnold, G. *et al.*, 1983; Flanagan, D. and Mercer, A. R., 1989a; Galizia, C. G. *et al.*, 1999b). Since each glomerulus has a distinct functional response spectrum (see below), the antennal tract segregation may have a functional significance. In honeybees, the morphology of the innervating OSN terminals differs between glomeruli innervated by the four antennal tracts (Mobbs, P. G., 1982). Furthermore, this segregation corresponds to distinct groups of PNs that leave the AL following different tracts (see below) (Abel, R. *et al.*, 2001; Kirschner, S. *et al.*, 2006).

Antennal nerves contain other axons too: mechanosensory and gustatory axons from the antenna travel along the AL, bypassing it toward the antennal mechanosensory and motor center (AMMC) in the dorsal lobe (DL) (Suzuki, H., 1975; Gewecke, M., 1979; Mobbs, P. G., 1982; Kloppenburg, P. *et al.*, 1997). In honeybees, these are tracts T5 and T6. Efferent axons for antennal muscles, originating in motor neurons in the DL, use these tracts to enter the antenna. Finally, axons from modulatory neurons, with their unpaired cell bodies in the subesophageal ganglion, also enter the antenna. These neurons most likely use biogenic amines as transmitters. While their function has not yet been elucidated directly, a modulatory effect of biogenic amines on OSNs has been shown (Pophof, B., 2002).

4.41.2.3.2 Olfactory sensory neuron numbers

The number of OSNs differs greatly among species, and within some species among sexes. Male honeybees (drones) have ~300 000 OSNs, while (female) worker bees have ~65 000, the difference being probably due to the male's sensitivity for the queen's sexual pheromone (Esslen, J. and Kaissling, K. E., 1976). In *Manduca*, sexual dimorphism is reflected in OSN response properties, and not their numbers: both males and females have ~300 000 OSNs on each antenna (Sanes, J. R. and Hildebrand, J. G., 1976c; Oland, L. A. and Tolbert, L. P., 1988). *Drosophila* has ~1200 OSNs in both sexes (Stocker, R. F. *et al.*, 1990). Adult cockroaches have ~150 000 OSNs (Ernst, K. D. *et al.*, 1977). As juveniles, cockroaches have less OSNs. As they grow, they increase the number of antennal segments and sensilla with each nymphal instar (Schafer, R. and Sanchez, T. V., 1973). The number of OSNs in locusts is between 50 000 (Ernst, K. D. *et al.*, 1977) and 105 000 (Anton, S. *et al.*, 2002) and also increases over developmental stages (Ochieng, S. A. *et al.*, 1998; Chapman, R. F., 2002).

4.41.2.3.3 Projection of olfactory sensory neurons into the antennal lobe

Generally, one OSN axon innervates a single ipsilateral glomerulus in the AL, where it branches and where it forms many synapses. It is unknown how many synapses a single axon forms within the glomerulus, but given the often extensive branching of these axons, the number is likely to be high. In most cases, branching is strongest in the outermost layer of the innervated glomerulus, but in some species (e.g., cockroaches) or some subpopulations of glomeruli (e.g., T4 in bees), OSN axons invade the entire glomerulus. In bees, there is a concentric topological arrangement of OSN input to glomeruli, with OSNs from the distal antennal segments innervating the outer layer of the glomerulus, and more proximal OSNs occupying more central layers (Pareto, A., 1972). These layers are, however, strongly overlapping and may be dictated by developmental constraints rather than by functional necessity. Antennotopic projections have also been found in *Manduca* (Christensen, T. A. *et al.*, 1995) and *P. americana* (Hösl, M., 1990). Synapses are formed onto both LNs and PNs and are often dyadic, that is, one presynaptic element with two postsynaptic elements,

or even more complex (Malun, D. 1991a; Distler, P. G. and Boeckh, J., 1996; Sun, X.-J. *et al.*, 1997). In flies, most axons innervate a bilateral pair of homologous glomeruli, and OSNs form an axonal commissure between the two ALs (Strausfeld, N. J., 1976; Stocker, R. F., 1994). Each bilaterally innervated glomerulus receives equal input from both antennae (Vosshall, L. B. *et al.*, 2000). Some glomeruli, however, are innervated only unilaterally; in *D. melanogaster*, these are V, VL1, VP1, as well as VP2 and VP3 that collect all input from sensilla located on the *Drosophila* arista (Stocker, R. F. *et al.*, 1983; Stocker, R. F., 2001).

In locusts, most OSN axons innervate several glomeruli ipsilaterally (Ernst, K. D. *et al.*, 1977), but some innervate only one glomerulus (Anton, S. *et al.*, 2002).

4.41.2.3.4 Targeting mechanisms of olfactory sensory neurons

Targeting of OSNs onto glomeruli is best understood in *Drosophila*. After the ORs were characterized (Clyne, P. J. *et al.*, 1999; Gao, Q. and Chess, A., 1999; Vosshall, L. B. *et al.*, 1999), the mapping of their target areas has been intensely pursued (Couto, A. *et al.*, 2005; Fishilevich, E. and Vosshall, L. B., 2005). Indeed, the nomenclature of olfactory glomeruli by spatial location (e.g., DM2 for glomerulus 2 in the dorsomedial area) might eventually be used synonymously with the name of the OR gene expressed in the OSNs innervating it (e.g., dOr22a for DM2). The current rule is that each OSN expresses only one OR and that OSNs expressing the same OR converge on a single glomerulus in each hemisphere (Vosshall, L. B. *et al.*, 2000), but there are exceptions: in transgenic animals, a few axons go astray to other glomeruli (Bhalerao, S. *et al.*, 2003). Some OSNs express more than one OR. For example, dOr22a and dOr22b are coexpressed in ab3a (for antennal basiconic sensillum 3, neuron a), and their axons converge onto glomerulus DM2 in the AL, but dOr22b does not seem to contribute to the olfactory response of those neurons (Dobritsa, A. A. *et al.*, 2003). In pb2a OSNs (palp basiconic type 2, neuron a), receptors dOr33c and dOr85e are coexpressed, and in this case, both contribute to these neurons' molecular response profiles (MRRs) (Goldman, A. L. *et al.*, 2005). Other OSN axon populations innervate two glomeruli even though expressing the same OR. For example, OSNs expressing dOr67d innervate the two glomeruli DA1 and VA6 (Fishilevich, E. and Vosshall, L. B., 2005). An almost complete mapping of dOrs and their target glomeruli is now available for adult *Drosophila* (Couto, A. *et al.*, 2005; Fishilevich, E. and Vosshall, L. B., 2005). From this it is clear that the general rule one OSN – one receptor – one glomerulus is valid in most cases, but not followed strictly, allowing for additional degrees of freedom in functionally organizing chemosensory responses. In addition, most but not all OSNs express an additional OR-like receptor, which is dOr83b in *Drosophila* (Larsson, M. C. *et al.*, 2004), and which has an ortholog receptor in all other insects investigated so far, including mosquitoes, bees, moths, and beetles (Krieger, J. *et al.*, 2003; Pitts, R. J. *et al.*, 2004; Jones, W. D. *et al.*, 2005). OR expression in *Drosophila* OSNs is discussed in more Chapter Phototransduction in Microvillar Photoreceptors of Drosophila and Other Invertebrates.

In mammals, ORs are important for OSN axon targeting to the appropriate glomerulus (Wang, F. *et al.*, 1998; Feinstein, P. and Mombaerts, P., 2004; Feinstein, P. *et al.*, 2004). In insects, the innervated glomerulus is independent of the OR that is expressed (Dobritsa, A. A. *et al.*, 2003). Other factors are required for correct OSN targeting in *Drosophila*, including the Src homology domain 2 (SH2)/SH3 adapter Dock (Ang, L. H. *et al.*, 2003), the serine/threonine kinase Pak (Ang, L. H. *et al.*, 2003), the cell surface proteins *N*-cadherin (Hummel, T. and Zipursky, S. L., 2004), the immunoglobulin Dscam (Hummel, T. *et al.*, 2003), and the POU domain transcriptional factor Acj6 (Komiyama, T. *et al.*, 2004). Many of these factors are only expressed in subpopulations, suggesting some sort of combinatorial mechanism. For example, Dscam disrupts OSN targeting in many OSN axons, but not in those expressing the receptors dOr22a, and only partially in some others (Hummel, T. *et al.*, 2003). All OSNs in the antenna express Acj6, but not all OSNs in the maxillary palps do. Furthermore, precise OSN targeting is not only regulated by intrinsic transcriptional control but also by axon–axon interaction (Komiyama, T. *et al.*, 2004) and interactions with glial cells (Tolbert, L. P. *et al.*, 2004). Glomerular identity appears to be determined before OSN ingrowth, with the participation of PNs forming protoglomeruli (Jefferis, G. *et al.*, 2004).

4.41.2.3.5 Olfactory sensory neuron odor responses

Responses in OSN axons to odorants originate from the response properties of the ORs expressed in that axon, and other interactions at the periphery including OBPs. Response properties measured at the periphery are covered in another chapter.

Functional response properties of olfactory glomeruli have been measured in several species using optical imaging techniques, notably flies (Ng, M. *et al.*, 2002; Fiala, A. *et al.*, 2002; Wang, J. W. *et al.*, 2003), bees (Galizia, C. G. and Menzel, R., 2001; Fiala, A. *et al.*, 2002; Sachse, S. and Galizia, C. G., 2002; 2003), moths (Galizia, C. G. *et al.*, 2000a; Carlsson, M. A. *et al.*, 2002; Skiri, H. T. *et al.*, 2004), and ants (Galizia, C. G. *et al.*, 1999a). In all cases, glomeruli had characteristic odor-response profiles, confirming that a single or at most very few ORs dictate their response properties. Consequently, also in species other than *Drosophila*, OSNs expressing the same OR are likely to converge generally onto a single glomerulus. Additional support comes from the observation that in the recently sequenced genome of the honeybee, *A. mellifera*, the number of OR genes is close to 160 (Robertson, H. M. and Wanner, K. W., 2006). This number matches closely the number of glomeruli found in this species. Thus, molecular and optophysiological data have superseded earlier models of AL innervation based on single-cell electrophysiology that assumed OSNs with equal response profiles to innervate several glomeruli, and each glomerulus to receive input from several OSN types (Boeckh, J. and Tolbert, L. P., 1993). For locusts, where individual OSN axons innervate several glomeruli, no data about OSN targeting are as yet available.

OSNs differ in how broad their response spectrum is. Narrowly tuned OSNs form a labeled line: each OSN responds only to a single substance, and thus when that OSN is active, animals can behave assuming that the substance is in the environment. Such a system is very specialized, and in its extreme form, the number of odors that can be coded corresponds to the number of OSNs with different response profile (which would be ~43 in the adult *Drosophila*). On the other hand, broadly tuned OSNs create a combinatorial code. Each odor activates many OSN types, and each OSN can be activated by many odors. Thus, the information carried by individual glomeruli becomes ambiguous. It is only by analyzing the pattern of active glomeruli that the animal can identify an odor. Experiments show that many OSNs respond to a variety of substances at high concentration but may be exquisitely sensitive to a few molecules at a concentration several orders of magnitude lower (Røstelien, T. *et al.*, 2000; Stensmyr, M. C. *et al.*, 2003; Pelz, D. *et al.*, 2006). Are they highly sensitive labeled lines, or rather units in a combinatorial code? Animals are exposed to odorants over a large range of concentrations in their natural environment. A honeybee, for example, can smell an odor source over large distances (low-concentration task) but also recognize it when sitting on a flower (high-concentration task). The olfactory system should therefore be capable of differentiating, for a given OSN, between the occurrence of a low-concentration best ligand and a high-concentration secondary ligand. This cannot be done on the basis of a single OSN response itself and must be done by a pattern analysis across several OSNs. Even for sexual pheromones, the labeled line at OSN level is converted into a combinatorial system for the next processing step. Pheromones consist of blends of several substances, and extraction of the correct pheromone blend information is done by a combinatorial analysis of the respective glomerular activities (Christensen, T. A. and Hildebrand, J. G., 2002; Shirokova, E. *et al.*, 2005). Some species, such as *Helicoverpa armigera* and *Helicoverpa assulta*, have pheromone blends consisting of the same substances, but in different relative concentrations, so that relative activity becomes important information (Berg, B. G. *et al.*, 2005).

Most OSN responses are temporally structured: some are inhibited by odors and show rebound excitation at the end of the stimulus, some fire for a long time irrespective of stimulus duration, others only fire for a very short time, and stop even if the stimulus continues (de Bruyne, M. *et al.*, 2001). Some but not all of these effects are due to adaptation of the OSNs (tonic versus phasic response properties). The consequence for the central nervous system is that it gets a temporally complex input from the OSNs. This is in addition to the intrinsic temporal complexity that air-borne odors always have (Murlis, J. *et al.*, 1992). The question as to whether these temporal structures are used for odor analysis and whether the periphery rather than the AL network may cause part of the temporal patterns observed within the AL is discussed below.

OSN responses can also be inhibitory. Because the background activity differs among OSN types, an inhibitory ligand might become evident only when an OSN is also activated by another ligand, resulting in nonlinear mixture interactions (de Bruyne, M. *et al.*, 2001).

4.41.2.3.6 Olfactory sensory neuron transmitters

The OSN transmitter is likely to be acetylcholine (ACh), which is the primary excitatory transmitter in the insect brain. The evidence, however, is not

conclusive yet, and mostly based on the detection of the ACh-synthesizing enzyme choline acetyltransferase (ChAT) (Kreissl, S. and Bicker, G., 1989; Bicker, G., 1999a). ACh is present in *Manduca* OSNs (Sanes, J. R. and Hildebrand, J. G., 1976a; Stengl, M. *et al.*, 1990). Pressure application of ACh leads to activity (depolarization and hyperpolarization) in moth AL neurons, mediated by nicotinic receptors (Waldrop, B. and Hildebrand, J. G., 1989). In *Drosophila*, a ChAT/lacZ tranformant labels OSNs (Yasuyama, K. *et al.*, 1995), but immunoreactivity for ACh is low (Yasuyama, K. and Salvaterra, P. M., 1999). In all species studied so far, however, the presence of ACh, ChAT, and α-bungarotoxin binding sites was heterogeneous among glomeruli, leaving the possibility that there might be another, as yet unknown, transmitter (or cotransmitter) in OSNs (Kreissl, S. and Bicker, G., 1989; Homberg, U. *et al.*, 1995; Homberg, U. and Müller, U., 1999) or that glomeruli differ in receptor and/or vesicle density.

In moths, OSN axons contain nitric oxide (NO) synthase and release NO when activated by odors (Gibson, N. J. and Nighorn, A., 2000). NO signaling stimulates glial migration, and blocking NO signaling in development disrupts proper glomerular development in the AL (see Section 4.41.2.7) (Gibson, N. J. *et al.*, 2001). NO is also present in honeybee ALs, but it is unclear whether NO is produced in OSNs or other cells (Hosler, J. S. *et al.*, 2000; Bicker, G., 2001). The NO/cGMP system is involved in olfactory habituation in honeybees (Müller, U. and Hildebrandt, H., 2002), and blocking NO activity in adult honeybees disrupts olfactory discrimination in a similar way as when chloride channels are blocked (Hosler, J. S. *et al.*, 2000). In cockroaches and locusts, NO is not synthesized in OSNs but is synthesized in LNs (Elphick, M. *et al.*, 1995; Seidel, C. and Bicker, G. 1997; Ott, S. R. and Elphick, M. R., 2002).

4.41.2.4 Local Neurons

LNs are defined as neurons whose branching patterns are limited to the AL alone. Their somata are located close to the AL, and their neurites branch among olfactory glomeruli, and within them. Many different morphologies have been described, and a variety of transmitters and expressed peptides are known. Synaptic connections among LNs and with other neurons have been analyzed in few species only. Descriptions from different species vary in approach and technique, making a thorough comparison difficult. It is clear that we are lacking considerable knowledge about LNs in insects.

4.41.2.4.1 Morphology of local neurons

Morphologically, LNs fall into two major classes. One type innervates most if not all glomeruli uniformly. These neurons have been named symmetrical LNs (Matsumoto, S. G. and Hildebrand, J. G., 1981; Ernst, K. D. and Boeckh, J., 1983; Anton, S. and Homberg, U., 1999) or, in bees, homogeneous LNs (homoLNs) (Flanagan, D. and Mercer, A. R., 1989b). Another type innervates only a small number of glomeruli. In bees, these heterogeneous LNs (heteroLNs) have one dominant glomerulus with dense innervation, and several glomeruli with very sparse innervation (Flanagan, D. and Mercer, A. R., 1989b; Sun, X.-J. *et al.*, 1993a). They branch only in the core of the sparsely innervated glomeruli but branch in the core and the outer cap of the densely innervated glomeruli (Fonta, C. *et al.*, 1993; Abel, R. *et al.*, 2001). In moths, all asymmetric neurons described so far innervate a small group of glomeruli sparsely (asymmetric LNs) without a single, dominant glomerulus (Matsumoto, S. G. and Hildebrand, J. G., 1981). Symmetric and asymmetric LNs together account for the vast majority of LNs in the AL, with heteroLNs (asymmetric) dominating in bees (Flanagan, D. and Mercer, A. R., 1989b; Fonta, C. *et al.*, 1993; Sun, X.-J. *et al.*, 1993a), and symmetric LNs dominating in moths (Christensen, T. A. *et al.*, 1993). Other morphological types are LNs that innervate some dorsal glomeruli of the AL and areas of the AMMC (which makes their definition as LNs questionable), so far published for bees (Flanagan, D. and Mercer, A. R., 1989b). A thin connection between the two ALs has been described in bees (Arnold, G. *et al.*, 1985; Mobbs, P. G., 1985), which appears to contain about 30 GABAergic fibers in immunohistochemical sections (Schäfer, S. and Bicker, G., 1986). These neurons are multiglomerular (Fonta, C. *et al.*, 1993) and may be related to bilateral comparisons, regulation, and inhibition of AL activity.

In *Drosophila*, two GAL4 lines that label two distinct sets of LNs have been described. Both consist of homogeneously branching LNs, but density, morphology, and location of branches within glomeruli differ (Ito, K., personal communication). The functional differences in these two lines are also unknown. A third group of LNs is cholinergic and mediates excitatory interactions within the AL (Shang, Y, *et al.*, 2007). LNs that bilaterally connect the two ALs are also found in *Drosophila* and at least

some of them innervate only glomerular subsets and not the entire AL (Stocker, R. F. *et al.*, 1990; Stocker, R. F., 1994).

4.41.2.4.2 Local neuron numbers

Counts of LNs in insects are difficult, and rarely better than a gross estimate. There are up to 4000 LNs in bees (see below), ~360 LNs in moths (*M. sexta*) (Homberg, U. *et al.*, 1988), and ~100 (GABAergic) LNs in *Drosophila* (Ng, M. *et al.*, 2002). The estimates for other species are ~300 LNs both in cockroaches and in locusts (Anton, S. and Homberg, U., 1999).

Honeybees have by far the highest number, with up to 4000 LNs. This count is based on about 7350 neurons in each deutocerebrum, that is, the AL and DL taken together, of which 4750 are directly associated with the AL (Witthöft, W., 1967). The vast majority of these are either LNs or PNs. Assuming 800 PNs (see below), this leaves almost 4000 LNs.

4.41.2.4.3 Transmitters used by local neurons

Most LNs are GABAergic, with GABA-like immunoreactivity shown in bees (Schäfer, S. and Bicker, G., 1986), moths (Hoskins, S. G. *et al.*, 1986), *Drosophila* (Jackson, F. R. *et al.*, 1990; Buchner, E., 1991), cockroaches (Malun, D., 1991b; Distler, P. G. *et al.*, 1998b), and locusts (Leitch, B. and Laurent, G., 1996; Ignell, R. *et al.*, 2001). LNs get synaptic input also from GABAergic LNs. In *Drosophila*, GABAergic LNs expressing the GABA biosynthetic enzyme glutamic acid decarboxylase also express GABA receptors, both metabotropic and ionotropic (Ito, K., personal communication).

In bees, ~750 LNs stain for GABA (Schäfer, S. and Bicker, G., 1986), which forms a rather low proportion of GABAergic interneurons as compared with other insects, where most LNs appear to be GABAergic. Knowledge about LNs that are nonGABAergic is limited, with the exception of a population of about 35 LNs in honeybees that stain for histamine as a transmitter (Bornhauser, B. C. and Meyer, E. P., 1997). Application of histamine blocks activity in the honeybee AL (Sachse, S. and Galizia, C. G., 2002), suggesting that it acts as an inhibitory transmitter. The function of histaminergic LNs with regard to odor coding and processing is still unknown and needs further investigation. Since OSNs in flies express G-protein-coupled glutamate receptors, there probably is a population of glutamatergic LNs that synapse onto (at least some) OSN terminals (Ramaekers, A. *et al.*, 2001).

A pharmacological analysis is difficult in insects, because receptor affinities are not well characterized for most artificial antagonists and agonists. Furthermore, the long evolutionary history of insects results in considerable diversity. For example, the $GABA_A$ antagonist bicucculine modifies AL activity in moths (Christensen, T. A. *et al.*, 1998b), but not in bees, flies (own observations), and locusts (MacLeod, K. and Laurent, G., 1996). The chloride channel blocker Picrotoxin has both a washable and a nonwashable effect in bees (Sachse, S. and Galizia, C. G., 2002), but only a nonwashable effect in moths (Waldrop, B. *et al.*, 1987). The $GABA_B$ blocker 2H-saclofen is effective in moths (Lei, H personal communication), and the $GABA_B$ blocker CGP54626 is effective in fruit flies (Wilson, R. I. and Laurent, G., 2005).

LNs differ in their expression of neuropeptides. The available data show that many, often small populations of LNs, express characteristic peptides, including but by far not limited to allatotropin, allatostatins, tachykinins, FMRFamide, and other RFamide peptides. The patterns of peptide antiserum stainings differ widely among the species (Homberg, U. *et al.*, 1990; Nässel, D. R., 1993; Davis, N. T. *et al.*, 1996; Homberg, U. and Müller, U., 1999; Nässel, D. R., 2000; Homberg, U., 2002; Nassel, D. R. 2002; Schachtner, J. *et al.*, 2004; Iwano, M. and Kanzaki, R., 2005). Some neuropeptides are coexpressed with GABA while others are not. In locusts, locustatachikinin is found in a population of about 20 GABAergic neurons (Ignell, R. *et al.*, 2001). Myotropic neuropeptides of the orcokinin family are found in cockroach and locust LNs, but not in moths, bees, and flies (Hofer, S. *et al.*, 2005).

4.41.2.4.4 Physiology of local neurons

LNs have action potentials (APs) in honeybees (Sun, X.-J. *et al.*, 1993a; Galizia, C. G. and Kimmerle, B., 2004), moths (Christensen, T. A. *et al.*, 1993), flies (Wilson, R. I. *et al.*, 2004), and cockroaches (Ernst, K. D. and Boeckh, J., 1983), but in locusts LNs are nonspiking (Laurent, G. and Davidowitz, H., 1994).

In species where LNs spike, they can be tonically active in the resting animal and increase or decrease their firing upon stimulation with odors. In bees and moths, most intracellular recordings from LNs show multiple spike amplitudes. This might indicate that LNs with complex branching patterns have multiple spike initiation zones or that LNs are electrically coupled. Alternatively, their fine processes might lead to artificial electrical connections created by

the penetrating sharp electrode, in which case multiple spike heights would be an experimental artifact (Galizia, C. G. and Kimmerle, B., 2004). HeteroLNs in honeybees have distinct odor-response profiles comparable to those of uniglomerular PNs. Generally, the odors they respond to correspond to the odors expected from the honeybee functional atlas, that is, LNs respond to those odors associated with its dominant glomerulus, suggesting that their morphologically dominant glomerulus is their input site (Galizia, C. G. and Kimmerle, B., 2004). In contrast, homoLNs studied in *Drosophila* have very broad response profiles, responding to most odors, with activity spread across their entire arborization (Ng, M. *et al.*, 2002; Wilson, R. I. *et al.*, 2004). Furthermore, *Drosophila* is the only species, so far, where both inhibitory and excitatory LNs have been characterized (Shang, Y. *et al.* 2007).

LNs influence the responses in PNs in at least two ways: first, with a very fast inhibition, mediated by GABA acting on ionotropic channels, and second, on a slower timescale, which leads to continuing inhibitions even after stimulus offset (Christensen, T. A. *et al.*, 1998a). Studies with pharmacological antagonists have shown that the fast GABA-mediated currents cause synchrony among PN spikes, and odor-evoked oscillations in the 20–30 Hz range (MacLeod, K. and Laurent, G., 1996). Furthermore, LNs also mediate a disinhibitory connection between OSNs and PNs, which leads to an excitatory response in PNs. In this sequential arrangement OSN–LN–LN–PN, a tonically active LN tonically inhibits a PN; upon OSN activity, another LN becomes active, inhibits this LN, and thereby releases the PN from its inhibition, resulting in PN activity (Av-ron, E. and Rospars, J. P., 1995).

Across insects, the available data are insufficient to draw firm conclusions about LN response profiles. The function that LNs play for olfactory coding is discussed below (Section 4.41.3.2).

4.41.2.5 Projection Neurons

PNs connect the AL to other brain areas. Uniglomerular neurons branch in a single glomerulus within the AL and have axons that lead from the AL to the MBs and to the LP. Multiglomerular neurons branch in several if not all glomeruli and generally have axons that do not innervate the MBs, but a variety of other areas in the protocerebrum, both lateral (close to and overlapping with the LP) and more central (surrounding the α-lobe of the MB). PNs have both input and output synapses within olfactory glomeruli. It is unclear, though, whether all PNs have output synapses within the AL or only some of them.

4.41.2.5.1 Projection neuron morphology and tracts

Nomenclature of PN tracts is inconsistent across insect species, reflecting both their morphological diversity and a lack of knowledge about the homology of the tracts involved. Morphologically, in most species there is a strong antennocerebralis tract (ACT) that travels along the brain midline (mACT (medial ACT) in bees and iACT (inner ACT) in most other species), and a generally smaller tract that travels close to the optic lobes (lACT (lateral ACT) in bees, oACT (outer ACT) in moth, and mACT in flies). In addition, there are several minor tracts that sometimes share parts with the lACT/oACT, and whose axons target different areas (multiglomerular ACTs (mlACTs) in bees and mACTs in most other species). I will therefore present different insects sequentially. Branching patterns of PNs in the MBs and the LP are discussed in their respective sections below.

In bees, uniglomerular PNs form two tracts, the lACT and the mACT (Mobbs, P. G., 1982). The mACT travels along the brain midline toward the MBs where collaterals enter into the MB calyces, and continues to end branching in the LP. PNs in the mACT originate from glomeruli of the T2, T3, or T4 group (Bicker, G. *et al.*, 1993; Abel, R. *et al.*, 2001; Kirschner, S. 2006) and have their somata in the ventrolateral and dorsal soma cluster of the AL (Bicker, G. *et al.*, 1993). The lACT leaves the AL dorsally and then travels on the lateral, or outer side, close to the optic lobes. Collaterals enter the LP, and the tract continues and also innervates the MB calyces. lACT PNs innervate T1 glomeruli and their somata lie in the anteroventral and lateral part of the AL (Schäfer, S. *et al.*, 1988). Thus, uniglomerular PNs separate in tracts according to their innervated glomerulus, and the separation corresponds to separate antennal tracts (T1–T4). The molecular mechanisms for this separation are unknown, but some insight comes from flies (see below). Uniglomerular PNs in honeybees have small branches at their exit points of the AL, which may form connections between cells outside their innervated glomeruli, but whose computational function is not yet understood (Müller, D. *et al.*, 2002; Galizia, C. G. and Kimmerle, B., 2004). The initial portion of the lACT is also shared by

multiglomerular fibers that innervate only the LP and the ring neuropil of the α-lobe (Abel, R. *et al.*, 2001). Most multiglomerular PNs, however, use the mlACT, which in fact consists of several small tracts. Their axons also innervate the LP and the neuropil around the α-lobe. Within the AL, they branch sparsely within glomeruli (Fonta, C. *et al.*, 1993; Abel, R. *et al.*, 2001). The number of glomeruli that each multiPN innervates within the AL varies, ranging from a few to many or possibly all.

In *Manduca*, tracts are iACT, mACT, and oACT (Homberg, U. *et al.*, 1988). Most neurons in the iACT are uniglomerular, while most neurons in mACT and oACT are multiglomerular. Axons in the iACT and oACT innervate MB calyces and the LP, while axons in the mACT innervate a variety of foci in the LP but not the MBs (Homberg, U. *et al.*, 1988).

Fly tracts are also named iACT, mACT, and oACT (and, as in other species, these may be subdivided further), but these do not correspond to the moth nomenclature. The inner tract (traveling along the brain midline) has the strongest input to the MB calyces. The medial tract has some axons that innervate the MB calyces, while most axons target only the LP. Axons in the oACT do not innervate the MB calyces. All tracts innervate the LP (Stocker, R. F. *et al.*, 1990; Stocker, R. F., 1994; Strausfeld, N. J. *et al.*, 2003). Thus, *Drosophila*'s iACT and mACT may correspond to the honeybee's mACT and lACT, or the moth's iACT and oACT, respectively. As in bees, glomerular identity and tract are probably related in flies: the GH146 line labels PNs with somata in the anterodorsal cluster (adPN) and lateral cluster (lPN), which have axons that use the iACT and send their dendrites to about 30–35 stereotypical glomeruli (Jefferis, G. *et al.*, 2001; Marin, E. C. *et al.*, 2002; Wong, A. M. *et al.*, 2002; Jefferis, G. S. *et al.*, 2007; Lin, H. H. *et al.*, 2007). The tract used by PNs innervating the remaining glomeruli is unknown. GH146 also labels at least four PNs that use the mACT and at least one PN that uses the oACT. The POU domain transcription factors, Acj6 and Drifter, are expressed in adPNs and lPNs, respectively, and are required for their dendritic targeting (Komiyama, T. *et al.*, 2003). Interestingly, these genes are also necessary for OSN targeting (see Section 4.41.2.3.4).

PN tracts in cockroaches follow an only partially similar nomenclature: the iACT travels along the brain midline, the oACT travels along the optic lobes, and intermediate tracts have been named ACT tracts II, III, and IV (Malun, D. *et al.*, 1993). PNs in iACT are uniglomerular and innervate both the MB calyces and the LP. Pheromone-sensitive PNs in male cockroaches only use the iACT (Malun, D. *et al.*, 1993). PNs in tract II are also uniglomerular and innervate both MB and LP. PNs in the other tracts are multiglomerular and innervate the LP only (tracts III and oACT) or several brain areas including the MBs (tract IV, which originates from the same root in the AL as the oACT) (Malun, D. *et al.*, 1993).

PNs in locusts have a different morphology from what has been described so far. No uniglomerular PNs have been reported yet; rather, within the AL, PNs branch in a limited number of glomeruli (Laurent, G. *et al.*, 1996; Anton, S. *et al.*, 2002). This is reminiscent of the multiple glomeruli innervated by individual OSNs, but the two do not form corresponding groups, that is, PNs innervate groups of glomeruli that do not correspond to groups innervated by an OSN (Anton, S. *et al.*, 2002). In other words, glomerular groups in locusts cannot be functionally analogous to single glomeruli in other insects. In locusts, only a single ACT close to the brain midline connects the ALs to the MB (Leitch, B. and Laurent, G., 1996), but minor tracts that connect the AL to other areas do exist (Ignell, R. *et al.*, 2001).

4.41.2.5.2 Projection neuron numbers

In honeybees, the lACT and mACT probably house about 400 fibers each, and the mlACT much less, giving a total of less than 1000 (Rybak, J., 1994). This figure may represent an upper limit, considering that the number of PNs has also been estimated at 500 (Bicker, G. *et al.*, 1993) or 800 PNs (Hammer, M., 1997).

Manduca has ~400 uniglomerular PNs in the iACT and ~340 in the oACT, and ~122 multiglomerular PNs in the mACT (Homberg, U. *et al.*, 1988).

In *Drosophila*, the GAL4 line that is most often used for investigating properties of PNs is GH146 (Heimbeck, G. *et al.*, 2001). This line labels about 80–90 PNs, of which 85 are uniglomerular and travel in the iACT, with somata in the anterodorsal (40–50) and lateral cluster (30–35), and 6–7 are multiglomerular, do not use iACT, do not innervate the MB, and have their somata in the ventral cluster (Jefferis, G. *et al.*, 2001; Wong, A. M. *et al.*, 2002). The total number of PNs in *Drosophila* is estimated to be 150–200 (Stocker, R. F. *et al.*, 1997). The proportion of multiglomerular PNs with respect to uniglomerular PNs is below 10% in *Drosophila*.

An estimate of cockroach PN number is 250 (Ernst, K. D. *et al.*, 1977). The number of PNs in

locusts is ~830 (Leitch, B. and Laurent, G., 1996), based on counting axon profiles in the main ACT tract.

4.41.2.5.3 Projection neuron transmitters

Most uniglomerular PNs have ACh as transmitter. In bees, mACT PNs are AchE-positive, showing that they use ACh (Kreissl, S. and Bicker, G., 1989). Furthermore, Kenyon cells (KCs) express nicotinic ACh receptors and are activated by ACh (Bicker, G. and Kreissl, S., 1994). Fibers in the honeybee lACT are not cholinergic; they are taurin-immunoreactive (Bicker, G. *et al.*, 1993). No responses to taurin application could yet be measured in cultured KCs (Grünewald, B., personal communication). In moths, ~67 somata associated with the AL stain for AChE, and the oACT leading to the LP and the MB is stained (Homberg, U. *et al.*, 1995). The situation in *Drosophila* is similar, with at least one tract strongly stained for AChE (Yasuyama, K. and Salvaterra, P. M., 1999). In locusts, the ACT tract stains for AChE (Homberg, U., 2002).

Multiglomerular PNs that are GABAergic have been shown in bees (Schäfer, S. and Bicker, G., 1986), moths (Hoskins, S. G. *et al.*, 1986), and flies (Ito, K., personal communication). No other transmitter has so far been associated with multiglomerular PNs.

4.41.2.5.4 Projection neuron physiology

Responses in insect PNs have been measured at the single-cell level with electrophysiological techniques in a variety of species (Hansson, B. S. *et al.*, 1991; Christensen, T. A. *et al.*, 1998a; 1998b; Abel, R. *et al.*, 2001; Müller, D. *et al.*, 2002; Galizia, C. G. and Kimmerle, B., 2004; Wilson, R. I. and Laurent, G., 2005). Optical methods were successful in bees after loading PNs with calcium-sensitive dyes (Sachse, S. and Galizia, C. G., 2002; 2003) and in flies after genetically expressing activity-sensitive proteins (Fiala, A. *et al.*, 2002; Ng, M. *et al.*, 2002; Wang, J. W. *et al.*, 2003; Yu, D. *et al.*, 2004). PNs are spontaneously active in insects, including honeybees (Abel, R. *et al.*, 2001; Galán, R. F. *et al.*, 2005), moths (Christensen, T. A. *et al.*, 1998b), *Drosophila* (Wilson, R. I. *et al.*, 2004), cockroaches (Boeckh, J. *et al.*, 1987), and locusts (Perez-Orive, J. *et al.*, 2002). Against this background, responses to odors can be both excitatory and inhibitory. Their responses are shaped by the AL network (Christensen, T. A. *et al.*, 1998a; Sachse, S. and Galizia, C. G., 2002; Wilson, R. I. and Laurent, G., 2005; Olsen, S. R. *et al.*, 2007; Schlief, M. L. and Wilson, R. I. 2007; Shang, Y. *et al.*, 2007).

Instantaneous response frequencies of excitatory responses can be several hundreds of Hertz and persist over the duration of a 2-s stimulus. In honeybees, lACT neurons tend to respond to many odors with excitation, whereas mACT neurons display more complex responses to different odors, including phases of excitation and inhibition (Abel, R. *et al.*, 2001; Müller, D. *et al.*, 2002). PN physiology is discussed below in more detail (see Section 4.41.3).

4.41.2.6 Feedback Neurons and Biogenic Amines

Neurons that branch in the AL and also in other brain areas have been found in many insect species. There are many different morphologies and biochemical profiles of these neurons, but part of the apparent variability among species might be due to limited knowledge of these cells. Many of these neurons stain with antibodies against biogenic amines (dopamine, serotonin, octopamine, and histamine) and are believed to have a modulatory function, including up- and downregulation, thresholding, motivational states, attention, and learning (Hammer, M. and Menzel, R., 1998; Bicker, G., 1999b; Homberg, U. and Müller, U., 1999). Other possible feedback neurons are the honeybee AL-1 neurons that originate in the MB α-lobe and project widely through the ALs (Rybak, J. and Menzel, R., 1993). Dye injections into single neurons have also revealed the existence of neurons with somata in the subesophageal ganglia (SEG), of which some innervate only a few glomeruli in the AL symmetrically on both sides, and send collaterals to the MB (Abel, R. *et al.*, 2001).

I review evidence for biogenic amines (Bicker, G., 1999b; Monastirioti, M., 1999; Homberg, U., 2002) in the order dopamine, octopamine (Stevenson, P. A. and Sporhase-Eichmann, U., 1995; Roeder, T., 1999; Pflüger, H. J. and Stevenson, P. A., 2005), serotonin (Homberg, U., 2002), and histamine (Nässel, D. R., 1999).

Dopamine: Dopamine has been found in many insect ALs, but there is considerable variation in its presence and distribution (Homberg, U. and Müller, U., 1999). In honeybees, four large dopamine-immunoreactive cells innervate the glomeruli and central neuropil of each AL. Two of their somata lie in the dorsolateral cell-body rind of the AL and the other two close to the dorsal rind of the SEG (Schäfer, S. and Rehder, V., 1989). These neurons form a fine plexus both in the central neuropil of the AL and in the glomeruli and also branch in the DL, the

protocerebrum, and the SEG. Within the glomeruli, they are restricted to the core (Schürmann, F. W. *et al.*, 1989). While there are dopaminergic neurons in moth brains, their precise morphology is not yet known (Mesce, K. A. *et al.*, 2001). No dopamine was found in fly ALs (Nässel, D. R. and Elekes, K., 1992; Friggi-Grelin, F. *et al.*, 2003). In cockroaches, there are dopaminergic centrifugal neurons, and in addition, some LNs are dopamine-positive (Distler, P. G., 1990). In locust ALs, no dopamine immunoreactivity was found (Wendt, B. and Homberg, U., 1992).

Octopamine: All honeybee glomeruli contain octopamine-immunoreactive fibers, deriving from very few profiles entering the AL from ventroposterior. Within the outer cap of the glomeruli, these fibers appear to be of considerably larger diameter than the very thin fibers in the glomerular centers (Kreissl, S. *et al.*, 1994). A neuron that most likely uses octopamine in honeybees is the ventral unpaired median cell of maxillary neuromere 1 (VUMmx1), which has an unpaired soma in the subesophageal ganglion. Apart from the AL, this neuron has branches in the subesophageal ganglion itself and in the protocerebrum (MB and LP). The input–output relationship in the innervated areas is unknown (Kreissl, S. *et al.*, 1994; Bicker, G., 1999b). Functionally, it represents (part of) the unconditioned stimulus (US) in an appetitive learning paradigm (Hammer, M., 1993). When a honeybee is presented an odor (conditioned stimulus, CS) and rewarded with sugar water (US), she will extend the proboscis to lick the sugar water (proboscis extension reflex (PER)). After the learning trial, odor alone elicits a PER (classical or Pavlovian conditioning). Replacing the US with a depolarization of VUMmx1 also leads to an association, and preventing VUMmx1 to spike by hyperpolarizing it during a sugar water stimulus impairs learning (Hammer, M., 1993). In honeybees, octopamine is also related to division of labor within the hive (Schulz, D. J. *et al.*, 2002).

Octopamine is also present in fine arborizations within the AL in moths (Homberg, U. and Müller, U., 1999). These arborizations probably derive from at least three VUM neurons that also innervate the MBs, somewhat reminiscent of VUMmx1 in honeybees (Dacks, A. M. *et al.*, 2005). However, the detailed anatomy of these neurons is quite different between bees and moths, leaving their homology in doubt (Dacks, A. M. *et al.*, 2005). In the moth's periphery, octopamine increases responses to pheromones, but not to general odors (Pophof, B., 2002). In flies, a cluster of neurons in the SEG (SM cells) has a similar morphology to the honeybee VUM neurons, also innervating the ALs (Monastirioti, M., 1999). Octopaminergic neurons in the cockroach AL branch similar as in honeybee (Sinakevitch, I. *et al.*, 2005). In locusts, octopamine is present in fine arborizations within the AL (Homberg, U. and Müller, U., 1999), probably from dorsal unpaired neurons (DUM) in the SEG (Bräunig, P., 1991; Stevenson, P. A. and Sporhase-Eichmann, U., 1995).

Serotonin: In honeybees, there are two paired neurons immunoreactive for serotonin (5-hydroxytryptamine (5HT)), one in each side of the body, called the deutocerebral giant (DCG) neurons, which innervate the ipsilateral AL, the DL, and the SEG and descend into the ventral nerve cord. Their somata lie in the dorsolateral cell body cluster of the AL (Rehder, V. *et al.*, 1987). Within the glomeruli, serotonergic fibers are restricted to the outer cap (Schürmann, F. W. and Klemm, N., 1984). Two serotonergic neurons in the moth *M. sexta* have been well characterized (Kent, K. S. *et al.*, 1987; Sun, X.-J. *et al.*, 1993b). These neurons have their soma close to the AL and branch in the core of all glomeruli within the contralateral AL, without forming overlap with OSN afferent fibers that innervate the outer cap. They receive input in the superior protocerebrum, the MB, and the lateral accessory lobes. This anatomy suggests a role as feedback neurons, or as centrifugal modulators of AL responses. In flies, there are two serotonergic neurons associated with each AL that branch in olfactory glomeruli (Nässel, D. R., 1988). A pair of serotonergic neurons is also found in cockroaches, where each neuron has a soma in the AL, extending a neurite to the protocerebrum including the MB and then back to the AL where it branches and makes output synapses in most if not all glomeruli (Salecker, I. and Distler, P., 1990). In locusts, there are three serotonin-positive cells in each AL, innervating all glomeruli. These neurons are multiglomerular PNs that project toward the MB, without entering them. One has an axon in the iACT, and the other in an intermediate ACT (dmACT) (Ignell, R. *et al.*, 2001).

Histamine: In the honeybee AL, there are ~35 LNs that are immunoreactive for histamine (Bornhauser, B. C. and Meyer, E. P., 1997). Histamine acts as an inhibitory transmitter in this species (Sachse, S. and Galizia, C. G., 2002). In moths, histamine is not present in LNs, but it is present in two centrifugal neurons that innervate both ALs each and that also arborize in the AMMC and the SEG (Homberg, U. and Hildebrand, J. G., 1991). There

are no histaminergic neurites in *Drosophila* ALs (Nässel, D. R., 1999). Histamine is found in cockroach LNs, with a few somata around the ALs, and possibly a tract connecting to the AL ventrally (Pirvola, U. *et al.*, 1988). In the locust, there is one histamine-positive neuron in each AL that projects to the LP (Ignell, R. *et al.*, 2001).

4.41.2.7 Glial Cells

Glial cells have been analyzed in several insect species, including bees (Hähnlein, I. and Bicker, G., 1996), *Drosophila* (Jhaveri, D. *et al.*, 2000; Jhaveri, D. and Rodrigues, V., 2002; Jhaveri, D. *et al.*, 2004), cockroaches (Prillinger, L., 1981), and locust ALs (Hähnlein, I. *et al.*, 1996). Glial cells are certainly best known in moths (Kretzschmar, D. and Pflugfelder, G. O., 2002; Oland, L. A. and Tolbert, L. P., 2003; Tolbert, L. P. *et al.*, 2004). The cells are prominent on the outside of the AL and form thin processes that digitate between glomeruli well into the AL, thus separating them from each other. Glial cells are invisible in light microscopy and difficult to discern in electron microscopy. In species where glomeruli are arranged around a central, nonglomerular neuropil (coarse neuropil, e.g., honeybees, moths) glial cells do not form a border between glomeruli and the central neuropil. It should be noted that there is no universal glial cell marker in insects and that glial fibrillary acidic protein (GFAP) does not label insect glial cells.

Several different types of glial cells are associated with the AL. Along the antennal nerve, glial cells with long processes and multiple expansions enwrap axon fascicles. OSN axons travel as parallel bundles within the antennal nerve, but as they approach the AL, they reach a so-called sorting zone, where they form a dense and complex network, which results in a rearrangement of neighborhood relationships that ultimately leads to appropriate glomerular targeting. Glial cells are necessary for this rearrangement to occur (Oland, L. A. *et al.*, 1988; Rössler, W. *et al.*, 1999b). Within the AL, there are at least two glial-cell types that form borders around glomeruli: one has large cell bodies and branching, vellate arbors and the other has multiple, mostly unbranched processes with many lamellate expansions along their length that surround glomeruli as part of a multilamellar envelope (Oland, L. A. *et al.*, 1999). Glia in the neuropil is instrumental for protoglomerulus formation and proper development of the AL (Baumann, P. M. *et al.*, 1996). These mechanisms are mediated by direct contact between the OSN axon growth cones and the glial cells themselves, as shown *in vitro* (Tucker, E. S. and Tolbert, L. P., 2003; Tucker, E. S. *et al.*, 2004).

In the adult, glial cells might help keeping neural activity separate between glomeruli, and thus increasing the discriminatory power of the system. Goriely and colleagues simulated the movement of K^+ ions within the AL in a mathematical diffusion model based on electron microscopic data and found that the glial envelope could efficiently reduce ion movement between glomeruli. Since K^+ accumulation in extracellular space causes cell depolarization, this barrier might prevent cross talk between adjacent glomeruli (Goriely, A. R. *et al.*, 2002). Glia might also form a sink for the gaseous messenger NO, given that NO is involved in glial cell physiology (Gibson, N. J. *et al.*, 2001).

4.41.2.8 Cellular Organization and Number Relationships

What is the numerical relationship of the different neuron types in the AL, and how many neurons of each type innervate each glomerulus? The numbers differ widely among insects. For example, a single honeybee glomerulus is innervated on average by almost 400 OSNs (60 000 OSNs onto 160 glomeruli), 1000 LNs (as a gross estimate, assuming a total of 4000 LNs, with each innervating an average of 40 glomeruli), and 5 PNs (800 PNs in 160 glomeruli). The fruit fly *D. melanogaster* has fewer OSNs, but since most OSNs project into the ALs of both sides, the relationship of OSNs and glomerulus is 50:1. Each glomerulus is innervated by three PNs, on average (Wong, A. M. *et al.*, 2002). These average considerations do not consider that OSNs of different classes vary greatly in number, and therefore, the convergence/divergence ratio might span a wide range in different glomeruli not only across species but also within a species.

4.41.3 Functional Organization in the Antennal Lobe

Is it possible to attribute functional tasks to each neuron type in the AL? In a greatly simplified picture, the answer is yes, as developed elsewhere (Sachse, S. and Galizia, C. G., 2005). An interpretation of the main cell types forming the AL circuitry could then be as follows (see below for more details).

1. Homogeneous LNs uniformly innervate the AL and accomplish a gain control function. They set the background activity close to the threshold, thus optimizing the system's sensitivity. They also protect the system from overloading and are ideal candidates for driving oscillations.
2. Heterogeneous or asymmetric LNs enhance the contrast of across-glomeruli patterns by unidirectional connections between input glomeruli and output glomeruli.
3. Excitatory LNs may distribute information accross glomarular boundaries or amplify responses within glomeruli (see above).
4. Multiglomerular PNs have access to the entire AL. They may respond to global activity and thus give information about stimulus timing (onset/offset) and concentration and would be ideal candidates for cellular learning in the AL.
5. Uniglomerular PNs extract the activity of single glomeruli and project to higher-order brain centers. The identity of an odor is encoded in the combinatorial activity pattern across their axons' identities.

4.41.3.1 Odor-Evoked Activity Across Glomeruli

When an animal is challenged with an odor, many different receptor neurons are activated. Their axons send that activity to the AL in the form of AP trains. Due to the convergence of functionally equivalent axons onto individual glomeruli, the result is a pattern of glomeruli that are activated to a varying degree. Therefore, activity patterns across glomeruli are not binary (on/off), but continuous (each glomerulus can be activated to varying degrees). The resulting combinatorial odor patterns are sufficient, in terms of the information contained in the patterns, to identify an odor, and therefore could represent the olfactory code. However, it is not known what information is really used by the brain, and therefore, the biological olfactory code remains to be deciphered.

Odor-evoked combinatorial patterns can be measured with imaging techniques, because this allows for measuring several combinatorial odor responses across glomeruli within individual animals. Unfortunately, the temporal resolution is not yet sufficient to resolve individual APs, and therefore, imaging studies are limited to measuring time-averages of neural activity.

Responses have been measured in *D. melanogaster* by using genetically encoded reporter proteins. synaptopHluorin was used to measure synaptic vesicle release (Ng, M. *et al.*, 2002; Yu, D. *et al.*, 2004) and cameleon or G-CaMP for intracellular calcium (Fiala, A. *et al.*, 2002; Wang, J. W. *et al.*, 2003; Suh, G. S. *et al.*, 2004). These proteins were expressed under the control of specific promoters, which allow for a good reproducibility of the measured cells. For example, using the GAL4 line GH146, a reporter protein can be expressed in a population of brain cells that within the AL only consists of PNs. Similarly, expressing the reporter in GABAergic cells allows to exclusively measure inhibitory cells (mostly LNs, and a subpopulation of PNs). However, the relative contribution of different cell groups labeled by the same genetic line cannot be separated if they overlap spatially. Currently, the clearest separation can be expected from OSN populations, where reporter proteins can be driven to be expressed in all cells that also express ORs, or just a particular OR.

In species that do not have the molecular power of *Drosophila*, synthetic reporters can be used to stain the cells. Bath application of calcium-sensitive dyes has revealed odor responses in bees (Joerges, J. *et al.*, 1997; Galizia, C. G. and Menzel, R., 2001), ants (Galizia, C. G. *et al.*, 1999a), and moths (Galizia, C. G. *et al.*, 2000a; Carlsson, M. A. *et al.*, 2002; Hansson, B. S. *et al.*, 2003). Because the dye is applied in the bath, the exact proportion of measured cells cannot be determined and might include all neuron types as well as glial cells, making a cellular interpretation of the results difficult. In bees, however, the response magnitude (though not the time course) is a good estimate of receptor neuron response for each glomerulus (Galizia, C. G. and Vetter, R. S., 2004). In moths, measurements of released NO closely mirror the activity patterns measured with bath-applied calcium dyes (Collmann, C. *et al.*, 2004). Since in moths NO is produced only by OSNs (Gibson, N. J. and Nighorn, A., 2000), this suggests that also in this species the (bath-applied) calcium indicator response magnitude can be used to estimate OSN activity for each glomerulus. Time courses of these calcium responses do not correspond to electrophysiological measurements of OSNs: they rise continuously during the stimulus and decay slowly following the shape of a mathematical α-function (Stetter, M. *et al.*, 2001). Odor responses can also be measured with voltage-sensitive dyes (VSDs) (Galizia, C. G. *et al.*, 1997; 2000b). PNs can be measured without a contribution from other cell types if they are backfilled from the protocerebrum (Sachse, S. and Galizia, C. G., 2002; 2003). These selective stainings lead to calcium

responses that are fast, with a steep rise at stimulus onset and a steep decay at stimulus offset. As in mammals (Xu, F. *et al*., 2000; Leon, M. and Johnson, B. A., 2003), the spatial odor-response patterns have also been recorded using 2-DG labeling in fruit flies (Buchner, E. and Rodrigues, V., 1983; Rodrigues, V. and Buchner, E., 1984) and in *Calliphora* (Distler, P. G. *et al*., 1998a). This brings the advantage of having a permanent preparation, but the disadvantage of having but one measurement per animal, and no dynamic information.

An important strength of insect preparations is that glomeruli can be identified among animals, given their small number and their characteristic arrangements. Using VSD in honeybees allows recognizing the glomerular layout very clearly in the staining pattern (Galizia, C. G. and Vetter, R. S., 2004). This shows that activity patterns are indeed glomerular, that is, that the boundaries of highly active regions coincide with the boundaries of individual glomeruli. With identifiable glomeruli, comparison and characterization is straightforward. Even in species where a morphological atlas of glomeruli is not yet available, or when identifying glomeruli is not possible, odor-evoked patterns are so stereotype among individuals that a direct quantification can often be achieved (Meijerink, J. *et al*., 2003; Skiri, H. T. *et al*., 2004).

A recent development in insect olfactory recordings is the use of multielectrode arrays, which allow the simultaneous extracellular recording of many neurons but do not allow identifying the neurons involved (Christensen, T. A. *et al*., 2000).

4.41.3.2 Processing in the Antennal Lobe

The only olfactory information that is available to the brain must be present in OSN activity. However, not all information present in the OSNs is kept in PNs. The cellular network formed by OSNs, LNs, and PNs extracts information and creates a modified odor representation. The activity patterns across PNs are combinatorial and temporally fluctuating.

4.41.3.2.1 Contrast enhancement in the antennal lobe

In the AL network, an input layer (OSN) is transformed by internal connections (LNs) into an output layer (PNs). This resembles a neural network as it is often used in computational neurobiology (Getz, W. M., 1991; Linster, C. *et al*., 1994; Getz, W. M. and Lutz, A., 1999; Brody, C. D. and Hopfield, J. J., 2003), and indeed, the AL has often been modeled as such (Getz, W. M., 1991; Linster, C. *et al*., 1994; Getz W. M. and Lutz, A., 1999; Rabinovich, M. I. *et al*., 2000; Bazhenov, M. *et al*., 2001). Since both input and output are organized in the same glomeruli, this network has the additional beauty of having equal dimensionality for input and output. Therefore, the question of what role the hidden layer plays can easily be addressed by comparing the glomerular activity of PNs with the glomerular activity in the OSNs. This approach has been taken in several studies, with surprisingly disparate results. In optical imaging studies in *Drosophila*, the difference between PNs and OSNs was so small that no apparent processing was deducible (Ng, M. *et al*., 2002; Wang, J. W. *et al*., 2003). In an electrophysiological study comparing the input and the output of glomerulus DM2, also in *Drosophila*, the response spectrum was apparently broader in PNs than in OSNs (Wilson, R. I. *et al*., 2004). Comparing the input and the output for odor-concentration dose–response curves in honeybees showed that glomeruli with a low threshold for an odor have almost identical dose–response curves in PNs and in OSNs, while less-sensitive glomeruli have a shifted dose–response curve in PNs, showing that at higher concentrations LNs suppress these PN responses (Sachse, S. and Galizia, C. G., 2003). Thus, within 2 years, publications suggesting no change, response broadening, and response sharpening have been published. One difficulty arises from comparing activity across different neuron populations (OSNs and PNs). Conceptionally, the quantitative interpretation of such a comparison is impossible, because the conversion rate of neural activity is unknown. In electrophysiological studies, an AP in an OSN has a different value from an AP in a PN, and therefore, comparing AP numbers *per se* is impossible. For example, one AP in an OSN might be sufficient to strongly depolarize the PNs in the innervated glomerulus (given the high convergence of many OSNs in that glomerulus and the many synapses made by each OSN axon), while even several APs in a PN might not represent a significant signal in the MBs (given the high spontaneous activity level in these neurons and the possible need for APs to synchronize with other APs). The same argument is valid when optical signals are measured: calcium measurements record changes due to several intracellular cascades of dendritic and presynaptic calcium, and the measurements of synaptic exocytosis are similarly affected. Furthermore, transfer functions among neurons are not linear, again clouding a quantitative comparison of different neuron populations.

Therefore, the question of what the population of LNs is computing within the AL has to be addressed with different techniques. Linster C. and coworkers (2005) created a computer model of the AL and ran experimental data from honeybees under different assumptions about the connectivity of the LN network, comparing three network types: one where LNs interconnect neighboring glomeruli, one with stochastic connections, and one based on the odor-response properties of glomeruli. This approach avoids comparing PN and OSN activity directly but rather compares different network architectures and finds the one that matches best with experimental data. The results show that, in honeybees, inhibitory connections are strongest among glomeruli that have similar odor-response profiles, and weakest among glomeruli that do not overlap in their odor-response profiles, irrespective of their spatial position (Linster, C. *et al.*, 2005). This leads to an optimization of odor responses in PNs across odors, by reducing response overlap to similar odors, and supports the theory that the AL sharpens odor-response profiles.

Such a glomerulus-specific network is likely to be realized by heteroLNs, which densely innervate one glomerulus and diffusely innervate a limited number of other glomeruli. Because these neurons are not symmetrical, a glomerulus A that inhibits a glomerulus B does not need to receive inhibitory input from B. Physiological evidence for such a nonsymmetrical connectivity has been found in bees (Sachse, S. and Galizia, C. G., 2002). Interestingly, in behavioral experiments where odor similarity was studied, such an asymmetry has also been found: similarity from an odor A to B does not imply the same similarity from odor B to A (Guerrieri, F. *et al.*, 2005).

4.41.3.2.2 Sensitivity optimization in the antennal lobe

Some OSNs are active even without a stimulus, but this activity is not temporally complex. On the other hand, many electrophysiological recordings show that PNs are spontaneously active with a pronounced temporal complexity. As a consequence, continuously changing glomerular activity patterns are seen across glomeruli (for example see Relevant Websites section) (Sachse, S. and Galizia, C. G., 2002; Galán, R. F. *et al.*, 2005). If the response strength were normalized, an experimenter would not be able to distinguish individual events of spontaneous activity from odor-evoked responses. The spontaneous activity might result from a mechanism that increases the sensitivity to weak odors (Sachse, S. and Galizia, C. G., 2005). In this model, PNs can be compared to a loaded spring. An inhibitory feedback loop of LNs keeps PNs at firing threshold, so that minimal olfactory stimuli will suffice to elicit an odor-evoked pattern. In order to maintain PNs at threshold, their depolarization must constantly be probed, which is apparent as spontaneous activity. Such a mechanism may seem to interfere with a reliable representation of odor concentration. However, measuring odor concentration is much more affected by odor adaptation at the periphery, a phenomenon known from all sensory systems. Due to the phasic response properties of OSNs, the olfactory system always measures concentration changes rather than absolute concentrations. In the adapted state, the loaded spring model of the AL therefore ensures that even small increases in odor concentration will lead to them being detected by the animal. The strength of the olfactory stimulus (i.e., the concentration change magnitude) remains reliably coded in the response magnitude change across olfactory glomeruli (Sachse, S. and Galizia, C. G., 2005).

4.41.3.2.3 Temporal activity structures

Odor responses are already temporally structured at the level of OSNs: some OSNs have phasic, some have tonic responses, some have activity that outlasts the odor stimulus, and some reduce activity upon olfactory stimulation (de Bruyne, M. *et al.*, 2001). As a consequence, an olfactory stimulus that is temporally uniform leads to a pattern of activity that is temporally complex. In addition, in the natural environment of insects, odors themselves are temporally complex due to air turbulence (Murlis, J. *et al.*, 1992; Justus, K. A. *et al.*, 2005). This complicates the analysis of temporal patterns within the brain, suggesting that slow patterns might predominantly reflect stimulus variation (Vickers, N. J. *et al.*, 2001).

Response properties on a fast temporal scale can only be measured with electrophysiological techniques. Single-cell recordings allow to fill neurons with a dye and then to identify the glomerulus that was innervated (Müller, D. *et al.*, 2002; Galizia, C. G. and Kimmerle, B., 2004). Slow temporal structures consisting of sequences of bursts and inhibitory events are found in PNs in all insects studied so far, including moths (Christensen, T. A. *et al.*, 1998b), locusts (Laurent, G., 1996), and honeybees (Abel, R. *et al.*, 2001; Müller, U. and Hildebrandt, H., 2002). In locusts and honeybees, blocking chloride channels with Picrotoxin does not prevent these slow temporal patterns (MacLeod, K. and Laurent, G., 1996;

Stopfer, M. *et al*., 1997) but modifies them (Sachse, S. and Galizia, C. G., 2002). This suggests that they may partially originate in the OSN input or from a Picrotoxin-insensitive inhibitory network.

Behavioral studies have shown that olfactory decisions are taken rapidly in rats (Uchida, N. and Mainen, Z. F., 2003; Abraham, N. M. *et al*., 2004) and in bees (Ditzen, M. *et al*., 2003). This time was ~200 ms for mice and ~690 ms for honeybees, which included the time needed for olfactory recognition as well as motor responses and physical displacement of the animal. The time needed for olfactory discrimination is not affected by the difficulty of the olfactory task in terms of odor similarity or concentration (Ditzen, M. *et al*., 2003; Uchida, N. and Mainen, Z. F., 2003), or the difference in time, when present, is small (Abraham, N. M. *et al*., 2004). Physiological studies of PN responses show that 200–300 ms in locusts (Stopfer, M. *et al*., 2003) and 400 ms in bees (Galán, R. F. *et al*., 2004) are needed to reach the most distinct odor classification in the AL irrespective of odor concentration. Therefore, the later phases of slow activity components cannot be behaviorally relevant for odor discrimination. However, these late activities might play a role in olfactory learning or other aspects of olfactory processing that might occur after discrimination has taken place. An argument in favor of this interpretation is that odor representation is ameliorated during the first 2 s after stimulus onset, leading to a clearer distinction of odors (Galizia, C. G. *et al*., 2000b; Friedrich, R. W. and Laurent, G., 2001).

Fast temporal structures are evident in odor-evoked oscillations, which are found almost ubiquitously in olfactory systems. So far, within insects, only *Drosophila* seems not to respond with oscillation (Wilson, R. I. *et al*., 2004), while cockroaches (27 Hz), locusts (22 Hz), bees (30 Hz), wasps (17 Hz) all do (Stopfer, M. *et al*., 1999), and moths also (Heinbockel, T. *et al*., 1998). Applying Picrotoxin abolishes these oscillations (MacLeod, K. and Laurent, G., 1996; Stopfer, M. *et al*., 1997) and also modifies the spatial activity patterns across glomeruli (Sachse, S. and Galizia, C. G., 2002). Oscillations originate from many PNs firing APs simultaneously, due to a rhythmical inhibition from LNs that branch over large areas within the AL and the brain. Because individual PNs do not fire in every oscillation cycle, and because some APs also occur out of the rhythmic synchrony pattern, a model of olfactory coding has been proposed where odor identity would be encoded in sequences of changing PN ensembles (Laurent, G., 1999). However, other interpretations for synchronized APs have also been proposed, where synchrony would be more related to odor concentration or intermittency rather than to odor quality (Christensen, T. A. *et al*., 2000).

4.41.3.3 Combinatorial Odor Codes

Odors evoke combinatorial patterns of activated glomeruli, with each glomerulus participating in activity to many odors. These patterns are conserved among individuals (Galizia, C. G. *et al*., 1999c; Wang, J. W. *et al*., 2003), which is a consequence of the innate mapping of OSNs that express a given OR to individual glomeruli (Vosshall, L. B. *et al*., 2000; Couto, A. *et al*., 2005; Fishilevich, E. and Vosshall, L. B., 2005). As a corollary, patterns are also bilaterally symmetrical (Galizia, C. G. *et al*., 1998).

MRRs are best described as (some more, some less) broadly tuned to a best molecule (Sachse, S. *et al*., 1999). Importantly, there are no glomeruli for functional groups or other chemical parameters (e.g., aldehyde or C6 carbon chain). While some glomeruli preferentially respond to one functional group rather than another when tested for aldehydes, ketones, alcohols, carbon acids, or alkanes, they always respond also to other functional groups, even though the response is weaker. Furthermore, they always have a particular preferred range of molecule size to which they respond. Therefore, the response profile of individual glomeruli is not determined by particular features of the odorant (sometimes referred to as odotopes), such as ketone group or aldehyde, and the olfactory code is not a building set, where 1-heptanol would be coded in an alcohol glomerulus plus a C7 aliphatic chain glomerulus.

4.41.3.4 Coding Odor Concentration and Odor Mixtures

With increasing concentration, activity increases both in magnitude and in number of active glomeruli. As a corollary, with decreasing concentration, activity decreases and consists of a single glomerulus being active at very low concentration. This is a direct consequence of the receptors' MRRs that form the input: each receptor has a few substances to which it responds with a higher affinity than any other receptor, and at its lowest effective concentration, that substance will elicit a combinatorial pattern of activity in the AL that consists of that single glomerulus being active, and all other glomeruli being silent. At higher concentrations, many glomeruli are active, and every glomerulus takes

part in activity patterns of several odors. Again, this is a direct consequence of the broadening MRR of receptors with increasing concentrations. PN responses in honeybees are qualitatively stable over a concentrations range of up to 4 log units, because higher odor concentrations increase total response intensity without changing the relative intensity across glomeruli; at the input level, however, the activity patterns are more affected by concentration differences (Sachse, S. and Galizia, C. G., 2003). Thus, the neural network within the AL contributes to concentration invariance.

Mixture coding is complex and far from understood in insects. Most naturally occurring odors consist of a large number of volatile compounds. Additionally, the turbulent nature of air leads to odor plumes being mixed in a chaotic fashion (Murlis, J. *et al.*, 1992). This creates a difficult task for the olfactory system: should it create a synthetic representation of the blend, or rather an analytical separation of the components, or both? Several studies have asked how many odors animals can differentiate in a mixture. However, results cannot be generalized: perfumers know that some odors do blend, while others do not. Therefore, the number of discriminable odors depends on the quality of the odors mixed. Electrophysiological studies have also shown different kinds of mixture interactions. The presence of an odor B can interfere with the normally strong response to an odor A, which is termed mixture suppression. Conversely, a neuron or glomerulus may respond to a binary mixture with a response that exceeds the summed responses to the single components, defined as synergism. An inhibitory network within the AL optimized for sharpening odor-response patterns should have the effect of creating stronger mixture interactions with similar odors than with odors that elicit nonoverlapping response patterns. Psychophysically, this implies that similar odors in a mixture compose a new odor, which should make it difficult for the olfactory system to extract the identity of the odor components (synthetic representation), while mixtures of dissimilar substances are represented as the sum of the optimized representation of each component (analytical representation) (Wilson, D. A. and Stevenson, R. J., 2003). Behavioral data in rats support this idea by showing that rats perceive binary mixtures composed of dissimilar odors as very similar to their components, whereas binary mixtures containing similar odors appeared dissimilar to the animal (Wiltrout, C. *et al.*, 2003). By increasing the number of components in an odor mixture, mixture interactions are likely to increase and further reduce the similarity to the single-component patterns (Deisig, N. *et al.*, 2003). With this coding strategy of odor mixtures, the olfactory system implements a logic that allows a unique representation of odor mixtures without saturating the olfactory code, at the expense of a loss in analytical capacity.

4.41.3.5 Coding of Special Odors

There are several chemosensory tasks that are special for olfactory systems. Among them are pheromones (which can be further subdivided into sexual and nonsexual pheromones), CO_2 concentration, humidity, and contact (nontaste) odors.

4.41.3.5.1 Sexual pheromones

The sexual pheromone system is the classic example for a labeled line system, with each OSN type, and consequently the corresponding glomerulus, representing a component of the pheromone blend. Glomeruli specific for sexual pheromones do not have a broad response spectrum in the natural environment of the species, because none of the other ligands that exist (and are known) occur in nature. For example, in *M. sexta*, the sexual pheromone is a blend of two chemicals, the main component (*E*,*Z*)-10,12-hexadecadienal and the secondary component (*E*,*E*,*Z*)-10,12,14-hexadecatrienal. A different and more stable molecule, (*E*,*Z*)-11,13-pentadecadienal, is a good mimic and is routinely used instead in physiological experiments (Christensen, T. A. and Hildebrand, J. G., 1997). However, because it does not occur in nature, this glomerular activity channel is uniquely activated by its natural ligand within a natural environment (Kaissling, K. E. *et al.*, 1989). Female moths do not have a macroglomerular complex, since they are not receptive to sexual pheromones. They do, however, have a group of large, female-specific glomeruli that respond to plant-derived odors and might also be involved in odor-driven navigation (Reisenman, C. E. *et al.*, 2004).

Sexual pheromones in *Drosophila* are not involved in long-distance navigation, but rather part of a close-encounter olfactory display, that is detected by contact chemoreceptors. The only candidate for a volatile pheromone is *cis*-vaccenyl acetate (Costa, R., 1989; Amrein, H., 2004). Its precise behavioral significance remains to be elucidated, and includes attractive, repellent, and sex specific effects. There are several OSNs sensitive to *cis*-vaccenyl acetate. Cells expressing dOr67d reside in T1 sensilla on

the antenna and mediate sex recognition (Xu, P. *et al.*, 2005; Kurtovic, A., *et al.*, 2007), while cells expressing dOr65a reside in T3 sensilla and mediate generalization of courtship learning (Ejima, A., *et al.*, 2007).

The sexual pheromone of bees consists of several substances, with 9-keto-2(*E*)-decenoic acid (9-ODA) as main component, often referred to as queen's substance. Drones find queens using both olfactory and visual cues, that is, they follow her scent trail, and they identify a dark spot against the bright sky. Mating occurs while flying. The male AL is entirely different from the female, with a limited number of ordinary glomeruli, and four large macroglomeruli (Arnold, G. *et al.*, 1985). Macroglomeruli have complex substructures. In optical imaging experiments, small areas within macroglomeruli respond to many odors, suggesting a more complex arrangement than just separation of sexual pheromone processing from other odors (Sandoz, J. C. and Galizia, C. G., unpublished data). Queen's substance is also a social pheromone within the hive and prevents the emergence of new queens when it is present (Moritz, R. F. A. and Southwick, E. E., 1992).

4.41.3.5.2 Nonsexual pheromones

Nonsexual pheromones differ chemically from sexual pheromones in that they are often less complex molecules that may also be encountered as environmental odors. They sometimes also act as kairomones, as for the case of alarm pheromones that can elicit alarm in sympatric species (Hölldobler, B. and Wilson, E. O., 1990). Ants have a well-developed intraspecific communication system based on pheromones, which they use to communicate food sources, trails, alarm, and more (Hölldobler, B. and Wilson, E. O., 1990). In the ant *Camponotus rufipes*, activity elicited by environmental odors and by pheromonal substances overlap in the AL, suggesting that the two systems share their olfactory circuitry (Galizia, C. G. *et al.*, 1999a).

Important nonsexual pheromones for bees are citral and geraniol, both components of the Nasanov gland, a gland important for the social cohesion of the hive (Free, J. B., 1987): isoamyl acetate, which is the major component of the alarm pheromone associated with the sting apparatus (Free, J. B., 1987; Nuñez, J. *et al.*, 1997), and the repellent scent-marker 2-heptanone, which bees use to mark already visited flowers, thus avoiding revisiting a depleted nectar source (Giurfa, M. and Nunez, J. A., 1992; Giurfa, M., 1993). All of these substances elicit activity in the same region as environmental odors (Joerges, J. *et al.*, 1997; Galizia, C. G. and Menzel, R., 2001). Isoamyl acetate elicits strong responses in several glomeruli, among which T1-48, a glomerulus that is also activated by orange, clove oil, limonene, and several plant extracts. It is unknown whether there is a parallel, more 'labeled line'-like pathway for nonsexual pheromones, reminiscent of the macroglomerular system for sexual pheromones. If there is, this system is certainly not in the T1 region, whose response profiles have already been well mapped but could be located in the T2, T3, or the T4 glomeruli.

Aggregation pheromones are also found, e.g., in male Colorado beetles (Dickens, J. C. *et al.*, 2002). Some aggregation pheromones are effectively sexual pheromones. For example, the ceranbycid beetle *Neoclytus acuminatur* releases a species-specific aggregation pheromone that attracts both sexes (Lacey, E. S. *et al.*, 2004). As with sexual pheromones, aggregation pheromones are quite different for closely related beetles and may be involved in species segregation (Symonds, M. R. and Elgar, M. A., 2004). This is different in fruit flies, where aggregation pheromones are also found but do not form boundaries among species (Symonds, M. R. and Wertheim, B., 2005).

4.41.3.5.3 Carbon dioxide

Carbon dioxide detection is widespread among arthropods, with a wide variability in structure and function (Bogner, F. *et al.*, 1986; Kleineidam, C. and Tautz, J., 1996; Stange, G. and Stowe, S., 1999). CO_2-sensitive sensilla can be hairs, pegs, plugged, or open grooves and can be on the surface or located within a depression or a pit with a restricted opening (Keil, T. A., 1996; Stange, G. and Stowe, S., 1999). Similarly, the functional context for CO_2 detection differs. In hematophagous insects, including Ixodidae and Diptera, CO_2 sensitivity might be related to finding the host (Grant, A. J. *et al.*, 1995; Dekker, T. *et al.*, 2002). Insects that live in confined spaces, such as centipedes or beetle larvae, are capable of sensing CO_2. Similarly, social insects that live in hives (ants, bees, and termites) monitor CO_2 with tonic receptors and control its concentration in a manner reminiscent of homeostatic control (Lacher, V., 1964; Stange, G. and Stowe, S., 1999; Weidenmüller, A. *et al.*, 2002). For moths, in particular nocturnal moths feeding on nectar, CO_2 might be a component of the attractive flower odor, given that flowers that produce high-quality nectar also release considerable amounts of metabolic CO_2 (Guerenstein, P. G. *et al.*, 2004; Raguso, R. A., 2004; Thom, C. *et al.*, 2004).

Drosophila is repelled by CO_2, and a role of this gas as a component of a stress signal has been suggested (Suh, G. S. *et al.*, 2004). However, CO_2 is also produced by rotting fruit, and by fly aggregations on such fruit that might indicate good ovipositioning sites. In the AL, CO_2 activates the V glomerulus. It is innervated by OSNs located on the maxillary palps. These OSNs express two receptors: dGR21a (de Bruyne, M. *et al.*, 2001; Suh, G. S. *et al.*, 2004) and dGr63a (Jones, W. D., *et al.*, 2007) and do not coexpress the otherwise common coreceptor dOR83b (Larsson, M. C. *et al.*, 2004). The innate avoidance behavior to CO_2 is abolished when these OSNs are silenced, suggesting that there is no parallel, additional CO_2 channel (Suh, G. S. *et al.*, 2004). A homologous glomerulus is present in mosquitoes, where it is innervated by OSNs on the mouthparts (Distler, P. G. and Boeckh, J., 1997b). Similarly, CO_2-sensitive OSNs are located in a pit organ on the labial palps in moths, and their axons form glomeruli in the dorsal area of the AL (Kent, K. S. *et al.*, 1986). In locusts and cockroaches, these fibers project close to the AL but do not form a glomerulus within the AL (Ernst, K. D. *et al.*, 1977; Ignell, R. *et al.*, 2001).

4.41.3.5.4 Humidity

Hygroreceptors are often found on insect antennae (Tominaga, Y. and Yokohari, F., 1982; Yokohari, F., *et al.*, 1982; Yokohari, F., 1983; Nishikawa, M. *et al.*, 1995; Shanbhag, S. R. *et al.*, 1995; Nishino, H. *et al.*, 2003; Tichy, H. 2007). Bees are known to control the humidity in their hives, and to carry water into the hive when they need it (von Frisch, K., 1966). The homeostatic nature of this water detection task makes it likely that humidity be coded in a nonadapting labeled line system, possibly with a single glomerulus. The function of this glomerulus would then be limited to integrating the signals from all hygroreceptors on the antenna, rather than taking part in across-glomeruli processing. However, experimental data do not support this view; bees can associate vapor with a sucrose reward, and reliably respond to it, just as they learn appetitive odors (Menzel, R., personal communication). In intracellular recordings from mlACT neurons, some PNs showed responses to water vapor, which was increased by association with sugar water (Abel, R., 1997). Therefore, the information channel for water must overlap with the circuits responsible for associative learning. No localization of the representation of humidity in the AL is possible from the data currently available, apart from some intracellular recordings of honeybee PNs that across the odors tested responded exclusively to vapor and branched in a glomerulus of the T2 tract (Müller, D., personal communication).

4.41.3.5.5 Other special odors

In ants, a sensillum that does not respond to nest mates but does respond to cuticular components of nonnest mates has recently been found (Ozaki, M. *et al.*, 2005). This sensillum contains about 200 OSNs. The projections of these OSNs are not known. Nestmate recognition is also found in honeybees, where guarding bees at the hive entrance attack approaching bees that do not have the nest's own cuticular odor (von Frisch, K., 1966). In Hymenoptera, this recognition relies on the mixture of hydro- carbons present on the animal's cuticle (Dani, F. R. *et al.*, 2005), which is often exploited by parasite species (Lenoir, A. *et al.*, 2001).

4.41.3.6 Effects of Memory

The AL is the first olfactory neuropil where substantial cellular interaction takes place. Some of that interaction is experience dependent. What, then, are the memory traces that can be found in the AL? Both nonassociative and associative effects have been found.

Nonassociative learning occurs as a consequence of odor exposure. When a locust is repeatedly exposed to an odor, odor responses in PNs change in a characteristic way: they have less APs, but these APs are more precisely timed, suggesting that odor coding is more efficient for the later puffs in the series (Stopfer, M. and Laurent, G., 1999). This sensory memory trace is already visible in the second and third puff and decays within 10–15 min after the last puff (Stopfer, M. and Laurent, G., 1999). A related effect was found in honeybees: even without an olfactory stimulus, PNs are spontaneously active, but there is no preferential pattern of activity. After a single odor exposure, however, a pattern corresponding to the experienced odor reoccurs repeatedly within the sequence of spontaneous events, showing that spontaneous activity within the AL network is temporarily biased toward this pattern (Galán, R. F. *et al.*, 2005).

Most studies investigating associative learning in the AL have looked at classical conditioning, in which an odor is associated with a punishment (e.g., electroshock and aversive learning) or a reward (e.g., sugar water and appetitive learning). In flies, after aversive conditioning, some glomeruli change their

odor responses for a short time window, that is, 3 min after conditioning (Yu, D. *et al.*, 2004). These experiments were done by optically measuring synaptic vesicle release within the AL using the reporter protein synaptopHluorin in the PN line GH146. Thus, the measurements monitored the feedback activity in PNs within the AL, in a population of mixed multiglomerular and uniglomerular PNs comprising approximately 60% of the total PN population.

Application of sucrose (or water) to the honeybee antenna elicits a transient increase of PKA activity in the AL, but odor stimulation alone does not (Hildebrandt, H. and Müller, U., 1995a; 1995b). This effect is mediated by octopamine and reverts to baseline within 3 s (Hildebrandt, H. and Müller, U., 1995b). The sugar water stimulus of the appetitive learning paradigm (the US) is also mediated by octopamine: it can be replaced by octopamine injections restricted to the AL (octopamine is the putative transmitter of VUMmx1, the neuron that mediates the US in the bee brain) (Hammer, M. and Menzel, R., 1998). Blocking octopaminergic transmission by injecting an octopamine receptor antagonist (mianserin) or by injecting double-stranded octopamine receptor RNA into the AL interferes both with odor memory acquisition and with its recall, suggesting that octopamine is important for memory consolidation but also that octopaminergic neurons become reactivated during memory recall (Farooqui, T. *et al.*, 2003). In honeybees, single-trial conditioning leads to short-term memory (STM), while multiple conditioning leads to LTM. In the AL, multiple conditioning trials lead to an elevated PKA response mediated by the NO/cGMP system. Artificially increasing PKA activity in the AL after single-trial learning elicits long-term memory (Müller, U., 2000), suggesting that the PKA level, rather than its presence alone, is important for a switch between STM and long-term memory. Bath application of a calcium-sensitive dye revealed an effect of differential conditioning (one odor was rewarded, the other not) in the time window of 5–15 min after conditioning, showing that learning modifies the odor representation in the AL (Faber, T. *et al.*, 1999). Similarly, extracellular recordings from moths showed a net recruitment of AL neurons activated by the rewarded odor and a net loss of neurons activated by the unrewarded odor (Daly, K. C. *et al.*, 2004).

Other studies have disputed the role of the AL in olfactory associative memory. In *Drosophila*, KCs have been shown to be necessary and sufficient for short-term learning of odors (see below), leaving no space for a memory trace in the AL (Gerber, B. *et al.*, 2004a). In honeybees, a subpopulation of PNs (the uniglomerular PNs from the lACT tract) have very stable odor responses that are not affected by single-odor training or differential appetitive training (Peele, P., *et al.*, 2006). These neurons might represent a learning-resistant channel for reliable transfer of odor-related information to higher-order brain centers.

Together, these studies show that odor learning in the AL is a complex process that might affect spike timing and/or relative activities to different odors. They also show that these effects only occur in very limited time windows and that not all cell populations are involved in these plastic processes.

Because the development of the olfactory system is not part of this review, developmental plasticity is also not treated, even though developmental experience does shape odor responses and AL morphology (Winnington, A. P. *et al.*, 1996; Sigg, D. *et al.*, 1997).

4.41.4 Cellular Organization of the Mushroom Bodies

Mushroom bodies (MBs) are multimodal structures and are involved in learning (Strausfeld, N. J. and Gilbert, C., 1992; Heisenberg, M., 2003; Davis, R. L., 2004). In most insects, they receive both olfactory and visual input (Strausfeld, N. J. *et al.*, 1998; Farris, S. M., 2005). MBs owe their names to massive peduncles with large cup-shaped protuberances, which are called the calyces.

4.41.4.1 Kenyon Cells

The intrinsic neurons in the MBs are the KCs. Their number differs widely among species: in honeybees, there are ~170 000 KCs in each hemisphere (Witthöft, W., 1967; Mobbs, P. G., 1982), and *Drosophila* counts give ~2500 KCs (Stocker, R. F., 1994). In adult cockroaches, the number is ~175 000 (Neder, R., 1959), but juveniles have much smaller numbers (Farris, S. M. and Strausfeld, N. J., 2001), and adult locusts have ~50 000 KCs (Farivar, S. S., 2005). KC somata are small and densely packed close to the MB calyces. Their axons are long and thin and form the peduncles. Most axons branch, so that the peduncle splits into two lobes: the vertical (α) lobe and the horizontal (β) lobe. In *Drosophila*, these lobes are accompanied by the α'- and the β'-lobes (Strausfeld, N. J. *et al.*, 2003). A third lobe, the γ-lobe, is morphologically distinct in *Drosophila*, but physically juxtaposed to the ventral

aspect of the vertical lobe (the α-lobe) in honeybees (Strausfeld, N. J., 2002; Farris, S. M. *et al.*, 2004). The γ-lobe is formed by axons of clawed KCs, which have been found in *Drosophila*, bees, and cockroaches (they are sometimes referred to as class II or type 5 KCs) (Mobbs, P. G., 1982; Rybak, J. and Menzel, R., 1993; Strausfeld, N. J., 2002; Farris, S. M. *et al.*, 2004). Their somata are located outside the calyx, unlike all other KCs that have their somata inside the calyces. The name clawed derives from the claw-like dendritic shapes within the calyces. These KCs are the first population to occur in development. While in a simplified view of the KCs, the calyces are the input region and the lobes the output region of these cells, input synapses are also found in the lobes, allowing for local feedback within the lobes (Strausfeld, N. J. *et al.*, 2003).

The calyces are subdividable: in hymenoptera, these subdivisions are lip, collar, and basal ring, which correspond to different layers in the lobes. In honeybees, KC from lip, collar, and basal ring project into three separate bands in the α-lobe (or vertical lobe). Similarly, in *Drosophila*, subdivisions from the calyces can be traced to a layered structure in the α'/β'-lobe, and to a concentrically circular arrangement in the α/β-lobe (Tanaka, N. K. *et al.*, 2004). These layers partially correspond to KCs that differ in their morphology and/or in what transmitters they use, or in other molecular markers. Glutamate has been found in a KC subpopulation of bees (Bicker, G. *et al.*, 1988). Aspartate, glutamate, and taurine immunocytochemistry leads to different KC populations being labeled in *Drosophila* (Strausfeld, N. J. *et al.*, 2003) and in cockroaches (Sinakevitch, I. *et al.*, 2001). In addition, in *Drosophila*, KCs produce NO (Schürmann, F. W., 2000), but ACh and GABA are excluded as KC transmitters (Yusuyama, K. *et al.*, 2002). The complexity in KC morphology, pharmacology, and peptide expression is considerable in all species studied so far (Iwasaki, M. *et al.*, 1999; Strausfeld, N. J. and Li, Y., 1999a; 1999b; Strausfeld, N. J. *et al.*, 2000; Sinakevitch, I. *et al.*, 2001; Strausfeld, N. J., 2002; Strausfeld, N. J. *et al.*, 2003).

4.41.4.2 Projection Neuron Input

Olfactory input to the MB calyces occurs via uniglomerular PNs. In honeybees, chemosensory input is targeted at the lip and the basal ring of the calyces, while the intermediate area, the collar, receives input from the optic lobes. Each of these input areas is further subdivided into segregated zones, suggesting the existence of several parallel channels (Gronenberg, W., 2001). Similar arrangements are also found in other hymenoptera (Gronenberg, W., 1999; 2001).

In *Drosophila*, each PN axon travels over large areas of the calyx, forming synapses with many intrinsic KCs (Marin, E. C. *et al.*, 2002; Wong, A. M. *et al.*, 2002). This is reminiscent of the situation in the mammalian olfactory cortex (Zou, Z. *et al.*, 2005) and allows for a combinatorial readout of PN response patterns. PNs within the MB calyx region occupy concentric layers (Tanaka, N. K. *et al.*, 2004). PNs from identified glomeruli branch in a stereotype manner within the MB calyces, and PNs from different glomeruli have distinct but overlapping branching patterns (Marin, E. C. *et al.*, 2002; Wong, A. M. *et al.*, 2002). On average, three uniglomerular PNs innervate each glomerulus, and these have the same projection pattern in MB and LP, suggesting that they are not functionally distinct (Wong, A. M. *et al.*, 2002). PNs with similar axon projection patterns in the LP tend to receive input from neighboring glomeruli in *Drosophila*, suggesting that the organization of the LP mirrors some aspects of the organization in the AL (Marin, E. C. *et al.*, 2002; Tanaka, N. K. *et al.*, 2004), but other studies have not found this relationship (Wong, A. M. *et al.*, 2002). However, whether such spatial correlations are dictated by developmental constraints or are the result of functional neuropil optimization, or both, remains to be investigated.

Schematically, MB input can be described as a scaffold, with arrays of PN axons running perpendicular to arrays of KCs, and forming synapses with some, but not all KCs (Heisenberg, M., 2003). This is an ideal arrangement for a combinatorial readout across PNs. In *Drosophila*, PN axons have large boutons, 2–7 µm in diameter, throughout all calycal subdivisions, which is a considerable size when compared to KC somata of about 4 µm (Yusuyama, K. *et al.*, 2002). PN boutons are multisynaptic, with GABAergic input and KC output connections arranged to form glomerular structures (see below). The detailed geometrical layout of this structure has led to comparisons with the mammalian cerebellum, where the GABAergic circuit in MBs would correspond to Golgi cells in the cerebellum (Yusuyama, K. *et al.*, 2002), but it is unclear whether this similarity includes the cerebellar specialization for precise AP timing. Others have likened the vertebrate cerebellum to the central complex, rather than to the mushroom bodies (Svidersky, V. L. and Plotnikova, S. I., 2004).

Although not all PNs may be cholinergic (see above), PNs are the only cholinergic input to the MBs in *Drosophila* (Yasuyama, K. and Salvaterra, P. M., 1999).

4.41.4.3 Local Inhibitory and Modulatory Neurons; Mushroom Body Glomeruli

Dense GABAergic processes invade the MBs (Yusuyama, K. *et al*., 2002). These synaptic arrangements form microglomeruli with very local computational capabilities. In *Drosophila*, each MB glomerulus comprises a large cholinergic bouton formed by a PN axon from the AL, which is surrounded by tiny vesicle-free KC dendrites and several GABAergic terminals (Yusuyama, K. *et al*., 2002). GABAergic terminals contact both KC dendrites and PN axon terminals, suggesting that PN input is modulated both pre- and postsynaptically (Yusuyama, K. *et al*., 2002). This electron microscopic arrangement is also found in bees (Ganeshina, O. and Menzel, R., 2001) and in locusts (Leitch, B. and Laurent, G., 1996). MB glomeruli have no glial sheath (Ganeshina, O. and Menzel, R., 2001; Yusuyama, K. *et al*., 2002). KC dendritic spines label for F-actin in all insects studied so far, while the PN terminal boutons do not (Frambach, I. *et al*., 2004). Physiological evidence for the functional role of this circuit is discussed below.

A second inhibitory circuit within the MBs consists of GABAergic feedback neurons from the MB lobes back onto their calyces (Bicker, G. *et al*., 1985). These neurons are few in number, in honeybees ~55. Each feedback neuron innervates a subcompartment in the calyx. Due to the arrangement of intrinsic KCs, each subcompartment in the calyx is connected to its specific, corresponding layer in the α-lobe (Grünewald, B., 1999b). These neurons are found in bees (Bicker, G. *et al*., 1985; Schäfer, S. and Bicker, G., 1986), moths (Homberg, U. and Hildebrand, J. G., 1994), *Drosophila* (Yusuyama, K. *et al*., 2002), cockroaches (Farris, S. M. and Strausfeld, N. J., 2001), and locusts (Leitch, B. and Laurent, G., 1996).

Octopaminergic cellular processes sparsely but uniformly innervate MB calyces (Strausfeld, N. J. *et al*., 2003). In honeybees, these are likely to be from the VUMmx1 neuron that represents the CS during olfactory learning (Hammer, M., 1997). VUMmx1 branches in the AL, the MB, and the LP and has been discussed in the Section 4.41.2.6.

4.41.4.4 Output Lobe Circuitry

In comparison with the many studies published about input connections to the MB calyces, about the internal organization between calyces and lobes, and about the feedback from the lobes back onto the calyces, what has been published about the MB output to the LP and other brain areas is little. These target areas probably include premotor areas, so that the loop OSN–AL–MB–LP–motor neuron may form a complete behaviorally significant neural control loop, paralleled by the direct AL–LP loop that bypasses the MBs. In the *Drosophila* brain, at least three areas are MB output regions: the superior medial protocerebrum, the inferior medial protocerebrum, and the superior lateral protocerebrum (Ito, K. *et al*., 1998; Tanaka, N. K. *et al*., 2004). However, the precise delimitations of these areas are still being worked out.

Honeybee MB output neurons include unilateral neurons as well as bilaterally innervating neurons (Rybak, J. and Menzel, R., 1993). A prominent large neuron in honeybee brains is PE1, which is a single neuron in each brain hemisphere and connects the α-lobe to the LP and the ring neuropil around the α-lobe (Rybak, J. and Menzel, R., 1998; Brandt, R. *et al*., 2005). Responses of this multimodal neuron are modified after olfactory learning (Mauelshagen, J., 1993).

4.41.5 Functional Organization of the Mushroom Bodies

4.41.5.1 Odor-Evoked Activity and Processing

There is a massive divergence between PNs and KCs. In honeybees, 800 PNs project onto 180 000 KCs, and this ratio is similar in other species. Patch-clamp recordings in locusts show that KC activity is rare as compared with PNs (Stopfer, M. *et al*., 2003): while PNs had a probability of $p = 0.64$ to respond to any of the tested panel of odors, KCs responded with $p = 0.11$ (Perez-Orive, J. *et al*., 2002). Furthermore, while PNs respond with trains of spikes, KCs often respond with single or very few spikes only. These results were confirmed in flies and honeybees using calcium imaging of PNs and KCs (Wang, Y. L. *et al*., 2004; Szyszka, P. *et al*., 2005). Thus, odor representation is sparse across KCs (Laurent, G., 2002), where sparse is used both as population sparseness (a low proportion of units active at any

time) and as lifetime sparseness (few spikes in each neuron with narrow tuning) (Olshausen, B. A. and Field, D. J., 2004). The transformation between PNs and KCs appears useful because it may facilitate the readout mechanism (Laurent, G., 2002) and may allow more efficient learning due to the perpendicular array structure between PNs and KCs, as noted above (Heisenberg, M., 2003).

A comparison of PN activity in the ALs with PN activity at the synaptic boutons in the MBs and with KC activity showed that this sparsening occurs progressively: activity trains arriving at the MB terminals are inhibited presynaptically within the MBs by GABAergic glomerular microcircuits, so that only the first APs are likely to drive activity in KCs (Szyszka, P. *et al.*, 2005). This mechanism implies that only the first activity wave of every odor response is relevant for decoding within the MBs. In addition, the inhibitory feedback loop from the MB output lobes onto the calyces further sharpens that response (Szyszka, P. *et al.*, 2005). This feedback loop also locks activity into a global oscillatory rhythm (Perez-Orive, J. *et al.*, 2002), which in turn favors the extraction of synchronized APs from PNs (Perez-Orive, J. *et al.*, 2004). In this framework, only spikes that are in phase with the oscillatory activity carry relevant olfactory information, and extracting them would reduce noise and optimize coding (Laurent, G., 2002).

4.41.5.2 Olfactory Coding

These studies result in two distinct models (that need not be entirely exclusive). In one, only the initial firing pattern is read out for each odor puff (Szyszka, P. *et al.*, 2005), in the other only APs in synchrony with oscillations are relevant (Laurent, G., 2002). In both, most APs of PNs are not involved in olfactory coding within the MB calyces. Therefore, the question arises whether the remaining APs are wasted. Given that firing APs is among the most energy-costly activities of the brain (Attwell, D. and Laughlin, S. B., 2001), such a waste would appear as quite inefficient. However, the surplus spikes may not be wasted at all: PNs make synaptic output not only in the MB but also within the AL and in the LP, and this output is not filtered by the MB circuitry. Therefore, APs that are ignored within the MBs could still be an important part for olfactory coding within the AL and the LP.

The olfactory system has been compared with a support vector machine (Galán, R. F. *et al.*, 2004). Assuming a simplified system that is based on a combinatorial readout without any time-dependent mechanisms, a recipient neuron that reads across PN activities can only perform a very limited classification, which statistically corresponds to a linear classification in a multidimensional space. However, the addition of the MB as an intermediate step changes this picture: with a relatively small number of PNs, combinatorially mapped onto a very large number of KCs, which then are combinatorially read out by very few recipient neurons, very complex pattern families can be extracted. The intermediate step of enormously expanding the number of units by a large number of KCs allows for the computation of highly nonlinear classification schemes across PNs, which is reminiscent of support vector machines (Huerta, R. *et al.*, 2004). By adding temporal complexity to the code, the theoretical capacity of the system increases even further (Laurent, G. *et al.*, 2001).

4.41.5.3 Effects of Memory

Early confirmation of the role that MBs play in olfactory memory came from cooling experiments in honeybees, where memory retrieval was impaired when the MBs were cooled (Erber, J. *et al.*, 1980). Similarly, *Drosophila* mutants where MB structure is altered (*MB deranged, mbd*, and *MB miniature, mbm*) have learning deficits (Heisenberg, M. *et al.*, 1985). When the MBs are chemically ablated by applying the DNA synthesis inhibitor hydroxyurea during the early proliferation phase of KCs, olfactory memory is impaired in *Drosophila* (de Belle, J. S. and Heisenberg, M., 1994). In honeybees, partial ablation of MBs does not impair easy learning tasks (Malun, D. *et al.*, 2002), but more complex tasks involving several odors are impaired (Komischke, B. *et al.*, 2005). Similarly, blocking synaptic activity or disrupting MB physiology also leads to memory deficits (Connolly, J. B. *et al.*, 1996; Dubnau, J. *et al.*, 2001; McGuire, S. E. *et al.*, 2001).

There are many olfactory tasks that do not require MBs, and indeed, fly mutants that lack MBs are remarkably normal: they court and copulate, feed, lay eggs, are alert, seem to be well oriented in space, and respond to odors (Heisenberg, M., 2003). Furthermore, MBs are necessary not only for olfactory tasks but also for spatial memory and navigation (Mizunami, M. *et al.*, 1998; Strausfeld, N. J. *et al.*, 1998; Kwon, H. W. *et al.*, 2004).

In honeybees, the VUMmx1 neuron that represents appetitive reinforcer also innervates the MB calyces, suggesting that coincidence detection for appetitive

olfactory learning in honeybees occurs in the MB input region (Menzel, R. and Giurfa, M., 2001), in contrast to findings from *Drosophila* (see below). Optical imaging experiments show that a rewarded odor leads to increased calcium responses in the MB calyces as compared to before learning (Faber, T. and Menzel, R., 2001). Experience leads to morphological changes in honeybee MBs: worker bees that forage have KC dendrites with more branches than age-matched bees that do not forage, while the density of dendritic spines remained constant (Farris, S. M. *et al.*, 2001).

The best mechanistical analysis of olfactory memory traces in MBs comes from *Drosophila* (Waddell, S. and Quinn, W. G., 2001; Dubnau, J. *et al.*, 2003; Heisenberg, M., 2003; Davis, R. L., 2004). Olfactory memory can be subdivided into at least four phases: STM decays within an hour, middle-term memory (MTM) within 3 h, while anesthesia-resistant memory (ARM) and long-term memory (LTM) are two forms of LTM that differ in their training procedures: ARM occurs after massed training, and the protein synthesis-dependent LTM occurs after spaced training, that is, a training protocol where individual learning events occur with longer intervals in between (Tully, T. *et al.*, 1994).

Based on our current knowledge, KCs are the cells where this memory is located (Gerber, B. *et al.*, 2004a). A necessary second messenger in STM is cyclic AMP, and mutants for the genes *dunce* (*dnc*, which is a cAMP phosphodiesterase), DC0 (which is a PKA catalytic subunit), or CREB (cAMP response element binding protein) all are impaired in memory tasks. The *Drosophila* gene *rutabaga* (*rut*) codes for a Ca/CaM-dependent adenylyl cyclase (Levin, L. R. *et al.*, 1992). When *rut* is mutated, olfactory learning is impaired, but when *rut* is expressed in a mutant background in MB cells only, learning is restored (Zars, T. *et al.*, 2000). Several lines were used in these experiments, and the clawed KCs were the set of cells common to all of the effective lines, suggesting that clawed KCs are sufficient for short-term olfactory learning. A selective loss-of-function study of these cells showed that they are also necessary for olfactory learning (Connolly, J. B. *et al.*, 1996). The function of *rut* is only necessary in adult animals, but not during development (McGuire, S. E. *et al.*, 2003; Mao, Z. *et al.*, 2004). Furthermore, it acts presynaptically at the output synapses of KCs, and blocking synaptic release of these cells impairs retrieval, but not acquisition (Dubnau, J. *et al.*, 2001; Schwaerzel, M. *et al.*, 2002).

The gene *amnesiac* (*amn*) is strongly expressed in two large neurons, the two dorsal paired medial (DPM) neurons, and codes for a neuropeptide PACAP (pituitary adenylate cyclase activating peptide) that modulates *rut* activity in KCs. Disruption of *amn* leads to loss of MTM, as does silencing of DPM neurons. For the odors octanol and methylcyclohexanol, DPM neuron activity is necessary during storage and possibly consolidation, but not during acquisition and recall. However, memories for benzaldehyde need DPM neuron activity during acquisition (Keene, A. C. *et al.*, 2004). These data show that olfactory memory is not only highly complex in terms of memory phases and neural and genetic networks, but also diverse with respect to the odors used, adding tremendous complexity to the system.

The MBs are also involved in the two forms of long-term memory, ARM and LTM. These memory stages are not sequential: ARM is formed even in *amn* mutants that show no MTM and at least partially also in *rut* mutants that show no STM (Isabel, G. *et al.*, 2004). STM/MTM and ARM/LTM possibly rely on different KC populations, that is, those from the γ-lobe and from the α/β-lobe, respectively (Zars, T. *et al.*, 2000; Pascual, A. and Preat, T., 2001; Isabel, G. *et al.*, 2004). Nevertheless, LTM and ARM are not independent pathways: rather, LTM leads to an active erasure of ARM memory (Isabel, G. *et al.*, 2004). The cAMP response element CREB appears to be related to LTM (Yin, J. C. and Tully, T., 1996), although the scientific evidence has recently been questioned (Perazzona, B. *et al.*, 2004).

Associative learning occurs when a CS (which in this case is an odor) is paired with a US in a way that the CS acts as an efficient predictor for the US. A positive reward as US, such as food, elicits an appetitive response, while a negative US, such as an electric shock, leads to aversive conditioning. The sensory input for the US and the behavioral responses of these two paradigms are clearly distinct. Therefore, the neuronal pathways should be different. Indeed, in *Drosophila* an appetitive US is mediated by octopaminergic neurons, while an aversive US is mediated by dopaminergic neurons (Schwaerzel, M. *et al.*, 2003). This is consistent with findings in honeybees, where appetitive learning is mediated by octopamine (Hammer, M. and Menzel, R., 1998).

4.41.6 Cellular and Functional Organization of the Lateral Protocerebrum

In insect olfaction, the LP is, unfortunately, the least studied area. A frequent belief is that this area is

more related to innate behavior control, and less plastic than the circuitry in the MBs (Tanaka, N. K. *et al.*, 2004). Several lines of evidence support this model: in *Drosophila*, individual PNs branch in a highly stereotype and genetically predetermined way in the LP, while their branching pattern in the MBs is less predictable (Marin, E. C. *et al.*, 2002), and animals with ablated MBs but intact LP are not impaired in innate odor responses (de Belle, J. S. and Heisenberg, M., 1994). Because LP areas inherit the plasticity that comes from plastic MB output neurons such as the PE1 neuron (Mauelshagen, J., 1993) and the PCT neurons in honeybees (Grünewald, B., 1999a), local circuits involved in learning are more difficult to identify. Within the LP, there are many subregions that receive olfactory information, some from the AL only, and some from both the AL and the MB (Ito, K. *et al.*, 1998; Tanaka, N. K. *et al.*, 2004). Furthermore, the ring neuropil surrounding the vertical lobe is densely innervated by olfactory neurons.

4.41.7 The Larval System

This review focuses on the olfactory system of adult insects. The larval system has recently started to receive closer attention (Cobb, M., 1999; Heimbeck, G. *et al.*, 1999; Stocker, R. F., 2001; Scherer, S. *et al.*, 2003; Kreher, S. A. *et al.*, 2005; Marin, E. C. *et al.*, 2005). Most importantly, the larval system is much simpler than the adult, in terms of both cell numbers and organization, but shares important principles of the adult (Python, F. and Stocker, R. F., 2002a; 2002b). Larvae are suited for complex behavioral assays, including learning experiments (Scherer, S. *et al.*, 2003; Gerber, B. *et al.*, 2004b; Hendel, T. *et al.*, 2005). OSN afferents to the larval AL also form glomeruli that are interconnected by LNs, even though each glomerulus only receives input from a single OSN axon and is innervated only by a single PN (Kreher, S. A. *et al.*, 2005; Ramaekers, A. *et al.*, 2005). In *Drosophila* larvae, there are about 21 OSNs and about 25 expressed OR genes, of which only 13 are expressed in adults (Kreher, S. A. *et al.*, 2005; Ramaekers, A. *et al.*, 2005). That indicates that the different environment to which the larva is adapted has led to evolving a dedicated chemosensory system. This is further substantiated by the larger number of gustatory neurons in larvae than in adults. The larval mushroom bodies also share many of the characteristics with its adult counterpart (Marin, E. C. *et al.*, 2005). Given its numerical simplicity, it is easy to predict that we will learn a lot more about the larval olfactory system in the near future.

4.41.8 Olfactory Behavior

Theodosius Dobzhansky (1900–1975) stated, "Nothing in biology makes sense except in the light of evolution." For the individual animal, this can be paraphrased to behavior, and the statement becomes even more relevant for the scientific approach to studying olfaction, because it is only through observing behavior that it is possible to judge and investigate how an animal is making use of olfactory cues.

Olfactory behavior in insects has been studied in many species. An extensive review is beyond the scope of this chapter. Therefore, I limit myself to list some types of behavior that impose different constraints and/or requirements onto olfactory processing. Generally, insects are considered as more genetically predetermined and less plastic in their behavior than mammals. However, there are some olfactory behaviors that are exquisitely plastic, and even cognitive capabilities can be found in insects.

4.41.8.1 Odor Learning

Olfactory learning in insects has been reviewed extensively (Menzel, R. and Müller, U., 1996; Dubnau, J. *et al.*, 2003; Giurfa, M., 2003a; Heisenberg, M., 2003; Davis, R. L., 2004; Gerber, B. *et al.*, 2004a; Giurfa, M. and Malun, D., 2004), having been studied in many insects, notably honeybees (von Frisch, K., 1966; Menzel, R. and Müller, U., 1996), bumblebees (Plowright, R. C. and Laverty, T. M., 1984), moths (Fan, R. J. *et al.*, 1997; Hartlieb, E. *et al.*, 1999; Daly, K. C. and Smith, B. H., 2000), cockroaches (Sakura, M. *et al.*, 2002; Watanabe, H. *et al.*, 2003), and crickets (Matsumoto, Y. and Mizunami, M., 2004). No olfactory learning studies with locusts have yet been published, although non-olfactory learning capacities have been shown in *Schistocerca* (Dukas, R. and Bernays, E. A., 2000). Interestingly, also animals for which the ecological relevance of learning is not fully understood can be trained, and the most important example of this category is appetitive learning in the fruit fly, *Drosophila*, which can be trained both as adult (Borst, A., 1983; Schwaerzel, M. *et al.*, 2003) and as larva (Scherer, S. *et al.*, 2003; Hendel, T. *et al.*, 2005).

The most powerful approach to study olfactory learning relies on classical conditioning, by pairing a US with an odor as CS. Appetitive training is commonly used in bees, and sugar water (as nectar surrogate) is used as US. Most (but not all) studies in *Drosophila* use aversive learning with electroshocks as US. At a cellular level, appetitive and aversive pathways are different (see above) (Schwaerzel, M. *et al*., 2003). Decay of memory over time appears as seamless. However, this is the result of overlapping distinct memory phases (ATM, MTM, ARM, and LTM, in *Drosophila*), which can be induced by different training protocols (massed versus spaced training, and/or number of trials), and which rely on different cellular mechanisms (transcription, translation only, and phosphorylation only, see above). For example, long-term memory depends on a distributed arrangement of repeated conditioning trials over time (spaced training), whereas the same number of conditioning trials induces STM if applied in rapid succession (i.e., massed training) (Tully, T. *et al*., 1994).

Classical conditioning experiments in insects show all characteristics studied in psychological learning theory: the CS and the US have to coincide within a critical time interval, and the CS has to precede the US (Sutton, R. S. and Barto, A. G., 1981; Giurfa, M., 2003b). Protocols investigating blocking, latent inhibition, negative patterning, and positive patterning all work in honeybees, and complex training protocols reveal that honeybees have almost cognitive capacities (Menzel, R. and Giurfa, M., 1999; Giurfa, M., 2003a), including the capacity to discriminate between 'same' and 'different' and to transfer this concept between the visual and the olfactory system (Giurfa, M. *et al*., 2001).

4.41.8.2 Attractive and Repulsive Odors

In appetitive training experiments in bees, not all odors are equally easy to learn, suggesting that some odors have an innate bias toward being attractive (Vareschi, E., 1971). Similarly, in *Drosophila*, some odors are attractive and others repellent, but almost all odors are repellent when tested at very high concentrations (Borst, A., 1983).

In some cases, adding a component to a mixture can create a repellent effect. For example, the commercially used substance *N*,*N*-diethyltoluamide (DEET) acts as a repellent for many insects including mosquitoes (Rutledge, L. C. *et al*., 1978). The mechanistic explanation for its activity is still missing. Its effect on many species would suggest that it acts physiologically on olfactory mechanisms rather than interfering with a behavioral pattern. In other cases, specialized communication channels can be disrupted by added odors, such as when additional substances are added to a sexual pheromone. For example, sympatric moth species often use similar substances in their sexual pheromone blends, and a small amount of a substance belonging to a sympatric species can already block the attractive action of a pheromone (Vickers, N. J. and Baker, T. C., 1997). Interestingly, adding such a behavioral antagonist to the environment has been tested as one means for mating disruption in pest control, but the effects are limited, suggesting that the plume structure from an individual source can be recognized even against the repellent signal from another source (Cardé, R. T. and Minks, A. K., 1995).

4.41.8.3 Social Communication – Pheromones

Social insects have a large number of olfactory-guided behaviors, many of which are controlled by pheromones. Honeybees use social pheromones such as aggregation pheromones and alarm pheromones, among others. Processing of these odors in the AL is treated above. The behavior elicited by social pheromones is a stereotypical and innate behavior. However, the behavior is not conditional on the odor only: individuals are receptive or not, depending on the circumstances. This is true both for the released pheromone itself, which can elicit different behaviors in different hive situations (e.g., for a stable hive, or when a hive is swarming), and for a chemical component (e.g., isoamyl acetate, which is a component of the alarm pheromone but does not elicit defensive behavior when it is the component of a flower odor). Whether these differences in elicited behavior are controlled within the olfactory system (e.g., by feedback neurons), or in multimodal brain centers, is unknown.

Social pheromones have been studied particularly well in ants (Hölldobler, B. and Wilson, E. O., 1990). Some pheromones have different behavioral effects with increasing distance from the releasing individual, either due to decreased odor concentration or because in a mixture different volatilities of the components lead to changing component ratios with increasing distances, thus creating unique odor fingerprints for distance. For example, the alarm secretion of the ant *Oecophylla longinoda* contains

several substances that are active in concentric circles: 2-butyl-2-octenal in the inner circle elicits biting, 2-undecanone in the next elicits attraction and biting, 1-hexanol in the third elicits attraction, while the fourth concentric circle, 1-hexanol, only elicits attraction – all circles together having a radius of <10 cm (Hölldobler, B. and Wilson, E. O., 1990). Such a separation of mixture components is only possible because, physically, the aerodynamics of an ant's olfactory environment is different from that of a flying insect: in the air layer immediately above ground, turbulence is almost irrelevant, and odor diffusion becomes dominant. Tropotaxis is common, that is, ants follow odor concentration gradients, and they compare bilateral olfactory input from their antennae. The olfactory environment of a cockroach is also a substrate-bound still-air environment, and much behavior is related to active antennal movement. Spatial sampling of the olfactory environment is common in cockroaches (Boeckh, J. and Tolbert, L. P., 1993). However, even flying insects such as *Drosophila* are capable of using concentration differences between the two antennae for orientation (Borst, A., 1983), although the ecological relevance of this behavior has not yet been analyzed.

4.41.8.4 Sexual Communication – Pheromones

Sexual pheromone-related behavior (best studied in moths) is fundamentally different. These free-flying animals follow pheromone plumes that are transported downwind over large distances. The nature of the trail is inherently turbulent (Murlis, J. *et al.*, 1992). Odor concentration varies greatly, but the relative ratio of pheromone components does not. Consequently, the olfactory system is optimized to recognize a particular, genetically determined blend of substances, and male moth ALs have a stereotypical macroglomerular complex with glomeruli specifically dedicated to their species' pheromone components and to behavioral antagonists, which often are pheromones of closely related, sympatric species. Moths do not follow concentration gradients of pheromones. Rather, when they encounter an odor plume, they fly upwind, and when contact with the pheromone stops, they fly sideways (casting behavior) (Willis, M. A. and Baker, T. C., 1984; Cardé, R. T., 1996). In other words, the odor gives the information of when to fly, and the wind gives the information of where to fly. Therefore, the olfactory system is optimized for detecting short bursts of odors, with high frequencies (Christensen, T. A. and Sorensen, P. W., 1996). These mechanisms are not universal: some moths, such as storage pests that live in enclosed environments, have lost the requirement for turbulent pheromone trails (Justus, K. A. *et al.*, 2005).

Some plants, notably orchids, have evolved the capacity to mimic sexual pheromones and attract insects to pseudocopulate with them, thus insuring pollination (Schiestl, F. P. *et al.*, 2000; Ayasse, M. *et al.*, 2003).

4.41.8.5 Navigation – Innate Odors

Navigation toward an odor source occurs not only in the context of sexual calling but also in other behavioral contexts, for example in food source finding. Innate odors that are used for navigation are likely to rely on genetically encoded, hardwired olfactory coding mechanisms. Alternative models are also possible, such as early olfactory imprinting, in particular for phytophagous insects where the feeding substrate of a larva might influence the olfactory preference of the ovipositioning adult female.

Female moths follow characteristic odor trails of their host plants for finding good oviposition sites. Possibly, the neural circuits responsible for this are related to those of the male moth finding the female pheromone trail, as suggested by cross-grafting of female antennae onto male moths and vice versa (Schneiderman, A. M. *et al.*, 1986; Rössler, W. *et al.*, 1999a). Plants produce the attractive odors. They are often part of their obligate metabolic processes, which means that they represent evolutionarily reliable signals. Plant odor preferences can cause sympatric speciation, as shown in *Rhagoletis* flies, where two hosts (apple and hawthorn) are visited by different fly populations that prefer the respective plant odor substances (Linn, C. *et al.*, 2003; Linn, C. E. *et al.*, 2004).

Some plants respond to insect challenge by releasing stress volatiles, which act as attractants for other insect species that parasitize on the phytophagous species, creating tritrophic interaction systems (Karban, R. and Baldwin, I. T., 1997; Pare, P. W. and Tumlinson, J. H., 1999). Olfactory orientation of the parasitoids themselves consists in being attracted to an innately attractive odor.

Mosquitoes find their blood meals following a combination of cues, including lactic acid, ammonia, and CO_2, which act synergistically (Kline, D. L., 1998; Geier, M. *et al.*, 1999a; 1999b; Costantini, C. *et al.*, 2001; Steib, B. M. *et al.*, 2001; Dekker, T. *et al.*, 2002; Dekker, T. *et al.*, 2005). Such synergistic effects

are caused by mixture interactions, but it remains to be elucidated where within the olfactory pathway these interactions occur. Interestingly, humans that are infected with malaria gametocytes (the transmissible stage) are particularly attractive for the mosquito vector *Anopheles gambiae*, suggesting that the parasite might induce a change in the olfactory signature of the human host (Lacroix, R. *et al.*, 2005).

Insects feeding on carrion (e.g., blowflies) are also attracted by specific, innate odor cues, which often act synergistically with other sensory cues, such as heat or color. Some flowers have evolved appropriate displays to mimic these signals and use carrion-feeding insects as pollinators (Angioy, A. M. *et al.*, 2004; Raguso, R. A., 2004).

Navigation for innate odors includes trail pheromone navigation, used in many ant species (Hölldobler, B. and Wilson, E. O., 1990).

4.41.8.6 Navigation – Learned Odors

Not all odors used for navigation are innate. Many pollinating insects learn which flower is currently in blossom and use this information to improve their foraging success. When an odor trail is used for navigation in these instances, the brain cannot rely on innate circuitry. Whether the behavioral strategies and the neural circuitries for finding the odor source are comparable with those used for innate odors is currently unknown.

Odors are not the only cues used for navigation. Bees learn both olfactory and visual elements of a flower. However, optical resolution is low, and odors are the only long-range signals that are available for a bee. The optical resolution of a bee allows to see an inflorescence of 8 cm at a distance of ~90 cm and to recognize its color at a distance of ~30 cm, leaving olfaction alone for everything farther away than 90 cm (Galizia, C. G. *et al.*, 2005). Honeybees also use their topographical knowledge of the landscape for navigating (Giurfa, M. and Capaldi, E. A., 1999; Menzel, R. *et al.*, 2000). Scout bees communicate the location of a new crop using the waggle dance (von Frisch, K., 1966). But even during the waggle dance, follower bees experience the flower's odor on the dancer's body and might use that odor as an additional clue for navigation. This has led to a long controversy among bee researchers, with some researchers advocating odors as the main navigation clue opposed to those arguing for the dominant role of the bees' waggle dances (Wenner, A. M. and Johnson, D. L., 1967; Wenner, A. M., 2002). Recent studies that monitored individual bees' flights after receiving information from recruiter bees have shown that the waggle dance is the dominant information used (Riley, J. R. *et al.*, 2005).

Some orchids mimic a rewarding flower. This situation is quite different from sexual pheromone mimicry, because flower odors consist in more complex mixtures than pheromones, and therefore, their reproduction by a deceiving plant may be biochemically more difficult. In at least one of these cases, the mimicry only involves visual parameters, while the long-range task of attracting pollinating bees is solved not by mimicry but by having a model inflorescence in close neighborhood (Galizia, C. G. *et al.*, 2005). In other words, these orchids hitchhike on their model's olfactory display and attract the pollinators at close range with their visual display only.

4.41.9 Limitations and Potential of Using Insects to Study Olfactory Coding

Some people argue that it becomes increasingly difficult to justify research in insect olfaction. The classical advantages of insect models are the limited number of neurons and even more so the possibility of identifying individual neurons, thus allowing for detailed analyses across animals. With the recent technological advances in mammals, both in recording techniques and in molecular and genetic manipulations, these advantages lose in importance: insects no longer are the simpler models for mammalian neurophysiological research.

However, insects remain important models on their own. The relative simplicity of their brains makes it possible to study many species in great detail and thus to understand not just one solution that evolution proposed for olfactory coding, but several solutions. This comparative approach is the main treasure that insect studies can contribute. However, it comes with a price, and the consequences of this price weaken the case for studying insect olfaction: because technical approaches and possibilities differ in different laboratories and species, our information is often insufficient for a thorough comparison among species. For example, as stated above, temporal aspects of odor responses in PNs are best studied in locusts, while across-PN patterns are best understood in honeybees and flies, with moths somewhere in between. This fragmentation of knowledge and research time severely limits

the conclusions that can be drawn, in particular with respect to understanding which mechanisms are universal and which are specific specializations. The massive advance in possibilities provided by molecular biology in *Drosophila*, and the concomitant increase in laboratories involved in studying fly olfaction, will help by creating a well-understood insect model species. However, it is important to realize that *Drosophila*, just as any other insect species, is not a good model for insect olfaction. The diversity among insects is enormous, and it is this treasure that we need to unearth for our understanding of the basic mechanisms in olfaction.

References

Abel, R., Rybak, J., and Menzel, R. 2001. Structure and response patterns of olfactory interneurons in the honeybee, *Apis mellifera*. J. Comp. Neurol. 437, 363–383.

Abraham, N. M., Spors, H., Carleton, A., Margrie, T. W., Kuner, T., and Schaefer, A. T. 2004. Maintaining accuracy at the expense of speed; stimulus similarity defines odor discrimination time in mice. Neuron 44, 865–876.

Amrein, H. 2004. Pheromone perception and behavior in Drosophila. Curr. Opin. Neurobiol. 14, 435–442.

Ang, L. H., Kim, J., Stepensky, V., and Hing, H. 2003. Dock and Pak regulate olfactory axon pathfinding in Drosophila. Development 130, 1307–1316.

Angioy, A. M., Stensmyr, M. C., Urru, I., Puliafito, M., Collu, I., and Hansson, B. S. 2004. Function of the heater: the dead horse arum revisited. Proc. Biol. Sci. 271(Suppl. 3), S13–S15.

Anton, S. and Hansson, B. S. 1996. Antennal lobe interneurons in the desert locust *Schistocerca gregaria* (Forskal): processing of aggregation pheromones in adult males and females. J. Comp. Neurol. 370, 85–96.

Anton, S. and Homberg, U. 1999. Antennal Lobe Structure. In: Insect Olfaction (*ed*. B. S. Hansson), pp. 97–124. Springer.

Anton, S., Ignell, R., and Hansson, B. S. 2002. Developmental changes in the structure and function of the central olfactory system in gregarious and solitary desert locusts. Microsc. Res. Tech. 56, 281–291.

Arnold, G., Masson, C., and Budharugsa, S. 1983. Spatial organization of the sensory antennal system in the honeybee by using a cobalt ions marketing method. Apidologie 14, 127–135.

Arnold, G., Masson, C., and Budharugsa, S. 1985. Comparative study of the antennal lobes and their afferent pathway in the worker bee and the drone (*Apis mellifera*). Cell Tissue Res. 242, 593–605.

Attwell, D. and Laughlin, S. B. 2001. An energy budget for signaling in the grey matter of the brain. J. Cereb. Blood Flow Metab. 21, 1133–1145.

Av-ron, E. and Rospars, J. P. 1995. Modeling insect olfactory neuron signaling by a network utilizing disinhibition. Biosystems 36, 101–108.

Ayasse, M., Schiestl, F. P., Paulus, H. F., Ibarra, F., and Francke, W. 2003. Pollinator attraction in a sexually deceptive orchid by means of unconventional chemicals. Proc. Biol. Sci. 270, 517–522.

Baumann, P. M., Oland, L. A., and Tolbert, L. P. 1996. Glial cells stabilize axonal protoglomeruli in the developing olfactory lobe of the moth *Manduca sexta*. J. Comp. Neurol. 373, 118–128.

Bazhenov, M., Stopfer, M., Rabinovich, M., Abarbanel, H. D., Sejnowski, T. J., and Laurent, G. 2001. Model of cellular and network mechanisms for odor-evoked temporal patterning in the locust antennal lobe. Neuron 30, 569–581.

de Belle, J. S. and Heisenberg, M. 1994. Associative odor learning in Drosophila abolished by chemical ablation of mushroom bodies. Science 263, 692–695.

Berg, B. G., Almaas, T. J., Bjaalie, J. G., and Mustaparta, H. 2005. Projections of male-specific receptor neurons in the antennal lobe of the oriental tobacco budworm moth, *Helicoverpa assulta*: a unique glomerular organization among related species. J. Comp. Neurol. 486, 209–220.

Berg, B. G., Galizia, C. G., Brandt, R., and Mustaparta, H. 2002. Digital atlases of the antennal lobe in two species of tobacco budworm moths, the Oriental *Helicoverpa assulta* (male) and the American *Heliothis virescens* (male and female). J. Comp. Neurol. 446, 123–134.

Bhalerao, S., Sen, A., Stocker, R., and Rodrigues, V. 2003. Olfactory neurons expressing identified receptor genes project to subsets of glomeruli within the antennal lobe of *Drosophila melanogaster*. J. Neurobiol. 54, 577–592.

Bicker, G. 1999a. Histochemistry of classical neurotransmitters in antennal lobes and mushroom bodies of the honeybee. Microsc. Res. Tech. 45, 174–183.

Bicker, G. 1999b. Biogenic amines in the brain of the honeybee: cellular distribution, development, and behavioral functions. Microsc. Res. Tech. 44, 166–178.

Bicker, G. 2001. Sources and targets of nitric oxide signalling in insect nervous systems. Cell Tissue Res. 303, 137–146.

Bicker, G. and Kreissl, S. 1994. Calcium imaging reveals nicotinic acetylcholine receptors on cultured mushroom body neurons. J. Neurophysiol. 71, 808–810.

Bicker, G., Kreissl, S., and Hofbauer, A. 1993. Monoclonal antibody labels olfactory and visual pathways in Drosophila and Apis brains. J. Comp. Neurol. 335, 413–424.

Bicker, G., Schäfer, S., and Kingan, T. G. 1985. Mushroom body feedback interneurones in the honeybee show GABA-like immunoreactivity. Brain Res. 360, 394–397.

Bicker, G., Schäfer, S., Ottersen, O. P., and Storm-Mathisen, J. 1988. Glutamate-like immunoreactivity in identified neuronal populations of insect nervous systems. J. Neurosci. 8, 2108–2122.

Boeckh, J. and Tolbert, L. P. 1993. Synaptic organization and development of the antennal lobe in insects. Microsc. Res. Tech. 24, 260–280.

Boeckh, J., Ernst, K. D., and Selsam, P. 1987. Neurophysiology and neuroanatomy of the olfactory pathway in the cockroach. Ann. N. Y. Acad. Sci. 510, 39–43.

Bogner, F., Boppre, M., Ernst, K. D., and Boeckh, J. 1986. CO2 sensitive receptors on labial palps of rhodogastria moths (Lepidoptera, Arctiidae) – physiology, fine-structure and central projection. J. Comp. Physiol. [A] 158, 741–749.

Bornhauser, B. C. and Meyer, E. P. 1997. Histamine-like immunoreactivity in the visual system and brain of an orthopteran and a hymenopteran insect. Cell Tissue Res. 287, 211–221.

Borst, A. 1983. Computation of olfactory signals in *Drosophila melanogaster*. J. Comp. Physiol. [A] 152, 373–383.

Brandt, R., Rohlfing, T., Rybak, J., Krofczik, S., Maye, A., Westerhoff, M., Hege, H. C., and Menzel, R. 2005. Three-dimensional average-shape atlas of the honeybee brain and its applications. J. Comp. Neurol. 492, 1–19.

Bräunig, P. 1991. Suboesophageal DUM neurons innervate the principal neuropiles of the locust brain. Philos. Trans. R. Soc. Lond. B 332, 221–240.

Brody, C. D. and Hopfield, J. J. 2003. Simple networks for spike-timing-based computation, with application to olfactory processing. Neuron 37, 843–852.
de Bruyne, M., Foster, K., and Carlson, J. R. 2001. Odor coding in the Drosophila antenna. Neuron 30, 537–552.
Buchner, E. 1991. Genes expressed in the adult brain of Drosophila and effects of their mutations on behavior: a survey of transmitter- and second messenger-related genes. J. Neurogenet. 7, 153–192.
Buchner, E. and Rodrigues, V. 1983. Autoradiographic localization of [3H]choline uptake in the brain of *Drosophila melanogaster*. Neurosci. Lett. 42, 25–31.
Cardé, R. T. 1996. Odour plumes and odour-mediated flight in insects. Ciba Found. Symp. 200, 54–66; discussion 66–70.
Cardé, R. T. and Minks, A. K. 1995. Control of moth pests by mating disruption: successes and constraints. Annu. Rev. Entomol. 40, 559–585.
Carlsson, M. A., Galizia, C. G., and Hansson, B. S. 2002. Spatial representation of odours in the antennal lobe of the moth *Spodoptera littoralis* (Lepidoptera: Noctuidae). Chem. Senses 27, 231–244.
Chapman, R. F. 2002. Development of phenotypic differences in sensillum populations on the antennae of a grasshopper, *Schistocerca americana*. J. Morphol. 254, 186–194.
Christensen, T. A. and Hildebrand, J. G. 1997. Coincident stimulation with pheromone components improves temporal pattern resolution in central olfactory neurons. J. Neurophysiol. 77, 775–781.
Christensen, T. A. and Hildebrand, J. G. 2002. Pheromonal and host-odor processing in the insect antennal lobe: how different? Curr. Opin. Neurobiol. 12, 393–399.
Christensen, T. A. and Sorensen, P. W. 1996. Pheromones as tools for olfactory research. Introduction. Chem. Senses 21, 241–243.
Christensen, T. A., Harrow, I. D., Cuzzocrea, C., Randolph, P. W, and Hildebrand, J. G. 1995. Distinct projections of two populations of olfactory receptor axons in the antennal lobe of the sphinx moth *Manduca sexta*. Chem. Senses 20, 313–323.
Christensen, T. A., Pawlowski, V. M., Lei, H., and Hildebrand, J. G. 2000. Multi-unit recordings reveal context-dependent modulation of synchrony in odor-specific neural ensembles. Nat. Neurosci. 3, 927–931.
Christensen, T. A., Waldrop, B. R., Harrow, I. D., and Hildebrand, J. G. 1993. Local interneurons and information processing in the olfactory glomeruli of the moth *Manduca sexta*. J. Comp. Physiol. [A] 173, 385–399.
Christensen, T. A., Waldrop, B. R., and Hildebrand, J. G. 1998a. GABAergic mechanisms that shape the temporal response to odors in moth olfactory projection neurons. Ann. N. Y. Acad. Sci. 855, 475–481.
Christensen, T. A., Waldrop, B. R., and Hildebrand, J. G. 1998b. Multitasking in the olfactory system: context-dependent responses to odors reveal dual GABA-regulated coding mechanisms in single olfactory projection neurons. J. Neurosci. 18, 5999–6008.
Clyne, P. J., Warr, C. G., Freeman, M. R., Lessing, D., Kim, J., and Carlson, J. R. 1999. A novel family of divergent seven-transmembrane proteins: candidate odorant receptors in *Drosophila*. Neuron 22, 327–338.
Cobb, M. 1999. What and how do maggots smell? Biol. Rev. 74, 425–459.
Collmann, C., Carlsson, M. A., Hansson, B. S., and Nighorn, A. 2004. Odorant-evoked nitric oxide signals in the antennal lobe of *Manduca sexta*. J. Neurosci. 24, 6070–6077.
Connolly, J. B., Roberts, I. J., Armstrong, J. D., Kaiser, K., Forte, M., Tully, T., and O'Kane, C. J. 1996. Associative learning disrupted by impaired Gs signaling in Drosophila mushroom bodies. Science 274, 2104–2107.
Costa, R. 1989. Esterase-6 and the pheromonal effects of cis-vaccenyl acetate in *Drosophila melanogaster*. J. Evol. Biol. 2, 395–407.
Costantini, C., Birkett, M. A., Gibson, G., Ziesmann, J., Sagnon, N. F., Mohammed, H. A., Coluzzi, M., and Pickett, J. A. 2001. Electroantennogram and behavioural responses of the malaria vector *Anopheles gambiae* to human-specific sweat components. Med. Vet. Entomol. 15, 259–266.
Couto, A., Alenius, M., and Dickson, B. J. 2005. Molecular, anatomical, and functional organization of the Drosophila olfactory system. Curr. Biol. 15, 1535–1547.
Dacks, A. M., Christensen, T. A., Agricola, H. J., Wollweber, L., and Hildebrand, J. G. 2005. Octopamine-immunoreactive neurons in the brain and subesophageal ganglion of the hawkmoth *Manduca sexta*. J. Comp. Neurol. 488, 255–268.
Daly, K. C. and Smith, B. H. 2000. Associative olfactory learning in the moth *Manduca sexta*. J. Exp. Biol. 203, 2025–2038.
Daly, K. C., Christensen, T. A., Lei, H., Smith, B. H., and Hildebrand, J. G. 2004. Learning modulates the ensemble representations for odors in primary olfactory networks. Proc. Natl. Acad. Sci. U. S. A. 101, 10476–10481.
Dani, F. R., Jones, G. R., Corsi, S., Beard, R., Pradella, D., and Turillazzi, S. 2005. Nestmate recognition cues in the honey bee: differential importance of cuticular alkanes and alkenes. Chem. Senses 30, 477–489.
Davis, R. L. 2004. Olfactory learning. Neuron 44, 31–48.
Davis, N. T., Homberg, U., Teal, P. E. A., Altstein, M., Agricola, H. J., and Hildebrand, J. G. 1996. Neuroanatomy and immunocytochemistry of the median neuroendocrine cells of the subesophageal ganglion of the tobacco hawkmoth, *Manduca sexta*: immunoreactivities to PBAN and other neuropeptides. Microsc. Res. Tech. 35, 201–229.
Deisig, N., Lachnit, H., Sandoz, J. C., Lober, K., and Giurfa, M. 2003. A modified version of the unique cue theory accounts for olfactory compound processing in honeybees. Learn. Mem. 10, 199–208.
Dekker, T., Geier, M., and Cardé, R. T. 2005. Carbon dioxide instantly sensitizes female yellow fever mosquitoes to human skin odours. J. Exp. Biol. 208, 2963–2972.
Dekker, T., Steib, B., Cardé, R. T., and Geier, M. 2002. L-lactic acid: a human-signifying host cue for the anthropophilic mosquito *Anopheles gambiae*. Med. Vet. Entomol. 16, 91–98.
Dickens, J. C., Oliver, J. E., Hollister, B., Davis, J. C., and Klun, J. A. 2002. Breaking a paradigm: male-produced aggregation pheromone for the Colorado potato beetle. J. Exp. Biol. 205, 1925–1933.
Distler, P. G. 1990. Synaptic connections of dopamine-immunoreactive neurons in the antennal lobes of *Periplaneta americana*. Colocalization with GABA-like immunoreactivity. Histochemistry 93, 401–408.
Distler, P. G. and Boeckh, J. 1996. Synaptic connection between olfactory receptor cells and uniglomerular projection neurons in the antennal lobe of the American cockroach, *Periplaneta americana*. J. Comp. Neurol. 370, 35–46.
Distler, P. G. and Boeckh, J. 1997a. Synaptic connections between identified neuron types in the antennal lobe glomeruli of the cockroach, *Periplaneta americana*: II. Local multiglomerular interneurons. J. Comp. Neurol. 383, 529–540.
Distler, P. G. and Boeckh, J. 1997b. Central projections of the maxillary and antennal nerves in the mosquito *Aedes aegypti*. J. Exp. Biol. 200, 1873–1879.
Distler, P. G., Bausenwein, B., and Boeckh, J. 1998a. Localization of odor-induced neuronal activity in the antennal

lobes of the blowfly *Calliphora vicina*: a [3H] 2-deoxyglucose labeling study. Brain Res. 805, 263–266.
Distler, P. G., Gruber, C., and Boeckh, J. 1998b. Synaptic connections between GABA-immunoreactive neurons and uniglomerular projection neurons within the antennal lobe of the cockroach, *Periplaneta americana*. Synapse 29, 1–13.
Ditzen, M., Evers, J. F., and Galizia, C. G. 2003. Odor similarity does not influence the time needed for odor processing. Chem. Senses 28, 781–789.
Dobritsa, A. A., van der Goes van Naters, W., Warr, C. G., Steinbrecht, R. A., and Carlson, J. R. 2003. Integrating the molecular and cellular basis of odor coding in the *Drosophila* antenna. Neuron 37, 827–841.
Dubnau, J., Chiang, A. S., and Tully, T. 2003. Neural substrates of memory: from synapse to system. J. Neurobiol. 54, 238–253.
Dubnau, J., Grady, L., Kitamoto, T., and Tully, T. 2001. Disruption of neurotransmission in Drosophila mushroom body blocks retrieval but not acquisition of memory. Nature 411, 476–480.
Dukas, R. and Bernays, E. A. 2000. Learning improves growth rate in grasshoppers. Proc. Natl. Acad. Sci. U. S. A. 97, 2637–2640.
Ejima, A., Smith, B. P., Lucas, C., van der Goes van Naters, W., Miller, C. J., Carlson, J. R., Kevine, J. D., and Griffith, L. C. 2007. Generalization of courtship learning in Drosophila is mediated by *cis*-vaccenyl acetate. Curr. Biol. 17, 599–605.
Elphick, M., Rayne, R., Riveros-Moreno, V. V., Moncada, S., and Shea, M. 1995. Nitric oxide synthesis in locust olfactory interneurones. J. Exp. Biol. 198, 821–829.
Erber, J., Masuhr, T., and Menzel, R. 1980. Localization of short-term-memory in the brain of the bee, *Apis mellifera*. Physiol. Entomol. 5, 343–358.
Ernst, K. D. and Boeckh, J. 1983. A neuroanatomical study on the organization of the central antennal pathways in insects. III. Neuroanatomical characterization of physiologically defined response types of deutocerebral neurons in *Periplaneta americana*. Cell Tissue Res. 229, 1–22.
Ernst, K. D., Boeckh, J., and Boeckh, V. 1977. A neuroanatomical study on the organization of the central antennal pathways in insects. Cell Tissue Res. 176, 285–306.
Esslen, J. and Kaissling, K. E. 1976. Number and distribution of sensilla on antennal flagellum of honeybee (*Apis mellifera* L.). Zoomorphologie 83, 227–251.
Faber, T. and Menzel, R. 2001. Visualizing mushroom body response to a conditioned odor in honeybees. Naturwissenschaften 88, 472–476.
Faber, T., Joerges, J., and Menzel, R. 1999. Associative learning modifies neural representations of odors in the insect brain. Nat. Neurosci. 2, 74–78.
Fan, R. J., Anderson, P., and Hansson, B. 1997. Behavioural analysis of olfactory conditioning in the moth *Spodoptera littoralis* (Boisd.) (Lepidoptera: noctuidae). J. Exp. Biol. 200 (Pt 23), 2969–2976.
Farivar, S. S. 2005. Cytoarchitecture of the Locust Olfactory System. PhD Thesis, http://resolver.caltech.edu/Caltech ETD:etd-04212005-143332.
Farooqui, T., Robinson, K., Vaessin, H., and Smith, B. H. 2003. Modulation of early olfactory processing by an octopaminergic reinforcement pathway in the honeybee. J. Neurosci. 23, 5370–5380.
Farris, S. M. 2005. Evolution of insect mushroom bodies: old clues, new insights. Arthropod Struct. Dev. 34, 211–234.
Farris, S. M. and Strausfeld, N. J. 2001. Development of laminar organization in the mushroom bodies of the cockroach: Kenyon cell proliferation, outgrowth, and maturation. J. Comp. Neurol. 439, 331–351.
Farris, S. M., Abrams, A. I., and Strausfeld, N. J. 2004. Development and morphology of class II Kenyon cells in the mushroom bodies of the honey bee, *Apis mellifera*. J. Comp. Neurol. 474, 325–339.
Farris, S. M., Robinson, G. E., and Fahrbach, S. E. 2001. Experience- and age-related outgrowth of intrinsic neurons in the mushroom bodies of the adult worker honeybee. J. Neurosci. 21, 6395–6404.
Feinstein, P. and Mombaerts, P. 2004. A contextual model for axonal sorting into glomeruli in the mouse olfactory system. Cell 117, 817–831.
Feinstein, P., Bozza, T., Rodriguez, I., Vassalli, A., and Mombaerts, P. 2004. Axon guidance of mouse olfactory sensory neurons by odorant receptors and the beta2 adrenergic receptor. Cell 117, 833–846.
Fiala, A., Spall, T., Diegelmann, S., Eisermann, B., Sachse, S., Devaud, J. M., Buchner, E., and Galizia, C. G. 2002. Genetically expressed cameleon in *Drosophila melanogaster* is used to visualize olfactory information in projection neurons. Curr. Biol. 12, 1877–1884.
Fishilevich, E. and Vosshall, L. B. 2005. Genetic and functional subdivision of the Drosophila antennal lobe. Curr. Biol. 15, 1548–1553.
Flanagan, D. and Mercer, A. R. 1989a. An atlas and 3-D reconstruction of the antennal lobes in the worker honey bee, *Apis mellifera* L. (Hymenoptera: Apidae). Int. J. Insect Morphol. Embryol. 18, 145–159.
Flanagan, D. and Mercer, A. R. 1989b. Morphology and response characteristics of neurones in the deutocerebrum of the brain in the honeybee *Apis mellifera*. J. Comp. Physiol. [A] 164, 483–494.
Fonta, C., Sun, X. J., and Masson, C. 1993. Morphology and spatial distribution of bee antennal lobe interneurones responsive to odours. Chem. Senses 18, 101–119.
Frambach, I., Rössler, W., Winkler, M., and Schurmann, F. W. 2004. F-actin at identified synapses in the mushroom body neuropil of the insect brain. J. Comp. Neurol. 475, 303–314.
Free, J. B. 1987. Pheromones of social bees. Comstock Pub. Associates.
Friedrich, R. W. and Laurent, G. 2001. Dynamic optimization of odor representations by slow temporal patterning of mitral cell activity. Science 291, 889–894.
Friggi-Grelin, F., Coulom, H., Meller, M., Gomez, D., Hirsh, J., and Birman, S. 2003. Targeted gene expression in Drosophila dopaminergic cells using regulatory sequences from tyrosine hydroxylase. J. Neurobiol. 54, 618–627.
von Frisch, K. 1966. The Dancing Bees: An Account of the Life and Senses of the Honey Bee, 2nd Edition. Methuen.
Galán, R. F., Sachse, S., Galizia, C. G., and Herz, A. V. 2004. Odor-driven attractor dynamics in the antennal lobe allow for simple and rapid olfactory pattern classification. Neural. Comput. 16, 999–1012.
Galán, R. F., Weidert, M., Menzel, R., Herz, A. V. M., and Galizia, C. G. 2006. Sensory memory for odors is encoded in spontaneous correlated activity between olfactory glomeruli. Neural Comput.,18, 10–25.
Galizia, C. G. and Kimmerle, B. 2004. Physiological and morphological characterization of honeybee olfactory neurons combining electrophysiology, calcium imaging and confocal microscopy. J. Comp. Physiol. [A] 190, 21–38.
Galizia, C. G. and Menzel, R. 2001. The role of glomeruli in the neural representation of odours: results from optical recording studies. J. Insect Physiol. 47, 115–130.
Galizia, C. G. and Vetter, R. S. 2004. Optical Methods for Analyzing Odor-Evoked Activity in the Insect Brain. In: Advances in Insect Sensory Neuroscience (*ed*. T. A. Christensen), pp. 349–392. CRC Press.
Galizia, C. G., Joerges, J., Küttner, A., Faber, T., and Menzel, R. 1997. A semi *in-vivo* preparation for optical recording of the insect brain. J. Neurosci. Methods 76, 61–69.

Galizia, C. G., Kunze, J., Gumbert, A., Borg-Karlson, A. K., Sachse, S., Markl, C., and Menzel, R. 2005. Relationship of visual and olfactory signal parameters in a food-deceptive flower mimicry system. Behav. Ecol. 16, 159–168.

Galizia, C. G., Küttner, A., Joerges, J., and Menzel, R. 2000b. Odour representation in honeybee olfactory glomeruli shows slow temporal dynamics: an optical recording study using a voltage-sensitive dye. J. Insect Physiol. 46, 877–886.

Galizia, C. G., McIlwrath, S. L., and Menzel, R. 1999b. A digital three-dimensional atlas of the honeybee antennal lobe based on optical sections acquired by confocal microscopy. Cell Tissue Res. 295, 383–394.

Galizia, C. G., Menzel, R., and Hölldobler, B. 1999a. Optical imaging of odor-evoked glomerular activity patterns in the antennal lobes of the ant *Camponotus rufipes*. Naturwissenschaften 86, 533–537.

Galizia, C. G., Nägler, K., Hölldobler, B., and Menzel, R. 1998. Odour coding is bilaterally symmetrical in the antennal lobes of honeybees (*Apis mellifera*). Eur. J. Neurosci. 10, 2964–2974.

Galizia, C. G., Sachse, S., and Mustaparta, H. 2000a. Calcium responses to pheromones and plant odours in the antennal lobe of the male and female moth *Heliothis virescens*. J. Comp. Physiol. [A] 186, 1049–1063.

Galizia, C. G., Sachse, S., Rappert, A., and Menzel, R. 1999c. The glomerular code for odor representation is species specific in the honeybee *Apis mellifera*. Nat. Neurosci. 2, 473–478.

Ganeshina, O. and Menzel, R. 2001. GABA-immunoreactive neurons in the mushroom bodies of the honeybee: an electron microscopic study. J. Comp. Neurol. 437, 335–349.

Gao, Q. and Chess, A. 1999. Identification of candidate *Drosophila* olfactory receptors from genomic DNA sequence. Genomics 60, 31–39.

Gascuel, J. and Masson, C. 1991. A quantitative ultrastructural study of the honeybee antennal lobe. Tissue and Cell 23, 341–355.

Geier, M., Bosch, O. J., and Boeckh, J. 1999a. Ammonia as an attractive component of host odour for the yellow fever mosquito, *Aedes aegypti*. Chem. Senses 24, 647–653.

Geier, M., Bosch, O. J., and Boeckh, J. 1999b. Influence of odour plume structure on upwind flight of mosquitoes towards hosts. J. Exp. Biol. 202, 1639–1648.

Gerber, B., Scherer, S., Neuser, K., Michels, B., Hendel, T., Stocker, R. F., and Heisenberg, M. 2004b. Visual learning in individually assayed Drosophila larvae. J. Exp. Biol. 207, 179–188.

Gerber, B., Tanimoto, H., and Heisenberg, M. 2004a. An engram found? Evaluating the evidence from fruit flies. Curr. Opin. Neurobiol. 14, 737–744.

Getz, W. M. 1991. A neural network for processing olfactory-like stimuli. Bull. Math. Biol. 53, 805–823.

Getz, W. M. and Lutz, A. 1999. A neural network model of general olfactory coding in the insect antennal lobe. Chem. Senses 24, 351–372.

Gewecke, M. 1979. Central projection of antennal afferents for the flight motor in *Locusta migratoria* (Orthoptera, Acrididae). Entomologia Generalis 5, 317–320.

Gibson, N. J. and Nighorn, A. 2000. Expression of nitric oxide synthase and soluble guanylyl cyclase in the developing olfactory system of *Manduca sexta*. J. Comp. Neurol. 422, 191–205.

Gibson, N. J., Rossler, W., Nighorn, A. J., Oland, L. A., Hildebrand, J. G., and Tolbert, L. P. 2001. Neuron-glia communication via nitric oxide is essential in establishing antennal-lobe structure in *Manduca sexta*. Dev. Biol. 240, 326–339.

Giurfa, M. 1993. The repellent scent-mark of the honeybee *Apis mellifera ligustica* and its role as communication cue during foraging. Insectes Sociaux 40, 59–67.

Giurfa, M. 2003a. Cognitive neuroethology: dissecting non-elemental learning in a honeybee brain. Curr. Opin. Neurobiol. 13, 726–735.

Giurfa, M. 2003b. The amazing mini-brain: lessons from a honey bee. Bee World 84, 5–18.

Giurfa, M. and Capaldi, E. A. 1999. Vectors, routes and maps: new discoveries about navigation in insects. Trends Neurosci. 22, 237–242.

Giurfa, M. and Malun, D. 2004. Associative mechanosensory conditioning of the proboscis extension reflex in honeybees. Learn. Mem. 11, 294–302.

Giurfa, M. and Nunez, J. A. 1992. Honeybees mark with scent and reject recently visited flowers. Oecologia 89, 113–117.

Giurfa, M., Zhang, S., Jenett, A., Menzel, R., and Srinivasan, M. V. 2001. The concepts of ''sameness'' and ''difference'' in an insect. Nature 410, 930–933.

Goldman, A. L., Van der Goes van Naters, W., Lessing, D., Warr, C. G., and Carlson, J. R. 2005. Coexpression of two functional odor receptors in one neuron. Neuron 45, 661–666.

Goriely, A. R., Secomb, T. W., and Tolbert, L. P. 2002. Effect of the glial envelope on extracellular K^+ diffusion in olfactory glomeruli. J. Neurophysiol. 87, 1712–1722.

Grant, A. J., Wigton, B. E., Aghajanian, J. G., and O'Connell, R. J. 1995. Electrophysiological responses of receptor neurons in mosquito maxillary palp sensilla to carbon dioxide. J. Comp. Physiol. [A] 177, 389–396.

Grimaldi, D. A. and Engel, M. S. 2004. Evolution of the Insects. Cambridge University Press.

Gronenberg, W. 1999. Modality-specific segregation of input to ant mushroom bodies. Brain Behav. Evol. 54, 85–95.

Gronenberg, W. 2001. Subdivisions of hymenopteran mushroom body calyces by their afferent supply. J. Comp. Neurol. 435, 474–489.

Grünbaum, L. and Müller, U. 1998. Induction of a specific olfactory memory leads to a long-lasting activation of protein kinase C in the antennal lobe of the honeybee. J. Neurosci. 18, 4384–4392.

Grünewald, B. 1999a. Physiological properties and response modulations of mushroom body feedback neurons during olfactory learning in the honeybee, *Apis mellifera*. J. Comp. Physiol. [A] 185, 565–576.

Grünewald, B. 1999b. Morphology of feedback neurons in the mushroom body of the honeybee, *Apis mellifera*. J. Comp. Neurol. 404, 114–126.

Guerenstein, P. G., Yepez, E. A., van Haren, J., Williams, D. G., and Hildebrand, J. G. 2004. Floral CO2 emission may indicate food abundance to nectar-feeding moths. Naturwissenschaften 91, 329–333.

Guerrieri, F., Schubert, M., Sandoz, J. C., and Giurfa, M. 2005. Perceptual and neural olfactory similarity in honeybees. PLoS Biol 3, e60.

Hähnlein, I. and Bicker, G. 1996. Morphology of neuroglia in the antennal lobes and mushroom bodies of the brain of the honeybee. J. Comp. Neurol. 367, 235–245.

Hähnlein, I., Hartig, W., and Bicker, G. 1996. Datura stramonium lectin staining of glial associated extracellular material in insect brains. J. Comp. Neurol. 376, 175–187.

Hammer, M. 1993. An identified neuron mediates the unconditioned stimulus in associative olfactory learning in honeybees. Nature 366, 59–63.

Hammer, M. 1997. The neural basis of associative reward learning in honeybees. Trends Neurosci. 20, 245–252.

Hammer, M. and Menzel, R. 1998. Multiple sites of associative odor learning as revealed by local brain microinjections of octopamine in honeybees. Learn. Mem. 5, 146–156.

Hansson, B. S., Carlsson, M. A., and Kalinova, B. 2003. Olfactory activation patterns in the antennal lobe of the sphinx moth, *Manduca sexta*. J. Comp. Physiol. [A] 189, 301–308.

Hansson, B. S., Christensen, T. A., and Hildebrand, J. G. 1991. Functionally distinct subdivisions of the macroglomerular complex in the antennal lobe of the male sphinx moth *Manduca sexta*. J. Comp. Neurol. 312, 264–278.

Hartlieb, E., Anderson, P., and Hansson, B. S. 1999. Appetitive learning of odours with different behavioural meaning in moths. Physiol. Behav. 67, 671–677.

Heimbeck, G., Bugnon, V., Gendre, N., Haberlin, C., and Stocker, R. F. 1999. Smell and taste perception in *Drosophila melanogaster* larva: toxin expression studies in chemosensory neurons. J. Neurosci. 19, 6599–6609.

Heimbeck, G., Bugnon, V., Gendre, N., Keller, A., and Stocker, R. F. 2001. A central neural circuit for experience-independent olfactory and courtship behavior in *Drosophila melanogaster*. Proc. Natl. Acad. Sci. U. S. A. 98, 15336–15341.

Heinbockel, T., Kloppenburg, P., and Hildebrand, J. G. 1998. Pheromone-evoked potentials and oscillations in the antennal lobes of the sphinx moth *Manduca sexta*. J. Comp. Physiol. [A] 182, 703–714.

Heisenberg, M. 2003. Mushroom body memoir: from maps to models. Nat. Rev. Neurosci. 4, 266–275.

Heisenberg, M., Borst, A., Wagner, S., and Byers, D. 1985. Drosophila mushroom body mutants are deficient in olfactory learning. J. Neurogenet. 2, 1–30.

Hendel, T., Michels, B., Neuser, K., Schipanski, A., Kaun, K., Sokolowski, M. B., Marohn, F., Michel, R., Heisenberg, M., and Gerber, B. 2005. The carrot, not the stick: appetitive rather than aversive gustatory stimuli support associative olfactory learning in individually assayed *Drosophila* larvae. J. Comp. Physiol. [A] 191, 265–279.

Hildebrand, J. G. and Shepherd, G. M. 1997. Mechanisms of olfactory discrimination: converging evidence for common principles across phyla. Annu. Rev. Neurosci. 20, 595–631.

Hildebrandt, H. and Müller, U. 1995a. PKA activity in the antennal lobe of honeybees is regulated by chemosensory stimulation in vivo. Brain Res. 679, 281–288.

Hildebrandt, H. and Müller, U. 1995b. Octopamine mediates rapid stimulation of protein kinase A in the antennal lobe of honeybees. J. Neurobiol. 27, 44–50.

Hofer, S., Dircksen, H., Tollback, P., and Homberg, U. 2005. Novel insect orcokinins: characterization and neuronal distribution in the brains of selected dicondylian insects. J. Comp. Neurol. 490, 57–71.

Hölldobler, B. and Wilson, E. O. 1990. The Ants. Belknap Press of Harvard University Press.

Homberg, U. 2002. Neurotransmitters and neuropeptides in the brain of the locust. Microsc. Res. Tech. 56, 189–209.

Homberg, U. and Hildebrand, J. G. 1991. Histamine immunoreactive neurons in the midbrain and subesophageal ganglion of the sphinx moth *Manduca sexta*. J. Comp. Neurol. 307, 647–657.

Homberg, U. and Hildebrand, J. G. 1994. Postembryonic development of gamma-aminobutyric acid-like immunoreactivity in the brain of the sphinx moth *Manduca-Sexta*. J. Comp. Neurol. 339, 132–149.

Homberg, U. and Müller, U. 1999. Neuroactive Substances in the Antennal Lobe. In: Insect Olfaction (*ed*. B. S. Hansson), pp. 181–206. Springer.

Homberg, U., Hoskins, S. G., and Hildebrand, J. G. 1995. Distribution of acetylcholinesterase activity in the deutocerebrum of the sphinx moth *Manduca sexta*. Cell Tissue Res. 279, 249–259.

Homberg, U., Kingan, T. G., and Hildebrand, J. G. 1990. Distribution of FMRFamide-like immunoreactivity in the brain and suboesophageal ganglion of the sphinx moth *Manduca sexta* and colocalization with SCPB-, BPP-, and GABA-like immunoreactivity. Cell Tissue Res. 259, 401–419.

Homberg, U., Montague, R. A., and Hildebrand, J. G. 1988. Anatomy of antenno-cerebral pathways in the brain of the sphinx moth *Manduca sexta*. Cell Tissue Res. 254, 255–281.

Hoskins, S. G., Homberg, U., Kingan, T. G., Christensen, T. A., and Hildebrand, J. G. 1986. Immunocytochemistry of GABA in the antennal lobes of the sphinx moth *Manduca sexta*. Cell Tissue Res. 244, 243–252.

Hösl, M. 1990. Pheromone-sensitive neurons in the deutocerebrum of *Periplaneta americana* – Receptive fields on the antenna. J. Comp. Physiol. [A] 167, 321–327.

Hosler, J. S., Buxton, K. L., and Smith, B. H. 2000. Impairment of olfactory discrimination by blockade of GABA and nitric oxide activity in the honey bee antennal lobes. Behav. Neurosci. 114, 514–525.

Huerta, R., Nowotny, T., Garcia-Sanchez, M., Abarbanel, H. D., and Rabinovich, M. I. 2004. Learning classification in the olfactory system of insects. Neural Comput. 16, 1601–1640.

Huetteroth, W. and Schachtner, J. 2005. Standard three-dimensional glomeruli of the *Manduca sexta* antennal lobe: a tool to study both developmental and adult neuronal plasticity. Cell Tissue Res. 319, 513–524.

Hummel, T. and Zipursky, S. L. 2004. Afferent induction of olfactory glomeruli requires *N*-cadherin. Neuron 42, 77–88.

Hummel, T., Vasconcelos, M. L., Clemens, J. C., Fishilevich, Y., Vosshall, L. B., and Zipursky, S. L. 2003. Axonal targeting of olfactory receptor neurons in Drosophila is controlled by Dscam. Neuron 37, 221–231.

Ignell, R. 2001. Monoamines and neuropeptides in antennal lobe interneurons of the desert locust, Schistocerca gregana: an immunocytochemical study. Cell Tissue Res. 306, 143–156.

Ignell, R., Dekker, T., Ghaninia, M., and Hansson, B. 2005. The neuronal architecture of the mosquito deutocerebrum. J. Comp. Neurol. 493, 207–240.

Isabel, G., Pascual, A., and Preat, T. 2004. Exclusive consolidated memory phases in Drosophila. Science 304, 1024–1027.

Ito, K., Suzuki, K., Estes, P., Ramaswami, M., Yamamoto, D., and Strausfeld, N. J. 1998. The organization of extrinsic neurons and their implications in the functional roles of the mushroom bodies in *Drosophila melanogaster* Meigen. Learn. Mem. 5, 52–77.

Iwano, M. and Kanzaki, R. 2005. Immunocytochemical identification of neuroactive substances in the antennal lobe of the male silkworm moth *Bombyx mori*. Zoolog. Sci. 22, 199–211.

Iwasaki, M., Mizunami, M., Nishikawa, M., Itoh, T., and Tominaga, Y. 1999. Ultrastructural analyses of modular subunits in the mushroom bodies of the cockroach. J. Electron Microsc. 48, 55–62.

Jackson, F. R., Newby, L. M., and Kulkarni, S. J. 1990. Drosophila GABAergic systems: sequence and expression of glutamic acid decarboxylase. J. Neurochem. 54, 1068–1078.

Jefferis, G., Marin, E. C., Stocker, R. F., and Luo, L. Q. 2001. Target neuron prespecification in the olfactory map of Drosophila. Nature 414, 204–208.

Jefferis, G. S., Potter, C. J., Chan, A. M., Marin, E. C., Rohlfing, T., Maurer, C. R., Jr., and Luo, L. 2007. Comprehensive maps of Drosophila higher olfactory centers: spatially segregated fruit and pheromone representation. Cell 128, 1187–1203.

Jefferis, G., Vyas, R. M., Berdnik, D., Ramaekers, A., Stocker, R. F., Tanaka, N. K., Ito, K., and Luo, L. Q. 2004. Developmental origin of wiring specificity in the olfactory system of Drosophila. Development 131, 117–130.

Jhaveri, D. and Rodrigues, V. 2002. Sensory neurons of the Atonal lineage pioneer the formation of glomeruli within the adult Drosophila olfactory lobe. Development 129, 1251–1260.

Jhaveri, D., Saharan, S., Sen, A., and Rodrigues, V. 2004. Positioning sensory terminals in the olfactory lobe of Drosophila by Robo signaling. Development 131, 1903–1912.

Jhaveri, D., Sen, A., and Rodrigues, V. 2000. Mechanisms underlying olfactory neuronal connectivity in Drosophila – The atonal lineage organizes the periphery while sensory neurons and glia pattern the olfactory lobe. Dev. Biol. 226, 73–87.

Joerges, J., Küttner, A., Galizia, C. G., and Menzel, R. 1997. Representations of odours and odour mixtures visualized in the honeybee brain. Nature 387, 285–288.

Jones, W. D., Cayirlioglu, P., Kadow, I. G., and Vosshall, L. B. 2007. Two chemosensory receptors together mediated carbon dioxide detection in Drosophila. Nature 445, 86–90.

Jones, W. D., Nguyen, T. A., Kloss, B., Lee, K. J., and Vosshall, L. B. 2005. Functional conservation of an insect odorant receptor gene across 250 million years of evolution. Curr. Biol. 15, R119–121.

Justus, K. A., Cardé, R. T., and French, A. S. 2005. Dynamic properties of antennal responses to pheromone in two moth species. J. Neurophysiol. 93, 2233–2239.

Kaissling, K. E., Hildebrand, J. G., and Tumlinson, J. H. 1989. Pheromone receptor cells in the male moth *Manduca sexta*. Arch. Insect Biochem. and Physiol. 10, 273–279.

Karban, R. and Baldwin, I. T. 1997. Induced Responses to Herbivory. University of Chicago Press.

Kasowski, H. J., Kim, H., and Greer, C. A. 1999. Compartmental organization of the olfactory bulb glomerulus. J. Comp. Neurol. 407, 261–274.

Keene, A. C., Stratmann, M., Keller, A., Perrat, P. N., Vosshall, L. B., and Waddell, S. 2004. Diverse odor-conditioned memories require uniquely timed dorsal paired medial neuron output. Neuron 44, 521–533.

Keil, T. A. 1996. Sensilla on the maxillary palps of Helicoverpa armigera caterpillars: in search of the CO_2-receptor. Tissue Cell 28, 703–717.

Kent, K. S., Harrow, I. D., Quartararo, P., and Hildebrand, J. G. 1986. An accessory olfactory pathway in Lepidoptera: the labial pit organ and its central projections in *Manduca sexta* and certain other sphinx moths and silk moths. Cell Tissue Res. 245, 237–245.

Kent, K. S., Hoskins, S. G., and Hildebrand, J. G. 1987. A novel serotonin-immunoreactive neuron in the antennal lobe of the sphinx moth *Manduca sexta* persists throughout postembryonic life. J. Neurobiol. 18, 451–465.

Kirschner, S., Kleineidam, C. J., Zube, C., Rybak, J., Grubewakd, B., and Rossler, W. 2006. Dual olfactoty pathway in the honeybee, *Apis mellifera*. J. Comp Neurol. 499, 933–952.

Kleineidam, C. and Tautz, J. 1996. Perception of carbon dioxide and other ''air-condition'' parameters in the leaf cutting ant *Atta cephalotes*. Naturwissenschaften 83, 566–568.

Kline, D. L. 1998. Olfactory responses and field attraction of mosquitoes to volatiles from Limburger cheese and human foot odor. J. Vector Ecol. 23, 186–194.

Kloppenburg, P., Camazine, S. M., Sun, X. J., Randolph, P., and Hildebrand, J. G. 1997. Organization of the antennal motor system in the sphinx moth *Manduca sexta*. Cell Tissue Res. 287, 425–433.

Komischke, B., Sandoz, J. C., Malun, D., and Giurfa, M. 2005. Partial unilateral lesions of the mushroom bodies affect olfactory learning in honeybees *Apis mellifera* L. Eur. J. Neurosci. 21, 477–485.

Komiyama, T., Carlson, J. R., and Luo, L. 2004. Olfactory receptor neuron axon targeting: intrinsic transcriptional control and hierarchical interactions. Nat. Neurosci. 7, 819–825.

Komiyama, T., Johnson, W. A., Luo, L., and Jefferis, G. S. 2003. From lineage to wiring specificity. POU domain transcription factors control precise connections of Drosophila olfactory projection neurons. Cell 112, 157–167.

Kreher, S. A., Kwon, J. Y., and Carlson, J. R. 2005. The molecular basis of odor coding in the Drosophila larva. Neuron 46, 445–456.

Kreissl, S. and Bicker, G. 1989. Histochemistry of acetylcholinesterase and immunocytochemistry of an acetylcholine receptor-like antigen in the brain of the honeybee. J. Comp. Neurol. 286, 71–84.

Kreissl, S., Eichmuller, S., Bicker, G., Rapus, J., and Eckert, M. 1994. Octopamine-like immunoreactivity in the brain and subesophageal ganglion of the honeybee. J. Comp. Neurol. 348, 583–595.

Kretzschmar, D. and Pflugfelder, G. O. 2002. Glia in development, function, and neurodegeneration of the adult insect brain. Brain Res. Bull. 57, 121–131.

Krieger, J., Klink, O., Mohl, C., Raming, K., and Breer, H. 2003. A candidate olfactory receptor subtype highly conserved across different insect orders. J. Comp. Physiol. [A] 189, 519–526.

Kurtovic, A., Widmer, A., and Dickson, B. J. 2007. A single class of olfactory neurons mediates behavioural responses to a Drosophila sex pheromone. Nature 446, 542–546.

Kwon, H. W., Lent, D. D., and Strausfeld, N. J. 2004. Spatial learning in the restrained American cockroach *Periplaneta americana*. J. Exp. Biol. 207, 377–383.

Lacey, E. S., Ginzel, M. D., Millar, J. G., and Hanks, L. M. 2004. Male-produced aggregation pheromone of the cerambycid beetle *Neoclytus acuminatus* acuminatus. J. Chem. Ecol. 30, 1493–1507.

Lacher, V. 1964. Elektrophysiologische Untersuchungen an einzelnen Rezeptoren für Geruch, Kohlendioxyd, Luftfeuchtigkeit und Temperatur auf den Antennen der Arbeitsbiene und der Drohne (*Apis mellifica* L.) [Electrophysiological single-receptor analysis for odor, CO_2, humidity and temperature on the antennae of worker and drone honeybees]. Zeitschrift für vergleichende Physiologie 48, 587–623.

Lacroix, R., Mukabana, W. R., Gouagna, L. C., and Koella, J. C. 2005. Malaria infection increases attractiveness of humans to mosquitoes. PLoS Biol. 3, e298.

Laissue, P. P., Reiter, C., Hiesinger, P. R., Halter, S., Fischbach, K. F., and Stocker, R. F. 1999. Three-dimensional reconstruction of the antennal lobe in *Drosophila melanogaster*. J. Comp. Neurol. 405, 543–552.

Larsson, M. C., Domingos, A. I., Jones, W. D., Chiappe, M. E., Amrein, H., and Vosshall, L. B. 2004. Or83b encodes a broadly expressed odorant receptor essential for *Drosophila* olfaction. Neuron 43, 703–714.

Laurent, G. 1996. Dynamical representation of odors by oscillating and evolving neural assemblies. Trends Neurosci. 19, 489–496.

Laurent, G. 1999. A systems perspective on early olfactory coding. Science 286, 723–728.

Laurent, G. 2002. Olfactory network dynamics and the coding of multidimensional signals. Nat. Rev. Neurosci. 3, 884–895.

Laurent, G. and Davidowitz, H. 1994. Encoding of olfactory information with oscillating neural assemblies. Science 265, 1872–1875.

Laurent, G., Stopfer, M., Friedrich, R. W., Rabinovich, M. I., Volkovskii, A., and Abarbanel, H. D. 2001. Odor encoding as an active, dynamical process: experiments, computation, and theory. Annu. Rev. Neurosci. 24, 263–297.

Laurent, G., Wehr, M., and Davidowitz, H. 1996. Temporal representations of odors in an olfactory network. J. Neurosci. 16, 3837–3847.

Leitch, B. and Laurent, G. 1996. GABAergic synapses in the antennal lobe and mushroom body of the locust olfactory system. J. Comp. Neurol. 372, 487–514.

Lenoir, A., D'Ettorre, P., Errard, C., and Hefetz, A. 2001. Chemical ecology and social parasitism in ants. Annu. Rev. Entomol. 46, 573–599.

Leon, M. and Johnson, B. A. 2003. Olfactory coding in the mammalian olfactory bulb. Brain Res. Brain Res. Rev. 42, 23–32.

Levin, L. R., Han, P. L., Hwang, P. M., Feinstein, P. G., Davis, R. L., and Reed, R. R. 1992. The Drosophila learning and memory gene rutabaga encodes a Ca^{2+}/Calmodulin-responsive adenylyl cyclase. Cell 68, 479–489.

Lin, H. H., Lai, J. S., Chin, A. L., Chen, Y. C., and Chiang, A. S. 2007. A map of olfactory representation in the Drosophila mushroom body. Cell 128, 1205–1217.

Linn, C. E., Jr., Dambroski, H. R., Feder, J. L., Berlocher, S. H., Nojima, S., and Roelofs, W. L. 2004. Postzygotic isolating factor in sympatric speciation in Rhagoletis flies: reduced response of hybrids to parental host-fruit odors. Proc. Natl. Acad. Sci. U. S. A. 101, 17753–17758.

Linn, C., Jr., Feder, J. L., Nojima, S., Dambroski, H. R., Berlocher, S. H., and Roelofs, W. 2003. Fruit odor discrimination and sympatric host race formation in Rhagoletis. Proc. Natl. Acad. Sci. U. S. A. 100, 11490–11493.

Linster, C., Kerszberg, M., and Masson, C. 1994. How neurons may compute: the case of insect sexual pheromone discrimination. J. Comput. Neurosci. 1, 231–238.

Linster, C., Sachse, S., and Galizia, C. G. 2005. Computational modeling suggests that response properties rather than spatial position determine connectivity between olfactory glomeruli. J. Neurophysiol. 93, 3410–3417.

MacLeod, K. and Laurent, G. 1996. Distinct mechanisms for synchronization and temporal patterning of odor-encoding neural assemblies. Science 274, 976–979.

Malun, D. 1991a. Inventory and distribution of synapses of identified uniglomerular projection neurons in the antennal lobe of *Periplaneta americana*. J. Comp. Neurol. 305, 348–360.

Malun, D. 1991b. Synaptic relationships between GABA-immunoreactive neurons and an identified uniglomerular projection neuron in the antennal lobe of *Periplaneta americana*: a double-labeling electron microscopic study. Histochemistry 96, 197–207.

Malun, D., Giurfa, M., Galizia, C. G., Plath, N., Brandt, R., Gerber, B., and Eisermann, B. 2002. Hydroxyurea-induced partial mushroom body ablation does not affect acquisition and retention of olfactory differential conditioning in honeybees. J. Neurobiol. 53, 343–360.

Malun, D., Waldow, U., Kraus, D., and Boeckh, J. 1993. Connections between the deutocerebrum and the protocerebrum, and neuroanatomy of several classes of deutocerebral projection neurons in the brain of male *Periplaneta americana*. J. Comp. Neurol. 329, 143–162.

Mao, Z., Roman, G., Zong, L., and Davis, R. L. 2004. Pharmacogenetic rescue in time and space of the rutabaga memory impairment by using Gene-Switch. Proc. Natl. Acad. Sci. U. S. A. 101, 198–203.

Marin, E. C., Jefferis, G. S., Komiyama, T., Zhu, H., and Luo, L. 2002. Representation of the glomerular olfactory map in the Drosophila brain. Cell 109, 243–255.

Marin, E. C., Watts, R. J., Tanaka, N. K., Ito, K., and Luo, L. Q. 2005. Developmentally programmed remodeling of the Drosophila olfactory circuit. Development 132, 725–737.

Masante-Roca, I., Gadenne, C., and Anton, S. 2005. Three-dimensional antennal lobe atlas of male and female moths, *Lobesia botrana* (Lepidoptera: Tortricidae) and glomerular representation of plant volatiles in females. J. Exp. Biol. 208, 1147–1159.

Matsumoto, S. G. and Hildebrand, J. G. 1981. Olfactory mechanisms in the moth *Manduca sexta* – response characteristics and morphology of central neurons in the antennal lobes. Proc. R. Soc. Lond. B Biol. Sci. 213, 249–277.

Matsumoto, Y. and Mizunami, M. 2004. Context-dependent olfactory learning in an insect. Learn. Mem. 11, 288–293.

Mauelshagen, J. 1993. Neural correlates of olfactory learning paradigms in an identified neuron in the honeybee brain. J. Neurophysiol. 69, 609–625.

McGuire, S. E., Le, P. T., and Davis, R. L. 2001. The role of Drosophila mushroom body signaling in olfactory memory. Science 293, 1330–1333.

McGuire, S. E., Le, P. T., Osborn, A. J., Matsumoto, K., and Davis, R. L. 2003. Spatiotemporal rescue of memory dysfunction in Drosophila. Science 302, 1765–1768.

Meijerink, J., Carlsson, M. A., and Hansson, B. S. 2003. Spatial representation of odorant structure in the moth antennal lobe: a study of structure-response relationships at low doses. J. Comp. Neurol. 467, 11–21.

Menzel, R. and Giurfa, M. 1999. Cognition by a mini brain. Nature 400, 718–719.

Menzel, R. and Giurfa, M. 2001. Cognitive architecture of a mini-brain: the honeybee. Trends Cogn. Sci. 5, 62–71.

Menzel, R. and Müller, U. 1996. Learning and memory in honeybees: from behavior to neural substrates. Annu. Rev. Neurosci. 19, 379–404.

Menzel, R., Brandt, R., Gumbert, A., Komischke, B., and Kunze, J. 2000. Two spatial memories for honeybee navigation. Proc. R. Soc. Lond. B Biol. Sci. 267, 961–968.

Mesce, K. A., DeLorme, A. W., Brelje, T. C., and Klukas, K. A. 2001. Dopamine-synthesizing neurons include the putative H-cell homologue in the moth *Manduca sexta*. J. Comp. Neurol. 430, 501–517.

Mizunami, M., Weibrecht, J. M., and Strausfeld, N. J. 1998. Mushroom bodies of the cockroach: their participation in place memory. J. Comp. Neurol. 402, 520–537.

Mobbs, P. G. 1982. The brain of the honeybee *Apis mellifera* 1. The connections and spatial organization of the mushroom bodies. Philos. R. Soc. Lond. B Biol. Sci. 298, 309–354.

Mobbs, P. G. 1985. Brain Structure. In: Comprehensive Insect Physiology Biochemistry and Pharmacology. In: Nervous System: Structure and Motor Function, Vol. 5, (*eds*. G. A. Kerkut and L. I. Gilbert), pp. 299–370. Pergamon Press.

Monastirioti, M. 1999. Biogenic amine systems in the fruit fly *Drosophila melanogaster*. Microsc. Res. Tech. 45, 106–121.

Moritz, R. F. A. and Southwick, E. E. 1992. Bees as Superorganisms: An Evolutionary Reality. Springer-Verlag.

Müller, U. 2000. Prolonged activation of cAMP-dependent protein kinase during conditioning induces long-term memory in honeybees. Neuron 27, 159–168.

Müller, U. and Hildebrandt, H. 2002. Nitric oxide/cGMP-mediated protein kinase A activation in the antennal lobes plays an important role in appetitive reflex habituation in the honeybee. J. Neurosci. 22, 8739–8747.

Müller, D., Abel, R., Brandt, R., Zockler, M., and Menzel, R. 2002. Differential parallel processing of olfactory information in the honeybee, *Apis mellifera* L. J. Comp. Physiol. [A] 188, 359–370.

Murlis, J., Elkinton, J. S., and Cardé, R. T. 1992. Odor plumes and how insects use them. Annu. Rev. Entomol. 37, 505–532.

Nässel, D. R. 1988. Serotonin and serotonin-immunoreactive neurons in the nervous system of insects. Prog. Neurobiol. 30, 1–85.

Nässel, D. R. 1993. Neuropeptides in the insect brain: a review. Cell Tissue Res. 273, 1–29.

Nässel, D. R. 1999. Histamine in the brain of insects: a review. Microsc. Res. Tech. 44, 121–136.
Nässel, D. R. 2000. Functional roles of neuropeptides in the insect central nervous system. Naturwissenschaften 87, 439–449.
Nässel, D. R. and Elekes, K. 1992. Aminergic neurons in the brain of blowflies and *Drosophila* – Dopamine-immunoreactive and tyrosine hydroxylase-immunoreactive neurons and their relationship with putative histaminergic neurons. Cell Tissue Res. 267, 147–167.
Neder, R. 1959. Allometrisches Wachstum von Hirnteilen bei drei verschieden grossen Schabenarten. (Allometric growth of brain structures in three cockroaches of different size). Zool. Jahrb. Anat. 77, 411–464.
Ng, M., Roorda, R. D., Lima, S. Q., Zemelman, B. V., Morcillo, P., and Miesenbock, G. 2002. Transmission of olfactory information between three populations of neurons in the antennal lobe of the fly. Neuron 36, 463–474.
Nishikawa, M., Yokohari, F., and Ishibashi, T. 1995. Central projections of the antennal cold receptor neurons and hygroreceptor neurons of the cockroach *Periplaneta americana*. J. Comp. Neurol. 361, 165–176.
Nishino, H., Yamashita, S., Yamazaki, Y., Nishikawa, M., Yokohari, F., and Mizunami, M. 2003. Projection neurons originating from thermo- and hygrosensory glomeruli in the antennal lobe of the cockroach. J. Comp. Neurol. 455, 40–55.
Nuñez, J., Almeida, L., Balderrama, N., and Giurfa, M. 1997. Alarm pheromone induces stress analgesia via an opioid system in the honeybee. Physiol. Behav. 63, 75–80.
Ochieng, S. A., Hallberg, E., and Hansson, B. S. 1998. Fine structure and distribution of antennal sensilla of the desert locust, *Schistocerca gregaria* (Orthoptera: Acrididae). Cell Tissue Res. 291, 525–536.
Oland, L. A. and Tolbert, L. P. 1988. Effects of hydroxyurea parallel the effects of radiation in developing olfactory glomeruli in insects. J. Comp. Neurol. 278, 377–387.
Oland, L. A. and Tolbert, L. P. 2003. Key interactions between neurons and glial cells during neural development in insects. Annu. Rev. Entomol. 48, 89–110.
Oland, L. A., Marrero, H. G., and Burger, I. 1999. Glial cells in the developing and adult olfactory lobe of the moth *Manduca sexta*. Cell Tissue Res. 297, 527–545.
Oland, L. A., Tolbert, L. P., and Mossman, K. L. 1988. Radiation-induced reduction of the glial population during development disrupts the formation of olfactory glomeruli in an insect. J. Neurosci. 8, 353–367.
Olsen, S. R., Bhandawat, V., and Wilson, R. I. 2007. Excitatory interactions between olfactory processing channels in the Drosophila antennal lobe. Neuron 54, 89–103.
Olshausen, B. A. and Field, D. J. 2004. Sparse coding of sensory inputs. Curr. Opin. Neurobiol. 14, 481–487.
Ott, S. R. and Elphick, M. R. 2002. Nitric oxide synthase histochemistry in insect nervous systems: methanol/formalin fixation reveals the neuroarchitecture of formaldehyde-sensitive NADPH diaphorase in the cockroach Periplaneta americana. J. Comp. Neurol. 448, 165–185.
Ozaki, M., Wada-Katsumata, A., Fujikawa, K., Iwasaki, M., Yokohari, F., Satoji, Y., Nisimura, T., and Yamaoka, R. 2005. Ant nestmate and non-nestmate discrimination by a chemosensory sensillum. Science 309, 311–314.
Pare, P. W. and Tumlinson, J. H. 1999. Plant volatiles as a defense against insect herbivores. Plant Physiol. 121, 325–332.
Pareto, A. 1972. Die zentrale Verteilung der Fühlerrafferenz bei Arbeiterinnen der Honigbiene, *Apis mellifera* L. [Spatial distribution of sensory antennal fibres in the central nervous system of worker bees]. Z Zellforsch Mikrosk Anat 131, 109–140.
Pascual, A. and Preat, T. 2001. Localization of long-term memory within the Drosophila mushroom body. Science 294, 1115–1117.
Peele, P., Ditzen, M., Menzel, R., and Galzia, C. G. 2006. Appetitive odor learning does not change olfactory coding in a subpopulation of honeybee antennal lobe neurons. J. Comp. Physiol. A 192, 1083–1103.
Pelz, D., Roeske, C., and Galizia, C. G. 2004. Odour response spectrum of a population of genetically identified olfactory sensory neurons: characterizing the input to a single glomerulus in *Drosophila melanogaster. ECRO*, Dijon, France.
Perazzona, B., Isabel, G., Preat, T., and Davis, R. L. 2004. The role of cAMP response element-binding protein in Drosophila long-term memory. J. Neurosci. 24, 8823–8828.
Perez-Orive, J., Bazhenov, M., and Laurent, G. 2004. Intrinsic and circuit properties favor coincidence detection for decoding oscillatory input. J. Neurosci. 24, 6037–6047.
Perez-Orive, J., Mazor, O., Turner, G. C., Cassenaer, S., Wilson, R. I., and Laurent, G. 2002. Oscillations and sparsening of odor representations in the mushroom body. Science 297, 359–365.
Pflüger, H. J. and Stevenson, P. A. 2005. Evolutionary aspects of octopaminergic systems with emphasis on arthropods. Arthropod Struct. Dev. 34, 379–396.
Pirvola, U., Tuomisto, L., Yamatodani, A., and Panula, P. 1988. Distribution of histamine in the cockroach brain and visual system: an immunocytochemical and biochemical study. J. Comp. Neurol. 276, 514–526.
Pitts, R. J., Fox, A. N., and Zwiebel, L. J. 2004. A highly conserved candidate chemoreceptor expressed in both olfactory and gustatory tissues in the malaria vector *Anopheles gambiae*. Proc. Natl. Acad. Sci. U. S. A. 101, 5058–5063.
Plowright, R. C. and Laverty, T. M. 1984. The ecology and sociobiology of bumble bees. Annu. Rev. Entomol. 29, 175–199.
Pophof, B. 2002. Octopamine enhances moth olfactory responses to pheromones, but not those to general odorants. J. Comp. Physiol. [A] 188, 659–662.
Prillinger, L. 1981. Postembryonic development of the antennal lobes in *Periplaneta americana* L. Cell Tissue Res. 215, 563–575.
Python, F. and Stocker, R. F. 2002a. Adult-like complexity of the larval antennal lobe of *D. melanogaster* despite markedly low numbers of odorant receptor neurons. J. Comp. Neurol. 445, 374–387.
Python, F. and Stocker, R. F. 2002b. Immunoreactivity against choline acetyltransferase, gamma-aminobutyric acid, histamine, octopamine, and serotonin in the larval chemosensory system of *Dosophila melanogaster*. J. Comp. Neurol. 453, 157–167.
Rabinovich, M. I., Huerta, R., Volkovskii, A., Abarbanel, H. D., Stopfer, M., and Laurent, G. 2000. Dynamical coding of sensory information with competitive networks. J. Physiol. Paris 94, 465–471.
Raguso, R. A. 2004. Flowers as sensory billboards: progress towards an integrated understanding of floral advertisement. Curr. Opin. Plant Biol. 7, 434–440.
Ramaekers, A., Magnenat, E., Marin, E. C., Gendre, N., Jefferis, G. S., Luo, L., and Stocker, R. F. 2005. Glomerular maps without cellular redundancy at successive levels of the Drosophila larval olfactory circuit. Curr. Biol. 15, 982–992.
Ramaekers, A., Parmentier, M. L., Lasnier, C., Bockaert, J., and Grau, Y. 2001. Distribution of metabotropic glutamate receptor DmGlu-A in *Drosophila melanogaster* central nervous system. J. Comp. Neurol. 438, 213–225.
Rehder, V., Bicker, G., and Hammer, M. 1987. Serotonin-immunoreactive neurons in the antennal lobes and suboesophageal ganglion of the honeybee. Cell Tissue Res. 247, 59–66.

Rein, K., Zockler, M., Mader, M. T., Grubel, C., and Heisenberg, M. 2002. The Drosophila standard brain. Curr. Biol. 12, 227–231.

Reisenman, C. E., Christensen, T. A., Francke, W., and Hildebrand, J. G. 2004. Enantioselectivity of projection neurons innervating identified olfactory glomeruli. J. Neurosci. 24, 2602–2611.

Riley, J. R., Greggers, U., Smith, A. D., Reynolds, D. R., and Menzel, R. 2005. The flight paths of honeybees recruited by the waggle dance. Nature 435, 205–207.

Robertson, H. M. and Wanner, K. W. 2006. The chemoreceptor superfamily in the honey bee, *Apis mellifera*: expansion of the odorant, but not gustatory, receptor family. Genome. Res. 16, 1395–1403.

Rodrigues, V. and Buchner, E. 1984. [3H]2-deoxyglucose mapping of odor-induced neuronal activity in the antennal lobes of *Drosophila melanogaster*. Brain Res. 324, 374–378.

Roeder, T. 1999. Octopamine in invertebrates. Prog. Neurobiol. 59, 533–561.

Rospars, J. P. 1988. Structure and development of the insect antennodeutocerebral system. Int. J. Insect Morphol. Embryol. 17, 243–294.

Rospars, J. P. and Hildebrand, J. G. 1992. Anatomical identification of glomeruli in the antennal lobes of the male sphinx moth *Manduca sexta*. Cell Tissue Res. 270, 205–227.

Rössler, W., Oland, L. A., Higgins, M. R., Hildebrand, J. G., and Tolbert, L. P. 1999b. Development of a glia-rich axon-sorting zone in the olfactory pathway of the moth *Manduca sexta*. J. Neurosci. 19, 9865–9877.

Rössler, W., Randolph, P. W., Tolbert, L. P., and Hildebrand, J. G. 1999a. Axons of olfactory receptor cells of transsexually grafted antennae induce development of sexually dimorphic glomeruli in *Manduca sexta*. J. Neurobiol. 38, 521–541.

Røstelien, T., Borg-Karlson, A. K., Fäldt, J., Jacobsen, U., and Mustaparta, H. 2000. The plant sesquiterpene germacrene D specifically activates a major type of antennal receptor neruons of the tobacco budworm moth *Heliothis virescens*. Chem. Senses 25, 141–148.

Rutledge, L. C., Moussa, M. A., Lowe, C. A., and Sofield, R. K. 1978. Comparative sensitivity of mosquito species and strains to the repellent diethyl toluamide. J. Med. Entomol. 14, 536–541.

Rybak, J. 1994. Die strukturelle Organisation der Pilzkîrper und synaptische Konnektivität protocerebraler Interneurone im Gehirn der Honigbiene, *Apis mellifera*. Eine licht- und elektronenmikroskopische Studie. Ph.D. thesis, Freie Universität Berlin.

Rybak, J. and Menzel, R. 1993. Anatomy of the mushroom bodies in the honey bee brain: the neuronal connections of the alpha-lobe. J. Comp. Neurol. 334, 444–465.

Rybak, J. and Menzel, R. 1998. Integrative properties of the Pe1 neuron, a unique mushroom body output neuron. Learn. Mem. 5, 133–145.

Sachse, S. and Galizia, C. G. 2002. Role of inhibition for temporal and spatial odor representation in olfactory output neurons: a calcium imaging study. J. Neurophysiol. 87, 1106–1117.

Sachse, S. and Galizia, C. G. 2003. The coding of odour-intensity in the honeybee antennal lobe: local computation optimizes odour representation. Eur. J. Neurosci. 18, 2119–2132.

Sachse, S. and Galizia, C. G. 2006. Topography and Dynamics of the Olfactory System. In Microcircuits: The Interface Between Neurons and Global Brain Function. Dahlem Workshop Report 93 (*ed*. S. Grillner), pp. 251–273. MIT Press.

Sachse, S., Rappert, A., and Galizia, C. G. 1999. The spatial representation of chemical structures in the antennal lobe of honeybees: steps towards the olfactory code. Eur. J. Neurosci. 11, 3970–3982.

Sakura, M., Okada, R., and Mizunami, M. 2002. Olfactory discrimination of structurally similar alcohols by cockroaches. J. Comp. Physiol. [A] 188, 787–797.

Salecker, I. and Distler, P. 1990. Serotonin-immunoreactive neurons in the antennal lobes of the American cockroach *Periplaneta americana*: light- and electron-microscopic observations. Histochemistry 94, 463–473.

Sanes, J. R. and Hildebrand, J. G. 1976a. Acetylcholine and its metabolic enzymes in developing antennae of moth, *Manduca sexta*. Dev. Biol. 52, 105–120.

Sanes, J. R. and Hildebrand, J. G. 1976b. Structure and development of antennae in a moth, *Manduca sexta*. Dev. Biol. 51, 282–299.

Sanes, J. R. and Hildebrand, J. G. 1976c. Origin and morphogenesis of sensory neurons in an insect antenna. Dev. Biol. 51, 300–319.

Schachtner, J., Schmidt, M., and Homberg, U. 2005. Organization and evolutionary trends of primary olfactory brain centers in Tetraconata (Crustacea + Hexapoda). Arthropod Struct. Dev. 34, 257–299.

Schachtner, J., Trosowski, B., D′Hanis, W., Stubner, S., and Homberg, U. 2004. Development and steroid regulation of RFamide inummoreactivity in antennal lobe neurons of the sphinx moth *Manduca sexta*. J. Exp. Biol. 207, 2389–2400.

Schäfer, S. and Bicker, G. 1986. Distribution of GABA-like immunoreactivity in the brain of the honeybee. J. Comp. Neurol. 246, 287–300.

Schäfer, S. and Rehder, V. 1989. Dopamine-like immunoreactivity in the brain and suboesophageal ganglion of the honeybee. J. Comp. Neurol. 280, 43–58.

Schafer, R. and Sanchez, T. V. 1973. Antennal sensory system of the cockroach, *Periplaneta americana*: postembryonic development and morphology of the sense organs. J. Comp. Neurol. 149, 335–354.

Schäfer, S., Bicker, G., Ottersen, O. P., and Storm-Mathisen, J. 1988. Taurine-like immunoreactivity in the brain of the honeybee. J. Comp. Neurol. 268, 60–70.

Scherer, S., Stocker, R. F., and Gerber, B. 2003. Olfactory learning in individually assayed *Drosophila* larvae. Learn. Mem. 10, 217–225.

Schief, M. L. and Wilson, R. I. 2007. Olfactory processing and behavior downstream from highly selective receptor neurons. Nat. Neurosci. 10, 623–630.

Schiestl, F. P., Ayasse, M., Paulus, H. F., Lofstedt, C., Hansson, B. S., Ibarra, F., and Francke, W. 2000. Sex pheromone mimicry in the early spider orchid (*Ophrys sphegodes*): patterns of hydrocarbons as the key mechanism for pollination by sexual deception. J. Comp. Physiol. [A] 186, 567–574.

Schneiderman, A. M., Hildebrand, J. G., Brennan, M. M., and Tumlinson, J. H. 1986. Transsexually grafted antennae alter pheromone directed behavior in a moth. Nature 323, 801–803.

Schulz, D. J., Barron, A. B., and Robinson, G. E. 2002. A role for octopamine in honey bee division of labor. Brain Behavior and Evolution 60, 350–359.

Schürmann, F. W. 2000. Acetylcholine, GABA, glutamate and NO as putative transmitters indicated by immunocytochemistry in the olfactory mushroom body system of the insect brain. Acta Biol. Hung. 51, 355–362.

Schürmann, F. W. and Klemm, N. 1984. Serotonin-immunoreactive neurons in the brain of the honeybee. J. Comp. Neurol. 225, 570–580.

Schürmann, F. W., Elekes, K., and Geffard, M. 1989. Dopamine-like immunoreactivity in the bee brain. Cell Tissue Res. 256, 399–410.

Schwaerzel, M., Heisenberg, M., and Zars, T. 2002. Extinction antagonizes olfactory memory at the subcellular level. Neuron 35, 951–960.

Schwaerzel, M., Monastirioti, M., Scholz, H., Friggi-Grelin, F., Birman, S., and Heisenberg, M. 2003. Dopamine and octopamine differentiate between aversive and appetitive olfactory memories in Drosophila. J. Neurosci. 23, 10495–10502.

Seidel, C. and Bicker, G. 1997. Colocalization of NADPH-diaphorase and GABA-immunoreactivity in the olfactory and visual system of the locust. Brain Res. 769, 273–280.

Shanbhag, S. R., Singh, K., and Singh, R. N. 1995. Fine-structure and primary sensory projections of sensilla located in the sacculus of the antenna of *Drosophila melanogaster*. Cell Tissue Res. 282, 237–249.

Shang, Y., Claridge-Chang, A., Sjulson, L., Oyoaert, M., and Miesenbock, G. 2007. Exciatory local circuits and their implications for olfactory processing in the fly antennal lobe. Cell 128, 601–612.

Shepherd, G. M. and Greer, C. A. 1998. Olfactory Bulb. In: The Synaptic Organization of the Brain, 4th ed. (*ed*. G. M. Shepherd), pp. 159–203. Oxford University Press.

Shirokova, E., Schmiedeberg, K., Bedner, P., Niessen, H., Willecke, K., Raguse, J. D., Meyerhof, W., and Krautwurst, D. 2005. Identification of specific ligands for orphan olfactory receptors. G protein-dependent agonism and antagonism of odorants. J. Biol. Chem. 280, 11807–11815.

Sigg, D., Thompson, C. M., and Mercer, A. R. 1997. Activity-dependent changes to the brain and behavior of the honey bee, *Apis mellifera* (L.). J. Neurosci. 17, 7148–7156.

Sinakevitch, I., Farris, S. M., and Strausfeld, N. J. 2001. Taurine-, aspartate- and glutamate-like immunoreactivity identifies chemically distinct subdivisions of Kenyon cells in the cockroach mushroom body. J. Comp. Neurol. 439, 352–367.

Sinakevitch, I., Niwa, M., and Strausfeld, N. J. 2005. Octopamine-like immunoreactivity in the honey bee and cockroach: comparable organization in the brain and subesophageal ganglion. J. Comp. Neurol. 488, 233–254.

Skiri, H. T., Galizia, C. G., and Mustaparta, H. 2004. Representation of primary plant odorants in the antennal lobe of the moth *Heliothis virescens* using calcium imaging. Chem. Senses 29, 253–267.

Skiri, H. T., Ro, H., Berg, B. G., and Mustaparta, H. 2005. Consistent organization of glomeruli in the antennal lobes of related species of heliothine moths. J. Comp. Neurol. 491, 367–380.

Stange, G. and Stowe, S. 1999. Carbon-dioxide sensing structures in terrestrial arthropods. Microsc. Res. Tech. 47, 416–427.

Steib, B. M., Geier, M., and Boeckh, J. 2001. The effect of lactic acid on odour-related host preference of yellow fever mosquitoes. Chem. Senses 26, 523–528.

Stengl, M., Homberg, U., and Hildebrand, J. G. 1990. Acetylcholinesterase activity in antennal receptor neurons of the sphinx moth *Manduca sexta*. Cell Tissue Res. 262, 245–252.

Stensmyr, M. C., Giordano, E., Balloi, A., Angioy, A. M., and Hansson, B. S. 2003. Novel natural ligands for Drosophila olfactory receptor neurones. J. Exp. Biol. 206, 715–724.

Stetter, M., Greve, H., Galizia, C. G., and Obermayer, K. 2001. Analysis of calcium imaging signals from the honeybee brain by nonlinear models. Neuroimage 13, 119–128.

Stevenson, P. A. and Sporhase-Eichmann, U. 1995. Localization of octopaminergic neurones in insects. Comp. Biochem. Physiol. A 110, 203–215.

Stocker, R. F. 1994. The organization of the chemosensory system in *Drosophila melanogaster*: a review. Cell Tissue Res. 275, 3–26.

Stocker, R. F. 2001. *Drosophila* as a focus in olfactory research: mapping of olfactory sensilla by fine structure, odor specificity, odorant receptor expression, and central connectivity. Microsc. Res. Tech. 55, 284–296.

Stocker, R. F., Heimbeck, G., Gendre, N., and de Belle, J. S. 1997. Neuroblast ablation in *Drosophila* P[GAL4] lines reveals origins of olfactory interneurons. J. Neurobiol. 32, 443–456.

Stocker, R. F., Lienhard, M. C., Borst, A., and Fischbach, K. F. 1990. Neuronal architecture of the antennal lobe in *Drosophila melanogaster*. Cell Tissue Res. 262, 9–34.

Stocker, R. F., Singh, R. N., Schorderet, M., and Siddiqi, O. 1983. Projection patterns of different types of antennal sensilla in the antennal glomeruli of *Drosophila melanogaster*. Cell Tissue Res. 232, 237–248.

Stopfer, M. and Laurent, G. 1999. Short-term memory in olfactory network dynamics. Nature 402, 664–668.

Stopfer, M., Bhagavan, S., Smith, B. H., and Laurent, G. 1997. Impaired odour discrimination on desynchronization of odour-encoding neural assemblies. Nature 390, 70–74.

Stopfer, M., Jayaraman, V., and Laurent, G. 2003. Intensity versus identity coding in an olfactory system. Neuron 39, 991–1004.

Stopfer, M., Wehr, M., MacLeod, K., and Laurent, G. 1999. Neural Dynamics, Oscillatory Synchronisation, and Odour Codes. In: Insect Olfaction (*ed*. B. S. Hansson), pp. 163–180. Springer.

Strausfeld, N. J. 1976. Atlas of an Insect Brain. Springer-Verlag.

Strausfeld, N. J. 2002. Organization of the honey bee mushroom body: representation of the calyx within the vertical and gamma lobes. J. Comp. Neurol. 450, 4–33.

Strausfeld, N. J. and Gilbert, C. 1992. Small-field neurons associated with oculomotor control in muscoid flies: cellular organization in the lobula plate. J. Comp. Neurol. 316, 56–71.

Strausfeld, N. J. and Hildebrand, J. G. 1999. Olfactory systems: common design, uncommon origins? Curr. Opin. Neurobiol. 9, 634–639.

Strausfeld, N. J. and Li, Y. 1999a. Representation of the calyces in the medial and vertical lobes of cockroach mushroom bodies. J. Comp. Neurol. 409, 626–646.

Strausfeld, N. J. and Li, Y. 1999b. Organization of olfactory and multimodal afferent neurons supplying the calyx and pedunculus of the cockroach mushroom bodies. J. Comp. Neurol. 409, 603–625.

Strausfeld, N. J., Hansen, L., Li, Y., Gomez, R. S., and Ito, K. 1998. Evolution, discovery, and interpretations of arthropod mushroom bodies. Learn. Mem. 5, 11–37.

Strausfeld, N. J., Homberg, U., and Kloppenburg, P. 2000. Parallel organization in honey bee mushroom bodies by peptidergic Kenyon cells. J. Comp. Neurol. 424, 179–195.

Strausfeld, N. J., Sinakevitch, I., and Vilinsky, I. 2003. The mushroom bodies of *Drosophila melanogaster*: an immunocytological and golgi study of Kenyon cell organization in the calyces and lobes. Microsc. Res. Tech. 62, 151–169.

Suh, G. S., Wong, A. M., Hergarden, A. C., Wang, J. W., Simon, A. F., Benzer, S., Axel, R., and Anderson, D. J. 2004. A single population of olfactory sensory neurons mediates an innate avoidance behaviour in Drosophila. Nature 431, 854–859.

Sun, X.-J., Fonta, C., and Masson, C. 1993a. Odour quality processing by bee antennal lobe interneurones. Chem. Senses 18, 355–377.

Sun, X.-J., Tolbert, L. P., and Hildebrand, J. G. 1993b. Ramification pattern and ultrastructural characteristics of the serotonin-immunoreactive neuron in the antennal lobe of the moth *Manduca sexta*: a laser scanning confocal and electron microscopic study. J. Comp. Neurol. 338, 5–16.

Sun, X.-J., Tolbert, L. P., and Hildebrand, J. G. 1997. Synaptic organization of the uniglomerular projection neurons of the antennal lobe of the moth *Manduca sexta*: a laser scanning confocal and electron microscopic study. J. Comp. Neurol. 379, 2–20.

Sutton, R. S. and Barto, A. G. 1981. Toward a modern theory of adaptive networks: expectation and prediction. Psychol. Rev. 88, 135–170.

Suzuki, H. 1975. Convergence of olfactory inputs from both antennae in the brain of the honeybee. J. Exp. Biol. 62, 11–26.

Svidersky, V. L. and Plotnikova, S. I. 2004. On structural-functional organization of dragonfly mushroom bodies and some general considerations about purpose of these formations. J. Evol. Biochem. Physiol. 40, 608–624.

Symonds, M. R. and Elgar, M. A. 2004. The mode of pheromone evolution: evidence from bark beetles. Proc. Biol. Sci. 271, 839–846.

Symonds, M. R. and Wertheim, B. 2005. The mode of evolution of aggregation pheromones in Drosophila species. J. Evol. Biol. 18, 1253–1263.

Szyszka, P., Ditzen, M., Galkin, A., Galizia, C. G., and Menzel, R. 2005. Sparsening and temporal sharpening of olfactory representations in the honeybee mushroom bodies. J. Neurophysiol. 94, 3303–3313.

Tanaka, N. K., Awasaki, T., Shimada, T., and Ito, K. 2004. Integration of chemosensory pathways in the Drosophila second-order olfactory centers. Curr. Biol. 14, 449–457.

Thom, C., Guerenstein, P. G., Mechaber, W. L., and Hildebrand, J. G. 2004. Floral CO_2 reveals flower profitability to moths. J. Chem. Ecol. 30, 1285–1288.

Tichy, H. 2007. Humidity-dependent cold cells on the antenna of the stick insect. J. Neurophysiol. 97, 3851–3858.

Toga, A. W. and Thompson, P. M. 2001. Maps of the brain. Anat. Rec. 265, 37–53.

Tolbert, L. P., Oland, L. A., Tucker, E. S., Gibson, N. J., Higgins, M. R., and Lipscomb, B. W. 2004. Bidirectional influences between neurons and glial cells in the developing olfactory system. Prog. Neurobiol. 73, 73–105.

Tominaga, Y. and Yokohari, F. 1982. External structure of the sensillum capitulum, a hygro- and thermoreceptive sensillum of the cockroach, *Periplaneta americana*. Cell Tissue Res. 226, 309–318.

Tucker, E. S. and Tolbert, L. P. 2003. Reciprocal interactions between olfactory receptor axons and olfactory nerve glia cultured from the developing moth *Manduca sexta*. Dev. Biol. 260, 9–30.

Tucker, E. S., Oland, L. A., and Tolbert, L. P. 2004. In vitro analyses of interactions between olfactory receptor growth cones and glial cells that mediate axon sorting and glomerulus formation. J. Comp. Neurol. 472, 478–495.

Tully, T., Preat, T., Boynton, S. C., and Del Vecchio, M. 1994. Genetic dissection of consolidated memory in Drosophila. Cell 79, 35–47.

Turin, L. 1996. A spectroscopic mechanism for primary olfactory reception. Chem. Senses 21, 773–791.

Uchida, N. and Mainen, Z. F. 2003. Speed and accuracy of olfactory discrimination in the rat. Nat. Neurosci. 6, 1224–1229.

Vareschi, E. 1971. Duftunterscheidung bei der Honigbiene. Einzelzellableitungen und Verhaltensreaktionen. (Odor discrimination in honeybees. Single cell recordings and behavioral studies). ZverglPhysiol 75, 143–173.

Vickers, N. J. and Baker, T. C. 1997. Chemical communication in heliothine moths. VII. correlation between diminished responses to point-source plumes and single filaments similarly tainted with a behavioral antagonist. J. Comp. Physiol. [A] 180, 523–536.

Vickers, N. J., Christensen, T. A., Baker, T. C., and Hildebrand, J. G. 2001. Odour-plume dynamics influence the brain's olfactory code. Nature 410, 466–470.

Vosshall, L. B., Amrein, H., Morozov, P. S., Rzhetsky, A., and Axel, R. 1999. A spatial map of olfactory receptor expression in the *Drosophila* antenna. Cell 96, 725–736.

Vosshall, L. B., Wong, A. M., and Axel, R. 2000. An olfactory sensory map in the fly brain. Cell 102, 147–159.

Wachowiak, M., Cohen, L. B., and Ache, B. W. 2002. Presynaptic inhibition of olfactory receptor neurons in crustaceans. Microsc. Res. Tech. 58, 365–375.

Waddell, S. and Quinn, W. G. 2001. Flies, genes, and learning. Annu. Rev. Neurosci. 24, 1283–1309.

Waldrop, B. and Hildebrand, J. G. 1989. Physiology and pharmacology of acetylcholinergic responses of interneurons in the antennal lobes of the moth *Manduca sexta*. J. Comp. Physiol. [A] 164, 433–441.

Waldrop, B., Christensen, T. A., and Hildebrand, J. G. 1987. GABA-mediated synaptic inhibition of projection neurons in the antennal lobes of the sphinx moth, *Manduca sexta*. J. Comp. Physiol. [A] 161, 23–32.

Wang, Y. L., Guo, H. F., Pologruto, T. A., Hannan, F., Hakker, I., Svoboda, K., and Zhong, Y. 2004. Stereotyped odor-evoked activity in the mushroom body of Drosophila revealed by green fluorescent protein-based Ca^{2+} imaging. J. Neurosci. 24, 6507–6514.

Wang, F., Nemes, A., Mendelsohn, M., and Axel, R. 1998. Odorant receptors govern the formation of a precise topographic map. Cell 93, 47–60.

Wang, J. W., Wong, A. M., Flores, J., Vosshall, L. B., and Axel, R. 2003. Two-photon calcium imaging reveals an odor-evoked map of activity in the fly brain. Cell 112, 271–282.

Watanabe, H., Kobayashi, Y., Sakura, M., Matsumoto, Y., and Mizunami, M. 2003. Classical olfactory conditioning in the cockroach *Periplaneta americana*. Zoolog. Sci. 20, 1447–1454.

Weidenmüller, A., Kleineidam, C., and Tautz, J. 2002. Collective control of nest climate parameters in bumblebee colonies. Anim. Behav. 63, 1065–1071.

Wendt, B. and Homberg, U. 1992. Immunocytochemistry of dopamine in the brain of the locust *Schistocerca gregaria*. J. Comp. Neurol. 321, 387–403.

Wenner, A. M. 2002. The elusive honey bee dance ''language'' hypothesis. J. Ins. Behav. 15, 859–878.

Wenner, A. M. and Johnson, D. L. 1967. Honeybees: do they use direction and distance information provided by their dancers? Science 158, 1072–1077.

Willis, M. A. and Baker, T. C. 1984. Effects of intermittent and continuous pheromone stimulation on the flight behavior of the oriental fruit moth, *Grapholita molesta*. Physiol. Entomol. 9, 341–358.

Wilson, R. I. and Laurent, G. 2005. Role of GABAergic inhibition in shaping odor-evoked spatiotemporal patterns in the Drosophila antennal lobe. J. Neurosci. 25, 9069–9079.

Wilson, D. A. and Stevenson, R. J. 2003. The fundamental role of memory in olfactory perception. Trends Neurosci. 26, 243–247.

Wilson, R. I., Turner, G. C., and Laurent, G. 2004. Transformation of olfactory representations in the Drosophila antennal lobe. Science 303, 366–370.

Wiltrout, C., Dogra, S., and Linster, C. 2003. Configurational and nonconfigurational interactions between odorants in binary mixtures. Behav. Neurosci. 117, 236–245.

Winnington, A. P., Napper, R. M., and Mercer, A. R. 1996. Structural plasticity of identified glomeruli in the antennal lobes of the adult worker honey bee. J. Comp. Neurol. 365, 479–490.

Witthöft, W. 1967. Absolute Anzahl und Verteilung der Zellen im Hirn der Honigbiene [Absolute number and distribution of cells in the brain of honeybees]. Z. Morphol. Tiere 61, 160–184.

Wong, A. M., Wang, J. W., and Axel, R. 2002. Spatial representation of the glomerular map in the *Drosophila* protocerebrum. Cell 109, 229–241.

Xu, P., Atkinson, R., Jones, D. N., and Smith, D. P. 2005. Drosophila OBP LUSH is required for activity of pheromone-sensitive neurons. Neuron 45, 193–200.
Xu, F., Greer, C. A., and Shepherd, G. M. 2000. Odor maps in the olfactory bulb. J. Comp. Neurol. 422, 489–495.
Yokohari, F. 1983. The coelocapitular sensillum, an antennal hygro- and thermoreceptive sensillum of the honey bee, *Apis mellifera* L. Cell Tissue Res. 233, 355–365.
Yasuyama, K. and Salvaterra, P. M. 1999. Localization of choline acetyltransferase-expressing neurons in Drosophila nervous system. Microsc. Res. Tech. 45, 65–79.
Yasuyama, K., Kitamoto, T., and Salvaterra, P. M. 1995. Localization of choline acetyltransferase-expressing neurons in the larval visual system of *Drosophila melanogaster*. Cell Tissue Res. 282, 193–202.
Yin, J. C. and Tully, T. 1996. CREB and the formation of long-term memory. Curr. Opin. Neurobiol. 6, 264–268.
Yokohari, F., Tominaga, Y., and Tateda, H. 1982. Antennal hygroreceptors of the honey bee, *Apis mellifera* L. Cell Tissue Res. 226, 63–73.
Yu, D., Ponomarev, A., and Davis, R. L. 2004. Altered representation of the spatial code for odors after olfactory classical conditioning; memory trace formation by synaptic recruitment. Neuron 42, 437–449.
Zars, T., Fischer, M., Schulz, R., and Heisenberg, M. 2000. Localization of a short-term memory in Drosophila. Science 288, 672–675.
Zou, Z., Li, F., and Buck, L. B. 2005. Odor maps in the olfactory cortex. Proc. Natl. Acad. Sci. U. S. A. 102, 7724–7729.

Further Reading

Yasuyama, K., Meinertzhagen, I. A., and Schurmann, F. W. 2002. Synaptic organization of the mushroom body calyx in *Drosophila melanogaster*. J. Comp. Neurol. 445, 211–226.

Relevant Websites

http://www.flybrain.org – An online database of *Drosophila* nervous system.

http://neuro.uni-konstanz.de – Research group in insect olfaction.

4.42 Odor Plumes and Animal Orientation

M A Willis, Case Western Reserve University, Cleveland, OH, USA

© 2008 Elsevier Inc. All rights reserved.

4.42.1	**Ubiquity of the Use of Olfaction to Locate Distant Resources**	772
4.42.2	**Distribution of Odorants in the Environment**	772
4.42.2.1	Diffusion versus Turbulent Diffusion	773
4.42.2.2	Environmental Effects on Odorant Distribution	775
4.42.3	**Plume Characteristics Important to Plume-Tracking Organisms**	775
4.42.3.1	Temporal/Spatial Structure	775
4.42.3.2	Quality	776
4.42.3.3	Quantity	776
4.42.4	**Tracking Odor Plumes Typically Requires Information from Multiple Senses**	777
4.42.4.1	Orientation to Flow	777
4.42.4.2	Orientation to Odors	777
4.42.4.2.1	Spatial comparisons of odor concentration (bilaterally symmetrical sensors)	777
4.42.4.2.2	Temporal comparisons of odor concentration (sensors small relative to the scale of the plume, memory required)	778
4.42.4.3	Importance of Active Sampling Behaviors to Odor Detection and Processing	778
4.42.5	**Man-Made Odor Tracking Systems**	779
4.42.6	**Conclusions**	779
References		780

Glossary

aesthetasc sensilla Peg-shaped sensillae on the antennules, or first antenna, of crustaceans that detect chemicals dissolved in the surrounding water. Each aesthetasc can contain dendrites from a few, to more than 100 olfactory receptor neurons.

boundary layer The layer of any fluid defined by the velocity gradient that begins at zero flow at the surface of an object and extends upward until the average ambient flow velocity is reached.

concha Several fine, narrow, and curled boney shelves that project into the nasal passages of mammals. Also known as turbinates.

epithelium A thin layer of cells that covers the outer surfaces and lines the inner surfaces of our bodies. A sensory epithelium is such an outer layer that lines a sensory structure and carries the sensory receptor cells embedded in it.

fluid dynamics The field of engineering involved in the description, characterization, and manipulation of the behavior of fluids, particularly water and air.

neuromast a sensory structure in the skin of fish that detects changes in the direction, or intensity of water movement.

The distribution of chemicals resulting from the interaction of flowing fluid with a source of volatile chemicals is commonly called a plume, which has a discontinuous patchy structure (Figure 1). The internal structure of odor plumes changes predictably with both distance downstream from the source and distance from centerline across the plume, and behavioral experiments indicate that odor-tracking animals alter their tracking behavior in response to these changes. In most organisms tested, odor-tracking behavior requires the intermittent olfactory stimulation generated by the patchy structure of the plume to generate upstream movement and successful location of the source. Neurons at all levels of the olfactory system are sensitive to intermittent stimulation, and some circuits appear to preserve the temporal activation patterns experienced

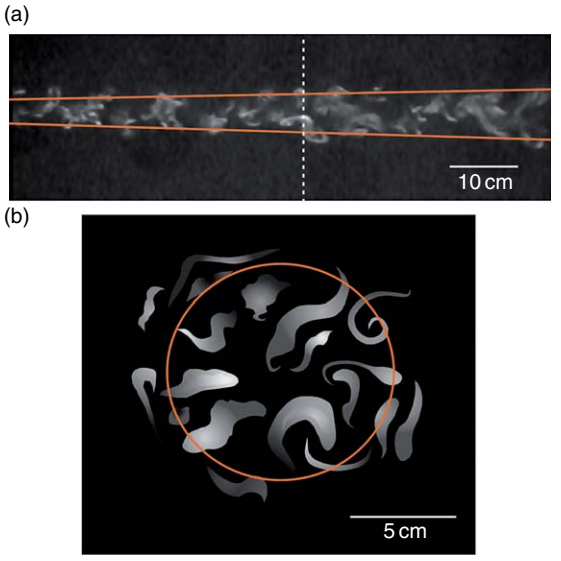

Figure 1 Two perspectives on instantaneous views of smoke visualizations of wind-borne odor plumes. (a) A single field from a video recording of a $TiCl_4$ smoke plume in a laboratory wind tunnel viewed from above. The time-averaged plume boundaries are represented by red lines running from the upwind to downwind side of the image (i.e., left to right). In this image, the wind is blowing from left to right at 75 cm s^{-1}, and the source is a 0.7 cm filter paper disk to which a drop of $TiCl_4$ has been applied. Since this is the same source used in insect odor-tracking experiments, according to the laws of fluid dynamics, the structure of the plume should be similar to the odor plume experienced by the insects. (b) A schematic approximation illustrating the tracker's eye view of the smoke plume visualization depicted in (a) above. The red circle represents an extension of the time-averaged plume boundaries in (a) onto this cross section. White dashed line is approximately 1 m downwind from the source. (a) Reproduced from Webb, B., Harrison, R. R., and Willis, M. A. 2004. Sensorimotor control of navigation in arthropod and artificial systems. Arthropod Struct. Dev. 33, 301–330, with permission from Elsevier.

in a plume and relay them to higher processing centers in the brain. Recent studies using simulation models and odor-guided robots are leading to tests of biological hypotheses that would be difficult or impossible to address with living organisms, and are also leading to the first man-made plume-tracking systems.

4.42.1 Ubiquity of the Use of Olfaction to Locate Distant Resources

Virtually every object on our planet, biotic or abiotic, sheds molecules into the environment. If these molecules are in high enough concentrations, they can be detected and processed by the olfactory systems of animals as they move through the environment, seeking opportunities to forage (Arbas, E. A. *et al.*, 1993; Weissburg, M. J. and Zimmer-Faust, R. K., 1994; Basil, J. A. *et al.*, 2000; Raguso, R. and Willis, M., 2002; Ferner and Weissburg, M. J., 2005; Raguso, R. and Willis, M., 2005), mate (Cardé, R. T. and Minks, A. K., 1997 and citations therein), locate home and appropriate territories (Wolf, H. and Wehner, R., 2000), and avoid predators (Susswein, A. J. *et al.*, 1982). The behavior of two fluids, air and water, dominates the distribution of these molecules, and to a large degree determines how living organisms are able to use this molecular information to adapt their behavior, increasing their probability of survival and reproduction (Vickers, N. J., 2000; Weissburg, M. J., 2000).

Flow-borne odor plumes provide information important for aquatic, marine, and terrestrial organisms that walk, fly, and swim to locate resources. Despite these seemingly different environments and modes of locomotion, the paths generated by these animals often appear remarkably similar (Figures 2 and 3). Whether this similarity in tracking trajectories stems from a similarity in underlying physiological and behavioral mechanisms is almost entirely unknown.

4.42.2 Distribution of Odorants in the Environment

Our understanding of how volatile chemicals are distributed in the environment and the effects that this has on the behavior of animals tracking odor plumes has advanced considerably in recent years. This has resulted from behavioral biologists working together with fluid dynamics engineers to study the fine structure of odor plumes in different and dynamically changing environments (Wright, R. H., 1958, Figure 1; Murlis, J. and Jones, C. D., 1981; Murlis, J. *et al.*, 1990; Weissburg, M. J. and Zimmer-Faust, R. K., 1993; Griffiths, N. and Brady, J., 1995; Murlis, J. *et al.*, 2000; Webster, D. R. and Weissburg, M. J., 2001). Odor plume structure has significant effects on the tracking behavior of almost every animal in which this has been tested (Vickers, N. J., 2000; Weissburg, M. J., 2000).

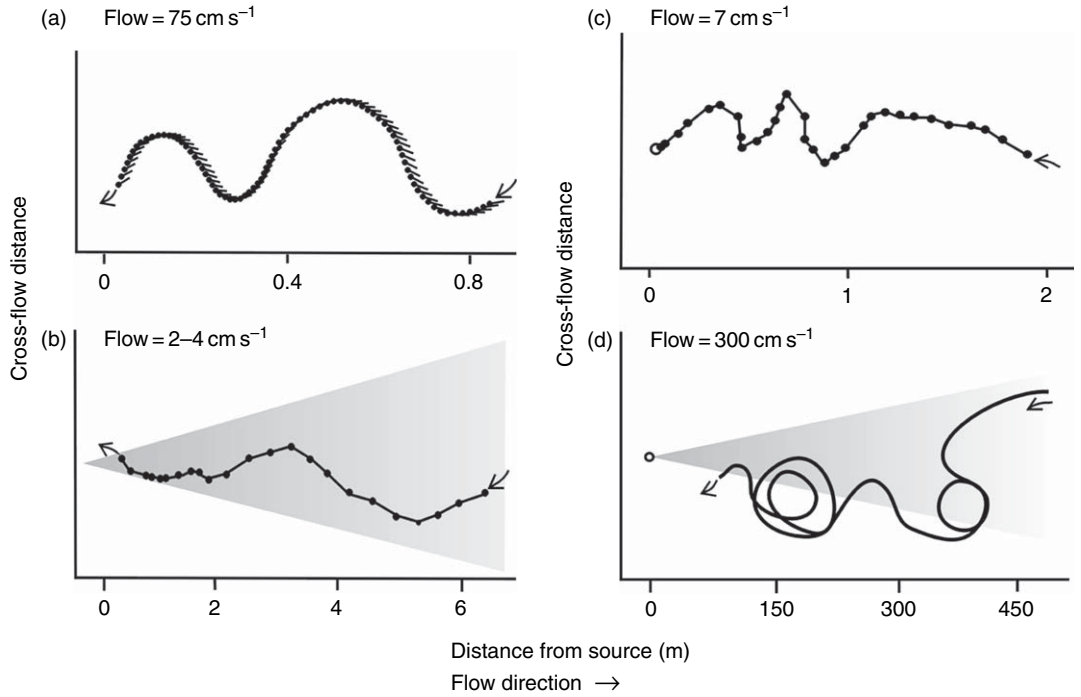

Figure 2 Movement paths of animals tracking plumes while supported by the fluid through which they are tracking, as viewed from above. (a) Flight path of a male moth, *Manduca sexta*, tracking an airborne plume of female sex-attractant pheromone in a laboratory wind tunnel. (b) Swimming path of the Antarctic fish, *Trematomus bernachii*, while tracking a water-borne plume of prey extract recorded in its natural environment. (c) Swimming path of the cephalopod mollusk, *Nautilus pompilus*, tracking a water-borne plume of prey extract recorded in a laboratory flume. (d) Observer's approximation of the flight path of a Turkey vulture, *Cathartes aura*, tracking an airborne plume of ethyl mercaptan, a volatile chemical associated with dead animals. In all images, the fluid flows from left to right, and the flow velocities for each example are presented in each panel. (a) Reproduced from Webb, B., Harrison, R. R., and Willis, M. A. 2004. Sensorimotor control of navigation in arthropod and artificial systems. Arthropod Struct. Dev. 33, 301–330, with permission from Elsevier. (b) Reproduced from Polar Biology, Vol. 21, 1999, pp. 151–154, Olfactory search tracks in the Antarctic fish. *Trematomous bernacchi*, Montgomery, J. C., Diebel, C., Halstead, M. B. D., and Downer, J., figure 1, with kind permission of Springer Science and Business Media and the authors. (c) Reproduced from Basil, J. A., Hanlon, R. T., Sheikh, S. I., and Atema, J. 2000. Three-dimentional odor tracking by *Nautilus pompilius*. J. Exp. Biol. 203, 1409–1414, with permission from the Company of Biologists Ltd. (d) Image was provided by Willis, unpublished data.

4.42.2.1 Diffusion versus Turbulent Diffusion

The distribution of volatile odorants in fluids is determined primarily by the processes of diffusion and turbulence (Murlis, J. *et al.*, 1990; Vogel, S., 1994; Weissburg, M. J., 2000). For animals larger than approximately 1 mm, turbulence is usually the more important of these two processes (Weissburg, M. J., 2000). According to the laws of fluid dynamics, the behavior of air and water are governed by similar constraints, and their behavior can be predicted depending on viscosity, flow velocity, and density (Vogel, S., 1994). Turbulence can be described as velocity variations in the flow itself or can result from velocity differences caused when flowing fluid interacts with fixed objects in the flow. From a fluid dynamical perspective, plumes are typically described by a statistical distribution that has been depicted as a smooth concentration gradient that diminishes both with distance downstream from the source and across the flow from the plume's centerline to the edges, both laterally and vertically (Bossert, W. H. and Wilson, E. O., 1963). However, a snapshot of an odor plume reveals a discontinuous structure composed of patches of odor separated by clean air (Figure 1).

The olfactory sensory cells and central processing circuitry of animals do not typically respond to distributions of odorants averaged over time. Rather, they respond to changes in sensory stimuli and initiate behavioral responses in tens or hundreds of

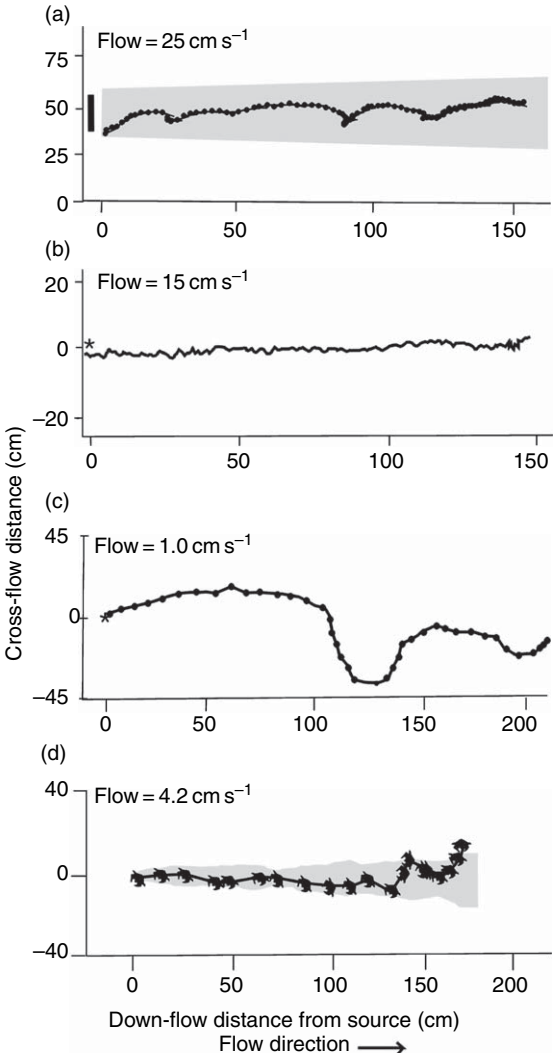

Figure 3 Movement paths of substrate-borne animals tracking air- and water-borne odor plumes as viewed from above. (a) Walking path of a male cockroach, *Periplaneta americana*, tracking an airborne plume of female sex attractant issuing from source 14.3 cm across in a laboratory wind tunnel. (a) Reproduced from Willis, M. A. and Avondet, J. L. 2005. Odor-modulated orientation in walking male cockroaches, *Periplaneta americana* (L.), and the effects of odor plumes of different structure. J. Exp. Biol. 208, 721–735, with permission from the Company of Biologists Ltd. (b) Crawling path of a predatory marine snail, *Busycon carica*, in a plume of prey odorant in a laboratory flume. (b) Reproduced from Ferner, M. C. and Weissburg, M. J. 2005. Slow-moving predatory gastropods track prey odors in fast and turbulent flow. J. Exp. Biol. 208, 809–819, with permission of the Company of Biologists Ltd. (c) Walking path of a lobster, *Homarus americanus*, tracking a water-borne plume of prey odorants in a laboratory flume. (c) Reproduced from J. Chem. Ecol., Vol. 17, 1991, pp. 1293–1307, Chemical orientation of lobsters, *Homarus americanus*, in turbulent odor plumes, Moore, P. A., Scholtz, N., and Atema, J., figure 5, with kind permission of Springer Science and Business Media. (d) Walking path of a blue crab, *Callinectes sapidus*, tracking prey odor in its natural environment. In all images, the fluid flows from left to right, and the flow velocities for each example are presented in each panel. (d) Reproduced from Zimmer-Faust, R. K., Finelli, C. M., Pentcheff, N. D., and Wethey, D. S. 1995. Odor plumes and animal navigation in turbulent water flow: A field study. Biol. Bull. 188, 111–116, with permission from Marine Biological Laboratory and the author.

milliseconds. High-frequency sampling of plumes performed in water (Moore, P. A. and Atema, J., 1991) and air (Vickers, N. J. *et al.*, 2001) reveals the structure underlying time-averaged plume statistics. Any tracker moving across the plume will have an increased probability of encountering filaments of higher concentration as it moves toward the plume centerline, across the flow, from any direction

(Figure 1(b)). Likewise, in both air (Murlis, J. and Jones, C. D., 1981; Murlis, J. *et al.*, 1990; 2000) and water (Webster, D. R. and Weissburg, M. J., 2001), a tracker will have an increased probability of encountering higher concentration plume filaments as it moves into the flow toward the source. The lateral and longitudinal decrease in concentration (i.e., molecules/volume of fluid) results primarily from turbulent mixing of the filaments within the plume, not diffusion. Behavioral experiments suggest that plume-tracking animals use these changes in plume structure to adapt their behavior. Considering the speed of most animal locomotion and fluid flow in most of earth's environments (i.e., tens of centimeters to meters/second) together with the small distances/time generated by diffusion (*c.* 9.5 cm in 1 h for a typical insect sex pheromone in air; Loudon, C., 2003), it is easy to understand that turbulence dominates the distribution of the stimulus and thus the structure of the tracking behavior observed from odor-tracking animals.

4.42.2.2 Environmental Effects on Odorant Distribution

Although we can measure the differences in plumes in different environments (Weissburg, M. J. and Zimmer-Faust, R. K., 1994; Griffiths, N. and Brady, J., 1995; Murlis, J. *et al.*, 2000), the primary significance of these differences stems from the fact that plume-tracking animals show dramatically different behavior and success at source location in different turbulent flows. Even though many organisms are superbly adapted to track plumes to their sources, ambient flow and turbulence conditions can exist in natural environments that make the task almost impossible to perform (Elkinton, J. S. *et al.*, 1987; Weissburg, M. J. and Zimmer-Faust, R. K., 1993; Griffiths, N. and Brady, J., 1995).

4.42.3 Plume Characteristics Important to Plume-Tracking Organisms

Behaviors that are initiated or modulated by olfactory information can be difficult to study because the primary stimulus is out of the control of the researchers almost as soon as it evaporates from the dispenser. However, even with this major difficulty, it is possible to define three broad categories of information known to be detected by plume-tracking organisms: (1) temporal/spatial structure of molecules distributed in the plume, (2) quality of the molecules in the plume, and (3) quantity of molecules in the plume. Experimental manipulation of variables in each of these three categories results in significant changes in the structure of the paths taken by odor-tracking organisms as they orient and move upstream or upwind toward the source (Belanger, J. H. and Willis, M. A., 1996).

4.42.3.1 Temporal/Spatial Structure

The patchy structure of odor plumes has been known to researchers studying olfactory orientation for some time (Wright, R. H., 1958), but its dramatic effect on orientation and tracking behavior has been fully appreciated only recently (Cardé, R. T. and Minks, A. K., 1997). The intermittent stimulation resulting from an odor plume is necessary for most animals tested to orient to odor, except for the fruit fly *Drosophila melanogaster* (Budick, S. A. and Dickinson, M. H., 2006), one species of moth (*Cadra cautella*; Justus, K. A. and Cardé, R. T., 2002), and small organisms in a detectable gradient (e.g., microorganisms, copepods; Weissburg, M. J., 2000). Recent results show that the temporal/spatial structure of an odor plume has a more dramatic effect on the structure of tracking behavior than any other known variable (Mafra-Neto, A. and Cardé, R. T., 1994; Vickers, N. J. and Baker, T. C., 1994). For example, it has been observed that sources emitting similar levels of chemicals but manipulated to generate structurally different plumes elicit characteristically different behavior from males approaching from downwind (Charlton, R. E. *et al.*, 1993; Mafra-Neto, A. and Cardé, R. T., 1994; Vickers N. J. and Baker T. C., 1994; Willis, M. A. *et al.*, 1994). A seminal study by Vickers N. J. and Baker T. C. (1992) showed that moths alter their tracking performance in response to both the timing of encounters with structural elements of the plume and the concentration detected from those elements. Their study used a puffing device to experimentally control the interval between puffs while they varied the concentration of the source independently. By altering these variables independently, Vickers N. J. and Baker T. C. (1992) demonstrated that decreasing the number of pheromone puffs encountered enabled their moths to track upwind to high concentrations that they normally could not.

Dogs challenged to track trails of odor deposited on the ground were more successful (over 90%) tracking a path of discontinuous patches (i.e., human foot steps) than a continuous trail of odor (Hepper, P. G. and Wells, D. L., 2005). So the combination of discrete

patches of odor with no odor in between, and the active sniffing behavior performed while tracking, results in an intermittent odor signal that appears to be required for dogs to track substrate-borne trails. In addition, recent measurements of respiratory air flow in dogs during the tracking of wind-borne odors, combined with modeling of the flow through the upper respiratory tract, suggest that a nearly continuous inflow of odor-bearing air over the olfactory epithelium is probable, even while running (Steen, J. B. *et al.*, 1996). Thus, in this situation, some if not all of the temporal/spatial structure of the odor might be preserved to be presented to the olfactory epithelium.

What effect does the sniffing behavior of vertebrate animals have on the structure of the plume? One possibility is that the increased flow velocity interacting with the concha in the nasal passages would result in increased turbulence and a completely mixed sample arriving at the olfactory epithelium. This could effectively smooth out the dramatic peaks and valleys in the odor signal caused by the filamentous structure of the plume. Whether this actually happens, and how it might affect the trackers' behavior, awaits further study.

Crustaceans also sniff as a way to enhance or alter their olfactory inputs (Schmidt, B. C. and Ache, B. W., 1979). When responding to odor, they move the olfactory part of their second antennae (i.e., antennules) through the water very rapidly (Schmidt, B. C. and Ache, B. W., 1979). Flicking behavior, as this is known, has been shown to decrease the boundary layer around the antennules and force the odor filaments into the array of odor-detecting sensilla (Koehl, M. A. R., 2006). The effect of the shallower boundary layer is to decrease the distance that the odor molecules must diffuse to reach the receptors and thus enhances the extraction of odor information from the environment. To date, the effects of flicking behavior on the perceived structure of an odor plume have not been measured directly, and how this could affect the animal's tracking behavior has not been determined.

4.42.3.2 Quality

In moths, the best-known example, detection of the number and type of molecules in an odorant plume is determined by the combination of peripheral sensory structures and central processing. This has been demonstrated in behavioral experiments by independently manipulating the structure of the plume and the chemical compounds making up that structure (Vickers, N. J. and Baker, T. C., 1992). Two sensory cells that detect the two components of the pheromone required for behavioral activity are housed a few microns apart in the same sensory hair on the antenna. Their spatial coincidence means that they are perfectly situated to detect temporal coincidences of odorant components in the pheromone. This arrangement of sensory structures, in combination with central coincidence detecting interneurons (Christensen, T. C. and Hildebrand, J. G., 1988), is capable of resolving spatial/temporal separation of structural elements in the plume in the millisecond (i.e., millimeter) range. At the wind speeds at which these experiments were performed, this resulted in male moths being able to discriminate between odorant encounters approximately 3 m apart (Baker, T. C. *et al.*, 1998). Thus, in a fundamental way, the ability of these animals to use blends of odorant compounds in a meaningful way may *require* the patchiness of the distribution and detection that characterizes plumes. The components of a behaviorally relevant blend of compounds must be detected nearly simultaneously to activate a behavioral response (Vickers, N. J. and Baker, T. C., 1992; Baker, T. C. *et al.*, 1998; Vickers, N. J., 2006).

4.42.3.3 Quantity

Concentration of chemicals in the plume or plume filaments is known to change predictably with distance from the source. As the individual filaments expand as a result of turbulence and, as the period from evaporation from the source to detection gets longer, the same amount of chemicals is spread over a larger space, that is, dilution, resulting in lower concentration. This will also result in the ratio of the peak concentration to the mean decreasing with distance from the source. Thus, the peak concentration will be lower, and the time from odor onset to peak concentration detected upon contacting a filament of odor will be longer as the plume moves farther and farther downwind. It is clear that animals modulate their behavior according to their distance from the source and, when tested independently, they modulate their behavior according to changes in concentration. Thus, plume-tracking animals appear to modulate their behavior according to both changes in odorant concentration and the spatial/temporal structure of those concentration differences, and these responses can operate independently (Vickers, N. J. and Baker, T. C., 1992).

4.42.4 Tracking Odor Plumes Typically Requires Information from Multiple Senses

In most known cases, plume-tracking animals require information from multiple sensory systems to successfully perform this task. The environmental cue that the tracking organism uses to orient its steering is the direction of the fluid flow, not a nonexistent odor gradient. The preferred direction of orientation with respect to the flow, if there is one, is usually modulated by the presence or absence of the odor.

4.42.4.1 Orientation to Flow

The direction of flow may be extracted from the environment directly by the deflection of a mechanosensory structure, for example, antennae and wind-sensitive hairs in arthropods (Arbas, E. A., 1986), superficial neuromast sensors in the lateral line system in fish (Baker, C. F. and Montgomery, J. C., 1999), feathers or wind-sensitive breast feathers in birds (Gewecke, M. and Woike, M., 1978), or facial whiskers in mammals (Dehnhardt, G. *et al.*, 1998). When the animal is in contact with a solid substrate, these sensors will provide the speed and direction of the flow. However, if the animal is suspended in the flow, like a swimming fish or flying bird or insect, the information provided by these sensors will be the speed of the organism with respect to the flow. Flying or swimming animals almost always detect the flow direction indirectly by determining how they are moving with respect to the nonmoving parts of their environment (e.g., the ground or trees). The single well-documented contradiction to this statement is the Mexican blind cave fish (Baker, C. F. and Montgomery, J. C., 1999). However, these results suggest that the lateral line system could provide flow direction to any fish.

All well-described examples of indirect detection of flow direction involve animals using visually detected movement with respect to an assumed stationary environment. In the case of flying moths, it is thought that they are able to compute the wind speed and direction by comparing their intended course to their realized course, with any difference between the two assumed to be caused by wind-induced drift (Marsh, D. *et al.*, 1978). This method of using visual information to steer with respect to the wind direction and speed while tracking an odor plume was first demonstrated by Kennedy J. S. (1940) in female mosquitoes tracking human breath. Kennedy and his co-workers went on to demonstrate that using visually perceived wind information to steer and control flight speed (known as optomotor anemotaxis) was ubiquitous in flying insects, whether or not they were tracking odor (Kennedy, J. S. and Marsh, D., 1974; Marsh, D. *et al.*, 1978; David, C. T., 1986). The use of visually detected flow information to control the speed and direction of movement has also been demonstrated clearly in male rainbow trout tracking female oviduct extract upstream (Emanuel, M. E. and Dodson, J. J., 1979).

4.42.4.2 Orientation to Odors

Animals that use odor cues to track plumes may use two hypothetical mechanisms to acquire chemical information on which to base their steering decisions: (1) spatial comparisons of odor inputs to bilaterally symmetrical sensors (i.e., antennae or nostrils), and (2) temporal comparisons of odor inputs sensed at different points in time (Frankel, G. S. and Gunn, D. L., 1961; Schöne, H., 1984; Dusenberry, D. B., 1992). It is possible that either of these two strategies may be more effective at tracking plumes generated under different environmental and flow conditions (Weissburg, M. J., 2000). These two hypotheses are typically referred to as spatial and temporal strategies respectively. Since the vast majority of odor-tracking animals have bilaterally symmetrical odor sensors, the possibility that both strategies could be operating at the same time, either synergistically or independently, has always been acknowledged (Frankel, G. S. and Gunn, D. L., 1961; Schöne, H., 1984). However, careful experiments necessary to resolve these questions have rarely been pursued (Martin, H., 1965; Hangartner, W., 1967; Bell, W. J. and Tobin, T. R., 1981; Borst, A. and Heisenberg, M., 1982; Johnsen, P. B. and Teeter, J. H., 1985).

4.42.4.2.1 Spatial comparisons of odor concentration (bilaterally symmetrical sensors)

Animals walking slowly through slower flows experience relatively less turbulent plumes because the surfaces they walk on damp its vertical component (Weissburg, M. J., 2000). Slow movement relative to the slowly moving plume may allow such plume trackers to steer to remain in the plume by using a spatial sampling strategy to experience the odor edges defined by the rapid drop of concentration at the lateral margins of the plume (Figure 1(b)). Chemical concentration differences that would inform these steering decisions could be sensed

instantaneously using bilateral sensors, or because of the relatively low encounter rate with odor structures in the plume, the same sensors could enable time averaging of concentration in the central nervous system. If an odor-tracking organism were using spatial comparisons to control its maneuvering, it would be possible, knowing the plume structure, to predict when and in what direction it would turn. Recent observations in plume-tracking cockroaches suggest that many, but perhaps not all, of the turns in their walking tracks may result from bilateral comparisons (Figure 4). Recent analyses indicate that knowledge

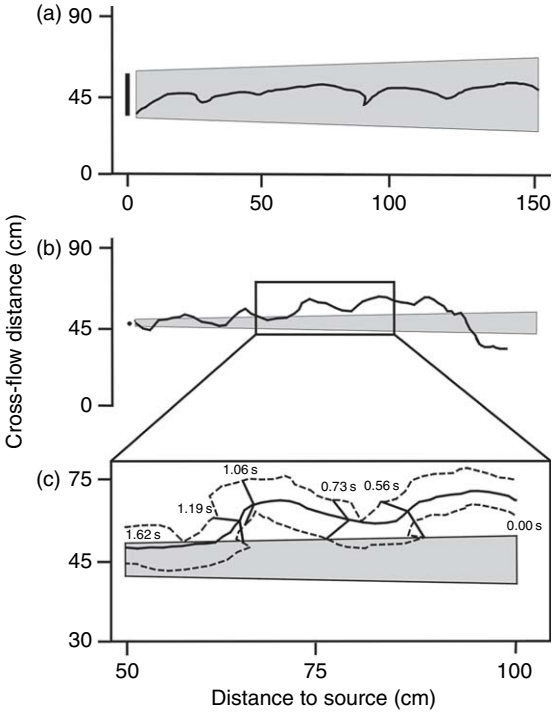

Figure 4 Movement paths of male cockroaches as they track female sex-attractant pheromone plumes of different structures. (a) Walking path of a male cockroach tracking a turbulent plume issuing from a 14.3 cm wide source in a laboratory wind tunnel. Note that the cockroach never approaches the lateral pheromone-clean air boundary of the plume. (b) Walking path of a male cockroach tracking a turbulent plume issuing from a source 0.7 cm wide (i.e., point-source plume). Note the regular sinusoidal zigzagging turning executed by this male as he tracked the plume upwind toward the source. (c) Detail of (b) above showing the position and orientation of the animal's antennae during a brief sequence of turning. In all images, the fluid flows from left to right, and the flow velocities for each example are presented in each panel. Reproduced from Willis, M. A. and Avondet, J. L. 2005. Odor-modulated orientation in walking male cockroaches, *Periplaneta americana* (L.), and the effects of odor plumes of different structure. J. Exp. Biol. 208, 721–735, with permission of the Company of Biologists Ltd.

of the plume structure should allow prediction of sensor spacing appropriate to support bilateral concentration comparisons (Webster, D. R. *et al.*, 2001).

4.42.4.2.2 Temporal comparisons of odor concentration (sensors small relative to the scale of the plume, memory required)

In contrast, animals swimming or flying are moving relatively more rapidly, through faster turbulent flows and thus experience an odor plume at a much faster rate (which makes it essentially a continuous series of pheromone-clean air edges). These animals may not have time to extract information about changes in the plume fast enough to support adaptive maneuvering using a spatial strategy. To a system focused on the timing of the odor inputs and not where it is, the edge of the plume is just another odor on–off in the sequence (Webster, D. R. *et al.*, 2001).

The inability, in most cases, to determine when and where an organism detects an odor plume, both in relation to the plume and in relation to the animals' own preceding and subsequent behavior, has made it almost impossible to determine which of the existing hypothetical mechanisms may underlie the behavior we observe. In only one case has the physiological response of the olfactory sensors to plume structure been measured during a plume-tracking performance (Vickers, N. J. and Baker, T. C., 1994). Even in this example, the olfactory responses were measured from a surgically detached antenna carried by the odor-tracking individual, not from the antennae of the individual actually performing the tracking behavior.

4.42.4.3 Importance of Active Sampling Behaviors to Odor Detection and Processing

Loudon C. and Koehl M. A. R. (2000) have shown that flows induced by pheromone-activated wing fanning behavior in *Bombyx mori* males may enhance the ability of the males to respond to pheromone during plume-tracking behavior. Measurements of air flow over the male moth's feathery antenna showed rhythmically varying velocities that matched the moths' wing beat frequency. Such a rhythmically varying flow would cause intermittent encounters between the antennae and any odor plume near enough to be drawn into the flow generated by the beating wings. When the wings of *B. mori* males were removed, their success at locating the females decreased (Ishida, H. *et al.*, 1996). Similar active sampling behaviors are generated by lobsters, crayfish,

and other crustaceans when they are tracking odors as they rapidly flex their antennules driving their chemosensors through the plume in a behavior known as flicking (Schmidt, B. C. and Ache, B. W., 1979; Koehl, M. A. R., 2006).

4.42.5 Man-Made Odor Tracking Systems

Although our knowledge and understanding of odor plumes and the neural and behavioral responses of plume-tracking organisms is far from complete, enough is known that some have begun to apply this knowledge to man-made odor-tracking systems. Some of the first robotic odor-tracking systems were conceived and fabricated by Russell R. A. (1999) to provide the chemical communication capabilities of social insects (e.g., ants and bees) to interacting robots. The idea was to use odor tracking in a manner similar to ants and termites, as a way to mark trails through the environment, to guide the foraging behavior of other members of a robot team. Russell's first attempts included fabricating the entire system, from the robot to the odor detectors (Russell, R. A., 1999). These early robots were able to track a volatile chemical trail deposited on the substrate for some time and distance. However, in both the robotic system and its insect model, the source of the odor (i.e., the odor trail) was always very close to the tracker. These initial experiments then led to the development of wind direction sensors and tracking algorithms that mimicked the pheromone-tracking behavior of male silk worm moths, *B. mori* (Russell, R. A. *et al.*, 1995). These new sensory and control systems performed well enough to guide a mobile robot around obstacles in a laboratory environment and successfully locate a source of volatile chemicals (Russell, R. A. *et al.*, 1995). Similar experiments were being conducted in other laboratories with similar results (Ishida, H. *et al.*, 1994).

To date, the most significant hindrances to the development of odor-tracking robots are the chemical detectors; the robots' olfactory sensors. None of the currently available off-the-shelf man-made odor detectors approach the temporal response or exquisite sensitivity of their biological precursors. In one series of experiments, this problem was overcome by surgically removing the biological odor detectors (i.e., the antennae of male moths) and mounting them on a mobile robot (Kuwana, Y. *et al.*, 1995). Although these experiments demonstrated the efficacy of interfacing living (i.e., dying) tissue with simple electronics, and generated predictable odor-activated steering responses, the relatively short life of the antenna after removal from the insect makes this alternative impractical.

Another approach has been to fabricate robotic odor-tracking systems explicitly as a means to test biological hypotheses about how animals track odor plumes (Grasso, F. W. *et al.*, 2000; Edwards, S. *et al.*, 2005). These robotic studies usually form part of a multipronged research program aimed at working iteratively between robotic or simulation experiments and animal studies. In these studies, simulation and mobile robot experiments are developed using new and existing biological knowledge, and their results then are used to inform the design and interpretation of the subsequent behavioral or neurophysiological studies. Results from some of these robotic experiments (Grasso, F. W. *et al.*, 2000; Edwards, S. *et al.*, 2005) have caused the reexamination of our previous understanding of odor tracking.

4.42.6 Conclusions

If we could know when the organisms detected an odor filament together with the preceding and subsequent behavior, we could begin to understand how the animals are using the information to control their behavior. Do they modify their tracking behavior based on each encounter with odor as suggested by recent experiments (Mafra-Neto, A. and Cardé, R. T., 1994; Vickers, N. J. and Baker, T. C., 1994), or do they continuously modulate an odor-activated internal program as proposed earlier (Kennedy, J. S., 1983). Or does the trackers' response change in a context-dependent manner? Do some animals have alternative tracking algorithms that are employed in different environmental conditions (i.e., different plumes structures) or does a single simple tracking algorithm yield apparently different but adaptive behavior as the animal actively interacts with different plume structures generated in different environmental conditions? Much is known about this interesting biological phenomenon, but many lacunae in our knowledge at all levels of organization, environmental, neural, and behavioral, remain to be filled before a complete understanding is revealed.

References

Arbas, E. A. 1986. Control of hindlimb posture by wind-sensitive hairs and antennae during locust flight. J. Comp. Physiol. A 159, 849–857.

Arbas, E. A., Willis, M. A., and Kanzaki, R. 1993. Organization of Goal-Oriented Locomotion: Pheromone-Modulated Flight Behavior of Moths. In: Biological Neural Networks in Invertebrate Neuroethology and Robotics (*eds*. R. D. Beer, R. E. Ritzmann, and T. McKenna). pp. 159–198. Academic Press.

Baker, C. F. and Montgomery, J. C. 1999. The sensory basis for rheotaxis in the blind Mexican cave fish, *Astynax fasciatus*. J. Comp. Physiol. A 184, 519–527.

Baker, T. C., Fadamiro, H. Y., and Cosse, A. A. 1998. Moths use fine tuning for odour resolution. Nature 393, 530.

Basil, J. A., Hanlon, R. T., Sheikh, S. I., and Atema, J. 2000. Three-dimentional odor tracking by *Nautilus pompilius*. J. Exp. Biol. 203, 1409–1414.

Belanger, J. H. and Willis, M. A., 1996. Adaptive control of odor-guided locomotion: behavioral flexibility as an antidote to environmental unpredictability. Adapt. Behav. 4, 217–253.

Bell, W. J. and Tobin, T. R. 1981. Orientation to sex pheromone in the American cockroach: analysis of chemo-orientation mechanisms. J. Insect Physiol. 27, 501–508.

Borst, A. and Heisenberg, M. 1982. Osmotropotaxis in *Drosophila melanogaster*. J. Comp. Physiol. 147, 479–484.

Bossert, W. H. and Wilson, E. O. 1963. The analysis of olfactory communication among animals. J. Theor. Biol. 48, 443–469.

Budick, S. A. and Dickinson, M. H. 2006. Free flight responses of *Drosophila melanogaster* to attractive odors. J. Exp. Biol. 209, 3001–3017.

Cardé, R. T. and Minks, A. K. 1997. Pheromone Research: New Directions. Chapman & Hall.

Charlton, R. E., Kanno, H., Collins, R. D., and Cardé, R. T. 1993. Influence of pheromone concentration and ambient temperature on the flight of the gypsy moth, *Lymantria dispar* (L), in a sustained-flight wind-tunnel. Physiol. Entomol. 18, 349–362.

Christensen, T. C. and Hildebrand, J. G. 1988. Frequency coding in central olfactory neurons in the sphinx moth, *Manduca sexta*. Chem. Senses 13, 23–30.

David, C. T. 1986. Mechanisms of Directional Flight in Wind. In: Mechanisms in Insect Olfaction (*eds*. T. L. Payne, M. C. Birch, and C. E. J. Kennedy), pp. 49–58. Clarendon.

Dehnhardt, G., Mauck, B., and Bleckmann, H. 1998. Seal whiskers detect water movements. Nature, 394, 235–236.

Dusenberry, D. B. 1992. Sensory Ecology., W.H. Freeman.

Edwards, S., Rutkowski, A., Quinn, R., and Willis, M. 2005. Moth-inspired plume tracking strategies in three-dimensions. Proceedings of the 2005 IEEE International Conference on Robotics and Automation, 1681–1686.

Elkinton, J. S., Schal, C., Ono, T., and Cardé, R. T. 1987. Pheromone puff trajectory and upwind flight of male gypsy moth in a forest. Physiol. Entomol. 12, 399–406.

Emanuel, M. E. and Dodson, J. J. 1979. Modification of the rheotropic behavior of male rainbow trout (*Salmo gairderi*) by ovarian fluid. J. Fish. Res. Board Can. 36, 63–68.

Ferner, M. C. and Weissburg, M. J. 2005. Slow-moving predatory gastropods track prey odors in fast and turbulent flow. J. Exp. Biol. 208, 809–819.

Frankel, G. S. and Gunn, D. L. 1961. The Orientation of Animals. Dover.

Gewecke, M. and Woike, M. 1978. Breast feathers as an air-current sense organ for the control of flight behaviour in a songbird (*Carduelis spinus*). Zietschrift für Tierpsychology 47, 293–298.

Grasso, F. W., Consi, T. R., Mountain, D. C., and Atema, J. 2000. Biomimetic robot lobster performs chemo-orientation in turbulence using a pair of spatially separated sensors: Progress and challenges. Robot. Auton. Syst. 30, 115–131.

Griffiths, N. and Brady, J. 1995. Wind structure in relation to odour plumes in tsetse fly habitats. Physiol. Entomol. 20, 286–292.

Hangartner, W. 1967. Spezifität und inaktivierung des spurpheromons von *Lasius fuliginosus* Latr. und orientierung der arbeiterinnen im duftfeld. Zeitschrift für Vergleichende Physiologie 57, 103–136.

Hepper, P. G. and Wells, D. L. 2005. How many footsteps do dogs need to determine the direction of an odor trail? Chem. Senses 30, 291–298.

Ishida, H., Hayashi, K., Takakusaki, M., Nakamoto, T., Moriizumi, T., and Kanzaki, R. 1996. Odour-source localization system mimicking behaviour of silkworm moth. Sens. Actuators A 99, 225–230.

Ishida, H., Suetsugu, T., Nakamoto, T., and Moriizumi, T. 1994. Study of autonomous mobile sensing system for localization of odor source using gas sensors and anemotactic sensors. Sensors and Actuators A 45, 154–157.

Johnsen, P. B. and Teeter, J. H. 1985. Behavioral responses of Bonnethead sharks (*Sphyrna tiburo*) to controlled olfactory stimulation. Mar. Behav. Physiol. 11, 283–291.

Justus, K. A. and Cardé, R. T. 2002. Flight behaviour of males of two moths, *Cadra cautella* and *Pectinophora gossypiella*, in homogeneous clouds of pheromone. Physiol. Entomol. 27, 67–75.

Kennedy, J. S. 1940. The visual responses of flying mosquitoes. Proceedings of the Zoological Society of London A 109, 221–242.

Kennedy, J. S. 1983. Zigzagging and casting as a response to wind-borne odor: a review. Physiol. Entomol. 8, 109–120.

Kennedy, J. S. and Marsh, D. 1974. Pheromone regulated anemotaxis in flying moths. Science 184, 999–1001.

Koehl, M. A. R. 2006. The fluid mechanics of arthropod sniffing in turbulent odor plumes. Chem. Senses 31, 93–105.

Kuwana, Y., Shimoyama, I., and Miura, H. 1995. Steering control of a mobile robot using insect antennae. IEEE/RSJ International Conference on Intelligent Robots and Systems, 2, 530–535.

Loudon, C. 2003. The Biomechanical Design of an Insect Antenna as an Odor Capture Device. In: Insect Pheromone Biochemistry and Molecular Biology (*eds*. G. J. Blomquist and R. G. Vogt), pp. 609–630. Elsevier Academic Press.

Loudon, C. and Koehl, M. A. R. 2000. Sniffing by a silkworm moth: wing fanning enhances air penetration through and pheromone interception by antennae. J. Exp. Biol. 203, 2977–2990.

Mafra-Neto, A. and Cardé, R. T. 1994. Fine-scale structure of pheromone plumes modulates upwind orientation of flying male moths. Nature 369, 142.

Marsh, D., Kennedy, J. S., and Ludlow, A. R. 1978. An analysis of anemotactic zigzagging flight in male moths stimulated by pheromone. Physiol. Entomol. 3, 221–240.

Martin, H. 1965. Osmotropotaxis in the honeybee. Nature 208, 59–63.

Moore, P. A. and Atema, J. 1991. Spatial information in the three-dimensional fine structure of an aquatic odor plume. Biol. Bull. 181, 408–418.

Moore, P. A., Scholtz, N., and Atema, J. 1991. Chemical orientation of lobsters, *Homarus americanus*, in turbulent odor plumes. J. Chem. Ecol. 17, 1293–1307.

Montgomery, J. C., Diebel, C., Halstead, M. D. B., and Downer, J. 1999. Olfactory search tracks in the Antarctic fish *Trematomus bernachii*. Polar Biol. 21, 151–154.

Murlis, J. and Jones, C. D. 1981. Fine-scale structure of odour plumes in relation to insect orientation to distant pheromone and other attractant sources. Physiol. Entomol. 6, 71–86.

Murlis, J., Willis, M. A., and Cardé, R. T. 1990. Odor Signals: Patterns in Time and Space. In: Proceedings of the X International Symposium on Olfaction and Taste, Oslo (*ed*. K. Døving).

Murlis, J., Willis, M. A., and Cardé, R. T. 2000. Spatial and temporal structure of pheromone plumes in fields and forests. Physiol. Entomol. 25, 211–222.

Raguso, R. and Willis, M. 2002. Synergy between visual and olfactory cues in nectar feeding by naïve hawkmoths. Anim. Behav. 64, 685–695.

Raguso, R. and Willis, M. 2005. Synergy between visual and olfactory cues in nectar feeding by wild hawkmoths, *Manduca sexta*. Anim. Behav. 69, 407–418.

Russell, R. A. 1999. Odour Detection by Mobile Robots. World Scientific Publishing.

Russell, R. A., Thiel, D., Deveza, R., and Mackay-Sim, A. 1995. A robotic system to locate hazardous chemical leaks. IEEE International Conference on Robotics and Automation, 1, 556–561.

Schmidt, B. C. and Ache, B. W. 1979. Olfaction: response enhancement by flicking in a decapod crustacean. Science 205, 204–206.

Schöne, H. 1984. Spatial Orientation. Princeton University Press.

Steen, J. B., Mohus, I., Kvesetberg, T., and Walløe, L. 1996. Olfaction in bird dogs during hunting. Acta Physiol. Scand. 157, 115–229.

Susswein, A. J., Cappell, M. S., and Bennett, M. V. L. 1982. Distance chemoreception in *Navanax inermis*. Marine Behav. Physiol. 8, 231–241.

Vickers, N. J. 2000. Mechanisms of animal navigation in odor plumes. Biol. Bull. 198, 203–212.

Vickers, N. J. 2006. Winging it: moth flight behavior and responses of olfactory neurons are shaped by pheromone plume dynamics. Chem. Senses 31, 155–166.

Vickers, N. J. and Baker, T. C. 1992. Male *Heliothis virescens* maintain upwind flight in response to experimentally pulsed filaments of their sex pheromone (Lepidoptera: Noctuidae). J. Insect Behav. 5, 669–687.

Vickers, N. J. and Baker, T. C. 1994. Reiterative responses to single strands of odor promote sustained upwind flight and odor source location by moths. Proc. Natl. Acad. Sci. U. S. A. 91, 5756–5760.

Vickers, N. J., Christensen, T. A., Baker, T. C, and Hildebrand, J. G. 2001. Odour-plume dynamics influence the brain's olfactory code. Nature 410, 466–470.

Vogel, S. 1994. Life in Moving Fluids, Princeton University Press.

Webb, B., Harrison, R. R., and Willis, M. A. 2004. Sensorimotor control of navigation in arthropod and artificial systems. Arthropod Struct. Dev. 33, 301–330.

Webster, D. R. and Weissburg, M. J. 2001. Chemosensory guidance cues in a turbulent odor plume. Limn. Oceanogr. 46, 1034–1047.

Webster, D. R., Rahman, S., and Dasi, L. P. 2001. On the usefulness of bilateral comparison to tracking turbulent chemical plumes. Limnol. Oceanogr. 46, 1048–1053.

Weissburg, M. J. 2000. The fluid dynamical context of chemosensory behavior. Biol. Bull. 198, 188–200.

Weissburg, M. J. and Zimmer-Faust, R. K. 1993. Life and death in moving fluids: Hydrodynamic effects on chemosensory-mediated predation. Ecology 74, 1428–1443.

Weissburg, M. J. and Zimmer-Faust, R. K. 1994. Odor plumes and how blue crabs use them in finding prey. J. Exp. Biol. 197, 349–375.

Willis, M. A. and Avondet, J. L. 2005. Odor-modulated orientation in walking male cockroaches, *Periplaneta americana* (L.), and the effects of odor plumes of different structure. J. Exp. Biol. 208, 721–735.

Willis, M. A., David, C. T., Murlis, J., and Cardé, R. T. 1994. Effects of pheromone plume structure and visual stimuli on the pheromone-modulated upwind flight of male gypsy moths (*Lymantria dispar* L.), in a forest. J. Insect Behav. 7, 385–409.

Wolf, H. and Wehner, R. 2000. Pinpointing food sources: Olfactory and anemotactic orientation in desert ants, *Cataglyphis fortis*. J. Exp. Biol. 203, 857–868.

Wright, R. H. 1958. The olfactory guidance of flying insects. The Can. Entomol. 90, 81–89.

Zimmer-Faust, R. K., Finelli, C. M., Pentcheff, N. D., and Wethey, D. S. 1995. Odor plumes and animal navigation in turbulent water flow: A field study. Biol. Bull. 188, 111–116.

4.43 Accessory Olfactory System

F Zufall and T Leinders-Zufall, University of Saarland School of Medicine, Homburg, Germany

A C Puche, University of Maryland School of Medicine, Baltimore, MD, USA

© 2008 Elsevier Inc. All rights reserved.

4.43.1	**Introduction**	784
4.43.2	**A Brief Historical Perspective**	785
4.43.3	**The Vomeronasal Organ**	786
4.43.3.1	Basic Anatomical Organization	786
4.43.3.2	Zonal Segregation of the Vomeronasal System	788
4.43.3.3	A Genetic Basis for Stimulus Detection	789
4.43.3.4	Molecular Physiology of Neuronal Sensing	789
4.43.3.5	Signal Transduction Mechanisms	791
4.43.3.6	The Search for Sensory Stimuli	794
4.43.3.6.1	Stimulus access	794
4.43.3.6.2	Complex stimuli	795
4.43.3.6.3	Urinary volatiles	795
4.43.3.6.4	General odors	796
4.43.3.6.5	Major histocompatibility complex peptide ligands	796
4.43.3.6.6	Other specific peptides	797
4.43.3.6.7	Proteins	797
4.43.3.7	Sensory Coding Strategies in the Vomeronasal Organ	798
4.43.4	**The Accessory Olfactory Bulb**	798
4.43.4.1	Inputs from the Vomeronasal Organ	798
4.43.4.2	Functional Organization of the Accessory Olfactory Bulb	799
4.43.4.2.1	Interneurons	801
4.43.4.2.2	Subdivisions	802
4.43.4.3	Outputs of the Accesory Olfactory Bulb	802
4.43.4.4	Centrifugal Afferents to the Accessory Olfactory Bulb	804
4.43.5	**Mechanisms of Behavior**	804
4.43.5.1	Detection of Heterospecific Signals	805
4.43.5.2	Male Aggression to Intruder Males	805
4.43.5.3	Maternal Aggression to Intruder Males	806
4.43.5.4	Male Mating Behavior	806
4.43.5.5	Male Ultrasonic Vocalizations	806
4.43.5.6	Timing of Puberty, Cyclicity, and Ovulation in Females	806
4.43.5.7	Hormonal Responses	807
4.43.5.8	Pregnancy Block and Individual Recognition in Females: The Bruce Effect	807
References		808

Glossary

aEPL Accessory external plexiform layer.
aGCL Accessory granule layer.
aGL Accessory glomerular layer.
aMCL Accessory mitral cell layer.
AOB Accessory olfactory bulb.
AOC Accessory olfactory cortex.
aONL Accessory olfactory nerve layer.
AONm Anterior olfactory nucleus, medial division.

AP Posterior amygdaloid nucleus.
APVH Anterior periventricular hypothalamus.
BAOT Bed nucleus of the accessory olfactory tract.
Bar Barrington's nucleus.
BST Bed nucleus of the stria terminalis.
CG Central (periaqueductal) gray.
CNGA2 Cyclic nucleotide-gated channel type A2.
DAG Diacylglycerol.
DB Nucleus of the diagonal band.
DR Dorsal raphe nucleus.
DT Dendritic tip.
EVG Electrovomeronasogram.
GC-D Guanylyl cyclase type D.
GG Grüneberg ganglion.
LC Locus coeruleus.
LOT Lateral olfactory tract.
LPO Lateral preoptic area.
MC Mitral cell.
Me Medial amygdaloid nucleus.
MHC Major histocompatibility complex.
MPO Medial preoptic area.
NSE Nonsensory epithelium.
P/Amb Nucleus ambiguous and periabigual area.
PDE4A Phosphodiesterase type 4A.
PG Periglomerular.
Pit Pituitary.
PMCo Posteromedial cortical amygdaloid nucleus.
RVL Rostroventrolateral medulla.
SAG 1-Stearoyl-2-arachidonoyl-*sn*-glycerol.
SC Sustentacular cell.
SCis Lumbosacral spinal cord.
SO Supraoptic nucleus.
SOM Septal organ of Masera.
TRP Transient receptor potential.
TRPC2 Canonical transient receptor potential channel type 2.
VB Vomer bone.
VMH Ventromedial hypothalamic nucleus.
VN Vomeronasal nerve.
VNO Vomeronasal organ.
VSN Vomeronasal sensory neuron.
V1R Vomeronasal receptor family type 1.
V2R Vomeronasal receptor family type 2.
wt Wild type.

4.43.1 Introduction

The majority of vertebrates have dual independent olfactory systems; possessing an accessory olfactory system (AOS) in addition to the main olfactory system. The AOS has attracted a great deal of attention in recent years because of a growing recognition of the essential role in chemical communication and the regulation of social behaviors this system plays. Key elements of the AOS (Figure 1) include

1. the vomeronasal organ (VNO), a chemoreceptive structure situated at the base of the nasal septum which houses the vomeronasal sensory neurons (VSNs);
2. the accessory olfactory bulb (AOB), a structure of the forebrain that receives input from the VNO serving as the first processing center of vomeronasal information; and
3. higher olfactory centers that receive direct or indirect information from the AOB.

These higher brain structures include, in mammals, the medial amygdala and parts of the cortical and posterior amygdala, the bed nucleus of the accessory olfactory tract (BAOT), the bed nucleus of the stria terminalis (BST), and the medial hypothalamus. The focus of this chapter will be on physiology and function of the VNO and AOB. Whenever possible, we attempt to link genetic information with anatomical, physiological, and behavioral approaches. Because the mouse has become the principal model system for a genetically driven, systems-oriented approach, the focus of this chapter will be on rodent AOS function. However, it is important to realize that the precise role of the AOS must be viewed in close relationship to species-specific adaptations. Indeed, the initial discovery of pheromonal–behavioral signaling through specific neural pathways was pioneered in invertebrate biology, and many of the fundamental concepts of VNO–AOB function have developed from research in nonmammalian species.

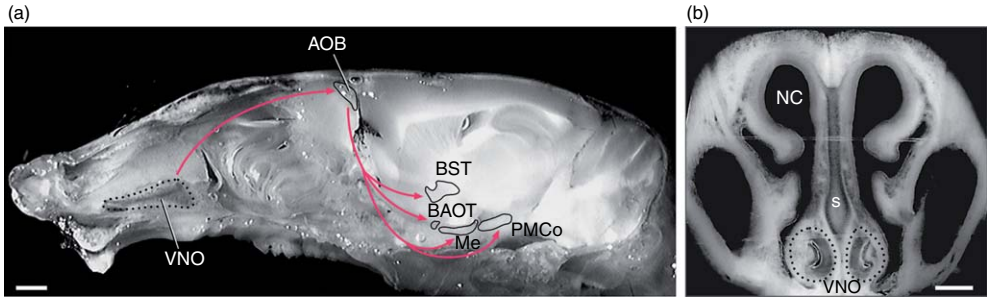

Figure 1 Anatomy of the accessory olfactory system. (a) Perisaggital view of the mouse head with a superimposed diagram representing the accessory olfactory pathway. Sensory inputs in the accessory olfactory system are detected by sensory neurons in the vomenonasal organ (VNO), a bilateral tubular structure in the anterior region of the nasal cavity (see (b)). An extensive network of blood sinuses is located at the lateral external wall of the organ. Together with a band of cavernous erectile tissue, it provides the hardware for a vomeronasal pump that aids in stimulus delivery. Axons of the vomeronasal sensory neurons (VSNs) project to the accessory olfactory bulb (AOB), which in turn transmits sensory information to the bed nucleus of the stria terminalis (BST), the bed nucleus of the accessory olfactory tract (BAOT), and the amygdala, that is, the medial amygdaloid nucleus (Me) as well as the posteromedial cortical amydaloid nucleus (PMCo). The information is then transmitted from the amygdala to specific nuclei of the hypothalamus. These tertiary projections to the hypothalamic region are also known as the neuroendocrine hypothalamus. This area controls the release of hormones by the pituitary and therefore modulates the endocrine status of the animal. As a reference for the location of the VNO, the septum was partially removed to reveal the turbinates of the main olfactory organ. Scale bar = 1.5 mm. (b) Transmitted light image of a coronal section through a postnatal day 7 mouse head showing the location of the bilateral VNO (dashed circles) at the base of the nasal septum (S). NC, nasal cavity. Scale bar = 200 μm.

4.43.2 A Brief Historical Perspective

The VNO was discovered by Ludvig Jacobson (and hence often referred to as Jacobson's organ) and was originally described in a Danish publication (Jacobson, L., 1813). This work has recently been translated into English and is thus accessible to a wider audience (Doving, K. B. and Trotier, D., 1998; Jacobson, L. *et al.*, 1998). Jacobson described the organ in a variety of domesticated mammals, some wild carnivores, ungulates, and marine mammals. He assumed that the organ was secretory in nature but suspected that it could also function as a sensory organ.

Balogh C. (1860), Klein E. (1881), Piana G. P. (1882), and Retzius G. (1894) observed similarities in the morphology of sensory neurons in the main olfactory epithelium and VNO, and proposed a common function between the cells. During the following years, the presence of the VNO was confirmed in most mammals (von Mihalkovics, V., 1899; Perlman, S. M., 1934). A review by Doving K. B. and Trotier D. (1998) has reproduced the excellent quality of cross sections of the mouse VNO originally published by von Mihalkovics V. (1899).

The existence of the AOB in mammals was recognized by von Gudden B. (1870). McCotter R. E. (1912) was the first to clearly demonstrate that the AOB is a brain structure dedicated to the reception of vomeronasal nerve (VN) fibers, and that it gives off fibers that join the lateral olfactory tract. He suggested that the olfactory system should be divided into two distinct subsystems, namely an ordinary and an AOS.

Beginning in the 1930s and extending to the 1950s, Lord Adrian began to use electrophysiological methods to record extracellular activity from the VNs of the rabbit. He was unable to show a reaction to chemical stimuli in the VNO, but he noted considerable rhythmic activity in response to localized pressure (Adrian, E. D., 1955).

During the 1950s and 1960s, an intense period of pheromone research began. Following the seminal work on insect pheromones (Karlson, P. and Lüscher, M., 1959), behavioral endocrinologists had discovered several pheromonal effects in mice and a consensus emerged that these effects require a functional olfactory system. Winans S. S. and Scalia F. (1970) suggested that some of these effects might depend on a functional AOS. This idea eventually led to the dual olfactory hypothesis (reviewed by Halpern, M., 1987), which proposed that distinct parallel pathways could be traced from the periphery of the main and AOSs into the telencephalon and diencephalon of all animals possessing these two chemoreceptive systems. As pointed out by Halpern M. (1987), a main corollary of this hypothesis is that each system should be involved in distinct behavioral

domains. During the 1970s and 1980s, research concentrated on testing this hypothesis and its corollary by using a combination of anatomical, behavioral, and physiological approaches. This work has been summarized in a number of excellent reviews (Burghardt, G. M., 1970; Madison, D. W., 1977; Keverne, B., 1979; Wysocki, C. J., 1979; Johnston, R. E., 1983; Keverne, E. B., 1983; Meredith, M., 1983; Halpern, M., 1987; Wysocki, C. J. and Meredith, M., 1987).

The 1990s saw an explosion of interest in AOS function triggered by the application of molecular biological and genetic approaches, together with the use of more sophisticated electrophysiological recording techniques. A significant finding was the segregation of the mouse and rat vomeronasal system into two major subsystems, each expressing distinct classes of signal transduction-related molecules (Halpern, M. *et al.*, 1995; Berghard, A. *et al.*, 1996; Jia, C. and Halpern, M., 1996). This was followed by the identification of the first (Dulac, C. and Axel, R., 1995) and second families of vomeronasal receptor genes (Herrada, G. and Dulac, C., 1997; Ryba, N. J. and Tirindelli, R., 1997; Matsunami, H. and Buck, L. B., 1997), and the cloning of the ion channel TRPC2 (canonical transient receptor potential channel type 2) (Liman, E. R. *et al.*, 1999). The first patch clamp recordings from single VSNs were carried out by Trotier D. *et al* (1993), Taniguchi, M. *et al.* (1995), and Liman E. R. and Corey D. P. (1996). In parallel, gene-targeting methods were developed by Mombaerts P. *et al.* (1996), which subsequently led to an analysis of the axonal projection patterns of specific subsets of VSNs (Belluscio, L. *et al.*, 1999; Rodriguez, I. *et al.*, 1999).

Since 2000, research activities aimed at understanding AOS function have further increased. The year 2000 saw the development of reduced mouse VNO preparations that allowed for simultaneous recording of stimulus-induced activity from hundreds of VSNs (Holy, T. E. *et al.*, 2000; Leinders-Zufall, T. *et al.*, 2000) leading to the identification of the first prospective pheromones acting on mammalian VSNs (Leinders-Zufall, T. *et al.*, 2000). Next came the targeted deletion of specific signal transduction genes, which enabled, for the first time in the AOS, a correlation between gene function, cellular activity, and behavioral changes (Del Punta, K. *et al.*, 2002a; Leypold, B. G. *et al.*, 2002; Stowers, L. *et al.*, 2002). Progress in understanding VSN signal transduction mechanisms (Lucas, P. *et al.*, 2003) was quickly followed by the finding that a subset of VSNs function as detectors of peptide ligands of the major histocompatibility complex (MHC), and that these peptides influence selective pregnancy termination (the Bruce effect) (Leinders-Zufall, T. *et al.*, 2004). In parallel, the first recordings from AOB neurons in freely behaving mice were undertaken, making it now possible to correlate neuronal activity in the AOB with specific behavioral changes (Luo, M. *et al.*, 2003). Several reviews have summarized these most recent aspects of AOS research (Dulac, C. and Torello, A. T., 2003; Brennan, P. A. and Keverne, E. B., 2004; Luo, M. and Katz, L. C., 2004; Mombaerts, P., 2004; Bigiani, A. *et al.*, 2005; Boehm, T. and Zufall, F., 2006). Halpern M. and Martínez-Marcos A. (2003) have provided the most comprehensive review on structure and function of the vomeronasal system published thus far.

4.43.3 The Vomeronasal Organ

4.43.3.1 Basic Anatomical Organization

The structure of the VNO and its neuroepithelium has been described in representatives from virtually every major vertebrate class at the light microscopic and ultrastructural level, demonstrating a remarkable conservation between different species. Many of these original studies have been summarized by Halpern M. (1987) and Halpern M. and Martínez-Marcos A. (2003) and the reader is referred to these extensive reviews. In mammals, the VNO is a bilateral, cigar-shaped organ that is located at the base of the nasal septum, anterior and ventral to the main olfactory epithelium (Figures 1 and 2). Each VNO is encased in a bony and/or cartilaginous capsule known as vomer bone capsule. Chemosensory stimuli gain access to the VNO through its single rostral opening which, in rodents, opens into the nasal cavity. The main structural elements of the VNO are best seen in coronal sections (Figures 2(b)–2(d) and 2(h)) and include a central lumen, a medially located crescent-shaped sensory epithelium, and a laterally located nonsensory epithelium together with an extensive network of blood sinuses surrounded by a band of cavernous tissue. These latter components provide the hardware for a vomeronasal pump that aids in stimulus delivery (Meredith, M. and O'Connell, R. J., 1979; Meredith, M. *et al.*, 1980) (see below).

The VNO sensory epithelium consists primarily of three cell types (Ciges, M. *et al.*, 1977; Vaccarezza, O. L. *et al.*, 1981; Garrosa, M. and Coca, S., 1991):

1. elongated glia-like supporting cells,
2. bipolar sensory cells known as VSNs, and
3. a sparse population of basal stem cells.

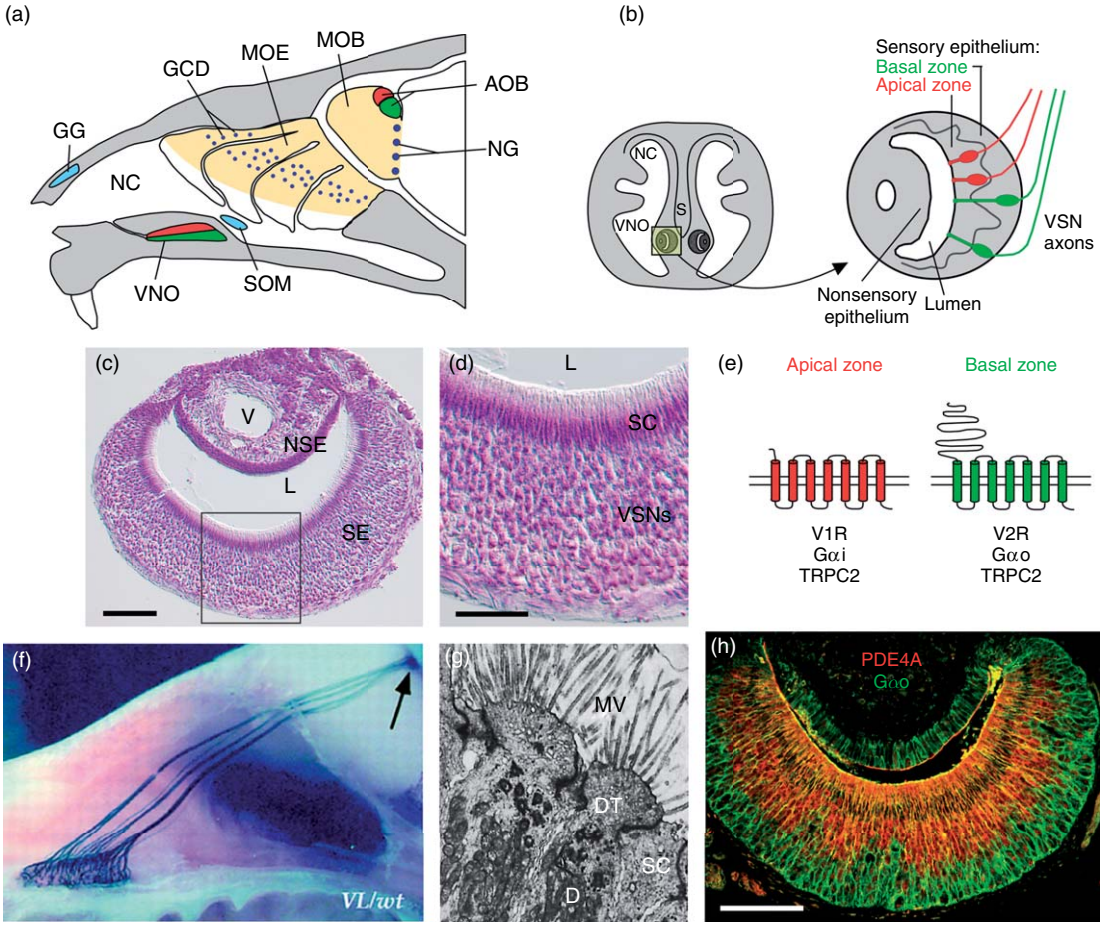

Figure 2 Organization of the sense of smell. (a) Midsagittal view of the rodent nasal cavity (NC) and forebrain. Vomeronasal sensory neurons (VSNs) in the vomeronasal organ (VNO), which is located at the base of the nasal septum (S), project to the anterior (red) or posterior (green) accessory olfactory bulb (AOB). Sensory neurons in the main olfactory epithelium (MOE) project their axons to glomeruli in the main olfactory bulb (MOB). These MOE neurons employ cyclic nucleotide-gated channels for sensory transduction. The septal organ of Masera (SOM) is an isolated island of olfactory sensory neurons that project axons to glomeruli in the ventromedial olfactory bulb. The Grüeneberg ganglion (GG) projects axons to specific glomeruli in the caudal region of the MOB. GCD (guanylyl cyclase D-expressing) neurons are located in the MOE, but project to a limited number of necklace glomeruli (NG) in the caudal MOB. (b–d) Coronal sectioning through the nasal cavity reveals the typical crescent-shaped organization of the VNO sensory epithelium (SE). The region delimited by the black box in (c) is shown at higher magnification in (d). L, lumen; NSE, nonsensory epithelium; SC, sustentacular cell; V, vein. Original sections in (c) and (d) are Nissl stains. Scale bars = 100 μm (c) and 50 μm (d). (e) The sensory epithelium is segregated into two distinct zones, both of which express a unique set of transduction-related molecules: (1) an apical zone (red VSNs) that expresses the G protein $G\alpha_{i2}$ as well as members of the V1R family of vomeronasal receptors, and (2) a basal zone that characteristically contains VSNs (green) that express $G\alpha_o$ and members of the V2R receptor family. Both neuron types express TRPC2. (f) Distribution and axonal projection pattern of a subpopulation of gene-targeted VSNs, showing that axon bundles (vomeronasal nerves) terminate in the AOB (arrow). To visualize this topography, a targeted mutation was generated that led to co expression of taulacZ in all VSNs expressing a distinct V1R receptor. (g) Electron micrograph of a transverse section through two mouse VSNs showing their dendritic process (D), which enlarges into a dendritic tip or knob (DT). From the knob emanate various microvilli (MV). (h) Visualization by confocal microscopy of the two principal expression zones of the VNO sensory epithelium using double-label immunohistochemistry with antibodies to phosphodiesterase type 4A (PDE4A, red) and $G\alpha_o$ (green). Scale bar = 100 μm. (a–e) Reprinted from Zufall, F., Ukhanov, K., Lucas, P., Liman, E., and Leinders-Zufall, T. 2005. Neurobiology of TRPC2: from gene to behavior. Pflügers Arch. 451, 61–71, with kind permission of Springer Science and Business Media. (f) Reprinted from Rodriguez, I., Feinstein, P., and Mombaerts, P. 1999. Variable patterns of axonal projections of sensory neurons in the mouse vomeronasal system. Cell 97, 199–208, with permission from Elsevier. (g) Reprinted from Ciges, M., Labella, T., Gayoso, M., Sanchez, G. 1977. Ultrastructure of the organ of Jacobson and comparative study with olfactory mucosa. Acta Otolaryngol. 83, 47–58, Taylor & Francis. (h) Reprinted with permission from Leinders-Zufall, T., Brennan, P., Widmayer, P., Prasanth Chandramani, S., Maul-Pavicic, A., Jager, M., Li, X. H., Breer, H., Zufall, F., and Boehm, T. 2004. MHC class I peptides as chemosensory signals in the vomeronasal organ. Science 306, 1033–1037, AAAS.

VSNs make up the majority of the cells in the sensory epithelium and are responsible for the detection of chemostimuli. VSNs extend a dendritic process to the luminal surface where it enlarges into an apical dendritic knob (Figure 2(g)). Unlike olfactory sensory neurons (OSNs), the dendritic knob of VSNs lacks cilia instead containing up to 100 microvilli (Figure 2(g)). In rat, VSN microvilli are 3–6 μm long and approximately 100 nm in diameter (Vaccarezza, O. L. *et al.*, 1981). The primary chemotransduction events are thought to take place in these microvilli. The most prominent feature of the dendritic knob is an extensive network of cisterns that appear as a series of small cylindrical rods without any specific orientation (Vaccarezza, O. L. *et al.*, 1981). Cisterns have not been detected in the microvilli. By contrast, the apical VSN dendrite has an extensive network of mitochondria and endoplasmic reticulum (Ciges, M. *et al.*, 1977; Vaccarezza, O. L. *et al.*, 1981). The mitochondria typically appear radially oriented in the dendrite and are generally parallel to the dendritic plasmalemma. The soma is characterized by its clear round nucleus and the extensive presence of rough endoplasmic reticulum. Particularly at the apical pole of the soma, where the dendrite begins to emerge, there is a complex stack of Golgi apparatus, rough endoplasmic reticulum, and a multivesicular body. Thus, organelles that could serve as intracellular Ca^{2+} stores are spatially compartmentalized in VSNs but, as far as we know, are not present in the microvilli. A single unmyelinated, axon emerges from the basal aspect of the soma of each VSN and exits the epithelium through the basal lamina. VSN axons coalesce to form the relatively long VNs that course along the septum, pass through the cribriform plate, and end in the glomeruli of the AOB, where they synapse onto second-order mitral cells (Halpern, M., 1987 and references therein). This axonal projection pattern is best observed in mutant mouse strains in which specific subpopulations of VSNs coexpress histological markers such as β-galactosidase or green fluorescent protein (Belluscio, L. *et al.*, 1999; Rodriguez, I. *et al.*, 1999) (Figure 2(f)).

The evolution of the VNO has been reviewed by Bertmar G. (1981) and Eisthen H. L. (1992; 1997). In general, the presence of a discrete VNO appears to be a derived character of tetrapods and did not arise as a terrestrial adaptation. VSNs are thought to first appear in amphibians, although a recent study using transgenic zebrafish in combination with VNO-specific markers showed the existence of a VNO-like subsystem of microvillous sensory neurons within the olfactory epithelium of fish (Sato, Y. *et al.*, 2005). Many reptiles possess a well-developed VNO; the VNO of the garter snake has become one of the best-studied model systems for understanding VNO function (Halpern, M. and Martinez-Marcos, A., 2003). The AOS has been lost independently in several taxa, including crocodilians, birds, some bats, and some primates (Eisthen, H. L., 1992). Among primates, New World monkeys possess VNOs whereas adult Old World monkeys do not appear to have well developed VNOs (Halpern, M. and Martinez-Marcos, A., 2003).

Do humans possess a functional VNO? While this question has been hotly debated for many years, a consensus is emerging (Meisami, E. and Bhatnagar, K. P., 1998; Trotier, D. *et al.*, 2000; Meredith, M., 2001; Dulac, C. and Torello, A. T., 2003; Halpern, M. and Martinez-Marcos, A., 2003; Wysocki, C. J. and Preti, G., 2004). At the anatomical level, bipolar receptor cells can be found within the VNO of the developing human fetus, but are absent in the adult (Boehm, N. and Gasser, B., 1993; Boehm, N. *et al.*, 1994; Wysocki, C. J. and Preti, G., 2004). More importantly, there appear to be no connections of the VNO with the adult brain, and in adult humans an anatomically distinct AOB cannot be located (Meisami, E. and Bhatnagar, K. P., 1998). Thus, any putative pheromonal responses by humans are likely mediated by the main olfactory system rather than by an AOS (Wysocki, C. J. and Preti, G., 2004). Consistent with a vestigial AOS in humans, most of the genes encoding vomeronasal classes of receptors are pseudogenes in humans (Dulac, C. and Torello, A. T., 2003).

4.43.3.2 Zonal Segregation of the Vomeronasal System

The VNO sensory epithelium of many mammals is not homogeneous, but it can be partitioned into at least two distinct zones or layers containing apical (superficial) and basal (deep) VSN populations, respectively (Halpern, M. *et al.*, 1998; Tirindelli, R. *et al.*, 1998; Dulac, C., 2000) (Figures 2(b), 2(e), and 2(h)). The two subsets of sensory neurons project their axons to segregated zones of the AOB (von Campenhausen, H. *et al.*, 1997; Mori, K. *et al.*, 2000; Halpern, M. and Martinez-Marcos, A., 2003). As will be summarized in subsequent sections of this chapter, it is becoming increasingly clear that this spatial segregation has important consequences for the handling of structurally and functionally

distinct sets of chemostimuli. The zonal separation was first recognized in the AOS of opossum, mouse, and rat by localization of the G protein subunits $G\alpha_{i2}$ and $G\alpha_o$ to two distinct zones: $G\alpha_{i2}$-positive VSNs define an apical zone whereas $G\alpha_o$-positive VSNs define a basal zone of the VNO epithelium (Halpern, M. *et al.*, 1995; Berghard, A. *et al.*, 1996; Jia, C. and Halpern, M., 1996) (Figures 2(e) and 2(h)).

As reviewed in detail by Halpern M. and Martínez-Marcos A. (2003), numerous other markers (often with unknown functions) are expressed in the VNO and AOB in a heterogeneous manner. For example, an axonal surface glycoprotein, olfactory cell adhesion molecule (OCAM), is expressed exclusively in apical VSNs (von Campenhausen, H. *et al.*, 1997; Yoshihara, Y. *et al.*, 1997). Likewise, the cAMP-specific phosphodiesterase type 4A (PDE4A) is found specifically in apical VSNs (Lau, Y. E. and Cherry, J. A., 2000) (Figure 2(h)). The axon guidance molecule neuropilin-2, a coreceptor for a subfamily of secreted guidance cues known as class 3 semaphorins, is also detected in VSNs of the apical layer (Walz, A. *et al.*, 2002). By contrast, olfactory marker protein (OMP), a 19 kDa cytoplasmic protein of unknown function, is usually present in all mature mammalian VSNs (Halpern, M. and Martinez-Marcos, A., 2003) (Figure 3(a)). Maybe most interestingly, the partitioning of the AOS is maintained at the level of different vomeronasal receptors, summarized in the next section.

4.43.3.3 A Genetic Basis for Stimulus Detection

Differential screening of cDNA libraries constructed from single rat VSNs led to the isolation of the first family of vomeronasal, G-protein-coupled receptor genes, the V1Rs (vomeronasal receptor family type 1) (Dulac, C. and Axel, R., 1995). These are completely distinct from the olfactory receptor superfamily. In the mouse genome, 293 V1R sequences have been identified of which 137 have uninterrupted full-length open reading frames. These are divided into 12 subfamilies that are considerably divergent from each other (Del Punta, K. *et al.*, 2000; Rodriguez, I. *et al.*, 2002). V1R genes are expressed in VSNs of the apical zone of the sensory epithelium (Figure 2(e)) and each individual receptor gene is expressed by only a small subset of VSNs (Dulac, C. and Axel, R., 1995) (Figures 3(b) and 3(c)). Evidence for a functional role of V1Rs in vomeronasal chemodetection comes from the observation that a mouse line lacking a cluster of V1Rs fails to respond to urinary chemicals with known pheromonal effects (6-hydroxy-6-methyl-3-heptanone, *n*-pentylacetate, and isobutylamine) (Del Punta, K. *et al.*, 2002a) (Figures 3(d) and 3(e)). In an alternative approach, green fluorescent protein-tagged VSNs that express the *V1rb2* gene have been shown to respond to the urinary compound 2-heptanone and this response was absent when *V1rb2* gene was deleted (Boschat, C. *et al.*, 2002). This result strongly implies that V1rb2 is a receptor for 2-heptanone.

A second large family of G-protein-coupled receptors expressed in the VNO is formed by the V2R (vomeronasal receptor family type 2) genes, which are expressed in VSNs of the basal zone (Herrada, G. and Dulac, C., 1997; Matsunami, H. and Buck, L. B., 1997; Ryba, N. J. and Tirindelli, R., 1997). With their large extracellular, N-terminal domain (Figure 2(e)), V2Rs resemble the calcium-sensing and metabotropic glutamate receptors rather than V1Rs and olfactory receptors. In the mouse, the V2R gene repertoire consists of 208 members of which only 61 exhibit an intact open reading frame (Yang, H. *et al.*, 2005). Although each V2R gene is generally expressed by only a small subset of VSNs, one subfamily of V2R genes is coexpressed broadly across basal VSNs (Martini, S. *et al.*, 2001). It still remains to be seen whether this results in the formation of functional homo- or heterodimeric receptor proteins (Bigiani, A. *et al.*, 2005).

VSNs in the basal layer express yet another multigene family representing nonclassical class Ib genes of the MHC (Ishii, T. *et al.*, 2003; Loconto, J. *et al.*, 2003). These seem to form multimolecular complexes with V2Rs and have been proposed to function as escort molecules in the transport of V2Rs to the cell surface (Loconto, J. *et al.*, 2003). These findings are intriguing in light of the evidence that subsets of basal VSNs are tuned to respond to class I MHC peptide ligands (Leinders-Zufall, T. *et al.*, 2004). However, a recent structural analysis of MHC class 1b proteins found no evidence for bound peptides, suggesting that class Ib molecules are unlikely to provide specific recognition of MHC peptide ligands in VSNs (Olson, R. *et al.*, 2005).

4.43.3.4 Molecular Physiology of Neuronal Sensing

Like OSNs, VSNs have evolved distinct ionic mechanisms that enable them to generate specific neural signals in response to chemostimulation. Recent years

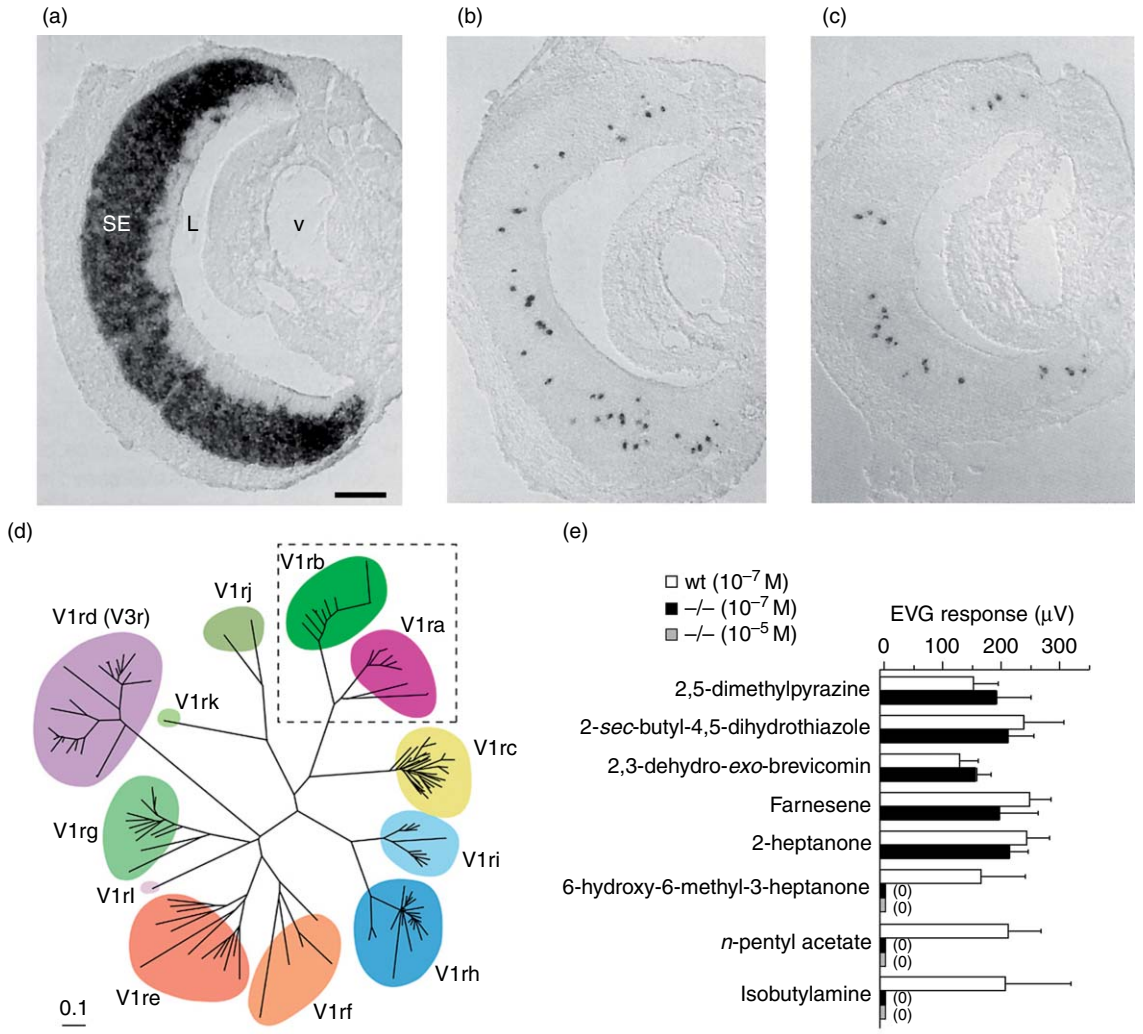

Figure 3 (a–c) Expression of Vr1 receptor RNA is restricted to a subset of vomeronasal sensory neurons (VSNs). Coronal sections of the vomeronasal organ (VNO) dissected from adult male rats were annealed with digoxigenin-labeled antisense RNA probes for olfactory marker protein (a). *In situ* hybridization to coronal sections of a dissected VNO using digoxigenin-labeled probes for rat Vr1 receptors VN1 (b) and VN3 (c). VNO cDNA clones 1 and 3 label 2.7% and 1.1% of cells in the rat sensory epithelium, respectively. L, lumen; SE, sensory epithelium; V, blood vessel. The two above-mentioned rat V1r genes have been predicted to belong to the V1ra group of vomeronasal receptors based on homology with the mouse V1r genes (Del Punta, K. *et al.*, 2000). (d) Unrooted tree representing the 137 mouse V1r genes, with 12 families readily distinguishable. Dashed lines enclose the V1ra and V1rb families of which most members were deleted from the germ line in the study shown in (e). (e) Histogram of electrovomeronasogram (EVG) responses (mean ± SD) from wild type (wt) and Δ*V1rab*Δ mutant mice. Both male and female mutant mice do not respond to 6-hydroxy-6-methyl-3-heptanone, *n*-pentyl acetate, and isobutylamine, but are otherwise normal in their responses to other tested compounds. This chemosensory deficiency supports a role of V1r receptors as pheromone receptors. Stimulus concentration, 10^{-7} M (white and black bars) or 10^{-5} M (gray bars). (a–c) Reprinted from Dulac, C. and Axel, R. 1995. A novel family of genes encoding putative pheromone receptors in mammals. Cell 83, 195–208, with permission from Elsevier. (d, e) reprinted from Del Punta, K., Leinders-Zufall, T., Rodriguez, I., Jukam, D., Wysocki, C. J., Ogawa, S., Zufall, F., and Mombaerts, P. 2002a. Deficient pheromone responses in mice lacking a cluster of vomeronasal receptor genes. Nature 419, 70–74, with permission from Nature Publishing Group.

have delivered significant progress in our ability to record physiological responses in VSNs and to analyze the ionic and molecular mechanisms underlying such responses.

Patch clamp recordings using individual VSNs from mouse, rat, frog, snake, turtle, or lizard – either freshly dissociated or in acute VNO tissue slices – have established that VSNs exhibit resting potentials,

ranging from −60 to −80 mV or even more negative (Trotier, D. *et al.*, 1993; Liman, E. R. and Corey, D. P. 1996; Trotier, D. and Doving, K. B., 1996; Inamura, K. and Kashiwayanagi, M., 2000; Taniguchi, M. *et al.*, 2000; Fadool, D. A. *et al.*, 2001; Fieni, F. *et al.*, 2003; Lucas, P. *et al.*, 2003; Leinders-Zufall, T. *et al.*, 2004; Labra, A. *et al.*, 2005). An electrogenic Na^+, K^+-ATPase appears to be essential in setting this resting potential (Trotier, D. and Doving, K. B., 1996). VSNs express a variety of voltage-dependent currents, including rapid, tetrodotoxin-sensitive Na^+ currents (Trotier, D. *et al.*, 1993; Liman, E. R. and Corey, D. P. 1996; Fieni, F. *et al.*, 2003), voltage- and Ca^{2+}-dependent K^+ currents (Trotier, D. *et al.*, 1993; Liman, E. R. and Corey, D. P., 1996; Inamura, K., *et al.*, 1997; Fadool, D. A. *et al.*, 2001; Labra, A. *et al.*, 2005), several types of voltage-activated Ca^{2+} currents (Trotier, D. *et al.*, 1993; Liman, E. R. and Corey, D. P., 1996; Fieni, F. *et al.*, 2003), and hyperpolarization-activated inward rectifying currents (Trotier, D. *et al.*, 1993; Liman, E. R. and Corey, D. P., 1996). A common feature of most VSNs analyzed thus far seems to be their high input resistance. Combined with a low threshold for action potential generation, this means that only a few picoampere of inward current are sufficient to evoke repetitive spiking in these neurons (Liman, E. R. and Corey, D. P., 1996; Inamura, K., *et al.*, 1997; Trotier, D., 1998; Taniguchi, M. *et al.*, 2000), an ability that has important consequences for the generation of ligand-induced responses in these cells. The biophysical features of VSNs differ considerably from those observed in supporting cells of the vomeronasal epithelium (Ghiaroni, V. *et al.*, 2003).

How do VSNs respond to chemical stimulation? Several laboratories used extracellular or whole-cell current clamp recordings to demonstrate that VSNs, at rest, maintain a relatively low spiking activity and that chemostimulation produces a transient increase in the rate of action potential firing (Trotier, D., 1998; Inamura, K. *et al.*, 1999; Holy, T. E. *et al.*, 2000; Leinders-Zufall, T. *et al.*, 2000; Lucas, P. *et al.*, 2003; Leinders-Zufall, T. *et al.*, 2004) (Figures 4(a) and 4(b)). This excitation is caused by the generation of a depolarizing receptor potential sufficient in size to activate voltage-gated Na^+ channels (Lucas, P. *et al.*, 2003) (Figure 4(c)). The ionic properties of this receptor potential are not yet fully understood, but it is clear that the receptor potential depends critically on the generation of a transient inward current in the distal dendrites and microvilli of VSNs which is associated with an increase in membrane conductance (Inamura, K. and Kashiwayanagi, M., 2000; Taniguchi, M. *et al.*, 2000; Lucas, P. *et al.*, 2003) (Figure 4(d)). The primary electrical events in VSN dendrites can also be monitored by placing micropipettes on VSN microvilli using a semi-intact VNO preparation and recording local field potentials that are known as an electrovomeronasogram (EVG) (Figures 4(e) and 4(f)). This technique has been very useful in the search for molecular cues acting on VSNs (Taniguchi, M. *et al.*, 1998; Leinders-Zufall, T. *et al.*, 2000; 2004) (Figure 4(f)), as well as for the phenotypic characterization of VSN responses in animals with targeted mutations (Del Punta, K. *et al.*, 2000; Leypold, B. G. *et al.*, 2002) (Figures 3(e) and 5(f)). Finally, it is important to note that chemostimulation also causes a transient rise in the intracellular Ca^{2+} concentration of VSNs (Leinders-Zufall, T. *et al.*, 2000; Cinelli, A. R. *et al.*, 2002; Spehr, M. *et al.*, 2002; Leinders-Zufall, T. *et al.*, 2004) (Figures 4(g) and 4(h)). This stimulus-evoked Ca^{2+} response is used increasingly to identify molecular cues recognized by the VSNs and to determine VNO coding mechanisms (Figure 4(i) and see below).

Although these basic response properties have now been observed independently by several investigators, other experiments suggest that there are also differences in the properties of VSN sensory responses amongst species. For example, VSNs from turtle and lizard, respectively, have been shown to exhibit both inward and outward currents in response to chemostimulation (Fadool, D. A. *et al.*, 2001; Labra, A. *et al.*, 2005). In particular, the properties of the voltage-activated K^+ currents differ between VSNs from male and female animals (Fadool, D. A. *et al.*, 2001). Thus, a modicum of caution needs to be used for extrapolating cellular mechanisms in response to chemostimulation across species.

4.43.3.5 Signal Transduction Mechanisms

How do VSNs transduce a sensory stimulus into a change in membrane conductance? Increasing evidence indicates that this process depends on a G-protein-coupled second messenger cascade that ultimately leads to the activation of specific ion channels. Here, we will summarize the key results that led to our current understanding of this signaling cascade (Halpern, M. and Martinez-Marcos, A., 2003; Bigiani, A. *et al.*, 2005; Zufall, F. *et al.*, 2005).

An important development during the mid 1990s was the demonstration that VSNs and OSNs differ in their chemosensory signal transduction pathways. Several molecules that are essential for transduction

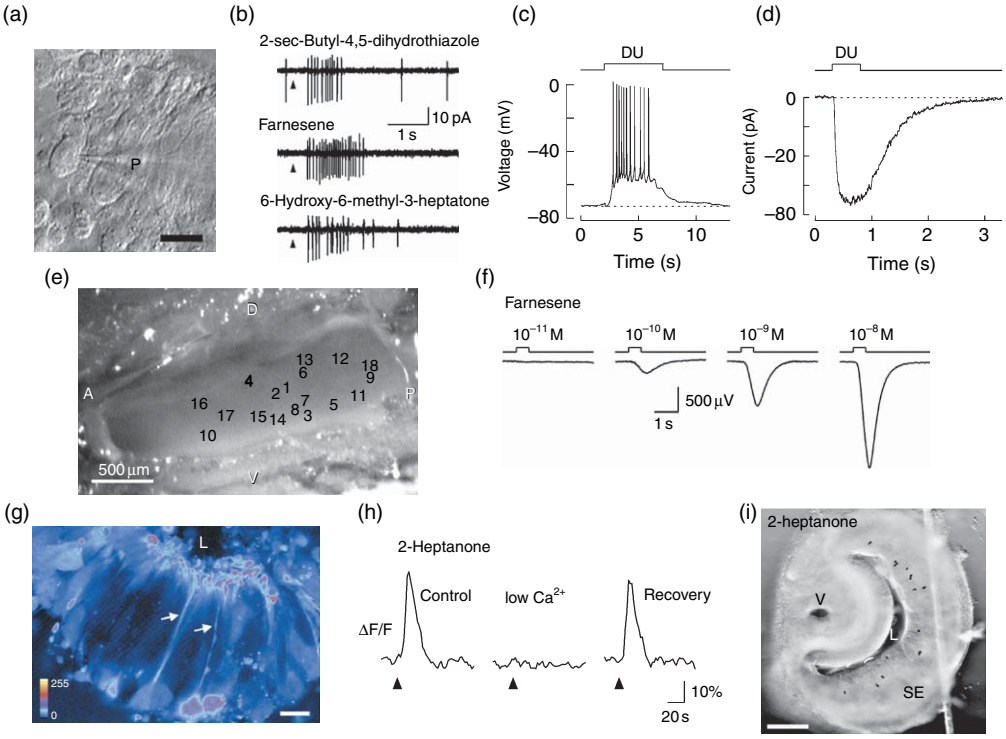

Figure 4 (a) Infrared–differential interference contrast micrograph showing a vomeronasal organ (VNO) tissue slice. Individual vomeronasal sensory neuron (VSN) somata are clearly visible. P, patch electrode. Scale bar = 10 µm. (b) Trains of extracellularly recorded, action-potential-driven, capacitive currents produced by bath application of 2-*sec*-butyl-4,5-dihydrothiazole, farnesene, or 6-hydroxy-6-methyl-3-heptanone (all at 10^{-7} M). Each response was from a different vomeronasal sensory neuron (VSN) using the approach shown in (a). Arrowheads, start of bath application (duration, 1–3 s). (c) Focal stimulation of a current-clamped VSN with dilute urine (DU) produces a depolarizing receptor potential leading to robust action potential discharges. (d) Under voltage clamp, 500-ms stimulation generates a rapidly activating and then deactivating inward current (the sensory current). Holding potential, −70 mV. (e, f) Image and electrovomeronasogram (EVG) responses of the microvillus surface of the vomeronasal sensory epithelium. Numbers in the image indicate the various sites at which field potentials (EVG responses) were recorded. 500-ms pulses of increasing concentrations of farnesene produced dose-dependent EVG responses. Ligands were focally applied to the microvillus surface of the sensory epithelium by a multibarreled stimulation pipette. A, anterior; D, dorsal; V, ventral; P, posterior. (g, h) Pheromone-induced Ca^{2+} elevations in single VSNs. (g) Confocal fluorescence image acquired at rest (pseudocolor scale) showing subcellular structures of VSNs such as single dendrites. Scale bar = 10 µm. (h) Waveform of somatic Ca^{2+} transient of a single VSN evoked by bath-applied 2-heptanone (10^{-7} M). The response was reversible abolished by lowering the Ca^{2+} concentration in the bath solution. (i) Spatial representation of functional, pheromone-induced activity in VNO. Reconstructed VSN response map ($\Delta F/F$ Ca^{2+} images digitally superimposed onto transmitted light image of the same slice) for 10^{-7} M 2-heptanone, showing that VSNs activated by this ligand (black dots) were interspersed within the apical zone of the sensory epithelium (SE). L, lumen; V, vein. Scale bar = 100 µm. (a, b, f, g, h, i) Reprinted from Leinders-Zufall, T., Lane, A. P., Puche, A. C., Ma, W., Novotny, M. V., Shipley, M. T., and Zufall, F. 2000. Ultrasensitive pheromone detection by mammalian vomeronasal neurons. Nature 405, 792–796, with permission from Nature Publishing Group. (c, d) Reprinted from Lucas, P., Ukhanov, K., Leinders-Zufall, T., and Zufall F. 2003. A diacylglycerol-gated cation channel in vomeronasal neuron dendrites is impaired in *TRPC2* mutant mice: mechanism of pheromone transduction. Neuron 40, 551–561, with permission from Elsevier. (e) Reprinted from Zufall, F., Kelliher, K. R., and Leinders-Zufall, T. 2002. Pheromone detection by mammalian vomeronasal neurons. Microsc. Res. Tech. 58, 251–260, with permission of Wiley.

in OSNs – the G protein G_{olf}, adenylyl cyclase type III, and the cyclic nucleotide-gated channel type A2 (CNGA2) subunit – are not present in the VNO sensory epithelium (Berghard, A. *et al.*, 1996; Wu, Y. *et al.*, 1996). Unlike OSNs, VSNs do not respond to cyclic nucleotides with a conductance change or Ca^{2+} rise (Liman, E. R. and Corey, D. P., 1996; Cinelli, A. R. *et al.*, 2002; but see also Taniguchi, M. *et al.*, 1996). The focus of interest therefore shifted toward the other major family of ion channels involved in sensory signal transduction, the transient receptor potential (TRP) channels. An important

advance came with the cloning of *TRPC2* from bovine, mouse, and rat (Wissenbach, U. *et al.*, 1998; Liman, E. R. *et al.*, 1999; Vannier, B. *et al.*, 1999; Hofmann, T. *et al.*, 2000). Because *TRPC2* encodes a protein that is expressed in all VSNs and specifically localized to the sensory microvilli of these cells (Figures 5(a) and 5(b)), it was proposed to participate in VSN sensory transduction (Liman, E. R. *et al.*, 1999; Menco, B. P. *et al.*, 2001). Many TRP channels, especially those of the classical TRPC subfamily, are known to depend on signaling pathways involving phospholipase C (PLC), an enzyme that hydrolyzes phosphatidylinositol-4,5-bisphosphate (PIP_2) into inositol 1,4,5-trisphosphate ($Ins(1,4,5)P_3$) and diacylglycerol (DAG) (Montell, C. *et al.*, 2002). Therefore, the localization of TRPC2 to VSN microvilli

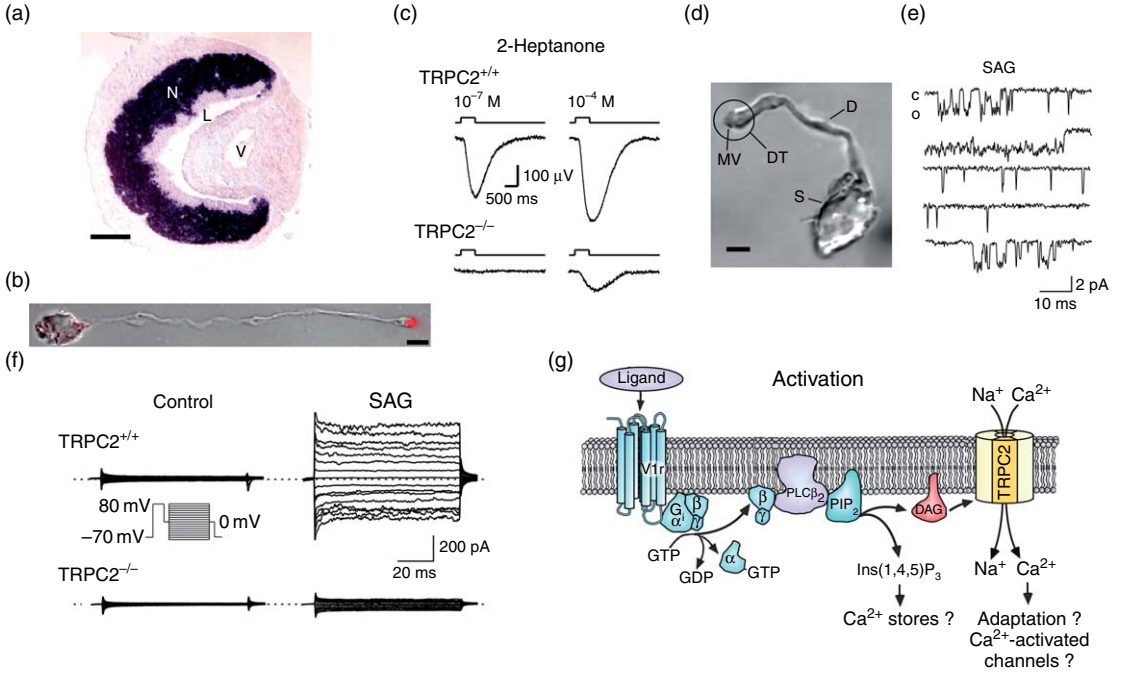

Figure 5 (a) Expression of TRPC2 in the vomeronasal organ (VNO). Labeling of a section of VNO from adult rat with a digoxigenin antisense probe directed against TRPC2 reveals strong expression (dark reaction product) of the TRPC2 mRNA in all VSNs (N). Scale bar = 100 μm. (b) In a singly dissociated vomeronasal sensory neuron (VSN), TRPC2 immunoreactivity (red) is clearly seen in the tuft of microvilli at the distal end of the dendrite. Scale bar = 5 μm. (c) Strongly diminished responses are observed in $TRPC2^{-/-}$ VSNs to 2-heptanone. Representative field potential responses from wild-type ($TRPC2^{+/}$) (upper) and $TRPC2^{-/-}$ mice (lower). Responses were induced by 500 ms pulses of 2-heptanone at 10^{-7} or 10^{-4} M, respectively. (d) Micrograph showing an isolated mouse VSN. D, dendrite; MV, microvilli; S, soma. Plasma membrane inside out patches were taken from the encircled area denoted as dendritic tip (DT) in experiments shown in (e). Scale bar = 3 μm. (e) The endogenous diacylglycerol analog 1-stearoyl-2-arachidonoyl-*sn*-glycerol (SAG) activates a 42-pS channel. Control recordings before SAG application showed no activity or only an occasional brief channel opening. Continuous application of SAG (10 μM) evoked single-channel events. (f) $TRPC2^{-/-}$ VSNs display a striking defect in the activation of the diacylglycerol-gated channel. Representative families of whole-cell currents to a series of depolarizing and hyperpolarizing voltage steps (as indicated in the figure) were recorded from an isolated wild-type (upper) and $TRPC2^{-/-}$ VSN (lower). VSNs were exposed successively to extracellular solution (control) and solution containing SAG (50 μM). Voltage-gated channels were blocked in these experiments. Dotted line, zero current level. (g) Schematic representation of pathways that might regulate the activity of the TRPC2 channel in the DT of a mammalian VSN. The model refers to VSNs of the apical zone of the VNO. Whether this applies also to VSNs of the basal zone remains to be investigated. (a, b) Reprinted from Liman, E. R., Corey, D. P., and Dulac, C. 1999. TRP2: a candidate transduction channel for mammalian pheromone sensory signaling. Proc. Natl. Acad. Sci. U. S. A. 96, 5791–5796, with permission from the publisher. (c) Reprinted from Leypold, B. G., Yu, C. R., Leinders-Zufall, T., Kim, M. M., Zufall, F., and Axel, R. 2002. Altered sexual and social behaviors in trp2 mutant mice. Proc. Natl. Acad. Sci. U. S. A. 99, 6376–6381, with permission from the publisher. (d–f) Reprinted from Lucas, P., Ukhanov, K., Leinders-Zufall, T., and Zufall F. 2003. A diacylglycerol-gated cation channel in vomeronasal neuron dendrites is impaired in TRPC2 mutant mice: mechanism of pheromone transduction. Neuron 40, 551–561, with permission from Elsevier. (g) Reprinted from Zufall, F., Ukhanov, K., Lucas, P., Liman, E., and Leinders-Zufall, T. 2005. Neurobiology of TRPC2: from gene to behavior. Pflügers Arch. 451, 61–71, with kind permission of Springer Science and Business Media.

suggested the use of a phosphoinositide signaling pathway for VSN transduction (Liman, E. R. *et al.*, 1999). Several studies have now provided evidence that PLC is indeed critical for the generation of sensory responses in VSNs (Inamura, K. *et al.*, 1997; Holy, T. E. *et al.*, 2000; Lucas, P. *et al.*, 2003).

Investigations of mice with targeted deletions in *TRPC2* have established an essential role of this gene in the detection of pheromonal stimuli by the VNO (Leypold, B. G. *et al.*, 2002; Stowers, L. *et al.*, 2002). In $TRPC2^{-/-}$ mice, pheromone-evoked EVG responses were either absent or strongly diminished, depending on stimulus concentration (Leypold, B. G. *et al.*, 2002) (Figure 5(c)). Likewise, action potential recordings showed that VSNs from $TRPC2^{-/-}$ mice are unable to respond to cues present in dilute urine (Stowers, L. *et al.*, 2002). Furthermore, $TRPC2^{-/-}$ mice showed striking defects in social behaviors (Leypold, B. G. *et al.*, 2002; Stowers, L. *et al.*, 2002), results that will be discussed in Section 4.43.5.

What kind of ion channel is formed by TRPC2? Although this question is still being investigated, evidence indicates that TRPC2 is required for a Ca^{2+}-permeable cation channel that is gated by the lipid messenger DAG or one of its endogenous analogs (Lucas, P. *et al.*, 2003). Excised patch recordings identified a 42-pS DAG-activated cation channel present in high density in the plasma membrane of dendritic knobs of VSNs and the activation of this channel is strongly defective in $TRPC2^{-/-}$ VSNs (Figures 5(d)–5(f)). Furthermore, the functional properties of this channel are consistent with those of the pheromone-evoked conductance (Lucas, P. *et al.*, 2003). Independent evidence that endogenously produced DAG may be a critical second messenger in the sensory response of VSNs comes from pharmacological blockade of DAG kinase, an enzyme involved in termination of DAG signaling (Lucas, P. *et al.*, 2003; Zufall, F. *et al.*, 2005). Thus a direct link between stimulus-induced PLC activity, gating of the TRPC2 channel by DAG, and the sensory current has been established (Figure 5(g)).

Several other second messengers such as Ca^{2+} or $Ins(1,4,5)P_3$ are likely to be involved in VSN signal transduction (Cinelli, A. R. *et al.*, 2002; Lucas, P. *et al.*, 2003). TRPC2 seems to form protein–protein interactions with the type III $Ins(1,4,5)P_3$ receptor (Brann, J. H. *et al.*, 2002) and biochemical studies in several species have reported increased $Ins(1,4,5)P_3$ levels in response to sensory stimulation of the VNO (Luo, Y. *et al.*, 1994; Kroner, C. *et al.*, 1996; Wekesa, K. S. and Anholt, R. R., 1997; Krieger, J. and Breer, H., 1999; Sasaki, K. *et al.*, 1999; Cinelli, A. R. *et al.*, 2002). Furthermore, flash photolysis of $Ins(1,4,5)P_3$ has been shown to excite frog VSNs (Gjerstad, J. *et al.*, 2003). One possibility is that $Ins(1,4,5)P_3$-induced Ca^{2+} release from intracellular stores (Lucas, P. *et al.*, 2003) leads to the opening of Ca^{2+}-dependent channels. These could be Ca^{2+}-activated cation channels, such as those found in hamster VSNs (Liman, E. R., 2003), or other Ca^{2+}-dependent channels. Such a mechanism could be involved in the primary sensory response, or it could mediate further amplification of this response. Even less clear than the roles of $Ins(1,4,5)P_3$ and Ca^{2+} are the proposed roles for arachidonic acid (Spehr, M. *et al.*, 2002) and cAMP (Halpern, M. and Martinez-Marcos, A., 2003) in VSN transduction. More information will be required to assess the precise function of these messenger molecules.

4.43.3.6 The Search for Sensory Stimuli

Understanding the functional role of the AOS requires identification of the sensory cues that are detected by the VSNs. It has been known since the 1970s that the mammalian VNO plays an essential role in the detection of stimuli of social nature, including some pheromone-like signals (Meredith, M. *et al.*, 1983; Halpern, M., 1987; Johnston, A. N. *et al.*, 1993); however, identification of the molecular nature of these stimuli proved surprisingly difficult. The advent of large-scale neurophysiological recording techniques in the VNO and AOB has enabled a more systematic search for vomeronasal stimuli. Surprisingly, the long held notion that VSNs detect only nonvolatile molecules appears an oversimplification of the systems function. VSNs show responses to a wider range of stimuli, including molecules that would not normally be categorized as pheromones. Additionally, it is now clear that many social recognition signals including some pheromones can also be detected by OSNs in the main olfactory system and that the mammalian main and AOSs detect, in part, overlapping sets of stimuli. Putatively, information about the same stimuli derived from each system is integrated in higher brain centers (Meredith, M., 1998; Boehm, T. and Zufall, F., 2006; Boehm, U. *et al.*, 2005; Shepherd, G. M., 2006; Spehr, M. *et al.*, 2006).

4.43.3.6.1 Stimulus access

Abundant evidence has shown that animals must actively enlarge the openings to the VNO and activate a pumping or suction mechanism to transport

chemical stimuli into the lumen of the VNO (Halpern, M., 1987; Wysocki, C. J. and Meredith, M., 1987). Work by Meredith and coworkers in hamster has established that the large blood vessels located within the VNO are capable of dilation and constriction and thus serve as a pumping mechanism that is activated in situations of novelty (Meredith, M., 1994). This vascular pump is under the control of sympathetic nerve fibers and interruption of these efferent nerves causes behavioral deficits similar to those produced by lesioning of the VNs (Meredith, M. and O'Connell, R. J., 1979; Meredith, M. *et al.*, 1980; Meredith, M. and O'Connell, J. M., 1988). There is now excellent evidence that activation of the VNO by appropriate stimuli can occur following direct physical contact of the nose with a stimulus source (Luo, M. *et al.*, 2003; Leinders-Zufall, T. *et al.*, 2004). Recordings from single neurons in the AOB of mice that were engaged in natural behaviors showed increased neuronal firing after physical contact with a conspecific (Luo, M. *et al.*, 2003) (see also Section 4.43.4). For nonvolatile cues such as peptide ligands, such physical contact is indeed required to reach sensory neurons in the nose in an *in vivo* situation (Leinders-Zufall, T. *et al.*, 2004; Spehr, M. *et al.*,2006). Volatile cues dissolved in bodily secretions will also reach the VNO following direct physical contact between the nose and a stimulus source. However, whether the VNO can detect such volatiles in the absence of direct physical contact remains debated (Luo, M. *et al.*, 2003; Trinh, K. and Storm, D. R., 2003). In at least one example, clear activation of the mouse AOB in vivo was observed in response to volatile stimuli that were delivered via the airstream (Xu, F. *et al.*, 2005).

4.43.3.6.2 Complex stimuli

To evoke sensory responses in the AOS, numerous researchers have tested complex natural communication stimuli such as urine, soiled bedding, vaginal secretion, and seminal fluid. Functional responses to these stimuli were monitored using a variety of techniques including immediate early gene expression in VNO and AOB (Halem, H. A. *et al.*, 1999; Kumar, A. *et al.*, 1999; Halem, H. A., *et al.*, 2001) or medial amygdala (Meredith, M. and Westberry, J. M., 2004), biochemical analysis of second messenger formation in VNO tissue (Wekesa, K. S. and Anholt, R. R., 1997), electrophysiological recording or Ca^{2+} imaging from single neurons in the VNO (Inamura, K. *et al.*, 1999; Holy, T. E. *et al.*, 2000; Spehr, M. *et al.*, 2002; Leinders-Zufall, T. *et al.*, 2004) or AOB (Luo, M. *et al.*, 2003), and functional magnetic resonance imaging (fMRI) of AOB (Xu, F. *et al.*, 2005). Although the details of the findings in these studies differ in many cases, taken together the evidence clearly shows that complex stimuli contain specific molecular cues that are recognized by VSNs. Particularly interesting data from single cell VSN recordings suggest that VSNs respond to cues present in urine that carry information about strain, species, and sex (Inamura, K. *et al.*, 1999; Holy, T. E. *et al.*, 2000). Recordings from single AOB neurons of freely behaving mice led to similar conclusions regarding the information content of vomeronasal stimuli (Luo, M. *et al.*, 2003). These latter authors also showed for the first time neuronal activity in response to active social investigation of anogenital or head/face regions of conspecifics of different genetic strains (Luo, M. *et al.*, 2003).

4.43.3.6.3 Urinary volatiles

Mouse urine contains hundreds of volatile compounds (Schwende, F. J. *et al.*, 1986; Novotny, M. V. *et al.*, 1999a) some of which have been associated with distinct endocrine or behavioral responses in conspecifics and are therefore considered prospective pheromones (see Section 4.43.5). A direct demonstration that at least some of these molecules directly activate VSNs came from a combination of EVG recording and Ca^{2+} imaging in VNO slices (Leinders-Zufall, T. *et al.*, 2000). The putative mouse pheromones 2,5-dimethylpyrazine, 2-*sec*-butyl-4,5-dihydrothiazole, 2,3-dehydro-*exo*-brevicomin, a mixture of E,E-α-farnesene and E-β-farnesene (referred to as farnesene), 2-heptanone, and 6-hydroxy-6-methyl-3-heptanone were potent sensory cues in the mouse VNO (Table 1) (Leinders-Zufall, T. *et al.*, 2000). VSNs responded to these compounds at nanomolar to subnanomolar concentrations, several orders of magnitude more sensitive than previously suspected. Activated VSNs were located in the apical, V1R-expressing layer of the VNO (Leinders-Zufall, T. *et al.*, 2000) (Figure 4(i)). Several other urinary volatiles including *n*-pentyl acetate and isobutylamine (Del Punta, K. *et al.*, 2002a; Trinh, K. and Storm, D. R., 2003) were subsequently identified as stimuli for mouse VSNs. Genetic ablation of a group of V1R genes showed an essential role for these receptors in the detection of 6-hydroxy-6-methyl-3-heptanone, *n*-pentyl acetate, isobutylamine, and 2-heptanone (Boschat, C. *et al.*, 2002; Del Punta, K. *et al.*, 2002a). Further evidence for the activity of these molecules derives from functional imaging in the AOB of intact mice showing that 2-heptanone activates the AOS (Xu, F. *et al.*, 2005).

Table 1 Structure, origin, and function of some urinary volatiles acting in the VNO

Name	*Chemical structure*	*Origin*	*Possible chemosignaling function in female mice*	*Detection threshold EVG response (M)*
2,5-Dimethylpyrazine		Female urine	Puberty delay[a]	10^{-8}–10^{-7}
2-*sec*-Butyl-4,5-dihydrothiazole	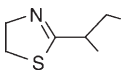	Male bladder, urine	Estrus synchronization[b], puberty acceleration[c]	10^{-10}–10^{-9}
2,3-Dehydro-*exo*-brevicomin	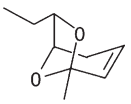	Male bladder, urine	Estrus synchronization[b], puberty acceleration[c]	10^{-10}–10^{-9}
α- and β-farnesenes	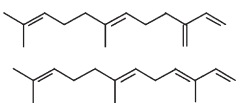	Male preputial gland	Puberty acceleration[c]	10^{-11}–10^{-10}
2-Heptanone	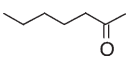	Female or male urine	Estrus extension[d]	10^{-11}–10^{-10}
6-Hydroxy-6-methyl-3-heptanone	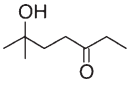	Male bladder urine	Puberty acceleration[e]	10^{-8}–10^{-7}

[a]Novotny M. *et al.* (1986).
[b]Jemiolo B. *et al.* (1986).
[c]Novotny M. V. *et al.* (1999b).
[e]Jemiolo B. *et al.* (1989).
[f]Novotny M. V. *et al.* (1999a).
EVG, electrovomeronasogram; VNO, vomeronasal organ.
Reprinted from Leinders-Zufall T., Lane A. P., Puche A. C., Ma W., Novotny M. V., Shipley M. T., and Zufall F. 2000. Ultrasensitive pheromone detection by mammalian vomeronasal neurons. Nature 405, 792–796, with permission from Nature Publishing Group.

4.43.3.6.4 General odors

Early studies indicated that VSNs are activated by a fraction of odorants without known pheromonal functions (Müller, W., 1971; Tucker, D., 1971). More recent investigations have confirmed and extended these findings (Sam, M. *et al.*, 2001; Trinh, K. and Storm, D. R., 2003). Functional imaging studies of the AOB used a mixture of six of the compounds reported by Sam M. *et al.* (2001) – methyl anisole, patchone, indole, helional, butyrophenone, and fenchone – to demonstrate that they stimulate the mouse AOB *in vivo* (Xu, F. *et al.*, 2005). Sam M. *et al.* (2001) suggested that these odorants could be released from plants or other animal species that may signal the presence of a predator or indicate the suitability of a particular site for feeding or nesting.

4.43.3.6.5 Major histocompatibility complex peptide ligands

A particularly surprising finding was the discovery that subsets of mouse VSNs are tuned to recognize members of a large family of immune system molecules known as the MHC peptide ligands (Leinders-Zufall, T. *et al.*, 2004). Together with the evidence presented above, this demonstrates that the mouse VNO can detect both volatile and nonvolatile cues. As pointed out by Boehm T. and Zufall F. (2006), MHC peptides are not considered pheromones according to the classical definition by Karlson P. and Lüscher M. (1959). Hence, the detection of MHC peptide ligands by VSNs shows that the VNO also plays important roles in the sensing of nonpheromonal chemical signals of social nature.

Table 2 Structure of peptide ligands acting in the VNO

MHC peptide ligands	*Other specific peptides*
AAPDNRETF[a]	SIPSKDALLK (sodefrin)[b]
SYFPEITHI[a]	SILSKDAQLK (silefrin)[c]
SYIPSAEKI[a]	1 ADQKTNHEADLKNPDPQEVQRALARILC ALGELDKLVKDQ 40
	41 ANAGQQEFKLPKDFTGRSK CRSLGRIK 67 (exocrine gland-secreting peptide 1)[d]

[a]Leinders-Zufall T. *et al.* (2004).
[b]Kikuyama S. *et al.* (1995).
[c]Yamamoto K. *et al.* (2000).
[d]Kimoto H. *et al.* (2005).
MHC, major histocompatibility complex; VNO, vomeronasal organ.

Immune system researchers have established a clear structural relationship between MHC molecules and their peptide ligands, which are usually nine amino acids long (Table 2; summarized in Boehm T. and Zufall F. 2006). MHC/peptide complexes present at the cell surface carry information about the genetic makeup of cells. They are shed from the cell surface and their fragments appear in bodily fluids such as serum, saliva, sweat, and urine (Singh, P. B. *et al.*, 1987). These truncated MHC molecules are thought to have a reduced affinity to their peptide ligands and are thus likely to release them into the extracellular space. The finding that the structural complexity of MHC peptide ligands can be sensed by neurons in the VNO suggests that this information is used for the sensory evaluation of the genotype of a conspecific, or in other words for the detection of genetic individuality (Boehm, T. and Zufall, F., 2006). Experiments in behaving mice strongly support this notion (Leinders-Zufall, T. *et al.*, 2004) (see Section 4.43.5). VSNs can sense MHC peptides at low concentrations, with detection thresholds near 10^{-12} M. Mapping studies in VNO slices combined with the use of immunocytochemical markers showed that MHC peptides are detected by VSNs in the basal layer (Leinders-Zufall, T. *et al.*, 2004). This indicates that VSNs of the apical and basal zones detect structurally and functionally distinct sets of molecular cues.

4.43.3.6.6 Other specific peptides

It is worth noting that a number of specific peptide pheromones have been identified previously in organisms as diverse as bacteria, fungi, mollusks, arthropods, and a variety of vertebrates (Altstein, M., 2004). Among vertebrates, maybe the best example comes from work in closely related newt species where the decapeptides sodefrin (SIPSKDALLK) and silefrin (SILSKDAQLK) have been shown to attract conspecific females (Kikuyama, S. *et al.*, 1995; Yamamoto, K. *et al.*, 2000) (Table 2), most likely via activation of their VNOs (Toyoda, F. and Kikuyama, S., 2000). More recently, in mice a male-specific 7 kDa peptide secreted from the extraorbital lacrimal gland has been shown to stimulate VSNs (Kimoto, H. *et al.*, 2005). This peptide (Table 2), which has been called exocrine gland-secreting peptide 1 (ESP1), seems to be encoded by a gene from a new multigene family consisting of at least 23 members (Kimoto, H. *et al.*, 2005). Although the behavioral role of ESP1 is not yet clear, these results together with those of Leinders-Zufall T. *et al.* (2004) indicate that social communication in mammals involves the detection of extended families of peptidergic chemosignals by the VNO.

4.43.3.6.7 Proteins

It has long been thought that VSNs can detect chemical signals of proteinaceous nature. The best evidence for protein detection by the VNO comes from work using snakes (Jiang, X. C. *et al.*, 1990; summarized in Halpern, M. and Martinez-Marcos, A., 2003) where a 20-kDa chemoattractant purified from earthworm shock secretions (known as ES20) has been shown to induce excitatory responses in VNO and AOB. This protein has been used extensively to characterize second messenger formation and signal transduction events in snake VSNs (Halpern, M. and Martinez-Marcos, A., 2003). Collectively, this work has shown that prey detection is a major function of the snake VNO. In a terrestrial salamander, a 22 kDa protein with structural homology to members of the interleukin-6 cytokine family has been shown to affect female receptivity but it is not yet clear whether this molecule is detected by the VNO (Rollmann, S. M. *et al.*, 1999).

Work in rodents also suggested an involvement of proteins in VNO sensing. Mouse urine contains a class of highly polymorphic proteins known as major urinary proteins (MUPs) that are implicated in individuality recognition (Hurst, J. L. *et al.*, 2001). It seems clear that MUPs bind urinary volatiles (Novotny, M. V. *et al.*, 1999a; Zidek, L. *et al.*, 1999) and release them from scent marks (Hurst, J. L. and Beynon, R. J., 2004). However, whether MUPs

devoid of their volatile ligands function as VSN stimuli as suggested by Mucignat-Caretta C. *et al.* (1995) and Cavaggioni A. and Mucignat-Caretta C. (2000) remains on open question (see Novotny, M. V. *et al.*, 1999a). Essentially, the same can be said about a protein isolated from hamster vaginal fluid known as aphrodisin (Singer, A. G. *et al.*, 1986). Like MUPs, aphrodisin belongs to the lipocalin superfamily and it remains unclear whether it functions as a carrier for small hydrophobic chemicals or as a pheromone in its own right (Briand, L. *et al.*, 2004a; 2004b).

4.43.3.7 Sensory Coding Strategies in the Vomeronasal Organ

In the main olfactory system, our current understanding is that OSNs respond to chemical epitopes that may be present on different odorant molecules, and that the tuning of main olfactory neurons is broad; that is, a single OSN responds to related chemical epitopes with different affinities. By contrast, mouse VSNs – at least those located in the apical layer of the VNO – show much narrower tuning properties. Specifically, VSN tuning curves to putative pheromone molecules do not seem to broaden with increasing concentrations of ligand and an increase in stimulus strength does not recruit activation of more neurons (Leinders-Zufall, T. *et al.*, 2000). Populations of VSNs also exhibit strong selectivity for either male or female urine, although the molecules underlying this response are unknown (Holy, T. E. *et al.*, 2000). Thus, if OSNs in the MOE are hypothesized to be epitope sensors, VSNs of the apical zone might be considered molecule detectors for single putative pheromones. However, not all VSNs in apical and basal zones may employ the same strategies for encoding socially relevant chemosignals. For example, work using the MHC peptide ligands as sensory stimuli has clearly shown that a given basal VSN can detect multiple peptides exhibiting distinct chemical structures (Leinders-Zufall, T. *et al.*, 2004). Furthermore, the vast structural repertoire of the family of MHC peptide ligands argues against a one cell–one receptor–one ligand strategy but rather for the existence of some kind of combinatorial coding mechanism in peptide-detecting VSNs. Thus, mammalian VSNs may employ a variety of coding strategies. Similar conclusions were reached by analyzing sensory responses to complex stimuli from lizard VSNs (Labra, A. *et al.*, 2005).

4.43.4 The Accessory Olfactory Bulb

4.43.4.1 Inputs from the Vomeronasal Organ

VSNs within the VNO project axons that traverse along the nasal septum, through the cribriform plate, along the medial surface of the main olfactory bulb (MOB), and terminate exclusively in the AOB (Figure 2(f)). In rodents, the AOB is located at a dorsocaudal position relative to the MOB (Figures 1(a), 2(a), and 2(f)). The fascicles of axons comprising this VN are distinct from those fascicles innervating the MOB (Halpern, M., 1987). These axons pass through the nerve fiber layer (aONL) of the AOB and converge to glomeruli in the accessory glomerular layer (aGL) (Figure 6). Unlike the MOB where glomeruli are large (50–100 μm diameter) and organized into a distinct layer one to two glomeruli thick segregated by numerous juxtaglomerular cells, AOB glomeruli are smaller (10–50 μm diameter), numerous, poorly separated by juxtaglomerular cells, and distributed in a loosely organized layer that is many glomeruli thick. Early studies using cell surface antigens showed that the projections from the VNO segregated into two zones, an anterior and a posterior zone (Mori, K. *et al.*, 1985; Mori, K., 1987; Schwarting, G. A. and Crandall, J. E., 1991; Takami, S. *et al.*, 1992b; Osada, T. *et al.*, 1994). Recent studies demonstrated that these anterior and posterior zones receive input from distinct classes of VSNs (Halpern, M. *et al.*, 1995; Rodriguez, I. *et al.*, 1999; Del Punta, K. *et al.*, 2002b). VSNs located apically in the VNO sensory epithelium expressing the V1R receptor family and the G protein $G\alpha_{i2}$ (described above) project to the anterior aGL domain, while VSNs located basal expressing the V2R receptor family and the $G\alpha_o$ G protein project axons into the posterior aGL domain.

In the main olfactory system, OSNs expressing the same odor receptor gene project to only two or a few glomeruli in each bulb (Rodriguez, I. *et al.*, 1999; Del Punta, K. *et al.*, 2002b). However, unlike the high degree of axon convergence in the MOB, VSNs expressing the same receptor gene project to multiple glomeruli in either the anterior or posterior domain of the AOB (six to 20 glomeruli per gene have been reported; Belluscio, L. *et al.*, 1999; Rodriguez, I. *et al.*, 1999; Del Punta, K. *et al.*, 2002b). The distribution of these multiple glomeruli within each domain exhibits a high degree of variability compared to the convergence and position of glomeruli in the MOB, but there is a general similarity across animals.

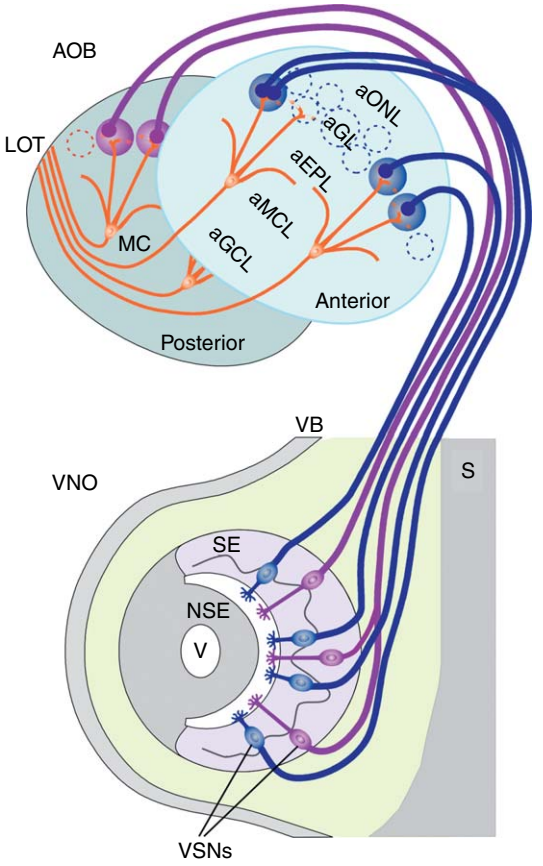

Figure 6 Diagram showing the mosaic projection of vomeronasal sensory neurons (VSNs). The sensory epithelium (SE) is segregated into two distinct zones, both of which express a unique set of transduction-related molecules: (1) an apical zone (blue VSNs) that expresses the G protein $G\alpha_{i2}$ as well as members of the V1R family of vomeronasal receptors, and (2) a basal zone that characteristically contains VSNs (purple) that express $G\alpha_o$ and members of the V2R receptor family. Unlike the main olfactory bulb, VSNs expressing the same receptors project to multiple glomeruli in the AOB, and AOB mitral cells (MC) innervate multiple glomeruli. The AOB can be further divided into mainly five layers depending on the cell types present, that is, the accessory olfactory nerve layer (aONL), accessory glomerular layer (aGL), the accessory external plexiform layer (aEPL), the accessory mitral cell layer (aMCL), and the accessory granule cell layer (aGCL). LOT, lateral olfactory tract; NSE, nonsensory epithelium; S, septum; V, blood vessel; VB, vomer bone.

4.43.4.2 Functional Organization of the Accessory Olfactory Bulb

With respect to circuit organization, the AOB appears quite similar to the MOB; however, there are points of significant differences in the arrangement of circuits in the AOB. Within each glomerulus, VSN axons synapse onto the dendrites of mitral, tufted, and juxtaglomerular neurons. Electrophysiological studies in tissue slices demonstrated that, similar to OSNs in the main olfactory system, glutamate is the primary VSN neurotransmitter (Dudley, C. A. and Moss, R. L., 1995; Jia, C. *et al.*, 1999). Glutamatergic transmission from the VSN to postsynaptic target neurons is heavily dependent on alpha-amino-3-hydroxy-5-methyl-4-isoxazolepropionic acid (AMPA)/kainate receptors for fast postsynaptic responses, and on *N*-methyl-D-aspartate (NMDA) receptors for slower components of the response (Dudley, C. A. and Moss, R. L., 1995; Jia, C. *et al.*, 1999). AOB mitral cell responses in the awake animal consist of a gradual elevation in firing rate over 2–5 s following contact with a stimulus, for example, anogenital investigation (Luo, M. *et al.*, 2003). The slowly evolving elevation of firing rate is in sharp contrast to other sensory systems such as vision, auditory or somatosensory where the precise timing of stimulus-triggered responses are highly conserved. However, the slow evolution of activity in the AOB mitral cell is consistent with the nature of odor access and receptor kinetics discussed above. The relatively slow characteristics of olfactory responses could allow for significant temporal evolution of local inhibitory feedback and cortical feedback during the detection event, as postulated by Laurent and coworkers for the main olfactory system (for a review, see Laurent, G., 2002).

VSNs expressing the same receptor gene project to the AOB in a complex, multiglomerular pattern, but how is this complex glomerular projection pattern read by the AOB? The major output neuron of the AOB, the mitral cell, has a strikingly different structure to mitral cells of the MOB. It has been known for nearly a century that AOB mitral cells possess multiple apical dendrites, upto five, that each ramify within a different glomerulus (Cajal, R. S., 1911; Takami, S. and Graziadei, P. P., 1990; 1991) (Figure 7(a)). It was thought for many years that this multiglomerular organization of mitral cell dendrites allowed for sampling from different glomeruli and thus presumably different olfactory specificity; a cross-modality model. A logical prediction of this idea is that AOB mitral cells would be broadly tuned, capable of responding and integrating different kinds of vomeronasal input. A blend of pheromonal compounds could thus be integrated in the context of relative intensity of input by concurrent activation of glomeruli with different receptor identity. A difficulty with such a model is the requirement that mitral cell dendritic connectivity between different glomeruli precisely match

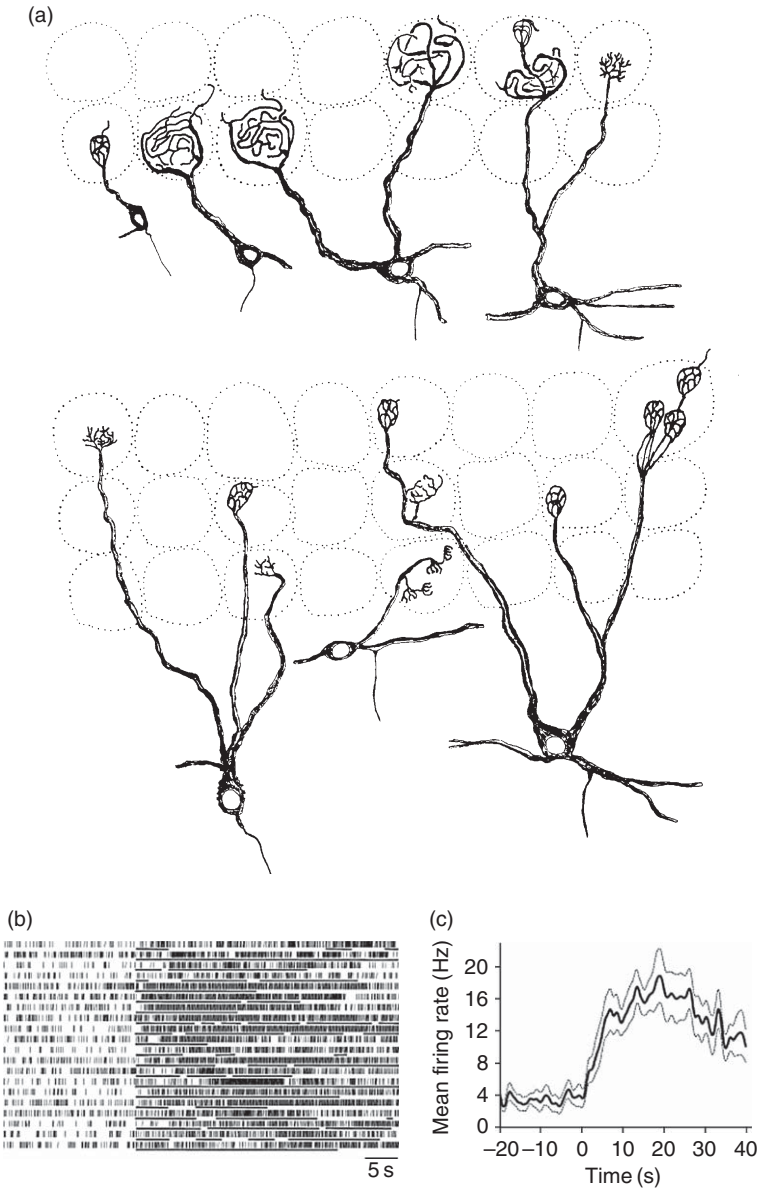

Figure 7 (a) Schematic drawing of accessory olfactory bulb (AOB) mitral and tufted cells. These cells have between one and five apical dendrites that terminate in different glomeruli. (b, c) Response kinetics of AOB neurons in the awake mouse. (b) Raster plots of the activation patterns of 14 AOB cells. Plots are aligned with the initiation of the first direct contact. Black bars beneath rasters represent periods of direct contact between the snout of test animals and the body of stimulus animals. (c) Plot of the mean firing rate (thick black line) from the AOB cells shown in (b). The thin gray lines represent ± 1 SEM. The activity of the AOB cells gradually increased following the initiation of active investigation, which is unlike the main olfactory bulb (MOB) neurons that respond invariably to odor ligands with rapid and abrupt changes in firing frequency. (a) Reprinted from Takami, S. and Graziadei, P. P.1991. Light microscopy Golgi study of mitral/tufted cells in the accessory olfactory bulb of the adult rat. J. Comp. Neurol. 311, 65–83, with permission from Wiley. (b, c) reprinted with permission from Luo, M., Fee, M. S., and Katz, L. C. 2003. Encoding pheromonal signals in the accessory olfactory bulb of behaving mice. Science 299, 1196–1201, AAAS.

biologically relevant pheromonal blends, a formidable problem of wiring specificity.

However, it was recently shown that the divergent pattern of VSN projections into the AOB could be rendered convergent due to the multiple glomerular projections of the mitral cell (Del Punta, K. *et al.*, 2002b). This study suggested that at least some of the mitral cell multiple processes, but not all, innervate glomeruli that receive axons from the same population of VSNs (Del Punta, K. *et al.*, 2002b).

The convergence of VSNs with the same receptor gene and presumably the same receptive field to a single mitral cell challenges the notion that AOB mitral cells would show a cross-modal response by integrating different sensory stimuli. Instead, AOB mitral cell response profiles may closely match those of the VSNs, modified by spatiotemporal circuit processing in the AOB; a labeled-line model. Because mouse VSNs, at least those of the apical layer, exhibit a narrow receptive field tuned to a single putative pheromone even at a wide range of concentrations (as discussed in the preceding section), a labeled line predicts that AOB mitral cells should thus exhibit similar narrow response profiles and that increasing concentrations of ligand will not recruit additional mitral cells. Elegant work by Luo M. and Katz L. C. (2004) in awake, behaving mice tested these predictions. Single unit recordings from the mitral cell layer of the awake, behaving mouse showed a high degree of selectivity for sex and strain of animal used as the stimulus (Luo, M. *et al.*, 2003; Luo, M. and Katz, L. C., 2004) (Figures 7(b) and 7(c)). The high selectivity of AOB mitral cell physiological responses supports the notion of a labeled line from VSN to AOB mitral cell.

What then is the benefit of a divergent VSN projection that is subsequently rendered, at least in part, convergent at the AOB mitral cell? One possibility is that the formation of multiple glomeruli of the same receptor type may be important for enhancing signal to noise via glomerular level lateral inhibition. Multiple small glomeruli of the same type are adjacent to a greater number of other receptor type glomeruli compared to a single large glomerulus such as present in the MOB. In the MOB an extensive lateral interglomerular network allows for integration between numerous different receptor type glomeruli (Aungst, J. L. *et al.*, 2003); however, there does not appear to be such a long-range interglomerular network in the AOB (unpublished observations). The ensemble of multiple glomeruli of the same receptor type with only short interglomerular neuronal connections would still have the potential for extensive and diverse lateral inhibition compared to a single glomerulus of larger size. Luo M. and Katz L. C. (2004) observed inhibition that does not require preceding excitation, suggesting the presence of selective lateral inhibition. The authors attribute this to selective lateral inhibition at the level of granule–mitral–granule cell connections (discussed below), but the observation is also consistent with glomerular lateral inhibition.

Together, the recent studies on VNO and AOB support the notion that VNO–AOB follows a labeled line neural encoding strategy rather than a cross modality, and that AOB mitral cells could act as functional modules. Further evidence for the role of AOB mitral cells as functional units comes from recent cellular physiology experiments (Lowe, G., 2003; Urban, N. N. and Castro, J. B., 2005). Calcium imaging and paired dendritic recordings were used to show action potentials in AOB mitral cells back propagate without attenuation through the entire dendritic tree (Ma, J. and Lowe, G., 2004). This active nondecremental back propagation could assist in coordinating activity of all the mitral cells projecting to the same glomerulus. In the MOB mitral cells projecting to the same glomerulus show synchronous membrane oscillations that are likely to depend on intraglomerular coupling between the cells (Carlson, G. C., *et al.*, 2000; Schoppa, N. E. and Westbrook, G. L., 2001; 2002). If a similar coupling exists in the AOB the nonattenuating back propagation of action potentials would contribute to binding all the mitral cells of that glomerulus into a single responsive unit.

4.43.4.2.1 Interneurons

The AOB contains a sparse population of juxtaglomerular cells located between glomeruli, although relatively little is known about these cells. Golgi studies show the dendrites of these AOB juxtaglomerular cells ramify in the aGL (Cajal, R. S., 1911) and can be categorized into periglomerular (PG) neurons and tufted cells. Immunohistochemistry shows the presence of larger glutamate containing cells, presumably the tufted cells, and smaller γ-aminobutyric acid (GABA)-containing cells, presumably the inhibitory PG neurons (Takami, S. *et al.*, 1992a; Quaglino, E. *et al.*, 1999). The role of these interneurons is presumed to be similar to the MOB, although no studies have yet examined these cells in detail. Any role of these cells is, however, likely to be local to one or neighboring glomeruli as there is no indication of the extensive interglomerular network present in the MOB (unpublished observations).

AOB granule cells are a numerous population of GABAergic inhibitory neurons located in the deep layers of the AOB. Unlike the MOB the mitral and granule cell layers are less distinct in the AOB, with mitral and granule cells intermingled through the broad mitral cell layer, and dispersed granule cells present throughout the deeper granule cell layer. In general, MOB olfactory bulb granule cells are thought to play

two roles in the olfactory circuit; feedback inhibition of mitral cells and lateral inhibition between mitral cells. AOB mitral cells have lateral dendrites that run for hundreds of microns, significantly shorter than the multimillimeter lengths of MOB mitral cell lateral dendrites (Cajal, R. S., 1911; Takami, S. and Graziadei, P. P., 1990; 1991). However, as the AOB is smaller than the MOB the fraction of AOB within reach of the mitral lateral dendrites is very high. AOB granule cell dendrodendritic connections with mitral cells can be formed with the lateral dendrites or with the basal portions of the apical dendrites which, given the considerable distances that these lateral/apical dendrites can project, still allows for either feedback or lateral inhibition between diverse AOB mitral cells. Shepherd and co-workers using field potential and whole-cell recordings in AOB slices showed activation of the VN results in a sequence of neural responses in the AOB that is consistent with VN stimulation of mitral cells, followed by mitral cell dendrodendritic excitation of granule cells and subsequent reciprocal inhibition of mitral cells by granule cell GABA release (Jia, C. *et al.*, 1999). This work demonstrated the basic reciprocal mitral–granule–mitral inhibition circuit follows the same principles as the MOB. Mitral–granule–mitral lateral inhibition is also present in the AOB. Mitral cell inhibitory responses can occur without a preceding excitatory response in that cell, consistent with lateral inhibition from a distant excited mitral cell (Luo, M. *et al.*, 2003).

There have been numerous studies examining the patterns of neural activation using increased expression of c-fos (an immediate early gene) as an activity marker following stimulation with different strain/sex mouse urine/odor (for review Halpern, M. and Martinez-Marcos, A., 2003 and reference therein). These stimuli evoke c-fos activity in cells across all layers of the bulb, particularly in the granule and mitral layers. The dispersed location of mitral cells together with the inherent difficulties of attributing c-fos staining in nuclei to a particular cell type, make the mapping of AOB mitral cell activity problematic. However, these studies clearly show extensive c-fos activity in the granule cell layer which is consistent with the notion that there is extensive feedback and lateral inhibition shaping AOB output.

4.43.4.2.2 Subdivisions

The anterior and posterior domains of the AOB receive input from different populations of VSNs that express different families of receptor genes; thus, it is seems likely that different stimuli may elicit responses from only one of the two AOB domains. Although c-fos responses to natural stimuli are generally dispersed throughout the AOB there are reports of preferential activity to a species/sex difference in the rostral domain (Matsuoka, M. *et al.*, 1999). Optical imaging and field potential recordings of AOB slices showed electrical stimulation of the anterior aONL elicited activity from the anterior internal plexiform layer. Stimulation of parts of the posterior aONL suggest this region is further subdivided into a rostral two-thirds and caudal one-third AOB domain (Sugai, T. *et al.*, 2000). Additional evidence for these further divisions comes from recent genetic tract tracing showing a VSN–VR population projecting into a restricted middle part of the bulb, putatively into the more rostral part of the posterior division (Mombaerts, unpublished observation).

4.43.4.3 Outputs of the Accesory Olfactory Bulb

Track tracing studies from the 1960s and 1970s demonstrated that the central connections of the AOB and MOB to higher order olfactory structures are essentially nonoverlapping. These observations lead to the hypothesis that the AOB and MOB pathways would serve different functional roles (Winans, S. S. and Scalia, F., 1970; Raisman, G., 1972; Scalia, F. and Winans, S. S., 1975). Subsequent research over the past 30 years has clarified many behavioral roles that are specific to vomeronasal function (several example effects are discussed in Section 4.43.5). The AOB has direct projections (Figure 8) to the medial (Me) and posteromedial cortical amygdaloid nucleus (PMCo), the BST, and the BAOT (Scalia, F. and Winans, S. S., 1975; de Olmos, J. *et al.*, 1978; Shipley, M. T. and Adamek, G. D., 1984). Together these structures can be called the accessory olfactory cortex (AOC). A recent examination of higher cortical projections from the anterior and posterior domains of the mouse AOB concluded both domains project into the same brain regions (Sugai, T. *et al.*, 2000). However, mitral cells in the opossum anterior AOB appear to project into deep cell layers of the medial amygdaloid complex (corresponding to the ventral division of the medial amygdala in rats) while the posterior AOB domain mitral cells project only into the superficial layers (Martinez-Marcos, A. and Halpern, M., 1999). Opossum mitral cell projections from the different domains of the AOB to the other AOC structures were essentially overlapping (Martinez-Marcos, A. and Halpern, M., 1999). These data show the

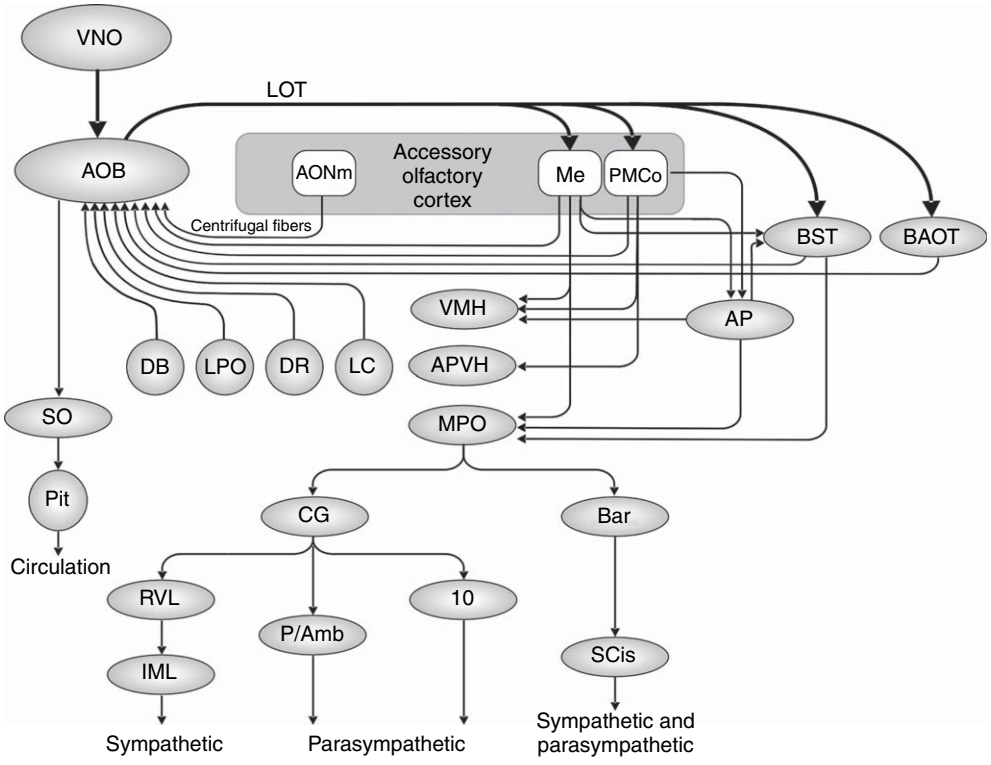

Figure 8 Diagrammatic representation of the connections of the accessory olfactory bulb (AOB) with cortical and subcortical structures. The major outputs of the AOB along the lateral olfactory tract (LOT) are shown at the upper part of the diagram. The major centrifugal inputs from the cortical regions back to the olfactory bulb are shown centrally along with higher-order connections. Emphasis is placed on possible circuits that mediate output responses such as autonomic, behavioral, or hormonal changes. 10, dorsal motor nucleus of the vagus; AOB, accessory olfactory bulb; AONm, anterior olfactory nucleus, medial division; AP, posterior amygdaloid nucleus; APVH, anterior periventricular hypothalamus; BAOT, bed nucleus of the lateral olfactory tract; Bar, Barrington's nucleus; BST, bed nucleus of the stria terminalis; CG, central (periaqueductal) gray; DB, nucleus of the diagonal band; DR, dorsal raphe nucleus; LC, locus coeruleus; LPO, lateral preoptic area; Me, medial amygdaloid nucleus; MPO, medial preoptic area; P/Amb, nucleus ambiguous and periambigual area; PMCo, posteromedial cortical amygdaloid nucleus; Pit, pituitary; RVL, rostroventrolateral medulla; SCis, lumbosacral spinal cord; SO, supraoptic nucleus; VMH, ventromedial hypothalamic nucleus; VNO, vomeronasal organ.

divergence into segregated pathways in the AOB generally, with some species differences, converge to the same higher brain regions.

The structures comprising the AOC are complex in organization and innervate many cortical and subcortical structures throughout the central nervous system (CNS). For example, the medial amygdala is a complex heterogeneous structure that is partitioned into at least four regions on the basis of cytoarchitecture, neurotransmitter content, hormone receptor expression, connections and putative functions (for a review, see Paxinos, G., 2004). The amygdala is a neural structure thought to be heavily involved in emotive states including behaviors such as mating and aggression behaviors in rat. The Me and PMCo have projections to other amygdaloid nuclei, notably the posterior amygdaloid nucleus (AP) (Canteras, N. S. *et al.*, 1992), and to the medial preoptic area and the hypothalamus (for a review, see Shiosaka, S. *et al.*, 1982). The AP appears to receive convergent input from both the Me and PMCo and projects heavily upon some of the same structures targeted by Me and PMCo, namely the medial preoptic area and the ventromedial hypothalamic nucleus. Some of these secondary olfactory connections strongly influence sexual drive. The posterodorsal part of Me (MePD) contains neurons that project to four cell groups that are known to be sexually dimorphic and differ in their roles in reproduction. The medial preoptic area (MPO) is one of the sexually dimorphic targets of MePD and lesions of MPO decreases male copulatory behavior (for review Simerly, R. B. *et al.*, 1989). These higher-order connections of the AOB are highly consistent with roles for VNO function in

mating, species recognition, and aggression. Indeed, studies of c-fos expression following mating in the AOB and higher brain regions by many investigators clearly establishes a link for vomeronasal activity in this behavior (Brennan, P. A. *et al.*, 1992; Fernandez-Fewell, G. D. and Meredith, M., 1994; Halem, H. A. *et al.*, 1999; Fewell, G. D. and Meredith, M., 2002).

4.43.4.4 Centrifugal Afferents to the Accessory Olfactory Bulb

The AOB receives heavy centrifugal inputs from higher brain regions (Figure 8), although from fewer sites than the MOB. The major olfactory cortex afferents to AOB are from the BST, the nucleus of the accessory olfactory tract, the Me, and the PMCo (de Olmos, J. *et al.*, 1978; Shipley, M. T. and Adamek, G. D., 1984). A restricted part of the medial division of AON sends a dense projection to the granule cell layer of AOB (Rizvi, T. A. *et al.*, 1992), but all other divisions of AON lack connections with AOB. Several of these structures (e.g., the amygdala) receive input from the AOB and thus are situated to provide a potential rapid feedback circuit with the AOB.

There are also extensive nonolfactory modulatory inputs to the AOB arising from the nucleus of the diagonal band (DB), lateral preoptic area, median and dorsal raphe, and the locus coeruleus (LC). The terminal distribution of these common inputs differs in AOB and MOB, especially with respect to the cholinergic inputs from the DB and serotonergic inputs from the LC. The cholinergic–serotonergic inputs to AOB are mainly to the granule cell layer and internal plexiform layer and only sparsely to the glomerular layer, whereas in the MOB glomeruli are heavily innervated (McLean, J. H. and Shipley, M. T., 1987; Le Jeune, H. and Jourdan, F., 1991). These fibers are thought to target PG cells in the MOB (McLean, J. H. and Shipley, M. T., 1987), as the AOB has fewer PG cells this may account for the paucity of serotonin and acetylcholine innervation of the AOB glomerular layer. The roles of these extensive centrifugal fiber tracts in circuit processing in the AOB (and the MOB) are largely unknown.

4.43.5 Mechanisms of Behavior

Following the pioneering work of Powers J. B. and Winans S. S. (1975), a vast number of studies have been published on the role of the VNO and AOS in behavioral responses using a variety of animal models such as hamsters, voles, mice, rats, farm animals, and reptiles. This work has been summarized previously and the reader is referred to several extensive reviews (Meredith, M., 1983; Wysocki, C. J. and Meredith, M., 1987; Halpern, M., 1987; Johnston, R. E., 2000; Halpern, M. and Martinez-Marcos, A., 2003). Here, we will focus on only a few selected functions of the AOS for which the evidence seems particularly well established. Most recently, it has become clear that the mammalian main and AOSs detect, at least in part, overlapping sets of sensory stimuli (see Spehr, M. *et al.*, 2006) and that both systems play important roles in the regulation of social behaviors and the sensing of pheromone-like chemical signals. Consequently, it has been suggested that the main olfactory and vomeronasal systems should be viewed as complementary rather than separate pathways for chemical communication (Brennan, P. A. and Keverne, E. B., 2004; Shepherd, G. M., 2006). Current work is focusing on a dissection of the different nasal subsystems in behavioral responses using a combination of gene-targeting methods and more classical lesioning approaches. However, this goal is proving more difficult than previously thought because of the growing complexity of the function of the mammalian nose in chemosensory communication and the fact that each method exhibits specific limitations. For example, surgical removal of the VNO (VNX) also leads to removal of the terminal nerve system (Wysocki, C. J. and Meredith, M., 1987; Wysocki, C. J. and Lepri, J. J., 1991) and lesioning of the MOE by application of zinc sulphate is often incomplete. Similarly, the use of gene-targeted animals can involve a number of limitations. For example, deletion of the ion channel TRPC2 causes a dramatic loss in VSN sensitivity rather than a total loss of function (Leypold, B. G. *et al.*, 2002) and deletion of the CNGA2 subunit as a method to disrupt signaling in the main olfactory epithelium is likely to cause other deficits in the CNS (Mandiyan, V S. *et al.*, 2005). Furthermore, the role of these signal transduction molecules in additional olfactory subsystems (Figure 2(a)) such as the guanylyl cyclase type (GC-D) cell system (Zufall, F. and Munger, S. D., 2001), the septal organ of Masera (Tian, H. and Ma, M., 2004), and the Grueneberg ganglion (Fuss, S. H. *et al.*, 2005; Storan, M. J. and Key, B., 2006) is not yet clear. Thus, we must be careful in the interpretation of behavioral results based on the use of either method and in most cases, only a combination of methodological approaches, together with parallel analysis at the cellular level, will provide definitive answers. Table 3 shows a comparison of behavioral impairments caused by surgical VNO ablation or genetic manipulation of VSNs.

Table 3 Behavioral impairments, relative to wild type, caused by surgical ablation of VNO or genetic manipulation of VSNs

Phenotype	*VNO ablation*[a]	*Trp2*$^{-/-}$[b,c]	*V1Rab*$^{-/-}$[d]	*β2m*$^{-/-}$[e]	$G\alpha_{i2}^{-/-}$[f]
Male sexual behavior directed to females	Reduced, fewer mounts and longer latency, experience-dependent	Normal	Reduced drive to initiate sexual behavior	Not reported	Normal
Male sexual behavior directed to males	Not reported	Increased	Normal/reduced	Normal	Normal
Male ultrasonic vocalizations to females	Eliminated/reduced, experience-dependent	Normal	Normal	Not reported	Not reported
Male ultrasonic vocalizations to males	Eliminated/reduced, experience-dependent	Increased	Not reported	Not reported	Not reported
Male aggression to intruder male	Eliminated	Eliminated	Normal	Eliminated	Reduced, depends on genetic background
Maternal aggression to intruder male	Eliminated	Eliminated	Eliminated	Not reported	Eliminated/reduced

[a]Lepri J. J. and Wysocki C. J. (1987).
[b]Leypold B. G. *et al.* (2002).
[c]Stowers L. *et al.* (2002).
[d]Del Punta K. *et al.* (2002a).
[e]Loconto J. *et al.* (2003).
[f]Norlin E. M. *et al.* (2003).
VNO, vomeronasal organ; VSN, vomeronasal sensory neuron.
Reprinted from Brennan, P. A. and Keverne, E. B. 2004. Something in the air? New insights into mammalian pheromones. Curr. Biol. R81–R89, with permission from Elsevier.

4.43.5.1 Detection of Heterospecific Signals

Work in the AOS of snakes has provided the best example that the VNO can be involved in the initiation of behavioral responses to both social and nonsocial chemical cues. The role of the snake VNO in prey recognition and response to prey odors has been especially well documented (Halpern, M., 1987; Halpern, M. and Martinez-Marcos, A., 2003; Baxi, K. N. *et al.*, 2006). Snakes with lesioned VNs stop following prey odor trails and eventually stop eating prey (Halpern, M., 1987). As pointed out by Baxi K. N. *et al.* (2006), heterospecific stimuli such as those involved in foraging cannot be considered pheromones.

4.43.5.2 Male Aggression to Intruder Males

In rodents, one of the best examples for a role of the VNO in the regulation of social behaviors comes from work on intermale aggression in mice using a resident–intruder assay. In this assay, a male intruder is added to the home cage of a singly housed test mouse. After initial olfactory exploration, a wild-type resident mouse will initiate vigorous attacks against the intruder. The involvement of the VNO in this type of aggression is clearly demonstrated by several studies using surgical VNO ablations (Clancy, A. N. *et al.*, 1984; Wysocki, C. J. and Lepri, J. J., 1991; Halpern, M. and Martinez-Marcos, A., 2003). An excellent correspondence (Table 3) exists between these studies and more recent work that employed mice with a targeted mutation in the cation channel gene TRPC2, also showing absence or strong reduction of male–male aggression (Leypold, B. G. *et al.*, 2002; Stowers, L. *et al.*, 2002). Consistent with these findings, TRPC2-deficient mice fail to establish territorial dominance relationships (Leypold, B. G. *et al.*, 2002). Together, these results demonstrate the importance of the VNO in sensing male chemosignals and initiating an appropriate aggressive response.

4.43.5.3 Maternal Aggression to Intruder Males

The correspondence between the behavioral effects of the TRPC2 deletion and surgical VNO ablation is also very good in the context of maternal aggression (Table 3). Female mice are usually not aggressive toward intruders, but lactating females vigorously attack intruder males (Gandelman, R. *et al.*, 1972). Ablation of the VNO eliminates the display of maternal aggression (Bean, N. J. and Wysocki, C. J., 1989; Wysocki, C. J. and Lepri, J. J., 1991) and this aggression is also absent in TRPC2$^{-/-}$ females (Leypold, B. G. *et al.*, 2002). Similarly, maternal aggression is substantially reduced in mice lacking a cluster V1R receptor genes (V1rab$^{-/-}$, Del Punta, K. *et al.*, 2002a) as well as in Gα_{i2} mutant mice (Norlin, E. M. *et al.*, 2003). Thus, it seems clear that the loss of specific sensory inputs in the VNO causes a loss of the display of maternal aggression in mice. Interestingly, although the V1rab$^{-/-}$ mice fail to initiate maternal aggression, there are no differences in male–male aggression compared with control mice (Del Punta, K. *et al.*, 2002a). This suggests that different male chemosignals might be responsible for triggering aggression in males and females (Brennan, P. A. and Keverne, E. B., 2004).

4.43.5.4 Male Mating Behavior

Although there is abundant evidence for an involvement of the rodent VNO in male sexual behavior (Wysocki, C. J. and Meredith, M., 1987; Halpern, M. and Martinez-Marcos, A., 2003) its exact role remains unclear, possibly due to complex interactions with other chemosensory systems, especially the main olfactory system (Brennan, P. A. and Keverne, E. B., 2004). Initial studies were done in hamster where approximately one-third of male hamsters with VN cuts developed a severe mating deficit (Powers, J. B. and Winans, S. S., 1975). Subsequently, Meredith M. (1986) showed that sexually inexperienced male hamsters are severely defective in male–female mating behavior when the VNO is removed, but that prior sexual experience can mitigate the lesion effects. Results in mice are less clear. Although several studies reported the importance of an intact VNO for the normal display of sexual behavior in male mice (Clancy, A. N. *et al.*, 1984; Bean, N. J. and Wysocki, C. J., 1989; Wysocki, C. J. and Lepri, J. J., 1991), a more recent study found that the rates of mounting and intromission and the timing of ejaculation are equivalent in sexually naive control and VNX mice (Pankevich, D. E. *et al.*, 2004).

In TRPC2$^{-/-}$ mice, sexual behavior toward females appears to be unaffected. Instead, TRPC2$^{-/-}$ males show abnormally high levels of mounting behavior toward other males (Leypold, B. G. *et al.*, 2002; Stowers, L. *et al.*, 2002), a phenotype not previously observed in surgical lesioning studies (Pankevich, D. E. *et al.*, 2004). It has been argued that the VNO plays an essential role in gender discrimination (Stowers, L. *et al.*, 2002), but this is currently debated (Pankevich, D. E. *et al.*, 2004).

4.43.5.5 Male Ultrasonic Vocalizations

Male mice emit 70 kHz precopulatory vocalizations in the presence of female mice or their chemical cues (Nyby, J. *et al.*, 1979; Wysocki, C. J. and Lepri, J. J., 1991). Deafferentation of the VNO abolishes vocalizing in sexually naïve males and reduces it in males that have had previous sexual experience (Wysocki, C. J. and Lepri, J. J., 1991). However, ultrasonic vocalizations persist in TRPC2$^{-/-}$ males and are not suppressed in the presence of male chemosignals (Stowers, L. *et al.*, 2002; Brennan, P. A. and Keverne, E. B., 2004). The discrepancies between the effects of surgical and genetic lesions might be explained, in part, by the result that the loss of TRPC2 does not cause a complete loss of function in the VNO (Leypold, B. G. *et al.*, 2002).

4.43.5.6 Timing of Puberty, Cyclicity, and Ovulation in Females

A vast literature exists on the role of the VNO in altering the course of puberty and modulating female cyclicity and ovulation in a variety of species (Meredith, M. *et al.*, 1983; Halpern, M., 1987; Halpern, M. and Martinez-Marcos, A., 2003). Among these effects, puberty acceleration (Vandenbergh, J. G., 1983), caused by exposure to male chemosignals during female development, represents one of the best examples for a clear dependence on an intact VNO (Kaneko, N. *et al.*, 1980; Lomas, D. E. and Keverne, E. B., 1982; Sanchez-Criado, J. E., 1982). Novotny and collaborators have identified several volatile urine constituents that are capable of accelerating puberty in female mice (Novotny, M. V. *et al.*, 1999a; 1999b). Other evidence suggests that the delay of the onset of puberty, observed in crowded female house mice, depends also upon

a functional VNO (Wysocki, C. J. and Lepri, J. J., 1991). Further work using animals with specific genetic deletions will be required to examine some of these effects.

4.43.5.7 Hormonal Responses

Some of the VNO-dependent functions summarized above depend on the coordination of neuroendocrine functions and the release of specific hormones. Significant efforts have been undertaken to establish a direct link between VNO stimulation and hormonal function (Keverne, E. B., 1983; Meredith, M. *et al.*, 1983). It is important to note that the level of reproductive hormones can also be influenced by the detection of chemosignals via the main olfactory system (Meredith, M., 1998) and current work is focusing on establishing neural connections between chemosensory neurons of the main and AOSs and neural circuits involved in hormone regulation (Boehm, U. *et al.*, 2005; Yoon, H. *et al.*, 2005; Shepherd, G. M., 2006). With respect to VNO stimulation, some of the best evidence comes from measurement of the gonadotropin luteinizing hormone (LH), which itself depends on the release of gonadotropin releasing hormone (GnRH, also known as luteinizing hormone releasing hormone (LHRH)) (Wysocki, C. J. and Meredith, M., 1987; Meredith, M., 1998; Halpern, M. and Martinez-Marcos, A., 2003). Female rats, when exposed to males or their odors, show a surge in LH and this effect is absent after removal of the VNO or lesioning of the AOB (Beltramino, C. and Taleisnik, S., 1983). Electrical stimulation of the AOB or medial (vomeronasal) amygdala produces a similar LH surge, whereas stimulation of the MOB or lateral (olfactory) amygdala does not elicit a facilitatory but rather an inhibitory effect (Beltramino, C. and Taleisnik, S., 1978; 1979).

Male mice exhibit a plasma testosterone surge after an encounter with strange females or their odors (Macrides, F. *et al.*, 1975). Removal of the VNO blocks this testosterone surge after exposure to an anesthetized female (Wysocki, C. J. *et al.*, 1983). Similarly, reflexive release of LH following exposure to female urine odor is blocked in VNO-lesioned male mice, although exposure to females did cause LH responses in these mice (Coquelin, A. *et al.*, 1984). These results stress the existence of multiple convergent pathways involved in LH regulation.

4.43.5.8 Pregnancy Block and Individual Recognition in Females: The Bruce Effect

One of the best-known examples of olfactory imprinting in adult vertebrates is the selective pregnancy block (or Bruce effect; Bruce, H. M., 1959) in the mouse, which depends on the formation and maintenance of a long-lasting odor recognition memory by the vomeronasal system (Brennan, P. *et al.*, 1990; Brennan, P. A. and Keverne, E. B., 1997; Halpern, M. and Martinez-Marcos, A., 2003). The Bruce effect occurs when a recently mated female mouse aborts if exposed to the urine odor of a male genetically different from the stud male (Figure 9). This unfamiliar male odor results in pregnancy block and return to estrus in the recently mated female. Keverne and colleagues suggest that the dendrodendritic synapse between granule cells and mitral cells in AOB may be critical for odor memory of the mate in the female (Keverne, E. B. and de la Riva, C., 1982; Rosser, A. E. and Keverne, E. B., 1985; Kaba, H. *et al.*, 1989). The Bruce effect can be abolished if noradrenergic centrifugal input to the female AOB is blocked immediately after mating, presumably before olfactory memories of the mate are formed (Keverne, E. B. and de la Riva, C., 1982; Rosser, A. E. and Keverne, E. B., 1985). Thus, noradrenalin appears to be important in strengthening the memory of the odor of the mating partner. Noradrenergic innervation of the AOB derives from LC projections primarily to the accessory granule layer (aGCL) and accessory mitral cell layer (aMCL) with lower density in the accessory external plexiform layer (aEPL) and aGL (McLean, J. H. *et al.*, 1989). Based on these light microscopic studies it was suggested that the major target of the noradrenalin input are granule cells (McLean, J. H. *et al.*, 1989). Thus, noradrenalin exciting granule cells and enhancing inhibition of a subset of mitral cells for several hours following mating may facilitate this selective odor memory.

The MHC peptide ligands are the first identified vomeronasal stimuli that can mediate the Bruce effect. To show that MHC peptides provide a crucial signal among the plethora of other cues present in male urine, peptides characteristic of a disparate MHC molecule were synthesized and added to the urine of a familiar male. Compared to the addition of cognate peptides, which had no effect, disparate peptides caused pregnancy block by otherwise familiar urine (Leinders-Zufall, T. *et al.*, 2004) (Figure 9). These results indicate that MHC peptides are recognized as natural odors and convey genotypic information in the context of a distinct social behavior (Boehm, T. and Zufall, F., 2006).

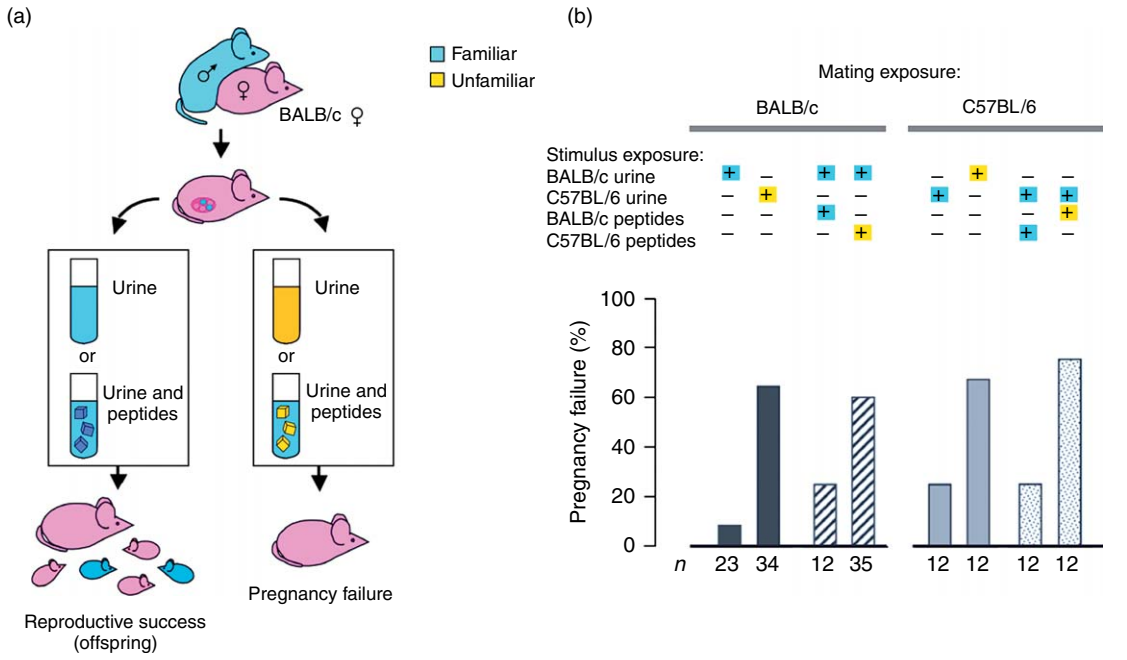

Figure 9 (a) Processing of major histocompatibility complex (MHC) peptide ligands via the accessory system provides a crucial signal in the pregnancy block paradigm of female mice (the Bruce effect), where disparate but not cognate peptides caused pregnancy block when added to otherwise familiar urine. (b) Percent pregnancy failure in female BALB/c (H-2d haplotype) mice mated with either BALB/c (H-2d haplotype) or C57BL/6 (H-2b haplotype) males. Exposure to different male urine types, which, in some cases, were supplemented with MHC class I peptides specific for BALB/c or C57BL/6 haplotypes is indicated. Reprinted with permission from Leinders-Zufall, T., Brennan, P., Widmayer, P., Chandramani, S. P., Maul-Pavicic, A., Jager, M., Li, X. H., Breer, H., Zufall, F., and Boehm, T. 2004. MHC class I peptides as chemosensory signals in the vomeronasal organ. Science 306, 1033–1037, AAAS.

In summary, it is now clear that the AOS is involved in a wide variety of functions including complex mechanisms such as those mediating the sensing of genome composition of a conspecific. The upcoming years, undoubtedly, will provide further exciting results with respect to the role of the VNO and AOS in chemical communication.

References

Adrian, E. D. 1955. Synchronised activity in the vomero-nasal nerves with a note on the function of the organ of Jacobsen. Pflugers Arch. 260, 188–192.

Altstein, M. 2004. Peptide pheromones: an overview. Peptides 25, 1373–1376.

Aungst, J. L., Heyward, P. M., Puche, A. C., Karnup, S. V., Hayar, A., Szabo, G., and Shipley, M. T. 2003. Centre-surround inhibition among olfactory bulb glomeruli. Nature 426, 623–629.

Balogh, C. 1860. Über das Jacobson'sche Organ des Schafes. Sitzungsbericht Akad. Wiss. Wien 42, 449–549.

Baxi, K. N., Dorries, K. M., and Eisthen, H. L. 2006. Is the vomeronasal system really specialized for detecting pheromones? Trends Neurosci. 29, 1–7.

Bean, N. J. and Wysocki, C. J. 1989. Vomeronasal organ removal and female mouse aggression: the role of experience. Physiol. Behav. 45, 875–882.

Belluscio, L., Koentges, G., Axel, R., and Dulac, C. 1999. A map of pheromone receptor activation in the mammalian brain. Cell 97, 209–220.

Beltramino, C. and Taleisnik, S. 1978. Facilitatory and inhibitory effects of electrochemical stimulation of the amygdala on the release of luteinizing hormone. Brain Res. 144, 95–107.

Beltramino, C. and Taleisnik, S. 1979. Effect of electrochemical stimulation in the olfactory bulbs on the release of gonadotropin hormones in rats. Neuroendocrinology 28, 320–328.

Beltramino, C. and Taleisnik, S. 1983. Release of LH in the female rat by olfactory stimuli. Effect of the removal of the vomeronasal organs or lesioning of the accessory olfactory bulbs. Neuroendocrinology 36, 53–58.

Berghard, A., Buck, L. B., and Liman, E. R. 1996. Evidence for distinct signaling mechanisms in two mammalian olfactory sense organs. Proc. Natl. Acad. Sci. U. S. A. 93, 2365–2369.

Bertmar, G. 1981. Evolution of vomeronasal organs in vertebrates. Evolution 35, 359–366.

Bigiani, A., Mucignat-Caretta, C., Montani, G., and Tirindelli, R. 2005. Pheromone reception in mammals. Rev. Physiol. Biochem. Pharmacol. 154, 1–35.

Boehm, N. and Gasser, B. 1993. Sensory receptor-like cells in the human foetal vomeronasal organ. Neuroreport 4, 867–870.

Boehm, T. and Zufall, F. 2006. MHC peptides and the sensory evaluation of genotype. Trends Neurosci. 29, 100–107.

Boehm, N., Roos, J., and Gasser, B. 1994. Luteinizing hormone-releasing hormone (LHRH)-expressing cells in the nasal septum of human fetuses. Brain Res. Dev. Brain Res. 82, 175–180.

Boehm, U., Zou, Z., and Buck, L. B. 2005. Feedback loops link odor and pheromone signaling with reproduction. Cell 123, 683–695.

Boschat, C., Pelofi, C., Randin, O., Roppolo, D., Luscher, C., Broillet, M. C., and Rodriguez, I. 2002. Pheromone detection mediated by a V1r vomeronasal receptor. Nat. Neurosci. 5, 1261–1262.

Brann, J. H., Dennis, J. C., Morrison, E. E., and Fadool, D. A. 2002. Type-specific inositol 1,4,5-trisphosphate receptor localization in the vomeronasal organ and its interaction with a transient receptor potential channel, TRPC2. J. Neurochem. 83, 1452–1460.

Brennan, P. A. and Keverne, E. B. 1997. Neural mechanisms of mammalian olfactory learning. Prog. Neurobiol. 51, 457–481.

Brennan, P. A. and Keverne, E. B. 2004. Something in the air? New insights into mammalian pheromones. Curr. Biol. 14, R81–R89.

Brennan, P. A., Hancock, D., and Keverne, E. B. 1992. The expression of the immediate-early genes c-fos, egr-1 and c-jun in the accessory olfactory bulb during the formation of an olfactory memory in mice. Neuroscience 49, 277–284.

Brennan, P., Kaba, H., and Keverne, E. B. 1990. Olfactory recognition: a simple memory system. Science 250, 1223–1226.

Briand, L., Blon, F., Trotier, D., and Pernollet, J. C. 2004a. Natural ligands of hamster aphrodisin. Chem. Senses 29, 425–430.

Briand, L., Trotier, D., and Pernollet, J. C. 2004b. Aphrodisin, an aphrodisiac lipocalin secreted in hamster vaginal secretions. Peptides 25, 1545–1552.

Bruce, H. M. 1959. An exteroceptive block to pregnancy in the mouse. Nature 184, 105.

Burghardt, G. M. 1970. Chemical Reception in Reptiles. In: Communication by Chemical Signals (*eds*. J. W. Johnson, D. R. Moulton, and A. Turk A), pp. 241–308. Appleton-Century-Crofts.

von Campenhausen, H., Yoshihara, Y., and Mori, K. 1997. OCAM reveals segregated mitral/tufted cell pathways in developing accessory olfactory bulb. Neuroreport 8, 2607–2612.

Cajal, R. S. 1911. Histologie du Systeme Neurveux de l'Hommes et des Vertebres. Maloine.

Canteras, N. S., Simerly, R. B., and Swanson, L. W. 1992. Connections of the posterior nucleus of the amygdala. J. Comp. Neurol. 324, 143–179.

Carlson, G. C., Shipley, M. T., and Keller, A. 2000. Long-lasting depolarizations in mitral cells of the rat olfactory bulb. J. Neurosci. 20, 2011–2021.

Cavaggioni, A. and Mucignat-Caretta, C. 2000. Major urinary proteins, alpha(2U)-globulins and aphrodisin. Biochim. Biophys. Acta 1482, 218–228.

Ciges, M., Labella, T., Gayoso, M., and Sanchez, G. 1977. Ultrastructure of the organ of Jacobson and comparative study with olfactory mucosa. Acta Otolaryngol. 83, 47–58.

Cinelli, A. R., Wang, D., Chen, P., Liu, W., and Halpern, M. 2002. Calcium transients in the garter snake vomeronasal organ. J. Neurophysiol. 87, 1449–1472.

Clancy, A. N., Coquelin, A., Macrides, F., Gorski, R. A., and Noble, E. P. 1984. Sexual behavior and aggression in male mice: involvement of the vomeronasal system. J. Neurosci. 4, 2222–2229.

Coquelin, A., Clancy, A. N., Macrides, F., Noble, E. P., and Gorski, R. A. 1984. Pheromonally induced release of luteinizing hormone in male mice: involvement of the vomeronasal system. J. Neurosci. 4, 2230–2236.

Del Punta, K., Leinders-Zufall, T., Rodriguez, I., Jukam, D., Wysocki, C. J., Ogawa, S., Zufall, F., and Mombaerts, P. 2002a. Deficient pheromone responses in mice lacking a cluster of vomeronasal receptor genes. Nature 419, 70–74.

Del Punta, K., Puche, A., Adams, N., Rodriguez, I., and Mombaerts, P. 2002b. A divergent pattern of sensory axonal projections is rendered convergent by second-order neurons in the accessory olfactory bulb. Neuron 35, 1057.

Del Punta, K., Rothman, A., Rodriguez, I., and Mombaerts, P. 2000. Sequence diversity and genomic organization of vomeronasal receptor genes in the mouse. Genome Res. 10, 1958–1967.

Doving, K. B. and Trotier, D. 1998. Structure and function of the vomeronasal organ. J. Exp. Biol. 201, 2913–2925.

Dudley, C. A. and Moss, R. L. 1995. Electrophysiological evidence for glutamate as a vomeronasal receptor cell neurotransmitter. Brain Res. 675, 208–214.

Dulac, C. 2000. Sensory coding of pheromone signals in mammals. Curr. Opin. Neurobiol. 10, 511–518.

Dulac, C. and Axel, R. 1995. A novel family of genes encoding putative pheromone receptors in mammals. Cell 83, 195–206.

Dulac, C. and Torello, A. T. 2003. Molecular detection of pheromone signals in mammals: from genes to behaviour. Nat. Rev. Neurosci. 4, 551–562.

Eisthen, H. L. 1992. Phylogeny of the vomeronasal system and of receptor cell types in the olfactory and vomeronasal epithelia of vertebrates. Microsc. Res. Tech. 23, 1–21.

Eisthen, H. L. 1997. Evolution of vertebrate olfactory systems. Brain Behav. Evol. 50, 222–233.

Fadool, D. A., Wachowiak, M., and Brann, J. H. 2001. Patch-clamp analysis of voltage-activated and chemically activated currents in the vomeronasal organ of *Sternotherus odoratus* (stinkpot/musk turtle). J. Exp. Biol. 204, 4199–4212.

Fernandez-Fewell, G. D. and Meredith, M. 1994. c-fos expression in vomeronasal pathways of mated or pheromone-stimulated male golden hamsters: contributions from vomeronasal sensory input and expression related to mating performance. J. Neurosci. 14, 3643–3654.

Fewell, G. D. and Meredith, M. 2002. Experience facilitates vomeronasal and olfactory influence on Fos expression in medial preoptic area during pheromone exposure or mating in male hamsters. Brain Res. 941, 91–106.

Fieni, F., Ghiaroni, V., Tirindelli, R., Pietra, P., and Bigiani, A. 2003. Apical and basal neurones isolated from the mouse vomeronasal organ differ for voltage-dependent currents. J. Physiol. 552, 425–436.

Fuss, S. H., Omura, M., and Mombaerts, P. 2005. The Grueneberg ganglion of the mouse projects axons to glomeruli in the olfactory bulb. Eur. J. Neurosci. 22, 2649–2654.

Gandelman, R., Zarrow, M. X., and Denenberg, V. H. 1972. Reproductive and maternal performance in the mouse following removal of the olfactory bulbs. J. Reprod. Fertil. 28, 453–456.

Garrosa, M. and Coca, S. 1991. Postnatal development of the vomeronasal epithelium in the rat: an ultrastructural study. J. Morphol. 208, 257–269.

Ghiaroni, V., Fieni, F., Tirindelli, R., Pietra, P., and Bigiani, A. 2003. Ion conductances in supporting cells isolated from the mouse vomeronasal organ. J. Neurophysiol. 89, 118–127.

Gjerstad, J., Valen, E. C., Trotier, D., and Doving, K. 2003. Photolysis of caged inositol 1,4,5-trisphosphate induces action potentials in frog vomeronasal microvillar receptor neurones. Neuroscience 119, 193–200.

von Gudden, B. 1870. Experimentaluntersuchung über das peripherische und centrale Nervensystem. Archiv. Psychol. 2, 699–720.

Halem, H. A., Cherry, J. A., and Baum, M. J. 1999. Vomeronasal neuroepithelium and forebrain Fos responses to male

pheromones in male and female mice. J. Neurobiol. 39, 249–263.
Halem, H. A., Cherry, J. A., and Baum, M. J. 2001. Central forebrain Fos responses to familiar male odours are attenuated in recently mated female mice. Eur. J. Neurosci. 13, 389–399.
Halpern, M. 1987. The organization and function of the vomeronasal system. Annu. Rev. Neurosci. 10, 325–362.
Halpern, M. and Martinez-Marcos, A. 2003. Structure and function of the vomeronasal system: an update. Prog. Neurobiol. 70, 245–318.
Halpern, M., Jia, C., and Shapiro, L. S. 1998. Segregated pathways in the vomeronasal system. Microsc. Res. Tech. 41, 519–529.
Halpern, M., Shapiro, L. S., and Jia, C. 1995. Differential localization of G proteins in the opossum vomeronasal system. Brain Res. 677, 157–161.
Herrada, G. and Dulac, C. 1997. A novel family of putative pheromone receptors in mammals with a topographically organized and sexually dimorphic distribution. Cell 90, 763–773.
Hofmann, T., Schaefer, M., Schultz, G., and Gudermann, T. 2000. Cloning, expression and subcellular localization of two novel splice variants of mouse transient receptor potential channel 2. Biochem. J. 351, 115–122.
Holy, T. E., Dulac, C., and Meister, M. 2000. Responses of vomeronasal neurons to natural stimuli. Science 289, 1569–1572.
Hurst, J. L. and Beynon, R. J. 2004. Scent wars: the chemobiology of competitive signalling in mice. Bioessays 26, 1288–1298.
Hurst, J. L., Payne, C. E., Nevison, C. M., Marie, A. D., Humphries, R. E., Robertson, D. H., Cavaggioni, A., and Beynon, R. J. 2001. Individual recognition in mice mediated by major urinary proteins. Nature 414, 631–634.
Inamura, K. and Kashiwayanagi, M. 2000. Inward current responses to urinary substances in rat vomeronasal sensory neurons. Eur. J. Neurosci. 12, 3529–3536.
Inamura, K., Kashiwayanagi, M., and Kurihara, K. 1997. Inositol-1,4,5-trisphosphate induces responses in receptor neurons in rat vomeronasal sensory slices. Chem. Senses 22, 93–103.
Inamura, K., Matsumoto, Y., Kashiwayanagi, M., and Kurihara, K. 1999. Laminar distribution of pheromone-receptive neurons in rat vomeronasal epithelium. J. Physiol. 517(Pt 3), 731–739.
Ishii, T., Hirota, J., and Mombaerts, P. 2003. Combinatorial coexpression of neural and immune multigene families in mouse vomeronasal sensory neurons. Curr. Biol. 13, 394–400.
Jacobson, L. 1813. Anatoisk beskrievelse over et nyt organ i huusdyrenes naese. Vet. Selsk. Skrift 2, 209–246.
Jacobson, L., Trotier, D., and Doving, K. B. 1998. Anatomical description of a new organ in the nose of domesticated animals by Ludvig Jacobson (1813) [classical article]. Chem. Senses 23, 743–754.
Jemiolo, B., Andreolini, F., Xie, T. M., Wiesler, D., and Novotny, M. 1989. Puberty-affecting synthetic analogs of urinary chemosignals in the house mouse, *Mus domesticus*. Physiol. Behav. 46, 293–298.
Jemiolo, B., Harvey, S., and Novotny, M. 1986. Promotion of the Whitten effect in female mice by synthetic analogs of male urinary constituents. Proc. Natl. Acad. Sci. U. S. A. 83, 4576–4579.
Jia, C. and Halpern, M. 1996. Subclasses of vomeronasal receptor neurons: differential expression of G proteins (Gi alpha 2 and G(o alpha)) and segregated projections to the accessory olfactory bulb. Brain Res. 719, 117–128.
Jia, C., Chen, W. R., and Shepherd, G. M. 1999. Synaptic organization and neurotransmitters in the rat accessory olfactory bulb. J. Neurophysiol. 81, 345–355.
Jiang, X. C., Inouchi, J., Wang, D., and Halpern, M. 1990. Purification and characterization of a chemoattractant from electric shock-induced earthworm secretion, its receptor binding, and signal transduction through the vomeronasal system of garter snakes. J. Biol. Chem. 265, 8736–8744.
Johnston, R. E. 1983. Chemical Signals and Reproductive Behavior. In: Pheromones and Reproduction in Mammals (*ed*. J. G. Vandenbergh), pp. 71–79. Academic Press.
Johnston, R. E. 2000. Chemical Communication and Pheromones: The Types of Chemical Signals and the Role of the Vomeronasal System. In: The Neurobiology of Taste and Smell (*eds*. T. E. Finger, W. L. Silver, and D. Restrepo), pp. 101–127. Wiley-Liss.
Johnston, A. N., Rogers, L. J., and Johnston, G. A. 1993. Glutamate and imprinting memory: the role of glutamate receptors in the encoding of imprinting memory. Behav. Brain Res. 54, 137–143.
Kaba, H., Rosser, A., and Keverne, B. 1989. Neural basis of olfactory memory in the context of pregnancy block. Neuroscience 32, 657–662.
Kaneko, N., Debski, E. A., Wilson, M. C., and Whitten, W. K. 1980. Puberty acceleration in mice. II. Evidence that the vomeronasal organ is a receptor for the primer pheromone in male mouse urine. Biol. Reprod. 22, 873–878.
Karlson, P. and Lüscher, M. 1959. Pheromones: a new term for a class of biologically active substances. Nature 183, 55–56.
Keverne, B. 1979. The Dual Olfactory Projections and Their Significance for Behaviour. In: Chemical Ecology: Odour Communication in Animals (*ed*. F. J. Ritter), pp. 75–83. Elsevier/North-Holland Biomed Press.
Keverne, E. B. 1983. Pheromonal influences on the endocrine regulation of reproduction. Trends Neurosci. 6, 381–384.
Keverne, E. B. and de la Riva, C. 1982. Pheromones in mice: reciprocal interaction between the nose and brain. Nature 296, 148–150.
Kikuyama, S., Toyoda, F., Ohmiya, Y., Matsuda, K., Tanaka, S., and Hayashi, H. 1995. Sodefrin: a female-attracting peptide pheromone in newt cloacal glands. Science 267, 1643–1645.
Kimoto, H., Haga, S., Sato, K., and Touhara, K. 2005. Sex-specific peptides from exocrine glands stimulate mouse vomeronasal sensory neurons. Nature 437, 898–901.
Klein, E. 1881. The organ of Jacobson in the rabbit. Q. J. Microsc. Sci. 21, 549–555.
Krieger, J. and Breer, H. 1999. Olfactory reception in invertebrates. Science 286, 720–723.
Kroner, C., Breer, H., Singer, A. G., and O'Connell, R. J. 1996. Pheromone-induced second messenger signaling in the hamster vomeronasal organ. Neuroreport 7, 2989–2992.
Kumar, A., Dudley, C. A., and Moss, R. L. 1999. Functional dichotomy within the vomeronasal system: distinct zones of neuronal activity in the accessory olfactory bulb correlate with sex-specific behaviors. J. Neurosci. 19, RC32.
Labra, A., Brann, J. H., and Fadool, D. A. 2005. Heterogeneity of voltage- and chemosignal-activated response profiles in vomeronasal sensory neurons. J. Neurophysiol. 94, 2535–2548.
Lau, Y. E. and Cherry, J. A. 2000. Distribution of PDE4A and G(o) alpha immunoreactivity in the accessory olfactory system of the mouse. Neuroreport 11, 27–32.
Laurent, G. 2002. Olfactory network dynamics and the coding of multidimensional signals. Nat. Rev. Neurosci. 3, 884–895.
Le Jeune, H. and Jourdan, F. 1991. Postnatal development of cholinergic markers in the rat olfactory bulb: a histochemical and immunocytochemical study. J. Comp. Neurol. 314, 383–395.

Leinders-Zufall, T., Brennan, P., Widmayer, P., Chandramani, S. P., Maul-Pavicic, A., Jäger, M., Li, X. H., Breer, H., Zufall, F., and Boehm, T. 2004. MHC class I peptides as chemosensory signals in the vomeronasal organ. Science 306, 1033–1037.

Leinders-Zufall, T., Lane, A. P., Puche, A. C., Ma, W., Novotny, M. V., Shipley, M. T., and Zufall, F. 2000. Ultrasensitive pheromone detection by mammalian vomeronasal neurons. Nature 405, 792–796.

Lepri, J. J. and Wysocki, C. J. 1987. Removal of the vomeronasal organ disrupts the activation of reproduction in female voles. Physiol. Behav. 40, 349–355.

Leypold, B. G., Yu, C. R., Leinders-Zufall, T., Kim, M. M., Zufall, F., and Axel, R. 2002. Altered sexual and social behaviors in trp2 mutant mice. Proc. Natl. Acad. Sci. U. S. A. 99, 6376–6381.

Liman, E. R. 2003. Regulation by voltage and adenine nucleotides of a Ca^{2+}-activated cation channel from hamster vomeronasal sensory neurons. J. Physiol. 548, 777–787.

Liman, E. R. and Corey, D. P. 1996. Electrophysiological characterization of chemosensory neurons from the mouse vomeronasal organ. J. Neurosci. 16, 4625–4637.

Liman, E. R., Corey, D. P., and Dulac, C. 1999. TRP2: a candidate transduction channel for mammalian pheromone sensory signaling. Proc. Natl. Acad. Sci. U. S. A. 96, 5791–5796.

Loconto, J., Papes, F., Chang, E., Stowers, L., Jones, E. P., Takada, T., Kumanovics, A., Fischer, L. K., and Dulac, C. 2003. Functional expression of murine V2R pheromone receptors involves selective association with the M10 and M1 families of MHC class Ib molecules. Cell 112, 607–618.

Lomas, D. E. and Keverne, E. B. 1982. Role of the vomeronasal organ and prolactin in the acceleration of puberty in female mice. J. Reprod. Fertil. 66, 101–107.

Lowe, G. 2003. Electrical signaling in the olfactory bulb. Curr. Opin. Neurobiol. 13, 476–481.

Lucas, P., Ukhanov, K., Leinders-Zufall, T., and Zufall, F. 2003. A diacylglycerol-gated cation channel in vomeronasal neuron dendrites is impaired in TRPC2 mutant mice: mechanism of pheromone transduction. Neuron 40, 551–561.

Luo, M. and Katz, L. C. 2004. Encoding pheromonal signals in the mammalian vomeronasal system. Curr. Opin. Neurobiol. 14, 428–434.

Luo, M., Fee, M. S., and Katz, L. C. 2003. Encoding pheromonal signals in the accessory olfactory bulb of behaving mice. Science 299, 1196–1201.

Luo, Y., Lu, S., Chen, P., Wang, D., and Halpern, M. 1994. Identification of chemoattractant receptors and G-proteins in the vomeronasal system of garter snakes. J. Biol. Chem. 269, 16867–16877.

Ma, J. and Lowe, G. 2004. Action potential backpropagation and multiglomerular signaling in the rat vomeronasal system. J. Neurosci. 24, 9341–9352.

Macrides, F., Bartke, A., and Dalterio, S. 1975. Strange females increase plasma testosterone levels in male mice. Science 189, 1104–1106.

Madison, D. W. 1977. Chemical Communication in Amphibians and Reptiles. In: Chemical Signals in Vertebrates (*eds*. D. Muller-Schwarze and M. M. Mozell), pp. 135–168. Plenum.

Mandiyan, V. S., Coats, J. K., and Shah, N. M. 2005. Deficits in sexual and aggressive behaviors in Cnga2 mutant mice. Nat. Neurosci. 8, 1660–1662.

Martinez-Marcos, A. and Halpern, M. 1999. Differential projections from the anterior and posterior divisions of the accessory olfactory bulb to the medial amygdala in the opossum, *Monodelphis domestica*. Eur. J. Neurosci. 11, 3789–3799.

Martini, S., Silvotti, L., Shirazi, A., Ryba, N. J., and Tirindelli, R. 2001. Co-expression of putative pheromone receptors in the sensory neurons of the vomeronasal organ. J. Neurosci. 21, 843–848.

Matsunami, H. and Buck, L. B. 1997. A multigene family encoding a diverse array of putative pheromone receptors in mammals. Cell 90, 775–784.

Matsuoka, M., Yokosuka, M., Mori, Y., and Ichikawa, M. 1999. Specific expression pattern of Fos in the accessory olfactory bulb of male mice after exposure to soiled bedding of females. Neurosci. Res. 35, 189–195.

McCotter, R. E. 1912. The connection of the vomeronasal nerves with the accessory olfactory bulb in the opossum and other mammals. Anat. Rec. 6, 299–318.

McLean, J. H. and Shipley, M. T. 1987. Serotonergic afferents to the rat olfactory bulb: II. Changes in fiber distribution during development. J. Neurosci. 7, 3029–3039.

McLean, J. H., Shipley, M. T., Nickell, W. T., Aston-Jones, G., and Reyher, C. K. 1989. Chemoanatomical organization of the noradrenergic input from locus coeruleus to the olfactory bulb of the adult rat. J. Comp. Neurol. 285, 339–349.

von Mihalkovics, V. 1899. Nasenhöhle und Jacobsonsches Organ. Anat. Embryol. (Berl.) 11, 1–108.

Meisami, E. and Bhatnagar, K. P. 1998. Structure and diversity in mammalian accessory olfactory bulb. Microsc. Res. Tech. 43, 476–499.

Menco, B. P., Carr, V. M., Ezeh, P. I., Liman, E. R., and Yankova, M. P. 2001. Ultrastructural localization of G-proteins and the channel protein TRP2 to microvilli of rat vomeronasal receptor cells. J. Comp. Neurol. 438, 468–489.

Meredith, M. 1983. Sensory Physiology of Pheromone Communication. In: Pheromones and Reproduction in Mammals (*ed*. J. G. Vandenbergh), pp. 199–252. Academic Press.

Meredith, M. 1986. Vomeronasal organ removal before sexual experience impairs male hamster mating behavior. Physiol. Behav. 36, 737–743.

Meredith, M. 1994. Chronic recording of vomeronasal pump activation in awake behaving hamsters. Physiol. Behav. 56, 345–354.

Meredith, M. 1998. Vomeronasal, olfactory, hormonal convergence in the brain. Cooperation or coincidence? Ann. N. Y. Acad. Sci. 855, 349–361.

Meredith, M. 2001. Human vomeronasal organ function: a critical review of best and worst cases. Chem. Senses 26, 433–445.

Meredith, M. and O'Connell, R. J. 1979. Efferent control of stimulus access to the hamster vomeronasal organ. J. Physiol. 286, 301–316.

Meredith, M. and O'Connell, J. M. 1988. HRP uptake by olfactory and vomeronasal receptor neurons: use as an indicator of incomplete lesions and relevance for non-volatile chemoreception. Chem. Senses 13, 487–515.

Meredith, M. and Westberry, J. M. 2004. Distinctive responses in the medial amygdala to same-species and different-species pheromones. J. Neurosci. 24, 5719–5725.

Meredith, M., Graziadei, P. P., Graziadei, G. A., Rashotte, M. E., and Smith, J. C. 1983. Olfactory function after bulbectomy. Science 222, 1254–1255.

Meredith, M., Marques, D. M., O'Connell, R. O., and Stern, F. L. 1980. Vomeronasal pump: significance for male hamster sexual behavior. Science 207, 1224–1226.

Mombaerts, P. 2004. Genes and ligands for odorant, vomeronasal and taste receptors. Nat. Rev. Neurosci. 5, 263–278.

Mombaerts, P., Wang, F., Dulac, C., Chao, S. K., Nemes, A., Mendelsohm, M., Edmondson, J., and Axel, R. 1996. Visualizing an olfactory sensory map. Cell 87, 675–686.

Montell, C., Birnbaumer, L., and Flockerzi, V. 2002. The TRP channels, a remarkably functional family. Cell 108, 595–598.

Mori, K. 1987. Monoclonal antibodies (2C5 and 4C9) against lactoseries carbohydrates identify subsets of olfactory and vomeronasal receptor cells and their axons in the rabbit. Brain Res. 408, 215–221.

Mori, K., von Campenhausen, H., and Yoshihara, Y. 2000. Zonal organization of the mammalian main and accessory olfactory systems. Philos. Trans. R. Soc. Lond. B Biol. Sci. 355, 1801–1812.

Mori, K., Fujita, S. C., Imamura, K., and Obata, K. 1985. Immunohistochemical study of subclasses of olfactory nerve fibers and their projections to the olfactory bulb in the rabbit. J. Comp. Neurol. 242, 214–229.

Mucignat-Caretta, C., Caretta, A., and Cavaggioni, A. 1995. Acceleration of puberty onset in female mice by male urinary proteins. J. Physiol. 486(Pt 2), 517–522.

Müller, W. 1971. Vergleichende elektrophysiologische Untersuchungen an den Sinnesepithelien des Jacobsonschen Organs und der Nase von Amphibien (Rana), Reptilien (Lacerta) und Säugetieren (Mus). Z. vergl. Physiologie 72, 370–385.

Norlin, E. M., Gussing, F., and Berghard, A. 2003. Vomeronasal phenotype and behavioral alterations in G alpha i2 mutant mice. Curr. Biol. 13, 1214–1219.

Novotny, M., Jemiolo, B., Harvey, S., Wiesler, D., and Marchlewska-Koj, A. 1986. Adrenal-mediated endogenous metabolites inhibit puberty in female mice. Science 231, 722–725.

Novotny, M. V., Jemiolo, B., Wiesler, D., Ma, W., Harvey, S., Xu, F., Xie, T. M., and Carmack, M. 1999a. A unique urinary constituent, 6-hydroxy-6-methyl-3-heptanone, is a pheromone that accelerates puberty in female mice. Chem. Biol. 6, 377–383.

Novotny, M. V., Ma, W., Wiesler, D., and Zidek, L. 1999b. Positive identification of the puberty-accelerating pheromone of the house mouse: the volatile ligands associating with the major urinary protein. Proc. Biol. Sci. 266, 2017–2022.

Nyby, J., Wysocki, C. J., Whitney, G., Dizinno, G., and Schneider, J. 1979. Elicitation of male mouse (*Mus musculus*) ultrasonic vocalizations I: urinary cues. J. Comp. Physiol. Psychol. 93, 957–975.

de Olmos, J., Hardy, H., and Heimer, L. 1978. The afferent connections of the main and the accessory olfactory bulb formations in the rat: an experimental HRP-study. J. Comp. Neurol. 181, 213–244.

Olson, R., Huey-Tubman, K. E., Dulac, C., and Bjorkman, P. J. 2005. Structure of a pheromone receptor-associated MHC molecule with an open and empty groove. PLoS Biol. 3, e257.

Osada, T., Kito, K., Ookata, K., Graziadei, P. P., Ikai, A., and Ichikawa, M. 1994. Monoclonal antibody (VOM2) specific for the luminal surface of the rat vomeronasal sensory epithelium. Neurosci. Lett. 170, 47–50.

Pankevich, D. E., Baum, M. J., and Cherry, J. A. 2004. Olfactory sex discrimination persists, whereas the preference for urinary odorants from estrous females disappears in male mice after vomeronasal organ removal. J. Neurosci. 24, 9451–9457.

Paxions, G. 2004. The Rat Nervous System, 3rd edn. London Academic Press.

Perlman, S. M. 1934. Jacobson's organ (organon vomero-nasale, Jacobsoni): its anatomy, gross, microscopic and comparative, with some observations as well on its function. Ann. Otol. Rhinol. Larangyol. 43, 739–768.

Piana, G. P. 1882. Contribuzioni alla conoscenza della strutture e della funzione dell' organo di Jacobson. Bologna 1880. Deusch Zeitsch Tiermedizin 7, 325–335.

Powers, J. B. and Winans, S. S. 1975. Vomeronasal organ: critical role in mediating sexual behavior of the male hamster. Science 187, 961–963.

Quaglino, E., Giustetto, M., Panzanelli, P., Cantino, D., Fasolo, A., and Sassoe-Pognetto, M. 1999. Immunocytochemical localization of glutamate and gamma-aminobutyric acid in the accessory olfactory bulb of the rat. J. Comp. Neurol. 408, 61–72.

Raisman, G. 1972. An experimental study of the projection of the amygdala to the accessory olfactory bulb and its relationship to the concept of a dual olfactory system. Exp. Brain Res. 14, 395–408.

Retzius, G. 1894. Die Riechzellen der Ophidier in der Riechschleimhaut und im Jacobson'schen Organ. Biol. Untersuch. Neue Folge 6, 48–51.

Rizvi, T. A., Ennis, M., and Shipley, M. T. 1992. Reciprocal connections between the medial preoptic area and the midbrain periaqueductal gray in rat: a WGA-HRP and PHA-L study. J. Comp. Neurol. 315, 1–15.

Rodriguez, I., Del Punta, K., Rothman, A., Ishii, T., and Mombaerts, P. 2002. Multiple new and isolated families within the mouse superfamily of V1r vomeronasal receptors. Nat. Neurosci. 5, 134–140.

Rodriguez, I., Feinstein, P., and Mombaerts, P. 1999. Variable patterns of axonal projections of sensory neurons in the mouse vomeronasal system. Cell 97, 199–208.

Rollmann, S. M., Houck, L. D., and Feldhoff, R. C. 1999. Proteinaceous pheromone affecting female receptivity in a terrestrial salamander. Science 285, 1907–1909.

Rosser, A. E. and Keverne, E. B. 1985. The importance of central noradrenergic neurones in the formation of an olfactory memory in the prevention of pregnancy block. Neuroscience 15, 1141–1147.

Ryba, N. J. and Tirindelli, R. 1997. A new multigene family of putative pheromone receptors. Neuron 19, 371–379.

Sam, M., Vora, S., Malnic, B., Ma, W., Novotny, M. V., and Buck, L. B. 2001. Odorants may arouse instinctive behaviours. Nature 412, 142.

Sanchez-Criado, J. E. 1982. Involvement of the Vomeronasal System in the Reproductive Physiology of the Rat. In: Olfaction and Endocrine Regulation (*ed*. W. Breipohl), pp. 209–217. IRL Press.

Sasaki, K., Okamoto, K., Inamura, K., Tokumitsu, Y., and Kashiwayanagi, M. 1999. Inositol-1,4,5-trisphosphate accumulation induced by urinary pheromones in female rat vomeronasal epithelium. Brain Res. 823, 161–168.

Sato, Y., Miyasaka, N., and Yoshihara, Y. 2005. Mutually exclusive glomerular innervation by two distinct types of olfactory sensory neurons revealed in transgenic zebrafish. J. Neurosci. 25, 4889–4897.

Scalia, F. and Winans, S. S. 1975. The differential projections of the olfactory bulb and accessory olfactory bulb in mammals. J. Comp. Neurol. 161, 31–55.

Schoppa, N. E. and Westbrook, G. L. 2001. Glomerulus-specific synchronization of mitral cells in the olfactory bulb. Neuron 31, 639–651.

Schoppa, N. E. and Westbrook, G. L. 2002. AMPA autoreceptors drive correlated spiking in olfactory bulb glomeruli. Nat. Neurosci. 5, 1194–1202.

Schwarting, G. A. and Crandall, J. E. 1991. Subsets of olfactory and vomeronasal sensory epithelial cells and axons revealed by monoclonal antibodies to carbohydrate antigens. Brain Res. 547, 239–248.

Schwende, F. J., Wiesler, D., Jorgenson, J. W., Carmack, M., and Novotny, M. 1986. Urinary volatile constituents of the house mouse, *Mus musculus*, and their endocrine dependency. J. Chem. Ecol. 12, 277–296.

Shepherd, G. M. 2006. Smells, brains and hormones. Nature 439, 149–151.

Shiosaka, S., Sakanaka, M., Inagaki, S., Senba, E., Hara, Y., Takatsuki, K., Takagi, H., Kawai, Y., and Tohyama, M. 1982. Putative Neurotransmitters in the Amygdaloid Complex With

Special Reference to Peptidergic Pathways. In: Chemical Neuroanatomy (*ed*. P. C. Emson), pp. 359–389. Raven Press.
Shipley, M. T. and Adamek, G. D. 1984. The connections of the mouse olfactory bulb: a study using orthograde and retrograde transport of wheat germ agglutinin conjugated to horseradish peroxidase. Brain Res. Bull. 12, 669–688.
Simerly, R. B., Young, B. J., Capozza, M. A., and Swanson, L. W. 1989. Estrogen differentially regulates neuropeptide gene expression in a sexually dimorphic olfactory pathway. Proc. Natl. Acad. Sci. U. S. A. 86, 4766–4770.
Singer, A. G., Macrides, F., Clancy, A. N., and Agosta, W. C. 1986. Purification and analysis of a proteinaceous aphrodisiac pheromone from hamster vaginal discharge. J. Biol. Chem. 261, 13323–13326.
Singh, P. B., Brown, R. E., and Roser, B. 1987. MHC antigens in urine as olfactory recognition cues. Nature 327, 161–164.
Spehr, M., Hatt, H., and Wetzel, C. H. 2002. Arachidonic acid plays a role in rat vomeronasal signal transduction. J. Neurosci. 22, 8429–8437.
Spehr, M., Kelliher, K. R., Li, X. H., Boehm, T., Leinders-Zufall, T., and Zufall, F. 2006. Essential role of the main olfactory system in social recognition of major histocompatibility complex peptide ligands. J. Neurosci. 26, 1961–1970.
Storan, M. J. and Key, B. 2006. Septal organ of Gruneberg is part of the olfactory system. J. Comp. Neurol. 494, 834–844.
Stowers, L., Holy, T. E., Meister, M., Dulac, C., and Koentges, G. 2002. Loss of sex discrimination and male-male aggression in mice deficient for TRP2. Science 295, 1493–1500.
Sugai, T., Sugitani, M., and Onoda, N. 2000. Novel subdivisions of the rat accessory olfactory bulb revealed by the combined method with lectin histochemistry, electrophysiological and optical recordings. Neuroscience 95, 23–32.
Takami, S. and Graziadei, P. P. 1990. Morphological complexity of the glomerulus in the rat accessory olfactory bulb – a Golgi study. Brain Res. 510, 339–342.
Takami, S. and Graziadei, P. P. 1991. Light microscopic Golgi study of mitral/tufted cells in the accessory olfactory bulb of the adult rat. J. Comp. Neurol. 311, 65–83.
Takami, S., Fernandez, G. D., and Graziadei, P. P. 1992a. The morphology of GABA-immunoreactive neurons in the accessory olfactory bulb of rats. Brain Res. 588, 317–323.
Takami, S., Graziadei, P. P., and Ichikawa, M. 1992b. The differential staining patterns of two lectins in the accessory olfactory bulb of the rat. Brain Res. 598, 337–342.
Taniguchi, M., Kashiwayanagi, M., and Kurihara, K. 1995. Intracellular injection of inositol 1,4,5-trisphosphate increases a conductance in membranes of turtle vomeronasal receptor neurons in the slice preparation. Neurosci. Lett. 188, 5–8.
Taniguchi, M., Kashiwayanagi, M., and Kurihara, K. 1996. Intracellular dialysis of cyclic nucleotides induces inward currents in turtle vomeronasal receptor neurons. J. Neurosci. 16, 1239–1246.
Taniguchi, M., Wang, D., and Halpern, M. 1998. The characteristics of the electrovomeronasogram: its loss following vomeronasal axotomy in the garter snake. Chem. Senses 23, 653–659.
Taniguchi, M., Wang, D., and Halpern, M. 2000. Chemosensitive conductance and inositol 1,4,5-trisphosphate-induced conductance in snake vomeronasal receptor neurons. Chem. Senses 25, 67–76.
Tian, H. and Ma, M. 2004. Molecular organization of the olfactory septal organ. J. Neurosci. 24, 8383–8390.
Tirindelli, R., Mucignat-Caretta, C., and Ryba, N. J. 1998. Molecular aspects of pheromonal communication via the vomeronasal organ of mammals. Trends Neurosci. 21, 482–486.
Toyoda, F. and Kikuyama, S. 2000. Hormonal influence on the olfactory response to a female-attracting pheromone, sodefrin, in the newt, *Cynops pyrrhogaster*. Comp. Biochem. Physiol. B Biochem. Mol. Biol. 126, 239–245.
Trinh, K. and Storm, D. R. 2003. Vomeronasal organ detects odorants in absence of signaling through main olfactory epithelium. Nat. Neurosci. 6, 519–525.
Trotier, D. 1998. Electrophysiological properties of frog olfactory supporting cells. Chem. Senses 23, 363–369.
Trotier, D. and Doving, K. B. 1996. Functional role of receptor neurons in encoding olfactory information. J. Neurobiol. 30, 58–66.
Trotier, D., Doving, K. B., and Rosin, J. F. 1993. Voltage-dependent currents in microvillar receptor cells of the frog vomeronasal organ. Eur. J. Neurosci. 5, 995–1002.
Trotier, D., Eloit, C., Wassef, M., Talmain, G., Bensimon, J. L., Doving, K. B., and Ferrand, J. 2000. The vomeronasal cavity in adult humans. Chem. Senses 25, 369–380.
Tucker, D. 1971. Nonolfactory Responses from the Nasal Cavity: Jacobson's Organ and the Trigeminal System. In: Handbook of Sensory Physiology (*ed*. L. M. Beidler), pp. 151–181. Springer Verlag.
Urban, N. N. and Castro, J. B. 2005. Tuft calcium spikes in accessory olfactory bulb mitral cells. J. Neurosci. 25, 5024–5028.
Vaccarezza, O. L., Sepich, L. N., and Tramezzani, J. H. 1981. The vomeronasal organ of the rat. J. Anat. 132, 167–185.
Vandenbergh, J. G. 1983. Social Factors Controlling Puberty in the Female Mouse. In: Hormones and Behaviours in Higher Vertebrates (*eds*. J. Balthazart, J. Prive, and R. Gilles), pp. 342–349. Springer Verlag.
Vannier, B., Peyton, M., Boulay, G., Brown, D., Qin, N., Jiang, M., Zhu, X., and Birnbaumer, L. 1999. Mouse trp2, the homologue of the human trpc2 pseudogene, encodes mTrp2, a store depletion-activated capacitative Ca^{2+} entry channel. Proc. Natl. Acad. Sci. U. S. A. 96, 2060–2064.
Walz, A., Rodriguez, I., and Mombaerts, P. 2002. Aberrant sensory innervation of the olfactory bulb in neuropilin-2 mutant mice. J. Neurosci. 22, 4025–4035.
Wekesa, K. S. and Anholt, R. R. 1997. Pheromone regulated production of inositol-(1, 4, 5)-trisphosphate in the mammalian vomeronasal organ. Endocrinology 138, 3497–3504.
Winans, S. S. and Scalia, F. 1970. Amygdaloid nucleus: new afferent input from the vomeronasal organ. Science 170, 330–332.
Wissenbach, U., Schroth, G., Philipp, S., and Flockerzi, V. 1998. Structure and mRNA expression of a bovine trp homologue related to mammalian trp2 transcripts. FEBS Lett. 429, 61–66.
Wu, Y., Tirindelli, R., and Ryba, N. J. 1996. Evidence for different chemosensory signal transduction pathways in olfactory and vomeronasal neurons. Biochem. Biophys. Res. Commun. 220, 900–904.
Wysocki, C. J. 1979. Neurobehavioral evidence for the involvement of the vomeronasal system in mammalian reproduction. Neurosci. Biobehav. Rev. 3, 301–341.
Wysocki, C. J. and Lepri, J. J. 1991. Consequences of removing the vomeronasal organ. J. Steroid Biochem. Mol. Biol. 39, 661–669.
Wysocki, C. J. and Meredith, M. 1987. The Vomeronasal System. In: Neurobiology of Taste and Smell (*eds*. T. E. Finger and W. L. Silver), pp. 125–150. Wiley and Sons.
Wysocki, C. J. and Preti, G. 2004. Facts, fallacies, fears, and frustrations with human pheromones. Anat. Rec. A Discov. Mol. Cell. Evol. Biol. 281, 1201–1211.
Wysocki, C. J., Katz, Y., and Bernhard, R. 1983. Male vomeronasal organ mediates female-induced testosterone surges in mice. Biol. Reprod. 28, 917–922.

Xu, F., Schaefer, M., Kida, I., Schafer, J., Liu, N., Rothman, D. L., Hyder, F., Restrepo, D., and Shepherd, G. M. 2005. Simultaneous activation of mouse main and accessory olfactory bulbs by odors or pheromones. J. Comp. Neurol. 489, 491–500.

Yamamoto, K., Kawai, Y., Hayashi, T., Ohe, Y., Hayashi, H., Toyoda, F., Kawahara, G., Iwata, T., and Kikuyama, S. 2000. Silefrin, a sodefrin-like pheromone in the abdominal gland of the sword-tailed newt, *Cynops ensicauda*. FEBS Lett. 472, 267–270.

Yang, H., Shi, P., Zhang, Y. P., and Zhang, J. 2005. Composition and evolution of the V2r vomeronasal receptor gene repertoire in mice and rats. Genomics 86, 306–315.

Yoon, H., Enquist, L. W., and Dulac, C. 2005. Olfactory inputs to hypothalamic neurons controlling reproduction and fertility. Cell 123, 669–682.

Yoshihara, Y., Kawasaki, M., Tamada, A., Fujita, H., Hayashi, H., Kagamiyama, H., and Mori, K. 1997. OCAM: A new member of the neural cell adhesion molecule family related to zone-to-zone projection of olfactory and vomeronasal axons. J. Neurosci. 17, 5830–5842.

Zidek, L., Stone, M. J., Lato, S. M., Pagel, M. D., Miao, Z., Ellington, A. D., and Novotny, M. V. 1999. NMR mapping of the recombinant mouse major urinary protein I binding site occupied by the pheromone 2-sec-butyl-4,5-dihydrothiazole. Biochemistry 38, 9850–9861.

Zufall, F. and Munger, S. D. 2001. From odor and pheromone transduction to the organization of the sense of smell. Trends Neurosci. 24, 191–193.

Zufall, F., Ukhanov, K., Lucas, P., Liman, E., and Leinders-Zufall, T. 2005. Neurobiology of TRPC2: from gene to behavior. Pflugers. Arch. 451, 61–71.

4.44 Genomics of Vomeronasal Receptors

I Rodriguez, University of Geneva, Geneva, Switzerland

© 2008 Elsevier Inc. All rights reserved.

4.44.1	**Introduction**	815
4.44.2	**V1r Receptors**	816
4.44.2.1	On the Size of the Repertoires	816
4.44.2.2	Remarkably Variable Repertoires	817
4.44.2.3	Clustered Gene Families	817
4.44.2.4	Monogenic and Monoallelic V1r Expression	817
4.44.2.5	V1rs as Chemodetectors and Guidance Molecules	818
4.44.3	**V2r Receptors**	818
4.44.3.1	Genomic Parallels and Divergences with V1rs	818
4.44.3.2	Immune Multigene Families and V2r-Expressing Sensory Neurons	819
4.44.4	**Perspective**	819
4.44.4.1	A Genomic Trail of Speciation Events	819
References		819

Glossary

vomeronasal organ (VNO) Sensory olfactory structure, physically separate from the main olfactory system and present in mammals, amphibians, and reptiles. Its function is often linked to pheromone perception.

V1r receptors Pheromone receptors expressed by vomeronasal sensory neurons present in the apical part of the vomeronasal sensory neuroepithelium in rodents.

V2r receptors Putative pheromone receptors expressed by vomeronasal sensory neurons present in the basal part of the vomeronasal sensory neuroepithelium in rodents.

4.44.1 Introduction

The survival of multicellular organisms depends on their ability to perceive and recognize the outside and their own inside worlds. The main tool selected by evolution to achieve these basic tasks is based on the expression of multiple and different receptors, in specific cells. These cells then either directly respond to the stimuli, or instead transmit the information to others, which process the signals. To achieve this general need for receptor variability, various strategies have been selected by different systems and species. The vertebrate immune system, for example, bases its T-cell receptor (TCR) and Ig remarkable diversity on genomic recombination between a relatively limited number of coding segments. Another inventive strategy, used by many life forms including viruses, achieves variability by random mutation of messenger RNA transcripts. A very different option, which is based neither on genome recombination nor on transcript alteration, is used by vertebrate chemosensory systems to face the outside world: they benefit from receptor gene repertoires of amazing size and diversity already present in the genomes, which directly translate into an exceptional variability of chemoreceptors. Thus, odorant, taste, and vomeronasal receptor genes represent a substantial part of the coding fraction of mammalian genomes.

Vomeronasal receptor genes will be discussed here. Although some of their characteristics may be shared by odorant and taste receptor genes, they should not be assumed to be so, since their likely direct involvement in pheromone perception involved specific evolutionary pressures, pressures probably different from those which affected other chemosensory receptor genes. Moreover, the signal transduction cascades of sensory cells expressing odorant or vomeronasal receptors, but also their

targets in the brain, two processes which directly involve the expressed chemoreceptors, are dissimilar.

In mammals, pheromones are mostly (but not only) perceived by the vomeronasal organ. Two large putative seven transmembrane receptor families, the V1r and V2r superfamilies (Dulac, C. and Axel, R., 1995; Herrada, G. and Dulac, C., 1997; Matsunami, H. and Buck, L. B., 1997; Ryba, N. J. and Tirindelli, R., 1997), are almost exclusively expressed by vomeronasal sensory neurons.

4.44.2 V1r Receptors

4.44.2.1 On the Size of the Repertoires

All mammalian genomes apparently contain V1r genes. V1r repertoire sizes can be relatively limited, such as in dogs, for example, with only 8–10 potentially functional V1r genes (Rodriguez, I., 2005; Young, J. M., 2005), or particularly expanded such as in mice, where V1rs number about 160 (Rodriguez, I. *et al.*, 2002; Zhang, X. *et al.*, 2004) (Figure 1). Other species, such as cows or opossums, possess V1r repertoires of intermediate size (Grus, W. *et al.*, 2005). A few potentially functional V1r genes (among many pseudogenes; Giorgi, D. *et al.*, 2000; Kouros-Mehr, H. *et al.*, 2001) have been reported in primates, including humans (Rodriguez, I. *et al.*, 2000; Rodriguez, I. and Mombaerts, P., 2002). This may appear surprising since catarrhine primates only possess a vestigial and thus likely nonfunctional vomeronasal organ after birth (Maier, W., 1997) (a situation thought to be a result of trichromatic vision acquisition; Liman, E. R. and Innan, H., 2003; Zhang, J. and Webb, D. M., 2003; Gilad, Y. *et al.*, 2004). Possibly explaining the presence of V1r genes without functional vomeronasal system, expression of V1r genes has been reported outside the vomeronasal organ, in the main olfactory epithelium, in some species (Rodriguez, I. *et al.*, 2000; Wakabayashi, Y. *et al.*, 2002; Karunadasa, D. K. *et al.*, 2006). Thus, despite our strong taste for clear-cut expression profiles, the exclusive association between V1r expression and vomeronasal function is incorrect. This parallels the wrongly assumed functional dichotomy between the main olfactory and the vomeronasal systems, supposedly exclusively responsible for odor and pheromone perception, respectively. The origin of V1rs dates back apparently over 450 million years ago, since V1rs have also been identified in teleost species (Pfister, P. and Rodriguez, I., 2005). In these species, however, and unlike all mammals that express numerous V1rs, a very limited number of V1r genes are present in the genome (Pfister, P. *et al.*, 2007; Shi, P. and Zhang, J., 2007). These observations argue both for the presence of V1rs in other vertebrate phyla such as reptiles, and for a specific advantage in non-teleost species to maintain large and diversified V1r repertoires.

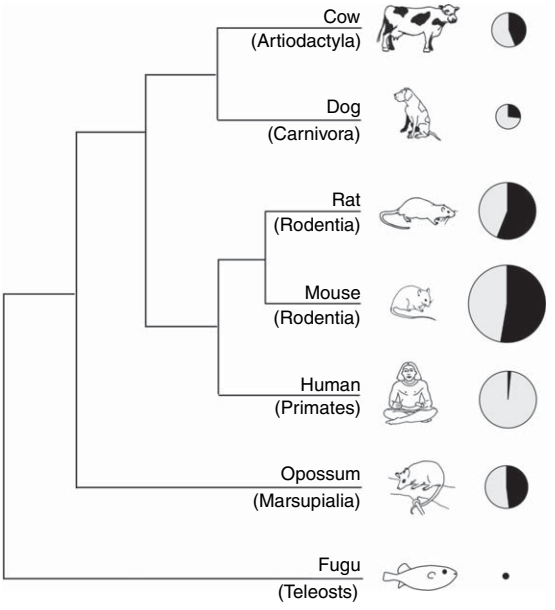

Figure 1 Variability of the V1r repertoire size between different vertebrate species. Pies represent the complete V1r repertoires corresponding to each species, and their surface the number of V1r genes. Black and gray indicate potentially functional V1r genes and pseudogenes, respectively. Adapted from Rodriguez, I. 2005. Remarkable diversity of mammalian pheromone receptor repertoires. Proc. Natl. Acad. Sci. U.S.A. 102, 6639–6640.

In addition to functional genes, a sizeable number of V1r pseudogenes are found in most species. Functional V1r genes are indeed sometimes less numerous than pseudogenic sequences, even in orders with well-developed vomeronasal systems such as rodents (Giorgi, D. and Rouquier, S., 2002; Rodriguez, I. *et al.*, 2002; Grus, W. E. and Zhang, J., 2004; Young, J. M. *et al.*, 2005) (Figure 1). Based on the sequence of their products, V1r genes can be divided into multiple, highly divergent families (12–15 in rodents), which only share a few common, highly conserved amino acids. Intrafamily homologies typically range from 40% to 98%, while interfamily identities can be as low as 15% (Rodriguez, I. *et al.*, 2002).

But does size matter? The very closely related and numerous V1r genes in a given family may each play a specific role and be responsible for the recognition of a narrow set of agonists; alternatively, these could represent a very redundant set of receptors with very little

evolutionary pressure to stay intact at the individual level, a view possibly supported by the large number of pseudogenes found in each family. Genetic experiments involving the partial deletion of defined V1r families, and the analysis of the potential resulting behavioral deficits have not yet settled this issue.

4.44.2.2 Remarkably Variable Repertoires

The recent sequencing of multiple mammalian genomes allowed the comparison of complete V1r repertoires between different species. These comparisons led to the surprising observation that V1r genes are not only highly variable inside the repertoire of a given species, but that repertoires of different species are also remarkably different (Lane, R. P. *et al.*, 2004). Thus, the parallel exploration of the cow, dog, opossum, and mouse V1r repertoires revealed species-specific expansions and absence of some V1r families (Grus, W. *et al.*, 2005). More unexpected, a similar observation was made when analyzing the mouse and rat V1r repertoires. Although both of these species are closely related and mostly express common V1r families, each also possesses their own V1r receptor families (Grus, W. E. and Zhang, J., 2004; Lane, R. P. *et al.*, 2004; Shi, P. *et al.*, 2005). V1r repertoires are thus characterized by rapid gene turnover and lineage-specific phylogenetic clustering, via gene duplications, deletions, and gene conversions.

A closer look at the evolutionary forces acting on these genes revealed that the diversification of the V1r repertoires, both inside a given species and between species, is at least partly the result of positive Darwinian selective pressure (i.e., the fixation of mutations that alter the translated sequence were favored over those which did not) (Mundy, N. I. and Cook, S., 2003; Lane, R. P. *et al.*, 2004; Shi, P. *et al.*, 2005). Positive selection has been observed in a few genes, evolving rapidly and often involved in the recognition of foreign molecules or cells, and usually related to the immune or fertilization processes. This latter function involves the recognition of same-species gametes, or the nonrecognition of gametes from different species: variability is there thought to provide postmating species barriers. One may suggest that V1r gene variability could similarly provide reproduction barriers, but in this case premating barriers, allowing only individuals possessing a given set of V1r receptors to adequately respond to the pheromonal blends of their own species. An attractive hypothesis would be to consider V1r diversity or novelty as potentially instrumental during speciation events, by their contribution to premating reproductive isolation. In favor of such possible role in speciation, V1r receptors are known to be narrowly tuned (Leinders-Zufall, T. *et al.*, 2000), unlike odorant receptors, and are therefore likely to dramatically alter perception and thus social behavior if lost or modified. In addition, in support of this view, a link between pheromone perception and speciation has been observed in a moth species (*Ostrinia*), in which changes in pheromone signaling and perception apparently allowed isolation and possibly speciation (Roelofs, W. L. *et al.*, 2002).

4.44.2.3 Clustered Gene Families

V1r families are often organized in clusters in the genome, and are present on virtually all autosomes in the few species where this was analyzed. These clusters result from multiple duplication events, possibly facilitated by Line1 repetitive elements, elements which are found at unusual high density in genomic regions harboring V1r genes (Lane, R. P. *et al.*, 2002; Lane, R. P. *et al.*, 2004), and whose retrotransposition apparently correlates with V1r duplications (Lane, R. P. *et al.*, 2004). Although V1rs are multiexonic genes (usually 2 or 3 exons), V1r coding sequences are entirely included in single exons (often the last one), similarly to many other G-coupled receptor genes. As previously mentioned, V1r families are organized, or better said found, in clusters; each of these contain multiple V1r units, whose transcription orientation is apparently random. Evidence for cluster-mediated regulatory mechanisms has recently been reported by us (Roppolo, D. *et al.*, 2007). Each V1r gene contains a relatively large segment of about 600 bp, located mostly upstream its transcription start site and overlapping slightly with the 5′-untranslated region, which is remarkably conserved (over 80%) between members of a given V1r family but not between different V1r family members (Lane, R. P. *et al.*, 2002; Lane, R. P. *et al.*, 2004). This observation contrasts with the poor promoter sequence conservation reported for odorant receptor genes. The role of these ultraconserved elements, largely more conserved than what one would expect from conventional promoters, is unknown.

4.44.2.4 Monogenic and Monoallelic V1r Expression

At the base of our current understanding of pheromone coding is the belief that each vomeronasal sensory neuron expresses a single (or a few) V1r receptor

genes (Dulac, C. and Axel, R., 1995), from a single, randomly chosen allele (Rodriguez, I. *et al.*, 1999). The perception of blends would thus involve a more central integration of multiple highly specific signals. Although monoallelic expression is experimentally well supported, the monogenic assumption still needs stronger experimental evidence. What is clear is that neurons expressing V1rs are not the same as those expressing V2rs. The first ones are expressed by sensory neurons located in the apical part of the pseudostratified vomeronasal epithelium, while the second ones are found in the more basal strata. The joined patterns of expression indicate that all mature sensory neurons express either V1r or V2r genes.

4.44.2.5 V1rs as Chemodetectors and Guidance Molecules

A remarkable dual role is apparently played by V1r receptors. First, not surprisingly, those expressed at the vomeronasal dendritic endings in contact with the outside world, play a role in chemodetection. This is supported by

1. a genetic approach in the mouse involving the deletion of an entire V1r cluster, and the observation of a correlated deficiency to perceive pheromones *in vitro*, and of inadequate behavior responses to specific interindividual interactions (Del Punta, K. *et al.*, 2000; Del Punta, K. *et al.*, 2002), and
2. by the identification of 2-heptanone, a molecule present in mouse urine, which plays a pheromonal role in this species, as an agonist for the V1rb2 receptor (Boschat, C. *et al.*, 2002).

Second, the expression of V1rs is instrumental in the elaboration of an adequate topographical map in the accessory olfactory bulb. Genetic experiments have shown that vomeronasal sensory neurons expressing a given V1r gene project their axons toward 10–20 neuropil-rich spherical structures, called glomeruli, in the caudal part of the olfactory bulb termed the accessory olfactory bulb (Belluscio, L. *et al.*, 1999; Rodriguez, I. *et al.*, 1999). Sensory neurons expressing other V1r receptors project to different glomeruli, leading to a complex topographical map of a few hundred glomeruli. The prevention of expression of a given V1r in a sensory neuron population leads to an altered axonal projection map, no longer convergent, which innervates glomeruli corresponding other receptors. This very particular dual role is also shared by odorant receptors, receptors that can even substitute for V1rs, in a vomeronasal context (Rodriguez, I. *et al.*, 1999). This and other observations in the olfactory system (Feinstein, P. *et al.*, 2004) suggest that very unrelated seven transmembrane receptors, in different systems, may also play a role in axonal targeting.

4.44.3 V2r Receptors

Three research groups independently identified V2rs in 1998 (Herrada, G. and Dulac, C., 1997; Matsunami, H. and Buck, L. B., 1997; Ryba, N. J. and Tirindelli, R., 1997). Our understanding of V2r biology, both in terms of role and expression in different species, lags behind the little we know about V1rs, likely for the simple reason that their identification postdates the one of V1rs. Unlike these latter, V2rs share strong homologies with well-known seven transmembrane G-coupled receptors, with long extracellular N-termini, including calcium-sensing and glutamate receptors.

4.44.3.1 Genomic Parallels and Divergences with V1rs

V2r genes have been identified in vertebrates, and are apparently restricted, as V1rs, to this subphylum. Numerous V2rs are found in frogs (Hagino-Yamagishi, K. *et al.*, 2004), and in teleost species (Cao, Y. *et al.*, 1998; Naito, T. *et al.*, 1998; Speca, D. J. *et al.*, 1999; Hashiguchi, Y. and Nishida, M., 2005), such as *Danio rerio*, for example, whose genome contains over 50 V2rs, (contrasting with the extremely limited number of V1rs in this species). In mammals such as mice and rats, 61 and 57 V2r genes with intact open reading frames have been reported, respectively (Yang, H. *et al.*, 2005). These numbers represent a strikingly low proportion (between 29% and 34%) of the complete, pseudogene-including V2r repertoire of these two species. The chromosomal distribution of these genes is wide, since in the mouse they are located on at least 12 chromosomes, including the X chromosome. V2rs tend, like V1rs, to be clustered in the genome, with no apparent specific organization within these clusters.

The exact number of different expressed receptors corresponding to the known V2r genes is difficult to evaluate, since the large extracellular part of V2r receptors is encoded by multiple exons that are often alternatively spliced, and which therefore lead to a corresponding expansion of the V2r

repertoires variability. In rodents, V2rs have been classified into three families, among which one, family C, is particularly distant from the others, a situation likely reflecting an ancient divergence with the other two families, predating the separation between teleosts and tetrapods (Yang, H. *et al.*, 2005). Repertoire comparisons between mouse and rat indicate that similarly to what is observed for V1rs, V2rs form species-specific clades, with the result that only a few rat–mouse orthologs can be identified. A more detailed analysis of the evolution of rodent V2rs suggests that most species-specific clades resulted from recent gene duplications/losses, with a minor role played by gene conversion events. Moreover, similarly to what was observed for V1rs, positive selection was detected for specific amino acids in V2rs (Yang, H. *et al.*, 2005), with the particularity that most of them were located on the N-terminal extracellular region of the receptor, a segment thought to mediate ligand/receptor interactions.

4.44.3.2 Immune Multigene Families and V2r-Expressing Sensory Neurons

Vomeronasal receptors are thought to interact with G proteins, respectively, the Gi2a and Goa subunits for V1rs and V2rs. An unexpected complex and nonrandom coexpression, and interaction, was recently reported between two unlikely partners: V2r receptors and major histocompatibility complex (MHC) molecules (Ishii, T. *et al.*, 2003; Loconto, J. *et al.*, 2003). Members of the nonclassical MHC class I M10 and M1 families (6 and 3 members, respectively), are exclusively expressed by vomeronasal sensory neurons. Genes encoding for these receptors are clustered on chromosome 17 in the mouse, and are part of the H2-M locus, the most distal segment encoding class I genes.

These MHC receptors are involved, via a still unknown mechanism, in the adequate export of at least some V2rs to the cellular membrane (Loconto, J. *et al.*, 2003). Reports suggest however, in addition, a more direct involvement of MHC molecules in pheromone perception. For example, MHC-diassortative pregnancy block and preferences have been demonstrated in multiple species and conditions. Moreover, some vomeronasal sensory neurons respond to class I, MHC-binding peptides (Leinders-Zufall, T. *et al.*, 2004). The presence of specific MHC molecules in the vomeronasal organ forces us to consider them as prime candidates for such interactions. Thus, it is possible that not only do MHC type I function as facilitators of V2r cell surface expression, but that they may be able to detect peptides (although crystal structure data does not support this hypothesis (Olson, R. *et al.*, 2005)) via the use of their binding grooves, a crucial tool used by their classical counterparts.

4.44.4 Perspective

4.44.4.1 A Genomic Trail of Speciation Events

A similar strategy has thus been selected by evolution to provide vertebrate pheromone-sensing systems with two large and diverse repertoires of chemoreceptors: rapid gene birth and death. We look today at a battlefield with hundreds of pseudogenic sequences, often more numerous than potentially functional ones. This represents an amazing source of information, and because of the speed at which the repertoires evolved, a unique recording of speciation events, including those that occurred relatively recently. We are now lacking data relative to the other side of the coin: the pheromones themselves. These are today, in vertebrates, still remarkably poorly described (insects got somehow more attention for once). Even in rodents, which are largely the best-studied mammals in the pheromone field, <10 compounds have been reported to mediate pheromonal interactions, a situation largely due to the tedious biochemical purifications involved in the identification of these chemicals. Thus, unless we benefit from a biochemical technical revolution allowing large-scale approaches similar to the one which makes today a quick survey of complete genomes an easy task, a global understanding of vertebrate pheromone perception at the peripheral level will be incomplete, for a long time.

References

Belluscio, L., Koentges, G., Axel, R., and Dulac, C. 1999. A map of pheromone receptor activation in the mammalian brain. Cell 97, 209–220.

Boschat, C., Pelofi, C., Randin, O., Roppolo, D., Luscher, C., Broillet, M. C., and Rodriguez, I. 2002. Pheromone detection mediated by a V1r vomeronasal receptor. Nat. Neurosci. 5, 1261–1262.

Cao, Y., Oh, B. C., and Stryer, L. 1998. Cloning and localization of two multigene receptor families in goldfish olfactory epithelium. Proc. Natl. Acad. Sci. U. S. A. 95, 11987–11992.

Del Punta, K., Leinders-Zufall, T., Rodriguez, I., Jukam, D., Wysocki, C. J., Ogawa, S., Zufall, F., and Mombaerts, P. 2002. Deficient pheromone responses in mice lacking a cluster of vomeronasal receptor genes. Nature 419, 70–74.

Del Punta, K., Rothman, A., Rodriguez, I., and Mombaerts, P. 2000. Sequence diversity and genomic organization of vomeronasal receptor genes in the mouse. Genome Res. 10, 1958–1967.

Dulac, C. and Axel, R. 1995. A novel family of genes encoding putative pheromone receptors in mammals. Cell 83, 195–206.

Feinstein, P., Bozza, T., Rodriguez, I., Vassalli, A., and Mombaerts, P. 2004. Axon guidance of mouse olfactory sensory neurons by odorant receptors and the beta2 adrenergic receptor. Cell 117, 833–846.

Gilad, Y., Wiebe, V., Przeworski, M., Lancet, D., and Pääbo, S. 2004. Loss of olfactory receptor genes coincides with the acquisition of full trichromatic vision in primates. PLoS Biol. 2, E5.

Giorgi, D. and Rouquier, S. 2002. Identification of V1R-like putative pheromone receptor sequences in non-human primates. Characterization of V1R pseudogenes in marmoset, a primate species that possesses an intact vomeronasal organ. Chem. Senses 27, 529–537.

Giorgi, D., Friedman, C., Trask, B. J., and Rouquier, S. 2000. Characterization of nonfunctional V1R-like pheromone receptor sequences in human. Genome Res. 10, 1979–1985.

Grus, W. E. and Zhang, J. 2004. Rapid turnover and species-specificity of vomeronasal pheromone receptor genes in mice and rats. Gene 340, 303–312.

Grus, W., Shi, P., Zhang, Y., and Zhang, J., 2005. Dramatic variation of the vomeronasal pheromone gene repertoire among five orders of placental and marsupial mammals. PNAS 102, 5767–5772.

Hagino-Yamagishi, K., Moriya, K., Kubo, H., Wakabayashi, Y., Isobe, N., Saito, S., Ichikawa, M., and Yazaki, K. 2004. Expression of vomeronasal receptor genes in *Xenopus laevis*. J. Comp. Neurol. 472, 246–256.

Herrada, G. and Dulac, C. 1997. A novel family of putative pheromone receptors in mammals with a topographically organized and sexually dimorphic distribution. Cell 90, 763–773.

Hashiguchi, Y. and Nishida, M. 2005. Evolution of vomeronasal-type odorant receptor genes in the zebrafish genome. Gene 362, 19–28.

Ishii, T., Hirota, J., and Mombaerts, P. 2003. Combinatorial coexpression of neural and immune multigene families in mouse vomeronasal sensory neurons. Curr. Biol. 13, 394–400.

Karunadasa, D. K., Chapman, C., and Bicknell, R. J. 2006. Expression of pheromone receptor gene families during olfactory development in the mouse: expression of a V1 receptor in the main olfactory epithelium. Eur. J. Neurosci. 23, 2563–2572.

Kouros-Mehr, H., Pintchovski, S., Melnyk, J., Chen, Y. J., Friedman, C., Trask, B., and Shizuya, H. 2001. Identification of non-functional human VNO receptor genes provides evidence for vestigiality of the human VNO. Chem. Senses 26, 1167–1174.

Lane, R. P., Cutforth, T., Axel, R., Hood, L., and Trask, B. J. 2002. Sequence analysis of mouse vomeronasal receptor gene clusters reveals common promoter motifs and a history of recent expansion. Proc. Natl. Acad. Sci. U. S. A. 99, 291–296.

Lane, R. P., Young, J., Newman, T., and Trask, B. J. 2004. Species specificity in rodent pheromone receptor repertoires. Genome Res. 14, 603–608.

Leinders-Zufall, T., Brennan, P., Widmayer, P. S. P. C., Maul-Pavicic, A., Jager, M., Li, X. H., Breer, H., Zufall, F., and Boehm, T. 2004. MHC class I peptides as chemosensory signals in the vomeronasal organ. Science 306, 1033–1037.

Leinders-Zufall, T., Lane, A. P., Puche, A. C., Ma, W., Novotny, M. V., Shipley, M. T., and Zufall, F. 2000. Ultrasensitive pheromone detection by mammalian vomeronasal neurons. Nature 405, 792–796.

Liman, E. R. and Innan, H. 2003. Relaxed selective pressure on an essential component of pheromone transduction in primate evolution. Proc. Natl. Acad. Sci. U. S. A. 100, 3328–3332.

Loconto, J., Papes, F., Chang, E., Stowers, L., Jones, E. P., Takada, T., Kumanovics, A., Fischer Lindahl, K., and Dulac, C. 2003. Functional expression of murine V2R pheromone receptors involves selective association with the M10 and M1 families of MHC class Ib molecules. Cell 112, 607–618.

Maier, W. 1997. The nasopalatine duct and the nasal floor cartilages in catarrhine primates. Z. Morphol. Anthropol. 81, 289–300.

Matsunami, H. and Buck, L. B. 1997. A multigene family encoding a diverse array of putative pheromone receptors in mammals. Cell 90, 775–784.

Mundy, N. I. and Cook, S. 2003. Positive selection during the diversification of class I vomeronasal receptor-like (V1RL) genes, putative pheromone receptor genes, in human and primate evolution. Mol. Biol. Evol. 20, 1805–1810.

Naito, T., Saito, Y., Yamamoto, J., Nozaki, Y., Tomura, K., Hazama, M., Nakanishi, S., and Brenner, S. 1998. Putative pheromone receptors related to the Ca^{2+}-sensing receptor in Fugu. Proc. Natl. Acad. Sci. U. S. A. 95, 5178–5181.

Olson, R., Huey-Tubman, K. E., Dulac, C., and Bjorkman, P. J. 2005. Structure of a pheromone receptor-associated MHC molecule with an open and empty groove. PLoS Biol. 3, e257.

Pfister, P. and Rodriguez, I. 2005. Olfactory expression of a single and highly variable V1r pheromone receptor-like gene in fish species. Proc. Natl. Acad. Sci. U. S. A. 102(15), 5489–5494.

Pfister, P., Randall, J., Montoya-Burgos, J. I., and Rodriguez, I. 2007. Divergent evolution among teleost V1r receptor genes. PLoS ONE 2, e379.

Rodriguez, I. 2005. Remarkable diversity of mammalian pheromone receptor repertoires. Proc. Natl. Acad. Sci. U. S. A. 102, 6639–6640.

Rodriguez, I. and Mombaerts, P. 2002. Novel human vomeronasal receptor-like genes reveal species-specific families. Curr. Biol. 12, R409–R411.

Rodriguez, I., Del Punta, K., Rothman, A., Ishii, T., and Mombaerts, P. 2002. Multiple new and isolated families within the mouse superfamily of V1r vomeronasal receptors. Nat. Neurosci. 5, 134–140.

Rodriguez, I., Feinstein, P., and Mombaerts, P. 1999. Variable patterns of axonal projections of sensory neurons in the mouse vomeronasal system. Cell 97, 199–208.

Rodriguez, I., Greer, C. A., Mok, M. Y., and Mombaerts, P. 2000. A putative pheromone receptor gene expressed in human olfactory mucosa. Nat. Genet. 26, 18–19.

Roelofs, W. L., Liu, W., Hao, G., Jiao, H., Rooney, A. P., and Linn, C. E., Jr. 2002. Evolution of moth sex pheromones via ancestral genes. Proc. Natl. Acad. Sci. U. S. A. 99, 13621–13626.

Roppolo, D., Vollery, S., Kan, C., Lüscher, C., Broillet, M. C., and Rodriguez, I. 2007. Gene cluster lock after pheromone receptor gene choice. EMBO J. (in press).

Ryba, N. J. and Tirindelli, R. 1997. A new multigene family of putative pheromone receptors. Neuron 19, 371–379.

Shi, P. and Zhang, J. 2007. Comparative genomic analysis identifies an evolutionary shift of vomeronasal receptor gene repertoires in the vertebrate transition from water to land. Genome Res. 17(2), 166–174.

Shi, P., Bielawski, J. P., Yang, H., and Zhang, Y. P. 2005. Adaptive diversification of vomeronasal receptor 1 genes in rodents. J. Mol. Evol. 60, 566–576.

Speca, D. J., Lin, D. M., Sorensen, P. W., Isacoff, E. Y., Ngai, J., and Dittman, A. H. 1999. Functional identification of a goldfish odorant receptor. Neuron 23, 487–498.

Wakabayashi, Y., Mori, Y., Ichikawa, M., Yazaki, K., and Hagino-Yamagishi, K. 2002. A putative pheromone receptor gene is expressed in two distinct olfactory organs in goats. Chem. Senses 27, 207–213.

Yang, H., Shi, P., Zhang, Y. P., and Zhang, J. 2005. Composition and evolution of the V2r vomeronasal receptor gene repertoire in mice and rats. Genomics 86, 306–315.

Young, J. M., Kambere, M., Trask, B. J., and Lane, R. P. 2005. Divergent V1R repertoires in five species: Amplification in rodents, decimation in primates, and a surprisingly small repertoire in dogs. Genome Res. 15, 231–240.

Zhang, J. and Webb, D. M. 2003. Evolutionary deterioration of the vomeronasal pheromone transduction pathway in catarrhine primates. Proc. Natl. Acad. Sci. U. S. A. 100, 8337–8341.

Zhang, X., Rodriguez, I., Mombaerts, P., and Firestein, S. 2004. Odorant and vomeronasal receptor genes in two mouse genome assemblies. Genomics 83, 802–811.

4.45 Human Olfactory Psychophysics

Brad Johnson, Rehan M Khan, and Noam Sobel, UC Berkeley, Berkeley, CA, USA

Published by Elsevier Inc.

4.45.1	**Introduction**	824
4.45.2	**Olfactory Detection**	826
4.45.2.1	Method of Odorant Delivery	826
4.45.2.1.1	Olfactometers	826
4.45.2.1.2	To sniff or not to sniff	828
4.45.2.1.3	Jars	828
4.45.2.2	The Assumed Threshold Model	829
4.45.2.3	Measuring the Threshold Model	830
4.45.2.4	Measuring Near-Threshold Performance	831
4.45.2.5	Nonolfactory Detection of Airborne Chemicals	831
4.45.2.6	Adaptation	832
4.45.2.7	Reported Absolute Thresholds	832
4.45.3	**Olfactory Discrimination**	836
4.45.3.1	Discriminating between Different Concentrations	837
4.45.3.2	Discriminating between Different Odorants	838
4.45.3.3	Speed of Olfactory Discrimination	840
4.45.4	**Olfactory Identification**	841
4.45.4.1	Language and Olfactory Identification	842
4.45.4.2	Identification of an Odor Rather than Its Parts	843
4.45.4.3	Nostril-Specific Odor Tuning	844
4.45.4.4	Identifying Odor Characteristics	847
4.45.4.5	Odor Space	848
4.45.4.5.1	Perception-based maps	848
4.45.4.5.2	Explicit similarity methods	848
4.45.4.5.3	Implicit similarity methods	849
4.45.4.6	Final Word	851
References		851

Glossary

2AFC Two-alternative forced-choice psychophysical paradigm in which a subject must choose which of two alternatives (one target and one distracter) is the target.

3AFC Three-alternative forced-choice psychophysical paradigm in which a subject must choose which of three alternatives (one target and two distracters) is the target.

adaptation The temporary diminution of response to successive repetitions of a stimulus.

adaptive staircase method A method for presenting stimuli to ascertain a detection threshold in which the choice of successive stimuli depends on prior responses.

anosmia A condition in which a subject cannot detect any odorant.

anosmia, specific An inability to detect a specific odorant in the absence of a general anosmia.

ascending method of limits A method for presenting stimuli in sequence from low to high concentration to determine detection threshold.

detection threshold The minimal concentration of an odorant sufficient for reliable detection.

JND Just noticeable difference. The smallest increment in the intensity of a stimulus that can be discerned.

magnitude estimation The assignment of a numerical value to the perceived intensity of a stimulus

MDS Multidimensional scaling. A technique for inferring a coordinate space in which objects whose pairwise distances are known can be placed.

method of constant stimuli A procedure for determining absolute or discrimination thresholds wherein a standard stimulus is presented repeatedly against distractors drawn one at a time from a set spanning a range of intensities and subjects make a forced-choice decision at each trial.
odorant Airborne molecule perceived as an odor.
olfactometer A device for the precise delivery of odorants to a subject.
osmic Able to smell, in contradistinction to anosmic.
power law A mathematical function that describes the relationship between a stimulus magnitude and its corresponding perceived magnitude.
psychometric function A function that relates a behavioral response (e.g., percent correct identification) to a stimuli to some parameter (usually a magnitude) of the stimulus.
psychophysics The precise measurement of perceptual phenomena in relation to their physical stimuli.
pure olfactant An odorant that activates only the olfactory and not the trigeminal system
signal detection theory A theory that describes how well a signal can be detected embedded within noise as a function of the signal strength and the detector's criterion or bias.
trigeminal odorant An odorant that stimulates the trigeminal system.
UPSIT University of Pennsylvania smell identification test. A standardized multiple-choice smell identification test that is used to identify olfactory function as a function of age.
vibrational theory A controversial theory of how molecules interact with olfactory receptors according to which receptors use a form of electron spectroscopy to measure the vibrational spectra of molecules.
Weber–Fechner law A law which states that the perceived magnitude of a stimulus is proportional to the logarithm of the intensity of the stimulus.
Weber fraction The minimal increment in a stimulus necessary to perceive a change. It is a constant proportion of the original comparator stimulus.

4.45.1 Introduction

The field of psychophysics deals with describing the relationship between physical stimuli and their resultant perceptual phenomena within a rigorous, quantifiable framework. The field of neuroscience is then tasked with elucidating the genetic, molecular, cellular, and system-level physiological mechanisms that underlie this psychophysical framework. This pattern whereby psychophysics guides physiological research has been central to our understanding of the physiology of vision and audition. For example, psychophysical studies in vision demonstrated that all perceived colors can result from the mixing of just three colors, and that these perceived colors are largely determined by the wavelength of the impinging light. This psychophysical trichromatic model of color perception was the impetus that guided physiologists in their discovery of the three receptor types in the retina that provide the basis for color perception (De Valois, R. L. and De Valois, K. K. 1993).

Similarly, olfactory psychophysics has provided a broad basis for understanding olfaction. Often, however, what is observed about olfactory psychophysics is not the great mass of knowledge, but rather one prominent lack: the core question in olfactory psychophysics, namely, which particular properties of airborne molecules give rise to particular odor qualities, remains unanswered. The reason for this lacuna is not, as we shall see in this chapter, want of industry, but rather the peculiar complexities of both the stimulus and the perceptual response. Sometimes characterized as the most primitive sense, olfaction has also proved itself to be the most stubbornly inaccessible. Undoubtedly, this is in part because the stimulus is more complex than that in other distal senses. In vision, three spatial dimensions, one of intensity and another of wavelength, do much to constrain the stimulus space. In audition a similar number of dimensions are sufficient to characterize the basic properties of the stimulus. In olfaction, the number of stimulus features necessary to characterize the countless discriminable odor molecules may well number in the hundreds, and so olfaction may well be orders of magnitude more intrinsically complex than the other distal senses. Notwithstanding all this, a

considerable body of psychophysics exists and provides important constraints on efforts to understand olfactory physiology.

Olfactory perception can be described as a hierarchical pyramid (Savic, I. *et al.*, 2000) building up from a base of olfactory detection, followed by olfactory discrimination, and culminating in olfactory identification. We consider these three levels of processing as hierarchical because of their pattern of exclusivity. One can have olfactory detection without olfactory discrimination and identification, but not vice versa. Likewise, one can have detection and discrimination between two odorants, without odorant identification. Finally, olfactory identification requires olfactory detection, implicitly entails olfactory discrimination, and represents the highest level of olfactory processing whereby an olfactory percept is matched to an olfactory memory and given a semantic label. In this chapter, we will use this hierarchy of olfactory processing as our organizational guide and describe what the psychophysical study of human olfaction has taught us regarding each of these three processing stages.

It is noteworthy that the above functional hierarchy is loosely related to a neuroanatomical structural hierarchy (Savic, I. *et al.*, 2000; Royet, J. P. *et al.*, 2001; Sabri, M. *et al.*, 2005). The first phase in olfactory processing consists of sniffing odorants (reviewed in Mainland, J. and Sobel, N. 2005) that then cross a mucous membrane (reviewed in Lewis, J. E. and Dahl, A. R. 1995) in order to interact with (in humans) ~14 million olfactory receptors of ~400 different types (Gilad, Y. and Lancet, D. 2003) that line the olfactory epithelium. Same receptor types then converge via the olfactory nerve onto unique locations in the olfactory bulb called glomeruli. Following some processing at the level of the olfactory bulb, information is conveyed via the olfactory tract to olfactory cortex, mostly inhabiting the ventral portion of the temporal lobe (reviewed in Price, J. L. 1990). From there, olfactory information is relayed throughout the brain to multiple sites, most notably the limbic system, the orbitofrontal gyri, and insular cortex (reviewed in Sobel, N. *et al.*, 2003).

The process of olfactory detection is largely linked to events at the level of the epithelium in that it reflects a nonspecific increase is system activation beyond noise levels. The process of olfactory discrimination is linked to both events at the epithelium and events in the bulb, in that it reflects specific rather than nonspecific patterns of activity. Discrimination is also linked to cortex in that it calls upon short-term memory (Wilson, D. A. and Stevenson, R. J. 2003a; 2003b). Finally, the process of olfactory identification is linked to events in the epithelium and bulb, and strongly linked to events in cortex, in that it reflects linking specific patterns of odorant-induced activity to previously stored information such as semantic representations (Haberly, L. B. and Bower, J. M. 1989; Stevenson, R. J. and Boakes, R. A. 2003). Some human lesion studies support this loose link between the structural and functional hierarchy of olfaction. For example, temporal lobe lesions hamper olfactory discrimination and identification, but not detection (Zatorre, R. J. and Jones-Gotman, M. 1991). This link, however, should be treated as a loose framework only, as even the basic process of olfactory detection is undoubtedly subserved by cortical mechanisms of attention and noise suppression.

Although in this chapter we will focus on basic psychophysical mechanisms, it is noteworthy that these basic mechanisms subserve an extraordinary human sense (Shepherd, G. M., 2004). Humans have superb olfaction. For example, it may not surprise many that dogs can recognize humans by their odor (Schoon, G. A. A. and Debruin, J. C., 1994), but it will probably surprise most that reciprocally, humans can identify dogs by their odor (Wells, D. L. and Hepper, P. G., 2000). Similarly, the dominance of olfactory cues in the interaction between a rabbit and its pups is common knowledge (Schaal, B. *et al.*, 2003), but not all are aware that human mothers can identify their babies by smell (Porter, R. H. *et al.*, 1983), and human babies can identify the smell of their breast-feeding mother by 6 days after birth (Macfarelane, A. 1975; Schaal, B. *et al.*, 1980). Finally, that a pig can locate a truffle by its smell (Ackerman, D., 1990) is appreciated by all who like to eat it (the truffle), but that humans can spatially localize an odorant in a laboratory setting (Békésy, G. V. 1964; Porter, J. *et al.*, 2005) (Figure 1), or track an odor trail in a field setting (Porter, J. *et al.*, 2007), is appreciated by only an esoteric few. These are only but a few of the extraordinary olfactory abilities of humans.

Finally, despite the temptation of digressing to relevant data from physiology and functional imaging, as well as data from nonhuman animals, in this chapter we will limit such excursions to the absolute minimum. Here, we concentrate on human olfactory psychophysics only, but we encourage the interested reader to pursue the relevant physiology and imaging literature.

Figure 1 Scent tracking in dogs and humans. The left panel consists of an image published in the 1978 National Geographic Survey on Smell. A dead pheasant was dragged along a field as denoted by the yellow line. A dog with light-emitting diodes on its collar was then released at the far end of the field. The time-lapsed image reveals the dog's tracking behavior. The right panel consists of data from ongoing experiments in our laboratory. The odorant track was made of a mixture of common odorants. All sensory input other than olfaction was prevented by opaque goggles, earmuffs, and thick gloves. A backpack was equipped with monitors that measured subject's nasal respiration in real time and monitored subject location with RTK-GPS offering 1 mm resolution. Although slow, human subjects were surprisingly good at tracking scent trails.

4.45.2 Olfactory Detection

A basic idea of psychophysics is that there is a minimum stimulus quantity that is needed for conscious perception of a sensory event (Herbart, J. F., 1824–1825). In olfaction, estimates of this minimal quantity vary across odorants and even for the same odorant have varied tremendously across laboratories (Laffort, P. 1963; Patte, F. *et al.*, 1975; Van Gemert, L. J. and Nettenbreijer, A. H., 1977; Fazzalari, F. A., 1978; Van Gemert, L. J. 1984). For example, Amoore J. E. and Hautala E. (1983) report 10^6-fold range in detection threshold across laboratories for some odorants. This state of affairs, understatedly described by Devos M. and Patte F. (1990) as disappointing, is mostly the result of several clearly understood extraneous sources of variance having to do with methods of stimulus generation and delivery. Thus, any reading of the olfactory psychophysics literature depends on an understanding of these extraneous sources, which we will first review.

4.45.2.1 Method of Odorant Delivery

4.45.2.1.1 Olfactometers

In an otherwise excellent review of olfactory psychophysics, Engen T. (1973) noted that "[a] great deal has been done recently in instrumentation of the presentation of odorants, enough surely to satisfy those who feel psychophysical research starts with the apparatus." Yet 30 years after this perhaps too optimistic appraisal, we find that there is still no uniform standard device for the delivery of odorants. Odorant delivery methods vary widely across laboratories, and even in those that expend the most effort (and funds) toward odorant generation, there is still no olfactory device on a par with the visual projector or auditory amplifier.

The two most commonly used methods of odorant delivery are either sniffing the headspace over an odorant-filled jar or delivery through a dedicated apparatus usually referred to as an olfactometer, a term coined by Hans Zwaardemaker, one of the first to build such a device (Zwaardemaker, H., 1889). Olfactometers range from simple devices such as squeezable bottles fitted with nose cones, to slightly more complex devices using solenoid valves to control odorized airflow, to sophisticated devices using computer-controlled mass flow controllers (MFCs) that allow for precise control over not only odorant concentration, but also timing, temperature, and humidity (reviewed in Prah, D. *et al.*, 1995). See Figure 2 for an example of such an olfactometer and associated imaging and psychophysics uses.

Regardless of complexity, most olfactometers odorize the airflow by flowing a carrier (clean air or nitrogen) either over an odorant within a canister of some sort or through an odorant-infused sponge-type media, or bubbling the carrier through liquid odorant in a canister. The latter enables obtaining higher overall concentrations of odorized airflows, but carries the risk of generating aerosols within the odorized airflow. Thus, flowing carrier over, rather than through the odorant, generates a far more stable stimulus and is the recommended approach whenever it is sufficient for generating a dynamic range of concentrations. Most current olfactometers are air-dilution olfactometers, which means that they obtain the intended odorant concentration by diluting an odorized airflow with a clean airflow. The ratio of dilution will determine the end concentration. This stands in contrast to simpler olfactometers in which the concentration of the resultant airflow is set by using different concentrations of odorant liquid within the odorant canisters. High-end air-dilution olfactometers also enable mixing different odorized airflows with each other in order to obtain air-dilution odorant mixtures. MFC-equipped olfactometers offer the highest level of control over airflow parameters, enable odorant delivery onset times within the millisecond range, have very high repeatability and stability, and when properly calibrated with analytical devices such as photoionization or flame-ionization detectors, offer accurate control over odorant concentration. Although all the above attributes of high-end

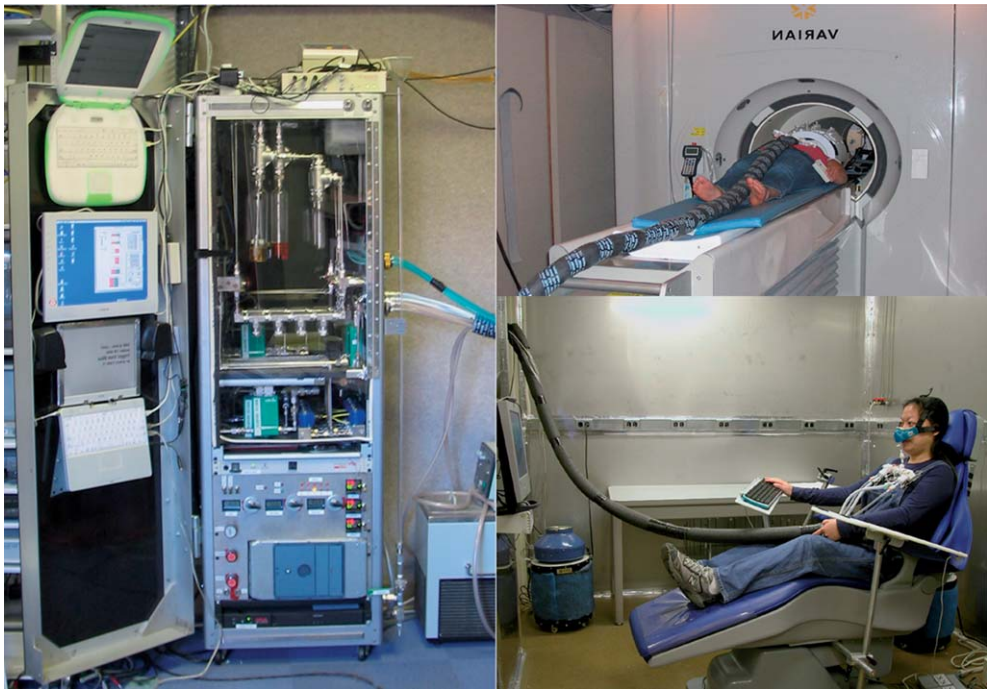

Figure 2 An air-dilution olfactometer. The olfactometer (left panel) is about 6 × 2 × 2 feet and weighs about 400 lbs. Using 13 MFCs and 18 solenoid valves, it delivers odorants to subjects in either the psychophysics laboratory (bottom right panel) or the fMRI scanner (top right panel) while simultaneously measuring airflow in each nostril separately. Although the olfactometer controls odorant temperature, humidity, flow rate, identity (one of five odorants, or any binary mixture thereof), intensity (verified by photoionization), and temporal resolution to the order of ~2 ms, it is still a far cry from a visual projector or auditory amplifier in its accuracy and versatility.

olfactometers render them the likely candidate for generating odorant stimuli when measuring absolute olfactory detection thresholds, these devices also suffer from typical drawbacks that hamper such efforts. Most prominent of these drawbacks is contamination. Within an olfactometer, odorized air passes through tubing before it reaches the sampling port, which may be in the form of a nasal mask, or tubes (canulas) that are inserted into the nostrils. Odorant molecules from ongoing experimental events tend to stick to these tubes, and then present themselves at unwanted times. Such contamination can be minimized by using nonstick tubing materials such as Teflon, glass, and stainless steel, but the contamination cannot be altogether eliminated. Considering the outstanding sensitivity of the human olfactory system, such contamination renders olfactometers a problematic device for the determination of absolute detection thresholds. Olfactometers remain, however, the preferred method of stimulus delivery for other olfactory tasks such as suprathreshold magnitude estimation, olfactory discrimination, identification, and so on.

4.45.2.1.2 To sniff or not to sniff

Olfaction is strongly dependent on a sensory-motor component, namely sniffing (Mainland, J. and Sobel, N. 2005). When using an olfactometer, one can eliminate sniffing by injecting the odorant into the nostrils of an otherwise passive subject. Furthermore, the subject can be trained in the behavior of velopharyngeal closure, whereby the soft palate elevates and lateral pharyngeal walls move medially to meet the soft palate to separate oral and nasal cavities, a method developed to reduce sniff-related artifacts that may be present in various methods of recording neural activity (Kobal, G. and Hummel, C., 1988). However, in most psychophysical studies, preventing sniffing significantly alters the behavior under investigation. Sniffs transport approximately 5–10% of the airflow entering the external nares to the epithelium (Keyhani, K. *et al.*, 1997). Sniff airflow velocity influences olfactory detection thresholds (Le Magnen, J., 1945; Laing, D. G., 1983; Sobel, N. *et al.*, 2000a) and olfactory intensity estimates (Rehn, T., 1978; Teghtsoonian, R. and Teghtsoonian, M., 1984; Youngentob, S. L. *et al.*, 1986; Hornung, D. E. *et al.*, 1997). Moreover, the somatosensory stimulation associated with airflow in the nose is represented by neural activity in both human olfactory bulb (Hughes, J. R. *et al.*, 1969) and olfactory cortex (Sobel, N. *et al.*, 1998), and it is necessary for olfactory perception. For example, when an odorant is injected intravenously into the bloodstream reaching the olfactory epithelium, it is not perceived as an odor. However, if the injection is simultaneously accompanied by a sniff of odorless air, or by a puff of odorless nitrogen into the nose, it is perceived as odor (Engen, T., 1973). In fact, a sniff may be sufficient to generate a rudimentary olfactory percept even in the absence of odorants. For example, when an early-type olfactometer that injected puffs of air into the nose (blast olfactometer) was tested, subjects responded to the blast pressure as an odor, even when odorant was not present (Wenzel, B. M. 1949; 1955). Similarly, when humans try to imagine an odor, they spontaneously sniff (Bensafi, M. *et al.*, 2003b), and if this spontaneous sniffing is prevented, the vividness of their olfactory imagery is reduced (Bensafi, M. *et al.*, 2005). All of this goes to show that sniffing is an integral and essential part of olfaction, and thus, when measuring olfactory behavior, sniffing should be enabled and measured whenever possible, even if it is avoidable through cannulated olfactometry.

4.45.2.1.3 Jars

An alternative to olfactometers is odor delivery by jars. Here the odorant is presented to the subject by smelling the headspace over a glass jar containing odorant at a given concentration, or by smelling the resultant airflow from a squeeze bottle similarly containing a fixed concentration of odorant. One can point to several disadvantages of this method in comparison with an olfactometer. In a high-end olfactometer equipped with an analytical device such as photoionization or flame ionization one has a dependable measure of odorant concentration in the vapor smelled by subjects. In contrast, when using jars, one can only estimate odor concentration based on the ideal gas law and Henry's law that assume proportionality of concentration in the headspace above a solution to the molar fraction within the solution. Unfortunately, due to various parameters such as interactions of the odorant with the diluents (e.g., mineral oil), the headspace concentration over a jar does not always match the theoretical expected concentration. Stone H. (1963) analytically measured the concentration of propionic acid within a mineral oil-based dilution series in jars and found that the actual headspace concentration deviated from the expected concentration, as deduced from the ideal gas law and Henry's law, by as much as two orders of magnitude (Stone, H., 1963; Haring, H. G. *et al.*, 1972). This limitation may be overcome by somehow

incorporating an analytical sampling protocol from jar headspace during jar delivery. However, besides the technical impracticality of such a solution, it would still not assure a controlled stimulus concentration. This is because factors such as variable distance of jar from nose across trials and across subjects, as well as variable sniffing behavior (Pfaffmann, C. 1951; Cain, W. S. and Engen, T. 1969), will all influence end concentrations. Jars have additional shortcomings in comparison with an olfactometer in the context of threshold testing. Whereas an air-dilution olfactometer can produce a very large number of discrete odorant concentrations, when using jars, one must have a separate jar for each concentration. This either limits the number of concentrations one can test, or requires use of many jars, a cumbersome arrangement indeed. In our experiments, we typically use ~25 jars in the process of a single odorant threshold determination. All that said, despite these and other drawbacks, the issue of olfactometer contamination renders jars the preferred method in our view for testing absolute detection threshold. Even having settled on jars another complication still looms large. When using jars, comparisons across groups (e.g., patients vs. healthy controls) or individuals within a laboratory are possible, but comparisons across laboratories are limited. Different laboratories use different type jars, different ratios in their dilution series, different diluents, and different methods for presentation of jar to nose. A solution that may minimize this variance may be found in two threshold test kits that have recently been made commercially available. One kit uses jars for presentations (The Smell Threshold Test, Sensonics) and the other uses odorant-pens (Sniffin' Sticks, Burghart Medical Technology) (Hummel, T. *et al.*, 1997; Kobal, G. *et al.*, 2000). Although these kits promise some uniformity across laboratories, they are each limited to one odorant, have rather widely spaced concentration intervals, and are expensive. An alternative to the commercial solution is for olfactory psychophysicists to finally agree on standards they will all use. The foundation for such an effort can be found in the work of groups such as Walker and colleagues (Walker, J. C. *et al.*, 2003) or Cometto-Muniz and their colleagues (Abraham, M. H. *et al.*, 2002; Cometto-Muniz, J. E. *et al.*, 2002; 2003), who have meticulously measured detection thresholds for many odorants (Cometto-Muniz, J. E. and Cain, W. S. 1990; Cometto-Muniz, J. E. *et al.*, 1998a; 1998b; 2001; 2002; 2003), and more critically, have described the relationship between liquid-phase and vapor-phase concentrations for many odorants (Cometto-Muniz, J. E. *et al.*, 2003).

4.45.2.2 The Assumed Threshold Model

Regardless of whether delivering odorants with olfactometers or jars, determination of detection threshold depends on the application of a particular sampling methodology and statistical criterion. In general, one assumes that detection around the threshold concentration conforms to a psychometric function, typically an S-shaped or ogive function wherein stimulus detectability increases continuously from chance to perfect accuracy over a range of stimulus concentrations. Such psychometric functions are prevalent across sensory modalities, and a typical example is shown in Figure 3. In the figure, stimulus intensity (concentration) is plotted on the abscissa and the observer's performance in a two-alternative forced-choice (2AFC) procedure is plotted on the ordinate. In this context, the observer's threshold is defined as some level of detectability, typically midway between chance and perfect performance, corresponding to 75% performance in the figure. Different procedures will define threshold at different levels of performance, accounting for some of the variance in results reported in the literature.

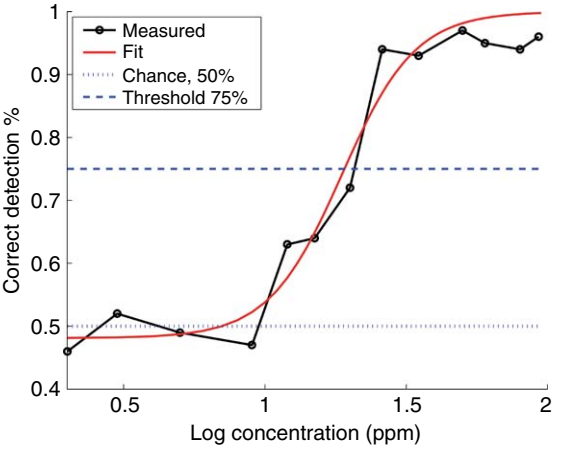

Figure 3 Detection threshold. Detection performance (percent correct in a two-alternative forced-choice (2AFC) task) is plotted as a function of odorant concentration. Raw data (black curve) are fitted with a Weibull psychometric function (red curve) which is used to determine the threshold detection value (value of the red curve at 75% correct performance; in this case ~1.3 log[ppm]). The use of a fitted curve allows more precise determination of thresholds than the raw data, which often has a fixed arbitrary step size.

A second source of variance is observer bias. An observer's response in the context of a threshold test is the product of (at least) two components, a sensory component reflecting the neural activity induced by the stimulus and a psychological component or bias reflecting the observer's predisposition to give one reply or another. This bias is usually different across observers and can also be modified by changing the task structure. For example, bias towards one response or another can change dramatically as a function of task contingencies, that is, the cost associated with making an error versus the benefit of making a correct selection. Methods of signal detection theory have been developed to control the influence of psychological bias on deduced detection thresholds. It is important to note, however, that complete disentanglement of these processes may be impossible, because psychological bias may influence not only the report of a sensory process, but also the sensory process itself. This is particularly true for olfaction that is typified by robust centrifugal projections from central brain structures to the periphery (Luskin, M. B. and Price, J. L., 1983). For example, the expectation of odor modifies patterns of neural activity in the olfactory bulb (Kay, L. M. and Laurent, G., 1999) and olfactory cortex (Zelano, C. *et al.*, 2005); thus, the bias of expectation will modify the sensory process of detection. With these issues in mind, we review methods for determining detection thresholds below.

4.45.2.3 Measuring the Threshold Model

The most widely used methods for measuring olfactory thresholds are the ascending method of limits (AML) (Cometto-Muniz, J. E. and Cain, W. S., 1998) and the adaptive staircase method (Dixon, W. J. and Massey, F. J., 1957; Cornsweet, T. N., 1962). A third method called the method of constant stimuli, which has been used in other sensory modalities, has been rarely used in olfaction, as the relatively large number of trials required by this method combined with the relatively large interstimulus intervals (ISIs) in olfaction make it prohibitive in most situations (Cain, W. S. *et al.*, 1988). In the AML, a sequence of concentrations of the odorant around the probable threshold concentration are prepared and trials are presented in sequence starting from the lowest and proceeding to the highest. Each trial consists of a 2AFC in which subjects are presented with the target odorant mixed in diluent and with just the diluent and are forced to indicate which of the two contained the odorant. If the subject is correct, another trial at the same concentration is initiated. If the subject is incorrect, the next highest concentration is used. The procedure is terminated when a predetermined number (typically five) (Cometto-Muniz, J. E. and Cain, W. S., 1998) of successive correct trials is achieved. Detection threshold is typically defined as the last concentration used.

The adaptive staircase is similar to the AML in that it too samples a predetermined series of concentrations with a 2AFC per trial procedure but differs in how it samples these concentrations and in its stopping rule. The staircase may be started at any trial, typically one is randomly chosen above the expected threshold, and then a rule is applied after each trial which determines the next concentration to use. In a typical staircase, a one-up two-down rule is used which means that after one incorrect trial the next highest concentration is used, and after two successive correct trials, the next lowest concentration is used. After a single correct trial, the same concentration is sampled again. Typical stopping rules for staircases include a predetermined number of sampling reversals, or a predetermined number of total trials (Linschoten, M. R. *et al.*, 2001). The data from the staircase are used to fit a psychometric function, typically an S-shaped function such as a logistic, cumulative normal, or Weibull function (see Figure 3). Threshold is defined as the concentration derived from the fitted function corresponding to performance halfway between chance and perfect performance, which is 75% correct in the case of a 2AFC. It should be noted that this definition of threshold differs from that used in the AML, which defines threshold as 100% performance, which explains why thresholds using AML are typically higher than those using staircases.

A variant of the adaptive staircase is the maximum likelihood adaptive staircase method (MLASM) in which a psychometric function is fit to all the data collected thus far after each trial, the threshold is estimated from this fitted function, and a concentration close to it is chosen for the next trial (Taylor, M. M. and Creelman, C. D., 1967). A number of procedures of MLASM are available (Linschoten, M. R. *et al.*, 2001). The method described by Linschoten M. R. *et al.* (2001) uses a logistic-function psychometric model and uses a sufficiently small error estimate on the estimated threshold as a stopping criterion. Their method compares favorably in terms of expected stopping time and accuracy of the estimated threshold with a one-up two-down staircase

method, and both methods outperform AML. It should be noted that this result is partly due to the different definitions of threshold employed, and because the AML method uses only a few data points rather than the whole set to estimate threshold. Indeed, when the same logistic function is fitted to the data collected from AML, i.e., when all the data collected are used to estimate the threshold rather than just the last few data points, the thresholds derived from the fit agree well with those derived from the staircase and MLASM methods (Linschoten, M. R. *et al.*, 2001). These results suggest that the method of sampling data around the threshold is less important than how this data are analyzed, i.e., when a proper psychometric function is fitted to the data and a common definition of threshold is applied (75% correct), all three methods are about equally useful. Indeed, using the AML procedure, while having the advantage of providing a threshold without recourse to computation, has little justification given the artificially large error of the method, and the trivial effort involved in significantly improving it. When a psychometric function is fit to all the data, the most significant factor in the precision of the estimated threshold is not the method of sampling concentration steps, but the step size between them (Linschoten, M. R. *et al.*, 2001). Considering all of the above, we recommend using the MLASM method and further recommend using the convenient shareware software available for this purpose called MLpest.

4.45.2.4 Measuring Near-Threshold Performance

Although determining a threshold concentration for detection or recognition is the most common question in research, a somewhat different procedure is needed to answer questions about near-threshold detection performance. In questions of absolute detectability, such as for example, whether a subject can truly detect the presence of a compound he or she appears to have no percept for, one might wish to use a procedure that explicitly incorporates a decision behavior model. The simplest and most widely used such procedure is derived from signal detection theory (Tanner, W. P. and Swets, J. A., 1954; Green, D. M. and Swets, J. A., 1966). In this model, the subject is presented with a large number of trials consisting of a single sample that either contains just the diluent or the diluent plus an odorant at some fixed concentration. The subject must indicate on every trial whether an odorant was present or not (yes or no). This results in four kinds of stimulus-response situations, which are conventionally called hits (stimulus present, yes), misses (stimulus present, no), correct rejections (stimulus absent, no), and false alarms (stimulus absent, yes). In this situation, different subjects may have different decision criteria or biases: a conservative subject may only indicate that the odorant is present only when he or she has high certainty resulting in relatively more misses and fewer false alarms, whereas a less conservative subject will indicate the presence of the odorant with significantly less certainty, resulting in relatively more false alarms and fewer misses. Signal detection theory provides a model of subject behavior that explicitly includes terms for the discriminability of the odorant from the diluent (termed d-prime), and for the subject bias or degree of conservatism (termed beta). These parameters are separable and subject to different manipulations: changes in the concentration of the olfactant will change d-prime, whereas differences in the rewards and penalties associated with correct and incorrect responses will change beta. Thus, subject bias may be factored out when discriminability is the issue, or conversely may be focused upon when it is the question of interest.

An example of the use of signal detection is found in a study by Bremner E. A. *et al.* (2003) in which eight putative nondetectors of the steroidal compound androstenone were tested on 74 yes/no detection trials. Although these putative nondetectors were determined to be insensitive to androstenone in a screening study, d-prime analysis of their yes/no trials revealed that seven of eight putative nondetectors could in fact detect androstenone. A second example from Sobel N. *et al.* (1999) found that eight subjects who reported no odor percept for a variant of the steroidal compound androstodienone were able to detect it in a signal detection experiment.

4.45.2.5 Nonolfactory Detection of Airborne Chemicals

The perception of smell is the result of odorant transduction at several types of nerve-endings, which will often occur in concert (Bojsen-Moller, F., 1975). An odorant that enters the nasal passage can stimulate both cranial nerves I (olfactory) and V (trigeminal), and most known odorants stimulate both. However, sensitivity and specificity are greater in the olfactory than the trigeminal nerve, and the latter conveys primarily nasal irritation (Cain, W. S.

and Murphy, C. L., 1980; Hummel, T., 2000). In this respect, the trigeminal system may serve as a nonspecific chemical warning device, rather than assist in olfactory discrimination and identification. There is some debate in the literature as to which odorants are pure olfactants, that is, stimulate the olfactory nerve only. There is, however, general agreement that vanillin is such an odorant (Doty, R. L. *et al.*, 1978; Doty, R. L., 1995). The odorants hydrogen sulfide, phenyl ethyl alcohol (PEA), and decanoic acid are also considered to have minimal trigeminal stimulation, if any (Doty, R. L. *et al.*, 1978; Livermore, A. *et al.*, 1992; Doty, R. L., 1995). By contrast, carbon dioxide can be considered a pure trigeminal in that it stimulates the trigeminal but not olfactory nerve (Hummel, T. *et al.*, 2003). Although most odorants will stimulate both systems, trigeminal thresholds are often several orders of magnitude higher in concentration than olfactory thresholds for the same odorants (Cometto-Muniz, J. E. and Cain, W. S., 1990). Thus, degree of trigeminal activation will have little influence on results of detection threshold studies, but may have significant impact on the results of studies using suprathreshold concentrations.

4.45.2.6 Adaptation

Any consideration of reported olfactory detection thresholds must consider the phenomenon of adaptation. Adaptation, in all sensory systems, is the waning of response with stimulus repetition. Adaptation can be viewed as either a limitation or advantage in sensory processing. It is a limitation in that the adapted sense may be unable to register the occurrence of an event that closely followed a previous, adapting event. By contrast, adaptation functions as gain control within sensory systems. This enables the system to detect changes under conditions of vastly differing background levels. Olfactory adaptation may result from mechanisms at every level of the olfactory process, starting from molecular mechanisms at the level of olfactory receptors, and on to cellular mechanisms at the level of olfactory bulb and cortex (Sobel, N. *et al.*, 2000b; Poellinger, A. *et al.*, 2001). Olfactory adaptation was first demonstrated by Zwaardemaker H. (1895) who found that during constant olfactory stimulation, detection threshold decreases linearly (Pfaffmann, C. 1951). Thus, in the context of determining absolute olfactory detection thresholds, one must consider adaptation in the experimental design. Specifically, an early trial within the threshold test may influence the outcome of the next trial. To minimize this, one must take the following two steps. Considering that adaptation is increased following exposure to higher concentration odorants (Berglund, B. *et al.*, 1971), one must use ascending concentrations within an olfactory threshold test. Pangborn R. M. *et al.* (1964) tested detection threshold for 2-heptanone three times, once in an ascending concentration order, once in a descending concentration order, and once in random order. Detection thresholds were lowest when tested with ascending concentrations and highest when tested with descending concentrations. A second step is to employ a sufficiently long ISI so as to minimize adaptation effects by allowing full recovery. Although most all published determinations of detection threshold employ ISIs in the range of 30–45 s, Koster E. P. (1971) reports that even ISIs of as long as 120 s do not allow for complete recovery at near-threshold levels. Effects on olfactory detection threshold can also result from the inverse of olfactory adaptation, namely olfactory facilitation. Facilitation consists of lower detection thresholds for one odorant after exposure to another (Engen, T. and Bosack, T. N., 1969). Interestingly, a determining factor on whether or not one odorant will facilitate the detection of another appears to be odorant solubility in water. When a significantly less soluble odorant is presented first, it facilitates the detectability of an ensuing more soluble odorant. By contrast, when a more soluble odorant is presented first, it reduces the detectability of an ensuing less soluble odorant, a phenomenon termed cross-adaptation. For example, using the long- and short-chain homologous alcohols C_3 (high solubility), C_4 (high solubility), and C_7 (low solubility), Corbit T. E. and Engen T. (1971) found that using C_7 as the adapting stimulus facilitated detection of C_3 and C_4, whereas using C_4 as the adapting stimulus inhibited detection of C_3. They hypothesized that these effects reflected the relative rates at which the odorants could cross the olfactory mucosa in order to then bind to receptors. Specifically, they argued that the low-solubility odorant changed the mucosal environment such that the higher-solubility odorants could then cross the mucosa more rapidly.

4.45.2.7 Reported Absolute Thresholds

Considering the above described sources of variance, namely method of odorant delivery, sniffing behavior, statistical analysis, nonolfactory effects, and

odorant order effects (adaptation and/or facilitation), it is not surprising that reports on absolute detection thresholds varied so widely across laboratories (Amoore, J. E. and Hautala, E., 1983). However, even data collected within laboratories initially suggested unusually high populational variance in olfactory detection thresholds. For example, detection threshold spans of as much as 5 (Brown, K. S. *et al.*, 1968) and 16 (Yoshida, M., 1984) log units within a homogeneous young and healthy population have been reported. Furthermore, the magnitude of this populational variance appears odorant dependent, significantly greater for some odorants than for others (Punter, P. H., 1983). In a critical study, Stevens and colleagues suggested that much of this variation may be explained by individual variation over time (Stevens, J. C. *et al.*, 1988). They tested three subjects on detection of three odorants over a period of 30 days. Every test consisted of an ascending staircase 2AFC paradigm, with five consecutive correct as criteria (plus an additional five correct for the next higher concentration). They found that the variability of each subject over time was similar to that seen in large groups at one point in time. In other words, they suggested that the dynamic properties of individual olfactory detection thresholds may underlie much of the apparent populational variance. However, when they pooled all their data for each of the three subjects, they found that the subjects were nearly identical. Taken together, these results suggest that the across-test variability reflected the poor power of the single test. Had the single test consisted of the 150 trials that contributed to each point in the pooled data, subjects' performance may have appeared stable. With this issue in mind, Walker J. C. *et al.* (2003) conducted repeated threshold testing using a 75 trial yes/no paradigm that took about 2.3 h to complete. Using such strict criteria, they failed to replicate the variability reported by Stevens J. C. *et al.* and concluded that thresholds are stable when meticulously determined. As concluded in this respect by Cain W. S. and Gent J. F. (1991), there is "little solace to those who may wish to measure quick and dirty olfactory thresholds".

In contrast to all of the above unintended sources of variance, olfactory thresholds are also influenced by various known factors. Principal amongst these is age. Olfactory detection thresholds are typically elevated two- to 15-fold in the healthy elderly in comparison with young adults (Schiffman, S. 1979; Cain, W. S. and Stevens, J. C. 1989; Doty, R. L. *et al.*, 1989; Cain, W. S. and Gent, J. F., 1991; Serby, M. *et al.*, 1991). This reduction in sensitivity is in fact clearly apparent by middle age (Cain, W. S. and Gent, J. F., 1991). In addition to age, detection thresholds are increased by exposure to environmental toxins, diseases that insult the peripheral components of the olfactory system (e.g., rhinitis), developmental diseases that insult the olfactory bulb (e.g., Kalmans), neurodegenerative diseases that may insult both peripheral and central components of the olfactory system (e.g., Parkinson's disease and Alzheimer's disease), and self-injurious behaviors such as excessive smoking or drinking of alcohol. Although reports of gender differences in olfactory detection thresholds have been mixed, a preponderance of evidence points to lower thresholds in women. Early studies by Bailey and colleagues suggested lower thresholds in men than in women (Bailey, E. H. S. and Nichols, E. L., 1884; Bailey, E. H. S. and Powell, L. M., 1885); however, later studies by Toulouse E. and Vaschide N. (1899) suggested the opposite. Still other studies found no difference between men and women in olfactory detection thresholds (Mesolella, V., 1934; Kloek, J., 1961; Matzker, J., 1965; Amoore, J. E. and Venstrom, D., 1966; Venstrom, D. and Amoore, J. E., 1968; Griffiths, N. M. and Patterson, R. L., 1970; Koelega, H. S. 1970;Koelega, H. S. and Koster, E. P., 1974; Dorries, K. M. *et al.*, 1989; Zatorre, R. J. and Jones-Gotman, M. 1990; Stevens, D. A. and O'Connell, R. J., 1991; Segal, N. *et al.*, 1995). In efforts to account for this variability, it has been suggested that a sex difference may be limited to specific odorants (Koelega, H. S. and Koster, E. P., 1974), or apparent only at particular points along the menstrual cycle. This too, however, has been a point of contention, with some studies suggesting lower (better) thresholds at time of ovulation (Le Magnen, J., 1952; Vierling, J. S. and Rock, J., 1967; Mair, R. G. *et al.*, 1978; Doty, R. L. *et al.*, 1981; 1982; Narita, S. *et al.*, 1992; Pause, B. M. *et al.*, 1996; 1999), others at the follicular phase (Henkin, R. I., 1974), others around menses (Koster, E. P., 1968; Doty R. L., 1976), or at menstruation (Le Magnen, J., 1952; Schneider, R. A. and Wolf, S., 1955; Good, P. R. *et al.*, 1976; Mair, R. G. *et al.*, 1978; Moriyama, M. and Kurahashi, T., 2000). Still other studies failed to find any differences across the menstrual cycle in olfactory detection thresholds (Amoore, J. E. *et al.*, 1975b; Herberhold, C. *et al.*, 1982; Filsinger, E. E. and Monte, W. C., 1986; Hummel, T. *et al.*, 1991; Kanamura, S. and Takashima, Y., 1991). Similarly, early pregnancy, which influences various aspects of olfactory perception, does not influence olfactory

detection threshold (Kolble, N. *et al.*, 2001). Whereas the bulk of the literature taken together may only imply lower thresholds in women, one recent study may have finally decided this issue. Dalton P. and colleagues (2002) measured detection threshold for benzaldehyde every 2 days, for 60 days. They found that whereas men's detection thresholds maintained a constant mean, women's thresholds decreased dramatically with time (Figure 4, middle panel). They both replicated this finding with an additional odorant (citralva) and demonstrated that it does not generalize to taste thresholds. In other words, whereas men and women had equal detection thresholds at baseline, they did not after training. This convincing study suggests that given the undertrained state of olfaction in most humans, differences between men and women are obscured (as reflected in the bulk of the literature). But once the full potential of the olfactory system is realized through training, women significantly outperform men in olfactory detection thresholds.

Training the olfactory system can serve not only to reduce detection threshold values from one concentration to a lower one, but can in fact also serve to enable detection of a previously completely undetectable odorant. The term specific anosmia is used to describe a state wherein a person with otherwise healthy olfaction is completely unable to detect a particular odorant, at any concentration. Although specific anosmia has been described for several odorants (Amoore, J. E., 1967; Amoore, J. E. *et al.*, 1975a; Amoore, J. E., 1977a; 1977b), it has been primarily studied with the odorant androstenone. Estimates of populational prevalence for androstenone anosmia range from ~2% to ~30% (review in Bremner, E. A. *et al.*, 2003). Considering that androstenone anosmia has a genetic component (Beets, M. G. J. and Theimer, E. T., 1970; Polak, E. H., 1973; Amoore, J. E., 1977a; 1977b), it has been considered as a possible psychophysical tool for probing the relationship between genetic makeup and specific olfactory abilities. One of the chief researchers of this phenomenon is Charles Wysocki. Wysocki, himself a nondetector of androstenone, noticed that after months of research and exposure, he had developed the ability to detect androstenone. In an effort to further explore this serendipitous observation, Wyscoki and colleagues systematically exposed androstenone nondetectors to androstenone (Wysocki, C. J. *et al.*, 1989). They found that repeated exposure induced detectability, which by 6 weeks of exposure was

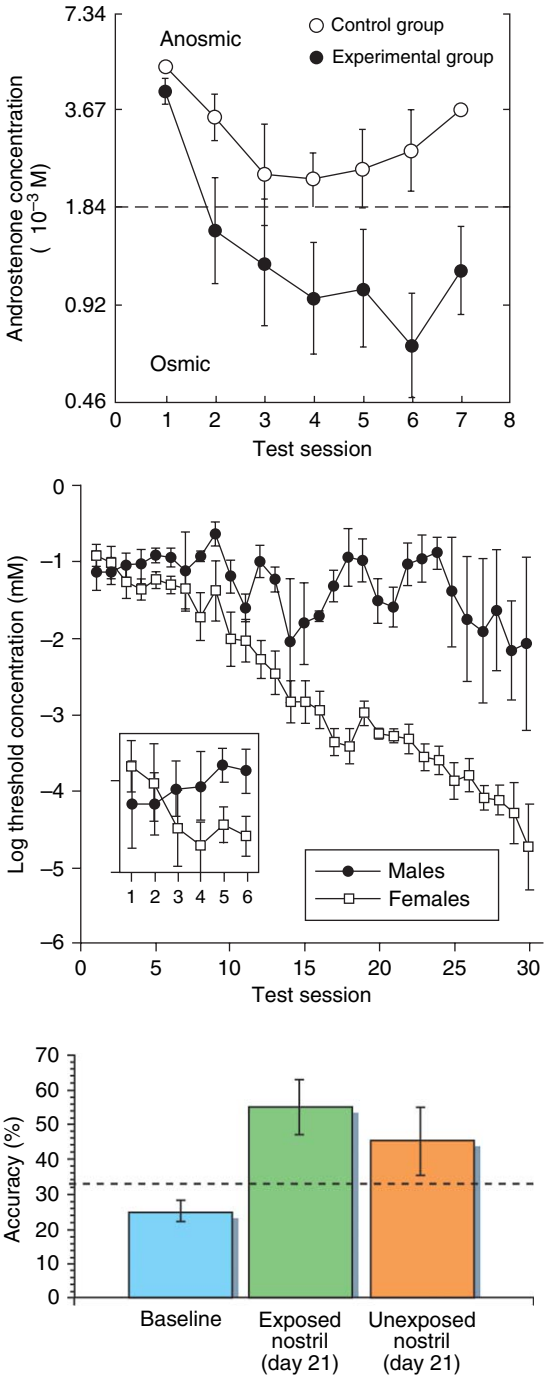

Figure 4 Improving olfactory detection threshold. The top panel depicts reductions in detection thresholds for androstenone during 6 weeks of exposure (Wysocki, C. J. *et al.*, 1989). The middle panel depicts reductions in detection threshold for benzaldehyde induced by 60 days of exposure in women but not men (Dalton, P. *et al.*, 2002). The bottom panel depicts detection of androstenone in the nostril that was exposed to androstenone vs. the unexposed nostril, following 21 days of exposure (Mainland, J. D. *et al.*, 2002).

significantly better than chance, and dramatically different from baseline (Figure 4, top panel).

What mechanisms underlie the plasticity evident in this and other studies where olfactory detection improved through practice? Was the improved performance the result of events in the nose or events in the brain? This question was addressed in experiments on rodents and humans. Yee K. K. and Wysocki C. J. (2001) surgically disconnected the epithelium from bulb in androstenone-anosmic mice. They then systematically exposed the now disconnected epithelium to androstenone over 10 days. When the epithelium-to-bulb connection regenerated 45–50 days later, they tested the mice for androstenone detection. Androstenone detection had improved significantly, leading the authors to suggest that plasticity underlying acquired olfactory abilities was peripheral, in the epithelium. Mainland J. D. *et al.* (2002) addressed the same question in humans. They repeatedly exposed only one nostril of androstenone nondetectors to androstenone, and then tested the unexposed nostril for detection. Following exposure, both the exposed and the naïve nostrils could detect androstenone, effectively doubling their detection accuracy (Figure 4, bottom panel). Since the two olfactory epithelia are not neurally connected at the peripheral level, Mainland J. D. *et al.* concluded that learning occurred via a central brain mechanism, such as olfactory bulb or cortex, which shared information from both nostrils. In contrast, Wang L. *et al.* (2004) conducted a study that led them to the opposite conclusion. These authors repeatedly measured olfactory evoked potentials (EOG) from the epithelium in the nose and olfactory event-related potentials (OERP) from the scalp concomitantly with an androstenone exposure paradigm. They found that increased androstenone detection was associated with changes in both the EOG and OERP. They concluded that a modified EOG necessarily implies plasticity and change at the level of the epithelium. A conclusion consistent with all the data is that exposure may induce changes at both the peripheral and central levels. Repeated exposure may indeed lead to increased expression of receptors at the epithelial level (Yee, K. K. and Wysocki, C. J., 2001), as well as to an increased ability of the brain to make sense of what was a previously senseless message (Mainland, J. D. *et al.*, 2002).

With all the confusion and disagreement regarding human olfactory detection thresholds, there is one fact that can be stated without controversy: human olfactory detection thresholds are exceedingly low, or in other words, the human olfactory system is a first-rate chemical detector. For example, the odorant ethyl mercaptan that is often added as a warning sign to propane can be detected at concentrations far below 1 part per billion (ppb), typically as low as 0.2 ppb (Whisman, M. *et al.*, 1978). This is equivalent to approximately three drops of odorant within an Olympic-size swimming pool – given two pools, a human could detect which pool contained the three drops of odorant! Finally, a report by the Japan Sanitation Center (Nagata, Y. and Takeuchi, N., 1990) suggests humans can detect isoamyl mercaptan at 0.77 parts per trillion (ppt)! This, to our knowledge, is the lowest reported human detection threshold (Figure 5).

How does this sensitivity compare with other mammals? The few direct within-experiment comparisons of olfaction in humans and other species have focused on tasks other than absolute detection threshold (Slotnick, B. M. and Ptak, J. E., 1977). Matthias Laska and colleagues have amassed detection thresholds across several species and have compared their data to that obtained by others from humans. In one such study, they measured detection threshold for the fox anal gland odorant 2,4,5-trimethylthiazoline (TMT) in rats, squirrel monkeys, and spider monkeys (Laska, M. *et al.*, 2005a). They found that whereas monkeys had thresholds comparable to those of previously found in humans (in the single ppb range) (Figure 6), rats detected TMT in

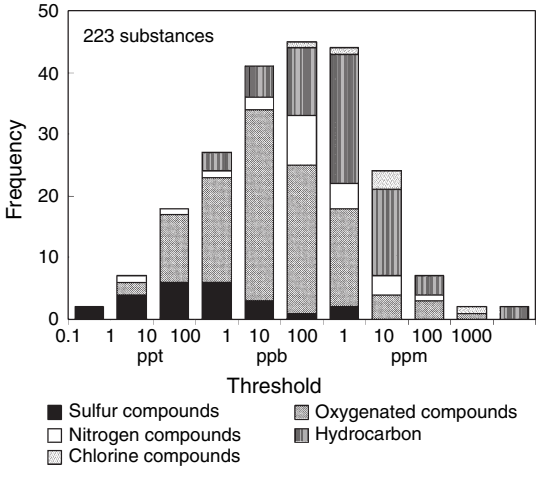

Figure 5 Human detection thresholds. Distribution of detection thresholds for different types of odorants. Humans can detect compounds containing sulfur in the ppt range (Nagata, Y. and Takeuchi, N., 1990).

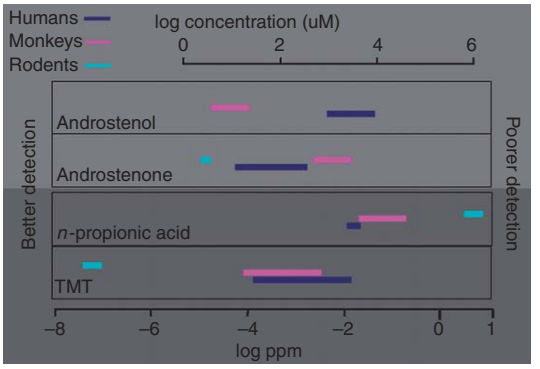

Figure 6 Detection thresholds across species. The data are amassed from studies by Laska and colleagues and are for detection of the fox odor 2,4,5-trimethylthiazoline (TMT), *n*-propionic acid, and the two steroidal compounds androstenol and androstenone. The two shades of gray distinguish the units in which results were reported, dark gray in log concentration of the vapor, and light gray in log concentration of the odorant liquid. The extent of the lines reflects the reported variance across studies. The important point illustrated is that each species excels at detecting particular odorants. For example, humans outperform rats and monkeys at detecting *n*-propionic acid. That said, one must keep in mind the limitation of comparing across studies that used different methods of delivery and statistical criteria.

the subpart per trillion (ppt) range (between 0.04 and 0.1 ppt). This is the lowest olfactory detection threshold ever reported for any animal.

This dramatic difference between rats on one hand and primates (including humans) and monkeys on the other seemingly supports the qualitative distinction considering rats and dogs as macrosmatic and primates and monkeys as microsmatic. However, Laska has suggested that this distinction may have been significantly influenced by the behavioral relevance of the odorants tested. Squirrel monkeys and pigtail macaques are better than rats at detecting a host of odorants that are not behaviorally significant to rats. For example, both squirrel monkeys and pigtail macaques outperformed rats by at least an order of magnitude at detecting *n*-propionic acid and *n*-pentanoic acid (Laska, M. *et al.*, 2004). Thus, one would like to see a comparison of detection thresholds for an odorant that is behaviorally significant to humans. Unlike the case of rats and TMT, however, humans are not faced with ongoing olfactory detection of predators, other than other humans. Indeed, although not in a predatory context, a host of steroidal compounds have been implicated in olfactory communication between humans (Monti-Bloch, L. *et al.*, 1998; Jacob, S. *et al.*, 2002; Bensafi, M. *et al.*, 2003a; 2004a; 2004b). Laska and colleagues measured detection thresholds for such compounds in monkeys (Laska, M. *et al.*, 2005b). In comparing their results to those obtained by others, they concluded that androstenone is best detected by mice, less so by monkeys, and even less by humans and pigs. In contrast, androstenol is better detected by humans than by monkeys (no data for mice and pigs). Summing up the efforts of Laska and colleagues, rodents outperform monkeys for some odorants, but monkeys outperform rodents for others. Similarly, monkeys outperform humans for some odorants, but humans outperform monkeys for others – these results are illustrated in Figure 6. Thus, any cross-species comparison of olfactory detection threshold must consider the behavioral relevance of the odorants tested. Furthermore, it is noteworthy that reported detection thresholds in nonhuman animals were obtained after hundreds, sometimes thousands of training trials. By contrast, most human thresholds were obtained after minimal training, if any. Considering the previously noted malleability of olfactory detection, it is tempting to consider the possibility that extensive training may induce/reveal detection thresholds in humans that rival those of macrosmatic mammals.

4.45.3 Olfactory Discrimination

One step up from olfactory detection in the hierarchy of olfaction is olfactory discrimination. Discrimination can be between two concentrations of the same odorant, or between two different odorants, at either the same or different concentrations. In order to discriminate between two odorants (smelled in succession), one must be able to detect them, form a neural representation of the first, and maintain this representation in short-term memory (Wilson, D. A. and Stevenson, R. J. 2003a; 2003b). The nature of this representation, however, is more akin to a sensory memory (Cowan, N., 1995) than a semantic or linguistically mediated memory, and discrimination is generally understood to occur without accessing long-term memory associations with the odorants, or semantic representations of the odorant, processes more properly associated with olfactory identification. The study of olfactory discrimination is susceptible to all the unwanted sources of variance described for the study of detection, namely methods of odorant delivery, sniffing behavior, statistical deduction, and experimental arrangement.

4.45.3.1 Discriminating between Different Concentrations

The simplest case of olfactory discrimination is that between two concentrations of the same odorant. Closely linked to the question of the minimal difference in concentration that can be discriminated is the nature of the relationship between odorant concentration and perception. In general, as the concentration of an odorant increases so does its perceived intensity (it is noteworthy that in some odorants, shifts in concentration are accompanied by shifts in odor quality as well) (Gross-Isseroff, R. and Lancet, D., 1988). The function that relates stimulus magnitude (concentration) to perceived magnitude (intensity) is a kind of psychometric function that can be measured. In this section, we will first describe how this psychometric function is estimated, and then describe how it is related to the issue of intensity discrimination.

The basic method for relating stimulus to perceived magnitude is referred to as magnitude estimation. Typically, many subjects are presented with many trials of an odorant stimulus, each trial at a different concentration. Subjects are asked to rate the intensity of each trial on a linear scale. Rating intensity can be achieved by assigning a number to the stimulus on a Likert scale (typically between 1 for low intensity and 9 for high intensity), or alternatively, by marking a line on a visual-analog scale (VAS). A VAS consists of a horizontal line presented on either paper or monitor, which is also accompanied by verbal descriptors at two or more points along the line. A typical VAS for intensity estimations may have the descriptor "barely detectable" at one end, and "the strongest smell I have ever experienced" at the other. On every trial, subjects cross the line at any location between these two extremes in a manner that reflects their perception. Using number assignment, Stevens S. S. (1957) and others found that the function which best describes the relation of odor concentration to perceived intensity was a simple power function defined as:

$$R = kS^b$$

Where R is perceived intensity, S is stimulus concentration, k is a constant for the logarithmic intercept, and b is a constant for the logarithmic slope. In logarithmic terms, the function is:

$$\mathrm{Log}R = b(\mathrm{Log}S) + \mathrm{Log}k$$

Figure 7 contains typical data from such an experiment. Power functions describe the relationship between perceived magnitude and stimulus magnitude in all sensory modalities including olfaction, and in all cases the slope is less than 1, so that successive increases in stimulus magnitude produce successively smaller and smaller increases in perceived magnitude. One implication of this saturating or compressed response is that doubling of stimulus magnitude will produce less than a doubling in its perceived intensity. Furthermore, the degree of this compression (i.e., the slope parameter) appears to be odorant specific. Cain W. S. (1969) demonstrated that this compression reflected an odorant's solubility in water. As odorant solubility increased, the degree of compression decreased. This, like the previously described effect on facilitation, may be the result of the higher rate at which more soluble odorants can cross the olfactory mucosa in order to bind to olfactory receptors (Mozell, M. M. and Jagodowicz, M., 1973). This predictable link between an odorant's solubility and the slope of it is power function forms, in our view, one of the most successful implementations of olfactory psychophysics in that is fulfils the previously mentioned goal of defining rules that link the physical stimulus to the resultant percept.

With an understanding of how odorant concentration is related to perceived intensity, we turn to the question of how discriminable different concentrations are from one another. The minimal perceptible change

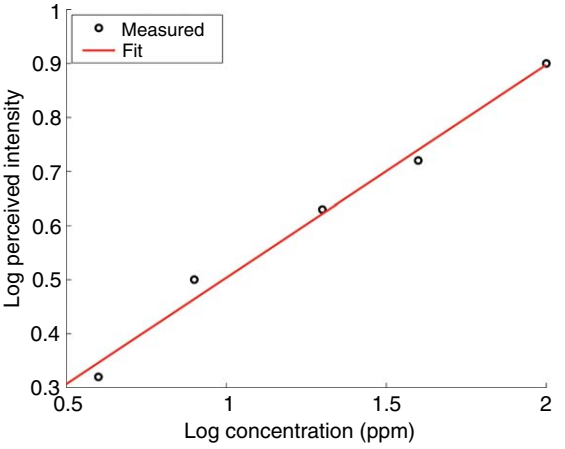

Figure 7 The relationship between odorant concentration and perceived intensity. As odorant concentration increases, so does perceived intensity. When expressing concentration and perception in log units, the relationship can be described by a power function, with a slope that is typically <1.

in stimulus magnitude is known as the just noticeable difference (JND) and follows the law of JND, which states that the minimum increase in a stimulus required for a subject to take notice (symbolized as ΔS) is in constant proportion to the initial stimulus (Fechner, G. T. 1860). This proportion, called the Weber fraction:

$$\Delta S = kS$$

where ΔS is the increment in S (JND), S is the standard stimulus, and k is Weber's fraction, is measured empirically by the method of constant stimuli. This equation implies the Weber–Fechner law:

$$R = k\log(S/S_a)$$

where R is the perceived magnitude and S_a is the absolute threshold for detection of the stimulus. Of course, this law applies only to detectable or suprathreshold stimuli.

In a typical JND experiment, a subject performs many trials in which they smell in rapid succession first a standard and then a comparison stimulus. Different comparison stimuli are used, some equal to the standard, and others differing by fixed proportions. The subject rates the two stimuli as either same or different. Typical Weber fractions for human vision and audition are in the 10% range (Mueller, C. G., 1951). In other words, reliable discrimination is achieved for a 10% increment from the standard. Initial experiments using the method of constant stimuli in olfaction suggested that olfaction indeed follows Weber's law, but that it is characterized by relatively high Weber fractions of between 25% and 33% (Gamble, R. C. 1899). This value was not only significantly higher than human auditory and visual Weber fractions, but also orders of magnitude higher than olfactory Weber fractions obtained in macrosmatic mammals. Slotnick B. M. and Ptak J. E. (1977) used a modified AML procedure to determine Weber fractions for the odorant amyl acetate in rats and humans within the same study. Similar to previous reports, they found human Weber fractions of ~30%, but rat Weber fractions of ~4%. However, in a landmark study, Cain W. S. (1977) found that the high Weber fractions reported for humans may have reflected fluctuations in the stimulus. Once the stimulus was carefully controlled, Cain revealed human olfactory Weber fractions of as low as 7% for some odorants (*n*-butyl alcohol), thus grouping olfaction together with vision and audition in its relative sensitivity, and reducing the implied magnitude of difference between humans and macrosmatic mammals in this respect.

4.45.3.2 Discriminating between Different Odorants

In the preceding section, the discriminability of two kinds of odor was parameterized in terms of the only difference between them, namely the concentration of the odorant. Concentration is a numerical scale, which permits us to define a metric on the difference in stimuli, and then relate the difference in perception to this stimulus difference. In comparing the discriminability of different odorants, that is, different species of molecules, there is no obvious metric that defines the extent of differences between them. For example, how different is methane from ammonia? How can we define this as a number? The question of how to define a metric of stimulus similarity against which to gauge discriminability is crucial to understanding olfactory discrimination. A variety of studies have used a variety of different chemical properties of odorants to define metrics of similarity to see how they affect discriminability. The ways in which molecules can change, however, number in the hundreds, and a systematic study of all of them with respect to discriminability, is close to impossible.

Beyond the essential question of how to define stimulus similarity, there are further issues involved in how to quantify discrimination. Discrimination between different odorants can be considered as an absolute binary decision, in which case it can be probed using 2AFC with same or different as answers, or three-alternative forced-choice (3AFC) where subjects select the odorant that is different from the two others (more than two others can also be used). Matthias Laska and colleagues have used such 3AFC paradigms to test discriminability of odorant molecules as a function of various aspects of their physical structure. They found that the greater the difference in carbon chain length between any two odorants, the easier they were to discriminate (Laska, M. and Freyer, D., 1997). Furthermore, they found that humans can discriminate aliphatic odorants equal in number of carbons, but different in oxygen moiety (Laska, M. *et al.*, 2000), and differences in structures that share a benzene ring rather than a linear and unbranched carbon chain (Laska, M., 2002). Laska and colleagues argued that such discrimination data can be used as a tool to probe the dimensionality of odor quality. Specifically, they assume that easier discrimination reflects greater perceptual difference. Thus, because discrimination

became easier as the difference in carbon chain length increased, they conclude that carbon chain length reflects a dimension of olfactory perception. Unfortunately, it is generally impossible to vary only a single parameter of variance across a molecule. For example, increasing odorant carbon chain length will decrease odorant solubility, which leads to a diminution in perceived intensity (Cain, W. S., 1969). Thus, when subjects are able to discriminate odorants of different carbon chain length, it is impossible to say whether the ability is due to differences in intensity, solubility, some other attribute, or chain length *per se*.

One class of molecular changes that avoids most of these confounding problems is that of enantiomeric pairs. Enantiomers are mirror-image or chiral molecular structures that under most circumstances will not differ in solubility or many other chemical properties. Humans can discriminate many enantiomers by smell (Jones, F. N. and Velasquez, V., 1974; Jones, F. N. and Elliot, D., 1975). However, some enantiomeric pairs are not easily discriminated (Theimer, E. T. *et al*., 1977; Laska, M. and Teubner, P. 1999), and still others are easily discriminated whereby one has a distinct odor and the other has no clear olfactory percept at all (Laska, M. and Teubner, P., 1999). Although these experiments reduce the potential sources of variance underlying discrimination, they still fail to link a particular molecular aspect of odorants to a particular olfactory percept or quality.

The overwhelming impression following review of the human olfactory discrimination literature is that humans can discriminate nearly any molecular change in odorant structure. An alternative strategy to probing the olfactory system through discrimination studies is to focus not on the incredible achievements of olfactory discrimination, but rather on those rare instances where the olfactory system fails to discriminate changes in odorant structure. Keller A. and Vosshall L. B. (2004) used discrimination studies to probe what has been termed the vibrational theory of olfaction. Specifically, the most widely accepted theory of olfaction holds that the molecular structure, or shape, of an odorant is the determining factor in its interaction with a receptor and hence in creating a percept. According to this theory, different receptors bind to particular structural elements of the odorant molecule, termed odotopes, creating a combinatorial pattern of neural activity across receptors that is the basis for the odor percept. A controversial alternative theory of olfaction suggests that olfactory receptors act as biological spectroscopes, encoding the vibrational spectrum of odorant molecules (Turin, L. 1996; 2002). Whereas the vibrational theory predicts that the shape of a molecule does not determine its percept, the simplest version of odotope theory predicts that the vibrational spectrum of a molecule does not determine its percept. These different predictions suggest a simple test of the two theories, namely locating a pair of molecules that are isoteric (same shape), yet whose vibrational spectra differ. The necessary pair of molecules can be made by isotope substitution; for example, substituting deuterium for hydrogen in one version of a molecule will change its vibrational spectrum but leave its shape unchanged. A simple version of odotope theory predicts these two molecules will smell the same, while the vibrational theory predicts they will smell different. In support of the vibrational theory, Luca Turin suggested that deuterated and undeuterated acetophenone smell quite different (Turin, L. 1996; 2002). To further address this, Keller and Vosshall systematically tested discriminability of these two odorants using several methods. They used a number-based similarity scale, and two variants of 3AFC, a triangle-test where subjects were asked to identify the one odorant jar of three that was different (two were indeed the same, either deuterated or undeuterated), and a duo-trio test where two stimuli were presented, and subjects were asked to match one to a third reference. Overall, subjects were unable to discriminate deuterated from undeuterated acetophenone, and Keller and Vosshall concluded that they found no psychophysical support for the vibrational theory.

Given the difficulties of determining how the myriad possible factors that vary across molecules might change perceptual qualities, that is, the difficulties in determining a similarity metric in the stimulus space, one possible strategy is to directly probe the similarity metric in the perceptual space. This is typically done by presenting pairs of stimuli and asking subjects to rate their similarity on a Likert scale or VAS (e.g., the question "how similar are these two odors?", with a line ranging from "not at all" to "identical"). A shortcoming of such scales is that they typical asymptote at both floor and ceiling, making them relatively insensitive for odors that are very similar or dissimilar. This limitation can in part be addressed using

performance-based measures of similarity scaling (Wise, P. *et al.*, 2000). For example, in both vision and audition, more difficult discriminations, namely discriminations between more similar stimuli, take longer. Thus, one can measure time-to-discrimination between various olfactory stimuli and assume that stimuli that take longer to discriminate are more similar in terms of olfactory quality (Wise, P. M. and Cain, W. S., 2000).

4.45.3.3 Speed of Olfactory Discrimination

Olfaction is not typically thought of as a rapid process. Indeed, when faced with olfactory discriminations, humans will typically take several sniffs, a sniffing bout, before they settle upon their discrimination judgment. Laing D. G. (1983) compared performance obtained in such natural sniffing bouts to that obtained in a single sniff. He found that for olfactory detection and intensity discrimination, one sniff produced results as good as those from a sniffing bout. In fact, a sniff as short as 400 ms was sufficient for maximal intensity discrimination accuracy. In a second study (Laing, D. G. 1986), subjects were trained to limit sniff duration to the sound of a buzzer. Sniffs lasting 420 ms were sufficient for 90% discrimination accuracy across different odorants. However, when odorant concentration was lowered to near-threshold, there was a time-accuracy trade-off in that shorter sniffs impaired discrimination accuracy. Whereas this experiment by Laing emphasized speed over accuracy, Wise and Cain emphasized accuracy over speed (Wise, P. M. and Cain, W. S., 2000). They compared discrimination times for perceptually similar (difficult comparison) and dissimilar (easy comparison) odorant pairs and found that latency decreased as accuracy increased. In other words, easy comparisons were made faster than difficult comparisons. These seemingly contradictory results (Figure 8) are simply two sides of the same coin, namely the speed-accuracy trade-off, which is affected by bias. If subjects are instructed to be fast, high speed will reflect inaccuracy. If subjects are instructed to be accurate, high speed will reflect accuracy. These contingencies are easily controlled in human experiments through appropriate instructions, but can be a cause for confusion in interpreting animal experiments (see Uchida, N. and Mainen, Z. F., 2003 vs. Abraham, M. H. *et al.*, 2004, compared in Khan, R. M. and Sobel, N., 2004).

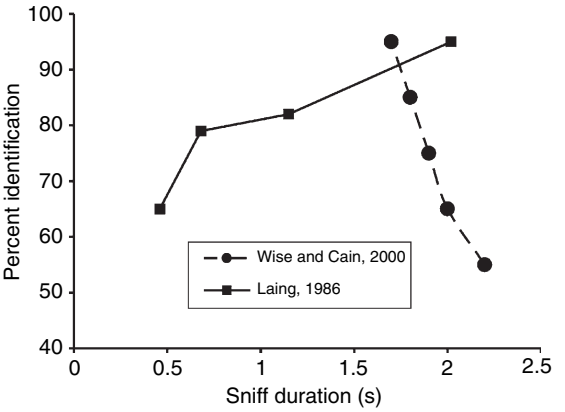

Figure 8 Time-accuracy trade-off. Behavior is modified by bias. Thus, when Laing D. G. (1986) stressed speed, the more subjects rushed, the less correct discriminations they made. In contrast, Wise and Cain stressed accuracy. Thus, when discriminations were easy and subjects were very confident, they answered at once. When discriminations were difficult, they took their time.

Finally, Johnson B. N. *et al.* (2003) used measurements of sniffing as an indirect performance-based measure to assess the latency-to-discrimination of differences in odorant intensity. Specifically, sniff vigor (flow rate, volume, and duration) is inversely proportional to odorant concentration (Laing, D. G. 1983; Warren, D. W. *et al.*, 1994; Sobel, N. *et al.*, 2001; Walker, J. C. *et al.*, 2001). Higher intensity odorants are sampled with reduced vigor, and lower intensity odorants are sampled with increased vigor. Johnson *et al.*, used careful recordings of sniff airflow combined with tight temporal control over odorant delivery. They found that sniffs start off with an extremely stereotyped structure, but are then modulated in accordance with odorant concentration by as early as 160 ms following sniff onset for an odorant that may have a trigeminal component, and 240 ms for a pure olfactant (Figure 9). These values are the lowest we are aware of for olfactory discrimination in humans and suggest that contrary to the common notion, olfaction is fast. Here a nonverbal measure of discrimination suggested that the olfactory system discriminated between two stimuli in less than 200 ms. Considering that odorant transduction alone is expected to account for at least ~150 ms of this latency (Firestein, S. *et al.*, 1990), this result suggests that the cognitive process of olfactory discrimination was extremely rapid.

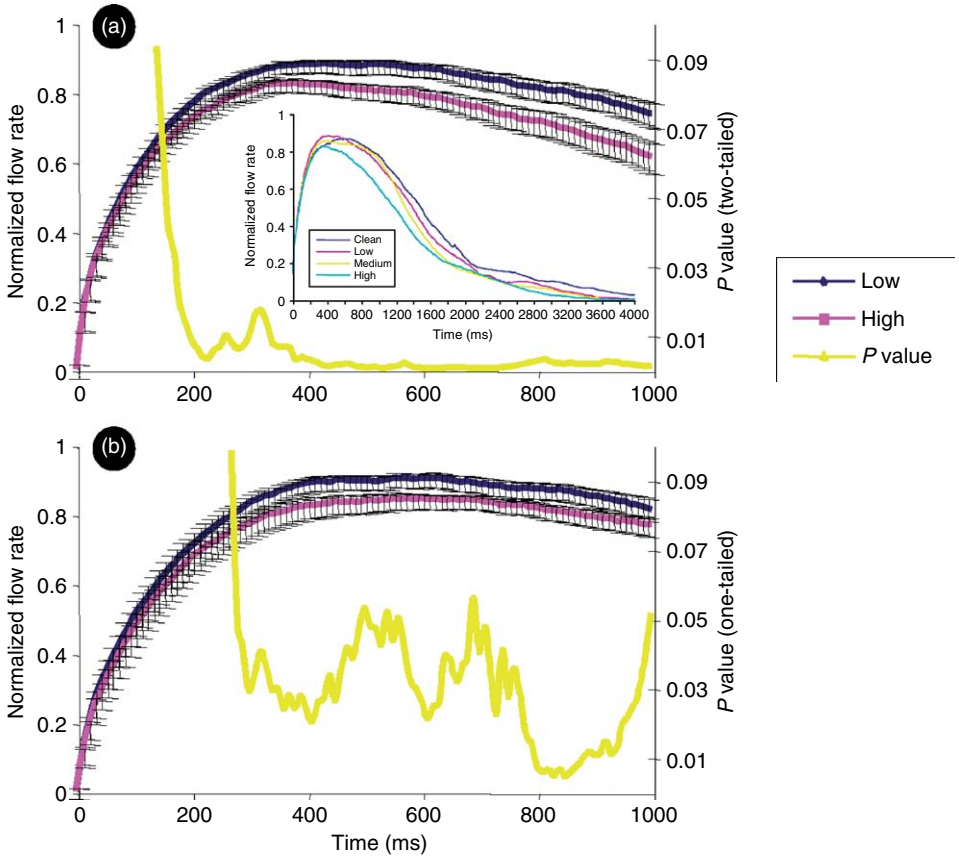

Figure 9 Speed of olfactory discrimination. Sniff magnitude serves as a nonverbal performance-based measure of discrimination. The inset depicts the full mean sniff of 28 subjects sniffing clean air, or one of three intensities of odor. Sniffs clearly separate as a function of odorant concentration. To probe the point of separation, only the first second of the sniff of 28 subjects for high and low concentration of propionic acid (a) and phenyl ethyl alcohol (PEA) (b) are depicted. The yellow line reflects a *t*-test between both traces. Sniff velocity drops when sniffing high as compared with low-concentration propionic acid by 160 ms after sniff onset and 240 ms for PEA.

4.45.4 Olfactory Identification

One step up from olfactory discrimination in the hierarchy of olfaction is olfactory identification. Whereas discrimination calls upon working memory to enable comparison of one odor with another, identification calls upon long-term memory in that in its explicit form, it consists of linking an odorant with a previously stored semantic representation. The study of olfactory identification is methodologically simpler than the study of detection and discrimination because the process of interest is slower and is mostly irrelevant at near-threshold concentrations. Despite this simpler methodological setting, olfactory identification remains the least understood perceptual process in olfaction. A basic goal of the study of olfactory psychophysics is a characterization of the structure of the perceptual space and its relation to the structure of the stimulus space. In vision, the laws of optics and the nature of light provide powerful constraints on the perceptual space: spatial location in the world is mapped onto spatial location in the retina which is subsequently preserved in subcortical and cortical processing, photon density maps onto brightness, and photon wavelength maps onto perceived color. Similarly in audition, characteristics of vibrations in the air can be mapped onto perceived qualities such as loudness, frequency, timbre, and so on. In olfaction, although there is agreement about the basic stimulus, namely relatively small molecules, there is surprisingly little consensus as to which aspects of the stimulus are connected with which aspects of perceptual experience. Indeed, there is not a perfumist or scientist who could predict the smell of a novel chemical structure, nor the chemical structure of a novel smell. This is unequivocally the

major question in the field of olfaction in general and olfactory perception in particular. Regarding this lacuna, Amoore, J. E. asked in 1970 "[h]ow can something *right in front of your nose* still remain a mystery while men are flying to the moon?" (Amoore, J. E., 1970). Now 35 years later, rovers are exploring mars, yet this question remains unanswered.

4.45.4.1 Language and Olfactory Identification

Free identification of odors is a surprisingly difficult task. Unprompted (without the use of multiple choices) odor identification accuracy of generally familiar odors is around 50% (Sumner, D., 1962; Lawless, H. T. and Engen, T., 1977; Cain, W. S., 1979; Engen, T., 1987; de Wijk, R. A. and Cain, W. S., 1994), although it can exceed 85% in experts (Bensafi, M. *et al.*, 2002b). Although odor familiarity can increase identification scores (Homewood, J. and Stevens, R. J., 2001), and discrimination sores (Savic, I. and Berglund, H. 2000), it does not always enable unprompted identification. Often subjects will acknowledge that the odor is familiar, but will be unable to name it. This situation has been named the tip-of-the-nose phenomenon (Lawless, H. T. and Engen, T., 1977), analogous to the tip-of-the-tongue phenomenon in word recall (Brown, R. and McNeill, D., 1966). Richardson J. T. and Zucco G. M. (1989) suggested that this phenomenon may result from subjects' tendency to use a small, impoverished set of verbal labels to encode odor memories, rather than precise and differentiating labels. When trying to recall a label at re-exposure to an odorant, the odor may be recognized, but may not activate a sufficiently precise differentiating label, leading to recognition without identification. To probe this issue, Cain W. S. (1979) trained participants to identify odors before testing them. Teaching subjects labels for odors over five sessions improved identification performance from 60% to 94%. In view of these results, Schab F. R. (1991) suggested that odor identification consists of two components, a perceptual process of odor encoding, and a verbal-semantic process that consists of the activation of potential labels in semantic memory, and the selection of the most appropriate label from those activated. On this account, the poor unprompted identification performance commonly observed might be explained by a limitation in odor encoding, or in the verbal-semantic treatment, or both (Schab, F. R., 1991; de Wijk, R. A., Schab, F. R. and Cain, W. S., 1995). Evidence for such a dual-component system can be seen in the influence of verbal context on olfactory perception. If the same odorant is presented within a positive versus negative verbal context, such as natural versus artificial, it is perceived as more pleasant (Herz, R. S., 2003). The magnitude of this effect can be significant. For example, Herz R. S. and von Clef J. (2001) presented subjects with a mixture of isovaleric acid and butyric acid labeled as either parmesan cheese or vomit. Using a 9-point pleasantness scale (9 = most pleasant), the same odorant was rated at 5.06 in the former condition and 1.68 in the latter. This result suggests an interesting interaction whereby odor perception is a poor generator of verbal labels (poorer than in other senses), yet verbal labels are a viable modifier of odor percepts (seemingly more so than in other senses).

Although the tip-of-the-nose phenomenon intuitively suggests that poor naming of odorants reflects failures at the level of verbal-semantic processing rather than perceptual processing, some lines of evidence suggest otherwise. For example, odor naming ability is highly correlated with odor discrimination ability, despite the latter's independence of semantic processes (de Wijk, R. A. and Cain, W. S., 1994). Jonsson, F. U. *et al.* (2005) further argued that the tip-of-the-nose phenomenon may not be as prevalent as one might think. These authors dissociated the tip-of-the-nose phenomenon from what they called a feeling of knowing, a sense of general familiarity that they argue reflects poor perceptual encoding of the odor. They presented subjects with 30 common odorants and collected subjective assessments from subjects regarding their experience during attempted identification. These subjective assessments were classified as either reflecting tip-of-the-nose phenomenon or feeling of knowing. They found that in failed identification, 4% of trials were accompanied by strong tip-of-the-nose phenomenon and 24% were accompanied by a strong feeling of knowing. From this, the authors argued that poor perceptual encoding accounts for a greater proportion of failed odor naming than does poor verbal-semantic processing.

The universally poor ability to freely recall odor names has shaped standard tests of olfactory identification, which generally eschew free recall in favor of forced multiple choice (Doty, R. L. *et al.*, 1984a; 1984b; Cain, W. S. *et al.*, 1988; Kobal, G. *et al.*, 1996; Hummel, T. *et al.*, 1997; Nordin, S. *et al.*, 1998). The most widely used of these tests is the University of Pennsylvania smell identification test (UPSIT) (Doty, R. L. *et al.*, 1984a; 1984b). This test consists of 40 microencapsulated odorants that subjects have

to scratch and sniff. For each odorant, their task is to choose among four alternative labels the one that best describes each odor (e.g., for the smell of pizza, the labels gasoline, pizza, peanuts, and lilac are proposed). The UPSIT may have some shortcomings as a scientific tool in that it was designed with clinical testing in mind. That said, it remains the only real standard test in olfaction and has proved enormously valuable in characterizing olfactory identification in both health and disease. The UPSIT and similar tests have revealed that olfactory identification is generally better in women than in men (Doty, R. L. *et al.*, 1985), that odor identification performance declines with age, usually following an inverted U-curve, best in young-adults and poorest in children and old-adults (Doty *et al.*, 1984c; Doty, R. L., 1989), and that olfactory identification declines in many diseases, to the extent that it may be diagnostic for some.

4.45.4.2 Identification of an Odor Rather than Its Parts

The nose is commonly thought of as a kind of chemical analyzer. As reviewed elsewhere in this book, specific chemicals are identified by specific receptors in a lock-and-key-type interaction based on receptor configuration and chemical functional groups. Furthermore, these individual chemicals are then represented in specific spatial patterns of activity on the surface of the olfactory bulb. In other words, the olfactory system is studied as a type of analytical tool, such as a chromatograph, which parses and stores information such that subcomponents may be identified from the original stimulus. Some behavioral researchers, however, hold a different view of olfactory processing. They believe that olfaction functions as a synthetic rather than an analytic process (Livermore, A. and Laing, D. G., 1998a; 1998b; Wilson, D. A. and Stevenson, R. J. 2003a; 2003b). By this, they mean that the olfactory system does not reduce the input into recognizable subcomponents but rather that it is the amalgam input that is recognized as a whole. The main line of evidence for this view is from the so-called gestalt aspect of olfaction evidenced in the perception of odor mixtures.

At the simplest level, human subjects are poor at determining whether an odor is a pure odorant (that we will refer to here as a simple odorant) or odorant mixture (that we will refer to here as a complex odorant) (Moskowitz, H. R. and Barbe, C. D., 1977). Furthermore, extensive characterization of odor mixture perception by Laing and colleagues has repeatedly found that humans cannot correctly identify the individual constituents of a mixture containing more than four or five constituents. In one study (Laing, D. G. and Francis, G. W., 1989), subjects were initially familiarized with seven odorants and their common names. Subjects were then asked to identify which of these seven components were in mixtures presented by an air-dilution olfactometer. Identification accuracy decreased as the number of components in the mixture increased. Performance was only marginally better than chance for four components and at chance for five components (Figure 10). As the actual number of components in the mixtures increased, the number of estimated components increased as well, but lagged behind the true number. Such performance is unlikely to be the result of inadequate experience as expert perfumers revealed very similar results (Livermore, A. and Laing, D. G., 1996). However, component identification is better for familiar than unfamiliar odors (Rabin, M. D., 1988).

Subjects' ability to identify mixture components when constituents were themselves complex odorants was at the same level of performance as when constituents were simple odorants (Livermore, A. and Laing, D. G., 1998a; 1998b). This critical result suggests that odorants were represented as irreducible objects that used equal neural processing capacity, whether they were simple or complex. This irreducibility was further evidenced in that subjects are worse at distinguishing the components of complex odors they had been trained to identify as a single odor, yet when presented with only some of

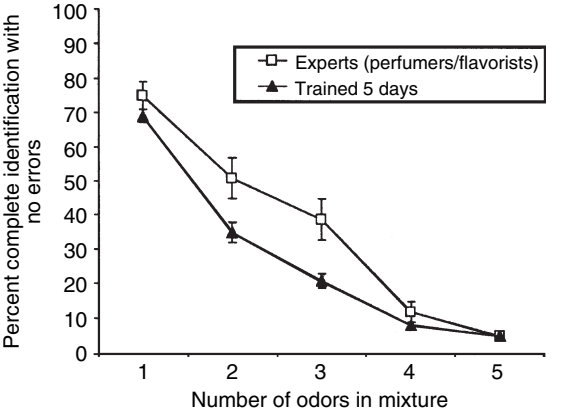

Figure 10 Odor mixture perception. Results from Laing and colleagues demonstrate that both expert perfumers and laypeople alike can identify up to four components of an odorant mixture.

the constituents of a learned odor object, they reported greater perception of qualities normally associated with the other constituents they had previously associated (Stevenson, R. J., 2001a; 2001b). This suggests that the mixed odorant is being represented as a single object, and when a portion of the object is presented the whole object is recalled.

These studies suggested that odorant qualities are blending together to decrease identification of components. To test this, Livermore A. and Laing D. G. (1998a; 1998b) tested mixture component identification using two sets of eight odorants chosen by a panel of expert perfumers as a set of bad blending odorants and a set of good blending odorants. As they predicted, component identification accuracy decreased with mixture complexity regardless of odorant group (good or bad blenders). Subjects were unable to identify more than three or four components in a mixture. However, subjects were significantly better at identifying components for the bad blending odorants than the good blending odorants.

Taken together, these experiments have been presented by some as evidence that olfaction is a synthetic rather than an analytic sense, which is to say that olfaction deals primarily with odor objects rather than odor molecules (Wilson, D. A. and Stevenson, R. J. 2003a; 2003b). It is clear, however, that olfaction, like all other senses, is both analytic and synthetic, and that these terms should be understood not as alternative construals but as descriptive of different levels of sensory processing. Consider an analogous situation in auditory processing. The sensory apparatus (the hair cells on the cochlea) is laid out to encode sound frequency in a linear fashion, and so the analytic basis set for audition is the set of pure tones within the audible range. As it is easy to generate pure tones (e.g., with tuning forks), we have the advantage of being able to probe the system with its analytic atoms. In olfaction, however, the basis set of the system is comprised of the few hundred different olfactory receptor types that are expressed in a particular organism. In general, each receptor responds to a range of molecules, and each molecule reacts with a number of receptors, so that individual molecular species are not the analytic atoms of the system. The set of atoms (or tuning forks) for olfaction would be a set of stimuli each of which reacted with only a single type of olfactory receptor. It is unlikely that many such olfactory stimuli exist. Continuing the comparison to audition, even an odorant composed of a single molecular type is thus analogous to a complex sound, not a pure tone. It is little surprise, on this view, that identification of complex and simple odors in mixtures is equal. Thus, to say that olfaction deals with olfactory objects rather than olfactory molecules is somewhat to have missed the point: molecules are not the analytic unit for olfaction but are themselves olfactory objects. Reverting to the analog in audition, if a viola is played simultaneously with a violin, a flute, a cello, and a trumpet, the ability of the system to distinguish the components (the particular instruments) from the mixture will be no better than the case of mixtures of molecules, and both may reflect fundamental information processing constraints.

Thus, in both audition and olfaction, the system begins with an analytic basis set, which must then be processed, in the light of much top-down information such as familiarity and learning the use of verbal labels, and attention to perceptual objects. The problem of mixture analysis in olfaction is akin to auditory scene analysis (Alain, C. and Arnott, S. R., 2000; Haykin, S. and Chen, Z., 2005) and should not be understood as a problem peculiar to olfaction. Inasmuch as the labels analytic and synthetic are useful, it is to remind us that olfaction, like all sensory modalities, is a complex, multilayered process.

4.45.4.3 Nostril-Specific Odor Tuning

Almost all odors that humans encounter in their environment are mixtures. Using mixture perception, Sobel N. *et al.* (1999) set out to ask whether the olfactory percept is equal across nostrils. Nostrils can be divided according to two criteria. One is the simple anatomical criterion, namely a left and right nostril. A second criterion is nasal airflow. In mammals, the rate of airflow is usually higher in one nostril than in the other. This occurs because a bilateral highly vascularized structure, the nasal turbinate, swells with blood flow in either one nostril or the other, increasing the resistance to airflow in one nostril in comparison to the other (Principato, J. J. and Ozenberger, J. M., 1970; Bojsen-Moller, F. and Fahrenkrug, J., 1971; Hasegawa, M. and Kern, E. B., 1977) (Figure 11(a)). The nostril with higher airflow, left or right, alternates on an ultradian rhythm of uncertain periodicity (Gilbert, A. N. and Rosenwasser, A. M., 1987; Mirza, N. et *al.*, 1997). Thus, nostrils can be designated either left and right or high flow (HF) and low flow (LF). However, in studies where one nostril was occluded in order to test the other, results regarding asymmetry in olfactory performance were mixed.

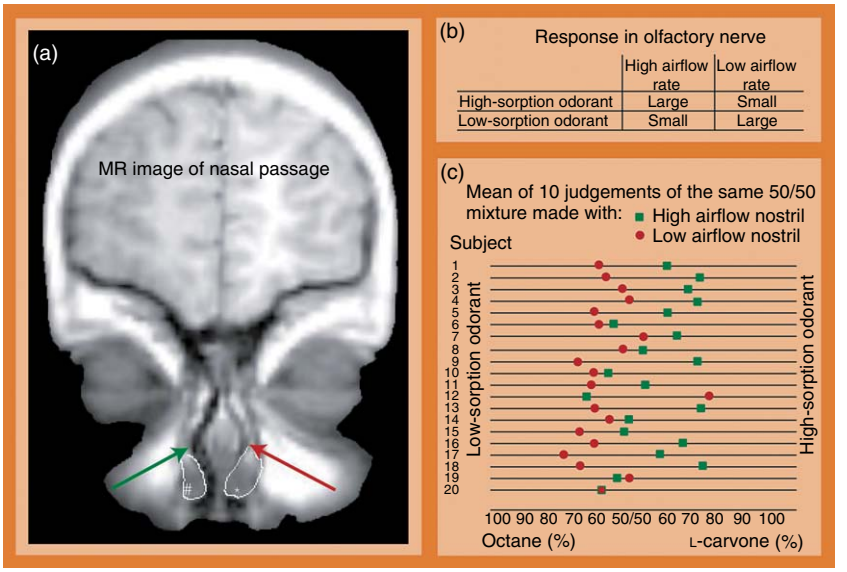

Figure 11 Nostril-specific odor tuning. (a) Magnetic resonance (MR) image of the nasal passage, which appears dark. The swollen (*) and relaxed (#) turbinates, outlined in white, result in an occluded right nostril (red arrow) and a clearer left nostril (green arrow). (b) The interaction between airflow rate and odorant sorption, which brings about a response in the olfactory nerve. (c) On each of ten trials, subjects were asked to smell an identical mixture of 50% octane and 50% L-carvone using either the left or right nostril. They were then given each individual odorant component to smell separately and judged the composition of the mixture by marking the line. Using the HF rate nostril (green), the average judgment was that the mixture consisted of 55% L-carvone and 45% octane. Using the LF rate nostril (red), the judgment was that it consisted of 61% octane and 39% L-carvone ($t(19) = 3.74$, $P = 0.001$).

Although some advantages have been suggested for right versus left nostril (Toulouse, E. and Vaschide, N., 1899; Koelega, H. S., 1979; Youngentob, S. L. *et al.*, 1982; Zatorre, R. J. and Jones-Gotman, M. 1990; Broman, D. A. *et al.*, 2001), and left versus right nostril (Homewood, J. and Stevens, R. J., 2001), no differences were found for HF versus LF nostrils (Eccles, R. *et al.*, 1989; Frye, R. E., 1995). This was paradoxical in view of the previously noted link between nasal airflow velocity and olfactory performance. Because increased velocity improves detection (Le Magnen, J., 1945; Laing, D. G. and Wilcox, M. E., 1983), and olfactory intensity estimates (Rehn, T., 1978; Teghtsoonian, R. and Teghtsoonian, M., 1984; Youngentob, S. L. *et al.*, 1986; Hornung, D. E. *et al.*, 1997), one would expect better olfactory performance in the HF nostril versus the LF nostril. Yet, no such differences were observed (Eccles, R. *et al.*, 1989; Frye, R. E., 1995). This paradox was resolved by Sobel N. *et al.* (2000a) who found that when humans are restricted to sniffing through one nostril only, if it is the LF nostril, they spontaneously increase sniff duration in that nostril so as to equate volume with the HF nostril. In other words, the olfactomotor system generates a compensatory sniff that accounts for the lower airflow in that nostril. Critically, Sobel N. *et al.*, found that once activation of this compensatory sniffing was prevented, olfactory performance was poorer in the LF nostril compared to the HF nostril (Sobel, N. *et al.*, 2000). Thus, the valid method for comparison of olfactory performance in the HF nostril versus the LF nostril is to assure that both sniff for the same duration (as they would have had one of them not been occluded for testing). This can be achieved by training subjects to match their sniff to either an auditory tone, or on-monitor measurement of nasal airflow (Mainland, J. D. *et al.*, 2005). With this in mind, Sobel N. *et al.* (1999) set out to test the hypothesis that the HF nostril and LF nostril would each be better tuned to a different aspect of an odor mixture. The framework for this hypothesis was set by the pioneering work of Mozell and colleagues, who demonstrated that odorants absorb in, and cross, the olfactory mucosa at different rates (Mozell, M. M. and Jagodowicz, M., 1973; Mozell, M. *et al.*, 1991). They established this phenomenon by measuring the relative sorption rates of 15 odorants across the mucosa of the bullfrog. Mozell and colleagues later found that the effect of an odorant on the magnitude of response in the olfactory nerve of the frog results from an interaction between the

particular sorption rate of that odorant and the flow rate at which it flows across the olfactory mucosa: a high-sorption rate odorant will induce a large response when delivered at a high airflow and a smaller response when delivered at a lower airflow. In contrast, a low-sorption rate odorant will induce a small response when delivered at a high airflow and a larger response when delivered at a lower airflow. A theoretical explanation to this is as follows: when a bolus of low-sorption odorant enters the nostril at a slow flow rate, there is a weak vector along the epithelium (slow flow) and a weak vector across the mucus (low sorption). This results in an even distribution of odorant molecules along the epithelium whereby a large epithelial surface area is affected, and the resulting response is large. In turn, when the same bolus of low-sorption odorant is flown rapidly across the mucosa, there is a strong vector along the epithelium (fast flow) and a weak vector across the mucus (low sorption). This results in a proportion of the molecules never sorbing before they are cleared into the respiratory system, an uneven distribution of odorant molecules along the epithelium whereby only the posterior end of the epithelial surface area is affected, and the resulting response is small. In contrast, when a bolus of high-sorption odorant enters the nostril at a slow flow rate, there is a weak vector along the epithelium (slow flow) and a strong vector across the mucus (high sorption). This results in an uneven distribution of odorant molecules along the epithelium whereby the full bolus saturates the anterior portion of the epithelium, a small epithelial surface area is affected, and the resulting response is small. In turn, when the same bolus of high-sorption odorant is flown rapidly across the mucosa, there is a strong vector along the epithelium (fast flow) and a strong vector across the mucus (high sorption) (Figure 11(b)). This results in an even distribution of odorant molecules along the epithelium whereby a large epithelial surface area is affected, and the resulting response is large.

The foregoing findings suggest that particular airflows will optimize perception for particular odorants. High airflows will optimize perception of higher-sorption rate odorants and low airflows will optimize perception of lower-sorption rate odorants. Considering these findings in the frog, one may predict that the difference in airflow rate between the nostrils in the human will result in a different olfactory percept in each nostril as a function of the interaction between airflow and odorant sorption rates. Accordingly, we hypothesized that the high-airflow nostril is better tuned to high-sorption rate odorants and the low-airflow nostril is better tuned to low-sorption rate odorants.

To test this, 20 subjects performed a task in which on each trial an olfactometer produced an equally proportioned mixture of the low-sorption rate odorant octane and the high-sorption rate odorant L-carvone (Figure 11(c)). Although subjects were deceived and told that the mixtures would be slightly different on every trial, they were actually identical mixtures. The subject then (1) took a monorhinal fixed-duration sniff of the mixture with either the HF rate nostril or LF rate nostril, (2) smelled each component odorant individually, and (3) judged the composition of the mixture on a proportion scale (ranging from 100% octane, to 50/50 octane/L-carvone to 100% L-carvone, as illustrated at bottom of Figure 11(c)). Each subject performed 20 trials with each nostril. All experimental components were counter-balanced to prevent confounds of cross-adaptation and learning.

Although the mixture was always the same, we predicted that when smelling the mixture with the high-airflow nostril, the high-sorption rate odorant would seem more prominent in the mixture, and when smelling the same mixture with the low-airflow nostril, the low-sorption rate odorant would seem more prominent. As predicted, 17 of the 20 subjects judged the same mixture to have a higher L-carvone content (high-sorption-rate odorant) when using the high-airflow nostril and a higher octane content (low-sorption-rate odorant) when using the low-airflow nostril (binomial, $P < .002$) (Figure 11(c)). This finding demonstrated that the olfactory content obtained from each nostril in a given sniff was different and related to sniff airflow. Each nostril was slightly better tuned to odorants that optimally sorb to the mucosa at the current flow rate in that nostril. This finding points to a fundamental commonality across distal sensory systems. In both vision and audition, the two sense organs simultaneously provide a slightly disparate image to the brain. In vision, this disparity is computationally manipulated to provide an additional dimension – depth. In audition, this disparity is computationally manipulated to provide an additional dimension – spatial location of sounds. We expect that the disparity of input across nostrils is similarly computationally manipulated to provide an additional dimension in olfaction. The nature of this olfactory dimension awaits characterization.

4.45.4.4 Identifying Odor Characteristics

Whereas odor identification can prove difficult, identifying particular odor characteristics or attributes is readily achieved. Even when they cannot identify an odor by name, subjects can generate descriptors for an odorant. Wise P. *et al.* (2000) have pointed to some limitations in assessing such behavior, such as (1) such judgments are difficult to verify, (2) different people may use widely different words to describe the same odors. This difference in language use across subjects can make it difficult to assess both interrater and intrarater agreement. Notwithstanding these issues, the analysis of subjective characteristics of odors provides a number of insights into how olfaction may be organized.

The most consistently agreed upon and meaningful characteristic of odors is their pleasantness, or valence as it is sometimes described. Whereas explicit identification, particularly of unfamiliar odors, can be relatively difficult, people can quite readily make judgments of odor pleasantness. Indeed, the primary perceptual aspect subjects use in odorant discrimination studies is odorant pleasantness (Schiffman, S. S. 1974; Godinot, N. and Sicard, G., 1995), and odor-grouping experiments show that pleasantness is the most salient dimension of olfaction (Berglund, B. *et al.*, 1973; Schiffman, S. *et al.*, 1977). Pleasant and unpleasant odors are evaluated at different speeds (Bensafi, M. *et al.*, 2002a) and act differentially on peripheral nervous responses (Jäncke, L. and Kaufmann, N., 1994; Brauchli, P. *et al.*, 1995; AlaouiIsmaili, O. *et al.*, 1997; AlaouiIsmaili, O. *et al.*, 1997; Bensafi, M., 2002b; 2002c; 2002d). Studies of startle reflexes suggest that unpleasant and pleasant smells might be mediated by at least two distinct fundamental emotional systems: an aversive system (associated with negative affects) and an appetitive one (associated with positive affects). According to Lang P. J. *et al.* (1990), activation of the aversive system might increase the magnitude of the startle reflex, while activation of the appetitive system might decrease the magnitude of the startle reflex. Odors have been used to produce positive and negative affective states during which unpleasant odors activate the aversive system and enhance startle reflexes (Miltner, W. *et al.*, 1994; Ehrlichman, H. *et al.*, 1995; 1997), whilst pleasant odors activate the appetitive system and attenuate startle reflexes (Ehrlichman, H. *et al.*, 1997). Startle in the presence of unpleasant odors may be a defensive behavior present early in life: in newborns, differential facial reactions have been found for pleasant and unpleasant odors (Steiner, J. E., 1979; Soussignan, R. *et al.*, 1997). The primacy of pleasantness judgments is also supported by electrophysiological recordings (Kobal, G. *et al.*, 1992; Pause, B. M. and Krauel, K. 2000; Masago, R. *et al.*, 2001) and functional neuroimaging studies (Zald, D. H. and Pardo, J. V., 1997; Fulbright, R. K. *et al.*, 1998; Crespo-Facorro, B. *et al.*, 2001; Henkin, R. I. and Levy, L. M., 2001; Gottfried, J. A. *et al.*, 2002a; 2002b).

Perceptually, odor valence is tightly linked with odorant intensity. In fact, the inverse correlation between odor intensity and valance is so pronounced that Henion K. E. (1971) suggested odor pleasantness and intensity are a single dimension. Henion based this claim on a study of a single odorant (*n*-amyl acetate). More comprehensive studies on the relationship between odor intensity and pleasantness, however, revealed a complex interaction whereby some odorants display a positive correlation (increased intensity leads to increased pleasantness), some an inverse correlation (increased intensity leads to decreased pleasantness), and yet others a variable inverted U-shaped correlation between pleasantness and intensity (Henion, K. E., 1971; Doty, R. L., 1975; Moskowitz, H. R. *et al.*, 1976; Distel, H. *et al.*, 1999) (Figure 12). The psychophysical data suggesting

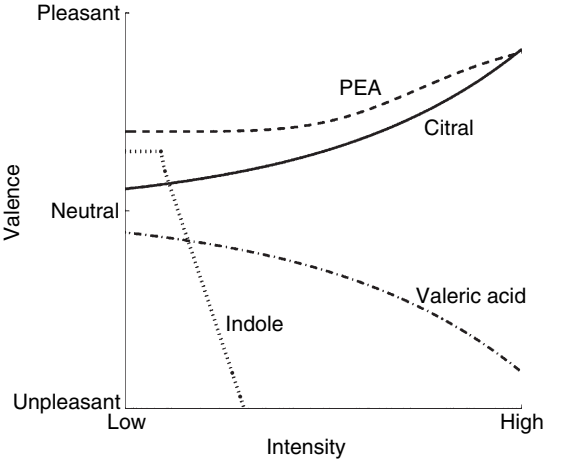

Figure 12 The relationship between intensity and valence. Different odors behave differently. Citral is pleasant, and as you increase its intensity, it becomes more pleasant. Valeric acid is unpleasant, and as you increase its intensity, it becomes more unpleasant. Phenyl ethyl alcohol (PEA) is pleasant, and this valence does not change much across a wide range of intensities, although it eventually does increase. Indole is pleasant at very low intensities, but even a relatively small increase in intensity shifts its percept to one that is extremely unpleasant.

intensity and valence are indeed dissociable constructs received support from neuroimaging studies that found olfactory intensity and valence are subserved by dissociable neural substrates (Gottfried, J. A. *et al.*, 2002b; Anderson, A. K. *et al.*, 2003; Anderson, A. K. and Sobel, N., 2003). Studies of olfactory psychophysics must consider this relationship in their design. For example, if one wants to probe intensity coding, one must keep valence constant, and vice versa.

4.45.4.5 Odor Space

In vision and audition, perceptual experience organizes itself, both through language and, directly, into an ordered space: perceptual events have a distinct relationship to one another that most people acknowledge. In vision, these organizational principles are so basic and ingrained, that they may scarcely need acknowledging: objects exist in a three-dimensional space with all the spatial relational operators, they have colors that can be ordered into a color wheel, so that colors themselves have a kind of spatial relationship. These basic facts arise from basic facts about the world: wavelengths of light, which map onto colors, themselves have an ordering, as does the nature of physical space. In audition, the sensory receptors are organized in the cochlea to map sound frequency onto a linear spatial gradient, and so within auditory perception, the experience of frequency has a linear ordering, namely pitch. That such a latent organization in the olfactory sensory apparatus may exist, and that it may map onto some intrinsic organizational principle within the set of olfactant molecules, has fueled numerous efforts to understand the olfactory odor space. These efforts are of two basic kinds: efforts to understand chemical features of molecules that may map onto perceptual differences and efforts to understand the structure of olfactory perceptual space itself, without reference to chemical properties. These different efforts are, of course, complementary, and the ultimate goal of each is to move from one to the other, so that specific changes in a perceptual space can be related to specific changes in molecular features. We will refer to these two kinds of efforts as stimulus-based maps and perception-based maps. We will first discuss the methods of acquiring feature information from these maps and subsequently discuss mathematical techniques usefully for reconstructing the maps from the information.

4.45.4.5.1 Perception-based maps

Attempts to assess the perceptual structure of olfaction have assumed there is an implicit set of features that are extracted by the nervous system from all odorants, and that these features can therefore be combined to form an olfactory space. The advantages of producing such maps is that from them unknown features of an odorant may be inferred from partial information, they can be used to investigate possible molecular features that correspond to underlying perceptual features, and they provide information about the possible organization of the olfactory nervous system.

All maps are connected to the idea of similarity: objects closer together in the perceptual space are more similar to each other than are objects further apart. Efforts to derive perceptual spaces can thus proceed in either of two ways: they can measure similarity between odorants directly and use this data to derive a map, or they can measure some other features of the objects and infer similarity from them indirectly and thus build a map. These two approaches can be thought of as explicit and implicit measures, depending on whether they measure or derive odorant similarity.

4.45.4.5.2 Explicit similarity methods

One approach to assessing similarity is having subjects group samples of odorants into categories. Odorants placed within the same category are judged to be more similar than odorants that span different categories. Subjects perform either a task where they place each odorant into one of the predefined categories to which it is most similar (Linneaus, C., 1756), or a task where they organize the odorants into any number of categories the subject deems appropriate (MacRae, A. W. *et al.*, 1990; 1992; Stevens, D. A. and O'Connell, R. J., 1996). The first method imposes a structure which may bias subjects and constrains the odor space (Lawless, H. T., 1989), but has the advantage of ensuring consistency of categories across subjects. Unrestricted sorting of odorants permits subjects greater freedom in expressing their perception, but there is greater intersubject variability, and the inconsistency of categories across subjects introduces further difficulties in combining subject data. However, this method appears reliable within subjects (MacRae, A. W. *et al.*, 1990; 1992), and certain differences in sorting might reflect true differences in perception by special subpopulations of subjects (Stevens, D. A. and O'Connell, R. J., 1996).

A second method is to present pairs of odorants and ask subjects to rate the similarity between them. The results from several such studies found considerable variability in judgments between subjects (Dimmick, F. L., 1927; Yoshida, M., 1964a; 1964b) but, as in the unrestricted sorting experiments, these differences may reflect true differences in perception (Dimmick, F. L., 1927; Gregson, R. M., 1972; Davis, R. G., 1979). Analysis of direct similarity scores suggest that in making judgments, subjects generally rely on a hedonic factor and several other factors which may vary across subjects (Yoshida, M., 1972a; 1972b; Moskowitz, H. R. and Gerbers, C. L., 1974; Schiffman, S. S. 1984). Part of this variability may result from a lack of specific instructions for similarity criteria (Wise, P. *et al.*, 2000). While useful for a relatively small set of odorants, the task becomes burdensome as the number of odorants increases, as the number of possible pairwise comparisons increases as the square of the number of odorants.

4.45.4.5.3 Implicit similarity methods

A second approach that is feasible for large sets of odorants is to instruct subjects to rate or rank odorants one at a time against a series of descriptors (e.g., verbal labels) (Dravnieks, A. *et al.*, 1978; Dravnieks, A., 1982; Laing, D. G. and Wilcox, M. E., 1983) and then inferring the similarity of pairs of odorants from their responses. This method assumes that similar odorants will have similar feature values, and thus will cluster together in the feature space. Dravnieks A. (1982) demonstrated that responses on a large set of semantic descriptors were stable across 150 subjects from 15 different locations across the United States. The use of a large set of descriptors reduces the concern that the choice of labels will limit the diversity of the method (Thiboud, M., 1991).

There are three large databases of odor category rankings available as commercial products – a strikingly small number considering the importance of such data and the uncertain reliability of these existing products. The largest and most comprehensive is the multivolume/compact-disc set by Steffen Actander. The Sigma-Aldrich Flavors & Fragrances Catalog contains a handful of odorant descriptors for each of 800 + chemicals. The most popular reference for obtaining odorant profiles is the Atlas of odor character profiles, which ranks 160 chemicals against each of the 146 descriptors (Dravnieks, A., 1985).

Once a full set of similarity data (either implicit or explicit) is available for a set of odorants, the organization of the result into a coherent odor space can be achieved through a variety of statistical methods. A common method for map reconstruction is with multidimensional scaling (MDS) (Kruskal, J. B. and Wish, M. 1978). We will only briefly introduce this method and leave the interested reader to seek out the provided references. The first step of MDS is to create an N by N distance matrix, where there are N odorants and the (i, j)th cell of the matrix contains the distance (the inverse of similarity) between the ith and jth odorants. The goal of MDS is to assign each odorant to a point in a metric space (typically Euclidean) so that the distance between odorants in this coordinate system preserves the distance structure in the original distance matrix (Figure 13). MDS is an iterative optimization algorithm that is often performed many times for high-dimensional spaces to reduce the chances of finding local minima. MDS is essential a data-compression technique, and there are many studies that set out to validate the technique for reducing olfactory perception data. The dimensionality of the constructed space must be specified as a prior constraint.

Using similarity ratings, several researchers found a primary pleasant–unpleasant dimension (Yoshida, M., 1972a; 1972b; Berglund, B. *et al.*, 1973;

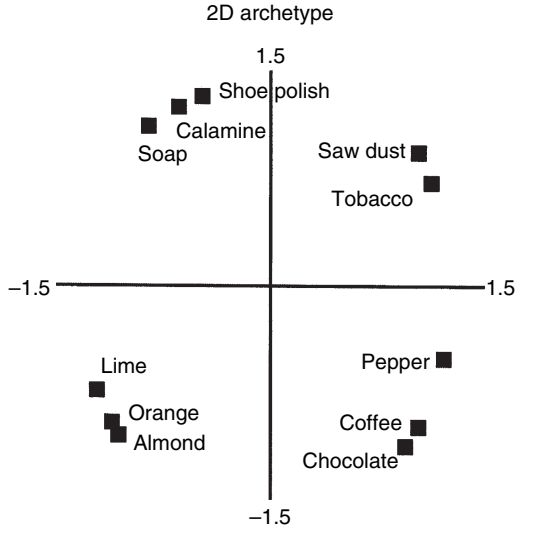

Figure 13 A two-dimensional multidimensional scaling (MDS) derived odor space for some common odors. The map is constructed from the similarity judgments of 110 subjects, so that the distances between odors in the MDS space is inversely proportional to perceived similarity. Although the axes are not meaningfully labeled, the odors cluster into sensible groups from Dawes, P. J. D., Dawes, M. T., *et al.* 2004. The smell map: commonality of odour perception confirmed. Clin. Otolaryngol. 29, 648–654.

Moskowitz, H. R. and Gerbers, C. L., 1974; Yoshida, M., 1975; Schiffman, S. *et al.*, 1977) and a secondary sweet-pungent dimension (Yoshida, M., 1964a; 1964b). The inability to associate more dimensions with perceptual qualities could be due to too few odorants or high subject variability that obscured everything except the most salient dimensions (e.g., hedonic value). Another weakness can be high between-subject variability for the underlying similarity ratings (Berglund, B. *et al.*, 1973). Cunningham M. and Crady C. A. (1971) used bipolar categories (e.g., pleasant or unpleasant or sour or sweet) instead of similarity ratings to probe the olfactory perceptual map and then used MDS to determine the most salient dimensions and found similar results in the salient dimensions.

Carrie S. *et al.* (1999) collected similarity reports for 20 normal and four hyposmic subjects on 11 common odors (i.e., coffee, chocolate, soap, and so on) and found very good agreement for the MDS maps of individual subjects. ALSCAL NMDS was used to compute a subject-weighted archetypal perception map. Individual subjects fit the archetypal map well, while the hyposmic did not. Dawes P. J. D. *et al.* (2004) repeated this experiment but used 110 new observers and found an almost identical MDS solution for the salient dimensions. However, the first three dimensions only accounted for 60% of response variance, suggesting either high variance between subjects, or that the odor space is in fact fairly high dimensional. Another source of this variance could be the known influence of olfactory sensitivity on perceptual quality (Stevens, D. A. and O'Connell, R. J., 1991).

Odor maps are also useful tools for understanding differences in perception across subjects. Stevens D. A. and O'Connell R. J. (1996) examined the perceptual map differences for three groups with differing sensitivity to the odorant pemenone. There are three typical perceptions of pemenone: putrid, nonputrid, and nondetection. Subjects responding in each of these ways were classified as osmic, allosmic, or anosmic, respectively. One hypothesis for these perceptual differences is differences in odorant receptor expression on the olfactory epithelium. Over 20 subjects from each group sorted 15 odorants (five putrid, five floral/fruity, and five wood/vegetable, note these are a priori groups created by the researchers and not based on the subjects) into any number of groups (e.g., free sorting). A similarity metric was created for each pair of odorants that was based on the percentage of subjects placing the pair in the same group. MDS was then used to project the distance matrix onto a three-dimensional space. The MDS created three clusters that reflected the three groups of odorants selected by the researchers (putrid, floral/fruity, and woody/vegetable). Additionally, the location of pemenone differed for each group of subjects. Pemenone was near the putrid cluster for osmics, near the vegetable/woody cluster for allosmics, and near the floral/fruity cluster for anosmics.

Perhaps the most extensive investigation of perceptual maps using MDS is by Chee-Ruiter and Madany-Mamlouk working in the laboratory of Jim Bower (Mamlouk, A. M., 2002; Mamlouk, A. M. *et al.*, 2003; Mamlouk, A. M. and Martinetz, T., 2004). Using the odor quality data in the Aldrich Flavor and Fragrances Catalog, Mamlouk computed the subdimensional distance (a weighted cross-entropy function) to estimate dissimilarity between the 851 odorants. The MDS solution suggested approximately 32 dimensions within the dissimilarity measurements, many more than typically presented in the MDS literature reviewed previously. When the solution was projected to a two-dimensional Euclidean space for visualization, distortions became apparent. Odorants that were not similar in the 32-dimensional solution became similar when collapsed, and some similarities were lost in the projection. In an interesting addition to the analysis, the number of nitrogen and sulfur atoms for each odorant emerged as the third dimension after the two-dimensional projection. The map shows that odorants containing nitrogen or sulfur were grouped together – supporting an eco-olfaction hypothesis in which metabolically relevant odorants are perceived similarly.

Altogether, efforts to understand the structure of the perceptual space reveal that a low dimensional description may be inadequate to capture the complexity of olfactory perception. Ultimately, the state of models of olfactory space is a half-finished project: the completion consists of connecting a space that represents meaningful features of perception with a physiological receptor space that represents the response of olfactory receptor cells to a given odor. This, of course, is no small task but is in fact tantamount to understanding a large part of all processing in the olfactory system. A fuller appreciation of the meaning of olfactory space models will emerge as progress towards this linkage bears fruit in future work.

4.45.4.6 Final Word

In this chapter, we have seen two things: first, that the human olfactory sensory system is an incredibly subtle molecular detector and discriminator; and second, that humans are an animal model particularly well suited for the study of what remains the biggest mystery in olfaction, namely the link between odorant structure and odorant percept. Whereas many other mammals exhibit olfactory detection and discrimination equal or better to that of humans, no other animal can convey its perception through language. Thus, for example, if one wanted to ask what properties of an odorant make it smell more like almonds, one could study nonhuman animals and devise complex behavioral tasks where one could only hope that decisions the animal would make (e.g., error rate or reaction time) might imply to what extent a given stimulus smells like almonds. However, any interpretation of animal behavior in this context is prone to error, as one can never be sure what stimulus features an animal is using in its decision process. This concern is increased due to the correlation between various olfactory features. For example, when studying intensity perception, how can we be sure that an animal is not basing its decisions in a task as a function of odorant valence rather than intensity, because these two dimensions of olfaction are tightly correlated. In contrast, when studying humans, the solution to such constraints is relatively easy. One can simply ask subjects: "which odorant smells more like almonds?". The power afforded by such a simple approach enables probing the more complex and essential questions of the qualities and similarities of odors. For these questions, the human model truly shines. With humans, not only can we learn much more about the percept because of language, but the datum of language use in connection with odors itself can be used to construct odor spaces that correlate with behavior. From the one side, the rules of biochemistry and physics govern how odorants react with olfactory receptors; from the other, there are rules of mind or perception. How they meet is the substance of psychophysics, and although the first bricks have been laid, the house remains to be built.

References

Abraham, M. H., Gola, J. M., *et al.* 2002. A model for odour thresholds. Chem. Senses 27(2), 95–104.

Abraham, N. M., Spors, H., *et al.* 2004. Maintaining accuracy at the expense of speed: stimulus similarity defines odor discrimination time in mice. Neuron 44(5), 865–876.

Ackerman, D. 1990. A Natural History of the Senses. Random House.

Alain, C. and Arnott, S. R. 2000. Selectively attending to auditory objects. Front. Biosci. 5, D202–212.

Alaouilsmaili, O., Robin, O., *et al.* 1997. Basic emotions evoked by odorants: Comparison between autonomic responses and self-evaluation. Physiol. Behav. 62(4), 713–720.

Alaouilsmaili, O., VernetMaury, E., *et al.* 1997. Odor hedonics: Connection with emotional response estimated by autonomic parameters. Chem. Senses 22(3), 237–248.

Amoore, J. E. 1967. Specific anosmia: a clue to the olfactory code. Nature 214(93), 1095–1098.

Amoore, J. E. 1970. The Molecular Basis of Odor, Charles C Thomas.

Amoore, J. E. 1977a. Specific anosmia and the concept of primary odors. Chem. Senses Flavor 2, 267–281.

Amoore, J. E. 1977b. Specific anosmias to 5-alpha-androst-16-en-3-one and omega-pentadecalactone: the urinous and musky primary odors. Chem. Senses Flavor 2, 401–425.

Amoore, J. E. and Hautala, E. 1983. Odor as an aid to chemical safety: odor thresholds compared with threshold limit values and volatilities for 214 industrial chemicals in air and water dilution. J. Appl. Toxicol. 3(6), 272–290.

Amoore, J. E. and Venstrom, D. 1966. Sensory analysis of odor qualities in terms of the stereochemical theory. J. Food Sci. 31, 118–128.

Amoore, J. E., Forrester, L. J., *et al.* 1975a. Specific anosmia to 1-pyrroline: the spermous primary odor. J. Chem. Ecol. 1(3), 299–310.

Amoore, J. E., Popplewell, J. R., *et al.* 1975b. Sensitivity of women to musk odor: no menstrual variation. J. Chem. Ecol. 1(3), 291–297.

Anderson, A. K. and Sobel, N. 2003. Dissociating intensity from valence as sensory inputs to emotion. Neuron 39(4), 581–583.

Anderson, A. K., Christoff, K., *et al.* 2003. Dissociated neural representations of intensity and valence in human olfaction. Nat. Neurosci. 6(2), 196–202.

Bailey, E. H. S. and Nichols, E. L. 1884. Preliminary notes on the delicacy of the special senses. NY Med. J. 40, 325.

Bailey, E. H. S. and Powell, L. M. 1885. Some special tests in regard to the delicacy of the sense of smell. Trans. Kans. Acad. Sci. 9, 100–101.

Beets, M. G. J. and Theimer, E. T. 1970. Odour Similarity between Structurally Unrelated Odorants. In: Taste and Smell in Vertebrates (*eds*. G. E. W. Wostenholme and J. Knight), pp. 313–323. J. & A. Churchill.

Békésy, G. V. 1964. Olfactory analogue to directional hearing. J. Appl. Physiol. 19, 369–373.

Bensafi, M., Brown, W. M., *et al.* 2003a. Sex-steroid derived compounds induce sex-specific effects on autonomic nervous system function in humans. Behav. Neurosci. 117(6), 1125–1134.

Bensafi, M., Brown, W. M., *et al.* 2004a. Sniffing human sex-steroid derived compounds modulates mood, memory and autonomic nervous system function in specific behavioral contexts. Behav. Brain Res. 152(1), 11–22.

Bensafi, M., Pierson, A., *et al.* 2002a. Modulation of visual event-related potentials by emotional olfactory stimuli. Neurophysiol. Clin. 32(6), 335–342.

Bensafi, M., Porter, J., *et al.* 2003b. Olfactomotor activity during imagery mimics that during perception. Nat. Neurosci. 6(11), 1142–1144.

Bensafi, M., Pouliot, S., *et al.* 2005. Odorant-specific patterns of sniffing during imagery distinguish ''bad'' and ''good'' olfactory imagers. Chem. Senses 30, 521–529.

Bensafi, M., Rouby, C., *et al.* 2002b. Do primacy, recency and experimental amnesia also exist for odor names? Curr. Psychol. Lett.: Behav. Brain Cogn. 8, 23–32.

Bensafi, M., Tsutsui, T., *et al.* 2004b. Sniffing a human sex-steroid derived compound affects mood and autonomic arousal in a dose-dependent manner. Psychoneuroendocrinology 29(10), 1290–1299.
Berglund, B., Berglund, U., *et al.* 1971. The effect of adaptation on odor detection. Percept. Psychophys. 9(5), 435–438.
Berglund, B., Berglund, U., *et al.* 1973. Multidimensional analysis of 21 odors. Scand. J. Psychol. 14(2), 131–137.
Bojsen-Moller, F. 1975. Demonstration of terminalis, olfactory, trigeminal and perivascular nerves in the rat nasal septum. J. Comp. Neurol. 159(2), 245–256.
Bojsen-Moller, F. and Fahrenkrug, J. 1971. Nasal swell-bodies and cyclic changes in the air passage of the rat and rabbit nose. J. Anat. 110(1), 25–37.
Brauchli, P., Ruegg, P. B., *et al.* 1995. Electrocortical and autonomic alteration by administration of a pleasant and an unpleasant odor. Chem. Senses 20(5), 505–515.
Bremner, E. A., Mainland, J. D., *et al.* 2003. The prevalence of androstenone anosmia. Chem. Senses 28(5), 423–432.
Broman, D. A., Olsson, M. J., *et al.* 2001. Lateralization of olfactory cognitive functions: effects of rhinal side of stimulation. Chem. Senses 26(9), 1187–1192.
Brown, R. and McNeill, D. 1966. The ''tip-of-the-tongue'' phenomenon. J. Verb. Learn. Verb. Behav. 5, 325–337.
Brown, K. S., Maclean, C. M., *et al.* 1968. Distribution of sensitivity to chemical odors in man. Hum. Biol. 40(4), 456–472.
Cain, W. S. 1969. Odor intensity. Differences in exponent of psychophysical function. Percept. Psychophys. 6(6A), 349–354.
Cain, W. S. 1977. Differential sensitivity for smell: ''noise'' at the nose. Science 195(4280), 796–798.
Cain, W. S. 1979. To know with the nose: keys to odor identification. Science 203(4379), 467–470.
Cain, W. S. and Engen, T. 1969. Olfactory Adaptation and the Scaling of Odor Intensity. International Symposium on Olfaction and Taste III. Academic Press.
Cain, W. S. and Gent, J. F. 1991. Olfactory sensitivity – reliability, generality, and association with aging. J. Exp. Psychol. Hum. Percept. Perform. 17(2), 382–391.
Cain, W. S. and Murphy, C. L. 1980. Interaction between chemoreceptive modalities of odour and irritation. Nature 284(5753), 255–257.
Cain, W. S. and Stevens, J. C. 1989. Uniformity of olfactory loss in aging. Ann. N. Y. Acad. Sci. 561, 29–38.
Cain, W. S., Gent, J. F., *et al.* 1988. Evaluation of olfactory dysfunction in the Connecticut Chemosensory Clinical Research Center. Laryngoscope 98(1), 83–88.
Carrie, S., Scannell, J. W., *et al.* 1999. The smell map: is there a commonality of odour perception? Clin. Otolaryngol. 24(3), 184–189.
Cometto-Muniz, J. E. and Cain, W. S. 1990. Thresholds for odor and nasal pungency. Physiol. Behav. 48(5), 719–725.
Cometto-Muniz, J. E. and Cain, W. S. 1998a. Trigeminal and olfactory sensitivity: comparison of modalities and methods of measurement. Int. Arch. Occup. Environ. Health 71(2), 105–110.
Cometto-Muniz, J. E., Cain, W. S., *et al.* 1998b. Nasal pungency and odor of homologous aldehydes and carboxylic acids. Exp. Brain Res. 118(2), 180–188.
Cometto-Muniz, J. E., Cain, W. S., *et al.* 2001. Ocular and nasal trigeminal detection of butyl acetate and toluene presented singly and in mixtures. Toxicol. Sci. 63(2), 233–244.
Cometto-Muniz, J. E., Cain, W. S., *et al.* 2002. Psychometric functions for the olfactory and trigeminal detectability of butyl acetate and toluene. J. Appl. Toxicol. 22(1), 25–30.
Cometto-Muniz, J. E., Cain, W. S., *et al.* 2003. Quantification of chemical vapors in chemosensory research. Chem Senses 28(6), 467–477.
Corbit, T. E. and Engen, T. 1971. Facilitation of olfactory detection. Percep. Psychophys. 10(6), 433–436.
Cornsweet, T. N. 1962. The staircase-method in psychophysics. Am. J. Psychol. 75, 485–491.
Cowan, N. 1995. Sensory memory and its role in information processing. Electroencephalogr. Clin. Neurophysiol. Suppl. 44, 21–31.
Crespo-Facorro, B., Paradiso, S., *et al.* 2001. Neural mechanisms of anhedonia in schizophrenia: a PET study of response to unpleasant and pleasant odors. JAMA 286(4), 427–435.
Cunningham, M. and Crady, C. A. 1971. Identification of olfactory dimensions by semantic differential technique. Psychon. Sci. 23(6), 387–388.
Dalton, P., Doolittle, N., *et al.* 2002. Gender-specific induction of enhanced sensitivity to odors. Nat. Neurosci. 5(3), 199–200.
Davis, R. G. 1979. Olfactory perceptual space model compared by quantitative methods. Chem. Senses Flavor 4, 21–33.
Dawes, P. J. D., Dawes, M. T., *et al.* 2004. The smell map: commonality of odour perception confirmed. Clin. Otolaryngol. 29, 648–654.
De Valois, R. L. and De Valois, K. K. 1993. A multi-stage color model. Vision Res. 33(8), 1053–1065.
de Wijk, R. A., Schab, F. R., and Cain, W. S. 1995. Odor identification. In: Odor Memory (*eds*. F. R. Schab and R. G. Crowder), pp. 21–37. Erlbaum.
Devos, M. and Patte, F. 1990. Standardized Human Olfactory Thresholds. Oxford University Press.
Dimmick, F. L. 1927. The investigation of the olfactory qualities. Psychol. Rev. 34(5), 321–335.
Distel, H., Ayabe-Kanamura, S., *et al.* 1999. Perception of everyday odors – correlation between intensity, familiarity and strength of hedonic judgement. Chem Senses 24(2), 191–199.
Dixon, W. J. and Massey, F. J. 1957. Introduction to Statistical Analysis. McGraw Hill.
Dorries, K. M., Schmidt, H. J., *et al.* 1989. Changes in sensitivity to the odor of androstenone during adolescence. Dev. Psychobiol. 22(5), 423–435.
Doty, R. L. 1975. An examination of relationships between the pleasantness, intensity and concentration of 10 odorous stimuli. Percept. Psychophysiol. 17, 492–496.
Doty, R. L. 1976. Reproductive Endocrine Influences upon Human Nasal Chemoreception: a Review. In: Mammalian Olfaction, Reproductive Processes and Behavior (*ed*. R. L. Doty), pp. 295–321. Academic Press.
Doty, R. L. 1989. Influence of age and age-related diseases on olfactory function. Ann. N. Y. Acad. Sci. 561, 76–86.
Doty, R. L. 1995. Intranasal Trigeminal Chemoreception: Anatomy, Physiology, and Psychophysics. In: Handbook of Olfaction and Gustation (*ed*. R. L. Doty), pp. 821–834. Marcel Dekker.
Doty, R. L., Brugger, W. E., *et al.* 1978. Intranasal trigeminal stimulation from odorous volatiles: psychometric responses from anosmic and normal humans. Physiol. Behav. 20(2), 175–185.
Doty, R. L., Hall, J. W., *et al.* 1982. Cyclical Changes in Olfactory and Auditory Sensitivity During the Menstrual Cycle: No Attenuation by Oral Contraceptive Medication. In: Olfaction and Endocrine Regulation (*ed*. W. Breipohl), IRL Press.
Doty, R. L., Riklan, M., *et al.* 1989. The olfactory and cognitive deficits of Parkinson's disease: evidence for independence. Ann. Neurol. 25(2), 166–171.
Doty, R. L., Shaman, P., and Dann, M. 1984a. Development of the University of Pennsylvania Smell Identification Test: a standardized microencapsulated test of olfactory function. Physiol. Behav. 32(3), 489–502.
Doty, R. L., Shaman, P., Kimmelman, C. P., and Dann, M. S. 1984b. University of Pennsylvania Smell Identification Test: a

rapid quantitative olfactory function test for the clinic. Laryngoscope 94(2 Pt 1), 176–178.
Doty, R. L., Snyder, P. L., *et al.* 1981. Endocrine, cardiovascular, and psychological correlates of olfactory sensitivity changes during the human menstrual cycle. J. Comp. Physiol. Psychol. 95, 45–60.
Dravnieks, A. 1982. Odor quality: semantically generated multidimensional profiles are stable. Science 218, 799–801.
Dravnieks, A. 1985. Atlas of Odor Character Profiles. ASTM Press.
Dravnieks, A., Bock, F. C., *et al.* 1978. Comparison of odors directly and through odor profiling. Chem. Senses 3, 191–220.
Eccles, R., Jawad, M. S., *et al.* 1989. Olfactory and trigeminal thresholds and nasal resistance to airflow. Acta Otolaryngol. 108(3–4), 268–273.
Ehrlichman, H., Brown, S., *et al.* 1995. Startle reflex modulation during exposure to pleasant and unpleasant odors. Psychophysiology 32(2), 150–154.
Ehrlichman, H., Kuhl, S. B., *et al.* 1997. Startle reflex modulation by pleasant and unpleasant odors in a between-subjects design. Psychophysiology 34(6), 726–729.
Engen, T. 1973. Sense of smell. Annu. Rev. Psychol. 24, 187–206.
Engen, T. 1987. Remembering odors and their names. Am. Sci. 75, 497–503.
Engen, T. and Bosack, T. N. 1969. Facilitation in olfactory detection. J. Comp. Physiol. Psychol. 68(3), 320–326.
Fazzalari, F. A. 1978. Compilation of Odor and Taste Threshold Values Data. ASTM Data Series DS4 8A.
Fechner, G. T. 1860. Elemente der psychophysik. Breitkopf and Harterl.
Filsinger, E. E. and Monte, W. C. 1986. Sex history, menstrual cycle, and psychophysical ratings of alpha androstenon, a possible human sex phermone. J. Sex Res. 22, 243–248.
Firestein, S., Shepherd, G. M., *et al.* 1990. Time course of the membrane current underlying sensory transduction in salamander olfactory receptor neurones. J. Physiol. 430, 135–158.
Frye, R. E. 1995. Nasal Airway Dynamics and Olfactory Function. In: Handbook of Olfaction and Gustation, Vol. 1 (*ed*. R. L. Doty), pp. 471–491. Marcel Dekker.
Fulbright, R. K., Skudlarski, P., *et al.* 1998. Functional MR imaging of regional brain responses to pleasant and unpleasant odors. AJNR Am. J. Neuroradiol. 19(9), 1721–1726.
Gamble, R. C. 1899. The applicability of Weber's lab to smell. Am. J. Psychol. 10, 82–143.
Gilad, Y. and Lancet, D. 2003. Population differences in the human functional olfactory repertoire. Mol. Biol. Evol. 20(3), 307–314.
Gilbert, A. N. and Rosenwasser, A. M. 1987. Biological rhythmicity of nasal airway patency: a re-examination of the 'nasal cycle'. Acta Otolaryngol. 104(1–2), 180–186.
Godinot, N. and Sicard, G. 1995. Odor categorization by human-subjects – an experimental approach. Chem. Senses 20(1), 101.
Good, P. R., Geary, N., *et al.* 1976. The effect of estrogen on odor detection. Chem. Senses Flavor 2, 45–50.
Gottfried, J. A., Deichmann, R., *et al.* 2002a. Functional heterogeneity in human olfactory cortex: an event-related functional magnetic resonance imaging study. J. Neurosci. 22(24), 10819–10828.
Gottfried, J. A., O'Doherty, J., *et al.* 2002b. Appetitive and aversive olfactory learning in humans studied using event-related functional magnetic resonance imaging. J. Neurosci. 22(24), 10829–10837.
Green, D. M. and Swets, J. A. 1966. Signal Detection Theory and Psychophysics. Wiley.
Gregson, R. M. 1972. Odour similarities and their multidimensional metric representation. Multivar. Behav. Res. 4, 165–175.
Griffiths, N. M. and Patterson, R. L. 1970. Human olfactory responses to 5-alpha-androst-16-en-3-one-principal component of boar taint. J. Sci. Food Agric. 21(1), 4–6.
Gross-Isseroff, R. and Lancet, D. 1988. Concentration-dependent changes of perceived odor quality. Chem. Senses 13(2), 191–204.
Haberly, L. B. and Bower, J. M. 1989. Olfactory cortex: model circuit for study of associative memory? Trends Neurosci. 12(7), 258–264.
Haring, H. G., Boelens, H., *et al.* 1972. Olfactory studies on enantiomeric eremophilane sesquiterpenoids. J. Agric. Food Chem. 20(5), 1018–1021.
Hasegawa, M. and Kern, E. B. 1977. The human nasal cycle. Mayo Clin. Proc. 52(1), 28–34.
Haykin, S. and Chen, Z. 2005. The cocktail party problem. Neural Comput. 17(9), 1875–1902.
Henion, K. E. 1971. Odor pleasantness and intensity: a single dimension? J. Exp. Psychol. 90(2), 275–279.
Henkin, R. I. 1974. Sensory Changes During the Menstrual Cycle. In: Biorhythms and Human Reproduction (*eds*. M. Ferin, F. Halberg, R. M. Richard and R. L. Vandewiele), pp. 277–285. Wiley.
Henkin, R. I. and Levy, L. M. 2001. Lateralization of brain activation to imagination and smell of odors using functional magnetic resonance imaging (fMRI): left hemispheric localization of pleasant and right hemispheric localization of unpleasant odors. J. Comput. Assist. Tomogr. 25(4), 493–514.
Herbart, J. F. 1824–1825. Psychologie als wissenschaft, neu gegrundet auf erfahrung, metaphysik und mathematik, Unzer.
Herberhold, C., Genkin, H., *et al.* 1982. Olfactory Threshold and Hormone Levels During the Human Menstrual Cycle. In: Olfaction and Endocrine Regulation (*ed*. W. Breipohl), pp. 343–351. IRL Press.
Herz, R. S. 2003. The effect of verbal context on olfactory perception. J. Exp. Psychol. Gen. 132(4), 595–606.
Herz, R. S. and von Clef, J. 2001. The influence of verbal labeling on the perception of odors: evidence for olfactory illusions?. Perception 30(3), 381–391.
Homewood, J. and Stevens, R. J. 2001. Differences in naming accuracy of odors presented to the left and right nostrils. Biol. Psychol. 58(1), 65–73.
Hornung, D. E., Chin, C., *et al.* 1997. Effect of nasal dilators on perceived odor intensity. Chem. Senses 22(2), 177–180.
Hughes, J. R., Hendrix, D. E., *et al.* 1969. Correlations Between Electrophysiological Activity from the Human Olfactory Bulb and the Subjective Response to Odoriferous Stimuli. International Symposium on Olfaction and Taste III, Academic Press.
Hummel, T. 2000. Assessment of intranasal trigeminal function. Int. J. Psychophysiol. 36(2), 147–155.
Hummel, T., Gollisch, R., *et al.* 1991. Changes in olfactory perception during the menstrual cycle. Experientia 47(7), 712–715.
Hummel, T., Mohammadian, P., *et al.* 2003. Pain in the trigeminal system: irritation of the nasal mucosa using short- and long-lasting stimuli. Int. J. Psychophysiol. 47(2), 147–158.
Hummel, T., Sekinger, B., *et al.* 1997. 'Sniffing' Sticks: olfactory performance assessed by the combined testing of odor identification, odor discrimination and olfactory threshold. Chem. Senses 22, 39–52.
Jacob, S., McClintock, M. K., *et al.* 2002. Paternally inherited HLA alleles are associated with women's choice of male odor. Nat. Genet. 30(2), 175–179.
Jäncke, L. and Kaufmann, N. 1994. Facial EMG responses to odors in solitude and with an audience. Chem. Senses 19, 99–111.

Johnson, B. N., Mainland, J. D., *et al.* 2003. Rapid olfactory processing implicates subcortical control of an olfactomotor system. J. Neurophysiol 90, 1084–1094.
Jones, F. N. and Elliot, D. 1975. Individual and substance differences in discriminability of optical isomers. Chem. Senses Flavour 1(3), 317–321.
Jones, F. N. and Velasquez, V. 1974. Effect of repeated discriminations on the identifiability of the enantiomers of carvone. Percept. Mot. Skills 38(3), 1001–1002.
Jonsson, F. U., Tchekhova, A., *et al.* 2005. A metamemory perspective on odor naming and identification. Chem. Senses 30, 353–365.
Kanamura, S. and Takashima, Y. 1991. Effect of the menstrual cycle on olfactory sensitivity. Chem. Senses 16, 202–203.
Kay, L. M. and Laurent, G. 1999. Odor- and context-dependent modulation of mitral cell activity in behaving rats. Nat. Neurosci. 2(11), 1003–1009.
Keller, A. and Vosshall, L. B. 2004. A psychophysical test of the vibration theory of olfaction. Nat. Neurosci. 7(4), 337–338.
Keyhani, K., Scherer, P. W., *et al.* 1997. A numerical model of nasal odorant transport for the analysis of human olfaction. J. Theor. Biol. 186(3), 279–301.
Khan, R. M. and Sobel, N. 2004. Neural processing at the speed of smell. Neuron 44(5), 744–747.
Kloek, J. 1961. The smell of some steroid sex-hormones and their metabolites. Psychiatr. Neurol. Neurochir. 64, 309–344.
Kobal, G. and Hummel, C. 1988. Cerebral chemosensory evoked potentials elicited by chemical stimulation of the human olfactory and respiratory nasal mucosa. Electroencephalogr. Clin. Neurophysiol. 71(4), 241–250.
Kobal, G., Hummel, T., Sekinger, B., Barz, S., Roscher, S., and Wolf, S. 1996. ''Sniffin' sticks'': screening of olfactory performance. Rhinology 34(4), 222–226.
Kobal, G., Hummel, T., *et al.* 1992. Differences in human chemosensory evoked-potentials to olfactory and somatosensory chemical stimuli presented to left and right nostrils. Chem. Senses 17(3), 233–244.
Kobal, G., Klimek, L., *et al.* 2000. Multi-center investigation of 1036 subjects using a standardized method for the assessment of olfactory function combining tests of odor identification, odor discrimination, and olfactory thresholds. Eur. Arch. Otorhnolaryngol. 257, 205–211.
Koelega, H. S. 1970. Extraversion, sex, arousal and olfactory sensitivity. Acta Psychol. (Amst.) 34(1), 51–66.
Koelega, H. S. 1979. Olfaction and sensory asymmetry. Chem. Senses 4, 89–95.
Koelega, H. S. and Koster, E. P. 1974. Some experiments on sex differences in odor perception. Ann. N. Y. Acad. Sci. 237(0), 234–246.
Kolble, N., Hummel, T., *et al.* 2001. Gustatory and olfactory function in the first trimester of pregnancy. Eur. J. Obstet. Gynecol. Reprod. Biol. 99(2), 179–183.
Koster, E. P. 1968. Olfactory sensitivity and the menstrual cycle. Olfactologia 1, 57–64.
Koster, E. P. 1971. In: Adaptation and cross-adaptation in olfaction: an experimental study with olfactory stimuli at low levels of intensity. Utrecht University: p. 211.
Kruskal, J. B. and Wish, M. 1978. Multidemensional Scaling, Sage Publications.
Laffort, P. 1963. Essai de standardisation des seuils olfactifs humains pour 192 corps pur. Arch. Sci. Physiol. 17, 75–105.
Laing, D. G. 1983. Natural sniffing gives optimum odour perception for humans. Perception 12(2), 99–117.
Laing, D. G. 1986. Identification of single dissimilar odors is achieved by humans with a single sniff. Physiol. Behav. 37(1), 163–170.
Laing, D. G. and Francis, G. W. 1989. The capacity of humans to identify odors in mixtures. Physiol. Behav. 46(5), 809–814.
Laing, D. G. and Wilcox, M. E. 1983. Perception of components in binary odour mixtures. Chem. Senses 7, 249–264.
Lang, P. J., Bradley, M. M., *et al.* 1990. Emotion, attention, and the startle reflex. Psychol. Rev. 97(3), 377–395.
Laska, M. 2002. Olfactory discrimination ability for aromatic odorants as a function of oxygen moiety. Chem. Senses 27(1), 23–29.
Laska, M. and Freyer, D. 1997. Olfactory discrimination ability for aliphatic esters in squirrel monkeys and humans. Chem. Senses 22(4), 457–465.
Laska, M. and Teubner, P. 1999. Olfactory discrimination ability of human subjects for ten pairs of enantiomers. Chem. Senses 24(2), 161–170.
Laska, M., Ayabe-Kanamura, S., *et al.* 2000. Olfactory discrimination ability for aliphatic odorants as a function of oxygen moiety. Chem. Senses 25(2), 189–197.
Laska, M., Fendt, M., *et al.* 2005a. Detecting danger – or just another odorant? Olfactory sensitivity for the fox odor component 2,4,5-trimethylthiazoline in four species of mammals. Physiol. Behav. 84(2), 211–215.
Laska, M., Wieser, A., *et al.* 2004. Olfactory sensitivity for carboxylic acids in spider monkeys and pigtail macaques. Chem. Senses 29(2), 101–109.
Laska, M., Wieser, A., *et al.* 2005b. Olfactory responsiveness to two odorous steroids in three species of nonhuman primates. Chem. Senses. 30(6), 505–511.
Lawless, H. T. 1989. Exploration of fragrance categories and ambiguous odors using multidimensional-scaling and cluster-analysis. Chem. Senses 14(3), 349–360.
Lawless, H. T. and Engen, T. 1977. Associations to odors: interference, mnemonics, and verbal labeling. J. Exp. Psychol. 3(1), 52–59.
Le Magnen, J. 1945. Etude des facteurs dynamiques de l'excitation olfactive. L'Année Psychologique. 6, 77–89.
Le Magnen, J. 1952. Les phénomènes olfacto-sexuels chez l'homme. Arch. Sci. Physiol. 6, 125–160.
Lewis, J. E. and Dahl, A. R. 1995. Olfactory Mucosa: Composition, Enzymatic Localization, and Metabolism. In: Handbook of Olfaction and Gustation (*ed*. R. L. Doty), pp. 33–52. Marcel Dekker.
Linneaus, C. 1756. Odores medicamentorum. Amoenitates Academicae 3, 183–201.
Linschoten, M. R., Harvey, L. O., Jr., *et al.* 2001. Fast and accurate measurement of taste and smell thresholds using a maximum-likelihood adaptive staircase procedure. Percept. Psychophys. 63(8), 1330–1347.
Livermore, A. and Laing, D. G. 1996. Influence of training and experience on the perception of multicomponent odor mixtures. J. Exp. Psychol. Hum. Percept. Perform. 22(2), 267–277.
Livermore, A. and Laing, D. G. 1998a. The influence of chemical complexity on the perception of multicomponent odor mixtures. Percept. Psychophys. 60(4), 650–661.
Livermore, A. and Laing, D. G. 1998b. The influence of odor type on the discrimination and identification of odorants in multicomponent odor mixtures. Physiol. Behav. 65(2), 311–320.
Livermore, A., Hummel, T., *et al.* 1992. Chemosensory event-related potentials in the investigation of interactions between the olfactory and the somatosensory (trigeminal) systems. Electroencephalogr. Clin. Neurophysiol. 83(3), 201–210.
Luskin, M. B. and Price, J. L. 1983. The topographic organization of associational fibers of the olfactory system in the rat, including centrifugal fibers to the olfactory bulb. J. Comp. Neurol. 216, 264–291.
Macfarelane, A. 1975. Olfaction in the development of social preferences in the human neonate. Ciba Found. Symp. 33, 103–117.

MacRae, A. W., Howgate, P., *et al.* 1990. Assessing the similarity of odors by sorting and by triadic comparison. Chem. Senses 15(6), 691–699.
MacRae, A. W., Rawcliffe, T., *et al.* 1992. Patterns of odor similarity among carbonyls and their mixtures. Chem. Senses 17(2), 119–125.
Mainland, J. and Sobel, N. 2006. The sniff is part of the olfactory percept. Chem. Senses 31(2), 181–196.
Mainland, J. D., Bremner, E. A., *et al.* 2002. Olfactory plasticity: one nostril knows what the other learns. Nature 419(6909), 802.
Mainland, J. D., Johnson, B. N., *et al.* 2005. Olfactory impairments in patients with unilateral cerebellar lesions are selective to inputs from the contralesion nostril. J. Neurosci. 25(27), 6362–6371.
Mair, R. G., Bouffard, J. A., *et al.* 1978. Olfactory sensitivity during the menstrual cycle. Sens. Processes 2(2), 90–98.
Mamlouk, A. M. 2002. Quantifying Olfactory Perception. Institute for Signal Processing.
Mamlouk, A. M. and Martinetz, T. 2004. On the dimensions of the olfactory perception space. Neurocomputing 58–60, 1019–1025.
Mamlouk, A. M., Chee-Ruiter, C., *et al.* 2003. Quantifying olfactory perception: mapping olfactory perception space by using multidimensional scaling and self-organizing maps. Neurocomputing 52–54, 591–597.
Masago, R., Shimomura, Y., *et al.* 2001. The effects of hedonic properties of odors and attentional modulation on the olfactory event-related potentials. J. Physiol. Anthropol. Appl. Hum. Sci. 20(1), 7–13.
Matzker, J. 1965. Riechen und Lebensalter-Riechen und Rauchen. Achiv. Ohren 185, 755–760.
Mesolella, V. 1934. L'ofatto nelle diverse eta. Arch. Ital. Otol. Rinol. Laring. 46, 43–62.
Miltner, W., Matjak, M., *et al.* 1994. Emotional qualities of odors and their influence on the startle reflex in humans. Psychophysiology 31(1), 107–110.
Mirza, N., Kroger, H., *et al.* 1997. Influence of age on the 'nasal cycle'. Laryngoscope 107(1), 62–66.
Monti-Bloch, L., Diaz-Sanchez, V., *et al.* 1998. Modulation of serum testosterone and autonomic function through stimulation of the male human vomeronasal organ (VNO) with pregna-4,20-diene-3,6-dione. J. Steroid Biochem. Mol. Biol. 65(1–6), 237–242.
Moriyama, M. and Kurahashi, T. 2000. Human olfactory contrast accompanies the menstrual cycle. Chem. Senses 25, 216.
Moskowitz, H. R. and Barbe, C. D. 1977. Profiling of odor components and their mixtures. Sens. Processes 1(3), 212–226.
Moskowitz, H. R. and Gerbers, C. L. 1974. Dimensional salience of odors. Ann. N. Y. Acad. Sci. 237(SEP27), 1–16.
Moskowitz, H. R., Dravnieks, A., *et al.* 1976. Odor intensity and pleasantness for a diverse set of odorants. Percept. Psychophysiol. 19, 122–128.
Mozell, M., Kent, P., *et al.* 1991. The effect of flow rate upon the magnitude of the olfactory response differs for different odorants. Chem. Senses 16(6), 631–649.
Mozell, M. M. and Jagodowicz, M. 1973. Chromatographic separation of odorants by the nose: retention times measured across in vivo olfactory mucosa. Science 181(106), 1247–1249.
Mueller, C. G. 1951. Frequency of seeing functions for intensity discrimination of various levels of adapting intensity. J. Gen. Physiol. 34(4), 463–474.
Nagata, Y. and Takeuchi, N. 1990. Measurement of odor threshold by triangle odor bag method. Bull. Jpn. Environ. Sanit. Cent. 17, 77–89.
Narita, S., Koama, T., *et al.* 1992. Variation of odor sensitivity and reaction time in menstrual cycle. Chem. Senses 17, 97.
Nordin, S., Bramerson, A., Liden, E., and Bende, M. 1998. The Scandinavian Odor-Identification Test: development, reliability, validity and normative data. Acta Otolaryngol. 118(2), 226–234.
Pangborn, R. M., Berg, H. W., *et al.* 1964. Influence of methodology on olfactory response. Percept. Motor Skills 18(1), 91–103.
Patte, F., Etcheto, M., *et al.* 1975. Selected and standardized values of suprathreshold odour intensities for 110 substances. Chem. Senses Flavour 1, 283–305.
Pause, B. M. and Krauel, K. 2000. Chemosensory event-related potentials (CSERP) as a key to the psychology of odors. Int. J. Psychophysiol. 36(2), 105–122.
Pause, B. M., Krauel, K., *et al.* 1999. Perception of HLA-Related Body Odors During the Course of the Menstrual Cycle. In: Advances in Chemical Signals in Vertebrates (*eds*. R. E. Johnston, D. Muller-Schwarze and P. W. Sorensen), pp. 201–207. Plenum.
Pause, B. M., Sojka, B., *et al.* 1996. Olfactory information processing during the course of the menstrual cycle. Biol. Psychol. 44(1), 31–54.
Pfaffmann, C. 1951. Taste and Smell. In: Handbook of Experimental Psychology (*ed*. S. W. Stevens). Wiley.
Poellinger, A., Thomas, R., *et al.* 2001. Activation and habituation in olfaction – an fMRI study. Neuroimage 13(4), 547–560.
Polak, E. H. 1973. Mutiple profile-multiple receptor site model for vertebrate olfaction. J. Theor. Biol. 40(3), 469–484.
Porter, J., Craven, B., Khan, R. M., Chang, S. J., Kang, I., Judkewitz, B., Volpe, J., Settles, G., and Sobel, N. 2007. Mechanisms of scent-tracking in humans. Nat Neurosci. 10(1), 27–29.
Porter, J., Anand, T., *et al.* 2005. Brain mechanisms for extracting spatial information from smell. Neuron 47, 581–592.
Porter, R. H., Cernoch, J. M., *et al.* 1983. Maternal recognition of neonates through olfactory cues. Physiol. Behav. 30(1), 151–154.
Prah, D., Sears, S., *et al.* 1995. Modern Approaches to Air Dilution Olfactometry. In: Handbook of Olfaction and Gustation, Vol. I (*ed*. R. L. Doty), pp. 227–257. Marcel Dekker, Inc.
Price, J. L. 1990. Olfactory System. In: The Human Nervous System (*ed*. G. Paxinos), pp. 979–1001. Academic Press.
Principato, J. J. and Ozenberger, J. M. 1970. Cyclical changes in nasal resistance. Arch. Otolaryngol. 91(1), 71–77.
Punter, P. H. 1983. Measurement of human olfactory thresholds for several groups of structurally related-compounds. Chem. Senses 7(3–4), 215–235.
Rabin, M. D. 1988. Experience facilitates olfactory discrimination and mixture component analysis by humans. Percept. Psychophys. 44(6), 532–540.
Rehn, T. 1978. Perceived odor intensity as a function of air flow through the nose. Sens. Processes 2(3), 198–205.
Richardson, J. T. and Zucco, G. M. 1989. Cognition and olfaction: a review. Psychol. Bull. 105(3), 352–360.
Royet, J. P., Hudry, J., *et al.* 2001. Functional neuroanatomy of different olfactory judgments. Neuroimage 13(3), 506–519.
Sabri, M., Radnovich, A. J., *et al.* 2005. Neural correlates of olfactory change detection. Neuroimage 25(3), 969–974.
Savic, I. and Berglund, H. 2000. Right-nostril dominance in discrimination of unfamiliar, but not familiar, odours. Chem. Senses 25(5), 517–523.
Savic, I., Gulyas, B., *et al.* 2000. Olfactory functions are mediated by parallel and hierarchical processing. Neuron 26(3), 735–745.
Schaal, B., Coureaud, G., *et al.* 2003. Chemical and behavioural characterization of the rabbit mammary pheromone. Nature 424(6944), 68–72.

Schaal, B., Montagner, H., *et al.* 1980. Olfactory stimulations in mother–child relations. Reprod. Nutr. Dev. 20(3B), 843–858.
Schab, F. R. 1991. Odor memory: taking stock. Psychol. Bull. 109(2), 242–251.
Schiffman, S. 1979. Changes in Taste and Smell with Age: Psychophysical Aspects. In: Sensory Systems and Communications in the Eldery: Aging, Vol. 10 (*eds*. J. M. Ordy and K. Brizzee), pp. 227–246. Raven Press.
Schiffman, S., Robinson, D. E., *et al.* 1977. Multidimensional-scaling of odorants – examination of psychological and physiochemical dimensions. Chem. Senses Flavour 2(3), 375–390.
Schiffman, S. S. 1974. Physicochemical correlates of olfactory quality. Science 185(146), 112–117.
Schiffman, S. S. 1984. Mathematical Approaches for Quantitative Design of Odorants and Tastants. In: Computers in Flavor and Fragrance Research (*eds*. C. Warren and J. Walradt), pp. 33–50. American Chemical Society.
Schneider, R. A. and Wolf, S. 1955. Olfactory perception thresholds for citral utilizing a new type olfactorium. 8, 337–342.
Schoon, G. A. A. and Debruin, J. C. 1994. The ability of dogs to recognize and cross-match human odors. Forensic Sci. Int. 69(2), 111–118.
Segal, N., Topolski, T. D., *et al.* 1995. Twin analysis of odor identification and perception. Physiol. Behav. 57, 605–609.
Serby, M., Larson, P., *et al.* 1991. The nature and course of olfactory deficits in Alzheimer's disease. Am. J. Psychiatr. 148(3), 357–360.
Shepherd, G. M. 2004. The human sense of smell: are we better than we think? PLoS Biol. 2(5), E146.
Slotnick, B. M. and Ptak, J. E. 1977. Olfactory intensity-difference thresholds in rats and humans. Physiol. Behav. 19(6), 795–802.
Sobel, N., Johnson, B. N., *et al.* 2003. Functional Neuroimaging of Human Olfaction. In: Handbook of Olfaction and Gustation (*ed*. R. L. Doty), pp. 251–273. Marcel Dekker, Inc.
Sobel, N., Khan, R. M., *et al.* 1999. The world smells different to each nostril. Nature 402(6757), 35.
Sobel, N., Khan, R. M., *et al.* 2000a. Sniffing longer rather than stronger to maintain olfactory detection threshold. Chem. Senses 25(1), 1–8.
Sobel, N., Prabhakaran, V., *et al.* 1998. Sniffing and smelling: separate subsystems in the human olfactory cortex. Nature 392(6673), 282–286.
Sobel, N., Prabhakaran, V., *et al.* 2000b. Time course of odorant-induced activation in the human primary olfactory cortex. J. Neurophysiol. 83(1), 537–551.
Sobel, N., Thomason, M. E., *et al.* 2001. An impairment in sniffing contributes to the olfactory impairment in Parkinson's disease. Proc. Natl. Acad. Sci. U. S. A. 98(7), 4154–4159.
Soussignan, R., Schaal, B., *et al.* 1997. Facial and autonomic responses to biological and artificial olfactory stimuli in human neonates: re-examining early hedonic discrimination of odors. Physiol. Behav. 62(4), 745–758.
Steiner, J. E. 1979. Human facial expressions in response to taste and smell stimulation. Adv. Child Dev. Behav. 13, 257–295.
Stevens, D. A. and O'Connell, R. J. 1991. Individual differences in thresholds and quality reports of human subjects to various odors. Chem. Senses 16(1), 57–67.
Stevens, D. A. and O'Connell, R. J. 1996. Semantic-free scaling of odor quality. Physiol. Behav. 60(1), 211–215.
Stevens, J. C., Cain, W. S., *et al.* 1988. Variability of olfactory thresholds. Chem. Senses 13(4), 643–653.
Stevens, S. S. 1957. On the psychophysical law. Psychol. Rev. 64(3), 153–181.
Stevenson, R. J. 2001a. The acquisition of odour qualities. Q. J. Exp. Psychol. Section a-Hum. Exp. Psychol. 54(2), 561–577.
Stevenson, R. J. 2001b. Associative learning and odor quality perception: how sniffing an odor mixture can alter the smell of its parts. Learn. Motiv. 32(2), 154–177.
Stevenson, R. J. and Boakes, R. A. 2003. A mnemonic theory of odor perception. Psychol. Rev. 110(2), 340–364.
Stone, H. 1963. Techniques for odor measurement – olfactometric vs. sniffing. J. Food Sci. 28(6), 719–725.
Sumner, D. 1962. On testing the sense of smell. Lancet 2, 895–897.
Tanner, W. P. and Swets, J. A. 1954. A decision-making theory of visual detection. Psychol. Rev. 61(6), 401–409.
Taylor, M. M. and Creelman, C. D. 1967. Pest – efficient estimates on probability functions. J. Acoust. Soc. Am. 41(4P1), 782–787.
Teghtsoonian, R. and Teghtsoonian, M. 1984. Testing a perceptual constancy model for odor strength: the effects of sniff pressure and resistance to sniffing. Perception 13(6), 743–752.
Theimer, E. T., Yoshida, T., and Klaiber, E. M. 1977. Olfaction and molecular shape. Chirality as a requisite for odor. J Agric Food Chem. 25(5), 1168–1177.
Thiboud, M. 1991. Empirical Classification of Odours. In: Perfumes: Art, Science, and Technology (*eds*. Müller P.M. and Lamparsky D.) pp. 253–286. Kluwer Academic Publishers.
Toulouse, E. and Vaschide, N. 1899. Mesure de l'odorat chez l'homme et chez la femme. Comp. Rend. Soc. Biol. 51, 381–383.
Turin, L. 1996. A spectroscopic mechanism for primary olfactory reception. Chem. Senses 21(6), 773–791.
Turin, L. 2002. A method for the calculation of odor character from molecular structure. J. Theor. Biol. 216(3), 367–385.
Uchida, N. and Mainen, Z. F. 2003. Speed and accuracy of olfactory discrimination in the rat. Nat. Neurosci. 6(11), 1224–1229.
Van Gemert, L. J. 1984. Compilations of odour threshold values in air. Supplement V. Report No 84.220 TNO-CIVO Food Analysis Institute.
Van Gemert, L. J. and Nettenbreijer, A. H. 1977. Compilation of odour threshold values in air and water. Central Institute for Nutrition and Food Research TNO and National Institute for Water Supply.
Venstrom, D. and Amoore, J. E. 1968. Olfactory threshold in relation to age, sex, or smoking. J. Food Sci. 33, 264–265.
Vierling, J. S. and Rock, J. 1967. Variations in olfactory sensitivity to exaltolide during the menstrual cycle. J. Appl. Physiol. 22, 311–315.
Walker, J. C., Hall, S. B., *et al.* 2003. Human odor detectability: new methodology used to determine threshold and variation. Chem. Senses 28(9), 817–826.
Walker, J. C., Kendal-Reed, M., *et al.* 2001. Human responses to propionic acid. II. Quantification of breathing responses and their relationship to perception. Chem. Senses 26(4), 351–358.
Wang, L., Chen, L., *et al.* 2004. Evidence for peripheral plasticity in human odour response. J. Physiol. 554, 236–244.
Warren, D. W., Walker, J. C., *et al.* 1994. Effects of odorants and irritants on respiratory behavior. Laryngoscope 104(5 Pt 1), 623–626.
Wells, D. L. and Hepper, P. G. 2000. The discrimination of dog odours by humans. Perception 29(1), 111–115.
Wenzel, B. M. 1949. Differential sensitivity in olfaction. J. Exp. Psychol. 39(2), 129–143.
Wenzel, B. M. 1955. Olfactometric method utilizing natural breathing in an odor-free environment. Science 121(3153), 802–803.

Whisman, M., Goetzinger, J., *et al.* 1978. Odorant evaluation: a study of ethanethiol and tetrahdrothiophene as warning agents in propane. Environ. Sci. Technol. 12, 1285–1288.
de Wijk, R. A. and Cain, W. S. 1994. Odor quality: discrimination versus free and cued identification. Percept. Psychophys. 56(1), 12–18.
Wilson, D. A. and Stevenson, R. J. 2003a. The fundamental role of memory in olfactory perception. Trends Neurosci. 26(5), 243–247.
Wilson, D. A. and Stevenson, R. J. 2003b. Olfactory perceptual learning: the critical role of memory in odor discrimination. Neurosci. Biobehav. Rev. 27(4), 307–328.
Wise, P., Olsson, M., *et al.* 2000. Quantification of odor quality. Chem. Senses 25(4), 429–443.
Wise, P. M. and Cain, W. S. 2000. Latency and accuracy of discriminations of odor quality between binary mixtures and their components. Chem. Senses 25(3), 247–265.
Wysocki, C. J., Dorries, K. M., *et al.* 1989. Ability to perceive androstenone can be acquired by ostensibly anosmic people. Proc. Natl. Acad. Sci. U. S. A. 86(20), 7976–7978.
Yee, K. K. and Wysocki, C. J. 2001. Odorant exposure increases olfactory sensitivity: olfactory epithelium is implicated. Physiol. Behav. 72(5), 705–711.
Yoshida, M. 1964a. Studies in psychometric classification of odors (4). Jpn. Psychol. Res. 6, 115–124.
Yoshida, M. 1964b. Studies in psychometric classification of odors (5). Jpn. Psychol. Res. 6, 145–154.
Yoshida, M. 1972a. Studies in psychometric classification of odors (6). Jpn. Psychol. Res. 14(2), 70–86.
Yoshida, M. 1972b. Studies in psychometric classification of odors (7). Jpn. Psychol. Res. 14(3), 101–108.
Yoshida, M. 1975. Psychometric classification of odors. Chem. Senses Flavour 1(4), 443–464.
Yoshida, M. 1984. Correlation analysis of detection threshold data for 'standard test' odors. Bull. Fac. Sci. Eng. 27, 343–353.
Youngentob, S. L., Kurtz, D. B., *et al.* 1982. Olfactory sensitivity: is there laterality? Chem. Senses 7(1), 11–21.
Youngentob, S. L. M., Stern, N. *et al.* 1986. Effect of airway resistance on perceived odor intensity. Am. J. Otolaryngol. 7(3), 187–193.
Zald, D. H. and Pardo, J. V. 1997. Emotion, olfaction, and the human amygdala: amygdala activation during aversive olfactory stimulation. Proc. Natl. Acad. Sci. U. S. A. 94(8), 4119–4124.
Zatorre, R. J. and Jones-Gotman, M. 1990. Right-nostril advantage for discrimination of odors. Percept. Psychophys. 47(6), 526–531.
Zatorre, R. J. and Jones-Gotman, M. 1991. Human olfactory discrimination after unilateral frontal or temporal lobectomy. Brain 114(Pt 1A), 71–84.
Zelano, C., Bensafi, M., *et al.* 2005. Attentional modulation in human primary olfactory cortex. Nat. Neurosci. 8(1), 114–120.
Zwaardemaker, H. 1889. On measurement of the sense of smell in clinical examination. Lancet i, 1300–1302.
Zwaardemaker, H. 1895. Die physiologie des geruchs. Wengelmann.

Relevant Websites

http://psych.colorado.edu – MLpest statistical thresholds.
http://shop.store.yahoo.com – Multivolume/compact-disc set of odor profiles by Steffen Actander.
http://www.sigmaaldrich.com – The Sigma-Aldrich Flavors & Fragrances Catalog.
http://www.smelltest.com – The Smell Threshold Test and the UPSIT, Sensonics;
http://www.burghart.net – Sniffin' Sticks, Burghart Medical Technology.

4.46 Disorders of Taste and Smell

R L Doty and K Saito, University of Pennsylvania, Philadelphia, PA, USA

S M Bromley, University of Pennsylvania, Philadelphia, PA, USA, UMDNJ-Robert Wood Johnson Medical School, Camden, NJ, USA

© 2008 Elsevier Inc. All rights reserved.

4.46.1	**Introduction**	864
4.46.2	**Anatomy of Human Taste and Smell Systems**	865
4.46.2.1	Olfactory Pathways	865
4.46.2.2	Gustatory Pathways	865
4.46.2.3	Trigeminal System	866
4.46.3	**Symptoms of Chemosensory Dysfunction**	866
4.46.4	**Clinical Evaluation of Chemosensory Disorders**	867
4.46.4.1	Medical History and Examination	867
4.46.4.2	Quantitative Chemosensory Testing	868
4.46.5	**Causes of Chemosensory Dysfunction**	868
4.46.5.1	Upper Respiratory and Oral Infections	870
4.46.5.2	Allergies and Rhinosinusitis	870
4.46.5.3	Disorders Influencing Airway Patency	871
4.46.5.4	Head Trauma	871
4.46.5.5	Iatrogenesis	872
4.46.5.6	Tumors and Central Nervous System Lesions	872
4.46.5.7	Drug Effects	874
4.46.5.8	Congenital and Inherited Disorders	874
4.46.5.9	Endocrine and Metabolic Diseases	875
4.46.5.9.1	Addison's disease	875
4.46.5.9.2	Cushing's syndrome	875
4.46.5.9.3	Diabetes	875
4.46.5.9.4	Hypothyroidism	875
4.46.5.9.5	Kallmann's syndrome	875
4.46.5.9.6	Kidney disease	876
4.46.5.9.7	Pseudohypoparathyroidism	876
4.46.5.9.8	Turner's syndrome	876
4.46.5.10	Psychiatric Disorders	876
4.46.5.10.1	Alcoholism	877
4.46.5.10.2	Anorexia and bulimia nervosa	877
4.46.5.10.3	Attention-deficit/hyperactivity disorder	877
4.46.5.10.4	Depression	877
4.46.5.10.5	Olfactory reference syndrome	877
4.46.5.10.6	Seasonal affective disorder	877
4.46.5.10.7	Schizophrenia	878
4.46.5.11	Neurodegenerative Diseases	878
4.46.5.11.1	Alzheimer's disease	878
4.46.5.11.2	Amyotrophic lateral sclerosis	879
4.46.5.11.3	Multiple sclerosis	879
4.46.5.11.4	Parkinson's disease	880
4.46.5.11.5	Progressive supranuclear palsy	880

4.46.5.12	Epilepsy	881
4.46.5.13	Migraine	882
4.46.6	**Treatment of Chemosensory Disorders**	882
4.46.7	**Summary**	883
References		884

Glossary

accessory nerve The 11th cranial nerve (CN XI). This nerve controls specific muscles of the neck, namely the sternocleidomastoid muscle and the upper part of the trapezius muscle.

Addison's disease A rare endocrine disorder, also termed chronic adrenal insufficiency or hypocorticism, in which the body produces insufficient amounts of adrenal steroid hormones (glucocorticoids and often mineralocorticoids).

adrencorticotropic hormone A hormone, also termed ACTH or corticotrophin, produced and secreted by the pituitary gland. This hormone stimulates the cortex of the cortex of the adrenal gland and boosts the synthesis of corticosteroids, mainly glucocorticoids, but also adrenal sex steroids (androgens).

adrenocortical insufficiency The inability of the adrenal gland to produce adequate amounts of cortisol in response to stress. Also termed hypocortisolism.

agenesis The failure of an organ to develop during embryonic growth and development. Agenesis of key organs such as the heart and brain is usually fatal. However, for those organs which occur in pairs, the loss of one member (i.e., unilateral agenesis) is not.

ageusia The loss of taste functions of the tongue, particularly the inability to detect sweetness, sourness, bitterness, saltiness, and umami (the taste of monosodium glutamate).

albright hereditary osteodystrophy A disorder, also known as Martin–Albright syndrome, characterized by a lack of renal responsiveness to parathyroid hormone, resulting in low serum calcium, high serum phosphate, and high serum parathyroid hormone. Patients with this disorder have short stature, characteristically shortened fourth and fifth metacarpals, and rounded facies.

Alzheimer's disease The most common cause of dementia. Characterized by progressive cognitive deterioration, mainly loss of memory, together with declining activities of daily living and neuropsychiatric symptoms or behavioral changes. Neuronal loss or atrophy occurs largely in the temporoparietal cortex but also in the frontal cortex. Pathologically defined by abnormal deposition of amyloid plaques and neurofibrillary tangles.

amyotrophic lateral sclerosis (ALS; also known as Lou Gehrig's Disease) A progressive and ultimately fatal neurodegenerative disease caused by the gradual degeneration of CNS nerve cells that control voluntary muscle movement. Both the upper motor neurons and the lower motor neurons degenerate or die, ceasing to send messages to muscles. The muscles gradually weaken, waste away (atrophy), and have fasciculations (twitches) because of denervation. Eventually, the brain completely loses its ability to initiate and control voluntary movement.

aneurysm A localized, blood-filled dilation (bulge) of a blood vessel caused by disease or weakening of the vessel wall. Cerebral aneurysms most commonly occur in arteries at the base of the brain (the circle of Willis).

angiotensin-converting enzyme An enzyme that catalyzes the conversion of angiotensin I to angiotensin II, a potent vasoconstrictor, and participates in the inactivation of bradykinin, a potent vasodilator. These two actions make it an ideal target in the treatment of conditions such as high blood pressure, heart failure, diabetic nephropathy, and type 2 diabetes mellitus.

anorexia nervosa An eating disorder characterized by low body weight and body image distortion with an obsessive fear of gaining weight. Individuals with anorexia often control body weight by voluntary starvation, purging, vomiting, excessive exercise, or other weight control measures, such as diet pills or diuretic drugs.

anosmia The lack of the ability to smell. It can be either temporary or permanent.

anterior olfactory nucleus A nucleus located in the posterior part of the olfactory bulb which serves as a relay between some projection neurons of the bulb and other brain regions, including the contralateral olfactory bulb and cortex.

antihyperlipidemic drugs A diverse group of lipid-lowering drugs used in the treatment of hyperlipidemias. There are several classes of antihypolipidemic drugs which differ in their impact on the cholesterol profile and in adverse side effects. Examples include statins, fibrates, niacin, bile acid sequestrants (resins), and drugs that inhibit cholesterol absorption.

antihypertensive drugs A class of drugs used in medicine and pharmacology to treat hypertension (high blood pressure). There are many classes of antihypertensives which act by varying means to lower blood pressure.

ataxia A neurological sign and symptom consisting of unsteady and clumsy motion of the limbs and torso, due to a failure of the gross coordination of muscle movements, most evident on standing and walking.

auriculotemporal nerve A branch of the mandibular nerve that runs with the superficial temporal artery and vein, and provides sensory innervation to various regions on the side of the head.

autonomic nervous system That part of the peripheral nervous system that controls homeostatic maintenance of the body's internal state. Also termed the visceral nervous system.

Bardet–Biedl syndrome A genetic multi-system disorder that can cause chronic and end-stage renal failure in children. It is characterized by obesity, limb deformities, cognitive impairment, and genitourinary tract malformations. Despite its rarity, this syndrome has come to recent prominence because of the primary cilia dysfunction underlying its pathogenesis.

basal ganglia A group of brain nuclei, sometimes termed the basal nuclei, which are interconnected with the cerebral cortex, thalamus, and brainstem. Mammalian basal ganglia are associated with a variety of functions, including motor control, cognition, emotions, and learning, and are known to be compromised in Parkinson's disease.

bulemia nervosa A psychological eating disorder in which recurrent binge eating is followed by intentional purging. This purging is done to compensate for the excessive intake of food, usually to prevent weight gain. Purging can take the form of vomiting; inappropriate use of laxatives, enemas, diuretics, or other medication; or excessive physical exercise.

burning mouth syndrome A condition, also termed glossodynia, characterized by a burning or tingling sensation on the lips, tongue, or entire mouth. Typically, there are no visual signs like discoloration to aid in the diagnosis.

chorda tympani nerve A branch of the facial nerve (cranial nerve VII) that carries sensory fibers providing taste sensation from the anterior two-thirds of the tongue, as well as presynaptic parasympathetic fibers to the submandibular ganglion that provide secretomotor innervation to the submandibular and sublingual salivary glands.

cribriform plate A portion of the ethmoid bone separating the brain cavity from the nasal cavity and through which the olfactory nerves project.

cryptorchidism The absence from the scrotum of one or both testes.

Cushing's syndrome A rare endocrine disorder caused by high blood levels of cortisol, a hormone relesed from the adrenal gland in response to ACTH from the pituitary gland. Also termed hypercortisolsim or hyperadrenocorticism.

Down syndrome A genetic disorder, previously termed mongolism, caused by the presence of all or part of an extra 21st chromosome (trisomy 21). Mental retardation and physical growth changes are typical characteristics.

dysgenesis Abnormal development of a tissue or other body part.

dysosmia A disordered smell quality, such as the odor of roses smelling like feces.

dysgeusia A disordered taste quality, such as salt tasting bitter.

ethmoidal Nerve A branch of the trigeminal nerve. The anterior ethmoidal nerve provides somatosensation to the nasal cavity.

facial nerve The 7th cranial nerve (CN VII). It emerges from the brainstem between the pons and the medulla. This nerve controls the muscles of facial expression and innervates the taste buds on the anterior two-thirds of the tongue via the chorda tympani nerve branch. It also supplies preganglionic parasympathetic fibers to several head and neck ganglia.

frontal lobe An area in the brain of vertebrates located at the front of each cerebral hemisphere. The frontal lobes play a part in impulse control, judgment, language production, working memory, motor function, problem solving, sexual behavior, socialization, and spontaneity, and are critical for normal planning, coordinating, controlling, and executing of a range of behaviors.

frontal operculum The most posterior portion of the inferior frontal gyrus of the frontal lobe. One famous part of the operculum is Broca's area which plays an important role in conversation or speech production, reading, and writing.

glossalgia Same as glossadynia; see burning mouth syndrome.

glossopharyngeal nerve The 9th cranial nerve. This nerve exits the brainstem from the sides of the upper medulla, just rostral (closer to the nose) to the vagus nerve. This nerve supplies the taste buds on the posterior third of the tongue.

Huntington's disease A rare inherited neurological disorder caused by a trinucleotide repeat expansion in the Huntingtin (Htt) gene. This expansion produces an altered form of the Htt protein, mutant Huntingtin (mHtt), which results in neuronal cell death in select areas of the brain. Its most obvious symptoms are abnormal body movements called chorea and a lack of coordination, but mentation and some aspects of personality also can be affected.

hypogeusia Diminished taste sensitivity.

hypoglossal nerve The 12th cranial nerve (XII). This nerve supplies motor fibres to all of the muscles of the tongue, except the palatoglossus muscle which is innervated by the vagus nerve (X) and the accessory nerve (XI).

hypogonadotropic hypogonadism A disorder characterized by a failure of the function of the gonads (ovaries or testes), resulting in hormonal deficiency and infertility. Deficiency of the sex hormones can result in defective primary or secondary sexual development, or withdrawal effects (e.g., premature menopause) in adults.

hypoparathyroidism Decreased function of the parathyroid glands, leading to decreased levels of parathyroid hormone (PTH). The consequence, hypocalcemia, is a serious medical condition.

hyposmia Diminished smell function.

hypothyroidism A disease state caused by insufficient production of thyroid hormone by the thyroid gland.

iatrogenesis Literally means ''brought forth by a healer'' (*iatros* means healer in Greek). As such, it can refer to good or bad effects, but it is almost exclusively used to refer to a state of ill health or adverse effect or complication caused by or resulting from medical treatment.

insular cortex A brain structure that lies deep to the brain's lateral surface within the lateral sulcus, a groove which separates the temporal lobe and inferior parietal cortex. The latter overlying cortical areas are known as opercula (meaning ''lids''), and parts of the frontal, temporal, and parietal lobes form opercula over the insular cortex (also termed insula).

internal capsule An area of brain white matter that separates the caudate nucleus and the thalamus from the lenticular nucleus. It consists of axonal fibers that run between the cerebral cortex and the pyramids of the medulla.

Kallmann syndrome A syndrome characterized by anosmia and hypogonadism (decreased functioning of the sex hormone-producing glands) caused by a deficiency of gonadotropin-releasing hormone (GnRH) in the hypothalamus. Also known as hypothalmic hypogonadism with anosmia, familial hypogonadism with anosmia, or hypogonadotropic hypogonadism with anosmia.

lingual nerve A branch of the mandibular nerve (CN V3), itself a branch of the trigeminal nerve. This nerve supplies sensory innervation to the mucous membrane of the anterior two-thirds of the tongue. It also carries non-trigeminal nerve fibers, including those responsible for taste sensation on the anterior tongue and both parasympathetic and sympathetic fibers to the submandibular ganglion, a structure suspended by two nerve filaments from the lingual nerve.

lymphedema A condition of localized fluid retention caused by a compromised lymphatic system. The lymphatic system (often referred to as the body's ''second'' circulatory system) collects and filters the interstitial fluid of the body.

magnetoencephalography An imaging technique used to measure the magnetic fields produced by electrical activity in the brain via extremely sensitive devices such as superconducting quantum Interference devices (SQUIDs). There are many uses for the MEG, including assisting surgeons in localizing a pathology, assisting researchers in determining the function of various parts of the brain, neurofeedback, and others.

meningioma Common benign tumors of the brain (95% of benign tumors) that can occasionally be malignant. They arise from the arachnoidal cap cells of the meninges and represent about 15% of all primary brain tumors.

midbrain The mesencephalon (or midbrain) is the middle of three vesicles that arise from the neural tube that forms the brain of developing animals.

Caudally the mesencephalon adjoins the pons (metencephalon) and rostrally it adjoins the diencephalons, a brain region containing the thalamus, hypothalamus, and other structures.

migraine A neurological disorder associated with an electrochemical change in the trigeminovascular regions of the brain. The most common symptom is an intense and disabling episodic headache. Migraine headaches are usually characterized by severe pain on one or both sides of the head as well as a multitude of potential neurological symptoms.

multiple sclerosis A chronic, inflammatory, demyelinating disease that affects the central nervous system (CNS). Symptoms can include sensory problems (most notably visual and balance problems), muscle weakness, depression, difficulties with coordination and speech, severe fatigue, cognitive impairment, overheating, and pain. MS causes impaired mobility and disability in more severe cases.

nucleus tractus solitarius The solitary nucleus and tract are structures in the brainstem that carry and receive visceral sensation and taste from the facial (VII), glossopharyngeal (IX), vagus (X) cranial nerves, as well as the cranial part of the accessory nerve (XI).

olfactory reference syndrome A psychiatric condition of excessive concern with odors, usually imagined. The disorder can be accompanied by shame, embarrassment, significant distress, avoidance behavior, and social isolation.

Parkinson's disease A degenerative disorder that often impairs motor skills and speech. It is classically characterized by muscle rigidity, tremor, a slowing of physical movement (bradykinesia) and, in extreme cases, a loss of physical movement (akinesia). The motor symptoms result from decreased dopamine within the basal ganglia, thereby reducting stimulation of the motor cortex. Secondary symptoms can include high level cognitive dysfunction and subtle language problems.

pons A central nervous system structure located on the brainstem above the medulla oblongata, below the midbrain, and anterior to the cerebellum. This structure relays sensory information between the cerebellum and cerebrum, and contains the pneumotaxic centers that regulate respiration. some theories pose that it has a role in dreaming.

postcentral gyrus The lateral postcentral gyrus is a prominent structure in the parietal lobe of the human brain and an important landmark. Often referred to as primary somatosensory cortex, as it received the bulk of the thalamocortical projection from the sensory input fields.

precentral gyrus The primary motor cortex (or M1) works in association with pre-motor areas to plan and execute movements. M1 contains large neurons known as Betz cells which send long axons down the spinal cord to synapse onto alpha motor neurons which connect to the muscles. Pre-motor areas are involved in planning actions (in concert with the basal ganglia) and refining movements based upon sensory input (this requires the cerebellum).

Primary olfactory cortex Cortical regions (e.g., entorhinocortex and pyriform cortex) that receive the initial projections from the olfactory bulb.

progressive supranuclear palsy A rare degenerative disorder involving the gradual deterioration and death of selected areas of the brain. The initial symptom in most cases is loss of balance and falls. Other common early symptoms are changes in personality or general slowing of movement. Later symptoms and signs are dementia (typically including loss of inhibition and ability to organize information), slurring of speech, difficulty swallowing, and difficulty moving the eyes, most specifically in the downward direction.

pseudohypoparathyroidism A condition caused by resistance to the parathyroid hormone. Patients have a low serum calcium and high phosphate, but the parathyroid hormone level is appropriately high.

schizophrenia A mental illness characterized by impairments in the perception or expression of reality, most commonly manifesting as auditory hallucinations, paranoid or bizarre delusions, or disorganized speech and thinking in the context of significant social or occupational dysfunction.

seasonal affective disorder An affective, or mood, disorder. Most sufferers experience normal mental health throughout most of the year, but experience depressive symptoms in the winter or summer.

sella turcica A saddle-shaped depression in the sphenoid bone at the base of the human skull. The seat of the saddle is known as the hypophyseal fossa which holds the pituitary gland.

striatum A subcortical part of the telencephalon. It is the major input station of the basal ganglia system. Anatomically, the striatum is comprised of the caudate and the putamen.

sulfhydryl group A functional group on a molecule composed of a sulfur and a hydrogen atom (–SH).
superior temporal gyrus The superior temporal gyrus is one of three (sometimes two) gyri in the temporal lobe of the human brain. A gyrus (plural gyri) is a bump or ridge on the surface of the brain.
temporal lobe These elements of the cerebrum lie at the sides of the brain, beneath the lateral or Sylvian fissure. Seen in profile, the human brain looks something like a boxing glove. The temporal lobes are where the thumbs would be. The temporal lobe is involved in sensory processing, as well as in semantics both in speech and vision. The temporal lobe contains the hippocampus and is therefore involved in memory formation as well.
thalamus A paired and symmetric deep portion of the brain which relays sensory information from sensory systems to various areas of the cortex. It constitutes the main part of the diencephalon.
trigeminal nerve The fifth cranial nerve (CN V). This nerve is responsible for sensation in the face, eyes, and oral cavity, and can respond to some chemicals, producing such sensations as cooling, sharpness, and warmth.
Turner syndrome This disorder occurs in 1 in 2500 female births. Instead of the normal XX sex chromosomes for a female, only one X chromosome is present and fully functional. A normal female karyotype is labeled 46, XX; individuals with Turner syndrome are 45, X (also labeled 45, X0 or less commonly X(,)) though other genetic variants occur. In Turner syndrome, female sexual characteristics are present but generally underdeveloped.
uremia A toxic condition resulting from renal failure, when kidney function is compromised and urea (a waste product normally excreted in the urine) is retained in the blood. Uremia can lead to disturbances in the platelets and hypersomnia, among other problems.
vagus nerve The 10th cranial nerve (CN X). This nerve starts in the brainstem (within the medulla oblongata) and extends, through the jugular foramen, down below the head, to the abdomen. The vagus nerve is responsible for such varied tasks as heart rate, gastrointestinal peristalsis, sweating, and quite a few muscle movements in the mouth, including speech (via the recurrent laryngeal nerve) and keeping the larynx open for breathing. It also receives some sensation from the outer ear, via the auricular branch (also known as Alderman's nerve) and part of the meninges. Taste buds at the back of the throat are innervated by this nerve.
vestibular nuclei The cranial nuclei for the vestibular nerve.

> ". . .smell and taste are in fact but a single composite sense, whose laboratory is the mouth and its chimney the nose. . .." Jean Anthelme Brillat-Savarin, 1826

4.46.1 Introduction

The senses of taste and smell warn us of toxins, such as spoiled food, leaking natural gas, polluted air, and smoke. Moreover, as noted above by Brillat-Savarin, author of *Physiologie du Gout*, these senses work together in their production of flavor sensations. This is why many people mistake the olfaction-related experiences derived from eating (e.g., the sensations of chocolate, strawberry, lemon, etc.), which depend upon stimulation of the olfactory receptors via the retronasal route, as emanating from the taste buds. In fact, taste buds only mediate the sensations of sweet, sour, salty, bitter, and possibly metallic (iron salts), umami (sodium salts), and chalky (calcium salts). Like primary colors, smell and taste sensations blend to create variable hues of chemosensory experience, and when combined with the sensory input from the trigeminal system, ingested substances acquire an aroma, texture, temperature, and spiciness, allowing for the overall perception of flavor.

Damage to the olfactory and gustatory systems can profoundly influence a patient's quality of life. Persons without a sense of smell can no longer enjoy the nuances of perfume, wine, and fine food, in some cases leading to depression and, depending upon the individual, weight loss or weight gain. Taste dysfunction, commonly presenting as an abnormal taste, may significantly affect food choices and adversely alter nutrient intake. Chemosensory dysfunction is particularly disabling for those who depend upon these

senses for their livelihood or safety, including plumbers, fire fighters, policemen, perfumers, and workers within the food and beverage industries. Surprisingly, disorders of taste and smell are common, being present in at least 1% of the population under the age of 65 years, and well over 50% of the population over the age of 65 years (Doty, R. L. *et al.*, 1984a; 1984b; Hoffman, H. J. *et al.*, 1998).

In this chapter, we review a number of human chemosensory disorders, present up-to-date practical techniques for their management and quantitative evaluation, and describe how they are classified, evaluated, and treated. This survey is not inclusive, and examples are presented only to show the relationship between specific disease states and chemosensory disturbances.

4.46.2 Anatomy of Human Taste and Smell Systems

Chemosensory dysfunction can arise from disorders that block delivery of stimuli to receptors, as well as from ones that damage neural processes at various levels of the sensory system. In the vast majority of cases of olfactory dysfunction, damage occurs to the olfactory membrane. The most typical site of taste dysfunction is generally less clear, although taste buds can be directly altered via injury to the lingual surfaces. Since the neural circuitry involved in olfactory and gustatory perception is complex, a basic overview of the anatomy of these systems is presented in this section to place clinical issues into perspective; more detailed descriptions of the biochemistry and physiology of these systems are found elsewhere in this volume.

4.46.2.1 Olfactory Pathways

Six to ten million olfactory receptor cells, collectively termed cranial nerve I (CN I), are located within the approximately $2\,cm^2$ pseudostratified columnar epithelium lining the region of the cribriform plate and sectors of the superior turbinate, middle turbinate, and superior septum. In the human, about 350 receptors are distributed across these millions of cells, localized to cilia extending from dendritic knobs into the overlying mucus (Rouquier, S. *et al.*, 2000). The axons of the receptor cells unite to form bundles of 30 to 50 fila ensheathed by glial cells that traverse the cribriform plate and pia matter to form the outermost layer of the olfactory bulb. The axons of the olfactory receptors enter the glomeruli of the second layer of the olfactory bulb, where they form multiple synapses with the dendrites of the mitral and tufted cells, the bulb's primary projection neurons. The olfactory bulb is a layered structure that serves as the first relay system in the olfactory pathway. The bulb transforms the incoming signal, sharpening the information relative to the mix of chemicals involved and bodily state (e.g., hunger). In addition to sending afferents directly to the olfactory cortex via the lateral olfactory tract, the mitral and tufted cells send collaterals that synapse within the periglomerular and external plexiform layers of the bulb, where efferent influences from central structures can occur.

The primary olfactory cortex (POC), the direct recipient of the bulbar afferents, is comprised of the anterior olfactory nucleus (AON), the piriform cortex, the olfactory tubercle, the entorhinal area, the periamygdaloid cortex, and the corticomedial amygdala (Figure 1). While the majority of olfactory bulb neurons project to the piriform cortex, found within the medial portion of the temporal lobe, other fibers project directly to structures of the limbic system involved in memory and emotion (e.g., entorhinal cortex, periamygdaloid complex, and subsequently the hippocampus). Some projections occur, via the anterior commissure, from pyramidal cells of the AON to contralateral elements of the POC. Contralateral, as well as ipsilateral, activity is present, although generally the ipsilateral activity is more intense and rapid, as measured, for example, by magnetoencephalography (MEG) (Tonoike, M. *et al.*, 1998). Olfaction differs from the other senses in sending projections to the cortex that do not relay first within the thalamus. Thalamic connections do exist, however, between projections to and from the primary and secondary olfactory cortices.

4.46.2.2 Gustatory Pathways

Taste receptors are mostly found within taste buds located on lingual protuberances, termed papillae. Some taste buds are found on the epiglottis and soft palate. The receptor elements within the buds are innervated by branches of the facial (CN VII), glossopharyngeal (IX), and vagus (CN X) nerves, depending upon the bud's location within the oral cavity (Figure 2). Unlike CN I, these cranial nerves are mixed motor and sensory nerves. This becomes important when considering clinical syndromes that involve taste dysfunction, since variable degrees of

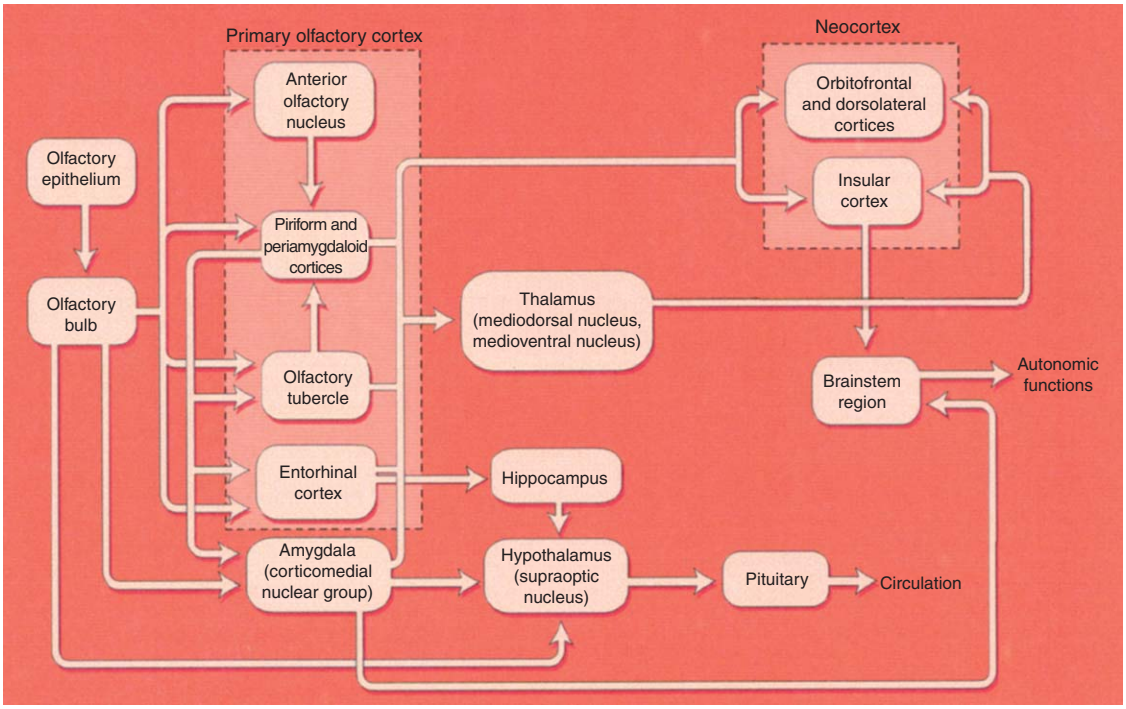

Figure 1 Primary afferent neural connections of the human olfactory system. Although olfactory fibers project from the amygdala to the feeding center of the hypothalamus, particularly the ventromedial and ventrolateral nuclei, it is unclear whether direct olfactohypothalamic routes are available in humans, as occurs in some other mammals. Copyright © 1996, Richard L. Doty.

either motor or sensory disturbance may be present depending upon where and to what extent the taste-mediating cranial nerve is injured.

All the peripheral gustatory fibers enter the brainstem and project to the nucleus of the tractus solitarius (NTS), which begins in the rosterolateral medulla and extends caudally along the ventral border of the vestibular nuclei. The major cortical projections from the NTS are to insular and perisylvian cortical regions, including the frontal operculum, superior temporal gyrus (opercular part), and inferior parts of the pre- and postcentral gyrus (Gloor, P., 1997; Faurion, A. *et al.*, 1998). A secondary cortical taste region is located in the caudomedial/caudolateral orbitofrontal cortex rostral to the primary taste cortex (Baylis, L. L. *et al.*, 1995). A number of such regions process touch and temperature, in addition to taste. The cells of the NTS also make viscerovisceral and viscerosomatic reflexive connections, via the interneurons of the reticular formation, with cranial nuclei that control (1) the muscles of facial expression; (2) taste-mediated behaviors, including chewing, licking, salivation, and swallowing; and (3) preabsorptive insulin release (Smith, D. V. and Shipley, M. T., 1992).

4.46.2.3 Trigeminal System

Free nerve endings from the trigeminal nerve (CN V) are found throughout the nasal and oral cavities. In the nose, they are responsible for somatosensory sensations induced by some odorants (e.g., stinging, sharpness, coolness, and warmth), whereas in the mouth, they contribute to the tactile, thermal, and spicy sensations essential for many flavor sensations. Anatomically, the anterior and lateral sectors of the nasal cavity are innervated by lateral and medial nasal branches of the ethmoidal nerve. The posterior region of the nasal cavity is innervated by the nasopalatine nerve. The gustatory fibers of the facial nerve (chorda tympani) travel in conjunction with the mandibular trigeminal fibers of the lingual nerve for a short distance near the tongue, making both of these nerves susceptible to orofacial causes of injury.

4.46.3 Symptoms of Chemosensory Dysfunction

The symptoms of chemosensory dysfunction can range from total loss of smell or taste perception

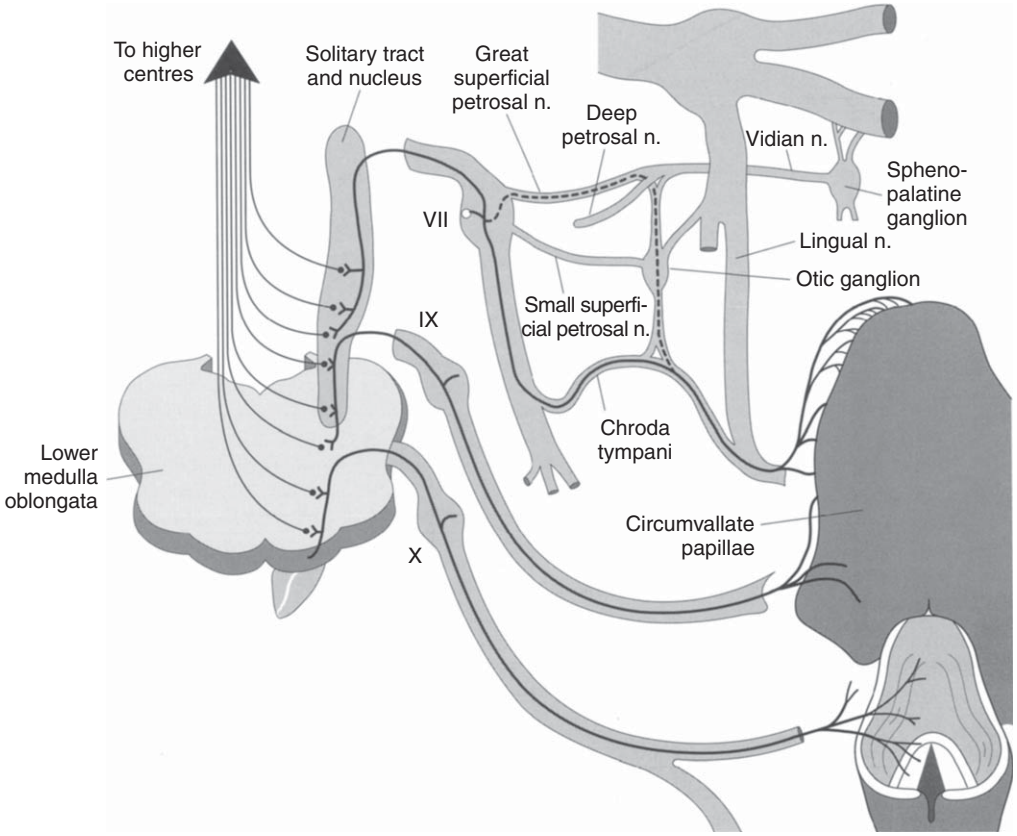

Figure 2 Distribution of cranial nerves to gustatory regions. CN VII fibers from the geniculate ganglion innervate taste buds on the anterior tongue and soft palate. CN IX fibers from cell bodies within the petrosal ganglion innervate taste bud on the lingual foliate and vallate papillae, as well as pharyngeal taste buds. CN X fibers from cell bodies in the nodose ganglion innervate taste buds on the epiglottis, larynx, and esophagus. Modified from Netter, F. H. 1964. The Ciba Collection of Medial Illustrations, Vol. 1, Nervous System. Ciba Pharmaceutical Corporation.

(termed anosmia and ageusia, respectively) to persistent and debilitating sensory disturbances, such as the presence of a strong and persistent salty taste (dysgeusia) or a bad smell (dysosmia). When such sensations appear without any apparent stimulus, they are termed phantogeusias or phantosmias, respectively. In most cases where a patient complains of chemosensory problems, some degree of smell or taste loss is apparent upon quantitative testing. In a few cases, however, disturbances in the perception of tastes or smells occur that cannot be objectively detected. A debilitating disorder, often associated with taste distortions that are not detectable by taste tests, is that of burning mouth syndrome (BMS; also known as glossodynia or glossalgia). In this syndrome, the patient experiences intense oral burning pain on the tongue or elsewhere within the oral cavity (Grushka, M. and Sessle, B. J., 1991).

4.46.4 Clinical Evaluation of Chemosensory Disorders

4.46.4.1 Medical History and Examination

The etiology of most cases of chemosensory dysfunction can be ascertained from carefully questioning the patient about the nature, timing, onset, duration, and pattern of symptoms, as well as a historical determination of antecedent events, such as head trauma, upper respiratory infections (URIs), toxic exposures, nasal or oral surgeries, and so on. A history of epistaxis, discharge (clear, purulent, or bloody), nasal obstruction, and somatic symptoms, including headache or irritation, may aid in establishing the probable etiology. Fluctuations in olfactory function usually reflect obstructive, rather than neural, factors. It is important to identify exacerbating or relieving foods or products, prior treatments and their efficacy

and comorbid medical conditions (e.g., liver disease, kidney disease, hypothyroidism, diabetes, and vitamin deficiencies). Delayed puberty in association with anosmia, with or without midline craniofacial abnormalities, deafness, and renal anomalies, suggests the possibility of Kallmann's syndrome or one of its variants. Patients who report never having had a sense of smell typically lack normal olfactory bulbs or tracts upon appropriate magnetic resonance imaging (MRI) studies (Li, C. *et al.*, 2003). Medications being used prior to or at the time of the symptom should be identified, particularly when taste, per se, appears to be altered. Such widely used drugs as statins, antifungal agents, and angiotensin-converting enzyme (ACE) inhibitors commonly cause chemosensory disturbances, most notably alterations in taste perception. Although dysosmias or phantosmias usually reflect alterations at the level of olfactory epithelium, in rare cases they signify central tumors or lesions that can be associated with tremor or seizure activity (e.g., automatisms, occurrence of black-outs, auras, and déjà vu).

Problems with speech articulation, salivation, chewing, swallowing, oral pain or burning, dryness of the mouth, periodontal disease, foul breath odor, recent dental procedures or surgeries, recent radiation exposure, medications, and bruxism can aid in establishing the basis of a taste problem. Inquiry into the patient's diet and oral habits may reveal exposure to oral irritants. Questions about hearing, tinnitus, and balance are important since the vestibulocochlear nerve (CN VIII) travels in close proximity to the facial nerve and can be susceptible to similar etiologies of disturbance (e.g., cerebellopontine angle tumors). Considering the occasional effect of gastroesophageal reflux on taste, asking about stomach problems may also be relevant. Constitutional symptoms – such as fever, malaise, headache and body pains, and rashes – may also be important since such symptoms often accompany cancers or systemic inflammatory conditions (e.g., lupus).

4.46.4.2 Quantitative Chemosensory Testing

A common error made on the part of clinicians is to accept a patient's report of olfactory dysfunction and to fail to objectively verify the presence or magnitude of the problem. Unfortunately, many persons are inaccurate in assessing the magnitude of their dysfunction, particularly the elderly or those with dementia. As noted in the introduction, a large number of patients confuse the loss of flavor sensations derived from the loss of olfactory function with taste, misleading themselves and their physicians as to the sensory system involved in their dysfunction (Figure 3). Some patients, particularly ones involved in litigation, attempt to malinger or overstate the nature of their dysfunction. Quantitative testing allows for a determination of the nature and degree of the chemosensory problem, the detection of malingering, and the tracking of changes in function over time and the efficacy of medical or surgical interventions.

Practical tests of smell function are now commercially available (for review, see Doty, R. L. 2001). The most widely used of such tests, the University of Pennsylvania smell identification test (UPSIT), has been administered to hundreds of thousands of patients and has been translated into a number of non-English languages. This test provides an indication of absolute smell loss, as well as the degree of smell loss relative to a patient's age and gender (i.e., percentile rank). The latter is critical, since smell ability decreases markedly in the later years (Figure 4). Electrophysiological tests, such as the odor event-related potential, can aid in the detection of malingering, although, unlike their auditory counterpart, they are presently unable to discern where in the olfactory pathway an anomaly exists. Although direct electrical recordings from the olfactory neuroepithelium can be made (termed the electro-olfactogram), such recordings can be misleading. Thus, anosmic patients lacking olfactory bulbs and tracts (e.g., those with Kallmann's syndrome), as well as patients with clearly determined psychophysical olfactory dysfunction (e.g., those with schizophrenia), commonly have clear electro-olfactograms.

Numerous taste tests are described in the literature that can be used to detect taste dysfunction, perhaps the most practical being that of electrogustometry. Testing of specific regions of the tongue is usually desired, since whole-mouth tests can be relatively insensitive to a number of gustatory alterations, given the redundancy of the innervation of the taste buds (for review, see Frank, M. E. *et al.*, 1995).

4.46.5 Causes of Chemosensory Dysfunction

Although there are reports of hundreds of disorders associated with chemosensory disturbance, a number of such reports are anecdotal and require empirical validation. Olfactory dysfunction can reflect, among other things, (1) altered airflow to the olfactory

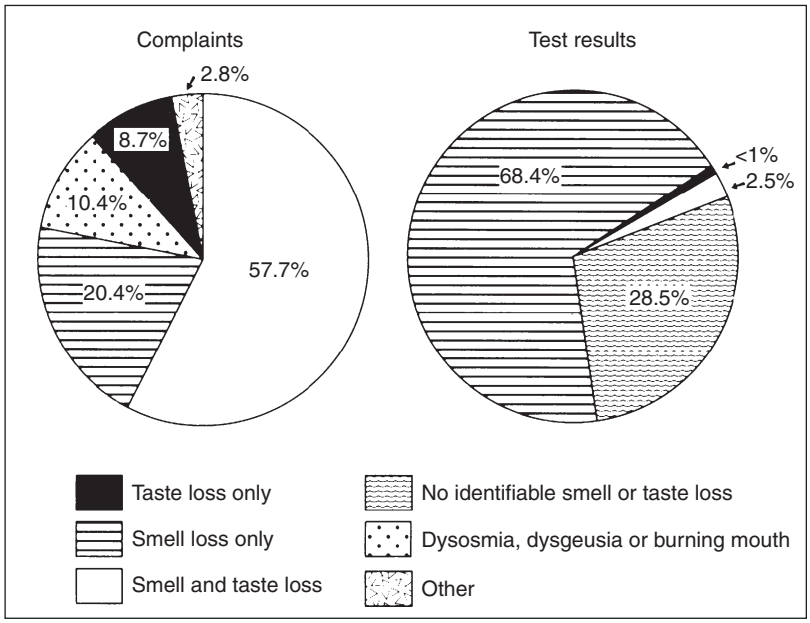

Figure 3 Distribution of primary chemosensory complaints (left diagram) and test results (right diagram) in 750 consecutive patients presenting to the University of Pennsylvania Smell and Taste Center for chemosensory evaluation. Note that the complaint categories of smell loss, taste loss, and smell and taste loss include some patients with secondary complaints of chemosensory distortion and burning mouth from Deems, D. A., Doty, R. L., Settle, R. G., Moore-Gillon, V., Shaman, P., Mester, A. F., *et al.*, 1991. Smell and taste disorders, a study of 750 patients from the University of Pennsylvania Smell and Taste Center. Arch. Otolaryngol. Head Neck Surg. 117, 519–528. Copyright © 1991, American Medical Association.

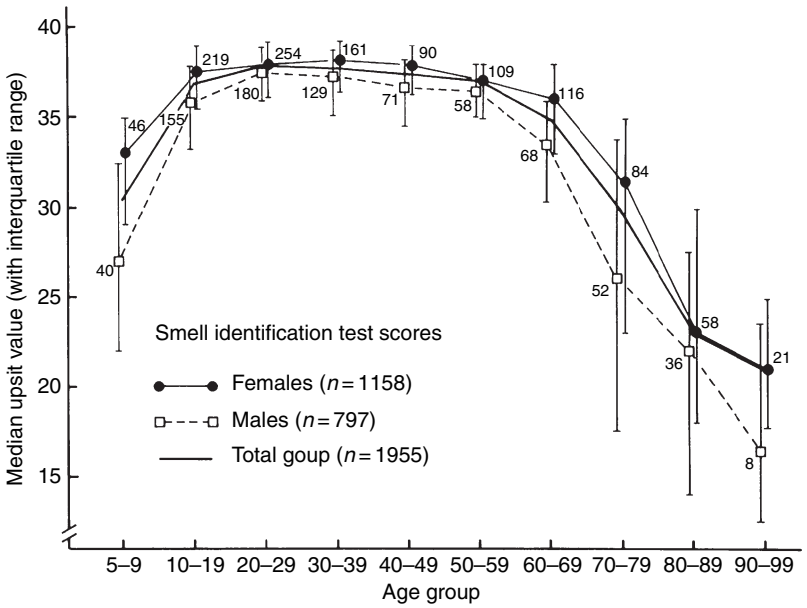

Figure 4 University of Pennsylvania smell identification test (UPSIT) scores as a function of age and gender. Numbers by data points indicate sample sizes modified from Doty, R. L., Shaman, P., Applebaum, S. L., Giberson, R., Siksorski, L., Rosenberg, *et al.* 1984a. Smell identification ability: changes with age. Science 226, 1441–1443; Doty, R. L., Shaman, P. and Dann, M. 1984b. Development of the University of Pennsylvania smell identification test: a standardized microencapsulated test of olfactory function. Physiol. Behav. 32, 489–502.

receptors (e.g., secondary to polyposis and excessive nasal engorgement), (2) damage to the olfactory membrane proper (e.g., from URIs, toxic chemical exposure, and occlusion of foramina through which the olfactory fila project), (3) damage to central nervous system (CNS) structures involved in olfactory transduction/processing (e.g., from strokes, epilepsy, and so on), and (4) systemic disturbances of metabolism or transduction (e.g., due to medications, hypothyroidism, diabetes, and liver or kidney disease). Approximately two-thirds of cases of chronic anosmia or hyposmia are due to prior URIs, rhinosinusitis, or head trauma (Deems, D. S. *et al.*, 1991). Mechanisms for the alteration of taste include (1) blockage of stimulus access to the taste buds (e.g., from damage to taste pores from caustic agents or burns, chronic lack of salivary proteins critical for taste bud maintenance), (2) the release of bad-tasting materials from dental appliances (e.g., bacterial infections, gingivitis, and purulent sialadenitis), (3) damage to one or more neural pathways or central brain regions (e.g., from epilepsy, tumors, strokes, viruses, occlusion of foramina through which nerves pass, and trauma), and (4) systemic disturbances of metabolism (e.g., medications, hypothyroidism, diabetes, and liver or kidney disease). Avitaminosis, particularly of the B group and C group, can result in pellagra, sprue, pernicious anemia, scurvy, or glossitis. Additionally, zinc and copper deficiencies are reportedly linked to taste disturbances (Mattes, R. D., 1995).

4.46.5.1 Upper Respiratory and Oral Infections

The most frequent cause of permanent smell loss in the adult human is an URI, such as associated with the common cold, influenza, pneumonia, or HIV+ (Deems, D. S. *et al.*, 1991). Often the respiratory illness is described as being more severe than usual, and in many cases dysosmia or phantosmia is present, at least initially. Most dysosmias subside over time, although some patients are left with a noticeable olfactory deficit. Such losses are most common in middle or older age, presumably reflecting cumulative insult and the challenge of epithelial regeneration in the face of reductions in the proliferation of basal cells and immature neurons. Evidence of damage to the olfactory epithelia from patients with post-URI anosmia includes extensive cicatrization, decreases in receptor cell number, absent or decreased numbers of cilia on remaining receptor cells, and replacement of sensory epithelium with respiratory-like epithelium (Yamagishi, M. *et al.*, 1994).

The taste system is similarly susceptible to damage from bacteria, viruses, and other agents. Some cases of Bell's palsy, for example, reflect viral damage to the facial nerve (e.g., from *Herpes simplex* virus-1), producing unilateral facial weakness, gustatory loss, and in some cases damage to the taste-salivary reflex, which is dependent upon a relay from the nucleus of the solitary tract to the parasympathetic fibers innervating the salivary glands (Murakami, S. *et al.*, 1996). Involvement of taste in Bell's palsy, which may involve over half the cases, localizes the lesion to the neural pathways from the pons, along the nervus intermedius portion of the facial nerve, through the geniculate ganglion, to the point where the chorda tympani joins the facial nerve in the facial canal. A more severe form of Bell's palsy, Ramsy–Hunt syndrome, results from an active *Herpes* infection of the geniculate ganglion and involves pain and vesicles in the external auditory canal or soft palate. Interestingly, dental procedures can activate viruses that, in turn, lead to infections that sometimes influence olfactory function.

4.46.5.2 Allergies and Rhinosinusitis

A significant number of patients with allergic rhinitis exhibit greater olfactory dysfunction than their nonallergic counterparts. In one study, for example, 23.1% of those with allergic rhinitis had a threshold at or above the 2½ percentile of the controls. The smell loss was associated with clinical or radiographic evidence of rhinosinusitis or nasal polyps. Thus, hyposmia was present in 42.9% of those with associated rhinosinusitis. The presence of hyposmia was only 14.3% in those with no associated rhinosinusitis (Cowart, B. J. *et al.*, 1993).

In general, olfactory dysfunction is related to the severity of rhinosinusitis [e.g., in one study, the mean UPSIT scores were 35, 31, 26, and 23 for Kennedy stages I to IV of the disease, respectively (Downey, L. L. *et al.*, 1996)]. While the smell loss associated with rhinosinusitis has been traditionally viewed as conductive (Figure 1), at best only weak associations have been found between quantitative olfactory test scores and measures of nasal airway patency (Cowart, B. J. *et al.*, 1993). Moreover, medical (e.g., administration of topical or systemic steroids) or surgical (e.g., excision of polyps) treatments rarely return olfactory function to normal, suggesting that the severity of histopathological changes within the olfactory mucosa may be the defining factor. Support for this hypothesis comes from

evidence that degree of epithelial inflammation is related to olfactory test scores in patients with chronic rhinosinusitis (Kern, R. C., 2000), and that olfactory epithelial biopsies from patients with nasal disease are less likely to yield olfactory-related tissue than those from controls (Feron, F. *et al.*, 1998). The same is true for anosmic vs. nonanosmic rhinosinusitis patients, the former of whom typically exhibit a more pathological epithelium (e.g., disordered arrangement of cells and more islands of respiratory-like epithelium) (Lee, S. H. *et al.*, 2000). While the taste system, per se, is not directly influenced by rhinosinusitis, unpleasant tasting discharge, e.g., from postnasal drip, is often present that is of significant concern to the patient.

4.46.5.3 Disorders Influencing Airway Patency

In addition to rhinosinusitis, other conditions that block or otherwise hinder airflow to the olfactory receptors can adversely influence the ability to smell. Children with choanal atresia, for example, suffer from smell loss. In this congenital disorder, the airway is obstructed by membranous or bony tissue. The limited data suggest that permanent olfactory dysfunction may occur in such patients, presumably reflecting the need for early exposure to odorants for normal olfactory system development. Thus, in one study, smell was tested before and after such repair in patients of relatively advanced age (8–31 years). Although one patient who had suffered from unilateral atresia had normal smell function, three others who had suffered from bilateral atresia had permanent olfactory loss (Gross-Isseroff, R. *et al.*, 1989). A reversible smell loss occurs in children whose nasal airflow is compromised by hypertrophied adenoid tissue (Figure 5) (Ghorbanian, S. N. *et al.*, 1983).

4.46.5.4 Head Trauma

Head trauma likely accounts for 10–20% of all smell and taste disorders (Deems, D. S. *et al.*, 1991). While there are studies that suggest between 4 and 7% of head trauma patients lose their sense of smell, incidence rates as high as 60% in cases of severe head injury have been reported. However, such high incidences are usually found in centers specializing in chemosensory disturbances and therefore are influenced by referral patterns (Doty, R. L. *et al.*, 1997c; Ogawa, T. and Rutka, J., 1999). In general, taste dysfunction resulting from trauma is much less common than posttraumatic smell dysfunction, with solitary ageusia of one or more primary taste modalities, as measured by whole-mouth testing, occurring in less than 1% of persons with major head injury (Deems, D. S. *et al.*, 1991). Only rarely are trauma-related taste disturbances unaccompanied by smell impairment.

A number of mechanisms have been implicated in trauma-related smell impairment, including (1) shearing injury to the olfactory nerve filaments of the cribriform plate as a result of brain movement relative to the skull, (2) damage to the nasal and sinus

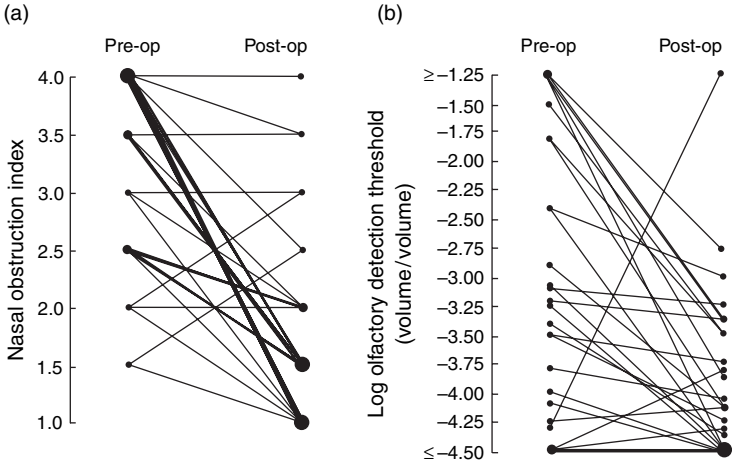

Figure 5 Nasal obstruction index (A) and olfactory detection threshold for phenyl ethyl alcohol (B) in 28 children before and after adenoidectomy. Each line joins preoperative (pre-op) and postoperative (post-op) values for an individual subject. Heavy lines denote confluence of several subjects who had the same preoperative and postoperative values (from Ghorbanian, S. N., Paradise, J. L., Doty, R. L. 1983. Odor perception in children in relation to nasal obstruction. Pediatrics 72, 510–516). Copyright © 1983 by the American Academy of Pediatrics.

architecture – with subsequent alteration of nasal airflow – without specific injury to the olfactory epithelium or neural projections, and (3) contusion or hemorrhage to central regions that mediate olfactory information (e.g., olfactory bulbs and tracts themselves, septal nuclei of the inferior frontal region, orbitofrontal territories, or the anteromedial temporal lobes). In addition to the severity of injury and loss of consciousness, there appear to be other factors associated with increased risk of developing anosmia after head trauma, including (1) anterior skull base fractures, (2) bilateral subfrontal lobe injury, (3) dural lacerations, and (4) cerebrospinal fluid leakage (Giasson, B. I. *et al.*, 2002). Occipital and lateral blows are more likely to result in anosmia than blows to the front of the head (Doty, R. L. *et al.*, 1997a; 1997b; 1997c). Compound fractures in the occipital, frontal, skull base, and mid-face are reported to be twice as likely as temporal and parietal fractures to result in olfactory alterations (Ogawa, T. and Rutka, J., 1999). In terms of facial fractures, nasozygomatic Le Fort fractures, fronto-orbital fractures, and pure La Fort fractures appear to most likely to be associated with smell disturbances (Horiguchi, T. *et al.*, 2003).

A strong correlate of head trauma-related anosmia is the severity of the injury (Doty, R. L. *et al.*, 1997a; 1997b; 1997c). Lower Glasgow coma scale ratings (GCS 3–8) are associated with a greater than 50% increase in the development of anosmia compared to moderate ratings (GCS 9–12) (Giasson, B. I. and Mushynski, W. E., 1996). Trauma-related loss of consciousness lasting 24 h or longer results in significantly more loss than that found in patients who have no loss of consciousness (Doty, R. L. *et al.*, 1997a; 1997b; 1997c).

The prognosis for posttraumatic ageusia is much better than for posttraumatic anosmia, and recovery from ageusia usually occurs in most patients over a period of a few weeks to months. The etiology of posttraumatic taste dysfunction varies. Head trauma that results in injury to the middle ear, a finding often encountered with temporal bone fractures, can result in both ipsilateral impairment of taste function and injury to the preganglionic parasympathetic fibers, thus preventing salivary secretion. Seven to 10% of temporal bone fractures reportedly result in facial nerve dysfunction (see Chang, C. Y. J. and Cass, S. P. 1999, for review). The lingual nerve, a branch of the mandibular division of the trigeminal nerve that subserves general somatic sensation and taste (due to coexisting chorda tympani fibers), can be damaged from trauma in and around the mouth and tongue, resulting in numbness and taste loss over the anterior tongue ispilateral to the side of injury. Trauma can produce Vernet's syndrome – a syndrome consisting of loss of taste in posterior third of tongue, paralysis of the vocal cord, palate, pharynx, trapezius, and sternocleidomastoid muscles secondary to lesions of the jugular foramen that affect CNs IX, X, and XI.

Isolated damage to the auriculotemporal nerve (ATN) can produce posttraumatic gustatory neuralgia, a taste-initiated, episodic, paroxysmal lancinating facial pain (often electric shock-like) in the cutaneous distribution of this nerve (Scrivani, S. J. *et al.*, 1998). Posttraumatic abnormalities involving the ATN, such as sweating and flushing following a taste stimulus, are termed Frey's syndrome. Although typically provoked by tastants, this syndrome can be elicited in some cases by the smell of food or emotional excitement (Scrivani, S. J. *et al.*, 1998).

4.46.5.5 Iatrogenesis

Head trauma is not the only type of trauma that can influence chemosensory function. In the case of olfaction, for example, various nasal and other surgical operations have been associated with smell loss (e.g., anterior ethmoidectomy, posterior ethmoidectomy, polypectomy, middle turbinate medialization, uncinectomy, sphenoidectomy, and anterior craniotomy). Although there are scattered reports of adverse influences of septoplasty and rhinoplasty on olfactory function, these operations only rarely influence smell function.

Trauma-related damage to the glossopharyngeal nerve, a nerve which is relatively well protected in comparison with the facial nerve, can occur from tonsillectomy, bronchoscopy, or laryngoscopy, reflecting the proximity of the lingual branch of this nerve to the muscle layer of the palatine tonsillar bed (Arnhold-Schneider, M. and Bernemann, D., 1987). Damage to this nerve is usually accompanied by damage to the nearby vagus, accessory, or hypoglossal nerves. Vernet's syndrome can also arise after parotid gland surgery, temporomandibular joint (TMJ) surgery, carotid endarterectomy, orthognathic surgery, and oncologic surgery.

4.46.5.6 Tumors and Central Nervous System Lesions

Damage to the olfactory bulbs and tracts can occur from numerous central tumors, including

meningiomas from the dura of the cribriform plate and surrounding regions (e.g., olfactory groove meningiomas, suprasellar ridge meningiomas), pituitary growths that extend above the sella turcica, and tumors within or around the third ventricle (for review, see Kern, R. C. and Mathog, R. H., 1991). Hyposmia or anosmia can be the principal or sole feature of an olfactory groove neoplasm. Unilateral and bilateral olfactory loss has been reported in frontal lobe glioma, suprasellar meningioma, and sphenoidal ridge meningioma, as well as in non-neoplastic space filling lesions, such as aneurysms of the anterior communicating bifurcation, large internal carotid aneurysms extending over the pituitary fossa, and hydrocephalus that forces the floor of the third ventricle downward (Graff-Radford, N. R. *et al.*, 1997). Removal of anterior skull base tumors via classical bifrontal craniotomy is commonly associated with postoperative anosmia and other complications (Jung, T. M. *et al.*, 1997).

Tumors growing anywhere along the path of the facial nerve – from the oral cavity, through the skull base, temporal bone and middle ear, to the cerebellopontine angle and the brainstem – can cause a mononeuropathy of the nerve and alterations in taste function. Nearly 10% of patients with surgically confirmed acoustic neuromas experience loss of taste as a primary complaint (Harner, S. G. and Laws, E. R., Jr., 1981). Lesions to brainstem structures that subserve taste can produce dysgeusia, although usually not without significant impairment of other cranial nerves or long tracts. Notable brainstem areas involved in taste that are susceptible to CNS lesions include the tractus solitarius and its nucleus (where injury produces ipsilateral deficits) and the pontine tegmentum (where injury produces bilateral deficits). Bilateral injury to the thalamus can result in ageusia, although unilateral lesions above the brainstem do not usually cause complete loss of function (likely due to the multiple areas involved in processing taste information). An isolated unilateral lesion to the thalamus or the parietal lobe may cause contralateral taste disturbance.

Gustatory perception may also be affected by cortical injury to areas of association cortex outside of the main gustatory processing regions. In a manner similar to that seen in the visual, auditory, tactile, and olfactory sensory systems, left unilateral neglect of taste sensations can result from contralateral injury to the right hemisphere (e.g., parietal lobe, thalamus, basal ganglia) (Bellas, D. N. *et al.*, 1988). In fact, a specific syndrome of buccal hemineglect exists in which patients neglect mouth and food products in the left half of the mouth and fail to initiate chewing and swallowing when food is in this location (Andre, J. M. *et al.*, 2000). This syndrome can result in choking or a socially embarrassing tendency to drool and regurgitate unnoticed food.

In a review of 15 reported cases, Onoda, K. and Ikeda, M. (1999) found that unilateral impairment of taste function occurs with injury to any one of several central locations, including the pons (eight cases), the thalamus (five cases), the midbrain (one case), and the internal capsule (one case). Based on the side of the respective central lesion and its effect on either unilateral or contralateral gustatory function, these authors surmised that the gustatory pathways ascend ipsilaterally from the medulla, cross over in their course from the pons to the midbrain, and synapse within the contralateral thalamus. Nonetheless, unilateral taste stimulation can reportedly evoke contralateral and bilateral cortical electrical responses (Kida, A., 1974), and one study suggests that taste information from both sides of the tongue must pass through the left insula for proper recognition to occur (Pritchard, T. C. *et al.*, 1999). In this study of six stroke patients with unilateral lesions of the insular cortex and three patients with brain damage outside the insula, damage to the right insula caused ipsilateral taste deficits in recognition and intensity, whereas damage to the left insula caused an ipsilateral deficit in taste intensity but a bilateral deficit in taste recognition.

Before the advent of modern imaging, olfactory tests were used to help diagnose and localize cribriform plate meningiomas and other tumors impacting the olfactory nerve (Elsberg, C. A., 1935a; 1935b). Olfactory recognition thresholds were reported to be elevated on the side where pressure was exerted on one olfactory nerve. When both nerves were involved, thresholds were bilaterally elevated, with more dysfunction on the most affected side. Expanding lesions on the ventral surfaces of the frontal cerebral lobes, as well as for suprasellar meningiomas and aneurysms of the internal carotid artery or the anterior part Willis' circle, produced such changes. Thresholds were uninfluenced by pituitary adenomas confined to the sella turcica, but were heightened if growth occurred above this bony structure. Tumors in or near the midline of the cranial cavity produced long-lasting adaptation (e.g., tumors of the corpus callosum, parasagital meningiomas, and infiltrating growths extending to the medial surface of a cerebral hemisphere). Decreased recognition threshold sensitivity sometimes is accompanied by generalized increased intracranial pressure

(Elsberg, C. A., 1935b). However, the findings of a recent study of ten patients with tumors localized to the left or right temporal or frontal lobes differed somewhat from these results (Daniels, C. *et al.*, 2001). Thus, patients with right-side tumors had odor discrimination deficits on both the left and the right. Those with left-side tumors exhibited attenuated function only when the odorant was presented to the left side, in accord with the notion that right hemisphere is more involved in olfactory processing than the left.

4.46.5.7 Drug Effects

Although both taste and smell can be altered by medications, drug-related taste disturbances occur much more frequently than drug-related olfactory disturbances. Over 250 medications reportedly alter the sense of taste, including antiproliferative drugs, antirheumatic drugs, antibiotic drugs, psychotrophic drugs, and drugs with sulfhydryl groups, such as penicillamine and captopril (Doty, R. L. and Bromley, S. M., 2004). Antihypertensive and antihyperlipidemic drugs, including ACE inhibitors, are commonly associated with taste disturbances, including hypogeusia and dysgeusia (Ackerman, B. H. and Kasbekar, N., 1997; Doty, R. L. *et al.*, 2003). Terbinafine, a commonly used antifungal medication, has been linked to taste disturbance that reportedly can last many months and, in some cases, for years (Doty, R. L. and Haxel, B. R. 2005). Among the medications used in the treatment of HIV and AIDS, the protease inhibitors have a taste themselves and appear to adversely modify the taste perception of other taste compounds (Schiffman, S. S. *et al.*, 1999). In a study of six psychotropic medications, including amytriptyline, clomipramine, desimpramine, imipramine, doxepin, and trifluoperazine, Schiffman, S. S. *et al.* (1998) found that these drugs do not only have a taste of their own, but alter the intensity of other tastants (such as salt and sugar).

Medication-related chemosensory changes can, in some instances, be reversed by discontinuance of the offending drug, by employing alternative medications, or by changing drug dosage. Unfortunately, many pharmacological agents appear to induce long-term alterations in taste that may take months to disappear even after drug discontinuance. Although the Physicians' Desk Reference (PDR) (2005) can be helpful in identifying medications that may result in drug-related chemosensory dysfunction, there is lack of uniformity and control in the acquisition of this information, and the relative influences on taste and smell can be confused.

4.46.5.8 Congenital and Inherited Disorders

The vast majority of idiopathic cases of apparent congenital anosmia exhibit agenesis or dysgenesis of the olfactory bulbs and stalks (Yousem, D. M. *et al.*, 1996). Several congenital olfactory syndromes are accompanied by endocrine dysfunction (e.g., Kallmann's syndrome), as discussed in the Section 4.46.5.9. Although most idiopathic congenital cases are presumably inherited, some may reflect early viral- or trauma-induced insults to the olfactory epithelium that produce regression of olfactory bulb/tract volume over time. Lygonis, C. S. (1969) reported total anosmia (without any apparent associated disorders) in members of four generations of a family living in an isolated island community and suggested that the pattern of inheritance was likely autosomal dominant. Singh, N., *et al.* (1970) described a familial anosmia loosely associated with premature baldness and vascular headaches, which appeared to be inherited as dominant with varying penetrance.

Recently, smell dysfunction has been reported in Bardet–Biedl syndrome (BBS), a rare pleiotropic genetic disorder associated with, among other things, retinal degeneration, obesity, limb anomalies, genitourinary abnormalities, and cognitive impairment (Iannaconne, A. *et al.*, 2005). Eight BBS genes have been cloned. One of these genes, the BBS4 gene, has been found in the olfactory neuroepithelium and plays a significant role in ciliary physiology. Interestingly, BBS4-knockout mice exhibit smell loss (Iannaconne, A. *et al.*, 2005).

Familial dysautononia (Riley–Day syndrome) is an autosomal recessively inherited disease with sensory neuropathy that mostly affects Ashkenazi Jewish patients. This disorder is associated with defective autonomic control, insensitivity to pain, hyporeflexia, and impaired lacrimation. Most notably for our purposes, patients with familial dysautonomia exhibit taste impairment secondary to the lack of fungiform papillae and lingual taste buds (Gadoth, N. *et al*, 1997). Taste dysfunction secondary to the absence of these structures was also described in two Japanese siblings who had late-onset progressive ataxia, global thermoanalgesia, sensorineural deafness, and mild autonomic disturbances (Fukutake, T. *et al*, 1996). This particular disease entity may represent a variant of late-onset hereditary spinocerebellar degeneration. More recently, Uchiyama, T. *et al.* (2001) described an individual with an apparently new variant of Machado–Joseph disease that lacked fungiform papillae.

4.46.5.9 Endocrine and Metabolic Diseases

A number of endocrine disorders have been associated with smell dysfunction. In general, the mechanisms responsible for the smell loss – aside from obvious anatomical alterations in the primary olfactory pathways – are poorly understood.

4.46.5.9.1 Addison's disease

One study has reported that patients with untreated adrenocortical insufficiency exhibit hypersensitivity to several odorants (e.g., pyridine, thiophene, and nitrobenzene), as well as to the vapors above aqueous solutions of six tastants (NaCl, KCl, HCl, $NaHCO_3$, sucrose, and urea) (Henkin, R. I. and Bartter, F. C. 1966). No overlap of the distribution of scores from the patient and control groups was observed, which is a remarkable finding. The patients detected differences between water and the tastant vapors at 1/10 000 the concentration of that observed for normals. The increased sensitivity was not influenced by daily 20 mg injections of deoxycorticosterone acetate (DOCA) for periods up to 10 days. In contrast, a similar regimen of 20 mg of the carbohydrate-active steroid prednisolone returned sensitivity to normal within 24 h.

Unfortunately, no attempts have been made to replicate this early work using more sophisticated sensory testing. If valid, the effects may reflect general processes, as hypersensitivity was also noted for pure-tone auditory thresholds and filtered and nonfiltered speech discrimination tests (Henkin, R. I. and Daly, R. L., 1968).

4.46.5.9.2 Cushing's syndrome

Cushing's syndrome is characterized by hypercortisolism, a chronic excessive secretion of adrenal corticosteroids. Adrenocorticotropic hormone (ACTH) hypersecretion occurs in approximately 80% of cases; the remaining approximately 20% reflect ACTH-independent etiologies (e.g., cortisol-secreting tumors or adrenal gland adenomas and carcinomas) (Ferrante, M. A., 1999). According to Henkin R. I. (1975), these patients have decreased sensitivity to odors, tastes, and sounds. In accord with this notion is a report by Ezeh P. I. *et al.* (1992) that dogs given chronic dexamethasone exhibit increased detection thresholds for benzaldehyde and eugenol (Ezeh, P. I. *et al.*, 1992).

4.46.5.9.3 Diabetes

A number of studies suggest that both taste and smell functions are altered by diabetes (for review, see Settle, R. G., 1991). In the case of smell, both threshold and suprathreshold deficits have been observed. One study found a correlation between smell identification scores and macrovascular disease in such patients (Weinstock, R. S. *et al.*, 1993). A progressive loss of taste beginning with glucose and extending to other sweeteners, salty stimuli, and then all stimuli has been noted (Hardy, S. L. *et al.*, 1981). In newly diagnosed noninsulin-dependent diabetics, quantifiable taste impairment exists that may be reversible, to some degree, with correction of the hyperglycemia (Perros, P. *et al.*, 1996). A subgroup of approximately 10% of first-degree relatives of noninsulin-dependent diabetics that have no neuropathies evidence taste dysfunction specific to glucose, but not other sugars such as fructose (Settle, R. G., 1981). It is not known if these individuals are the ones who go on to later develop diabetes, but this would seem quite possible.

4.46.5.9.4 Hypothyroidism

One might expect hypothyroidism to influence taste and smell functions, since this disease produces alterations in other sensory systems. Thus, 36–83% of hypothyroid patients are said to experience somesthetic disturbances, and 25–45% auditory or visual dysfunction, with night blindness reportedly being a common feature of the disorder (Mattes, R. D. *et al.*, 1986). In fact, dysgeusias appear to be disproportionately represented in hypothyroid patients (Deems, D. S. *et al.*, 1991). McConnell, R. J. *et al.* (1975) reported that seven of 18 patients with untreated primary hypothyroidism (39%) were cognizant of some alteration in their sense of smell, with three (17%) experiencing dysosmia. Lewitt M. S. *et al.* (1989) noted that 11 of 16 (69%) hypothyroid patients complained of alterations in taste and smell, although no detection threshold differences between the patients and controls were found for the odorant phenyl ethyl alcohol. Pittman J. A. and Beschi R. J. (1967) reported no influences of hypothyroidism on taste thresholds. Although experimentally induced hypothyroidism in rats fails to alter detection sensitivity to either tastes or odors, taste preferences are significantly effected, suggesting that thyroid disease may influence qualitative sensations, rather than sensitivity, per se (Brosvic, G. M. *et al.*, 1996).

4.46.5.9.5 Kallmann's syndrome

Kallmann's syndrome, which is more prevalent in men than in women, is defined as anosmia accompanied by idiopathic hypogonadotrophic hypogonadism (IHH).

This autosomal dominant disorder has incomplete expressivity and can be accompanied by cryptorchidism, deafness, midline craniofacial abnormalities, tooth agenesis, and renal anomalies. Relatives may be normal, may have anosmia unaccompanied by gonadal dysfunction, or may have anosmia and hypogonadism. Kallmann's syndrome patients typically have bilateral agenesis or dysgenesis of the olfactory bulbs and tracts, although lateralized variability may be present (Yousem, D. M. *et al.*, 1993).

The anosmia of Kallmann's syndrome is not reversed by either gonadotropin or gonadal steroid therapy, reflecting its anatomical basis. Given that testicular derangement can be largely reversed by hormones when given at the appropriate time, it is important to detect the endocrine problem as early as possible to prevent the possible development of irreversible atrophic changes and to minimize social consequences. Unfortunately, routine pediatric examinations do not test for olfactory function, and many individuals lacking such function, particularly children, do not seek help for this difficulty.

4.46.5.9.6 Kidney disease

Chronic renal failure is associated with alterations in smell and taste function, and in some circumstances, transplantation may improve the function. For example, Griep, M. I. *et al.* (1997) determined amyl acetate detection thresholds on 101 patients with chronic renal failure. Patients with cognitive deficits were excluded from analysis. No differences were noted for patients on peritoneal and hemodialysis, or for a subgroup of patients tested before and after hemodialysis. However, transplanted patients had better odor perception relative to matched dialysis controls. Significant negative correlations were noted between threshold sensitivity and serum concentrations of urea and phosphorus, as well as between such sensitivity and protein catabolic rates.

In patients younger than 55 years with uremia, a significant impairment of taste recognition was reported for salty, sweet, bitter, and sour agents relative to controls (Ciechanover, M. *et al.*, 1980). This impairment for sour and bitter, however, was found to show improvement immediately after dialysis. These uremic patients reportedly showed no signs of zinc deficiency.

4.46.5.9.7 Pseudohypoparathyroidism

Pseudohypoparathyroidism (PHP) is characterized by deficient responsiveness to, but not deficient production of, parathyroid hormone. Type Ia PHP exhibits generalized hormone resistance, a deficiency of the alpha chain of the stimulatory guanine nucleotide-binding protein ($G_s\alpha$) of adenylyl cyclase, and a constellation of developmental and skeletal anomalies termed Albright hereditary osteodystrophy (AHO). Type Ia patients exhibit obesity, short stature, brachydactyly, round faces, and subcutaneous ossifications. In contrast, type Ib patients have a specific hormone resistance to parathyroid hormone and lack a deficiency in $G_s\alpha$ protein activity. They also do not have AHO.

Patients with type Ia PHP, but not type Ib PHP, were reported, in the 1980s, to have olfactory dysfunction (Weinstock, R. S. *et al.*, 1986). The problem was attributed to the $G_s\alpha$ protein deficiency, since G_s proteins are involved in the first stages of olfactory transduction (Weinstock, R. S. *et al.*, 1986). More recent work, however, found type 1b patients to have similar olfactory dysfunction, making it unlikely that the PHP-related deficit reflects a $G_s\alpha$ protein deficiency (Doty, R. L. *et al.*, 1997a). In this same study, patients with pseudopseudohypoparathyroidism (PPHP), a disorder found in some relatives of patients with type Ia PHP, were found to have relatively normal smell function. Like type Ia PHP, PPHP is accompanied by a $G_s\alpha$ protein deficiency and by AHO, but not by a generalized end-organ hormone insensitivity. These findings suggest that the smell loss of PHP type Ia patients is unlikely due to $G_s\alpha$ deficiency. More work is clearly needed to determine the basis of the olfactory deficits in some patients with PHP.

4.46.5.9.8 Turner's syndrome

Chromatin-negative gonadal dysgenesis (Turner's syndrome) results from a X-chromosomal monosomy (i.e., 45,X karyotype). This disorder is characterized by a feminized phenotype, a short and sometimes webbed neck, small stature, low-set ears, a high-arched palate, shield-like chest, and sexual infantilism. Congenital lymphedema, cardiac deficits, and renal deficits are also sometimes found. Such patients reportedly have elevated detection and recognition thresholds to pyridine, thiophene, and nitrobenzene (Henkin, R. I., 1967). Gonadal hormone therapy was found to reverse the chemosensory deficits. A genetic basis for the chemosensory disorder is suggested by the fact that the mothers of the patients exhibited similar olfactory abnormalities.

4.46.5.10 Psychiatric Disorders

Several psychiatric disorders are associated with altered chemosensation. Such disorders include severe

stage anorexia nervosa, alcoholism with or without Wernicke–Korsakoff syndrome, seasonal affective disorder (SAD), attention-deficit/hyperactivity disorder (ADHD), depression, olfactory reference syndrome (ORS), schizophrenia, and chronic hallucinatory psychoses.

4.46.5.10.1 Alcoholism

Olfactory function is depressed in chronic alcoholics, particularly those whose alcoholism has led to vitamin deficiencies and the Wernicke–Korsakoff syndrome (Mair, R. G. *et al.*, 1986). For example, DiTraglia, G. M. *et al.* (1991) found alcoholics to have lower UPSIT scores than nonalcoholic controls; thus, 32% of 37 alcoholics exhibited scores within the clinically impaired range, as compared with 5% of 21 controls. A significant correlation was found between UPSIT scores and cortical sulcal volumes. In a follow-up study of 23 alcoholic subjects, those who had remained abstinent ($n = 15$) had significantly higher UPSIT scores than those who had not ($n = 8$). Subsequent studies by this group found impairment on the UPSIT to be associated with elevated cortical and ventricular CSF volumes, as well as with reduced cortical and subcortical gray matter volumes (Shear, P. K. *et al.*, 1992). Moreover, thalamic volume was found to be a significant unique predictor of UPSIT scores.

4.46.5.10.2 Anorexia and bulimia nervosa

Anorexia is associated with loss of olfactory function. Fedoroff, I. C. *et al.* (1995) administered the UPSIT and the phenyl ethyl alcohol threshold test to 55 eating-disordered hospitalized women. Very low-weight anorexics ($n = 11$) exhibited statistically significant deficits, although the magnitude of the losses was relative small, being approximately 3 UPSIT points and approximately 1.25 log vol/vol dilution units. The problem remained even after considerable weight has been regained at the time of discharge (although ideal body weight had not yet been achieved), suggesting the possibility that the effect may be long lasting.

4.46.5.10.3 Attention-deficit/hyperactivity disorder

Olfactory dysfunction has been associated with some forms of ADHDs. For example, Gansler, D. A. *et al.* (1998) found that patients diagnosed with ADHD/inattentive type (ADHD–) exhibited, among other things, odor identification deficits and deficits on a test of working memory, whereas those diagnosed with ADHD/hyperactive impulsive type (ADHD+) exhibited relatively more dysfunction on the Wisconsin card sorting test. These authors suggested that such differences may be linked to dysregulation of separate frontal neurotransmitter systems and/or brain regions.

4.46.5.10.4 Depression

Although persons with olfactory dysfunction often are depressed, the reverse is rarely true (i.e., depression does not cause smell loss). Thus, Amsterdam, J. D. *et al.* (1987) administered the UPSIT to 51 unmediated patients with well-documented moderate-to-severe depression and to 51 age-, race-, and gender-matched controls. No differences were observed between the scores of the two groups, a finding that has been replicated by others using this same test (Kopala, L. C. *et al.*, 1994).

Electrogustometric thresholds do not differ between depressed and nondepressed subjects (Scinska, A. *et al.*, 2004). Nevertheless, clinically depressed patients sometimes complain of an unpleasant or diminished taste that is not readily explainable by medications or other causes (Miller, S. M. and Naylor, G. J., 1989). Paradoxically, pleasantness ratings are higher in depressed patients than in controls for high concentrations of sucrose (Amsterdam, J. D. *et al.*, 1987; Kavaliers, M., 1989).

4.46.5.10.5 Olfactory reference syndrome

Patients with ORS believe that unpleasant or unhealthy smells emanate from their body (intrinsic hallucinations) or from some external source (extrinsic hallucinations). In cases where the hallucinations are minimal, patients complain about the odor but do not take steps to remove it. In other cases, the odor is so problematic that reasonable steps are taken to eliminate the odor (e.g., complaining to authorities or plugging up the chimney with newspapers). Compulsive washing behavior, changing clothes, and restriction of social activity is common in intrinsic hallucinatory cases. Some cases of ORC seem closely linked with an obsessive compulsive disorder and are amenable to treatment with serotonin uptake inhibitors (Dominguez, R. A. and Puig, A., 1997). ORS is generally viewed as distinct from schizophrenic or affective disorders (Pryse-Phillips, W., 1971; Bishop, E. R. 1980).

4.46.5.10.6 Seasonal affective disorder

There is some suggestion that SAD is associated with enhanced olfactory sensitivity. Thus, lower detection thresholds for the odorant phenyl ethyl alcohol have been reported in such patients relative to controls

(Postolache, T. T. *et al.*, 2002). This effect occurred regardless of whether the testing was done in the summer and winter, and no evidence of seasonal changes was found. However, a subsequent report, in which both UPSIT and threshold measures were determined for each side of the nose separately, found no differences between SAD patients and controls. Interestingly, however, depression scores were negatively correlated with right-, but not left-side UPSIT scores, suggesting the possibility of some laterality in affective state that influences smell function (Postolache, T. T. *et al.*, 1999).

4.46.5.10.7 Schizophrenia

Patients with schizophrenia exhibit moderate bilateral losses in olfactory function. In a comprehensive meta-analytic study, the median UPSIT score from 13 SZ studies was 32.5 (Moberg, P. J. *et al.*, 1999). The median effect size (i.e., the mean difference between patient and control groups expressed in SD units) for 17 SZ studies employing the UPSIT was 0.92. This deficit is clearly less, on average, than that seen in such neurodegenerative disorders as Alzheimer's disease (AD) and Parkinson's disease (PD) (see Section 4.46.5.11), where median effect sizes for eight AD and four PD studies have been reported as 2.01 and 1.66, respectively (Mesholam, R. I. *et al.*, 1998). In a recent study from our center, 23% of a group of 41 patients with SZ exhibited UPSIT scores indicative of microsmia or anosmia, in contrast to 94.4% of a group of 18 AD patients and 96.3% of a group of 54 PD patients (Moberg, P. J. *et al.*, unpublished data).

The olfactory decrement of SZ appears early in the disease process and, in fact, is found in many patients who may be prone to SZ, such as those with schizotypy or with family histories positive for significant mental illness (Park, S. and Schoppe, S., 1997; Kopala, L. C. *et al.*, 1998). This deficit appears to be more strongly related to neuropsychological measures of frontal lobe function (e.g., problems in executive function) than to measures of medial temporal lobe function (e.g., memory) (Pantelis, C. and Brewer, W. J., 1995); functional imaging studies report hypometabolism or decreased activation within the subtemporal and subfrontal lobes, particularly on the right (Buchsbaum, M. S. *et al.*, 1991). The olfactory bulbs and tracts are reduced in patients with SZ, as well as in their first-order relatives (Turetsky, B. I. *et al.*, 2003), although the significance of such reduction is not entirely clear. The smell loss of SZ correlates with negative, but not positive, symptoms of the disorder (Brewer, W. J. *et al.*, 1996). UPSIT scores are inversely and significantly correlated with disease duration, suggesting that some progression of pathology may be occurring somewhere in the olfactory pathways (Moberg, P. J. *et al.*, 1997). This phenomenon appears to be independent of medication history and gender. Presently, odor identification ability appears to be the only neuropsychological marker known to correlate with disease duration in SZ.

4.46.5.11 Neurodegenerative Diseases

The ability to smell is compromised in a number of neurodegenerative diseases, including AD, Down's syndrome (DS), Huntington's disease (HD), idiopathic PD, multi-infarct dementia (MID), multiple sclerosis (MS), Pick's disease, restless leg syndrome, and the parkinsonism–dementia complex of Guam (PDC) (for recent review, see Doty, R. L., 2003). The degree of olfactory dysfunction differs, on average, amongst most of these disorders. For example, as discussed in more detail below, AD, PD, and PDC are accompanied by marked alterations in the ability to smell, whereas HD and MID are accompanied by more moderate alterations. Essential tremor, progressive supranuclear palsy (PSP), and 1-methyl-4-phenyl-l,2,3,6-tetrahydropyridine-induced parkinsonism (MPTP-P) are associated with no, or only minor, changes in the ability to smell, in spite of the fact that they share major clinical features with PD.

4.46.5.11.1 Alzheimer's disease

The smell dysfunction of AD, although prevalent and marked (present in 85–90% of patients), is usually not total. Indeed, many patients are unaware of their disorder until after being tested ((Doty, R. L. *et al.*, 1987). The loss affects both nasal chambers in the earliest disease stages, including some cases of questionable AD, and appears to increase in magnitude with time. In a meta-analysis of 11 olfactory/AD studies, effect sizes ranging from 0.98 to 12.15 (median = 2.17) were noted (Mesholam, R. I. *et al.*, 1998). The olfactory dysfunction is reflected by decreased odor-related activation of central structures (e.g., subfrontal temporal lobe), as measured by positron emission tomography (PET; Figure 6) (Kareken, D. A. *et al.*, 2001).

Olfactory dysfunction – particularly in conjunction with other risk factors – appears to be a predictor of subsequent development of AD in older persons. For example, Graves, A. B. *et al.* (1999) administered a 12-item smell identification test to 1604 nondemented community-dwelling senior citizens 65 years of age or

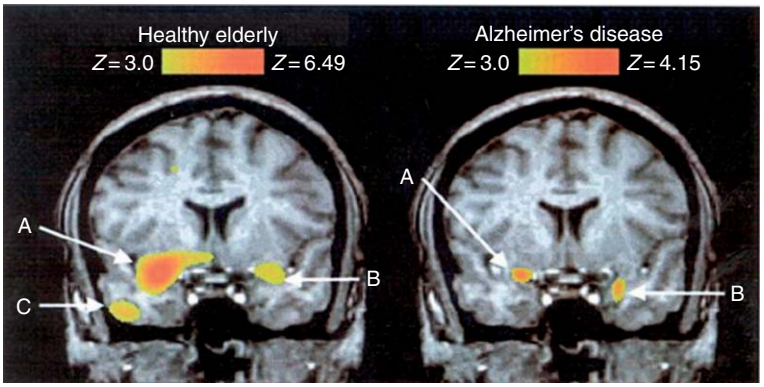

Figure 6 Left: Whole brain subtraction of olfactory stimulation minus control stimulation in healthy elderly control participants, coregistered on a T1-weighted reference magnetic resonance image ($n = 7$), accounting for one control participant whose right temporal lobe fell outside the scanner field of view. Right and left are reversed. Regions of interest are as follows: (a) Right frontotemporal junction (piriform area); (b) Left piriform area; (c) Right anterior-ventral temporal lobe (Brodmann 20). Right: Same whole-brain subtraction in patients with Alzheimer's disease. Regions of interest are as follows: A. 7 mm anterior to the frontotemporal junction (piriform) region in the control participants' image; B. Left amygdala-uncus (from Kareken, D. A., Doty, R. L., Moberg, P. J., Mosnik, D., Chen, S. H., Farlow, M. R., *et al*. 2001. Olfactory-evoked regional cerebral blood flow in Alzheimer's disease. Neuropsychology 15, 18–29). Copyright © 2001 by the American Psychological Association.

older. Over a subsequent 2 year time period, the identification test scores proved to be a better predictor of cognitive decline than global cognitive test scores. Anosmics who possessed at least one APOE-4 allele had 4.9 times the risk of having cognitive decline than normosmics not possessing this allele. This is in contrast to a 1.23 times greater risk for cognitive decline in normosmic individuals possessing at least one such APOE allele. Anosmic women who possessed at least one APOE-4 allele had an odds ratio of 9.71, compared to an odds ratio of 1.90 for women who were normosmic and possessed at least one allele. The corresponding odds ratios for men were 3.18 and 0.67, respectively. This study, along with similar longitudinal studies (e.g., Tabert, M. H. *et al*., 2005), strongly suggests that olfactory testing is a useful aid in determining those at-risk individuals who are most likely to develop AD.

4.46.5.11.2 Amyotrophic lateral sclerosis

Amyotrophic lateral sclerosis (ALS), traditionally viewed as a motor neuron disease, is associated with olfactory dysfunction. The degree of dysfunction is less than that seen in AD or PD, with average UPSIT scores falling around 30. One study of 58 patients with motor neuron disease reported that only bulbar patients exhibit significant deficits (Hawkes, C. H. *et al*., 1998). Another study of 37 ALS patients found that nearly half had UPSIT scores that fell within the normal range (Sajjadian, A. *et al*., 1994). Nonetheless, in the latter study, 75.7% of the patients scored below their individually matched controls. Only 11% of the ALS patients had total or near-total anosmia. Although no sex differences or laterality in the ALS-related test scores were observed, an age-related decrement was present. Interestingly, significant correlations were found between UPSIT scores and peripheral nerve conductance measures. One histological study of the olfactory bulbs from eight ALS patients revealed excessive lipofuscin deposition in all eight cases, suggesting subclinical neuronal damage (Hawkes, C. H. *et al*., 1998).

4.46.5.11.3 Multiple sclerosis

Although rare, smell loss can be a presenting symptom of MS (Constantinescu, C. S. *et al*., 1994). About a quarter of MS patients appear to exhibit olfactory dysfunction at any one time (Doty, R. L. *et al*., 1984b). The demyelinating plaques appear to be the basis of the disorder, as strong inverse correlations have been found between odor identification test scores and the number of plaques within the subfrontal and subtemporal lobes (Doty, R. L. *et al*., 1997b; Zorzon, M. *et al*., 2000). No such relationship is present in other brain regions. Longitudinal studies suggest that olfactory function waxes and wanes in relation to the exacerbation and remission of plaques within subtemporal and subfrontal lobes (Doty, R. L. *et al*., 1999). Evidence that MS alters taste function is limited,

although suprathreshold deficits have been observed for both tests of identification and perceived intensity (Catalanotto, F. A. *et al.*, 1984).

4.46.5.11.4 Parkinson's disease

Parkinson's disease, which is classically considered a motor disorder, is accompanied by smell loss with a prevalence rate greater than tremor, one of the cardinal signs of the disorder (Doty, R. L. *et al.*, 1988). As in AD, total anosmia is not the rule. Thus, only 38.3% of 81 patients evaluated in one study had UPSIT scores suggestive of anosmia, and only 13% of 38 patients who received an odor detection threshold test were unable to detect the highest odorant concentration presented (Doty, R. L. *et al.*, 1988). Moreover, all but one of 41 PD patients asked whether an odor was present on each of 40 UPSIT items answered affirmatively to 35 or more of the items, even though most were unable to identify the majority of the odors or felt that the perceived sensation did not correspond to the response alternatives. While olfactory loss is generally bilateral, there can be slight individual differences in the degree to which the left and right sides of the nose are involved. No association exists, however, between the side of relatively greater involvement and the side of hemiparkinsonism, as might be expected if asymmetrical damage to striatal dopamine systems were involved in the olfactory problem (Doty, R. L. *et al.*, 1992). The smell loss is unrelated to the magnitude of the motor symptoms, as well as a range of neuropsychological measures (Doty, R. L. *et al.*, 1989), although subtle variations among so-called benign vs. malignant forms may be present (Stern, M. B. *et al.*, 1994). Anti-PD medications (e.g., L-dopa, dopamine agonists, and anticholinergic compounds) have no influence on the smell deficit, which occurs as severely in nonmediated or nevermedicated patients as in medicated ones (Doty, R. L. *et al.*, 1992). A correlation between striatal dopamine transport activity, an index of the health of a neuron, and smell function has been recently reported (Siderowf, A. *et al.*, 2005).

The PD-related smell loss appears in both familial and sporadic forms and may be a sign of the preclinical disease state (Markopoulou, K. *et al.*, 1997; Berendse, H. W. B., 2001). As in the case with AD, some asymptomatic first-degree relatives of patients with either familial or sporadic forms of PD appear to exhibit olfactory dysfunction (Montgomery, E. B. *et al.*,. 1999). Recently, Berendse, H. W. B. (2001) administered tests of odor detection, identification, and discrimination to 250 relatives of PD patients (approximately 84% children, approximately 16% siblings, and one parent). In 25 hyposmic and 23 normosmic individuals sampled from this group, nigrostriatal dopaminergic function was assessed using single-photon emission computer tomography (SPECT) with [^{125}I]β-CIT as a dopamine transporter ligand. An abnormal reduction in striatal dopamine transporter binding was present in four of the 25 (16%) hyposmic relatives, two of whom subsequently developed clinical parkinsonism, and in none of the 23 normosmic relatives. Significant reductions in dopamine transporter binding were found only in hyposmic relatives of PD patients, suggesting olfactory dysfunction may precede clinical motor signs in PD. Such findings reiterate the point that olfactory testing, in conjunction with other measures, is likely useful in the early detection of PD.

Although the basis of the PD-related olfactory loss has been debated, Braak *et al.* present anatomical evidence suggesting that first CNS lesions of PD develop simultaneously within (a) the olfactory bulb and related portions of the AON and (b) the dorsal motor nucleus of the vagus nerve and adjoining intermediate reticular zone (Figure 7) (Del Tredici, K. *et al.*, 2002; Braak, H. *et al.*, 2003b). Cell types that succumb to PD-related development of inclusion bodies are primarily unmyelinated or poorly myelinated projection neurons with disproportionately long axons in relation to their somata (Braak, H. *et al.*, 2003b). It is noteworthy that dopamine-containing cells within the olfactory bulb are increased twofold in PD, at least in its later stages, despite the bulb's early involvement in the degenerative process and evidence of altered function (Huisman, E. *et al.*, 2004). The reason for this paradoxical finding is not known, although it may relate to the repopulation of periglomerular cells from progenitors within the anterior subventricular zone that migrate to the olfactory bulb via the rostral migratory stream (Saino-Saito, S. *et al.*, 2004).

4.46.5.11.5 Progressive supranuclear palsy

PSP, a disorder that accounts for approximately 4% of patients with parkinsonian symptoms, is commonly misdiagnosed as PD since it shares many motor features with PD. Unlike PD, however, tremor is rarely present in this disorder, and the parkinsonian features are less responsive to anti-PD medications (Jackson, J. A. *et al.*, 1983). Compared to PD, PSP is typically characterized by more frontal lobe dysfunction, more neuronal degeneration within the basal ganglia and upper brain

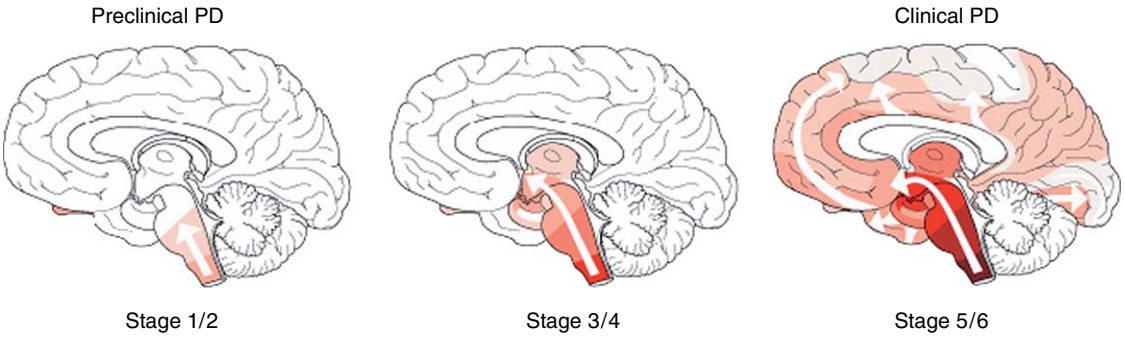

Figure 7 Parkinson's disease (PD)-related Lewy body pathology evolves in predictable stages. According to the staging system of Braak, Lewy bodies (LB) first form within in the olfactory bulb and dorsal motor nucleus of the vagal nerve (stage 1). In stage 2 and stage 3, LB pathology expands from these induction sites into additional brain stem nuclei (e.g., locus coeruleus and substantia nigra) and then into the amygdala. In stage 5 to stage 6, the pathology extends into the cerebral cortex. Clinical symptoms arise during stage 4 to stage 6 when the pathology involves significant regions of the substantia nigra and related brain areas (from Thal, D. R., Del, T. K., and Braak, H. 2004. Neurodegeneration in normal brain aging and disease 15. Sci. Aging Knowledge Environ. e26.).

stem, and less involvement of mesolimbic and mesocortical dopamine systems (Jankovic, J., 1989). Conceivably because of this difference in distribution of pathology, about half of PSP patients have a normal sense of smell, with the remainder having slight-to-moderate dysfunction. In one study of 22 PSP patients, for example, the mean PSP UPSIT score was approximately 32, compared to a mean PD UPSIT score of approximately 19 and a mean control UPSIT score of approximately 36.

4.46.5.12 Epilepsy

It is widely recognized that olfactory and gustatory auras can occur secondary to seizure activity within the temporal lobes and, more rarely, within the orbitofrontal lobes (Acharya, V. *et al.*, 1998). Examples of taste sensations that have been reported in such cases include peculiar, rotten, sweet, like a cigarette, like rotten apples, and like vomitus (for review, see (West, S. E. and Doty, R. L., 1995). However, some of these tastes likely represent smell sensations that are miscategorized as tastes by both the patients and their physicians.

A number of early olfactory threshold studies reported heightened overall bilateral olfactory sensitivity in patients with epilepsy, particularly prior to an ictal event. More recent studies, however, have not reported such hypersensitivity, conceivably reflecting (1) mitigating influences of modern anti-seizure medications or (2) evaluation of more severe and largely intractable cases. For example, one study reported normal bilaterally determined *n*-butanol odor detection thresholds in 18 epileptic patients relative to 17 controls (Eskenazi, B. *et al.*, 1986), a finding that was confirmed for unilaterally determined odor detection thresholds in 21 epileptic patients (Martinez, B. A. *et al.*, 1993). Similarly, another study of 16 patients with left foci and 14 patients with right foci found no detection threshold deficits on either side of the nose to the odorant phenyl ethyl alcohol (West, S. E. and Doty, R. L. 1995). In contrast to threshold studies, suprathreshold deficits have been reported in epileptic patients, including deficits in odor identification, discrimination, and both short- and long-term memory (e.g., Martinez, B. A. *et al.* (1993) . Prolonged odor event-related potential latencies have also been noted in patients with right-side foci after right-side odorant stimulation, and in patients with left-side foci after left-side odorant stimulation (Hummel, T. *et al.*, 1995).

Small, D. M., *et al.* (1997) observed that patients who had a right anterior temporal lobectomy had elevated citric acid recognition thresholds, but normal detection thresholds, relative to both controls and patients who had undergone left temporal lobectomy. Employing PET, these researchers noted that orally presented citric acid increased regional cerebral blood flow (rCBF) bilaterally in the caudolateral orbitofrontal cortex, but relatively more in the right anteromedial temporal lobe and in the right caudomedial orbitofrontal cortex. They speculated that (1) damage to the area corresponding to the rCBF increase in right anterior medial temporal lobe in normal subjects may account for elevation in taste recognition thresholds in lobectomized patients and (2) taste recognition requires

further processing by structures located in the anteromedial temporal lobe.

4.46.5.13 Migraine

The limited evidence suggests that 20–50% of migraineurs experience olfactory auras, osmophobia (intolerance of odors), and/or taste abnormalities during migraine attacks (Diamond, S. *et al.*, 1985). Moreover, both odorants and tastants can trigger migraine attacks in susceptible individuals (Blau, J. N. and Solomon, F., 1985). Unfortunately, few empirical studies of chemosensory function have been made in migraine sufferers, and consensus is lacking as to the direction of the effects. Hirsch, A. R. (1992) reported that of 67 migraineurs, 12 were either hyposmic or anosmic, a percentage much higher than that expected in the general population. No controls were tested. More recently, Snyder, R. D. and Drummond, P. D. (1997) determined odor recognition thresholds to acetone and vanillin in 20 migraine suffers and 21 controls. Rather than decreased sensitivity, these authors found heightened sensitivity (i.e., lower thresholds) in the migraineurs for the odor of vanillin. Although this was not the case for the odor of acetone, those migraineurs who reported that odors generally seemed stronger during migraine attacks exhibited lower acetone thresholds than those exhibited by the others. Hedonic ratings for concentrated acetone did not differ between the migraineurs and the controls.

4.46.6 Treatment of Chemosensory Disorders

Meaningful treatments are available for some, but not all, patients whose olfactory dysfunction is conductive, including dysfunction resulting from blockage of airflow to the olfactory neuroepithelium or from inflammation within the olfactory membrane proper (for review, see Doty, R. L. and Mishra, A., 2001). Thus, surgical procedures that reduce nasal obstruction can improve olfactory function in some patients. Effective therapies for olfactory loss secondary to allergic rhinitis include allergy management, topical cromolyn, topical and systemic corticosteroid therapies, and surgical procedures to reduce inflammation or obstructions. A brief course of systemic steroid therapy can be useful in distinguishing between conductive and sensorineural olfactory loss, since those with conductive loss will often respond to treatment. However, longer term systemic steroid therapy is not advised. Topical nasal steroids are often ineffectual in returning smell function because the steroid fails to reach the affected regions in the upper nasal passages. Increased efficacy presumably occurs when nasal steroid drops or sprays are administered in the head-down Moffett's position. In patients with obstructive inflammatory disease, swelling of the ostiomeatal complex can prevent drainage from the sinuses causing chronic sinusitis. Antibiotic therapy in combination with control of the allergic symptoms underlying the inflammation is effective in many of these cases. Resistant cases typically require surgery to improve drainage and clear infection (Bromley, S. M. and Doty, R. L., 2002).

It is an empirical question as to whether exercising the olfactory system by repeatedly exposing it to odorants improves olfactory function over time. Animal studies suggest that repeated presentations of an odor may alter detection thresholds (Doty, R. L. and Ferguson-Segall, M., 1989), as well as functional connectivity in higher brain regions (Wilson, D. A. *et al.*, 1985). Moreover, there is evidence, in humans, that repeated presentation of odorants increases sensitivity to them (Doty, R. L. *et al.*, 1981). A recently clinical study on this topic, which is unpublished, suggested that some benefit may accrue by exposing hyposmic subjects to a set of odorants in the morning and evening, although the degree of benefit was small and an atypically low spontaneous return of function was present in the control group (Hummel, T. *et al.*, 2005).

Currently, there are no treatment options for smell loss secondary to congenital or other malformations of the olfactory bulbs or stalks. In general, olfactory dysfunction due to sensorineural causes is difficult to manage, and the prognosis for patients suffering from long-standing anosmia due to upper respiratory illness or head trauma is relatively poor. Most patients who recover smell function subsequent to head trauma do so within 12 weeks of injury (Costanzo, R. M. *et al.*, 1995). Although there are no verified treatments for trauma-related olfactory loss, anti-inflammatory agents may minimize post-traumatic sequelae in some cases. Rat research suggests that application of nerve growth factor onto the olfactory epithelium may alleviate axotomy-induced degenerative changes in the olfactory receptor neurons, although it is not known whether this has any functional consequence or if such a procedure in humans would be efficacious (Yasuno, H. *et al.*, 2000). Rat studies also suggest that estrogens may offer some prophylaxis to neurotoxin-related damage to the olfactory receptor region (Dhong, H. J. *et al.*, 1999).

CNS tumors that impinge upon the olfactory bulbs and tracts, as well as sclerotic tissue within the medial temporal lobes, can be resected in some instances with a resultant improvement in olfaction. Although permanent sensory abnormalities can result from damage to a peripheral nerve supplying taste (e.g., lingual nerve and facial nerve), such damage is amenable to surgical repair, particularly in the first months after the injury (Robinson, P. P. *et al.*, 2000). However, the degree of return of function is highly variable and return of normal function is rare. In a series of 53 patients with prior lingual nerve injury who underwent direct reapposition of the nerve with epineurial sutures, Robinson, P. P. *et al.* (2000) found that 41% more patients could detect some taste solutions postoperatively.

A number of oral infections and inflammatory problems that alter taste function can be treated with appropriate antibiotic or anti-inflammatory medication. Even though a number of dysgeusias spontaneously remit with time (Deems, D. S. *et al.*, 1996), this is not true in all cases, and several interventions have been reported to aid in their resolution. First, those dysgeusias due to medications, such as salty or bitter tastes secondary to the use of drugs (e.g., ACE inhibitors and antifugals), commonly resolve following drug discontinuance, although such resolution may require months after cessation. Second, some pharmacological treatments are available for dysgeusias. Thus, low doses of anticonvulsants can eliminate dysgeusias due to central causes, such as partial seizures. Over-the-counter antioxidants or mineral supplements, such as alpha lipoic acid and zinc gluconate ($140\,\mathrm{mg\,day^{-1}}$), may mitigate some dysgeusias (Femiano, F. *et al.*, 2002; Heckmann, S. M. *et al.*, 2005), although zinc therapies are generally ineffectual for most chemosensory disturbances in the absence of frank zinc deficiencies such as occur in liver and kidney disease (Price, S., 1986). Tricyclic antidepressants (e.g., amitriptyline, desipramine, and nortriptyline) and benzodiazepines are reportedly useful as therapy in some cases. Specialized mouthwashes have been reported to provide symptomatic relief in some patients (e.g., chlorhexidine digluconate, dyclonine HCl) (Lang, N. P. *et al.*, 1988). In cases of dysgeusia or taste loss secondary to hypothyroidism, thyroxin replacement therapy is likely beneficial. Mucosal function and comfort can be provided to some patients with xerostomia and excessive dryness using artificial salivas (e.g., Xerolube) (Bromley, S. M. and Doty, R. L., 2003).

There is some rationale to controlling dysgeusias by applying a local anesthetic, such as a lidocaine or cancor sore solution, to selected sectors of the tongue. One basis for this approach comes from studies by Bartoshuk *et al.* (e.g., Yanagisawa, K. *et al.*, 1998). These authors found that anesthetizing one chorda tympani nerve increases the perceived intensity of bitter substances, such as quinine, applied to taste fields innervated by the contralateral glossopharyngeal nerve. In contrast, perceived intensity of NaCl applied to an area innervated by the ipsilateral glossopharyngeal nerve is decreased. When both chorda tympani nerves are anesthetized, the taste of quinine is intensified and the taste of NaCl diminished in areas innervated by the glossopharyngeal on both sides of the tongue. In about 40% of their subjects, a phantom dysgeusia, usually localized to the posterior tongue contralateral to the anesthesia, appeared in the absence of stimulation. This phantom taste was eliminated when the region of origin was anesthetized.

4.46.7 Summary

Possibly owing to the fact that, historically, most disorders of smell and taste have been difficult to diagnose and treat, physicians often downplay these senses in the routine neurological examination. This is unfortunate when one considers that such disorders are common and profoundly affect a patient's quality of life. The chemical senses largely determine the flavor of foods and beverages and provide an early warning for leaking natural gas, spoiled food, fire, and other adverse environmental situations. Importantly, olfactory disturbances can be an early sign of a number of serious diseases or anomalies, including AD, PD, epilepsy, MS, and schizophrenia. Although some patients initially present with a frank complaint of a smell disturbance, others are unaware of their dysfunction, pointing out the need for routine clinical quantitative assessment, which is now easily performed in the office.

In this chapter, we (1) reviewed the anatomy of the human taste and smell systems, (2) described the major symptoms experienced by patients suffering from chemosensory disorders, (3) described the major causes of chemnosensory dysfunction, and (4) presented up-to-date practical techniques for their management and quantitative evaluation. It is clear from the material reviewed that chemosensory disorders are varied in nature and can result from a

wide range of diseases and disturbances, including such common neurological disorders as AD and idiopathic PD. It is also apparent that while some types of chemosensory disturbances can be treated medically or surgically, in many cases treatment options are limited or nonexistent. Accurate assessment of the dysfunction is of value to both the patient and physician, allowing for a determination of the relative degree of dysfunction and whether the alteration is abnormal relative to a patient's age and gender.

References

Acharya, V., Acharya, J., and Luders, H. 1998. Olfactory epileptic auras. Neurology, 51, 56–61.

Ackerman, B. H. and Kasbekar, N. 1997. Disturbances of taste and smell induced by drugs. Pharmacotherapy, 17, 482–496.

Amsterdam, J. D., Settle, R. G., Doty, R. L., Abelman, E., and Winokur, A. 1987. Taste and smell perception in depression. Biol. Psychiatry, 22, 1481–1485.

Andre, J. M., Beis, J. M., Morin, N., and Paysant, J. 2000. Buccal hemineglect. Arch. Neurol. 57, 1734–1741.

Arnhold-Schneider, M. and Bernemann, D. 1987. Uber die Haufigkeit von Geschmacksstorungen nach Tonsillektomie. HNO, 35, 195–198.

Baylis, L. L., Rolls, E. T., and Baylis, G. C. 1995. Afferent connections of the caudolateral orbitofrontal cortex taste area of the primate. Neuroscience 64, 801–812.

Bellas, D. N., Novelly, R. A., Eskenazi, B., and Wasserstein, J. 1988. The nature of unilateral neglect in the olfactory sensory system. Neuropsychologia 26, 45–52.

Berendse, H. W. B. 2001. Subclinical dopaminergic dysfunction in asymptomatic Parkinson's disease patients' relatives with a decreased sense of smell. Ann. Neurol. 50, 34–41.

Bishop, E. R. 1980. An olfactory reference syndrome – monosymptomatic hypochondriasis. J. Clin. Psychiatry 41, 57–59.

Blau, J. N. and Solomon, F. 1985. Smell and other sensory disturbances in migraine. J. Neurol. 232, 275–276.

Braak, H., Del Tredici, K., Rub, U., De Vos, R. A., Jansen Steur, E. N., and Braak, E. 2003a. Staging of brain pathology related to sporadic Parkinson's disease. Neurobiol. Aging 24, 197–211.

Braak, H., Rub, U., Gai, W. P., and Del, T. K. 2003b. Idiopathic Parkinson's disease: possible routes by which vulnerable neuronal types may be subject to neuroinvasion by an unknown pathogen. J. Neural Transm. 110, 517–536.

Brewer, W. J., Edwards, J., Anderson, V., Robinson, T., and Pantelis, C. 1996. Neuropsychological, olfactory, and hygiene deficits in men with negative symptom schizophrenia. Biol. Psychiatry 40, 1021–1031.

Bromley, S. M. and Doty, R. L. 2002. Taste. In: *Diseases of the Nervous System: Clinical Neuroscience and Therapeutic Principles* (*eds*. A. K. Asbury, G. M. McKhann, W. I. McDonald, P. J. Goadsby, and J. C. McArthur), 3rd ed., pp. 610–620. Cambridge University Press.

Bromley, S. M. and Doty, R. L. 2003. Clinical disorders affecting taste: evaluation and management. In: *Handbook of Olfaction and Gustation* (*ed*. R. L. Doty), 2nd ed., pp. 935–957. Marcel Dekker.

Brosvic, G. M., Risser, J. M., Mackay-Sim, A., and Doty, R. L. 1996. Odor detection performance in hypothyroid and euthyroid rats. Physiol. Behav. 59, 117–121.

Buchsbaum, M. S., Kesslak, J. P., Lynch, G., Chui, H., Wu, J., Sicotte, N., *et al.* 1991. Temporal and hippocampal metabolic rate during an olfactory memory task assessed by positron emission tomography in patients with dementia of the Alzheimer type and controls. Preliminary studies. Arch. Gen. Psychiatry 48, 840–847.

Catalanotto, F. A., Dore-Duffy, P., Donaldson, J. O., Testa, M., Peterson, M., and Ostrom, K. M. 1984. Quality-specific taste changes in multiple sclerosis. Ann. Neurol. 16, 611–615.

Chang, C. Y. J. and Cass, S. P. 1999. Management of facial nerve injury due to temporal bone trauma. Amer. J. Otology. 20, 96–111.

Ciechanover, M., Peresecenschi, G., Aviram, A., and Steiner, J. E. 1980. Malrecognition of taste in uremia. Nephron 26, 20–22.

Constantinescu, C. S., Raps, E. C., Cohen, J. A., West, S. E., and Doty, R. L. 1994. Olfactory disturbances as the initial or most prominent symptom of multiple sclerosis. J. Neurol. Neurosurg. Psychiatry 57, 1011–1012.

Costanzo, R. M., DiNardo, L. J., and Zasler, N. D. 1995. Head injury and olfaction. In: *Handbook of Olfaction and Gustation* (*ed*. R. L. Doty), pp. 493–502. Marcel Dekker.

Cowart, B. J., Flynn-Rodden, K., McGeady, S. J., and Lowry, L. D. 1993. Hyposmia in allergic rhinitis. J. Allergy Clin. Immunol. 91, 747–751.

Daniels, C., Gottwald, B., Pause, B. M., Sojka, B., Mehdorn, H. M., and Ferstl, R. 2001. Olfactory event-related potentials in patients with brain tumors. Clin. Neurophysiol. 112, 1523–1530.

Deems, D. A., Doty, R. L., Settle, R. G., Moore-Gillon, V., Shaman, P., Mester, A. F., *et al.* 1991. Smell and taste disorders, a study of 750 patients from the University of Pennsylvania Smell and Taste Center. Arch. Otolaryngol. Head Neck Surg. 117, 519–528.

Deems, D. A., Yen, D. M., Kreshak, A., and Doty, R. L. 1996. Spontaneous resolution of dysgeusia. Arch. Otolaryngol. Head Neck Surg. 122, 961–963.

Del Tredici, K., Rub, U., De Vos, R. A., Bohl, J. R., and Braak, H. 2002. Where does Parkinson disease pathology begin in the brain? J. Neuropathol. Exp. Neurol. 61, 413–426.

Dhong, H. J., Chung, S. K., and Doty, R. L. 1999. Estrogen protects against 3-methylindole-induced olfactory loss. Brain Res. 824, 312–315.

Diamond, S., Freitag, F. G., Prager, J., and Gandi, S. 1985. Olfactory aura in migraine. N. Engl. J. Med. 312, 1390–1391.

DiTraglia, G. M., Press, D. S., Butters, N., Jernigan, T. L., Cermak, L. S., Velin, R. A., *et al.* 1991. Assessment of olfactory deficits in detoxified alcoholics. Alcohol 8, 109–115.

Dominguez, R. A. and Puig, A. 1997. Olfactory reference syndrome responds to clomipramine but not fluoxetine: a case report. J. Clin. Psychiatry 58, 497–498.

Doty, R. L. 2001. Olfaction. Annu. Rev. Psychol. 52, 423–452.

Doty, R. L. 2003. Odor perception in neurodegenerative diseases. In: *Handbook of Olfaction and Gustation* (*ed*. R. L. Doty), 2nd ed., pp. 479–502. Marcel Dekker.

Doty, R. L. and Bromley, S. M. 2004. Effects of drugs on olfaction and taste. Otolaryngol. Clin. North Am. 37, 1229–1254.

Doty, R. L. and Ferguson-Segall, M. 1989. Influence of adult castration on the olfactory sensitivity of the male rat: a signal detection analysis. Behav. Neurosci. 103, 691–694.

Doty, R. L. and Haxel, B. R. 2005. Objective assessment of terbinafine-induced taste loss. Laryngoscope 115, 2035–2037.

Doty, R. L. and Mishra, A. 2001. Olfaction and its alteration by nasal obstruction, rhinitis, and rhinosinusitis. Laryngoscope 111, 409–423.

Doty, R. L., Deems, D. A., and Stellar, S. 1988. Olfactory dysfunction in parkinsonism: a general deficit unrelated to

neurologic signs, disease stage, or disease duration. Neurology 38, 1237–1244.
Doty, R. L., Fernandez, A. D., Levine, M. A., Moses, A., and McKeown, D. A. 1997a. Olfactory dysfunction in type I pseudohypoparathyroidism: dissociation from Gs alpha protein deficiency. J. Clin. Endocrinol. Metab. 82, 247–250.
Doty, R. L., Li, C., Mannon, L. J., and Yousem, D. M. 1997b. Olfactory dysfunction in multiple sclerosis. N. Engl. J. Med. 336, 1918–1919.
Doty, R. L., Li, C., Mannon, L. J., and Yousem, D. M. 1999. Olfactory dysfunction in multiple sclerosis: relation to longitudinal changes in plaque numbers in central olfactory structures. Neurology 53, 880–882.
Doty, R. L., Philip, S., Reddy, K., and Kerr, K. L. 2003. Influences of antihypertensive and antihyperlipidemic drugs on the senses of taste and smell: a review. J. Hypertens. 21, 1805–1813.
Doty, R. L., Reyes, P. F., and Gregor, T. 1987. Presence of both odor identification and detection deficits in Alzheimer's disease. Brain Res. Bull. 18, 597–600.
Doty, R. L., Riklan, M., Deems, D. A., Reynolds, C., and Stellar, S. 1989. The olfactory and cognitive deficits of Parkinson's disease: evidence for independence. Ann. Neurol. 25, 166–171.
Doty, R. L., Shaman, P., and Dann, M. 1984b. Development of the University of Pennsylvania smell identification test: a standardized microencapsulated test of olfactory function. Physiol. Behav. 32, 489–502.
Doty, R. L., Shaman, P., Applebaum, S. L., Giberson, R., Siksorski, L., Rosenberg, *et al.* 1984a. Smell identification ability: changes with age. Science 226, 1441–1443.
Doty, R. L., Snyder, P. J., Huggins, G. R., and Lowry, L. D. 1981. Endocrine, cardiovascular, and psychological correlated of olfactory sensitivity changes during the human menstrual cycle. J. Comp. Physiol. Psychol. 95, 45–60.
Doty, R. L., Stern, M. B., Pfeiffer, C., Gollomp, S. M., and Hurtig, H. I. 1992. Bilateral olfactory dysfunction in early stage treated and untreated idiopathic Parkinson's disease. J. Neurol. Neurosurg. Psychiatry 55, 138–142.
Doty, R. L., Yousem, D. M., Pham, L. T., Kreshak, A. A., Geckle, R., and Lee, W. W. 1997c. Olfactory dysfunction in patients with head trauma. Arch. Neurol. 54, 1131–1140.
Downey, L. L., Jacobs, J. B., and Lebowitz, R. A. 1996. Anosmia and chronic sinus disease. Otolaryngol. Head Neck Surg 115, 24–28.
Elsberg, C. A. 1935a. XI. The value of quantitative olfactory tests for the localization of supratentorial tumors of the brain. A preliminary report. Bull. Neurol. Inst. NY 4, 511–522.
Elsberg, C. A. 1935b. XII. The localization of tumors of the frontal lobe of the brain by quantitative olfactory tests. Bull. Neurol. Inst. NY 4, 535–543.
Eskenazi, B., Cain, W. S., Novelly, R. A., and Mattson, R. 1986. Odor perception in temporal lobe epilepsy patients with and without temporal lobectomy. Neuropsychologia 24, 553–562.
Ezeh, P. I., Myers, L. J., Hanrahan, L. A., Kemppainen, R. J., and Cummins, K. A. 1992. Effects of steroids on the olfactory function of the dog. Physiol. Behav. 51, 1183–1187.
Faurion, A., Cerf, B., Le, B. D., and Pillias, A. M. 1998. fMRI study of taste cortical areas in humans. Ann. NY Acad. Sci. 855, 535–545.
Fedoroff, I. C., Stoner, S. A., Andersen, A. E., Doty, R. L., and Rolls, B. J. 1995. Olfactory dysfunction in anorexia and bulimia nervosa. Int. J. Eating Disord 18, 71–77.
Femiano, F., Scully, C., and Gombos, F. 2002. Idiopathic dysgeusia; an open trial of alpha lipoic acid (ALA) therapy. Int. J. Oral Maxillofac. Surg. 31, 625–628.
Feron, F., Perry, C., McGrath, J. J., and Mackay, S. 1998. New techniques for biopsy and culture of human olfactory epithelial neurons. Arch. Otolaryngol. Head Neck Surg. 124, 861–866.
Ferrante, M. A. 1999. Endogenous metabolic disorders. In: *Textbook of Clinical Neurology* (*eds*. C. G. Goetz and E. J. Pappert), pp. 731–767. W.B. Saunders Company.
Frank, M. E., Hettinger, T. P., and Clive, J. M. 1995. Current trends in measuring taste. In: *Handbook of Olfaction and Gustation* (*ed*. R. L. Doty), pp. 669–688. Marcel Dekker.
Funkutake, T., Kita, KI., Sakakibara, R., Takagi, K., Tokumaru, Y., Kojima, J., Hattari, T., and Hirayana, K. 1996. Late-onset hereditary ataxia with global thermoanalgesia and absence of fungiform papillae on the tongue in a Japanese family. Brain 119, 1011–1021.
Gadoth, N., Mass, E., Gordon, C. R., *et al.* 1997. Taste and smell in familial dysautonomia. Dev. Med. Child. Neurol. 39, 393–397.
Gansler, D. A., Fucetola, R., Krengel, M., Stetson, S., Zimering, R., and Makary, C. 1998. Are there cognitive subtypes in adult attention deficit/hyperactivity disorder? J. Nerv. Ment. Dis. 186, 776–781.
Ghorbanian, S. N., Paradise, J. L., and Doty, R. L. 1983. Odor perception in children in relation to nasal obstruction. Pediatrics 72, 510–516.
Giasson, B. I. and Mushynski, W. E. 1996. Aberrant stress-induced phosphorylation of perikaryal neurofilaments. J. Biol. Chem. 271, 30404–30409.
Giasson, B. I., Sampathu, D. M., Wilson, C. A., Vogelsberg-Ragaglia, V., Mushynski, W. E., and Lee, V. M. 2002. The environmental toxin arsenite induces tau hyperphosphorylation. Biochemistry 41, 15376–15387.
Gloor, P. 1997. *The Temporal Lobe and the Limbic System*. Oxford University Press.
Graff-Radford, N. R., Lin, S. C., Brazis, P. W., Bolling, J. P., Liesegang, T. J., Lucas, J. A., *et al.* 1997. Tropicamide eyedrops cannot be used for reliable diagnosis of Alzheimer's disease. [see comments]. Mayo Clin. Proc. 72, 495–504.
Graves, A. B., Bowen, J. D., Rajaram, L., McCormick, W. C., McCurry, S. M., Schellenberg, G. D., *et al.* 1999. Impaired olfaction as a marker for cognitive decline: interaction with apolipoprotein E epsilon4 status. Neurology 53, 1480–1487.
Griep, M. I., Van der, N. P., Sennesael, J. J., Mets, T. F., Massart, D. L., and Verbeelen, D. L. 1997. Odour perception in chronic renal disease. Nephrol. Dial. Transplant. 12, 2093–2098.
Gross-Isseroff, R., Ophir, D., Marshak, G., Ganchrow, J. R., Beizer, M., and Lancet, D. 1989. Olfactory function following late repair of choanal atresia. Laryngoscope 99, 1165–1166.
Grushka, M. and Sessle, B. J. 1991. Burning mouth syndrome. [Review] [101 refs]. Dent. Clin. North Am. 35, 171–184.
Hardy, S. L., Brennand, C. P., and Wyse, B. W. 1981. Taste thresholds of individuals with diabetes mellitus and of control subjects. J. Am. Diet. Assoc. 79, 286–289.
Harner, S. G. and Laws, E. R., Jr. 1981. Diagnosis of acoustic neurinoma. Neurosurgery 9, 373–379.
Hawkes, C. H., Shephard, B. C., Geddes, J. F., Body, G. D., and Martin, J. E. 1998. Olfactory disorder in motor neuron disease. Exp. Neurol. 150, 248–253.
Heckmann, S. M., Hujoel, P., Habiger, S., Friess, W., Wichmann, M., Heckmann, J. G., *et al.* 2005. Zinc gluconate in the treatment of dysgeusia – a randomized clinical trial. J. Dent. Res. 84, 35–38.
Henkin, R. I. 1967. Abnormalities of taste and olfaction in patients with chromatin negative gonadal dysgenesis. J. Clin. Endocrinol. Metab. 27, 1436–1440.
Henkin, R. I. 1975. The Role of Adrenal Corticosteroids in Sensory Processes. In: *Handbook of Physiology* (*eds*. H. Blaschko, A. D. Smith, and G. Sayers), pp. 209–230. American Physiological Society.
Henkin, R. I. and Bartter, F. C. 1966. Studies on olfactory thresholds in normal man and in patients with adrenal

cortical insufficiency: the role of adrenal cortical steroids and of serum sodium concentration. J. Clin. Invest. 45, 1631–1639.
Henkin, R. I. and Daly, R. L. 1968. Auditory detection and perception in normal man and in patients with adrenal cortical insufficiency: effect of adrenal cortical steroids. J. Clin. Invest. 47, 1269–1280.
Hirsch, A. R. 1992. Olfaction in migraineurs. Headache 32, 233–236.
Hoffman, H. J., Ishii, E. K., and Macturk, R. H. 1998. Age-related changes in the prevalence of smell/taste problems among the United States adult population. Results of the 1994 disability supplement to the National Health Interview Survey (NHIS). Ann. NY Acad. Sci. 855, 716–722.
Horiguchi, T., Uryu, K., Giasson, B. I., Ischiropoulos, H., LightFoot, R., Bellmann, C., *et al.* 2003. Nitration of tau protein is linked to neurodegeneration in tauopathies.[erratum appears in Am. J. Pathol. 2003 Dec; 163(6), 2645] . Am. J. Pathol. 163, 1021–1031.
Huisman, E., Uylings, H. B. M., and Hoogland, P. V. 2004. A 100% increase of 687 dopaminergie cells in the olfactory bulb may explain hyposmia in parkinson's disease. Mov. Disord. 19, 687–692.
Hummel, T., Pauli, E., Schuler, P., Kettenmann, B., Stefan, H., and Kobal, G. 1995. Chemosensory event-related potentials in patients with temporal lobe epilepsy. Epilepsia 36, 79–85.
Hummel, T., Risson, K., Muller, A., Reden, J., Weidenbecher, M., and Huttenbrink, K. B. 2005. ''Olfactory training'' in patients with olfactory loss. Presented at the Association for Chemoreception Sciences XXVII Annual Meeting. In Sarasota, Florida.
Iannaconne, A., Mykytyn, K., Persico, A. M., Searby, C. C., Baldi, A., Jablonski, M. M., *et al.* 2005. Clinical evidence of decreased olfaction in Bardet–Biedl syndrome caused by a deletion in the *BBS4* gene. Am. J. Med. Genet. 132A, 343–346.
Jackson, J. A., Jankovic, J., and Ford, J. 1983. Progressive supranuclear palsy: Clinical features and response to treatment in 16 patients. Ann. Neurol. 13, 273–278.
Jankovic, J. 1989. Parkinsonism-plus syndromes. Mov. Disord. 4, S95–S119.
Jung, T. M., TerKonda, R. P., Haines, S. J., Strome, S., and Marentette, L. J. 1997. Outcome analysis of the transglabellar/subcranial approach for lesions of the anterior cranial fossa: a comparison with the classic craniotomy approach. Otolaryngol. Head Neck Surg. 116, 642–646.
Kareken, D. A., Doty, R. L., Moberg, P. J., Mosnik, D., Chen, S. H., Farlow, M. R., *et al.* 2001. Olfactory-evoked regional cerebral blood flow in Alzheimer's disease. Neuropsychology 15, 18–29.
Kavaliers, M. 1989. Beta-funaltrexamine disrupts the day-night rhythm of nociception in mice. Brain Res. Bull. 22, 783–785.
Kern, R. C. 2000. Chronic sinusitis and anosmia: pathologic changes in the olfactory mucosa. Laryngoscope 110, 1071–1077.
Kern, R. C. and Mathog, R. H. 1991. Neoplasms of the nose and paranasal sinuses. In: *Smell and Taste in Health and Disease* (*eds*. T. V. Getchell, R. L. Doty, L. M. Bartoshuk, and J. B. Snow, Jr.), pp. 599–620. Raven Press.
Kida, A. 1974. Relations between the taste evoked potential and the background brain wave. J. Nihon Univ. Med. Assoc., 34, 43–52.
Kopala, L. C., Good, K. P., and Honer, W. G. 1994. Olfactory hallucinations and olfactory identification ability in patients with schizophrenia and other psychiatric disorders. Schizophr. Res. 12(3), 205–211.
Kopala, L. C., Good, K. P., Torrey, E. F., and Honer, W. G. 1998. Olfactory function in monozygotic twins discordant for schizophrenia. Am. J. Psychiatry 155, 134–136.
Lang, N. P., Catalanotto, F. A., Knopfli, R. U., and Antczak, A. A. A. 1988. Quality-specific taste impairment following the application of chlorhexidine digluconate mouth rinses. J. Clin. Periodontol. 15, 43–48.
Lee, S. H., Lim, H. H., Lee, H. M., Park, H. J., and Choi, J. O. 2000. Olfactory mucosal findings in patients with persistent anosmia after endoscopic sinus surgery. Ann. Otol. Rhinol. Laryngol. 109, 720–725.
Lewitt, M. S., Laing, D. G., Panhuber, H., Corbett, A., and Carter, J. N. 1989. Sensory perception and hypothyroidism. Chem. Senses 14, 537–546.
Li, C., Doty, R. L., Kennedy, D. W., and Yousem, D. M. 2003. Evaluation of olfactory deficits by structural medical imaging. In: *Handbook of Olfaction and Gustation* (*ed*. R. L. Doty), 2nd edn., pp. 593–613. Marcel Dekker.
Lygonis, C. S. 1969. Familial absence of olfaction. Heredity 61, 413–416.
Mair, R. G., Doty, R. L., Kelly, K. M., Wilson, C. S., Langlais, P. J., McEntee, W. J., *et al.* 1986. Multimodal sensory discrimination deficits in Korsakoff's psychosis. Neuropsychologia 24, 831–839.
Markopoulou, K., Larsen, K. W., Wszolek, E. K., Denson, M. A., Lang, A. E., Pfeiffer, R. F., *et al.* 1997. Olfactory dysfunction in familial parkinsonism. Neurology 49, 1262–1267.
Martinez, B. A., Cain, W. S., de Wijk, R. A., Spencer, D. D., Novelly, R. A., and Sass, K. J. 1993. Olfactory functioning before and after temporal lobe resection for intractable seizures. Neuropsychology 7, 351–363.
Mattes, R. D. 1995. Nutritional implications of taste and smell. In: *Handbook of Olfaction and Gustation* (*ed*. R. L. Doty), pp. 731–744. Marcel Dekker.
Mattes, R. D., Heller, A. D., and Rivlin, R. S. 1986. Abnormalities in suprathreshold taste function in early hypothyroidism in humans. In: *Clinical Measurement of Taste and Smell* (*eds*. H. L. Meiselman, and R. S. Rivlin), pp. 467–486. Macmillan Publishing Company.
McConnell, R. J., Menendez, C. E., Smith, F. R., Henkin, R. I., and Rivlin, R. S. 1975. Defects of taste and smell in patients with hypothyroidism. Am. J. Med. 59, 354–364.
Mesholam, R. I., Moberg, P. J., Mahr, R. N., and Doty, R. L. 1998. Olfaction in neurodegenerative disease: a meta-analysis of olfactory functioning in Alzheimer's and Parkinson's diseases. Arch. Neurol. 55, 84–90.
Miller, S. M. and Naylor, G. J. 1989. Unpleasant taste: A neglected symptom in depression. J. Affect. Disord. 17, 291–293.
Moberg, P. J., Agrin, R., Gur, R. E., Gur, R. C., Turetsky, B. I., and Doty, R. L. 1999. Olfactory dysfunction in schizophrenia: a qualitative and quantitative review. [Review] [90 refs]. Neuropsychopharmacology 21, 325–340.
Moberg, P. J., Doty, R. L., Turetsky, B. I., Arnold, S. E., Mahr, R. N., Gur, R. C., *et al.* 1997. Olfactory identification deficits in schizophrenia: correlation with duration of illness. Am. J. Psychiatry 154, 1016–1018.
Montgomery, E. B., Jr., Baker, K. B., Lyons, K., and Koller, W. C. 1999. Abnormal performance on the PD test battery by asymptomatic first-degree relatives. Neurology 52, 757–762.
Murakami, S., Mizobuchi, M., Nakashiro, Y., Doi, T., Hato, N., and Yanagihara, N. 1996. Bell palsy and herpes simplex virus: identification of viral DNA in endoneurial fluid and muscle [see comments]. Ann. Int. Med. 124, 27–30.
Netter, F. H. 1964. The Ciba Collection of Medial Illustrations, Vol. 1, Nervous System. Ciba Pharmaceutical Corporation. .
Ogawa, T. and Rutka, J. 1999. Olfactory dysfunction in head injured workers. Acta Otolaryngol. 540, 50–57.
Onoda, K. and Ikeda, M. 1999. Gustatory disturbance due to cerebrovascular disorder. Laryngoscope 109, 123–128.
Pantelis, C. and Brewer, W. J. 1995. Neuropsychological and olfactory dysfunction in schizophrenia: relationship of frontal

syndromes to syndromes of schizophrenia. Schizophr. Res. 17, 35–45.
Park, S. and Schoppe, S. 1997. Olfactory identification deficit in relation to schizotypy. Schizophr. Res. 26, 191–197.
Perros, P., MacFarlane, T. W., Counsell, C., and Frier, B. M. 1996. Altered taste sensation in newly-diagnosed NIDDM. Diabetes Care 19, 768–770.
Pittman, J. A. and Beschi, R. J. 1967. Taste thresholds in hyper- and hypothyroidism. J. Clin. Endocrinol. Metab. 27, 895–896.
Physicians' Desk Reference. 2005. (59th ed.) Montvale, N.J: Medical Economics Company, Inc.
Postolache, T. T., Doty, R. L., Wehr, T. A., Jimma, L. A., Han, L., Turner, E. H., *et al.* 1999. Monorhinal odor identification and depression scores in patients with seasonal affective disorder. J. Affect. Disord. 56, 27–35.
Postolache, T. T., Wehr, T. A., Doty, R. L., Sher, L., Turner, E. H., Bartko, J. J., *et al.* 2002. Patients with seasonal affective disorder have lower odor detection thresholds than control subjects. Arch. Gen. Psychiatry 59, 1119–1122.
Price, S. 1986. The role of zinc in taste and smell. In: *Clinical Measurement of Taste and Smell* (*eds*. H. L. Meiselman and R. S. Rivlin), pp. 443–445. MacMillan.
Pritchard, T. C., Macaluso, D. A., and Eslinger, P. J. 1999. Taste perception in patients with insular cortex lesions. Behav. Neurosci. 113, 663–671.
Pryse-Phillips, W. 1971. An olfactory reference syndrome. Acta Psychiatr. Scand. 47, 484–509.
Robinson, P. P., Loescher, A. R., and Smith, K. G. 2000. A prospective, quantitative study on the clinical outcome of lingual nerve repair. Br. J. Oral Maxillofac. Surg. 38, 255–263.
Rouquier, S., Blancher, A., and Giorgi, D. 2000. The olfactory receptor gene repertoire in primates and mouse: evidence for reduction of the functional fraction in primates. Proc. Natl Acad Sci. U.S.A. 97, 2870–2874.
Saino-Saito, S., Sasaki, H., Volpe, B. T., Kobayashi, K., Berlin, R., and Baker, H. 2004. Differentiation of the dopaminergic phenotype in the olfactory system of neonatal and adult mice 3. J. Comp. Neurol. 479, 389–398.
Sajjadian, A., Doty, R. L., Gutnick, D. N., Chirurgi, R. J., Sivak, M., and Perl, D. 1994. Olfactory dysfunction in amyotrophic lateral sclerosis. Neurodegeneration 3, 153–157.
Schiffman, S. S., Graham, B. G., Suggs, M. S., and Sattely-Miller, E. A. 1998. Effect of psychotropic drugs on taste responses in young and elderly persons. Ann. NY Acad. Sci. 855, 732–737.
Schiffman, S. S., Zervakis, J., Heffron, S., and Heald, A. E. 1999. Effect of protease inhibitors on the sense of taste. Nutrition 15, 767–772.
Scinska, A., Sienkiewicz-Jarosz, H., Kuran, W., Ryglewicz, D., Rogowski, A., Wrobel, E., *et al.* 2004. Depressive symptoms and taste reactivity in humans. Physiol. Behav. 82, 899–904.
Scrivani, S. J., Keith, D. A., Kulich, R., Mehta, N., and Maciewicz, R. J. 1998. Posttraumatic gustatory neuralgia: a clinical model of trigeminal neuropathic pain. J. Orofac. Pain 12, 287–292.
Settle, R. G. 1981. Suprathreshold glucose and fructose sensitivity in individuals with different family histories of non-insulin-dependent diabetes mellitus. Chem. Senses 6, 435–443.
Settle, R. G. 1991. The chemical senses in diabetes mellitus. In: *Smell and Taste in Health and Disease* (*eds*. T. V. Getchell, R. L. Doty, L. M. Bartoshuk, and J. B. Snow, Jr.), pp. 829–843. Raven Press.
Shear, P. K., Butters, N., Jernigan, T. L., DiTraglia, G. M., Irwin, M., Schuckit, M. A., *et al.* 1992. Olfactory loss in alcoholics: correlations with cortical and subcortical MRI indices. Alcohol 9, 247–255.
Siderowf, A., Newberg, A., Chou, K. L., Lloyd, M., Colcher, A., Hurtig, H. I., *et al.* 2005. [99mTc]TRODAT-1 SPECT imaging correlates with odor identification in early Parkinson disease. Neurology 64, 1716–1720.
Singh, N., Grewal, M. S., and Austin, J. H. 1970. Familial anosmia. Arch. Neurol. 22, 40–44.
Small, D. M., Jones-Gotman, M., Zatorre, R. J., Petrides, M., and Evans, A. C. 1997. A role for the right anterior temporal lobe in taste quality recognition. J. Neurosci. 17, 5136–5142.
Smith, D. V. and Shipley, M. T. 1992. Anatomy and physiology of taste and smell. J. Head Trauma Rehabil. 7, 1–14.
Snyder, R. D. and Drummond, P. D. 1997. Olfaction in migraine. [see comment]. Cephalalgia 17, 729–732.
Stern, M. B., Doty, R. L., Dotti, M., Corcoran, P., Crawford, D., McKeown, D. A., *et al.* 1994. Olfactory function in Parkinson's disease subtypes. Neurology 44, 266–268.
Tabert, M. H., Liu, X., Doty, R. L., Serby, M., Zamora, D., Pelton, G. H., *et al.* 2005. A 10-item smell identification scale related to risk for Alzheimer's disease. Ann. Neurol. 58, 155–160.
Thal, D. R., Del, T. K., and Braak, H. 2004. Neurodegeneration in normal brain aging and disease 15. Sci. Aging Knowledge Environ. e26.
Tonoike, M., Yamaguchi, M., Kaetsu, I., Kida, H., Seo, R., and Koizuka, I. 1998. Ipsilateral dominance of human olfactory activated centers estimated from event-related magnetic fields measured by 122-channel whole-head neuromagnetometer using odorant stimuli synchronized with respirations. Ann. NY Acad. Sci. 855, 579–590.
Turetsky, B. I., Moberg, P. J., Arnold, S. E., Doty, R. L., and Gur, R. E. 2003. Low olfactory bulb volume in first-degree relatives of patients with schizophrenia. Am. J. Psychiatry 160, 703–708.
Uchiyama, T., Fukutake, T., Arai, K., *et al.* 2001. Machado-Joseph disease associated with an absence of fungiform papillae on the tongue. Neurology 56, 558–560.
Weinstock, R. S., Wright, H. N., and Smith, D. U. 1993. Olfactory dysfunction in diabetes mellitus. Physiol. Behav. 53, 17–21.
Weinstock, R. S., Wright, H. N., Spiegel, A. M., Levine, M. A., and Moses, A. M. 1986. Olfactory dysfunction in humans with deficient guanine nucleotide-binding protein. Nature 322, 635–636.
West, S. E. and Doty, R. L. 1995. Influence of epilepsy and temporal lobe resection on olfactory function. Epilepsia 36, 531–542.
Wilson, D. A., Sullivan, R. M., and Leon, M. 1985. Odor familiarity alters mitral cell response in the olfactory bulb of neonatal rats. Brain Res. 354, 314–317.
Yamagishi, M., Fujiwara, M., and Nakamura, H. 1994. Olfactory mucosal findings and clinical course in patients with olfactory disorders following upper respiratory viral infection. Rhinology 32, 113–118.
Yanagisawa, K., Bartoshuk, L. M., Catalanotto, F. A., Karrer, T. A., and Kveton, J. F. 1998. Anesthesia of the chorda tympani nerve and taste phantoms. Physiol. Behav. 63, 329–335.
Yasuno, H., Fukazawa, K., Fukuoka, T., Kondo, E., Sakagami, M., and Noguchi, K. 2000. Nerve growth factor applied onto the olfactory epithelium alleviates degenerative changes of the olfactory receptor neurons following axotomy. Brain Res. 887, 53–62.
Yousem, D. M., Geckle, R. J., Bilker, W., McKeown, D. A., and Doty, R. L. 1996. MR evaluation of patients with congenital hyposmia or anosmia. AJR 166, 439–443.
Yousem, D. M., Turner, W. J., Li, C., Snyder, P. J., and Doty, R. L. 1993. Kallmann syndrome: MR evaluation of olfactory system. [see comments]. AJNR Am. J. Neuroradiol. 14, 839–843.
Zorzon, M., Ukmar, M., Bragadin, L. M., Zanier, F., Antonello, R. M., Cazzato, G., *et al.* 2000. Olfactory dysfunction and extent of white matter abnormalities in multiple sclerosis: a clinical and MR study. Mult. Scler. 6, 386–390.

5.01 The Adequate Stimulus

R D Treede, Johannes Gutenberg-University, Mainz, Germany

© 2008 Elsevier Inc. All rights reserved.

5.01.1	Noxious Stimulus	1
5.01.2	Nociceptive Stimulus	3
References		3

Glossary

nociception The processes of encoding and processing of noxious stimuli by the nervous system.

nociceptive stimulus An actually or potentially tissue damaging event that is encoded by primary nociceptive afferents. Although actual or potential tissue damage is the common denominator of those stimuli that may cause pain, there are some types of tissue damage that are not detected by any afferents, and thus do not cause pain. Therefore, not all noxious stimuli are adequate stimuli of nociceptive afferents. The adequate stimuli of nociceptors are termed nociceptive stimuli, which is a subset of noxious stimuli.

nociceptor A primary afferent nerve fiber that is capable of encoding noxious stimuli. All non-nociceptive afferents (e.g., tactile receptors, warm receptors) do respond to noxious stimuli (mechanical or thermal, respectively), because these stimuli are way above their respective thresholds. But only nociceptors are capable of encoding the relevant properties of those stimuli (e.g., sharpness, heat intensity in the painful range).

noxious stimulus An actual or potential tissue damaging event. This was found to be the common denominator of those stimuli that may cause pain. But there are some types of tissue damage that are not detected by any afferents, and thus do not cause pain. See nociceptive stimulus.

The term adequate stimulus (Kandel, E. R. *et al*., 2000) is used in sensory physiology to describe the class of environmental phenomena that requires the least amount of energy in order to elicit a percept mediated by a particular sensory system, for example, a visual percept can be elicited by a punch to the eye, but light from a television screen needs much less energy for this purpose. The implication from such observations in subjective sensory physiology is that the receptive organs of each sensory system are specialized to detect a corresponding class of environmental phenomena (i.e., photoreceptors in the eye are specialized to detect photons).

It was difficult to transfer this concept to the perception of pain and to the nociceptive system. Many different stimuli may cause pain (e.g., pin prick, burn injury, freeze injury, and inflammation), none of which needs particularly low amounts of energy. Sherrington is credited with identifying the common denominator of those stimuli as being tissue damage (in Greek: νοξη Noxe) or environmental phenomena that threaten to cause such damage. Hence, the adequate stimulus to elicit pain is traditionally called a noxious stimulus. It may be defined as follows.

5.01.1 Noxious Stimulus

A noxious stimulus is an actual or potential tissue damaging event. Noxious stimuli may belong to thermal, mechanical, or chemical modalities of energy supply. Therefore, the sensory organs of the nociceptive system, free nerve endings of thinly myelinated Aδ fibers, and unmyelinated C fibers in the skin and most other tissues, have a characteristic property: most of them are polymodal, that is, they respond to more than one modality of stimulus energy. Some nociceptive nerve endings, particularly those of Aδ fibers, are specialized to be most sensitive to one particular stimulus modality (e.g., either heat or pin prick). The differential

sensitivity spectra of nociceptive afferents suggest that pain quality may be encoded by a similar population code in the nociceptive system as taste quality in the gustatory system (Treede, R. D. *et al.*, 1998).

Polymodality is not the result of a primitive nonspecific responsivity to tissue damage. Instead, it is mediated by specialized signal transduction pathways, some of which have been elucidated at the molecular level (Julius, D. and Basbaum, A. I., 2001). One member of the gene family of transient receptor potential channels (TRPV1), for example, is specifically activated by moderate heat stimuli, low tissue pH, and a class of irritant substances called vanilloids. For most inflammatory mediators, specific receptor molecules are present in the membranes of nociceptive nerve endings.

The topic of this volume of the *Handbook of the Senses* is pain. The taxonomy of the International Association for the Study of Pain (IASP) defines pain as, "An unpleasant sensory and emotional experience associated with actual or potential tissue damage, or described in terms of such damage" (Merskey, H. *et al.*, 1979). This definition implicitly refers to the adequate stimulus as identified by Sherrington, in its extended form including potential tissue damage rather than calling for outright tissue damage. There are two good reasons for this extension. First, a system that only responds after tissue damage has occurred, cannot subserve a warning function for the organism. The sensory system that mediates pain sensation (the nociceptive system), however, provides even primitive organisms with an array of protective reflexes that can flexibly respond to threatening environmental challenges. Such a system needs to be sensitive enough to signal impending tissue damage before it occurs. Second, although primary nociceptive afferents, the sensory organs of the nociceptive system, encode different intensities of manifest tissue damage as graded action potential discharge rates (Raja, S. N. *et al.*, 1999), the nociceptor activation thresholds were found to be clearly lower than the intensity needed to damage the skin. In humans as well as many animal species, heating the skin to above 40 °C, cooling to below 30 °C, or punctate pressure around 1–5 bars activates nociceptors, but none of these stimuli damages the skin. In fact, for most people these stimuli are not even painful.

The relatively low peripheral nociceptor activation thresholds allow the nociceptive system to subserve its warning function in a highly flexible and plastic way. The peripheral input can be shut down by descending inhibition, if there is an *a priori* reason to ignore the warning signal. The system can also enhance its response to the warning signal by enhancing the efficacy of its central synapses. This process is called central sensitization and may be considered to be one of the phylogenetically oldest mechanisms of learning and memory (Woolf, C. J. and Walters, E. T., 1991). Primary nociceptive afferents may also enhance their responsiveness to their adequate stimuli, a process called peripheral sensitization (Raja, S. N. *et al.*, 1999). Both peripheral and central sensitization contribute to the warning function of the nociceptive system.

As a warning system, the nociceptive system has gaps in its sensitivity: there are some types of tissue damage that are not detected by any afferents, and thus do not cause pain or any protective behavior. This is a well-known phenomenon in internal organs such as the liver or the brain, where a malignant tumor may cause extensive damage without being noticed by the patient. There is an even more common phenomenon of tissue damage that goes unnoticed by the nociceptive system: damage by ultraviolet radiation (Figure 1). The pain of sunburn always comes too late, after the skin has

Figure 1 The concept of the adequate stimulus to activate the nociceptive system and to elicit pain can be illustrated by this scene. Ultraviolet radiation causes tissue damage, but this noxious stimulus is not detected by the nociceptive nerve endings. Only the inflammatory response of the skin leads to adequate activation of nociceptive nerve endings via chemical mediators, which serve as nociceptive stimuli.

already been damaged. This pain does not signal the initial damage but the body's response by an inflammatory reaction. The ensuing peripheral and central sensitization of the nociceptive system lead to pronounced hyperalgesia of the injured skin to heat and mechanical stimuli, which then serves to protect the skin from further damage. These observations have led to the introduction of a new term, nociceptive stimulus (Cervero, F. and Merskey, H., 1996).

5.01.2 Nociceptive Stimulus

A nociceptive stimulus is an actual or potential tissue damaging event that is encoded by primary nociceptive afferents. In summary, the adequate stimulus to activate the receptive organs of the nociceptive system consists of either actual or potential tissue damage (noxious stimulus). However, not all noxious stimuli are detected by the nociceptive system. Therefore, the adequate stimulus for this system in the strict sense is that subset of noxious stimuli that can be encoded by the nociceptive system (nociceptive stimuli). It is not unusual for a sensory system to encode only a part of the range of environmental phenomena that its receptive organs are specialized for: visual stimuli consist of a restricted range of wavelengths of electromagnetic waves, and auditory stimuli consist of a restricted frequency range of pressure waves in the air. Likewise, nociceptive stimuli consist of a restricted range of actually or potentially tissue-damaging events. Linguistically, the term nociceptive stimulus may appear to be a little odd, as it also implies reception rather than just stimulation, but for exactly that reason it fits well into the broader system of terms in sensory physiology.

According to the concept of the adequate stimulus, nociceptive stimuli are encoded by the nociceptive system, just as visual stimuli are encoded by the visual system and auditory stimuli are encoded by the auditory system. However, a full appreciation of our senses goes beyond these aspects of sensory physiology (Bieri, P., 1995; Metzinger, T., 2000): seeing comprises more than vision, hearing comprises more than audition, and pain comprises more than nociception. This is reflected in the definition of pain as given above that does not relate to any objective observable measure, but refers to the subjective experience of the person in pain.

References

Bieri, P. 1995. Pain a Case Study for the Mind–Body Problem. In: Pain and the Brain: From Nociception to Cognition (*eds*. B. Bromm and J. E. Desmedt), pp. 99–110. Raven Press.

Cervero, F. and Merskey, H. 1996. What is a noxious stimulus? Pain Forum 5, 157–161.

Julius, D. and Basbaum, A. I. 2001. Molecular mechanisms of nociception. Nature 413, 203–210.

Kandel, E. R, Schwartz, J. H, and Jessell, T. M 2000. Principles of Neural Science. 4th edn., p. 414. McGraw-Hill.

Merskey, H., Albe-Fessard, D., Bonica, J. J., Carmon, A., Dubner, R., Kerr, F. W. L., Lindblom, U., Mumford, J. M., Nathan, P. W., Noordenbos, W., Pagni, C. A., Renaer, M. J., Sternbach, R. A., and Sunderland, S. 1979. Pain terms: a list with definitions and notes on usage. Recommended by the IASP subcommittee on taxonomy. Pain 6, 249–252.

Metzinger, T. 2000. The Subjectivity of Subjective Experience: A Representationalist Analysis of the First-Person Perspective. In: Neural Correlates of Consciousness: Empirical and Conceptual Questions (*ed*. T. Metzinger), pp. 285–306. MIT Press.

Raja, S. N., Meyer, R. A., Ringkamp, M., and Campbell, J. N. 1999. Peripheral Neural Mechanisms of Nociception. In: Textbook of Pain (*eds*. P. D. Wall and R. Melzack), 4th edn, pp. 11–57. Churchill Livingstone.

Treede, R. D., Meyer, R. A., and Campbell, J. N. 1998. Myelinated mechanically insensitive afferents from monkey hairy skin: heat response properties. J. Neurophysiol. 80, 1082–1093.

Woolf, C. J. and Walters, E. T. 1991. Common patterns of plasticity contributing to nociceptive sensitization in mammals and aplysia. Trends Neurosci. 14, 74–78.

5.02 Pain Theories

F Cervero, McGill University, Montreal, QC, Canada

© 2008 Elsevier Inc. All rights reserved.

References 9

From the beginning of scientific enquiry there have been two opposing views on the biological meaning of pain. One view proposes that pain is a sense similar to vision or hearing, a component of the sensory repertoire of most animals that warns us of impending damage, gives accurate information to the brain about injuries, and helps us to heal. The inclusion of pain in *The Senses: A Comprehensive Reference,* alongside vision, hearing, or olfaction shows that this view is persuasive. But there has always been an alternative interpretation of pain that denies it being a sense like vision or hearing and attaches to both pain and its opposite pleasure fundamental roles in shaping the emotions and behaviors of the individual. Pain is seen as a trigger of emotional states, a behavioral drive, and a highly effective learning tool. Aristotle, who was the originator of this view, made it very clear: there are only five senses – vision, hearing, touch, taste, and smell. Pain and pleasure are not senses but passions of the soul.

Whether or not pain is a sense like the others is not just an academic exercise. The experimental paradigms used to study the nervous system can be fundamentally different depending on the theoretical approach to the object of the study. If pain is regarded as a sense, like vision or hearing, then we will look for sensors that are activated selectively by painful stimuli and for sensory pathways in the brain and spinal cord that carry pain information much in the same way as we identify photoreceptors in the retina and a visual pathway to the cortex. This approach has generated an interpretation of pain mechanisms known as the specificity theory, which maintains that there are elements of the peripheral and central nervous system (CNS) specifically and exclusively dedicated to the processing of pain-related information.

However, if pain is not a sense like vision or hearing, then we do not need to look for a specific neural machinery for its processing but for patterns of activation, spatial or temporal, in neurons that do not necessarily have time-locked responses to painful stimuli. If pain is a passion of the soul then we need distributed networks and interactive parallel processing and not a pain pathway. This view has been articulated throughout the last 100 years as the pattern theory of pain, denying the existence of dedicated sensory elements for pain processing and attributing the perception of pain to interactions between patterns of impulses in nonspecific neuronal networks. The influential gate theory of pain (Melzack, R. and Wall, P. D., 1965) is the best contemporary example of such an interpretation.

The specificity theory of pain was a natural development of the Doctrine of Specific Nerve Energies put forward by the German physiologist Johannes Müller in the nineteenth century. The basic proposal of Müller's doctrine is that each sensory modality is the result of the activation of a specific neural system in the brain. If we are able to perceive touch it is because we have a subset of cells in our peripheral and CNS that respond to touch; if an animal can perceive infrared light or an electromagnetic field then it must have a subset of neurons capable of sensing and processing these stimuli. As he put it: "Sensation is not the conduction of a quality or state of external bodies to consciousness, but the conduction of a quality or state of our nerves to consciousness, excited by an external cause" (Müller, J., 1835–1840). At the end of the nineteenth century, von Frey M. (1895) extended Müller's doctrine to pain sensation, thus reinforcing a strict sensory interpretation of pain. He proposed that the fine nerve endings of unmyelinated afferents were the pain receptors in the periphery and that there was a specific pain pathway taking their signals to the brain. This influential proposal is responsible for the well-known model of pain mechanisms often found in textbooks whereby a pain receptor in the periphery is activated by a noxious stimulus and sends impulses to the spinal cord and from there to the thalamus and cortex via a crossed spinothalamic

pathway. In other words, a relatively simple and straight forward pain pathway (Figure 1(a)).

In contrast, the pattern theory of pain represents a development of the Aristotelian concept of pain as a passion of the soul and was articulated in modern form by Goldscheider A. (1898) at the turn of the nineteenth century. The basic proposal is that pain is the result of intense stimulation of peripheral receptors, regardless of modality and tissue origin. For the pattern theory the neural substrate of pain perception consists of sequences of impulses in peripheral and central neurons that lead to pain sensations when certain spatial and temporal patterns of activity are produced. The emphasis of this interpretation is on patterns of neural activity evoked in the brain by a painful stimulus. In the 1960s, the gate theory of pain proposed a specific neural mechanism located at the first afferent relay in the spinal cord to illustrate how patterns of impulses in sensory receptors could lead to the modulation of pain sensation (Figure 1(b)). The gate theory emphasized the dynamic and plastic components of pain sensations and drew attention to pain modulation as opposed to an interpretation of pain exclusively as an alarm system. It also focused the attention of many researches on the clinical aspects of pain, away from physiological pain, which contributed a surge of studies on the effects of neuropathic lesions and on the development of animal models of inflammatory and pathological pain (see Cervero, F., 2005 for a recent discussion on the gate theory).

The considerable amount of new information about pain mechanisms gathered in the last 40 years has relegated the specificity versus pattern argument to a secondary role. It is now well established that there are specialized sensors in the skin, muscles, and viscera of most animals that are activated exclusively by stimuli that cause injury and whose excitation leads to the sensation of pain (Belmonte, C. and Cervero, F., 1996). It is also known that pain cannot be evoked, under normal circumstances, by changing the patterns of activation of tactile sensory receptors (Ochoa, J. and Torebjork, E., 1983; 1989). There are also substantial data showing that there are neurons in the spinal cord and brain driven mainly or exclusively by nociceptive stimuli (Hunt, S. P. and Mantyh, P. W., 2001). However, there is also significant experimental evidence in favor of plasticity in the nociceptive sensory channel and of the existence of dynamic processes that can alter profoundly the functional properties of peripheral nociceptors and of nociceptive central neurons (Treede, R. D. *et al.*, 1992; Hunt, S. P. and Mantyh, P. W., 2001; Julius, D. and Basbaum, A. I., 2001). It has also been demonstrated that following a peripheral injury or inflammation, the activation of tactile afferents from uninjured skin can evoke pain sensations (see Cervero,

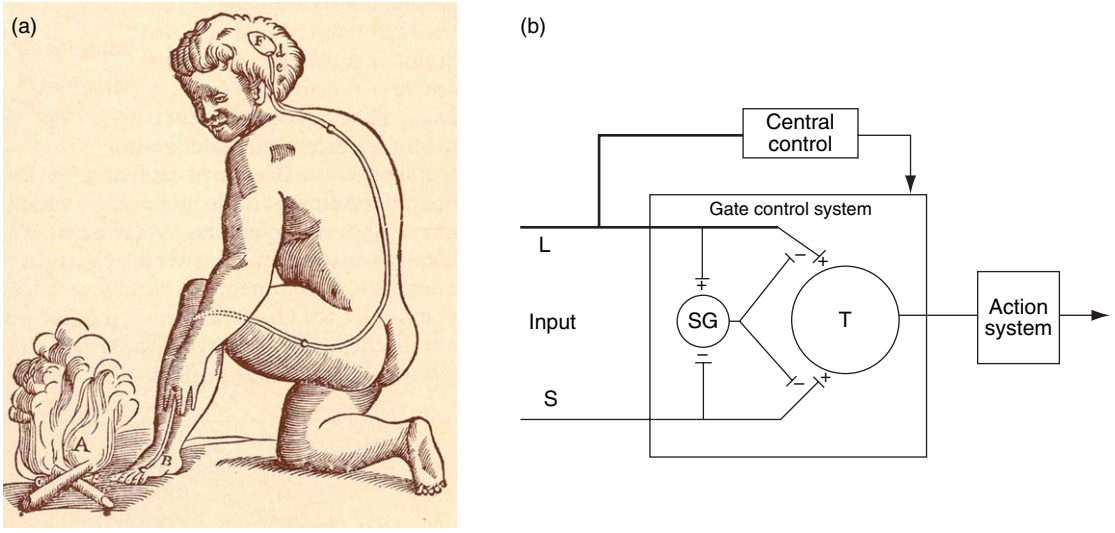

Figure 1 (a) Descartes' drawing of a pathway-oriented pain mechanism. The fire activates pain nerves in the foot of the child and these signals are transmitted to the brain where they are reflected into motor nerves that draw the foot away from the fire. (b) Schematic diagram of the gate theory of pain mechanisms. The diagram shows the presynaptic interaction model between large (L) and small (S) afferent fibers and the key role of substantia gelatinosa (SG) neurons controlling the activity of transmission (T) cells. (a) From Descartes, R. 1664. L'homme. Chez Jacques Le Gras. (b) Reprinted with permission from AAAS from Melzack, R. and Wall, P.D. 1965. Pain mechanisms: a new theory. Science 150, 971–979.

F. and Laird, J. M. A., 1996). Clearly, a point has been reached where neither a strict specificity nor a pattern interpretation can account for all that it is known about pain mechanisms.

We now realize that there are many different forms of pain (acute, traumatic, inflammatory, and neuropathic) and that pain is a dynamic process that cannot be explained with a single theory or a unique mechanism. One of the most striking expressions of the dynamic nature of pain sensation is its lack of adaptation. A continuous and uniform visual or auditory stimulus leads to sensory adaptation; we simply stop feeling this stimulus after a few seconds or minutes. However, the sensation of pain not only does not adapt to a continuous noxious stimulus but gets progressively worse so that, after a few minutes of persistent stimulation with a relatively mild painful stimulus, the sensation becomes unbearable. This change in pain sensitivity generates a state of pain amplification or hyperalgesia that is normally triggered and maintained by a persistent noxious stimulus but that can, under pathological circumstances, appear without an obvious cause so that the normal relationship between injury and pain is lost. Hyperalgesia and allodynia are the main symptoms of many chronic pain states and is the property of pain sensation that makes it particularly unpleasant and often unbearable.

In psychophysical terms a hyperalgesic state is represented by a leftward shift that occurs, following a peripheral injury, in the curve that relates stimulus intensity to pain sensation (Cervero, F. and Laird, J. M. A., 1996) (Figure 2). This shift causes the lower portion of the pain curve to fall in the innocuous stimulus intensity range (allodynia or pain produced by an innocuous stimulus) whereas the top portion shows an increased pain sensation to noxious stimuli (hyperalgesia proper or increased pain sensitivity to a noxious stimulus). Allodynia and hyperalgesia provide protective mechanisms to the organism, preventing the individual from stimulating an injured area and in so doing helping the healing process.

There are two forms of hyperalgesia: primary and secondary. Primary hyperalgesia is an increased pain sensitivity that occurs at the site of injury and it is the consequence of nociceptor sensitization, that is, the increased firing of peripheral nociceptors at the site of injury whose excitability has been increased by a number of locally released sensitizing agents. These sensitized nociceptors send enhanced afferent discharges to the CNS thus evoking increased pain from the primary hyperalgesic area and contributing

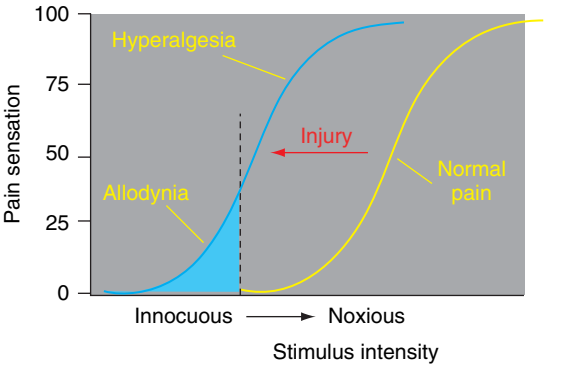

Figure 2 Diagram illustrating the changes in pain sensation induced by injury. The normal relationship between stimulus intensity and the magnitude of pain sensation is represented by the curve at the right-hand side of the figure. Pain sensation is only evoked by stimulus intensities in the noxious range (the vertical dotted line indicates the pain threshold). Injury provokes a leftward shift in the curve relating stimulus intensity to pain sensation. Under these conditions, innocuous stimuli evoke pain (allodynia). Reproduced From Cervero, F. and Laird, J. M. A. 1996. Mechanisms of touch-evoked pain (allodynia): a new model. Pain 68, 13–23, used with permission.

to the alterations in central processing that are, in turn, responsible for secondary hyperalgesia (Treede, R. D. *et al.*, 1992).

Secondary hyperalgesia is defined as an increased sensitivity to pain occurring in areas adjacent or even remote to the site of injury. For instance, following an injury to the hand an area of hyperalgesia may develop covering the entire arm or an inflammation of the gastrointestinal tract or the bladder may produce an area of hyperalgesia in the abdominal or pelvic regions. Secondary hyperalgesia is the result of an alteration in the processing by the CNS of impulses from low-threshold mechanoreceptors, such that, these impulses are able to activate nociceptive neurons and evoke pain. This central alteration is initially triggered and later maintained by the enhanced afferent discharges from the primary hyperalgesic area (Treede, R. D. *et al.*, 1992).

Different forms of pain are mediated by different mechanisms which participate in various ways in the generation of pain and hyperalgesia (Cervero, F. and Laird, J. M. A., 1991; Klein, T. *et al.*, 2005). Generally speaking we can identify three different forms of pain taking into account the relationship between noxious stimulus and pain sensation: nociceptive, inflammatory, and neuropathic (also called phase 1, 2, and 3 pains by Cervero, F. and Laird, J. M. A., 1991) (Figure 3). Nociceptive pain refers to the processing

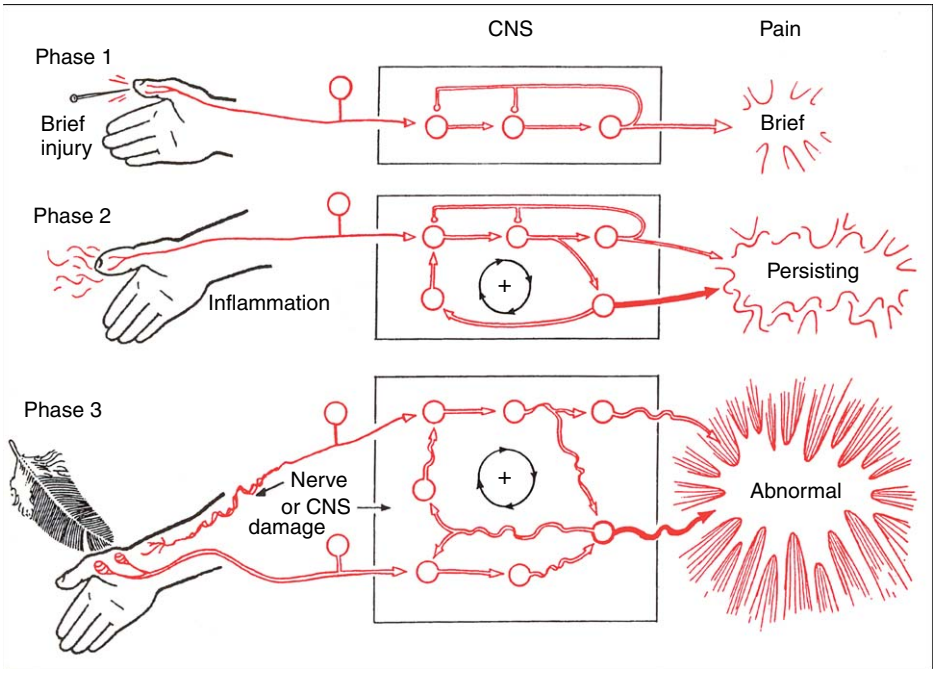

Figure 3 Diagram showing the three models of pain processing for the three main types of pain (nociceptive, inflammatory, and neuropathic or phases 1, 2, and 3). See text for further explanation. Reproduced from Cervero, F. and Laird, J. M. A. 1991 One pain or many pains? A new look at pain mechanisms. News Physiol. Sci. 6, 268–273, used with permission.

of brief noxious stimuli; inflammatory pain is the consequence of prolonged noxious stimulation leading to tissue damage; and neuropathic pain is the consequence of neurological damage, including peripheral neuropathies and central pain states.

Nociceptive pain is a protective sensation needed for the survival and well-being of the individual. The mechanisms subserving the processing of brief noxious stimuli can be viewed as a fairly simple pathway that carries impulses in peripheral nociceptors centrally toward the thalamus and cortex and leads to brief pain perception. In contrast, injury and tissue damage evoke an inflammatory reaction as part of the healing process and generate a pain state different from nociceptive pain as the response properties of the various components of the nociceptive system change. These changes include nociceptor sensitization and recruitment of populations of previously unresponsive receptors. In turn, CNS neurons show an amplification of their excitability expressed as increases in receptive field size and greater spontaneous and evoked firing. All of these changes indicate that the CNS has moved to a new, more excitable state as a result of the noxious input generated by tissue injury and inflammation. Under these conditions, an immediate correlation between discharges in peripheral nociceptors and pain perception is lost.

Neuropathic pain syndromes are the consequence of damage to peripheral nerves or to the CNS itself and produce pain sensations well outside the range of the sensations produced by the normal nociceptive system, even after serious peripheral injury or inflammation. These include spontaneous pain, greatly reduced pain thresholds, and mechanical allodynia. Neuropathic pain states are characterized by an almost complete lack of correlation between peripheral noxious stimuli and pain sensation and are produced by neurological lesions that cause abnormal impulse activity generated in nerve sprouts, neuromas, or in dorsal root ganglion cells, ephaptic coupling between adjacent nerve fibers and abnormal responses of peripheral nociceptors and CNS neurons. Nociceptive and inflammatory pains are symptoms of peripheral injury, whereas neuropathic pain is a symptom of neurological disease.

Whereas the specificity theory can explain fairly well the simpler forms of pain, such as a pin prick or the acute pain of a minor burn, complex pain experiences, including hyperalgesic states require substantial peripheral and central plasticity such that low-intensity stimuli evoke pain (i.e., secondary

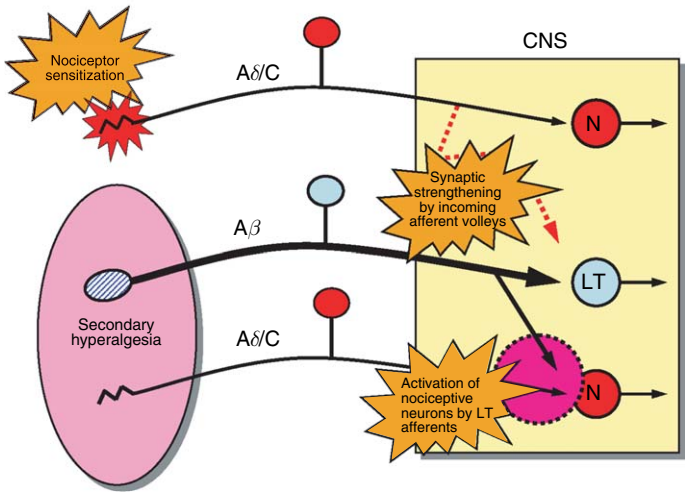

Figure 4 Diagram representing the basic mechanisms of primary and secondary hyperalgesia and the three key processes implicated in their generation. Primary hyperalgesia is produced by the stimulation of nociceptors connected to Aδ- and C-afferent fibers which activate nociceptive CNS pathways (N). Secondary hyperalgesia is produced by stimulation of tactile receptors connected to Aβ-afferents which normally activate low-threshold (LT) pathways but that as a consequence of the amplification of the nociceptive input from the injured area can now access nociceptive neurons (N). See text for further explanation.

hyperalgesia or touch-evoked allodynia). It is very likely that both specific and nonspecific nociceptive systems participate in the generation and maintenance of different pain states.

We can currently identify three key processes in the neurobiological approach to the mechanisms of pain and hyperalgesia: (1) the process of nociceptor activation and sensitization, responsible for the initial signaling of injury and the peripheral changes in the nociceptive system induced by a noxious stimulus; (2) the process of central amplification of nociceptive signals, known as central sensitization, generated by synaptic strengthening of connections between CNS neurons and responsible for the enhanced excitability that accompanies persistent pain states; and (3) the process whereby activity in low-threshold sensory receptors from undamaged peripheral areas can access the nociceptive system and evoke pain sensations and hyperalgesic states (e.g., touch-evoked pain, tactile allodynia) (Figure 4).

The analysis of these three processes supersedes interpretations of pain based on a specificity or pattern approach as all three contain elements that require the existence of groups of neurons dedicated to the processing of nociceptive signals as well as the expression of functional changes induced by afferent activity. Several of these changes can lead to major alterations of pain sensitivity through quite separate mechanisms. For instance, touch-evoked pain can be the result of sensitization of peripheral nociceptors leading to decreases in their activation threshold or be mediated by a purely central mechanism whereby low-threshold mechanoreceptors access nociceptive neurons. The emphasis has moved from theoretical interpretations based on a specific pain channel or on patterns of impulses to the in depth analysis of the functional processes that may cause the different pain and hyperalgesic states. Neither the specificity nor the pattern theories have been able to provide workable models for all forms of pain sensation. They still offer a useful theoretical framework for some of our observations but the weight of work has shifted to studying those processes that will help the development of effective pain relief therapies.

References

Belmonte, C. and Cervero, F. 1996. Neurobiology of Nociceptors. Oxford University Press.

Cervero, F. 2005. The Gate Theory Then and Now. In: The Paths of Pain (*eds*. H. Mershey, J. De Loeser, and R. Dubner), pp. 33–48. IASP Press.

Cervero, F. and Laird, J. M. A. 1991. One pain or many pains? A new look at pain mechanisms. News Physiol. Sci. 6, 268–273.

Cervero, F. and Laird, J. M. A. 1996. Mechanisms of touch-evoked pain (allodynia): a new model. Pain 68, 13–23.

Descartes, R. 1664. L'homme. Chez Jacques Le Gras.

Goldschaider, A. 1898. Über den Schmerz: Gesammelte Abhandlungen. Ambros.

Hunt, S. P. and Mantyh, P. W. 2001. The molecular dynamics of pain control. Nature Rev. Neurosci. 2, 83–91.
Julius, D. and Basbaum, A. I. 2001. Molecular mechanisms of nociception. Nature 413, 203–210.
Klein, T., Magerl, W., Rolke, R., and Treede, R. D. 2005. Human surrogate models of neuropathic pain. Pain 115, 227–233.
Melzack, R. and Wall, P. D. 1965. Pain mechanisms: a new theory. Science 150, 971–979.
Müller, J. 1835–1840. Handbuch der Physiologie des Menschen für Vorlesungen. J. Hölscher.
Ochoa, J. and Torebjork, E. 1983. Sensations evoked by intraneural microstimulation of single mechanoreceptor units innervating the human hand. J. Physiol. 342, 633–654.
Ochoa, J. and Torebjork, E. 1989. Sensations evoked by intraneural microstimulation of C nociceptor fibres in human skin nerves. J. Physiol. 415, 583–599.
Treede, R. D., Meyer, R. A., Raja, S. N., and Campbell, J. N. 1992. Peripheral and central mechanisms of cutaneous hyperalgesia. Prog. Neurobiol. 38, 397–421.
von Frey, M. 1895. Beitrage zur sinnesphysiologie der haut. Ber. Sachs. Ges. Wiss. 47, 166–184.

5.03 Anatomy of Nociceptors

S Mense, Institut für Anatomie und Zellbiologie, Universität Heidelberg, Heidelberg, Germany

© 2008 Elsevier Inc. All rights reserved.

5.03.1	**Introduction**	12
5.03.2	**General Morphological Features of Nociceptors**	14
5.03.2.1	Light Microscopic Structure	14
5.03.2.2	Ultrastructure	15
5.03.3	**Nociceptors in Various Tissues**	17
5.03.3.1	Skin	17
5.03.3.1.1	Light microscopy	18
5.03.3.1.2	Electron microscopy	19
5.03.3.2	Cornea	20
5.03.3.2.1	Light microscopy	20
5.03.3.2.2	Electron microscopy	21
5.03.3.3	Deep Somatic Tissues	22
5.03.3.3.1	Muscle pain compared to cutaneous pain	22
5.03.3.3.2	Nociceptors in muscle and tendon	22
5.03.3.3.3	Nociceptors in joints and ligaments	25
5.03.3.3.4	Tooth pulp	27
5.03.3.3.5	Dura mater encephali	32
5.03.3.4	Visceral Organs	33
5.03.3.4.1	Visceral pain	33
5.03.3.4.2	Testis	34
5.03.4	**Neuropeptide Content of Nociceptors**	34
5.03.4.1	General Remarks	34
5.03.4.2	Neuropeptides in Afferent Units of Different Tissues	35
5.03.4.3	Neuropeptides in Nociceptors and Other Types of Free Nerve Ending	36
5.03.5	**Efferent Function of Nociceptors**	37
5.03.5.1	Release of Neuropeptides from the Nociceptive Ending	37
5.03.5.2	The Axon Reflex	37
5.03.5.3	Neurogenic Inflammation	37
5.03.6	**Receptor Molecules in the Membrane of Nociceptors**	38
References		38

Glossary

anterograde transport Intra-axonal transport in the distal direction (away from the soma) of substances synthesized in (or injected into) spinal or cranial ganglion cells. The transport is brought about by molecules (kinesin for anterograde, and dynein for retrograde, transport) that bind substances and vesicles and move along the microtubules in the axoplasm.

axon reflex Release of neuropeptides from a branch of a nociceptor when the branch is invaded antidromically (against the normal direction of propagation) by action potentials. The released neuropeptides influence the microcirculation in the vicinity of the ending.

deep somatic tissues All subcutaneous tissues that are not viscera, namely tendon, fascia, muscles, ligaments, and joints.

epitendineum (peritendineum externum) Dense connective tissue with blood vessels, lymphatic vessels, and nerve fibers surrounding a tendon.

group I–IV fibers Nomenclature for afferent fibers that originate in deep somatic tissues. Group IV fibers correspond to C-fibers from the skin, and group III to Aδ-fibers. Group I fibers comprise the primary endings from muscle spindles (Ia-fibers) and Ib-fibers from Golgi tendon organs. Group II fibers and cutaneous Aβ-fibers are largely identical. The denominations using roman numerals are based on the diameter of the nerve fibers, those using arabic letters on the conduction velocity.

noceffector This term was coined by Kruger L. (1988) for nociceptors in the tooth; it emphasizes the efferent function of the receptor. Efferent function means that the receptor is involved in the maintenance of the tissue under normal and pathological circumstances by releasing substances stored in the ending. One aspect of such a noceffector role in the skin would be regulation of Langerhans cell type expression and proliferation of keratinocytes. Under pathophysiological circumstances, the effector role of a nociceptor is reflected in the axon reflex (see above) and neurogenic inflammation.

paciniform corpuscle A rapidly adapting mechanoreceptor with a morphology similar to that of a Pacinian corpuscle. It consists of a layered capsule that surrounds a central receptive core. The capsule is derived from the perineurium; the central core contains the receptive portion of the axon with Schwann cells around it. Compared to the Pacinian corpuscle, the paciniform corpuscle is smaller and has fewer laminae in its capsule. In skeletal muscle, it is often supplied by a group III fiber.

primary afferent unit The first sensory neuron in the body periphery. It includes the receptive ending, the afferent fiber, the soma in the spinal or cranial ganglion, and the central process in the dorsal root and the central nervous system (CNS).

receptor matrix An arrangement of cell organelles (mitochondria, vesicles, and axonal reticulum, i.e., a network of fluid-filled vacuoles) embedded in a granulated axonal cytoplasm.

Ruffini corpuscle A flat, encapsulated mechanoreceptor supplied by several myelinated nerve fibers. The fibers form a dense arborization within a capsule of connective tissue.

sensory terminal tree The preterminal axon and its branches. The term is part of the concept that both group III and IV endings do not have just one sensory site, but possess several branches with many receptive loci that together enhance the sensitivity of the free nerve ending as a sense organ.

varicosity An expansion of the preterminal axon of a slowly conducting sensory fiber (Aδ- or C-fiber). The varicosity contains mitochondria, vesicles, and other cell organelles. It is discussed as a receptive site. The varicosities of a free nerve ending are connected by thin stretches of axon; this arrangement causes the beaded appearance of a free nerve ending and the preterminal axon under the light microscope.

5.03.1 Introduction

Originally, pain was assumed to be an emotion like pleasure and fear. In the nineteenth century, this concept was replaced by the view that pain is due to activation of a set of specialized nerve endings. Von Frey M. (1894) was the first to link pain to fine nerve terminals in the skin. The functional term nociceptor is derived from the Latin word *noxius* for damaging or harmful. It denotes a sensory ending that detects actual or potential tissue damage. When activated, it may cause pain in humans and pain-related reflexes in animals. Another definition of a nociceptor is an ending that by its discharge behavior is capable of distinguishing between an innocuous and a noxious stimulus. An important point for the understanding of the function of nociceptors is that their stimulation threshold is just below tissue-damaging intensity. The function of nociceptors is not to signal existing tissue damage, but to inform the central nervous system (CNS) when stimuli approach tissue-threatening intensities.

Nociceptive endings are present in almost all tissues and organs of the organism. However, the fact that lesions of the brain and parenchyma of the lung, liver, and cartilage are not painful suggests that in

these tissues nociceptors are not present. Conversely, by stimulation of cornea, dura mater, and tooth pulp, pain is the predominant or only sensation that can be elicited. These observations led to the assumption that these tissues are equipped exclusively with nociceptors.

The available clinical and experimental evidence indicates that small-diameter afferent fibers have to be activated in order to elicit pain. These fibers conduct action potentials at a relatively slow velocity (below 30 m s^{-1} in the cat); histologically they comprise either thin myelinated (Aδ- or group III) fibers or nonmyelinated (C- or group IV) fibers. However, there are also nociceptors supplied by faster-conducting thick myelinated Aα/β-fibers: in the rat, approximately 20% of all Aα/β-fibers are nociceptive (for review, see Djouhri, L. and Lawson, S. N., 2004). The nomenclature with roman numerals (group I–IV fibers) was developed by Lloyd D. P. C. (1943) for muscle afferent fibers. It is now being used for afferent fibers from muscle, joint, tendons, and fascia (the so-called deep somatic tissues).

Generally, there is a negative relationship between mechanical threshold and conduction velocity (CV) of sensory afferents: the higher the CV, the lower the mechanical threshold (Burgess, R. P. and Perl, E. R., 1967). In the dorsal root ganglion (DRG), the correlation between soma diameter and axonal CV is weaker than generally thought. In Figure 1 (Hoheisel, U. and Mense, S., 1987), this correlation is shown for intracellularly stained DRG cells of the cat. For group III units (those having CVs between 2.5 and 30 ms^{-1}), there was no significant correlation between soma size and CV, and for group IV units (conducting at <2.5 ms^{-1}), the correlation was negative. Thus, from the soma size in the DRG, the diameter or CV of group III and IV afferent fibers cannot be inferred. Generally, the majority of nociceptive free nerve endings will originate from small-diameter DRG cells, but there are also relatively large somata that supply nociceptive terminals. Conversely, not all the small DRG cells supply nociceptive endings.

In morphological studies on the endings of unmyelinated fibers, the first hurdle to be taken is the distinction between efferent and afferent units, because postganglionic sympathetic fibers may look identical to unmyelinated afferent ones, except that the former have a larger mean diameter (Heppelmann, B. *et al.*, 1988). The presence of

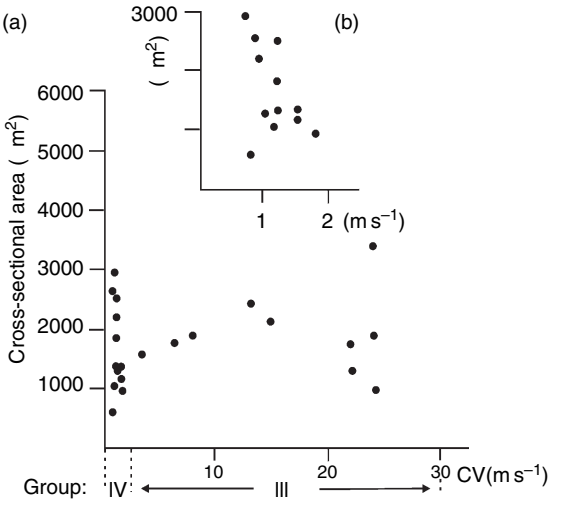

Figure 1 Relationship between cross-sectional area of dorsal root ganglion (DRG) cells and conduction velocity (CV) of the peripheral axon. (a) Data from 12 unmyelinated (C- or group IV) fibers and 10 thin myelinated (Aδ- or group III) fibers. (b) Data from the unmyelinated units at an expanded scale of the abscissa. There was no significant correlation between soma size and CV within group III fibers, and for group IV units the correlation was negative. (Modified from Hoheisel, U. and Mense, S., 1987, with permission).

neuropeptides may be helpful, since for instance CGRP is absent from postganglionic sympathetic fibers (Ju, G. *et al.*, 1987). However, postganglionic parasympathetic fibers have also been shown to contain neuropeptides. Therefore, if neuropeptide-immunoreactive (ir) free nerve endings are being studied, one has to assume that a certain (probably small) proportion of the endings originate from autonomic efferent fibers. Of course, the best way of eliminating this problem is to cut the autonomic supply to the studied body region.

Not all small-diameter, slowly conducting afferent fibers are nociceptive. In cutaneous nerves, there are thermoreceptors and low-threshold mechanoreceptors that have unmyelinated afferent fibers, and also in skeletal muscle low-threshold mechanoreceptors with group IV afferents can be found (Light, A. R. and Perl, E. R., 2003; Hoheisel, U. *et al.*, 2005). The presence of certain neuropeptides such as CGRP does not distinguish between high- and low-threshold mechanosensitive (HTM and LTM) group IV units, because the neuropeptide was found in both functional types (Hoheisel, U. *et al.*, 1994).

The development of myelinated nociceptors has been reported to depend upon the presence of trkA (tyrosin kinase A) and trkC receptors in the DRG, but not upon trkB receptors (Ichikawa, H. *et al.*, 2004). The trk receptors bind neurotrophins (NTs) selectively; the ligand for trkA is nerve growth factor (NGF), that for trkB, brain-derived neurotrophic factor (BDNF), and that for trkC, NT-3.

Even though several groups have studied and described the structure of putative nociceptors, clear morphological (light or electron microscopic) differences between the various functional types of nociceptor are not apparent. The functional differences are probably due to the equipment of the endings with different sets of receptor molecules (Cesare, P. and McNaughton, P., 1997).

In neurophysiological experiments on cats and rats, an unexpected finding was that many unmyelinated afferent units had two receptive fields (RFs), i.e., the same fiber could be activated by applying stimuli to more than one location. In the deep tissues of the cat tail, afferent units were found that had one RF in deep tissues (muscle, joint, and periosteum) and another one in the skin distal to the deep RF (Mense, S. *et al.*, 1981). Sometimes, the distance between the RFs could be several centimeters. The anatomical basis of this feature may be branching of the afferent fiber close to its area of termination. Anatomical and neurophysiological studies (Devor, M. *et al.*, 1984; Pierau, E.-K. *et al.*, 1984) have shown that afferent units with long branched axons are rare (a few percent of all afferent fibers), but they may be functionally relevant, since they are likely to reduce the spatial resolution of the nociceptive system, and thus could contribute to the diffuse nature of deep pain.

The data that are most important to this chapter were obtained in studies employing a combination of electrophysiological and neuroanatomical techniques, because otherwise one does not know if a given free nerve ending in a histological section has a nociceptive function. However, many purely morphological investigations on free nerve endings yielded results that are relevant to this chapter, even though the evidence for a nociceptive function is indirect. Therefore, many of these studies are included below.

The main emphasis of this chapter is on nociceptors or free nerve endings, respectively, in skin, muscle/joint, tooth pulp, and testis, because large sets of data are available from these tissues.

5.03.2 General Morphological Features of Nociceptors

5.03.2.1 Light Microscopic Structure

Morphologically, a nociceptor is a free nerve ending that is usually connected to the CNS through thin myelinated or unmyelinated nerve fibers. (As stated above, there are also nociceptors with thick myelinated fibers.) C- or group IV fibers are assumed to terminate exclusively in free nerve endings while group III fibers supply both free nerve endings and other types of receptors (for instance in muscle paciniform corpuscles; Barker, D., 1967; Stacey, M. J., 1969). A frequent location of free nerve endings is the wall of arterioles and the surrounding connective tissue; the capillaries proper do not have a rich supply with these endings (Stacey, M. J., 1969; Reinert, A. *et al.*, 1998). The marked sensitivity of free nerve endings to chemical stimuli, particularly to those associated with disturbances of the microcirculation, may be related to their location in or close to the wall of blood vessels.

The term free nerve ending or unencapsulated ending is derived from the fact that in the light microscope this type of ending lacks a visible (corpuscular) receptive structure (Stacey, M. J., 1969). Typically, such an ending consists of several branches or terminals that altogether form the receptor in the morphological sense. An afferent fiber together with its receptive ending is an afferent unit. In the fluorescence microscope, the receptive ending and the preterminal axon look like a string of beads with relatively wide diameter (so-called varicosities) connected by very thin stretches of axon. The diameter of a branch of a free nerve ending is 0.5–1.0 μm, i.e., at the limits of the resolution of the light microscope. Figure 2 shows a free nerve ending in a rat

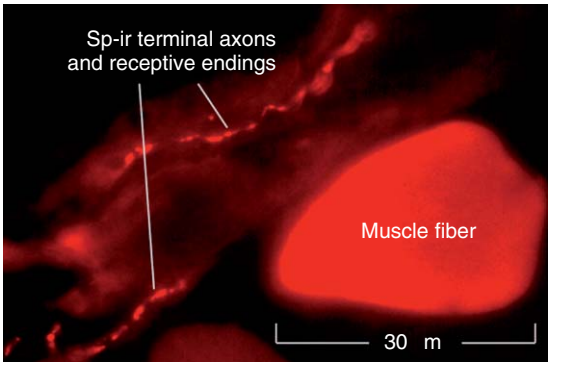

Figure 2 Histological section from rat gastrocnemius muscle showing two nerve fibers with varicosities visualized with fluorescent antibodies to substance P (SP; U. Hoheisel and S. Mense, unpublished data).

skeletal muscle after labeling with fluorescent antibodies to SP.

Most of the unmyelinated afferents enter the spinal cord via the dorsal root. However, there are also unmyelinated afferent fibers in the ventral root: approximately 30% of all ventral root fibers are unmyelinated and 50% of these fibers survive in the distal stump after cutting the ventral root. Therefore, they were assumed to be afferent with their soma located in the DRG (Applebaum, M. L. *et al.*, 1976).

In immunohistochemical studies, sensory free nerve endings have been described as either peptidergic or lectin-positive, the latter being largely peptide free. The lectin-positive endings possess membrane-associated glycoconjugates that bind the plant lectin *Griffonia simplicifolia* isolectin B4 (IB4). They are assumed to be identical to the fluoride-resistant acid phosphatase (FRAP) endings. Many of the IB4-positive endings express the purinergic P2X3receptor. In contrast, the peptidergic endings are equipped with the vanilloid receptor TRPV1 (transient receptor potential subtype V1). These cytochemical differences led to the hypothesis that the IB4-positive and -negative endings represent two functionally distinct classes of nociceptors. (Snider, W. E. and McMahon, S. B., 1998; Stucky, C. L. and Lewin, G. R., 1999). Recent evidence indicates that the peptidergic endings express trkA receptors, are dependent on NGF in their development, and express predominantly tetrodotoxin (TTX)- sensitive Na^+ channels, whereas the nonpeptidergic IB4-positive endings depend on glial cell–derived neurotrophic factor (GDNF) in their development and express more TTX-resistant Na^+ channels than the IB4-negative fibers (Wu, Z.-Z. and Pan, H.-L., 2004). Another difference between these two types of putative nociceptors is that the IB4-positive endings terminate freely in the tissue without close spatial relationship to blood vessels, whereas the peptidergic fibers are often associated with blood vessels (Silverman, J. D. and Kruger, L., 1988; Figure 3). At present, however, the assumption prevails that the separation between these two postulated types is probably not that sharp and that IB4-positive endings may also express TRPV1 receptors.

In experiments employing a combination of electrophysiological and immunohistochemical techniques to study functionally identified DRG cells, Lawson S. N. *et al.* (1997) reported that cells terminating in cutaneous nociceptive endings showed a strong tendency to express SP, particularly if they had a slow CV or small somata in the DRG.

5.03.2.2 Ultrastructure

In electron microscopic studies, often uncertainties remain as to the identity of the ending. Even when in combined electrophysiological–morphological investigations an ending is first functionally characterized and then morphologically reconstructed, it is sometimes difficult to make sure that a given ending in a histological section is the one that was studied functionally.

The published findings demonstrated that free nerve endings are not free in the strict sense, because the majority are ensheathed by Schwann cells (therefore, the term free nerve ending is a misnomer). Exceptions to this rule are endings in the epidermis

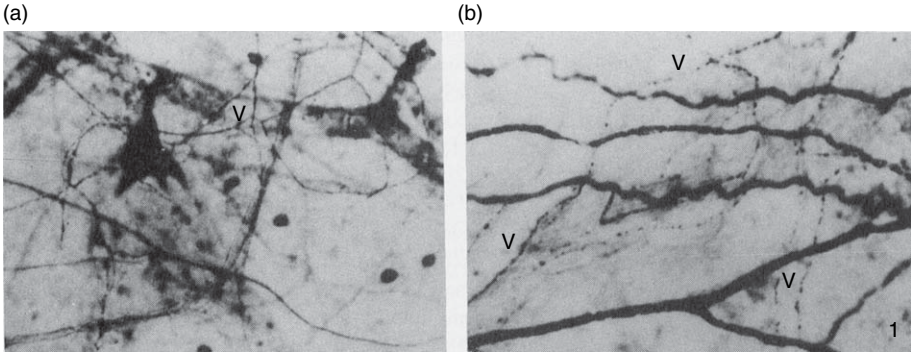

Figure 3 Testicular whole-mount preparation of the rat epididymal tunica vasculosa stained with Griffonia simplicifolia A-B4 lectin (a) and antibodies to calcitonin gene-related peptide (CGRP; (b)). Slender lectin-stained axonal bundles and terminals distribute freely throughout the tissue (a). The lectin-labeled axons bear little relation to blood vessels (V) whose endothelial basal lamina is also lectin-stained. In contrast, CGRP immunoreactivity is evident as heavily labeled coarse nerve bundles from which one can trace fine granular axons running closely adherent to blood vessels (V). (From Silverman, J. D. and Kruger, L., 1988, with permission.)

that lose their Schwann cell covering, when they pass the basal lamina of the epidermal layer (see below). Usually, also the receptive terminals are ensheathed by Schwann cells, and only small areas of the axonal membrane remain uncovered by Schwann cell processes. These areas are separated from the interstitial fluid only by the basal lamina that spans the exposed axonal membrane areas (Andres, K. H. *et al.*, 1985; Heppelmann, B. *et al.*, 1990a; 1990b; Messlinger, K., 1997). The varicosities in the exposed membrane areas are supplied with mitochondria and vesicles and show other structural specializations characteristic of receptive structures, and together with the end bulb they are assumed to be the site where external stimuli act. A reconstruction of such an ending is shown in Figure 4.

The arrangement of cell organelles (mitochondria, vesicles, and axonal reticulum, i.e., a network of fluid-filled vacuoles) embedded in a granulated axonal cytoplasm was called receptor matrix by Andres K. H. and von Düring M. (1973). Often, nociceptive endings exhibit granular or dense-core vesicles containing neuropeptides. However, vesicles containing catecholamines can have the same appearance, so that dense-core vesicles are not an unambiguous sign of a nociceptive ending. The function of the round clear vesicles in the peripheral ending is still obscure. They may contain the same transmitters as the central synaptic terminal (e.g., glutamate). Recent reports have shown that glutamate is an effective stimulant for nociceptive endings in the body periphery (Svensson, P. *et al.*, 2003). Therefore, it is conceivable that nociceptors enhance their own excitation by releasing glutamate when they are activated.

In a recent survey, Kruger L. *et al.* (2003a) list some features that were considered characteristic for nociceptive terminals in the body periphery:

(1) An axonal reticulum that may be derived from the smooth endoplasmic reticulum.
(2) Vesicle aggregates embedded in a granular axonal matrix that may be identical to the receptor matrix described by Andres K. H. and von Düring M. (1973).
(3) Exposed membrane areas that are not ensheathed by Schwann cells and directly contact the basal lamina.

The receptive terminal as a whole consists of several branches equipped with many receptive sites that have the appearance of varicosities. Together the branches constitute a sensory tree as shown in Figure 5 (Messlinger, K., 1996).

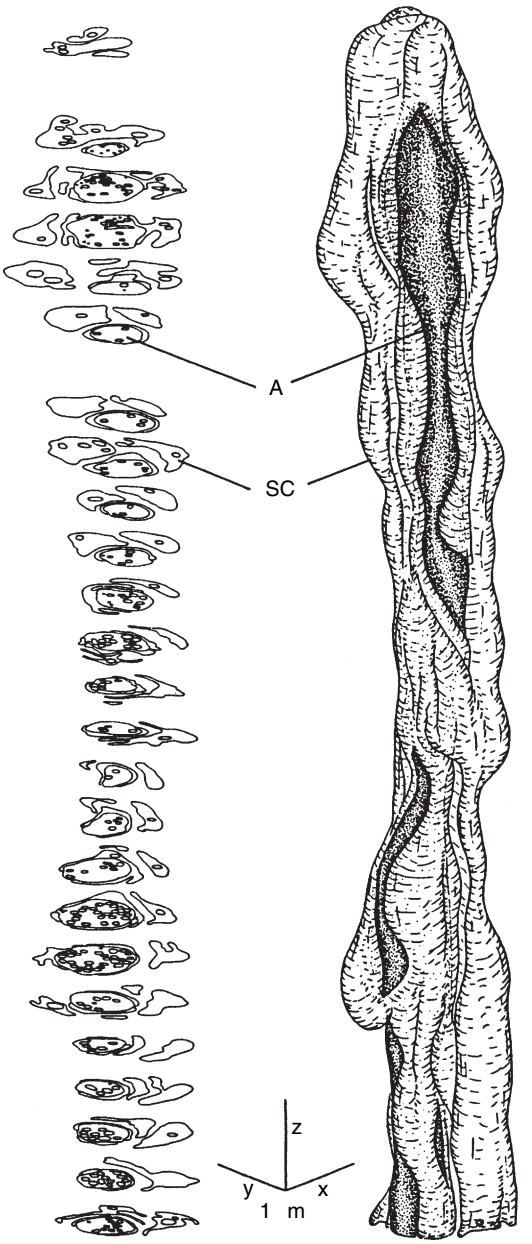

Figure 4 Reconstruction of an end branch of an articular group III ending. *Left*: Contours of the cross-sectioned nerve fiber at a distance of 1 μm each (computer-aided reconstruction). *Right*: Hand drawing based on the stack of sections showing the surface of the end branch. The bare axon areas (A) are densely dotted; SC, Schwann cell. (From Messlinger, K. *et al.*, 1995, with permission.)

It is important to note that the above features cannot be found at the synaptic terminal of the same neuron, i.e., the central and distal terminals of

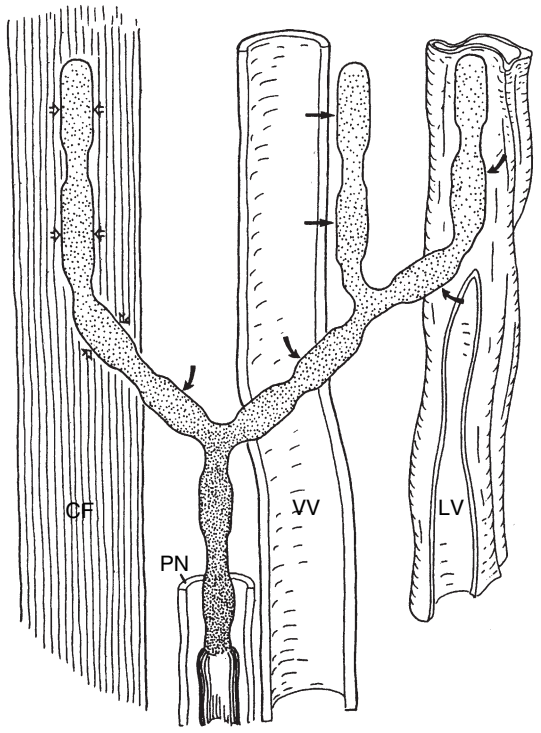

Figure 5 So-called sensory terminal tree of a group III fiber (schematic representation) as a possible morphological basis for sensitization of polymodal nociceptors. The summation of local receptive potentials created in perivascular (chemoreceptive) branches at venous vessels (VV) or lymphatic vessels (LV) in combination with the local potentials of mechanoreceptive branches in collagenous tissue (CF) may lead to a suprathreshold excitation at the basis of the sensory terminal tree within the perineurium (PN). (From Messlinger, K., 1996, with permission.)

a sensory neuron exhibit morphological differences. Small clear vesicles are present at both terminals, but at the peripheral terminal they show diversities in size, shape, and electron lucency, which are not present at the central terminal. The differences in vesicle content between the peripheral and the central terminal are difficult to explain, because if the vesicles are synthesized in the soma, as is generally assumed, a complicated sorting process is required. This is not impossible, because at least for channel proteins an exclusive transport to the peripheral terminal has been reported (Garcia-Anoveros, J. *et al.*, 2001). Another explanation would be that the small clear vesicles in the distal terminal are synthesized in the ending itself, but at present this appears unlikely. As the origin and the contents of the small clear vesicles in the peripheral terminal are unknown, the function of these vesicles is likewise obscure.

One of the characteristic functional properties of a nociceptor is its relatively high mechanical stimulation threshold. The high mechanical threshold is surprising, considering the fact that a free nerve ending is a fragile structure with a semifluid membrane. One factor that may be responsible for the high mechanical threshold is a special mechanosensitive ion channel, the transient receptor potential subunit V4 (TRPV4; Liedtke, W., 2005).

5.03.3 Nociceptors in Various Tissues

A complete overview of all tissues is not attempted. Only those organs/tissues for which comprehensive sets of data are available are addressed below.

5.03.3.1 Skin

The cutaneous nociceptors are generally subdivided into several types according to the fibers supplying them, namely Aδ/β- or C-fibers. Among the receptors supplied by myelinated fibers are (data from monkey, after Djouhri, L. and Lawson, S. N., 2004):

- Type I A mechano-heat receptors (AMH, supplied by Aδ- and Aβ-fibers). They have a relatively low mechanical, but a high thermal, threshold. They are called moderate pressure receptors by some.
- Type II A mechano-heat nociceptors (AMHs, supplied by Aδ-fibers). They have high mechanical and low thermal thresholds.

Among the receptors supplied by C-fibers, which are by far more frequent, are

- C-fiber mechano-heat nociceptors (CMHs), which have little sensitivity to algesic agents
- Cold nociceptors
- Polymodal nociceptors that respond to all noxious stimuli including algesic chemical stimuli

In a cutaneous nerve of the cat, approximately 50% of all unmyelinated afferent fibers were found to have a high mechanical threshold in the noxious range (Bessou, P. and Perl, E. R., 1969). These units also responded to noxious heat and irritant chemicals and therefore were considered to be polymodal nociceptors.

The measured size of the RF of a single unmyelinated fiber supplying a polymodal nociceptor depends on the thickness of the probe used for mechanical stimulation: Thick probes yielded areas of 6–32 mm^2 (mean 18 mm^2) in the rabbit, whereas

with small probes mean areas of 7.5 mm^2 were measured, which consisted of several mechanosensitive spots that could be activated independently from each other (Kenins, P., 1988).

5.03.3.1.1 Light microscopy

The nociceptive endings of the skin can extend in the epidermis to just beneath the surface. This explains why superficial abrasions of the skin can cause pain but no bleeding, because there are no blood vessels in the epidermis.

A study of the distribution of CGRP-ir fibers in the rat glabrous skin (Kruger, L. *et al.*, 1989) revealed a dense network in the subpapillary layer largely confined to dermal blood vessels and sweat glands. The intraepidermal fibers branched extensively in the stratum spinosum, but some extended nearly to the stratum corneum (Figures 6 and 7). These fibers were considered to fulfill a noceffector role rather than a nociceptive one. Noceffector means that these fibers have an efferent function and are involved in the maintenance of the tissue under normal and pathological circumstances (Kruger, L., 1988). One aspect of such a noceffector role in the skin would be regulation of Langerhans cell type expression and proliferation of keratinocytes (Kruger, L. and Halata, Z., 1996). In hairy skin of the rat, a similar arrangement of CGRP-ir fibers was found with the additional feature that the lower portion of each hair follicle exhibited an extensive innervation. Sebaceous glands and arrector pili muscles were not supplied with CGRP-ir fibers.

To find out if the effect of capsaicin treatment of skin pain (e.g., erythralgia) is due to a desensitization or destruction of nociceptive nerve fibers, Simone and coworkers (Simone, D. A. *et al.*, 1998) performed a light microscopic study of capsaicin effects in skin biopsies of human skin. In the epidermal layer of intact skin, mainly fibers ir for PGP 9.5 (protein gene product 9.5, a general marker for nerve fibers) were found, whereas in the dermis a dense innervation of CGRP- and SP-ir fibers was present. After topical capsaicin treatment, the CGRP- and PGP-ir fibers were almost completely gone, but the SP-ir fibers were less affected. Simultaneously, heat pain and pain produced by sharp objects were markedly reduced. This finding is surprising, because most SP-ir fibers are assumed to be nociceptive (Lawson, S. N. *et al.*, 1997).

Recently, unmyelinated fibers stained for PGP 9.5 in the skin of human biopsy material have been studied using confocal microscopy (Kennedy, W. R., 2004). Of interest in the context of the present chapter are fibers that penetrated the basal lamina and branched in the epidermis, because they can be assumed to be free nerve endings. The PGP 9.5-positive fibers in the epidermis had an appearance similar to that described in other reports: From a subepidermal plexus single fibers coursed in the epidermis, where they could be easily counted (Figure 8(a)). In skin biopsies of patients with diabetic neuropathy, the density of the epidermal

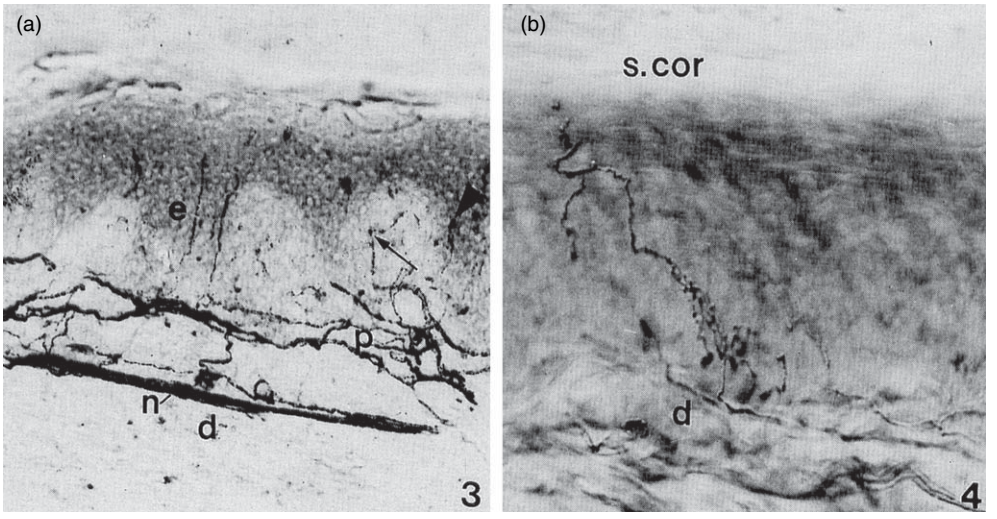

Figure 6 Digital glabrous skin. (a) A dermal (d) cutaneous nerve gives rise to an extensive calcitonin gene-related peptide-immunoreactive (CGRP-ir) subpapillary nerve plexus (p) from which individual axons can be traced into epidermal pegs (e) and dermal papillae (arrow). Some branches appear to end at varying depths within the stratum spinosum revealing terminal expansions (arrowhead) (×63). (b) Branched CGRP-ir axons in palmar glabrous skin extending from the dermis (d) nearly to the stratum corneum (s.cor) (×320). (From Kruger, L. *et al.*, 1989, with permission.)

Figure 7 A dermal calcitonin gene-related peptide-immunoreactive (CGRP-ir) axon terminating as a free nerve ending with a bulbous enlargement (arrow) (×320). (From Kruger, L. *et al.*, 1989, with permission.)

branches was much less, and some fibers showed swellings that were interpreted as an indication of de- or regeneration (Figure 8(b)).

5.03.3.1.2 Electron microscopy

In a combined electrophysiological–electron microscopic study on mechanical nociceptors in the cat skin (Kruger, L. *et al.*, 1981), single receptive endings were first identified functionally in electrophysiological recordings and then examined morphologically. Mechano-nociceptors had RFs consisting of several sensitive spots with relatively insensitive areas in between. After functional identification, the location of the mechanosensitive spots was marked with fine steel pins and the tissue processed for light and electron microscopy. The study focused on afferent units conducting at 20–30 $m\,s^{-1}$, i.e., on myelinated mechano-nociceptors. Some of the thin myelinated fibers approached the papillary layer of the corium (dermis), lost their myelin sheath in this area but retained their Schwann cell layer, and penetrated the epidermal basal layer. The penetration site was considered to be the receptive portion of the ending; here the axons exhibited mitochondria, clear round and dense-core vesicles. Most of the axons that penetrated into the epidermal layer still had a Schwann cell covering (Figure 9), but in some cases the Schwann cell sheath was lost and the basal lamina of the axon fused with that of keratinocytes (Cauna, N., 1966).

Nociceptive endings originating from Aδ-fibers have been reported to terminate in the basal layer of the epidermis, i.e., they do not penetrate into the

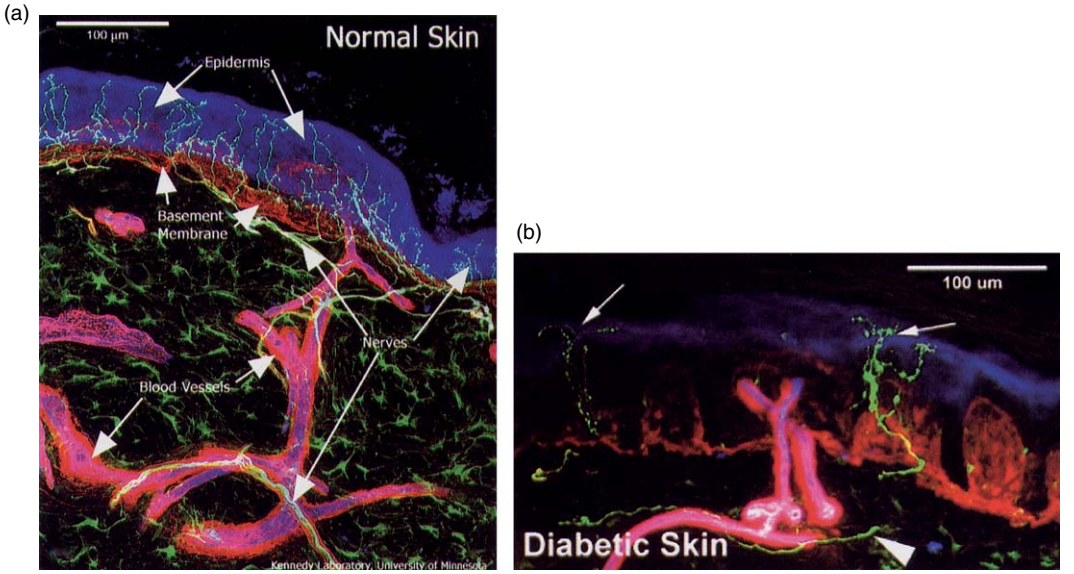

Figure 8 (a) Normal human epidermal and papillary dermis innervation. Nerve fibers (green and yellow) course in bundles through the dermis and branch into the papillary dermis to form the subepidermal neural plexus. Fibers from this plexus penetrate the epidermal–dermal basement membrane (red) to enter the epidermis (blue). Note that the basement membrane surrounding capillaries also appears red and some nonneuronal fibroblasts appear green. Epidermal nerve fibers are abundant and uniformly distributed. (b) Diabetic skin. Two tufts (arrows) arise from the subepidermal neural plexus (arrowhead). Nerve fibers comprising the right tuft have many swellings. Irregular distribution characterized by tufting and clustering of nerve fibers and the presence of swelling is distinctive of neuropathy. (From Kennedy, W. R., 2004, with permission.)

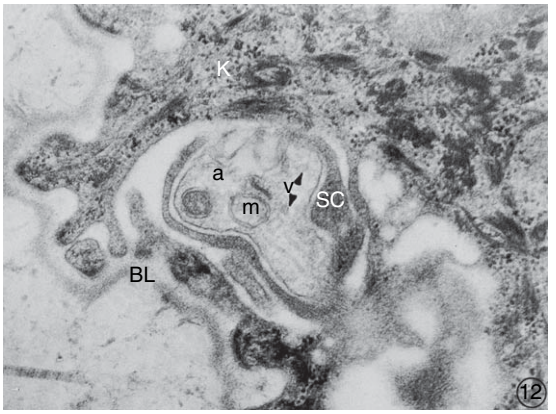

Figure 9 Cat hairy skin. An intradermal axon (a) containing mitochondria (m) and clear vesicles (v) (arrowheads) enclosed by a Schwann cell (SC). The basal lamina (BL) of the keratinocyte (K) is not shared by the Schwann cell, which lacks a basal lamina only within the epidermis (×40 000). (From Kruger, L. *et al.*, 1981, with permission.)

upper epidermal layer (Kruger, L. and Halata, Z., 1996). At present, these endings cannot be morphologically distinguished from cutaneous cold receptors that have the same location (Hensel, H. *et al.*, 1974).

Du J. *et al.* (2003) reported that nociceptive unmyelinated endings in the rat digital nerves exhibit *N*-methyl-D-aspartate (NMDA) receptor molecules type 1 (NMDAR1) and can be excited by glutamate. These data support those of Svensson P. *et al.* (2003). The NMDAR1 were assumed to contribute to the sensitization of nociceptors in inflamed tissue, because they showed an increased expression 7 days after induction of an experimental inflammation.

5.03.3.2 Cornea

Hundred years ago, von Frey assumed that from the cornea only pain can be evoked, but later several reports were published indicating that also sensation of touch, warmth, and cold can be elicited. The corneal epithelium is one of the tissues with the highest innervation density of the body and in this regard is comparable with the tooth pulp.

In an electrophysiological study on fine nerve fibers of the cornea *in vitro*, Aδ-fibers were described that were sensitive to mechanical and heat stimuli. These units were situated in the basal epithelial layer, whereas polymodal C-fiber endings were found in the superficial layers (MacIver, M. G. and Tanelian, D. L., 1993).

Recordings from single corneal sensory fibers demonstrated that the RFs of LTM endings were relatively large with a size of 50–200 mm^2 in the cat (Tower, S., 1940). Most of the slowly conducting (Aδ- or C-) fibers of the cornea were found to be polymodal and responded to mechanical, thermal, and chemical stimuli. They had a smaller RF size of ∼25 mm^2. Acidic solutions were used to test these units, and the endings responded readily to a pH of 5 to 4.5 with a discharge that was nearly proportional to the proton concentration. Capsaicin – a specific ligand for the TRPV1 receptor – was also excitatory for slowly conducting corneal afferents (Belmonte, C. *et al.*, 1991).

In contrast to most other body regions, the cornea is not supplied by blood vessels. Therefore, after a lesion has occurred, blood cells have no rapid access to the damaged area. In this case, lesion-induced sensitization of corneal nociceptors can occur through activation of tissue cyclooxygenase and lipoxygenase-generating prostaglandins (PGs) and other sensitizing agents.

An interesting feature of corneal sensory endings is that the continuous shedding of epithelial cells on the surface of the cornea changes the morphology of the nerve terminals. This results in a rearrangement of the arborization pattern of superficial terminals within 1 week. Also after a relatively mild injury, a remodeling of the corneal sensory ending takes place, and this remodeling is associated with an increased expression of the growth-associated protein (GAP)-43 in the corneal afferents (Belmonte, C. and Gallar, J., 1996). This protein is known to be involved in the development and regeneration of neurons; it is also present in growth cones of regenerating nerve fibers.

5.03.3.2.1 Light microscopy

Light microscopic investigations showed that corneal afferents were either thin myelinated or unmyelinated. As in the skin, they formed a dense plexus in the stroma from which branches ascended through the basal epithelial layer and terminated in bulb-like structures just underneath the corneal surface. In the electrophysiological study mentioned above (MacIver, M. G. and Tanelian, D. L., 1993) the fibers differed in their morphology: Aδ-fibers looked like leashes and polymodal C-fiber terminals like stranded endings under epifluorescence.

As in free nerve endings of other tissues, neuropeptides such as SP and CGRP are present in corneal terminals. Interestingly, in the cornea SP has a trophic effect on the corneal epithelium. The healing of a corneal wound is promoted by external

administration of SP. Conversely, the healing process is delayed if SP is missing in the corneal terminals, e.g., after injection of capsaicin into the retrobulbar space to deplete SP-containing fibers. Generally, SP appears to promote mitosis in epithelial cells of the cornea, while CGRP inhibits it. After corneal irritation or damage, signs of neurogenic inflammation occur such as edema, conjunctivial vasodilatation, and photophobia. These symptoms are attributed to the release of neuropeptides from the sensory corneal terminals (e.g., SP and CGRP).

5.03.3.2.2 *Electron microscopy*

Electron microscopic studies showed that thin fibers entering the epithelium lost their Schwann cell covering, often branched and exhibited varicosities that contained mitochondria, neurofilaments and round clear vesicles (Figures 10 and 11; Belmonte, C. and Gallar, J., 1996; Müller, L. J. *et al.*, 1996). Terminals containing granular vesicles were numerous only at the limbus of the cornea. These endings disappeared after sympathectomy and, therefore, were considered to be adrenergic terminals. Sensory endings (i.e., those having their somata in the trigeminal ganglion) were often ir to SP and CGRP. Hoyes A. D. and Barber P. (1976) distinguished between two types of sensory free nerve endings that originated from unmyelinated corneal fibers:

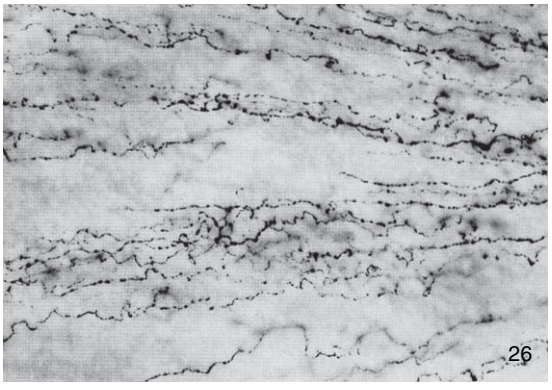

Figure 10 Flat mount preparation of cornea. The focal plane is through the base of the corneal epithelium, which is heavily innervated by varicose calcitonin gene-related peptide-immunoreactive (CGRP-ir) axons coursing radially inward from the limbus. Branches can be traced in more superficial focal planes ascending perpendicularly between epithelial cells to approach the epithelial surface (×200). (From Silverman, J. D. and Kruger, L., 1988, with permission.)

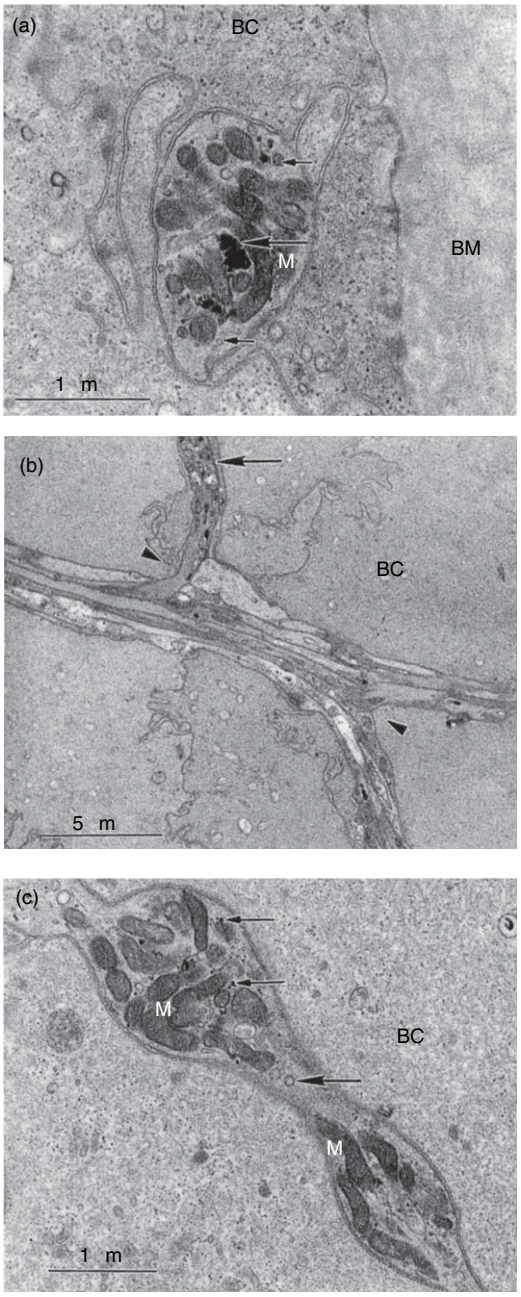

Figure 11 Nerve fibers in the epithelium of the human cornea. (a) Cross section of a single nerve fiber at the level of an axonal expansion (a bead), showing numerous mitochondria (M), glycogen particles (large arrow), and vesicles (small arrow) (×16576). (b) Frontal section of a nerve filament that bifurcates at the points indicated by the arrowheads. The single fiber running in the upper part of the picture has a bead filled with mitochondria (large arrow) (×3000). (c) Frontal section of a single fiber, showing two beads filled with numerous dark mitochondria (M), glycogen particles (small arrows), and vesicles (large arrow) (×12544). BC, basal cell; BM, Bowman's membrane. (From Müller, L. J. *et al.*, 1996, with permission.)

(1) Units that contained many mitochondria and were considered to be mechano- or thermoreceptors.
(2) Units exhibiting clear and dense-core vesicles. These units were assumed to be nociceptive afferents; they were concentrated in the central parts of the cornea where no blood vessels are present. The majority of this fiber type had an intraepithelial location.

Attempts to correlate morphology with function in corneal receptive endings did not yield unequivocal results. Therefore, in their review, Belmonte C. and Gallar J. (1996) stated that "no morphological specialization has been found in corneal nerve terminals associated with the various functional classes of corneal afferents."

5.03.3.3 Deep Somatic Tissues

5.03.3.3.1 Muscle pain compared to cutaneous pain

Muscle pain is less well localized than cutaneous pain. One reason for this difference may be the fact that muscle pain – but not cutaneous pain – is often referred to sites distant from the lesion. Another possible reason is the lower innervation density of muscle tissue. Direct quantitative comparisons between the innervation density of muscle and skin have not been published so far and are difficult to make, because muscle tissue is 3D and skin largely 2D.

Free nerve endings in muscle are partly nociceptive and partly nonnociceptive. The latter ones have a low mechanical threshold and are assumed to mediate pressure and tension sensations from muscle tissue. Another important function for these nonnociceptive endings in muscle is to control the adjustment of circulation and respiration to the requirements of muscle work. They are activated by physiological degrees of exercise and send their information to the circulatory and respiratory centers in the medulla (McCloskey, D. I. and Mitchell, J. H., 1972).

5.03.3.3.2 Nociceptors in muscle and tendon

Several studies on the response properties of unmyelinated afferent fibers from cat and dog muscle demonstrated that a subpopulation of these afferents are excited by stimuli (strong mechanical and algesic chemical) that are known to elicit pain (Kumazawa, T. and Mizumura, K., 1977; Mense, S., 1977; Mense, S. and Meyer, H., 1985).

Besides capsaicin, ATP (binding to the purinergic P2X3 receptor), NGF, and protons (acting through TRPV1 and acid-sensing ion channels (ASICs)) are effective stimulants for muscle nociceptors (Hoheisel, U. *et al.*, 2004; 2005). Similar to nociceptive afferents from the skin, afferent fibers from nociceptors in rat muscle are equipped with TTX-resistant (TTX-r) Na^+ channels (Steffens, H. *et al.*, 2003).

5.03.3.3.2.(i) Light microscopy In a quantitative evaluation of neuropeptide-ir free nerve endings and preterminal axons (both characterized by varicosities) in the gastrocnemius–soleus muscle of the rat, most endings were found around small blood vessels (arterioles or venules), whereas capillaries and the muscle cells were not supplied by these endings. Most numerous were the CGRP-ir endings followed by endings with SP-immunoreactivity (IR), VIP-IR, NGF-IR, and GAP-43-IR (Reinert, A. *et al.*, 1998). Many endings exhibited IR for more than one peptide, e.g., for SP and CGRP or SP and VIP (Figure 12).

After 12 days of an experimental myositis, the innervation density of the muscle with neuropeptide-ir free nerve endings was significantly increased. The effect was particularly marked for endings with SP-IR, GAP-43-IR, and NGF-IR (Reinert, A. *et al.*, 1998; Figure 13 (b and c)). The density of the SP-ir fibers doubled in inflamed muscle. Of course the question arose if this increase was due to inflammation-induced sprouting of the nerve fibers or due to an increase in the neuropeptide content of the individual fiber so that a higher proportion of fibers were above the detection threshold in the fluorescence microscope. The finding that the density of NGF-ir and GAP-43-ir fibers increased together with that of SP-ir endings was interpreted that sprouting had occurred, because NGF and GAP-43 are strongly expressed in growth cones.

Free nerve endings in the calcaneal tendon of the rat showed IR to the same neuropeptides, but the distribution of the fibers was different from muscle. In the epitendineum, the fibers formed a much denser network than in muscle, but the collagen fiber bundles in the center of the tendon were largely free from free nerve endings (Reinert, A. and Mense, S. unpublished data). This finding may explain why chronic mechanical stress to the epitendineum can be very painful, whereas ruptures of collagen bundles within the tendon may occur without pain.

5.03.3.3.2.(ii) Electron microscopy

5.03.3.3.2.(ii).(a) Muscle The first comprehensive report on the morphology of free nerve endings

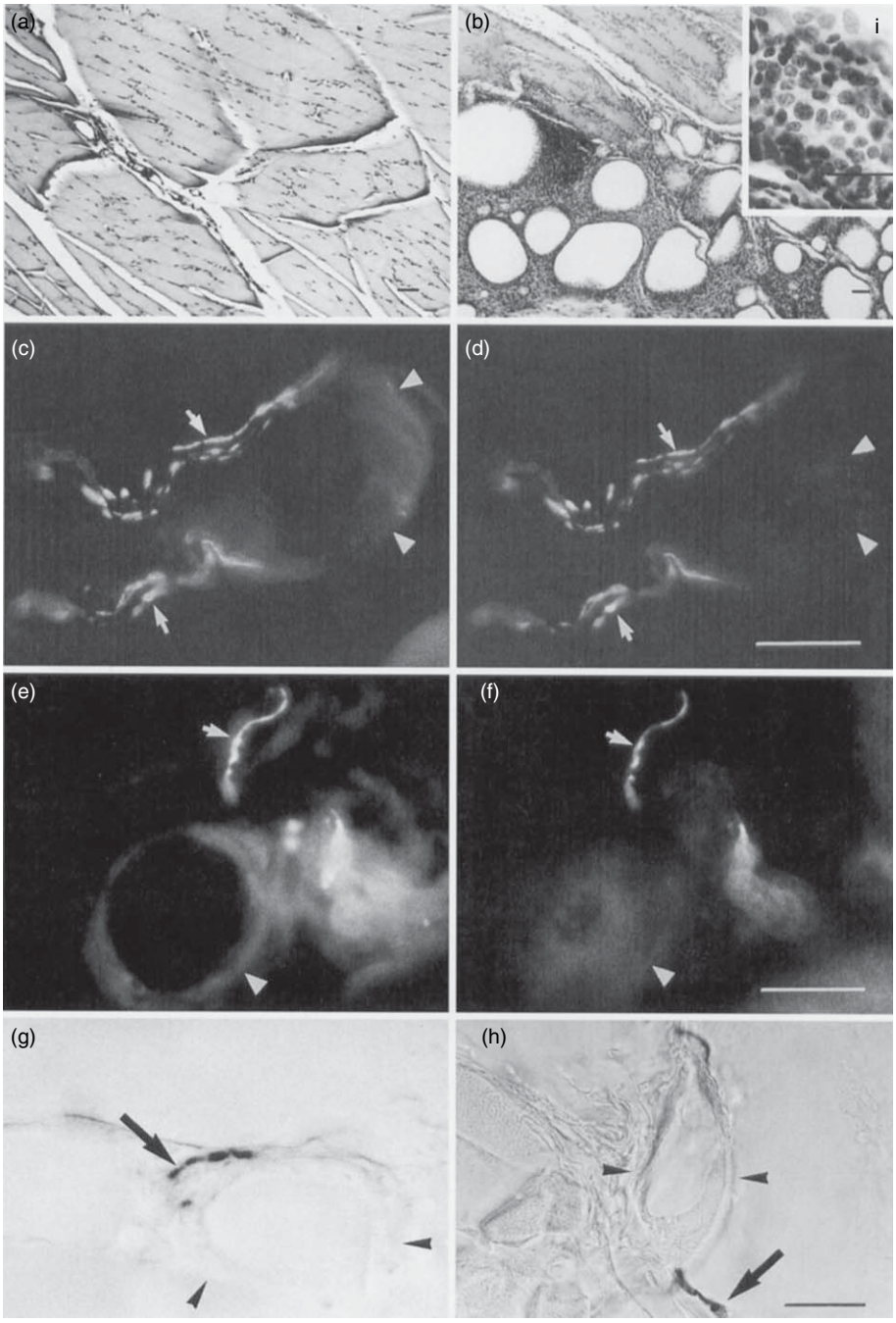

Figure 12 (a and b) Sections of intact (a) and persistently inflamed (b) muscle. Scale bar = 100 μm. The insert (i) in (b) shows lymphoid cells between vacuoles at a higher magnification. Scale bar = 50 μm. (c–f) Neuropeptide-ir nerve fibers in muscle. (c) Varicose SP-ir fibers (arrows) in the adventitia of an artery (arrowheads). (d) The fibers shown in (c) double-labeled for calcitonin gene-related peptide (CGRP). (e) Perivascular SP-ir fiber that is also ir for vasoactive intestinal polypeptide (VIP; (f)). (g) Perivascular fiber in inflamed muscle exhibiting immunoreactivity for NGF (arrow, same magnification as in (h)). (h) Growth-associated protein 43 (GAP 43)-ir fiber (arrow) in the wall of an artery (arrowheads). Scale bar = 25 μm (c–h). (From Reinert, A. *et al.*, 1998, with permission.)

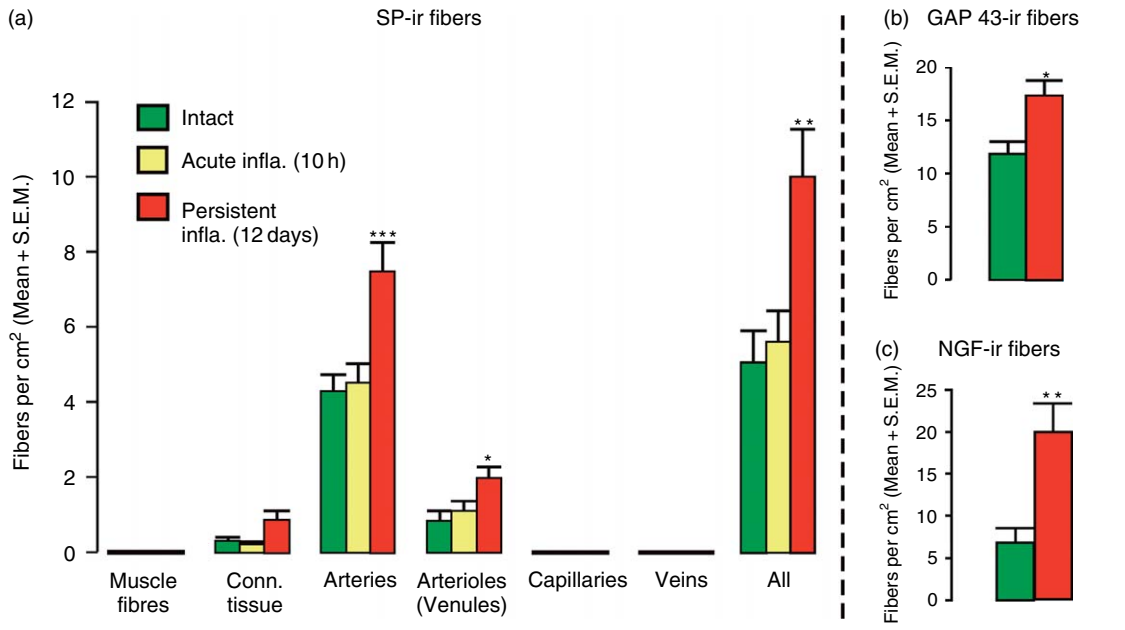

Figure 13 Innervation density of substance P-immunoreactive (SP-ir), growth-associated protein 43 (GAP 43)-ir, and nerve growth factor (NGF)-ir fibers in intact and inflamed muscle. Acute inflammation (yellow bars), duration 10 h; persistent inflammation (red bars), duration 12 days. (a) Distribution of SP-ir fibers in the components of muscle tissue. Note that no fibers were found close to muscle fibers and capillaries. Asterisks mark the level of significance compared to intact muscle. $^{*}p < 0.05$; $^{**}p < 0.01$; $^{***}p < 0.001$, *U* test. (Modified after Reinert, A. *et al.*, 1998.)

in skeletal muscle of the cat was published by Stacey M. J. (1969). He used the silver impregnation technique in sympathectomized animals and focused on endings supplied by group III and IV fibers. The majority of the latter had a diameter of 0.35 µm; the unmyelinated afferents outnumbered the myelinated ones by a factor of 2. A prominent location of free nerve endings supplied by group IV fibers was the adventitia of arterioles and venules. Myelinated (group II and III) afferents generated not only free nerve endings but also paciniform corpuscles, whereas unmyelinated fibers terminated exclusively in free nerve endings.

In another study on sympathectomized cats, von Düring M. and Andres K. H. (1990) reported that the predominant location of group III and IV endings was in the perimysium surrounding larger or smaller bundles of muscle fibers. Other locations were the adventitia of arterioles, venules, and lymphatic vessels (LV), and finally the endoneurium of nerve fiber bundles. The latter terminals were assumed to belong to nervi nervorum. In muscle, the terminals of group III fibers were generally larger than those of group IV fibers, and they contained more mitochondria and a more distinct receptor matrix. Figure 14 shows a group IV terminal in the endomysium around the precapillary segment of a blood vessel in the soleus muscle. The ending contained clear and dense-core vesicles and had exposed membrane areas. The authors suggested that those terminals (mainly originating from group III fibers) that had a close association with connective tissue may have a mechanoreceptive function mediating stretch or pressure, whereas endings that lacked this feature but had a spatial relation to mast cells were nociceptors.

5.03.3.3.2.(ii).(b) Tendon The electron microscopic reconstruction of free endings in the calcaneal tendon of the cat yielded various morphological types of free nerve endings connected to group III and IV afferent fibers (Andres, K. H. *et al.*, 1985). Based on morphological criteria or the location in the tissue, the authors distinguished five types of free nerve endings supplied by group III fibers: Type 1 terminated in venous vessels (VV) (called the lanceolate type); it was special in that it had a flattened profile in cross sections and possessed exposed receptive areas on its edges. Type 2 ended in the wall of LV. Types 3 and 4 supplied the connective tissue around blood vessels, and one of these types had contacts to collagen fiber bundles. The collagen bundles were assumed to transfer mechanical forces to

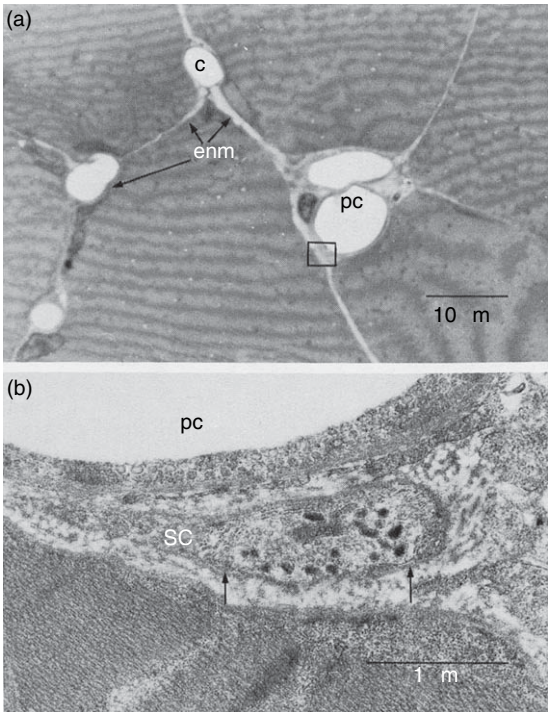

Figure 14 Nerve terminal of a group IV fiber in the soleus muscle of the cat. Rectangle in (a) represents the area of the receptor shown in (b). The terminal axon contains numerous dense-core and clear vesicles. pc, precapillary segment; c, capillary; SC, Schwann cell. Arrows indicate exposed axonal membrane areas. (From von Düring, M. and Andres, K. H., 1990, with permission.)

the receptive ending and, therefore, the endings were viewed as mechanoreceptors. The fifth type of group III ending innervated the endoneural connective tissues of small nerve fiber bundles (Figure 15).

In the same study, two types of free nerve endings of group IV fibers were described; both were located in the connective tissue of blood vessels, and some of the fibers contained granulated vesicles. The terminals showed penicillate formations (Figure 16).

5.03.3.3.3 Nociceptors in joints and ligaments

5.03.3.3.3.(i) Pain from joints In humans, experimental joint pain has been evoked by administration of noxious mechanical and chemical stimuli to the articular capsule and ligaments. No pain is elicited by stimulation of cartilage, because cartilage is not innervated. Joint inflammation is characterized by hyperalgesia and persistent pain at rest. The discharge properties of joint nociceptors largely reflect these subjective phenomena of joint pain (Guilbaud, G. *et al.*, 1985; Schaible, H.-G. and Schmidt, R. F., 1985; Schaible, H.-G. and Grubb, B. D., 1993; Schaible, H.-G., 2006). In inflamed joint, initially mechanoinsensitive afferents (silent nociceptors) are sensitized and may become mechanosensitive (Schaible, H.-G. and Schmidt, R. F., 1988).

5.03.3.3.3.(ii) Ultrastructure of articular free nerve endings In a thorough investigation of articular endings, Heppelmann B. *et al.* (1990a) studied free nerve endings from the knee joint of the cat in sympathectomized animals. Figure 17 shows the reconstruction of group III and IV nerve endings from the joint capsule of the cat's knee joint. As in other tissues, free nerve endings in joint were ensheathed by Schwann cells, and only some sites were not covered. Usually, these exposed areas were located in the varicosities of the ending (the beads) and the end bulb, here the axon, often directly abutted the basal lamina. The exposed membrane areas were assumed to be the receptive sites of the fibers; they exhibited structures that are often associated with receptive sites: aggregates of mitochondria, glycogen particles, vesicles in the axoplasm, and an electron-dense filamentous structure of the axoplasm (the receptor matrix). The end bulb, i.e., the most distal beaded end of the fiber (Figure 18 shows the end bulb of one branch of the group III unit reconstructed in Figure 17), had generally the same structure as the axonal beads, except that the mitochondria showed a special arrangement: the organelles were not oriented in parallel as in the axonal beads but pointed with their axis in all possible directions.

In the cat's knee joint capsule, free nerve endings generated by group III fibers were smaller in axon diameter and had shorter branches (up to 200 μm) than those supplied by group IV fibers (more than 300 μm). The main difference between group III and IV endings was that the latter never had a neurofilament core in their axoplasm, which was present in all axons and axonal beads of group III fibers (but not in the end bulbs). The functional significance of the neurofilament core is obscure; one possible function is mechanical stabilization of the group III endings that usually have a more unfavorable quantitative relation between the fluid axoplasm and the more rigid axolemma.

The authors of these and similar data (Heppelmann, B. *et al.*, 1990a; 1990b; Messlinger, K., 1996) put forward the concept that both group III and IV fibers form sensory terminal trees that consist of the preterminal axon and its branches (Figure 5). The

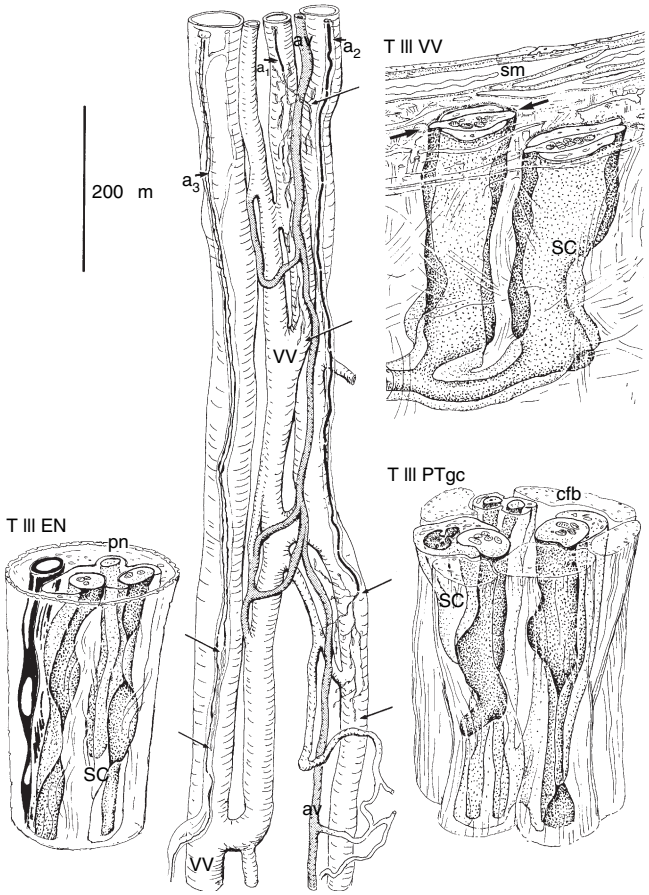

Figure 15 Group III fiber terminals in cat calcaneal tendon. Reconstruction of a series of sections over a length of 1 mm showing three different terminals of group III afferents. A fascicle of arterial vessels (av) and venous vessels (VV) with some arterio-venous anastomoses is accompanied by small nerve fiber bundles of which the myelinated axons (a_1, a_2, a_3) are reconstructed. The schematic drawings show segments of three different terminals at a higher magnification (T III VV, T III PTgc, and T III EN) with their typical relations to the surrounding tissue structures. Axon membrane segments without any Schwann cell (SC) covering are marked by higher contrast. The terminal of the a_1 axon is the T III VV type with two lanceolate terminals in the adventitia of the vessel. The arrows indicate the free edges of the terminal. Smooth muscle cell (sm). The terminal of the a_2 axon is type T III PTgc in the connective tissue of the vessel–nerve–fiber fascicle. The terminals are oriented to collagen fiber bundles (cfb). The terminal of the a_3 axon is the T III EN type. The terminals ramify within the endoneural space. Another small myelinated axon passes the terminals. Perineural sheath (pn). The length of the receptive areas of each myelinated axon is indicated in the reconstruction by arrows. (From Andres, K. H. *et al.*, 1985, with permission.)

terminal tree is not covered by myelin (in group III endings) and lacks a perineurial sheath (in both group III and IV endings); it is assumed to form the sensory ending proper.

Considerations on the space constant of free nerve endings prompted Heppelmann B. *et al.* (1990a; 1990b) to hypothesize that the distance from the end bulb as the main receptive region to the regenerative region – where the action potential originates – may be dangerously great for a safe transformation of the receptor potential into an action potential. Therefore, the axonal beads may not only serve as receptive sites but also as amplifiers of the receptor potential.

The group IV endings terminating in the medial collateral ligament (Figure 19) exhibited the same features as the terminals in the joint capsule: They had exposed membrane areas and contained mitochondria, glycogen particles, and vesicles (Heppelmann, B. *et al.*, 1990b; Messlinger, K., 1996).

Group III and IV fibers of the joint terminate as free nerve endings in the fibrous capsule, adipose tissue, ligaments, menisci, and periosteum. Staining

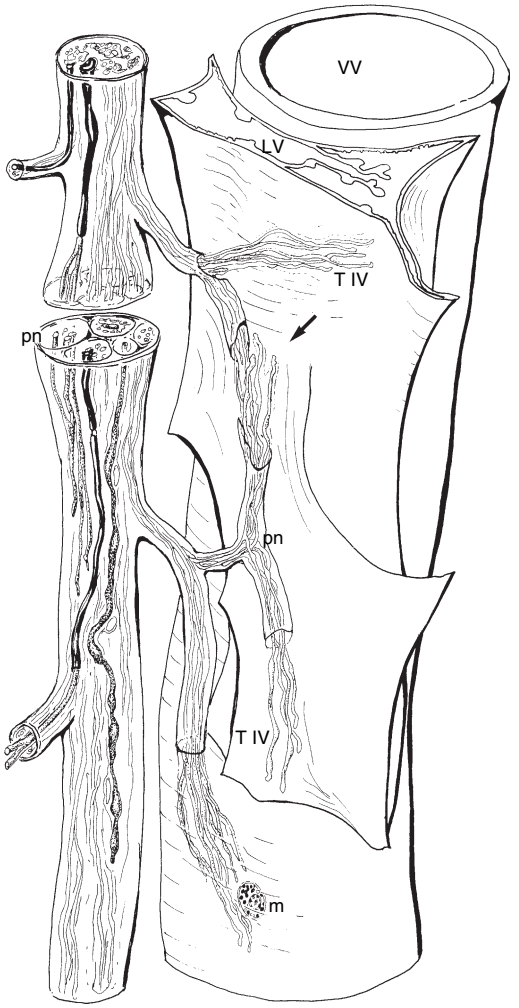

Figure 16 Group IV fiber terminals (T IV) in cat calcaneal tendon. Schematic drawing of group IV fibers and their sensory regions in the surrounding connective tissue of venous (VV) and lymphatic (LV) vessels. Perineural sheath (pn). The various parts of the scheme are not to scale. The terminal bundles end in penicillate formations. (From Andres, K. H. *et al.*, 1985, with permission.)

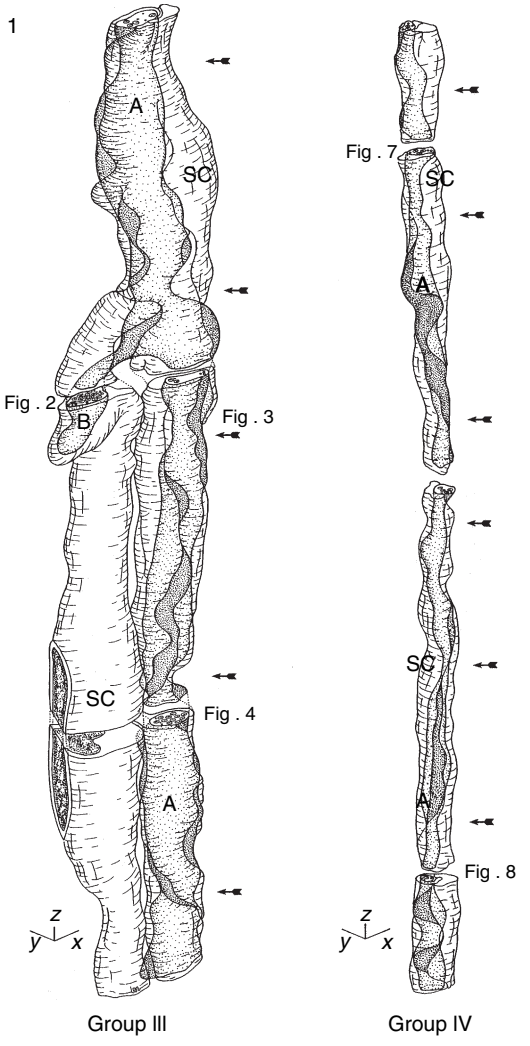

Figure 17 Sensory endings in the knee joint capsule of the cat. Reconstructions based on ultrathin sections at 1-μm intervals. Areas of bare axolemma without Schwann cell covering are marked by dense stippling. A, sensory axon; SC, Schwann cell; arrows, thin segments between axonal beads (×6000). *x*, *y*, *z* bars, 1 μm. *Left*: group III fiber, length of reconstructed fiber 70 μm. *Right*: group IV fiber. The axonal beads are shorter and the thin segments longer than in group III fibers. Areas of bare axolemma are interrupted by axon segments with complete Schwann cell wrapping. (From Heppelmann, B. *et al.*, 1990b, with permission.)

for nerve fibers and neuropeptides also demonstrated endings in the synovial layer. Interestingly, a few group IV endings terminated in the perineurium (PN) of the articular nerve. Assuming that these endings are nociceptors, they might be responsible for neuropathic pain originating in the joint.

The major neuropeptides in small-diameter joint afferents were SP, CGRP, and somatostatin (SOM). Neurokinin (NK)-A, galanin, enkephalins, and neuropeptide Y have also been localized to joint afferents (Schaible, H.-G. and Grubb, B. D., 1993; Schaible, H.-G., 2006).

5.03.3.3.4 Tooth pulp

5.03.3.3.4.(i) Toothache In psychophysiological studies, electrical stimulation of the tooth pulp has been reported to elicit pain exclusively (Andersson, S. A. *et al.*, 1973). Therefore, the free nerve endings in the pulp were assumed to be either nociceptors or sympathetic postganglionic fibers. Rats show aversive behavior when capsaicin is applied to the exposed

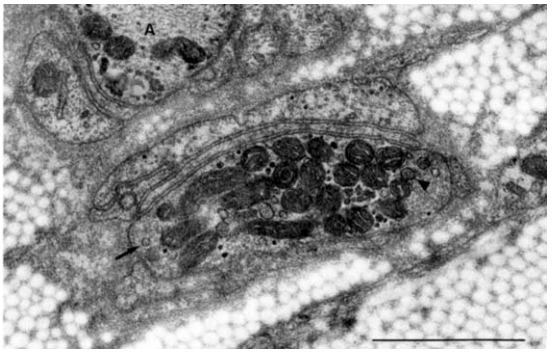

Figure 18 Axonal end bulb of an articular group III fiber in the cat. In addition to mitochondria and glycogen particles, the end bulb contains several clear vesicles (arrow) and larger dense-core vesicles (arrowhead). In contrast to more proximal axonal beads, microtubules and a neurofilament core are missing in the end bulb. (From Heppelmann, B. *et al.*, 1990a, with permission.)

dentine of the incisors (Chidiac, J. J. *et al.*, 2002; Rifai, K. *et al.*, 2004). The latter observation indicates that nociceptive afferents of the tooth pulp are equipped with the TRPV1 receptor for which capsaicin is a specific ligand.

Functional studies of the receptive properties of single unmyelinated tooth pulp afferents are scarce. The published data show that slowly conducting afferent units from cat are sensitive to stimuli that are known to elicit pain in humans (hot and cold, local administration of bradykinin (BK), and mechanical stimulation) (Jyväsjärvi, E. and Kniffki, K. D., 1992). Many of the recorded units responded to more than one stimulus and thus behaved like polymodal nociceptors. In another study, the sensitivity to capsaicin of Aβ-, Aδ-, and C-fibers was compared in cat tooth pulp afferents. Not only C-fiber endings were excited but also Aδ-units, albeit at a smaller proportion. None of the Aβ-endings responded to the stimulant (Ikeda, H. *et al.*, 1997).

No studies combining electrophysiological and morphological techniques were conducted on teeth. Therefore, in morphological investigations a possible nociceptive function of the free nerve endings can be discussed, but is not sure.

5.03.3.3.4.(ii) Light and electron microscopy

Data are available from many species including man. The morphology of the free nerve endings is similar to that described above for other tissues in more detail. In the following paragraph, possible differences between nerve fibers in mature and continuously growing teeth (e.g., mice incisors) are not considered.

(1) The great majority (56–79.6% in the cat mandibular canine tooth; Holland, G. R. and Robinson, P. P., 1983) of the fibers supplying the tooth pulp are unmyelinated with a mean diameter of 0.4 μm in man (Koling, A., 1985); they often branch and form a dense subodontoblastic plexus (the peripheral plexus of Raschkow, see Byers, M. R., 1984, for review) in the apex of the tooth. Between the plexus and the odontoblast layer, there is the cell-free zone of Weil. Figure 20 shows an overview of the afferent fibers in the root and coronal pulp of a rat molar. The data were obtained in experiments in which the trigeminal ganglion was injected with an anterogradely transported marker (WGA-HRP) to visualize afferent fibers only (Ibuki, T. *et al.*, 1996). In the subodontoblastic region, axo-axonal appositions and appositions between axons and odontoblasts have been described by some authors, but others could not support this finding. The other pulpal afferents conduct in the Aδ-range; Aβ-fibers are sparse.

(2) Many axons are incompletely ensheathed by Schwann cells (Figure 21); they sometimes leave the Schwann cell sheath completely to terminate as naked axons in the extracellular space. In those fibers that do have a sheath, the Schwann cells often lack a basal lamina (Figure 22; Byers, M. R. *et al.*, 1982). The majority of the afferent fibers form beaded free nerve endings in odontoblast layer, predentin, and in dentinal tubules, many of which are innervated. The intradentinal endings extend only 100–200 μm into the dentin, and sometimes more than one axon accompanies an odontoblast process (Figure 23). Gunji T. (1982) put forward the concept that the odontoblast processes and the axons in the dentinal tubules form a mechanoreceptive complex. In contrast to the intradentinal axons, the odontoblast processes reach the dentin–enamel border and could be deformed by mechanical stimuli. The mechanical movements or deformations of the processes may then excite the sensory axons that do not penetrate that far into the dentinal tubules.

(3) The varicosities of the free nerve endings exhibited specializations known from nociceptors in other tissue such as mitochondria, small clear and large dense-core vesicles, smooth endoplasmic reticulum, and few microtubules and neurofilaments (Figure 24; Byers, M. R., 1984; Ibuki, T. *et al.*, 1996). Ibuki T. *et al.* (1996) distinguished between

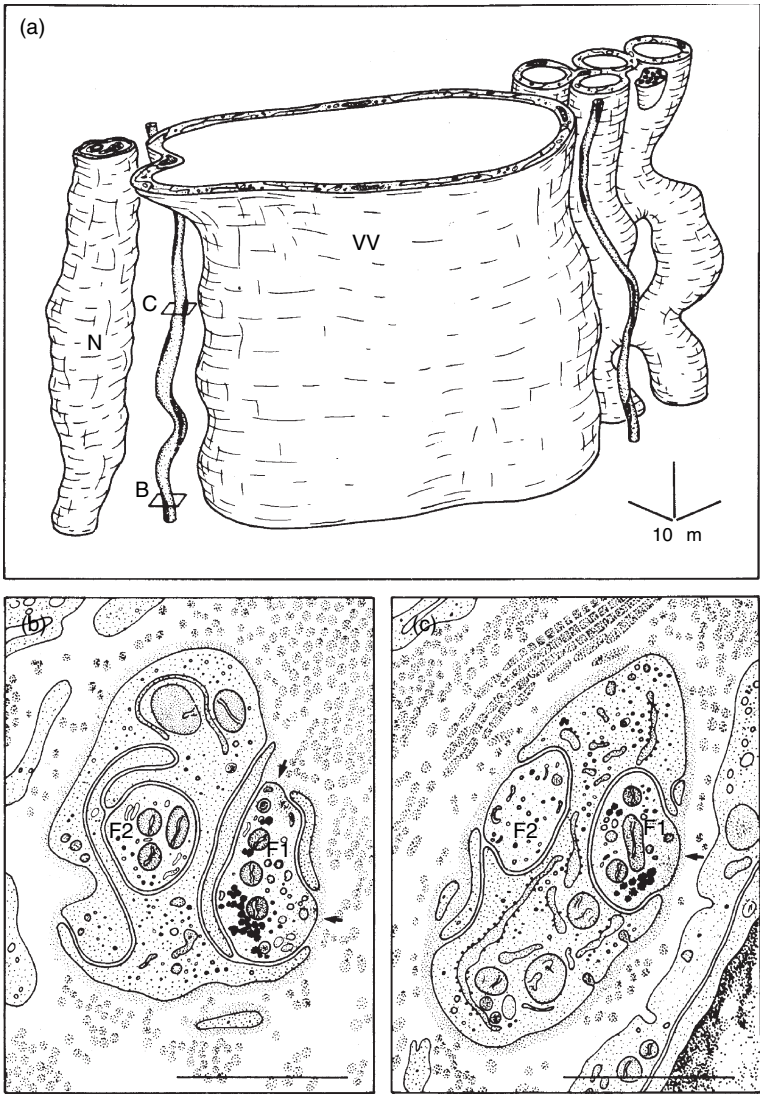

Figure 19 Group IV fiber endings at a venous vessel (VV) in the medial collateral ligament of the cat. (a) Reconstruction based on serial semi- and ultrathin sections. Besides a small peripheral nerve (N), two terminal nerve fiber bundles without perineurial sheath that enclose two group IV fibers (*left*) and one single fiber (*right*) run along the VV. (b and c) Cross sections of the nerve fiber bundle with two group IV fibers as marked in Figure 3(a) at high magnification. Drawings from original electron micrographs. Scale bar = 1 μm. (b) Cross section showing a bulge of one of the nerve fibers (Fl) with bare areas of the axolemma (arrows), mitochondria, glycogen particles, and vesicles. The other nerve fiber (F2) is completely ensheathed by the Schwann cell. C, cross section 40 μm distal from that of Figure 3(b) showing the final thickening of the nerve fiber Fl with bare area of axolemma (arrow). The second nerve fiber (F2) continues. (From Heppelmann, B. *et al.*, 1990b, with permission.)

two types of varicosity: one contained many mitochondria, while the other was characterized by the presence of large dense-core and small clear vesicles. Generally, a rich supply with mitochondria and glycogen particles is interpreted as an indication of high energy demands and, therefore is likely to occur in endings with a low mechanical threshold and high firing probability, while nociceptive endings have a lower probability of being excited, and therefore need less mitochondria.

(4) Besides a nociceptive function many of the small-caliber tooth afferents may have a trophic influence on blood vessels in the pulp or on odontoblasts. They may be necessary for repair or normal growth, as in continuously growing teeth. The finding that the anterograde marker

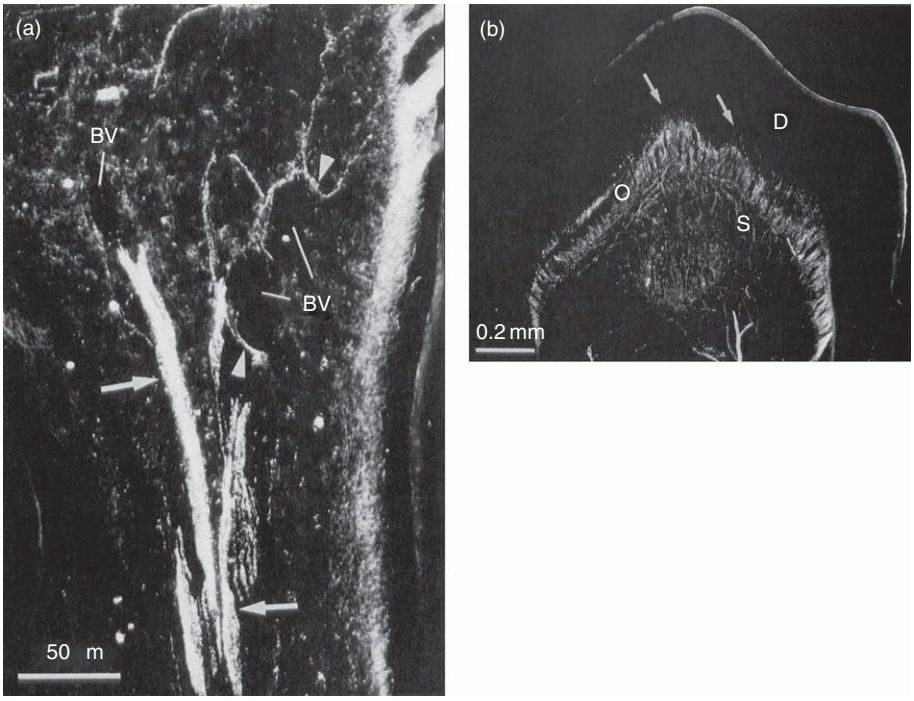

Figure 20 Innervation of root pulp (a) and coronal pulp (b) in a rat tooth. The fibers were labeled anterogradely from the trigeminal ganglion. (a) Bundles of labeled fibers (arrows) run along the blood vessels (BV) of the root pulp. Some fibers surround the blood vessels (arrowheads). (b) The fibers form a subodontoblast plexus (S) and penetrate the dentin (arrows). D, dentin; O, odontoblast. (From Ibuki, T. *et al.*, 1996, with permission.)

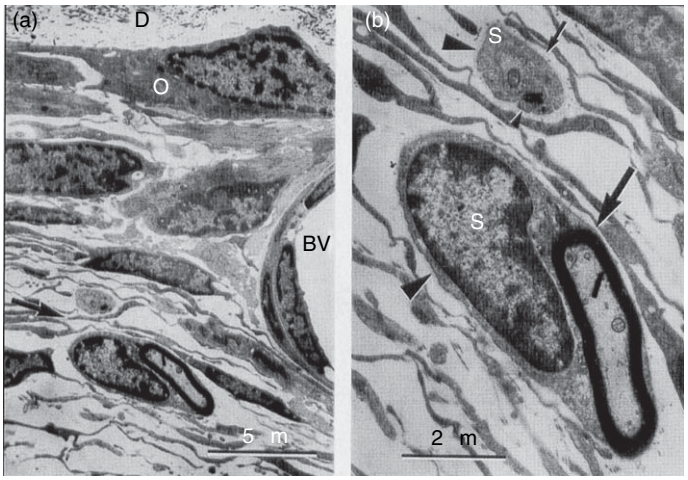

Figure 21 (a) Fibers labeled anterogradely with horseradish peroxidase in the subodontoblastic region of the tooth. BV, blood vessel; D, dentin; O, odontoblast. (b) High magnification of the area marked by an arrow in (a). Horseradish peroxidase reaction product is present in the myelinated Aδ-axon (large arrow) and unmyelinated axons (small arrow). The unmyelinated axon has partially lost its Schwann cell sheath (arrowheads). S, Schwann cell. (From Ibuki, T. *et al.*, 1996, with permission.)

(WGA-HRP) injected into the trigeminal ganglion by Ibuki T. *et al.* (1996) was found not only within the axons but also outside between the axons and the odontoblast processes (Figure 24) was assumed to reflect a release process that normally supplies the odontoblasts with trophic substances. This hypothesis resembles the nocefector concept of Kruger.

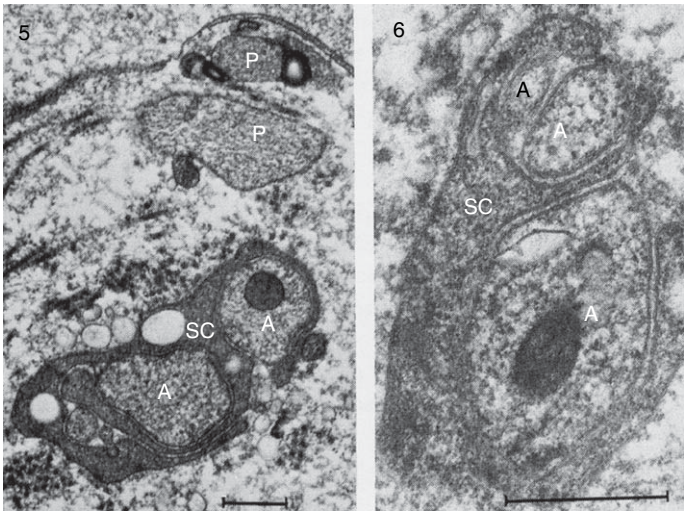

Figure 22 Nerve fibers in the cell-free zone of the tooth pulp. Unmyelinated axons (A) were identified in this zone when surrounded by a Schwann cell (SC), but no basal lamina accompanied the Schwann cell. Other cell processes (P) could be axons or fibroblasts. Scale bars, 0.5 μm (×42300). (From Byers, M. R. *et al.*, 1982, with permission.)

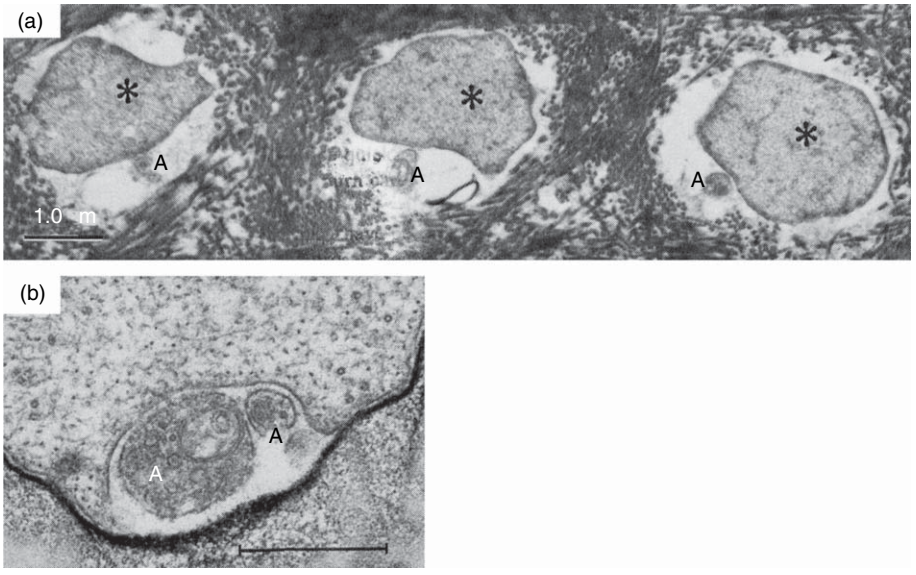

Figure 23 Axons in dentinal tubules. (a) A cluster of adjacent dentinal tubules at the predentin–dentin border. Each tubule contains an axon (A) and an odontoblast process (*) (×10350). (b) Two adjacent axons in the same dentinal tubule. (From Byers, M. R. *et al.*, 1982, with permission.)

5.03.3.3.4.(iii) Neuropeptide content and equipment with receptor molecules Sensory dental axons contain many neuropeptides (SP, CGRP, VIP, enkephalin), the most interesting one being SP because of its relation to a nociceptive function. A particularly rich innervation with CGRP-ir fibers was found in the subodontoblast layer and the dentinal tubules (Kruger, L. and Halata, Z., 1996). These endings were thought to have a noceffector function (Kruger, L., 1988).

SP-ir fibers predominated in the center of the tooth pulp. The expression of SP in carious human teeth has been found to be increased, and the increase was larger in symptomatic than in asymptomatic teeth. This finding parallels the results obtained from inflamed muscle (see above) and suggests that

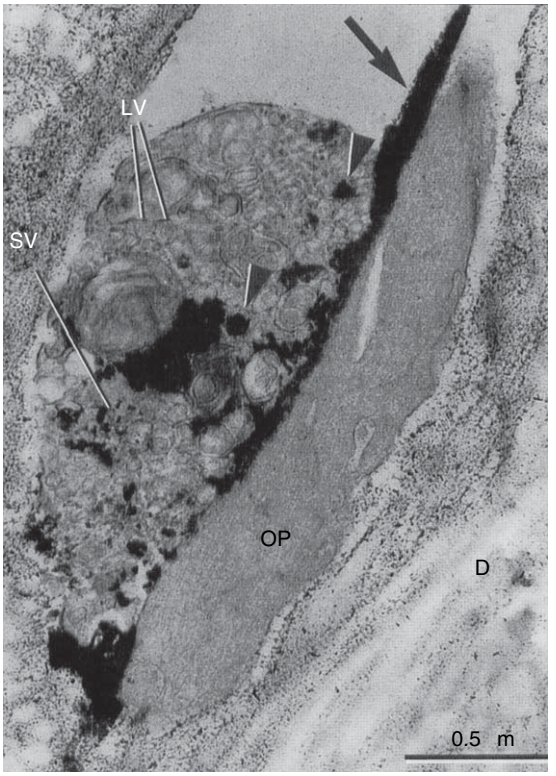

Figure 24 Anterogradely labeled sensory varicosity adjacent to an odontoblast process (OP) in dentin. The varicosity is full of large dense-core vesicles (LV) and small clear vesicles (SV). Some vesicles (arrowheads) contain the horseradish peroxidase reaction product used for anterograde labeling. The reaction product is also present in the extracellular space (arrow). D, dentin. (From Ibuki, T. *et al.*, 1996, with permission.)

SP plays an important role in the mediation of toothache (Rodd, H. D. and Boissonade, F. M., 2000). In one patient with hereditary sensory and autonomic neuropathy, CGRP- and SP-ir fibers were completely missing, which could explain the sensory deficit associated with this condition (Rodd, H. D. *et al.*, 1998). The lack of CGRP- and SP-ir fibers was accompanied by an upregulation of neuropeptide Y.

The nerve endings in the tooth pulp have been shown to be equipped with receptor molecules that are thought to be associated with a nociceptive function, e.g., P2X3, TRPV1 (Renton, T. *et al.*, 2003), and the vanilloid receptor-like protein, VRL1. In rat molar tooth pulp, fibers ir to trkB (the receptor for BDNF and NT-4) were found. These fibers included both unmyelinated and myelinated units. This and other findings were interpreted as indicating that BDNF and/or NT-4 are involved in the development, differentiation, or regeneration of the tooth pulp innervation (Foster, E. *et al.*, 1995).

However, not all free nerve endings can be considered to be nociceptive; in the tooth pulp many endings appear to supply blood vessels (Zhang, J. Q. *et al.*, 1998). The vascular innervation with neuropeptide-ir nerve endings is largely restricted to arterioles; capillaries and lymphatics were mostly devoid of an innervation. This distribution pattern resembles that of skeletal muscle. Substances involved in the vascular and cellular regulation of the tooth pulp in the rat are SP, NK-A, and CGRP, which are thought to be released from nerve endings. This function was inferred from the finding that pulpal hard tissue cells, blood vessels, and fibroblasts were equipped with NK-1 and NK-2 receptors (for SP and NK-A, respectively) as well as CGRP1 receptors (Fristad, I. *et al.*, 2003).

5.03.3.3.5 Dura mater encephali

5.03.3.3.5.(i) Headache Generally, those types of headache that are associated with vascular changes in the meninges (e.g., migraine) are being attributed to the activation of para- or perivascular nociceptive endings by agents released from the nerve terminals. Among these substances are SP, CGRP, and NK-1. Observations supporting this assumption are that – when tested in awake subjects – meninges are most painful close to blood vessels, and that migraine pain is most intense during the phase of vasodilatation and increase of vascular permeability.

5.03.3.3.5.(ii) Light and electron microscopy In their light and electron microscopic study on receptive endings in the dura mater of the rat, Andres K. H. *et al.* (1987) described terminals of myelinated and unmyelinated fibers. The tissue around postcapillary blood vessels and the superior sagittal sinus exhibited a particularly high innervation density of endings. Contrary to former belief, the dura also contained LV (Figure 25). These vessels were innervated mainly by endings from unmyelinated fibers.

Some of the myelinated fibers terminated in Ruffini-like nerve endings, while most of the myelinated and all of the unmyelinated fibers terminated in free nerve endings. The Ruffini-like receptors were located close to collagen fiber bundles of the wall of the sagittal sinus and of other blood and LV. They were viewed as stretch receptors.

Among the free nerve endings formed by unmyelinated fibers, one type was located very close (at a distance of $<1\,\mu m$) to the endothelial cells of the

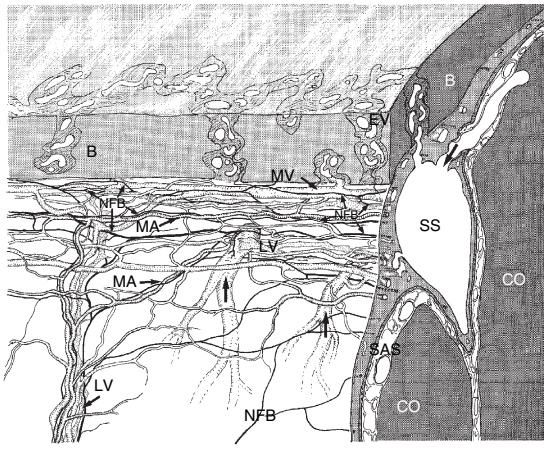

Figure 25 Vascular bed of the dura underneath the parietal bone (B) and dorsal to the sagittal sinus (SS). Arrows, entrance of the superior cerebral veins into the sagittal sinus; MA, branches of meningeal artery; MV, branches of meningeal vein; EV, emissary vein; LV, lymphatic vessels; NFB, nerve fiber bundles exhibiting a terminal plexus; CO, cortex; SAS, subarachnoidal space. (From Andres, K. H. *et al.*, 1987, with permission.)

postcapillary venules. It had the typical appearance of free nerve endings in other tissues with exposed membrane areas, mitochondria, vesicles, and a receptor matrix. The endings that were located close to the wall of blood vessels would be in a good position to monitor the composition of the interstitial fluid in the vicinity of the vessels (Figure 26). They could well perform nociceptive functions, for instance in cases of headache when sensitizing and pain-producing substances are released from the blood plasma and afferent nerve fibers.

Many of the nerve fibers accompanying blood vessels contained CGRP or SP (Figure 27; Hanesch, U., 1996). Like in other tissues, SP-ir fibers were less numerous than CGRP-ir ones. While SP-IR was located inside the axoplasm, the SP receptor NK-1 was found on the outer membrane of the Schwann cells surrounding the axons.

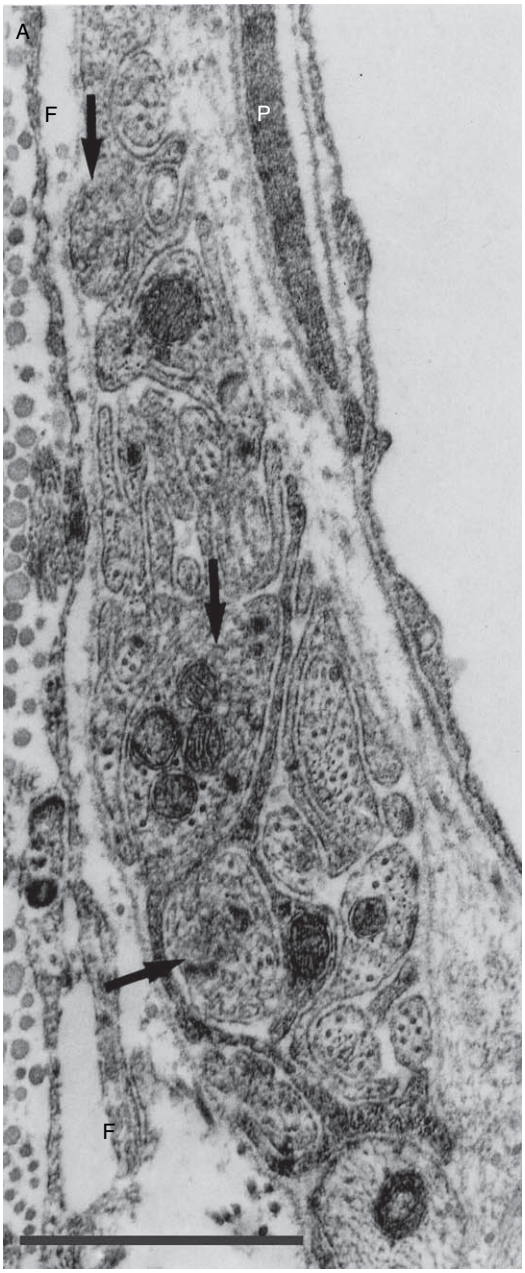

Figure 26 Nerve terminations in the dura at the wall of a venous vessel. Axon profiles with vesicles and receptor matrix are indicated (arrows); the other axons exhibit cytoskeletal elements (×45000). Scale bar = 1 μm. The gap between the terminal and the postcapillary venule with endothelial fenestration is <1 μm. F, process of fibrocyte; P, pericyte. (From Andres, K. H. *et al.*, 1987, with permission.)

5.03.3.4 Visceral Organs

5.03.3.4.1 Visceral pain

The mechanisms of visceral pain are still poorly understood. Apparently, some inner organs are equipped with specific nociceptors (HTM and polymodal ones; Jänig W. (1996), for review), but their existence has not been proven for all viscera. It is conceivable that the pain from some viscera is mediated not by specific nociceptors but is encoded in the pattern of discharge in populations of relatively unspecific visceral afferents. The clinical observation that a small cut into the gut is not painful, but spasm or ischemia of a larger area causes strong

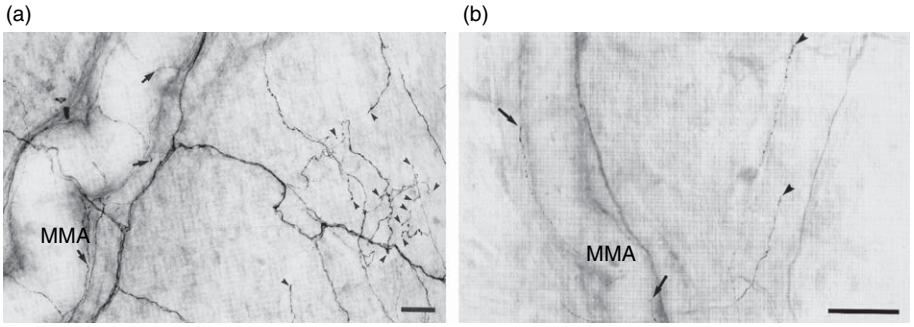

Figure 27 Neuropeptide-ir nerve fibers in the dura mater of the rat. (a) CGRP-ir fibers accompany and cross the middle meningeal artery (MMA). Small bundles of fibers branch off the main bundle and terminate in the connective tissue thereby forming tree-like endings (arrowheads). Some fibers end at the artery (arrows). (b) SP-ir fibers accompanying the MMA. Single beaded nerve fibers terminate at the vessel wall (arrows) or in the connective tissue between blood vessels (arrowheads). (From Hanesch, U., 1996, with permission.)

pain, is generally attributed to the low innervation density of the inner organs.

5.03.3.4.2 Testis

Electrophysiological studies by Kumazawa and coworkers (Kumazawa, T. and Mizumura, K., 1980; Kumazawa, T. *et al*., 1987) have shown that in the tissue layers covering the seminiferous tubules in the rat, endings with unmyelinated afferent fibers are present that behave like polymodal nociceptors in that they can be activated by mechanical stimuli, pain-producing substances, and heat. The innervation density of the tissue is low, and the receptive endings are located directly underneath the tunica albuginea. These properties made it possible to relate the mechanosensitive spots found in electrophysiological experiments to structures in histological specimen.

Kruger L. and coworkers (2003b) used this approach to elucidate the ultrastructure of nociceptive endings of the testis. In the electrophysiological experiments, the location of the receptive ending was marked with insect pins. The endings were reconstructed from serial electron microscopic sections (Figure 28), and in general they showed the features described above for putative nociceptors in other tissues. The preterminal axon had expansions (varicosities) with axonal constrictions in between. Approaching the terminal proper, the axons often lost their microtubules and neurofilaments. Instead, a network of axonal reticulum (probably endoplasmic reticulum) appeared that was embedded in a granular matrix (similar to the receptor matrix of Andres, K. H. and von Düring, M., 1973). This arrangement of an axonal reticulum in a granular matrix (Figure 29) has not been described by other authors, but it is unclear if this arrangement is special for testicular nociceptors, or if it had been overlooked in other tissues.

In the distal tip of the axon, the axolemma exhibited a greater number of exposed areas that directly contacted the basal lamina. The authors stress the presence of clusters of small spherical vesicles, aggregates of mitochondria, and axonal reticulum in a granular matrix in this part of the axon that apparently forms the receptive terminal (Figure 30). Interspersed between the spherical vesicles were so-called granular vesicles that differed somewhat from the dense-core vesicles of endings containing catecholamines and, therefore, could be distinguished from sympathetic nerve endings.

The functional interpretation of the ultrastructure of the terminal poses some problems: Even though it is characterized by special features (vesicle clusters, mitochondria, and exposed axolemma), the axonal zones close to the terminal likewise exhibited some of these specializations. Therefore, it is difficult to decide if only the ultimate terminal is the receptive site where the electrical receptor potential originates or if also other parts of the preterminal branches can be viewed as receptive, as in the sensory tree concept. An important question in this context is where the generator portion of the nociceptor axon is located and if it exhibits structural specializations different from those of the receptive terminal.

5.03.4 Neuropeptide Content of Nociceptors

5.03.4.1 General Remarks

In many cells, neurotransmitters coexist with neuropeptides, or one neuron contains more than

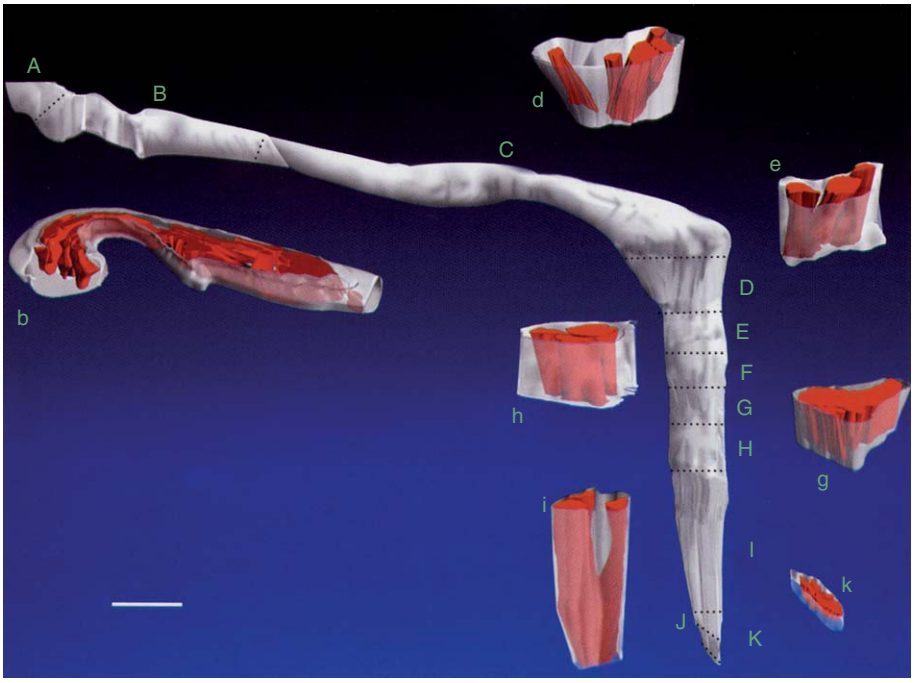

Figure 28 Three-dimensional reconstruction of a pin-marked receptive field (RF) identified from a physiologically characterized nociceptor polymodal fiber discharge in an *in vitro* canine testicular preparation based on a series of semithin (~1 μm) sections from which ultrathin sections were obtained in each of the sectors, labeled A–K. In the segments indicated in lower case, axons are shown in red and Schwann cell basal lamina boundaries in white. Scale bar = 1 μm. (From Kruger, L. *et al.*, 2003b, with permission.)

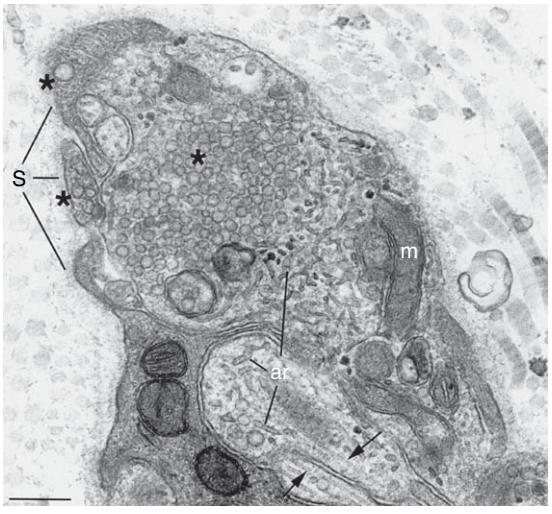

Figure 29 Electron micrograph (from sector E of Figure 28) displaying a putative receptive terminal containing a characteristic preterminal array of axonal reticulum (ar), microtubules (arrows), glycogen granules, and spherical vesicles (asterisks) embedded in a granular matrix and clustered below a surface ensheathed by dark Schwann cell processes (S) and containing vesicles. The bare upper axolemma is in direct contact with the basal lamina. Scale bar = 0.5 μm. (From Kruger, L. *et al.*, 2003, with permission.)

one neuropeptide. It is well known that a large proportion of SP-expressing DRG neurons also contain glutamate. Another example is that almost all DRG cells that are ir for CGRP also exhibit IR for SP and other neuropeptides (Ju, G. *et al.*, 1987). It is generally assumed that glutamate acts as the main neurotransmitter in nociceptive afferents, whereas the neuropeptides function as neuromodulators that – with few exceptions – enhance the central nervous effects of peripheral noxious stimuli (Hökfelt, T. *et al.*, 1980; Kow, L.-M. and Pfaff, D. W., 1988). The peptides are synthesized in the somata of the DRG or in ganglion cells of cranial nerves. They are transported to both the central and the peripheral terminal of the primary afferent unit.

5.03.4.2 Neuropeptides in Afferent Units of Different Tissues

No neuropeptide has been found that can be considered specific for afferent fibers from a particular tissue. DRG cells projecting in a cutaneous nerve

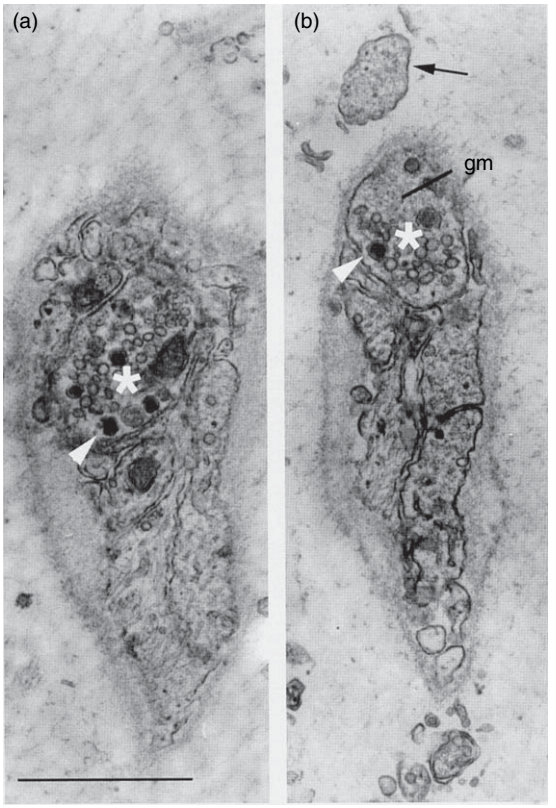

Figure 30 Electron micrograph of the final traced portion of the marked receptive field (RF) indicated in sector K of Figure 28 containing the final vesicle-rich axonal profiles, including several dense-core vesicles (arrowheads), all within a granular matrix (gm) exposed in b to the basal lamina. Arrow, additional unidentified profile. Scale bar = 1 μm. (From Kruger, L. *et al.*, 2003b, with permission.)

have been shown to contain SP, CGRP, and SOM and thus present a peptide pattern similar to that of muscle nerves, whereas visceral afferent units lack IR to SOM (Molander, C. *et al.*, 1987; O'Brien, C. *et al.*, 1989). In comparison to skin nerves, muscle nerves have been reported to contain less SP. This finding has been teleologically explained by assuming that the vasodilatation and plasma extravasation caused by the release of SP and CGRP from afferent fibers would be deleterious for skeletal muscle, since it is surrounded by a tight fascia. Because of the fascia, an SP-induced muscle edema would result in a high increase in interstitial pressure and could cause muscle necrosis. On the other hand, there can be no doubt that a considerable proportion of free nerve endings in muscle exhibit IR to SP and CGRP (Reinert, A. *et al.*, 1998). Therefore, SP and CGRP are likely to be involved in painful alterations of muscle tissue.

5.03.4.3 Neuropeptides in Nociceptors and Other Types of Free Nerve Ending

Whether or not a particular neuropeptide or combination of neuropeptides is associated with a particular type of receptor is obscure. There is evidence from studies on DRG cells (Lawson, S. N. *et al.*, 1997; Djouhri, L. and Lawson, S. N., 2004) indicating that SP-like IR (SP-LI) – and to a lesser extent, also CGRP-LI – was present predominantly in nociceptive units. Arguments supporting a nociceptive function of SP are that noxious stimulation is followed by a release of SP in the dorsal horn, and that the mRNA for SP and other tachykinins is upregulated under these circumstances. On the other hand, there is also evidence speaking against such a relation between the nociceptive function and the presence of SP. In a study by Leah J. D. *et al.* (1985), the great majority (10 out of 12) of individually identified nociceptive DRG cells of the cat did not exhibit SP-LI. Virtually all primary afferent units with SP-LI also exhibited CGRP-LI (Garry, M. G. *et al.*, 1989); both peptides are presumably released together when the fiber is active. In the spinal cord, CGRP has been reported to prolong the action of SP by inhibiting its degradation and to facilitate synaptic transmission in general by enhancing the calcium influx into afferent fibers.

Data from experiments in which single DRG cells with receptive endings in muscle were first functionally identified and then injected with a dye, showed that at least some cell bodies whose peripheral processes terminated in muscle HTM (presumably nociceptive) receptors exhibited CGRP-LI (Hoheisel, U. *et al.*, 1994). However, IR to SP, CGRP, and other neuropeptides was not only present in nociceptive units but also in other types of muscle receptors (e.g., in some muscle spindles and other LTM units). For instance, SP-LI has been found in LTM receptors, e.g., in nerve fibers from Krause corpuscles in the dog's tongue. Most of the cutaneous and deep receptor types studied so far showed CGRP-LI in some of their cell bodies in the DRG (Hoheisel, U. and Mense, S., 1987). The only condition for the presence of CGRP-LI seemed to be that the afferent unit had a small soma size and/or a slow CV.

5.03.5 Efferent Function of Nociceptors

5.03.5.1 Release of Neuropeptides from the Nociceptive Ending

Neuropeptides (e.g., SP, CGRP, VIP, and SOM) are stored in vesicles in the varicosities of the peripheral terminal. Whenever a nociceptor is excited, it releases neuropeptides into the interstitial tissue. SP then releases histamine from mast cells, and together with CGRP these agents cause vasodilatation and an increase in vascular permeability of the blood vessels around the active ending. The result is a shift of blood plasma from the intravascular to the interstitial space. Outside the blood vessel, BK is cleaved from the plasma protein kallidin, and serotonin (5-HT) is set free from platelets and PGs (particularly PG E2) from endothelial and other tissue cells. All these substances sensitize nociceptors. Thus, the main tissue alteration induced by a nondestructive noxious mechanical stimulus is a localized region of vasodilatation, edema, and sensitized nociceptors.

5.03.5.2 The Axon Reflex

The release of neuropeptides from an activated nociceptor is an essential aspect of its function. A nociceptor is not a passive sensor for tissue-threatening stimuli; it actively influences the microcirculation and chemical composition of the interstitial space around it. The morphological basis of the axon reflex is that the branches of a single nociceptive ending can extend over a relatively large area (several hundred micrometers). If a noxious stimulus activates only parts of the ending, the action potentials originating in the regenerative region of the ending can invade antidromically (against the normal direction of propagation) those branches of the ending that were not excited by the stimulus. These antidromic action potentials release neuropeptides from the unstimulated branches. The whole process is called axon reflex. It is assumed to be the reason for the wheal and flare around a cutaneous lesion. The vascular permeability is increased mainly by SP (and by the NK-A and -B; Gamse, R. and Saria, A., 1985), whereas CGRP is assumed to act primarily as a vasodilatator. There is evidence showing that CGRP enhances the plasma extravasation induced by SP and NK-A and -B, but reduces the vasodilatory action of SP by desensitizing muscle arterioles to the peptide (Öhlén, A. *et al.*, 1988).

The area of wheal and flare after a localized damage to the skin – for instance around a needle prick – could be an indicator of the extent of the excited nociceptive ending. Of course, this is true only if a single ending is stimulated and if the distance covered by diffusion of the neuropeptides is constant.

The size of the RFs of cutaneous polymodal nociceptors was found to be $<2\ mm^2$ in cat (Bessou, P. and Perl, E. R., 1969) and $6–32\ mm^2$ in rabbit (Kenins, P., 1988). These figures are greater than the reported length of the branches of a nociceptor ending (a few hundred micrometers). The difference may be due to the fact that nociceptors can be excited from a certain distance, particularly when coarse probes are used. For a muscle nociceptor, the size of the RF can be determined only with limitations, particularly if it is located deep within the muscle. The reported sizes of superficially located fields or the projections of deep RFs on the muscle surface range from spotlike to several square centimeters in the gastrocnemius muscle of the cat and dog (Kumazawa, T. and Mizumura, K., 1977; Mense, S. and Meyer, H., 1985).

5.03.5.3 Neurogenic Inflammation

The release of SP, CGRP, NK-A, and other agents from nociceptors is the central factor in the cascade of events that lead to neurogenic inflammation in the periphery (Lembeck, F. and Holzer, P., 1979). Neurogenic inflammation is characterized by tissue edema and infiltration by immune cells after antidromic activation of nociceptive nerve endings, i.e., when action potentials are generated somewhere along the course of primary afferent units (spinal nerve or dorsal root). The action potentials propagate to both the CNS (causing pain) and the peripheral ending (causing release of neuropeptides and neurogenic inflammation). The published data indicate that vasodilatation can be elicited by antidromic stimulation of both Aδ- and C-fibers, but increase in vascular permeability and plasma extravasation by stimulation of C-fibers only. Neuropathies and radiculopathies and other pathological conditions that are associated with antidromic activity in sensory nerve fibers are examples of such events. Neurogenic inflammation is likely to increase the dysesthesias and pain of patients suffering from neuropathies.

Neuropeptides also influence immune cells (for a review, see Morley, J. E. *et al.*, 1987) and synoviocytes. These actions may be of particular importance for the

development and maintenance of chronic arthritis and other inflammatory disorders of deep somatic tissues.

5.03.6 Receptor Molecules in the Membrane of Nociceptors

Classic stimulants for nociceptors are endogenous pain-producing (algesic) substances such as BK, 5-HT, and high concentrations of potassium ions. Injections of hypertonic NaCl solutions (4.5–6.0%) have been used for many decades to elicit pain from deep somatic tissues. Similar to potassium, the stimulating effects of hypertonic NaCl are considered to be unspecific (i.e., not mediated by a receptor–ligand interaction).

The effects of BK on nerve endings are mediated by G protein-coupled B1 and B2 receptors. Binding of the ligands to this and other receptors of this type results in changes of the state of activation of intracellular second messenger systems such as phospholipase C (PLC), cyclic adenosine monophosphate (cAMP), cyclic guanosin monophosphate (cGMP), and protein kinases (PK). One possible sequel of the activation of these messengers is the phosphorylation of ion channels. This increases the opening time or opening probability of the channels. Collectively, the processes lead either to direct excitation of the ending or to a changed reaction of the nerve ending to external stimuli (sensitization or desensitization).

In intact tissue, the discharges evoked in nerve endings by BK are mainly due to the activation of the BK receptor B2, whereas under pathological conditions the receptor B1 is the predominant one (for a review of receptor molecules mediating the effects of pain-producing substances, see Kumazawa, T., 1996). It is often overlooked that the above substances, particularly BK, excite not only nociceptors but also nonnociceptive endings with thin myelinated and unmyelinated afferent fibers. Therefore, BK cannot be considered a specific excitant of nociceptors. However, muscle receptors with group I and II afferents (e.g., muscle spindles and tendon organs) are not excited by BK.

The stimulating effects of serotonin on nociceptive terminals in the body periphery are largely mediated by the 5-HT3 receptor. Similar to PGE2, which binds to a G protein-coupled prostanoid receptor (EP2), serotonin sensitizes nociceptors rather than exciting them under (patho)physiological circumstances. The reason is that in damaged tissue concentrations of 5-HT and PGE2 are released, which are sufficient for sensitizing, but not for activating, nociceptors.

Novel stimulants for nociceptors are ATP, capsaicin, low pH, and NGF (Caterina, M. J. and David, J., 1999). ATP binds to purinergic receptors (in nociceptive endings, the P2X3 receptor; Ding, Y. *et al.*, 2000) and opens a cation channel. Animal experiments have shown that nociceptors respond to ATP in concentrations that are present in tissue cells. This means that every time a cell is damaged (by trauma or a pathological process), it releases ATP in amounts that can cause pain. For this reason, ATP has been considered a general signal substance for tissue trauma (Cook, S. P. and McCleskey, E. W., 2002).

Capsaicin, the active ingredient of chilli peppers, is a natural stimulant for the vanilloid receptor VR1, now called TRPV1 (Caterina, M. J. and Julius, D., 2001). The receptor is also sensitive to an increase in H^+ concentration and to heat with a threshold of approximately 39 °C. The sensitivity of this receptor to protons is important under conditions in which the pH of the tissue is lowered (exhaustive muscle work, ischemia, and inflammation). TRPV2 is present mainly in myelinated heat nociceptors that have a thermal threshold above 52 °C, and TRPV4 is being discussed as the main receptor of mechano-nociceptors (Liedtke, W., 2005).

A special feature of nociceptive afferent fibers are TTX-r sodium channels. TTX is a neurotoxin that blocks TTX-sensitive sodium channel and thus inhibits conduction in nerve fibers that possess this type of Na^+ channel (mostly large-diameter fibers). Nociceptive fibers are equipped with TTX-r channels; therefore, TTX has no blocking action. Two TTX-r Na^+ channels that are important for nociception are the voltage-gated sodium channels (Na_v) 1.9 and 1.8. Na_v 1.9 has been found exclusively in nociceptive primary afferent neurons, whereas Na_v 1.8 is present in both nociceptive and nonnociceptive ones (for review, Djouhri, L. and Lawson, S. N., 2004).

References

Andersson, S. A., Ericson, T., Holmgren, E., and Lindqvist, G. 1973. Electro-acupuncture. Effect on pain threshold measured with electrical stimulation of teeth. Brain Res. 63, 393–396.

Andres, K. H. and von Düring, M. 1973. Morphology of cutaneous receptors. In: Handbook of Sensory Physiology, Vol II, Somatosensory System (*ed*. A. Iggo), pp. 3–28, Springer.

Andres, K. H., von Düring, M., Muszynski, K., and Schmidt, R. F. 1987. Nerve fibres and their terminals of the dura mater encephali in the rat. Anat. Embryol. 175, 289–301.

Andres, K. H., von Düring, M., and Schmidt, R. F. 1985. Sensory innervation of the Achilles tendon by group III and IV afferent fibers. Anat. Embryol. 172, 145–156.

Applebaum, M. L., Clifton, G. L., Coggeshall, R. E., Coulter, J. D., Vance, W. H., and Willis, W. D. 1976. Unmyelinated fibres in the sacral 3 and caudal 1 ventral root of the cat. J. Physiol. 256, 557–572.

Barker, D. 1967. The innervation of mammalian skeletal muscle. In: CIBA Foundation Symposium on Myotatic, Kinesthetic and Vestibular Mechanisms (*eds*. A. V. S. DeReuck and J. Knight), pp. 3–19, Little Brown.

Belmonte, C. and Gallar, J. 1996. Corneal nociceptors. In: Neurobiology of Nociceptors. (*eds*. C. Belmonte and F. Cervero), pp. 146–183, Oxford University Press.

Belmonte, C., Gallar, J., Pozo, M. A., and Rebollo, I. 1991. Excitation by irritant substances of sensory afferent units in the cat's cornea. J. Physiol. 437, 709–725.

Bessou, P. and Perl, E. R. 1969. Response of cutaneous sensory units with unmyelinated fibers to noxious stimuli. J. Neurophysiol. 32, 1025–1043.

Burgess, P. R. and Perl, E. R. 1967. Myelinated afferent fibers responding specifically to noxious stimulation of the skin. J. Physiol. 190, 541–562.

Byers, M. R. 1984. Dental sensory receptors. Intern. Rev. Neurobiol. 25, 39–94.

Byers, M. R., Neuhaus, S. J., and Gehrig, J. D. 1982. Dental sensory receptor structure in human teeth. Pain 13, 221–235.

Caterina, M. J. and David, J. 1999. Sense and specificity: a molecular identity for nociceptors. Curr. Opin. Neurobiol. 9, 525–530.

Caterina, M. J. and Julius, D. 2001. The vanilloid receptor: a molecular gateway to the pain pathway. Ann. Rev. Neurosci. 24, 487–517.

Cauna, N. 1966. Fine Structure of the Receptor Organs and Its Probable Functional Significance. In: Touch, Heat and Pain (*eds*. A. V. S. DeReuck and J. Knight), pp. 117–127, Churchill.

Cesare, P. and McNaughton, P. 1997. Peripheral pain mechanisms. Curr. Opin. Neurobiol. 7, 493–499.

Chidiac, J. J., Rifai, K., Hawwa, N. N., Massaad, C. A., Jurjus, A. R., Jabbur, S. J., and Saade, N. E. 2002. Nociceptive behaviour induced by dental application of irritants to rat incisors: a new model for tooth inflammatory pain. Eur. J. Pain 6, 55–67.

Cook, S. P. and McCleskey, E. W. 2002. Cell damage excites nociceptors through release of cytosolic ATP. Pain 95, 41–47.

Devor, M., Wall, P. D., and McMahon, S. B. 1984. Dichotomizing somatic nerve fibers exist in rats but they are rare. Neurosci. Lett. 49, 187–192.

Ding, Y., Cesare, P., Drew, L., Nikitaki, D., and Wood, J. N. 2000. ATP, P2X receptors, and pain pathways. J. Auton. Nerv. Syst. 81, 289–294.

Djouhri, L. and Lawson, S. N. 2004. Aβ-fiber nociceptive primary afferent neurons: a review of incidence and properties in relation to other afferent A-fiber neurons in mammals. Brain Res. Rev. 46, 131–145.

Du, J., Zhou, S., Coggeshall, R. E., and Carlton, S. M. 2003. N-methyl-D-aspartate-induced excitation and sensitization of normal and inflamed nociceptors. Neuroscience 118, 547–562.

von Düring, M. and Andres, K. H. 1990. Topography and Ultrastructure of Group III and IV Nerve Terminals of the Cat's Gastrocnemius-Soleus Muscle. In: The Primary Afferent Neuron (*eds*. W. Zenker and W. L. Neuhuber), pp. 35–41, Plenum Press.

Foster, E., Risling, M., and Fried, K. 1995. TrkB-like immunoreactivity in trigeminal sensory nerve fibers of the rat molar tooth pulp: development and response to nerve injury. Brain Res. 686, 123–133.

von Frey, M. 1894. Beiträge zur Physiologie des Schmerzsinns. Königl. Sächs. Ges. Wiss., Math. Phys. Klasse 46, 185–196.

Fristad, I., Vandevska-Radunovic, V., Fjeld, K., Wimalawansa, S. F., and Hals Kvinnsland, I. 2003. NK1, NK2, NK3 and CGRP1 receptors identified in rat oral soft tissues and in bone and dental hard tissue cells. Cell Tiss. Res. 311, 383–391.

Gamse, R. and Saria, A. 1985. Potentiation of tachykinin-induced plasma protein extravasation by calcitonin gene-related peptide. Eur. J. Pharmacol. 114, 61–66.

Garcia-Anoveros, J., Samad, T. A., Zuvela-Jelaska, L., Woolf, C. J., and Corey, D. P. 2001. Transport and localization of the DEG/ENaC ion channel BNaC1alpha to peripheral mechanosensory terminals of dorsal root ganglia neurons. J. Neurosci. 21, 2678–2686.

Garry, M. G., Miller, K. E., and Seybold, V. S. 1989. Lumbar dorsal root ganglia of the cat: a quantitative study of peptide immunoreactivity and cell size. J. Comp. Neurol. 284, 36–47.

Guilbaud, G., Iggo, A., and Tegner, R. 1985. Sensory receptors in ankle joint capsules of normal and arthritic rats. Exp. Brain Res. 58, 29–40.

Gunji, T. 1982. Morphological research on the sensitivity of dentin. Arch. Histol. Jpn. 45, 45–67.

Hanesch, U. 1996. Neuropeptides in Dural Fine Sensory Nerve Endings-Involvement in Neurogenic Inflammation? In: Progress in Brain Research, Vol. 113 (*eds*. T. Kumazawa, L. Kruger, and K. Mizumura), pp. 299–317. Elsevier Science.

Hensel, H., Andres, K. H., and von Düring, M. 1974. Structure and function of cold receptors. Pflügers Arch. 352, 1–10.

Heppelmann, B., Heuss, C., and Schmidt, R. F. 1988. Fiber size distribution of myelinated and unmyelinated axons in the medial and posterior articular nerves of the cat's knee joint. Somatosens. Res. 5, 273–281.

Heppelmann, B., Messlinger, K., Neiss, W., and Schmidt, R. F. 1990a. Ultrastructural three-dimensional reconstruction of group III and group IV sensory nerve endings (free nerve endings) in the knee joint capsule of the rat: evidence for multiple receptive sites. J. Comp. Neurol. 292, 103–116.

Heppelmann, B, Messlinger, K., Neiss, W. F., and Schmidt, R. F. 1990b. The Sensory Terminal Tree of 'Free Nerve Endings' in the Articular Capsule of the Knee. In: The Primary Afferent Neuron (*eds*. W. Zenker and W. L. Neuhuber), pp. 73–85, Plenum Press.

Hoheisel, U. and Mense, S. 1987. Observations on the morphology of axons and somata of slowly conducting dorsal root ganglion cells in the cat. Brain Res. 423, 269–278.

Hoheisel, U., Mense, S., and Scherotzke, R. 1994. Calcitonin gene-related peptide-immunoreactivity in functionally identified primary afferent neurones in the rat. Anat. Embryol. 189, 41–49.

Hoheisel, U., Reinöhl, J., Unger, T., and Mense, S. 2004. Acidic pH and capsaicin activate mechanosensitive group IV muscle receptors in the rat. Pain 110, 149–157.

Hoheisel, U., Unger, T., and Mense, S. 2005. Excitatory and modulatory effects of inflammatory cytokines and neurotrophins on mechanosensitive group IV muscle afferents in the rat. Pain 114, 168–176.

Hökfelt, T., Johansson, O., Ljungdahl, Å, Lundberg, J. M., and Schultzberg, M. 1980. Peptidergic neurones. Nature 284, 515–521.

Holland, G. R. and Robinson, P. P. 1983. The number and size of axons at the apex of the cat's canine tooth. Anat. Rec. 205, 215–222.

Hoyes, A. D. and Barber, P. 1976. Ultrastructure of the corneal nerves in the rat. Cell Tiss. Res. 172, 133–144.

Ibuki, T., Kido, M. A., Kiyoshima, T., Terada, Y., and Tanaka, T. 1996. An ultrastructural study of the relationship between sensory trigeminal nerves and odontoblasts in rat dentin/pulp as demonstrated by the anterograde transport of wheat germ agglutinin-horseradish peroxidase (WGA-HRP). J. Dent. Res. 75, 1963–1970.

Ichikawa, H., Matsuo, S., Silos-Santiago, I., Jacquin, M. F., and Sugimoto, T. 2004. The development of myelinated nociceptors is dependent upon trks in the trigeminal ganglion. Acta Histochem. 106, 337–343.

Ikeda, H., Tokita, Y., and Suda, H. 1997. Capsaicin-sensitive A delta fibers in cat tooth pulp. J. Dent. Res. 76, 1341–1349.

Jänig, W. 1996. Neurobiology of visceral afferent neurons: neuroanatomy, functions, organ regulations and sensations. Biol. Psychol. 42, 29–51.

Ju, G., Hökfelt, T., Brodin, E., Fahrenkrug, F. J., Fischer, J. A., Frey, P., Elde, R. P., and Brown, J. C. 1987. Primary sensory neurons of the rat showing calcitonin gene-related peptide immunoreactivity and their relation to substance P-, somatostatin-, galanin-, vasoactive intestinal polypeptide-, and cholecystokinin-immunoreactive ganglion cells. Cell Tiss. Res. 247, 417–431.

Jyväsjärvi, E. and Kniffki, K. D. 1992. Studies on the presence and functional properties of afferent C-fibers in the cat's dental pulp. Proc. Finn. Dent. Soc. 88(Suppl. 1), 533–542.

Kenins, P. 1988. The functional anatomy of the receptive fields of rabbit C polymodal nociceptors. J. Neurophysiol. 59, 1098–1115.

Kennedy, W. R. 2004. Opportunities afforded by the study of unmyelinated nerves in skin and other organs. Muscle Nerve 29, 756–767.

Koling, A. 1985. Freeze-fracture electron microscopy of non-myelinated nerve fibres in the human dental pulp. Arch. Oral Biol. 30, 685–690.

Kow, L.-M. and Pfaff, D. W. 1988. Neuromodulatory actions of peptides. Ann. Rev. Pharmacol. Toxicol. 28, 163–188.

Kruger, L. 1988. Morphological features of thin sensory afferent fibers: a new interpretation of 'nociceptor' function. Progr. Brain Res. 74, 253–257.

Kruger, L. and Halata, Z. 1996. Structure of nociceptor 'endings'. In: Neurobiology of Nociceptors (*eds*. C. Belmonte and F. Cervero), pp. 37–71, Oxford University Press.

Kruger, L., Kavookjian, A. M., Kumazawa, T., Light, A. R., and Mizumura, K. 2003b. Nociceptor structural specialization in canine and rodent testicular ''free'' nerve endings. J. Comp. Neurol. 463, 197–211.

Kruger, L., Light, A. R., and Schweizer, F. E. 2003a. Axonal terminals of sensory neurons and their morphological diversity. J. Neurocytol. 32, 205–216.

Kruger, L., Perl, E. R., and Sedivec, M. J. 1981. Fine structure of myelinated mechanical nociceptor endings in cat hairy skin. J. Comp. Neurol. 198, 137–154.

Kruger, L., Silverman, J. D., Mantyh, P. W., Sternini, C., and Brecha, N. C. 1989. Peripheral patterns of calcitonin-gene-related peptide general somatic sensory innervation: cutaneous and deep terminations. J. Comp. Neurol. 280, 291–302.

Kumazawa, T. 1996. The Polymodal Receptor Bio-Warning and Defense System. In: Progress in Brain Research, Vol. 113 (*eds*. T. Kumazawa, L. Kruger, and K. Mizumura), pp. 3–18, Elsevier Science.

Kumazawa, T. and Mizumura, K. 1977. Thin-fibre receptors responding to mechanical, chemical and thermal stimulation in the skeletal muscle of the dog. J. Physiol. 273, 179–194.

Kumazawa, T. and Mizumura, K. 1980. Chemical responses of polymodal receptors of the scrotal contents in dogs. J. Physiol. 299, 219–231.

Kumazawa, T., Mizumura, K., and Sato, J. 1987. Response properties of polymodal receptors studied using in vitro testis superior spermatic nerve preparations of dogs. J. Neurophysiol. 57, 702–711.

Lawson, S. N., Crepps, B. A., and Perl, E. R. 1997. Relationship of substance P to afferent characteristics of dorsal root ganglion neurons in guinea-pig. J. Physiol. 505, 177–191.

Leah, J. D., Cameron, A. A., and Snow, P. J. 1985. Neuropeptides in physiologically identified mammalian sensory neurones. Neurosci. Lett. 56, 257–263.

Lembeck, F. and Holzer, P. 1979. Substance P as neurogenic mediator of antidromic vasodilation and neurogenic plasma extravasation, Naunyn-Schmiedeb. Arch. Pharmacol. 310, 175–183.

Liedtke, W. 2005. TRPV4 plays an evolutionary conserved role in the transduction of osmotic and mechanical stimuli in live animals. J. Physiol. 567, 53–58.

Light, A. R. and Perl, E. R. 2003. Unmyelinated afferent fibers are not only for pain anymore. J. Comp. Neurol. 461, 137–139.

Lloyd, D. P. C. 1943. Neuron patterns controlling transmission of ipsilateral hind limb reflexes in cat. J. Neurophysiol. 6, 293–315.

MacIver, M. G. and Tanelian, D. L. 1993. Structural and functional specialization of Aδ and C fiber free nerve endings innervating rabbit corneal epithelium. J. Neurosci. 13, 4511–4524.

McCloskey, D. I. and Mitchell, J. H. 1972. Reflex cardiovascular and respiratory responses originating in exercising muscle. J. Physiol. 224, 173–186.

Mense, S. 1977. Nervous outflow from skeletal muscle following chemical noxious stimulation. J. Physiol. 267, 75–88.

Mense, S. and Meyer, H. 1985. Different types of slowly conducting afferent units in cat skeletal muscle and tendon. J. Physiol. 363, 403–417.

Mense, S., Light, A. R., and Perl, E. R. 1981. spinal Terminations of Subcutaneous High-Threshold Mechanoreceptors. In: Spinal Cord Sensation (*eds*. A. G. Brown and M. Réthelyi), pp. 79–86, Scottish Academic Press.

Messlinger, K. 1996. Functional Morphology of Nociceptive and Other Fine Sensory Endings (Free Nerve Endings) in Different Tissues. In: Progress in Brain Research, Vol. 113 (*eds*. T. Kumazawa, L. Kruger, and K. Mizumura), pp. 273–298. Elsevier Science.

Messlinger, K. 1997. Was ist ein Nozizeptor? Schmerz 5, 353–367.

Molander, C., Ygge, I., and Dalsgaard, C.-J. 1987. Substance P-, somatostatin-, and calcitonin gene-related peptide-like immunoreactivity and fluoride resistant acid phosphatase-activity in relation to retrogradely labeled cutaneous, muscular and visceral primary sensory neurons in the rat. Neurosci. Lett. 74, 37–42.

Morley, J. E., Kay, N. E., Solomon, G. F., and Plotnikoff, N. P. 1987. Neuropeptides: conductors of the immune orchestra. Life Sci. 41, 527–544.

Müller, L. J., Pels, L., and Vrensen, G. F. 1996. Ultrastructural organization of human corneal nerves. Invest. Ophthal. Vis. Sci. 37, 476–488.

O'Brien, C., Woolf, C. J., Fitzgerald, M., Lindsay, R. M., and Molander, C. 1989. Differences in the chemical expression of rat primary afferent neurons which innervate skin, muscle or joint. Neuroscience 32, 493–502.

Öhlén, A., Wiklund, N. P., Persson, M. G., and Hedqvist, P. 1988. Calcitonin gene-related peptide desensitizes skeletal muscle arterioles to substance P in vivo. Br. J. Pharmacol. 95, 673–674.

Pierau, F.-K., Fellmer, G., and Taylor, D. C. M. 1984. Somato-visceral convergence in cat dorsal root ganglion neurones demonstrated by double-labelling with fluorescent tracers. Brain Res. 321, 63–70.

Reinert, A., Kaske, A., and Mense, S. 1998. Inflammation-induced increase in the density of neuropeptide-immunoreactive nerve endings in rat skeletal muscle. Exp. Brain Res. 121, 174–180.

Renton, T., Yiangou, Y., Baecker, P. A., Ford, A. P., and Anand, P. 2003. Capsaicin receptor VR1 and ATP purinoceptor P2X3 in painful and nonpainful human tooth pulp. J. Orofac. Pain 17, 245–250.

Rifai, K., Chidiac, J. J., Hawwa, N., Baliki, M., Jabbur, S. J., and Saade, N. E. 2004. Occlusion of dentinal tubules and selective block of pulp innervation prevent the nociceptive behaviour induced in rats by intradental application of irritants. Arch. Oral Biol. 49, 457–468.

Rodd, H. D. and Boissonade, F. M. 2000. Substance P expression in human tooth pulp in relation to caries and pain experience. Eur. J. Oral Sci. 108, 467–474.

Rodd, H. D., Loescher, A. R., and Boissonade, F. M. 1998. Immunocytochemical and electron-microscopic features of tooth pulp innervation in hereditary sensory and autonomic neuropathy. Arch. Oral Biol. 43, 445–454.

Schaible, H.-G. 2005. Basic Mechanisms of Deep Somatic Pain. In: Textbook of Pain (*eds*. S. B. McMahon and M. Koltzenburg), pp. 621–633. Churchill Livingstone.

Schaible, H.-G. and Grubb, B. D. 1993. Afferent and spinal mechanisms of joint pain. Pain 55, 45–54.

Schaible, H.-G. and Schmidt, R. F. 1985. Effects of an experimental arthritis on the sensory properties of fine articular afferent units. J. Neurophysiol. 54, 1109–1122.

Schaible, H.-G. and Schmidt, R. F. 1988. Time course of mechanosensitivity changes in articular afferents during a developing experimental arthritis. J. Neurophysiol. 60, 2180–2195.

Silverman, J. D. and Kruger, L. 1988. Lectin and neuropeptide labeling of separate populations of dorsal root ganglion neurons and associated 'nociceptor' thin axons in rat testis and cornea whole-mount preparations. Somatosens. Res. 5, 259–267.

Simone, D. A., Nolano, M., Johnson, T., Wendelschafer-Crabb, G., and Kennedy, W. R. 1998. Intradermal injection of capsaicin in humans produces degeneration and subsequent reinnervation of epidermal nerve fibers: correlation with sensory function. J. Neurosci. 18, 8947–8959.

Snider, W. E. and McMahon, S. B. 1998. Tackling pain at the source: new ideas about nociceptors. Neuron 20, 629–632.

Stacey, M. J. 1969. Free nerve endings in skeletal muscle of the cat. J. Anat. 105, 231–254.

Steffens, H., Eek, B., Trudrung, P., and Mense, S. 2003. Tetrodotoxin block of A-fibre afferents from skin and muscle – A tool to study pure C-fibre effects in the spinal cord. Pflügers Arch. 445, 607–613.

Stucky, C. L. and Lewin, G. R. 1999. Isolectin B(4)-positive and –negative nociceptors are functionally distinct. J. Neurosci. 19, 6497–6505.

Svensson, P., Cairns, B. E., Wang, K., Hu, J. W., Graven-Nielsen, T., Arendt-Nielsen, L., and Sessle, B. J. 2003. Glutamate-evoked pain and mechanical allodynia in the human masseter muscle. Pain 101, 221–227.

Tower, S. 1940. Unit for sensory reception in cornea. With notes on nerve impulses from sclera, iris and lens. J. Neurophysiol. 3, 486–500.

Wu, Z.-Z. and Pan, H.-L. 2004. Tetrodotoxin-sensitive and –resistant Na+ channel currents in subsets of small sensory neurons of rats. Brain Res. 1029, 251–258.

Zhang, J. Q., Nagata, K., and Iijima, T. 1998. Scanning electron microscopy and immunohistochemical observations of the vascular nerve plexuses in the dental pulp of rat incisor. Anat. Rec. 251, 214–220.

Further Reading

Heppelmann, B, Messlinger, K., Neiss, W. F., and Schmidt, R. F. 1994. Mitochondria in fine afferent nerve fibres of the knee joint in the cat: a quantitative electron-microscopical examination. Cell Tiss. Res. 275, 493–501.

Heppelmann, B., Pfeffer, H.-G., Schaible, H.-G., and Schmidt, R. F. 1986. Effects of acetylsalicylic acid and indomethacin on single groups III and IV sensory units from acutely inflamed joints. Pain 26, 337–351.

Messlinger, K., Pawlak, M., Steinbach, H., Trost, B., and Schmidt, R. F. 1995. A new combination of methods for localization, identification, and three-dimensional reconstruction of the sensory endings of articular afferents characterized by electrophysiology. Cell Tiss. Res. 281, 283–294.

Yeh, Y. and Byers, M. R. 1983. Fine structure and axonal transport labeling of intraepithelial sensory nerve endings in anterior hard palate of the rat. Somatosens. Res. 1, 1–19.

5.04 Molecular Biology of the Nociceptor/Transduction

M S Gold, University of Pittsburgh, Pittsburgh PA, USA

M J Caterina, Johns Hopkins School of Medicine, Baltimore, MD, USA

© 2008 Elsevier Inc. All rights reserved.

5.04.1	**Introduction**	44
5.04.1.1	Structure Dictates Function: The Anatomy of the Nociceptor	45
5.04.1.2	Nociceptor Inputs and Outputs: More than Meets the Eye	47
5.04.1.2.1	The onset of nociceptor excitation: hyperpolarization versus depolarization	47
5.04.1.2.2	Efferent function	47
5.04.1.2.3	Spike integration within the cell body	48
5.04.1.2.4	Slow axonal transport	48
5.04.2	**The Molecular Toolbox of Sensory Neurons**	49
5.04.2.1	Ion Channels Involved in the Transduction of Extracellular Signals	49
5.04.2.1.1	P2X adenosine triphosphate-gated ion channels	49
5.04.2.1.2	Proton-gated ion channels	50
5.04.2.1.3	Transient receptor potential ion channels	51
5.04.2.2	Ion Channels Influencing Passive Membrane Properties: Membrane Resistance	53
5.04.2.3	Ion Channels Underlying Active Membrane Processes	54
5.04.2.3.1	Action potential upstroke	54
5.04.2.3.2	Action potential downstroke	54
5.04.2.3.3	After potential	55
5.04.2.3.4	Action potential threshold	56
5.04.2.3.5	High-threshold voltage-gated Ca^{2+} current	57
5.04.2.4	Membrane Receptors that Indirectly Alter Nociceptor Function	57
5.04.2.4.1	G-protein-coupled receptors	57
5.04.2.4.2	Neurotrophin receptors	58
5.04.3	**Additive and Emergent Properties of Nociceptor Membrane Proteins**	59
5.04.3.1	Introduction	59
5.04.3.2	Shared Modalities and Polymodality	59
5.04.3.3	Functional Interactions between Nociceptor Proteins	60
5.04.4	**Injury-Induced Plasticity in Transduction**	61
5.04.4.1	Introduction	61
5.04.4.2	Inflammation-Induced Changes in Nociceptor Sensory function – Inflammatory Pain	61
5.04.4.3	Changes in Nociceptor Function Following Traumatic Nerve Injury – Neuropathic Pain	62
5.04.4.3.1	Nerve injury-induced changes in transduction	62
5.04.4.3.2	Changes in membrane stability	63
5.04.4.3.3	Mechanisms underlying nerve injury-induced changes in transduction	64
5.04.5	**Conclusion**	64
References		65

Glossary

action potential A characteristic pattern of neuronal depolarization and hyperpolarization that mediates transmission of information along the length of the neuron and triggers communication with synaptically connected neurons.

afterpotential The change in membrane potential that follows the action potential.

cable properties Passive electrophysiological properties of a neuron that influence the movement of charge, and therefore the spread of a change in

membrane potential, along a neuron. These properties include internal resistance (influenced by the diameter of the neural process), membrane resistance (influenced by the number of open ion channels in the membrane), and membrane capacitance (determined by the total membrane surface area).

generator potential Membrane depolarization resulting from the transduction of environmental stimuli (i.e., thermal, mechanical, or chemical). This transduction results in a change in membrane conductance that underlies the change in membrane potential.

G-protein-coupled receptors A diverse family of membrane proteins that trigger changes in cell function by signaling through intracellular guanine nucleotide-binding proteins.

hyperalgesia A state in which the sensitivity of nociceptive signaling pathways to environmental stimuli is enhanced.

inflammatory pain Spontaneous pain or hypersensitivity to environmental stimuli arising from inflammation in areas innervated by nociceptive neurons.

length constant A measure of the distance over which a current injected at a point source will spread within a neuron.

neurotrophins A diverse family of soluble signaling molecules that promote the differentiation, survival, and/or function of neurons.

nociceptor Specialized sensory neuron whose activation signals the presence of noxious, or potentially damaging stimuli. These neurons are selectively activated by noxious stimuli, under normal circumstances, or by molecules released once tissue damage has already occurred.

neuropathic pain Spontaneous pain or hypersensitivity to environmental stimuli arising from damage to neural tissue.

receptive field The area in or on the body within which adequate stimuli are capable of generating activity in a given neuron.

polymodality The ability of a molecule or neuron to be activated by more than one type (modality) of stimulus (e.g., mechanical and chemical).

tranduction A process in which environmental stimuli evoke conformational changes in the structure of specific proteins located on nociceptor terminals that directly or indirectly (i.e., via cellular signaling cascades) trigger the opening or closing of ion channels.

transient receptor potential A historically based name for a family of related iron channels that are prevalent in nociceptive neurons and other sensory neuron subtypes.

5.04.1 Introduction

The perception of pain is usually triggered when mechanical, chemical, or thermal stimuli of high intensity or a particular quality are detected by a specialized subpopulation of sensory neurons referred to as nociceptors. Although the term nociceptor has probably outlived its utility, we will use it here as a means of distinguishing afferents capable of responding to tissue damage from those that normally only encode innocuous stimuli. Nociceptor activation typically begins with transduction, a process in which environmental stimuli evoke conformational changes in the structure of specific proteins located on nociceptor terminals that directly or indirectly (i.e., via cellular signaling cascades) trigger the opening or closing of ion channels. The resulting changes in ionic flow across the plasma membrane produce a change in membrane potential, referred to as a generator potential. If the generator potential reaches a critical threshold, action potential firing ensues. In order for these action potentials to trigger a perception of pain, however, they must be propagated to the central terminal of the sensory neuron and subsequently evoke neurotransmitter release in sufficient quantities to activate postsynaptic spinal cord neurons. Thus, there are multiple critical steps in the afferent transmission of nociceptive information, each of which involves a unique compilation of specialized proteins. We will begin this chapter by describing several important but sometimes overlooked anatomical and physiological features of nociceptive neurons. We will then introduce some of the major protein classes that contribute to transduction and, to a more limited extent, the ensuing neurophysiological processes that result in the transmission of nociceptive information to the spinal cord. Subsequently, we will provide a glimpse at how such variables as molecular heterogeneity,

intermolecular interactions, posttranslational modifications, and ion channel distribution can vastly expand the sensory versatility of the nociceptive neurons. Finally, we will describe in greater detail a few of the changes that underlie nociceptor signaling plasticity in the context of inflammation and nerve injury. Although neurotransmission within the spinal cord dorsal horn represents another important function of nociceptors, we will defer a description of this process to other chapters of this volume.

5.04.1.1 Structure Dictates Function: The Anatomy of the Nociceptor

Sensory neurons are referred to as pseudounipolar neurons because they start out during development as bipolar neurons with a central process extending into the spinal or trigeminal dorsal horn and a peripheral process extending out to peripheral targets. During development, the initial segment of these two processes merges to form a T junction, leaving the cell body attached to peripheral and central processes via a single short length of axon (Fitzgerald, M., 2005) (Figure 1). Both central and peripheral processes terminate in a branching pattern referred to as a terminal arbor (Figure 1). The extent of the peripheral arbor depends on the afferent type and site of innervation. For example, afferents innervating the fingertips may innervate a square millimeter or less of skin, and therefore appear to have relatively few terminal branches (Darian-Smith, I. *et al.*, 1980; Andrew, D. and Greenspan, J. D., 1999). In contrast, afferents innervating a visceral structure such as the colon may have an extensive terminal arborization that extends over many centimeters of tissue (Berthoud, H. R. *et al.*, 2004). Afferents responsible for the transduction of low-threshold mechanical stimuli such as brush or vibration terminate in specialized structures such as Rufinni endings or Merkel discs that are critical for mediating the appropriate response to these stimuli (Mearow, K. M. and

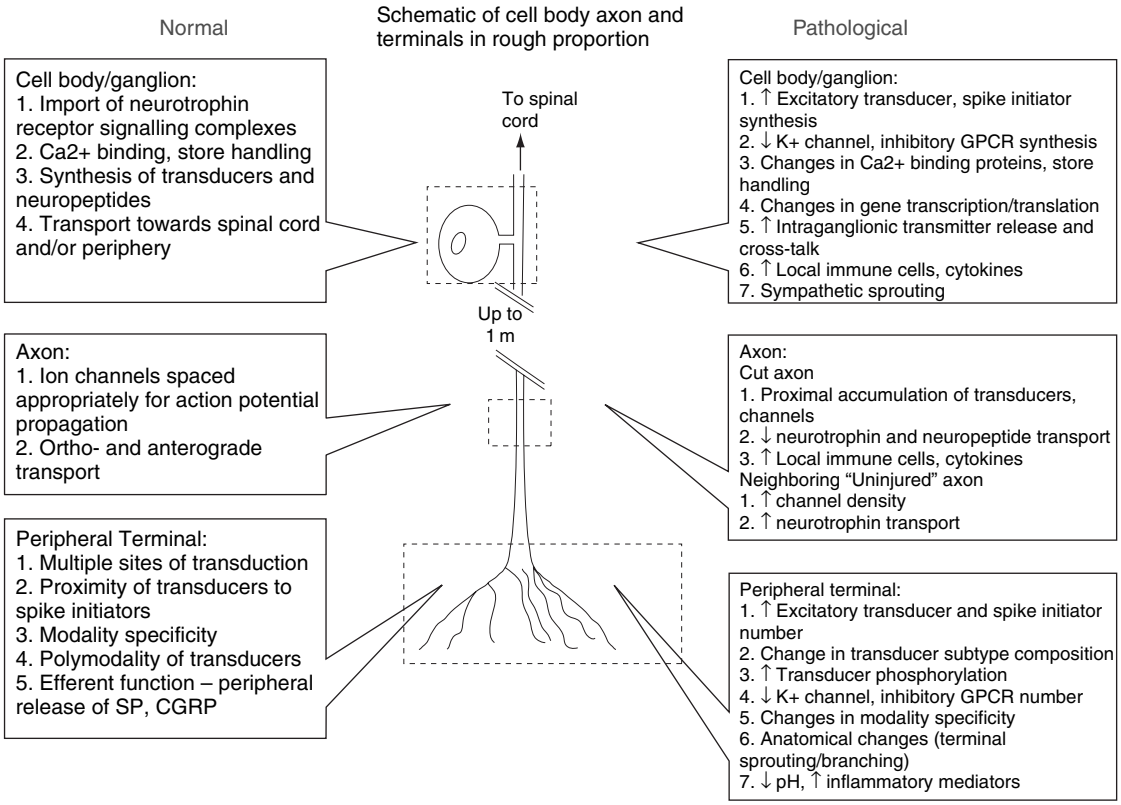

Figure 1 Schematic diagram of three major peripheral compactments of a nociceptive neuron: the cell body (top), axon (middle), and peripheral terminal arbor (bottom). Blowups at left: functional and anatomical properties of these compartments under normal conditions. Blowups at right: characteristic changes associated with nerve injury or inflammation.

Diamond, J., 1988; Johnson, K. O., 2001). In contrast, nociceptors are said to have free nerve endings, because peripheral terminals of these afferents do not appear to be associated with any specific cell type (Kruger, L. *et al*., 2003a). Further description of this anatomical arrangment can be found in the chapter by Mense in this volume (Chapter Anatomy of Nociceptors).

There are at least three important implications of the observation that peripheral terminals of nociceptors are free. First, while recent evidence suggests that transduction may occur in cells surrounding nociceptive terminals (i.e., urothelial cells (Birder, L. A., 2005) or keratinocytes (Guler, A. D. *et al*., 2002; Peier, A. M. *et al*., 2002b; Khodorova, A. *et al*., 2003; Wu, G. *et al*., 2004a) (see below)), the fact that nociceptive terminals are generally not associated with specialized cells suggests that these neurons themselves possess the machinery necessary for transduction. Consistent with this suggestion, the isolated cell bodies of putative nociceptors *in vitro* have been show to respond to thermal (Cesare, P. and McNaughton, P., 1996; Reichling, D. B. and Levine, J. D., 1997; Reid, G. and Flonta, M., 2001; Thut, P. D. *et al*., 2003), mechanical (McCarter, G. C. *et al*., 1999), and various chemical (Baccaglini, P. I. and Hogan, P. G., 1983) stimuli. Second, if transduction machinery is present in nociceptive terminals, transduction may occur whenever and wherever a transducer is properly positioned in the cell membrane. The result is that transduction can and probably does occur at multiple sites in a peripheral arbor (Gover, T. D. *et al*., 2003; Zhao, J. *et al*., 2006). This has important implications for spike initiation and integration of stimuli applied throughout a receptive field (Darian-Smith, I. *et al*., 1980). It also has important implications for the generation of ectopic activity in the presence of injury as there is evidence that the cut ends of axons may rapidly develop mechanical, thermal, and chemical sensitivity (Michaelis, M. *et al*., 1999) and that spontaneous activity may arise from within sensory ganglia following nerve injury (Kajander, K. C. *et al*., 1992). Third, because nerve endings are not only free of an association with a specific cell type, but free of even perineurial encapsulation (Devor, M., 1999), these endings are not only accessible to the chemical milieu of the tissue, but may be accessible to therapeutic interventions.

Both light and electron micrographic analyses of nociceptive terminals reveal complex anatomical structures. As suggested above, the structure of the terminal arbor varies with target of innovation. There is also evidence that subpopulations of nociceptive afferents have distinct terminal arbor patterns within the same structure. For example, the terminal arbor morphology of cutaneous C fibers varies according to whether the C fiber is peptidergic (i.e., expresses substance P or calcitonin gene-related peptide (CGRP)) or expresses the mas-related gene (mrg), MrgD (Zylka, M. J. *et al*., 2005). Furthermore, in the cornea, the terminal arbor of C-fiber afferents is distinct from that of Aδ fibers (MacIver, M. B. and Tanelian, D. L., 1993). At an ultrastructural level, nociceptive terminals appear to have beaded endings with clusters of organelles such as mitochondria at sites of swelling (Kruger, L. *et al*., 2003b). While the functional implications of this beaded structure remain to be determined, it has been suggested that swellings may be sites for transduction and/or the peripheral release of transmitter.

Finally, it is clear that active membrane properties, and therefore the nature of the afferent signal, are influenced by an interaction between the distribution, density, and biophysical properties of ion channels and transducers present in afferent terminals and the morphological features of the terminal arbor. Cable theory describes the impact of leak channels, terminal branch points, and irregularities in membrane shape such as those associated with the beaded pattern described above. As a first pass, all of these features, in addition to the relatively large surface-to-volume ratio associated with fine terminals suggest that the length constant, a measure of the distance over which a current injected at a point source will spread within the terminal, is quite small in nociceptive terminals. This implies that there are likely to be multiple sites of spike initiation throughout the terminal arbor. Importantly, it is likely that the cable properties, and therefore length constant, of nociceptive terminals are dynamically regulated. This notion is based on the observation that potassium leak currents, which determine membrane resistance, may be regulated by a number of factors such as transmitters and second messengers (Maingret, F. *et al*., 2000). Furthermore, evidence from dorsal horn neurons (Mantyh, P. W. *et al*., 1995) suggests that terminal morphology may be rapidly altered. Importantly, a change in a length constant may influence active membrane properties such as action potential threshold and spike accommodation.

5.04.1.2 Nociceptor Inputs and Outputs: More than Meets the Eye

The major focus of this chapter is on molecules involved in the initiation of fast orthograde electrical signaling by nociceptors to the central nervous system. However, several physiological features of nociceptors fall outside this conventional framework but are important within the larger context of sensory transduction. Therefore, before we dissect the mechanisms of nociceptor stimulus transduction, action potential generation, and action potential propagation in any detail, it is worth considering a few of these features.

5.04.1.2.1 The onset of nociceptor excitation: hyperpolarization versus depolarization

Sensory transduction in the mammalian nervous system can arise from either membrane hyper-polarization or membrane depolarization. The visual system utilizes the former while the somatosensory system utilizes the latter. Consequently, in the absence of stimuli, the resting membrane potential of nociceptive afferents is relatively hyperpolarized, with little, if any spontaneous activity (Rose, R. D. *et al.*, 1986; Ritter, A. M. and Mendell, L. M., 1992). This resting membrane potential appears to reflect a relatively large K^+ conductance through both voltage-insensitive (Baumann, T. K. *et al.*, 2004) and voltage-gated K^+ channels (Kirchhoff, C. *et al.*, 1992). However, this K^+ conductance appears to be working against a relatively high membrane permeability to depolarizing cations (i.e., Na^+ and Ca^{2+}), at least in cutaneous afferents (Kirchhoff, C. *et al.*, 1992). Data from studies of the isolated sensory neuron cell body *in vitro* suggest that a significant depolarizing conductance may be present in a relatively large percentage of putative nociceptive afferents (Viana, F. *et al.*, 2002).

There are at least two implications of a significant depolarizing conductance in nociceptive afferents. First, it suggests that a viable mode of transduction may involve the closing of a K^+ channel. In the absence of a depolarizing conductance, closing a K^+ channel in a membrane in which K^+ conductance is the only major conductance responsible for the establishment of the resting membrane potential, will result in little, if any change in membrane potential. Consistent with the suggestion that there is a significant depolarizing conductance in putative nociceptive afferents, there is evidence that some forms of cold transduction reflect the closing of a K^+ channel (Reid, G. and Flonta, M., 2001; Viana, F. *et al.*, 2002). Second, the presence of a significant depolarizing conductance in nociceptive afferents suggests that the resting membrane potential will be relatively depolarized. This has been observed repeatedly in studies on dissociated sensory neurons, where the resting membrane potential of putative nociceptive afferents is more depolarized than that of putative non-nociceptive afferents (see Gold, M. S. *et al.*, 1996a). There is evidence that intact nociceptive terminals *in situ* may be depolarized as well (Brock, J. A. *et al.*, 2001). As mentioned above, resting membrane potential may influence not only transduction, given the voltage dependence of several transducers (see below), but also spike initiation.

5.04.1.2.2 Efferent function

It is clear that nociceptor afferent neurotransmission contributes to the perception of pain associated with tissue injury (Treede, R. D. *et al.*, 1992). However, it is also clear there are tissues distributed throughout the body that are heavily innervated by nociceptive afferents, but that will never give rise to the sensation of pain in many of us. For example, even though pericardial tissue receives nociceptive innervation thought to be responsible for pain associated with cardiac ischemia (Immke, D. C. and McCleskey, E. W., 2001), the majority of us will never experience discomfort arising from this structure. What might be the function(s) of nociceptors in these locations? One potential answer to this question stems from the ability of many nociceptors to release bioactive substances with the potential to exert trophic and/or inflammatory effects on targets of innervation. For example, CGRP, which can be released by many nociceptive neurons, has been shown to regulate cellular activity underlying bone formation and resorption, two processes critical to the maintenance of healthy bone (Lerner, U. H., 2002). Such seemingly paradoxical efferent nociceptor activity is particularly important in tissues subjected to injury. Under these circumstances, the release of transmitters from the peripheral nociceptor terminals has been shown to contribute to local hyperemia and plasma extravasation (hallmarks of the so-called neurogenic inflammation), to the orchestration of tissue repair, and to the initiation and maintenance of pain and hyperalgesia (Willis, W. D., 1999). Much of the focus in this area has been on nociceptor release of CGRP and another peptide transmitter, substance P (Figure 1). However, it is now clear that glutamate is also released into the periphery, where it appears

able to act in an autocrine fashion to further activate and/or sensitize nociceptive afferents (deGroot, J. *et al*., 2000). Appreciation of these efferent capabilities has led to the suggestion that a better name for nociceptive sensory neurons might be noceffector afferents (Kruger, L., 1988).

Three mechanisms have been described that may contribute to the injury-induced efferent release of neurotransmitter. One is the axon reflex, thought to be mediated by action potential spread from one branch in a terminal arbor to other branches (Lewis, T., 1935). A second, relatively rare, mechanism is axonal coupling, in which axons traveling in the same bundle may, as a result of injury, come into such close proximity that activity in one axon is able to initiate activity in a second axon (Meyer, R. A. *et al*., 1985). A third mechanism actually involves the initiation of action potentials in the central terminals of nociceptive afferents within the spinal cord dorsal horn that are propagated antidromically out into the periphery (Sluka, K. A. *et al*., 1995). While the exact mechanism of this activation is still debated, there is evidence that in the presence of inflammation there is a change in presynaptic gamma-aminobutyric acid (GABA) ergic input, such that primary afferent-driven GABA release from interneurons is capable of action potential generation at central terminals (Sluka, K. A. *et al*., 1995). A fourth mechanism, often overlooked in this discussion, involves the possible direct coupling between calcium-permeable transducers and transmitter release. Such a mechanism appears to contribute to the inflammation associated with capsaicin-induced activation of its receptor transient receptor potential vanilloid 1 (TRPV1) (see below).

5.04.1.2.3 Spike integration within the cell body

There is evidence indicating that once the T junction is formed within the sensory ganglia, action potentials need not invade the sensory neuron cell body (Amir, R. and Devor, M., 2003). This observation begs the question of why action potentials invade the cell body at all. One answer to this question appears to be that the invading action potential provides a mechanism for the recruitment of additional activity. The term cross-excitation has been used to describe the observation that activity in one axon can induce activity in neighboring axons (Devor, M. and Wall, P. D., 1990). Interestingly, the prevalence of cross-excitation increases in the presence of tissue injury, providing a mechanism for peripherally mediated secondary hyperalgesia (Devor, M. and Wall, P. D., 1990). While the exact mechanisms underlying such cross talk have yet to be completely worked out (Amir, R. and Devor, M., 1996), there is evidence that the sensory neuron cell body is capable of releasing transmitter (Huang, L. Y. and Neher, E., 1996) and that peripheral nerve stimulation results in the release of transmitter within the ganglia (Matsuka, Y. *et al*., 2001).

More relevant to the issue of transduction, however, is the observation that afferent activity is capable of driving changes in gene transcription (Figure 1). For example, there is evidence that electrical activity in sensory neurons is capable of changing Na^+ channel expression (Klein, J. P. *et al*., 2003). Interestingly, the pattern of activity appears to influence the pattern of gene transcription (Fields, R. D. *et al*., 2005). The result may be as profound as to determine whether or not sprouting axons are able to coalesce into a nerve. One mediator that appears to be critical for the integration of activity within the cell body is Ca^{2+}, acting through a number of Ca^{2+}-dependent molecules (Eshete, F. and Fields, R. D., 2001). Thus, the transduction of activity within the sensory neuron cell body involves the influx of Ca^{2+}, which then initiates a number of cellular processes including gene transcription.

5.04.1.2.4 Slow axonal transport

Another general mechanism critical to nociceptive signaling involves axonal transport to the cell body, rather than action potential propagation. This is a remarkable process, given the tremendous length of sensory nerve axons (up to 1 m), relative to their soma size (~18–30 μm). Among the primary functions of this form of signaling, which may take hours to days, are the maintenance of nociceptor survival during development, the maintenance of nociceptive phenotype and function in the adult, and orchestration of the afferent response to tissue injury (Koltzenburg, M., 1999). The best-studied example of signaling via slow axonal transport is that of neurotrophic factors bound to their receptors (Figure 1) (Zweifel, L. S. *et al*., 2005). However, slow axonal transport can also lead to signaling in the distant sensory neuron cell body following ligand-dependent internalization of G-protein-coupled receptors (GPCRs) (e.g., those for neurokinins, opioids, and extracellular proteases) (Tseng, L. F. and Narita, M., 1995; Vergnolle, N. *et al*., 2001). In addition, transcription factors, second messenger molecules, cell surface glycoproteins, and foreign particles such as plant lectins, toxins, and viruses can all be transported retrogradely from peripheral sensory

neuron terminals toward the cell body (Wang, H. F. *et al.*, 1998; Vulchanova, L. *et al.*, 2001; Tarpley, J. W. *et al.*, 2004; Yeomans, D. C. *et al.*, 2005; Mata, M. *et al.*, 2006). In what has been a boon to researchers, there are some molecules that are selectively taken up by subpopulations of sensory neurons, and have therefore been used to characterize innervation patterns (see Wang, H. F. *et al.*, 1998). Sensory neurons also appear to be able to take up inflammatory mediators such as TNFα (Schafers, M. *et al.*, 2002). Exactly how sensory neurons use the information associated with the presence or absence of various molecules transported back to the cell body remains to be determined. However, the internalization and transport of molecules present at sensory neuron terminals appears to be a mechanism for sensory neurons to monitor tissue integrity and adjust to changes in the local environment.

5.04.2 The Molecular Toolbox of Sensory Neurons

Sensory neurons express a multitude of cell surface proteins that serve anatomically as markers of neuronal subtypes and functionally as mediators of the fundamental signaling and transmission functions outlined in the previous section. Three classes of sensory neuron cell surface proteins have been studied in the greatest detail: ion channels, metabotropic GPCRs, and receptors for neurotrophins or cytokines. Together, these proteins endow sensory afferents with responsiveness to a qualitatively and quantitatively diverse collection of environmental variables and dictate the passive and active properties essential for converting a generator potential into a signal that reaches the spinal cord. As detailed below, certain membrane proteins found in nociceptors (e.g., P2X3, TRPM8, mrgA, and NaV1.8) are expressed within subsets of sensory neurons at levels much higher than anywhere else in the body. Such enriched expression has provided reagents that can be used for sensory neuron- or nociceptor-specific gene disruption or transgene expression in the laboratory setting. More importantly, it provides at least the theoretical opportunity to develop antinociceptive drugs that have minimal effects on other cell types. A few of the more prominent classes of cell surface proteins expressed in sensory neurons are described below.

5.04.2.1 Ion Channels Involved in the Transduction of Extracellular Signals

5.04.2.1.1 P2X adenosine triphosphate-gated ion channels

Extracellular adenosine triphosphate (ATP), released upon cell damage, has been recognized as a nociceptive stimulus ever since the demonstration that application of this molecule to a blister base produces pain in human psychophysical studies (Bleehan, T. and Keele, C. A., 1977). At least one mechanism by which ATP activates nociceptors is via activation of ATP-gated ion channels of the P2X family. These channels are comprised of a heterotrimer of P2X subunits, each with two transmembrane domains and a large extracellular loop that contains the ATP binding site. Seven P2X subtypes have been cloned in mammals. They differ with respect to their sensitivity to ATP or ATP analogs, as well as the kinetics of their ATP-evoked currents. For example, homomeric P2X3 is responsive to α,β-methylene ATP, and exhibits a rapidly desensitizing current response, whereas homomeric P2X2 exhibits slowly desensitizing currents that are α,β-methylene ATP insensitive. When coassembled, these channels form an α,β-methylene sensitive, slowly desensitizing heteromultimeric channel. P2X channels are typically nonselective cation channels that exhibit considerable permeability to both Na^+ and Ca^{2+} ions. In several cases, however, (P2X2, P2X4, and P2X7) protracted stimulation of these channels can lead to an apparent dilation of the channel pore, such that much larger organic cations such as *N*-methyl D-glucamine are able to permeate the channel. The significance of this dynamic ion selectivity remains unclear (North, R. A., 2002).

Although mRNAs encoding P2X1 through P2X6 have all been detected in sensory neurons, P2X2 and P2X3 appear to be expressed most prominently in these cells. P2X2 is expressed in neurons with a wide range of cell body sizes. In contrast, at least in skin, P2X3 expression appears to be confined to a subpopulation of small-diameter sensory neurons that bind isolectin B4 (IB4) and that project to inner lamina II of the spinal cord dorsal horn (North, R. A., 2002). It is important to note, however, that the precise relationship between P2X3 expression and IB4 binding may vary between cutaneous afferents with their cell bodies in dorsal root ganglia and other nociceptor populations such as those in the trigeminal ganglion (Ambalavanar, R. *et al.*, 2005). Genetic disruption of both P2X3 and P2X2 results

in elimination of all transient ATP-evoked currents and all but a small persistent ATP-evoked current in cultured sensory neurons (Cockayne, D. A. *et al.*, 2005).

P2X channels also contribute to pain sensation *in vivo*. For example, although application of P2X3 antagonists (Jarvis, M. F. *et al.*, 2002; McGaraughty, S. *et al.*, 2003) or antisense oligodeoxynucleotide-mediated knockdown of P2X3 (Barclay, J. *et al.*, 2002; Honore, P. *et al.*, 2002) have no apparent effect on acute nociceptive responses to mechanical or thermal stimuli, both interventions have been shown to reduce thermal and/or mechanical hyperalgesia associated with complete Freund's adjuvant (CFA) administration into the paw and several models of neuropathic pain, as well as reducing the extent of the first and second phases of paw licking following intraplantar formalin injection. Gene knockout of P2X3 or P2X2/3 receptors in mice has also been reported to diminish formalin-evoked nocifensive behavior. However, these knockout animals exhibit a perplexing mixture of pain-related phenotypes, including paradoxically enhanced behavioral avoidance of heat and cold stimuli (Cockayne, D. A. *et al.*, 2000; Souslova, V. *et al.*, 2000; Cockayne, D. A. *et al.*, 2005; Shimizu, I. *et al.*, 2005). In visceral structures, epithelial cells appear capable of the storage and Ca^{2+}-dependent release of ATP in response to mechanical and chemical stimuli. P2X3 and P2X2/3 receptors on primary afferent terminals enable visceral afferents to respond to this released ATP, perhaps contributing to visceral pain sensation (Cockayne, D. A. *et al.*, 2000; Vlaskovska, M. *et al.*, 2001; Andersson, K. E., 2002; Birder, L. A., 2005). A similar mechanism may underlie ATP-mediated stimulus transduction in cutaneous tissue in the presence of inflammation (Wu, G. *et al.*, 2004a). P2X receptors contribute to nociceptive neurotransmission in a number of other ways, as well. In the spinal cord, for example, activation of presynaptic P2X3-containing channels and postsynaptic P2X channels of other subtypes, modulates neurotransmitter release and excitability, respectively (Gu, J. G. and MacDermott, A. B., 1997; Nakatsuka, T. and Gu, J. G., 2001; Nakatsuka, T. *et al.*, 2003; Tsuzuki, K. *et al.*, 2003). In addition, although it appears not to be expressed within neurons themselves, P2X7 is necessary for normal inflammation, nerve injury-induced hyperalgesia (Chessell, I. P. *et al.*, 2005), and CFA-induced hyperalgesia in rats (Dell'Antonio, G. *et al.*, 2002a; 2002b), probably owing to its role in cytokine release from inflammatory cells (Labasi, J. M. *et al.*, 2002).

5.04.2.1.2 Proton-gated ion channels

Reductions in tissue pH, as might occur during ischemia or inflammation, can potently activate nociceptors and sensitize them to heat and other stimuli. *In vitro*, low pH activates cationic channels in sensory neurons that can exhibit transient, sustained, or biphasic kinetics (Bevan, S. and Yeats, J., 1991). At least some of these responses can be attributed to the acid-sensing ion channel (ASIC) family. These multimeric ion channels are comprised of subunits that topologically resemble the P2X channels, with two transmembrane domains each and an extracellular ligand (H^+) binding domain. Five ASIC subtypes have been cloned, of which four (ASIC1–4) are expressed in peripheral sensory neurons (Waldmann, R. *et al.*, 1999; Waldmann, R., 2001). Splice variants of several subtypes add to the overall complexity, and one such variant, ASIC1β, appears to be selectively enriched in sensory neurons (Chen, C. C. *et al.*, 1998). Upon activation by low pH (from <7 to <4, depending on the subtype) ASICs typically mediate a prominent and rapidly desensitizing Na^+ current. However, some subtypes (e.g., ASIC3), exhibit a biphasic current consisting of an initial desensitizing sodium current, followed by a more sustained current that includes Ca^{2+} ions (Waldmann, R. *et al.*, 1999; Waldmann, R., 2001).

Several lines of evidence support the participation of ASIC channels in acid responsiveness of sensory neurons. First, the kinetics of sensory neuron responses to a pH 6 stimulus are altered in neurons isolated from ASIC1, ASIC2, or ASIC3 knockout mice or in wild-type neurons exposed to APETx2, an ASIC3-selective antagonist from sea anemone (Price, M. P. *et al.*, 2001; Benson, C. J. *et al.*, 2002; Xie, J. *et al.*, 2002; Diochot, S. *et al.*, 2004). Second, pH 5-evoked C-fiber responses are reduced in *ex vivo* skin–nerve explants derived from ASIC3 knockout mice (Price, M. P. *et al.*, 2001). Third, mice lacking ASIC3 exhibit defects in the ipsilateral mechanical hyperalgesia that typically develops 4 h after injection of acid to the gastrocnemius muscle (Price, M. P. *et al.*, 2001) as well as defects in the bilateral hyperalgesia that develops after two intramuscular acid injections, 5 days apart (Sluka, K. A. *et al.*, 2003). Interestingly, no changes in behavioral responses to acute subcutaneous acid injection have been reported in these knockout studies. However, ASIC3 may be particularly important for sensing reductions in muscle pH during ischemia (Immke and McCleskey 2001).

In addition to acid detection, ASICs have also been implicated in mechanosensation. This

hypothesis was initially based upon the recognition that ASICs bear structural and pharmacological similarities (i.e., amiloride sensitivity) to degenerins, cationic channels identified in genetic screens for mechanosensory defects in the nematode, *Cenorhabditis elegans* (O'Hagan, R. and Chalfie, M., 2005). The immunolocalization of ASIC2 and 3 to sensory afferent terminals (Price, M. P. *et al.*, 2000; Garcia-Anoveros, J. *et al.*, 2001; Price, M. P. *et al.*, 2001) and the systematic examination of mechanosensation in ASIC knockout mice have lent support to this notion. Mice lacking ASIC1 were recently reported to exhibit no detectable changes in mechanoreceptor properties in the skin–nerve preparation. However, there was an enhancement of mechanically evoked firing rate in gastrointestinal afferents in these mice, accompanied by a reduction in gastric emptying rate (Page, A. J. *et al.*, 2004). Studies of ASIC2 KO mice have yielded somewhat conflicting results. In one study, these mice were reported to exhibit reduced mechanically evoked firing rate of rapidly adapting Aβ mechanoreceptors (RAM), without a change in RAM threshold (Price, M. P. *et al.*, 2000). In another study, however, no change in RAM response characteristics was observed (Roza, C. *et al.*, 2004). ASIC3 KO mice were reported to exhibit decreased sensitivity of Aδ mechanoreceptors but increased sensitivity of RAM, together with increased behavioral withdrawal from mechanical stimulation after carageenan (Price, M. P. *et al.*, 2001).

In contrast to the situation for acid detection, it has been relatively difficult to correlate mechanically evoked currents with the presence of particular ASIC subunits. Indeed a recent *in vitro* study of mechanically evoked currents revealed no differences between wild type and ASIC2 knockout, ASIC3 knockout, or ASIC2/3 double knockout mice. Instead, the authors of this study observed that the cationic dye, ruthenium red, could inhibit mechanosensitive currents, suggesting the possible participation of transient receptor potential (TRP) channels (see below) (Drew, L. J. *et al.*, 2004).

5.04.2.1.3 Transient receptor potential ion channels

One early clue that nociceptive neurons might express signaling proteins distinct from those of other neuronal subtypes was the observation that exposure of neonatal rats to capsaicin, the main pungent ingredient in hot peppers, produces a lifelong depletion of small-diameter sensory neurons, with no such effects on larger-diameter neurons. As adults, these animals exhibit diminished responsiveness not only to subsequent capsaicin challenge, but also to other painful stimuli (Jancso, G. *et al.*, 1977). The highly enriched expression of a vanilloid receptor in nociceptive neurons appears to underlie these incredibly selective effects of capsaicin and related vanilloid compounds (Szallasi, A. and Blumberg, P. M., 1999). This conclusion was corroborated by the molecular cloning of a capsaicin-gated ion channel named TRPV1 (Caterina, M. J. *et al.*, 1997).

TRPV1 belongs to the TRP family, which in mammals contains approximately 30 members. TRP channel subunits have six transmembrane domains and intracellular N- and C-termini, and apparently form tetrameric channels on the cell surface. A remarkable feature of TRPV1 is that, in addition to vanilloid compounds, it can be activated by a number of other stimuli, including protons (pH < 5) (Tominaga, M. *et al.*, 1998), certain endogenous arachidonic acid derivatives (anandamide, *N*-arachidonyl dopamine, and 12-HPETE) (Zygmunt, P. M. *et al.*, 1999; Hwang, S. W. *et al.*, 2000; Huang, S. M. *et al.*, 2002) and even noxious heat (>42 °C) (Caterina, M. J. *et al.*, 1997). Nonvanilloid exogenous chemicals capable of activating TRPV1 include ethanol (Trevisani, M. *et al.*, 2002), camphor (Xu, H. *et al.*, 2005), and 2-aminoethoxydiphenyl borate (2-APB) (Hu, H. Z. *et al.*, 2004).

Sensory neurons derived from TRPV1 knockout mice not only are devoid of vanilloid responsiveness but also exhibit deficits in current responses evoked by pH 5 or moderate heat (45–50 °C) stimuli. All *in vivo* vanilloid-evoked responses are correspondingly absent in TRPV1 knockout mice. These animals also exhibit modestly reduced (but not absent) behavioral responses to acute noxious heat. A far more striking nociceptive phenotype is apparent in these mice following cutaneous inflammation by mustard oil, carageenan, or complete Freund's adjuvant or following surgical incision of the skin. Under these conditions, almost none of the thermal hyperalgesia typically exhibited by wild-type mice is observed in mice lacking TRPV1, although mechanical hyperalgesia is unaffected (Caterina, M. J. *et al.*, 2000; Davis, J. B. *et al.*, 2000; Pogatzki-Zahn, E. M. *et al.*, 2005). More recent pharmacological studies have further supported a role for TRPV1 in inflammatory thermal hyperalgesia (Pomonis, J. D. *et al.*, 2003; Gavva, N. R. *et al.*, 2004; Honore, P. *et al.*, 2005). However, the degree to which this channel may or may not participate in neuropathic pain states is much less clear. Although some pharmacological

studies using TRPV1 antagonists with significant potential for off-target effects have suggested a possible role (Pomonis, J. D. *et al.*, 2003; Walker, K. M. *et al.*, 2003), mice lacking TRPV1 exhibit apparently normal thermal hyperalgesia following partial ligation of the sciatic nerve (Caterina, M. J. *et al.*, 2000). The recent availability of more selective TRPV1 antagonists promises to resolve this issue (Rami, H. K. and Gunthorpe, M. J., 2004). One particularly promising recent finding was that a TRPV1-selective antagonist was shown to partially attenuate the mechanical hyperalgesia associated with experimental bone cancer pain (Ghilardi, J. R. *et al.*, 2005).

Following the identification of TRPV1, a host of other TRP channels were found to be expressed in sensory ganglia. Like TRPV1, many of these channels are polymodal, exhibiting responsiveness to a multiple physical and chemical stimuli (Jordt, S. E. *et al.*, 2003; Patapoutian, A. *et al.*, 2003). Whereas TRPV1 appears to be the only member of this family gated by capsaicin, TRPV2, TRPV3, and TRPV4, like TRPV1, can be activated by elevated ambient temperatures. TRPV2 is expressed most prominently in a subpopulation of neurons with medium- to large-diameter cell bodies. Based on their size, expression of CGRP and neurofilament proteins, and projection pattern within the spinal cord, many of these neurons are likely to correspond to Aδ neurons. However, some presumably Aβ neurons that project within the dorsal columns also appear to express TRPV2. Heterologously expressed TRPV2 can be activated by temperatures >52 °C, a thermal response pattern reminiscent of those exhibited by Type II Aδ fibers in peripheral nerve recording studies and by a subpopulation of medium-diameter, capsaicin-insensitive dorsal root ganglion (DRG) neurons in isolated cultures (Caterina, M. J. *et al.*, 1999). TRPV2 can alternatively be activated by hypo-osmolarity (Iwata, Y. *et al.*, 2003), cell stretch (Muraki, K. *et al.*, 2003), or 2-APB (Hu, H. Z. *et al.*, 2004).

TRPV3 is activated by warm temperatures (>34–37 °C), although its thermal responsiveness extends well into the noxious range (Peier, A. M. *et al.*, 2002b; Smith, G. D. *et al.*, 2002; Xu, H. *et al.*, 2002). This channel can, alternatively, be activated by certain exogenous chemical substances (camphor, 2-APB) (Chung, M. K. *et al.*, 2004b; Hu, H. Z. *et al.*, 2004; Moqrich, A. *et al.*, 2005). The expression pattern of TRPV3 remains somewhat controversial. Although there are reports of TRPV3 mRNA or protein expression in sensory neurons (Smith, G. D. *et al.*, 2002; Xu, H. *et al.*, 2002), its expression in these cells is far less clear than in skin keratinocytes (Peier, A. M. *et al.*, 2002b), where TRPV3-mediated current responses can be readily generated (Chung, M. K. *et al.*, 2004a; Moqrich, A. *et al.*, 2005). These findings have led to the notion that TRPV3 may signal the presence of cutaneous warmth via keratinocyte–sensory neuron communication. Support for a role of TRPV3 in thermosensation has come from the observation that in mice lacking this protein, heat-evoked nociception is blunted in the hot plate and tail immersion assays. In addition, on a thermal gradient, selection of preferred floor temperatures is slowed, but not absent, in these mice (Moqrich, A. *et al.*, 2005).

TRPV4 can be gated by warm temperatures (>32 °C), hypo-osmolarity, cytochrome P450 metabolites of arachidonic acid, or the synthetic phorbol ester, 4α-phorboldibutyryl didecanoate (Nilius, B. *et al.*, 2004). Like TRPV3, TRPV4 is expressed more prominently in keratinocytes than in sensory afferents (Guler, A. D. *et al.*, 2002), although there is evidence for low-level TRPV4 protein expression in a population of medium- to large-diameter sensory afferents (Liedtke, W. and Friedman, J. M., 2003). Mice lacking TRPV4 exhibit reduced sensitivity to noxious mechanical or hypertonic stimuli, prolonged tail immersion latencies at modestly hot temperatures, and a shift in thermal selection behavior toward floor temperatures warmer than those selected by wild-type mice (Liedtke, W. and Friedman, J. M., 2003; Suzuki, M. *et al.*, 2003; Alessandri-Haber, N. *et al.*, 2005; Lee, H. *et al.*, 2005b).

Just as heat can activate TRPV1–TRPV4, cold temperatures have been reported to activate at least two other TRP channels. TRPM8 was identified on the basis of its responsiveness to the cold-mimetic agent, menthol. Examination of its thermosensory responsiveness revealed, however, that it could alternatively be activated by modest reductions in ambient temperature (<22 °C) (McKemy, D. D. *et al.*, 2002; Peier, A. M. *et al.*, 2002a). Another cold-mimetic agent, icilin, can also activate TRPM8, but only when intracellular Ca^{2+} levels are elevated (McKemy, D. D. *et al.*, 2002; Chuang, H. H. *et al.*, 2004). TRPM8 is expressed in a subset of small-diameter neurons that lack expression of TRPV1, substance P or Isolectin B4 (Peier, A. M. *et al.*, 2002a).

Another icilin-sensitive TRP channel that has been implicated in cold sensation is TRPA1. This channel is expressed in a subpopulation of small-diameter sensory neurons and is commonly coexpressed with TRPV1. In some studies, recombinant TRPA1 has been reported to be responsive to intense cooling (<18 °C) (Story, G. M. *et al.*, 2003). Consistent with

this finding, mice lacking TRPA1 were recently reported to exhibit reduced withdrawal behavior on a cold plate or in response to acetone-mediated cooling of the hind paw (Kwan, K. Y. *et al.*, 2006). However, the cold sensitivity of TRPA1 is not universally accepted, since other investigators have failed to detect such responses and have reported normal cold-evoked behavioral responses in a distinct line of TRPA1 null mice (Jordt, S. E. *et al.*, 2004). Another point of contention revolves around the potential contributions of TRPA1 to mechanosensation, which is supported by immunolocalization studies (Nagata, K. *et al.*, 2005) and by analysis of one knockout mouse line (Kwan, K. Y. *et al.*, 2006) but not another (Bautista, D. M. *et al.*, 2006). The basis for these apparent discrepancies remains unclear. However, there is uniform consensus that TRPA1 is a mediator of nociceptive responses to certain irritant chemicals, including mustard oil (allyl isothiocyanate), cinnamaldehyde, and acrolein and that it serves as a downstream target following the activation of bradykinin receptors (Bandell, M. *et al.*, 2004; Jordt, S. E. *et al.*, 2004; Bautista, D. M. *et al.*, 2006; Kwan, K. Y. *et al.*, 2006). Indeed, both lines of TRPA1 null mice were found to be defective in nocifensive behavioral responses to mustard oil injection, mustard oil-evoked allodynia, and bradykinin-evoked pain-like behavior (Bautista, D. M. *et al.*, 2006; Kwan, K. Y. *et al.*, 2006).

Thus far, the examination of TRP channels within sensory neurons has been confined largely to those that either exhibit preferentially high expression in these cells or have been identified as being responsive to chemical stimuli with recognizable sensory effects. However, other TRP channels are known to be expressed quite broadly in neuronal and non-neuronal cells, where they participate in numerous functions that are important to sensory neuron biology (e.g., store-operated Ca^{2+} entry, Mg^{2+} uptake, mechanosensation, axon guidance) (Ramsey, I. S. *et al.*, 2006). Therefore, studies aimed at the analysis of those channels in sensory ganglia may yield further important insights.

5.04.2.2 Ion Channels Influencing Passive Membrane Properties: Membrane Resistance

While a number of channels contribute to the establishment of input resistance, two general classes have been described at a molecular level. One class includes the two-pore K^+ channels. These channels have no intrinsic voltage sensitivity and are active at resting membrane potentials thereby contributing to resting input resistance. TWIK related potassium channel (TREK-1) was the first of these K^+ channels to be identified in sensory neurons. TWIK stands for tandem of P domains in a weak inward rectifier potassium channel (Patel, A. J. and Honore, E., 2001). TREK-1 was cloned in 1996 based on homology to TWIK. While TREK-1 was originally shown to be activated by arachidonic acid and inhibited by cAMP, it was subsequently demonstrated that TREK-1 was activated by membrane stretch, osmotic welling as well as molecules that caused membrane crenation. Two more mechanosensitive two-pore potassium channels, TREK-2 and TRAAK were subsequently described (Maingret, F. *et al.*, 1999; Bang, H. *et al.*, 2000), both of which are also activated by membrane stretch and crenators and both of which are present in sensory ganglia (Kang, D. and Kim, D., 2006). Nevertheless, it remains to be determined whether any of these channels underlies the mechanosensitivity of primary afferent neurons (Patel, A. J. and Honore, E., 2001).

A second class of ion channel that may also contribute to resting input resistance is a member of the voltage-gated Na^+ channel family. One member of this family, NaV1.9 appears to encode a voltage-gated channel with unique gating properties (Cummins, T. R. *et al.*, 1999). The channel has a very low threshold for activation, activates very slowly upon membrane depolarization, and undergoes very little inactivation with small membrane depolarizations. These gating properties have two important consequences. First, it is likely that this channel contributes little, if anything to the rapid upstroke of the action potential. Second, the channel should, in theory, contribute a depolarizing drive at resting membrane potentials (Herzog, R. I. *et al.*, 2001). The problem with this theory is that biophysical analysis of persistent Na^+ currents in sensory neurons (putative NaV1.9-mediated currents) (Priest, B. T. *et al.*, 2005) indicate that this current is subject to a profound slow inactivation (Cummins, T. R. *et al.*, 1999). This voltage and time-dependent process is associated with a channel transition from a closed state, from which it could be activated with membrane depolarization, to an inactivated state, from which the channel is no longer available for activation. The extent of slow inactivation of NaV1.9 is such that there is virtually no detectable persistent current evoked from a typical resting membrane potential (i.e., -60 mV). There is evidence suggesting that the voltage dependence of

slow inactivation is influenced by recording conditions, such that the use of fluoride-based electrode solutions results is a hyperpolarizing shift in the voltage dependence of this process (Coste, B. *et al.*, 2004). Consequently, the extent of inactivation may be overestimated when the whole-cell patch configuration is used, if stability of the internal milieu is as important for the stability of NaV1.9 as it is for other ion channels (Kepplinger, K. J. *et al.*, 2000). Either way, what is clear is that even a few NaV1.9 channels active at rest could have a profound influence on neuronal excitability (Herzog, R. I. *et al.*, 2001).

5.04.2.3 Ion Channels Underlying Active Membrane Processes

5.04.2.3.1 Action potential upstroke

Voltage-gated Na^+ channels are critical for the upstroke, or rapid depolarization, phase of the neuronal action potential. Typical voltage-gated Na^+ channels consist of an α-subunit and two β-subunits (Catterall, W. A., 1992). The α-subunit contains everything necessary for a functional voltage-gated channel, including the ion pore, voltage sensor, and inactivation gate. β-subunits appear to both influence channel gating as well as play a major role in channel trafficking (Isom, L. L., 2001). Recent evidence suggests that one of the β-subunits may also influence channel inactivation (Grieco, T. M. *et al.*, 2005). Nine α-subunits have been cloned and clearly demonstrated to underlie voltage-gated Na^+ currents (Catterall, W. A. *et al.*, 2005a). A tenth α-subunit has been identified that is distantly related to the other nine and has been suggested to function as a Na^+ transporter rather than a voltage-gated channel (Goldin, A. L. *et al.*, 2000). Four β-subunits have been cloned (Goldin, A. L. *et al.*, 2000; Yu, F. H. *et al.*, 2003). There is evidence that eight of the nine α-subunits and all four β-subunits are present in sensory neurons (Black, J. A. *et al.*, 1996; Shah, B. S. *et al.*, 2000; Renganathan, M. *et al.*, 2002; Takahashi, N. *et al.*, 2003). α-subunits are differentially distributed both between and within sensory neurons. For example, NaV1.7, 1.8, and 1.9 are preferentially expressed in putative nociceptive afferents (Fang, X. *et al.*, 2002; Djouhri, L. *et al.*, 2003a; 2003b), while NaV1.1 is preferentially expressed in non-nociceptive afferents (Black, J. A. *et al.*, 1996). Within nociceptive afferents, NaV1.8 appears to be normally localized to the cell body and terminal arbor (Ritter, A. M. and Mendell, L. M., 1992; Jeftinija, S., 1994; Gu, J. G. and MacDermott, A. B., 1997; Brock, J. A. *et al.*, 1998; Khasar, S. G. *et al.*, 1998), while NaV1.6 is present along the axons (Rios, J. C. *et al.*, 2003). Furthermore, there is evidence that channel expression is developmentally regulated. For example, in the rat, expression levels of NaV1.3 and 1.5 are high during development, and then reduced to almost undetectable levels after birth (Waxman, S. G. *et al.*, 1994; Renganathan, M. *et al.*, 2002). Importantly, the pattern of both α- and β-subunit expression is altered both within and between neurons following injury, changes that are thought to play a significant role in pain and hyperalgesia associated with tissue injury.

Voltage-gated Na^+ currents in sensory neurons are generally described in terms of their sensitivity to tetrodotoxin (TTX) where currents are TTX-sensitive (NaV1.1, 1.2, 1.3, 1.6, and 1.7), TTX-insensitive (NaV1.5), or TTX-resistant (NaV1.8 and 1.9). The TTX-resistant currents are further subdivided into inactivating (NaV1.8) and persistent current (NaV1.9). Based on data from biophysical characterization of these subunits and toxin sensitivity, NaV1.8 appears to be largely responsible for spike initiation in the terminals and cell body of nociceptive afferents (Gold, M. S., 2000a), while the TTX-sensitive channels, NaV1.6 and NaV1.7, are likely to underlying action potential conduction. Recent evidence from the NaV1.7 null mutant mouse suggests that NaV1.7 may also play a significant role in action potential generation in nociceptive afferent terminals (Nassar, M. A. *et al.*, 2004). A small cohort of individuals was also recently identified who do not experience pain in response to noxious stimuli, even though they appear to be aware of stimuli that should produce pain, exhibiting few, if any detectable somatosensory abnormalities (Cox, J. J. *et al.*, 2006). All of these individuals possess loss of function mutations in NaV1.7, indicating that this channel is necessary for the stimulus evoked perception of pain.

5.04.2.3.2 Action potential downstroke

The falling phase of the action potential is the result of two processes. One is the inactivation of voltage-gated Na^+ channels and the second is the activation of K^+ channels. One class of channels that plays a major role in controlling the rate of membrane repolarization are the sustained (i.e., delayed rectifier type) voltage-gated K^+ channels (Werz, M. A. and MacDonald, R. L., 1983). There appear to be at least three types of sustained voltage-gated K^+ currents present in sensory neurons based on biophysical and pharmacological properties

(Gold, M. S. *et al.*, 1996c). While the K^+ channel subunits underlying these currents have yet to be conclusively identified, immunohistochemical data have implicated several possible candidates (Rasband, M. N. *et al.*, 1998).

Another class of channel that contributes to membrane repolarization is the large conductance Ca^{2+}-modulated K^+ channel, (i.e., BK or Maxi-K channel). These channels are encoded by a single α-subunit (*slo*, which has several splice variants), whose gating properties, Ca^{2+} sensitivity, and pharmacological sensitivity is influenced by the presence of one of four distinct β-subunits (Wallner, M. *et al.*, 1998). While these channels have intrinsic voltage sensitivity, the voltage dependence of activation is such that in the absence of Ca^{2+}, it is unlikely that these channels would be sufficiently activated to contribute to the downstroke of the action potential (Wallner, M. *et al.*, 1998). This suggests that there is sufficient Ca^{2+} entry via voltage-gated Ca^{2+} channels during the action potential (Blair, N. T. and Bean, B. P., 2002), to enable activation of BK channels. The nature of the association between BK channels and voltage-gated Ca^{2+} channels in afferent terminals has yet to be described. However, the timing of BK current activation in the cell body suggests that there is a relatively tight association between the two.

5.04.2.3.3 After potential

The after potential is the change in membrane potential that follows an action potential. This is generally a membrane hyperpolarization (more negative than resting membrane potential), but may also be a depolarizing after potential (DAP). Two different mechanisms have been described that contribute to the DAP. One mechanism involves a high density of low threshold, or T-type voltage-gated Ca^{2+} channels (White, G. *et al.*, 1989). The biophysical properties of these channels are such that if present at a high enough density, they are able to depolarize the membrane following an action potential, providing enough depolarizing drive to evoke a burst of action potentials. The second current suggested to contribute to a DAP is a Ca^{2+}-dependent Cl^- current (Mayer, M., 1985). As the name implies, activation of this current requires sufficient Ca^{2+} entry during the action potential. It also requires the intracellular Cl^- concentration is such that the equilibrium concentration for Cl^- is depolarized.

In the majority of nociceptive sensory neurons, the somatic action potential is followed by an after hyperpolarization (AHP). In fact, a distinguishing feature of nociceptive afferents is that the somatic action potential is associated with a relatively long AHP (McLachlan, E. M. *et al.*, 1993; Villiere, V. and McLachlan, E. M., 1996; Djouhri, L. *et al.*, 2003a). A number of distinct currents have been suggested to influence the magnitude and duration of the AHP. Furthermore, because of differences between currents with respect to biophysical properties of channel gating, changes in intracellular Ca^{2+} concentrations, etc., the relative contribution of different ion channels to the AHP changes with time. Because of this feature, investigators have often divided the AHP into fast (early), intermediate, and slow (late) AHP. Channels mediating the fast AHP are generally those that contributed to the downstroke of the action potential (i.e., sustained voltage-gated K^+ and BK currents). These channels generally deactivate (i.e., close) rapidly and therefore do not generally contribute to the AHP for more than several of milliseconds (Fowler, J. C. *et al.*, 1985a).

The hyperpolarization associated with the fast AHP may result in the activation of three additional types of currents that have opposing influences on membrane potential. First, there may be the activation of inward rectifying K^+ currents (Scroggs, R. S. *et al.*, 1994). These currents appear to activate and inactivate rapidly in sensory neurons and therefore appear to primarily influence the fast AHP. Second, there may be the activation of low-threshold inactivating or A-type voltage-gated K^+ currents (Cardenas, C. G. *et al.*, 1995). These channels are largely inactivated at rest. However, there may be enough membrane hyperpolarization associated with the fast AHP to enable recovery from inactivation of a number of A-type K^+ channels. Because these channels have a low threshold for activation, once recovered from inactivation, the channels will open and therefore prolong the decay of the AHP. Because A-type currents in sensory neurons may inactivate slowly (i.e., with time constants of decay will over 100 ms (Gold, M. S. *et al.*, 1996c)), these channels can and do contribute significantly to the intermediate AHP (Harriott, A. *et al.*, 2006). As such, these channels play a significant role in regulating interspike interval (Connor, J. A. and Stevens, C. F., 1971; Yoshimura, N. and de Groat, W. C., 1999). Importantly, persistent inflammation and nerve injury have been shown to result in a decrease in these currents, which is associated with a concomitant increase in membrane excitability (Yoshimura, N. and de Groat, W. C., 1999; Moore, B. A. *et al.*, 2002; Stewart, T. *et al.*, 2003; Dang, K. *et al.*, 2004; Harriott, A.

et al., 2006). Third, there may be the activation of hyperpolarization-activated cationic current (Ih). These currents, carried by family channels called hyperpolarization-activated cyclic nucleotide-gated (HCN) channels, are nonselective cationic currents (Robinson, R. B. and Siegelbaum, S. A., 2003). Consequently, activation of these channels results in a depolarizing current, which, if of sufficient magnitude, may contribute to spike initiation. A high density of these channels can result in membrane oscillations and spontaneous activity. Indeed, there is evidence that these currents are upregulated in the presence of injury, a change that has been suggested to contribute to spontaneous afferent activity observed following nerve injury (Chaplan, S. R. *et al.*, 2003). Furthermore, there is evidence that blocking these channels attenuates mechanical hypersensitivity observed following nerve injury (Lee, D. H. *et al.*, 2005a). These channels are also modulated by cyclic nucleotides (Ingram, S. L. and Williams, J. T., 1994; Robinson, R. B. and Siegelbaum, S. A., 2003), which suggests that they may contribute to the increased excitability observed in the presence of inflammation as well, given that many inflammatory mediators induce an increase in cAMP concentrations (Levine, J. D. *et al.*, 1993).

In a subpopulation of sensory neurons, a slow AHP has also been described (Fowler, J. C. *et al.*, 1985a; 1985b; Weinreich, D. and Wonderlin, W. F., 1987). This AHP apparently reflects the activation of a Ca^{2+}-dependent K^+ channel that takes several hundred milliseconds to activate, but once activated takes several seconds to close (Cordoba-Rodriguez, R. *et al.*, 1999). Consequently, activation of these channels has a profound influence of spike accommodation. The slow AHP has been well described in nodose ganglion neurons, where it appears to be a target for inflammatory mediators that are able to block it in a cAMP dependent manner. The result is a dramatic increase in excitability (Weinreich, D. and Wonderlin, W. F., 1987). While there is evidence that a similar channel may be present in DRG neurons, it does not appear to play a major role in inflammatory mediator-induced sensitization of nociceptive afferents (Gold, M. S. *et al.*, 1996d). Four Ca^{2+}-dependent but voltage-independent channels have been cloned and are referred to as SK1–4, in reference to their small single-channel conductance (Bond, C. T. *et al.*, 2005). There is immunohistochemical evidence for the presence of these SK1 in sensory neurons (Boettger, M. K. *et al.*, 2002) and we have data from a single-cell PCR experiment suggesting that others are expressed as well (Gold, M. S., unpublished observation). It remains to be determined which if any of the SK channels mediates the slow AHP given several striking differences between the SK channels and the slow AHP in terms of pharmacological sensitivity, Ca^{2+} dependence and gating properties (Cordoba-Rodriguez, R. *et al.*, 1999).

5.04.2.3.4 Action potential threshold

The action potential threshold is where the various influences of all the ion channels in the membrane come into play. The magnitude and nature of leak conductance determines membrane resistance and the impact a generator current will have on the membrane potential. The biophysical properties of voltage-gated K^+ currents will determine the magnitude of the K^+ conductance associated with membrane depolarization as well as the impact of resting membrane potential on that value. Similarly, the biophysical properties of voltage-gated Na^+ currents will determine the voltage at which these channels begin to open, the rate at which they open and the rate at which they inactivate in the face of slow membrane depolarizations. Given the fact that there is considerable variation in the biophysical properties of Na^+ channels depending on which α- and β-subunits are present, the relative density of these subunits will have a significant impact on action potential threshold (Matzner, O. and Devor, M., 1992).

Another class of ion channels that may contribute to the action potential threshold are the low threshold (i.e., T-type) voltage-gated Ca^+ channels. As with voltage-gated Na^+ channels, T-type channels consist of an α-subunit that contains the channel-pore, voltage-sensing, and inactivation gates, and ancillary subunits that influence channel gating and trafficking (Catterall, W. A. *et al.*, 2005b). Three α-subunit genes have been cloned that encode for T-type currents. T-type currents appear to be present in a low density in putative nociceptive afferents (Scroggs, R. S. and Fox, A. P., 1992). While the activation rate of these channels does not appear to be sufficient to enable these channels to contribute to the action potential upstroke, the low threshold for activation enables these currents to amplify the effects of small membrane depolarizations. Consequently, an increase in the density of these channels can have a significant influence on membrane excitability. In support of this suggestion, these channels have recently been implicated in epileptogenisis (Czapinski, P. *et al.*, 2005). More recent

evidence suggests that they may contribute to the sensitization of nociceptive afferents in the presence of tissue injury (Barton, M. E. *et al.*, 2005).

5.04.2.3.5 High-threshold voltage-gated Ca^{2+} current

The structure of high-threshold voltage-gated Ca^{2+} channels is analogous to that of voltage-gated Na^{+} channels and T-type Ca^{2+} channels, with a single α-subunit that contains the ion pore, voltage-sensor, etc., and several different ancillary subunits that influence channel gating (i.e., the β-subunit) and/or channel trafficking (i.e., the $\alpha 2\delta$-subunit complex) (Catterall, W. A. *et al.*, 2005b). Seven α-subunits encoding high-threshold channels have been cloned, resulting in four currents that are distinguishable on the basis of unique pharmacological sensitivity. Molecular biological and pharmacological analyses indicate that all four current types are likely present in nociceptive afferents (Kostyuk, P. G. *et al.*, 1981; Scroggs, R. S. and Fox, A. P., 1992; Kim, D. S. *et al.*, 2001; Yusaf, S. P. *et al.*, 2001; Wu, Z. Z. *et al.*, 2004b). While these channels are critical for transmitter release, their role in direct regulation of excitability is less clear. On the one hand, they enable inward current that contributes to membrane depolarization and prolongation of the action potential. On the other hand, they enable activation of K^{+} and Cl^{-} currents that may be inhibitory. Thus, the site of channel activation is critical. Of note, in studies involving the isolated sensory neuron cell body, there is evidence to suggest that inflammatory mediators decrease the density of high-threshold voltage-gated currents (Borgland, S. L. *et al.*, 2002), and in the presence of nerve injury, there is a decrease in the density of high-threshold voltage-gated currents as well (Baccei, M. L. and Kocsis, J. D., 2000; Hogan, Q. H. *et al.*, 2000; Kim, D. S. *et al.*, 2001). Authors of both the studies suggested that these changes may contribute to pain associated with tissue injury and all are certainly correct on this point.

5.04.2.4 Membrane Receptors that Indirectly Alter Nociceptor Function

5.04.2.4.1 G-protein-coupled receptors

Many of the cell surface proteins that define the functional and histological identity of sensory neurons are the so-called GPCRs. These proteins, which possess seven transmembrane domains, an extracellular amino terminus, and an intracellular carboxyl terminus, signal by catalyzing the dissociation of guanosine diphosphate (GDP) from the α-subunit of heterotrimeric G proteins associated with the intracellular face of the plasma membrane. As a consequence of its dissociation, GDP is replaced with guanosine triphosphate (GTP), causing the heterotrimer to dissociate into a GTP-bound α-subunit and a free $\beta\gamma$ dimer. Both the GTP-bound α-subunit and the free $\beta\gamma$ dimer have specific cellular targets through which they are able to activate or inhibit signaling cascades and/or directly modify the activity of specific ion channels (Gilman, A. G., 1987; Pierce, K. L. *et al.*, 2002). This versatile signal transduction strategy is used by at least 1000 different GPCRs expressed throughout the body, and dozens of these are expressed by nociceptors and other sensory neurons. A few notable examples include B1 and B2 receptors for bradykinin (Steranka, L. R. *et al.*, 1988), P2Y2 receptors for ATP (Tominaga, M. *et al.*, 2001), PAR2 protease-activated receptors (Vergnolle, N. *et al.*, 2001), EP1 EP3C and EP4 receptors for prostaglandin E2 (Ferreira, S. H. *et al.*, 1978; Sugimoto, Y. *et al.*, 1994; Oida, H. *et al.*, 1995), mu, kappa, and delta opioid receptors (Dado, R. J. *et al.*, 1993; Arvidsson, U. *et al.*, 1995), several subtypes of metabotropic glutamate receptor (Bhave, G. *et al.*, 2001; Yang, D. and Gereau, R. W. T., 2002), and at least seven subtypes of 5HT receptor (Nicholson, R. *et al.*, 2003). One recently discovered family of apparently pronociceptive GPCRs are those of the so-called mrg or sensory neuron specific (SNS) family (Dong, X. *et al.*, 2001; Lembo, P. M. *et al.*, 2002; Zylka, M. J. *et al.*, 2003). The expression pattern of this GPCR family exhibits remarkable species-specific heterogeneity, as there appear to be at least 50 members in mice, but only four in rat and only a few distantly related homolog in humans (Zylka, M. J. *et al.*, 2003).

GPCRs expressed in sensory ganglia can be broadly classified into those that enhance nociceptor excitability and those that diminish it. Sensitizing receptors tend to couple to either Gq (e.g., B2, P2Y2, PAR2, and EP1) or Gs (e.g., EP3C, EP4). The activated α-subunit of Gq activates phospholipase C (PLC), an enzyme that catalyzes cleavage of the membrane phospholipid phosphatidylinositol bisphosphate to inositol 1,3,5-trisphosphate (IP3) and diacylglycerol (DAG). IP3 evokes the release of Ca^{2+} ions from intracellular stores that, together with DAG, go on to trigger the plasma membrane localization and activation of protein kinase C (PKC) (Gilman, A. G., 1987). Multiple PKC isoforms (α, δ, ε, and μ) have been shown to facilitate nociceptor

sensitization through their phosphorylation of ion channels and other target proteins (Cesare, P. *et al.*, 1999; Khasar, S. G. *et al.*, 1999; Olah, Z. *et al.*, 2002; Wang, Y. *et al.*, 2004). Ca^{2+} ions can also act in many other ways, such as by binding to proteins such as calmodulin that can allosterically regulate ion channels and intracellular enzymes in a Ca^{2+}-dependent manner (Numazaki, M. *et al.*, 2003). The GTP-bound Gαs subunit activates the enzyme adenylyl cyclase, which catalyzes the generation of cyclic adenosine monophosphate (cAMP) from ATP (Gilman, A. G., 1987). cAMP, in turn, activates cAMP-dependent protein kinase (protein kinase A, PKA), which can also phosphorylate and augment the responsiveness of certain ligand-, heat-, or voltage-gated channels (Gold, M. S. *et al.*, 1998; Bhave, G. and Gereau, R. W. T., 2004). Another intracellular enzyme recently implicated in nociception is the cAMP-activated guanine nucleotide exchange protein, Epac, which couples intracellular cAMP generation to the PLC-dependent sensitization of TTX-resistant sodium channels (Hucho, T. B. *et al.*, 2005). Interestingly, although all of the actions of pronociceptive GPCRs on excitability are indirect, through their actions on downstream signaling mechanisms, activation of some (e.g., bradykinin receptors) is sufficient to trigger action potential firing, whereas activation of others (e.g., prostaglandin receptors) primarily enhances neuronal responsiveness to other exogenous stimuli (Birrell, G. J. *et al.*, 1991; 1993; Kumazawa, T. *et al.*, 1996). This distinction may reflect differences in signal amplification or differences in the proximity of a given GPCR, its target enzymes, and a given depolarizing ion channel.

In contrast to the pronociceptive receptors, GPCRs that couple to Gi or Go proteins (e.g., μ-opioid receptor, type II metabotropic glutamate receptors) tend to suppress neuronal activity. This outcome results from inhibition of adenylyl cyclase (to diminish PKA phosphorylation of target proteins), inhibition of voltage-gated Ca^{2+} channels, and/or activation of hyperpolarizing G-protein-coupled inwardly rectifying K^+ channels (GIRKs of the Kv4 family) (McFadzean, I., 1988; Bhave, G. and Gereau, R. W. T., 2004).

5.04.2.4.2 Neurotrophin receptors

As described in detail elsewhere in this chapter, neurotrophins are also important regulators of sensory neuron development, survival, and excitability. One major class of neurotrophic factors that carry out these functions is the nerve growth factor (NGF) family (NGF, BDNF, neurotrophin-3, and neurotrophin-4). The receptors for this family of nociceptors fall into two categories: a low-affinity receptor p75, which appears to bind all members of the family, and homodimeric high-affinity receptors that are specific for each of the family members (TrkA, TrkB, or TrkC) (Huang, E. J. and Reichardt, L. F., 2001). Interestingly, one p75 monomer and one Trk dimer can apparently bind the same neurotrophin dimer simultaneously (He, X. L. and Garcia, K. C., 2004). During development, all sensory neurons destined to become nociceptors are dependent on NGF for survival. However, with maturation, only a subset of nociceptive afferents continues to express the high-affinity NGF receptor, TrkA. In these neurons, continued access to NGF is no longer necessary for survival, but remains essential for the maintenance of the afferent phenotype, which includes peptide expression and the specific composition of ion channels and transducers. Afferents have continued access to NGF produced by target tissue, but the amount of NGF available is critical: a decrease in access to NGF appears to result in the loss of nociceptive phenotype, while increased access to NGF results in an increase in the expression of nociceptive markers (Koltzenburg, M., 1999). BDNF and neurotrophin-3 can also alter nociceptor function (Shu, X. Q. and Mendell, M. L., 1999).

Transduction of the signal arising from the binding of NGF family members to their receptors consists of both slow processes requiring internalization of the neurotrophin–receptor complex and rapid signaling processes that occur at the nociceptor terminal. In both cases, NGF binding drives the dimerization of the TrkA receptor, resulting in TrkA autophosphorylation and the recruitment of a complex of molecules that signal through distinct enzymatic pathways. These include, but are not limited to, pathways involving phospho-inositol 3 kinase (PI3K), ras-mitogen-associated protein kinase (MAPK), and PLC γ. The activated complex with NGF-bound TrkA at its core is internalized into a specialized endosomal vesicle and transported along microtubules to the cell body, where signaling from this complex can trigger changes in transcription, translation, and protein trafficking (Zweifel, L. S. *et al.*, 2005). For many years, this slow retrograde process was viewed as the predominant mode of neurotrophin signaling in sensory neurons. More recently, however, it has become evident that NGF–TrkA activation of PI3K, MAPK, and PLCγ

produces rapid effects at the nociceptor terminal by altering ion channel sensitivity and plasma membrane localization within seconds, chiefly via receptor phosphorylation (Shu, X. and Mendell, M. L., 2001; Bonnington, J. K. and McNaughton, P. A., 2003; Zhang, X. *et al*., 2005). These events will be described in greater detail in the final section of this chapter. The p75 receptor is associated with the activation of a distinct set of second messenger pathways, including one involving the activation of sphingomyelinase and the liberation of ceramide (Zhang, Y. H. *et al*., 2002; Zhang, Y. H. and Nicol, G. D., 2004).

Nociceptive afferents expressing TrkA constitute a subpopulation of nociceptive afferents. Other subpopulations of nociceptive afferents express receptors for other neurotrophic factors. For example, one subpopulation of nociceptive afferents that do not express the neuropeptides substance P or CGRP, lose their NGF dependence during early postnatal life and begin to express a receptor for glial cell-derived neurotrophic factor (GDNF) (Molliver, D. C. *et al*., 1997). GDNF is a member of a second family of neurotrophins that includes neuturin, artemin, and persephin. As with NGF in TrkA-expressing neurons, the amount of GDNF to which these nonpeptidergic nociceptive afferents have access influences their phenotypic properties (see Fjell, J. *et al*., 1999a). GDNF signaling involves a specific GDNF family receptor (GFR), which acts in conjunction with another receptor tyrosine kinase, ret, that is shared by all members of this family. Interestingly, GDNF signaling involves second messenger pathways similar to those underling the actions of NGF, including PLC-γ, MAPK, and PI3K (Airaksinen, M. S. and Saarma, M., 2002). Thus, the phenotype of subpopulations of nociceptive afferents is regulated by different receptor systems that appear to ultimately use similar transduction cascades.

5.04.3 Additive and Emergent Properties of Nociceptor Membrane Proteins

5.04.3.1 Introduction

It should be evident from the preceding section that sensory afferents have, at their disposal, an extensive repertoire of cell surface proteins with diverse stimulus specificities and signaling capabilities. However, a full mechanistic understanding of nociceptive signal transduction, action potential generation, and spike propagation will require that pain biologists move beyond a mere itemization of the contents of this toolbox to an appreciation of the additive and emergent properties that can arise from the polymodal nature of some of these molecules, their posttranslational modulation, their interactions, and their spatial distribution. In this section, we attempt to illustrate these principles using a few specific examples, some well established, and others more speculative in nature.

5.04.3.2 Shared Modalities and Polymodality

One source of signaling complexity and heterogeneity among sensory neurons is the existence of multiple transducers for a given stimulus modality. For example, as described above, at least six TRP channels expressed in sensory neurons can be gated by heat or cold. Although each channel exhibits a characteristic temperature range over which it is thermally responsive, in many cases these ranges overlap, theoretically allowing continuous recognition of the thermal environment. At the same time, the largely nonoverlapping expression patterns of TRPM8, TRPV1, and TRPV2 lend some credence to the labeled-line hypothesis, which states that distinct sensory modalities (innocuous cold, pain, itch, etc.) are conveyed by anatomically distinct subsets of sensory afferents with specific central projection patterns (Craig, A. D., 2002). However, it should be noted that this segregation of thermotransduction mechanisms is not absolute. For example, some polymodal nociceptors exhibit paradoxical dual responsiveness to both intense heat and intense cold (Dodt, E. and Zotterman, Y., 1952). Even at the molecular level, TRPV1 and TRPA1 are coexpressed in a significant fraction of small-diameter sensory neurons. Though the implications for thermosensation remain controversial, such coexpression appears to be critical for full responsiveness to bradykinin, perhaps owing to the potentiation of TRPA1 by Ca^{2+} ions flowing through TRPV1 (Bautista, D. M. *et al*., 2006). Thus, while the labeled line hypothesis may adequately address some aspects of thermosensation, the overall situation may be more complex.

Mechanotransduction represents an even more extreme example of likely complementarity and redundancy among transducing molecules. Members

of both the ASIC and the TRP families have been implicated in this process, but only modest deficits in mechanotransduction have been reported in animals lacking any single putative mechanosensory protein (Price, M. P. *et al.*, 2000; Liedtke, W. and Friedman, J. M., 2003; Suzuki, M. *et al.*, 2003; Page, A. J. *et al.*, 2004; Kwan, K. Y. *et al.*, 2006). One interpretation of these findings is that mechanotransduction involves complexes of intracellular, transmembrane, and extracellular molecules, and that multiple interchangeable ion channel subunits can contribute to the ion permeation pathways of these transduction complexes.

Another source of complexity in sensory nerve signal transduction is responsiveness to multiple modalities within a single transduction molecule. One of the best-studied examples of this phenomenon is the capsaicin receptor, TRPV1. This channel protein can be activated by a diverse list of chemical or thermal stimuli (Caterina, M. J. and Julius, D., 2001). In addition, there is evidence that this channel or its splice variants may participate in osmotic or mechanical sensitivity in osmosensory regions of the brain and in non-neuronal cells of the urinary bladder (Birder, L. A., 2005; Naeini, R. S. *et al.*, 2006). Such polymodal responsiveness provides ample opportunities for convergent stimuli to combine additively or even supraadditively to produce greater nociceptor activation than any single stimulus. For example, even a modest reduction in pH (to 6.4) can drop the apparent thermal threshold for TRPV1 activation to near body temperature, possibly leading to spontaneous pain in the context of inflammation or ischemia (Tominaga, M. *et al.*, 1998).

5.04.3.3 Functional Interactions between Nociceptor Proteins

Interactions between different proteins on the surface of the nociceptor terminal can also have profound effects on nociceptors transduction and therefore function. Sometimes, these interactions are direct, as in the case of ion channel or GPCR heteromultimerization. In other cases, second messenger molecules and intracellular enzymes facilitate functional interactions among membrane proteins. Recently, for example, it was demonstrated that TRPM8 can activate Ca^{2+}-dependent phospholipases that, in turn, cleave the phosphatidyl inositol bisphosphate that inhibits or activates a host of channels, including inwardly rectifying potassium channels, as well as TRPM8, itself (Rohacs, T. *et al.*, 2005). Similarly, TRPV1 can activate MAPK signaling pathways (Zhuang, Z. Y. *et al.*, 2004). An additional interaction mechanism that has been reported in other types of sensory neurons, but could also conceivably occur in nociceptors, is the stimulation of Ca^{2+}-activated K^+ channels by the Ca^{2+} ions that flow through ligand-gated ion channels (Yuhas, W. A. and Fuchs, P.A., 1999; Isaacson, J. S. and Murphy, G. J., 2001). This arrangement has the potential to shape the amplitude, duration, and even the direction of generator potential.

Active membrane properties are also strongly dependent upon the interaction, at multiple levels, between the ion channels and the other membrane proteins underlying transduction and those regulating action potential initiation and propagation. For example, even small changes in resting membrane potential or generator potential will dramatically influence the availability of different voltage-gated ion channels. Similarly, the second messenger pathways activated by GPCRs and neurotrophin receptors can impact many facets of action potential generation and propagation, as described in the final section of this chapter. The spatial distribution of ion channels underlying each of the steps in afferent signaling is another critical determinant of whether or not there will be successful transmission of sensory information. The ion channels underlying spike initiation must be close enough to the ion channels underlying stimulus transduction that the generator potential pushes the membrane potential above the action potential threshold (Figure 1). Similarly, the ion channels underlying action potential propagation must be close enough to the site of spike initiation, that the action potential is faithfully propagated toward the central nervous system. In addition, action potential threshold may be relatively high in nociceptors that utilize the high-threshold voltage-gated Na^+ channel NaV1.8 for spike initiation, whereas action potential burst duration may be relatively short in nociceptors in which Ca^{2+}-dependent K^+ channels are present in high densities.

One implication of the precise nature of these spatial relationships between of ion channels within sensory neurons is that cellular processes underlying the trafficking and anchoring of ion channels within sensory neurons must be tightly regulated. While there is much to be learned about the distribution and anchoring of ion channels in sensory neurons, the observation that it is possible to induce modality

specific sensitization in polymodal nociceptors, raises the possibility that ion channels and/or transducers are differentially distributed throughout the terminal arbor. Adaptor/scaffold proteins can also shape nociceptor responsiveness by bridging ion channels or GPCRs with intracellular enzymes or with proteins that regulate intracellular transport. For example, PICK1, a PDZ domain-containing protein, appears to regulate the subcellular trafficking of ASIC channel subunits (Duggan, A. *et al.*, 2002), while annexin has been demonstrated to regulate surface expression and function of NaV1.8 (Okuse, K. *et al.*, 2002).

In summary, signaling heterogeneity, convergence of function, protein–protein interactions, and cytosolic signaling, as well as spatiotemporal organization of ion channels allow an already complex set of membrane proteins to vastly expand the sensory and coding capacity of nociceptive neurons.

5.04.4 Injury-Induced Plasticity in Transduction

5.04.4.1 Introduction

Research into the underlying mechanisms of pain associated with tissue injury has revealed that while there are a number of key players that are involved with a wide range of injury types the nature of the contribution of these players varies as a function of the type of injury. For example, acute, phosphorylation-dependent modulation of the voltage-gated Na^+ channel NaV1.8 (Fitzgerald, E. M. *et al.*, 1999), results in an increase in current that contributes to an inflammation-induced increase in nociceptors excitability (England, S. *et al.*, 1996; Gold, M. S. *et al.*, 1996b). In contrast, following traumatic nerve injury, redistribution of NaV1.8 to the axons of uninjured afferents appears to be necessary for the expression of mechanical hypersensitivity associated with nerve injury (Gold, M. S. *et al.*, 2003). There are many such examples, a number of which have been alluded to in the preceding discussion. However, while it is beyond the scope of the present chapter to detail the array of injury-induced changes in mechanisms underlying stimulus transduction, it is informative to consider several specific examples of modulatory events that occur in the context of inflammation and nerve injury. A few of these mechanisms are illustrated schematically in Figure 1.

5.04.4.2 Inflammation-Induced Changes in Nociceptor Sensory function – Inflammatory Pain

One of the best examples of injury-induced changes in the transduction properties of nociceptive neurons is the enhanced responsiveness to heat that occurs following tissue inflammation. As indicated in Section 5.04.2 of this chapter, the thermal hyperalgesia associated with several distinct inflammatory insults (CFA, carageenan, and mustard oil) or specific inflammatory mediators (bradykinin, NGF, ATP, proteases, and prostaglandin E2) depends strongly on the presence of TRPV1. Consistent with this observation, TRPV1 ion channel activity can be sensitized by these various agents in dissociated DRG neurons or heterologous expression systems (Lopshire, J. C. and Nicol, G. D., 1998; Shu,X. and Mendell, M. L., 2001; Vellani, V. *et al.*, 2001; Bonnington, J. K. and McNaughton, P. A., 2003). One lesson emerging from these studies, however, is that TRPV1 sensitization by inflammatory mediators can proceed via a number of alternative mechanisms.

The most direct mechanism by which inflammatory mediators can sensitize TRPV1 is by evoking the generation or liberation of TRPV1 coagonists, such as protons (Caterina, M. J. *et al.*, 1997) or arachidonic acid metabolites (Hwang, S. W. *et al.*, 2000; Huang, S. M. *et al.*, 2002). Convergent interactions of TRPV1 with multiple stimulators result in channel activity levels greater than those evoked by one agonist alone. Another extensively studied TRPV1 sensitization mechanism involves direct phosphorylation of this channel by serine/threonine kinases (PKC, PKA, Ca^{2+}/calmodulin-dependent protein kinase II) (Bhave, G. and Gereau, R. W. T., 2004) or the src tyrosine kinase (Zhang, X. *et al.*, 2005). Although there is some overlap in their recognition sequences, each kinase apparently targets a different collection of phosphorylation sites, resulting in the generation of distinct phospho-TRPV1 species. In the case of ser/thr kinases, phosphorylation appears to enhance TRPV1 sensitivity to its chemical and thermal agonists and/or reverse TRPV1 desensitization (Bhave, G. and Gereau, R. W. T., 2004). In contrast, TRPV1 phosphorylation by src kinase, which is activated by NGF–trkA signaling, leads within 10 min to a translocation of TRPV1 from an intracellular compartment to the plasma membrane, resulting in an increase in the overall number of TRPV1 channels on the cell surface (Zhang, X.

et al., 2005). The MAPK, p38, has also been shown to participate in NGF-stimulated facilitation of TRPV1 signaling during inflammation. Although the relevant target of p38 phosphorylation is not known, the end result is an apparent enhancement of TRPV1 translation and/or trafficking to peripheral nociceptor terminals that requires 1–2 days (Ji, R. R. *et al.*, 2002).

A third general mechanism by which TRPV1 can be modulated in the context of inflammation is by alterations in membrane phospholipid content. For example, it has been proposed that phosphatidylinositol bisphosphate exerts a tonic inhibition on TRPV1 activity and that its hydrolysis by PLC relieves that inhibition (Chuang, H. H. *et al.*, 2001; Prescott, E. D. and Julius, D., 2003). The effects of PIP2 on TRPV1 may be complex, however, given that this phospholipid is also required for resensitization of TRPV1 following agonist-dependent desensitization (Liu, B. *et al.*, 2005). More recently, work from several laboratories has provided evidence that phosphorylation of PIP2 to PIP3 by PI3 kinase to form PIP3 represents yet another mechanism for TRPV1 sensitization (Bonnington, J. K. and McNaughton, P. A., 2003; Zhuang, Z. Y. *et al.*, 2004; Zhang, X. *et al.*, 2005). Although the precise basis for this effect remains unclear, one intriguing suggestion is that it is due to the effects of PIP3 on src activity, thus potentially linking lipid-based and protein kinase-based sensitization events (Zhuang, Z. Y. *et al.*, 2004). Much remains to be learned about the relative importance of and interactions between these different processes. However, it is clear that nociceptors have developed multiple means of responding to tissue inflammation by becoming hypersensitive.

5.04.4.3 Changes in Nociceptor Function Following Traumatic Nerve Injury – Neuropathic Pain

Pain and hyperalgesia arising from direct damage to sensory neurons come under the heading of neuropathic pain. One of the most dramatic and common features of neuropathic pain is the presence of ongoing pain (Backonja, M. M. and Stacey, B., 2004). This feature is distinct from inflammatory pain, where it is often possible to relieve pain if it is possible to eliminate stimuli that impact the inflamed tissue. There is compelling evidence to suggest that ongoing pain associated with peripheral nerve injury is the result of aberrant and/or ongoing activity in both injured afferents and their uninjured neighbors (Gold, M. S., 2000b). Most compelling are the observations that ongoing neuropathic pain may be blocked with the administration of local anesthetics (Gracely, R. H. *et al.*, 1992). However, there is also a very tight correlation between the development of nociceptive behaviors and the emergence of ongoing afferent activity in animal models of neuropathic pain (Liu. C. N. *et al.*, 2000). Because of this association between ongoing afferent activity and ongoing pain, considerable effort has been dedicated to the identification of mechanisms that may contribute to this activity. Central to this search is the question of whether the activity is driven by stimulus transduction, or whether there are changes in the relative contribution of ion channels resulting in membrane potential instability, the emergence or amplification of membrane potential oscillations that are capable of driving action potential generation. There is evidence for both sources of activity.

5.04.4.3.1 Nerve injury-induced changes in transduction

Several nerve injury-induced changes in transduction have been identified. These can be loosely grouped into those involving aberrant expression of transducers normally present in peripheral nerve, aberrant coupling between the transducers and cellular pathways and the emergence of inappropriate sources of stimulation. The list of tranducers aberrantly expressed following nerve injury has grown as fast as transducers have been identified. Aberrant expression comes in at least three forms. One is the expression of transducers in the wrong place within a neuron. The most dramatic example of this is the emergence of mechanical and thermal sensitivity at the cut end of a peripheral axon (Michaelis, M. *et al.*, 1999). More recently, it have been demonstrated that compression of a nerve is sufficient to alter the distribution of tranducers in the membrane (Ma, C. *et al.*, 2006). Importantly, aberrant expression patterns are not restricted to the point of compression or injury as a cut axon will result in increased mechanical sensitivity of the sensory neuron soma (Howe, J. F. *et al.*, 1977). Two consequences of these changes are the emergence of mechanical sensitivity at sites that are normally mechanically insensitive and mechanical allodynia, a situation in which a mechanical stimulus, such as that associated with movement, that is normally not painful, becomes a source of pain. Worse still, mechanical stimuli associated with physiological functions, such as movement of tissue associated with blood flow, may also become a source of stimuli for these transducers. A

second form of aberrant expression is the emergence of transducers in the wrong neurons. For example, as indicated above, TRPV1 is primarily expressed in nociceptive afferents. However, following nerve injury, this transducer is expressed in what were previously low-threshold non-nociceptive afferents (Rashid, M. H. *et al.*, 2003). A third form of aberrant expression is a change in the levels of expression of transducers normally present in a neuron. There is evidence for both decreases in inhibitory transducers and increases in excitatory transducers. For example, nerve injury is associated with a decrease in the expression of opioid receptors (Kohno, T. *et al.*, 2005), which are the transducers for the inhibitory signal of both endogenous and exogenous opioids. The result is a decrease in the efficacy of mechanisms normally involved in attenuating pronociceptive processes. An example of an increase in an excitatory transducer is an increase in the expression of the ATP receptor, P2X3 (Fukuoka, T. *et al.*, 2002). The combination of these changes in expression levels is a net increase in afferent excitability.

Evidence in support of aberrant coupling between transducers and signaling pathways following nerve injury is less compelling but should be mentioned. The pathway that has received the greatest attention is the adrenergic system, largely as a result of the observation that pain associated with nerve injury may be sympathetically dependent. What most pain scientists agree on, is that in normal tissue, activation of the sympathetic nervous system is not painful. In fact, primary afferent neurons express adrenergic receptors that are critical for the antinociceptive actions of spinally administered adrenergic agonists. However, following nerve injury, adrenergic agonists may become excitatory (Sato, J. and Perl, E. R., 1991; Devor, M. *et al.*, 1994; Chen, Y. *et al.*, 1996; Liu, X. *et al.*, 1999; Moon, D. E. *et al.*, 1999). Mechanisms of this excitation are still debated, but there is evidence to support at least two mechanisms. One is that there is a change in adrenergic receptor expression and/or coupling such that activation of adrenergic receptors on primary afferent becomes excitatory (Davis, K. D. *et al.*, 1991; Birder, L. A. and Perl, E. R., 1999). A second is that there is a change in the signaling pathway underlying the actions of adrenergic agonists at autoreceptors on the sympathetic postganglionic neuron terminals: in the presence of elevated levels of intracellular Ca^{2+}, norepinephrine becomes capable of driving the release of arachidonic acid metabolites such as prostaglandin E2 (Gonzales, R. *et al.*, 1989; 1991), which then act directly on the primary afferent.

The emergence of inappropriate sources of stimulation may involve sources that are both expected and those that are much less so. Following nerve injury, there are a number of changes that occur in both the injured axon and the surrounding tissue that facilitate restoration of the normal innervation pattern (see Murinson, B. B. *et al.*, 2005). Injured nerves extend processes, which if scar tissue forms at the same time, may not be able to access former nerve tracks. The result may be the formation of a neuroma. Thus, an expected source of stimulation would be mechanical stimulation of the neuroma associated with traction of the surrounding scar tissue. Interestingly, nerve injury may also be associated with the sprouting of sympathic postganglionic terminals into the sensory ganglia (McLachlan, E. M. *et al.*, 1993). This striking observation provided anatomical evidence of sympathic/afferent coupling within the sensory ganglia. While many details about the mechanisms underlying this sprouting have yet to be determined, access to NGF appears to be a regulating factor (Ramer, M. S. and Bisby, M. A., 1999).

5.04.4.3.2 Changes in membrane stability

As emphasized above, the distribution, expression levels and biophysical properties of ion channels in a neural membrane are critical to the maintenance of a given level of membrane excitability. Change in any of these parameters may have profound effects. Not surprisingly, nerve injury is associated with changes in all three, with clear examples of changes in distribution (Gold, M. S. *et al.*, 2003), expression levels (Waxman, S. G. *et al.*, 1994; Dib-Hajj, S. *et al.*, 1996; Decosterd, I. *et al.*, 2002), and biophysical properties (Cummins, T. R. and Waxman, S. G., 1997) of ion channels in both injured neurons and their uninjured neighbors. One of the more striking ramifications of changes in all three of these properties is the emergence and/or amplification of membrane potential oscillations which, it has been argued, are sufficient to drive ongoing activity following nerve injury (Amir, R. *et al.*, 1999). Two critical players have been identified. One is a voltage-gated Na^+ channel with appropriate biophysical properties to sustain the upstroke of the oscillation. The second is a K^+ leak current that drives the downstroke of the oscillation (Amir, R. *et al.*, 1999). While the K^+ channels have yet to be identified, several different Na^+ channels have been implicated. One possibility is a TTX-resistant channel such as NaV1.8 or NaV1.9. This would be consistent with the observation that the upstroke of the oscillation in

trigeminal neurons is TTX-resistant (Puil, E. *et al.*, 1989) as well as the biophysical properties of the current implicated in studies of isolated DRG neurons (Liu, C. N. *et al.*, 2002). However, spontaneous activity in injured afferents is most robust in sensory neurons with a large cell body diameter giving rise to myelinated axons (Liu, C. N. *et al.*, 2000); neither TTX-resistant channel is present in this subpopulation of sensory neurons and both are dramatically downregulated in injured neurons (Dib-Hajj, S. *et al.*, 1996; Decosterd, I. *et al.*, 2002). Another channel that has received a lot of attention is NaV1.3. This channel is upregulated in the presence of injury (Waxman, S. G. *et al.*, 1994; Black, J. A. *et al.*, 1999) and appears to have biophysical properties consistent with ongoing high-frequency activity (Cummins, T. R. and Waxman, S. G., 1997; Cummins, T. R. *et al.*, 2001). There is evidence for the accumulation of TTX-sensitive Na^+ channels at sites of nerve injury (Devor, M. *et al.*, 1993). Furthermore, there is evidence that at least some of the oscillatory activity in sensory neurons is sensitive to TTX (Amir, R. *et al.*, 1999). However, antisense knockdown of this channel has no impact on nociceptive behavior associated with nerve injury (Lindia, J. A. *et al.*, 2005).

Recent evidence from a cohort of individuals who suffer from a paroxysmal pain disorder raise the possibility that NaV1.7 may contribute to nerve injury-induced increases in afferent excitability. Sufferers of this disorder appear to share gain of function mutations in NaV1.7, decreasing the rate and/or extent of channel inactivation (Fertleman, C. R. *et al.*, 2006). While the link between neuropathic pain and paroxysmal pain disorder is tenuous, manifestations of this disorder share similarities with signs and symptoms neuropathic pain, most notably a sensitivity to the membrane stabilizer carbamazepine. A different set of NaV1.7 mutations appears to underlie primary erythermalgia (Yang, Y. *et al.*, 2004), a rare pain disorder associated with pain and redness in the feet and hands. Mutations in NaV1.7 associated with erythermalgia contribute to an increase in the excitability of primary afferent neurons (Rush, A. M. *et al.*, 2006), but they also appear to result in a decrease in the excitability of sympathetic postganglionic neurons, and it is likely the combination of these changes in excitability that appear to mediate the unique symptoms of the disorder. At least two lines of evidence argue against a role for NaV1.7 in pain associated with traumatic nerve injury. First, in patients with peripheral nerve injury NaV1.7 protein appears to decrease in the DRG neurons and remains undetectable in injured peripheral nerve (Coward, K. *et al.*, 2001). Second, there appears to be no deficit in the nerve injury-induced hypersensitivity in an NaV1.7 null mutant mouse (Nassar, M. A. *et al.*, 2005). Thus, while the specific channels underlying nerve injury-induced increases in afferent excitability have yet to be conclusively identified, it is clear that ion channels alone may become a generator of ongoing activity in injured neurons.

5.04.4.3.3 Mechanisms underlying nerve injury-induced changes in transduction

While many of the mechanistic details underlying nerve injury-induced changes in transducer and/or ion channels have yet to be identified, it is clear that changes in access to trophic factors plays a major role in the process (Waxman, S. G. *et al.*, 1999; Sah, D. W. *et al.*, 2003). Following nerve injury, different groups of afferents may either be deprived of access to neurotrophic factors or bathed in excess levels with those that are injured being deprived and those that remain being bathed in excess. The suggestion that access to neurotrophic factors plays a critical role in driving nerve injury-induced changes is supported by the observation that exogenous application of factors such as NGF or GDNF to injured neurons restores ion channel expression levels and may eliminate ongoing activity. Exogenous NGF restores expression levels of NaV1.8 and NaV1.9 and reduces expression levels of NaV1.3 (Black, J. A. *et al.*, 1997; Fjell, J. *et al.*, 1999b). GDNF has also been shown to differentially regulate expression levels of NaV1.3 (Boucher, T. J. *et al.*, 2000; Leffler, A. *et al.*, 2002). Similarly, the peripheral administration of NGF results in the sensitization of nociceptive afferents and increases in the expression of many proteins that are increased in uninjured afferents following nerve injury (e.g., TRPV1) (Ji, R. R. *et al.*, 2002; Rashid, M. H. *et al.*, 2003). Attenuation of neurotrophin signaling through antibodies or antagonist has also been shown to reverse inflammation-induced changes in afferent excitability (McMahon, S. B., 1996; Koltzenburg, M. *et al.*, 1999).

5.04.5 Conclusion

Adequate treatment of chronic pain in the absence of serious side effects remains an elusive goal for patients, clinicians, and basic researchers. What should be clear from the preceding discussion is that the identification of effective therapeutic interventions has been hampered by the realization that the system is far more

complex than ever imagined. The redundancy of signaling molecules, the promiscuity of receptors, and the delicate balance of both inhibitory and facilitatory processes have all kept the silver bullet frustratingly out of reach. However, identification of proteins highly enriched in nociceptive afferents that are critical for the transmission of nociceptive information to the central nervous system, an understanding of how these molecules function within the larger context of molecules in and around the afferent, all coupled with the early success of selective blockers of these compounds in clinical trials, suggests that truly novel and effective therapeutic interventions may not be far off.

References

Airaksinen, M. S. and Saarma, M. 2002. The GDNF family: signalling, biological functions and therapeutic value. Nat. Rev. Neurosci. 3, 383–394.

Alessandri-Haber, N., Joseph, E., Dina, O. A., Liedtke, W., and Levine, J. D. 2005. TRPV4 mediates pain-related behavior induced by mild hypertonic stimuli in the presence of inflammatory mediator. Pain 118, 70–79.

Ambalavanar, R., Moritani, M., and Dessem, D. 2005. Trigeminal P2X3 receptor expression differs from dorsal root ganglion and is modulated by deep tissue inflammation. Pain 117, 280–291.

Amir, R. and Devor, M. 1996. Chemically mediated cross-excitation in rat dorsal root ganglia. J. Neurosci. 16, 4733–4741.

Amir, R. and Devor, M. 2003. Electrical excitability of the soma of sensory neurons is required for spike invasion of the soma, but not for through-conduction. Biophys. J. 84, 2181–2191.

Amir, R., Michaelis, M., and Devor, M. 1999. Membrane potential oscillations in dorsal root ganglion neurons: role in normal electrogenesis and neuropathic pain. J. Neurosci. 19, 8589–8596.

Andersson, K. E. 2002. Bladder activation: afferent mechanisms. Urology 59, 43–50.

Andrew, D. and Greenspan, J. D. 1999. Mechanical and heat sensitization of cutaneous nociceptors after peripheral inflammation in the rat. J. Neurophysiol. 82, 2649–2656.

Arvidsson, U., Dado, R. J., Riedl, M., Lee, J. H., Law, P. Y., Loh, H. H., Elde, R., and Wessendorf, M. W. 1995. Delta-opioid receptor immunoreactivity: distribution in brainstem and spinal cord, and relationship to biogenic amines and enkephalin. J. Neurosci. 15, 1215–1235.

Baccaglini, P. I. and Hogan, P. G. 1983. Some rat sensory neurons in culture express characteristics of differentiated pain sensory cells. Proc. Natl. Acad. Sci. U. S. A. 80, 594–598.

Baccei, M. L. and Kocsis, J. D. 2000. Voltage-gated calcium currents in axotomized adult rat cutaneous afferent neurons. J. Neurophysiol. 83, 2227–2238.

Backonja, M. M. and Stacey, B. 2004. Neuropathic pain symptoms relative to overall pain rating. J. Pain. 5, 491–497.

Bandell, M., Story, G. M., Hwang, S. W., Viswanath, V., Eid, S. R., Petrus, M. J., Earley, T. J., and Patapoutian, A. 2004. Noxious cold ion channel TRPA1 is activated by pungent compounds and bradykinin. Neuron 41, 849–857.

Bang, H., Kim, Y., and Kim, D. 2000. TREK-2, a new member of the mechanosensitive tandem-pore K^+ channel family. J. Biol. Chem. 275, 17412–17419.

Barclay, J., Patel, S., Dorn, G., Wotherspoon, G., Moffatt, S., Eunson, L., Abdel'al, S., Natt, F., Hall, J., Winter, J., *et al.* 2002. Functional downregulation of P2X3 receptor subunit in rat sensory neurons reveals a significant role in chronic neuropathic and inflammatory pain. J. Neurosci. 22, 8139–8147.

Barton, M. E., Eberle, E. L., and Shannon, H. E. 2005. The antihyperalgesic effects of the T-type calcium channel blockers ethosuximide, trimethadione, and mibefradil. Eur. J. Pharmacol. 521, 79–85.

Baumann, T. K., Chaudhary, P., and Martenson, M. E. 2004. Background potassium channel block and TRPV1 activation contribute to proton depolarization of sensory neurons from humans with neuropathic pain. Eur. J. Neurosci. 19, 1343–1351.

Bautista, D. M., Jordt, S. E., Nikai, T., Tsuruda, P. R., Read, A. J., Poblete, J., Yamoah, E. N., Basbaum, A. I., and Julius, D. 2006. TRPA1 mediates the inflammatory actions of environmental irritants and proalgesic agents. Cell 124, 1269–1282.

Benson, C. J., Xie, J., Wemmie, J. A., Price, M. P., Henss, J. M., Welsh, M. J., and Snyder, P. M. 2002. Heteromultimers of DEG/ENaC subunits form H^+-gated channels in mouse sensory neurons. Proc. Natl. Acad. Sci. U. S. A. 99, 2338–2343.

Berthoud, H. R., Blackshaw, L. A., Brookes, S. J., and Grundy, D. 2004. Neuroanatomy of extrinsic afferents supplying the gastrointestinal tract. Neurogastroenterol. Motil. 16(Suppl. 1), 28–33.

Bevan, S. and Yeats, J. 1991. Protons activate a cation conductance in a subpopulation of rat dorsal root ganglion neurones. J. Physiol. 433, 145–161.

Bhave, G. and Gereau, R. W. T. 2004. Posttranslational mechanisms of peripheral sensitization. J. Neurobiol. 61, 88–106.

Bhave, G., Karim, F., Carlton, S. M., and Gereau, R. W. T. 2001. Peripheral group I metabotropic glutamate receptors modulate nociception in mice. Nat. Neurosci. 4, 417–423.

Birder, L. A. 2005. More than just a barrier: urothelium as a drug target for urinary bladder pain. Am. J. Physiol. Renal Physiol. 289, F489–F495.

Birder, L. A. and Perl, E. R. 1999. Expression of alpha2-adrenergic receptors in rat primary afferent neurones after peripheral nerve injury or inflammation. J. Physiol. 515, 533–542.

Birrell, G. J., McQueen, D. S., Iggo, A., Coleman, R. A., and Grubb, B. D. 1991. PGI2-induced activation and sensitization of articular mechanonociceptors. Neurosci. Lett. 124, 5–8.

Birrell, G. J., McQueen, D. S., Iggo, A., and Grubb, B. D. 1993. Prostanoid-induced potentiation of the excitatory and sensitizing effects of bradykinin on articular mechanonociceptors in the rat ankle joint. Neuroscience 54, 537–544.

Black, J. A., Cummins, T. R., Plumpton, C., Chen, Y. H., Hormuzdiar, W., Clare, J. J., and Waxman, S. G. 1999. Upregulation of a silent sodium channel after peripheral, but not central, nerve injury in DRG neurons. J. Neurophysiol. 82, 2776–2785.

Black, J. A., Dib-Hajj, S., McNabola, K., Jeste, S., Rizzo, M. A., Kocsis, J. D., and Waxman, S. G. 1996. Spinal sensory neurons express multiple sodium channel alpha-subunit mRNAs. Brain. Res. Mol. Brain Res. 43, 117–131.

Black, J. A., Langworthy, K., Hinson, A. W., Dib-Hajj, S. D., and Waxman, S. G. 1997. NGF has opposing effects on Na^+ channel III and SNS gene expression in spinal sensory neurons. Neuroreport 8, 2331–2335.

Blair, N. T. and Bean, B. P. 2002. Roles of tetrodotoxin (TTX)-sensitive Na^+ current, TTX-resistant Na^+ current, and Ca^{2+} current in the action potentials of nociceptive sensory neurons. J. Neurosci. 22, 10277–10290.

Bleehan, T. and Keele, C. A. 1977. Observations on the algogenic actions of adenosine compounds on the human blister base preparation. Pain 3, 367–377.

Boettger, M. K., Till, S., Chen, M. X., Anand, U., Otto, W. R., Plumpton, C., Trezise, D. J., Tate, S. N., Bountra, C., Coward, K., *et al.* 2002. Calcium-activated potassium channel SK1- and IK1-like immunoreactivity in injured human sensory neurones and its regulation by neurotrophic factors. Brain 125, 252–263.

Bond, C. T., Maylie, J., and Adelman, J. P. 2005. SK channels in excitability, pacemaking and synaptic integration. Curr. Opin. Neurobiol. 15, 305–311.

Bonnington, J. K. and McNaughton, P. A. 2003. Signalling pathways involved in the sensitisation of mouse nociceptive neurones by nerve growth factor. J. Physiol. 551, 433–446.

Borgland, S. L., Connor, M., Ryan, R. M., Ball, H. J., and Christie, M. J. 2002. Prostaglandin E(2) inhibits calcium current in two sub-populations of acutely isolated mouse trigeminal sensory neurons. J. Physiol. 539, 433–444.

Boucher, T. J., Okuse, K., Bennett, D. L., Munson, J. B., Wood, J. N., and McMahon, S. B. 2000. Potent analgesic effects of GDNF in neuropathic pain states. Science 290, 124–127.

Brock, J. A., McLachlan, E. M., and Belmonte, C. 1998. Tetrodotoxin-resistant impulses in single nociceptor nerve terminals in guinea-pig cornea. J. Physiol. (Lond.) 512, 211–217.

Brock, J. A., Pianova, S., and Belmonte, C. 2001. Differences between nerve terminal impulses of polymodal nociceptors and cold sensory receptors of the guinea-pig cornea. J. Physiol. 533, 493–501.

Cardenas, C. G., Del Mar, L. P., and Scroggs, R. S. 1995. Variation in serotonergic inhibition of calcium channel currents in four types of rat sensory neurons differentiated by membrane properties. J. Neurophysiol. 74, 1870–1879.

Caterina, M. J. and Julius, D. 2001. The vanilloid receptor: a molecular gateway to the pain pathway. Ann. Rev. Neurosci. 24, 487–517.

Caterina, M. J., Leffler, A., Malmberg, A. B., Martin, W. J., Trafton, J., Petersen-Zeitz, K. R., Koltzenburg, M., Basbaum, A. I., and Julius, D. 2000. Impaired nociception and pain sensation in mice lacking the capsaicin receptor (see comments). Science 288, 306–313.

Caterina, M. J., Rosen, T. A., Tominaga, M., Brake, A. J., and Julius, D. 1999. A capsaicin receptor homologue with a high threshold for noxious heat. Nature 398, 436–441.

Caterina, M. J., Schumacher, M. A., Tominaga, M., Rosen, T. A., Levine, J. D., and Julius, D. 1997. The capsaicin receptor: a heat-activated ion channel in the pain pathway. Nature 389, 816–824.

Catterall, W. A. 1992. Cellular and molecular biology of voltage-gated sodium channels. Physiol. Rev. S15–S48.

Catterall, W. A., Goldin, A. L., and Waxman, S. G. 2005a. International Union of Pharmacology. XLVII. Nomenclature and structure–function relationships of voltage-gated sodium channels. Pharmacol. Rev. 57, 397–409.

Catterall, W. A., Perez-Reyes, E., Snutch, T. P., and Striessnig, J. 2005b. International Union of Pharmacology. XLVIII. Nomenclature and structure–function relationships of voltage-gated calcium channels. Pharmacol. Rev. 57, 411–425.

Cesare, P. and McNaughton, P. 1996. A novel heat-activated current in nociceptive neurons and its sensitization by bradykinin. Proc. Natl. Acad. Sci. U. S. A. 93, 15435–15439.

Cesare, P., Dekker, L. V., Sardini, A., Parker, P. J., and McNaughton, P. A. 1999. Specific involvement of PKC-epsilon in sensitization of the neuronal response to painful heat. Neuron 23, 617–624.

Chaplan, S. R., Guo, H. Q., Lee, D. H., Luo, L., Liu, C., Kuei, C., Velumian, A. A., Butler, M. P., Brown, S. M., and Dubin, A. E. 2003. Neuronal hyperpolarization-activated pacemaker channels drive neuropathic pain. J. Neurosci. 23, 1169–1178.

Chen, C. C., England, S., Akopian, A. N., and Wood, J. N. 1998. A sensory neuron-specific, proton gated ion channel. Proc. Natl. Acad. Sci. U. S. A. 95, 10240–10245.

Chen, Y., Michaelis, M., Janig, W., and Devor, M. 1996. Adrenoreceptor subtype mediating sympathetic-sensory coupling in injured sensory neurons. J. Neurophysiol. 76, 3721–3730.

Chessell, I. P., Hatcher, J. P., Bountra, C., Michel, A. D., Hughes, J. P., Green, P., Egerton, J., Murfin, M., Richardson, J., Peck, W. L., *et al.* 2005. Disruption of the P2X7 purinoceptor gene abolishes chronic inflammatory and neuropathic pain. Pain 114, 386–396.

Chuang, H. H., Neuhausser, W. M., and Julius, D. 2004. The super-cooling agent icilin reveals a mechanism of coincidence detection by a temperature-sensitive TRP channel. Neuron 43, 859–869.

Chuang, H. H., Prescott, E. D., Kong, H., Shields, S., Jordt, S. E., Basbaum, A. I., Chao, M. V., and Julius, D. 2001. Bradykinin and nerve growth factor release the capsaicin receptor from PtdIns(4,5)P2-mediated inhibition. Nature 411, 957–962.

Chung, M. K., Lee, H. A. M., Suzuki, M., and Caterina, M. J. 2004a. TRPV3 and TRPV4 mediate warmth-evoked currents in primary mouse keratinocytes. J. Biol. Chem. 279, 21569–21575.

Chung, M. K., Lee, H. A. M., Suzuki, M., and Caterina, M. J. 2004b. 2-aminonethoxydiphenyl borate activates and sensitizes the heat-gated ion channel, TRPV3. J. Neurosci. 24, 5177–5182.

Cockayne, D. A., Dunn, P. M., Zhong, Y., Rong, W., Hamilton, S. G., Knight, G. E., Ruan, H. Z., Ma, B., Yip, P., Nunn, P., *et al.* 2005. P2X2 knockout mice and P2X2/P2X3 double knockout mice reveal a role for the P2X2 receptor subunit in mediating multiple sensory effects of ATP. J. Physiol. 567, 621–639.

Cockayne, D. A., Hamilton, S. G., Zhu, Q. M., Dunn, P. M., Zhong, Y., Novakovic, S., Malmberg, A. B., Cain, G., Berson, A., Kassotakis, L., *et al.* 2000. Urinary bladder hyporeflexia and reduced pain-related behaviour in P2X3-deficient mice. Nature 407, 1011–1015.

Connor, J. A. and Stevens, C. F. 1971. Voltage clamp studies of a transient outward membrane current in gastropod neural somata. J. Physiol. 213, 21–30.

Cordoba-Rodriguez, R., Moore, K. A., Kao, J. P., and Weinreich, D. 1999. Calcium regulation of a slow post-spike hyperpolarization in vagal afferent neurons. Proc. Natl. Acad. Sci. U. S. A. 96, 7650–7657.

Coste, B., Osorio, N., Padilla, F., Crest, M., and Delmas, P. 2004. Gating and modulation of presumptive NaV1.9 channels in enteric and spinal sensory neurons. Mol. Cell Neurosci. 26, 123–134.

Coward, K., Aitken, A., Powell, A., Plumpton, C., Birch, R., Tate, S., Bountra, C., and Anand, P. 2001. Plasticity of TTX-sensitive sodium channels PN1 and brain III in injured human nerves. Neuroreport 12, 495–500.

Cox, J. J., Reimann, F., Nicholas, A. K., Thornton, G., Roberts, E., Springell, K., Karbani, G., Jafri, H., Mannan, J., Raashid, Y., *et al.* 2006. An SCN9A channelopathy causes congenital inability to experience pain. Nature 444, 894–898.

Craig, A. D. 2002. How do you feel? Interoception: the sense of the physiological condition of the body. Nat. Rev. Neurosci. 3, 655–666.

Cummins, T. R. and Waxman, S. G. 1997. Downregulation of tetrodotoxin-resistant sodium currents and upregulation of a rapidly repriming tetrodotoxin-sensitive sodium current in small spinal sensory neurons after nerve injury. J. Neurosci. 17, 3503–3514.

Cummins, T. R., Aglieco, F., Renganathan, M., Herzog, R. I., Dib-Hajj, S. D., and Waxman, S. G. 2001. Nav1.3 sodium channels: rapid repriming and slow closed-state inactivation display quantitative differences after expression in a mammalian cell line and in spinal sensory neurons. J. Neurosci. 21, 5952–5961.

Cummins, T. R., Dib-Hajj, S. D., Black, J. A., Akopian, A. N., Wood, J. N., and Waxman, S. G. 1999. A novel persistent tetrodotoxin-resistant sodium current in SNS-null and wild-type small primary sensory neurons. J. Neurosci. 19, RC43.

Czapinski, P., Blaszczyk, B., and Czuczwar, S. J. 2005. Mechanisms of action of antiepileptic drugs. Curr. Top. Med. Chem. 5, 3–14.

Dado, R. J., Law, P. Y., Loh, H. H., and Elde, R. 1993. Immunofluorescent identification of a delta (delta)-opioid receptor on primary afferent nerve terminals. Neuroreport 5, 341–344.

Dang, K., Bielefeldt, K., and Gebhart, G. F. 2004. Gastric ulcers reduce A-type potassium currents in rat gastric sensory ganglion neurons. Am. J. Physiol. Gastrointest. Liver. Physiol. 286, G573–G579.

Darian-Smith, I., Davidson, I., and Johnson, K. O. 1980. Peripheral neural representation of spatial dimensions of a textured surface moving across the monkey's finger pad. J. Physiol. 309, 135–146.

Davis, J. B., Gray, J., Gunthorpe, M. J., Hatcher, J. P., Davey, P. T., Overend, P., Harries, M. H., Latcham, J., Clapham, C., Atkinson, K., *et al.* 2000. Vanilloid receptor-1 is essential for inflammatory thermal hyperalgesia. Nature 405, 183–187.

Davis, K. D., Treede, R. D., Raja, S. N., Meyer, R. A., and Campbell, J. N. 1991. Topical application of clonidine relieves hyperalgesia in patients with sympathetically maintained pain. Pain 47, 309–317.

Decosterd, I., Ji, R. R., Abdi, S., Tate, S., and Woolf, C. J. 2002. The pattern of expression of the voltage-gated sodium channels Na(v)1.8 and Na(v)1.9 does not change in uninjured primary sensory neurons in experimental neuropathic pain models. Pain 96, 269–277.

De Groot, J., Zhou, S., and Carlton, S. M. 2000. Peripheral glutamate release in the hindpaw following low and high intensity sciatic stimulation. Neuroreport 11, 497–502.

Dell'Antonio, G., Quattrini, A., Cin, E. D., Fulgenzi, A., and Ferrero, M. E. 2002a. Relief of inflammatory pain in rats by local use of the selective P2X7 ATP receptor inhibitor, oxidized ATP. Arthritis Rheum. 46, 3378–3385.

Dell'Antonio, G., Quattrini, A., Dal Cin, E., Fulgenzi, A., and Ferrero, M. E. 2002b. Antinociceptive effect of a new P(2Z)/P2X7 antagonist, oxidized ATP, in arthritic rats. Neurosci. Lett. 327, 87–90.

Devor, M. 1999. Unexplained peculiarities of the dorsal root ganglion. Pain Suppl. 6, S27–S35.

Devor, M. and Wall, P. D. 1990. Cross-excitation in dorsal root ganglia of nerve-injured and intact rats. J. Neurophysiol. 64, 1733–1746.

Devor, M., Govrin, L. R., and Angelides, K. 1993. Na^+ channel immunolocalization in peripheral mammalian axons and changes following nerve injury and neuroma formation. J. Neurosci. 13, 1976–1992.

Devor, M., Janig, W., and Michaelis, M. 1994. Modulation of activity in dorsal root ganglion neurons by sympathetic activation in nerve-injured rats. J. Neurophysiol. 71, 38–47.

Dib-Hajj, S., Black, J. A., Felts, P., and Waxman, S. G. 1996. Down-regulation of transcripts for Na channel alpha-SNS in spinal sensory neurons following axotomy. Proc. Natl. Acad. Sci. U. S. A. 93, 14950–14954.

Diochot, S., Baron, A., Rash, L. D., Deval, E., Escoubas, P., Scarzello, S., Salinas, M., and Lazdunski, M. 2004. A new sea anemone peptide, APETx2, inhibits ASIC3, a major acid-sensitive channel in sensory neurons. EMBO J. 23, 1516–1525.

Djouhri, L., Fang, X., Okuse, K., Wood, J. N., Berry, C. M., and Lawson, S. N. 2003a. The TTX-resistant sodium channel Nav1.8 (SNS/PN3): expression and correlation with membrane properties in rat nociceptive primary afferent neurons. J. Physiol. 550, 739–752.

Djouhri, L., Newton, R., Levinson, S. R., Berry, C. M., Carruthers, B., and Lawson, S. N. 2003b. Sensory and electrophysiological properties of guinea-pig sensory neurones expressing Nav 1.7 (PN1) Na^+ channel alpha subunit protein. J. Physiol. 546, 565–576.

Dodt, E. and Zotterman, Y. 1952. The discharge of specific cold fibers at high temperatures (paradoxical cold.). Acta Physiol. Scand. 26, 358–365.

Dong, X., Han, S., Zylka, M. J., Simon, M. I., and Anderson, D. J. 2001. A diverse family of GPCRs expressed in specific subsets of nociceptive sensory neurons. Cell 106, 619–632.

Drew, L. J., Rohrer, D. K., Price, M. P., Blaver, K. E., Cockayne, D. A., Cesare, P., and Wood, J. N. 2004. Acid-sensing ion channels ASIC2 and ASIC3 do not contribute to mechanically activated currents in mammalian sensory neurones. J. Physiol. 556, 691–710.

Duggan, A., Garcia-Anoveros, J., and Corey, D. P. 2002. The PDZ domain protein PICK1 and the sodium channel BNaC1 interact and localize at mechanosensory terminals of dorsal root ganglion neurons and dendrites of central neurons. J. Biol. Chem. 277, 5203–5208.

England, S., Bevan, S., and Docherty, R. J. 1996. PGE2 modulates the tetrodotoxin-resistant sodium current in neonatal rat dorsal root ganglion neurones via the cyclic AMP-protein kinase A cascade. J. Physiol. 495(Pt 2), 429–440.

Eshete, F. and Fields, R. D. 2001. Spike frequency decoding and autonomous activation of Ca^{2+}-calmodulin-dependent protein kinase II in dorsal root ganglion neurons. J. Neurosci. 21, 6694–6705.

Fang, X., Djouhri, L., Black, J. A., Dib-Hajj, S. D., Waxman, S. G., and Lawson, S. N. 2002. The presence and role of the tetrodotoxin-resistant sodium channel Na(v)1.9 (NaN) in nociceptive primary afferent neurons. J. Neurosci. 22, 7425–7433.

Ferreira, S. H., Nakamura, M., and de Abreu Castro, M. S. 1978. The hyperalgesic effects of prostacyclin and prostaglandin E2. Prostaglandins 16, 31–37.

Fertleman, C. R., Baker, M. D., Parker, K. A., Moffatt, S., Elmslie, F. V., Abrahamsen, B., Ostman, J., Klugbauer, N., Wood, J. N., Gardiner, R. M., and Rees, M. 2006. SCN9A mutations in paroxysmal extreme pain disorder: allelic variants underlie distinct channel defects and phenotypes. Neuron 52, 767–774.

Fields, R. D., Lee, P. R., and Cohen, J. E. 2005. Temporal integration of intracellular Ca^{2+} signaling networks in regulating gene expression by action potentials. Cell Calcium 37, 433–442.

Fitzgerald, M. 2005. The development of nociceptive circuits. Nat. Rev. Neurosci. 6, 507–520.

Fitzgerald, E. M., Okuse, K., Wood, J. N., Dolphin, A. C., and Moss, S. J. 1999. cAMP-dependent phosphorylation of the tetrodotoxin-resistant voltage-dependent sodium channel SNS. J. Physiol. 516(Pt 2), 433–446.

Fjell, J., Cummins, T. R., Dib-Hajj, S. D., Fried, K., Black, J. A., and Waxman, S. G. 1999a. Differential role of GDNF and NGF in the maintenance of two TTX-resistant sodium channels in adult DRG neurons. Brain. Res. Mol. Brain Res. 67, 267–282.

Fjell, J., Cummins, T. R., Fried, K., Black, J. A., and Waxman, S. G. 1999b. *In vivo* NGF deprivation reduces SNS expression and TTX-R sodium currents in IB4-negative DRG neurons. J. Neurophysiol. 81, 803–810.

Fowler, J. C., Greene, R., and Weinreich, D. 1985a. Two calcium-sensitive spike after-hyperpolarizations in visceral sensory neurones of the rabbit. J. Physiol. (Lond.) 365, 59–75.

Fowler, J. C., Wonderlin, W. F., and Weinreich, D. 1985b. Prostaglandins block Ca^{2+}-dependent slow afterhyperpolarization independent of effects on Ca^{2+} influx in visceral afferent neurons. Brain Res. 345, 345–349.

Fukuoka, T., Tokunaga, A., Tachibana, T., Dai, Y., Yamanaka, H., and Noguchi, K. 2002. VR1, but not P2X(3), increases in the spared L4 DRG in rats with L5 spinal nerve ligation. Pain 99, 111–120.

Garcia-Anoveros, J., Samad, T. A., Zuvela-Jelaska, L., Woolf, C. J., and Corey, D. P. 2001. Transport and localization of the DEG/ENaC ion channel BNaC1alpha to peripheral mechanosensory terminals of dorsal root ganglia neurons. J. Neurosci. 21, 2678–2686.

Gavva, N. R., Klionsky, L., Qu, Y., Shi, L., Tamir, R., Edenson, S., Zhang, T. J., Viswanadhan, V. N., Toth, A., Pearce, L. V., *et al.* 2004. Molecular determinants of vanilloid sensitivity in TRPV1. J. Biol. Chem. 279, 20283–20295.

Ghilardi, J. R., Rohrich, H., Lindsay, T. H., Sevcik, M. A., Schwei, M. J., Kubota, K., Halvorson, K. G., Poblete, J., Chaplan, S. R., Dubin, A. E., *et al.* 2005. Selective blockade of the capsaicin receptor TRPV1 attenuates bone cancer pain. J. Neurosci. 25, 3126–3131.

Gilman, A. G. 1987. G proteins: transducers of receptor-generated signals. Annu. Rev. Biochem. 56, 615–649.

Gold, M. S. 2000a. Sodium channels and pain therapy. Cur. Opin. Anaesthesiol. 13, 565–572.

Gold, M. S. 2000b. Spinal nerve ligation: what to blame for the pain and why. Pain 84, 117–120.

Gold, M. S., Dastmalchi, S., and Levine, J. D. 1996a. Co-expression of nociceptor properties in dorsal root ganglion neurons from the adult rat *in vitro*. Neuroscience 71, 265–275.

Gold, M. S., Levine, J. D., and Correa, A. M. 1998. Modulation of TTX-R INa by PKC and PKA and their role in PGE2-induced sensitization of rat sensory neurons *in vitro*. J. Neurosci. 18, 10345–10355.

Gold, M. S., Reichling, D. B., Shuster, M. J., and Levine, J. D. 1996b. Hyperalgesic agents increase a tetrodotoxin-resistant Na^+ current in nociceptors. Proc. Natl. Acad. Sci. U. S. A. 93, 1108–1112.

Gold, M. S., Shuster, M. J., and Levine, J. D. 1996c. Characterization of six voltage-gated K^+ currents in adult rat sensory neurons. J. Neurophysiol. 75, 2629–2646.

Gold, M. S., Shuster, M. J., and Levine, J. D. 1996d. Role of a slow Ca^{2+}-dependent slow afterhyperpolarization in prostaglandin E2-induced sensitization of cultured rat sensory neurons. Neurosci. Lett. 205, 161–164.

Gold, M. S., Weinreich, D., Kim, C. S., Wang, R., Treanor, J., Porreca, F., and Lai, J. 2003. Redistribution of Na(V)1.8 in uninjured axons enables neuropathic pain. J. Neurosci. 23, 158–166.

Goldin, A. L., Barchi, R. L., Caldwell, J. H., Hofmann, F., Howe, J. R., Hunter, J. C., Kallen, R. G., Mandel, G., Meisler, M. H., Netter, Y. B., *et al.* 2000. Nomenclature of voltage-gated sodium channels. Neuron 28, 365–368.

Gonzales, R., Goldyne, M. E., Taiwo, Y. O., and Levine, J. D. 1989. Production of hyperalgesic prostaglandins by sympathetic postganglionic neurons. J. Neurochem. 53, 1595–1598.

Gonzales, R., Sherbourne, C. D., Goldyne, M. E., and Levine, J. D. 1991. Noradrenaline-induced prostaglandin production by sympathetic postganglionic neurons is mediated by $alpha_2$-adrenergic receptors. J. Neurochem. 57, 1145–1150.

Gover, T. D., Kao, J. P., and Weinreich, D. 2003. Calcium signaling in single peripheral sensory nerve terminals. J. Neurosci. 23, 4793–4797.

Gracely, R. H., Lynch, S. A., and Bennett, G. J. 1992. Painful neuropathy: altered central processing maintained dynamically by peripheral input. Pain 51, 175–194.

Grieco, T. M., Malhotra, J. D., Chen, C., Isom, L. L., and Raman, I. M. 2005. Open-channel block by the cytoplasmic tail of sodium channel beta4 as a mechanism for resurgent sodium current. Neuron 45, 233–244.

Gu, J. G. and MacDermott, A. B. 1997. Activation of ATP P2X receptors elicits glutamate release from sensory neuron synapses. Nature 389, 749–753.

Guler, A. D., Lee, H., Iida, T., Shimizu, I., Tominaga, M., and Caterina, M. 2002. Heat-evoked activation of the ion channel, TRPV4. J. Neurosci. 22, 6408–6414.

Harriott, A., Dessem, D., and Gold, M. S. 2006. Inflammation increases the excitability of masseter muscle afferents. Neuroscience 141(1), 433–442.

He, X. L. and Garcia, K. C. 2004. Structure of nerve growth factor complexed with the shared neurotrophin receptor p75. Science 304, 870–875.

Herzog, R. I., Cummins, T. R., and Waxman, S. G. 2001. Persistent TTX-resistant Na+ current affects resting potential and response to depolarization in simulated spinal sensory neurons. J. Neurophysiol. 86, 1351–1364.

Hogan, Q. H., McCallum, J. B., Sarantopoulos, C., Aason, M., Mynlieff, M., Kwok, W., and Bosnjak, Z. J. 2000. Painful neuropathy decreases membrane calcium current in mammalian primary afferent neurons. Pain 86, 43–53.

Honore, P., Kage, K., Mikusa, J., Watt, A. T., Johnston, J. F., Wyatt, J. R., Faltynek, C. R., Jarvis, M. F., and Lynch, K. 2002. Analgesic profile of intrathecal P2X(3) antisense oligonucleotide treatment in chronic inflammatory and neuropathic pain states in rats. Pain 99, 11–19.

Honore, P., Wismer, C. T., Mikusa, J. P., Zhu, C. Z., Zhong, C., Gauvin, D. M., Gomtsyan, A., El Kouhen, R., Lee, C. H., Marsh, K., Sullivan, J. P., Faltynek, C. R., and Jarvis, M. F. 2005. A-425619, [1-isoquindin-5-yl-3-(4-trifluromethyl-benzyl)-urea], a novel transient receptor potential type V1 receptor antagonist, relieves pathophysiological pain associated with inflammation and tissue injury in rats. J. Pharmacol. Exp. Ther. 314(1), 410–421.

Howe, J. F., Loeser, J. D., and Calvin, W. H. 1977. Mechanosensitivity of dorsal root ganglia and chronically injured axons: a physiological basis for the radicular pain of nerve root compression. Pain 3, 25–41.

Hu, H. Z., Gu, Q., Wang, C., Colton, C. K., Tang, J., Kinoshita-Kawada, M., Lee, L. Y., Wood, J. D., and Zhu, M. X. 2004. 2-aminoethoxydiphenyl borate is a common activator of TRPV1, TRPV2, and TRPV3. J. Biol. Chem. 279, 35741–35748.

Huang, L. Y. and Neher, E. 1996. Ca(2+)-dependent exocytosis in the somata of dorsal root ganglion neurons. Neuron 17, 135–145.

Huang, E. J. and Reichardt, L. F. 2001. Neurotrophins: roles in neuronal development and function. Annu. Rev. Neurosci. 24, 677–736.

Huang, S. M., Bisogno, T., Trevisani, M., Al-Hayani, A., De Petrocellis, L., Fezza, F., Tognetto, M., Petros, T. J., Krey, J. F., Chu, C. J., *et al.* 2002. An endogenous capsaicin-like substance with high potency at recombinant and native vanilloid VR1 receptors. Proc. Natl. Acad. Sci. U. S. A. 99, 8400–8405.

Hucho, T. B., Dina, O. A., and Levine, J. D. 2005. Epac mediates a cAMP-to-PKC signaling in inflammatory pain: an isolectin

B4(+) neuron-specific mechanism. J. Neurosci. 25, 6119–6126.
Hwang, S. W., Cho, H., Kwak, J., Lee, S. Y., Kang, C. J., Jung, J., Cho, S., Min, K. H., Suh, Y. G., Kim, D., and Oh, U. 2000. Direct activation of capsaicin receptors by products of lipoxygenases: endogenous capsaicin-like substances. Proc. Natl. Acad. Sci. U. S. A. 97, 6155–6160.
Immke, D. C. and McCleskey, E. W. 2001. ASIC3: a lactic acid sensor for cardiac pain. ScientificWorldJournal 1, 510–512.
Ingram, S. L. and Williams, J. T. 1994. Opioid inhibition of Ih via adenylyl cyclase. Neuron 13, 179–186.
Isaacson, J. S. and Murphy, G. J. 2001. Glutamate-mediated extrasynaptic inhibition: direct coupling of NMDA receptors to Ca(2+)-activated K^+ channels. Neuron 31, 1027–1034.
Isom, L. L. 2001. Sodium channel beta subunits: anything but auxiliary. Neuroscientist 7, 42–54.
Iwata, Y., Katanosaka, Y., Arai, Y., Komamura, K., Miyatake, K., and Shigekawa, M. 2003. A novel mechanism of myocyte degeneration involving the Ca^{2+}-permeable growth factor-regulated channel. J. Cell. Biol. 161, 957–967.
Jancso, G., Kiraly, E., and Jancso-Gabor, A. 1977. Pharmacologically induced selective degeneration of chemosensitive primary sensory neurons. Nature 270, 741–743.
Jarvis, M. F., Burgard, E. C., McGaraughty, S., Honore, P., Lynch, K., Brennan, T. J., Subieta, A., Van Biesen, T., Cartmell, J., Bianchi, B., *et al.* 2002. A-317491, a novel potent and selective non-nucleotide antagonist of P2X3 and P2X2/3 receptors, reduces chronic inflammatory and neuropathic pain in the rat. Proc. Natl. Acad. Sci. U. S. A. 99, 17179–17184.
Jeftinija, S. 1994. The role of tetrodotoxin-resistant sodium channels of small primary afferent fibers. Brain Res. 639, 125–134.
Ji, R. R., Samad, T. A., Jin, S. X., Schmoll, R., and Woolf, C. J. 2002. p38 MAPK activation by NGF in primary sensory neurons after inflammation increases TRPV1 levels and maintains heat hyperalgesia. Neuron 36, 57–68.
Johnson, K. O. 2001. The roles and functions of cutaneous mechanoreceptors. Curr. Opin. Neurobiol. 11, 455–461.
Jordt, S. E., Bautista, D. M., Chuang, H. H., McKemy, D. D., Zygmunt, P. M., Hogestatt, E. D., Meng, I. D., and Julius, D. 2004. Mustard oils and cannabinoids excite sensory nerve fibres through the TRP channel ANKTM1. Nature 427, 260–265.
Jordt, S. E., McKemy, D. D., and Julius, D. 2003. Lessons from peppers and peppermint: the molecular logic of thermosensation. Curr. Opin. Neurobiol. 13, 487–492.
Kajander, K. C., Wakisaka, S., and Bennett, G. J. 1992. Spontaneous discharge originates in the dorsal root ganglion at the onset of a painful peripheral neuropathy in the rat. Neurosci. Lett. 138, 225–228.
Kang, D. and Kim, D. 2006. TREK-2(K2P10.1) and TRESK (K2P18.1) are major background K^+ channels in dorsal root ganglion neurons. Am. J. Physiol. Cell Physiol. 291(1), C138–C146.
Kepplinger, K. J., Forstner, G., Kahr, H., Leitner, K., Pammer, P., Groschner, K., Soldatov, N. M., and Romanin, C. 2000. Molecular determinant for run-down of L-type Ca^{2+} channels localized in the carboxyl terminus of the 1C subunit. J. Physiol. 529(Pt 1), 119–130.
Khasar, S. G., Gold, M. S., and Levine, J. D. 1998. A tetrodotoxin-resistant sodium current mediates inflammatory pain in the rat. Neurosci. Lett. 256, 17–20.
Khasar, S. G., Lin, Y. H., Martin, A., Dadgar, J., McMahon, T., Wang, D., Hundle, B., Aley, K. O., Isenberg, W., McCarter, G., *et al.* 1999. A novel nociceptor signaling pathway revealed in protein kinase C epsilon mutant mice. Neuron 24, 253–260.
Khodorova, A., Navarro, B., Jouaville, L. S., Murphy, J. E., Rice, F. L., Mazurkiewicz, J. E., Long-Woodward, D., Stoffel, M., Strichartz, G. R., Yukhananov, R., and Davar, G. 2003. Endothelin-B receptor activation triggers an endogenous analgesic cascade at sites of peripheral injury. Nat. Med. 9, 1055–1061.
Kim, D. S., Yoon, C. H., Lee, S. J., Park, S. Y., Yoo, H. J., and Cho, H. J. 2001. Changes in voltage-gated calcium channel alpha(1) gene expression in rat dorsal root ganglia following peripheral nerve injury. Brain Res. Mol. Brain Res. 96, 151–156.
Kirchhoff, C., Leah, J. D., Jung, S., and Reeh, P. W. 1992. Excitation of cutaneous senory nerve endings in the rat by 4-aminopyridine and tetraethylammonium. J. Neurophysiol. 67, 125–131.
Klein, J. P., Tendi, E. A., Dib-Hajj, S. D., Fields, R. D., and Waxman, S. G. 2003. Patterned electrical activity modulates sodium channel expression in sensory neurons. J. Neurosci. Res. 74, 192–198.
Kohno, T., Ji, R. R., Ito, N., Allchorne, A. J., Befort, K., Karchewski, L. A., and Woolf, C. J. 2005. Peripheral axonal injury results in reduced mu opioid receptor pre- and post-synaptic action in the spinal cord. Pain 117, 77–87.
Koltzenburg, M. 1999. The changing sensitivity in the life of the nociceptor. Pain Suppl. 6, S93–S102.
Koltzenburg, M., Bennett, D. L., Shelton, D. L., and McMahon, S. B. 1999. Neutralization of endogenous NGF prevents the sensitization of nociceptors supplying inflamed skin. Eur. J. Neurosci. 11, 1698–1704.
Kostyuk, P. G., Veselovsky, N. S., and Fedulova, S. A. 1981. Ionic currents in the somatic membrane of rat dorsal root ganglion neurons-II. Calcium currents. Neuroscience 6, 2431–2437.
Kruger, L. 1988. Morphological features of thin sensory afferent fibers: a new interpretation of 'nociceptor' function. Prog. Brain Res. 74, 253–257.
Kruger, L., Kavookjian, A. M., Kumazawa, T., Light, A. R., and Mizumura, K. 2003a. Nociceptor structural specialization in canine and rodent testicular ''free'' nerve endings. J. Comp. Neurol. 463, 197–211.
Kruger, L., Light, A. R., and Schweizer, F. E. 2003b. Axonal terminals of sensory neurons and their morphological diversity. J. Neurocytol. 32, 205–216.
Kumazawa, T., Mizumura, K., Koda, H., and Fukusako, H. 1996. EP receptor subtypes implicated in the PGE2-induced sensitization of polymodal receptors in response to bradykinin and heat. J. Neurophysiol. 75, 2361–2368.
Kwan, K. Y., Allchorne, A. J., Vollrath, M. A., Christensen, A. P., Zhang, D. S., and Corey, D. P. 2006. TRPA1 contributes to cold, mechanical, and chemical nociception, but is not essential for hair cell transduction. Neuron 50, 277–289.
Labasi, J. M., Petrushova, N., Donovan, C., McCurdy, S., Lira, P., Payette, M. M., Brissette, W., Wicks, J. R., Audoly, L., and Gabel, C. A. 2002. Absence of the P2X7 receptor alters leukocyte function and attenuates an inflammatory response. J. Immunol. 168, 6436–6445.
Lee, D. H., Chang, L., Sorkin, L. S., and Chaplan, S. R. 2005a. Hyperpolarization-activated, cation-nonselective, cyclic nucleotide-modulated channel blockade alleviates mechanical allodynia and suppresses ectopic discharge in spinal nerve ligated rats. J. Pain 6, 417–424.
Lee, H., Iida, T., Mizuno, A., Suzuki, M., and Caterina, M. J. 2005b. Altered thermal selection behavior in mice lacking transient receptor potential vanilloid 4. J. Neurosci. 25, 1304–1310.
Leffler, A., Cummins, T. R., Dib-Hajj, S. D., Hormuzdiar, W. N., Black, J. A., and Waxman, S. G. 2002. GDNF and NGF reverse changes in repriming of TTX-sensitive Na(+) currents following axotomy of dorsal root ganglion neurons. J. Neurophysiol. 88, 650–658.

Lembo, P. M., Grazzini, E., Groblewski, T., O'Donnell, D., Roy, M. O., Zhang, J., Hoffert, C., Cao, J., Schmidt, R., Pelletier, M., *et al.* 2002. Proenkephalin A gene products activate a new family of sensory neuron-specific GPCRs. Nat. Neurosci. 5, 201–209.

Lerner, U. H. 2002. Neuropeptidergic regulation of bone resorption and bone formation. J. Musculoskelet. Neuronal Interact 2, 440–447.

Levine, J. D., Basbaum, A. I., and Fields, H. L. 1993. Peptides and primary afferent nociceptors. J. Neurosci. 13, 2273–2286.

Lewis, T. 1935. Experiments relating to cunateous hyperalgesia and its spread through somatic fibers. Clinical Sci. 2, 373–423.

Liedtke, W. and Friedman, J. M. 2003. Abnormal osmotic regulation in trpv4–/– mice. Proc. Natl. Acad. Sci. U. S. A. 100, 13698–13703.

Lindia, J. A., Kohler, M. G., Martin, W. J., and Abbadie, C. 2005. Relationship between sodium channel Na(V)1.3 expression and neuropathic pain behavior in rats. Pain 117, 145–153.

Liu, X., Chung, K., and Chung, J. M. 1999. Ectopic discharges and adrenergic sensitivity of sensory neurons after spinal nerve injury. Brain Res. 849, 244–247.

Liu, C. N., Devor, M., Waxman, S. G., and Kocsis, J. D. 2002. Subthreshold oscillations induced by spinal nerve injury in dissociated muscle and cutaneous afferents of mouse DRG. J. Neurophysiol. 87, 2009–2017.

Liu, C. N., Wall, P. D., Ben-Dor, E., Michaelis, M., Amir, R., and Devor, M. 2000. Tactile allodynia in the absence of C-fiber activation: altered firing properties of DRG neurons following spinal nerve injury. Pain 85, 503–521.

Liu, B., Zhang, C., and Qin, F. 2005. Functional recovery from desensitization of vanilloid receptor TRPV1 requires resynthesis of phosphatidylinositol 4,5-bisphosphate. J. Neurosci. 25, 4835–4843.

Lopshire, J. C. and Nicol, G. D. 1998. The cAMP transduction cascade mediates the prostaglandin E_2 enhancement of the capsaicin-elicited current in rat sensory neurons: whole cell and single-channel studies. J. Neurosci. 18, 6081–6092.

Ma, C., Greenquist, K. W., and Lamotte, R. H. 2006. Inflammatory mediators enhance the excitability of chronically compressed dorsal root ganglion neurons. J. Neurophysiol. 95, 2098–2107.

MacIver, M. B. and Tanelian, D. L. 1993. Free nerve ending terminal morphology is fiber type specific for A delta and C fibers innervating rabbit corneal epithelium. J. Neurophysiol. 69, 1779–1783.

Maingret, F., Fosset, M., Lesage, F., Lazdunski, M., and Honore, E. 1999. TRAAK is a mammalian neuronal mechano-gated K^+ channel. J. Biol. Chem. 274, 1381–1387.

Maingret, F., Patel, A. J., Lesage, F., Lazdunski, M., and Honore, E. 2000. Lysophospholipids open the two-pore domain mechano-gated K(+) channels TREK-1 and TRAAK. J. Biol. Chem. 275, 10128–10133.

Mantyh, P. W., DeMaster, E., Malhotra, A., Ghilardi, J. R., Rogers, S. D., Mantyh, C. R., Liu, H., Basbaum, A. I., Vigna, S. R., Maggio, J. E., *et al.* 1995. Receptor endocytosis and dendrite reshaping in spinal neurons after somatosensory stimulation. Science 268, 1629–1632.

Mata, M., Chattopadhyay, M., and Fink, D. J. 2006. Gene therapy for the treatment of sensory neuropathy. Expert. Opin. Biol. Ther. 6, 499–507.

Matsuka, Y., Neubert, J. K., Maidment, N. T., and Spigelman, I. 2001. Concurrent release of ATP and substance P within guinea pig trigeminal ganglia *in vivo*. Brain Res. 915, 248–255.

Matzner, O. and Devor, M. 1992. Na^+ conductance and the threshold for repetitive neuronal firing. Brain Res. 597, 92–98.

Mayer, M. 1985. A calcium-activated chloride current generates the after-depolarization of rat sensory neurons in culture. J. Physiol. 364, 217–239.

McCarter, G. C., Reichling, D. B., and Levine, J. D. 1999. Mechanical transduction by rat dorsal root ganglion neurons *in vitro*. Neurosci. Lett. 273, 179–182.

McFadzean, I. 1988. The ionic mechanisms underlying opioid actions. Neuropeptides 11, 173–180.

McGaraughty, S., Wismer, C. T., Zhu, C. Z., Mikusa, J., Honore, P., Chu, K. L., Lee, C. H., Faltynek, C. R., and Jarvis, M. F. 2003. Effects of A-317491, a novel and selective P2X3/P2X2/3 receptor antagonist, on neuropathic, inflammatory and chemogenic nociception following intrathecal and intraplantar administration. Br. J. Pharmacol. 140, 1381–1388.

McKemy, D. D., Neuhausser, V. M., and Julius, D. 2002. Identification of a cold receptor reveals a general role for TRP channels in thermosensation. Nature 416, 52–58.

McLachlan, E. M., Jang, W., Devor, M., and Michaelis, M. 1993. Peripheral nerve injury triggers noradrenergic sprouting within dorsal root ganglia. Nature 363, 543–546.

McMahon, S. B. 1996. NGF as a mediator of inflammatory pain. Philos. Trans. R. Soc. Lond. B Biol. Sci. 351, 431–440.

Mearow, K. M. and Diamond, J. 1988. Merkel cells and the mechanosensitivity of normal and regenerating nerves in *Xenopus* skin. Neuroscience 26, 695–708.

Meyer, R. A., Raja, S. N., and Campbell, J. N. 1985. Coupling of action potential activity between unmyelinated fibers in the peripheral nerve of monkey. Science 227, 184–187.

Michaelis, M., Blenk, K. H., Vogel, C., and Janig, W. 1999. Distribution of sensory properties among axotomized cutaneous C-fibres in adult rats. Neuroscience 94, 7–10.

Molliver, D. C., Wright, D. E., Leitner, M. L., Parsadanian, A. S., Doster, K., Wen, D., Yan, Q., and W.D. S. 1997. IB4-binding neurons switch from NGF to GDNF dependence in early postnatal life. Neuron 19, 849–861.

Moon, D. E., Lee, D. H., Han, H. C., Xie, J., Coggeshall, R. E., and Chung, J. M. 1999. Adrenergic sensitivity of the sensory receptors modulating mechanical allodynia in a rat neuropathic pain model. Pain 80, 589–595.

Moore, B. A., Stewart, T. M., Hill, C., and Vanner, S. J. 2002. TNBS ileitis evokes hyperexcitability and changes in ionic membrane properties of nociceptive DRG neurons. Am. J. Physiol. Gastrointest. Liver Physiol. 282, G1045–G1051.

Moqrich, A., Hwang, S. W., Earley, T. J., Petrus, M. J., Murray, A. N., Spencer, K. S., Andahazy, M., Story, G. M., and Patapoutian, A. 2005. Impaired thermosensation in mice lacking TRPV3, a heat and camphor sensor in the skin. Science 307, 1468–1472.

Muraki, K., Iwata, Y., Katanosaka, Y., Ito, T., Ohya, S., Shigekawa, M., and Imaizumi, Y. 2003. TRPV2 is a component of osmotically sensitive cation channels in murine aortic myocytes. Circ. Res. 93(9), 829–838.

Murinson, B. B., Archer, D. R., Li, Y., and Griffin, J. W. 2005. Degeneration of myelinated efferent fibers prompts mitosis in remak Schwann cells of uninjured C-fiber afferents. J. Neurosci. 25, 1179–1187.

Naeini, R. S., Witty, M. F., Seguela, P., and Bourque, C. W. 2006. An N-terminal variant of Trpv1 channel is required for osmosensory transduction. Nat. Neurosci. 9, 93–98.

Nagata, K., Duggan, A., Kumar, G., and Garcia-Anoveros, J. 2005. Nociceptor and hair cell transducer properties of TRPA1, a channel for pain and hearing. J. Neurosci. 25, 4052–4061.

Nakatsuka, T. and Gu, J. G. 2001. ATP P2X receptor-mediated enhancement of glutamate release and evoked EPSCs in dorsal horn neurons of the rat spinal cord. J. Neurosci. 21, 6522–6531.

Nakatsuka, T., Tsuzuki, K., Ling, J. X., Sonobe, H., and Gu, J. G. 2003. Distinct roles of P2X receptors in modulating

glutamate release at different primary sensory synapses in rat spinal cord. J. Neurophysiol. 89, 3243–3252.
Nassar, M. A., Levato, A., Stirling, L. C., and Wood, J. N. 2005. Neuropathic pain develops normally in mice lacking both Nav1.7 and Nav1.8. Mol. Pain 1, 24.
Nassar, M. A., Stirling, L. C., Forlani, G., Baker, M. D., Matthews, E. A., Dickenson, A. H., and Wood, J. N. 2004. Nociceptor-specific gene deletion reveals a major role for Nav1.7 (PN1) in acute and inflammatory pain. Proc. Natl. Acad. Sci. U. S. A. 101, 12706–12711.
Nicholson, R., Small, J., Dixon, A. K., Spanswick, D., and Lee, K. 2003. Serotonin receptor mRNA expression in rat dorsal root ganglion neurons. Neurosci. Lett. 337, 119–122.
Nilius, B., Vriens, J., Prenen, J., Droogmans, G., and Voets, T. 2004. TRPV4 calcium entry channel: a paradigm for gating diversity. Am. J. Physiol. Cell Physiol. 286, C195–C205.
North, R. A. 2002. Molecular physiology of P2X receptors. Physiol. Rev. 82, 1013–1067.
Numazaki, M., Tominaga, T., Takeuchi, K., Murayama, N., Toyooka, H., and Tominaga, M. 2003. Structural determinant of TRPV1 desensitization interacts with calmodulin. Proc. Natl. Acad. Sci. U. S. A. 100, 8002–8006.
O'Hagan, R. and Chalfie, M. 2005. Mechanosensation in *Caenorhabditis elegans*. Int. Rev. Neurobiol. 69, 169–203.
Oida, H., Namba, T., Sugimoto, Y., Ushikubi, F., Ohishi, H., Ichikawa, A., and Narumiya, S. 1995. *In situ* hybridization studies of prostacyclin receptor mRNA expression in various mouse organs. Br. J. Pharmacol. 116, 2828–2837.
Okuse, K., Malik-Hall, M., Baker, M. D., Poon, W. Y., Kong, H., Chao, M. V., and Wood, J. N. 2002. Annexin II light chain regulates sensory neuron-specific sodium channel expression. Nature 417, 653–656.
Olah, Z., Karai, L., and Iadarola, M. J. 2002. Protein kinase C(alpha) is required for vanilloid receptor 1 activation. Evidence for multiple signaling pathways. J. Biol. Chem. 277, 35752–35759.
Page, A. J., Brierley, S. M., Martin, C. M., Martinez-Salgado, C., Wemmie, J. A., Brennan, T. J., Symonds, E., Omari, T., Lewin, G. R., Welsh, M. J., and Blackshaw, L. A. 2004. The ion channel ASIC1 contributes to visceral but not cutaneous mechanoreceptor function. Gastroenterology 127, 1739–1747.
Patapoutian, A., Peier, A. M., Story, G. M., and Viswanath, V. 2003. ThermoTRP channels and beyond: mechanisms of temperature sensation. Nat. Rev. Neurosci. 4, 529–539.
Patel, A. J. and Honore, E. 2001. Properties and modulation of mammalian 2P domain K^+ channels. Trends Neurosci. 24, 339–346.
Peier, A. M., Moqrich, A., Hergarden, A. C., Reeve, A. J., Andersson, D. A., Story, G. M., Earley, T. J., Dragoni, I., McIntyre, P., Bevan, S., and Patapoutian, A. 2002a. A TRP channel that senses cold stimuli and menthol. Cell 108, 705–715.
Peier, A. M., Reeve, A. J., Andersson, D. A., Moqrich, A., Earley, T. J., Hergarden, A. C., Story, G. M., Colley, S., Hogenesch, J. B., McIntyre, P., *et al.* 2002b. A heat-sensitive TRP channel expressed in keratinocytes. Science 296, 2046–2049.
Pierce, K. L., Premont, R. T., and Lefkowitz, R. J. 2002. Seven-transmembrane receptors. Nat. Rev. Mol. Cell Biol. 3, 639–650.
Pogatzki-Zahn, E. M., Shimizu, I., Caterina, M., and Raja, S. N. 2005. Heat hyperalgesia after incision requires TRPV1 and is distinct from pure inflammatory pain. Pain 115, 296–307.
Pomonis, J. D., Harrison, J. E., Mark, L., Bristol, D. R., Valenzano, K. J., and Walker, K. 2003. *N*-(4-Tertiarybutylphenyl)-4-(3-cholorphyridin-2-yl)tetrahydropyrazine-1(2H)-carbox-amide (BCTC), a novel, orally effective vanilloid receptor 1 antagonist with analgesic properties: II. *in vivo* characterization in rat models of inflammatory and neuropathic pain. J. Pharmacol. Exp. Ther. 306, 387–393.
Prescott, E. D. and Julius, D. 2003. A modular PIP2 binding site as a determinant of capsaicin receptor sensitivity. Science 300, 1284–1288.
Price, M. P., Lewin, G. R., McIlwrath, S. L., Cheng, C., Xie, J., Heppenstall, P. A., Stucky, C. L., Mannsfeldt, A. G., Brennan, T. J., Drummond, H. A., *et al.* 2000. The mammalian sodium channel BNC1 is required for normal touch sensation. Nature 407, 1007–1011.
Price, M. P., McIlwrath, S. L., Xie, J., Cheng, C., Qiao, J., Tarr, D. E., Sluka, K. A., Brennan, T. J., Lewin, G. R., and Welsh, M. J. 2001. The DRASIC cation channel contributes to the detection of cutaneous touch and acid stimuli in mice. Neuron 32, 1071–1083.
Priest, B. T., Murphy, B. A., Lindia, J. A., Diaz, C., Abbadie, C., Ritter, A. M., Liberator, P., Iyer, L. M., Kash, S. F., Kohler, M. G., *et al.* 2005. Contribution of the tetrodotoxin-resistant voltage-gated sodium channel NaV1.9 to sensory transmission and nociceptive behavior. Proc. Natl. Acad. Sci. U. S. A. 102, 9382–9387.
Puil, E., Miura, R. M., and Spigelman, I. 1989. Consequences of 4-aminopyridine applications to trigeminal root ganglion neurons. J. Neurophysiol. 62, 810–820.
Ramer, M. S. and Bisby, M. A. 1999. Adrenergic innervation of rat sensory ganglia following proximal or distal painful sciatic neuropathy: distinct mechanisms revealed by anti-NGF treatment. Eur. J. Neurosci. 11, 837–846.
Rami, H. K. and Gunthorpe, M. J. 2004. The therapeutic potential of TRPV1 (VR1) antagonists: clinical answers await. Drug Discov. Today: Therapeutic Strategies. DOI: 10.1016/j.ddstr.2004.08.020.
Ramsey, I. S., Delling, M., and Clapham, D. E. 2006. An introduction to trp channels. Annu. Rev. Physiol. 68, 619–647.
Rasband, M. N., Trimmer, J. S., Schwarz, T. L., Levinson, S. R., Ellisman, M. H., Schachner, M., and Shrager, P. 1998. Potassium channel distribution, clustering, and function in remyelinating rat axons. J. Neurosci. 18, 36–47.
Rashid, M. H., Inoue, M., Kondo, S., Kawashima, T., Bakoshi, S., and Ueda, H. 2003. Novel expression of vanilloid receptor 1 on capsaicin-insensitive fibers accounts for the analgesic effect of capsaicin cream in neuropathic pain. J. Pharmacol. Exp. Ther. 304, 940–948.
Reichling, D. B. and Levine, J. D. 1997. Heat transduction in rat sensory neurons by calcium-dependent activation of a cation channel. Proc. Natl. Acad. Sci. U. S. A. 94, 7006–7011.
Reid, G. and Flonta, M. 2001. Cold transduction by inhibition of a background potassium conductance in rat primary sensory neurones. Neurosci. Lett. 297, 171–174.
Renganathan, M., Dib-Hajj, S., and Waxman, S. G. 2002. Na(v)1.5 underlies the 'third TTX-R sodium current' in rat small DRG neurons. Brain Res. Mol. Brain Res. 106, 70–82.
Rios, J. C., Rubin, M., St Martin, M., Downey, R. T., Einheber, S., Rosenbluth, J., Levinson, S. R., Bhat, M., and Salzer, J. L. 2003. Paranodal interactions regulate expression of sodium channel subtypes and provide a diffusion barrier for the node of Ranvier. J. Neurosci. 23, 7001–7011.
Ritter, A. M. and Mendell, L. M. 1992. Somal membrane properties of physiologically identified sensory neurons in the rat: effects of nerve growth factor. J. Neurophysiol. 68, 2033–2041.
Robinson, R. B. and Siegelbaum, S. A. 2003. Hyperpolarization-activated cation currents: from molecules to physiological function. Annu. Rev. Physiol. 65, 453–480.

Rohacs, T., Lopes, C. M., Michailidis, I., and Logothetis, D. E. 2005. PI(4, 5)P2 regulates the activation and desensitization of TRPM8 channels through the TRP domain. Nat. Neurosci. 8, 626–634.

Rose, R. D., Koerber, H. R., Sedivec, M. J., and Mendell, L. M. 1986. Somal action potential duration differs in identified primary afferents. Neurosci. Lett. 63, 259–264.

Roza, C., Puel, J. L., Kress, M., Baron, A., Diochot, S., Lazdunski, M., and Waldmann, R. 2004. Knockout of the ASIC2 channel in mice does not impair cutaneous mechanosensation, visceral mechanonociception and hearing. J. Physiol. 558, 659–669.

Rush, A. M., Dib-Hajj, S. D., Liu, S., Cummins, T. R., Black, J. A., and Waxman, S. G. 2006. A single sodium channel mutation produces hyper- or hypoexcitability in different types of neurons. Proc. Natl. Acad. Sci. U. S. A. 103, 8245–8250.

Sah, D. W., Ossipo, M. H., and Porreca, F. 2003. Neurotrophic factors as novel therapeutics for neuropathic pain. Nat. Rev. Drug Discov. 2, 460–472.

Sato, J. and Perl, E. R. 1991. Adrenergic excitation of cutaneous pain receptors induced by peripheral nerve injury. Science 251, 1608–1610.

Schafers, M., Geis, C., Brors, D., Yaksh, T. L., and Sommer, C. 2002. Anterograde transport of tumor necrosis factor-alpha in the intact and injured rat sciatic nerve. J. Neurosci. 22, 536–545.

Scroggs, R. S. and Fox, A. P. 1992. Calcium current variation between acutely isolated adult rat dorsal root ganglion neurons of different size. J. Physiol. 445, 639–658.

Scroggs, R. S., Todorovic, S. M., Anderson, E. G., and Fox, A. P. 1994. Variation in IH, IIR, and ILEAK between acutely isolated adult rat dorsal root ganglion neurons of different size. J. Neurophysiol. 71, 271–279.

Shah, B. S., Stevens, E. B., Gonzalez, M. I., Bramwell, S., Pinnock, R. D., Lee, K., and Dixon, A. K. 2000. beta3, a novel auxiliary subunit for the voltage-gated sodium channel, is expressed preferentially in sensory neurons and is upregulated in the chronic constriction injury model of neuropathic pain. Eur. J. Neurosci. 12, 3985–3990.

Shimizu, I., Iida, T., Guan, Y., Zhao, C., Raja, S. N., Jarvis, M. F., Cockayne, D. A., and Caterina, M. J. 2005. Enhanced thermal avoidance in mice lacking the ATP receptor P2X3. Pain 116, 96–108.

Shu, X. and Mendell, L. M. 2001. Acute sensitization by NGF of the response of small-diameter sensory neurons to capsaicin. J. Neurophysiol. 86, 2931–2938.

Shu, X. Q. and Mendell, L. M. 1999. Neurotrophins and hyperalgesia. Proc. Natl. Acad. Sci. U. S. A. 96, 7693–7696.

Sluka, K. A., Price, M. P., Breese, N. M., Stucky, C. L., Wemmie, J. A., and Welsh, M. J. 2003. Chronic hyperalgesia induced by repeated acid injections in muscle is abolished by the loss of ASIC3, but not ASIC1. Pain 106, 229–239.

Sluka, K. A., Willis, W. D., and Westlund, K. N. 1995. The role of dorsal root reflexes in neurogenic inflammation. Pain Forum 4, 141–149.

Smith, G. D., Gunthorpe, M. J., Kelsell, R. E., Hayes, P. D., Reilly, P., Facer, P., Wright, J. E., Jerman, J. C., Walhin, J. P., Ooi, L., *et al.* 2002. TRPV3 is a temperature-sensitive vanilloid receptor-like protein. Nature 418, 186–190.

Souslova, V., Cesare, P., Ding, Y., Akopian, A. N., Stanfa, L., Suzuki, R., Carpenter, K., Dickenson, A., Boyce, S., Hill, R., *et al.* 2000. Warm-coding deficits and aberrant inflammatory pain in mice lacking P2X3 receptors. Nature 407, 1015–1017.

Steranka, L. R., Manning, D. C., DeHaas, C. J., Ferkany, J. W., Borosky, S. A., Connor, J. R., Vavrek, R. J., Stewart, J. M., and Snyder, S. H. 1988. Bradykinin as a pain mediator: receptors are localized to sensory neurons, and antagonists have analgesic actions. Proc. Natl. Acad. Sci. U. S. A. 85, 3245–3249.

Stewart, T., Beyak, M. J., and Vanner, S. 2003. Ileitis modulates potassium and sodium currents in guinea pig dorsal root ganglia sensory neurons. J. Physiol. 552, 797–807.

Story, G. M., Peier, A. M., Reeve, A. J., Eid, S. R., Mosbacher, J., Hricik, T. R., Earley, T. J., Hergarden, A. C., Andersson, D. A., Hwang, S. W., *et al.* 2003. ANKTM1, a TRP-like channel expressed in nociceptive neurons, is activated by cold temperatures. Cell 112, 819–829.

Sugimoto, Y., Shigemoto, R., Namba, T., Negishi, M., Mizuno, N., Narumiya, S., and Ichikawa, A. 1994. Distribution of the messenger RNA for the prostaglandin E receptor subtype EP3 in the mouse nervous system. Neuroscience 62, 919–928.

Suzuki, M., Mizuno, A., Kodaira, K., and Imai, M. 2003. Impaired pressure sensation in mice lacking TRPV4. J. Biol. Chem. 278, 22664–22668.

Szallasi, A. and Blumberg, P. M. 1999. Vanilloid (Capsaicin) receptors and mechanisms. Pharmacol. Rev. 51, 159–212.

Takahashi, N., Kikuchi, S., Dai, Y., Kobayashi, K., Fukuoka, T., and Noguchi, K. 2003. Expression of auxiliary beta subunits of sodium channels in primary afferent neurons and the effect of nerve injury. Neuroscience 121, 441–450.

Tarpley, J. W., Kohler, M. G., and Martin, W. J. 2004. The behavioral and neuroanatomical effects of IB4-saporin treatment in rat models of nociceptive and neuropathic pain. Brain Res. 1029, 65–76.

Thut, P. D., Wrigley, D., and Gold, M. S. 2003. Cold transduction in rat trigeminal ganglia neurons *in vitro*. Neuroscience 119, 1071–1083.

Tominaga, M., Caterina, M. J., Malmberg, A. B., Rosen, T. A., Gilbert, H., Skinner, K., Raumann, B. E., Basbaum, A. I., and Julius, D. 1998. The cloned capsaicin receptor integrates multiple pain-producing stimuli. Neuron 21, 1–20.

Tominaga, M., Wada, M., and Masu, M. 2001. Potentiation of capsaicin receptor activity by metabotropic ATP receptors as a possible mechanism for ATP-evoked pain and hyperalgesia. Proc. Natl. Acad. Sci. U. S. A. 98, 6951–6956.

Treede, R. D., Davis, K. D., Campbell, J. N., and Raja, S. N. 1992. The plasticity of cutaneous hyperalgesia during sympathetic ganglion blockade in patients with neuropathic pain. Brain 115(Pt 2), 607–621.

Trevisani, M., Smart, D., Gunthorpe, M. J., Tognetto, M., Barbieri, M., Campi, B., Amadesi, S., Gray, J., Jerman, J. C., Brough, S. J., *et al.* 2002. Ethanol elicits and potentiates nociceptor responses via the vanilloid receptor-1. Nat. Neurosci. 5, 546–551.

Tseng, L. F. and Narita, M. 1995. Use of d-antisense oligo in the study of turnover of the d-opioid receptors in the spinal cord of the mice. Soc. Neurosci. Abstr. 21, 1363.

Tsuzuki, K., Ase, A., Seguela, P., Nakatsuka, T., Wang, C. Y., She, J. X., and Gu, J. G. 2003. TNP-ATP-resistant P2X ionic current on the central terminals and somata of rat primary sensory neurons. J. Neurophysiol. 89, 3235–3242.

Vellani, V., Mapplebeck, S., Moriondo, A., Davis, J. B., and McNaughton, P. A. 2001. Protein kinase C activation potentiates gating of the vanilloid receptor VR1 by capsaicin, protons, heat and anandamide. J. Physiol. (Lond.) 543, 813–825.

Vergnolle, N., Wallace, J. L., Bunnett, N. W., and Hollenberg, M. D. 2001. Protease-activated receptors in inflammation, neuronal signaling and pain. Trends Pharmacol. Sci. 22, 146–152.

Viana, F., de la Pena, E., and Belmonte, C. 2002. Specificity of cold thermotransduction is determined by differential ionic channel expression. Nat. Neurosci. 5, 254–260.

Villiere, V. and McLachlan, E. M. 1996. Electrophysiological properties of neurons in intact rat dorsal root ganglia classified by conduction velocity and action potential duration. J. Neurophysiol. 76, 1924–1941.

Vlaskovska, M., Kasakov, L., Rong, W., Bodin, P., Bardini, M., Cockayne, D. A., Ford, A. P., and Burnstock, G. 2001. P2X3 knock-out mice reveal a major sensory role for urothelially released ATP. J. Neurosci. 21, 5670–5677.

Vulchanova, L., Olson, T. H., Stone, L. S., Riedl, M. S., Elde, R., and Honda, C. N. 2001. Cytotoxic targeting of isolectin IB4-binding sensory neurons. Neuroscience 108, 143–155.

Waldmann, R. 2001. Proton-gated cation channels – neuronal acid sensors in the central and peripheral nervous system. Adv. Exp. Med. Biol. 502, 293–304.

Waldmann, R., Champigny, G., Lingueglia, E., De Weille, J. R., Heurteaux, C., and Lazdunski, M. 1999. H(+)-gated cation channels. Ann. N. Y. Acad. Sci. 868, 67–76.

Walker, K. M., Urban, L., Medhurst, S. J., Patel, S., Panesar, M., Fox, A. J., and McIntyre, P. 2003. The VR1 antagonist capsazepine reverses mechanical hyperalgesia in models of inflammatory and neuropathic pain. J. Pharmacol. Exp. Ther. 304, 56–62.

Wallner, M., Pratap, M., and Toro, L. 1998. Ca^{2+}-Dependent K^+ Channels in Muscle and Brain: Molecular Structure, Function and Diseases. In: Current Topics in Membranes, Vol. 46, Potassium Ion Channels: Molecular Structure, Function and Diseases (*eds*. Y. Kurachi, L. Y. Jan, and M. Lazdunski), pp. 117–140. Academic Press.

Wang, Y., Kedei, N., Wang, M., Wang, Q. J., Huppler, A. R., Toth, A., Tran, R., and Blumberg, P. M. 2004. Interaction between protein kinase Cmu and the vanilloid receptor type 1. J. Biol. Chem. 279(51), 53674–53682.

Wang, H. F., Shortland, P., Park, M. J., and Grant, G. 1998. Retrograde and transganglionic transport of horseradish peroxidase-conjugated cholera toxin B subunit, wheatgerm agglutinin and isolectin B4 from Griffonia simplicifolia I in primary afferent neurons innervating the rat urinary bladder. Neuroscience 87, 275–288.

Waxman, S. G., Dib-Hajj, S., Cummins, T. R., and Black, J. A. 1999. Sodium channels and pain. Proc. Natl. Acad. Sci. U. S. A. 96, 7635–7639.

Waxman, S. G., Kocsis, J. D., and Black, J. A. 1994. Type III sodium channel mRNA is expressed in embryonic but not adult spinal sensory neurons, and is reexpressed following axotomy. J. Neurophysiol. 72, 466–470.

Weinreich, D. and Wonderlin, W. F. 1987. Inhibition of calcium-dependent spike after-hyperpolarization increases excitability of rabbit visceral sensory neurones. J. Physiol. 394, 415–427.

Werz, M. A. and MacDonald, R. L. 1983. Opioid peptides selective for Mu- and Delta- opiate receptors reduce calcium-dependent action potential duration by increasing potassium conductance. Neurosci. Lett. 42, 173–178.

White, G., Lovinger, D. M., and Weight, F. F. 1989. Transient low-threshold Ca^{2+} current triggers burst firing through an afterdepolarizing potential in an adult mammalian neuron. Proc. Natl. Acad. Sci. 86, 6802–6806.

Willis, W. D., Jr. 1999. Dorsal root potentials and dorsal root reflexes: a double-edged sword. Exp. Brain Res. 124, 395–421.

Wu, Z. Z., Chen, S. R., and Pan, H. L. 2004b. Differential sensitivity of N- and P/Q-type Ca^{2+} channel currents to a mu opioid in isolectin B4-positive and -negative dorsal root ganglion neurons. J. Pharmacol. Exp. Ther. 311, 939–947.

Wu, G., Whiteside, G. T., Lee, G., Nolan, S., Niosi, M., Pearson, M. S., and Ilyin, V. I. 2004a. A-317491, a selective P2X3/P2X2/3 receptor antagonist, reverses inflammatory mechanical hyperalgesia through action at peripheral receptors in rats. Eur. J. Pharmacol. 504, 45–53.

Xie, J., Price, M. P., Berger, A. L., and Welsh, M. J. 2002. DRASIC contributes to pH-gated currents in large dorsal root ganglion sensory neurons by forming heteromultimeric channels. J. Neurophysiol. 87, 2835–2843.

Xu, H., Blair, N. T., and Clapham, D. E. 2005. Camphor activates and strongly desensitizes the transient receptor potential vanilloid subtype 1 channel in a vanilloid-independent mechanism. J. Neurosci. 25, 8924–8937.

Xu, H., Ramsey, I. S., Kotecha, S. A., Moran, M. M., Chong, J. A., Lawson, D., Ge, P., Lilly, J., Silos-Santiago, I., Xie, Y., *et al.* 2002. TRPV3 is a calcium-permeable temperature-sensitive cation channel. Nature 418, 181–186.

Yang, D. and Gereau, R. W. T. 2002. Peripheral group II metabotropic glutamate receptors (mGluR2/3) regulate prostaglandin E2-mediated sensitization of capsaicin responses and thermal nociception. J. Neurosci. 22, 6388–6393.

Yang, Y., Wang, Y., Li, S., Xu, Z., Li, H., Ma, L., Fan, J., Bu, D., Liu, B., Fan, Z., *et al.* 2004. Mutations in SCN9A, encoding a sodium channel alpha subunit, in patients with primary erythermalgia. J. Med. Genet. 41, 171–174.

Yeomans, D. C., Levinson, S. R., Peters, M. C., Koszowski, A. G., Tzabazis, A. Z., Gilly, W. F., and Wilson, S. P. 2005. Decrease in inflammatory hyperalgesia by herpes vector-mediated knockdown of Nav1.7 sodium channels in primary afferents. Hum. Gene. Ther. 16, 271–277.

Yoshimura, N. and de Groat, W. C. 1999. Increased excitability of afferent neurons innervating rat urinary bladder after chronic bladder inflammation. J. Neurosci. 19, 4644–4653.

Yu, F. H., Westenbroek, R. E., Silos-Santiago, I., McCormick, K. A., Lawson, D., Ge, P., Ferriera, H., Lilly, J., DiStefano, P. S., Catterall, W. A., *et al.* 2003. Sodium channel beta4, a new disulfide-linked auxiliary subunit with similarity to beta2. J. Neurosci. 23, 7577–7585.

Yuhas, W. A. and Fuchs, P. A. 1999. Apamin-sensitive, small-conductance, calcium-activated potassium channels mediate cholinergic inhibition of chick auditory hair cells. J. Comp. Physiol. [A] 185, 455–462.

Yusaf, S. P., Goodman, J., Pinnock, R. D., Dixon, A. K., and Lee, K. 2001. Expression of voltage-gated calcium channel subunits in rat dorsal root ganglion neurons. Neurosci. Lett. 311, 137–141.

Zhang, Y. H. and Nicol, G. D. 2004. NGF-mediated sensitization of the excitability of rat sensory neurons is prevented by a blocking antibody to the p75 neurotrophin receptor. Neurosci. Lett. 366, 187–192.

Zhang, X., Huang, J., and McNaughton, P. A. 2005. NGF rapidly increases membrane expression of TRPV1 heat-gated ion channels. EMBO J. 24, 4211–4223.

Zhang, Y. H., Vasko, M. R., and Nicol, G. D. 2002. Ceramide, a putative second messenger for nerve growth factor, modulates the TTX-resistant Na(+) current and delayed rectifier K(+) current in rat sensory neurons. J. Physiol. 544, 385–402.

Zhao, J., Gover, T. D., Muralidharan, S., Auston, D. A., Weinreich, D., and Kao, J. P. 2006. Caged vanilloid ligands for activation of TRPV1 receptors by 1- and 2-photon excitation. Biochemistry 45, 4915–4926.

Zhuang, Z. Y., Xu, H., Clapham, D. E., and Ji, R. R. 2004. Phosphatidylinositol 3-kinase activates ERK in primary sensory neurons and mediates inflammatory heat hyperalgesia through TRPV1 sensitization. J. Neurosci. 24, 8300–8309.

Zweifel, L. S., Kuruvilla, R., and Ginty, D. D. 2005. Functions and mechanisms of retrograde neurotrophin signalling. Nat. Rev. Neurosci. 6, 615–625.

Zygmunt, P. M., Petersson, J., Andersson, D. A., Chuang, H., Sorgard, M., Di Marzo, V., Julius, D., and Hogestatt, E. D. 1999. Vanilloid receptors on sensory nerves mediate the vasodilator action of anandamide. Nature 400, 452–457.

Zylka, M. J., Dong, X., Southwell, A. L., and Anderson, D. J. 2003. Atypical expansion in mice of the sensory neuron-specific Mrg G protein-coupled receptor family. Proc. Natl. Acad. Sci. U. S. A. 100, 10043–10048.

Zylka, M. J., Rice, F. L., and Anderson, D. J. 2005. Topographically distinct epidermal nociceptive circuits revealed by axonal tracers targeted to Mrgprd. Neuron 45, 17–25.

5.05 Zoster-Associated Pain and Nociceptors

H Maija, Helsinki University Hospital, Helsinki, Finland

© 2008 Elsevier Inc. All rights reserved.

5.05.1	Epidemiology and Course of Herpes Zoster and Postherpetic Neuralgia	75
5.05.2	Neuropathology of Herpes Zoster and Postherpetic Neuralgia	77
5.05.3	Mechanisms of Acute Zoster Pain	77
5.05.4	Pathophysiology of Postherpetic Neuralgia	78
References		79

Glossary

allodynia Painful response to normally pain-free stimulus on the skin.

herpes zoster (HZ) Usually painful reactivation of varicella-zoster virus.

postherpetic neuralgia (PHN) Prolonged pain after herpes zoster.

varicella-zoster virus (VZV) The causative agent of herpes zoster.

5.05.1 Epidemiology and Course of Herpes Zoster and Postherpetic Neuralgia

Postherpetic neuralgia (PHN) is a painful aftermath of herpes zoster (HZ), an acute inflammation of spinal nerves due to reactivation of varicella-zoster virus (VZV) residing dormant in sensory ganglia. HZ is the most common neurological disorder with a cumulative lifetime incidence of 10–20% in general population, and as high as 50% of a cohort surviving to 85 years of age (Dworkin, R. H. and Schmader, K. E., 2001). Surveys from two United Kingdom general-practice populations reported annual incidence rates of 3.4–4.8 per 1000 persons (McGregor, R. M., 1957; Hope-Simpson, R. E., 1965). Two population-based studies of epidemiology of HZ have been published from Rochester, Minnesota (Ragozzino, M. W. *et al.*, 1982; Donahue, J. G. *et al.*, 1995) and reported the annual age-adjusted incidences of 1.3 and 2.1 per 1000. About 50% of the HZ cases are thoracic, whereas trigeminal, cervical, and lumbar locations represent each 10–15% of the cases and sacral dermatomes about 5% of the cases. The distribution of HZ reflects the initial virus burden to sensory ganglia (Hope-Simpson, R. E., 1965).

In HZ, viral replication first causes ganglionitis followed by infection of the corresponding nerve and skin dermatome. Pain and unilateral dermatomal rash are the typical symptoms, often accompanied by paresthesias and itching. Patients with HZ affecting the extremities can have complex regional painlike symptoms (color changes, skin temperature changes, edema, weakness, and extradermatomal involvement), and the risk of PHN is high in these cases (Berry, J. D. *et al.*, 2004). Most patients experience pain during HZ, with only about 10% remaining pain-free. Pain precedes rash in 75% of cases (Haanpää, M. *et al.*, 1999a; Chidiac, C. *et al.*, 2001), lasting usually for some days, but in some cases weeks and even months before the eruption of rash (Gilden, D. H. *et al.*, 1991). Zoster pain tends to resolve spontaneously with time, but a minority of patients continue to have pain after the healing of rash. Retrospective epidemiological studies based on help-seeking behavior reported that about 10% of the patients have pain after the healing of rash, 5% of the patients have pain at 3 months, and 2% have pain at 1 year (Burgoon, C. F. *et al.*, 1957; Hope-Simpson, R. E., 1965; Ragozzino, M. W. *et al.*, 1982). A prospective long-term follow-up study from Iceland reported that 19% of the patients have pain at 1 month, 7% at 3 months, and 3% at 1 year (Helgason, S. *et al.*, 2000). A prospective observational community study reported pain in 30% of the patients at 6 weeks, 27% at 12 weeks, 16% at 6 months, and 9% at 1 year (Scott, F. T. *et al.*, 2003). The most important risk factors for PHN are old age and severe acute pain. Other predictors of PHN are severe rash, presence of prodromal pain, viremia at

presentation (Scott, F. T. *et al.*, 2003), and more pronounced immune response (Sato-Takeda, M. *et al.*, 2004), which reflect more severe acute disease. Mechanical allodynia, that is, painful response to normally pain-free mechanical stimulus on the skin, and pinprick hypoesthesia in acute HZ are associated with PHN at 3 months, but due to their insufficient sensitivity and specificity, they cannot be used as predictors of PHN for an individual patient (Haanpää, M. *et al.*, 2000). Abnormal findings in quantitative sensory testing (QST) are common in HZ: warm and cold thresholds are elevated in 20%, heat pain thresholds are lowered in 10%, and tactile thresholds are elevated in 25% of the patients with HZ. All somatosensory abnormalities tend to normalize with time. The abnormal QST findings are associated neither with the severity of acute pain nor with the development of PHN (Haanpää, M. *et al.*, 1999b).

HZ has been regarded as a simple model of peripheral unilateral neuritis caused by VZV, but evidence from neuropathological reports suggest that viral invasion and inflammation may extend to the central nervous system (CNS) as well (Denny-Brown, D. *et al.*, 1944; Watson, C. P. N. *et al.*, 1991). In a study with 56 immunocompetent HZ patients without clinical symptoms of CNS infection, cerebrospinal fluid (CSF) samples were obtained from 46 patients on days 1–18 from the eruption of rash, and 16 consecutive patients with cranial or cervical HZ underwent magnetic resonance imaging (MRI) 1–5 weeks following rash (Haanpää, M. *et al.*, 1998). In 35% of the patients there was evidence of VZV in the CSF either in the form of a positive polymerase chain reaction (PCR) or anti-VZV-immunoglobulin G (IgG). Leucocytosis (range 5–1440 μL^{-1}) was found in 46% of the patients. These changes were more common in patients with complications (e.g., peripheral motor paresis or ophthalmic complications) but they did not predict PHN. Zoster-related MRI changes were found in the brainstem in 56% of the patients and in the cervical cord in two. Three patients had enhancement of the trigeminal nerve in addition to the brainstem lesions. The presence of brainstem lesions in MRI was associated with the development of PHN at 3 months but not with the severity of acute pain.

Those who continue to suffer from prolonged pain after HZ describe three types of pain: a constant deep aching or burning pain, an intermittent pain with a lancinating quality, and allodynia of the skin. In an individual patient, any component can be the most distressing feature of the pain. Itching and dysesthetic sensations may also be present, being in some patients even more annoying than the pain itself (Oaklander, A. L. *et al.*, 2003). Normal sensory function is often altered in PHN. Mechanical allodynia is reported in 65–87% of patients with PHN (Watson, C. P. N. *et al.*, 1988; Nurmikko, T. and Bowsher, D., 1990; Pappagallo, M. *et al.*, 2000), and some patients have cold allodynia (Bowsher, D., 1996). The patients may experience paradoxical sensations in the affected skin area: hot may be felt cold or vice versa, and although light touch may be unpleasant or painful, firm pressure may attenuate pain (Nurmikko, T., 1994). Noordenbos W. (1959) investigated the skin of the patients with PHN and noted that there were areas of major sensory loss as well as minimal sensory loss in the affected region. Others have suggested that extreme allodynia to light touch is often restricted to areas surrounding scarred skin or lying at the border of affected and unaffected dermatomes. Allodynic areas may be often warm termographically, while scarred areas with maximal sensory loss are cool (Rowbotham, M. C. and Fields, H. L., 1989). When tested with conventional clinical methods, hypoesthesia to touch was present in 90% and hypoesthesia to pinprick in 92% of the patients in a pain clinic series (Watson, C. P. N. *et al.*, 1988). In another case series, 94% of the patients had impaired temperature and/or pinprick sensation and/or allodynia, and about 33% had also tactile deficit (Bowsher, D., 1996).

In QST, marked threshold elevations within the affected dermatome compared with the mirror-image site have been found for touch, pinprick, vibration, warmth, and cold (Bjerring, P. *et al.*, 1990; Nurmikko, T. and Bowsher, D., 1990; Eide, P. K. *et al.*, 1994; Rowbotham, M. C. and Fields, H. L., 1996; Rowbotham, M. C. *et al.*, 1996a; Choi, B. and Rowbotham, M. C., 1997; Attal N. *et al.*, 1999; Pappagallo, M. *et al.*, 2000). This indicates damage to unmyelinated and myelinated sensory fibers. Heat pain hypoesthesia is common in patients with PHN, but a minority of patients has heat pain hyperalgesia (Nurmikko, T. and Bowsher, D., 1990; Rowbotham, M. C. and Fields, H. L., 1996; Rowbotham, M. C. *et al.*, 1996a; Choi, B. and Rowbotham, M. C., 1997). In some patients with PHN, no asymmetry was found in warmth or heat pain thresholds, while the greatest threshold difference observed between the affected and contralateral dermatomes was as high as 12.2 °C for warmth and 9.6 °C for heat pain (Choi, B. and Rowbotham, M. C., 1997). However, noticeable asymmetry in thresholds between the affected site

and its mirror-image site was found in different modalities from 5% to 13% of HZ patients not developing PHN (Nurmikko, T. and Bowsher, D., 1990). Hence, it seems possible to have sensory threshold abnormality without PHN, and PHN without sensory threshold abnormality in the affected dermatome after HZ.

5.05.2 Neuropathology of Herpes Zoster and Postherpetic Neuralgia

The classic report of Head H. and Campbell A. W. (1900) is the most comprehensive study of the neuropathology of HZ, but it does not report the possible presence of PHN. Despite it and later studies, our understanding of the pathophysiology of PHN is far from complete. In acute HZ the dorsal root ganglion shows hemorrhagic inflammation and subsequent scarring (Head, H. and Campbell, A. W., 1900; Denny-Brown, D. *et al.*, 1944; Reske-Nielsen, E. *et al.*, 1986; Schmidbauer, M. *et al.*, 1992). Typically, only one ganglion is severely affected, while mild patchy inflammatory changes can be found in the neighboring ganglia (Denny-Brown, D. *et al.*, 1944; Schmidbauer, M. *et al.*, 1992). Ganglion cell necrosis is followed by secondary degeneration and fibrosis in the sensory root and the peripheral nerve. Direct inflammation can also damage the root and nerve (Head, H. and Campbell, A. W., 1900; Denny-Brown, D. *et al.*, 1944; Zacks, S. L. *et al.*, 1964; Watson, C. P. N. *et al.*, 1991; Schmidbauer, M. *et al.*, 1992). VZV has been shown in ganglial and satellite cells; in damaged nerve roots; in the vasa nervorum; in the distal peripheral nerve endoneurally, perineurally, and epineurally; and in Schwann cells (Schmidbauer, M. *et al.*, 1992). Inflammation in peripheral nerves may persist from weeks to months, which can eventually lead to noticeable fibrosis (Head, H. and Campbell, A. W., 1900; Zacks, S. L. *et al.*, 1964; Watson, C. P. N. *et al.*, 1991).

Only a few studies compare the neuropathological findings of those who recover with the finding of those who have PHN. In four patients who had HZ and went on to develop PHN, atrophy of the dorsal horn was found at autopsy whereas those without PHN did not show similar changes (Watson, C. P. N. *et al.*, 1991). However, one patient without PHN showed subacute myelopathy. The investigators found no difference in substance P, calcitonin gene-related peptide, a marker for norepinephrine, or in opioid receptor binding studies (Watson, C. P. N. *et al.*, 1991). After HZ, a preponderance of small-diameter fibers in the surviving fiber population in peripheral nerves is suggested (Noordenbos, W., 1959; Zacks, S. L. *et al.*, 1964; Watson, C. P. N. *et al.*, 1991), but the significance of this finding is ambiguous, as the fibers in question have not been fully identified. Loss of myelin combined with the preservation of axons has also been described (Fabian, V. A. *et al.*, 1997). Loss of axons and myelin in the peripheral nerve is similar in cases with and without PHN (Zacks, S. L. *et al.*, 1964).

Three studies using skin biopsies report that HZ lowers the innervation density of skin (Rowbotham, M. C. *et al.*, 1996a; Oaklander, A. L. *et al.*, 1998; Oaklander, A. L., 2001). These changes are more profound in patients with PHN, possibly because the absence of pain requires the preservation of a minimum density of primary nociceptive neurons (Oaklander, A. L., 2001). The severity of allodynia is nevertheless associated with well-preserved fiber density (Rowbotham, M. C. *et al.*, 1996a). The results of Oaklander A. L. *et al.* (1998) suggest that unilateral HZ can cause bilateral segmental damage to primary sensory neurons. It is of interest that changes in the epidermal innervation in the contralateral unaffected skin in patients with PHN correlate with the presence and severity of pain, but the pathophysiological explanation for this is unknown.

5.05.3 Mechanisms of Acute Zoster Pain

Mechanisms of acute zoster pain are not fully established. It is obvious that acute zoster pain represents a combination of nociceptive and neuropathic pain. The nociceptive component is caused by inflammation of the skin, which leads to excitation and sensitization of nociceptors. Increased afferent activity transmitted to the spinal cord creates a state of central hyperexcitability in the dorsal horn neurons, which resolves gradually in concert with the healing of tissue damage in a majority of patients. The neuropathic component is caused by direct viral damage and inflammation in the dorsal ganglion, peripheral nerve, and in some cases also in the dorsal root and spinal cord. According to the study of acute HZ, preherpetic pain is not associated with the severity of rash or QST changes, which suggests that virus-induced irritation in the afferent pathways rather than dermal inflammation or axonal damage is more salient in preherpetic pain (Haanpää, M. *et al.*, 1999a).

Because the abnormal QST findings are not associated with the severity of acute zoster pain, dysfunction of the thin fibers per se seems not to be the dominating factor in acute zoster pain. The presence of severe acute pain in acute HZ is associated with the presence of mechanical allodynia but not with severe rash, which implies a neuropathic character of allodynia in acute HZ rather than hyperesthesia or hyperalgesia due to cutaneous inflammation (Haanpää, M. *et al.*, 2000). It is not known to what extent the mechanisms of allodynia in acute HZ are the same as the mechanisms of allodynia in PHN. The extension of allodynia and somatosensory changes outside the affected dermatome is not uncommon in acute HZ, which indicates that the CNS is quite frequently involved even in mild cases of HZ (Haanpää, M. *et al.*, 1999a; 1999b; 2000). Although QST changes are common in HZ, they are not associated with the development of PHN. Hence, the prolonged pain in HZ cannot be explained by as a simple consequence of either axonal damage (represented as threshold elevation) or sensitization of the nociceptive system (represented as heat pain hyperalgesia). Transition from acute zoster-associated pain to PHN is likely to be a multifactorial process, perhaps involving both peripheral and central changes. The genetic factors regulating the inflammatory responses may play an important role in this process (Sato-Takeda, M. *et al.*, 2004).

5.05.4 Pathophysiology of Postherpetic Neuralgia

Patients with PHN have been studied using quantitative testing of the primary afferent function, skin biopsies, and controlled treatment trials. In studies of patients with allodynic PHN, the results concerning the role of C-nociceptors in PHN are conflicting. Using indirect assessment of C-fibers by quantifying the axon reflex reactions induced by histamine iontophoresis, Baron R. and Saguer M. (1993) found that histamine responses were reduced or abolished within allodynic areas, indicating degeneration of C-fibers. Patients, who had recovered from HZ without PHN, had bilaterally identical histamine responses, indicating complete recovery of C-fibers. Additionally, impairment of the C-fiber function correlated positively with the intensity of postherpetic pain. In contrast, Rowbotham M. C. and Fields H. L. (1996) found, using QST measurements, that in the allodynic area of PHN patients, pain severity correlated with the preservation of thermal sensory function. The same conclusion was drawn from the study using skin punch biopsies; the loss of cutaneous innervation correlated inversely with allodynia, and pain intensity was strongly related to the severity of allodynia (Rowbotham, M. C. *et al.*, 1996a). In another study, significant correlation was found between the intensity of ongoing pain and mechanical allodynia in patients with short-lasting (<1 year) but not in patients with long-lasting (≥1 year) PHN (Pappagallo, M. *et al.*, 2000). According to these results, the underlying pathophysiology may vary from patient to patient and with the duration of PHN.

In PHN, three subtypes have been suggested (Table 1): the irritable nociceptor subtype, the deafferented allodynic subtype, and the deafferented nonallodynic subtype (Fields, H. L. *et al.*, 1998; Petersen, K. *et al.*, 2000; Rowbotham, M. and Petersen, K., 2001). In patients with anatomically intact primary afferent nociceptors, pain and allodynia may be due to abnormal hyperactivity of the nociceptors and subsequent central sensitization, respectively (irritable nociceptor type). The topical capsaicin application test can be used to identify PHN patients in whom the mechanism of pain involves sensitization of peripheral afferents (Petersen, K. *et al.*, 2000;

Table 1 Proposed subtypes of PHN

Subtype	*Thermal sensory deficit*	*Allodynia*	*Anesthetic infiltration*	*Capsaicin sensitivity*
Irritable nociceptors	Minimal deficit or hyperalgesic to heat pain	Marked	Prolonged relief	Severe burning pain
Deafferented nonallodynic subtype	Marked to all modalities	None	No change	No sensation
Deafferented allodynic subtype	Marked to all modalities	Variable	Relief of allodynia short duration	Variably reduced

Fields, H. L., Rowbotham, M., and Baron, R. 1998. Postherpetic neuralgia: irritable nociceptors and deafferentation. Neurobiol. Dis. 5, 209–227 and Rowbotham, M. C., Petersen, K. L., and Feilds, H. L. Is postherpetic neuralgia more than one disorder. 1999. IASP New. Let. 3–7.

Petersen, K. *et al.*, 2002). In patients with loss of cutaneous C-nociceptor function, evaluated either by using QST of thermal thresholds (Nurmikko, T. and Bowsher, D., 1990; Nurmikko, T., 1994; Choi, B. and Rowbotham, M. C., 1997), C-fiber axon reflex (Baron, R. and Saquer, M., 1993), or capsaicin-induced flare (Morris, G. C. *et al.*, 1995), deafferentation and central reorganization may explain the PHN pain (Fields, H. L. *et al.*, 1998). If tactile (Aβ) fibers are preserved, allodynia may result from sprouting of the spinal terminals of Aβ mechanoreceptors into contact with the pain transmission neurons. These cases represent the deafferented allodynic subtype. In patients of deafferented nonallodynic subtype, pain may result from the activation of the CNS pain transmission neurons (Nurmikko, T. and Bowsher, D., 1990; Fields, H. L. *et al.*, 1998). In a study of 63 PHN patients, 25% of the cases were of irritable nociceptor type, 50% were of deafferentation with allodynia type, and 25% were of deafferentation without allodynia type (Pappagallo, M. *et al.*, 2000).

Pain relief of peripherally acting treatments, that is, topical agents, supports the role of peripheral nociceptors in PHN. Topical lidocaine, when used as a 5% gel under an occlusive dressing (Rowbotham, M. C. *et al.*, 1995) or as 5% patch (Rowbotham, M. C. *et al.*, 1996b; Galer, B. *et al.*, 1999) reduces pain and allodynia in PHN. Because it produces clinically insignificant serum levels, it is thought to relieve pain by reducing ectopic discharges in the affected peripheral afferent fibers by blocking upregulated sodium channels. Topical capsaicin has been studied in two randomized controlled trials (Bernstein, J. E. *et al.*, 1989; Watson, C. P. N. *et al.*, 1993). Capsaicin binds to nociceptors in the skin, causing excitation of neurons and a period of enhanced sensitivity perceived as itching, pricking, or burning, with cutaneous vasodilatation. This is followed by a refractory period with reduced sensitivity to, and after repeated applications, persistent desensitization (Nolano, M. *et al.*, 1999). The efficacy of topical capsaicin appears limited: the decrease of pain intensity was a maximum of 23% in one trial (Watson, C. P. *et al.*, 1993) and 30% in the other (Bernstein, J. E. *et al.*, 1989).

The question of the role of the sympathetic nervous system in PHN is ambiguous. In a double-blind study, the cutaneous infiltration of an adrenergic agonist into PHN skin caused only a modest increase of pain and allodynia severity (Choi, B. and Rowbotham, M. C., 1997). The role of sympathetic blocks in HZ and PHN remains controversial, and direct evidence of a major sympathetic contribution to PHN is nonexistent (Wu, C. L. *et al.*, 2000).

The treatment of HZ aims at minimizing the neural damage with antiviral drugs, maximal pain relief with analgesic drugs, and prevention of PHN. For those who continue to have prolonged pain, the current armamentarium of medical treatments, that is, tricyclic antidepressants, gabapentinoids, opioids, and topical lidocaine should be tested (Dubinsky, R. M. *et al.*, 2004). The possibility of multiple mechanisms in the same patient may explain why response to any single treatment is so often partial and forms a logic base for polytherapy. The detailed information of the efficacy of the treatments on the various components of PHN is lacking.

References

Attal, N., Brasseur, L., Chauvin, M., and Bouhassira, D. 1999. Effects of a single and repeated applications of a eutectic mixture of local anaesthetics (EMLA^{R}) cream on spontaneous and evoked pain in post-herpetic neuralgia. Pain 81, 203–209.

Baron, R. and Saguer, M. 1993. Postherpetic neuralgia: are C-nociceptors involved in signalling and maintenance of tactile allodynia? Brain 116, 1477–1496.

Bernstein, J. E., Korman, N. J., Bickers, D. R., Dahl, M. V., and Millikan, L. E. 1989. Topical capsaicin treatment of chronic postherpetic neuralgia. J. Am. Acad. Dermatol. 21, 265–270.

Berry, J. D., Rowbotham, M. C., and Petersen, K. L. 2004. Complex regional pain syndrome-like symptoms during herpes zoster. Pain 110, 1–12.

Bjerring, P., Arendt-Nielsen, L., and Soderberg, U. 1990. Argon laser induced cutaneous sensory and pain thresholds in post-herpetic neuralgia. Quantitative modulation by topical capsaicin. Acta Derm. Venereol. (Stockholm) 70, 121–125.

Bowsher, D. 1996. Postherpetic neuralgia and its treatment: a retrospective survey of 191 patients. J. Pain Symptom Manage. 12, 290–299.

Burgoon, C. F., Burgoon, J. S., and Baldridge, C. D. 1957. The natural history of herpes zoster. JAMA 164, 265–269.

Chidiac, C., Bruxelle, J., Daures, J. P., Hoang-Xuan, T., Morel, P., Leplege, A., El Hasnaoui, A., and de Labareyre, C. 2001. Characteristics of patients with herpes zoster on presentation to practitioners in France. Clin. Infect. Dis. 33, 62–69.

Choi, B. and Rowbotham, M. C. 1997. Effect of adrenergic receptor activation on post-herpetic neuralgia pain and sensory disturbances. Pain 69, 55–63.

Denny-Brown, D., Adams, R. D., and Fitzgerald, P. J. 1944. Pathologic features of herpes zoster. A note on geniculate herpes. Arch. Neurol. Psychiatry 51, 216–231.

Donahue, J. G., Choo, P. W., Manson, J. E., and Platt, R. 1995. The incidence of herpes zoster. Arch. Intern. Med. 155, 1605–1609.

Dubinsky, R. M., Kabbani, H., El-Chami, Z., Boutwell, C., and Ali, H. 2004. Practice parameter: treatment of postherpetic neuralgia. An evidence based report of the Quality Standards Subcommittee of the American Academy of Neurology. Neurology 63, 959–965.

Dworkin, R. H. and Schmader, K. E. 2001. The Epidemiology and Natural History of Herpes Zoster and Postherpetic Neuralgia. In: Herpes Zoster and Postherpetic Neuralgia, 2nd edn. (*eds*. C. P. N. Watson and A. A. Gershorn), pp. 39–64. Elsevier.

Eide, P. K., Jorum, E., Stubhaug, A., Bremnes, J., and Breivik, H. 1994. Relief of post-herpetic neuralgia with the N-methyl-D-aspartic acid receptor antagonist ketamine: a double-blind, cross-over comparison with morphine and placebo. Pain 58, 347–354.

Fabian, V. A., Wood, B., Crowley, B., and Kakulas, B. A. 1997. Herpes zoster brachial neuritis. Clin. Neuropathol. 16, 61–64.

Fields, H. L., Rowbotham, M., and Baron, R. 1998. Postherpetic neuralgia: irritable nociceptors and deafferentation. Neurobiol. Dis. 5, 209–227.

Galer, B. S., Rowbotham, M. C., Perander, J., and Friedman, E. 1999. Topical lidocaine patch relieves postherpetic neuralgia more effectively than a vehicle topical patch: results of an enriched enrollment study. Pain 80, 533–538.

Gilden, D. H., Dueland, A. N., Cohrs, R., Martin, J. R., Kleinschmidt-DeMasters, B. K., and Mahalingham, R. 1991. Preherpetic neuralgia. Neurology 41, 1215–1218.

Haanpää, M., Dastidar, P., Weinberg, A., Levin, M., Miettinen, A., Lapinlampi, A., Laippala, P., and Nurmikko, T. 1998. CSF and MRI findings in patients with acute herpes zoster. Neurology 51, 1405–1411.

Haanpää, M., Laippala, P., and Nurmikko, T. 1999a. Pain and somatosensory dysfunction in acute herpes zoster. Clin. J. Pain 15, 78–84.

Haanpää, M., Laippala, P., and Nurmikko, T. 1999b. Thermal and tactile perception thresholds in patients with herpes zoster. Eur. J. Pain 3, 375–386.

Haanpää, M., Laippala, P., and Nurmikko, T. 2000. Allodynia and pinprick hypoaesthesia in acute herpes zoster, and the development of postherpetic neuralgia. J. Pain Symptom Manage. 20, 50–58.

Head, H. and Campbell, A. W. 1900. The pathology of herpes zoster and its bearing on sensory localisation. Brain 23, 353–523.

Hope-Simpson, R. E. 1965. The nature of herpes zoster: a long-term study and a new hypothesis. Proc. R. Soc. Med. 58, 9–20.

McGregor, R. M. 1957. Herpes zoster, chicken pox and cancer in general practice. BMJ 1, 84–87.

Morris, G. C., Gibson, S. J., and Helme, R. D. 1995. Capsaicin-induced flare and vasodilatation in patients with post-herpetic neuralgia. Pain 63, 93–101.

Nolano, M., Simone, D. A., Wenderscharfer-Crabb, G., Johnson, T., Hazen, E., and Kennedy, W. R. 1999. Topical capsaicin in humans: parallel loss of epidermal nerve fibers and pain sensation. Pain 81, 135–145.

Noordenbos, W. 1959. Pain: Problems Pertaining to the Transmission of Nerve Impulses Which Give Rise to Pain. Elsevier.

Nurmikko, T. 1994. Sensory Dysfunction in Postherpetic Neuralgia. In: Touch, Temperature and Pain in Health and Disease, Progress in Pain Research and Management, Vol. 3 (*eds*. J. Boivie, P. Hansson, and U. Lindblom), pp. 133–141. IASP Press.

Nurmikko, T. and Bowsher, D. 1990. Somatosensory findings in postherpetic neuralgia. J. Neurol. Neurosurg. Psychiatry 53, 135–141.

Oaklander, A. L., Romans, K., Horasek, S., Stocks, A., Hauer, P., and Meyer, R. A. 1998. Unilateral postherpetic neuralgia is associated with bilateral sensory neuron damage. Ann. Neurol. 44, 789–795.

Oaklander, A. L. 2001. The density of remaining nerve endings in human skin with and without postherpetic neuralgia after shingles. Pain 92, 139–145.

Oaklander, A. L., Bowsher, D., Galer, B., Haanpää, M., and Jensen, M. P. 2003. Herpes zoster itch: preliminary epidemiological data. J. Pain 6, 338–343.

Pappagallo, M., Oaklander, A., Quatrano-Piacentini, A., Clark, M., and Raja, S. 2000. Heterogenous patterns of sensory dysfunction in postherpetic neuralgia suggest multiple pathophysiologic mechanisms. Anesthesiology 92, 691–698.

Petersen, K., Fields, H., Brennum, J., Sandroni, P., and Rowbotham, M. 2000. Capsaicin evoked pain and allodynia in post-herpetic neuralgia. Pain 88, 125–133.

Petersen, K. L., Rice, F. L., Suess, F., Berro, M., and Rowbotham, M. C. 2002. Relief of post-herpetic neuralgia by surgical removal of painful skin. Pain 98, 119–126.

Ragozzino, M. W., Melton, L. J., Kurland, L. T., Chu, C. P., and Perry, H. O. 1982. Population-based study on herpes zoster and its sequelae. Medicine 61, 310–316.

Reske-Nielsen, E., Oster, S., and Pedersen, B. 1986. Herpes zoster ophthalmicus and the mesencephalic nucleus. Acta Pathol. Microbiol. Immunol. Scand. 94, 263–269.

Rowbotham, M. and Petersen, K. 2001. Zoster-associated pain and neural dysfunction. Pain 93, 1–5.

Rowbotham, M. C. and Fields, H. L. 1989. Post-herpetic neuralgia: the relation of pain complaint, sensory disturbance, and skin temperature. Pain 39, 129–144.

Rowbotham, M. C. and Fields, H. L. 1996a. The relationship of pain, allodynia and thermal sensation in post-herpetic neuralgia. Brain 119, 347–354.

Rowbotham, M. C., Davies, P. S., and Fields, H. L. 1995. Topical lidocaine gel relieves postherpetic neuralgia. Ann. Neurol. 37, 246–253.

Rowbotham, M. C., Davies, P. S., Verkempinck, C., and Galer, B. S. 1996b. Lidocaine patch: double-blind controlled study of a new treatment method for post-herpetic neuralgia. Pain 65, 39–44.

Rowbotham, M. C., Yosipovitch, G., Connolly, M. K., Finlay, D., Forde, G., and Fields, H. L. 1996. Cutaneous innervation density in the allodynic form of postherpetic neuralgia. Neurobiol. Dis. 3, 205–214.

Rowbotham, M. C., Petersen, K. L., and Feilds, H. L. 1999. Is postherpetic neuralgia more than one disorder. IASP New. Let. 3–7.

Sato-Takeda, M., Ihn, H., Ohashi, J., Tsuchiya, N., Satake, M., Arita, H., Tamaki, K., Hanaoka, K., Tokunaga, K., and Yabe, T. 2004. The human histocompatibility leukocyte antigen (HLA) haplotype is associated with the onset of postherpetic neuralgia after herpes zoster. Pain 110, 329–336.

Schmidbauer, M., Budka, H., Pilz, P., Kurata, T., and Hondo, R. 1992. Presence, distribution and spread of productive varicella zoster virus infection in nervous tissue. Brain 115, 383–398.

Scott, F. T., Leedham-Green, M. E., Barrett-Muir, W. Y., Hawrami, K., Gallagher, W. J., Johnson, R., and Breuer, J. 2003. A study of shingles and the development of postherpetic neuralgia in East London. J. Med. Virol. 70 Suppl 1, S24–S30.

Watson, C. P. N., Evans, R., Watt, V. R., and Birkett, N. 1988. Post-herpetic neuralgia: 208 cases. Pain 35, 289–297.

Watson, C. P. N., Deck, H. J., Morshead, C., Van der Kooy, D., and Evans, R. J. 1991. Post-herpetic neuralgia: further post-mortem studies of cases with and without pain. Pain 44, 105–117.

Watson, C. P., Tyler, K. L., Bickers, D. R., Millikan, L. E., Smith, S., and Coleman, E. 1993. A randomized vehicle-controlled trial of topical capsaicin in the treatment of postherpetic neuralgia. Clin. Ther. 15, 510–526.

Wu, C. L., Marsh, A., and Dworkin, R. H. 2000. The role of sympathetic blocks in herpes zoster and postherpetic neuralgia. Pain 87, 121–129.

Zacks, S. L., Langfitt, T. W., and Elliott, F. A. 1964. Herpetic neuritis: a light and electron microscopic study. Neurology 14, 744–750.

Further Reading

Helgason, S., Petursson, G., Gudmundsson, S., and Sigurdsson, J. A. 2000. Prevalence of postherpetic neuralgia after a first episode of herpes zoster: prospective study with long term follow up. BMJ 321, 794–796.

Relevant Websites

http://www.iasp-pain.org – International Association for the Study of Pain.

http://www.vzvfoundation.org – VZN Research Foundation.

5.06 Ectopic Generators

M Devor, Hebrew University of Jerusalem, Jerusalem, Israel

© 2008 Elsevier Inc. All rights reserved.

5.06.1	**Introduction**	83
5.06.2	**Nerve Injury and Disease Trigger Ectopia**	83
5.06.2.1	Precipitating Factors	83
5.06.2.2	Spontaneous Ectopic Discharge	84
5.06.2.3	Ectopic Mechanosensitivity	84
5.06.2.4	Abnormal Response to Other Stimuli	85
5.06.3	**Ectopic Firing Contributes to Pain Sensation in Several Ways**	85
5.06.3.1	Ongoing Pain, Tender-Points, and Other Sensitivities	85
5.06.3.2	Allodynia – Pain Evoked by Stimulation of Residual Uninjured Afferents	86
5.06.4	**Cellular Mechanisms of Ectopic Impulse Generation**	86
5.06.4.1	Resonance	86
5.06.4.2	The Development of Ectopic Pacemaker Capability	87
References		87

Glossary

ectopic generator Pathophysiological site of electrical impulse generation in the peripheral nervous system (PNS) or central nervous system (CNS). Ectopic excludes locations of impulse generation in normal, healthy tissue. Examples are nerve-end neuromas and dorsal root ganglia (DRGs) in the event of nerve injury.

electrogenesis The process of electrical impulse generation in nervous system tissue. Electrogenesis usually includes two phases: formation of a generator depolarization (sensory transduction in the case of afferent endings) and encoding of the generator depolarization into an impulse train.

microneurographic recording An electrophysiological technique in which a fine wire microelectrode is inserted transcutaneously into the peripheral nerve, permitting recording of impulse activity in individual nerve fibers. This minimally invasive procedure can be applied to awake humans.

5.06.1 Introduction

Normally, sensation originates in impulse discharge generated at sensory endings in skin, viscera, and other peripheral tissues. When there has been injury to peripheral nerves, neuropathic pain may arise as a result of abnormal impulse discharge generated at ectopic sites. The most common locations of ectopic impulse generation are the site of injury and associated dorsal root ganglia (DRGs). This chapter will touch on the characteristics of ectopic impulse generation (ectopia), the ways in which ectopia contributes to neuropathic pain sensation, and the cellular mechanisms that underlie it.

5.06.2 Nerve Injury and Disease Trigger Ectopia

5.06.2.1 Precipitating Factors

Ectopic impulse generation develops secondary to frank injury of the axon or soma of sensory neurons, or disruption of the myelin sheath that surrounds many axons (dysmyelination and demyelination). Disruption of the Schwann cell sheath that embraces bundles of nonmyelinated axons (Remak bundles) may also be a cause. It is fairly obvious why damage or disease that disrupts the ability of axons to conduct nerve impulses should cause negative sensory abnormalities such as hypoesthesia and numbness. It

is much less obvious why neural pathology causes positive sensory symptoms and signs such as ongoing and evoked paresthesias, dysesthesias, and pain. The link is the emergence of ectopia. If the axotomy happens suddenly, there may be a brief period of injury discharge. In general, however, ectopia results from secondary changes that develop over time (Devor, M., 2006a). The pathophysiological changes that induce ectopia can be precipitated by a wide variety of events including trauma (frequently iatrogenic), nerve entrapment, infection (bacterial or viral), sterile inflammation, metabolic abnormalities, malnutrition, vascular abnormalities, neurotoxins (including many chemotherapeutic agents), radiation, inherited mutations, and autoimmune attack.

5.06.2.2 Spontaneous Ectopic Discharge

A considerable fraction of injured sensory neurons, as many as one-third in some experimental preparations, begin to fire spontaneously in the hours and days following injury. Microneurographic recordings in patients with nerve injury have revealed similar results (Nordin, M. *et al.*, 1984; Devor, M., 2006a). The origin of the activity has been identified as the swollen endbulbs that form in the neuroma just proximal to sites of axonal transection (Fried, K. *et al.*, 1991), outgrowing sprouts, plaques of demyelination, and the cell soma in the DRG. In the event of sudden traumatic neuropathy activity usually begins earliest in myelinated axons (A-fibers), sometimes as soon as 16 h after axotomy, with a preference for muscle over cutaneous afferents. Activity in unmyelinated (C-) fibers tends to appear in earnest later, after a few weeks. Specific parameters vary with the type of injury, source (axon or soma), and strain and species of animal.

Firing pattern is usually tonic-rhythmic (i.e., continuous), bursty, or irregular, with the occasional neuron showing complex, often cyclic variations in firing pattern. The instantaneous firing rate of tonic-rhythmic and bursty activity is typically 15–40 impulses per second (ips), with bursts typically occurring at intervals of between a few per second and one every few seconds (Figure 1). Irregular firing of single spikes occurs at the same relatively slow rate as bursting. The reason for these patterns is now known (Amir, R. *et al.*, 2002b). The basic clock driving ectopia triggers activity at the slow rate. Some cells render only singlet spikes. In others, an iterative process based on postspike depolarizing afterpotentials (DAPs) yields a short rhythmic burst upon each trigger event, resulting in bursty discharge. Tonic autorhythmicity reflects an unending burst, which can occur in cells that generate DAPs but in which the mechanism for ending bursts is relatively ineffective. Interestingly, observations in nerves in which only a part of the axons have been severed show that spontaneous ectopic activity may also develop in neighboring uninjured axons, particularly in C-fibers (Wu, G. *et al.*, 2001; Shim, B. *et al.*, 2005).

5.06.2.3 Ectopic Mechanosensitivity

Gentle percussion over sites of nerve injury, areas of entrapment or neuromas for example, typically evokes an intense stabbing or electric shocklike sensation. This is the Tinel sign. Similar sensations can be evoked by other maneuvers that apply mechanical force to injured

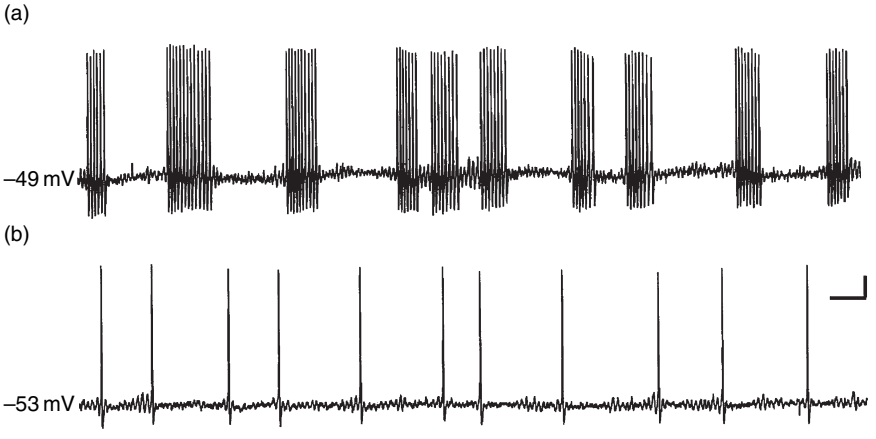

Figure 1 Typical patterns of spike activity generated at ectopic pacemaker sites. (a) Bursty discharge. (b) Irregular singlet firing. Subthreshold oscillations are visible in the baseline traces. Calibrations: 5 mV/100 ms.

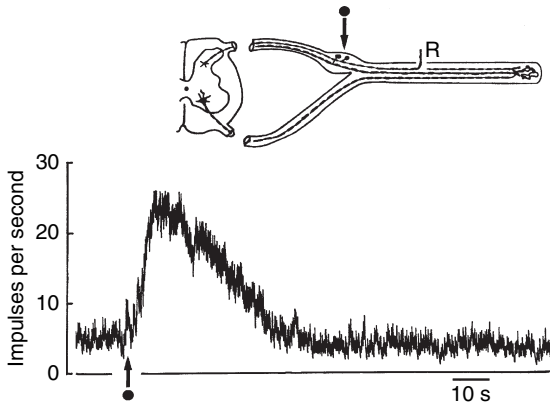

Figure 2 Mechanical afterdischarge. A weak, momentary stimulus to the surface of the DRG triggered a prolonged, self-sustained ectopic discharge burst.

nerves or spinal roots such as straight leg lifting in sciatica (Lasègue's sign), and the signs of Spurling and L'hermitte. Momentary mechanical stimulation of this sort frequently evokes ectopic discharge that outlasts the stimulus itself (afterdischarge), with corresponding aftersensation (Figure 2). This indicates that the underlying process is not just activation of sensitized nociceptors, or signal amplification, but the triggering of autonomous repetitive firing at ectopic pacemaker sites. The nature of this local electrical hyperexcitability is discussed below.

In the event of injuries that leave the nerve in-continuity, such as crush or freeze lesions, there is usually a second Tinel sign that advances with time, marking the farthest position reached by regenerating sprouts. In some conditions (e.g., diabetic neuropathy) paresthesias and pain may occur on tapping anywhere along the course of a nerve. This occurs when there are scattered outgrowing sprouts, demyelination plaques, or mechanosensitive end-bulbs resulting from axonal dying back. Although direct evidence has not yet been sought systematically in humans, it follows logically from studies in animals that pain evoked by deep palpation at tender spots, such as in fibromyalgia, might reflect ectopic mechanosensitivity at locations where small nerve branches cross through fascial planes, under tendons, or are otherwise at risk of being locally pinched.

5.06.2.4 Abnormal Response to Other Stimuli

Ectopic pacemaker sites also develop abnormal sensitivity to other depolarizing stimuli. Notable among these are response to circulating catecholamines and noradrenalin released from nearby (injured) postganglionic sympathetic axons (Devor, M. and Janig, W., 1981). Ectopic adrenosensitivity of sensory neurons yields sympathetic–sensory coupling, a likely substrate of sympathetically maintained chronic pain states. Afferent response to local and circulating inflammatory mediators is a second example of ectopic chemosensitivity. Abnormal discharge may also arise from temperature changes, ischemia, hypoxia, hypoglycemia, and other conditions capable of locally depolarizing afferent neurons at the sites at which they have developed local ectopic pacemaker capability (Devor, M., 2006a). Whereas intact sensory endings may be sensitive to these chemical and physical stimuli, axons in healthy nerve trunks and cell bodies in sensory ganglia are not. The key change in neuropathy is not the presence of excitatory stimuli but rather the ectopic emergence of sensitivity to them.

5.06.3 Ectopic Firing Contributes to Pain Sensation in Several Ways

5.06.3.1 Ongoing Pain, Tender-Points, and Other Sensitivities

The presence of ongoing ectopic discharge under circumstances in which ongoing dysesthesias and pain are present, and their simultaneous exacerbation by the same factors (e.g., mechanical stimulation, sympathetic efferent activity), constitutes *a priori* evidence that the ectopia is the cause of the pain. This conclusion is further supported by the observation that (diagnostic) nerve blocks using local anesthetics reliably obtund pain sensation in cases where the block is placed central to the site of nerve injury (Devor, M., 2006a). An interesting test case often raised as a counterexample is phantom limb pain in amputees. Although this pain is frequently eliminated (transiently) by blocking stump neuromas, there are reports of phantom limb pain persisting despite peripheral nerve block, and this observation has formed the basis for the widely held belief that phantom limb pain reflects abnormal neural activity originating in the cerebral cortex (Melzack, R., 1989; Flor, H. *et al.*, 1995). This conclusion is potentially flawed, however, because it ignores ectopic electrical impulse generation (electrogenesis) in sensory cell somata in the DRG. Amputation stump revision surgery is a common procedure, and is usually done under foramenal or spinal block. Although little published documentation is available (Tessler, M. J. and

Kleiman, S. J., 1994), experienced clinicians insist that these blocks reliably eliminate phantom limb pain for the duration of the pharmacological action of the local anesthetic agent. This would not occur if the pain signal originated supraspinally.

5.06.3.2 Allodynia – Pain Evoked by Stimulation of Residual Uninjured Afferents

Pain in response to light touch of the skin, tactile allodynia, is a common symptom in neuropathy. The simplest explanation is reduced response threshold in nociceptive C-fiber afferents, the classic excitable nociceptor hypothesis. This explanation is probably valid for heat allodynia. However, while neuropathy (and pronociceptive inflammatory mediators) can significantly reduce mechanical thresholds of sensory endings, few fibers that were originally nociceptors come to respond to the very weak tactile stimuli that are typically sufficient to evoke allodynia (Banik, R. K. and Brennan, T. J., 2004; Schlegel, T. *et al.*, 2004; Shim, B. *et al.*, 2005). Moreover, the response to painful touch in allodynic skin is rapid. There is no indication of the long delay between stimulus and response that would be expected from conduction in sensitized C-fibers, although sensitized Aδ nociceptors, if they exist, could contribute.

There is considerable evidence that cutaneous tactile allodynia in neuropathy (and inflammation) is primarily a sensory response to impulse activity in low-threshold mechanosensitive Aβ touch afferents abnormally amplified in the spinal cord (Campbell, J. N. *et al.*, 1988; Torebjork, H. *et al.*, 1992). The altered signal processing responsible for this Aβ pain is believed to result from one or a combination of numerous central nervous system (CNS) changes collectively called central sensitization (Woolf, C. J., 1983; Devor, M., 2006b). Central sensitization, which also amplifies ectopic afferent signals (spontaneous and evoked), is a dynamic process triggered and maintained by ongoing nociceptive input from the periphery. When the maintaining peripheral drive is eliminated, central sensitization fades, along with tactile allodynia. In neuropathy, sustained ectopic discharge can maintain central sensitization indefinitely, and with it Aβ pain and tactile allodynia (Gracely, R. *et al.*, 1992; Koltzenburg, M. *et al.*, 1994). This constitutes a second role of ectopia, in addition to providing a primary pain signal.

In contrast to the skin, it is likely that peripherally sensitized nociceptors play an important role in pain evoked by mechanical stimuli in inflamed viscera and deep somatic tissues such as muscles and joints. Reduced mechanical thresholds, including the recruitment of previously silent C-nociceptors, render the sensory endings of these afferents responsive to the (substantial) forces present during weight bearing, for example, or joint rotation (Schmidt, R., 1996). There is also good evidence for a contribution of central sensitization in deep tissue pain (Banic, B. *et al.*, 2004). Relatively little is known about changes in the response of injured afferent neurons, or the sensory endings of residual noninjured afferents, in the presence of neuropathy affecting nerves that supply deep tissues.

5.06.4 Cellular Mechanisms of Ectopic Impulse Generation

5.06.4.1 Resonance

The emergence of ectopic hyperexcitability in neuropathy is not a simple matter of lowered spike threshold. Rather, it reflects a more fundamental, qualitative change in the injured neuron's electrical characteristics. Most intact sensory neurons are incapable of generating sustained impulse discharge in midnerve or from within sensory ganglia, even in the presence of a strong sustained depolarizing stimulus. They are designed to fire exclusively in response to stimuli applied to the sensory ending in skin, muscle, etc., where the neuronal membrane is specialized for electrogenesis. Alterations in three cellular processes, gene expression, protein trafficking, and channel kinetics (below), actually create repetitive firing capability *de novo* at ectopic locations.

Ectopic repetitive firing capability (pacemaker capability) derives from electrical resonance that emerges in the cell membrane of the injured afferents, and resultant subthreshold oscillations in their normally stable resting potential (Amir, R. *et al.*, 1999; Wu, N. *et al.*, 2001). Subthreshold oscillations drive sustained ectopic discharge. This takes the form of irregular singlet spikes in some cells, and as repetitive bursting in others, depending on the ability of the cell to generate DAPs (Figure 1). Due to subthreshold oscillations, ectopic generator sites become responsive to slow onset and tonic depolarizing stimuli, which previously did not evoke sustained discharge. Some begin to fire spontaneously at rest, in the absence of stimulation. The biophysical processes that lead to membrane resonance, repetitive firing capability, ectopic discharge, and neuropathic pain are slowly coming into focus. Briefly, resonance in neuropathy appears to reflect reciprocation between inward Na^+

current carried by fast-activating, inactivating, and repriming tetrodotoxin (TTX)-sensitive Na^+ channels, and K^+ current passing through one or more voltage-insensitive K^+ leak channels, perhaps of the KCNK K2p family (Abdulla, F. A. and Smith, P. A., 2002; Amir, R. *et al.*, 2002a; Waxman, S. G., 2002). Voltage-sensitive K^+ channels tend to hold resonance in check, and their downregulation after axotomy is probably an important adjunct to ectopia (Kocsis, J. D. and Devor, M., 2000). Other channel types/conductances that might contribute to resonance characteristics of primary sensory neurons include certain Ca^{2+} channels, HCN (the Ih pacemaker channel), KCNQ-type K^+ channels, the β4 subunit-associated resurgent Na^+ current, and a persistent Na^+ conductance (gNaP), but their role, at this stage, is speculative. Many of the first-line analgesic agents used in the treatment of neuropathic pain (McQuay, M. and Moore, A., 1998), including (certain) anticonvulsants, tricyclic antidepressants, systemic local anesthetics, and (certain) antiarrhythmics are thought to act by stabilizing membrane resonance (Catterall, W. A., 1987; Deffois, A. *et al.*, 1996).

5.06.4.2 The Development of Ectopic Pacemaker Capability

The cascade of cellular events that lead to pacemaker capability and ectopic neuronal discharge begins with the injured primary sensory neuron. Our current understanding of the process is as follows. Axonal transection blocks the normal retrograde flow of neurotrophic signaling molecules (glial cell-derived neurotrophic factor (GDNF), nerve growth factor (NGF), and perhaps others) between the periphery and the sensory cell body. This triggers a change in the quantity of various proteins expressed by the cell body and exported by anterograde axoplasmic transport to both peripheral and central axon endings; some are upregulated and others downregulated (Boucher, T. J. and McMahon, S. B., 2001; Costigan, M. *et al.*, 2002; Xiao, H. S *et al.*, 2002). These changes alter the phenotype of the injured neuron, increasing its intrinsic resonance and supporting the emergence of ectopic electrogenesis.

In addition to changes in gene expression in injured sensory neurons, the delivery (trafficking) of transported molecules is disrupted. The most important change of this sort is the accumulation or depletion of molecules of excitability at ectopic generator sites (Figure 3), notably the accumulation of Na^+ channels (Devor, M., *et al.*, 1989; Devor, M., 2006a). Na^+ channels, for example, accumulate in neuroma endbulbs and sprouts, and in areas of demyelination. A third process that contributes to ectopic electrogenesis is altered channel kinetics. It is not ion channel proteins themselves that determine cell excitability but the ionic currents they carry. Increasing mean channel open time, for example, can have much the same effect on excitability as increasing the number of channels present. Proinflammatory cytokines and other mediators associated with neuropathy can affect channel kinetics in this way. For example, cAMP-dependent phosphorylation of Na^+ channel molecules reduces Na^+ current, while dephosphorylation returns it to normal (e.g., Li, M. *et al.*, 1992; Gold, M. S. *et al.*, 1996). Because certain hormones, trophic factors, cytokines, and other inflammatory mediators (notably prostaglandins) can activate protein kinases (PKA, PKC), they are positioned to affect the basic excitability of afferents, and not just to depolarize and excite sensory endings.

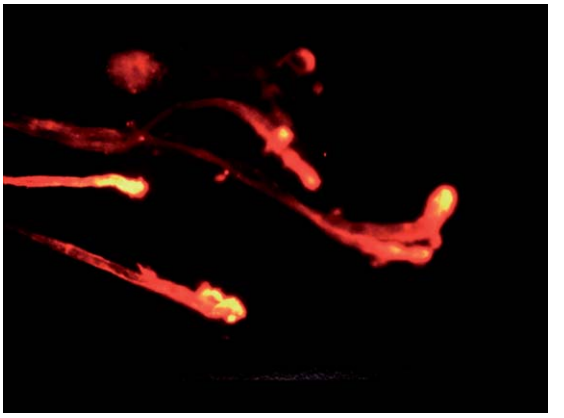

Figure 3 Immunolabeling shows the accumulation of Na^+ channels at the chronic cut end of hyperexcitable injured axons in an experimental nerve-end neuroma (for details see Devor, M. *et al.*, 1989).

References

Abdulla, F. A. and Smith, P. A. 2002. Changes in Na^+ channel currents of rat dorsal root ganglion neurons following axotomy and axotomy-induced autotomy. J. Neurophysiol. 88, 2518–2529.

Amir, R., Liu, C. N., Kocsis, J. D., and Devor, M. 2002a. Oscillatory mechanism in primary sensory neurones. Brain 125, 421–435.

Amir, R., Michaelis, M., and Devor, M. 1999. Membrane potential oscillations in dorsal root ganglion neurons: role in normal electrogenesis and in neuropathic pain. J. Neurosci. 19, 8589–8596.

Amir, R., Michaelis, M., and Devor, M. 2002b. Burst discharge in primary sensory neurons: triggered by subthreshold oscillations, maintained by depolarizing afterpotentials. J. Neurosci. 22, 1187–1198.

Banic, B., Petersen-Felix, S., Andersen, O. K., Radanov, B. P., Villiger, P. M., Arendt-Nielsen, L., and Curatolo, M. 2004. Evidence for spinal cord hypersensitivity in chronic pain after whiplash injury and in fibromyalgia. Pain 107, 15–17.

Banik, R. K. and Brennan, T. J. 2004. Spontaneous discharge and increased heat sensitivity of rat C-fiber nociceptors are present *in vitro* after plantar incision. Pain 112, 204–213.

Boucher, T. J. and McMahon, S. B. 2001. Neurotrophic factors and neuropathic pain. Curr. Opin. Pharmacol. 1, 66–72.

Campbell, J. N., Raja, S. N., Meyer, R. A., and MacKinnon, S. E. 1988. Myelinated afferents signal the hyperalgesia associated with nerve injury. Pain 32, 89–94.

Catterall, W. A. 1987. Common modes of drug action on Na^+ channels: local anaesthetics, antiarrhythmics and anticonvulsants. Trends Pharmacol. Sci. 8, 57–65.

Costigan, M., Befort, K., Karchewski, L., Griffin, R. S., D'Urso, D., Allchorne, A., Sitarski, J., Mannion, J. W., Pratt, R. E., and Woolf, C. J. 2002. Replicate high-density rat genome oligonucleotide microarrays reveal hundreds of regulated genes in the dorsal root ganglion after peripheral nerve injury. BMC Neurosci. 3, 16–28.

Deffois, A., Fage, D., and Carter, C. 1996. Inhibition of synaptosomal veratridine-induced sodium influx by antidepressants and neuroleptics used in chronic pain. Neurosci. Lett. 220, 117–120.

Devor, M. 2006a. Response of Nerves to Injury in Relation to Neuropathic Pain. In: Wall and Melzack's Textbook of Pain, 5th edn (*eds*. S. L. McMahon and M. Koltzenburg), Chapter 58, pp. 905–927. Churchill Livingstone.

Devor, M. 2006b. Central Changes after Peripheral Nerve Injury. In: Encyclopedia of Pain (*eds*. R. F. Schmidt and W. M. Willis), pp. 306–311. Springer.

Devor, M. and Janig, W. 1981. Activation of myelinated afferents ending in a neuroma by stimulation of the sympathetic supply in the rat. Neurosci. Lett. 24, 43–47.

Devor, M., Keller, C. H., Deerinck, T., Levinson, S. R., and Ellisman, M. H. 1989. Na^+ channel accumulation on axolemma of afferents in nerve end neuromas in Apteronotus. Neurosci. Lett. 102, 149–154.

Flor, H., Elbert, T., Knecht, S., Wienbruch, C., Pantev, C., Birbaumer, N., Larbig, W., and Taub, E. 1995. Phantom-limb pain as a perceptual correlate of cortical reorganization following arm amputation. Nature 375, 482–484.

Fried, K., Govrin-Lippmann, R., Rosenthal, F., Ellisman, M., and Devor, M. 1991. Ultra-structure of afferent axon endings in a neuroma. J. Neurocytol. 20, 682–701.

Gold, M. S., Reichling, D. B., Shuster, M. J., and Levine, J. D. 1996. Hyperalgesic agents increase a tetrodotoxin-resistant Na+ current in nociceptors. Proc. Nat. Acad. Sci. U. S. A. 93, 1108–1112.

Gracely, R., Lynch, S., and Bennett, G. 1992. Painful neuropathy: altered central processing, maintained dynamically by peripheral input. Pain 51, 175–194.

Kocsis, J. D. and Devor, M. 2000. Altered Excitability of Large Diameter Cutaneous Afferents Following Nerve Injury: Consequences For Chronic Pain. In: Proceedings of the 9th World Congress on Pain. Progress in Pain Research and Management (*eds*. M. Devor, M. C. Rowbotham, and Z. Wiesenfeld-Hallin). Vol. 16, pp. 119–135. IASP Press.

Koltzenburg, M., Torebjork, H., and Wahren, L. 1994. Nociceptor modulated central sensitization causes mechanical hyperalgesia in acute chemogenic and chronic neuropathic pain. Brain 117, 579–591.

Li, M., West, J. W., Lai, Y., Scheuer, Y., and Catterall, W. A. 1992. Functional modulation of brain sodium channels by cAMP-dependent phosphorylation. Neuron 8, 1151–1159.

McQuay, M. and Moore, A. 1998. An Evidence-Based Resource for Pain Relief, p. 264. Oxford University Press.

Melzack, R. 1989. Phantom limbs, the self and the brain. Can. Psychol. 30, 1–16.

Nordin, M., Nystrom, B., Wallin, U., and Hagbarth, K.-E. 1984. Ectopic sensory discharges and paresthesiae in patients with disorders of peripheral nerves, dorsal roots and dorsal columns. Pain 20, 231–245.

Schlegel, T., Sauer, S. K., Handwerker, H. O., and Reeh, P. W. 2004. Responsiveness of C-fiber nociceptors to punctate force-controlled stimuli in isolated rat skin: lack of modulation by inflammatory mediators and flurbiprofen. Neurosci. Lett. 361, 163–167.

Schmidt, R. 1996. The articular polymodal nociceptor in health and disease. Prog. Brain Res. 113, 53–81.

Shim, B., Kim, D. W., Kim, B. H., Nam, T. S., Leem, J. W., and Chung, J. M. 2005. Mechanical and heat sensitization of cutaneous nociceptors in rats with experimental peripheral neuropathy. Neuroscience 132, 193–201.

Tessler, M. J. and Kleiman, S. J. 1994. Spinal anaesthesia for patients with previous lower limb amputations. Anaesthesia 49, 439–441.

Torebjork, H., Lundberg, L., and LaMotte, R. 1992. Central changes in processing of mechanoreceptive input in capsaicin-induced secondary hyperalgesia in humans. J. Physiol. (Lond.) 448, 765–780.

Waxman, S. G. (*ed*.) 2002. Sodium channels and neuronal hyperexcitability. Novartis Found. Symp. 241, 232.

Woolf, C. J. 1983. Evidence for a central component of postinjury pain hypersensitivity. Nature 306, 686–688.

Wu, G., Ringkamp, M., Hartke, T. V., Murinson, B. B., Campbell, J. N., Griffin, J. W., and Meyer, R. A. 2001. Early onset of spontaneous activity in uninjured C-fiber nociceptors after injury to neighboring nerve fibers. J. Neurosci. 21, RC140.

Wu, N., Hsiao, C.-F., and Chandler, S. 2001. Membrane resonance and subthreshold membrane oscillations in mesencephalic V neurons: participants in burst generation. J. Neurosci. 21, 3729–3739.

Xiao, H. S., Huang, Q. H., Zhang, F. X., Bao, L., Lu, Y. J., Guo, C., Yang, L., Huang, W. J., Fu, G., Xu, S. H., Cheng, X. P., Yan, Q., Zhu, Z. D., Zhang, X., Chen, Z., Han, Z. G., and Zhang, X. 2002. Identification of gene expression profile of dorsal root ganglion in the rat peripheral axotomy model of neuropathic pain. Proc. Natl. Acad. Sci. U. S. A. 99, 8360–8365.

5.07 Sodium Channels

John N Wood, University College London, London, UK

© 2008 Elsevier Inc. All rights reserved.

5.07.1	How Do Sodium Channels Work?	89
5.07.2	Sodium Channels and Pain Pathways	92
5.07.3	$Na_v1.3$ and Neuropathic Pain	92
5.07.4	$Na_v1.7$ and Inflammation	93
5.07.5	$Na_v1.8$ and Nociception	93
5.07.6	The Diversity of Sodium Channel Subtypes	94
5.07.6.1	Selective Sodium Channel Blockers as Drugs	95
References		95

5.07.1 How Do Sodium Channels Work?

All sodium channels are single proteins made up of α-subunits that contain four homologous domains and form a voltage-gated sodium-selective aqueous pore (Figure 1). They comprise a family of nine structurally related α-subunits (Table 1). They are more than 75% identical over the amino acid sequences comprising the transmembrane and extracellular domains (Yu, F. H. and Catterall, W. A., 2003). The α-subunits show distinct patterns of expression, and are associated with accessory β-subunits that modify channel properties and interact with cytoskeletal and extracellular matrix proteins. The mechanism of channel gating involves the movement of voltage sensors (shown with positive charges in Figure 1) in response to changes in membrane potential. Lysine or arginine residues are found at intervals of three amino acids to produce a linear array of positive charges in the α-helical S4 transmembrane segments, and the movement of these charged areas of the channel opens the sodium-selective pore, defined by residues within the channel atrium. An intracellular loop lying between transmembrane domains 3 and 4 containing the tripeptide isoleucine phenylalanine methionine (IFM) is subsequently responsible for channel inactivation on a millisecond timescale. Sodium channel subtypes can be pharmacologically distinguished by their susceptibility to block by tetrodotoxin (TTX), a toxin isolated from puffer fish, which binds to the ion selectivity pore of some channels (Hille, B., 2002). Most sodium channels are blocked by nanomolar concentrations of TTX and are defined as TTX-sensitive (TTXs) whilst others are resistant to micromolar TTX and are defined as TTX-resistant (TTXr).

A short sequence found upstream of neuronal sodium channel genes (as well as other neuronal genes) was identified and named neuron-restricted silencing element (NRSE) or repressor element 1(RE-1). Transcription factors that bound to the motif were found to act as inhibitors of gene expression in nonneuronal cells. These proteins were named RE-1 silencing transcription factor (REST) or neuron-restrictive silencer factor (NRSF) and mutational analysis identified a single zinc finger motif in the carboxyl-terminal domain of the factor as essential for repressing sodium channel-derived reporter genes (Kraner, S. D. *et al.*, 1992). The inhibitory activity of the complex can be further modulated by double-stranded RNA molecules that have the same sequence as NRSE/RE-1, and are found in developing neuronal precursors. These regulatory RNA molecules are able to switch the repressor function of the complex to an ac activator role (Kuwabara, T. *et al.*, 2004). In this way, the assumption of a neuronal phenotype seems to depend in part upon regulatory RNAs driving gene expression downstream of NRSE/RE1 motifs. Sodium channels are known to be expressed at the very earliest stages of the appearance of a neuronal phenotype in the mouse. These studies highlight the significance of sodium channel expression in neuronal function throughout development.

The α-subunits of the voltage-gated sodium channel that form the sodium pore are associated with accessory β-subunits that modulate channel properties and interact with cytoskeletal and extracellular

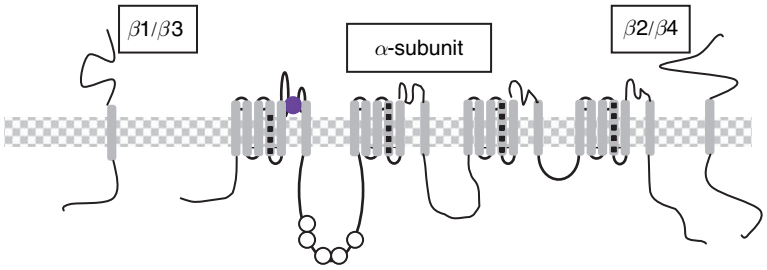

Figure 1 Structure of sodium channels. Voltage-gated sodium channels comprise a single functional α-subunit, which is tethered by associated accessory subunits to subcellular locations determined by both extracellular and intracellular proteins. Phosphorylation sites are shown on intracellular loop 2, and the serine residues in domain 1 that confers tetrodotoxin sensitivity is highlighted.

Table 1 Names and properties of voltage-gated sodium channel α-subunits

Type	*Gene symbol*	*Name*	*Tissue*	*TTX-sensitive*
$Na_V1.1$	SCN1A	Type I	CNS/PNS	+
$Na_V1.2$	SCN2A	Type II	CNS	+
$Na_V1.3$	SCN3A	Type III	CNS	+
$Na_V1.4$	SCN4A	SKM1	Skeletal muscle	+
$Na_V1.5$	SCN5A	SKMII	Heart/CNS	−
$Na_V1.6$	SCN8A	Nach6	CNS/glia	+
$Na_V1.7$	SCN9A	PN1	DRG	+
$Na_V1.8$	SCN10	SNS	DRG	−
$Na_V1.9$	SCN11	NAN	DRG	−

The nomenclature for sodium channel α-subunits, combined with their main site of expression (CNS – central nervous system, PNS – peripheral nervous system) and their sensitivity to block by tetrodotoxin (TTX), is shown.

matrix proteins. β-subunits are single transmembrane domain proteins that contain an extracellular domain that is homologous to the V-set of the immunoglobulin superfamily that includes cell adhesion molecules (Isom, L. L., 2002). The biochemical purification of two proteins, β1 and β2, that associate with α-subunits allowed the properties of these accessory factors to be investigated in heterologous expression systems. Molecular cloning has identified a β1-like member of the family named β3 and β2-like subunit named β4, as well as a splice variant of β1, β1A.

β1 and β1A are structurally homologous in the extracellular immunoglobulin-like loop region. β1A mRNA is expressed during embryonic development, and becomes undetectable after birth, concomitant with the onset of β1 expression. Immunocytochemical analysis of β1A expression revealed selective expression in brain and spinal cord neurons, with high expression in heart and all dorsal root ganglia neurons. Coexpression of $Na_v1.2A$ and β1A-subunits results in a 2.5-fold increase in sodium current density as a result of an increase in the level of functional sodium channels in expressing cells. β1A-expressing cell lines also revealed subtle differences in sodium channel activation and inactivation. β3 most closely related to β1 is the product of a separate gene localized to human chromosome 11q23.3. The expression pattern of β3 differs significantly from β1.

Coexpression of the β-subunits with sodium channel α-subunits in *Xenopus* oocytes or mammalian cell lines accelerates channel activation, and shifts the voltage dependence of inactivation to more negative potentials, indicating that β-subunits are important in the assembly, expression, and functional modulation of the rat brain sodium channel heterotrimeric complex (Isom, L. L., 2002). However, β-subunits do not appear to modulate the biophysical properties of all sodium channel α-subunits. $Na_v1.8$ α-subunits show aberrant properties when expressed in heterologous cells, but coexpression with β1, β1A, or β3 does not recapitulate normal channel behavior. The existence of factors other than accessory β-subunits that can alter inactivation kinetics has also been suggested by studies in which sodium channel α-subunits are expressed in cells lacking endogenous sodium channel β-subunits. Expression of rat cardiac $Na_v1.5$ and rat brain $Na_v1.2$ sodium channels in mammalian cell lines results in sodium channels

with rapid activation and inactivation characteristic of native neuronal sodium channel.

An additional function of β-subunits as cell adhesion molecules has been demonstrated by the ability of β-subunits to mediate homophilic interactions via their extracellular immunoglobulin-like repeats (Isom, L. L., 2002). Interacting β-subunits also recruit the cytoskeletal protein ankyrin-G to the cell surface via an interaction with their cytoplasmic domains, suggesting that these subunits link sodium channel α-subunits indirectly both to the cytoskeleton and to the extracellular matrix proteins, such as tenascin-R. Tenascin-R is an extracellular matrix molecule that is secreted by oligodendrocytes during myelination and that binds F3-contactin. Transfected cells stably expressing β1- or β2-subunits initially recognize and then are repelled from substrates containing tenascin-R. The cysteine-rich amino-terminal domain of tenascin-R appears to be responsible for the repellent effect on β-subunit-expressing cells. Application of the cysteine-rich N-terminal domain of tenascin-R to channels expressed in *Xenopus* oocytes potentiates expressed sodium currents. The binding of neuronal sodium channels to extracellular matrix molecules such as tenascin-R may thus play a role both in functional regulation and in localizing sodium channels in high density at nodes of Ranvier.

β-subunits also interact with the ankyrin-G membrane skeletal protein that is associated with spectrin–actin networks and also binds to integral membrane proteins including the L1 CAM family of cell adhesion molecules. Ankyrin-G is highly concentrated along with the L1CAM family members neurofascin and NrCAM at nodes of Ranvier and axon initial segments. Voltage-gated sodium channels are thus likely to associate in a complex containing neurofascin/NrCAM and ankyrin-G in myelinated neurons.

As well as the accessory subunits that link sodium channels to cytoskeletal and extracellular elements, other proteins are associated with sodium channels. Voltage-gated sodium channels in brain neurons were found to associate with receptor protein tyrosine phosphatase-β (RPTP-β) (Catterall 200. Both the extracellular domain and the intracellular catalytic domain of RPTP-β interact with sodium channels. Sodium channels were found to be tyrosine phosphorylated and dephosphorylation slowed $Na_v1.1$ inactivation, positively shifting voltage dependence and increasing whole-cell sodium current.

Regulation of sodium channels by protein kinases (PK) has already been demonstrated in a number of systems. Protein kinase A (PKA) can decrease or increase sodium currents by phosphorylation at consensus sites in the cytoplasmic domain I–II linker. Effects on membrane trafficking may also be mediated through phosphorylation. In the case of the cardiac channel, activation of PKA causes a slow increase in sodium current in *Xenopus* oocytes. Chloroquine and monensin, both compounds that disrupt plasma membrane recycling, reduce sodium currents. Preincubation with these agents also prevented the PKA-mediated rise in sodium current, indicating that this effect likely resulted from an increased number of channels in the plasma membrane.

There is strong evidence for specialized roles of the various sodium channel isoforms based on human genetic studies as well as the production of knockout mice. A perinatal lethal phenotype occurs in the $Na_v1.2$ sodium channel mouse knockout, which shows severe hypoxia as a result of brain stem apoptosis. $Na_v1.8$ channel knockouts have selective deficiencies in pain pathways (Akopian, A. N. *et al.*, 1999). Nax, a non-voltage-gated sodium channel homologue has been shown to play an important role in salt homeostasis, whilst loss of $Na_v1.6$ in the natural *med* mutant has been shown to lead to ataxia, dystonia, and paralysis. The deletion of accessory β-subunits, already known to play an important role in regulating functional channel expression and tethering α-subunits to specific subcellular locations, leads to a complex phenotype resulting in seizures and epileptogenic activity.

Naturally occurring mutations in both sodium channel α- and β-subunits have been implicated in various inherited disorders, many of which have been characterized in muscle sodium channel isoforms. Brugada syndrome, characterized by ventricular fibrillation, heart failure, and sudden death, is associated with mutations in the cardiac sodium channel $Na_v1.5$. Hyperkalemic periodic paralysis is associated with mutations in the skeletal muscle channel $Na_v1.4$. However, there is also evidence of a role for neuronal sodium channels and β-subunits in a variety of pathologies, including epilepsy, autism, and pain perception. Generalized epilepsy with febrile seizures (GEFS) is associated with mutations in either the β1-subunit (type I) or the α-subunit $Na_v1.1$ (type II). Some forms of autism associate with mutations in SCN1-3A sodium channel genes. The peripheral neuron-associated sodium channel $Na_v1.7$ encoded by gene SCN9A has been shown to be the site of mutations that lead to the chronic familial pain disorder primary erythermalgia (Yang, Y. *et al.*, 2004). This dominant condition is characterized by burning

in the extremities, pain evoked by standing and a generalized inflammatory phenotype. Interestingly, systemic treatment with the sodium channel blockers lidocaine or mexiletine leads to dramatic improvements in the symptoms associated with this disease.

Neuronal excitability depends to a considerable extent on sodium channel trafficking, distribution and density, as well as the intrinsic properties of the channels themselves in terms of thresholds of activation and repriming characteristics. The repertoire of sodium channels expressed by sensory neurons and the alterations that occur in pain states are now well documented (Waxman, *et al.*, 2002, Wood, J. N. *et al.*, 2004). Unmyelinated C-fiber-associated dorsal root ganglion (DRG) neurons are usually nociceptive whilst thinly myelinated Aδ-fibers also mediate fast pain, and a subset of myelinated Aβ-fibers are also nociceptive. TTXr sodium channels are present on C-fibers and seem to play a significant role in nociception (Akopian, A. N. *et al.*, 1999).

5.07.2 Sodium Channels and Pain Pathways

Acute, inflammatory, and neuropathic pain can all be attenuated or abolished by local treatment with sodium channel blockers such as lidocaine. The peripheral input that drives pain perception thus depends on the presence of functional voltage-gated sodium channels. Remarkably, two voltage-gated sodium channel genes ($Na_v1.8$ and $Na_v1.9$) are expressed selectively in damage-sensing peripheral neurons, whilst a third channel ($Na_v1.7$) is found predominantly in sensory and sympathetic neurons. An embryonic channel ($Na_v1.3$) is also upregulated in damaged peripheral nerves and associated with increased electrical excitability in neuropathic pain states. A combination of antisense and knockout studies support a specialized role for these sodium channels in pain pathways.

Small-diameter sensory neurons express a variety of sodium channel transcripts as well as a repertoire of electrophysiological and pharmacologically distinct type of sodium currents. Persistent sodium channels that are resistant to TTX are probably encoded for by $Na_v1.9$ channels, whilst the major transient TTXr channel isotype present predominantly in nociceptors is $Na_v1.8$. TTXs currents are encoded by a number of genes including $Na_v1.1$, $Na_v1.7$, and $Na_v1.6$. The current–voltage relationship of these different sorts of sodium channels found in DRG sensory neurons is shown in Figure 2. The persistent current activates at voltages close to the resting potential and is likely to play a role in setting thresholds of activation.

Evidence that altered sodium channel activity in peripheral neurons is associated with the development of inflammatory and neuropathic pain is strong. Altered patterns of sodium channel transcripts as well as changes in posttranslational modifications have been observed. Neuropathic pain that results from direct damage to peripheral nerves is the most problematic condition in terms of analgesic therapy. The pain evoked by these conditions seems to result initially from enhanced neuronal excitability that can be blocked by low-dose TTX.

5.07.3 $Na_v1.3$ and Neuropathic Pain

$Na_v1.3$ is widely expressed in the adult human central nervous system but is normally present at low levels in adult peripheral nervous system. Axotomy or other forms of nerve damage lead to the reexpression of $Na_v1.3$ and the associated $\beta3$-subunit in sensory neurons, but not in primary motor neurons (Waxman, S. G. *et al.*, 1994). This event can be reversed *in vitro* and *in vivo* by treatment with high levels of exogenous glial cell-derived neurotrophic factor (GDNF). $Na_v1.3$ is known to recover (reprime) rapidly from inactivation (Cummins *et al.*, 2001). Axotomy has been shown to induce the expression of rapidly repriming TTXs sodium channels in damaged neurons, and this event can also be reversed by the combined actions of GDNF and nerve growth factor (NGF). Concomitant with the reversal of $Na_v1.3$ expression by GDNF, ectopic action potential generation is diminished and thermal and mechanical pain-related behavior in a rat chronic constriction injury model is reversed. Moreover, $Na_v1.3$ is upregulated in dorsal horn neurons following experimental spinal cord injury and this upregulation is associated with hyperexcitability of these nociceptive neurons and pain; antisense knockdown of $Na_v1.3$ (and probably other sodium channels) attenuates the dorsal horn neuron hyperexcitability and the pain behaviors in spinal cord-injured animals (Hains, B. C. *et al.*, 2003). It therefore seems likely that $Na_v1.3$ reexpression may play a role in increasing neuronal excitability that contributes to neuropathic pain after nerve and spinal cord injury.

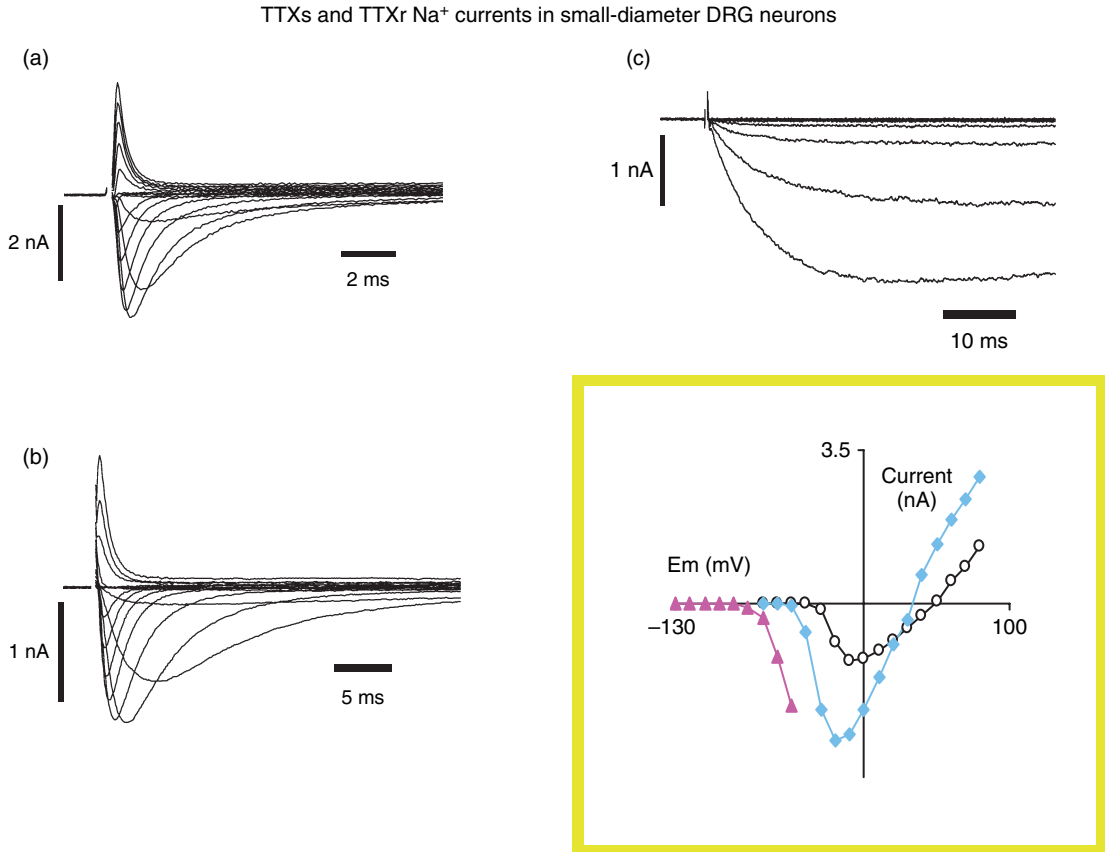

Figure 2 (a) TTX-sensitive (b) -resistant, and (c) persistent currents are shown. Note the different timescales for inactivation of the currents. The voltage at which the different types of channels activate is shown in panel 4 (red channel (c), blue channel (a), and black channel (b)). Although those channels that activate at the most negative potentials might seem to render other channels redundant, the ability to recover from inactivation is also an important determinant of neuronal excitability.

5.07.4 $Na_v1.7$ and Inflammation

$Na_v1.7$ encodes a TTXs channel found predominantly in peripheral sensory and sympathetic neurons. Interestingly, this channel is located at the terminal of sensory neurons, and is regulated in its expression by inflammatory mediators such as NGF, probably through mechanisms that involve the control of trafficking. The fact that a chronic inflammatory dominant human disease, primary erythermalgia, maps to this gene SCN10A suggests that this channel may have an important role in inflammatory pain (Yang, Y. *et al.*, 2004). Tissue-specific deletion in mouse nociceptors shows that $Na_v1.7$ plays a major role in inflammatory pain (Nassar, M. A. *et al.*, 2004). Low-dose lidocaine both inhibits the pain associated with primary erythermalgia and unmasks the phenotype of the $Na_v1.8$ null, further supporting a role for $Na_v1.7$ in inflammatory pain. $Na_v1.7$ mRNA contributes to an increase in TTXs sodium current in caraggeenan-inflamed rats, further implying a role in altering inflammatory pain thresholds. Recently humans with a loss of functional $Na_v1.7$ have been found to be completely pain free (Cox, J. J. *et al.*, 2006). Not surprisingly, this has stimulated major interest in developing an $Na_v1.7$-specific channel blocker.

5.07.5 $Na_v1.8$ and Nociception

$Na_v1.8$ is a TTXr sensory neuron-specific channel mainly expressed in nociceptive neurons. This channel contributes much of the sodium current underlying the depolarizing phase of the action potential in cells in which it is present and knockout mice lose all the inactivating TTXr sodium channel activity in DRG neurons (Akopian, A. N. *et al.*, 1999).

$Na_v1.8$ thus underlies the inactivating TTXr sodium currents that have been found to play a critical role in many aspects of nociceptor function. Functional expression of TTXr currents encoded by this channel is regulated by inflammatory mediators, including NGF. Both antisense and knockout studies support a role for the channel in contributing to inflammatory pain, as PGE_2-induced hyperalgesia is inhibited by antisense oligonucleotides. Antisense studies have also suggested a role for this protein in the development of neuropathic pain (Lai, J. *et al.*, 2002). A late-onset deficit in ectopic action propagation has been described in the $Na_v1.8$-null mutant mouse together with deficits in mechanohypersensitivity. A redistribution of immunoreactive $Na_v1.8$-like material has also been described in animal models of neuropathic pain, further supporting the lobby for $Na_v1.8$ as a key molecule in the pathogenesis of neuropathic pain. However, neuropathic pain behavior at early time points seems to be normal in the $Na_v1.8$-null mutant mouse.

Inflammatory mediators are known to alter the level of TTXr channel expression, and shift their threshold of activation to more negative potentials through the activation of PKA. Prostaglandin E_2, adenosine, and serotonin all increased the magnitude of $Na_v1.8$-mediated currents, shifted its conductance–voltage relation in a hyperpolarizing direction, and increased the rates of activation and inactivation of sodium channels in small-diameter sensory neurons in culture. These phenomena can be replicated *in vitro* with heterologously expressed $Na_v1.8$ channels, implicating this TTXr channel in setting peripheral pain thresholds. In support of a role for the $Na_v1.8$ channel in pain pathways, an $Na_v1.8$-null mutant shows deficits in inflammatory pain processing, in contrast to its responses to neuropathic damage (Akopian, A. N. *et al.*, 1999).

This channel also appears to have an important role in visceral pain. TTXr sodium currents were present in every colonic DRG neuron studied (Gold, *et al.*, 2002). Modulation of TTXr I(Na) in colonic afferents may be an underlying mechanism of hyperalgesia and pain associated with inflammation of the colon. Consistent with this, the $Na_v1.8$-null mutant has deficits in visceral pain and referred hyperalgesia.

Several strands of evidence also support a role for $Na_v1.9$ as an important contributor to the control of excitability in nociceptive afferents. The gene is expressed predominantly in neurons functionally defined as nociceptors. However, the phenotype of a mouse $Na_v1.9$ knockout is essentially normal.

5.07.6 The Diversity of Sodium Channel Subtypes

Given the fairly similar properties of voltage-gated sodium channels why are there so many different types of α-subunits present in nociceptive sensory neurons? A number of explanations are possible:

Firstly, the trafficking in sensory neurons of different sodium channels to distinct cellular locations (terminals, nodes of Ranvier, etc.) and the regulation of this process may provide a number of options to control neuronal excitability in different physiological contexts. Thus trafficking of $Na_v1.8$ into the cell membrane through its interaction with p11, which is massively upregulated by NGF, could play an important role in inflammatory pain – other channels do not show this behavior. It is important to remember that there are no external cues such as nodes of Ranvier to define the topological organization of sodium channels in C-fibers – the relatively even distribution of sodium channels to promote electrical propagation along the length of a very long axon is a process that is not understood, and altered channel density particularly at C-fiber terminals can have important effects on excitability. The two sodium channels that are uniquely associated with C-fibers may be involved in these processes.

Secondly, different structural features of the channels means that their response to posttranslational modification by enzymes such as PK is quite distinct. Phosphorylation on intracellular serines in $Na_v1.8$ increases peak current density, whilst in other channels present in DRG neurons, for example $Na_v1.7$, peak current diminishes. Primary sequence also determines the repriming characteristics of the different channels as well as their threshold of activation, which are crucial determinants of peripheral pain thresholds.

Thirdly, the topological relationship between different sodium channels and channels involved in sensing noxious stimuli may also play a role in setting thresholds of activation and thus pain thresholds. As noxious mechanosensation but not heat sensing is deficient in $Na_v1.8$-null mutant mice, we may argue that this channel is closely apposed to potential mechanosensors through a sequence-specific interaction with a macromolecular complex, and local depolarizations cause this channel to activate first to generate action potentials. Heat sensors may be linked

with other sodium channel subtypes. If true, this would suggest that molecules that disrupt specialized nociceptive complexes at the terminals of sensory neurons may have a useful analgesic effect. There is already evidence that disruption of the cytoskeleton has antihyperalgesic effects.

5.07.6.1 Selective Sodium Channel Blockers as Drugs

Tetrodotoxin has proved invaluable in discriminating between two classes of sodium channels. The $Na_v1.5$ channel, as well as the peripheral neuron-specific channel $Na_v1.8$, is a subfamily of TTXr sodium channels, including the evolutionarily earliest sodium channel $Na_v1.9$. However, little progress has been made in developing specific subtype selective channel blockers. Conotoxins provide a possible route to this goal. The venom from marine predatory cone shell snails (*Conus*) contains a complex cocktail of neurotoxic disulfide-rich peptides, termed conotoxins. Conotoxins produce their toxic effects via the targeted modulation of specific ion channels, and there is some evidence that they target specific sodium channels.

Sodium channel subtypes are thus differentially regulated in different pain states. New subtype selective blockers should therefore prove useful as both research tools and potential analgesic drugs. The presence of DRG-specific sodium channel isoforms presents an exciting opportunity to develop new classes of analgesic drugs that may have quite novel properties from present-day analgesics with utility in some conditions of intractable or chronic pain.

Acknowledgments

We thank the Wellcome Trust, the BBSRC, and the MRC for support.

References

Akopian, A. N., Souslova, V., England, S., Okuse, K., Ogata, N., Ure, J., Smith, A., Kerr, B. J., McMahon, S. B., Boyce, S., Hill, R., Stanfa, L. C., Dickenson, A. H., and Wood, J. N. 1999. The TTX-R sodium channel SNS has a specialized function in pain pathways. Nat. Neurosci. 2, 541–5489.

Cox, J. J., Reimann, F., Nicholas, A. K., Thornton, G., Roberts, E., Springell, K., Karbani, G., Jafri, H., Mannan, J., Raashid, Y., Al-Gazali, L., Hamamy, H., Valente, E. M., Gorman, S., Williams, R., McHale, D. P., Wood, J. N., Gribble, F. M., and Woods, C. G. 2006. An SCN9A channelopathy causes congenital inability to experience pain. Nature 444(7121), 894–898.

Cummins, T. R., Aglieco, F., Renganathan, M., Herzog, R. I., Dib-Hajj, S. D., and Waxman, S. G. 2001. Nav1.3 sodium channels: rapid repriming and slow closed-state inactivation display quantitative differences after expression in a mammalian cell line and in spinal sensory neurons. J. Neurosci. 21(16), 5952–5961.

Gold, M. S., Zhang, L., Wrigley, D. L., and Traub, R. J. 2002. Prostaglandin E(2) modulates TTX-RI(Na) in rat colonic sensory neurons. J. Neurophysiol. 88(3), 1512–1522.

Hains, B. C., Klein, J. P., Saab, C. Y., Craner, M. J., Black, J. A., and Waxman, S. G. 2003. Upregulation of sodium channel Nav1.3 and functional involvement in neuronal hyperexcitability associated with central neuropathic pain after spinal cord injury. J. Neurosci. 23(26), 8881–8892.

Hille, B. 2002. Ion Channels of Excitable Membranes. Sinauer.

Isom, L. L. 2002. Beta subunits: players in neuronal hyperexcitability? Novartis Found. Symp. 241, 124–138; discussion 138–143, 226–232.

Kraner, S. D., Chong, J. A., Tsay, H. J., and Mandel, G. 1992. Silencing the type II sodium channel gene: a model for neural-specific gene regulation. Neuron 9(1), 37–44.

Kuwabara, T., Hsieh, J., Nakashima, K., Taira, K., and Gage, F. H. 2004. A small modulatory dsRNA specifies the fate of adult neural stem cells. Cell 116(6), 779–793.

Lai, J., Lai, J., Gold, M. S., Kim, C. S., Bian, D., Ossipov, M. H., Hunter, J. C., and Porreca, F. 2002. Inhibition of neuropathic pain by decreased expression of the tetrodotoxin-resistant sodium channel, Nav1.8. Pain 95(1–2), 143–152.

Nassar, M. A., Stirling, L. C., Forlani, G., Baker, M. D., Matthews, E. A., Dickenson, A. H., and Wood, J. N. 2004. Nociceptor-specific gene deletion reveals a major role for Nav1.7 (PN1) in acute and inflammatory pain. Proc. Natl. Acad. Sci. U. S. A. 101(34), 12706–12711.

Ratcliffe, C. F., Qu, Y., McCormick, K. A., Tibbs, V. C., Dixon, J. E., Scheuer, T., and Catterall, W. A. 2000. A sodium channel signaling complex: Modulation by associated receptor protein tyrosine phosphatase beta. Nat. Neurosci. 3(5), 437–444.

Waxman, S. G., Cummins, T. R., Dib-Hajj, S. D., and Black, J. A. 2000. Voltage-gated sodium channels and the molecular pathogenesis of pain: A review. J. Rehabil. Res. Dev. 37(5), 517–528.

Waxman, S. G., Kocsis, J. D., and Black, J. A. 1994. Type III sodium channel mRNA is expressed in embryonic but not adult spinal sensory neurons, and is re-expressed following axotomy. J. Neurophysiol. 72(1), 466–470.

Wood, J. N., Boorman, J. P., Okuse, K., and Baker, M. D. 2004. Voltage-gated sodium channels and pain pathways. J. Neurobiol. 61(1), 55–71.

Yang, Y., Wang, Y., Li, S., Xu, Z., Li, H., Ma, L., Fan, J., Bu, D., Liu, B., Fan, Z., Wu, G., Jin, J., Ding, B., Zhu, X., and Shen, Y. 2004. Mutations in SCN9A, encoding a sodium channel alpha subunit, in patients with primary erythermalgia. J. Med. Genet. 41(3), 171–174.

Yu, F. H. and Catterall, W. A. 2003. Overview of the voltage-gated sodium channel family. Genome Biol. 4(3), 207.

Further Reading

Fauchier, L., Babuty, D., and Cosnay, P. 2000. Epilepsy, Brugada syndrome and the risk of sudden unexpected death. J. Neurol. 247(8), 643–644.

5.08 Physiology of Nociceptors

M Ringkamp and R A Meyer, Johns Hopkins University, Baltimore, MD, USA

© 2008 Elsevier Inc. All rights reserved.

5.08.1	**Introduction**	98
5.08.2	**Nociceptors in Uninjured Skin**	98
5.08.2.1	C-Fiber Nociceptors	98
5.08.2.2	A-Fiber Nociceptors	102
5.08.2.3	Classification of Nociceptors Based on Molecular Markers	103
5.08.3	**Efferent and Trophic Functions of Nociceptors**	104
5.08.4	**Acute Pain Sensations and Nociceptor Activity**	105
5.08.4.1	Pain from Heat Stimuli	105
5.08.4.1.1	Heat pain from glabrous skin is signaled by C-fiber nociceptors	105
5.08.4.1.2	First pain to heat on hairy skin is signaled by type II A-fiber nociceptors	106
5.08.4.1.3	Pain to prolonged heat stimuli is signaled by type I A-fiber nociceptors	108
5.08.4.2	Pain from Controlled Mechanical Stimuli	108
5.08.4.2.1	Sharp pain is signaled by A-fiber nociceptors	108
5.08.4.2.2	Pain from tonic pressure is signaled by C-fiber MIAs	108
5.08.4.3	Cold Pain Sensation	108
5.08.4.4	Capsaicin-Evoked Pain	108
5.08.5	**Hyperalgesia**	109
5.08.5.1	Primary Hyperalgesia	109
5.08.5.1.1	Hyperalgesia to heat is mediated by primary afferent sensitization	109
5.08.5.1.2	Hyperalgesia to mechanical stimuli	109
5.08.5.1.3	Inflammatory mediators and nociceptor sensitization	111
5.08.5.2	Secondary Hyperalgesia	112
5.08.5.2.1	Sensitization of primary afferent nociceptors does not occur	112
5.08.5.2.2	Central mechanisms of secondary hyperalgesia	112
References		113

Glossary

AMH A-fiber mechanoheat-sensitive nociceptor responsive to mechanical and heat stimuli.

central sensitization An enhanced neural response that occurs in the central nervous system (CNS).

CMH C-fiber mechanoheat-sensitive nociceptor responsive to mechanical and heat stimuli.

fatigue Decrement in response to repeated stimuli.

hyperalgesia Enhanced stimulus-evoked pain.

MIA Mechanically insensitive afferent.

MSA Mechanically sensitive afferent.

nociceptor Neuron responsive to noxious or injurious stimuli.

primary hyperalgesia Hyperalgesia that develops at the site of injury. Mechanical and thermal hyperalgesia are present at the zone of primary hyperalgesia following a cutaneous injury.

receptive field Area over which neuron is responsive to mechanical, thermal, chemical, or electrical stimulation.

secondary hyperalgesia Hyperalgesia that develops in an uninjured tissue surrounding a site of injury. Only mechanical hyperalgesia is present at the zone of secondary hyperalgesia.

sensitization Enhanced neural response.

5.08.1 Introduction

A vital function of the sensory nervous system is to signal the threat or occurrence of tissue injury. A specialized class of afferents performs this function. These afferents respond preferentially to noxious or injurious stimuli and are called nociceptors. Nociceptors are found in virtually every organ (except the brain), and activity in nociceptive afferents is thought to lead to the percept of pain. In this chapter, we will focus on nociceptors innervating skin. Nociceptors from other somatic tissues have similar properties.

The skin contains a number of distinct sensory receptors that respond selectively to different types of innocuous stimuli and encode different aspects of the sensory experience. For example, several types of low-threshold mechanoreceptors signal different aspects of touch sensation. Receptors that are exquisitely sensitive to gentle warming or gentle cooling are responsible for the percepts of warmth and cooling, respectively.

Nociceptors are distinguished from these innocuous receptors by their relatively high threshold for activation. Unlike innocuous receptors, nociceptors often respond to more than one energy form – that is, they are polymodal. Nociceptors are often subclassified based on the conduction velocity of their parent axon. C-fiber nociceptors are associated with unmyelinated fibers and have conduction velocities less than $2\ m\ s^{-1}$. A-fiber nociceptors are associated with myelinated fibers and have conduction velocities greater than $2\ m\ s^{-1}$.

We will first consider the properties of nociceptors from uninjured skin and how their response is related to sensations of acute pain. We will then consider the effects of skin injury on the response of nociceptors and how this is related to enhanced pain sensitivity called hyperalgesia. Where possible, electrophysiological responses to noxious stimuli will be compared to psychophysical measures of pain.

5.08.2 Nociceptors in Uninjured Skin

In experimental studies of nociceptors, the first task is to identify where on the skin the afferent is responsive. This area is called the receptive field. The receptive field is often located based on its response to mechanical stimuli (e.g., gentle pinching), and then the border is mapped with flexible small-diameter cylindrical probes that exert a relatively constant force when they bend (called von Frey probes). Quantitative stimuli of different energy modalities are then applied to this mechanical receptive field. In early studies, the response of nociceptors to heat and mechanical stimuli was tested leading to the nomenclature of C-fiber (CMH) or A-fiber mechanoheat nociceptors (AMH) corresponding to C-fiber or A-fiber nociceptors responsive to heat and mechanical stimuli. Most of these nociceptors also respond to chemical and/or cold stimuli and therefore are polymodal.

Nociceptors that respond to mechanical stimuli are also called mechanically sensitive nociceptive afferents (MSAs). Recently, it has become apparent that afferents exist that either are insensitive to mechanical stimuli or have extremely high mechanical thresholds; these afferents are called mechanically insensitive afferents (MIAs) or silent nociceptors. These afferents were missed in earlier studies of nociceptors that relied on mechanical techniques to search for the receptive field. MIAs have been identified in many different tissues including skin, cornea, knee joint, and viscera. In the skin, electrocutaneous stimulation can be used to search for the receptive field of MIAs (see Box 1). As will become apparent below, cutaneous MIAs differ from MSAs not only in their response to mechanical stimuli but also in their response to other stimulus modalities.

5.08.2.1 C-Fiber Nociceptors

The response of a typical CMH to a stepped increase in temperature in the receptive field is shown in Figure 1. For stimuli applied to the skin, there are five processes that occur to achieve this heat response. First, the heat stimulus needs to be absorbed by the skin. Second, the energy must be transmitted to the receptor terminal that sits below the skin surface. Third, the energy must be converted (or transduced) into a change in membrane potential at the terminal of the nociceptor. Molecular mechanisms of heat transduction are described in Chapter Molecular Biology of the Nociceptor/Transduction. Fourth, the increase in membrane potential must be sufficient to generate an action potential. Finally, the action potential must propagate orthodromically to the central nervous system (CNS) (and to the recording electrode).

Thermal modeling studies combined with electrophysiological recordings indicate that the heat threshold of CMHs in monkeys depends on the temperature at the depth of the receptor terminal and not on the rate of temperature change (Tillman, D. B. *et al.*, 1995). Based on this analysis, the majority of CMHs have heat thresholds between 39 and 41 °C. However, the depth of the heat-responsive terminal

Box 1 Mapping mechanically insensitive afferents

Mechanically insensitive afferents (MIAs) either are completely unresponsive to mechanical stimuli or have such a high threshold for activation that they cannot be activated by light pinch stimuli applied to the skin. Mechanical stimuli are inadequate to locate the cutaneous receptive field of these afferents. Furthermore, repetitive noxious mechanical and heat stimuli could sensitize the nociceptive endings over the course of an electrophysiological experiment. Also, the use of mechanical and thermal stimuli bias the study toward those afferents that are responsive to these stimuli. Because of these reasons, a different search strategy has been developed that allows the receptive fields of afferents, including MIAs, to be localized in an unbiased manner. Instead of using natural stimuli, an electrical stimulus is applied to the skin (see adjacent figure).

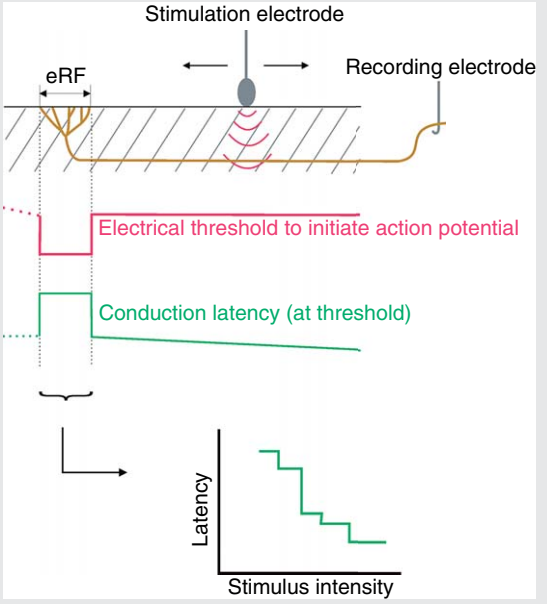

A saline-soaked cotton swap is used as a monopolar cathotic search electrode to locate the receptive field. Electrical stimuli are applied through the cotton swap at the skin over the presumed path of the cutaneous nerve from which the recordings are obtained. In response to the electrical stimulus, the afferent nerve fiber is excited and an action potential is generated and conducted to the recording electrode. The latency depends on the conduction velocity of the nerve fiber and the conduction distance. When the stimulation electrode is moved further distally along the peripheral nerve, the conduction latency (green line) of the unit increases due to the increase in conduction length. By moving the electrode further distally, the path of the unit can be traced peripherally toward its receptive field. The receptive field has been located when three phenomena occur. First, the threshold electrical stimulus intensity (pink line) that is needed to excite the afferent transcutaneously drops to its minimum. This drop is most likely due to the fact that the afferent nerve fiber ends in peripheral terminals that are located in the superficial layers of the skin. Therefore, the distance between the stimulation electrode and the nerve endings is minimized. Second, at stimulation threshold, the conduction latency of the action potential increases to its maximum, since the action potential is generated at the most distal part of the axon, that is, its peripheral ending. This latency increase is not continuous but a step increase. Third, within the electrical receptive field (eRF), the latency of the action potential decreases in discrete steps as the stimulus intensity increases. These sudden latency jumps are thought to be due to a switch of the action potential initiation site, for example, from a distal site of the axon (like the most distal ending) to a more proximal site (like a branch point) when the stimulus intensity is increased. Skin sites at which the conduction latency decreases in discrete steps with increasing stimulus intensity belong to the eRF of the unit under study. The described technique can therefore be used to locate the peripheral receptive field and to delineate its borders.

varies widely (from 20 to 570 µm below the skin surface). Since the tissue at the depth of the receptor heats more slowly than the skin surface due to thermal inertia, the heat threshold as measured by the surface temperature of the skin can vary greatly.

The heat response of CMHs increases monotonically with skin temperature above threshold. This suprathreshold response varies directly with the rate of temperature change at the receptor – slow temperature changes give lower instantaneous discharge frequencies than fast temperature changes.

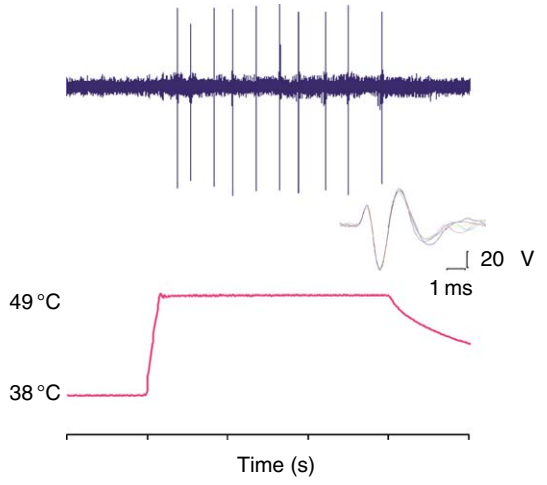

Figure 1 Response of a typical C-fiber mechanoheat-sensitive afferent (CMH) to a heat stimulus. A laser thermal stimulator was used to deliver a constant temperature stimulus (from a 38 °C baseline to 49 °C for 3 s) to the receptive field of a CMH on the hairy skin of the hand of an anesthetized monkey. The large action potential waveform corresponds to a CMH that responded with 10 action potentials to this stimulus. Inset: High-resolution recording of action potential waveforms.

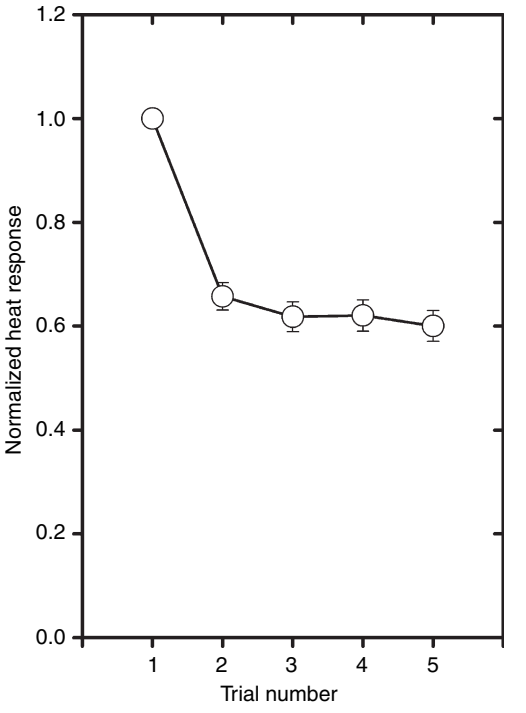

Figure 2 C-fiber mechanoheat-sensitive afferents (CMHs) exhibit fatigue to repeated heat stimuli. Identical heat stimuli were presented every 60 s to the receptive field of CMHs recorded from the anesthetized monkey. The response decreased significantly to the second stimulus and reached a plateau after several stimuli. Data were normalized by dividing by the response to the first stimulus. Adapted from Peng, Y. B., Ringkamp, M., Meyer, R. A., and Campbell, J. 2003. Fatigue and paradoxical enhancement of heat response in C-fiber nociceptors from cross-modal excitation. J. Neurosci. 23, 4766–4774, copyright 2003 by the society for Neuroscience, with permission.

The heat response of CMHs is strongly influenced by stimulus history. For example, when identical heat stimuli are repeated every 60 s, the response to the second stimulus is about 66% of the response to the first (Figure 2). This decrement in response is called fatigue. The amount of fatigue is inversely related to the interstimulus interval (i.e., shorter intervals lead to more fatigue) and directly related to the magnitude of the preceding stimulus (i.e., the larger the preceding stimulus, the greater the fatigue). As a result of fatigue, the shape of the stimulus–response function can also vary with stimulus history. Fatigue can also greatly influence threshold measurements. Complete recovery from fatigue takes more than 10 min.

A decrease in the heat response can also be produced by mechanical stimulation of the receptive field or electrical stimulation of the parent axon (Peng, Y. B. *et al.*, 2003). Thus, fatigue to one stimulus modality can be produced by a stimulus of a different modality. Interestingly, recovery from cross-modal fatigue is much faster than recovery from fatigue produced by the same stimulus modality. This suggests that cross-modal fatigue does not effect the stimulus transduction apparatus in the same way as unimodal fatigue.

In contrast to fatigue, which leads to a decreased response, the response of nociceptors can also be enhanced, for example, by tissue injury. This sensitization may account for aspects of hyperalgesia and is discussed in more detail later in this chapter.

CMHs do not respond to mechanical stimulation with blunt objects but respond well to application of sharp objects. Their mean mechanical threshold to von Frey probes is 2.2 bars. The receptive field size is around 20 mm^2 in monkeys but can be much larger in humans. The receptive field typically consists of multiple punctate regions of high mechanical sensitivity surrounded by areas of lesser sensitivity. Presumably these hot spots correspond to the locations of the receptor terminals.

For cylindrical probes, the response at a given force increases as the size of the probe decreases (Garell, P. C. *et al.*, 1996). This relationship scales inversely with a linear dimension of the probe (i.e.,

probe circumference) not probe area. Thus, the adequate stimulus for activating nociceptors appears to be related to force per unit length, and activation of the receptor terminals appears to occur at the edge of the probe where the strain is the greatest.

C-fiber MIAs are by definition insensitive to mechanical stimuli but are more responsive to chemical stimuli than CMHs and may be considered as chemosensors. For example, microneurographic recordings in human subjects (see Box 2) have shown that capsaicin (the active ingredient in hot peppers) evokes a vigorous response in C-fiber MIAs. Histamine also vigorously activates a subpopulation of C-MIAs. In contrast, histamine and capsaicin evoke weak responses in CMHs. Interestingly, MIAs can develop a response to mechanical stimuli after skin injury (discussed in more detail below).

C-MIAs also differ from C-MSAs with regard to their conductive properties. Most unmyelinated fibers exhibit a slowing of conduction with repetitive electrical stimulation that is called activity-dependent slowing. C-MIAs show significantly more slowing than C-MSAs (Weidner, C. *et al.*, 1999). One possible explanation for this finding is that the relative distribution of ion channels involved with conduction is different in these two classes of afferents.

C-fiber afferents with extremely low thresholds to mechanical stimuli have been identified in the hairy skin of rodents, monkeys, and humans (Nordin, M., 1990). These afferents are responsive to light stroking of the skin but not to heat. They are thought to be involved in the sensation of pleasant touch and therefore may play a role in affiliative behavior.

C-fiber afferents with extremely low thresholds to heat are prevalent in all species. These afferents do not respond to mechanical stimuli but have ongoing activity at room temperature and respond to gentle warming of the skin (Darian-Smith, I. *et al.*, 1979).

Box 2 Marking technique

The marking technique is used in recordings that are hampered by a small signal-to-noise ratio that makes the identification of an action potential based on its waveform impractical. The marking technique is commonly used in human microneurography experiments, in which the signal-to-noise ratio is usually small. To use the marking technique, the primary afferent is electrically activated at a constant frequency (e.g., one stimulus every 4 s) through a pair of needle electrodes that are inserted intradermally close to the receptive field of the unit. In response to the ongoing low-frequency electrical stimulation, an action potential can be recorded at the recording electrode at a constant, fixed conduction latency (see the following figure).

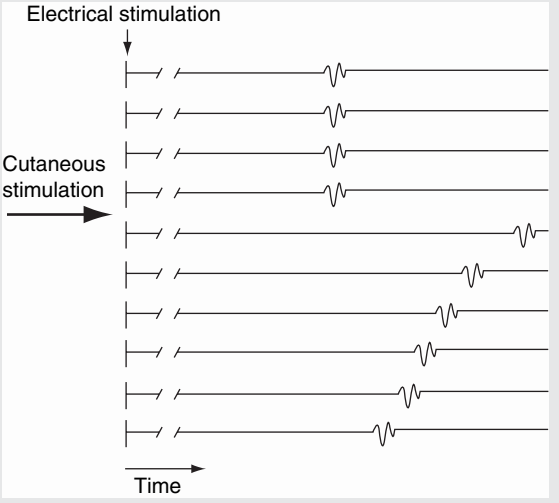

If the unit is also activated by a cutaneous (mechanical, thermal, and chemical) stimulus (see arrow), the conduction latency of the following electrically induced action potential will increase. This increase in conduction latency marks the unit as being activated by the stimulus applied to the receptive field. With ongoing electrical stimulation, the conduction latency slowly recovers to the original latency. Marking obviously indicates slowing of conduction along the course of the axon and is thought to be due to the additional action potentials that were initiated by the mechanical (or heat or chemical) stimulus and were conducted along the axon. Due to these additional action potentials, more sodium channels along the axonal membrane will be in an inactivated state when the next action potential induced by the ongoing electrical stimulation is generated and conducted. As a consequence of this inactivation, the conduction velocity for this action potential is decreased, leading to an increase in conduction latency.

Table 1 Properties of type I and type II A-fiber nociceptors

Property	*Type I*	*Type II*
Heat threshold (short-duration stimuli)	High	Low
Heat threshold (long-duration stimuli)	Low	Low
Response to heat	Slow onset, slowly increasing	Fast onset, rapidly adapting
Mechanical threshold	Low (mostly MSAs)	High (mostly MIAs)
Conduction velocity	Aδ and Aß fibers	Aδ fibers
Sensitization after heat injury	Yes	No
Location	Hairy and glabrous skin	Hairy skin

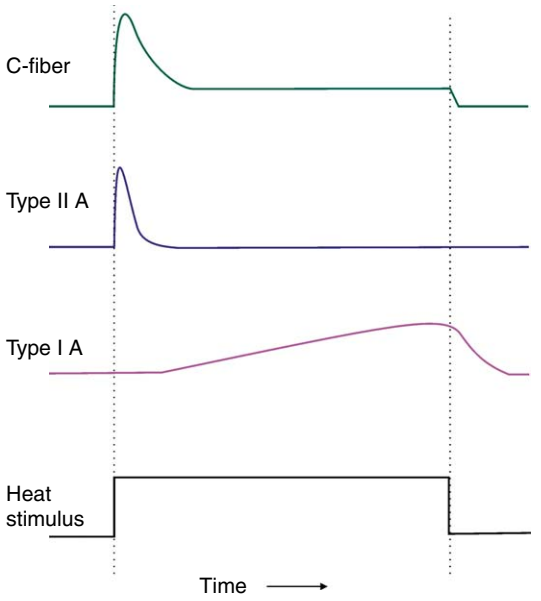

Figure 3 Response of nociceptors to a long-duration intense heat stimulus. The response of C-fiber nociceptors is quick and slowly adapts. The response of type II A-fibers is also quick but quickly adapts. The response of type I A-fibers is slow and builds during the stimulus.

The ongoing activity is suppressed by cooling. These afferents are thought to serve the percept of warmth and are often referred to as warm fibers.

5.08.2.2 A-Fiber Nociceptors

Two distinct types of heat-sensitive A-fiber nociceptors have been described (Table 1) (Treede, R.-D. *et al.*, 1998). Type I fibers are responsive to mechanical and chemical stimuli but have relatively high heat thresholds when short-duration stimuli are used. For this reason, they have also been called high-threshold mechanoreceptors (HTMs). However, most type I A-fibers respond to long-duration heat stimuli (Figure 3), and their thresholds to long-duration heat stimuli are low. In addition, they develop a response to short-duration heat stimuli after injury. Heat transduction in type I afferents is thought to be subserved by the transient receptor potential channel V2 (TRPV2) ion channel. The mechanical threshold and receptive field size for type I AMHs are comparable to those of CMHs. The mean conduction velocity of type I fibers is around 25 m s^{-1} with some fibers having conduction velocities as high as 55 m s^{-1}. Thus, their conduction velocity overlaps the traditional Aß and Aδ myelinated fiber range. Type I AMHs are found in both hairy and glabrous skin.

Type II A-fiber nociceptors are characterized by a fast response to heat stimuli that quickly adapts (Figure 3). Their heat thresholds to short-duration stimuli are much lower than those of type I AMHs. Most type II fibers have very high mechanical thresholds or do not respond to mechanical stimuli and therefore are MIAs. Their mean conduction velocity (15 m s^{-1}) places them within the Aδ myelinated fiber range. In monkeys, they are only found in hairy skin.

Similar to CMHs, A-fiber nociceptors do not respond to mechanical stimulation with blunt object but respond well to sharp objects. The response to mechanical stimuli varies with position in the receptive field. When a 100 µm wide blade is systematically moved to different positions within the receptive field, highly reproducible receptive field response maps can be obtained that contain multiple peaks and valleys (Slugg, R. M. *et al.*, 2004). As the force increases, the response and width of the peaks increase, the response in the valleys increases, and new peaks emerge (Figure 4(a)). Although the response increases with force in most positions in the receptive field, there are positions where the response reaches a plateau at higher forces (Figure 4(b)). The averaged response across the receptive field provides an estimate for the response in the population of nociceptors that innervates a particular location (Figure 4(c)). The population response function for A- and C-fiber nociceptors

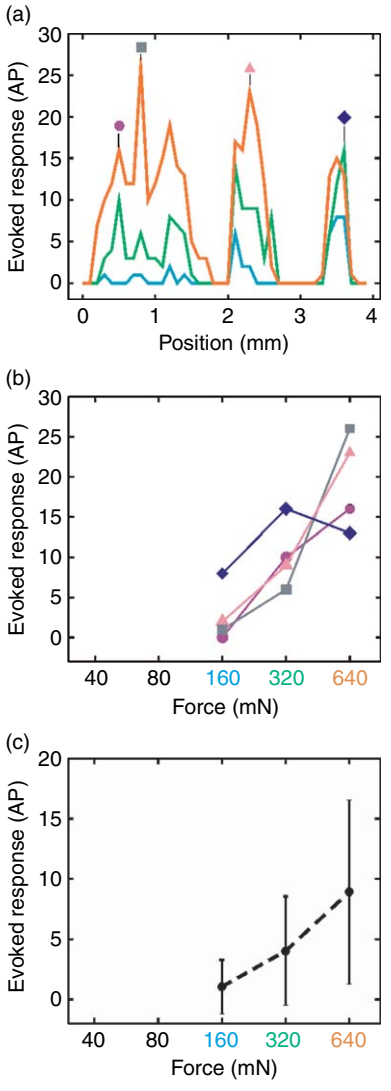

Figure 4 Response of a type I A-fiber nociceptor to a blade stimulus. (a) Maps of response as a function of position and force. A 100 μm wide blade was systematically applied to every position across the receptive field. The response shows peaks and valleys that grow in height and width as the stimulus strength increased (forces: 160, 320, and 640 mN). (b) Stimulus–response function varied with position in the receptive field. In most positions, the response increased monotonically with force, but in one position shown the response reached a plateau at the higher forces. (Symbols in (a) indicate the positions plotted.) (c) The average response across the receptive field is plotted. This provides an estimate of how the population of nociceptors that innervate a single spot on the skin would respond to the stimulus. Adapted from Slugg, R. M., Campbell, J. N., and Meyer, R. A. 2004. The population response of A- and C-fiber nociceptors in monkey ncodes high-intensity mechanical stimuli. J. Neurosci. 24, 4649–4656, copyright 2004 by the Society for Neuroscience, with permission.

increases monotonically with force. The main differences between A- and C-fiber nociceptors are (1) A-fibers in general exhibit a larger response than C-fibers, (2) the population response of A-fibers quadruples with every doubling of force, whereas the response of C-fibers doubles with every doubling of force, and (3) the A-fibers exhibit a better differential response with respect to different probe sizes and forces (Garell, P. C. *et al.*, 1996; Slugg, R. M. *et al.*, 2000).

Aδ-fiber afferents with ongoing activity are present in monkeys and humans. The neural activity in these afferents increases with gentle cooling and decreases with gentle warming (Darian-Smith, I. *et al.*, 1973). These afferents do not respond to mechanical stimulation with thermally neutral probes. These afferents are thought to subserve the percept of cool.

5.08.2.3 Classification of Nociceptors Based on Molecular Markers

In addition to a classification that is based on receptive properties, nociceptive afferents can be categorized using molecular markers that are expressed in their cell bodies or on their cell membrane. Markers that have been used for this purpose include neuropeptides, enzymes, and proteins involved in signal transduction, receptors for growth factors, and other molecules on the cell surface.

The somata of slowly conducting nociceptive afferents are small. In contrast to large cells that can be labeled with RT97, an antibody that is directed against neurofilament protein (NF200), only some of the small cells can be labeled with RT97. Small, RT97-positive neurons most likely represent the somata of Aδ nociceptive fibers. RT97-negative cells likely represent unmyelinated neurons.

Nociceptive afferents are commonly classified as peptidergic or nonpeptidergic (Figure 5). Peptidergic cells express substance P (SP) and/or calcitonin gene-related peptide (CGRP) or somatostatin (SOM). In rats, about 50% of neurons are peptidergic (Lawson, S. N., 1992). Peptidergic cells also express the tyrosine kinase receptor A (TrkA), the receptor for nerve growth factor (NGF), suggesting that they are NGF dependent. In addition, peptidergic cells express the TRPV1 channel that is activated by noxious heat stimuli and protons and also mediates the responsiveness to vanilloids (capsaicin and resiniferatoxin). Centrally, peptidergic neurons project to lamina I and the outer lamina II of the dorsal horn.

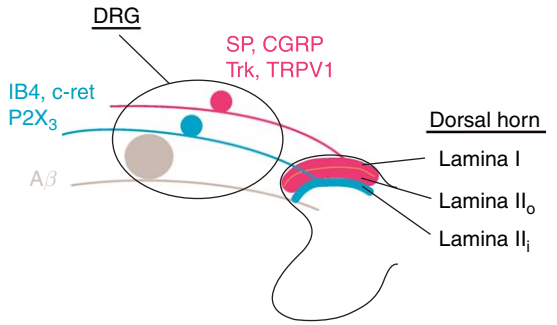

Figure 5 Small-diameter dorsal root ganglion neurons can be divided into two classes based on molecular markers in their cell bodies. The neurons in one class (shown in pink) are tyrosine kinase receptor A (TrkA), transient receptor potential V1 (TRPV1) channel, calcitonin gene-related peptide (CGRP), and substance P (SP)-positive and project to lamina I and lamina II_o of the dorsal horn. The neurons in the other class (shown in blue) are IB4, c-ret, and $P2X_3$ positive and project to lamina II_i.

Nonpeptidergic cells contain fluoride-resistant acid phospatase (FRAP) and bind the plant lectin IB4 from *Griffonia simplicifolia*. About 50% of dorsal root ganglion cells are IB4 positive ($IB4^+$). In contrast to peptidergic cells, $IB4^+$ neurons depend on glial cell-derived neurotrophic factor (GDNF) and they express the necessary receptors, tyrosine kinase Ret (c-ret), and glial cell-derived neurotrophic factor receptors (GDNFRα1–4). $IB4^+$ cells express the $P2X_3$ receptor, a purinergic ligand-gated ion channel that is activated by adenosine triphospate (ATP). The central terminals of $IB4^+$ neurons terminate in the inner sheet of lamina II. Some $IB4^+$ neurons also express *m*as-*r*elated *g*enes A and D (mrgA and mrgD) or *m*as-*r*elated *G p*rotein-coupled *r*eceptors A and D (mrgprA and mrgprD) (Dong, X. *et al.*, 2001). $IB4^+$ and $mrgA^+$ neurons are mostly $P2X_3^-$ and express c-ret only at a low level. In contrast, $IB4^+$ and $mrgD^+$ neurons are also $P2X_3^+$ and express high levels of c-ret (Dong, X. *et al.*, 2001). $IB4^+$ fibers innervate many tissues of the body, including muscle and visceral organs. However, $IB4^+/mrgpd^+$ fibers are exclusively found in skin, where they terminate in the stratum granulosum of the epidermis, whereas CGRP-containing nerve fibers end less superficial in the stratum spinosum (Zylka, M. J. *et al.*, 2005). In addition, $IB4^+/mrgpd^+$ neurons appear to project to a distinct lamina of the dorsal horn, that is, between the outer and the inner sheet of lamina II. Thus peptidergic and nonpeptidergic nociceptive neurons appear to differ in growth factor dependency, in ion channel expression involved in signal transduction, in their peripheral terminations, and in their central, dorsal horn projections.

While the classification into peptidergic and nonpeptidergic cells is commonly used, it should be emphasized that there is an overlap of marker expression between peptidergic and nonpeptidergic neurons. For example, some $IB4^+$ neurons express TRPV1or CGRP. Furthermore, there are considerable species differences in the expression and coexpression of these markers. For example, in mice only a minority of $IB4^+$ cells express TRPV1 (Zwick, M. *et al.*, 2002), whereas in rats the majority of $IB4^+$ and $IB4^-$ cells express TRPV1 (Michael, G. JC. and Priestley, J. V., 1999). Finally, the expression of these markers is not rigid but changes during development and after injury. Thus, peripheral inflammation increases the proportion of cells expressing neuropeptides, whereas following nerve injury, the proportion of cells expressing neuropeptides decreases.

5.08.3 Efferent and Trophic Functions of Nociceptors

In addition to serving the afferent function of signaling pain sensation, nociceptors also mediate efferent effects such as the flare that surrounds an injury site. This flare is thought to be due to an axonreflex mechanism, since the flare is absent in denervated tissue but present when a cutaneous nerve is blocked at a proximal location. When an action potential is initiated in the cutaneous terminals, it propagates not only orthodromically up the axons toward the CNS but also antidromically into peripheral branches of the nerve fiber where it causes the release of neuropeptides that are present in the terminals (Figure 6). Since afferent and efferent paths of this reflex arc are within the same axon, this reflex has been coined an axon reflex. The peripherally released neuropeptides include SP, neurokinin A (NKA), CGRP, vasoactive intestinal polypeptide (VIP), and SOM.

In animals, SP and CGRP are released from capsaicin-sensitive nerve endings and may induce vasodilation and plasma extravasation. These neuropeptides are also thought to stimulate epidermal cells (e.g., Langerhans' cells and kerotinocytes) and to play a role in immunological processes such as the migration of leukocytes at sites of tissue injury. In human skin, the antidromic release of neuropeptides is thought to lead to vasodilation, but not plasma extravasation (Schmelz, M. and Petersen, L. J., 2001). The area of the axon reflexive flare in humans is much

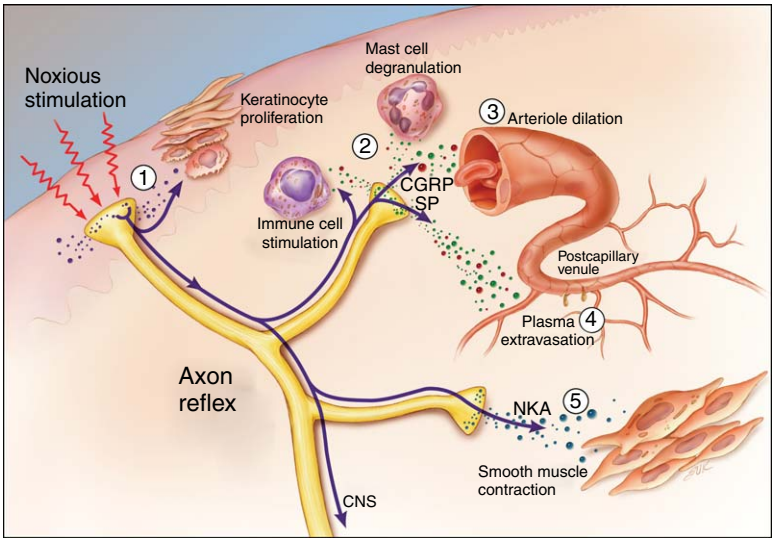

Figure 6 Nociceptors have an efferent function. Noxious stimulation of the nociceptor terminals leads to action potential propagation not only to the CNS but also into other peripheral branches of the nociceptor where they cause the release of neuropeptides such as calcitonin gene-related peptide (CGRP), SP, or NKA. The release of neuropeptides from nociceptors can lead to (1) proliferation of keratinocytes, (2) stimulation of immune cells or degranulation of mast cells, (3) vasodilation, (4) plasma extravasation, and (5) smooth muscle contraction. Artwork by Ian Suk, Johns Hopkins University. Reproduced from Meyer, R. A., Ringkamp, R., Campbell, J. N., and Raja, S. N. 2005. Peripheral Mechanisms of Cutaneous Nociception. In: Wall and Melzack's Textbook of Pain, 5 edn. (*ed*. M. K. S. McMahon), pp. 3–34. Elsevier, with permission from Elsevier.

Table 2 Roles of different afferents in acute pain sensation

Percept	*Afferents responsible*
Heat pain on glabrous skin	CMHs
First pain to heat on hairy skin	Type II A-fibers
Second pain to heat on hairy skin	CMHs
Pain to sustained heat stimulus	Type I AMHs
Pain to sharp mechanical stimulus	A-fiber nociceptors
Pain to sustained pressure	C-MIAs
Pain to capsaicin	C-MIAs, A-MIAs

larger than the receptive field size of CMHs. C-MIAs have large receptive field sizes and could therefore account for the large area of flare. The high threshold needed to induce flare by electrocutaneous stimulation is also consistent with mediation by MIAs (Schmelz, M. *et al*., 2000).

5.08.4 Acute Pain Sensations and Nociceptor Activity

We now address the role of different classes of nociceptors in acute pain sensation (Table 2). To do this, psychophysical measurements of pain intensity in human subjects are compared to the neuronal response in nociceptors when both are exposed to identical stimuli. A number of different scaling techniques can be used by humans including a visual analog scale (VAS) and the magnitude estimation technique (see Box 3)

5.08.4.1 Pain from Heat Stimuli

5.08.4.1.1 Heat pain from glabrous skin is signaled by C-fiber nociceptors

Near pain threshold, only two classes of fibers respond to heat stimuli applied to the glabrous skin, warm fibers, and CMHs. Type II A-fiber nociceptors are not found on glabrous skin, and type I AMHs have high heat thresholds. Warm fibers respond to gentle warming, but their response reaches a peak at temperatures at or below the threshold for pain (Figure 7) and then decreases for higher temperatures. In contrast, the response of CMHs starts at or below the heat pain threshold, and the response increases with temperature into the painful range. The stimulus–response functions for CMHs and for human pain ratings match well (Figure 7, Box 3).

There are a number of additional lines of corroborating evidence that CMHs encode heat pain sensation from glabrous skin: First, the long reaction time in human subjects to step increases in temperature is

Box 3 Psychophysical measurements of pain

A number of different techniques exist to measure the intensity of pain in human subjects. One of the most commonly used techniques is the visual analog scale (VAS) in which descriptors of pain are placed along the edge of the scale. This technique is very useful for measuring moderate levels of pain but suffers from ceiling effects for high levels of pain (i.e., once the subjects rates a given stimulus near the top of the scale, there is little room left for stimuli that may be much more intense).

Another method that is extremely useful for correlations with neural responses is the technique of magnitude estimation. In this procedure, the subjects are presented a moderately painful stimulus and asked to assign a number (e.g., 100) to their perceived intensity of that stimulus. Subsequent stimuli are then rated relative to this modulus. For example, if the next stimulus is twice as intense, the rating would be 200; half as intense, the rating would be 50. This technique does not suffer from ceiling effects, since the subject can use whatever numbers are needed to indicate the relative intensity of the stimulus. This is basically a ratio scale, since all ratings are made relative to the modulus. Ideally, the modulus is repeated during the course of the experiment to refresh the subject's memory.

An example of the use of the magnitude estimation technique to measure the intensity of heat pain in human subjects is shown in the figure.

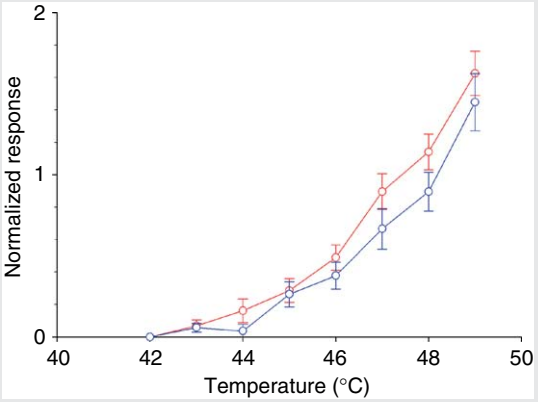

In this experiment, the glabrous skin of the hand was exposed to a random presentation of temperatures ranging from 41 to 49 °C in 1 °C increments. The random sequence was preceded by the presentation of a 45 °C stimulus that was used by the subjects to establish the reference rating (i.e., their modulus). To combine data across subjects who used different numbers for their modulus, data were normalized by dividing the ratings to a given stimulus by the ratings to the first stimulus. An identical sequence of temperatures was presented to the receptive field of CMHs recorded from the anesthetized monkey. The data across the population of CMHs were normalized by dividing the response of the nociceptors to a given temperature by the response to the initial 45 °C stimulus. The close correlation between the psychophysical data and the electrophysiological data provides strong evidence that CMHs encode heat pain from glabrous skin. Figure reproduced from Meyer, R. A. and Campbell, J. N. 1981b. Peripheral neural coding of pain sensation. Johns Hopkins APL Tech. Dig. 2, 164–171, with permission from APLTD.

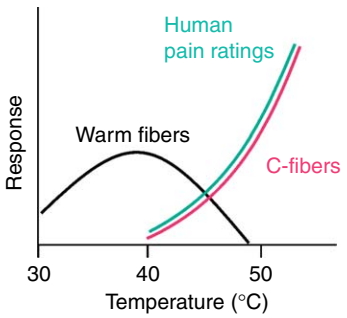

Figure 7 C-fiber nociceptors signal heat pain sensation from the glabrous skin. The response of warm fibers reaches a peak at relatively low temperatures and decreases as the temperature approaches the painful range. The response of C-fiber nociceptors starts near the pain threshold and increases with temperature. The pain ratings of human subjects closely matches the response profile of C-fiber nociceptors.

consistent with peripheral action potential propagation in the slowly conducting unmyelinated fibers. Second, selective blockade of peripheral conduction in myelinated fibers does not abolish heat pain sensation. Third, the fatigue to repeated heat stimuli described above for CMHs is also observed in psychophysical studies of pain to repeated heat stimuli. Fourth, in human microneurography experiments, intraneural electrical stimulation of presu-mably single CMHs elicits pain sensations.

5.08.4.1.2 First pain to heat on hairy skin is signaled by type II A-fiber nociceptors

In the hairy skin of the arm, stepped increases in temperature lead to a double pain sensation; an initial pricking pain is followed after a short lull by a

burning sensation (Figure 8). The reaction time to the pricking pain sensation is too short for conduction by slowly conducting unmyelinated fibers in the periphery. In addition, first pain sensation is blocked during a selective blockade of myelinated fibers.

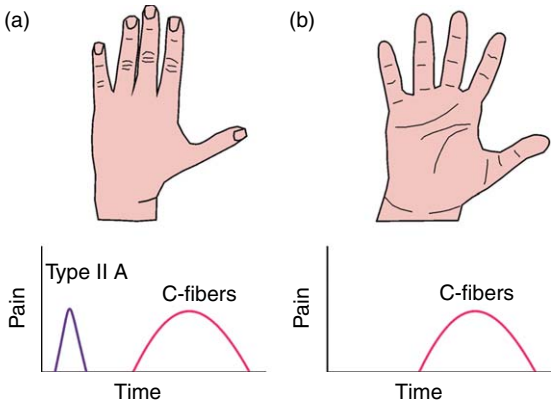

Figure 8 Heat pain on hairy and glabrous skin. (a) A heat stimulus on hairy skin leads to a dual pain sensation, an initial pricking pain followed by a burning pain. This is consistent with the finding that type II A-fiber nociceptors are found on hairy skin. (b) A heat stimulus on glabrous skin leads to burning pain only. Type II A-fibers are not found on glabrous skin.

These findings suggest that the first pain sensation to heat is mediated by myelinated afferents.

The type II A-fiber nociceptors are ideally suited to signal first pain sensation. The quick burst in action potential activity at the onset of a heat stimulus seen in type II A-fiber nociceptors is consistent with the percept of a short-lasting pricking sensation. The heat threshold of type II A-fiber nociceptors is also near the heat threshold for first pain sensation. The lack of type II fibers in glabrous skin is consistent with the absence of first pain to heat on the glabrous skin (Figure 8).

Figure 9 illustrates the neural responses to stepped increases in temperature in hairy skin. The heat stimulus activates a population of CMHs and type II A-fiber nociceptors with receptive fields that overlap the area of the heat stimulus. At the cutaneous terminals, both classes of fibers respond relatively quickly to the heat stimulus, but the response of the type II A-fibers rapidly adapts. As the neural signal propagates up to the CNS, these responses separate in time due to the conduction velocity differences of the myelinated and unmyelinated fibers. The signal from the type II fibers arrives at the CNS much sooner than the response of the

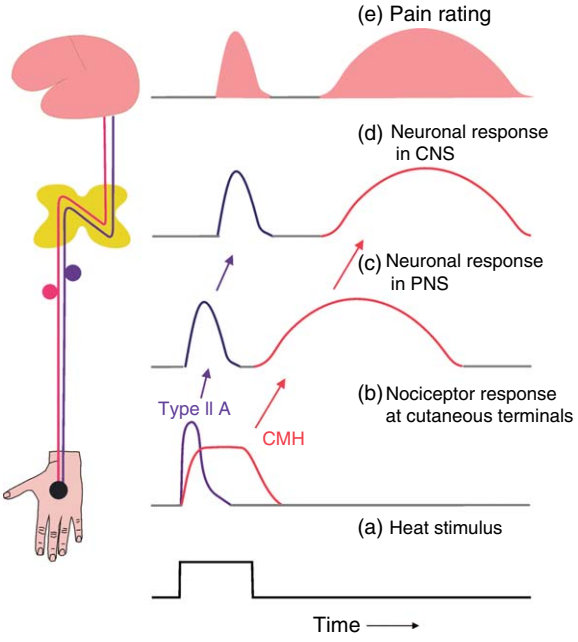

Figure 9 First pain to heat on hairy skin is signaled by A-fiber nociceptors. A stepped heat stimulus on hairy skin (a) leads to a dual pain sensation, a sharp pain followed after a lull by a burning pain (e). Heat stimuli near pain threshold activate two classes of nociceptors on hairy skin, type II A-fibers and C-fiber mechanoheat-sensitive afferents (CMHs) (b). The signal that reaches the central nervous system (CNS) is both delayed and broader than the signal at the receptor terminals. The A-fibers have a faster conduction velocity than the C-fibers and therefore their signals arrive at the CNS with less delay. The broadening of the signal is due to the variation in conduction velocity across the population of fibers that respond.

CMHs. In addition, the signals from each class of afferents become broader because of the variation in conduction velocity in each population of fibers that respond to the stimulus. The double pain response reflects the different arrival times at the CNS of neural signals from these two classes of afferents. This difference in arrival time is more apparent for stimuli applied to the distal extremities where the conduction lengths are long. A double pain sensation is not as apparent at more rostral locations (e.g., the face) where the conduction distances are short.

5.08.4.1.3 Pain to prolonged heat stimuli is signaled by type I A-fiber nociceptors

A long-duration heat stimulus applied to the glabrous skin produces pain that lasts through out the stimulus. However, the response of CMHs adapts to a long heat stimulus. In contrast, the response of type I A-fiber nociceptors builds during the course of a prolonged heat stimulus (Figure 3). Therefore, type I A-fiber nociceptors are thought to account for the pain to sustained high-intensity heat stimuli.

5.08.4.2 Pain from Controlled Mechanical Stimuli

5.08.4.2.1 Sharp pain is signaled by A-fiber nociceptors

The force thresholds for sharpness and pain from cylindrical objects increase in direct proportion with the circumference of the probe (Greenspan, J. D. and McGillis, S. L. B., 1991). As noted above, a similar relationship exists between probe circumference and the response of nociceptors. Sharp pain sensation is dramatically reduced in the presence of a selective blockade of A-fiber conduction. In addition, the reaction time for perception of sharp pain is short. Thus, A-fiber nociceptors appear to be primarily responsible for encoding the percept of sharp pain. Prolonged topical application of capsaicin leads to a substantial decrease in heat pain sensitivity but does not greatly affect mechanical pain sensibility (Magerl, W. *et al.*, 2001). This suggests that the A-fibers involved in sharp pain are insensitive to capsaicin (likely, type I AMHs).

5.08.4.2.2 Pain from tonic pressure is signaled by C-fiber MIAs

Firm pressure does not hurt if applied for short periods of time but becomes painful when sustained for long periods of time. The response of mechanically sensitive nociceptors adapts to a constant mechanical stimulus. In contrast, C-fiber MIAs develop a response during a maintained stimulus (Schmidt, R. *et al.*, 2000). In addition, the pain to tonic pressure does not disappear during a selective A-fiber block (Andrew, D. and Greenspan, J. D., 1999). Thus, it appears that C-fiber MIAs encode the pain to tonic pressure.

5.08.4.3 Cold Pain Sensation

The threshold for cold pain sensation is around 14 °C on hairy skin. This is much farther from resting skin temperature (33 °C) than the threshold for heat pain (around 45 °C). In addition, the slope of the stimulus–response function for cold pain is shallower than that for heat pain (Morin, C. and Bushnell, M. C., 1998). Cold pain appears to be signaled, at least in part, from deep receptors since topical anesthetics do not abolish it and the latency for the perception of cold pain is long.

The majority of nociceptors respond to ice applied to the receptive field. A nonselective cation channel (TRPA1) has been identified that has an activation threshold (18 °C) near the cold pain threshold and is found in a subset of nociceptors (Story, G. M. *et al.*, 2003). However, the role of this channel in signaling the pain to a noxious cold stimulus is controversial (Bautista, D. M. *et al.*, 2006; Kwan, K. Y. *et al.*, 2006). In the presence of an A-fiber block, gentle cooling stimuli become painful. It is thought that cold-evoked activity in A-delta cold fibers normally inhibits pain produced by activation of nociceptors.

5.08.4.4 Capsaicin-Evoked Pain

Capsaicin, the active ingredient in hot peppers, produces a burning percept upon contact with mucous membranes and produces intense pain that lasts for several minutes when injected into the skin. Topical or intradermal capsaicin can also lead to a marked desensitization to heat stimuli. The TRPV1 channel expressed by many nociceptors is thought to be responsible for the pungency of capsaicin. Injection of capsaicin into the receptive field of CMHs produces a weak response and can lead to a desensitization of the afferent to heat. Injection of capsaicin into the receptive field of A-fiber and C-fiber MIAs produces a long-lasting, strong response, suggesting that these afferents are responsible for the pain from capsaicin.

5.08.5 Hyperalgesia

A tissue injury can lead to an enhancement of pain sensibility called hyperalgesia. Hyperalgesia is characterized by a leftward shift in the stimulus–response function relating pain intensity to stimulus intensity (Figure 10(a)). There is a decrease in the threshold for pain, an increase in the pain to suprathreshold stimuli, and ongoing pain. The electrophysiological correlate for hyperalgesia is sensitization of nociceptive neurons (Figure 10(b)), either of peripheral nociceptors (peripheral sensitization) or of central neurons involved in processing nociceptive input (central sensitization) or both. Sensitization is characterized by a leftward shift in the neural response at different stimulus intensities. There is a decrease in the threshold for eliciting a response, an increase in the response to suprathreshold stimuli, and spontaneous activity.

Two zones of hyperalgesia are readily identified (Figure 11). Primary hyperalgesia occurs at the site of injury and is characterized by hyperalgesia to both heat and mechanical stimuli. Secondary hyperalgesia occurs in the uninjured tissue surrounding the site of injury and is characterized by hyperalgesia to mechanical but not heat stimuli. This dichotomy provides evidence that the mechanisms for primary and secondary hyperalgesia differ.

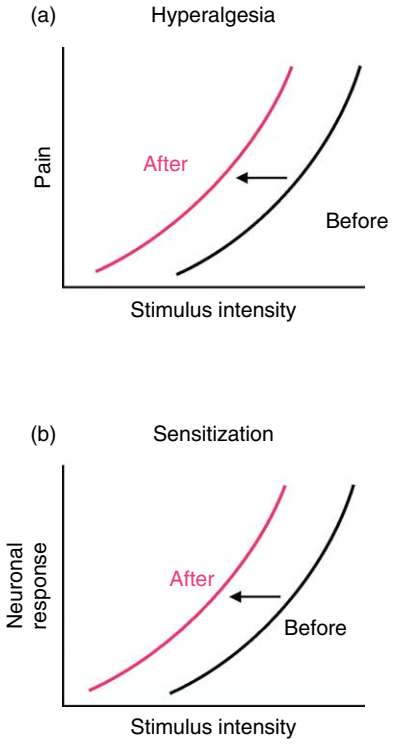

Figure 10 Hyperalgesia and sensitization. (a) Hyperalgesia is characterized by a leftward shift in the stimulus function relating pain intensity to stimulus intensity. (b) Sensitization is characterized by a leftward shift in the stimulus function relating neural response to stimulus intensity.

5.08.5.1 Primary Hyperalgesia

5.08.5.1.1 Hyperalgesia to heat is mediated by primary afferent sensitization

Hyperalgesia to heat is prevalent after a cutaneous injury and after inflammation. Substantial evidence indicates that sensitization of primary afferent nociceptors to heat accounts for this hyperalgesia. For example, a burn injury to the glabrous skin of the hand leads to marked hyperalgesia to heat and sensitization of type I AMHs to heat (Figure 12). Although a burn to the glabrous skin does not lead to sensitization of CMHs, a burn injury to the hairy skin does. This suggests that the propensity to sensitize is a function of skin type. Whether this is due to differences in the milieu or due to differences in the properties of the neurons is not known.

Hyperalgesia to heat can also develop after inflammation. When a cocktail of inflammatory mediators is injected into the receptive field of nociceptive afferents, marked sensitization to heat stimuli is observed.

5.08.5.1.2 Hyperalgesia to mechanical stimuli

Hyperalgesia to mechanical stimuli also occurs after a cutaneous injury and after inflammation. A number of possible mechanisms may account for this mechanical hyperalgesia.

Nociceptor sensitization. Although a burn injury leads to sensitization of nociceptors to heat stimuli, the mechanical threshold of nociceptors is not lowered, suggesting that this injury does not produce sensitization to mechanical stimuli. However, nociceptors are sensitized to mechanical stimuli in situations of inflammation. For example, injection into the receptive field of inflammatory substances leads to a sensitization of MIAs to mechanical stimuli. Inflammation of the knee joint also leads to a sensitization of MIAs to mechanical stimuli.

Spatial summation. When a burn injury is applied at the edge of the receptive field of a nociceptor, the receptive field expands into the area of injury. As a result, a mechanical stimulus in the area of injury evokes a response in a greater number of nociceptive

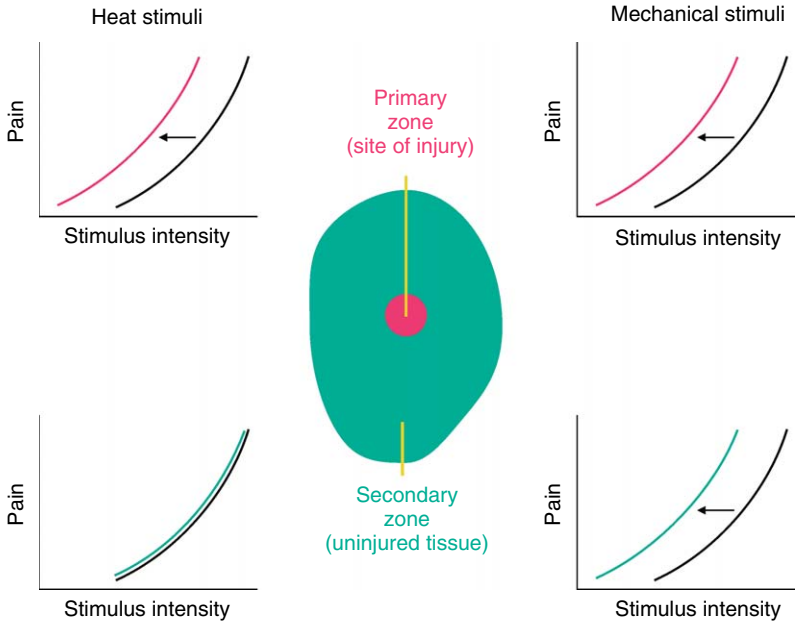

Figure 11 Primary and secondary hyperalgesia. There are two forms of hyperalgesia. Primary hyperalgesia occurs at the site of injury and is characterized by hyperalgesia to both mechanical and heat stimuli. Secondary hyperalgesia occurs in the uninjured tissue surrounding the injury site and is characterized by hyperalgesia to mechanical but not heat stimuli.

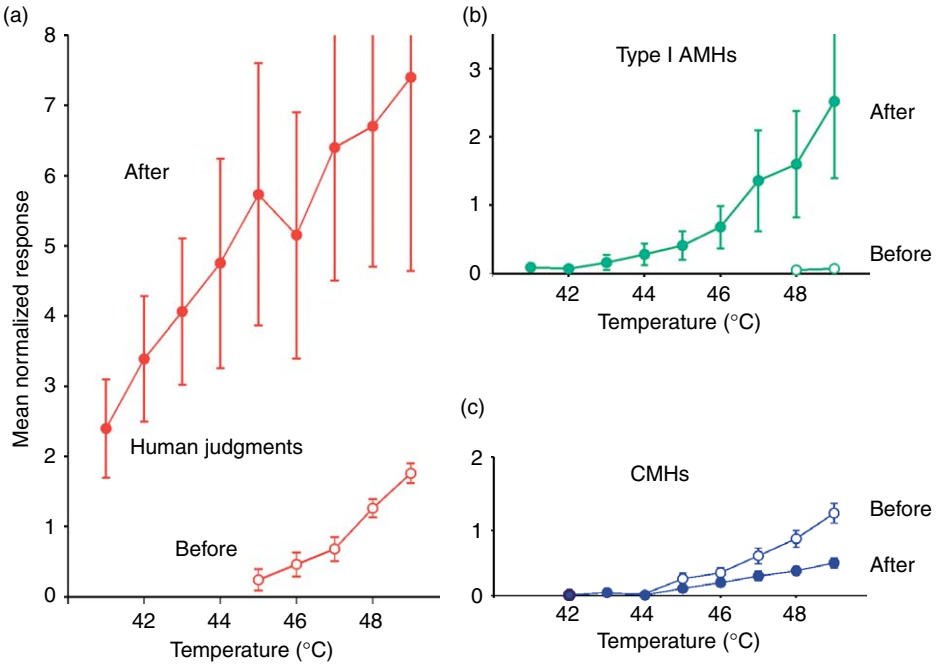

Figure 12 Primary hyperalgesia to heat is signaled by sensitization of primary afferent nociceptors. (a) A burn injury to the glabrous skin of human subjects leads to a dramatic increase in pain ratings to heat stimuli. (b) The same burn injury leads to a marked sensitization of type I AMHs in the anesthetized monkey. (c) This burn injury led to a desensitization of CMHs on glabrous skin. However, burn injuries to CMHs on hairy skin do lead to sensitization. Adapted from Meyer, R. A. and Campbell, J. N. 1981a. Myelinated nociceptive afferents account for the hyperalgesia that follows a burn to the hand. Science 213, 1527–1529, with permission from AAAS.

afferents. This will lead to spatial summation in the CNS that would be expected to produce more pain.

Central sensitization. Peripheral sensitization appears to account, at least in part, for hyperalgesia to mechanical stimuli. In addition, the central sensitization phenomena to be described below for secondary hyperalgesia may also play a role in primary hyperalgesia to mechanical stimuli.

5.08.5.1.3 Inflammatory mediators and nociceptor sensitization

Injury leads to the local release of various endogenous substances that excite or modulate the terminals of primary-afferent nociceptors (Figure 13). For example, bradykinin is released on tissue injury (e.g., from the plasma) and can excite and sensitize nociceptor terminals. Intradermal injection of bradykinin produces pain and hyperalgesia. Serotonin, histamine, and prostaglandin can also be released from mast cells and alter nociceptor terminal sensitivity. Tissue injury can also lead to the release or leakage of adenosine and its derivatives (e.g., ATP) into the extracellular space and could therefore activate sensory terminals. Low pH levels found in inflammed tissue activate and modulate nociceptor terminals. During inflammation, cytokines (e.g., interleukins and tumor necrosis factor alpha) are released by a variety of cells (e.g., macrophages) and are not only involved in regulating the inflammatory process but may also act as algesic substances either by directly activating nociceptive endings or by increasing their sensitivity to natural stimuli.

As illustrated in Figure 13, these agents can act directly at specialized receptors on the nociceptor terminal to excite the ending or to alter the sensitivity of the ending. The molecular mechanisms of transduction and sensitization are discussed in more detail in Chapter Molecular Biology of the Nociceptor/Transduction.

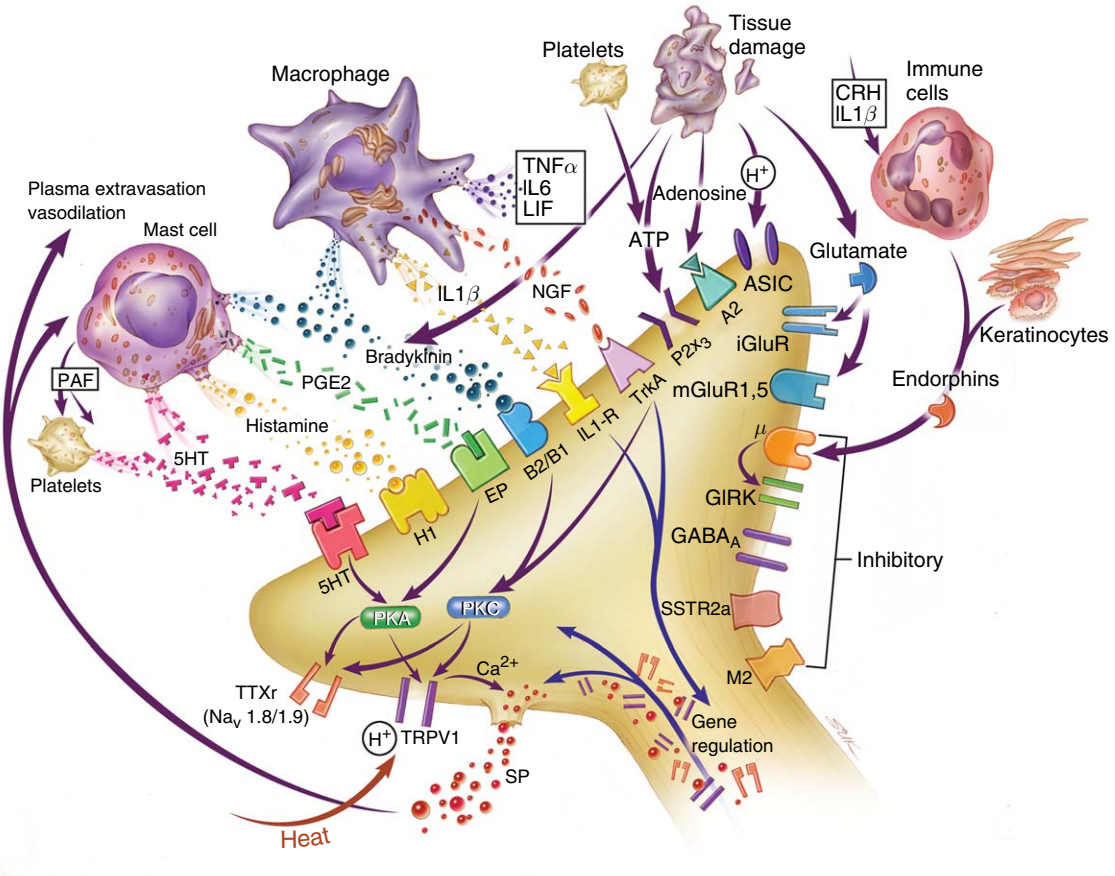

Figure 13 Inflammatory mediators act on specific receptors located at the nociceptor terminals. Artwork by Ian suk, Johns Hopkins University. Reproduced from Meyer, R. A., Ringkamp, R., Campbell, J. N., and Raja, S. N. 2005. Peripheral Mechanisms of Cutaneous Nociception. In: Wall and Melzack's Textbook of Pain, 5 edn. (*ed*. M. K. S. McMahon), pp. 3–34. Elsevier.

5.08.5.2 Secondary Hyperalgesia

Secondary hyperalgesia is characterized by hyperalgesia to mechanical but not heat stimuli. Two distinct forms of mechanical hyperalgesia have been reported (Figure 14). Punctate hyperalgesia (or static hyperalgesia) is characterized by hyperalgesia to sharp stimuli that normally cause pain (e.g., stiff von Frey probes and pin prick). Stroking hyperalgesia (or dynamic hyperalgesia or allodynia) is characterized by pain to a light moving touch (e.g., stroking of the skin with a soft brush) but not blunt pressure.

5.08.5.2.1 Sensitization of primary afferent nociceptors does not occur

One possible explanation for secondary hyperalgesia is that the sensitization process that occurs at the site of injury spreads to adjacent uninjured tissue. In a manner similar to that described above for the axon-reflexive flare response, the nerve endings could release not only vasoactive substances but also substances that produce sensitization of nociceptive terminals. However, a number of lines of evidence suggest that spreading sensitization does not occur. For example, burn or mechanical injuries or mustard oil application to one half of the receptive field of nociceptors lead to sensitization of that part of the receptive field but not of the uninjured part of the receptive field. In addition, antidromic electrical stimulation of nociceptors, which should lead to the release of these putative sensitizing substances from the terminals, does not lead to sensitization. Also, the area of flare is generally smaller than the area of hyperalgesia. In addition, flare can be induced by substances (e.g., histamine injection) that do not lead to the development of hyperalgesia. Finally, flare can spread across the midline of the body, but hyperalgesia does not.

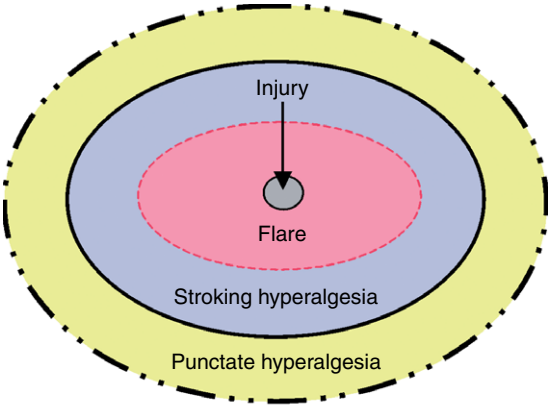

	Stroking hyperalgesia (allodynia)	Punctate hyperalgesia (static hyperalgesia)
Adequate stimulus	Light stroking	Punctate stimuli
Area	Small	Large
Duration	Short	Long
Central sensitization	Yes	Yes
Primary afferent signal	Low-threshold mechano-receptors	Nociceptors

Figure 14 Two forms of secondary hyperalgesia to mechanical stimuli. The properties of punctate and stroking hyperalgesia are different, suggesting that the neural mechanisms may differ.

5.08.5.2.2 Central mechanisms of secondary hyperalgesia

The preponderance of experimental data indicate that secondary hyperalgesia is the result of plasticity in the CNS often called central sensitization (Figure 15). This central sensitization is initiated by

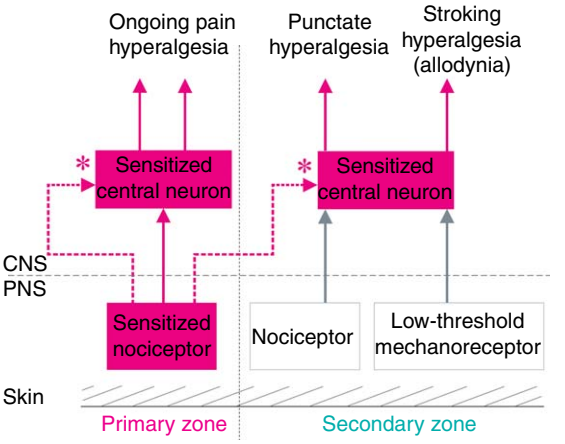

Figure 15 Secondary hyperalgesia is due to central sensitization. An injury or inflammation leads to activation and sensitization of nociceptors in the zone of primary hyperalgesia. Activity in the peripheral nociceptors produces a state of central plasticity in the CNS called central sensitization (*). This sensitization spreads to central neurons with input from adjacent, uninjured afferents. Sensitization to input from nociceptors accounts for punctate hyperalgesia. Sensitization to input from low-threshold mechanoreceptors accounts for stroking hyperalgesia (or allodynia).

neural activity in primary-afferent nociceptors and is already apparent at the level of the dorsal horn.

Compelling evidence for central sensitization comes from an experiment in which capsaicin was injected into both the forearms of human volunteers (LaMotte, R. H. *et al.*, 1991). In the control arm, the capsaicin injection produced intense pain and led to the development of a flare and a large zone of secondary hyperalgesia. In the test arm, the nerve supplying the forearm was anesthetized at a proximal site prior to the injection. The injection did not hurt but did lead to the development of an axon-reflexive flare, indicating that the nociceptors had been activated and were able to release vasoactive substances (and also putative sensitizing substances). Three hours after the capsaicin injection, there was no hyperalgesia on the test arm, but the control arm still had a large zone of secondary hyperalgesia.

The characteristics of stroking and punctate hyperalgesia are different, suggesting that the neural mechanisms are different (Figure 14). For example, the area of punctate hyperalgesia is typically larger than the area of stroking hyperalgesia. In addition, the duration of punctate hyperalgesia is longer than the duration of stroking hyperalgesia. Stroking hyperalgesia appears to be more dependent on ongoing input from nociceptors, since cooling or anesthetizing the site of injury substantially reduces the zone of stroking hyperalgesia without greatly affecting the zone of punctate hyperalgesia. As described below, both forms of secondary hyperalgesia are thought to be due to central sensitization mechanisms.

Stroking hyperalgesia appears to be due to central sensitization to input from low-threshold myelinated mechanoreceptors (Figure 15). The light stroking stimulus that produces pain in the secondary zone readily activates low-threshold mechanoreceptors but not nociceptors. Compelling evidence comes from an experiment in which intraneural microstimulation was performed in human volunteers (Torebjörk, H. E. *et al.*, 1992). A low-intensity, fixed-frequency electrical stimulus produced a tactile percept referred to a small area on the foot. Capsaicin was then injected adjacent to this area and produced secondary hyperalgesia that spread into this area. When the electrical stimulation was repeated at the same intensity and frequency, it now produced pain. This electrical stimulation of myelinated fibers bypassed the natural transduction apparatus and indicates that there was central sensitization to input from myelinated fibers. Additional evidence comes from studies which show that selective peripheral blockade of myelinated fibers (with conduction maintained in unmyelinated fibers) leads to the disappearance of stroking hyperalgesia.

Punctate hyperalgesia appears to be due to central sensitization to input from nociceptors (Figure 15). Punctate hyperalgesia, and not stroking hyperalgesia, developed when capsaicin was injected into the arm of a patient with a selective, large-fiber neuropathy, indicating that small myelinated or unmyelinated fibers are involved. In addition, enhanced pain to woolen fabrics is observed in the zone of secondary hyperalgesia. Since the prickliness of woolen fabrics is encoded by activity in nociceptors, not mechanoreceptors, activity in nociceptors likely accounts for this hyperalgesia. Selective nerve blocks revealed that punctate hyperalgesia disappeared when Aδ nerve fibers were blocked, suggesting that Aδ nociceptors are important. The nociceptors appear to be capsaicin insensitive since topical application of capsaicin produced desensitization to heat but did not eliminate punctate hyperalgesia produced by a subsequent injection of capsaicin adjacent to the treated area (Magerl, W. *et al.*, 2001).

Acknowledgments

This research was supported in part by the National Institutes of Health (NS-14447 and NS-026363) and by a Stuart S. Janney Fellowship from the Applied Physics Laboratory (RAM).

References

Andrew, D. and Greenspan, J. D. 1999. Peripheral coding of tonic mechanical cutaneous pain: comparison of nociceptor activity in rat and human psychophysics. J. Neurophysiol. 82, 2641–2648.

Bautista, D. M., Jordt, S. E., Nikai, T., Tsuruda, P. R., Read, A. J., Poblete, J., Yamoah, E. N., Basbaum, A. I., and Julius, D. 2006. TRPA1 mediates the inflammatory actions of environmental irritants and proalgesic agents. Cell 124, 1269–1282.

Darian-Smith, I., Johnson, K. O., and Dykes, R. 1973. "Cold" fiber population innervating palmar and digital skin of the monkey: responses to cooling pulses. J. Neurophysiol. 36, 325–346.

Darian-Smith, I., Johnson, K. O., LaMotte, C., Shigenaga, Y., Kenins, P., and Champness, P. 1979. Warm fibers innervating palmar and digital skin of the monkey: responses to thermal stimuli. J. Neurophysiol. 42, 1297–1315.

Dong, X., Han, S., Zylka, M. J., Simon, M. I., and Anderson, D. J. 2001. A diverse family of GPCRs expressed in specific subsets of nociceptive sensory neurons. Cell 106, 619–632.

Garell, P. C., McGillis, S. L. B., and Greenspan, J. D. 1996. Mechanical response properties of nociceptors innervating feline hairy skin. J. Neurophysiol. 75, 1177–1189.

Greenspan, J. D. and McGillis, S. L. B. 1991. Stimulus features relevant to the perception of sharpness and mechanically evoked cutaneous pain. Somatosens. Motor Res. 8, 137–147.

Kwan, K. Y., Allchorne, A. J., Vollrath, M. A., Christensen, A. P., Zhang, D. S., Woolf, C. J., and Corey, D. P. 2006. TRPA1 contributes to cold, mechanical, and chemical nociception but is not essential for hair-cell transduction. Neuron 50, 277–289.

LaMotte, R. H., Shain, C. N., Simone, D. A., and Tsai, E.-F. P. 1991. Neurogenic hyperalgesia: psychophysical studies of underlying mechanisms. J. Neurophysiol. 66, 190–211.

Lawson, S. N. 1992. Morphological and Biochemical Cell Types of Sensory Neurons. In: Sensory Neurons (*ed*. S. A. Scott), pp. 27–59. Oxford University Press.

Magerl, W., Fuchs, P. N., Meyer, R. A., and Treede, R.-D. 2001. Roles of capsaicin-insensitive nociceptors in cutaneous pain and secondary hyperalgesia. Brain 124, 1754–1764.

Meyer, R. A. and Campbell, J. N. 1981a. Myelinated nociceptive afferents account for the hyperalgesia that follows a burn to the hand. Science 213, 1527–1529.

Meyer, R. A. and Campbell, J. N. 1981b. Peripheral neural coding of pain sensation. Johns Hopkins APL Tech. Dig. 2, 164–171.

Meyer, R. A., Ringkamp, R., Campbell, J. N., and Raja, S. N. 2005. Peripheral Mechanisms of Cutaneous Nociception. In: Wall and Melzack's Textbook of Pain, 5 edn. (*ed*. M. K. S. McMahon), pp. 3–34. Elsevier.

Michael, G. J. and Priestley, J. V. 1999. Differential expression of the mRNA for the vanilloid receptor subtype 1 in cells of the adult rat dorsal root and nodose ganglia and its downregulation by axotomy. J. Neurosci. 19, 1844–1854.

Morin, C. and Bushnell, M. C. 1998. Temporal and qualitative properties of cold pain and heat pain: a psychophysical study. Pain 74, 67–73.

Nordin, M. 1990. Low-threshold mechanoreceptive and nociceptive units with unmyelinated (C) fibres in the human supraorbital nerve. J. Physiol. (Lond.) 426, 229–240.

Peng, Y. B., Ringkamp, M., Meyer, R. A., and Campbell, J. 2003. Fatigue and paradoxical enhancement of heat response in C-fiber nociceptors from cross-modal excitation. J. Neurosci. 23, 4766–4774.

Schmelz, M. and Petersen, L. J. 2001. Neurogenic inflammation in human and rodent skin. News Physiol. Sci. 16, 33–37.

Schmelz, M., Michael, K., Weidner, C., Schmidt, R., Torebörk, H. E., and Handwerker, H. O. 2000. Which nerve fibers mediate the axon reflex flare in human skin? Neuroreport 11, 645–648.

Schmidt, R., Schmelz, M., Torebjörk, H. E., and Handwerker, H. O. 2000. Mechano-insensitive nociceptors encode pain evoked by tonic pressure to human skin. Neuroscience 98, 793–800.

Slugg, R. M., Campbell, J. N., and Meyer, R. A. 2004. The population response of A- and C-fiber nociceptors in monkey encodes high-intensity mechanical stimuli. J. Neurosci. 24, 4649–4656.

Slugg, R. M., Meyer, R. A., and Campbell, J. N. 2000. Response of cutaneous A- and C-fiber nociceptors in the monkey to controlled-force stimuli. J. Neurophysiol. 83, 2179–2191.

Story, G. M., Peier, A. M., Reeve, A. J., Eid, S. R., Mosbacher, J., Hricik, T. R., Earley, T. J., Hergarden, A. C., Andersson, D. A., Hwang, S. W., McIntyre, P., Jegla, T., Bevan, S., and Patapoutian, A. 2003. ANKTM1, a TRP-like channel expressed in nociceptive neurons, is activated by cold temperatures. Cell 112, 819–829.

Tillman, D. B., Treede, R.-D., Meyer, R. A., and Campbell, J. N. 1995. Response of C fibre nociceptors in the anaesthetized monkey to heat stimuli: estimates of receptor depth and threshold. J. Physiol. 485(Pt. 3), 753–765.

Torebjörk, H. E., Lundberg, L. E. R., and LaMotte, R. H. 1992. Central changes in processing of mechanoreceptive input in capsaicin-induced secondary hyperalgesia in humans. J. Physiol. (Lond.) 448, 765–780.

Treede, R.-D., Meyer, R. A., and Campbell, J. N. 1998. Myelinated mechanically insensitive afferents from monkey hairy skin: heat-response properties. J. Neurophysiol. 80, 1082–1093.

Weidner, C., Schmelz, M., Schmidt, R., Hansson, B., Handwerker, H. O., and Torebjork, H. E. 1999. Functional attributes discriminating mechano-insensitive and mechano-responsive C nociceptors in human skin. J. Neurosci. 19, 10184–10190.

Zwick, M., Davis, B. M., Woodbury, C. J., Burkett, J. N., Koerber, H. R., Simpson, J. F., and Albers, K. M. 2002. Glial cell line-derived neurotrophic factor is a survival factor for isolectin B4-positive, but not vanilloid receptor 1-positive, neurons in the mouse. J. Neurosci. 22, 4057–4065.

Zylka, M. J., Rice, F. L., and Anderson, D. J. 2005. Topographically distinct epidermal nociceptive circuits revealed by axonal tracers targeted to Mrgprd. Neuron 45, 17–25.

5.09 Itch

E Carstens, University of California, Davis, CA, USA

© 2008 Elsevier Inc. All rights reserved.

5.09.1	Introduction and Definition of Itch	115
5.09.2	Is Itch Distinct from Pain?	116
5.09.3	Pain Inhibition of Itch	117
5.09.4	Peripheral and Spinal Mechanisms of Itch	117
5.09.5	Alloknesis (Itchy Skin) and Sensitization	119
5.09.6	Central Representation of Itch	120
5.09.7	Animal Models of Itch	120
5.09.8	Itch Mediators	121
References		123

Glossary

allodynia Pain due to a stimulus that does not normally provoke pain.
alloknesis Itch elicited by light touching or stroking.
hyperalgesia An increased response to a stimulus which is normally painful.
hyperknesis Itch elicited by strong mechanical stimulation.
itch Unpleasant sensation associated with the desire to scratch.
nociceptor A receptor preferentially sensitive to a noxious stimulus or to a stimulus, which would become noxious if prolonged.
pain An unpleasant sensory and emotional experience associated with actual or potential tissue damage, or described in terms of such damage.
pruriceptor A sensory receptor preferentially sensitive to a pruritic stimulus.

5.09.1 Introduction and Definition of Itch

Itch is widely considered to be an unpleasant sensation associated with the desire to scratch. The definition of itch has recently been refined to include the following subcategories: pruriceptive (originating from skin damage), neuropathic (originating from nerve damage), neurogenic (originating centrally), and psychogenic (Yosipovitch, G. *et al.*, 2003). Itch is frequently associated with common insect bites or exposure to plants, providing a warning signal to remove the offending stimulus by scratching or rubbing the affected skin area. Itch can be experimentally elicited by cutaneous histamine and other chemicals (Schmelz, M. *et al.*, 2003b) and by electrical surface stimulation of the skin (Tuckett, R. P., 1982; Ikoma, A. *et al.*, 2005). However, itch also commonly occurs under a variety of skin conditions such as dry skin and contact or atopic dermatoses (eczema). Moreover, a variety of systemic disorders also have itching as a symptom (Krajnik, M. and Zbigniew, Z., 2001), in particular, liver dysfunctions such as cholestasis or biliary cirrhosis (Bergasa, N. V. *et al.*, 2000), and renal failure (Murphy, M. and Carmichael, A. J., 2000). Neuropathic itch is less commonly associated with lesions of the spinal cord (Dey, D. D. *et al.*, 2005) or other central structures. While itch associated with, for example, urticaria (hives) can be relieved by antihistamines acting at the H1 histamine receptor, itch associated with other skin conditions and systemic diseases is often refractory to antihistamines. This suggests that there may be other itch mediators and mechanisms in addition to histamine, the prototypical itch mediator in normal human skin.

Itch has historically been considered by some to be a low level of pain, and perhaps for this reason

the experimental study of itch has until now received much less attention compared to pain. Nevertheless, recent studies have provided exciting new evidence for the existence of itch-selective peripheral receptors and central pathways separate from those mediating pain (for recent reviews, see Stander, S. *et al.*, 2003; Twycross, R. *et al.*, 2003; Yosipovitch, G. *et al.*, 2003; 2004; Biro, T. *et al.*, 2005). This vignette will describe some of the recent advances in our understanding of itch mechanisms. An overview of the neural basis for itch versus pain is provided first, followed by consideration of animal itch models and, finally, possible itch mediators and mechanisms based on human and animal research.

5.09.2 Is Itch Distinct from Pain?

The concept that itch is on a continuum with pain prompted the frequency theory (von Frey, M., 1922), depicted schematically in Figure 1(a). A low firing rate in cutaneous nociceptors connected to a common central pathway elicits a sensation of itch, while high-frequency firing elicits pain. This idea is supported by observations that numerous stimuli, including histamine (Broadbent, J. L., 1955) elicit itch at low intensities and pain at higher intensities, and that both pain and itch are conveyed via the spinothalamic tract (White, J. C. and Sweet, W. H., 1969). The notion that itch and pain are conveyed by a common set of neurons, however, is belied by the following observations. Most importantly, itch can be elicited by focal electrical stimulation of the skin surface (Tuckett, R. P., 1982; Ikoma, A. *et al.*, 2005) or by intraneural microstimulation (Schmidt, R. *et al.*, 1993) and the itch becomes more intense but never takes on a painful quality as the stimulus frequency is increased. Conversely, pain elicited by intraneural stimulation never transforms to itch at lower frequencies (Ochoa, J. and Torebjörk, E., 1989; Handwerker, H. O. *et al.*, 1991). Furthermore, itch and pain rarely coexist and concurrent noxious stimulation, such as scratching, is well known to inhibit itch. Morphine and other opioids depress pain but frequently elicit or exacerbate itch, as discussed further below. Also, the behavioral manifestation of itch, scratching, is very different from manifestations of pain that often include withdrawal of the stimulated limb and/or escape reactions. Withdrawal from a noxious stimulus serves a protective function to prevent tissue damage, whereas scratching may represent an attempt to remove a pruritic stimulus that has already impinged upon tissue. In this regard, humans can localize the site of itch elicited by focal histamine application with errors of less than 10 mm, comparable to localization of punctate painful stimuli and only slightly worse than localization of tactile stimuli (Koltzenburg, M. *et al.*, 1993). This would aid the accuracy of scratches directed to an itchy site. However, two-point discrimination for histamine-induced itch is fairly poor, approximately 12–15 cm on forearm skin (Wahlgren, C. F and Ekblom, A., 1996) consistent with the very large

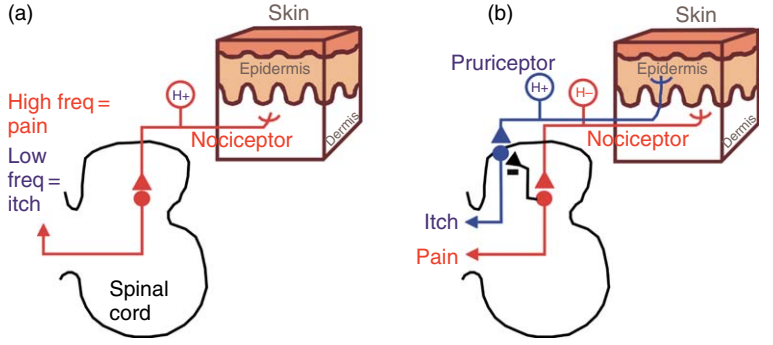

Figure 1 Theories of itch transmission. (a) Frequency theory. Both pruritic and noxious stimuli excite polymodal nociceptors in skin, which project to a common population of neurons in the spinal cord. These neurons signal itch at a low firing rate, and pain at a higher firing rate. H+: responsive to histamine. (b) Specificity (or selectivity) theory. Pruritic stimuli excite a selective population of pruriceptors in superficial epidermis that are histamine-sensitive (H+), and that project to a select population of spinal neurons (blue) in the superficial dorsal horn. Activity in this pathway signals itch. Dermal nociceptors project to a separate population of pain-signaling spinal neurons (red). Incorporated in this schematic is an inhibitory connection (black) from pain- to itch-transmitting neurons, reflecting the ability of noxious counterstimuli to inhibit itch.

innervation territories of putative pruriceptors (Schmelz, M. *et al.*, 1997) (see below).

For the reasons noted above, it has long been postulated that itch and pain are conveyed via separate central pathways, with pain capable of inhibiting itch transmission. This concept is depicted in Figure 1(b). The separate pathways for itch and pain constitute the classic specificity theory. Given recent evidence showing a relative, rather than absolute, sensitivity of potential itch-signaling fibers to pruritics, the term selectivity is more appropriate. The ability of pain to inhibit itch is incorporated by the black inhibitory neuron shown in Figure 1(b), although interactions between nociceptive and pruriceptive systems may conceivably occur at supraspinal as well as spinal levels.

5.09.3 Pain Inhibition of Itch

Numerous experimental studies have demonstrated suppression of itch in humans by a variety of counterstimuli including cooling, mustard oil, and electrical cutaneous field stimulation (Bickford, R. G., 1937; Gammon, G. D. and Starr, I., 1941; Murray, F. S. and Weaver, M. M., 1975; Frustorfer, H. *et al.*, 1986; Ward, L. *et al.*, 1996; Nilsson, H. J. *et al.*, 1997). This suppression undoubtedly underlies the antipruritic effect of scratching. Opioids acting at the μ -opioid receptor depress pain, yet frequently induce or exacerbate itch in human patients (Bromage, P., 1981; Bromage, P. R. *et al.*, 1982; Morgan, M., 1987; Ballantyne, J. C. *et al.*, 1988), suggesting that inhibition of tonic nociceptive activity facilitates itch transmission. Consistent with this, μ-opioid antagonists reduce histamine-induced itch (Heyer, G. *et al.*, 1997a). Intradermal injection of histamine at a site previously anesthetized by local anesthetic in human subjects resulted in markedly enhanced itch (Atanassoff, P. G. *et al.*, 1999). The authors postulated that histamine excites two types of peripheral receptor, one conveying itch and the other being antipruritic (i.e., exciting central itch-inhibitory neurons). Preferential local anesthetic blockade of the antipruritic fibers would unmask pruriceptive input leading to increased itch.

Scratching behavior in mice and monkeys induced by μ-opioids is reduced by κ-opioid agonists in mice (Togashi, Y. *et al.*, 2002; Umeuchi, H. *et al.*, 2003) and monkeys (Ko, M. C. *et al.*, 2003). The κ agonists are also analgesic, suggesting a complex interaction between pro- and antipruritic opioid receptor-mediated central mechanisms. One possible scenario consistent with this interplay between μ- and κ-opioids is shown in Figure 2.

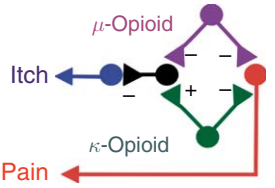

Figure 2 Schematic of opioid interactions with itch- and pain-signaling spinal neurons. μ-Opioid agonists (purple) inhibit pain and can induce or exacerbate itch, possibly by inhibiting interneurons (black) that tonically inhibit itch-transmitting neurons (blue), i.e., disinhibition. κ-Opioid agonists (dark green) also inhibit pain and may excite the inhibitory interneuron (black), thus inhibiting itch.

5.09.4 Peripheral and Spinal Mechanisms of Itch

Recent studies have provided evidence favoring the selectivity theory of itch depicted in Figure 1(b). Human microneurographic studies have uncovered a class of mechanically insensitive cutaneous receptors with slowly conducting unmyelinated afferent fibers that respond to cutaneous histamine over a time course that closely matches that of concomitant itch sensation (Figure 3; Schmelz, M. *et al.*, 1997). These potential itch receptors are called pruriceptors. Such histamine-responsive fibers also responded more weakly to prostaglandin E_2, serotonin, and acetylcholine, which were capable of inducing weak itch when delivered intradermally via microdialysis (Schmelz, M. *et al.*, 2003b). However, the fibers were not exclusively pruriceptive, as they also responded to capsaicin and bradykinin, which induce burning pain (Schmelz, M. *et al.*, 2003b), indicating that these fibers are itch-selective rather than itch-specific. These fibers could also be excited by electrical skin stimulation; however, the current intensities were much higher compared to electrical currents eliciting itch from the wrist (Ikoma, A. *et al*, 2005) suggesting that there may be additional pruriceptor subtypes.

Following the discovery of histamine-selective pruriceptors, a subpopulation of mechanically insensitive spinothalamic tract neurons in the cat superficial dorsal horn (lamina I) with temporally similar responses to histamine was identified (Andrew, D. and Craig, A. D., 2001) (Figure 3). Chemical selectivity was tested in four cases, with two additionally responding to mustard oil (which elicits burning pain) while the

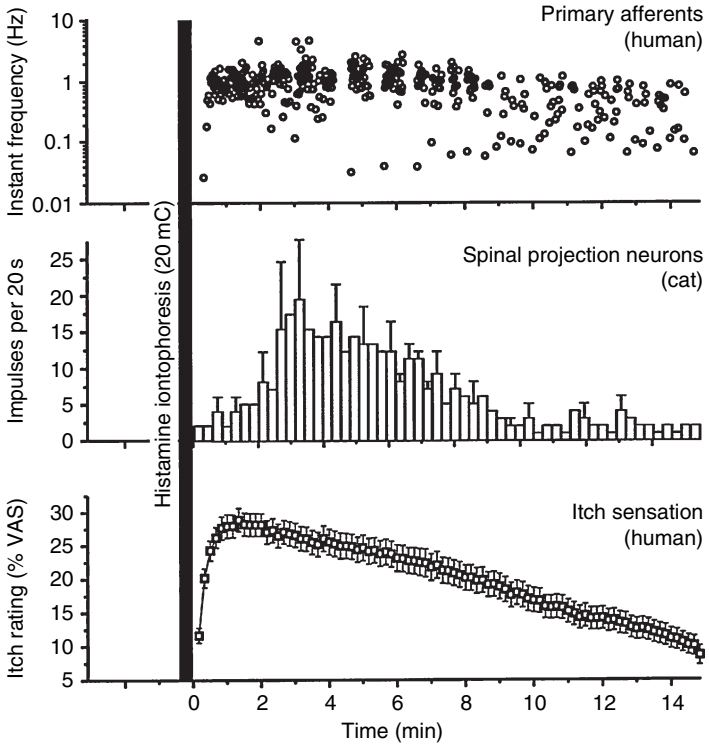

Figure 3 Time course of histamine-evoked response of an unmyelinated primary afferent fiber (upper panel), and mean responses of lamina I spinothalamic tract neurons (middle panel) in relation to itch sensation (lower panel). Vertical bar indicates time of delivery of histamine by iontophoresis to the skin. Adapted from Schmelz, M., Schmidt, R., Bickel, A., Forster, C., Handwerker, H. O., and Torebjork, H. E. 1997. Specific C-receptors for itch in human skin. J. Neurosci. 17, 8003–8008 and Andrew, D. and Craig, A. D. 2001. Spinothalamic lamina I neurons selectively sensitive to histamine: a central neural pathway for itch. Nat. Neurosci. 4, 72–76, with permission from Nature Publishing Group.

other two did not. These latter two units may be histamine-selective, while the units sensitive to both histamine and mustard oil resemble lamina I units in rats that gave prolonged response to serotonin (5-HT; also a pruritic) but usually also exhibited phasic responses to mustard oil, capsaicin, and other algogens (Jinks, S. L. and Carstens, E., 2002). An older study reported a fraction of wide dynamic range (WDR)-type neurons to respond to cutaneous application of cowhage (Wei, J. Y. and Tuckett, R. P., 1991). A recent study of identified spinothalamic tract neurons in primate found that about half responded to intradermal histamine, with all additionally responding to capsaicin (Simone, D. A. *et al.*, 2004). Moreover, neuronal responses to light mechanical stroking were unchanged after histamine, arguing against a role in alloknesis for these neurons. The authors conclude that such neurons are more likely to signal pain than itch. Similar findings were reported in the rat for neurons not identified by ascending projections (Carstens, E., 1997). Intradermal histamine produced an *N*-methyl-D-aspartic acid (NMDA) receptor-dependent expansion of lumbar neuronal receptive fields (Jinks, S. L. and Carstens, E., 1998) possibly reflecting central sensitization of pain rather than itch, as histamine may be algesic rather than pruritic in rats (see below; Jinks, S. L. and Carstens, E., 2002). Thus, the bulk of current evidence favors the concept of an itch-selective pathway, originating from mechanically insensitive, pruritogen-selective C-fiber afferents which project to lamina I spinothalamic tract neurons that, in turn, convey itch signals to the lateral thalamus and cortex (Figure 1(b)).

An alternative view is that spinal WDR neurons may also contribute to itch, much as they are thought to contribute to signaling pain together with nociceptive-specific neurons. Both pruritic (serotonin, histamine) and algesic chemicals (capsaicin, nicotine, formalin) excited neurons in overlapping regions of the superficial dorsal horn (laminae I–II) as assessed by c-fos (Jinks, S. L. *et al.*, 2002; Nojima, H. *et al.*, 2003b). The vast majority of single WDR neurons recorded in rat superficial dorsal horn responded to both pruritic and algesic chemical stimuli as well as

noxious heat (Jinks, S. L. and Carstens, E., 2000; 2002). Importantly, superficial dorsal horn neurons gave prolonged responses to serotonin that corresponded with the time course of serotonin-evoked scratching behavior in rats (Jinks, S. L. and Carstens, E., 2002) (Figure 4). The neuronal discharge rate during the response to serotonin was much lower compared to the phasic responses evoked by capsaicin and other algesic stimuli. Serotonin elicits dose-related scratching in rodents that was significantly reduced by opioid antagonists (Yamaguchi, T. *et al.*, 1999; Nojima, H. and Carstens, E., 2003a; Nojima, H. *et al.*, 2003b). Furthermore, c-fos expression in the superficial dorsal horn elicited by intradermal capsaicin, but not serotonin, was attenuated by morphine (Nojima, H. *et al.*, 2003b), consistent with serotonin being pruritic rather than algesic. If this is the case, then one must consider the possibility that pruriceptive information is being signaled by superficial WDR neurons, consistent with the frequency theory of itch.

In conclusion, exciting new information strongly favors the existence of an itch-selective pathway, but it would probably be wise not to completely discount the possible added contribution of nonselective neurons until more complete details about itch signaling have emerged. Future efforts to characterize itch-signaling neurons should test the following properties consistent with itch:

- Responses inhibited by scratching and other antipruritic counterstimuli.
- Responses facilitated by morphine (Jinks, S. L. and Carstens, E., 2000).
- Morphine facilitation blocked by κ-opioid antagonists.
- Responses inhibited by μ-opioid antagonists.
- Increased mechanical sensitivity consistent with alloknesis.

5.09.5 Alloknesis (Itchy Skin) and Sensitization

Intradermal injection of histamine elicits itch sensation, a wheal at the injection site, and a surrounding flare reaction due to histamine-evoked release of vasodilatory peptides (substance P (SP), calcitonin gene-related peptide). Light stroking in a broad area of normal skin surrounding the histamine injection can elicit itch, a phenomenon called itchy skin or alloknesis (Simone, D. A. *et al.*, 1991). The spread of alloknesis was prevented by local anesthesic block adjacent to the site of histamine injection, indicating that alloknesis is of neurogenic origin (Simone, D. A. *et al.*, 1991). Noxious punctuate stimulation in and around the region of alloknesis also elicits itch (hyperknesis) (Atanassoff, P. G. *et al.*, 1999).

The chronic itch of skin conditions such as atopic dermatitis suggests the possibility of peripheral or central sensitization along the itch-signaling pathway (Ikoma, A. *et al.*, 2004). Moreover, noxious stimuli such as acetylcholine, acid, heat, and pinprick, which normally evoke pain, instead elicit itch in atopic dermatitis patients (Vogelsang, M. *et al.*, 1995; Ikoma, A. *et al.*, 2004). A peripheral sensitization of

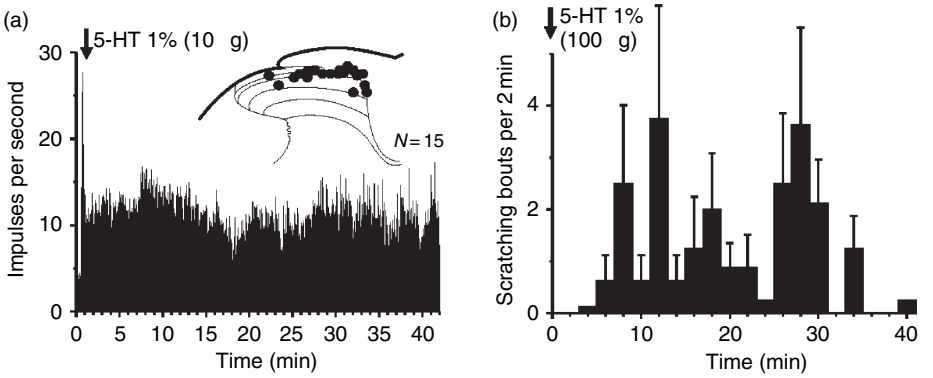

Figure 4 Prolonged responses of superficial dorsal horn neurons to 5-HT compared with scratching. (a) Averaged peristimulus–time histogram (PSTH, bin width: 1 s) of responses of superficial dorsal horn neurons to intradermal microinjection of 5-HT (60 mM; 1 μl) at arrow in pentobarbital-anesthetized rats. Inset shows recordings sites (dots) compiled on section through L5 dorsal horn. (b) Graph plots mean number of hindlimb scratching bouts (error bars: SEM) directed toward the site of injection of 5-HT in the nape of the neck in Sprague-Dawley rats. Scratching bouts were counted in 2 min intervals. Adapted from Jinks, S. L. and Carstens, E. 2002. Prolonged responses of superficial dorsal horn neurons to intracutaneous serotonin and other irritant chemicals: comparison with scratching behavior. J. Neurophysiol. 87, 1280–1289.

pruriceptors is suggested by microneurographic recordings from an atopic dermatitis patient, revealing a subset of mechanically insensitive C-fiber afferents that exhibited irregular patterns of spontaneous activity; two of these were activated by pruritic stimulation (Schmelz, M. *et al.*, 2003a). Since mechanically insensitive, histamine-responsive C-fibers normally do not exhibit any spontaneous activity (Schmelz, M. *et al.*, 1997), their increased firing in atopic dermatitis may represent sensitization that contributes to spontaneous itch. Central sensitization is also likely to contribute to pathological itch (Ikoma, A. *et al.*, 2004). Central sensitization of pain is mediated partly via excessive excitation of spinal neurons by nociceptors releasing glutamate and SP, which act at postsynaptic NMDA and neurokinin-1 receptors to initiate Ca^{2+}-dependent intracellular events resulting in enhanced neuronal excitability (Ji, R. R. *et al.*, 2003). Central sensitization is associated with hyperalgesia (increased pain), allodynia (pain from a normally nonpainful stimulus), and expansion of mechanosensitive receptive fields. It is conceivable that conditions associated with chronic itch may induce central sensitization of itch-signaling neurons via mechanisms similar to those for central sensitization of pain (Ikoma, A. *et al.*, 2004).

5.09.6 Central Representation of Itch

Using positron emission tomography (PET), histamine injection in the right upper arm differentially activated the contralateral anterior cingulate cortex, ipsilateral inferior parietal lobule, as well as bilateral supplementary and premotor cortical areas (Hsieh, J. C. *et al.*, 1994). Activation of the ipsilateral premotor cortical areas was suggested to represent an urge to scratch. A more recent PET study using histamine pin prick on the right arm reported dose-related activation in premotor and supplementary motor areas and anterior cingulate gyrus, as well as in contralateral primary (but not secondary) somatosensory and primary motor cortex, prefrontal cortex and contralateral insula, and prefrontal and superior temporal cortex (Drzezga, A. *et al.*, 2001). While there was some overlap in cortical areas activated by itch versus pain, there were notable differences, particularly in the activation of secondary somatosensory cortex and thalamus by pain but not itch (Drzezga, A. *et al.*, 2001). A third recent PET study also reported dose-related activation in many of the same cortical areas by iontophoretically applied histamine, but notably also in thalamus. Simultaneous application of a noxious cold (5 °C) stimulus reduced the degree of histamine-evoked cortical activation. Interestingly, coapplication of noxious cold and histamine revealed significant activation in midbrain periaqueductal gray (PAG). This suggests that in addition to the well-known role of the PAG in pain modulation, it may also play a role in modulation of itch (Carstens, E., 1997; Mochizuki, H. *et al.*, 2003). These studies indicate that noxious and pruritic stimuli activate overlapping as well as separate cortical and subcortical regions, lending partial support for separate central pathways mediating itch versus pain.

5.09.7 Animal Models of Itch

Scratching directed toward a site of pruritic stimulation in rodents is thought to reflect itch sensation (Berendsen, H. H. G. and Broekkamp, C. L. E., 1991; Kuraishi, Y. *et al.*, 1995). However, scratching is a normal grooming behavior and in some cases may reflect pain rather than itch (DeCastro-Costa, M. *et al.*, 1987). Moreover, hindlimb scratching is elicited by intrathecal injection of numerous agents including neurokinins, capsaicin, and morphine (Frenk, H. *et al.*, 1988; Wilcox, G. L., 1988; Ko, M. C. and Naughton, N. N., 2000), even in spinalized animals (Bossut, D. *et al.*, 1988) suggesting direct activation of motor scratch reflex circuits. Facial scratching is also elicited by intracerebroventricular and intramedullary injection of opiates (Königstein, H., 1948; Thomas, D. A. *et al.*, 1993; Thomas, D. A. and Hammond, D. L., 1995; Tohda, C. *et al.*, 1997b; Johnson, M. D. *et al.*, 1999; Kuraishi, Y. *et al.*, 2000) and other substances including adrenocorticotropic hormone (ACTH) and many neuropeptides (Share, N. N. and Rackham, A., 1981; Van Wimersma Greidanus, T. B., 1986; Van Wimersma Greidanus, T. B. *et al.*, 1987; Van Wimersma Greidanus, T. B. and Maigret, C., 1988; Van Wimersma Greidanus, T. B. *et al.*, 1988; Van Wimersma Greidanus, T. B. and Maigret, C., 1991; Johnson, M. D. *et al.*, 1999).

Despite the caveats noted above, there is good evidence that hindlimb scratching may distinguish between itch and pain. Substances that induce itch in humans, including SP (Hagermark, O. *et al.*, 1978), the mast cell degranulator compound 48/80 (Fjellner, B. and Hägermark, O., 1982), serotonin (5-HT; Weisshaar, E. *et al.*, 1997), and platelet activating factor (PAF, Fjellner, B. and Hägermark, O., 1985), elicit dose-related scratching in rodents (Berendsen, H. H. G and Broekkamp, C. L. E, 1991; Kuraishi, Y. *et al.*, 1995;

Woodward, D. F. *et al.*, 1995; Yamaguchi, T. *et al.*, 1999; Thomsen J. S. *et al.*, 2001; Jinks, S. L. and Carstens, E., 2002). In contrast, capsaicin and formalin, which induce burning pain, elicit little or no scratching (Kuraishi, Y. *et al.*, 1995; Yamaguchi, T. *et al.*, 1999; Jinks, S. L. and Carstens, E., 2002). One notable difference is histamine, which is the definitive pruritogen in humans (Simone, D. A. *et al.*, 1987; 1991; Hagermark, O., 1995) yet does not elicit scratching in several strains of mice (Kuraishi, Y. *et al.*, 1995; Yamaguchi, T. *et al.*, 1999; Inagaki, N. *et al.*, 2001) or Sprague-Dawley rats (Thomsen, J. S. *et al.*, 2001; Jinks, S. L. and Carstens, E., 2002). This might be explained by the much lower concentration of histamine in cutaneous mast cells of rodents (Gustafsson, B., 1980; Graziano, F. M., 1988; Purcell, W. M. *et al.*, 1989) in favor of 5-HT which induces scratching via the 5-HT_2 receptor (Yamaguchi, T. *et al.*, 1999; Nojima, H. and Carstens, E., 2003b). However, other rodent strains including the ICR mouse (Maekawa, T. *et al.*, 2000) and hairless guinea-pig (Woodward, D. F. *et al.*, 1995) exhibit dose-related scratching to histamine, indicating the existence of strain differences in the scratch-inducing potency of itch mediators.

Importantly, opiate antagonists significantly attenuated hindlimb scratching elicited by 5-HT (Yamaguchi, T. *et al.*, 1999; Nojima, H. and Carstens, E., 2003a; Nojima, H. *et al.*, 2003b) or SP (Andoh, T. *et al.*, 1998). This is consistent with the report that opiate antagonists reduce histamine-induced itch in humans (Heyer, G. *et al.*, 1997a) and further supports scratching as an itch-related response.

Additional animal models of acute itch include hindlimb scratching directed toward the eye in albino guinea-pigs (Woodward, D. F. *et al.*, 1995). In this model, histamine, 5-HT, PAF, and prostaglandin E_2 elicited significant, dose-related ocular scratching while even high concentrations of the algesic agents bradykinin, acetic acid, or saline did not. Another model is biting directed toward the site of 5-HT injected into the hind paw of mice (Hagiwara, K. *et al.*, 1999). 5-HT (60–100 nmol) elicited approximately equal numbers of licks and bites, but only biting was significantly attenuated by both naloxone and the 5-HT antagonist, methysergide. In contrast, formalin elicited hind paw licking but no biting. These results suggest that biting represents a means of noxious counterstimulation of the paw to relieve itch.

Animal models of acute allergic (e.g., Inagaki, N. *et al.*, 2000; Ohtsuka, E. *et al.*, 2001; Nojima, H. and Carstens, E., 2003b) and dry-skin itch (Miyamoto, T. *et al.*, 2002b; Nojima, H. *et al.*, 2003a; Nojima, H. *et al.*, 2004) have also been developed. One model that most people can relate to is mosquito-bite-induced itch. Initial exposure of ICR mice to mosquito bites did not result in scratching. However, twice-weekly exposure of the mice to mosquito bites resulted in a progressive increase in scratching. Naïve mice sensitized by injection of female mosquito salivary gland extract (the presumed antigen) exhibited marked scratching upon the first mosquito bite, indicating that it triggered an acute allergic reaction and associated itch (Ohtskua, E. *et al.*, 2001).

A potential model of chronic itch is the NC/jic mouse (Tohda, C. *et al.*, 1997a; Yamaguchi, T. *et al.*, 2001). Within 2–6 months after birth, a majority of these animals spontaneously develop skin lesions (eczema, bleeding, alopecia) associated with excessive scratching that is naloxone-sensitive. These animals did not develop skin lesions, scratching, or increased plasma immonoglobulin G levels when reared in a specific pathogen-free environment, but did so within 4 weeks after being transferred to a conventional environment. The NC/jic mouse may represent an animal model of itch associated with chronic dermatitis, affording the possibility to develop novel antipruritic treatment strategies for clinical cases of itch that are poorly treated by antihistamines.

5.09.8 Itch Mediators

Histamine is the most important mediator of normal human itch. It is localized in cutaneous mast cells along with a variety of other chemicals including serotonin, chymase, and tryptase. Intradermal histamine primarily elicits a dose-dependent sensation of itch (Melton, F. M. and Shelly, W. P., 1950; Keele, C. A. and Armstrong, D., 1964; Handwerker, H. O. *et al.* 1987; Simone, D. A. *et al.* 1987; 1991). Microdialysis of histamine in the skin elicited almost exclusively, itch sensation and strongly excited mechanically insensitive C-fibers that are considered to be pruriceptors as discussed earlier (Schmelz, M. *et al.*, 2003b). The itch sensation evoked by histamine and other pruritic chemicals (e.g., serotonin, SP, PAF, vasoactive intestinal polypeptide) is in nearly all cases prevented by pretreatment with H_1 receptor antagonists (Hagermark, O., 1992; Heyer, G. and Magerl, W., 1995), suggesting a common action via histamine released by mast cell degranulation. However, other mediators might act independently of histamine release to induce itch, as discussed further below.

More than 50 years ago, Arthur R. P. and Shelley W. B. (1955) reported the itch-inducing effects of proteases including mucunain (Shelley W. B. and Arthur, R. P., 1955), a peptidase extracted from spicules of the velvet bean plant, cowhage, which elicit itch upon contact with skin. The serine proteases trypsin and chymase and the cystein protease papain induce itch that may be independent of histamine (Rajka, G., 1969; Hagermark, O. *et al.*, 1972). Mast cell chymase elicited scratching in mice, and a chymase inhibitor reduced allergic scratching (Imada, T. *et al.*, 2002). An exciting new development is the discovery of the proteinase-activated receptor (PAR). One subtype, PAR-2, is targeted by trypsin and mast cell tryptase, is expressed in sensory neurons and other tissues (Steinhoff, M. and Roosterman, D., 2005) and may be involved in itch (Steinhoff, M. *et al.*, 2003). In particular, PAR-2 expression is increased fourfold in patients with atopic dermatitis, and these patients experience itch upon intralesional application of PAR-2 agonists that is histamine-independent (Steinhoff, M. *et al.*, 2003). Thus, PAR-2 represents a novel target for antipruritic drugs, particularly for conditions like atopic dermatitis in which the itch is refractory to antihistamines.

Serotonin (5-HT) delivered to the skin induces weak itch in humans (Hagermark, O., 1992; Weisshaar, E. *et al.*, 1997) and may be involved in the pruritus of polycythemia vera (Fjellner, B. and Hagermark, O., 1979; Fitzsimons, E. J. *et al.*, 1981) and cholestasis (Schworer, H. *et al.*, 1995; Weisshaar, E. *et al.*, 1999; Jones, E. A. and Bergasa, N. V., 2000). Intradermal microdialysis of 5-HT elicited weak-to-moderate itch in some subjects and pain in others, but excited mechanically insensitive, histamine-sensitive C-fiber pruriceptors (Schmelz, M. *et al.*, 2000b; 2003a) in support of a role as itch mediator. As noted earlier, 5-HT potently induces scratching in rodents via the 5-HT_2 receptor (Yamaguchi, T. *et al.*, 1999; Nojima, H. and Carstens, E., 2003b), whereas the 5-HT_3 receptor may be involved under certain chronic itch conditions in humans (Schworer, H. *et al.*, 1995; Weisshaar, E. *et al.*, 1999).

Intradermal injection (Hagermark, O. and Strandberg, K., 1977) or microdialysis (Neisius, U. *et al.*, 2002; Schmelz, M. *et al.*, 2003) of prostaglandin E_2 also elicited weak itch in some subjects and strongly excited histamine-sensitive C-fiber pruriceptors (Schmelz, M. *et al.*, 2003).

Acetylcholine normally elicits pain, but instead induced itch in patients with atopic dermatitis (Heyer, G. *et al.*, 1997b). Intradermal microdialysis of acetylcholine induced itch in some subjects but more frequently pain, and excited most histamine-sensitive C-fiber pruriceptors tested (Schmelz, M. *et al.*, 2003). Cholinergic agonists elicited dose-related scratching in mice that was reduced by opiate and muscarinic M3 receptor antagonists; nicotine did not elicit scratching (Miyamoto,T. *et al.*, 2002).

Intradermal injection of the neuropeptide SP elicits itch (Hagermark, O. *et al.*, 1978; Thomsen, D. A. *et al.*, 2002) via mast cell degranulation (Hagermark, O. *et al.*, 1978). However, a recent study reported no itch or pain sensations with up to 10^{-5} M SP delivered by intradermal microdialysis, and concluded that physiological levels of SP are insufficient to induce mast cell degranulation (Weidner, C. *et al.*, 2000). In rodents, SP elicited dose-dependent scratching that was reduced by opiate and neurokinin-1 antagonists, and was at least partly independent of mast cell degranulation (Andoh, T. *et al.*, 1998).

A variety of other mediators may also have some role in itch. PAF elicits histamine-dependent itch in humans (Fjellner, B. and Hagermark, O., 1985), and scratching behavior in guinea-pigs, which, however, was reduced by PAF antagonists but not by histamine H1 antagonists (Woodward, D. F. *et al.*, 1995). Leukotriene B_4 (LTB_4) elicited scratching in mice that was attenuated by an LTB_4 antagonist (Andoh, T. and Kuraishi, Y., 1998). LTB_4 also plays a role in scratching elicited by intradermal injection of SP (Andoh, T. *et al.*, 2001) and nociceptin (Andoh, T. *et al.*, 2004). Endothelin delivered by intradermal microdialysis or injection induced short-lasting burning itch accompanied by release of histamine and nitric oxide (Wenzel, R. R *et al.*, 1998; Katugampola, R. *et al.*, 2000). Interleukin-2 (IL-2), but not tumor necrosis factor-alpha, given intradermally induced weak itch (Wahlgren, C. F. *et al.*, 1995; Darsow, U. *et al.*, 1997) and there is indirect evidence that IL-4 and IL-6 may also have some role in pathological itch (Nordlind, K. *et al.*, 1996; Chan, L. S. *et al.*, 2001).

The preceding list is by no means comprehensive, but certainly we have now at least scratched the surface in terms of identifying peripheral mediators, receptors, and neural pathways involved in signaling the enigmatic sensory quality of itch.

Acknowledgments

The author's work has been supported by research grants from the NIH (#DE13685) and the State of California Tobacco-Related Disease Research Program (#11RT-0053).

References

Andoh, T. and Kuraishi, Y. 1998. Intradermal leukotriene B_4, but not prostaglandin E_2, induces itch-associated responses in mice. Eur. J. Pharmacol. 353, 93–96.

Andoh, T., Katsube, N., Maruyama, M., and Kuraishi, Y. 2001. Involvement of leukotriene B4 in substance P-induced itch-associated response in mice. J. Invest. Dermatol. 117, 1621–1626.

Andoh, T., Nagasawa, T., Satoh, M., and Kuraishi, Y. 1998. Substance P induction of itch-associated response mediated by cutaneous NK1 tachykinin receptors in mice. J. Pharmacol. Exp. Ther. 286, 1140–1145.

Andoh, T., Yageta, Y., Takeshima, H., and Kuraishi, Y. 2004. Intradermal nociceptin elicits itch-associated responses through leukotriene B(4) in mice. J. Invest. Dermatol. 123, 196–201.

Andrew, D. and Craig, A. D. 2001. Spinothalamic lamina I neurons selectively sensitive to histamine: a central neural pathway for itch. Nat. Neurosci. 4, 72–76.

Arthur, R. P. and Shelley, W. B. 1955. The role of proteolytic enzymes in the production of pruritus in man. J. Invest. Dermatol. 25, 341–346.

Atanassoff, P. G., Brull, S. J., Zhang, J., Greenquist, K., Silverman, D. G., and LaMotte, R. H. 1999. Enhancement of experimental pruritus and mechanically evoked dysesthesiae with local anesthesia. Somatosens. Motor Res. 16, 291–298.

Ballantyne, J. C., Loach, A. B., and Carr, D. B. 1988. Itching after epidual and spinal opiates. Pain 33, 149–160.

Berendsen, H. H. G. and Broekkamp, C. L. E. 1991. A peripheral 5-HT_{1D}-like receptor involved in serotonergic induced hindlimb scratching in rats. Eur. J. Pharmacol. 194, 201–208.

Bergasa, N. V., Mehlman, J. K., and Jones, E. A. 2000. Pruritus and fatigue in primary biliary cirrhosis. Bailliere's Best Pract. Res. Clin. Gastroenterol. 14, 643–655.

Bickford, R. G. 1937. Experiments relating to the itch sensation, its peripheral mechanism and central pathway. Clin. Sci. 3, 377–386.

Biro, T., Ko, M. C., Bromm, B., Wei, E. T., Bigliardi, P., Siebenhaar, F., Hashizume, H., Misery, L., Bergasa, N. V., Kamei, C., Schouenborg, J., Roostermann, D., Szabo, T., Maurer, M., Bigliardi-Qi, M., Meingassner, J. G., Hossen, M. A., Schmelz, M., and Steinhoff, M. 2005. How best to fight that nasty itch – from new insights into the neuroimmunological, neuroendocrine, and neurophysiological bases of pruritus to novel therapeutic approaches. Exp. Dermatol. 14, 225–240.

Bossut, D., Frenk, H., and Mayer, D. J. 1988. Is substance P a primary afferent neurotransmitter for nociceptive input? II. Spinalization does not reduce and intrathecal morphine potentiates behavioral responses to substance P. Brain Res. 445, 232–239.

Broadbent, J. L. 1955. Observations on histamine-induced pruritis and pain. Br. J. Pharmacol. 10, 183–185.

Bromage, P. 1981. The price of intraspinal narcotic analgesia: basic constraints. Anesth. Analg. 60, 461–463.

Bromage, P. R., Camporesi, E. M., Durant, P. A., and Nielsen, C. H. 1982. Nonrespiratory side effects of epidural morphine. Anesth. Analg. 61, 490–495.

Carstens, E. 1997. Responses of rat spinal dorsal horn neurons to intracutaneous microinjection of histamine, capsaicin, and other irritants. J. Neurophysiol. 77, 2499–2514.

Chan, L. S., Robinson, N., and Xu, L. 2001. Expression of interleukin-4 in the epidermis of transgenic mice results in a pruritic inflammatory skin disease: an experimental animal model to study atopic dermatitis. J. Invest. Dermatol. 117, 977–983.

Darsow, U., Scharein, E., Bromm, B., and Ring, J. 1997. Skin testing of the pruritogenic activity of histamine and cytokines (interleukin-2 and tumour necrosis factor-alpha) at the dermal–epidermal junction. Br. J. Dermatol. 137, 415–417.

DeCastro-Costa, M., Gybels, J., Kupers, R., and Van Hees, J. 1987. Scratching behaviour in arthritic rats: a sign of chronic pain or itch? Pain 29, 123–131.

Dey, D. D., Landrum, O., and Oaklander, A. L. 2005. Central neuropathic itch from spinal-cord cavernous hemangioma: a human case, a possible animal model, and hypotheses about pathogenesis. Pain 113, 233–237.

Drzezga, A., Darsow, U., Treede, R. D., Siebner, H., Frisch, M., Munz, F., Weilke, F., Ring, J., Schwaiger, M., and Bartenstein, P. 2001. Central activation by histamine-induced itch: analogies to pain processing: a correlational analysis of O-15 H_2O positron emission tomography studies. Pain 92, 295–305.

Fitzsimons, E. J., Dagg, J. H., and McAllister, E. J. 1981. Pruritus of polycythaemia vera: a place for pizotifen? Br. Med. J. 283, 277.

Fjellner, B. and Hagermark, O. 1979. Pruritus in polycythemia vera: treatment with aspirin and possibility of platelet involvement. Acta Derm. Venereol. 59, 505–512.

Fjellner, B. and Hägermark, O. 1982. Influence of ultraviolet light on itch and flare reactions in human skin induced by histamine and the histamine liberator compound 48/80. Acta Derm. Venereol. 62, 137–140.

Fjellner, B. and Hägermark, O. 1985. Experimental pruritus evoked by platelet activating factor (PAF-acether) in human skin. Acta Derm. Venereol. 65, 409–412.

Frenk, H., Bossut, D., Urca, G., and Mayer, D. J. 1988. Is substance P a primary afferent neurotransmitter for nociceptive input? I. Analysis of pain-related behaviors resulting from intrathecal administration of substance P and 6 excitatory compounds. Brain Res. 455, 223–231.

Frustorfer, H, Hermanns, M., and Latzke, L. 1986. The effects of thermal stimulation on clinical and experimental itch. Pain 24, 259–269.

Gammon, G. D. and Starr, I. 1941. Studies on the relief of pain by counterirritation. J. Clin. Invest. 20, 13–20.

Graziano, F. M. 1988. Mast cells and mast cell products. Methods Enzymol. 162, 501–522.

Gustafsson, B. 1980. Cytofluorometric analysis of anaphylactic secretion of 5-hydroxytryptamine and heparin from rat mast cells. Int. Arch Allergy Appl. Immunol. 63, 121–128.

Hagermark, O. 1992. Peripheral and central mediators of itch. Skin Pharmacol. 5, 1–8.

Hägermark, O. 1995. Itch mediators. Sem. Dermatol. 14, 271–276.

Hagermark, O. and Strandberg, K. 1977. Pruritogenic activity of prostaglandin E2. Acta Derm. Venereol. 57, 37–43.

Hagermark, O., Hokfelt, T., and Pernow, B. 1978. Flare and itch induced by substance P in human skin. J. Invest. Dermatol. 71, 233–235.

Hagermark, O., Rajka, G., and Bergvist, U. 1972. Experimental itch in human skin elicited by rat mast cell chymase. Acta Derm. Venereol. 152, 25–128.

Hagiwara, K, Nojima, H., and Kuraishi, Y. 1999. Serotonin-induced biting of the hind paw is itch-related response in mice. Pain Res. 14, 53–59.

Handwerker, H. O., Forster, C., and Kirchoff, C. 1991. Discharge patterns of human C-fibers induced by itching and burning stimuli. J. Neurophysiol. 66, 307–315.

Handwerker, H. O., Magerl, W., Klemm, F., Land, E., and Westerman, R. A. 1987. Quantitative Evaluation of Itch Sensation. In: Fine Afferent Nerve Fibers and Pain (*eds*. R. F. Schmidt, H.-G. Schaible, and C. Vahle-Hinz), pp. 462–473. VCH.

Heyer, G. and Magerl, W. 1995. Skin Reactions and Sensations Induced by Intradermal Injection of Substance P into

Compound 48/80 Pretreated Skin. In: Wound Healing and Skin Physiology (*ed*. M. Altmeyer), pp. 335–344. Springer.
Heyer, G., Dotzer, M., Diepgen, T. L., and Handwerker, H. O. 1997a. Opiate and H1 antagonist effects on histamine induced pruritus and alloknesis. Pain 73, 239–243.
Heyer, G., Vogelgsang, M., and Hornstein, O. P. 1997b. Acetylcholine is an inducer of itching in patients with atopic eczema. J. Dermatol. 24, 621–625.
Hsieh, J. C., Hagermark, O., Stahle-Backdahl, M., Ericson, K., Eriksson, L., Stone-Elander, S., and Ingvar, M. 1994. Urge to scratch represented in the human cerebral cortex during itch. J. Neurophysiol. 72, 3004–3008.
Ikoma, A., Fartasch, M., Heyer, G., Miyachi, Y., Handwerker, H., and Schmelz, M. 2004. Painful stimuli evoke itch in patients with chronic pruritus: central sensitization for itch. Neurology 62, 212–217.
Ikoma, A., Handwerker, H., Miyachi, Y., and Schmelz, M. 2005. Electrically evoked itch in humans. Pain 113, 148–154.
Imada, T., Komorita, N., Kobayashi, F., Naito, K., Yoshikawa, T., Miyazaki, M., Nakamura, N., and Kondo, T. 2002. Therapeutic potential of a specific chymase inhibitor in atopic dermatitis. Jpn. J. Pharmacol. 90, 214–217.
Inagaki, N., Nagao, M., Igeta, K., Kawasaki, H., Kim, J. F., and Nagai, H. 2001. Scratching behavior in various strains of mice. Skin Pharmacol. Appl. Skin Physiol. 14, 87–96.
Inagaki, N., Nakamura, N., Nagao, M., Kawasaki, H., and Nagai, H. 2000. Inhibition of passive cutaneous anaphylaxis-associated scratching behavior by mu-opioid receptor antagonists in ICR mice. Int. Arch. Allergy Immunol. 123(4), 365–368.
Ji, R. R., Kohno, T., Moore, K. A., and Woolf, C. J. 2003. Central sensitization and LTP: do pain and memory share similar mechanisms? Trends Neurosci. 26, 696–705.
Jinks, S. L. and Carstens, E. 1998. Spinal NMDA receptor involvement in expansion of dorsal horn neuronal receptive field area produced by intracutaneous histamine. J. Neurophysiol. 79, 1613–1618.
Jinks, S. L. and Carstens, E. 2000. Superficial dorsal horn neurons identified by intracutaneous histamine: chemonociceptive responses and modulation by morphine. J. Neurophysiol. 84, 616–627.
Jinks, S. L. and Carstens, E. 2002. Prolonged responses of superficial dorsal horn neurons to intracutaneous serotonin and other irritant chemicals: comparison with scratching behavior. J. Neurophysiol. 87, 1280–1289.
Jinks, S. L., Simons, C. T., Dessirier, J. M., Carstens, M. I., Antognini, J. F., and Carstens, E. 2002. C-fos induction in rat superficial dorsal horn following cutaneous application of noxious chemical or mechanical stimuli. Exp. Brain Res. 145, 261–269.
Johnson, M. D., Ko, M., Choo, K. S., Traynor, J. R., Mosberg, H. I., Naughton, N. N., and Woods, J. H. 1999. The effects of the phyllolitorin analogue [desTrp(3), Leu(8)]phyllolitorin on scratching induced by bombesin and related peptides in rats. Brain Res. 839, 194–198.
Jones, E. A. and Bergasa, N. V. 2000. Evolving concepts of the pathogenesis and treatment of the pruritus of cholestasis. Can. J. Gastroenterol. 14, 33–40.
Katugampola, R., Church, M. K., and Clough, G. F. 2000. The neurogenic vasodilator response to endothelin-1: a study in human skin *in vivo*. Exp. Physiol. 85, 839–844.
Keele, C. A. and Armstrong, D. 1964. Substances Producing Pain and Itch. Williams and Wilkins.
Ko, M. C. and Naughton, N. N. 2000. An experimental itch model in monkeys: characterization of intrathecal morphine-induced scratching and antinociception. Anesthesiology 92, 795–805.
Ko, M. C., Lee, H., Song, M. S., Sobczyk-Kojiro, K., Mosberg, H. I., Kishioka, S., Woods, J. H., and Naughton, N. N. 2003. Activation of kappa-opioid receptors inhibits pruritus evoked by subcutaneous or intrathecal administration of morphine in monkeys. J. Pharmacol. Exp. Ther. 305, 173–179.
Koltzenburg, M., Handwerker, H. O., and Torebjörk, H. E. 1993. The ability of humans to localise noxious stimuli. Neurosci. Lett. 150, 219–222.
Königstein, H. 1948. Experimental study of itch stimuli in animals. Arch. Derm. Syphilol. 57, 829–849.
Krajnik, M. and Zbigniew, Z. 2001. Understanding pruritis in systemic disease. J. Pain Symptom Manage. 21, 151–168.
Kuraishi, Y., Nagasawa, T., Hayashi, K., and Satoh, M. 1995. Scratching behavior induced by pruritogenic but not algesiogenic agents in mice. Eur. J. Pharmacol. 275, 229–233.
Kuraishi, Y., Yamaguchi, T., and Miyamoto, T. 2000. Itch-scratch responses induced by opioids through central mu opioid receptors in mice. J. Biomed. Sci. 7, 248–252.
Maekawa, T., Nojima, H., and Kurahishi, Y. 2000. Itch-associated responses of afferent nerve innervating the murine skin: different effects of histamine and serotonin in ICR and ddY mice. Jpn. J. Pharmacol. 84, 462–466.
Melton, F. M. and Shelly, W. P. 1950. The effect of topical antipruritic therapy on experimentally induced pruritis in man. J. Invest. Dermatol. 15, 325–332.
Miyamoto, T., Nojima, H., and Kuraishi, Y. 2002a. Cholinergic agonists induce itch-associated response via M3 muscarinic acetylcholine receptors in mice. Jpn. J. Pharmacol. 88, 351–354.
Miyamoto, T., Nojima, H., Shinkado, T., Nakahashi, T., and Kuraishi, Y. 2002b. Itch-associated response induced by experimental dry skin in mice. Jpn. J. Pharmacol. 88, 285–292.
Mochizuki, H., Tashiro, M., Kano, M., Sakurada, Y., Itoh, M., and Yanai, K. 2003. Imaging of central itch modulation in the human brain using positron emission tomography. Pain 105, 339–346.
Morgan, M. 1987. Epidural and intrathecal opioids. Anaesth. Intensive Care 15, 60–67.
Murphy, M. and Carmichael, A. J. 2000. Renal itch. Clin. Exp. Dermatol. 25, 103–106.
Murray, F. S. and Weaver, M. M. 1975. Effects of ipsilateral and contralateral counterirritation on experimentally induced itch in human beings. J. Comp. Physiol. Psychol. 89, 819–826.
Neisius, U., Olsson, R., Rukwied, R., Lischetzki, G., and Schmelz, M. 2002. Prostaglandin E2 induces vasodilation and pruritus, but no protein extravasation in atopic dermatitis and controls. J. Am. Acad. Dermatol. 47, 28–32.
Nilsson, H. J., Levinsson, A., and Schouenborg, J. 1997. Cutaneous field stimulation (CFS): a new powerful method to combat itch. Pain 71, 49–55.
Nojima, H. and Carstens, E. 2003a. Quantitative assessment of directed hind limb scratching behavior as a rodent itch model. J. Neurosci. Methods 126, 137–143.
Nojima, H. and Carstens, E. 2003b. Serotonin 5-HT_2 receptor involvement in acute 5-HT-evoked scratching but not in allergic pruritus induced by dinitrofluorobenzene in rats. J. Pharmacol. Exp. Ther. 306, 245–252.
Nojima, H., Cuellar, J. M., Simons, C. T., Iodi Carstens, M., and Carstens, E. 2004. Spinal *c-fos* expression associated with spontaneous biting in a mouse model of dry skin pruritus. Neurosci. Lett. 361, 79–82.
Nojima, H., Iodi Carstens, M., and Carstens, E. 2003a. *c-fos* expression in superficial dorsal horn of cervical spinal cord associated with spontaneous scratching in rats with dry skin. Neurosci. Lett. 347, 62–64.
Nojima, H., Simons, C. T., Cuellar, J. M., Carstens, M. I., Moore, J. A., and Carstens, E. 2003b. Opioid modulation of

scratching and spinal c-fos expression evoked by intradermal serotonin. J. Neurosci. 23, 10784–10790.
Nordlind, K., Chin, L. B., Ahmed, A. A., Brakenhoff, J., Theodorsson, E., and Liden, S. 1996. Immunohistochemical localization of interleukin-6-like immunoreactivity to peripheral nerve-like structures in normal and inflamed human skin. Arch. Dermatol. Res. 288, 431–435.
Ochoa, J. and Torebjork, E. 1989. Sensations evoked by intraneural microstimulation of C nociceptor fibres in human skin nerves. J. Physiol. Lond. 415, 583–599.
Ohtsuka, E., Kawai, S., Ichikawa, T., Nojima, H., Kitagawa, K., Shirai, Y., Kamimura, K., and Kuraishi, Y. 2001. Roles of mast cells and histamine in mosquito bite-induced allergic itch-associated responses in mice. Jpn. J. Pharmacol. 86, 97–105.
Purcell, W. M., Cohen, D. L., and Hanahoe, T. H. 1989. Comparison of histamine and 5-hydroxytryptamine content and secretion in rat mast cells isolated from different anatomical locations. Int. Arch. Allergy Applied Immunol. 90, 382–386.
Rajka, G. 1969. Latency and duration of pruritus elicited by trypsin in aged patients with itching eczema and psoriasis. Acta. Derm. Venereol. 49, 401–403.
Schmelz, M., Hilliges, M., Schmidt, R., Orstavik, K., Vahlquist, C., Weidner, C., Handwerker, H. O., and Torebjork, H. E. 2003a. Active ''itch fibers'' in chronic pruritus. Neurology 61, 564–566.
Schmelz, M., Schmidt, R., Bickel, A., Forster, C., Handwerker, H. O., and Torebjork, H. E. 1997. Specific C-receptors for itch in human skin. J. Neurosci. 17, 8003–8008.
Schmelz, M., Schmidt, R., Weidner, C., Hilliges, M., Torebjork, H. E., and Handwerker, H. O. 2003b. Chemical response pattern of different classes of C-nociceptors to pruritogens and algogens. J. Neurophysiol. 89, 2441–2448.
Schmidt, R., Torebjork, E., and Jorum, E. 1993. Pain and itch from intraneural microstimulation. *Abstracts of the 7th World Congress on Pain*, Paris, 143.
Schworer, H., Hartmann, H., and Ranadori, G. 1995. Relief of cholestatic pruritus by a novel class of drugs: 5-hydroxytryptamine type 3 (5-HT_3) receptor antagonists: effectiveness of ondansetron. Pain 61, 33–37.
Share, N. N. and Rackham, A. 1981. Intracerebral substance P in mice: behavioral effects and narcotic agents. Brain Res. 211, 379–386.
Shelley, W. B. and Arthur, R. P. 1955. Mucunain, the active pruritogenic proteinase of cowhage. Science 122, 469–470.
Simone, D. A., Alreja, M., and LaMotte, R. H. 1991. Psychophysical studies of the itch sensation and itchy skin (''alloknesis'') produced by intracutaneous injection of histamine. Somatosens. Motor Res. 8, 271–279.
Simone, D. A., Nigeow, J. Y. F., Whitehouse, J., Becerra-Cabal, L., Putterman, G. J., and LaMotte, R. H. 1987. The magnitude and duration of itch produced by intracutaneous injections of histamine. Somatosens. Res. 5, 81–92.
Simone, D. A., Zhang, X., Li, J., Zhang, J. M., Honda, C. N., LaMotte, R. H., and Giesler, G. J., Jr. 2004. Comparison of responses of primate spinothalamic tract neurons to pruritic and algogenic stimuli. J. Neurophysiol. 91(1), 213–222.
Stander, S., Steinhoff, M., Schmelz, M., Weisshaar, E., Metze, D., and Luger, T. 2003. Neurophysiology of pruritus: cutaneous elicitation of itch. Arch. Dermatol. 139, 1463–1470.
Steinhoff, M. and Roosterman, D. 2005. Viewpoint 5. Exp. Dermatol. 14, 231–233.
Steinhoff, M., Neisius, U., Ikoma, A., Fartasch, M., Heyer, G., Skov, P. S., Luger, T. A., and Schmelz, M. 2003. Proteinase-activated receptor-2 mediates itch: a novel pathway for pruritus in human skin. J. Neurosci. 23, 6176–6180.
Thomas, D. A. and Hammond, D. L. 1995. Microinjection of morphine into the rat medullary dorsal horn produces a dose-dependent increase in facial scratching. Brain Res. 695, 267–270.
Thomas, D. A., Williams, G. M., Iwata, K., Kenshalo, D. R., Jr., and Dubner, R. 1993. The medullary dorsal horn. A site of action of morphine in producing facial scratching in monkeys. Anesthesiology 9, 548–554.
Thomsen, J. S., Petersen, M. B., Benfeldt, E., Jensen, S. B., and Serup, J. 2001. Scratch induction in the rat by intradermal serotonin: a model for pruritus. Acta Derm. Venereol. 81, 250–254.
Thomsen, J. S., Sonne, M., Benfeldt, E., Jensen, S. B., Serup, J., and Menne, T. 2002. Experimental itch in sodium lauryl sulphate-inflamed and normal skin in humans: a randomized, double-blind, placebo-controlled study of histamine and other inducers of itch. Br. J. Dermatol. 146, 792–800.
Togashi, Y., Umeuchi, H., Okano, K., Ando, N., Yoshizawa, Y., Honda, T., Kawamura, K., Endoh, T., Utsumi, J., Kamei, J., Tanaka, T., and Nagase, H. 2002. Antipruritic activity of the kappa-opioid receptor agonist, TRK-820. Eur. J. Pharmacol. 435, 259–264.
Tohda, C., Yamaguchi, T., and Kuraishi, Y. 1997a. Increased expression of mRNA for myocyte-specific enhancer binding factor (MEF) 2C in the cerebral cortex of the itching mouse. Neurosci. Res. 29, 209–215.
Tohda, C., Yamaguchi, T., and Kuraishi, Y. 1997b. Intracisternal injection of opioids induces itch-associated response through mu-opioid receptors in mice. Jpn. J. Pharmacol. 74, 77–82.
Tuckett, R. P. 1982. Itch evoked by electrical stimulation of the skin. J. Invest. Dermatol. 79, 368–373.
Twycross, R., Greaves, M. W., Handwerker, H., Jones, E. A., Libretto, S. E., Szepietowski, J. C., and Zylicz, Z. 2003. Itch: scratching more than the surface. QJM 96, 7–26.
Umeuchi, H., Togashi, Y., Honda, T., Nakao, K., Okano, K., Tanaka, T., and Nagase, H. 2003. Involvement of central mu-opioid system in the scratching behavior in mice, and the suppression of it by the activation of kappa-opioid system. Eur. J. Pharmacol. 477, 29–35.
Van Wimersma Greidanus, T. B. 1986. Effects of naloxone and neurotensin on excessive grooming behavior of rats induced by bombesin, beta-endorphin and ACTH. NIDA Res Monogr. 75, 477–480.
Van Wimersma Greidanus, T. B. and Maigret, C. 1988. Grooming behavior induced by substance P. Eur. J. Pharmacol. 154, 217–220.
Van Wimersma Greidanus, T. B. and Maigret, C. 1991. Neuromedin-induced excessive grooming/scratching behavior is suppressed by naloxone, neurotensin and a dopamine D1 receptor antagonist. Eur. J. Pharmacol. 209, 57–61.
Van Wimersma Greidanus, T. B., Maigret, C., and Krechting, B. 1987. Excessive grooming induced by somatostatin or its analog SMS 201-995. Eur. J. Pharmacol. 144, 277–285.
Van Wimersma Greidanus, T. B., Maigret, C., Rinkel, G. J., Metzger, P., Panis, M., Van Zinnicq Bergmann, F. E., Poelman, J., and Colbern, D. L. 1988. Some characteristics of TRH-induced grooming behavior in rats. Peptides 9, 283–288.
Vogelsang, M., Heyer, G., and Hornstein, O. P. 1995. Acetylcholine induces different cutaneous sensations in atopic and non-atopic subjects. Acta Derm. Venereol. 75, 434–436.
Von Frey, M. 1922. Zur Physiologie der Juckempfindung. Arch. Neerland. Physol. 7, 142–145.
Ward, L, Wright, E., and McMahon, S. B. 1996. A comparison of the effects of noxious and non-noxious counterstimuli on experimentally induced itch and pain. Pain 64, 129–138.

Wahlgren, C. F. and Ekblom, A. 1996. Two-point discrimination of itch in patients with atopic dermatitis and healthy subjects. Acta Derm. Venereol. 76, 48–51.

Wahlgren, C. F, Tengvall Linder, M., Hagermark, O., and Scheynius, A. 1995. Itch and inflammation induced by intradermally injected interleukin-2 in atopic dermatitis patients and healthy subjects. Arch. Dermatol. Res. 287, 572–580.

Wei, J. Y. and Tuckett, R. P. 1991. Response of cat ventrolateral spinal axons to an itch-producing stimulus (cowhage). Somatosens Mot. Res. 8, 227–239.

Weidner, C., Klede, M., Rukwied, R., Lischetzki, G., Neisius, U., Skov, P. S., Petersen, L. J., and Schmelz, M. 2000. Acute effects of substance P and calcitonin gene-related peptide in human skin – a microdialysis study. J. Invest. Dermatol. 115, 1015–1020.

Weisshaar, E., Ziethen, B., and Gollnick, H. 1997. Can a serotonin type 3 (5-HT3) receptor antagonist reduce experimentally-induced itch? Inflamm. Res. 46, 412–416.

Weisshaar, E., Ziethen, B., Rohl, F. W., and Gollnick, H. 1999. The antipruritic effect of a 5-HT_3 receptor antagonist (tropisetron) is dependent on mast cell depletion: an experimental study. Exp. Dermatol. 8, 254–260.

Wenzel, R. R., Zbinden, S., Noll, G., Meier, B., and Luscher, T. F. 1998. Endothelin-1 induces vasodilation in human skin by nociceptor fibres and release of nitric oxide. Br. J. Clin. Pharmacol. 45, 441–446.

White, J. C. and Sweet, W. H. 1969. Pain and the Neurosurgeon: A Forty Year Experience. Thomas.

Wilcox, G. L. 1988. Pharmacological studies of grooming and scratching behavior elicited by spinal substance P and excitatory amino acids. Ann. N. Y. Acad. Sci. 525, 228–236.

Woodward, D. F., Nieves, A. L., Spada, C. S., Williams, L. S., and Tuckett, R. P. 1995. Characterization of a behavioral model for peripherally evoked itch suggests platelet-activating factor as a potent pruritogen. J. Pharmacol. Exp. Ther. 272, 758–765.

Yamaguchi, T., Maekawa, T., Nishikawa, Y., Nojima, H., Kaneko, M., Kawakita, T., Miyamoto, T., and Kuraishi, Y. 2001. Characterization of itch-associated responses of NC mice with mite-induced chronic dermatitis. J. Dermatol. Sci. 25, 20–28.

Yamaguchi, T., Nagasawa, T., Satoh, M., and Kuraishi, Y. 1999. Itch-associated response induced by intradermal serotonin through 5-HT_2 receptors in mice. Neurosci. Res. 35, 77–83.

Yosipovitch, G., Greaves, M. W., Fleischer, A. B., and McGlone, F. 2004. Itch: Basic Mechanisms and Therapy. Marcel Dekker.

Yosipovitch, G., Greaves, M. W., and Schmelz, M. 2003. Itch. Lancet 361, 690–694.

5.10 Thermal Sensation (Cold and Heat) through Thermosensitive TRP Channel Activation

Makoto Tominaga, National Institutes of Natural Sciences, Okazaki, Japan

© 2008 Elsevier Inc. All rights reserved.

5.10.1	**Introduction**	127
5.10.2	**Heat Receptors**	127
5.10.2.1	TRPV1 (VR1)	127
5.10.2.1.1	Cloning of TRPV1 and its characterization	127
5.10.2.1.2	Reduction of temperature threshold for TRPV1 activation: A mechanism for inflammatory pain	128
5.10.2.2	TRPV2 (VRL-1)	129
5.10.2.3	TRPV3 and TRPV4	129
5.10.3	**Cold Receptors**	129
5.10.3.1	TRPM8	129
5.10.3.2	TRPA1	130
5.10.4	**Thermonociception by Non-TRP Proteins**	130
5.10.5	**Conclusion**	130
References		131

5.10.1 Introduction

We feel a wide range of temperatures spanning from cold to heat. Within this range, temperatures over about 43 °C and below about 15 °C evoke not only a thermal sensation, but also a feeling of pain. The neurons that allow us to sense temperatures are located in the dorsal root ganglia (DRG) and within cranial nerve ganglia such as trigeminal ganglion (TG). It has been hypothesized that cutaneous nociceptor endings detect temperature and other physical stimuli by means of ion channels responsive to these stimuli. Insight into the molecular nature of the temperature-activated channels came with the cloning of the capsaicin receptor, TRPV1 (Caterina, M. J. *et al.*, 1997). TRPV1 is a member of the TRP (transient receptor potential) superfamily of ion channels, whose prototypical member, TRP, was found to be deficient in a *Drosophila* mutant exhibiting abnormal responsiveness to continuous light (Montell, C., 2005). Three other TRPV channels, TRPV2, TRPV3, and TRPV4, have been cloned and characterized as heat thermosensors (Jordt, S. E. *et al.*, 2003; Patapoutian, A. *et al.*, 2003). The threshold temperatures for activation of these channels range from relatively warm (TRPV3 and TRPV4) to extremely hot (TRPV2). In contrast to the four thermosensitive TRPV channels, two other TRP channels, TRPM8 and TRPA1, have been found to be activated by cold stimuli (Jordt, S. E. *et al.*, 2003; Patapoutian, A. *et al.*, 2003). Between the two channels, TRPA1 is perhaps more likely to be involved in nociception because the temperature threshold for its activation is about 17 °C, close to the reported threshold for cold nociceptors.

5.10.2 Heat Receptors

5.10.2.1 TRPV1 (VR1)

5.10.2.1.1 Cloning of TRPV1 and its characterization

One characteristic shared by many nociceptive neurons is sensitivity to capsaicin, the main pungent ingredient of hot chili peppers (Szallasi, A. and Blumberg, P. M., 1999). A capsaicin receptor was isolated in 1997 and designated vanilloid receptor subtype 1 (VR1) (Caterina, M. J. *et al.*, 1997), and now it is called TRPV1 in TRPV subfamily of a large TRP ion channel superfamily (Figure 1). Patch-clamp recordings (Caterina, M. J. *et al.*, 1997; Tominaga, M. *et al.*, 1998) revealed that TRPV1 is a nonselective cation channel with high Ca^{2+} permeability and that TRPV1 can be activated not only by capsaicin but also by protons and heat over 43 °C, all of which are known to cause pain *in vivo*. Single channel openings of TRPV1 by any of the three

(a)

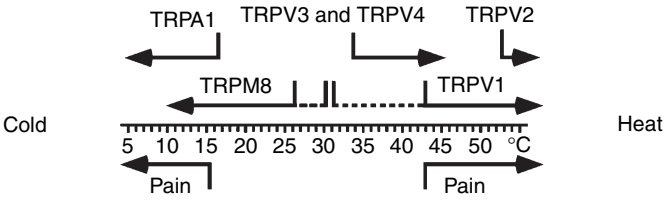

(b)

Receptor	Temperature threshold for activation	Expression	Other effective stimuli
TRPV1	>43 °C	Sensory neurons brain/ skin?	Capsaicin/ proton lipids 2-Aminoethoxydiphenyl borate (2APB)
TRPV2	>52 °C	Sensory neurons/ brain/ spinal cord/ lung/ liver/ spleen/ colon	Mechanical stimulus 2-Aminoethoxydiphenyl borate (2APB)
TRPV3	>32–39 °C	Sensory neurons/ brain/ spinal cord/ skin/ stomach/ colon	2-Aminoethoxydiphenyl borate (2APB) camphor
TRPV4	>27–35 °C	Sensory neurons/ hypothalamus/ skin/ kidney/ lung/ inner ear	Hypotonic stimulus/ 4αPDD Mechanical stimulus Epoxyeicosatrienoic acids
TRPM8	<25–28 °C	Sensory neurons	Menthol/ icilin
TRPA1	<17 °C	Sensory neurons	Allyl isothiocyanate Δ^9-tetrahydrocannabinol cinnamaldehyde mechanical stimulus

Figure 1 (a) Temperatures causing pain and activating six thermosensitive transient receptor potential (TRP) channels. Dotted lines indicate that threshold temperatures for activation of TRPV1 and TRPM8 are not fixed but changeable in the presence of other stimuli (see text). (b) Comparison of the mammalian six thermosensitive TRP channels.

stimuli in a membrane-delimited fashion indicate that the three stimuli gate TRPV1 directly and that TRPV1 is, itself, a heat sensor. These stimuli are likely to work in concert to regulate the activity of TRPV1 *in vivo*, especially under pathological conditions where tissue acidosis and elevated temperature may come into play. TRPV1 transcript and protein were found to be most highly expressed in sensory neurons (Caterina, M. J. *et al.*, 1997; Tominaga, M. *et al.*, 1998). Moreover, *in situ* hybridization and immunostaining revealed that, within DRG and TG, TRPV1 expression predominated in small-diameter cell bodies, most of which give rise to unmyelinated C fibers.

To determine whether TRPV1 really contributes to the detection of these noxious stimuli *in vivo*, mice lacking this protein were generated and analyzed for nociceptive function. Sensory neurons from mice lacking TRPV1 were deficient in their responses to each of the reported noxious stimuli – capsaicin, proton, and heat (Caterina, M. J. *et al.*, 2000). Consistent with this observation, behavioral responses to capsaicin were absent, and responses to acute thermal stimuli were diminished in these mice. The most prominent feature of the knockout mouse thermosensory phenotype was a virtual absence of thermal hypersensitivity in the setting of inflammation. These findings indicate that TRPV1 is essential for selective modalities of pain sensation and for tissue injury-induced thermal hyperalgesia.

5.10.2.1.2 Reduction of temperature threshold for TRPV1 activation: A mechanism for inflammatory pain

Inflammatory pain is characterized by hypersensitivity both at the site of damage and in the adjacent tissue, and one underlying mechanism is the modulation (sensitization) of ion channels such as TRPV1. Sensitization is triggered by extracellular inflammatory mediators that are released *in vivo* from surrounding damaged or inflamed tissues and from nociceptive neurons themselves (Julius, D. and Basbaum, A. I., 2001). Tissue acidification is also induced in pathological conditions such as ischemia or inflammation, and such acidification exacerbates or causes pain. Among the inflammatory mediators, extracellular ATP, bradykinin, prostaglandins (PGE_2 and PGI_2), or tryptase or trypsin have been reported to potentiate TRPV1 responses through their

Gq-coupled $P2Y_2$, B_2, EP_1, IP, or PAR2 (proteinase activated receptor 2) receptors, respectively, mainly in a protein kinase C (PKC)-dependent manner in both a heterologous expression system and native DRG neurons (Tominaga, M. and Caterina, M. J., 2004; Moriyama, T. *et al.*, 2005). In addition to potentiating capsaicin- or proton-evoked currents, in the presence of the inflammatory mediators, the threshold temperature for heat activation of TRPV1 was reduced to as low as 30 °C, such that normally nonpainful thermal stimuli (i.e., normal body temperature) are capable of activating TRPV1. Under these circumstances, the inflammatory mediators seem to act as direct activators of TRPV1. This represents a novel mechanism through which the large amounts of the mediators released from different cells in inflammation might trigger a sensation of pain. Interactions between the Gq-coupled receptors and TRPV1 in relation to inflammatory pain have been proven at behavioral level using the Gq-coupled receptor- or TRPV1-deficient mice (Tominaga, M. and Caterina, M. J., 2004; Moriyama, T. *et al.*, 2005). A PKA-dependent and PIP_2-mediated pathways also seem to be involved in TRPV1 sensitization (Tominaga, M. and Caterina, M. J., 2004).

Tissue acidification is induced in pathological conditions such as ischemia or inflammation, and such acidification exacerbates or causes pain. In addition to the direct activation of TRPV1, acidification also shifts temperature–response curve of TRPV1 to the left so that the channel can be activated at lower temperatures (lower than body temperature) and responses to heat are bigger at a given suprathreshold temperature (Tominaga, M. *et al.*, 1998). This phenomenon might also contribute to inflammatory pain.

5.10.2.2 TRPV2 (VRL-1)

A protein, which is 49% identical to TRPV1, was isolated and designated VRL-1 and later renamed TRPV2 (Caterina, M. J. *et al.*, 1999; Jordt, S. E. *et al.*, 2003; Patapoutian, A. *et al.*, 2003; Tominaga, M. and Caterina, M. J., 2004) (Figure 1). TRPV2 can be activated by high temperatures with a threshold of ~52 °C. TRPV2 currents showed similar properties to those of TRPV1 such as high Ca^{2+} permeability.

Intense TRPV2 immunoreactivity was observed in medium- to large-diameter cells in rat DRG neurons (Caterina, M. J. *et al.*, 1999). Together with the fact that many of the TRPV2 immunoreactive cells in rat DRG costained with the marker for myelinated neurons, it was concluded that TRPV2 is preferentially expressed in Aδ fibers. TRPV2 transcript and protein were found not only in sensory neurons but also in motoneurons and in many nonneuronal tissues that are unlikely to be exposed to temperatures above 50 °C (Caterina, M. J. *et al.*, 1999). These results indicate that TRPV2 undoubtedly contributes to numerous functions in addition to nociceptive processing.

5.10.2.3 TRPV3 and TRPV4

TRPV3 and TRPV4 have been found to be activated by warm temperatures, ~34–38 °C for TRPV3 and ~27–35 °C for TRPV4, in heterologous expression systems and mouse keratinocytes, and to be expressed in multiple tissues, including, among others, sensory and hypothalamic neurons and keratinocytes (Jordt, S. E. *et al.*, 2003; Patapoutian, A. *et al.*, 2003; Tominaga, M. and Caterina, M. J., 2004) (Figure 1). Among the tissues, both TRPV3 and TRPV4 were most predominantly expressed in the skin keratinocytes and have been reported to be involved in thermosenation by keratinocytes, based on the studies using wildtype and TRPV3- or TRPV4-deficient keratinocytes (Chung, M. K. *et al.*, 2004; Lee, H. *et al.*, 2005; Moqrich, A. *et al.*, 2005). Thermosensing ability of TRPV3 or TRPV4 were proven at animal level because both TRPV3- and TRPV4-deficient mice exhibited some different thermal preference from that in wildtype mice. TRPV4 has also been shown to be involved in mechanical stimulus- and hypotonicity-induced nociception in rodents at baseline or following hypersensitivity induced by prostaglandin injection or taxol hypersensitivity. Furthermore, TRPV4-deficient mice reportedly exhibit deficits in inflammation-induced thermal hyperalgesia (Todaka, H. *et al.*, 2004). TRPV3 has been reported to function as a camphor receptor (Moqrich, A. *et al.*, 2005).

5.10.3 Cold Receptors

5.10.3.1 TRPM8

The cooling sensation of menthol, a chemical agent found in mint, is well established, and both cooling and menthol have been suggested to be transduced through a nonselective cation channel in DRG neurons (Figure 1). Two groups independently cloned and characterized a cold receptor, TRPM8, which can be also activated by menthol (McKemy, D. D.

et al., 2002; Peier, A. M. *et al.*, 2002). In heterologous expression systems, TRPM8 could be activated by menthol or by cooling, with an activation temperature of ~25–28 °C. TRPM8 could alternatively be activated by other cooling compounds, such as menthone, eucalyptol, and icilin. There also appears to be interaction between effective stimuli for TRPM8, in that subthreshold concentrations of menthol increased the temperature threshold for TRPM8 activation from 25 °C to 30 °C. This is reminiscent of TRPV1, whose activation temperature is reduced under mildly acidic conditions that do not open TRPV1 alone (Tominaga, M. *et al.*, 1998). Whole-cell recording in HEK293 cells expressing TRPM8 revealed that TRPM8 is a nonselective cation channel with relatively high Ca^{2+} permeability.

TRPM8 is expressed in a subset of DRG and TG neurons that can be classified as small-diameter C fiber-containing neurons (McKemy, D. D. *et al.*, 2002; Peier, A. M. *et al.*, 2002). Interestingly, however, TRPM8 is not coexpressed with TRPV1.

5.10.3.2 TRPA1

TRPA1 was reported as a distantly related TRP channel which is activated by cold with a lower activation threshold as compared with TRPM8 (Story, G. M. *et al.*, 2003) (Figure 1). In heterologous expression systems, TRPA1 was activated by cold stimuli with an activation temperature of about 17 °C, which is close to the reported noxious cold threshold. This finding led to the suggestion that TRPA1 is involved in cold nociception. Whole-cell recording in Chinese hamster ovary (CHO) cells expressing TRPA1 revealed cationic permeability with similar preferences for monovalent and divalent cations. Whether TRPA1 is gated directly by cold remains to be elucidated. A study from another group failed to reproduce cold responsiveness in TRPA1 (Jordt, S. E. *et al.*, 2004). The reason for this apparent discrepancy is unclear. However, both groups have demonstrated that TRPA1 can be activated by pungent isothiocyanate compounds such as those found in wasabi, horseradish, cinammon, and mustard oil (Tominaga, M. and Caterina, M. J., 2004). Thus, several of the thermosensitive TRP channels likely to be involved in nociception can be activated by stimuli other than temperature.

Unlike TRPM8, TRPA1 is specifically expressed in a subset of sensory neurons that express the nociceptive markers CGRP and substance P (Story, G. M. *et al.*, 2003). Furthermore, TRPA1 is frequently coexpressed with TRPV1, raising the possibility that TRPA1 and TRPV1 mediate the function of a class of polymodal nociceptors. Such coexpression might also explain the paradoxical hot sensation experienced when one is exposed to a very cold stimulus.

5.10.4 Thermonociception by Non-TRP Proteins

The discovery of thermosensitive TRP channels indicates that thermosensation is mediated in part by a common molecular mechanism involving ion channels such as TRP channels as primary transducers of thermal stimuli. However, it is still possible that other proteins are involved in thermosensation and thermonociception. Indeed, TREK-1, a member of a family of mammalian two-pore domain K^+ channels, is expressed in mouse DRG neurons and activated by heat. Because opening of TREK-1 causes hyperpolarization of the membrane potential by efflux of K^+ ions, TREK-1 might be involved in pain relief through the reduction of firing upon noxious heat stimulus. Alternatively, inhibition of TREK-1 by cold stimuli might lead to nociception through depolarization. Further studies will be necessary to determine whether TREK-1 is involved in thermonociception. In addition to K^+ channels, other membrane proteins such as Na^+/K^+ ATPase, members of degenerin/epithelial sodium channels (DEG/ENaC), and $P2X_3$ receptors have been reported to be thermosensative. However, the involvement of those proteins in thermonociception remains to be established.

5.10.5 Conclusion

Significant advances in thermonociception research have been made in the last several years with the cloning and characterization of thermosensitive TRP channels. It is not known how multiple thermosensitive TRP channels are used within the same or different sensory neurons to provide us with the ability to evaluate temperature precisely over a broad range. Central integration of the thermal information acquired by peripheral nerve endings is almost certainly a critical component of this process. Furthermore, regulatory mechanisms similar to those emerging for TRPV1 are likely to exist for most of the thermosensitive TRP channels. Therefore, an

understanding of the molecules surrounding thermosensitive TRP channels from the periphery to the central nervous system will be indispensable to a complete understanding of thermonociception.

References

Caterina, M. J., Leffler, A., Malmberg, A. B., Martin, W. J., Trafton, J., Petersen-Zeitz, K. R., Koltzenburg, M., Basbaum, A. I., and Julius, D. 2000. Impaired nociception and pain sensation in mice lacking the capsaicin receptor. Science 288, 306.

Caterina, M. J., Rosen, T. A., Tominaga, M., Brake, A. J., and Julius, D. 1999. A capsaicin-receptor homologue with a high threshold for noxious heat. Nature 398, 436.

Caterina, M. J., Schumacher, M. A., Tominaga, M., Rosen, T. A., Levine, J. D., and Julius, D. 1997. The capsaicin receptor: a heat-activated ion channel in the pain pathway. Nature 389, 816.

Chung, M. K., Lee, H., Mizuno, A., Suzuki, M., and Caterina, M. J. 2004. TRPV3 and TRPV4 mediate warmth-evoked currents in primary mouse keratinocytes. J. Biol. Chem. 279, 21569.

Jordt, S. E., Bautista, D. M., Chuang, H. H., McKemy, D. D., Zygmunt, P. M., Hogestatt, E. D., Meng, I. D., and Julius, D. 2004. Mustard oils and cannabinoids excite sensory nerve fibres through the TRP channel ANKTM1. Nature 427, 260.

Jordt, S. E., McKemy, D. D., and Julius, D. 2003. Lessons from peppers and peppermint: the molecular logic of thermosensation. Curr. Opin. Neurobiol. 13, 487.

Julius, D. and Basbaum, A. I. 2001. Molecular mechanisms of nociception. Nature 413, 203.

Lee, H., Iida, T., Mizuno, A., Suzuki, M., and Caterina, M. J. 2005. Altered thermal selection behavior in mice lacking transient receptor potential vanilloid 4. J. Neurosci. 25, 1304.

McKemy, D. D., Neuhausser, W. M., and Julius, D. 2002. Identification of a cold receptor reveals a general role for TRP channels in thermosensation. Nature 416, 52.

Montell, C. 2005. The TRP superfamily of cation channels. Sci. STKE 2005, re3.

Moqrich, A., Hwang, S. W., Earley, T. J., Petrus, M. J., Murray, A. N., Spencer, K. S., Andahazy, M., Story, G. M., and Patapoutian, A. 2005. Impaired thermosensation in mice lacking TRPV3, a heat and camphor sensor in the skin. Science 307, 1468.

Moriyama, T., Higashi, T., Togashi, K., Iida, T., Segi, E., Sugimoto, Y., Tominaga, T., Narumiya, S., and Tominaga, M. 2005. Sensitization of TRPV1 by EP1 and IP reveals peripheral nociceptive mechanism of prostaglandins. Mol. Pain 1, 3.

Patapoutian, A., Peier, A. M., Story, G. M., and Viswanath, V. 2003. ThermoTRP channels and beyond: mechanisms of temperature sensation. Nat. Rev. Neurosci. 4, 529.

Peier, A. M., Moqrich, A., Hergarden, A. C., Reeve, A. J., Andersson, D. A., Story, G. M., Earley, T. J., Dragoni, I., McIntyre, P., Bevan, S., and Patapoutian, A. 2002. A TRP channel that senses cold stimuli and menthol. Cell 108, 705.

Story, G. M., Peier, A. M., Reeve, A. J., Eid, S. R., Mosbacher, J., Hricik, T. R., Earley, T. J., Hergarden, A. C., Andersson, D. A., Hwang, S. W., McIntyre, P., Jegla, T., Bevan, S., and Patapoutian, A. 2003. ANKTM1, a TRP-like channel expressed in nociceptive neurons, is activated by cold temperatures. Cell 112, 819.

Szallasi, A. and Blumberg, P. M. 1999. Vanilloid (Capsaicin) receptors and mechanisms. Pharmacol. Rev. 51, 159.

Todaka, H., Taniguchi, J., Satoh, J., Mizuno, A., and Suzuki, M. 2004. Warm temperature-sensitive transient receptor potential vanilloid 4 (TRPV4) plays an essential role in thermal hyperalgesia. J. Biol. Chem. 279, 35133.

Tominaga, M. and Caterina, M. J. 2004. Thermosensation and pain. J. Neurobiol. 61, 3.

Tominaga, M., Caterina, M. J., Malmberg, A. B., Rosen, T. A., Gilbert, H., Skinner, K., Raumann, B. E., Basbaum, A. I., and Julius, D. 1998. The cloned capsaicin receptor integrates multiple pain-producing stimuli. Neuron 21, 531.

5.11 The Development of Nociceptive Systems

G J Hathway and M F Fitzgerald, University College London, London, UK

© 2008 Elsevier Inc. All rights reserved.

5.11.1	The Development of Nociceptors and Their Peripheral and Spinal Connections	133
5.11.2	The Development of Spinal Nociceptive Circuits	135
5.11.3	The Development of Ascending Pain Pathways	136
5.11.4	Pain and the Developing Cortex	136
5.11.5	Pain and the Developing Limbic System	137
5.11.6	The Development of Descending Pain Pathways	137
5.11.7	Development of Neurotransmitter/Receptor Function in Descending Pathways	138
5.11.8	The Development of Persistent Pain	140
5.11.9	Concluding Remarks	140
References		141

Glossary

A fibers Large-diameter myelinated primary afferent sensory fibers with large cell bodies in the dorsal root ganglion. The largest diameter Aβ fibers are mainly low-threshold mechanoceptors and the smaller Aδ fibers are both mechanoreceptors and nociceptors.

C fibers Small-diameter unmyelinated primary afferent sensory fibers with small cell bodies in the dorsal root ganglion. The majority are nociceptors. They divide into a neuropeptide containing, Trk-receptor expressing group and a lectin IB4 binding group although the functional implications of this are still unclear.

embryonic (E) age These are dated from the time of fertilization. Rat gestation is 21.5 days, mouse a little shorter. Rats are born relatively early in terms of CNS development and the early postnatal period is often paralleled with the final gestation of development in man.

receptive field The area on the body surface that when stimulated evokes action potentials in a given neuron.

periaqueductal gray An area of the brainstem that surrounds the aqueduct connecting the third and fourth ventricles. This area projects to the medullary raphe region, which in turn sends projections down the dorsolateral funiculus of the spinal cord to the dorsal horn. This pathway is known to strongly modulate spinal pain processing.

receptor subunits Ion channels are generally made up of several glycoprotein subunits around a central pore. These subunits can confer special characteristics upon a channel, such as increased calcium permeability or longer opening times. The subunits of many channels change with development, thereby altering the channel properties.

5.11.1 The Development of Nociceptors and Their Peripheral and Spinal Connections

Pain is usually, although not always, triggered by tissue damage and consequently a discussion of developing nociceptive pathways begins with the maturation of primary sensory neurons in the dorsal root ganglia (DRG) and their peripheral and central connections. The two main subtypes of primary sensory neurons, A cells and C cells (future nociceptors) are specified at an early stage of development under the control of specific transcription factors. In the rat, lumbar DRG cells are born in two waves from embryonic day (E)12–E15 (gestation 21.5 days); C cells are born in the second wave, later than the larger-diameter A cells. There is evidence also that the future peptidergic nociceptors are born before the nonpeptidergic group (Hall, A. K.

et al., 1997; Jackman, A. and Fitzgerald, M., 2000). Young C cells immediately send out centrally and peripherally directed processes, again lagging some days behind A cells. However, from the time that they innervate peripheral skin, nociceptors are capable of transmitting information about noxious cutaneous stimulation (Box 1).

The study of sensory neurogenesis, axon outgrowth, and target finding is a fast-moving and exciting area of developmental biology. Not only are there a number of key regulatory genes controlling these events but the many aspects of nociceptor development are dependent upon access to neurotrophic factors (Fitzgerald, M., 2005). A key neurotrophic factor affecting nociceptor development is nerve growth factor, NGF, which not only determines nociceptor fate but is also critically required for nociceptor survival (Davies, A. M., 2000; Fitzgerald, M., 2005) during embryonic life and continues to influence nociceptor development postnatally by

1. NGF regulates axon outgrowth, independently of cell survival (Markus, A. *et al.*, 2002).
2. NGF determines nociceptor physiological properties. NGF signaling in the early postnatal period is required for C nociceptors to respond to noxious heat and for the normal development of myelinated high-threshold mechanoreceptors (Aδ fibers) (Ritter, A. M. *et al.*, 1991; Lewin, G. R. and Mendell, L. M., 1994).
3. NGF influences nociceptor expression of the neuropeptides substance P (SP) and calcitonin-gene-related peptide (CGRP) (Davies, A. M., 2000; Hall, A. K. *et al.*, 2001).
4. NGF regulates skin innervation density. Excess epidermal NGF leads to hyperinnervation (Davis, B. M. *et al.*, 1997).

The growth of C-fiber terminals into the spinal dorsal horn occurs just before birth in the rat and from the outset, these fibers terminate in a somatotopically precise manner in laminae I–II of the dorsal horn. Neuropeptide containing nocieptive terminals in laminae I and II can be detected prenatally, steadily increasing in density over the first 10 postnatal days, while IB4+ve terminals appear a few days later, suggesting that these fibers may form central connections later than peptidergic fibers and indeed be involved in a separate central pain pathway (Braz, J. M. *et al.*, 2005).

The immature C-fiber terminals are functional at birth but neurotransmitter release is of low frequency and the synapses are too immature to evoke substantial spike activity *in vivo* until the second postnatal week. This in contrast to the A fiber which, when stimulated, can evoke robust action potentials in dorsal horn cells from before birth (Fitzgerald, M. and Jennings, E., 1999; Baccei, M. L. *et al.*, 2003). As in the adult, immature C fibers terminate exclusively in laminae I and II. However, in the first postnatal weeks, they share this termination area with large-diameter Aβ afferents whose terminals extend dorsally into laminae II and I and form transient synaptic connections. This is followed by a gradual withdrawal from the superficial laminae over the first 3 postnatal weeks (Fitzgerald, M. *et al.*, 1994). The postnatal withdrawal of Aβ fibers from the superficial dorsal horn is an activity-dependent process, which that can be prevented by intrathecal application of the NMDA receptor antagonist MK801 (Beggs, S. *et al.*, 2002). The functional implications of the presence of A fibers in newborn lamina II are not known but they may contribute to the larger receptive fields and increased excitability to tactile stimulation described below.

Box 1 Postnatal development of C nociceptor properties

Although all of the broad functional classes of primary afferents are present in the rat hindlimb at birth, the maturation process varies according to the individual stimulus modality (Koltzenburg, M., 1999). From birth, polymodal nociceptors respond to noxious chemical, mechanical, and thermal stimuli with thresholds and firing frequencies that are characteristic of mature C fibers (Fitzgerald, M., 1987; Keller, A. F. *et al.*, 2004). This is consistent with early expression of TRPV1, critical for the detection of painful thermal and chemical stimuli, and the ATP-gated $P2X_3$ receptor (Guo, A. *et al.*, 2001) that plays an important role in thermal and mechanical hyperalgesia following inflammation or nerve injury and the tetrodotoxin-resistant sodium channel Nav1.8, necessary for the normal detection of noxious mechanical and thermal stimuli and the sensitization of nociceptive sensory neurons (Benn, S. C. *et al.*, 2001).

Nociceptive cells require activation of trkA receptors by nerve growth factor (NGF) for survival during the embryonic period, but during the postnatal period, a subset of these neurons downregulate trkA and become dependent on glial-cell-line-derived neurotrophic factor (GDNF) via the expression of the GDNF receptor Ret (Bennett, D. L. *et al.*, 1996; Molliver, D. C. *et al.*, 1997). Thus the clear distinction between (1) the trkA+ve, neuropeptide containing C fibers and (2) the IB4+ve, nonpeptidergic nociceptors appears postnatally, although the functional implications of this in terms of nociception is not clear.

5.11.2 The Development of Spinal Nociceptive Circuits

At birth, strong spinal nociceptive reflexes can be evoked by mechanical stimulation, which are exaggerated compared to the adult for the first 2–3 postnatal weeks (Ekholm, J., 1967; Fitzgerald, M. *et al.*, 1988) with lower thresholds and larger, more synchronized and prolonged muscle contractions. A prick on the hind foot in the newborn rat can evoke limb withdrawal, wriggling, rolling, and simultaneous responses from all four limbs. Receptive fields of hindlimb flexor muscles are large and disorganized such that the limb withdrawal can be evoked that is not always appropriate to the stimulus (Holmberg, H. and Schouenborg, J., 1996). As the pup matures, the response decreases in magnitude and becomes restricted to an isolated leg or foot movement. Thresholds for withdrawal from heat stimuli are also lower in younger animals. In contrast with mechanical reflexes, but consistent with the slow synaptic maturation of C-fiber-evoked responses, cutaneous application of the selective C-fiber irritant, mustard oil, evokes little or no spinal reflex response until postnatal day 10 (Baccei, M. L. and Fitzgerald, M., 2005).

The excitability of mechanical neonatal cutaneous reflexes is attributable to underlying changes in dorsal horn sensory processing and is likely to be due to absence of fine-tuning of sensory and nociceptive neuronal circuitry in the newborn. The earlier maturation and widespread presence of functional A-fiber terminals in both the substantia gelatinosa and deeper laminae in the first weeks of life appear to adequately compensate for the weak C-fiber input and dominate the physiological responses of dorsal horn neurons, fewer of which are nociceptive in the newborn cord, especially of the wide dynamic range (WDR) variety. Receptive field areas of dorsal horn cells, mapped by natural mechanical stimulation of skin, are large at birth and decrease in size with age. Pinching or brushing the receptive field of many neonatal dorsal horn cells results in long-lasting after-discharges (30–90 s) which on days 0–3 may be more pronounced than the initial evoked response but which decrease in duration and amplitude of these responses with age (Fitzgerald, M. and Jennings, E., 1999; Torsney, C. and Fitzgerald, M., 2002). This predominantly A-fiber-induced spike activity appear to have a critical role in the formation of nociceptive circuits. Newborn rat pups have a high error rate in the direction of a tail flick on noxious stimulation than adults, which gradually improves over 3 weeks (Waldenstrom, A. *et al.*, 2003). The maturation is unaffected by daily noxious stimulation but blocking low-intensity tactile inputs from the tail with local anesthetic, during the critical 10-day period, prevents this postnatal tuning. Low-intensity tactile input from, for example, spontaneous twitching during sleep could play a role in shaping nociceptive circuits in early life (Petersson, P. *et al.*, 2003).

Postnatal maturation and tuning of nociceptive circuits critically depends upon the postnatal development of excitatory and inhibitory neurotransmitter/receptor function in the neonatal dorsal horn. The developmental pharmacology of spinal pain pathways has been an area of intense recent interest (Pattinson, D. and Fitzgerald, M., 2004; Fitzgerald, M., 2005) and some important features are shown in Box 2. The properties of immature

Box 2 The development of excitatory and inhibitory transmission in developing spinal pain circuits

Glutamate AMPA and NMDA receptors are highly expressed in the newborn dorsal horn and their expression decreases and becomes spatially organized with age. This is accompanied by changes in subunit composition leading to greater AMPA-dependent Ca^{2+} influx, altered receptor kinetics, greater NMDA receptor affinity, and increased Mg^{2+} sensitivity in neonatal spinal neurons (Watanabe, M. *et al.*, 1994; Jakowec, M. W. *et al.*, 1995; Albuquerque, C. *et al.*, 1999; Bardoni, R., 2001; Green, G. M. and Gibb, A. J., 2001; Stegenga, S. L. and Kalb, R. G., 2001). Presynaptic Ca^{2+}-permeable KA receptors found on IB4+ve C cells switch to a Ca^{2+}-impermeable form early in the first postnatal week (Lee, C. J. *et al.*, 2001).

Despite early expression of GABA and glycine and their receptors, newborn lamina II neurons exhibit only GABA mIPSCs (Baccei, M. L. and Fitzgerald, M., 2004) probably due to low levels of gephyrin, the postsynaptic scaffolding protein (Bremner *et al.*, 2005). There is also a fourfold acceleration in the decay rate of GABA mIPSCs in laminae I–II neurons between P8 and P23 triggered by local neurosteroid release (Keller, A. F. *et al.*, 2004). $GABA_AR$ activation in the developing dorsal horn can be excitatory rather than inhibitory, due to the high intracellular Cl^- concentration in immature neurons producing a positive E_{Cl}. $GABA_AR$ activation depolarizes some lamina II cells but the response becomes exclusively hyperpolarizing by P6–P7 (Baccei, M. L. and Fitzgerald, M., 2004). This is probably due to the onset of expression of the K^+–Cl^- cotransporter KCC2 which decreases $[Cl]_i$ over the postnatal period. However, E_{Cl} is always more negative than action potential threshold at P0–P1 suggesting that GABA will still inhibit the firing of newborn superficial dorsal horn neurons (albeit less effectively than in the adult).

Both presynaptic and postsynaptic $GABA_BRs$ are functional from birth in the neonatal dorsal horn, but seem to be regulated differently over the early postnatal period (Baccei, M. L. and Fitzgerald, M., 2004).

synaptic transmission tends to enhance calcium influx into developing dorsal horn neurons compared to adult neurons, which may be important for a variety of developmental processes including synapse formation and remodeling.

5.11.3 The Development of Ascending Pain Pathways

Following integration in the dorsal horn, sensory and nociceptive information is conducted to supraspinal centers via ascending tracts to targets in the brainstem, midbrain, hypothalamus, thalamus, and amygdala. A key ascending pathway involved in pain and hyperalgesia arises from lamina I of the dorsal horn of the spinal cord, particularly neurokinin 1 (NK1) expressing neurons receiving Aδ- and C-fiber nociceptive input, which project to the parabrachial area of the brainstem. These neurons then project to the amygdala (affective components of pain) and the hypothalamus (autonomic functions such as changes in heart rate and blood pressure). Outputs from these structures are passed via the periaqueductal gray (PAG), which in turn sends descending projections back to the dorsal horn in a spinobulbar spinal loop. Descending projections to the dorsal horn arise from the brainstem nuclei, nucleus raphe magnus (NRM), raphe dorsalis, reticularis, paragigantocellularis (NRPG), as well as locus coeruleus, PAG, and mesencephalic reticular formation (Todd, A. J. *et al.*, 2000; Mantyh, P. W. and Hunt, S. P., 2004; Suzuki, R. *et al.*, 2004; Ding, Y. Q. *et al.*, 1995; Marshall, G. E. *et al.*, 1996).

Little is known about the development of ascending spinothalamic and spinoparabrachial tracts. In the rat, neurogenesis of dorsal horn projection neurons is complete by E16 having followed a systematic pattern of migration and settlement in the dorsal horn related to their axon trajectories (Nissen, U. V. *et al.*, 2005). The projecting axons grow up the spinal cord prenatally (Bice, T. N. and Beal, J. A., 1997); spinothalamic tract fibers reach the thalamus just before birth at E19. In the rat, afferents appear to reach the thalamus by E19 (Higashi, S. *et al.*, 2002) while in the sheep, projection fibers from dorsal horn cells are in the thalamus approximately two-thirds through gestation (Rees, S. *et al.*, 1994; Ding, Y. Q. *et al.*, 1995). The thalamocortical axon (TCA) projection originates in dorsal thalamus, conveys sensory input to the neocortex, and has a critical role in cortical development. Information about the development of these pathways is entirely from visual and somatosensory (whisker) pathways in rodents and their relevance to nociceptive processing can only be inferred. Recently, however, a study by Man S. H. *et al.* (2005) has shown the presence at birth of the NK1+ve lamina 1 ascending projection from the DH to the parabrachial area of the brainstem using retrograde tracing and c-fos immunostaining. The outgrowth of axons from the thalamus to the cortex begins at E13–E14 in rodents just before the arrival of the first cells migrating into the preplate zone. The migration of cortical neurons from the proliferative neuroepithelium lining the telencephalic ventricle to the cortical plate is highly complex and tightly regulated (Meyer, G., 2001). Thalamic axons and preplate fibers meet in the lateral part of the internal capsule at E15 and grow in association with early corticofugal axons, right up to the cortical subplate. The topography of thalamic axons is maintained throughout the pathway and they reach the cortex by associating with the projections of a number of preexisting cells, including the preplate scaffold. These cells invade the cortical plate 24–48 h later and form functional synaptic connections in the cortical plate around E18–E19. At birth, thalamic axons have extended into cortical layers IV, V, and VI in a topographically precise manner and exhibit a periphery-related pattern in layer IV (Schlaggar, B. L. and O'Leary, D. D., 1994; Molnar, Z. *et al.*, 2003). The spatial distribution of thalamic synapses onto cortical neurons (predominantly found at dendritic spines) is established at least as early as P11 in the somatosensory cortex of the mouse (Lev, D. L. *et al.*, 2002).

5.11.4 Pain and the Developing Cortex

The development of specific cortical areas is dependent upon both extrinsic influences from thalamocortical input and intrinsic genetic controls such as the transcription factors Emx2 and Pax6 (O'Leary, D. D. and Nakagawa, Y., 2002). This process extends over several months in man compared to the mouse cortex that requires a week (Angevine, J. B. and Sidman, R. L., 1961). In man, the generation and migration of cortical neurons begins in the fifth gestational week (O'Rahilly, R. and Muller, F., 1994) and continues until week 22 (Sidman, R. L. and Rakic, P., 1973). Following the arrival of neurons at their correct destination, they begin to differentiate and to extend dendritic fields. It is in the last 2 months of gestation that the characteristic folding of the cortex

into sulci and gyri takes place (Fees-Higgins, A. and Larroche, J. C., 1987).

One area of interest is the anterior cingulate cortex (ACC) that appears to play an important role in the affective and cognitive aspects of pain, but little is known of the development of this region. Ultrasonic scans taken from preterm neonates have confirmed that at week 28 the ACC is fully developed (Huang, C. C., 1991).

Subplate neurons (SPn) play an important role in the formation of thalamocortical connections during early development and show glutamatergic and GABAergic spontaneous synaptic activity. Whole-cell recordings from SPn in somatosensory cortical slices of postnatal day 0–3 rats, showed that SPn receive distinct functional synaptic inputs arising from the thalamus, cortical plate, and other SPn mediated by AMPA and NMDA receptors (Hanganu, I. L. *et al.*, 2002; Luhmann, H. J. *et al.*, 2003). GABA activity is depolarizing at this age (see Box 2). Electrophysiological analysis of cortical cells at P7 shows them to be organized in columns as in the adult but to have larger receptive fields, similar to that discussed above for the spinal cord (Armstrong-James, M. A., 1970; Armstrong-James, M., 1975). Human somatosensory potentials evoked by electrical stimulation are observed at 29 weeks (Klimach, V. J. and Cooke, R. W., 1988) while preliminary studies using infrared spectroscopy during routine clinical heel lances suggest that a cortical blood flow response is present as early as 25 weeks (Slater, R. *et al.*, 2006).

While axonal growth and early topographic arrangement of thalamocortical fiber pathways do not rely on activity-dependent mechanisms requiring evoked neurotransmitter release (Molnar, Z. *et al.*, 2002), the formation of cortical circuits is highly dependent upon normal sensory experience. The postnatal plasticity of cortical circuits has been studied in great detail for the visual (Yao, H. and Dan, Y., 2005) and somatosensory whisker barrel cortex (Fox, K., 2002), but little is known about the effect of nociceptive activity upon cortical development (Anand, K. J., 2000).

5.11.5 Pain and the Developing Limbic System

The amygdala is a part of the limbic system and plays a key role in the emotional evaluation of sensory stimuli (Davis, M., 1998a; Aggleton, J. P., 1999; Gallagher, M. and Schoenbaum, G., 1999; Maren, S., 1999; Ledoux, J. E., 2000b; Cardinal, R. N. *et al.*, 2002; Davidson, R. J., 2002; Zald, D. H., 2003). In the rat, the amygdala is a complex of 13 nuclei and cortical regions and their subdivisions. There is some debate as to whether the amygdala should be considered a single entity or as a collection of functionally diverse nuclei that share some anatomical and physiological similarities (Aggleton, J. P. and Saunders, R. C., 2000). There are both direct and indirect nociceptive inputs to the laterocapsular part of the central nucleus of the amygdala (the nociceptive amygdala) and the whole central area supplies the major output forming widespread connections with forebrain areas, the hypothalamus and the brainstem (Pitkanen, A. *et al.*, 1998; Davis, M., 1998b; Aggleton, J. P. and Saunders, R. C., 2000; Ledoux, J. E., 2000a; Bourgeais, S. *et al.*, 2001; Neugebauer, V. and Li, W., 2002; 2003; Li, W. and Neugebauer, V., 2004).

Neurons in the amygdala of the rhesus monkey are generated during a 3-week period very early in gestation (E30–E50 of a 165-day gestation; Kordower, J. H. *et al.*, 1992). This neurogenesis appears to occur simultaneously within all the amygdalal nuclei. This pattern has also been reported in humans (Humphrey, T., 1968; Nikolic, I. and Kostovic, I., 1986). In the rodent, LOM-homeodomain genes have been shown to play a role in the segregation of embryonic amygdalal cells into appropriate groupings and this family of genes plays a fundamental role in the development of every single amygdalal nucleus (Remedios, R. *et al.*, 2004). The distribution of opiate receptors in the amygdala of a 1-week-old monkey appears the same as in the adult indicating early neurochemical maturation (Bachevalier, J. *et al.*, 1986). Widespread connections to and from the monkey amygdala at 1 week of age appear to be pruned over the postnatal period (Webster, M. J. *et al.*, 1991). The same connections are likely to occur over the first 2 postnatal weeks in rats.

5.11.6 The Development of Descending Pain Pathways

Brainstem descending pathways form a major mechanism in the control of pain transmission (Pitkanen, A. *et al.*, 1998; Ren, K. and Dubner, R., 2002; Gebhart, G. F., 2004) and there is more known about the development of these descending controls compared to the ascending systems.

Brainstem nuclei differentiate between E11 and E16 in the rat and all other major brain systems are morphologically identifiable by E18 (Altman, J. and Bayer, S. A., 1984; Momose-Sato, Y. *et al.*, 2001). In the rat embryo, the parabrachial area can be visualized histochemically from at least E17 (Cholley, B. *et al.*, 1989) (Figure 1).

As with ascending tracts, axons from brainstem nuclei appear to grow down the spinal cord well before birth (Cabana, T. and Martin, G. F., 1984). Injections of horseradish peroxidase into lumbosacral spinal cord of the neonatal rat label brainstem nuclei with similar density to that seen in the adult (Leong, S. K., 1983; Fitzgerald, M. *et al.*, 1987) but it is unclear at what stage these axons begin producing collaterals that innervate the dorsal horn and make synapses with their target cells. Mapping degenerating axons and synaptic endings following thoracic hemisections

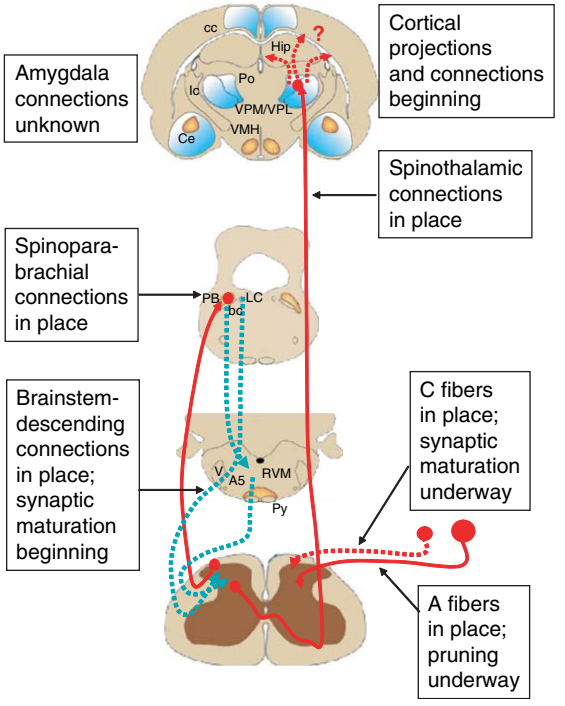

Figure 1 Diagram summarizing the state of development of ascending and descending pathways involved in the transmission of pain in the newborn rat. It is important to remember that changes in the anatomy of the pathways depicted here are also accompanied by changes in the physiology and neurochemistry of these pathways also. Additionally, the maturation of human nociceptive pathways occurs over different and as yet unknown time courses from those discussed here. Adapted from Hunt, S. and Mantyh, P. 2001. The molecular dynamics of pain control. Nat. Rev. Neurosci. 2, 83–91.

of the spinal cord at various postnatal stages suggests that descending axon collaterals innervate the intermediate and central gray from birth but that they are not found in the dorsal horn until P15 (Gilbert, M. and Stelzner, D. J., 1979).

Descending inhibitory pathways traveling from the brainstem via the dorsolateral funiculus of the spinal cord to the dorsal horn grow down the spinal cord early in fetal life, but they do not extend collateral branches into the dorsal horn for some time. Stimulation of the dorsolateral funiculi (DLF) fails to produce descending inhibition of C-fiber-evoked activity in neonatal rats before P9, but high-intensity stimulation produced descending inhibition at P18. By P22–P24 more typical adult responses were observed (Fitzgerald, M. and Koltzenburg, M., 1986). Similarly, the inhibition of C and Aδ activity in the dorsal horn by PAG stimulation via the DLF that is clearly observed in adults (Basbaum, A. I. and Fields, H. L., 1978) cannot be produced in rat pups before P21 (van Praag, H. and Frenk, H., 1991). Diffuse noxious inhibitory control (DNIC), measured as a reduction in noxious-evoked dorsal horn c-fos expression in the presence of an inflammatory stimulus elsewhere on the body, also develops between P12 and P21 (Boucher, T. *et al.*, 1998).

The delayed postnatal onset of functional descending inhibition, despite the presence of DLF terminals in the dorsal horn may be due to immaturity of neurotransmitter/receptor interactions (see below) or delayed maturation of critical interneurons. It has been suggested that the maturation of descending inhibition is dependent upon afferent C-fiber activity, because rats treated with capsaicin at birth have reduced inhibitory controls as adults (Cervero, F. and Plenderleith, M. B., 1985). The lack of descending inhibition in the neonatal dorsal horn means that there is no endogenous analgesic system to dampen noxious inputs as they enter the CNS and their effects may therefore be more profound than in the adult. It also explains why stimulus-produced analgesia from the PAG is not effective until P21 in rats (van Praag, H. and Frenk, H., 1991).

5.11.7 Development of Neurotransmitter/Receptor Function in Descending Pathways

It is widely accepted that 5-HT is the most relevant neurotransmitter with respect to the descending control of spinal cord excitability. Descending

serotonergic pathways predominantly mediate descending inhibitory control over spinal cord excitability, but 5-HT is involved in both antinociceptive and pronociceptive effects depending upon the subtype of receptor that it is acting upon (Millan, M. J., 2002; Gebhart, G. F., 2004). An excitatory, pronociceptive role has been attributed to the 5-HT_3 receptor (Suzuki, R. *et al.*, 2002). In the adult, descending inhibition and excitation are conveyed rostrocaudally via different spinal pathways, the DLF and ventral/ventrolateral funiculi (VLF), respectively (Millan, M. J., 2002), and since both of these tracts appear in the embryonic period, both types of control may also be possible in the newborn. Neurons that produce 5-HT (serotonin) are amongst the earliest to be detected in the developing CNS (Rubenstein, J. L., 1998) with the mesencephalon containing detectable levels by E12 (E12; Aitken, A. R. and Tork, I., 1988). 5-HT containing descending neurons is present in the rat between E15 and E19 (Lidov, H. G. and Molliver, M. E., 1982; Lakke, E. A., 1997), those arising from the raphe nuclei are present in the cervical cord by E14 and in the lumbar cord by E16–E17. 5-HT fibers were not found to innervate the dorsal horn until E19 (Rajaofetra, N. *et al.*, 1989). Examination of the pre- and postnatal development of the descending serotonergic pathways to the spinal cord show that the maturation of 5-HT terminals occurs in a ventral to dorsal direction such that innervation of the lumbar dorsal horn does not occur until P14 and the adult pattern of high-density terminals in lamina II at P21 (Bregman, B. S., 1987). Direct application of 5-HT to the neonatal spinal cord *in vitro* is effective in very young superficial dorsal horn cells, suggesting that at least some 5-HT receptors are functional from birth (Li, P. and Zhuo, M., 1998).

Although 5-HT is the most important neurotransmitter, other monoaminergic and peptidergic compounds must also be considered with regard to the descending control of spinal cord excitability. The major noradrenergic input to the dorsal horn is from the locus coeruleus (LC) and adjacent noradrenergic nuclei in the brainstem. Activation of this pathway leads to the release of noradrenaline that acts postsynaptically on α_2-adrenergic receptors to produce a decrease in excitability and a concomitant analgesia (Sagen, J. and Proudfit, H. K., 1984; Jones, B. E. 1991; Jasmin, L. *et al.*, 2002). Noradrenaline containing terminals appear earlier in the dorsal horn than serotonin (Loizou, L. A., 1972; Commissiong, J. W., 1983) and levels are generally mature by 2 weeks postnatally. As with 5-HT, the development of the noradrenergic system in the ventral horn precedes that in the dorsal horn. Expression of the α2A receptor mRNA is observed in high levels in the dorsal horn from E19 and is downregulated postnatally (Winzer-Serhan, U. H. *et al.*, 1997), which has led to the proposal that noradrenaline has a trophic role in the developing cord (Huang, Y. *et al.*, 2002). Recent functional studies have shown that the local spinal cord application dexmedetomidine, the potent α2A agonist, has antinociceptive and antihyperalgesic actions from at least P3 (Walker, S. 2005).

Dopamine is also released by descending tracts; the main source is from the A11 (posterior) region of the hypothalamus (Commissiong, J. W. *et al.*, 1978; Commissiong, J. W. and Neff, N. H., 1979; Swanson, L. W. and Kuypers, H. G., 1980), which provide extensive networks of dopamine-containing fibers in the dorsal horn and lamina X of the spinal cord (Skagerberg, G. *et al.*, 1982; 1988). In the rat, dopamine containing neurons appear in the mesencephalon at E12–E13 (Olson, L. and Seiger, A., 1972) and levels of dopmaine appear to increase throughout development with particularly high levels being found in the solitary tract in the brainstem (Moore, R. Y. and Bloom, F. E., 1978).

Numerous other nonmonoaminergic transmitters are found in the terminals of descending pathways in the spinal cord including histamine, vasopressin, and oxytocin. Other transmitters released by descending projections are also present in intrinsic DH neurons. Of these, acetylcholine is the most prominent, having both a pro- and antinociceptive effect depending on the subtype of the receptor activated. Other neurotransmitters in the category are GABA and glycine. Cholinergic neurons in the brainstem generally develop later than catecholaminergic systems with levels of cholinergic markers such as choline acetyltransferase being only a few percent of the levels seen in the adult rat at birth but start to increase rapidly after P10 (Diebler, M. F. *et al.*, 1979).

A major peptidergic descending input from the brainstem to the dorsal horn of the spinal cord is via enkephalin and other opioid peptides (pre-proenkephalin, pre-prodynorphin, pre-proendomorphin, pre-pro-opiomelanocortin (POMC), and orphaninFQ). Opioids play an important role in pain transmission both by initiating the descending controls from the brainstem and by directly reducing the evoked activity of C and Aδ fibers in the dorsal horn via presynaptic opiate receptors. There is considerable postnatal development of this receptor

expression, with neonatal rats not only having a higher density but also a less selective distribution of μ-opioid receptors on DRG cells (Nandi, R. *et al.*, 2004). Morphine has a markedly higher analgesic efficacy in young rats in mechanical but not thermal noxious tests but it is not known whether this results from central or peripheral regulation of opioid pathways (Nandi, R. and Fitzgerald, M., 2005).

5.11.8 The Development of Persistent Pain

While it is essential to understand the underlying development of nociception, tissue injury, inflammation, and nerve damage can lead to more persistent pain that lasts for days, weeks, or months. Such pains arise from central sensitization and changes in gene expression as triggered by intense and sensitized peripheral nociceptor inputs (Woolf, C. J. and Salter, M. W., 2000).

Cutaneous mechanical thresholds fall in neonatal rat pups following local carrageenan injection (Marsh, D. *et al.*, 1999) and mustard oil application (Jiang, M. C. and Gebhart, G. F., 1998) but the effect is less at P3 than at P21. This may partly reflect peripheral nociceptor terminal immaturity. C fibers are capable of peripheral sensitization from before birth (Koltzenburg M., and Lewin, G. R., 1997) but peripheral C-fiber terminals do not release sufficient SP to produce neurogenic extravasation until P10 (Fitzgerald, M., and Gibson, S., 1984). Electrophysiological studies *in vivo* show that sensitization of dorsal horn cells can be observed 2–5 h after carageenan inflammation of the hindpaw at all ages although the exact pattern of effects is age dependent (Fitzgerald, M. and Jennings, E., 1999; Torsney, C. and Fitzgerald, M., 2003). In slice preparations, NMDA-dependent C-fiber-evoked depolarization of spinal cord cells and windup of cells to repeated C-fiber stimulation has been demonstrated in the young (8–14 days) spinal cord (Sivilotti, L. G, *et al.*, 1993). Recently, the role of descending brainstem excitatory pathways in maintaining persistent pain have been emphasized (Gebhart, G. F., 2004), but the developmental regulation of this system has not been investigated.

In adults, partial nerve injury can trigger neuropathic pain, charcterized by a lowered mechanical sensitivity or allodynia. In postnatal animal models of neuropathic pain, this allodynia is not observed until the animals are over 3 weeks old (Howard, R. F. *et al.*, 2001). This is interesting in view of the substantial cell death that occurs in the DRG of axons damaged in early life compared to adults (Yip, H. K. *et al.*, 1984; Benn, S. C. *et al.*, 2002) followed by transganglionic degeneration and subsequent withdrawal of central terminals (Bondok, A. A. and Sansone, F. M., 1984; Aldskogius, H. and Risling, M., 1989), sprouting of adjacent, intact axon collaterals into the denervated region (Fitzgerald, M., 1985; Fitzgerald, M. *et al.*, 1990; Shortland, P. and Fitzgerald, M., 1994) and disruption of the somatotopic organization of central terminals within the dorsal horn and cortex (Kaas, J. H. *et al.*, 1983). Clearly these changes do not trigger pain. One possibility is that the central microglial and immune responses that follow nerve injury in the adult and may contribute to neuropathic pain (Marchand, F. *et al.*, 2005) are not activated in the immature spinal cord.

There is also evidence that injury at a critical period of development may lead to long-term alterations in sensory processing resulting in hypo- or hyperalgesia (Lidow, M. S., 2002). The mechanisms underlying this are poorly understood. It is possible that early tissue damage, which is known to release excess neurotrophins into the wounded area (Constantinou, J. *et al.*, 1994) not only sensitizes peripheral nociceptors, but also permanently influences nociceptor development as described above. Alternatively central changes in activity-dependent connectivity are produced because of the increased barrage of C-fiber nociceptor input at a time when synapses are still forming (Fitzgerald, M. and Walker, S. M., 2003). Central changes in transmitter–receptor expression may also occur. Early inflammatory pain leads to an increase in expression in the PAG of serotonin receptors (5HT1A, 5HT1D, 5HT2A, 5HT2C, 5HT4), NR2D and NR3A subunits of the NMDA receptor, $GABA_A\gamma 2$ and $GABA_A\theta$ subunits, the NK1, and the CCK-2 receptor. As well as being hypoalgesic, these animals exhibited decreased anxiety and greater stress-coping ability; this was indexed by better performance on the elevated plus maze and decreased basal and stress-induced neuroendocrine markers of anxiety and stress (Anseloni, V. C. *et al.*, 2005). For further review of this area, see Baccei M. L. and Fitzgerald M. (2005).

5.11.9 Concluding Remarks

In this chapter we have attempted to briefly review what is currently known about the development and maturation of pain pathways. While our knowledge of

Box 3 Development of pain pathways in humans

Because human infants cannot report pain, we have to use indirect physiological and behavioral methods to assess its existence and severity and there is considerable debate on how best to measure pain in infants (Stevens, B. J. and Franck, L. S., 2001).

From 23 weeks of gestational age, human fetuses mount a hormonal response when needles are inserted into the innervated intrahepatic vein (Giannakoulopoulos, X. *et al.*, 1994). Noxious activation of nerve endings stimulates central pathways (most likely through the fetal hypothalamic–pituitary–adrenal axis), producing a biochemical stress response, although the link between perceived pain and the hormonal stress response is unpredictable, even in adults. Hormonal responses are also used to measure pain in the youngest preterm infants (~24–26 weeks), along with many other physiological measures such as heart rate variability, crying and palmar sweating and motor activity (Stevens, B. J. and Franck, L. S., 2001), and characteristic facial expressions (Craig, K. D. *et al.*, 2002). Many of these measures can be applied to pain related to a particular noxious event, such as a needle prick, but are harder to use for persistent pain. Studies using cutaneous reflexes evoked by stimulation in and around an area of injury, show that infants display cutaneous sensitization or hyperalgesia lasting days and weeks (Andrews, K. and Fitzgerald, M., 2002; Andrews, K. *et al.*, 2002), consistent with laboratory studies. Nothing is known of the maturation of descending brainstem controls in human infants.

True pain experience requires functional maturation of higher brain centers and recent studies using infrared spectroscopy during routine clinical heel lances suggest that a cortical blood flow response is present as early as 25 weeks (Slater, R. *et al.*, 2006).

the development of spinal nociceptive pathways has increased considerably in recent years (Fitzgerald, M., 2005), the understanding of the structural and functional maturation of supraspinal centers involved in the affective and nociceptive components of pain is severely lacking. With rapid improvements in medical knowledge and technologies, it is now possible to treat children born at increasing premature stages of development. This requires long periods of hospitalization and large numbers of often invasive procedures that in an adult or older child would be considered painful (Box 3), leading to the administration of analgesic and sedative compounds. We know that neonates respond to pain but the pathways differ in important ways from those in adults. Until we understand more of the functional development and maturation of the central neuronal elements involved in the experience of pain, the best course of analgesic action in infancy remains unclear.

Acknowledgments

The authors would like to thank The Wellcome Trust, The Wellcome London Pain Consortium, and Professor S. P. Hunt (UCL).

References

Aggleton, J. P. 1999. Mapping recognition memory in the primate brain: why it's sometimes right to be wrong. Brain Res. Bull. 50, 447–448.

Aggleton, J. P. and Saunders, R. C. 2000. The Amygdala, 2nd edn. Oxford University Press.

Aitken, A. R. and Tork, I. 1988. Early development of serotonin-containing neurons and pathways as seen in wholemount preparations of the fetal rat brain. J. Comp. Neurol. 274, 32–47.

Albuquerque, C., Lee, C. J., Jackson, A. C., and MacDermott, A. B. 1999. Subpopulations of GABAergic and non-GABAergic rat dorsal horn neurons express Ca^{2+}-permeable AMPA receptors. Eur. J. Neurosci. 11, 2758–2766.

Aldskogius, H. and Risling, M. 1989. Number of dorsal root ganglion neurons and axons in cats of different ages. Exp. Neurol. 106, 70–73.

Altman, J. and Bayer, S. A. 1984. The development of the rat spinal cord. Adv. Anat. Embryol. Cell Biol. 85, 1–164.

Anand, K. J. 2000. Pain, plasticity, and premature birth: a prescription for permanent suffering? Nat. Med. 6, 971–973.

Andrews, K. and Fitzgerald, M. 2002. Wound sensitivity as a measure of analgesic effects following surgery in human neonates and infants. Pain 99, 185–195.

Andrews, K. A., Desai, D., Dhillon, H. K., Wilcox, D. T., and Fitzgerald, M. 2002. Abdominal sensitivity in the first year of life: comparison of infants with and without prenatally diagnosed unilateral hydronephrosis. Pain 100, 35–46.

Angevine, J. B. and Sidman, R. L. 1961. Autoradiogrpahic study of cell migration suring histogenesis of cerebral cortex in the mouse. Nature 192, 766–768.

Anseloni, V. C., He, F., Novikova, S. I., Turnbach, R. M., Lidow, I. A., Ennis, M., and Lidow, M. S. 2005. Alterations in stress-associated behaviors and neurochemical markers in adult rats after neonatal short-lasting local inflammatory insult. Neuroscience 131, 635–645.

Armstrong-James, M. A. 1970. Spontaneous and evoked single unit activity in 7-day rat cerebral cortex. J. Physiol. 208, 10P–11P.

Armstrong-James, M. 1975. The functional status and columnar organization of single cells responding to cutaneous stimulation in neonatal rat somatosensory cortex S1. J. Physiol. 246, 501–538.

Baccei, M. L. and Fitzgerald, M. 2004. Development of GABAergic and glycinergic transmission in the neonatal rat dorsal horn. J. Neurosci. 24, 4749–4757.

Baccei, M. L. and Fitzgerald, M. 2005. In: The Textbook of Pain, 5th edn. (eds McMahon and Koltzenburg), Chapter 8, pp.143–158. Elsevier.

Baccei, M. L., Bardoni, R., and Fitzgerald, M. 2003. Development of nociceptive synaptic inputs to the neonatal

rat dorsal horn: glutamate release by capsaicin and menthol. J. Physiol. 549, 231–242.
Bachevalier, J., Ungerleider, L. G., O'Neill, J. B., and Friedman, D. P. 1986. Regional distribution of [3H]naloxone binding in the brain of a newborn rhesus monkey. Brain Res. 390, 302–308.
Bardoni, R. 2001. Excitatory synaptic transmission in neonatal dorsal horn: NMDA and ATP receptors. News Physiol. Sci. 16, 95–100.
Basbaum, A. I. and Fields, H. L. 1978. Endogenous pain control mechanisms: review and hypothesis. Ann. Neurol. 4, 451–462.
Beggs, S., Torsney, C., Drew, L. J., and Fitzgerald, M. 2002. The postnatal reorganization of primary afferent input and dorsal horn cell receptive fields in the rat spinal cord is an activity-dependent process. Eur. J. Neurosci. 16, 1249–1258.
Benn, S. C., Costigan, M., Tate, S., Fitzgerald, M., and Woolf, C. J. 2001. Developmental expression of the TTX-resistant voltage-gated sodium channels Nav1.8 (SNS) and Nav1.9 (SNS2) in primary sensory neurons. J. Neurosci. 21, 6077–6085.
Benn, S. C., Perrelet, D., Kato, A. C., Scholz, J., Decosterd, I., Mannion, R. J., Bakowska, J. C., and Woolf, C. J. 2002. Hsp27 upregulation and phosphorylation is required for injured sensory and motor neuron survival. Neuron 36, 45–56.
Bennett, D. L., Averill, S., Clary, D. O., Priestley, J. V., and McMahon, S. B. 1996. Postnatal changes in the expression of the trkA high-affinity NGF receptor in primary sensory neurons. Eur. J. Neurosci. 8, 2204–2208.
Bice, T. N. and Beal, J. A. 1997. Quantitative and neurogenic analysis of neurons with supraspinal projections in the superficial dorsal horn of the rat lumbar spinal cord. J. Comp. Neurol. 388, 565–574.
Bondok, A. A. and Sansone, F. M. 1984. Retrograde and transganglionic degeneration of sensory neurons after a peripheral nerve lesion at birth. Exp. Neurol. 86, 322–330.
Boucher, T., Jennings, E., and Fitzgerald, M. 1998. The onset of diffuse noxious inhibitory controls in postnatal rat pups: a C-Fos study. Neurosci. Lett. 257, 9–12.
Bourgeais, L., Gauriau, C., and Bernard, J. F. 2001. Projections from the nociceptive area of the central nucleus of the amygdala to the forebrain: a PHA-L study in the rat. Eur. J. Neurosci. 14, 229–255.
Braz, J. M., Nassar, M. A., Wood, J. N., and Basbaum, A. I. 2005. Parallel ''pain'' pathways arise from subpopulations of primary afferent nociceptor. Neuron 47, 787–793.
Bregman, B. S. 1987. Development of serotonin immunoreactivity in the rat spinal cord and its plasticity after neonatal spinal cord lesions. Brain Res. 431, 245–263.
Bremner, L., Fitzgerald, M., and Baccei, M. 2006. The functional GABA(A)-receptor mediated inhibition in the neonatal dorsal horn. J. Neurophysiol. 95(6), 3893–3897.
Cabana, T. and Martin, G. F. 1984. Developmental sequence in the origin of descending spinal pathways. Studies using retrograde transport techniques in the North American opossum (*Didelphis virginiana)*. Brain Res. 317, 247–263.
Cardinal, R. N., Parkinson, J. A., Lachenal, G., Halkerston, K. M., Rudarakanchana, N., Hall, J., Morrison, C. H., Howes, S. R., Robbins, T. W., and Everitt, B. J. 2002. Effects of selective excitotoxic lesions of the nucleus accumbens core, anterior cingulate cortex, and central nucleus of the amygdala on autoshaping performance in rats. Behav. Neurosci. 116, 553–567.
Cervero, F. and Plenderleith, M. B. 1985. C-fibre excitation and tonic descending inhibition of dorsal horn neurones in adult rats treated at birth with capsaicin. J. Physiol. 365, 223–237.
Cholley, B., Wassef, M., Arsénio-Nunes, L., Brehier, A., and Sotelo, C. 1989. Proximal trajectory of the brachium conjunctivum in rat fetuses and its early association with the parabrachial nucleus. A study combining *in vitro* HRP anterograde axonal tracing and immunocytochemistry. Brain Res. Dev. Brain Res. 45, 185–202.
Commissiong, J. W. 1983. The development of catecholaminergic nerves in the spinal cord of rat. II. Regional development. Brain Res. 313, 75–92.
Commissiong, J. W. and Neff, N. H. 1979. Current status of dopamine in the mammalian spinal cord. Biochem. Pharmacol. 28, 1569–1573.
Commissiong, J. W., Galli, C. L., and Neff, N. H. 1978. Differentiation of dopaminergic and noradrenergic neurons in rat spinal cord. J. Neurochem. 30, 1095–1099.
Constantinou, J., Reynolds, M. L., Woolf, C. J., Safieh-Garabedian, B., and Fitzgerald, M. 1994. Nerve growth factor levels in developing rat skin: upregulation following skin wounding. Neuroreport 5, 2281–2284.
Craig, K. D., Korol, C. T., and Pillai, R. R. 2002. Challenges of judging pain in vulnerable infants. Clin. Perinatol. 29, 445–457.
Davidson, R. J. 2002. Anxiety and affective style: role of prefrontal cortex and amygdala. Biol. Psychiatry 51, 68–80.
Davis, M. 1998a. Are different parts of the extended amygdala involved in fear versus anxiety? Biol. Psychiatry 44, 1239–1247.
Davis, M. 1998b. Are different parts of the extended amygdala involved in fear versus anxiety? Biol. Psychiatry 44, 1239–1247.
Davies, A. M. 2000. Neurotrophins: more to NGF than just survival. Curr. Biol. 10, R374–R376.
Davis, B. M., Fundin, B. T., Albers, K. M., Goodness, T. P., Cronk, K. M., and Rice, F. L. 1997. Overexpression of nerve growth factor in skin causes preferential increases among innervation to specific sensory targets. J. Comp. Neurol. 387, 489–506.
Diebler, M. F., Farkas-Bargeton, E., and Wehrle, R. 1979. Developmental changes of enzymes associated with energy metabolism and the synthesis of some neurotransmitters in discrete areas of human neocortex. J. Neurochem. 32, 429–435.
Ding, Y. Q., Takada, M., Shigemoto, R., and Mizumo, N. 1995. Spinoparabrachial tract neurons showing substance P receptor-like immunoreactivity in the lumbar spinal cord of the rat. Brain Res. 674, 336–340.
Ekholm, J. 1967. Postnatal changes in cutaneous reflexes and in the discharge pattern of cutaneous and articular sense organs. A morphological and physiological study in the cat. Acta. Physiol. Scand. Suppl. 297, 1–130.
Fees-Higgins, A. and Larroche, J. C. 1987. Development of The Human Foetal Brain: An Anatomical Atlas. INSERM.
Fitzgerald, M. 1985. The post-natal development of cutaneous afferent fibre input and receptive field organization in the rat dorsal horn. J. Physiol. 364, 1–18.
Fitzgerald, M. 1987. Cutaneous primary afferent properties in the hind limb of the neonatal rat. J. Physiol. 383, 79–92.
Fitzgerald, M. 2005. The development of nociceptive circuits. Nat. Rev. Neurosci. 6, 507–520.
Fitzgerald, M. and Gibson, S. 1984. The postnatal physiological and neurochemical development of peripheral sensory C fibres. Neuroscience 13, 933–944.
Fitzgerald, M. and Jennings, E. 1999. The postnatal development of spinal sensory processing. Proc. Natl. Acad. Sci. U. S. A. 96, 7719–7722.
Fitzgerald, M. and Koltzenburg, M. 1986. The functional development of descending inhibitory pathways in the dorsolateral funiculus of the newborn rat spinal cord. Brain Res. 389, 261–270.
Fitzgerald, M. and Walker, S. M. 2003. The Role of Activity in Developing Pain Pathways. In: Proceedings of the 10th

World Congress on Pain (*eds*. J. Dostrovsky, D. Carr, and M. Koltzenburg), pp. 185–196. IASP Press.
Fitzgerald, M., Butcher, T., and Shortland, P. 1994. Developmental changes in the laminar termination of A fibre cutaneous sensory afferents in the rat spinal cord dorsal horn. J. Comp. Neurol. 348, 225–233.
Fitzgerald, M., King, A. E., Thompson, S. W., and Woolf, C. J. 1987. The postnatal development of the ventral root reflex in the rat; a comparative *in vivo* and *in vitro* study. Neurosci. Lett. 78, 41–45.
Fitzgerald, M., Shaw, A., and MacIntosh, N. 1988. Postnatal development of the cutaneous flexor reflex: comparative study of preterm infants and newborn rat pups. Dev. Med. Child Neurol. 30, 520–526.
Fitzgerald, M., Woolf, C. J., and Shortland, P. 1990. Collateral sprouting of the central terminals of cutaneous primary afferent neurons in the rat spinal cord: pattern, morphology, and influence of targets. J. Comp. Neurol. 300, 370–385.
Fox, K. 2002. Anatomical pathways and molecular mechanisms for plasticity in the barrel cortex. Neuroscience 111, 799–814.
Gallagher, M. and Schoenbaum, G. 1999. Functions of the amygdala and related forebrain areas in attention and cognition. Ann. N. Y. Acad. Sci. 877, 397–411.
Gebhart, G. F. 2004. Descending modulation of pain. Neurosci. Biobehav. Rev. 27, 729–737.
Giannakoulopoulos, X., Sepulveda, W., Kourtis, P., Glover, V., and Fisk, N. M. 1994. Fetal plasma cortisol and beta-endorphin response to intrauterine needling. Lancet 344, 77–81.
Gilbert, M. and Stelzner, D. J. 1979. The development of descending and dorsal root connections in the lumbosacral spinal cord of the postnatal rat. J. Comp. Neurol. 184, 821–838.
Green, G. M. and Gibb, A. J. 2001. Characterization of the single-channel properties of NMDA receptors in laminae I and II of the dorsal horn of neonatal rat spinal cord. Eur. J. Neurosci. 14, 1590–1602.
Guo, A., Simone, D. A., Stone, L. S., Fairbanks, C. A., Wang, J., and Elde, R. 2001. Developmental shift of vanilloid receptor 1 (VR1) terminals into deeper regions of the superficial dorsal horn: correlation with a shift from TrkA to Ret expression by dorsal root ganglion neurons. Eur. J. Neurosci. 14, 293–304.
Hall, A. K., Ai, X., Hickman, G. E., MacPhedran, S. E., Nduaguba, C. O., and Robertson, C. P. 1997. The generation of neuronal heterogeneity in a rat sensory ganglion. J. Neurosci. 17, 2775–2784.
Hall, A. K., Dinsio, K. J., and Cappuzzello, J. 2001. Skin cell induction of calcitonin gene-related peptide in embryonic sensory neurons in vitro involves activin. Dev. Biol. 229, 263–270.
Hanganu, I. L., Kilb, W., and Luhmann, H. J. 2002. Functional synaptic projections onto subplate neurons in neonatal rat somatosensory cortex. J. Neurosci. 22, 7165–7176.
Higashi, S., Molnar, Z., Kurotani, T., and Toyama, K. 2002. Prenatal development of neural excitation in rat thalamocortical projections studied by optical recording. Neuroscience 115, 1231–1246.
Holmberg, H. and Schouenborg, J. 1996. Postnatal development of the nociceptive withdrawal reflexes in the rat: a behavioural and electromyographic study. J. Physiol. 493(Pt 1), 239–252.
Howard, R. F., Hatch, D. J., Cole, T. J., and Fitzgerald, M. 2001. Inflammatory pain and hypersensitivity are selectively reversed by epidural bupivacaine and are developmentally regulated. Anesthesiology 95, 421–427.
Huang, C. C. 1991. Sonographic cerebral sulcal development in premature newborns. Brain Dev. 13, 27–31.
Huang, Y., Stamer, W. D., Anthony, T. L., Kumar, D. V., St, J. P., and Regan, J. W. 2002. Expression of alpha(2)-adrenergic receptor subtypes in prenatal rat spinal cord. Brain Res. Dev. Brain Res. 133, 93–104.
Humphrey, T. 1968. The development of the human amygdala during early embryonic life. J. Comp. Neurol. 132, 135–165.
Hunt, S. and Mantyh, P. 2001. The molecular dynamics of pain control. Nat. Rev. Neurosci. 2, 83–91.
Jackman, A. and Fitzgerald, M. 2000. Development of peripheral hindlimb and central spinal cord innervation by subpopulations of dorsal root ganglion cells in the embryonic rat. J. Comp. Neurol. 418, 281–298.
Jakowec, M. W., Fox, A. J., Martin, L. J., and Kalb, R. G. 1995. Quantitative and qualitative changes in AMPA receptor expression during spinal cord development. Neuroscience 67, 893–907.
Jasmin, L., Tien, D., Weinshenker, D., Palmiter, R. D., Green, P. G., Janni, G., and Ohara, P. T. 2002. The NK1 receptor mediates both the hyperalgesia and the resistance to morphine in mice lacking noradrenaline. Proc. Natl. Acad. Sci. U. S. A. 99, 1029–1034.
Jiang, M. C. and Gebhart, G. F. 1998. Development of mustard oil-induced hyperalgesia in rats. Pain 77, 305–313.
Jones, B. E. 1991. Noradrenergic locus coeruleus neurons: their distant connections and their relationship to neighboring (including cholinergic and GABAergic) neurons of the central gray and reticular formation. Prog. Brain Res. 88, 15–30.
Kaas, J. H., Merzenich, M. M., and Killackey, H. P. 1983. The reorganization of somatosensory cortex following peripheral nerve damage in adult and developing mammals. Annu. Rev. Neurosci. 6, 325–356.
Keller, A. F., Breton, J. D., Schlichter, R., and Poisbeau, P. 2004. Production of 5alpha-reduced neurosteroids is developmentally regulated and shapes GABA(A) miniature IPSCs in lamina II of the spinal cord. J. Neurosci. 24, 907–915.
Klimach, V. J. and Cooke, R. W. 1988. Maturation of the neonatal somatosensory evoked response in preterm infants. Dev. Med. Child Neurol. 30, 208–214.
Koltzenburg, M. 1999. The changing sensitivity in the life of the nociceptor. Pain Suppl. 6, S93–S102.
Koltzenburg, M. and Lewin, G. R. 1997. Receptive properties of embryonic chick sensory neurons innervating skin. J. Neurophysiol. 78, 2560–2568.
Kordower, J. H., Piecinski, P., and Rakic, P. 1992. Neurogenesis of the amygdaloid nuclear complex in the rhesus monkey. Brain Res. Dev. Brain Res. 68, 9–15.
Lakke, E. A. 1997. The projections to the spinal cord of the rat during development: a timetable of descent. Adv. Anat. Embryol. Cell Biol. 135, 1–143.
Ledoux, J. E. 2000a. Emotion circuits in the brain. Annu. Rev. Neurosci. 23, 155–184.
Ledoux, J. E. 2000b. Emotion circuits in the brain. Annu. Rev. Neurosci. 23, 155–184.
Lee, C. J., Kong, H., Manzini, M. C., Albuquerque, C., Chao, M. V., and MacDermott, A. B. 2001. Kainate receptors expressed by a subpopulation of developing nociceptors rapidly switch from high to low Ca^{2+} permeability. J. Neurosci. 21, 4572–4581.
Leong, S. K. 1983. Localizing the corticospinal neurons in neonatal, developing and mature albino rat. Brain Res. 265, 1–9.
Lev, D. L., Weinfeld, E., and White, E. L. 2002. Synaptic patterns of thalamocortical afferents in mouse barrels at postnatal day. J. Comp. Neurol. 442, 63–77.
Lewin, G. R. and Mendell, L. M. 1994. Regulation of cutaneous C-fibre heat nociceptors by nerve growth factor in the developing rat. J. Neurophysiol. 71, 941–949.
Li, W. and Neugebauer, V. 2004. Differential roles of mGluR1 and mGluR5 in brief and prolonged nociceptive processing in central amygdala neurons. J. Neurophysiol. 91, 13–24.
Li, P. and Zhuo, M. 1998. Silent glutamatergic synapses and nociception in mammalian spinal cord. Nature 393, 695–698.

Lidov, H. G. and Molliver, M. E. 1982. Immunohistochemical study of the development of serotonergic neurons in the rat CNS. Brain Res. Bull. 9, 559–604.

Lidow, M. S. 2002. Long-term effects of neonatal pain on nociceptive systems. Pain 99, 377–383.

Loizou, L. A. 1972. The postnatal ontogeny of monoamine-containing neurones in the central nervous system of the albino rat. Brain Res. 40, 395–418.

Luhmann, H. J., Hanganu, I., and Kilb, W. 2003. Cellular physiology of the neonatal rat cerebral cortex. Brain Res. Bull. 60, 345–353.

Man, S. H., Wong, Y. M., Fitzgerald, M. F., and Hunt, S. P. 2005. Postnatal development of excitatory link between lamina I and the brainstem. Proceedings of the International Society for the Study of Pain. Abstract.

Mantyh, P. W. and Hunt, S. P. 2004. Setting the tone: superficial dorsal horn projection neurons regulate pain sensitivity. Trends Neurosci. 27, 582–584.

Marchand, F., Perretti, M., and McMahon, S. B. 2005. Role of the immune system in chronic pain. Nat. Rev. Neurosci. 6, 521–532.

Maren, S. 1999. Long-term potentiation in the amygdala: a mechanism for emotional learning and memory. Trends Neurosci. 22, 561–567.

Markus, A., Zhong, J., and Snider, W. D. 2002. Raf and akt mediate distinct aspects of sensory axon growth. Neuron 35, 65–76.

Marsh, D., Dickenson, A., Hatch, D., and Fitzgerald, M. 1999. Epidural opioid analgesia in infant rats II: responses to carrageenan and capsaicin. Pain 82, 33–38.

Marshall, G. E., Shehab, S. A., Spike, R. C., and Todd, A. J. 1996. Neurokinin-1 receptors on lumbar spinothalamic neurons in the rat. Neuroscience 72, 255–263.

Meyer, G. 2001. Human neocortical development: the importance of embryonic and early fetal events. Neuroscientist 7, 303–314.

Millan, M. J. 2002. Descending control of pain. Prog. Neurobiol. 66, 355–474.

Molliver, D. C., Wright, D. E., Leitner, M. L., Parsadanian, A. S., Doster, K., Wen, D., Yan, Q., and Snider, W. D. 1997. IB4-binding DRG neurons switch from NGF to GDNF dependence in early postnatal life. Neuron 19, 849–861.

Molnar, Z., Kurotani, T., Higashi, S., Yamamoto, N., and Toyama, K. 2003. Development of functional thalamocortical synapses studied with current source-density analysis in whole forebrain slices in the rat. Brain Res. Bull. 60, 355–371.

Molnar, Z., Lopez-Bendito, G., Small, J., Partridge, L. D., Blakemore, C., and Wilson, M. C. 2002. Normal development of embryonic thalamocortical connectivity in the absence of evoked synaptic activity. J. Neurosci. 22, 10313–10323.

Momose-Sato, Y., Sato, K., and Kamino, K. 2001. Optical approaches to embryonic development of neural functions in the brainstem. Prog. Neurobiol. 63, 151–197.

Moore, R. Y. and Bloom, F. E. 1978. Central catecholamine neuron systems: anatomy and physiology of the dopamine systems. Annu. Rev. Neurosci. 1, 129–169.

Nandi, R. and Fitzgerald, M. 2005. Opioid analgesia in the newborn. Eur. J. Pain 9, 105–108.

Nandi, R., Beacham, D., Middleton, J., Koltzenburg, M., Howard, R. F., and Fitzgerald, M. 2004. The functional expression of mu opioid receptors on sensory neurons is developmentally regulated; morphine analgesia is less selective in the neonate. Pain 111, 38–50.

Neugebauer, V. and Li, W. 2002. Processing of nociceptive mechanical and thermal information in central amygdala neurons with knee-joint input. J. Neurophysiol. 87, 103–112.

Neugebauer, V. and Li, W. 2003. Differential sensitization of amygdala neurons to afferent inputs in a model of arthritic pain. J. Neurophysiol. 89, 716–727.

Nikolic, I. and Kostovic, I. 1986. Development of the lateral amygdaloid nucleus in the human fetus: transient presence of discrete cytoarchitectonic units. Anat. Embryol. (Berl.) 174, 355–360.

Nissen, U. V., Mochida, H., and Glover, J. C. 2005. Development of projection-specific interneurons and projection neurons in the embryonic mouse and rat spinal cord. J. Comp. Neurol. 483, 30–47.

O'Leary, D. D. and Nakagawa, Y. 2002. Patterning centers, regulatory genes and extrinsic mechanisms controlling arealization of the neocortex. Curr. Opin. Neurobiol. 12, 14–25.

Olson, L. and Seiger, A. 1972. Early prenatal ontogeny of central monoamine neurons in the rat: fluorescence histochemical observations. Z. Anat. Entwicklungsgesch 137, 301–316.

O'Rahilly, R. and Muller, F. 1994. Neurulation in the normal human embryo. Ciba Found. Symp. 181, 70–82.

Pattinson, D. and Fitzgerald, M. 2004. The neurobiology of infant pain: development of excitatory and inhibitory neurotransmission in the spinal dorsal horn. Reg. Anesth. Pain Med. 29, 36–44.

van Praag, H. and Frenk, H. 1991. The development of stimulation-produced analgesia (SPA) in the rat. Brain Res. Dev. Brain Res. 64, 71–76.

Petersson, P., Waldenstrom, A., Fahraeus, C., and Schouenborg, J. 2003. Spontaneous muscle twitches during sleep guide spinal self-organization. Nature 424, 72–75.

Pitkanen, A., Savander, V., and Ledoux, J. E. 1998. Organization of intra-amygdaloid circuitries in the rat: an emerging framework for understanding functions of the amygdala. Trends Neurosci. 20(11), 517–523 Abstract.

Rajaofetra, N., Sandillon, F., Geffard, M., and Privat, A. 1989. Pre- and post-natal ontogeny of serotonergic projections to the rat spinal cord. J. Neurosci. Res. 22, 305–321.

Rees, S., Nitsos, I., and Rawson, J. 1994. The development of cutaneous afferent pathways in fetal sheep: a structural and functional study. Brain Res. 661, 207–222.

Remedios, R., Subramanian, L., and Tole, S. 2004. LIM genes parcellate the embryonic amygdala and regulate its development. J. Neurosci. 24, 6986–6990.

Ren, K. and Dubner, R. 2002. Descending modulation in persistent pain: an update. Pain 100, 1–6.

Ritter, A. M., Lewin, G. R., Kremer, N. E., and Mendell, L. M. 1991. Requirement for nerve growth factor in the development of myelinated nociceptors *in vivo*. Nature 350, 500–502.

Rubenstein, J. L. 1998. Development of serotonergic neurons and their projections. Biol. Psychiatry 44, 145–150.

Sagen, J. and Proudfit, H. K. 1984. Effect of intrathecally administered noradrenergic antagonists on nociception in the rat. Brain Res. 310, 295–301.

Schlaggar, B. L. and O'Leary, D. D. 1994. Early development of the somatotopic map and barrel patterning in rat somatosensory cortex. J. Comp. Neurol. 346, 80–96.

Shortland, P. and Fitzgerald, M. 1994. Neonatal sciatic nerve section results in a rearrangement of the central terminals of saphenous and axotomized sciatic nerve afferents in the dorsal horn of the spinal cord of the adult rat. Eur. J. Neurosci. 6, 75–86.

Sidman, R. L. and Rakic, P. 1973. Neuronal migration, with special reference to developing human brain: a review. Brain Res. 62, 1–35.

Sivilotti, L. G., Thompson, S. W., and Woolf, C. J. 1993. Rate of rise of the cumulative depolarization evoked by repetitive stimulation of small-caliber afferents is a predictor of action potential windup in rat spinal neurons *in vitro*. J. Neurophysiol. 69, 1621–1631.

Skagerberg, G., Bjorklund, A., Lindvall, O., and Schmidt, R. H. 1982. Origin and termination of the diencephalo-spinal dopamine system in the rat. Brain Res. Bull. 9, 237–244.

Skagerberg, G., Meister, B., Hokfelt, T., Lindvall, O., Goldstein, M., Joh, T., and Cuello, A. C. 1988. Studies on dopamine-, tyrosine hydroxylase- and aromatic L-amino acid decarboxylase-containing cells in the rat diencephalon: comparison between formaldehyde-induced histofluorescence and immunofluorescence. Neuroscience 24, 605–620.

Slater, R., Cantarella, A., Gallella, S., Worley, A., Boyd, S., Meek, J., and Fitzgerald, M. 2006. Cortical pain responses in human infants. J. Neurosci. 26(14), 3662–3666.

Stegenga, S. L. and Kalb, R. G. 2001. Developmental regulation of *N*-methyl-D-aspartate- and kainate-type glutamate receptor expression in the rat spinal cord. Neuroscience 105, 499–507.

Stevens, B. J. and Franck, L. S. 2001. Assessment and management of pain in neonates. Paediatr. Drugs 3, 539–558.

Suzuki, R., Morcuende, S., Webber, M., Hunt, S. P., and Dickenson, A. H. 2002. Superficial NK1-expressing neurons control spinal excitability through activation of descending pathways. Nat. Neurosci. 5, 1319–1326.

Suzuki, R., Rygh, L. J., and Dickenson, A. H. 2004. Bad news from the brain: descending 5-HT pathways that control spinal pain processing. Trends Pharmacol. Sci. 25, 613–617.

Swanson, L. W. and Kuypers, H. G. 1980. The paraventricular nucleus of the hypothalamus: cytoarchitectonic subdivisions and organization of projections to the pituitary, dorsal vagal complex, and spinal cord as demonstrated by retrograde fluorescence double-labeling methods. J. Comp. Neurol. 194, 555–570.

Todd, A. J., McGill, M. M., and Shehab, S. A. 2000. Neurokinin 1 receptor expression by neurons in laminae I, III and IV of the rat spinal dorsal horn that project to the brainstem. Eur. J. Neurosci. 12, 689–700.

Torsney, C. and Fitzgerald, M. 2002. Age-dependent effects of peripheral inflammation on the electrophysiological properties of neonatal rat dorsal horn neurons. J. Neurophysiol. 87, 1311–1317.

Torsney, C. and Fitzgerald, M. 2003. Spinal dorsal horn cell receptive field size is increased in adult rats following neonatal hindpaw skin injury. J. Physiol. 550, 255–261.

Waldenstrom, A., Thelin, J., Thimansson, E., Levinsson, A., and Schouenborg, J. 2003. Developmental learning in a pain-related system: evidence for a cross-modality mechanism. J. Neurosci. 23, 7719–7725.

Walker, S. 2005. Modulation of pain by alpha 2 agonists – effect of developmental age. Ph.D. thesis, University College London.

Watanabe, M., Mishina, M., and Inoue, Y. 1994. Distinct spatiotemporal distributions of the *N*-methyl-D-aspartate receptor channel subunit mRNAs in the mouse cervical cord. J. Comp. Neurol. 345, 314–319.

Webster, M. J., Ungerleider, L. G., and Bachevalier, J. 1991. Lesions of inferior temporal area TE in infant monkeys alter cortico-amygdalar projections. Neuroreport 2, 769–772.

Winzer-Serhan, U. H., Raymon, H. K., Broide, R. S., Chen, Y., and Leslie, F. M. 1997. Expression of alpha 2 adrenoceptors during rat brain development – I. Alpha 2A messenger RNA expression. Neuroscience 76, 241–260.

Woolf, C. J. and Salter, M. W. 2000. Neuronal plasticity: increasing the gain in pain. Science 288, 1765–1769.

Yao, H. and Dan, Y. 2005. Synaptic learning rules, cortical circuits, and visual function. Neuroscientist 11, 206–216.

Yip, H. K., Rich, K. M., Lampe, P. A., and Johnson, E. M., Jr. 1984. The effects of nerve growth factor and its antiserum on the postnatal development and survival after injury of sensory neurons in rat dorsal root ganglia. J. Neurosci. 4, 2986–2992.

Zald, D. H. 2003. The human amygdala and the emotional evaluation of sensory stimuli. Brain Res. Brain Res. Rev. 41, 88–123.

5.12 Appropriate/Inappropriate Developed Pain Paths

J Schouenborg, Lund University, Lund, Sweden

© 2008 Elsevier Inc. All rights reserved.

5.12.1	General Background	147
5.12.2	Modular Organization of Sensorimotor Circuits in the Spinal Cord	147
5.12.3	Action-Based Sensory Encoding	149
5.12.4	Functional Adaptation of Sensorimotor Circuits During Development	149
5.12.5	Concluding Remarks	152
References		152

5.12.1 General Background

The topographical organization of the somatosensory input to the spinal cord has traditionally been regarded as a somatotopically organized map of the body (Molander, C. and Grant, G., 1985; Mirnics, K. and Koerber, H. R., 1995; Silos-Santiago, I. *et al.*, 1995; Wilson, P. and Kitchener, P. D., 1996; Brown, P. B. *et al.*, 1997; 2004; 2005), with different body parts represented in different central nervous system (CNS) areas and the size of the representation being a function of receptor density and, to some extent, practise (see Blake, D. T., *et al.*, 2002). Most studies on the body representation have been focused on the sensory discriminative aspects (Brown, P. B. *et al.*, 2004; 2005). However, a major function of the spinal cord is to use the sensory information to control skeletal muscles. It has therefore been suggested that the somatosensory input may be primarily organized in a motor frame of reference (Levinsson, A. *et al.*, 2002). Such a view might explain some of the oddities with the known topography. For example, in the dorsal horn, there is an extensive overlap of afferent terminals from different body parts, and the sequence of the representation from distal to proximal body parts is neither continuous nor sequential (Levinsson, A. *et al.*, 2002). Moreover, the phenomenon of somatotopically inappropriate terminations, that is, primary afferents terminating outside the main projection area, might be explained if different motor systems requiring sensory information from same body region have different locations in the spinal cord.

To be useful in motor control, somatosensory information must be encoded with respect to body anatomy and movement patterns produced by the sensorimotor circuits. This is a computationally demanding task since the multisensory information (nociception, pressure, temperature, joint angles, muscle force, and length) arises from a complex body constitution. Understanding how sensory information is processed by spinal sensorimotor circuits and how the adult organization emerges during development is therefore a major task. This review will deal with the current literature on the modular organization of the spinal cord and the role of somatosensory imprinting in establishing an action-based sensory encoding in these modules.

5.12.2 Modular Organization of Sensorimotor Circuits in the Spinal Cord

During the last 10 years, the concept of a modular organization of the spinal cord has grown stronger. The idea of a modular organization of motor circuits in CNS is not new and, for the spinal cord, was proposed already in 1981 by Grillner, S. for locomotor circuits (unit bursters causing rhythmic activity around a joint) and later for circuits controlling scratch reflexes in the turtle (Mortin, L. I. *et al.*, 1985; Stein, P. S. *et al.*, 1998; Berkowitz, A., 2001). However, although a modular organization is conceivable, it is not yet clear exactly what constitutes a module in these rhythm-generating systems, the extent to which the different modules overlap in space, and how sensory information is related to the function of these modules (Tresch, M. C. *et al.*, 2002).

A modular type of reflex organization in the mammalian spinal cord was first demonstrated for the nociceptive withdrawal reflex (NWR) system in the rat (Schouenborg, J. and Kalliomäki, J., 1990; Schouenborg, J. *et al.*, 1992), but subsequently also in cats (Levinsson, A. *et al.*, 1999), mice (Thelin, J. M. and Schouenborg, J., 2003), and humans

(Sonnenborg, F. A. *et al.*, 2000). Here, the word modular is used synonymous to the term functional unit of a system, that is, not alluding to the existence of different motor systems, such as stepping, standing, scratching, or withdrawal reflex systems. For the NWR system, each excitatory module preferentially acts on a single muscle and performs a detailed sensorimotor transformation resulting in a graded withdrawal of the limb (or part of the limb) from its receptive field. For each excitatory NWR module, the input strength has a characteristic pattern on the skin that mimics the pattern of withdrawal efficacy in a standing position when the principal output muscle of the module contracts (Figure 1; Schouenborg, J. and Weng, H.-R., 1994). In a sense, the pattern of withdrawal (or unloading) efficacy is imprinted on the receptive field of the module. Neurones that encode sensory input in this motor frame of reference, termed reflex encoders (Schouenborg, J. *et al.*, 1995), are mainly located in deep dorsal horn laminae IV–VI. These neurones receive and weight the multisensory input from both tactile Aβ and nociceptive Aδ and C afferent fibers in proportion to the withdrawal/unloading action of the modules in a standing position (Figure 2). It is worth noting that, although the nociceptive input is stronger than that from tactile input, the strength of the input mediated by different types of afferent fibers is weighted in the same way. In fact, a large proportion of the wide dynamic range neurones, that is, neurones receiving a convergent input from tactile and nociceptive receptors, often referred to as wide dynamic range neurons, in the deep layers of the fifth lumbar segment, appear to be of the reflex encoder type. Within the L4–5 segments, reflex encoders for the interossei, flexor digitorum longus, gastrocnemius, peronei, and extensor digitorum longus muscles are located in a mediolateral sequence reminiscent of the corresponding topographical organization of the motoneuron columns in the ventral horn. Hence, the reflex encoders appear to be located in discrete pools that have a musculotopic organization.

A corresponding set of inhibitory reflex modules also exists. In this case, the receptive fields correspond to the graded movement of the skin area toward external stimulation (i.e., increase in load) on contraction of the muscle in the module (Weng, H.-R. and Schouenborg, J., 1996). As a result of this organization, the excitatory and inhibitory modules are engaged to a degree that is proportional to their respective withdrawal/loading efficacy on skin stimulation.

The same principles of sensorimotor transformation as found for rat withdrawal reflexes also apply to the cat, mice, and humans (Levinsson, A. *et al.*, 1999 in cats; Sonnenborg, F. A. *et al.*, 2000; Thelin, J. M. and Schouenborg, J., 2003). Interestingly, muscles with different function in two different species exhibit corresponding differences in the receptive fields of the withdrawal reflexes. Thus, withdrawal reflexes elicited in dorsiflexors are much weaker in the cat than in the rat and vice versa for reflexes to plantar flexors. Cats stand on their digits, whereas rats stand on the whole plantar surface. In the standing position, the dorsiflexors of cat digits are much less effective in withdrawing the plantar skin than the corresponding muscles in rats and vice versa for plantar flexors. These findings are consistent with the view that these reflexes consist of adaptive modules (see Section 5.12.4).

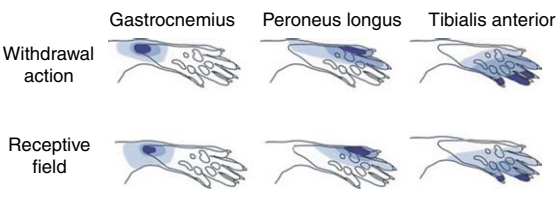

Figure 1 Action-based sensory encoding. Typical distributions of sensitivity and corresponding withdrawal action for three muscles are shown. Low, medium, and high dot density indicates areas of the skin from which the evoked responses were 0–30%, 30–70%, and 70–100% of maximal response, respectively. Adapted from Schouenborg, J. and Weng, H.-R. 1994. Sensorimotor transformation in a spinal motor system. Exp. Brain. Res. 100, 170–174.

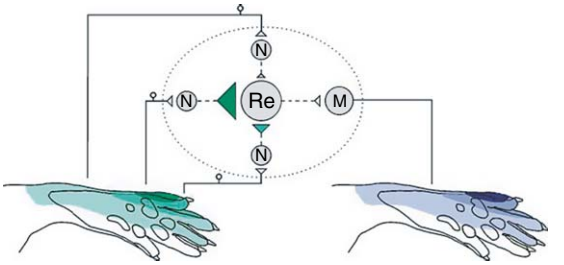

Figure 2 Schematic circuitry organization of a withdrawal reflex module. Nociceptive afferents from the receptive field (right) synapse with nociceptive neurones (N) in the superficial laminae of the dorsal horn. Reflex encoder neurones (Re) receive a weighted nociceptive input from superficially located neurones. Re project either directly or indirectly to motoneurones essentially controlling the action of a single muscle. Withdrawal efficacy of the module is shown to the right. Sensitivity in strength of primary afferent input and sensitivity in receptive fields is coded by color intensity. Tactile input is omitted for clarity.

Based on microstimulation in the dorsal horn of the spinal cord, a somewhat different modular organization of sensorimotor circuits acting on synergistic muscle groups was later proposed in frogs and rats (Tresch, M. C. and Bizzi, E., 1999; Bizzi, E. *et al.*, 2000, Saltiel, P. *et al.*, 2001). According to these authors, electrical and glutamatergic stimulation of the deep dorsal horn often results in a movement toward an equilibrium point, independent of the starting position of the limb. Here, the output of a module would include activity in two or more different muscles. Whether these findings reflect the existence of a fundamentally different type of reflex system than that of the withdrawal reflex system or the outcome of a combined stimulation of many withdrawal reflex modules is not clear at present. In a recent study, Avella and colleagues suggested, by analyzing electromyography (EMG) in frog hindlimbs during kicking, that a combination of a limited number of synergistic units was used for this behaviour (Avella, A. *et al.*, 2003).

5.12.3 Action-Based Sensory Encoding

By mapping tactile input to the dorsal horn, longitudinal cigar-shaped zones that weight the monosynaptic cutaneous input as a function of the unloading pattern caused by individual modules were found (Figure 3; Levinsson, A. *et al.*, 2002). This was a surprising finding in that it indicates that sensory input to the spinal cord gets organized and weighted in a motor frame of reference already at the level of the first-order synapses and that there may, consequently, not be a true 'map' of the body in the spinal cord as previously thought (Molander, C. and Grant, G., 1985; Mirnics, K. and Koerber, H. R., 1995; Silos-Santiago, I. *et al.*, 1995; Brown, P. B. *et al.*, 1997). Given that a main function of the spinal cord is to translate sensory information into movement corrections, an action-based sensory encoding do, however, appear to be an economical and fast way of processing the sensory information.

There are many reasons to think that action-based sensory encoding is fundamental also for higher-order motor systems. For example, the C1, C3, and X zones in the anterior cerebellar lobe is divided into microzones, where each microzone is defined by its climbing fibre input from a specific receptive field on the skin (Garwicz, M., 2002; Garwicz, M. *et al.*, 2002; Apps, R. and Garwicz, M., 2005). These climbing fibers encode the sensory input in the same way as individual spinal modules, that is, as a function of the unloading pattern caused by single muscle contraction.

5.12.4 Functional Adaptation of Sensorimotor Circuits During Development

Given that the adult sensorimotor transformations performed by the spinal withdrawal reflex circuits reflect precisely weighted connections in modules, how can this weighting be achieved during development? While the gross topographical organization of interneurons of the spinal cord is likely to be guided by gradients of trophic substances during the development (Albright, T. D. *et al.*, 2000, Chen, A. I. *et al.*, 2006; Chen, C. L. *et al.*, 2006; Kramer, I. *et al.*, 2006), it is difficult to see how such mechanisms could encode the detailed strength of every connection in the networks. Recent studies on the NWR system provide some clues to this problem. The sensorimotor transformations performed by its modules are functionally adapted during the first postnatal weeks in the rat (Holmberg, H. and Schouenborg, J., 1996a). During this time, the strength of the erroneous (or inappropriate) connections becomes weaker, whereas the strength of the adequate connections becomes proportional to the unloading effect on the skin of muscle contraction. Moreover, during this time, NWR can adapt to both altered innervation of the skin caused by nerve sections (Holmberg, H. and Schouenborg, J., 1996b) and to altered movement patterns caused by tendon transfer in the neonatal rat (Holmberg, H. *et al.*, 1997). Blocking the sensory input during the time of functional adaptation abolishes the learning (Waldenström, A. *et al.*, 2003), indicating a role for sensory input. Notably, a selective block of the nociceptive input by EMLA salve did not have an effect as compared with vehicle treatment. The functional adaptation is not blocked unless tactile input is also blocked, indicating a key role for tactile input in tuning nociceptive connections (Figure 4(a)). This conclusion is strongly supported by the finding that tactile feedback ensuing on spontaneous motility in spinal sensorimotor circuits alters the nociceptive connection strengths in NWR modules during postnatal development (Figures 4(b)–4(c)); Petersson, P. *et al.*, 2003). Thus, the pattern of tactile inputs arriving in conjunction with the spontaneous movements has an instructive

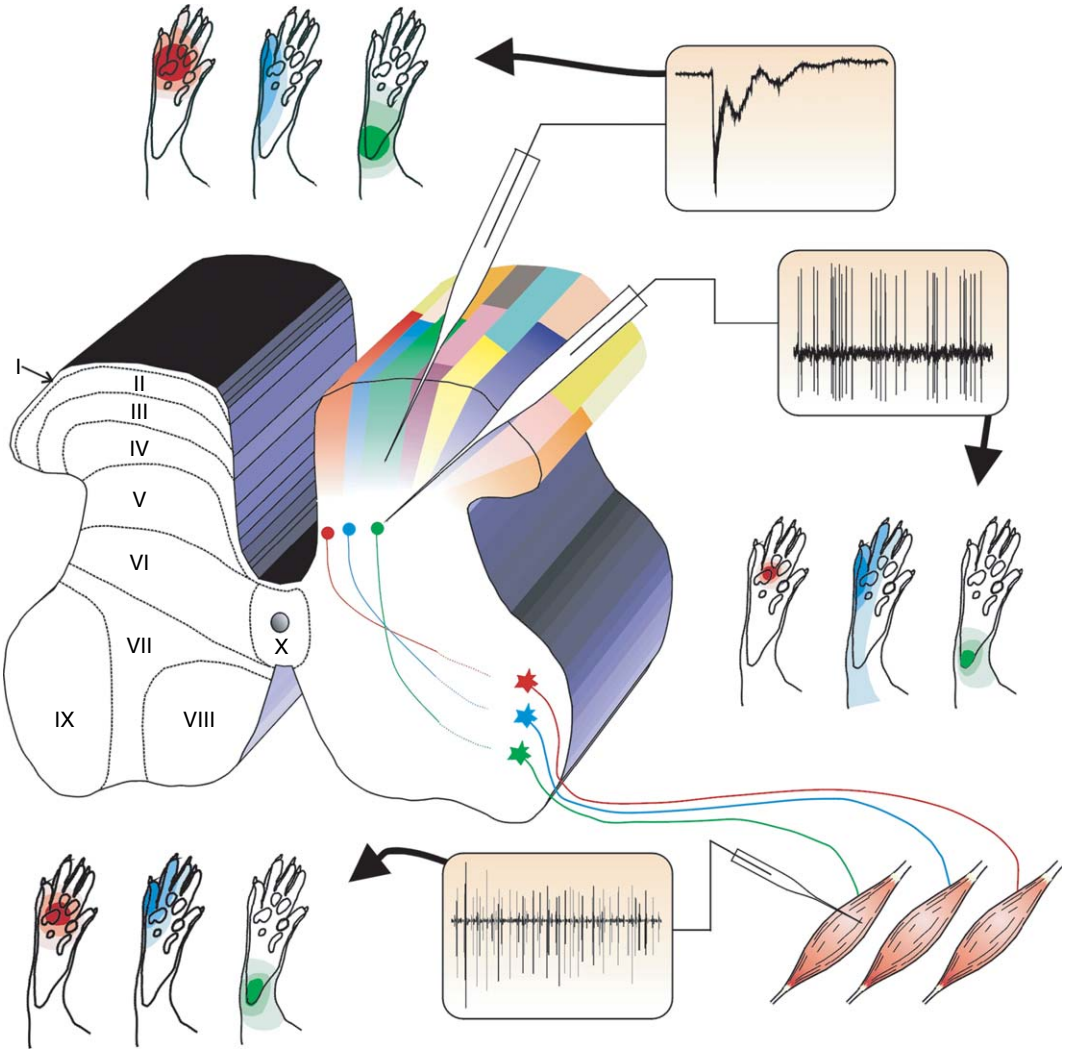

Figure 3 Schematic figure of proposed modular organization of the spinal cord. Columns of the dorsal horn receive a cutaneous input that has a specific weight distribution. This weight distribution is the same as that of nociceptive input to reflex encoders (interneurones that can encode the withdrawal reflex strength of individual modules) in deep dorsal horn. The reflex encoders are assumed to project to single muscles and weight the input according to the withdrawal efficacy of the output muscle. Sensitivity in strength of primary afferent input and sensitivity in receptive fields is coded by color intensity. Upper recordings, receptive fields of monosynaptic tactile field potentials; middle recordings, receptive fields of reflex encoders, bottom recordings, receptive fields of single muscles. Schematic indication of Rexed's laminae to the left.

role in the functional adaptation of the reflex modules. Uncorrelated input (given at random time points) does not cause a learning effect. Since this learning process results in an imprint of the withdrawal efficacy on the reflex modules, it was termed somatosensory imprinting (Holmberg, H. *et al.*, 1997; Petersson, P. *et al.*, 2003).

The finding that the strength of the nociceptive connections to the NWR network can be functionally adapted by tactile input discloses a hitherto unknown form of cross-modality learning in the spinal cord that solves the puzzle of how a pain-related system can be learned during postnatal development, despite the rare occurrence of noxious events. Notably, this novel form of unsupervised learning occurs during active sleep, characterized by atonia in the musculature. This state may be particularly advantageous for learning since the sensory feedback on muscle contraction stands out from a more or less silent background.

A hitherto neglected problem is how the myriad of different types of somatosensory primary afferents, conveying information from different sensory

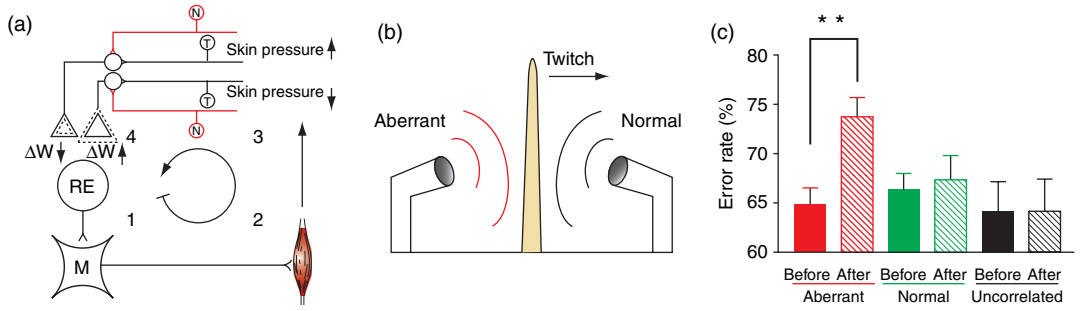

Figure 4 Somatosensory imprinting. (a) Proposed learning cycle underlying somatosensory imprinting. A learning cycle consists of the following chain of events. (1) Spontaneous bursts in reflex encoders (REs). (2) Motoneuron (M) activation leading to a muscle twitch that causes skin movement. (3) Increased or decreased skin pressure resulting in altered sensory input to pre-reflex encoder interneurons. Black lines (T) represent afferents from skin areas from where an increase and decrease, respectively, in low-threshold mechanoreceptor input would occur. Red lines (N) symbolize nociceptive afferents. (4) The strengths of erroneous connections (receiving increased tactile input) between pre-RE interneurons and REs are weakened and that of appropriate ones (receiving reduced tactile input) is strengthened (Dw = change in connection strength) (modified from Waldenström, A. *et al*., 2003). (b) Behavioural experiments. Schematic training set-up depicting aberrant and normal training protocol. Distal tail of a sleeping rat pup is shown. Air puffs directed to the skin surface moving toward or away from the air stream is termed aberrant or normal conditioning, respectively. One session of conditioning stimulation lasted for 2 h. Arrow indicates direction of spontaneous tail flick (modified from Petersson, P. *et al*., 2003). (c) The nociceptive withdrawal reflex (NWR) error rate (%) before and after aberrant or normal tactile stimulation (mean SE). The NWR error rate was significantly increased (Kruskal–Wallis and Dunnett's test $P < 0.01$) in rats given aberrant tactile feedback for 2 h (47 training sessions). Normal air-puff stimulation (53 training sessions) had no effect. Control experiments, using random air-puff stimulation (23 training sessions) or no stimulation (23 training sessions) did not affect NWR adaptation (Wilcoxon signed rank test $P = 0.65$ and $P = 0.37$, respectively), ruling out direct effects of the set-up, test stimulations, or of uncorrelated stimulation. (Adapted from Petersson, P., Waldenström, A., Fåhreaus, C., and Schouenborg, J. 2003. Spontaneous muscle twitches during sleep guide spinal self-organization. Nature 424(6244), 72–75.

modalities and locations, gets organized in the dorsal horn so that spinal multisensory modules receive topographically ordered information. Considering the apparent lack of somatotopic organization in the dorsal root ganglia and that different nerve fibre types enter the spinal cord by different routes and at different times during development, this is not a trivial problem. Indeed, recent data indicate that the adult body representation in the dorsal horn arises from an initially floating and plastic organization with many inappropriate connections through profound activity-dependent rewiring, involving both sprouting and elimination of afferent connections. In this process, tactile input seems to guide the alignment of tactile and nociceptive termination since disturbed tactile input patterns results in disturbed termination patterns of both tactile and nociceptive afferent fibers (Granmo, G. *et al*., 2002; Petersson, P. *et al*., 2004; Granmo, G. *et al*., 2005; 2007). The activity-dependent changes in the organization of the primary afferent termination in the spinal cord including changes in laminar termination patterns of tactile afferents are paralleled in time by reflex sensorimotor transformations, suggesting that the emerging action-based body representation is at least partly imprinted on the first-order synapses. Importantly, these findings suggest that the adult action-based sensory encoding emerges by sensorimotor circuits probing the patterns of tactile input that ensue on movements caused by the effector muscles.

Spontaneous movements are a ubiquitous phenomenon during embryonic development in all vertebrates and mammals (De Vries, J. I. *et al*., 1982; Blumberg, M. S. and Lucas, D. E., 2000). However, while a role in maturation of motoneurones, motoneuronal axonal path finding, and contacts with skeletal muscles appears likely (Hanson, M. G. and Landmesser, L. T., 2004; 2006), their role in the CNS and for sensorimotor learning in particular has, however, not been known. The activity appears to be caused by spontaneous endogenous activity in neuronal circuits in the spinal cord and brain stem (Blumberg, M. S. and Lucas, D. E., 2000). Although present classifications tend to lump the spontaneous motility broadly into a few categories, detailed studies in humans distinguished 16 different types (De Vries, J. I. *et al*., 1982). The prevalence and complexity of these movements lead us to suggest that all major spinal motor systems contribute to the spontaneous movements during development. Furthermore, since somatosensory imprinting is

highly effective, it may well be that all major groups of spinal motor systems learn relevant aspects of the body anatomy and biomechanics during development by probing the sensory feedback after spontaneous endogenous activation. It has also been suggested that the sensory input arising after spontaneous movements guide the tuning of the somatotopic organization of the somatosensory cortex during development (Khazipov, R. *et al.*, 2004). It may thus be proposed that sensory input arising as a consequence of spontaneous movements during development plays a key role also in the organization of higher-order sensorimotor systems.

As yet, little is known about the molecular mechanisms underlying somatosensory imprinting. While calcium transients (Perrier, J. F. and Hounsgaard, J., 2000; Russier, M. *et al.*, 2003) and/or spontaneous fluctuations of glutamate release (O'Donovan, M. J. *et al.*, 1998; O'Donovan, M. J., 1999) have been suggested to play a role for the initiation of spontaneous movements, *N*-methyl-D-aspartate (NMDA) receptors may also be involved in the learning mechanisms since the rewiring of the tactile afferent fiber termination in the dorsal horn during development is blocked by topically applied MK-801 (Mendelson, B., 1994; Beggs, S. *et al.*, 2002; Granmo, G. *et al.*, 2002; 2005). Moreover, mice with a disturbed long-term potentiation (LTP) in the hippocampus exhibit disturbed receptive fields of NWR, suggesting that LTP-like mechanisms in the spinal cord may be involved in somatosensory imprinting (Thelin, J. M., 2005). To further unravel the mechanisms that underlie the somatosensory imprinting is clearly an important task in future.

5.12.5 Concluding Remarks

The embryonic development of the spinal cord is characterized by a ventral to dorsal temporal sequence. Appearance of motoneurons precedes that of interneurons which in turn precedes primary afferent ingrowth (Altman, J. and Bayer, S. A., 1984). It is thus of interest that there is a specific spatial relation between the topography of motoneuron pools and lamina V reflex encoders (Schouenborg, J. *et al.*, 1995) and between the weight distribution of cutaneous input to the dorsal horn and the receptive fields of the reflex encoders. Taken together, these findings indicate an instrumental role of motoneurons and the patterns of sensory feedback caused by spontaneous motility during development in the functional assembly of the dorsal horn. The elimination of inappropriate connections and strengthening of appropriate connections that normally occurs during development is likely to be a reflection of such a learning-dependent process.

Besides providing insights into how the wiring of the spinal cord is accomplished, the reviewed findings may well have clinical relevance. While the repair of the spinal cord after injury has so far been relatively unsuccessful, some advances indicate that regeneration across spinal lesions is possible and that some functional recovery may occur after such regeneration (Li, Y. *et al.*, 1997; Zgraggen, W. J. *et al.*, 1998; Levinsson, A. *et al.*, 2000). A major problem, once the obstacle of limited regeneration has been overcome, will be to eliminate the erroneous connections arising from regeneration (Bareyre, F. M. *et al.*, 2004). Such connections may be devastating for the patient. For example, patients with partially transected spinal cords often report chronic pain that is very difficult to alleviate (Sjölund, B. H., 2002). If adaptive mechanisms, such as somatosensory imprinting, which decrease the gain in erroneous connections and increase the gain in adequate connections can be utilized, true functional recovery may be attainable also from chaotically regenerated connections. A combination therapy based on training using feedback stimulation to tune the regenerated connections and pharmacological treatment that disinhibits regeneration might thus prove to be extremely useful.

Acknowledgments

This work was supported by Swedish MRC project no 01013 and a Linné grant, Knut and Alice Wallenbergs Foundation, Kocks Foundation.

References

Albright, T. D., Jessell, T. M., Kandel, E. R., and Posner, M. I. 2000. Neural science: a century of progress and the mysteries that remain. Neuron 25, (Suppl.), S1–S55. Review.

Altman, J. and Bayer, S. A. 1984. The development of the rat spinal cord. Adv. Anat. Embryol. Cell Biol. 85, 1–166.

Apps, R. and Garwicz, M. 2005. Anatomical and physiological foundations of cerebellar information processing. Nat. Rev. Neurosci. Apr: 6(4), 297–311. Review.

Avella, A., Saltiel, P., and Bizzi, E. 2003. Combinations of muscle synergies in the construction of a natural motor behavior. Nat. Neurosci. 6, 300–308.

Bareyre, F. M., Kerschensteiner, M., Raineteau, O., Mettenleiter, T. C., Weinmann, O., and Schwab, M. E. 2004.

The injured spinal cord spontaneously forms a new intraspinal circuit in adult rats. Nat. Neurosci. 7, 269–277.
Beggs, S., Torsney, C., Drew, L. J., and Fitzgerald, M. 2002. The postnatal reorganization of primary afferent input and dorsal horn cell receptive fields in the rat spinal cord is an activity-dependent process. Eur. J. Neurosci. 16, 1249–1258.
Berkowitz, A. 2001. Broadly tuned spinal neurons for each form of fictive scratching in spinal turtles. J. Neurophysiol. 86, 1017–1025.
Bizzi, E., Tresch, M. C., Saltiel, P., and d'Avella, A. 2000. New perspectives on spinal motor systems. Nat. Rev. Neurosci. 1, 101–108.
Blake, D. T., Byl, N. N., and Merzenich, M. M. 2002. Representation of the hand in the cerebral cortex. Behav. Brain Res. 135(1–2), 179–184.
Blumberg, M. S. and Lucas, D. E. 2000. Dual mechanisms of twitching during sleep in neonatal rats. Behav. Neurosci. 108, 1196–1202.
Brown, P. B., Harton, P., Millecchia, R., Lawson, J. J., Brown, A. G., Koerber, H. R., Culberson, J., and Stephens, S. 2005. From innervation density to tactile acuity 2: Embryonic and adult pre- and postsynaptic somatotopy in the dorsal horn. Brain Res. 1055, 36–59.
Brown, P. B., Koerber, H. R., and Millecchia, R. 1997. Assembly of the dorsal horn somatotopic map. Somatosens. Mot. Res. 14, 93–106.
Brown, P. B., Koerber, H. R., and Millecchia, R. 2004. From innervation density to tactile acuity. 1. Spatial representation. Brain Res. 1011, 14–32.
Chen, A. I., de Nooij, J. C., and Jessell, T. M. 2006. Graded activity of transcription factor Runx3 specifies the laminar termination pattern of sensory axons in the developing spinal cord. Neuron 49, 395–408.
Chen, C. L., *et al.* 2006. Runx1 determines nociceptive sensory neuron phenotype and is required for thermal and neuropathic pain. Neuron 49, 365–377.
De Vries, J. I., Visser, G. H., and Prechtl, H. F. 1982. The emergence of fetal behaviour. I. Qualitative aspects. Early Hum. Dev., 7, 301–322.
Garwicz, M. 2002. Spinal reflexes provide motor error signals to cerebellar modules – relevance for motor coordination. Brain Res. Rev. 40, 152–165.
Garwicz, M., Levinsson, A., and Schouenborg, J. 2002. Common principles of sensory encoding spinal reflex modules and cerebellar climbing fibres. J. Physiol. 540, 1061–1069.
Granmo, G., Jensen, T., Lind, G., and Schouenborg, J. 2005. NMDA dependent changes in dorsal horn somatotopy in the developing rat. IASP 11th World Congress on Pain, Sydney. Abstract.
Granmo, M., Levinsson, A., and Schouenborg, J. 2002. Postnatal changes in dorsal horn somatotopy in the rat. IASP 10th World Congress on Pain, 77–P73. Abstract.
Granmo, G., Petersson, P., and Schouenborg, J. Establishment of an action based body representation in the spinal cord. Submitted for publication.
Grillner, S. 1981. Control of locomotion in bipeds, tetrapods, and fish. In: *Handbook of Physiology* (*ed*. V. B. Brooks), Vol. 2, American Physiological Society, Bethesda, pp. 1179–1236, Section 1.
Hanson, M. G. and Landmesser, L. T. 2004. Normal patterns of spontaneous activity are required for correct motor axon guidance and the expression of specific guidance molecules. Neuron 43(5), 687–701.
Hanson, M. G. and Landmesser, L. T. 2006. Increasing the frequency of spontaneous rhythmic activity disrupts pool-specific axon fasciculation and pathfinding of embryonic spinal motoneurons. J. Neurosci. 26(49), 12769–12780.
Holmberg, H. and Schouenborg, J. 1996a. Postnatal development of the nociceptive withdrawal reflexes in the rat: a behavioural and electromyographic study. J. Physiol. 493, 239–252.
Holmberg, H. and Schouenborg, J. 1996b. Developmental adaptation of withdrawal reflexes to early alteration of peripheral innervation in the rat. J. Physiol. 495, 399–409.
Holmberg, H., Schouenborg, J., Yu, Y., and Weng, H.-R. 1997. Developmental adaptation of rat nociceptive withdrawal reflexes after neonatal tendon transfer. J. Neurosci. 17, 2071–2078.
Khazipov, R., Sirota, A., Leinekugel, X., Holmes, G. L., Ben-Ari, Y., and Buzsaki, G. 2004. Early motor activity drives spindle bursts in the developing somatosensory cortex. Nature 432(7018), 758–761.
Kramer, I., *et al.* 2006. A role for Runx transcription factor signaling in dorsal root ganglion sensory neuron diversification. Neuron 49, 379–393.
Levinsson, A., Garwicz, M., and Schouenborg, J. 1999. Sensorimotor transformation in cat nociceptive withdrawal reflex system. Eur. J. Neurosci. 11, 4327–4332.
Levinsson, A., Holmberg, H., Broman, J., Zhang, M., and Schouenborg, J. 2002. Spinal sensorimotor transformation: Relation between cutaneous somatotopy and a reflex network. J. Neurosci. 22, 8170–8182.
Levinsson, A., Holmberg, H., Schouenborg, J., Seiger, A., Aldskogius, H., and Kozlova, E. N. 2000. Functional connections are established in the deafferented rat spinal cord by peripherally transplanted human embryonic sensory neurons. Eur. J. Neurosci. 12, 3589–3595.
Li, Y., Field, P. M., and Raisman, G. 1997. Repair of adult rat corticospinal tract by transplants of olfactory ensheating cells. Science 277, 2000–2002.
Mendelson, B. 1994. Chronic embryonic MK-801 exposure disrupts the somatotopic organization of cutaneous nerve projections in the chick spinal cord. Brain Res. Dev. Brain Res. 82, 152–166.
Mirnics, K. and Koerber, H. R. 1995. Prenatal development of rat primary afferent fibers: II. Central projections. J. Comp. Neurol. 355, 601–614.
Molander, C. and Grant, G. 1985. Cutaneous projections from the rat hindlimb foot to the substantia gelatinosa of the spinal cord studied by transganglionic transport of WGA-HRP conjugate. J. Comp. Neurol. 237, 476–484.
Mortin, L. I., Keifer, J., and Stein, P. S. G. 1985. Three forms of the scratch reflex in the spinal turtle: movement analyses. J. Neurophysiol., 53, 1501–1516.
O'Donovan, M. J. 1999. The origin of spontaneous activity in developing networks of the vertebrate nervous system. Curr. Opin. Neurobiol., 9, 94–104.
O'Donovan, M. J., Wenner, P., Chub, N., Tabak, J., and Rinzel, J. 1998. Mechanisms of spontaneous activity in the developing spinal cord and their relevance to locomotion. Ann. NY Acad. Sci. 860, 130–141.
Perrier, J. F. and Hounsgaard, J. 2000. Development and regulation of response properties in spinal cord motoneurones. Brain Res. Bull. 53, 529–535.
Petersson, P., Mundt-Petersen, K. and Schouenborg, J. 2004. Changes in primary afferent termination patterns accompany functional adaptation of nociceptive withdrawal reflexes. Society for Neuroscience Congress, Abstract 177.3.
Petersson, P., Waldenström, A., Fåhreaus, C., and Schouenborg, J. 2003. Spontaneous muscle twitches during sleep guide spinal self-organization. Nature 424(6944), 72–75.
Russier, M., Carlier, E., Ankri, N., Fronzaroli, L., and Debanne, D. 2003. A-, T-, and H-type currents shape intrinsic firing of developing rat abducens motoneurons. J. Physiol. (Lond.) 549, 21–36.
Saltiel, P., Wyler-Duda, K., D'Avella, A., Tresch, M. C., and Bizzi, E. 2001. Muscle synergies encoded within the spinal

cord: evidence from focal intraspinal NMDA iontophoresis in the frog. J. Neurophysiol. 85, 605–619.
Schouenborg, J. and Kalliomäki, J. 1990. Functional organization of the nociceptive withdrawal reflexes. I. Activation of hindlimb muscles in the rat. Exp. Brain Res. 83, 67–78.
Schouenborg, J. and Weng, H.-R. 1994. Sensorimotor transformation in a spinal motor system. Exp. Brain. Res. 100, 170–174.
Schouenborg, J., Holmberg, H., and Weng, H. R. 1992. Functional organization of the nociceptive withdrawal reflexes. II. Changes of excitability and receptive fields after spinalization in the rat. Exp. Brain Res. 90, 469–478.
Schouenborg, J., Weng, H. R., Kalliomäki, J., and Holmberg, H. 1995. A survey of spinal dorsal horn neurones encoding the spatial organization of withdrawal reflexes in the rat. Exp. Brain Res. 106, 19–27.
Silos-Santiago, I., Jeng, B., and Snider, W. D. 1995. Sensory afferents show appropriate somatotopy at the earliest stage of projection to dorsal horn. Neuroreport 6, 861–865.
Sjölund, B. H. 2002. Pain and rehabilitation after spinal cord injury – the case of sensory spasticity? Brain Res. Rev. 40, 250–256.
Sonnenborg, F. A., Andersen, O. K., and Arendt-Nielsen, L. 2000. Modular organization of excitatory and inhibitory reflex receptive fields elicited by electrical stimulation of the foot sole in man. Clin. Neurophysiol. 111(12), 2160–2169.
Stein, P. S., McCullough, M. L., and Currie, S. N. 1998. Spinal motor patterns in the turtle. Ann. NY Acad. Sci. 16, 142–154.
Thelin, J. M. 2005. Plasticity in mice nociceptive spinal circuits – role of cell adhesion molecules Lund University, Faculty of Medicine Doctoral Dissertation Series, 94 ISSN 1652-8220, ISBN: 91-85439-95-9.
Thelin, J. M. and Schouenborg, J. 2003. Postnatal learning in nociceptive withdrawal reflexes in different mouse strains. Program No. 260.18. 2003. Abstract Viewer/Itinerary Planner. Washington, DC: Society for Neuroscience Congress.
Tresch, M. C. and Bizzi, E. 1999. Responses to spinal microstimulation in the chronically spinalized rat and their relationship to spinal systems activated by low threshold cutaneous stimulation. Exp. Brain Res. 129, 401–416.
Tresch, M. C., Saltiel, P., D'Avella, A., and Bizzi, E. 2002. Coordination and localization in spinal motor systems. Brain Res. Rev. 40, 66–79.
Waldenström, A., Thelin, J., Thimansson, E., Levinsson, A., and Schouenborg, J. 2003. Developmental learning in a pain-related system: evidence for a cross-modality mechanism. J. Neurosci., 23, 7719–7725.
Weng, H.-R. and Schouenborg, J. 1996. Cutaneous inhibitory receptive fields of withdrawal reflexes in the decerebrate spinal rat. J. Physiol. (Lond.) 493, 253–265.
Wilson, P. and Kitchener, P. D. 1996. Plasticity of cutaneous primary afferent projections to the spinal dorsal horn. Prog. Neurobiol. 48, 105–129.
Zgraggen, W. J., Metz, G. A. S., Kartje, G. L., Thallmair, M., and Schwab, M. E. 1998. Functional recovery and enhanced corticofugal plasticity after unilateral pyramidal tract lesion and blockade of myelin-associated neurite growth inhibitors in adult rats. J. Neurosci., 18, 4744–4757.

Further Reading

Brown, P. B., Harton, P., Millecchia, R., Lawson, J. J., Kunjarana-ayudhya, T., Stephens, S., Miller, M. A., Hicks, L., and Culberson, J. 2000. Spatial convergence and divergence between cutaneous afferent axons and dorsal horn cells are not constant. J. Comp. Neurol. 420, 277–290.
Schouenborg, J. 2003. Somatosensory imprinting in spinal reflex modules. J. Rehab. Med. 41(Suppl.), 73–80 Review.

5.13 Pain Control: A Child-Centered Approach

Patricia A McGrath, The University of Toronto, Toronto, ON, Canada

© 2008 Elsevier Inc. All rights reserved.

5.13.1	Introduction	155
5.13.2	Modifying a Child's Pain	155
5.13.3	Guidelines for Treating Acute Pain	157
5.13.4	Guidelines for Treating Chronic Pain	161
References		163

Glossary

behavioral factors These factors refer to the specific behaviors of children, parents, and staff during pain episodes and also to parents' and children's broader actions in response to a chronic pain problem.

cognitive factors These factors include parents' and children's understanding of the pain problem, knowledge of effective therapies, and expectations for continuing pain or pain relief.

emotional factors These factors include parent's and children's feelings about the pain itself or responsible health condition and its adverse impact on the family, as well as any associated emotional disorders (such as anxiety or depression).

situational factors These factors represent a unique interaction between the child and the context in which the pain is experienced; they can vary dynamically, depending on the specific circumstances and setting.

5.13.1 Introduction

During the last two decades, unprecedented scientific and clinical attention has focused on the unique pain problems of infants, children, and adolescents (Schechter, N. L. *et al.*, 2003; McGrath, P. A., 2005; Schechter, N. L., 2007). Our knowledge of how children perceive pain and how we can alleviate their suffering has dramatically improved. Like adults, children's pain is modified both by ascending systems activated by sensory stimuli and by descending pain-suppressing systems activated by psychological factors. However, children's pain seems more plastic or modifiable in comparison to adults', so that environmental and psychological factors may exert a more powerful influence on children's pain perceptions (McGrath, P. A. and Dade, L. A., 2004).

Plasticity, from both a biological and a psychological perspective, is an essential concept in treating a child's pain. Our treatment approach has shifted from an almost exclusive disease-centered focus – detecting and treating the putative source of tissue damage – to a broader child-centered perspective, assessing the child with pain, identifying contributing psychological and contextual factors, and then targeting interventions accordingly. This chapter describes such a treatment approach, based on the unique factors that modify a child's pain.

5.13.2 Modifying a Child's Pain

Certain modifying factors are relevant for all children's pain experiences, irrespective of etiology. The model shown in Figure 1 lists the key factors that can increase pain, intensify distress, and exacerbate pain-related disability. A child's characteristics, such as cognitive level, sex, gender, temperament, previous pain experience, family, and cultural background (listed in the shaded box), generally shape how children interpret and cope with pain (Blount, R. L. *et al.*, 1991; Schechter, N. L. *et al.*, 1991; Bennett-Branson, S. and Craig, K., 1993; Schanberg, L. E. *et al.*, 1998; Chambers, C. T., 2003, Uman, L. S. and Chambers, C. T., 2007). However, other factors (listed in the open boxes) represent a

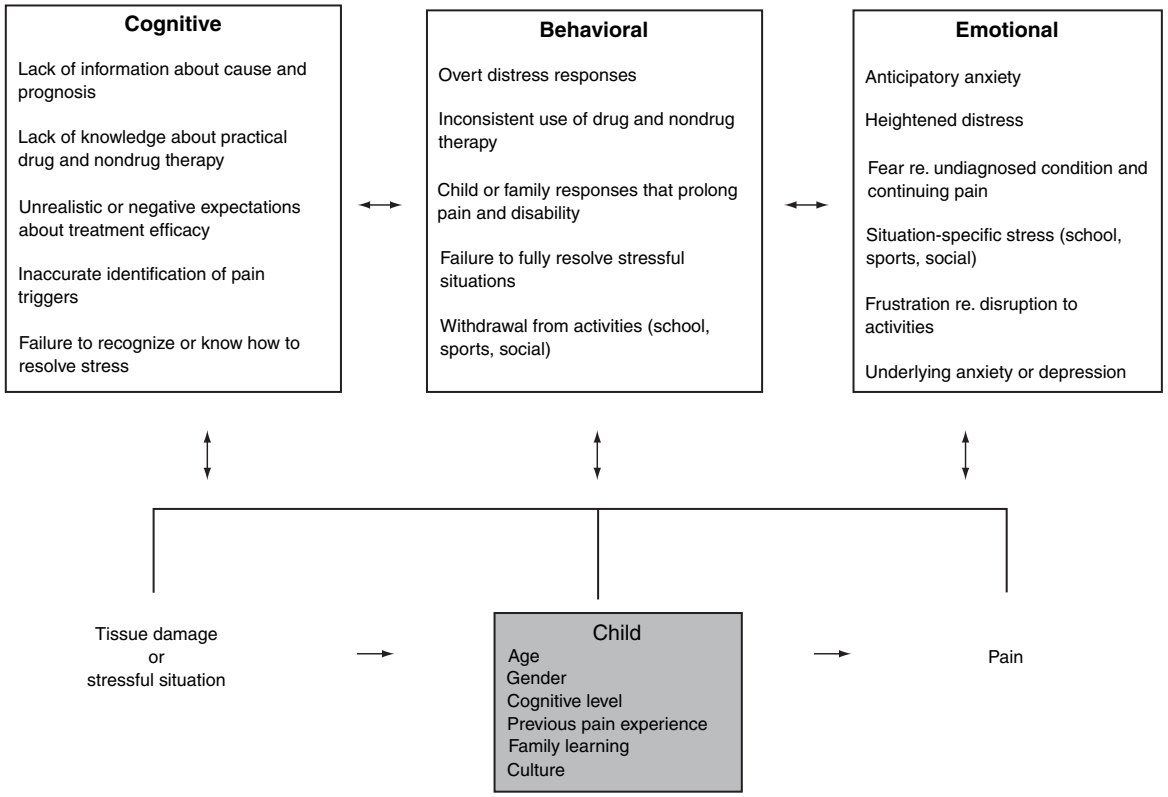

Figure 1 Biopsychosocial model for pain.

unique interaction between the child and the context in which the pain is experienced. These situational factors can vary dynamically, depending on the specific circumstances and setting. For example, a child receiving treatment for cancer may have repeated injections, central venous port access, or lumbar punctures, any of which can cause pain. Yet, even when tissue damage from these procedures is consistent, the situational factors present for a particular treatment are unique for each child.

The beliefs, behaviors, and emotional states of the children, parents, and clinicians all play important roles in modifying children's pain. Certain factors can intensify pain and distress, whereas others can eventually trigger pain episodes, prolong pain-related disability, or maintain the cycle of repeated pain episodes for children with recurrent pain syndromes (McGrath, P. A. and Hillier, L. M., 2003). While they may be unable to change the more stable child characteristics, health care providers can dramatically improve children's pain by modifying situational factors. Cognitive factors include parents' and children's understanding of the pain problem, knowledge of effective therapies, and expectations for continuing pain or pain relief. Behavioral factors refer to the specific behaviors of children, parents, and staff during pain episodes and also to parents' and children's broader actions in response to a chronic pain problem. Emotional factors include parent's and children's feelings about the pain itself or responsible health condition and its adverse impact on the family, as well as any associated emotional disorders (such as anxiety or depression). Parents' understanding of the cause of pain, possible treatments, and long-term prognosis guides their behaviors toward children and shapes children's emotional responses to the pain problem.

Situational factors may affect children even more than adults. Adults typically have experienced a wide variety of pains differing in etiology, intensity, and quality; their diverse experiences create a broad base of knowledge, realistic expectations, and versatile coping behaviors. In contrast, children, especially very young children, have considerably limited pain experience. They rely mainly on information conveyed within the immediate situation to interpret pain and to respond appropriately. Thus, children are particularly sensitive to environmental cues and to the behaviors of the adults who are present. A child's pain

is not predetermined by the extent of injury, disease progression, or invasiveness of a medical procedure. When health care providers ignore the powerful mediating impact of situational factors, they can easily, albeit inadvertently, increase a child's distress and pain. Generally, accurate information, realistic expectations, choices, control, and the use of some independent pain-reducing strategies will result in less pain.

5.13.3 Guidelines for Treating Acute Pain

Although distraction and parental support can minimize the pain caused by minor bumps and scrapes of childhood, pharmacological therapy (analgesics, adjunct analgesics, anesthetics, anxiolytics, and sedatives, as reviewed in other chapters) is the foundation for controlling children's acute pain (Finley, G. A. and McGrath, P. J., 2001; Dalens, B., 2003; Krane, E. J. *et al.*, 2003; Maunuksela, E.-L. and Olkkola, K. T., 2003; Yaster, M., 2003; Wilder, R. T., 2003; Brown, S. C. *et al.*, 2005; Bean-Lijewski, J. D., 2007; Schneeweiss, S., 2007). Children require appropriate analgesics, i.e., drugs selected according to type and severity of pain, doses determined by a child's weight based on the drug's duration of action to provide consistent pain relief and prevent breakthrough pain throughout the recovery period, and doses administered at regular dosing intervals. (For dosing guidelines, please see Finley, G. A. and McGrath, P. J., 2001; Krane, E. J. *et al.*, 2003; Brown, S. C. 2006.) Premature and term newborns show reduced clearance of most opioids (Wong, C. M. *et al.*, 2003). The differences in pharmacokinetics and pharmacodynamics among neonates, preterm infants, and full-term infants warrant special dosing considerations for infants and close monitoring when they receive opioids.

Recommended starting doses for analgesic medications for children are listed in Tables 1 and 2. Starting doses for adjuvant analgesic medications to control pain, drug-related side effects, and other symptoms are listed in Table 3.

Analgesics should be complemented by a practical cognitive-behavioral approach to ensure optimal pain relief, especially when treating acute pain from invasive medical procedures. First, health care providers should appreciate that children learn about pain because of their own injury-related acute pains. They perceive acute pains more as the occasionally inevitable result of daily activities than as something to fear. They quickly learn that pain is caused by injury, often easily visible, is relatively brief, and is relieved by many drug and nondrug interventions. Thus, they usually have accurate developmentally appropriate information about why something hurts and positive expectations for pain relief. In contrast, when children experience pain during invasive medical and dental procedures or after surgery, they often feel that they have no control, they may not know what to expect, and they may not know any simple pain control methods that they can use in these

Table 1 Nonopioid drugs to control pain in children

Drug	*Dosage*	*Comments*
Acetaminophen	10–15 mg kg^{-1} PO, every 4–6 h	Lacks gastrointestinal and hematological side effects; lacks anti-inflammatory effects (may mask infection-associated fever) Dose limit of 65 mg kg^{-1} day^{-1} or 4 g day^{-1}, whichever is less
Ibuprofen	5–10 mg kg^{-1} PO, every 6–8 h	Anti-inflammatory activity Use with caution in patients with hepatic or renal impairment, compromised cardiac function or hypertension (may cause fluid retention, edema), history of GI bleeding or ulcers, may inhibit platelet aggregation Dose limit of 40 mg kg^{-1} day^{-1}; maximum dose of 2400 mg day^{-1}
Naproxen	10–20 mg kg^{-1} day^{-1} PO, divided every 12 h	Anti-inflammatory activity. Use with caution and monitor closely in patients with impaired renal function. Avoid in patients with severe renal impairment Dose limit of 1 g day^{-1}
Diclofenac	1 mg kg^{-1} PO, every 8–12 h	Anti-inflammatory activity. Similar GI, renal, and hepatic precautions as noted above for ibuprofen and naproxen Dose limit of 50 mg dose^{-1}

Note: Increasing the dose of nonopioids beyond the recommended therapeutic level produces a ceiling effect, in that there is no additional analgesia but there are major increases in toxicity and side effects.
PO, by mouth; GI, gastrointestinal.
Brown, S. C. and McGrath, P. A. In Press. Pain Control in Children. In: Oxford Textbook of Palliative Medicine 4/e (*eds.* G. Hanks, N. Cherny, N. Christakis, M. Fallon, S. Kaasa, R. Portenoy). Oxford University Press.

Table 2 Opioid analgesics – usual starting doses for children

Drug	*Equianalgesic dose (parenteral)*	*Starting Dose IV*	*IV:PO ratio*	*Starting dose PO/ transdermal*	*Duration of action*
Morphine	10 mg	Bolus dose = 0.05–0.1 mg kg^{-1} every 2–4 h Continuous infusion = 0.01–0.04 mg kg^{-1} h^{-1}	1:3	0.15–0.3 mg kg^{-1} $dose^{-1}$ every 4 h	3–4 h
Hydromorphone	1.5 mg	0.015–0.02 mg kg^{-1} every 4 h	1:5	0.06 mg kg^{-1} every 3–4 h	2–4 h
Codeine	120 mg	Not recommended		1.0 mg kg^{-1} every 4 h (dose limit 1.5 mg $kg^{-1}dose^{-1}$)	3–4 h
Oxycodone	5–10 mg	Not recommended		0.1–0.2 mg kg^{-1} every 3–4 h	3–4 h
Meperidine[a]	75 mg	0.5–1.0 mg kg^{-1} every 3–4 h	1:4	1.0–2.0 mg kg^{-1} every 3–4 h (dose limit 150 mg)	1–3 h
Fentanyl[b]	100 μg	1–2 μg $kg^{-1}h^{-1}$ as continuous infusion		25 μg patch	72 h (patch)

[a]Avoid use in renal impairment. Metabolite may cause seizures.
[b]Potentially highly toxic. Not for use in acute pain control.
Principles of opioid administration:
1. If inadequate pain relief and no toxicity at peak onset of opioid action, increase dose in 50% increments.
2. Avoid IM administration.
3. Whenever using continuous infusion, plan for hourly rescue doses with short onset opioids if needed. Rescue dose is usually 50–200% of continuous hourly dose. If greater than 6 rescues are necessary in 24-h period, increase daily infusion total by the total amount of rescues for previous 24 h/24. An alternative is to increase infusion by 50%.
4. To change opioids because of incomplete cross-tolerance: if changing between opioids with short duration of action, start new opioid at 50% of equianalgesic dose. Titrate to effect.
5. To taper opioids – anyone on opioids over 1 week must be tapered to avoid withdrawal: taper by 50% for 2 days, and then decrease by 25% every 2 days. When dose is equianalgesic to an oral morphine dose of 0.6 mg kg^{-1} day^{-1}, it may be stopped. Some patients on opioids for prolonged periods may require much slower weaning.
PO, by mouth; IV, intravenous.
Brown, S. C. and McGrath, P. A. In Press. Pain Control in Children. In: Oxford Textbook of Palliative Medicine 4/e (*eds.* G. Hanks, N. Cherny, N. Christakis, M. Fallon, S. Kaasa, and R. Portenoy). Oxford University Press.
NOTE: Doses are for opioid-naive patients. For infants under 6 months, start at one-quarter to one-third the suggested dose and titrate to effect.

new situations. In fact, health care providers may instruct children how to cope (i.e., behave) during a painful procedure in a manner that makes it easier for the person administering the procedure, but does not necessarily make it better for the child.

Health care providers often focus on explaining to parents and inadvertently neglect the child. Time constraints necessitate juggling who has priority and, understandably, concerned parents are a priority. Yet, children should remain the number 1 priority because it is their pain that is directly modified. Every word and action conveys powerful information to children. As an example, a young boy became very distressed when he learned that a local anesthetic should freeze his arm so he wouldn't feel anything. Finally, he explained that he was afraid his arm would become like a Popsicle. Health care providers have tremendous power in influencing what children know, how they can respond, and the relevance of the situation (i.e., injury, disease, treatment) and consequent pain. The manner in which health care providers introduce themselves, the words they choose to explain what will happen, and whether they confidently show children what they could do to lessen the pain profoundly impact what children will experience.

These situational factors can intensify children's pain and distress, even when children receive anxiolytics and analgesics. As an example, when children with cancer at our center first started receiving topical anesthetic creams before intravenous insertions and portacather injections, considerably more children were referred to our pain clinic. We learned that busy clinical staff no longer focused on an individual child in the manner that they had previously – encouraging the child to understand from their specific perspective (i.e., age, gender, culture) and use their preferred 'close your pain gate' methods.

Table 3 Adjuvant analgesics – doses for children

Drug category	*Drug, dosage*	*Indications*	*Comments*
Antidepressants	Amitriptyline, 0.2–0.5 mg kg^{-1} PO.	Neuropathic pain (i.e., vincristine-induced, radiation plexopathy, tumor invasion, CRPS-1)	Usually improved sleep and pain relief within 3–5 days
	Titrate upward by 0.25 mg kg^{-1} every 2–3 days	Insomnia	Anticholinergic side effects are dose-limiting. Use with caution for children with increased risk for cardiac dysfunction
	Maintenance: 0.2–3.0 mg kg^{-1}		
	Alternatives: nortriptyline, doxepin, imipramine		
Anticonvulsants	Gabapentin, 5 mg $kg^{-1}day^{-1}$ PO.	Neuropathic pain, especially shooting, stabbing pain.	Side effects: gastrointestinal upset, ataxia, dizziness, disorientation, somnolence
	Titrate upward over 3–7 days. Maintenance: up to 15–50 mg $kg^{-1}day^{-1}$ PO divided TID.		Monitor for hematological, hepatic, and allergic reactions with carbamazepine
	Carbamazepine, initial dosing: 10 mg $kg^{-1}day^{-1}$ PO divided OD or BID. Maintenance: up to 20–30 mg $kg^{-1}day^{-1}$ PO divided every 8 h. Increase dose gradually over 2–4 weeks.		
	Alternatives: phenytoin, clonazepam		

(*Continued*)

Table 3 (Continued)

Drug category	*Drug, dosage*	*Indications*	*Comments*
Sedatives, hypnotics, anxiolytics	Diazepam, 0.025–0.2 mg kg^{-1} PO every 6 h.	Acute anxiety, muscle spasm	Sedative effect may limit opioid use. Other side effects include depression and dependence with prolonged use
	Lorazepam, 0.05 mg $kg^{-1}dose^{-1}$ SL	Premedication for painful procedures	
	Midazolam, 0.5 mg $kg^{-1}dose^{-1}$ PO administered 15–30 min prior to procedure; 0.05 mg $kg^{-1}dose^{-1}$ IV for sedation		
Antihistamines	Hydroxyzine, 0.5 mg kg^{-1} PO every 6 h.	Opioid-induced pruritus, anxiety, nausea	Sedative side effects may be helpful
	Diphenhydramine, 0.5−1.0 mg kg^{-1} PO/IV every 6 h		
Psychostimulants	Dextroamphetamine, methylphenidate, 0.1–0.2 mg kg^{-1} BID.	Opioid-induced somnolence	Side effects include agitation, sleep disturbance, and anorexia.
	Escalate to 0.3−0.5 mg kg^{-1} as needed	Potentiation of opioid analgesia	Administer second dose in afternoon to avoid sleep disturbances
Corticosteroids	Prednisone, prednisolone, and dexamethasone dosage depends on clinical situation (i.e. dexamethasone initial dosing: 0.2 mg kg^{-1} IV. Dose limit 10 mg. Subsequent dose 0.3 mg $kg^{-1}day^{-1}$ IV divided every 6 h)	Headache from increased intracranial pressure, spinal or nerve compression; widespread metastases	Side effects include edema, dyspeptic symptoms, and occasional gastrointestinal bleeding

CRPS-1, complex regional pain syndrome, type 1; PO, by mouth; IV, intravenous; SL, sublingual.

Brown, S. C. and McGrath, P. A. In Press. Pain Control in Children. In: Oxford Textbook of Palliative Medicine 4/e (*eds.* G. Hanks, N. Cherny, N. Christakis, M. Fallon, S. Kaasa, and R. Portenoy). Oxford University Press.

Instead, they applied the magic cream and sent children to a play area until it was time to conduct the invasive procedure. Despite the proven anesthetic properties of the cream, many children reported increased pain and exhibited increased distress in comparison to their pretopical procedures (McGrath, P. A., 1990).

Although psychological therapies are reviewed in other chapters, even the simple provision of information about what is happening, why the procedure is conducted in a certain manner, what equipment will be used, who will be present, the nature of the child's sensations during different phases of the procedure, and some straightforward instructions about how a child might lessen pain will dramatically reduce the pain caused by any invasive procedure to minimize anxiety and pain. As listed in Table 4, health care providers should explain what will happen and emphasize what sensations a child may feel, e.g., warmth, coolness, pressure, rather than the frightening label of pain. They should teach children a few basic attention and distraction methods to reduce pain and guide families to recognize the particular circumstances that exacerbate pain and distress.

Children who receive multiple invasive procedures over a prolonged period are at particular risk for developing anxiety and fear. Inaccurate understanding of the disease or injury, parents' anxiety about the underlying condition and painful treatments, inconsistency in treatment administration, lack of control and coping strategies, and fears about the effects of the disease or side effects of treatment can intensify a child's treatment-related pain. Regrettably, some inconsistencies in how procedures are conducted are common in clinical practice. The more procedures a child has, the more likely that they will experience a difficult procedure – more pain, more nausea, etc. A child then becomes fearful and expects that another difficult procedure is inevitable and a cycle of heightened anxiety, increased pain, and emotional distress ensues.

Many cognitive-behavioral programs have been designed to complement drug therapies for children with cancer (Hilgard, J. R. and LeBaron, S., 1984; LeBaron, S. and Zeltzer, L. K., 1996; Olness, K. and Kohen, D. P., 1996; Liossi, C., 2002; Collins, J. and Weisman, S. J., 2003; Kuttner, L. and Solomon, R., 2003). These child-centered programs usually combine basic education with psychological therapies (i.e., attention and distraction, hypnosis or hypnotic-like suggestions for analgesia, desensitization procedures, behavioral management, relaxation exercises, and biofeedback) to minimize children's anxiety and pain. The specific program components vary for different children because therapies are selected to target the unique child, family, and situational factors that were identified from the child's pain assessment as the factors that intensified children's pain, anxiety, and distress. Generally, as children receive developmentally appropriate accurate information, gain realistic expectations, have more choices and control, and use independent pain control strategies, they have less pain and distress.

5.13.4 Guidelines for Treating Chronic Pain

Effective treatment of chronic pain usually requires an integrated treatment approach comprising drug therapy, physical therapy, and psychological counseling, rather than a single therapy. Chronic pain generally has multiple sources affecting both peripheral and central nervous systems, with both nociceptive and neuropathic components. Certain cognitive, behavioral, and emotional factors may intensify pain, increase distress, and exacerbate a

Table 4 Preparing children for invasive procedures

Remember that anxiety and distress can increase pain.
Explain what will happen clearly, in simple developmentally appropriate language.
Emphasize the qualities of the sensations they may experience such as cold, sharp, tingling, and pressure so that children focus on what they are feeling, rather than only on the hurting aspect.
If the procedure will hurt, describe what children might feel using more familiar examples of pains that they have experienced during play and sports.
Use versatile pain control methods that involve children such as attention and distraction, deep breathing, counting exercises, or guided imagery.
Give children as many choices and as much control as possible such as choosing which arm for injections, whether to watch or look away, and which pain control method to use.

child's disability. The pain adversely affects all aspects of children's lives. Parents are distressed by the pain itself, its implications for their children's future, its life-threatening potential (if any), and the prospect of continuing pain and progressive disability. Parents and adolescents tend to emphasize and fear the future consequences of children's physical condition, whereas young children are more preoccupied by the immediate consequences and disruption to their daily activities. The dynamics within the family (both for siblings and for extended family members) inevitably change as chronic pain prevents children from pursing their normal activities and as family schedules adjust accordingly to the health care needs of the child with pain (for review, please see McGrath, P. J. and Finley, G. A., 1999; Berde, C. B. *et al.*, 2003; McGrath, P. A. and Dade, L. A., 2004).

In order to treat chronic pain effectively, health care providers should carefully determine the physical etiology (if possible) and also critically appraise the unique situational factors that may influence pain. Interdisciplinary teams, comprising physicians, nurses, psychologists, psychiatrists, and physical therapists, are better equipped to conduct a more comprehensive biopsychosocial assessment than a single pain specialist. After consultation among members, the team should provide a diagnosis that includes both the etiology and the relevant factors influencing children's pain. The biopsychosocial model shown in Figure 1 provides a concrete framework for explaining these factors and subsequently presenting the rationale for an integrated treatment approach comprising pharmacology, physiotherapy, and psychology. The specific drugs and therapies within this child-centered approach derive from the assessment results and are selected to target the responsible central and peripheral mechanisms and to mitigate the pain-exacerbating impact of situational factors.

NSAIDs and opioids in effective doses and regular dosing schedules can relieve pain with a primary nociceptive etiology. Drugs should be selected according to their analgesic potency based on the child's pain level – acetaminophen to control mild pain, codeine to control moderate pain, and morphine for strong pain (World Health Organization, 1998). Even when children require opioid analgesics, they should continue to receive acetaminophen (and NSAIDs, if appropriate) as supplemental analgesics. Health care providers should monitor a child's pain regularly and adjust analgesic doses as necessary to control the pain. The effective opioid dose to relieve pain varies widely among different children or in the same child at different times. To relieve ongoing pain, opioid doses should be increased steadily until comfort is achieved, unless the child experiences unacceptable side effects such as somnolence or respiratory depression. Adjuvant analgesics (especially gabapentin and tricyclic antidepressants) have become the main drugs for treating neuropathic pain (Berde, C. B. *et al.*, 2003).

Some children, irrespective of what may have caused their pain initially, develop significant functional disability that far exceeds their reported pain level. These children do not attend school, participate in sports, or socialize with peers. Families are frustrated because they may have tried to follow treatment recommendations and reintegrate children back into their normal activities. Parents may believe that health care providers do not believe the child and do not understand the severity of the pain problem. Families believe that children will return to normal (even when children have been disabled for years) as soon as health care providers cure the pain problem. A futile cycle ensues, with health care providers attempting to restore normal functioning and families refusing to cooperate until the pain is relieved. Children with severe disability constitute a unique clinical challenge. Gradually, I have learned to identify the problem to families as twofold – a chronic pain problem and a disability problem. Usually disability is the more serious problem. Thus, treatment should immediately focus on the both aspects – we must deal with the pain, but, concurrently, we must deal with the increasing disability. Almost all children who have a major disability problem will require additional psychological treatment and assistance to reenter school and resume their previous activities.

For any child with chronic pain, health care provides should recognize the common situational factors that influence parents' responses to children's continuing pain complaints, especially when pain is not caused by active disease or injury. Parents usually try to understand their child's pain from an acute disease perspective, where pain is due to a single cause and can be relieved by a single treatment. They do not understand that chronic pain, unlike most pains that they have already experienced, may have several interrelated causes. Thus, parents request further medical investigations as they search for the clear-cut physical etiology and concentrate on finding one treatment that will immediately stop the pain. Parents may reject potentially effective

treatments after only one attempt, even though the treatment would address some of the causes and might lessen children's pain over time. Some parents expect that their child will remain very disabled until the one right treatment is found and believe that they have no control in changing the future course of continuing pain and disability.

To mitigate the factors that can intensify a child's chronic pain or exacerbate disability, health care providers should "Stop, Look, & Listen": Stop an exclusive disease focus; Look at the big picture, i.e., assess the child with pain; and Listen to the child's pain history, appreciating the potential impact of situational factors (McGrath, P. A. and Dade, L. A., 2004). The diagnosis is a critical component of pain management. Even when some aspects of the pain condition are puzzling, health care providers should honestly describe what they know and explain what they need to explore further in a straightforward and reassuring manner. Accurate information about the pain source(s) can mitigate the increased distress caused by a family's misinterpretations and anxieties. Moreover, since expectancies can profoundly affect treatment effectiveness, health care providers should build on this knowledge and directly address their patients' expectancies within the diagnostic appointment.

An accurate diagnosis should include information about both the primary causes and the secondary contributing factors so that treatments can be targeted at each relevant factor. Since these factors may vary over time, pain assessment remains a critical component of any treatment regimen. The focus of continuing assessment is the child with pain – not only the pain features but also the situational factors that modulate pain. Even when pain is due to actively progressing disease such as for children with advanced cancer, many other factors can affect their pain and suffering. Health care providers should assess these factors and target treatments accordingly. The treatment rationale is on the multifactorial etiology of pain and recommendations for a multimodal treatment approach. This is in direct contrast to the single cause and single treatment approach normally adequate for relieving acute pain.

References

Bean-Lijewski, J. D. 2007. Acute Pain in Children – Post-operative Pain. In: Encyclopedic Reference of Pain (*eds*. R. F. Schmidt and W. D. Willis), pp. 16–28. Springer-Verlag.

Bennett-Branson, S. and Craig, K. 1993. Post-operative pain in children: developmental and family influences on spontaneous coping strategies. Can. J. Behav. Sci. 25, 355–383.

Berde, C. B., Lebel, A. A., and Olsson, G. 2003. Neuropathic Pain in Children. In: Pain in Infants, Children, and Adolescents (*eds*. N. L. Schechter, C. B. Berde, and M. Yaster), 2nd edn., pp. 620–638. Lippincott Williams and Wilkins.

Blount, R. L., Landolf-Fritsche, B., Powers, S. W., and Sturges, J. W. 1991. Differences between high and low coping children and between parent and staff behaviors during painful medical procedures. J. Pediatr. Psychol. 16, 795–809.

Brown, S. C. 2006. Cancer pain and palliative care in children. In: Encyclopedic Reference of Pain (*eds*. R. F. Schmidt and W. D. Willis), pp. 220–224. Springer-Verlag.

Brown, S. C., McGrath, P. A., and Krmpotic, K. 2005. Pain in Children. In: Neurologic Basis of Pain (*ed*. M. Pappagallo), pp. 225–242. McGraw-Hill.

Chambers, C. T. 2003. The Role of Family Factors in Pediatric Pain. In: Pediatric Pain: Biological and Social Context, Progress in Pain Research and Management, Vol. 26. (*eds*. P. J. McGrath and G. A. Finley), pp. 99–130. IASP Press.

Collins, J. and Weisman, S. J. 2003. Management of Pain in Childhood Cancer. In: Pain in Infants, Children, and Adolescents (*eds*. N. L. Schechter, C. B. Berde, and M. Yaster), 2nd edn., pp. 517–538. Lippincott Williams and Wilkins.

Dalens, B. 2003. Peripheral Nerve Blockade in the Management of Postoperative Pain in Infants, Children, and Adolescents (*eds*. N. L. Schechter, C. B. Berde, and M. Yaster), 2nd edn., pp. 363–395. Lippincott Williams and Wilkins.

Finley, G. A. and McGrath, P. J. (*eds.*) 2001. Acute and Procedure Pain in Infants and Children. Progress in Pain Research and Management. IASP Press.

Hilgard, J. R. and LeBaron, S. 1984. Hypnotherapy of Pain in Children with Cancer. William Kaufman.

Krane, E. J. *et al.* 2003. Treatment of Pediatric Pain with Nonconventional Analgesics. In: Pain in Infants, Children, and Adolescents (*eds*. N. L. Schechter, C. B. Berde, and M. Yaster), 2nd edn., pp. 225–240. Lippincott Williams and Wilkins.

Kuttner, L. and Solomon, R. 2003. Hypnotherapy and Imagery for Managing Children's Pain. In: Pain in Infants, Children, and Adolescents (*eds*. N. L. Schechter, C. B. Berde, and M. Yaster), 2nd edn., pp. 317–328. Lippincott Williams and Wilkins.

LeBaron, S. and Zeltzer, L. K. 1996. Children in Pain. In: Hypnosis and Suggestion in the Treatment of Pain: A Clinical Guide (*eds*. J. Barber and C. J. Bejenke), pp. 305–340. W. W. Norton.

Liossi, C. 2002. Procedure-Related Cancer Pain in Children. Radcliffe Medical Press Ltd.

Maunuksela, E.-L. and Olkkola, K. T. 2003. Nonsteroidal Anti-inflammatory Drugs in Pediatric Pain Management. In: Pain in Infants, Children, and Adolescents (*eds*. C. B. Berde, N. L. Schechter, and, M. Yaster), pp. 171–180. Lippincott Williams and Wilkins.

McGrath, P. A. 1990. Pain in Children: Nature, Assessment and Treatment. Guilford Press.

McGrath, P. A. 2005. Children – Not Simply ''Little Adults''. In: Paths of Pain 1975–2005 (*eds*. H. Merskey, J. D. Loeser, and R. Dubner), pp. 433–446. IASP Press.

McGrath, P. A. and Dade, L. A. 2004. Effective Strategies to Decrease Pain and Minimize Disability. In: Psychological Modulation of Pain: Integrating Basic Science and Clinical Perspectives (*eds*. D. D. Price and M. C. Bushnell), pp. 73–96. IASP Press.

McGrath, P. J. and Finley, G. A. 1999. Chronic and Recurrent Pain in Children and Adolescents. IASP Press.

McGrath, P. A. and Hillier, L. M. 2003. Modifying the Psychological Factors that Intensify Children's Pain and Prolong Disability. In: Pain in Infants, Children, and Adolescents (*eds*. N. L. Schechter, C. B. Berde, and M. Yaster), 2nd edn., pp. 85–104. Lippincott Williams and Wilkins.

Olness, K. and Kohen, D. P. 1996. Hypnosis and Hypnotherapy with Children, 3rd edn. Guilford Press.

Schanberg, L. E., Keefe, F. J., Lefebvre, J. C., Kredich, D. W., and Gil, K. M. 1998. Social context of pain in children with juvenile primary fibromyalgia syndrome: parental pain history and family environment. Clin. J. Pain 14, 107–115.

Schechter, N. L. 2007. Evolution of Pediatric Pain Treatment. In: Encyclopedic Reference of Pain (*eds*. R. F. Schmidt and W. D. Willis), pp. 749–752. Springer-Verlag.

Schechter, N. L., Berde C. B., and Yaster, M. (*eds*.) 2003. Pain in Infants, Children, and Adolescents, 2nd edn. Lippincott Williams and Wilkins.

Schechter, N. L., Bernstein, B. A., Beck, A., Hart, L., and Scherzer, L. 1991. Individual differences in children's response to pain: role of temperament and parental characteristics. Pediatrics 87, 171–177.

Schneeweiss, S. 2007. Pain and Sedation of Children in the Emergency Setting. In: Encyclopedic Reference of Pain (*eds*. R. F. Schmidt and W. D. Willis), pp. 1637–1641. New York. Springer-Verlag.

Uman, L. S. and Chambers, C. T. 2007. Impact of Familial Factors on Children's Chronic Pain. In: Encyclopedic Reference of Pain (*eds*. R. F. Schmidt and W. D. Willis), pp. 961–964. Springer-Verlag.

Wilder, R. T. 2003. Regional Anesthetic Techniques for Chronic Pain Management. In: Pain in Infants, Children, and Adolescents (*eds*. N. L. Schechter, C. B. Berde, and M. Yaster), 2nd edn., pp. 396–416. Lippincott Williams and Wilkins.

Wong, C. M., *et al.* 2003. The Pain (and Stress) in Infants in a Neonatal Intensive Care Unit. In: Pain in Infants, Children, and Adolescents (*eds*. N. L. Schechter, C. B. Berde, and M. Yaster), 2nd edn., pp. 669–692. Lippincott Williams and Wilkins.

World Health Organization 1998. Cancer Pain Relief and Palliative Care in Children. World Health Organization, Geneva.

Yaster, M. 2003. Clinical Pharmacology. In: Pain in Infants, Children and Adolescents (*eds*. N. L. Schechter, C. B. Berde, and M. Yaster), pp. 71–84. Lippincott Williams and Wilkins.

Further Reading

Brown, S. C. and McGrath, P. A. (In Press). Pain Control in Children. In: Oxford Textbook of Palliative Medicine 4/e (*eds.* G. Hanks, N. Cherny, N. Christakis, M. Fallon, S. Kaasa, and R. Portenoy). Oxford University Press.

Schanberg, L. E., Gil, K. M., Anthony, K. K., Yow, E., and Rochon, J. 2005. Pain, stiffness, and fatigue in juvenile polyarticular arthritis: contemporaneous stressful events and mood as predictors. Arthritis Rheum. 52(4), 1196–1204.

5.14 Assaying Pain-Related Genes: Preclinical and Clinical Correlates

V E Scott, R Davis-Taber, and P Honore, Global Pharmaceutical Research and Development, Abbott Park, IL, USA

© 2008 Elsevier Inc. All rights reserved.

5.14.1	Introduction	165
5.14.2	Microarray Analysis of Whole Dorsal Root Ganglion from the Spinal Nerve Ligation Model	165
5.14.3	Microarray Data Analysis and Follow-up Studies	167
5.14.4	Microarray Analysis of Subpopulations of Neurons Isolated from Dorsal Root Ganglion	167
5.14.5	Evaluation of Additional Neuropathic Pain Models by Microarray	169
5.14.6	The Strengths and Limitations of Microarray Analysis for Pain Research	170
5.14.7	The Genetics of Pain	171
References		172

5.14.1 Introduction

Microarray gene chip technology is a powerful tool to evaluate changes in multiple transcript levels simultaneously in different tissue preparations. In the pain field, efforts have focused on characterizing gene transcript changes that occur in chronic pain states such as neuropathic pain (Wang, H. *et al.*, 2002; Xiao, H. S. *et al.*, 2002; Davis-Taber, R. *et al.*, 2003; Thimmapaya, R. *et al.*, 2003; Valder, C. R. *et al.*, 2003; Davis-Taber, R. *et al.*, 2004) and this will be the main focus of this chapter. Neuropathic pain is initiated or caused by a primary lesion or dysfunction of the nervous system. As this technology emerged, it was anticipated that it could be used to determine the key molecular players in both the development and maintenance of neuropathic pain, which would enhance our understanding of this disease and provide insights into the identification of potential therapeutic targets for the treatment of pain. Prior to microarray approaches, studies were limited to evaluation of a set of specific preselected genes/proteins in samples from animal pain models or human tissues using techniques such as quantitative reverse transcriptase polymerase chain reaction (RT-PCR), Western blot analysis, and immunocytochemistry. Dependent upon the gene chips used, this analysis permits evaluation of both known and unknown gene transcripts (expressed sequence tags (ESTs)) using relatively small amounts of RNA. In each of the studies highlighted in this chapter a wealth of transcriptional information was obtained. However, determination of which gene product would offer the best therapeutic potential will require extensive additional follow-up studies. Microarray studies are clearly just the starting point. This chapter will be divided into sections detailing the studies that have been reported evaluating gene expression changes from neuropathic pain models using microarray gene chip analysis, including discussion in each section on study design, sample selection, isolation of RNA, choice of microarray gene chip platforms, and data analysis. The follow-up to microarray studies outlining the expectations and limitations of these studies will also be described. Lastly, the use of microarray gene chips for pinpointing genetic variation in disease states that will direct suitable therapeutics based upon genetic predispositions for specific patient populations will be discussed.

5.14.2 Microarray Analysis of Whole Dorsal Root Ganglion from the Spinal Nerve Ligation Model

Several different studies have evaluated the expression changes that occur in the rat whole dorsal root ganglion (DRG; Wang, H. *et al.*, 2002; Thimmapaya, R. *et al.*, 2003; Valder, C. R. *et al.*, 2003) and dorsal horn of the spinal cord (Sun, H. *et al.*, 2002; Wang, H. *et al.*, 2002) following spinal nerve ligation (SNL) using microarray analysis. The overall goal of each of these studies was to obtain a better understanding of the molecular pathophysiology of neuropathic pain and through this analysis identify potential new targets for the treatment of this chronic pain state. In some studies following tight ligation of the lumbar 5 (L5) and

lumbar 6 (L6) DRG, the development of allodynia was shown to develop 3 days following surgery and remained established for weeks ipsilateral to the insult (Wang, H. *et al.*, 2002; Valder, C. R. *et al.*, 2003). In these studies each animal was assessed for the development of tactile allodynia by behavioral testing prior to being included/excluded from the study. This was performed using von Frey filaments and to be included in the study animals needed to have a paw withdrawal threshold of less than 3 g in the neuropathic rats and greater than 10 g in the control rats. While some studies focused on evaluating the changes that occur both during the development and in fully established neuropathic pain (Wang, H. *et al.*, 2002), others assessed only established pain (Sun, H. *et al.*, 2002; Thimmapaya, R. *et al.*, 2003; Valder, C. R. *et al.*, 2003; Davis-Taber *et al.*, 2003). Several experimental design differences exist in each of these reports. In some studies since the contralateral paw did not display significant allodynia similarly to the sham animals, the L4/L5/L6 (Wang, H. *et al.*, 2002) or L5/L6 (Valder, C. R. *et al.*, 2003) DRG contralateral to the injury were selected for comparison with the equivalent injured DRGs from the same animals. In a parallel study to avoid any potential issues that could arise during surgery to alter gene expression contralateral to the injury and not revealed by allodynia assessment, the L5/L6 ipsilateral to the surgery were compared with the L5/L6 from sham-operated animals (Thimmapaya, R. *et al.*, 2003).

Another interesting comparison examined the expression differences between the injured L5/L6 DRG from Harlan and Holtzman Sprague-Dawley rats (Valder, C. R. *et al.*, 2003). The Holtzman rats were selected for this analysis as they do not develop the tactile allodynia observed in Harlan rats following SNL (Luo, Z. D. *et al.*, 1999). The goal of this study was to compare the expression profiles between these two strains and then extend these analyses to assess changes that were regulated following injury in one or both strains. This study did identify differentially expressed genes in the two strains, providing new information on neuroplasticity in DRG of these rats in response to nerve injury (Valder, C. R. *et al.*, 2003) in addition to those associated with neuropathic pain. However, cautious analysis of these data is important since similar regulation of gene changes in both strains is not an eliminating factor in defining whether the altered gene transcript is related to neuropathic pain development. Several transcripts that are known to be centrally involved in pain processing did change in both strains, that is, Nav1.8 and protein kinase C epsilon highlighting the limitations of this study.

A critical consideration when designing these experiments is to ensure that sufficient samples are collected to reflect the true changes that arise due to neuropathic pain and animal variation accurately. To this end assessment of DRG from L5/L6 region was performed using at least ten animals that were pooled prior to isolation of RNA for each of these studies. The comparison was made between the injured L5/L6 and either the contralateral L5/L6 (Wang, H. *et al.*, 2002) or sham L5/L6 (Thimmapaya, R. *et al.*, 2003). In one of the spinal cord studies nine animals were divided into three groups and in each group the dorsal and ventral spinal cords were pooled separately to form each pair of samples (three pairs). The comparison that was made in this tissue was between the dorsal and ventral spinal cord of neuropathic rats (Wang, H. *et al.*, 2002). In the other study, the global gene expression in the ipsilateral lumbar spinal cord was compared with the contralateral lumbar spinal cord from the neuropathic rats and to the sham control (Sun, H. *et al.*, 2002).

Typically protocols for isolating total RNA have been comparable throughout these studies using the TRizol protocol (Life Technologies/Invitrogen; Carlsbad, CA, USA) followed by RNeasy (Qiagen; Valencia, CA, USA) RNA clean-up step. The RNA quality was assessed either by denatured gel electrophoresis or capillary electrophoresis on the Agilent 2100 Bioanalyzer (Applied Biosystems; Foster City, CA, USA) to ensure that the 28S:18S ribosomal RNA (rRNA) ratio was greater than 1.0 for each sample, indicating that the sample was pure.

The microarray gene chip platform that was selected for each of these studies was the Affymetrix rat RG-U34a GeneChip®. On these microarray chips, each gene transcript is represented by probe sets containing 16 oligonucleotides, eight of which are matched and eight mismatched to the sequence of the transcript of interest. The oligonucleotides are 20 base pairs long, with a 3′ bias and may be to the coding and noncoding regions of the gene. Hybridization probes from each of these samples were generated and hybridized to the chips as recommended by Affymetrix. The microarray data was analyzed using the SAFER algorithm (Holder, D. *et al.*, 2002), Microarray Suite Expression Algorithm (Affymetrix; Santa Clara, CA, USA) or Rosetta Resolver (Rosetta Biosoftware; Seattle, WA, USA). Several microarray analysis software packages are available. Some utilize only a statistical algorithm (Affymetrix analysis software) while other analysis packages incorporate error models for normalization

of intensity between arrays and adjustments for probe-specific biases (SAFER and Resolver). Following a paired *t*-test and analysis of variance (ANOVA) analysis to determine a ratio for the expression changes between both samples a *P* value is generated and represents the probability that an observed gene expression change was due to a measurement error. To be considered significant, the change in gene expression had to occur in each microarray experiment and had to exhibit a value of $P \leq 0.05$ within each experiment. Another consideration that has been shown in each of these studies is how much does the transcript need to change to be considered significant enough to play a role in pain? In all the studies discussed in this chapter a cut-off of twofold was selected. This arbitrary cut-off was chosen since a large number of significant changes were observed but it is known that the expression of $P2X_3$, a validated pain target, only changed by 1.8-fold and would be excluded from this analysis. Therefore it is important not to exclude all small changes due to magnitude but if their changes are significant with $P \leq 0.05$, further analysis is warranted.

5.14.3 Microarray Data Analysis and Follow-up Studies

Following microarray analysis, the changes that were observed must be confirmed using either quantitative RT-PCR (Q-RTPCR), *in situ* hybridization, or, if reagents are available, immunocytochemistry. The latter two are preferable as the microarray studies described so far have all examined heterogeneous populations of cells (neurons and glial cells) and evaluation of specific tissue sections would provide a more precise profile of where the expression changes have occurred. Following confirmation of a subset of transcripts identified by microarray, data analysis has focused on classifying the gene transcripts into groups based upon the function of the gene product if known. An example of such a classification comes from the studies examining the changes in the L5/L6 DRG following SNL compared to sham L5/L6 DRG whereby gene products were grouped into cellular homeostasis and remodeling, ion channels and receptors, enzymes, immune response, neuronal markers, synaptic plasticity, transcription factors, and a miscellaneous category (Thimmapaya, R. *et al.*, 2003). Following this classification, it became evident that several examples of genes involved in synaptic plasticity (e.g., Narp and synaptobrevin) were downregulated, whereas genes involved in the immune response (e.g., MHCII) and cell regeneration/proliferation (e.g., Reg-2 and GADD45) were upregulated. A similar pattern of changes has been observed in the different neuropathic pain studies reported (Wang, H. *et al.*, 2002; Xiao, H. S. *et al.*, 2002; Valder, C. R. *et al.*, 2003).

5.14.4 Microarray Analysis of Subpopulations of Neurons Isolated from Dorsal Root Ganglion

All the studies described above examine the gene changes that occur in the entire DRG, which is composed of heterogenous subpopulations of cells (neurons and glial cells). Examining specific subpopulations of neurons would provide more precise information on the transcript expression changes. To accomplish this, LCM was used. This is a novel technology that permits the isolation and capture of specific cells from a tissue such as DRG in a native state. Determining the gene expression profile of different cell types has been hampered until recently by the inability to recover enough high-quality RNA from these cells for use in microarray experiments. Application of a new technique, antisense RNA (aRNA) amplification, has increased the yield of RNA to accommodate the requirements necessary for complementary DNA (cDNA) spotted and high-density oligonucleotide microarrays. DRG are composed of multiple neuronal and glial cell types and in particular, small-diameter neurons mediate nociceptive responses whereas large neurons facilitate mechanosensation. Two studies have profiled the differential gene expression of these nociceptive and mechanosensitive naive neurons by microarray (Luo, L. *et al.*, 1999; Davis-Taber, R. *et al.*, 2003). DRGs were flash frozen in cryomolds, sectioned to ~8 μm thickness and visualized with a Nissl (cresyl violet) stain to identify the neurons. Naive small (<25 μm and an identifiable nucleus) and large (>40 μm) diameter neurons were captured (PixCell II LCM system; Arcturus, Mountain View, CA, USA) and total RNA extracted from cellular material adherent to the thermoplastic film on the LCM caps. Multiple RNA isolation and amplification reagents and kits are commercially available from a variety of vendors (e.g., Arcturus, Mountain View, CA, USA; Stratagene, San Diego, CA, USA; Epicentre Technologies, Madison, WI, USA). aRNA was amplified two to three times prior to

hybridization onto a custom cDNA spotted array or an Affymetrix high-density oligonucleotide GeneChip® array (Luo, L. *et al.*, 1999; Davis-Taber, R. *et al.*, 2003).

There are several aspects of experimental design that should be considered prior to initiation of an LCM microarray study. First, a sufficient number of cells should be captured. For each of the LCM studies discussed, approximately 1000 small and 1000 large DRG neurons were isolated for microarray profiling. An alternative to capturing a greater amount of cellular material is increasing the number of rounds of RNA amplification. One trade-off to higher yields is a shortening of the RNA transcripts with each successive round of amplification. One other consideration is the 3′ bias of the aRNA transcripts generated. This is important when determining the microarray platform to use. Many high-density oligonucleotide arrays already incorporate a 3′ bias in their probe design (e.g., Affymetrix) but this issue may be more significant when using custom spotted arrays.

The initial studies profiling naive small and large DRG neurons observed a differential gene expression pattern for these two neuronal subpopulations. In the first study, naive cervical DRG aRNA from adult rats were hybridized to a custom cDNA spotted microarray (Luo, L. *et al.*, 1999). The microarray chip had 477 cDNAs that were obtained from two differential display experiments: (1) identified genes uniquely expressed in DRG compared to brain, liver, and kidney; and (2) genes that were differentially expressed in L5/L6 between ipsilateral (SNL) and contralateral (control). Approximately 40 genes were found to be enriched in either neuronal subpopulation with a greater majority detected in the small DRG neurons. The second study collected similar sized neuronal cells from rat lumbar L5/L6 DRG and hybridized the aRNA to the Affymetrix Neurobiology GeneChip® (Davis-Taber, R. *et al.*, 2003). In the small and large DRG neurons, ∼100 genes were detected and classified into functional groups (channels and receptors, enzymes, cell signaling, and cytoskeletal). In the categories of cell signaling and channels and receptors, there was an equal number of genes differentially enriched in each neuronal subpopulation, however, large DRG neurons predominantly expressed cytoskeletal proteins and enzymes. Examining the results reported in both experiments has shown that similar expression patterns and fold enrichment were observed for both neuronal subpopulations. A lack of glial-specific gene expression suggests that there was minimal glial contamination in the capturing process.

To understand the gene expression changes that occur in neuropathic pain states further, neuronal subpopulations were isolated from DRG following SNL or sham surgery and profiled by microarray. Similar to the naive DRG studies, small (∼1000 cells) and large (∼1000 cells) neurons were captured from SNL and sham L5/L6 ipsilateral DRGs (∼4000 total) by LCM and evaluated by Affymetrix rat RG-U34a GeneChip® arrays (Davis-Taber, R. *et al.*, 2004). Microarray analysis showed altered expression patterns between SNL and sham animals especially in large DRG neurons where the majority of gene changes occurred. Although some genes showed a common expression signature across both small and large neurons, a number of genes were dysregulated in only one neuronal subtype. A comparison of the whole DRG SNL microarray data (Thimmapaya, R. *et al.*, 2003) with the SNL small and large DRG neuron study revealed only a small number of genes that were commonly altered in all three samples. Also, only a small percentage of gene expression changes observed in the small (35%) or large (22%) neurons were dysregulated in the whole DRG microarray study. This suggests that within the individual neuronal subtypes, the distinct expression patterns that were observed may have been masked or minimized in the whole DRG microarray study. Microarray analysis of the small and large DRG neuronal subpopulations isolated from the injured DRG following SNL has provided a deeper understanding of the differential gene expression associated with neuropathic pain (Davis-Taber, R. *et al.*, 2004).

A potential limitation of the LCM microarray studies is the ability to collect a pure subpopulation of neurons. The time constraints of standard immunohistochemical staining procedures would allow tissue sections to rehydrate which could hinder precise capture of individual cells so a modified cresyl violet staining protocol developed by Arcturus Engineering, Mountain View, CA, USA, was used to visualize both small and large diameter DRG neurons. Without a way to distinguish the different small DRG neuron subtypes, a mixed population of peptidergic and non-peptidergic neurons were captured and pooled together. TRPV1 expression is an example of this limitation whereby it was shown to be downregulated in the L5/L6 small DRG neurons in the LCM SNL study but was not detected in the naive, L5/L6 small DRG neurons. Localization studies have shown that TRPV1 is found on peptidergic small-diameter

neurons and the receptor's inconsistent detection may result from the level of sensitivity of RNA amplification and microarray techniques from a mixed population of small DRG neurons. However, evaluation of the expression levels of RNA from subpopulations of neurons has provided a depth of information on transcripts that was previously not possible when whole DRG samples were assessed.

5.14.5 Evaluation of Additional Neuropathic Pain Models by Microarray

In addition to studies on the expression changes in DRG from SNL model of neuropathic pain, microarray analysis has also been performed on DRG following peripheral axotomy. In one study a custom microarray chip was generated that contained genes that were overexpressed in DRG 14 days following axotomy (Xiao, H. S. *et al*., 2002). The L4/L5 DRG were then probed against this chip at various timepoints to assess the changes in expression that occur both during the development and following established pain. Some genes changed expression immediately by day 2 (neuropeptide Y, heat shock protein 27, LIM domain protein CLP36) while others showed a more significant change at 14 days (neuronal nitric oxide synthase (nNOS), calcitonin gene-related peptide (CGRP)) following axotomy. The changes were confirmed for a subset of genes by *in situ* hybridization. Interestingly many of the genes that changed expression were the same as those observed in the SNL model (Table 1) indicating that these neuropathic pain models share some underlying molecular components. A second study used the Affymetrix rat RG-U34a GeneChip® gene chip and also examined the L4/L5 DRG following sciatic nerve axotomy over a time course of 1–14 days postinjury (Costigan, M. *et al*., 2002). This

Table 1 Representative gene expression changes identified by microarray analysis from rat L5/L6 DRG following peripheral nerve injury

Accession number	*Description*	*SNL (L5/L6) (Thimmapaya, R. et al., 2003)*	*Published changes: preclinical neuropathic models*
X59864	ASM15	4.84	↑ Valder C. R. *et al*. (2003)
AI009268	Ca^{2+}/calmodulin-dependent protein kinase 2 delta	2.29	↑ Xiao H. S. *et al*. (2002)
X81193	Cysteine-rich protein 3 (muscle LIM protein)	42.57	↑ Wang H. *et al*. (2002); ↑ Xiao H. S. *et al*. (2002); ↑ Valder C. R. *et al*. (2003)
L21192	GAP43	2.76	↑ Wang H. *et al*. (2002); ↑ Xiao H. S. *et al*. (2002); ↑ Valder C. R. *et al*. (2003)
AF028784	Glial fibrillary acidic protein (GFAP)	5.54	↑ Valder C. R. *et al*. (2003)
M98049	Pancreatitis-associated protein (Reg-2)	20.36	↑ Wang H. *et al*. (2002); ↑ Valder C. R. *et al*. (2003)
AA799645	Phospholemman chloride channel	2.45	↑ Costigan M. *et al*. (2002)
X80290	Pituitary adenylate cyclase activating peptide (PACAP)	3.04	↑ Costigan M. *et al*. (2002); ↑ Wang H. *et al*. (2002); ↑ Xiao H. S. *et al*. (2002)
M18331	Protein kinase C epsilon	−5.55	↑ Xiao H. S. *et al*. (2002); ↓ Valder C. R. *et al*. (2003)
U48246	Protein kinase C-binding protein NELL1	−12.15	↓ Wang H. *et al*. (2002); ↑ Xiao H. S. *et al*. (2002); ↓ Valder C. R. *et al*. (2003)
AB003991	SNAP-25A	−2.50	↓ Costigan M. *et al*. (2002); ↓ Wang H. *et al*. (2002); ↓ Xiao H. S. *et al*. (2002); ↓ Valder C. R. *et al*. (2003)
AF059030	Sodium voltage-gated channel, $Na_v1.9$	−23.85	↓ Wang H. *et al*. (2002); ↓ Valder C. R. *et al*. (2003)
X52772	Synaptotagmin I	−3.03	↔ Xiao H. S. *et al*. (2002)
X59737	Ubiquitous mitochondrial creatine kinase	−6.33	↓ Wang H. *et al*. (2002)

Genes that show enhanced or diminished expression from injured dorsal root ganglia (DRG) versus sham-operated DRG with a twofold change and $P \leq 0.05$. The fold increases and decreases in gene expression observed with DRG from spinal nerve ligated (SNL) rats are given, together with published microarray analysis of gene changes from preclinical neuropathic pain models (Xiao, H. S. *et al*., 2002, axotomy; Wang, H. *et al*., 2002, SNL; Costigan, M. *et al*., 2002, axotomy; Valder, C. R. *et al*., 2003, SNL). Genes were upregulated (↑), downregulated (↓), or unchanged (↔).

analysis compared naive DRG to the injured DRG and focused on the evaluation of data following this comparison. The data presented supported the use of a $P < 0.05$ significance threshold for detecting regulated genes. When a cut-off of a twofold change in expression was applied to select gene transcripts to assess, this led to an estimated error rate of 16%. Combining a more than 1.5-fold expression change and a $P < 0.05$ reduced the estimated error to 5%. Using the latter analysis, 240 genes changed expression significantly and many had not been previously described as changing following axotomy. Changes in expression of a subset of the genes were confirmed by *in situ* and Northern blots analysis. This study also identified increases in gene expression of genes mostly involved in immune responses and inflammation and decreases in those involved in neurotransmission similar to that reported for the SNL model of neuropathic pain. Taken together the microarray studies identified genes that are dysregulated in neuropathic pain states from different pain models providing an opportunity to unveil potential neuropathic molecular signatures that are common between these models.

5.14.6 The Strengths and Limitations of Microarray Analysis for Pain Research

Our knowledge of the complexity of neuropathic pain has heightened following the use of microarray gene chip technology. This approach provided opportunities to examine multiple gene transcripts simultaneously in pain states. Interestingly in these different studies similar gene changes have been observed in the DRG from diverse peripheral nerve injury models. A subset of these changes are given in Table 1, which shows that in most cases the gene products were dysregulated in a similar direction. However, in a couple of examples the transcripts were altered differently between the different models (Nell1; protein kinase C epsilon). The studies that have been performed have focused on gene changes that occur in the spinal cord and DRG but it is also known that areas of the brain are important for pain processing. Changes in gene expression can also occur in brain areas such as the rostral ventral medulla and periaqueductal gray, which participate in ascending and descending nociceptive signaling (Miki, K. *et al.*, 2002) in chronic pain states.

In addition to the strengths of microarray analysis detailed above there are also limitations. These assays are not suitable for detection of post-translational modifications of functional proteins including phosphorylation/dephosphorylation of ion channels, membrane proteins, and transcription factors. Functional modifications of pain-relevant proteins that do not alter their transcriptional levels include activation of *N*-methyl-D-aspartate receptors by injury-induced protein kinase C-mediated phosphorylation (Chen, L. and Huang, L. Y., 1992) and the downstream regulatory element antagonistic modulator (DREAM)-mediated derepression of prodynorphin expression that is regulated by elevated intracellular calcium and protein kinase A activation (Carrion, A. M. *et al.*, 1998). DREAM-deficient mice have been shown to have elevated spinal cord prodynorphin levels and reduced inflammatory pain behaviors (Cheng, H. Y. *et al.*, 2002).

Additionally, translation of the data arising from these studies to identify potential novel therapeutic targets is also a challenge. The approach undertaken in the studies highlighted in this chapter, has been to examine the literature for any data that would indicate that the protein encoded by a dysregulated transcript plays a role in pain. A complicating factor studying nociception and associated gene regulation in pain states is that unlike metabolic diseases where pathways are well understood, little is known about the specific pathways underlying pain. Application of programs that assess gene ontology (i.e., GenMAPP, GoSurfer, GOTM, WebGestalt, GoMiner, OntoExpress, and ErmineJ) and known pathways (i.e., Pathway Assist) can provide some insights into nociceptive signaling.

As mentioned earlier, microarray studies have generated a wealth of information but to understand the role of each gene product in pain will require extensive follow-up studies. Another approach that could be taken would be to evaluate the effects of administering target specific agonists or antagonists in preclinical pain models to determine if these proteins offer potential opportunities for novel therapeutic intervention if such agents already exist. Gene silencing using antisense or small interfering RNA (siRNA) approaches would also be other ways to establish if a protein that was dysregulated in a pain state would be a useful pain target (Hemmings-Mieszczak, M. *et al.*, 2003; Tan, P. H. *et al.*, 2005). Pain microarray studies as predicted have deepened our understanding of key players in neuropathic pain. However, deciphering the precise role of specific gene products in pain and identification of novel therapeutic targets awaits further investigation and is eagerly anticipated.

5.14.7 The Genetics of Pain

The pain microarray gene chip analysis detailed earlier in this chapter provides a snapshot of the changes in gene expression that occur in chronic pain states with the ultimate goal of understanding pain mechanisms and identifying potential novel therapeutic targets for pain treatment. Additional efforts to identify human genes associated with pain have examined congenital insensitivity to pain (CIP) that has been linked to the gene encoding serine palmitoyl-transferase (Nagasako, E. M. *et al.*, 2003). A subtype of this disorder CIP IV has been linked to single changes in nucleotide sequence (single nucleotide polymorphisms (SNPs)) of the TrkA receptor rendering the protein nonfunctional (Indo, Y. *et al.*, 1996). While nerve growth factor binding to the TrkA receptor is known to contribute to the survival and regulation of small diameter neurons, loss-of-function phenotypes observed in these individuals with SNPs are similar to the knockout animals. Another example is the gene responsible for familial hemiplegic migraine that has been linked to human chromosome 19p13 and more recently identified as the gene encoding a calcium channel α-subunit (CACNA1A; Joutel, A. *et al.*, 1993). Specific patients suffering from migraines have been shown to have missense mutations in this gene that lead to gain-of-function phenotypes. This calcium channel has been shown to be associated with serotonin release, magnesium levels, and the phenomenon of cortical spreading depression, each of which contribute to the pathophysiology of migraine (Ophoff, R. A. *et al.*, 1996).

Differences in human pain perception have also been associated to a common SNP (V158M) in the gene of the enzyme catechol-*o*-methyltransferase (COMT). Individuals homozygous for the Met^{158} allele of COMT showed diminished regional μ-opioid responses to pain compared with heterozygotes, which was opposite to the effects observed with the Val^{158} homozygote (Zubieta, J. K. *et al.*, 2003). Individuals with the more active form of the enzyme (Val^{158}) are less susceptible to pain than people with Met^{158} at the same position. COMT activity is also associated with a pathological pain condition known as temporomandibular joint disorder (TMD) that impacts 5–15% of the adult population. The relationship between COMT polymorphism, pain sensitivity, and risk of TMD development has recently been reported (Diatchenko, L. *et al.*, 2005). Three genetic variants (haplotypes) of the COMT gene, designated as low-pain sensitivity, average-pain sensitivity, and high-pain sensitivity were identified, that encompass 96% of the examined genotypes and lead to altered enzyme activity. The more active the COMT enzyme inversely correlated with pain susceptibility and the lower risk of developing TMD (Diatchenko, L. *et al.*, 2005).

Another interesting aspect of human genetics examined the sex differences in pain and analgesic sensitivity has been an area of research focus and increasing amounts of evidence suggest that sex differences may reflect the activation of gender-specific neural mechanisms. Since clinically κ-opioid receptor agonists show more efficacy in women than men, a recent report investigated the possible sex specificity of the genetic mediation of κ-opioid analgesia in mice using quantitative trait locus (QTL) mapping (Mogil, J. S. *et al.*, 2003). QTL mapping is a technique in which the co-inheritance of continuous traits and polymorphic DNA markers (e.g., microsatellites or SNPs) can be used to broadly identify the chromosomal location of genes responsible for trait variability (Lander, E. S. and Schork, N. J., 1994). Three convergent lines of evidence point to the mouse melanocortin-1 (*MCR1*) gene as the female-specific QTL. Furthermore analysis of women with red hair and fair skin containing two variant *MCR1* alleles displayed significantly greater analgesia from the κ-opioid pentazocine than all other groups (Mogil, J. S. *et al.*, 2003).

With the completion of the human genome project and ongoing efforts to sequence the genomes of a variety of other species, a plethora of sequence information is now available. New microarray applications and chip platforms are being developed to pinpoint genetic variation in disease states, isolate biomarkers that may indicate a predisposition for a given disease and identify treatment strategies and/or drug candidates that would have maximal benefit for a patient population with a specific genetic make-up.

The first of these new array platforms are comparative genomic hybridization (CGH) arrays. These microarrays are designed across large areas of sequence (i.e., a single chromosome) and even an entire genome to provide broad coverage for genotyping. CGH arrays have been generated from bacterial artificial chromosome (BAC) clones containing large genomic inserts and require a reference genome for comparison to the sample genome (Herr, A. *et al.*, 2005). These arrays have been used to determine differences in copy number

of particular genes and identify chromosomal imbalances found in cancer, genetic disorders, and deletion mutants with unique phenotypes used for scientific research (Hughes, T. R. *et al.*, 2000; Bruder, C. E. G. *et al.*, 2001; Herr, A. *et al.*, 2005). In contrast, to CGH arrays, resequencing and genome tiling arrays are designed to smaller, specific regions of a chromosome or genomic sequence and have been used to detect unknown mutations or to narrow down the area where a mutation may occur (Chee, M. *et al.*, 1996; Galvin, P. *et al.*, 2004; Lin, S. M. *et al.*, 2006). Resequencing arrays have probes designed to a particular sequence which when combined together will encompass all of the sequence within a specified region. Tiling arrays are designed to walk along a section of sequence with each probe representing one of the four nucleotides at a single nucleotide position. The probes are designed in sets of four. At a certain nucleotide position in the middle of the probe, each of the four probes will represent a different nucleotide (A, C, G, or T). The next four overlapping probes will have a mismatch (A, C, G, or T) at the next nucleotide position in succession from the mismatch in the previous probe set. The overall result from both these array platforms is a lack of hybridization and a subsequent decrease in signal intensity for the probes surrounding a mutation or polymorphism.

Linkage analysis studies using restriction-fragment length polymorphisms (RFLP) and polymorphic microsatellites have been useful in understanding mendelian-linked diseases. However, these tools have proven less consistent for mapping more complex disorders (i.e., schizophrenia, manic depression, and multiple sclerosis) that may have greater genetic heterogeneity or nonmendelian inheritance (Risch, N. J., 2000). More recently, SNPs, single nucleotide changes in DNA sequence, have been identified and catalogued in a number of genomic databases. Several SNP microarray chips have been developed (e.g., Affymetrix GeneChip Human Mapping 10K array) and used in concert with high-density microsatellite linkage sets to identify susceptibility or candidate genes that may be associated with the phenotype of a specific disease (Riley, J. H. *et al.*, 2000; Risch, N. J., 2000; Roses, A. D., 2000; Sawcer, S. J. *et al.*, 2004; Schaid, D. J. *et al.*, 2004).

Microarray can be a powerful tool, but also a hindrance. This technology can quickly and efficiently generate large amounts of data. However, excavating through this mass of information can be a time-consuming and possibly fruitless process without the proper analysis tools. With the implementation of these new array platforms, software has also been designed to aid in genotyping and linkage mapping studies. In the future, microarray may deepen our understanding of the genomic landscape and perhaps shed light on the origins of disease states. This genetic-driven trend could lead to individualized medical diagnoses and therapeutic treatment strategies.

References

Bruder, C. E. G., Hirvela, C., Tapia-Paez, I., Fransson, I., Segraves, R., Hamilton, G., Zhang, X. X., Evans, D. G., Wallace, A. J., Baser, M. E., Zucman-Rossi, J., Hergersberg, M., Boltshauser, E., Papi, L., Rouleau, G. A., Poptodorov, G., Jordanova, A., Rask-Andersen, H., Kluwe, L., Mautner, V., Sainio, M., Hung, G., Mathiesen, T., Moller, C., Pulst, S. M., Harder, H., Heiberg, A., Honda, M., Niimura, M., Sahlen, S., Blennow, E., Albertson, D. G., Pinkel, D., and Dumanski, J. P. 2001. High resolution deletion analysis of constitutional DNA from neurofibromatosis type 2 (NF2) patients using microarray-CGH. Hum. Mol. Genet. 10, 271–282.

Carrion, A. M., Mellstrom, B., and Naranjo, J. R. 1998. Protein kinase A-dependent derepression of the human prodynorphin gene via differential binding to an intragenic silencer element. Mol. Cell. Biol. 18, 6921–6929.

Chee, M., Yang, R., Hubbell, E., Berno, A., Huang, X. C., Stern, D., Winkler, J., Lockhart, D. J., Morris, M. S., and Fodor, S. P. A. 1996. Accessing genetic information with high-density DNA arrays. Science 274, 610–614.

Chen, L. and Huang, L. Y. 1992. Protein kinase C reduces Mg^{2+} block of NMDA-receptor channels as a mechanism of modulation. Nature 356, 521–523.

Cheng, H. Y., Pitcher, G. M., Laviolette, S. R., Whishaw, I. Q., Tong, K. I., Kockeritz, L. K., Wada, T., Joza, N. A., Crackower, M., Goncalves, J., Sarosi, I., Woodgett, J. R., Oliveira-dos-Santos, A. J., Ikura, M., van der Kooy, D., Salter, M. W., and Penninger, J. M. 2002. DREAM is a critical transcriptional repressor for pain modulation. Cell 108, 31–43.

Costigan, M., Befort, K., Karchewski, L., Griffin, R. S., D'Urso, D., Allchorne, A., Sitarski, J., Mannion, J. W., Pratt, R. E., and Woolf, C. J. 2002. Replicate high-density rat genome oligonucleotide microarrays reveal hundreds of regulated genes in the dorsal root ganglion after peripheral nerve injury. BMC Neurosci. 3, 16.

Davis-Taber, R., Choi, W., Kroeger, P., Seiler, F., Gagne, G., Kage, K., Faltynek, C., Gopalakrishnan, M., and Scott, V. 2003. Differential gene expression in small and large diameter DRG neurons isolated by laser capture microdissection. Am. Pain Soc. 2003; poster .

Davis-Taber, R., Choi, W., Vos, M., Zhu, C., Seiler, F., Gagne, G., Kage, K., Kroeger, K., Honore, P., Fagerland, J., Faltynek, C., Gopalakrishnan, M., Surowy, C., and Scott, V. E. 2004. Transcriptional profiling in small and large DRG neurons from a neuropathic pain model using LCM. Am. Pain Soc. 2004; poster .

Diatchenko, L., Slade, G. D., Nackley, A. G., Bhalang, K., Sigurdsson, A., Belfer, I., Goldman, D., Xu, K., Shabalina, S. A., Shagin, D., Max, M. B., Makarov, S. S., and Maixner, W. 2005. Genetic basis for individual variations in

pain perception and the development of a chronic pain condition. Hum. Mol. Genet. 14(1), 135–143.

Galvin, P., Clarke, L. A., Harvey, S., and Amaral, M. D. 2004. Microarray analysis in cystic fibrosis. J. Cyst Fibros. 3 (Suppl 2), 29–33.

Hemmings-Mieszczak, M., Dorn, G., Natt, F. J., Hall, J., and Wishart, W. L. 2003. Independent combinatorial effect of antisense oligonucleotides and RNAi-mediated specific inhibition of the recombinant rat P2X3 receptor. Nucl. Acids Res. 31, 2117–2126.

Herr, A., Grutzmann, R., Matthaei, A., Artelt, J., Schrock, E., Rump, A., and Pilarsky, C. 2005. High-resolution analysis of chromosomal imbalances using the Affymetrix 10K SNP genotyping chip. Genomics 85, 392–400.

Holder, D., Pikounis, V., Raubertas, R., Svetnik, V., and Soper, K. 2002. Statistical Analysis of High Density Oligonucleotide Arrays: A SAFER Approach. In: Proceedings of the American Statistical Association, Atlanta, Georgia.

Hughes, T. R., Roberts, C. J., Dai, H., Jones, A. R., Meyer, M. R., Slade, D., Burchard, J., Dow, S., Ward, T. R., Kidd, M. J., Friend, S. H., and Marton, M. J. 2000. Widespread aneuploidy revealed by DNA microarray expression profiling. Nature Genet. 25, 333–337.

Indo, Y., Tsuruta, M., Hayashida, Y., Karim, M. A., Ohta, K., Kawano, T., Mitsubuchi, H., Tonoki, H., Awaya, Y., and Matsuda, I. 1996. Mutations in the TRKA/NGF receptor gene in patients with congenital insensitivity to pain with anhidrosis. Nat. Genet. 13(4), 485–488.

Joutel, A., Bousser, M. G., Biousse, V., Labauge, P., Chabriat, H., Nibbio, A., Maciazek, J., Meyer, B., Bach, M. A., Weissenbach, J., *et al.* 1993. A gene for familial hemiplegic migraine maps to chromosome 19. Nat. Genet. 5(1), 40–45.

Lander, E. S. and Schork, N. J. 1994. Genetic dissection of complex traits. Science 265(5181), 2037–2048.

Lin, S. M., Devakumar, J., and Kibbe, W. A. 2006. Improved prediction of treatment response using microarrays and existing biological knowledge. Pharmacogenomics 7, 495–501.

Luo, L., Salunga, C., Guo, H., Bittner, A., Joy, K., Galindo, J., Xiao, H., Rogers, K., Wan, J., Jackson, M., and Erlander, M. 1999. Gene expression profiles of laser-captured adjacent neuronal subtypes. Nature Med. 5, 117–122.

Luo, Z. D., Chaplan, S. R., Scott, B. P., Cizkova, D., Calcutt, N. A., and Yaksh, T. L. 1999. Neuronal nitric oxide synthase mRNA upregulation in rat sensory neurons after spinal nerve ligation: lack of a role in allodynia development. J. Neurosci. 19, 9201–9208.

Miki, K., Zhou, Q. Q., Guo, W., Guan, Y., Terayama, R., Dubner, R., and Ren, K. 2002. Changes in gene expression and neuronal phenotype in brain stem pain modulatory circuitry after inflammation. J. Neurophysiol. 87, 750–760.

Mogil, J. S., Wilson, S. G., Chesler, E. J., Rankin, A. L., Nemmani, K. V., Lariviere, W. R., Groce, M. K., Wallace, M. R., Kaplan, L., Staud, R., Ness, T. J., Glover, T. L., Stankova, M., Mayorov, A., Hruby, V. J., Grisel, J. E., and Fillingim, R. B. 2003. The melanocortin-1 receptor gene mediates female-specific mechanisms of analgesia in mice and humans. Proc. Natl. Acad. Sci. U. S. A. 100(8), 4867–4872.

Nagasako, E. M., Oaklander, A. L., and Dworkin, R. H. 2003. Congenital insensitivity to pain: an update. Pain 101(3), 213–219.

Ophoff, R. A., Terwindt, G. M., Vergouwe, M. N., van Eijk, R., Oefner, P. J., Hoffman, S. M., Lamerdin, J. E., Mohrenweiser, H. W., Bulman, D. E., Ferrari, M., Haan, J., Lindhout, D., van Ommen, G. J., Hofker, M. H., Ferrari, M. D., and Frants, R. R. 1996. Familial hemiplegic migraine and episodic ataxia type-2 are caused by mutations in the Ca^{2+} channel gene CACNL1A4. Cell 87(3), 543–552.

Riley, J. H., Allan, C. J., Lai, E., and Roses, A. 2000. The use of single nucleotide polymorphisms in the isolation of common disease genes. Pharmacogenomics 1, 39–47.

Risch, N. J. 2000. Searching for genetic determinants in the new millennium. Nature 405, 847–856.

Roses, A. D. 2000. Pharmacogenetics and the practice of medicine. Nature 405, 857–865.

Sawcer, S. J., Maranian, M., Singlehurst, S., Yeo, T., Compston, A., Daly, M. J., De Jager, P. L., Gabriel, S., Hafler, D. A., Ivinson, A. J., Lander, E. S., Rioux, J. D., Walsh, E., Gregory, S. G., Schmidt, S., Pericak-Vance, M. A., Barcellos, L., Hauser, S. L., Oksenberg, J. R., Kenealy, S. J., and Haines, J. L. 2004. Enhancing linkage analysis of complex disorders: an evaluation of high density genotyping. Hum. Mol. Genet. 13, 1943–1949.

Schaid, D. J., Guenther, J. C., Christensen, G. B., Hebbring, S., Rosenow, C., Hilker, C. A., McDonnell, S. K., Cunningham, J. M., Slager, S. L., Blute, M. L., and Thibodeau, S. N. 2004. Comparison of microsatellites versus single-nucleotide polymorphisms in a genome linkage screen for prostate cancer-susceptibility loci. Am. J. Hum. Genet. 75, 948–965.

Sun, H., Xu, J., Della Penna, K. B., Benz, R. J., Kinose, F., Holder, D. J., Koblan, K. S., Gerhold, D. L., and Wang, H. 2002. Dorsal horn-enriched genes identified by DNA microarray, *in situ* hybridization and immunohistochemistry BMC Neurosci. 3, 11–23.

Tan, P. H., Yang, L. C., Shih, H. C., Lan, K. C., and Cheng, J. T. 2005. Gene knockdown with intrathecal siRNA of NMDA receptor NR2B subunit reduces formalin-induced nociception in the rat. Gene Ther. 12, 59–66.

Thimmapaya, R., Davis-Taber, R., Choi, W., Zhu, C., Gubbins, E., Vos, M., Helfrich, R., Kage, K., Daza, A., Donnelly-Roberts, D., Harris, R., Surowy, C., Honore, P., Kroeger, P., Faltynek, C., Gopalakrishnan, M., and Scott, V. E. 2003. Gene expression profiling in the spinal nerve ligation model of neuropathic pain using microarray technology. Soc. Neurosci. 2003; poster .

Valder, C. R., Liu, J. J., Song, Y. H., and Luo, Z. D. 2003. Coupling gene chip analyses and rat genetic variances in identifying potential target genes that may contribute to neuropathic allodynia development. J. Neurochem. 87, 560–573.

Wang, H., Sun, H., Della Penna, K., Benz, R. J., Xu, J., Gerhold, D. L., Holder, D. J., and Koblan, K. S. 2002. Chronic neuropathic pain is accompanied by global changes in gene expression and shares pathobiology with neurodegenerative diseases. Neuroscience 114, 529–546.

Xiao, H. S., Huang, Q. H., Zhang, F. X., Bao, L., Lu, Y. J., Guo, C., Yang, L., Huang, W. J., Fu, G., Xu, S. H., Cheng, X. P., Yan, Q., Zhu, Z. D., Zhang, X., Chen, Z., Han, Z. G., and Zhang, X. 2002. Identification of gene expression profile of dorsal root ganglion in the rat peripheral axotomy model of neuropathic pain. Proc. Natl. Acad. Sci. U. S. A. 99, 8360–8365.

Zubieta, J. K., Heitzeg, M. M., Smith, Y. R., Bueller, J. A., Xu, K., Xu, Y., Koeppe, R. A., Stohler, C. S., and Goldman, D. 2003. COMT val158met genotype affects mu-opioid neurotransmitter responses to a pain stressor. Science 299(5610), 1240–3.

5.15 Evolutionary Aspects of Pain

E T Walters, University of Texas at Houston, Medical School, Houston, TX, USA

© 2008 Elsevier Inc. All rights reserved.

5.15.1	**Introduction**	176
5.15.2	**Evolution of Nociceptive Mechanisms**	176
5.15.2.1	Nociceptors	176
5.15.2.1.1	Identification of nociceptors in diverse phyla	176
5.15.2.1.2	Conserved mechanisms of nociceptive transduction	177
5.15.2.1.3	Nociceptor-specific gene expression	178
5.15.2.2	Nociceptive Networks and Antinociceptive Modulation	178
5.15.2.2.1	Common nociceptive functions mediated by diverse neural circuits	178
5.15.2.2.2	Widespread occurrence of antinociceptive mechanisms	179
5.15.2.2.3	Recent evolution of opiate systems	179
5.15.2.3	Nociceptive Plasticity and Sensitization	179
5.15.2.3.1	*N*-Methyl-D-asparate-receptor-dependent long-term synaptic potentiation	180
5.15.2.3.2	Activation of the transcription factor, Ca^{2+} and cAMP Response Element-Binding Protein	180
5.15.2.3.3	Local protein synthesis and primitive memory mechanisms	180
5.15.3	**Evolution of Emotional Components of Pain**	181
5.15.3.1	Emotional Awareness is not Required for Nociceptive Responses	181
5.15.3.2	Even Snails Display Complex Motivational Effects after Noxious Stimulation	181
5.15.3.3	Cognitive and Emotional Responses to Noxious Stimulation Differ across Species	181
5.15.4	**Conclusions**	182
References		182

Glossary

CREB Ca^{2+} and cAMP response element-binding protein, a transcription factor that binds to specific enhancer elements in DNA and enhances the expression of corresponding genes when certain Ca^{2+}- or cAMP-activated protein kinases, such as CaMK or PKA, phosphorylate the CREB protein.

degenerin/epithelial Na^+ (DEG/ENaC) channels A family of ion channels that conduct Na^+ ions and can be constitutively active or gated by mechanical distention or protons. Channels that are gated by protons are called acid-sensing ion channels (ASICs).

MAPK (ERK) Mitogen-activated protein kinase, a family of protein kinases that includes the extracellular signal-regulated kinase (ERK). ERK has many functions related to neural plasticity, both in the cytoplasm and nucleus.

MRG Mas-related genes, a family of genes encoding G-protein-coupled receptors, some of which are expressed selectively in mammalian nociceptors. Also called sensory neuron-specific G-protein-coupled receptors (SNSRs).

NMDA-receptor-dependent LTP *N*-Methyl-D asparate-receptor-dependent long-term synaptic potentiation, a form of use-dependent synaptic plasticity induced by Ca^{2+} influx through the class of glutamate receptors that is selectively activated (pharmacologically) by the drug, NMDA.

RFamide peptides A family of peptide neurotransmitters sharing the same C terminal RFamide (arginine-phenylalanine-NH_2) sequence.

transient receptor potential (TRP) A family of ion channels, many of which conduct cations nonselectively. Different channels in this family are opened by various inputs, including heat, cooling, protons, and intracellular signals.

TTX-resistant, voltage-gated Na^+ channels Members of the voltage-gated Na^+ channel family that are relatively insensitive to blockade by the specific antagonist, tetrodotoxin (TTX). These channels (NaV1.8 and NaV1.9) are expressed selectively in nociceptive dorsal root ganglion neurons.

5.15.1 Introduction

Pain, according to a widely accepted definition (Merskey, H. and Bogduk, N., 1994), is an unpleasant sensory and emotional experience associated with actual or potential tissue damage. This definition is intended to capture essential features of human experiences linked to tissue damage and makes no claims about the evolutionary roots or possible biological functions of pain. Nonetheless, it raises two distinct sets of evolutionary questions. First, how did sensory responses to actual or potential tissue damage evolve? What biological adaptations do these responses represent, and to what extent are the underlying mechanisms conserved across the animal kingdom? Second, how did the unpleasant emotional components of pain evolve? This essay considers comparative functional and molecular findings from diverse species in the animal kingdom that begin to address these questions. Because this task requires reference to far more reports than can be cited in a brief account, citations are made primarily to review articles or to recent reports that provide additional references to this diverse literature. Although no recent, comprehensive review of nociceptive biology in invertebrates exists, highly comprehensive reviews of nociceptive mechanisms in mammals can be found in other chapters in this volume, and in a recent book (Willis, W. D. and Coggeshall, R. E., 2004).

5.15.2 Evolution of Nociceptive Mechanisms

Because an animal's reproductive success is clearly enhanced if it can detect and avoid pervasive threats to its structural integrity that otherwise would impair or end its ability to reproduce, selection pressures for mechanisms that recognize noxious stimuli and trigger adaptive physiological and behavioral responses must be very strong (Walters, E. T., 1994). Indeed, animals in several phyla have now been shown to possess nociceptors connected to neural networks controlling defensive responses, and these varied nociceptive systems share numerous features including distinctive forms of plasticity. Common properties in diverse species are of interest for evolutionary questions because they point to (1) common selection pressures that have shaped similar but independently derived (analogous) adaptations; and/or (2) the conservation of homologous mechanisms descending from common ancestors. Figure 1 shows a simplified view of evolutionary relationships among selected species mentioned in this essay that have been used to study nociceptive biology. Those that have had their genome completely sequenced are indicated by asterisks (human, mouse, fruit fly, and roundworm). The current explosion of molecular genetic information from a growing number of species promises to illuminate evolutionary relationships among nociceptive mechanisms with a level of detail and precision that could only be dreamed of a few years ago.

5.15.2.1 Nociceptors

Nociceptors are defined as sensory neurons that are activated preferentially by tissue-damaging stimuli, either immediately or when a noxious stimulus is sufficiently prolonged. Because of the medical, social, and economic importance of pain, most studies of nociceptors have been in selected mammalian species rather than animals more distantly related to humans. Thus, the comparative physiological and molecular information needed to discern evolutionary patterns in nociceptive function is still quite limited. However, the availability of extensive genomic and proteomic data from a growing number of species should soon shed light on the evolution of specific molecular components of nociceptive systems.

5.15.2.1.1 Identification of nociceptors in diverse phyla

Physiological identification and characterization of nociceptors is challenging because the somata are usually dispersed among those of many other types of neurons, and the fine peripheral and central fibers are essentially inaccessible for direct intracellular examination in living preparations. Nevertheless, nociceptors have now been demonstrated convincingly in representatives of all the major animal phyla (Figure 1), including nematode worms (Tobin, D. M. and Bargmann, C. I., 2004), leeches (Nicholls, J. G. and Baylor, D. A., 1968), insects (Tracey, W. D. Jr., *et al.*, 2003), mollusks (Illich, P. A. and Walters, E. T., 1997), and various chordates, including fish (Sneddon, L. U. *et al.*, 2003), amphibians (Lynn, B. and O'Shea, N. R., 1998), reptiles (Liang, Y. F. *et al.*, 1995), birds (Holloway, J. A. *et al.*, 1980), and mammals (Light, A. R., 1992). Additional species, including snails (Malyshev, A. Y. and Balaban, P. M.,

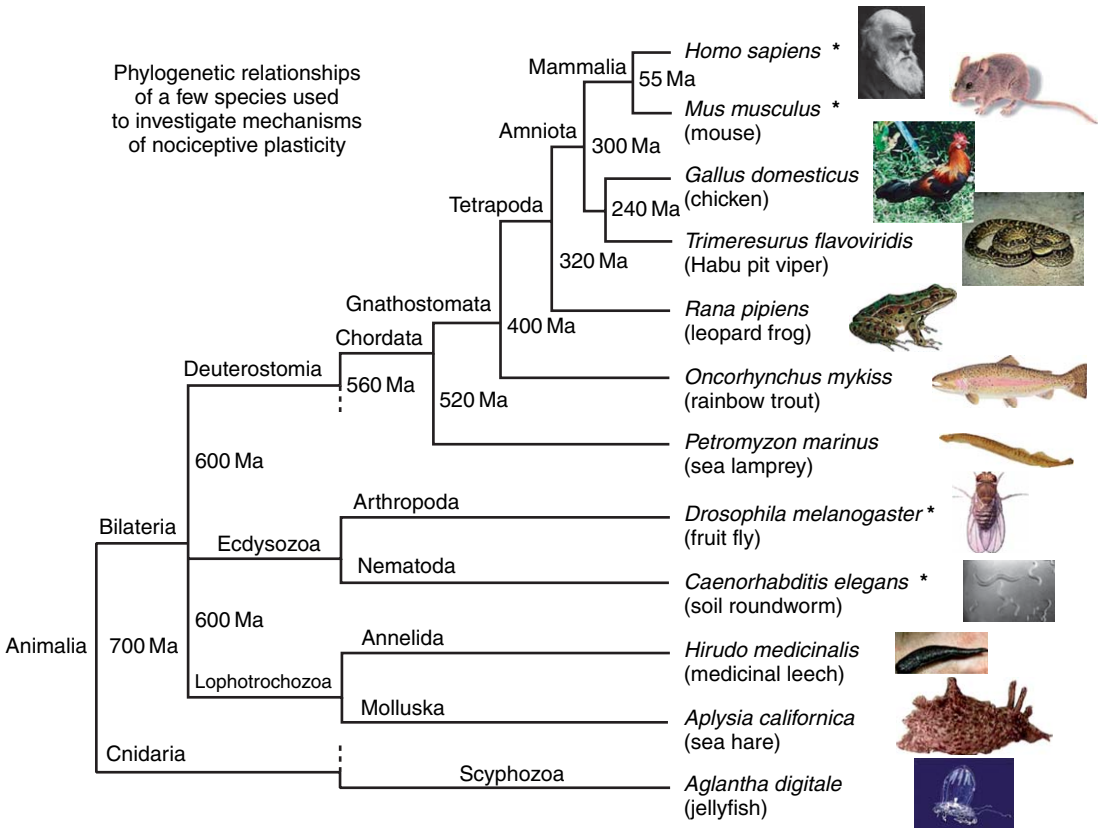

Figure 1 Greatly simplified phylogeny of a few selected species (right) that have been used to investigate nociceptive biology. Numbers indicate approximate time of divergence (millions of years ago, Ma) of the indicated groups (Dawkins, R., 2004). Groupings reflect recent molecular phylogenetics rather than traditional views based on morphological evidence. The traditional phyla indicated on this chart are chordata, arthropoda, nematoda, annelida, molluska, and cnidaria. Because of the paucity of fossil evidence prior to the Cambrian period (more than 540 Ma) and uncertainties in molecular clocks over longer periods, the older times of divergence on the chart are much rougher estimates than the more recent ones. Asterisks indicate species for which complete genome sequence information is currently available.

2002) and lampreys (Christenson, J. et al., 1988) have mechanosensory neurons that are likely to be nociceptive, despite their relatively low mechanical thresholds, because the tissue they innervate is delicate enough to be damaged by modest pressures (see Illich, P. A. and Walters, E. T., 1997).

5.15.2.1.2 Conserved mechanisms of nociceptive transduction

Tissue damage can be produced by various mechanical forces and chemical agents as well as by excessive temperature changes, so one would expect that nociceptors utilize diverse stimulus transduction mechanisms. Combined molecular and physiological analyses of nociceptive transduction have revealed important mechanisms in a few species. Many forms of mechanotransduction, perhaps including the transduction of noxious forces in some cells, depend upon depolarizing current entry through channels in the degenerin/epithelial Na^+ channel (DEG/ENaC) family. Several of these channels are required for activation of low-threshold mechanosensory neurons in the nematode, *C. elegans* (Tobin, D. M. and Bargmann, C. I., 2004), while in mice some channel subunits within this same family are acid sensitive (DRASIC/ASIC3) and contribute to the responses of some nociceptive neurons both to acid and to noxious pinch (Price, M. P. *et al.*, 2001). Another family of channels, the transient receptor potential (TRP) superfamily, has demonstrated its importance for nociceptive transduction in both vertebrates and invertebrates. TRPV channels in *C. elegans* are required for nociceptive, osmosensory, mechanosensory, and some chemosensory responses (Tobin, D. M. and Bargmann, C. I., 2004). In mammals, TRPV1 channels in sensory neurons are activated by heat, acid, capsaicin (the pungent vanilloid

ingredient of chili peppers), and other chemicals (Krause, J. E. *et al.*, 2005). Mice lacking TRPV1 channels show impaired sensory and behavioral responses to heat, vanilloids, and inflammation (Caterina, M. J. *et al.*, 2000). TRP channels also transduce noxious stimuli in the fly, *Drosophila*; mutations of the painless gene (which encodes a TRPA family member) nearly eliminate nociceptive behavioral responses of larvae to noxious heat or mechanical stimuli (Tracey, W. D., Jr., *et al.*, 2003). TRPA family channels are found in vertebrate nociceptors as well, where they are activated by noxious cold, various pungent compounds, and bradykinin (Bandell, M. *et al.*, 2004). These recent results show that nociceptive transduction in at least three different phyla makes use of shared families of ion channels, notably TRPV and TRPA channels, and perhaps DEG/ENaC channels. However, these channel families are not specific to nociception; each family also has members that are involved in innocuous mechanosensation (including hearing in *Drosophila*) and various forms of chemosensation (Tobin, D. M. and Bargmann, C. I., 2004). Thus, nociception has exploited a number of ancient and versatile ion channel families that have also been used during evolution for additional forms of sensory transduction.

5.15.2.1.3 Nociceptor-specific gene expression

Although evolution is opportunistic and tends to find multiple uses for individual gene products, some remain functionally specialized. Several genes have been found to be expressed relatively selectively in mammalian nociceptors, suggesting specialized functions related to nociceptive processing. These include the TTX-resistant, voltage-gated Na^+ channels, NaV1.8 and NaV1.9, which show alterations after nerve injury that are likely to contribute to neuropathic pain (Lai, J. *et al.*, 2004). They also include a family of receptors called Mas-related genes (MRG) (Dong, X. *et al.*, 2001) or sensory neuron-specific G-protein-coupled receptors (SNSR) (Lembo, P. M. et al., 2002). These sensory neuron receptors have displayed exceptionally rapid recent evolution in some mammals (Choi, S. S. and Lahn, B. T., 2003), and might have first appeared in the chordate lineage. Rapid changes within the MRG family are illustrated dramatically by the variation in nociceptor-specific MRG genes within a single mammalian order; mice have 22 MRGA and 14 MRGC genes, whereas gerbils, and rats only have one of each (Zylka, M. J. *et al.*, 2003). Only six of the 13 MRG genes in humans are clearly orthologous (displaying sequence homology across species) with mice MRG genes. Little is known about the functions of these receptors, although the diversity of ligands implicated for them include a variety of RFamide peptides thought to be antinociceptive (Dong, X. *et al.*, 2001 and see below). The recency and rapidity of change in the MRG family suggests that strong selection pressures may be acting on antinociceptive modulation of nociceptors in vertebrates, including primates (Choi, S. S. and Lahn, B. T., 2003; Zylka, M. J. *et al.*, 2003; Zhang, L. *et al.*, 2005). Further investigation of the distribution – across diverse taxa – of genes found to be preferentially expressed in mammalian nociceptors should provide interesting insights into the evolution of nociceptive systems.

5.15.2.2 Nociceptive Networks and Antinociceptive Modulation

The capability for rapid detection of noxious stimuli could only have been selected during evolution if systems to translate this information into adaptive behavior had also been selected. Almost every animal that has been examined, from jellyfish to humans, displays withdrawal and/or escape responses to noxious stimulation (Walters, E. T., 1994), although these responses are inhibited under some circumstances (see further ahead).

5.15.2.2.1 Common nociceptive functions mediated by diverse neural circuits

Nociceptive responses are mediated by neural circuits that range enormously in complexity across different animals. In cnidarians (hydra, jellyfish, sea anemones), some simple withdrawal reflexes may be mediated in part by just a two-cell pathway involving a multifunction sensory-motor neuron synaptically connected to epithelial-muscular cells. However, even in cnidarians, which lack a brain or central ganglia, relatively complex withdrawal and escape responses can be mediated by a neural net containing sensory, motor, and interneurons (e.g., Mackie, G. O., 2004). At the other end of the behavioral spectrum, nociceptive circuits in mammals involve not only diverse types of sensory, motor, and interneurons at the spinal level, but vast numbers of neurons in higher brain structures (e.g., Craig, A. D., 2003). Different populations of neurons process nociceptive sensory information, generate defensive motor patterns, and modulate nociceptive responses depending upon the state of the organism and its previous experience. These basic nociceptive/defensive tasks

are also mediated by functionally similar, but much simpler, neural circuits in several invertebrate species that have been investigated, including *C. elegans* (Wittenburg, N. and Baumeister, R., 1999), the medicinal leech (Shaw, B. K. and Kristan, W. B., Jr. , 1995), and several gastropod mollusks – *Aplysia* (Cleary, L. J. et al., 1995), *Tritonia* (Getting, P. A., 1977), and *Helix* (Balaban, P. M., 2002). Although the organization of these circuits differs greatly among the mammalian and invertebrate species examined, common mechanisms of nociceptive plasticity appear to be shared by these diverse animals (see further ahead).

5.15.2.2.2 Widespread occurrence of antinociceptive mechanisms

One of the most important functions of nociceptive circuits is to modulate nociceptive responses, so that the threshold, selection, and intensity of defensive responses are well matched to the nature and context of a noxious threat. The form of modulation that has received the most experimental attention in nociceptive systems is antinociception, which produces analgesia or hypoalgesia in humans. Many authors have argued that it is adaptive for an animal to inhibit responses, including pain and recuperative responses evoked by injury, during active defense in life-threatening encounters with predators or aggressive conspecifics (see Walters, E. T., 1994). Indeed, most animals examined thus far, including various invertebrates, transiently suppress appetitive, recuperative, and other nondefensive behaviors that might compete with urgent fight-or-flight responses evoked immediately by noxious stimuli. In mammals (Light, A. R., 1992) and at least one invertebrate, *Aplysia* (Cleary, L. J. *et al.*, 1995), inhibitory effects of noxious stimulation are exerted at multiple stages within sensory-motor pathways. Strong pre- and/or postsynaptic inhibition during noxious stimulation occurs at the first synapse in these pathways (from somatic primary afferent neurons) in various species, including mammals (Light, A. R., 1992) and *Aplysia* (Mackey, S. L. *et al.*, 1987).

5.15.2.2.3 Recent evolution of opiate systems

There has been much interest in the phylogenetic distribution of antinociceptive neuropeptides, and especially the opioid family because of its well-known analgesic functions in humans. Pharmacological, immunocytochemical, and biochemical studies have suggested that opiate-like substances and opiate receptors occur in nervous and immune systems of diverse species, including invertebrates and even unicellular organisms (Stefano, G. B. *et al.*, 2003). However, genes within the opioid/orphanin family have not been detected in the genomes of *C. elegans* or *Drosophila* (nor have genes within the corresponding melanocortin receptor family), which supports the hypothesis that this gene family first appeared in a deuterostome ancestor around the time that the chordate lineage diverged (Dores, R. M. *et al.*, 2002) (Figure 1). The only invertebrate opioids that have been sequenced are proteins related to pro-opiomelanocortin (POMC), which have been found in immunocytes in a leech (Salzet, M. *et al.*, 1997) and in the mussel, *Mytilus edulis* (Stefano, G. B. *et al.*, 1999). Paradoxical features of these POMC sequences led to the suggestion that the vertebrate-like POMC in these invertebrates may have come somehow by cross-phylum gene transfer (Dores, R. M. *et al.*, 2002), and these unusual features reinforce indications that antinociceptive opioids may be a chordate innovation. In contrast, another neuropeptide family having antinociceptive functions is widespread in the animal kingdom: the RFamide family which is expressed in many phyla, including cnidarians, nematodes, arthropods, mollusks, and chordates (Li, C. *et al.*, 1999; Nichols, R., 2003). In mammals some RFamides activate MRG receptors (Dong, X. *et al.*, 2001) (and see above), while in *Aplysia* FMRFamide can produce both short-term and long-term inhibition of synaptic transmission from nociceptive sensory neurons (Montarolo, P. G. *et al.*, 1988). However, RFamides also have pronociceptive actions (Yudin, Y. K. *et al.*, 2004) as well as many actions unrelated to nociceptive modulation.

5.15.2.3 Nociceptive Plasticity and Sensitization

As just discussed, many animals show a transient reduction in responsiveness to somatic stimuli during active defensive behavior. However, if an animal is injured and escapes, it often displays enhanced responsiveness to somatosensory stimuli while it recuperates. This nociceptive sensitization (and hyperalgesia in some species) is targeted to the injured region and can be very long lasting. It facilitates defensive responses, helping to protect an injured animal during a period when it may be weakened and emitting wound-related signals that can attract the attention of predators, parasites, and aggressive competitors (Walters, E. T., 1994). The persistence of nociceptive sensitization during recuperation periods that can last weeks or longer raises

the possibility that nociceptive sensitization may utilize mechanisms that are shared with other long-lasting neural alterations, such as learning and memory. Demonstrations that the same plasticity mechanisms contribute both to nociceptive sensitization and to learning and memory, and evidence that these mechanisms have common functions in very distantly related animal species, indicate that evolutionary links between injury and memory may be quite primitive (Walters, E. T., 1994; Weragoda, R. M. *et al.*, 2004). Of several apparent commonalities between injury-induced and learning-related mechanisms in diverse phyla, three will be considered here.

5.15.2.3.1 *N*-Methyl-D-asparate-receptor-dependent long-term synaptic potentiation

As in mammals (Ji, R. R. *et al.*, 2003), somatosensory afferents in several intensively studied invertebrate species appear to release glutamate, which acts upon both NMDA and non-NMDA postsynaptic receptors. These invertebrates include *C. elegans* (Brockie, P. J. *et al.*, 2001), *Aplysia* (Dale, N. and Kandel, E. R., 1993), *Helix* (another snail) (Bravarenko, N. I. *et al.*, 2003), and the leech (Burrell, B. D. and Sahley, C. L., 2004). In mammals (Ji, R. R. *et al.*, 2003), *Aplysia* (Lin, X. Y. and Glanzman, D. L., 1994), *Helix* (Nikitin, V. P. *et al.*, 2002), and the leech (Burrell, B. D. and Sahley, C. L., 2004), intense activation of a sensory pathway (which under normal conditions would occur during noxious stimulation of the periphery) strongly depolarizes second-order neurons and activates NMDA receptors, leading to LTP in the nociceptive pathway, which contributes to nociceptive sensitization. As in mammals (Martin, S. J. *et al.*, 2000), in *Aplysia* (Murphy, G. G. and Glanzman, D. L., 1997), *Helix* (Nikitin, V. P. *et al.*, 2002), and the leech (Burrell, B. D. and Sahley, C. L., 2004), NMDA-receptor-dependent LTP has been implicated as a mechanism of learning and memory.

5.15.2.3.2 Activation of the transcription factor, Ca^{2+} and cAMP Response Element-Binding Protein

A second commonality is a role for a transcription factor, the Ca^{2+} and cAMP response element-binding protein (CREB), in inducing long-term neuronal alterations that require changes in gene transcription and protein synthesis. A key role for this transcription factor was first implicated in long-term memory formation in *Aplysia*, *Drosophila*, mice, and rats (Silva, A. J. *et al.*, 1998; Kandel, E. R., 2001). Later, hyperalgesia was found to be accompanied by CREB phosphorylation in the rat spinal cord (Ji, R. R. and Rupp, F., 1997), and interference with CREB binding to DNA was shown to attenuate sensitized behavioral responses in a rat neuropathic pain model (Ma, W. et al., 2003). Interestingly, the sensory neurons from *Aplysia* originally used to demonstrate possible roles of CREB in long-term memory formation (Kandel, E. R., 2001) are nociceptive and exhibit long-term hyperexcitability following noxious cutaneous stimulation, and this hyperexcitability is blocked by injection of CRE oligonucleotides to prevent CREB binding (Lewin, M. R. and Walters, E. T., 1999). Cellular signals involved in activating CREB are also common to both memory and nociceptive sensitization/hyperalgesia in various phyla. Particular attention has been paid to the roles of PKA and MAPK (ERK) in CREB-related plasticity in mammalian hippocampus and forebrain (Waltereit, R. and Weller, M., 2003), mammalian spinal cord (Kawasaki, Y. *et al.*, 2004), and *Aplysia* sensory neurons (Kandel, E. R., 2001).

5.15.2.3.3 Local protein synthesis and primitive memory mechanisms

The observations mentioned above suggest that evolution made use of common basic mechanisms, including NMDA-receptor-dependent LTP and CREB-dependent transcriptional regulation, to induce long-lasting neuronal alterations underlying quite different functions: nociceptive sensitization and learning. Because strong selection pressures would have favored adaptive responses to peripheral injury at the earliest stages of animal evolution (prior to the evolution of brains complex enough for associative learning), it has been suggested that adaptive responses to peripheral injury, including nociceptive sensitization, emerged first as an adaptation to tissue damage and later evolved into mechanisms of learning and memory (Walters, E. T., 1994). In ancient, soft-bodied animals that were ancestral to most contemporary animals (Figure 1), some of these mechanisms may have functioned initially at sites of peripheral injury in axons and terminals. A vestige of early memory-like mechanisms linked to peripheral injury might be represented today by localized, long-term hyperexcitability of peripheral axon segments of nociceptive sensory neurons found in *Aplysia* (Weragoda, R. M. *et al.*, 2004). This sensitizing axonal alteration is induced by nerve crush or local depolarization and, like the late phase of LTP in mammalian

hippocampus (Tang, S. J. *et al.*, 2002), it requires local, rapamycin-sensitive protein synthesis (Weragoda, R. M. *et al.*, 2004). It has not yet been determined whether this apparently primitive mechanism contributes to neuropathic pain in mammals, but evidence for intra-axonal protein synthesis following peripheral nerve injury has been found in axons of mammalian DRG neurons (e.g. Zheng, J. Q. *et al.*, 2001).

5.15.3 Evolution of Emotional Components of Pain

Perhaps the most commonly asked question related to the evolution of pain is one that has yet to be answered by scientists: Which animals feel pain? This question is critical for animal welfare issues, and is also of considerable philosophical interest (Allen, C., 2004). Many philosophers of science have argued that a human observer cannot know for sure whether another being or species has subjective, conscious experiences such as pain. The existence of emotional pain in other species may defy proof, but evolutionary and neurobiological considerations indicate strongly that these components of pain did not emerge *de novo* in humans, while also suggesting that the capacity to experience subjective pain is not a universal animal trait.

5.15.3.1 Emotional Awareness is not Required for Nociceptive Responses

As discussed above, most animals have nociceptive systems that detect noxious stimuli and activate defensive responses. Nociceptive reflexes and even nociceptive plasticity, however, can almost certainly operate without conscious, emotional experience because these responses are expressed not only in the simplest animals but also in greatly simplified physiological preparations, such as a spinalized rat or an *Aplysia* ganglion connected to part of the animal's tail. Moreover, in human patients nociceptive reflexes can be expressed without conscious awareness below the level of a spinal transection.

5.15.3.2 Even Snails Display Complex Motivational Effects after Noxious Stimulation

In addition to the abilities to detect noxious stimuli and activate defensive responses, adaptations to actual or incipient tissue damage include motivational responses, and these too can be observed throughout the animal kingdom. Pain motivates humans and other mammals to avoid contexts or actions associated with the onset of the pain, and similar motivational effects of noxious stimulation (often electric shock that activates nociceptors) have been used experimentally to produce aversive learning in a wide variety of invertebrates, including flies, worms, and snails (reviewed by Krasne, F. B. and Glanzman, D. L., 1995; Waddell, S. and Quinn, W. G., 2001; Rankin, C. H., 2004). Some of these motivational effects appear remarkably similar to those produced by noxious stimuli in mammals. For example, pairing an odor with strong cutaneous shock causes the previously neutral odor to evoke a conditioned fear-like state in *Aplysia*, so that the odor comes to evoke a freezing response, inhibit appetitive responses, and facilitate defensive responses to tactile stimuli (Walters, E. T. *et al.*, 1981).

5.15.3.3 Cognitive and Emotional Responses to Noxious Stimulation Differ across Species

Although relatively simple invertebrates show functional similarities to vertebrates (sometimes with conserved molecular mechanisms) in detecting noxious stimuli, activating defensive behavior, and motivating learned and unlearned responses to a noxious event, vast differences in the size and structure of their brains indicate that major differences exist between most invertebrates and many vertebrates in the cognitive and possible emotional processing of information about tissue damage. For example, in *Aplysia*, the body surface is represented by a somatotopic map formed by nociceptor somata in central ganglia (Walters, E. T. *et al.*, 2004), and peripheral injury causes nociceptor soma hyperexcitability selectively in nociceptors representing the injured region. These and other sensory changes are sufficient to alter reflexive responses to stimuli received by the injured region, but they do not cause these normally silent sensory neurons to become spontaneously active. If one assumes that ongoing pain requires ongoing neural activity somewhere in a nervous system, then an absence of ongoing activity may be taken as evidence that tissue damage fails to produce long-lasting, pain-like states. In relatively simple invertebrates, one can systematically sample the activity of individual neurons and use optical imaging methods to sample the activity of populations of neurons to test this possibility following strong noxious stimulation. Although

many more neurons need to be sampled before firm conclusions can be made, preliminary observations in *Aplysia* suggest that a persistent (lasting days or longer) increase in ongoing neural activity within the CNS does not accompany long-term, nociceptive sensitization of defensive reflexes. Instead, sensitization lasting days or weeks appears to be maintained largely by synaptic facilitation and hyperexcitability of sensory neurons, which remain silent in the absence of peripheral stimulation. An apparent lack of ongoing activity in the *Aplysia* CNS would contrast with increases in neural activity that probably occur in some regions of the human brain during persistent pain states (Casey, K. L., 2000).

Investigating the evolution of emotional aspects of pain is an enormous challenge because the biological functions of conscious pain (as opposed to unconscious nociceptive responses) are not obvious and the neural substrates are very difficult to define. Nevertheless, there are many intriguing observations in these areas. For example, much research has been stimulated by the suggestion that conscious awareness of an animal's own bodily states might help it predict the behavioral states (read the mind) of other animals (Keenan, J. *et al.*, 2003). Conscious awareness of bodily states, including the emotional awareness of pain, involves dynamic neural representations of the body (e.g. Craig, A. D., 2003). Even the most complex brains of invertebrates, such as the octopus or honeybee, as well as the brains of non-mammalian vertebrates, have much smaller numbers of neurons and less obviously organized brain structures than found in behaviorally sophisticated mammals such as primates and cetaceans, and thus presumably less capacity for such representations. Indeed, extremely complex neuroanatomical substrates support the multiple representations and meta-representations of the body that are associated with emotional awareness and suffering in humans, which has suggested to some that these aspects of pain may not occur in animals lacking, for example, an equivalent to the anterior insular cortex of primates (Craig, A. D., 2003). Although direct measurement of subjective pain in animals is not possible, clues about the evolution of this capacity may still come from comparing across a broad range of species possible functions of emotional awareness as well as the neural substrates critical for expressing signs of such awareness.

5.15.4 Conclusions

Nociceptive mechanisms that permit an animal to detect, respond to, and remember peripheral injury are found throughout the animal kingdom. Some of these are likely to represent convergent (analogous) evolutionary responses to similar injury-related selection pressures in diverse organisms, which may depend upon different molecular substrates in different animal groups. For example, while most animals show transient, antinociceptive responses to noxious stimulation, the use of opiates and melanocortin receptors for antinociception may largely be restricted to vertebrates. On the other hand, emerging molecular genetic information indicates that other nociceptive mechanisms have been highly conserved from mechanisms that must have already been present around 600 million years ago in worm-like animals that were the last common ancestors of modern roundworms, flies, leeches, snails, mice, and humans (Figure 1). Conserved (homologous) nociceptive mechanisms that have been revealed thus far are related to nociceptive transduction (e.g., TRP channels), plasticity of nociceptor synapses (e.g., NMDA-receptor-dependent LTP), and regulation of gene transcription in nociceptive pathways (e.g., CREB activation). Because of dramatic increases in molecular genetic information from all the major phyla and the coupling of this information with continuing physiological studies of various species, it seems likely that knowledge gained from investigating highly conserved mechanisms in disparate creatures will provide insights that might help control intransigent pain states in humans. Comparative studies may also shed some light on the selection pressures that shaped the evolution of emotional aspects of pain, even though the subjective experience of pain may not be amenable to direct experimental investigation in other species.

References

Allen, C. 2004. Animal pain. Nous 38, 617–643.

Balaban, P. M. 2002. Cellular mechanisms of behavioral plasticity in terrestrial snail. Neurosci. Biobehav. Rev. 26, 597–630.

Bandell, M., Story, G. M., Hwang, S. W., Viswanath, V., Eid, S. R., Petrus, M. J., Earley, T. J., and Patapoutian, A. 2004. Noxious cold ion channel TRPA1 is activated by pungent compounds and Bradykinin. Neuron 41, 849–57.

Bravarenko, N. I., Korshunova, T. A., Malyshev, A. Y., and Balaban, P. M. 2003. Synaptic contact between mechanosensory neuron and withdrawal interneuron in

terrestrial snail is mediated by L-Glutamate-like transmitter. Neurosci. Lett. 341, 237–240.
Brockie, P. J., Madsen, D. M., Zheng, Y., Mellem, J., and Maricq, A. V. 2001. Differential expression of glutamate receptor subunits in the nervous system of Caenorhabditis elegans and their regulation by the homeodomain protein unc-42. J. Neurosci. 21, 1510–1522.
Burrell, B. D. and Sahley, C. L. 2004. Multiple forms of long-term potentiation and long-term depression converge on a single interneuron in the leech cns. J. Neurosci. 24, 4011–4019.
Casey, K. L. 2000. Concepts of pain mechanisms: the contribution of functional imaging of the human brain. Prog. Brain. Res. 129, 277–287.
Caterina, M. J., Leffler, A., Malmberg, A. B., Martin, W. J., Trafton, J., Petersen-Zeitz, K. R., Koltzenburg, M., Basbaum, A. I., and Julius, D. 2000. Impaired nociception and pain sensation in mice lacking the capsaicin receptor. Science 288, 306–313.
Choi, S. S. and Lahn, B. T. 2003. Adaptive evolution of MRG, a neuron-specific gene family implicated in nociception. Genome Res. 13, 2252–2259.
Christenson, J., Boman, A., Lagerback, P., and Grillner, S. 1988. The dorsal cell, one class of primary sensory neuron in the lamprey spinal cord. i. touch, pressure but no nociception - a physiological study. Brain Res. 440, 1–8.
Cleary, L. J., Byrne, J. H., and Frost, W. N. 1995. Role of interneurons in defensive withdrawal reflexes of *Aplysia*. Learn. Mem. 2, 133–151.
Craig, A. D. 2003. Pain mechanisms: labeled lines versus convergence in central processing. Annu. Rev. Neurosci. 26, 1–30.
Dale, N. and Kandel, E. R. 1993. L-Glutamate may be the fast excitatory transmitter of aplysia sensory neurons. Proc. Natl. Acad. Sci. USA 90, 7163–7167.
Dawkins, R. 2004. The Ancestor's Tale: a Pilgrimage to the Dawn of Evolution, Houghton Mifflin.
Dong, X., Han, S., Zylka, M. J., Simon, M. I., and Anderson, D. J. 2001. A diverse family of gpcrs expressed in specific subsets of nociceptive sensory neurons. Cell 106, 619–632.
Dores, R. M., Lecaude, S., Bauer, D., and Danielson, P. B. 2002. Analyzing the evolution of the opioid/orphanin gene family. Mass Spectrom Rev. 21, 220–243.
Getting, P. A. 1977. Neuronal organization of escape swimming in *Tritonia*. J. Comp. Physiol. 121, 325–342.
Holloway, J. A., Trouth, C. O., Wright, L. E., and Keyser, G. F. 1980. Cutaneous receptive field characteristics of primary afferents and dorsal horn cells in the avian (*Gallus domesticus*). Exp. Neurol. 68, 477–488.
Illich, P. A. and Walters, E. T. 1997. Mechanosensory neurons innervating *Aplysia* siphon encode noxious stimuli and display nociceptive sensitization. J. Neurosci. 17, 459–469.
Ji, R. R. and Rupp, F. 1997. Phosphorylation of transcription factor CREB in rat spinal cord after formalin-induced hyperalgesia: relationship to c-fos induction. J. Neurosci. 17, 1776–1785.
Ji, R. R., Kohno, T., Moore, K. A., and Woolf, C. J. 2003. Central sensitization and ltp: do pain and memory share similar mechanisms? Trends Neurosci. 26, 696–705.
Kandel, E. R. 2001. The molecular biology of memory storage: a dialogue between genes and synapses. science 294, 1030–1038.
Kawasaki, Y., Kohno, T., Zhuang, Z. Y., Brenner, G. J., Wang, H., Van Der Meer, C., Befort, K., Woolf, C. J., and Ji, R. R. 2004. ionotropic and metabotropic receptors, protein kinase a, protein kinase c, and src contribute to c-fiber-induced ERK activation and cAMP response element-binding protein phosphorylation in dorsal horn neurons, leading to central sensitization. J. Neurosci. 24, 8310–8321.
Keenan, J., Gallup, G. G., and Falk, D. 2003. The Face in the Mirror: The Search for the Origins of Consciousness. HarperCollins Publishers.
Krasne, F. B. and Glanzman, D. L. 1995. What we can learn from invertebrate learning. Annu. Rev. Psychol. 46, 585–624.
Krause, J. E., Chenard, B. L., and Cortright, D. N. 2005. Transient receptor potential ion channels as targets for the discovery of pain therapeutics. Curr. Opin. Investig. Drugs 6, 48–57.
Lai, J., Porreca, F., Hunter, J. C., and Gold, M. S. 2004. Voltage-gated sodium channels and hyperalgesia. Annu. Rev. Pharmacol. Toxicol. 44, 371–97.
Lembo, P. M., Grazzini, E., Groblewski, T., O'Donnell, D., Roy, M. O., Zhang, J., Hoffert, C., Cao, J., Schmidt, R., Pelletier, M., Labarre, M., Gosselin, M., Fortin, Y., Banville, D., Shen, S. H., Strom, P., Payza, K., Dray, A., Walker, P., and Ahmad, S. 2002. Proenkephalin a gene products activate a new family of sensory neuron–specific Gpcrs. Nat. Neurosci. 5, 201–209.
Lewin, M. R. and Walters, E. T. 1999. Cyclic GMP pathway is critical for inducing long-term sensitization of nociceptive sensory neurons. Nature Neurosci. 2, 18–23.
Li, C., Kim, K., and Nelson, L. S. 1999. FMRFamide-related neuropeptide gene family in caenorhabditis elegans. Brain Res. 848, 26–34.
Liang, Y. F., Terashima, S., and Zhu, A. Q. 1995. Distinct morphological characteristics of touch, temperature, and mechanical nociceptive neurons in the crotaline trigeminal ganglia. J. Comp. Neurol. 360, 621–633.
Light, A. R. 1992. The Initial Processing of Pain and Its Descending Control: Spinal and Trigeminal Systems Karger.
Lin, X. Y. and Glanzman, D. L. 1994. Hebbian induction of long-term potentiation of *Aplysia* synapses: partial requirement for activation of an NMDA-related receptor. Proc. R. Soc. Lond. B 255, 215–221.
Lynn, B. and O'Shea, N. R. 1998. Inhibition of forskolin-induced sensitisation of frog skin nociceptors by the cyclic AMP-Dependent Protein Kinase A Antagonist H-89. Brain Res. 780, 360–362.
Ma, W., Hatzis, C., and Eisenach, J. C. 2003. Intrathecal injection of cAMP response element binding protein (CREB) antisense oligonucleotide attenuates tactile allodynia caused by partial sciatic nerve ligation. Brain Res. 988, 97–104.
Mackey, S. L., Glanzman, D. L., Small, S. A., Dyke, A. M., Kandel, E. R., and Hawkins, R. D. 1987. Tail shock produces inhibition as well as sensitization of the siphon-withdrawal reflex of Aplysia: possible behavioral role for presynaptic inhibition mediated by the peptide Phe-Met-Arg-Phe-Nh2. Proc. Natl. Acad. Sci. USA 84, 8730–8734.
Mackie, G. O. 2004. Central neural circuitry in the jellyfish aglantha: a model 'simple nervous system'. Neurosignals 13, 5–19.
Malyshev, A. Y. and Balaban, P. M. 2002. Identification of mechanoafferent neurons in terrestrial snail: response properties and synaptic connections. J. Neurophysiol. 87, 2364–2371.
Martin, S. J., Grimwood, P. D., and Morris, R. G. 2000. Synaptic plasticity and memory: an evaluation of the hypothesis. Annu. Rev. Neurosci. 23, 649–711.
Merskey, H. and Bogduk, N. 1994. Classification of Chronic Pain, Second Edition, IASP Task Force on Taxonomy. IASP Press.
Montarolo, P. G., Kandel, E. R., and Schacher, S. 1988. Long-Term Heterosynaptic Inhibition in Aplysia. Nature 333, 171–174.
Murphy, G. G. and Glanzman, D. L. 1997. Mediation of classical conditioning in aplysia californica by long-term potentiation of sensorimotor synapses. Science, 278, 467–471.
Nicholls, J. G. and Baylor, D. A. 1968. Specific modalities and receptive fields of sensory neurons in cns of the leech. J. Neurophysiol. 31, 740–756.

Nichols, R. 2003. Signaling pathways and physiological functions of Drosophila Melanogaster FMRFamide-related Peptides. Annu. Rev. Entomol. 48, 485–503.

Nikitin, V. P., Koryzev, S. A., and Shevelkin, A. V. 2002. Selective effects of an NMDA glutamate receptor antagonist on the sensory input from chemoreceptors in the snail's head during acquisition of nociceptive sensitization. Neurosci. Behav. Physiol. 32, 129–134.

Price, M. P., McIlwrath, S. L., Xie, J., Cheng, C., Qiao, J., Tarr, D. E., Sluka, K. A., Brennan, T. J., Lewin, G. R., and Welsh, M. J. 2001. The DRASIC cation channel contributes to the detection of cutaneous touch and acid stimuli in mice. Neuron 32, 1071–1083.

Rankin, C. H. 2004. Invertebrate learning: what can't a worm learn? Curr. Biol. 14, R617–R618.

Salzet, M., Salzet-Raveillon, B., Cocquerelle, C., Verger-Bocquet, M., Pryor, S. C., Rialas, C. M., Laurent, V., and Stefano, G. B. 1997. Leech immunocytes contain proopiomelanocortin: nitric oxide mediates hemolymph proopiomelanocortin processing. J. Immunol. 159, 5400–5411.

Shaw, B. K. and Kristan, W. B., Jr. 1995. The whole-body shortening reflex of the medicinal leech: motor pattern, sensory basis, and interneuronal pathways. J. Comp. Physiol. A 177, 667–681.

Silva, A. J., Kogan, J. H., Frankland, P. W., and Kida, S. 1998. CREB and memory. Annu. Rev. Neurosci. 21, 127–148.

Sneddon, L. U., Braithwaite, V. A., and Gentle, M. J. 2003. Do fishes have nociceptors? evidence for the evolution of a vertebrate sensory system. Proc. R. Soc. Lond. B. Biol. Sci. 270, 1115–1121.

Stefano, G. B., Salzet-Raveillon, B., and Salzet, M. 1999. Mytilus edulis hemolymph contains pro-opiomelanocortin: LPS and morphine stimulate differential processing. Brain Res. Mol. Brain Res. 63, 340–350.

Stefano, G. B., Cadet, P., Rialas, C. M., Mantione, K., Casares, F., Goumon, Y., and Zhu, W. 2003. Invertebrate opiate immune and neural signaling. Adv. Exp. Med. Biol. 521, 126–147.

Tang, S. J., Reis, G., Kang, H., Gingras, A. C., Sonenberg, N., and Schuman, E. M. 2002. A rapamycin-sensitive signaling pathway contributes to long-term synaptic plasticity in the hippocampus. Proc. Natl. Acad. Sci. USA 99, 467–472.

Tobin, D. M. and Bargmann, C. I. 2004. Invertebrate nociception: behaviors, neurons and molecules. J. Neurobiol. 61, 161–174.

Tracey, W. D., Jr., Wilson, R. I., Laurent, G., and Benzer, S. 2003. Painless, a Drosophila gene essential for nociception. Cell 113, 261–273.

Waddell, S. and Quinn, W. G. 2001. Flies, genes, and learning. Annu. Rev. Neurosci. 24, 1283–1309.

Waltereit, R. and Weller, M. 2003. Signaling from cAMP/PKA to MAPK and synaptic plasticity. Mol. Neurobiol. 27, 99–106.

Walters, E. T. 1994. Injury-related behavior and neuronal plasticity: an evolutionary perspective on sensitization, hyperalgesia and analgesia. Int. Rev. Neurobiol. 36, 325–427.

Walters, E. T., Bodnarova, M., Billy, A. J., Dulin, M. F., Diaz-Rios, M., Miller, M. W., and Moroz, L. L. 2004. Somatotopic organization and functional properties of mechanosensory neurons expressing sensorin-A mRNA in *Aplysia californica*. J. Comp. Neurol. 471, 219–240.

Walters, E. T., Carew, T. J., and Kandel, E. R. 1981. Associative learning in *Aplysia*: evidence for conditioned fear in an invertebrate. Science 211, 504–506.

Weragoda, R. M., Ferrer, E., and Walters, E. T. 2004. Memory-like alterations in *Aplysia* axons after nerve injury or localized depolarization. J. Neurosci. 24, 10393–10401.

Willis, W. D. and Coggeshall, R. E. 2004. Sensory Mechanisms of the Spinal Cord: Primary Afferent Neurons and the Spinal Dorsal Horn. Kluwer Academic/Plenum Publishers.

Wittenburg, N. and Baumeister, R. 1999. Thermal avoidance in *Caenorhabditis elegans*: an approach to the study of nociception. Proc. Natl. Acad. Sci. U. S. A. 96, 10477–10482.

Yudin, Y. K., Tamarova, Z. A., Ostrovskaya, O. I., Moroz, L. L., and Krishtal, O. A. 2004. RFa-related peptides are algogenic: evidence in vitro and in vivo. Eur. J. Neurosci. 20, 1419–1423.

Zhang, L., Taylor, N., Xie, Y., Ford, R., Johnson, J., Paulsen, J. E., and Bates, B. 2005. Cloning and expression of MRG receptors in macaque, mouse, and human. Brain Res. Mol. Brain Res. 133, 187–197.

Zheng, J. Q., Kelly, T. K., Chang, B., Ryazantsev, S., Rajasekaran, A. K., Martin, K. C., and Twiss, J. L. 2001. A functional role for intra-axonal protein synthesis during axonal regeneration from adult sensory neurons. J. Neurosci. 21, 9291–9303.

Zylka, M. J., Dong, X., Southwell, A. L., and Anderson, D. J. 2003. Atypical expansion in mice of the sensory neuron-specific MRG G protein-coupled receptor family. Proc. Natl. Acad. Sci. USA 100, 10043–10048.

5.16 Redheads and Pain

J S Mogil, McGill University, Montreal, QC, Canada

© 2008 Elsevier Inc. All rights reserved.

5.16.1	Finding Genes Associated with Phenotypic Variability	185
5.16.2	MC1R and the Melanocortin-1 Receptor	185
5.16.3	MC1R and Analgesia	186
5.16.4	MC1R and Anesthesia	188
5.16.5	MC1R and Pain	188
5.16.6	Future Directions	190
References		190

Glossary

allele One possible form (or variant) of a gene, defined by its particular nucleotide sequence.

genotype The inherited alleles (one from each parent) at a genetic locus (e.g., a gene).

phenotype An observable or measurable biological trait.

pleiotropy The involvement of a single gene in more than one phenotype

polymorphism see Allele.

5.16.1 Finding Genes Associated with Phenotypic Variability

With recent developments in classical and molecular genetic techniques, identifying genes, and the DNA sequence variants in or near them, responsible for disease susceptibility and normal variation in biological phenotypes is becoming increasingly tractable. Two main methodologies are employed to this end: genetic linkage mapping and genetic association studies (see Lander, E. S. and Schork, N. J., 1994). These approaches have begun to be applied to the study of pain (see Mogil, J. S., 2004). For example, variable sensitivity of humans to experimental and clinical pain has been provisionally associated with the genes *COMT* (catechol-*O*-methyltransferase) (Zubieta, J. K. *et al.*, 2003; Diatchenko, L. *et al.*, 2005), *OPRD* (δ-opioid receptor; Kim, H. *et al.*, 2004), *TRPV1* (transient receptor potential vanilloid type 1; Kim, H. *et al.*, 2004), *OPRM* (μ-opioid receptor gene) (Klepstad, P. *et al.*, 2004; Fillingim, R. B. *et al.*, 2005), *IL6* (interleukin-6; Noponen-Hietala, N. *et al.*, 2005), *IL1* (interleukin-1; Solovieva, S. *et al.*, 2004), and others. These association studies were inspired in some cases by a mouse linkage mapping finding, in others by the phenotype of a null mutant (transgenic knockout) mouse, and in others simply by the known involvement of the protein in pain processing.

There are a finite number of human genes, current estimates are less than 30 000, but a virtually unlimited number of biological phenotypes. It is thus necessarily true that every gene will eventually be shown to be genetically associated with multiple (and possibly unrelated) traits. This principle is known as pleiotropy. Currently, one of the best-known examples of a gene with pleiotropic effects is *MC1R*, the gene coding for the melanocortin-1 receptor (MC1R).

5.16.2 MC1R and the Melanocortin-1 Receptor

The melanocortin receptor family consists of five subtypes, MC1R–MC5R. These receptors bind the melanocortin peptides, including α-melanocyte-stimulating hormone (α-MSH), β-MSH, γ-MSH, and adrenocorticotrophic hormone (ACTH), all cleaved from the proopiomelanocortin (*POMC*) gene along with β-endorphin (see Tatro, J. B., 1996; Wikberg, J. E. S., 1999; Abdel-Malek, Z. A., 2001; Starowicz, K. and Przewlocka, B., 2003). The

receptors are transcribed from five separate genes, and each receptor has differential tissue distributions and affinities for the melanocortins. All melanocortin receptor subtypes couple positively to adenylate cyclase when activated (Chhajlani, V. and Wikberg, J. E. S., 1992). The MC1R, previously known as the α-MSH receptor, actually has equal affinity for ACTH, and is found primarily in melanocytes of the skin. It is also been demonstrated in a variety of glial cells, the testes, placenta, pituitary (see Tatro, J. B., 1996; Wikberg, J. E. S., 1999; Abdel-Malek, Z. A., 2001; Starowicz, K. and Przewlocka, B., 2003), and in neurons of the midbrain periaqueductal gray (Xia, Y. *et al.*, 1995). The role of α-MSH acting on melanocyte MC1Rs to regulate pigmentation of skin and hair by stimulation of eumelanin synthesis has been understood in great detail for some time (see Eberle, A. N., 1988). Other α-MSH effects are also well known, and have been attributed to actions at the MC1R. For example, α-MSH has potent anti-inflammatory and antipyretic activity (see Tatro, J. B., 1996), and may play a role in nerve regeneration (see Starowicz, K. and Przewlocka, B., 2003) and female sexual behavior (Pfaus, J. G. *et al.*, 2004). Injection of α-MSH (or ACTH) into the brain has been reported to affect nociceptive sensitivity (see Starowicz, K. and Przewlocka, B., 2003), usually in a manner opposed to the actions of endogenous opioids, although the literature is contradictory. It is possible that some or all of these effects are mediated at spinal MC4Rs, since the MC4R-selective antagonist, SHU9119, reduces neuropathic hypersensitivity states when injected into the spinal cord (Vrinten, D. H. *et al.*, 2001).

Given the known role of MC1Rs in pigmentation and the highly polymorphic nature of *MC1R*, the hypothesis that the *MC1R* gene might be associated with variability in human hair color and skin tone was palpable. Indeed, Valverde P. *et al.* (1995) demonstrated that the inheritance of loss-of-function *MC1R* alleles was genetically associated with red hair and fair skin in humans. Subsequent work has determined that approximately 60–85% of natural redheads are so because of their inheritance of variant alleles of *MC1R*, especially those producing the very common Arg151Cys, Arg160Trp, and Asp294His amino acid substitutions (see Schaffer, J. V. and Bolognia, J. L., 2001). Red hair is much more likely if multiple alleles are inherited, and the number of variant alleles is important in determining the precise shade of red. In addition, it has been subsequently demonstrated that *MC1R* is the major gene responsible for solar lentigines (i.e., freckles; Bastiaens, M. *et al.*, 2001a), reduced tanning ability (Healy, E. *et al.*, 2000), and skin cancer (malignant melanoma, squamous cell, and basal cell carcinoma) susceptibility even in individuals without red hair (Palmer, J. S. *et al.*, 2000; Bastiaens, M. *et al.*, 2001b). It should be noted that *MC1R* genetics is rather complex, with a large number of known rare (<1% allele frequency) mutations and at least three common variants (Val60Leu, Val92Met, and Arg163Gln) that are only partially penetrant or completely silent, producing no impairment of MC1R functioning (see Schaffer, J. V. and Bolognia, J. L., 2001).

5.16.3 MC1R and Analgesia

Using genetic linkage (formally, quantitative trait locus or QTL) mapping, a gene affecting the magnitude of swim stress-induced analgesia (SIA) in female but not male mice was localized to distal mouse chromosome 8 (Mogil, J. S. *et al.*, 1997). This SIA was previously demonstrated to be sex-specific in its neurochemical mediation (e.g., Mogil, J. S. *et al.*, 1993; Kavaliers, M. and Galea, L. A. M., 1995). Specifically, pharmacological blockade of the *N*-methyl-D-aspartate (NMDA) excitatory amino acid receptor abolishes SIA in male rodents, but does not do so (at any dose or in any estrous phase) in females. Kavaliers M. and Choleris E. (1997) found that analgesia from a κ-opioid-selective agonist, NPC12626, was similarly sexually dimorphic in its neurochemical mediation, being blocked by NMDA antagonists only in males. The possible sex-specificity of κ-opioid analgesia was then a hot topic, as data from Gear R. W. *et al.* (1996) suggested that κ-opioid-acting drugs may only produce efficacious analgesia, in the third molar extraction model, in women. Mogil J. S. *et al.* (2003) hypothesized that if SIA and κ-opioid analgesia were both sexually dimorphic, and a female-specific linkage on chromosome 8 had been already demonstrated for SIA, one would likely be seen for κ-opioid analgesia as well. This was quickly confirmed using the κ-opioid-selective compound, U50,488 (Mogil, J. S. *et al.*, 2003), but the confidence interval containing the gene(s) responsible for the linkage was quite large. Of the ~200 murine genes in this region, however, one emerged as a high-probability candidate: *Mc1r*. Evidence for its candidacy included the possible role of α-MSH and/or ACTH as antiopioid peptides (see above) and the demonstration of neuronal MC1Rs in the periaqueductal gray (Xia, Y. *et al.*, 1995),

a supraspinal region of well-known importance in pain modulation (see Basbaum, A. I. and Fields, H. L., 1984). It should also be noted that dynorphin can bind with reasonable affinity in *in vitro* assays to MC1R (Quillan, J. M. and Sadee, W., 1997).

Using a three-pronged strategy, Mogil J. S. and colleagues have provided considerable supporting evidence that the mouse *Mc1r* gene is indeed the female-specific QTL for U50,488 analgesia. First, null mutant recessive yellow (C57BL/6-*Mc1r*$^{e/e}$, or *e/e*) mice, which arose spontaneously rather than being engineered using transgenic technology (see Cone, R. D. *et al.*, 1996), were tested for U50,488 analgesia along with their C57BL/6 wild-type controls. We found that female but not male *e/e* mutants displayed significantly greater U50,488 analgesia (see Figure 1(a)),

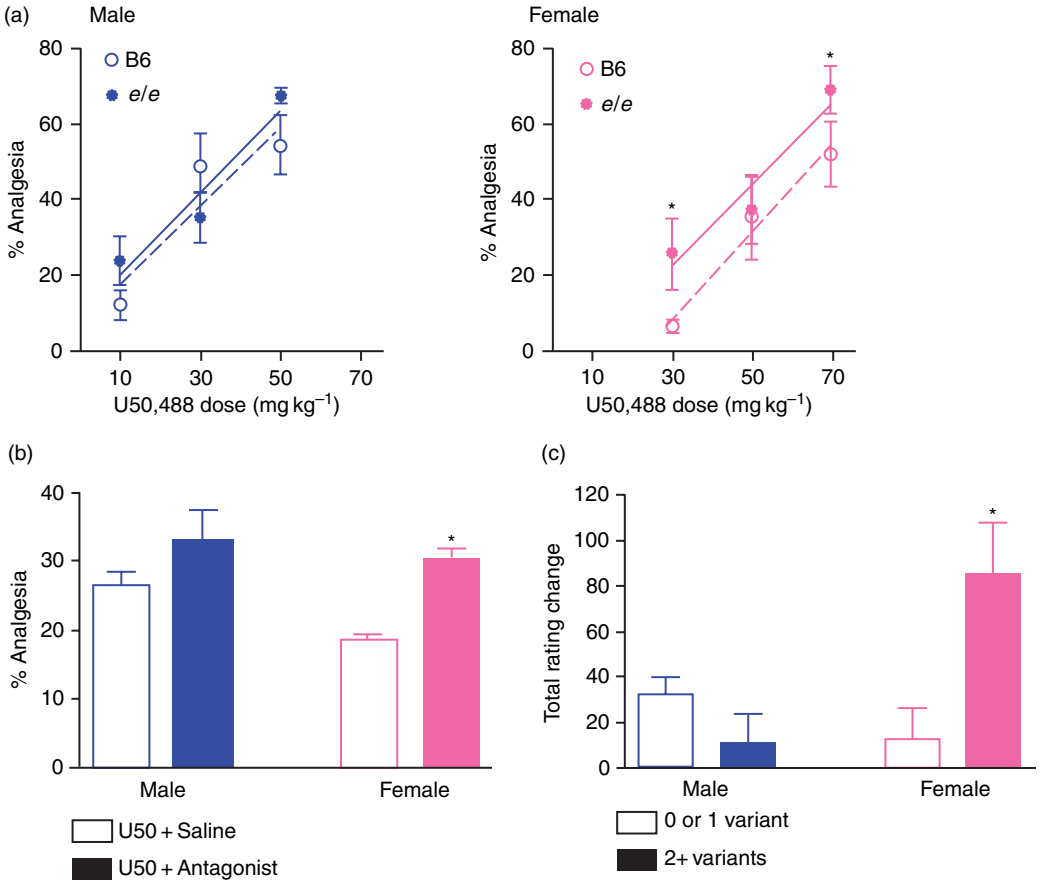

Figure 1 Female-specific effect of MC1R functional status on κ-opioid analgesia in mice and humans. (a) Response on the 49 °C tail-withdrawal test to systemic injection of various doses (10–70 mg kg^{-1}, subcutaneous (s.c.)) of the selective κ-opioid agonist, U50,488, in male and female spontaneous mutant recessive yellow (*e/e*) mice and their wild-type counterparts, C57BL/6 (B6). The *e/e* mutants of both sexes have nonfunctional MC1Rs due to a frameshift mutation at position 183. Symbols represent mean ± standard error of the mean (SEM) percent of total analgesia (based on area under the time–effect curve) over a 60 min testing period postdrug administration. (b) Female-specific potentiation of U50,488 (U50) analgesia (70 mg kg^{-1}, s.c.), on the 49 °C tail-withdrawal test, by injection of a peptidergic MC1R antagonist, Ac-Nle-Asp-Trp-DPhe-Nle-Trp-Lys-NH_2 (20 μg/mouse in 2.5 μl), into the lateral ventricles of outbred mice. Bars represent mean ± SEM percent of total analgesia (based on area under the time–effect curve) over a 60-min testing period postdrug administration. (c) Female-specific influence of *MC1R* genotype on pentazocine (0.5 mg kg^{-1}, intravenous) analgesia in humans. Subjects of both sexes were studied in two experimental sessions as described in detail in Mogil J. S. *et al.* (2003). Bars represent mean ± SEM difference scores for summed pain intensity ratings (0–100; 5 ×) during the ischemic pain procedure, computed by subtracting postdrug from predrug ratings, in subjects with consensus sequence or one *MC1R* variant (0 or 1 variant) and subjects with two or more *MC1R* variants (2+ variants). The 2+ variant subjects possessed nonfunctional MC1Rs, and were unanimously redheaded. *$P < 0.05$ compared to other condition within-sex. Adapted from Mogil, J. S. *et al.* 2003. The melanocortin-1 receptor gene mediates female-specific mechanisms of analgesia in mice and humans. Proc. Natl. Acad. Sci. U. S. A. 100, 4867–4872.

and perhaps more importantly, that this analgesia was sensitive to NMDA blockade in the female mutants, suggesting that they had switched over to the malelike system (Mogil, J. S. *et al.*, 2003). This switching has been observed before and since with other hormonal disruptions of the female system (Mogil, J. S. *et al.*, 1993; Kavaliers, M. and Galea, L. A. M., 1995; Sternberg, W. F. *et al.*, 2004). Second, injection of a selective peptidergic MC1R antagonist, Ac-Nle-Asp-Trp-DPhe-Nle-Trp-Lys-NH_2, into the cerebral ventricles of (outbred) male and female mice produced a potentiation of U50,488 analgesia only in females (see Figure 1(b)), and furthermore rendered that analgesia newly sensitive to inhibition by an NMDA antagonist (Mogil, J. S. *et al.*, 2003). Finally, Austin and Mogil have demonstrated sex and strain differences in periaqueductal gray expression of the *Mc1r* gene using quantitative polymerase chain reaction (J. S. Austin and J. S. Mogil, unpublished data) in directions entirely consistent with the hypothesis that lower MC1R functionality is associated with higher κ-opioid analgesia.

These data, supportive of the sex-specific involvement of *Mc1r* in κ-opioid analgesia in the mouse, inspired a small association study in humans designed to test the same hypothesis in our species. College-age subjects were tested for thermal and ischemic pain before and after administration of pentazocine (Talwin®; 0.5 mg kg^{-1}) or saline, and then genotyped at the human *MC1R* gene by direct sequencing of exons containing common variants. We found that pentazocine analgesia was modest in all male subjects, and also in women with functional MC1Rs (i.e., those with the consensus DNA sequence or only one variant). Women with nonfunctional MC1Rs (i.e., those with two or more variants; all phenotypic redheads) displayed robust pentazocine analgesia (Mogil, J. S. *et al.*, 2003; see Figure 1(c)).

These data represent the first time a genetic finding in the mouse has ever been directly translated to humans within a single published study. More importantly, though, the data are the first to suggest that, like the mouse, humans possess qualitatively (i.e., neurochemically) distinct mechanisms of pain modulation, since the functional status of the MC1R affected analgesic output in one sex but not the other. A follow-up study was performed, in order to determine whether *Mc1r* and *MC1R* play a role in μ-opioid analgesia in mice and humans, respectively. μ-Opioid analgesia is of much greater clinical relevance than κ-opioid analgesia due to the high μ-selectivity of most clinically used opiate drugs. In addition to differences in pain sensitivity *per se* (see Section 5.16.5 below), we found that *e/e* mice were significantly more sensitive to analgesia from both morphine and its bioactive metabolite, morphine-6β-glucuronide (Mogil, J. S. *et al.*, 2005a). Curiously, the effect of MC1R functional status on μ-opioid analgesia did not appear to be sex-specific, with both male and female mutants showing increased sensitivity (see Figure 2(b)). Again, data collected in humans were entirely analogous, with redheads of both sexes showing robustly higher morphine-6β-glucuronide inhibition of noxious electrical stimuli (Mogil, J. S. *et al.*, 2005a; see Figure 2(d)).

5.16.4 MC1R and Anesthesia

It has long been clinical lore among anesthesiologists that redheads are harder to anesthetize with inhalant anesthetics than others, but these anecdotal impressions were never tested experimentally until recently. Liem E. B. *et al.* (2004) recruited 20 young adult women (10 with red hair, 10 with dark hair), and studied the minimum alveolar concentration of desflurane required to prevent movement in response to intradermal electrical stimulation of the anterior thigh. They found that red-haired women required almost 20% more anesthetic to abolish responding. This finding regarding anesthetic sensitivity cannot easily be reconciled with the aforementioned findings regarding analgesia. If the greater response of *MC1R* mutants (i.e., redheads) to κ- and μ-opioid analgesics is reflective of higher endogenous activity of a tonically active analgesic system, one might have expected red-haired women to require less anesthetic, not more. Unfortunately, only women were tested in the study by Liem E. B. *et al.* (2004), so sex differences could not be evaluated. In apparent support of this finding, this same group tested *e/e* mutants for sensitivity to four inhaled anesthetic compounds (isoflurane, sevoflurane, desflurane, and halothane), and found that although mutant mice were not significantly less sensitive to any one anesthetic compared to controls, when data from all anesthetics were combined the genotypic difference achieved statistical significance ($P = 0.023$; Xing, Y. *et al.*, 2004).

5.16.5 MC1R and Pain

One limitation of the study by Liem E. B. *et al.* (2004) is that no attempt was made to study nociceptive sensitivity of the subjects in the absence of anesthetic,

so it was impossible to tell whether the differences observed involved differential sensitivity among genotypes to the anesthetic, or differential sensitivity to the noxious stimulus itself. It has recently been demonstrated in mice that the latter can easily be confused for the former (Mogil, J. S. *et al.*, 2005b). In a recently published follow-up study by their group (Liem, E. B. *et al.*, 2005), women (30 with red hair, 30 with dark hair) were tested for sensory thresholds, pain thresholds, and pain tolerance to electrical and thermal stimulation. No differences were seen in sensitivity to electrical stimulation, but heat and cold pain perception was higher in redheads. Redheads were also found to be resistant to subcutaneous (but not liposomal) lidocaine anesthesia against electrical stimulation (Liem, E. B. *et al.*, 2005).

These data are in contrast with an earlier study, showing no *MC1R* genotypic differences in thermal pain sensitivity (Mogil, J. S. *et al.*, 2003), although that study was probably too lightly powered to assess the issue. However, the data of Liem E. B. *et al.* (2005) are also entirely contradictory with a larger follow-up study (Mogil, J. S. *et al.*, 2005a), which observed in *e/e* mutant mice of both sexes (across a broad range of noxious stimulus modalities) and humans of both sexes a decreased sensitivity to noxious electrical stimulation (see Figures 2(a) and 2(b)). There are a number of possible reasons for the discrepancy. Methodological differences can be found between the three experiments, of course. It is difficult to blind experimenters to hair color, and it is possible that this lack of blinding was a greater issue in one

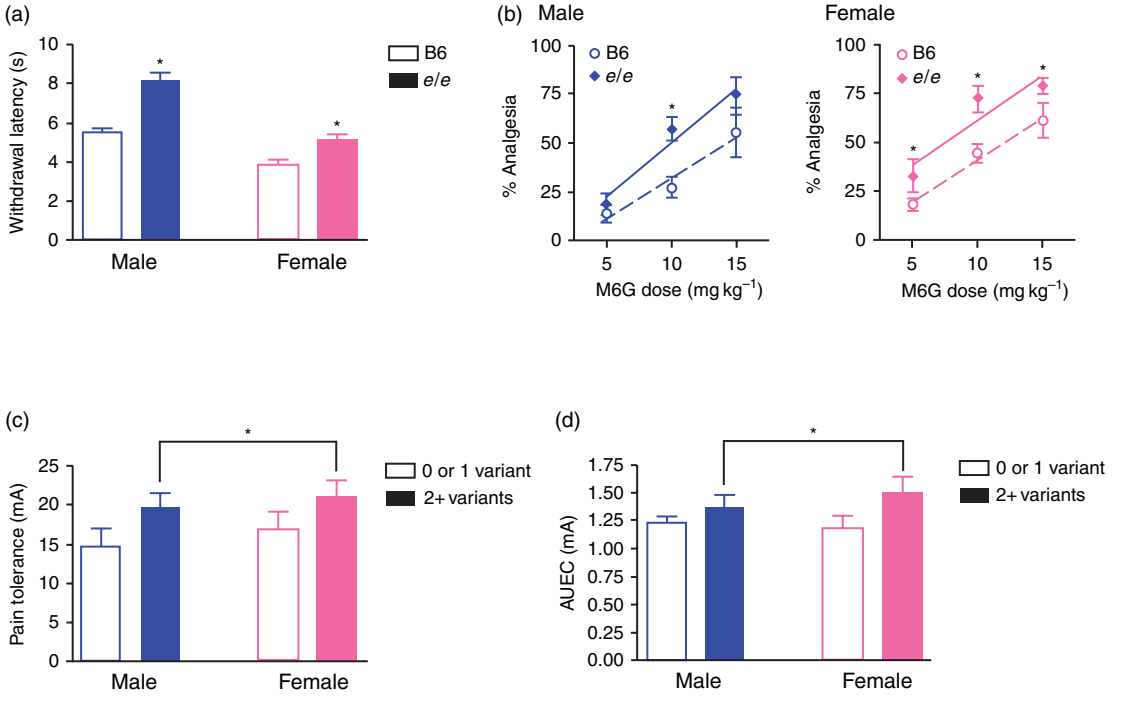

Figure 2 Effect of MC1R functional status on pain sensitivity and μ-opioid analgesia in mice and humans of both sexes. (a) Sensitivity of male and female spontaneous mutant recessive yellow (*e/e*) mice and their wildtype counterparts, C57BL/6 (B6), on the thermal paw-withdrawal test. Bars represent mean ± standard error of the mean (SEM) latency (in s) to withdraw from a radiant heat stimulus positioned under the ventral hind paws (right and left hind paw data combined). (b) Response of B6 and *e/e* mutants on the 49 °C tail-withdrawal test to systemic injection of various doses (5–15 mg kg^{-1}, subcutaneous) of the selective μ-opioid agonist (and morphine metabolite), morphine-6β-glucuronide (M6G). Symbols represent mean ± SEM percent of total analgesia (based on area under the time–effect curve) over a 300-min testing period postdrug administration. (c) Baseline tolerance to electrical current (10 Hz; 0.1 ms; increased by 0.5-mA steps) applied to the skin in men and women with functional (0 or 1 variant) or nonfunctional (2+ variants) MC1Rs. Bars represent mean ± SEM tolerated stimulus intensity. (d) Influence of *MC1R* genotype on M6G analgesia (0.3 mg kg^{-1}, intravenous) in men and women. Subjects were studied as described in detail in Mogil J. S. *et al.* (2005a). Bars represent mean ± SEM analgesia as expressed as area under the time–effect curve (AUEC relative to baseline current shown in (c)). *$P < 0.05$ compared to other genotype. Adapted from Mogil, J. S. *et al.* 2005a. Melanocortin-1 receptor gene variants affect pain and μ-opioid analgesia in mice and humans. J. Med. Genet. 42, 583–587.

study than another. Liem E. B. and colleagues studied women only, whereas Mogil J. S. and colleagues studied men and women. Most importantly, perhaps, Liem E. B. and colleagues compared phenotypes (women with dark or red hair) whereas Mogil J. S. and colleagues compared *MC1R* genotypes (subjects with functional or nonfunctional MC1Rs). It is not the case that all redheads are so because of inheritance of *MC1R* variants (see Section 5.16.2 above); that needs to be determined empirically by sequencing. Thus it is possible that some subjects in Liem E. B. *et al.* (2005) were misclassified in their inferred genotype.

Finally, a human genetic association study has revealed a possible association with *MC1R* variants and vulvar vestibulitis, with sufferers 3.5-fold more likely to carry loss-of-function alleles at the *MC1R* (Foster, D. C. *et al.*, 2004). It is unclear whether this risk is related to altered pain processing or, as suggested by the authors, to the known anti-inflammatory role of MC1Rs.

5.16.6 Future Directions

It is obvious that future work is needed to resolve the true directions of *MC1R* genotypic effect on pain and pain inhibition phenotypes, and to clarify which phenotypes are sex-specific and which are not. Nonetheless, the fact that a gene like *MC1R* would be involved in pain, analgesia, or anesthesia should be considered quite a surprise. It does not appear on any lists of highly probable candidate genes for mediating pain traits (Belfer, I. *et al.*, 2004), and was considered by many to be a gene whose function was already annotated, or solved. The unearthing of *MC1R*'s role in this particular biological domain highlights the advantages for gene discovery of both mouse genetic linkage mapping and bedside-to-bench strategies.

References

Abdel-Malek, Z. A. 2001. Melanocortin receptors: their functions and regulation by physiological agonists and antagonists. Cell. Mol. Life Sci. 58, 434–441.

Basbaum, A. I. and Fields, H. L. 1984. Endogenous pain control systems: brainstem spinal pathways and endorphin circuitry. Annu. Rev. Neurosci. 7, 309–338.

Bastiaens, M., ter Huurne, J., Gruis, N., Bergman, W., Westendorp, R., Vermeer, B. J., and Bavinck, J. N. B. 2001a. The melanocortin-1-receptor gene is the major freckle gene. Hum. Mol. Genet. 10, 1701–1708.

Bastiaens, M. T., ter Huurne, J. A. C., Kielich, C., Gruis, N. A., Westendorp, R. G. J., Vermeer, B. J., and Bavinck, J. N. B. 2001b. Melanocortin-1 receptor gene variants determine the risk of nonmelanoma skin cancer independently of fair skin and red hair. Am. J. Hum. Genet. 68, 884–894.

Belfer, I., Wu, T., Kingman, A., Krishnaraju, R. K., Goldman, D., and Max, M. B. 2004. Candidate gene studies of human pain mechanisms: a method for optimizing choice of polymorphisms and sample size. Anesthesiology 100, 1562–1572.

Chhajlani, V. and Wikberg, J. E. S. 1992. Molecular cloning and expression of the human melanocyte stimulating hormone receptor. FEBS Lett. 309, 417–420.

Cone, R. D., Lu, D., Koppula, S., Vage, D. I., Klungland, H., Boston, B., Chen, W., Orth, D. N., Pouton, C., and Kesterson, R. A. 1996. The melanocortin receptors: agonists, antagonists, and the hormonal control of pigmentation. Rec. Prog. Horm. Res. 51, 287–317.

Diatchenko, L., Slade, G. D., Nackley, A. G., Bhalang, K., Sigurdsson, A., Belfer, I., Goldman, D., Xu, K., Shabalina, S. A., Shagin, D., Max, M. B., Makarov, S. S., and Maixner, W. 2005. Genetic basis for individual variations in pain perception and the development of a chronic pain condition. Hum. Mol. Genet. 14, 135–143.

Eberle, A. N. 1988. The Melanotropins. Chemistry, Physiology and Mechanisms of Action. S. Karger.

Fillingim, R. B., Kaplan, L., Staud, R., Ness, T. J., Glover, T. L., Campbell, C. M., Mogil, J. S., and Wallace, M. R. 2005. The A118G single nucleotide polymorphism of the mu-opioid receptor gene (OPRM1) is associated with pressure pain sensitivity in humans. J. Pain 6, 159–167.

Foster, D. C., Sazenski, T. M., and Stodgell, C. J. 2004. Impact of genetic variation in interleukin-1 receptor antagonist and melanocortin-1 receptor genes on vulvar vestibulitis syndrome. J. Reprod. Med. 49, 503–509.

Gear, R. W., Miaskowski, C., Gordon, N. C., Paul, S. M., Heller, P. H., and Levine, J. D. 1996. Kappa-opioids produce significantly greater analgesia in women than in men. Nature Med. 2, 1248–1250.

Healy, E., Flanagan, N., Ray, A., Todd, C., Jackson, I. J., Matthews, J. N. S., Birch-Machin, M. A., and Rees, J. L. 2000. Melanocortin-1-receptor gene and sun sensitivity in individuals without red hair. Lancet 355, 1072–1073.

Kavaliers, M. and Choleris, E. 1997. Sex differences in *N*-methyl-D-aspartate involvement in κ opioid and non-opioid predator-induced analgesia in mice. Brain Res. 768, 30–36.

Kavaliers, M. and Galea, L. A. M. 1995. Sex differences in the expression and antagonism of swim stress-induced analgesia in deer mice vary with the breeding season. Pain 63, 327–334.

Kim, H., Neubert, J. K., San Miguel, A., Xu, K., Krishnaraju, R. K., Iadarola, M. J., Goldman, D., and Dionne, R. A. 2004. Genetic influence on variability in human acute experimental pain sensitivity associated with gender, ethnicity and psychological temperament. Pain 109, 488–496.

Klepstad, P., Rakvag, T. T., Kaasa, S., Holthe, M., Dale, O., Borchgrevink, P. C., Baar, C., Vikan, T., Krokan, H. E., and Skorpen, F. 2004. The 118 A > G polymorphism in the human μ-opioid receptor gene may increase morphine requirements in patients with pain caused by malignant disease. Acta Anaesthesiol. Scand. 48, 1232–1239.

Lander, E. S. and Schork, N. J. 1994. Genetic dissection of complex traits. Science 265, 2037–2048.

Liem, E. B., Joiner, T. V., Tsueda, K., and Sessler, D. I. 2005. Increased sensitivity to thermal pain and reduced subcutaneous lidocaine efficacy in redheads. Anesthesiology 102, 509–514.

Liem, E. B., Lin, C. M., Suleman, M. I., Doufas, A. G., Gregg, R. G., Veauthier, J. M., Loyd, G., and Sessler, D. I.

2004. Anesthetic requirement is increased in redheads. Anesthesiology 101, 279–283.

Mogil, J. S. (*ed*.) 2004. The Genetics of Pain, p. 349. IASP Press.

Mogil, J. S., Richards, S. P., O'Toole, L. A., Helms, M. L., Mitchell, S. R., Kest, B., and Belknap, J. K. 1997. Identification of a sex-specific quantitative trait locus mediating nonopioid stress-induced analgesia in female mice. J. Neurosci. 17, 7995–8002.

Mogil, J. S., Ritchie, J., Smith, S. B., Strasburg, K., Kaplan, L., Wallace, M. R., Romberg, R. R., Bijl, H., Sarton, E. Y., Fillingim, R. B., and Dahan, A. 2005a. Melanocortin-1 receptor gene variants affect pain and μ-opioid analgesia in mice and humans. J. Med. Genet. 42, 583–587.

Mogil, J. S., Smith, S. B., O'Reilly, M. K., and Plourde, G. 2005b. Influence of nociception and stress-induced antinociception on genetic variation in isoflurane anesthetic potency among mouse strains. Anesthesiology 103, 751–758.

Mogil, J. S., Sternberg, W. F., Kest, B., Marek, P., and Liebeskind, J. C. 1993. Sex differences in the antagonism of swim stress-induced analgesia: effects of gonadectomy and estrogen replacement. Pain 53, 17–25.

Mogil, J. S., Wilson, S. G., Chesler, E. J., Rankin, A. L., Nemmani, K. V. S., Lariviere, W. R., Groce, M. K., Wallace, M. R., Kaplan, L., Staud, R., Ness, T. J., Glover, T. L., Stankova, M., Mayorov, A., Hruby, V. J., Grisel, J. E., and Fillingim, R. B. 2003. The melanocortin-1 receptor gene mediates female-specific mechanisms of analgesia in mice and humans. Proc. Natl. Acad. Sci. U. S. A. 100, 4867–4872.

Noponen-Hietala, N., Virtanen, I., Karttunen, R., Schwenke, S., Jakkula, E., Li, H., Merikivi, R., Barral, S., Ott, J., Karppinen, J., and Ala-Kokko, L. 2005. Genetic variations in *IL6* associate with intervertebral disc disease characterized by sciatica. Pain 114, 186–194.

Palmer, J. S., Duffy, D. L., Box, N. F., Aitken, J. F., O'Gorman, L. E., Green, A. C., Hayward, N. K., Martin, N. G., and Sturm, R. A. 2000. Melanocortin-1 receptor polymorphisms and risk of melanoma: is the association explained solely by pigmentation phenotype. Am. J. Hum. Genet. 66, 176–186.

Pfaus, J. G., Shadiack, A., Van Soest, T., Tse, M., and Molinoff, P. B. 2004. Selective facilitation of sexual solicitation in the female rat by a melanocortin receptor agonist. Proc. Natl. Acad. Sci. U. S. A. 101, 10201–10204.

Quillan, J. M. and Sadee, W. 1997. Dynorphin peptides: antagonists of melanocortin receptors. Pharm. Res. 14, 713–719.

Schaffer, J. V. and Bolognia, J. L. 2001. The melanocortin-1 receptor: red hair and beyond. Arch. Dermatol. 137, 1477–1485.

Solovieva, S., Leino-Arjas, P., Saarela, J., Luoma, K., Raininko, R., and Riihimaki, H. 2004. Possible association of interleukin 1 gene locus polymorphisms with low back pain. Pain 109, 8–19.

Starowicz, K. and Przewlocka, B. 2003. The role of melanocortins and their receptors in inflammatory processes, nerve regeneration and nociception. Life Sci. 73, 823–847.

Sternberg, W. F., Chesler, E. J., Wilson, S. G., and Mogil, J. S. 2004. Acute progesterone can recruit sex-specific neurochemical mechanisms mediating swim stress induced and kappa-opioid analgesia in mice. Horm. Behav. 46, 467–473.

Tatro, J. B. 1996. Receptor biology of the melanocortins, a family of neuroimmunomodulatory peptides. Neuroimmunomodulation 3, 259–284.

Valverde, P., Healy, E., Jackson, I., Rees, J. L., and Thody, A. J. 1995. Variants of the melanocyte-stimulating hormone receptor gene are associated with red hair and fair skin in humans. Nat. Genet. 11, 328–330.

Vrinten, D. H., Adan, R. A. H., Groen, G. J., and Gispen, W. H. 2001. Chronic blockade of melanocortin receptors alleviates allodynia in rats with neuropathic pain. Anesth. Analg. 93, 1572–1577.

Wikberg, J. E. S. 1999. Melanocortin receptors: perspectives for novel drugs. Eur. J. Pharmacol. 375, 295–310.

Xia, Y., Wikberg, J. E. S., and Chhajlani, V. 1995. Expression of melanocortin 1 receptor in periaqueductal gray matter. Neuroreport 6, 2193–2196.

Xing, Y., Sonner, J. M., Eger, E. I., II, Cascio, M., and Sessler, D. I. 2004. Mice with a melanocortin 1 receptor mutation have a slightly greater minimum alveolar concentration than control mice. Anesthesiology 101, 544–546.

Zubieta, J. K., Heitzeg, M. M., Smith, Y. R., Bueller, J. A., Xu, K., Xu, Y., Koeppe, R. A., Stohler, C. S., and Goldman, D. 2003. COMT *val158met* genotype affects μ-opioid neurotransmitter responses to a pain stressor. Science 299, 1240–1243.

5.17 Autonomic Nervous System and Pain

Wilfrid Jänig, Physiologisches Institut, Christian-Albrechts-Universität zu Kiel, Germany

© 2008 Elsevier Inc. All rights reserved.

5.17.1	**Introduction**	194
5.17.2	**Neurobiology of the Autonomic Nervous System and Pain**	196
5.17.2.1	Reactions of the Sympathetic Nervous System in Pain	196
5.17.2.2	Visceral Afferents, Autonomic Nervous System, and Pain	198
5.17.2.3	Hyperalgesia and Sympathetically Mediated Changes in Referred Zones During Visceral Pain	199
5.17.3	**Role of the Sympathetic Nervous System in the Generation of Pain**	201
5.17.3.1	Clinical Background: Sympathetically Maintained Pain	201
5.17.3.2	Sympathetically Maintained Pain Following Nerve Lesion Simulated in Behavioral Animal Models	202
5.17.3.3	Direct Involvement of the Sympathetic Nervous System in the Generation of Pain Following Nerve Trauma	205
5.17.3.3.1	Coupling between lesioned postganglionic and afferent nerve terminals	205
5.17.3.3.2	Coupling between unlesioned postganglionic and afferent nerve terminals following partial nerve lesion	206
5.17.3.3.3	Coupling in the dorsal root ganglion and collateral sprouting following peripheral nerve lesion	206
5.17.3.3.4	Adrenoceptors involved in chemical sympathetic afferent coupling following nerve lesion	208
5.17.3.3.5	Synopsis	208
5.17.3.4	Indirect Involvement of the Sympathetic Nervous System in the Generation of Pain	209
5.17.3.4.1	Changes of neurovascular transmission and development of hyperreactivity of blood vessels	209
5.17.3.4.2	Sensitization of nociceptors mediated by sympathetic terminals independent of excitation and release of noradrenaline	211
5.17.3.4.3	Sensitization of nociceptors initiated by nerve growth factor or cytokines possibly mediated by sympathetic terminals	212
5.17.3.4.4	Sympatho-adrenal system and nociceptor sensitization	213
5.17.4	**Sympathetic Nervous System and Central Integrative Mechanisms in the Control of Hyperalgesia and Inflammation**	216
5.17.4.1	The Complex Regional Pain Syndrome Type I as Model	216
5.17.4.2	Sympathetic Nervous System and Acute Experimental Inflammation	218
5.17.4.3	Sympathetic Nervous System and Immune System	221
References		221

Glossary

allodynia, hyperalgesia Hyperalgesia denotes increased pain generated by a stimulus that is normally painful and excites nociceptors. It has a peripheral (sensitization of nociceptors) and/or a central component (sensitization of central neurons, e.g., in the dorsal horn of the spinal cord). Allodynia is pain generated by stimuli that activate low-threshold mechanoreceptors (mechanical allodynia) or cold receptors (cold allodynia). The mechanism of allodynia is central (central sensitization generated by persistent excitation of nociceptors). Secondary allodynia is pain elicited by stimulation of low-threshold mechanoreceptors in an area of skin that surrounds a territory with sensitized nociceptors (e.g., generated by inflammation) (Merskey, H. and Bogduk, H., 1994; Meyer, R. A. *et al.*, 2005).

causalgia See Chapter Complex Regional Pain Syndromes.
complex regional pain syndrome See Chapter Neuropathic Pain: Clinical.
enteric nervous system The enteric nervous system (Jänig, W., 2006).
homeostasis The maintenance of physiological parameters such as concentration of ions, blood glucose, arterial blood gases, and body core temperature in a narrow range and around predetermined set-points is called homeostasis. Homeostatic regulation involves autonomic systems, endocrine systems, and the respiratory system (Jänig, W., 2006).
neuropathic pain See Chapters Neuropathic Pain: Basic Mechanisms (Animal) and Complex Regional Pain Syndromes.
referred pain Pain from a particular visceral organ or a particular deep somatic structure is perceived to arise from the body surface (skin), from deep somatic structures, or from other viscera. The area or deep body structures where the pain is referred to is innervated by nerves of the same spinal segments as the affected deep body structures (Giamberardino, M. A., 1999; Jänig, W., 1993; Jänig, W. and Häbler, H. J., 2002).
sympathetic block, sympathectomy See Chapter Sprouting in Dorsal Root Ganglia.
sympathetically maintained pain (SMP) See Chapter Complex Regional Pain Syndromes.
sympatho-adrenal system The sympatho-adrenal system is the adrenal medulla and its innervation by sympathetic preganglionic neurons. The adrenal medulla consists of cells that release either adrenaline or noradrenaline upon impulses in the preganglionic neurons. The sympatho-adrenal system is functionally distinct from the various types of sympatho-neural systems (Jänig, W., 2006).
viscero-somatic convergent neurons (dorsal horn of the spinal cord) See Chapter Spinal Cord Mechanisms of Hyperalgesia and Allodynia.

5.17.1 Introduction

Research on the relationship between the autonomic nervous system and pain is a controversial field with many interesting facets that are important from the biological, pathobiological, and clinical point of view. (I prefer to use the terms biology and pathobiology, instead of physiology and pathophysiology, because they include physiological, morphological, biochemical, and molecular aspects.) I will discuss this field in a broad context and focus mainly on the sympathetic nervous system. I will argue that the peripheral sympathetic noradrenergic neuron may have, in addition to its conventional function to transmit signals generated in the brain to peripheral target cells (e.g., smooth muscle cells, secretory epithelia, heart cells, and neurons of the enteric nervous system), quite different functions that are directly or indirectly related to protection of body tissues and pain. These functions have not been studied as extensively as those related to the regulation of autonomic target cells (Jänig, W., 2006). The parasympathetic nervous system is not involved in the generation of pain, yet it may also be important in protection of body tissues (e.g., the gastrointestinal tract (GIT)). Vagal afferents are involved in integrative aspects of pain, hyperalgesia, and inflammation. This is discussed elsewhere (Jänig, W., 2005; Jänig, W. and Levine, J. D., 2006) and summarized in Jänig W. (2007).

The topic *Autonomic Nervous System and Pain* cannot be reduced to peripheral local processes in which peripheral nociceptive afferent fibers (sensitization of nociceptors and generation of ectopic impulses after nerve lesion), sympathetic fibers, and nonneural cells (e.g., cells of the immune system and the vasculature) are involved. The question to be asked is: How are the cellular and subcellular processes that lead to ongoing pain, allodynia, and hyperalgesia in neuropathic pain and inflammatory pain orchestrated by the brain in the continuous protection of the body against agents from outside as well as from within the body? The brain is an important player to organize and control these protective body reactions via neuroendocrine (hypothalamo-pituitary-adrenocortical and sympatho-adrenal) and autonomic (preferentially the sympathetic) systems. Feedback to the brain occurs via various signaling molecules (e.g., interleukines), hard-wired nociceptive afferents, and other afferent neurons (Figure 1). Table 1 lists different functions of the sympathetic nervous system related to pain and protection of body tissues in biological and pathobiological

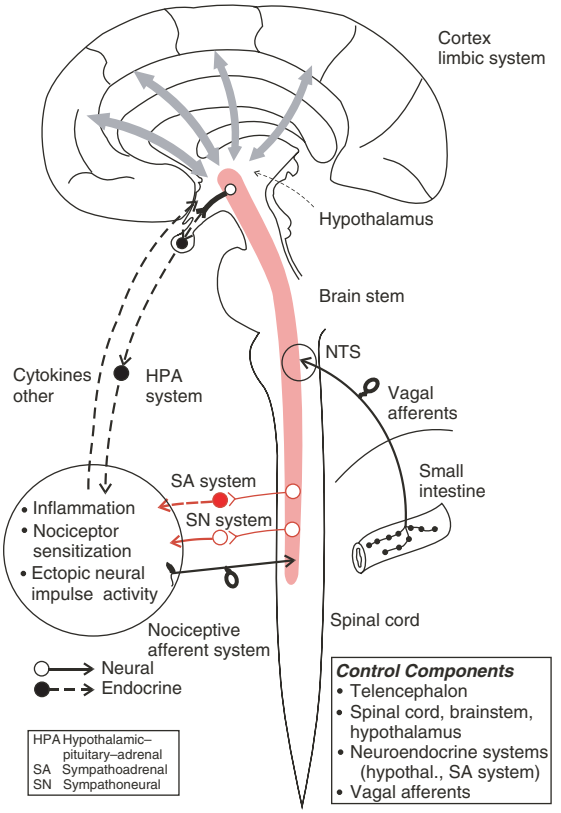

Figure 1 Spinal cord, brainstem, and hypothalamus contain neuronal circuits (pink shaded area) that modulate nociceptor sensitivity, inflammation, and ectopic activity in lesioned afferent neurons in the periphery of the body via the sympatho-adrenal (SA) system, the sympatho-neural system, and the hypothalamic–pituitary–adrenal (HPA) system. Feedback information from the peripheral inflammatory process occurs via nociceptive primary afferent neurons and cytokines. Abdominal vagal afferents signal events from the inner defense line of the body (GALT, gut-associated lymphoid tissue) to the lower brainstem (NTS, nucleus tractus solitarii). The telencephalon controls inflammation and sensitivity of nociceptors via the circuits in the neuraxis (see shaded double arrows).

conditions. It shows that peripheral as well as central mechanisms have to be considered and that the topic includes not only pain and hyperalgesia but also neural and neuroendocrine regulation of inflammation and the immune system.

The integration of the control of protective neural, endocrine, and immune mechanisms occurs in the brain (brainstem, hypothalamus, limbic system, and neocortex). Perception of sensations, feeling of emotions, autonomic, endocrine, and somatomotor responses are coordinated and are, therefore, parallel readouts of the central representations, although the evolvement of feelings of emotions may require explicitly the afferent feedback from body responses generated by the efferent neural autonomic and somatomotor signals (Damasio, A., 2003). These central representations act back on the peripheral tissues, the immune and nociceptive primary afferent neurons, via the endocrine and autonomic nervous systems (Figure 1). The central circuits are also the origin of illness responses that include aversive feelings, pain, and hyperalgesia. This central integration is related or identical to the integrative processes, involving neuroendocrine, immune, and neural systems, occurring during environmental challenges such as viral and bacterial infection (Arkins, S. *et al.*, 2001; Miller, A. H. *et al.*, 2001). Thus, the autonomic nervous system is one component in the generation of pain and protective body reactions that are organized and regulated by the brain and disease occurs when this neural regulation fails.

I will distinguish three aspects of the topic Sympathetic nervous system and pain (Table 1):

1. Reactions of the sympathetic nervous system during pain. This includes the autonomic integrated and adaptive reactions during pain, reflexes to noxious stimulation, and reactions mediated by sympathetic systems in referred zones.
2. Coupling (cross-talk) from sympathetic (noradrenergic) neurons to afferent neurons in the generation of pain. Four broad categories of coupling will be discussed: Direct coupling related to excitation of the sympathetic postganglionic neurons and release of noradrenaline; indirect coupling related to influence of inflammatory processes by the sympathetic nervous system; coupling independent of excitation and noradrenaline release by sympathetic neurons. A fourth category is the effect of adrenaline released by the adrenal medulla on the sensitivity of nociceptors.
3. Sympathetic nervous system and central mechanisms. Based on observations made on patients and animal experimentation, it is likely that activity in sympathetic noradrenergic neurons or in the sympatho-adrenal system, both generated in the brain, contributes directly or indirectly to pain. This central aspect includes the various forms of sympathetic afferent coupling discussed before.

The role of the sympathetic nervous system and its transmitters in chronic inflammation (such as rheumatoid diseases) or in systemic chronic pain diseases (e.g., fibromyalgia) and its interaction with the peptidergic afferent innervation as well as the

Table 1 Sympathetic nervous system and pain

Reactions of the sympathetic nervous system in pain[a]
Protective spinal reflexes
Fight, flight, and quiescence organized at the level of the periaqueductal gray
Hyperalgesia and sympathetically mediated changes in referred zones during visceral pain
Role of the sympathetic nervous system in the generation of pain[b]
Sympathetic–afferent coupling in the periphery
Coupling after nerve lesion (noradrenaline, α-adrenoceptors)
Coupling via the micromilieu of the nociceptor and the vascular bed
Sensitization of nociceptors mediated by sympathetic terminals independent of excitation and release of noradrenaline
Sensitization of nociceptors initiated by cytokines or nerve growth factor and mediated by sympathetic terminals
Sympatho-adrenal system and nociceptor sensitization
Sympathetic nervous system and central mechanisms[c]
Control of inflammation and hyperalgesia by sympathetic and neuroendocrine mechanisms
Complex regional pain syndrome and sympathetic nervous system
Immune system and sympathetic nervous system
Rheumatic diseases and sympathetic nervous system
Systemic chronic pain (e.g., fibromyalgia) and sympathetic nervous system

[a]Bandler R. and Shipley M. T. (1994); Bandler R. *et al.* (2000a; 2000b); Jänig W. (1993; 2006).
[b]Jänig W. and Baron R. (2001); Jänig W. (2005); Jänig W. and Häbler H. J. (2000b); Jänig W. and Koltzenburg M. (1991); Jänig W. and Levine J. D. (2005).
[c]Jänig W. and Baron R. (2002; 2003; 2004); Jänig W. and Häbler H. J. (2000a); Jänig W. *et al*. (2000); Jänig W. and Levine J. D. (2005); Straub R. H. and Härle P. (2005); Straub R. H. *et al*. (2005); Vierck C. J. Jr. (2006).

hypothalamo-pituitary-adrenal (HPA) system will not be discussed. We are at the beginning of the experimental investigation of these control mechanisms (Straub, R. H. and Härle, P., 2005; Straub, R. H. *et al*., 2005; Vierck, C. J. Jr., 2006).

5.17.2 Neurobiology of the Autonomic Nervous System and Pain

The peripheral autonomic nervous system is by definition an efferent system consisting of many functionally distinct pathways that transmit the impulse activity from the spinal cord or brainstem to the effector cells. These pathways are separate from each other and functionally distinct with respect to the effector cells, as is the impulse transmission in the autonomic ganglia and at the neuroeffector junctions to the effector cells. Each peripheral sympathetic or parasympathetic pathway is connected to distinct neuronal networks in the spinal cord, brainstem, and hypothalamus that generate the typical discharge patterns in the autonomic neurons and are responsible for the precise regulation of the target organs (cardiovascular regulation, thermoregulation, regulation of pelvic organs, regulation of GIT, and so forth). The autonomic regulations are represented in these central networks. The anatomical, histochemical, and functional organization of the autonomic nervous system, in particular of the sympathetic nervous system, in the periphery and in the brain, mostly receives insufficient attention in studies of the functioning of this system under pathobiological conditions. I emphasize three points (Jänig, W. and McLachlan, E. M., 2002; Jänig, W., 2006): First, the sympathetic nervous system is functionally as well differentiated as the parasympathetic nervous system. It does not react as a unitary system under normal physiological conditions. Second, the terms sympathetic and parasympathetic are defined anatomically and not functionally. Thus, to use these terms functionally is misleading. Third, the long-held view that sympathetic and parasympathetic nervous system function universally antagonistically is also misleading. Both systems complement each other in their functions.

5.17.2.1 Reactions of the Sympathetic Nervous System in Pain

Any acute, but possibly also chronic tissue-damaging stimulus affects the sympathetic nervous system. Neurons of sympathetic systems exhibit generalized and specific reactions to these stimuli. The generalized reactions probably occur only in certain types of sympathetic system (e.g., muscle vasoconstrictor, visceral vasoconstrictor, sudomotor neurons, or sympathetic cardiomotor neurons) but are weak or absent in other systems (e.g., sympathetic systems to pelvic

organs). They are organized in spinal cord, brainstem (medulla oblongata and mesencephalon), and hypothalamus and can be conceptualized as component parts of the different patterns of defense behavior, such as confrontational defense, flight, or quiescence (Figure 2). Confrontational defense and flight are typical of an active defense strategy when animals encounter threatening stimuli that are potentially injurious for the body, the former potentially leading to fight and the latter to forward avoidance. Both patterns are represented in the lateral and dorsolateral periaqueductal gray of the mesencephalon, activated from the body surface or cortex, and associated with endogenous nonopioid analgesia, hypertension, and tachycardia. Quiescence is similar to the natural reactions of mammals to serious injury and chronic pain occurring particularly in the deep and visceral body domains. It is represented in the ventrolateral periaqueductal gray, activated from the deep (somatic and visceral) body domains, and consists of hyporeactivity, hypotension, bradycardia, and an endogenous opioid analgesia. These stereotyped preprogrammed elementary behaviors and their association with the endogenous control of analgesia enable the organism to cope with dangerous situations that are always accompanied by pain or impending pain. The dorsolateral, lateral, and ventrolateral columns of the periaqueductal gray have distinct reciprocal connections with the autonomic centers in the lower brainstem and hypothalamus that differentially regulate the activity in neurons of the autonomic pathways. They are under differential

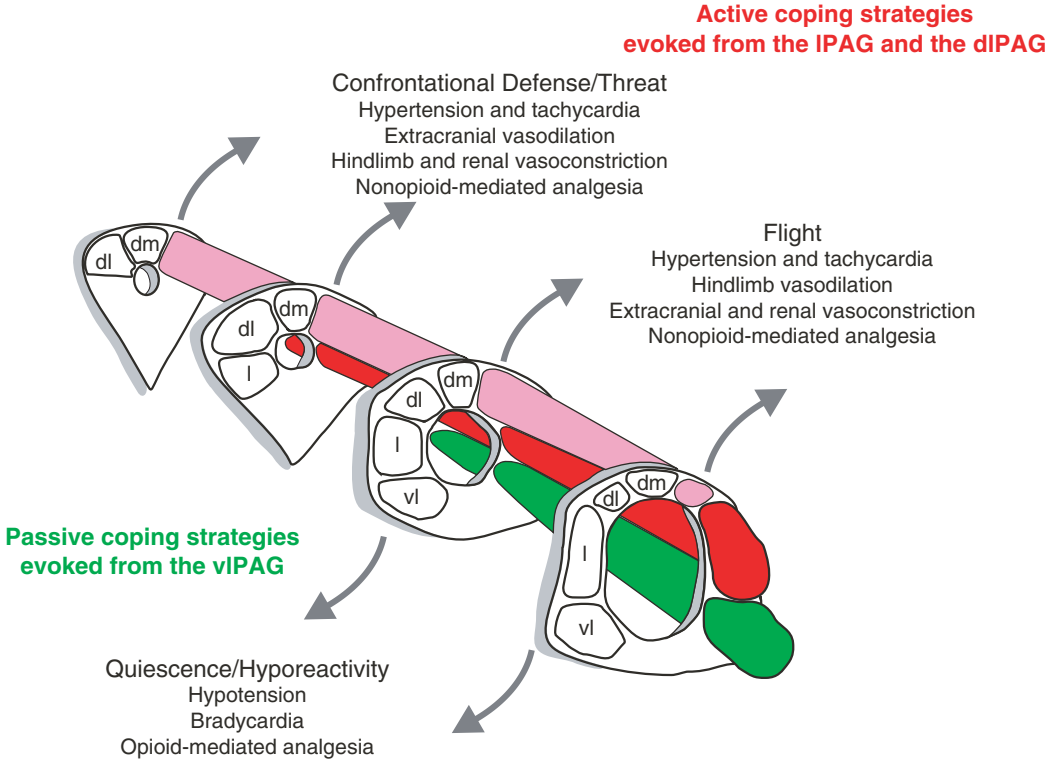

Figure 2 Representation of defense behaviors in the dorsolateral, lateral, and ventrolateral periaqueductal gray. Schematic illustration of the dorsolateral (dl), lateral (l), and ventrolateral (vl) columns within the rostral, intermediate, and caudal periaqueductal gray (PAG). The dorsomedial neural PAG columns are indicated too. Stimulation of neuron populations in the dlPAG, lPAG, and vlPAG by microinjections of the excitatory amino acid glutamate that excites only cell bodies of neurons but not axons evokes distinct defense behaviors: Confrontational defense is elicited from the rostral portion of the dlPAG and lPAG; flight is elicited from the caudal part of the dlPAG and lPAG; quiescence (cessation of spontaneous motor activity) is elicited from the vlPAG in the caudal portion of the PAG. These defense behaviors include typical autonomic cardiovascular reactions (changes of blood pressure, heart rate, and blood flows) and sensory changes (nonopioid- or opioid-mediated analgesia). The representations of confrontational defense and flight are the basis for active coping strategies produced by the cortex. The representation of quiescence is the basis for passive coping strategies produced by the cortex. Modified from Bandler R. and Shipley M. T. (1994) and Bandler R. *et al.* (2000b).

control of the medial and orbital prefrontal cortex and other telencephalic centers (Bandler, R. and Shipley, M. T., 1994; Bandler, R. *et al.*, 2000a; 2000b; Keay, K. A. and Bandler, R., 2004).

There also exist more localized reactions of the sympathetic nervous system to noxious stimuli that are organized within the spinal cord and trigeminal nucleus and in the periphery. These localized reactions are reflected in various somato-sympathetic and viscero-sympathetic reflexes, the afferent neurons of these reflexes are nociceptive (skin, deep somatic tissues, and viscera) and the efferent neurons sympathetic innervating blood vessels (in skin, deep somatic tissues, and viscera), sweat glands, erector pili muscles, enteric nervous system, or other effectors in the viscera. Both afferent neurons and efferent pathways are synaptically connected by various groups of interneurons, establishing circuits that probably are the basis of the changes occurring in referred zones during chronic stimulation of deep nociceptive primary afferents (see below). For example, cutaneous vasoconstrictor neurons exhibit distinct inhibitory reflexes to noxious stimuli of the territories innervated by these neurons.

The hypothalamo-mesencephalic and the spinal level of integration are presumably protective under normal biological conditions and are associated with the activation of the hypothalamo-pituitary adrenocortical system (Jänig, W., 2006).

5.17.2.2 Visceral Afferents, Autonomic Nervous System, and Pain

Visceral organs in the thoracic, abdominal, and pelvic cavities are innervated by two sets of extrinsic primary afferent neurons: spinal visceral afferent neurons and vagal visceral afferent neurons (the latter also including afferent neurons from arterial baro- and chemoreceptors that project through the glossopharyngeal nerve). Spinal visceral afferent neurons have their cell bodies in the dorsal root ganglia (DRG) and vagal afferent neurons in the inferior (nodose) ganglion of the vagus nerve (a few in the superior (jugular) ganglion of the vagus nerve and some arterial baro- and chemoreceptor afferents in the petrosal ganglion). Visceral afferent neurons are involved in specific organ regulations, multiple organ reflexes, neuroendocrine regulations, and visceral sensations (including visceral pain), shaping and eliciting emotional feelings and other functions. They monitor the inner state of the body and serve to maintain homeostasis and to adapt the internal milieu and the regulation of the organs to the behavior of the organism. They are anatomically and functionally closely associated with the autonomic nervous system. However, they should not be labeled sympathetic, parasympathetic, or autonomic afferent neurons. These functional labels are misleading since they imply that the visceral afferent neurons have functions that uniquely pertain to the sympathetic or parasympathetic autonomic nervous system, the exception being that afferent neurons of the enteric nervous system are per definition enteric afferent neurons. No functional, morphological, histochemical, or other criteria do exist to associate any type of visceral afferent neuron with only one autonomic system (Jänig, W., 2006).

Usually, vagal afferent neurons are described and characterized by adequate physiological stimuli exciting them and by the main reflexes associated with the cardiovascular system, respiratory system, GIT, or other regulatory systems (Undem, B. J. and Weinreich, D., 2005). However, several observations show that groups of vagal afferents innervating visceral organs in the thoracic and abdominal cavity are involved in the control of nociception and pain, in neuroendocrine control of nociceptors, in the control of inflammation, and in the control of general protective body reactions including illness responses. Subgroups of vagal afferent neurons may signal events from visceral organs, in particular those occurring at the internal defense line of the body in the GIT represented in the liver and in the small intestine (which contains the largest immune system of the body, the gut associated lymphoid tissue (GALT)), to the central nervous system that triggers protective body reactions not only in the viscera but also in the superficial and deep somatic body tissues (see Chapters Visceral Pain; Vagal Afferent Neurons and Pain; Jänig, W., 2005). These vagal afferent neurons may be activated or sensitized by cellular processes of these inner body defense lines and their signaling molecules. Stimulation of vagal afferents may generate sickness behavior that is characterized by several protective illness responses (immobility, decreased social interaction, decrease in food intake and of digestion, formation of taste aversion against novel food, loss of weight, fever, increase of sleep, change in endocrine functions (e.g., of the activation of the hypothalamic–pituitary system), malaise; Watkins, L. R. *et al.*, 1995; Maier, S. F. and Watkins, L. R., 1998; Watkins, L. R. and Maier, S. F., 1999; 2000; Goehler, L. E. *et al.*, 2000), activates the inhibitory control of nociceptive impulse transmission

in the spinal and trigeminal dorsal horn (Foreman, R. D., 1989; Randich, A. and Gebhart, G. F., 1992; Jänig, W., 2005), inhibits nociceptive–neuroendocrine reflex circuits that control inflammation (via the sympatho-adrenal system and the hypothalamic–pituitary system (Green, P. G. *et al.*, 1995; 1997; Jänig, W. *et al.*, 2000; Miao, F. J.-P. *et al.*, 2000; 2001)), and inhibits the central circuits that control via the adrenal medulla and release of adrenaline the sensitivity of nociceptors (Khasar, S. G. *et al.*, 1998a; 1998b; Jänig, W. *et al.*, 2000; Khasar, S. G. *et al.*, 2003; Jänig, W. *et al.*, 2006; see below). For these hypothetic functions of vagal afferents involving neuroendocrine and autonomic systems, in the protection of the body, an umbrella concept in the frame of body protection, pain, and inflammation has to be formulated. This has to include the central circuits (see Jänig, W., 2005; Jänig, W. and Levine, J. D., 2006).

5.17.2.3 Hyperalgesia and Sympathetically Mediated Changes in Referred Zones During Visceral Pain

Chronic stimulation of spinal afferents from visceral organs may elicit pain, hyperalgesia, and allodynia in the referred zones of the body surface and of the deep somatic domain (skin, subcutaneous tissue, musculature, tendons, fascia, and bones). Hyperalgesia and allodynia that are elicited in the superficial and deep somatic domains by visceral diseases are equivalent to secondary hyperalgesia and allodynia in the skin caused by ongoing activity in polymodal C-nociceptors (Cervero, F. and Jänig, W., 1992; Vecchiet, L. *et al.*, 1993). The degree and spatial spread of referred pain, hyperalgesia, and allodynia depend on the intensity and duration of the visceral stimulation and the type of visceral organ. They are abolished after blockade of the impulse traffic in spinal visceral afferents to the spinal cord. They may be generated by sensitization of neurons in the spinal cord that are involved in the generation of sensations (e.g., spinothalamic tract neurons), in the descending control of spinal circuits (e.g., spinal neurons projecting to the brainstem or interneurons mediating signals of the endogenous control system), and in the regulation of sympathetic target organs and skeletal musculature constituting spinal and supraspinal viscero-sympathetic and viscero-somatic reflex pathways (Figure 3). The most likely candidate of these neurons is the broad class of viscero-somatic convergent neurons in the spinal cord (Cervero, F. and Jänig, W., 1992; Cervero, F., 1995; Bielefeldt, T. K. and Gebhart, G. F., 2006).

Little attention has been given to the generation of autonomic changes (reflected in changes of blood flow, sweating, and piloerection) and of trophic changes in the skin and its appendages, subcutis, joint capsules, and fascia of the referred hyperalgesic (Head's) zones during visceral diseases (Jänig, W. and Morrison, S. F., 1986). These changes are very variable between individuals but reported to be relatively stable for each individual. The clinical diagnosis of a visceral disease (e.g., in the GIT, of the evacuative organs, or of the heart) may be predicted from these changes with a probability of about 70% (Beal, M. C., 1983; Cox, J. M. *et al.*, 1983; Beal, M. C., 1985; Nicholas, A. S. *et al.*, 1985).

It is important to note that the trophic changes occur in regions that are outside of the site of injury or trauma, that the first sign of the trophic changes is probably the edema, and that the severe signs of these changes develop relatively slowly and late. These changes are believed to be generated by the segmental sympathetic outflow to the visceral reference zones at the trunk. However, the trophic changes in the referred zones may also or additionally be related to changes in the retrograde axonal transport in afferent neurons that innervate the referred zones (see discussion in Jänig, W., 1993). We need more reliable and quantitative data about the changes occurring in the referred somatic zones in patients with various visceral diseases to develop testable hypotheses.

The mechanisms explaining referred visceral pain and the changes observed in the referred zones that probably are associated with the sympathetic neurons are barely understood. Classical central theories trying to explain referred visceral pain are the convergence-projection theory of Ruch T. C. (1965) and the convergence-facilitation theory of MacKenzie, J. (1920). (The convergence-projection theory of Ruch T. C. (1965) is based on the concept that spinal neurons in the dorsal horn projecting to the thalamus obtain convergent synaptic input from primary afferent neurons innervating viscera or somatic body tissues. The telencephalon localizes the pain generated by activity in visceral afferents erroneously into somatic tissues of the corresponding dermatomes, myotomes, and sklerotomes. The convergence-facilitation theory of MacKenzie J. (1920) proposes that afferent inputs from the viscera to the spinal cord are not directly related to pain sensation but that they produce a generalized increase of excitability in the area of the spinal cord, which is related to the respective visceral organ generating

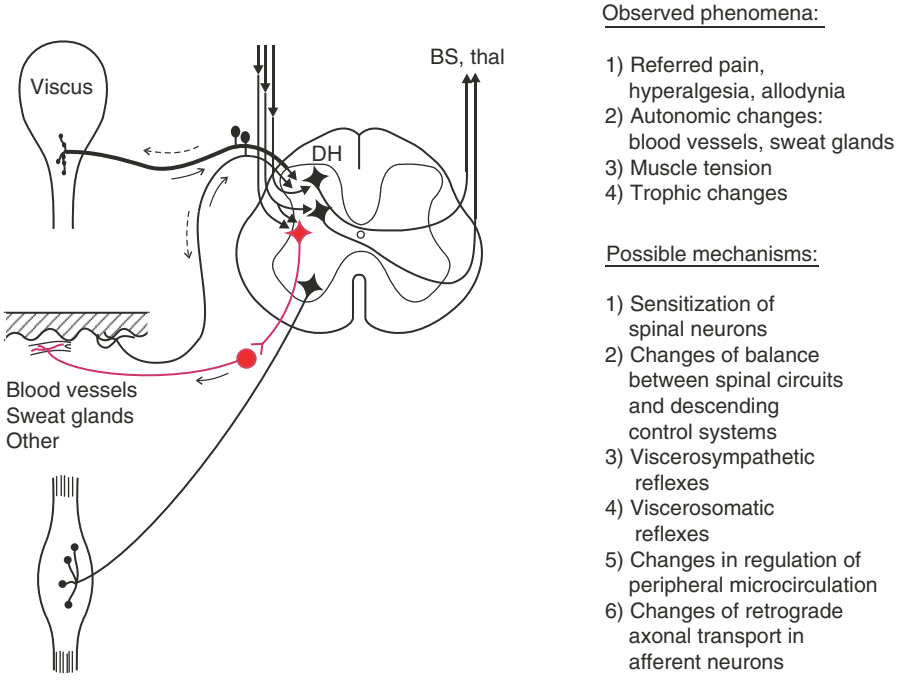

Figure 3 Observed phenomena generated in referred zones during visceral trauma (e.g., inflammation) and the putative mechanisms underlying these changes. Sympathetic pathways (indicated in red) mediate changes of blood flow, sweating, or piloerection and possibly changes of tissue structure (edema, trophic changes). The mechanisms underlying the latter are not understood. Continuous arrows, excitation; dashed arrows, retrograde axonal transport. BS, brainstem; DH, dorsal horn; thal, thalamus. Modified from Jänig W. (1993).

an irritable focus. This was to promote activity in neurons projecting to the thalamus and obtaining convergent synaptic input from somatic tissue (leading to referred pain and referred hyperalgesia), in motoneurons (leading to muscle spasms), and in sympathetic neurons (leading to autonomic changes in the referred zones) (Ness, T. J., 1995).) However, both theories explain the mechanisms underlying referred pain rather incompletely and the mechanisms of the other changes in the referred zones in which the sympathetic nervous system is involved not at all (see Ness, T. J. and Gebhart, G. F., 1990; Jänig, W. and Koltzenburg, M., 1993; Vecchiet, L. *et al.*, 1993; Ness, T. J., 1995; Giamberardino, M. A., 1999, for discussion). It is suggested that persistent sensitization and activation of visceral afferent neurons (e.g., during chronic inflammation) sensitize the second-order viscero-somatic convergent neurons in the dorsal horn of the spinal cord that can be synaptically activated from viscera as well as from somatic tissues (skin and deep somatic tissues). However, it has not been convincingly demonstrated that these viscero-somatic convergent neurons can be sensitized by activity in visceral afferents (Herrero, J. F. *et al.*, 2000; Jänig, W. and Häbler, H. J., 2002).

This invites speculation that not only spinal mechanisms but also, or in particular, supraspinal mechanisms are responsible to explain the phenomenology of referred pain. Supraspinal mechanisms controlling synaptic impulse transmission in the dorsal horn are inhibitory or excitatory (Urban, M. O. and Gebhart, G. F., 1999; Porreca, F. *et al.*, 2002). These mechanisms are represented in the periaqueductal gray, the caudal raphe nuclei, the ventromedial medulla, and the dorsolateral pontine tegmentum (Fields, H. L. *et al.*, 2006). They do control not only nociceptive impulse transmission in the dorsal horn but also various autonomic regulations and possibly neuroendocrine regulations (Mason, P., 2001) and are in turn under the control of the cerebral hemispheres. Thus, the reference of visceral affections (e.g., chronic inflammation in the viscera) into somatic zones may be dependent on these endogenous protective control systems. These referred phenomena (that include sensory, autonomic, and motor changes) may therefore be the biological

expression of protective mechanisms operating in spinal cord and brainstem in the somatic body domains.

5.17.3 Role of the Sympathetic Nervous System in the Generation of Pain

5.17.3.1 Clinical Background: Sympathetically Maintained Pain

Pain being dependent on activity in sympathetic neurons is called sympathetically maintained pain (SMP). SMP is a symptom and includes generically spontaneous pain and pain evoked by mechanical or thermal stimuli. It may be present in the complex regional pain syndrome (CRPS) type I and type II and in other pain syndromes. The idea about the involvement of the (efferent) sympathetic nervous system in the generation of pain is based on various clinical observations that have been documented in the literature since tens of years (Bonica, J. J., 1990). Representative for these multiple observations on patients with pain in which the sympathetic nervous system is causally involved are experimental investigation on patients with CRPS who had SMP (1–4) and other less well-controlled observations on patients with pain.

1. Spontaneous pain, mechanical allodynia, and cold allodynia in the upper extremity of patients with CRPS II, which are alleviated by stellate ganglion block, can be rekindled, under the condition of sympathetic block, by injection of noradrenaline into the skin area that was painful before sympathetic block (Figure 4; Torebjörk, H. E. *et al.*, 1995). By the same token, it has been shown in patients with causalgia, who had been successfully treated either by sympathectomy or by transcutaneous nerve stimulation, that ionophoretic application of noradrenaline to the previously causalgic skin area rekindles spontaneous pain and mechanical allodynia (Wallin, G. *et al.*, 1976). Rekindling of spontaneous and evoked pain or enhancement of both by noradrenaline injected into the skin area, which was painful before sympathetic block or before successful treatment, took 10 min or longer to develop (Figure 4b). This long latency indicates that noradrenaline does not act possibly directly on the afferent fiber terminals, but by some unknown mechanism via changes in the micromilieu of the nociceptors.
2. Intradermal injection of noradrenaline in physiologically relevant doses in patients with SMP evokes greater pain in the affected limb regions than in the contralateral unaffected limb or in control subjects. Most patients whose pain increased after injection of noradrenaline in the affected extremity report a decrease in pain following systemic injection of the α-adrenoceptor blocker phentolamine (Ali, Z. *et al.*, 2000; see also Arnér, S., 1991).
3. In CRPS type I patients with SMP, pain is relieved after blockade of sympathetic activity to the affected extremity by a local anesthetic applied to the appropriate sympathetic paravertebral ganglia. This pain relief lasts significantly longer than the short-lasting pain-relieving effect of saline injected close to the same paravertebral ganglia (control injection) in the same group of CRPS patients showing that the real pain-relieving effect generated by blockade of sympathetic activity can be discriminated from the placebo effect and the duration of pain relief outlasts the duration of conduction block generated by the local anesthetic by an order of magnitude (Price, D. D. *et al.*, 1998; see Figure 15).
4. Pain (spontaneous, mechanical allodynia) in the hand of chronic CRPS I patients with SMP, which is clamped to a temperature of about 36 °C, is enhanced when activity in cutaneous vasoconstrictor neurons is increased by central cooling (Figure 5), yet not in chronic CRPS I patients without SMP (Baron, R. *et al.*, 2002). This experiment demonstrates that an increase of activity in sympathetic neurons by a physiological intervention (central cooling) can increase pain, possibly independent of a vascular component. An important side effect of this experimental investigation is that the peripheral mechanisms underlying SMP in CRPS I patients occur mainly in deep somatic tissues.
5. Injection of adrenaline around a stump neuroma that has developed long after limb amputation may be intensely painful (Chabal, C. *et al.*, 1992).
6. In patients with CRPS II, but not in those with hyperhidrosis, intraoperative electrical stimulation of the sympathetic chain may increase spontaneous pain (Walker, A. E. and Nulsen, F., 1948; White, J. C. and Sweet, W. H., 1969).
7. In patients with SMP phentolamine (α-adrenoceptor blocker) given intravenously may relieve pain but not propranolol (β-adrenoceptor blocker) (Arnér, S., 1991; Raja, S. N. *et al.*, 1991; Dellemijn, P. L. *et al.*, 1994).

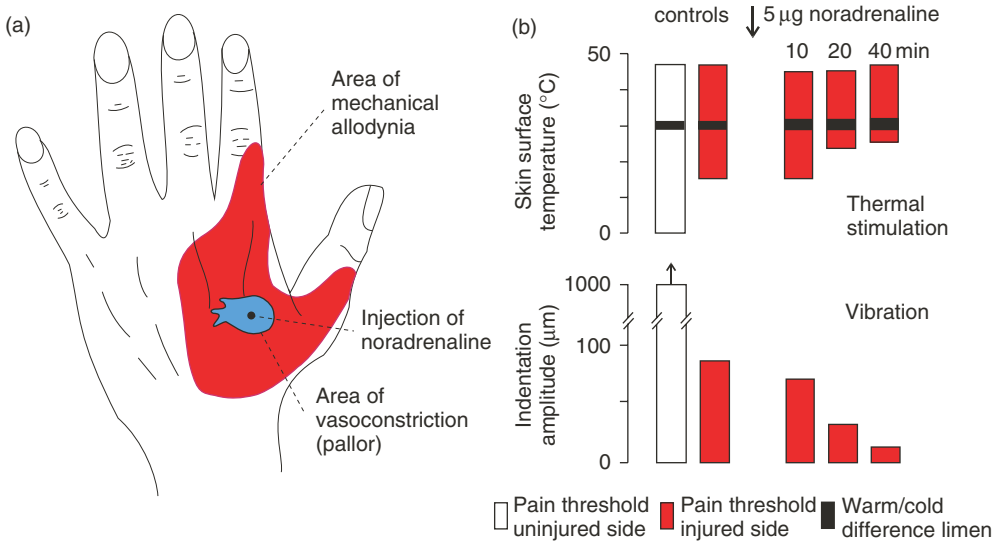

Figure 4 Mechanical and cold allodynia in CRPS type II patients with sympathetically maintained pain (SPM) elicited by intradermal injection of noradrenaline. Noradrenaline was injected intradermally at the site of mechanical and cold allodynia when the patients were temporarily relieved from their pain by a stellate ganglion block with lidocaine (1%) or bupivacaine (0.25%). (a) Area of pallor and mechanical allodynia 20 min after intradermal injection of 2 µg noradrenaline. (b) Sequential quantitative sensory testing of patients before and after intradermal injection of 5 µg noradrenaline during a time without blockade of the stellate ganglion. This patient had mechanical allodynia (indentation amplitude of a mechanical vibration stimulus to evoke pain about 90 µm, *lower panel*) and cold hyperalgesia/allodynia (cold pain threshold about 15 °C, *upper panel*). The mechanical allodynia (further decrease of indentation amplitude to elicit pain) and cold allodynia (further decrease of cold pain threshold) progressively worsened starting approximately 20 min after intradermal injection of 5 µg noradrenaline. Modified from Torebjörk H. E. *et al.* (1995) with permission.

8. In some patients with postherpetic neuralgia, spontaneous pain and mechanical allodynia are enhanced after intracutaneous injection of adrenaline or the α1-adrenoceptor agonist phenylephrine (Choi, B. and Robotham, M. C., 1997).

I recommend to read Mitchell S. W. (1872), Livingston W. K. (1943/1976; here in particular chapters 5, 6, 14, and 15), and Bonica J. J. (1953; Chapter 28). These texts are not only of historical interest (here the literature before 1953 is discussed) but also the reader will find (1) a wealth of carefully reported clinical observations and (2) ideas developed on the basis of these clinical observations that are still quite modern, showing that the progress in this field is not as impressive as it appears to be.

These key experiments conducted on human patients with SMP demonstrate that (1) activation of sympathetic postganglionic neurons can produce pain, (2) blockade of sympathetic activity can relieve the pain, (3) noradrenaline injected intracutaneously rekindles the pain, and (4) α-adrenoceptor blockers or guanethidine (which depletes noradrenaline from its stores) can relieve the pain (Jänig, W. and Baron, R., 2001; 2002; Jänig, W., 2002; Jänig, W. and Baron, R., 2003).

The interpretation of these data is that the nociceptors are excited and possibly sensitized by noradrenaline released by the sympathetic fibers. Either the nociceptors have expressed adrenoceptors or the excitatory effect is generated indirectly, e.g., via changes in blood flow and subsequent ischemia or by other components modulated by sympathetic fibers. The ways of sympathetic afferent coupling to be discussed are illustrated in Figure 6. Sympathetically maintained activity in nociceptive neurons may generate and maintain a state of central sensitization/hyperexcitability, leading to spontaneous pain and secondary evoked pain (mechanical and possibly cold allodynia). This is schematically illustrated in Figure 7.

5.17.3.2 Sympathetically Maintained Pain Following Nerve Lesion Simulated in Behavioral Animal Models

In animals (rats), signs of pain are measured by quantifiable behavioral components, e.g., paw-withdrawal latency to thermal noxious stimulation (heat and cold), frequency and threshold of paw withdrawal to mechanical stimulation, degree of self-mutilation

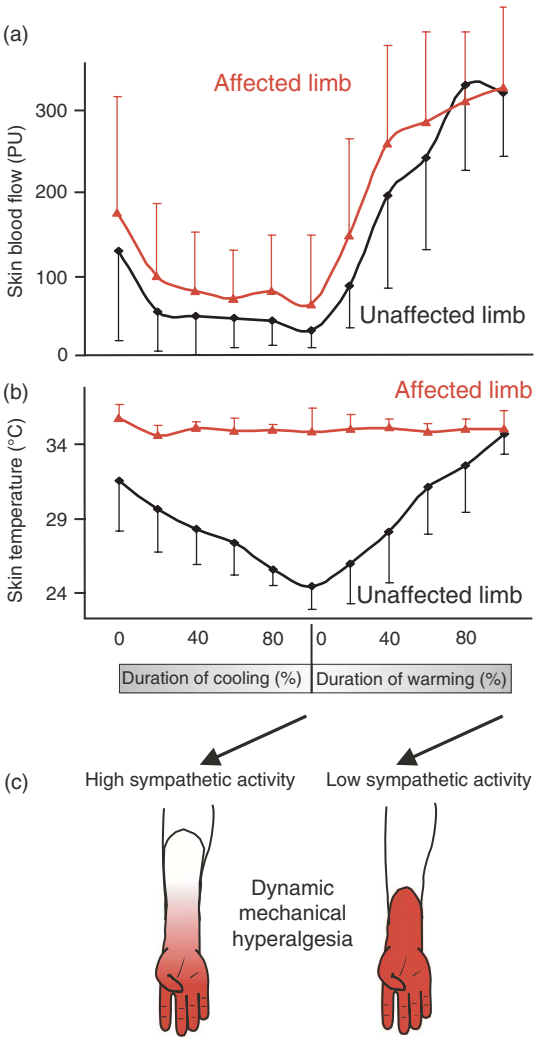

Figure 5 Experimental changes of activity in cutaneous sympathetic vasoconstrictor neurons by physiological thermoregulatory reflex stimuli in 13 complex regional pain syndrome (CRPS) patients. With the help of a thermal suit, whole-body cooling and warming was performed to alter sympathetic skin nerve activity. The subjects were lying in a suit supplied by tubes, in which running water at 12 °C and 50 °C, respectively (inflow temperature), was used to cool or warm the whole body. By these means, sympathetic activity can be switched on and off. (a) High sympathetic vasoconstrictor activity during cooling induces considerable drop in skin blood flow on the affected and unaffected extremity (laser Doppler flowmetry). Measurements were taken at 5-min intervals (mean + SD). (b) On the unaffected side, a secondary decrease of skin temperature was documented. On the affected side, the forearm temperature was clamped at 35 °C by a feedback-controlled heat lamp to exclude temperature effects on the sensory receptor level. Measurements were taken at 5-min intervals (mean + SD). (c) Effect of cutaneous sympathetic vasoconstrictor activity on dynamic mechanical hyperalgesia in one CRPS patient with sympathetically maintained pain (SMP). Activation of sympathetic neurons (during cooling) leads to an increase of the area of dynamic mechanical hyperalgesia. Reprinted with permission from Baron R. *et al.* (2002).

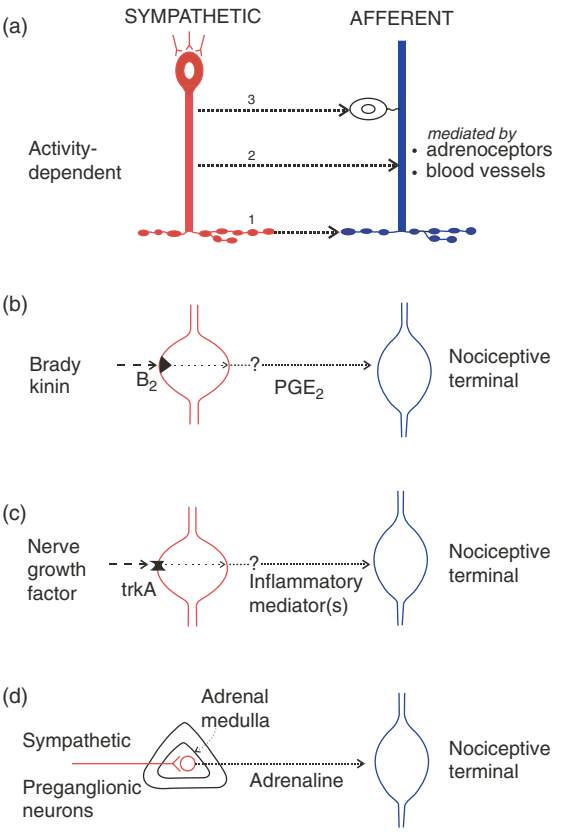

Figure 6 Ways hypothesized to couple sympathetic and primary afferent neurons following peripheral nerve lesion (a) or during inflammation (b–d). (a) These types of coupling depend on the activity in the sympathetic neurons and on the expression of functional adrenoceptors by the afferent neurons or mediation indirectly via the blood vessels (blood flow). It can occur in the periphery (1), in the dorsal root ganglion (3), or possibly also in the lesioned nerve (2). (b) The inflammatory mediator bradykinin acts at B_2 receptors in the membrane of the sympathetic varicosities or in cells upstream of these varicosities, inducing release of prostaglandin E_2 (PGE_2) and sensitization of nociceptors. This way of coupling is probably not dependent on activity in the sympathetic neurons. (c) Nerve growth factor released during an experimental inflammation reacts with the high-affinity receptor trkA, in the membrane of the sympathetic varicosities, inducing release of an inflammatory mediator or inflammatory mediators and sensitization of nociceptors. This effect is probably not dependent on activity in the sympathetic neurons. (d) Activation of the adrenal medulla by sympathetic preganglionic neurons leads to release of adrenaline that generates sensitization of nociceptors. The ? in (b) and (c) indicates that PGE_2 or other inflammatory mediators may be released by cells other than the sympathetic varicosities. Modified from Jänig W. and Häbler H. J. (2000b).

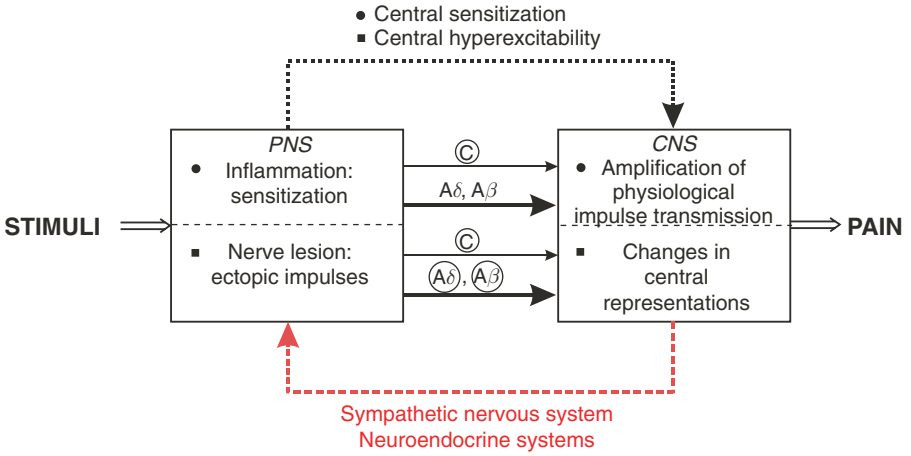

Figure 7 Concept of generation of peripheral and central hyperexcitability during inflammatory pain and neuropathic pain. The upper interrupted arrow indicates that the central changes are generated (and possibly maintained) (a) by persistent activation of nociceptors with C-fibers (e.g., during chronic inflammation) called here central sensitization or (b) after trauma with nerve lesion by ectopic activity and other changes in lesioned afferent neurons called here central hyperexcitability. The lower interrupted arrow indicates the efferent feedback via the sympathetic nervous system and neuroendocrine systems (e.g., the sympatho-adrenal system). Primary afferent nociceptive neurons (in particular those with C-fibers) are sensitized during inflammation. After nerve lesion, all lesioned primary afferent neurons (unmyelinated as well as myelinated ones) undergo biochemical, physiological, and morphological changes that become irreversible with time. These peripheral changes entail changes of the central representation (of the somato-sensory system) that become irreversible if no regeneration of primary afferent neurons to their target tissue occurs. The central changes, induced by persistent activity in afferent nociceptive neurons during inflammation or induced after nerve lesion, are also reflected in the efferent feedback systems that may establish positive feedback loops to the primary afferent neurons.

(autotomy), or spontaneous lifting and licking of paw. These reactions are interpreted as equivalent to mechanical or thermal hyperalgesia or allodynia or spontaneous pain in humans. Behavioral models allow to test whether the sympathetic nervous system contributes to these hyperalgesic/allodynic behaviors or to spontaneous pain behavior. Animals are given clinically relevant nerve lesions, and behavioral experiments are performed before and after interventions aimed at the sympathetic supply of the affected extremity. The strength of these models includes the range of possible experimental manipulations performed at the sympathetic nervous system and the use of different strains of animals or transgenic animals. Quantitative data obtained in these behavioral experiments lead to the formulation of hypotheses that can be tested in reduced experiments *in vivo* and *in vitro* using various methodical approaches.

Several rat models of neuropathic pain involving controlled nerve lesions have been used to determine the contribution of the sympathetic nervous system to neuropathic pain. The results obtained in these experiments are summarized in Table 2. The interventions include surgical or chemical sympathectomy, systemic or local application of adrenoceptor blockers (e.g., phentolamine (α_1,α_2), prazosin (α_1), or yohimbin (α_2)) or of adrenoceptor agonists (e.g., phenylephrine (α_1) and clonidine (α_2)), and intraperitoneal application of guanethidine (that is taken up by the noradrenergic terminals and depletes noradrenaline).

Overall, the results obtained on these rat behavioral models of nerve injury are somewhat disappointing since they did not lead to straightforward answers. Thus, the controversial results on these models provide conflicting evidence on the role of the sympathetic nervous system in generating pain behavior, indicating that behavioral animal models must be designed with utmost care. Small changes in the experimental procedures may create major behavioral changes. Behavioral testing should be performed in a blinded fashion if possible, and the models must be designed in close association with the clinical situation to be certain to test what is intended to be tested. The results of systemic pharmacological interventions (e.g., application of adrenoceptor agonists or antagonists, guanethidine, or chemical sympathectomy with 5-hydroxy-dopamine) do not necessarily allow functional interpretations, partly because of the widespread systemic effects of these agents. Finally, the controversial results obtained from the animal behavior

Table 2 Nerve lesion animal (rat) models to study sympathetically maintained pain (SMP)

Model	*Nerve lesion*	*Behavioral measurements*	*Interventions at the sympathetic supply*	*Results*
1. Autotomy model[a]	Ligation and transection of sciatic and saphenous nerve	Autotomy of affected paw (self-mutilation)	Intraperitoneal guanethidine	Autotomy ↓
			Subcutaneous noradrenaline	Autonomy ↑
2. Partial lesion of the sciatic nerve[b]	Ligation of 33–50% of sciatic nerve	Heat HA/ mechanical HA	Intraperitoneal guanethidine, Noradrenaline local	Heat HA ↓, Mechanical HA ø, Heat HA ↑, Mechanical HA ↑
3. Chronic constriction injury of the sciatic nerve[c]	Loose ligation of sciatic nerve	Heat HA/ mechanical HA	Surgical sympathectomy, intraperitoneal guanethidine	Heat HA ↓, Mechanical HA (↓), ø
4. Spinal nerve ligation model[d]	Ligation and transection of spinal nerve L5, L5/L6	Mechanical HA/ allodynia heat HA	Surgical sympathectomy	Mechanical HA ↓ or ø[f] heat HA ↓
5. Cryolysis of the sciatic nerve[e]	Cryolysis of sciatic nerve	Mechanical allodynia	Surgical sympathectomy	Mechanical allodynia ø

[a]Wall P. D. *et al.* (1979a; 1979b); Coderre T. J. *et al.* (1984; 1986); Coderre T. J. and Melzack R. (1986).
[b]Seltzer Z. *et al.* (1990); Shir Y. and Seltzer Z. (1991); Tracey D. J. *et al.* (1995).
[c]Bennett G. J. and Xie Y. K. (1988); Neil A. *et al.* (1991); Desmeules J. A. *et al.* (1995); Kim K. J. *et al.* (1997).
[d]Kim S. H. and Chung J. M. (1991); Kim S. H. *et al.* (1993); Kim K. J. *et al.* (1997); Kinnman E. and Levine J. D. (1995); Ringkamp M. *et al.* (1999).
[e]Willenbring S. *et al.* (1995).
[f]The negative effects of surgical sympathectomy reported by Ringkamp M. *et al.* (1999: Pain 79, 142) were obtained independently by two different groups.
HA, hyperalgesia; ↓, decrease; ↑, increase; ø, no effect.

models may argue that the models do not reflect SMP as defined clinically.

This controversial situation does not mean that behavioral animal models are useless and cannot simulate the clinical situation. On the contrary, we are dependent on the design of these animal models if we want to unravel the mechanisms behind the different types of pathological pain in which the sympathetic nervous system is involved. However, the same model cannot be expected to represent SMP in different groups of patients. Furthermore, the animal models so far tested are related to nerve lesions. Rat models simulating SMP in patients with pain states developing after trauma without nerve lesion (Table 1) practically do not exist (e.g., for patients with CRPS I).

5.17.3.3 Direct Involvement of the Sympathetic Nervous System in the Generation of Pain Following Nerve Trauma

Under physiological conditions, there exists almost no acute influence of sympathetic postganglionic neurons on sensory neurons projecting to skin or deep somatic tissues in mammals. The effects that have been measured under experimental conditions on sensory receptors with myelinated or unmyelinated axons were weak and can in part be explained by changes of the effector organs (erector pili muscles and blood vessels) induced by the activation of sympathetic neurons. These rather negative results do not rule out that noradrenaline or colocalized substances released by the postganglionic terminals have secondary long-term effects on the excitability of sensory receptors although we have no experimental evidence for this (Jänig, W. and Koltzenburg, M., 1991).

5.17.3.3.1 Coupling between lesioned postganglionic and afferent nerve terminals

Coupling may occur between sympathetic fibers and afferent terminals in a neuroma, following nerve section or ligation. Some myelinated as well as unmyelinated nerve fibers in the neuroma can be excited following electrical stimulation of the sympathetic supply or by noradrenaline or adrenaline injected systemically. The coupling has been

observed in young neuromas but less so in old ones, weeks and months after nerve lesion. Furthermore, the frequency of electrical stimulation applied to the sympathetic trunk in order to excite the lesioned afferent nerve fibers was high, generating activity in the sympathetic neurons that does not occurs under physiological conditions (Jänig, W., 2006). This corresponds to the clinical experience showing that neuroma pain is usually not dependent on sympathetic activity. It also corresponds to histological observations showing that catecholamine-containing axon profiles are rare within the neuroma and for several centimeters proximal to it but may be present in the scar tissue around the neuroma), many weeks after cutting and ligating the nerve (McLachlan, E. M., unpublished data). Thus, this coupling is chemical and occurs via noradrenaline acting on α-adrenoceptors, although other mediator substances may also be involved (Jänig, W., 1990). Ephaptic coupling between sympathetic fibers and afferent fibers has so far not been observed in a neuroma (Devor, M. and Jänig, W., 1981; Blumberg, H. and Jänig, W., 1982; 1984; Jänig, W. and Koltzenburg, M., 1991).

The situation is different when afferent and sympathetic fibers are allowed to regenerate to the target tissue. This has been shown experimentally for the chronic situation more than a year after cross-union of nerves (e.g., adaptation of the proximal stump of the sural or superficial peroneal nerve to the distal stump of the tibial nerve, in the cat) and after reinnervation of appropriate and inappropriate target tissues. Now unmyelinated afferent fibers may be vigorously excited by electrical low-frequency stimulation of the sympathetic supply (Häbler, H. J. *et al.*, 1987). Also this excitation is adrenoceptor-mediated (Figure 8). It can be mimicked by adrenaline or noradrenaline and blocked by α-adrenoceptor blockers (e.g., phentolamine).

5.17.3.3.2 Coupling between unlesioned postganglionic and afferent nerve terminals following partial nerve lesion

Intact C-fiber polymodal nociceptors in the skin may develop sensitivity to catecholamines following partial nerve injury. Sympathetic nerve stimulation and noradrenaline may excite the polymodal nociceptors or sensitize them for heat stimuli. The activation and sensitization is already seen 4–10 days after partial nerve lesion and is maintained for at least 150 days. This sympathetic afferent coupling apparently involves the nonlesioned polymodal nociceptive afferent axons that project through the lesion site and nonlesioned postganglionic axons. It is suggested that the unlesioned unmyelinated afferents develop hyper-reactivity to catecholamines following degeneration of the sympathetic postganglionic axons. Expression of adrenoceptors in afferent fibers may be triggered by collateral sprouting of both afferent fibers and postganglionic fibers in the target tissue (Sato, J. and Perl, E. R., 1991). However, sympathetic afferent coupling leading to activation or sensitization of nociceptors requires sympathetic stimulation at high nonphysiological frequencies.

5.17.3.3.3 Coupling in the dorsal root ganglion and collateral sprouting following peripheral nerve lesion

Chemical sympathetic afferent coupling following peripheral nerve lesion (e.g., a spinal nerve, the sciatic nerve, or another hindlimb nerve) may occur proximally to the injury site in the nerve or in the DRG (Figure 6a3). Sympathetic postganglionic fibers reach the spinal nerves via gray rami. Most of these fibers project distally to peripheral target cells, and others project proximally (e.g., to the DRG) and are normally found along blood vessels. This situation changes after an experimental nerve lesion (e.g., transection and ligation of the sciatic nerve in rats). Now many perivascular catecholamine-containing axons of the unlesioned proximally projecting neurons start to sprout in the DRGs that contain somata with lesioned axons. The extent of this collateral sprouting increases with time after nerve lesion. Some somata are partially or almost completely surrounded by varicose catecholaminergic terminals several weeks after nerve lesion; the frequency of these catecholamine-fluorescent structures increases for more than 70 days after nerve lesion. The noradrenergic axons sprout preferentially to axotomized large-diameter afferent cell bodies (McLachlan, E. M. *et al.*, 1993; Chapter Sprouting in Dorsal Root Ganglia).

Neurophysiological experiments on rats with nerve lesion (ligation and transection of a spinal nerve, the sciatic nerve, or other hindlimb nerves) show that afferent neurons projecting in the lesioned nerve can be excited or depressed in their activity affected via the DRG by electrical stimulation of sympathetic neurons and by catecholamines: (1) In the first 2 to 3 weeks after nerve lesion, most A-fiber neurons with spontaneous activity and only very few silent A-fiber neurons are excited. At later time periods, when the catecholaminergic sprouting in the

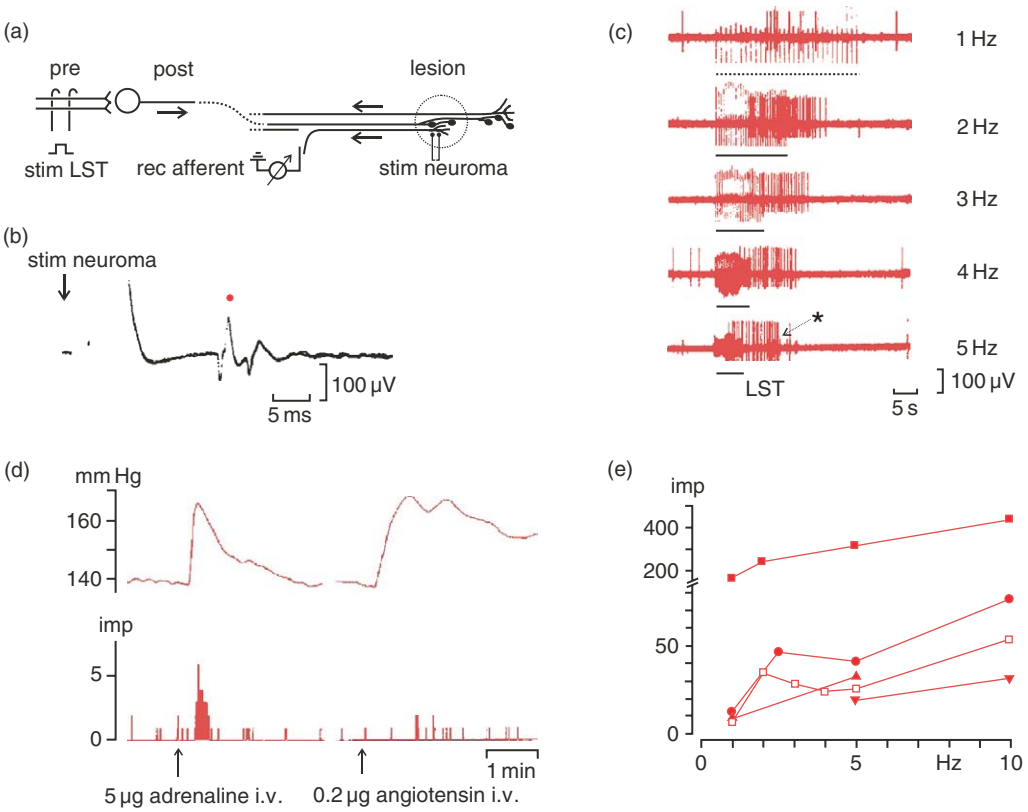

Figure 8 Sympathetic afferent coupling after nerve lesion with subsequent fiber regeneration. Excitation of unmyelinated afferent fibers by electrical stimulation of sympathetic fibers following nerve injury. Unmyelinated primary afferents were recorded in cats 11–20 months following a nerve lesion. The central cut stump of a cutaneous nerve innervating hairy skin (sural or superficial peroneal nerve) had been imperfectly adapted to the distal stump of a transected mixed nerve (tibial nerve). This preparation was designed to mimic the consequences of lesion of a mixed nerve. A neuroma-in-continuity at the lesion site was present and cutaneous nerve fibers had regenerated into skin and deep somatic tissue supplied by the mixed nerve. (a) Experimental setup. post, postganglionic; pre, preganglionic; LST, lumbar sympathetic trunk. (b) The afferent fibers were identified as unmyelinated by electrical stimulation of the neuroma with single impulses. The signal indicated by the dot was recorded from the same afferent fiber as in (c) and (d); the afferent fiber conducted at 1.3 m s^{-1}. (c) Record from a single unmyelinated afferent unit. Supramaximal stimulation of the LST with trains of 30 pulses at 1–5 Hz (trains and stimulation artifacts indicated by bars). Note that the afferent unit had some low rate of ongoing activity (impulses before the trains at 1 and 4 Hz) and a second fiber was activated at 5 Hz stimulation (marked by an asterisk). (d) Adrenaline (5 µg injected i.v.) activated the fiber. Angiotensin (0.2 µg injected i.v.) generated a large increase of blood pressure (MAP, mean arterial blood pressure) but did not activate the afferent fiber. (e) Stimulus response curves for the single unit (□) and four filaments containing two to three (●, ▲/▼) or more than five (■) afferent units. Ordinate scale is the total number of impulses exceeding ongoing activity in response to variable stimulation frequency of the LST. Modified from Häbler H. J. *et al.* (1987).

DRG is more prominent, most spontaneously active A-fiber neurons are inhibited during stimulation of the sympathetic supply but rarely excited. (2) Only very few afferent neurons with unmyelinated axons respond to electrical stimulation of the sympathetic trunk; most of them are inhibited in their activity (McLachlan, E. M. *et al.*, 1993; Devor, M. *et al.*, 1994; Michaelis, M. *et al.*, 1996). (3) The coupling from sympathetic postganglionic fibers to the afferent cell bodies in the DRG probably occurs only to spontaneously active muscle afferent neurons with Aδ-fibers (Michaelis, M. *et al.*, 2000). (4) Activation of the afferent neurons, via the DRG, requires high-frequency stimulation of the sympathetic neurons at 5 to 20 Hz. Sympathetic pre- and postganglionic neurons rarely discharge at these frequencies under physiological conditions. (5) Mechanical allodynic and hyperalgesic behavior shown by rats with L5 spinal nerve injury (transection and ligation) is not dependent on the innervation of the DRG by sympathetic neurons (Ringkamp, M. *et al.*, 1999; see point 4 in Table 2). The rate of ectopic activity originating in

the DRG, 15 to 45 days after spinal nerve injury, is not maintained by activity in sympathetic neurons (Liu, X. *et al*., 2000). (6) Afferent neurons in the DRG may be activated indirectly by ischemia generated by decrease of blood flow during vasoconstriction in the DRG following electrical stimulation of the sympathetic trunk and not directly via adrenoceptors expressed in the DRG cells (Häbler, H.-J. *et al*., 2000). (7) Axotomized medium- to large-diameter DRG neurons express α_{2A}-adrenoceptors after sciatic nerve injury (Birder, L. A. and Perl, E. R., 1999). However, these upregulated adreceptors disappear after several weeks as perineural catecholaminergic sprouting develops and only small depolarizations can be generated by high concentrations of noradrenaline in axotomized DRG somata (Lopez de Armentia, M. *et al*., 2003).

The mechanism leading to the collateral sprouting of postganglionic noradrenergic fibers in the DRG is possibly related to neurotrophic signals and their receptors generated by afferent cells with lesioned axons in the DRG and the surrounding satellite glia cells (Chapter Sprouting in Dorsal Root Ganglia). Whether these aberrant pathological connections can account for spontaneous pain and allodynia in some patients after peripheral nerve lesions is doubtful and awaits further investigations (Jänig, W. *et al*., 1996).

5.17.3.3.4 Adrenoceptors involved in chemical sympathetic afferent coupling following nerve lesion

Excitation or depression of lesioned primary afferent neurons (in the DRG, in their lesioned terminals in the neuroma or in their regenerating sprouts), or of unlesioned collaterally sprouting primary afferents generated by activation of the sympathetic innervation, is mimicked by systemic injection of noradrenaline or adrenaline and prevented by blockade of α-adrenoceptors (e.g., phentolamine). Thus, both excitation and depression are suggested to be mediated by α-adrenoceptors. The cellular mechanisms underlying the increased sensitivity are unknown. Novel expression or upregulation of adrenoceptors occurs; alternatively, normally present adrenoreceptors that are not functional become uncovered and effective during the response to damage. The subtype of α-adrenoreceptor being involved in the sympathetic–afferent coupling in the different rat models is predominantly α_2 (Chen, Y. *et al*., 1996). Knowledge about the subtypes of adrenoceptor following nerve trauma may turn out to be useful in the design of more specific treatment modalities for neuropathic pain conditions involving sympathetic efferent activity (Jänig, W. *et al*., 1996; Jänig, W. and Häbler, H. J., 2000b).

5.17.3.3.5 Synopsis

Peripheral trauma with nerve injury may lead to sensitization and activation of nociceptive and activation of other primary afferent neurons. These processes may depend on and are maintained by the sympathetic nervous system. Several ways of coupling between sympathetic postganglionic neurons and primary afferent neurons are possible and have been worked out experimentally on animal models with controlled nerve lesions, showing that there may develop intimate relationships between sympathetic and afferent neurons under pathophysiological conditions (Figure 9):

1. The sympathetic postganglionic neuron may develop chemically mediated cross talk to primary afferent neurons. Whether this occurs probably depends on the time after nerve lesion as well as on the type of nerve lesion (partial or complete).
2. Following peripheral nerve lesion, remote collateral sprouting of unlesioned postganglionic fibers occurs in the DRG, preferentially toward the large-diameter sensory cells. Collateral sprouting of unlesioned postganglionic fibers may also occur in the peripheral target tissue (in particular after partial nerve lesion).
3. The transmission from sympathetic neurons to afferent neurons is mediated by noradrenaline, but additional mediator substances cannot be excluded.
4. Primary afferent neurons express functional adrenoceptors. The type of adrenoceptor involved is preferentially α_2 in animal models.
5. The signals that initiate the sprouting and the functional expression of adrenoceptors in the afferent neurons may be related to neurotrophic substances that derive from the Schwann cells or other cells. Their upregulation is related to the plastic changes of the primary afferent and sympathetic postganglionic neurons and possibly to decrease of the density of the noradrenergic innervation and/or to activity in the afferent and sympathetic neurons (see Chapter Sprouting in Dorsal Root Ganglia).

These plastic changes of primary afferent and sympathetic postganglionic neurons following peripheral trauma with nerve lesion may explain some of the

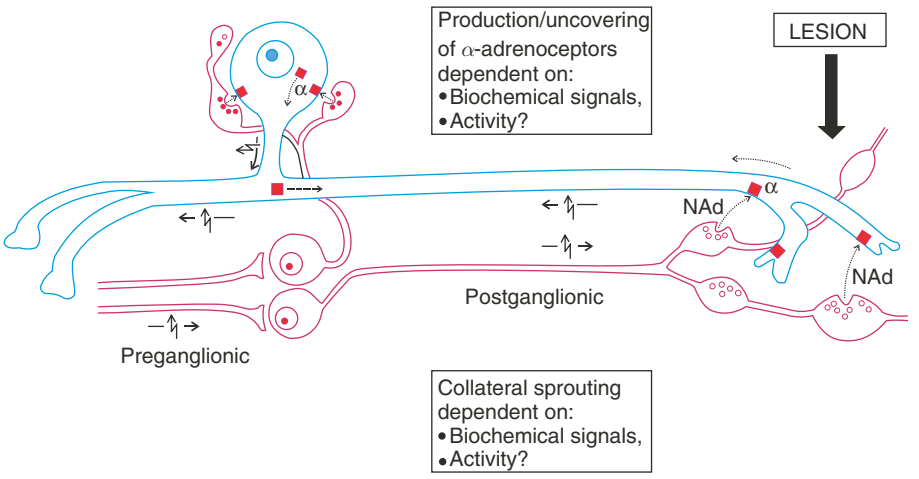

Figure 9 Relation between afferent and sympathetic neurons following peripheral nerve lesion. Collateral sprouting of unlesioned sympathetic neurons in the dorsal root ganglion (DRG) and in the peripheral target tissue. Upregulation or uncovering of functional adrenoceptors (α) by afferent neurons after nerve lesion. It is unclear in which way these processes are related to the biochemical signals (e.g., neurotrophins) synthesized by neurons, Schwann cells, and other cells in the DRG and the expression of their receptors. In which way are these processes dependent on activity in the afferent neurons, on the presence/absence of postganglionic noradrenergic neurons, or on the activity in the postganglionic neurons? NAd, noradrenaline. Modified from Jänig W. *et al.* (1996).

clinical sensory phenomena in patients with SMP, e.g., in CRPS type II. However, they do not explain (1) the slow development of spontaneous pain and allodynia after noradrenaline is injected into the skin that was painful before sympathetic block or before sympathectomy (Torebjörk, H. E. *et al.*, 1995) (Figure 4); (2) the long-lasting pain relief in patients with SMP after sympathetic blocks Figure 15 and (3) the mechanism of SMP in patients without nerve lesion, e.g., in patients with CRPS type I.

5.17.3.4 Indirect Involvement of the Sympathetic Nervous System in the Generation of Pain

Nociceptive afferents are embedded in a complex micromilieu (Figure 10). The state of this micromilieu surrounding the receptive terminals depends on mediator substances that are released during inflammatory processes following trauma from non-neural cells such as mast cells, polymorphonuclear leucocytes, macrophages, fibroblasts, endothelial cells, or other cells. The microcirculation is under neural control of sympathetic vasoconstrictor neurons. Moreover, activation of subgroups of nociceptive primary afferents causes not only orthodromic impulse traffic but also arteriolar (precapillary) vasodilation and (in most tissues, but not in human skin) venular plasma extravasation by release of neuropeptides from the receptive terminals (e.g., substance P (SP) and calcitonin-gene-related peptide (CGRP)). Both afferent-induced changes are called neurogenic inflammation (McDonald, D. M., 1997; Holzer, P., 1998). Thus, there are possibilities for indirect coupling between sympathetic and afferent nerve terminals (Figure 10): (1) Vascular perfusion of the micromilieu surrounding the nociceptors after nerve trauma may change as consequences of denervation and reinnervation by postganglionic vasoconstrictor neurons and afferent nociceptive neurons and hyper-reactivity of blood vessels to nerve impulses and circulating catecholamines may develop (Jobling, P. *et al.*, 1992; Koltzenburg, M. *et al.*, 1995). (2) Nociceptors may be sensitized by inflammatory mediators such as prostaglandins and interleukins, the release of which from nonneuronal cells of the micromilieu may be mediated by noradrenergic nerve terminals.

5.17.3.4.1 Changes of neurovascular transmission and development of hyperreactivity of blood vessels

Neural control of blood vessels can change dramatically after trauma with nerve lesion, but possibly also after trauma without (Koltzenburg, M. *et al.*, 1995):

1. Cutaneous blood vessels that are reinnervated after a nerve lesion exhibit stronger than normal

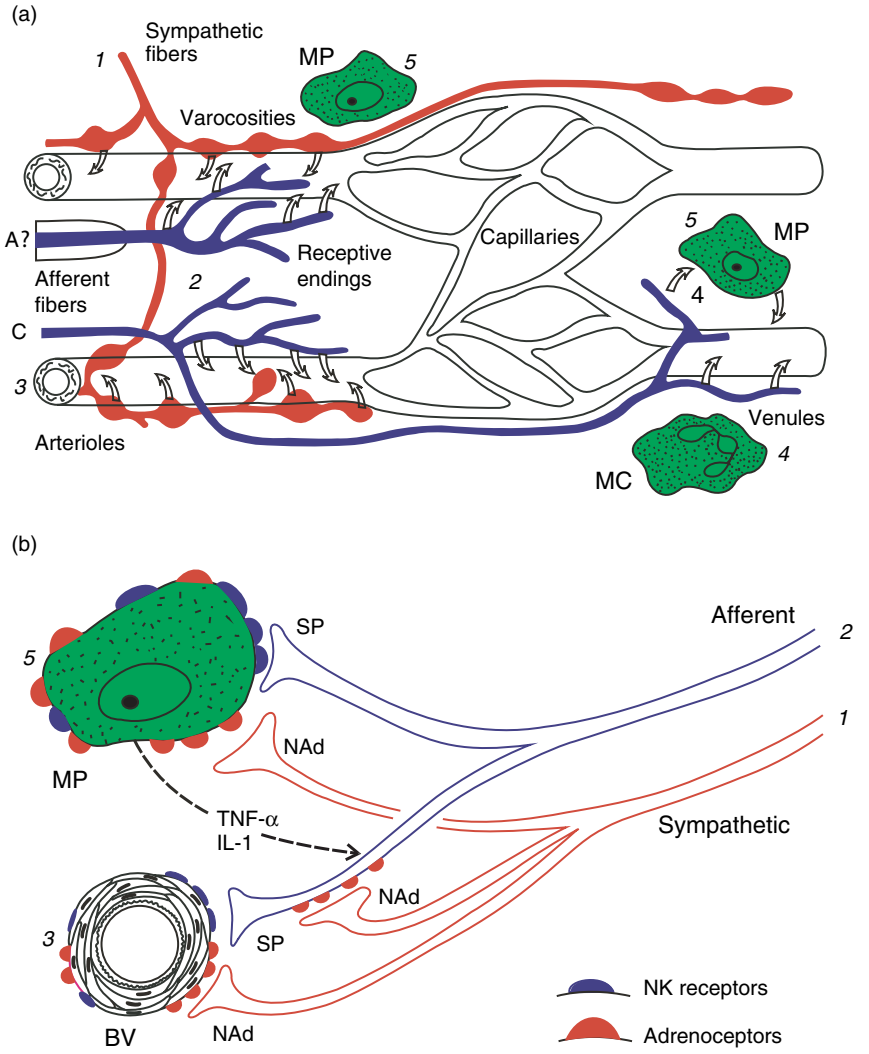

Figure 10 (a) The micromilieu of nociceptors. The microenvironment of primary afferents is thought to affect the properties of the receptive endings of myelinated (Aδ) and unmyelinated (C) afferent fibers. This has been particularly documented for inflammatory processes, but one may speculate that pathological changes in the direct surroundings of primary afferents may contribute to other pain states as well. The vascular bed consists of arterioles (directly innervated by sympathetic and afferent (Aδ, C) fibers), capillaries (not innervated and not influenced by nerve fibers), and venules (not directly innervated but influenced by nerve fibers). The micromilieu depends on several interacting components: Neural activity in postganglionic noradrenergic fibers (*1*) supplying blood vessels (*3*, BV) causes release of noradrenaline (NAd) and possibly other substances causing vasoconstriction. Excitation of primary afferents (Aδ- and C-fibers) (*2*) causes vasodilation in precapillary arterioles and plasma extravasation in postcapillary venules (C-fibers only) by the release of SP and other vasoactive compounds (e.g., calcitonin gene-related peptide, CGRP). Some of these effects may be mediated by nonneuronal cells such as mast cells (MC, *4*) and macrophages (MP, *5*). Other factors that affect the control of the microcirculation are the myogenic properties of arterioles (*3*) and more global environmental influences such as a change of the temperature and the metabolic state of the tissue (modified from Jänig, W. and Koltzenburg, M., 1991). (b) Hypothetical relation between sympathetic noradrenergic nerve fibers (*1*), peptidergic afferent nerve fibers (*2*), blood vessels (*3*, BV), and macrophages (*4*, MP). The activated and sensitized afferent nerve fibers activate macrophages (via SP release). The immune cells start to release cytokines, such as tumor necrosis factor α (TNF-α) and interleukin 1 (IL-1), which further activate afferent fibers by enhancing sodium influx into the cells. SP (and CGRP) released from the afferent nerve fibers reacts with neurokinin 1 (NK1) receptors (CGRP receptors) in the blood vessels (arteriolar vasodilation, venular plasma extravasation; neurogenic inflammation). The sympathetic nerve fibers interact with this system potentially on three levels: (1) via adrenoceptors (mainly α) on the blood vessels (vasoconstriction), (2) via adrenoceptors (mainly β) on macrophages (further release of cytokines), and (3) via adrenoceptors (mainly α) on afferents (further sensitization of these fibers). Modified from Jänig W. and Baron R. (2003).

vasoconstriction to impulses in sympathetic neurons.

2. The sympathetically reinnervated cutaneous blood vessels show stronger than normal vasoconstrictions to systemic catecholamines and appear to be hyper-reactive.
3. Blood vessels exhibit changes in vasodilation to antidromic activation of reinnervated peptidergic unmyelinated afferents.

The reinnervated blood vessels may therefore be under stronger than normal vasoconstrictor influence that can no longer be counteracted by an afferent-mediated vasodilation (see Häbler, H. J., *et al.*, 1997). *In vitro* investigation of the rat tail artery has shown that the functional recovery of neurovascular transmission is permanently disturbed after a nerve lesion (Jobling, P. *et al.*, 1992).

The altered neural and nonneural control of blood vessels, following trauma with nerve lesion, can contribute to the abnormal regulation of blood flow through skin and deep somatic tissues and possibly to the trophic changes (including the edema) that are seen in patients with CRPS. They may furthermore be a permissive factor in the generation of afferent nociceptive impulse activity and therefore in the sensitization of nociceptors and in the generation of pain.

Finally, it is commonly believed that skin temperature changes observed in painful disorders following trauma with or without nerve lesion (e.g., in CRPS I or II) reflect changes of activity in cutaneous vasoconstrictor neurons, in the sense that cold skin is associated with a high level and warm skin with a low level of activity in these neurons. This is probably a misconception, and there is no proof for this relation between skin temperature and activity in sympathetic neurons under these pathophysiological conditions.

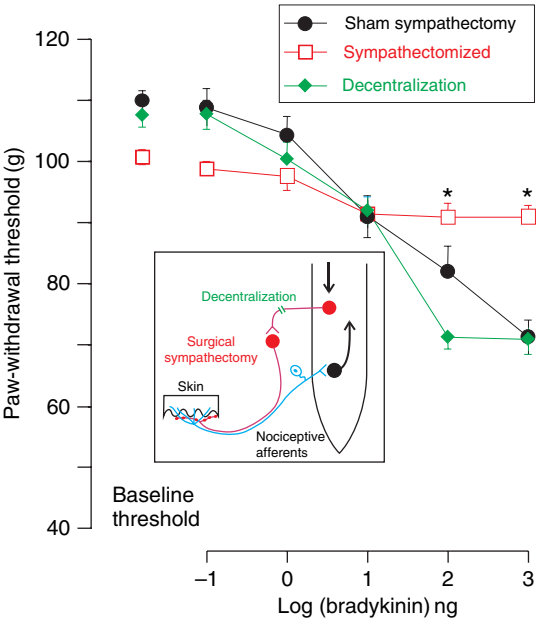

Figure 11 Mechanical hyperalgesic behavior and sympathetic innervation. Cutaneous nociceptors on the dorsum of the paw are stimulated by a linearly increasing mechanical force. Paw-withdrawal threshold (PWT) is defined as the mean (±SEM) minimum force (in grams, ordinate scale) at which the rat withdraws its paw. Abscissa scale: log dose of bradykinin (BK, in nanograms) injected in a volume of 2.5 µl of saline into the dermis of the skin. Decrease of PWT to mechanical stimulation induced by intradermal injection of BK in sham-sympathectomized (control) rats (●, 6 hindpaws), in surgically sympathectomized rats (lumbar paravertebral ganglia L2 – L4 removed 8 days before; □, 12 hindpaws), and in rats with decentralized lumbar sympathetic chains (white rami with preganglionic axons to paravertebral ganglia L2 and L3 and chain rostral to ganglion L2 transected 8 days before; ◆, 10 paws). Abscissa scale: log dose of BK (in nanograms). Sham sympathectomy and sympathetic decentralization were both significantly different from sympathectomy groups at doses of BK of 10^2 and 10^3 ng (*, $P < 0.01$). Modified from Khasar S. G. *et al.* (1998a).

5.17.3.4.2 Sensitization of nociceptors mediated by sympathetic terminals independent of excitation and release of noradrenaline

Withdrawal threshold to stimulation of the rat hindpaw with a linearly increasing mechanical stimulus applied to the dorsum of the paw decreases dose-dependently after intradermal injection of the inflammatory mediator bradykinin (an octapeptide cleaved from plasma α_2-globulins, by kallikreins circulating in the plasma) (Figure 11). Following a single injection of bradykinin, this decrease lasts for more than 1 h for mechanical stimulation. This type of mechanical hyperalgesic behavior is mediated by the B_2 bradykinin-receptor and is not present when bradykinin is injected subcutaneously (Khasar, S. G. *et al.*, 1993; 1995; Jänig, W. and Häbler, H. J., 2000b). In normal rat, bradykinin-induced hyperalgesic behavior is blocked by the cyclooxygenase inhibitor indomethacin and therefore mediated by a prostaglandin (probably PGE_2) that sensitizes nociceptors for mechanical stimulation. However, in vagotomized rats in which the bradykinin-induced

mechanical hyperalgesia is significantly enhanced (by activation of the adrenal medulla, see below and Figure 13a), indomethacin has almost no effect on bradykinin-induced hyperalgesia. This failure is not related to a switch from B2- to B1-receptor subtype because the selective B1-receptor agonist des-Arg9-bradykinin fails to produce hyperalgesia in vagotomized rats (Khasar, S. G. *et al.*, 1998a). The same applies to rats that were sound-stressed for 4 days (Khasar, S. G. *et al.*, 2005). Thus, bradykinin-induced hyperalgesia may not be mediated by prostanoids in vagotomized or sound-stressed rats. Furthermore, convincing sensitization to mechanical stimulation by bradykinin has only been demonstrated for afferent fibers innervating the cat knee joint (Neugebauer, V. *et al.*, 1989) or the cat skeletal muscle (Mense, S. and Meyer, H., 1988). Manning D. C. *et al.* (1991) demonstrated in humans that intradermal injection of bradykinin (100 ng to 10 µg) generates hyperalgesia to heat stimulation but not to mechanical stimulation.

The decrease in paw-withdrawal threshold to mechanical stimulation generated by intradermal injection of bradykinin is significantly reduced after surgical sympathectomy. Decentralization of the lumbar paravertebral sympathetic ganglia (denervating the postganglionic neurons by cutting the preganglionic sympathetic axons) does not abolish the bradykinin-induced mechanical hyperalgesic behavior (Figure 11). This indicates that the sensitizing effect of bradykinin is not dependent on activity in the sympathetic neurons innervating skin and therefore not on release of noradrenaline (Khasar, S. G. *et al.*, 1998a) and that bradykinin stimulates the release of prostaglandin from the sympathetic terminals or from other cells in association with the sympathetic terminals in the skin (Figure 6b).

Mechanical hyperalgesic behavior generated by intracutaneous injection of bradykinin and its dependence on the sympathetic innervation of the skin is an interesting phenomenon. However, that mechanical hyperalgesia is due to prostanoids sensitizing nociceptors since indomethacin prevents it appears to be too simple. The reasons are (1) the finding that sympathetic fibers mediate this hyperalgesia independent of neural activity and release of noradrenaline; (2) indomethacin does not block this behavior under certain conditions (e.g., when the adrenal medullae are activated after vagotomy (see below) or after sound stress); (3) sensitization of nociceptive afferents innervating deep somatic tissues by bradykinin to mechanical stimulation has been demonstrated in neurophysiological experiments in the cat, not yet in humans for cutaneous pain (Manning, D. C. *et al.*, 1991); (4) in skin there is a spatial dissociation between afferent nociceptive fibers and sympathetic fibers, many of the former ending in the epidermis and subepidermal plexus, whereas most of the latter terminate in deeper dermal layer, raising the question as to the nature of the interaction between both groups of fibers.

These points argue that the dependence of bradykinin-induced cutaneous mechanical behavior on the sympathetic innervation has to be reinvestigated using a rigorous experimental approach. Neurophysiological experiments are required to demonstrate that sensitization of nociceptors by bradykinin is dependent on the presence of sympathetic terminals.

5.17.3.4.3 Sensitization of nociceptors initiated by nerve growth factor or cytokines possibly mediated by sympathetic terminals

5.17.3.4.3.(i) Nerve growth factor Systemic injection of nerve growth factor (NGF) is followed by a transient thermal and mechanical hyperalgesia in rats (Lewin, G. R. *et al.*, 1993; 1994) and humans (Petty, B. G. *et al.*, 1994). During experimental inflammation (evoked by Freund's adjuvant in the rat hindpaw), NGF increases in the inflamed tissue paralleled by the development of thermal and mechanical hyperalgesia. Both are prevented by anti-NGF antibodies (Lewin, G. R. *et al.*, 1994). The mechanisms responsible are sensitization of nociceptors via high-affinity NGF-receptors (trkA receptors) and an increased synthesis of CGRP and SP in the afferent cell bodies induced by NGF taken up by the afferent terminals and transported to the cell bodies. The NGF-induced sensitization of nociceptors or part of it seems to be mediated indirectly by the sympathetic postganglionic terminals. In rats, heat and mechanical hyperalgesic behavior generated by local injection of NGF into the skin is prevented or significantly reduced after chemical or surgical sympathectomy (Woolf, C. J. *et al.*, 1996). These experiments suggest that the NGF released during inflammation by inflammatory cells acts on the sympathetic terminals via high-affinity trkA receptors, inducing the release of inflammatory mediators (the source of which is unknown) and subsequently sensitization of nociceptors for mechanical and heat stimuli (Figure 6c; McMahon, S. B., 1996; Woolf, C. J., 1996; Jänig, W. and Häbler, H. J., 2000b). It is unclear whether this sensitization of nociceptors mediated by terminal sympathetic nerve fibers (1) is dependent on activity

in the sympathetic neurons and release of noradrenaline and on adrenoceptors expressed in the nociceptive afferent neurons or (2) is independent of neural activity and release of noradrenaline.

5.17.3.4.3.(ii) Proinflammatory cytokines Based on behavioral experiments conducted on rats (studying mechanical and heat hyperalgesia), it has been shown that tissue injury, injection of the bacterial cell wall endotoxin lipopolysaccharide, or injection of carrageenan (a plant polysaccharide) stimulates tissue inflammation and leads to sensitization of nociceptors. Systematic pharmacological interventions using blockers or inhibitors of the various mediators demonstrate that the proinflammatory cytokines, tumor necrosis factor α (TNF-α), interleukin-1 (IL-1), IL-6, and IL-8 may be involved in this process of nociceptor sensitization and therefore in the generation of hyperalgesia (Woolf, C. J. *et al.*, 1996; 1997; Poole, S. *et al.*, 1999). Pathogenic stimuli lead to activation of resident cells and release of the inflammatory mediator bradykinin and other mediators. The inflammatory mediators and the pathogenic stimuli themselves activate macrophages, monocytes, and other immune-related cells that release TNF-alpha. Nociceptors are believed to be sensitized by two possible pathways (Figure 12): (1) TNF-α induces production of IL-6 and IL-1β by immune cells, whereby IL-6 enhances the production of IL-1β. These interleukins stimulate cyclooxygenase 2 (COX 2) and the production of prostaglandins (PGE_2, PGI_2) that in turn react with the nociceptive terminal via E-type prostaglandin receptors. (2) TNF-α induces the release of IL-8 from endothelial cells and macrophages. IL-8 reacts with the sympathetic terminals that are supposed to mediate sensitization of nociceptive afferent terminals by release of noradrenaline to act via β_2-adrenoceptors. These two peripheral pathways by which nociceptive afferents are hypothesized to be sensitized involving cytokines are under inhibitory control of circulating glucocorticoids (indicated by asterisks in Figure 12) and of other, anti-inflammatory, interleukins (e.g., IL-4 and IL-10 indicated by # in Figure 12).

It is important to emphasize that the mechanisms of sensitization of nociceptive afferents, involving NGF, proinflammatory cytokines, and noradrenergic sympathetic postganglionic fibers, have been deduced on the basis of behavioral and pharmacological experiments. Proof of such interaction by directly assessing the activity of nociceptors with electrophysiological techniques and of the effect of noradrenergic nerve fibers on the afferent nerve fibers are lacking. These experiments have to be done.

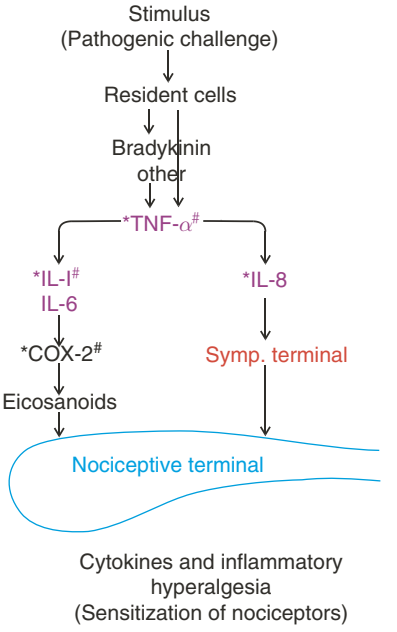

Figure 12 Hypothetical role of cytokines in sensitization of nociceptors during inflammation and the underlying putative peripheral mechanisms leading to hyperalgesia. Pathogenic stimuli activate resident cells and lead to release of inflammatory mediators (such as bradykinin). Proinflammatory cytokines are synthesized and released by macrophages and other immune or immune-related cells. Nociceptors are postulated to be sensitized by two pathways involving the cytokines: (1) Tumor necrosis factor α (TNF-α) induces synthesis and release of interleukin 1 (IL-1) and IL-6 which, in turn, induce the release of eicosanoids (prostaglandin E_2 and I_2 (PGE_2, PGI_2)) by activating cyclooxygenase-2 (COX-2). (2) TNF-α induces synthesis and release of IL-8. IL-8 activates sympathetic terminals that sensitize nociceptors via β_2-adrenoceptors. Glucocorticoids inhibit the synthesis of the cytokines and the activation of COX-2 (indicated by asterisks). Anti-inflammatory cytokines (such as IL-4 and IL-10) that are also synthesized and released by immune cells inhibit the synthesis and release of proinflammatory cytokines (indicated by #). This scheme is fully dependent on behavioral experiments and pharmacological interventions. The different steps will need to be verified experimentally using neurophysiological experiments. Modified from Poole S. *et al.* (1999).

5.17.3.4.4 Sympatho-adrenal system and nociceptor sensitization

Activity of the sympatho-adrenal system (adrenal medulla) is regulated by central circuits that are different from those regulating other sympathetic systems (Morrison, S. F. and Cao, W. H., 2000;

Morrison, S. F., 2001; Jänig, W., 2006). Activation of this system (e.g., by release of the central sympathetic circuits, connected to preganglionic neurons that innervate the adrenal medulla, from vagal inhibition by subdiaphragmatic vagotomy (Figure 13c; Khasar, S. G. *et al.*, 1998a; 1998b), but not of the sympatho-neural system, generates mechanical hyperalgesia and enhances bradykinin-induced mechanical hyperalgesia (decrease of paw-withdrawal threshold to mechanical stimulation of the skin, compare closed circles with open triangles in Figure 13a). Both develop slowly over 7 to 14 days during continuous activation of the adrenal medullae (e.g., induced by subdiaphragmatic vagotomy) and are maintained over 5 weeks tested (open triangles in Figure 13b). In rats with denervated adrenal medullae (adrenal nerves with preganglionic axons innervating the cells of the adrenal medulla sectioned (Figure 13c)), subdiaphragmatic

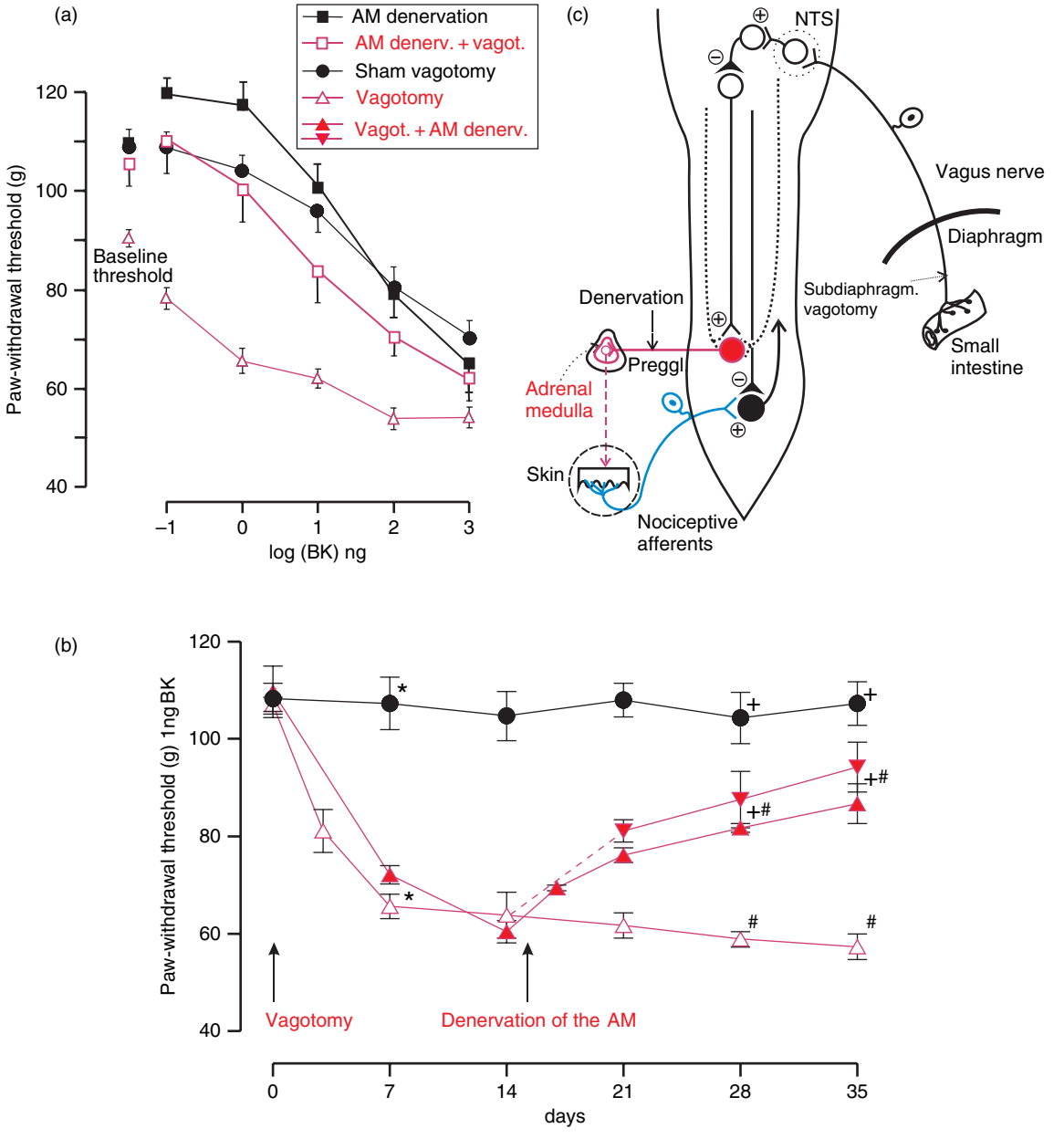

vagotomy has only a small effect (compare open squares with closed squares in Figure 13a). This decrease of paw-withdrawal threshold can be explained by removal of inhibition of nociceptive impulse transmission in the spinal dorsal horn (Figure 13c; see Randich, A. and Gebhart, G. F., 1992; see Chapter Descending Control Mechanisms). Denervation of the adrenal medullae, 14 days after vagotomy when the decrease of paw-withdrawal threshold is maximal, is followed by a slow increase of paw-withdrawal threshold taking more than 3 weeks (compare closed triangles with open triangles in Figure 13b). Thus, the decrease of paw-withdrawal threshold following vagotomy is reversed after denervation of the adrenal medullae. Application of adrenaline through a minipump for 3 to 14 days slowly enhances the development of mechanical hyperalgesia induced by bradykinin injected intradermally. Furthermore, continuous application of a β_2-adrenoceptor blocker over 7–14 days by way of a minipump prevents the enhancement of this hyperalgesic behavior generated by activation of the adrenal medullae (Khasar, S. G. *et al.*, 2003).

The results of this experiment are interpreted in the following way: Adrenaline released by persistent activation of the adrenal medullae sensitizes cutaneous nociceptors for mechanical stimuli. This sensitization of nociceptors and its reversal are slow and take days to develop. The slow time course implies that the nociceptor sensitization cannot be acutely blocked by an adrenoceptor antagonist given intracutaneously or systemically. Adrenaline probably does not act directly on the cutaneous nociceptors but on cells in the microenvironment of the nociceptors inducing slow changes, which result in nociceptor sensitization. Candidate cells may be mast cells, macrophages, or keratinocytes, which then release substances that generate sensitization (Khasar, S. G. *et al.*, 1998b; Jänig, W. *et al.*, 2000; Jänig, W. and Häbler, H. J., 2000b). The change of sensitivity of a population of nociceptors generated by adrenaline released by the adrenal medullae that is regulated by the brain would be a novel mechanism of sensitization. This novel mechanism would be different from mechanisms that lead to activation and/or sensitization of nociceptors by sympathetic afferent coupling as discussed above (Figure 6d).

This peripheral mechanism of pain and hyperalgesia involving adrenaline released by the sympatho-adrenal system and acting on nociceptors may operate in ill-defined pain syndromes such as irritable bowel syndrome, functional dyspepsia, fibromyalgia, and chronic fatigue syndrome (Wolfe, F. *et al.*, 1990; Mayer, E. A. *et al.*, 1995; Clauw, D. J. and Chrousos, G. P., 1997). The conclusions about long-term sensitization of nociceptors for mechanical stimulation by adrenaline fully rest on behavioral experiments. Neurophysiological experiments *in vivo* on primary afferent nociceptive neurons are required to test directly whether all or only a subpopulation of nociceptors are sensitized.

Figure 13 Long-term enhancement of bradykinin (BK)-induced mechanical hyperalgesia after vagotomy and its disappearance after denervation of the adrenal medullae (AM). (a) Decrease of paw withdrawal threshold (PWT) to mechanical stimulation of the dorsum of the rat hindpaw induced by BK injected intradermally (BK-induced behavioral mechanical hyperalgesia), in sham-vagotomized rats (●, $n = 18$), in vagotomized rats (△, $n = 16$; 7 days after subdiaphragmatic vagotomy), in rats with denervated adrenal medullae (■, $n = 6$), and in vagotomized rats with denervated AM (□, $n = 6$). For details see legend of Figure 11. (b) Total change of PWT (baseline plus BK-induced) in response to intradermal injection of 1 ng BK in rats before and 7 to 35 days after vagotomy (△, $n = 6$), before and 7 to 35 days after sham vagotomy (●, $n = 8$) and in rats whose AM are denervated 14 days after vagotomy and measurements taken up to 35 days after initial surgery (▲, rats tested after vagotomy and denervation of the AM ($n = 6$); ▼, rats only tested after additional denervation of the AM ($n = 4$)). Note that 1ng BK injected intradermally does not significantly change the PWT in rats with intact vagus nerves (see (a)). $^{*}P < 0.01$, ▲/△ versus ● on day 7; $^{+}P > 0.05$ ▲/▼ versus ● on days 28 and 35; $^{\#}P < 0.01$, ▲/▼ versus △ on days 28 and 35. (c) Schematic diagram showing the proposed neural circuits in spinal cord and brainstem which modulate nociceptor sensitivity via the sympatho-adrenal system. Sensitivity of cutaneous nociceptors for mechanical stimulation is modulated by adrenaline released by the AM. Activation of the AM increases the sensitivity of the nociceptors. Activity in preganglionic neurons innervating the AM depends on activity in vagal afferents from the small intestine that has an inhibitory influence on the central pathways to these preganglionic (preggl) neurons. Thus, interruption of the vagal afferents leads to activation of the AM. It is hypothesized that these neuronal (reflex) circuits in the brainstem are under the control of upper brainstem, hypothalamus, and telencephalon. Dotted thin lines: Axons of sympathetic premotor neurons in the brainstem that project through the dorsolateral funiculi of the spinal cord to the preganglionic neurons of the AM. ⊕, excitation; ⊖, inhibition. Modified from Khasar S. G. *et al.* (1998b).

5.17.4 Sympathetic Nervous System and Central Integrative Mechanisms in the Control of Hyperalgesia and Inflammation

The brain is suggested to modulate inflammation via the sympatho-neural and/or the sympatho-adrenal system although the mechanisms underlying these influences are little understood. Any influence of this type will affect indirectly the sensitivity of nociceptors. Here I will briefly discuss the hypothetical role of both sympathetic systems: (1) in CRPS that is characterized by a peripheral inflammatory process (in addition to changes in the central nervous system) suggested to be dependent on the sympathetic nervous system; (2) in experimental inflammation (bradykinin-induced synovial plasma extravasation); and (3) in the potential modulation of the immune tissue.

5.17.4.1 The Complex Regional Pain Syndrome Type I as Model

CRPS are painful disorders that may develop as a consequence of trauma typically affecting the limbs. Clinically, they are characterized by pain (spontaneous, hyperalgesia, and allodynia), active and passive movement disorders including an increased physiological tremor, abnormal regulation of blood flow and sweating, edema of skin and subcutaneous tissues, and trophic changes of skin, appendages of skin, and subcutaneous tissues (Stanton-Hicks, M. *et al.*, 1995; Jänig, W. and Stanton-Hicks, M., 1996; Harden, R. N. *et al.*, 2001; Jänig, W. and Baron, R., 2002; 2003). CRPS type I (previously called reflex sympathetic dystrophy) usually develops after minor trauma with a small or no obvious nerve lesion at an extremity (e.g., bone fracture, sprains, bruises or skin lesions, and surgeries) and rarely also after remote trauma in the visceral domain or after a lesion of the central nervous system (e.g., stroke). An important feature of CRPS I is that the severity and combination of clinical symptoms are disproportionate to the severity and type of trauma with a tendency to spread in the affected distal limb. The symptoms are not confined to the innervation zone of an individual nerve. CRPS type II (previously called causalgia) develops after trauma with a mostly large nerve lesion (Stanton-Hicks, M. *et al.*, 1995; Jänig, W. and Stanton-Hicks, M., 1996; Harden, R. N. *et al.*, 2001).

On the basis of clinical observations and research on human patients and animals, the hypothesis has been put forward that CRPS (in particular type I) is a systemic disease involving the central and peripheral nervous system (Figure 14). Various traumas can trigger variable combinations of clinical phenomena in which the somatosensory system, the sympathetic nervous system, the somatomotor system, and peripheral (vascular and inflammatory) systems are involved (Harden, R. N. *et al.*, 2001; Jänig, W. and Baron, R., 2002; 2003). The central changes are reflected in changes of somatic sensations (increase of detection thresholds for mechanical, cold, warm, and heat stimuli), of motor performances, and of neural regulation of sympathetic effector systems (vasculature, sweat glands, inflammatory cells, etc.). Thus, it is hypothesized that the central representations of the sensory, motor, and sympathetic systems are changed. The peripheral changes consist of inflammation involving blood vessels, inflammatory cells, peptidergic afferent nerve fibers, and sympathetic afferent coupling (see above and Figures 6 and 10). The peripheral changes cannot be seen independently of the central ones; both interact with each other via afferent and efferent signals. Furthermore, the mechanisms that underlie CRPS cannot be reduced to one system or to one mechanism only (e.g., to sympathetic afferent coupling, to an adrenoceptor disease, to a peripheral inflammatory disease, and to a psychogenic disease) (Harden, R. N. *et al.*, 2001; Jänig, W. and Baron, R., 2002; 2003).

The centrally generated activity in sympathetic neurons may be involved in various ways in the pathogenesis of CRPS type I, the main argument being that the peripheral changes are reversed or aggravated after intervention at the peripheral sympathetic nervous system (sympathetic blocks, stimulation of the sympathetic innervation; Figure 14). Three points that are relevant in the present context of sympathetic nervous system, pain, and body protection need to be emphasized for CRPS type I with SMP:

- In a subgroup of CRPS I patients, pain or a component of pain is obviously dependent on activity in sympathetic neurons and related to activation or sensitization of nociceptors by noradrenaline released by the sympathetic fibers (SMP). The nociceptors have expressed adrenoceptors and/or the excitatory effect is generated indirectly, e.g., by way of changes in blood flow in deep somatic tissues of an extremity (Baron, R. *et al.*, 2002). Sympathetically

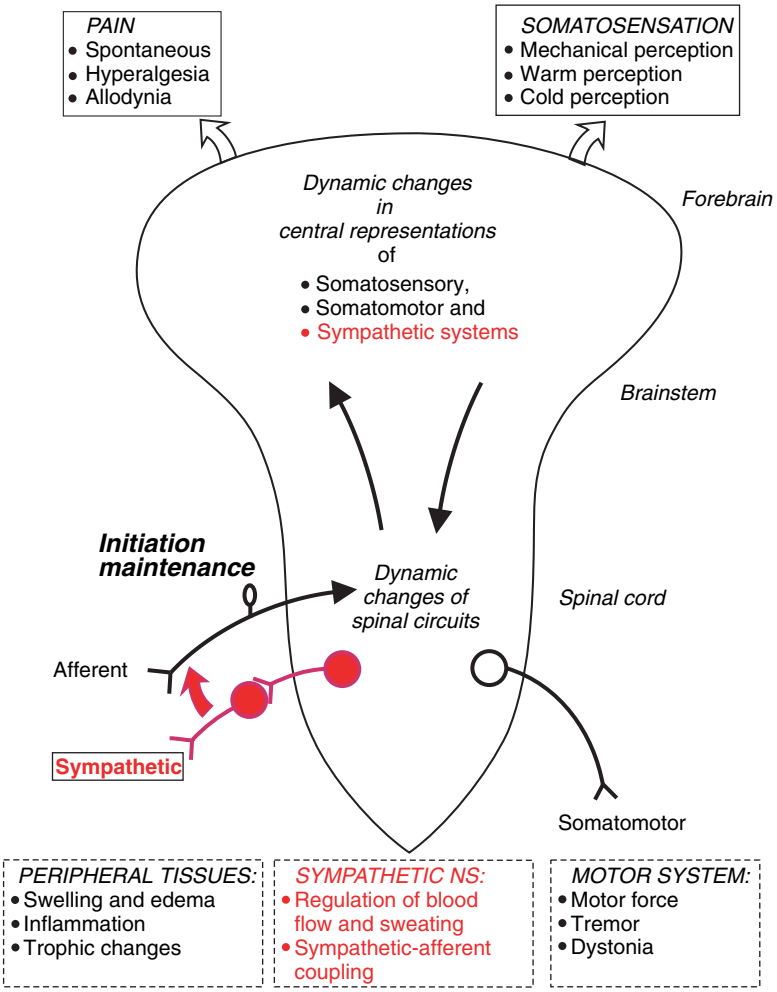

Figure 14 Schematic diagram summarizing the sensory, autonomic, and somatomotor changes in complex regional pain syndrome I (CRPS I) patients. The figure symbolizes the CNS (forebrain, brainstem, and spinal cord). Changes occur in the central representations of the somatosensory, the motor, and the sympathetic nervous system (which include the spinal circuits) and are reflected in the changes of the sensory painful and nonpainful perceptions, of cutaneous blood flow and sweating, and of motor performances. They are triggered and possibly maintained by the nociceptive afferent input from the somatic and visceral body domains. It is unclear whether these central changes are reversible in chronic CRPS I patients. These central changes affect the endogenous control system of nociceptive impulse transmission possibly too. Coupling between the sympathetic neurons and the afferent neurons in the periphery (see red arrow) is one component of the pain in CRPS I patients with sympathetically maintained pain (SMP). However, it seems to be unimportant in CRPS I patients without SMP. Modified from Jänig W. and Baron R. (2002; 2003).

maintained activity in nociceptive neurons may generate a state of central sensitization/hyperexcitability that is responsible for spontaneous pain and secondary evoked pain (mechanical and cold allodynia; see above and Figures 5 and 7).

- Swelling (edema) and inflammation may be generated by sympathetic and peptidergic afferent fibers interacting with each other at the arteriolar site (influencing blood flow) and venular site (influencing plasma extravasation) of the vascular bed. Sympathetic fibers are suggested to influence inflammatory cells (macrophages and mast cells) by way of noradrenaline and adrenoceptors on the inflammatory cells (Figure 10) (Jänig, W. and Baron, R., 2002; 2003).
- Trophic changes in skin, appendages of skin, and subcutaneous tissues (including joints and so forth) are believed to be dependent, at least in part, on the sympathetic innervation. The nature of this neural influence on the tissue structure is unknown (Jänig, W. and Stanton-Hicks, M., 1996; Harden, R. N. *et al.*, 2001; Jänig, W. and Baron, R., 2003).

These three groups of observation made on patients with CRPS I (who have no nerve lesion and therefore by definition not neuropathic pain) argue that the change of activity in sympathetic neurons entails peripheral changes which in turn may result in secondary activation and/or sensitization of primary afferent nociceptive neurons. The underlying mechanism(s) of this activation/sensitization of nociceptive afferent neurons may involve short- and long-term processes as discussed above

As already mentioned above, an important observation, in CRPS I patients with SMP (but possibly also in CRPS II patients with SMP), is that pain relief following conduction block of sympathetic neurons by a local anesthetic applied to the sympathetic chain mostly outlasts the conduction block by at least an order of magnitude (days) (Figure 15; Price, D. D. *et al.*, 1998). The long-lasting pain-relieving effect of sympathetic blocks suggests that activity in sympathetic neurons, which is of central origin, maintains a positive feedback circuit via the primary afferent neurons that are probably nociceptive in function. This positive feedback circuit maintains a central state of hyperexcitability (e.g., of neurons in the spinal dorsal horn; Figure 7), via excitation of afferent neurons started by an intense noxious event. The persistent afferent activity needed to maintain such a state of central hyperexcitability is switched off during temporary block of conduction in the sympathetic chain lasting only a few hours and cannot be immediately switched on again when the conduction block wears off and the activity in the sympathetic postganglionic neurons (and therefore probably also the sympathetically induced activity in afferent neurons) returns. It is hypothesized that the afferent activity has to act over a long time period to initiate and maintain the central state of hyperexcitability (via the positive feedback). The mechanism underlying this important and interesting phenomenon needs to be studied experimentally in patients with SMP as well as in animal models that have to be designed.

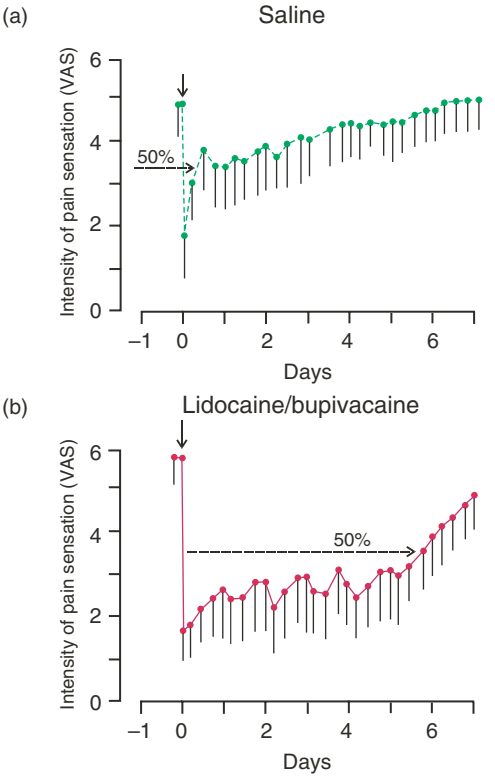

Figure 15 Effect of sympathetic blocks with a local anesthetic (lidocaine/bupivacaine) or of injection of saline close to the corresponding paravertebral sympathetic ganglia on pain in seven patients with CRPS I. Double-blind crossover study. Effect on pain following both interventions at the sympathetic supply was measured in the same group of CRPS I patients. Pain was systematically measured repeatedly using the visual analogue scale (VAS) on the day of the injection and on 7 days after the injection. Both interventions produced pain relief (see 50% value of pain relief). However, the mean relief of pain to injection of the local anesthetic lasted for 6 days and was significantly longer than the mean pain relief following local injection of saline that lasted for 6 h (placebo block). The initial maximal peaks of analgesia were statistically not different. Means + SEM. Modified from Price D. D. *et al.* (1998).

5.17.4.2 Sympathetic Nervous System and Acute Experimental Inflammation

Inflammation of body tissues is accompanied by sensitization of nociceptors leading to ongoing pain and hyperalgesia (Figure 7). The sensitization of nociceptors is generated by various signaling molecules released by the inflammatory cells including cells of the immune system (Figures 10 and 12; McMahon, S. B. *et al.*, 2006; Meyer, R. A. *et al.*, 2005). Inflammation is potentially controlled by the brain via the HPA system, the sympatho-neural system, and the sympatho-adrenal system (Figure 16c), resulting in an enhancement or inhibition of the inflammatory (protective) responses depending on the behavioral state of the organism. Any change in neural and neuroendocrine control of inflammation should indirectly affect the sensitization of nociceptors innervating the inflamed tissue and therefore ongoing pain and hyperalgesia. Although we know relatively little about the role of both sympathetic systems in the

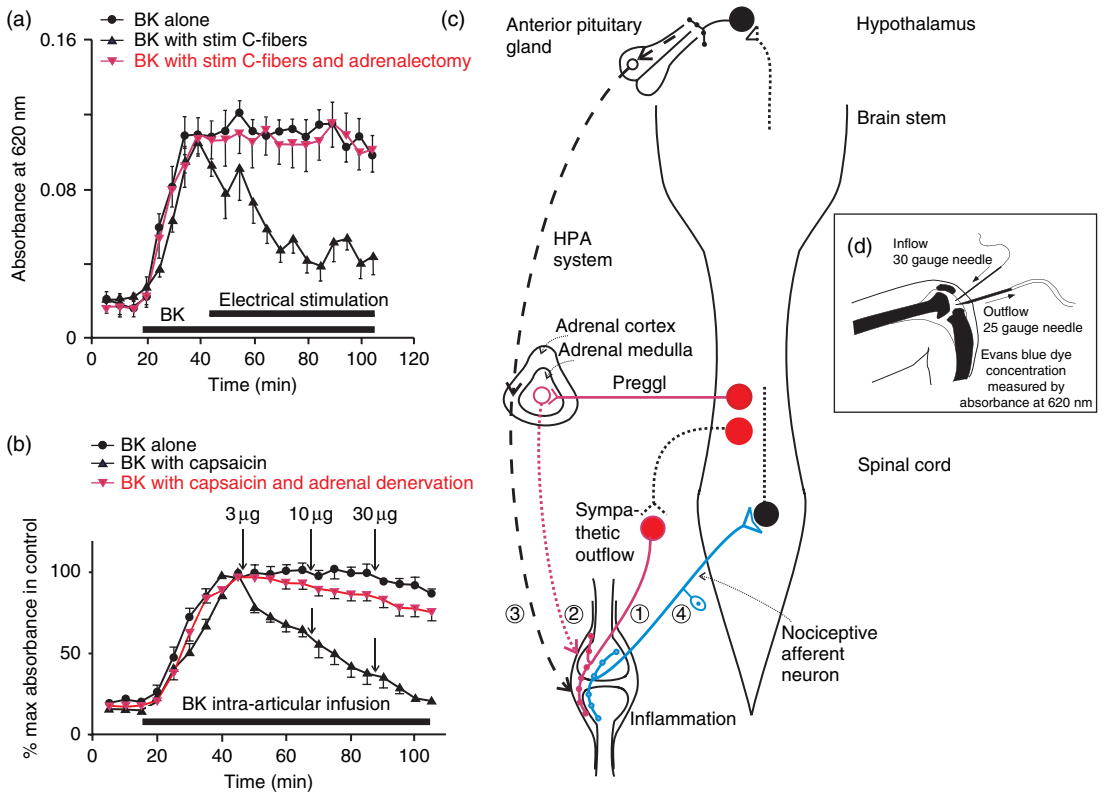

Figure 16 Experimental inflammation is controlled by the hypothalamo-pituitary system and the sympatho-adrenal system. Bradykinin (BK)-induced plasma extravasation (PE) was determined in the knee joint of anesthetized rats (d). Skin overlying the knee was excised to expose the joint capsule, and rats were then given an intravenous injection of Evans blue dye (50 mg kg $^{-1}$). The 30-gauge inflow and 25-gauge outflow needles were then inserted into the knee joint cavity for the inflow of perfusion fluid (0.9% saline at 250 µl min^{-1}). Perfusion fluid was collected over 5-min periods for up to 120 min and dye concentration determined spectrophotometrically at 620 nm. The absorbance at this wavelength is linearly related to the dye concentration and therefore to the degree of PE of the synovia (see ordinate scales in (a) and (b)). Following collection of the first three samples to establish baseline PE levels when the joint cavity is perfused with saline, BK (160 nM; and other substances) is (are) added to the perfusing fluid. This produces a rapid and sustained increase in the magnitude of PE (● in (a) ($n = 8$) and (b) ($n = 16$)). (a) Noxious transcutaneous electrical stimulation (25 mA, 3 Hz, 0.25 ms pulses) exciting C-fibers applied to the contralateral hindpaw after sample 8 produces a rapid decrease in the magnitude of PE (▲, $n = 7$). This inhibition produced by noxious electrical stimulation is prevented in rats in which the adrenal gland had been removed 1 week prior to the perfusion study (▼, $n = 7$). (b) Stimulation of cutaneous nociceptors by capsaicin injected into the palmar skin of the rat forepaw (3, 10, 30 µg in 2.5 µl) decreased the magnitude of PE (▲, $n = 8$). This inhibition produced by capsaicin was prevented in rats with denervated adrenal medullae (section of the adrenal nerves; ▼, $n = 8$). The rats were vagotomized. (c) Schematic diagram showing the neural and neuroendocrine components being involved in the control of BK-induced synovial PE: (*1*) Terminals of sympathetic postganglionic neurons mediate 60–70% of BK-induced synovial PE and the inhibitory effect of corticosterone on BK-induced synovial PE. (*2*, *3*) Control of BK-induced PE by the HPA system and the sympatho-adrenal system. (*4*) Change of sensitivity of nociceptive afferents during inflammation as well as modulation of experimental inflammation by peptides released these afferents. The central nociceptive–neuroendocrine reflex circuits are not shown (see Green, P. G. *et al.*, 1995; Miao, F. J.-P. *et al.*, 2000; 2001). Mean + SEM in (a) and (b). (a) after Green P. G. *et al.* (1995); (b) after Miao F. J.-P. *et al.* (2000); (d) after Jänig W. *et al.* (2006).

control of inflammation (see Straub, R. H. *et al.*, 2005; Straub, R. H. and Härle, P., 2005), I will summarize the role of both systems in the control of acute experimental inflammation generated in the rat knee joint perfused with the inflammatory mediator bradykinin (bradykinin-induced plasma extravasation).

Continuous perfusion of bradykinin through the rat knee joint (Figure 16d) produces a large, sustained increase in plasma extravasation with a decay of about 10% over 1–2 h (Figure 16a and b, filled circles). This bradykinin-induced plasma extravasation response is largely dependent on the postganglionic

sympathetic neuron terminal: surgical sympathectomy reduces the magnitude of response by 60–70%, but acute sympathetic decentralization (section of the preganglionic axons) has no significant effect. Similarly, acute interruption of the lumbar sympathetic chains during ongoing bradykinin-induced plasma extravasation does not reduce this extravasation. Finally, the sodium channel blocker tetrodotoxin coperfused with bradykinin into the knee joint cavity does not reduce the plasma extravasation (Miao, F. J.-P. *et al.*, 1996a; 1996b). Thus, bradykinin-induced synovial plasma extravasation is dependent on the presence of sympathetic terminals in the synovia, but not on activity in these terminals and not on release of noradrenaline (function *1* in Figure 16c). This dependence on the sympathetic terminals is particularly large at bradykinin concentrations that have been measured in inflamed tissues (10^{-8} to 10^{-7} M; Hargreaves, K. M. *et al.*, 1993; Swift, J. Q. *et al.*, 1993). This is a novel peripheral function of postganglionic sympathetic fibers, at least in the context of the model of synovial inflammation, produced by the potent endogenous inflammatory mediator bradykinin. This function occurs at the postcapillary venules by release of a chemical substance (possibly prostaglandin E2 and/or related substances), which is independent of the electrical activity in the sympathetic neurons. Whether this substance is released by the sympathetic terminals or by other cells in association with these terminals is unknown. Future investigations will have to show whether this unusual function of sympathetic postganglionic terminals also applies to other inflammatory models.

Bradykinin-induced synovial plasma extravasation is under control of the brain mediated by the sympatho-adrenal system and the HPA system (functions *2* and *3* in Figure 16c). Both the neuroendocrine control systems can be reflex activated by noxious stimuli. The HPA system is most efficiently activated by continuous transcutaneous electrical stimulation of afferent C-fibers and the sympatho-adrenal system during stimulation of nociceptors by capsaicin (e.g., injected into the plantar or palmar skin or into the peritoneal cavity).

The differential activation of both neuroendocrine systems, the hypothalamic–pituitary system and the sympatho-adrenal system, generated by the modes of afferent stimulation is interesting but puzzling. During transcutaneous electrical stimulation, C-fibers are stimulated continuously and synchronously at 1–4 Hz together with A-fibers. This activation of C-fibers is certainly unphysiological. Capsaicin injected into the skin or into the peritoneal cavity excites only C-fibers (and a few Aδ-fibers; but not Aβ-fibers) asynchronously. This activation is similar to physiological activation, e.g., by heat. These modes of afferent stimulation can be used to differentially activate both neuroendocrine systems experimentally whatever the central underlying mechanisms are for this differential activation.) The nociceptive–neuroendocrine reflex circuits in spinal cord and brainstem are enhanced after subdiaphragmatic vagotomy; thus, they are under inhibitory control of central circuits activated by abdominal vagal afferents. Both the central nociceptive–neuroendocrine reflex circuits and their inhibitory control exerted by activity in abdominal vagal afferents are described elsewhere (Miao, F. J.-P. *et al.*, 1997a; 1997b; 2000; 2001; 2003).

Transcutaneous electrical stimulation of C-fibers inhibits bradykinin-induced plasma extravasation (normal triangles in Figure 16a). This inhibition is mediated by the HPA system since it can be prevented by removal of the adrenal glands (inverted triangles in Figure 16a), by hypophysectomy, by blockade of the corticosterone metabolism, and by blockade of corticosterone receptors. It can be mimicked by intravenous infusion of corticosterone (Green, P. G. *et al.*, 1997). The inhibition of bradykinin-induced plasma extravasation generated by activation of the HPA system or by intravenous infusion of corticosterone is dependent on the presence of sympathetic postganglionic nerve fibers in the synovia: The bradykinin-induced plasma extravasation remaining after sympathectomy (removal of paravertebral ganglia) cannot any longer be inhibited by activation of the hypothalamic–pituitary system or by corticosterone injected intravenously. This shows that the sympathetic fibers are in a strategic, yet unexpected, position in the control of synovial plasma extravasation by the brain (Green, P. G. *et al.*, 1997).

Reflex inhibition of bradykinin-induced plasma extravasation generated by stimulation of nociceptors by capsaicin (normal triangles in Figure 16b) is prevented by denervation of the adrenal medullae (inverted triangles in Figure 16b). Thus, it is mediated by adrenaline released by the adrenal medullae.

The mechanisms by which corticosterone released by the adrenal cortex and adrenaline released by the adrenal medulla depress bradykinin-induced synovial plasma extravasation and the role of the sympathetic nerve fibers innervating the synovia in this depression are unknown. Corticosterone seems to act via the peptide annexin possibly released by inflammatory cells in

the synovia (Green, P. G. *et al.*, 1998). Here it is important to emphasize that the control of experimental synovial inflammation by both neuroendocrine systems affects indirectly the sensitivity of nociceptors innervating the knee joint and, therefore, also pain and hyperalgesia and that this change of sensitivity is therefore under the control of the brain.

5.17.4.3 Sympathetic Nervous System and Immune System

The hypothalamus can influence the immune system by way of the sympathetic nervous system and can therefore control protective mechanisms of the body at the cellular level (Besedovsky, H. O. and del Rey, A., 1995; Hori, T. *et al.*, 1995; Madden, K. S. and Felten, D. L., 1995; Madden, K. S. *et al.*, 1995). The parameters of the immune tissues potentially controlled are proliferation, trafficking and circulation of lymphocytes, functional activity of lymphoid cells (e.g., activity of natural killer cells) and cytokine production, hematopoesis of bone marrow, mucosal immunity, thymocyte development, etc. (for details of potential mechanisms, see Elenkov, I. J. *et al.*, 2000). The mechanisms of this influence remain largely unsolved (Ader, A. and Cohen, N., 1993; Saphier, D., 1993; Besedovsky, H. O. and del Rey, A., 1995). It is unknown (1) whether there exists a functionally distinct sympathetic system from the brain to the immune system or (2) whether the modulation of the immune system is a general function of the sympathetic nervous system. The more likely hypothesis favored by me is that the immune system is modulated by the brain by way of a functionally and anatomically distinct sympathetic pathway (Figure 17; for discussion, see Jänig, W. and Häbler, H. J., 2000a; Jänig, W., 2006). The reflex discharge characteristics of the neurons of this hypothetical sympathetic pathway innervating the immune tissue and the neural circuits in spinal cord, brainstem, and hypothalamus being involved in regulation of the activity of this pathway should be different from those of other sympathetic pathways (Jänig, W., 2006). In fact a hypothalamo-sympathetic neural system that controls the immune system has been postulated (Hori, T. *et al.*, 1995). In both cases it is hypothesized that activity in the sympathetic neurons supplying the immune system entails indirect modulation of the sensitivity of nociceptors involving various types of immune-related cells and their signaling molecules (e.g., cytokines, see above and Jänig, W. and Levine, J. D., 2006).

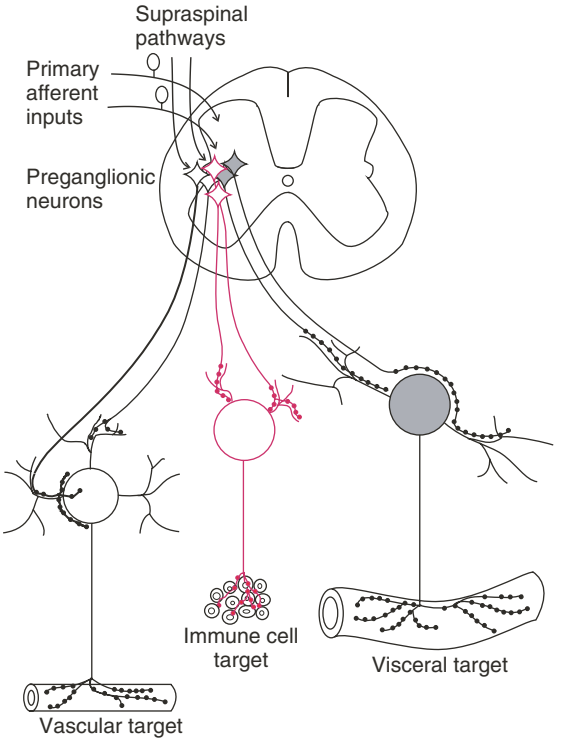

Figure 17 A separate sympathetic pathway to the immune tissue: a hypothesis. Demonstrated are three functional types of sympathetic pathway, one each to the vasculature (e.g., to blood vessels in skeletal muscle or skin or viscera), to the viscera (e.g., to the gastrointestinal tract being involved in the regulation of motility or secretion), or to the immune tissue. This neural link to the immune tissue may indirectly lead to sensitization of nociceptors and pain (modified from Jänig, W., 2006).

Acknowledgment

Supported by the Deutsche Forschungsgemeinschaft and the German Ministry of Research and Education (German Research Network on Neuropathic Pain).

References

Ader, A. and Cohen, N. 1993. Psychoneuroendocrinology: conditioning and stress. Annu. Rev. Physiol. 44, 53–85.

Ali, Z., Raja, S. N., Wesselmann, U., Fuchs, P. N., Meyer, R. A., and Campbell, J. N. 2000. Intradermal injection of norepinephrine evokes pain in patients with sympathetically maintained pain. Pain 88, 161–168.

Arkins, S., Johnson, R. W., Minshall, C., Dantzer, R., and Kelley, K. W. 2001. Immunophysiology: The Interaction of Hormones, Lymphohemopoietic Cytokines, and the Neuroimmune Axis. In: Handbook of Physiology. Section 7: The Endocrine System. Vol. IV: Coping with the Environment: Neural and Neuroendocrine Mechanisms (*ed*. B. S. McEwen), pp. 469–495. Oxford University Press.

Arnér, S. 1991. Intravenous phentolamine test: diagnostic and prognostic use in reflex sympathetic dystrophy. Pain 46, 17–22.

Bandler, R. and Shipley, M. T. 1994. Columnar organization in the midbrain periaqueductal gray: modules for emotional expression? Trends Neurosci. 17, 379–389.

Bandler, R., Keay, K. A., Floyd, N., and Price, J. 2000a. Central circuits mediating patterned autonomic activity during active vs. passive emotional coping. Brain Res. Bull. 53, 95–104.

Bandler, R., Price, J. L., and Keay, K. A. 2000b. Brain mediation of active and passive emotional coping. Prog. Brain Res. 122, 333–349.

Gebhart G. Mechanisms Underlying Complex Regional Pain Syndrome. Role of the Sympathetic Nervous System. In: Autonomic Failure (*eds*. C.J. Mathias and R. Bannister). Oxford University Press.

Baron, R., Schattschneider, J., Binder, A., Siebrecht, D., and Wasner, G. 2002. Relation between sympathetic vasoconstrictor activity and pain and hyperalgesia in complex regional pain syndromes: a case-control study. Lancet 359, 1655–1660.

Beal, M. C. 1983. Palpatory testing for somatic dysfunction in patients with cardiovascular disease. J. Am. Osteopath. Assoc. 82, 822–831.

Beal, M. C. 1985. Viscerosomatic reflexes: a review. J. Am. Osteopath. Assoc. 85, 786–801.

Bennett, G. J. and Xie, Y. K. 1988. A peripheral mononeuropathy in rat that produces disorders of pain sensation like those seen in man. Pain 33, 87–107.

Besedovsky, H. O. and del Rey, A. 1995. Immune-neuroendocrine interactions: facts and hypotheses. Endocr. Rev. 17, 64–102.

Bielefeldt, T. K. and Gebhart, G. F. 2006. Visceral Pain: Basic Mechanisms. In: Wall and Melzack's Textbook of Pain, 5th edn (*eds*. S. B. McMahon and M. Koltzenburg), pp. 721–736. Elsevier Churchill Livingstone.

Birder, L. A. and Perl, E. R. 1999. Expression of alpha2-adrenergic receptors in rat primary afferent neurones after peripheral nerve injury or inflammation. J. Physiol. 515, 533–542.

Blumberg, H. and Jänig, W. 1982. Activation of fibers via experimentally produced stump neuromas of skin nerves: ephaptic transmission or retrograde sprouting? Exp. Neurol. 76, 468–482.

Blumberg, H. and Jänig, W. 1984. Discharge pattern of afferent fibers from a neuroma. Pain 20, 335–353.

Bonica, J. J. 1953. Causalgia and Other Reflex Sympathetic Dystrophies. In: The Management of Pain, Chapter 28 (*ed*. J. J. Bonica), pp. 913–978. Lea and Febiger.

Bonica, J. J. 1990. Causalgia and Other Reflex Sympathetic Dystrophies. In: The Management of Pain, 2nd edn (*ed*. J. J. Bonica), pp. 220–243. Lea and Febiger.

Cervero, F. 1995. Mechanisms of Visceral Pain: Past and Present. In: Visceral Pain (*ed*. G. F. Gebhart), pp. 25–41. IASP Press.

Cervero, F. and Jänig, W. 1992. Visceral nociceptors: a new world order? Trends Neurosci. 15, 374–378.

Chabal, C., Jacobson, L., Russell, L. C., and Burchiel, K. J. 1992. Pain response to perineuromal injection of normal saline, epinephrine, and lidocaine in humans. Pain 49, 9–12.

Chen, Y., Michaelis, M., Jänig, W., and Devor, M. 1996. Adrenoreceptor subtype mediating sympathetic-sensory coupling in injured sensory neurons. J. Neurophysiol. 76, 3721–3730.

Choi, B. and Rowbotham, M. C. 1997. Effect of adrenergic receptor activation on post-herpetic neuralgia pain and sensory disturbances. Pain 69, 55–63.

Clauw, D. J. and Chrousos, G. P. 1997. Chronic pain and fatigue syndromes: overlapping clinical and neuroendocrine features and potential pathogenic mechanisms. Neuroimmunomodulation 4, 134–153.

Coderre, T. J. and Melzack, R. 1986. Procedures which increase acute pain sensitivity also increase autotomy. Exp. Neurol. 92, 713–722.

Coderre, T. J., Abbott, F. V., and Melzack, R. 1984. Effects of peripheral antisympathetic treatments in the tail-flick, formalin and autotomy tests. Pain 18, 13–23.

Coderre, T. J., Grimes, R. W., and Melzack, R. 1986. Deafferentation and chronic pain in animals: an evaluation of evidence suggesting autotomy is related to pain. Pain 26, 61–84.

Cox, J. M., Gorbis, S., Dick, L. M., Rogers, J. C., and Rogers, F. J. 1983. Palpable musculoskeletal findings in coronary artery disease: results of a double-blind study. J. Am. Osteopath. Assoc. 82, 832–836.

Damasio, A. 2003. Looking for Spinoza. Joy, Sorrow, and the Feeling Brain. Harvest Books, Harcourt, Inc.

Dellemijn, P. L., Fields, H. L., Allen, R. R., McKay, W. R., and Rowbotham, M. C. 1994. The interpretation of pain relief and sensory changes following sympathetic blockade. Brain 117, 1475–1487.

Desmeules, J. A., Kayser, V., Weil-Fuggaza, J., Bertrand, A., and Guilbaud, G. 1995. Influence of the sympathetic nervous system in the development of abnormal pain-related behaviours in a rat model of neuropathic pain. Neuroscience 67, 941–951.

Devor, M. and Jänig, W. 1981. Activation of myelinated afferents ending in a neuroma by stimulation of the sympathetic supply in the rat. Neurosci. Lett. 24, 43–47.

Devor, M., Jänig, W., and Michaelis, M. 1994. Modulation of activity in dorsal root ganglion neurons by sympathetic activation in nerve-injured rats. J. Neurophysiol. 71, 38–47.

Elenkov, I. J., Wilder, R. L., Chrousos, G. P., and Vizi, E. S. 2000. The sympathetic nerve – an integrative interface between two supersystems: the brain and the immune system. Pharmacol. Rev. 52, 595–638.

Fields, H. L., Basbaum, A. I., and Heinricher, M. M. 2006. In: Central nervous system mechanisms of pain modulation (*eds*. S. B. McMahon and M. Koltzenburg), pp. 125–142. Elsevier Churchill Livingstone.

Foreman, R. D. 1989. Organization of the spinothalamic tract as a relay for cardiopulmonary sympathetic afferent fiber activity. Prog. Sensory Physiol. 9, 1–51.

Gebhart, G. F. 2007. In: The Senses: A Comprehensive References. In: Pain, Vol. 3 (*eds*. C. Bushnell and A. I. Basbaum). Elsevier.

Giamberardino, M. A. 1999. Recent and forgotten aspects of visceral pain. Eur. J. Pain 3, 77–92.

Goehler, L. E., Gaykema, R. P., Hansen, M. K., Anderson, K., Maier, S. F., and Watkins, L. R. 2000. Vagal immune-to-brain communication: a visceral chemosensory pathway. Auton. Neurosci. 85, 49–59.

Green, P. G., Jänig, W., and Levine, J. D. 1997. Sympathetic terminal: target for negative feedback neuroendocrine control of inflammatory response in the rat. J. Neurosci. 17, 3234–3238.

Green, P. G., Miao, F. J.-P., Jänig, W., and Levine, J. D. 1995. Negative feedback neuroendocrine control of the inflammatory response in rats. J. Neurosci. 15, 4678–4686.

Green, P. G., Strausbaugh, H. J., and Levine, J. D. 1998. Annexin I is a local mediator in neural-endocrine feedback control of inflammation. J. Neurophysiol. 80, 3120–3126.

Häbler, H.-J., Eschenfelder, S., Liu, X.-G., and Jänig, W. 2000. Sympathetic-sensory coupling after L5 spinal nerve lesion in the rat and its relation to changes in dorsal root ganglion blood flow. Pain 87, 335–345.

Häbler, H. J., Jänig, W., and Koltzenburg, M. 1987. Activation of unmyelinated afferents in chronically lesioned nerves by adrenaline and excitation of sympathetic efferents in the cat. Neurosci. Lett. 82, 35–40.

Häbler, H. J., Wasner, G., and Jänig, W. 1997. Interaction of sympathetic vasoconstriction and antidromic vasodilatation in the control of skin blood flow. Exp. Brain Res. 113, 402–410.

Harden, R.N., Baron, R., and Jänig, W. (*eds.*). 2001 Complex Regional Pain Syndrome. IASP Press.

Hargreaves, K. M., Roszkowski, M. T., and Swift, J. Q. 1993. Bradykinin and inflammatory pain. Agents Actions Suppl. 41, 65–73.

Herrero, J. F., Laird, J. M., and Lopez-Garcia, J. A. 2000. Wind-up of spinal cord neurones and pain sensation: much ado about something? Prog. Neurobiol. 61, 169–203.

Holzer, P. 1998. Neurogenic vasodilatation and plasma leakage in the skin. Gen. Pharmacol. 30, 5–11.

Hori, T., Katafuchi, T., Take, S., Shimizu, N., and Niijima, A. 1995. The autonomic nervous system as a communication channel between the brain and the immune system. Neuroimmunomodulation 2, 203–215.

Jänig, W. 1990. Activation of afferent fibers ending in an old neuroma by sympathetic stimulation in the rat. Neurosci. Lett. 111, 309–314.

Jänig, W. 1993. Spinal Visceral Afferents, Sympathetic Nervous System and Referred Pain. In: New Trends in Referred Pain and Hyperalgesia. Pain Research and Clinical Management, Vol. 7 (*eds*. L. Vecchiet, D. Albe-Fessard, U. Lindblom, and M. A. Giamberardino), pp. 83–89. Elsevier Science Publishers.

Jänig, W. 2002. Pain in the Sympathetic Nervous System: Pathophysiological Mechanisms. In: Autonomic Failure, 4th edn (*eds*. C. J. Mathias and R. Bannister), pp. 99–108. Oxford University Press.

Jänig, W. 2005. Vagal Afferents and Visceral Pain. Advances in Vagal Afferent Neurobiology (*eds*. B. Undem and D. Weinreich), pp. 465–493. CRC Press.

Jänig, W. 2006. The Integrative Action of the Autonomic Nervous System. Neurobiology of Homeostasis. Cambridge University Press.

Jänig, W. and Baron, R. 2001. The Role of the Sympathetic Nervous System in Neuropathic Pain: Clinical Observations and Animal Models. In: Neuropathic Pain: Pathophysiology and Treatment (*eds*. P. T. Hansson, H. L. Fields, R. G. Hill, and P. Marchettini), pp. 125–149. IASP Press.

Jänig, W. and Baron, R. 2002. Complex regional pain syndrome is a disease of the central nervous system. Clin. Auton. Res. 12, 150–164.

Jänig, W. and Baron, R. 2003. Complex regional pain syndrome: mystery explained? Lancet Neurol. 2, 687–697.

Janig, W. and Baron, R. 2004. Experimental approach to CRPS. Pain 108, 3–7.

Jänig, W. and Häbler, H. J. 2000a. Specificity in the organization of the autonomic nervous system: a basis for precise neural regulation of homeostatic and protective body functions. Prog. Brain Res. 122, 351–367.

Jänig, W. and Häbler, H. J. 2000b. Sympathetic nervous system: contribution to chronic pain. Prog. Brain Res. 129, 451–468.

Jänig, W. and Häbler, H. J. 2002. Physiologie und Pathophysiologie viszeraler Schmerzen [Physiology and pathophysiology of visceral pain]. Schmerz 16, 429–446.

Jänig, W. and Koltzenburg, M. 1991. What Is the Interaction Between the Sympathetic Terminal and the Primary Afferent Fiber? In: Towards a New Pharmacotherapy of Pain (*eds*. A. I. Basbaum and J. -M. Besson), pp. 331–352. Dahlem Workshop Reports. John Wiley and Sons.

Jänig, W. and Koltzenburg, M. 1993. Pain Arising from the Urogenital Tract. In: Nervous Control of the Urogenital Tract. Vol. 3. The Autonomic Nervous System (*eds*. G. Burnstock and C. A. Maggi), pp. 523–576. Harwood Academic Publisher.

Jänig, W. and Levine, J. D. 2006. Autonomic–endocrine–immure interactions in acute nd chronic pain. In: Wall and Melzack's Textbook of Pain, 5th edn (*eds*. S. B. McMahon and M. Koltzenburg), pp. 205–218. Elsevier. Churchill Livingstone.

Jänig, W. and McLachlan, E. M. 2002. Neurobiology of the Autonomic Nervous System. In: Autonomic Failure, 5th edn (*eds*. C. J. Mathias and R. Bannister), pp. 3–15. Oxford University Press.

Jänig, W. and Morrison, J. F. B. 1986. Functional properties of spinal visceral afferents supplying abdominal and pelvic organs, with special emphasis on visceral nociception. Prog. Brain Res. 67, 87–114.

Jänig, W. and Stanton-Hicks, M. (*eds.*). 1996 Reflex Sympathetic Dystrophy – A Reappraisal. IASP Press.

Jänig, W., Chapman, C. R., and Green, P. G. 2006. Pain and Body Protection: Sensory, Autonomic, Neuroendocrine and Behavioral Mechanisms. In: The Control of Inflammation and Hyperalgesia. In Proceedings of the 11th World Congress on Pain (*eds*. H. Flor, E. Kalso, and J. O. Dostrovsky), pp. 331–347. IASP Press.

Jänig, W., Khasar, S. G., Levine, J. D., and Miao, F. J.-P. 2000. The role of vagal visceral afferents in the control of nociception. Prog. Brain Res. 122, 273–287.

Jänig, W., Levine, J. D., and Michaelis, M. 1996. Interactions of sympathetic and primary afferent neurons following nerve injury and tissue trauma. Prog. Brain Res. 112, 161–184.

Jobling, P., McLachlan, E. M., Jänig, W., and Anderson, C. R. 1992. Electrophysiological responses in the rat tail artery during reinnervation following lesions of the sympathetic supply. J. Physiol. 454, 107–128.

Keay, K. A. and Bandler, R. 2004. Periaqueductal gray. In: The Rat Nervous System, 3rd edn (*ed*. G. Paxinos), pp. 243–257. Academic Press.

Khasar, S. G., Green, P. G., and Levine, J. D. 1993. Comparison of intradermal and subcutaneous hyperalgesic effects of inflammatory mediators in the rat. Neurosci. Lett. 153, 215–218.

Khasar, S. G., Green, P. G., and Levine, J. D. 2005. Repeated sound stress enhances inflammatory pain in the rat. Pain 116, 79–86.

Khasar, S. G., Green, P. G., Miao, F. J.-P., and Levine, J. D. 2003. Vagal modulation of nociception is mediated by adrenomedullary epinephrine in the rat. Eur. J. Neurosci. 17, 909–915.

Khasar, S. G., Miao, F. J.-P., Jänig, W., and Levine, J. D. 1998a. Modulation of bradykinin-induced mechanical hyperalgesia in the rat skin by activity in the abdominal vagal afferents. Eur. J. Neurosci. 10, 435–444.

Khasar, S. G., Miao, F. J.-P., Jänig, W., and Levine, J. D. 1998b. Vagotomy-induced enhancement of mechanical hyperalgesia in the rat is sympathoadrenal-mediated. J. Neurosci. 18, 3043–3049.

Khasar, S. G., Miao, F. J.-P., and Levine, J. D. 1995. Inflammation modulates the contribution of receptor-subtypes to bradykinin-induced hyperalgesia in the rat. Neuroscience 69, 685–690.

Kim, S. H. and Chung, J. M. 1991. Sympathectomy alleviates mechanical allodynia in an experimental animal model for neuropathy in the rat. Neurosci. Lett. 134, 131–134.

Kim, S. H., Na, H. S., Sheen, K., and Chung, J. M. 1993. Effects of sympathectomy on a rat model of peripheral neuropathy. Pain 55, 85–92.

Kim, K. J., Yoon, Y. W., and Chung, J. M. 1997. Comparison of three rodent neuropathic pain models. Exp. Brain Res. 113, 200–206.

Kinnman, E. and Levine, J. D. 1995. Sensory and sympathetic contributions to nerve injury-induced sensory abnormalities in the rat. Neurosci. 64, 751–767.

Koltzenburg, M., Häbler, H.-J., and Jänig, W. 1995. Functional reinnervation of the vasculature of the adult cat paw pad by axons originally innervating vessels in hairy skin. Neuroscience 67, 245–252.

Lewin, G. R., Ritter, A. M., and Mendell, L. M. 1993. Nerve growth factor-induced hyperalgesia in the neonatal and adult rat. J. Neurosci. 13, 2136–2148.

Lewin, G. R., Rueff, A., and Mendell, L. M. 1994. Peripheral and central mechanisms of NGF-induced hyperalgesia. Eur. J. Neurosci. 6, 1903–1912.

Lopez de Armentia, M., Leeson, A. H., Stebbing, M. J., Urban, L., and McLachlan, E. M. 2003. Responses to sympathomimetics in rat sensory neurones after nerve transection. Neuroreport 14, 9–13.

Livingston, W. K. 1943. Pain Mechanisms. A Physiological Interpretation of Causalgia and Its Related States. Macmillan (reprinted by Plenum Press [1976]).

Liu, X., Eschenfelder, S., Blenk, K. H., Jänig, W., and Häbler, H. 2000. Spontaneous activity of axotomized afferent neurons after L5 spinal nerve injury in rats. Pain 84, 309–318.

MacKenzie, J. 1920. Symptoms and Their Interpretation, 4th edn. Shaws and Sons.

Madden, K. S. and Felten, D. L. 1995. Experimental basis for neural-immune interactions. Physiol. Rev. 75, 77–106.

Madden, K. S., Sanders, K., and Felten, D. L. 1995. Catecholamine influences and sympathetic modulation of immune responsiveness. Rev. Pharmacol. Toxicol. 35, 417–448.

Maier, S. F. and Watkins, L. R. 1998. Cytokines for psychologists: implications of bidirectional immune-to-brain communication for understanding behavior, mood, and cognition. Psychol. Rev. 105, 83–107.

Manning, D. C., Raja, S. N., Meyer, R. A., and Campbell, J. N. 1991. Pain and hyperalgesia after intradermal injection of bradykinin in humans. Clin. Pharmacol. Ther. 50, 721–729.

Mason, P. 2001. Contributions of the medullary raphe and ventromedial reticular region to pain modulation and other homeostatic functions. Annu. Rev. Neurosci. 24, 737–777.

Mayer, E. A., Munakata, J., Mertz, H., Lembo, T., and Bernstein, C. N. 1995. Visceral Hyperalgesia and Irritable Bowel Syndrome. In: Visceral Pain (*ed*. G. F. Gebhart), pp. 429–468. IASP Press.

McDonald, D. M. 1997. Neurogenic Inflammation in the Airways. In: Autonomic Control of the Respiratory System (*ed*. P. J. Barnes), pp. 249–289. Harwood Academic Publishers GmbH.

McLachlan, E. M., Jänig, W., Devor, M., and Michaelis, M. 1993. Peripheral nerve injury triggers noradrenergic sprouting within dorsal root ganglia. Nature 363, 543–546.

McMahon, S. B. 1996. NGF as a mediator of inflammatory pain. Philos. Trans. R. Soc. Lond. B Biol. Sci. 351, 431–440.

McMahon, S. B., Bennett, D. L. H., and Bevan, S. 2006. Inflammatory Mediators and Modulators of Pain. In: Wall and Melzack's Textbook of Pain, 5th edn (*eds*. S. B. McMahon and M. Koltzenburg), pp. 49–72. Elsevier Churchill Livingstone.

Mense, S. and Meyer, H. 1988. Bradykinin-induced modulation of the response behaviour of different types of feline group III and IV muscle receptors. J. Physiol. 398, 49–63.

Merskey, H. and Bogduk, H. 1994. Classification of Chronic Pain: Description of Chronic Pain Syndromes and Definition of Pain Terms, 2nd edn. IASP Press.

Meyer, R. A., Ringkamp, M., Campbell, J. N., and Raja, S. N. 2006. Peripheral Mechanisms of Cutaneous Nociception. In: Wall and Melzack's Textbook of Pain, 5th edn (*eds*. S. B. McMahon and M. Koltzenburg), pp. 3–34. Elsevier Churchill Livingstone.

Miao, F. J.-P, Green, P. G., Coderre, T. J., Jänig, W., and Levine, J. D. 1996a. Sympathetic-dependence in bradykinin-induced synovial plasma extravasation is dose-related. Neurosci. Lett. 205, 165–168.

Miao, F. J.-P., Jänig, W., Green, P. G., and Levine, J. D. 1997a. Inhibition of bradykinin-induced synovial plasma extravasation produced by noxious cutaneous and visceral stimuli and its modulation by activity in the vagal nerve. J. Neurophysiol. 78, 1285–1292.

Miao, F. J.-P., Jänig, W., Jasmin, L., and Levine, J. D. 2001. Spino-bulbo-spinal pathway mediating vagal modulation of nociceptive-neuroendocrine control of inflammation in the rat. J. Physiol. 532, 811–822.

Miao, F. J.-P., Jänig, W., Jasmin, L., and Levine, J. D. 2003. Blockade of nociceptive inhibition of plasma extravasation by opioid stimulation of the periaqueductal gray and its interaction with vagus-induced inhibition in the rat. Neuroscience 119, 875–885.

Miao, F. J.-P., Jänig, W., and Levine, J. D. 1996b. Role of sympathetic postganglionic neurons in synovial plasma extravasation induced by bradykinin. J. Neurophysiol. 75, 715–724.

Miao, F. J.-P., Jänig, W., and Levine, J. D. 1997b. Vagal branches involved in inhibition of bradykinin-induced synovial plasma extravasation by intrathecal nicotine and noxious stimulation in the rat. J. Physiol. 498, 473–481.

Miao, F. J.-P., Jänig, W., and Levine, J. D. 2000. Nociceptive-neuroendocrine negative feedback control of neurogenic inflammation activated by capsaicin in the skin: role of the adrenal medulla. J. Physiol. 527, 601–610.

Michaelis, M., Devor, M., and Jänig, W. 1996. Sympathetic modulation of activity in rat dorsal root ganglion neurons changes over time following peripheral nerve injury. J. Neurophysiol. 76, 753–763.

Michaelis, M., Liu, X., and Jänig, W. 2000. Axotomized and intact muscle afferents but no skin afferents develop ongoing discharges of dorsal root ganglion origin after peripheral nerve lesion. J. Neurosci. 20, 2742–2748.

Miller, A. H., Pearce, B. D., Ruzek, M. C., and Biron, C. A. 2001. Interactions Between the Hypothalamic-Pituitary-Adrenal Axis and Immune System During Viral Infection: Pathways for Environmental Effects on Disease Expression. In: Handbook of Physiology. Section 7: The Endocrine System. Vol. IV: Coping with the Environment: Neural and Neuroendocrine Mechanisms (*ed*. B. S. McEwen), pp. 425–450. Oxford University Press.

Mitchell, S. W. 1872. Injuries of Nerves and Their Consequences. J. P. Lippincott.

Morrison, S. F. 2001. Differential control of sympathetic outflow. Am. J. Physiol. Regul. Integr. Comp. Physiol. 281, R683–R698.

Morrison, S. F. and Cao, W. H. 2000. Different adrenal sympathetic preganglionic neurons regulate epinephrine and norepinephrine secretion. Am. J. Physiol. Regul. Integr. Comp. Physiol. 279, R1763–R1775.

Neil, A., Attal, N., and Guilbaud, G. 1991. Effects of guanethidine on sensitization to natural stimuli and self-mutilating behaviour in rats with a peripheral neuropathy. Brain Res. 565, 237–246.

Ness, T. J. 1995. Historical and Clinical Perspectives of Visceral Pain. In: Visceral Pain. Progress in Pain Research and Management, Vol. 5 (*ed*. G. F. Gebhart), pp. 3–23. IASP Press.

Ness, T. J. and Gebhart, G. F. 1990. Visceral pain: a review of experimental studies. Pain 41, 167–234.

Neugebauer, V., Schaible, H. G., and Schmidt, R. F. 1989. Sensitization of articular afferents to mechanical stimuli by bradykinin. Pflügers Arch. 415, 330–335.

Nicholas, A. S., DeBias, D. A., Ehrenfeuchter, W., England, K. M., England, R. W., Greene, C. H., *et al.* 1985. A somatic component to myocardial infarction. Br. Med. J. 291, 13–17.

Petty, B. G., Cornblath, D. R., Adornato, B. T., Chaudhry, V., Flexner, C., Wachsman, M., *et al.* 1994. The effect of systemically administered recombinant human nerve growth factor in healthy human subjects. Ann. Neurol. 36, 244–246.

Poole, S., Cunha, F. Q., and Ferreira, S. H. 1999. Hyperalgesia from Subcutaneous Cytokines. In: Cytokines and Pain (*eds*. L. R. Watkins and S. F. Maier), pp. 59–87. Birkhäuser Verlag.

Porreca, F., Ossipov, M. H., and Gebhart, G. F. 2002. Chronic pain and medullary descending facilitation. Trends Neurosci. 25, 319–325.

Price, D. D., Long, S., Wilsey, B., and Rafii, A. 1998. Analysis of peak magnitude and duration of analgesia produced by local anesthetics injected into sympathetic ganglia of complex regional pain syndrome patients. Clin. J. Pain 14, 216–226.

Raja, S. N., Treede, R. D., Davis, K. D., and Campbell, J. N. 1991. Systemic alpha-adrenergic blockade with phentolamine: a diagnostic test for sympathetically maintained pain. Anesthesiology 74, 691–698.

Randich, A. and Gebhart, G. F. 1992. Vagal afferent modulation of nociception. Brain Res. Rev. 17, 77–99.

Ringkamp, M., Eschenfelder, S., Grethel, E. J., Häbler, H.-J., Meyer, R. A., Jänig, W., and Raja, S. N. 1999. Lumbar sympathectomy failed to reverse mechanical allodynia- and hyperalgesia-like behavior in rats with L5 spinal nerve injury. Pain 79, 143–153.

Ruch, T. C. 1965. Pathophysiology of Pain. In: Physiology and Biophysics (*eds*. T. C. Ruch and H. D. Patton), pp. 345–363. Saunders.

Saphier, D. 1993. Psychoimmunology: The Missing Link. In: Hormonally Induced Changes in Mind and Brain (*ed*. J. Schulkin), pp. 191–224. Academic Press.

Sato, J. and Perl, E. R. 1991. Adrenergic excitation of cutaneous pain receptors induced by peripheral nerve injury. Science 251, 1608–1610.

Seltzer, Z., Dubner, R., and Shir, Y. 1990. A novel behavioral model of neuropathic pain disorders produced in rats by partial sciatic nerve injury. Pain 43, 205–218.

Shir, Y. and Seltzer, Z. 1991. Effects of sympathectomy in a model of causalgiform pain produced by partial sciatic nerve injury in rats. Pain 45, 309–320.

Stanton-Hicks, M., Jänig, W., Hassenbusch, S., Haddox, J. D., Boas, R., and Wilson, P. 1995. Reflex sympathetic dystrophy, changing concepts and taxonomy. Pain 63, 127–133.

Straub, R. H. and Härle, P. 2005. Sympathetic neurotransmitters in joint inflammation. Rheum. Dis. Clin. North Am. 31, 43–59.

Straub, R. H., Baerwald, C. G., Wahle, M., and Jänig, W. 2005. Autonomic dysfunction in rheumatic diseases. Rheum. Dis. Clin. North Am. 31, 61–75.

Swift, J. Q., Garry, M. G., Roszkowski, M. T., and Hargreaves, K. M. 1993. Effect of flurbiprofen on tissue levels on immunoreactive bradykinin and acute postoperative pain. J. Oral. Max. Surg. 51, 112–117.

Torebjörk, H. E., Wahren, L. K., Wallin, B. G., Hallin, R., and Koltzenburg, M. 1995. Noradrenaline-evoked pain in neuralgia. Pain 63, 11–20.

Tracey, D. J., Cunningham, J. E., and Romm, M. A. 1995. Peripheral hyperalgesia in experimental neuropathy: mediation by alpha 2-adrenoreceptors on post-ganglionic sympathetic terminals. Pain 60, 317–327.

Undem, B. J. and Weinreich, D. (*eds.*). 2005. Advance in Vagal Afferent Neurobiology. CRC Press.

Urban, M. O. and Gebhart, G. F. 1999. Supraspinal contributions to hyperalgesia. Proc. Natl. Acad. Sci. U. S. A. 96, 7687–7692.

Vecchiet, L., Albe-Fessard, D., Lindblom, U., and Giamberardino, M.A. (*eds.*). 1993. New Trends in Referred Pain and Hyperalgesia. Pain Research and Clinical Management, Vol. 7. Elsevier Science Publishers.

Vierck, C. J., Jr. 2006. Mechanisms underlying development of spatially distributed chronic pain (fibromyalgia). Pain 124, 242–263.

Walker, A. E. and Nulsen, F. 1948. Electrical stimulation of the upper thoracic portion of the sympathetic chain in man. Arch. Neurol. Psychiatry 59, 559–560.

Wall, P. D., Devor, M., Inbal, R., Scadding, J. W., Schonfeld, D., Seltzer, Z., and Tomkiewicz, M. M. 1979a. Autotomy following peripheral nerve lesions: experimental anaesthesia dolorosa. Pain 7, 103–111.

Wall, P. D., Scadding, J. W., and Tomkiewicz, M. M. 1979b. The production and prevention of experimental anesthesia dolorosa. Pain 6, 175–182.

Wallin, G., Torebjörk, E., and Hallin, R. 1976. Preliminary Observations on the Pathophysiology of Hyperalgesia in the Causalgic Pain Syndrome. In: Sensory Functions of the Skin in Primates (*ed*. Y. Zottermann), pp. 489–499. Pergamon Press.

Watkins, L.R. and Maier, S.F. (*eds.*). 1999. Cytokines and Pain, Birkhäuser Verlag.

Watkins, L. R. and Maier, S. F. 2000. The pain of being sick: implications of immune-to-brain communication for understanding pain. Annu. Rev. Psychol. 51, 29–57.

Watkins, L. R., Maier, S. F., and Goehler, L. E. 1995. Immune activation: the role of pro-inflammatory cytokines in inflammation, illness responses and pathological pain states. Pain 63, 289–302.

White, J. C. and Sweet, W. H. 1969. Pain and the Neurosurgeon: A Forty Year Experience. Springfield.

Willenbring, S., Beauprie, I. G., and DeLeo, J. A. 1995. Sciatic cryoneurolysis in rats: a model of sympathetically independent pain. Part 1: Effects of sympathectomy. Anesth. Analg. 81, 544–548.

Wolfe, F., Smythe, H. A., Yunus, M. B., Bennett, R. M., Bombardier, C., Goldenberg, D. L., *et al.* 1990. The American College of Rheumatology (1990) Criteria for the Classification of Fibromyalgia. Report of the Multicenter Criteria Committee. Arthritis Rheum. 33, 160–172.

Woolf, C. J. 1996. Phenotypic modification of primary sensory neurons: the role of nerve growth factor in the production of persistent pain. Phil. Trans. R. Soc. Lond. B 351, 441–448.

Woolf, C. J., Allchorne, A., Safieh-Garabedian, B., and Poole, S. 1997. Cytokines, nerve growth factor and inflammatory hyperalgesia: the contribution of tumour necrosis factor alpha. Br. J. Pharmacol. 121, 417–424.

Woolf, C. J., Ma, Q.-P., Allchorne, A., and Poole, S. 1996. Peripheral cell types contributing to the hyperalgesic action of nerve growth factor in inflammation. J. Neurosci. 16, 2716–2723.

Further Reading

Miao, F. J.-P., Green, P. G., and Levine, J. D. 2004. Mechanosensitive duodenal afferents contribute to vagal modulation of inflammation in the rat. J. Physiol. 554, 227–235.

5.18 Sympathetic Blocks for Pain

A Sharma, Columbia University, New York, NY, USA

J N Campbell and S N Raja, Johns Hopkins University, Baltimore, MD, USA

© 2008 Elsevier Inc. All rights reserved.

5.18.1	**Introduction**	227
5.18.1.1	Sympathetically Maintained Pain	228
5.18.2	**Techniques of Sympathetic Blockade**	229
5.18.3	**Sympathetic Block for Diagnosis**	229
5.18.3.1	Local Anesthetic Sympathetic Blocks	230
5.18.3.2	Intravenous Regional Sympathetic Blockade	231
5.18.3.3	Systemic Alpha-Adrenergic Blockade	231
5.18.4	**Sympathetic Block for Therapy of Chronic Pain States**	232
5.18.4.1	Local Anesthetic Sympathetic Blocks and Intravenous Regional Sympathetic Blockade	232
5.18.4.2	Spinal Cord Stimulation	233
5.18.4.3	Chemical Neurolysis and Radiofrequency Denervation Techniques	233
5.18.4.4	Surgical Sympathectomy	233
5.18.5	**Conclusions**	234
References		234

5.18.1 Introduction

Traditionally, the sympathetic nervous system (SNS) is considered as an efferent system that controls peripheral blood flow, sweating, and piloerection. This autonomic part of the nervous system, however, may play a pivotal role in certain pain conditions. Over the last decade, much knowledge has been gained on the mechanisms of interaction between the sensory afferent and sympathetic efferent systems. Pain dependent on the discharge of sympathetic nerves is referred to as sympathetically maintained pain (SMP). Insights into the pathophysiology of SMP help its treatment. The concept of SMP stemmed from clinical observations that certain patients with persistent pain after traumatic nerve lesions received dramatic pain relief from blockade of sympathetic ganglion with local anesthetic agents or perivascular sympathectomy.

A pain syndrome often associated with SMP is now termed complex regional pain syndrome (CRPS). Only subsets of patients with CRPS have SMP. Formerly termed as reflex sympathetic dystrophy (RSD), CRPS is an incompletely understood pain disorder that usually results from a traumatic injury and clinically presents as nondermatomal distribution of pain and sensory abnormalities in an extremity. Symptoms and signs include hyperalgesia and allodynia (enhanced pain to natural stimuli such as a pin prick or light stroking of the skin, respectively), autonomic features, and motor dysfunction. Some patients in addition have a motor impairment not readily explained by a lesion in the peripheral nervous system. Edema at the time of presentation or at an earlier time point is a common feature. CRPS may be present in cases with (CRPS type II) or without a nerve lesion (CRPS type I). After the initial description of this disease by Weir Mitchell in 1864 (who called it causalgia) and decades later by Paul Sudeck (Sudeck's syndrome), Leriche advocated its treatment by sympathetic interruption in 1916. Leriche (vicious cycle hypothesis, 1939) and Mandl (1947) were pioneers in proposing the connection between pain and SNS. The concept that the SNS was involved in the mechanisms of pain in CRPS was further propagated by Evans, who coined the term reflex sympathetic dystrophy. In view of the explosion of research regarding mechanisms of pain in RSD and lack of uniform diagnostic criteria, major taxonomical changes were proposed by the International Association for the Study of Pain (IASP) Consensus Team, and the term complex regional pain syndrome was introduced (Stanton-Hicks, M. *et al.*, 1995). According to the IASP classification, two distinct subtypes are now identified. Patients in whom the above-described

conglomeration of symptoms and signs develop after injury to a major peripheral nerve are considered to have CRPS type II (previously known as causalgia). The remaining patients in whom injuries to a limb or lesions in remote body areas precede the onset of symptoms without any identifiable nerve damage are classified as CRPS type I (previously termed reflex sympathetic dystrophy) (Merskey, H. and Bogduk, N., 1995). Since the initial proposal of diagnostic criteria for CRPS, further modifications have been made (Harden, R. N. and Bruehl, S. P., 2006). Presently, the clinical signs and symptoms of CRPS are grouped into the following categories:

1. Positive sensory abnormalities (spontaneous pain, mechanical, somatic or deep somatic hyperalgesia).
2. Vascular abnormalities (vasodilation or vasoconstriction, skin temperature asymmetries, or skin color changes).
3. Sudomotor abnormalities (swelling, hyper-, or hyperhidrosis).
4. Motor changes (weakness, tremor, dystonia, or coordination deficits) and trophic changes (nail or hair changes, skin atrophy, joint stiffness, or soft-tissue changes).

The criteria are being further validated as no gold standard diagnostic tool has been established for CRPS (Baron, R. and Jänig, W., 2004; Harden, R. N. and Bruehl, S. P., 2006). The 1993 IASP consensus team also acknowledged the term sympathetically maintained pain (SMP) and defined it as "Pain that is maintained by sympathetic efferent innervation or by circulating catecholamines." A role for circulating catecholamines has not been clearly established though. SMP is traditionally diagnosed by relief of allodynia, hyperalgesia, ongoing pain, and a selective blockade of sympathetic function. Notably, patients with CRPS, as previously indicated, may have both SMP and sympathetically independent pain (SIP) in varying proportions (Stanton-Hicks, M. *et al.*, 1995).

Even after decades of animal and human research, the pathophysiology of CRPS remains uncertain. Though it is common to refer to CRPS as a neuropathic pain disorder, it is not clear that pathology of the nervous system is at the root of this disorder as patients with or without nervous system lesions may manifest with symptoms of CRPS (Jänig, W. and Baron, R., 2002; 2003; 2004). Moreover, it is clear that CRPS is a diagnosis of exclusion, as other diseases (e.g., nerve entrapment and diabetic neuropathy) may present with similar signs and symptoms.

5.18.1.1 Sympathetically Maintained Pain

The clinical picture of CRPS with vascular (vasodilation or vasoconstriction, skin temperature asymmetries, or skin color changes) and sudomotor abnormalities (swelling, hyper-, or hypohidrosis) perhaps promoted the initial idea of SNS dysfunction as the primary etiology of the disease. Several lines of evidence suggest a dysregulation of autonomic function in the initial phase of the disease. Furthermore, enhancement of spontaneous pain and hyperalgesia after physiological activation of SNS (Baron, R. *et al.*, 2002; Drummond, P. D. and Finch, P. M., 2004) and resolution of pain, physiological tremor, and swelling in some patients after sympathetic blocks strengthen this view. The detection of autoantibodies against the autonomic nervous system in certain CRPS patients provides further evidence to this concept.

The relief of pain by blockade of the SNS initially invited speculation of an increased SNS discharge as a potential mechanism for SMP. Several observations were against this hypothesis. First, patients with SMP, particularly in the early period of the disease, may present with warm rather than cold skin. Under conditions of increased sympathetic discharge, vasoconstriction should lead to a cold skin. Also others noted that catecholamine levels in the venous return of the affected extremity were below those in normal subjects or their unaffected side.

In 1948, Walker *et al.* made an important clinical observation that provided convincing evidence for SMP. At that time, sympathectomy was performed to treat limb ischemia and also to relieve pain in patients with causalgia. Walker and colleagues performed a preganglionic sympathectomy and placed electrodes on the ganglion. Postoperatively, the ganglion was stimulated. Since the ganglion was dissociated from the spinal cord, electrical stimulation would only induce an efferent discharge in the peripheral sympathetic fibers. Stimulation induced pain in patients with causalgia, but not in patients with limb ischemia. This indicated that SMP was due to efferent function of the SNS. In a further experiment performed decades later, norepinephrine was injected in patients with SMP. In these patients, the sympathetic ganglia were blocked with local anesthetic. If SNS dysfunction does exist, does it involve under- or overactivity? Earlier description of the disease promoted the concept of distinct phases with an initial phase involving warm, erythematous skin (stage I or acute stage) presumably due to SNS underactivity, an intermittent phase of both warm and cold sensation

(stage II or dystrophic stage) followed by chronic cold sensation (stage III or atrophic stage) due to SNS hyperactivity. Although the existence of distinct phases of CRPS is debated at present (Bruehl, S. *et al.*, 2002), many studies have shown that vasomotor tone is reduced in very early stages of CRPS (Kurvers, H. A. *et al.*, 1995; Wasner, G. *et al.*, 2001), but not in later stages. The finding of reduced plasma norepinephrine and neuropeptide Y concentration on the affected extremity in early phase of the disease confirms this proposition (Raja, S. N. *et al.*, 1995). It seems that the apparent increase in vasomotor tone in later stages of CRPS (as evident by vasoconstriction or cold skin) is due to increased sensitivity (hyper- or supersensitivity) of skin microvessels to catecholamines (Kurvers, H. A. *et al.*, 1995) or secondary changes in neurovascular transmission while actual sympathetic tone is still depressed. Possible mechanisms for this supersensitivity might be decreased neuronal uptake of norepinephrine in the sympathetic neuroeffector junction (Raja, S. N. *et al.*, 1995) or increased number of peripheral α-receptors (Davis, K. D. *et al.*, 1991; Ali, Z. *et al.*, 2000). Studies in experimental animals report an increased expression of α-adrenoceptors in the neuromas that develop after nerve damage. Norepinephrine causes increased excitation of the neuroma afferents. Peripheral nerve injury may also result in sprouting of adrenergic fibers into the dorsal root ganglion and forms contact with sensory neurons. Thus, sympathetic afferent interactions might exist in the vicinity of the sensory receptors in partially denervated peripheral tissues, the peripheral nerve at the site of injury, and the dorsal root ganglion where cell bodies of injured sensory nerves are located.

Although SNS dysfunction is a fascinating concept, it does not explain all features of CRPS. Inflammatory and central origin of pain in CRPS patients has been suggested, and significant animal and human research support their contributions. The readers are advised to review the articles by Jänig W. and Baron R. (2003; 2004) for further understanding in this matter. Readers are also encouraged to read the conflicting views of Ochoa J. and Verdugo R. J. (2001) on the existence of SMP as well as the value of diagnostic phentolamine test or sympathetic blocks. The authors have negated the existence of SMP based on their own studies (Verdugo, R. J. and Ochoa, J. L., 1994), which in our opinion, had methodological deficiencies. A detailed discussion of these mechanisms and opposing views is beyond the scope of this chapter.

5.18.2 Techniques of Sympathetic Blockade

The techniques to achieve sympathetic blockade include the following:

1. Local anesthetic regional block (LASB) of sympathetic ganglion or trunk, for example, stellate ganglion block or lumbar sympathetic block.
2. Neuraxial techniques, for example, epidural or spinal block.
3. Intravenous regional sympathetic blockade (IRSB) with phentolamine, guanethidine, bretylium, clonidine, or lidocaine using tourniquet (Bier block technique).
4. Intravenous infusion of systemic alpha-adrenergic antagonists.
5. Radiofrequency denervation of sympathetic ganglion or trunk.
6. Surgical sympathectomy.

While LASB, IRSB with sympatholytic or local anesthetic medications, neuraxial techniques, and intravenous infusion of adrenergic antagonist can be used for both diagnostic and therapeutic benefits, neurolytic procedures (e.g., 5 and 6) are reserved for treatment of selected patients who show consistent but short-lasting response to initial diagnostic modalities.

5.18.3 Sympathetic Block for Diagnosis

The effectiveness of any diagnostic test or procedure is measured by its sensitivity and specificity. A good diagnostic test, when performed appropriately, should give consistent results in a given patient and should help guide therapy or predict outcome. Before any meaningful conclusions can be drawn from a sympathetic block by any technique, optimum inhibition of sympathetic outflow to the involved extremity needs to be achieved. This requires knowledge of the anatomical distribution of sympathetic innervation and the common pitfalls associated with the conduct and interpretation of these procedures. For instance, in performing stellate ganglion block to achieve an upper extremity sympathetic blockade, it is imperative to block contributions from upper thoracic ganglions that are anatomically separate from the stellate ganglion. This could be achieved by modifications in the previous technique. Similarly, injection of local anesthetic solution into nearby

vascular structures could cause failure to achieve sympatholysis. This can be avoided with the use of intravenous contrast agent and live fluoroscopy to rule out intravascular placement of needle tip.

Following sympathetic blockade, determination of adequacy of sympatholysis is imperative. Monitoring skin temperature change is commonly used in clinical practice. Adequate sympathetic blockade is inferred by approximation of core body temperature and skin temperature of the ipsilateral limb. Accepting a rise in skin temperature by an arbitrary number in comparison with the contralateral limb leads to higher false-positive blocks (Schurmann, M. *et al.*, 2001), probably due to bilateral increase in blood flow following sympathetic block techniques. Many authors recommend further assessment of sympathetic function by sweat test (Stevens, R. A. *et al.*, 1998) or skin conductance response.

5.18.3.1 Local Anesthetic Sympathetic Blocks

LASBs are technically challenging procedures that require training. They have the advantage of selectively blocking stellate or lumbar sympathetic ganglion and/or chain with a small dose of local anesthetic solution without concomitant blockade of sensory or motor fibers (Table 1). Using fluoroscopic or CT guidance, the needle tip is positioned in close proximity to the sympathetic ganglia and a local anesthetic solution is injected. Although numerous complications of LASB have been reported in the literature, these techniques are safe in experienced hands. Efficacy of the block is assessed as previously described by monitoring objective evidence of sympathetic blockade, for example, cutaneous temperature monitoring. The patient is asked to report the intensity of pain using a numeric

Table 1 Comparison of diagnostic modalities for sympathetically maintained pain

Technique	*Advantages*	*Disadvantages*
Interventional regional sympathetic block with local anesthetic agents (LASBs)	1. Well-localized sympathetic ganglion or chain can be anesthetized (blocked). Objective signs of sympathectomy are seen with small doses of LA 2. Systemic side effects from intravenous medications are avoided	1. Requires technical expertise and has higher cost 2. Requires fluoroscopy or CT guidance 3. Complication from contrast or medication allergy 4. Complication from technical reasons; e.g., infection, bleeding, and nerve damage 5. Poorly tolerated in pediatric population and patients with needle phobia 6. Sedatives used during the interventional technique might hinder with postprocedure pain responses 7. False negative • LA fails to anesthetize the sympathetic ganglion adequately • Intravascular injection • Central sympathetic–nociceptive interactions may be missed 8. False positive • LA anesthetizing somatic afferent fibers in the vicinity and causing pain relief from concurrent somatic blockade • Regional ischemic pain will improve with sympathetic block • Placebo effect
Intravenous regional sympathetic blockade (IRSB)	1. Easy to perform 2. Better patient acceptance 3. Low cost 4. Intravenous medications like phentolamine can cross blood–brain barrier and act on spinal cord α-2 adrenergic receptors, which are involved in pain modulation	1. Side effects of medications, e.g., phentolamine can cause positive chrontropic and inotrophic effects 2. Achieving complete sympathectomy at clinically tolerable doses might be difficult 3. Placebo effect cannot be ruled out

pain score before and after sympathetic blockade. The response is usually considered to be positive when a 50% or greater improvement in pain scores is reported in the light of adequate sympathectomy. LASB is traditionally considered as the gold standard against which other techniques have been tested in past (Dellemijn, P. L. *et al.*, 1994). Beyond CRPS, LASBs are also used to block efferent sympathetic fibers at thoracic sympathetic trunk, celiac plexus, superior hypogastric plexus, and ganglion impar to confirm improvement in pain prior to more invasive therapeutic blocks. These invasive procedures are used in the treatment of cancer pain, which may be somatic or visceral, and neuropathic or mixed in nature. A positive response to a temporary diagnostic local anesthetic block is a useful predictor of the success of subsequent neurodestructive procedures. Differential spinal or epidural blocks have also been described to distinguish somatic or central mechanisms from sympathetic etiologies. However, it is difficult to achieve selective sympathetic blockade with these techniques.

5.18.3.2 Intravenous Regional Sympathetic Blockade

Intravenous regional anesthesia, a technique described by August Bier in 1908, involves injection of a local anesthetic solution in a limb, isolated by tourniquet. Based on this concept, Hannington-Kiff proposed IRSB using guanethidine. Initially, guanethidine (with or without a local anesthetic agent) was used to perform this block and later other medications were tried. These include sympatholytics like reserpine, bretylium, or clonidine; local anesthetics like prilocaine or lidocaine; and others like kitanserin (5-HT2 antagonist). Although IRSBs have been used therapeutically in SMP, their use in diagnostic blocks has been limited. The ischemic tourniquet used during the procedure can itself relieve hyperalgesia in neuropathic pain patient (Campbell, J. N. *et al.*, 1988) and cause false-positive results. Certain patients tolerate tourniquet poorly. With IRSBs, guanethidine is often coinjected with local anesthetics since the release of norepinephrine by guanethidine is usually associated with the exacerbation of pain. As a result, diagnosis is often confounded by the effects of local anesthetics. Sudden release of tourniquet might release high doses of medications in systemic circulation and cause significant side effects. This technique is, hence, not useful as a diagnostic tool.

5.18.3.3 Systemic Alpha-Adrenergic Blockade

Intravenous alpha-adrenergic blockade with phentolamine (Phentolamine block, PhB) has been proposed as a safe and effective method of diagnosing SMP (Raja, S. N. *et al.*, 1991; Dellemijn, P. L. *et al.*, 1994). This technique is different from IRSB as no tourniquet is used to isolate the affected limb. In the initial study by Raja S. N. *et al.* (1991), 20 patients were randomly assigned to 25–35 mg of intravenous phentolamine (being administered in a double-blinded fashion) or LASB with 0.25% bupivacaine, and similar pain relief patterns were observed. Although 5–7 °C temperature difference was seen following LASB, the changes in cutaneous temperature after PhB were variable (1.8 ± 0.7 °C). Similar results were obtained by Dellemijn P. L. *et al.* (1994) who concluded that phentolamine infusion is less sensitive but more specific test of SMP than LASB. Both groups (Raja, S. N. *et al.*, 1991; Dellemijn, P. L. *et al.*, 1994) mentioned that the mechanism of pain relief during sympathetic blockade was independent of cutaneous vasodilatation or skin temperature changes. In an attempt to find optimum test dose, Raja S. N. *et al.* (1996) then compared the effect of two different doses of phentolamine (0.5 and 1 mg kg^{-1}) on skin blood flow (using a laser Doppler blood flow monitor) and sympathetically mediated vasoconstrictor response (a reflex decrease in peripheral blood flow in response to deep inhalation) (Raja, S. N. *et al.*, 1996). They concluded that the higher dose of phentolamine (1 mg kg^{-1} over 10 min) resulted in more complete adrenoceptor blockade and recommended this higher dose with cutaneous temperature monitoring to evaluate the sympathetically mediated component in neuropathic pain states.

There is a paucity of research in recognition of placebo responsiveness to sympathetic blocks. Randomization of patients for interventional techniques not only is difficult but also has ethical implications. Clinical observation frequently shows prolonged benefit in some patients beyond the duration of action of local anesthetic agents. Although reversal of central sensitization in the spinal cord and reduced coupling of sympathetic and sensory neurons have been put forward as a possible explanation, other possibilities need further consideration. In order to reduce placebo responsiveness, patients should have different diagnostic procedures like LASB and PhB on separate days. These two

procedures provide complementary information and both may be needed to confirm the diagnosis of SMP (Dellemijn, P. L. *et al.*, 1994).

5.18.4 Sympathetic Block for Therapy of Chronic Pain States

In the past, once diagnosis of SMP was established, patients were often offered a series of regional or intravenous blocks in attempt to reduce pain and vasomotor symptoms. At present, they are considered as an element of multidisciplinary treatment plans. Patients who get significant benefit from initial blocks are often subjected to more aggressive interventional therapies. These treatment modalities are presumed to have enduring sympathectomy or modulation of SNS. They include spinal cord (dorsal column) stimulation, chemical neurolytic procedures, radiofrequency denervation of sympathetic trunk, or even surgical sympathectomy.

5.18.4.1 Local Anesthetic Sympathetic Blocks and Intravenous Regional Sympathetic Blockade

LASBs provide short-term benefits in relieving spontaneous and evoked pain and reducing vasomotor symptoms. Their long-term efficacy is unproven. In contrast, IRSB does not require any special expertise, is easier to perform and, comparatively, has better patient acceptance (Table 1). These procedures have the risk of tourniquet-related pain (if used) and significant side effects from the medications. Both techniques can get false-positive results from placebo effect.

Randomized controlled trials (RCTs) are considered as gold standard to evaluate the efficacy of any therapeutic modality, but not many of these studies have been conducted to assess the usefulness of LASB in SMP. Most randomized trials have been done in CRPS patients (includes both SMP and SIP patients) and not specifically in SMP states. SIP patients are not expected to get any long-term benefits from sympathetic blocks and their inclusion in the study biases the results. Cepeda M. S. *et al.* (2002) attempted a systematic review of RCTs of the effect of LASB in CRPS (not SMP) patients but were unable to pool data due to significant differences in their design. The authors then reviewed nonrandomized controlled studies, case series, and RCTs with acceptable designs, published in English-language peer review journals from 1916 through 1999. Only 29 studies met the inclusion criteria of a sample size of at least 10 patients undergoing LASB with convincible evidence of CRPS. Interestingly, of these 29 studies, only 10 studies evaluated the technical success of block and only two of those assessed pain and outcome. Based on the data from 14 studies (454 patients) that quantified the magnitude of patient's responses and also reported the number of patients with different degrees of responses, authors found that 29% patients undergoing LASB obtain full pain relief (>75% improvement) while 41% obtain partial relief (25–75% improvement). Authors concluded that less than one-third positive response (full pain relief) is consistent with placebo effect and that the efficacy of sympathetic blocks for treatment of CRPS is inconclusive. Many of these 14 studies were published prior to 1960 and only two actually identified technical success of block and pain scores.

Long-term usefulness of IRSB is even less certain. Jadad A. R. *et al.* (1995) attempted a small RCT (nine patients) of the effects of repeated intravenous guanethidine blocks on pain intensity and relief, adverse effects, mood, duration of analgesia, and global scores. The trial was stopped prematurely because of the severity of the adverse effects (hypotension). No significant difference was found between guanethidine and placebo on any of the outcome measures. The authors also presented a systematic review of seven studies on the effects of IRSB in CRPS. Two of these studies, one using ketanserin and one bretylium, with 17 patients in total, showed some advantage over control but few other RCTs showed lack of efficacy of guanethidine. Authors concluded that the use of guanethidine in IRSBs for patients with CRPS was not supported by any available literature. A recent study by Livingstone *et al.* again showed no significant analgesic advantage of guanethidine over a normal saline placebo block in the treatment of early CRPS type I.

Difficulty in conducting RCTs for LASBs or IRSBs for treatment of CRPS or SMP is explicable. Randomization to placebo is almost impossible. Patients or physicians cannot be blinded as outcomes of adequate sympathectomy are obvious. Also, ethical issues might arise in performing technically challenging procedures like stellate ganglion block with saline. But randomization can be done in a different fashion. The new concept of expertise-based RCTs might be useful in this condition when patient outcomes can be compared between physicians who perform repeat LASBs or IVRBs to those who solely

impose conservative management. But again, such studies should compare patients with documented diagnosis of SMP and not CRPS. Based on available data in literature, efficacy and duration of LASB is variable and, indeed, unpredictable. Short duration of pain relief and reduction in vasomotor symptoms is often seen in clinical practice and should be utilized to improve mobility, range of motion, and motor strength by physiotherapy. Repeated blocks are beneficial in selected patients with willingness to actively participate in physiotherapy and are showing signs of continuing improvement.

5.18.4.2 Spinal Cord Stimulation

Spinal cord stimulation (SCS) has recently gained acceptance for a wide variety of neuropathic pain syndromes. A recent RCT (Kemler, M. A. *et al.*, 2004) and meta-analysis of literature (Grabow, T. S. *et al.*, 2003) showed that SCS results in a long-term pain reduction and health-related quality-of-life improvement, but no clinically important improvement of functional status, in chronic RSD. The technique is more effective and less expensive when compared with the standard treatment protocol for chronic CRPS (Mekhail, N. A. *et al.*, 2004). The mechanism of action by which the device provides pain relief is unclear. In general, patients with good response to sympathetic blocks are likely to have long-term pain relief (Hord, E. D. *et al.*, 2003) with SCS, although it does not affect skin microcirculation. The readers are encouraged to read a recent review on this subject for a detailed discussion (Meyerson, B. and Linderoth, B., 2001).

5.18.4.3 Chemical Neurolysis and Radiofrequency Denervation Techniques

Patients who show good response to initial sympathetic blocks are often subjected to radiofrequency denervation or chemical neurolytic destruction of sympathetic innervation. The technique of radiofrequency denervation has gone through various modifications by Noe *et al.*, Rocco, and Sluitjer. At present, destruction of T2 and T3 ganglions is recommended for upper extremity involvement while guidelines for lower extremity vary. Most authors suggest destruction of at least the first three ganglions (L1, L2, and L3), whereas others believe that the L4 and even L5 must be included for good long-term results. Complications of neurodestructive procedures include postsympathectomy sympathalgia, compensatory hyperhidrosis, Horner's syndrome, wound infection, and spinal cord injury. There is a theoretical advantage of lesser incidence of postsympathetic neuralgia and more precise sympatholysis with radiofrequency technique in comparison with chemical neurolysis. Outcome data for these techniques vary. While Wilkinson H. A. (1996) reported almost 90% partial or complete evidence of sympathectomy after 2 years, most authors report sustained pain relief in less than two-thirds of patients at 2 years, and about one-third at 5 years. In a systematic review of the effects of percutaneous neurodestructive procedures for neuropathic pain, Mailis A. and Furlan A. (2003) concluded that the practice of surgical and chemical sympathectomy is based on poor quality evidence, uncontrolled studies, and personal experience. Therefore, more clinical trials of sympathectomy are required to establish the overall effectiveness and potential risks of this procedure. Because of the limited long-term outcomes, consideration should be given to neuromodulatory methods for SMP involving extremities. For other SMP syndromes, like visceral neuropathic pain in pancreatic cancer, chemical neurolyis continues to be the procedure of choice.

5.18.4.4 Surgical Sympathectomy

Surgical sympathectomy has been tried in patients who achieve good pain relief with a series of sympathetic block. Better outcomes are predicted when sympathectomy is performed early in the disease. Concerns about recurrence or development of new CRPS or disabling compensatory sweating syndrome have been raised after surgical sympathectomy, but current data suggests low incidence (7%) of these complications (Bandyk, D. F. *et al.*, 2002). Other disturbing complication includes transient (<3 months) postprocedural sympathalgia (in one-third of the patients following cervicodorsal sympathectomy and 20% of the patients after lumbar sympathectomy). At 1 year postprocedure, one-quarter of the patients are expected to continue experience significant improvement (pain severity score <3) and an additional 50% of the patients would have continued but reduced pain severity and an increase in daily/work activities (Bandyk, D. F. *et al.*, 2002). Many surgeons prefer video-assisted minimally invasive techniques instead of open sympathectomy to reduce other complication rates and promote early postoperative recovery. With the increasing popularity of radiofrequency procedure, rates of surgical sympathectomy have decreased.

5.18.5 Conclusions

SNS plays an intriguing role in maintaining pain in certain conditions. Complex regional pain syndromes are prime example of such states. Selective sympathetic blocks are commonly used to diagnose a subset of patients with a predominant sympathetically maintained pain state. In order to avoid false-positive diagnosis, at least two different diagnostic tests should be implicated on separate days to confirm the diagnosis. Treatment options that have shown some promising results include local anesthetic sympathetic blocks, SCS, radiofrequency techniques, and surgical sympathectomy in early stages. Visceral pain of pancreatic origin responds well to chemical neurolytic blocks. More randomized trials are warranted to prove long-term efficacy of neuromodulation as well as neurodestructive techniques.

References

Ali, Z., Raja, S. N., Wesselmann, U., Fuchs, P. N., Meyer, R. A., and Campbell, J. N. 2000. Intradermal injection of norepinephrine evokes pain in patients with sympathetically maintained pain. Pain 88(2), 161–168.

Bandyk, D. F., Johnson, B. L., Kirkpatrick, A. F., Novotney, M. L., and Back, M. R. 2002. Surgical sympathectomy for reflex sympathetic dystrophy syndromes. J. Vasc. Surg. 35(2), 269–277.

Baron, R. and Jänig, W. 2004. Complex regional pain syndromes – how do we escape the diagnostic trap? Lancet 364(9447), 1739–1741.

Baron, R., Schattschneider, J., Binder, A., Siebrecht, D., and Wasner, G. 2002. Relation between sympathetic vasoconstrictor activity and pain and hyperalgesia in complex regional pain syndromes: a case-control study. Lancet 359(9318), 1655–1660.

Bruehl, S., Harden, R. N., Galer, B. S., Saltz, S., Backonja, M., and Stanton-Hicks, M. 2002. Complex regional pain syndrome: are there distinct subtypes and sequential stages of the syndrome? Pain 95(1–2), 119–124.

Campbell, J. N., Raja, S. N., Meyer, R. A., and Mackinnon, S. E. 1988. Myelinated afferents signal the hyperalgesia associated with nerve injury. Pain 32(1), 89–94.

Cepeda, M. S., Lau, J., and Carr, D. B. 2002. Defining the therapeutic role of local anesthetic sympathetic blockade in complex regional pain syndrome: a narrative and systematic review. Clin. J. Pain 18(4), 216–233.

Davis, K. D., Treede, R. D., Raja, S. N., Meyer, R. A., and Campbell, J. N. 1991. Topical application of clonidine relieves hyperalgesia in patients with sympathetically maintained pain. Pain 47(3), 309–317.

Dellemijn, P. L., Fields, H. L., Allen, R. R., McKay, W. R., and Rowbotham, M. C. 1994. The interpretation of pain relief and sensory changes following sympathetic blockade. Brain 117(Pt 6), 1475–1487.

Drummond, P. D. and Finch, P. M. 2004. Persistence of pain induced by startle and forehead cooling after sympathetic blockade in patients with complex regional pain syndrome. J. Neurol. Neurosurg. Psychiatry 75(1), 98–102.

Grabow, T. S., Tella, P. K., and Raja, S. N. 2003. Spinal cord stimulation for complex regional pain syndrome: an evidence-based medicine review of the literature. Clin. J. Pain 19(6), 371–383.

Harden, R. N. and Bruehl, S. 2006. Diagnosis of complex regional pain syndrome: signs, symptons, and new empirically derived diagnostic criteria. Clin. J. Pain 22(5), 415–419.

Hord, E. D., Cohen, S. P., Cosgrone, G. R., Ahmed, S. U., Vallejo, R., Chang, Y., and Stojanovic, M. P. 2003. The predictive value of sympathetic block for the success of spinal cord stimulation. Neurosurgery 53(3), 626–632.

Jadad, A. R., Carroll, D., Glynn, C. J., and McQuay, H. J. 1995. Intravenous regional sympathetic blockade for pain relief in reflex sympathetic dystrophy: a systematic review and a randomized, double-blind crossover study. J. Pain Symp. Manage. 10(1), 13–20.

Jänig, W. and Baron, R. 2002. Complex regional pain syndrome is a disease of the central nervous system. Clin. Auton. Res. 12(3), 150–164.

Jänig, W. and Baron, R. 2003. Complex regional pain syndrome: mystery explained? Lancet Neurol. 2(11), 687–697.

Jänig, W. and Baron, R. 2004. Experimental approach to CRPS. Pain Mar. 108(1–2), 3–7.

Kemler, M. A., De Vet, H. C., Barendse, G. A., Van Den Wildenberg, F. A., and Van Kleef, M. 2004. The effect of spinal cord stimulation in patients with chronic reflex sympathetic dystrophy: two years' follow-up of the randomized controlled trial. Ann. Neurol. 55(1), 13–18.

Kurvers, H. A., Jacobs, M. J., Beuk, R. J., Van den Wildenberg, F. A., Kitslaar, P. J., Slaaf, D. W., and Reneman, R. S. 1995. Reflex sympathetic dystrophy: evolution of microcirculatory disturbances in time. Pain 60(3), 333–340.

Mailis, A. and Furlan, A. 2003. Sympathectomy for neuropathic pain. Cochrane Database Syst. Rev. (2), CD002918.

Mekhail, N. A., Aeschbach, A., and Stanton-Hicks, M. 2004. Cost benefit analysis of neurostimulation for chronic pain. Clin. J. Pain 20(6), 462–468.

Merskey, H. and Bogduk, N. 1995. Classification of Chronic Pain: Descriptions of Chronic Pain Syndromes and Definition of Terms. IASP Press.

Meyerson, B. and Linderoth, B. 2001. Spinal Cord Stimulation. In: Bonica's Management of Pain, 3rd edn. (*eds*. J. D. Loeser, S. D. Butler, C. R. Chapman, *et al.*), pp. 1857–1876. Lippincott Williams and Wilkins.

Ochoa, J. and Verdugo, R. J. 2001. Mechanisms of neuropathic pain: nerve, brain, and psyche: perhaps the dorsal horn but not the sympathetic system. Clin. Auton. Res. 11(6), 335–339.

Raja, S. N., Choi, Y., Asano, Y., Holmes, C., and Goldstein, D. S. 1995. Arteriovenous differences in plasma concentrations of catechols in rats with neuropathic pain. Anesthesiology 83(5), 1000–1008.

Raja, S. N., Treede, R. D., Davis, K. D., and Campbell, J. N. 1991. Systemic alpha-adrenergic blockade with phentolamine: a diagnostic test for sympathetically maintained pain. Anesthesiology 74(4), 691–698.

Raja, S. N., Turnquist, J. L., mEleka, S., and Campbell, J. N. 1996. Monitoring adequacy of alpha-adrenoceptor blockade following systemic phentolamine administration. Pain 64(1), 197–204.

Schurmann, M., Gradl, G., Wizgal, I., Tutic, M., Moser, C., Azad, S., and Beyer, A. 2001. Clinical and physiologic evaluation of stellate ganglion blockade for complex regional pain syndrome type I. Clin. J. Pain 17(1), 94–100.

Stanton-Hicks, M., Jänig, W., Hassenbusch, S., Haddox, J. D., Boas, R., and Wilson, P. 1995. Reflex sympathetic dystrophy: changing concepts and taxonomy. Pain 63(1), 127–133.

Stevens, R. A., Stotz, A., Kao, T. C., Powar, M., Burgen, S., and Kleinman, B. 1998. The relative increase in skin temperature after stellate ganglion block is predictive of a complete sympathectomy of the hand. Reg. Anesth. Pain Med. 23(3), 266–270.

Verdugo, R. J and Ochoa, J. L. 1994. 'Sympathetically maintained pain'. I. Phentolamine block questions the concept. Neurology 44(6), 1003–1010.

Verdugo, R. J., Campero, M., and Ochoa, J. L. 1994. Phentolamine sympathetic block in painful polyneuropathies. II. Further questioning of the concept of 'sympathetically maintained pain'. Neurology 44(6), 1010–1014.

Wasner, G., Schattschneider, J., Heckmann, K., Maier, C., and Baron, R. 2001. Vascular abnormalities in reflex sympathetic dystrophy (CRPS I): mechanisms and diagnostic value. Brain. 124(Pt 3), 587–599.

Wilkinson, H. A. 1996. Percutaneous radiofrequency upper thoracic sympathectomy. Neurosurgery 38(4), 715–725.

Further Reading

Jänig, W., Levine, J. D., and Michaelis, M. 1996. Interactions of sympathetic and primary afferent neurons following nerve injury and tissue trauma. Prog. Brain Res. 113, 161–184.

Nathan, P. W. 1983. Pain and the sympathetic system. J. Auton. Nerv. Syst. 7(3–4), 363–370.

5.19 Sprouting in Dorsal Root Ganglia

E M McLachlan, Prince of Wales Medical Research Institute, Randwick, NSW, Australia

© 2008 Elsevier Inc. All rights reserved.

5.19.1	The Discovery	238
5.19.2	Sprouting of Sympathetic Axons within Dorsal Root Ganglia	239
5.19.3	Sprouting of Primary Afferent Neurons within Dorsal Root Ganglia	239
5.19.4	Formation of Perineuronal Rings or Baskets	239
5.19.5	Underlying Cellular Mechanisms	240
5.19.6	Other Functional Considerations	241
5.19.7	Other Forms of Sympathetic Plasticity after Nerve Injury	241
References		242

Glossary

Aβ nociceptors They have often been ignored but there is accumulating evidence that a subpopulation of large-diameter fast-conducting (A) sensory neurons are nociceptive (Djouhri, L. and Lawson, S. N., 2004).

calcitonin gene-related peptide (CGRP) It is a neuropeptide present in the majority of peptidergic primary afferent nociceptor neurons. CGRP is also expressed in some medium to large diameter afferent neurons and appears *de novo* in others. including gracile-projecting mechanosensitive neurons, after nerve injuries (Ma, W. *et al.*, 1999).

galanin It is a neuropeptide present in a subpopulation of CGRP-containing primary afferent nociceptor neurons. It is upregulated both in these neurons and in sympathetic postganglionic neurons after a peripheral nerve injury.

neuropeptide Y (NPY) It is a neuropeptide that is present in many sympathetic postganglionic vasoconstrictor neurons in most species. It is upregulated in gracile-projecting low-threshold mechanosensitive primary afferent neurons after peripheral nerve lesions.

nonpeptidergic sensory neurons These are small-diameter dorsal root ganglion neurons that lack any known neuropeptide but express GFRα1-2 and c-RET, components of the receptor complex for glial-derived neurotrophic factor, and bind isolectin B4 (derived from *Griffonia simplicifolia*) (Bennett, D. L. *et al.*, 1998), neither of which are features of peptidergic sensory neurons. Nonpeptidergic sensory neurons are usually nociceptive (Lawson, S. N., 2002).

p75 It is the low-affinity nerve growth factor (NGF) receptor recognized by NGF, brain-derived neurotrophic factor (BDNF), neurotrophin-3 (NT-3), and neurotrophin-4/5 (NT-4/5). p75 interacts with each neurotrophin but with slightly different binding properties. It has striking structural homology with a family of receptors, including tumor necrosis factor (TNF) receptors, CD40, and Fas, consistent with it having many functions.

peptidergic sensory neurons These are small-diameter dorsal root ganglion neurons that contain a known neuropeptide (such as substance P, calcitonin gene-related peptide, galanin, somatostatin, and vasoactive intestinal polypeptide) and are usually nociceptors (Lawson, S. N., 2002).

perineuronal rings or baskets These are arrangements of varicose nerve terminals formed by the endings of sympathetic neurons and peptidergic and nonpeptidergic sensory neurons within dorsal root ganglia that project into a lesioned nerve trunk.

retrograde reaction Refers to the response in the soma of a neuron when its axon is severed. Following axotomy, either a positive signal of injury or the arrest of the normal retrograde traffic from the axon terminals reaches the soma within a few hours via the retrograde axoplasmic transport mechanism. The neuron soma swells and the nucleus may assume an eccentric position. These structural changes are referred to chromatolysis as the chromophilic Nissl bodies are disrupted. Protein synthesis is modified so that synthesis of neurotransmitter substances is reduced and other

activities such as regeneration are supported. The satellite glia around the soma also respond and begin to release cytokines and chemokines. They proliferate and start to synthesize neurotrophins.

satellite glia These are the support cells that surround the cell bodies of primary afferent neurons within dorsal root ganglia. They normally express low levels of glial fibrillary acidic protein (GFAP) which is upregulated after nerve injury prior to the cells proliferating around damaged neurons.

substance P (SP) It is a neuropeptide present in a subpopulation of peptidergic primary afferent nociceptor neurons. It is upregulated in gracile-projecting low-threshold mechanosensitive primary afferent neurons after peripheral nerve lesions.

5.19.1 The Discovery

Clinicians observe that, in a subgroup of patients with chronic neuropathic pain after peripheral nerve injury of varying degrees of severity, sympathetic activity exacerbates or initiates pain, usually described as burning or stabbing (Bonica, J. J., 1990). The pain can be referred to superficial and/or deep sites and is often associated with allodynia and hyperalgesia. It has been postulated that, after the injury, nociceptors are activated by norepinephrine released by sympathetic activity, for example, during emotional stress or exposure to low environmental temperatures. This idea was based on evidence that pain was relieved by blockade of (1) the activity of sympathetic postganglionic neurons by injecting local anesthetics into paravertebral ganglia supplying the affected limb (Bonica, J. J., 1990), (2) norepinephrine release by injecting guanethidine into the limb (Wahren, L. K. *et al.*, 1991), or (3) the effects of norepinephrine by injecting α-adrenoceptor antagonists such phentolamine intravenously (Raja, S. N. *et al.*, 1991). Sympathetically maintained pain usually develops days to weeks after the injury.

These observations are mysterious because sympathetic nerve terminals are not co-located with nociceptor neurons or their terminals. In the skin, sympathetic axons terminate on arteriolar vessels deep within the dermis whereas nociceptor terminals lie below and within the epidermis. Sensory and sympathetic terminals do not usually co-locate in deeper tissues, other than rare axons containing substance P (SP) and calcitonin gene-related peptide (CGRP) that run among the sympathetic perivascular terminals on blood vessels (Holzer, P., 1992). There is no evidence for α-adrenoceptors on nociceptor terminals in normal skin and subcutaneous introduction of norepinephrine produces blanching but no pain.

Following early studies triggered by military injuries, an explosion of research in the last 25 years has utilized mainly rodents with injuries to one sciatic nerve that lead to diverse alterations in the damaged neurons, their supporting glia, the tissues they previously supplied, and the related vasculature. In addition inflammatory cells invade, not only the lesion site, but also retrogradely along the nerve trunk and within L4/5 dorsal root ganglia (DRGs), L3/4 sympathetic paravertebral ganglia, and the ventral horn of L4/5 spinal cord (Aldskogius, H. and Kozlova, E. N., 1998; Hu, P. and McLachlan, E. M., 2002; 2004). These changes persist for many months unless the damaged axons can regenerate to their target tissues.

Of relevance to injury-induced spontaneous pain is the generation of spontaneous activity in 20–30% of primary afferents within the damaged nerve. This activity is thought to contribute to central sensitization in the dorsal horn leading to abnormal discharge of nociceptive pathways (Mannion, R. J. and Woolf, C. J., 2000). The ectopic activity arises at two sites: in unmyelinated (C) neurons, it is initiated at the site of the injury (Michaelis, M. *et al.*, 1995); in myelinated (A) neurons, it arises from oscillations in the membrane potential of the somata in the DRG (Kajander, K. C. *et al.*, 1992; Liu, C. N. *et al.*, 2000). When the DRG and its connections are intact *in vivo*, activity in A axons arises in muscle but not cutaneous afferents (Michaelis, M. *et al.*, 2000).

The ectopic discharge in some DRG neurons can be generated or modulated by sympathetic activity. Wilfrid Jänig recorded from single myelinated afferent axons projecting down a ligated sciatic nerve (McLachlan, E. M. *et al.*, 1993). Stimulation of the sympathetic supply at high frequency (50 Hz for 10 s) excited a subgroup of afferents. Intravenous application of phentolamine completely inhibited the response, confirming that the sympathetic-sensory link was

located proximally. Histochemical demonstration of norepinephrine revealed perivascular terminals outside the ganglion sprouting through the DRG (McLachlan, E. M. *et al.*, 1993). After a few weeks, some sprouting axons had formed interwoven baskets or rings of varicose terminals around a few large-diameter neurons. These novel structures appeared to be the anatomical basis for a functional link between sympathetic and sensory systems after injury.

5.19.2 Sprouting of Sympathetic Axons within Dorsal Root Ganglia

Sprouting of norepinephrine-containing terminals into DRGs after injury was soon confirmed in many laboratories (e.g., Chung, K. *et al.*, 1996; Kim, H. J. *et al.*, 1996; Ramer, M. S. and Bisby, M. A., 1997), mainly using immunohistochemistry to demonstrate tyrosine hydroxylase (TH), the rate-limiting enzyme for the synthesis of norepinephrine. The time course of development of sprouts varies with the site and nature of the lesion (Ramer, M. S. *et al.*, 1999). In rats, the sprouts develop over a few weeks after sciatic transection and form increasing numbers of perineuronal rings after ~4 weeks. The number of rings reaches a maximum (~2.5% of neurons or ~7.5% of A neurons) between 8 and 12 weeks and then gradually declines over 1 year or more (Hu, P. and McLachlan, E. M., 2001). While sympathetic sprouts appear in normal aged animals (Ramer, M. S. and Bisby, M. A., 1998b), this cannot account for the raised proportion of rings on the side ipsilateral to the lesion. Some perineuronal rings may persist indefinitely after injury, probably accounting for their presence in humans as described by Ramon y Cajal (Garcia-Poblete, E. *et al.*, 2003). The extent of sprouting is generally greater if the lesion is closer to the DRG (Kim, H. J. *et al.*, 1996; Ramer, M. S. and Bisby, M. A., 1998a) and if more axons are cut (Kim, H. J. *et al.*, 2001), although the relationships are not linear and may depend on the proportions of cutaneous and muscle axons involved (Hu, P. and McLachlan, E. M., 2003). Sprouting of sympathetic terminals into DRGs after sciatic transection does not occur in guinea-pigs that lack sympathetic terminals on nearby vessels (Hu, P. and McLachlan, E. M., 2000).

Sympathetic sprouts are already quite extensive after 7 days if the spinal nerve is transected (Chung, K. *et al.*, 1996; Ramer, M. S. *et al.*, 1998). Cutting L5 spinal nerve leads to hyperalgesia within a few days in the territory of the intact root (L4). Sympathetic sprouts appear sooner and are more prolific when the sciatic nerve is only partially transected (Shir, Y. and Seltzer, Z., 1991) or subjected to chronic constriction (CCI) (Bennett, G. J. and Xie, Y. K., 1988) rather than transection. These injuries, like spinal nerve transection, leave intact axons lying in regions of Wallerian degeneration and the ensuing inflammatory reaction damages more axons. Such injuries produce mechanical allodynia and thermal hyperalgesia within a few days.

5.19.3 Sprouting of Primary Afferent Neurons within Dorsal Root Ganglia

One possible trigger for sprouting of perivascular terminals is an increased local concentration of neurotrophins, such as nerve growth factor (NGF) (Herzberg, U. *et al.*, 1997; see below). Consistent with this, sensory neurons containing SP and CGRP which bear the appropriate receptors (trkA) sprout within the lesioned DRG, forming similar numbers of perineuronal rings (McLachlan, E. M. and Hu, P., 1998). Galanin appears in some sprouts of both sympathetic and peptidergic origin (Hu, P. and McLachlan, E. M., 2001).

There is one report (Li, L. and Zhou, X. F., 2001) that the nonpeptidergic primary afferent axons that bind *Griffonia simplicifolia* I isolectin B4 (IB4) also sprout within L5 DRG after spinal nerve transection. Increasingly from 5 weeks after the lesion, IB4+ axons were found to encircle mainly large-diameter neuron somata where they were intermingled with proliferated satellite cells that also bound IB4. In some cases, TH+ axons were present around the same neurons. What is amazing is that tenfold more neurons received IB4+ perineuronal rings than TH+, CGRP+, or galanin+ rings at the same postoperative time (McLachlan, E. M. and Hu, P., 1998; Hu, P. and McLachlan, E. M., 2001). However, only a few of the IB4+ axons also stained for protein gene product (PGP) 9.5, a pan-neuronal marker (ubiquitin C-terminal hydroxylase).

5.19.4 Formation of Perineuronal Rings or Baskets

Perineuronal rings form more often at either pole of the DRG where large-diameter neurons are clustered (McLachlan, E. M. *et al.*, 1993). The neurons that receive them can be axotomized or intact (Jones, M. G. *et al.*, 1999; Hu, P. and

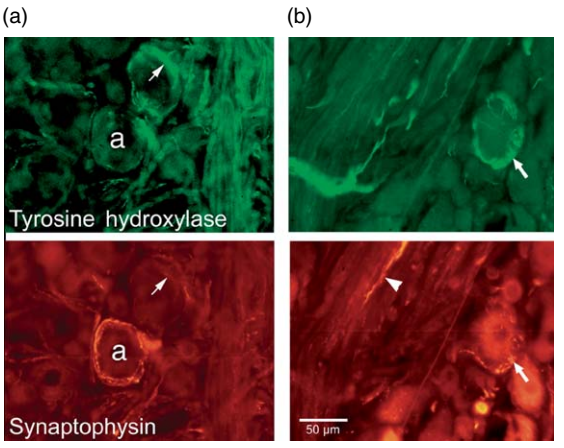

Figure 1 Perineuronal rings in rat L5 dorsal root ganglia 10 weeks after sciatic nerve transection and ligation. Two pairs of micrographs (a) and (b) show immunofluorescence for tyrosine hydroxylase (TH, green) and synaptophysin (Syn, red). (a) TH+ terminals that lack Syn (thin arrows) wrap around a neuron soma adjacent to another (A) that bears a dense basket of Syn+ terminals. (b) A neuron receives a TH+/Syn+ perineuronal ring (thick arrows). TH+ axons in the small nerve bundle to the left in (b) do not express Syn but a sprouting axon in the main axon bundle (arrowhead) is Syn+.

McLachlan, E. M., 2003). The varicose terminals intertwine around the somata but normally remain within the layers of proliferated satellite glia, very rarely forming contact with neuron somata (Chung, K. *et al.*, 1997; Shinder, V. *et al.*, 1999).

Sometimes isolated neurons are targeted, or more than one type of axon can encircle the same neuron (McLachlan, E. M. and Hu, P., 1998) or, in other cases, adjacent neurons receive a ring from one or other axon type (Figure 1). Synaptophysin, a non-specific marker of sprouting axons, appears in rings at a similar density to those with TH, CGRP, or galanin (Hu, P. and McLachlan, E. M., 2003). This may result because synaptophysin is only partly co-located with these substances or because of nonpeptidergic axon sprouts. As synaptophysin is also a synaptic vesicle protein, its presence in some but not all varicosities within rings supports them being release sites. Unfortunately, it is likely to be impossible to measure release directly from these terminals.

5.19.5 Underlying Cellular Mechanisms

Systemic lidocaine is successful in treating some forms of neuropathic pain (Wallace, M. S. *et al.*, 2000). Delivery of lidocaine by osmotic pump to rats with nerve transection reduced the amount of sympathetic sprouting and the number of TH+ rings (Zhang, J. M. *et al.*, 2004), as did its application locally at the time of the lesion. These data suggest that activity derived from the neuroma is important for initiating the sprouting response.

Sympathetic axons sprout from two sources: (1) from intact perivascular terminals, which occur after a distant lesion, and are dependent on NGF and (2) by retrograde growth along the spinal nerve, which occurs when anterograde growth is obstructed at the lesion, and is NGF-independent. The former predominates after a distant injury, and the latter after spinal nerve ligation (Ramer, M. S. and Bisby, M. A., 1999). However, a common response to axotomy is the sprouting of collaterals from a transected axon within a short distance from the soma (Kelly, M. E. M. *et al.*, 1989) and this may occur after lesions to either sympathetic or sensory axons.

Upregulation of neurotrophin messenger ribonucleic acid (mRNA) by satellite glia leads to their local production within the DRG, stimulating growth of axons bearing appropriate receptors. This has been shown for NGF and neurotrophin-3 (NT-3) which are synthesized by the proliferated satellite glia that surround large-diameter neurons. Treatment with antibodies to NGF or NT-3 reduces the length of TH+ sprouts after a spinal nerve lesion (Ramer, M. S. and Bisby, M. A., 1999; Zhou, X. F. *et al.*, 1999) as both trkA and trkC are present on sympathetic and sensory axons. Brain-derived neurotrophic factor (BDNF) is upregulated in lesioned DRG neurons and antibodies to BDNF also inhibit sympathetic sprouting (Deng, Y. S. *et al.*, 2000). These approaches do not seem to have been applied to examine sprouting of sensory neurons. Glial cell-derived neurotrophic factor (GDNF) mRNA is present in satellite cells in DRGs and is upregulated after injury (Hammarberg, H. *et al.*, 1996), providing a basis for the sprouting of IB4+ axons (Li, L. and Zhou, X. F., 2001). Intrathecal GDNF does not elicit sympathetic sprouts (Jones, M. G. *et al.*, 1999) but leukemia inhibitory factor does (Thompson, S. W. and Majithia, A. A., 1998), perhaps by an effect that modifies NGF production.

The formation of perineuronal rings has been studied in trigeminal ganglia of transgenic mice. When these animals overexpress NGF (Davis, B. M. *et al.*, 1994), TH+ terminals preferentially target trkA+ CGRP+ sensory neurons that contain NGF (Walsh, G. S. and Kawaja, M. D., 1998; Walsh, G. S. *et al.*, 1999). The data indicate that CGRP+ axons do not

sprout in these animals. If NGF or trkA is deleted, the TH+ axons do not enter the ganglion. If p75 is deleted but NGF is overexpressed, abundant TH+ sprouts wander through the DRG without associating with specific neuron somata (Walsh, G. S. *et al.*, 1999).

These elegant experiments do not help to explain sprouting or the formation of rings after nerve injury in normal adult animals. As mentioned above, NGF is synthesized by satellite glia that express p75 whereas trkA is downregulated on neuron somata (Verge, V. M. *et al.*, 1989). Further, no sprouts appear in the rat trigeminal ganglion after transection of the infraorbital or inferior alveolar nerve quite close to the ganglion (Bongenhielm, U. *et al.*, 1999) or chronic constriction injury (CCI) of the mental nerve (Grelik, C. *et al.*, 2005). This seems surprising as sympathetic axons join the nerve immediately distal to the trigeminal ganglion as for the DRG. Perhaps the absence of large-diameter proprioceptive neurons (located in the mesencephalic nucleus V) prevents the changes that trigger sympathetic sprouting in lesioned DRGs. Whether peptidergic neurons in trigeminal ganglia sprout after nerve lesions does not seem to have been examined.

Nevertheless it seems likely that the expression of p75 on proliferated glia in rat DRGs is important for ring formation. In guinea-pigs, in which sympathetic sprouting does not occur (see above), peptidergic axons sprout into the DRG but do not form perineuronal rings after sciatic transection. This might be explained by both the absence of glial reaction to axotomy (i.e., no upregulation of glial fibrillary acidic protein) and the failure of glia to express p75 in this species (Hu, P. and McLachlan, E. M., 2000).

What initiates neurotrophin production? It might follow the retrograde reaction in satellite glia and the subsequent invasion of the DRG by macrophages and lymphocytes (Hu, P. and McLachlan, E. M., 2002). Following sciatic transection, macrophage and T-cell density peaks after 1 week and remains raised for several months. Lymphocytes and macrophages secrete neurotrophins and proinflammatory cytokines. Neurotrophins trigger sprouting and cytokines sensitize DRG neurons. Further, T cells contribute to injury-induced pain (Moalem, G. *et al.*, 2004).

5.19.6 Other Functional Considerations

The somata around which perineuronal rings form have been thought to be low-threshold mechanoreceptors. The absence of sympathetic rings around peptidergic neurons (Ramer, M. S. and Bisby, M. A., 1998c) excludes the gracile-projecting A neurons which express SP, CGRP, NPY, and galanin several weeks after a peripheral injury (Zhang, X. *et al.*, 1993; Noguchi, K. *et al.*, 1995; Ma, W. and Bisby, M. A., 1997; Ma, W. *et al.*, 1999). Varicose peptidergic rings do not form around peptidergic neurons (McLachlan, E. M. and Hu, P., 1998). However, ~20% of A neurons in rat L5 DRG are Aβ-nociceptors (Djouhri, L. and Lawson, S. N., 2004) that is, 6% of all neurons, and at least some have large diameters. Allowing that TH+ terminals make up only ~50% of rings, rings may occur on 6% of neurons, making it feasible that Aβ-nociceptor neurons are the targets. While trkA is currently the only specific marker of these Aβ-neurons (Fang, X. *et al.*, 2005), this is downregulated after axotomy (Verge, V. M. *et al.*, 1989; Li, L. *et al.*, 2000) so that it may not be possible to test this idea.

Despite evidence that α-adrenoceptors are expressed *de novo* by a small proportion of largely medium-diameter neurons in lesioned DRGs (Birder, L. A. and Perl, E. R., 1999), there is limited evidence that norepinephrine can excite lesioned A neurons. Although norepinephrine can depolarize a small proportion of both control and damaged neurons in intact DRGs *in vitro* (Jones, M. G. *et al.*, 1999), this does not seem to be α-adrenoceptor mediated (Lopez de Armentia, M. *et al.*, 2003; cf. Xing, J. L. *et al.*, 2003). For neuropeptides, neuron somata with myelinated axons lack CGRP binding sites (Segond von Banchet, G. *et al.*, 2002), although they can develop sensitivity to galanin and SP after axotomy (Xu, Z. Q. *et al.*, 1997; Abdulla, F. A. *et al.*, 2001). This has not been demonstrated *in situ*.

5.19.7 Other Forms of Sympathetic Plasticity after Nerve Injury

Is there another explanation for the enhanced responses to sympathetic activation after injury? The normal consequence of sympathetic activity is vasoconstriction which is abolished by phentolamine. Stimulation paradigms that excite DRG neurons (>10 Hz) elicit marked vasoconstriction in most vascular beds. Stimulation of the lumbar sympathetic chain augmented discharge in a proportion of myelinated dorsal root axons from spinal nerve-injured rats only when vascular resistance in the

DRG was near maximal (Häbler, H. J. *et al.*, 2000). Discharge was also increased by vasoconstrictor agents and blockade of nitric oxide synthase. These data imply that enhanced neurovascular responses after a lesion jeopardize perfusion of the DRG, and raise the possibility that ischemia may be responsible for increasing excitability of sensory neurons.

Finally, the phenomenon of sympathetic sprouting in lesioned DRGs has had attention because of its possible relation to sympathetically maintained neuropathic pain. It is, however, important to note the failure of sympathectomy to modify ectopic activity in anesthetized rats (Liu, X. G. *et al.*, 2000) or mechanical allodynia (Ringkamp, M. *et al.*, 1999), and the lack of relation between the extent of sympathetic sprouting and pain behavior (Kim, H. J. *et al.*, 1999). Thus, although sympathetic perineuronal rings have been postulated to underlie ectopic activity, evidence for this in experimental animals is not convincing. Nevertheless the experiments on sprouting have provided insights into plasticity in the damaged nervous system.

Acknowledgments

Work in the author's laboratory was supported by the National Health & Medical Research Council and the Motor Accidents Authority of New South Wales.

References

Abdulla, F. A., Stebbing, M. J., and Smith, P. A. 2001. Effects of substance P on excitability and ionic currents of normal and axotomized rat dorsal root ganglion neurons. Eur. J. Neurosci. 13, 545–562.

Aldskogius, H. and Kozlova, E. N. 1998. Central neuron–glial and glial–glial interactions following axon injury. Prog. Neurobiol. 55, 1–26.

Bennett, D. L., Michael, G. J., Ramachandran, N., Munson, J. B., Averill, S., Yan, Q., McMahon, S. B., and Priestley, J. V. 1998. A distinct subgroup of small DRG cells express GDNF receptor components and GDNF is protective for these neurons after nerve injury. J. Neurosci. 18, 3059–3072.

Bennett, G. J. and Xie, Y. K. 1988. A peripheral mononeuropathy in rat that produces disorders of pain sensation like those seen in man. Pain 33, 87–107.

Birder, L. A. and Perl, E. R. 1999. Expression of alpha2-adrenergic receptors in rat primary afferent neurons after peripheral nerve injury or inflammation. J. Physiol. 515, 533–542.

Bongenhielm, U., Biossonade, F. M., Westermark, A., Robinson, P. P., and Fried, K. 1999. Sympathetic nerve sprouting fails to occur in the trigeminal ganglion after peripheral nerve injury in the rat. Pain 82, 283–288.

Bonica, J. J. 1990. The Management of Pain. Lea and Febiger.

Chung, K., Lee, B. H., Yoon, Y. W., and Chung, J. M. 1996. Sympathetic sprouting in the dorsal root ganglia of the injured peripheral nerve in a rat neuropathic pain model. J. Comp. Neurol. 376, 241–252.

Chung, K., Yoon, Y. W., and Chung, J. M. 1997. Sprouting sympathetic fibers form synaptic varicosities in the dorsal root ganglion of the rat with neuropathic injury. Brain Res. 751, 275–280.

Davis, B. M., Albers, K. M., Seroogy, K. B., and Katz, D. M. 1994. Overexpression of nerve growth factor in transgenic mice induces novel sympathetic projections to primary sensory neurons. J. Comp. Neurol. 349, 464–474.

Deng, Y. S., Zhong, J. H., and Zhou, X. F. 2000. Effects of endogenous neurotrophins on sympathetic sprouting in the dorsal root ganglia and allodynia following spinal nerve injury. Exp. Neurol. 164, 344–350.

Djouhri, L. and Lawson, S. N. 2004. Aβ-fiber nociceptive primary afferent neurons: a review of incidence and properties in relation to other afferent A-fiber neurons in mammals. Brain Res. Rev. 46, 131–145.

Fang, X., Djouhri, L., McMullan, S., Berry, C., Okuse, K., Waxman, S. G., and Lawson, S. N. 2005. trkA is expressed in nociceptive neurons and influences electrophysiological properties via Nav1.8 expression in rapidly conducting nociceptors. J. Neurosci. 25, 4868–4878.

Garcia-Poblete, E., Fernandez-Garcia, H., Moro-Rodriguez, E., Catala-Rodriguez, M., Rico-Morales, M. L., Garcia-Gomez-de-las-Heras, S., and Palomar-Gallego, M. A. 2003. Sympathetic sprouting in dorsal root ganglia (DRG): a recent histological finding? Histol. Histopathol. 18, 575–586.

Grelik, C., Bennett, G. J., and Ribeiro-da-Silva, A. 2005. Autonomic fibre sprouting and changes in nociceptive sensory innervation in the rat lower lip skin following chronic constriction injury. Eur. J. Neurosci. 21, 2475–2487.

Häbler, H. J., Eschenfelder, S., Liu, X. G., and Jänig, W. 2000. Sympathetic-sensory coupling after L5 spinal nerve lesion in the rat and its relation to changes in dorsal root ganglion blood flow. Pain 87, 335–345.

Hammarberg, H., Piehl, F., Cullheim, S., Fjell, J., Hokfelt, T., and Fried, K. 1996. GDNF mRNA in Schwann cells and DRG satellite cells after chronic sciatic nerve injury. Neuroreport 7, 857–860.

Herzberg, U., Eliav, E., Dorsey, J. M., Gracely, R. H., and Kopin, I. J. 1997. NGF involvement in pain induced by chronic constriction injury of the rat sciatic nerve. Neuroreport 8, 1613–1618.

Holzer, P. 1992. Peptidergic sensory neurons in the control of vascular functions: mechanisms and significance in the cutaneous and splanchnic vascular beds. Rev. Physiol. Biochem. Pharmacol. 121, 49–146.

Hu, P. and McLachlan, E. M. 2000. Distinct sprouting responses of sympathetic and peptidergic sensory axons proximal to a sciatic nerve transection in guinea pigs and rats. Neurosci. Lett. 295, 59–63.

Hu, P. and McLachlan, E. M. 2001. Long-term changes in the distribution of galanin in dorsal root ganglia after sciatic or spinal nerve transection in rats. Neuroscience 103, 1059–1071.

Hu, P. and McLachlan, E. M. 2002. Macrophage and lymphocyte invasion of dorsal root ganglia after peripheral nerve lesions in the rat. Neuroscience 112, 23–38.

Hu, P. and McLachlan, E. M. 2003. Selective reactions of cutaneous and muscle afferent neurons to peripheral nerve transection in rats. J. Neurosci. 23, 10559–10567.

Hu, P. and McLachlan, E. M. 2004. Inflammation in sympathetic ganglia proximal to sciatic nerve transection in rats. Neurosci. Lett. 365, 39–42.

Jones, M. G., Munson, J. B., and Thompson, S. W. 1999. A role for nerve growth factor in sympathetic sprouting in rat dorsal root ganglia. Pain 79, 21–29.

Kajander, K. C., Wakisaka, S., and Bennett, G. J. 1992. Spontaneous discharge originates in the dorsal root ganglion at the onset of a painful peripheral neuropathy in the rat. Neurosci. Lett. 138, 225–228.

Kelly, M. E. M., Bulloch, A. G. M., Lukowiak, K., and Bisby, M. A. 1989. Regeneration of frog sympathetic neurons is accompanied by sprouting and retraction of intraganglionic neurites. Brain Res. 477, 363–368.

Kim, H. J., Na, H. S., Back, S. K., and Hong, S. K. 2001. Sympathetic sprouting in sensory ganglia depends on the number of injured neurons. Neuroreport 12, 3529–3532.

Kim, H. J., Na, H. S., Nam, H. J., Park, K. A., Hong, S. K., and Kang, B. S. 1996. Sprouting of sympathetic nerve fibers into the dorsal root ganglion following peripheral nerve injury depends on the injury site. Neurosci. Lett. 212, 191–194.

Kim, H. J., Na, H. S., Sung, B., Nam, H. J., Chung, Y. J., and Hong, S. K. 1999. Is sympathetic sprouting in the dorsal root ganglia responsible for the production of neuropathic pain in a rat model? Neurosci. Lett. 269, 103–106.

Lawson, S. N. 2002. Phenotype and function of somatic primary afferent nociceptive neurons with C-, Adelta- or Aalpha/beta-fibres. Exp. Physiol. 87, 239–244.

Li, L. and Zhou, X. F. 2001. Pericellular Griffonia simplicifolia I isolectin B4-binding ring structures in the dorsal root ganglia following peripheral nerve injury in rats. J. Comp. Neurol. 439, 259–274.

Li, L., Deng, Y. S., and Zhou, X. F. 2000. Downregulation of TrkA expression in primary sensory neurons after unilateral lumbar spinal nerve transection and some rescuing effects of nerve growth factor infusion. Neurosci. Res. 38, 183–191.

Liu, C. N., Michealis, M., Amir, R., and Devor, M. 2000. Spinal nerve injury enhances subthreshold membrane potential oscillations in DRG neurons: relation to neuropathic pain. J. Neurophysiol. 84, 205–215.

Liu, X. G., Eschenfelder, S., Blenk, K. H., Jänig, W., and Häbler, H. J. 2000. Spontaneous activity of axotomized afferent neurons after L5 spinal nerve injury in the rats. Pain 84, 309–318.

Lopez de Armentia, M., Leeson, A. H., Stebbing, M. J., Urban, L., and McLachlan, E. M. 2003. Responses to sympathomimetics in rat sensory neurons after nerve transection. Neuroreport 14, 9–13.

Ma, W. and Bisby, M. A. 1997. Differential expression of galanin immunoreactivities in the primary sensory neurons following partial and complete sciatic nerve injuries. Neuroscience 79, 1183–1195.

Ma, W., Ramer, M. S., and Bisby, M. A. 1999. Increased calcitonin gene-related peptide immunoreactivity in gracile nucleus after partial sciatic nerve injury: age-dependent and originating from spared sensory neurons. Exp. Neurol. 159, 459–473.

Mannion, R. J. and Woolf, C. J. 2000. Pain mechanisms and management: a central perspective. Clin. J. Pain 16, S144–S156.

McLachlan, E. M. and Hu, P. 1998. Axonal sprouts containing calcitonin gene-related peptide and substance P form pericellular baskets around large diameter neurons after sciatic nerve transection in the rat. Neuroscience 84, 961–965.

McLachlan, E. M., Jänig, W., Devor, M., and Michaelis, M. 1993. Peripheral nerve injury triggers noradrenergic sprouting within dorsal root ganglia. Nature 363, 543–546.

Michaelis, M., Blenk, K. H., Janig, W., and Vogel, C. 1995. Development of spontaneous activity and mechanosensitivity in axotomized afferent nerve fibers during the first hours after nerve transection in rats. J. Neurophysiol. 74, 1020–1027.

Michaelis, M., Liu, X., and Jänig, W. 2000. Axotomized and intact muscle afferents but no skin afferents develop ongoing discharges of dorsal root origin after peripheral nerve lesion. J. Neurosci. 20, 2742–2748.

Moalem, G., Xu, K., and Yu, L. 2004. T lymphocytes play a role in neuropathic pain following peripheral nerve injury in rats. Neuroscience 129, 767–777.

Noguchi, K., Kawai, Y., Fukuoka, T., Senba, E., and Miki, K. 1995. Substance P induced by peripheral nerve injury in primary afferent sensory neurons and its effect on dorsal column nucleus neurons. J. Neurosci. 15, 7633–7643.

Raja, S. N., Treede, R. D., Davis, K. D., and Campbell, J. N. 1991. Systemic alpha-adrenergic blockade with phentolamine: a diagnostic test for sympathetically maintained pain. Anesthesiology 74, 691–698.

Ramer, M. S. and Bisby, M. A. 1997. Rapid sprouting of sympathetic axons in dorsal root ganglia of rats with a chronic constriction injury. Pain 70, 237–244.

Ramer, M. S. and Bisby, M. A. 1998a. Differences in sympathetic innervation of mouse DRG following proximal or distal nerve lesions. Exp. Neurol. 152, 197–207.

Ramer, M. S. and Bisby, M. A. 1998b. Normal and injury-induced sympathetic innervation of rat dorsal root ganglia increases with age. J. Comp. Neurol. 394, 38–47.

Ramer, M. S. and Bisby, M. A. 1998c. Sympathetic axons surround neuropeptide-negative axotomized sensory neurons. Neuroreport 9, 3109–3113.

Ramer, M. S. and Bisby, M. A. 1999. Adrenergic innervation of rat sensory ganglia following proximal or distal painful sciatic neuropathy: distinct mechanisms revealed by anti-NGF treatment. Eur. J. Neurosci. 11, 837–846.

Ramer, M. S., Murphy, P. G., Richardson, P. M., and Bisby, M. A. 1998. Spinal nerve lesion-induced mechanoallodynia and adrenergic sprouting in sensory ganglia are attenuated in interleukin-6 knockout mice. Pain 78, 115–121.

Ramer, M. S., Thompson, S. W. N., and McMahon, S. B. 1999. Causes and consequences of sympathetic basket formation in dorsal root ganglia. Pain 6, S111–S120.

Ringkamp, M., Eschenfelder, S., Grethel, E. J., Häbler, H. J., Meyer, R. A., Jänig, W., and Raja, S. N. 1999. Lumbar sympathectomy failed to reverse mechanical allodynia- and hyperalgesia-like behavior in rats with L5 spinal nerve injury. Pain 79, 143–153.

Segond von Banchet, G., Pastor, A., Biskup, C., Schlegel, K., Benndorf, K., and Schaible, H. G. 2002. Localization of functional calcitonin gene-related peptide binding sites in a subpopulation of cultured dorsal root ganglion neurons. Neuroscience 110, 131–145.

Shinder, V., Govrin-Lippmann, R., Cohen, S., Belenky, M., Ilin, P., Fried, K., Wilkinson, H. A., and Devor, M. 1999. Structural basis of sympathetic-sensory coupling in rat and human dorsal root ganglia following peripheral nerve injury. J. Neurocytol. 28, 743–761.

Shir, Y. and Seltzer, Z. 1991. Effects of sympathectomy in a model of causalgiform pain produced by partial sciatic nerve injury in rats. Pain 45, 309–320.

Thompson, S. W. and Majithia, A. A. 1998. Leukemia inhibitory factor induces sympathetic sprouting in intact dorsal root ganglia in the adult rat *in vivo*. J. Physiol. 506, 809–816.

Verge, V. M., Riopelle, R. J., and Richardson, P. M. 1989. Nerve growth factor receptors on normal and injured sensory neurons. J. Neurosci. 9, 914–922.

Wahren, L. K., Torebjork, E., and Nystrom, B. 1991. Quantitative sensory testing before and after regional guanethidine block in patients with neuralgia in the hand. Pain 46, 23–30.

Wallace, M. S., Ridgeway, B. M., Leung, A. Y., Gerayli, A., and Yaksh, T. L. 2000. Concentration-effect relationship of intravenous lidocaine on the allodynia of complex regional pain syndrome types I and II. Anesthesiology 92, 75–83.

Walsh, G. S. and Kawaja, M. D. 1998. Sympathetic axons surround nerve growth factor-immunoreactive trigeminal neurons: observations in mice overexpressing nerve growth factor. J. Neurobiol. 34, 347–360.

Walsh, G. S., Krol, K. M., and Kawaja, M. D. 1999. Absence of the p75 neurotrophin receptor alters the pattern of sympathosensory sprouting in the trigeminal ganglia of mice overexpressing nerve growth factor. J. Neurosci. 19, 258–273.

Xing, J. L., Hu, S. J., Jian, Z., and Duan, J. H. 2003. Subthreshold membrane potential oscillation mediates the excitatory effect of norepinephrine in chronically compressed dorsal root ganglion neurons in the rat. Pain 105, 177–183.

Xu, Z. Q., Zhang, X., Grillner, S., and Hökfelt, T. 1997. Electrophysiological studies on rat dorsal root ganglion neurons after peripheral axotomy: changes in responses to neuropeptides. Proc. Nat. Acad. Sci. U. S. A. 94, 13262–13266.

Zhang, J. M., Li, H., and Munir, M. A. 2004. Decreasing sympathetic sprouting in pathologic sensory ganglia: a new mechanism for treating neuropathic pain using lidocaine. Pain 109, 143–149.

Zhang, X., Meister, B., Elde, R., Verge, V. M., and Hokfelt, T. 1993. Large calibre primary afferent neurons projecting to the gracile nucleus express neuropeptide Y after sciatic nerve lesions: an immunohistochemical and in situ hybridization study in rats. Eur. J. Neurosci. 5, 1510–1519.

Zhou, X. F., Deng, Y. S., Chie, E., Xue, Q., Zhong, J. H., McLachlan, E. M., Rush, R. A., and Xian, C. 1999. Satellite cell-derived nerve growth factor and neurotrophin-3 are involved in noradrenergic sprouting in the dorsal root ganglia following peripheral nerve injury in the rat. Eur. J. Neurosci. 11, 1711–1722.

5.20 Vagal Afferent Neurons and Pain

W Jänig, Christian-Albrechts-Universität zu Kiel, Kiel, Germany

© 2008 Elsevier Inc. All rights reserved.

5.20.1	**Introduction**	246
5.20.2	**Vagal Afferents, Pain, and Nociception**	246
5.20.2.1	Thoracic Visceral Organs	246
5.20.2.2	Pelvic and Abdominal Organs	247
5.20.3	**Abdominal Vagal Afferents, Protection of the Body, and Illness Responses**	247
References		249

Glossary

allodynia, hyperalgesia See Chapter Autonomic Nervous System and Pain.

angina (pectoris) A paroxysmal thoracic pain, with a feeling of suffocation and impending death, due, most often but not always, to anoxia of the myocardium.

GALT (gut-associated lymphoid tisue) Immune system of the gastrointestinal tract, in particular in the small intestine. It includes the immune cells of Peyer´s patches, M-cells of the epithelial lining modified entestinal epithelial cells (enterocytes), lyphocytes in the almina propria, macrophages, and mast cells. Its function is to defend the body against invading antigens from food, bacteria, parasites, and toxins.

neurogenic inflammation Peptidergic primary afferent neurons with unmyelinated fibers (some with small-diameter myelinated (A delta) fibers) generate upon excitation precapillary (arteriolar) vasodilation (by release of calcitonin gene-related peptide (CGRP) supported by release of substance P and neurokinin A) and postcapillary (venular) plasma extravasation (by release of substance P and neurokinin A). Originally venular plasma extravasation was called neurogenic inflammation, but both precapillary vasodilation and postganglionic plasma extravasation are collectively now called neurogenic inflammation.

referred pain See Chapter Autonomic Nervous System and Pain.

vagal afferents Afferents projecting through the vagal nerves. Most of their cell bodies are located in the inferior vagal (nodose) ganglion and a few in the superior vagal (jugular) ganglion.

1. Vagal afferents innervating the heart may be involved in pain during angina referred to the upper cervical dermatomes and myotomes.
2. Vagal afferents innervating the stomach and being excited by acid are involved in nociceptive protective reactions, but probably not in conscious perception of pain.
3. Transmission of nociceptive impulses in the spinal or trigeminal dorsal horn is under inhibitory control generated by activity in cardiopulmonary and/or abdominal vagal afferents.
4. Vagal afferents innervating the liver (thus passing through the hepatic branch of the abdominal vagus nerves) are involved in illness responses generated by lipopolysaccharides (LPS) (bacterial antigens) or proinflammatory cytokines (e.g., interleukin-1β (IL-1β) or tumor necrosis factor α (TNF-α)) into the peritoneal cavity. One component of the illness responses is hyperalgesic behavior.
5. Activity in abdominal vagal afferents innervating the small intestine and probably sensing toxic and other events in the gastrointestinal tract (GIT) may be involved in reflex modulation of inflammation and sensitivity of nociceptors in somatic tissues via the sympatho-adrenal system (releasing adrenaline) and possibly the hypothalamo-pituitary–adrenal system.

The response properties of vagal afferents to physiological stimuli being involved in the reflex modulation of nociception, pain, hyperalgesia, inflammation, and illness responses are unknown. It

is likely that not one functionally specific type of vagal afferent neuron is involved but several different types.

5.20.1 Introduction

The vagus nerves contain 80–85% visceral afferent fibers, most of them innervating the GIT, and 15–20% preganglionic parasympathetic fibers, at least in rats (Precht, J. C. and Powley, T. L., 1990; Berthoud, H. R. *et al.*, 1991). These afferent neurons are involved not only in organ regulation by the autonomic nervous system (Jänig, W., 2006) but also in the control of protective body reactions that include nociception and pain. These functions are inferred from various types of experimental investigations and from some clinical observations. It is unclear whether functionally specific groups of vagal afferents are involved in protective body reactions or whether vagal afferents being involved in organ regulation are also responsible for protective body reactions. In this chapter I will summarize:

1. data related to the role of vagal afferents in generating pain and in modulating central processing of nociceptive impulse activity and
2. data about the role of vagal afferents in protective reactions of the body including inflammation and hyperalgesia (Jänig, W., 2005; Jänig, W. and Levine, J. D., 2006).

5.20.2 Vagal Afferents, Pain, and Nociception

5.20.2.1 Thoracic Visceral Organs

Pain elicited from the proximal esophagus and proximal trachea is probably mediated by vagal afferents innervating the mucosa of these organs. These afferents are peptidergic (i.e., contain calcitonin gene related peptide (CGRP) and/or substance P); their cell bodies are probably located in the jugular ganglion (superior vagal ganglion; see Berthoud, H. R. and Neuhuber, W. L., 2000) cells in the nodose ganglion (inferior vagal ganglion) are almost exclusively peptide-negative, whereas neurons in the jugular ganglion may contain peptides). Activation of these afferents generates neurogenic inflammation in the mucosa (venular plasma extravasation and vasodilation (McDonald, D. M. *et al.*, 1988; McDonald, D. M., 1990)). Pain elicited from the more distal sections of esophagus and trachea as well as from the bronchi may be generated by stimulation of spinal visceral afferent neurons yet not of vagal afferents. However, this situation is unclear and needs further experimentation.

Cardiac pain (e.g., during ischemic heart disease) is considered to be mediated by activation of spinal visceral afferents having their cell bodies in the dorsal root ganglia C8–T9 (mainly T2–6). However, attempts to relieve cardiac angina pain by surgical interventions (cervico-thoracic sympathectomy, dorsal rhizotomy, injection of alcohol into the sympathetic chain) consistently showed that only 50–60% of patients report complete relief from angina while the remaining patients report either partial relief or no relief at all. Some failures to relief pain may have been attributed to incomplete spinal denervation of the heart; but vagal afferents innervating particularly the inferior–posterior part of the heart may mediate cardiac pain too (see Meller, S. T. and Gebhart, G. F., 1992).

Electrical stimulation of cervical vagal afferent fibers in rats modulates the nociceptive tail reflex as well as the responses of dorsal horn neurons in the lumbar spinal cord. Low-intensity electrical vagal stimulation, probably exciting mainly myelinated afferents, facilitates both whereas high-intensity stimulation, probably exciting mainly C-fibers, attenuates both (Randich, A. and Gebhart, G. F., 1992; Ren, K. *et al.*, 1993). Nociceptive reflexes in neurons of the trigeminal nucleus caudalis or oralis of rats were mainly suppressed during electrical stimulation of cervical vagal afferents (Bossut, D. F. and Maixner, W., 1996; Takeda, M. *et al.*, 1998). Neurophysiological investigations in monkeys and rats show that some spino-thalamic tract (STT) neurons in the superficial dorsal horn and deeper laminae of the cervical segments C1–C2 (C3) can be synaptically activated by electrical stimulation of cardiopulmonary spinal and vagal afferents or by injection of algogenic chemicals in the pericardial sac via both afferent pathways. The activation of the STT neurons by vagal afferents is relayed through the nucleus tractus solitarii. These STT neurons are also synaptically activated by mechanical stimulation of the somatic receptive fields in the corresponding segments from the head, jaw, neck, and shoulder (dermatomes, myotomes); this is fully in line with clinical observations showing that cardiac pain may be referred to neck, shoulder, and jaw (Lindgren, I. and Olivecrona, H., 1947; White, J. C. and Bland, E. F., 1948; Meller, S. T. and Gebhart, G. F., 1992). The dorsal horn of the same high cervical spinal

segments contains neurons with similar convergent synaptic inputs from vagal, spinal visceral, and somatic afferents that project to more caudal spinal thoracic, lumbar, and sacral segments. These dorsal horn neurons are involved in the inhibitory control of nociceptive impulse transmission (see Foreman, R. D., 1999; Chandler, M. J. *et al.*, 2002; see also Section 5.20.3, point 2).

Experimental studies on animals showing that nociceptive behavior and inhibition of nociceptive impulse transmission in the spinal and trigeminal dorsal horn is inhibited by electrical stimulation of the cervical vagus nerve have led to the idea that continuous electrical stimulation of vagal afferents could be used to treat chronic pain syndromes in patients. Electrical stimulation of the vagus nerve via a pair of electrodes implanted at the left cervical vagus nerve has been used recently in patients with some success to treat drug-resistant refractory epilepsy. The mechanisms underlying this antiepileptic effect are unknown (Schachter, S. C., 2005). A few experimental studies have been conducted on these patients to test whether experimental pain can be attenuated by vagal nerve stimulation. Furthermore, in patients with chronic headache (migraine, tension-type headache, cluster headache) electrodes have been implanted at the left cervical vagus nerve. In these experiments, in pilot studies, as well as in some case reports it has been shown that electrical vagal nerve stimulation may reduce experimental pain or relieve chronic headache (for literature and discussion see Multon, S. and Schoenen, J., 2005).

5.20.2.2 Pelvic and Abdominal Organs

Visceral pain elicited from pelvic and most abdominal organs is triggered by stimulation of spinal visceral afferent neurons and not by stimulation of vagal afferent neurons (Cervero, F., 1994; see Chapter Spinal Cord Mechanisms of Hyperalgesia and Allodynia). However, the situation is not entirely clear for the gastroduodenal section of the GIT. Whether patients with complete interruption of spinal ascending impulse transmission at the thoracic level T1 or at a more rostral segmental level can experience pain from the gastroduodenal section (e.g., during gastritis, a peptic ulcer, or distension of the stomach) has never been systematically investigated. Patients with complete lesion of the cervical spinal cord experience abdominal hunger, dread, and nausea (Crawford, J. P. and Frankel, H. L., 1971). Furthermore, these patients may experience vague sensations of fullness after a hot meal. But acid reflux or an obstructed or distended viscus usually does not generate discomfort and pain (Juler, G. L. and Eltorai, I. M., 1985; Strauther, G. R. *et al.*, 1999). An acute perforation of a duodenal ulcer may be accompanied by violent pain in the right or left shoulder (page 284 in Guttmann, L., 1976), indicating that vagal afferents may be involved.

It is generally accepted that stimulation of vagal afferents innervating the stomach elicits emesis, bloating, and nausea, all three being protective reactions. Experiments on rats show that influx of acid into and other chemical insults of the gastroduodenal mucosa lead to a host of locally and centrally organized protective reactions that are mediated by spinal visceral and vagal afferent neurons. Activation of vagal afferents by these chemical stimuli excites neurons in the nucleus tractus solitarii, area postrema, lateral parabrachial nucleus, subceruleus nucleus, thalamic and hypothalamic paraventricular nuclei, supraoptic nucleus, and central amygdala, but not in the insular cortex (the major central representation area of the stomach) as shown by the expression of the marker protein Fos (Michl, T. *et al.*, 2001). Furthermore, neurons in the spinal dorsal horn do not seem to be activated. Thus, vagal afferents innervating the gastroduodenal mucosa (Holzer, P. and Maggi, C. A., 1998; Holzer, P.; 2002; 2003; 2006) (1) seem to be involved in chemonociception, local protective reactions, and generation of autonomic, endocrine, and behavioral protective reactions but (2) not in pain perception, yet in the emotional aspect of pain and therefore indirectly in upper abdominal hyperalgesia.

These fascinating ideas, formulated by Holzer, need verification by further experimentation. For example, it is unclear in which way (1) activity in spinal visceral afferents and vagal afferents is centrally integrated *in vivo* so as to elicit the protective reflexes, protective behavior, and pain sensations including visceral hyperalgesia and (2) activity in vagal afferents is responsible for the emotional aspects of visceral pain, but spinal visceral afferents for the conscious perception of visceral pain.

5.20.3 Abdominal Vagal Afferents, Protection of the Body, and Illness Responses

The small intestine and liver are very vulnerable portals of entries into the body. Both have potent local defense systems and serve as internal defense

lines of the body. The small intestine contains a powerful immune system (the gut associated lymphoid tissue (GALT) (Shanahan, F., 1994)) that is innervated by vagal afferents projecting through the celiac branches of the abdominal vagus nerve. Specific modulation of activity in these afferents in conjunction with the reaction of the GALT may act as an early warning system to the rest of the body by transmitting important information to the brain about toxic events and agents in the small intestine that are dangerous for the organism (Berthoud, H. R. and Neuhuber, W. L., 2000). Thus, particularly vagal afferents in the celiac branches of the abdominal vagus nerves that innervate the small intestine (in addition to the distal duodenum and the proximal colon) and vagal afferents in the hepatic branch that innervate the liver (in addition to the proximal duodenum, pancreas, and pylorus) may be important for protective functions of the GIT and the body:

1. Vagal afferents in the celiac branches of the abdominal vagus nerve monitor chemical and mechanical events that occur in the intestine under physiological and pathophysiological conditions (for review see Grundy, D. and Scratcherd, T., 1989), that is, are related to meals, ingestion of toxic substances, inflammation, obstruction. These afferents respond to distension or contraction of the small intestine or to intraluminal chemical stimulation (e.g., maltose, glucose, protein products of long-chain lipids, or intraluminal osmotic stimuli). The responses to chemical stimuli are mediated by enterochromaffin cells releasing 5-HT and by 5-HT_3 receptors on the terminals of the vagal afferents (Zhu, J. X. *et al.*, 2001) or enteroendocrine cells releasing cholecystokinin (CCK) and the CCK_A receptor on the terminals of the vagal afferent neurons (Richards, W. *et al.*, 1996; Lal, S. *et al.*, 2001). Vagal afferent neurons may be associated with the GALT and may be excited by inflammatory processes and toxic processes, also probably mediated by enterochromaffin cells releasing serotonin (5-HT), enteroendocrine cells releasing CCK, or mast cells releasing histamine and other compounds (Kirkup, A. J. *et al.*, 2001; Kreis, M. E. *et al.*, 2002). The functional specificity of these afferents with respect to the different types of intraluminal stimuli is unknown. The vagal afferents are important for preabsorptive detection of energy-yielding molecules and probably for other properties of nutrient solutions that are toxic and deleterious for the GIT and for the body (Walls, E. K. *et al.*, 1995a; 1995b). Additionally, some vagal afferents that innervate the small intestine and the liver respond to cytokines (e.g., IL-1β); these afferents may encode events that are related to the immune system of the GIT and liver (Niijima, A., 1996).
2. Electrical stimulation of abdominal vagal afferents exerts inhibition or facilitation of central nociceptive impulse transmission in the spinal dorsal horn and depresses nociceptive behavior depending on as to whether unmyelinated or myelinated vagal afferents are excited (Randich, A. and Gebhart, G. F., 1992). Electrical stimulation of cervical vagal afferents in monkeys suppresses transmission of impulse activity in STT neurons with nociceptive function at all levels of the spinal cord. Electrical stimulation of subdiaphragmatic vagal afferents has no effect on STT neurons in this species, arguing that particularly cardiopulmonary vagal afferents are involved in this inhibitory control. The central pathways mediating the inhibitory effect are neurons in the subceruleus–parabrachial complex (noradrenergic) and neurons in the nucleus raphe magnus of the rostroventromedial medulla (serotonergic) that project to the spinal cord (Foreman, R. D., 1989). The central pathways mediating the facilitatory effect are mediated by suprapontine pathways (Gebhart, G. F. and Randich, A., 1992; Randich, A. and Gebhart, G. F., 1992). The functional types of vagal afferents being involved in inhibitory and facilitatory control of nociceptive impulse transmission are unknown.
3. Activity in vagal afferents innervating the small intestine (i.e., projecting through the celiac branches of the abdominal vagus nerves) is important in reflex modulation of inflammatory processes (e.g., in the knee joint) and mechanical hyperalgesic behavior (by sensitization of nociceptors) in remote body tissues involving the sympatho-adrenal system and possibly the hypothalamo-pituitary–adrenal system (Green, P. G. *et al.*, 1995; 1997; Miao, F. J.-P. *et al.*, 1997a;1997b; Khasar, S. G. *et al.*, 1998a; 1998b; Jänig, W. *et al.*, 2000; Miao, F. J. -P. *et al.*, 2000, Miao; F. J. -P.*et al.*, 2001; Khasar, S. G. *et al.*, 2003; Miao, F. J. -P. *et al.*, 2003a; 2003b; see Section 5.17.3.4.4 and 5.17.4 in Chapter Autonomic Nervous System and Pain.
4. Intraperitoneal injection of illness-inducing agents, such as the bacterial cell wall endotoxin LPS in rats, produces behavioral hyperalgesia.

This is mediated by activity in subdiaphragmatic vagal afferents, specifically afferents running in the hepatic branch. It is suggested that LPS activates hepatic macrophages (Kupffer cells), dendritic cells, and leukocytes that release IL-1β and TNF-α. This in turn activates vagal afferents from the liver. IL-1β and TNF-α injected intraperitoneally themselves generate behavioral hyperalgesia that is abolished by vagotomy (Watkins, L. R. *et al.*, 1994a; 1994b; 1995a; 1995b; 1995c; 1995d). The proinflammatory cytokines either activate the vagal afferents directly or bind to glomus cells in the abdominal paraganglia that are innervated by vagal afferents; the activated vagal afferents signal the peripheral events to the brain, leading to hyperalgesia (as shown by an enhanced thermal nociceptive tail-flick reflex).

5. Pain behavior mediated by vagal afferents, activated by intraperitoneal injection of LPS or of proinflammatory cytokines, is part of a general sickness behavior characterized by various protective illness responses (e.g., immobility, decreased social interaction, decrease in food intake, formation of taste aversion to novel foods, decrease of digestion, loss of weight (anorexia), fever, increase of sleep, change in endocrine functions (activation of the hypothalamo–pituitary–adrenal axis), malaise) and is correlated with marked alterations of brain functions. For example, food aversion and anorexia generated in rats by intraperitoneal TNF-α are abolished or attenuated by subdiaphragmatic vagotomy (Bret-Dibat, J. L. *et al.*, 1995; Bernstein, I. L., 1996). Endotoxin, IL-1β, or TNF-α injected intraperitoneally activate nodose ganglion cells (Gaykema, R. P. *et al.*, 1998) and various brain areas in rodents (nucleus tractus solitarii, parabrachial nuclei, and hypothalamic supraoptic and paraventricular nuclei) as well as induce IL-1β mRNA in the pituitary gland, hypothalamus, and hippocampus. These changes do not occur or are significantly attenuated in subdiaphragmatically vagotomized animals (Ericsson, A. *et al.*, 1994; Wan, W. *et al.*, 1994; Layé, S. *et al.*, 1995; see Sawchenko, P. E. *et al.*, 1996; Dantzer, R. *et al.*, 1998; 2000).
6. Watkins, Maier, and coworkers have developed the idea that vagal abdominal afferents projecting through the hepatic branch of the abdominal vagus nerves form an important neural interface between the immune system and the brain. Activation of these afferents by signals from the immune system (proinflammatory cytokines IL-1β, TNF-α, IL-6) trigger via different centers in brain stem and hypothalamus illness responses, one component being pain and hyperalgesia. The underlying mechanisms of these illness responses have been discussed (Maier, S. F. and Watkins, L. R., 1998; Watkins, L. R. and Maier, S. F., 1999, Goehler, L. E. *et al.*, 2000; Watkins, L. R. and Maier, S. F., 2000). The physiology of the vagal afferents involved in the communication between the immune system, which operates as a diffuse sensory system to detect chemical constituents associated with dangerous microorganisms and their toxins, and the brain has to be worked out.

Acknowledgments

Supported by the Deutsche Forschungsgemeinschaft and the German Ministry of Research and Education (German Research Network on Neuropathic Pain).

References

Bernstein, I. L. 1996. Neural mediation of food aversions and anorexia induced by tumor necrosis factor and tumors. Neurosci. Biobehav. Rev. 20, 177–181.

Berthoud, H. R. and Neuhuber, W. L. 2000. Functional and chemical anatomy of the afferent vagal system. Auton. Neurosci. 85, 1–17.

Berthoud, H. R., Carlson, N. R., and Powley, T. L. 1991. Topography of efferent vagal innervation of the rat gastrointestinal tract. Am. J. Physiol. 260, R200–R207.

Bossut, D. F. and Maixner, W. 1996. Effects of cardiac vagal afferent electrostimulation on the responses of trigeminal and trigeminothalamic neurons to noxious orofacial stimulation. Pain 65, 101–109.

Bret-Dibat, J. L., Bluthe, R. M., Kent, S., Kelley, K. W., and Dantzer, R. 1995. Lipopolysaccharide and interleukin-1 depress food-motivated behavior in mice by a vagal-mediated mechanism. Brain Behav. Immun. 9, 242–246.

Cervero, F. 1994. Sensory innervation of the viscera: peripheral basis of visceral pain. Physiol. Rev. 74, 95–138.

Chandler, M. J., Zhang, J., Qin, C., and Foreman, R. D. 2002. Spinal inhibitory effects of cardiopulmonary afferent inputs in monkeys: neuronal processing in high cervical segments. J. Neurophysiol. 87, 1290–1302.

Crawford, J. P. and Frankel, H. L. 1971. Abdominal 'visceral' sensation in human tetraplegia. Paraplegia 9, 153–158.

Dantzer, R., Bluthe, R. M., Gheusi, G., Cremona, S., Laye, S., Parnet, P., and Kelley, K. W. 1998. Molecular basis of sickness behavior. Ann. N. Y. Acad. Sci. 856, 132–138.

Dantzer, R., Konsman, J. P., Bluthe, R. M., and Kelley, K. W. 2000. Neural and humoral pathways of communication from the immune system to the brain: parallel or convergent? Auton. Neurosci. 85, 60–65.

Ericsson, A., Kovacs, J. C., and Sawchenko, P. E. 1994. A functional anatomical analysis of central pathways

subserving the effects of interleukin-1 on stress-related neuroendocrine neurons. J. Neurosci. 14, 897–913.
Foreman, R. D. 1989. Organization of the spinothalamic tract as a relay for cardiopulmonary sympathetic afferent fiber activity. Prog. Sens. Physiol. 9, 1–51.
Foreman, R. D. 1999. Mechanisms of cardiac pain. Annu. Rev. Physiol. 61, 143–167.
Gaykema, R. P., Goehler, L. E., Tilders, F. J., Bol, J. G., McGorry, M., Fleshner, M., Maier, S. F., and Watlans, L. R. 1998. Bacterial endotoxin induces fos immunoreactivity in primary afferent neurons of the vagus nerve. Neuroimmunomodulation 5, 234–240.
Gebhart, G. F. and Randich, A. 1992. Vagal modulation of nociception. APS J. 1, 26–32.
Goehler, L. E., Gaykema, R. P., Hansen, M. K., Anderson, K., Maier, S. F., and Watkins, L. R. 2000. Vagal immune-to-brain communication: a visceral chemosensory pathway. Auton. Neurosci. 85, 49–59.
Green, P. G., Jänig, W., and Levine, J. D. 1997. Sympathetic terminal: target for negative feedback neuroendocrine control of inflammatory response in the rat. J. Neurosci. 17, 3234–3238.
Green, P. G., Miao, F. J. P., Jänig, W., and Levine, J. D. 1995. Negative feedback neuroendocrine control of the inflammatory response in rats. J. Neurosci. 15, 4678–4686.
Grundy, D. and Scratcherd, T. 1989. Sensory Afferents from the Gastrointestinal Tract. In: Handbook of Physiology, The Gastrointestinal System (*ed*. J. D. Wood), pp. 593–620. Am. Physiol. Soc.
Guttmann, L. 1976. Spinal Cord Injuries. Comprehensive Management and Research. Blackwell Scientific Publications.
Holzer, P. 2002. Sensory neurone responses to mucosal noxae in the upper gut: relevance to mucosal integrity and gastrointestinal pain. Neurogastroenterol. Motil. 14, 459–475.
Holzer, P. 2003. Afferent signalling of gastric acid challenge. J. Physiol. Pharmacol. 54(Suppl. 4), 43–53.
Holzer, P. 2006. Efferent-like roles of afferent neurons in the gut: Blood flow regulation and tissue protection. Auton. Neurosci. 125, 70–75.
Holzer, P. and Maggi, C. A. 1998. Dissociation of dorsal root ganglion neurons into afferent and efferent-like neurons. J. Neurosci. 86, 389–398.
Jänig, W. 2005. Vagal Afferents and Visceral Pain. In: Advances in Vagal Afferent Neurobiology (*eds*. B. Undem and D. Weinreich), pp. 465–493. CRC Press.
Jänig, W. 2006. The Integrative Action of the Autonomic Nervous System. Neurobiology of Homeostasis. Cambridge University Press.
Jänig, W. and Levine, J. D. 2006. Autonomic-Neuroendocrine-Immune Responses in Acute and Chronic Pain. In: Wall & Melzack's Textbook of Pain, 5th edn. (*eds*. S. B. McMahon and M. Koltzenburg), pp. 205–218. Elsevier Churchill Livingstone.
Jänig, W., Khasar, S. G., Levine, J. D., and Miao, F. J.-P. 2000. The role of vagal visceral afferents in the control of nociception. Prog. Brain Res. 122, 273–287.
Juler, G. L. and Eltorai, I. M. 1985. The acute abdomen in spinal cord injury patients. Paraplegia 23, 118–123.
Khasar, S. G., Green, P. G., Miao, F. J.-P., and Levine, J. D. 2003. Vagal modulation of nociception is mediated by adrenomedullary epinephrine in the rat. Eur. J. Neurosci. 17, 909–915.
Khasar, S. G., Miao, F. J.-P., Jänig, W., and Levine, J. D. 1998a. Modulation of bradykinin-induced mechanical hyperalgesia in the rat skin by activity in the abdominal vagal afferents. Eur. J. Neurosci. 10, 435–444.
Khasar, S. G., Miao, F. J.-P., Jänig, W., and Levine, J. D. 1998b. Vagotomy-induced enhancement of mechanical hyperalgesia in the rat is sympathoadrenal-mediated. J. Neurosci. 18, 3043–3049.
Kirkup, A. J., Brunsden, A. M., and Grundy, D. 2001. Receptors and transmission in the brain-gut axis: potential for novel therapies. I. Receptors on visceral afferents. Am. J. Physiol. Gastrointest. Liver Physiol. 280, G787–G794.
Kreis, M. E., Jiang, W., Kirkup, A. J., and Grundy, D. 2002. Cosensitivity of vagal mucosal afferents to histamine and 5-HT in the rat jejunum. Am. J. Physiol. Gastrointest. Liver Physiol. 283, G612–G617.
Lal, S., Kirkup, A. J., Brunsden, A. M., Thompson, D. G., and Grundy, D. 2001. Vagal afferent responses to fatty acids of different chain length in the rat. Am. J. Physiol. Gastrointest. Liver Physiol. 281, G907–G915.
Layé, S., Bluthe, R. M., Kent, S., Combe, C., Medina, C., Parnet, P., Kelley, K. and Dantzer, R. 1995. Subdiaphragmatic vagotomy blocks induction of IL-1 beta mRNA in mice brain in response to peripheral LPS. Am. J. Physiol. 268, R1327–R1331.
Lindgren, I. and Olivecrona, H. 1947. Surgical treatment of angina pectoris. J. Neurosurg. 4, 19–39.
Maier, S. F. and Watkins, L. R. 1998. Cytokines for psychologists: implications of bidirectional immune-to-brain communication for understanding behavior, mood, and cognition. Psychol. Rev. 105, 83–107.
McDonald, D. M. 1990. The ultrastructure and permeability of tracheobronchial blood vessels in health and disease. Eur. Respir. J. (Suppl.)12, 572s–585s.
McDonald, D. M., Mitchell, R. A., Gabella, G., and Haskell, A. 1988. Neurogenic inflammation in the rat trachea. II. Identity and distribution of nerves mediating the increase in vascular permeability. J. Neurocytol. 17, 605–628.
Meller, S. T. and Gebhart, G. F. 1992. A critical review of the afferent pathways and the potential chemical mediators involved in cardiac pain. J. Neurosci. 48, 501–524.
Miao, F. J.-P., Green, P. G., and Levine, J. D. 2003b. Mechano-sensitive duodenal afferents contribute to vagal modulation of inflammation in the rat. J. Physiol. (Lond.) 554, 227–235.
Miao, F. J.-P., Jänig, W., and Levine, J. D. 1997a. Vagal branches involved in inhibition of bradykinin-induced synovial plasma extravasation by intrathecal nicotine and noxious stimulation in the rat. J. Physiol. (Lond.) 498, 473–481.
Miao, F. J.-P., Jänig, W., and Levine, J. D. 2000. Nociceptive-neuroendocrine negative feedback control of neurogenic inflammation activated by capsaicin in the skin: role of the adrenal medulla. J. Physiol. (Lond.) 527, 601–610.
Miao, F. J.-P., Jänig, W., Green, P. G., and Levine, J. D. 1997b. Inhibition of bradykinin-induced synovial plasma extravasation produced by noxious cutaneous and visceral stimuli and its modulation by activity in the vagal nerve. J. Neurophysiol. 78, 1285–1292.
Miao, F. J.-P., Jänig, W., Jasmin, L., and Levine, J. D. 2001. Spino-bulbo-spinal pathway mediating vagal modulation of nociceptive-neuroendocrine control of inflammation in the rat. J. Physiol. (Lond.) 532, 811–822.
Miao, F. J.-P., Jänig, W., Jasmin, L., and Levine, J. D. 2003a. Blockade of nociceptive inhibition of plasma extravasation by opioid stimulation of the periaqueductal gray and its interaction with vagus-induced inhibition in the rat. Neurosci. 119, 875–885.
Michl, T., Jocic, M., Heinemann, A., Schuligoi, R., and Holzer, P. 2001. Vagal afferent signaling of a gastric mucosal acid insult to medullary, pontine, thalamic, hypothalamic and limbic, but not cortical, nuclei of the rat brain. Pain 92, 19–27.
Multon, S. and Schoenen, J. 2005. Pain control by vagus nerve stimulation: from animal to man . . . and back. Acta Neurol. Belg. 105, 62–67.

Niijima, A. 1996. The afferent discharge from sensors for interleukin-1 beta in the hepatoportal system in the anesthetized rat. J. Auton. Nerv. Syst. 61, 287–291.

Precht, J. C. and Powley, T. L. 1990. The fibre composition of the abdominal vagus in the rat. Anat. and Embryol. 181, 101–115.

Randich, A. and Gebhart, G. F. 1992. Vagal afferent modulation of nociception. Brain Res. Rev. 17, 77–99.

Ren, K., Zhuo, M., Randich, A., and Gebhart, G. F. 1993. Vagal afferent stimulation-produced effects on nociception in capsaicin-treated rats. J. Neurophysiol. 69, 1530–1540.

Richards, W., Hillsley, K., Eastwood, C., and Grundy, D. 1996. Sensitivity of vagal mucosal afferents to cholecystokinin and its role in afferent signal transduction in the rat. J. Physiol. (Lond.) 497, 473–481.

Sawchenko, P. E., Brown, E. R., Chan, R. K., Ericsson, A., Li, H. Y., Roland, B. L., and Kovacs, K. J. 1996. The paraventricular nucleus of the hypothalamus and the functional neuroanatomy of visceromotor responses to stress. Prog. Brain Res. 107, 201–222.

Schachter, S. C. 2005. Electrical Stimulation of the Vagus Nerve for the Treatment of Epilepsy. In: Advances in Vagal Afferent Neurobiology (*eds*. B. J. Undem and D. Weinreich), pp. 495–510. CRC Press.

Shanahan, F. 1994. The Intestinal Immune System. Physiology of the Gastrointestinal Tract (*ed*. L. R. Johnson), pp. 643–684. Raven Press.

Strauther, G. R., Longo, W. E., Virgo, K. S., and Johnson, F. E. 1999. Appendicitis in patients with previous spinal cord injury. Am. J. Surg. 178, 403–405.

Takeda, M., Tanimoto, T., Ojima, K., and Matsumoto, S. 1998. Suppressive effect of vagal afferents on the activity of the trigeminal spinal neurons related to the jaw-opening reflex in rats: involvement of the endogenous opioid system. Brain Res. Bull. 47, 49–56.

Walls, E. K., Phillips, R. J., Wang, F. B., Holst, M. C., and Powley, T. L. 1995b. Suppression of meal size by intestinal nutrients is eliminated by celia vagal deafferentation. Am. J. Physiol. 269, R1410–1419.

Walls, E. K., Wang, F. B., Holst, M. C., Phillips, R. J., Voreis, J. S., Perkins, A. R., Pollard, L. E. and Powley, T. L. 1995a. Selective vagal rhizotomies: a new dorsal surgical approach used for intestinal deafferentations. Am. J. Physiol. 269, R1279–1288.

Wan, W., Wetmore, L., Sorensen, C. M., Greenberg, A. H., and Nance, D. M. 1994. Neural and biochemical mediators of endotoxin and stress-induced c-fos expression in the rat brain. Brain Res. Bull. 34, 7–14.

Watkins, L.R. and Maier, S. F. (*eds.*) 1999. Cytokines and Pain. Birkhäuser Verlag.

Watkins, L. R. and Maier, S. F. 2000. The pain of being sick: implications of immune-to-brain communication for understanding pain. Annu. Rev. Psychol. 51, 29–57.

Watkins, L. R., Goehler, L. E., Relton, J., Brewer, M. T., and Maier, S. F. 1995a. Mechanisms of tumor necrosis factor-alpha (TNF-alpha) hyperalgesia. Brain Res. 692, 244–250.

Watkins, L. R., Goehler, L. E., Relton, J. K., Tartaglia, N., Silbert, L., Martin, D., and Maier, S. F. 1995b. Blockade of interleukin-1 induced hyperthermia by sub-diaphragmatic vagotom: evidence for vagal mediation of immune-brain communication. Neurosci. Lett. 183, 27–31.

Watkins, L. R., Maier, S. F., and Goehler, L. E. 1995c. Cytokine-to-brain communication: a review & analysis of alternative mechanisms. Life Sci. 57, 1011–1026.

Watkins, L. R., Maier, S. F., and Goehler, L. E. 1995d. Immune activation: the role of pro-inflammatory cytokines in inflammation, illness responses and pathological pain states. Pain 63, 289–302.

Watkins, L. R., Wiertelak, E. P., Goehler, L. E., Mooney-Heiberger, K., Martinez, J., Furness, L. Smith, K. P. and Maier, S. F. 1994a. Neurocircuitry of illness-induced hyperalgesia. Brain Res. 639, 283–299.

Watkins, L. R., Wiertelak, E. P., Goehler, L. E., Smith, K. P., Martin, D., and Maier, S. F. 1994b. Characterization of cytokine-induced hyperalgesia. Brain Res. 654, 15–26.

White, J. C. and Bland, E. F. 1948. The surgical relief of severe angina pectoris. Medicine 27, 1–42.

Zhu, J. X., Zhu, X. Y., Owyang, C., and Li, Y. 2001. Intestinal serotonin acts as a paracrine substance to mediate vagal signal transmission evoked by luminal factors in the rat. J. Physiol. (Lond.) 530, 431–442.

5.21 Sex, Gender, and Pain

R B Fillingim, University of Florida College of Dentistry, Community Dentistry and Behavioral Science Gainesville, FL, USA

© 2008 Elsevier Inc. All rights reserved.

5.21.1	Sex Differences in Pain Responses	253
5.21.2	Sex Differences in Responses to Pain Treatment	253
5.21.3	Mechanisms Underlying Sex Differences in Pain	254
5.21.4	Conclusions and Future Directions	255
References		255

Glossary

biopsychosocial model A model of pain that posits that the experience of and response to pain results from complex, dynamic interactions among biological, psychological, and sociocultural variables.

gender A person's self-representation as male or female, or how that person is responded to by social institutions on the basis of that individual's gender presentation.

sex The classification of living things, generally as male or female, according to their reproductive organs and functions assigned by the chromosomal complement.

5.21.1 Sex Differences in Pain Responses

Considerable evidence suggests that females and males differ in their experience of both clinical and experimentally induced pain (for reviews, see Fillingim, R. B. and Maixner, W., 1995; Unruh, A. M., 1996; Berkley, K. J., 1997; LeResche, L., 1999; Fillingim, R. B., 2003). For example, several chronic pain disorders are more prevalent among women, and in population surveys women report more pain than men (Fillingim, R. B. and Maixner, W., 1995; Unruh, A. M., 1996; Berkley, K. J., 1997). Moreover, some evidence indicates that clinical pain may be more severe for women than men. For example, women have reported greater postsurgical pain than men in some (Savedra, M. C. *et al.*, 1993; Averbuch, M. and Katzper, M., 2000; Coulthard, P. *et al.*, 2000; Taenzer, A. H. *et al.*, 2000; Morin, C. *et al.*, 2000; Averbuch, M. and Katzper, M., 2001; Kalkman, C. J. *et al.*, 2003) but not all (e.g., Gordon, N. C. *et al.*, 1995; Gear, R. W. *et al.*, 1996a; Chia, Y. Y. *et al.*, 2002) studies. Women have also reported higher pain ratings in acute cancer-related pain (Cepeda, M. S. *et al.*, 2003), procedural pain such as colonoscopy (Froehlich, F. *et al.*, 1997), and conditions presented in emergency rooms (Boccardi, L. and Verde, M., 2003). In addition, women display greater perceptual responses to laboratory-induced pain relative to men, although the magnitude of these differences varies across studies, perhaps due to methodological differences (e.g., pain assay, stimulus characteristics, sample selection; Fillingim, R. B. and Maixner, W., 1995; Riley, J. L. *et al.*, 1998). Interestingly, consistent with the human literature, greater behavioral responses to noxious stimuli have been reported among female compared to male rodents (e.g., Barrett, A. C. *et al.*, 2002b; 2003; Terner, J. M. *et al.*, 2003; also for reviews, see Bodnar, R. J. *et al.*, 1988; Berkley, K. J., 1997), with some exceptions (Mogil, J. S. *et al.*, 1993; Kayser, V. *et al.*, 1996). In general, these findings suggest that females exhibit greater perceptual responses to pain than males; however, the mechanisms underlying these sex differences have not been determined.

5.21.2 Sex Differences in Responses to Pain Treatment

In addition to basal pain sensitivity, sex-related influences on responses to pharmacologic and nonpharmacologic pain treatments have received

increasing attention in recent years. The rodent literature fairly consistently demonstrates greater analgesic responses to opioid agonists among males versus female animals (Bodnar, R. J. *et al.*, 1988; Kepler, K. L. *et al.*, 1989; 1991; Kiefel, J. M. and Bodnar. R. J., 1992; Islam, A. K. *et al.*, 1993; Cicero, T. J. *et al.*, 1996a; 1997; Kest, B. *et al.*, 2000; Craft, R. M., 2003a; 2003b). However, the human literature regarding sex differences in analgesic responses has shown mixed results. Some clinical studies demonstrate greater analgesic responses among women, others show no sex differences, and others report greater analgesia among men (Fillingim, R. B. and Gear, R. W., 2004). Among the most consistent findings is a series of studies indicating more robust analgesic responses κ-opioid-acting drugs after oral surgery (Gear, R. W. *et al.*, 1996a; 1996b; 1999; 2003). Laboratory studies in humans have shown mixed results, as well (Sarton, E. *et al.*, 2000; Fillingim, R. B. *et al.*, 2004; Romberg, R. *et al.*, 2004; Olofsen, E. *et al.*, 2005; Fillingim, R. B. *et al.*, 2005c). Sex differences in response to nonpharmacologic interventions for pain has received less empirical attention, though a few laboratory (Keogh, E. *et al.*, 2000; Sternberg, W. F. *et al.*, 2001) and clinical (Hansen, F. R. *et al.*, 1993; Krogstad, B. S. *et al.*, 1996; Jensen, I. B. *et al.*, 2001) studies suggest that sex differences in treatment responses may emerge. It is possible that the consistent sex differences in analgesic responses are specific to the oral surgery pain model, perhaps due to its inflammatory component or based on interactions with other medications administered perioperatively. The clinical relevance of these results beyond this acute pain model remains unknown, and this is an area ripe for future investigation.

5.21.3 Mechanisms Underlying Sex Differences in Pain

It is important to recognize that sex differences in pain are inevitably determined by interactions among multiple biopsychosocial processes. While these mechanisms are typically described as either psychosocial or biological, this dualistic conceptualization is artificial and potentially counterproductive. For instance, sex differences in expression of pain are often attributed to the effects of stereotypic sex roles, typically considered a psychosocial issue. However, neurobiological and hormonal correlates of masculine versus feminine sex roles may well contribute to differences in nociceptive processing. Thus, various psychosocial and biological mechanisms underlying sex differences in pain responses could refer to the same fundamental processes described at different levels of analysis.

Several biological variables have been implicated in sex differences in both clinical and experimental pain responses. Abundant preclinical and clinical evidence suggests that gonadal hormones are important, because hormonal influences on basal pain sensitivity as well as responses to analgesic compounds have been well documented (Riley, J. L. III. *et al.*, 1999; Fillingim, R. B. and Ness, T. J., 2000; Bodnar. R. J. *et al.*, 2002). Also, endogenous pain inhibitory systems may function differently in females and males, including the endogenous opioid system. Zubieta and colleagues have reported sex differences in both basal and pain-evoked μ-opioid receptor binding in certain brain regions (Zubieta, J. K. *et al.*, 1999; 2002). Genetic factors may also contribute to sex differences in pain. In rodents, sex differences in nociceptive and antinociceptive responses are often strain-dependent (Mogil, J. S. *et al.*, 2000; Barrett, A. C. *et al.*, 2002a; Terner, J. M. *et al.*, 2003), and pain-related quantitative trait loci (QTLs) are often sex-specific (Mogil, J. S. *et al.*, 1997; Mogil, J. S., 2000). Recent findings provide corroborating results in humans (Kim, H. *et al.*, 2004). Also, Mogil J. S. *et al.* (2003) demonstrated in both mice and humans that the melanocortin-1-receptor gene (*MC1R*) was associated with analgesic responses to κ-opioids among females but not males. Also, the A118G single nucleotide polymorphism of the μ-opioid receptor gene (*OPRM1*) was significantly associated with pressure pain thresholds, but this association was only significant among males (Fillingim, R. B. *et al.*, 2005b). Thus, several biological factors may contribute to sex differences in pain.

Numerous psychosocial variables also contribute to sex differences in pain responses. Anxiety and other negative emotions have been more strongly related with both clinical and experimental pain responses among men than women (Fillingim, R. B. *et al.*, 1996; Edwards, R. R. *et al.*, 2000; Riley, J. L., III *et al.*, 2001; Jones, A. and Zachariae, R., 2002; Robinson, M. E. *et al.*, 2005) Moreover, positive affect predicted lower experimental pain sensitivity and fewer side effects in responses to pentazocine (a mixed action opioid) among men, but not women (Fillingim, R. B. *et al.*, 2005a). Additional psychosocial factors that may contribute to sex differences in pain include cognitive and behavioral pain coping strategies (Affleck, G. *et al.*, 1999; Unruh, A. M. *et al.*, 1999; Keefe, F. J. *et al.*, 2000; Mercado, A. C. *et al.*, 2000; Osman, A. *et al.*, 2000), gender roles (Otto, M. W. and

Dougher, M. J., 1985; Myers, C. D. *et al.*, 2001; Robinson, M. E. *et al.*, 2003), and family history of pain (Edwards, P. W. *et al.*, 1985; Fillingim, R. B. *et al.*, 2000).

5.21.4 Conclusions and Future Directions

The evidence reviewed indicates consistent sex differences in pain-related responses, to which multiple biopsychosocial factors contribute. The literature focuses more heavily on quantitative sex differences (i.e., does the magnitude of pain or analgesia differ in women vs. men?); however, of equal if not greater importance are qualitative sex differences (i.e., are the mediators of pain and analgesia different in women vs. men?). Some examples are provided above, including findings demonstrating sex-specific genetic and psychosocial associations with pain. The clearest challenge for the future is to determine the practical significance of these sex differences and to integrate this information into clinical practice. It seems plausible that expanding research into qualitative sex differences may be more informative in this regard, because such differences imply that some components of the pain processing system may be fundamentally different in women versus men, which calls for sex-specific treatment approaches. It is hoped that continued research into sex, gender and pain will ultimately enhance pain management for both women and men.

Acknowledgment

This work was supported by NIH grant NS41670.

References

Affleck, G., Tennen, H., Keefe, F. J., Lefebvre, J. C., Kashikar-Zuck, S., Wright, K., Starr, K., and Caldwell, D. S. 1999. Everyday life with osteoarthritis or rheumatoid arthritis: independent effects of disease and gender on daily pain, mood, and coping. Pain 83, 601–609.

Averbuch, M. and Katzper, M. 2000. A search for sex differences in response to analgesia. Arch. Intern. Med. 160, 3424–3428.

Averbuch, M. and Katzper, M. 2001. Gender and the placebo analgesic effect in acute pain. Clin. Pharmacol. Ther. 70, 287–291.

Barrett, A. C., Cook, C. D., Terner, J. M., Roach, E. L., Syvanthong, C., and Picker, M. J. 2002a. Sex and rat strain determine sensitivity to kappa opioid-induced antinociception. Psychopharmacology (Berl.) 160, 170–181.

Barrett, A., Smith, E., and Picker, M. 2002b. Sex-related differences in mechanical nociception and antinociception produced by mu- and kappa-opioid receptor agonists in rats. Eur. J. Pharmacol. 452, 163.

Barrett, A. C., Smith, E. S., and Picker, M. J. 2003. Capsaicin-induced hyperalgesia and μ-opioid-induced antihyperalgesia in male and female Fischer 344 rats. J. Pharmacol. Exp. Ther. 307, 237–245.

Berkley, K. J. 1997. Sex Differences in Pain. Behav. Brain Sci. 20, 371–380.

Boccardi, L. and Verde, M. 2003. Gender differences in the clinical presentation to the emergency department for chest pain. Ital. Heart J. 4, 371–373.

Bodnar, R. J., Commons, K., and Pfaff, D. W. 2002. Central Neural States Relating Sex and Pain. Johns Hopkins University Press.

Bodnar, R. J., Romero, M. T., and Kramer, E. 1988. Organismic variables and pain inhibition: roles of gender and aging. Brain Res. Bull. 21, 947–953.

Cepeda, M. S., Africano, J. M., Polo, R., Alcala, R., and Carr, D. B. 2003. Agreement between percentage pain reductions calculated from numeric rating scores of pain intensity and those reported by patients with acute or cancer pain. Pain 106, 439–442.

Chia, Y. Y., Chow, L. H., Hung, C. C., Liu, K., Ger, L. P., and Wang, P. N. 2002. Gender and pain upon movement are associated with the requirements for postoperative patient-controlled iv analgesia: a prospective survey of 2,298 Chinese patients. Can. J. Anaesth. 49, 249–255.

Cicero, T. J., Nock, B., and Meyer, E. R. 1996. Gender-related differences in the antinociceptive properties of morphine. J. Pharmacol. Exp. Ther. 279, 767–773.

Cicero, T. J., Nock, B., and Meyer, E. R. 1997. Sex-related differences in morphine's antinociceptive activity: relationship to serum and brain morphine concentrations. J. Pharmacol. Exp. Ther. 282, 939–944.

Coulthard, P., Pleuvry, B. J., Dobson, M., and Price, M. 2000. Behavioural measurement of postoperative pain after oral surgery. Br. J. Oral Maxillofac. Surg. 38, 127–131.

Craft, R. M. 2003a. Sex differences in drug- and non-drug-induced analgesia. Life Sci. 72, 2675–2688.

Craft, R. M. 2003b. Sex differences in opioid analgesia: from mouse to man. Clin. J. Pain 19, 175–186.

Edwards, R. R., Augustson, E., and Fillingim, R. B. 2000. Sex-specific effects of pain-related anxiety on adjustment to chronic pain. Clin. J. Pain 16, 46–53.

Edwards, P. W., Zeichner, A., Kuczmierczyk, A. R., and Boczkowski, J. 1985. Familial pain models: the relationship between family history of pain and current pain experience. Pain 21, 379–384.

Fillingim, R. B. 2003. Sex-related influences on pain: a review of mechanisms and clinical implications. Rehabil. Psychol. 48, 165–174.

Fillingim, R. B. and Gear, R. W. 2004. Sex differences in opioid analgesia: clinical and experimental findings. Eur. J. Pain 8, 413–425.

Fillingim, R. B. and Maixner, W. 1995. Gender differences in the responses to noxious stimuli. Pain Forum 4, 209–221.

Fillingim, R. B. and Ness, T. J. 2000. Sex-related hormonal influences on pain and analgesic responses. Neurosci. Biobehav. Rev. 24, 485–501.

Fillingim, R. B., Edwards, R. R., and Powell, T. 2000. Sex-dependent effects of reported familial pain history on clinical and experimental pain responses. Pain 86, 87–94.

Fillingim, R. B., Hastie, B. A., Ness, T. J., Glover, T. L., Campbell, C. M., and Staud, R. 2005a. Sex-related psychological predictors of baseline pain perception and analgesic responses to pentazocine. Biol. Psychol. 69, 97–112.

Fillingim, R. B., Kaplan, L., Staud, R., Ness, T. J., Glover, T. L., Campbell, C. M., Mogil, J. S., and Wallace, M. R. 2005b. The A118G single nucleotide polymorphism of the mu-opioid receptor gene (OPRM1) is associated with pressure pain sensitivity in humans. J. Pain 6, 159–167.

Fillingim, R. B., Keefe, F. J., Light, K. C., Booker, D. K., and Maixner, W. 1996. The influence of gender and psychological factors on pain perception. J. Gender Cult. Health 1, 21–36.

Fillingim, R. B., Ness, T. J., Glover, T. L., Campbell, C. M., Hastie, B. A., Price, D. D., and Staud, R. 2005c. Morphine responses and experimental pain: sex differences in side effects and cardiovascular responses but not analgesia. J. Pain 6, 116–124.

Fillingim, R. B., Ness, T. J., Glover, T. L., Campbell, C. M., Price, D. D., and Staud, R. 2004. Experimental pain models reveal no sex differences in pentazocine analgesia in humans. Anesthesiology 100, 1263–1270.

Froehlich, F., Thorens, J., Schwizer, W., Preisig, M., Kohler, M., Hays, R. D, Fried, M., and Gonvers, J. J. 1997. Sedation and analgesia for colonoscopy: patient tolerance, pain, and cardiorespiratory parameters. Gastrointest. Endosc. 45, 1–9.

Gear, R. W., Gordon, N. C., Heller, P. H., Paul, S., Miaskowski, C., and Levine, J. D. 1996a. Gender difference in analgesic response to the kappa-opioid pentazocine. Neurosci. Lett. 205, 207–209.

Gear, R. W., Gordon, N. C., Miaskowski, C., Paul, S. M., Heller, P. H., and Levine, J. D. 2003. Sexual dimorphism in very low dose nalbuphine postoperative analgesia. Neurosci. Lett. 339, 1–4.

Gear, R. W., Miaskowski, C., Gordon, N. C., Paul, S. M., Heller, P. H., and Levine, J. D. 1999. The kappa opioid nalbuphine produces gender- and dose-dependent analgesia and antianalgesia in patients with postoperative pain. Pain 83, 339–345.

Gear, R. W., Miaskowski, C., Gordon, N. C., Paul, S. M., Heller, P. H., and Levine, J. D. 1996b. Kappa-opioids produce significantly greater analgesia in women than in men. Nat. Med. 2, 1248–1250.

Gordon, N. C., Gear, R. W., Heller, P. H., Paul, S., Miaskowski, C., and Levine, J. D. 1995. Enhancement of morphine analgesia by the GABAB agonist baclofen. Neuroscience 69, 345–349.

Hansen, F. R., Bendix, T., Skov, P., Jensen, C. V., Kristensen, J. H., Krohn, L., and Schioeler, H. 1993. Intensive, dynamic back-muscle exercises, conventional physiotherapy, or placebo-control treatment of low-back pain. A randomized, observer-blind trial. Spine 18, 98–108.

Islam, A. K., Beczkowska, I. W., and Bodnar, R. J. 1993. Interactions among aging, gender, and gonadectomy effects upon naloxone hypophagia in rats. Physiol. Behav. 54, 981–992.

Jensen, I. B., Bergstrom, G., Ljungquist, T., Bodin, L., and Nygren, A. L. 2001. A randomized controlled component analysis of a behavioral medicine rehabilitation program for chronic spinal pain: are the effects dependent on gender? Pain 91, 65–78.

Jones, A. and Zachariae, R. 2002. Gender, anxiety, and experimental pain sensitivity: an overview. J. Am. Med. Womens Assoc. 57, 91–94.

Kalkman, C. J., Visser, K., Moen, J., Bonsel, G. J., Grobbee, D. E., and Moons, K. G. 2003. Preoperative prediction of severe postoperative pain. Pain 105, 415–423.

Kayser, V., Berkley, K. J., Keita, H., Gautron, M., and Guilbaud, G. 1996. Estrous and sex variations in vocalization thresholds to hindpaw and tail pressure stimulation in the rat. Brain Res. 742, 352–354.

Keefe, F. J., Lefebvre, J. C., Egert, J. R., Affleck, G., Sullivan, M. J., and Caldwell, D. S. 2000. The relationship of gender to pain, pain behavior, and disability in osteoarthritis patients: the role of catastrophizing. Pain 87, 325–334.

Keogh, E., Hatton, K., and Ellery, D. 2000. Avoidance versus focused attention and the perception of pain: differential effects for men and women. Pain 85, 225–230.

Kepler, K. L., Kest, B., Kiefel, J. M., Cooper, M. L., and Bodnar, R. J. 1989. Roles of gender, gonadectomy and estrous phase in the analgesic effects of intracerebroventricular morphine in rats. Pharmacol. Biochem. Behav. 34, 119–127.

Kepler, K. L., Standifer, K. M., Paul, D., Kest, B., Pasternak, G. W., and Bodnar, R. J. 1991. Gender effects and central opioid analgesia. Pain 45, 87–94.

Kest, B., Sarton, E., and Dahan, A. 2000. Gender differences in opioid-mediated analgesia: animal and human studies. Anesthesiology 93, 539–547.

Kiefel, J. M. and Bodnar, R. J. 1992. Roles of gender and gonadectomy in pilocarpine and clonidine analgesia in rats. Pharmacol. Biochem. Behav. 41, 153–158.

Kim, H., Neubert, J. K., San, M. A., Xu, K., Krishnaraju, R. K., Iadarola, M. J., Goldman, D., and Dionne, R. A. 2004. Genetic influence on variability in human acute experimental pain sensitivity associated with gender, ethnicity and psychological temperament. Pain 109, 488–496.

Krogstad, B. S., Jokstad, A., Dahl, B. L., and Vassend, O. 1996. The reporting of pain, somatic complaints, and anxiety in a group of patients with TMD before and 2 years after treatment: sex differences. J. Orofac. Pain 10, 263–269.

LeResche, L. 1999. Gender Considerations in the Epidemiology of Chronic Pain. In: Epidemiology of Pain (*ed*. I. K. Crombie), pp. 43–52. IASP Press.

Mercado, A. C., Carroll, L. J., Cassidy, J. D., and Cote, P. 2000. Coping with neck and low back pain in the general population. Health Psychol. 19, 333–338.

Mogil, J. S. 2000. Interactions Between Sex and Genotype in the Mediation and Modulation of Nociception in Rodents. In: Sex, Gender, and Pain (*ed*. R. B. Fillingim), pp. 25–40. IASP Press.

Mogil, J. S., Chesler, E. J., Wilson, S. G., Juraska, J. M., and Sternberg, W. F. 2000. Sex differences in thermal nociception and morphine antinociception in rodents depend on genotype. Neurosci. Biobehav. Rev. 24, 375–389.

Mogil, J. S., Richards, S. P., O'Toole, L. A., Helms, M. L., Mitchell, S. R., and Belknap, J. K. 1997. Genetic sensitivity to hot-plate nociception in DBA/2J and C57BL/6J inbred mouse strains: possible sex-specific mediation by delta2-opioid receptors. Pain 70, 267–277.

Mogil, J. S., Sternberg, W. F., Kest, B., Marek, P., and Liebeskind, J. C. 1993. Sex differences in the antagonism of stress-induced analgesia: effects of gonadectomy and estrogen replacement. Pain 53, 17–25.

Mogil, J. S., Wilson, S. G., Chesler, E. J., Rankin, A. L., Nemmani, K. V., Lariviere, W. R., Groce, M. K., Wallace, M. R., Kaplan, L., Staud, R., Ness, T. J., Glover, T. L., Stankova, M., Mayorov, A., Hruby, V. J., Grisel, J. E., and Fillingim, R. B. 2003. The melanocortin-1 receptor gene mediates female-specific mechanisms of analgesia in mice and humans. Proc. Natl. Acad. Sci. U. S. A. 100, 4867–4762.

Morin, C., Lund, J. P., Villarroel, T., Clokie, C. M., and Feine, J. S. 2000. Differences between the sexes in post-surgical pain. Pain 85, 79–85.

Myers, C. D., Robinson, M. E., Riley, J. L., III, and Sheffield, D. 2001. Sex, gender, and blood pressure: contributions to experimental pain report. Psychosom. Med. 63, 545–550.

Olofsen, E., Romberg, R., Bijl, H., Mooren, R., Engbers, F., Kest, B., and Dahan, A. 2005. Alfentanil and placebo analgesia: no sex differences detected in models of experimental pain. Anesthesiology 103, 130–139.

Osman, A., Barrios, F. X., Gutierrez, P. M., Kopper, B. A., Merrifield, T., and Grittmann, L. 2000. The Pain Catastrophizing Scale: further psychometric evaluation with adult samples. J. Behav. Med. 23, 351–365.

Otto, M. W. and Dougher, M. J. 1985. Sex differences and personality factors in responsivity to pain. Percept. Mot. Skills 61, 383–390.

Riley, J. L., III, Robinson, M. E., Wade, J. B., Myers, C. D., and Price, D. D. 2001. Sex differences in negative emotional responses to chronic pain. J. Pain 2, 354–359.

Riley, J. L., III, Robinson, M. E., Wise, E. A., Myers, C. D., and Fillingim, R. B. 1998. Sex differences in the perception of noxious experimental stimuli: a meta-analysis. Pain 74, 181–187.

Riley, J. L. I., Robinson, M. E., Wise, E. A., and Price, D. D. 1999. A meta-analytic review of pain perception across the menstrual cycle. Pain 81, 225–235.

Robinson, M. E., Dannecker, E. A., George, S. Z., Otis, J., Atchison, J. W., and Fillingim, R. B. 2005. Sex differences in the associations among psychological factors and pain report: a novel psychophysical study of patients with chronic low back pain. J. Pain 6, 463–470.

Robinson, M. E., Gagnon, C. M., Riley, J. L., III, and Price, D. D. 2003. Altering gender role expectations: effects on pain tolerance, pain threshold, and pain ratings. J. Pain 4, 284–288.

Romberg, R., Olofsen, E., Sarton, E., den, Hartigh J., Taschner, P. E., and Dahan, A. 2004. Pharmacokinetic–pharmacodynamic modeling of morphine-6-glucuronide-induced analgesia in healthy volunteers: absence of sex differences. Anesthesiology 100, 120–133.

Sarton, E., Olofsen, E., Romberg, R., den Hartigh, J., Kest, B., Nieuwenhuijs, D., Burm, A., Teppema, L., and Dahan, A. 2000. Sex differences in morphine analgesia: an experimental study in healthy volunteers. Anesthesiology 93, 1245–1254.

Savedra, M. C., Holzemer, W. L., Tesler, M. D., and Wilkie, D. J. 1993. Assessment of postoperation pain in children and adolescents using the adolescent pediatric pain tool. Nurs. Res. 42, 5–9.

Sternberg, W. F., Bokat, C., Kass, L., Alboyadjian, A., and Gracely, R. H. 2001. Sex-dependent components of the analgesia produced by athletic competition. J. Pain 2, 65–74.

Taenzer, A. H., Clark, C., and Curry, C. S. 2000. Gender affects report of pain and function after arthroscopic anterior cruciate ligament reconstruction. Anesthesiology 93, 670–675.

Terner, J. M., Lomas, L. M., Smith, E. S., Barrett, A. C., and Picker, M. J. 2003. Pharmacogenetic analysis of sex differences in opioid antinociception in rats. Pain 106, 381–391.

Unruh, A. M. 1996. Gender variations in clinical pain experience. Pain 65, 123–167.

Unruh, A. M., Ritchie, J., and Merskey, H. 1999. Does gender affect appraisal of pain and pain coping strategies? Clin J. Pain 15, 31–40.

Zubieta, J. K., Dannals, R. F., and Frost, J. J. 1999. Gender and age influences on human brain mu-opioid receptor binding measured by PET. Am. J. Psychiatry 156, 842–848.

Zubieta, J. K., Smith, Y. R., Bueller, J. A., Xu, Y., Kilbourn, M. R., Jewett, D. M., Meyer, C. R., Koeppe, R. A., and Stohler, C. S. 2002. mu-Opioid receptor-mediated antinociceptive responses differ in men and women. J. Neurosci. 22, 5100–5107.

5.22 Neurotrophins and Pain

Lorne M Mendell, State University of New York, Stony Brook, NY, USA

© 2008 Elsevier Inc. All rights reserved.

5.22.1	The Neurotrophin Family and Its Receptors	260
5.22.2	Neurotrophins and Development of Nociceptors	260
5.22.3	Nerve Growth Factor Affects Electrophysiological Properties of Nociceptors that Express TrkA	262
5.22.4	Exogenous Nerve Growth Factor Elicits Hyperalgesia	262
5.22.4.1	Chronic Changes	262
5.22.4.2	Acute Changes	262
5.22.4.3	Mechanisms of Nerve Growth Factor Action in the Skin	263
5.22.5	Acute Sensitization by Nerve Growth Factor of the Response of Dissociated Nociceptors	264
5.22.6	TrkA Signaling Pathways Responsible for Acute Effects of Nerve Growth Factor	265
5.22.7	p75 Receptor Influence on Sensory Neuron Function	266
5.22.8	Effects of Nerve Growth Factor on Expression of Channels and Receptors in Nociceptors	267
5.22.8.1	TRPV1 Receptors	267
5.22.8.2	P2X3 Receptors	268
5.22.8.3	ASIC Channels	268
5.22.8.4	BK Receptors	268
5.22.8.5	Na^+ Channels	268
5.22.8.6	PGE2 Receptors	269
5.22.9	Neurotrophins and Sensitization of Tissues Other than Skin	269
5.22.9.1	Visceral Structures	269
5.22.9.2	Muscle Afferents	269
5.22.9.3	Joint Receptors	269
5.22.10	Nerve Growth Factor, Enhances Peptide Expression in the Dorsal Root Ganglion, and Central Sensitization	270
5.22.11	Role of Brain-Derived Neurotrophic Factor, Neurotrophin-4, and Neurotrophin-3 in Peripheral Sensitization	270
5.22.12	Neurotrophins and Neuropathic Pain	271
5.22.13	Neurotrophins and the Clinic	272
5.22.14	Discussion, Conclusions, and Open Questions	272
References		273

Glossary

immunoadhesin A chimeric molecule consisting of a IgG backbone (Fc region) linked to the binding site of a receptor that binds to a molecule to be sequestered, e.g., trkA-IgG binds nerve growth factor (NGF).

keratinocyte Immune-competent cell in the epidermis.

mast cell Immune-competent cell that stores inflammatory mediators.

neutrophil A type of white blood cell that phagocytoses microorganisms (i.e., due to infection) and breaks them down.

skin nerve preparation *In vitro* preparation in which the skin is removed with its nerve supply (e.g., ankle skin and saphenous nerve) and placed in a chamber. The nerve is led into a second chamber separated from the skin chamber so that the skin can be maintained in oxygenated Ringer, whereas the nerve can be placed in oil for extracellular recording.

tachyphylaxis A process whereby the response to an agent applied repeatedly becomes smaller and smaller.

5.22.1 The Neurotrophin Family and Its Receptors

Neurotrophin molecules are 13.5-kDa proteins that come in four major forms that show a substantial overlap in their primary structure. These are known as nerve growth factor (NGF), brain-derived neurotrophic factor (BDNF), neurotrophin-3 (NT-3), and neurotrophin-4 (also known neurotrophin-5 or neurotrophin-4/5, NT-4/5). The molecular biology underlying the synthesis of these molecules has been reviewed elsewhere (Teng, K. K. and Hempstead, B. L., 2004). Neurotrophins bind to two classes of receptors: the tropomyosin-related kinase (trk) receptors, trkA, trkB, and trkC, as well as the p75 receptor that is a member of the tumor necrosis factor (TNF) superfamily. Although these two receptor types are often considered to function together as a complex (Chao, M. V. and Hempstead, B. L., 1995; He, X. L. and Garcia, K. C., 2004), there is also evidence that they can function independently (see Section 5.22.7).

The trk receptors are known as the high-affinity neurotrophin receptors and selectively bind the different neurotrophin molecules. NGF binds selectively to trkA, BDNF and NT-4/5 to trkB, and NT-3 to trkC (Huang, E. J. and Reichardt, L. F., 2001). Some cross-binding with lower affinity also occurs (Barbacid, M., 1994). The p75 receptor is generally known as the low-affinity receptor, although it actually binds neurotrophins with high affinity but with rapid kinetics. It binds all known neurotrophins with similar affinity. Thus, the selective expression of trk receptors in different cell types (MCMahon, S. B. *et al.*, 1994) is a major factor underlying the selective effects of neurotrophins in the nervous system.

Ligands binding to the extracellular component of trk receptors induce autophosphorylation of the trk molecule, which leads to downstream effects via multiple signaling pathways (Kaplan, D. R. and Miller, F. D., 2000). For example, phospholipase Cγ (PLCγ) is phosphorylated subsequent to its recruitment to the cell membrane as a consequence of phosphorylation of tyrosine 785 on trkA (Obermeier, A. *et al.*, 1993). This is very likely an important mechanism in mediating neurotrophin-induced effects (see below). However, other intracellular signaling pathways are also activated by neurotrophin binding to trk receptors including the Ras–Raf–Mek–Erk pathway and the PI-3K pathway (Kaplan, D. R. and Cooper, E., 2001). Some of these have also been implicated in mediating the functional effects of neurotrophins (see Section 5.22.6).

5.22.2 Neurotrophins and Development of Nociceptors

The early history of the discovery of NGF has been extensively reviewed (Cowan, W. M., 2001). It began with the observation that extracts from mouse salivary glands induce proliferation of processes of explanted dorsal root ganglion (DRG) and sympathetic ganglion cells. Later, biochemical studies revealed that the active factor is a peptide that became known as nerve growth factor. NGF was subsequently identified as an important factor assuring survival of developing sensory neurons since its absence induced by treating the animal with an NGF antibody resulted in the survival of fewer cells in the DRG as well as in sympathetic ganglia. This led to the neurotrophic hypothesis (Davies, A. M., 1996), which states that a soluble trophic factor is present in limiting amounts in the target tissue of a population of neurons, which require it in order to survive. Nerve terminals that are successful in internalizing this factor and transporting it to the cell body for its metabolic use survive; the unsuccessful ones die. More detailed studies of the DRG revealed that selective neutralization of NGF via its antibody results in depletion of a limited population of DRG cells, specifically those that express peptides such as substance P and calcitonin gene-related peptide (CGRP) and project into superficial laminae of the spinal cord. i.e., those that are identified with nociception (reviewed in Mendell, L. M., 1995). Animals treated in this way exhibit a higher threshold for painful stimuli. Genetically modified animals have proven very useful in demonstrating these relationships with those under- or overexpressing NGF in the skin being hypo- or hyperalgesic, respectively (Davis, B. M. *et al.*, 1993), and those underexpressing the NGF receptor trkA being hypoalgesic (Smeyne, R. J. *et al.*, 1994).

In all these manipulations, NGF was considered to affect the number of nociceptors, permitting more or fewer to survive. However, it has become apparent that NGF influences the properties of nociceptors in the immediate postnatal period, beyond the time it can affect DRG cell number. Ritter A. M. *et al.* (1991; see also Lewin, G. R. *et al.*, 1992a) demonstrated that a class of nociceptors known as Aδ high-threshold mechanoreceptors (HTMRs) is severely depleted in rats treated postnatally with an antibody to NGF (anti-NGF). The proportion of Aδ low-threshold mechanoreceptors known as down hair receptors (D hairs) is elevated by a similar proportion.

Significantly, the proportion of a third population of afferent fibers also conducting in the Aδ range and innervating subcutaneous tissues is unchanged. Thus, HTMRs are not selectively depleted since if this occurs, the proportion of all other fiber types would be expected to increase. Furthermore, when cell counts were undertaken in the DRG, no change in cell number was noted. Consistent with these findings, the magnitude of the vasodilator response elicited by antidromic activation of cutaneous nerves is reduced in proportion to the depletion of Aδ HTMRs (Lewin, G. R. *et al.*, 1992b).

These findings suggest that the postnatal development of nociceptors depends on the availability of NGF and that in its absence sensory neurons normally destined to be HTMRs become D hairs. This has been referred to as a phenotypic shift (Lewin, G. R. *et al.*, 1992a). Cell number in the DRG declines if the antibody is delivered between P0 and P2, whereas the phenotypic shift from HTMR to D hair occurs after anti-NGF treatment between P4 and P11. Attention was drawn to evidence that sensory axons normally first innervate the epidermis, with many terminals later withdrawing to the dermal layer as hair follicles and other structures develop (Reynolds, M. L. *et al.*, 1991). NGF is expressed by a limited population of cells in the epidermis, for example in basal keratinocytes (Di Marco, E. *et al.*, 1991), and it was hypothesized that the availability of NGF there would cause trkA-expressing neurons to differentiate into nociceptors with epidermal terminals. In the absence of NGF due to anti-NGF treatment, these terminals would recede into the dermal layers of the skin, as occurred with most non-trkA-expressing neurons (reviewed in Lewin, G. R. and Mendell L. M., 1993; Mendell, L. M. *et al.*, 1999).

Exogenous NGF delivered postnatally does not elevate the relative proportion of HTMRs (Lewin, G. R. *et al.*, 1993). However, enhancing NGF levels in the skin beginning during development (E11) in transgenic mice via the keratin promoter increases the number of sensory neurons well above normal levels (Albers, K. M. *et al.*, 1994). Electrophysiological studies have confirmed that nociceptors are selectively rescued by the availability of the additional NGF (Stucky, C. L. *et al.*, 1999).

The DRG cell population undergoes substantial changes in the expression of trkA postnatally. A substantial number lose trkA expression over the first 3 postnatal weeks, and there is a parallel increase in the number of cells exhibiting receptors for glial-derived neurotrophic factor (GDNF) (Molliver, D. C. *et al.*, 1997). Cells undergoing this conversion do not express p75 even in neonates, i.e., they are $p75^{-}/trkA^{+}$ as distinct from cells that are $p75^{+}/trkA^{+}$ (Figure 1). Receptors for GDNF consist of an intracellular signaling receptor domain RET, which is a tyrosine kinase receptor. There are four different ligand-binding domains, GFR1–GFR4, that bind different members of the GDNF family. GDNF itself binds to GFRα1. Other agonists are neurturin (NTN) binding to GFRα2, artemin binding to GFRα3 and persepherin that binds to GFRα4 (Saarma, M.

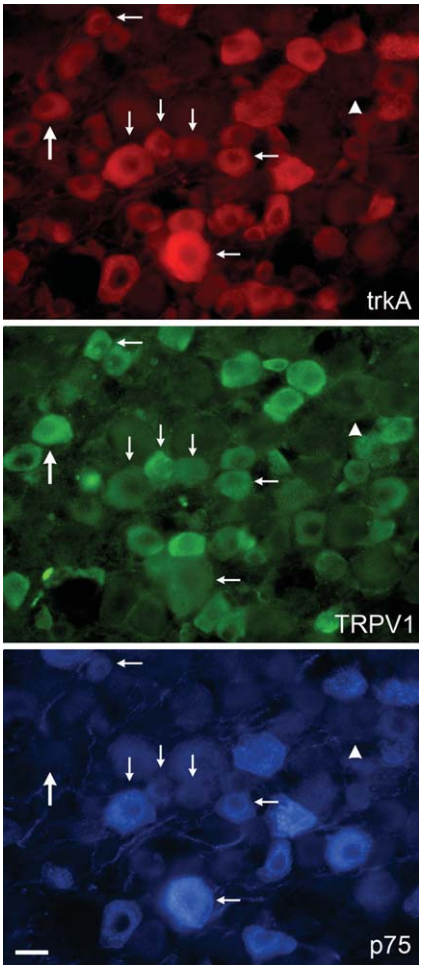

Figure 1 Dorsal root ganglion (DRG) tissue section from 10-day-old rat immunostained for trkA (red), TRPV1 (green), and p75 (blue). Most small cells are at least weakly positive for trkA, TRPV1, and p75 (small down and horizontal arrows). In one case (large up arrow), the cell was $trkA^{+}/TRPV1^{+}/p75^{-}$; this cell was likely to lose its trkA expression and gain receptors for GDNF. The cell denoted by an arrowhead is negative for all three markers used. Scale bar (*lower left*) is 20 μm. Data from Petruska J. C. and Mendell L. M. (unpublished).

and Sariola, H., 1999). In rats, the population expressing cRet also express the lectin IB4 (in adults $trkA^+$ cells are $IB4^-$). In mice, this separation is not as distinct. In rats, $IB4^+/cret^+/trkA^-$ cells have been shown to project more deeply into lamina II (lamina IIi) and are considered to be sensitive to nonnoxious stimulation. These neurons, unlike $trkA^+/IB4^-$ neurons, do not contain CGRP. GDNF has actions on GFR/Ret-expressing nociceptors that only partially overlap those of NGF on trkA-expressing nociceptors (see Section 5.22.8).

5.22.3 Nerve Growth Factor Affects Electrophysiological Properties of Nociceptors that Express TrkA

The finding that treatment with anti-NGF affects properties of nociceptors suggested that trkA is expressed selectively in nociceptors. This has been confirmed in a number of electrophysiological studies (Ritter, A. M. and Mendell, L. M., 1992; Djouhri, L. *et al.*, 2001) where application of NGF or anti-NGF was found to affect properties of the action potential in nociceptors only, regardless of axon size (Aβ, Aδ, or C). Interestingly, both these studies found effects on action potential fall time although the effects differed, probably because of the very different conditions of the experiments. Both studies also revealed that NGF does not affect the duration of after hyperpolarization. The selective expression of trkA in electrophysiologically characterized nociceptors has recently been confirmed directly by Fang X. *et al.* (2005).

5.22.4 Exogenous Nerve Growth Factor Elicits Hyperalgesia

5.22.4.1 Chronic Changes

Neonatal rats are more sensitive to being handled after an initial injection of NGF (Lewin, G. R. *et al.*, 1993). It was surmised that changes had occurred in the nociceptive system. Behavioral studies in 5-week-old rats treated with NGF every other day from birth revealed both mechanical and thermal hyperalgesia (Lewin, G. R. *et al.*, 1993). Additional studies with serial observations on rats treated either as neonates (0–2 weeks old) or as juveniles (2–5 weeks old) demonstrated that the sensitizing effect of NGF lasts several weeks after the end of treatment.

Individual Aδ HTMRs in rats treated systemically over the first 2 postnatal weeks with NGF exhibit a significantly diminished mechanical threshold (i.e., are more sensitive) up to 9 weeks of age after which it returns to control values (Lewin, G. R. *et al.*, 1993). Neonatal treatment with anti-NGF elevates mechanical threshold (Lewin, G. R. *et al.*, 1992). Treatment of older rats with NGF has no measurable effect on mechanical threshold. A similar study on C-fibers (Lewin, G. R. and Mendell, L. M., 1994) has revealed that treatment with NGF increases the fraction sensitive to noxious heat, whereas anti-NGF reduces it. Unlike the changes in mechanical sensitivity in Aδ-fibers, these changes are apparently permanent. The mechanical sensitivity of these C-fiber units is unchanged, although a population of mechanically sensitive units with an unusually low threshold is observed in anti-NGF-treated preparations. Reducing NGF levels in the skin in adult rats using the immunoadhesin trkA-IgG 10–12 days before recording (Bennett, D. L. *et al.*, 1998a) also causes a substantial decline in the response of individual units to noxious heat with no change in the response to mechanical stimulation. The number of units sensitive to bradykinin also decreases after trkA-IgG treatment, suggesting an important contribution of NGF to bradykinin sensitivity of nociceptors (see Section 5.22.8.4).

5.22.4.2 Acute Changes

Examination of the acute effects of a single administration of NGF (i.p.) in adult rats revealed that thermal hyperalgesia becomes significant virtually immediately, unlike mechanical hyperalgesia that develops gradually and reaches significance only after a few hours. Hyperalgesia elicited by a single i.p. injection of NGF lasts several days. Localized small injections of NGF into the skin elicit thermal and mechanical hyperalgesia of much shorter duration (Woolf, C. J. *et al.*, 1994; Shu, X. *et al.*, 1999). These local injections indicate the likelihood that NGF can act directly on cells located in the skin. NGF itself does not evoke any behavioral response; it merely sensitizes the response to subsequent nociceptive stimuli.

Although administration of NGF to the skin elicits hyperalgesia, it does not cause inflammation. On the other hand, treatments or injuries that elicit inflammation, such as complete Freund's adjuvant (CFA), enhance NGF levels in the skin (Weskamp, G. and Otten, U., 1987; Aloe, L. *et al.*, 1992).

Inflammatory cytokines, specifically TNFα and IL-1β, known to be expressed during inflammation, enhance NGF levels when delivered separately into the skin (Woolf, C. J. *et al.*, 1997). These studies have suggested a temporal sequence: TNF$\alpha \rightarrow$ IL-1$\beta \rightarrow$ NGF (Figure 2). Cells responsible for producing NGF include keratinocytes (Di Marco, E. *et al.*, 1991) and mast cells (Leon, A. *et al.*, 1994).

The requirement for NGF as an essential intermediate in causing inflammatory hyperalgesia has been demonstrated in experiments where its levels are experimentally diminished using an antibody to NGF (Lewin, G. R. *et al.*, 1994; Woolf, C. J. *et al.*, 1994) or an immunoadhesin such as trkA-IgG (McMahon, S. B. *et al.*, 1995; Koltzenburg, M. *et al.*, 1999), both of which deplete endogenous NGF. These agents prevent the development of hyperalgesia to mechanical or thermal stimuli in response to inflammatory agents such as CFA. In the case of thermal hyperalgesia, these agents can also substantially reduce ongoing inflammatory pain within an hour. However, mechanical hyperalgesia is reduced only after 24–48 h (Woolf, C. J. *et al.*, 1994; 1996). This difference between thermal and mechanical hyperalgesia is consistent with the conclusion, based on the latency of onset after exposure to NGF, that thermal hyperalgesia is due to a peripheral action, whereas the mechanical hyperalgesia is indirect, probably involving transcriptional changes at the level of the DRG (but see Section 5.22.7).

Rueff A. and Mendell L. M. (1996) recorded the activity of single nociceptor axons in an excised skin nerve preparation with the corium side up where NGF could be applied directly to the electrophysiologically identified receptive field of the fiber. They tested the response to noxious heat and mechanical stimulation under control conditions and 10 min later with NGF applied to the corium surface of the unit or under control conditions (no NGF). They observed a significant decline in threshold to noxious heat, but no acute change in threshold to mechanical stimulation. The sensitivity to NGF was abolished if mast cells were degranulated over a period of several days prior to treatment (see Section 5.22.4.3).

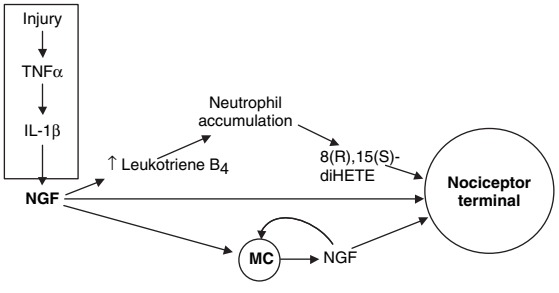

Figure 2 Major mechanisms underlying acute action of nerve growth factor (NGF) on sensory neurons. Exogenous NGF sensitizes sensory neurons via neutrophils, mast cells (MCs), and perhaps directly. Other possible mechanisms are mentioned in the text. NGF is released endogenously after injury via the action of cytokines TNFα and IL-1β (rectangle).

5.22.4.3 Mechanisms of Nerve Growth Factor Action in the Skin

A number of pharmacological approaches have been undertaken to explore the identity of cells and mechanisms underlying sensitization of nociceptive responses by NGF. A contribution by the sympathetic nervous system to the sensitizing effect of NGF has been identified since guanethidine treatment substantially reduces NGF's acute hyperalgesic effect (Andreev, N. Yu. *et al.*, 1995) by delaying its onset (Woolf, C. J. *et al.*, 1996).

Mast cells also participate in NGF-induced sensitization, particularly of noxious thermal stimuli. Mast cells express trkA receptors (Horigome, K. *et al.*, 1993), and NGF causes them to degranulate their contents consisting of serotonin, histamine, and NGF itself (reviewed in Mendell, L. M. *et al.*, 1999). Degranulation of mast cells in advance of NGF administration delays the development of thermal hyperalgesia for about 3 h but does not prevent the later phase of thermal hyperalgesia, nor does it abolish mechanical hyperalgesia (Lewin, G. R. *et al.*, 1994; see also Woolf, C. J. *et al.*, 1996). Behavioral experiments using pharmacological antagonists indicate that serotonin is an important contributor to mast cell-mediated sensitization initiated by NGF (Lewin, G. R. *et al.*, 1994). Under some special conditions, NGF can elicit sensitization in the absence of mast cell activity (Amann, R. *et al.*, 1996a), suggesting the existence of other pathways (Figure 2), or perhaps that NGF acts directly on trkA receptors expressed by other cells, for example, the nociceptors themselves (Averill, S. *et al.*, 1995; Galoyan, S. M. *et al.*, 2003; see Section 5.22.5).

Another action of NGF is enhancement of the level of leukotrienes, specifically leukotriene B_4 (LTB_4), via upregulation of the enzyme 5-lipoxygenase (Amann, R. *et al.*, 1996b; Bennett, G. *et al.*, 1998b). Leukotrienes are known to sensitize nociceptors (Martin, H. A. *et al.*, 1988). This occurs as a result of neutrophil accumulation and their subsequent

release of 8(R), 15(S)-diHETE. If neutrophils are depleted pharmacologically, NGF-induced hyperalgesia is abolished (Bennett, G. *et al.*, 1998b).

Keratinocytes may also play an important role in NGF-induced hyperalgesia. These cells are known to express trkA receptors and to contain NGF (Terenghi, G. *et al.*, 1997) and thus may act in a manner similar to that described for mast cells (see above). They are also known to release ATP (Koizumi, S. *et al.*, 2004) that activates nociceptor terminals (Cook, S. P. and McCleskey, E. W., 2002). Enhancement of NGF expression in these cells in genetically modified mice enhances nociceptive behavior (Davis, B. M. *et al.*, 1993).

The multiplicity of cell types that express trkA receptors and the number of substances capable of sensitizing nociceptors released by these cells in response to NGF indicate the complexity of peripheral sensitization by neurotrophins. They also indicate the difficulty of using behavioral methods and preparations such as the skin nerve preparation, where all these cells remain in close contiguity, to arrive at cellular mechanisms of sensitization. Thus, many studies have made use of dissociated DRG cells to examine the effects of NGF directly on trkA-expressing neurons. Such studies have the obvious advantage of providing a relatively unobstructed view of cellular mechanisms but at the expense of the intercellular interactions that take place *in vivo*.

5.22.5 Acute Sensitization by Nerve Growth Factor of the Response of Dissociated Nociceptors

Shu X. Q. and Mendell L. M. (1999a; 1999b) have investigated the effect of NGF on the response of small (<30 μm) dissociated DRG cells to capsaicin, known to elicit the sensation of noxious heat (Lamotte, R. H. *et al.*, 1992) via the VR1 (now referred to as TRPV1) receptor (Caterina, M. J. *et al.*, 1997). NGF sensitizes the response to capsaicin (Shu, X. and Mendell, L. M., 1999b), measured as an increased inward current in the presence of NGF, in a dose-dependent manner over the range of 2–100 ng ml^{-1}. Its effect is blocked by the protein kinase inhibitor K252a known to antagonize the response of trkA, although not in a highly selective manner (Knusel, B. and Hefti, F., 1992). Not all cells tested are sensitized by NGF, indicating that not all these small cells express the trkA receptor, as predicted from immunohistochemical studies (Averill, S. *et al.*, 1995; Bennett, D. L. *et al.*, 1996a; Figures 1 and 3).

The duration of NGF action is difficult to determine because the test input, capsaicin, is associated with long-lasting tachyphylaxis. To circumvent this problem, Shu X. and Mendell L. M. (2001) have examined the duration of NGF action under conditions of reduced Ca^{2+} that eliminates tachyphylaxis

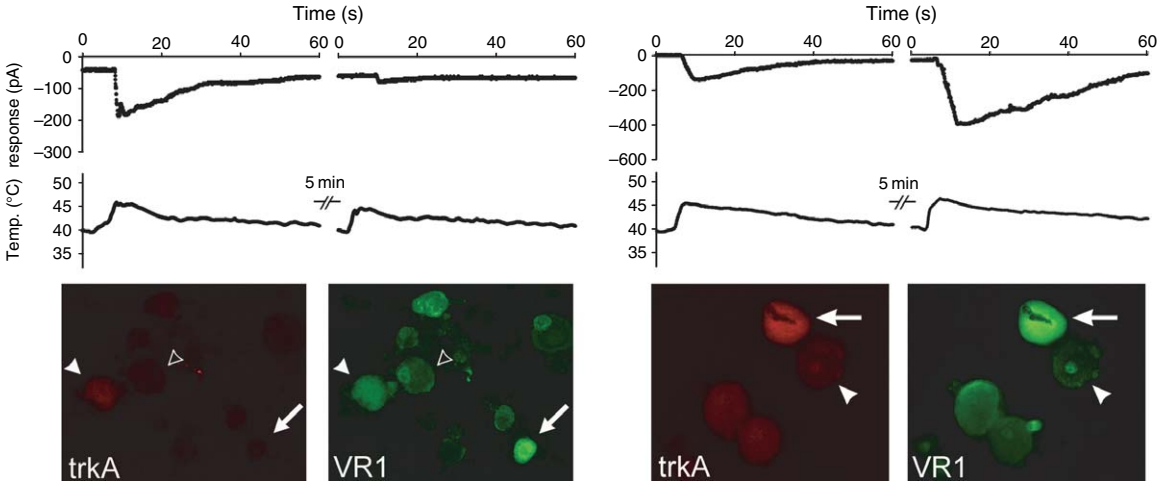

Figure 3 The response of two dissociated dorsal root ganglion (DRG) cells to administration of nerve growth factor (NGF) and demonstration that sensitization of the response requires expression of trkA. Cell on left was tested with two heat pulses (*bottom traces*). The second response 5 min later exhibited tachyphylaxis despite the presence of NGF in the bathing solution for 5 min between heat pulses. The cell (diameter 26 μm; thick arrow) was recovered and immunostained for TRPV1 and trkA. It was classified as $TRPV1^{+}/trkA^{-}$. Another cell in the same field denoted by white arrowhead is $trkA^{+}/TRPV1^{+}$ and a third cell denoted by white-bordered arrowhead is classified $trkA^{-}/TRPV1^{-}$. Cell on right showed sensitization of the response to heat after 5 min exposure to NGF. The cell (diameter 25 μm; arrow) was recovered, immunostained, and classified $trkA^{+}/TRPV1^{+}$. Cell denoted by arrowhead was $trkA^{-}/TRPV1^{-}$. Adapted from Galoyan *et al.* (2003) with permission.

(Koplas, P. A. *et al.*, 1997). They found that a 10-min exposure to NGF sensitizes a neuron to repeated puffs of capsaicin for as long as 70 min, suggesting that the effect of NGF involves more than a direct action on the conductance of a membrane channel or the sensitivity of a receptor (see Section 5.22.6).

Galoyan S. M. *et al.* (2003) have carried out similar experiments in small dissociated DRG cells from adult rats using noxious heat instead of capsaicin as the test stimulus (Figure 3). One advantage of the noxious heat stimulus over capsaicin is the ease with which threshold can be established. These cells respond an inward current whose threshold is 43–44 °C which is characteristic of the TRPV1 receptor expressed in hetrologous cells (caterina, M. J., *et al.*, 1997). NGF-induced sensitization of the response to noxious heat has properties that are similar to sensitization of the response to capsaicin. NGF does not alter temperature threshold; its major effect is to enhance the magnitude of the heat evoked current. Recent studies suggest that the acute increase of TRPV1 current elicited by exposure to NGF is due to increased trafficking and subsequent insertion of the additional TRPV1 receptors into the plasma membrane rather than an increase in channel unitary conductance (Zhang, X., *et al.*, 2005; Stein, A. T., *et al.*, 2006). These cells respond with a threshold of about 43–44 °C, which is characteristic of the TRPV1 receptor (Caterina, M. J. *et al.*, 1997). NGF-induced sensitization of the response to noxious heat has properties that are similar to sensitization of the response to capsaicin. One of the advantages of noxious heat over capsaicin as the stimulus is the ability to establish a threshold value. This has permitted the conclusion that NGF does not alter temperature threshold; its major effect is to enhance the magnitude of the heat-evoked current.

As observed with capsaicin, NGF does not sensitize the heat-evoked response in some neurons. Immunohistochemical characterization of the recorded cells has revealed that the NGF-induced sensitization of the heat-evoked inward current is closely associated with the expression of trkA (Figure 3). This is not unexpected since studies in heterologous cells have demonstrated that the ability for NGF to sensitize the TRPV1 response requires that the cell express trkA (Chuang, H. H. *et al.*, 2001).

Zhu W. *et al.* (2004) have recently demonstrated that the capsaicin- or noxious heat-induced TRPV1 response in DRG cells isolated from neonatal rats cannot be sensitized by NGF unlike the response in cells from adults. Thus, in neonates, there is no close correspondence between the expression of trkA and the ability of NGF to sensitize the TRPV1 response, i.e., trkA is expressed in cells that fail to be sensitized by NGF. However, cells in neonates failing to be sensitized by NGF can be sensitized by bradykinin, i.e., the failure for NGF to sensitize the cells is not a generalized failure for sensitization to occur. It is not presently known what factor develops during the neonatal period that permits NGF to sensitize the heat-evoked response.

NGF-induced sensitization develops gradually from P4 to P10 (Zhu, W. *et al.*, 2004). This is the time at which trkA-expressing cells lose their requirement for NGF in order to survive (Lewin, G. R. *et al.*, 1992). It has been hypothesized that the inability for NGF to sensitize cells in neonates may be a protective mechanism to prevent undue nociceptive input due to sensitization at a time that NGF is required to assure survival of nociceptors (Zhu, W. *et al.*, 2004).

GDNF, like NGF, acutely elevates cytosolic Ca^{2+} in DRG cells (Lamb, K. and Bielefeldt, K., 2003). Recent experiments suggest that exposure of dissociated sensory neurons to GDNF, neurturin or artermin for several minutes rapidly enhances the sensitivity of TRPV1 receptors to capsaicin in isolated DRG cells (Malin, S. A., *et al.*, 2006). Artemin mRNA, but not neurturin or GDNF, is upregulated in the skin in response to inflammatory conditions; its expression increases faster, and to a greater extent, than that of NGF. Administration of these agents elicits thermal hyperalgesia lasting several hours which is substantially prolonged if NGF is co-injected. These findings broaden our understanding of the role of trophic factors in sensitization of nociceptors.

5.22.6 TrkA Signaling Pathways Responsible for Acute Effects of Nerve Growth Factor

Signaling initiated by trk receptor activation is diverse, and for a general treatment of this subject from a more molecular perspective, the reader is referred to a recent review (e.g., Huang, E. J. and Reichardt, L. F., 2001; Nicol, G. D. and Vasko, M. R., 2007). Many studies carried out on NGF-induced signaling have been directed toward determining the signaling pathways involved in cell survival and axon outgrowth. Here, we provide a more focused

treatment related to NGF's role as a sensitizing agent in sensory neurons.

Chuang H. H. *et al.* (2001) reported that phosphatidyl-4.5-inositol biphosphate (PtdIns(4,5)P_2 – PIP_2) exerts a tonic inhibitory effect on the inward current produced by TRPV1 via its interaction with the C-terminal domain of TRPV1. They suggested that NGF sensitizes TRPV1 by activating PLC which inhibits PIP_2, thereby disinhibiting TRPV1, a mechanism corroborated by the demonstration that the PLC inhibitor U-73122 antagonizes the sensitizing effect of NGF in adult rat DRG neurons (Galoyan, S. M., *et al.*, 2003). This mechanism has not been confirmed in subsequent studies (see below). Furthermore, recent findings suggest that PIP_2 facilitates rather than inhibits TRPV1 receptor activity (Stein, A. T. *et al.*, 2006). A related finding indicates that PIP_2 is required for recovery from desensitization (Lin, B., *et al.*, 2005) known to occur after TRPV1 receptor activation.

Chuang H. H. and coworkers pointed out that the activation of PLC would also be expected to enhance levels of protein kinase C (PKC) via diacylglycerol (DAG). However, they found that inhibitors of PKC fail to abolish NGF-induced sensitization of TRPV1. This has been confirmed by Shu X. and Mendell L. M. (2001) in adult rat DRG cells using a different pair of PKC blockers. Interestingly, other investigators working in dissociated DRG neurons have obtained very different results on the signaling pathways involved in NGF-induced sensitization. Bonnington J. K. and McNaughton P. A. (2003), working in neonatal mouse DRG cells, used a different inhibitor of PLC, neomycin, and found no inhibition of NGF-induced sensitization of the capsaicin response and also that the most robust inhibition of NGF-induced potentiation occurred by blocking the activity of PI-3K and PKC, the latter in contrast to the earlier findings (see above). Zhuang Z.-Y. *et al.* (2004), working in adult rat (see also Zhu, W. and Oxford, G. S., 2007) have confirmed the role for PI-3K in NGF-induced sensitization, agreeing with Bonnington J. K. and McNaughton P. A., but also reported that the MEK inhibitor PD98059 blocked the effect of NGF unlike the findings of both Bonnington J. K. and McNaughton P. A. (2003) and Shu X. and Mendell L. M. (2001).

It is important to note that there are several differences among these experiments including the use of rats and mice of different strains, cell culture conditions, protocols (e.g., number of capsaicin pulses), different assays such as Ca^{2+} imaging, and membrane current. These studies point out the complexity of studies on signaling pathways, specifically the need to define the conditions under which they are investigated. It may be necessary to carry out such studies *in vivo* where conditions are more tightly regulated in order to understand which of the many possible pathways are operating under physiological conditions.

5.22.7 p75 Receptor Influence on Sensory Neuron Function

The p75 receptor is expressed in all cells that also express trkA and trkB receptors, but in only about half the cells expressing trkC. Cells not expressing trk do not express p75 (Wright, D. E. and Snider, W. D., 1995). p75 binds all neurotrophins (see reviews by Patapoutian, A. and Reichardt, L. F., 2001; Huang, E. J. and Reichardt, L. F., 2001). The functional role of trk and p75 in mediating the effects of neurotrophins has received greatest attention in developmental studies as determinants of neuronal survival and apoptosis (Hempstead, B. L. *et al.*, 1991; Miller, F. D. and Kaplan, D. R., 2001). For example, p75 acts as a mediator of sympathetic neuron apoptosis, whereas trkA mediates cell survival (Majdan, M. *et al.*, 2001).

Relatively little attention was paid to the p75 receptor initially in evaluating the physiological effects of NGF because of evidence that sensitization to noxious heat by NGF is normal in p75 knockouts (Bergmann, I. *et al.*, 1998, but see von Schack, D. *et al.*, 2001, for evidence that this knockout is not complete). However, the finding that activation of p75 enhances ceramide via activation of the sphingomyelin pathway (Dobrowsky, R. T. *et al.*, 1994) prompted a search for physiological effects elicited by NGF binding to the p75 receptor (reviewed by Nicol, G. D. and Vasko, M. R., 2007). Zhang Y. H. *et al.* (2002) reported that NGF-induced activation of the ceramide pathway via the p75 receptor enhances membrane excitability (membrane gain-number of APs per nanoampere of current applied across the cell membrane) in capsaicin-sensitive DRG neurons (presumptive nociceptors) by enhancing a TTX-insensitive Na^+ conductance and decreasing the magnitude of the K^+-rectifier. These experiments were carried out first by short circuiting p75 by administering ceramide itself, and second by demonstrating that the effects of NGF could be blocked by administering glutathione, an inhibitor of neutral sphingomyelinase, the enzyme responsible for

producing ceramide (Liu, B. and Hannun, Y. A., 1997). A p75 blocking antibody also prevents ceramide facilitation of membrane gain (Zhang, Y. H. and Nicol, G. D., 2004). Thus, NGF might sensitize the response of the cell by enhancing its depolarization (trkA) and independently by increasing the number of action potentials produced per unit of depolarization (p75) (Mendell, L. M., 2002). In this context, it is interesting that one of the major deficits in p75-knockout mice is a substantial reduction of discharge frequency of certain mechanoreceptors (Stucky, C. L. and Koltzenburg, M., 1997).

Cellular mechanisms for interaction between p75 and trkA have also been described. Working in human neuroblastoma cells, Plo I. *et al.* (2004) reported that activation of trkA reduces sphingomyelinase levels and thus reduces ceramide production (i.e., reduced p75 signaling) via PKC. Similarly, Bilderback T. R. *et al.* (2001) demonstrated in PC12 cells that PI-3K, activated by NGF via trkA, acutely inhibits acidic sphingomyelinase activated by NGF via the p75 receptor. Since PI-3K under certain conditions has also been shown to play a role in NGF-induced activation of TRPV1 via trkA (see Section 5.22.6), NGF appears to have the potential to affect cell discharge in a complex manner involving interaction of the signaling pathways activated by p75 and trkA. Also in PC12 cells, MacPhee I. and Barker P. A. (1997; 1999) demonstrated a reciprocal action of NGF, i.e., brief activation of p75 acutely reduces trkA activity via a ceramide-dependent mechanism, whereas extended p75 activation facilitates trkA. Another recent report (He, X. L. and Garcia, K. C., 2004) suggests that NGF can bind to p75 in a 2:1 molecular ratio and that this complex might bind to trkA. Such a scheme would predict cooperativity between p75 and trkA at the level of the cell surface in addition to intracellular signaling. Furthermore, there is now evidence that p75 can modulate the action of the trk receptors by increasing trk receptor autophosphorylation (Berg, M. M. *et al.*, 1991; Verdi, J. M. *et al.*, 1994), by increasing the concentration of the neurotrophin in the vicinity of its trk receptor (Barker, P. A. and Shooter, E. M., 1994), and/or by increasing the selectivity of the trk receptor for its ligand (Rodriguez-Tebar, A. *et al.*, 1992; Benedetti, M. *et al.*, 1993). Thus, even though there is evidence for independent effects of neurotrophins via trkA and p75, the possibility that these pathways could interact in nociceptive neurons must be considered.

5.22.8 Effects of Nerve Growth Factor on Expression of Channels and Receptors in Nociceptors

The acute changes in sensory neuron function considered heretofore are very rapid and hence considered to be posttranscriptional changes. However, there is now substantial evidence that NGF can also regulate the expression of numerous receptors and channels via transcriptional mechanisms and in this way exert much more profound and long-lasting effects on the properties of nociceptors (Figure 4). Furthermore, in the case of several of the channels (TRPV1, BK, P2X3, and TTX-resistant Na^+ channels), there is evidence for differential regulation by NGF and GDNF.

5.22.8.1 TRPV1 Receptors

Chronic exposure of DRG cells in culture to NGF increases their response to capsaicin (Bevan, S. and Winter, J., 1995; Ganju, P. *et al.*, 1998); this is attributed to an increase in expression of TRPV1 associated with enhanced levels of TRPV1 mRNA (Winston, J. *et al.*, 2001). *In vivo* studies have documented that peripheral administration of NGF enhances expression of TRPV1 via activation of p^{38} MAP kinase in trkA+ sensory neurons in the DRG and in sciatic nerve and especially in the skin by selective centrifugal transport (Ji, R. R. *et al.*, 2002). A recent report (Amaya, F. *et al.*, 2004) has shown that the elevated expression of TRPV1 begins 1 day after CFA administration into the paw and lasts for up to 1 week, returning to normal at 2 weeks. Both NGF and GDNF levels increase in DRG neurons after CFA treatment, with NGF

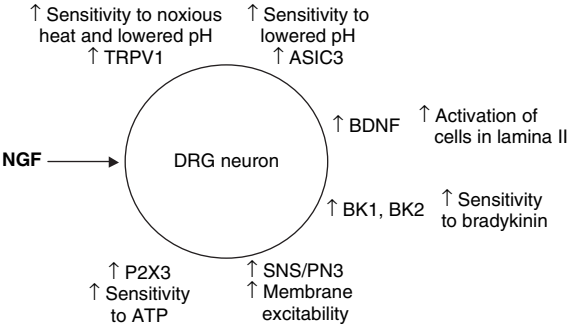

Figure 4 The variety of possible long-term actions of nerve growth factor (NGF) on expression of various channels, receptors, and neurotrophins in nociceptors. In each case, the major functional effect is listed. Further details in text.

exhibiting a relatively rapid rise and fall (peak at 1 day) and GDNF reaching its peak level at 1 week and falling to control levels by the second week. Selectively interfering with NGF and GDNF upregulation using antibodies has clarified that NGF and GDNF elevate TRPV1 expression in different populations of nociceptive sensory neurons, $trkA^+$ and $IB4^+$ neurons, respectively. Furthermore, restricting elevation of TRPV1 expression to either population of DRG cells reduces the thermal nociception elicited during CFA-induced inflammation.

5.22.8.2 P2X3 Receptors

NGF also enhances expression of the P2X3 receptor (Bradbury, E. J. *et al.*, 1998; Ramer, M. S. *et al.*, 2001) considered important in pain produced by ATP (Cook, S. P. and McCleskey, E. W., 2002). One week after intrathecal administration, GDNF elevates P2X3 expression in spinal terminals of Ret/$IB4^+$ neurons in which it is normally expressed. NGF has a more profound effect since it causes novel expression of P2X3 in neurons terminating in more superficial laminae of the spinal cord where P2X3 is normally not expressed. Although these latter changes are relatively small, it was concluded that they might be a significant component in NGF-mediated inflammatory pain.

5.22.8.3 ASIC Channels

ASIC channels are Na channels gated by H^+. The ASIC3 isoform is expressed in DRG cells identified as nociceptors by coexpression of markers characteristic of such neurons. Along with TRPV1 receptors, ASIC3 receptors are considered to be important mediators of the pain associated with tissue acidosis (Voilley, N. *et al.*, 2001). Mamet J. *et al.* (2003) have shown in culture that NGF enhances the expression of the ASIC3 isoform in DRG cells. They describe a physiological control mechanism, suggesting that low levels of NGF regulate ASIC3 expression via trkA and the PLC/PKC signaling pathway. During inflammation, NGF levels rise and the increased activation of p75 removes inhibition of the downstream effects of JNK and p38 that are also activated by NGF via trkA (Ji, R. R. *et al.*, 2002). Since these downstream effects include expression of ASIC3, this mechanism can act as a switch whereby the enhanced level of NGF switches on production of ASIC3 by removing tonic inhibition of JNK and p38.

5.22.8.4 BK Receptors

Another receptor upregulated by NGF is a member of the bradykinin (BK) receptor family. Nociceptors express the B2 form of the BK receptor constitutively; the B1 form is expressed only after inflammation (Dray, A. and Perkins, M., 1993). McNaughton P. A. and coworkers have reported that freshly dissociated mouse DRG cells undergo upregulation of B2 mRNA (confirmed at the protein level immunocytochemically) when exposed to NGF for 3 days; GDNF is much less effective (Lee, Y. J. *et al.*, 2002). These studies are consistent with previous observations that cultured cells are more responsive to bradykinin when cultured in the presence of NGF (Petersen, M. *et al.*, 1998). The identity of the receptor responsible for this action of NGF (trkA or p75) is controversial (see discussion in Lee, Y. J. *et al.*, 2002). Interestingly, expression of the B1 receptor can be enhanced in cultured DRG neurons in the presence of GDNF but not NGF (Vellani, V. *et al.*, 2004). However, *in vivo* the effects of NGF may be much more complex as suggested by Rueff A. *et al.* (1996) who hypothesized that NGF might indirectly cause upregulation of B1 receptors on DRG neurons via release of cytokines such as TNFα and IL-1β from inflammatory cells.

5.22.8.5 Na^+ Channels

Waxman, S. G., Kocsis, J. D., and coworkers have shown that NGF can affect Na^+ and K^+ channel expression of nociceptive afferent fibers (Fjell, J. *et al.*, 1999; Everill, B. and Kocsis, J. D., 2000). Fjell J. and coworkers noted changes in the properties of small-diameter DRG cells after peripheral axotomy that could be reversed by administration of NGF. Specifically, they observed that axotomy diminishes the TTX-resistant Na current in these neurons and that provision of NGF partially reverses this decline due to an effect on SNS/PN3 TTX-resistant Na^+ channel (Na_v 1.8). NGF is unable to reverse the axotomy-induced attenuation of activity in NaN, another TTX-resistant Na^+ channel (Na_v 1.9). However, GDNF is able to reverse the decline in both NaN and SNS/PN3. Interestingly, GDNF but not NGF enhances TTX-resistant currents in small DRG neurons studied in culture, suggesting that the ability to restore function after axotomy does not predict effects under all conditions. However, given the likely importance of TTX-resistant Na^+ channels in the function of nociceptors (Ritter, A. M. and

Mendell, L. M., 1992; Fang, X. *et al.*, 2005), the finding that neurotrophins can influence their function makes this system a potentially important target in achieving pain control.

5.22.8.6 PGE2 Receptors

The multiplicity of channels affected by NGF suggests that this growth factor acts as a master switch in regulating the sensitivity of sensory neurons to nociceptive stimuli. However, its control is not universal since NGF does not control expression of the PGE2 receptor (Southall, M. D. and Vasko, M. R., 2000) that mediates the hyperalgesia caused by prostaglandins.

5.22.9 Neurotrophins and Sensitization of Tissues Other than Skin

The skin has attracted most of the attention in studies of the peripheral effects of neurotrophins. This is in keeping with the focus on this organ in investigations of somatosensory mechanisms. However, there is considerable evidence that NGF contributes to the sensitization of other tissues, specifically viscera, muscle, and joints, all of which are sites where inflammatory pain can occur.

5.22.9.1 Visceral Structures

Several investigators have observed enhanced levels of NGF in the bladder in models of interstitial cystitis, a normally painful condition (Oddiah, D. *et al.*, 1998; Toma, H. *et al.*, 2000; Bielefeldt, K. *et al.*, 2003). In human studies, the level of NGF determined in bladder biopsies was found to be higher in individuals whose condition is painful (Lowe, E. M. *et al.*, 1997). Using viral transfer methods, Lamb K. *et al.* (2004) demonstrated that enhancing NGF levels in rat bladder leads to overactivity measured cystometrographically. If NGF is neutralized using immunological methods, the bladder overactivity produced by external irritants is reduced (Lamb, K. *et al.*, 2003). NGF has also been demonstrated to be upregulated in other visceral organs such as the bowel in association with inflammatory conditions (di Mola, F. F. *et al.*, 2000) or in an animal model of pancreatitis (Toma, H. *et al.*, 2000).

5.22.9.2 Muscle Afferents

Recent studies have indicated that neurotrophins can influence the discharge of small-diameter muscle afferents. Hoheisel U. *et al.* (2005) evaluated the effect of intramuscular NGF on the discharge of small-diameter (Group IV) muscle afferents and found that only units with high mechanical threshold are facilitated. They reported that threshold is unchanged, but discharge frequency in response to adequate stimulation increases virtually immediately after NGF (0.8 μM) administration. Interestingly, they also observed that administration of BDNF (1 μM) causes a decline in discharge frequency, but only several minutes after administration.

The sensitization of high-threshold muscle afferents is consistent with the sensitization observed in response to intramuscular administration of NGF to the masseter muscle in humans (Svensson, P. *et al.*, 2003). Changes were observed 1 and 7 days after administration but not after 1 h and were described as consisting of both mechanical allodynia and hyperalgesia. Under pathological conditions, it seems likely that the cytokine TNFα is upregulated in muscle and that this leads to production of NGF (Schafers, M. *et al.*, 2003).

5.22.9.3 Joint Receptors

Synovial fluid from arthritic joints in humans expresses elevated levels of NGF (Falcini, F. *et al.*, 1996; Halliday, D. A. *et al.*, 1998), which has been attributed to elevated levels of cytokines such as TNFα and IL1-β (Manni, L. *et al.*, 2003), much as has been reported in skin (see Section 5.22.4.3). There have been no reports of enhanced sensitivity of joint afferents to mechanical stimulation in response to NGF although sensitization is known to occur in models of experimental arthritis (Schaible, H. G. and Schmidt, R. F., 1985). Joints treated with CFA have a more extensive innervation (Shinoda, M. *et al.*, 2003), possibly as a result of the enhanced levels of NGF known to promote terminal axonal sprouting in the skin (Diamond, J. *et al.*, 1992). An enhancement in peripheral axon terminals of trkA$^+$ nociceptive afferents might be expected to increase sensitivity to peripheral stimuli as a result of increased numbers of receptor molecules. Recently, Shelton D. L. *et al.* (2005) have demonstrated that administration of a monoclonal antibody against NGF (mAb 911, Rinat Neuroscience) can eliminate the pain associated with an experimental autoimmune arthritic condition in rats.

5.22.10 Nerve Growth Factor, Enhances Peptide Expression in the Dorsal Root Ganglion, and Central Sensitization

The ability of NGF to elicit rapid sensitization via posttranscriptional changes and to increase the expression of receptors and channels involved in setting the sensitivity and activity of nociceptors is indicative of its ability to enhance peripheral sensitization. However, NGF also elevates expression of peptides in the DRG ganglion and these are believed to enhance the central effects of glutamate released by nociceptors, i.e., to contribute to central sensitization (McMahon, S. B. *et al.*, 1993). Lindsay R. M. and Harmar A. J. (1989) were among the first to demonstrate that DRG cells maintained in culture exhibit enhanced levels of substance P and CGRP after exposure to NGF in the medium. These peptides are considered to be important mediators in central sensitization because of the very long-lasting depolarization that they produce in postsynaptic cells, leading to activation of the NMDA receptor (McMahon, S. B. *et al.*, 1993). Both NGF and GDNF enhance capsaicin-stimulated release of CGRP from cultured trigeminal ganglion neurons; however, the effect of GDNF is due entirely to the greater survival of these neurons in its presence (i.e., no change in response of individual neurons to capsaicin), whereas the effect of NGF is attributed in part to increased CGRP release per neuron, i.e., NGF sensitizes the response to capsaicin (Price, T. J. *et al.*, 2005).

The possibility for direct participation of neurotrophins in central sensitization was initially advanced by the finding *in vivo* that BDNF is also upregulated in the cell body of trkA receptor-expressing DRG cells several hours to days after exposure to NGF (Apfel, S. C. *et al.*, 1996; Michael, G. J. *et al.*, 1997). This suggested that BDNF would be released into the spinal cord, a prediction that has been borne out experimentally (Lever, I. J. *et al.*, 2001). The high-affinity receptor for BDNF, trkB, is found on neurons throughout the superficial dorsal horn (Bradbury, E. J. *et al.*, 1998; Garraway, S. M. *et al.*, 2003). A physiological role for BDNF has been established in models of inflammatory pain by demonstrating that sequestration of spinal BDNF using intrathecally delivered trkB-IgG diminishes the response to noxious heat (Kerr, B. J. *et al.*, 1999; Mannion, R. J. *et al.*, 1999; Pezet, S. *et al.*, 2002). In these experiments, it was also demonstrated that NGF has no central action, i.e., different neurotrophins act to promote peripheral and central sensitization (but see Section 5.22.11, indicating that BDNF and NT-4 can also elicit peripheral sensitization).

Direct physiological evidence for the action of BDNF in the superficial dorsal horn has come from experiments in spinal slices where it has been reported that BDNF facilitates the synaptic response of cells in lamina II to electrical stimulation of C-fibers both in neonates (Garraway, S. M. *et al.*, 2003) and in adults (Garraway, S. M. *et al.*, 2005). This facilitation of AMPA/kainate responses (measured in voltage clamp) is virtually immediate after superfusion of BDNF ($100\,\mathrm{ng\,ml^{-1}}$) and lasts for at least a few hours after washout of the BDNF. The effect of BDNF requires participation of NMDA receptors since it is blocked by APV. Additional pharmacological experiments have demonstrated a role for PKC in this process and also that administration of BDNF results in phosphorylation of the NMDA receptor in neurons in the superficial dorsal horn (Slack, S. E. *et al.*, 2004). It is important to note that BDNF itself does not elicit any detectable effect on lamina II neurons; it only acts to sensitize the response to stimulation of small-diameter sensory afferents. The neurotrophin effect is specific; superfusion of NT-3 does not sensitize this response (Garraway, S. M. *et al.*, 2003).

The requirement for functional NMDA receptors in order for BDNF to be effective in sensitizing the response of lamina II neurons to C-fiber input is consistent with the behavioral finding that pretreating rats for several days with systemic MK-801, an antagonist of NMDA receptors, selectively blocks the late phase of thermal and mechanical hyperalgesia elicited by NGF (Lewin, G. R. *et al.*, 1994). This late phase was attributed to central sensitization, whereas the acute phase, not affected by MK-801 treatment, was identified with peripheral sensitization. Thus, NGF exerts its effects by peripheral and central sensitization which together have been advanced as mechanisms to explain different components of hyperalgesia (McMahon, S. B. *et al.*, 1993).

5.22.11 Role of Brain-Derived Neurotrophic Factor, Neurotrophin-4, and Neurotrophin-3 in Peripheral Sensitization

There is increasing evidence that acute sensitization of nociceptors can be affected by neurotrophins other than NGF. Specifically, BDNF and NT-4 sensitize

nociceptive function acutely at the behavioral level (Shu, X. *et al.*, 1999), at the level of nociceptor discharge measured in isolated skin nerve preparations (Rueff, A. and Mendell, L. M., 1996; Shu, X. *et al.*, 1999), and at the level of capsaicin-activated TRPV1 currents measured in dissociated cells (Shu, X. and Mendell, L. M., 1999b). The proportion of small cells ($d \leq 30\,\mu m$) sensitized by NT-4 is similar to that sensitized by NGF. Therefore, it seems unlikely that trkA expression is required for cells to be sensitized by NT-4 since as a population, relatively few (10%) small $trkA^+$ sensory neurons also express trkB (Karchewski, L. A. *et al.*, 1999). Thus, activation of trkB alone can sensitize the response to capsaicin.

It is not known where trkB ligands would come from naturally in the periphery since there is no evidence at present that BDNF or NT-4 is upregulated in the skin immediately after inflammation. However, BDNF is upregulated in nerves undergoing Wallerian degeneration, opening the possibility that trkB ligands sensitize neurons after damage to neighboring nerve trunks. Another possibility is that BDNF, which is known to be released from the central terminals of nociceptors, would also be released from their peripheral terminals in the skin and that this would be the normal source of trkB ligands. Such a line of reasoning suggests that BDNF might act peripherally to reinforce the central sensitization it also elicits.

NT-3 does not elicit any acute sensitization of the response to noxious heat measured either electrophysiologically or behaviorally (Shu, X. *et al.*, 1999; Shu, X. and Mendell, L. M., 1999b) despite evidence that it can bind to trkA (Lindsay, R. M., 1996). However, 7-day exposure of $trkA^+/trkC^-$sensory neurons to NT-3 results in a substantial reduction in trkA receptor expression (Gratto, K. A. and Verge, V. M., 2003). Accompanying this loss of trkA is a decline in substance P levels. These studies suggest that NT-3 might have therapeutic value in diminishing painful states initiated by the activation of trkA.

5.22.12 Neurotrophins and Neuropathic Pain

Most considerations of neurotrophins and pain have centered on their role in inflammatory pain since they are naturally upregulated in the both periphery and DRG and play a prominent role in peripheral and central sensitization. However, there is also evidence that neurotrophins may contribute to the pain associated with nerve manipulations that are accepted as models for neuropathic pain. Thus, Zhou X. F. *et al.* (2000) have demonstrated that antibodies to NGF, BDNF, and NT-3 delivered to the DRG can reduce the pain associated with spinal nerve axotomy. Interestingly, antibodies to NGF elicit their effect in the early stages after injury, whereas BDNF and NT-3 antibodies exert their effects only later. In addition, Zhou X. F. *et al.* demonstrated that BDNF and NGF, but not NT-3, delivered to the DRG in intact preparations elicit mechanical allodynia. It is worth contrasting these findings with those of Kerr B. J. *et al.* (1999; see above) who showed that NGF delivered intrathecally elicits no nociceptive behavior. These differences presumably reflect the differences in the expression of trkA that is known to be present in the DRG, but not in the spinal cord. Theodosiou M. *et al.* (1999) carried out similar experiments with neurotrophin antibodies in rats subject to chronic partial axotomy of the sciatic nerve. They observed both mechanical and thermal hyperalgesia in these rats that could be relieved by antibodies to NGF or BDNF but not NT-3.

Fukuoka T. *et al.* (2001) have studied uninjured neurons in the L4 DRG in rats subjected to L5 spinal nerve ligation (Chung model). They observed an increase in BDNF mRNA levels in L4 associated with increased levels of expression as well as recruitment of additional neurons into the population of DRG neurons expressing BDNF mRNA. They also found that the enhanced sensitivity to noxious heat associated with this injury could be diminished temporarily by intrathecal application of an antibody to BDNF. Significantly, NGF appears to play a role in this enhancement of BDNF levels since NGF is increased in the DRG whose spinal nerve is ligated, and an antibody to NGF delivered to the injured DRG can prevent the upregulation of BDNF in the neighboring ganglion as well as the associated thermal hyperalgesia.

A recent study (Wilson-Gerwing, T. D. *et al.*, 2005) indicates that NT-3 can prevent the long-lasting increased expression of TRPV1 observed in the chronic constriction injury (CCI) model of neuropathic pain. They further demonstrated that NT-3 reduces expression of p38 MAPK shown to be a primary factor in the delayed elevation of TRPV1 expression in the skin (Ji, R. R. *et al.*, 2002). Treatment with NT-3-reduced thermal hyperalgesia, but not the mechanical hypersensitivity associated with CCI.

A different role for neurotrophins in neuropathic pain was reported by Bennett D. L. *et al.* (1996b) who

demonstrated that sprouting of peripherally axotomized Aβ-fibers into the superficial laminae of the spinal cord, considered to be a possible mechanism for neuropathic pain after such damage (Woolf, C. J. *et al.*, 1995), is reduced by application of NGF to the damaged nerve. They argued that this was not a direct effect of NGF on the sprouting of A-fibers since it would imply that sprouting is paradoxically reduced by administration of NGF. Also, large non-nociceptive Aβ-fibers do not express trkA, and so it is not clear how NGF would affect their sprouting. They proposed that NGF elicits sprouting of axotomized C-fibers that would reverse the A-fiber sprouting caused initially by the peripheral axotomy.

The pain associated with peripheral nerve damage has been shown to also have a microglial component. ATP released from damaged nociceptive afferents activates microglial P2 × 4 receptors; the activated microglia release BDNF which inhibits the KCC2 chloride transporter in lamin I cells (Coull, J. A., *et al.*, 2005). This shifts the chloride equilibrium potential in the depolarizing direction which changes the sign of inhibitory input toward excitation. This increases activity in nociceptive pathways contributing to pain. Thus, microglial BDNF as well as neuronal (DRG) BDNF can contribute to central sensitization. Interaction between these two sources of BDNF remains to be discovered.

Despite the lack of consistency, these experiments indicate several potential roles for neurotrophins in neuropathic pain. These are based on their ability to directly sensitize neuronal responses as well as their ability to elicit structural changes in the sensory nervous system.

5.22.13 Neurotrophins and the Clinic

The very strong sensitizing effect of neurotrophins on nociceptive pathways both peripherally and in the spinal cord has given them a very high profile in pain research. One of the earliest indications of a clinical effect emerged from Phase I clinical trials to determine the safety of NGF delivered systemically (Petty, B. G. *et al.*, 1994). NGF was administered subcutaneously or intramuscularly in human volunteers in amounts ranging from 0.03 to 1.0 $\mu g\,kg^{-1}$, dosages that are much lower than typically used in rats (1 $\mu g\,g^{-1}$). These subjects experienced myalgia in truncal and bulbar muscles as well as hyperalgesia at the site of injection. The latter could persist for up to 7 weeks. Similar human trials using single localized injections of NGF (1–3 μg per patient) in the arm resulted in localized allodynia and thermal hyperalgesia lasting several weeks (Dyck, P. J. *et al.*, 1997). These experiments in humans with verbal reports provide significant confirmation of the results from animal experiments. They also suggest that the use of NGF to increase cell survival or for other purposes will require measures to overcome the nociceptive side effects.

As discussed above, peripheral NGF levels are upregulated as a consequence of inflammation resulting in hyperalgesia. Furthermore, the hyperalgesia associated with inflammation can be largely eliminated by reducing NGF levels using either a sequestering antibody or a trkA immunoadhesin. This has prompted the development of NGF antibodies for eventual use in humans. Recently, Sevcik M. A. *et al.* (2005) reported that an antibody mAb 911 (Rinat Neuroscience Corporation) is effective in attenuating the pain in a mouse model of bone cancer whose sarcoma tumor cells are a source of high levels of NGF. As shown above (Section 5.22.9), bladder pain associated with models of cystitis is also associated with elevated expression of NGF, as is arthritic pain. Thus, we can expect that clinical trials using will be undertaken as soon as antibodies have been rendered safe for human use.

Several clinical conditions reported to be associated with alterations in NGF or trkA expression have been reviewed by Anand P. (2004). The trkA receptor is dysfunctional in individuals with congenital insensitivity to noxious stimulation, probably as a result of a mutation. Leprosy, a condition associated with hypoalgesia, is accompanied by reduced expression of NGF. Similar findings have been made in diabetic neuropathy. Conversely, the pain associated with injury to nerves has been correlated with enhanced expression of NGF in the associated nerve trunks. Together, these findings suggest that manipulation of neurotrophin levels may turn out to be a useful therapeutic approach to various conditions associated with disorders of nociception.

5.22.14 Discussion, Conclusions, and Open Questions

The past 15 years have seen an important expansion in our understanding of the role of neurotrophins as it has become generally accepted that they function throughout the life of the animal, not only during development. With regard to their effect on

nociception, it is clear that the survival of nociceptors is dependent on the integrity of the NGF/trkA system during the perinatal period. Beyond this period, the influence of NGF on nociceptors is very wide ranging (Petruska, J. C. and Mendell, L. M., 2004). NGF sensitizes nociceptors both acutely via post-transcriptional mechanisms (Figure 2) and chronically by enhancing the expression of numerous channels associated with nociceptors (Figure 4). These effects are exerted on nociceptors innervating many different tissues, including skin, muscle, joints, and viscera although at this time it is not yet known whether these neurons are regulated identically by NGF.

The discovery of the capsaicin receptor VR1/TRPV1 (Caterina, M. J. *et al.*, 1997), the revelation that this receptor mediated the response to noxious heat (Tominaga, M. *et al.*, 1998), and the finding that NGF could sensitize the response to capsaicin (Shu, X. and Mendell, L. M., 1999b) or to noxious heat (Galoyan, S. M. *et al.*, 2003) seemed to be entirely consistent with the behavioral evidence that NGF sensitizes the response to noxious heat. However, several experiments have raised difficulties with this simple picture. A substantial fraction of cell membrane patches from small-diameter sensory neurons were found to be sensitive to capsaicin (indicating TRPV1 expression) or noxious heat, but not both (Nagy, I. and Rang, H. P., 1999), suggesting that the receptor for capsaicin and for noxious heat are not the same. Furthermore, although two studies in dissociated cells from TRPV1$^{-/-}$ mice revealed the expected deficit in noxious heat sensitivity (Caterina, M. J. *et al.*, 2000; Davis, J. B. *et al.*, 2000), the same reports demonstrated that less reduced preparations (skin nerve or *in vivo* preparations) displayed considerable residual sensitivity to noxious heat. This raises questions concerning our model of how NGF acts to sensitize the response to noxious heat – specifically whether other noxious heat receptors exist (Woodbury, C. J. *et al.*, 2004) and whether these are affected by neurotrophins.

The finding that activation of the p75 receptor enhances membrane gain via by increasing TTX-insensitive Na current and decreasing the strength of K-rectification (see Section 5.22.7) expands possible mechanisms for sensitization by NGF. It also opens the possibility for sensitizing effects of other neurotrophins since p75, unlike trkA, trkB, and trkC, binds all the neurotrophins. The role of p75 in mediating the functional effects of NGF is still largely unknown.

Finally, the fact that NGF has so many different possible actions on nociceptive function in terms of the variety of cells that express trkA (Section 5.22.4.3) as well as the multiple effects that NGF can elicit in individual nociceptors (Sections 5.22.8 and 5.22.10) raises important questions about how all these mechanisms interact to cause sensitization. If the scheme outlined in Figure 2 is a complete representation of the peripheral mechanism of NGF action, one would expect that elimination of mast cells would reduce but not abolish NGF-induced sensitization. However, acute sensitization is abolished (Lewin, G. R. *et al.*, 1994), suggesting that NGF activation of the neutrophil pathway (Bennett, G. *et al.*, 1998b) or direct activation of nociceptor terminals is not sufficient to mediate the acute phase of NGF-induced hyperalgesia. Similarly, inhibiting neutrophil accumulation completely eliminates the hyperalgesic effect of NGF (Bennett, G. *et al.*, 1998b), indicating that the mast cell or direct effects are not sufficient either. Together, these findings suggest an interaction between these different mechanisms, and it will be important to dissect these interactions in order to more fully understand how NGF (and neurotrophins more generally) acts as a sensitizing agent for nociceptors. In view of increasing interest in manipulating NGF levels in a clinical setting, it will be necessary to understand its physiology at a more integrative level.

Acknowledgment

I thank Dr. Jeff Petruska for useful comments on an early draft of the manuscript and for help with figures. The author's research was supported by NIH (NS39420; NS16996) and the Christopher Reeve Paralysis Foundation Consortium on Spinal Injury.

References

Albers, K. M., Wright, D. E., and Davis, B. M. 1994. Overexpression of nerve growth factor in epidermis of transgenic mice causes hypertrophy of the peripheral nervous system. J. Neurosci. 14, 1422–1432.

Aloe, L., Tuveri, M. A., and Levi-Montalcini, R. 1992. Studies on carrageenan-induced arthritis in adult rats: presence of nerve growth factor and role of sympathetic innervation. Rheumatol. Internat. 12, 213–216.

Amann, R., Schuligoi, R., Herzeg, G., and Donnerer, J. 1996a. Intraplantar injection of nerve growth factor into the rat hind paw: local edema and effects on thermal nociceptive threshold. Pain 64, 323–329.

Amann, R., Schuligoi, R., Lanz, I., and Peskar, B. A. 1996b. Effect of a 5-lipoxygenase inhibitor on nerve growth factor-

induced thermal hyperalgesia in the rat. Eur. J. Pharmacol. 306, 89–91.
Amaya, F., Shimosato, G., Nagano, M., Ueda, M., Hashimoto, S., Tanaka, Y., Suzuki, H., and Tanaka, M. 2004. NGF and GDNF differentially regulate TRPV1 expression that contributes to development of inflammatory thermal hyperalgesia. Eur. J. Neurosci. 20, 2303–2310.
Anand, P. 2004. Neurotrophic factors and their receptors in human sensory neuropathies. Prog. Brain Res. 146, 477–492.
Andreev, N. Yu., Dimitrieva, N., Koltzenburg, M., and McMahon, S. B. 1995. Peripheral administration of nerve growth factor in the adult rat produces a thermal hyperalgesia that requires the presence of sympathetic post-ganglionic neurones. Pain 63, 109–115.
Apfel, S. C., Wright, D. E., Wiideman, A. M., Dormia, C., Snider, W. D., and Kessler, J. A. 1996. Nerve growth factor regulates the expression of brain-derived neurotrophic factor mRNA in the peripheral nervous system. Mol. Cell. Neurosci. 7, 134–142.
Averill, S., McMahon, S. B., Clary, D. O., Reichardt, L. F., and Priestley, J. V. 1995. Immunocytochemical localization of trkA receptors in chemically identified subgroups of adult rat sensory neurons. Eur. J. Neurosci. 7, 1484–1494.
Barbacid, M. 1994. The Trk family of neurotrophin receptors. J. Neurobiol. 25, 1386–1403.
Barker, P. A. and Shooter, E. M. 1994. Disruption of NGF binding to the low affinity neurotrophin receptor p75LNTR reduces NGF binding to TrkA on PC12 cells. Neuron 13, 203–215.
Benedetti, M., Levi, A., and Chao, M. V. 1993. Differential expression of nerve growth factor receptors leads to altered binding affinity and neurotrophin responsiveness. Proc. Natl. Acad. Sci. U. S. A. 90, 7859–7863.
Bennett, D. L., Averill, S., Clary, D. O., Priestley, J. V., and McMahon, S. B. 1996a. Postnatal changes in the expression of the trkA high-affinity NGF receptor in primary sensory neurons. Eur. J. Neurosci. 8, 2204–2208.
Bennett, D. L., French, J., Priestley, J. V., and McMahon, S. B. 1996b. NGF but not NT-3 or BDNF prevents the A fiber sprouting into lamina II of the spinal cord that occurs following axotomy. Mol. Cell Neurosci. 8, 211–220.
Bennett, D. L., Koltzenburg, M., Priestley, J. V., Shelton, D. L., and McMahon, S. B. 1998a. Endogenous nerve growth factor regulates the sensitivity of nociceptors in the adult rat. Eur. J. Neurosci. 10, 1282–1291.
Bennett, G., al-Rashed, S., Hoult, J. R., and Brain, S. D. 1998b. Nerve growth factor induced hyperalgesia in the rat hind paw is dependent on circulating neutrophils. Pain 77, 315–322.
Berg, M. M., Sternberg, D. W., Hempstead, B. L., and Chao, M. V. 1991. The low-affinity p75 nerve growth factor (NGF) receptor mediates NGF-induced tyrosine phosphorylation. Proc. Natl. Acad. Sci. U. S. A. 88, 7106–7110.
Bergmann, I., Reiter, R., Toyka, K. V., and Koltzenburg, M. 1998. Nerve growth factor evokes hyperalgesia in mice lacking the low-affinity neurotrophin receptor p75. Neurosci. Lett. 255, 87–90.
Bevan, S. and Winter, J. 1995. Nerve growth factor (NGF) differentially regulates the chemosensitivity of adult rat cultured sensory neurons. J. Neurosci. 15, 4918–4926.
Bielefeldt, K., Ozaki, N., and Gebhart, G. F. 2003. Role of nerve growth factor in modulation of gastric afferent neurons in the rat. Am. J. Physiol. Gastrointest. Liver Physiol. 284, G499–G507.
Bilderback, T. R., Gazula, V. R., and Dobrowsky, R. T. 2001. Phosphoinositide 3-kinase regulates crosstalk between Trk A tyrosine kinase and p75(NTR)-dependent sphingolipid signaling pathways. J. Neurochem. 76, 1540–1551.
Bonnington, J. K. and McNaughton, P. A. 2003. Signalling pathways involved in the sensitisation of mouse nociceptive neurones by nerve growth factor. J. Physiol. 551(Pt 2), 433–446.
Bradbury, E. J., King, V., Simmons, L. J., Priestley, J. V., and McMahon, S. B. 1998. NT-3, but not BDNF, prevents atrophy and death of axotomized spinal cord projection neurons. Eur. J. Neurosci. 10, 3058–3068.
Caterina, M. J., Lefler, A., Malmberg, A. B., Martin, W. J., Trafton, J., Petersen-Zeitz, K. R., Koltzenburg, M., Basbaum, A. I., and Julius, D. 2000. Impaired nociception and pain sensation in mice lacking the capsaicin receptor. Science 288, 306–313.
Caterina, M. J., Schumacher, M. A., Tominaga, M., Rosen, T. A., Levine, J. D., and Julius, D. 1997. The capsaicin receptor: a heat activated ion channel in the pain pathway. Nature 389, 816–824.
Chao, M. V. and Hempstead, B. L. 1995. p75 and Trk: a two-receptor system. Trends Neurosci. 18, 321–326.
Chuang, H. H., Prescott, E. D., Kong, H., Shields, S., Jordt, S. E., Basbaum, A. I., Chao, M. V., and Julius, D. 2001. Bradykinin and nerve growth factor release the capsaicin receptor from PtdIns(4,5)P2-mediated inhibition. Nature 411, 957–962.
Cook, S. P. and McCleskey, E. W. 2002. Cell damage excites nociceptors through release of cytosolic ATP. Pain 95, 41–47.
Coull, J. A., Beggs, S., Boudreau, D., Boivin, D., Tsuda, M., Inoue, K., Gravel, C., Salter, M. W., and De Koninck, Y. 2005. BDNF from microglia causes the shift in neuronal anion gradient underlying neuropathic pain. Nature 438, 1017–1021.
Cowan, W. M. 2001. Viktor Hamburger and Rita Levi-Montalcini: the path to the discovery of nerve growth factor. Annu. Rev. Neurosci. 24, 551–600.
Davies, A. M. 1996. The neurotrophic hypothesis: where does it stand? Philos. Trans. R. Soc. Lond. B Biol. Sci. 351, 389–394.
Davis, J. B., Gray, J., Gunthorpe, M. J., Hatcher, J. P., Davey, P. T., Overend, P., Harries, M. H., Latcham, J., Clapham, C., Atkinson, K., Hughes, S. A., Rance, K., Grau, E., Harper, A. J., Pugh, P. L., Rogers, D. C., Bingham, S., Randall, A., and Sheardown, S. A. 2000. Vanilloid receptor-1 is essential for inflammatory thermal hyperalgesia. Nature 405, 183–187.
Davis, B. M., Lewin, G. R., Mendell, L. M., Jones, M. E., and Albers, K. M. 1993. Altered expression of nerve growth factor in the skin of transgenic mice leads to changes in response to mechanical stimuli. Neuroscience 56, 789–792.
Di Marco, E., Marchisio, P. C., Bondanza, S., Franzi, A. T., Cancedda, R., and De Luca, M. 1991. Growth-regulated synthesis and secretion of biologically active nerve growth factor by human keratinocytes. J. Biol. Chem. 266, 21718–21722.
Diamond, J., Holmes, M., and Coughlin, M. 1992. Endogenous NGF and nerve impulses regulate the collateral sprouting of sensory axons in the skin of the adult rat. J. Neurosci. 12, 1454–1466.
Djouhri, L., Dawbarn, D., Robertson, A., Newton, R., and Lawson, S. N. 2001. Time course and nerve growth factor dependence of inflammation-induced alterations in electrophysiological membrane properties in nociceptive primary afferent neurons. J. Neurosci. 21, 8722–8733.
Dobrowsky, R. T., Werner, M. H., Castellino, A. M., Chao, M. V., and Hannun, Y. A. 1994. Activation of the sphingomyelin cycle through the low-affinity neurotrophin receptor. Science 265, 1596–1599.
Dray, A. and Perkins, M. 1993. Bradykinin and inflammatory pain. Trends Neurosci. 16, 99–104.

Dyck, P. J., Peroutka, S., Rask, C., Burton, E., Baker, M. K., Lehman, K. A., Gillen, D. A., Hokanson, J. L., and O'Brien, P. C. 1997. Intradermal recombinant human nerve growth factor induces pressure allodynia and lowered heat-pain threshold in humans. Neurology 48, 501–505.

Everill, B. and Kocsis, J. D. 2000. Nerve growth factor maintains potassium conductance after nerve injury in adult cutaneous afferent dorsal root ganglion neurons. Neuroscience 100, 417–422.

Falcini, F., Matucci Cerinic, M., Lombardi, A., Generini, S., Pignone, A., Tirassa, P., Ermini, M., Lepore, L., Partsch, G., and Aloe, L. 1996. Increased circulating nerve growth factor is directly correlated with disease activity in juvenile chronic arthritis. Ann. Rheum. Dis. 55, 745–748.

Fang, X., Djouhri, L., McMullan, S., Berry, C., Okuse, K., Waxman, S. G., and Lawson, S. N. 2005. trkA is expressed in nociceptive neurons and influences electrophysiological properties via Nav1.8 expression in rapidly conducting nociceptors. J. Neurosci. 25, 4868–4878.

Fjell, J., Cummins, T. R., Dib-Hajj, S. D., Fried, K., Black, J. A., and Waxman, S. G. 1999. Differential role of GDNF and NGF in the maintenance of two TTX-resistant sodium channels in adult DRG neurons. Brain Res. Mol. Brain Res. 67, 267–282.

Fukuoka, T., Kondo, E., Dai, Y., Hashimoto, N., and Noguchi, K. 2001. Brain-derived neurotrophic factor increases in the uninjured dorsal root ganglion neurons in selective spinal nerve ligation model. J. Neurosci. 21, 4891–4900.

Galoyan, S. M., Petruska, J. C., and Mendell, L. M. 2003. Mechanisms of sensitization of the response of single dorsal root ganglion cells from adult rat to noxious heat. Eur. J. Neurosci. 18, 535–541.

Ganju, P., O'Bryan, J. P., Der, C., Winter, J., and James, I. F. 1998. Differential regulation of SHC proteins by nerve growth factor in sensory neurons and PC12 cells. Eur. J. Neurosci. 10, 1995–2008.

Garraway, S. M., Anderson, A. J., and Mendell, L. M. 2005. BDNF-induced facilitation of afferent evoked responses in lamina II neurons is reduced following neonatal spinal cord contusion injury. J. Neurophysiol. [Epub ahead of print].

Garraway, S. M., Petruska, J. C., and Mendell, L. M. 2003. BDNF sensitizes the response of lamina II neurons to high threshold primary afferent inputs. Eur. J. Neurosci. 18, 2467–2476.

Gratto, K. A. and Verge, V. M. 2003. Neurotrophin-3 down-regulates trkA mRNA, NGF high-affinity binding sites, and associated phenotype in adult DRG neurons. Eur. J. Neurosci. 18, 1535–1548.

Halliday, D. A., Zettler, C., Rush, R. A., Scicchitano, R., and McNeil, J. D. 1998. Elevated nerve growth factor levels in the synovial fluid of patients with inflammatory joint disease. Neurochem. Res. 23, 919–922.

He, X. L. and Garcia, K. C. 2004. Structure of nerve growth factor complexed with the shared neurotrophin receptor p75. Science 304, 870–875.

Hempstead, B. L., Martin-Zanca, D., Kaplan, D. R., Parada, L. F., and Chao, M. V. 1991. High-affinity NGF binding requires coexpression of the trk proto-oncogene and the low-affinity NGF receptor. Nature 350, 678–683.

Hoheisel, U., Unger, T., and Mense, S. 2005. Excitatory and modulatory effects of inflammatory cytokines and neurotrophins on mechanosensitive group IV muscle afferents in the rat. Pain 114, 168–176.

Horigome, K., Pryor, J. C., Bullock, E. D., and Johnson, E. M., Jr. 1993. Mediator release from mast cells by nerve growth factor. J. Biol. Chem. 268, 14881–14887.

Huang, E. J. and Reichardt, L. F. 2001. Neurotrophins: roles in neuronal development and function. Annu. Rev. Neurosci. 24, 677–736.

Ji, R. R., Samad, T. A., Jin, S. X., Schmoll, R., and Woolf, C. J. 2002. p38 MAPK activation by NGF in primary sensory neurons after inflammation increases TRPV1 levels and maintains heat hyperalgesia. Neuron 36, 57–68.

Kaplan, D. R. and Cooper, E. 2001. PI-3 kinase and IP3: partners in NT3-induced synaptic transmission. Nat. Neurosci. 4, 5–7.

Kaplan, D. R. and Miller, F. D. 2000. Neurotrophin signal transduction in the nervous system. Curr. Opin. Neurobiol. 10, 381–391.

Karchewski, L. A., Kim, F. A., Johnston, J., McKnight, R. M., and Verge, V. M. 1999. Anatomical evidence supporting the potential for modulation by multiple neurotrophins in the majority of adult lumbar sensory neurons. J. Comp. Neurol. 413, 327–341.

Kerr, B. J., Bradbury, E. J., Bennett, D. L., Trivedi, P. M., Dassan, P., French, J., Shelton, D. B., McMahon, S. B., and Thompson, S. W. 1999. Brain-derived neurotrophic factor modulates nociceptive sensory inputs and NMDA-evoked responses in the rat spinal cord. J. Neurosci. 19, 5138–5148.

Knusel, B. and Hefti, F. 1992. K-252 compounds: modulators of neurotrophin signal transduction. J. Neurochem. 59, 1987–1996.

Koizumi, S., Fujishita, K., Inoue, K., Shigemoto-Mogami, Y., Tsuda, M., and Inoue, K. 2004. Ca^{2+} waves in keratinocytes are transmitted to sensory neurons: the involvement of extracellular ATP and P2Y2 receptor activation. Biochem. J. 380, 329–338.

Koltzenburg, M., Bennett, D. L., Shelton, D. L., and McMahon, S. B. 1999. Neutralization of endogenous NGF prevents the sensitization of nociceptors supplying inflamed skin. Eur. J. Neurosci. 11, 1698–1704.

Koplas, P. A., Rosenberg, R. L., and Oxford, G. S. 1997. The role of calcium in the desensitization of capsaicin responses in rat dorsal root ganglion neurons. J. Neurosci. 17, 3525–3537.

Lamb, K. and Bielefeldt, K. 2003. Rapid effects of neurotrophic factors on calcium homeostasis in rat visceral afferent neurons. Neurosci. Lett. 336, 9–12.

Lamb, K., Gebhart, G. F., and Bielefeldt, K. 2004. Increased nerve growth factor expression triggers bladder overactivity. J. Pain 5, 150–156.

Lamb, K., Kang, Y. M., Gebhart, G. F., and Bielefeldt, K. 2003. Nerve growth factor and gastric hyperalgesia in the rat. Neurogastroenterol. Motil. 15, 355–361.

LaMotte, R. H., Lundberg, L. E., and Torebjork, H. E. 1992. Pain, hyperalgesia and activity in nociceptive C units in humans after intradermal injection of capsaicin. J. Physiol. 448, 749–764.

Lee, Y. J., Zachrisson, O., Tonge, D. A., and McNaughton, P. A. 2002. Upregulation of bradykinin B2 receptor expression by neurotrophic factors and nerve injury in mouse sensory neurons. Mol. Cell Neurosci. 19, 186–200.

Leon, A., Buriani, A., Dal Toso, R., Fabris, M., Romanello, S., Aloe, L., and Levi-Montalcini, R. 1994. Mast cells synthesize, store, and release nerve growth factor. Proc. Natl. Acad. Sci. U. S. A. 91, 3739–3743.

Lever, I. J., Bradbury, E. J., Cunningham, J. R., Adelson, D. W., Jones, M. G., McMahon, S. B., Marvizon, J. C., and Malcangio, M. 2001. Brain-derived neurotrophic factor is released in the dorsal horn by distinctive patterns of afferent fiber stimulation. J. Neurosci. 21, 4469–4477.

Lewin, G. R. and Mendell, L. M. 1993. Nerve growth factor and nociception. Trends Neurosci. 16, 353–359.

Lewin, G. R. and Mendell, L. M. 1994. Regulation of cutaneous C-fibre nociceptors by nerve growth factor in the developing rat. J. Neurophysiol. 71, 941–949.

Lewin, G. R., Lisney, S. J., and Mendell, L. M. 1992b. Neonatal anti-NGF treatment reduces the A delta- and C-fibre evoked vasodilator responses in rat skin: evidence that nociceptor afferents mediate antidromic vasodilatation. Eur. J. Neurosci. 4, 1213–1218.

Lewin, G. R., Ritter, A. M., and Mendell, L. M. 1992a. On the role of nerve growth factor in the development of myelinated nociceptors. J. Neurosci. 12, 1896–1905.

Lewin, G. R., Ritter, A. M., and Mendell, L. M. 1993. Nerve growth factor-induced hyperalgesia in the neonatal and adult rat. J. Neurosci. 13, 2136–2148.

Lewin, G. R., Rueff, A., and Mendell, L. M. 1994. Peripheral and central mechanisms of NGF-induced hyperalgesia. Eur. J. Neurosci. 6, 1903–1912.

Lindsay, R. M. 1996. Role of neurotrophins and trk receptors in the development and maintenance of sensory neurons: an overview. Philos. Trans. R. Soc. Lond. B Biol. Sci. 351, 365–373.

Lindsay, R. M. and Harmar, A. J. 1989. Nerve growth factor regulates expression of neuropeptide genes in adult sensory neurons. Nature 337, 362–364.

Liu, B. and Hannun, Y. A. 1997. Inhibition of the neutral magnesium-dependent sphingomyelinase by glutathione. J. Biol. Chem. 272, 16281–16287.

Liu, B., Zhang, C., and Qin, F. 2005. Functional recovery from desensitization of vanilloid receptor TRPV1 requires resynthesis of phosphatidylinositol 4,5-bisphosphate. J. Neurosci. 25, 4835–4843.

Lowe, E. M., Anand, P., Terenghi, G., Williams-Chestnut, R. E., Sinicropi, D. V., and Osborne, J. L. 1997. Increased nerve growth factor levels in the urinary bladder of women with idiopathic sensory urgency and interstitial cystitis. Br. J. Urol. 79, 572–577.

MacPhee, I. J. and Barker, P. A. 1997. Brain-derived neurotrophic factor binding to the p75 neurotrophin receptor reduces TrkA signaling while increasing serine phosphorylation in the TrkA intracellular domain. J. Biol. Chem. 272, 23547–23551.

MacPhee, I. and Barker, P. A. 1999. Extended ceramide exposure activates the trkA receptor by increasing receptor homodimer formation. J. Neurochem. 72, 1423–1430.

Majdan, M., Walsh, G. S., Aloyz, R., and Miller, F. D. 2001. TrkA mediates developmental sympathetic neuron survival in vivo by silencing an ongoing p75NTR-mediated death signal. J. Cell Biol. 155, 1275–1285.

Malin, S. A., Molliver, D. C., Koerber, H. R., Cornuet, P., Frye, R., Albers, K. M., and Davis, B. M. 2006. Glial cell line-derived neurotrophic factor family members sensitize nociceptors in vitro and produce thermal hyperalgesia *in vivo*. J. Neurosci. 26, 8588–8599.

Mamet, J., Lazdunski, M., and Voilley, N. 2003. How nerve growth factor drives physiological and inflammatory expressions of acid-sensing ion channel 3 in sensory neurons. J. Biol. Chem. 278, 48907–48913.

Manni, L., Lundeberg, T., Fiorito, S., Bonini, S., Vigneti, E., and Aloe, L. 2003. Nerve growth factor release by human synovial fibroblasts prior to and following exposure to tumor necrosis factor-alpha, interleukin-1 beta and cholecystokinin-8: the possible role of NGF in the inflammatory response. Clin. Exp. Rheumatol. 21, 617–624.

Mannion, R. J., Costigan, M., Decosterd, I., Amaya, F., Ma, Q. P., Holstege, J. C., Ji, R. R., Acheson, A., Lindsay, R. M., Wilkinson, G. A., and Woolf, C. J. 1999. Neurotrophins: peripherally and centrally acting modulators of tactile stimulus-induced inflammatory pain hypersensitivity. Proc. Natl. Acad. Sci. U. S. A. 96, 9385–9390.

Martin, H. A., Basbaum, A. I., Goetzl, E. J., and Levine, J. D. 1988. Leukotriene B4 decreases the mechanical and thermal thresholds of C-fiber nociceptors in the hairy skin of the rat. J. Neurophysiol. 60, 438–445.

di Mola, F. F., Friess, H., Zhu, Z. W., Koliopanos, A., Bley, T., Di Sebastiano, P., Innocenti, P., Zimmermann, A., and Buchler, M. W. 2000. Nerve growth factor and Trk high affinity receptor (TrkA) gene expression in inflammatory bowel disease. Gut 46, 670–679.

McMahon, S. B., Armanini, M. P., Ling, L. H., and Phillips, H. S. 1994. Expression and coexpression of trk receptors in subpopulations of adult primary sensory neurons projecting to identified peripheral targets. Neuron 12, 1161–1171.

McMahon, S. B., Bennett, D. L., Priestley, J. V., and Shelton, D. L. 1995. The biological effects of endogenous nerve growth factor on adult sensory neurons revealed by a trkA-IgG fusion molecule. Nat. Med. 1, 774–780.

McMahon, S. B., Lewin, G. R., and Wall, P. D. 1993. Central hyperexcitability triggered by noxious inputs. Curr. Opin. Neurobiol. 3, 602–610.

Mendell, L. M. 1995. Neurotrophic factors and the specification of neural function. Neuroscientist 1, 26–34.

Mendell, L. M. 2002. Does NGF binding to p75 and trkA receptors activate independent signaling pathways to sensitize nociceptors? J. Physiol. (Perspective) 544, 333.

Mendell, L. M., Albers, K. M., and Davis, B. M. 1999. Neurotrophins, nociceptors and pain. Microsc. Res. Tech. 45, 252–261.

Michael, G. J., Averill, S., Nitkunan, A., Rattray, M., Bennett, D. L., Yan, Q., and Priestley, J. V. 1997. Nerve growth factor treatment increases brain-derived neurotrophic factor selectively in TrkA-expressing dorsal root ganglion cells and in their central terminations within the spinal cord. J. Neurosci. 17, 8476–8490.

Miller, F. D. and Kaplan, D. R. 2001. Neurotrophin signalling pathways regulating neuronal apoptosis. Cell Mol. Life Sci. 58, 1045–1053.

Molliver, D. C., Wright, D. E., Leitner, M. L., Parsadanian, A. S., Doster, K., Wen, D., Yan, Q., and Snider, W. D. 1997. IB4-binding DRG neurons switch from NGF to GDNF dependence in early postnatal life. Neuron 19, 849–861.

Nagy, I. and Rang, H. P. 1999. Similarities and differences between the responses of rat sensory neurons to noxious heat and capsaicin. J. Neurosci. 19, 647–655.

Nicol, G. D. and Vasko, M. R. 2007. Unraveling the story of NGF-mediated sensitization of nociceptive sensory neurons: ON or OFF the Trks? Mol Interv. 7, 26–41.

Obermeier, A., Halfter, H., Wiesmuller, K. H., Jung, G., Schlessinger, J., and Ullrich, A. 1993. Tyrosine 785 is a major determinant of Trk–substrate interaction. EMBO J. 12, 933–941.

Oddiah, D., Anand, P., McMahon, S. B., and Rattray, M. 1998. Rapid increase of NGF, BDNF and NT-3 mRNAs in inflamed bladder. Neuroreport 9, 1455–1458.

Patapoutian, A. and Reichardt, L. F. 2001. Trk receptors: mediators of neurotrophin action. Curr. Opin. Neurobiol. 11, 272–280.

Petersen, M., Klusch, A., and Eckert, A. 1998. The proportion of isolated rat dorsal root ganglion neurones responding to bradykinin increases with time in culture. Neurosci. Lett. 252, 143–146.

Petruska, J. C. and Mendell, L. M. 2004. The many functions of nerve growth factor: multiple actions on nociceptors. Neurosci. Lett. 361, 168–171.

Petty, B. G., Cornblath, D. R., Aldornato, B. T., Chaudhry, V., Flexner, C., Wachsman, M., Sinicropi, D., Burton, L. E., and Peroutka, S. J. 1994. The effect of systemically administered recombinant human nerve growth factor in healthy human subjects. Ann. Neurol. 36, 244–246.

Pezet, S., Cunningham, J., Patel, J., Grist, J., Gavazzi, I., Lever, I., and Malcangio, M. 2002. BDNF modulates sensory neuron synaptic activity by a facilitation of GABA transmission in the dorsal horn. Mol. Cell. Neurosci. 21, 51–62.

Plo, I., Bono, F., Bezombes, C., Alam, A., Bruno, A., and Laurent, G. 2004. Nerve growth factor-induced protein

kinase C stimulation contributes to TrkA-dependent inhibition of p75 neurotrophin receptor sphingolipid signaling. J. Neurosci. Res. 77, 465–474.

Price, T. J., Louria, M. D., Candelario-Soto, D., Dussor, G. O., Jeske, N. A., Patwardhan, A. M., Diogenes, A., Trott, A. A., Hargreaves, K. M., and Flores, C. M. 2005. Treatment of trigeminal ganglion neurons in vitro with NGF, GDNF or BDNF: effects on neuronal survival, neurochemical properties and TRPV1-mediated neuropeptide secretion. BMC Neurosci. 6, 4.

Ramer, M. S., Bradbury, E. J., and McMahon, S. B. 2001. Nerve growth factor induces P2X(3) expression in sensory neurons. J. Neurochem. 77, 864–875.

Ramer, M. S., Bradbury, E. J., Michael, G. J., Lever, I. J., and McMahon, S. B. 2003. Glial cell line-derived neurotrophic factor increases calcitonin gene-related peptide immunoreactivity in sensory and motoneurons in vivo. Eur. J. Neurosci. 18, 2713–2721.

Reynolds, M. L., Fitzgerald, M., and Benowitz, L. I. 1991. GAP-43 expression in developing cutaneous and muscle nerves in the rat hindlimb. Neuroscience 41, 201–211.

Ritter, A. M. and Mendell, L. M. 1992. Somal membrane properties of physiologically identified sensory neurons in the rat: effects of nerve growth factor. J. Neurophysiol. 68, 2033–2041.

Ritter, A. M., Lewin, G. R., Kremer, N. E., and Mendell, L. M. 1991. Requirement for nerve growth factor in the development of myelinated nociceptors in vivo. Nature 350, 500–502.

Rodriguez-Tebar, A., Dechant, G., Gotz, R., and Barde, Y. A. 1992. Binding of neurotrophin-3 to its neuronal receptors and interactions with nerve growth factor and brain-derived neurotrophic factor. EMBO J. 11, 917–922.

Rueff, A. and Mendell, L. M. 1996. Nerve growth factor and NT-5 induce increased thermal sensitivity of cutaneous nociceptors in vitro. J. Neurophysiol. 76, 3593–3596.

Rueff, A., Dawson, A. J., and Mendell, L. M. 1996. Characteristics of nerve growth factor induced hyperalgesia in adult rats: dependence on enhanced bradykinin-1 receptor activity but not neurokinin-1 receptor activation. Pain 66, 359–372.

Saarma, M. and Sariola, H. 1999. Other neurotrophic factors: glial cell line-derived neurotrophic factor (GDNF). Microsc. Res. Tech. 45, 292–302.

Stein, A. T., Ufret-Vincenty, C. A., Hua, L., Santana, L. F., and Gordon, S. E. 2006. Phosphoinositide 3-kinase binds to TRPV1 and mediates NGF-stimulated TRPV1 trafficking to the plasma membrane. J. Gen. Physiol. 128, 509–522.

von Schack, D., Casademunt, E., Schweigreiter, R., Meyer, M., Bibel, M., and Dechant, G. 2001. Complete ablation of the neurotrophin receptor p75NTR causes defects both in the nervous and the vascular system. Nat. Neurosci. 4, 977–978.

Schafers, M., Sorkin, L. S., and Sommer, C. 2003. Intramuscular injection of tumor necrosis factor-alpha induces muscle hyperalgesia in rats. Pain 104, 579–588.

Schaible, H. G. and Schmidt, R. F. 1985. Effects of an experimental arthritis on the sensory properties of fine articular afferent units. J. Neurophysiol. 54, 1109–1122.

Sevcik, M. A., Ghilardi, J. R., Peters, C. M., Lindsay, T. H., Halvorson, K. G., Jonas, B. M., Kubota, K., Kuskowski, M. A., Boustany, L., Shelton, D. L., and Mantyh, P. W. 2005. Anti-NGF therapy profoundly reduces bone cancer pain and the accompanying increase in markers of peripheral and central sensitization. Pain 115, 128–141.

Shelton, D. L., Zeller, J., Ho, W. H., Pons, J., and Rosenthal, A. 2005. Nerve growth factor mediates hyperalgesia and cachexia in auto-immune arthritis. Pain. [Epub ahead of print].

Shinoda, M., Honda, T., Ozaki, N., Hattori, H., Mizutani, H., Ueda, M., and Sugiura, Y. 2003. Nerve terminals extend into the temporomandibular joint of adjuvant arthritic rats. Eur. J. Pain. 7, 493–505.

Shu, X. Q. and Mendell, L. M. 1999a. Neurotrophins and hyperalgesia. Proc. Natl. Acad. Sci. U. S. A. 96, 7693–7696.

Shu, X. and Mendell, L. M. 1999b. Nerve growth factor acutely sensitizes the response of adult rat sensory neurons to capsaicin. Neurosci. Lett. 274, 158–162.

Shu, X. and Mendell, L. M. 2001. Acute sensitization by NGF of the response of small-diameter sensory neurons to capsaicin. J. Neurophysiol. 86, 2931–2938.

Shu, X., Llinas, A., and Mendell, L. M. 1999. Effects of trkB and trkC neurotrophin receptor agonists on thermal nociception: a behavioural and electrophysiological study. Pain 80, 463–470.

Slack, S. E., Pezet, S., McMahon, S. B, Thompson, S. W., and Malcangio, M. 2004. Brain-derived neurotrophic factor induces NMDA receptor subunit one phosphorylation via ERK and PKC in the rat spinal cord. Eur. J. Neurosci. 20, 1769–1778.

Smeyne, R. J., Klein, R., Schnapp, A., Long, L. K., Bryant, S., Lewin, A., Lira, S. A., and Barbacid, M. 1994. Severe sensory and sympathetic neuropathies in mice carrying a disrupted Trk/NGF receptor gene. Nature 368, 246–249.

Southall, M. D. and Vasko, M. R. 2000. Prostaglandin E(2)-mediated sensitization of rat sensory neurons is not altered by nerve growth factor. Neurosci. Lett. 287, 33–36.

Stucky, C. L. and Koltzenburg, M. 1997. The low-affinity neurotrophin receptor p75 regulates the function but not the selective survival of specific subpopulations of sensory neurons. J. Neurosci. 11, 4398–4405.

Stucky, C. L., Koltzenburg, M., Schneider, M., Engle, M. G., Albers, K. M., and Davis, B. M. 1999. Overexpression of nerve growth factor in skin selectively affects the survival and functional properties of nociceptors. J. Neurosci. 19, 8509–8516.

Svensson, P., Cairns, B. E., Wang, K., and Arendt-Nielsen, L. 2003. Injection of nerve growth factor into human masseter muscle evokes long-lasting mechanical allodynia and hyperalgesia. Pain 104, 241–247.

Teng, K. K. and Hempstead, B. L. 2004. Neurotrophins and their receptors: signaling trios in complex biological systems. Cell Mol. Life Sci. 61, 35–48.

Terenghi, G., Mann, D., Kopelman, P. G., and Anand, P. 1997. trkA and trkC expression is increased in human diabetic skin. Neurosci. Lett. 228, 33–36.

Theodosiou, M., Rush, R. A., Zhou, X. F., Hu, D., Walker, J. S., and Tracey, D. J. 1999. Hyperalgesia due to nerve damage: role of nerve growth factor. Pain 181, 245–255.

Toma, H., Winston, J., Micci, M. A., Shenoy, M., and Pasricha, P. J. 2000. Nerve growth factor expression is up-regulated in the rat model of L-arginine-induced acute pancreatitis. Gastroenterology 119, 1373–1381.

Tominaga, M., Caterina, M. J., Malmberg, A. B., Rosen, T. A., Gilbert, H., Skinner, K., Raumann, B. E., Basbaum, A. I., and Julius, D. 1998. The cloned capsaicin receptor integrates multiple pain-producing stimuli. Neuron 21, 531–543.

Vellani, V., Zachrisson, O., and McNaughton, P. A. 2004. Functional bradykinin B1 receptors are expressed in nociceptive neurones and are upregulated by the neurotrophin GDNF. J. Physiol. 560, 391–401.

Verdi, J. M., Birren, S. J., Ibanez, C. F., Persson, H., Kaplan, D. R., Benedetti, M., Chao, M. V., and Anderson, D. J. 1994. p75LNGFR regulates Trk signal transduction and NGF-induced neuronal differentiation in MAH cells. Neuron 12, 733–745.

Voilley, N., de Weille, J., Mamet, J., and Lazdunski, M. 2001. Nonsteroid anti-inflammatory drugs inhibit both the activity

and the inflammation-induced expression of acid-sensing ion channels in nociceptors. J. Neurosci. 21, 8026–8033.
Weskamp, G. and Otten, U. 1987. An enzyme-linked immunoassay for nerve growth factor (NGF): a tool for studying regulatory mechanisms involved in NGF production in brain and in peripheral tissues. J. Neurochem. 48, 1779–1786.
Wilson-Gerwing, T. D., Dmyterko, M. V., Zochodne, D. W., Johnston, J. M., and Verge, V. M. 2005. Neurotrophin-3 suppresses thermal hyperalgesia associated with neuropathic pain and attenuates transient receptor potential vanilloid receptor-1 expression in adult sensory neurons. J. Neurosci. 25, 758–767.
Winston, J., Toma, H., Shenoy, M., and Pasricha, P. J. 2001. Nerve growth factor regulates VR-1mRNA levels in cultures of adult dorsal root ganglion neurons. Pain 89, 181–186.
Woodbury, C. J., Zwick, M., Wang, S., Lawson, J. J., Caterina, M. J., Koltzenburg, M., Albers, K. M., Koerber, H. R., and Davis, B. M. 2004. Nociceptors lacking TRPV1 and TRPV2 have normal heat responses. J. Neurosci. 24, 6410–6415.
Woolf, C. J., Allchorne, A., Safieh-Garabedian, B., and Poole, S. 1997. Cytokines, nerve growth factor and inflammatory hyperalgesia: the contribution of tumour necrosis factor alpha. Br. J. Pharmacol. 121, 417–424.
Woolf, C. J., Ma, Q. P., Allchorne, A., and Poole, S. 1996. Peripheral cell types contributing to the hyperalgesic action of nerve growth factor in inflammation. J. Neurosci. 16, 2716–2723.
Woolf, C. J., Safieh-Garabedian, B., Ma, Q.-P., Crilly, P., and Winter, J. 1994. Nerve growth factor contributes to the generation of inflammatory sensory hypersensibility. Neuroscience 62, 327–331.
Woolf, C. J., Shortland, P., Reynolds, M., Ridings, J., Doubell, T., and Coggeshall, R. E. 1995. Reorganization of central terminals of myelinated primary afferents in the rat dorsal horn following peripheral axotomy. J. Comp. Neurol. 360, 121–134.
Wright, D. E. and Snider, W. D. 1995. Neurotrophin receptor mRNA expression defines distinct populations of neurons in rat dorsal root ganglia. J. Comp. Neurol. 351, 329–338.
Zhang, Y. H. and Nicol, G. D. 2004. NGF-mediated sensitization of the excitability of rat sensory neurons is prevented by a blocking antibody to the p75 neurotrophin receptor. Neurosci. Lett. 366, 187–192.
Zhang, X., Huang, J., and McNaughton, P. A. 2005. NGF rapidly increases membrane expression of TRPV1 heat-gated ion channels. EMBO J. 24, 4211–4223.
Zhang, Y. H., Vasko, M. R., and Nicol, G. D. 2002. Ceramide, a putative second messenger for NGF, modulates the TTX-resistant $Na^{\cdot}$ current and delayed rectifier K current in rat sensory neurons. J. Physiol. (Lond.) 544, 385–402.
Zhou, X. F., Deng, Y. S., Xian, C. J., and Zhong, J. H. 2000. Neurotrophins from dorsal root ganglia trigger allodynia after spinal nerve injury in rats. Eur. J. Neurosci. 12, 100–105.
Zhu, W. and Oxford, G. S. 2007. Phosphoinositide-3-kinase and mitogen activated protein kinase signaling pathways mediate acute NGF sensitization of TRPV1. Mol. Cell. Neurosci. 34, 689–700.
Zhu, W., Galoyan, S. M., Petruska, J. C., Oxford, G. S., and Mendell, L. M. 2004. A developmental switch in acute sensitization of small dorsal root ganglion (DRG) neurons to capsaicin or noxious heating by NGF. J. Neurophysiol. 92, 3148–3152.
Zhuang, Z.-Y., Xu, H., Clapham, D. E., and Ji, R.-R. 2004. Phosphatidylinositol 3-kinase activates ERK in primary sensory neurons and mediates inflammatory heat hyperalgesia through TRPV1 sensitization. J. Neurosci. 24, 8300–8309.

5.23 Morphological and Neurochemical Organization of the Spinal Dorsal Horn

A Ribeiro-da-Silva, McGill University, Montreal, QC, Canada

Y De Koninck, Centre de recherche Université Laval Robert-Giffard, Québec, QC, Canada

© 2008 Elsevier Inc. All rights reserved.

5.23.1	**Introduction**	280
5.23.2	**Overall Organization of Dorsal Horn: Rexed Lamination**	280
5.23.3	**Primary Afferent Fibers**	283
5.23.3.1	Types of Afferents, Neurochemistry, and Termination in Spinal Cord	283
5.23.3.2	Synaptic Arrangements of Primary Afferents	284
5.23.3.3	Receptors on Primary Sensory Fibers	286
5.23.3.4	Expression of Voltage-Gated Sodium Channels by Sensory Fibers	288
5.23.4	**Dorsal Horn Neurons**	288
5.23.4.1	Lamina I Neurons	289
5.23.4.1.1	Morphological classification of lamina I neurons	289
5.23.4.1.2	Correspondence with function	289
5.23.4.1.3	Expression of NK-1r in subpopulations of lamina I neurons	291
5.23.4.2	Lamina II Neurons	292
5.23.4.3	Laminae III–VI	293
5.23.4.4	Neurochemistry of Dorsal Horn Neurons	294
5.23.4.4.1	Neurokinins	294
5.23.4.4.2	Neurokinin receptors	295
5.23.4.4.3	CGRP and CGRP receptors	295
5.23.4.4.4	Somatostatin	295
5.23.4.4.5	Opioid peptides	295
5.23.4.4.6	Opioid receptors	296
5.23.4.4.7	Glutamate	296
5.23.4.4.8	Glutamate receptors	297
5.23.4.4.9	Inhibitory amino acids	297
5.23.4.4.10	GABA and glycine receptors	298
5.23.4.4.11	Other classical transmitters and other neuropeptides	298
5.23.5	**Identified Neuronal Circuits**	299
5.23.6	**Conclusion and Future Directions**	301
References		302

Glossary

bouton Dilated portion of an axon possessing synaptic vesicles and establishing synapses with adjacent dendrites or other neuronal components. Synonyms – axonal varicosity or axon terminal.

presynaptic dendrite Dendrite possessing synaptic vesicles, and which is presynaptic to other neuronal processes, mainly dendrites. In the dorsal horn, presynaptic dendrites occur in islet cells.

substantia gelatinosa (of Rolando) Synonym of lamina II of Rexed. So named because of the translucent and gelatinous appearance when examined in fresh tissue.

superficial dorsal horn Region of the dorsal horn corresponding to laminae I and II of Rexed.

synaptic glomerulus (of the spinal cord) Complex synaptic arrangement in which a central axonal bouton, of primary sensory afferent origin, establishes synaptic contacts with several processes from dorsal horn neurons.

5.23.1 Introduction

The superficial laminae of the dorsal horn of the spinal cord, particularly the marginal layer (or lamina I of Rexed) and the substantia gelatinosa (or lamina II of Rexed), represent the area of the central nervous system (CNS) where the first modulation of pain-related information occurs. Although some progress has been made in recent years concerning our knowledge of the anatomical and neurochemical characteristics of the relevant cells and systems, our understanding of this area is far from complete. In particular, despite significant recent progress, our understanding of the synaptic circuitry and how neurotransmitters/neuromodulators in this region interact with their receptors is still incomplete, and even less is known about the changes that occur in acute and chronic pain (for recent review see Todd, A. J. and Ribeiro-da-Silva, A., 2005). This chapter presents an overview of what is known concerning the morphology and neurochemistry of the spinal dorsal horn, attempting to extract an emerging integrated view of the morphological and neurochemical organization in this area of the CNS from the available literature.

Because most of the work on the structure of the spinal cord has been carried out on the rat, we have based our description on this species, but when possible have made comparison to other species. We have focused on the superficial dorsal horn because of its relevance in the transmission and modulation of pain-related information.

5.23.2 Overall Organization of Dorsal Horn: Rexed Lamination

The first subdivision of the dorsal horn into horizontal laminae, based on the morphological properties of the cells in a Nissl-type staining, was performed in the cat dorsal horn (Rexed, B., 1952; 1954). It was later verified that this lamination could be adapted with minor modifications to almost any mammalian species. In particular, it has been adapted to the monkey (Ralston, H. J., III, 1979), human (Harmann, P. A. *et al.*, 1988), rat (Steiner, T. J. and Turner, L. M., 1972; Molander, C. *et al.*, 1984; 1989), and mouse (Ma, W. Y. *et al.*, 1995), besides nonmammalian species such as the pigeon (Leonard, R. B. and Cohen, D. H., 1975). Through a correlation of light and electron microscopy, it has been possible since the 1970s to establish criteria to identify the laminae at the ultrastructural level (for reviews see Light, A. R., 1992; Ribeiro-da-Silva, A., 2004).

Despite some recent criticism (Woodbury, C. J. *et al.*, 2000), the Rexed lamination remains the reference. Unfortunately, it is not always followed accurately, and many published micrographs show laminar limits that were based more on speculation rather than on objective evaluation using the proper approaches. This is true particularly for ultrastructural studies and also for those using radioactive ligand binding. This is unfortunate because, as we will discuss below, it is easy to set up the limits of the laminae with acceptable accuracy (see Figures 1 and 2 and below).

Besides neuroglia and vessels, the spinal dorsal horn contains several elements of neuronal origin: (a) the final arborization and termination of primary afferent fibers; (b) local circuit neurons, some excitatory and others inhibitory; (c) projection neurons to the brain; (d) propriospinal neurons, which interconnect different levels of the spinal cord; and (e) descending axons from several supraspinal sources.

Lamina I of the dorsal horn is also known as the marginal layer and lamina II as the substantia gelatinosa (of Rolando). These two laminae together represent what is frequently called the superficial dorsal horn and are of particular importance for the spinal processing of pain-related information and its forwarding to higher levels. This is true in particular for lamina I and the outer 2/3 of lamina II, as the inner 1/3 is mostly nonnociceptive. In contrast, laminae III–IV represent what is called the nucleus proprius, which was thought to represent a nonnociceptive region of the spinal cord. While this view is mostly valid, this region does contain neurons that are known to respond to noxious stimuli and project to the brain, which were initially thought to occur only in lamina V (De Koninck, Y. *et al.*, 1992; Ma, W. *et al.*, 1996).

Figure 1 shows the laminar organization of the rat spinal cord at the C4 level, as detected using a Nissl method on thick sections, and the correlation with laminae detected on semithin plastic sections. Although the criteria are quite different, there is a very good match between the laminae when identified by the Nissl approach and the semithin sections approach. When using a Nissl staining, lamina I can be recognized by a rather low cell density (Figure 1(a) and (1b)), with an occasional large neuron among mostly small cells. Lamina II is a layer with a higher density of cells than lamina I; these cells

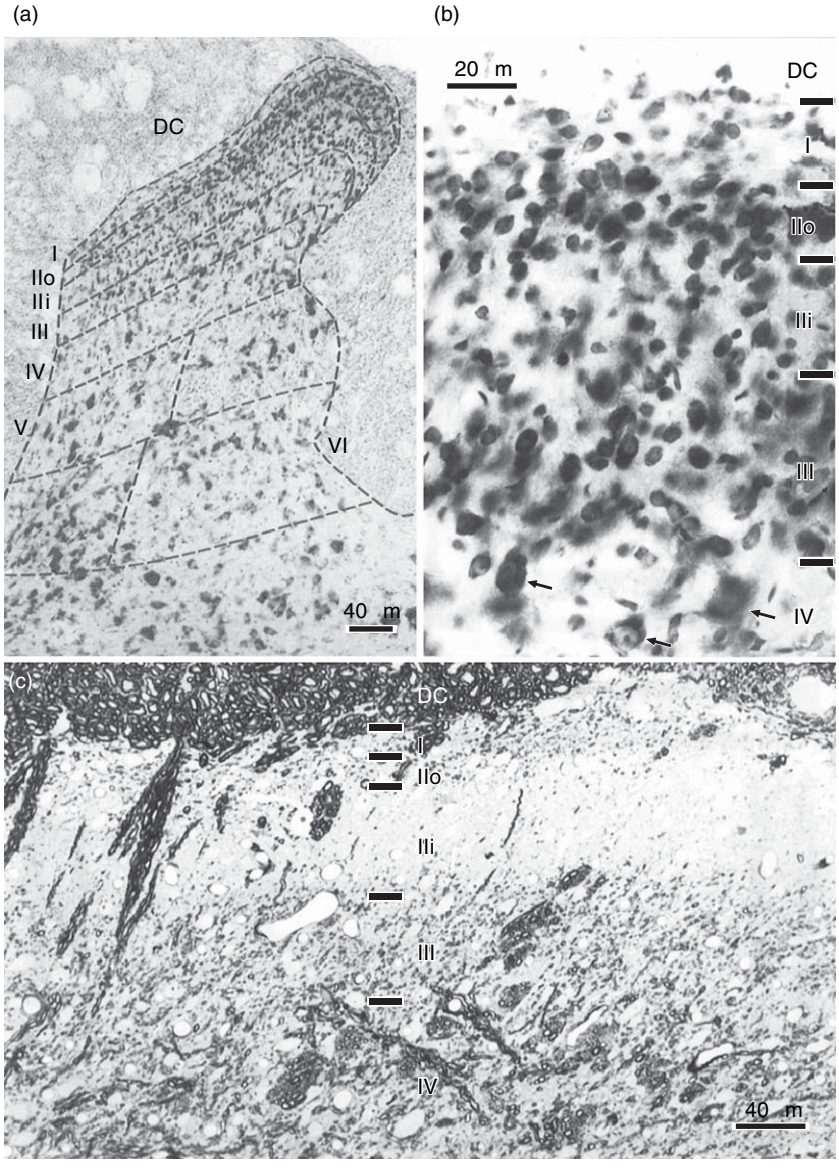

Figure 1 Rexed's laminae at the C4 level of the adult rat spinal cord. (a) and (b) represent micrographs from frozen cross sections, 50 μm in thickness, stained with toluidine blue as described by Rexed B. (1952). In (a), note the overall laminar organization of the dorsal horn. In (b), note that lamina I (I) has a low density of cells, whereas outer lamina II (LIIo) stands out because of the clustering of small neurons, which differentiate it from the inner part of lamina II (IIi). Both LIIo and inner lamina II (LIIi) have numerous small neurons, of rather uniform size. The presence of some slightly larger neurons separates lamina III from LIIi, whereas lamina IV can be easily distinguished from lamina III by the lower cell density and the presence of some large neurons. (c) represents a micrograph from an Epon-embedded semithin (2 μm thick) transverse section of the rat dorsal horn at the C4 level, stained with toluidine blue and Azur II, to illustrate that Rexed's laminae can be identified in these sections, which are used as reference for ultrastructural observations; notably, lamina IIi can be clearly delineated from lamina III by the absence of myelin (see text for details). DC, dorsal columns.

are rather small in size and occur in a considerably higher density in outer lamina II (LIIo) than in inner lamina II (LIIi). It should be noted that in many articles the subdivision of lamina II into outer and inner parts does not follow a cytoarchitectonic scheme as it should and some authors simply consider LIIo as the dorsal half of lamina II. Although in rat we have used lamina IIA to refer to LIIo and lamina IIB to refer to LIIi (see Ribeiro-da-Silva, A., 2004, for rationale), in the current chapter we will use

the nomenclature followed in most of the literature. The border between LIIi and lamina III is difficult to distinguish in Nissl-type preparations, as the main features are similar except for the presence of some larger cells in lamina III. Lamina IV, in contrast, is easy to distinguish from lamina III because of the lower cell density and the presence of some rather large neurons (Figure 1(b)).

The superficial laminae can also be recognized in Epon-embedded 1–2-μm-thick semithin sections stained with toluidine blue, as this approach has been validated by integrated light and electron microscopic studies (Ribeiro-da-Silva, A. and Coimbra, A., 1982). In these preparations, lamina I can be distinguished from LIIo by the presence of a higher density of small myelinated fibers, whereas LIIi is virtually devoid of myelin (Figure 1(c)). In contrast, lamina III is easily distinguished from IIi by the appearance of numerous thinly myelinated fibers (Figure 1(c)).

At mid-lumbar levels, which represent the region innervating the hind limbs and which has been studied extensively, the thickness of the superficial laminae is greater in the medial 2/3 than in the lateral third. Overall the thickness of LI and LIIo is twice the value of mid-cervical levels. Figure 2 illustrates the laminar subdivisions at the level of the L5 segment of the young rat spinal cord.

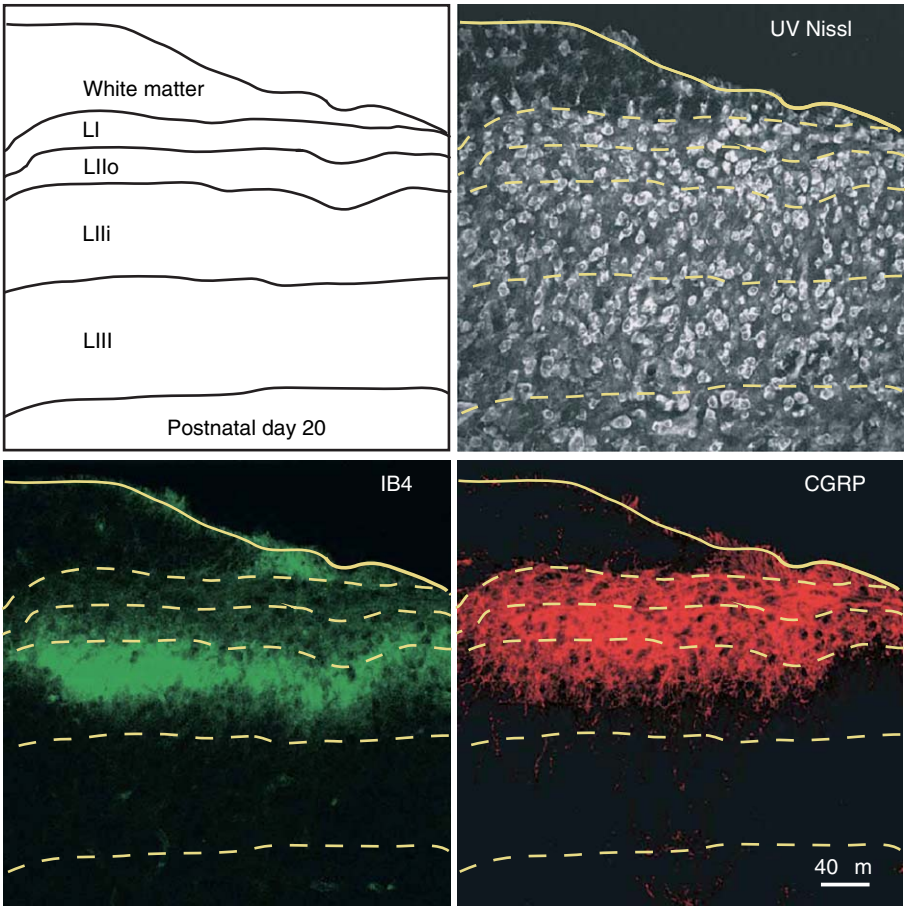

Figure 2 Rexed's laminae at the L5 level of the spinal cord of a young rat (20-day old). Micrographs represent confocal images that result from the fusion of several optical sections obtained using a multitrack approach on a 50-μm-thick transverse section. Section was immunostained for calcitonin gene-related peptide (CGRP) and incubated for IB4 binding and a Nissl-type labeling using an ultraviolet fluorescent marker. The Nissl-type labeling was used to identify the Rexed's laminae and to create an overlay, which was applied to the other images, and is shown isolated in the upper left picture. This figure clearly illustrates that CGRP immunostaining occurs in lamina I (LI), outer lamina II (LIIo), and part of inner lamina II (LIIi), whereas IB4 labeling is most intense in the dorsal part of LIIi. Because the thickness of each lamina is rather constant at the same level of the spinal cord, overlays created like this are useful to identify the laminae even in material not stained with a Nissl method.

5.23.3 Primary Afferent Fibers

5.23.3.1 Types of Afferents, Neurochemistry, and Termination in Spinal Cord

The great majority of afferents that transmit pain-related information (nociception) are of small diameter and have unmyelinated (C) or thinly myelinated (Aδ) axons. Most such small-diameter fibers convey pain-related information and, therefore, are often named nociceptors. These small-diameter fibers represent the central processes of pseudounipolar neurons of small or medium size located in the dorsal root ganglia (DRG) and terminate in the superficial laminae of the dorsal horn of the spinal cord (for reviews see Grant, G. and Robertson, B., 2004; Ribeiro-da-Silva, A., 2004). The smaller-diameter (unmyelinated) nociceptive afferents can be divided into two major subpopulations, the peptidergic and the nonpeptidergic. The peptidergic expresses substance P (SP) and calcitonin gene-related peptide (CGRP), and the nonpeptidergic possesses fluoride-resistant acid phosphatase (FRAP) activity, binds the lectin GSA-IB4, and expresses purinergic $P2X_3$ receptors (Hunt, S. P. and Rossi, J., 1985; Alvarez, F. J. and Fyffe, R. E., 2000; Hunt, S. P. and Mantyh, P. W., 2001). These two populations differ in neurotrophic support in the adult. In fact, during development, both populations require nerve growth factor (NGF) for survival, but shortly after birth only the peptidergic continues to respond to NGF, whereas the nonpeptidergic population starts to respond instead to glial cell line-derived neurotrophic factor (GDNF) (Bennett, D. L. H. *et al.*, 1998). Accordingly, the peptidergic population expresses the NGF high-affinity receptor, trkA, whereas the nonpeptidergic expresses GDNF receptors. It has also been shown that the latter population expresses the purinergic receptor $P2X_3$ (Bradbury, E. J. *et al.*, 1998; Snider,W. D. and McMahon, S. B., 1998). Although the distinction between two populations of primary sensory fibers, peptidergic and nonpeptidergic, seems attractive, it is not fully accurate as a small proportion of peptidergic sensory fibers (those that colocalize CGRP and somatostatin (SOM)) do not respond to NGF in the adult and bind the lectin GSA-IB4 (Alvarez, F. J. and Fyffe, R. E., 2000; Priestley, J. V. *et al.*, 2002). It should be noted that, in all of the above putative nociceptive fibers, the classical synaptic transmitter is very likely glutamate (Battaglia, G. and Rustioni, A., 1988; De Biasi, S. and Rustioni, A., 1988; Merighi, A. *et al.*, 1991). In the spinal cord, sensory fibers that express SP and CGRP terminate mostly in laminae I, outer II, and lamina V; those that colocalize CGRP and SOM terminate in laminae I and II, and those that contain FRAP, bind the lectin GSA-IB4 or express the purinergic $P2X_3$ receptor, terminate mostly in the middle third of lamina II (see Figure 2; for reviews see Bradbury, E. J. *et al.*, 1998; Ribeiro-da-Silva, A., 2004). Not all the nociceptive afferents that express SP are C fibers; some are thinly myelinated (Aδ) afferents. There is a significant population of nociceptive fibers that are Aδ and were shown to represent high-threshold mechanoreceptors (HTM) after being characterized electrophysiologically and filled intracellularly with horseradish peroxidase in cat and monkey; they were shown to terminate in laminae I and V (Light, A. R. and Perl, E. R., 1979). The morphological and neurochemical identification of these Aδ HTM fibers is difficult because they do not contain peptides, do not bind IB4, and do not express $P2X_3$ receptors. However, there is evidence from an *in situ* hybridization study that the 5-HT3 may be highly expressed by Aδ HTM fibers (Zeitz, K. P. *et al.*, 2002). Although the prevailing view is that Aβ fibers are nonnociceptive, it has been suggested that some of the myelinated nociceptors conduct in the Aβ range. In rat, these Aβ nociceptors might represent up to 20% of all Aβ somatic afferents according to some reports (for review see Djouhri, L and Lawson, S. N., 2004).

Although a small number of C fibers are nonnociceptive and convey either innocuous mechanical or thermal information, most nonnociceptive mechanosensitive afferents are either thinly myelinated (Aδ) or thick afferents (Aβ) (Alvarez, F. J. and Fyffe, R. E., 2000). Most innocuous Aδ afferents innervate down hairs (D hair afferents) and terminate in the deeper part of lamina II and in lamina III, a distribution that contrasts with the preferential termination of nociceptive Aδ afferents in laminae I and V (Light, A. R. and Perl, E. R., 1979). Like the nociceptive fibers, the nonnociceptive afferents are glutamatergic (Battaglia, G. and Rustioni, A., 1988; De Biasi, S. and Rustioni, A., 1988; Merighi, A. et al., 1991). Curiously, the T-type calcium channel Cav3.2 seems to be expressed exclusively by D hair afferents, as detected by in situ hybridization at the level of the DRG (Shin, J. B. et al., 2003).

It should be noted that other neuropeptides have been localized in the fibers that contain SP and CGRP: neurokinin A (Dalsgaard, C. J. *et al.*, 1985), galanin (Ju, G. *et al.*, 1987; Zhang, X. *et al.*, 1993), and

Table 1 Overview of the classical transmitter and peptidergic innervation of the spinal dorsal horn of the rat, as described in text

Origin of neurotransmitter/neuropeptide			
>Primary afferents	***Local circuit neurons***	***Neurons projecting to brain***	***Descending fibers***
Glu + SP[a] + CGRP + End-2 + (Gal[b]) + (CCK[c]) + (VIP[c])	Glu + SP + ENK	Glu + SP + ENK	5-HT + SP + TRH
Glu + SOM + CGRP	Glu + NKB	Glu + dynorphins (?)	5-HT + ENK
Glu + dynorphin B (at sacral levels) + ?	Glu + SOM	Glu + Gal + CCK	GABA
Glu + ?	Endomorphin-1 + ?		GABA + Gly
Glu + (NPY[c])	GABA + ENK		Noradrenaline
	GABA + Ach		
	GABA + NPY		
	Glu + Gal + CCK (?)		
	Glu + dynorphins (?)		
	Glu + neurotensin		

[a]All neurons that express SP colocalize NKA in rat. Neurochemical in parenthesis are not expressed or expressed in a reduced number of afferents in the absence of lesion.
[b]Galanin is strongly upregulated after nerve lesion.
[c]These peptides are expressed only in a significant number of primary afferents following peripheral nerve lesion.
This table does not intend to be a complete list. It is restricted to the peptides mentioned in the text.
Abbreviations: Ach, acetylcholine; CCK, cholecystokinin; CGRP, calcitonin gene-related peptide; End-2, endomorphin 2; ENK, enkephalin; Gal, galanin; Glu, glutamate; NKA, neurokinin A; NKB, neurokinin B; NPY, neuropeptide Y; SP, substance P; SOM, somatostatin; TRH, thyrotropin-releasing hormone; VIP, vasocative intestinal peptide.

the opioid peptide endomorphin-2 (Martin-Schild, S. *et al*., 1997; Martin-Schild, S. *et al*., 1998). Dynorphin B has been detected in some primary sensory fibers from visceral afferents from pelvic viscera at sacral levels in the cat (Basbaum, A. I. *et al*., 1986). Some neuropeptides are not expressed in any significant amount in primary sensory fibers in naïve rats but are upregulated following peripheral axotomy: vasoactive intestinal peptide (VIP) and cholecystokinin (CCK) appear on small, peptidergic afferents, whereas neuropeptide Y (NPY) appears in large-diameter afferents (for review see Hökfelt, T. *et al*., 1994). Table 1 gives an overview of classical transmitters and peptides in the dorsal horn, including those in the terminals of primary sensory fibers.

5.23.3.2 Synaptic Arrangements of Primary Afferents

In the dorsal horn, primary afferent boutons establish mostly simple axodendritic, and to a lesser extent, axosomatic synapses. However, a significant proportion of primary afferent endings participate in complex arrangements named synaptic glomeruli, where they form the central terminal (Coimbra, A. *et al*., 1974; Ribeiro-da-Silva, A. and Coimbra, A., 1982). Glomeruli represent multiplier systems, i.e., devices that transmit sensory information to several dorsal horn neurons. They also constitute important modulatory devices as the primary afferent terminals are often postsynaptic to other neuronal profiles. Since the central terminals of glomeruli are all of primary afferent origin, as has been shown by their complete disappearance following multiple dorsal rhizotomies (Coimbra, A. *et al*., 1984), they provide a very useful means of identifying these afferents with electron microscopy, without the need for transported or immunocytochemical markers. The detailed features of synaptic glomeruli in the rat have been reviewed in a recent publication (Ribeiro-da-Silva, A., 2004). To be classified as a synaptic glomerulus, a synaptic arrangement must meet simultaneously all of following criteria when viewed in a single ultrathin section: (a) it should possess a central terminal (C) with round synaptic vesicles; (b) this C terminal has to be surrounded by at least four neuronal profiles, representing either dendritic profiles or axonal bouton profiles; (c) there have to be at least two visible synaptic contacts between the central bouton profiles and the peripheral profiles. Two main types of synaptic glomeruli have been identified in rat by Ribeiro-da-Silva A. and Coimbra A. (1982), and are named type I and type II. Glomeruli of type I have a central bouton of scalloped contour, with an electrondense matrix, with rather densely packed synaptic vesicles and a low density of mitochondria, whereas type II

glomeruli are larger and possess a central terminal, which has a rounder contour, a lighter cytoplasmatic matrix, synaptic vesicles, which are more uniform in size and less densely packed, and a higher density of mitochondria (Ribeiro-da-Silva, A. and Coimbra, A., 1982). This classification is applicable to the mouse and, with some modifications, to the cat and the monkey (unpublished observations). A comparable classification was established for the monkey dorsal horn (Knyihár-Csillik, E. *et al.*, 1982b), in which three glomerular types were described, based on the properties of their central terminals. Of the three types described in the monkey by Knyihár-Csillik E. *et al.* (1982b), the dense sinusoid axon (DSA) type corresponds to the type I of Ribeiro-da-Silva A. and Coimbra A. (1982) and the regular synaptic vesicles (RSV) type corresponds to type II. Although the large dense-core vesicle (LDCV) type of Knyihár-Csillik E. *et al.* (1982b) has apparently no equivalent in the classification of Ribeiro-da-Silva A. and Coimbra A. (1982), this type has been considered in rat as a subtype of type I (subtype Ib), as in this species most of their central terminals share the dark axoplasm, the sinuous contour, and small size with type I central boutons, although they display numerous dense-core vesicles (Ribeiro-da-Silva, A. *et al.*, 1989; Ribeiro-da-Silva, A., 2004). However, the incorporation of these glomeruli with dense-core vesicles in type I is not legitimate in cat and monkey, as in these species they have larger central boutons, with more mitochondria and a lighter matrix than in rat. Therefore, for the sake of simplicity, we propose that in cat and primates, glomeruli can be classified into type I, type II, and peptide-type (because all the central boutons of this later type express neuropeptides – see below). In rat both type Ia and type II glomeruli have complex synaptic arrangements in which the central bouton is postsynaptic to presynaptic dendrites and axonal boutons and presynaptic to both normal dendrites and presynaptic dendrites (see Figure 3 for details). One main feature of peptide-type synaptic glomeruli (type Ib in rat) is that their central terminal is seldom postsynaptic to presynaptic dendrites and peripheral axons.

Of the nociceptive afferents, the nonpeptidergic, IB4-binding afferents terminate mostly as central boutons of synaptic glomeruli of type I (or more precisely in rat of subtype Ia), whereas the peptidergic endings are glomerular in only a small proportion, particularly in rat (Ribeiro-da-Silva, A. *et al.*, 1989); when they are glomerular, the central boutons (subtype Ib) contain dense-core vesicles and peptide immunoreactivity (CGRP, together with either SP or SOM; Ribeiro-da-Silva, A., 1995). Concerning nonnociceptive boutons, many terminate as central boutons of type II synaptic glomeruli (e.g., the D-hair afferents), but many are nonglomerular, including the ones corresponding to the termination of G-hair afferents, based on the data obtained in the cat (for review see Maxwell, D. J. and Réthelyi, M., 1987). Figure 4 shows a diagrammatic representation of the different types and subtypes of synaptic glomeruli in rat. There are considerable species differences in the type of synaptic arrangements of primary sensory fibers. For instance, lamina I and LIIo are virtually devoid of synaptic glomeruli in rat (Ribeiro-da-Silva, A. and Coimbra, A., 1982), but not in cat or monkey; in this latter species, there are, in laminae I and IIo, numerous type II glomeruli corresponding to the termination of the HTM myelinated nociceptors (Réthelyi, M. *et al.*, 1982), which are nonglomerular in rat, as well as a considerable number of peptide-type glomeruli (Knyihár-Csillik, E. *et al.*, 1982b), which are sparse in rat.

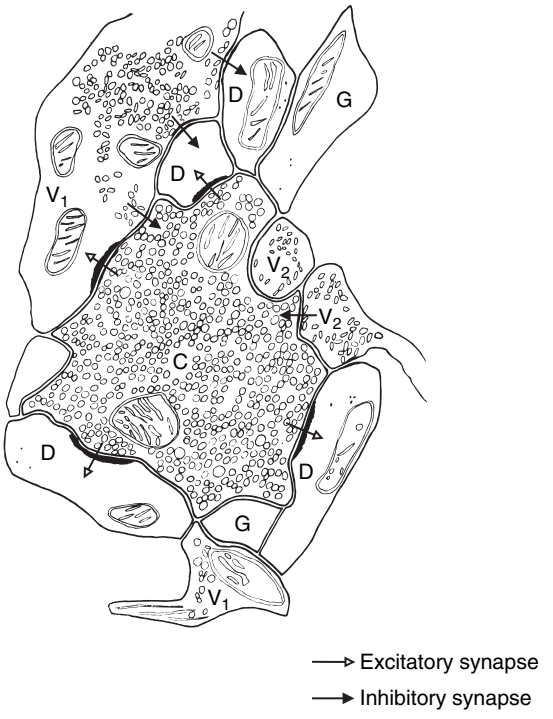

Figure 3 Diagram of a synaptic glomerulus of type Ia, with representation of the complex synaptic arrangements of the triadic type. The drawing was inspired by an electron micrograph of a type Ia glomerulus and shows the morphological features and the synaptic circuits involving the central bouton, of primary sensory origin, and the peripheral profiles. C, Central bouton; D, regular dendrite; V_1, presynaptic dendrite; V_2, peripheral axonal bouton; G, glial profile.

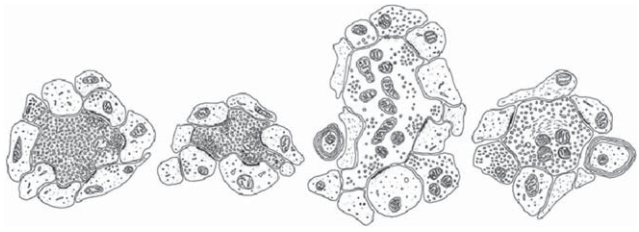

	Type Ia	Type Ib	Type IIa	Type IIb
I				
IIo	++	+		
IIIdorsal	++++++	++	+	
IIIventral	+++		+++++	++
III			++++	++++
Afferent innervation	Nonpeptidergic C fibers (IB4 and P2X3)	Peptidergic (CGRP + SP CGRP + SOM)	Aδ fibers D-Hair (?)	Aβ fibers (?)

Figure 4 Types of synaptic glomeruli and their laminar incidence in laminae I–III of the rat dorsal horn. The drawings on top were inspired by actual electron micrographs of representative samples of each glomerular type. Note that in rat, lamina I (I) is virtually devoid of glomeruli and that outer lamina II (LIIo) has only a low number of them. This is a considerable difference when comparing to the cat and primate, which have glomeruli in significant numbers in lamina I and outer II. In contrast, the other laminae have abundant synaptic glomeruli. Most type Ia glomeruli are condensed in a rather narrow band (~20 μm thick at cervical levels), which represents the dorsal part of inner lamina II (III_{dorsal}). Most of the inner lamina II ($III_{ventral}$) has a predominance of type IIa glomeruli, whereas lamina III is normally devoid of type I glomeruli and has similar numbers of both subtypes of type II glomeruli. The data concerning laminar incidence of glomeruli are semiquantitative and are based on the data collected from other publications (Ribeiro-da-Silva, A. and Coimbra, A., 1982; Ribeiro-da-Silva, A. *et al.*, 1989). The information on the types of afferent fibers, which terminate as central boutons of each type of glomerulus, is either based on evidence obtained in rat (for type I glomeruli) or extrapolated from the data obtained in cat and primate. See text for details on glomerular classification.

It is important to stress that of the populations of nociceptive primary sensory fibers, the peptidergic is not postsynaptic to GABAergic neurons in the species studied (Alvarez, F. J. *et al.*, 1993; Ribeiro-da-Silva, A., 2004). In contrast, in rat, the IB4-binding population (which terminates as central boutons of glomeruli of type Ia) is postsynaptic to GABAergic neurons (Todd, A. J. and Lochhead, V., 1990; Ribeiro-da-Silva, A., 2004). In cat and primates, the HTM myelinated nociceptors that terminate in synaptic glomeruli are also postsynaptic to dorsal horn neurons at synapses, which have the morphological properties of inhibitory junctions or in which the profiles have been shown to express GABA (Réthelyi, M. *et al.*, 1982; Alvarez, F. J. *et al.*, 1992). There seem to be species differences though, as a primate study has shown that the terminals that have the morphology of the IB4 nonpeptidergic population of the rat did not show them to be involved in axo- or dendroaxonic synapses (Knyihár-Csillik, E. *et al.*, 1982a). Similarly, in rat the HTM myelinated nociceptors are not glomerular and not postsynaptic to other structures. The above indicates different presynaptic control of the different type of nociceptive inputs, as well as likely species differences in such presynaptic control.

5.23.3.3 Receptors on Primary Sensory Fibers

Receptors expressed on primary afferent terminals in the spinal dorsal horn include neurotransmitter/modulator receptors and neurotrophic factor receptors. It is important to point out that most of the past studies of the neurotransmitter/modulator receptors on primary afferents have been performed in the dorsal root ganglia. Information on localization of receptors on the terminals of primary sensory fibers in the spinal cord is recent and still rather limited as it

required the development of specific antibodies against the neurotransmitter/modulator receptors.

Concerning glutamate receptors, α-amino-3-hydroxy-5-methylisoxazole-4-propionic acid (AMPA) receptors have a widespread distribution in DRG neurons (Tachibana, M. *et al.*, 1994; Lu, C. R. *et al.*, 2002). It has been shown at the light and ultrastructural levels that *N*-methyl-D-aspartic acid (NMDA) receptors occur in sensory fibers in the dorsal horn (Liu, H. *et al.*, 1994b). A presynaptic localization of sensory fibers in the dorsal horn has also been shown for kainate (Hwang, S. J. *et al.*, 2001) and metabotropic glutamate receptors (Ohishi, H. *et al.*, 1995). It is important to note that while ionotropic glutamate receptors are typically viewed as excitatory, their activation on primary afferent terminals leads to inhibition of transmitter release, likely via primary afferent terminal depolarization (PAD) akin to the action of presynaptic $GABA_A$ receptors (Kerchner, G. A. *et al.*, 2001; Lee, C. J. *et al.*, 2002; Bardoni, R. *et al.*, 2004). This contrasts with the apparent excitatory role that glutamate receptors appear to play at the peripheral endings of primary afferents (Cairns, B. E. *et al.*, 1998; Svensson, P. *et al.*, 2003). To further complicate the matter, PAD appears to have an opposite effect on spontaneous transmitter release (facilitation) versus evoked release (inhibition) (for review see Engelman, H. S. and MacDermott, A. B., 2004). Subunits of the $GABA_A$ receptor have also been identified by *in situ* hybridization in DRG neurons (Persohn, E. *et al.*, 1991), consistent with the functional evidence of a role for these receptors in presynaptic inhibition of primary afferents (for review see Rudomin, P. and Schmidt R. F., 1999). Intriguingly, however, to date it has not yet been possible to immunocytochemically label $GABA_A$ receptor subunits at axoaxonic synapses in the dorsal horn, although they have been labeled in dorsal horn neurons (Alvarez, F. J. *et al.*, 1996; Todd, A. J. *et al.*, 1996). There also appears to be a difference in the strength of $GABA_A$ receptor-mediated responses between subtypes of small-diameter afferents (Labrakakis, C. *et al.*, 2003). Subunits of the metabotropic $GABA_B$ receptor have been identified in DRG neurons and, in the dorsal horn, in dendrites and central boutons of glomeruli (Poorkhalkali, N. *et al.*, 2000; Ribeiro-da-Silva and Shigemoto, unpublished observations).

Concerning opioid receptors, it is well established that they occur in primary sensory fibers. The evidence originates from studies using radioactive ligand binding, which show that both μ- and δ-opioid receptors in the dorsal horn are reduced following dorsal rhizotomy (Fields, H. L. *et al.*, 1980), and from *in situ* hybridization studies, which have shown that mRNA for each of the main opioid receptors (μ, δ, and κ) occurs in DRG neurons (Minami, M. *et al.*, 1995).

There is both immunocytochemical and *in situ* hybridization evidence that the SP receptor, the neurokinin 1 receptor (NK-1r), occurs in DRG cells and on sensory fibers in the periphery (Ruocco, I. *et al.*, 1997; Li, H. S. and Zhao, Z. Q., 1998). Surprisingly, the NK-1r cannot be detected by immunocytochemistry on terminals of primary sensory fibers in the spinal dorsal horn, an observation that suggests that the NK-1r synthesized in DRG neurons is targeted preferentially toward the periphery. In contrast, the NK-1r occurs in well-defined populations of dorsal horn neurons, as described below.

The capsaicin receptor, TRPV1, previously named VR1 (Caterina, M. J., 2003), occurs in small diameter primary sensory afferents. Unfortunately, there is conflicting evidence in the literature regarding which afferent populations express the receptor. The *in situ* hybridization data of Michael G. J. and Priestley J. V. (1999) concluded that it is expressed by the majority of small- and medium-sized dorsal root ganglion neurons, which label with the lectin IB4 or are CGRP-immunoreactive (IR). In contrast, using immunocytochemistry Guo A. *et al.* (1999) concluded that TRPV1 occurred mainly in the nonpeptidergic, IB4-binding afferents, and to a minor extent in the peptidergic as well. An important observation is that there was a phenotypic switch in the postnatal period leading to the progressive expression of TRPV1 in DRG neurons that bind the lectin IB4, whereas the population that colocalized peptides did not change (Guo, A. *et al.*, 2001). Furthermore, a very significant species difference does occur because in mouse TRPV1 is not expressed by the IB4-binding population of afferents but rather by the peptidergic population (Zwick, M. *et al.*, 2002), suggesting that the phenotypic switch, which occurs postnatally in the rat, does not take place in the mouse. This is a particularly important point as it suggests that the results obtained with TRPV1 knockout mice are not transposable to the rat.

The purinergic receptor $P2X_3$ has been detected in the nonpeptidergic population of nociceptive afferents (Bradbury, E. J. *et al.*, 1998) and, in agreement with this, in the central boutons of glomeruli of type I (Llewellyn-Smith, I. J. and Burnstock, G., 1998). Because of the variability with the conditions of incubation in a number of afferents that are labeled by IB4 binding (see Alvarez, F. J. and Fyffe, R. E.,

2000, for a discussion), $P2X_3$ immunostaining may represent a better way of identifying the nonpeptidergic subpopulation of C fibers.

Concerning cholinergic receptors on primary sensory fibers, both nicotinic and muscarinic receptors have been identified (Flores, C. M. *et al.*, 1996; Haberberger, R. *et al.*, 1999). Concerning adrenergic receptors, both $\alpha 1$ and $\alpha 2$ receptors have also been localized in the DRG neurons (Kinnman, E. *et al.*, 1997; Birder, L. A. and Perl, E. R., 1999; Xie, J. *et al.*, 2001), and there is also some evidence that they occur in nociceptive primary afferents in the spinal cord (Stone, L. S. *et al.*, 1998). Because α-adrenergic receptors in the DRG are upregulated after peripheral nerve lesion, these receptors may be implicated in the sensitization of primary afferents in sympathetically maintained pain.

There is abundant literature on the expression of trophic factor receptors by primary sensory fibers (for review see Priestley, J. V. *et al.*, 2002). All three high-affinity neurotrophin receptors, trkA, trkB. and trkC, have been detected in DRG neurons. Of these, trkB and trkC occur in large-diameter neurons, corresponding to low-threshold mechanoreceptors, whereas trkA is found in nociceptive neurons that express the neuropeptides CGRP and SP. The low-affinity neurotrophin receptor, p75, has been identified in the populations of DRG neurons that express one of the high-affinity neurotrophin receptors. The nonpeptidergic, IB4-binding population, including its subpopulation that colocalizes CGRP and SOM, expresses in the adult components of the GDNF receptor family, but not in neurotrophin receptors (Alvarez, F. J. and Fyffe, R. E., 2000).

5.23.3.4 Expression of Voltage-Gated Sodium Channels by Sensory Fibers

In recent years, there has been a developing interest on voltage-gated sodium channels expressed by primary sensory fibers, as changes in some have been linked to pain states (for review see Wood, J. N. *et al.*, 2004). Channels with α subunits coded by the $Na_v1.8$ and $Na_v1.9$ genes are sensory neuron-specific and commonly referred to as tetrodotoxin (TTX)-resistant because higher doses of TTX are required to block them (Amaya, F. *et al.*, 2000). Although the two channels are mostly colocalized in the same DRG neurons in the rat (Amaya, F. *et al.*, 2000), the $Na_v1.8$ channel also occurs in some larger-diameter afferents, as was demonstrated in a study in which the physiological properties of the neurons expressing it was studied in the DRG (Djouhri, L. *et al.*, 2003) and by immunocytochemistry, which shows that $Na_v1.9$ channel immunoreactivity is restricted to laminae I–II whereas some $Na_v1.8$ signal was detected in the deeper laminae as well (Amaya, F. *et al.*, 2000). Regarding small-diameter afferents that express these channels, both channels seem to be expressed equally by peptidergic and nonpeptidergic (IB4-positive) afferents, although such expression was present only in about 50% of trkA-positive and 50% IB4-positive neurons (Amaya, F. *et al.*, 2000). However, a recent study in the mouse indicated that, in this species, the $Na_v1.8$ channel is expressed by 80% of the IB4-binding population of sensory fibers and only by 20% of the CGRP-IR (Braz, J. M. *et al.*, 2005), which would suggest that there are significant species differences in the relative expression of these channels. Of the TTX-sensitive channels, the $Na_v1.7$ channel is also expressed selectively in nociceptive, small-diameter afferents, although it also occurs in sympathetic neurons, and seems to play a major role in acute and inflammatory pain (Nassar, M. A. *et al.*, 2004). Interestingly, mutations that cause loss of function of $Na_v1.7$ were recently found in three consanguineous families from northern Pakistan characterized by complete inability to sense pain (Cox, J. J. *et al.*, 2006).

5.23.4 Dorsal Horn Neurons

The great majority of neurons in each lamina of the dorsal horn are local circuit neurons (interneurons), with axons that remain in the spinal cord. It should be noted that laminae I and V also possess predominantly interneurons, despite the fact that they are normally regarded as the origin of major ascending nociceptive pathways to the brain. These interneurons participate in synaptic circuits, which unfortunately are still very incompletely known. To complicate matters, there is evidence of considerable interspecies differences. These differences affect the distribution and synaptic connections of primary sensory fibers as well as the neurotransmitter/neuropeptide colocalization and the ascending pathways. It certainly does not help that most immunocytochemical studies on physiologically characterized, intracellularly filled neurons were performed in the cat, whereas most of those based on a combination of tract tracing and immunocytochemistry are from the rat and the monkey, and studies on transgenic animals were performed in the mouse.

The primary sensory fibers terminate in the dorsal horn in contact with both interneurons and projection neurons. Unfortunately, our knowledge concerning the details of the termination of specific fiber populations on identified dorsal horn neurons is extremely limited, because a systematic study combining intracellular recordings and labeling of sensory fibers with labeling of dorsal horn neurons has never been done for the nociceptive afferents. This lack of information from intracellular techniques is not a major issue for the SP afferents that innervate neurons that express the NK-1r because the available antibodies label the NK-1r-IR dorsal horn neurons extremely well, in a Golgi-like manner, which allows their morphological characterization. Because of this, we have rather detailed information on NK-1r-positive neurons innervated directly by SP, including their supraspinal projection sites (for recent review see Todd, A. J. and Ribeiro-da-Silva, A., 2005). Unfortunately, the same is not true for the termination of the nonpeptidergic population of nociceptive fibers in the dorsal horn, despite the fact that their endings can be identified directly on electron micrographs (EM) without the need of any label, because of their unique morphology as type I glomeruli central boutons (Ribeiro-da-Silva, A., 2004). In fact, it is still unknown if the central boutons of type I glomeruli synapse directly on the projection neurons or if there is an interposed interneuron. Recent evidence demonstrates a pathway for nonpeptidergic afferents connecting to lamina I neurons via lamina IIi interneurons (Lu, Y. and Perl, E. R., 2005) (given that the great majority of the C fibers that innervate lamina IIi are from the nonpeptidergic subpopulation; see also below). A challenging alternative has been proposed recently in a study using a transgenic mouse endogenously expressing a tracer transported transsynaptically in the nonpeptidergic afferents that express the $Na_V1.8$ channel. This study has shown that these afferents are connected to lamina II interneurons that link primarily to lamina V projection neurons that, in turn, target fourth-order neurons in the amygdala, hypothalamus, bed nucleus of the stria terminalis, and globus pallidus (Braz, J. M. *et al.*, 2005). The $Na_V1.8$ subclass of nonpeptidergic, IB4-binding afferents demonstrated in mice would thus likely be distinct from the putative subclass that would connect to lamina I via lamina IIi based on the studies by Lu Y. and Perl E. R. (2003; 2005) in the rat. It remains to be determined whether this is a species difference and how these pathways transpose to other species.

5.23.4.1 Lamina I Neurons

5.23.4.1.1 Morphological classification of lamina I neurons

Four morphological types of neurons have been described in the rat by Lima D. and Coimbra A. (1983; 1986): fusiform, flattened, multipolar, and pyramidal (Figure 5). Most of these neurons have their perikarya and dendritic arborization extending predominantly in the rostrocaudal axis, but with some processes extending along the mediolateral axis. For most cells, the dendrites remain within the limits of lamina I. However, some specific cell subtypes have been described with dendrites extending into laminae II and III (Figure 6); these represent a small proportion of the total number of cells that may represent local circuit neurons (Yu, X. H. *et al.*, 2005), although the possibility remains that they project to another supraspinal site different from the thalamus and the parabrachial nucleus (Lima, D. and Coimbra, A., 1990; Almarestani, L. *et al.*, 2007). Antidromic recording and retrograde labeling with horseradish peroxidase or cholera toxin subunit b have demonstrated that lamina I neurons project to several supraspinal areas including the thalamus, the periaqueductal gray, and the parabrachial nucleus (for reviews see Lima, D. and Coimbra, A., 1988; Spike, R. C. *et al.*, 2003; Yu, X. H. *et al.*, 2005). A comparable classification of lamina I projection neurons has been carried out in the cat (Zhang, E. T. *et al.*, 1996) and the monkey (Zhang, E. T. and Craig, A. D., 1997; Yu, X. H. *et al.*, 1999) based on the analysis of horizontal sections (Figure 5). In this latter classification, the multipolar and flattened types were merged into one category (multipolar neurons). Because of the correlation with classifications done in other species and correlation with function (see below), we have found it more appropriate to classify lamina I neurons in rat into the general types of fusiform, multipolar, and pyramidal (Yu, X. H. *et al.*, 1999; 2005; Almarestani, L. *et al.*, 2007) (Figure 6). While to a large extent these cell types can be recognized in horizontal sections (Figure 5), complete classification of these cells require a 3D reconstruction of their dendritic tree (Figures 5 and 6) (Yu, X. H. *et al.*, 1999; 2005).

5.23.4.1.2 Correspondence with function

Recent evidence suggests a correspondence between the morphological characteristics of lamina I neurons and their functional properties (Han, Z. S. *et al.*, 1998). Three main functional types of lamina I neurons

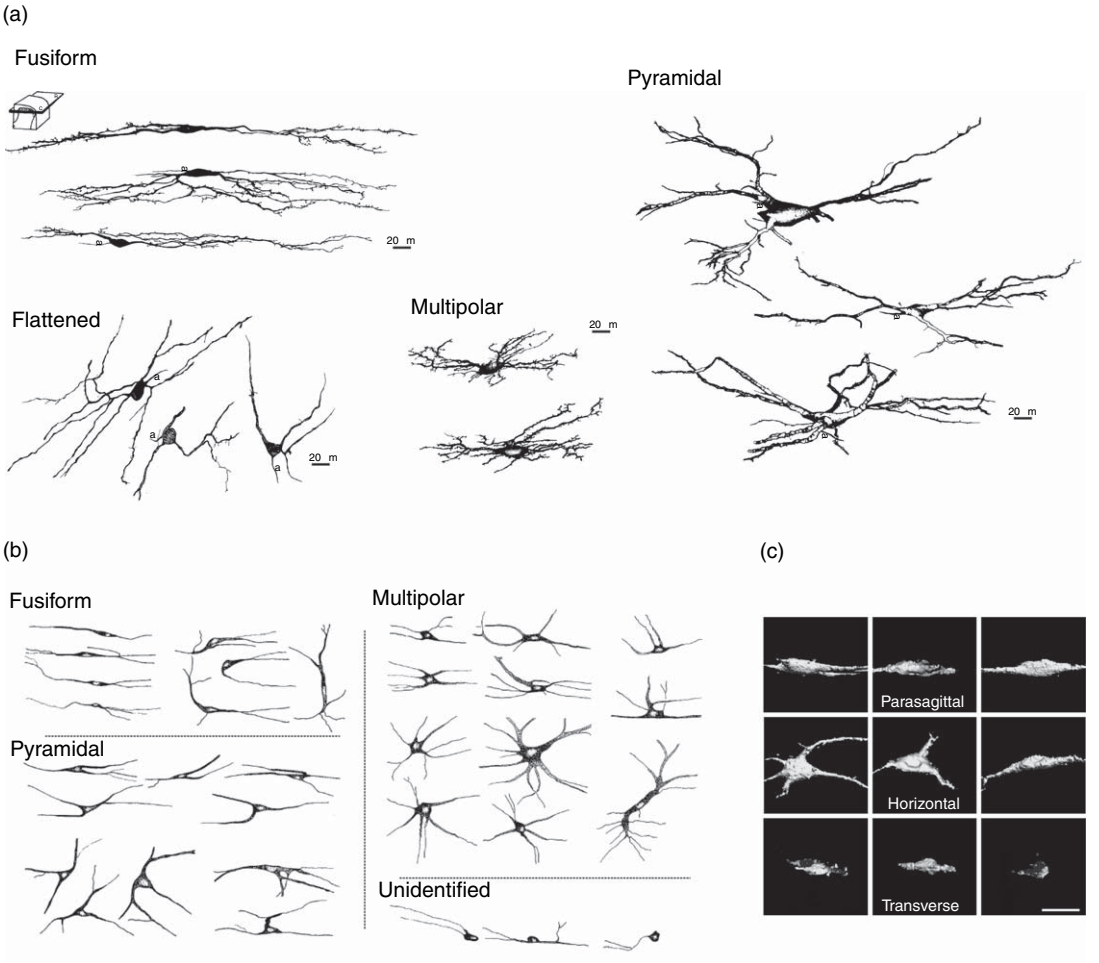

Figure 5 Representative drawings of lamina I neurons in the rat and the monkey spinal dorsal horn. The drawings in (a) are based on camera lucida reconstructions from Golgi-impregnated cells viewed in the horizontal plane (modified from Lima, D. and Coimbra, A., 1986). (b) The basic scheme was extended to higher species, such as the monkey, with minor nomenclature adjustments (modified from Zhang, E. T. and Craig, A. D., 1997; see text). (c) Three-dimensional reconstructions from serial confocal images of retrogradely labeled lamina I spinothalamic neurons in rats (from Yu, X. H. *et al.*, 2005). Note that lamina I projection neurons in rat (Yu, X. H. *et al.*, 2005), cat (Zhang, E. T. *et al.*, 1996; Han, Z. S. *et al.*, 1998), and monkey (Zhang, E. T. and Craig, A. D., 1997) do not appear to have ventrally directed dendrites (see also text) and are thus properly identified only in the horizontal plane as shown in (c) (modified from Yu, X. H. *et al.*, 2005).

have been identified on the basis of their response to cutaneous sensory inputs: nociceptive-specific (NS) neurons, responsive only to noxious heat and pinch; polymodal nociceptive neurons, responsive to noxious heat and pinch as well as to innocuous and noxious cold (HPC); and innocuous thermoreceptive neurons responsive only to innocuous cooling (COLD) (Craig, A. D. and Kniffki, A. I., 1985; Craig, A. D. and Bushnell, M. C., 1994; Dostrovsky, J. O. and Craig, A. D., 1996; Han, Z. S. *et al.*, 1998). A correspondence between these functional classes of lamina I and the morphological types (fusiform, pyramidal, and multipolar) has been found in the cat whereby fusiform cells were all NS, pyramidal cells were all COLD, and multipolar cells were divided between HPC and NS (Han, Z. S. *et al.*, 1998). These results are also consistent with previous reports that many pyramidal and multipolar cells possess large axons in the cat (Gobel, S., 1978a) and the rat (Lima, D. and Coimbra, A., 1986). In contrast, fusiform cells are characterized by thin, likely unmyelinated axons (Lima, D. and Coimbra, A., 1986), consistent with the observation that HPC and COLD cells have faster antidromic conduction velocities (Craig, A. D. and Kniffki, K. D., 1985) than NS neurons (Craig, A. D. and Kniffki, K. D., 1985). Recent evidence using

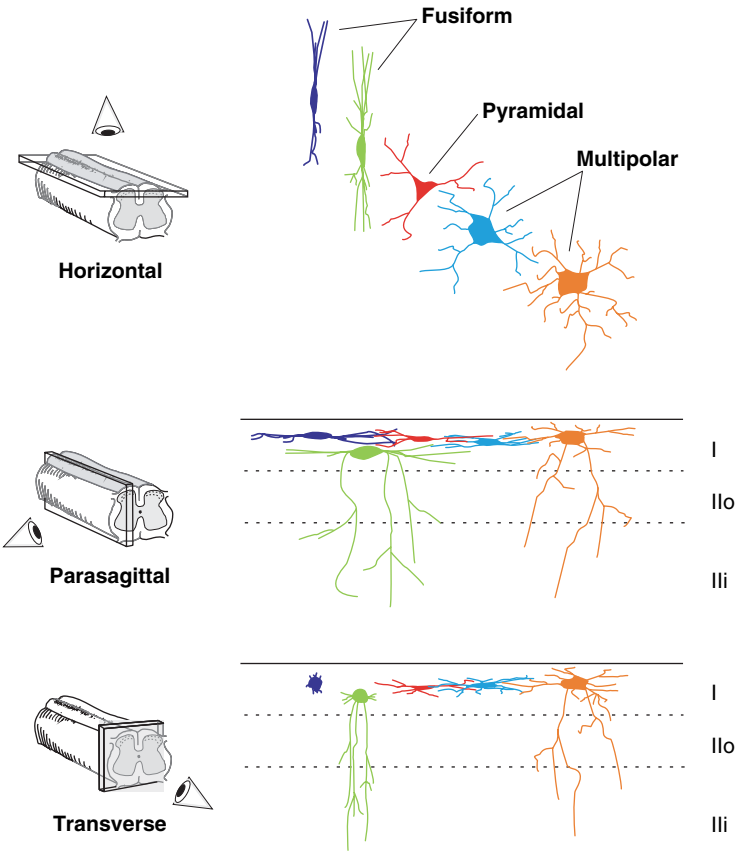

Figure 6 Morphological classification of the neuronal populations in lamina I. The classification is mainly based on cell body shape and primary dendrite orientation. Adaptation of the original classification by Lima D. and Coimbra A. (1986) to take into account recent findings on projection neurons (see Figure 5 and text) and interneurons (see text). Most cells types (especially the projection neurons) are best identified in the horizontal plane. Sagittal and transverse views may be useful to test for ventrally directed dendrites.

whole cell recording in slices indicates the presence of distinct classes of lamina I neurons on the basis of their intrinsic firing properties (Prescott, S. A. and De Koninck, Y., 2002; Ruscheweyh, R. *et al.*, 2004). In addition, a correspondence between intrinsic electrophysiological properties and morphology in lamina I has been shown in rat (Prescott, S. A. and De Koninck, Y., 2002) whereby tonic cells were typically fusiform, phasic cells were pyramidal, and delayed onset and single spike cells were multipolar. In the latter study, the multipolar cell subtype probably correspond to the small multipolar subtype with ventrally directed dendrites and therefore are likely not projection neurons.

5.23.4.1.3 Expression of NK-1r in subpopulations of lamina I neurons

The finding that pyramidal neurons corresponded to a class of lamina I neurons that only respond to innocuous thermal stimuli was of particular interest because of the evidence that nonnociceptive neurons fail to respond to SP (Henry, J. L., 1976) and do not receive significant amount of SP input (De Koninck, Y. *et al.*, 1992; Ma, W. *et al.*, 1996). We therefore decided to test whether pyramidal neurons express NK-1r (Yu, X. H. *et al.*, 1999). The results indicated that, while normally one-third of lamina I neurons are pyramidal in the cervical and lumbar enlargements of the spinal cord (Zhang, E. T. *et al.*, 1996; Zhang, E. T. and Craig, A. D., 1997; Yu, X. H. *et al.*, 1999), only ~5% of the NK-1r-expressing neurons in these areas were pyramidal, most being either fusiform or multipolar. This type of differential distribution gives further support to the concept that there is a correlation between the functional properties of neurons and their morphological features. In a recent study (Yu, X. H. *et al.*, 2005), we obtained data in the rat consistent with that in the

monkey whereby retrogradely labeled lamina I spinothalamic tract (STT) cells were evenly distributed among the three main cell types (Zhang, E. T. and Craig, A. D., 1997; Yu, X. H. *et al.*, 1999), and NK-1r immunoreactivity was also preferentially expressed in fusiform and multipolar lamina I STT neurons.

A high proportion (60–80%), but not all, of lamina I projection neurons are IR for NK-1r (Marshall, G. E. *et al.*, 1996; Yu, X. H. *et al.*, 1999; 2005). In contrast, however, only a subset of NK-1r-IR neurons are projection neurons (49% after the injection of tracer in the thalamus; Yu, X. H. *et al.*, 2005). A large proportion of lamina I neurons project to the parabrachial nucleus. Importantly, although it had been reported that very few lamina I neurons in rat project to the thalamus at lumbar levels (Spike, R. C. *et al.*, 2003), we found that a significant number, about 9%, of lamina I neurons project to the thalamus (Yu, X. H. *et al.*, 2005), a figure comparable to that found in primate by us (Yu, X. H. *et al.*, 1999) and others (Andrew, D. *et al.*, 2003). Our recent data on spinoparabrachial neurons also indicate that most pyramidal cells in this subpopulation do not express NK-1r (Almarestani, L. *et al.*, 2007).

5.23.4.2 Lamina II Neurons

Lamina II neurons have been classified originally by Ramón y Cajal (1909) into two main types, the central cell, which occurs throughout the lamina, and the limiting cell, which is restricted to a region close to the laminae I–II border. These same morphological types were identified in the cat by Gobel S. (1975; 1978b), and were renamed islet cells and stalked cells, respectively. A Golgi method study by Todd A. J. and Lewis S. G. (1986) identified cells with the characteristics of stalked and islet cells, as described by Gobel, in lamina II of the rat (Figure 7). Concerning incidence of these cells, the stalked cells were shown to represent about half of the stained cells in LIIo; in contrast, islet cells were found throughout lamina II and corresponded to about one-third of the entire stained neuronal population (Todd, A. J. and Lewis, S. G., 1986). It should be noted that these authors reported other cell types in lamina II; in fact, about half of the cells in the ventralmost part of lamina II did not fit in either the stalked or islet cell categories, although they could be subdivided into groups based on their dendritic arborization. The axons of these cells either crossed to lamina III or remained within the limits of lamina II. Some of these neurons may correspond to the stellate and laminae II–III border cells described in other species (Todd, A. J. and Lewis, S. G., 1986).

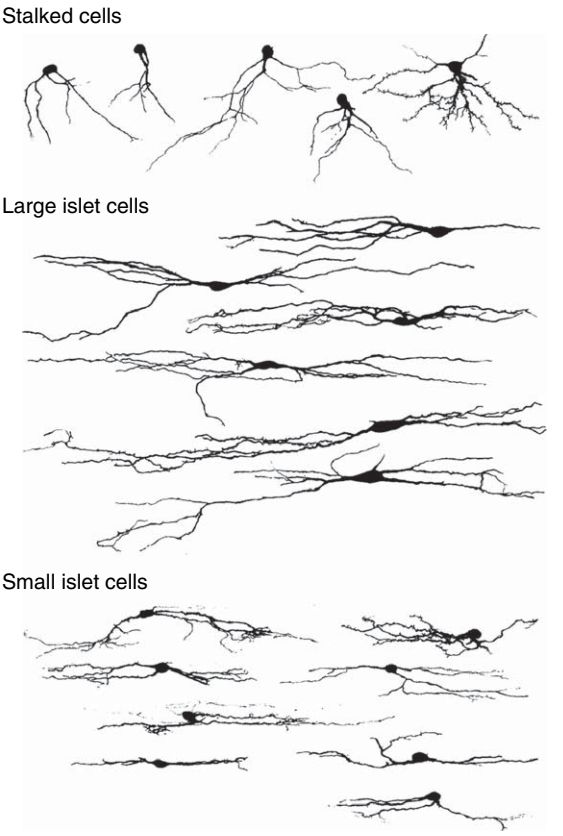

Figure 7 Representative drawings of lamina II neurons in the rat spinal dorsal horn. Three main cell types are represented in these camera lucida drawings of Golgi-impregnated cells: the stalked, small islet, and large islet cells (see text for further details). Modified from Todd A. J. and Spike R. C. (1993).

Recently, Grudt T. J. and Perl E. R. (2002) performed a detailed morphological analysis of the different cells types in lamina II following intracellular labeling in spinal cord slices of the hamster. They identified five morphological types of lamina II neurons: islet, central, medial–lateral, radial, and vertical (Figure 8). Most of lamina II neurons had dendritic arbors that were primarily orientated in the rostrocaudal dimension and relatively flattened in the mediolateral and dorsoventral directions (consistent with Scheibel, M. E. and Scheibel, A. B., 1968). The islet cells of Grudt T. J. and Perl E. R. (2002) appear to correspond well with the islet cells of Gobel S. (1975; 1978b) and the large islet cells of Todd A. J. and Lewis S. G. (1986) (Figures 7 and 8); the radial cells resembled the star-shape neurons of Bicknell H. R. and Beal J. A. (1984); or the stellate

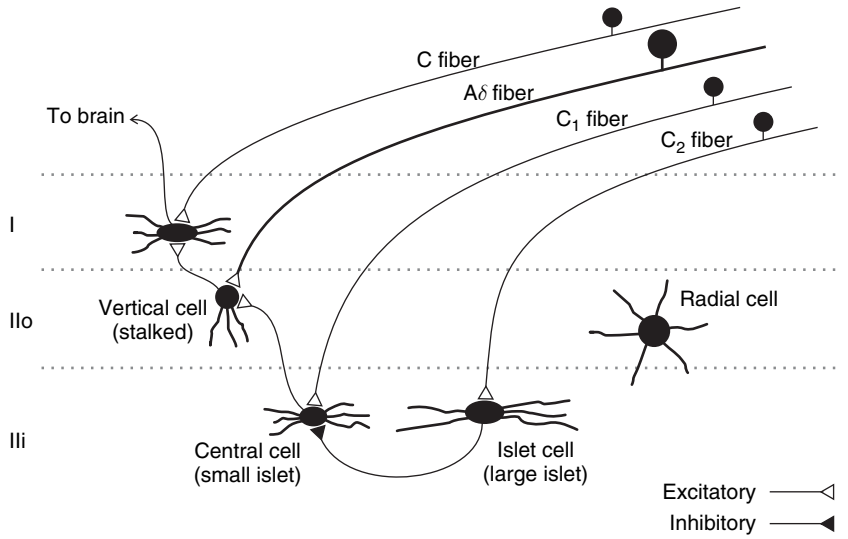

Figure 8 Diagrammatic representation of morphological types of neuron in lamina II and their primary afferent input and interconnections. A correspondence between the classification by Todd A. J. and Spike R. C. (1993) (words in parenthesis) and that of Grudt T. J. and Perl E. R. (2002) and Lu Y. and Perl E. R. (2003; 2005) is attempted as described in the text. Scheme for interconnection is based on Lu Y. and Perl E. R. (2003; 2005) (see text for a complete description). Note that distinct classes of C fibers appear to contact the two classes of islet cells based on the conduction velocity data. Note also the feed-forward inhibition between the islet cell and the central cell, which is unidirectional (Lu, Y. and Perl, E. R., 2003).

neurons described by Schoenen J. (1982). The central cells were similar to islet cells, but with a much smaller dendritic expansion in the rostrocaudal direction, thus appearing to correspond to Ramon y Cajal's central cells and Todd's small islet cells (Figures 7 and 8). The medial–lateral cells were the sole type with dendrites extending substantially in the mediolateral axis. The vertical cells appear to correspond to the limitroph neurons of Ramon y Cajal and stalked cells of Gobel.

Using paired recordings in slices and stimulation of primary afferents in rat spinal cord slices, Lu Y. and Perl E. R. (2003; 2005) were able to describe a specific connection path between subclasses of C-fiber afferents and the network of large islet cells, small islet cells (central), and stalked cells (vertical), as summarized in Figure 8. Notably, their results show that distinct subclasses of C fibers connect to different laminae II neurons subtypes and that stalked cells are indeed feed-forward excitatory cells to lamina I neurons, confirming what had been postulated in previous reports (Bennett, G. J. *et al.*, 1980; Gobel, S. *et al.*, 1980).

Concerning islet cells, it has been found that their electrophysiological properties differed depending on their localization in lamina II, as those situated in deep lamina II were nonnociceptive, while those in LIIo were nociceptive (Bennett, G. J. *et al.*, 1980; Gobel, S. *et al.*, 1980). These findings concur with previous studies in the cat by Light A. R. *et al.* (1979). It interesting to note that in the cat, according to Light A. R. and collaborators (1979), the type of response elicited from lamina II cells, either nociceptive or nonnociceptive, had little correlation with their morphology but was related to where the dendritic tree arborized. This observation was interpreted as a consequence of the type of primary sensory fibers, which contacted the dendrites of the cells, as the afferents that terminated in deep lamina II did not seem to be nociceptive in the cat (Light, A. R. and Perl, E. R., 1979).

5.23.4.3 Laminae III–VI

Laminae III–VI possess both interneurons and projection neurons and have a rather heterogeneous population of cells with dendrites that cut across these laminae (Brown, A. G., 1982). Cells of some of the major ascending pathways (spinothalamic, spinocervical, and dorsal column postsynaptic pathway) have cell bodies located in these laminae (Brown, A. G., 1982). Lamina III can be considered as a continuation of the ventralmost part of lamina II, with some small neurons with characteristics similar to those of that part of lamina II, as described in one study (Wall, P. D. *et al.*, 1979). In cat, cells in lamina

III have been described as nonnociceptive and heterogeneous (Maxwell, D. J. *et al.*, 1983) based on intracellular injections of physiologically characterized neurons. However, this concept that all lamina III cells are nonnociceptive is not correct based on the detection of wide dynamic range cells in this laminae III–IV of the cat, which possess dorsally oriented dendrites branching in the superficial laminae (De Koninck, Y. *et al.*, 1992; Ribeiro-da-Silva, A. *et al.*, 1992; Ma, W. *et al.*, 1996; 1997), as well as on the detection of neurons in the same laminae of the rat, which express the NK-1r and possess dorsally oriented dendrites that branch into laminae I and II (Liu, H. *et al.*, 1994a; Brown, J. L. *et al.*, 1995; Littlewood, N. K. *et al.*, 1995; Naim, M. *et al.*, 1997).

5.23.4.4 Neurochemistry of Dorsal Horn Neurons

In spite of a large number of studies that identified neurochemicals in dorsal horn neurons, the available information is less than satisfactory because, with a few exceptions, the information on the morphological properties of the neurons is either incomplete or simply lacking. This is a consequence of the fact that, in most cases, little more is known than the size and the localization of the neurochemically characterized cell bodies. There are some exceptions, however. The most striking exception is likely the excellent characterization of the population that expresses the NK-1r because a Golgi-like staining of the cells is obtained. With most neurochemicals, either the staining is inadequate to allow a proper characterization of the cell (e.g., cell body faintly labeled) or the number of immunolabeled cells is so high that it is impossible to characterize individual cells. In the case of *in situ* hybridization studies, only cell bodies are labeled, and therefore the information obtained with the use of this approach is significant but limited. The only approaches that can deliver an integrative view of morphological and neurochemical properties of the cells are those that involve the combination of intracellular filling of neurons with immunocytochemistry, but they have been sparsely used to date. Therefore, in the text below little correlation to cell populations described above will be made because such data are simply lacking. Table 1 gives an overview of classical transmitter/neuropeptide colocalizations in the dorsal horn, as described in the text.

5.23.4.4.1 Neurokinins

All three main mammalian neurokinins (SP, neurokinin A, and neurokinin B (NKB)) occur in dorsal horn neurons. SP-containing cell bodies have been detected in laminae I and II, both with immunocytochemistry (Ljungdahl, A. *et al.*, 1978; Ribeiro-da-Silva, A. *et al.*, 1991) and *in situ* hybridization (Warden, M. K. and Young, W. S., 1988). It is interesting to note that most, if not all, SP-IR cell bodies in the rat dorsal horn colocalize enkephalin (ENK) immunoreactivity (Ribeiro-da-Silva, A. *et al.*, 1991), and they seem to be glutamatergic as well because they express the vesicular glutamate transporter 2 (VGLUT2) (Todd, A. J. *et al.*, 2003). It has been speculated in the past that some of these neurons colocalizing SP and enkephalin immunoreactivities represent stalked cells, based on their laminar localization in LIIo, absence of presynaptic dendrites, and synapses on lamina I neurons (Ribeiro-da-Silva, A. *et al.*, 1991). However, neurons colocalizing SP and enkephalin likely belong to other cell types as well and some of these project to higher levels. In particular, SP-IR lamina I and lamina V cells have been shown to project to the thalamus in rat and cat (Battaglia, G. and Rustioni, A., 1992), and it is possible that they also project to other targets such as the midbrain parabrachial nucleus. Based on the finding that spinal cord SP-IR neurons normally colocalize enkephalin and glutamate, we can speculate that such projection neurons colocalize all three neurochemicals.

Virtually all SP-containing neurons in the rat express neurokinin A (NKA) as well (Carter, M. S. and Krause, J. E., 1990), which means that their distribution is essentially the same. This applies to the primary sensory fibers that also express SP, which represent the main source of SP in the dorsal horn (see Section Types of Afferents, Neurochemistry, and Termination in Spinal Cord). Another source of SP and NKA in the dorsal horn are axons originating from cell bodies located in the brain stem (Hökfelt, T. *et al.*, 1978; Gilbert, R. F. *et al.*, 1982); although most such fibers terminate in the ventral horn, some terminate in the dorsal horn.

NKB derives from a different precursor, and in contrast to SP and NKA, does not occur in primary sensory neurons (Ogawa, T. *et al.*, 1985). A light and electron microscopic immunocytochemical study using a marker of NKB neurons revealed that the signal occurs in axon terminals in laminae I–II, with a peak in lamina IIi, and in cell bodies and dendrites mostly in lamina IIi (McLeod, A. L. *et al.*, 2000).

Lamina III showed much less immunolabeling. Signal for NKB was detected in dendrites of type I glomeruli, suggesting a participation in the modulation of nociception (McLeod, A. L. *et al.*, 2000). Neurons expressing NKB seem to be excitatory and glutamatergic (Polgár, E. *et al.*, 2006).

5.23.4.4.2 Neurokinin receptors

Originally, NK-1r immunoreactivity was described in neurons with cell bodies residing in lamina I and in laminae III–IV, but not in lamina II (Liu, H. *et al.*, 1994a; Nakaya, Y. *et al.*, 1994). More recent studies, however, have identified NK-1r immunoreactivity in some neurons in LIIo (McLeod, A.L. *et al.*, 1998; Ribeiro-da-Silva, A. *et al.*, 2000). Most of the NK-1r-IR neurons project to higher levels, having targets such as the thalamus (Marshall, G. E. *et al.*, 1996), the parabrachial nucleus (Ding, Y.-Q. *et al.*, 1995; Todd, A. J. *et al.*, 2000), the lateral reticular nucleus, the dorsal part of caudal medulla, and, to a minor extent, the periaqueductal gray (Todd, A. J. *et al.*, 2000).

The receptor for neurokinin A (the neurokinin-2 receptor) hardly occurs in the CNS (for review see Ribeiro-da-Silva, A. *et al.*, 2000). Immunoreactivity for the neurokinin-2 receptor in the superficial spinal dorsal horn was rather weak and restricted to a narrow band in the lateral part of lamina I, and seemed to be localized in glial cells (Zerari, F. *et al.*, 1998). This is an unexpected finding that indicates that either neurokinin A acts through another receptor in the CNS or that it acts mainly in the periphery. There is evidence that NKA coreleased with SP from primary sensory fibers acts through the NK-1r and may be an important component of signaling through peptidergic afferent fibers (Trafton, J. A. *et al.*, 2001).

The preferential receptor for NKB, the neurokinin-3 receptor, was identified in cell bodies located in lamina I and, mostly, in lamina II (Ding, Y. Q. *et al.*, 1996; Zerari, F. *et al.*, 1997; Mileusnic, D. *et al.*, 1999; Ding, Y. Q. *et al.*, 2002). Interestingly, the cell populations that express the neurokinin-3 receptor coexpress either the μ-opioid receptor or GABA and nitric oxide synthase (NOS) (Ding, Y. Q. *et al.*, 2002).

5.23.4.4.3 CGRP and CGRP receptors

Immunoreactivity for CGRP in the spinal dorsal horn is restricted to primary sensory fibers in rodents, and likely in others species as well. Concerning CGRP receptors, their distribution has been studied with ligand binding and have been shown to occur in high density in lamina I and in deeper laminae but were sparse in lamina II (Yashpal, K. *et al.*, 1992). Curiously, following peripheral nerve lesion, CGRP receptors were upregulated in lamina II, indicating that lamina II cells have the capacity to synthesize the receptor (Kar, S. *et al.*, 1994).

5.23.4.4.4 Somatostatin

The neuropeptide SOM occurs both in primary sensory fibers (see above) and in dorsal horn neurons (Hökfelt, T. *et al.*, 1976; Alvarez, F. J. and Priestley, J. V., 1990; Ribeiro-da-Silva, A. and Cuello, A. C., 1990b). Cells bodies from SOM-IR neurons occur mainly in lamina II (Alvarez, F. J. and Priestley, J. V., 1990; Ribeiro-da-Silva, A. and Cuello, A. C., 1990b) and seem to be glutamatergic as they also express VGLUT2 (Todd, A. J. *et al.*, 2003). The receptors for SOM are G protein-coupled and form a family of five receptors (sst1 to sst5) (Dournaud, P. *et al.*, 2000). The distribution of these receptor subtypes has been studied with immunocytochemistry, and they have been found in cell bodies and processes in the superficial dorsal horn (Schulz, S. *et al.*, 1998; Von Banchet, G. S. *et al.*, 1999).

5.23.4.4.5 Opioid peptides

5.23.4.4.5.(i) Enkephalins Although there are two main enkephalins, met- and leu-enkephalin, no differences in distribution have been detected with antibodies generated against each of the two, and as they share a common precursor, *in situ* hybridization studies do not reveal differences in distribution either. Therefore, as in most studies, we refer to enkephalin immunoreactivity, not discriminating whether studies were done with antibodies raised against leu- or met-enkephalin. Enkephalin immunoreactivity is intense in axons and cell processes in laminae I and II (Hökfelt, T. *et al.*, 1977; Hunt, S. P. *et al.*, 1981) and has also been detected in neuronal cell bodies in laminae I–III (Del Fiacco, M. and Cuello, A. C., 1980; Hunt, S. P. *et al.*, 1981; Miller and Seybold, 1989). *In situ* hybridization studies have not detected any significant evidence for the presence of the enkephalin precursor signal in DRG neurons, beyond a few isolated cells (Ruda, M. A. *et al.*, 1989), and sensory deafferentation does not result in any decrease of enkephalin levels in the dorsal horn (Ruda, M. A. *et al.*, 1986). Therefore, almost all the enkephalin in the dorsal horn seems to be from local circuit neurons, with a minor component colocalized in axons from serotonergic neurons of the raphe nuclei that project to the spinal cord (Hökfelt, T. *et al.*, 1979); most such axons,

however, terminate in the ventral horn (Tashiro, T. *et al*., 1988; Menétrey, D. and Basbaum, A. I., 1987). A small percentage of enkephalinergic neurons project to the brain (Standaert, D. G. *et al*., 1986). Concerning enkephalin in neurons with cell bodies located in the dorsal horn, it occurs in two different populations of neurons: (a) cells that are SP-IR (Tashiro, T. *et al*., 1987; Senba, E. *et al*., 1988; Ribeiro-da-Silva, A. *et al*., 1991) and that likely are glutamatergic (Todd, A. J. *et al*., 2003); and (b) cells that are GABAergic (Todd, A. J. *et al*., 1992b). An interesting conclusion is that as all SP-IR neurons in the dorsal horn seem to possess enkephalin immunoreactivity, the colocalization of both peptides can be used as a marker to identify SP-IR fibers that are intrinsic to the dorsal horn (Ribeiro-da-Silva, A., 2004). The ultrastructural studies of SP and enkephalin double labeling have confirmed the colocalization of the two peptides in both rat and cat and provided evidence that enkephalin-IR boutons or presynaptic dendrites are never presynaptic to SP-IR boutons (Ribeiro-da-Silva, A. *et al*., 1991; Ma, W. *et al*., 1997). In the cat, enkephalin-IR boutons have been shown to contact spinothalamic neurons (Ruda, M. A. *et al*., 1984) and neurons of the dorsal column postsynaptic pathway (Nishikawa, N. *et al*., 1983). Our own data on physiologically characterized, intracellularly filled dorsal horn neurons, some of which likely projected to the brain, has shown that these cells had appositions from boutons colocalizing SP and enkephalin immunoreactivities and from boutons IR for only one of the peptides, which likely represented the population colocalizing enkephalin and GABA and the population colocalizing SP and CGRP (primary sensory in origin) (Ma, W. *et al*., 1997).

5.23.4.4.5.(ii) Dynorphins Most of the dynorphin in the dorsal horn is from spinal cord neurons, with a minor component at sacral levels from visceral afferents (see above). The distribution of the dynorphins in the dorsal horn has been studied both by immunocytochemistry with antibodies raised against dynorphin A and dynorphin B as well as by *in situ* hybridization using probes for the dynorphin precursor. The available data indicate that the dynorphins occur in axons and cells bodies in laminae I, IIo, and V, in both rat and cat (Cruz, L. and Basbaum, A. I., 1985; Miller, K. E. and Seybold, V. S., 1987; Leah, J. *et al*., 1988; Ruda, M. A. *et al*., 1988; Cho, H. J and Basbaum, A. I., 1989). These neurons have been reported as forming an heterogeneous population, although some neurons in LIIo resembled stalked cells (Cruz, L. and Basbaum, A. I., 1985; Cho, H. J. and Basbaum, A. I., 1989). The dynorphins are not restricted to local circuits neurons, as some of the neurons that express them project to the parabrachial nucleus (Standaert, D. G. *et al*., 1986).

5.23.4.4.5.(iii) Endormorphins Of the two endomorphins, endomorphin-2 is restricted to primary sensory fibers, where it is colocalized with SP (Martin-Schild, S. *et al*., 1998; Sanderson Nydahl K., *et al*., 2004). In contrast, endomorphin-1 is intrinsic to the CNS and occurs in fibers in laminae I and II (Martin-Schild, S. *et al*., 1999).

5.23.4.4.6 Opioid receptors

Besides occurring on primary sensory fibers (see above), opioid receptors are located on dorsal horn neurons as well. *In situ* hybridization cytochemistry has confirmed the occurrence of opioid receptors in dorsal horn neurons (Minami, M. and Satoh, M., 1995). The δ-opioid receptor occurs both on cell bodies and dendrites of dorsal horn neurons and in axon terminals (Cheng, P. Y. *et al*., 1995; 1997); some of the axon terminals expressing the receptor colocalize enkephalin (Cheng, P. Y. *et al*., 1995). In contrast, the κ receptor has been localized mostly in dendrites and cell bodies (Arvidsson, U. *et al*., 1995). Immunoreactivity for the μ receptor occurs mostly in lamina II (Honda, C. N. and Arvidsson, U., 1995; Kemp, T. *et al*., 1996), axon terminals, dendritic profiles, and cell bodies (Cheng, P. Y. *et al*., 1996; 1997). Most of the cell bodies displaying μ-opioid receptor immunoreactivity are located in lamina II and do not colocalize GABA or glycine immunoreactivities, which suggests that the neurons that express the μ receptor may be mostly excitatory interneurons (Kemp, T. *et al*., 1996).

5.23.4.4.7 Glutamate

It has been known for a long time that a high percentage of neurons in the dorsal horn are glutamatergic. However, the evidence was mostly indirect, as glutamate immunostaining is not a reliable marker of glutamatergic cells bodies (Ottersen, O. P. and Storm-Mathisen, J., 1984). Currently, the most reliable way of identifying glutamatergic dorsal horn neurons is the immunocytochemical detection of one of the vesicular glutamate transporters. However, because the immunoreactivity is located mostly in axonal terminals and is low in dendrites and cell bodies, we have to rely on colocalization studies to identify the glutamatergic neurons.

Colocalization studies have revealed that most non-primary sensory axonal varicosities in the dorsal horn that expressed SP, SOM, or neurotensin were IR for the vesicular glutamate transporter (VGLUT2), strongly indicating that these cell populations are glutamatergic (Todd, A. J. *et al.*, 2003). It is also assumed that most of the projection neurons, including the cells of lamina I, are glutamatergic, although direct immunocytochemical evidence is lacking. Systematic studies combining *in situ* hybridization for vesicular glutamate transporters are required to confirm this point.

5.23.4.4.8 Glutamate receptors

Besides occurring in primary sensory fibers (see section Receptors on Primary Sensory Fibers above), glutamate receptors have also been identified in dorsal horn neurons. Concerning the ionotropic glutamate receptors, their distribution has been studied with both *in situ* hybridization and immunocytochemistry. The predominant subunits of AMPA receptors in the dorsal horn are GluR1 and GluR2 (Furuyama, T. *et al.*, 1993; Jakowec, M. W. *et al.*, 1995a; 1995b), and the labeling of many cell bodies has been detected by immunocytochemistry. An interesting observation is that the GluR1 subunit is particularly associated with GABAergic neurons, while the GluR2 is mainly found in cells that lack GABA (Spike, R. C. *et al.*, 1998). Concerning NMDA receptors, the NR1 subunit is highly expressed in dorsal horn neurons (Tölle, T. R. *et al.*, 1993; Watanabe, M. *et al.*, 1994) and may be expressed by all cells. Less is known about the expression of the NR2 subunit of the NMDA receptor and of kainate receptors (Furuyama, T. *et al.*, 1993; Tölle, T. R. *et al.*, 1993; Watanabe, M. *et al.*, 1994). Metabotropic glutamate receptors are also expressed by dorsal horn neurons and of these the mGluR5 is the most prevalent (Berthele, A. *et al.*, 1999; Jia, H. *et al.*, 1999).

5.23.4.4.9 Inhibitory amino acids

5.23.4.4.9.(i) GABA The distribution of GABAergic neurons in the dorsal horn was originally studied by autoradiography using ^{3}H-GABA high-affinity uptake and by immunocytochemistry using anti-glutamic acid decarboxylase (GAD) antibodies (Ribeiro-da-Silva, A. and Coimbra, A., 1980; Hunt, S. P. *et al.*, 1981; Barber, R. P. *et al.*, 1982). Later studies used immunoreactivity for GABA itself (Todd, A. J. and McKenzie, J., 1989). A study in rat showed that GABAergic neurons were evenly distributed in laminae I–III, where they represented 24–33% or 28–46% of the overall neuronal population (Todd, A. J. and McKenzie, J., 1989; Todd, A. J. and Sullivan, A. C., 1990). Through a combination of GABA immunostaining and the Golgi method, some of the GABAergic neurons of lamina II were identified as islet cells, but never as stalked cells (Todd, A. J. and McKenzie, J., 1989). This observation is consistent with the observation of islet cells with presynaptic dendrites (Gobel, S. *et al.*, 1980; Spike, R. C. and Todd, A. J., 1992), which indicate an inhibitory function. Results from Lu Y. and Perl E. R. (2003; 2005) suggest that only the large islet cells of Todd A. J. (1986) (Figures 7 and 8) are GABAergic while small islet cells (central cell) are glutamatergic. Large islet cells appear to act as feed-forward inhibitory neurons to small islet cells (Lu, Y. and Perl, E. R., 2003) (Figure 8).

In the spinal cord, GABA participates in both presynaptic inhibition on terminals of primary afferents and postsynaptic inhibition of dorsal horn neurons. Morphological support for the involvement of GABAergic interneurons in presynaptic inhibition was obtained by demonstrating that these are presynaptic to primary sensory fibers; this evidence was obtained by means of a combination of GAD immunocytochemistry with nerve lesions in the rat (Barber, R. P. *et al.*, 1978) or with the intracellular filling of identified afferent fibers in the cat (Maxwell, D. J. and Noble, R., 1987). The identification of both presynaptic dendrites and peripheral axons in glomeruli presynaptic to their central bouton, of known primary sensory origin, provided further morphological support to the participation of GABAergic dorsal horn neurons in the presynaptic inhibition of primary sensory fibers (Todd, A. J., 1996; Ribeiro-da-Silva, A., 2004). In these presynaptic structures, GABA is colocalized with other neurochemicals, such as enkephalin, acetylcholine (Ribeiro-da-Silva, A., 2004), glycine (Todd, A. J., 1991; 1996), NPY, or galanin (Polgár, E. *et al.*, 1999b). A minor component of the GABAergic terminals in the dorsal horn originates from the brain stem (Antal, M. *et al.*, 1996), and a recent *in vivo* electrophysiological study provides evidence for descending monosynaptic GABAergic and/or glycinergic inputs from the rostral ventromedial medulla to the substantia gelatinosa (Kato, G. *et al.*, 2006).

5.23.4.4.9.(ii) Glycine Glycinergic neurons are found in most laminae of the dorsal horn; in laminae I–III, their proportion in the overall is considerably higher in lamina III (30%) than in lamina I (9%) or in

lamina II (14%) (Todd, A. J. and Sullivan, A. C., 1990). Virtually all glycinergic neurons in laminae I–III are also GABAergic (Todd, A. J. and Sullivan, A. C., 1990; Todd, A. J., 1991); however, only about half of the GABAergic cells colocalize glycine immunoreactivity (Todd, A. J. and Sullivan, A. C., 1990; Todd, A. J., 1991). Terminals colocalizing GABA and glycine immunoreactivities are presynaptic mostly to dendrites and cell bodies, except in LIIi and deeper dorsal horn where they are also presynaptic to primary sensory fibers in type II but not in type I glomeruli (Todd, A. J., 1996). There is indirect evidence that glycine is likely colocalized with GABA in some descending fibers from the brain stem (Kato, G. *et al.*, 2006).

5.23.4.4.10 GABA and glycine receptors

$GABA_A$ receptors seem to be ubiquitous in dorsal horn neurons, where their subunit precursors have been identified by *in situ* hybridization (Persohn, E. *et al.*, 1991) and their proteins by immunocytochemistry (Alvarez, F. J. *et al.*, 1996; Bohlhalter, S. *et al.*, 1996). The combination of $\alpha 3$, $\beta 3$, and $\gamma 2$ subunits appears to occur in cells throughout the dorsal horn, while $\alpha 1$ subunits are expressed by neurons in deeper laminae (Bohlhalter, S. *et al.*, 1996). An electron microscopic study using an antibody-recognizing subunits $\beta 2$–$\beta 3$ of the $GABA_A$ receptor revealed predominantly dendrite and cell body staining, with no direct evidence of labeling of sensory fibers (Alvarez, F. J. *et al.*, 1996).

A study of the distribution of immunoreactivity for the two subunits of the metabotropic $GABA_B$ receptor, $GABA_BR1$ and $GABA_BR2$, revealed that they occurred in highest concentrations in laminae I and II, where they were detected both in cell bodies and in the neuropile (Margeta-Mitrovic, M. *et al.*, 1999). The localization of the cell bodies that express the subunits of the $GABA_B$ receptor was confirmed by *in situ* hybridization (Towers, S. *et al.*, 2000).

Interestingly, in the dorsal horn, glycine receptors seem restricted to intrinsic neurons. Glycine receptors are ionotropic receptors made up of a combination of α and β subunits. The initial studies were performed with antibodies against gephyrin (a glycine- and GABA receptor-associated protein). These studies were performed at the time when it was thought that this protein was associated only with the glycine receptor. Surprisingly, these studies were rather accurate, as in the spinal cord, gephyrin-IR sites match the distribution of glycine receptors more closely than that of $GABA_A$ receptors (see e.g. Mitchell, K. *et al.*, 1993). One of the glycine receptor subunits (GlyR $\alpha 3$) has been found to be specifically expressed in the superficial laminae of the spinal dorsal horn, particularly in lamina II (Harvey, R. J. *et al.*, 2004), although the most abundant subunit in the adult spinal cord is the $\alpha 1$ (Becker, C. M. *et al.*, 1988). One interesting feature relative to the distribution of GABA and glycine receptors in the spinal cord is that many synapses colocalize GABA and glycine, and the specificity of the mixed GABA/glycine synapses seems to be determined by the expression, properties, and the subsynaptic localization of the $GABA_A$, $GABA_B$, and glycine receptors in the target cells (Chéry, N. and De Koninck, Y., 1999; 2000) and their changes during development (Keller, A. F. *et al.*, 2001).

It should be kept in mind that the great majority of GABA- and glycine-containing terminals are presynaptic to spinal neurons, not to primary afferent terminals (Todd, A. J. and Spike, R. C., 1993), and GABAergic and glycinergic interneurons control an important network of polysynaptic connections between primary afferents and dorsal horn neurons. For example, blockade of GABAergic and glycinergic inhibition unmasks low-threshold input to dorsal horn neurons that do not receive monosynaptic input from low-threshold afferents (Baba, H. *et al.*, 2003; Torsney, C. and MacDermott, A. B., 2006). Impaired inhibition is thus a likely substrate for cross talk between sensory modalities and appear to underlie allodynia characteristic of neuropathic pain syndromes (Moore, K. A. *et al.*, 2002; Coull, J. A. *et al.*, 2003; Coull, J. A. *et al.*, 2005).

5.23.4.4.11 Other classical transmitters and other neuropeptides

One of the better-defined transmitter-specific systems in the dorsal horn is the cholinergic one. In fact, neuronal perikarya IR for choline acetyltransferase (ChAT) have been identified in the spinal dorsal horn (Kimura, H. *et al.*, 1981; Barber, R. P. *et al.*, 1984; Todd, A. J., 1991). These neurons are not numerous, occur mainly in laminae III–IV, and are presynaptic to primary sensory fibers in synaptic glomeruli and to neurons (Ribeiro-da-Silva, A. and Cuello, A. C., 1990a). Interestingly, as mentioned above, most, if not all, of these cholinergic cell bodies and boutons colocalize GABA.

Regarding other transmitters, spinal serotonin originates from neurons with cell bodies in the brain stem (for review see Ruda, M. A. *et al.*, 1986). Interestingly, in the cat, these serotonin-IR profiles

have been shown to synapse on projection neurons (Ruda, M. A., 1986). These fibers colocalizes other transmitters such as enkephalin (Hökfelt, T. *et al.*, 1979) (see above) or SP and thyrotropin-releasing hormone (TRH) (Johansson, O. *et al.*, 1981). Another transmitter-specific system originating from the brain stem is the noradrenergic one. Although their light microscopic distribution and their origin in the brain stem are well known (Westlund, K. N. *et al.*, 1983; Fritschy, J. M. and Grzanna, R., 1990), there is still not much information about these noradrenergic fibers except that they are presynaptic to spinal dorsal horn neurons (Hagihira, S. *et al.*, 1990; Doyle, C. A. and Maxwell, D. J., 1991). Interestingly, noradrenergic analgesia appears to involve presynaptic inhibition of glutamate release from α2c-adrenergic terminals of local excitatory interneurons (Olave, M. J. and Maxwell, D. J., 2002; 2003a) contacting NK-1r-IR projection neurons (Olave, M. J. and Maxwell, D. J., 2003b). Neurotensin immunoreactivity occurs in neurons in laminae I and II (Hunt, S. P. *et al.*, 1981; Seybold, V. S. and Elde, R. P., 1982), which do not colocalize GABA (Todd, A. J. *et al.*, 1992a) but do express VGLUT2, and are likely glutamatergic (Todd, A. J. *et al.*, 2003). Furthermore, most of the neurotensin-IR neurons in LIIi express protein kinase C gamma (Polgár, E. *et al.*, 1999a).

5.23.5 Identified Neuronal Circuits

While our knowledge of synaptic circuits in the dorsal horn remains limited, some patterns are emerging based on recent findings. Figure 9 attempts to summarize some observations described above. It should be noted here that there are significant interspecies differences in the neurochemical and anatomical organization of the region. Thus some of the proposed circuits may not hold across all species.

One should stress here that, while we propose well-defined circuits, not all chemical communication involves hard-wired synapses (Zoli, M. *et al.*, 1999). Nonsynaptic or paracrine transmission is thought to occur particularly with peptides and monoamines; however, it probably occurs for amino acid transmitters also acting both on their ionotropic and metabotropic receptors (Rossi, D. and Hamann, M., 1998; Chéry, N. and De Koninck, Y., 1999; 2000). Whereas under physiological conditions, most interneuronal communication in the dorsal horn probably takes place either at synapses or close to the site of release, diffusion of neurochemicals over longer distances cannot be excluded, particularly in the case of neuropeptides. Nevertheless, it should be kept in mind that the neuropile represents a significant diffusion barrier, and it is unlikely that even peptides diffuse large distances when released at physiological concentrations. Therefore, a detailed description of the chemical neuroanatomy of the dorsal horn circuits is important to understand sensory processing.

As most synapses in the dorsal horn are axodendritic, it is not surprising that the majority of interneurons appear to act on their targets through a postsynaptic mechanism; however, some cells clearly participate in presynaptic interactions. GABAergic axons, which are thought to originate from local interneurons, establish axoaxonic synapses on the central boutons of synaptic glomeruli, except for those in peptidergic (type Ib) glomeruli that are seldom postsynaptic to other profiles. There is a fundamental difference between the types of GABAergic neurons that innervate type Ia and type II glomeruli, because boutons containing GABA and glycine are presynaptic to the central boutons of type II, but not to type Ia glomeruli (Todd, A. J., 1996). In contrast, neurons colocalizing GABA and enkephalin immunoreactivities seem to innervate central axons of type I and II glomeruli equally (through both axoaxonic and dendroaxonic synapses) (Ribeiro-da-Silva, A., 2004). The population of neurons with GABA and ChAT is relatively small (Todd, A. J., 1991); however, their axons contribute a significant contingent of axoaxonic synapses in type II, and to a lesser extent in type Ia, glomeruli (Ribeiro-da-Silva, A. and Cuello, A. C., 1990a; Ribeiro-da-Silva, A., 2004). The neurons with GABA and acetylcholine (revealed by ChAT immunoreactivity) have cell bodies in laminae III and IV and dendrites that extend superficially, where they receive synaptic input from primary afferents in both type Ia and type II glomeruli. Cells that colocalize GABA and NPY appear to selectively target NK-1r-IR laminae III/IV projection neurons, with which they make numerous axodendritic and axosomatic synapses (Polgár, E. *et al.*, 1999b).

As discussed above, most (if not all) of the SP-containing neurons in the superficial laminae are also enkephalin-IR (Ribeiro-da-Silva, A. *et al.*, 1991). They are located in laminae I and II and receive synaptic input from nonpeptidergic C fibers in type Ia glomeruli and from SP-containing afferents outside glomeruli. Interestingly, based on evidence

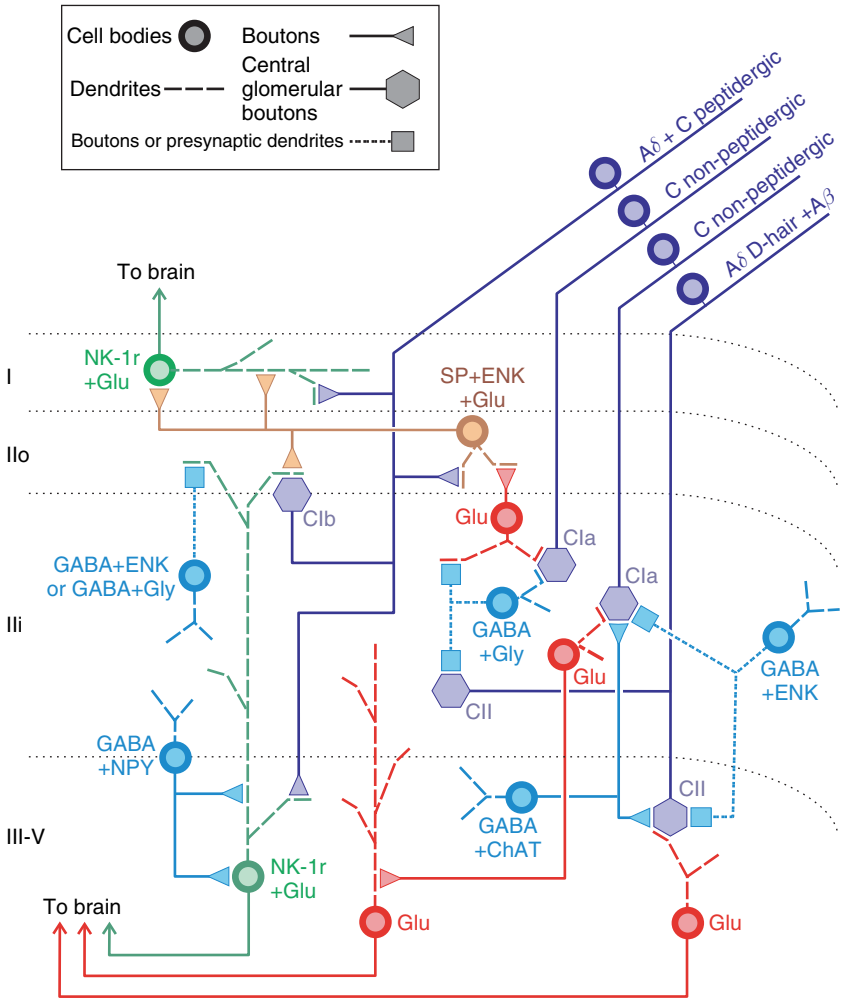

Figure 9 Summary diagram of neuronal circuits in the dorsal horn. Different synaptic arrangements involve the different classes of primary afferents endings in the dorsal horn (glomerular and nonglomerular). In particular, the glomerular structures are exquisite sites of presynaptic modulation of afferent inputs. Yet, it should be kept in mind that, while this diagram highlights the different presynaptic arrangements in which the different populations of GABAergic interneurons are involved, most GABAergic and glycinergic synapses remain axodendritic and axosomatic in the dorsal horn. While physiological studies indicate that Aδ high-threshold mechanoreceptors (HTM) provide input to laminae I and V, further information on the synaptic arrangements they are involved in is unavailable due to the lack of specific markers for these types of afferents. Peptidergic Aδ and C nociceptors are known to contact spinal projection neurons that express the NK-1 receptor both in laminae I and V. The substance P (SP)–enkephalin (ENK)–Glu interneuron positioned in lamina IIo represents a prototype stalked cell, which, for the sake of simplicity, accounts for both the circuitry illustrated in Figure 8 based on the physiological data (see Lu, Y. and Perl, E. R., 2003; 2005) and that based on what is known of the peptidergic circuitry (Ribeiro-da-Silva, A. *et al.*, 1991). It remains to be confirmed, however, whether a single type of stalked cell, expressing SP, ENK, and glutamate, constitutes a common pathway to lamina I projection neurons or whether parallel circuits are involved. Two nonpeptidergic afferent pathways are illustrated to account for the possibility that parallel circuits with no cross talk at the level of the dorsal horn may connect to ascending pathways (see text for further details; Braz, J. M. *et al.*, 2005).

from studies in the cat (Ma, W. *et al.*, 1997), these neurons seem to preferentially innervate nociceptive neurons in lamina I and in the deep dorsal horn, which probably express the NK-1r (Figure 9).

Finally, these findings, together with those of Lu Y. and Perl E. R. (2003; 2005) and the evidence of a parallel pathway via laminae II–V (Braz, J. M. *et al.*, 2005) (see above) that exclude NK-1r-expressing cells, suggest that distinct subclasses of nonpeptidergic afferents connect to laminae I and V ascending pathways with virtually no cross talk at the level of the dorsal horn (Figure 9).

5.23.6 Conclusion and Future Directions

An important conclusion of this review is that, despite all the progress, we are still unable to answer a few very basic questions regarding the synaptic organization of the dorsal horn. This is in part a consequence of the heterogeneity of neuronal populations in each layer and therefore the difficulty to properly identify subtypes of neurons in functional studies (in contrast with highly organized structures like the cerebellum, hippocampus, and even neocortex).

For example, while a significant amount of data on the organization of inhibitory circuits is available from purely morphological and immunocytochemical studies, little is known at the functional level, in part because of the difficulty to identify GABAergic and glycinergic interneurons for targeted electrophysiological recording. This is likely to change, thanks to the growing availability of transgenic mice that express enhanced green fluorescent protein (GFP) in specific subpopulations of inhibitory interneurons (e.g., under the control of the promoter for glutamic acid decarboxylase or the glycine transporter 2) (Hantman, A. W. *et al.*, 2004; Heinke, B. *et al.*, 2004; Dougherty, K. J. *et al.*, 2005; Zeilhofer, H. U. *et al.*, 2005). The same is true for subpopulations of interneurons that are associated with other specific markers (e.g., neuropeptides and calbindin).

Emerging classification schemes, based on combinations of morphological features, transmitter and receptor phenotypes, and electrophysiological properties (Thomson, A. M. *et al.*, 1989; Yoshimura, M. and Jessell, T. M. 1989; Lopez-Garcia, J. A. and King, A. E., 1994; Han, Z. S. *et al.*, 1998; Jo, Y. H. *et al.*, 1998; Yu, X. H. *et al.*, 1999; Grudt, T. J. and Perl, E. R., 2002; Prescott, S. A. and De Koninck, Y., 2002; Ruscheweyh, R. and Sandkuhler, J., 2002; Ruscheweyh, R. *et al.*, 2004; Hantman, A. W. and Perl, E. R., 2005; Yu, X. H. *et al.*, 2005), will also be critical to better understand the organization of neuronal circuits in the dorsal horn. Indeed, studies combining electrophysiological recording and intracellular labeling with immunocytochemistry remain critical to obtain a finer identification of neuronal subpopulations and their function as well as to obtain a more complete picture of the afferent and efferent connections of transmitter-specific interneurons; however, such approaches are technically demanding and remain insufficiently used (De Koninck, Y. *et al.*, 1992; Ribeiro-da-Silva, A. *et al.*, 1992; Ma, W. *et al.*, 1996; 1997; Lawson, S. N. *et al.*, 1997; 2002).

An important challenge for the future will also be to better unravel the functional significance of the multiple transmitter signals originating from the same cells and the same synaptic terminals. For example, the functional meaning of the corelease of GABA and glycine (Chéry, N. and De Koninck, Y., 1999) – two very similar neurotransmitters – from the same terminals remains elusive in a large part. Several synapses also appear to use opposing transmitters, such as SP and enkephalin (Ribeiro-da-Silva, A. *et al.*, 1991) or GABA and ATP (Jo, Y. H. and Schlichter, R., 1999); whether these involve local feedback systems, differential release conditions, or nonlinear modes of action (Kupfermann, I., 1991; Nusbaum, M. P. *et al.*, 2001) remains to be determined. Several of these questions continue to be elusive simply because the modes of action of several neuropeptides remain incompletely understood. Target-selective expression of receptors may determine the functional meaning of the mixed transmitter signals released from the same neuron. For example, when GABA and glycine are colocalized in axoaxonic contacts with primary afferent terminals, only $GABA_A$ and $GABA_B$ are expressed on those terminals; the glycinergic signal must only be meaningful at other synapses from the same presynaptic neuron or acting on receptors located on dendrites neighboring the release site (Rossi, D. and Hamann, M., 1998). In the same line, fine subcellular segregation of receptors in the target cells may have very significant impact on how mixed transmitter signals are decoded by the postsynaptic cell (see e.g., Chéry, N. and De Koninck, Y., 1999; 2000; Keller, A. F. *et al.*, 2001).

While important information has arisen from the use of markers of specific primary afferent subclasses, it is necessary to develop more refined classification schemes. For example, both on anatomical and physiological grounds, the current classification schemes of peptidergic and nonpeptidergic C-fiber afferents (e.g., binding IB4 or expressing CGRP) remains too general to account for the existing diversity of subclasses. The search for newer cell surface markers or the development of transgenic models expressing GFP in specific subpopulations of cells will be important to unravel the synaptic circuitry and functional role of each subclass of afferents and their spinal dorsal horn targets.

An important issue to keep in mind that may be an important limitation in our current understanding is the occurrence of interspecies differences. For

example, many of the original studies on neurons characterized physiologically and labeled intracellularly with injections of markers have been performed in the cat, whereas tract-tracing and immunocytochemical studies have generally been carried out in the rat and the monkey, while studies relying on transgenic tools have to be conducted in the mouse. Many of these species differences have been described earlier in this chapter. One difference that may be worth stressing again is the fact that the TRPV1 receptor is restricted to the peptidergic afferents in the mouse, but not in the rat (see above), raising concerns about the use of mouse transgenic models to study the function of this and other receptors.

While currently much emphasis is naturally placed on studying direct interactions between pairs of neurons to unravel the synaptic circuitry in the dorsal horn, a better understanding of the organization of the network will eventually require the integrative study of polysynaptic pathways (e.g., from primary afferents to spinal projection neurons). For example, cross talk between ascending pathways by means of polysynaptic connections regulated by local inhibitory circuits in the dorsal horn is likely a critical element underlying plasticity and pathology of the pain system (Yaksh, T. L., 1989; Sherman, S. E. and Loomis, C.W., 1994; Baba, H. *et al.*, 2003; Torsney, C. and MacDermott, A. B., 2006).

In summary, novel tools are emerging to allow us to improve our understanding of the structural and functional organization of the dorsal horn. These include novel markers, especially markers compatible with live cell studies such as transgenic animals expressing GFP in specific cell types (Hantman, A. W. *et al.*, 2004; Heinke, B. *et al.*, 2004; Dougherty, K. J. *et al.*, 2005; Zeilhofer, H. U. *et al.*, 2005) and the use of specific fluorescent ligands compatible with live cell studies (see e.g., Labrakakis, C. *et al.*, 2003; Labrakakis, C. and MacDermott, A. B., 2003). Novel methods are also emerging to identify neuronal pathways such as transsynaptic markers (Jasmin, L. *et al.*, 1997; Kissa, K. *et al.*, 2002; Braz, J. M. *et al.*, 2005). It also remains critical to combine these tools with other approaches to establish correlations between different identifiers of cell structure and function (e.g., morphology, transmitter/receptor phenotype, and electrophysiological properties). These steps are important to obtain a better grasp of the organization of the dorsal horn, which remains an essential condition for the understanding of nociceptive processing as well as of the neural basis of altered nociception in chronic pain conditions.

References

Almarestani, L., Waters, S. M., Krause, J. E., Bennett, G. J., and Ribeiro-da-Silva, A. 2007. Morphological characterization of spinal cord dorsal horn lamina I neurons projecting to the parabrachial nucleus in the rat. J. Comp. Neurol., in press.

Alvarez, F. J. and Fyffe, R. E. 2000. Nociceptors for the 21st century. Curr. Rev. Pain 4, 451–458.

Alvarez, F. J. and Priestley, J. V. 1990. Anatomy of somatostatin-immunoreactive fibres and cell bodies in the rat trigeminal subnucleus caudalis. Neuroscience 38, 343–357.

Alvarez, F. J., Kavookjian, A. M., and Light, A. R. 1992. Synaptic interactions between GABA-immunoreactive profiles and the terminals of functionally defined myelinated nociceptors in the monkey and cat spinal cord. J. Neurosci. 12, 2901–2917.

Alvarez, F. J., Kavookjian, A. M., and Light, A. R. 1993. Ultrastructural morphology, synaptic relationships, and CGRP immunoreactivity of physiologically identified C-fiber terminals in the monkey spinal cord. J. Comp. Neurol. 329, 472–490.

Alvarez, F. J., Taylor-Blake, B., Fyffe, R. E. W., de Blas, A. L., and Light, A. R. 1996. Distribution of immunoreactivity for the β_2 and β_3 subunits of the $GABA_A$ receptor the mammalian spinal cord. J. Comp. Neurol. 365, 392–412.

Amaya, F., Decosterd, I., Samad, T. A., Plumpton, C., Tate, S., Mannion, R. J., Costigan, M., and Woolf, C. J. 2000. Diversity of expression of the sensory neuron-specific TTX-resistant voltage-gated sodium ion channels SNS and SNS2. Mol. Cell Neurosci. 15, 331–342.

Andrew, D., Krout, K. E., and Craig, A. D. 2003. Differentiation of lamina I spinomedullary and spinothalamic neurons in the cat. J. Comp. Neurol. 458, 257–271.

Antal, M., Petko, M., Polgár, E., Heizmann, C. W., and Storm-Mathisen, J. 1996. Direct evidence of an extensive GABAergic innervation of the spinal dorsal horn by fibres descending from the rostral ventromedial medulla. Neuroscience 73, 509–518.

Arvidsson, U., Riedl, M., Chakrabarti, S., Vulchanova, L., Lee, J.-H., Nakano, A. H., Lin, X., Loh, H. H., Law, P.-Y., Wessendorf, M. W., and Elde, R. 1995. The kappa-opioid receptor is primarily postsynaptic: combined immunohistochemical localization of the receptor and endogenous opioids. Proc. Natl. Acad. Sci. U. S. A. 92, 5062–5066.

Baba, H., Ji, R. R., Kohno, T., Moore, K. A., Ataka, T., Wakai, A., Okamoto, M., and Woolf, C. J. 2003. Removal of GABAergic inhibition facilitates polysynaptic A fiber-mediated excitatory transmission to the superficial spinal dorsal horn. Mol. Cell Neurosci. 24, 818–830.

Barber, R. P., Phelps, P. E., Houser, C. R., Crawford, G. D., Salvaterra, P. M., and Vaughn, J. E. 1984. The morphology and distribution of neurons containing choline acetyltransferase in the adult rat spinal cord: an immunohistochemical study. J. Comp. Neurol. 229, 329–346.

Barber, R. P., Vaughn, J. E., and Roberts, E. 1982. The cytoarchitecture of GABAergic neurons in rat spinal cord. Brain Res. 238, 305–328.

Barber, R. P., Vaughn, J. E., Saito, K., McLaughlin, B. J., and Roberts, E. 1978. GABAergic terminals are presynaptic to

primary afferent terminals in the substantia gelatinosa of the rat spinal cord. Brain Res. 141, 35–55.
Bardoni, R., Torsney, C., Tong, C. K., Prandini, M., and MacDermott, A. B. 2004. Presynaptic NMDA receptors modulate glutamate release from primary sensory neurons in rat spinal cord dorsal horn. J. Neurosci. 24, 2774–2781.
Basbaum, A. I., Cruz, L., and Weber, E. 1986. Immunoreactive dynorphin B in sacral primary afferent fibers of the cat. J. Neurosci. 6, 127–133.
Battaglia, G. and Rustioni, A. 1988. Coexistence of glutamate and substance P in dorsal root ganglion neurons of the rat and monkey. J. Comp. Neurol. 277, 302–312.
Battaglia, G. and Rustioni, A. 1992. Substance P innervation of the rat and cat thalamus. II. Cells of origin in the spinal cord. J. Comp. Neurol. 315, 473–486.
Becker, C. M., Hoch, W., and Betz, H. 1988. Glycine receptor heterogeneity in rat spinal cord during postnatal development. EMBO J. 7, 3717–3726.
Bennett, G. J., Abdelmoumene, M., Hayashi, H., and Dubner, R. 1980. Physiology and morphology of substantia gelatinosa neurons intracellularly stained with horseradish peroxidase. J. Comp. Neurol. 194, 809–827.
Bennett, D. L. H., Michael, G. J., Ramachandran, N., Munson, J. B., Averill, S., Yan, Q., McMahon, S. B., and Priestley, J. V. 1998. A distinct subgroup of small DRG cells express GDNF receptor components and GDNF is protective for these neurons after nerve injury. J. Neurosci. 18, 3059–3072.
Berthele, A., Boxall, S. J., Urban, A., Anneser, J. M., Zieglgänsberger, W., Urban, L., and Tölle, T. R. 1999. Distribution and developmental changes in metabotropic glutamate receptor messenger RNA expression in the rat lumbar spinal cord. Dev. Brain Res. 112, 39–53.
Bicknell, H. R. and Beal, J. A. 1984. Axonal and dendritic development of substantia gelatinosa neurons in the lumbosacral spinal cord of the rat. J. Comp. Neurol. 226, 508–522.
Birder, L. A. and Perl, E. R. 1999. Expression of α_2-adrenergic receptors in rat primary afferent neurones after peripheral nerve injury or inflammation. J. Physiol. (Lond.) 515, 533–542.
Bohlhalter, S., Weinmann, O., Mohler, H., and Fritschy, J. M. 1996. Laminar compartmentalization of $GABA_A$-receptor subtypes in the spinal cord: an immunohistochemical study. J. Neurosci. 16, 283–297.
Bradbury, E. J., Burnstock, G., and McMahon, S. B. 1998. The expression of $P2X_3$ purinoreceptors in sensory neurons: Effects of axotomy and glial-derived neurotrophic factor. Mol. Cell. Neurosci. 12, 256–268.
Braz, J. M., Nassar, M. A., Wood, J. N., and Basbaum, A. I. 2005. Parallel ''pain'' pathways arise from subpopulations of primary afferent nociceptor. Neuron 47, 787–793.
Brown, A. G. 1982. The dorsal horn of the spinal cord. Q. J. Exp. Physiol. 67, 193–212.
Brown, J. L., Liu, H., Maggio, J. E., Vigna, S. R., Mantyh, P. W., and Basbaum, A. I. 1995. Morphological characterization of substance P receptor-immunoreactive neurons in the rat spinal cord and trigeminal nucleus caudalis. J. Comp. Neurol. 356, 327–344.
Cairns, B. E., Sessle, B. J., and Hu, J. W. 1998. Evidence that excitatory amino acid receptors within the temporomandibular joint region are involved in the reflex activation of the jaw muscles. J. Neurosci. 18, 8056–8064.
Carter, M. S. and Krause, J. E. 1990. Structure, expression, and some regulatory mechanisms of the rat preprotachykinin gene encoding substance P, neurokinin A, neuropeptide K, and neuropeptide gamma. J. Neurosci. 10, 2203–2214.
Caterina, M. J. 2003. Vanilloid receptors take a TRP beyond the sensory afferent. Pain 105, 5–9.
Cheng, P. Y., Liu-Chen, L. Y., and Pickel, V. M. 1997. Dual ultrastructural immunocytochemical labeling of μ and δ opioid receptors in the superficial layers of the rat cervical spinal cord. Brain Res. 778, 367–380.
Cheng, P. Y., Moriwaki, A., Wang, J. B., Uhl, G. R., and Pickel, V. M. 1996. Ultrastructural localization of μ-opioid receptors in the superficial layers of the rat cervical spinal cord: Extrasynaptic localization and proximity to Leu^5-enkephalin. Brain Res. 731, 141–154.
Cheng, P. Y., Svingos, A. L., Wang, H., Clarke, C. L., Jenab, S., Beczkowska, I. W., Inturrisi, C. E., and Pickel, V. M. 1995. Ultrastructural immunolabeling shows prominent presynaptic vesicular localization of δ-opioid receptor within both enkephalin- and nonenkephalin-containing axon terminals in the superficial layers of the rat cervical spinal cord. J. Neurosci. 15, 5976–5988.
Chéry, N. and De Koninck, Y. 1999. Junctional versus extrajunctional glycine and $GABA_A$ receptor-mediated IPSCs in identified lamina I neurons of the adult rat spinal cord. J. Neurosci. 19, 7342–7355.
Chéry, N. and De Koninck, Y. 2000. $GABA_B$ receptors are the first target of released GABA at lamina I inhibitory synapses in the adult rat spinal cord. J. Neurophysiol. 84, 1006–1011.
Cho, H. J. and Basbaum, A. I. 1989. Ultrastructural analysis of dynorphin B-immunoreactive cells and terminals in the superficial dorsal horn of the deafferented spinal cord of the rat. J. Comp. Neurol. 281, 193–205.
Coimbra, A., Ribeiro-da-Silva, A., and Pignatelli, D. 1984. Effects of dorsal rhizotomy on the several types of primary afferent terminals in laminae I–III of the rat spinal cord. An electron microscope study. Anat. Embryol. (Berl.) 170, 279–287.
Coimbra, A., Sodré-Borges, B. P., and Magalhães, M. M. 1974. The substantia gelatinosa Rolandi of the rat. Fine structure, cytochemistry (acid phosphatase) and changes after dorsal root section. J. Neurocytol. 3, 199–217.
Coull, J. A., Beggs, S., Boudreau, D., Boivin, D., Tsuda, M., Inoue, K., Gravel, C., Salter, M. W., and De Koninck, Y. 2005. BDNF from microglia causes the shift in neuronal anion gradient underlying neuropathic pain. Nature 438, 1017–1021.
Coull, J. A., Boudreau, D., Bachand, K., Prescott, S. A., Nault, F., Sik, A., De Koninck, P., and De Koninck, Y. 2003. Trans-synaptic shift in anion gradient in spinal lamina I neurons as a mechanism of neuropathic pain. Nature 424, 938–942.
Cox, J. J., Reimann, F., Nicholas, A. K., Thornton, G., Roberts, E., Springell, K., Karbani, G., Jafri, H., Mannan, J., Raashid, Y., Al-Gazali, L., Hamamy, H., Valente, E. M., Gorman, S., Williams, R., McHale, D. P., Wood, J. N., Gribble, F. M., and Woods, C. G. 2006. An SCN9A channelopathy causes congenital inability to experience pain. Nature 444, 894–898.
Craig, A. D. and Bushnell, M. C. 1994. The thermal grill illusion: unmasking the burn of cold pain. Science 265, 252–255.
Craig, A. D. and Kniffki, K. D. 1985. Spinothalamic lumbosacral lamina I cells responsive to skin and muscle stimulation in the cat. J. Physiol. (Lond.) 365, 197–221.
Cruz, L. and Basbaum, A. I. 1985. Multiple opioid peptides and the modulation of pain: immunohistochemical analysis of dynorphin and enkephalin in the trigeminal nucleus caudalis and spinal cord of the cat. J. Comp. Neurol. 240, 331–348.
Dalsgaard, C. J., Haegerstrand, A., Theodorsson-Norheim, E., Brodin, E., and Hökfelt, T. 1985. Neurokinin A-like immunoreactivity in rat primary sensory neurons; coexistence with substance P. Histochemistry 83, 37–39.
De Biasi, S. and Rustioni, A. 1988. Glutamate and substance P coexist in primary afferent terminals in the superficial laminae of spinal cord. Proc. Natl. Acad. Sci. U. S. A. 85, 7820–7824.

De Koninck, Y., Ribeiro-da-Silva, A., Henry, J. L., and Cuello, A. C. 1992. Spinal neurons exhibiting a specific nociceptive response receive abundant substance P-containing synaptic contacts. Proc. Natl. Acad. Sci. U. S. A. 89, 5073–5077.

Del Fiacco, M. and Cuello, A. C. 1980. Substance P-and enkephalin-containing neurones in the rat trigeminal system. Neuroscience 5, 803–815.

Ding, Y. Q., Lu, C. R., Wang, H., Su, C. J., Chen, L. W., Zhang, Y. Q., and Ju, G. 2002. Two major distinct subpopulations of neurokinin-3 receptor-expressing neurons in the superficial dorsal horn of the rat spinal cord. Eur. J. Neurosci. 16, 551–556.

Ding, Y. Q., Shigemoto, R., Takada, M., Ohishi, H., Nakanishi, S., and Mizuno, N. 1996. Localization of the neuromedin K receptor (NK3) in the central nervous system of the rat. J. Comp. Neurol. 364, 290–310.

Ding, Y.-Q., Takada, M., Shigemoto, R., and Mizuno, N. 1995. Spinoparabrachial tract neurons showing substance P receptor- like immunoreactivity in the lumbar spinal cord of the rat. Brain Res. 674, 336–340.

Djouhri, L. and Lawson, S. N. 2004. A beta-fiber nociceptive primary afferent neurons: a review of incidence and properties in relation to other afferent A-fiber neurons in mammals. Brain Res. Rev. 46, 131–145.

Djouhri, L., Fang, X., Okuse, K., Wood, J. N., Berry, C. M., and Lawson, S. N. 2003. The TTX-resistant sodium channel Nav1.8 (SNS/PN3): expression and correlation with membrane properties in rat nociceptive primary afferent neurons. J. Physiol 550, 739–752.

Dostrovsky, J. O. and Craig, A. D. 1996. Cooling-specific spinothalamic neurons in the monkey. J. Neurophysiol. 76, 3656–3665.

Dougherty, K. J., Sawchuk, M. A., and Hochman, S. 2005. Properties of mouse spinal lamina I GABAergic interneurons. J. Neurophysiol. 94, 3221–3227.

Dournaud, P., Slama, A., Beaudet, A., and Epelbaum, J. 2000. Somatostatin Receptors. In: Peptide Receptors, Part 1 (*eds*. R. Quirion, A. Björklund, and T. Hökfelt), pp. 1–43. Elsevier Science.

Doyle, C. A. and Maxwell, D. J. 1991. Ultrastructural analysis of noradrenergic nerve terminals in the cat lumbosacral spinal dorsal horn: A dopamine-β- hydroxylase immunocytochemical study. Brain Res. 563, 329–333.

Engelman, H. S. and MacDermott, A. B. 2004. Presynaptic ionotropic receptors and control of transmitter release. Nat. Rev. Neurosci. 5, 135–145.

Fields, H. L., Emson, P. C., Leigh, B. K., Gilbert, R. F., and Iversen, L. L. 1980. Multiple opiate receptor sites on primary afferent fibres. Nature 284, 351–353.

Flores, C. M., DeCamp, R. M., Kilo, S., Rogers, S. W., and Hargreaves, K. M. 1996. Neuronal nicotinic receptor expression in sensory neurons of the rat trigeminal ganglion: demonstration of $\alpha 3\beta 4$, a novel subtype in the mammalian nervous system. J. Neurosci. 16, 7892–7901.

Fritschy, J. M. and Grzanna, R. 1990. Demonstration of two separate descending noradrenergic pathways to the rat spinal cord: evidence for an intragriseal trajectory of locus coeruleus axons in the superficial layers of the dorsal horn. J. Comp. Neurol. 291, 553–582.

Furuyama, T., Kiyama, H., Sato, K., Park, H. T., Maeno, H., Takagi, H., and Tohyama, M. 1993. Region-specific expression of subunits of ionotropic glutamate receptors (AMPA-type, KA-type and NMDA receptors) in the rat spinal cord with special reference to nociception. Mol. Brain Res. 18, 141–151.

Gilbert, R. F., Emson, P. C., Hunt, S. P., Bennett, G. W., Marsden, C. A., Sandberg, B. E., Steinbusch, H. W., and Verhofstad, A. A. 1982. The effects of monoamine neurotoxins on peptides in the rat spinal cord. Neuroscience 7, 69–87.

Gobel, S. 1975. Golgi studies of the substantia gelatinosa neurons in the spinal trigeminal nucleus. J. Comp. Neurol. 162, 397–416.

Gobel, S. 1978a. Golgi studies of the neurons in layer I of the dorsal horn of the medulla (trigeminal nucleus caudalis). J. Comp. Neurol. 180, 375–393.

Gobel, S. 1978b. Golgi studies of the neurons in layer II of the dorsal horn of the medulla (trigeminal nucleus caudalis). J. Comp. Neurol. 180, 395–414.

Gobel, S., Falls, W. M., Bennett, G. J., Abdelmoumene, M., Hayashi, H., and Humphrey, E. 1980. An EM analysis of the synaptic connections of horseradish peroxidase-filled stalked cells and islet cells in the substantia gelatinosa of the adult cat spinal cord. J. Comp. Neurol. 194, 781–807.

Grant, G. and Robertson, B. 2004. Primary Afferent Projections to the Spinal Cord. In: The Rat Nervous System (*ed*. G. Paxinos), pp. 111–119. Elsevier Academic Press.

Grudt, T. J. and Perl, E. R. 2002. Correlations between neuronal morphology and electrophysiological features in the rodent superficial dorsal horn. J. Physiol. (Lond.) 540, 189–207.

Guo, A., Simone, D. A., Stone, L. S., Fairbanks, C. A., Wang, J., and Elde, R. 2001. Developmental shift of vanilloid receptor 1 (VR1) terminals into deeper regions of the superficial dorsal horn: correlation with a shift from TrkA to Ret expression by dorsal root ganglion neurons. Eur. J. Neurosci. 14, 293–304.

Guo, A., Vulchanova, L., Wang, J., Li, X., and Elde, R. 1999. Immunocytochemical localization of the vanilloid receptor 1 (VR1): relationship to neuropeptides, the $P2X_3$ purinoceptor and IB4 binding sites. Eur. J. Neurosci. 11, 946–958.

Haberberger, R., Henrich, M., Couraud, J. Y., and Kummer, W. 1999. Muscarinic M2-receptors in rat thoracic dorsal root ganglia. Neurosci. Lett. 266, 177–180.

Hagihira, S., Senba, E., Yoshida, S., Tohyama, M., and Yoshiya, I. 1990. Fine structure of noradrenergic terminals and their synapses in the rat spinal dorsal horn: an immunohistochemical study. Brain Res. 526, 73–80.

Han, Z. S., Zhang, E. T., and Craig, A. D. 1998. Nociceptive and thermoreceptive lamina I neurons are anatomically distinct. Nat. Neurosci. 1, 218–225.

Hantman, A. W. and Perl, E. R. 2005. Molecular and genetic features of a labeled class of spinal substantia gelatinosa neurons in a transgenic mouse. J. Comp. Neurol. 492, 90–100.

Hantman, A. W., van den Pol, A. N., and Perl, E. R. 2004. Morphological and physiological features of a set of spinal substantia gelatinosa neurons defined by green fluorescent protein expression. J. Neurosci. 24, 836–842.

Harmann, P. A., Chung, K., Briner, R. P., Westlund, K. N., and Carlton, S. M. 1988. Calcitonin gene-related peptide (CGRP) in the human spinal cord: a light and electron microscopic analysis. J. Comp. Neurol. 269, 371–380.

Harvey, R. J., Depner, U. B., Wassle, H., Ahmadi, S., Heindl, C., Reinold, H., Smart, T. G., Harvey, K., Schutz, B., bo-Salem, O. M., Zimmer, A., Poisbeau, P., Welzl, H., Wolfer, D. P., Betz, H., Zeilhofer, H. U., and Muller, U. 2004. GlyR alpha3: an essential target for spinal PGE2-mediated inflammatory pain sensitization. Science 304, 884–887.

Heinke, B., Ruscheweyh, R., Forsthuber, L., Wunderbaldinger, G., and Sandkuhler, J. 2004. Physiological, neurochemical and morphological properties of a subgroup of GABAergic spinal lamina II neurones identified by expression of green fluorescent protein in mice. J. Physiol. 560, 249–266.

Henry, J. L. 1976. Effects of substance P on functionally identified units in cat spinal cord. Brain Res. 114, 439–451.

Hökfelt, T., Elde, R., Johansson, O., Luft, R., Nilsson, G., and Arimura, A. 1976. Immunohistochemical evidence for

separate populations of somatostatin-containing and substance P-containing primary afferent neurons in the rat. Neuroscience 1, 131–136.

Hökfelt, T., Ljungdahl, A., Steinbusch, H. W., Verhofstad, A. N., Nilsson, G., Brodin, E., Pernow, B., and Goldstein, M. 1978. Immunohistochemical evidence of substance P-like immunoreactivity in some 5-hydroxytryptamine-containing neurons in the rat central nervous system. Neuroscience 3, 517–538.

Hökfelt, T., Ljungdahl, A., Terenius, L., Elde, R., and Nilsson, G. 1977. Immunohistochemical analysis of peptide pathways possibly related to pain and analgesia: enkephalin and substance P. Proc. Natl. Acad. Sci. USA 74, 3081–3085.

Hökfelt, T., Terenius, L., Kuypers, H. G. J. M., and Dann, O. 1979. Evidence for enkephalin immunoreactive neurons in the medulla oblongata projecting to the spinal cord. Neurosci. Lett. 14, 55–60.

Hökfelt, T., Zhang, X., and Wiesenfeld-Hallin, Z. 1994. Messenger plasticity in primary sensory neurons following axotomy and its functional implications. Trends Neurosci. 17, 22–30.

Honda, C. N. and Arvidsson, U. 1995. Immunohistochemical localization of delta- and mu-opioid receptors in primate spinal cord. NeuroReport 6, 1025–1028.

Hunt, S. P. and Mantyh, P. W. 2001. The molecular dynamics of pain control. Nat. Rev. Neurosci. 2, 83–91.

Hunt, S. P. and Rossi, J. 1985. Peptide- and non-peptide-containing unmyelinated primary sensory afferents: the parallel processing of nociceptive information. Philos. Trans. R. Soc. Lond. [Biol.] 308, 283–289.

Hunt, S. P., Kelly, J. S., Emson, P. C., Kimmel, J. R., Miller, R. J., and Wu, J.-Y. 1981. An immunohistochemical study of neuronal populations containing neuropeptides or gamma-aminobutyrate within the superficial layers of the rat dorsal horn. Neuroscience 6, 1883–1898.

Hwang, S. J., Pagliardini, S., Rustioni, A., and Valtschanoff, J. G. 2001. Presynaptic kainate receptors in primary afferents to the superficial laminae of the rat spinal cord. J. Comp. Neurol. 436, 275–289.

Jakowec, M. W., Fox, A. J., Martin, L. J., and Kalb, R. G. 1995a. Quantitative and qualitative changes in AMPA receptor expression during spinal cord development. Neuroscience 67, 893–907.

Jakowec, M. W., Yen, L., and Kalb, R. G. 1995b. *In situ* hybridization analysis of AMPA receptor subunit gene expression in the developing rat spinal cord. Neuroscience 67, 909–920.

Jasmin, L., Burkey, A. R., Card, J. P., and Basbaum, A. I. 1997. Transneuronal labeling of a nociceptive pathway, the spino-(trigemino-)parabrachio-amygdaloid, in the rat. J. Neurosci. 17, 3751–3765.

Jia, H., Rustioni, A., and Valtschanoff, J. G. 1999. Metabotropic glutamate receptors in superficial laminae of the rat dorsal horn. J. Comp. Neurol. 410, 627–642.

Jo, Y. H. and Schlichter, R. 1999. Synaptic corelease of ATP and GABA in cultured spinal neurons. Nat. Neurosci. 2, 241–245.

Jo, Y. H., Stoeckel, M. E., and Schlichter, R. 1998. Electrophysiological properties of cultured neonatal rat dorsal horn neurons containing GABA and met-enkephalin-like immunoreactivity. J. Neurophysiol. 79, 1583–1586.

Johansson, O., Hökfelt, T., Pernow, B., Jeffcoate, S. L., White, N., Steinbusch, H. W., Verhofstad, A. A., Emson, P. C., and Spindel, E. 1981. Immunohistochemical support for three putative transmitters in one neuron: coexistence of 5-hydroxytryptamine, substance P- and thyrotropin releasing hormone-like immunoreactivity in medullary neurons projecting to the spinal cord. Neuroscience 6, 1857–1881.

Ju, G., Hökfelt, T., Brodin, E., Fahrenkrug, J., Fischer, J. A., Frey, P., Elde, R. P., and Brown, J. C. 1987. Primary sensory neurons of the rat showing calcitonin gene-related peptide immunoreactivity and their relation to substance P-, somatostatin-, galanin-, vasoactive intestinal polypeptide- and cholecystokinin-immunoreactive ganglion cells. Cell Tissue Res. 247, 417–431.

Kar, S., Rees, R. G., and Quirion, R. 1994. Altered calcitonin gene-related peptide, substance P and enkephalin immunoreactivities and receptor binding sites in the dorsal spinal cord of the polyarthritic rat. Eur. J. Neurosci. 6, 345–354.

Kato, G., Yasaka, T., Katafuchi, T., Furue, H., Mizuno, M., Iwamoto, Y., and Yoshimura, M. 2006. Direct GABAergic and glycinergic inhibition of the substantia gelatinosa from the rostral ventromedial medulla revealed by in vivo patch-clamp analysis in rats. J. Neurosci. 26, 1787–1794.

Keller, A. F., Coull, J. A., Chéry, N., Poisbeau, P., and De Koninck, Y. 2001. Region-specific developmental specialization of GABA-glycine cosynapses in laminas I–II of the rat spinal dorsal horn. J. Neurosci. 21, 7871–7880.

Kemp, T., Spike, R. C., Watt, C., and Todd, A. J. 1996. The μ-opioid receptor (MOR1) is mainly restricted to neurons that do not contain GABA or glycine in the superficial dorsal horn of the rat spinal cord. Neuroscience 75, 1231–1238.

Kerchner, G. A., Wilding, T. J., Li, P., Zhuo, M., and Huettner, J. E. 2001. Presynaptic kainate receptors regulate spinal sensory transmission. J. Neurosci. 21, 59–66.

Kimura, H., McGeer, P. L., Peng, J. H., and McGeer, E. G. 1981. The central cholinergic system studied by choline acetyltransferase immunohistochemistry in the cat. J. Comp. Neurol. 200, 151–201.

Kinnman, E., Nygårds, E. B., and Hansson, P. 1997. Peripheral α-adrenoreceptors are involved in the development of capsaicin induced ongoing and stimulus evoked pain in humans. Pain 69, 79–85.

Kissa, K., Mordelet, E., Soudais, C., Kremer, E. J., Demeneix, B. A., Brulet, P., and Coen, L. 2002. In vivo neuronal tracing with GFP-TTC gene delivery. Mol. Cell Neurosci. 20, 627–637.

Knyihár-Csillik, E., Csillik, B., and Rakic, P. 1982a. Periterminal synaptology of dorsal root glomerular terminals in the substantia gelatinosa of the spinal cord in the rhesus monkey. J. Comp. Neurol. 210, 376–399.

Knyihár-Csillik, E., Csillik, B., and Rakic, P. 1982b. Ultrastructure of normal and degenerating glomerular terminals of dorsal root axons in the substantia gelatinosa of the rhesus monkey. J. Comp. Neurol. 210, 357–375.

Kupfermann, I. 1991. Functional studies of cotransmission. Physiol. Rev. 71, 683–732.

Labrakakis, C. and MacDermott, A. B. 2003. Neurokinin receptor 1-expressing spinal cord neurons in lamina I and III/IV of postnatal rats receive inputs from capsaicin sensitive fibers. Neurosci. Lett. 352, 121–124.

Labrakakis, C., Tong, C. K., Weissman, T., Torsney, C., and MacDermott, A. B. 2003. Localization and function of ATP and $GABA_A$ receptors expressed by nociceptors and other postnatal sensory neurons in rat. J. Physiol. 549, 131–142.

Lawson, S. N., Crepps, B. A., and Perl, E. R. 1997. Relationship of substance P to afferent characteristics of dorsal root ganglion neurones in guinea-pig. J. Physiol. (Lond.) 505, 177–191.

Lawson, S. N., Crepps, B., and Perl, E. R. 2002. Calcitonin gene-related peptide immunoreactivity and afferent receptive properties of dorsal root ganglion neurones in guinea-pigs. J. Physiol. 540, 989–1002.

Leah, J., Menétrey, D., and De Pommery, J. 1988. Neuropeptides in long ascending spinal tract cells in the rat: evidence for parallel processing of ascending information. Neuroscience 24, 195–207.

Lee, C. J., Bardoni, R., Tong, C. K., Engelman, H. S., Joseph, D. J., Magherini, P. C., and MacDermott, A. B. 2002. Functional expression of AMPA receptors on central terminals of rat dorsal root ganglion neurons and presynaptic inhibition of glutamate release. Neuron 35, 135–146.

Leonard, R. B. and Cohen, D. H. 1975. A cytoarchitectonic analysis of the spinal cord of the pigeon (*Columba livia*). J. Comp. Neurol. 163, 159–180.

Li, H. S. and Zhao, Z. Q. 1998. Small sensory neurons in the rat dorsal root ganglia express functional NK-1 tachykinin receptor. Eur. J. Neurosci. 10, 1292–1299.

Light, A. R. 1992. Organization of the Spinal Cord. In: The Initial Processing of Pain and its Descending Control: Spinal and Trigeminal Systems. Pain and Headache Series, Vol.12 (Series ed. P. L. Gildenberg) (*ed*. A. R. Light), pp. 75–86. Basel.

Light, A. R. and Perl, E. R. 1979. Spinal termination of functionally identified primary afferent neurons with slowly conducting myelinated fibers. J. Comp. Neurol. 186, 133–150.

Light, A. R., Trevino, D. L., and Perl, E. R. 1979. Morphological features of functionally defined neurons in the marginal zone and substantia gelatinosa of the spinal dorsal horn. J. Comp. Neurol. 186, 151–172.

Lima, D. and Coimbra, A. 1983. The neuronal population of the marginal zone (lamina I) of the rat spinal cord. A study based on reconstructions of serially sectioned cells. Anat. Embryol. (Berl.) 167, 273–288.

Lima, D. and Coimbra, A. 1986. A Golgi study of the neuronal population of the marginal zone (lamina I) of the rat spinal cord. J. Comp. Neurol. 244, 53–71.

Lima, D. and Coimbra, A. 1988. The spinothalamic system of the rat: structural types of retrogradely labelled neurons in the marginal zone (lamina I). Neuroscience 27, 215–230.

Lima, D. and Coimbra, A. 1990. Structural types of marginal (lamina I) neurons projecting to the dorsal reticular nucleus of the medulla oblongata. Neuroscience 27, 591–606.

Littlewood, N. K., Todd, A. J., Spike, R. C., Watt, C., and Shehab, S. A. S. 1995. The types of neuron in spinal dorsal horn which possess neurokinin-1 receptors. Neuroscience 66, 597–608.

Liu, H., Brown, J. L., Jasmin, L., Maggio, J. E., Vigna, S. R., Mantyh, P. W., and Basbaum, A. I. 1994a. Synaptic relationship between substance P and the substance P receptor: Light and electron microscopic characterization of the mismatch between neuropeptides and their receptors. Proc. Natl. Acad. Sci. U. S. A. 91, 1009–1013.

Liu, H., Wang, H., Sheng, M., Jan, L. Y., Jan, Y. N., and Basbaum, A. I. 1994b. Evidence for presynaptic *N*-methyl-D-aspartate autoreceptors in the spinal cord dorsal horn. Proc. Natl. Acad. Sci. U. S. A. 91, 8383–8387.

Ljungdahl, A., Hökfelt, T., and Nilsson, G. 1978. Distribution of substance P-like immunoreactivity in the central nervous system of the rat - I. Cell bodies and nerve terminals. Neuroscience 3, 861–943.

Llewellyn-Smith, I. J. and Burnstock, G. 1998. Ultrastructural localization of $P2X_3$ receptors in rat sensory neurons. NeuroReport 9, 2545–2550.

Lopez-Garcia, J. A. and King, A. E. 1994. Membrane properties of physiologically classified rat dorsal horn neurons *in vitro*: correlation with cutaneous sensory afferent input. Eur. J. Neurosci. 6, 998–1007.

Lu, Y. and Perl, E. R. 2003. A specific inhibitory pathway between substantia gelatinosa neurons receiving direct C-fiber input. J. Neurosci. 23, 8752–8758.

Lu, Y. and Perl, E. R. 2005. Modular organization of excitatory circuits between neurons of the spinal superficial dorsal horn (laminae I and II). J. Neurosci. 25, 3900–3907.

Lu, C. R., Hwang, S. J., Phend, K. D., Rustioni, A., and Valtschanoff, J. G. 2002. Primary afferent terminals in spinal cord express presynaptic AMPA receptors. J. Neurosci. 22, 9522–9529.

Ma, W., Ribeiro-da-Silva, A., De Koninck, Y., Radhakrishnan, V., Cuello, A. C., and Henry, J. L. 1997. Substance P and enkephalin immunoreactivities in axonal boutons presynaptic to physiologically identified dorsal horn neurons. An ultrastructural multiple-labelling study in the cat. Neuroscience 77, 793–811.

Ma, W., Ribeiro-da-Silva, A., De Koninck, Y., Radhakrishnan, V., Henry, J. L., and Cuello, A. C. 1996. Quantitative analysis of substance P immunoreactive boutons on physiologically characterized dorsal horn neurons in the cat lumbar spinal cord. J. Comp. Neurol. 376, 45–64.

Ma, W. Y., Ribeiro-da-Silva, A., Noel, G., Julien, J.-P., and Cuello, A. C. 1995. Ectopic substance P and calcitonin gene-related peptide immunoreactive fibres in the spinal cord of transgenic mice over-expressing nerve growth factor. Eur. J. Neurosci. 7, 2021–2035.

Margeta-Mitrovic, M., Mitrovic, I., Riley, R. C., Jan, L. Y., and Basbaum, A. I. 1999. Immunohistochemical localization of $GABA_B$ receptors in the rat central nervous system. J. Comp. Neurol. 405, 299–321.

Marshall, G. E., Shehab, S. A. S., Spike, R. C., and Todd, A. J. 1996. Neurokinin-1 receptors on lumbar spinothalamic neurons in the rat. Neuroscience 72, 255–263.

Martin-Schild, S., Gerall, A. A., Kastin, A. J., and Zadina, J. E. 1998. Endomorphin-2 is an endogenous opioid in primary sensory afferent fibers. Peptides 19, 1783–1789.

Martin-Schild, S., Gerall, A. A., Kastin, A. J., and Zadina, J. E. 1999. Differential distribution of endomorphin 1- and endomorphin 2-like immunoreactivities in the CNS of the rodent. J. Comp. Neurol. 405, 450–471.

Martin-Schild, S., Zadina, J. E., Gerall, A. A., Vigh, S., and Kastin, A. J. 1997. Localization of endomorphin-2-like immunoreactivity in the rat medulla and spinal cord. Peptides 18, 1641–1649.

Maxwell, D. J. and Noble, R. 1987. Relationship between hair-follicle afferent terminations and glutamic acid decarboxylase-containing boutons in cat's spinal cord. Brain Res. 408, 308–312.

Maxwell, D. J. and Réthelyi, M. 1987. Ultrastructure and synaptic connections of cutaneous afferent fibres in the spinal cord. Trends Neurosci. 10, 117–123.

Maxwell, D. J., Fyffe, R. E. W., and Réthelyi, M. 1983. Morphological properties of physiologically characterized lamina III neurones in the cat spinal cord. Neuroscience 10, 1–22.

McLeod, A. L., Krause, J. E., Cuello, A. C., and Ribeiro-da-Silva, A. 1998. Preferential synaptic relationships between substance P-immunoreactive boutons and neurokinin 1 receptor sites in the rat spinal cord. Proc. Natl. Acad. Sci. U. S. A. 95, 15775–15780.

McLeod, A. L., Krause, J. E., and Ribeiro-da-Silva, A. 2000. Immunocytochemical localization of neurokinin B in the rat spinal dorsal horn and its association with substance P and GABA: an electron microscopic study. J. Comp. Neurol. 420, 349–362.

Menétrey, D. and Basbaum, A. I. 1987. The distribution of substance P-, enkephalin- and dynorphin-immunoreactive neurons in the medulla of the rat and their contribution to bulbospinal pathways. Neuroscience 23, 173–187.

Merighi, A., Polak, J. M., and Theodosis, D. T. 1991. Ultrastructural visualization of glutamate and aspartate immunoreactivities in the rat dorsal horn, with special reference to the co-localization of glutamate, substance P and calcitonin- gene related peptide. Neuroscience 40, 67–80.

Michael, G. J. and Priestley, J. V. 1999. Differential expression of the mRNA for the vanilloid receptor subtype 1 in cells of

the adult rat dorsal root and nodose ganglia and its downregulation by axotomy. J. Neurosci. 19, 1844–1854.
Mileusnic, D., Lee, J. M., Magnuson, D. J., Hejna, M. J., Krause, J. E., Lorens, J. B., and Lorens, S. A. 1999. Neurokinin-3 receptor distribution in rat and human brain: an immunohistochemical study. Neuroscience 89, 1269–1290.
Miller, K. E. and Seybold, V. S. 1987. Comparison of met-enkephalin-, dynorphin A-, and neurotensin immunoreactive neurons in the cat and rat spinal cords: I. Lumbar cord. J. Comp. Neurol. 255, 293–304.
Miller, K. E. and Seybold, V. S. 1989. Comparison of met-enkephalin, dynorphin A, and neurotensin immunoreactive neurons in the cat and rat spinal cords: II. Segmental differences in the marginal zone. J. Comp. Neurol. 279, 619–628.
Minami, M. and Satoh, M. 1995. Molecular biology of the opioid receptors: Structures, functions and distributions. Neurosci. Res. 23, 121–145.
Minami, M., Maekawa, K., Yabuuchi, K., and Satoh, M. 1995. Double *in situ* hybridization study on coexistence of μ-, δ- and kappa-opioid receptor mRNAs with preprotachykinin A mRNA in the rat dorsal root ganglia. Mol. Brain Res. 30, 203–210.
Mitchell, K., Spike, R. C., and Todd, A. J. 1993. An immunocytochemical study of glycine receptor and GABA in laminae I–III of rat spinal dorsal horn. J. Neurosci. 13, 2371–2381.
Molander, C., Xu, Q., and Grant, G. 1984. The cytoarchitectonic organization of the spinal cord in the rat. I. The lower thoracic and lumbosacral cord. J. Comp. Neurol. 230, 133–141.
Molander, C., Xu, Q., Rivero-Melian, C., and Grant, G. 1989. Cytoarchitectonic organization of the spinal cord in the rat: II. The cervical and upper toracic spinal cord. J. Comp. Neurol. 289, 375–385.
Moore, K. A., Kohno, T., Karchewski, L. A., Scholz, J., Baba, H., and Woolf, C. J. 2002. Partial peripheral nerve injury promotes a selective loss of GABAergic inhibition in the superficial dorsal horn of the spinal cord. J. Neurosci. 22, 6724–6731.
Naim, M., Spike, R. C., Watt, C., Shehab, S. A., and Todd, A. J. 1997. Cells in laminae III and IV of the rat spinal cord that possess the neurokinin-1 receptor and have dorsally directed dendrites receive a major synaptic input from tachykinin-containing primary afferents. J. Neurosci. 17, 5536–5548.
Nakaya, Y., Kaneko, T., Shigemoto, R., Nakanishi, S., and Mizuno, N. 1994. Immunohistochemical localization of substance P receptor in the central nervous system of the adult rat. J. Comp. Neurol. 347, 249–274.
Nassar, M. A., Stirling, L. C., Forlani, G., Baker, M. D., Matthews, E. A., Dickenson, A. H., and Wood, J. N. 2004. Nociceptor-specific gene deletion reveals a major role for Nav1.7 (PN1) in acute and inflammatory pain. Proc. Natl. Acad. Sci. U. S. A. 101, 12706–12711.
Nishikawa, N., Bennett, G. J., Ruda, M. A., Lu, G. W., and Dubner, R. 1983. Immunocytochemical evidence for a serotoninergic innervation of dorsal column postsynaptic neurons in cat and monkey: light- and electron-microscopic observations. Neuroscience 10, 1333–1340.
Nusbaum, M. P., Blitz, D. M., Swensen, A. M., Wood, D., and Marder, E. 2001. The roles of co-transmission in neural network modulation. Trends Neurosci. 24, 146–154.
Ogawa, T., Kanazawa, I., and Kimura, S. 1985. Regional distribution of substance P, neurokinin α and neurokinin β in rat spinal cord, nerve roots and dorsal root ganglia, and the effects of dorsal root section or spinal transection. Brain Res. 359, 152–157.
Ohishi, H., Nomura, S., Ding, Y. Q., Shigemoto, R., Wada, E., Kinoshita, A., Li, J. L., Neki, A., Nakanishi, S., and Mizuno, N. 1995. Presynaptic localization of a metabotropic glutamate receptor, mGluR7, in the primary afferent neurons: An immunohistochemical study in the rat. Neurosci. Lett. 202, 85–88.
Olave, M. J. and Maxwell, D. J. 2002. An investigation of neurones that possess the alpha 2C-adrenergic receptor in the rat dorsal horn. Neuroscience 115, 31–40.
Olave, M. J. and Maxwell, D. J. 2003a. Axon terminals possessing the alpha 2c-adrenergic receptor in the rat dorsal horn are predominantly excitatory. Brain Res. 965, 269–273.
Olave, M. J. and Maxwell, D. J. 2003b. Neurokinin-1 projection cells in the rat dorsal horn receive synaptic contacts from axons that possess alpha2C-adrenergic receptors. J. Neurosci. 23, 6837–6846.
Ottersen, O. P. and Storm-Mathisen, J. 1984. Glutamate- and GABA-containing neurons in the mouse and rat brain, as demonstrated with a new immunocytochemical technique. J. Comp. Neurol. 229, 374–392.
Persohn, E., Malherbe, P., and Richards, J. G. 1991. *In situ* hybridization histochemistry reveals a diversity of $GABA_A$ receptor subunit mRNAs in neurons of the rat spinal cord and dorsal root ganglia. Neuroscience 42, 497–507.
Polgár, E., Fowler, J. H., McGill, M. M., and Todd, A. J. 1999a. The types of neuron which contain protein kinase C gamma in rat spinal cord. Brain Res. 833, 71–80.
Polgár, E., Furuta, T., Kaneko, T., and Todd, A. J. 2006. Characterization of neurons that express preprotachykinin B in the dorsal horn of the rat spinal cord. Neuroscience 1–27
Polgár, E., Shehab, S. A. S., Watt, C., and Todd, A. J. 1999b. GABAergic neurons that contain neuropeptide Y selectively target cells with the neurokinin 1 receptor in laminae III and IV of the rat spinal cord. J. Neurosci. 19, 2637–2646.
Poorkhalkali, N., Juneblad, K., Jönsson, A. C., Lindberg, M., Karlsson, O., Wallbrandt, P., Ekstrand, J., and Lehmann, A. 2000. Immunocytochemical distribution of the $GABA_B$ receptor splice variants $GABA_B$ R1a and R1b in the rat CNS and dorsal root ganglia. Anat. Embryol. (Berl.) 201, 1–13.
Prescott, S. A. and De Koninck, Y. 2002. Four cell types with distinctive membrane properties and morphologies in lamina I of the spinal dorsal horn of the adult rat. J. Physiol. 539, 817–836.
Priestley, J. V., Michael, G. J., Averill, S., Liu, M., and Willmott, N. 2002. Regulation of nociceptive neurons by nerve growth factor and glial cell derived neurotrophic factor. Can. J. Physiol. Pharmacol. 80, 495–505.
Ralston, H. J., III 1979. The fine structure of laminae I, II and III of the macaque spinal cord. J. Comp. Neurol. 184, 619–642.
Ramón y Cajal, S. 1909. Histologie du Système Nerveux de l'Homme et des Vertébrés. Vol. 1. Transl. L. Azoulay. A. Maloine.
Réthelyi, M., Light, A. R., and Perl, E. R. 1982. Synaptic complexes formed by functionally defined primary sensory afferent units with fine myelinated fibers. J. Comp. Neurol. 207, 381–393.
Rexed, B. 1952. The cytoarchitectonic organization of the spinal cord in the cat. J. Comp. Neurol. 96, 415–495.
Rexed, B. 1954. A cytoarchitectonic atlas of the spinal cord in the cat. J. Comp. Neurol. 100, 297–397.
Ribeiro-da-Silva, A. 1995. Ultrastructural features of the colocalization of calcitonin gene related peptide with substance P or somatostatin in the dorsal horn of the spinal cord. Can. J. Physiol. Pharmacol. 73, 940–944.
Ribeiro-da-Silva, A. 2004. Substantia Gelatinosa of the Spinal Cord. In: The Rat Nervous System (*ed*. G. Paxinos), pp. 129–148. Elsevier Academic Press.
Ribeiro-da-Silva, A. and Coimbra, A. 1980. Neuronal uptake of ^{3}H-GABA and ^{3}H-glycine in laminae I–III substantia gelatinosa Rolandi) of the rat spinal cord. An autoradiographic study. Brain Res. 188, 449–464.

Ribeiro-da-Silva, A. and Coimbra, A. 1982. Two types of synaptic glomeruli and their distribution in laminae I–III of the rat spinal cord. J. Comp. Neurol. 209, 176–186.

Ribeiro-da-Silva, A. and Cuello, A. C. 1990a. Choline acetyltransferase-immunoreactive profiles are presynaptic to primary sensory fibers in the rat superficial dorsal horn. J. Comp. Neurol. 295, 370–384.

Ribeiro-da-Silva, A. and Cuello, A. C. 1990b. Ultrastructural evidence for the occurrence of two distinct somatostatin-containing systems in the substantia gelatinosa of rat spinal cord. J. Chem. Neuroanat. 3, 141–153.

Ribeiro-da-Silva, A., De Koninck, Y., Cuello, A. C., and Henry, J. L. 1992. Enkephalin-immunoreactive nociceptive neurons in the cat spinal cord. NeuroReport 3, 25–28.

Ribeiro-da-Silva, A., McLeod, A. L., and Krause, J. E. 2000. Neurokinin Receptors in the CNS. In: Handbook of Chemical Neuroanatomy, Vol. 16: Peptide Receptors, Part I (*eds*. R. Quirion, A. Björklund, and T. Hökfelt), pp. 195–240. Elsevier Science.

Ribeiro-da-Silva, A., Pioro, E. P., and Cuello, A. C. 1991. Substance P- and enkephalin-like immunoreactivities are colocalized in certain neurons of the substantia gelatinosa of the rat spinal cord. An ultrastructural double-labeling study. J. Neurosci. 11, 1068–1080.

Ribeiro-da-Silva, A., Tagari, P., and Cuello, A. C. 1989. Morphological characterization of substance P-like immunoreactive glomeruli in the superficial dorsal horn of the rat spinal cord and trigeminal subnucleus caudalis: a quantitative study. J. Comp. Neurol. 281, 497–415.

Rossi, D. J. and Hamann, M. 1998. Spillover-mediated transmission at inhibitory synapses promoted by high affinity α6 subunit $GABA_A$ receptors and glomerular geometry. Neuron 20, 783–795.

Ruda, M. A. 1986. The Pattern and Place of Nociceptive Modulation in the Dorsal Horn. A Discussion of the Anatomically Characterized Neural Circuitry of Enkephalin, Serotonin, and Substance P. In: Spinal Afferent Processing (*ed*. T. L. Yaksh), pp. 141–164. Plenum Press.

Ruda, M. A., Bennett, G. J., and Dubner, R. 1986. Neurochemistry and neural circuitry in the dorsal horn. Prog. Brain Res. 66, 219–268.

Ruda, M. A., Coffield, J., and Dubner, R. 1984. Demonstration of postsynaptic opioid modulation of thalamic projection neurons by the combined techniques of retrograde horseradish peroxidase and enkephalin immunocytochemistry. J. Neurosci. 4, 2117–2132.

Ruda, M. A., Cohen, L. V., Shiosaka, S., Takahashi, T., Allen, B., Humphrey, E., and Iadarola, M. J. 1989. *In situ* Hybridization Histochemical and Immunocytochemical Analysis of Opioid Gene Products in a Rat Model of Peripheral Inflammation. In: Processing of Sensory Information in the Superficial Dorsal Horn of the Spinal Cord (*eds*. F. Cervero, G. J. Bennett, and P. M. Headley), pp. 383–394. Plenum Press.

Ruda, M. A., Iadarola, M. J., Cohen, L. V., and Young, W. S. 1988. *In situ* hybridization histochemistry and immunocytochemistry reveal an increase in spinal dynorphin biosynthesis in a rat model of peripheral inflammation and hyperalgesia. Proc. Natl. Acad. Sci. U. S. A. 85, 622–626.

Rudomin, P. and Schmidt, R. F. 1999. Presynaptic inhibition in the vertebrate spinal cord revisited. Exp. Brain Res. 129, 1–37.

Ruocco, I., Krause, J. E., and Ribeiro-da-Silva, A. 1997. Anatomical localization of substance P and the neurokinin-1 receptor in the skin of the rat lower lip: an electron microscopy study. Soc. Neurosci. Abst. 23, 1490. Ref Type: Abstract

Ruscheweyh, R. and Sandkuhler, J. 2002. Lamina-specific membrane and discharge properties of rat spinal dorsal horn neurones *in vitro*. J. Physiol. 541, 231–244.

Ruscheweyh, R., Ikeda, H., Heinke, B., and Sandkuhler, J. 2004. Distinctive membrane and discharge properties of rat spinal lamina I projection neurones *in vitro*. J Physiol 555, 527–543.

Sanderson Nydahl K., Skinner, K., Julius, D., and Basbaum, A. I. 2004. Co-localization of endomorphin-2 and substance P in primary afferent nociceptors and effects of injury: a light and electron microscopic study in the rat. Eur. J. Neurosci. 19, 1789–1799.

Scheibel, M. E. and Scheibel, A. B. 1968. Terminal axonal patterns in the cat spinal cord. II. The dorsal horn. Brain Res. 9, 32–58.

Schoenen, J. 1982. The dendritic organization of the human spinal cord: the dorsal horn. Neuroscience 7, 2057–2087.

Schulz, S., Schreff, M., Schmidt, H., Händel, M., Przewlocki, R., and Höllt, V. 1998. Immunocytochemical localization of somatostatin receptor sst_{2A} in the rat spinal cord and dorsal root ganglia. Eur. J. Neurosci. 10, 3700–3708.

Senba, E., Yanaihara, C., Yanaihara, N., and Tohyama, M. 1988. Co-localization of substance P and Met-enkephalin-Arg^6-Gly^7-Leu^8 in the intraspinal neurons of the rat, with special reference to the neurons in the substantia gelatinosa. Brain Res. 453, 110–116.

Seybold, V. S. and Elde, R. P. 1982. Neurotensin immunoreactivity in the superficial laminae of the dorsal horn of the rat: I. Light microscopic studies of cell bodies and proximal dendrites. J. Comp. Neurol. 205, 89–100.

Sherman, S. E. and Loomis, C. W. 1994. Morphine insensitive allodynia is produced by intrathecal strychnine in the lightly anesthetized rat. Pain 56, 17–29.

Shin, J. B., Martinez-Salgado, C., Heppenstall, P. A., and Lewin, G. R. 2003. A T-type calcium channel required for normal function of a mammalian mechanoreceptor. Nat. Neurosci. 6, 724–730.

Snider, W. D. and McMahon, S. B. 1998. Tackling pain at the source: new ideas about nociceptors. Neuron 20, 629–632.

Spike, R. C. and Todd, A. J. 1992. Ultrastructural and immunocytochemical study of lamina II islet cells in rat spinal dorsal horn. J. Comp. Neurol. 323, 359–369.

Spike, R. C., Kerr, R., Maxwell, D. J., and Todd, A. J. 1998. GluR1 and GluR2/3 subunits of the AMPA-type glutamate receptor are associated with particular types of neurone in laminae I–III of the spinal dorsal horn of the rat. Eur. J. Neurosci. 10, 324–333.

Spike, R. C., Puskár, Z., Andrew, D., and Todd, A. J. 2003. A quantitative and morphological study of projection neurons in lamina I of the rat lumbar spinal cord. Eur. J. Neurosci. 18, 2433–2448.

Standaert, D. G., Watson, S. J., Houghten, R. A., and Saper, C. B. 1986. Opioid peptide immunoreactivity in spinal and trigeminal dorsal horn neurons projecting to the parabrachial nucleus in the rat. J. Neurosci. 6, 1220–1226.

Steiner, T. J. and Turner, L. M. 1972. Cytoarchitecture of the rat spinal cord. J. Physiol. (Lond.) 222, 123P–125P.

Stone, L. S., Broberger, C., Vulchanova, L., Wilcox, G. L., Hökfelt, T., Riedl, M. S., and Elde, R. 1998. Differential distribution of α_{2A} and α_{2C} adrenergic receptor immunoreactivity in the rat spinal cord. J. Neurosci. 18, 5928–5937.

Svensson, P., Cairns, B. E., Wang, K., Hu, J. W., Graven-Nielsen, T., rendt-Nielsen, L., and Sessle, B. J. 2003. Glutamate-evoked pain and mechanical allodynia in the human masseter muscle. Pain 101, 221–227.

Tachibana, M., Wenthold, R. J., Morioka, H., and Petralia, R. S. 1994. Light and electron microscopic immunocytochemical localization of AMPA-selective glutamate receptors in the rat spinal cord. J. Comp. Neurol. 344, 431–454.

Tashiro, T., Satoda, T., Takahashi, O., Matsushima, R., and Mizuno, N. 1988. Distribution of axons exhibiting both

enkephalin- and serotonin- like immunoreactivities in the lumbar cord segments: an immunohistochemical study in the cat. Brain Res. 440, 357–362.

Tashiro, T., Takahashi, O., Satoda, T., Matsushima, R., and Mizuno, N. 1987. Immunohistochemical demonstration of coexistence of enkephalin- and substance P-like immunoreactivities in axonal components in the lumbar segments of cat spinal cord. Brain Res. 424, 391–395.

Thomson, A. M., West, D. C., and Headley, P. M. 1989. Membrane characteristics and synaptic responsiveness of superficial dorsal horn neurons in a slice preparation of adult rat spinal cord. Eur. J. Neurosci. 1, 479–488.

Todd, A. J. 1991. Immunohistochemical evidence that acetylcholine and glycine exist in different populations of GABAergic neurons in lamina III of rat spinal dorsal horn. Neuroscience 44, 741–746.

Todd, A. J. 1996. GABA and glycine in synaptic glomeruli of the rat spinal dorsal horn. Eur. J. Neurosci. 8, 2492–2498.

Todd, A. J. and Lewis, S. G. 1986. The morphology of Golgi-stained neurons in lamina II of the rat spinal cord. J. Anat. 149, 113–119.

Todd, A. J. and Lochhead, V. 1990. GABA-like immunoreactivity in type I glomeruli of rat substantia gelatinosa. Brain Res. 514, 171–174.

Todd, A. J. and McKenzie, J. 1989. GABA-immunoreactive neurons in the dorsal horn of the rat spinal cord. Neuroscience 31, 799–806.

Todd, A. J. and Ribeiro-da-Silva, A. 2005. Molecular Architecture of the Dorsal Horn. In: Neurobiology of Pain (*eds*. S. P. Hunt and M. Koltzenburg), pp. 65–94. Oxford University Press.

Todd, A. J. and Spike, R. C. 1993. The localization of classical transmitters and neuropeptides within neurons in laminae I–III of the mammalian spinal dorsal horn. Prog. Neurobiol. 41, 609–638.

Todd, A. J. and Sullivan, A. C. 1990. Light microscope study of the coexistence of GABA-like and glycine-like immunoreactivities in the spinal cord of the rat. J. Comp. Neurol. 296, 496–505.

Todd, A. J., Hughes, D. I., Polgár, E., Nagy, G. G., Mackie, M., Ottersen, O. P., and Maxwell, D. J. 2003. The expression of vesicular glutamate transporters VGLUT1 and VGLUT2 in neurochemically defined axonal populations in the rat spinal cord with emphasis on the dorsal horn. Eur. J. Neurosci. 17, 13–27.

Todd, A. J., McGill, M. M., and Shehab, S. A. 2000. Neurokinin 1 receptor expression by neurons in laminae I, III and IV of the rat spinal dorsal horn that project to the brainstem. Eur. J. Neurosci. 12, 689–700.

Todd, A. J., Russell, G., and Spike, R. C. 1992a. Immunocytochemical evidence that GABA and neurotensin exist in different neurons in laminae II and III of rat spinal dorsal horn. Neuroscience 47, 685–691.

Todd, A. J., Spike, R. C., Russell, G., and Johnston, H. M. 1992b. Immunohistochemical evidence that Met-enkephalin and GABA coexist in some neurones in rat dorsal horn. Brain Res. 584, 149–156.

Todd, A. J., Watt, C., Spike, R. C., and Sieghart, W. 1996. Colocalization of GABA, glycine, and their receptors at synapses in the rat spinal cord. J. Neurosci. 16, 974–982.

Tölle, T. R., Berthele, A., Zieglgänsberger, W., Seeburg, P. H., and Wisden, W. 1993. The differential expression of 16 NMDA and non-NMDA receptor subunits in the rat spinal cord and in periaqueductal gray. J. Neurosci. 13, 5009–5028.

Torsney, C. and MacDermott, A. B. 2006. Disinhibition opens the gate to pathological pain signaling in superficial neurokinin 1 receptor-expressing neurons in rat spinal cord. J. Neurosci. 26, 1833–1843.

Towers, S., Princivalle, A., Billinton, A., Edmunds, M., Bettler, B., Urban, L., Castro-Lopes, J., and Bowery, N. G. 2000. GABAB receptor protein and mRNA distribution in rat spinal cord and dorsal root ganglia. Eur. J. Neurosci. 12, 3201–3210.

Trafton, J. A., Abbadie, C., and Basbaum, A. I. 2001. Differential contribution of substance P and neurokinin A to spinal cord neurokinin-1 receptor signaling in the rat. J. Neurosci. 21, 3656–3664.

Von Banchet, G. S., Schindler, M., Hervieu, G. J., Beckmann, B., Emson, P. C., and Heppelmann, B. 1999. Distribution of somatostatin receptor subtypes in rat lumbar spinal cord examined with gold-labelled somatostatin and anti-receptor antibodies. Brain Res. 816, 254–257.

Wall, P. D., Merrill, E. G., and Yaksh, T. L. 1979. Responses of single units in laminae 2 and 3 of cat spinal cord. Brain Res. 160, 245–260.

Warden, M. K. and Young, W. S. 1988. Distribution of cells containing mRNAs encoding substance P and neurokinin B in the rat central nervous system. J. Comp. Neurol. 272, 90–113.

Watanabe, M., Mishina, M., and Inoue, Y. 1994. Distinct spatiotemporal distributions of the N-methyl-D-aspartate receptor channel subunit mRNAs in the mouse cervical cord. J. Comp. Neurol. 345, 314–319.

Westlund, K. N., Bowker, R. M., Ziegler, M. G., and Coulter, J. D. 1983. Noradrenergic projections to the spinal cord of the rat. Brain Res. 263, 15–31.

Wood, J. N., Boorman, J. P., Okuse, K., and Baker, M. D. 2004. Voltage-gated sodium channels and pain pathways. J. Neurobiol. 61, 55–71.

Woodbury, C. J., Ritter, A. M., and Koerber, H. R. 2000. On the problem of lamination in the superficial dorsal horn of mammals: a reappraisal of the substantia gelatinosa in postnatal life. J. Comp. Neurol. 417, 88–102.

Xie, J., Ho, L. Y., Wang, C., Mo, C. J., and Chung, K. 2001. Differential expression of alpha1-adrenoceptor subtype mRNAs in the dorsal root ganglion after spinal nerve ligation. Mol. Brain Res. 93, 164–172.

Yaksh, T. L. 1989. Behavioral and autonomic correlates of the tactile evoked allodynia produced by spinal glycine inhibition: effects of modulatory receptor systems and excitatory amino acid antagonists. Pain 37, 111–123.

Yashpal, K., Kar, S., Dennis, T., and Quirion, R. 1992. Quantitative autoradiographic distribution of calcitonin gene-related peptide (hCGRPα) binding sites in the rat and monkey spinal cord. J. Comp. Neurol. 322, 224–232.

Yoshimura, M. and Jessell, T. M. 1989. Primary afferent evoked synaptic responses and slow potential generation in rat substantia gelatinosa neurons *in vitro*. J. Neurophysiol. 62, 96–108.

Yu, X. H., Ribeiro-da-Silva, A., and De Koninck, Y. 2005. Morphology and NK-1 receptor expression of spinothalamic lamina I neurons in the rat spinal cord. J. Comp. Neurol. 491, 56–68.

Yu, X. H., Zhang, E. T., Craig, A. D., Shigemoto, R., Ribeiro-da-Silva, A., and De Koninck, Y. 1999. NK-1 receptor immunoreactivity in distinct morphological types of lamina I neurons of the primate spinal cord. J. Neurosci. 19, 3545–3555.

Zeilhofer, H. U., Studler, B., Arabadzisz, D., Schweizer, C., Ahmadi, S., Layh, B., Bosl, M. R., and Fritschy, J. M. 2005. Glycinergic neurons expressing enhanced green fluorescent protein in bacterial artificial chromosome transgenic mice. J. Comp. Neurol. 482, 123–141.

Zeitz, K. P., Guy, N., Malmberg, A. B., Dirajlal, S., Martin, W. J., Sun, L., Bonhaus, D. W., Stucky, C. L., Julius, D., and Basbaum, A. I. 2002. The 5-HT3 subtype of serotonin receptor contributes to nociceptive processing via a novel subset of myelinated and unmyelinated nociceptors. J. Neurosci. 22, 1010–1019.

Zerari, F., Karpitskiy, V., Krause, J., Descarries, L., and Couture, R. 1997. Immunoelectron microscopic localization of NK-3 receptor in the rat spinal cord. NeuroReport 8, 2661–2664.

Zerari, F., Karpitskiy, V., Krause, J., Descarries, L., and Couture, R. 1998. Astroglial distribution of neurokinin-2 receptor immunoreactivity in the rat spinal cord. Neuroscience 84, 1233–1246.

Zhang, E. T. and Craig, A. D. 1997. Morphology and distribution of spinothalamic lamina I neurons in the monkey. J. Neurosci. 17, 3274–3284.

Zhang, E. T., Han, Z. S., and Craig, A. D. 1996. Morphological classes of spinothalamic lamina I neurons in the cat. J. Comp. Neurol. 367, 537–549.

Zhang, X., Nicholas, A. P., and Hökfelt, T. 1993. Ultrastructural studies on peptides in the dorsal horn of the spinal cord–I. Co-existence of galanin with other peptides in primary afferents in normal rats. Neuroscience 57, 365–384.

Zoli, M., Jansson, A., Sykova, E., Agnati, L. F., and Fuxe, K. 1999. Volume transmission in the CNS and its relevance for neuropsychopharmacology. Trends Pharmacol. Sci. 20, 142–150.

Zwick, M., Davis, B. M., Woodbury, C. J., Burkett, J. N., Koerber, H. R., Simpson, J. F., and Albers, K. M. 2002. Glial cell line-derived neurotrophic factor is a survival factor for isolectin B4-positive, but not vanilloid receptor 1-positive, neurons in the mouse. J. Neurosci. 22, 4057–4065.

5.24 Spinal Cord Physiology of Nociception

A R Light, University of Utah, Salt Lake City, UT, USA

S Lee, Korea Institute of Science and Technology, Seoul, Korea

© 2008 Elsevier Inc. All rights reserved.

5.24.1	**Organization of the Spinal Cord**	311
5.24.2	**Ventral Horn: Motor**	312
5.24.3	**Dorsal Horn: Sensory**	312
5.24.4	**Laminar Organization**	312
5.24.5	**Laminae I and II (the Substantia Gelatinosa)**	312
5.24.6	**The Adequate Stimulus**	313
5.24.7	**Physiology of Neurons in the Dorsal Horn by Laminae**	313
5.24.8	**Lamina I**	313
5.24.8.1	Modality of Input to Lamina I	313
5.24.8.2	Receptive Field Characteristics	314
5.24.9	**Projections and Function of Lamina I Neurons**	315
5.24.10	**Lamina II**	316
5.24.11	**Outer Lamina II**	316
5.24.11.1	Modality of Input to Outer Lamina II	316
5.24.11.2	Receptive Field Characteristics	316
5.24.12	**Projections and Function of Outer Lamina II Neurons**	319
5.24.12.1	Inner Lamina II (II_i)	320
5.24.12.1.1	Projections and function of inner lamina II neurons	320
5.24.12.2	Lamina III	320
5.24.12.3	Lamina IV	321
5.24.12.4	Lamina V	321
5.24.13	**The Ventral Horn**	321
5.24.14	**Somatotopic Organization**	322
5.24.15	**Physiological Properties of Spinal Neurons**	323
5.24.16	**Intrinsic Properties of Spinal Dorsal Horn Neurons**	323
5.24.16.1	Burst Firing Neurons	325
5.24.16.2	Delayed-Onset Firing Neurons	325
5.24.16.3	Gap Firing Neurons	325
5.24.16.4	Phasic Firing Neurons	326
5.24.16.5	Single-Spike Firing Neurons	326
5.24.17	**Relationship between Intrinsic Firing Patterns and Physiological Types of Dorsal Horn Neurons**	326
5.24.18	**Summary**	327
References		327

5.24.1 Organization of the Spinal Cord

The spinal cord consists of a wrapping of axons inside of which are neurons comprising the first relay for sensory information and motoneurons with axons that connect directly with skeletal muscles. In addition to sensory and motor integration, considerable sympathetic nervous system integration occurs in this structure. The neurons of the spinal cord are clustered together in a butterflylike arrangement, with the each of the two wings containing neurons representing or controlling muscles and skin in the right or left side of the body, respectively. The more posterior (or dorsal) portion of each wing is specialized for sensory function and is called the dorsal horn, while the more anterior (or ventral) portion is specialized for motor function and is called the ventral horn (see Figures 1 and 2).

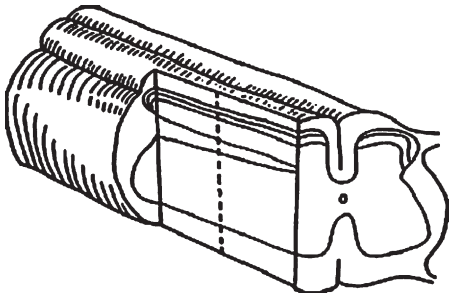

Figure 1 Cut-away view of lumbar spinal cord. From Light, A.R. 1992. Pain and Headache (Vol. 12): the Initial Processing of Pain and its Descending Control: Spinal and Trigeminal Systems. Karger, with permission.

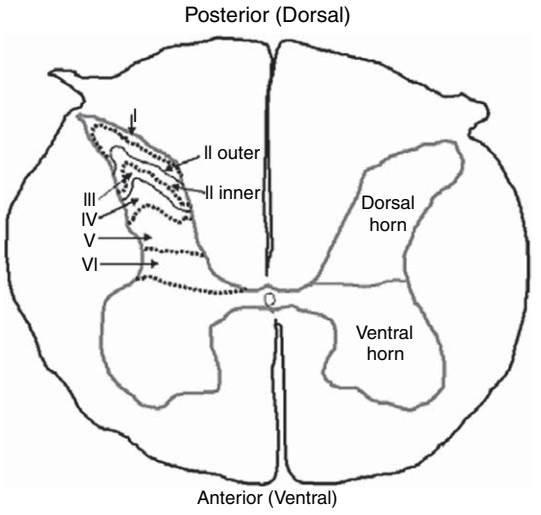

Figure 2 Laminae of the spinal cord dorsal horn.

5.24.2 Ventral Horn: Motor

The ventral horn contains all of the motoneurons whose axons leave the ventral horn in the ventral roots and directly innervate skeletal muscles of the body. However, most of the neurons in the ventral horn have axons that remain in the spinal cord and are, therefore, interneurons and are involved in motor integration. For the purposes of this chapter, the ventral horn is most important for the integration of reflexes. The most important of which are nociceptive reflexes. The most notable of the nociceptive reflexes is the flexion reflex which is often used as a surrogate for a response to pain, although the flexion reflex can often be regulated in different ways than the perception of pain (Mauderli, A. P. *et al.*, 2000). This chapter will not consider the ventral horn in detail. The axons surrounding the ventral gray matter are of interest in the physiology of pain systems, as the axons of many nociceptive (and non-nociceptive) neurons in the dorsal horn travel in the white matter of the ventral horn. Some ascend all the way to the thalamus, or even hypothalamus.

5.24.3 Dorsal Horn: Sensory

The dorsal horn consists of the terminations of primary afferent neurons whose cell bodies lie in the dorsal root ganglia, and many interneurons with terminations within the spinal cord. The dorsal horn also contains many transmission neurons with axons that leave the spinal cord and terminate in the brainstem (medulla and pons), thalamus, and hypothalamus (see Chapter Ascending Pathways: Anatomy and Physiology for more information on the ascending pathways originating from the spinal cord).

The dorsal horn also receives many inputs from higher brain centers that can modify, or in some cases, completely inhibit transmission from primary afferent neurons to other brain centers, including the ventral horn (see Chapter Descending Control Mechanisms for more information on descending modulatory pathways).

5.24.4 Laminar Organization

Many scientists have described the organization of the dorsal horn as laminar. Rexed B. (1952) divided the dorsal horn into six layers or laminae defined by the sizes and shapes of the cells within them (see Figure 2). Other defining characteristics of these laminae are the orientation of axons and dendrites of the neurons within them, and the amount of myelin that coats the axons in each layer (Clarke, J. L., 1859). The most dorsal, or superficial laminae (laminae I and II) as well as one of the deepest layers (lamina V) are most often associated with nociception (Light, A. R., 1992). While these laminae were originally defined using anatomical criteria (see chapter 9) they prove to also segregate some of the physiology of sensory systems of the spinal cord.

5.24.5 Laminae I and II (the Substantia Gelatinosa)

Because of its peculiar appearance in fresh tissue, the gelatinous translucent region that caps the dorsal horn has been called the substantia gelatinosa. This

region was defined as lamina II by Rexed B. (1952). Capping the substantia gelatinosa is the even more superficial lamina I, also called the substantia spongiosa or marginal zone (Waldeyer, W., 1889; Ramon Y Cajal, S., 1909). These regions have been associated with nociception since at least the time of Ranson (Ranson, S. W., 1913; 1914; 1915; Ranson, S. W. and von Hess, C. L., 1915; Ranson, S. W. and Billingsley, P. R., 1916; Ranson, S. W. and Davenport, H. K., 1931). Ranson made the association between the translucent appearance of these regions and the lack of myelinated axon terminations in these regions and the likely termination of unmyelinated axons, which even then he associated with pain.

Fifty years later, lamina I and II were definitively shown to contain neurons that specifically responded to noxious (noxious meaning tissue damaging) stimuli and others responding to innocuous thermal stimuli (Christensen, B. N. and Perl, E. R., 1969; 1970; Mosso, J. A. and Kruger, L., 1973). Some of these neurons were shown to project through the anterolateral tract to the thalamus (Kumazawa, T. *et al.*, 1971; 1975; Craig, A. D. and Kniffki, K. D., 1985). However, these investigators also showed that laminae I and II integrated more than purely nociceptive inputs with innocuous thermal neurons found in lamina I and innocuous mechanical neurons found in lamina II.

5.24.6 The Adequate Stimulus

Physiological descriptions of nociceptive neurons in the spinal cord dorsal horn are often based on the adequate stimulus (see chapter 2 for a thorough discussion of the adequate stimulus). We define this as the best (most effective) natural (most likely to occur in an environment not manipulated by humans) stimulus that excites (evokes action potentials) in a neuron. For example, while punctate pressure that does not cause immediate harm to the skin may occasionally evoke an action potential in a spinal neuron, if that neuron fires a train of action potentials at 100 Hz to punctuate pressure that damages the skin, then the adequate stimulus is presumed to be noxious mechanical stimulation. If this same neuron responds to electrical shock, its adequate stimulus is not presumed to be electrical stimulation. Electrical shock is unlikely to occur in a world without human intervention.

5.24.7 Physiology of Neurons in the Dorsal Horn by Laminae

Being largely sensory in nature, the types of peripheral stimuli that activate the intrinsic neurons of the dorsal horn are strongly related to the physiological types of primary afferents that synapse on the spinal neurons. A discussion of the properties of nociceptive primary afferents and their responses to peripheral stimuli of various types is found in chapter 4. Integration of these primary afferent inputs occurs to various degrees in the spinal neurons. Some neurons retain the modality selectivity of the primary afferents, while others integrate the input of more than one type of primary afferent.

5.24.8 Lamina I

5.24.8.1 Modality of Input to Lamina I

Most investigators agree that a substantial portion of lamina I (see Figure 2 for location in spinal cord) neurons respond specifically or preferentially to various forms of noxious stimuli (Light, A. R., 1992). In studies using cats, Light A. R. found that 63% of neurons identified as lamina I neurons by intracellular labeling were nociceptive while 12% responded to innocuous cooling (4%) or warming (cooling and warming neurons are referred to collectively as thermoreceptive neurons); 14% responded to innocuous mechanical stimuli, and 5% responded to both innocuous mechanical stimuli and noxious stimuli. Of the neurons with nociceptive inputs, 28% responded only to noxious mechanical stimuli while 35% responded to noxious mechanical stimuli, and also to noxious heat and chemical stimuli. Only some of these neurons were tested with noxious cold. Figure 3 shows some characteristic responses of lamina I cells.

Andrew D. and Craig A. D. (2002) determined that the types of inputs observed for lamina I neurons projecting to the thalamus were similar to those described for unidentified lamina I neurons. Some differences for identified spinothalamic neurons were a disproportionate percentage of neurons with thermal inputs in the spinothalamic population. Of 125 lamina I spinothalamic neurons, 61% were nociceptive and 39% were thermoreceptive (most responded to cooling, 35%, with the rest responding to innocuous warming, 4%). Andrew D. and Craig A. D. also found that the nociceptive neurons were classifiable into

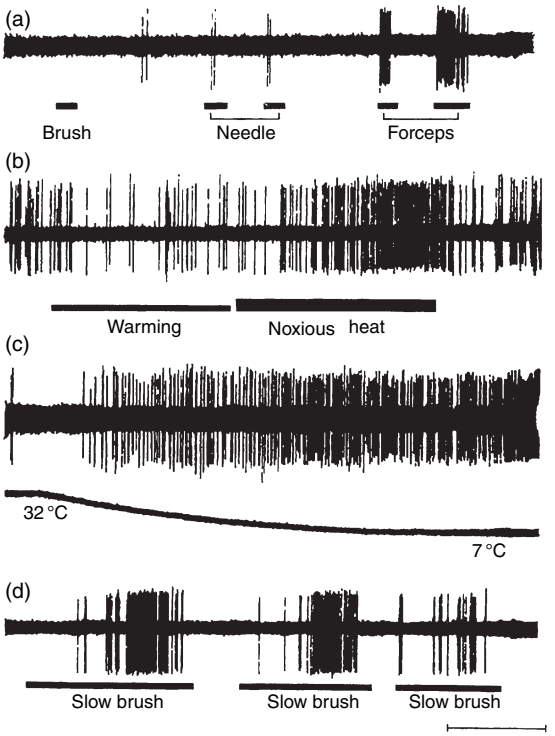

Figure 3 Responses of lamina I neurons (a) Neuron activated only by noxious mechanical stimulation of skin. (b) Neuron activated by both noxious mechanical stimuli (not shown) and noxious heating of the skin. (c) Neuron activated only by innocuous cooling of the skin. (d) Neurons activated only by innocuous mechanical stimulation of the skin. This neuron responded only to brushing at less than 10 cm s^{-1}. Scale bar = 10 s for (a), (b), and (d); 20 s for (c). From Light, A. R. 1992. Pain and Headache (Vol. 12): the Initial Processing of Pain and its Descending Control: Spinal and Trigeminal Systems. Karger. Reprinted with permission from Light, A. R., Trevino, D. L., and Perl, E. R. 1979. Morphological features of functionally defined neurons in the marginal zone and substantia gelatinosa of the spinal dorsal horn. J. Comp. Neurol. 186, 151–171. Copyright 1979, Wiley-Liss of John Wiley & Sons, Inc.

somewhat different groups than those summarized by Light A. R. (1992). Of the 61% nociceptive neurons, a minority (43%) were described as nociceptive specific. Of the nociceptive-specific neurons, most (80%) were responsive to both noxious mechanical and noxious heat stimuli, with only 20% responsive to only mechanical stimuli. The majority (57%) of the nociceptive neurons was classified as responding to heat, pressure, and cold (HPC). These neurons responded not only to noxious mechanical pressure, but also responded to innocuous cooling temperatures. Craig (Andrew, D. and Craig, A. D., 2002) has also determined the quantitative response properties of lamina I nociceptive neurons (see Figure 4). The data presented in these publications clearly indicate that lamina I neurons are capable of reliably detecting and transmitting precise quantitative information about noxious pressure to higher centers (Craig, A. D. and Andrew, D., 2002). These authors showed the quantitative responses of lamina I neurons to activation by noxious heat. The responses correlate very well with human pain ratings of the same stimuli (see Figure 5).

In addition to nociceptive and thermal inputs, lamina I neurons also encode stimuli interpreted as itch and metabolic signals produced by contracting muscles.

Craig's laboratory reported recording neurons in lamina I that specifically respond to stimuli provoking itch (Andrew, D. and Craig, A. D., 2001; see Figure 6), and others that responded only to actively contracting muscles (Wilson, L. B. *et al.*, 2002; see Figure 7). Some of the neurons responding only to actively contracting muscles may represent metaboreceptors that encode the metabolites produced by actively contracting muscles, and may be the peripheral receptors that are capable of encoding the signals interpreted as muscle fatigue, and/or muscle pain. These neurons may also be the sensory arm of sympathetic reflexes known to be activated by actively contracting muscles (Rotto, D. M. and Kaufman, M. P., 1988).

While the detailed neuronal properties presented here were obtained from recordings in cats, similar percentages of these various types of neurons in lamina I have been found in monkeys (Kumazawa, T. *et al.*, 1975; Kumazawa, T. and Perl, E. R., 1978; Light, A. R. *et al.*, 1979; Price, D. D. *et al.*, 1979; Chung, J. M. *et al.*, 1986; Craig, A. D., 2004) and rats (Giesler, G. J., Jr. *et al.*, 1976; Menetrey, D. *et al.*, 1977; Light, A. R. and Willcockson, H. H., 1999) although some of those referenced here report many more neurons responding to both noxious and non-noxious stimuli in the wide-dynamic-range (WDR) fashion (see chapter 10.1 for more information). Very recently, similar types of neurons have also been reported in lamina I of the mouse, in an *ex vivo* preparation in mouse (Koerber, H. R., personal communication, 2007).

5.24.8.2 Receptive Field Characteristics

The receptive fields of lamina I neurons range from quite small (1 mm^2) to quite large (1000 mm^2) depending on the body part encoded. The smallest receptive fields are found on the digits, while the

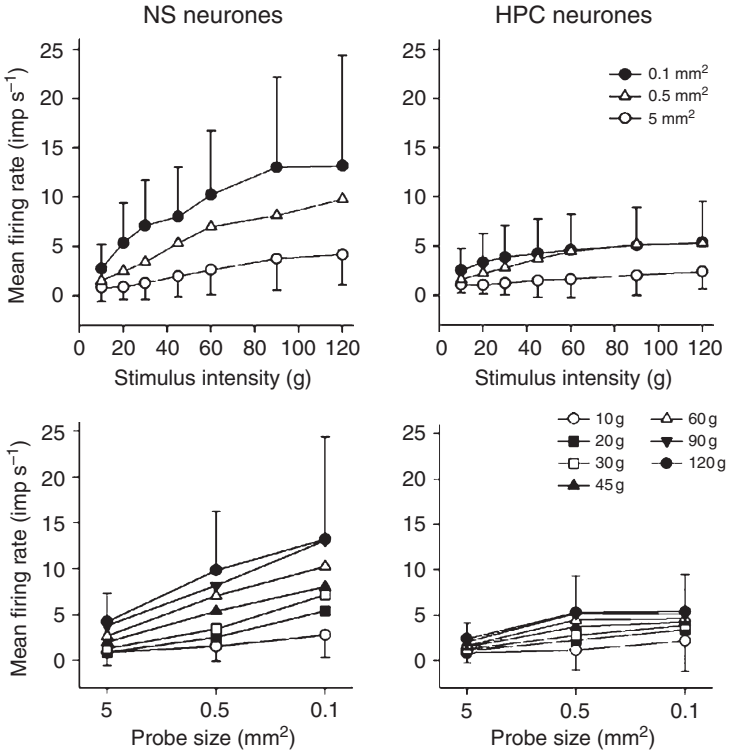

Figure 4 Quantitative responses of lamina I neurons Mean population stimulus–response curves to graded mechanical stimulation (10–120 g) for NS ($n = 20$) and HPC ($n = 19$) neurones (top row). The same data replotted with respect to toprobe size are shown in the bottom row. NS, nociceptive-specific neurons; HPC, heat, pressure, and cold. From Andrew, D. and Craig, A. D. 2002. Quantitative responses of spinothalamic lamina I neurones to graded mechanical stimulation in the cat. J. Physiol. 545, 913–931, reprinted with permission.

largest are found on the back and hip. The receptive field sizes and pattern indicates considerable convergence from primary afferent neurons. Thus, the smallest excitatory receptive fields for lamina I neurons can approximate the size of C-primary afferent polymodal nociceptors (<1 mm). The largest excitatory receptive fields, however, are many times the size of the largest primary afferent receptive field. Lamina I neurons with A-fiber nociceptive input do not have the spotlike receptive fields of the primary afferents, but have a more uniform receptive field, indicating convergence of several A-nociceptors onto the lamina I neurons.

Excitatory receptive fields often have an inhibitory surround region, stimulation of which with noxious stimuli causes inhibitory post synaptic potentials (IPSPs)in the recorded neuron and can inhibit activation induced by stimulation of the more central excitatory receptive field (see Figure 8 for explanation of how these receptive fields are formed).

5.24.9 Projections and Function of Lamina I Neurons

While many of the neurons in lamina I most likely function as integrative interneurons within lamina I, a large proportion of these neurons project to other spinal cord and brain regions.

Many of the neurons in lamina I have been shown to project to higher brain centers including the thalamus, the parabrachial region, the medullary reticular formation, and even the hypothalamus (see chapter 14 for more on this topic). A much larger proportion of lamina I cells have been shown to project to higher brain centers than neurons located in laminae II-IV. Craig A. D. (1996; 2003) has also found lamina I projection neurons responding specifically to itch inputs, and others responding specifically to ergoreception (inputs from actively contracting muscles; see above). He has attempted to generalize these inputs as homeostasis inputs, that is, inputs necessary to maintain body integrity.

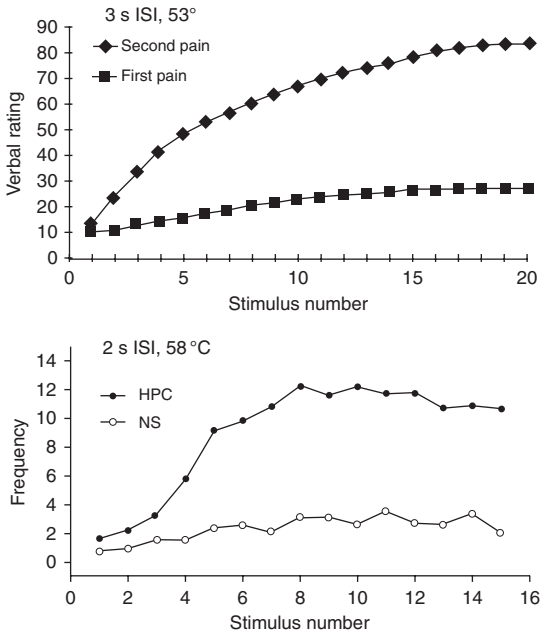

Figure 5 Comparison of the mean response curves of heat, pressure, and cold (HPC) and nociceptive-specific (NS) lamina I spinothalamic tract cells (bottom) to the maximal repeated brief contact heat stimulus trial with the mean report of human subjects to the maximal trial in the study of Vierck *et al*. (1997) (top). In the top panel, 53 DEG = 53°C; ISI = Interstimulus interval. From Craig, A. D. and Andrew, D. 2002. Responses of spinothalamic lamina I neurons to repeated brief contact heat stimulation in the cat. J. Neurophysiol. 87, 1902–1914, reprinted with permission.

Thus, one of the major functions of lamina I is to convey information about nociceptive inputs, itch, and thermal inputs, to higher brain centers . Lamina I also integrates and relays inputs necessary for sympathetic functions. Craig has grouped these functions as homeostatic and suggests the view that lamina I is critical for relatively objective information about body integrity necessary to maintain homeostasis, and thus, life (Craig, A. D., 1996; 2003).

5.24.10 Lamina II

Almost 30 years after the first definitive recordings were made from the substantia gelatinosa, the function of this region is still not understood. Recordings combined with intracellular labeling suggested that the anatomically observable division of lamina II into an inner and outer region had an apparent functional correlation.

5.24.11 Outer Lamina II

5.24.11.1 Modality of Input to Outer Lamina II

The outer region contains mostly nociceptive neurons while the inner region contains mostly innocuous mechanically responsive neurons (see Figure 9 for recordings of common responses). This relationship has been shown in cats, monkeys, and rats (Kumazawa, T. and Perl, E. R., 1978; Bennett, G. J. *et al*., 1979; Light, A. R. *et al*., 1979; Bennett, G. J. *et al*., 1980; Light, A. R. *et al*., 1981; Light, A. R. and Kavookjian, A. M., 1984; Steedman, W. M. *et al*., 1985; Light, A. R. and Willcockson, H. H., 1999).

In a summary of data from experiments in the Light and Perl laboratory (Light, A. R., 1992), 70% of the neurons identified as having cell bodies in lamina IIo were nociceptive. Forty-eight per cent responded only to mechanical nociceptive inputs, while 32% responded to at least noxious heat and noxious mechanical inputs, and many that were tested, also responded to noxious chemicals, making them polymodal nociceptive inputs. Of the remainder, 20% responded to both innocuous and noxious mechanical inputs and 5% each were thermoreceptive (most to cooling) and 5% responded only to innocuous mechanoreceptive stimuli.

The neurons in the outer region of lamina II have small receptive fields, and neurons can receive only noxious mechanical inputs, only noxious heat or cold inputs, and mixtures of mechanical and heat, and noxious chemical inputs. Summarizing data from several publications (Light, A. R. *et al*., 1979; Light, A. R. and Kavookjian, A. M., 1984; Light, A. R. and Kavookjian, A. M., 1988; Light, A. R. and Willcockson, H. H., 1999), some 70% of lamina IIo neurons are nociceptive, 5% are thermoreceptive, 5% are responsive to innocuous mechanical stimuli, and 20% respond to both innocuous mechanical stimuli and nociceptive stimuli. Similar to lamina I neurons, some of the nociceptive neurons respond selectively to noxious mechanical inputs, with perhaps more of these than other types. Other nociceptive neurons respond to noxious heat as well as to noxious mechanical stimuli.

5.24.11.2 Receptive Field Characteristics

The receptive fields of lamina IIo neurons tend to be smaller than those of the overlying lamina I

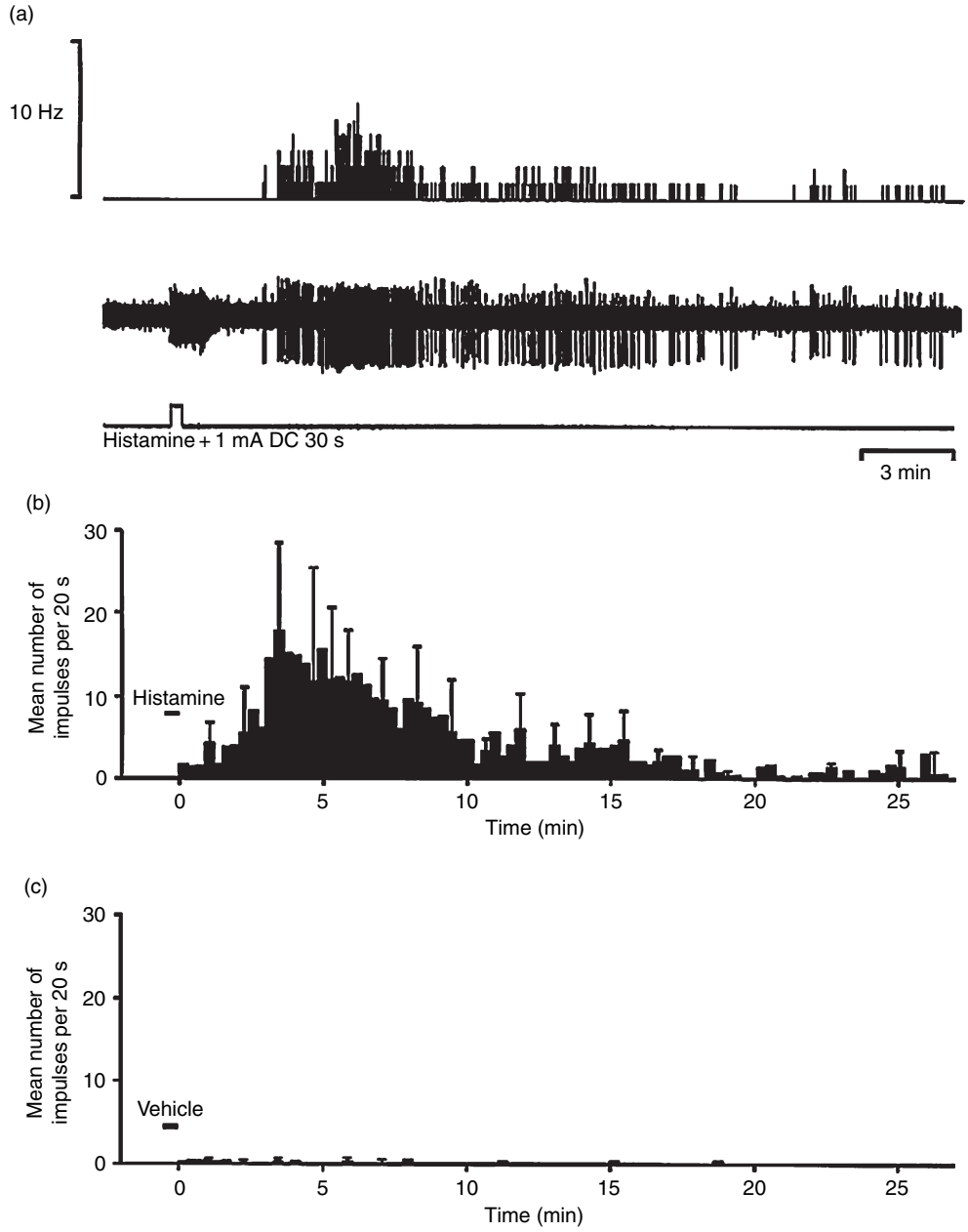

Figure 6 Histamine- and vehicle-evoked responses from histamine-sensitive lamina I spinothalamic tract neurons. (a) The response of a single neuron to histamine. Top histogram, binned firing rate of the neuron (1-s bins). The middle trace shows the analog record of neuronal activity; the thickening of the baseline in this record during the iontophoresis (indicated by the lower trace) is due to the current-evoked activation of several neighboring neurons. (b) Mean response of all 10 histamine-sensitive lamina I spinothalamic tract neurons to histamine application. (c) Mean responses of the same 10 neurons to vehicle application. Error bars, 1 standard deviation; bin size, 20 s; DC, direct current. With permission from Andrew, D. and Craig, A. D. 2001. Spinothalamic lamina I neurons selectively sensitive to histamine: a central neural pathway for itch. Nat. Neurosci. 4, 72–77.

neurons (Price, D. D. *et al.*, 1979). This may be due to the less extensive mediolateral spread of dendrites of lamina II neurons (see chapter 9). Lamina II neurons may also have fewer complex receptive fields, sometimes lacking an inhibitory surround region. These two observations, along with some

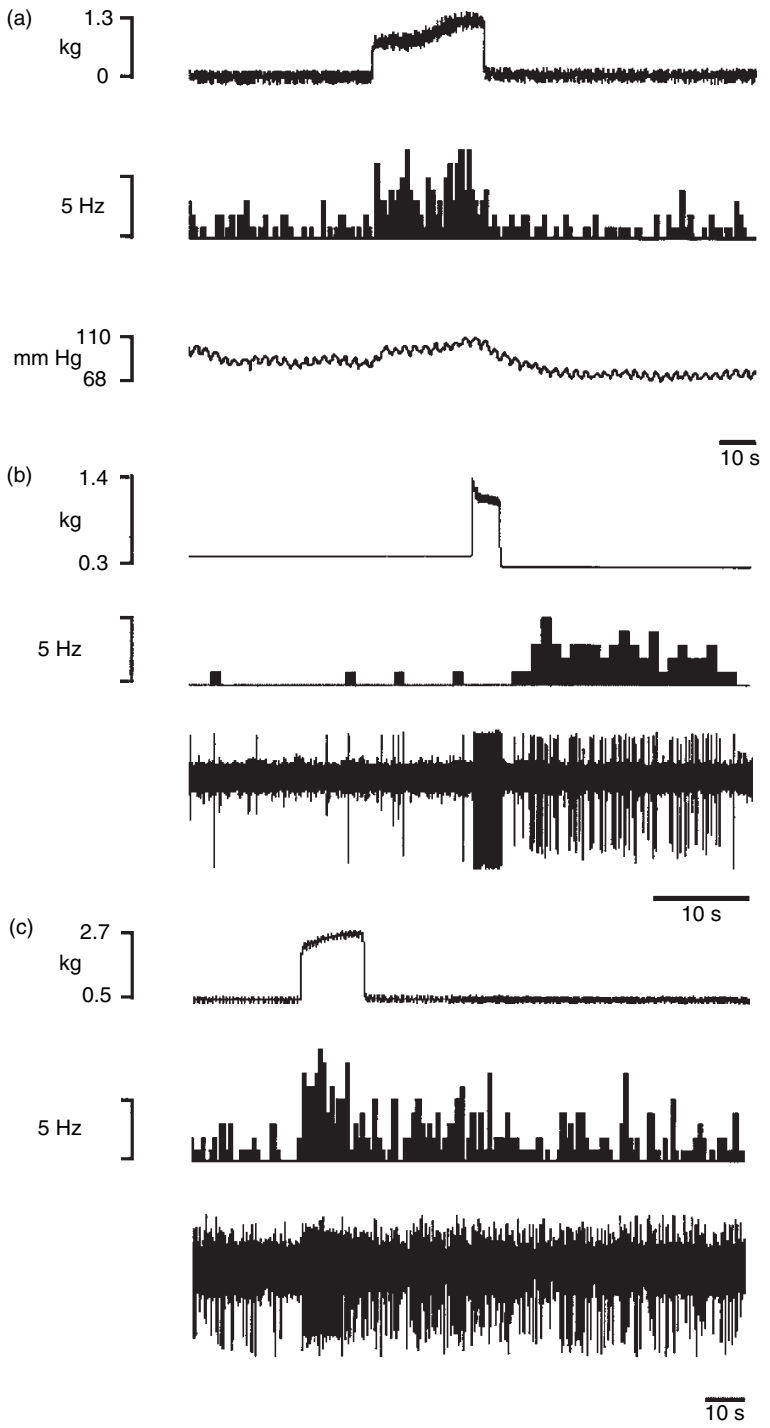

Figure 7 Examples of the variety of responses of lamina I neurons that were excited by muscle contraction. The traces show from the top downward: the tension developed in the triceps surae muscle, the discharge of the single neuron histogrammed in 1 s bins and either mean blood pressure (a) or the neural recording ((b) and (c)). (a) Response from a heat, pressure, and cold (HPC) lamina I neuron with unidentified projections that was excited by contraction that paralleled the tension developed in the muscle and the centrally evoked cardiovascular reflex. (b) Response of another HPC lamina I neuron with unidentified projections that was only excited after the contraction. (c) Response of a spinobulbar lamina I neuron (central conduction velocity 2.2 m s^{-1}) that was excited during and after the contraction; this neuron had no identifiable cutaneous receptive field but responded to stretching the triceps muscle and also to rhythmic contractions at 5 Hz. From Wilson, L. B., Andrew, D., and Craig, A. D. 2002. Activation of spinobulbar lamina I neurons by static muscle contraction. J. Neurophysiol. 87, 1641–1645, reprinted with permission.

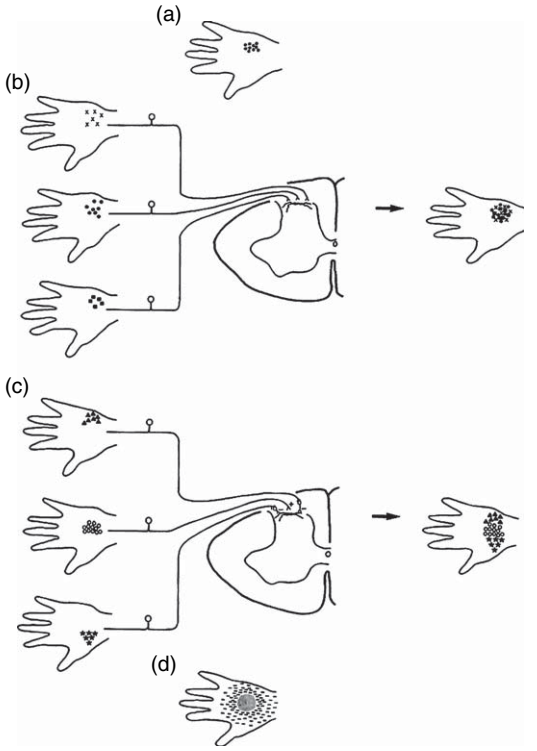

Figure 8 Diagram of mechanisms of integration of nociceptive inputs in lamina I neurons. (a) Indicates the receptive field of a single primary afferent nociceptor with an Aδ axon. Each spot represents a point at which noxious mechanical stimulation evokes a discharge. (b) Left panel indicates the receptive fields of three mechanical nociceptors with overlapping receptive fields. The three primary afferents terminate on the same lamina I neuron in the middle panel. The right panel indicates the resulting receptive field. The receptive field is somewhat larger, and more responsive points are found within the responsive area. Thus, unlike primary afferent receptors, spinal nociceptive neurons have nearly continuous receptive fields with less unresponsive regions between responsive spots. (c) Left panel indicates the receptive fields of three nonoverlapping primary afferent mechanical nociceptors. The middle panel indicates that the lamina I neuron receives excitatory input from the axons whose receptive field is indicated with open circles. The other two axons excite inhibitory neurons (this is a simplification), and in all cases, both excitatory and inhibitory neurons are excited by all primary afferent neurons). The result is that the receptive field of the lamina I neuron, shown at right, consists of inhibitory inputs (shown with filled symbols) and excitatory inputs (shown with open symbols). (d) This receptive field is typical for spinal cord nociceptive neurons and indicates both of the processes described in (a)–(c). The central crosshatched region is the excitatory receptive field in which noxious mechanical stimulation causes excitation of the spinal neuron. Noxious mechanical stimulation of the region outside the excitatory receptive field causes inhibition and is indicated by minus signs. This inhibitory field fades out gradually as the distance from the excitatory field increases. Adapted from Light, A. R. 1992. Pain and Headache (Vol. 12): the Initial Processing of Pain and its Descending Control: Spinal and Trigeminal Systems. Karger, reprinted with permission.

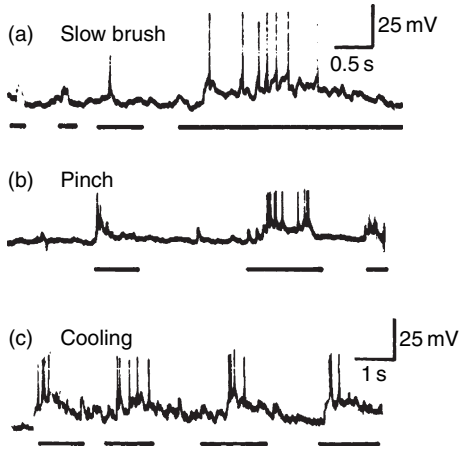

Figure 9 Low-gain, direct-current patch-clamp recordings *in vivo* from the most common types of responsive neurons encountered in the substantia gelatinosa of rats. Examples of slow brush (a), pinch (b), and innocuous cooling (c) (ethyl chloride spray applied to brush and brushed on skin) responsive neurons. From Light, A. R. and Willcockson, H. H. 1999. Spinal laminae I–II neurons in rat recorded in vivo in whole cell, tight seal configuration: properties and opioid responses. J. Neurophysiol. 82, 3316–3326, reprinted with permission.

anatomical findings (see chapter 9) suggest that at least some lamina II neurons project inputs to overlying lamina I neurons.

5.24.12 Projections and Function of Outer Lamina II Neurons

In addition to projections to lamina I, lamina IIo neurons have been shown to project to deeper laminae, including laminae III, IV, and V (Light, A. R. and Kavookjian, A. M., 1988; Eckert, W. A., III, *et al.*, 2003). Substantial intralaminar projects have also been noted for many years (Szentagothai, J., 1964; Matsushita, M., 1969; Rethelyi, M. and Szentagothai, J., 1969; Rethelyi, M. *et al.*, 1981; 1983; 1989). Both inhibitory and excitatory intralaminar, as well as extralaminar connections, are possible (Lu, Y. and Perl, E. R., 2005). A few neurons in lamina II have also been shown to project long connections to the thalamus (Giesler, G. J., Jr. *et al.*, 1978; Willis, W. D. *et al.*, 1978). Whether these projections represent ectopic lamina I neurons, or more projections of this variety have yet to be detected is unknown.

Thus, lamina IIo neurons may function both as inhibitory neurons helping to create the inhibition surround receptive fields described above, and as

excitatory relay neurons for convergence of receptive fields and possible amplification of the excitatory signal (see Figure 8).

5.24.12.1 Inner Lamina II (II_i)

The inner division of lamina II has many neurons that respond to innocuous mechanical stimuli (Light, A. R. *et al.*, 1979; Price, D. D. *et al.*, 1979; Woolf, C. J. and Fitzgerald, M., 1983; Light, A. R. and Kavookjian, A. M., 1988; Light, A. R. and Willcockson, H. H., 1999). A detailed analysis of the types of inputs to this lamina has not been made. One survey (Light, A. R., 1992) found that between 50% and 80% of the neurons responded only to innocuous mechanical stimuli. A very common response was a preferential response to a very slowly moving stimulus (e.g., see Figure 9(a)). The response to mechanical stimulation often adapts with very few repetitions of the stimulus, sometimes after only a single stimulation. Responses of this type do not relate directly to any known type of primary afferent input. Intracellular analysis of these response properties identified a prominent IPSP evoked by innocuous mechanical stimulation that was capable of inhibiting nearly all action potential generation (Light, A. R. *et al.*, 1979). Neurons with these types of inputs seem to dominate this sublamina.

However, in addition to innocuous mechanical inputs, considerable circumstantial evidence suggests that nociceptive inputs should also reach inner lamina II. First, a few neurons in this layer have been found to be activated preferentially by nociceptive stimuli. Second, primary afferents labeling with isolectin B4 (IB4) terminate heavily in inner lamina II. At least some of the IB4-positive afferents have been identified as nociceptive, and eliminating IB4-containing primary afferents reduced inflammatory pain in rats. vanilloid receptor like 1 (VRL-1 also called TRPV2)also labels inner lamina II suggesting that a population of myelinated nociceptor may selectively terminate in this region (Lewinter, R. D. *et al.*, 2004). Neurons in lamina IIi show increases in protein kinase Cγ (PKCγ) following inflammation which results in allodynia (Martin, W. J. *et al.*, 1999; 2001). At least a few nociceptive primary afferent fibers have shown extensive terminations in lamina IIi (Sugiura, Y. *et al.*, 1986; Koerber H. R. *et al.*, personal communication, 2004). Finally, either muscle nociceptive input to laminae IIi cells, and/or muscle metaboreceptor input to this layer is predicted by the terminations of single group IV muscle afferents in this layer (Ling, L. J. *et al.*, 2003).

Potentially then, nociceptive neurons, and possibly, metaboreceptive neurons should be found in inner lamina II. Whether these neurons represent special types of nociceptive inputs (such as inputs sensitive to inflammation) or have nociceptive inputs (such as muscle nociceptive inputs) that have not been found in recording studies thus far remains to be examined.

5.24.12.1.1 Projections and function of inner lamina II neurons

Like other neurons in lamina II, lamina IIi has substantial axonal projections to other regions of lamina II (Szentagothai, J., 1964; Matsushita, M., 1969; Rethelyi, M. and Szentagothai, J., 1969; Rethelyi, M. *et al.*, 1981; 1983; 1989). In addition, at least some of these neurons project axons to deeper laminae, where they synapse with other spinal cord neurons (Light, A. R. and Kavookjian, A. M., 1988; Eckert, W. A., III, *et al.*, 2003). Basbaum's laboratory has also recently proposed that neurons in this region project to lamina V neurons which subsequently project to higher brain regions, not usually considered in nociceptive processing (Braz, J. M. *et al.*, 2005).

The innocuous responses of lamina IIi neurons seems most related to sensuous touch (Olausson, H. *et al.*, 2002) or tickle. As these neurons have not been shown to project in large numbers to the thalamus or other brain regions rostral to the spinal cord, it is unknown how these inputs are relayed to higher brain centers. However, it is interesting that some have noted that tickle is abolished following lesions of the anterolateral tract (Lahuerta, J. *et al.*, 1990).

5.24.12.2 Lamina III

Lamina III mostly contains neurons that receive only innocuous mechanical inputs (Pomeranz, B. *et al.*, 1968; Price, D. D. and Mayer, D. J., 1974; Wall, P. D. *et al.*, 1979; Light, A. R. and Durkovic, R. G., 1984). However, at least some nociceptive neurons can be found here. Nociceptive neurons in lamina III may respond only to noxious mechanical stimuli, or to noxious thermal and chemical stimuli as well as to noxious mechanical stimuli (Brown, A. G. and Fyffe, R. E., 1981; Maxwell, D. J. *et al.*, 1983; Maxwell, D. J. and Koerber, H. R., 1987). Most investigators have reported that neurons that do respond to noxious stimuli, also respond to innocuous stimuli, albeit with much lower action potential frequency. The importance of lamina III in nociception is unknown. In cats, many lamina III

neurons project to the lateral cervical nucleus. In rats and primates, at least some of these neurons project to the dorsal column nuclei (Rustioni, A. *et al.*, 1979; Giesler, G. J., Jr. *et al.*, 1984). As with lamina IIi, PKCγ is upregulated in lamina III neurons following nerve injury and inflammation (Polgar, E. *et al.*, 1999; Miletic, V. *et al.*, 2000), suggesting at least inflammatory inputs, if not nociceptive inputs to this lamina.

5.24.12.3 Lamina IV

Lamina IV neurons are also dominated by responses to innocuous mechanical stimuli (Armett, C. J. *et al.*, 1962; Pomeranz, B. *et al.*, 1968; Price, D. D. and Browe, A. C., 1973). Many other neurons, however, respond more vigorously to noxious stimuli (both mechanical and thermal) than to innocuous stimuli (the WDR response). In cats, for example, Light A. R. and Durkovic R. G. (1984) found that 56% of the recorded neurons responded only to innocuous mechanical stimuli, while 37% responded to innocuous stimuli, but increased their response rate to noxious stimuli. Only 6% of the neurons responded only to noxious stimuli. In cats, a substantial number of lamina IV neurons project to the lateral cervical nucleus and are, therefore, spinocervical neurons (Brown, A. G., 1968; Brown, A. G. and Franz, D. N., 1969; Bryan, R. N. *et al.*, 1973; 1974). At least some of these neurons encode some aspects of noxious stimuli. The proportion of spinocervical neurons in primates appears to be less than in cats (Bryan, R. N. *et al.*, 1974). Again some of these neurons encode noxious stimuli (Brown, A. G., 1968; Brown, A. G. and Franz, D. N., 1969; Bryan, R. N. *et al.*, 1973; 1974; Kajander, K. C. and Giesler, G. J., Jr., 1987). Specific functions for noxious inputs relayed via the spinocervical tract are unknown, but may represent an alternative pathway for pain transmission, separate from the spinothalamic tract (Willis, W. D. and Westlund, K. N., 1997). Finally, at least some lamina IV neurons project to the thalamus (Trevino, D. L. *et al.*, 1973; Albe-Fessard, D. *et al.*, 1974; Trevino, D. L. *et al.*, 1974; Willis, W. D. *et al.*, 1974; Price, D. D. and Mayer, D. J., 1975).

5.24.12.4 Lamina V

A very large literature exists on the nociceptive properties of neurons in lamina V (Wall, P. D., 1967; Mendell, L. M. and Wall, P. D., 1965; Hillman, P. and Wall, P. D., 1969; Wall, P. D., 1973; Price, D. D. and Dubner, R., 1977; Dubner, R., 1978; Dubner, R. and Bennett, G. J., 1983; Willis, W. D., 1985; 1988). This is partly due to the relative ease of recording the larger neurons located in this layer, and partly due to its known large projection to the thalamus, making it a large contributor to the spinothalamic tract and this tract has long been implicated as a pain transmission pathway.

Lamina V contains many neurons that respond to both noxious and innocuous stimuli, and also neurons that respond selectively to noxious stimuli. Innocuous mechanoreceptive neurons are also found in this lamina (Mendell, L. M. and Wall, P. D., 1965; Hillman, P. and Wall, P. D., 1969; Light, A. R. and Durkovic, R. G., 1984).

The receptive fields of lamina V neurons tend to be larger than neurons with similar modalities in lamina I–IV. A common feature of the receptive fields, like those in lamina I, is a zone of inhibitory influence surrounding the excitatory receptive field (inhibition surround). Typically, the most effective stimulus for eliciting inhibition is the same as that of the excitatory region (Hillman, P. and Wall, P. D., 1969).

The response characteristics of at least some lamina V neurons correlate well with human estimates of pain intensity and with reflex response of animals to noxious stimuli (Dubner, R. *et al.*, 1977; 1980; Casey, K. L., 1982; Dubner, R. *et al.*, 1989; e.g., see figure 10). This, along with the fact that many lamina V neurons project in the anterolateral tract to the thalamus, both of which are implicated in pain transmission, indicate that lamina V neurons are important in at least some aspects of pain perception. The likely contribution of lamina V neurons to the flexion reflex pathway probably contributes to the observations that lamina V neuron responses are similar to nociceptive reflexes (Light, A. R. and Durkovic, R. G., 1984; Morgan, M. M., 1998).

The presence of innocuous activation of many lamina V neurons in addition to nociceptive activation requires additional mechanisms to allow discrimination between innocuous and noxious stimuli.

5.24.13 The Ventral Horn

The ventral horn contains many neurons that project to the thalamus. However, the properties of these spinal neurons suggest a role in proprioception, rather than in nociceptive processing (Menetrey, D. *et al.*, 1984; Ammons, W. S., 1987; Craig, A. D., Jr. *et al.*, 1989).

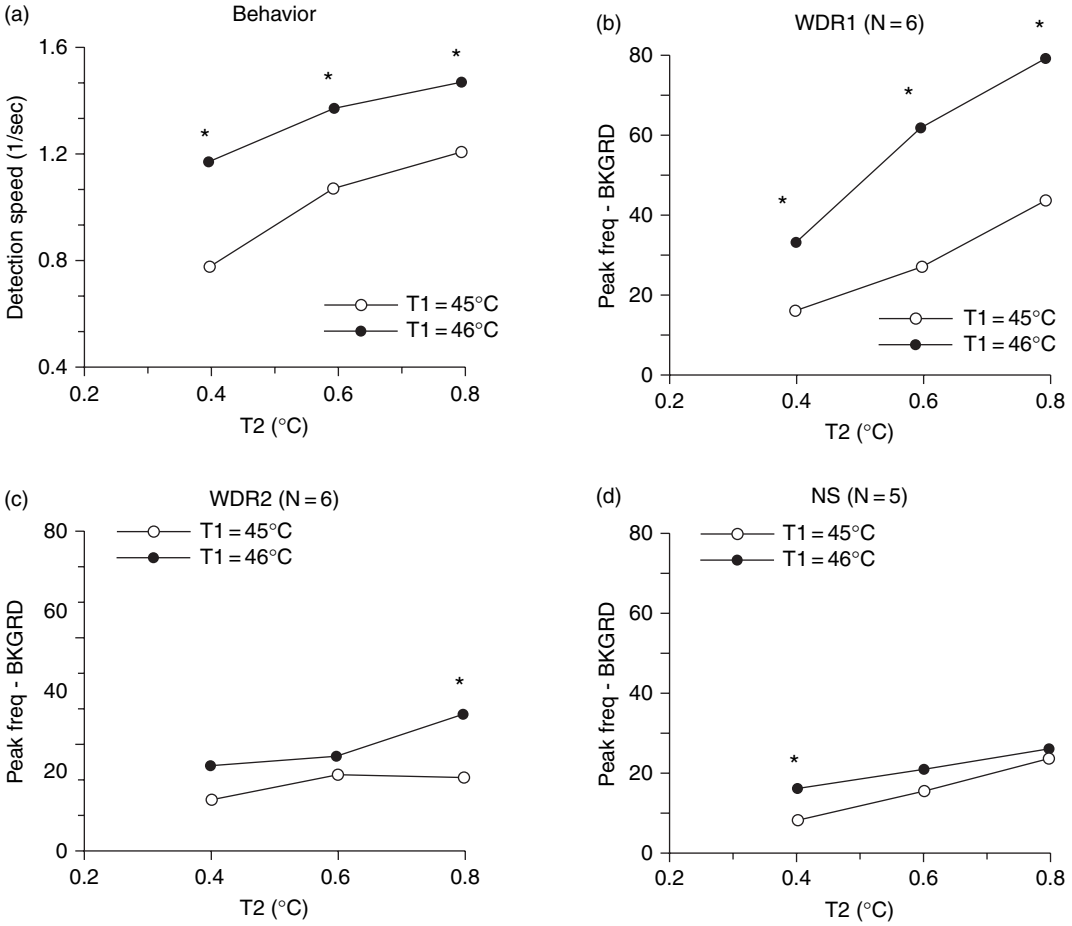

Figure 10 (a) Detection speeds in response to 0.4, 0.6, and 0.8 °C T2 stimuli from T1s of 45 and 46 °C while recording from wide-dynamic range (WDR)1, WDR2, and nociceptive-specific (NS) neurons. There was a significant increase in detection speed for each T2 temperature when Tl was 46 °C ($P < 0.01$). Each point represents the average of four trials from each of 17 neurons. (b)–(d) Responses of WDRl (b), WDR2(c), and NS (d) neurons to the same stimuli as in (a). Asterisks indicate significant increases ($P < 0.01$) in neuronal discharge when Tl was 46 °C. Each point represents the average of four trials per neuron. From Dubner, R., Kenshalo, D.R., Jr., Maixner, W., Bushnell, M. C., and Oliveras, J. L. 1989. The correlation of monkey medullary dorsal horn neuronal activity and the perceived intensity of noxious heat stimuli. J. Neurophysiol. 62, 450–457, reprinted with permission.

5.24.14 Somatotopic Organization

Submodality is encoded by neurons in different laminae. However, spatial encoding of the body surface is encoded in the medial-lateral and rostral-caudal planes (Brown, P. B. and Fuchs, J. L., 1975; Koerber, H. R. and Brown, P. B., 1977; Light, A. R. and Durkovic, R. G., 1984; Ritz, L. A. *et al.*, 1985; Brown, P. B. *et al.*, 1997; 2005). The overall map of the body surface is similar in all laminae. Figures 11 and 12 show the overall somatotopic map and more detail of the lumbar region. Overall, the map follows the segmental body plan. However, the map is distorted in the regions that encode the highly innervated digits and feet with a much greater representation of these body regions than the neck and trunk regions. The distortions in this map also represent the density of primary afferent innervation of the skin, with digits being much more densely innervated than proximal limb regions and trunk regions. These distortions are correlated to nociceptive discrimination of these same body regions with greater discrimination possible at the tips of the digits, and less on the trunk.

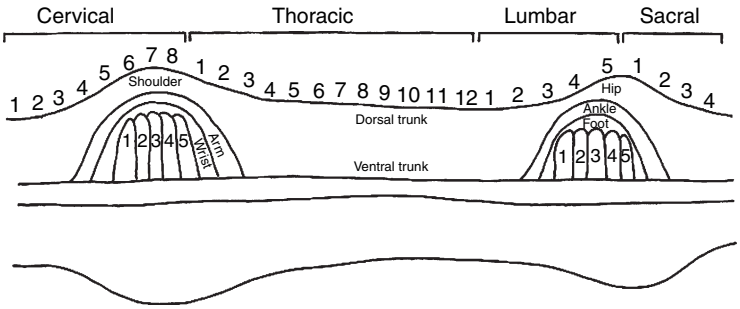

Figure 11 Somatotopic map of representation of body surface in primal spinal cord gray matter. Cervical, thoracic, lumber, and sacral segments are indicated. Maps of this sort are somewhat misleading in that receptive fields often encompass more than one of the body regions indicated on the map. For example, in the lumbar cord, receptive fields notes as hip may be restricted to the hip, but others may include a strip that includes the entire leg including the toes as well as the hip. From Light, A. R. 1992. Pain and Headache (Vol. 12): the Initial Processing of Pain and its Descending Control: Spinal and Trigeminal Systems. Karger, reprinted with permission.

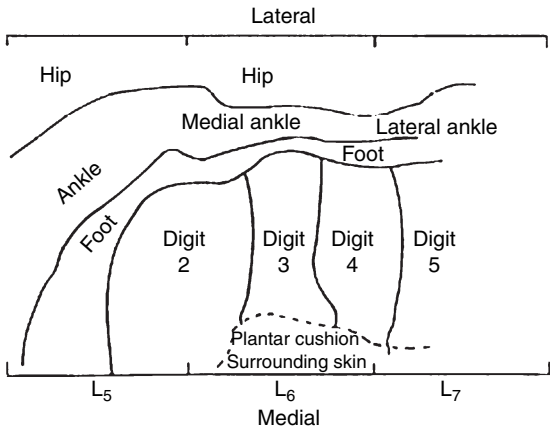

Figure 12 Somatopic organization of the foot representation in the spinal cord of cats. Most medial toe designated as toe 2; most lateral toe designated as toe 5. Map depicts density centers and does not indicate the overlapping of cell groups that have different receptive field locations. From Light, A. R. and Kavookjian, A. M. 1984. Substantia gelatinosa neurons with axons projecting to other dorsal horn laminae. Soc. Neurosci. Abstr. 10, 489, reprinted with permission.

5.24.15 Physiological Properties of Spinal Neurons

Considerable detail of the physiological properties of the intrinsic neurons of the spinal cord has been obtained by using recordings from spinal cord slices. These preparations have the advantage of a known a stable milieu surrounding the neurons. In addition, access to neurons in either the transverse or horizontal slice is less problematic because less white matter tissue must be traversed with a microelectrode before attaining recordings from the cell bodies. Because access is easier, whole-cell patch clamp of the spinal cord neurons can be readily accomplished in slice preparations. Recordings in this mode are more stable, details of synaptic inputs more easily observed, and membrane currents rather than voltage changes can be measured.

The major disadvantage, however, is that except for very recent recordings (Koerber, personal communication, 2006) the inputs to the spinal cord are removed. Thus, the adequate stimulus for the neurons is unknown in slice recordings. Since neurons are heterologous with respect to their inputs in all areas of the spinal cord, the physiological properties obtained from slice preparations can only be related to the types of inputs they receive in a broad fashion, drawing on what is know about the most common types of neurons found in the specific laminae. With these limitations in mind, still, much useful knowledge has been obtained from slice preparations. Where possible, we relate the properties observed in slice preparations to those obtained from intact preparations.

5.24.16 Intrinsic Properties of Spinal Dorsal Horn Neurons

In the spinal dorsal horn, using sharp electrode and whole-cell patch clamp recording several types of neurons have been distinguished on the basis of their intrinsic firing properties. However, these firing types and the relative numbers of each type vary depending on the experimental conditions and

species. Seven types of firing have been identified. Tonic, burst, delayed onset, gap, phasic, and single spike. These are shown in Figure 13.

Tonically firing neurons have repetitive action potentials with little frequency adaptation and little amplitude attenuation during sustained depolarization. (Figures 13 (Aa) and 13 (Ca)). The majority of tonic neurons are either WDR or nociceptive-specific neurons (Lopez-Garcia, J. A. and King, A. E., 1994). The ion channels expressed by tonic neurons that

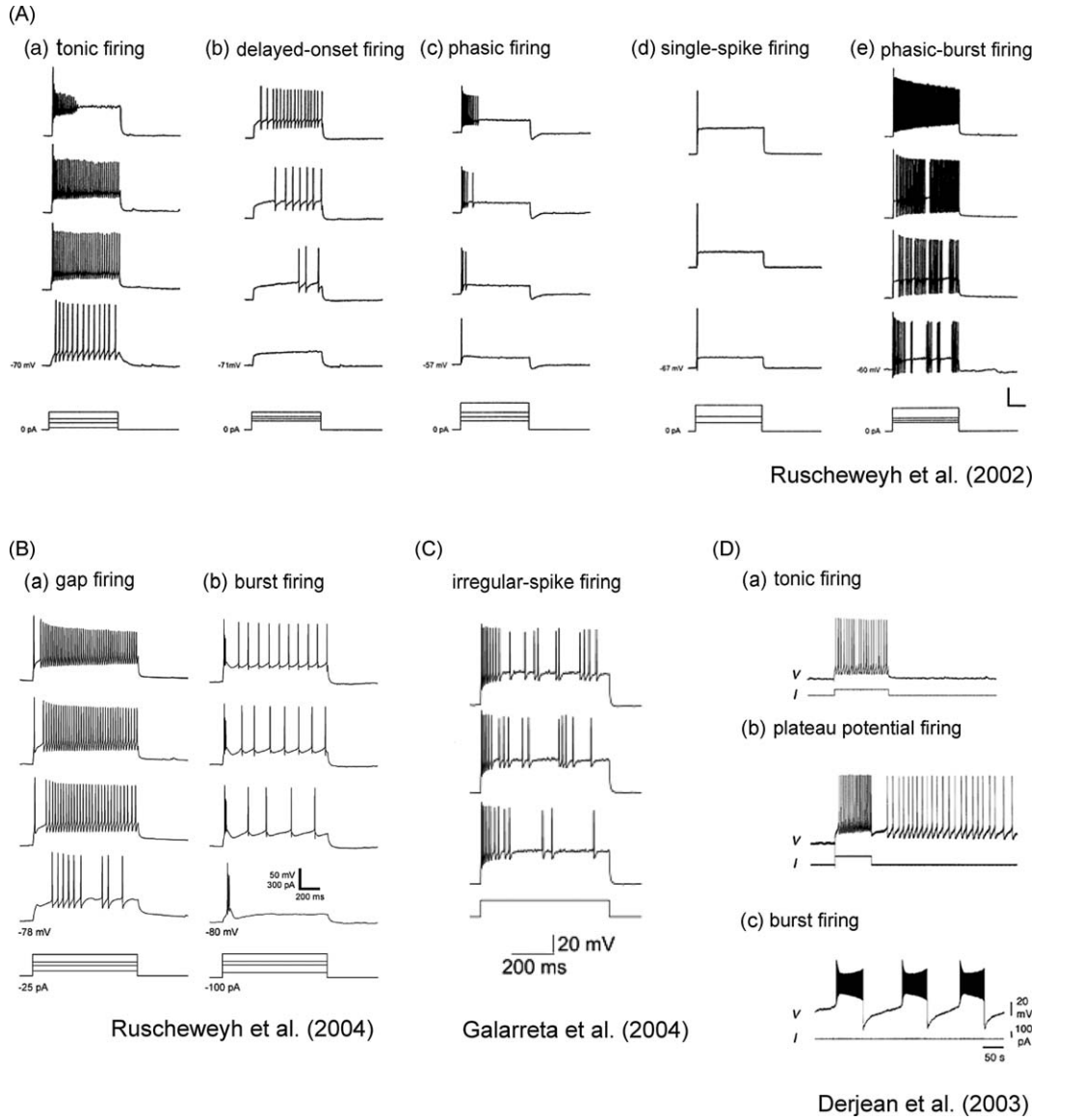

Figure 13 Firing patterns of neurons. (A) Five patterns of rat spinal dorsal horn neurons. Firing patterns were obtained in response to 1-s injections of depolarizing current (25–350 pA, 25-pA steps) at resting membrane potential. Bottom traces in (a)–(e), injected currents. (B) Typical firing patterns of lamina I projection neurons. Firing patterns were obtained in response to depolarizing current injection from hyperpolarized holding potentials. C: Deep dorsal horn neurons show three modes of firing. A: from Ruscheweyh, R. and Sandkuhler, J. 2002. Lamina-specific membrane and discharge properties of rat spinal dorsal horn neurones in vitro. J. Physiol. 541, 231–244, reprinted with permission; B: from Dahlhaus, A., Ruscheweyh, R., and Sandkuhler, J. 2005. Synaptic input of rat spinal lamina I projection and unidentified neurones in vitro. J. Physiol. 566(Pt 2), 355–368, reprinted with permission; C: from Derjean, D., Bertrand, S., Le Masson, G., Landry, M., Morisset, V., and Nagy, F. 2003. Dynamic balance of metabotropic inputs causes dorsal horn neurons to switch functional states. Nat. Neurosci. 6(3), 274–281, reprinted with permission.

shape this response pattern are only partly understood. It has been suggested that a voltage gated Na^+ current in combination with a pronounced delayed rectifier K^+ (K_{DR}) current and absent or weak A-type K^+ (K_A) current help to generate the basic tonic firing pattern (Ruscheweyh, R. and Sandkuhler, J., 2002; Melnick, I. V. *et al.*, 2004b). A Ca^{2+}-dependent K^+ (K_{Ca}) conductance that is sensitive to apamin regulates the discharge frequency, prolonging interspike intervals, and stabilizing firing pattern evoked by sustained membrane depolarization (Melnick, I. V. *et al.*, 2004a).

Tonic firing neurons in lamina I display prolonged excitatory postsynaptic potentials (EPSPs). The mechanisms for these prolonged EPSPs appears not to be a property of the presynaptic release, but are mediated by a persistent sodium current, $I_{Na,p}$ that amplifies and prolongs the depolarization caused by brief stimulation, combined with a persistent calcium current, $I_{Ca.p}$, that contributes to the prolongation, but not the amplification (Prescott, S. A. and De Koninck, Y., 2005). The net result is that these currents can increase integration time and encourage temporal summation of inputs, at the expense of reduced ability to encode the timing of synaptic inputs. Thus, the tonic firing neurons operate as integrators of synaptic inputs.

5.24.16.1 Burst Firing Neurons

Burst firing neurons exhibit a high-frequency barrage of action potentials that ride on the peak of a low-threshold Ca^{2+} spike (Figure 13 (Bb)). In the superficial dorsal horn (laminae I and II), the burst firing pattern was characterized by a short burst of two to four action potentials riding on a slow depolarizing wave at the onset of a depolarizing current pulse (Ruscheweyh, R. *et al.*, 2004; see Figure 13 (Bb)). With stronger current injections, this pattern could be converted to the tonic pattern (Ruscheweyh, R. and Sandkuhler, J., 2002). The burst pattern was evident only if the neuron was held more negative than −60 mV in whole-cell recordings. The current causing the bursting pattern was not affected by tetrodotoxin, but was partially blocked by Ni^{2+} and Cd^{2+}. Interestingly, the burst firing occurred almost exclusively in projection neurons and was nearly absent in nonprojection neurons, and found more often in neurons projecting to the periaqueductal gray than neurons projecting to the parabrachial region (Ruscheweyh, R. *et al.*, 2004).

The potential function of burst firing for dorsal horn nociceptive neurons is not currently understood. However, some have suggested that this pattern could contribute to the distortion of nociceptive processing in the dorsal horn that is associated with persistent pathological pain (Herrero, J. F. *et al.*, 2000). An example of an animal model of this is that increased burst firing of neurons in the spinal cord was correlated with the induction of recurrent autotomy in nerve injured rats (Asada, H. *et al.*, 1996).

5.24.16.2 Delayed-Onset Firing Neurons

Delayed-onset firing neurons demonstrate a slow ramp depolarization in response to subthreshold depolarizing current pulses (Yoshimura, M. and Jessell, T. M., 1989; Grudt, T. J. and Perl, E. R., 2002; Prescott, S. A. and De Koninck, Y., 2002; Ruscheweyh, R. and Sandkuhler, J., 2002). With higher current injections, a delay between the onset of the depolarizing current and the first action potentials gradually shortens. Repetitive firing is less regular than in tonic firing neurons, and often, the firing rate increases during the current pulse (Prescott, S. A. and De Koninck, Y., 2002; Ruscheweyh, R. and Sandkuhler, J., 2002). Yoshimura M. and Jessell T. M. (1989a) and Ruscheweyh R. and Sandkuhler J. (2002) suggested that the transient outward rectifying current (I_A) was involved in the response of neurons to sudden depolarization and served to delay the onset of the first action potentials.

Delayed-onset neurons were found almost entirely in lamina I and II, and not in deeper laminae. Whether these neurons are nociceptive, and the functional relevance of this firing pattern is not known.

5.24.16.3 Gap Firing Neurons

Gap firing neurons, also called late spiking neurons, are characterized by a considerably delayed-onset first spike flowed by tonic firing after week current pulses. With stronger current pulses, a long interval occurs between the first and second spike apparently due to a transient hyperpolarization occurring after the onset of the first depolarizing impulse (see Figure 13 (Ba)). Ruscheweyh R. *et al.* (2004) suggested that this firing pattern could be evoked only if the neuron was held at a negative potential more negative than −75 mV. They also suggested that gap firing and burst firing are the most common patterns of projection neurons with less excitable membranes having a broad action potential duel to a hump in the falling phase of the action potential. They determined that gap firing neurons preferentially project to the parabrachial region of the

brainstem, with fewer projecting to the periaqueductal gray region. Apparently, a slow I_A is required for the appearance of gap firing (Ruscheweyh, R. *et al.*, 2004).

5.24.16.4 Phasic Firing Neurons

Phasic firing neurons (Figure 13Ac) generate a short burst of action potentials during sustained depolarization. They have been reported by several groups (Thomson, A. M. *et al.*, 1989; Lopez-Garcia, J. A. and King, A. E., 1994; Prescott, S. A. and De Koninck, Y., 2002; Ruscheweyh, R. and Sandkuhler, J., 2002; Melnick, I. V. *et al.*, 2004b). The phasic pattern may be related to the density of Na^+ channels, and their voltage dependency, which may be shifted towards more positive potentials. Melnick I. V. *et al.*, (2004a) found that phasic neurons were found in the lateral part of lamina II. Lopez-Garcia J. A. and King A. E. (1994) classified most phasic neurons as nociceptive specific.

5.24.16.5 Single-Spike Firing Neurons

Single-spike firing neurons (Figure 13(Ad)) typically generate only one action potential at the onset of a current pulse, regardless of the intensity of the current pulse. A transient, voltage-dependent outward current may be involved in generating the single spike pattern. 4-aminopyridine (a K_v blocker) converts single-spike firing to tonic firing (Ruscheweyh, R. and Sandkuhler, J., 2002).

5.24.17 Relationship between Intrinsic Firing Patterns and Physiological Types of Dorsal Horn Neurons

Very few investigators have attempted to relate the firing patterns described above to the types of adequate stimuli that normally activate these neurons. Figure 14 demonstrates the data from one such attempt in rats. As this figure indicates Lopez-Garcia J. A. and King A. E. (1994) determined that the majority (81%) of WDR neurons responded with tonic firing, while nociceptive-specific neurons were mostly phasic firing neurons. Low-threshold mechanoreceptor (LTM) neurons were of both the tonic and phasic firing types. Neurons that were not fired by adequate stimuli, but demonstrated subthreshold inputs were either tonic firing or single spike type of neurons. In contrast to their conclusions, Graham B. A. *et al.* (2004) using whole-cell recordings in adult mice *in vivo* did not

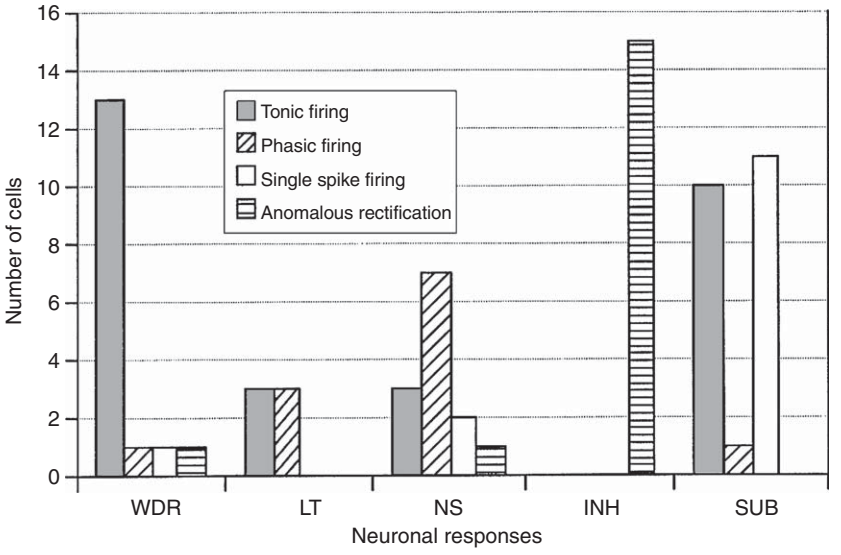

Figure 14 Distribution of electrophysiological groups from a hemisected slice preparation from rats with hindlimb attached. The number of physiologically classified wide-dynamic range neurons (WDR), low-threshold neurons (LT), nociceptive-specific neurons (NS), and neurons displaying inhibitory events (INH) are shown along with the firing type. SUB, subthreshold for firing action potentials. Adapted from Lopez-Garcia, J. A. and King, A. E. 1994. Membrane properties of physiologically classified rat dorsal horn neurons in vitro: correlation with cutaneous sensory afferent input. Eur. J. Neurosci. 6, 998–1007, with permission.

find a consistent relationship between any of the firing pattern types of neurons and physiological inputs.

Lu Y. and Perl E. R. (2003) also found that all lamina II neurons receiving inhibitory inputs from other lamina II neurons were of the phasic firing type, indicating at least some functional organization is related to the firing pattern of lamina II neurons.

Clearly, the firing patterns described here reflect specific currents mediated by specific ion channels. These specific ion channels can be altered by a number of pharmacologic agents, endogenous neurotransmitters and neuromodulators. The specificity of neurons for these channels could convey specificity of drug action on particular functional types of neurons. Some of this is the topic of Chapter 20, and much of this will be the subject of future investigations into the rich modulatory capacity of sensory neurons in the dorsal horn of the spinal cord.

5.24.18 Summary

The spinal cord dorsal horn contains the first relay for afferent inputs from the skin, muscles, and viscera of the body. The superficial dorsal horn contains at least some neurons that maintain the selectivity for modalities encoded by the primary afferent endings. These include a number of different modalities including innocuous warming, innocuous cooling, noxious mechanical, noxious thermal, noxious chemical, prurigenic (itch producing), metabolic (non-noxious signals from actively contracting muscles), and innocuous mechanical stimuli of various forms as well as other inputs from autonomic sensory neurons.

In the majority of neurons in the dorsal horn, various combinations of these inputs are integrated to allow detection of features (such as edges, speed of movement, location on the skin, noxious hot objects, etc.). Such integration allows for useful motor outputs to be generated to compensate for the inputs received, e.g., moving a limb away from a hot object, scratching a biting insect, or wiping away an insect crawling on the skin.

Many neurons in the dorsal horn also transmit selective afferent inputs, or integrated inputs to other regions of the central nervous system, including other parts of the spinal cord, the medulla, midbrain, and thalamus as well as the hypothalamus. Thus, the dorsal horn serves as the first integration and relay center for nociceptive as well as a variety of non-nociceptive inputs.

Dorsal horn neurons are modulated by inputs from higher brain centers. Inputs from other centers can greatly modify the amplitude of signals relayed from primary afferent neurons.

Dorsal horn neurons are quite heterogeneous with respect to the types of inputs that they encode, and with respect to their intrinsic membrane properties. In at least some cases, it appears that the intrinsic membrane properties are associated with the types of inputs they receive, and these intrinsic properties may allow the neurons to better integrate certain types of inputs.

References

Albe-Fessard, D., Levante, A., and Lamour, Y. 1974. Origin of spino-thalamic tract in monkeys. Brain Res. 65, 503–509.

Ammons, W. S. 1987. Characteristics of spinoreticular and spinothalamic neurons with renal input. J. Neurophysiol. 58, 480–495.

Andrew, D. and Craig, A. D. 2001. Spinothalamic lamina I neurons selectively sensitive to histamine: a central neural pathway for itch. Nat. Neurosci. 4, 72–77.

Andrew, D. and Craig, A. D. 2002. Quantitative responses of spinothalamic lamina I neurones to graded mechanical stimulation in the cat. J. Physiol. 545, 913–931.

Armett, C. J., Gray, J. A. B., Hunsperger, R. W., and Lal, K. B. 1962. The transmission of information in primary receptor neurones and second-order neurones of a phasic system. J. Physiol. 164, 395–421.

Asada, H., Yamaguchi, Y., Tsunoda, S., and Fukuda, Y. 1996. The role of spinal cord activation before neurectomy in the development of autotomy. Pain 64, 161–167.

Bennett, G. J., Abdelmoumene, M., Hayashi, H., and Dubner, R. 1980. Physiology and morphology of substantia gelatinosa neurons intracellularly stained with horseradish peroxidase. J. Comp. Neurol. 194, 809–827.

Bennett, G. J., Hayashi, H., Abdelmoumene, M., and Dubner, R. 1979. Physiological properties of stalked cells of the substantia gelatinosa intracellularly stained with horseradish peroxidase. Brain Res. 164, 285–289.

Braz, J. M., Nassar, M. A., Wood, J. N., and Basbaum, A. I. 2005. Parallel ''pain'' pathways arise from subpopulations of primary afferent nociceptor. Neuron 47, 787–793.

Brown, A. G. 1968. Single unit activity in the spinocervical tract of the cat. J. Physiol. (Lond.) 198, 62passim–62pas63p.

Brown, A. G. and Franz, D. N. 1969. Responses of spinocervical tract neurones to natural stimulation of identified cutaneous receptors. Exp. Brain Res. 7, 231–249.

Brown, A. G. and Fyffe, R. E. 1981. Form and function of dorsal horn neurones with axons ascending the dorsal columns in cat. J. Physiol. (Lond.) 321, 31–47.

Brown, P. B. and Fuchs, J. L. 1975. Somatotopic representation of hindlimb skin in cat dorsal horn. J. Neurophysiol. 38, 1–9.

Brown, P. B., Koerber, H. R., and Millecchia, R. 1997. Assembly of the dorsal horn somatotopic map. Somatosens. Mot. Res. 14, 93–106.

Brown, P. B., Millecchia, R., Lawson, J. J., Brown, A. G., Koerber, H. R., Culberson, J., and Stephens, S. 2005. From innervation density to tactile acuity 2: embryonic and adult pre- and postsynaptic somatotopy in the dorsal horn. Brain Res. 1055, 36–59.

Bryan, R. N., Coulter, J. D., and Willis, W. D. 1974. Cells of origin of the spinocervical tract in the monkey. Exp. Neurol. 42, 574–586.

Bryan, R. N., Trevino, D. L., Coulter, J. D., and Willis, W. D. 1973. Location and somatotopic organization of the cells of origin of the spino-cervical tract. Exp. Brain Res. 17, 177–189.

Casey, K. L. 1982. Neural mechanisms of pain: an overview. Acta Anaesthesiol. Scand. Suppl. 74, 13–20.

Christensen, B. N. and Perl, E. R. 1969. Unique excitation of cells at the margin of the spinal dorsal horn by cutaneous nociceptors. Fed. Proc. 28, 276.

Christensen, B. N. and Perl, E. R. 1970. Spinal neurons specifically excited by noxious or thermal stimuli: marginal zone of the dorsal horn. J. Neurophysiol. 33, 293–307.

Chung, J. M., Surmeier, D. J., Lee, K. H., Sorkin, L. S., Honda, C. N., Tsong, Y., and Willis, W. D. 1986. Classification of primate spinothalamic and somatosensory thalamic neurons based on cluster analysis. J. Neurophysiol. 56, 308–327.

Clarke, J. L. 1859. Further researches on the grey substance of the spinal cord. Phil. Trans. 149, 437–467.

Craig, A. D. 1996. An ascending general homeostatic afferent pathway originating in lamina I. Prog. Brain Res. 107, 225–242 [Review; 78 references]

Craig, A. D. 2003. A new view of pain as a homeostatic emotion. Trends Neurosci. 26, 303–307.

Craig, A. D. 2004. Lamina I, but not lamina V, spinothalamic neurons exhibit responses that correspond with burning pain. J. Neurophysiol. 92, 2604–2609.

Craig, A. D. and Andrew, D. 2002. Responses of spinothalamic lamina I neurons to repeated brief contact heat stimulation in the cat. J. Neurophysiol. 87, 1902–1914.

Craig, A. D. and Kniffki, K. D. 1985. Spinothalamic lumbosacral lamina I cells responsive to skin and muscle stimulation in the cat. J. Physiol. (Lond.) 365, 197–221.

Craig, A. D., Jr., Linington, A. J., and Kniffki, K. D. 1989. Cells of origin of spinothalamic tract projections to the medial and lateral thalamus in the cat. J. Comp. Neurol. 289, 568–585.

Dahlhaus, A., Ruscheweyh, R., and Sandkuhler, J. 2005. Synaptic input of rat spinal lamina I projection and unidentified neurones in vitro. J. Physiol. 566(Pt 2), 355–368.

Derjean, D., Bertrand, S., Le Masson, G., Landry, M., Morisset, V., and Nagy, F. 2003. Dynamic balance of metabotropic inputs causes dorsal horn neurons to switch functional states. Nat. Neurosci. 6(3), 274–281.

Dubner, R. 1978. Neurophysiology of pain. Dent. Clin. North. Am. 22, 11–30.

Dubner, R. and Bennett, G. J. 1983. Spinal and trigeminal mechanisms of nociception. Ann. Rev. Neurosci. 381–418.

Dubner, R., Hayes, R. L., and Hoffman, D. S. 1980. Neural and behavioral correlates of pain in the trigeminal system. Res. Publ. Assoc. Res. Nerv. Ment. Dis. 58, 63–72.

Dubner, R., Kenshalo, D. R., Jr., Maixner, W., Bushnell, M. C., and Oliveras, J. L. 1989. The correlation of monkey medullary dorsal horn neuronal activity and the perceived intensity of noxious heat stimuli. J. Neurophysiol. 62, 450–457.

Dubner, R., Price, D. D., Beitel, R. E., and Hu, J. W. 1977. Peripheral Neural Correlates of Behavior in Monkey and Human Related to Sensory-Discriminative Aspects of Pain. In: Pain in the Trigeminal Region (*eds*. D. J. Anderson and B. Matthews), pp. 57–66. Elsevier.

Eckert, W. A., III, McNaughton, K. K., and Light, A. R. 2003. Morphology and axonal arborization of rat spinal inner lamina II neurons hyperpolarized by mu-opioid-selective agonists. J. Comp. Neurol. 458, 240–256.

Giesler, G. J., Jr., Cannon, J. T., Urca, G., and Liebeskind, J. C. 1978. Long ascending projections from substantia gelatinosa Rolandi and the subjacent dorsal horn in the rat. Science 202, 984–986.

Giesler, G. J., Menetrey, D., Guilbaud, G., and Besson, J. M. 1976. Lumbar cord neurons at the origin of the spinothalamic tract in the rat. Brain Res. 118, 320–324.

Giesler, G. J., Jr., Nahin, R. L., and Madsen, A. M. 1984. Postsynaptic dorsal column pathway of the rat. I. Anatomical studies. J. Neurophysiol. 51, 260–275.

Graham, B. A., Brichta, A. M., and Callister, R. J. 2004. An in vivo mouse spinal cord preparation for patch-clamp analysis of nociceptive processing. J. Neurosci. Methods 136, 221–228.

Grudt, T. J. and Perl, E. R. 2002. Correlations between neuronal morphology and electrophysiological features in the rodent superficial dorsal horn. J. Physiol. 540, 189–207.

Herrero, J. F., Laird, J. M., and Lopez-Garcia, J. A. 2000. Wind-up of spinal cord neurones and pain sensation: much ado about something? Prog. Neurobiol. 61, 169–203.

Hillman, P. and Wall, P. D. 1969. Inhibitory and excitatory factors influencing the receptive fields of lamina 5 spinal cord cells. Exp. Brain Res. 9, 284–306.

Kajander, K. C. and Giesler, G. J., Jr. 1987. Responses of neurons in the lateral cervical nucleus of the cat to noxious cutaneous stimulation. J. Neurophysiol. 57, 1686–1704.

Koerber, H. R. and Brown, P. B. 1977. Somatotopic organization of the brachial cord of cat. Soc. Neurosci. Abstr. 3, 485.

Kumazawa, T. and Perl, E. R. 1978. Excitation of marginal and substantia gelatinosa neurons in the primate spinal cord: indications of their place in dorsal horn functional organization. J. Comp. Neurol. 177, 417–434.

Kumazawa, T., Perl, E. R., Burgess, P. R., and Whitehorn, D. 1971. Excitation of posteromarginal cells (lamina I) in monkey and their projection in lateral spinal tracts. Proc. Intl. Union Physiol. Sci. 9, 328.

Kumazawa, T., Perl, E. R., Burgess, P. R., and Whitehorn, D. 1975. Ascending projections from marginal zone (lamina I) neurons of the spinal dorsal horn. J. Comp. Neurol. 162, 1–11.

Lahuerta, J., Bowsher, D., Campbell, J., and Lipton, S. 1990. Clinical and instrumental evaluation of sensory function before and after percutaneous anterolateral cordotomy at cervical level in man. Pain 42, 23–30.

Lewinter, R. D., Skinner, K., Julius, D., and Basbaum, A. I. 2004. Immunoreactive TRPV-2 (VRL-1), a capsaicin receptor homolog, in the spinal cord of the rat. J. Comp. Neurol. 470, 400–408.

Light, A. R. 1992. Pain and Headache (Vol. 12): the Initial Processing of Pain and its Descending Control: Spinal and Trigeminal Systems. Karger.

Light, A. R. and Durkovic, R. G. 1984. Features of laminar and somatotopic organization of lumbar spinal cord units receiving cutaneous inputs from hindlimb receptive fields. J. Neurophysiol. 52, 449–458.

Light, A. R. and Kavookjian, A. M. 1984. Substantia gelatinosa neurons with axons projecting to other dorsal horn laminae. Soc. Neurosci. Abstr. 10, 489.

Light, A. R. and Kavookjian, A. M. 1988. Morphology and ultrastructure of physiologically identified substantia gelatinosa (lamina II) neurons with axons that terminate in deeper dorsal horn laminae (III–V). J. Comp. Neurol. 267, 172–189.

Light, A. R., Rethelyi, M., and Perl, E. R. 1981. Ultrastructure of Functionally Identified Neurones in the Marginal Zone and the Substantia Gelatinosa. In: Spinal Cord Sensation (*eds*. A. G. Brown and M. Rethelyi), pp. 97–102. Scottish Academic Press.

Light, A. R., Trevino, D. L., and Perl, E. R. 1979. Morphological features of functionally defined neurons in the marginal zone and substantia gelatinosa of the spinal dorsal horn. J. Comp. Neurol. 186, 151–171.

Light, A. R. and Willcockson, H. H. 1999. Spinal laminae I–II neurons in rat recorded in vivo in whole cell, tight seal configuration: properties and opioid responses. J. Neurophysiol. 82, 3316–3326.

Ling, L. J., Honda, T., Shimada, Y., Ozaki, N., Shiraishi, Y., and Sugiura, Y. 2003. Central projection of unmyelinated (C) primary afferent fibers from gastrocnemius muscle in the guinea pig. J. Comp. Neurol. 461, 140–150.

Lopez-Garcia, J. A. and King, A. E. 1994. Membrane properties of physiologically classified rat dorsal horn neurons in vitro: correlation with cutaneous sensory afferent input. Eur. J. Neurosci. 6, 998–1007.

Lu, Y. and Perl, E. R. 2003. A specific inhibitory pathway between substantia gelatinosa neurons receiving direct C-fiber input. J. Neurosci. 23, 8752–8758.

Lu, Y. and Perl, E. R. 2005. Modular organization of excitatory circuits between neurons of the spinal superficial dorsal horn (laminae I and II). J. Neurosci. 25, 3900–3907.

Martin, W. J., Liu, H., Wang, H., Malmberg, A. B., and Basbaum, A. I. 1999. Inflammation-induced up-regulation of protein kinase Cγ immunoreactivity in rat spinal cord correlates with enhanced nociceptive processing. Neuroscience 88, 1267–1274.

Martin, W. J., Malmberg, A. B., and Basbaum, A. I. 2001. PKCgamma contributes to a subset of the NMDA-dependent spinal circuits that underlie injury-induced persistent pain. J. Neurosci. 21, 5321–5327.

Matsushita, M. 1969. Some aspects of interneuronal connections cat's spinal gray matter. J. Comp. Neurol. 136, 57–80.

Mauderli, A. P., Acosta-Rua, A., and Vierck, C. J. 2000. An operant assay of thermal pain in conscious, unrestrained rats. J. Neurosci. Methods 97, 19–29.

Maxwell, D. J. and Koerber, H. R. 1987. Morphologically unusual feline spinocervical tract neurons. Exp. Neurol. 95, 521–524.

Maxwell, D. J., Fyffe, R. E., and Rethelyi, M. 1983. Morphological properties of physiologically characterized lamina III neurones in the cat spinal cord. Neuroscience 10, 1–22.

Melnick, I. V., Santos, S. F., and Safronov, B. V. 2004a. Mechanism of spike frequency adaptation in substantia gelatinosa neurones of rat. J. Physiol. 559, 383–395.

Melnick, I. V., Santos, S. F., Szokol, K., Szucs, P., and Safronov, B. V. 2004b. Ionic basis of tonic firing in spinal substantia gelatinosa neurons of rat. J. Neurophysiol. 91, 646–655.

Mendell, L. M. and Wall, P. D. 1965. Responses of single dorsal cord cells to peripheral cutaneous unmyelinated fibres. Nature 206, 97–99.

Menetrey, D., de Pommery, J., and Roudier, F. 1984. Properties of deep spinothalamic tract cells in the rat, with special reference to ventromedial zone of lumbar dorsal horn. J. Neurophysiol. 52, 612–624.

Menetrey, D., Giesler, G. J., Jr., and Besson, J. M. 1977. An analysis of response properties of spinal cord dorsal horn neurones to nonnoxious and noxious stimuli in the spinal rat. Exp. Brain Res. 27, 15–33.

Miletic, V., Bowen, K. K., and Miletic, G. 2000. Loose ligation of the rat sciatic nerve is accompanied by changes in the subcellular content of protein kinase C beta II and gamma in the spinal dorsal horn. Neurosci. Lett. 288, 199–202.

Morgan, M. M. 1998. Direct comparison of heat-evoked activity of nociceptive neurons in the dorsal horn with the hindpaw withdrawal reflex in the rat. J. Neurophysiol. 79, 174–180.

Mosso, J. A. and Kruger, L. 1973. Receptor categories represented in spinal trigeminal nucleus caudalis. J. Neurophysiol. 36, 472–488.

Olausson, H., Lamarre, Y., Backlund, H., Morin, C., Wallin, B. G., Starck, G., Ekholm, S., Strigo, I., Worsley, K., Vallbo, A. B., and Bushnell, M. C. 2002. Unmyelinated tactile afferents signal touch and project to insular cortex. Nat. Neurosci. 5, 900–904.

Polgar, E., Fowler, J. H., McGill, M. M., and Todd, A. J. 1999. The types of neuron which contain protein kinase C gamma in rat spinal cord. Brain Res. 833, 71–80.

Pomeranz, B., Wall, P. D., and Weber, W. V. 1968. Cord cells responding to fine myelinated afferents from viscera, muscle, and skin. J. Physiol. (Lond.) 199, 511–532.

Prescott, S. A. and De Koninck, Y. 2002. Four cell types with distinctive membrane properties and morphologies in lamina I of the spinal dorsal horn of the adult rat. J. Physiol. 539, 817–836.

Prescott, S. A. and De Koninck, Y. 2005. Integration time in a subset of spinal lamina I neurons is lengthened by sodium and calcium currents acting synergistically to prolong subthreshold depolarization. J. Neurosci. 25, 4743–4754.

Price, D. D. and Browe, A. C. 1973. Responses of spinal cord neurons to graded noxious and non-noxious stimuli. Brain Res. 64, 425–429.

Price, D. D. and Dubner, R. 1977. Neurons that subserve the sensory-discriminative aspects of pain. Pain 3, 307–338.

Price, D. D. and Mayer, D. J. 1974. Physiological laminar organization of the dorsal horn of M. mulatta. Brain Res. 79, 321–325.

Price, D. D. and Mayer, D. J. 1975. Neurophysiological characterization of the anterolateral quadrant neurons subserving pain in M. mulatta. Pain 1, 59–72.

Price, D. D., Hayashi, H., Dubner, R., and Ruda, M. A. 1979. Functional relationships between neurons of marginal and substantia gelatinosa layers of primate dorsal horn. J. Neurophysiol. 42, 1590–1608.

Ramon Y, and Cajal, S. 1909. Histologie du Systeme Nerveux de l'Homme et des Vertebres. Maloine.

Ranson, S. W. 1913. The course within the spinal cord of the non-medullated fibers of the dorsal roots: a study of Lissauer's tract in the cat. J. Comp. Neurol. 23, 259–281.

Ranson, S. W. 1914. The tract of Lissauer and the substantia gelatinosa Rolandi. Am. J. Anat. 16, 97–126.

Ranson, S. W. 1915. Unmyelinated nerve-fibres as conductors of protopathic sensation. Brain 38, 381–389.

Ranson, S. W. and Billingsley, P. R. 1916. The conduction of painful afferent impulses in the spinal nerves. Am. J. Physiol. 40, 571–584.

Ranson, S. W. and Davenport, H. K. 1931. Sensory unmyelinated fibers in the spinal nerves. Am. J. Anat. 48, 331–353.

Ranson, S. W. and von Hess, C. L. 1915. The conduction within the spinal cord of the afferent impulses producing pain and the vasomotor reflexes. Am. J. Physiol. 38, 128–152.

Rethelyi, M. and Szentagothai, J. 1969. The large synaptic complexes of the substantia gelatinosa. Exp. Brain Res. 7, 258–274.

Rethelyi, M., Light, A. R., and Perl, E. R. 1981. Synapses made by nociceptive laminae I and II neurones. Pain suppl. S127.

Rethelyi, M., Light, A. R., and Perl, E. R. 1983. Synapses made by nociceptive laminae I and II neurons. In: (*eds*. J. J. Bonica, U. Lindblom, and A. Iggo),Advances in Pain Research and Therapy, Vol. 5, pp. 111–118. Raven Press.

Rethelyi, M., Light, A. R., and Perl, E. R. 1989. Synaptic ultrastructure of functionally and morphologically characterized neurons of the superficial spinal dorsal horn of cat. J. Neurosci. 9, 1846–1863.

Rexed, B. 1952. The cytoarchitectonic organization of the spinal cord in the cat. J. Comp. Neurol. 96, 415–466.

Ritz, L. A., Culberson, J. L., and Brown, P. B. 1985. Somatotopic organization in cat spinal cord segments with fused dorsal horns: caudal and thoracic levels. J. Neurophysiol. 54, 1167–1177.

Rotto, D. M. and Kaufman, M. P. 1988. Effect of metabolic products of muscular contraction on discharge of group III and IV afferents. J. Appl. Physiol. 64, 2306–2313.

Ruscheweyh, R. and Sandkuhler, J. 2002. Lamina-specific membrane and discharge properties of rat spinal dorsal horn neurones in vitro. J. Physiol. 541, 231–244.

Ruscheweyh, R., Ikeda, H., Heinke, B., and Sandkuhler, J. 2004. Distinctive membrane and discharge properties of rat spinal lamina I projection neurones *in vitro*. J. Physiol. 555, 527–543.

Rustioni, A., Hayes, N. L., and O'Neill, S. 1979. Dorsal column nuclei and ascending spinal afferents in macaques. Brain 102, 95–125.

Steedman, W. M., Molony, V., and Iggo, A. 1985. Nociceptive neurones in the superficial dorsal horn of cat lumbar spinal cord and their primary afferent inputs. Exp. Brain Res. 58, 171–182.

Sugiura, Y., Lee, C. L., and Perl, E. R. 1986. Central projections of identified, unmyelinated (C) afferent fibers innervating mammalian skin. Science 234, 358–361.

Szentagothai, J. 1964. Neuronal and synaptic arrangement in the substantia gelatinosa Rolandi. J. Comp. Neurol. 122, 219–239.

Thomson, A. M., West, D. C., and Headley, P. M. 1989. Membrane characteristics and synaptic responsiveness of superficial dorsal horn neurons in a slice preparation of adult rat spinal cord. Eur. J. Neurosci. 1, 479–488.

Trevino, D. L., Coulter, J. D., and Willis, W. D. 1973. Location of cells of origin of spinothalamic tract in lumbar enlargement of the monkey. J. Neurophysiol. 36, 750–761.

Trevino, D. L., Coulter, J. D., Maunz, R. A., and Willis, W. D. 1974. Location and functional properties of spinothalamic cells in the monkey. Adv. Neurol. 4, 167–170.

Vierck, C. J., Jr., Cannon, R. L., Fry, G., Maixner, W., and Whitsel, B. L. 1997. Characteristics of temporal summation of second pain sensations elicited by brief contact of glabrous skin by a preheated thermode. J. Neurophysiol. 78, 992–1002.

Waldeyer, W. 1889. Das Gorilla-Ruckenmark. Acedemie der Wissenschaften.

Wall, P. D. 1967. The laminar organization of dorsal horn and effects of descending impulses. J. Physiol. (Lond.) 188, 403–423.

Wall, P. D. 1973. Dorsal Horn Electrophysiology. In: Handbook of Sensory Physiology. Somatosensory System (*ed*. A. Iggo), pp. 253–270. Springer-Verlag.

Wall, P. D., Merrill, E. G., and Yaksh, T. L. 1979. Responses of single units in laminae 2 and 3 of cat spinal cord. Brain Res. 160, 245–260.

Willis, W. D. 1985. The Pain System: the Neural Basis of Nociceptive Transmission in the Mammalian Nervous System. Karger.

Willis, W. D., Jr. 1988. Dorsal horn neurophysiology of pain. Ann. N. Y. Acad. Sci. 531, 76–89.

Willis, W. D. and Westlund, K. N. 1997. Neuroanatomy of the pain system and of the pathways that modulate pain. J. Clin. Neurophysiol. 14, 2–31. [Review; 393 references]

Willis, W. D., Leonard, R. B., and Kenshalo, D. R., Jr. 1978. Spinothalamic tract neurons in the substantia gelatinosa. Science 202, 986–988.

Willis, W. D., Trevino, D. L., Coulter, J. D., and Maunz, R. A. 1974. Responses of primate spinothalamic tract neurons to natural stimulation of hindlimb. J. Neurophysiol. 37, 358–372.

Wilson, L. B., Andrew, D., and Craig, A. D. 2002. Activation of spinobulbar lamina I neurons by static muscle contraction. J. Neurophysiol. 87, 1641–1645.

Woolf, C. J. and Fitzgerald, M. 1983. The properties of neurones recorded in the superficial dorsal horn of the rat spinal cord. J. Comp. Neurol. 221, 313–328.

Yoshimura, M. and Jessell, T. M. 1989. Primary afferent-evoked synaptic responses and slow potential generation in rat substantia gelatinosa neurons *in vitro*. J. Neurophysiol. 62, 96–108.

5.25 What is a Wide-Dynamic-Range Cell?

D Le Bars, INSERM U-713, Paris, France

S W Cadden, University of Dundee, Dundee, UK

© 2008 Elsevier Inc. All rights reserved.

5.25.1	Introduction	332
5.25.2	Segmental Excitatory Receptive Fields	332
5.25.2.1	General	332
5.25.2.2	Plasticity	333
5.25.3	Segmental Inhibitory Receptive Field	335
5.25.3.1	General	335
5.25.3.2	Plasticity	335
5.25.4	Perturbance of the Basic Somesthetic Activity by a Painful Focus	335
5.25.5	Multiple or Vast Painful Foci	336
5.25.6	Summary and Conclusions	337
References		337

Glossary

allodynia Pain caused by stimuli which would not normally cause pain (i.e., non-noxious stimuli).

angina pectoris Chest pain from cardiac ischemia.

basic somesthetic activity Description of the ongoing activity in somatosensory pathways in the absence of any deliberate stimuli.

bistable A mechanism which can essentially be in one of two states (e.g., on or off)

body image Conscious mental representation of the body.

body schema Unconscious model of the body in the brain.

bulbo-spinal control A neural control mechanism originating in the brainstem and projecting to the spinal cord.

dermatome Area of skin innervated by nerves from a given segment of the spinal cord.

diffuse noxious inhibitory controls (DNIC) Neural controls triggered by noxious stimulation of widespread areas of the body which exert an inhibitory influence on wide-dynamic-range neurons.

dorsal column stimulation Technique for inducing analgesia/hypoalgesia by electrically stimulating the dorsal columns of the spinal cord.

excitatory receptive field Area of the body (surface or interior) which when stimulated will produce excitation of a given neuron.

hyperalgesia Increased level of pain felt in response to a noxious stimulus (cf. allodynia).

hypoalgesic Pertaining to a reduction of pain.

inhibitory receptive field Area of the body (surface or interior) which when stimulated will produce inhibitory effects on the activity of a given neuron.

microelectrophoretic application Application of a substance in its ionic form from a microelectrode by the application of electrical current.

monoarthritis Inflammation of a single joint.

nociceptive stimulus Stimulus which activates nociceptive afferents (which could be a noxious stimulus (see below) or an electrical stimulus).

noxious stimulus Stimulus which causes or threatens to cause tissue damage.

polyarthritis Inflammation of several joints.

propriospinal mechanism Neural mechanism mediated entirely within the spinal cord.

radiating pain Pain which spreads from the area of stimulation to adjacent areas.

referred pain Pain which is felt in areas remote to the area of stimulation (as well as or instead of from the area of stimulation).

supraspinal mechanism Neural mechanism which at least in part, involves structures above the spinal cord.
transcutaneous electrical nerve stimulation Technique for inducing analgesia/hypoalgesia by electrically stimulating peripheral nerves through the skin (i.e., with electrodes placed on the skin).
trigeminal nucleus caudalis Most caudal part of the trigeminal sensory nuclear complex (or of the trigeminal spinal nucleus); also sometimes called the medullary dorsal horn.

5.25.1 Introduction

Wide-dynamic-range (WDR) neurons (various other names have been used by different authors for these neurones, e.g., trigger, lamina V-type, class 2, multireceptive, and convergent neurones) are found in the spinal dorsal horn (and its medullary homolog, trigeminal nucleus caudalis), both in the superficial layers and more so in deeper areas centered on lamina V. They are activated by both nociceptive and non-nociceptive stimuli and include interneurons involved in polysynaptic reflexes and neurons projecting in pathways such as the spinothalamic and spinoreticular tracts (Willis, W. D. and Coggeshall, R. E., 1991). For various reasons, these neurons are believed to play a key role in pain. For example, many procedures used to alleviate pain in man (e.g., systemic or intrathecal morphine, transcutaneous electrical nerve stimulation, and dorsal column stimulation), also result in a reduction in the responses of WDR cells to nociceptive stimuli. Indeed, some WDR neurons show patterns of activity which are more reminiscent of certain types of pain than activity in peripheral nociceptive nerves (Adriaensen, H. *et al.*, 1984; Cervero, F. *et al.*, 1988). For example, a WDR neuron may remain active after removal of a stimulus from its peripheral excitatory field (e.g., Wagman, I. H. and Price, D. D., 1969) while conversely it may remain inactive following the brief activation of inhibitory mechanisms even if there is still a stimulus on the excitatory field (Cadden, S. W., 1993). Such bistable patterns of activity might be explained by inherent properties of WDR neurons (e.g., Morisset, V. and Nagy, F., 1996) and/or their involvement in positive feedback circuits (see Cadden, S. W., 1993).

WDR neurons also constitute a site where excitatory and inhibitory influences converge. This chapter focuses on the properties of WDR neurons under physiological conditions, and most particularly, on the concept that they exhibit whole body receptive fields. One consequence of this unusual property is that it necessitates consideration of the output of the whole population of these neurons (Le Bars, D., 2002). The extent of a nociceptive focus can differ greatly depending on its cause, and consequently the global volume of information sent to the brain will also vary. Although *a priori* this volume of information is determined by the intensity, duration, and area being stimulated, it can also be altered profoundly by past and present experiences.

5.25.2 Segmental Excitatory Receptive Fields

5.25.2.1 General

WDR neurons receive information from all three groups of cutaneous afferents, that is, Aβ-, Aδ-, and C-fibers (e.g., Wagman, I. H. and Price, D. D., 1969; Menétrey, D. *et al.*, 1977). The excitatory receptive fields from which this information arises are fairly restricted in size (Figure 1). Studies in conscious monkeys illustrate that these receptive fields can expand or contract depending on the attentional state of the animal (e.g., Dubner, R. *et al.*, 1981). Although the receptive fields are usually larger than those of nociceptive-specific neurons, they can still provide useful information regarding stimulus location. Usually, these receptive fields exhibit a gradient of sensitivity: in the center even light mechanical stimuli can activate the neuron, while at the periphery only intense stimuli elicit responses (e.g., Menétrey, D. *et al.*, 1977).

When increasing intensities of mechanical or thermal stimuli are applied to the center of the receptive field, the rate and duration of neuronal firing increases (see insert in Figure 1). In this respect, these neurons seem better than nociceptive-specific neurons at encoding intensities of

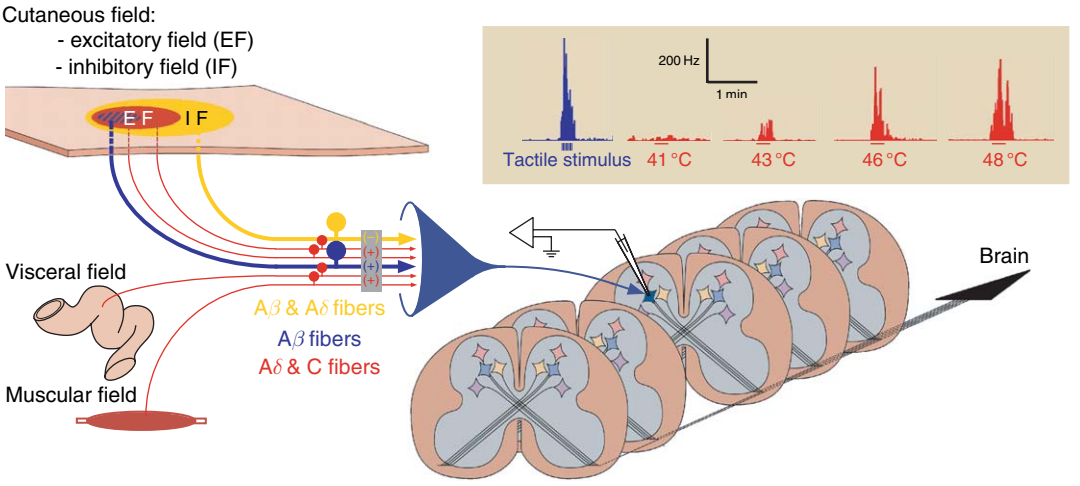

Figure 1 Schematic organization of the segmental receptive field of a wide-dynamic-range (WDR) neuron. The principal part on the skin is made up of an excitatory (EF) and an inhibitory (IF) field. The center of the EF can be activated by both innocuous and nociceptive stimuli (blue and red stripes, respectively). The periphery of the EF is activated only by nociceptive stimuli (red). The inhibitory field (yellow) is activated mainly by non-nociceptive stimuli. As shown, the receptive field may also include visceral and/or muscular components thus completing a convergence of excitatory (+) and inhibitory (−) information onto a single neuron. A ratemeter recording from a WDR neuron in the rat lumbar cord (insert, top right) shows responses to stimuli applied to the center of the excitatory field: repetitive innocuous (light pressure) stimuli produced a high level of firing while applications of radiant heat (indicated by bars with temperatures achieved) evoked responses which increased with temperature within the noxious range. Adapted from Le Bars, D. and Chitour, D. 1983. Do convergent neurons in the spinal cord discriminate nociceptive from non-nociceptive information? Pain 17, 1–19.

noxious stimuli (Hoffman, D. S. *et al.*, 1981). It is often believed that WDR neurons respond more strongly to noxious stimulation than to any form of innocuous stimulation. However, this is not quite true. In fact, the responses evoked in WDR neurons by noxious heat can be exceeded by repetitively applied innocuous mechanical stimuli (insert of Figure 1) (see Le Bars, D. and Chitour, D., 1983). Thus, firing frequency alone cannot distinguish between non-noxious and noxious stimuli. How can this fact be reconciled with WDR neurons having a central role in pain processing? It seems that the meaningful signal is the pattern of activity from the whole population of WDR cells and not simply the signals from each individual neuron. As their receptive fields overlap one another, the organization of spatial convergence from WDR neurons must be taken into account. This is illustrated by the fact that when a tactile stimulus is applied to a given territory, it activates only the few WDR neurons whose excitatory fields have centers in the territory. However, a noxious stimulus applied in the same place, will activate not only the same WDR neurons, but also those whose excitatory fields have peripheries in the territory (Figure 2).

Moreover, some WDR neurons are activated from more than one type of tissue (e.g., cutaneous and visceral or cutaneous and muscular). This convergence helps explain clinical curiosities such as radiating or referred pain, for example, to the left arm in angina pectoris. Indeed, WDR neurons can capture all the information coming from interfaces with both the external environment (the skin) and the internal milieu (viscera, muscles, etc.). This information constitutes a basic somesthetic activity. Thus, it is possible that these neurons are not involved exclusively in pain and, by transmitting this basic somesthetic activity, inform the brain that the organism is suffering no special perturbation from either external or internal sources.

5.25.2.2 Plasticity

The convergence onto a single WDR neuron is actually greater than is observed under normal conditions. This discrepancy is such that on fringes of the excitatory field, there is a zone which when stimulated will trigger a depolarization of the WDR neuron (Figure 2(c)) which normally will be insufficient to elicit action potentials. This is consistent with the observation that cutaneous receptive fields of WDR neurons are apparently smaller when mapped using natural as opposed to electrical stimulation (e.g., Mendell, L. M., 1984), given that the electrical stimuli produce more synchronized afferent activity which results in more effective

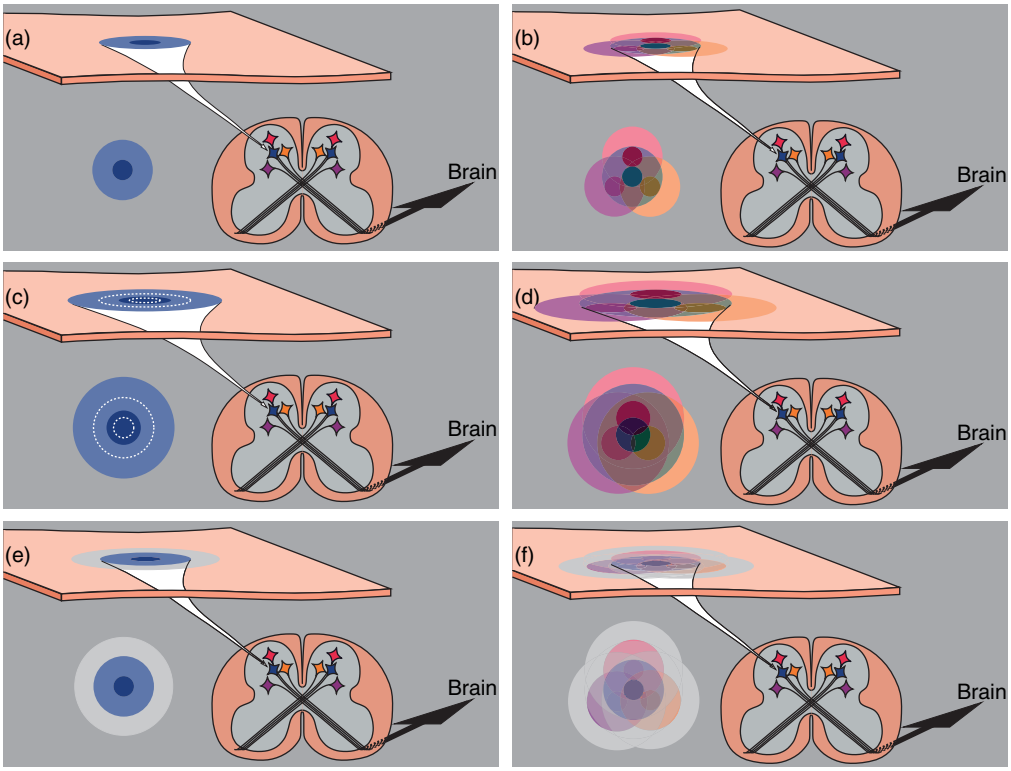

Figure 2 (a) When recordings are made from an individual wide-dynamic-range (WDR) neuron (the blue neuron in the diagram), activation by noxious stimuli applied to any part of its excitatory receptive field can be observed (blue surface on the skin). Its center (blue dark) is also sensitive to low-intensity stimuli. (b) The excitatory fields of adjacent WDR neurons overlap one another, so that a noxious stimulus will activate not only the center of some receptive fields (blue area) but also the edges of others (pale surfaces colored red, purple, and yellow). Thus, when applied to a given surface area (here the center of the blue field), a noxious stimulus will activate many neurons (four in this case) whereas a non-noxious stimulus will activate far fewer (here only one). (c) In fact the surface potentially covered by the excitatory receptive field of a WDR neuron is larger than that observed under physiological conditions. If the neuron (blue) from which recordings are being made is partially depolarized (e.g., by microelectrophoretically applying an excitatory amino acid to its membrane), an enlargement of the excitatory receptive field can be observed. This means that the span of the excitatory receptive fields is potentially much greater than shown in (a) (as indicated by the broken white lines). This is probably what occurs under inflammatory conditions. (d) Thus, considering four neurons, it can be seen that a non-noxious stimulus applied to the center of the blue field will now be able to activate the red, purple, and yellow neurons as well (cf. (b)). (e) At the periphery of their excitatory fields, WDR neurons have an inhibitory field (white zone). When mechanical stimuli are applied to this area, the neuron is inhibited. (f) The inhibitory fields of a population of adjacent WDR neurons substantially overlap one another. Thus in the center of the red field, mechanical stimuli activate the red neuron but inhibit the purple and yellow neurons. When tactile stimuli are applied to a large surface, they will not only activate the centers of excitatory fields and potentially generate a false nociceptive signal, they will also activate inhibitory fields with a resulting attenuation of the global response. This is the basis for some physical methods of pain-relief (see text).

summation of excitatory postsynaptic potentials. The concept of quiescent synapses (e.g., Wall, P. D., 1977) developed with the idea that in some conditions, this fringe of the receptive field can produce significant information transfer, that is, trigger action potentials. Such synapses can be made more efficacious experimentally by partially depolarizing a neuron using microelectrophoretic application an excitatory amino acid (Zieglgänsberger, W. and Herz, A., 1971) or pharmacologically blocking inhibitory transmitter mechanisms (e.g., Yokota, T. and Nishikawa, Y., 1979). Under these circumstances, the receptive fields enlarge and this is also seen after transient electrical stimulation of C-fibers, injury, noxious pinch, intradermal injection of capsaicin, or noxious stimulation of viscera or muscle.

Such plasticity may be triggered naturally by peripheral or central pathologies. In general, sensitization of excitatory mechanisms or a deficiency of inhibitory ones will produce both increased activity in the neuronal population associated with a painful focus and a growth of this population (Figure 2(d)). This is

illustrated by the increased size of excitatory receptive fields during acute or chronic inflammation (e.g., Grubb, B. D. *et al.*, 1993). The resulting increased information is transmitted to, and decoded in, the brain where it constitutes a form of hyperalgesia. This increase in nociceptive information varies with the volume of the body affected by the lesion (i.e., in a three-dimensional way) and also has a temporal dimension.

5.25.3 Segmental Inhibitory Receptive Field

5.25.3.1 General

WDR neurons frequently exhibit not only excitatory cutaneous receptive fields, but also inhibitory fields that are often situated proximally (e.g., Hillman, P. and Wall, P. D., 1969). When applied to this area, most mechanical stimuli, notably those of low intensity, inhibit the activity of WDR neurons. It is often implied that these phenomena are triggered only by the activation of Aβ-fibers. However, numerous studies have demonstrated that activation of Aδ-fibers results in more powerful inhibitions (e.g., Chung, J. M. *et al.*, 1984). Thus the activation of a pool of Aδ-fiber terminals will both activate those WDR neurons with excitatory receptive fields in this particular area and inhibit those with overlapping inhibitory receptive fields. As described below, the final output from these neurons constitutes a contrasted picture reminiscent of the lateral inhibition described in other systems (e.g., visual and touch).

5.25.3.2 Plasticity

It is important to consider the overlap of excitatory and inhibitory fields of neighboring WDR neurons (Figures 2(e) and 2(f)). The organization of the inhibitory fields offers an explanation for how, at least in nonpathological conditions, the high levels of activity produced in individual neurons by application of multiple non-nociceptive stimuli to large surface areas (incorporating numerous centers of excitatory fields) do not constitute a nociceptive signal. Such an eventuality is prevented by the concomitant stimulation of numerous inhibitory fields which attenuates the overall response of the neuronal population. in contrast, a deficit of such inhibitory effects will result in a greater amount of activity being produced by harmless stimuli. Once transmitted to and decoded by the brain, such information could constitute a form of allodynia such as that triggered by brushing the skin with cotton wool, which is characteristic of some neuropathies.

The convergence of excitatory and inhibitory influences may also explain the hypoalgesic effects of stimulating parts of the body close to a painful focus, for example, by rubbing or transcutaneous electrical nerve stimulation (TENS). Indeed, the fact that large and fine cutaneous afferent fibers interact with this potential effect has been known for a long time (e.g., Head, H. *et al.*, 1905; Noordenbos, W., 1959; Melzack, R. and Wall, P. D., 1965).

5.25.4 Perturbance of the Basic Somesthetic Activity by a Painful Focus

In addition to the segmental inhibitory influences discussed above, WDR neurons are inhibited by nociceptive stimulation of areas of the body remote from their segmental receptive fields. These effects involve propriospinal and supraspinal mechanisms. The former can be observed in the dorsal horn of spinal animals (e.g., Gerhart, K. D. *et al.*, 1981) but the underlying mechanisms have not been investigated in detail. The supraspinal mechanisms are observed in intact but not in spinalized animals and have been studied more extensively (see Chapter Diffuse Noxious Inhibitory Controls (DNIC)).

In fact, any noxious stimulus will activate descending bulbo-spinal controls and these will strongly depress the activity of neurons in the spinal dorsal horn and its trigeminal homolog. In several species, the vast majority of WDR neurons (and some nociceptive-specific neurons) are profoundly inhibited by noxious stimulation of any part of the body provided it is not the neuron's own excitatory receptive field. In effect, the receptive fields of these neurons are made up by the whole body – mainly in the form of an inhibitory receptive field except in its own neural segment where both inhibitory and excitatory fields exist. These whole body phenomena which have been termed diffuse noxious inhibitory controls (DNIC) work by hyperpolarizing WDR neurons (see Chapter Diffuse Noxious Inhibitory Controls (DNIC)).

In summary, a noxious focus activates a segmental subset of WDR neurons and inhibits all other WDR neurons (Figure 3(b)). This mechanism effectively improves the signal-to-noise ratio by increasing the contrast between the activities of the excited neurons and the depressed activity of the remainder.

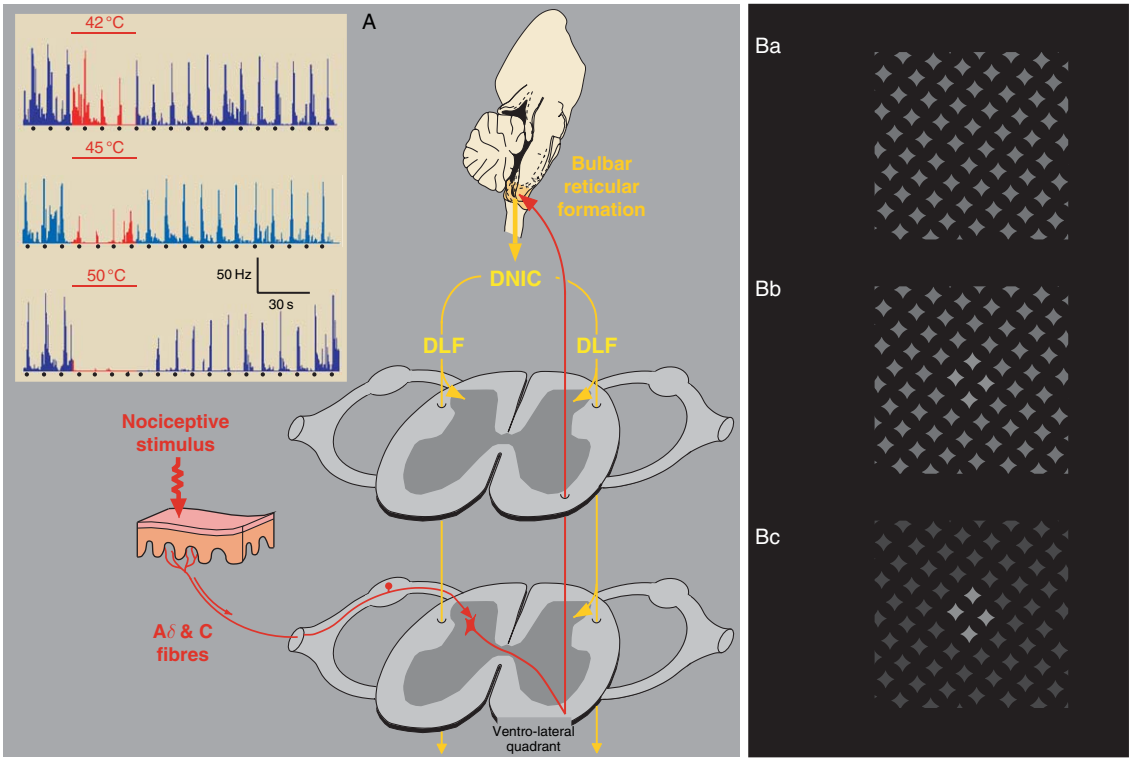

Figure 3 (A) Triggering of descending inhibitory controls by nociceptive stimuli. One consequence of a painful focus is the modification of activity of a whole population of WDR neurons. Nociceptive signals pass up the ventrolateral quadrant to activate structures in the bulbar reticular formation. These structures in turn send signals down the dorsolateral cord to trigger powerful inhibitory mechanisms in all segments not concerned with the initial stimulus. The insert (top left) shows a recording from a WDR neuron in the rat lumbar cord whose receptive field on the extremity of a hindpaw, was mechanically stimulated by a paint brush once every 10 s (indicated by black spots). The resulting activity was inhibited by the application of remote noxious stimuli (immersion of the tail in 42, 45, or 50 °C water). This inhibition increased with the water temperature. (B) Schematization of the activity of all WDR neurons: (Ba) in the absence of a painful focus, these neurons produce the basic somaesthetic information, consisting of signals from the body about its immediate environment; (Bb) as a consequence of a painful focus, some of these neurons are activated (four of them in the center of this diagram), but it is difficult to extract this information because of the background noise; (Bc) however the inhibition of the other neurons by the mechanisms described in (a), makes it possible for the brain to extract the information about the painful focus due to the contrast between the activated and the inhibited neurons. DLF, dorsolateral funiculus; DNFC, diffuse noxious inhibitory control.

Interestingly, DNIC are exacerbated in experimental models of clinical pain (e.g., monoarthritis, polyarthritis, and peripheral mononeuropathies; e.g., Danziger, N. *et al.*, 2000).

5.25.5 Multiple or Vast Painful Foci

If it is accepted that WDR neurons are important in pain, then interactions between nociceptive signals from separate parts of the body must result in interactions between the corresponding pains. In fact, a painful stimulus can decrease or even mask pain arising from another part of the body (see Chapter Diffuse Noxious Inhibitory Controls (DNIC)).

The size of a painful focus can vary greatly depending on the underlying pathology and consequently the volume of nociceptive information sent to the brain will also vary. How do WDR neurons behave when noxious stimuli are applied to increasingly large surface areas? In fact, two opposite effects are observed: up to a particular area of stimulation – approximately twice that of the neuron's excitatory field – there is an accelerating transfer function; however for larger surface areas, the responses gradually diminish (Bouhassira, D. *et al.*, 1995). This is consistent with findings in humans that noxious thermal stimulation of increasingly large areas of skin causes an increasingly painful sensation only over a restricted range of surface areas (e.g., Hardy, J. D.

et al., 1952) and that painful thermal stimuli evoke pleasant warmth when applied to larger areas (Melzack, R. *et al.*, 1962). The classical poor correlation between the extent of an injury and the intensity of pain may also involve such mechanisms.

Thus it seems that a painful focus activates a negative feedback loop affecting WDR neurons only when it generates a sufficient volume of nociceptive information. This volume is undoubtedly determined by the intensity of the stimulus, the area to which it is applied, and its duration. In this respect, the role of temporal summation in triggering inhibitory bulbo-spinal mechanisms must be addressed (Gozariu, M. *et al.*, 1997).

5.25.6 Summary and Conclusions

The global population of WDR neurons is activated continuously but unpredictably by all the non-noxious stimuli provided by the environment. The resulting basic somaesthetic activity can constitute either noise from which the brain may have difficulty extracting a clear signal, or a significant message. According to modern neuropsychological concepts, this on-going information from the whole body, along with that from other sensory systems, notably the vestibular and visual systems, is integrated to generate a permanent, unconscious, representation of the physiological reality of self. At the beginning of the twentieth century, the great neurologist Henry Head proposed that our brains contain two schemas – "a postural model of ourselves and another schema allowing the recognition of the locality of the stimulated spot" (Head, H. and Holmes, G., 1911). However, following Schilder P. (1950), the simple term body schema is usually used to refer to both models. Even though the terms are sometimes used interchangeably, it is advisable to distinguish body schema which is an unconscious cerebral model of the body, from body image which is a conscious mental representation. WDR neurons are good candidates for constructing and endlessly rebuilding the memory of one's physical self (Le Bars, D., 2002). Previous experiences, be they neutral, pleasant, or unpleasant (e.g., pain), contribute to the building of this memory; all will have activated WDR neurons. Intense or long-lasting pains are probably among the physical causes which most commonly disturb the body schema: they generate a painful body by focusing attention on one part of the body to the detriment of the others. The body schema then emerges from relative unconsciousness and the painful focus becomes pre-eminent and relatively oversized. Spino-bulbo-spinal mechanisms could underlie this over-representation by providing a filter which imposes the nociceptive signal to the detriment of information from the rest of the body.

After all, this is what happens within any large gathering: silence is necessary if a speaker is to be heard. DNIC establish such silence among spinal neurons. Conversely, a hubbub does not reduce the speaker to silence, but drowns his speech to the extent that he cannot be heard. This is one way in which morphine works – and DNIC are extremely sensitive to low doses of morphine (see Le Bars, D. *et al.*, 1995).

In summary, WDR neurons do not constitute a single-channel transmission network. Nociceptive information is processed by complex mechanisms which can modify the gain of the system. The modulation of this gain is determined by the three-dimensional characteristics of the painful focus – not only its intensity and duration but also its surface area. Beyond a critical level, an increase in the number of activated noci-responsive neurons is associated with a decrease in their individual responses.

A complete analysis of nociceptive processes must consider not only a large population of neurons but also their interactions. Pain in clinical practice is not punctuate and involves a large number of excitatory receptive fields of peripheral fibers and central neurons. When several foci coexist, the global signal from WDR neurons may be polymorphic with the resulting pain showing fluctuations, instability, or even versatility due to the resulting interactions.

References

Adriaensen, H., Gybels, J., Handwerker, H. O., and Van Hees, J. 1984. Nociceptor discharges and sensations due to prolonged noxious mechanical stimulation: a paradox. Human Neurobiol. 3, 53–58.

Bouhassira, D., Gall, O., Chitour, D., and Le Bars, D. 1995. Dorsal horn convergent neurones: negative feed-back triggered by spatial summation of nociceptive afferents. Pain 62, 195–200.

Cadden, S. W. 1993. The ability of inhibitory controls to 'switch-off' activity in dorsal horn convergent neurones in the rat. Brain Res. 628, 65–71.

Cervero, F., Handwerker, H. O., and Laird, J. M. 1988. Prolonged noxious mechanical stimulation of the rat's tail: responses and encoding properties of dorsal horn neurones. J. Physiol. 404, 419–436.

Chung, J. M., Fang, Z. R., Hori, Y., Lee, K. H., and Willis, W. D. 1984. Prolonged inhibition of primate spinothalamic tract cells by peripheral nerve stimulation. Pain 19, 259–275.

Danziger, N., Le Bars, D., and Bouhassira, D. 2000. Diffuse Noxious Inhibitory Controls and Arthritis in the Rat. In: Pain and Neuroimmune Interactions (*eds*. N. E. Saadé, A. V. Apkarian, and S. J. Jabbur), pp. 69–78. Kluwer Academic Press.

Dubner, R., Hoffman, D. S., and Hayes, R. L. 1981. Neuronal activity in medullary dorsal horn of awake monkeys trained in a thermal discrimination task. III. Task-related responses and their functional role. J. Neurophysiol. 46, 444–464.

Gerhart, K. D., Yezierski, R. P., Giesler, G. J., Jr., and Willis, W. D. 1981. Inhibitory receptive fields of primate spinothalamic tract cells. J. Neurophysiol. 46, 1309–1325.

Gozariu, M., Bragard, D., Willer, J. C., and Le Bars, D. 1997. Temporal summation of C-fiber afferent inputs: competition between facilitatory and inhibitory effects on C-fiber reflex in the rat. J. Neurophysiol. 78, 3165–3179.

Grubb, B. D., Stiller, R. U., and Schaible, H. G. 1993. Dynamic changes in the receptive field properties of spinal cord neurons with ankle input in rats with chronic unilateral inflammation in the ankle region. Exp. Brain Res. 92, 441–452.

Hardy, J. D., Woolf, H. G., and Goodel, H. 1952. Pain Sensations and Reactions. William and Wilkins.

Head, H. and Holmes, G. 1911. Sensory disturbances from cerebral lesions. Brain 34, 102–245.

Head, H., Rivers, W. H. R., and Sherren, J. 1905. The afferent nervous system from a new aspect. Brain 28, 99–115.

Hillman, P. and Wall, P. D. 1969. Inhibitory and excitatory factors influencing the receptive fields of lamina 5 spinal cord cells. Exp. Brain Res. 9, 284–306.

Hoffman, D. S., Dubner, R., Hayes, R. L., and Medlin, T. P. 1981. Neuronal activity in medullary dorsal horn of awake monkeys trained in a thermal discrimination task. I. Responses to innocuous and noxious thermal stimuli. J. Neurophysiol. 46, 409–427.

Le Bars, D. 2002. The whole body receptive field of dorsal horn multireceptive neurones. Brain Res. Rev. 40, 29–44.

Le Bars, D. and Chitour, D. 1983. Do convergent neurons in the spinal cord discriminate nociceptive from non-nociceptive information? Pain 17, 1–19.

Le Bars, D., Bouhassira, D., and Villanueva, L. 1995. Opioids and Diffuse Noxious Inhibitory Controls in the Rat. In: Pain and the Brain: From Nociceptor to Cortical Activity (*eds*. B. Bromm and J. E. Desmedt), Advances in Pain Research and Therapy, Vol. 22, pp. 517–539. Raven Press.

Melzack, R. and Wall, P. D. 1965. Pain mechanisms: a new theory. Science 150, 971–979.

Melzack, R., Rose, G., and McGinty, D. 1962. Skin sensitivity to thermal stimuli. Exp. Neurol. 6, 300–314.

Mendell, L. M. 1984. Modifiability of sipnal synapses. Physiol. Rev. 64, 260–324.

Menétrey, D., Giesler, G. J., Jr., and Besson, J. M. 1977. An analysis of response properties of spinal cord dorsal horn neurones to nonnoxious and noxious stimuli in the spinal rat. Exp. Brain Res. 27, 15–33.

Morisset, V. and Nagy, F. 1996. Modulation of regenerative membrane properties by stimulation of metabotropic glutamate receptors in rat deep dorsal horn neurons. J. Neurophysiol. 76, 2794–2798.

Noordenbos, W. 1959. Pain. Elsevier.

Schilder, P. 1950. The Image and Appearance of the Human Body. International Universities Press.

Wagman, I. H. and Price, D. D. 1969. Responses of dorsal horn cells of *M. Mulatta* to cutaneous and sural A and C fiber stimuli. J. Neurophysiol. 32, 803–817.

Wall, P. D. 1977. The presence of ineffective synapses and the circumstances which unmask them. Philos. Trans. R Soc. London Ser. B 278, 361–372.

Willis, W. D. and Coggeshall, R. E. 1991. Sensory Mechanisms of the Spinal Cord. Plenum.

Yokota, T. and Nishikawa, Y. 1979. Actions of picrotoxin upon trigeminal subnucleus caudalis neurons in the monkey. Brain Res. 171, 369–373.

Zieglgänsberger, W. and Herz, A. 1971. Changes of cutaneous receptive fields of spino-cervical tract neurones and other dorsal horn neurones by microelectrophoretically administered amino acids. Exp. Brain Res. 13, 111–126.

5.26 Spinal Cord Mechanisms of Hyperalgesia and Allodynia

T J Coderre, McGill University, Montreal, QC, Canada

© 2008 Elsevier Inc. All rights reserved.

5.26.1	**Characteristics of Hyperalgesia**	341
5.26.1.1	Definition and Historical Background	341
5.26.1.2	Precipitating Conditions for Hyperalgesia and Evidence of Central Sensitization	341
5.26.1.2.1	Cutaneous injury	341
5.26.1.2.2	Peripheral nerve stimulation	342
5.26.1.2.3	Inflammation	343
5.26.1.2.4	Peripheral nerve injury	343
5.26.1.2.5	Spinal cord injury	344
5.26.1.2.6	Illness-induced hyperalgesia	345
5.26.1.2.7	Chronic opiate exposure	345
5.26.2	**Alterations in Spinal Cord Dorsal Horn**	345
5.26.2.1	Alterations in Transmitter or Growth Factor Expression or Release	345
5.26.2.1.1	Neuropeptides	345
5.26.2.1.2	Excitatory amino acids	346
5.26.2.1.3	Other transmitters	349
5.26.2.1.4	Neurotrophins	349
5.26.2.1.5	Phenotype switch	350
5.26.2.2	Expression of Second Messengers and Transcription Factors	350
5.26.2.2.1	Second messengers	350
5.26.2.2.2	Transcription factors	353
5.26.2.3	Alterations in Receptor and Ion Channel Expression, Activity, or Cellular Location	354
5.26.2.3.1	Neuropeptide receptors	354
5.26.2.3.2	Excitatory amino acid receptors	354
5.26.2.3.3	Other receptors	355
5.26.2.3.4	Scaffolding and adaptor proteins	356
5.26.2.3.5	Ion channels	356
5.26.2.4	Alterations in Transporter Activity	358
5.26.2.4.1	Glutamate transporters	358
5.26.2.4.2	Cation chloride transporters	358
5.26.2.5	Glial Cell Alterations	358
5.26.2.5.1	Microglia	358
5.26.2.5.2	Astrocytes	359
5.26.2.5.3	Neuron–glial interactions	359
5.26.2.6	Descending Facilitation	360
5.26.2.7	Anatomical Changes	360
5.26.2.7.1	Cell death and apoptotic genes	360
5.26.2.7.2	Sprouting	361
5.26.3	**Conclusion**	362
References		362

Glossary

adaptor protein A protein which is accessory to main proteins in a signal transduction pathway. These proteins often lack any intrinsic enzymatic activity themselves, but instead mediate specific protein-protein interactions that drive the formation of protein complexes.

allodynia Pain due to a stimulus that does not normally provoke pain.

antisense oligonucleotides Single strands of DNA or RNA that are complementary to a chosen sequence. Antisense RNAs prevent translation of complementary RNA strands by binding to them.

apoptosis An orchestrated series of biochemical events leading to cell death.

carrageenan A linear sulphated polysaccharide extracted from red seaweeds that is used as an inflammatory agent.

central sensitization Activity- or injury-dependent changes in the excitability of central nervous system (CNS) neurons, typically in pain pathways, and is reflected by increased spontaneous activity, reduced thresholds or increased responsiveness to afferent inputs, prolonged after- discharges to repeated stimulation, and the expansion of the peripheral receptive fields of central neurons.

complete Freund's adjuvant An antigen solution composed of inactivated and dried *Mycobacterium tuberculosis* emulsified in mineral oil, used as an immunopotentiator (booster of the immune system) and inflammatory agent.

2-deoxy-D-glucose A marker for tissue glucose use.

excitatory amino acids Amino acid neurotransmitters that include aspartate and glutamate. Glutamate is the most abundant fast excitatory neurotransmitter in the mammalian nervous system.

excitatory postsynaptic potential (EPSP) Is a temporary increase in postsynaptic membrane potential caused by the flow of positively charged ions into the postsynaptic cell.

glial cells Commonly called neuroglia or simply glia, are non-neuronal cells that provide support and nutrition, maintain homeostasis, form myelin, and participate in signal transmission in the nervous system.

homosynaptic sensitization Facilitation of activity occuring at the synapses that connect two neurons.

hyperalgesia An increased response to a stimulus which is normally painful. Primary hyperalgesia occurs at the site of injury, and secondary hyperalgesia in adjacent, or sometimes remote, uninjured tissue.

inhibitory postsynaptic potential (IPSP) Is the change in membrane voltage of a postsynaptic neuron which results from synaptic activation of inhibitory neurotransmitter receptors.

ion channels Pore-forming proteins that help to establish and control the small voltage gradient across the plasma membrane of all living cells by allowing the flow of ions down their electrochemical gradient.

long-term potentiation (LTP) An increase in the strength of a chemical synapse that lasts from minutes to several days.

neuropeptides A variety of peptides found in neural tissue.

neurotrophins Also called ''neurotrophic factors'', are a family of protein which induce the survival of neurons. They belong to a family of growth factors, secreted proteins which are capable of signaling particular cells to survive, or differentiate, or grow.

phenotype switch A process by which neurons change their phenotype and begin to produce and release substances they normally do not produce.

protein kinase Is a kinase enzyme that modifies other proteins by chemically adding phosphate groups to them (phosphorylation).

protein tyrosine phophatase (PTP) An enzyme that remove phosphate groups from phosphorylated tyrosine residues on proteins.

scaffold proteins Proteins that bring together various other proteins in a signaling pathway and allows for their interaction. They recruit downstream effectors in a pathway and enhance specificity of the signal.

secondary messengers Secondary messengers are a component of signal transduction cascades that utilize receptors on the surface of the plasma membrane which are generally coupled to a kinase on the interior surface of the membrane. The kinase then phosphorylates another molecule which carries out another action.

transcription factor A protein that works in concert with other proteins to either increase or decrease the transcription of genes.

transporters Membrane-bound pumps that move biochemicals and other atomic or molecular substances across membranes.

wide dynamic range A property of spinal cord dorsal horn neurons (typically in lamina V) that exhibit graded responses to non-noxious and noxious stimuli since they receive convergent input from non-nociceptive and nociceptive primary afferent fibers.

wind-up Cumulative depolarization, action potential bursting and afterdischarges in spinal cord dorsal horn neurons following high frequency, C-fiber strength electrical stimulation or intensely noxious natural stimuli.

5.26.1 Characteristics of Hyperalgesia

5.26.1.1 Definition and Historical Background

The term hyperalgesia was first coined by Gowers in the 1800s, and is often still used as a term to define what Hardy J. D. (1956) described as "a state of increased pain sensation induced by either noxious or ordinarily nonnoxious stimulation of peripheral tissue." The International Association for the Study of Pain (IASP) currently uses separate terms for the two reactions Hardy described. Thus, hyperalgesia is defined as "an increased response to a stimulus which is normally painful," while "pain due to a stimulus that does not normally provoke pain" is known as allodynia (IASP website). Over the years, hyperalgesia (not distinguished from allodynia) has been further separated into primary and secondary hyperalgesia; primary hyperalgesia occurs at the site of injury, and secondary hyperalgesia in adjacent, or sometimes remote, uninjured tissue. Primary hyperalgesia is reflected by a hypersensitivity to thermal and mechanical stimuli, and is driven largely by sensitization of peripheral nociceptors. Secondary hyperalgesia is predominantly characterized by hypersensitivity to mechanical stimuli, and likely involves central sensitization. Central sensitization refers to activity- or injury-dependent changes in the excitability of central nervous system (CNS) neurons, typically in pain pathways, and is reflected by increased spontaneous activity, reduced thresholds or increased responsiveness to afferent inputs, prolonged after-discharges to repeated stimulation, and the expansion of the peripheral receptive fields of central neurons (Woolf, C. J. *et al.*, 1988; Coderre, T. J. *et al.*, 1993). Although central sensitization has been demonstrated in neurons throughout the somatosensory nervous system, the mechanisms underlying central sensitization have been largely generated from studies concentrating on spinal cord dorsal horn neurons. The characteristics and underlying mechanisms of central sensitization in spinal cord dorsal horn neurons will be the main focus of the remaining sections of this chapter, and will be a recurring theme in various chapters of this volume that address alterations in pain processing associated with injury or disease of peripheral tissue, primary afferent nerves, or CNS structures.

5.26.1.2 Precipitating Conditions for Hyperalgesia and Evidence of Central Sensitization

5.26.1.2.1 Cutaneous injury

5.26.1.2.1.(i) Heat injury Considerable evidence demonstrates that heat injury of the skin produces a sensitization of peripheral nociceptors. Peripheral sensitization occurs both in Aδ and C-fiber nociceptors (Beitel, R. E. and Dubner, R., 1976; Fitzgerald, M. and Lynn, B., 1977), and largely accounts for primary hyperalgesia (Meyer, R. A. and Campbell, J. N., 1981; Torebjörk, H. E. *et al.*, 1984). In addition, dorsal horn neurons fire with increasing frequency in response to repeated applications of a noxious heat stimulus (Perl, E. R. *et al.*, 1976, Kenshalo, D. R. *et al.*, 1979) or following thermal injury (Price, D. D. *et al.*, 1978; Kenshalo, D. R. *et al.*, 1982), indicative of central sensitization. In addition to the sensitization and prolonged excitation of dorsal horn cells, noxious stimulation associated with tissue injury also produces an expansion of the receptive fields of dorsal horn neurons. Thus, neurons in the dorsal horn of the spinal cord with receptive fields adjacent to a cutaneous heat injury expand their receptive fields to incorporate the site of injury (McMahon, S. B. and Wall, P. D., 1984).

Evidence that central sensitization contributes to secondary hyperalgesia after heat injury was supported initially by reports that heat injury-induced cutaneous hyperalgesia spreads well beyond the area of nociceptor sensitization. Thalhammer J. G. and Lamotte R. H. (1982) found that a heat injury in one half of a cutaneous nociceptor's receptive field did not produce heat sensitization in the other half, despite the fact that hyperalgesia spread into this area. Typically, nociceptor sensitization associated with injury is restricted to about 5–10 mm of the site of injury (Fitzgerald, M., 1979) while, in contrast, cutaneous hyperalgesia spreads as far as 10–20 cm beyond the site of injury (Hardy, J. D. *et al.*, 1950).

Although it is commonly reported that there is mechanical, but not heat hyperalgesia in the secondary zone (Raja, S. N. *et al.*, 1984), secondary heat hyperalgesia has been reported in some cases (Pedersen, J. L. and Kehlet, H. 1998). Importantly, secondary heat hyperalgesia is significantly reduced when lidocaine is administered i.v. prior to heat injury (Holthusen, H. *et al.*, 2000), suggesting that central sensitization plays a role in its initiation. Animal behavioral studies support this conclusion, as the spread of hyperalgesia to the rat hind paw

contralateral to the paw that received a thermal injury is unaffected by either deafferentation or anesthetic blocks of the injured hind paw following the injury, but is prevented if deafferentation or anesthetic block precedes the injury (Coderre, T. J. and Melzack, R., 1985; 1987).

5.26.1.2.1.(ii) Mechanical injury Mechanical injury of the skin also produces both primary and secondary hyperalgesia, as has been demonstrated in the rat plantar incision model (Brennan, T. J. *et al.*, 1996), as well as following incision of human skin (Kawamata, M. *et al.*, 2002a). Although both pre- and postincisional administration of intrathecal (i.t.) morphine or bupivacaine reduce secondary hyperalgesia in the rat model (Zahn, P. K. and Brennan, T. J., 1999), only preincisional administration of s.c. or i.v. lidocaine reduce secondary hyperalgesia in humans (Kawamata, M. *et al.*, 2002a). These results again support a role for central sensitization in the initiation of secondary hyperalgesia after mechanical skin injury. This conclusion is also consistent with the finding that rat plantar incisions or other mechanical injuries produce an increase in the responsiveness of spinal wide dynamic range (WDR) neurons to innocuous and noxious stimuli, as well as increases in their receptive fields (Cervero, F. *et al.*, 1988; Kawamata, M. *et al.*, 2002b).

5.26.1.2.1.(iii) Capsaicin Capsaicin, the active ingredient of hot chilli peppers, produces hyperalgesia in both animals (Gilchrist, H. D. *et al.*, 1996) and humans (Carpenter, S. E. and Lynn, B., 1981) when injected or applied to the skin. Evidence that capsaicin-induced hyperalgesia depends on central sensitization initially came from animal studies that showed that intradermal injections of capsaicin produced enhanced excitability of spinal cord dorsal horn neurons in cats (Simone, D. A. *et al.*, 1989) and monkeys (Dougherty, P. M. and Willis, W. D., 1992). In both monkeys (Baumann, T. K. *et al.*, 1991) and humans (Lamotte, R. H. *et al.*, 1992), capsaicin injections produce extensive, spreading hyperalgesia without producing the same degree of spreading sensitization of primary afferent nociceptors. Indeed, capsaicin caused the spread of both brush allodynia and pinprick hyperalgesia beyond the borders of the territory of the nerve which innervates the injected skin area (Sang, C. N. *et al.*, 1996), suggesting that there is extraterritorial pain that is dependent on central sensitization. Furthermore, in humans, hyperalgesia to punctate mechanical stimuli, which develops after intradermal injection of capsaicin, is maintained even after anesthetizing the region where capsaicin was injected (Lamotte, R. H. *et al.*, 1991). However, if the skin region is anesthetized prior to capsaicin injection, cutaneous hyperalgesia does not develop. Furthermore, hyperalgesic responses to capsaicin can be prevented if the area of skin where the injection is made is rendered anesthetic by a proximal anesthetic block of the peripheral nerve which innervates it. Thus, for hyperalgesia to develop it is critical that initial inputs from the injury reach the CNS. However, once hyperalgesia is established, it does not need to be maintained by inputs from the injured peripheral tissue. In support of this, Torebjörk H. E. *et al.* (1992) have shown that pain thresholds to intraneural electrical stimulation of afferent fibers are dramatically reduced following intradermal capsaicin injection in the skin from which the stimulated nerve emanates: neural stimulation which was felt as tactile before administration of capsaicin, was painful after capsaicin. Importantly, this reduced pain threshold is evident even when the sensory projected field of the afferent nerve is anesthetized after the capsaicin injection. Again, a state of central sensitization is indicated since once they have established their effects, inputs from the injured region are not required to maintain the lowered threshold.

5.26.1.2.2 Peripheral nerve stimulation

Much of the early evidence that spinal mechanisms contribute to hyperalgesia and allodynia came from studies that used peripheral nerve stimulation as a conditioning stimulus, and assessed the influence of the conditioning on spinal function or the function of spinal output neurons. Early studies showed that repeated high-frequency C-fiber afferent stimulation sequentially increases dorsal horn activity resulting in a prolonged discharge of the cell, lasting from seconds to minutes poststimulation (Mendell, L. M. and Wall, P. D., 1965; Mendell, L. M., 1966). This phenomenon, which has been labeled as windup, results from a homosynaptic sensitization (Woolf, C. J. *et al.*, 1988) of dorsal horn neurons, and likely represents a short-term sensitization of dorsal horn neurons that underlies the intense reactions and lingering after sensations to stimuli at the pain tolerance level. Although windup is not synonymous with central sensitization (Woolf, C. J., 1996), stimulation that causes windup can produce some of the classical characteristics of central sensitization including expansion of dorsal horn neuronal receptive fields and enhanced spinal neuronal

responses to C-fiber, but not A-fiber electrical stimulation (Li, J. *et al.*, 1999).

In early studies of central mechanisms of hyperalgesia, it was shown that noxious electrical stimulation of cutaneous and muscle afferent nerves (Woolf, C. J., 1983; Wall, P. D. and Woolf, C. J., 1984), as well as cutaneous (Woolf, C. J., 1983) and deep (Woolf, C. J. and McMahon, S. B., 1985) tissue injury, produce an increase in the excitability of the ipsilateral and contralateral flexor efferent nerves in response to noxious mechanical stimulation of the hind paw. Because the increased excitability in the contralateral flexor efferent nerve is maintained even after inputs from the injured paw are blocked by local anesthesia, the results suggest that central, not peripheral, changes underlie this effect.

Although typically associated with hippocampal neurons, evidence suggests that the phenomenon long-term potentiation (LTP) can also be elicited in spinal cord dorsal horn neurons after stimulation of primary afferents in transverse spinal cord slices (Randic, M. *et al.*, 1993; Lozier, A. P. and Kendig, J. J., 1995), as well as *in vivo* after electrical nerve stimulation (Svendsen, F. *et al.*, 1997; 1999) or intense natural noxious stimulation (Rygh, L. J. *et al.*, 1999). Importantly, LTP induced by electrical nerve stimulation or noxious stimulation is maintained after lidocaine block distal to the stimulation site in the sciatic nerve (Svendsen, F. *et al.*, 1999) or proximal to the site of noxious stimulation (Rygh, L. J. *et al.*, 1999).

5.26.1.2.3 Inflammation

5.26.1.2.3.(i) Subcutaneous inflammation Subcutaneous injections of inflammatory substances such as carrageenan and complete Freund's adjuvant (CFA) in the rat hind paw produce thermal hyperalgesia and mechanical allodynia (Buritova, J. *et al.*, 1996; Arevalo, M. I. *et al.*, 2003), as well as a sensitization of peripheral nociceptors (Kocher, L. *et al.*, 1987; Andrew, D. and Greenspan, J. D., 1999). There is also evidence of central sensitization associated with peripheral inflammation. Subcutaneous carrageenan injections produce increased excitability of rat spinal cord neurons as shown by increased responses to mechanical and electrical stimulation, enhanced windup, expanded receptive fields (Hedo, G. *et al.*, 1999; Torsney, C. and Fitzgerald, M., 2002), and increased flexor efferent neuron responsiveness (Xu, X.-J. *et al.*, 1995). Subcutaneous injections of CFA in rats also produce central sensitization, as evidenced by the enhancement of dorsal horn neurons spontaneous activity and increased responsiveness to thermal, mechanical and electrical nerve stimulation (Hylden, J. L. K. *et al.*, 1989; Ren, K. *et al.*, 1992). After subcutaneous CFA, there is also an increased ability to induce LTP (Vikman, K. S. *et al.*, 2003), expanded receptive fields in rat dorsal horn neurons (Hylden, J. L. K. *et al.*, 1989; Ren, K. *et al.*, 1992), and an increase in the excitability of flexor efferent neurons (Seybold, V. S. *et al.*, 2003).

5.26.1.2.3.(ii) Joint inflammation Injection of kaolin and carrageenan into the rat knee joint produces limping and guarding of the limb (Sluka, K. A. and Westlund, K. N., 1993), as well as a sensitization of peripheral nociceptors (Neugebauer, V. and Schaible, H. G., 1988). The same stimulus produces enhanced responsiveness of spinal cord dorsal horn neurons to normal movement or tactile stimulation of the knee joint (Neugebauer, V. and Schaible, H. G., 1988; 1990), as well as an expansion of the receptive field of dorsal horn neurons that respond to joint input (Neugebauer, V. and Schaible, H. G., 1990). There is also an expansion of dorsal horn neuron receptive fields following the induction of polyarthritis in multiple joints three weeks or more following CFA injections to the rat tail (Menétrey, D. and Besson, J. M. 1982; Calvino, B. *et al.*, 1987).

5.26.1.2.4 Peripheral nerve injury

Traumatic (Bennett, G. J. and Xie, Y. K., 1988; Seltzer, Z. *et al.*, 1990; Kim, S. H. and Chung, J. M., 1992; Decosterd, I. and Woolf, C. J., 2000), inflammatory (Eliav, E. *et al.*, 1999; Milligan, E. D. *et al.*, 2003), or chemical (Tanner, K. D. *et al.*, 1998; Polomano, R. C. *et al.*, 2000) injury of peripheral nerves induces heat and/or mechanical hyperalgesia, or mechanical and/or cold allodynia in animal models. While there is an established contribution of peripheral pathology to hyperalgesia and allodynia in these models (Chen, Y. and Devor, M., 1998; Liu, X. *et al.*, 1999), it is also clear that central sensitization plays a critical role. Thus, 9–11 days after chronic constriction injury (CCI) of the rat sciatic nerve, lumbar spinal cord dorsal horn neurons exhibit abnormal characteristics including spontaneous activity, exaggerated, and prolonged responses to noxious and innocuous mechanical stimulation (Laird, J. M. and Bennett, G. J., 1993), with prolonged after-discharges more prevalent in WDR neurons, as opposed to nociceptive-specific neurons (Sotgiu, M. L. *et al.*, 1995; Pitcher, G. M. and Henry, J. L., 2000). Two weeks after L5/L6 spinal nerve ligation (SNL), rat dorsal horn neurons also show increased spontaneous firing with irregular firing patterns (Suzuki, R. and Dickenson, A. H., 2005).

Thresholds for excitatory postsynaptic potentials (EPSPs) of lamina II neurons are dramatically lower after CCI, and spared nerve injury (Kohno, T. *et al.*, 2003), and there is a long-lasting posttetanic potentiation of sciatic-evoked A-fiber superficial dorsal horn field potentials that is present over the same time course as thermal hyperalgesia in CCI rats (Draganic, P. *et al.*, 2001). Tight ligation of the L5/L6 spinal nerve also results in a lower threshold for activation of C-fiber-driven dorsal horn field potentials, and for the induction of LTP in dorsal horn neurons (Xing, G. *et al.*, 2003).

Increases in spontaneous and evoked activity in dorsal horn neurons of CCI rats are paralleled by increases in [^{14}C]-2-deoxyglucose metabolic activity throughout the lumbar spinal dorsal horn, with greater increases in the medial portion of the ipsilateral dorsal horn (Mao, J. *et al.*, 1992a). Fos protein expression, often used as a measure of neuronal activation, is also increased in the spinal cord dorsal horn of CCI rats (Ro, L. S. *et al.*, 2004). Importantly, Fos protein expression is elevated throughout the dorsal horn (lamina I–VI) of the entire lumbar spinal cord, and like [^{14}C]-2-deoxyglucose activity, significant but lower increases were found in the contralateral dorsal horn. Thus, for both the [^{14}C]-2-deoxyglucose and Fos protein expression measures, there is a spread of neuronal activity to spinal regions outside of the normal central terminations of the sciatic nerve. This may explain why abnormal pain sensations are sometimes exhibited contralaterally, or in body areas that do not correspond with the terminations of an injured peripheral nerve (Koltzenburg, M. *et al.*, 1999; Ro, L. S. *et al.*, 2004).

In addition to enhanced spontaneous and evoked activity, spinal cord dorsal horn neurons of CCI rats are also found to have expanded receptive fields (Pitcher, G. M. and Henry, J. L., 2000). Rats with diabetic neuropathy following treatment with streptozotocin are also found to have dorsal horn neurons with high level of spontaneous activity and with expanded receptive fields (Chen, S. R. and Pan, H. L., 2002). A recent study measured dorsal horn neuronal activity in neuropathic pain patients undergoing surgery for ablation of the dorsal root entry zone (Guenot, M. *et al.*, 2003). These authors found similar alterations in dorsal horn neuron activity including bursting activity (in patients with deafferentation pain after brachial plexus avulsion) and nonrandom patterns of spontaneous discharge (in patients with peripheral nerve injury).

The enhanced spontaneous or evoked activity of dorsal horn neurons likely contribute to hyperalgesia and allodynia since systemic low-dose lidocaine reduces both spontaneous activity in WDR neurons (Sotgiu, M. L. *et al.*, 1992) and the thermal hyperalgesia (Abram, S. E. and Yaksh, T. L., 1994) in CCI rats. Mechanical allodynia induced by partial sciatic nerve lesion or SNL is also attenuated by i.t. treatment with very low doses of lidocaine that are not effective when given systemically (Ma, W. *et al.*, 2003a). The hyperalgesia after CCI depends partly on an injury discharge at the time of surgery, since the onset of thermal hyperalgesia in CCI rats was delayed by treating the nerve with bupivacaine 15 min before, but not 15 min after nerve constriction (Yamamoto, T. *et al.*, 1993).

5.26.1.2.5 Spinal cord injury

Animal models of central pain have been generated following traumatic, inflammatory, or excitotoxic injury of the spinal cord (see Vierck, C. J. and Light, A. R., 2000 or Yezierski, R. P., 2000 for reviews). Traumatic (Christensen, M. D. *et al.*, 1996; Christensen, M. D. and Hulsebosch, C. E., 1997; Bruce, J. C. *et al.*, 2002), inflammatory (Cahill, C. M. *et al.*, 1998), and excitotoxic (Yezierski, R. P. *et al.*, 1998) injury of spinal cord produces mechanical and thermal allodynia and/or hyperalgesia in rat hind paws. Spinal cord injury also results in a sensitization of spinal cord dorsal horn neurons as indicated by increased spontaneous activity, increased evoked responses to mechanical stimuli, and increased duration of after-discharges and enhanced windup (Yezierski, R. P. and Park, S. H., 1993; Christensen, M. D. and Hulsebosch, C. E., 1997; Wang, J. *et al.*, 2005; Zhang, H. *et al.*, 2005). It was recently demonstrated that spinal sensitization (enhanced spontaneous and evoked activity and enhanced windup in dorsal horn neurons), as well as hind paw thermal and mechanical allodynia, are reduced in spinal cord injured rats that are treated spinally with bupivacaine at the time of the injury (Zhang, H. *et al.*, 2005), suggesting that spinal sensitization underlies the development of allodynia/hyperalgesia after spinal cord injury. Spinal treatment with morphine also reduces the enhanced mechanically evoked responses of WDR neurons in the spinal cord dorsal horn of spinal cord injured rats (Wang, J. *et al.*, 2005). Consistent with these findings, it has recently been shown that central pain (spontaneous pain, mechanical allodynia, and/or mechanical hyperalgesia) associated with spinal cord injury in

rats is reduced by intravenous lidocaine administration (Attal, N. *et al.*, 2000; Finnerup, N. B. *et al.*, 2005).

5.26.1.2.6 Illness-induced hyperalgesia

Thermal hyperalgesia is also induced by intraperitoneal (i.p.) injection of agents that induce illness including lithium chloride and the bacterial cell wall endotoxin lipopolysaccharide (LPS) (Wiertelak, E. P. *et al.*, 1994; Watkins, L. R. *et al.*, 1994a). Illness-induced hyperalgesia has been shown to be dependent on spinal mechanisms that are activated by a descending pain facilitatory pathway (see below) that projects from the nucleus raphe magnus (NRM) through the dorsolateral funiculus to the spinal cord dorsal horn. The NRM has also been shown to be activated by brain regions that receive inputs from hepatic vagal afferent nerves (Watkins, L. R. *et al.*, 1994b).

5.26.1.2.7 Chronic opiate exposure

Thermal and/or mechanical hyperalgesia are observed in rats after repeated high-dose morphine treatment (Kayan, S. *et al.*, 1971; Mao, J. and Mayer, D. J., 2001) or in some cases after administration of low doses of morphine (Holtman, J. R., Jr. and Wala, E. P., 2005). This phenomenon mirrors a trend that has been observed in clinics in which chronic pain patients are treated with morphine (Jacobsen *et al.*, 1995). Mao J. *et al.* (1995a) and Mayer D. J. *et al.* (1999) have noted a parallel between hyperalgesia that occurs after repeated morphine exposure and that produced by neuropathic injury, each causing the activation of similar intracellular signaling pathways and the appearance of dark neurons in spinal cord dorsal horn. It is also significant that expression of the transcription factor Fos, which is commonly used as an indicator of neuronal activation, is upregulated in the spinal dorsal horn of rats that are morphine dependent and have withdrawal precipitated by injection of naltrexone (Rohde, D. S. *et al.*, 1996).

5.26.2 Alterations in Spinal Cord Dorsal Horn

5.26.2.1 Alterations in Transmitter or Growth Factor Expression or Release

5.26.2.1.1 Neuropeptides

Several lines of evidence suggest that C-fiber neuropeptides are involved in triggering CNS plasticity following injury or noxious stimulation. A role for C-fiber neuropeptides in nociception is suggested as noxious stimulation or peripheral inflammation causes the release of substance P (SP) (Go, V. L. and Yaksh, T. L., 1987; Oku, R. *et al.*, 1987; Duggan, A. W. *et al.*, 1988), neurokinin (NK) A (Hua, X. Y. *et al.*, 1986; Duggan, A. W. *et al.*, 1990), somatostatin (Kuraishi, Y. *et al.*, 1985; Morton, C. R. *et al.*, 1988), calcitonin gene-related peptide (CGRP) (Saria, A. *et al.*, 1986), dynorphin 1–17 (Parra, M. C. *et al.*, 2002), and galanin (Morton, C. R. and Hutchison, W. D., 1990; Colvin, L. A. and Duggan, A. W. *et al.*, 1998) in spinal cord dorsal horn. Spontaneous and noxious stimulus-evoked release of neuropeptide Y (NPY) is enhanced in the dorsal horn of rats with CCI of the sciatic nerve (Mark, M. A. *et al.*, 1998). Furthermore, the iontophoretic application of SP and other NKs produces an excitation of dorsal horn neurons (Henry, J. L., 1976; Willcockson, W. S. *et al.*, 1984a), while i.t. treatment produces behavioral hyperalgesia (Moochhala, S. M. and Sawynok, J., 1984; Cridland, R. A. and Henry, J. L., 1986) or nociceptive behaviors (Hylden, J. L., and Wilcox, G. L., 1981; Seybold, V. S. *et al.*, 1982; Gamse, R. and Saria, A., 1986) in rodents.

There is a decrease in immunoreactive staining for the neuropeptides SP and CGRP in the superficial dorsal horn of rats with experimental arthritis (Sluka, K. A. *et al.*, 1992). While the decrease in these neuropeptides occurs early (4–8 h) after knee inflammation, substance P and CRGP are increased after 5–7 days in the dorsal root ganglia and spinal cord of rats with inflammation of the knee (Sluka, K. A. and Westlund, K. N., 1993) or hind paw (Donnerer, J. *et al.*, 1993). Conversely, and spinal cord dorsal horn substance P and CGRP are decreased in the weeks after CCI of the sciatic nerve (Cameron, A. A. *et al.*, 1991). There is also a decrease in both mRNA and peptide levels of SP, somatostatin and CGRP in the DRG after peripheral nerve section (Jessell, T. M. *et al.*, 1979; Nielsch, V. *et al.*, 1987; Noguchi, K. *et al.*, 1989, 1990, 1993; Henken, D. B. *et al.*, 1990; Baranowsli, A. P. *et al.*, 1993), whereas the levels of cholecystokinin (CCK), galanin, pituitary adenylate cyclase activating peptide (PACAP), vasoactive intestinal polypeptide (VIP) and NPY are increased (Shehab, S. A. and Atkinson, M. E., 1986; Hokfelt, T. *et al.*, 1987; Villar, M. J. *et al.*, 1989; Noguchi, K. *et al.*, 1989, 1993; Wakisaka, S. *et al.*, 1991, 1992; Zhang, X. *et al.*, 1993b, Zhang, Y. Z., 1996). Dynorphin mRNA is also increased in the spinal dorsal horn following traumatic spinal cord injury (Tachibana, T. *et al.*, 1998).

For SP, the decreased immunoreactivity may reflect increased neuropeptide release since *in vivo* microdialysis studies show that spinal SP is increased

following partial sciatic nerve ligation (Wallin, J. and Schott, E., 2002). The increased levels of galanin may play an antinociceptive role as galanin overexpressing mice have attenuated mechanical and heat hyperalgesia after partial ischemic injury (Hygge-Blakeman, K. *et al.*, 2004) or CCI (Eaton, M. J. *et al.*, 1999) of the sciatic nerve. Spinal administration of galanin also produces an inhibition of dorsal horn neuronal responses to natural and electrical stimuli in rats with SNL (Flatters, S. J. *et al.*, 2002). In contrast, galanin knockout mice have attenuated responses to hind paw formalin injections (Kerr, B. J. *et al.*, 2001a), and have reduced thermal hyperalgesia after intraplantar injection of carrageenan (Kerr, B. J. *et al.*, 2001a) or partial sciatic nerve transection (Kerr, B. J. *et al.*, 2000). In addition, both windup and the facilitation of spinal reflexes following conditioning stimulation are significantly reduced in galanin knockout mice with sciatic nerve transections (Kerr, B. J. *et al.*, 2001b). Upregulated CCK may contribute to mechanical hypersensitivity as allodynia induced by spinal ischemic injury is reduced following administration of a CCK-B receptor antagonist (Wiesenfeld-Hallin, Z. *et al.*, 1997). Prodynorphin knockout mice or mice receiving dynorphin A antisera do not develop mechanical and thermal hyperalgesia after SNL (Gardell, L. R. *et al.*, 2004), suggesting that upregulated dynorphin contributes to nerve injury-induced hyperalgesia. Indeed, elevated spinal dynorphin content associated with SNL has been demonstrated to be coincident with the onset of mechanical allodynia and thermal hyperalgesia (Malan, T. P. *et al.*, 2000). Although the release of both VIP and NPY are elevated in the deep dorsal horn of rats with spinal nerve transection, the increases do not appear to be related to neuropathic pain as increases were observed even in rats that did not exhibit behavioral signs of hyperalgesia (Kim, H. J. *et al.*, 2003).

A role of C-fiber neuropeptides in noxious stimulus-induced plasticity is further suggested by several findings. Repetitive stimulation of dorsal roots elicits a slow depolarization in dorsal horn neurons which is mimicked by SP (Murase, K. and Randic, M., 1984), NK A (Murase, K. *et al.*, 1989), CGRP (Ryu, P. D. *et al.*, 1988), VIP (Urban, L. and Randic, M., 1984), or CCK (Murase, K. *et al.*, 1987), and is blocked by SP antagonists or capsaicin applied to the tissue bath (Urban, L. and Randic, M., 1984). Iontophoretic application of neuropeptides, such as SP, produces enhanced dorsal horn neuron responses to noxious thermal and mechanical stimulation (Henry, J. L., 1976; Randic, M. and Miletic, V., 1977). Dorn horn neuronal LTP induced *in vivo* by high-intensity, high-frequency tetanic afferent nerve stimulation is blocked by i.v. administration of NK-1) or NK-2 antagonists (Liu, X. and Sandkuhler, J., 1997). Knockout of the preprotackykinin-A gene, from which SP and NKA are derived, results in a reduction in the time course over which dorsal horn WDR neurons are sensitized following mustard oil application to the mice hind paw, as well as a reduction in the magnitude of poststimulus discharges of WDR neurons (Martin, W. J. *et al.*, 2004).

The increased excitability in flexor efferents, induced either by C-fiber electrical stimulation or by the application of chemical irritants, is blocked by pretreatment of the sciatic and saphenous nerves with the C-fiber neurotoxin capsaicin (Woolf, C. J. and Wall, P. D., 1986) or by the SP antagonist spantide II (Wiesenfeld-Hallin, Z. *et al.*, 1990). I.t. application of the C-fiber neuropeptides SP (Woolf, C. J. and Wiesenfeld-Hallin, Z., 1986), NK A (Xu, X.-J. *et al.*, 1991), CGRP (Woolf, C. J. and Wiesenfeld-Hallin, Z., 1986), VIP (Wiesenfeld-Hallin, Z., 1987), somatostatin (Wiesenfeld-Hallin, Z., 1985), and galanin (Wiesenfeld-Hallin, Z. *et al.*, 1989) produces prolonged enhancements in the excitability of the flexion reflex.

In addition, the hyperalgesia that develops in the hind paw contralateral to a thermal injury is mimicked by i.t. treatment with SP and NKA, and reversed by pretreatment with a SP antagonist (Coderre, T. J. and Melzack, R., 1991). Subcutaneous injection of formalin, which elicits a persistent nociceptive response associated with central changes (Coderre, T. J. *et al.*, 1990), evokes an immediate, intense barrage of C-fiber afferent activity (McCall, W. D. *et al.*, 1996), and produces an increase in SP in the cerebrospinal fluid (Kuraishi, Y. *et al.*, 1989). Furthermore, nociceptive responses to formalin are significantly suppressed in rats pretreated with peptide (Murray, C. W. *et al.*, 1991) and nonpeptide (Yamamoto, T. and Yaksh, T. L., 1991; Yashpal, K. *et al.*, 1993) NK-1 receptor antagonists, as well as the C-fiber neurotoxin capsaicin (Dray A. and Dickenson, A. H., 1991). Finally, various nonpeptide NK-1 receptor antagonists attenuate allodynia and hyperalgesia that is evoked by CCI of the sciatic nerve (Cumberbatch, M. J. *et al.*, 1998; Cahill, C. M. and Coderre, T. J., 2002).

5.26.2.1.2 *Excitatory amino acids*

Additional evidence implicates a contribution of excitatory amino acids (EAAs) to injury-induced

neuroplasticity. EAAs have widespread activity in the CNS including the spinal cord (Watkins, J. C. and Evans, R. H., 1981; Davies, J. and Watkins, J. C., 1983) and thalamus (Eaton, S. A. and Salt, T. E., 1990). The role of EAAs in nociception is suggested since noxious stimulation or peripheral inflammation causes the release of glutamate and aspartate in spinal cord dorsal horn (Skilling, S. R. *et al.*, 1988; Sorkin, L. S. *et al.*, 1992). The dorsal horn synaptosomal level of EAAs is increased in rats with CCI of the sciatic nerve (Somers, D. L. and Clemente, F. R., 2002), and dorsal horn levels of EAAs are increased in rats with a plantar incision (Zahn, P. K. *et al.*, 2002) or CCI of the sciatic nerve (al-Ghoul, W. M. *et al.*, 1993; Kawamata, M. and Omote, K., 1996). Furthermore, iontophoretic application of EAAs produces an excitation of dorsal horn neurons (Curtis, D. R. and Watkins, J. C., 1960; Willcockson, W. S. *et al.*, 1984b; Schneider, S. P. and Perl, E. R., 1988), while i.t. treatment produces both behavioral hyperalgesia and spontaneous nociceptive behaviors (Aanonsen, L. M. and Wilcox, G. L., 1986; 1987).

A role of EAAs in noxious stimulus-induced plasticity is further suggested by several findings. The windup of dorsal horn neuron activity after frequency C-fiber stimulation is mimicked by the application of L-glutamate or *N*-methyl-D-aspartate (NMDA) (Gerber, G. and Randic, M., 1989), and blocked by application of either competitive (Dickenson, A. H. and Sullivan, A. F., 1987; Thompson, S. W. *et al.*, 1990) or noncompetitive (Davies, S. N. and Lodge, D., 1987; Thompson, S. W. *et al.*, 1990) NMDA antagonists. Iontophoretic application of EAAs produces receptive field changes in dorsal horn neurons (Zieglgansberger, W. and Herz, A., 1971), as well as enhanced dorsal horn neuron responses to nonnoxious and noxious mechanical stimulation (Aanonsen, L. M. *et al.*, 1990; Dougherty, P. M. and Willis, W. D., 1991). Dorsal horn neurons that are sensitized following peripheral tissue injury/inflammation show increased responsiveness to the iontophoretic application of EAAs (Dougherty, P. M. and Willis, W. D., 1992; Dougherty, P. M. *et al.*, 1992b), and exhibit a reduction in responsiveness or sensitization following intravenous administration of ketamine or iontophoretic application of NMDA antagonists (Schaible, H.-G. *et al.*, 1991), or the administration of α-amino-3-hydroxy-5-methylisoxazole-4-propionic acid (AMPA) or NMDA antagonists to dorsal horn neurons by reverse microdialysis (Dougherty, P. M. *et al.*, 1992a).

I.t. administration of the EAAs L-glutamate or L-aspartate produces an increase in the excitability of flexor efferents (Woolf, C. J. and Wiesenfeld-Hallin, Z., 1986), while competitive or noncompetitve NMDA antagonists reduce the facilitation of flexion reflexes induced by electrical (C-fiber) stimulation or cutaneous application of the chemical irritant mustard oil (Woolf, C. J. and Thompson, S. W., 1991). Hyperalgesia that develops in the hind paw contralateral to a thermal injury is both mimicked following i.t. treatment with NMDA, and reversed by an NMDA receptor antagonist (Coderre, T. J. and Melzack, R. 1991). Studies in humans (Kristensen, J. D. *et al.*, 1992), show that i.t. treatment with the competitive NMDA receptor antagonist 3-(2-carboxypiperazin-4-yl)-propyl-1-phosphonic acid (CPP) abolished after-discharges and spreading pain and hyperalgesia (symptoms proposed to be associated with windup) in a patient with neuropathic pain.

A contribution of ionotropic glutamate receptors (iGluRs) to nociceptive processing was originally suggested by the ability of AMPA/kainate, and particularly NMDA, receptor antagonists to produce analgesic effects in both phasic and tonic nociceptive tests in rats (Cahusac, P. M. *et al.*, 1984; Nasstrom, J. *et al.*, 1992). In addition, AMPA antagonists have been found to produce an inhibition of miniature endplate potentials in dorsal horn neurons (Hori, Y. and Endo, K., 1992) and dorsal root potentials evoked by single shock C-fiber stimulation (Thompson, S. W. *et al.*, 1992). Furthermore, tetanic electrical stimulation of the primary afferent fibers *in vitro* (Randic, M. *et al.*, 1993) or *in vivo* (Liu, X. G. and Sandkuhler, J., 1995) induces a LTP of the C-fiber-evoked potentials in dorsal horn neurons that is prevented by superfusion with NMDA antagonists.

NMDA antagonists have been particularly effective at reducing persistent pain associated with central sensitization. The noncompetitive NMDA antagonist MK-801 reduces the hyperalgesia which develops in rats with peripheral neuropathy (Davar, G. *et al.*, 1991; Mao, J. *et al.*, 1992c) or adjuvant-induced inflammation (Ren, K. *et al.*, 1992) and reduces autotomy behavior in rats with peripheral nerve sections (Seltzer, Z. *et al.*, 1991). Various competitive and noncompetitive NMDA receptor antagonists reduce the enhanced after-discharges, windup, and thermal- and mechanical-evoked responses of spinal dorsal horn neurons in rats with SNL (Leem, J. W. *et al.*, 1996; Suzuki, R. *et al.*, 2001). MK-801 has been found to reduce the increases in intracellular calcium ion (Ca^{2+}) concentration in spinal dorsal horn slices of rats which had CCI of the sciatic nerve (Kawamata, M. and Omote, K., 1996), as well as reducing increased Fos protein expression in response to

nonnoxious mechanical stimulation of the hind paw of CCI rats (Kosai, K. *et al.*, 2001). MK-801 also reduces the adjuvant inflammation-induced expansion of the receptive fields of nociceptive neurons in spinal cord dorsal horn (Dubner, R. and Ruda, M. A., 1992). In humans, ischemic and postoperative pain is suppressed by subanesthetic doses of ketamine (Maurset, A. *et al.*, 1989), while in the rat the increased activity in dorsal horn in response to ischemia associated with femoral artery occlusion is inhibited by i.t. application of an NMDA antagonist (Sher, G. and Mitchell, D., 1990). Subcutaneous injection of formalin evokes an increased release of glutamate and aspartate in spinal cord dorsal horn (Skilling, S. R. *et al.*, 1988), while the sustained responses of spinal nociceptive cells to noxious peripheral stimulation produced by subcutaneous formalin injection are reduced by i.t. administration of selective NMDA antagonists (Haley, J. E. *et al.*, 1990). Nociceptive responses to formalin are also both enhanced by pretreatment with the EAA agonists, L-glutamate and L-aspartate, as well as combinations of NMDA + AMPA or NMDA + trans-1-aminocyclopentane-1,3-dicarboxylate (ACPD) (Coderre, T. J. and Melzack, R., 1992a), and suppressed by pretreatment with NMDA antagonists (Murray, C. W. *et al.*, 1991; Coderre, T. J. and Melzack, R., 1992a).

Evidence suggests that in addition to iGluRs, metabotropic glumate receptors (mGluRs) also play a significant role in nociception. Unlike iGluRs, which gate cation channels, mGluRs are coupled by G proteins to various intracellular messengers (Pin, J. P. and Duvoisin, R., 1995). Molecular cloning techniques have identified eight subtypes of mGluRs to date, some of which include splice variants (Pin, J. P. *et al.*, 1992; Hollmann, M. and Heinemann, S. F., 1994). The eight subtypes of mGluRs are divided into three groups based on sequence homology, signal transduction mechanisms, and ligand selectivites (Nakanishi, S., 1992). Group I includes mGluR1 and 5 which stimulate phospholipase C (PLC), leading to protein kinase C (PKC) activation, phosphoinositide (PI) hydrolysis, and intracellular Ca^{2+} mobilization (Houamed, K. M. *et al.*, 1991; Masu, M. *et al.*, 1991; Abe, T. *et al.*, 1992).

The nonselective mGluR antagonist L-AP3 attenuates rat dorsal horn neuronal activity associated with repeated mustard oil application (Young, M. R. *et al.*, 1994; 1995) and knee joint inflammation (Neugebauer, V. *et al.*, 1994). Furthermore, the nonselective mGluR agonists trans-ACPD or 1*S*,3*R*-ACPD produce a depolarization (Young, M. R. *et al.*, 1994; 1995) or increased evoked responses (Palecek, J. *et al.*, 1994) in dorsal horn neurons. 1*S*,3*R*-ACPD also produces a ventral root (VR) depolarization in neonatal rat spinal cord *in vitro* (Boxall, S. J. *et al.*, 1996; 1998). The VR depolarization produced by 1*S*,3*R*-ACPD and windup after stimulation of dorsal roots, or capsaicin application, are blocked by the mGluR antagonist (+/−)-alpha-methyl-4-carboxphenylglycine (MCPG) (Boxall, S. J. *et al.*, 1996).

Selective group I mGluR antagonists also reduce rat dorsal horn neuronal activity evoked by hind paw mustard oil (Boxall, S. J. *et al.*, 1996) or capsaicin (Neugebauer, V. *et al.*, 1999). Furthermore, dorsal horn neuronal activity is increased by spinal administration of the group I mGluR agonist dihydroxyphenylglycine (DHPG) (Young, M. R. *et al.*, 1997; Neugebauer, V. *et al.*, 1999); although see Chen Y. *et al.* (2000). DHPG may act primarily at mGluR1, as agonists of mGluR5 (*trans*-ADA, CHPG) have either less (Young, M. R. *et al.*, 1997) or no (Neugebauer, V. *et al.*, 1999) excitatory effects. However, 1*S*,3*R*-ACPD, DHPG, and CHPG all produce a long-lasting potentiation of polysynaptic EPSPs in dorsal horn cells receiving C-fiber afferent input (Zhong, J. *et al.*, 2000). The neuronal activation evoked by spinal DHPG, or hind paw application of mustard oil or capsaicin, is also reduced by mGluR1-selective antagonists (Young, M. R. *et al.*, 1997; Neugebauer, V. *et al.*, 1999). However, a selective mGluR5 antagonist 2-methyl-6-(phenylethynyl)-pyridine (MPEP) attenuates shock-induced VR potentials and windup in isolated spinal cords (Bordi, F. and Ugolini, A., 2000), as well as reducing the enhanced spontaneous and noxious-stimulus-evoked activity in spinal cord neurons of rats with CCI of the sciatic nerve (Sotgiu, M. L. *et al.*, 2003). Alternatively, group II and III mGluR agonists depress spinal reflexes or activity in isolated spinal cords (Saitoh, T. *et al.*, 1998; Gerber, G. *et al.* 2000; Krieger, P. and El Manira, A., 2002), and reverse the hypersensitivity of dorsal horn neurons after skin capsaicin treatment (Neugebauer, V. *et al.*, 2000) or SNL (Chen, S. R. and Pan, H. L., 2005).

Behavioral studies also suggest mGluRs influence nociception. I.t. quisqualate, an mGluR and AMPA receptor agonist, produces hyperalgesia (Aanonsen, L. M. *et al.*, 1990; Kolhekar, R. and Gebhart, G. F., 1994), as well as nociceptive behaviors (Sun, X. and Larson, A. A. 1991) in rodents. The mGluR agonist 1*S*,3*R*-ACPD (Fisher, K. and Coderre, T. J., 1996a)

produces similar behaviors, implicating mGluRs in these responses. Furthermore, nociceptive behaviors and hyperalgesia are also produced by i.t. DHPG (Fisher, K. and Coderre, T. J., 1996a; 1998; Dolan, S. and Nolan, A. M., 2000; Hama, A. T., 2003), but importantly, not by the selective mGluR5 agonist trans-ADA (Fisher, K. and Coderre, T. J., 1996a). This suggests a pronociceptive role of spinal mGluR1. Conversely, i.t. administration of trans-ACPD, and a group II mGluR agonist (L-CCG-I), produce increased mechanical withdrawal thresholds, that are blocked by a group II mGluR antagonist (Chen, S. R. and Pan, H. L., 2005). This suggests an antinociceptive role for group II mGluRs.

Group I mGluRs are also implicated in the development of hyperalgesia and persistent pain associated with inflammatory or chemical injury. Thus, nonselective and group I selective mGluR antagonists (Walker, K. *et al.*, 2001; Zhang, L. *et al.*, 2002; Zhu, C. Z. *et al.*, 2004), and group I mGuR antisense oligonucleotides (Fundytus, M. E. *et al.*, 2002) reduce hyperalgesia in rats with hind paw inflammation. Furthermore, formalin nociception is enhanced by spinal i.t. 1*S*,3*R*-ACPD (Coderre, T. J. and Melzack, R., 1992a) and DHPG (Fisher, K. and Coderre, T. J., 1996b), and nociception associated with hind paw formalin (Fisher, K. and Coderre, T. J., 1996b; Varty, G. B. *et al.*, 2005) and i.p. acetic acid injections are reduced by group I mGluR antagonists (Chen, Y. *et al.*, 2000; Zhu, C. Z. *et al.*, 2004). Formalin nociception is also reduced by group II and III mGluR agonists (Fisher, K. and Coderre, T. J., 1996b; Simmons, R. M. A. *et al.*, 2002), and by enhancing an endogenous group II mGluR agonist (Yamamoto, T. *et al.*, 2004). Thus, while Group I activation is nociceptive, activation of Group II or III mGluRs is antinociceptive. Indeed, group I mGluR-linked intracellular messengers (i.e., PKC, IP_3 (inositol trisphosphate), and $_{i}Ca^{2+}$) contribute to nociception (Igwe, O. J. and Ning, L., 1994; Mao, J. *et al.*, 1995b), while events linked to group II/III mGluR (i.e., decreased cyclic adenosine monophosphate (cAMP) production) produce antinociception (Gereau, R. W. and Conn, P. J., 1994; Shen, J. *et al.*, 2000).

mGluRs also influence hyperalgesia induced by nerve injury. Group I mGluR antagonists reduce hyperalgesia in CCI-injured rats (Fisher, K. *et al.*, 1998). CCI-induced hyperalgesia is also reduced by selective mGluR1 and mGluR5 antagonists (Fisher, K. *et al.*, 2002; Zhu, C. Z. *et al.*, 2004), as well as group II (2R,4R-APDC) and III (L-AP4) mGluR agonists (Fisher, K. *et al.*, 2002), and by antisense oligonucleotides to mGluR1 and mGluR5 (Fundytus, M. E. *et al.*, 2001). Hyperalgesia after SNL is reduced by group I mGluR antagonists (Dogrul, A. *et al.*, 2000; Zhu, C. Z. *et al.*, 2004; Varty, G. B. *et al.*, 2005) and group II and III agonists (Simmons, R. M. A. *et al.*, 2002; Chen, S. R. and Pan, H. L., 2005). Tactile allodynia after spinal cord injury is also reduced by the mGluR1 antagonist (RS)-1-aminoindan-1,5-dicarboxylic acid (AIDA) (Mills, C. D. *et al.*, 2000), as well as group II and III mGluR agonists (Mills, C. D. *et al.*, 2002). Group II (mGluR3,4) and group III (mGluR4, 6, 7, 8) result in reduced production of cyclic adenosine monophosphate (cAMP) (Schoepp, D. D. *et al.*, 1995; Tanabe, Y. et al., 1993).

5.26.2.1.3 Other transmitters

The expression of a variety of other transmitters are affected following inflammatory or nerve injuries that produce hyperalgesia and allodynia. Thus, there is a reduction in the number of gamma-aminobutyric acid (GABA)- and glutamate decarboxylase (GAD)-, the synthetic enzyme for GABA, immunoreactive cells in the spinal cord of rats with CCI of the sciatic nerve (Eaton, M. J. *et al.*, 1998). There is also a reduction in the level of GABA in spinal cord microdialysates taken form rats with a partial constriction of the sciatic nerve that exhibit allodynia (Stiller, C. O., *et al.*, 1996). Recent studies also indicate that there is a reduction in endomorphin-2 immunoreactivity in the superficial dorsal horn of mice with a partial ligation of the sciatic nerve, which paralleled the development of thermal hyperalgesia (Smith, R. R. *et al.*, 2001).

5.26.2.1.4 Neurotrophins

Neurotrophins (NTs) are growth factors which stimulate neuronal growth in embryonic development, and maintain neuronal viability in adult tissues. NTs include nerve growth factor (NGF) that acts selectively at tyrosine kinase receptor A (TrkA), brain-derived neurotrophic factor (BDNF), NT-4, and NT-5, which act at TrkB receptors, and NT-3 that acts at TrkC receptors in spinal cord. An additional NT, glial-derived neurotrophic factor (GDNF), binds to the receptor GFR-alpha1. Small diameter unmyelinated primary afferent fibers generally fall into two groups: one which contains CGRP, SP, and TrkA receptors, and depends on NGF for its development; a second contains the lectin IB-4 and TrkB receptors, and is dependent on GDNF for its

development (McMahon, S. B. *et al.*, 1994). Importantly, these neurotrophic factors are not only required for neuronal development; they continue to be produced by numerous types of cells, produce excitatory effects on primary afferent fibers, and are required to maintain normal neuronal function of primary afferent fibers. BDNF has been found to be expressed in primary afferent fibers (particularly C fibers containing CGRP and SP) (Barakat-Walter, I., 1996), and to act in the spinal cord to enhance neuronal excitability (Kerr, B. J. *et al.*, 1999; Thompson, S. W. *et al.*, 1999).

It has been hypothesized that hyperalgesia after inflammatory injury is influenced by an upregulation of BDNF in primary afferent fibers that occurs in response to peripheral stimulation of primary afferent fibers with NGF (Thompson, S. W. *et al.*, 1999). Thus, inflammation leads to increased production of NGF in peripheral tissue, which stimulates TrkA receptors on the first group of primary afferent fibers (peptidergic fibers) described above (Apfel, S. C., 2000). The stimulation of TrkA receptors results in increased BDNF production in this group of C fibers (Apfel, S. C. *et al.*, 1996; Michael, G. J. *et al.*, 1997), and precipitates enhanced BDNF release, and a subsequent sensitization of dorsal horn neurons (Thompson, S. W. *et al.*, 1999). Noxious thermal, mechanical, and chemical stimuli, but not innocuous stimuli, also causes activation of spinal TrkB receptors as shown by increased Trk phosphorylation and increased extracellular signal-regulated kinase (ERK) activation (see below) in dorsal horn, which is blocked by sequestering BDNF with a TrKB–IgG fusion molecule (Pezet, S. *et al.*, 2002).

Importantly, BDNF protein and mRNA expression is increased in rat DRG and spinal dorsal horn following hind paw injection of CFA (Cho, H. J. *et al.*, 1997a; 1997b). BDNF protein levels are increased in DRG and spinal cord dorsal after CCI of the sciatic nerve (Ha, S. O. *et al.*, 2001; Miletic, G. and Miletic, V., 2002), while BDNF mRNA and or protein is also increased in uninjured L4 DRG and dorsal horn following L5 SNL (Fukuoka, T. *et al.*, 2001; Ha, S. O. *et al.*, 2001). I.t. administration of antibodies to BDNF attenuate thermal hyperalgesia in rats with L5 SNL (Fukuoka, T. *et al.*, 2001), while BDNF antisense olgionucleotides and the BDNF-scavenging protein TrkB–IgG attenuates carrageenan-induced thermal hyperalgesia (Kerr, B. J. *et al.*, 1999; Groth, R. and Aanonsen, L. M., 2002). Conversely, i.t. administration of BDNF and NT-4/5, which act at TrkB, but not the TrkC agonist NT-3, produce thermal hyperalgesia, while antisense to TrkB attenuates carrageenan-induced thermal hyperalgesia in rats (Groth, R. and Aanonsen, L. M., 2002). In contrast, antisense oliginucleotides to NT-3 have been found to attenuate mechanical allodynia in rats with partial sciatic nerve ligation (White, D. M., 2000). Alternatively, rats intrathecally treated with adenovirus to produce a spinal cord overexpression of BDNF (Eaton, M. J. *et al.*, 2002), or transgenic mice that overexpress NT-3 in muscle (Gandhi, R. *et al.*, 2004), each exhibit reduced mechanical allodynia and thermal hyperalgesia, after CCI of the sciatic nerve or acid injection into the gastrocnemius muscle, respectively. Protein and mRNA levels of GDNF and GFRα-1 are significantly increased in DRGs of rats with CCI of the sciatic nerve, and thermal hyperalgesia in CCI rats is significantly enhanced by i.t. administration of GFRα-1 antisense oligonucleotides, suggesting that GDNF may act at GFRα-1 to produce antihyperalgesic effects (Dong, Z. Q. *et al.*, 2005).

5.26.2.1.5 Phenotype switch

Evidence suggests that specific primary afferent fibers may be able to switch their phenotype following intense noxious stimulation. Thus, it has been shown that after inflammatory injury Aβ fibers begin to produce and release SP (which they normally do not contain) (Neumann, S. *et al.*, 1996); a phenomenon that has important implications for the development of mechanical allodynia (which is believed to mediated largely by Aβ fibers). Evidence suggests that growth factors or NTs may play a critical role in the development of these injury-induced phenotype changes (Woolf, C. J., 1996). The NT BDNF itself has been shown to undergo a phenotype switch after nerve injury as there is a shift in the size distribution of rat DRG neurons that contain BDNF after sciatic nerve lesions, so that large neurons, which do not initially express BDNF, start to express more than small neurons (Zhou, X. F. *et al.*, 1999a). Large DRG neurons also exhibit a phenotype switch when they start to express both BDNF (Ohtori, S. *et al.*, 2002) and CGRP (Ohtori, S. *et al.*, 2001) after CFA-induced inflammation of the lumbar facet joint.

5.26.2.2 Expression of Second Messengers and Transcription Factors

5.26.2.2.1 Second messengers

A growing body of literature suggests that intracellular messengers linked with various ionotropic and metabotropic receptors contribute to synaptic

plasticity in spinal cord dorsal horn. Ca^{2+} is a key intracellular messenger that is elevated in the cytoplasm of neurons following influx through receptor-operated and voltage-gated Ca^{2+} channels, or following release from intracellular stores. Glutamate and aspartate stimulate the influx of Ca^{2+} through NMDA receptor-operated channels (MacDermott, A. B. *et al.*, 1986). SP produces an elevation in intracellular Ca^{2+} by mobilizing its release from intracellular stores (Womack, M. D. *et al.*, 1988), while both SP (Womack, M. D. *et al.*, 1989) and CGRP (Oku, R. *et al.*, 1988) increase Ca^{2+} influx through voltage-gated Ca^{2+} channels. Activity at either NK-1 receptors by SP (Mantyh, P. W. *et al.*, 1984), or at metabotropic EAA receptors by glutamate and aspartate (Sugiyama, H. *et al.*, 1987), stimulates the hydrolysis of inositol phospholipids by activating a polyphosphoinositide-specific PLC. PLC is an enzyme which catalyzes the hydrolysis of polyphosphatidylinositol into the intracellular messengers IP_3 and diacylglycerol (DAG). Following its production, IP_3 stimulates the release of Ca^{2+} from internal stores; on the other hand, DAG stimulates the translocation and activation of PKC.

Gerber G. *et al.* (1989) showed that activators of PKC enhance the basal and evoked release of glutamate and aspartate in the spinal cord slice, as well as the depolarizing responses of dorsal horn neurons to exogenous glutamate and NMDA. Furthermore, Chen L. and Huang L.-Y. M. (1992) demonstrated that PKC increases NMDA-activated currents in isolated trigeminal cells by increasing the probability of channel openings and by reducing the voltage-dependent Mg^{2+} block of NMDA receptor channels. PKC is involved in synaptic plasticity causing a phosphorylation of both group I mGluR (Alaluf, S. *et al.*, 1995) and NMDA receptors (Chen, L. and Huang, L.-Y. M., 1992). Enhanced spinal PKC activity is observed following inflammatory (Yashpal, K. *et al.*, 1995; 2001; Sweitzer, S. M. *et al.*, 2004b) and nerve injury (Mao, J. *et al.*, 1992b; Miletic, V. *et al.*, 2000; Fundytus, M. E. *et al.*, 2001; Yashpal, K. *et al.*, 2001) and PKC inhibitors reduce pain induced by hind paw injection of noxious chemicals (Yashpal, K. *et al.*, 1995; 2001; Li, K. C. and Chen, J., 2003; Sweitzer, S. M. *et al.*, 2004b) and nerve injury (Hua, X. Y. *et al.*, 1999b; Miletic, V. *et al.*, 2000; Yajima, Y. *et al.*, 2003). PKC also enhances NMDA receptor activity (Liao, G. Y. *et al.*, 2001; Skeberdis, V. A. *et al.*, 2001) and NMDA receptor trafficking to neuronal plasma membranes (Lan, J. Y. *et al.*, 2001). PKC has several different isoforms, and evidence suggests that PKCγ is increased in the rat spinal cord dorsal horn after CCI of the sciatic nerve (Mao, J. *et al.*, 1995b), and the synaptosomal membrane fraction of both PKCγ and PKCβ-II is increased in the spinal cord dorsal of CCI rats (Miletic, V. *et al.*, 2000). Importantly, PKCγ knockout mice exhibit reduced mechanical allodynia and thermal hyperalgesia after partial sciatic nerve ligation (Malmberg, A. B. *et al.*, 1997a). PKCε is also upregulated in rat DRG following hind paw injections of carrageenan or CFA, in a manner that is correlated with the development of inflammatory hyperalgesia (Zhou, Y. *et al.*, 2003).

Increased neuronal Ca^{2+} infux also activates phospholipase A2 that triggers the production of arachidonic acid (Dumuis, A. *et al.*, 1988; 1990), which is metabolized into various eicosanoids, including prostaglandins (PGs). Further increases in arachidonic acid occur following the breakdown of DAG (Gammon, C. M. *et al.*, 1989), which is produced following stimulation of PLC with activity at various metabotropic receptors. Spinal administration of PGE_2 enhances the responsiveness and receptive field sizes of rat spinal dorsal horn neurons (Vasquez, E. *et al.*, 2001), as well as producing mechanical allodynia and thermal hyperalgesia in mice (Minami, T. *et al.*, 1994a; 1994b). There is an increase in the levels of PGE_2 in CSF of rat after knee joint injection of carrageenan/kaolin (Yang, L. C. *et al.*, 1996) or i.t. injection of SP (Hua, X. Y. *et al.*, 1999a). The breakdown of arachidonic acid into PGs in inhibited by nonsteroidal anti-inflammatory drugs (NSAIDs), and i.t. administration of NSAIDs produces analgesia in animals subjected to i.p. acetic acid or hind paw formalin injections (Yaksh, T. L., 1982; Malmberg, A. B. and Yaksh, T. L., 1992a), as well as reducing enhanced flexor reflexes in rats with hind paw injections of CFA (Seybold, V. S. *et al.*, 2003). I.t. NSAIDs block thermal hyperalgesia induced by i.t. treatment with NMDA or SP (Malmberg, A. B. and Yaksh, T. L., 1992b). There is also an elevation of the enzyme cyclooxygenase-2 (COX-2) in the spinal CSF of rats with hind paw carrageenan injections (Ibuki, T. *et al.*, 2003) or in the spared nerve injury model (Broom, D. C., *et al.*, 2004). Furthermore, thermal hyperalgesia associated with carrageenan injection is attenuated by i.t. treatment with a selective inhibitor of COX-2 (Dirig, D. M. *et al.*, 1998; Ibuki, T. *et al.*, 2003), but not COX-1 (Yaksh, T. L. *et al.*, 2001). I.t. COX-2 inhibitors are found to relieve hyperalgesia in a model of hind paw inflammation, but not in the spared nerve injury model (Broom *et al.*, 2004).

Elevation in intracellular Ca^{2+} in neurons also leads to increases in additional protein kinases such as Ca^{2+}/calmodulin-dependent protein kinase (CaMK) (Kennedy, M. B. *et al.*, 1983). There is an increased expression and phosphorylation of CaMK-II in rat spinal cord dorsal horn after hind paw injection of capsaicin, while i.t. administration of a CaMK-II inhibitor reduces enhanced dorsal horn neuronal responsiveness and behavioral responses after hind paw capsaicin (Fang, L. *et al.*, 2002), as well as reducing mechanical allodynia and thermal hyperalgesia in CCI mice (Garry, E. M. *et al.*, 2003). Mice with a mutation of the alpha-CaMK-II gene, which prevents autophosphorylation of CaMK-II, also have diminished nociceptive responses to hind paw formalin injections (Zeitz, K. P. *et al.*, 2004).

The binding of Ca^{2+} to calmodulin activates nitric oxide (NO) synthase, which generates NO from free L-arginine (Garthwaite, J. *et al.*, 1988), which in turn activates soluable guanylate cyclase and increases cGMP (Southam, E. *et al.*, 1991). Intracellularly the Ca^{2+} binds to calmodulin which activates NO synthase. NO synthase converts L-arginine to NO, and the released NO stimulates the production of cGMP from soluable guanylate cyclase (Synder, S. H., 1992). The levels of neuronal NO synthase, as well as NADPHd and [^{3}H]citrulline staining (markers of NO activity), are increased in the rat DRG and spinal cord dorsal horn after CCI or transection of the sciatic nerve (Cizkova, D. *et al.*, 2002a; Lukacova, N. *et al.*, 2003), SNL (Steel, J. H., *et al.*, 1994), or hind paw formalin injection (Lam, H. H. *et al.*, 1996). There is also increased cGMP in the spinal dorsal horn of rats with CCI of the sciatic nerve that parallels the development of mechanical allodynia and thermal hyperalgesia (Siegan, J. B. *et al.*, 1996). In addition, NO synthase inhibitors or an inhibitor of soluable guanylate cyclase reduce the thermal hyperalgesia that develops in rats with chronic nerve constriction injury (Meller, S. T. *et al.*, 1992) or hind paw carrageenan (Meller, S. T. *et al.*, 1994; Osborne, M. G. and Coderre, T. J., 1999).

Mediators such as NO, which increase neuronal cGMP, stimulate the production of cAMP-dependent protein kinase (PKG) (Scott, J. D., 1991). The spinal dorsal horn levels of PKG1α are increased in response to hind paw injection of formalin, and i.t. administration of PKG inhibitors reduces nociceptive responses to formalin (Tao, Y. X. *et al.*, 2000; Schmidtko, A. *et al.*, 2003). I.t. treatment with a PKG inhibitor also reverses mechanical allodynia observed in rats with a hind paw injection of capsaicin (Sluka, K. A. and Willis, W. D., 1997), and thermal hyperalgesia induced by i.t. injections of NMDA or an NO donor (Tao, Y. X. and Johns, R. A., 2000). I.t. administration of a PKG activator produces mechanical allodynia which is absent in PKG-I knockout mice, further implicating a role for spinal PKG in allodynia (Tegeder, I. *et al.*, 2004a).

Activity at various neuropeptide receptors leads to increased levels of adenylate cyclase in spinal cord neurons (see Millan, M. J., 1999 for a review). The enzyme adenylate cyclase increases cAMP and its associated kinase, protein kinase A (PKA), which causes membrane phosphorylation that enhances Na^+ and Ca^{2+} currents, and decreases K^+ currents in primary afferent fibers (Vanegas, H. and Schaible, H. G., 2001). Enhancing the spinal cord levels of PKA leads to a sensitization of dorsal horn neurons to noxious mechanical stimulation (Lin, Q. *et al.*, 2002), and i.t. administration of PKA inhibitors attenuate the mechanical allodynia induced by hind paw injection of capsaicin (Sluka, K. A. and Willis, W. D., 1997). There is also a reduction in thermal hyperalgesia associated with hind paw inflammation in mice with a target mutation of the type I regulatory subunit of PKA (Malmberg, A. B. *et al.*, 1997b).

Activity of growth factors and various hormones leads to the activation of a mitogen-activated protein kinase (MAPK) pathway through stimulation of a GTP-binding protein Ras and protein kinases, such as PKC (Davis, R. J., 1993). A growing body of literature suggests that MAPK, including ERK, p38 MAPK, and c-Jun N-terminal kinase (JNK) contribute to spinal nociceptive processing. Recent studies have shown ERK activity is observed in lamina I and IIo of the ipsilateral dorsal horn after noxious thermal stimulation of the hind paw or C-fiber electrical nerve stimulation, but not after nonnoxious thermal or A fiber electrical stimulation (Ji, R. R. *et al.*, 1999). ERK activity is also observed in rodent DRG or spinal cord dorsal horn in response to hind paw injections of carrageenan (Galan, A. *et al.*, 2002), CFA (Ji, R. R. *et al.*, 2002a, Obata, K. *et al.*, 2003), formalin (Ji, R. R. *et al.*, 1999, Karim, F. *et al.*, 2001), or capsaicin (Ji, R. R. *et al.*, 1999), or to sciatic nerve transection (Obata, K. *et al.*, 2003), CCI (Obata, K. *et al.*, 2004a) partial sciatic nerve ligation (Ma, W. and Quirion, R., 2002) or L5 SNL (Obata, K. *et al.*, 2004b). Inhibitors of ERK have been found to reduce nociception induced by formalin (Ji, R. R. *et al.*, 1999, Karim, F. *et al.*, 2001), and hyperalgesia or allodynia after hind paw injection of carrageenan (Sammons, M. J. *et al.*, 2000), CFA (Ji, R. R. *et al.*, 2002a) or

capsaicin (Kawasaki, Y. *et al.*, 2004), and in rats with CCI of the sciatic nerve (Ciruela, A. *et al.*, 2003) or L5 SNL (Obata, K. *et al.*, 2004b). Recently, it has been shown that stimulation of group I mGluRs leads to activation of ERK in spinal cord dorsal horn, and that antagonists of group I mGluRs produce a reduction in formalin-stimulated ERK activation (Karim, F. *et al.*, 2001). Adwanikar, H. *et al.* (2004) has also shown that ERK inhibitors significantly reduce DHPG-induced spontaneous nociceptive behaviors (SNBs) in mice that have received a prior hind paw injection of CFA.

Recent evidence indicates there is an increase in phosphorylated p38 MAPK in DRG neurons and microglia of the DRG and spinal cord following hind paw injection of formalin (Kim, S. Y. *et al.*, 2002) or capsaicin (Sweitzer, S. M. *et al.*, 2004a; Mizushima, T. *et al.*, 2005) or CCI of the sciatic nerve (Kim, S. Y. *et al.*, 2002; Obata, K. *et al.*, 2004a). I.t. treatment with a p38 MAPK inhibitor reverses thermal hyperalgesia produced by hind paw capsaicin injection (Sweitzer, S. M. *et al.*, 2004a; Mizushima, T. *et al.*, 2005) or in CCI rats (Obata, K. *et al.*, 2004a). There is also increased p38 MAPK activity in neurons of both the injured L5 and the uninjured L4 DRG after L5 SNL, and i.t. treatment with a p38 MAPK inhibitor reverses mechanical allodynia and thermal hyperalgesia in L5 SNL rats (Obata, K. *et al.*, 2004b). In contrast, JNK activity is increased only in L5 DRG neurons after L5 SNL, and i.t. administration of a JNK inhibitor reverses only mechanical allodynia in rats with L5 SNL (Obata, K. *et al.*, 2004b). JNK activity is also increased in the spinal cord dorsal horn of rats with partial sciatic nerve ligation (Ma, W. and Quirion, R., 2002).

It is now evident that activity of the NMDA receptor is regulated by the protein tyrosine kinases (PTKs), Src and Fyn, which phosphorylate the NMDA channel and enhance its activity (Yu, X. M. *et al.*, 1997; Tezuka, T. *et al.*, 1999; Yu, X. M. and Salter, M. W., 1999). Evidence that this process might contribute to hyperalgesia after nerve injury is suggested as phosphotyrosine staining is increased in the spinal cord dorsal horn following sciatic nerve transection (Eckert, W. A. *et al.*, 1994). Furthermore, i.t. administration of nonselective PTK inhibitors, reduce hind paw mechanical and thermal hyperalgesia produced by injection of carrageenan and kaolin to the base of the rat tail, or following i.t. injection of NMDA (Sato, E. *et al.*, 2003), as well as reducing thermal hyperalgesia in rats with partial sciatic nerve ligation (Yajima, Y. *et al.*, 2002). I.t. treatment with a selective Src inhibitor delays the onset of mechanical allodynia and hyperalgesia induced by hind paw injection of CFA (Guo, W. *et al.*, 2002), as well as reducing capsaicin-induced ERK activation in spinal cord slices (Kawasaki, Y. *et al.*, 2004). In contrast to the effects of PTKs, NMDA receptors currents have been shown to be inhibited by protein tyrosine phosphatases (PTPs) (Wang, Y. T. *et al.*, 1996). Recent studies have shown that i.t. administration of PTP inhibitors produces an enhancement of mechanical allodynia and hyperalgesia induced by hind paw injection of capsaicin (Zhang, X. *et al.*, 2003). Studies using selective inhibitors or antisense oligonucleotides have also implicated various other kinases including: IkappaB kinase (Tegeder, I. *et al.*, 2004b), cyclin-dependent kinase 5 (Cdk5) (Wang, C. H. *et al.*, 2005), and Rho kinase (Tatsumi, S. *et al.*, 2005) in nociception or hyperalgesia associated with hind paw formalin or zymosan injection or CCI of the sciatic nerve.

5.26.2.2.2 Transcription factors

Noxious stimulation leads to the expression of proto-oncogenes and their protein products which act as transcription factors. Hunt S. P. *et al.* (1987) first demonstrated that the c-fos protein product Fos is expressed in postsynaptic dorsal horn neurons following noxious thermal or chemical stimulation of the skin. The expression of Fos has also been demonstrated in rat spinal dorsal horn in response to noxious pinch of the hind paws (Bullitt, E., 1989), the injection of formalin (Presley, R. W. *et al.*, 1990) or carrageenan (Draisci, G. and Iadorola, M. J., 1989) into a hind paw or sodium urate crystals into joints (Menétrey, D. *et al.*, 1989), the injection of acetic acid into viscera (Menétrey, D. *et al.*, 1989), the induction of polyarthritis with CFA (Menétrey, D. *et al.*, 1989). Fos expression in the rat spinal dorsal horn is also increased after transection (Chi, S. I. *et al.*, 1993), CCI (Kajander, K. C. *et al.*, 1996; Catheline, G. *et al.*, 1999) or partial ligation (Delander, G. E. *et al.*, 1997) of the sciatic nerve. Importantly, there is a strong correlation between pain behavior and the number of cells expressing Fos (Presley, R. W. *et al.*, 1990). The time course of Fos expression after peripheral inflammation (Draisci, G. and Iadorola, M. J., 1989) or nerve injury (Delander, G. E. *et al.*, 1997) has been found to be correlated with the development of hyperalgesia. Moreover, morphine pretreatment produces a dose-dependent suppression of Fos expression which corresponds with its analgesic effects (Presley, R. W. *et al.*, 1990; Tolle, T. R. *et al.*, 1990).

An increase in phosphorylated cyclic AMP response element binding (pCREB) protein is observed in the spinal cord dorsal horn of rats with partial ligation or CCI of the sciatic nerve (Ma, W. and Quirion, R., 2001; Miletic, G. *et al.*, 2002, 2004b) or hind paw injections of capsaicin (Kawasaki, Y. *et al.*, 2004; Fang, L. *et al.*, 2005). Elevation in spinal pCREB associated with nerve injury, hind paw capsaicin, or electrical nerve stimulation has been found to be dependent on the activation of PKA, PKC, ERK, or CaMK (Kawasaki, Y. *et al.*, 2004; Miletic, G. *et al.*, 2004b; Fang, L. *et al.*, 2005; Miyabe, T. and Miletic, V., 2005). I.t. treatment with antisense oligonucleotides to CREB reduces the mechanical allodynia in rats with partial sciatic nerve ligation (Ma, W. *et al.*, 2003b).

Noxious stimulation, inflammatory, or nerve injury also leads to the spinal cord expression of other transcription factors, including Fos B, Jun, Jun B, Jun C, Jun D (Herdegen, T. *et al.*, 1991a; 1991b; Delander, G. E. *et al.*, 1997), NGFI-A/Krox 24, NGFI-B, serum response factor (Herdegen, T. *et al.*, 1990; Wisden, W. *et al.*, 1990), FRA-1, FRA-2 (Munglani, R. and Hunt, S. P., 1995), AP-1, nuclear factor kappa B, octamer factors (Chan, C. F. *et al.*, 2000; Pollock, G. *et al.*, 2005), activating transcription factor 3 (Tsujino, H. *et al.*, 2000), cyclic AMP responsive element modulator (Naranjo, J. R. *et al.*, 1997), and peroxisome proliferators-activated receptor-alpha (Benani, A. *et al.*, 2004).

5.26.2.3 Alterations in Receptor and Ion Channel Expression, Activity, or Cellular Location

5.26.2.3.1 Neuropeptide receptors

Recent studies show that there is an increase in the internalization of NK-1 receptors in the spinal cord dorsal horn following electrical nerve or noxious peripheral stimulation, and that this internalization is enhanced in rats with inflammatory or nerve injuries (Allen, B. J. *et al.*, 1999). There is also an upregulation of NK-1 receptors in the spinal cord dorsal horn in response to hind paw inflammation induced by CFA and following sciatic nerve transection (Aanonsen, L. M. *et al.*, 1992). Importantly, upregulation of dorsal horn NK-1 mRNA after partial sciatic nerve ligation is significantly correlated with the development of thermal hyperalgesia (Taylor, B. K. and McCarson, K. E., 2004). The importance of NK-1 receptors to the development of hyperalgesia after tissue injury is also highlighted by the finding that destruction of neurons with NK-1 receptors with the toxin saporin bound to SP abolishes the development of mechanical and thermal hyperalgesia following intraplantar capsaicin injection (Khasabov, S. G. *et al.*, 2002). NK-1 knockout mice also have attenuated dorsal horn neuronal responses to suprathreshold stimuli and a reduction of windup of deep dorsal horn neurons after C-fiber electrical nerve stimulation (Suzuki, R. *et al.*, 2003).

As for other neuropeptide receptors, it has been shown that sciatic nerve transection produces a marked increase if CCK-B receptor mRNA in the dorsal root ganglia (Zhang, X. *et al.*, 1993a). Although there is no change in the expression of the VIP/PACAP receptor PAC1, there is a decrease in VPAC1 and an increase in VPAC2 in the dorsal horn following CCI of the sciatic nerve.

5.26.2.3.2 Excitatory amino acid receptors

The NMDA receptor has two subunits NMDAR1 (NR1) and NMDAR2 (NR2), with four splice variants of the NR2 subunit (NR2A–D). Two of the NR2 subunits are heavily expressed in the spinal cord dorsal horn and have been studied in respect to plasticity associated with nociception. Recent evidence indicates that there is enhanced phosphorylation of the NR1 subunit of rat dorsal horn neurons after intradermal injection of capsaicin (Zou, X. *et al.*, 2000) or after noxious heat stimulation of the hind paw (Brenner, G. J., *et al.*, 2004), effects which depends on the activation of kinases, including PKA and/or PKC. Elevated levels of phosphorylated NR1 is also found in the spinal dorsal horn of rats with an excitotoxic injury of the spinal cord that causes central neuropathic pain (Caudle, R. M. *et al.*, 2003), or following hind paw inflammation with carrageenan (Caudle, R. M. *et al.*, 2005).

There is also a prolonged increase in the phosphorylation of NR2B subunits in rat spinal dorsal horn after inflammation induced by hind paw injection of CFA, that is dependent on activation of PKC and Src kinase (Guo, W. *et al.*, 2002), although decreases in rat spinal NR2B phosphorylation have also been observed after hind paw inflammation (Caudle, R. M. *et al.*, 2005). Increased phosphorylation of NR2B in spinal dorsal horn has also been observed in mice with transected sciatic nerves. The increased phosphorylated NR2B was attenuated by administration of a NR2B selective antagonist and in mice lacking Fyn kinase, a Src-family kinase (Abe, T. *et al.*, 2005). Recently, the C-fiber-stimulated windup of spinal dorsal horn

neurons was shown to be attenuated by i.v. administration of a selective NR2B antagonist (Kovacs, G. *et al.*, 2004). The importance of phosphorylation of spinal NR subunits to central sensitization is based on now long established evidence that such phosphorylation produces an enhancement of Ca^{2+} currents at NMDA receptor channels (Chen, L. and Huang, L.-Y. M., 1992). Thus, PKC activation, initiated by glutamate- or aspartate-induced PLC activity and Ca^{2+} influx through NMDA channels, leads to further influx of Ca^{2+} through NMDA channels, creating a positive feedback loop for glutamate and aspartate neurotransmission. As described above, a similar mechanism has been demonstrated for pathways that involve Src or Fyn kinase (Yu, X. M. *et al.*, 1997; Tezuka, T. *et al.*, 1999).

A recent question concerning synaptic activity at glutamate synapses is the issue of possible alterations in the trafficking of glutamate receptor to the plasma membrane and synapses of postsynaptic neurons. In recent years it has been established that glutamate receptors move between the cell cytoplasm and the plasma membrane, altering the number of receptors that are available to respond to glutamate and aspartate. Generally referred to as receptor trafficking, glutamate receptors are inserted into and removed from the plasma membrane by exocytosis and endocytosis (or internalization), respectively, and diffused laterally within the plasma membrane (Collingridge, G. L. *et al.*, 2004). Recent studies have implicated trafficking of AMPA (Malinow, R. R., and Malenka, R. C., 2002), kainite (Jaskolski, F. *et al.*, 2005), and NMDA (Carroll, R. C. and Zukin, R. S., 2002) receptors as key processes in regulating synaptic plasticity.

Alterations in the activity of AMPA receptors are implicated in plasticity associated with nociception. AMPA receptors in lamina III–IV of the dorsal horn are upregulated following dorsal rhizotomy (Carlton, S. M. *et al.*, 1998). There are four subunits of AMPA receptors, known as GluR1–4, some of which have splice variants, and GluR1 and GluR2 are predominant in the spinal cord (Nagy, G. G. *et al.*, 2004). It has recently been shown that there is a PKA- and PKC-dependent upregulation of phosphorylated GluR1 in the spinal cord dorsal horn of rats that have received a hind paw injection of capsaicin or noxious stimulation (Fang, L. *et al.*, 2003; Nagy, G. G. *et al.*, 2004). Recent evidence also indicates that GluR1 receptors are trafficked to the plasma membrane of dorsal horn neurons in response to visceral inflammation (Galan, A. *et al.*, 2004), via a CaMK-II-dependent mechanism. This raises the possibility that noxious stimulation may lead to a recruitment of functional AMPA receptors to the postsynaptic membrane and synapses of spinal neurons that normally do not have functional AMPA receptors. The phenomenom of silent synapses has been demonstrated in cultured hippocampal neurons exposed to stimuli that produce LTP (Liao, D. *et al.*, 1995), and may contribute to hyperexcitability of dorsal horn neurons in persistent pain conditions (Kerchner, G. A. *et al.*, 1999).

Recent studies have demonstrated alterations in the expression of various mGluRs in the DRG and dorsal horn of rats following nerve injury or persistent pain. There is a dramatic downregulation of mGluR1 mRNA in rat L5 DRG cells following tibial nerve axotomy (Hofmann, H. A. *et al.*, 2001). In contrast, mGluR5 immunoreactivity is increased in L4 and L5 DRGs of rats with L5 SNL (Hudson, L. J. *et al.*, 2002), and in the rat spinal cord dorsal horn after hind paw carrageenan injection (Dolan, S. *et al.*, 2003). There is also increased mGluR3 mRNA in the dorsal horn of rats with their hind paws exposed to ultraviolet irradiation (Boxall, S. J. *et al.*, 1998), and an upregulation of both mGluR3 and mGluR5 mRNA in the dorsal horn of sheep with chronic hindlimb inflammation (Dolan, S. *et al.*, 2003). Upregulations of mGluR2, 3, and 5 mRNA in the dorsal horn have also been reported a sheep model of postsurgical pain (Dolan, S. *et al.*, 2004). Spinal mGluR1, but not mGluR5, mRNA is also upregulated in response to spinal cord injury, while group II mGluRs are downregulated (Mills, C. D. *et al.*, 2001).

5.26.2.3.3 Other receptors

In addition to effects on neuropeptides and EAA receptors, inflammatory and nerve injuries that produce hyperalgesia are known to produce alterations in various other transmitter receptors and ion channels in neurons in spinal cord dorsal horn or DRG neurons. Sciatic nerve transection produces an upregulation of GABA-A and a downregulation of GABA-B receptors in the rat spinal cord dorsal horn (Castro-Lopes, J. M. *et al.*, 1995). A similar downregulation of GABA-B receptors occurs after joint inflammation induced by CFA injection in the rat knee, but no change in GABA-A receptors was found (Castro-Lopes, J. M. *et al.*, 1995). There is also a downregulation of μ-opioid receptor immunoreactivity in the rat and monkey spinal cord dorsal horn following peripheral nerve axotomy (Zhang, X. *et al.*, 1998). In addition, there is an increase in phosphorylated μ-opioid receptors following sciatic nerve ligation (Narita, M. *et al.*, 2004). The reduction in

number of μ-opioid receptors or the phosphorylation of remaining receptors may explain why morphine-induced antinociception (Ossipov, M. H. *et al.*, 1995; Narita, M. *et al.*, 2004) and the presynaptic inhibitory effects of μ-opioids (Kohno, T. *et al.*, 2005) are reduced in mice and rats with peripheral nerve injury, although see also Suzuki R. *et al.* (1999). There is, however, also an increase in the levels of phosphorylated κ-opioid receptors in the spinal cord dorsal horn of mice with a partial sciatic nerve lesion, an effect that is not shown in prodynorphin knockout mice that have enhanced tactile allodynia and thermal hyperalgesia (Xu, M. *et al.*, 2004). These findings suggest that the loss of endogenous dynorphin activity at κ-opioid receptors may also contribute to allodynia and hyperalgesia after nerve injury.

In contrast to the effects of opioid receptors, CCI of the sciatic nerve leads to a MAPK-dependent upregulation of spinal cannabinoid-1 (CB-1) receptors (Lim, G. *et al.*, 2003). The upregulation of spinal CB-1 was determined to be responsible for the anti-allodynic and antihyperalgesic effects of a CB-1 agonist in CCI rats, as the reduction in mechanical allodynia and thermal allodynia produced by Win 55,212-2 was lost in rats pretreated with an ERK inhibitor (PD98059) that blocked the spinal CB-1 upregulation (Lim, G. *et al.*, 2003). CCI of the rat sciatic nerve also leads to an upregulation of P2X3 receptors in spinal cord dorsal horn (Novakovic, S. D. *et al.*, 1999). This upregulation may contribute to hyperalgesia and allodynia, as an adenosine kinase inhibitor produces a greater inhibition of post-discharge, windup, and C-fiber-evoked responses in spinal cord neurons of rat with SNLs than in sham controls. Recent studies also indicate that there is an upregulation of $\alpha 3$ and $\alpha 5$ spinal nicotinic acetylcholine (nAcH) receptors following rat SNL (Vincler, M. and Eisenach, J. C., 2004), and an increase in spinal melanocortin (MC) receptors after CCI of the rat sciatic nerve (Vrinten, D. H. *et al.*, 2000). It is expected that upregulated $\alpha 5$ nAcH and MC receptors may contribute to allodynia after nerve injuries, as an $\alpha 5$ nAcH antisense olgionucleotides and an MC receptor antagonist significantly attenuate mechanical allodynia in SNL and CCI rats, respectively (Vrinten, D. H. *et al.*, 2000; Vincler, M. A. and Eisenach, J. C., 2005).

5.26.2.3.4 Scaffolding and adaptor proteins

NMDA receptors bind directly to membrane-associated guanylate kinases (MAGUKs) that regulate surface and synaptic NMDAR trafficking in the CNS (Ponting, C. P. *et al.*, 1997). MAGUKs include the adaptor proteins known as postsynaptic density proteins 93 and 95 (PSD-93, PSD-95), which are abundantly expressed in the spinal cord dorsal horn (Garry, E. M. *et al.* 2003; Tao, Y. X. *et al.*, 2003). Knockout of PSD-93 reduces surface NR2A and NR2B, lowers NMDA receptor-mediated postsynaptic currents and potentials, and reduces hyperalgesia and/or allodynia in mice with SNL or hind paw injection of CFA (Tao, Y. X. *et al.*, 2003). Antisense knockdown of spinal cord PSD-93 also reduces mechanical allodynia and thermal hyperalgesia in rats with hind paw CFA injection or following peripheral nerve injury (Zhang, B. *et al.*, 2003). Knockout or knockdown of PSD-95 also reduces hyperalgesia and allodynia in CCI mice or in rats with L5 SNL, respectively (Tao, F. *et al.*, 2001; Garry, E. M. *et al.*, 2003).

Homer is an intracellular scaffolding protein that is implicated in the intracellular retention and trafficking of group I mGluRs (Roche, K. W. *et al.*, 1999; Ango, F. *et al.*, 2000). Homer proteins also interact with the postsynaptic density protein Shank, a PDZ domain-containing protein binding to the PSD-95/NMDA receptor complex (Naisbitt, S. *et al.*, 1999; Tu, J. C. *et al.*, 1999). There are increases in the levels of both Homer and Shank in spinal cord dorsal horn in rats with CCI of the sciatic nerve at the time points when they exhibit mechanical allodynia and thermal hyperalgesia (Miletic, G. *et al.*, 2005). Another scaffolding protein, neurofilament light chain (NFL) protein, is downregulated in the DRG and spinal dorsal horn of rats with inflammation after a hind paw injection of zymosan (Kunz, S. *et al.*, 2004), the breakdown of NFL protein and inflammatory hyperalgesia were blocked with an inhibitor of the protease calpain. The cell adhesion molecule E-cadherin is dramatically downregulated in spinal cord dorsal horn in response to sciatic nerve transection (Brock, J. H. *et al.*, 2004), while the microtubule associated protein 1B is upregulated (Soares, S. *et al.*, 2002). The presynaptic vesicle protein synaptophysin is increased in spinal dorsal horn in parallel with thermal hyperalgesia in CCI rats (Chou, A. K. *et al.*, 2002).

5.26.2.3.5 Ion channels

Inflammatory and nerve injuries lead to alterations in sensory neuron ion channel expression, distribution and function that contribute to hyperalgesia and allodynia. In particular, evidence indicates that various sodium (Na^+) channels subtypes are altered in

association with inflammation or neuropathy. There is an upregulation of the Na^+ channel subunit $Na_V1.3$ in DRG neurons or spinal cord dorsal horn neurons following peripheral nerve axotomy (Waxman, S. G. *et al.*, 1994), traumatic spinal cord injury (Hains, B. C. *et al.*, 2003) and CCI of the sciatic nerve (Hains, B. C. *et al.*, 2004), as well as hind paw injection of carrageenan (Black, J. A. *et al.*, 2004). In the case of CCI, a spinal upregulation likely contributes to hyperalgesia/allodynia, as i.t. administration of antisense oligonucleotides to $Na_V1.3$ decreased expression to normal levels and decreased the enhanced spontaneous activity and evoked responses of dorsal horn neurons, as well as reducing thermal hyperalgesia and mechanical allodynia in CCI rats (Hains, B. C. *et al.*, 2004).

There is also an upregulation of Na_V 1.7 and $Na_V1.8$, but not $Na_V1.9$, in DRG in response to hind paw injection of carrageenan (Tanaka, M. *et al.*, 1998; Black, J. A. *et al.*, 2004). Hyperalgesia in response to hind paw inflammation is reduced or delayed in rats treated with $Na_V1.8$ antisense oligonucleotides (Khasar, S. G. *et al.*, 1998) or in $Na_V1.8$ knockout mice (Akopian, A. N. *et al.*, 1999). Although $Na_V1.8$ channels are not upregulated in DRG after nerve injury (Okuse, K. *et al.*, 1997; Novakovic, S. D. *et al.*, 1998), antisense oligonucleotide knockdown of $Na_V1.8$ attenuates neuropathic pain in rats with SNL (Lai, J. *et al.*, 2002; Gold, M. S. *et al.*, 2003). The effectiveness of the knockdown may be explained by findings that there is a redistribution of $Na_V1.8$ channels in injured nerves with an accumulation of these channels at the site of the nerve injury (Novakovic, S. D. *et al.*, 1998; Gold, M. S. *et al*, 2003).

As for $Na_V1.9$, it has been shown that knockdown of its protein has no influence on allodynia or hyperalgesia in SNL rats (Porreca, F. *et al.*, 1999), while disruption of the SCN11A gene, which encodes $Na_V1.9$, attenuates thermal hyperalgesia and spontaneous pain after peripheral inflammation (Priest, B. T. *et al.*, 2005).

Ca^{2+} channels also show changes in expression following nerve injury. Thus, after axotomy or partial nerve ligation of the sciatic nerve there is an upregulation of $Ca_V1.2$ (L-type α1C) and $Ca_V2.3$ (R-type α1E) (Yang, L. *et al.*, 2004; Dobremez, E. *et al.*, 2005). Evidence suggests that L-type Ca^{2+} channels contribute to tonic nociception (Del Pozo, E. *et al.*, 1987; Coderre, T. J. and Melzack, R., 1992b), and recent evidence indicates that $Ca_V2.3$ knockout mice have reduced responses to inflammatory pain (Saegusa, H. *et al.*, 2000), suggesting that R-type Ca^{2+} channels may also play a role in hyperalgesia/allodynia. There is also an upregulation of $Ca_V2.2$ (N-type Ca^{2+} channels α1B) in both DRG and spinal dorsal horn after hind paw injection of carrageenan (Yokoyama, K. *et al.*, 2003) or CCI of the sciatic nerve (Cizkova, D. *et al.*, 2002b). Many preclinical studies have shown that antagonists of N-type Ca^{2+} channels reduce allodynia or hyperalgesia associated with inflammatory or nerve injuries, and suggest that $Ca_V2.2$ is a key target (see Winquist, R. J. *et al.*, 2005 for a review). There is also a reduction of tactile allodynia and thermal hyperalgesia associated with SNL in $Ca_V2.2$ knockout mice (Saegusa, H. *et al.*, 2001). Although the P-type Ca^{2+} channel have also been implicated in the development of hyperalgesia, the effects of their antagonists have been less effective (Sluka, K. A., 1998; Matthews, E. A. and Dickenson, A. H., 2001), and a selective Q-type antagonist was ineffective (Nebe, J. *et al.*, 1997). In addition, others have found in response to axotomy or CCI of the sciatic nerve there is a downregulation of $Ca_V1.2$ (L-type α1C), $Ca_V1.3$ (L-type α1D), $Ca_V3.2$ (T-type α1H) and $Ca_V3.3$ (T-type α1I) mRNA expression in rat DRG (Kim, D. S. *et al.*, 2001). A role for T-type channels in hyperalgesia is suggested since antisense knockdown of $Ca_V3.2$ reduces both hyperalgesia and allodynia in rats with CCI of the sciatic nerve (Bourinet, E. *et al.*, 2004).

Recent studies also show there is an upregulation of $\alpha_2\delta$ Ca^{2+} channel auxillary subunits found in the DRG and spinal dorsal horn of rats after SNL and to a lesser extent CCI of the sciatic nerve (Luo, Z. D. *et al.*, 2001; 2002). The upregulation of $\alpha_2\delta$ subunits is temporally related to the development of tactile allodynia after SNL, and i.t. treatment of antisense oligonucleotide to $\alpha_2\delta$ diminishes the tactile allodynia in SNL rats (Li, C. Y. *et al.*, 2004). The importance of this subunit to hyperalgesia and allodynia is also highlighted by the fact that the $\alpha_2\delta$ subunit is the only known binding site for gabapentin and pregabalin which are effective antihyperalgesic agents for many neuropathic pain patients (Frampton, J. E. and Foster, R. H., 2005; Wiffen, P. J. *et al.*, 2005).

There is considerable evidence that sensory neuron vanilloid receptors, including TRPV1 (VR-1) and TRPV2 (VRL-1), play a critical role in the transduction of noxious heat (Caterina, M. J. and Julius, D., 2001). An up-regulation of TRPV1 has also been found in the spared L4 DRG following L5 SNL (Hudson, L. J. *et al.*, 2001) and CCI (Wilson-Gerwing, T. D. *et al.*, 2005). Importantly, the upregulation of L4 DRG TRPV1 correlates

temporally with the development and maintenance of thermal hyperalgesia after L5 SNL (Fukuoka, T. *et al*., 2002). I.t. administration of NT-3 reduces thermal hyperalgesia as well as reducing the elevated DRG TRPV1 expression in CCI rats (Wilson-Gerwing, T. D. *et al*., 2005). Systemic treatment with a TRPV1 antagonist reduces thermal hyperalgesia induced by hindpaw capsaicin, carrageenan or CFA, as well as mechanical hyperalgesia after partial sciatic nerve lesion in the guinea pig (Walker, K. M. *et al*., 2003), and carrageenan-induced thermal hyperalgesia is absent in TRPV1 knock-out mice (Davis, J. B. *et al*., 2000). In contrast, i.t. administration of a TRPV1 antagonist is less effective at reducing noxious stimulus-evoked dorsal horn neuronal responses in SNL rats as compared to sham controls (Kelly, S. and Chapman, V., 2002). Evidence suggests that there is also an up-regulation of TRPV1 in DRG associated with peripheral inflammation, and that the upregulation is associated with thermal hyperalgesia and depends on p38 MAPK activation (Ji, R. R. *et al*., 2002b). Recent evidence indicates that while the levels of TRPV2 receptors in DRG are not affected by peripheral nerve axotomy, their levels in sympathetic post-ganglionic neurons are upregulated after nerve sections (Gaudet, A. D. *et al*., 2004).

5.26.2.4 Alterations in Transporter Activity

5.26.2.4.1 Glutamate transporters

Glutamate transporters are critical for the reuptake of transmitter in glutamate synapses, and the major ones include vesicular glutamate transporters VGluT1-3 and EAAC1 and glial glutamate transporters (GLAST and GLT-1) (Shigeri, Y. *et al*., 2004). There is a downregulation of EAAC1, GLAST, and GLT-1 is the spinal cord dorsal horn of CCI rats at time points when they exhibit mechanical allodynia and thermal hyperalgesia (Sung, B. *et al*., 2003). The EAAC1, GLAST, and GLT-1 downregulation in rats with taxol-induced neuropathy is paralleled by increases in spontaneous activity, prolonged afterdischarges, and windup in dorsal horn neurons (Cata, J. P. *et al*., 2005; Weng, H. R. *et al*., 2005). Dorsal horn EAAC1, GLAST, and GLT-1 are also all downregulated in chronic morphine-treated rats in a manner that is temporally correlated with the development of thermal hyperalgesia (Mao, J. *et al*., 2002a; Lim, G. *et al*., 2005). I.t. administration of inhibitors of glutamate transporters has also been shown to produce mechanical allodynia and thermal hyperalgesia (Mao, J. *et al*., 2002a; Liaw, W. J. *et al*., 2005). Finally, using *in vivo* voltametry and pressure-ejected glutamate, it has been shown that the uptake of glutamate is significantly reduced in the spinal cord dorsal horn of rats with SNL (Binns, B. C. *et al*., 2005), illustrating the impact of glutamate transporter suppression.

5.26.2.4.2 Cation chloride transporters

Recent studies suggest that alterations in the function of cation chloride cotransporters may play a role in hyperalgesia states by modulating the chloride concentration inside nociceptive cells. Galan A. and Cervero F. (2005) report that there is a 50% increase in the Na^+–Cl^-–K^+ isoform 1 (NKCC1) in the dorsal horn of mice after intracolonic capsaicin injection, as well as an increase in the phosphorylation of NKCC1. In addition, NKCC1 knockout mice have a reduction in mechanical allodynia to stroking induced by intradermal capsaicin (Laird, J. M. *et al*., 2004). They propose that increased NKCC-1 shifts the anion gradient and alters normal presynaptic inhibition in dorsal horn by producing an increase in the intracellular concentration of chloride and an enhanced GABA-mediated primary afferent depolarization that leads to mechanical allodynia (Galan, A. and Cervero, F., 2005). Thus, GABAergic depolarization in primary afferents will lead to a cross excitation between low- and high-threshold afferents that produce allodynia by reducing GABA-mediated presynaptic inhibition (Price, T. J. *et al*., 2005).

Furthermore, Coull J. A. *et al*. (2003) found a reduction in the potassium chloride exporter (KCC2) in the spinal dorsal horn of CCI rats. This decrease was paralleled by a shift in the transmembrane anion gradient that caused normally inhibitory anion synaptic currents to be excitatory, and an increase in the net excitability of lamina I dorsal horn neurons in CCI rats (Coull, J. A. *et al*., 2003). In addition, blockade or knockdown of spinal KCC2 in intact rats produced mechanical allodynia, suggesting that disruption of anion homeostatis could be responsible for allodynia in neuropathic rats (Coull, J. A. *et al*., 2003). The decrease in spinal KCC2 is proposed then to result in a loss of GABA-/glycinergic inhibitory tone and, in some cases, inverting its action into net excitation that causes allodynia after nerve injury (Price, T. J. *et al*., 2005).

5.26.2.5 Glial Cell Alterations

5.26.2.5.1 Microglia

Activation of microglial and the release of proinflammatory cytokines from these cells was originally

found to play a significant role in illness-induced hyperalgesia, including that produced by bacterial endotoxins and viruses such as HIV-1 (see Watkins, L. R. and Maier, S. F., 1999 for a review). There is also an increase in activated microglia, as indicated by increased complement receptor C3bi (OX-42) immunoreactivity in rat spinal cord dorsal horn following sciatic nerve transection (Eriksson, N. P. *et al.*, 1993). There is an increase in immunoreactivity for microglial markers OX-42 and histocompatibility complex II (OX-6), as well, in the dorsal horn of rats with partial sciatic nerve ligation (Coyle, D. E., 1998), with a linear correlation between increased mechanical allodynia and increased OX-42 staining. OX-42 is also increased in dorsal horn following injury of spinal nerve roots, and is accompanied by increases in expression of the interleukin 1β (IL-1β) (Hashizume, H. *et al.*, 2000) and the fractalkine receptor X3CR1 in dorsal horn microglia (Verge, G. M. *et al.*, 2004; Lindia, J. A. *et al.*, 2005). Peripheral inflammation induced by hind paw CFA injections also leads to increases in microglial markers, including OX-42, Mac-1, TLR4, and CD14 in spinal dorsal horn (Raghavendra, V. *et al.*, 2004). I.t. administration of an inhibitor of microglial cell activation attenuates mechanical allodynia in rats with sciatic nerve inflammation, as well as reducing the expression of the proinflammatory cytokines IL-1β and tumor necrosis factor alpha (TNFα) and their converting enzymes in spinal dorsal horn after sciatic nerve inflammation (Milligan, E. D. *et al.*, 2003; Ledeboer, A. *et al.*, 2005). A glial metabolic inhibitor also reduces C-fiber afferent-stimulated LTP in spinal cord dorsal horn neurons (Ikeda, H. and Murase, K., 2004).

Mechanical allodynia in ipsilateral and contralateral hind paws of rats with a unilateral inflammation of the sciatic nerve is also reduced following i.t. treatment with antagonists of the proinflammatory cytokines IL-1β, IL-6, and TNFα (Milligan, E. D. *et al.*, 2003). I.t. administration of the cytokine fractalkine produces mechanical allodynia and thermal hyperalgesia that is blocked by an inhibitor of microglial activation, as well as an antagonist of IL-1 and antibodies to IL-6 (Milligan, E. D. *et al.*, 2004; 2005). In contrast, a neutralizing antibody of the fractalkine receptor (CX3CR1) delays the development of mechanical allodynia and thermal hyperalgesia in rats with CCI or inflammatory injury of the sciatic nerve (Milligan, E. D. *et al.*, 2004). Increased cytokine activity in spinal nerve injured rats leads to a phosphorylation of p38 MAPK in dorsal horn microglia, and a p38 MAPK inhibitor reduces mechanical allodynia in neuropathic rats (Inoue, K. *et al.*, 2003; Tsuda, M. *et al.*, 2004). The expression of the P2X4 receptor, a subtype of ATP receptors, is also enhanced in rat spinal microglia after SNL, and ATP acting at P2X4 receptor on microglia leads to the release of cytokines which activate p38 MAPK (Inoue, K., 2006). Pharmacological blockade or knockdown of P2X4 receptors reverse mechanical allodynia after SNL in rats, while i.t. administration of microglia activated by P2X4 receptor stimulation produces mechanical allodynia in naïve rats (Tsuda, M. *et al.*, 2003).

5.26.2.5.2 Astrocytes

There is also an increase in activated astrocytes as indicated by increased staining of glial fibrillary acidic protein (GFAP) in rat spinal cord dorsal horn following sciatic nerve transection (Eriksson, N. P. *et al.*, 1993) or partial sciatic nerve ligation (Ma, W. and Quirion, R., 2002). The degree of thermal hyperalgesia or mechanical allodynia in rats with CCI of the sciatic nerve (Garrison, C. J. *et al.*, 1991) and injury of spinal nerve roots (Hashizume, H. *et al.*, 2000) or partial sciatic nerve injury (Coyle, D. E., 1998), respectively, is correlated with the magnitude of GFAP staining in the spinal cord dorsal horn. GFAP is also increased in dorsal horn following SNL, and is accompanied by increases expression the cytokine fibroblast growth factor-2 (Madiai, F. *et al.*, 2003) and increases in fractalkine (CX3CL1) in astrocytes (Lindia, J. A. *et al.*, 2005). Hind paw injection of CFA also produces spinal astrocyte activation as indicated by increased GFAP and S100B expression in the dorsal horn (Raghavendra, V. *et al.*, 2004). There is also an increase in MAPK activity in astrocytes as indicated by increases in phosphorylated ERK and JNK in cells that colocalize GFAP (Ma, W. and Quirion, R., 2002).

5.26.2.5.3 Neuron–glial interactions

Many of the factors released by glial cells discussed in the two above sections (particularly cytokines) act to sensitize neurons and represent neuron–glial interactions that contribute to hyperalgesia and/or allodynia. A recent study by Coull J. A. *et al.* (2005) provides an excellent example of a neuronal–glial interactive pathway that has been implicated in the development of allodynia and hyperalgesia in nerve-injured rats. These authors have shown that ATP-stimulated microglia cause a shift in the anion reversal potential in spinal lamina I neurons similar to that observe in rats with sciatic nerve injury. The

shift inverts the polarity of GABA currents so that GABA produces excitation rather than the normal inhibition of lamina I neurons. In addition, they showed that applying BDNF mimics the alteration in anion gradient, that ATP stimulation evokes the release of BDNF from microglia, and that blocking BDNF effects on TrkB receptors reverses allodynia and anion gradient shifts that follow nerve injury or administration of ATP-stimulated microglia (Coull, J. A. *et al.*, 2005). This study illustrates the importance of neuron–glial interactions to allodynia in neuropathic rats, and indicates that BDNF is a crucial signalling molecule between microglia and neurons.

5.26.2.6 Descending Facilitation

Sensitization of spinal cord dorsal horn neurons is not only enabled by increased input from primary afferent nociceptors, but also by a decrease in descending inhibitory controls and a phenomenon known as descending facilitation. The role of descending facilitation was reported by Watkins L. R. *et al.* (1994b) who found lesions of the NRM reduced illness-induced hyperalgesia. Pertovaara, A. (1998) further reported that mustard oil application to the rat hind paw produced a facilitation of evoked nociceptive responses of dorsal horn neurons that was attenuated by spinal transection or lidocaine block of the rostroventromedulla (RVM). Descending facilitation of spinal neurons has also been observed through a pathway that involves the nucleus reticularis gigantocellularis (Zhuo, M. and Gebhart, G. F. 1992). Spinal cord transection or RVM blocks, as well as inhibition of RVM NMDA receptors or NO synthase, also prevent the development of secondary hyperalgesia in rats after topical mustard oil, carrageenan inflammation and SNL (see Urban, M. O. and Gebhart, G. F., 1999). Mechanical allodynia after SNL in rats is reversed by ipsilateral dorsal column lesions of by administration of lidocaine into the ipsilateral nucleus gracilis, suggesting that descending facilitation from supraspinal sites depends on afferent signals transmitted by large myelinated fibers in the dorsal column pathway (Sun, H. *et al.*, 2001). Importantly, large myelinated fibers projecting to the nucleus gracilis have been found to change their phenotype and express SP following sciatic nerve transection, and NK-1 receptor antagonists suppress stimulus-induced Fos expression in the gracile nucleus in sciatic nerve lesioned rats (Noguchi, K. *et al.*, 1995). It has also been suggested that a descending facilitatory serotonergic pathway is activated by superficial dorsal horn neurons that express NK-1 (Suzuki, R. *et al.*, 2002).

5.26.2.7 Anatomical Changes

5.26.2.7.1 Cell death and apoptotic genes

5.26.2.7.1.(i) Cell death Transection of the sciatic nerve results in transganglionic degeneration atrophy and signs of Wallerian degeneration in the monkey spinal cord (Knyihar-Csillik, E. *et al.*, 1987). In rats, there is a dramatic increase of terminal deoxynucleotidyl transferase-mediated biotinylated UTP nick end labeling (TUNEL)-stained interneurons in superficial (Azkue, J. J. *et al.*, 1998) and deep (Oliveira, A. L. *et al.*, 1997) dorsal horn neurons after sciatic nerve transection, indicating that apoptotic mechanisms are involved in the cell death process. CCI of the rat sciatic nerve also leads to degenerative changes in spinal cord with the appearance of hyperchromatic or dark neurons (Sugimoto, T. *et al.*, 1990; Nachemson, A. K. and Bennett, G. J., 1993) and TUNEL-labeled neurons (Whiteside, G. T. and Munglani, R., 2001; Maione, S. *et al.*, 2002) in the dorsal horn. The apoptotic degeneration after nerve injury appears to depend on EAA-induced excitotoxicity since premptive treatment with NMDA or mGluR5 antagonists reduces TUNEL staining after transection (Azkue, J. J. *et al.*, 1998) or CCI (Whiteside, G. T. and Munglani, R., 2001; de Novellis, V. *et al.*, 2004) of the sciatic nerve. Reducing neuronal apopotosis in spinal dorsal horn by administration of erythroprotein also prevents mechanical allodynia in rats with spinal nerve root crush injury (Sekiguchi, Y. *et al.*, 2003).

Recent evidence suggest that there is a decrease in GABA-A-mediated inhibitory postsynaptic potentials (IPSPs) in rats with spared nerve injury or CCI (Moore, K. A. *et al.*, 2002), suggesting a reduction in the presynaptic release of GABA after nerve injury. Partial nerve injured was also found to produce a reduction in the GABA synthesizing enzyme glutamic acid decarboxylase (GAD) as well as increased TUNEL staining indicative of apoptosis in dorsal horn (Moore, K. A. *et al.*, 2002), although it has been recently suggested that most TUNEL staining is in microglia and not neurons (Polgar, E. *et al.*, 2005). Blocking apoptosis with a caspase inhibitor prevents the loss of spinal GABAergic interneurons, the reduction in spinal IPSCs, and mechanical and cold allodynia after CCI or partial sciatic nerve injury (Scholz, J. *et al.*, 2005). Furthermore, rats with SNL

have alterations in the normal inhibition of C-fiber-evoked activity by GABA-A agonists (Kontinen, V. K. and Dickenson, A. H., 2000; Sokal, D. M. and Chapman, V., 2003), and spinal cord injured rats with allodynia do not exhibit the normal increases in evoked responses of dorsal horn neurons after ionotophorectic application of GABA-A antagonists (Drew, G. M. *et al.*, 2004). In addition, a reduction in the glycinergic inhibitory control of spinal neurons occurs after CFA-induced inflammation of the hind paw as reflected by a reduced mean frequency of glycine-mediated miniature IPSCs in lamina I neurons (Muller, F. *et al.*, 2003). All these findings point to a potentially important contribution to hyperalgesia and/or allodynia of cell death of inhibitory neurons.

5.26.2.7.1.(ii) Apoptotic genes Recent research suggests that chronic pain produces alterations in apoptotic and antiapoptotic genes either following gene transcription or by posttranslational mechanisms. CCI of the sciatic nerve leads to alterations of dorsal horn levels of various members of Bcl-2 gene family, including an upregulation of the proapoptotic gene Bax and the antiapoptotic genes Bcl-2 and Bcl-xL, and a downregulation of Bcl-xS (Maione, S. *et al.*, 2002; de Novellis, V. *et al.*, 2004). Importantly, spinal neuron apoptosis indicated by TUNEL staining, thermal, and mechanical hyperalgesia and the alterations in apoptotic genes were all reversed by treatment with an mGluR5 antagonist (de Novellis, V. *et al.*, 2004). There is also an upregulation of the proapoptotic protein Bax and caspase 3, and a downregulation of the antiapopototic protein Bcl-2 in chronic morphine-treated rats that exhibit thermal hyperalgesia (Mao, J. *et al.*, 2002b). Neuronal apopotosis in dorsal horn and thermal hyperalgesia in chronic morphine-treated rats are attenuated by i.t. administration of a nonselective caspase and a caspase-3-selective inhibitor (Mao, J. *et al.*, 2002b). I.t. quisqualic acid-induced excitotoxic spinal cord injury produces pain-related behaviors and increased expression of CD-95 or Fas ligand and TNF-related apoptotis-inducing ligand (TRAIL), and i.t. treatment with IL-10, an anti-inflammatory cytokine, reduced pain-related behaviors in spinal injured rats (Plunkett, J. A. *et al.*, 2001). Furthermore, inhibition of activator (1,2,8, and 9) and effector (3) caspases attenuates neuropathic pain induced in rats by cancer and HIV/AIDS chemotherapeutic agents, as well as pain-related behavior induced by TNFα (Joseph, E. K. and Levine, J. D., 2004). A caspase inhibitor also reduces mechanical and cold allodynia in rats with partial nerve injury (Scholz, J. *et al.*, 2005), while an inhibitor of poly(ADP-ribose) synthetase, an enzyme involved in glutamate-induced neurotoxicity, reduces the expression of dark neurons and allodynia and hyperalgesia in CCI rats (Mao, J. *et al.*, 1997). Galectin-1, a member of the family of β-galactoside-binding animal lectins, has been shown to be a proapoptotic factor, and is increased in spinal cord dorsal horn after peripheral nerve transection (Imbe, H. *et al.*, 2003; McGraw, J. *et al.*, 2005). I.t. treatment with antibodies to galectin-1 attenuates the mechanical allodynia in the spared nerve injury model (Imbe, H. *et al.*, 2003).

5.26.2.7.2 Sprouting

5.26.2.7.2.(i) Sympathetic fibers Although controversial, there is long-standing evidence that alterations in sympathetic nervous system function plays a role in hyperalgesia and allodynia following nerve injury (Janig, W. *et al.*, 1996). Sympathetic activity may influence inputs to spinal cord dorsal horn following the development of abnormal connectivity between sympathetic efferent fibers and primary afferent fibers. McLachlan E. M. *et al.* (1993) showed that sympathetic axons sprout into the DRGs of rats with sciatic nerve transection and form basket-like structures around large neurons. Similar sympathetic fiber sprouting is observed after SNL (Chung, K. *et al.*, 1993) and partial ligation (Lee, B. H. *et al.*, 1998) or CCI of the sciatic nerve (Ramer, M. S. and Bisby, M. A., 1997). Mechanical and allodynia in SNL rats is abolished after sympathectomy, which eliminates most sprouting fibers (Chung, K. *et al.*, 1996). Sympathetic sprouting, mechanical allodynia, and thermal hyperalgesia after CCI depends on the occurrence of Wallerian degeneration (Ramer, M. S. *et al.*, 1997) and an upregulation of NGF (Ramer, M. S. and Bisby, M. A., 1997) in DRG neurons. There is also and upregulation of NGF and NT-3 in glial cells of the DRG in SNL rats, and antibodies to NGF, BDNF, and NT-3 reduce sympathetic sprouting in rat DRG and thermal hyperalgesia after SNL (Zhou, X. F. *et al.*, 1999b; Deng, Y. S. *et al.*, 2000). Sympathetic sprouting and mechanical allodynia after SNL are attenuated in IL-6 knockout mice, implicating cytokines as key factors contributing to these changes (Ramer, M. S. *et al.*, 1998).

5.26.2.7.2.(ii) Aβ fibers It it difficult to explain the development of allodynia in response to activity-

drive plasticity as Aβ fibers, which transmit low-threshold touch inputs generally do not terminate on spinal nociceptive neurons. Evidence generated over the past 15 years suggests, however, that allodynia may be partly explained the nerve injury-induced sprouting of the terminals of Aβ fibers into dorsal horn lamina I and IIo where they are able to contact spinal nociceptive neurons (Woolf, C. J. *et al.*, 1992; Shortland, P. and Woolf, C. J., 1993). It has been suggested that regenerating Aβ fibers exhibit collateral sprouting into superficial dorsal horn lamina after the terminal arbors of small Aδ and C fibers degenerate following peripheral nerve injury (Wilson, P. and Kitchener, P. D., 1996), a theory that is supported by evidence of similar Aβ fiber sprouting after local application of the C-fiber neurotoxin capsaicin to the sciatic nerve (Mannion, R. J. *et al.*, 1996). Aβ fiber sprouting into rat spinal lamina II has also been observed in rats with SNL or CCI of the sciatic nerve (Shortland, P. *et al.*, 1997; Nakamura, S. and Myers, R. R., 1999) or even chronic inflammation of the rat hind paw (Ma, Q. P. and Tian, L., 2002). Lekan H. A. *et al.* (1997) also found increased Aβ fibers in dorsal roots despite overall decreases in rat DRG cells after SNL. Both the sprouting of Aβ fibers into lamina II and mechanical allodynia after sciatic nerve injury are absent in mice lacking membrane-type 5 matrix metalloproteinase (Komori, K. *et al.*, 2004), and the sprouting is accompanied by *de novo* expression of SP, somatostatin, and PACAP in deeper lamina (Jongsma, H. *et al.*, 2000; Swamydas, M. *et al.*, 2004). The conclusions of these studies have been questioned, however, by evidence that after nerve injury Aδ fibers (Ma, Q. P. and Tian, L., 2001) or even C fibers (Tong, Y. G. *et al.*, 1999; Shehab, S. A. *et al.*, 2003) may begin to uptake the cholera toxin B subunit that has been used in the previous studies as a selective marker of Aβ fibers.

5.26.3 Conclusion

Hyperalgesia and allodynia are consequences of cutaneous or deep tissue and nerve injury and depend on both peripheral and central sensitization. Central sensitization relies on various alterations in both presynaptic DRG cells, interneurons and postsynaptic spinal cord dorsal horn neurons, as well as satellite cells in the dorsal horn and DRG. There are changes in the expression of receptors and ion channels, as well as alterations in their cellular location within neurons. There is evidence that changes in scaffolding proteins, kinases and phosphatases, and transporters influence the synaptic activity and anion gradients of pre- and postsynaptic neurons in the spinal cord dorsal horn. Activation of microglial and astrocytes and the release of mediators such as cytokines and neurotrophins result in neuron–glial interactions that also contribute to increased excitability in the spinal cord. Finally there is evidence of cell death, trans-synaptic degeneration, and the sprouting of sympathetic efferent fibers in DRG and A-fiber primary afferent fibers in the dorsal horn which contribute to central sensitization and the development and/or maintenance of hyperalgesia and allodynia.

Acknowledgments

This work is supported by grants form CIHR, NSERC, and FRSQ to T. J. C.

References

Aanonsen, L. M. and Wilcox, G. L. 1986. Phencyclidine selectively blocks a spinal action of *N*-methyl-D-aspartate in mice. Neurosci. Lett. 67, 191–197.

Aanonsen, L. M. and Wilcox, G. L. 1987. Nociceptive action of excitatory amino acids in the mouse: effects of spinally administered opioids, phencyclidine and sigma agonists. J. Pharmacol. Exp. Ther. 243, 9–19.

Aanonsen, L. M., Lei, S., and Wilcox, G. L. 1990. Excitatory amino acid receptors and nociceptive neuro-transmission in rat spinal cord. Pain 41, 309–321.

Aanonsen, L. M., Kajander, K. C., Bennett, G. J., and Seybold, V. S. 1992. Autoradiographic analysis of 125I-substance P binding in rat spinal cord following chronic constriction injury of the sciatic nerve. Brain Res. 596, 259–268.

Abe, T., Matsumura, S., Katano, T., Mabuchi, T., Takagi, K., Xu, L., Yamamoto, A., Hattori, K., Yagi, T., Watanabe, M., Nakazawa, T., Yamamoto, T., Mishina, M., Nakai, Y., and Ito, S. 2005. Fyn kinase-mediated phosphorylation of NMDA receptor NR2B subunit at Tyr1472 is essential for maintenance of neuropathic pain. Eur. J. Neurosci. 22, 1445–1454.

Abe, T., Sugihara, H., Nawa, H., Shigemoto, R., Mizuno, N., and Nakanishi, S. 1992. Molecular characterization of a novel metabotropic glutamate receptor mGluR5 coupled to inositol phosphate/Ca^{2+} signal transduction. J. Biol. Chem. 267, 13361–13368.

Abram, S. E. and Yaksh, T. L. 1994. Systemic lidocaine blocks nerve injury-induced hyperalgesia and nociceptor-driven spinal sensitization in the rat. Anesthesiology 80, 383–391.

Adwanikar, H., Karim, F., and Gereou, R. W., 4th 2004. Inflammation persistently enhances nocifensive behaviors mediated by spinal group I mglurs through sustained ERK activation. pain 111, 125–135.

Akopian, A. N., Souslova, V., England, S., Okuse, K., Ogata, N., Ure, J., Smith, A., Kerr, B. J., McMahon, S. B., Boyce, S., Hill, R., Stanfa, L. C., Dickenson, A. H., and Wood, J. N.

1999. The tetrodotoxin-resistant sodium channel SNS has a specialized function in pain pathways. Nat. Neurosci. 2, 541–548.

Alaluf, S., Mulvihill, E. R., and McIlhinney, A. J. 1995. Rapid agonist mediated phosphorylation of the metabotropic glutamate receptor 1a by protein kinase C in permanently transfected BHK cells. FEBS Lett. 367, 301–305.

Allen, B. J., Li, J., Menning, P. M., Rogers, S. D., Ghilardi, J., Mantyh, P. W., and Simone, D. A. 1999. Primary afferent fibers that contribute to increased substance P receptor internalization in the spinal cord after injury. J. Neurophysiol. 81, 1379–1390.

Andrew, D. and Greenspan, J. D. 1999. Mechanical and heat sensitization of cutaneous nociceptors after peripheral inflammation in the rat. J. Neurophysiol. 82, 2649–2656.

Ango, F., Pin, J. P., Tu, J. C., Xiao, B., Worley, P. F., Bockaert, J., and Fagni, L. 2000. Dendritic and axonal targeting of type 5 metabotropic glutamate receptor is regulated by homer1 proteins and neuronal excitation. J. Neurosci. 20, 8710–8716.

Apfel, S. C. 2000. Neurotrophic factors and pain. Clin. J. Pain 16, S7–S11.

Apfel, S. C., Wright, D. E., Wiideman, A. M., Dormia, C., Snider, W. D., and Kessler, J. A. 1996. Nerve growth factor regulates the expression of brain-derived neurotrophic factor mRNA in the peripheral nervous system. Mol. Cell. Neurosci. 7, 134–142.

Arevalo, M. I., Escribano, E., Caleno, A., Domenech, J., and Queralt, J. 2003. Thermal hyperalgesia and light touch allodynia after intradermal *Mycobacterium butyricum* administration in rat. Inflammation 27, 293–299.

Attal, N., Gaude, V., Brasseur, L., Dupuy, M., Guirimand, F., Parker, F., and Bouhassira, D. 2000. Intravenous lidocaine in central pain: a double-blind, placebo-controlled, psychophysical study. Neurology 54, 564–574.

Azkue, J. J., Zimmermann, M., Hsieh, T. F., and Herdegen, T. 1998. Peripheral nerve insult induces NMDA receptor-mediated, delayed degeneration in spinal neurons. Eur. J. Neurosci. 10, 2204–2206.

Barakat-Walter, I. 1996. Brain-derived neurotrophic factor-like immunoreactivity is localized mainly in small sensory neurons of rat dorsal root ganglia. J. Neurosci. Methods 68, 281–288.

Baranowsli, A. P., Priestley, J. V., and McMahon, S. 1993. Substance P in cutaneous primary sensory neurons-a comparison of models of nerve injury that allow varying degrees of regeneration. Neuroscience 55, 1025–1036.

Baumann, T. K., Simone, D. A., Shain, C. N., and LaMotte, R. H. 1991. Neurogenic hyperalgesia: the search for the primary cutaneous afferent fibers that contribute to capsaicin-induced pain and hyperalgesia. J. Neurophysiol. 66, 212–227.

Beitel, R. E. and Dubner, R. 1976. Response of unmyelinated (C) polymodal nociceptors to thermal stimuli applied to monkey's face. J. Neurophysiol. 39, 1160–1175.

Benani, A., Heurtaux, T., Netter, P., and Minn, A. 2004. Activation of peroxisome proliferator-activated receptor alpha in rat spinal cord after peripheral noxious stimulation. Neurosci. Lett. 369, 59–63.

Bennett, G. J. and Xie, Y. K. 1988. A peripheral mononeuropathy in rat produces disorders of pain sensation like those seen in man. Pain 33, 87–107.

Binns, B. C., Huang, Y., Goettl, V. M., Hackshaw, K. V., and Stephens, R. L. Jr. 2005. Glutamate uptake is attenuated in spinal deep dorsal and ventral horn in the rat spinal nerve ligation model. Brain Res. 1041, 38–47.

Black, J. A., Liu, S., Tanaka, M., Cummins, T. R., and Waxman, S. G. 2004. Changes in the expression of tetrodotoxin-sensitive sodium channels within dorsal root ganglia neurons in inflammatory pain. Pain 108, 237–247.

Bordi, F. and Ugolini, A. 2000. Involvement of mGluR(5) on acute nociceptive transmission. Brain Res. 871, 223–233.

Bourinet, E., Alloui, A., Monteil, A., Barrere, C., Couette, B., Poirot, O., Pages, A., McRory, J., Snutch, T. P., Eschalier, A., and Nargeot, J. 2004. Silencing of the Cav3.2 T-type calcium channel gene in sensory neurons demonstrates its major role in nociception. EMBO J. 24, 315–324.

Boxall, S. J., Berthele, A., Laurie, D. J., Sommer, B., Zieglgansberger, W., Urban, L., and Tolle, T. R. 1998. Enhanced expression of metabotropic glutamate receptor 3 messenger RNA in the rat spinal cord during ultraviolet irradiation induced peripheral inflammation. Neuroscience 82, 591–602.

Boxall, S. J., Thompson, S. W., Dray, A., Dickenson, A. H., and Urban, L. 1996. Metabotropic glutamate receptor activation contributes to nociceptive reflex activity in the rat spinal cord in vitro. Neuroscience 74, 13–20.

Brennan, T. J., Vandermeulen, E. P., and Gebhart, G. F. 1996. Characterization of a rat model of incisional pain. Pain 64, 493–501.

Brenner, G. J., Ji, R. R., Shaffer, S., and Woolf, C. J. 2004. Peripheral noxious stimulation induces phosphorylation of the NMDA receptor NR1 subunit at the PISC-dependent site, serine-896, in spinal cord dorsal horn neurons. Eur. J. Neurosci. 20, 375–384.

Brock, J. H., Elste, A., and Huntley, G. W. 2004. Distribution and injury-induced plasticity of cadherins in relationship to identified synaptic circuitry in adult rat spinal cord. J. Neurosci. 24, 8806–8817.

Broom, D. C., Samad, T. A., Kohno, T., Tegeder, I., Geisslinger, G., and Woolf, C. J. 2004. Cyclooxygenase 2 expression in the spared nerve injury model of neuropathic pain. Neuroscience 124, 891–900.

Bruce, J. C., Oatway, M. A., and Weaver, L. C. 2002. Chronic pain after clip-compression injury of the rat spinal cord. Exp. Neurol. 178, 33–48.

Bullitt, E. 1989. Induction of c-fos-like protein within the lumbar spinal cord and thalamus of the rat following peripheral stimulation. Brain Res. 493, 391–397.

Buritova, J., Fletcher, D., Honore, P., and Besson, J. M. 1996. Effects of local anaesthetics on carrageenan-evoked inflammatory nociceptive processing in the rat. Br. J. Anaesth. 77, 645–652.

Cahill, C. M. and Coderre, T. J. 2002. Attenuation of hyperalgesia in a rat model of neuropathic pain after intrathecal pre- or post-treatment with a neurokinin-1 antagonist. Pain 95, 277–285.

Cahill, C. M., Dray, A., and Coderre, T. J. 1998. Priming enhances endotoxin-induced thermal hyperalgesia and mechanical allodynia in rats. Brain Res. 808, 13–22.

Cahusac, P. M., Evans, R. H., Hill, R. G., Rodriquez, R. E., and Smith, D. A. 1984. The behavioural effects of an *N*-methylaspartate receptor antagonist following application to the lumbar spinal cord of conscious rats. Neuropharmacology 23, 719–724.

Calvino, B., Villanueva, L., and LeBars, D. 1987. Dorsal horn (convergent) neurones in the intact anaesthetized arthritic rat. II. Heterotopic inhibitory influences. Pain 28, 81–98.

Cameron, A. A., Cliffer, K. D., Dougherty, P. M., Willis, W. D., and Carlton, S. M. 1991. Changes in lectin, GAP-43 and neuropeptide staining in the rat dorsal horn following experimental peripheral neuropathy. Neurosci. Lett. 131, 249–252.

Carlton, S. M., Hargett, G. L., and Coggeshall, R. E. 1998. Plasticity in alpha-amino-3-hydroxy-5-methyl-4-isoxazolepropionic acid receptor subunits in the rat dorsal horn following deafferentation. Neurosci. Lett. 242, 21–24.

Carpenter, S. E. and Lynn, B. 1981. Vascular and sensory responses of human skin to mild injury after topical treatment with Capsaicin. Br. J. Pharmacol. 73, 755–758.

Carroll, R. C. and Zukin, R. S. 2002. NMDA-receptor trafficking and targeting: implications for synaptic transmission and plasticity. Trends Neurosci. 25, 571–577.

Castro-Lopes, J. M., Malcangio, M., Pan, B. H., and Bowery, N. G. 1995. Complex changes of GABAA and GABAB receptor binding in the spinal cord dorsal horn following peripheral inflammation or neurectomy. Brain Res. 679, 289–297.

Cata, J. P., Weng, H. R., Chen, J. H., and Dougherty, P. M. 2006. Altered discharges of spinal wide dynamic range neurons and down-regulation of glutamate transporter expression in rats with paclitaxel-induced hyperalgesia. Neuroscience 138, 329–338.

Caterina, M. J. and Julius, D. 2001. The vanilloid receptor: a molecular gateway to the pain pathway. Annu. Rev. Neurosci. 24, 487–517.

Catheline, G., Le Guen, S., Honore, P., and Besson, J. M. 1999. Are there long-term changes in the basal or evoked Fos expression in the dorsal horn of the spinal cord of the mononeuropathic rat? Pain 80, 347–357.

Caudle, R. M., Perez, F. M., Del Valle-Pinero, A. Y., and Iadarola, M. J. 2005. Spinal cord NR1 serine phosphorylation and NR2B subunit suppression following peripheral inflammation. Mol. Pain 1, 25.

Caudle, R. M., Perez, F. M., King, C., Yu, C. G., and Yezierski, R. P. 2003. *N*-methyl-D-aspartate receptor subunit expression and phosphorylation following excitotoxic spinal cord injury in rats. Neurosci. Lett. 349, 37–40.

Cervero, F., Handwerker, H. O., and Laird, J. M. A. 1998. Prolonged noxious stimulation of the rat's tail: responses and encoding properties of dorsal horn neurons. J. Physiol. (Lond.) 404, 419–436.

Chan, C. F., Sun, W. Z., Lin, J. K., and Lin-Shiau, S. Y. 2000. Activation of transcription factors of nuclear factor kappa B, activator protein-1 and octamer factors in hyperalgesia. Eur. J. Pharmacol. 402, 61–68.

Chen, Y. and Devor, M. 1998. Ectopic mechanosensitivity in injured sensory axons arises from the site of spontaneous electrogenesis. Eur. J. Pain 2, 165–178.

Chen, L. and Huang, L.-Y. M. 1992. Protein kinase C reduces Mg^{2+} block of NMDA-receptor channels as a mechanism of modulation. Nature 356, 521–523.

Chen, S. R. and Pan, H. L. 2002. Hypersensitivity of spinothalamic tract neurons with diabetic neuropathic pain in rats. J. Neurophysiol. 87, 2726–2733.

Chen, S. R. and Pan, H. L. 2005. Distinct roles of group III metabotropic receptors in control of nociception and dorsal horn neurons in normal and nerve-injured rats. J. Pharmacol. Exp. Ther. 312, 120–126.

Chen, Y., Bacon, G., Sher, E., Clark, B. P., Kallman, M. J., Wright, R. A., Johnson, B. G., Schoepp, D. D., and Kingston, A. E. 2000. Evaluationof the activity of a novel metabotropic glutamate receptor antagonist (+/−)-2-amino-2-(3-*cis* and *trans*-carboxycyclobutyl-3-(9-thioxanthyl)propionic acid) in the *in vitro* neonatal spinal cord and in an in vivo pain model. Neuroscience 95, 787–793.

Chi, S. I., Levine, J. D., and Basbaum, A. I. 1993. Peripheral and central contributions to the persistent expression of spinal cord fos-like immunoreactivity produced by sciatic nerve transection in the rat. Brain Res. 617, 225–237.

Cho, H. J., Kim, S. Y., Park, M. J., Kim, D. S., Kim, J. K., and Chu, M. Y. 1997a. Expression of mRNA for brain-derived neurotrophic factor in the dorsal root ganglion following peripheral inflammation. Brain Res. 749, 358–362.

Cho, H. J., Kim, J. K., Zhou, X. F., and Rush, R. A. 1997b. Increased brain-derived neurotrophic factor immunoreactivity in rat dorsal root ganglia and spinal cord following peripheral inflammation. Brain Res. 764, 269–272.

Chou, A. K., Muhammad, R., Huang, S. M., Chen, J. T., Wu, C. L., Lin, C. R., Lee, T. H., Lin, S. H., Lu, C. Y., and Yang, L. C. 2002. Altered synaptophysin expression in the rat spinal cord after chronic constriction injury of sciatic nerve. Neurosci. Lett. 333, 155–158.

Christensen, M. D. and Hulsebosch, C. E. 1997. Chronic central pain after spinal injury. J. Neurotrauma 14, 517–537.

Christensen, M. D., Everhart, A. W., Pickelman, J. T., and Hulsebosch, C. E. 1996. Mechanical and thermal allodynia in chronic central pain following spinal cord injury. Pain 68, 97–107.

Chung, K., Kim, H. J., Na, H. S., Park, M. J., and Chung, J. M. 1993. Abnormalities of sympathetic innervation in the area of an injured peripheral nerve in a rat model of neuropathic pain. Neurosci. Lett. 162, 85–88.

Chung, K., Lee, B. H., Yoon, Y. W., and Chung, J. M. 1996. Sympathetic sprouting in the dorsal root ganglia of the injured peripheral nerve in a rat neuropathic pain model. J. Comp. Neurol. 376, 241–252.

Ciruela, A., Dixon, A. K., Bramwell, S., Gonzalez, M. I., Pinnock, R. D., and Lee, K. 2003. Identification of MEK1 as a novel target for the treatment of neuropathic pain. Br. J. Pharmacol. 138, 751–756.

Cizkova, D., Lukacova, N., Marsala, M., and Marsala, J. 2002a. Neuropathic pain is associated with alterations of nitric oxide synthase immunoreactivity and catalytic activity in dorsal root ganglia and spinal dorsal horn. Brain Res. Bull. 58, 161–171.

Cizkova, D., Marsala, J., Lukacova, N., Marsala, M., Jergova, S., Orendacova, J., and Yaksh, T. L. 2002b. Localization of N-type Ca2+ channels in the rat spinal cord following chronic constrictive nerve injury. Exp. Brain Res. 147, 456–463.

Coderre, T. J. and Melzack, R. 1985. Increased pain sensitivity following heat injury involves a central mechanism. Behav. Brain Res. 15, 259–262.

Coderre, T. J. and Melzack, R. 1987. Cutaneous hyperalgesia: contributions of the peripheral and central nervous systems to the increase in pain sensitivity after injury. Brain Res. 404, 95–106.

Coderre, T. J. and Melzack, R. 1991. Central neural mediators of secondary hyperalgesia following heat injury in rats: neuropeptides and excitatory amino acids. Neurosci. Lett. 131, 71–74.

Coderre, T. J. and Melzack, R. 1992a. The contribution of excitatory amino acids to central sensitization and persistent nociception after formalin-induced tissue injury. J. Neurosci. 12, 3665–3670.

Coderre, T. J. and Melzack, R. 1992b. The role of NMDA receptor-operated calcium channels in persistent nociception after formalin-induced tissue injury. J. Neurosci. 12, 3671–3675.

Coderre, T. J., Katz, J., Vaccarino, A. L., and Melzack, R. 1993. Contribution of central neuroplasticity to pathological pain: review of clinical and experimental evidence. Pain 52, 259–285.

Coderre, T. J., Vaccarino, A. L., and Melzack, R. 1990. Central nervous system plasticity in the tonic pain response to subcutaneous formalin injection. Brain Res. 535, 155–158.

Collingridge, G. L., Isaac, J. T. R., and Wang, Y. T. 2004. Receptor trafficking and synaptic plasticity. Nat. Rev. Neurosci. 5, 952–961.

Colvin, L. A. and Duggan, A. W. 1998. Primary afferent-evoked release of immunoreactive galanin in the spinal cord of the neuropathic rat. Br. J. Anaesth. 81, 436–443.

Coull, J. A., Beggs, S., Boudreau, D., Boivin, D., Tsuda, M., Inoue, K., Gravel, C., Salter, M. W., and De Koninck, Y. 2005. BDNF from microglia causes the shift in neuronal anion gradient underlying neuropathic pain. Nature 438, 1017–1021.

Coull, J. A., Boudreau, D., Bachand, K., Prescott, S. A., Nault, F., Sik, A., De Koninck, P., and De Koninck, Y. 2003. Trans-synaptic shift in anion gradient in spinal lamina I neurons as a mechanism of neuropathic pain. Nature 424, 938–942.

Coyle, D. E. 1998. Partial peripheral nerve injury leads to activation of astroglia and microglia which parallels the development of allodynic behavior. Glia 23, 75–83.

Cridland, R. A. and Henry, J. L. 1986. Comparison of the effects of substance P, neurokinin A, physalaemin and eledoisin in facilitating a nociceptive reflex in the rat. Brain Res. 381, 93–99.

Cumberbatch, M. J., Carlson, E., Wyatt, A., Boyce, S., Hill, R. G., and Rupniak, N. M. 1998. Reversal of behavioural and electrophysiological correlates of experimental peripheral neuropathy by the NK1 receptor antagonist GR205171 in rats. Neuropharmacology 37, 1535–1543.

Curtis, D. R. and Watkins, J. C. 1960. The excitation and depression of spinal neurones by structurally related amino acids. J. Neurochem. 6, 117–141.

Davar, G., Hama, A., Deykin, A., Vos, B., and Maciewicz, R. 1991. MK-801 blocks the development of thermal hyperalgesia in a rat model of experimental painful neuropathy. Brain Res. 553, 327–330.

Davies, S. N. and Lodge, D. 1987. Evidence for involvement of N-methylaspartate receptors in 'wind-up' of class 2 neurones in the dorsal horn of the rat. Brain Res. 424, 402–406.

Davies, J. and Watkins, J. C. 1983. Role of excitatory amino acid receptors in mono- and polysynaptic excitation in the cat spinal cord. Exp. Brain Res. 49, 280–290.

Davis, R. J. 1993. The mitogen-activated protein kinase signal transduction pathway. J. Biol. Chem. 268, 14553–14556.

Davis, J. B., Gray, J., Gunthorpe, M. J., Hatcher, J. P., Davey, P. T., Overend, P., Harries, M. H., Latcham, J., Clapham, C., Atkinson, K., Hughes, S. A., Rance, K., Grau, E., Harper, A. J., Pugh, P. L., Rogers, D. C., Bingham, S., Randall, A., and Sheardown, S. A. 2000. Vanilloid receptor-1 is essential for inflammatory thermal hyperalgesia. Nature 405, 183–187.

Decosterd, I. and Woolf, C. J. 2000. Spared nerve injury: an animal model of persistent peripheral neuropathic pain. Pain 87, 149–158.

Del Pozo, E., Caro, G., and Baeyens, J. M. 1987. Analgesic effects of several calcium channel blockers in mice. Eur. J. Pharmacol. 137, 155–160.

Delander, G. E., Schott, E., Brodin, E., and Fredholm, B. B. 1997. Spinal expression of mRNA for immediate early genes in a model of chronic pain. Acta Physiol. Scand. 161, 517–525.

Deng, Y. S., Zhong, J. H., and Zhou, X. F. 2000. Effects of endogenous neurotrophins on sympathetic sprouting in the dorsal root ganglia and allodynia following spinal nerve injury. Exp. Neurol. 164, 344–350.

Dickenson, A. H. and Sullivan, A. F. 1987. Evidence for a role of the NMDA receptor in the frequency dependent potentiation of deep rat dorsal horn nociceptive neurones following C fibre stimulation. Neuropharmacology 26, 1235–1238.

Dirig, D. M., Isakson, P. C., and Yaksh, T. L. 1998. Effect of COX-1 and COX-2 inhibition on induction and maintenance of carrageenan-evoked thermal hyperalgesia in rats. J. Pharmacol. Exp. Ther. 285, 1031–1038.

Dobremez, E., Bouali-Benazzouz, R., Fossat, P., Monteils, L., Dulluc, J., Nagy, F., and Landry, M. 2005. Distribution and regulation of L-type calcium channels in deep dorsal horn neurons after sciatic nerve injury in rats. Eur. J. Neurosci. 21, 3321–3333.

Dogrul, A., Ossipov, M. H., Lai, J., Malan, T. P., Jr., and Porreca, F. 2000. Peripheral and spinal antihyperalgesic activity of SIB-1757, a metabotropic glutamate receptor (mGLUR(5)) antagonist, in experimental neuropathic pain in rats. Neurosci. Lett. 292, 115–118.

Dolan, S. and Nolan, A. M. 2000. Behavioural evidence supporting a differential role for group I and II metabotropic glutamate receptors in spinal nociceptive transmission. Neuropharmacology 39, 1132–1138.

Dolan, S., Kelly, J. G., Monteiro, A. M., and Nolan, A. M. 2003. Up-regulation of metabotropic glutamate receptor subtypes 3 and 5 in spinal cord in a clinical model of persistent inflammation and hyperalgesia. Pain 106, 501–512.

Dolan, S., Kelly, J. G., Monteiro, A. M., and Nolan, A. M. 2004. Differential expression of central metabotropic glutamate receptor (mGluR) subtypes in a clinical model of post-surgical pain. Pain 110, 369–377.

Dong, Z. Q., Ma, F., Xie, H., Wang, Y. Q., and Wu, G. C. 2006. Down-regulation of GFRalpha-1 expression by antisense oligodeoxynucleotide attenuates electroacupuncture analgesia on heat hyperalgesia in a rat model of neuropathic pain. Brain Res. Bull. 69, 30–36.

Donnerer, J., Schuligoi, R., Stein, C., and Amann, R. 1993. Upregulation, release and axonal transport of substance P and calcitonin gene-related peptide in adjuvant inflammation and regulatory function of nerve growth factor. Regul Pept 46, 50–154.

Dougherty, P. M. and Willis, W. D. 1991. Enhancement of spinothalamic neuron responses to chemical and mechanical stimuli following combined microiontophoretic application of *N*-methyl-D-aspartic acid and substance P. Pain 47, 85–93.

Dougherty, P. M. and Willis, W. D. 1992. Enhanced responses of spinothalamic tract neurons to excitatory amino acids accompany capsaicin-induced sensitization in the monkey. J. Neurosci. 12, 883–894.

Dougherty, P. M., Palecek, J., Paleckova, V., Sorkin, L. S., and Willis, W. D. 1992a. The role of NMDA and non-NMDA excitatory amino acid receptors in the excitation of primate spinothalamic tract neurons by mechanical, thermal and electrical stimuli. J. Neurosci. 12, 3025–3041.

Dougherty, P. M., Sluka, K. A., Sorkin, K. N., Westlund, K. N., and Willis, W. D. 1992b. Neural changes in acute arthritis in monkeys. I. Parallel enhancement of responses of spinothalamic tract neurons to mechanical stimulation and excitatory amino acids. Brain Res. Rev. 17, 1–13.

Draganic, P., Miletic, G., and Miletic, V. 2001. Changes in post-tetanic potentiation of A-fiber dorsal horn field potentials parallel the development and disappearance of neuropathic pain after siatic nerve ligation in rats. Neurosci. Lett. 301, 127–130.

Draisci, G. and Iadarola, M. J. 1989. Temporal analysis of increases in c-fos, preprodynorphin and preproenkephalin mRNAs in rat spinal cord. Brain Res. Mol. Brain Res. 6, 31–37.

Dray, A. and Dickenson, A. 1991. Systemic capsaicin and olvanil reduce the acute algogenic and the late inflammatory phase following formalin injection into rodent paw. Pain 47, 79–83.

Drew, G. M., Siddall, P. J., and Duggan, A. W. 2004. Mechanical allodynia following contusion injury of the rat spinal cord is associated with loss of GABAergic inhibition in the dorsal horn. Pain 109, 379–388.

Dubner, R. and Ruda, M. A. 1992. Activity-dependent neuronal plasticity following tissue injury and inflammation. Trends Neurosci. 15, 96–103.

Duggan, A. W., Hendry, I. A., Mortom, C. R., Hutchison, W. D., and Zhao, Z. Q. 1988. Cutaneous stimuli releasing immunoreactive substance P in the dorsal horn of the cat. Brain Res. 451, 261–273.

Duggan, A. W., Hope, P. J., Jarrott, B., Schaible, H. -G., and Fleetwood-Walker, S. M. 1990. Release, spread and persistence of immunoreactive neurokinin A in the dorsal horn of the cat following noxious cutaneous stimulation. Studies with antibody microprobes. Neuroscience 35, 195–202.

Dumuis, A., Pin, J. -P., Oomagari, K., Sebben, M., and Bockaert, J. 1990. Arachidonic acid released from striatal neurons by joint stimulation of ionotropic and metabotropic quisqualate receptors. Nature 347, 182–184.

Dumuis, A., Sebben, M., Haynes, L., Pin, J. -P., and Bockaert, J. 1988. NMDA receptors activate the arachidonic acid cascade system in striatal neurons. Nature 336, 68–70.

Eaton, S. A. and Salt, T. E. 1990. Thalamic NMDA receptors and nociceptive sensory synaptic transmission. Neurosci. Lett. 110, 297–302.

Eaton, M. J., Blits, B., Ruitenberg, M. J., Verhaagen, J., and Oudega, M. 2002. Amelioration of chronic neuropathic pain after partial nerve injury by adeno-associated viral (AAV) vector-mediated over-expression of BDNF in the rat spinal cord. Gene Ther. 9, 1387–1395.

Eaton, M. J., Karmally, S., Martinez, M. A., Plunkett, J. A., Lopez, T., and Cejas, P. J. 1999. Lumbar transplant of neurons genetically modified to secrete galanin reverse pain-like behaviors after partial sciatic nerve injury. J. Peripher. Nerv. Syst. 4, 245–257.

Eaton, M. J., Plunkett, J. A., Karmally, S., Martinez, M. A., and Montanez, K. 1998. Changes in GAD- and GABA-immunoreactivity in the spinal dorsal horn after peripheral nerve injury and promotion of recovery by lumbar transplant of immortalized serotonergic precursors. J. Chem. Neuroanat. 16, 57–72.

Eckert, W. A., Valtschanoff, J. G., Otey, C. A., Rustioni, A., and Weinberg, R. J. 1994. Tyrosine phosphorylation in rat spinal cord after sciatic nerve transection. Neuroreport 5, 1289–1292.

Eliav, E., Herzberg, U., Ruda, M. A., and Bennet, G. J. 1999. Neuropathic pain from an experimental neuritis of the rat sciatic nerve. Pain 83, 169–182.

Eriksson, N. P., Persson, J. K., Svensson, M., Arvidsson, J., Molander, C., and Aldskogius, H. 1993. A quantitative analysis of the microglial cell reaction in central primary sensory projection territories following peripheral nerve injury in the adult rat. Exp. Brain Res. 96, 19–27.

Fang, L., Wu, J., Lin, Q., and Willis, W. D. 2002. Calcium-calmodulin-dependent protein kinase II contributes to spinal cord central sensitization. J. Neurosci. 22, 4196–4204.

Fang, L., Wu, J., Lin, Q., and Willis, W. D. 2003. Protein kinases regulate the phosphorylation of the GluR1 subunit of AMPA receptors of spinal cord in rats following noxious stimulation. Brain Res. Mol. Brain Res. 118, 160–165.

Fang, L., Wu, J., Zhang, X., Lin, Q., and Willis, W. D. 2005. Calcium/calmodulin dependent protein kinase II regulates the phosphorylation of cyclic AMP-responsive element-binding protein of spinal cord in rats following noxious stimulation. Neurosci. Lett. 374, 1–4.

Finnerup, N. B., Biering-Sorensen, F., Johannesen, I. L., Terkelsen, A. J., Juhl, G. I., Kristensen, A. D., Sindrup, S. H., Bach, F. W., and Jensen, T. S. 2005. Intravenous lidocaine relieves spinal cord injuriy pain: a randomized controlled trial. Anesthesiology 105, 1023–1030.

Fisher, K. and Coderre, T. J. 1996a. Comparison of nociceptive effects produced by intrathecal administration of mGluR agonists. Neuroreport 7, 2743–2747.

Fisher, K. and Coderre, T. J. 1996b. The contribution of metabotropic glutamate receptors (mGluRs) to formalin-induced nociception. Pain 68, 255–263.

Fisher, K. and Coderre, T. J. 1998. Hyperalgesia and allodynia induced by intrathecal (*RS*)-dihydroxyphenylglycine in rats. Neuroreport 9, 1169–1172.

Fisher, K., Fundytus, M. E., Cahill, C. M., and Coderre, T. J. 1998. Intrathecal administration of the mGluR compound, (*S*)-4CPG, attenuates hyperalgesia and allodynia associated with sciatic nerve constriction injury in rats. Pain 77, 59–66.

Fisher, K., Lefebvre, C. D., and Coderre, T. J. 2002. The effects of intrathecal administration of selective metabotropic glutamate receptor compounds in a rat model of neuropathic pain. Pharmacol. Biochem. Behav. 73, 411–418.

Fitzgerald, M. 1979. The spread of sensitization of polymodal nociceptors in the rabbit from nearby injury and by antidromic nerve stimulation. J. Physiol. 297, 207–216.

Fitzgerald, M. and Lynn, B. 1977. The sensitization of high threshold mechanoreceptors with myelinated axons by repeated heating. J. Physiol. 265, 549–563.

Flatters, S. J., Fox, A. J., and Dickenson, A. H. 2002. Nerve injury induces plasticity that results in spinal inhibitory effects of galanin. Pain 98, 249–258.

Frampton, J. E. and Foster, R. H. 2005. Pregabalin: in the treatment of postherpetic neuralgia. Drugs 65, 111–118; discussion 119–120.

Fukuoka, T., Kondo, E., Dai, Y., Hashimoto, N., and Noguchi, K. 2001. Brain-derived neurotrophic factor increases in the uninjured dorsal root ganglion neurons in selective spinal nerve ligation model. J. Neurosci. 21, 4891–4900.

Fundytus, M. E., Osborne, M. G., Henry, J. L., Coderre, T. J., and Dray, A. 2002. Antisense oligonucleotide knockdown of mGluR1 alleviates hyperalgesia and allodynia associated with chronic inflammation. Pharmacol. Biochem. Behav. 73, 401–410.

Fundytus, M. E., Yashpal, K., Chabot, J. G., Osborne, M. G., Lefebvre, C. D., Dray, A., Henry, J. L., and Coderre, T. J. 2001. Knockdown of spinal metabotropic glutamate receptor 1 (mGluR(1)) alleviates pain and restores opioid efficacy after nerve injury in rats. Br. J. Pharmacol. 132, 354–367.

Galan, A. and Cervero, F. 2005. Painful stimuli induce in vivo phosphorylation and membrane mobilization of mouse spinal cord NKCC1 co-transporter. Neuroscience 133, 245–252.

Galan, A., Laird, J. M., and Cervero, F. 2004. *In vivo* recruitment by painful stimuli of AMPA receptor subunits to the plasma membrane of spinal cord neurons. Pain 112, 315–323.

Galan, A., Lopez-Garcia, J. A., Cervero, F., and Laird, J. M. 2002. Activation of spinal extracellular signaling-regulated kinase-1 and -2 by intraplantar carrageenan in rodents. Neurosci. Lett. 322, 37–40.

Gammon, C. M., Allen, A. C. C., and Morell, P. 1989. Bradykinin stimulates phosphoinositide hydrolysis and mobilization of arachidonic acid in dorsal root ganglion neurons. J. Neurochem. 53, 95–101.

Gamse, R. and Saria, A. 1986. Nociceptive behavior after intrathecal injections of substance P, neurokinin A and calcitonin gene-related peptide in mice. Neurosci. Lett. 70, 143–147.

Gandhi, R., Ryals, J. M., and Wright, D. E. 2004. Neurotrophin-3 reverses chronic mechanical hyperalgesia induced by intramuscular acid injection. J. Neurosci. 24, 9405–9413.

Gardell, L. R., Ibrahim, M., Wang, R., Wang, Z., Ossipov, M. H., Malan, T. P., Jr., Porreca, F., and Lai, J. 2004. Mouse strains that lack spinal dynorphin upregulation after peripheral nerve injury do not develop neuropathic pain. Neuroscience 123, 43–52.

Garrison, C. J., Dougherty, P. M., Kajander, K. C., and Carlton, S. M. 1991. Staining of glial fibrillary acidic protein (GFAP) in lumbar spinal cord increases following a sciatic nerve constriction injury. Brain Res. 565, 1–7.

Garry, E. M., Moss, A., Delaney, A., O'Neill, F., Blakemore, J., Bowen, J., Husi, H., Mitchell, R., Grant, S. G., and Fleetwood-Walker, S. M. 2003. Neuropathic sensitization of behavioral reflexes and spinal NMDA receptor/CaM kinase II interactions are disrupted in PSD-95 mutant mice. Curr. Biol. 13, 321–328.

Garthwaite, J., Charles, S. L., and Chess-Williams, R. 1988. Endothelium-derived relaxing factors released on activation of NMDA receptors suggests role as intracellular messenger in the brain. Nature 336, 385–388.

Gaudet, A. D., Williams, S. J., Hwi, L. P., and Ramer, M. S. 2004. Regulation of TRPV2 by axotomy in sympathetic, but not sensory neurons. Brain Res. 1017, 155–162.

Gerber, G. and Randic, M. 1989. Participation of excitatory amino acid receptors in the slow excitatory synaptic transmission in the rat spinal cord *in vitro*. Neurosci. Lett. 106, 220–228.

Gerber, G., kangrga, I., Ryu, P-D., Larew, J. S., and Randic, M. 1989. Multiple effect of phorbol esters in the rat spinal dorsal horn. J. Neurosci. 9, 3606–3617.

Gerber, G., Zhong, J., Youn, D., and Randic, M. 2000. Group II and group III metabotropic glutamate receptor agonists depress synoptic transmission in the rat spinal cord dorsal horn. Neuroscience 100, 393–406.

Gereau, R. W. and Conn, P. J. 1994. Potentiation of cAMP responses by metabotropic glutamate receptors depresses excitatory synaptic transmission by a kinase-independent mechanism. Neuron 12, 1121–1129.

al-Ghoul, W. M., Volsi, G. L., Weinberg, R. J., and Rustioni, A. 1993. Glutamate immunocytochemistry in the dorsal horn after injury or stimulation of the sciatic nerve of rats. Brain Res. Bull. 30, 453–459.

Gilchrist, H. D., Allard, B. L., and Simone, D. A. 1996. Enhanced withdrawal responses to heat and mechanical stimuli following interplantar injection of capsaicin in rats. Pain 67, 179–188.

Go, V. L. and Yaksh, T. L. 1987. Release of substance P from the cat spinal cord. J. Physiol. 391, 141–167.

Gold, M. S., Weinreich, D., Kim, C. S., Wang, R., Treanor, J., Porreca, F., and Lai, J. 2003. Redistribution of Na(V)1.8 in uninjured axons enables neuropathic pain. J. Neurosci. 23, 158–166.

Groth, R. and Aanonsen, L. 2002. Spinal brain-derived neurotrophic factor (BDNF) produces hyperalgesia in normal mice while antisense directed against either BDNF or trkB, prevent inflammation-induced hyperalgesia. Pain 100, 171–181.

Guenot, M., Bullier, J., Rospars, J. P., Lansky, P., Mertens, P., and Sindou, M. 2003. Single-unit analysis of the spinal dorsal horn in patients with neuropathic pain. J. Clin. Neurophysiol. 20, 143–150.

Guo, W., Zou, S., Guan, Y., Ikeda, T., Tal, M., Dubner, R., and Ren, K. 2002. Tyrosine phosphorylation of the NR2B subunit of the NMDA receptor in the spinal cord during the development and maintenance of inflammatory hyperalgesia. J. Neurosci. 22, 6208–6217.

Ha, S. O., Kim, J. K., Hong, H. S., Kim, D. S., and Cho, H. J. 2001. Expression of brain-derived neurotrophic factor in rat dorsal root ganglia, spinal cord and gracile nuclei in experimental models of neuropathic pain. Neuroscience 107, 301–309.

Hains, B. C., Klein, J. P., Saab, C. Y., Craner, M. J., Black, J. A., and Waxman, S. G. 2003. Upregulation of sodium channel Nav1.3 and functional involvement in neuronal hyperexcitability associated with central neuropathic pain after spinal cord injury. J. Neurosci. 23, 8881–8892.

Hains, B. C., Saab, C. Y., Klein, J. P., Craner, M. J., and Waxman, S. G. 2004. Altered sodium channel expression in second-order spinal sensory neurons contributes to pain after peripheral nerve injury. J. Neurosci. 24, 4832–4839.

Haley, J. E., Sullivan, A. F., and Dickenson, A. H. 1990. Evidence for spinal *N*-methyl-D-aspartate receptor involvement in prolonged chemical nociception in the rat. Brain Res. 518, 218–226.

Hama, A. T. 2003. Acute activation of the spinal cord metabotropic glutamate subtype-5 receptor leads to cold hypersensitivity in the rat. Neuropharmacology 44, 423–430.

Hardy, J. D. 1956. The nature of pain. J. Chronic. Dis. 4, 22–51.

Hardy, J. D., Wolff, H. G., and Goodell, H. 1950. Experimental evidence on the nature of cutaneous hyperalgesia. J. Clin. Invest. 29, 115–140.

Hashizume, H., DeLeo, J. A., Colburn, R. W., and Weinstein, J. N. 2000. Spinal glial activation and cytokine expression after lumbar root injury in the rat. Spine 25, 1206–1217.

Hedo, G., Laird, J. M., and Lopez-Garcia, J. A. 1999. Time-course of spinal sensitization following carrageenan-induced inflammation in the young rat: a comparative electrophysiological and behavioural study *in vitro* and *in vivo*. Neuroscience 92, 309–318.

Henken, D. B., Battisti, W. P., Chesselet, M. E., Murray, M., and Tessler, A. 1990. Expression of B-preprotachykinin mRNA and tachykinins in rat dorsal root ganglion cells following peripheral or central axotomy. Neuroscience 39, 733–742.

Henry, J. L. 1976. Effects of substance P on functionally identified units in cat spinal cord. Brain Res. 114, 439–451.

Herdegen, T., Leah, J. D., Manisali, A., Bravo, R., and Zimmermann, M. 1991a. c-JUN-like immunoreactivity in the CNS of the adult rat: basal and transynaptically induced expression of an immediate-early gene. Neuroscience 41, 643–654.

Herdegen, T., Tolle, T. R., Bravo, R., Zieglgansberger, W., and Zimmermann, M. 1991b. Sequential expression of JUN B, JUN D and FOS B proteins in rat spinal neurons: cascade of transcriptional operations during nociception. Neurosci. Lett. 129, 1–4.

Herdegen, T., Walker, T., Leah, J. D., Bravo, R., and Zimmermann, M. 1990. The KROX-24 protein, a new transcription regulating factor: expression in the rat central nervous system following afferent somatosensory stimulation. Neurosci. Lett. 120, 21–24.

Hofmann, H. A., Siegling, A., Denzer, D., Spreyer, P., and De Vry, J. 2001. Metabotropic glutamate mGluR1 receptor mRNA expression in dorsal root ganglia of rats after peripheral nerve injury. Eur. J. Pharmacol. 429, 135–138.

Hokfelt, T., Wiesenfeld-Hallin, X., Villar, M. J., and Melander, T. 1987. Increase of galanin-like immunoreactivity in rat dorsal root ganglion cells after peripheral axotomy. Neurosci. Lett. 83: 217–220.

Hollmann, M. and Heinemann, S. F. 1994. Cloned glutamate receptors. Annu. Rev. Neurosci. 17, 31–108.

Holthusen, H., Irsfeld, S., and Lipfert, P. 2000. Effect of pre- or post-traumatically applied i.v. lidocaine on primary and secondary hyperalgesia after experimental heat trauma in humans. Pain 88, 295–302.

Holtman, J. R., Jr. and Wala, E. P. 2005. Characterization of morphine-induced hyperalgesia in male and female rats. Pain 114, 62–70.

Hori, Y. and Endo, K. 1992. Miniature postsynaptic currents recorded from identified rat spinal dorsal horn projection neurons in thin-slice preparations. Neurosci. Lett. 142, 191–195.

Houamed, K. M., Kuijper, J. L., Gilbert, T. L., Haldeman, B. A., O'Hara, P. J., Mulvihill, E. R., Almers, W., and Hagen, F. S. 1991. Cloning, expression, and gene structure of a G

protein-coupled glutamate receptor from rat brain. Science 252, 1318–1321.
Hua, X. Y., Chen, P., Marsala, M., and Yaksh, T. L. 1999a. Intrathecal substance P-induced thermal hyperalgesia and spinal release of prostaglandin E2 and amino acids. Neuroscience 89, 525–534.
Hua, X. Y., Chen, P., and Yaksh, T. L. 1999b. Inhibition of spinal protein kinase C reduces nerve injury-induced tactile allodynia in neuropathic rats. Neurosci. Lett. 276, 99–102.
Hua, X. Y., Saria, A., Gamse, R., Theodorsson-Norheim, E., Brodin, E., and Lundberg, J. M. 1986. Capsaicin-induced released of multiple tachykinins (substance P, neurokinin A and eledoisin-like material) from guinea-pig spinal cord and ureter. Neuroscience 19, 313–319.
Hudson, L. J., Bevan, S., McNair, K., Gentry, C., Fox, A., Kuhn, R., and Winter, J. 2002. Metabotropic receptor 5 upregulation in A-fibers after spinal nerve injury: 2-methyl-6-(phenylethynyl)-pyridine (MPEP) reverses the induced thermal hyperalgesia. J. Neurosci. 22, 2660–2668.
Hudson, L. J., Bevan, S., Wotherspoon, G., Gentry, C., Fox, A., and Winter, J. 2001. VR1 protein expression increases in undamaged DRG neurons after partial nerve injury. Eur. J. Neurosci. 13, 2105–2114.
Hunt, S. P., Pini, A., and Evan, G. 1987. Induction of c-fos-like protein in spinal cord neurones following sensory stimulation. Nature 328, 632–634.
Hygge-Blakeman, K., Brumovsky, P., Hao, J. X., Xu, X. J., Hokfelt, T., Crawley, J. N., and Wiesenfeld-Hallin, Z. 2004. Galanin over-expression decreases the development of neuropathic pain-like behaviors in mice after partial sciatic nerve injury. Brain Res. 1025, 152–158.
Hylden, J. L. and Wilcox, G. L. 1981. Intrathecal substance P elicits a caudally-directed biting and scratching behavior in mice. Brain Res. 217, 212–215.
Hylden, J. L. K., Nahin, R. L., Traub, R. J., and Dubner, R. 1989. Expansion of receptive fields of spinal lamina 1 projection neurones in rats with unilateral adjuvant-induced inflammation: the contribution of dorsal horn mechanisms. Pain 37, 229–243.
Ibuki, T., Matsumura, K., Yamazaki, Y., Nozaki, T., Tanaka, Y., and Kobayashi, S. 2003. Cyclooxygenase-2 is induced in the endothelial cells throughout the central nervous system during carrageenan-induced hind paw inflammation; its possible role in hyperalgesia. J. Neurochem. 86, 318–328.
Igwe, O. J. and Ning, L. 1994. Regulation of the second-messenger systems in the rat spinal cord during prolonged peripheral inflammation. Pain 58, 63–75.
Ikeda, H. and Murase, K. 2004. Glial nitric oxide-mediated long-term presynaptic facilitation revealed by optical imaging in rat spinal dorsal horn. J. Neurosci. 24, 9888–9896.
Imbe, H., Okamoto, K., Kadoya, T., Horie, H., and Senba, E. 2003. Galectin-1 is involved in the potentiation of neuropathic pain in the dorsal horn. Brain Res. 993, 72–83.
Inoue, K. 2006. The function of microglia through purinergic receptors: neuropathic pain and cytokine release. Pharmacol. Ther. 109, 210–226.
Inoue, K., Koizumi, S., Tsuda, M., and Shigemoto-Mogami, Y. 2003. Signaling of ATP receptors in glia-neuron interaction and pain. Life Sci. 74, 189–197.
Jacobsen, L. S., Olsen, A. K., Sjogren, P., and Jensen, N. H. 1995. Morphine-induced hyperalgesia, allodynia and myoclonus – new side-effects of morphine? Vgeskr Laeger 157, 3307–3310.
Janig, W., Levine, J. D., and Michaelis, M. 1996. Interactions of sympathetic and primary afferent neurons following nerve injury and tissue trauma. Prog. Brain Res. 113, 161–184.
Jaskolski, F., Coussen, F., and Mulle, C. 2005. Subcellular localization and trafficking of kainite receptors. Trends Pharmacol. Sci. 26, 20–26.
Jessell, T., Tsunoo, A., Kanazawa, I., and Otsuka, M. 1979. Substance P: depletion in the dorsal horn of the rat spinal cord after section of the peripheral processes of primary sensory neurons. Brain Res. 168, 247–259.
Ji, R. R., Baba, H., Brenner, G. J., and Woolf, C. J. 1999. Nociceptive-specific activation of ERK in spinal neurons contributes to pain hypersensitivity. Nat. Neurosci. 2, 1114–1119.
Ji, R. R., Befort, K., Brenner, G. J., and Woolf, C. J. 2002a. ERK/MAP kinase activation in superficial spinal cord neurons induces prodynorphin and NK-1 upregulation and contributes to persistent inflammatory pain hypersensitivity. J. Neurosci. 22, 478–485.
Ji, R. R., Samad, T. A., Jin, S. X., Schmoll, R., and Woolf, C. J. 2002b. p38 MAPK activation by NGF in primary sensory neurons after inflammation increases TRPV1 levels and maintains heat hyperalgesia. Neuron 36, 57–68.
Jongsma, H., Danielsen, N., Sundler, F., and Kanje, M. 2000. Alteration of PACAP distribution and PACAP receptor binding in the rat sensory nervous system following sciatic nerve transection. Brain Res. 853, 186–196.
Joseph, E. K. and Levine, J. D. 2004. Caspase signalling in neuropathic and inflammatory pain in the rat. Eur. J. Neurosci. 20, 2896–2902.
Kajander, K. C., Madsen, A. M., Iadarola, M. J., Draisci, G., and Wakisaka, S. 1996. Fos-like immunoreactivity increases in the lumbar spinal cord following a chronic constriction injury to the sciatic nerve of rat. Neurosci. Lett. 206, 9–12.
Karim, F., Wang, C. C., and Gereau, R. W. 2001. Metabotropic glutamate receptor subtypes 1 and 5 are activators of extracellular signal-regulated kinase signaling required for inflammatory pain in mice. J. Neurosci. 21, 3771–3779.
Kawamata, M. and Omote, K. 1996. Involvement of increased excitatory amino acids and intracellular Ca^{2+} concentration in the spinal dorsal horn in an animal model of neuropathic pain. Pain 68, 85–96.
Kawamata, M., Watanabe, H., Nishikawa, K., Takahashi, T., Kozuka, Y., Kawamata, T., Omote, K., and Namiki, A. 2002a. Different mechanisms of development and maintenance of experimental incision-induced hyperalgesia in human skin. Anesthesiology 97, 550–559.
Kawamata, M., Takahashi, T., Kozuka, Y., Nawa, Y., Nishikawa, K., Narimatsa, E., Watanabe, H., and Namiki, A. 2002b. Experimental incision-induced pain in human skin: effects of systemic lidocaine on flare formation and hyperalgesia. Pain 100, 77–89.
Kawasaki, Y., Kohno, T., Zhuang, Z. Y., Brenner, G. J., Wang, H., Van Der Meer, C., Befort, K., Woolf, C. J., and Ji, R. R. 2004. Ionotropic and metabotropic receptors, protein kinase A, protein kinase C, and Src contribute to C-fiber-induced ERK activation and cAMP response element-binding protein phosphorylation in dorsal horn neurons, leading to central sensitization. J. Neurosci. 24, 8310–8321.
Kayan, S., Woods, L. A., and Mitchell, C. L. 1971. Morphine-induced hyperalgesia in rats tested on the hot plate. J. Pharmacol. Exp. Ther. 177, 509–513.
Kelly, S. and Chapman, V. 2002. Effects of peripheral nerve injury on functional spinal VR1 receptors. Neuroreport 13, 1147–1150.
Kennedy, M. B., McGuinness, T., and Greengard, P. 1983. A calcium/calmodulin-dependent protein kinase from mammalian brain that phosphorylates Synapsin I: partial purification and characterization. J. Neurosci. 3, 818–831.
Kenshalo, D. R. Jr., Leonard, R. B., Chung, J. M., and Willis, W. D. 1979. Responses of primate spinothalamic neurons to graded and to repeated noxious heat stimuli. J. Neurophysiol. 42, 1370–1389.
Kenshalo, D. R., Jr., Leonard, R. B., Chung, J. M., and Willis, W. D. 1982. Facilitation of the responses of primate

spinothalamic cells to cold and mechanical stimuli by noxious heating of the skin. Pain 12, 141–152.
Kerchner, G. A., Li, P., and Zhuo, M. 1999. Speaking out of turn: a role for silent synapses in pain. IUBMB Life 48, 251–256.
Kerr, B. J., Bradbury, E. J., Bennett, D. L., Trivedi, P. M., Dassan, P., French, J., Shelton, D. B., McMahon, S. B., and Thompson, S. W. 1999. Brain-derived neurotrophic factor modulates nociceptive sensory inputs and NMDA-evoked responses in the rat spinal cord. J. Neurosci. 19, 5138–5148.
Kerr, B. J., Cafferty, W. B., Gupta, Y. K., Bacon, A., Wynick, D., McMahon, S. B., and Thompson, S. W. 2000. Galanin knockout mice reveal nociceptive deficits following peripheral nerve injury. Eur. J. Neurosci. 12, 793–802.
Kerr, B. J., Gupta, Y., Pope, R., Thompson, S. W., Wynick, D., and McMahon, S. B. 2001a. Endogenous galanin potentiates spinal nociceptive processing following inflammation. Pain 93, 267–277.
Kerr, B. J., Thompson, S. W., Wynick, D., and McMahon, S. B. 2001b. Endogenous galanin is required for the full expression of central sensitization following peripheral nerve injury. Neuroreport 12, 3331–3334.
Khasabov, S. G., Rogers, S. D., Ghilardi, J. R., Peters, C. M., Mantyh, P. W., and Simone, D. A. 2002. Spinal neurons that possess the substance P receptor are required for the development of central sensitization. J. Neurosci. 22, 9086–9098.
Khasar, S. G., Gold, M. S., and Levine, J. D. 1998. A tetrodotoxin-resistant sodium current mediates inflammatory pain in the rat. Neurosci. Lett. 256, 17–20.
Kim, S. H. and Chung, J. M. 1992. An experimental model for peripheral neuropathy produced by segmental spinal nerve ligation in the rat. Pain 50, 355–363.
Kim, H. J., Back, S. K., Kim, J., Sung, B., Hong, S. K., and Na, H. S. 2003. Increases in spinal vasoactive intestinal polypeptide and neuropeptide Y are not sufficient for the genesis of neuropathic pain in rats. Neurosci. Lett. 342, 109–113.
Kim, S. Y., Bae, J. C., Kim, J. Y., Lee, H. L., Lee, K. M., Kim, D. S., and Cho, H. J. 2002. Activation of p38 MAP kinase in the rat dorsal root ganglia and spinal cord following peripheral inflammation and nerve injury. Neuroreport 13, 2483–2486.
Kim, D. S., Yoon, C. H., Lee, S. J., Park, S. Y., Yoo, H. J., and Cho, H. J. 2001. Changes in voltage-gated calcium channel alpha(1) gene expression in rat dorsal root ganglia following peripheral nerve injury. Brain. Res. Mol. Brain Res. 96, 151–156.
Knyihar-Csillik, E., Rakic, P., and Csillik, B. 1987. Transganglionic degenerative atrophy in the substantia gelatinosa of the spinal cord after peripheral nerve transection in rhesus monkeys. Cell Tissue Res. 247, 599–604.
Kocher, L., Anton, F., Reeh, P. W., and Handwerker, H. O. 1987. The effect of carrageenan-induced inflammation on the sensitivity of unmyelinated skin nociceptors in the rat. Pain 29, 363–373.
Kohno, T., Ji, R. R., Ito, N., Allchorne, A. J., Befort, K., Karchewski, L. A., and Woolf, C. J. 2005. Peripheral axonal injury results in reduced mu opioid receptor pre- and post-synaptic action in the spinal cord. Pain 117, 77–87.
Kohno, T., Moore, K. A., Baba, H., and Woolf, C. J. 2003. Peripheral nerve injury alters excitatory synaptic transmission in lamina II of the rat dorsal horn. J. Physiol. 548, 131–138.
Kolhekar, R. and Gebhart, G. F. 1994. NMDA and quisqualate modulation of visceral nociception in the rat. Brain Res. 651, 215–226.
Koltzenburg, M., Wall, P. D., and McMahon, S. B. 1999. Does the right side know what the left is doing? Trends Neurosci. 22, 122–127.
Komori, K., Nonaka, T., Okada, A., Kinoh, H., Hayashita-Kinoh, H., Yoshida, N., Yana, I., and Seiki, M. 2004. Absence of mechanical allodynia and Abeta-fiber sprouting after sciatic nerve injury in mice lacking membrane-type 5 matrix metalloproteinase. FEBS Lett. 557, 125–128.
Kontinen, V. K. and Dickenson, A. H. 2000. Effects of midazolam in the spinal nerve ligation model of neuropathic pain in rats. Pain 85, 425–431.
Kosai, K., Tateyama, S., Ikeda, T., Uno, T., Nishimori, T., and Takasaki, M. 2001. MK-801 reduces non-noxious stimulus-evoked Fos-like immunoreactivity in the spinal cord of rats with chronic constriction nerve injury. Brain Res. 910, 12–18.
Kovacs, G., Kocsis, P., Tarnow, J., Horvath, C., Szombathelyi, Z., and Farisas, S 2004. NR2B containing NMDA receptor dependent windup of single spinal neurons. Neuropharmacology 46, 23–30.
Krieger, P. and El Manira, A. 2002. Group II mGluR-mediated depression of sensory synaptic transmission. Brain Res. 937, 41–44.
Kristensen, J. D., Svensson, B., and Gordh, T., Jr. 1992. The NMDA-receptor antagonist CPP abolishes neurogenic 'wind-up pain' after intrathecal administration in humans. Pain 51, 249–253.
Kunz, S., Niederberger, E., Ehnert, C., Coste, O., Pfenninger, A., Kruip, J., Wendrich, T. M., Schmidtko, A., Tegeder, I., and Geisslinger, G. 2004. The calpain inhibitor MDL 28170 prevents inflammation-induced neurofilament light chain breakdown in the spinal cord and reduces thermal hyperalgesia. Pain 110, 409–418.
Kuraishi, Y., Hirota, N., Sato, Y., Hanashima, N., Takagi, H., and Satoh, M. 1989. Stimulus specificity of peripherally evoked substance P release from the rabbit dorsal horn *in situ*. Neuroscience 30, 241–250.
Kuraishi, Y., Hirota, N., Sato, Y., Hino, Y., Satoh, M., and Takagi, H. 1985. Evidence that substance P and somatostatin transmit separate information related to pain in the spinal dorsal horn. Brain Res. 325, 294–298.
Lai, J., Gold, M. S., Kim, C. S., Bian, D., Ossipov, M. H., Hunter, J. C., and Porreca, F. 2002. Inhibition of neuropathic pain by decreased expression of the tetrodotoxin-resistant sodium channel, NaV1.8. Pain 95, 143–152.
Laird, J. M. and Bennett, G. J. 1993. An electrophysiological study of dorsal horn neurons in the spinal cord of rats with an experimental peripheral neuropathy. J. Neurophysiol. 69, 2072–2085.
Laird, J. M., Garcia-Nicas, E., Delpire, E. J., and Cervero, F. 2004. Presynaptic inhibition and spinal pain processing in mice: a possible role of the NKCC1 cation-chloride co-transporter in hyperalgesia. Neurosci. Lett. 361, 200–203.
Lam, H. H., Hanley, D. F., Trapp, B. D., Saito, S., Raja, S., Dawson, T. M., and Yamaguchi, H. 1996. Induction of spinal cord neuronal nitric oxide synthase (NOS) after formalin injection in the rat hind paw. Neurosci. Lett. 210, 201–204.
LaMotte, R. H., Lundberg, L. E. R., and Torebjörk, H. E. 1992. Pain, hyperalgesia and activity in nociceptive C units in humans after intradermal injection of capsaicin. J. Physiol. 448, 749–764.
LaMotte, R. H., Shain, C. N., Simone, D. A., and Tsai, E. F. 1991. Neurogenic hyperalgesia: psychophysical studies of underlying mechanisms. J. Neurophysiol. 66, 190–211.
Lan, J. Y., Skeberdis, V. A., Jover, T., Grooms, S. Y., Lin, Y., Araneda, R. C., Zheng, X., Bennett, M. V., and Zukin, R. S. 2001. Protein kinase C modulates NMDA receptor trafficking and gating. Nat. Neurosci. 4, 382–390.
Ledeboer, A., Sloane, E. M., Milligan, E. D., Frank, M. G., Mahony, J. H., Maier, S. F., and Watkins, L. R. 2005. Minocycline attenuates mechanical allodynia and proinflammatory cytokine expression in rat models of pain facilitation. Pain 115, 71–83.

Lee, B. H., Yoon, Y. W., Chung, K., and Chung, J. M. 1998. Comparison of sympathetic sprouting in sensory ganglia in three animal models of neuropathic pain. Exp. Brain Res. 120, 432–438.

Leem, J. W., Choi, E. J., Park, E. S., and Paik, K. S. 1996. *N*-methyl-D-aspartate (NMDA) and non-NMDA glutamate receptor antagonists differentially suppress dorsal horn neuron responses to mechanical stimuli in rats with peripheral nerve injury. Neurosci. Lett. 211, 37–40.

Lekan, H. A., Chung, K., Yoon, Y. W., Chung, J. M., and Coggeshall, R. E. 1997. Loss of dorsal root ganglion cells concomitant with dorsal root axon sprouting following segmental nerve lesions. Neuroscience 81, 527–534.

Li, C. Y., Song, Y. H., Higuera, E. S., and Luo, Z. D. 2004. Spinal dorsal horn calcium channel alpha2delta-1 subunit upregulation contributes to peripheral nerve injury-induced tactile allodynia. J. Neurosci. 24, 8494–8499.

Li, J., Simone, D. A., and Larson, A. A. 1999. Windup leads to characteristics of central sensitization. Pain 79, 75–82.

Li, K. C. and Chen, J. 2003. Differential roles of spinal protein kinases C and A in development of primary heat and mechanical hypersensitivity induced by subcutaneous bee venom chemical injury in the rat. Neurosignals 12, 292–301.

Liao, D., Hessler, N. A., and Malinow, R. 1995. Activation of postsynaptically silent synapses during pairing-induced LTP in CA1 region of hippocampal slice. Nature 375, 400–404.

Liao, G. Y., Wagner, D. A., Hsu, M. H., and Leonard, J. P. 2001. Evidence for direct protein kinase-C mediated modulation of *N*-methyl-D-aspartate receptor current. Mol. Pharmacol. 59, 960–964.

Liaw, W. J., Stephens, R. L. Jr., Binns, B. C., Chu, Y., Sepkuty, J. P., Johns, R. A., Rothstein, J. D., and Tao, Y. X. 2005. Spinal glutamate uptake is critical for maintaining normal sensory transmission in rat spinal cord. Pain 115, 60–70.

Lim, G., Sung, B., Ji, R. R., and Mao, J. 2003. Upregulation of spinal cannabinoid-1-receptors following nerve injury enhances the effects of Win 55,212-2 on neuropathic pain behaviors in rats. Pain 105, 275–283.

Lim, G., Wang, S., and Mao, J. 2005. cAMP and protein kinase A contribute to the downregulation of spinal glutamate transporters after chronic morphine. Neurosci. Lett. 376, 9–13.

Lin, Q., Wu, J., and Willis, W. D. 2002. Effects of protein kinase a activation on the responses of primate spinothalamic tract neurons to mechanical stimuli. J. Neurophysiol. 88, 214–221.

Lindia, J. A., McGowan, E., Jochnowitz, N., and Abbadie, C. 2005. Induction of CX3CL1 expression in astrocytes and CX3CR1 in microglia in the spinal cord of a rat model of neuropathic pain. J. Pain 6, 434–438.

Liu, X. G. and Sandkuhler, J. 1995. Long-term potentiation of C-fiber-evoked potentials in the rat spinal dorsal horn is prevented by spinal *N*-methyl-D-aspartic acid receptor blockage. Neurosci. Lett. 191, 43–46.

Liu, X. and Sandkuhler, J. 1997. Characterization of long-term potentiation of C-fiber-evoked potentials in spinal dorsal horn of adult rat: essential role of NK1 and NK2 receptors. J. Neurophysiol. 78, 1973–1982.

Liu, X., Chung, K., and Chung, J. M. 1999. Ectopic discharges and adrenergic sensitivity of sensory neurons after spinal nerve injury. Brain Res. 849, 244–247.

Lozier, A. P. and Kendig, J. J. 1995. Long-term potentiation in an isolated peripheral nerve–spinal cord preparation. J. Neurophysiol. 74, 1001–1009.

Lukacova, N., Cizkova, D., Krizanova, O., Pavel, J., Marsala, M., and Marsala, J. 2003. Peripheral axotomy affects nicotinamide adenine dinucleotide phosphate diaphorase and nitric oxide synthases in the spinal cord of the rabbit. J. Neurosci. Res. 71, 300–313.

Luo, Z. D., Calcutt, N. A., Higuera, E. S., Valder, C. R., Song, Y. H., Svensson, C. I., and Myers, R. R. 2002. Injury type-specific calcium channel alpha 2 delta-1 subunit up-regulation in rat neuropathic pain models correlates with antiallodynic effects of gabapentin. J. Pharmacol. Exp. Ther. 303, 1199–1205.

Luo, Z. D., Chaplan, S. R., Higuera, E. S., Sorkin, L. S., Stauderman, K. A., Williams, M. E., and Yaksh, T. L. 2001. Upregulation of dorsal root ganglion (alpha)2(delta) calcium channel subunit and its correlation with allodynia in spinal nerve-injured rats. J. Neurosci. 21, 1868–1875.

Ma, Q. P. and Tian, L. 2001. A-fibres sprouting from lamina I into lamina II of spinal dorsal horn after peripheral nerve injury in rats. Brain Res. 904, 137–140.

Ma, Q. P. and Tian, L. 2002. Cholera toxin B subunit labeling in lamina II of spinal cord dorsal horn following chronic inflammation in rats. Neurosci. Lett. 327, 161–164.

Ma, W. and Quirion, R. 2001. Increased phosphorylation of cyclic AMP response element-binding protein (CREB) in the superficial dorsal horn neurons following partial sciatic nerve ligation. Pain 93, 295–301.

Ma, W. and Quirion, R. 2002. Partial sciatic nerve ligation induces increase in the phosphorylation of extracellular signal-regulated kinase (ERK) and c-Jun N-terminal kinase (JNK) in astrocytes in the lumbar spinal dorsal horn and the gracile nucleus. Pain 99, 175–184.

Ma, W., Du, W., and Eisenach, J. C. 2003a. Intrathecal lidocaine reverses tactile allodynia caused by nerve injuries and potentiates the antiallodynic effect of the COX inhibitor ketorolac. Anesthesiology 98, 203–208.

Ma, W., Hatzis, C., and Eisenach, J. C. 2003b. Intrathecal injection of cAMP response element binding protein (CREB) antisense oligonucleotide attenuates tactile allodynia caused by partial sciatic nerve ligation. Brain Res. 988, 97–104.

MacDermott, A. B., Mayer, M. L., Westbrook, G. L., Smith, S. J., and Barker, J. L. 1986. NMDA-receptor activation increases cytoplasmic calcium concentration in cultured spinal cord neurons. Nature 321, 519–522.

Madiai, F., Hussain, S. R., Goettl, V. M., Burry, R. W., Stephens, R. L., Jr., and Hackshaw, K. V. 2003. Upregulation of FGF-2 in reactive spinal cord astrocytes following unilateral lumbar spinal nerve ligation. Exp. Brain Res. 148, 366–376.

Maione, S., Siniscalco, D., Galderisi, U., de Novellis, V., Uliano, R., Di Bernardo, G., Berrino, L., Cascino, A., and Rossi, F. 2002. Apoptotic genes expression in the lumbar dorsal horn in a model neuropathic pain in rat. Neuroreport 13, 101–106.

Malan, T. P., Ossipov, M. H., Gardell, L. R., Ibrahim, M., Bian, D., Lai, J., and Porreca, F. 2000. Extraterritorial neuropathic pain correlates with multisegmental elevation of spinal dynorphin in nerve-injured rats. Pain 86, 185–194.

Malinow, R. and Malenka, R. C. 2002. AMPA receptor trafficking and synaptic plasticity. Annu. Rev. Neurosci. 25, 103–126.

Malmberg, A. B. and Yaksh, T. L. 1992a. Antinociceptive actions of spinal nonsteroidal anti-inflammatory agents on the formalin test in the rat. J. Pharmacol. Exp. Ther. 263, 136–146.

Malmberg, A. B. and Yaksh, T. L. 1992b. Hyperalgesia mediated by spinal glutamate or substance P receptor blocked by spinal cyclooxygenase inhibition. Science 257, 1276–1279.

Malmberg, A. B., Brandon, E. P., Idzerda, R. L., Liu, H., McKnight, G. S., and Basbaum, A. I. 1997a. Diminished inflammation and nociceptive pain with preservation of neuropathic pain in mice with a targeted mutation of the type I regulatory subunit of cAMP-dependent protein kinase. J. Neurosci. 17, 7462–7470.

Malmberg, A. B., Chen, C., Tonegawa, S., and Basbaum, A. I. 1997b. Preserved acute pain and reduced neuropathic pain in mice lacking PKCgamma. Science 278, 279–283.

Mannion, R. J., Doubell, T. P., Coggeshall, R. E., and Woolf, C. J. 1996. Collateral sprouting of uninjured primary afferent A-fibers into the superficial dorsal horn of the adult rat spinal cord after topical capsaicin treatment to the sciatic nerve. J. Neurosci. 16, 5189–5195.

Mantyh, P. W., Pinnock, R. D., Downes, C. P., Goedert, M., and Hunt, S. P. 1984. Correlation between inositol phospholipid hydrolysis and substance P receptors in rat CNS. Nature 309, 795–797.

Mao, J. and Mayer, D. J. 2001. Spinal cord neuroplasticity following repeated opioid exposure and its relation to pathological pain. Ann. N. Y. Acad. Sci. 933, 175–184.

Mao, J., Price, D. D., Coghill, R. C., Mayer, D. J., and Hayes, R. L. 1992a. Spatial patterns of spinal cord [^{14}C]-2-deoxyglucose metabolic activity in a rat model of painful peripheral mononeuropathy. Pain 50, 89–100. Erratum in: Pain 1992 51, 389.

Mao, J., Price, D. D., and Mayer, D. J. 1995a. Mechanisms of hyperalgesia and morphine tolerance: a current view of their possible interactions. Pain 62, 259–274.

Mao, J., Price, D. D., Mayer, D. J., and Hayes, R. L. 1992b. Pain-related increases in spinal cord membrane-bound protein kinase C following peripheral nerve injury. Brain Res. 588, 144–149.

Mao, J., Price, D. D., Mayer, D. J., Lu, J., and Hayes, R. L. 1992c. Intrathecal MK-801 and local nerve anesthesia synergistically reduce nociceptive behaviours in rats with experimental peripheral mononeuropathy. Brain Res. 576, 254–262.

Mao, J., Price, D. D., Phillips, L. L., Lu, J., and Mayer, D. J. 1995b. Increases in protein kinase C gamma immunoreactivity in the spinal cord dorsal horn of rats with painful mononeuropathy. Neurosci. Lett. 198, 75–78.

Mao, J., Price, D. D., Zhu, J., Lu, J., and Mayer, D. J. 1997. The inhibition of nitric oxide-activated poly(ADP-ribose) synthetase attenuates transsynaptic alteration of spinal cord dorsal horn neurons and neuropathic pain in the rat. Pain 72, 355–366.

Mao, J., Sung, B., Ji, R. R., and Lim, G. 2002a. Chronic morphine induces downregulation of spinal glutamate transporters: implications in morphine tolerance and abnormal pain sensitivity. J. Neurosci. 22, 8312–8323.

Mao, J., Sung, B., Ji, R. R., and Lim, G. 2002b. Neuronal apoptosis associated with morphine tolerance: evidence for an opioid-induced neurotoxic mechanism. J. Neurosci. 22, 7650–7661.

Mark, M. A., Colvin, L. A., and Duggan, A. W. 1998. Spontaneous release of immunoreactive neuropeptide Y from the central terminals of large diameter primary afferents of rats with peripheral nerve injury. Neuroscience 83, 581–589.

Martin, W. J., Cao, Y., and Basbaum, A. I. 2004. Characterization of wide dynamic range neurons in the deep dorsal horn of the spinal cord in preprotachykinin-a null mice *in vivo*. J. Neurophysiol. 91, 1945–1954.

Masu, M., Tanabe, Y., Tsuchida, K., Shigemoto, R., and Nakanishi, S. 1991. Sequence and expression of a metabotropic glutamate receptor. Nature 349, 760–765.

Matthews, E. A. and Dickenson, A. H. 2001. Effects of spinally delivered N- and P-type voltage-dependent calcium channel antagonists on dorsal horn neuronal responses in a rat model of neuropathy. Pain 92, 235–246.

Maurset, A., Skoglund, L. A., Hustveit, O., and Oye, I. 1989. Comparison of ketamine and pethidine in experimental and postoperative pain. Pain 36, 37–41.

Mayer, D. J., Mao, J., Holt, J., and Price, D. D. 1999. Cellular mechanisms of neuropathic pain, morphine tolerance, and their interactions. Proc. Natl. Acad. Sci. U. S. A. 96, 7731–7736.

McCall, W. D., Tanner, K. D., and Levine, J. D. 1996. Formalin induces biphasic activity in C-fibers in the rat. Neurosci. Lett. 208, 45–48.

McGraw, J., Gaudet, A. D., Oschipok, L. W., Kadoya, T., Horie, H., Steeves, J. D., Tetzlaff, W., and Ramer, M. S. 2005. Regulation of neuronal and glial galectin-1 expression by peripheral and central axotomy of rat primary afferent neurons. Exp. Neurol. 195, 103–114.

McLachlan, E. M., Janig, W., Devor, M., and Michaelis, M. 1993. Peripheral nerve injury triggers noradrenergic sprouting within dorsal root ganglia. Nature 363, 543–546.

McMahon, S. B. and Wall, P. D. 1984. Receptive fields of rat lamina 1 projection cells move to incorporate a nearby region of injury. Pain 19, 235–247.

McMahon, S. B., Armanini, M. P., Ling, L. H., and Phillips, H. S. 1994. Expression and coexpression of Trk receptors in subpopulations of adult primary sensory neurons projecting to identified peripheral targets. Neuron 12, 1161–1171.

Meller, S. T., Cummings, C. P., Traub, R. J., and Gebhart, G. F. 1994. The role of nitric oxide in the development and maintenance of the hyperalgesia produced by intraplanter injection of carrageenan in the rat. Neuroscience 60, 367–374.

Meller, S. T., Pechman, P. S., Gebhart, G. F., and Maues, T. J. 1992. Nitric oxide mediates the thermal hyperalgesia produced in a model of neuropathic pain in the rat. Neuroscience 50, 7–10.

Mendell, L. M. 1966. Physiological properties of unmyelinated fiber projections to the spinal cord. Exp. Neurol. 16, 316–332.

Mendell, L. M. and Wall, P. D. 1965. Responses of single dorsal cord cells to peripheral cutaneous unmyelinated fibres. Nature 206, 97–99.

Menétrey, D. and Besson, J. M. 1982. Electrophysiological characteristics of dorsal horn cells in rats with cutaneous inflammation resulting from chronic arthritis. Pain 13, 343–364.

Menétrey, D., Gannon, A., Levine, J. D., and Basbaum, A. I. 1989. Expression of c-fos protein in interneurons and projection neurons of the rat spinal cord in response to noxious somatic, articular, and visceral stimulation. J. Comp. Neurol. 285, 177–195.

Meyer, R. A. and Campbell, J. N. 1981. Myelinated nociceptive afferents account for the hyperalgesia that follows a burn to the hand. Science 213, 1527–1529.

Michael, G. J., Averill, S., Nitkunan, A., Rattray, M., Bennett, D. L., Yan, Q., and Priestley, J. V. 1997. Nerve growth factor treatment increases brain-derived neurotrophic factor selectively in TrkA-expressing dorsal root ganglion cells and in their central terminations within the spinal cord. J. Neurosci. 17, 8476–8490.

Miletic, G. and Miletic, V. 2002. Increases in the concentration of brain derived neurotrophic factor in the lumbar spinal dorsal horn are associated with pain behavior following chronic constriction injury in rats. Neurosci. Lett. 319, 137–140.

Miletic, G., Hanson, E. N., Savagian, C. A., and Miletic, V. 2004b. Protein kinase A contributes to sciatic ligation-associated early activation of cyclic AMP response element binding protein in the rat spinal dorsal horn. Neurosci. Lett. 360, 149–152.

Miletic, G., Miyabe, T., Gebhardt, K. J., and Miletic, V. 2005. Increased levels of Homer1b/c and Shank1a in the post-synaptic density of spinal dorsal horn neurons are associated with neuropathic pain in rats. Neurosci. Lett. 386, 189–193.

Miletic, G., Pankratz, M. T., and Miletic, V. 2002. Increases in the phosphorylation of cyclic AMP response element binding protein (CREB) and decreases in the content of calcineurin accompany thermal hyperalgesia following chronic constriction injury in rats. Pain 99, 493–500.

Miletic, V., Bowen, K. K., and Miletic, G. 2000. Loose ligation of the rat sciatic nerve is accompanied by changes in the subcellular content of protein kinase C beta II and gamma in the spinal dorsal horn. Neurosci. Lett. 288, 199–202.

Mills, C. D., Johnson, K. M., and Hulsebosch, C. E. 2002. Role of group II and group III metabotropic glutamate receptors in spinal cord injury. Exp. Neurol. 173, 153–167.

Millan, M. J. 1999. The induction of pain: an integrative review. Prog. Neurobiol. 57, 1–164.

Milligan, E. D., Twining, C., Chacur, M., Biedenkapp, J., O'Connor, K., Poole, S., Tracey, K., Martin, D., Maier, S. F., and Watkins, L. R. 2003. Spinal glia and proinflammatory cytokines mediate mirror-image neuropathic pain in rats. J. Neurosci. 23, 1026–1040.

Milligan, E. D., Zapata, V., Chacur, M., Schoeniger, D., Biedenkapp, J., O'Connor, K. A., Verge, G. M., Chapman, G., Green, P., Foster, A. C., Naeve, G. S., Maier, S. F., and Watkins, L. R. 2004. Evidence that exogenous and endogenous fractalkine can induce spinal nociceptive facilitation in rats. Eur. J. Neurosci. 20, 2294–2302.

Milligan, E. D., Zapata, V., Schoeniger, D., Chacur, M., Green, P., Poole, S., Martin, D., Maier, S. F., and Watkins, L. R. 2005. An initial investigation of spinal mechanisms underlying pain enhancement induced by fractalkine, a neuronally released chemokine. Eur. J. Neurosci. 22, 2775–2782.

Mills, C. D., Fullwood, S. D., and Hulsebosch, C. E. 2001. Changes in metabotropic glutamate receptor expression following spinal cord injury. Exp. Neurol. 170, 244–257.

Mills, C. D., Xu, G. Y., Johnson, K. M., McAdoo, D. J., and Hulsebosch, C. E. 2000. AIDA reduces glutamate release and attenuates mechanical allodynia after spinal cord injury. Neuroreport 11, 3067–3070.

Minami, T., Nishihara, I., Uda, R., Ito, S., Hyodo, M., and Hayaishi, O. 1994a. Characterization of EP-receptor subtypes involved in allodynia and hyperalgesia induced by intrathecal administration of prostaglandin E2 to mice. Br. J. Pharmacol. 112, 735–740.

Minami, T., Uda, R., Horiguchi, S., Ito, S., Hyodo, M., and Hayaishi, O. 1994b. Allodynia evoked by intrathecal administration of prostaglandin E2 to conscious mice. Pain 57, 217–223.

Miyabe, T. and Miletic, V. 2005. Multiple kinase pathways mediate the early sciatic ligation-associated activation of CREB in the rat spinal dorsal horn. Neurosci. Lett. 381, 80–85.

Mizushima, T., Obata, K., Yamanaka, H., Dai, Y., Fukuoka, T., Tokunaga, A., Mashimo, T., and Noguchi, K. 2005. Activation of p38 MAPK in primary afferent neurons by noxious stimulation and its involvement in the development of thermal hyperalgesia. Pain 113, 51–60.

Moochhala, S. M. and Sawynok, J. 1984. Hyperalgesia produced by intrathecal substance P and related peptides: desensitization and cross desensitization. Br. J. Pharmacol. 82, 381–388.

Moore, K. A., Kohno, T., Karchewski, L. A., Scholz, J., Baba, H., and Woolf, C. J. 2002. Partial peripheral nerve injury promotes a selective loss of GABAergic inhibition in the superficial dorsal horn of the spinal cord. J. Neurosci. 22, 6724–6731.

Morton, C. R. and Hutchison, W. D. 1990. Release of sensory neuropeptides in the spinal cord: studies with calcitonin gene-related peptide and galanin. Neuroscience 31, 807–815.

Morton, C. R., Hutchison, W. D., and Hendry, I. A. 1988. Release of immunoreactive somatostatin in the spinal dorsal horn of the cat. Neuropeptides 12, 189–197.

Muller, F., Heinke, B., and Sandkuhler, J. 2003. Reduction of glycine receptor-mediated miniature inhibitory postsynaptic currents in rat spinal lamina I neurons after peripheral inflammation. Neuroscience 122, 799–805.

Munglani, R. and Hunt, S. P. 1995. Molecular biology of pain. Br. J. Anaesth. 75, 186–192.

Murase, K. and Randic, M. 1984. Actions of substance P on rat spinal dorsal horn neurones. J. Physiol. 346, 203–217.

Murase, K., Randic, M., Ryu, P. D., and Usui, S. 1987. Substance P and Cholecystokinin Octapeptide Modify a Slow Inward Calcium-Sensitive Current Relaxation in Rat Spinal Cord Dorsal Horn Neurones. In: Fine Afferent Nerve Fibers and Pain (*eds*. R. F. Schmidt, H. G. Schaible, and C. Vahle-Hinz), pp. 265–271. VCH Verlagsgesellschaft.

Murase, K., Ryu, P. D., and Randic, M. 1989. Tachykinins modulate multiple ionic conductances in voltage-clamped rat spinal dorsal horn neurons. J. Neurophysiol. 61, 854–865.

Murray, C. W., Cowan, A., and Larson, A. A. 1991. Neurokinin and NMDA antagonists (but not a kainic acid antagonist) are antinociceptive in the mouse formalin model. Pain 44, 179–185.

Nachemson, A. K. and Bennett, G. J. 1993. Does pain damage spinal cord neurons? Transsynaptic degeneration in rat following a surgical incision. Neurosci. Lett. 162, 78–80.

Nagy, G. G., Al-Ayyan, M., Andrew, D., Fukaya, M., Watanabe, M., and Todd, A. J. 2004. Widespread expression of the AMPA receptor GluR2 subunit at glutamatergic synapses in the rat spinal cord and phosphorylation of GluR1 in response to noxious stimulation revealed with an antigen-unmasking method. J. Neurosci. 24, 5766–5777.

Naisbitt, S., Kim, E., Tu, J. C., Xiao, B., Sala, C., Valtschanoff, J., Weinberg, R. J., Worley, P. F., and Sheng, M. 1999. Shank, a novel family of postsynaptic density proteins that binds to the NMDA receptor/PSD-95/GKAP complex and cortactin. Neuron 23, 569–582.

Nakamura, S. and Myers, R. R. 1999. Myelinated afferents sprout into lamina II of L3-5 dorsal horn following chronic constriction nerve injury in rats. Brain Res. 818, 285–290.

Nakanishi, S. 1992. Molecular diversity of glutamate receptors and implications for brain function. Science 258, 579–603.

Naranjo, J. R., Mellstrom, B., Carrion, A. M., Lucas, J. J., Foulkes, N. S., and Sassone-Corsi, P. 1997. Peripheral noxious stimulation induces CREM expression in dorsal horn: involvement of glutamate. Eur. J. Neurosci. 9, 2778–2783.

Narita, M., Kuzumaki, N., Suzuki, M., Narita, M., Oe, K., Yamazaki, M., Yajima, Y., and Suzuki, T. 2004. Increased phosphorylated-mu-opioid receptor immunoreactivity in the mouse spinal cord following sciatic nerve ligation. Neurosci. Lett. 354, 148–152.

Näsström, J., Karlsson, U., and Post, C. 1992. Antinociceptive actions of different classes of excitatory amino acid receptor antagonists in mice. Eur. J. Pharmacol. 212, 21–29.

Nebe, J., Vanegas, H., Neugebauer, V., and Schaible, H. G. 1997. Omega-agatoxin IVA, a P-type calcium channel antagonist, reduces nociceptive processing in spinal cord neurons with input from the inflamed but not from the normal knee joint – an electrophysiological study in the rat *in vivo*. Eur. J. Neurosci. 9, 2193–2201.

Neugebauer, V. and Schaible, H. G. 1988. Peripheral and spinal components of the sensitization of spinal neurons during an acute experimental arthritis. Agents Actions 25, 234–236.

Neugebauer, V. and Schaible, H. G. 1990. Evidence for a central component in the sensitization of spinal neurons with joint input during development of acute arthritis in cat's knee. J. Neurophysiol. 64, 299–311.

Neugebauer, V., Chen, P. S., and Willis, W. D. 1999. Role of metabotropic glutamate receptor subtype mGluR1 in brief nociception and central sensitization of primate STT cells. J. Neurophysiol. 82, 272–282.

Neugebauer, V., Chen, P. S., and Willis, W. D. 2000. Groups II and III metabotropic glutamate receptors differentially modulate brief and prolonged nociception in primate STT cells. J. Neurophysiol. 84, 2998–3009.

Neugebauer, V., Lucke, T., and Schaible, H. G. 1994. Requirement of metabotropic glutamate receptors for the generation of inflammation-evoked hyperexcitability in rat spinal cord neurons. Eur. J. Neurosci. 6, 1179–1186.

Neumann, S., Doubell, T. P., Leslie, T., and Woolf, C. J. 1996. Inflammatory pain hypersensitivity mediated by phenotypic switch in myelinated primary sensory neurons. Nature 384, 360–364.

Nielsch, V., Bisby, M. A., and Keen, P. 1987. Effect of cutting or crushing the rat sciatic nerve on synthesis of substance P by isolated L5 dorsal root ganglia. Neuropeptides 10, 137–145.

Noguchi, K., De Leon, M., Nahin, R. L., Senba, E., and Ruda, M. A. 1993. Quantification of axotomy-induced alteration of neuropeptide mRNAs in dorsal root ganglion neurons with special reference to neuropeptide Y mRNA and the effects of neonatal capsaicin treatment. J. Neurosci. Res. 35, 54–66.

Noguchi, K., Kawai, Y., Fukuoka, T., Senba, E., and Miki, K. 1995. Substance P induced by peripheral nerve injury in primary afferent sensory neurons and its effect on dorsal column nucleus neurons. J. Neurosci. 15, 7633–7643.

Noguchi, K., Senba, E., Morita, Y., Sato, M., and Tohyama, M. 1989. Prepro-VIP and preprotachykinin mRNAs in the rat dorsal root ganglion cells following peripheral axotomy. Mol. Brain Res. 6, 327–330.

Noguchi, K., Senba, E., Morita, Y., Sato, M., and Tohyama, M. 1990. Alpha-CGRP and beta-CGRP mRNAs are differentially regulated in the rat spinal cord and dorsal root ganglion. Mol. Brain Res. 7, 299–304.

Novakovic, S. D., Kassotakis, L. C., Oglesby, I. B., Smith, J. A., Eglen, R. M., Ford, A. P., and Hunter, J. C. 1999. Immunocytochemical localization of P2X3 purinoceptors in sensory neurons in naive rats and following neuropathic injury. Pain 80, 273–282.

Novakovic, S. D., Tzoumaka, E., McGivern, J. G., Haraguchi, M., Sangameswaran, L., Gogas, K. R., Eglen, R. M., and Hunter, J. C. 1998. Distribution of the tetrodotoxin-resistant sodium channel PN3 in rat sensory neurons in normal and neuropathic conditions. J. Neurosci. 18, 2174–2187.

de Novellis, V., Siniscalco, D., Galderisi, U., Fuccio, C., Nolano, M., Santoro, L., Cascino, A., Roth, K. A., Rossi, F., and Maione, S. 2004. Blockade of glutamate mGlu5 receptors in a rat model of neuropathic pain prevents early over-expression of pro-apoptotic genes and morphological changes in dorsal horn lamina II. Neuropharmacology 46, 468–479.

Obata, K., Yamanaka, H., Dai, Y., Mizushima, T., Fukuoka, T., Tokunaga, A., and Noguchi, K. 2004a. Differential activation of MAPK in injured and uninjured DRG neurons following chronic constriction injury of the sciatic nerve in rats. Eur. J. Neurosci. 20, 2881–2895.

Obata, K., Yamanaka, H., Dai, Y., Tachibana, T., Fukuoka, T., Tokunaga, A., Yoshikawa, H., and Noguchi, K. 2003. Differential activation of extracellular signal-regulated protein kinase in primary afferent neurons regulates brain-derived neurotrophic factor expression after peripheral inflammation and nerve injury. J. Neurosci. 23, 4117–4126.

Obata, K., Yamanaka, H., Kobayashi, K., Dai, Y., Mizushima, T., Katsura, H., Fukuoka, T., Tokunaga, A., and Noguchi, K. 2004b. Role of mitogen-activated protein kinase activation in injured and intact primary afferent neurons for mechanical and heat hypersensitivity after spinal nerve ligation. J. Neurosci. 24, 10211–10222.

Ohtori, S., Takahashi, K., Chiba, T., Yamagata, M., Sameda, H., and Moriya, H. 2001. Phenotypic inflammation switch in rats shown by calcitonin gene-related peptide immunoreactive dorsal root ganglion neurons innervating the lumbar facet joints. Spine 26, 1009–1013.

Ohtori, S., Takahashi, K., and Moriya, H. 2002. Inflammatory pain mediated by a phenotypic switch in brain-derived neurotrophic factor-immunoreactive dorsal root ganglion neurons innervating the lumbar facet joints in rats. Neurosci. Lett. 323, 129–132.

Oku, R., Nanayama, T., and Sato, M. 1988. Calcitonin gene-related peptide modulates calcium mobilization in synaptosomes of rat spinal dorsal horn. Brain Res. 475, 356–360.

Oku, R., Satoh, M., and Takagi, H. 1987. Release of substance P from the spinal dorsal horn is enhanced in polyarthritic rats. Neurosci. Lett. 74, 315–319.

Okuse, K., Chaplan, S. R., McMahon, S. B., Luo, Z. D., Calcutt, N. A., Scott, B. P., Akopian, A. N., and Wood, J. N. 1997. Regulation of expression of the sensory neuron-specific sodium channel SNS in inflammatory and neuropathic pain. Mol. Cell Neurosci. 10, 196–207.

Oliveira, A. L., Risling, M., Deckner, M., Lindholm, T., Langone, F., and Cullheim, S. 1997. Neonatal sciatic nerve transection induces TUNEL labeling of neurons in the rat spinal cord and DRG. Neuroreport 8, 2837–2840.

Osborne, M. G. and Coderre, T. J. 1999. Effects of intrathecal administration of nitric oxide synthase inhibitors on carrageenan-induced thermal hyperalgesia. Br. J. Pharmacol. 126, 1840–1846.

Ossipov, M. H., Lopez, Y., Nichols, M. L., Bian, D., and Porreca, F. 1995. Inhibition by spinal morphine of the tail-flick response is attenuated in rats with nerve ligation injury. Neurosci. Lett. 199, 83–86.

Palecek, J., Paleckova, V., Dougherty, P. M., and Willis, W. D. 1994. The effect of trans-ACPD, a metabotropic excitatory amino acid receptor agonist, on the responses of primate spinothalamic tract neurons. Pain 56, 261–269.

Parra, M. C., Nguyen, T. N., Hurley, R. W., and Hammond, D. L. 2002. Persistent inflammatory nociception increases levels of dynorphin 1-17 in the spinal cord, but not in supraspinal nuclei involved in pain modulation. J. Pain 3, 330–336.

Pedersen, J. L. and Kehlet, H. 1998. Secondary hyperalgesia to heat stimuli after burn injury in man. Pain 76, 377–384.

Perl, E. R., Kumazawa, T., Lynn, B., and Kenins, P. 1976. Sensitization of high threshold receptors with unmyelinated (C) afferent fibers. Prog. Brain Res. 43, 263–277.

Pertovaara, A. 1998. A neuronal correlate of secondary hyperalgesia in the rat spinal dorsal horn is submodality selective and facilitated by supraspinal influence. Exp. Neurol. 149, 193–202.

Pezet, S., Malcangio, M., Lever, I. J., Perkinton, M. S., Thompson, S. W., Williams, R. J., and McMahon, S. B. 2002. Noxious stimulation induces Trk receptor and downstream ERK phosphorylation in spinal dorsal horn. Mol. Cell Neurosci. 21, 684–695.

Pin, J. P. and Duvoisin, R. 1995. The metabotropic glutamate receptors: structure and functions. Neuropharmacology 34, 1–26.

Pin, J. P., Waeber, C., Prezeau, L., Bockaert, J., and Heinemann, S. F. 1992. Alternative splicing generates metabotropic glutamate receptors inducing different patterns of calcium release in Xenopus oocytes. Proc. Natl. Acad. Sci. U. S. A. 89, 10331–10335.

Pitcher, G. M. and Henry, J. L. 2000. Cellular mechanisms of hyperalgesia and spontaneous pain in a spinalized rat model

of peripheral neuropathy: changes in myelinated afferent inputs implicated. Eur. J. Neurosci. 12, 2006–2020.

Plunkett, J. A., Yu, C. G., Easton, J. M., Bethea, J. R., and Yezierski, R. P. 2001. Effects of interleukin-10 (IL-10) on pain behavior and gene expression following excitotoxic spinal cord injury in the rat. Exp Neurol 168, 144–154.

Polgar, E., Hughes, D. I., Arham, A. Z., and Todd, A. J. 2005. Loss of neurons from laminas I-III of the spinal dorsal horn is not required for development of tactile allodynia in the spared nerve injury model of neuropathic pain. J. Neurosci. 25, 6658–6666.

Pollock, G., Pennypacker, K. R., Memet, S., Israel, A., and Saporta, S. 2005. Activation of NF-kappaB in the mouse spinal cord following sciatic nerve transection. Exp. Brain Res. 165, 470–477.

Polomano, R. C., Mannes, A. J., Clark, U. S., and Bennett, G. J. 2000. A painful peripheral neuropathy in the rat produced by the chemotherapeutic drug, paclitaxel. Pain 94, 293–304.

Ponting, C. P., Phillips, C., Davies, K. E., and Blake, D. J. 1997. PDZ domains: targeting signalling molecules to sub-membranous sites. Bioessays 19, 469–479.

Porreca, F., Lai, J., Bian, D., Wegert, S., Ossipov, M. H., Eglen, R. M., Kassotakis, L., Novakovic, S., Rabert, D. K., Sangameswaran, L., and Hunter, J. C. 1999. A comparison of the potential role of the tetrodotoxin-insensitive sodium channels, PN3/SNS and NaN/SNS2, in rat models of chronic pain. Proc. Natl. Acad. Sci. U. S. A. 96, 7640–7644. Erratum in: Proc. Natl. Acad. Sci. U. S. A. 96, 10548.

Presley, R. W., Menétrey, D., Levine, J. D., and Basbaum, A. I. 1990. Systemic morphine supresses noxious stimulus-evoked Fos protein-like immunoreactivity in the rat spinal cord. J. Neurosci. 10, 323–335.

Price, D. D., Hayes, R. L., Ruda, M., and Dubner, R. 1978. Spatial and temporal transformations of input to spinothalamic tract neurons and their relation to somatic sensations. J. Neurophysiol. 41, 933–946.

Price, T. J., Cervero, F., and de Koninck, Y. 2005. Role of cation-chloride-cotransporters (CCC) in pain and hyperalgesia. Curr. Top. Med. Chem. 5, 547–555.

Priest, B. T., Murphy, B. A., Lindia, J. A., Diaz, C., Abbadie, C., Ritter, A. M., Liberator, P., Iyer, L. M., Kash, S. F., Kohler, M. G., Kaczorowski, G. J., MacIntyre, D. E., and Martin, W. J. 2005. Contribution of the tetrodotoxin-resistant voltage-gated sodium channel NaV1.9 to sensory transmission and nociceptive behavior. Proc. Natl. Acad. Sci. U. S. A. 102, 9382–9387.

Raghavendra, V., Tanga, F. Y., and DeLeo, J. A. 2004. Complete Freund's adjuvant-induced peripheral inflammation evokes glial activation and proinflammatory cytokine expression in the CNS. Eur. J. Neurosci. 20, 467–473.

Raja, S. N., Campbell, J. N., and Meyer, R. A. 1984. Evidence for different mechanisms of primary and secondary hyperalgesia following heat injury to the glabrous skin. Brain 107, 1179–1188.

Ramer, M. S. and Bisby, M. A. 1997. Rapid sprouting of sympathetic axons in dorsal root ganglia of rats with a chronic constriction injury. Pain 70, 237–244.

Ramer, M. S., French, G. D., and Bisby, M. A. 1997. Wallerian degeneration is required for both neuropathic pain and sympathetic sprouting into the DRG. Pain 72, 71–78.

Ramer, M. S., Murphy, P. G., Richardson, P. M., and Bisby, M. A. 1998. Spinal nerve lesion-induced mechanoallodynia and adrenergic sprouting in sensory ganglia are attenuated in interleukin-6 knockout mice. Pain 78, 115–121.

Randic, M. and Miletic, V. 1977. Effect of substance P in cat dorsal horn neurones activated by noxious stimuli. Brain Res. 128, 164–169.

Randic, M., Jiang, M. C., and Cerne, R. 1993. Long-term potentiation and long-term depression of primary afferent neurotransmission in the rat spinal cord. J. Neurosci. 13, 5228–5241.

Ren, K., Hylden, J. L. K., Williams, G. M., Ruda, M. A., and Dubner, R. 1992. The effects of a non-competitive NMDA receptor antagonist, MK-801, on behavioral hyperalgesia and dorsal horn neuronal activity in rats with unilateral inflammation. Pain 50, 331–344.

Ro, L. S., Li, H. Y., Huang, K. F., and Chen, S. T. 2004. Territorial and extra-territorial distribution of Fos protein in the lumbar spinal dorsal horn neurons in rats with chronic constriction nerve injuries. Brain Res. 1004, 177–187.

Roche, K. W., Tu, J. C., Petralia, R. S., Xiao, B., Wenthold, R. J., and Worley, P. F. 1999. Homer 1b regulates the trafficking of group I metabotropic glutamate receptors. J. Biol. Chem. 274, 25953–25957.

Rohde, D. S., Detweiler, D. J., and Basbaum, A. I. 1996. Spinal cord mechanisms of opioid tolerance and dependence: fos-like immunoreactivity increases in subpopulations of spinal cord neurons during withdrawal. Neuroscience 72, 233–242.

Rygh, L. J., Svendsen, F., Hole, K., and Tjolsen, A. 1999. Natural noxious stimulation can induce long-term increase of spinal nociceptive responses. Pain 82, 305–310.

Ryu, P. D., Gerber, G., Murase, K., and Randic, M. 1988. Calcitonin gene related peptide enhances calcium current of rat dorsal root ganglion neurons and spinal excitatory synaptic transmission. Neurosci. Lett. 89, 305–312.

Saegusa, H., Kurihara, T., Zong, S., Kazuno, A., Matsuda, Y., Nonaka, T., Han, W., Toriyama, H., and Tanabe, T. 2001. Suppression of inflammatory and neuropathic pain symptoms in mice lacking the N-type Ca^{2+} channel. EMBO J. 20, 2349–2356.

Saegusa, H., Kurihara, T., Zong, S., Minowa, O., Kazuno, A., Han, W., Matsuda, Y., Yamanaka, H., Osanai, M., Noda, T., and Tanabe, T. 2000. Altered pain responses in mice lacking alpha 1E subunit of the voltage-dependent Ca^{2+} channel. Proc. Natl. Acad. Sci. U. S. A. 97, 6132–6137.

Saitoh, T., Ishida, M., and Shinozaki, H. 1998. Potentiation by DL-alpha-aminopimelate of the inhibitory action of a novel mGluR agonist (L-F2CCG-I) on monosynaptic excitation in the rat spinal cord. Br. J. Pharmacol. 123, 771–779.

Sammons, M. J., Raval, P., Davey, P. T., Rogers, D., Parsons, A. A., and Bingham, S. 2000. Carrageenan-induced thermal hyperalgesia in the mouse: role of nerve growth factor and the mitogen-activated protein kinase pathway. Brain Res. 876, 48–54.

Sang, C. N., Gracely, R. H., Max, M. B., and Bennett, G. J. 1996. Capsaicin-evoked mechanical allodynia and hyperalgesia cross nerve territories. Evidence for a central mechanism. Anesthesiology 85, 491–496.

Saria, A., Gamse, R., Petermann, J., Fischer, J. A., Theorodorsson-Norheim, E., and Lundeberg, J. M. 1986. Stimultaneous release of several tachykinins and calcitonin gene-related peptide from rat spinal cord. Neurosci. Lett. 63, 310–314.

Sato, E., Takano, Y., Kuno, Y., Takano, M., and Sato, I. 2003. Involvement of spinal tyrosine kinase in inflammatory and *N*-methyl-D-aspartate-induced hyperalgesia in rats. Eur. J. Pharmacol. 468, 191–198.

Schaible, H.-G., Grubb, B. D., Neugebauer, V., and Oppmann, M. 1991. The effects of NMDA antagonists on neuronal activity in cat spinal cord evoked by acute inflammation in the knee joint. Eur. J. Neurosci. 3, 981–991.

Schmidtko, A., Ruth, P., Geisslinger, G., and Tegeder, I. 2003. Inhibition of cyclic guanosine 5′-monophosphate-dependent protein kinase I (PKG-I) in lumbar spinal cord reduces formalin-induced hyperalgesia and PKG upregulation. Nitric Oxide 8, 89–94.

Schneider, S. P. and Perl, E. R. 1988. Comparison of primary afferent and glutamate excitation of neurons in the mammalian spinal dorsal horn. J. Neurosci. 8, 2062–2073.

Schoepp, D. D., Johnson, B. G., Salhoff, C. R., Valli, M. J., Desai, M. A., Burnett, J. P., Mayne, N. G., and Monn, J. A. 1995. Selective inhibition of forskolin-stimulated cyclic AMP formation in rat hippocampus by a novel mGluR agonist, 2R, 4R-4-amino-pyrrolidine-2,4- dicarboxylate. Neuropharmacology 34, 843–850.

Scholz, J., Broom, D. C., Youn, D. H., Mills, C. D., Kohno, T., Suter, M. R., Moore, K. A., Decosterd, I., Coggeshall, R. E., and Woolf, C. J. 2005. Blocking caspase activity prevents transsynaptic neuronal apoptosis and the loss of inhibition in lamina II of the dorsal horn after peripheral nerve injury. J. Neurosci. 25, 7317–7323.

Scott, J. D. 1991. Cyclic nucleotide-dependent protein kinases. Pharmacol. Ther. 50, 123–145.

Sekiguchi, Y., Kikuchi, S., Myers, R. R., and Campana, W. M. 2003. ISSLS prize winner: erythropoietin inhibits spinal neuronal apoptosis and pain following nerve root crush. Spine 28, 2577–2584.

Seltzer, Z., Cohn, S., Ginzburg, R., and Beilin, B. Z. 1991. Modulation of neuropathic pain behavior in rats by spinal disinhibition and NMDA receptor blockade of injury discharge. Pain 45, 69–75.

Seltzer, Z., Dubner, R., and Shir, Y. 1990. A novel behavioral model of neuropathic pain disorders produced in rats by partial sciatic nerve injury. Pain 43, 205–218.

Seybold, V. S., Hylden, J. K. L., and Wilcox, G. L. 1982. Intrathecal substance P and somatostatin in rats: behaviors indicative of sensation. Peptides 3, 49–54.

Seybold, V. S., Jia, Y. P., and Abrahams, L. G. 2003. Cyclo-oxygenase-2 contributes to central sensitization in rats with peripheral inflammation. Pain 105, 47–55.

Shehab, S. A. and Atkinson, M. E. 1986. Vasoactive intestinal polypeptide (VIP) increases in the spinal cord after peripheral axotomy of the sciatic nerve originate from primary afferent neurons. Brain Res. 372, 37–44.

Shehab, S. A., Spike, R. C., and Todd, A. J. 2003. Evidence against cholera toxin B subunit as a reliable tracer for sprouting of primary afferents following peripheral nerve injury. Brain Res. 964, 218–227.

Shen, J., Benedict Gomes, A., Gallagher, A., Stafford, K., and Yoburn, B. C. 2000. Role of cAMP-dependent protein kinase (PKA) in opioid agonist-induced mu-opioid receptor downregulation and tolerance in mice. Synapse 38, 322–327.

Sher, G. and Mitchell, D. 1990. *N*-methyl-D-aspartate receptors mediate responses of rat dorsal horn neurons to hindlimb ischemia. Brain Res. 522, 55–62.

Shigeri, Y., Seal, R. P., and Shimamoto, K. 2004. Molecular pharmacology of glutamate transporters, EAATs and VGLUTs. Brain Res. Brain Res. Rev. 45, 250–265.

Shortland, P. and Woolf, C. J. 1993. Chronic peripheral nerve section results in a rearrangement of the central axonal arborizations of axotomized A beta primary afferent neurons in the rat spinal cord. J. Comp. Neurol. 330, 65–82.

Shortland, P., Kinman, E., and Molander, C. 1997. Sprouting of A-fibre primary afferents into lamina II in two rat models of neuropathic pain. Eur. J. Pain 1, 215–227.

Siegan, J. B., Hama, A. T., and Sagen, J. 1996. Alterations in rat spinal cord cGMP by peripheral nerve injury and adrenal medullary transplantation. Neurosci. Lett. 215, 49–52.

Simmons, R. M. A., Webster, A. A., Kalra, A. B., and Iyenger, S. 2002. Group II mGluR receptor agonists are effective I persistent and neuropathic pain models in rats. Pharmacol. Biochem. Behav. 73, 419–427.

Simone, D. A., Baumann, T. K., Collins, J. G., and LaMotte, R. H. 1989. Sensitization of cat dorsal horn neurons to innocuous mechanical stimulation after intradermal injection of capsaicin. Brain Res. 486, 185–189.

Skeberdis, V. A., Lan, J., Opitz, T., Zheng, X., Bennett, M. V., and Zukin, R. S. 2001. mGluR1-mediated potentiation of NMDA receptors involves a rise in intracellular calcium and activation of protein kinase C. Neuropharmacology 40, 856–865.

Skilling, S. R., Smullin, D. H., and Larson, A. A. 1988. Extracellular amino acid concentrations in the dorsal spinal cord of freely moving rats following veratridine and nociceptive stimulation. J. Neurochem. 51, 127–132.

Sluka, K. A. 1998. Blockade of N- and P/Q-type calcium channels reduces the secondary heat hyperalgesia induced by acute inflammation. J. Pharmacol. Exp. Ther. 287, 232–237.

Sluka, K. A. and Westlund, K. N. 1993. Behavioral and immunohistochemical changes in an experimental arthritis model in rats. Pain 55, 367–377.

Sluka, K. A. and Willis, W. D. 1997. The effects of G-protein and protein kinase inhibitors on the behavioral responses of rats to intradermal injection of capsaicin. Pain 71, 165–178.

Sluka, K. A., Dougherty, P. M., Sorkin, L. S., Willis, W. D., and Westlund, K. N. 1992. Neural changes in acute arthritis in monkeys III. Changes in substance P, calcitonin gene-related peptide and glutamate in the dorsal horn of the spinal cord. Brain Res. Rev. 17, 29–38.

Smith, R. R., Martin-Schild, S., Kastin, A. J., and Zadina, J. E. 2001. Decreases in endomorphin-2-like immunoreactivity concomitant with chronic pain after nerve injury. Neuroscience 105, 773–778.

Soares, S., von Boxberg, Y., Lombard, M. C., Ravaille-Veron, M., Fischer, I., Eyer, J., and Nothias, F. 2002. Phosphorylated MAP1B is induced in central sprouting of primary afferents in response to peripheral injury but not in response to rhizotomy. Eur. J. Neurosci. 16, 593–606.

Sokal, D. M. and Chapman, V. 2003. Effects of spinal administration of muscimol on C- and A-fibre evoked neuronal responses of spinal dorsal horn neurones in control and nerve injured rats. Brain Res. 962, 213–220.

Somers, D. L. and Clemente, F. R. 2002. Dorsal horn synaptosomal content of aspartate, glutamate, glycine and GABA are differentially altered following chronic constriction injury to the rat sciatic nerve. Neurosci. Lett. 323, 171–174.

Sorkin, L. S., Westlund, K. N., Sluka, K. A., Dougherty, P. M., and Willis, W. D. 1992. Neural changes in acute arthritis in monkeys. IV. Time course of amino acid release into the lumbar dorsal horn. Brain Res. Rev. 17, 39–50.

Sotgiu, M. L., Bellomi, P., and Biella, G. E. 2003. The mGluR5 selective antagonist 6-methyl-2-(phenylethynyl)-pyridine reduces the spinal neuron pain-related activity in mononeuropathic rats. Neurosci. Lett. 342, 85–88.

Sotgiu, M. L., Biella, G., and Riva, L. 1995. Poststimulus afterdischarges of spinal WDR and NS units in rats with chronic nerve constriction. Neuroreport 6, 1021–1024.

Sotgiu, M. L., Lacerenza, M., and Marchettini, P. 1992. Effect of systemic lidocaine on dorsal horn neuron hyperactivity following chronic peripheral nerve injury in rats. Somatosens. Mot. Res. 9, 227–233.

Southam, E., East, S. J., and Garthwaite, J. 1991. Excitatory amino acid receptors coupled to the nitric oxide: cyclic GMP pathway in rat cerebellum during development. J. Neurochem. 56, 2072–2081.

Stiller, C. O., Cui, J. G., O'Connor, W. T., Brodin, E., Meyerson, B. A., and Linderoth, B. 1996. Release of gamma-aminobutyric acid in the dorsal horn and suppression of tactile allodynia by spinal cord stimulation in mononeuropathic rats. Neurosurgery 39, 367–374.

Steel, J. H., Terenghi, G., Chung, J. M., Na, H. S., Carlton, S. M., and Polak, J. M. 1994. Increased nitric oxide synthase immunoreactivity in rat dorsal root ganglia in a neuropathic pain model. Neurosci. Lett. 169, 81–84.

Sugimoto, T., Bennett, G. J., and Kajander, K. C. 1990. Transsynaptic degeneration in the superficial dorsal horn after sciatic nerve injury: effects of a chronic constriction injury, transection, and strychnine. Pain 42, 205–213.

Sugiyama, H., Ito, I., and Hirono, C. 1987. A new type of glutamate receptor linked to inositol phospholipid metabolism. Nature 325, 531–533.

Sun, X. and Larson, A. A. 1991. Behavioral sensitization to kainic acid and quisqualic acid in mice: comparison to NMDA and substance P responses. J. Neurosci. 11, 3111–3123.

Sun, H., Ren, K., Zhong, C. M., Ossipov, M. H., Malan, T. P., Lai, J., and Porreca, F. 2001. Nerve injury-induced tactile allodynia is mediated via ascending spinal dorsal column projections. Pain 90, 105–111.

Sung, B., Lim, G., and Mao, J. 2003. Altered expression and uptake activity of spinal glutamate transporters after nerve injury contribute to the pathogenesis of neuropathic pain in rats. J. Neurosci. 23, 2899–2910.

Suzuki, R. and Dickenson, A. H. 2006. Differential pharmacological modulation of the spontaneous stimulus-independent activity in the rat spinal cord following peripheral nerve injury. Exp. Neurol. 198, 72–80.

Suzuki, R., Chapman, V., and Dickenson, A. H. 1999. The effectiveness of spinal and systemic morphine on rat dorsal horn neuronal responses in the spinal nerve ligation model of neuropathic pain. Pain 80, 215–228.

Suzuki, R., Matthews, E. A., and Dickenson, A. H. 2001. Comparison of the effects of MK-801, ketamine and memantine on responses of spinal dorsal horn neurones in a rat model of mononeuropathy. Pain 91, 101–109.

Suzuki, R., Morcuende, S., Webber, M., Hunt, S. P., and Dickenson, A. H. 2002. Superficial NK1-expressing neurons control spinal excitability through activation of descending pathways. Nat. Neurosci. 5, 1319–1326.

Suzuki, R., Hunt, S. P., and Diusenson, A. H. 2003. The coding of noxious mechanical and thermal stimuli of deep dorsal horn neurones is attenuated in NK1 knockout mice. Neuropharmacology 45, 1093–1100.

Svendsen, F., Tjolsen, A., Gjerstad, J., and Hole, K. 1999. Long term potentiation of single WDR neurons in spinalized rats. Brain Res. 816, 487–492.

Svendsen, F., Tjolsen, A., and Hole, K. 1997. LTP of spinal A beta and C-fibre evoked responses after electrical sciatic nerve stimulation. Neuroreport 8, 3427–3430.

Swamydas, M., Skoff, A. M., and Adler, J. E. 2004. Partial sciatic nerve transection causes redistribution of pain-related peptides and lowers withdrawal threshold. Exp. Neurol. 188, 444–451.

Sweitzer, S. M., Peters, M. C., Ma, J. Y., Kerr, I., Mangadu, R., Chakravarty, S., Dugar, S., Medicherla, S., Protter, A. A., and Yeomans, D. C. 2004a. Peripheral and central p38 MAPK mediates capsaicin-induced hyperalgesia. Pain 111, 278–285.

Sweitzer, S. M., Wong, S. M., Peters, M. C., Mochly-Rosen, D., Yeomans, D. C., and Kendig, J. J. 2004b. Protein kinase C epsilon and gamma: involvement in formalin-induced nociception in neonatal rats. J. Pharmacol. Exp. Ther. 309, 616–625.

Synder, S. H. 1992. Nitric oxide: first in a new class of neurotransmitters. Science 257, 494–496.

Tachibana, T., Miki, K., Fukuoka, T., Arakawa, A., Taniguchi, M., Maruo, S., and Noguchi, K. 1998. Dynorphin mRNA expression in dorsal horn neurons after traumatic spinal cord injury: temporal and spatial analysis using *in situ* hybridization. J. Neurotrauma 15, 485–494.

Tanabe, Y., Nomura, A., Masu, M., Shigemoto, R., Mizuno, N., and Nakanishi, S. 1993. Signal transduction, pharmacological properties, and expression patterns of two rat metabotropic glutamate receptors, mGluR3 and mGluR4. J. Neurosci. 13, 1372–1378.

Tanaka, M., Cummins, T. R., Ishikawa, K., Dib-Hajj, S. D., Black, J. A., and Waxman, S. G. 1998. SNS Na^+ channel expression increases in dorsal root ganglion neurons in the carrageenan inflammatory pain model. Neuroreport 9, 967–972.

Tanner, K. D., Reichling, D. B., and Levine, J. D. 1998. Nociceptor hyper-responsiveness during vincristine-induced painful peripheral neuropathy in the rat. J. Neurosci. 18, 6480–6491.

Tao, Y. X. and Johns, R. A. 2000. Activation of cGMP-dependent protein kinase Ialpha is required for *N*-methyl-D-aspartate- or nitric oxide-produced spinal thermal hyperalgesia. Eur. J. Pharmacol. 392, 141–145.

Tao, Y. X., Hassan, A., Haddad, E., and Johns, R. A. 2000. Expression and action of cyclic GMP-dependent protein kinase Ialpha in inflammatory hyperalgesia in rat spinal cord. Neuroscience 95, 525–533.

Tao, Y. X., Rumbaugh, G., Wang, G. D., Petralia, R. S., Zhao, C., Kauer, F. W., Tao, F., Zhuo, M., Wenthold, R. J., Raja, S. N., Huganir, R. L., Bredt, D. S., and Johns, R. A. 2003. Impaired NMDA receptor-mediated postsynaptic function and blunted NMDA receptor-dependent persistent pain in mice lacking postsynaptic density-93 protein. J. Neurosci. 23, 6703–6712.

Tao, F., Tao, Y. X., Gonzalez, J. A., Fang, M., Mao, P., and Johns, R. A. 2001. Knockdown of PSD-95/SAP90 delays the development of neuropathic pain in rats. Neuroreport 12, 3251–3255.

Tatsumi, S., Mabuchi, T., Katano, T., Matsumura, S., Abe, T., Hidaka, H., Suzuki, M., Sasaki, Y., Minami, T., and Ito, S. 2005. Involvement of Rho-kinase in inflammatory and neuropathic pain through phosphorylation of myristoylated alanine-rich C-kinase substrate (MARCKS). Neuroscience 131, 491–498.

Taylor, B. K. and McCarson, K. E. 2004. Neurokinin-1 receptor gene expression in the mouse dorsal horn increases with neuropathic pain. J. Pain 5, 71–76.

Tegeder, I., Del Turco, D., Schmidtko, A., Sausbier, M., Feil, R., Hofmann, F., Deller, T., Ruth, P., and Geisslinger, G. 2004a. Reduced inflammatory hyperalgesia with preservation of acute thermal nociception in mice lacking cGMP-dependent protein kinase I. Proc. Natl. Acad. Sci. U. S. A. 101, 3253–3257.

Tegeder, I., Niederberger, E., Schmidt, R., Kunz, S., Guhring, H., Ritzeler, O., Michaelis, M., and Geisslinger, G. 2004b. Specific Inhibition of IkappaB kinase reduces hyperalgesia in inflammatory and neuropathic pain models in rats. J. Neurosci. 24, 1637–1645.

Tezuka, T., Umemori, H., Akiyama, T., Nakanishi, S., and Yamamoto, T. 1999. PSD-95 promotes Fyn-mediated tyrosine phosphorylation of the *N*-methyl-D-aspartate receptor subunit NR2A. Proc. Natl. Acad. Sci. U. S. A. 96, 435–440.

Thalhammer, J. G. and LaMotte, R. H. 1982. Spatial properties of nociceptor sensitization following heat injury of the skin. Brain Res. 231, 257–265.

Thompson, S. W., Bennett, D. L., Kerr, B. J., Bradbury, E. J., and McMahon, S. B. 1999. Brain-derived neurotrophic factor is an endogenous modulator of nociceptive responses in the spinal cord. Proc. Natl. Acad. Sci. U. S. A. 96, 7714–7718.

Thompson, S. W., Gerber, G., Sivilotti, L. G., and Woolf, C. J. 1992. Long duration ventral root potentials in the neonatal rat spinal cord *in vitro*; the effects of ionotropic and metabotropic excitatory amino acid receptor antagonists. Brain Res. 595, 87–97.

Thompson, S. W. N., King, A. E., and Woolf, C. J. 1990. Activity-dependent changes in rat ventral horn neurones in vitro; summation of prolonged afferent evoked postsynaptic depolarizations produce a d-APV sensitive windup. Eur. J. Neurosci. 2, 638–649.

Tolle, T. R., Castro-Lopes, J. M., Coimbra, A., and Zieglgansberger, W. 1990. Opiates modify induction of c-fos proto-oncogene in the spinal cord of the rat following noxious stimulation. Neurosci. Lett. 111, 46–51. Erratum in: Neurosci. Lett. 1990, 114, 239.

Tong, Y. G., Wang, H. F., Ju, G., Grant, G., Hokfelt, T., and Zhang, X. 1999. Increased uptake and transport of cholera toxin B-subunit in dorsal root ganglion neurons after peripheral axotomy: possible implications for sensory sprouting. J. Comp. Neurol. 404, 143–158.

Torebjörk, H. E., LaMotte, R. H., and Robinson, C. J. 1984. Peripheral neural correlation of magnitude of cutaneous pain and hyperalgesia: simultaneous recordings in humans of sensory judgements of pain and evoked response in nociceptors with C-fibres. J. Neurophysiol. 51, 325.

Torebjörk, H. E., Lundeberg, L., and LaMotte, R. H. 1992. Central changes in processing of mechanoreceptive input in capsaicin-induced secondary hyperalgesia in humans. J. Physiol. 448, 765–780.

Torsney, C. and Fitzgerald, M. 2002. Age-dependent effects of peripheral inflammation on the electrophysiological properties of neonatal rat dorsal horn neurons. J. Neurophysiol. 87, 1311–1137.

Tsuda, M., Mizokoshi, A., Shigemoto-Mogami, Y., Koizumi, S., and Inoue, K. 2004. Activation of p38 mitogen-activated protein kinase in spinal hyperactive microglia contributes to pain hypersensitivity following peripheral nerve injury. Glia 45, 89–95.

Tsuda, M., Shigemoto-Mogami, Y., Koizumi, S., Mizokoshi, A., Kohsaka, S., Salter, M. W., and Inoue, K. 2003. P2X4 receptors induced in spinal microglia gate tactile allodynia after nerve injury. Nature 424, 778–783.

Tsujino, H., Kondo, E., Fukuoka, T., Dai, Y., Tokunaga, A., Miki, K., Yonenobu, K., Ochi, T., and Noguchi, K. 2000. Activating transcription factor 3 (ATF3) induction by axotomy in sensory and motoneurons: a novel neuronal marker of nerve injury. Mol. Cell Neurosci. 15, 170–182.

Tu, J. C., Xiao, B., Naisbitt, S., Yuan, J. P., Petralia, R. S., Brakeman, P., Doan, A., Aakalu, V. K., Lanahan, A. A., Sheng, M., and Worley, P. F. 1999. Coupling of mGluR/Homer and PSD-95 complexes by the Shank family of postsynaptic density proteins. Neuron 23, 583–592.

Urban, M. O. and Gebhart, G. F. 1999. Supraspinal contributions to hyperalgesia. Proc. Natl. Acad. Sci. U. S. A. 96, 7687–7692.

Urban, L. and Randic, M. 1984. Slow excitatory transmission in rat dorsal horn: possible mediation by peptides. Brain Res. 290, 336–341.

Vanegas, H. and Schaible, H. G. 2001. Prostaglandins and cyclooxygenases [correction of cycloxygenases] in the spinal cord. Prog. Neurobiol. 64, 327–363. Erratum in: Prog. Neurobiol. 2001 65, 609.

Varty, G. B., Grilli, M., Forlani, A., Fredduzzi, S., Grzelak, M. E., Guthrie, D. H., Hodgson, R. A., Lu, S. X., Nicolussi, E., Pond, A. J., Parker, E. M., Hunter, J. C., Higgins, G. A., Reggiani, A., and Bertorelli, R. 2005. The antinociceptive and anxiolytic-like effects of the metabotropic glutamate receptor 5 (mGluR5) antagonists, MPEP and MTEP, and the mGluR1 antagonist, LY456236, in rodents: a comparison of efficacy and side-effect profiles. Psychopharmacology (Berl.) 179, 207–217.

Vasquez, E., Bar, K. J., Ebersberger, A., Klein, B., Vanegas, H., and Schaible, H. G. 2001. Spinal prostaglandins are involved in the development but not the maintenance of inflammation-induced spinal hyperexcitability. J. Neurosci. 21, 9001–9008.

Verge, G. M., Milligan, E. D., Maier, S. F., Watkins, L. R., Naeve, G. S., and Foster, A. C. 2004. Fractalkine (CX3CL1) and fractalkine receptor (CX3CR1) distribution in spinal cord and dorsal root ganglia under basal and neuropathic pain conditions. Eur. J. Neurosci. 20, 1150–1160.

Vierck, C. J., Jr. and Light, A. R. 2000. Allodynia and hyperalgesia within dermatomes caudal to a spinal cord injury in primates and rodents. Prog. Brain Res. 129, 411–428.

Vikman, K. S., Duggan, A. W., and Siddall, P. J. 2003. Increased ability to induce long-term potentiation of spinal dorsal horn neurones in monoarthritic rats. Brain Res. 990, 51–57.

Villar, M. J., Cortes, R., Theodorsson, E., Wiesenfeld-Hallin, Z., Schalling, M., Fahrenkrug, J., Emson, P. C., and Hokfelt, T. 1989. Neuropeptide expression in rat dorsal root ganglion cells and spinal cord after peripheral nerve injury with special reference to galanin. Neuroscience 33, 587–604.

Vincler, M. and Eisenach, J. C. 2004. Plasticity of spinal nicotinic acetylcholine receptors following spinal nerve ligation. Neurosci. Res. 48, 139–145.

Vincler, M. A. and Eisenach, J. C. 2005. Knock down of the alpha 5 nicotinic acetylcholine receptor in spinal nerve-ligated rats alleviates mechanical allodynia. Pharmacol. Biochem. Behav. 80, 135–143.

Vrinten, D. H., Gispen, W. H., Groen, G. J., and Adan, R. A. 2000. Antagonism of the melanocortin system reduces cold and mechanical allodynia in mononeuropathic rats. J. Neurosci. 20, 8131–8137.

Wakisaka, S., Kajander, K. C., and Bennett, G. J. 1991. Increased neuropeptide Y (NPY)-like immunoreactivity in rat sensory neurons following peripheral axotomy. Neurosci. Lett. 124, 200–203.

Wakisaka, S., Kajander, K. C., and Bennett, G. J. 1992. Effects of peripheral nerve injuries and tissue inflammation on the levels of neuropeptide Y-like immunoreactivity in rat primary afferent neurons. Brain Res. 598, 349–352.

Walker, K., Bowes, M., Panesar, M., Davis, A., Gentry, C., Kesingland, A., Gasparini, F., Spooren, W., Stoehr, N., Pagano, A., Flor, P. J., Vranesic, I., Lingenhoehl, K., Johnson, E. C., Varney, M., Urban, L., and Kuhn, R. 2001. mGluR5 receptors and nociceptive function I. Selective blockade of mGluR5 receptors in models of acute, persistent and chronic pain. Neuropharmacology 40, 1–9.

Walker, K. M., Urban, L., Medhurst, S. J., Patel, S., Panesar, M., Fox, A. J., and McIntyre, P. 2003. The VR1 antagonist capsazepine reverses mechanical hyperalgesia in models of inflammatory and neuropathic pain. J. Pharmacol. Exp. Ther. 304, 56–62.

Wall, P. D. and Woolf, C. J. 1984. Muscle but not cutaneous C-afferent input produces prolonged increases in the excitability of the flexion reflex in the rat. J. Physiol. (Lond.) 356, 443–458.

Wallin, J. and Schott, E. 2002. Substance P release in the spinal dorsal horn following peripheral nerve injury. Neuropeptides. 36, 252–256.

Wang, C. H., Chou, W. Y., Hung, K. S., Jawan, B., Lu, C. N., Liu, J. K., Hung, Y. P., and Lee, T. H. 2005. Intrathecal administration of roscovitine inhibits Cdk5 activity and attenuates formalin-induced nociceptive response in rats. Acta Pharmacol. Sin. 26, 46–50.

Wang, J., Kawamata, M., and Namiki, A. 2005. Changes in properties of spinal dorsal horn neurons and their sensitivity to morphine after spinal cord injury in the rat. Anesthesiology 102, 152–164.

Wang, Y. T., Yu, X. M., and Salter, M. W. 1996. Ca(2+)-independent reduction of *N*-methyl-D-aspartate channel activity by protein tyrosine phosphatase. Proc. Natl. Acad. Sci. U. S. A. 93, 1721–1725.

Watkins, J. C. and Evans, R. H. 1981. Excitatory amino acid transmitters. Annu. Rev. Pharmacol. Toxicol. 21, 165–204.

Watkins, L. R. and Maier, S. F. 1999. Implications of immune-to-brain communication for sickness and pain. Proc. Natl. Acad. Sci. U. S. A. 96, 7710–7713.

Watkins, L. R., Wiertelak, E. P., Furness, L. E., and Maier, S. F. 1994a. Illness-induced hyperalgesia is mediated by spinal neuropeptides and excitatory amino acids. Brain. Res. 664, 17–24.

Watkins, L. R., Wiertelak, E. P., Goehler, L. E., Mooney-Heiberger, K., Martinez, J., Furness, L., Smith, K. P., and Maier, S. F. 1994b. Neurocircuitry of illness-induced hyperalgesia. Brain Res. 639, 283–299.

Waxman, S. G., Kocsis, J. D., and Black, J. A. 1994. Type III sodium channel mRNA is expressed in embryonic but not adult spinal sensory neurons, and is reexpressed following axotomy. J. Neurophysiol. 72, 466–470.

Weng, H. R., Aravindan, N., Cata, J. P., Chen, J. H., Shaw, A. D., and Dougherty, P. M. 2005. Spinal glial glutamate transporters downregulate in rats with taxol-induced hyperalgesia. Neurosci. Lett. 386, 18–22.

White, D. M. 2000. Neurotrophin-3 antisense oligonucleotide attenuates nerve injury-induced Abeta-fibre sprouting. Brain Res. 885, 79–86.

Whiteside, G. T. and Munglani, R. 2001. Cell death in the superficial dorsal horn in a model of neuropathic pain. J. Neurosci. Res. 64, 168–173.

Wiertelak, E. P., Furness, L. E., Watkins, L. R., and Maier, S. F. 1994. Illness-induced hyperalgesia is mediated by a spinal NMDA–nitric oxide cascade. Brain Res. 664, 9–16.

Wiesenfeld-Hallin, Z. 1985. Intrathecal somatostatin modulates spinal sensory and reflex mechanisms: behavioral and electrophysiological studies in the rat. Neurosci. Lett. 62, 69–74.

Wiesenfeld-Hallin, Z. 1987. Intrathecal vasoactive intestinal polypeptide modulates spinal reflex excitability primarily to cutaneous thermal stimuli in rats. Neurosci. Lett. 80, 293–297.

Wiesenfeld-Hallin, Z., Aldskogius, H., Grant, G., Hao, J. X., Hokfelt, T., and Xu, X. J. 1997. Central inhibitory dysfunctions: mechanisms and clinical implications. Behav. Brain. Sci. 20, 420–425.

Wiesenfeld-Hallin, Z., Villar, M. J., and Hokfelt, T. 1989. The effects of intrathecal galanin and C-fibre stimulation on the flexor reflex in the rat. Brain Res. 486, 205–213.

Wiesenfeld-Hallin, Z., Xu, X. J., Hakanson, R., Feng, D. M., and Folkers, K. 1990. Plasticity of the peptidergic mediation of spinal reflex facilitation after peripheral nerve section in the rat. Neurosci. Lett. 116, 293–298.

Wiffen, P. J., McQuay, H. J., Edwards, J. E., and Moore, R. A. 2005. Gabapentin for acute and chronic pain. Cochrane Database Syst. Rev. 20, CD005452. Review.

Willcockson, W. S., Chung, J. M., Hori, Y., Lee, K. H., and Willis, W. D. 1984a. Effects of iontophorectically released peptides on primate spinothalamic tract cells. J. Neurosci. 4, 741–750.

Willcockson, W. S., Chung, J. M., Hori, Y., Lee, K. H., and Willis, W. D. 1984b. Effects of iontophorectically released amino acids and amines on primate spinothalamic tract cells. J. Neurosci. 4, 732–740.

Wilson, P. and Kitchener, P. D. 1996. Plasticity of cutaneous primary afferent projections to the spinal dorsal horn. Prog. Neurobiol. 48, 105–129.

Wilson-Gerwing, T. D., Dmyterko, M. V., Zochodne, D. W., Johnston, J. M., and Verge, V. M. 2005. Neurotrophin-3 suppresses thermal hyperalgesia associated with neuropathic pain and attenuates transient receptor potential vanilloid receptor-1 expression in adult sensory neurons. J. Neurosci. 25, 758–767.

Winquist, R. J., Pan, J. Q., and Gribkoff, V. K. 2005. Use-dependent blockade of Cav2.2 voltage-gated calcium channels for neuropathic pain. Biochem. Pharmacol. 70, 489–499.

Wisden, W., Errington, M. L., Williams, S., Dunnett, S. B., Waters, C., Hitchcock, D., Evan, G., Bliss, T. V., and Hunt, S. P. 1990. Differential expression of immediate early genes in the hippocampus and spinal cord. Neuron 4, 603–614.

Womack, M. D., MacDermott, A. B., and Jessell, T. M. 1988. Sensory transmitters regulate intracellular calcium in dorsal horn neurons. Nature 334, 351–353.

Womack, M. D., MacDermott, A. B., and Jessell, T. M. 1989. Substance P increases [Ca2+]i in dorsal horn neurons via two distinct mechanisms. Soc. Neurosci. Abstr. 15, 184.

Woolf, C. J. 1983. Evidence for a central component of post-injury pain hypersensitivity. Nature 306, 686–688.

Woolf, C. J. 1996. Windup and central sensitization are not equivalent. Pain 66, 105–108.

Woolf, C. J. and McMahon, S. B. 1985. Injury-induced plasticity of the flexor reflex in chronic decerebrate rats. Neuroscience 16, 395–404.

Woolf, C. J. and Thompson, S. W. 1991. The induction and maintenance of central sensitization is dependent on *N*-methyl-D-aspartic acid receptor activation; implications for the treatment of post-injury pain hypersensitivity states. Pain 44, 293–299.

Woolf, C. J. and Wall, P. D. 1986. Relative effectiveness of C primary afferent fibers of different origins in evoking a prolonged facilitation of the flexor reflex in the rat. J. Neurosci. 6, 1433–1442.

Woolf, C. J. and Wiesenfeld-Hallin, Z. 1986. Substance P and calcitonin gene-related peptide synergistically modulate the gain of the nociceptive flexor withdrawal reflex in the rat. Neurosci. Lett. 66, 226–230.

Woolf, C. J., Shortland, P., and Coggeshall, R. E. 1992. Peripheral nerve injury triggers central sprouting of myelinated afferents. Nature 355, 75–78.

Woolf, C. J., Thompson, S. W., and King, A. E. 1988–1989. Prolonged primary afferent induced alterations in dorsal horn neurones, an intracellular analysis *in vivo* and *in vitro*. J. Physiol. (Paris) 83, 255–266.

Xing, G., Liu, F., Yao, L., Wan, Y., and Han, J. 2003. Changes in long-term synaptic plasticity in the spinal dorsal horn of neuropathic pain rats. Beijing Da Xue Xue Bao 35, 226–230.

Xu, X. J., Elfvin, A., and Wiesenfeld-Hallin, Z. 1995. Subcutaneous carrageenan, but not formalin, increases the excitability of the nociceptive flexor reflex in the rat. Neurosci. Lett. 196, 116–118.

Xu, X.-J., Maggi, C. A., and Wiesenfeld-Hallin, Z. 1991. On the role of NK-2 tachykinin receptors in the mediation of spinal reflex excitability in the rat. Neuroscience 44, 483–490.

Xu, M., Petraschka, M., McLaughlin, J. P., Westenbroek, R. E., Caron, M. G., Lefkowitz, R. J., Czyzyk, T. A., Pintar, J. E., Terman, G. W., and Chavkin, C. 2004. Neuropathic pain activates the endogenous kappa opioid system in mouse spinal cord and induces opioid receptor tolerance. J. Neurosci. 24, 4576–4584.

Yajima, Y., Narita, M., Narita, M., Matsumoto, N., and Suzuki, T. 2002. Involvement of a spinal brain-derived neurotrophic factor/full-length TrkB pathway in the development of nerve injury-induced thermal hyperalgesia in mice. Brain Res. 958, 338–346.

Yajima, Y., Narita, M., Shimamura, M., Narita, M., Kubota, C., and Suzuki, T. 2003. Differential involvement of spinal protein kinase C and protein kinase A in neuropathic and inflammatory pain in mice. Brain Res. 992, 288–293.

Yaksh, T. L. 1982. Central and Peripheral Mechanisms for the Antialgesic Action of Acetylsalicylic Acid. In: Acetylsalicylic

Acid: New Uses for an Old Drug (*eds*. H. J. M. Barett, J. Hirsh, and J. F. Mustard), pp. 137–151. Raven Press.

Yaksh, T. L., Dirig, D. M., Conway, C. M., Svensson, C., Luo, Z. D., and Isakson, P. C. 2001. The acute antihyperalgesic action of nonsteroidal, anti-inflammatory drugs and release of spinal prostaglandin E2 is mediated by the inhibition of constitutive spinal cyclooxygenase-2 (COX-2) but not COX-1. J. Neurosci. 21, 5847–5853.

Yamamoto, T. and Yaksh, T. L. 1991. Stereospecific effects of a nonpeptide NK-1 selective antagonist, CP-96,345: antinociception in the absence of motor dysfunction. Life Sci. 49, 1955–1963.

Yamamoto, T., Hirasawa, S., Wroblewska, B., Grajkowska, E., Zhou, J., Kozikowski, A., Wroblewski, J., and Neale, J. H. 2004. Antinociceptive effects of *N*-acetylaspartylglutamate (NAAG) peptidase inhibitors ZJ-11, ZJ-17 and ZJ-43 in the rat formalin test and in the rat neuropathic pain model. Eur. J. Neurosci. 20, 484–494.

Yamamoto, T., Shimoyama, N., and Mizuguchi, T. 1993. Role of the injury discharge in the development of thermal hyperesthesia after sciatic nerve constriction injury in the rat. Anesthesiology 79, 993–1002.

Yang, L., Zhang, F. X., Huang, F., Lu, Y. J., Li, G. D., Bao, L., Xiao, H. S., and Zhang, X. 2004. Peripheral nerve injury induces trans-synaptic modification of channels, receptors and signal pathways in rat dorsal spinal cord. Eur. J. Neurosci. 19, 871–883.

Yang, L. C., Marsala, M., and Yaksh, T. L. 1996. Characterization of time course of spinal amino acids, citrulline and PGE2 release after carrageenan/kaolin-induced knee joint inflammation: a chronic microdialysis study. Pain 67, 345–354.

Yashpal, K., Fisher, K., Chabot, J.-G., and Coderre, T. J. 2001. Differential effects of NMDA and group I mGluR antagonists on both nociception and spinal cord protein kinase C translocation in the formalin test and a model of neuropathic pain in rats. Pain 94, 17–29.

Yashpal, K., Pitcher, G. M., Parent, A., Quirion, R., and Coderre, T. J. 1995. Noxious thermal and chemical stimulation induce increases in 3H-Phorbol 12, 13-dibutyrate binding in spinal cord dorsal horn as well as persistent pain and hyperalgesia, which is reduced by inhibition of protein kinase C. J. Neurosci. 15, 3263–3272.

Yashpal, K., Radhakrishnan, V., Coderre, T. J., and Henry, J. L. 1993. CP-96,345, but not its stereoisomer, CP-96,344, blocks the nociceptive responses to intrathecally administered substance P and to noxious thermal and chemical stimuli in the rat. Neuroscience 52, 1039–1047.

Yezierski, R. P. 2000. Pain following spinal cord injury: pathophysiology and central mechanisms. Prog. Brain Res. 129, 429–449.

Yezierski, R. P. and Park, S. H. 1993. The mechanosensitivity of spinal sensory neurons following intraspinal injections of quisqualic acid in the rat. Neurosci. Lett. 157, 115–119.

Yezierski, R. P., Liu, S., Ruenes, G. L., Kajander, K. J., and Brewer, K. L. 1998. Excitotoxic spinal cord injury: behavioral and morphological characteristics of a central pain model. Pain 75, 141–155.

Yokoyama, K., Kurihara, T., Makita, K., and Tanabe, T. 2003. Plastic change of N-type Ca channel expression after preconditioning is responsible for prostaglandin E2-induced long-lasting allodynia. Anesthesiology 99, 1364–1370.

Young, M. R., Fleetwood-Walker, S. M., Dickinson, T., Blackburn-Munro, G., Sparrow, H., Birch, P. J., and Bountra, C. 1997. Behavioural and electro-physiological evidence supporting a role for group I metabotropic glutamate receptors in the mediation of nociceptive inputs to the rat spinal cord. Brain Res. 777, 161–169.

Young, M. R., Fleetwood-Walker, S. M., Mitchell, R., and Dickinson, T. 1995. The involvement of metabotropic glutamate receptors and their intracellular signalling pathways in sustained nociceptive transmission in rat dorsal horn neurons. Neuropharmacology 34, 1033–1041.

Young, M. R., Fleetwood-Walker, S. M., Mitchell, R., and Munro, F. E. 1994. Evidence for a role of metabotropic glutamate receptors in sustained nociceptive inputs to rat dorsal horn neurons. Neuropharmacology 33, 141–144.

Yu, X. M. and Salter, M. W. 1999. Src, a molecular switch governing gain control of synaptic transmission mediated by *N*-methyl-D-aspartate receptors. Proc. Natl. Acad. Sci. U. S. A. 96, 7697–7704.

Yu, X. M., Askalan, R., Keil, G. J., 2nd, and Salter, M. W. 1997. NMDA channel regulation by channel-associated protein tyrosine kinase Src. Science 275, 674–678.

Zahn, P. K. and Brennan, T. J. 1999. Primary and secondary hyperalgesia in a rat model for human postoperative pain. Anesthesiology 90, 863–872.

Zahn, P. K., Sluka, K. A., and Brennan, T. J. 2002. Excitatory amino acid release in the spinal cord caused by plantar incision in the rat. Pain 100, 65–76.

Zeitz, K. P., Giese, K. P., Silva, A. J., and Basbaum, A. I. 2004. The contribution of autophosphorylated alpha-calcium-calmodulin kinase II to injury-induced persistent pain. Neuroscience 128, 889–898.

Zhang, X., Dagerlind, A., Elde, R. P., Castel, M. N., Broberger, C., Wiesenfeld-Hallin, Z., and Hokfelt, T. 1993a. Marked increase in cholecystokinin B receptor messenger RNA levels in rat dorsal root ganglia after peripheral axotomy. Neuroscience 57, 227–233.

Zhang, X., Bao, L., Shi, T. J., Ju, G., Elde, R., and Hokfelt, T. 1998. Down-regulation of mu-opioid receptors in rat and monkey dorsal root ganglion neurons and spinal cord after peripheral axotomy. Neuroscience 82, 223–240.

Zhang, Y. Z., Hannibal, J., Zhao, Q., Moller, K., Danielsen, N., Fahrenkrug, J., and Sundler, F. 1996. Pituitary adenylate cyclase activating peptide expression in the rat dorsal root ganglia: up-regulation after peripheral nerve injury. Neuroscience 74, 1099–1110.

Zhang, L., Lu, Y., Chen, Y., and Westlund, K. N. 2002. Group I metabotropic glutamate receptor antagonists block secondary thermal hyperalgesia in rats with knee joint inflammation. J. Pharmacol. Exp. Ther. 300, 149–156.

Zhang, X., Meister, B., Elde, R., Verge, V. M., and Hokfelt, T. 1993b. Large calibre primary afferent neurons projecting to the gracile nucleus express neuropeptide Y after sciatic nerve lesions: an immunohistochemical and in situ hybridization study in rats. Eur. J. Neurosci. 5, 1510–1519.

Zhang, B., Tao, F., Liaw, W. J., Bredt, D. S., Johns, R. A., and Tao, Y. X. 2003. Effect of knock down of spinal cord PSD-93/chapsin-110 on persistent pain induced by complete Freund's adjuvant and peripheral nerve injury. Pain 106, 187–196.

Zhang, X., Wu, J., Fang, L., and Willis, W. D. 2003. The effects of protein phosphatase inhibitors on nociceptive behavioral responses of rats following intradermal injection of capsaicin. Pain 106, 443–451.

Zhang, H., Xie, W., and Xie, Y. 2005. Spinal cord injury triggers sensitization of wide dynamic range dorsal horn neurons in segments rostral to the injury. Brain Res. 1055, 103–110.

Zhong, J., Gerber, G., Kojic, L., and Randic, M. 2000. Dual modulation of excitatory synaptic transmission by agonists at group I metabotropic glutamate receptors in the rat spinal dorsal horn. Brain Res. 887, 359–377.

Zhou, X. F., Chie, E. T., Deng, Y. S., Zhong, J. H., Xue, Q., Rush, R. A., and Xian, C. J. 1999a. Injured primary sensory neurons switch phenotype for brain-derived neurotrophic factor in the rat. Neuroscience 92, 841–853.

Zhou, X. F., Deng, Y. S., Chie, E., Xue, Q., Zhong, J. H., McLachlan, E. M., Rush, R. A., and Xian, C. J., 1999b. Satellite-cell-derived nerve growth factor and neurotrophin-3

are involved in noradrenergic sprouting in the dorsal root ganglia following peripheral nerve injury in the rat. Eur. J. Neurosci. 11, 1711–1722.
Zhou, Y., Li, G. D., and Zhao, Z. Q. 2003. State-dependent phosphorylation of epsilon-isozyme of protein kinase C in adult rat dorsal root ganglia after inflammation and nerve injury. J. Neurochem. 85, 571–580.
Zhu, C. Z., Wilson, S. G., Mikusa, J. P., Wismer, C. T., Gauvin, D. M., Lynch, J. J., III, Wade, C. L, Decker, M. W., and Honore, P. 2004. Assessing the role of metabotropic glutamate receptor 5 in multiple nociceptive modalities. Eur. J. Pharmacol. 506, 107–118.
Zhuo, M. and Gebhart, G. F. 1992. Characterization of descending facilitation and inhibition of spinal nociceptive transmission from the nuclei reticularis gigantocellularis and gigantocellularis pars alpha in the rat. J. Neurophysiol. 67, 1599–1614.
Zieglgansberger, W. and Herz, A. 1971. Changes of cutaneous receptive fields of spino-cervical-tract neurones and other dorsal horn neurones by microelectrophoretically administered amino acids. Exp. Brain Res. 13, 111–126.
Zou, X., Lin, Q., and Willis, W. D. 2000. Enhanced phosphorylation of NMDA receptor 1 subunits in spinal cord dorsal horn and spinothalamic tract neurons after intradermal injection of capsaicin in rats. J. Neurosci. 20, 6989–6997.

Further Reading

Abbadie, C., Brown, J. L., Mantyh, P. W., and Basbaum, A. I. 1996. Spinal cord substance P receptor immunoreactivity increases in both inflammatory and nerve injury models of persistent pain. Neuroscience 70, 201–209.
Barbour, B., Szatkowski, M., Ingledew, N., and Attwell, D. 1989. Arachidonic acid induces a prolonged inhibition of glutamate uptake into glial cells. Nature 342, 918–920.
Miletic, G., Hanson, E. N., and Miletic, V. 2004a. Brain-derived neurotrophic factor-elicited or sciatic ligation-associated phosphorylation of cyclic AMP response element binding protein in the rat spinal dorsal horn is reduced by block of tyrosine kinase receptors. Neurosci. Lett. 361, 269–271.
Watkins, L. R., Martin, D., Ulrich, P., Tracey, K. J., and Maier, S. F. 1997. Evidence for the involvement of spinal cord glia in subcutaneous formalin induced hyperalgesia in the rat. Pain 71, 225–235.

Relevant Website

http://www.iasp-pain.org/terms-p.html

5.27 Glycine Receptors

H U Zeilhofer, University of Zurich, Zurich, Switzerland

© 2008 Elsevier Inc. All rights reserved.

5.27.1	Molecular Architecture of Glycine Receptors	381
5.27.2	Glycinergic Innervation in the Spinal Cord Dorsal Horn	381
5.27.3	Inhibitory Glycine Receptors and Spinal Pain Control	382
5.27.3.1	Glycine Receptors in the Spinal Control of Inflammatory Pain	382
5.27.3.2	Glycine Receptors in the Spinal Control of Neuropathic Pain	383
5.27.3.3	Transmitters Facilitating Glycinergic Inhibition	384
References		384

Glossary

GABA Gamma aminobutyric acid; fast inhibitory neurotransmitter in the mammalian CNS.

GABA$_A$ receptor Chloride channel-coupled GABA receptor blocked by bicuculline.

glycine Fast inhibitory neurotransmitter in the spinal cord and brain stem.

gephyrin Postsynaptic protein mediating the clustering of $GABA_A$ and glycine receptors in the postsynaptic membrane.

cyclooxygenase-2 Inducible enzyme mediating the production of prostaglandin precursors.

EGFP Enhanced green fluorescent protein used, for example to label cells *in vitro* and *in vivo*.

KCC2 Potassium/chloride exporter protein, needed for central neurons to reduce their intracellular chloride concentration to physiological levels.

5.27.1 Molecular Architecture of Glycine Receptors

Glycine is the major inhibitory neurotransmitter in the spinal cord and brain stem. In addition, glycine is an obligatory co-agonist at excitatory glutamate receptors of the *N*-methyl-D-aspartate (NMDA) subtype. This chapter focuses on inhibitory (strychnine-sensitive) glycine receptors. These glycine receptors are heteropentameric chloride-permeable ion channels composed of α and β subunits (Legendre, P., 2001). Four different genes (*glra1–glra4*) encode for the glycine-binding α subunits and one gene (*glrb*) encodes for the so-called structural β subunit. α Subunits carry the glycine binding site and are capable of forming functional homomeric receptor channels. The β subunit permits postsynaptic clustering of glycine receptors through an interaction with the postsynaptic density protein gephyrin. Most glycine receptors in the adult are heteromeric receptors composed of $\alpha 1$ and β subunits. GlyR$\alpha 2$ forms homomeric receptor channels during embryonic development and in early postnatal life. In most organs GlyR$\alpha 2$ homomers are replaced by GlyR$\alpha 1/\beta$ heteromers during postnatal maturation. GlyR$\alpha 3$ is another adult glycine receptor subunit but much less abundant than GlyR$\alpha 1$. GlyR$\alpha 4$ is probably not expressed in humans because of a premature stop codon in the *GLRA4* gene.

5.27.2 Glycinergic Innervation in the Spinal Cord Dorsal Horn

Immunofluorescence studies have shown that markers of glycinergic innervation are abundant in the spinal cord dorsal horn (Todd, A. J. and Sullivan, A. C., 1990). Glycine receptors are found throughout the dorsal horn. As in other regions of the central nervous system (CNS), most glycine receptors in the adult spinal cord are $\alpha 1/\beta$ heteromeric receptor channels. However, in the superficial layers of the dorsal horn, where most nociceptive afferents terminate, glycine receptors contain GlyR$\alpha 3$ in addition to GlyR$\alpha 1$ and GlyRβ (Figure 1) (Harvey, R. J. *et al.*, 2004). The prominent

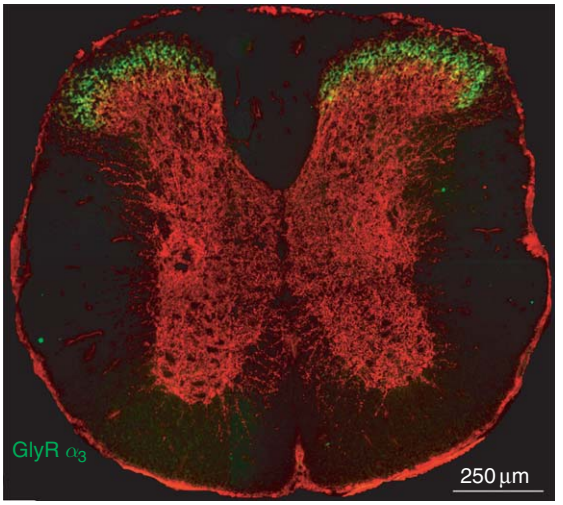

Figure 1 Expression of GlyRα3 in the spinal cord dorsal horn. GlyRα3 (green) is distinctly expressed in the superficial layers where nociceptive afferents terminate, whereas gephyrin (red), a marker for glycinergic and GABAergic synapses, is found throughout the spinal cord. Adapted from Harvey, R. J., Depner, U. B., Wässle, H., Ahmadi, S., Heindl, C., Reinold, H., Smart, T. G., Harvey, K., Schütz, B., Abo-Salem, O. M., Zimmer, A., Poisbeau, P., Welzl, H., Wolfer, D. P., Betz, H., Zeilhofer, H. U., and Müller, U. 2004. GlyR α3: an essential target for spinal inflammatory pain sensitization. Science 304, 884–887; with permission.

expression of glycine receptors in the spinal cord is accompanied by dense glycinergic innervation. Glycinergic axon terminals, characterized by the expression of the neuronal glycine transporter isoform GlyT2, and glycinergic cell bodies, identified by their immunoreactivity against glycine, are widely distributed in the dorsal horn. Recently, mice expressing enhanced green fluorescent protein (EGFP) under the transcriptional control of the GlyT2 gene have been generated (Zeilhofer, H. U. *et al.*, 2005). In the dorsal horn of these mice, numerous glycinergic (EGFP/GlyT2-positive) neurons are found in the deeper dorsal horn (laminae III–V) and in lamina I, whereas relatively few glycinergic neurons are seen in lamina II. In addition to these local inhibitory interneurons, descending antinociceptive glycinergic fiber tracts (Antal, M. *et al.*, 1996; Kato, G. *et al.*, 2006) probably contribute to the glycinergic innervation of the dorsal horn.

5.27.3 Inhibitory Glycine Receptors and Spinal Pain Control

Plenty of information meanwhile indicates that relief from synaptic inhibition by spinal blockade of glycine (and also of $GABA_A$) receptors can elicit and exaggerate nociceptive responses (for a recent review see Zeilhofer, H. U., 2005). Several groups have meanwhile demonstrated that relief from inhibition also occurs endogenously during inflammation and possibly also after peripheral nerve injury.

5.27.3.1 Glycine Receptors in the Spinal Control of Inflammatory Pain

Inflammatory pain originates to a large extent from prostaglandins, which are produced in response to inflammation and tissue damage mainly by inducible cyclooxygenase-2 (COX-2). The pivotal role of prostaglandins for pain sensitization is obvious from our everyday experience that profound analgesia can be achieved through inhibition of prostanoid formation either by the classical nonspecific cyclooxygenase (COX) inhibitors (aspirin and related drugs) or by the more recently developed COX-2-specific inhibitors (Brune, K. and Zeilhofer, H. U., 2005).

For a long time it was widely believed that prostaglandins sensitize the nociceptive system only at the level of the peripheral nociceptor. This long-held view has changed significantly since the mid-1990s when several groups demonstrated that inflammation induces COX-2 expression not only in the peripheral inflamed tissue, but also in the CNS, in particular in the spinal cord dorsal horn. A central action of prostaglandins and accordingly also a central mode of action for the analgesic action of COX inhibitors are meanwhile generally accepted (Malmberg, A. B. and Yaksh, T. L., 1992; Samad, T. A. *et al.*, 2002).

Electrophysiological experiments have shown that PGE_2 reduces inhibitory glycinergic neurotransmission in the spinal cord dorsal horn, but does not interfere with GABAergic or glutamatergic neurotransmission (Figure 2) (Ahmadi, S. *et al.*, 2002). This inhibition is (at least in adult animals) specific for neurons in the superficial layers of the dorsal horn and for PGE_2 (PGD_2, PGI_2, and $PGF_{2\alpha}$ are without effect). It involves activation of postsynaptic prostaglandin E receptors of the EP2 subtype and a specific protein kinase A (PKA)-dependent phosphorylation of GlyRα3-containing receptors, which are in the spinal cord distinctly expressed in the superficial layers (Harvey, R. J. *et al.*, 2004). Subsequent experiments using site-directed mutagenesis have shown that GlyRα3 is phosphorylated at serine 346 in the long intracellular loop between transmembrane regions 3 and 4. Figure 3 shows a schematic

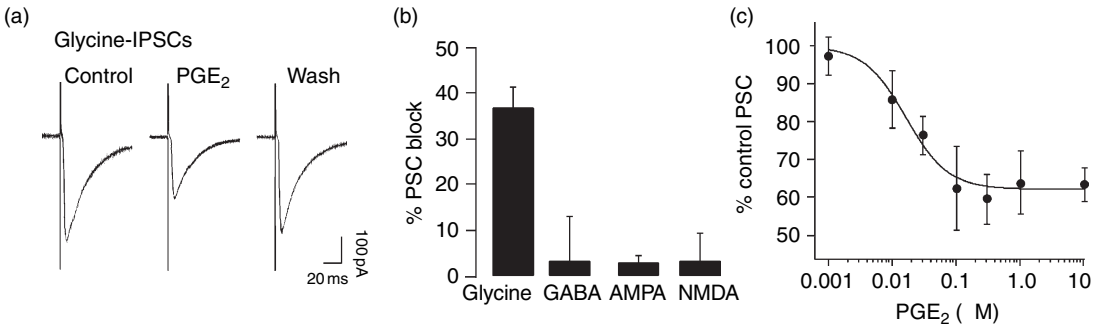

Figure 2 PGE_2 selectively inhibits glycinergic neurotransmission onto spinal cord dorsal horn neurons. (a) Averaged inhibitory postsynaptic current (IPSC) traces recorded from a neuron in the superficial dorsal horn under control conditions, in the presence of PGE_2, and after its removal. (b) Statistical analysis (mean ± SEM). Significant inhibition by PGE_2 occurred only for glycinergic IPSCs, GABAergic IPSCs, and excitatory postsynaptic currents mediated by glutamate receptors of the alpha-amino-3-hydroxy-5-methyl-4-isoxazolepropionic acid (AMPA) or *N*-methyl-D-aspartate (NMDA) type remained unchanged. (c) Concentration–response curve. Significant inhibition of glycinergic IPSC occurred at low nanomolar concentrations. Adapted from Ahmadi, S., Lippross, S., Neuhuber, W. L., and Zeilhofer, H. U. 2002. PGE_2 selectively blocks inhibitory glycinergic neurotransmission onto rat superficial dorsal horn neurons. Nat. Neurosci. 5, 34–40, with permission from Nature Publishing Group.

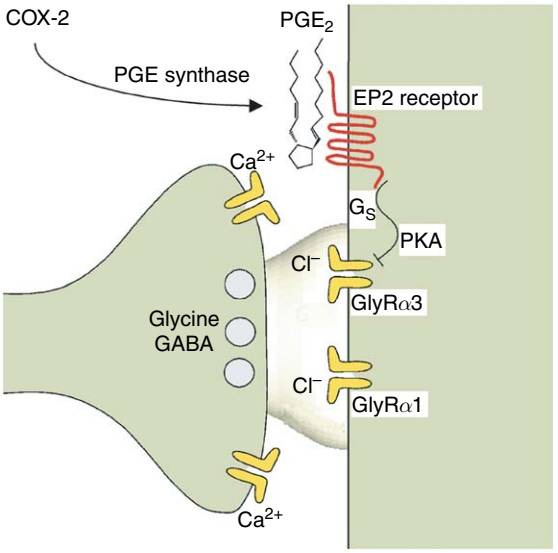

Figure 3 Schematic representation of the intracellular pathway leading to inhibition of glycinergic neurotransmission by PGE_2. PGE_2 activates E-type prostaglandin receptors of the EP2 subtype, which subsequently lead to an increase in intracellular camp and activate protein kinase A (PKA). PKA finally phosphorylates and inhibits GlyRα3. Adapted from Progress in Pain research and Management, vol. 30.

representation of the intracellular pathway that underlies inhibition of glycine receptors by PGE_2. Unlike GlyRα3-containing receptors, homomeric glycine receptors formed by GlyRα1 and heteromeric channels composed of GlyRα1 and GlyRβ are not inhibited by PKA activation and mice carrying a loss-of-function mutation in the GlyRα1 subunit lack a nociceptive phenotype.

Mice lacking GlyRα3 (or EP2 receptors) not only exhibit a nearly complete loss of pain sensitization by spinal PGE_2 but also display nearly identical nociceptive phenotypes in models of inflammatory pain (Figure 4) (Harvey, R. J. *et al.*, 2004, Reinold, H. *et al.*, 2005; see also Zeilhofer, H. U., 2005). Both types of knockout mice develop normal initial thermal and mechanical sensitization, but recover much faster from hyperalgesia than wild-type mice. Inhibition of glycinergic neurotransmission by PGE_2 thus is a key event in the generation of inflammatory pain.

5.27.3.2 Glycine Receptors in the Spinal Control of Neuropathic Pain

A role for cyclooxygenase products has also been proposed for neuropathic pain originating from peripheral nerve injury. However, a significant contribution of prostaglandins to this pain form is discussed controversially and other mechanisms leading to a similar relief from inhibition may be more important (Hösl, K. *et al.*, 2006). Possible mechanisms include an inhibition of synaptic glycine release, reduced responsiveness of postsynaptic glycine receptors, a reduction in the transmembrane chloride gradient rendering the inhibitory tone of GABAergic and glycinergic synaptic input less efficient, and a loss of inhibitory innervation, for

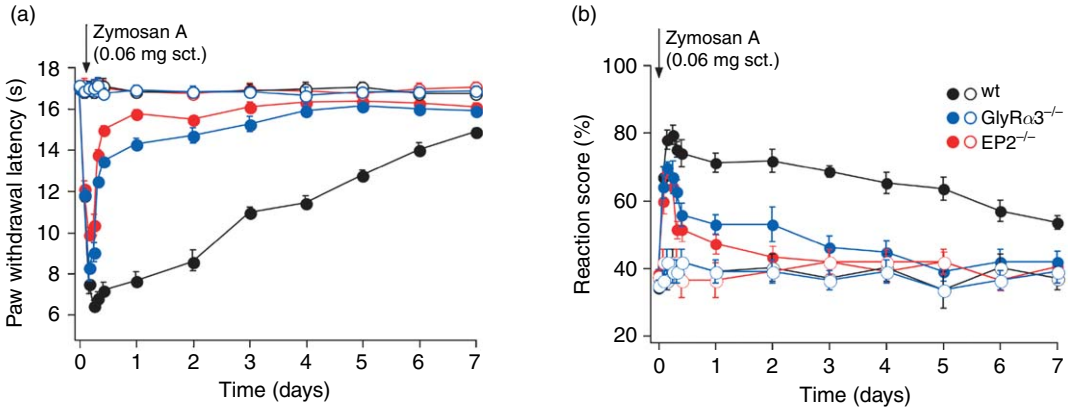

Figure 4 Inflammatory pain sensitization in mice lacking PGE_2-mediated inhibition of glycinergic neurotransmission. An inflammatory response was induced by subcutaneous injection by a yeast extract (zymosan A) into one hind paw. Inflammatory hyperalgesia was assessed by stimulating the inflamed paw either with noxious heat or mechanically with calibrated von Frey filaments. Both mice lacking the EP2 receptor ($EP2^{-/-}$ mice) and mice deficient in GlyRα3 ($GlyR\alpha3^{-/-}$ mice) recovered quickly from inflammatory hyperalgesia. Adapted from Zeilhofer, H. U. 2005. The glycinergic control of spinal pain processing. Cell Mol. Life Sci. 62, 2027–2035.

example due to a selective death of GABAergic or glycinergic interneurons.

There is indeed experimental evidence for all three possibilities, but their contribution to neuropathic pain is not clear. A reduction in the transmembrane chloride gradient in dorsal horn neurons following peripheral nerve injury has been reported by Coull J. A. *et al.* (2003). Peripheral nerve trauma reduced the expression of the potassium chloride exporter KCC2 in dorsal horn neurons. This induced a shift of the chloride equilibrium potential to more depolarized values and rendered inhibitory GABAergic and glycinergic input less efficient. Another extensively discussed report suggests that peripheral nerve injury induces a specific loss of spinal inhibitory GABAergic neurotransmission in the dorsal horn of rats in the chronic constriction injury model and the spared nerve injury model of neuropathic pain (Moore, K. A. *et al.*, 2002). This original report has proposed that the loss of GABAergic input was due to the selective apoptotic death of GABAergic interneurons. Subsequent studies have however suggested that such a loss may not be necessary for the development of hyperalgesia in the chronic nerve injury model of neuropathic pain (Polgar, E. *et al.*, 2003; 2004). Finally, the neuropeptide nocistatin is a specific inhibitor of GABA and glycine release in the spinal cord dorsal horn (Zeilhofer, H. U. *et al.*, 2000) and it increases nociceptive responses in the rat formalin test and in the chronic constriction injury of neuropathic pain after intrathecal injection.

5.27.3.3 Transmitters Facilitating Glycinergic Inhibition

Given that a relief from glycinergic and/or GABAergic inhibition underlies inflammatory and neuropathic pain, one might speculate that transmitters, which facilitate inhibitory transmission might contribute to endogenous antinociception. Several transmitters including ATP (Jang, I. S. *et al.*, 2001; Rhee, J. S. *et al.*, 2000) and norepinephrine (Baba, H. *et al.*, 2000a; 2000b) facilitate glycine release through the activation of P2X receptors and $\alpha2$ adrenoceptors in the spinal cord, respectively. In rat sacral commissural neurons (lamina X) glycinergic membrane currents are potentiated by norepinephrine acting on $\alpha2$ adrenoceptors through a postsynaptic mechanism (Nabekura, J. *et al.*, 1999). These and possibly other similar processes may contribute to endogenous pain-controlling processes. Unfortunately, only very few drugs target glycine receptors and most of them lack the isoform specificity (Laube, B. *et al.*, 2002).

References

Ahmadi, S., Lippross, S., Neuhuber, W. L., and Zeilhofer, H. U. 2002. PGE_2 selectively blocks inhibitory glycinergic neurotransmission onto rat superficial dorsal horn neurons. Nat. Neurosci. 5, 34–40.

Antal, M., Petko, M., Polgar, E., Heizmann, C. W., and Storm-Mathisen, J. 1996. Direct evidence of an extensive GABAergic innervation of the spinal dorsal horn by fibres

descending from the rostral ventromedial medulla. Neuroscience 73, 509–518.
Baba, H., Goldstein, P. A., Okamoto, M., Kohno, T., Ataka, T., Yoshimura, M., and Shimoji K. 2000a. Norepinephrine facilitates inhibitory transmission in substantia gelatinosa of adult rat spinal cord (part 2): effects on somatodendritic sites of GABAergic neurons. Anesthesiology 92, 485–492.
Baba, H., Shimoji, K., and Yoshimura, M. 2000b. Norepinephrine facilitates inhibitory transmission in substantia gelatinosa of adult rat spinal cord (part 1): effects on axon terminals of GABAergic and glycinergic neurons. Anesthesiology 92, 473–484.
Brune, K. and Zeilhofer, H. U. 2005. Antipyretic Analgesics – Basic Aspects. In: Melzack and Wall's Textbook of Pain, 5th edn. (*eds*. S. McMahon and M. Koltzenburg), pp. 459–469. Churchill Livingstone.
Coull, J. A., Boudreau, D., Bachand, K., Prescott, S. A., Nault, F., Sik, A., De Koninck, P., and De Koninck, Y. 2003. Trans-synaptic shift in anion gradient in spinal lamina I neurons as a mechanism of neuropathic pain. Nature 424, 938–942.
Harvey, R. J., Depner, U. B., Wässle, H., Ahmadi, S., Heindl, C., Reinold, H., Smart, T. G., Harvey, K., Schütz, B., Abo-Salem, O. M., Zimmer, A., Poisbeau, P., Welzl, H., Wolfer, D. P., Betz, H., Zeilhofer, H. U., and Müller, U. 2004. GlyR α3: an essential target for spinal inflammatory pain sensitization. Science 304, 884–887.
Hösl, K., Reinold, H., Harvey, R. J., Müller, U., Narumiya, S., and Zeilhofer, H. U. 2006. Spinal prostaglandin E receptors of the EP2 subtype and the glycine receptor α3 subunit, which mediate central inflammatory hyperalgesia, do not contribute to pain after peripheral nerve injury or formalin injection. Pain 126, 46–53.
Jang, I. S., Rhee, J. S., Kubota, H., Akaike, N., and Akaike, N. 2001. Developmental changes in P2X purinoceptors on glycinergic presynaptic nerve terminals projecting to rat substantia gelatinosa neurones. J. Physiol. 536, 505–519.
Kato, G., Yasaka, T., Katafuchi, T., Furue, H., Mizuno, M., Iwamoto, Y., and Yoshimura, M. 2006. Direct GABAergic and glycinergic inhibition of the substantia gelatinosa from the rostral ventromedial medulla revealed by *in vivo* patch-clamp analysis in rats. J. Neurosci. 26, 1787–1794.
Laube, B., Maksay, G., Schemm, R., and Betz, H. 2002. Modulation of glycine receptor function: a novel approach for therapeutic intervention at inhibitory synapses? Trends Pharmacol. Sci. 23, 519–527.
Legendre, P. 2001. The glycinergic inhibitory synapse. Cell. Mol. Life Sci. 58, 760–793.
Malmberg, A. B. and Yaksh, T. L. 1992. Hyperalgesia mediated by spinal glutamate or substance P receptor blocked by spinal cyclooxygenase inhibition. Science 257, 1276–1279.
Moore, K. A., Kohno, T., Karchewski, L. A., Scholz, J., Baba, H., and Woolf, C. J. 2002. Partial peripheral nerve injury promotes a selective loss of GABAergic inhibition in the superficial dorsal horn of the spinal cord. J. Neurosci. 22, 6724–6731.
Nabekura, J., Xu, T. L., Rhee, J. S., Li, J. S., and Akaike, N. 1999. Alpha2-adrenoceptor-mediated enhancement of glycine response in rat sacral dorsal commissural neurons. Neuroscience 9, 29–41.
Polgar, E., Gray, S., Riddell, J. S., and Todd, A. J. 2004. Lack of evidence for significant neuronal loss in laminae I–III of the spinal dorsal horn of the rat in the chronic constriction injury model. Pain 111, 144–150.
Polgar, E., Hughes, D. I., Riddell, J. S., Maxwell, D. J., Puskar, Z., and Todd, A. J. 2003. Selective loss of spinal GABAergic or glycinergic neurons is not necessary for development of thermal hyperalgesia in the chronic constriction injury model of neuropathic pain. Pain 104, 229–239.
Reinold, H., Ahmadi, S., Depner, U. B., Layh, B., Heindl, C., Hamza, M., Pahl, A., Brune, K., Narumiya, S., Müller, U., and Zeilhofer, H. U. 2005. Spinal inflammatory hyperalgesia is mediated by prostaglandin E receptors of the EP2 subtype. J. Clin. Invest. 115, 673–679.
Rhee, J. S., Wang, Z. M., Nabekura, J., Inoue, K., and Akaike, N. 2000. ATP facilitates spontaneous glycinergic IPSC frequency at dissociated rat dorsal horn interneuron synapses. J. Physiol. 524, 471–483.
Samad, T. A., Sapirstein, A., and Woolf, C. J. 2002. Prostanoids and pain: unraveling mechanisms and revealing therapeutic targets. Trends Mol. Med. 8, 390–396.
Todd, A. J. and Sullivan, A. C. 1990. Light microscope study of the coexistence of GABA-like and glycine-like immunoreactivities in the spinal cord of the rat. J. Comp. Neurol. 296, 496–505.
Zeilhofer, H. U. 2005. The glycinergic control of spinal pain processing. Cell Mol. Life Sci. 62, 2027–2035.
Zeilhofer, H. U., Muth-Selbach, U., Gühring, H., Erb, K., and Ahmadi, S. 2000. Selective suppression of inhibitory synaptic transmission by nocistatin in the rat spinal cord dorsal horn. J. Neurosci. 20, 4922–4999.
Zeilhofer, H. U., Studler, B., Arabadzisz, D., Schweizer, C., Ahmadi, S., Layh, B., Bösl, M. R., and Fritschy, J. M. 2005. Glycinergic neurons expressing enhanced green fluorescent protein in bacterial artificial chromosome transgenic mice. J. Comp. Neurol. 482, 123–141.

Further Reading

Baba, H., Kohno, T., Moore, K. A., and Woolf, C. J. 2001. Direct activation of rat spinal dorsal horn neurons by prostaglandin E2. J. Neurosci. 21, 1750–1756.
Sherman, S. E., Luo, L., and Dostrovsky, J. O. 1997. Spinal strychnine alters response properties of nociceptive-specific neurons in rat medial thalamus. J. Neurophysiol. 78, 628–637.
Sivilotti, L. and Woolf, C. J. 1994. The contribution of $GABA_A$ and glycine receptors to central sensitization: disinhibition and touch-evoked allodynia in the spinal cord. J. Neurophysiol. 72, 169–179.

5.28 Pain Following Spinal Cord Injury

R P Yezierski, Comprehensive Center for Pain Research and The McKnight Brain Institute, University of Florida, Gainesville, FL, USA

© 2008 Elsevier Inc. All rights reserved.

5.28.1	The Condition of Pain Following Spinal Cord Injury	387
5.28.2	Clinical Characteristics of Spinal Injury Pain	388
5.28.3	The Research Challenge of Spinal Injury Pain	389
5.28.4	Pathophysiology of Spinal Cord Injury	390
5.28.5	Mechanism(s) of Pain Following Spinal Injury	391
5.28.5.1	Loss of Inhibitory Tone	392
5.28.5.2	Pattern Generators of Pain	393
5.28.5.3	Cell Signaling Pathways: Synaptic Plasticity and Functional State	394
5.28.5.4	Supraspinal Changes Following Spinal Cord Injury	395
5.28.6	Future Directions	395
References		396

Glossary

at-level pain Pain condition associated with spinal cord injury. Located in dermatomes associated with spinal segments immediately adjacent to the site of injury. Characteristics typically include elevated sensitivity to mechanical and thermal stimuli. Spontaneous sensations (i.e., tingling, numbness, burning) can also be associated with this condition of abnormal sensation. Believed to have a predominately spinal mechanism.

below-level pain Pain condition associated with spinal cord injury. Located in dermatomes associated with spinal segments below the level of injury. Pain is typically spontaneous with characteristics of burning, stabbing, and shooting sensations. Mechanism of below-level pain is believed to involve spinal as well as supraspinal mechanisms.

central injury cascade Pathological events triggered by injury to the central nervous system. Initial events include the extracellular release of excitatory amino acids and the initiation of excitotoxic and inflammatory cascades. Included in this cascade are neurochemical and molecular changes that ultimately lead to changes in the functional properties of spinal and supraspinal sensory neurons.

central sensitization Change in the functional state of central neurons secondary to persistent input or injury-induced elevations of excitatory amino acids leading to the activation of cellular signaling pathways. The end result of this change in functional state is an increase in excitability that can lead to clinical symptoms of allodynia, hyperalgesia, or pain.

pattern generators of pain Dysfunctional neurons with increased excitability are capable of producing abnormal discharges. Collectively the discharges generated from a large population of neurons can form the substrate responsible for the perception of pain.

secondary injury Following an initial mechanical or vascular insult to the brain or spinal cord there is a series of events that are components of the central injury cascade. These events lead to the spread of pathological damage of central neurons beyond the primary insult.

5.28.1 The Condition of Pain Following Spinal Cord Injury

Pain following spinal cord injury (SCI) is one of many challenges associated with the life-threatening consequences of SCI. Over the past 15 years clinical and preclinical studies related to at- and below-level pain have provided an understanding of the spinal and supraspinal mechanism(s) responsible for these conditions. In spite of the fact that loss of sensory and motor function below the level of injury are regarded as the most significant consequences of SCI, the condition of pain has a direct relationship with the ability of patients to regain an optimal level of activity, return to work, and achieve an acceptable quality of life. The impact of spinal injury pain on the healthcare community is evident from studies reporting the incidence of painful sensations at a rate of 60–80% for all SCI patients with nearly 40% reporting severe pain to the extent they would trade any chance of recovering motor function for relief of pain (Nepomuceuno, C. *et al*., 1979; Beric, A., 1990; Britell, C. W. and Mariano, A. J., 1991; Tasker, R. R. *et al*., 1991; Beric, A., 1992; Widerstrom-Noga, E. G. *et al*., 1999a). The functional impact of pain following SCI is further demonstrated by a report describing the challenge of dealing with pain is only surpassed by the decreased ability to walk, loss of sexual function, and bladder and bowel dysfunction (Widerstrom-Noga, E. G. *et al*., 1999b).

5.28.2 Clinical Characteristics of Spinal Injury Pain

Pain associated with SCI is typically bilateral and perceived in anesthetic regions at and below the level of injury. Although changes in sensation above the injury have been reported, there is little evidence supporting the clinical significance of this type of altered sensation. The more common at- and below-level conditions are often referred to as deafferentation pain, dysesthetic pain, or central dysesthesia syndrome (Beric, A. *et al*., 1988; Bonica, J. J., 1991; Yezierski, R. P., 2002). A characteristic of SCI pain that has been consistently documented is the detrimental impact across multiple quality of life domains, including life satisfaction, physical health, and overall handicap. Commonly used descriptors of SCI pain include burning, tingling, numbness, aching, and throbbing. Although it is often difficult to classify different categories of pain, below-level neuropathic pain is the most common and most difficult to treat (Finnerup, N. M. *et al*., 2002). When discussing different classifications of pain it is helpful to have a standard taxonomy. A Task Force of the International Association for the Study of Pain proposed a taxonomy for SCI pain based on the type of pain, location, and putative mechanism of pain onset (Siddall, P. J. *et al*., 2002; Table 1). Having a taxonomy that is accepted and used by clinical and basic research specialists in the fields of pain and spinal injury is essential to achieving a better understanding of different pain conditions.

Table 1 International Association for the Study of Pain proposed classification of spinal cord injury pain

Broad type (tier one)	*Broad system (tier two)*	*Specific structures/pathology (tier three)*
Nociceptive	Musculoskeletal	Bone, joint, muscle trauma, or inflammation
		Mechanical instability
		Muscle spasm
		Secondary overuse syndromes
	Visceral	For example, Renal calculus, bowel dysfunction
		Dysreflexic headache
Neuropathic	(above level)	Compressive mononeuropathies
		Complex regional pain syndromes
	(at level)	Nerve root compression, cauda equina
		Syringomyelia
		Spinal cord trauma/ischaemia
		Dual level cord and root trauma
	(below level)	Spinal cord trauma/ischaemia

Adapted from Siddall, P. J., Yezierski, R. P., and Loeser, J. D. 2002. Taxonomy and Epidemiology of Spinal Cord Injury. In: Spinal Cord Injury Pain: Assessment, Mechanisms, Management (*eds*. R. P. Yezierski and K. Burchiel), pp. 9–24. IASP Press, with permission from International Association for the Study of pain.

The condition of pain following spinal injury has a variable onset depending on the type of pain. Siddall P. J. *et al.* (2003) described the prevalence and onset of different types of pain in a cohort of 100 patients. Musculoskeletal pain (59%) was the most common type of pain followed by at-level (41%) and below-level (34%) neuropathic pain, with visceral pain (5%) the least common type of pain experienced. The mean onset time for any type of pain was 1.6 years with at-level and musculoskeletal pain having the shortest onset times, 1.2 and 1.3 years, respectively. Below-level pain generally had a longer onset time (1.8 years) and visceral pain had the longest (4.2 years). While there has been considerable effort to identify physical factors such as completeness and level of injury that correlate with pain onset, few consistent predictors have been identified (Siddall, P. J. *et al.*, 1999a; Werhagen, L. *et al.*, 2004). A positive relationship between the higher incidence of pain in patients with thoroacolumbar and incomplete lesions has been described (Demirel, G. *et al.*, 1998).

5.28.3 The Research Challenge of Spinal Injury Pain

A major challenge in the study of altered sensation following SCI is the development of appropriate injury models that parallel the human condition. The study of SCI pain has seen the use of several different models, including mechanical trauma, isolated lesions, complete transection, chemical lesions, and ischemic injury, each with pathological components found in the human condition (Wiesenfeld-Hallin, Z. *et al.*, 1994; Siddall, P. J. *et al.*, 1995; Christensen, M. D. and Hulsebosch, C. E., 1997; Yezierski, R. P. *et al.*, 1998; Bruce, J. C. *et al.*, 2002; Scheifer, C. *et al.*, 2002). Behavioral outcome measures used to evaluate injury-induced changes in sensation represents another critical factor in the study of spinal and supraspinal mechanisms of different pain conditions. The majority of behavioral measures used in the study of spinal injury pain rely on responses to mechanical and thermal stimuli to evaluate changes in nociceptive sensitivity. These studies have used a variety of nociceptive reflexes, such as hindpaw withdrawal, that are regulated by segmentally organized spinal mechanisms and are present in spinalized animals. Lick and guard responses have also been used and these responses to nociceptive input depend on spino-bulbo-spinal circuits and are present in decerebrate animals (Woolf, C. J., 1984). Reflex responses are important measures of nociception that have the potential to reveal changes in excitability of spinal circuits, an important consequence of spinal injury. Enhancement of flexion/withdrawal reflexes as reported in the spastic syndrome, however, can be dissociated from chronic below-level pain in individual cases of subtotal SCI (Vierck, C. J. *et al.*, 2002a; 2002). These responses do not represent the component of pain perception that requires cerebral processing of sensation (Mauderli, A. P. *et al.*, 2000) and are more likely to apply to the study of at-level pain that is thought to depend on a spinal mechanism. A misconception in the preclinical study of SCI pain is that stimulation of peripheral dermatomes below the lesion to elicit a reflex response is thought to qualify as the study of below-level pain. The fact is below-level pain is likely to involve supraspinal mechanisms and therefore cannot be studied with reflex-based outcome measures.

Another strategy of behavioral assessment is the use of operant tests that require discrimination between nociceptive and non-nociceptive stimulation and the organization of complex behavioral adaptations to specific environmental contingencies. This approach is believed to provide a more accurate assessment of the pain experience (Vierck, C. J. *et al.*, 2002). The challenge of selecting appropriate behavioral measures is especially evident in the study of below-level pain. If it is assumed that this type of pain requires cortical involvement then to study this type of pain effectively a behavioral measure that relies on activation of cortical structures must be used. The only measures to fit these criteria are operant behaviors that rely on cortical processing for the perception of nociceptive stimuli as well as the planning and execution of learned responses. Acceptance of the differences between responses obtained with operant versus reflex measures represents a major challenge in the study of spinal injury pain, especially studies related to at- and below-level pain.

By far the most significant sensory consequence of spinal injury is below-level pain. This condition has been difficult to study in preclinical models as the pain is typically spontaneous and occurs in parts of the body that are anesthetic. Below-level pain has been attributed to white matter damage, although evidence supports the presence of abnormal activity within the gray matter contributing to below-level hyperalgesia and spontaneous pain behavior. This was demonstrated in experiments with rats and monkeys in which ischemic involvement of spinal gray matter was a critical factor in the development of hyperalgesia after interruption of the spinothalamic tract (Vierck, C. J. *et al.*, 2000). Similarly, quisqualic acid injections in

the spinal gray matter produce below-level hyperalgesia and spontaneous pain behavior without damage to surrounding gray matter (Yezierski, R. P. *et al*., 1998; King, C. D. *et al*., 2006). Clinically, results of a magnetic resonance imaging study in patients with and without below-level pain showed the most common pathological feature of patients with below-level pain was the presence of lesions that included the central core of spinal gray matter (Finnerup, N. M. *et al*., 2003b).

5.28.4 Pathophysiology of Spinal Cord Injury

In order to understand the mechanisms responsible for SCI pain it is important to acknowledge that associated with spinal injury is a cascade of biochemical, molecular, and anatomical changes that collectively impact the survivability and functional integrity of spinal neurons (Figure 1). The clinical consequences associated with SCI, including at- and below-level pain, are believed to result from the influence of this cascade on the functional state of spinal and supraspinal neurons. Therefore to understand the end result (i.e., pain), it is important to appreciate the basic biology of secondary events that precede this condition.

The most obvious pathological changes associated with traumatic or ischemic injury to the spinal cord include, but are by no means limited to, the loss of neurons, damage to surrounding white matter, astrocytic scarring, syrinx formation, and breakdown of the spinal blood–brain barrier (Kakulas, B. A. *et al*., 1990; Bunge, R. P. *et al*., 1993). Also contributing to the progression of tissue damage are secondary injury cascades that include excitotoxic and inflammatory processes (Young, W., 1987; Tator, C. H. and

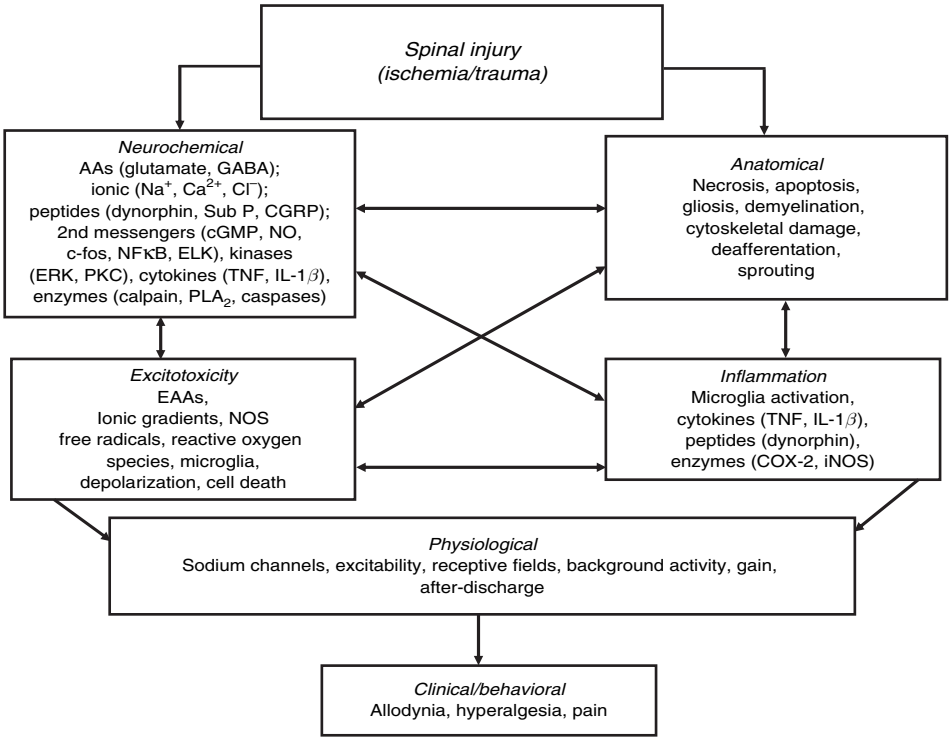

Figure 1 Components of the spinal injury cascade that contribute to the mechanism responsible for the development of pain. Evidence supporting the involvement of this cascade comes from results of clinical and experimental studies involving mechanical, ischemic, and/or chemical models of spinal injury (see text for details). The four major components of the cascade (neurochemical, excitotoxicity, anatomical, and inflammation) are represented as interactive and collectively lead to conditions producing functional changes in spinal and supraspinal neurons. The endpoint of the cascade is the onset of clinical and behavioral symptoms, e.g., allodynia, hyperalgesia, and pain. AAs, amino acids; cGMP, cyclic guanidine monophosphate; CGRP, calcium gene-related peptide; COX-2, cyclo-oxygenase-2; EAA, excitatory amino acid; ELK, ets-like gene; ERK, extracellular signal-regulated kinase; GABA, gamma-aminobutyric acid; IL-1β, interleukin-1β; iNOS, inducible nitric oxide synthase; NFkB, nuclear factor kappa B; NO, nitric oxide; PKC, protein kinase C; PLA_2, phospholipase A2; Sub P, substance P; TNF, tumor necrosis factor. Reproduced from Yezierski, R. P. 2006. Pain Following Spinal Cord Injury: Central Mechanisms. In: Handbook of Clinical Neurology (*eds*. F. Cervero and T. S. Jensen), Vol. 81, pp. 293–307, with permission from Elsevier.

Fehlings, M. G., 1991; Hsu, C. Y. *et al.*, 1994; Regan, R. and Choi, D. W., 1994; Bethea, J. R. *et al.*, 1999). Excitotoxic events following spinal injury are initiated by the well-documented effects of excitatory amino acids (EAAs) that are involved in the secondary pathology, including neuronal degeneration (Faden, A. I. and Simon, R. P., 1988; Nag, S. and Riopelle, R. J., 1990; Hao, J. X. *et al.*, 1991; Yezierski, R. P. *et al.*, 1993; Regan, R. and Choi, D. W., 1994; Wrathall, J. R. *et al.*, 1994). For this reason glutamate has been viewed as one of several putative chemical mediators contributing to the central cascade of secondary pathological changes following injury (Tator, C. H. and Fehlings, M. G., 1991). Inflammation is another major contributor to secondary injury (Bethea, J. R. and Dietrich, W. D., 2002). With the aid of specific histological and immunohistological stains the temporal profile of glia activation (astrocytes, microglial) and the infiltration of macrophages and other inflammatory cell types can be followed. Upregulation of messenger RNA (mRNA) for c-fos, tumor necrosis factor (TNF)-α and dynorphin have also been described following SCI (Yakovlev, A. G. and Faden, A. I., 1994). From this discussion it should be clear that the pathological sequela of SCI is by no means simple neither is it restricted to the site of insult as pathological consequences of SCI have been observed throughout the full extent of the neuraxis (Brewer, K. L. *et al.*, 1997; Jain, N. *et al.*, 1998; Morrow, T. J. *et al.*, 2000).

One of the earliest responses to spinal injury is the breakdown of cellular membranes and subsequent activation of phospholipases. Within minutes of injury, lipid peroxidation and membrane hydrolysis release polyunsaturated fatty acids capable of causing damage, through arachidonic acid and eicosanoid pathways (Anderson, D. and Hall, E., 1993; Tator, C., 1995). Reactive oxygen species (ROS) likewise trigger excitotoxic reactions (glutamate and quinolinate); catecholamine oxidation; mitochondrial breakdown; oxidation of extravasated hemoglobin; neutrophil infiltration; microglial activation; and release of nitric oxide, cytokines, and growth factors. Thus, ROS contribute to the development of a permissive environment for pain following SCI (Kim, H. K. *et al.*, 2004; Hains, B. C. and Waxman, S. G., 2006; Peng, X. M. *et al.*, 2006). Other changes associated with different models of SCI include: afferent sprouting in distant segments (Ondarza, A. B. *et al.*, 2003), upregulation of vanilloid receptor expression (Zhou, Y. *et al.*, 2002), changes in expression of metabotropic glutamate receptors (Mills, C. D. *et al.*, 2001), activation of protein kinases and transcription factors associated with the MAPK signaling pathway (Crown, E. D. *et al.*, 2005; Yu, C. G. and Yezierski, R. P., 2005a), increased NR1 serine phosphorylation of the NMDA receptor (Caudle, R. M. *et al.*, 2003), changes in galanin immunoreactivity (Zvarova, K. *et al.*, 2004), and increased expression of c-fos mRNA (Yakovlev, A. G. and Faden, A. I., 1994; Siddall, P. J. *et al.*, 1999b; Abraham, K. E. and Brewer, K. L., 2001). Furthermore, analysis of molecular events using DNA microarray analysis has shown that 1 h after spinal trauma there are changes in mRNA levels for 165 genes (Nesic, O. *et al.*, 2002; 2005), including those regulating transcription factors, inflammatory processes, cell survival, and membrane excitability. In spite of the wide range of changes associated with spinal injury, the challenge remains to determine which ones have a causal relationship with the mechanism of pain onset, as opposed to being secondary events associated with the process of injury.

An important consideration in the progression of pathological changes associated with spinal injury is the longitudinal extent over which spinal tissue is influenced by the central injury cascade. In a study using agents with neuroprotective properties it was shown that limiting the spread of injury had a significant impact on the expression of pain-related behaviors (Yu, C. G. *et al.*, 2003). This study led to the proposal of a spatial threshold in which a critical distance of spinal tissue must be affected by the secondary injury cascade in order for pain behaviors to develop. Therefore, a critical determinant underlying the expression of pain following SCI may be a combination of specific injury related events together with the longitudinal spread of these events within the cord (Yezierski, R. P., 2000; Gorman, A. L. *et al.*, 2001). Identifying the mechanism responsible for the spread of injury may provide valuable insight into the development of different pain conditions. Given the permissive microenvironment for the development of pain associated with the wide spectrum of molecular, anatomical, neurochemical, and functional changes that occur following spinal injury it is not surprising that pain is a common clinical finding following injury.

5.28.5 Mechanism(s) of Pain Following Spinal Injury

The precise mechanism(s) underlying different types of neuropathic pain (at- and below-level) associated with spinal injury remain to be determined. While

below-level pain is considered to have a central mechanism involving cortical and subcortical structures, at-level pain may have peripheral and central components. Unfortunately, little is known about the potential peripheral contribution to spinal injury pain. Little is also known about the role of the autonomic nervous system (ANS) in the development of different pain conditions following injury. Given the likely damage to sympathetic and parasympathetic neurons following injury and the contribution of the ANS to chronic pain states, there is a need for studies focusing on the role of autonomic dysfunction in the development of spinal injury pain.

Results of experimental studies have provided evidence to construct a working model for at- and below-level behavioral effects of SCI. This model includes a combination of six conditions: (1) loss of spinal inhibitory neurons, (2) emergence of spinal generators and supraspinal amplifiers of abnormal activity, (3) dependence on a population of NK-1R expressing neurons in the superficial dorsal horn, (4) longitudinal progression of a secondary injury cascade, (5) reorganization of supraspinal structures, and (6) activation of the MAPK cell signaling pathway (Figure 2).

5.28.5.1 Loss of Inhibitory Tone

A critical factor in the onset of painlike behaviors following SCI is the loss of inhibitory influences within the injured spinal cord (Wiesenfeld-Hallin, Z., *et al.* 1994). The loss of inhibitory control allows for the recruitment of surrounding neurons and intensification and spread of abnormal sensations, including pain. Support for this conclusion comes from four lines of evidence: (1) following ischemic injury there is an increased excitability of WDR neurons that is reversed by the $GABA_B$ receptor agonist baclofen (Hao, J. X. *et al.*, 1992), (2) hypersensitivity to peripheral stimuli can be produced in normal animals by the intrathecal administration of gamma-aminobutyric acid (GABA) receptor antagonists (Yaksh, T. L., 1989; Hao, J.-X. *et al.*, 1994),

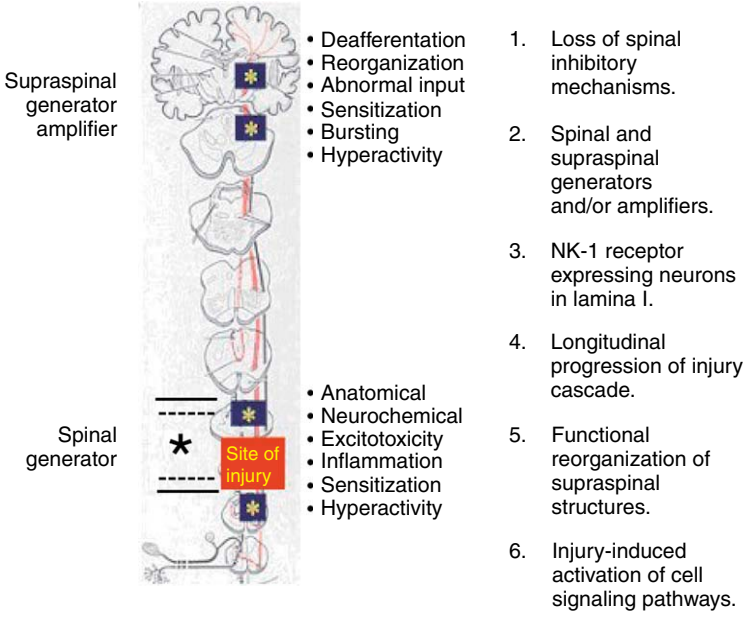

Figure 2 Summary of six different injury-induced changes contributing to the development of at- and below-level pain associated with spinal cord injury. A spinal pain generator evolves due to the collective impact of anatomical, neurochemical, inflammatory, and excitotoxic changes that result in the increased excitability of spinal sensory neurons. Specific changes contributing to the development of the spinal generator include loss of inhibitory mechanisms, the longitudinal progression of the spinal injury cascade, and the injury-induced activation of cell-signaling pathways. At supraspinal levels the presence of a generator/amplifier mechanism emerges as a result of the loss of afferent input from spinal segments below the level of injury (deafferentation). The functional impact of this and other injury-induced changes at supraspinal levels (e.g., sprouting, unmasking of connections) results in the activation of supraspinal regions by input from somatotopically inappropriate regions of the cord and the referral of pain sensations to dermatomes below the level of injury. Reproduced from Yezierski, R. P. 2006. Pain Following Spinal Cord Injury: Central Mechanisms. In: Handbook of Clinical Neurology (*eds*. F. Cervero and T. S. Jensen), Vol. 81, pp. 293–307, with permission from Elsevier.

(3) decreased numbers of GABA-positive neurons following ischemic spinal injury (Zhang, A.-L. *et al.*, 1999), and (4) administration of drugs that prolong the action of inhibitory neurotransmitters (i.e., tricyclic antidepressants) are effective in the short-term treatment of spinal injury pain (Tunks, E., 1986; Lejon, G. and Boivie, J., 1991; Boivie, J., 1994). Although existing evidence supports the decreased inhibitory influence of GABAergic neurotransmission in altering the functional properties of neurons in the injured cord, not to be overlooked in this process is a decreased influence of supraspinal inhibitory pathways that may be disrupted following injury. Alterations in descending serotonergic projections above and below the site of injury have led to the suggestion that loss of inhibitory influences below the injury may contribute to the increased excitability of neurons while an increase in serotonergic projections above the injury may contribute, through descending facilitation, to a change in functional state of neurons above the level of injury (Oatway, M. A. *et al.*, 2004).

5.28.5.2 Pattern Generators of Pain

Another component of the pathophysiological sequela of SCI that is thought to contribute to the onset of altered sensations is the emergence of a pattern generating mechanism (spinal and supraspinal). Several observations are consistent with the pattern generating hypothesis: (1) existence of focal regions of hyperactivity in the spinal cord and thalamus of spinal injured patients (Loeser, J. D. *et al.* 1968; Edgar, R. E. *et al.*, 1993; Lenz, F. A. *et al.*, 2000); (2) effectiveness of spinal anesthesia in alleviating pain when delivered proximal to the site of injury (Pollock, L. J. *et al.*, 1951; Botterell, E. H. *et al.*, 1953; Loubser, P. G. and Donovan, W. H., 1991); and (3) sensitization and prolonged after-discharges of spinal and supraspinal sensory neurons following SCI (Hao, J. X. *et al.*, 1992; Yezierski, R. P. and Park, S. H., 1993; Lenz, F. A. *et al.*, 2000; Drew, G. M. *et al.*, 2001; Hains, B. C. *et al.*, 2003b; Hoheisel, U. *et al.*, 2003; Hao, J. X. *et al.*, 2004; Hains, B. C. *et al.*, 2005). Consistent with an involvement of neuronal hyperexcitability as a component of the spinal and possibly supraspinal mechanism of SCI pain are results of pharmacological studies. For example, lidocaine and ketamine, two drugs that reduce membrane excitability and glutamate receptor activation are effective in treating SCI pain (Loubser, P. G. and Donovan, W. H., 1991; Eide, P. K. *et al.*, 1995; Attal, N. *et al.*, 2000). Efforts to increase inhibition with either baclofen or propofol are also effective (Herman, R. M. *et al.*, 1992; Canavero, S. *et al.*, 1995). The anticonvulsant lamotrigine that affects sodium channels involved in hyperexcitability is also suggested to be effective in SCI patients with spontaneous and evoked pain (Finnerup, N. M. *et al.*, 2002).

Consistent with the excitability hypothesis and involvement of neurons in the superficial dorsal horn in spontaneous and evoked pain behaviors, are clinical reports of abnormal focal hyperactivity within the superficial laminae of the injured cord (Edgar, R. E. *et al.*, 1993). Microcoagulation of these hyperactive areas in the dorsal root entry zone (DREZ) at depths of 1–2 mm, representing Rexed's laminae I–II, results in a significant diminution of pain. A variant of the DREZ technique utilizing intramedullary recordings of C-fiber evoked responses to guide DREZ lesioning allows for the somatotopic mapping of the DREZ with regard to the generation of central deafferentation pain. In 25 patients where this technique was used, 84% received complete pain relief (Falci, S. *et al.*, 2002). An involvement of this region in the generation of pain is further supported by a report where elimination of NK-1R-expressing neurons in the superficial dorsal horn resulted in not only the prevention of spontaneous pain behavior, but also the reversal of the behavior once it had been initiated (Yezierski, R. P. *et al.*, 2004).

Injury-induced changes contributing to increased excitability of spinal circuitry has also been attributed to an increased expression of the $Na_v1.3$ sodium channel in spinal segments L3–L5 following contusion injury at T9 (Hains, B. C. *et al.*, 2003a). Upregulation of $Na_v1.3$ expression at sites remote from the epicenter of injury was shown to have a significant role in producing increased excitability of spinal multireceptive neurons recorded in L3–L5. Efforts to block these changes after injury showed that responses of neurons in animals treated intrathecally with antisense oligodeoxynucleotides targeting $Na_v1.3$ decreased expression of $Na_v1.3$ mRNA and protein, reduced hyperexcitability of multireceptive neurons, and attenuated mechanical allodynia and thermal hyperalgesia after SCI. Similarly, upregulation of $Na_v1.3$ sodium channels in thalamic neurons has also been shown to contribute to changes in the electrophysiological properties of these neurons (Hains, B. C. *et al.*, 2005). Thus, changes in the functional state of sensory neurons secondary to upregulation of sodium channels provides the mechanism for a pain generator in the injured cord as well as an amplifier of abnormal activity in thalamus.

The contribution of abnormal spinal input together with the effects of deafferentation (secondary to loss of spinal projection neurons) and upregulation of sodium channels could result in the development of abnormal generators or amplifiers of spinal input at supraspinal sites (Vierck, C. J., Jr., 1991). The transient relief of below-level pain in humans following application of local anesthetic to the proximal stump of a spinal lesion (Pollock, L. J. *et al.*, 1951) suggests that the presence of a spinal generator plays a significant role in maintaining chronic below-level pain. Thus, a combination of supraspinal changes secondary to deafferentation, and the emergence of a spinal generator of abnormal activity are two significant events that may contribute to the development and maintenance of below-level pain. Recently, the report of elevated blood flow in thalamic nuclei (possibly reflecting changes in the functional state of neurons) lend additional support to the thalamic involvement in the supraspinal response to SCI and to the mechanism of injury-induced pain (Morrow, T. J. *et al.*, 2000).

5.28.5.3 Cell Signaling Pathways: Synaptic Plasticity and Functional State

Another consideration for the mechanism of chronic pain following spinal injury is synaptic plasticity and changes in the functional state of spinal neurons. A significant response to injury of central or peripheral origin is the cellular response believed to contribute to the sensitization of spinal neurons (Woolf, C. J. and Csotigan, M., 1999; Woolf, C. J., 1992; Willis, W. D., 2002). Synaptic plasticity in the central nervous system is thought to be part of central sensitization and together with the long-term changes in functional state of spinal sensory neurons represents a potential mechanism for persistent pain (Ji, R. R. *et al.*, 2003). Unfortunately, we are only at the beginning of understanding the biochemical and molecular events underlying long-term functional plasticity and their role in chronic pain. Included in the events thought to be involved in producing long-term changes are: (1) phosphorylation of regulatory proteins (as well as dephosphorylation of others), (2) positive and negative regulation of gene transcription, (3) injury-induced synthesis of proteins (as well as reduced synthesis of others), (4) strengthening of some and weakening of other connections (synaptic long-term potentiation, sprouting, and pruning), and (5) the death or rescuing of neurons. These neuronal changes share initiating events such as glutamate-induced elevations in calcium, maintaining events (nitric oxide synthesis, activation of protein kinases), perpetuating forces (activation of cyclic AMP response element-binding (CREB), nuclear factor kappa B (NF-κB), and terminal results (altered synaptic efficacy). In contrast to cellular events underlying persistent pain of peripheral origin, the mechanism underlying long-term plasticity associated with pain of central origin remains largely unexplored.

Important events contributing to the development of injury-induced pain are found in a construct of central sensitization and plasticity (Woolf, C. J. and Csotigan, M., 1999; Ji, R. R. and Woolf, C. J., 2001; Ji, R. R. *et al.*, 2003). Hypersensitivity is believed to be a consequence of early posttranslational changes as well as later transcription-dependent changes in effector genes. Neuroplasticity resulting from these events includes activity-dependent changes in neurons and specific signaling molecules in signal transduction pathways. These changes likely contribute to alterations in the basal state of excitability that ultimately contributes to the development of spinal pain generators and possibly supraspinal amplifiers.

Examples of cell signaling events following spinal injury were described in a study of changes in the mitogen-activated protein kinase (MAPK) signaling pathway following excitotoxic spinal injury including: (1) increased phosphorylation of ERK1/2, (2) increased activation of NF-κB and phosphorylation of ELK-1, and (3) increased gene expression for the NK-1 receptor and NR1 and NR-2A subunits of the NMDA receptor (Yu, C. G. and Yezierski, R. P., 2005a). Blockade of the MAPK cascade with the MEK inhibitor PD98059 inhibited phosphorylation of ELK-1, activation of NF-κB, and gene expression of NR1, NR-2A, and NK-1R, and prevented the development of spontaneous pain behavior. Injury-induced elevations in spinal levels of EAAs thus lead to the activation of the ERK → ELK-1 and NF-κB signaling cascades and the transcriptional regulation of receptors important in the development of chronic pain. Blockade of these intracellular kinase cascades prevents the onset of injury-induced pain behavior. Similar changes in different components of the MAPK signaling pathway have been described in the diencephalon following injury (Yu, C.-G. and Yezierski, R. P., 2005b). The persistent upregulation of CREB in spinothalamic tract cells is another example of how cell signaling events are affected by SCI (Crown, E. D. *et al.*, 2005).

The above results suggest that many of the same molecular changes described as activity-dependent following peripheral nerve and tissue injury can also

be induced following central injury, that is, injury dependent. This suggests that the mechanism responsible for the increased excitability of spinal neurons following spinal injury may be similar to the well-documented activity-dependent mechanism induced by damage to peripheral tissue and/or nerves, a mechanism resulting in the activation of intracellular kinase cascades and ultimately long-term changes in synaptic efficacy and neuronal excitability. The end result of these events is the emergence of a hyperexcitable pain-generating mechanism.

5.28.5.4 Supraspinal Changes Following Spinal Cord Injury

One cannot discuss SCI without acknowledging the most fundamental of all anatomical facts and that is the connection between the brain and spinal cord. Following injury to the cord it has been well documented that there are multiple changes (e.g., anatomical, molecular, functional) that occur within cortical and subcortical structures. Changes in supraspinal structures could potentially contribute to the central mechanism responsible for the onset and progression of injury-induced pain behaviors. Studies carried out include an evaluation of changes in forebrain blood flow (Morrow, T. J. *et al.*, 2000), and evaluation of opiate transmitters in selected supraspinal sites (Abraham, K. E. *et al.*, 2001). In the study by Morrow T. J. *et al.* (2000) significant increases in regional cerebral blood flow were found in seven of 22 supraspinal structures examined, including the arcuate nucleus, hindlimb region of S1 cortex, parietal cortex and the thalamic posterior, ventral posterior medial and lateral nuclei. All of these structures have well-documented roles in sensory processing. These studies complement clinical observations showing similar changes in thalamic blood flow following SCI (Ness, T. J. *et al.*, 1998), alterations in the chemical profile of ventroposterolateral thalamus in patients with SCI pain (Pattany, P. M. *et al.*, 2002), and reports of hyperactive foci of thalamic activity in SCI patients with spontaneous burning pain (Lenz, F. A. *et al.*, 2000; Ohara, S. *et al.*, 2002).

Additional support for supraspinal changes contributing to the mechanism of spinal injury pain is the work from Brewer and colleagues focusing on changes in peptidergic transmitter systems at supraspinal levels following excitotoxic SCI (Abraham, K. E. *et al.*, 2001). Preproenkephalin (PPE) and preprodynorphin (PPD) expression was shown to increase in cortical regions associated with nociceptive function; PPE in the cingulate cortex and PPD in the parietal cortex, both ipsilateral and contralaterally at various timepoints following injury. Increases in PPD were significant in animals that developed spontaneous pain behaviors versus those that did not. PPE expression in the anterior cingulate cortex and PPD expression in the contralateral parietal cortex were significantly higher in animals with spontaneous pain behaviors versus those without pain behaviors. The important conclusion from these reports is that following spinal injury there are significant changes in selected supraspinal sites including somatosensory structures putatively involved in pain processing. These results are consistent with a recent report in humans using proton magnetic resonance spectroscopy showing changes in the thalamic concentrations of selected metabolites in SCI patients with pain (Pattany, P. M. *et al.*, 2002). Thus there is likely to be a significant supraspinal component to the mechanism responsible for the development of below-level SCI pain. Understanding the role of these supraspinal changes in the development of pain, especially below-level, remains a challenge for future studies.

5.28.6 Future Directions

An important realization of clinical and experimental studies directed toward understanding the mechanism(s) of SCI pain is the importance of identifying the critical events responsible for the onset of this condition. Continued studies focusing on different components of secondary excitotoxic and inflammatory cascades ultimately responsible for the dysfunction of spinal and supraspinal neurons are essential to the design of more effective interventions. The condition of pain associated with spinal injury is unlikely to have a simple mechanism that relies exclusively on any one consequence of injury. It is more probable that several components of a central injury cascade contribute to the development and maintenance of different pain states. The precise mechanism is likely to depend on the nature of the injury and progression of pathological and biochemical changes along the rostrocaudal axis of the cord, and include anatomical, molecular, and functional changes occurring in supraspinal structures. The mechanism is likely to include the combination of deafferentation resulting from spinal lesions combined with tonic excitatory input from a generator of abnormal activity in or around the epicenter of gray matter damage, that is, penumbral region. This

input reaches deafferented supraspinal processing centers (via undamaged projections or multisynaptic pathways) and contributes to the abnormal discharge and/or amplification of activity ultimately leading to the perception of pain (at- or below-level).

In conclusion, well-established animal models indicate that at-level SCI pain results from excitotoxic/ischemic damage to the spinal gray and white matter. Experimental models have identified putative mechanisms for generation of at-level pain and have suggested a number of potential therapeutic approaches, including pharmacological strategies targeting inhibitory systems or spinal mediators of cell survival. Of special importance is control over secondary signaling pathways along with injury-induced chemical and molecular changes that modulate neuronal excitability. Additionally, current evidence suggests that restricting the extent of excitotoxic injury after traumatic SCI might prevent the development of below-level neuropathic pain, both by reducing excitatory influences and by limiting gray matter damage. In contrast, below-level neuropathic pain does not appear to result only from interruption of spinothalamic projections to rostral targets, but is potentiated by interruption and/or activation of other pathways, including propriospinal systems. Important questions related to different pain conditions associated with SCI include the role of glia activation and descending modulation (i.e., facilitation) in the initiation and maintenance of different pain states. It will also be important to determine if there are autonomic and peripheral components to the mechanism of SCI pain. Central and/or peripheral contributions to injury-induced visceral pain is another area requiring additional study. Continued use of available animal models of at- and below-level pain should provide an increasingly precise definition of mechanism(s) and potential therapeutic targets for these conditions.

Acknowledgments

This work was supported by NS40096 (RPY).

References

Abraham, K. E. and Brewer, K. L. 2001. Expression of c-fos mRNA is increased and related to dynorphin mRNA expression following excitotoxic spinal cord injury in the rat. Neurosci. Lett. 307, 187–191.

Anderson, D. and Hall, E. 1993. Pathophysiology of spinal cord trauma. Ann. Emerg. Med. 22, 987–992.

Attal, N., Gaude, V., Brasseur, L., Dupuy, M., Guirimand, F., Parker, F., and Bouhassira, D. 2000. Intravenous lidocaine in central pain: a double-blind, placebo controlled, psychophysical study. Neurology 54, 564–574.

Beric, A. 1990. Altered Sensation and Pain in Spinal Cord Injury. In: Recent Achievements in Restorative Neurology (*eds*. M. R. Dimitrijevic, P. D. Wall, and U. Lindblom), pp. 27–36. Karger.

Beric, A. 1992. Pain in Spinal Cord Injury. In: Spinal Cord Dysfunction (*ed*. L. S. Illis), pp. 156–165. Oxford University Press.

Beric, A., Dimitrijevic, M., and Lindblom, U. 1988. Central dysesthesia syndrome in SCI patients. Pain 34, 109–116.

Bethea, J. R. and Dietrich, W. D. 2002. Targeting the host inflammatory response in traumatic spinal cord injury. Curr. Opin. Neurol. 15, 355–360.

Bethea, J. R., Yu, C.-G., Plunkett, J. A., and Yezierski, R. P. 1999. Effects of interleukin-10 (IL-10) on pain behaviors following excitotoxic spinal cord injury. Soc. Neurosci. Abstr. 25, 1443.

Boivie, J. 1994. Central Pain. In: Textbook of Pain, 4rd edn. (*eds*. P. D. Wall and R. Melzack), Churchill Livingston. 871–902.

Bonica, J. J. 1991. Semantic, Epidemiologic and Educational Issues of Central Pain. In: Pain and Central Nervous System Disease: the Central Pain Syndromes (*ed*. K. L. Casey), pp. 13–29. Raven Press.

Botterell, E. H., Callaghan, H. C., and Jousse, A. T. 1953. Pain in paraplegia: clinical management and surgical treatment. Proc. R. Soc. Med. 47, 281–288.

Brewer, K., Yezierski, R. P., and Bethea, J. R. 1997. Excitotoxic spinal cord injury induces diencephalic changes in gene expression. Soc. Neurosci. Abstr. 23, 438.

Britell, C. W. and Mariano, A. J. 1991. Chronic pain in spinal cord injury. Phys. Med. Rehab. 5, 71–82.

Bruce, J. C., Oatway, M. A., and Weaver, L. C. 2002. Chronic pain after clip-compression injury of the rat spinal cord. Exp. Neurol. 178, 33–48.

Bunge, R. P., Puckett, W. R., Becerra, J. L., Marcillo, A., and Quencer, R. M. 1993. Observations on the pathology of human spinal cord injury. A review and classification of 22 new cases with details from a case of chronic cord compression with extensive focal demyelination. Adv. Neurol. 59, 75–89.

Canavero, S., Bonicalzi, V., Pagni, C. A., *et al.* 1995. Propofol analgesia in central pain: preliminary clinical observations. J. Neurol. 242, 561–567.

Caudle, R. M., Perez, F. M., King, C., Yu, C. G., and Yezierski, R. P. 2003. *N*-methyl-D-aspartate receptor subunit expression and phosphorylation following excitotoxic spinal cord injury in rats. Neurosci. Lett. 349, 37–40.

Christensen, M. D. and Hulseboch, C. E. 1997. Chronic central pain after spinal cord injury. J. Neurotrauma 14, 517–537.

Crown, E. D., Ye, Z., Johnson, K. M., Xu, G. Y., McAdoo, D. J., Westlund, K. N., and Hulsebosch, C. E. 2005. Upregulation of the phosphorylated form of CREB in spinothalamic tract cells following spinal cord injury: relation to central neuropathic pain. Neurosci. Lett. 384, 139–144.

Demirel, G., Yllmas, H., Gencosmanoglu, B., and Kesiktas, N. 1998. Pain following spinal cord injury. Spinal Cord. 36, 25–28.

Drew, G. M., Siddall, P. J., and Duggan, A. W. 2001. Responses of spinal neurons to cutaneous and dorsal root stimuli in rats with mechanical allodynia after contusive spinal cord injury. Br. Res. 893, 59–69.

Edgar, R. E., Best, L. G., Quail, P. A., and Obert, A. D. 1993. Computer-assisted DREZ microcoagulation: posttraumatic spinal deafferentation pain. J. Spinal Dis. 6, 48–56.

Eide, P. K., Stubhaug, A., and Stenehjem, A. E. 1995. Central dysesthesia pain after traumatic spinal cord injury is

dependent on *N*-methyl-D-aspartate receptor activation, Neurosurgery 37, 1080–1087.
Faden, A. I. and Simon, R. P. 1988. A potential role for excitotoxins in the pathophysiology of spinal cord injury. Ann. Neurol, 24, 623–626.
Falci, S., Best, L., Bayles, R., Lammertse, D., and Starnes, C. 2002. Dorsal root entry zone microcoagulation for spinal cord injury-related central pain: operative intramedullary electrophysiological guidance and clinical outcome. J. Neurosurg. 97, 193–200.
Finnerup, N. M., Gyldensted, C., Nielsen, E., Kristensen, A. D., Back, F. W., and Jensen, T. S. 2003. MRI in chronic spinal cord injury patients with and without central pain. Neurology 61, 1569–1575.
Finnerup, N. B., Johannesen, I. L., Sindrup, S. H., Bach, F. W., and Jensen, T. S. 2002. Pharmacological Treatment of Spinal Cord Injury Pain. In: Spinal Cord Injury Pain: Assessment, Mechanisms, Management (*eds*. R. P. Yezierski and K. Burchiel), pp. 341–351. IASP Press.
Gorman, A. L., Yu, C. G., Sanchez, D., Ruenes, G. R., Daniels, L., and Yezierski, R. P. 2001. Conditions affecting the onset, severity, and progression of a spontaneous pain-like behavior after excitotoxic spinal cord injury. J. Pain 2, 229–240.
Hains, B. C. and Waxman, S. G. 2006. Activated microglia contribute to the maintenance of chronic pain after spinal cord injury. J. Neurosci. 26, 4308–4317.
Hains, B. C., Klein, J. P., Saab, C. Y., Craner, M. J., Black, J. A., and Waxman, S. G. 2003a. Upregulation of sodium channel $Na_V1.3$ and functional involvement in neuronal hyperexcitability associated with central neuropathic pain after spinal cord injury. J. Neurosci. 23, 8881–8892.
Hains, B. C., Saab, C. Y., and Waxman, S. G. 2005. Changes in electrophysiological properties and sodium channel Nav1.3 expression in thalamic neurons after spinal cord injury. Brain 128, 2359–2371.
Hains, B. C., Willis, W. D., and Hulsebosch, C. E. 2003b. Temporal plasticity of dorsal horn somatosensory neurons after acute and chronic spinal cord hemisection in rat. Brain Res. 970, 238–241.
Hao, J. X., Xu, X. J., Aldskogius, H., Seiger, Å., and Wiesenfeld-Hallin, Z. 1991. The excitatory amino acid receptor antagonist MK-801 prevents the hypersensitivity induced by spinal cord ischemia in the rat. Exp. Neurol. 114, 182–191.
Hao, J.-X., Xu, X.-J., and Wiesenfeld-Hallin, Z. 1994. Intrathecal-aminobutyric acidB ($GABA_B$) receptor antagonist CGP 45448 induces hypersensitivity to mechanical stimuli in the rat. Neurosci. Lett. 182, 299–302.
Hao, J. X., Xu, X. J., Yu, Y. X, Seiger, Å., and Wiesenfeld-Hallin, Z. 1992. Baclofen reverses the hypersensitivity of dorsal horn wide dynamic range neurons to mechanical stimulation after transient spinal cord ischemia: implications for a tonic GABAergic inhibitory control of myelinated fiber input. Neurophysiology 68, 392–396.
Hao, J. X., Kupers, R. C., and Xu, X. J. 2004. Response characteristics of spinal cord dorsal horn neurons in chronic allodynic rats after spinal cord injury. J. Neurophysiol. 92, 1391–1399.
Herman, R. M., D'Luzansky, S. C., and Ippoliti, R. 1992. Intrathecal baclofen suppresses central pain in patients with spinal lesions: a pilot study. Clin. J. Pain 8, 338–345.
Hoheisel, U., Scheifer, C., Trudrung, P., Unger, T., and Mense, S. 2003. Pathophysiological activity in rat dorsal horn neurones in segments rostral to a chronic spinal cord injury. Br. Res. 974, 134–145.
Hsu, C. Y., Lin, T. N., Xu, J., Chao, J., and Hogan, E. L. 1994. Kinins and Related Inflammatory Mediators in Central Nervous System Injury. In: The Neurobiology of Central Nervous System Trauma (*eds*. S. K. Salzman and A. L. Faden), pp. 145–154. Oxford Press.
Jain, N., Florence, S., and Kaas, J. H. 1998. Reorganization of somatosensory cortex after nerve and spinal cord injury. News Physiol. Sci. 14, 144–149.
Ji, R. R. and Woolf, C. J. 2001. Neuronal plasticity and signal transduction in nociceptive neurons: implications for the initiation and maintenance of pathological pain. Neurobiol. Dis. 8, 1–10.
Ji, R. R., Kohno, T., Moore, K. A., and Woolf, C. J. 2003. Central sensitization and LTP: do pain and memory share similar mechanisms? Trends Neurosci. 26, 696–705.
Kakulas, B. A., Smith, E., Gaekwad, U. F., Kaelan, C., and Jacobsen, P. 1990. The Neuropathology of Pain and Abnormal Sensations in Human Spinal Cord Injury Derived from the Clinicopathological Data Base at the Royal Perth Hospital. In: Recent Achievements in Restorative Neurology, (*eds*. M. R. Dimitrijevic, P. D. Wall, and U. Lindblom) Karger, pp. 37–41.
Kim, H. K., Kwon, P. S., Zhou, J. L., Taglialatela, G., Kyungsoon, C., Coggeshall, R. E., and Chung, J. M. 2004. Reactive oxygen species (ROS) play an important role in a rat model of neuropathic pain. Pain 111, 116–124.
King, C. D., Vierck, C. J., Berens, S., and Yezierski, R. P. 2006. Acute stress enhances below-level pain after spinal cord injury. Soc. Neurosci. Meeting, Atlanta, GA.
Leijon, G. and Boivie, J. 1991. Pharmacological Treatment of Central Pain. In: Pain and the Central Nervous System Disease: The Central Pain Syndromes (*ed*. K. L. Casey), pp. 257–266. Raven Press.
Lenz, F. A., Lee, J. I., and Dougherty, P. M. 2000. Human Thalamus Reorganization Related to Nervous System Injury and Dystonia. In: Nervous System Plasticity and Chronic Pain (*eds*. J. Sandkühler, B. Bromm, and G. F. Gebhart),Prog. Brain Res. Vol. 129, pp. 259–273. Elsevier.
Loeser, J. D., Ward, A. A., and White, L. E. 1968. Chronic deafferentation of human spinal cord neurons. J. Neurosurg. 29, 48–50.
Loubser, P. G. and Donovan, W. H. 1991. Diagnostic spinal anesthesia in chronic spinal cord injury pain. Paraplegia 29, 25–36.
Mauderli, A. P., Acosta-Rua, A., and Vierck, C. J. 2000. A conscious behavioral assay of thermal pain in rodents. J. Neurosci. Methods 97, 19–29.
Mills, C. D., Fullwood, S. D., and Hulsebosch, C. E. 2001. Changes in metabotropic receptor expression following spinal cord injury. Exp. Neurol. 170, 244–257.
Morrow, T. J., Paulson, P. E., Brewer, K. L., Yezierski, R. P., and Casey, K. L. 2000. Chronic, selective forebrain responses to excitotoxic dorsal horn injury. Exp. Neurol. 161, 220–226.
Nag, S. and Riopelle, R. J. 1990. Spinal neuronal pathology associated with continuous intrathecal infusion of *N*-methyl-D-aspartate in the rat. Acta Neuropathol. 81, 7–13.
Nepomuceno, C., Fine, P. R., Richards, J. S., Gowens, H., Stover, S. L., Rantanuabol, U., and Houston, R. 1979. Pain in patients with spinal cord injury. Arch. Phys. Med. Rehabil. 60, 605–609.
Nesic, O., Svrakic, N. M., Xu, G. Y., McAdoo, D., Westlund, K. N., Hulsebosch, C. E., Galante, A., Soteropoulos, P., Tolias, P., Young, W., Hart, R. P., and Perez-Polo, J. R. 2002. DNA microarray analysis of the contused spinal cord: effect of NMDA receptor inhibition. J. Neurosci. Res. 68, 406–423.
Nesic, O., Lee, J., Johnson, K. M., Ye, Z., Xu, G. Y., Unaia, G. C., Wood, T. G., McAdoo, D. J., Westlund, K. N., Hulsebosch, C. E., and Perez-Polo, J. R. 2005. Transcriptional profiling of spinal cord injury-induced central neuropathic pain. J. Neurochem. 95, 998–1014.
Ness, T. J., Pedro, E. C. S., Richards, J. S., Kezar, L., Liu, H.-G., and Mountz, J. M. 1998. A case of spinal cord injury-related

pain with baseline rCBF brain SPECT imaging and beneficial response to gabapentin. Pain 78, 139–143.
Ohara, S., Garonzik, I., Hua, S., and Lenz, F. A. 2002. Microelectrode Studies of the Thalamus in Patients with Central Pain and in Control Patients with Movement Disorders. In: Spinal Cord Injury Pain: Assessment, Mechanisms, Management, Prog. Pain Res. Manage., Vol. 23, pp. 219–236 IASP Press.
Oatway, M. A., Chen, Y., and Weaver, L. C. 2004. The 5-HT_3 receptor facilitates at-level mechanical allodynia following spinal cord injury. Pain 110, 259–268.
Ondarza, A. B., Ye, Z., and Hulsebosch, C. E. 2003. Direct evidence of primary afferent sprouting in distant segments following spinal cord injury in rat: colocalization of GAP-43 and CGRP. Exp. Neurol. 184, 373–380.
Pattany, P. M., Yezierski, R. P., Widerstrom-Noga, E. G., Bowen, B. C., Martinez-Arizala, A., Garcia, B. R., and Quencer, R. M. 2002. Proton magnetic resonance spectroscopy of the thalamus: evaluation of patients with chronic neuropathic pain following spinal cord injury. Am. J. Neuroradiology 23, 901–905.
Peng, X. M., Zhou, Z. G., Glorioso, J. C., Fink, D. J., and Mata, M. 2006. Tumor necrosis factor-alpha contributes to below-level neuropathic pain after spinal injury. Ann. Neurol. 59, 843–851.
Pollock, L. J., Brown, M., Boshes, B., Finkelman, I., Chor, H., Arieff, A. J., and Finkel, J. R. 1951. Pain below the level of injury of the spinal cord. AMA Arch. Neurol. Psychiat. 65, 319–322.
Regan, R. and Choi, D. W. 1994. Excitoxicity and Central Nervous System Trauma. In: The Neurobiology of Central Nervous System Trauma (*eds*. S. K. Salzman and A. L. Faden), pp. 173–181. Oxford Press.
Scheifer, C., Hoheisel, U., Trudrung, P., Unger, T., and Mense, S. 2002. Rats with chronic spinal cord transection as a possible model for the at-level pain of paraplegic patients. Neurosci. Lett. 323, 117–120.
Siddall, P., Xu, C. L., and Cousins, M. 1995. Allodynia following traumatic spinal cord injury in the rat. Neuroreport 6, 1241–1244.
Siddall, P. J., McClelland, J. M., Rutkowski, S. B., and Cousins, M. J. 2003. A longitudinal study of the prevalence and characteristics of pain in the first five years following spinal cord injury. Pain 103, 249–257.
Siddall, P. J., Taylor, D., McClelland, J., Rutkowski, S., and Cousins, M. 1999a. Pain report and the relationship of pain to physical factors in the first 6 months following spinal cord injury. Pain 81, 187–197.
Siddall, P. J., Xu, C. L., Floyd, N., and Keay, K. A. 1999b. C-fos expression in the spinal cord in rats exhibiting allodynia following contusive spinal cord injury. Brain Res. 851, 281–286.
Siddall, P. J., Yezierski, R. P., and Loeser, J. D. 2002. Taxonomy and Epidemiology of Spinal Cord Injury. In: Spinal Cord Injury Pain: Assessment, Mechanisms, Management (*eds*. R. P. Yezierski and K. Burchiel), pp. 9–24. IASP Press.
Tator, C. H. and Fehlings, M. G. 1991. Review of the secondary injury theory of acute spinal cord trauma with emphasis on vascular mechanisms. J. Neurosurg. 75, 15–26.
Tator, C. 1995. Update on the pathophysiology and pathology of acute spinal cord injury. Brain Pathol. 5, 407–413.
Tasker, R. R., de Carvalho, G., and Dostrovsky, J. O. 1991. The History of Central Pain Syndromes, with Observations Concerning Pathophysiology and Treatment. In: Pain and Central Nervous System Disease: The Central Pain Syndromes (*ed*. K. L. Casey), pp. 31–58. Raven Press.
Tunks, E. 1986. Pain in Spinal Cord Injured Patients. In: Management of Spinal Cord Injuries (*eds*. R. F. Bloch and M. Basbaum), pp. 180–211. William and Wilkins.
Vierck, C. J., Jr. 1991. Can Mechanisms of Central Pain Syndromes be Investigated in Animal Models? In: Pain and Central Nervous System Disease: The Central Pain Syndromes (*ed*. K. L. Casey), pp. 129–141. Raven Press.
Vierck, C. J., Siddall, P. J., and Yezierski, R. P. 2000. Pain following spinal cord injury: animal models and mechanistic studies. Pain 89, 1–5.
Vierck, C. J., Cannon, R. L., Stevens, K. A., Acosta-Ru, A. J., and Wirth, E. D. 2002. Mechanisms of Increased Pain Sensitivity Within Dermatomes Remote from an Injured Segment of the Spinal Cord. In: Spinal Cord Injury Pain: Assessment, Mechanisms, Management (*eds*. R. P. Yezierski and K. Burchiel), pp. 155–173. IASP Press.
Werhagen, L., Budh, C. N., Hutling, C., and Molander, C. 2004. Neuropathic pain after traumatic spinal cord injury – relations to gender, spinal, level, completeness, and age at the time of injury. Spinal Cord 42, 665–673.
Widerstrom-Noga, E. G., Cuervo, E., Broton, J. G., Duncan, R. C., and Yezierski, R. P. 1999a. Self-reported consequences of spinal cord injury: results of a postal survey. Arch. Phys. Med. Rehab. 80, 580–586.
Widerstrom-Noga, E. G., Cuevo, E. F., Broton, J. G., Duncan, R. C., and Yezierski, R. P. 1999b. Perceived difficulty in dealing with consequences of SCI. Arch. Phys. Med. Rehab. 80, 580–586.
Wiesenfeld-Hallin, Z., Hao, J. X., Aldskogius, H., Seiger, Å., and Xu, X. J. 1994. Allodynia-Like Symptoms in Rats After Spinal Cord Ischemia: An Animal Model of Central Pain. In: Touch, Temperature and Pain in Health and Disease: Mechanisms and Assessments (*eds*. J. Boivie, P. Hansson, and U. Lindblom), Vol. 4, pp. 455–472. IASP Press.
Willis, W. D. 2002. Long-term potentiation in spinothalamic neurons. Brain Res. Rev. 40, 202–214.
Woolf, C. J. 1984. Long term alterations in the excitability of the flexion reflex produced by peripheral tissue injury in the chronic decerebrate rat. Pain 18, 325–343.
Woolf, C. J. and Csotigan, M. 1999. Transcriptional and posttranslational plasticity and the generation of inflammatory pain. Proc. Natl. Acad. Sci. U. S. A. 96, 7723–7730.
Woolf, C. J., Shortland, P., and Loggeshall, R. E. 1992. Peripheral nerve injury triggen central sprouting of myelinated afferents. Nature 355, 75–78.
Wrathall, J. R., Choiniere, D., and Teng, Y. D. 1994. Dose dependent reduction of tissue loss and functional impairment after spinal cord trauma with the AMPA/kainate antagonist NBQX. J. Neurosci. 14, 6598–6607.
Yakovlev, A. G. and Faden, A. I. 1994. Sequential expression of c-fos protooncogene, TNF-alpha, and dynorphin genes in spinal cord following experimental traumatic injury. Mol. Chem. Neuropath. 24, 179–190.
Yaksh, T. L. 1989. Behavioral and autonomic correlates of the tactile evoked allodynia produced by spinal glycine inhibition: effects of modulatory receptor systems and excitatory amino acid antagonists. Pain 47, 111–123.
Yezierski, R. P. 2000. Pain Following Spinal Cord Injury: Pathophysiology and Central Mechanisms. In: Nervous System Plasticity and Chronic Pain (*eds*. J. Sandkühler, B. Bromm, and G. F. Gebhart), Vol. 129, pp. 429–449. Elsevier.
Yezierski, R. P. 2002. Central Neuropathic Pain. In: Surgical Management of Pain (*ed*. K. Burchiel), pp. 42–64. Thieme Medical Publishers.
Yezierski, R. P. 2006. Pain Following Spinal Cord Injury: Central Mechanisms. In: Handbook of Clinical Neurology (*eds*. F. Cervero and T. S. Jensen), Vol. 81, pp. 293–307. Elsevier.
Yezierski, R. P. and Park, S. H. 1993. The mechanosensitivity of spinal sensory neurons following intraspinal injections of quisqualic acid in the rat. Neurosci. Lett. 157, 115–119.

Yezierski, R. P., Liu, S., Ruenes, G. L., Kajander, K. J., and Brewer, K. L. 1998. Excitotoxic spinal cord injury: behavioral and morphological characteristics of a central pain model. Pain 75, 141–155.
Yezierski, R. P., Santana, M., Park, D. H., and Madsen, P. W. 1993. Neuronal degeneration and spinal cavitation following intraspinal injections of quisqualic acid in the rat. J. Neurotrauma 10, 445–456.
Yezierski, R. P., Yu, C. G., Mantyh, P. W., Vierck, C. J., and Lappi, D. A. 2004. Spinal neurons involved in the generation of at-level pain following spinal injury in the rat. Neurosci. Lett. 361, 232–236.
Young, W. 1987. The post-injury responses in trauma and ischemia: secondary injury or protective mechanism. CNS Trauma 4, 27–52.
Yu, C. G. and Yezierski, R. P. 2005a. Activation of the ERK 1/2 signaling cascade by excitotoxic spinal cord injury. Brain Res. Mol. Brain Res. 138, 244–255.
Yu, C.-G. and Yezierski, R. P. 2005b. Effects of Excitotoxic Spinal Cord Injury on Thalamic MAPK and $GABA_A$ Receptors, IASP Meeting, Sydney, Australia.
Yu, C. G., Fairbanks, C. A., Wilcox, G. L., and Yezierski, R. P. 2003. Effects of agmatine, interleukin-10 and cyclosporin on spontaneous pain behavior following excitotoxic spinal cord injury in rats. J. Pain 4, 129–140.
Zhang, A.-L., Hao, J.-X., Seiger, Å, Xu, X.-J., Wiesenfeld-Hallin, Z., Grant, G., and Aldskogius, H. 1999. Decreased GABA immunoreactivity in spinal cord dorsal horn neurons after transient spinal cord ischemia in the rat. Brain Res. 656, 187–190.
Zhou, Y., Wang, Y., Abdelhady, M., Mourad, M. S., and Hassouna, M. M. 2002. Change of vanilloid receptor 1 following neuromodulation in rats with spinal cord injury. J. Surg. Res. 107, 140–144.
Zvarova, K., Murray, E., and Vizzard, M. A. 2004. Changes in galanin immunoreactivity in rat lumbosacral spinal cord and dorsal root ganglia after spinal cord injury. J. Comp. Neurol. 475, 590–603.

Further Reading

Aimone, J. B., Leasure, J. L., Perreau, V. M., and Thallmair, M. 2004. Spatial and temporal gene expression profiling of the contused rat spinal cord. Exp. Neurol. 189, 204–221.
Bethea, J., Castro, M., Lee, T. T., Dietrich, W. D., and Yezierski, R. 1998. Traumatic spinal cord injury induces nuclear factor kappa B activation. J. Neurosci. 18, 3251–3260.
Brewer, K. L., Bethea, J. R., and Yezierski, R. P. 1999. Neuroprotective effects of interleukin-10 following excitotoxic spinal cord injury. Exp. Neurol. 159, 484–493.
Brewer, K. L., McMillan, D., Nolan, T., and Shum, K. 2003. Cortical changes in cholecystokinin mRNA are related to spontaneous pain behaviors following spinal cord injury in the rat. Molec. Brain Res. 118, 171–174.
Christensen, M. D., Everhart, A. W., Pickeman, J., and Hulsebosch, C. E. 1996. Mechanical and thermal allodynia in chronic central pain following spinal cord injury. Pain 68, 97–107.
Davidoff, G. and Roth, E. 1991. Clinical Characteristics of Central (Dysesthetic) Pain in Spinal Cord Injury Patients. In: Pain and Central Nervous System Disease: The Central Pain Syndromes (*ed*. K. L. Casey), pp. 77–83. Raven Press.
Davidoff, G., Roth, E., Guarracini, M., Sliwa, J., and Yarkony, G. 1987. Function limiting dysesthetic pain syndrome among traumatic SCI patients: a cross sectional study. Pain 29, 39–48.
Eide, P. K. 1998. Pathophysiological mechanisms of central neuropathic pain after spinal cord injury. Spinal Cord 36, 601–612.
Finnerup, N. M. and Jensen, T. S. 2004. Spinal cord injury pain – mechanisms and treatment. Eur. J. Neurol. 11, 73–82.
Finnerup, N. B., Johannesen, I. L., Fuglsang-Frederiksen, A., Bach, F. W., and Jensen, T. S. 2003a. Sensory function in spinal cord injury patients with and without central pain. Brain 126, 57–70.
Gerke, M. B., Duggan, A. W., and Siddall, P. J. 2003. Thalamic neuronal activity in rats with mechanical allodynia following contusive spinal cord injury. Neuroscience 117, 715–722.
Gris, D., Marsh, M. A., Oatway, M. A., Chen, Y., Hamilton, E. F., Dekaban, G. A., and Weaver, L. C. 2004. Transient blockade of the CD11d/CD18 integrin reduces secondary damage after spinal cord injury, improving sensory, autonomic and motor function. J. Neurosci. 24, 4043–4051.
Hains, B. C., Everhart, A. W., Fullwood, S. T., and Hulsebosch, C. E. 2002. Changes in serotonin, serotonin transporter expression and serotonin denervation supersensitivity: involvement in chronic central pain after spinal hemisection in the rat. Exp. Neurol. 175, 347–362.
Hains, B. C., Saab, C. Y., and Waxman, S. G. 2006. Alterations in burst firing of thalamic VPL neurons and reversal by $Na_v1.3$ antisense following spinal cord injury. J. Neurophysiol. 95, 3343–3352.
Hayashi, M., Ueyama, T., Nemoto, K., Tamaki, T., and Senba, E. 2000. Sequential mRNA expression for immediate early genes, cytokines and neurotrophins in spinal cord injury. J. Neurotrauma 17, 203–218.
Koetzner, L., Hua, X. Y., Lai, J., Porreca, F., and Yaksh, T. 2004. Nonopioid actions of intrathecal dynorphin evoke spinal excitatory amino acid and prostaglandin E2 release mediated by cyclooxygnease-1 and -2. J. Neurosci. 24, 1451–1458.
Melzack, R. and Loeser, J. D. 1978. Phantom body pain in paraplegics: evidence for a central ''pattern generating mechanism'' for pain. Pain 4, 195–210.
Moore, C. I., Stern, C. E., Dunbar, C., Kostyk, S. K., Gehi, A., and Corkin, S. 2000. Referred phantom sensations and cortical reorganization after spinal cord injury in humans. Proc. Natl. Acad. Sci. U. S. A. 97, 14703–14708.
Plunkett, J. A., Yu, C. G., Bethea, J. R., and Yezierski, R. P. 2001. Effects of interleukin-10 (IL-10) on pain behavior and gene expression following excitotoxic spinal cord injury in the rat. Exp. Neurol. 169, 144–154.
Porreca, F., Ossipov, M. H., and Gebhart, G. F. 2002. Chronic pain and medullary descending facilitation. Trends Neurosci. 25, 319–325.
Rintala, D. H., Loubser, P. G., Castro, J., Hart, K. A., and Fuhrer, M. J. 1998. A comprehensive assessment of chronic pain in a community-based sample of men with spinal cord injury. J. Phys. Med. Rehab. 79, 604–614.
Siddall, P. J. 2002. Spinal Drug Administration in the Treatment of Spinal Cord Injury Pain. In: Spinal Cord Injury Pain: Assessment, Mechanisms, Management (*eds*. R. P. Yezierski and K. Burchiel), pp. 353–364. IASP Press.
Summers, J. D., Rapoff, M. A., Varghese, G., Porter, K., and Palmer, R. E. 1991. Psychosocial factors in chronic spinal cord injury pain. Pain 47, 183–189.
Vierck, C. J. and Light, A. R. 2002. Assessment of Pain Sensitivity in Dermatomes Caudal to Spinal Cord Injury in Rats. In: Spinal Cord Injury Pain: Assessment, Mechanisms, Management (*eds*. R. P. Yezierski and K. Burchiel), pp. 137–154. IASP Press.
Vierck, C. J., Jr. and Light, A. R. 2000. Allodynia and Hyperalgesia within Dermatomes Caudal to a Spinal Cord Injury in Primates and Rodents. In: Nervous System Plasticity and Chronic Pain (*eds*. J. Sandkuhler, B. Bromm, and G. Gebhart), Vol. 129, pp. 411–428. Elsevier.

Xu, X. J., Hao, J. X., and Wiesenfeld-Hallin, Z. 2002. Physiological and Pharmacological Characterization of a Rat Model of Spinal Cord Injury Pain After Spinal Ischemia. In: Spinal Cord Injury Pain: Assessment, Mechanisms, Management (*eds*. R. P. Yezierski and K. Burchiel), pp. 175–187. IASP Press.

Yezierski, R. P. 2002. Pathophysiology and Animals Models of Spinal Cord Injury Pain. In: Spinal Cord Injury Pain: Assessment, Mechanisms, Management (*eds*. R. P. Yezierski and K. Burchiel), Prog. Pain Res. Manage. Vol. 23, pp. 117–136. IASP Press.

R. P. Yezierski and K. J. Burchiel *(eds).* 2002. Spinal Cord Injury Pain: Assessment, Mechanisms, Management IASP Press.

Zhang, A. L., Hao, J. X., Seiger, Å., Xu, X. J., Wiesenfeld-Hallin, Z., Grant, G., and Aldskogius, H. 1999. Decreased GABA immunoreactivity in spinal cord dorsal horn neurons after transient spinal cord ischemia in the rat. Brain Res. 656, 187–190.

5.29 Long-Term Potentiation in Pain Pathways

J Sandkühler, Medical University of Vienna, Vienna, Austria

© 2008 Elsevier Inc. All rights reserved.

5.29.1	Introduction	401
5.29.2	Induction of Long-Term Potentiation in Pain Pathways	402
5.29.3	Signal Transduction Pathways	403
5.29.3.1	Long-Term Potentiation Induction is Context Sensitive	404
5.29.4	Prevention of Long-Term Potentiation	404
5.29.5	Reversal of Long-Term Potentiation	405
5.29.6	Functional Consequences of Long-Term Potentiation in Pain Pathways	405
5.29.7	Conclusions	405
References		405

Glossary

synaptic efficacy, syn. synaptic strength Magnitude of postsynaptic current or potential in response to a presynaptic action potential. Synaptic strength may be modified by pre- and/or postsynaptic modulation.

long-term potentiation (LTP) Enduring increase in synaptic efficacy.

long-term depression (LTD) Enduring decrease in synaptic efficacy of a putatively nonpotentiated synapse.

depotentiation Enduring decrease of synaptic efficacy of a previously potentiated synapse, that is, reversal of LTP.

LTP induction Cellular signal transduction pathways which lead to LTP.

LTP maintenance Cellular signal transduction pathways which are involved in stabilizing established LTP.

spinal field potential Extracelluar electrical field which is mainly generated by simultaneous postsynaptic currents in spinal cord neurons in response to a brief stimulus, similar to evoked potentials in cerebral cortex.

5.29.1 Introduction

Long-term potentiation (LTP) is defined as the persistent increase in synaptic strength (Bliss, T. V. P. and Collingridge, G. L., 1993; Malenka, R. C. and Nicoll, R. A., 1999). Repetitive use of a synapse often leads to LTP which may last for a few hours only or for days to months. Synaptic strength may also be reduced for prolonged periods of time which is called long-term depression (LTD) when induced in a normal synapse or depotentiation when elicited in a previously potentiated synapse, that is, in the maintenance phase of LTP (Huang, C. C. and Hsu, K. S., 2001).

LTP has been most intensively studied in hippocampus where it is considered a fundamental cellular model of learning and memory formation (Bliss, T. V. P. and Collingridge, G. L., 1993; Malenka, R. C. and Nicoll, R. A., 1999). LTP has also been shown in pain pathways at synapses between primary afferent Aδ- or C-fibers and spinal dorsal horn neurons and is one of the proposed cellular mechanisms of pain amplification (Moore, K. A. *et al.*, 2000; Sandkühler, J., 2000). The potential consequences of LTP in pain pathways are manifold: (1) after LTP is established, suprathreshold excitatory input will now evoke stronger excitation of nociceptive neurons. Thus, LTP at nociceptive synapses may underlie hyperalgesia; (2) previously subthreshold excitatory input, from the subliminal fringe of a neurons' receptive field may now elicit action potential firing. This may widen painful areas and contribute to hyperalgesia as well; and (3) some spinal dorsal horn neurons receive subthreshold input from somatotopically inappropriate body areas, for example, the contralateral body half. LTP anywhere

along this subliminal input path may cause mirror image pain or radiating pain. LTP at nociceptive synapses may, however, not significantly lower pain thresholds and is therefore not considered a likely mechanism of allodynia.

The most direct way to ascertain LTP in pain pathways is to measure monosynaptically evoked postsynaptic currents or potentials. So far this has only been done *in vitro* by recording Aδ- or C-fiber-evoked excitatory postsynaptic currents or potentials from dorsal horn neurons in response to electrical stimulation of dorsal roots. When postsynaptic currents are elicited synchronously in a sufficient number of neighboring neurons, electrical field potential are generated which are strong enough to be detected with extracellular microelectrodes (Schouenborg, J., 1984). Thus, to evaluate changes in synaptic strength, C-fiber-evoked field potentials can be recorded in superficial spinal dorsal horn *in vivo* and *in vitro* in response to supramaximal electrical stimulation of a dorsal root or a sensory nerve, for example, the sciatic nerve. If, however, events downstream to postsynaptic currents are recorded, such as action potential discharges, polysynaptically evoked responses, withdrawal reflexes or pain ratings, LTP can no longer be assessed directly. These measures are, however, indispensable to evaluate the functional consequences of LTP in pain pathways. This is discussed in greater detail elsewhere (Sandkühler, J., 2007).

5.29.2 Induction of Long-Term Potentiation in Pain Pathways

In superficial spinal lamina I, LTP is selectively induced in a group of nociceptive specific neurons which express the NK1 receptor for substance P and which project to the brain (see Figure 1; Ikeda, H. *et al.*, 2003; Ikeda, H. *et al.*, 2006). This group of neurons plays a key role in hyperalgesia following inflammation and nerve injury (Mantyh, P. W. *et al.*, 1997). In spinal cord LTP can be induced in different ways, for example, by electrical nerve stimulation , by nerve injury, or peripheral noxious events. Stimulation within the innervation territory of a sensory nerve, for example, with chemical irritants, or by inflammation may also trigger LTP at C-fiber synapses. All conditioning stimuli tested so far which induce LTP at Aδ-synapses (Randic, M. *et al.*, 1993) and/ or C-fiber synapses (Liu, X. G. and Sandkühler, J., 1995) may also cause hyperalgesia in experimental animals.

1. Electrical nerve stimulation: LTP has been induced by conditioning high intensity, high frequency burst-like stimulation (HFS, typically given as 50–100 Hz bursts for 1 s at C-fiber strength) *in vitro* (Randic, M. *et al.*, 1993; Hamba, M. *et al.*, 2000; Ikeda, H. *et al.*, 2000; Ikeda, H. *et al.*, 2003) and *in vivo* (Liu, X. G. and Sandkühler, J., 1997; Miletic, G. and Miletic, V., 2000; Ma, J. Y. and Zhao, Z. Q., 2001; Zhang, H. M. *et al.*, 2001). Stimulation intensity must be sufficient to recruit C-fibers; stimulation at A-fiber intensity is ineffective to induce LTP at C-fiber synapses (Liu, X. G. and Sandkühler, J., 1997). C-fibers do, however, discharge at such high frequencies only rarely. Thus, the pathological relevance of HFS-induced LTP can be challenged.
2. Recent studies show that not only HFS but also conditioning low frequency stimuli at 2–10 Hz which is well within the frequency band of C-fiber discharges during inflammation or tissue injury causes robust LTP, both, *in vivo* and *in vitro* (Terman, G. W. *et al.*, 2001; Ikeda, H. *et al.*, 2006)/electrical stimulation of sciatic nerve at C-fiber intensity (2 Hz, 2 min) induces robust LTP to 300% of control values which is not reversible within the recording periods of up to 18 h (Figure 1; Ikeda, H. *et al.*, 2006).
3. Electrical stimulation of nerves evokes regular and highly synchronous discharges which is not typical for naturally occurring, irregular nonsynchronous discharge patterns. Thus, it was important to show that LTP can also be induced by excitation of sensory nerve endings, for example, by subcutaneous injection of either capsaicin or formalin. In animals with spinal cord and descending pathways intact, intraplantar, s.c. injections of capsaicin or formalin induce slowly rising LTP (Figure 1; Ikeda, H. *et al.*, 2006).
4. Finally, with descending spinal pathways interrupted noxious skin heating and acute nerve injury also causes LTP at C-fiber synapses (Sandkühler, J. and Liu, X., 1998). This demonstrates that naturally occurring, low frequency, irregular, and nonsynchronous afferent barrage can cause synaptic plasticity in pain pathways.

LTP of C-fiber-evoked spinal field potentials can also be induced pharmacologically. In spinalised rats, topical application of *N*-methyl-D-aspartate (NMDA), substance P or neurokinin A induces LTP (Liu, X. G. and Sandkühler, J., 1998). In intact animals, spinal

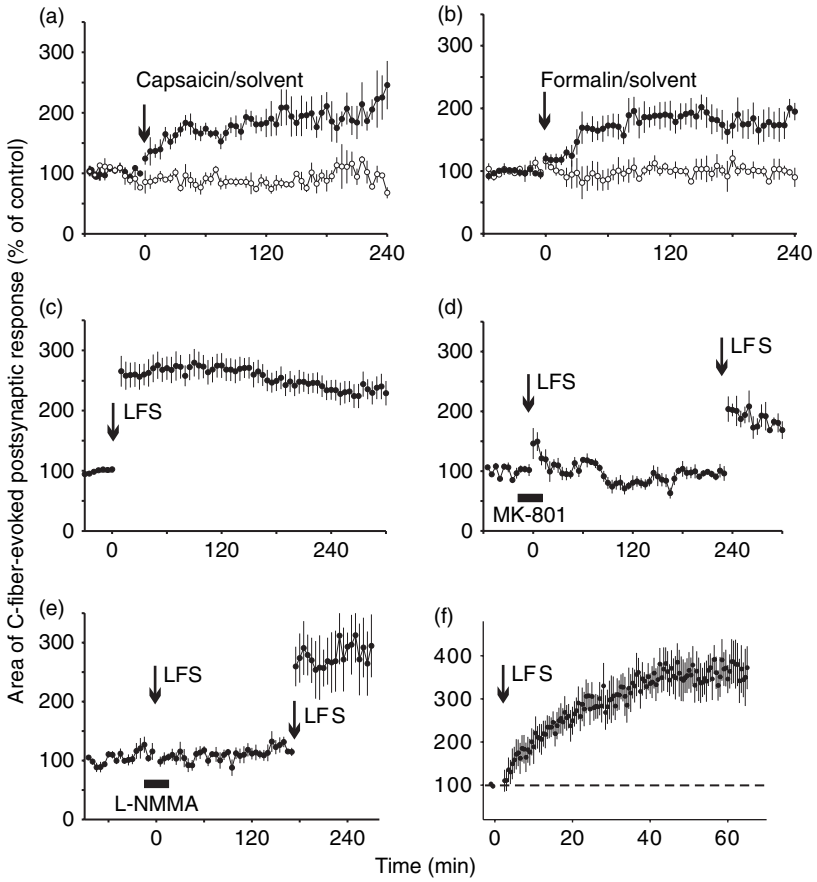

Figure 1 LTP can be induced by natural, low-frequency afferent barrage evoked by inflammation of peripheral tissue *in vivo* and by low-frequency stimulation of dorsal root afferents *in vitro*. Mean time courses of C-fiber-evoked field potentials recorded extracellulary in superficial spinal dorsal horn in response to electrical stimulation of left sciatic nerve of deeply anaesthetized adult rats with spinal cords and afferent nerves intact (a)–(e). Subcutaneous injections of transient receptor potential vanilloid 1 channel agonist capsaicin (1%, 100 µl, $n = 5$, (a) or formalin (5%, 100 µl, $n = 6$), (b) into the glabrous skin at the ipsilateral hind paw, within the innervation territory of the sciatic nerve at time zero (arrows) induced LTP (closed circles), while injections of the respective solvents (open circles) had no effects ($n = 3$ in each group). Conditioning electrical LFS (2 Hz, 2 min at C-fiber intensity) of sciatic nerve at time zero (arrow) also induced LTP ($n = 28$), (c) which was prevented by NMDA receptor antagonist MK-801 (3 mg kg^{-1}, i.v.-infusion over 30 min: horizontal bar, $n = 5$); (d) a second conditioning LFS four hours later (arrow) was partially effective in inducing LTP. NOS inhibitor L-NMMA (100 mg kg^{-1} h^{-1}, i.v., horizontal bar, $n = 5$); (e) also blocked LTP induction. This block was fully reversible as shown by a second LFS 3 h later (arrow). Similarly, LFS of dorsal roots at C-fibre strength induces robust LTP at synapses between C-fibre afferents and lamina I neurons with a projection to the midbrain periaqueductal gray (PAG) in a rat spinal cord–dorsal root preparation ($n = 18$). Adapted from Ikeda, H., Stark, J., Fischer, H., Wagner, M., Drdla, R., Jäger, T., and Sandkühler, J. 2006. Synaptic amplifier of inflammatory pain in the spinal dorsal horn. Science 312, 1659–1662.

application of dopamine D1/D5 or protein kinase A activators but not D2 receptor agonists selectively induces protein synthesis-dependent late phase of LTP (Yang, H. W. *et al.*, 2005).

5.29.3 Signal Transduction Pathways

The signal transduction pathways which lead to LTP in spinal dorsal horn largely overlap with those involved in hyperalgesia in behaving animals. At C-fiber synapses, LTP induction requires co-activation of ionotropic glutamate receptors of the NMDA type (Randic, M. *et al.*, 1993; Liu, X. G. and Sandkühler, J., 1995; Ikeda, H. *et al.*, 2003; 2006; see, however, Hamba, M. *et al.* 2000) and group I but not group II or group III metabotropic glutamate receptors (mGluRs) (Hamba, M. *et al.*, 2000; Zhong, J. *et al.*, 2000; Azkue, J. J. *et al.*, 2003). LTP-inducing conditioning stimuli release substance P in spinal cord (Afrah, A. W. *et al.*, 2002) and activation of

NK1 receptors for substance P and NK2 receptors for neurokinin A are required for LTP induction (Liu, X. G. and Sandkühler, J., 1997). Opening of T-type voltage gated calcium channels is also necessary (Ikeda, H. *et al.*, 2003; 2006). All this leads to an activity-dependent rise in intracellular calcium ion concentration and activation of calcium-dependent signal transduction. The magnitude of HFS-induced LTP of C-fiber-evoked responses is linearly correlated with the rise in postsynaptic $[Ca^{2+}]_i$ (Ikeda, H. *et al.*, 2003). Blockade of calcium rise in the postsynaptic neuron or calcium-calmodulin-dependent protein kinase II prevents LTP induction (Ikeda, H. *et al.*, 2003; see, however, Hamba, M. *et al.*, 2000; Yang, H. W. *et al.*, 2004). Activation of group I mGluRs may activate phospholipase C (PLC) pathway leading to either protein kinase C activation or formation of inositol-1,4,5-trisphosphate (IP_3). Blockade of either PLC, PKC, or IP_3 receptors all abolish LTP induction (Ikeda, H. *et al.*, 2003).

Activation of NMDA, NK1, or NK2 receptors is not necessary for maintenance of LTP (Liu, X. G. and Sandkühler, J., 1997). Maintenance of the late phase of LTP which starts about 3 h after induction requires, however, *de novo* protein synthesis (Hu, N. W. *et al.*, 2003).

5.29.3.1 Long-Term Potentiation Induction is Context Sensitive

Induction of LTP not only depends upon the activity patterns at the presynaptic terminals, but also on the functional state of the postsynaptic neurons, namely the level of postsynaptic inhibition. Under conditions of impaired inhibition, previously ineffective presynaptic activity may now induce LTP and protocols which normally induce LTD may then cause LTP. *In vitro*, both, Aδ-fiber-evoked (Randic, M. *et al.*, 1993) and C-fiber-evoked (Ikeda, H. *et al.*, 2003) responses are potentiated by conditioning 100 Hz stimulation of dorsal roots when postsynaptic neurons are mildly depolarized to −70 to −60 mV. The same conditioning stimulation induces, however, LTD of Aδ-fiber-evoked responses if cells are hyperpolarized to −85 mV, suggesting that the direction of synaptic plasticity is voltage dependent (Randic, M. *et al.*, 1993).

Spinal Aβ-/Aδ-fiber-evoked field potentials are depressed by conditioning 50 Hz stimulation of sciatic nerve. After blockade of $GABA_A$ receptors with bicuculline the same conditioning stimulus now produces LTP rather than LTD (Miletic, G. and Miletic, V., 2001). In animals with a nerve injury, inhibition in spinal cord may be impaired. Conditioning stimulation at 50 Hz produces a short lasting potentiation followed by LTD in control animals but LTP in animals with a chronic constriction injury of sciatic nerve (Miletic, G. and Miletic, V., 2000). Topical application of muscimol (10 μg) to spinal cord prevents tetanus-induced LTP of A-fiber-evoked field potentials in animals with a nerve injury. In the presence of $GABA_A$ receptor agonist muscimol the same conditioning stimulation evokes an LTD rather than an LTP (Miletic, G. *et al.*, 2003).

Pharmacological activation of spinal NMDA receptors and NK1 or NK2 receptors is insufficient to induce LTP in intact animals. When descending pathways, which are mainly inhibitory in acute preparations, are cut, then the same receptor agonists now trigger LTP (Liu, X. G. and Sandkühler, J., 1998). This confirms that level of postsynaptic inhibition regulates induction and polarity of synaptic plasticity. Some pharmacological induction protocols do not require any presynaptic stimulation which suggests that LTP can be induced in the absence of presynaptic activity. This may be relevant when neuromodulators such as substance P diffuse to distant, inactive synapses (volume transmission), which is a potential mechanism of spreading synaptic plasticity in the spinal cord.

Functional blockade of glial cells by i.t. administration of fluorocitrate changes the direction of HFS induced plasticity of C-fiber-evoked potentials. When HFS is given 1 h, but not 3 h after fluorocitrate LTD rather than LTP is induced (Ma, J. Y. and Zhao, Z. Q., 2002). The mechanism of this switch in polarity of synaptic plasticity is presently unknown but recent evidence suggests that glial cell-derived nitric oxide is liberated via activation of type 1 mGluRs and triggers LTP (Ikeda, H. and Murase, K., 2004).

5.29.4 Prevention of Long-Term Potentiation

LTP of C-fiber-evoked field potentials *in vivo* is not affected by deep (surgical) level of anesthesia with urethane, isoflurane, or sevoflurane in mature rats (Benrath, J. *et al.*, 2004). LTP is, however, prevented by low-dose intravenous infusion of μ-opioid receptor agonist fentanyl (Benrath, J. *et al.*, 2004). Similarly, spinal field potentials elicited by stimulation in the tract of Lissauer in spinal cord slices is blocked by DAMGO, a more specific agonist at these receptors

(Terman, G. W. *et al.*, 2001). Spinal application of Zn^{2+} also blocked LTP induction *in vivo* (Ma, J. Y. and Zhao, Z. Q., 2001).

5.29.5 Reversal of Long-Term Potentiation

Brief, high-frequency conditioning of sciatic nerve at Aδ-fiber intensity partially and temporarily reverses LTP of C-fiber-evoked field potentials when given 15 or 60 min but not 3 h after LTP induction (Liu, X. G. *et al.*, 1998;Zhang, H. M., *et al.*, 2001). Similarly, blockade of either protein kinase C, calcium-calmodulin-dependent protein kinase II or protein kinase A before or up to 30–60 min after conditioning stimulation abolishes LTP induction. Kinase blockers are, however, ineffective, when applied 3 h after induction. Inhibition of *de novo* protein synthesis in spinal dorsal horn during high frequency stimulation of sciatic nerve selectively blocked late phase of LTP but not its early phase lasting for about 3 h (Hu, N. W. *et al.*, 2003).

5.29.6 Functional Consequences of Long-Term Potentiation in Pain Pathways

A number of studies provide convergent evidence that LTP at spinal synapses of nociceptive Aδ- or C-fibers facilitates downstream processing of pain-related information. This includes action potential firing in superficial and deep dorsal horn neurons (Svendsen, F. *et al.*, 1999; Willis, W. D., 2002; Wallin, J. *et al.*, 2003; Twining, C. M. *et al.*, 2004; Pedersen, L. M. *et al.*, 2005) and pain perception in human subjects (Klein, T. *et al.*, 2004). Induction protocols signal transduction pathways and pharmacology of LTP and facilitation of C-fiber-evoked discharges largely overlap, which is in line with the hypothesis that LTP underlies these facilitations. Under some pathological conditions facilitation of C-fiber-evoked action potential discharges is enhanced, for example, when descending pathways are interrupted (Gjerstad, J. *et al.*, 2001) or if a joint is inflamed (Vikman, K. S. *et al.*, 2003). Induction of LTP of A-fiber-evoked field potentials by high frequency conditioning stimulation is facilitated in animals with a loose ligation of sciatic nerve (Miletic, G. and Miletic, V., 2000). One study reported reduced facilitation in animals with spinal nerve ligations (Rygh, L. J. *et al.*, 2000).

5.29.7 Conclusions

Induction protocols signal transduction pathways and pharmacology of LTP and some forms of hyperalgesia are virtually identical, rendering LTP in spinal dorsal horn an attractive cellular model of hyperalgesia.

References

Afrah, A. W., Fiska, A., Gjerstad, J., Gustafsson, H., Tjølsen, A., Olgart, L., Stiller, C. O., Hole, K., and Brodin, E. 2002. Spinal substance P release *in vivo* during the induction of long-term potentiation in dorsal horn neurons. Pain 96, 49–55.

Azkue, J. J., Liu, X. G., Zimmermann, M., and Sandkühler, J. 2003. Induction of long-term potentiation of C fibre-evoked spinal field potentials requires recruitment of group I, but not group II/III metabotropic glutamate receptors. Pain 106, 373–379.

Benrath, J., Brechtel, C., Martin, E., and Sandkühler, J. 2004. Low doses of fentanyl block central sensitization in the rat spinal cord *in vivo*. Anesthesiology 100, 1545–1551.

Bliss, T. V. P. and Collingridge, G. L. 1993. A synaptic model of memory: long-term potentiation in the hippocampus. Nature 361, 31–39.

Gjerstad, J., Tjølsen, A., and Hole, K. 2001. Induction of long-term potentiation of single wide dynamic range neurones in the dorsal horn is inhibited by descending pathways. Pain 91, 263–268.

Hamba, M., Onodera, K., and Takahashi, T. 2000. Long-term potentiation of primary afferent neurotransmission at trigeminal synapses of juvenile rats. Eur. J. Neurosci. 12, 1128–1134.

Hu, N. W., Zhang, H. M., Hu, X. D., Li, M. T., Zhang, T, Zhou, L. J., and Liu, X. G. 2003. Protein synthesis inhibition blocks the late-phase LTP of C-fiber evoked field potentials in rat spinal dorsal horn. J. Neurophysiol. 89, 2354–2359.

Huang, C. C. and Hsu, K. S. 2001. Progress in understanding the factors regulating reversibility of long-term potentiation. Rev. Neurosci. 12, 51–68.

Ikeda, H. and Murase, K. 2004. Glial nitric oxide-mediated long-term presynaptic facilitation revealed by optical imaging in rat spinal dorsal horn. J. Neurosci. 24, 9888–9896.

Ikeda, H., Asai, T., and Murase, K. 2000. Robust changes of afferent-induced excitation in the rat spinal dorsal horn after conditioning high-frequency stimulation. J. Neurophysiol. 83, 2412–2420.

Ikeda, H., Heinke, B., Ruscheweyh, R., and Sandkühler, J. 2003. Synaptic plasticity in spinal lamina I projection neurons that mediate hyperalgesia. Science 299, 1237–1240.

Ikeda, H., Stark, J., Fischer, H., Wagner, M., Drdla, R., Jäger, T., and Sandkühler, J. 2006. Synaptic amplifier of inflammatory pain in the spinal dorsal horn. Science 312, 1659–1662.

Klein, T., Magerl, W., Hopf, H. C., Sandkühler, J., and Treede, R. D. 2004. Perceptual correlates of nociceptive long-term potentiation and long-term depression in humans. J. Neurosci. 24, 964–971.

Liu, X. G. and Sandkühler, J. 1995. Long-term potentiation of C-fiber-evoked potentials in the rat spinal dorsal horn is prevented by spinal *N*-methyl-D-aspartic acid receptor blockage. Neurosci. Lett. 191, 43–46.

Liu, X. G. and Sandkühler, J. 1997. Characterization of long-term potentiation of C-fiber-evoked potentials in spinal dorsal horn of adult rat: essential role of NK1 and NK2 receptors. J. Neurophysiol. 78, 1973–1982.

Liu, X. G. and Sandkühler, J. 1998. Activation of spinal *N*-methyl-D-aspartate or neurokinin receptors induces long-term potentiation of spinal C-fibre-evoked potentials. Neuroscience 86, 1209–1216.

Liu, X. G., Morton, C. R., Azkue, J. J., Zimmermann, M., and Sandkühler, J. 1998. of C-fibre-evoked spinal field potentials by stimulation of primary afferent Aδ-fibres in the adult rat. Eur. J. Neurosci. 10, 3069–3075.

Ma, J. Y. and Zhao, Z. Q. 2001. The effects of Zn^{2+} on long-term potentiation of C fiber-evoked potentials in the rat spinal dorsal horn. Brain Res. Bull. 56, 575–579.

Ma, J. Y. and Zhao, Z. Q. 2002. The involvement of glia in long-term plasticity in the spinal dorsal horn of the rat. Neuroreport 13, 1781–1784.

Malenka, R. C. and Nicoll, R. A. 1999. Long-term potentiation– a decade of progress? Science 285, 1870–1874.

Mantyh, P. W., Rogers, S. D., Honoré, P., Allen, B. J., Ghilardi, J. R., Li, J., Daughters, R. S., Lappi, D. A., Wiley, R. G., and Simone, D. A. 1997. Inhibition of hyperalgesia by ablation of lamina I spinal neurons expressing the substance P receptor. Science 278, 275–279.

Miletic, G. and Miletic, V. 2000. Long-term changes in sciatic-evoked A-fiber dorsal horn field potentials accompany loose ligation of the sciatic nerve in rats. Pain 84, 353–359.

Miletic, G. and Miletic, V. 2001. Contribution of GABA-A receptors to metaplasticity in the spinal dorsal horn. Pain 90, 157–162.

Miletic, G., Draganic, P., Pankratz, M. T., and Miletic, V. 2003. Muscimol prevents long-lasting potentiation of dorsal horn field potentials in rats with chronic constriction injury exhibiting decreased levels of the GABA transporter GAT-1. Pain 105, 347–353.

Moore, K. A., Baba, H., and Woolf, C. J. 2000. Synaptic Transmission and Plasticity in the Superficial Dorsal Horn. In: Nervous System Plasticity and Chronic Pain, (*eds*. J. Sandkühler, B. Bromm, and G. F. Gebhart), Vol. 129, pp. 63–81. Elsevier.

Pedersen, L. M., Lien, G. F., Bollerud, I., and Gjerstad, J. 2005. Induction of long-term potentiation in single nociceptive dorsal horn neurons is blocked by the CaMKII inhibitor AIP. Brain Res. 1041, 66–71.

Randic, M., Jiang, M. C., and Cerne, R. 1993. Long-term potentiation and long-term depression of primary afferent neurotransmission in the rat spinal cord. J. Neurosci. 13, 5228–5241.

Rygh, L. J., Kontinen, V. K., Suzuki, R., and Dickenson, A. H. 2000. Different increase in C-fibre evoked responses after nociceptive conditioning stimulation in sham-operated and neuropathic rats. Neurosci. Lett. 288, 99–102.

Sandkühler, J. 2000. Learning and memory in pain pathways. Pain 88, 113–118.

Sandkühler, J. 2007. Understanding LTP in pain pathways. Mol. Pain 3, 9.

Sandkühler, J. and Liu, X. 1998. Induction of long-term potentiation at spinal synapses by noxious stimulation or nerve injury. Eur. J. Neurosci. 10, 2476–2480.

Schouenborg, J. 1984. Functional and topographical properties of field potentials evoked in rat dorsal horn by cutaneous C-fibre stimulation. J. Physiol. 356, 169–192.

Svendsen, F., Tjølsen, A., Rygh, L. J., and Hole, K. 1999. Expression of long-term potentiation in single wide dynamic range neurons in the rat is sensitive to blockade of glutamate receptors. Neurosci. Lett. 259, 25–28.

Terman, G. W., Eastman, C. L., and Chavkin, C. 2001. Mu opiates inhibit long-term potentiation induction in the spinal cord slice. J. Neurophysiol. 85, 485–494.

Twining, C. M., Sloane, E. M., Milligan, E. D., Chacur, M., Martin, D., Poole, S., Marsh, H., Maier, S. F., and Watkins, L. R. 2004. Peri-sciatic proinflammatory cytokines, reactive oxygen species, and complement induce mirror-image neuropathic pain in rats. Pain 110, 299–309.

Vikman, K. S., Duggan, A. W., and Siddall, P. J. 2003. Increased ability to induce long-term potentiation of spinal dorsal horn neurones in monoarthritic rats. Brain Res. 990, 51–57.

Wallin, J., Fiska, A., Tjølsen, A., Linderoth, B., and Hole, K. 2003. Spinal cord stimulation inhibits long-term potentiation of spinal wide dynamic range neurons. Brain Res. 973, 39–43.

Willis, W. D. 2002. Long-term potentiation in spinothalamic neurons. Brain Res. Rev. 40, 202–214.

Yang, H. W., Zhou, L. J., Hu, N. W., Xin, W. J., and Liu, X. G. 2005. Activation of spinal D1/D5 receptors induces latep hase LTP of c-fiber evoked field potentials in rat spinal dorsal horn. J. Neurophysiol. 94, 961–967.

Yang, H. W., Hu, X. D., Zhang, H. M., Xin, W. J., Li, M. T., Zhang, T., Zhou, L. J., and Liu, X. G. 2004. Roles of CaMKII, PKA and PKC in the induction and maintenance of LTP of C-Fiber evoked field potentials in rat spinal dorsal horn. J. Neurophysiol. 91, 1122–1133.

Zhang, H. M., Qi, Y. J., Xiang, X. Y., Zhang, T., and Liu, X. G. 2001. Time-dependent plasticity of synaptic transmission produced by long-term potentiation of C-fiber evoked field potentials in rat spinal dorsal horn. Neurosci. Lett. 315, 81–84.

Zhong, J., Gerber, G., Kojic, L., and Randic, M. 2000. Dual modulation of excitatory synaptic transmission by agonists at group I metabotropic glutamate receptors in the rat spinal dorsal horn. Brain Res. 887, 359–377.

5.30 Immune System, Pain and Analgesia

H L Rittner, H Machelska, and C Stein, Charité – Universitätsmedizin Berlin, Campus Benjamin Franklin, Berlin, Germany

© 2008 Elsevier Inc. All rights reserved.

5.30.1	Introduction	407
5.30.2	Proalgesic Mechanisms	408
5.30.2.1	Proinflammatory Cytokines	408
5.30.2.1.1	Tumor necrosis factor-α	409
5.30.2.1.2	Interleukin-1β	410
5.30.2.1.3	Interleukin-6	411
5.30.2.1.4	Interleukin-18	412
5.30.2.2	Chemokines	412
5.30.2.3	Nerve Growth Factor	413
5.30.2.4	Other Mediators: Bradykinin	414
5.30.2.5	Clinical Implications and Perspectives	415
5.30.3	Analgesic Mechanisms	415
5.30.3.1	Anti-Inflammatory Cytokines	415
5.30.3.2	Opioid Peptides	416
5.30.3.2.1	Peripheral opioid receptors	416
5.30.3.2.2	Opioid peptides produced by immune cells	417
5.30.3.2.3	Migration of opioid-containing immune cells to inflamed tissue	418
5.30.3.2.4	Release of opioid peptides from immune cells	420
5.30.3.2.5	Analgesia produced by immune-derived opioid peptides	420
5.30.3.2.6	Clinical implications	422
5.30.3.2.7	Perspectives	422
References		423

Glossary

CFA Complete Freund's adjuvant.
CCR/CXCR Chemokine receptor.
CRF Corticotropin releasing factor.
COX Cyclooxygenase.
CXCL1 KC keratinocyte-derived chemokine.
CXCL2/3 MIP-2 macrophage inflammatory protein.
CXCL8 IL-8.
DRG Dorsal root ganglion.
GDNF Glial cell-line-derived neurotrophic factor.
ICAM-1 Intercellular adhesion molecule-1.
IL Interleukin.
IL-1ra IL-1 receptor antagonist.
NGF Nerve growth factor.
NMDA *N*-methyl-D-aspartate.
PC Prohormone convertase.
PECAM-1 Platelet-endothelial cell adhesion molecule-1.
PENK Proenkephalin.
POMC Proopiomelanocortin.
SRIF Somatotropin release inhibiting factor (somatostatin).
TNF-α Tumor necrosis factor-α.
TrkA Tyrosine receptor kinase A.
TRPV1 Vanilloid receptor-1 (transient receptor potential vanilloid 1).
TTX Tetrodotoxin.

5.30.1 Introduction

Tissue destruction or inflammation are accompanied by an invasion of immune cells and liberation of numerous mediators. While these mediators contribute to the body's ability to counteract the destruction of tissue integrity, they also elicit pain by activation of specialized primary afferent neurons called nociceptors (reviewed in Julius, D. and Basbaum, A. I., 2001). They are defined as "receptors preferentially sensitive to a noxious stimulus or to a stimulus which would become noxious if prolonged" (definition of the International Association for the Study of Pain, IASP) (Merskey, H. and Bogduk, N., 1994). Trigeminal and dorsal root ganglia (DRG) contain nociceptor cell bodies which give rise to myelinated Aδ and unmyelinated C fibers. Aδ and C fibers transduce and propagate noxious stimuli to the dorsal horn of the spinal cord from where these stimuli are transmitted to the brain. At the level of the spinal cord and at supraspinal sites, various neurotransmitters come into plays which, together with environmental and cognitive factors, contribute to the eventual sensation of pain (Scholz, J. and Woolf, C. J., 2002). Strictly speaking, analgesia is defined as the inhibition of pain in man, while antinociception is defined as the inhibition of behavioral responses to noxious stimuli in animals. Although central mechanisms also play a prominent role, the following chapter will focus on the peripheral injured tissue itself.

5.30.2 Proalgesic Mechanisms

Inflammatory pain is characterized by an increased response to mechanical and heat stimuli, which are normally painful (Merskey, H. and Bogduk, N., 1994). This is called mechanical or thermal hyperalgesia, respectively. After tissue injury, local tissue macrophages and dendritic cells are activated. The inflammatory response is amplified by migration of leukocytes into the inflamed tissue, by production of inflammatory mediators as well as tissue acidification. Several agents are used experimentally to induce nonspecific inflammation in experimental animals. The most widely used are carrageenan and complete Freund's adjuvant (CFA) injected into the hindpaw of rodents. Carrageenan is used for short-term inflammation, while CFA is used to model longer time courses of tissue injury. Less frequently used agents include lipopolysaccharide, zymosan injection, or peritoneal inflammation using acetic acid or glycogen.

Neuropathic pain can arise following injury of peripheral nerves, when damaged or neighboring undamaged nerve fibers are sensitized or fire ectopically. It is also characterized by mechanical and thermal hyperalgesia. In addition, animals with neuropathy are sensitive to stimuli that do not evoke pain behavior under normal conditions, e.g., to touch, cooling, or warming. This is called allodynia (Merskey, H. and Bogduk, N., 1994). The most common models of neuropathic pain are tight ligation of spinal nerves and tight or loose ligation of the sciatic nerve. These models differ in the degree of neuronal damage but all resemble human neuropathy resulting from trauma-induced injury of peripheral nerves (e.g. entrapment, chronic nerve compression) (Bennet, G. J., 1994).

In the following section the effects of different mediators including cytokines, chemokines, nerve growth factor (NGF), and bradykinin are discussed in three aspects: injection of the mediator into non-inflamed tissue, blocking the mediator in models of inflammatory pain, and the role of the mediator in neuropathic pain.

5.30.2.1 Proinflammatory Cytokines

Cytokines are small proteins produced in the inflamed tissue as well as in lymphoid organs with stimulatory or inhibitory properties on immune function. Cytokines act through high-affinity receptors. Among the many different cytokines, the type I cytokines have a similar four α helical bundle structure. Their receptors correspondingly share characteristic features that have led to their description as the cytokine receptor superfamily, or type I cytokine receptors. Cytokine receptors in general are characterized by low abundance and a multisubunit structure yielding low- and high-affinity receptor forms. They are integral membrane glycoproteins with the N-terminal outside and a single membrane-spanning domain. Unlike growth factors that contain an instrinsic tyrosine kinase in their cytoplasmic domain, cytokine receptors induce tyrosine phosphorylation via additional molecules. Multiple signaling pathways/molecules have been observed for various cytokines. Collectively, these include the Jak-STAT pathway, the Ras–mitogen-activated protein (MAP) kinase pathway, Src and ZAP70 and related proteins, phosphatidylinositol 3-kinase

(PI3K), insulin receptor substrates 1 and 2 (IRS-1 and IRS-2), and phosphatases.

Cytokines are produced on demand and travel only over short distances. *In vivo* concentrations are in the range of a few picograms to nanograms per milliliter. Cytokines are pleiotropic and redundant, they influence mostly immune cells and the inflammatory response. Recently, however, cytokines have been shown to link the immune system and the nervous system and they seem to modulate pain and hyperalgesia.

5.30.2.1.1 Tumor necrosis factor-α

The tumor necrosis factor (TNF) recptor superfamily is comprised of at least 19 genes encoding 20 type II (i.e., intracellular N-terminus, extracellular C-terminus) transmembrane proteins. Included are several well-known ligands such as TNF-α, TNF-β (lymphotoxin-α, LT-α), Fas ligand, and CD40 ligand, as well as an increasing number of newly described mediators. TNF-α is the prototypic proinflammatory cytokine due to its role in initiating a cascade of cytokines and growth factors in the inflammatory response. Intraplantar injection of TNF-α into non-inflamed paws produced a short-lived dose-dependent mechanical hyperalgesia in rats (Cunha, F. Q. *et al.*, 1992). TNF-α seems to have indirect as well as direct hyperalgesic properties. Indirect action is supported by the following evidence: inhibitors of prostaglandin synthesis via cyclooxygenase (COX) inhibitors, and antagonists of adrenergic receptors can attenuate TNF-α-induced hyperalgesia in rats. In mice, TNF-α action is only dependent on the prostaglandin pathway (Cunha, T. M. *et al.*, 2005). Interestingly, the actions of TNF-α seem to be longer lasting if TNF-α is administered repetitively. Such treatment resulted in hyperalgesia lasting up to 30 days after cessation of the daily TNF-α injections in rats (Sachs, D. *et al.*, 2002). TNF-α-induced hyperalgesia in this study was again dependent on release of prostaglandins, as well as sympathetic amines, because blockade of either reduced hyperalgesia. Other groups have demonstrated a role of NGF in TNF-α-induced hyperalgesia. Pretreatment of rats with anti-NGF antiserum significantly attenuated TNF-α-induced mechanical and thermal hyperalgesia (Woolf, C. J. *et al.*, 1997). A direct action on nociceptors was postulated in electrophysiological studies (Sorkin, L. S. *et al.*, 1997; Junger, H. and Sorkin, L. S., 2000). TNF-α applied onto the sciatic nerve or injected subcutaneously into normal paws produced aberrant electrophysiological activity and dose dependently sensitized nociceptors to mechanical stimuli. This effect was restricted to Aδ and C fibers and no effect was seen in Aβ mechanoreceptive fibers. Interestingly, however, higher doses of TNF-α produced lower responses (U-shaped dose–response). The authors postulated that this was related to TNF-α-induced release of anti-inflammatory cytokines (Sorkin, L. S. *et al.*, 1997; Junger, H. and Sorkin, L. S., 2000).

TNF-α exerts its effects through two known receptors, TNFR1 and TNFR2. Expression of both was evaluated in DRG from rats (Li, Y. *et al.*, 2004): TNFR1 mRNA was expressed in virtually all neurons and in nonneuronal cells with increased levels in models of peripheral inflammation. TNFR2 was exclusively expressed and regulated in nonneuronal cells. *In situ* hybridization revealed varying levels of TNFR1 mRNA in virtually all DRG neurons including putative nociceptive neurons coding for calcitonin gene-related peptide, substance P, or vanilloid receptor 1 (transient receptor potential vanilloid 1; TRPV1). Similarly, expression of TNFR1 and TNFR2 protein was seen in rat DRG neurons and their axons and increased in models of neuropathic pain (Shubayev, V. I. and Myers, R. R., 2001; Schäfers, M. *et al.*, 2003c). In contrast, TNFR1 is not expressed in DRG neurons from normal mice but is seen in mice with nerve injury (Ohtori, S. *et al.*, 2004). TNFR localization on peripheral endings has not been examined but seems likely because of expression in DRG and its presence in axons.

Some studies are available regarding the role of endogenous TNF-α in inflammatory hyperalgesia. In one study, antisera against TNF-α could completely block hyperalgesia induced by intraplantar carrageenan injection (Cunha, F. Q. *et al.*, 1992). Similar results are seen in lipopolysaccharide-induced inflammation (Ferreira, S. H. *et al.*, 1993). A third study examined TNF-α in CFA-induced hindpaw inflammation (Woolf, C. J. *et al.*, 1997). Here, a single injection of anti-TNF-α serum before CFA application significantly delayed the onset of the resultant inflammatory hyperalgesia and reduced interleukin (IL)-1β but not NGF levels measured 24 h later. A role for TNF-α in inflammatory pain has also been confirmed in mice using TNFR1 knockout mice (Cunha, T. M. *et al.*, 2005). The intensity of hyperalgesia after intraplantar carrageenan injection was significantly lower in these animals. Therefore, TNF-α seems to be an endogenous mediator in inflammatory pain in mice and in rats. Monocytes and tissue macrophages are the primary

sources for TNF-α synthesis. TNF-α synthesis is stimulated by a wide variety of agents. In macrophages, it is induced by biological, chemical, and physical stimuli such as viruses, bacterial and parasitic products, tumor cells, complement, cytokines, ischemia, trauma, and irradiation (Figure 1) (Cunha, F. Q. and Ferreira, S. H., 2003; Cunha, T. M. *et al.*, 2005). In peripheral tissues of rats, TNF-α activity is followed by increases in IL-6 and IL-8, and IL-6 is followed by IL-1β and then by NGF. All of these finally mediate their effects through prostaglandins or sympathetic amines. This cascade is also seen with few modifications in mice (Cunha, T. M. *et al.*, 2005).

The role of TNF-α has also been studied in neuropathic pain. TNF-α mRNA was upregulated in the sciatic nerve at 2 weeks after its loose ligation (a chronic constriction injury model) (Okamoto, K. *et al.*, 2001). Also, TNF-α protein was detected in inflammatory cells accumulating at the ligated sciatic nerve (Cui, J. G. *et al.*, 2000; Schäfers, M. *et al.*, 2003a). Treatment of animals with neuropathic injury using anti-TNF-α antibodies and especially with the combination of anti-TNF-α and anti-IL-1β antibodies significantly reduced signs of neuropathic pain (Schäfers, M. *et al.*, 2001). In another model, treatment starting 2 days before spinal nerve ligation with the TNF-α receptor antagonist etanercept attenuated mechanical allodynia (Schäfers, M. *et al.*, 2003d). *In vivo* studies have recently been substantiated by electrophysiological studies. *In vitro* perfusion of DRG cells with TNF-α elicits neuronal discharges in Aδ and C fibers, which are markedly higher and longer lasting after nerve injury (Schäfers, M. *et al.*, 2003b). This demonstrates an increased sensitivity of injured neurons to TNF-α. TNF-α-induced hyperalgesia in this model is mediated via TNFR1 (Schäfers, M. *et al.*, 2003c). Downstream effectors of TNF-α include the p38 MAP kinase pathway. Intrathecal infusion of a p38 inhibitor reduced neuropathic pain if it was started before but not 7 days after spinal nerve ligation. Cessation of therapy resulted in increased allodynia.

In summary, TNF-α has hyperalgesic properties if injected exogenously. It also has endogenous hyperalgesic actions in inflammatory and neuropathic pain. The effect seems to be mediated in part indirectly via prostaglandins and sympathetic amines. Recent data also suggest direct sensitizing effects on sensory neurons.

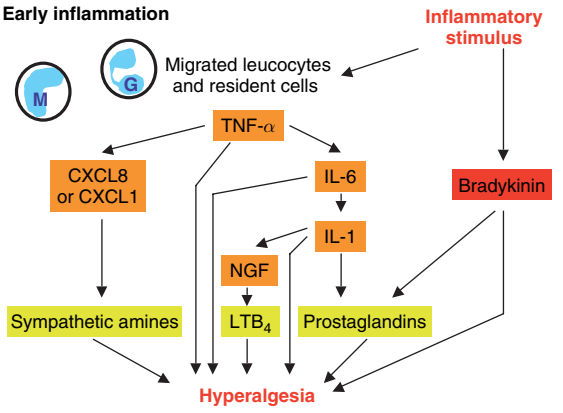

Figure 1 Hyperalgesic mechanisms in early inflammation. An inflammatory agent stimulates the migration of leukocytes, e.g., granulocytes (G) and monocytes (M), into the inflamed tissue. In the tissue, these leukocytes as well as resident cells initiate a cascade of cytokines including tumor necrosis factor-α (TNF-α) and interleukins (ILs), chemokines (CXCL8, CXCL1), nerve growth factor (NGF), bradykinin, and secondary mediators like sympathetic amines, leukotriene B_4 (LTB_4), and prostaglandins culminating in hyperalgesia. TNF-α, IL-6, IL-1, and bradykinin can also have direct hyperalgesic effects on nociceptors.

5.30.2.1.2 *Interleukin-1β*

IL-1 and its family members are primarily proinflammatory cytokines. They can stimulate the expression of genes associated with inflammation and autoimmune diseases. The most salient and relevant properties of IL-1 in inflammation are the initiation of COX, type 2 phospholipase A, and inducible nitric oxide synthase. Hyperalgesic effects of IL-1 have first been demonstrated by injection into hindpaws of rats without inflammation or nerve injury (Ferreira, S. H. *et al.*, 1988): in contrast to IL-1α, IL-1β is able to sensitize nociceptors. Several mechanisms have been proposed to mediate this indirect action, including prostaglandins, nitric oxide, NGF, and bradykinin. The hyperalgesic effect of IL-1β is blocked by treatment with indomethacin, a nonselective COX inhibitor reducing the formation of prostaglandins (Figure 1) (Ferreira, S. H. *et al.*, 1988). In mice, IL-1β also induces prostaglandin formation mediating hyperalgesia (Cunha, T. M. *et al.*, 2005). Injection of IL-1β into normal tissue induces thermal hyperalgesia and the production of NGF. The thermal hyperalgesia but not the NGF production can be prevented by pretreatment with recombinant IL-1 receptor antagonist (IL-1ra). There is also evidence of a direct action of IL-1β on nociceptors: intraplantar injection of IL-1β potentiates action potentials in rat DRG neurons in response to thermal or mechanical stimuli, and a decrease of the mechanical threshold for nerve firing was observed

after local injection of IL-1β (Fukuoka, H. *et al.*, 1994). In the *in vitro* skin–nerve preparation brief exposure to IL-1β facilitates the heat-induced release of calcitonin gene-related peptide (a pronociceptive mediator) from peptidergic sensory neurons (Opree, A. and Kress, M., 2000). This was confirmed by a follow-up study (Obreja, O. *et al.* 2002a). IL-1 potentiated heat-activated inward currents and shifted the activation threshold towards lower temperature without altering intracellular calcium currents.

Intracellular mediators of these effects included protein tyrosine kinases and protein kinase C. One of the IL-1 receptors subtypes, the IL-1RI, was expressed in DRG cells as shown by polymerase chain reaction and *in situ* hybridization. The authors propose that recruitment of tyrosine kinases and downstream activation of protein kinase C phosphorylate TRPV1 to cause heat hyperalgesia. Both mRNA and IL-1RI protein are found in DRG neurons and glial cells (Li, M. *et al.*, 2005) of rats with and without paw inflammation. However IL-1RI localization has not been shown on peripheral nerve terminals. Using autoradiography, we did not detect IL-1 binding on nerves in either inflamed or noninflamed paws, but on immune cells in inflamed paws (Mousa, S. A. *et al.*, 1996). Therefore, IL-1 receptor expression in the periphery requires further studies.

IL-1β also has an endogenous hyperalgesic role in inflammatory as well as in neuropathic pain. In hindpaw inflammation induced by carrageenan or lipopolysaccharide IL-1ra can reduce, by not completely block, hyperalgesia in rats and in mice (Ferreira, S. H. *et al.*, 1993; Cunha, J. M. *et al.*, 2000; Cunha, T. M. *et al.*, 2005). The same effect can be seen in CFA-induced hindpaw inflammation or in mice after intraperitoneal injection of acetic acid (Safieh-Garabedian, B. *et al.*, 1995; Cunha, J. M. *et al.*, 2000). In CFA-induced inflammation, the authors propose that the effect is mediated by NGF, because treatment with IL-1ra also reduced the local production of NGF (Safieh-Garabedian, B. *et al.*, 1995). Interestingly, our group has shown analgesic effects of IL-1β via release of opioid peptides from immune cells in CFA-induced inflammation (see Analgesic Effects of Corticotropin Releasing Factor, Interleukin-1β, and Noradreline for discussion).

In neuropathic pain models, the role of IL-1 has not been thoroughly examined. Expression of IL-1β is seen in inflammatory cells accumulating at the sciatic nerve in ligation and inflammatory models of neuropathy as assesed by immunohistochemistry and by polymerase chain reaction (Gazda, L. S. *et al.*, 2001; Okamoto, K. *et al.*, 2001). Blocking of IL-1R in mice with chronic constriction injury reduces thermal hyperalgesia, mechanical allodynia, and also immunoreactivity for TNF-α (Sommer, C. *et al.*, 1999). However, the mechanisms remain unclear. So far, no study has demonstrated IL-1R expression in neuropathy. In summary, IL-1β seems to have hyperalgesic actions in different models of pain. The mechanism – direct or indirect – still needs to be clarified.

5.30.2.1.3 Interleukin-6

IL-6 is a one of the major proinflammatory cytokines. Its level is below detection under physiological conditions but is rapidly and strongly upregulated in early inflammation and can be detected early in the serum. Intraplantar injection of IL-6 induces hyperalgesia in normal rats (Poole, S. *et al.*, 1995). An indirect mechanism of this effect is supported by data showing inhibition of IL-6-induced hyperalgesia when animals are treated with COX blockers (Cunha, F. Q. *et al.*, 1992) (Figure 1). However, so far it is not known which cells and receptors are involved.

Direct effects have been proposed by other groups: In the rat *in vitro* skin–nerve preparation basal and heat-evoked release of calcitonin gene-related peptide from nociceptors was measured. IL-6 did not induce heat sensitization, when applied alone, but was effective in the presence of soluble IL-6 receptor (sIL-6R) (Opree, A. and Kress, M., 2000). sIL-6R is needed for cells that express only the signaling receptor unit gp130. The complex of sIL-6R and IL-6 can then induce a signal to activate cells. This so-called *trans*-signaling expands the spectrum of cells responsive to IL-6 to include neurons. IL-6, in combination with its soluble receptor, can sensitize nociceptors to heat, providing evidence for the constitutive expression of gp130, but not of the IL-6-membrane-bound (specific) receptor, in nociceptors (Obreja, O. *et al.*, 2002b). Hyper-IL-6 (HIL-6), a fusion protein of IL-6 and sIL-6R, was designed to mimic the effects of the IL-6–sIL-6R complex. *In vitro* exposure of DRG neurons to HIL-6 potentiated heat-activated inward currents and shifted the activation thresholds towards lower temperatures without affecting intracellular calcium levels (Obreja, O. *et al.*, 2005). This effect was reduced by a Janus tyrosine kinase inhibitor, a selective protein kinase C inhibitor as well as a selective blocker of the protein kinase C delta isoform, but not by the COX inhibitor indomethacin. *In situ* hybridization and reverse transcription-polymerase chain

reaction revealed expression of the signal-transducing beta subunit of gp130 in neuronal somata but not in satellite cells in DRG from normal rats (Gadient, R. A. and Otten, U., 1996; Obreja, O. *et al.*, 2005). These data suggest a direct activation of sensory neurons by IL-6–sIL-6R.

As seen for IL-1β and TNF-α, endogenous IL-6 is also important for the development of hyperalgesia: Antisera neutralizing IL-6 inhibited lipopolysaccharide-induced hyperalgesia in rats (Ferreira, S. H. *et al.*, 1993). IL-6 knockout mice were shown to have reduced thermal and mechanical hyperalgesia after injection of carrageenan into the hindpaw (Xu, X. J. *et al.*, 1997). In this study, however, IL-6 knockout mice without inflammation displayed baseline hyperalgesia, which could not be explained by the authors.

In neuropathic mice, IL-6 mRNA levels were upregulated in DRG and correlated well with the development of nerve injury-induced thermal hyperalgesia and mechanical allodynia (Murphy, P. G. *et al.*, 1999). IL-6 knockout mice had reduced thermal and mechanical hyperalgesia in the chronic constriction injury model. In summary, IL-6 belongs to the group of proinflammatory hyperalgesic cytokines with direct as well as indirect effects on neurons, similar to IL-1β and TNF-α.

5.30.2.1.4 Interleukin-18

IL-18 is a member of the IL-1 ligand superfamily and is expressed in various cell types including macrophages and dendritic cells. Its biological functions include stimulation of activated T cells and enhancement of natural killer cell lytic activity. Furthermore, IL-18 activates and attracts neutrophils by inducing the production of TNF-α and subsequently leukotriene B_4. Injection of IL-18 into normal paws caused time and dose-dependent mechanical hyperalgesia (Verri, W. A., Jr. *et al.*, 2004) Interestingly, only morphine and dexamethasone blocked IL-18-induced hyperalgesia, whereas blockade of the prostaglandin or sympathetic pathway had no effect. In fact, the hyperalgesia elicited by IL-18 seems to be mediated via endothelin receptors, because it was abolished by blockage of endothelin receptor B (Verri, W. A., Jr. *et al.*, 2004).

5.30.2.2 Chemokines

Chemokines (CC and CXC) are chemotatic mediators produced in inflamed tissue. They control trafficking of leukocytes under physiological and inflammatory conditions, angiogenesis, and wound healing. They can be divided into subfamilies based on their structural motifs (the position of cysteine residues located near the N-terminus of the protein: CC, CXC, and CX_3C). Chemokines bind to a group of chemokine receptors (CCR, CXCR, and CX_3CR; seven transmembrane-spanning G_i protein-coupled receptors) expressed on leukocytes. Although each receptor subtype typically binds multiple chemokines, the specificity is defined by a chemokine subfamily. Recently, chemokines and their receptors have been detected on cells in the central and peripheral nervous system.

Several observations indicate a role of chemokines in hyperalgesia. Chemokine receptors such as CXCR4 and CCR4 are expressed on subpopulations of DRG neurons and their corresponding ligands can induce calcium influx (Oh, S. B. *et al.*, 2001). However, in neonates the percentage of neurons responding to chemokine stimulation was significantly lower than the percentage responding to bradykinin or capsaicin. Direct intraplantar injection of some chemokines (CCL5, CXCL12, and CCL22) induces hyperalgesia in normal animals (Oh, S. B. *et al.*, 2001). In addition, some chemokines (human CXCL8 (IL-8) or rat CXCL1 (KC keratinocyte-derived chemokine)) can indirectly cause hyperalgesia through release of sympathetic amines when applied subcutaneously into the hindpaw (Lorenzetti, B. B. *et al.*, 2002; Cunha, F. Q. and Ferreira, S. H., 2003). Hyperalgesic effects of CXCL1 were further examined in mice (Cunha, T. M. *et al.*, 2005). Intraplantar injection of a small dose of CXCL1 induced hyperalgesia with a peak between 3 and 5 h returning to normal after 24 h. Pretreatment of mice with indomethacin, a COX inhibitor, or guanethidine, a blocker of sympathetic amines, reduced the hyperalgesia. An almost complete blockade was achieved if both agents were combined. Interestingly, CXCL1-induced hyperalgesia could also be inhibited by IL-1ra but no change was seen in TNFR1 knockout mice. Therefore, IL-1β seems to be downstream of CXCL1, whereas TNF-α is upstream. In contrast, our own unpublished data suggest that intraplantar injection of CXCL1 as well as CXCL2/3 (MIP-2 macrophage inflammatory protein) in normal rats does not evoke thermal or mechanical hyperalgesia for up to 12 h postinjection despite significant recruitment of granulocytes. Differences could be explained by the doses or the behavioral test used (see below). Doses producing maximal chemokine-induced granulocyte recruitment do not induce hyperalgesia in our model Rittner, H. L., *et al.* 2006.

In a recent study, a connection between chemokines and TRPV1 was shown (Zhang, N. *et al.*, 2005). CCL3 (macrophage inflammatory protein 1α) that binds to CCR1 was tested *in vitro* and *in vivo*. Activation of CCR1 resulted in increases in TRPV1-mediated Ca^{2+} influx and increased sensitivity of TRPV1 to its ligand capsaicin. *In vivo* the latency in the mouse hot plate test was reduced for up to 45 min after a local injection of CCL3. Thus, CCL3 seems to be capable of enhancing the sensitivity of TRPV1, possibly through a G protein-dependent signaling pathway.

The endogenous role of chemokines was studied in rats and mice in carrageenan-induced hindpaw inflammation. In studies by Ferreira *et al.*, human CXCL8 and rat CXCL1 were shown to contribute to carrageenan-induced hyperalgesia in rats (Cunha, F. Q. *et al.*, 1991; Lorenzetti, B. B. *et al.*, 2002; Sachs, D. *et al.*, 2002). Similarly, injection of carrageenan elicited hyperalgesia, which could be reduced by pretreatment with anti-CXCL1 antibodies in mice (Cunha, T. M. *et al.*, 2005). Therefore, part of the hyperalgesia seen in carrageenan inflammation is dependent directly or indirectly on certain chemokines. However, our own studies in CFA-induced inflammation suggest an additional role of chemokines in counteracting inflammatory pain. In this model, concomitant injection of CXCL2/3 and CFA induced a threefold increase in the number of neutrophils in the inflamed paw after 2 h, while mechanical and thermal hyperalgesia was not changed (Brack, A. *et al.*, 2004d). Furthermore, inhibition of CXCL1 and CXCL2/3 in inflamed paws had no effect on mechanical hyperalgesia despite significant reduction of the number of infiltrating neutrophils after 2 h (Brack, A. *et al.*, 2004c) (see also Analgesic Effects of Corticotropin Releasing Factor, Interleukin-1β, and Noradreline and Endogenous Opoid Analgesia). The differences between our studies and those by Cunha *et al.*, might be related to the model of inflammation (CFA versus carrageenan) or to the type of behavioral test used. While we determined the amount of mechanical pressure required for the rat to withdraw its paw (modified Randall–Selitto method), Cunha *et al.*, used a substantially more painful stimulus that induced sympathetic activation with a freezing reaction and apnea.

In neuropathic pain the role of chemokines has not been thoroughly examined. Disruption of the gene for CCR2 prevented mechanical allodynia in the chronic constriction injury model (Abbadie, C. *et al.*, 2003). CCR2, activated by CCL2 (monocyte chemotrattractant protein-1), is responsible for attracting monocytes into inflamed tissue. Therefore the authors conclude that the decreased number of monocytes is responsible for the reduced pain in this model. In summary, the contribution of chemokines to hyperalgesia may depend on their type, the model of pain, the time frame and the dose of chemokine used. Some of the indirect effects are mediated by the ability of chemokines to attract monocytes.

5.30.2.3 Nerve Growth Factor

NGF belongs to the family of neurotrophic proteins, together with brain-derived neurotrophic factor (BDNF), neurotrophin-3 (NT-3), NT-4/5, and NT-6. NGF governs the innervation of target tissues during development and plays an important role in neuronal survival and maintenance of connectivity. Besides its action on neurons, NGF also has immunomodulatory effects in different inflammatory diseases including asthma, arthritis, and psoriasis. NGF is constitutively expressed in keratinocytes in normal skin. However, many cells including all subtypes of leukocytes as well as sensory neurons can express NGF in inflammation (Vega, J. A. *et al.*, 2003). After binding to its high-affinity receptor tyrosine receptor kinase A (trkA) on peripheral terminals of sensory neurons, NGF is internalized and retrogradely transported to the somata in the DRG. NGF is a potent regulator of gene expression of neuropeptides like calcitonin gene-related peptide and substance P, of receptors like TRPV1 and of ion channels like tetrodotoxin (TTX)-resistant sodium channels. The role of endogenous NGF has mostly been examined using proteins that block the bioactivity of NGF because deletion of NGF or trkA in mice is lethal within the first week of life.

Injection of NGF into the normal rat paw induces a long-lasting thermal as well as mechanical hyperalgesia (Lewin, G. R. *et al.*, 1994). These effects seem to be in part dependent on mast cells and on a central component involving *N*-methyl-D-aspartate (NMDA) receptors. Nociceptor sensitization was also observed *in vitro* in a skin–nerve preparation (Rueff, A. and Mendell, L. M., 1996). Infusion of trkA–IgG into the noninflamed rat paw to block local NGF diminished thermal hyperalgesia and decreased calcitonin gene-related peptide content in DRG neurons (McMahon, S. B. *et al.*, 1995). The detection of sensitizing properties of NGF has been corroborated by the analysis of transgenic mice overexpressing NGF in the epidermis (Stucky, C. L. *et al.*, 1999). These animals developed hyperalgesia without any signs of inflammation of the

skin. In electrophysiological studies unmyelinated nociceptors responded with a fourfold intensity to heat stimuli in comparison to wild-type mice. Moreover, almost every C fiber responded to heat in NGF overexpressing animals in contrast to only half of the C fibers in wild-type animals. No enhanced response to mechanical stimuli was seen. Together, this provides supporting evidence for the heat-sensitizing property of NGF. Importantly, endogenous NGF seems to be responsible for maintenance of the sensitivity of nociceptors as application of trkA–IgG fusion molecule to the innervation territory of the cutaneous saphenous nerve resulted in a reduction of innervation density of the epidermis and of the percentage of neurons responding to heat or bradykinin (Bennett, D. L. *et al.*, 1998).

Blocking of NGF by trkA–IgG in carrageenan-induced inflammation prevents the development of thermal hyperalgesia and the sensitization of nociceptors despite normal development of inflammation as measured by tissue edema (McMahon, S. B. *et al.*, 1995; Koltzenburg, M. *et al.*, 1999). Similarly, injection of anti-NGF antibodies blocks the development of thermal hyperalgesia in CFA-induced inflammation (Lewin, G. R. *et al.*, 1994). Thus, NGF seems to be part of the inflammatory cascade involving initially inflammatory cytokines like IL-1β and TNF-α and subsequently NGF (Figure 1) (Cunha, T. M. *et al.*, 2005).

Neuropathic pain is also influenced by NGF; however, the data seem to be controversial. Treatment with anti-NGF in the chronic constriction injury model reduced hyperalgesia but the effect showed a delayed onset, short duration, and dependency on the dosage (Ro, L. S. *et al.*, 1999). In a recent paper the role of NGF and glial cell-line-derived neurotrophic factor (GDNF) on nociceptor function was examined (Zwick, M. *et al.*, 2003). Two lines of transgenic mice that contained an increased number of either NGF- or GDNF-dependent neurons were used. These mice were tested in a model of inflammatory pain (CFA) and neuropathic pain (spinal nerve ligation model). Contrary to expectations, neither line of transgenic mice became more hyperalgesic following induction of persistent pain. In fact, NGF-overexpressing mice recovered more rapidly from initial inflammatory hyperalgesia and became hypoalgesic despite extensive paw swelling in the inflammatory model. In the neuropathic model, only wild-type mice became hyperalgesic. mRNA expression of opioid receptors, NMDA receptors, metabolic glutamate receptor, sodium channels and vanilloid receptors showed marked differences in DRG neurons but not in the spinal cord between wild-type and NGF- or GDNF-overexpressing animals. This suggested that the somatosensory system is capable of producing normal pain behavior despite significant modification of nociceptors.

NGF blockade seems to produce analgesia also in other pain states. In a model of bone cancer pain, osteosarcoma tumor cells are injected into the intramedullary space of the mouse femur. In a recent study, the authors focused on a novel NGF-sequestering antibody and demonstrated that two administrations produce a profound reduction in both ongoing and movement-evoked bone cancer pain-related behaviors that was greater than that achieved with acute administration of 10 or 30 mg kg^{-1} of morphine (Sevcik, M. A. *et al.*, 2005). In summary, neutralization of NGF produces analgesia in most pain models studied.

5.30.2.4 Other Mediators: Bradykinin

Bradykinin is a nonapeptide generated from high-molecular-weight kininogen through cleavage by kallikrein under inflammatory conditions in plasma. It is also released from mast cells during asthma attacks and within the gut as a gastrointestinal vasodilator. Bradykinin is rapidly generated after tissue injury and seems to modulate most of the events observed during the inflammatory process including vasodilatation, increase of vascular permeability, plasma extravasation, and cell migration (reviewed in Calixto, J. B. *et al.*, 2000). It is also one of the most potent endogenous proalgesic mediators (Ferreira, S. H. *et al.*, 1993). It directly activates bradykinin receptors on primary afferent neurons or sensitizes nociceptors indirectly through release of prostaglandins, nitric oxide, neurokinins, calcitonin gene-related peptide, cytokines, and histamine (Figure 1), or via alterations of vanilloid receptor channel gating (Chuang, H. H. *et al.*, 2001). In fact, lipopolysaccharide- or carrageenan-induced inflammation triggers the TNF-α-driven cytokine cascade via the release of bradykinin (references in Cunha, F. Q. and Ferreira, S. H., 2003). Bradykinin is released at the beginning of the inflammation because delayed treatment with bradykinin receptor antagonists 2 h after injection of lipopolysaccharide or carrageenan has no effect on hyperalgesia or inflammation.

Bradykinin also plays a role in neuropathic pain. Ablation of the gene for the bradykinin receptor 1 resulted in a significant reduction of mechanical allodynia and thermal hyperalgesia in early stages of

nerve injury (Ferreira, J. *et al.*, 2005). Furthermore, systemic treatment with the bradykinin receptor 1-selective antagonist des-Arg9-[Leu8]-bradykinin reduced the established mechanical allodynia observed 7–28 days after nerve lesion in wild-type mice. Nonpeptidic orally active bradykinin receptor 1 and 2 antagonists are currently being developed as peripheral analgesics (Sawynok, J., 2003; Marceau, F. and Regoli, D., 2004).

5.30.2.5 Clinical Implications and Perspectives

A myriad of peripheral mediators is involved in inflammatory as well as neuropathic pain. The most frequently used pain medications are selective or nonselective inhibitors of COX. These nonsteroidal anti-inflammatory drugs inhibit the common final pathway of most proalgesic compounds, the production of prostaglandins. However, these drugs have serious side effects such as gastrointestinal ulcer formation, bleeding and/or, thromboembolic events. Because of the multitude of proinflammatory and proalgesic mediators the development of new analgesics is difficult. Inhibiting one pathway may still leave other mediators available. On the other hand, cytokine antagonists such as the TNF-α receptor antagonist etanercept have been developed for treatment of autoimmune disease like rheumatoid arthritis and have been shown to produce analgesia in patients (Sommer, C. *et al.*, 2001). Despite the almost innumerable number of mediators new treatments are under current investigation including, e.g., the blockade of the bradykinin system (Sawynok, J., 2003; Marceau, F. and Regoli, D., 2004). The development of peripherally acting drugs would have advantages such as the avoidance of central side effects. For example, the localized (e.g., topical) administration of drugs can potentially optimize drug concentrations at the site of injury without systemically active drug levels and fewer adverse systemic effects, fewer drug interactions, and no need to titrate doses into a therapeutic range compared with systemic administration.

5.30.3 Analgesic Mechanisms

Leukocytes are the source not only of hyperalgesic mediators but also of antinociceptive mediators. The best-characterized and clinically tested compounds are the endogenous opioid peptides. Other analgesic mediators include anti-inflammatory cytokines, somatostatin (somatotropin release inhibiting factor; SRIF), and the endocannabinoids.

5.30.3.1 Anti-Inflammatory Cytokines

In later stages of inflammation cytokines are produced, which limit inflammation and counteract hyperalgesia (references in Cunha, F. Q. and Ferreira, S. H., 2003). For example, IL-4, IL-10, IL-13, and IL-1ra can produce analgesia (Figure 2) (Cunha, F. Q. *et al.*, 1999; Cunha, J. M. *et al.*, 2000; Cunha, F. Q. and Ferreira, S. H., 2003). IL-4 and IL-13 are produced by Th_2 lymphocytes and mast cells and suppress the production of proinflammatory mediators such as IL-1, TNF-α, interferon-γ, and CXCL8. In addition, inhibition of COX-2 is observed. IL-10 is a product of T-lymphocytes and monocytes and inhibits the production of Th_1 proinflammatory cytokines including IL-1, IL-6, IL-8, and TNF-α. Besides, it upregulates IL-1ra. These effects are also seen in models of pain. Pretreatment with IL-4, IL-10, and IL-13 dose dependently blocked hyperalgesia induced by carrageenan, bradykinin, and TNF-α but did not affect hyperalgesia induced by CXCL8 and prostaglandins. Furthermore, the endogenous role of anti-inflammatory cytokines to limit hyperalgesia was demonstrated by application of antisera against IL-4, IL-10, and IL-13. They potentiated hyperalgesia induced by carrageenan, bradykinin,

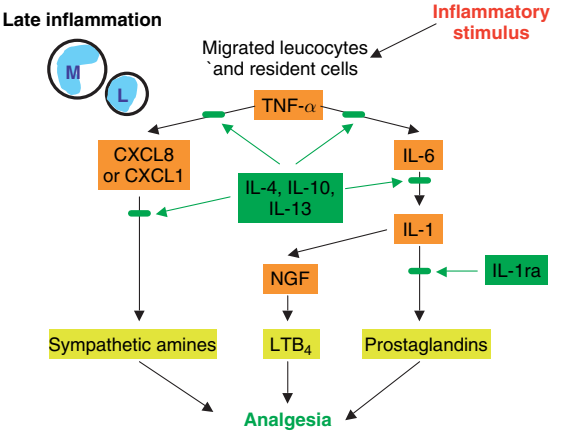

Figure 2 Analgesic cytokines in late inflammation. During ongoing inflammation leukocytes, e.g., lymphocytes (L) and monocytes/macrophages (M), start to produce anti-inflammatory cytokines like interleukin-4 (IL-4), IL-10, IL-13, and IL-1 receptor antagonist (IL-1ra). These cytokines inhibit the proinflammatory cytokines such as TNF-α, IL-1, and IL-6, and block the cascade.

and TNF-α. This effect was not seen in athymic and mast-cell-depleted rats. Thus, it seems that endogenous sources of IL-4 and IL-13 are mast cells and lymphocytes, respectively. Analgesic actions of IL-4, IL-10, and IL-13 are not only seen in paw inflammation but also in models of peritonitis and knee joint incapacitation induced by zymosan. Analgesic properties of anti-inflammatory cytokines are independent of endogenous production of opioid peptides (Vale, M. L. *et al.*, 2003). In summary, during ongoing inflammation analgesic cytokines are produced which counteract the effects of the proinflammatory hyperalgesic cytokines generated in the early stages.

5.30.3.2 Opioid Peptides

5.30.3.2.1 Peripheral opioid receptors

5.30.3.2.1.(i) Localization Opioid peptides are the natural ligands at opioid receptors. Three cDNAs and their genes have been identified, encoding the μ-, δ-, and κ-opioid receptor (MOP, DOP, and KOP), respectively (Kieffer, B. L. and Gaveriaux-Ruff, C., 2002). All three receptors can mediate pain inhibition and they are found throughout the nervous system, including somatic and visceral sensory neurons, spinal cord projection and interneurons, midbrain, and cortex. Recent interest has focused on the identification of opioid receptors on peripheral processes of sensory neurons. The cell bodies of these neurons in DRG express all three mRNAs and receptor proteins (Stein, C. *et al.*, 2001). Opioid receptors are intraaxonally transported into the neuronal processes and are detectable on peripheral sensory nerve terminals in animals and in humans. Colocalization studies confirmed the presence of opioid receptors on neurons expressing substance P and/or calcitonin gene-related peptide in DRG small- and medium-sized neurons and in their central and peripheral terminals (Dado, R. J. *et al.*, 1993; Zhang, X. *et al.*, 1998; Wenk, H. N. and Honda, C. N., 1999; Guan, J. S. *et al.*, 2005). Further, anatomical and electrophysiological studies showed expression of opioid receptors on unmyelinated C and on myelinated Aδ fibers (i.e., nociceptors) (Beland, B. and Fitzgerald, M., 2001; Pare, M. *et al.*, 2001; Suzuki, R. and Dickenson, A. H., 2002) but not on large myelinated Aβ fibers (Arvidsson, U. *et al.*, 1995; Beland, B. and Fitzgerald, M., 2001). However, after nerve injury morphine depressed responses of Aβ fibers (Suzuki, R. and Dickenson, A. H., 2002), and expression δ-receptors on the A$\alpha\beta$ fibers in Meissner corpuscules in glaborus skin has been recently reported (Pare, M. *et al.*, 2001). The binding characteristics (affinity) of peripheral and central opioid receptors are similar but the molecular masses of peripheral and central μ-receptors appear to be different (references in Stein, C. *et al.*, 2003). If these findings are confirmed, a search for selective ligands at such distinct receptors may be warranted.

It has been suggested that opioid receptors are also located on sympathetic postganglionic neuron terminals. However, there are reports arguing against this notion and studies attempting the direct demonstration of opioid receptor mRNA in sympathetic ganglia have produced negative results. In addition, thorough morphological investigations have clearly demonstrated the presence of δ-receptors on unmyelinated primary afferent neurons and the absence of such receptors on postganglionic sympathetic neurons in skin, lip, and cornea. Moreover, chemical sympathectomy with 6-hydroxydopamine does not change the expression of opioid receptors in the DRG or the peripheral analgesic effects of μ-, δ-, and κ-receptor agonists in a model of inflammatory pain. Together, these findings have corroborated the notion that peripheral opioid receptors mediating analgesia are exclusively localized on primary sensory neurons (references in Stein, C. *et al.*, 2001).

Opioid binding sites and the expression of opioid receptor transcripts have also been demonstrated in immune cells. Opioid-mediated modulation of the proliferation of these cells and of their functions (e.g., chemotaxis, superoxide and cytokine production, mast cell degranulation) has been reported. These immunomodulatory actions can be stimulatory as well as inhibitory and have been ascribed to the activation of opioid receptors (Sacerdote, P. *et al.*, 2003; Sharp, B. M., 2003). However, the significance of such effects with regard to pain transmission has not been investigated as yet.

5.30.3.2.1.(ii) Opioid receptor signaling in sensory neurons All three types of opioid receptors mediate the inhibition of high-voltage-activated calcium currents in cultured primary afferent neurons. These effects are transduced by G proteins (G_i and/or G_o) (references in Stein, C. *et al.*, 2001; 2003). Although it is well-known that opioids induce membrane hyperpolarization due to increased potassium currents in central neurons, this could not be detected in DRG neurons so far (Akins, P. T. *et al.*, 1993). Thus, the modulation of calcium channels appears to be the primary mechanism for the inhibitory effects of opioids on peripheral sensory neurons. In addition,

opioids – via inhibition of adenylyl cyclase – suppress TTX-resistant sodium- and nonselective cation currents stimulated by the inflammatory agent prostaglandin E_2 (Ingram, S. L. and Williams, J. T., 1994; Gold, M. S. and Levine, J. D., 1996). Interestingly, TTX-resistant sodium channels are selectively expressed in nociceptors, they are important for impulse initiation and action potential conductance, they mediate spontaneous activity in sensitized nociceptors and they accumulate at the site of injury in damaged nerves leading to ectopic impulse generation (Porreca, F. *et al.*, 1999; Laird, J. M. *et al.*, 2002). The latter observations may explain the notable efficacy of peripheral opioids in inflammatory and neuropathic pain (Stein, C. *et al.*, 2001; 2003). Consistent with their effects on ion channels, opioids attenuate the excitability of peripheral nociceptor terminals, the propagation of action potentials, the release of excitatory proinflammatory neuropeptides (substance P, calcitonin gene-related peptide) from peripheral sensory nerve endings, and vasodilatation evoked by stimulation of C fibers (references in Stein, C. *et al.*, 2001). All of these mechanisms result in analgesia and/or anti-inflammatory actions.

5.30.3.2.1.(iii) Peripheral opioid receptors and inflammation Peripheral opioid analgesic effects are augmented under conditions of tissue injury such as inflammation, neuropathy, or bone damage (Stein, C. *et al.*, 2001; 2003). One underlying mechanism is an increased number (upregulation) of peripheral opioid receptors. In neuronal cell cultures, μ-receptor transcription is upregulated by the cytokine IL-4 through binding of STAT6 transcription factors to the μ-receptor gene promoter (Kraus, J. *et al.*, 2001). In DRG, the synthesis and expression of opioid receptors can be increased by peripheral tissue inflammation (Ji, R. R. *et al.*, 1995; Zöllner, C. *et al.*, 2003). Subsequently, the axonal transport of opioid receptors is greatly enhanced leading to their upregulation and to enhanced agonist efficacy at peripheral nerve terminals (Jeanjean, A. P. *et al.*, 1995; Mousa, S. A. *et al.*, 2001). In addition, the specific milieu (low pH, prostanoid release) of inflamed tissue may increase opioid agonist efficacy by enhanced G protein coupling and by increased neuronal cyclic adenosine monophosphate levels (Selley, D. E. *et al.*, 1993; Ingram, S. L. and Williams, J. T., 1994; Zöllner, C. *et al.*, 2003). Inflammation also leads to an increase in the number of sensory nerve terminals (sprouting) and disrupts the perineurial barrier, thus facilitating the access of opioid agonists to their receptors (Stein, C. *et al.*, 2001; 2003).

5.30.3.2.2 Opioid peptides produced by immune cells

Three families of opioid peptides are well characterized in the central nervous and neuroendocrine systems (Akil, H. *et al.*, 1998). Each family derives from a distinct gene and from one of the three precursor proteins proopiomelanocortin (POMC), proenkephalin (PENK), or prodynorphin, respectively. Appropriate processing yields their respective representative opioid peptides, the endorphins, enkephalins, and dynorphins (Table 1). These peptides exhibit different affinity and selectivity for the three opioid receptors μ (endorphins, enkephalins), δ (enkephalins, endorphins), and κ (dynorphin). Two additional endogenous opioid peptides have been isolated from bovine brain: endomorphin-1 and endomorphin-2 (Table 1). Both peptides are considered highly selective μ-receptor ligands. Their precursors are not known yet. All of these opioid peptides have been detected in immune cells but the POMC and PENK families have been studied most extensively.

5.30.3.2.2.(i) Proopiomelanocortin-derived opioid peptides POMC-related opioid peptides have been found in immune cells of many vertebrates and nonvertebrates (references in Machelska, H. *et al.*, 2002). To determine whether these immune-competent cells actually synthesize POMC rather than simply absorb related peptides from plasma,

Table 1 Structure of endogenous opioid peptides

β-Endorphin	Tyr-Gly-Gly-Phe-Met-Thr-Ser-Glu-Lys-Ser-Gln-Thr-Pro-Leu-Val-Thr-Leu-Phe-Lys-Asn-Ala-Ile-Val-Lys-Asn-Ala-His-Lys-Lys-Gly-Gln-OH
Methionine-enkephalin	Tyr-Gly-Gly-Phe-Met-OH
Leucine-enkephalin	Tyr-Gly-Gly-Phe-Leu-OH
Dynorphin A	Tyr-Gly-Gly-Phe-Leu-Arg-Arg-Ile-Arg-Pro-Lys-Leu-Lys-Tyr-Asp-Asn-Gln-OH
Endomorphin-1	Tyr-Pro-Trp-Phe-OH
Endomorphin-2	Tyr-Pro-Phe-Phe-OH

mRNA encoding POMC was sought for and demonstrated in many of these studies. The pituitary POMC gene is organized into three exons separated by intervening sequences which are removed during processing following transcription to produce the full-length, 1200-nt transcript. Initially, truncated POMC transcripts were found in leukocytes (references in Machelska, H. *et al.*, 2002). Lyons P. D. and Blalock J. E. (1997) reexamined the question of POMC mRNA expression using novel polymerase chain reaction procedures. With this exacting and sensitive methodology, they found expression of full-length transcripts encoding all three POMC exons in rat mononuclear leukocytes. This POMC transcript is spliced in the same way as the pituitary transcript and contains the sequence for the signal peptide, which is necessary for the correct routing into the regulated secretory pathway. The POMC protein is also proteolytically processed in a way consistent with the pituitary gland (Lyons, P. D. and Blalock, J. E., 1997; Mousa, S. A. *et al.*, 2004). These results unequivocally demonstrate that immune cells can produce full-length POMC transcripts. Apparently, this production is stimulated by various immune and inflammatory mediators (Smith, E. M., 2003).

5.30.3.2.2.(ii) Proenkephalin-derived opioid peptides PENK-derived opioid peptides have also been detected in human and rodent immune cells. Both the mRNA and methionine (Met)-enkephalin protein were detected. Preproenkephalin mRNA was found in T- and B-cells, macrophages, and mast cells. In subpopulations of immune cells this mRNA was shown to be highly homologous to brain PENK mRNA, abundant and apparently translated, as immunoreactive enkephalin is present and/or released. The appropriate enzymes necessary for posttranslational processing of PENK have also been identified in immune cells (references in Machelska, H. *et al.*, 2002).

5.30.3.2.2.(iii) Immune-derived opioid peptides in inflammation Immune-derived opioid peptides apparently play a substantial role in the modulation of inflammatory pain (Machelska, H. *et al.*, 2002; Stein, C. *et al.*, 2003). POMC mRNA and β-endorphin, as well as Met-enkephalin and dynorphin were found in cells derived from lymph nodes, and in leukocytes in the blood and within inflamed tissue in CFA model of inflammatory pain (Cabot, P. J. *et al.*, 1997; 2001; Machelska, H. *et al.*, 2003; Mousa, S. A. *et al.*, 2004). In the pituitary, POMC processing begins as the nascent polypeptide enters the endoplasmic reticulum directed by the signal peptide, and POMC cleavage begins in the *trans*-Golgi network (references in Mousa, S. A. *et al.*, 2004). The POMC prohormone is directed to the regulated secretory pathway at the *trans*-Golgi network by binding to a sorting receptor, membrane-bound carboxypeptidase E. The prohormone convertases PC1 (also called PC1/3) and PC2 cleave POMC within the *trans*-Golgi network. PC1 mediates the initial cleavage into adrenocorticotropic and β-lipotropic hormones. The inactive pro-PC2 is bound to 7B2 (a chaperone-like binding protein) and is transported from the endoplasmic reticulum to later compartments of the secretory pathway, where it matures to active PC2; thereafter, PC2 converts β-lipotropic hormone into β-melanocyte stimulating hormone and β-endorphin (references in Mousa, S. A. *et al.*, 2004). Recently, we detected β-endorphin and POMC alone and colocalized with PC1, PC2, carboxypeptidase E, and 7B2 in leukocytes in the blood and within inflamed paw tissue (Mousa, S. A. *et al.*, 2004). This demonstrates that immune cells express the entire machinery required for POMC processing into functionally active β-endorphin.

In this CFA model, mRNAs encoding POMC and PENK and the corresponding opioid peptides β-endorphin and Met-enkephalin are abundant in cells of inflamed but not in noninflamed tissue (Przewlocki, R. *et al.*, 1992). Histomorphological procedures and flow cytometry have identified the opioid-containing cells as T- and B-lymphocytes, granulocytes, and monocytes/macrophages (Przewlocki, R. *et al.*, 1992; Rittner, H. L. *et al.*, 2001). Also, it was shown that β-endorphin is present in activated/memory T-cells within inflamed tissue (Cabot, P. J. *et al.*, 1997; Mousa, S. A. *et al.*, 2001). Thus, opioid peptides are processed and present both in circulating and inflammatory cells infiltrating injured tissue.

5.30.3.2.3 Migration of opioid-containing immune cells to inflamed tissue

The recruitment of leukocytes from the circulation into areas of inflammation begins with the attachment of these cells to vascular endothelium, followed by their transmigration into the tissue. This is mediated by specific cell adhesion and chemoattractant/activator molecules. Leukocytes are recruited from the circulation by a well-orchestrated set of events. They undergo multiple attachments to and detachments from the vessel's endothelial cells prior

to transendothelial migration. This includes slowing and rolling along the endothelial cell wall that is mediated predominantly by the interaction of selectins expressed on leukocytes (L-selectin) and on endothelial cells (P- and E-selectin) with their ligands on endothelium or immune cells, respectively. The rolling leukocytes can then be activated by chemoattractants such as chemokines released from inflammatory cells and presented on endothelium. This leads to the upregulation and increased avidity of integrins. These mediate the firm adhesion of leukocytes to endothelial cells via ligands of the immunoglobulin superfamily, e.g., intercellular adhesion molecule-1 (ICAM-1). Finally, the immune cells transmigrate through the endothelial wall mediated by immunoglobulin superfamily members (e.g., platelet-endothelial adhesion molecule-1; PECAM-1) and are directed to the sites of inflammation to initiate a host defense (reviewed by Petruzzelli, L. *et al.*, 1999; von Andrian, U. H. and Mackay, C. R., 2000).

Recent findings indicate that these events can also be involved in the endogenous control of inflammatory pain. In the model of unilateral hind paw inflammation with CFA we have shown that integrin α_4 and the chemokines CXCL2 and CXCL1 are expressed by leukocytes, while adhesion molecules such as P- and E-selectins, ICAM-1, and PECAM-1 are upregulated on endothelium in inflamed paw tissue (Mousa, S. A. *et al.*, 2000; Machelska, H. *et al.*, 2002; Brack, A. *et al.*, 2004; Machelska, H. *et al.*, 2004) (Figure 3). Expression of CXCL1 and CXCL2 mRNAs and protein contents significantly increased in inflamed tissue during the course of inflammation (Brack, A. *et al.*, 2004). Importantly, L-selectin, integrins β_2, and the CXC chemokine receptor 2 (CXCR2) are coexpressed by opioid-containing leukocytes, which have migrated to inflamed subcutaneous paw tissue (Mousa, S. A. *et al.*, 2000; Brack, A. *et al.*, 2004; Machelska, H. *et al.*, 2004). Furthermore, pretreatment of rats with a selectin blocker (fucoidin), selective antibodies against

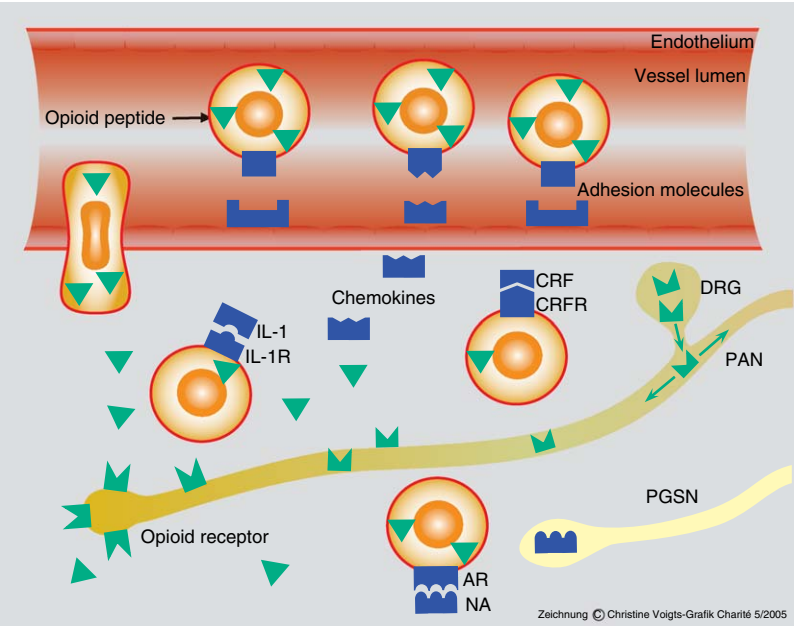

Figure 3 Migration of opioid-producing cells and opioid secretion within inflamed tissue. Adhesion molecules are upregulated on vascular endothelium and are coexpressed by circulating immune cells producing opioid peptides. These cells coexpress receptors for chemokines, which are presented on endothelium. Certain adhesion molecules mediate rolling of opioid-containing leukocytes along the endothelium. The rolling leukocytes can then be activated by chemokines, which upregulate another class of adhesion molecules mediating adhesion. Finally cells transmigrate through the endothelium. Once extravasated, these cells can be stimulated by stress or releasing agents such as corticotropin releasing factor (CRF), interleukin-1β (IL-1β), chemokines, and noradrenaline (NA) to secrete opioid peptides. CRF, IL-1, and NA (the latter derived from postganglionic sympathetic neurons; PGSN) elicit opioid release by activating CRF receptors (CRFR), IL-1 receptors (IL-1R), and adrenergic receptors (AR) on immune cells, respectively. Opioids bind to peripheral opioid receptors (produced in dorsal root ganglia (DRG) and transported to peripheral endings of primary afferent neurons; PAN) and lead to analgesia.

ICAM-1, integrins α_4 and β_2, or chemokines CXCL1 and CXCL2 substantially decreases the number of opioid-containing leukocytes infiltrating the inflamed tissue (Machelska, H. *et al.*, 1998; Machelska, H. *et al.*, 2002; Brack, A. *et al.*, 2004; Machelska, H. *et al.*, 2004) and in consequence abolishes endogenous peripheral opioid analgesia (see Endogenous Opoid Analgesia). This suggests that circulating opioid-producing immune cells home to inflamed tissue where they secrete the opioids to inhibit pain. Afterward, they travel to the regional lymph nodes, depleted of the opioid peptides (Cabot, P. J. *et al.*, 1997; 2001). Thus, local signals apparently not only stimulate the synthesis of opioid peptides in resident inflammatory cells but also attract opioid-containing cells from the circulation to the site of injury to reduce pain. This is controlled by specific chemotactic and adhesive mechanisms.

5.30.3.2.4 Release of opioid peptides from immune cells

Regulated secretion of peptides requires secretory granules deriving from the Golgi network for transport to the cell membrane. As discussed in Immune-Derived Opoid Peptides in Inflammation immune cells in the blood and in inflamed tissue coexpress the entire machinery required for POMC processing into functionally active β-endorphin (Mousa, S. A. *et al.*, 2004). Furthermore, our ultrastructural observations show that β-endorphin-expressing macrophages, monocytes, granulocytes, and lymphocytes, contain rough endoplasmic reticulum and Golgi apparatus, similar to pituitary cells. Immunostaining of β-endorphin was detectable in secretory granules, which were grouped in small or large membranous vesicular structures. The smaller β-endorphin-immunoreactive secretory granules were localized within cytoplasm, and the larger ones were arranged at the cell periphery ready for the exocytosis, similar to the pituitary (Mousa, S. A. *et al.*, 2004). In the pituitary, β-endorphin and other POMC-derived peptides are released by corticotropin releasing factor (CRF) and IL-1β (references in Schäfer, M., 2003). Similar mechanisms can trigger opioid release within peripheral inflamed tissue (Figure 3). CRF is present in immune cells, fibroblasts and vascular endothelium and peripheral CRF expression is enhanced in inflamed synovial and subcutaneous tissue of animals and humans (Schäfer, M. *et al.*, 1996). CRF and IL-1β receptors and their upregulation were demonstrated in inflamed lymph nodes and paw tissue in CFA model. Their pharmacological characteristics were similar to the high-affinity CRF- and IL-1β-binding sites in the pituitary (Mousa, S. A. *et al.*, 1996). Furthermore, the coexpression of CRF-1 and CRF-2 receptors with β-endorphin in monocytes/macrophages, granulocytes and lymphocytes were recently shown in the blood and in inflamed paw tissue (Mousa, S. A. *et al.*, 2003). In contrast, CRF receptors were not detected on peripheral sensory nerves. (Mousa, S. A. *et al.*, 1996; Mousa, S. A. *et al.*, 2003). The activation of CRF and IL-1β receptors on cells from lymph nodes results in the secretion of opioid peptides *in vitro*. In those studies β-endorphin, Met-enkephalin, and dynorphin were dose dependently released by CRF, while IL-1β released β-endorphin and dynorphin but not Met-enkephalin. These effects were specific to CRF and IL-1β receptors (Schäfer, M. *et al.*, 1994; Cabot, P. J. *et al.*, 1997; 2001; Mamet, J. *et al.*, 2002). Moreover, this release of opioid peptides was calcium-dependent and mimicked by elevated extracellular concentrations of potassium. This is consistent with a regulated pathway of release from secretory vesicles, as in neurons and endocrine cells (Cabot, P. J. *et al.*, 1997; 2001).

Adrenergic receptor agonists have also been shown to secrete β-endorphin from human peripheral blood mononuclear cells (Kavelaars, A. *et al.*, 1990). Similar mechanisms are involved in β-endorphin release from leukocytes in the rat CFA model of inflammatory pain (Binder, W. *et al.*, 2004) (Figure 3). Double labeling demonstrated adrenergic α_1-, β_2-, and, to a lesser degree, α_2 receptors expressed on β-endorphin-containing leukocytes in inflamed paw tissue. β-endorphin-containing and adrenergic α_1- and β_2-receptor-expressing immune cells were localized in close proximity to sympathetic nerve fibers, and chemical ablation of these fibers abolished intrinsic opioid analgesia. Finally, noradrenaline induced adrenergic receptor-specific release of β-endorphin from immune cells *in vitro* (Binder, W. *et al.*, 2004). Taken together, CRF, IL-1β, and sympathetic neuron-derived noradrenaline can act on their respective receptors on immune cells resulting in release of opioid peptides (Figure 3).

5.30.3.2.5 Analgesia produced by immune-derived opioid peptides

5.30.3.2.5.(i) Analgesic effects of corticotropin releasing factor, interleukin-1β, and noradrenaline

CRF-, IL-1β-, and noradrenaline-induced release of opioids from immune cells also occurs *in vivo*

(Figure 3). CRF and IL-1β injected into inflamed paws in CFA model produce dose-dependent analgesia reversible by their respective antagonists (Schäfer, M. *et al.*, 1994). CRF can produce analgesia both in early and late stages of inflammation (2 h and 6 days) and, in accord with anatomical findings (see Release of Opoid Peptides from Immune Cells), CRF analgesia involves both CRF-1 and CRF-2 receptors (Machelska, H. *et al.*, 2003; Mousa, S. A. *et al.*, 2003; Brack, A. *et al.*, 2004c). Intravenous administration of these agents in locally effective doses does not change pain thresholds, demonstrating a peripheral site of action (Schäfer, M. *et al.*, 1994; Machelska, H. *et al.*, 2003; Mousa, S. A. *et al.*, 2003; Brack, A. *et al.*, 2004c). Leukocytes apparently are the target for CRF and IL-1β because immunosuppression with cyclosporine A, depletion of granulocytes, blockade of chemokines (CXCL1 and CXCL2/3), as well as anti-selectin and anti-ICAM-1 treatments result in a significant reduction of opioid-containing immune cells and of CRF- or IL-1β-induced analgesia (Schäfer, M. *et al.*, 1994; Machelska, H. *et al.*, 1998; 2002; Brack, A. *et al.*, 2004c). Also, cyclosporine A-induced attenuation of CRF analgesia could be restored by injection of activated lymphocytes (Hermanussen, S. *et al.*, 2004). CRF- and IL-1β-induced analgesia is blocked by an antibody against β-endorphin, suggesting that this opioid plays a major role. In addition, Met-enkephalin appears to be involved in CRF-, and dynorphin in IL-1β-induced analgesia (Schäfer, M. *et al.*, 1994).

These results are in line with other studies on local analgesic effects of CRF (Hargreaves, K. M. *et al.*, 1989; McLoon, L. K. *et al.*, 2002) and of the cytokines IL-6 and TNF-α (Czlonkowski, A. *et al.*, 1993) but are in contrast to hyperalgesia mediated by IL-1β, IL-6, and TNF-α discussed in Cunha F. Q. and Ferreira S. H. (2003). Importantly, however, the latter hyperalgesic effects of exogenous cytokines were observed after injections into noninflamed tissue (Cunha, F. Q. *et al.*, 1992; Poole, S. *et al.*, 1995; Safieh-Garabedian, B. *et al.*, 1995; Woolf, C. J. *et al.*, 1997; Cunha, T. M. *et al.*, 2005). Apparently, hyperalgesia in highly inflamed tissue (4 days after CFA) has already reached a ceiling effect (Machelska, H. *et al.*, 2003) and therefore cannot be further increased. Instead, in such tissue opioid-containing immune cells became the predominant target for cytokines to produce analgesia. Contribution of endogenous proinflammatory cytokines to the generation of pain was mostly observed either in early stages (3–6 h) when cytokine blockade preceded induction of CFA inflammation (Woolf, C. J. *et al.*, 1997) or in short-lasting (30 min to 3 h) inflammation, e.g., induced with carrageenan, lipopolysaccharide, or acetic acid (Cunha, F. Q. *et al.*, 1992; Ferreira, S. H. *et al.*, 1993; Cunha, J. M. *et al.*, 2000; Cunha, T. M. *et al.*, 2005). Thus, the presence or absence of inflammation, the duration and/or model of inflammatory pain are factors to be taken into consideration.

Noradrenaline administered directly into inflamed tissue has been shown to produce analgesia, reversible by α_1-, α_2-, and β_2-adrenergic receptor antagonists in CFA model. Further, this effect was dose dependently blocked by μ and δ receptor antagonists and antibody against β-endorphin (Binder, W. *et al.*, 2004). These data suggest that this catecholamine produces analgesia via opioid peptides activating peripheral opioid receptors. In noninflamed tissue, noradrenaline did not influence pain behavior in this model, consistent with the lack of opioid-containing cells and with the scarcity of adrenergic receptors (Binder, W. *et al.*, 2004). However, the role of peripheral adrenergic receptors in nociception appears controversial. In noninflamed tissue, noradrenaline has been shown to produce hyperalgesia via α_2-adrenergic receptors. Others found that α_2-agonists could also produce peripheral analgesia. It has even been postulated that hyperalgesia is mediated via α_{2B} and analgesia is mediated via α_{2C} receptors (references in Binder, W. *et al.*, 2004). Thus, different receptor subtypes, receptor localization, microenvironment, and the presence or absence of inflammation are important parameters to be considered.

5.30.3.2.5.(ii) Endogenous opioid analgesia Stress is a natural stimulus triggering inhibition of pain (Willer, J. C. *et al.*, 1981; Terman, G. W. *et al.*, 1984). In rats, stress induced by cold water (4 °C) swim (for 1 min) elicits potent analgesia in inflamed but not in noninflamed paws in CFA model (Stein, C. *et al.*, 1990a; Machelska, H. *et al.*, 2003). In early inflammation (6 h), this swim stress-induced analgesia was only partially attenuated by peripherally selective doses of different opioid peptide antibodies and receptor antagonists but was fully reversed by centrally acting doses of an opioid receptor antagonist (Machelska, H. *et al.*, 2003). At later stages of inflammation (4–6 days), swim stress analgesia was completely abolished by peripherally selective doses of antibody against β-endorphin and by μ and δ-antagonists (Stein, C. *et al.*, 1990a). Together, these data indicate that at early stages of CFA-induced inflammation all three families of opioid

peptides and receptors are involved, while at later stages β-endorphin acting at μ- and δ-receptors dominates. Whereas at early stages both peripheral and central opioid receptors are involved, at later stages endogenous analgesia is mediated exclusively by peripheral opioid receptors. Thus, peripheral opioid mechanisms of pain control become more prevalent with the duration and severity of inflammation. Endogenous triggers of swim stress-induced analgesia are locally produced CRF and sympathetic nerve-derived catecholamines because this effect is abolished by local neutralization of CRF (Schäfer, M. *et al.*, 1996; Machelska, H. *et al.*, 2003), and by sympathetic blockade (Binder, W. *et al.*, 2004).

Various types of immune cells are the source of opioids as demonstrated by the abolishment of stress-induced analgesia by immunosuppression with cyclosporine A or whole-body irradiation and by depletion of monocytes/macrophages (Stein, C. *et al.*, 1990b; Przewlocki, R. *et al.*, 1992; Brack, A. *et al.*, 2004a). Moreover, this effect is also extinguished by inhibiting the extravasation of β-endorphin-containing immune cells following blockade of L- and P-selectins, α_4 and β_2 integrins or of ICAM-1 (Machelska, H. *et al.*, 1998; 2002; 2004). These adhesion molecules apparently regulate the migration of opioid-containing immune cells and the subsequent generation of intrinsic pain control in inflamed tissue (Figure 3).

A future challenge is to identify factors that will increase homing of opioid-containing cells to injured tissue and will enhance analgesia. To this end, we have shown that hematopoetic growth factors strongly mobilized granulocytes in the blood but resulted only in a minor increase in the number of opioid-containing leukocytes in inflamed paws and in no change of CRF- and swim stress-induced analgesia (Brack, A. *et al.*, 2004b). Another approach was to increase the migration of opioid-containing cells to inflamed tissue with local injections of CXCL2. However, this did not result in stronger CRF- or swim stress-induced analgesia either, most probably as a result of the small number of peripheral opioid receptors at this very early (2 h) stage of inflammation (Brack, A. *et al.*, 2004d). Indeed, previous studies had shown that intrinsic analgesia increases with the duration of inflammation (2 h to 4 days), in parallel with the number of opioid-containing leukocytes, with the number of peripheral opioid receptors and with the efficacy of opioid receptor–G protein coupling in sensory neurons (Mousa, S. A. *et al.*, 2001; Rittner, H. L. *et al.*, 2001; Zöllner, C. *et al.*, 2003).

5.30.3.2.6 Clinical implications

Peripheral endogenous opioid analgesia has found many clinical applications. Opioid receptors have been demonstrated on peripheral terminals of sensory nerves in human synovia (Stein, C. *et al.*, 1996) and these receptors mediate analgesia in patients with various types of pain (e.g., in chronic rheumatoid arthritis and osteoarthritis, bone pain, after dental, laparoscopic, urinary bladder, and knee surgery) (references in Stein, C. *et al.*, 2003). Opioid peptides are found in human synovial lining cells, mast cells, lymphocytes, and macrophages. The prevailing peptides are β-endorphin and Met-enkephalin, while only minor amounts of dynorphin are detectable (Stein, C. *et al.*, 1993; 1996). The interaction of synovial opioids with peripheral opioid receptors was examined in patients undergoing knee surgery. Blocking intraarticular opioid receptors by the local administration of naloxone resulted in significantly increased postoperative pain (Stein, C. *et al.*, 1993). Taken together, these findings suggest that in a stressful (e.g., postoperative) situation, opioids are tonically released from inflamed tissue and activate peripheral opioid receptors to attenuate clinical pain. Importantly, these endogenous opioids do not interfere with exogenous morphine, i.e., intraarticular morphine is an equally potent analgesic in patients with and without opioid-producing inflammatory synovial cells (Stein, C. *et al.*, 1996). This suggests that, in contrast to the rapid development of tolerance in the central nervous system, the immune cell-derived opioids do not readily produce cross-tolerance to morphine at peripheral opioid receptors.

5.30.3.2.7 Perspectives

Effective control of inflammatory pain can result from interactions between leukocyte-derived opioid peptides and their receptors on peripheral sensory neurons. These findings provide new insights into intrinsic mechanisms of pain control and open strategies to develop new drugs and alternative approaches to treatment of pain. Immunocompromised patients (e.g., in AIDS, cancer, diabetes) frequently suffer from painful neuropathies, which can be associated with intra- and perineural inflammation, with reduced intraepidermal nerve fiber density and with low $CD4^+$ lymphocyte counts (Polydefkis, M. *et al.*, 2002). Thus it may be interesting to investigate the opioid

production/release and the migration of opioid-containing leukocytes in these patients. The important role of certain adhesion molecules and chemokines in the trafficking of opioid-containing cells to injured tissues indicates that antiadhesion or antichemokine strategies for the treatment of inflammatory diseases may in fact carry a significant risk to exacerbate pain. It would be highly desirable to identify stimulating factors and strategies that selectively attract opioid-producing cells and increase peripheral opioid receptor numbers in damaged tissue. Augmenting the synthesis and/or secretion of opioid peptides and opioid receptor numbers within injured tissue may be accomplished by gene therapy: delivery of PENK, POMC, and of μ receptor cDNAs have been shown to decrease chronic pain and inflammation (Braz, J. *et al*., 2001; Lu, C. Y. *et al*., 2002; Xu, Y. *et al*., 2003).

Importantly, opioid analgesia resulting from neuroimmune interactions occurs in peripheral tissues and therefore is devoid of central opioid side effects (such as depression of breathing, nausea, clouding of consciousness, addiction, and high rate of tolerance) and of typical side effects produced by COX inhibitors (such as gastric erosions, ulcers, bleeding, diarrhea, thromboembolic events, and renal toxicity). Many efforts are currently undertaken to develop peripherally acting analgesics by aiming at individual excitatory receptors or channels on sensory neurons (Simonin, F. and Kieffer, B. L., 2002). The major advantage of targeting opioid receptors is their mechanism of action: the inhibition of calcium (and possibly sodium) channels simply renders the nociceptor less excitable to the plethora of stimulating molecules expressed in damaged tissue. Thus, peripherally acting opioids can prevent and reverse the action of multiple excitatory agents simultaneously, in contrast to blocking only one single noxious stimulus. Uncovering mechanisms that can enhance the availability of endogenous opioids within injured tissue and the signal transduction of peripheral opioid receptors will open exciting possibilities for pain research and therapy.

References

Abbadie, C., Lindia, J. A., Cumiskey, A. M., Peterson, L. B., Mudgett, J. S., Bayne, E. K., DeMartino, J. A., MacIntyre, D. E., and Forrest, M. J. 2003. Impaired neuropathic pain responses in mice lacking the chemokine receptor CCR2. Proc. Natl. Acad. Sci. U. S. A. 100, 7947–7952.

Akil, H., Owens, C., Gutstein, H., Taylor, L., Curran, E., and Watson, S. 1998. Endogenous opioids: overview and current issues. Drug Alcohol Depend. 51, 127–140.

Akins, P. T. and McCleskey, E. W. 1993. Characterization of potassium currents in adult rat sensory neurons and modulation by opioids and cyclic AMP. Neuroscience 56, 759–769.

von Andrian, U. H. and Mackay, C. R. 2000. T-cell function and migration. Two sides of the same coin. N. Engl. J. Med. 343, 1020–1034.

Arvidsson, U., Riedl, M., Chakrabarti, S., Lee, J. H., Nakano, A. H., Dado, R. J., Loh, H. H., Law, P. Y., Wessendorf, M. W., and Elde, R. 1995. Distribution and targeting of a mu-opioid receptor (MOR1) in brain and spinal cord. J. Neurosci. 15, 3328–3341.

Beland, B. and Fitzgerald, M. 2001. Mu- and delta-opioid receptors are downregulated in the largest diameter primary sensory neurons during postnatal development in rats. Pain 90, 143–150.

Bennet, G. J. 1994. Animal Models of Neuropathic Pain. In: Proceedings of the 7th World Congress on Pain, Progress in Pain Research and Management (*eds*. G. F. Gebhart, D. L. Hammond, and T. S. Jensen), pp. 495–510. IASP Press.

Bennett, D. L., Koltzenburg, M., Priestley, J. V., Shelton, D. L., and McMahon, S. B. 1998. Endogenous nerve growth factor regulates the sensitivity of nociceptors in the adult rat. Eur. J. Neurosci. 10, 1282–1291.

Binder, W., Mousa, S. A., Sitte, N., Kaiser, M., Stein, C., and Schafer, M. 2004. Sympathetic activation triggers endogenous opioid release and analgesia within peripheral inflamed tissue. Eur. J. Neurosci. 20, 92–100.

Brack, A., Labuz, D., Schiltz, A., Rittner, H. L., Machelska, H., Schäfer, M., Reszka, R., and Stein, C. 2004a. Tissue monocytes/macrophages in inflammation: hyperalgesia versus opioid-mediated peripheral antinociception. Anesthesiology 101, 204–211.

Brack, A., Rittner, H. L., Machelska, H., Beschmann, K., Sitte, N., Schäfer, M., and Stein, C. 2004b. Mobilization of opioid-containing polymorphonuclear cells by hematopoetic growth factors and influence on inflammatory pain. Anesthesiology 100, 149–157.

Brack, A., Rittner, H. L., Machelska, H., Shaqura, M., Mousa, S. A., Labuz, D., Zöllner, C., Schäfer, M., and Stein, C. 2004c. Control of inflammatory pain by chemokine-mediated recruitment of opioid-containing polymorphonuclear cells. Pain 112, 229–238.

Brack, A., Rittner, H. L., Machelska, H., Shaqura, M., Mousa, S. A., Labuz, D., Zöllner, C., Schäfer, M., and Stein, C. 2004d. Endogenous peripheral antinociception in early inflammation is not limited by the number of opioid-containing leukocytes but by opioid receptor expression. Pain 108, 67–75.

Braz, J., Beaufour, C., Coutaux, A., Epstein, A. L., Cesselin, F., Hamon, M., and Pohl, M. 2001. Therapeutic efficacy in experimental polyarthritis of viral-driven enkephalin overproduction in sensory neurons. J. Neurosci. 21, 7881–7888.

Cabot, P. J., Carter, L., Gaiddon, C., Zhang, Q., Schäfer, M., Loeffler, J. P., and Stein, C. 1997. Immune cell-derived beta-endorphin. Production, release, and control of inflammatory pain in rats. J. Clin. Invest. 100, 142–148.

Cabot, P. J., Carter, L., Schäfer, M., and Stein, C. 2001. Methionine-enkephalin- and Dynorphin A-release from immune cells and control of inflammatory pain. Pain 93, 207–212.

Calixto, J. B., Cabrini, D. A., Ferreira, J., and Campos, M. M. 2000. Kinins in pain and inflammation. Pain 87, 1–5.

Chuang, H. H., Prescott, E. D., Kong, H., Shields, S., Jordt, S. E., Basbaum, A. I., Chao, M. V., and Julius, D. 2001.

Bradykinin and nerve growth factor release the capsaicin receptor from PtdIns(4,5)P2-mediated inhibition. Nature 411, 957–962.

Cui, J. G., Holmin, S., Mathiesen, T., Meyerson, B. A., and Linderoth, B. 2000. Possible role of inflammatory mediators in tactile hypersensitivity in rat models of mononeuropathy. Pain 88, 239–248.

Cunha, F. Q. and Ferreira, S. H. 2003. Peripheral hyperalgesic cytokines. Adv. Exp. Med. Biol. 521, 22–39.

Cunha, J. M., Cunha, F. Q., Poole, S., and Ferreira, S. H. 2000. Cytokine-mediated inflammatory hyperalgesia limited by interleukin-1 receptor antagonist. Br. J. Pharmacol. 130, 1418–1424.

Cunha, F. Q., Lorenzetti, B. B., Poole, S., and Ferreira, S. H. 1991. Interleukin-8 as a mediator of sympathetic pain. Br. J. Pharmacol. 104, 765–767.

Cunha, F. Q., Poole, S., Lorenzetti, B. B., and Ferreira, S. H. 1992. The pivotal role of tumour necrosis factor alpha in the development of inflammatory hyperalgesia. Br. J. Pharmacol. 107, 660–664.

Cunha, F. Q., Poole, S., Lorenzetti, B. B., Veiga, F. H., and Ferreira, S. H. 1999. Cytokine-mediated inflammatory hyperalgesia limited by interleukin-4. Br. J. Pharmacol. 126, 45–50.

Cunha, T. M., Verri, W. A., Jr., Silva, J. S., Poole, S., Cunha, F. Q., and Ferreira, S. H. 2005. A cascade of cytokines mediates mechanical inflammatory hypernociception in mice. Proc. Natl. Acad. Sci. U. S. A. 102, 1755–1760.

Czlonkowski, A., Stein, C., and Herz, A. 1993. Peripheral mechanisms of opioid antinociception in inflammation: involvement of cytokines. Eur. J. Pharmacol. 242, 229–235.

Dado, R. J., Law, P. Y., Loh, H. H., and Elde, R. 1993. Immunofluorescent identification of a delta (delta)-opioid receptor on primary afferent nerve terminals. Neuroreport 5, 341–344.

Ferreira, J., Beirith, A., Mori, M. A., Araujo, R. C., Bader, M., Pesquero, J. B., and Calixto, J. B. 2005. Reduced nerve injury-induced neuropathic pain in kinin B1 receptor knock-out mice. J. Neurosci. 25, 2405–2412.

Ferreira, S. H., Lorenzetti, B. B., Bristow, A. F., and Poole, S. 1988. Interleukin-1 beta as a potent hyperalgesic agent antagonized by a tripeptide analogue. Nature 334, 698–700.

Ferreira, S. H., Lorenzetti, B. B., and Poole, S. 1993. Bradykinin initiates cytokine-mediated inflammatory hyperalgesia. Br. J. Pharmacol. 110, 1227–1231.

Fukuoka, H., Kawatani, M., Hisamitsu, T., and Takeshige, C. 1994. Cutaneous hyperalgesia induced by peripheral injection of interleukin-1 beta in the rat. Brain Res. 657, 133–140.

Gadient, R. A. and Otten, U. 1996. Postnatal expression of interleukin-6 (IL-6) and IL-6 receptor (IL-6R) mRNAs in rat sympathetic and sensory ganglia. Brain Res. 724, 41–46.

Gazda, L. S., Milligan, E. D., Hansen, M. K., Twining, C. M., Poulos, N. M., Chacur, M., KA, O. C., Armstrong, C., Maier, S. F., Watkins, L. R., and Myers, R. R. 2001. Sciatic inflammatory neuritis (SIN): behavioral allodynia is paralleled by peri-sciatic proinflammatory cytokine and superoxide production. J. Peripher. Nerv. Syst. 6, 111–129.

Gold, M. S. and Levine, J. D. 1996. DAMGO inhibits prostaglandin E2-induced potentiation of a TTX-resistant Na^+ current in rat sensory neurons *in vitro*. Neurosci. Lett. 212, 83–86.

Guan, J. S., Xu, Z. Z., Gao, H., He, S. Q., Ma, G. Q., Sun, T., Wang, L. H., Zhang, Z. N., Lena, I., Kitchen, I., Elde, R., Zimmer, A., He, C., Pei, G., Bao, L., and Zhang, X. 2005. Interaction with vesicle luminal protachykinin regulates surface expression of delta-opioid receptors and opioid analgesia. Cell 122, 619–631.

Hargreaves, K. M., Dubner, R., and Costello, A. H. 1989. Corticotropin releasing factor (CRF) has a peripheral site of action for antinociception. Eur. J. Pharmacol. 170, 275–279.

Hermanussen, S., Do, M., and Cabot, P. J. 2004. Reduction of beta-endorphin-containing immune cells in inflamed paw tissue corresponds with a reduction in immune-derived antinociception: reversible by donor activated lymphocytes. Anesth. Analg. 98, 723–729.

Ingram, S. L. and Williams, J. T. 1994. Opioid inhibition of Ih via adenylyl cyclase. Neuron 13, 179–186.

Jeanjean, A. P., Moussaoui, S. M., Maloteaux, J. M., and Laduron, P. M. 1995. Interleukin-1 beta induces long-term increase of axonally transported opiate receptors and substance P. Neuroscience 68, 151–157.

Ji, R. R., Zhang, Q., Law, P. Y., Low, H. H., Elde, R., and Hokfelt, T. 1995. Expression of mu-, delta-, and kappa-opioid receptor-like immunoreactivities in rat dorsal root ganglia after carrageenan-induced inflammation. J. Neurosci. 15, 8156–8166.

Julius, D. and Basbaum, A. I. 2001. Molecular mechanisms of nociception. Nature 413, 203–210.

Junger, H. and Sorkin, L. S. 2000. Nociceptive and inflammatory effects of subcutaneous TNFalpha. Pain 85, 145–151.

Kavelaars, A., Ballieux, R. E., and Heijnen, C. J. 1990. *In vitro* beta-adrenergic stimulation of lymphocytes induces the release of immunoreactive beta-endorphin. Endocrinology 126, 3028–3032.

Kieffer, B. L. and Gaveriaux-Ruff, C. 2002. Exploring the opioid system by gene knockout. Prog. Neurobiol. 66, 285–306.

Koltzenburg, M., Bennett, D. L., Shelton, D. L., and McMahon, S. B. 1999. Neutralization of endogenous NGF prevents the sensitization of nociceptors supplying inflamed skin. Eur. J. Neurosci. 11, 1698–1704.

Kraus, J., Borner, C., Giannini, E., Hickfang, K., Braun, H., Mayer, P., Hoehe, M. R., Ambrosch, A., Konig, W., and Hollt, V. 2001. Regulation of mu-opioid receptor gene transcription by interleukin-4 and influence of an allelic variation within a STAT6 transcription factor binding site. J. Biol. Chem. 276, 43901–43908.

Laird, J. M., Souslova, V., Wood, J. N., and Cervero, F. 2002. Deficits in visceral pain and referred hyperalgesia in Nav1.8 (SNS/PN3)-null mice. J. Neurosci. 22, 8352–8356.

Lewin, G. R., Rueff, A., and Mendell, L. M. 1994. Peripheral and central mechanisms of NGF-induced hyperalgesia. Eur. J. Neurosci. 6, 1903–1912.

Li, Y., Ji, A., Weihe, E., and Schafer, M. K. 2004. Cell-specific expression and lipopolysaccharide-induced regulation of tumor necrosis factor alpha (TNFalpha) and TNF receptors in rat dorsal root ganglion. J. Neurosci. 24, 9623–9631.

Li, M., Shi, J., Tang, J. R., Chen, D., Ai, B., Chen, J., Wang, L. N., Cao, F. Y., Li, L. L., Lin, C. Y., and Guan, X. M. 2005. Effects of complete Freund's adjuvant on immunohistochemical distribution of IL-1beta and IL-1R I in neurons and glia cells of dorsal root ganglion. Acta Pharmacol. Sin. 26, 192–198.

Lorenzetti, B. B., Veiga, F. H., Canetti, C. A., Poole, S., Cunha, F. Q., and Ferreira, S. H. 2002. CINC-1 mediates the sympathetic component of inflammatory mechanical hypersensitivity in rats. Eur. Cytokine Netw. 13, 456–461.

Lu, C. Y., Chou, A. K., Wu, C. L., Yang, C. H., Chen, J. T., Wu, P. C., Lin, S. H., Muhammad, R., and Yang, L. C. 2002. Gene-gun particle with pro-opiomelanocortin cDNA produces analgesia against formalin-induced pain in rats. Gene Ther. 9, 1008–1014.

Lyons, P. D. and Blalock, J. E. 1997. Pro-opiomelanocortin gene expression and protein processing in rat mononuclear leukocytes. J. Neuroimmunol. 78, 47–56.

Machelska, H., Brack, A., Mousa, S. A., Schopohl, J. K., Rittner, H. L., Schäfer, M., and Stein, C. 2004. Selectins and

integrins but not platelet-endothelial cell adhesion molecule-1 regulate opioid inhibition of inflammatory pain. Br. J. Pharmacol. 142, 772–780.

Machelska, H., Cabot, P. J., Mousa, S. A., Zhang, Q., and Stein, C. 1998. Pain control in inflammation governed by selectins. Nat. Med. 4, 1425–1428.

Machelska, H., Mousa, S. A., Brack, A., Schopohl, J. K., Rittner, H. L., Schäfer, M., and Stein, C. 2002. Opioid control of inflammatory pain regulated by intercellular adhesion molecule-1. J. Neurosci. 22, 5588–5596.

Machelska, H., Schopohl, J. K., Moussa, S. A., Schäfer, M., and Stein, C. 2003. Different mechanisms of intrinsic pain inhibition in early and late inflammation. J. Neuroimmuno 14, 30–39.

Mamet, J., Baron, A., Lazdunski, M., and Voilley, N. 2002. Proinflammatory mediators, stimulators of sensory neuron excitability via the expression of acid-sensing ion channels. J. Neurosci. 22, 10662–10670.

Marceau, F. and Regoli, D. 2004. Bradykinin receptor ligands: therapeutic perspectives. Nat. Rev. Drug. Discov. 3, 845–852.

McLoon, L. K., Sandnas, A. M., Nockleby, K. J., and Wirtschafter, J. D. 2002. Reduction in vesicant-induced cellular inflammation and hyperalgesia by local injection of corticotropin releasing factor in rabbit eyelid. Inflamm. Res. 51, 16–23.

McMahon, S. B., Bennett, D. L., Priestley, J. V., and Shelton, D. L. 1995. The biological effects of endogenous nerve growth factor on adult sensory neurons revealed by a trkA–IgG fusion molecule. Nat. Med. 1, 774–780.

Merskey, H. and Bogduk, N. 1994. Pain Terminology. In: Classification of Chronic Pain. IASP Task Force on Taxonomy (*eds*. H. Merskey and N. Bogduk), pp. 209–214. IASP Press.

Mousa, S. A., Bopaiah, C. P., Stein, C., and Schäfer, M. 2003. Involvement of corticotropin-releasing hormone receptor subtypes 1 and 2 in peripheral opioid-mediated inhibition of inflammatory pain. Pain 106, 297–307.

Mousa, S. A., Machelska, H., Schafer, M., and Stein, C. 2000. Co-expression of beta-endorphin with adhesion molecules in a model of inflammatory pain. J. Neuroimmunol. 108, 160–170.

Mousa, S. A., Schafer, M., Mitchell, W. M., Hassan, A. H., and Stein, C. 1996. Local upregulation of corticotropin-releasing hormone and interleukin-1 receptors in rats with painful hindlimb inflammation. Eur. J. Pharmacol. 311, 221–231.

Mousa, S. A., Shakibaei, M., Sitte, N., Schafer, M., and Stein, C. 2004. Subcellular pathways of beta-endorphin synthesis, processing, and release from immunocytes in inflammatory pain. Endocrinology 145, 1331–1341. Epub 2003 Nov 1320.

Mousa, S. A., Zhang, Q., Sitte, N., Ji, R., and Stein, C. 2001. beta-Endorphin-containing memory-cells and mu-opioid receptors undergo transport to peripheral inflamed tissue. J. Neuroimmunol. 115, 71–78.

Murphy, P. G., Ramer, M. S., Borthwick, L., Gauldie, J., Richardson, P. M., and Bisby, M. A. 1999. Endogenous interleukin-6 contributes to hypersensitivity to cutaneous stimuli and changes in neuropeptides associated with chronic nerve constriction in mice. Eur. J. Neurosci. 11, 2243–2253.

Obreja, O., Biasio, W., Andratsch, M., Lips, K. S., Rathee, P. K., Ludwig, A., Rose-John, S., and Kress, M. 2005. Fast modulation of heat-activated ionic current by proinflammatory interleukin 6 in rat sensory neurons. Brain 128, 1634–1641.

Obreja, O., Rathee, P. K., Lips, K. S., Distler, C., and Kress, M. 2002a. IL-1 beta potentiates heat-activated currents in rat sensory neurons: involvement of IL-1RI, tyrosine kinase, and protein kinase C. FASEB J. 16, 1497–1503.

Obreja, O., Schmelz, M., Poole, S., and Kress, M. 2002b. Interleukin-6 in combination with its soluble IL-6 receptor sensitises rat skin nociceptors to heat, *in vivo*. Pain 96, 57–62.

Oh, S. B., Tran, P. B., Gillard, S. E., Hurley, R. W., Hammond, D. L., and Miller, R. J. 2001. Chemokines and glycoprotein120 produce pain hypersensitivity by directly exciting primary nociceptive neurons. J. Neurosci. 21, 5027–5035.

Ohtori, S., Takahashi, K., Moriya, H., and Myers, R. R. 2004. TNF-alpha and TNF-alpha receptor type 1 upregulation in glia and neurons after peripheral nerve injury: studies in murine DRG and spinal cord. Spine 29, 1082–1088.

Okamoto, K., Martin, D. P., Schmelzer, J. D., Mitsui, Y., and Low, P. A. 2001. Pro- and anti-inflammatory cytokine gene expression in rat sciatic nerve chronic constriction injury model of neuropathic pain. Exp. Neurol. 169, 386–391.

Opree, A. and Kress, M. 2000. Involvement of the proinflammatory cytokines tumor necrosis factor-alpha, IL-1 beta, and IL-6 but not IL-8 in the development of heat hyperalgesia: effects on heat-evoked calcitonin gene-related peptide release from rat skin. J. Neurosci. 20, 6289–6293.

Pare, M., Elde, R., Mazurkiewicz, J. E., Smith, A. M., and Rice, F. L. 2001. The Meissner corpuscle revised: a multiafferented mechanoreceptor with nociceptor immunochemical properties. J. Neurosci. 21, 7236–7246.

Petruzzelli, L., Takami, M., and Humes, H. D. 1999. Structure and function of cell adhesion molecules. Am. J. Med. 106, 467–476.

Polydefkis, M., *et al.*, 2002. Reduced intraepidermal nerve fiber density in HIV-associated sensory neuropathy. Neurology 58, 115–119.

Poole, S., Cunha, F. Q., Selkirk, S., Lorenzetti, B. B., and Ferreira, S. H. 1995. Cytokine-mediated inflammatory hyperalgesia limited by interleukin-10. Br. J. Pharmacol. 115, 684–688.

Porreca, F., Lai, J., Bian, D., Wegert, S., Ossipov, M. H., Eglen, R. M., Kassotakis, L., Novakovic, S., Rabert, D. K., Sangameswaran, L., and Hunter, J. C. 1999. A comparison of the potential role of the tetrodotoxin-insensitive sodium channels, PN3/SNS and NaN/SNS2, in rat models of chronic pain. Proc. Natl. Acad. Sci. U. S. A. 96, 7640–7644.

Przewlocki, R., Hassan, A. H., Lason, W., Epplen, C., Herz, A., and Stein, C. 1992. Gene expression and localization of opioid peptides in immune cells of inflamed tissue: functional role in antinociception. Neuroscience 48, 491–500.

Rittner, H. L., Brack, A., Machelska, H., Mousa, S. A., Bauer, M., Schäfer, M., and Stein, C. 2001. Opioid peptide-expressing leukocytes: identification, recruitment, and simultaneously increasing inhibition of inflammatory pain. Anesthesiology 95, 500–508.

Rittner, H. L., Mousa, S. A., Labuz, D., Beschmann, K., Schäfer, M., Stein, C., and Brack, A. 2006. Selective local PMN recruitment by CXCL1 or CXCL2/3 injection does not cause inflammatory pain. J. Leuk. Biol. 79, 1022–1032.

Ro, L. S., Chen, S. T., Tang, L. M., and Jacobs, J. M. 1999. Effect of NGF and anti-NGF on neuropathic pain in rats following chronic constriction injury of the sciatic nerve. Pain 79, 265–274.

Rueff, A. and Mendell, L. M. 1996. Nerve growth factor NT-5 induce increased thermal sensitivity of cutaneous nociceptors *in vitro*. J. Neurophysiol. 76, 3593–3596.

Sacerdote, P., Limiroli, E., and Gaspani, L. 2003. Experimental evidence for immunomodulatory effects of opioids. Adv. Exp. Med. Biol. 521, 106–116.

Sachs, D., Cunha, F. Q., Poole, S., and Ferreira, S. H. 2002. Tumour necrosis factor-alpha, interleukin-1beta and interleukin-8 induce persistent mechanical nociceptor hypersensitivity. Pain 96, 89–97.

Safieh-Garabedian, B., Poole, S., Allchorne, A., Winter, J., and Woolf, C. J. 1995. Contribution of interleukin-1 beta to the inflammation-induced increase in nerve growth factor levels and inflammatory hyperalgesia. Br. J. Pharmacol. 115, 1265–1275.

Sawynok, J. 2003. Topical and peripherally acting analgesics. Pharmacol. Rev. 55, 1–20.

Schäfer, M. 2003. Cytokines and peripheral analgesia. Adv. Exp. Med. Biol. 521, 40–50.

Schäfer, M., Carter, L., and Stein, C. 1994. Interleukin 1 beta and corticotropin-releasing factor inhibit pain by releasing opioids from immune cells in inflamed tissue. Proc. Natl. Acad. Sci. U. S. A. 91, 4219–4223.

Schäfer, M., Mousa, S. A., Zhang, Q., Carter, L., and Stein, C. 1996. Expression of corticotropin-releasing factor in inflamed tissue is required for intrinsic peripheral opioid analgesia. Proc. Natl. Acad. Sci. U. S. A. 93, 6096–6100.

Schäfers, M., Brinkhoff, J., Neukirchen, S., Marziniak, M., and Sommer, C. 2001. Combined epineurial therapy with neutralizing antibodies to tumor necrosis factor-alpha and interleukin-1 receptor has an additive effect in reducing neuropathic pain in mice. Neurosci. Lett. 310, 113–116.

Schäfers, M., Geis, C., Svensson, C. I., Luo, Z. D., and Sommer, C. 2003a. Selective increase of tumour necrosis factor-alpha in injured and spared myelinated primary afferents after chronic constrictive injury of rat sciatic nerve. Eur. J. Neurosci. 17, 791–804.

Schäfers, M., Lee, D. H., Brors, D., Yaksh, T. L., and Sorkin, L. S. 2003b. Increased sensitivity of injured and adjacent uninjured rat primary sensory neurons to exogenous tumor necrosis factor-alpha after spinal nerve ligation. J. Neurosci. 23, 3028–3038.

Schäfers, M., Sorkin, L. S., Geis, C., and Shubayev, V. I. 2003c. Spinal nerve ligation induces transient upregulation of tumor necrosis factor receptors 1 and 2 in injured and adjacent uninjured dorsal root ganglia in the rat. Neurosci. 347, 179–182.

Schäfers, M., Svensson, C. I., Sommer, C., and Sorkin, L. S. 2003d. Tumor necrosis factor-alpha induces mechanical allodynia after spinal nerve ligation by activation of p38 MAPK in primary sensory neurons. J. Neurosci. 23, 2517–2521.

Scholz, J. and Woolf, C. J. 2002. Can we conquer pain? Nat. Neurosci. 5(Suppl.), 1062–1067.

Selley, D. E., Breivogel, C. S., and Childers, S. R. 1993. Modification of G protein-coupled functions by low-pH pretreatment of membranes from NG108-15 cells: increase in opioid agonist efficacy by decreased inactivation of G proteins. Mol. Pharmacol. 44, 731–741.

Sevcik, M. A., Ghilardi, J. R., Peters, C. M., Lindsay, T. H., Halvorson, K. G., Jonas, B. M., Kubota, K., Kuskowski, M. A., Boustany, L., Shelton, D. L., and Mantyh, P. W. 2005. Anti-NGF therapy profoundly reduces bone cancer pain and the accompanying increase in markers of peripheral and central sensitization. Pain 115, 128–141.

Sharp, B. M. 2003. Opioid receptor expression and intracellular signaling by cells involved in host defense and immunity. Adv. Exp. Med. Biol. 521, 98–105.

Shubayev, V. I. and Myers, R. R. 2001. Axonal transport of TNF-alpha in painful neuropathy: distribution of ligand tracer and TNF receptors. J. Neuroimmunol. 114, 48–56.

Simonin, F. and Kieffer, B. L. 2002. Two faces for an opioid peptide – and more receptors for pain research. Nature 5, 185–186.

Smith, E. M. 2003. Opioid peptides in immune cells. Adv. Exp. Med. Biol. 521, 51–68.

Sommer, C., Petrausch, S., Lindenlaub, T., and Toyka, K. V. 1999. Neutralizing antibodies to interleukin 1-receptor reduce pain associated behavior in mice with experimental neuropathy. Neurosci. Lett. 270, 25–28.

Sommer, C., Schäfers, M., Marziniak, M., and Toyka, K. V. 2001. Etanercept reduces hyperalgesia in experimental painful neuropathy. J. Peripher. Nerv. Syst. 6, 67–72.

Sorkin, L. S., Xiao, W. H., Wagner, R., and Myers, R. R. 1997. Tumour necrosis factor-alpha induces ectopic activity in nociceptive primary afferent fibres. Neuroscience 81, 255–262.

Stein, C., Gramsch, C., and Herz, A. 1990a. Intrinsic mechanisms of antinociception in inflammation: local opioid receptors and beta-endorphin. J. Neurosci. 10, 1292–1298.

Stein, C., Hassan, A. H., Lehrberger, K., Giefing, J., and Yassouridis, A. 1993. Local analgesic effect of endogenous opioid peptides. Lancet 342, 321–324.

Stein, C., Hassan, A. H., Przewlocki, R., Gramsch, C., Peter, K., and Herz, A. 1990b. Opioids from immunocytes interact with receptors on sensory nerves to inhibit nociception in inflammation. Proc. Natl. Acad. Sci. U. S. A. 87, 5935–5939.

Stein, C., Machelska, H., and Schafer, M. 2001. Peripheral analgesic and antiinflammatory effects of opioids. Z. Rheumatol. 60, 416–424.

Stein, C., Pfluger, M., Yassouridis, A., Hoelzl, J., Lehrberger, K., Welte, C., and Hassan, A. H. 1996. No tolerance to peripheral morphine analgesia in presence of opioid expression in inflamed synovia. J. Clin. Invest. 98, 793–799.

Stein, C., Schäfer, M., and Machelska, H. 2003. Attacking pain at its source: new perspectives on opioids. Nat. Med. 9, 1003–1008.

Stucky, C. L., Koltzenburg, M., Schneider, M., Engle, M. G., Albers, K. M., and Davis, B. M. 1999. Overexpression of nerve growth factor in skin selectively affects the survival and functional properties of nociceptors. J. Neurosci. 19, 8509–8516.

Suzuki, R. and Dickenson, A. H. 2002. Nerve injury-induced changes in opioid modulation of wide dynamic range dorsal column nuclei neurones. Neuroscience 111, 215–228.

Terman, G. W., Shavit, Y., Lewis, J. W., Cannon, J. T., and Liebeskind, J. C. 1984. Intrinsic mechanisms of pain inhibition: activation by stress. Science 226, 1270–1277.

Vale, M. L., Marques, J. B., Moreira, C. A., Rocha, F. A., Ferreira, S. H., Poole, S., Cunha, F. Q., and Ribeiro, R. A. 2003. Antinociceptive effects of interleukin-4, -10, and -13 on the writhing response in mice and zymosan-induced knee joint incapacitation in rats. J. Pharmacol. Exp. Ther. 304, 102–108.

Vega, J. A., Garcia-Suarez, O., Hannestad, J., Perez-Perez, M., and Germana, A. 2003. Neurotrophins and the immune system. J. Anat. 203, 1–19.

Verri, W. A., Jr., Schivo, I. R., Cunha, T. M., Liew, F. Y., Ferreira, S. H., and Cunha, F. Q. 2004. Interleukin-18 induces mechanical hypernociception in rats via endothelin acting on ETB receptors in a morphine-sensitive manner. J. Pharmacol. Exp. Ther. 310, 710–717.

Wenk, H. N. and Honda, C. N. 1999. Immunohistochemical localization of delta opioid receptors in peripheral tissues. J. Comp. Neurol. 408, 567–579.

Willer, J. C., Dehen, H., and Cambier, J. 1981. Stress-induced analgesia in humans: endogenous opioids and naloxone-reversible depression of pain reflexes. Science 212, 689–691.

Woolf, C. J., Allchorne, A., Safieh-Garabedian, B., and Poole, S. 1997. Cytokines, nerve growth factor and inflammatory hyperalgesia: the contribution of tumour necrosis factor alpha. Br. J. Pharmacol. 121, 417–424.

Xu, Y., Gu, Y., Xu, G. Y., Wu, P., Li, G. W., and Huang, L. Y. 2003. Adeno-associated viral transfer of opioid receptor gene to primary sensory neurons: a strategy to increase opioid antinociception. Proc. Natl. Acad. Sci. U. S. A. 100, 6204–6209.

Xu, X. J., Hao, J. X., Andell-Jonsson, S., Poli, V., Bartfai, T., and Wiesenfeld-Hallin, Z. 1997. Nociceptive responses in interleukin-6-deficient mice to peripheral inflammation and peripheral nerve section. Cytokine 9, 1028–1033.

Zhang, X., Bao, L., Arvidsson, U., Elde, R., and Hokfelt, T. 1998. Localization and regulation of the delta-opioid receptor in dorsal root ganglia and spinal cord of the rat and monkey: evidence for association with the membrane of large dense-core vesicles. Neuroscience 82, 1225–1242.

Zhang, N., Inan, S., Cowan, A., Sun, R., Wang, J. M., Rogers, T. J., Caterina, M., and Oppenheim, J. J. 2005. A proinflammatory chemokine, CCL3, sensitizes the heat- and capsaicin-gated ion channel TRPV1. Proc. Natl. Acad. Sci. U. S. A. 102, 4536–4541.

Zöllner, C., Shaqura, M. A., Bopaiah, C. P., Mousa, S. A., Stein, C., and Schäfer, M. 2003. Painful inflammation induced increase in μ opioid receptor binding and G-protein coupling in primary afferent neurons. Mol. Pharm. 64, 202–210.

Zwick, M., Molliver, D. C., Lindsay, J., Fairbanks, C. A., Sengoku, T., Albers, K. M., and Davis, B. M. 2003. Transgenic mice possessing increased numbers of nociceptors do not exhibit increased behavioral sensitivity in models of inflammatory and neuropathic pain. Pain 106, 491–500.

Further Reading

Machelska, H. and Stein, C. 2002. Immune mechanisms in pain control. Anesth. Analg. 95, 1002–1008.

Relevant Website

http://www.iasp.pain.org – International Association for the Study of Pain.

5.31 Mechanisms of Glial Activation after Nerve Injury

L R Watkins, E D Milligan, and S F Maier, University of Colorado at Boulder, Boulder, CO, USA

© 2008 Elsevier Inc. All rights reserved.

5.31.1	Introduction	429
5.31.2	Glial Activation in Response to Neurotransmitters	429
5.31.3	Glial Activation in Response to Neuromodulators	430
5.31.4	Glial Activation by Unique Neuron-to-Glia Signals	430
5.31.5	Beyond Neuropathic Pain: Glial Activation in Response to Opioids	431
5.31.6	Conclusions	432
References		432

5.31.1 Introduction

It has been known since the early 1970s that peripheral nerve injury leads to the activation of glia in anatomically linked regions of the brain and spinal cord (Aldskogius, H. and Kozlova, E. N., 1998). In these studies, glial activation was inferred by upregulation of the so-called glial activation markers. These signs that glial activation has occurred can be visualized under the microscope using immunohistochemistry to detect cell-type specific changes (e.g., increased expression of glial fibrillary acidic protein by astrocytes; increased expression of complement type 2 receptors by microglia). Such studies revealed that damage of sensory afferent nerves activates glia in the region of the afferent terminations in the central nervous system (CNS). Likewise, damage of motor efferents activates glia in the CNS in the region of the involved motor neuron cell bodies (Aldskogius, H. and Kozlova, E. N., 1998). While this early literature documented the phenomenon of glial activation in CNS following peripheral nerve injury, the mechanisms underlying such activation remained obscure.

Two decades later, glial activation was linked to neuropathic pain. This link was again initially based on the upregulation of glial activation markers (Garrison, C. J. *et al.*, 1991; 1994). Pharmacology, anatomy, and molecular biology studies that followed documented that microglia and then astrocytes are sequentially activated in response to inflammation and damage to peripheral nerves (Raghavendra, V. *et al.*, 2003; Ledeboer, A. *et al.*, 2005). Indeed, studies of p38 mitogen-activated protein (MAP) kinase activation demonstrated that microglial activation occurs with remarkable rapidity following nerve injury (Svensson, C. I. *et al.*, 2004). Upon activation, neuroexcitatory products that glia release are importantly involved in the initiation and maintenance of neuropathic pain, via their actions on neurons of the pain pathway (Watkins, L. R. *et al.*, 2001; Watkins, L. R. and Maier, S. F., 2003). Thus, converging lines of evidence utilizing a variety of techniques all support the conclusion that glia are key players in neuropathic pain.

However, what is known to date regarding glial involvement in neuropathic pain begs a fundamentally important question: how do glia know to become activated? That is, what message(s) do glia receive that trigger their transition from basal to activated states? This will be discussed first in the context of glial activation in response to injury or inflammation of peripheral nerves, and then more broadly in the context of glial activation in response to analgesics used clinically to treat chronic pain, such as morphine and methadone.

5.31.2 Glial Activation in Response to Neurotransmitters

Given that (1) glia become activated in response to inflammation and damage of peripheral tissues and peripheral nerves and (2) this activation occurs within the somatotopically appropriate region of spinal cord, this suggests that glia may be activated by neurotransmitters released by nocisponsive primary afferents. Indeed, calcitonin gene-related peptide (CGRP) (Haas, C. A. *et al.*, 1991; Reddington, M. *et al.*, 1995), adenosine triphosphate (ATP) (Araque, A. *et al.*, 1999; Tsuda, M. *et al.*, 2003), glutamate (Araque, A. *et al.*, 1999; Tsuda, M. *et al.*, 2003), and substance P

(Svensson, C. I. *et al.*, 2003; Marriott, I., 2004) can each activate microglia and astrocytes. Such neurotransmitter-driven glial activation can be relevant for pain facilitation. For example, pain facilitation that is normally produced upon intrathecal administration of the excitatory amino acid, *N*-methyl-D-aspartate (NMDA), is abolished by blocking microglial activation (Hua, X.-Y. *et al.*, 2005).

Regarding substance P, studies of spinal cord glia have demonstrated that it can activate both astrocytes and microglia. Astrocytes isolated from spinal cord (but not from other brain regions) release prostaglandins upon exposure to substance P (Marriott, D. R. *et al.*, 1991). Substance P can also stimulate the production of proinflammatory cytokines in both astrocytes (Martin, F. C. *et al.*, 1992; Palma, C. *et al.*, 1997; Lieb, K. *et al.*, 1998) and microglia (Martin, F. C. *et al.*, 1993; Luber-Narod, J. *et al.*, 1994). When substance P is injected intrathecally in rats, this activates spinal cord microglia as reflected by phosphorylation (activation) of microglial p38 MAP kinase, a signaling pathway linked to pain facilitation (Svensson, C. I. *et al.*, 2004). Interestingly, microglia can also produce substance P, suggesting that these glial cells may potentially contribute to substance P-mediated pain signaling (Lai, J. P. *et al.*, 2002).

ATP has also recently attracted attention as a neurotransmitter that can enhance pain via the activation of glia. Microglia (but not neurons or astrocytes) express an ionotropic ATP receptor subtype called P2X4 whose expression can become dramatically upregulated in response to peripheral nerve injury (Tsuda, M. *et al.*, 2003). Pharmacological blockade of spinal P2X4 receptors and knockdown of P2X4 receptors using antisense oligodeoxynucleotides each reverse neuropathy-induced tactile allodynia (Tsuda, M. *et al.*, 2003). Intriguingly, activation of microglia by ATP is sufficient to cause pain facilitation. That is, microglia that are first stimulated *in vitro* by ATP, and then injected intrathecally in rats, induces mechanical allodynia (Tsuda, M. *et al.*, 2003).

While, at first glance, it would seem logical that glia must become activated in response to neurotransmitters released as a consequence of peripheral nerve injury, one must remember the literature of the 1970s. That is, if one damages a pure motor nerve, glia are activated surrounding the motor neuron cell bodies within the CNS. In this case, there is no damage to sensory afferent fibers. So, despite there being no neurotransmitter release, glia are still being intensely activated. Thus, while glia do express receptors for neurotransmitters and can respond to them, they are not required for glial activation to take place. This predicts that other signals, beyond neurotransmitters, must exist which can trigger the activation of glia.

5.31.3 Glial Activation in Response to Neuromodulators

Neuromodulators, such as prostaglandins and nitric oxide (NO) are well documented to enhance pain (Woolf, C. J. and Salter, M. W., 2000). In addition to direct excitatory effects on neurons, these substances can also activate glia. Using NO as the example, NO induces calcium oscillations in astrocytes, a marker of activation in this cell type. In turn, NO-induced calcium oscillations causes a nondecrementing, rapid spread of excitation to surrounding astrocytes through cell-to-cell low-resistance connections called gap junctions (Heidemann, A. C. *et al.*, 2004; Sul, J. *et al.*, 2004). Thus NO-excited astrocytes lead to the excitation of a much larger population of astrocytes. Once activated, these glia can then begin releasing neuroexcitatory substances (Araque, A. *et al.*, 1999). In addition, NO induces the release of glutamate, ATP, and prostaglandins from astrocytes (Molina-Holgado, F. *et al.*, 1995; Bal-Price, A. *et al.*, 2002) and stimulates the production of proinflammatory cytokines in both microglia and astrocytes (Sun, D. *et al.*, 1998). Regarding actions in spinal cord, NO has recently been demonstrated to drive the production and release of proinflammatory cytokines in response to intrathecally administered gp120, a protein expressed on the surface of the acquired immune deficiency syndrome (AIDS) virus that activates glia (Holguin, A. *et al.*, 2004). As gp120-induced proinflammatory cytokines induce mechanical allodynia, it would be predicted that NO synthesis inhibitors would block such pain changes concomitant with blocking NO-induced production of these cytokines. Indeed, that was the result found (Holguin, A. *et al.*, 2004).

5.31.4 Glial Activation by Unique Neuron-to-Glia Signals

Beyond neurotransmitters and neuromodulators classically known for their pain-enhancing effects, glia can also be activated by substances novel to the pain field. This class includes fractalkine and substances released by damaged cells. Regarding fractalkine, it is a protein expressed on the extracellular surface of both sensory afferent neurons and

neurons intrinsic to the spinal cord (Verge, G. M. *et al.*, 2004; Lindia, J. A. *et al.*, 2005). Fractalkine is tethered to the neurons in such a way as to be enzymatically released under strong neuroexcitatory conditions. Upon release, fractalkine acts as a diffusible signaling molecule (Chapman, G. *et al.*, 2000). Intriguingly, under basal conditions, the receptor for fractalkine is expressed predominantly by spinal microglia (Verge, G. M. *et al.*, 2004; Lindia, J. A. *et al.*, 2005). Thus, upon insult to the body, released fractalkine serves as a neuron-to-microglial signal. In response to peripheral nerve inflammation and injury, there is an increase in fractalkine receptor expression by microglia in the dorsal horn and microglia remain the sole apparent source of fractalkine receptor expression (Verge, G. M. *et al.*, 2004; Lindia, J. A. *et al.*, 2005). Under some (but not all) neuropathic conditions, astrocytes may begin producing fractalkine, suggestive that astrocytes also stimulate microglia via the release of fractalkine, so to maintain microglial activation under such conditions (Verge, G. M. *et al.*, 2004; Lindia, J. A. *et al.*, 2005).

Regarding the role of fractalkine in pain facilitation, what is known to date is that fractalkine upregulates P2X4 receptors in dorsal spinal cord microglia (Wieseler-Frank, J. *et al.*, 2004). As reviewed above, this microglia-specific ATP receptor is implicated in the induction of mechanical allodynia (Tsuda, M. *et al.*, 2003). When fractalkine is injected intrathecally, it induces both mechanical allodynia and thermal hyperalgesia, via the release of proinflammatory cytokines (Johnston, I. N. *et al.*, 2004; Milligan, E. D. *et al.*, 2004; 2005). Importantly, endogenous fractalkine enhances pain. That is, blocking fractalkine actions both delays and reverses neuropathic pain (Milligan, E. D. *et al.*, 2004). This suggests that peripheral nerve injury causes perseverative release of fractalkine and this release contributes to the induction and maintenance of neuropathic pain.

Lastly, glia can be activated by substances that signal neuronal damage. Microglia, like other immune cells, express evolutionarily conserved receptors for detecting cell damage, as well as for detecting pathogens such as bacteria and viruses. The genes for these receptors are homologous to the Toll gene in *Drosophila* and have therefore come to be referred to as Toll-like receptors (TLRs). One TLR subtype, TLR4, has been clearly implicated in pain facilitation (Tanga, F. Y. *et al.*, 2005). TLR4 knockout mice show reduced neuropathic pain in response to L5 nerve transection, as do rats treated with TLR4 antisense oligodeoxynucleotide to reduce the expression of spinal TLR4. This treatment also decreased expression of spinal microglial markers and proinflammatory cytokines, compared to controls (Tanga, F. Y. *et al.*, 2005). While TLR4 is best known as the receptor that recognizes bacterial endotoxin (lipopolysaccharide), it also binds endogenous substances associated with cell damage. These include members of the heat shock protein family and proteoglycans.

The potential link to heat shock proteins is especially intriguing. Heat shock proteins are classically thought of as intracellular proteins that aid in cell survival after stress or trauma (Costigan, M. *et al.*, 1998). However, heat shock proteins are also released by damaged and dying cells and such extracellular heat shock proteins can activate glia (Kakimura, J. *et al.*, 2002; Takata, K. *et al.*, 2003). Indeed, heat shock proteins are known to be upregulated for months in the spinal processes of sensory neurons whose peripheral axons are damaged (Costigan, M. *et al.*, 1998). Preliminary data suggest that heat shock proteins can synergize with other glial excitatory stimuli to enhance the production of proinflammatory cytokines by dorsal spinal cord microglia (Wieseler-Frank, J. *et al.*, 2004).

5.31.5 Beyond Neuropathic Pain: Glial Activation in Response to Opioids

While the focus to this point has been on endogenous signals that activate glia, it is also noteworthy that glia are activated by opioids, including morphine (Song, P. and Zhao, Z. Q., 2001; Raghavendra, V. *et al.*, 2002; Johnston, I. N. *et al.*, 2004; Shavit, Y. *et al.*, 2004) and methadone (Hutchinson, M. R. *et al.*, 2005). The results for morphine that have been reported across labs to date are remarkably consistent in demonstrating that spinal cord glia become progressively more activated by morphine upon repeated administration and that morphine-induced glial activation leads to the production and release of proinflammatory cytokines. This opioid-induced proinflammatory cytokine release has been linked, using diverse methodologies, to an attenuation of acute morphine analgesia, to the development of morphine tolerance, and to the expression of withdrawal-induced thermal hyperalgesia and mechanical allodynia (for a review, see Watkins, L. R. *et al.*, 2005). What is important about this line of research is that it documents that glia are not only activated in response to peripheral injury and inflammation, but also by first-line opioids used for clinical pain control. Thus, glial activation becomes a

double-edged sword, occurring both in response to situations that induce pathological pain and in response to drugs intended to treat it.

5.31.6 Conclusions

It is clear from the studies reviewed above that spinal cord glia can become activated in response to a wide array of chemical signals. Some are neurotransmitters and neuromodulators naturally released in spinal cord dorsal horn in response to inflammation and damage in the body, others are unique neuron-to-glia signals released by activated and damaged neurons, and surprisingly some are drugs commonly used for clinical pain control. Regardless of what the activating stimulus is, the end result is strikingly similar. That is, activated glia begin producing and releasing an array of neuroexcitatory substances, including proinflammatory cytokines. Taken together, these studies clearly predict that targeting spinal cord glia and glial proinflammatory products should suppress pain facilitation induced by inflammation and damage to peripheral tissues and enhance the clinical efficacy of opioids.

References

Aldskogius, H. and Kozlova, E. N. 1998. Central neuron–glial and glial–glial interactions following axon injury. Prog. Neurobiol. 55, 1–26.

Araque, A., Parpura, V., Sanzgiri, R. P., and Haydon, P. G. 1999. Tripartite synapses: glia, the unacknowledged partner. Trends Neurosci. 22, 208–215.

Bal-Price, A., Moneer, Z., and Brown, G. C. 2002. Nitric oxide induces rapid, calcium-dependent release of vesicular glutamate and ATP from cultured rat astrocytes. Glia 40, 312–323.

Chapman, G., Moores, K., Harrison, D., Campbell, C. A., Stewart, B. R., and Strijbos, P. J. L. M. 2000. Fractalkine cleavage from neuronal membranes represents an acute event in the inflammatory response to excitotoxic brain damage. J. Neurosci. 20(RC87), 1–5.

Costigan, M., Mannion, R. J., Kendall, G., Lewis, S. E., Campagna, J. A., Coggeshall, R. E., Meridith-Middleton, J., Tate, S., and Woolf, C. J. 1998. Heat shock protein 27: developmental regulation and expression after peripheral nerve injury. J. Neurosci. 18, 5891–5900.

Garrison, C. J., Dougherty, P. M., and Carlton, S. M. 1994. GFAP expression in lumbar spinal cord of naive and neuropathic rats treated with MK-801. Exp. Neurol. 129, 237–243.

Garrison, C. J., Dougherty, P. M., Kajander, K. C., and Carlton, S. M. 1991. Staining of glial fibrillary acidic protein (GFAP) in lumbar spinal cord increases following a sciatic nerve constriction injury. Brain Res. 565, 1–7.

Haas, C. A., Reddington, M., and Kreutzberg, G. W. 1991. Calcitonin gene-related peptide stimulates the induction of c-fos gene expression in rat astrocyte cultures. Eur. J. Neurosci. 3, 708–712.

Heidemann, A. C., Schipke, C. G., Peters, O., and Kettenmann, H. 2004. Nitric oxide triggers repetitive calcium transients in astrocytes in mouse cortical slices. Proc. Soc. Neurosci. 34, 405–407.

Holguin, A., Biedenkapp, J., Campisi, J., Wieseler-Frank, J., O'Connor, K. A., Milligan, E. D., Maksimova, E., Bravmann, C., Hansen, M. K., Martin, D., Fleshner, M., Maier, S. F., and Watkins, L. R. 2004. HIV-1 gp120 stimulates proinflammatory cytokine-mediated pathological pain via activation of nitric oxide synthase-I (nNOS). Pain 110, 517–530.

Hua, X.-Y., Svensson, C. I., Matsui, T., Fitzsimmons, B., Yaksh, T. L., and Webb, M. 2005. Intrathecal minocycline attenuates peripheral inflammation-induced hyperalesia by inhibiting p38 MAPK in spinal microglia. Eur. J. Neurosci. 22, 2431–2440.

Hutchinson, M. R., Milligan, E. D., Maier, S. F., and Watkins, L. R. 2005. Interleukin-1 receptor antagonist (IL1ra) ''unmasks'' analgesia following both R- & S-methadone: evidence for induction of spinal proinflammatory cytokines (PICs) via non-classical opioid receptors. Proc. Soc. Neurosci. abstract no. 49.11.

Johnston, I. N., Milligan, E. D., Wieseler-Frank, J., Frank, M. G., Zapata, V., Campisi, J., Langer, S., Martin, D., Green, P., Fleshner, M., Leinwand, L., Maier, S. F., and Watkins, L. R. 2004. A role for proinflammatory cytokines and fractalkine in analgesia, tolerance, and subsequent pain facilitation induced by chronic intrathecal morphine. J. Neurosci. 24, 7353–7365.

Kakimura, J., Kitamura, Y., Takata, K., Umeki, M., Suzuki, S., Shibagaki, K., Taniguchi, T., Nomura, Y., Gebicke-Haerter, P. J., Smith, M. A., Perry, G., and Shimohama, S. 2002. Microglial activation and amyloid-beta clearance induced by exogenous heat-shock proteins. FASEB J. 16, 601–603.

Lai, J. P., Douglas, S. D., Shaheen, F., Pleasure, D. E., and Ho, W. Z. 2002. Quantification of substance p mRNA in human immune cells by real-time reverse transcriptase PCR assay. Clin. Diagn. Lab. Immunol. 9, 138–143.

Ledeboer, A., Sloane, E. M., Milligan, E. D., Frank, M., Maier, S. F., and Watkins, L. R. 2005. Selective inhibition of spinal cord microglial activation attenuates mechanical allodynia and proinflammatory cytokine expression in rat models of pain facilitation. Pain 115, 71–83.

Lieb, K., Schaller, H., Bauer, J., Berger, M., Schulze-Osthoff, K., and Fiebich, B. L. 1998. Substance P and histamine induce interleukin-6 expression in human astrocytoma cells by a mechanism involving protein kinase C and nuclear factor-IL-6. J. Neurochem. 70, 1577–1583.

Lindia, J. A., McGowan, E., Jochnowitz, N., and Abbadie, C. 2005. Induction of CX3CL1 expression in astrocytes and CX3CR1 in microglia in the spinal cord of a rat model of neuropathic pain. J. Pain 6, 434–438.

Luber-Narod, J., Kage, R., and Leeman, S. E. 1994. Substance P enhances the secretion of tumor necrosis factor-alpha from neuroglial cells stimulated with lipopolysaccharide. J. Immunol. 152, 819–824.

Marriott, I. 2004. The role of tachykinins in central nervous system inflammatory responses. Front. Biosci. 9, 2153–2165.

Marriott, D. R., Wilkin, G. P., and Wood, J. N. 1991. Substance P-induced release of prostaglandins from astrocytes: regional specialisation and correlation with phosphoinositol metabolism. J. Neurochem. 56, 259–265.

Martin, F. C., Anton, P. A., Gornbein, J. A., Shanahan, F., and Merrill, J. E. 1993. Production of interleukin-1 by microglia in response to substance P: role for a non-classical NK-1 receptor. J. Neuroimmunol. 42, 53–60.

Martin, F. C., Charles, A. C., Sanderson, M. J., and Merrill, J. E. 1992. Substance P stimulates IL-1 production by astrocytes via intracellular calcium. Brain Res. 599, 13–18.

Milligan, E. D., Zapata, V., Chacur, M., Schoeniger, D., Biedenkapp, J., O'Connor, K., Verge, G. M., Chapman, G., Green, P., Foster, A. C., Naeve, G. S., Maier, S. F., and Watkins, L. R. 2004. Evidence that exogenous and endogenous fractalkine can induce spinal nociceptive facilitation. Eur. J. Neurosci. 20, 2294–2302.

Milligan, E. D., Zapata, V., Schoeniger, D., Chacur, M., Green, P., Poole, S., Martin, D., Maier, S. F., and Watkins, L. R. 2005. An initial investigation of spinal mechanisms underlying pain enhancement induced by fractalkine, a neuronally-released chemokine. Eur. J. Neurosci. 22, 2775–2782.

Molina-Holgado, F., Lledo, A., and Guaza, C. 1995. Evidence for cyclooxygenase activation by nitric oxide in astrocytes. Glia 15, 167–172.

Palma, C., Minghetti, L., Atolfi, M., Ambrosini, E., Silberstein, F. C., manzini, S., Levi, G., and Aloisi, F. 1997. Functional characterization of substance P receptors on cultured human spinal cord astrocytes: synergism of substance P with cytokines in inducing interleukin-6 and prostaglandin E2 production. Glia 21, 183–193.

Raghavendra, V., Rutkowski, M. D., and DeLeo, J. A. 2002. The role of spinal neuroimmune activation in morphine tolerance/hyperalgesia in neuropathic and sham-operated rats. J. Neurosci. 22, 9980–9989.

Raghavendra, V., Tanga, F., and DeLeo, J. A. 2003. Inhibition of microglial activation attenuates the development but not existing hypersensitivity in a rat model of neuropathy. J. Pharmacol. Exp. Ther. 306, 624–630.

Reddington, M., Priller, J., Treichel, J., Haas, C., and Kreutzberg, G. W. 1995. Astrocytes and microglia as potential targets for calcitonin gene related peptide in the central nervous system. Can. J. Physiol. Pharmacol. 73, 1047–1049.

Shavit, Y., Wolf, G., Goshen, I., Livshits, D., and Yirmiya, R. 2004. Interleukin-1 antagonizes morphine analgesia and underlies morphine tolerance. Pain 115, 50–59.

Song, P. and Zhao, Z. Q. 2001. The involvement of glial cells in the development of morphine tolerance. Neurosci. Res. 39, 281–286.

Sul, J., Legresley, A., Ellis-Davies, G., and Haydon, P. G. 2004. Photoreleased nitric oxide regulates glial calcium signaling. Proc. Soc. Neurosci., 34, 405–409.

Sun, D., Coleclough, C., Cao, L., Hu, X., Sun, S., and Whitaker, J. N. 1998. Reciprocal stimulation between TNF-alpha and nitric oxide may exacerbate CNS inflammation in experimental autoimmune encephalomyelitis. J. Neuroimmunol. 89, 122–130.

Svensson, C. I., Fitzsimmons, B., Azizi, S., Powell, H. C., Hua, X.-Y., and Yaksh, T. L. 2004. Spinal p38beta isoform mediates tissue injury-induced hyperalgesia and spinal sensitization. J. Neurochem. 92, 1508–1520.

Svensson, C. I., Marsala, M., Westerlund, A., Calcutt, N. A., Campana, W. M., Freshwater, J. D., Catalano, R., Feng, Y., Protter, A. A., Scott, B., and Yaksh, T. L. 2003. Activation of p38 mitogen-activated protein kinase in spinal microglia is a critical link in inflammation-induced spinal pain processing. J. Neurochem. 86, 1534–1544.

Takata, K., Kitamura, Y., Tsuchiya, D., Kawasaki, T., Taniguchi, T., and Shimohama, S. 2003. Heat shock protein-90-induced microglial clearance of exogenous amyloid-beta1-42 in rat hippocampus *in vivo*. Neurosci. Lett. 344, 87–90.

Tanga, F. Y., Nutile-McMenemy, N., and DeLeo, J. A. 2005. The CNS role of Toll-like receptor 4 in innate neuroimmunity and painful neuropathy. Proc. Natl. Acad. Sci. U. S. A. 102, 5856–5861.

Tsuda, M., Shigemoto-Mogami, Y., Koizumi, S., Mizokoshi, A., Kohsaka, S., Slater, M. W., and Inoue, K. 2003. P2X4 receptors induced in spinal microglia gate tactile allodynia after nerve injury. Nature 424, 778–783.

Verge, G. M., Milligan, E. D., Maier, S. F., Watkins, L. R., Naeve, G. S., and Foster, A. C. 2004. Fractalkine (CX3CL1) and fractalkine receptor (CX3CR1) distribution in spinal cord and dorsal root ganglia under basal versus neuropathic pain conditions. Eur. J. Neurosci. 20, 1150–1160.

Watkins, L. R. and Maier, S. F. 2003. Glia: a novel drug discovery target for clinical pain. Nat. Rev. Drug. Discov. 2, 973–985.

Watkins, L. R., Hutchinson, M. R., Johnston, I., and Maier, S. F. 2005. Glia: novel counter-regulators of opioid analgesia. Trends Neurosci. 28, 661–669.

Watkins, L. R., Milligan, E. D., and Maier, S. F. 2001. Glial activation: a driving force for pathological pain. Trends Neurosci. 24, 450–455.

Wieseler-Frank, J., Kwiecien, O., Jekich, B., Maier, S. F., and Watkins, L. R. 2004. Putative neuron-to-glia signals synergize to enhance interleukin-1 production by rat dorsal spinal cord glial cells *in vitro*. Proc. Soc. Neurosci. abstract no. 518.11.

Woolf, C. J., and Salter, M. W. 2000. Neuronal plasticity: increasing the gain in pain. Science 288, 1765–1769.

5.32 Trigeminal Mechanisms of Nociception: Peripheral and Brainstem Organization

D A Bereiter, University of Minnesota, Minneapolis, MN, USA

K M Hargreaves, University of Texas Health Science Center, San Antonio, TX, USA

J W Hu, University of Toronto, Toronto, ON, Canada

© 2008 Elsevier Inc. All rights reserved.

5.32.1	Introduction	435
5.32.2	The Peripheral Trigeminal Nerve System	438
5.32.2.1	General Features	438
5.32.2.2	Neurochemical and Molecular Properties of Trigeminal Ganglion Neurons	439
5.32.3	Central Aspects of Trigeminal Organization	441
5.32.3.1	Somatotopy	442
5.32.3.2	Intersubnuclear Connections	443
5.32.3.3	Relationship to the Autonomic Nervous System	443
5.32.3.4	Neurochemical Markers	444
5.32.3.5	Efferent Projections	446
5.32.4	Functional Considerations	447
5.32.4.1	Ocular Pain Processing	448
5.32.5	Chronic Craniofacial Pain	448
References		450

5.32.1 Introduction

At first glance the trigeminal nerve (Vn), the largest cranial nerve, serves many of the same functions as spinal nerves for lower parts of the body by relaying innocuous and noxious mechanical, thermal and chemical sensory information from all tissues of the head and oral cavity to the brain (Figure 1). Although there are many similarities, peripheral and central aspects of the Vn system are organized quite differently from the spinal system (see Table 1). A primary function of the Vn system is to detect damaging or potentially damaging environmental challenges to the head and oral cavity and one obvious distinction from spinal systems is the diversity of specialized craniofacial tissues innervated by the Vn that provide such detection. Tissues such as the dental pulp, cornea, and dura lack appreciable innervation by large diameter afferent fibers and generally evoke only pain sensation to natural stimuli (Feindel, W. *et al*., 1960; Kenshalo, D. R., 1960; Beuerman, R. W. and Tanelian, D. L., 1979; Trowbridge, H. O. *et al*., 1980). Sensory afferents that innervate mucosal tissues of the eye, nose, and oral cavity have a high sensitivity to airborne chemicals (Cometto-Muniz, J. E. and Cain, W. S., 1995) and are thought to underlie the common chemical sense in mammals (see Bryant, B. and Silver, W. L., 2000). The Vn also supplies all specialized receptor regions of the head including the fungiform taste papillas (Whitehead, M. C. *et al*., 1999), cochlea (Vass, Z. *et al*., 1997) and the eye (Belmonte, C. *et al*., 1997). In some mammals and lower vertebrates the Vn relays sensory information unrelated to nociception from unique peripheral structures over distinct central pathways to meet environmental demands. For example, Vn afferents that supply the pit organ of crotaline snakes, a highly sensitive thermal receptor with broad spectral tuning that complements visual input, do not respond to capsaicin (Moiseenkova, V. *et al*., 2003) and project to separate regions of the trigeminal brainstem complex (Molenaar, G. J., 1978). The skin of the bill of the platypus contains some 30 000–40 000 mucous sensory glands innervated by small myelinated trigeminal afferent fibers that detect electromagnetic radiation emitted by prey and used for underwater navigation (Proske, U. *et al*., 1998). The whisking of mystacial vibrissas on the face of rodents provides essential textural and perceptual information for exploration and food-gathering in a frequency-dependent manner (Petersen, C. C., 2003; Moore, C. I., 2004), whereas the trigeminal innervation of the snout of the coati mundi (Barker, D. J. and Welker,

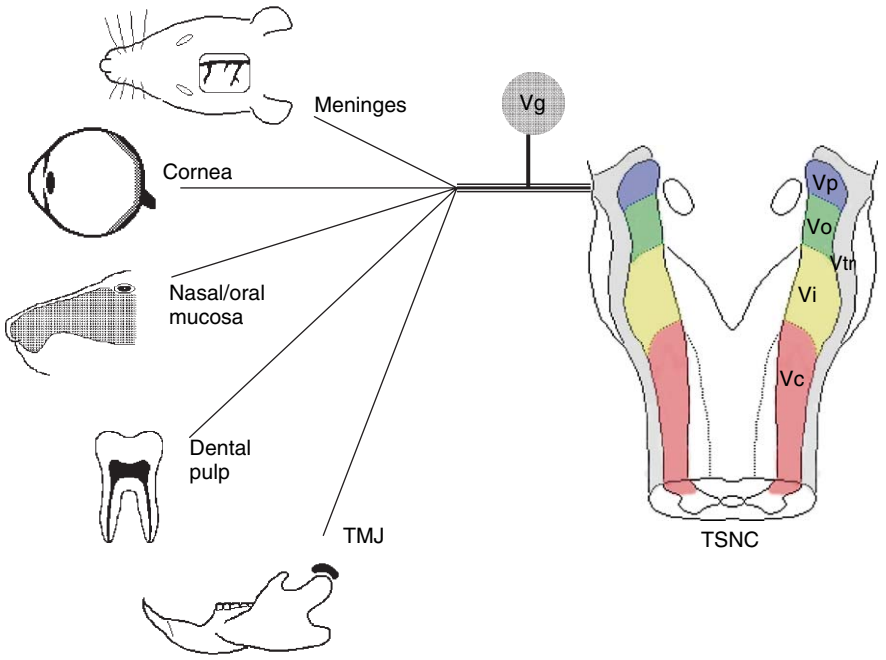

Figure 1 Unique craniofacial tissues supplied by the Trigeminal Nerve.

W. I., 1969) and Eimer's organ of the appendages of the star-nosed mole (Catania, K. C., 1999) relay highly refined tactile information and appear more analogous to somatosensory receptors of the hands than face of primates. Thus, a significant feature of the peripheral Vn is its association with highly specialized sensory functions of craniofacial and oral tissues.

The organization of the central Vn system also displays unusual features distinct from spinal systems that may be relevant to pain processing. At the level of the initial synapse, the trigeminal sensory brainstem nuclear complex (TSNC), craniofacial tissues are represented somatotopically at multiple, and in some cases discontinuous levels, while spinal nerves project to a few dominant contiguous segments (see Renehan, W. E. and Jacquin, M. F., 1993; Bereiter, D. A. *et al.*, 2000; Sessle, B. J., 2000). The importance of multiple representation remains uncertain; however, based on encoding properties and efferent projections, this feature may reflect the segregation of neuronal populations that serve different aspects of trigeminal function. Although the representation of craniofacial tissues accounts for a relatively large area of sensory thalamus and somatosensory cortex, a feature that has long been appreciated since the classic studies of Penfield W. and Rasmussen T. (1950), the cortical representation of some specialized craniofacial tissues is organized in unusual patterns (e.g., teeth) and not always proportional to innervation density (e.g., ocular surface). In lower mammals, peripheral and central specializations can lead to remarkable magnification of the cortical representation of orofacial tissues such as the nasal appendages of the star-nosed mole which accounts for over 50% of the area of primary somatosensory cortex (SmI; Catania, K. C. and Kaas, J. H., 1997). Similarly, the representation of the enlarged incisors of the naked mole rat used for tunneling and underground navigation accounts for over 30% of SmI (Catania, K. C. and Remple, M. S., 2002). In the albino rat the face occupies more than 60% of SmI with a large area devoted to the cortical barrels and mystacial vibrissae (Welker, C., 1971), whereas a significant portion of the lateral somatosensory cortex is devoted to the teeth (Remple, M. S. *et al.*, 2003). Cortical representation of craniofacial tissues in primates is much reduced compared to lower mammals; however, in select regions such as area 3b, the representation of the face and oral cavity remains unexpectedly large, though curiously, the ocular surface with its high innervation density is represented only weakly (Manger, P. R. *et al.*, 1995; Jain, N. *et al.*, 2001). Beyond the biological importance of protecting the head and oral cavity from damaging stimuli, the Vn is critical for preserving normal eating and sleeping habits, while the emotional

Table 1 General distinctive features of the trigeminal sensory system

Factor	*Details*	*References*
Peripheral trigeminal system		
Sensory innervation of specialized tissues	Cavernous sinus, cornea/conjunctiva, dental pulp, lacrimal gland, nasal mucosa, pineal gland, salivary glands, temporomandibular joint, tongue, vibrissae	Rozsa A. J. and Beuerman R. W. (1982), Anggard A. *et al.* (1983), Byers M. R. (1984), Kido M. A. *et al.* (1995), Bleys R. L. *et al.* (1996), Reuss S. (1999), Cheng S. B. *et al.* (2000), Muller L. J. *et al.* (2003), Kawabata A. *et al.* (2004)
Somatotopy within TG	TG neurons from major Vn branches (ophthalmic, maxillary and mandibular) distributed from anteromedial to posterolateral, respectively	Kerr F. W. L. (1963), Marfurt C. F. (1981), Arvidsson J. *et al.* (1992), Aigner M. *et al.* (2000)
Mesencephalic nucleus of V (Vmes)	Vmes within the CNS; jaw muscle spindle and periodontal ligament afferents only	Cody F. W. *et al.* (1972), Linden R. W. (1978)
Muscle innervation	Sparse or misshaped muscle spindles in lip, extraocular and jaw opening muscles of humans	Lennartsson B. (1979), Bruenech J. R. and Ruskell G. L. (2001)
Embryonic origin	Ophthalmic division of TG from neurogenic placodes maxillary, mandibular divisions of TG from neural crest	Noden D. M. (1991), Artinger K. B. *et al.* (1998), Baker C. V. *et al.* (2002)
Sensory axon diameter	% A-δ fibers > % C-fibers	Young R. F. and King R. B. (1973), Holland G. R. and Robinson P. P. (1992)
Sensory fiber bifurcation	Descending branch of Vtr: % C-fibers > A-δ-fibers	Tashiro T. *et al.* (1984)
Sensory fiber termination	Direct sensory fiber projection to autonomic relay nuclei (e.g., NTS)	Jacquin M. F. *et al.* (1983), Marfurt C. F. and Rajchert D. M. (1991), Panneton W. M. *et al.* (1994)
Linkage to parasympathetic outflow	Cutaneous vasodilatation, hypotension and bradycardia to TG stimuli	Kumada M. *et al.* (1977), Drummond P. D. (1992), Ramien M. *et al.* (2004)
Sympathetic fibers	Vn << spinal nerves	Hoffmann K. D. and Matthews M. A. (1990)
Central trigeminal system		
Facial dermatomes	Representation of orofacial tissues at multiple levels of TSNC	Marfurt C. F. (1981), Panneton W. M. and Burton H. (1981), Shigenaga Y. *et al.* (1986b), Ma P. M. (1991)
Onion skin organization	Perioral and midline tissues represented more rostral than lateral tissues	Jacquin M. F. *et al.* (1986), Shigenaga Y. *et al.* (1986a)
Sensory convergence	Termination of cranial nerves V, VII, IX, X, and upper cervical rootlets in caudal Vc	Kerr F. W. L. (1961), Beckstead R. M. and Norgren R. (1979), Hu J. W. *et al.* (2005)
Intersubnuclear connections	Lissauer's tract equivalent plus deep bundles	Gobel S. and Purvis M. B. (1972), Kruger L. *et al.* (1977), Ikeda M. *et al.* (1984), Jacquin M. F. *et al.* (1990)

CNS, central nervous system; NTS, nucleus tractus solitarius; TG, trigeminal ganglion; TSNC, trigeminal sensory brainstem nuclear complex.

significance of protecting one's face and self-image suggests that the Vn system has evolved features that set it apart from spinal systems.

Chronic orofacial pain is a significant public health concern that affects more than 20% of the population in western societies (Macfarlane, T. V. *et al.*, 2002b). Persistent orofacial pain has profound effects on eating and sleeping patterns, a strong association with depression, and a reduced sense of wellbeing (Korszun, A., 2002). Many common forms of chronic orofacial pain such as headache, temporomandibular disorders (TMD), odontalgia, and dry eye are difficult to treat clinically and may be associated with lower pain thresholds elsewhere in the body (Burstein, R. *et al.*, 2000; Sarlani, E. and Greenspan, J. D., 2003; Van Bijsterveld, O. P., *et al.*, 2003). Moreover, epidemiological studies indicate that many chronic craniofacial pain conditions are more prevalent and occur with greater intensity in women than men (Lipton, J. A. *et al.*, 1993; Sandstedt, P. and Sorensen, S., 1995;

LeResche, L., 1997; Rasmussen, B. K., 2001; Wolf, E. *et al*., 2001). This review highlights several neurobiological aspects of the Vn system that differ from spinal systems and may contribute to the pattern and magnitude of craniofacial pain.

5.32.2 The Peripheral Trigeminal Nerve System

5.32.2.1 General Features

The sensory portion of the Vn consists of three main nerve branches: ophthalmic, maxillary, and mandibular. Proprioceptive afferents from select craniofacial muscles and periodontal ligaments travel within the Vn, however; the cell bodies are located in the mesencephalic nucleus of V (Vme) in the rostral pons (Cody, F. W. *et al*., 1972; Linden, R. W., 1978). Unlike the spinal dorsal root ganglion (DRG) that has no apparent intraganglionic organization, the somata of neurons giving rise to the three branches of Vn are somatotopically arranged within the trigeminal ganglion (TG; Kerr, F. W. L., 1963; Marfurt, C. F., 1981; Arvidsson, J. *et al*., 1992; Aigner, M. *et al*., 2000). Table 1 lists several features of the peripheral Vn system that differ from the spinal system. Differences relevant to pain processing include the innervation of specialized tissues, composition, and central termination of afferents; relationship of sensory nerves to sympathetic efferent outflow; and neurochemical markers in ganglion cells. The Vn innervates a heterogeneous and unique group of craniofacial tissues well associated with pain sensation. The cornea is the most densely innervated tissue of the body, supplied exclusively by small diameter fibers (Rozsa, A. J. and Beuerman, R. W., 1982); is the only tissue in which nerve fibers penetrate the outer epithelial layers (Hoyes, A. D. and Barber, P., 1976; Muller, L. J. *et al*., 1996); and responds to very small changes in ocular surface temperature, moisture status, or foreign bodies (Belmonte, C. *et al*., 1997). The oral mucosal epithelium also is densely innervated by polymodal small diameter Vn afferents with relatively large receptive fields (RFs) compared to cutaneous receptors (Toda, K. *et al*., 1997) that provide proprioceptive information on lip/tongue position necessary for eating and speech as well as detecting noxious stimuli within the mouth (Trulsson, M. and Johansson, R. S., 2002). By contrast, the dental pulp is well insulated from the exterior environment and, while pain is the predominant sensation relayed by pulpal afferents, dental afferents respond best to natural stimuli after injury (Byers, M. R., 1984; Hildebrand, C. *et al*., 1995). Specialized transduction processes also are associated with these unique tissues such as the proposed hydrodynamic movement of fluid as the basis for dentinal pain (Brannstrom, M., 1986).

Peripheral Vn afferents are subject to frequent injury due to trauma, infection, or iatrogenic damage following surgery that can lead to peripheral sensitization. Indeed, one of the first demonstrations of enhanced peripheral C-fiber activity due to injury was reported for facial afferents in the monkey (Beitel, R. E. and Dubner, R., 1976). Since peripheral sensitization of small myelinated A-δ versus unmyelinated C-fibers does not occur uniformly, but rather varies for different tissue types and depends on the nature of the injury (see Meyer, R. A. *et al*., 2006), it may be significant that the sensory root of the Vn has a greater percentage of A-δ fibers than C-fibers compared to spinal nerves as determined by counts of axons (Young, R. F. and King, R. B., 1973; Holland, G. R. and Robinson, P. P., 1992) or lectin staining for C-fibers (Ambalavanar, R. and Morris. R., 1992; Wang, H. *et al*., 1994). Correspondingly, corneal (Belmonte, C. *et al*., 1997) and dural afferents (Levy, D. and Strassman, A. M., 2002) conducting in the A-δ range display greater sensitization than more slowly conducting C-fibers.

Complex regional pain syndrome (CRSP), formerly referred to as causalgia, is a neuropathic pain condition with sympathetic involvement, often resulting from trauma or bone fracture to the distal limbs (see Wasner, G. *et al*., 1998). The incidence of CRSP-like symptoms following trauma to craniofacial tissues is relatively low compared to injury of other tissues (Matthews, B., 1989). The exact reason for this observation is not certain; however, fewer sympathetic efferent fibers course within sensory branches of Vn compared to spinal nerves, and instead these fibers travel along the arteries that supply the head and oral cavity (Hoffmann, K. D. and Matthews, M. A., 1990; Maklad, A. *et al*., 2001). Spinal nerve injury induces sprouting of noradrenergic fibers into the DRG (McLachlan, E. M. *et al*., 1993), whereas comparable injury to Vn produces no such sprouting into the TG (Bongenhielm, U. *et al*., 1999; Benoliel, R. *et al*., 2001). Furthermore, cervical sympathectomy does not alter the development of ectopic discharge or increased mechanical sensitivity after inferior alveolar nerve transection (Bongenhielm, U. *et al*., 1998). Since the basis for sprouting into the DRG following nerve injury is thought to involve neurotrophins (Davis, B. M. *et al*., 1994), it is interesting to note that the number of trkA-positive corneal and dental sensory TG

neurons is significantly less (< 10%, Mosconi, T. *et al.*, 2001) than for spinal DRG neurons (40%, Molliver, D. C. and Snider, W. D., 1997). Failure to observe sympathetic sprouting may be specific for nerve injury, since central administration of nerve growth factor (NGF) induces significant sprouting into the TG and spinal DRG (Nauta, H. J. *et al.*, 1999).

5.32.2.2 Neurochemical and Molecular Properties of Trigeminal Ganglion Neurons

Although this review emphasizes comparisons of the TG and DRG systems in the adult, significant developmental differences also exist. While the functional significance of developmental differences (e.g., neurogenic placode vs. neural crest) may not be obvious in the healthy adult, many responses to injury recapitulate developmental differences and thus may have implications in the injured adult nervous system. Studies reporting similarities in development of the TG and DRG systems have included: P2X3 receptor expression (Ruan, H. Z. *et al.*, 2004); phenotype expression in trkB knockout mice (Klein, R. *et al.*, 1993; Gonzalez-Martinez, T. *et al.*, 2004); vesicular monoamine transporter levels (Hansson, S. R. *et al.*, 1998); the apoptotic enzyme, CPP32/apopain (Mukasa, T. *et al.*, 1997); neuronal tyrosine hydroxylase (Son *et al.*, 1996; Kim, S. J. *et al.*, 1997); six 4/ARECC3 mRNA (Esteve, P. and Bovolenta, P., 1999); the transcription factor, retinoid-X receptor γ (Georgiades, P. *et al.*, 1998); guanosine triphosphate (GTP)-binding protein G-α z (Kelleher, K. L. *et al.*, 1998); the fetal plasma glycoprotein, fetuin (Kitchener, P. D. *et al.*, 1997); FGF receptor mRNA (Wanaka, A. *et al.*, 1991); and the large zinc finger protein, KRC (Hicar, M. D. *et al.*, 2002). By contrast, studies reporting significant differences in the developing TG and DRG systems have included: expression of trkC at day 12.5 (DRG: yes, TG: no; Elkabes, S. *et al.*, 1994); requirement for NGF at day E16.5 (DRG > TG; Goedert, M. *et al.*, 1984); and sensitivity to cadmium-induced neurotoxicity (TG > DRG; Arvidson, B., 1983). Thus, developmental biology indicates some similarities with notable differences in the responsiveness to certain neurotrophic factors.

Table 2 summarizes results from studies comparing adult TG and DRG systems under basal (naive) conditions. These studies reveal many similarities among markers associated with nociception such as the percentage of TRPV1-positive neurons (Ambalavanar, R. *et al.*, 2005) and expression of P2X receptor subtypes (Collo, G. *et al.*, 1996; Cook, S. P. *et al.*, 1997; Xiang, Z. *et al.*, 1998). However, substantial differences also are observed that include: the percentage of neurons stained for substance P and somatostatin (TG > DRG; Kai-Kai, M. A., 1989), trkA receptor (DRG > TG; Mosconi, T. *et al.*, 2001), galectin-1 (DRG >> TG; Akazawa, C. *et al.*, 2004), μ- and δ-opioid receptors (DRG > TG; Buzas, B. and Cox, B. M., 1997), CCK (DRG > TG; Ghilardi, J. R. *et al.*, 1992), cytokeratin (TG >> DRG; Okabe, H. *et al.*, 1997), and neuropeptide Y (NPY)-binding sites (TG > DRG; Mantyh, P. W. *et al.*, 1994). In addition, TG and DRG systems display a differential sensitivity to ganglion cell labeling by selected anatomical tracers in which the TG system has a greater uptake of Fluoro-Gold than DRG but not of Fast Blue (Yoshimura, N. *et al.*, 1994).

Differences in cellular properties between the TG and DRG systems under naive conditions may contribute to differential responses to tissue injury. For example, sprouting of sympathetic nerve terminals into the DRG (McLachlan, E. M. *et al.*, 1993), but not the TG after nerve injury (Bongenhielm, U. *et al.*, 1999; Benoliel, R. *et al.*, 2001) is consistent with findings that trkA-positive neurons are more numerous in the DRG than TG (Mosconi, T. *et al.*, 2001). Comparison of nerve injury-induced changes for a majority of neuropeptides associated nociception such as substance P, TRPV1, P2X3, and NPY appear similar for TG and DRG systems (Zhang, X. *et al.*, 1996; Okuse, K. *et al.*, 1997; Eriksson, J. *et al.*, 1998; Elcock, C. *et al.*, 2001; Tsuzuki, K. *et al.*, 2001; Stenholm, E. *et al.*, 2002; Tsuzuki, K. *et al.*, 2003). However, species differences have been reported such as a decrease in galanin in TG of ferret (Elcock, C. *et al.*, 2001) compared to an increase in rat (Zhang, X. *et al.*, 1996) after Vn injury, similar to the increase in galanin in rat DRG after spinal nerve injury (Villar, M. J. *et al.*, 1989). Nerve injury causes higher spontaneous discharge rates and greater rhythmic firing patterns in DRGs than TGs (Tal, M. and Devor, M., 1992), effects often associated with sodium channel activity (see Wood, J. N. *et al.*, 2004). However, the basis for this difference is not certain since changes in the expression of the tetrodotoxin (TTX)-resistant sodium channel, NaV1.8, appear comparable for DRG and TG systems (Dib-Hajj, S., *et al.*, 1996; Bongenhielm, U. *et al.*, 2000). Susceptibility to infection also may differ between TG and DRG systems, since injection of herpes simplex virus (HSV) to the left ear pinna in

Table 2 Comparison of trigeminal (TG) and dorsal root ganglion (DRG) systems under naive conditions

Factor	*Details*	*References*
Substance P	TG $\geq$ DRG	Kai-Kai M. A. (1989)
Somatostatin	TG $\geq$ DRG	Kai-Kai M. A. (1989)
$P2X_1$, $P2X_2$, $P2X_3$, $P2X_4$, $P2X_5$, $P2X_6$ mRNA	TG $\sim$ DRG; no P2X2, P2X3 in Vme	Collo G. *et al.* (1996), Cook S. P. *et al.* (1997) Xiang Z. *et al.* (1998)
$P2X_3$-isolectin B4 co-expression	DRG >> TG	Ambalavanar R. *et al.* (2005)
TRPV1	TG $\sim$ DRG	Guo A. *et al.* (1999)
trkA	DRG > TG; $\sim$ 40% DRG versus 10–15% of TG neurons innervating pulp or cornea	Mosconi T. *et al.* (2001)
Arginine vasopressin	DRG > TG About 40% AVP is in capsaicin-sensitive neurons in both ganglia	Kai-Kai M. A. and Che Y. M. (1995)
$5\text{-}HT_{1d}$	TG $\sim$ DRG	Potrebic S. *et al.* (2003)
Oxytocin	TG > DRG	Kai-Kai M. A. (1989)
NADPH-diaphorase	DRG: T5–L1 >> C1-T4 = L2–S = TG	Aimi Y. *et al.* (1991)
CCK mRNA in monkey	DRG = 20%; TG = 10% of neurons	Verge V. M. *et al.* (1993)
CCK(B) receptor	Rat, rabbit: TG $\sim$ DRG Monkey: DRG > TG (nondetectable)	Ghilardi J. R. *et al.* (1992)
PYY binding sites (NPY receptor)	TG $\geq$ DRG	Mantyh P. W. *et al.* (1994)
Galectin-1 mRNA	DRG >> TG (nondetectable)	Akazawa C. *et al.* (2004)
Oncostatin M (OSM-β)	DRG > TG (OSMr-β coexpressed in TRPV1-positive neurons)	Tamura S. *et al.* (2003)
glycogen phosphorylase	DRG > TG	Pfeiffer B. *et al.* (1995)
Cytokeratin (AE1 and CAM5.2)	TG >> DRG	Okabe H. *et al.* (1997)
Glucocorticoid receptor (GR)	TG: GR expressed in substance P, CGRP, but not galanin-positive neurons DRG: GR expressed in substance P, CGRP, and galanin-positive neurons	DeLeon M. *et al.* (1994)
MOR mRNA	DRG: lumbar > thoracic $\sim$ cervical > TG	Buzas B. and Cox B. M. (1997)
DOR mRNA	DRG: lumbar $\sim$ thoracic $\sim$ cervical > TG	Buzas B. and Cox B. M. (1997)
TGF-α mitogenic effect *in vitro*	DRG: Yes TG: No	Chalazonitis A. *et al.* (1992)
Parvalbumin	TG smaller size than DRG, but both populations have high expression of carbonic anhydrase and low expression of CGRP	Ichikawa H. *et al.* (1994)
Osteocalcin $\pm$ parvalbumin	TG: 25% of neurons (31% express parvalbumin) Vme: 63% of neurons (>90% express parvalbumin) DRG: 16% of neurons (>90% express parvalbumin)	Ichikawa H. *et al.* (1999)
Osteocalcin and TRPV1 coexpression	TG = 14% DRG = none	Ichikawa H. and Sugimoto T. (2002)
Calretinin	TG: neurons mostly < 800 μm^2 and 34% positive for tachykinin DRG: neurons mostly > 800 μm^2 and 7% positive for tachykinin	Ichikawa H. *et al.* (1993)
S100 calcium-binding protein	TG: 59% (> 90% coexpress parvalbumin and calbindin D-28k) DRG: 44% (> 90% coexpress parvalbumin, none with calbindin D-28k)	Ichikawa H. *et al.* (1997)

(*Continued*)

Table 2 (Continued)

Factor	*Details*	*References*
tr7kC at day E12.5 of development	DRG: Yes TG: No	Elkabes S. *et al.* (1994)
NT-3 overexpression	TG > DRG for responsiveness	Albers K. M. *et al.* (1996)
Neonatal anti-NGF antisera at E16.5	DRG > TG for loss of substance P- and somatostatin-positive neurons	Goedert M. *et al.* (1984)
Uptake of fluorescent dyes	TG ~ DRG uptake of Fast Blue TG > DRG uptake of Fluoro-Gold	Yoshimura N. *et al.* (1994)

5-HT_{1d}, serotonin receptor subtype; CCK, cholecystokinin; CGRP, calcitonin gene-related peptide; DOR, δ-opioid receptor; DRG, dorsal root ganglion; MOR, μ-opioid receptor, messenger RNA; NADPH, nicotinamide adenine dinucleotide phosphate hydrogen; ; NGF, nerve growth factor; NPY, neuropeptide Y; P2X, ATP receptor; PYY, polypeptide Y; TG, trigeminal ganglion; TGF, tumor growth factor; trkA, tyrosine kinase A receptor subtype; TRPV1, vanilloid receptor.

mice produces 100% HSV infection in both the ipsilateral TG and cervical DRG. Interestingly, 70% of the TGs contralateral to injection, while only 10% of contralateral DRGs were infected (Thackray, A. M. and Field, H. J., 1996). Interhemispheric neural communication likely contributes to the progression of joint-related pain in trigeminal (see Bereiter, D. A. *et al.*, 2005b) as well as spinal systems (Levine, J. D. *et al.*, 1985; Shenker, N. *et al.*, 2003). The responsiveness to viral vectors in the Vn system has prompted recent efforts to deliver targeted transgene-derived products for control of trigeminal neuropathic pain (Meunier, A. *et al.*, 2005). Collectively, these studies reveal significant differences in peripheral Vn and spinal systems under naïve and injured conditions, differences that could not be predicted on the basis of results from spinal sensory systems alone.

5.32.3 Central Aspects of Trigeminal Organization

Noxious sensory information is relayed from Vn afferents to second-order neurons in the TSNC and the upper cervical spinal cord. The TSNC is the initial site of synaptic integration for sensory input from the head and oral cavity and shares this feature with the spinal dorsal horn and dorsal column nuclei that receive sensory input from the rest of the body (Figure 1). However, unlike the spinal cord, the TSNC is comprised of several cell groups with distinct cytological and organizational features (see Darian-Smith, I., 1973; Kruger, L. and Young, R. F., 1981) yet each cell group receives direct primary afferent projections from specific craniofacial tissues. The TSNC consists of: the principal nucleus (Vp), supratrigeminal region (Vsup) lying dorsal to Vp, an elongated spinal nucleus (Vsp) extending from the pons to the upper cervical spinal cord, and the interstitial islands or the paratrigeminal region (Pa5) embedded within the spinal trigeminal tract, dorsal and lateral to the caudal Vsp (Figure 2; see Kruger, L. and Young, R. F., 1981; Renehan, W. E. and Jacquin, M. F., 1993). The Vsp is further subdivided, from rostral to caudal, into subnucleus oralis (Vo), subnucleus interpolaris (Vi), and a laminated trigeminal subnucleus caudalis (Vc) as described originally by Olszewski J. (1950). Although nociceptive neurons in the caudal laminated portion of the TSNC, Vc, display properties similar to those at spinal levels (Price, D. D. *et al.*, 1976; Dubner, R. and Bennett, G. J., 1983) consistent with a prominent role in nociceptive processing (see also Bereiter, D. A. *et al.*, 2000; Sessle, B. J., 2000), the contribution of rostral portions of the TSNC to orofacial pain is less certain.

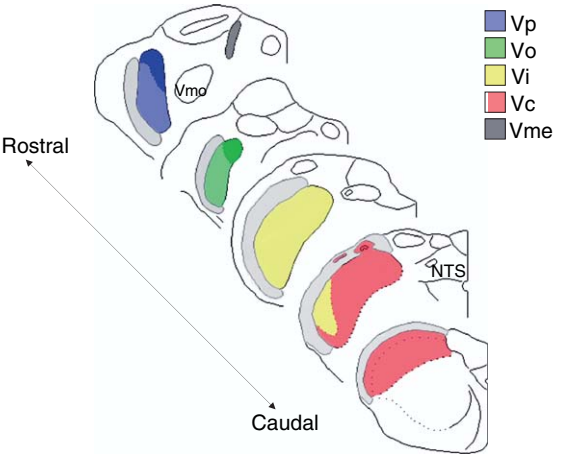

Figure 2 Trigeminal brainstem sensory complex.

5.32.3.1 Somatotopy

Somatotopy is a key feature of the trigeminal system and is seen within the TG as well as the TSNC distinct from the spinal cord. Craniofacial tissues are represented at multiple levels of the TSNC, while sensory afferents from other body loci terminate at several contiguous spinal segments of the spinal dorsal horn. Also, at caudal levels of the TSNC craniofacial tissues are represented in a series of semicircular bands that converge at the rostral midline of the face, often referred to as an onion-skin arrangement and by a medial-lateral representation in which the head is inverted (Jacquin, M. F. *et al.*, 1986; Shigenaga, Y. *et al.*, 1986a). Although somatotopy along the mediolateral axis is preserved at all levels of the TSNC, the onion-skin arrangement is most apparent in Vc. The implications of this organization for facial pain have been debated since an early report by Sjoqvist O. (1938) that trigeminal tractotomy at the level of rostral Vc reduced the pain of trigeminal neuralgia, while preserving the sense of temperature and touch on the face. It is understood that rostral portions of TSNC play a more prominent role in dental and intraoral pain than caudal portions (Young, R. F. and Perryman, K. M., 1984; see Sessle, B. J., 2000); however, the importance of multiple representation of extraoral tissues for other forms of craniofacial pain is not well understood. One reason for this uncertainty may be due to the fact that many craniofacial tissues are represented in a discontinuous manner along the rostrocaudal extent of the TSNC as summarized in Table 3. Although a small percentage of Vn afferents projects to both rostral and caudal portions of the TSNC (Silverman, J. D. and Kruger, L., 1985; Li, Y. Q. *et al.*, 1992), most fibers either ascend in a short sensory root to terminate in Vp or descend to give off branches to Vo, Vi, Vc, and the upper cervical dorsal horn. Several aspects of the afferent input pattern to TSNC are notable. First, the superficial laminas in Vc receive substantial input from all specialized tissues well associated with craniofacial pain conditions (e.g., cornea, dura, teeth, temporomandibular joint (TMJ)), while afferents from structures with no known relationship to pain perception (vibrissas) do not project to this region. Second, dental pulp afferents are the

Table 3 Summary of the relative density of trigeminal primary afferent terminals within different portions of the sensory trigeminal sensory nuclear complex.

	Vp		*Vo*					*Vc*			
	dm	*vl*	*dm*	*vl*	*Vi*	*dPa5*	*Vi/Vc*	*I–II*	*III–IV*	*V*	*References*
Cornea	−	+	−	+	+	−	+++	++	−	−	Panneton W. M. and Burton H. (1981), Marfurt C. F. and del Toro D. R. (1987), Marfurt C. F. and Echtenkamp S. F. (1988)
Nasal mucosa	−	+	+	+	++	−	+++	+++	+	+	Anton F. and Peppel P. (1991); Panneton W. M. (1991)
Dura	−	−	−	−	+	−	+++	+++	+	−	Arbab M. A. *et al.* (1988), Liu Y. *et al.* (2004)
Teeth	++	+	+++	+	+	+++	−	++	−	+	Marfurt C. F. and Turner D. F. (1984), Shigenaga Y. *et al.* (1986c); Takemura M. *et al.* (1993)
Masseter muscle	+	−	+	−	++	++	−	++	−	+	Nishimori T. *et al.* (1986), Shigenaga Y. *et al.* (1988), Arvidsson J. and Raappana P. (1989)
TMJ	+	−	+	−	++	++	−	+++	−	+	Jacquin M. F. *et al.* (1983); Shigenaga Y. *et al.* (1986a), (1986b), Capra N. F. (1987), Takemura M. *et al.* (1987)
Vibrissae	−	+++	−	+	+++	−	−	−	++	−	Jacquin M. F. *et al.* (1986), Nomura S. *et al.* (1986), Arvidsson J. (1982)

−, very few or none; +,++,+++, weak, moderate and dense terminal distribution; dPa5, dorsal paratrigeminal region; TMJ, temporomandibular joint; Vc, subnucleus caudalis; Vi, subnucleus interpolaris; Vo, subnucleus oralis; Vp, principal sensory nucleus.

only group of putative nociceptive fibers with a substantial projection to rostral portions of the TSNC, namely, to the dorsomedial portions of Vp and Vo, thus supporting the role for these regions in intraoral pain (Marfurt, C. F. and Turner, D. F., 1984; Shigenaga, Y. *et al.*, 1986c). Also, compared to other orofacial tissues associated with pain sensation, the termination pattern of dental afferents is particularly widespread along the rostrocaudal extent of the TSNC. Third, input from structures supplied by the ophthalmic branch of the Vn (e.g., cornea, nasal dura) project only sparsely to rostral portions of the TSNC suggesting that these regions play a lesser role than Vc in mediating pain due to uveitis, dry eye, sinusitis, or headache. Fourth, discontinuous representation is not unique to tissues supplied by the ophthalmic division (e.g., cornea, dura, nasal cavity) since the auriculotemporal nerve, a major source of innervation for the TMJ region also displays an uneven terminal distribution in the TSNC (Shigenaga, Y. *et al.*, 1986a; 1986b). In rodents vibrissae afferents project to most levels of the TSNC (Arvidsson, J., 1982; Nomura, S. *et al.*, 1986); however, the architectonic representation of the vibrissae fields, the so-called barrelettes, are well delineated in Vp, Vi, and Vc, but not Vo (Ma, P. M., 1991), supporting the notion that different levels of the TSNC mediate different aspects of sensory processing of innocuous as well as noxious inputs.

5.32.3.2 Intersubnuclear Connections

Rostral and caudal portions of the TSNC are connected by a rich longitudinal fiber network coursing within spinal trigeminal tract and through the deep bundles that extend from Vp to the upper cervical spinal cord (Gobel, S. and Purvis, M. B., 1972; Kruger, L. *et al.*, 1977; Ikeda, M. *et al.*, 1984; Jacquin, M. F. *et al.*, 1990). Although propriospinal-like connections of the TSNC share anatomical similarities with those at lower spinal levels, intersubnuclear connections in the TSNC link spatially distinct brainstem regions with common somatotopic representation of facial fields. The implications of this organization for facial pain remain to be determined; however, results from numerous animal studies support the clinical findings of Sjoqvist O. (1938) and indicate that ascending connections from caudal Vc generally facilitate the activity of neurons in more rostral portions within the TSNC. Lesion or chemical blockade of caudal Vc reduced the excitability of rostral trigeminal neurons responsive to noxious stimulation of tooth pulp (Greenwood, L. F. and Sessle, B. J., 1976; Chiang, C. Y. *et al.*, 2002), dura (Davis, K. D. and Dostrovsky, J. O., 1988), and cornea (Hirata, H. *et al.*, 2003). By contrast, innocuous sensory input from facial skin (Greenwood, L. F. and Sessle, B. J., 1976) and vibrissae (Hallas, B. H. and Jacquin, M. F., 1990) often was enhanced. Fewer studies have assessed the influence of rostral TSNC regions on caudal Vc neural activity, though in a recent study, muscimol blockade of the Vi/Vc transition region facilitated cornea-responsive neurons in laminas I–II of caudal Vc (Hirata, H. *et al.*, 2003). These results suggest that ascending as well as descending connections within the TSNC contribute to the integration of sensory inputs relevant for craniofacial pain.

5.32.3.3 Relationship to the Autonomic Nervous System

The trigeminal system is closely linked to brain regions that control autonomic outflow, especially parasympathetic outflow and vagus nerve activity. This linkage likely contributes to craniofacial pain conditions such as primary headache (Edvinsson, L. and Uddman, R., 2005) and dry eye (Hocevar, A. *et al.*, 2003), sudden bradycardia and asystole during maxillofacial surgery (Schaller, B., 2004), and the so-called diving reflex in infant humans (Goksor, E. *et al.*, 2002) and aquatic mammals (Butler, P. J. and Jones, D. R., 1997). Even facial skin differs from other cutaneous regions in that it is well supplied by parasympathetic fibers (Ramien, M. *et al.*, 2004). Under experimental conditions noxious stimulation of craniofacial tissues in humans evokes long-lasting vasodilatation in orofacial regions (Drummond, P. D., 1992; Izumi, H., 1999) that differs from responses evoked by stimulation of other body regions consistent with the existence of specialized trigeminal vasodilator reflex mechanisms (Kemppainen, P. *et al.*, 2001). Two aspects of the relationship between autonomic nerves and the trigeminal system are distinct from spinal cord and deserve special mention. Unlike at spinal levels where nearly all sensory nerves relay initially in the dorsal horn or dorsal column nuclei, many Vn afferents, especially those from the mandibular branch, project directly to brainstem nuclei that control autonomic outflow such as the nucleus tractus solitarius (NTS), parabrachial complex, and ventrolateral medulla (Kerr, F. W. L., 1961; Jacquin, M. F. *et al.*, 1983; Marfurt, C. F. and Rajchert, D. M., 1991; Panneton, W. M., 1991; Panneton, W. M. *et al.*, 1994). Also, unlike lower portions of the spinal cord, there is an extensive convergence of Vn, facial, glossopharyngeal, and vagal afferents to common laminae of

the lower TSNC and upper cervical dorsal horn (Denny-Brown, D. and Yanagisawa, N., 1973; Beckstead, R. M. and Norgren, R., 1979; Contreras, R. J. *et al.*, 1982; Altschuler, S. M. *et al.*, 1989; McNeill, D. L. *et al.*, 1991). The dorsal paratrigeminal region (dPa5) also receives inputs from multiple cranial nerves and upper cervical rootlets, has widespread connections to central autonomic pathways and other regions of the TSNC, and may be a key site of somatic–autonomic integration for cutaneous and visceral sensory input and control of homeostasis (Panneton, W. M. and Burton, H., 1985; Saxon, D. W. and Hopkins, D. A., 1998; Caous, C. A. *et al.*, 2001). Considerable evidence suggests that the Vc/upper cervical cord (Vc/C2) junction region differs from lower spinal cord. In addition to receiving convergent input from multiple cranial nerves and upper cervical rootlets (Pfaller, K. and Arvidsson, J., 1988; Neuhuber, W. L. and Zenker, W., 1989), second-order Vc/C2 neurons have widespread ascending connections to the hypothalamus (Burstein, R. *et al.*, 1990) and periaqueductal gray (PAG; Keay, K. A. *et al.*, 1997), brainstem regions well associated with control of autonomic outflow, and endogenous pain modulation circuits. The Vc/C2 junction also sends long-range descending projections to the lower spinal cord and is a critical region for visceral sensory, particularly vagus nerve, modulation of somatic input to lower spinal segments (Chandler, M. J. *et al.*, 2002). Although vagus nerve stimulation generally is associated with antinociception in humans (Kirchner, A. *et al.*, 2000) and animals (Randich, A. and Gebhart, G. F., 1992; Khasar, S. G. *et al.*, 1998), the relationship between vagus nerve activity and facial pain may be more complex. For example, increased vagal afferent activity has been suggested as one source of facial pain referred from the lung in cancer patients (see Sarlani, E. *et al.*, 2003), whereas in animal studies increased vagal activity inhibits painlike behavior and c-fos expression after formalin injection into facial skin (Bohotin, C. *et al.*, 2003) and tooth pulp-evoked activity of Vc/C2 dorsal horn neurons (Tanimoto, T. *et al.*, 2002). The effects of vagus nerve stimulation have been tested mainly on neurons in the caudal portions of the TSNC; however, vagal stimulation also inhibits tooth pulp-evoked digastric reflexes (Bossut, D. F. *et al.*, 1992) suggesting that modulation of neurons in rostral portions of the TSNC is possible. Given the extensive convergence and efferent projections of second-order neurons at the dPa5 and Vc/C2 regions, it is tempting to speculate that trigeminal–vagal interactions play a significant role in modulating pain above as well as below the neck.

5.32.3.4 Neurochemical Markers

The role of central neurons in mediating the various aspects of pain (e.g., sensation, autonomic control, motor reflexes) can be predicted, in part, on the basis of key factors such as the nature of the sensory input, encoding properties, response to analgesic agents, efferent projections (Price, D. D. and Dubner, R., 1977; Price, D. D. *et al.*, 2003), and, more recently, the distribution of a growing list of neurochemical markers associated with nociceptive processing (Woolf, C. J. and Salter, M. W., 2000; Julius, D. and Basbaum, A. I., 2001; Lewin, G. R. *et al.*, 2004). The data provided in Tables 4 (neurochemical markers) and 5 (efferent projections) are consistent with the notion that different portions of the TSNC contribute to different aspects of craniofacial pain. However, these data derive from results in naïve animals and do not specifically indicate which regions respond with phenotypic or long-term structural changes during chronic pain (see Basbaum, A. I., 1999; Hunt, S. P. and Mantyh, P. W., 2001; Scholz, J. and Woolf, C. J., 2002), changes that likely occur unequally in different portions of the TSNC.

Table 4 summarizes the pattern of distribution of selected neurochemical markers with known association to nociceptive processing and/or its modulation. The most striking aspect of these data is the dense and almost universal distribution of all markers within the superficial laminae of Vc, while only weak labeling is seen in laminae not associated with nociceptive processing (laminae III–IV). In rostral portions of the TSNC the density of different markers is more varied than in Vc. For example, the dorsomedial portions of Vp and Vo, regions that have a high density of afferent terminals from tooth pulp nerves, also display intense labeling for calcitonin gene-related peptide (CGRP) and trkA, whereas labeling for substance P and inositol 1,4,5 triphosphate (IP3) receptor are relatively weak and that for MOR1, the μ-opioid receptor, is absent. Interestingly, selective agonists for the 5-HT_{1B} receptor, a serotonergic receptor subtype that binds sumatriptan, an effective therapeutic agent for migraine, displays moderate density in the dorsomedial portions of Vp and Vo, yet neither region receives significant input from meningeal afferents. Although the laminar distribution of most neurochemical markers in Vc and the spinal dorsal horn are similar, significant differences have been reported for IB4 (Sugimoto, T. *et al.*, 1997a) and TRPV1 (Bae, Y. C. *et al.*, 2004), where spinal lamina IIi contains a greater expression of both markers than lamina IIo, while the reverse is seen in Vc. Also, the distribution of CGRP and substance P appears

Table 4 Summary of the distribution of neurochemical markers associated with nociceptive processing in different portions of the trigeminal sensory nuclear complex

	Vp		*Vo*					*Vc*			
	dm	*vl*	*dm*	*vl*	*Vi*	*dPa5*	*Vi/Vc*	*I–II*	*III–IV*	*V*	*References*
IB4	+	−	+	−	+	++	−	+++	−	−	Sugimoto T. *et al.* (1997a)
TRPV1	+	−	+	−	+	+++	++	+++	−	−	Bae Y. C. *et al.* (2004)
SP	+	−	+	−	+	++	++	+++	−	+	Boissonade F. M. *et al.* (1993), Sugimoto T. *et al.* (1997b)
NK1	+	−	+	−	+	+	+	+++	+	+	Nakaya Y. *et al.* (1994)
CGRP	++	−	+++	−	+	++	++	+++	−	+	Henry M. A. *et al.* (1996), Kruger L. *et al.* (1988), Sugimoto T. *et al.* (1997b)
$P2X_2$	+	+	+	++	++	+	++	++	+	+	Kanjhan R. *et al.* (1999)
trkA	+++	+	++	+	++	++	++	+++	+	−	Pioro E. P. and Cuello A. C. (1990), Sobreviela T. *et al.* (1994)
BDNF	+	−	+	−	+	++	++	+++	−	−	Connor J. M. *et al.* (1997)
trkB	++	++	++	++	++	++	++	+++	+	+	Yan Q. *et al.* (1997)
EP3	−	−	−	−	−	−	−	+++	−	−	Nakamura K. *et al.* (2000)
ChAT	+	−	+	−	+	−	−	++	−	−	Tatehata T. *et al.* (1987)
nNOS	+	−	+	−	+	++	+	+++	+	−	Dohrn C. S. *et al.* (1994), Rodrigo J. *et al.* (1994)
NR1	++	+	++	+	++	+++	++	+++	+	+	Petralia R. S. *et al.* (1994)
mGluR2	+	+	+	+	+	++	+	++	+	+	Ohishi H. *et al.* (1998)
GABA	+	+	++	+	+	+	++	+++	++	+	Ginestal E. and Matute C. (1993)
GABAaR	+	+	+	+	++	+	++	++	+	++	Fritschy J. M. and Mohler H. (1995), Pirker S. *et al.* (2000)
GABAbR	+	+	+	+	+	++	++	+++	+	+	Margeta-Mitrovic M. *et al.* (1999)
NE/DA	−	+	+	+	+	−	+	+	+	+	Kitahama K. *et al.* (2000), Levitt P. and Moore R. Y. (1979)
$AR\alpha/\beta$	+	+	+	+	+	+	+	++	+	+	Talley E. M. *et al.* (1996)
5-HT	+	+	+	+	+	+	++	+++	+	+	Harding A. *et al.* (2004), Steinbusch H. W. M. (1981)
$5\text{-}HT_{1B/1D}$	++	−	++	−	+	++	+	+++	+	+	Potrebic S. *et al.* (2003, Thor K. B. *et al.* (1992)
IP_3R	−	+	−	+	+	−	+	++	−	−	Rodrigo J. *et al.* (1993)
Calcineurin	−	+	−	+	+	−	+	+++	+	−	Strack S. *et al.* (1996)
Osteocalcin	−	+	−	+	+	++	+	+++	+	−	Ichikawa H. and Sugimoto T. (2002)
Endo2	−	−	+	−	+	++	+	+++	−	−	Martin–Schild S. *et al.* (1999)
MOR1	−	−	−	−	−	++	+	+++	−	−	Bereiter D. A. and Bereiter D. F. (2000), Ding Y. Q. *et al.* (1996)
ER_α	−	−	−	−	−	−		−	+++	+	Bereiter D. A. *et al.* (2005a)

−, very weak or no staining; +,++,+++, weak, moderate and dense staining; 5-HT, serotonin; $5HT_{1/2}$, serotonin receptor subtypes; $AR_{\alpha/\beta}$, adrenergic receptor subtypes; BDNF, brain-derived neurotrophic factor; CGRP, calcitonin gene-related peptide; ChAT, choline acetyltransferase; dPa5, dorsal paratrigeminal region; Endo2, endomorphin 2; EP3, prostaglandin receptor; ER_α, estrogen receptor alpha subtype; GABA, gamma-aminobutyric acid; GABAaR, GABA receptor α subtype, b2/3 subunit; GABAbR, GABA receptor β subtype, R1a/b subunit; IB4, isolectin B4; IP_3R, inositol triphosphate receptor; MOR1, μ-opioid receptor; NE/DA, norepinephrine/dopamine; NK1, neurokinin 1 receptor; nNOS, neuronal nitric oxide synthase; NR1, N-methyl-D-aspartic acid (NMDA) receptor subunit; $P2X_2$, ATP receptor; SP, substance P; trkA, tyrosine kinase A receptor subtype; trkB, tyrosine kinase B receptor subtype; TRPV1, vanilloid receptor; Vc, subnucleus caudalis; Vi, subnucleus interpolaris; Vo, subnucleus oralis; Vp, principal sensory nucleus.

more widely distributed across laminae I–III in Vc than in spinal dorsal horn where both neuropeptides are restricted to laminae I and IIo. The functional significance of these differences are not certain; however, the high degree of convergence of afferents from multiple sensory ganglion sources (e.g., trigeminal, nodose, cervical dorsal root) to the caudal Vc may underlie the poor localization and spreading of pain for many craniofacial pain conditions.

5.32.3.5 Efferent Projections

Table 5 summarizes major efferent projection targets of trigeminal neurons in different portions of the

Table 5 Summary of efferent projections from different portions of the trigeminal sensory nuclear complex to thalamic, pontine and medullary targets associated with various aspects of nociception

	Vp		Vo					Vc			
	dm	vl	dm	vl	Vi	dPa5	Vi/Vc	I–II	III–IV	III–IV	References
Thalamus											
VPM	+++	+++	+	+	++	+	+	++	+	++	Shigenaga Y. *et al.* (1983), Bruce L. L. *et al.* (1987); Mantle-St. John L. A. and Tracey D. J. (1987)
PO	−	+	−	++	++	−	+	+++	+	+	Dado R. J. and Giesler G. J. (1990), Guy N. *et al.* (2005)
SM	−	−	−	−	+	−	+++	++	−	−	Craig A. D. and Burton H. (1981), Dado R. J. and Giesler G. J. (1990), Yoshida A. *et al.* (1991)
Pf	+	−	+	−	+	−	+	−	−	++	Krout K. E. *et al.* (2002)
Hypothalamus											
VMH	−	−	+	+	+	−	++	+++	+	++	Malick A. and Burstein R. (1998)
LH	+	−	+	−	+	++	++	++	+	++	Malick A. and Burstein R. (1998), Ikeda T. *et al.* (2003)
Tectum											
APT	−	+	−	+	++	−	++	−	−	−	Yoshida A. *et al.* (1992)
SC	−	++	−	++	++	−	++	++	+	−	Bruce L. L. *et al.* (1987), Ndiaye A. *et al.* (2002)
PAG	−	−	−	−	−	−	−	++	−	+	Beitz A. J. (1982), Mantyh P. W. (1982), Wiberg M *et al.* (1986), Keay K. A. *et al.* (1997)
PBA	+	−	++	+	+	+++	++	+++	−	++	Panneton W. M. *et al.* (1994), Feil K. and Herbert H. (1995), Allen G. V. *et al.* (1996)
NTS	+	−	+	+	+	+++	+	++	−	−	Menetrey D. and Basbaum A. I. (1987), Zerari-Mailly F. *et al.* (2005)
ION	−	−	−	+	++	−	+	+	+	−	Huerta M. F. *et al.* (1985), Van Ham J. J. and Yeo C. H. (1992), Yatim N. *et al.* (1996)

−, very weak or no staining; +,++,+++, weak, moderate, and dense staining; APT, anterior pretectal nucleus; dPa5, dorsal paratrigeminal region; ION, inferior olivary nucleus; LH, lateral hypothalamic area; NTS, nucleus tractus solitarius; PAG, periaqueductal gray region; PBA, parabrachial region; Pf, medial and lateral parafascicular nuclei; PO, posterior thalamic nucleus; SC, superior colliculus; SM, nucleus submedius of thalamus; Vc, subnucleus caudalis; VMH, ventromedial hypothalamic area; Vi, subnucleus interpolaris; Vo, subnucleus oralis; Vp, principal sensory nucleus; VPM, ventroposteromedial nucleus of thalamus.

TSNC independent of the functional class (i.e., nociceptive versus innocuous sensory encoding). These data derive largely from studies in rodents; however, the qualitative pattern of efferent projections from the TSNC is similar across species, although there are significant quantitative species differences for some targets. Efferent projections from second-order neurons to the sensory thalamus have commanded considerable attention. The main sources of projections from the TSNC to the ventral posterior medial nucleus (VPM) arise from Vp and Vi, which in the case of rodents and most carnivores, is due to a heavy projection from vibrissae-driven rather than nociceptive neurons (Veinante, P. *et al.*, 2000). Nociceptive neurons in Vc that project to VPM originate mainly in laminae I and V (Ikeda, M. *et al.*, 2003) and moreover, the majority of projection neurons are found in rostral Vc rather than near the Vc/C2 junction region (Guy, N. *et al.*, 2005). Lamina I of Vc projects heavily to the posterior thalamus (PO); however, ventrolateral portions of Vo also provide a significant input to PO (Guy, N. *et al.*, 2005). Both Vc and spinal dorsal horn lamina I cells project to similar though adjacent regions of PO (Gauriau, C. and Bernard, J. F., 2004). Projections to parafascicular thalamic nuclei from Vc are sparse compared to spinal dorsal horn (Craig, A. D., 2004; Gauriau, C. and Bernard, J. F., 2004). Trigeminal projections to thalamic nucleus submedius (SM) reveal a unique pattern that differs markedly from spinal cord and exhibits significant species differences. In the rat the majority of SM projections arise from the ventrolateral portion of the Vi/Vc transition region with only weak input from lamina I and V of caudal Vc, while spinal projections to SM originate mainly from laminae V–VII (Dado, R. J. and Giesler, G. J., 1990; Yoshida, A. *et al.*, 1991). By contrast, in cat and monkey lamina I cells in Vc and spinal cord provide a significant direct input to SM with Vc displaying a somewhat more extensive projection (Craig A. D. and Burton, H., 1981). Trigeminal projections to autonomic control regions such as hypothalamus, parabrachial area, and NTS derive mainly from the dPa5, the Vi/Vc transition and lamina I of Vc, while more rostral regions of the TSNC provide relatively sparse input. This pattern is consistent with the dPa5 and lamina I of Vc receiving direct input from the vagus nerve. Spinal lamina I cells also project heavily to similar autonomic control regions of the brainstem (Cechetto, D. F. *et al.*, 1985; Menetrey, D. and Basbaum, A. I., 1987; Westlund, K. N. and Craig, A. D., 1996). Although nociceptive neurons in Vc (Sessle, B. J. *et al.*, 1981; Chiang, C. Y. *et al.*, 1994) and Vo (Chiang, C. Y. *et al.*, 1989) are markedly inhibited by direct stimulation of PAG or rostral ventromedial medulla (RVM), the afferent pathways from second-order TSNC neurons to these endogenous pain control regions are not well defined. Compared to the significant input from upper cervical levels of spinal cord (Keay, K. A. *et al.*, 1997) projections from TSNC to PAG are sparse (Beitz, A. J., 1982). These results add substantial support to the notion that laminae I–II of Vc are critical regions for processing nociceptive information relevant for multiple aspects of craniofacial pain. Behavioral evidence, though less extensively tested compared to spinal pain models, indicates that the Vc is necessary for opioid modulation of cutaneous facial pain (Oliveras, J. L. *et al.*, 1986) and that levels of attention markedly influence Vc nociceptive neurons and behavioral responsiveness (Hayes, R. L. *et al.*, 1981).

5.32.4 Functional Considerations

Recent developments in methods that assess neural activity and encoding properties provide the strongest evidence regarding the functional role of different regions of the TSNC in craniofacial pain. Advances in neuroimaging can distinguish somatotopic and simultaneous activation of brainstem and cortical responses to trigeminal stimuli in conscious humans (DaSilva, A. F. *et al.*, 2002), though resolution is not yet sufficient to discern the relative activation of different portions of the TSNC. Nociceptive neurons in the TSNC have been identified and their properties determined mainly on the basis of electrophysiological recording and, more recently, immediate early gene expression such as c-*fos*. Immunostaining for Fos, the protein product of c-*fos*, is a reliable method to identify populations of nociceptive central neurons at the single cell level (see Bullitt, E., 1990), an advantage not readily achieved by electrophysiology. Although there are examples of mismatches, properly designed c-*fos* studies generally complement electrophysiological results and have shed new light on long-standing controversies in trigeminal physiology. For example, a role for Vo in dental pain is suggested by: a dense terminal pattern in dorsomedial Vo from tooth pulp afferents (Marfurt, C. F. and Turner, D. F., 1984), a moderate-to-high density of CGRP staining (Sugimoto, T. *et al.*, 1997b), and behavioral studies revealing preservation of dental pain after trigeminal

tractotomy at the level of caudal Vi (Young, R. F. and Perryman, K. M., 1984). By contrast, few Vo neurons can be driven by natural stimulation of the tooth pulp compared to Vc (Hu, J. W. and Sessle, B. J., 1984) and few Fos-positive neurons are found in Vo after acute thermal stimulation of teeth (Chattipakorn, S. C. *et al.*, 1999). Thus, despite the fact that many Vo cells can be classified as nociceptive on the basis of cutaneous RF properties (Dallel, R. *et al.*, 1990), display wind-up to repeated cutaneous stimulation (Dallel, R. *et al.*, 1999), and are inhibited by systemic morphine (Dallel, R. *et al.*, 1996), the role of Vo in acute dental pain remains uncertain. It is possible that the Vo acts as a silent pain relay in the TSNC and becomes active only after persistent tissue damage since Fos-positive cells first appear in Vo only several days after molar tooth pulp exposure (Byers, M. R. *et al.*, 2000) and Vo neurons display sensitization provided input from Vc remains intact (Chiang, C. Y. *et al.*, 2002; Hu, B. *et al.*, 2002). Alternatively, rostral TSNC contributions to intraoral sensation and homeostasis may involve nonpulpal tissues (e.g., periodontal, muscosal receptors) and mediate select aspects of craniofacial pain (e.g., somatomotor reflexes).

5.32.4.1 Ocular Pain Processing

Ascribing a role for different portions of the TSNC in ocular pain appears more straightforward than for dental pain.

Corneal afferents terminate mainly in ventrolateral portions of caudal Vi and Vc with few fibers projecting to more rostral regions (Panneton, W. M. and Burton, H., 1981; Marfurt, C. F. and del Toro, D. R., 1987; Marfurt, C. F. and Echtenkamp, S. F., 1988). Acute stimulation of the ocular surface in the rat evokes a high density of Fos-positive cells at the Vi/Vc transition and caudal Vc and none in rostral regions of TSNC (Lu, J. *et al.*, 1993; Strassman, A. M. and Vos, B. P., 1993; Bereiter, D. A. *et al.*, 1994; Meng, I. D. and Bereiter, D. A., 1996). Converging lines of evidence support the notion that the Vi/Vc transition and caudal Vc serve different aspects of ocular pain.

All ocular cells in laminae I–II at the Vc/C2 junction are classified as nociceptive (wide-dynamic range (WDR), nociceptive specific (NS)), while many cells at the Vi/Vc transition have no cutaneous RF (Meng, I. D. *et al.*, 1997; Hirata, H. *et al.*, 1999). Many cells at the Vi/Vc transition are sensitive to the moisture status of the ocular surface, while few such neurons are found in caudal Vc, suggesting that this region is critical for reflex lacrimation (Hirata, H. *et al.*, 2004).

Repeated ocular surface stimulation evokes a wind-up like response among caudal Vc units, while Vi/Vc cells rapidly become desensitized (Meng, I. D. *et al.*, 1997). In a model for endotoxin-induced uveitis, at 7days after ocular inflammation convergent cutaneous RF areas become enlarged and responsiveness to ocular surface stimulation is enhanced among caudal Vc neurons, while Vi/Vc transition cells display no evidence of hyperalgesia (Bereiter, D. A. *et al.*, 2005c).

Systemic morphine inhibits all ocular cells at the caudal Vc, while nearly 30% of Vi/Vc cells are enhanced; an effect that can be produced by microinjection of μ-opioid receptor agonists directly into the caudal Vc (Meng, I. D. *et al.*, 1998; Hirata, H. *et al.*, 2000).

The modality of ocular units at the Vi/Vc and caudal Vc predicts, in part, the efferent projections to PO or salivatory nucleus in the brainstem (Hirata, H. *et al.*, 2000). The Vi/Vc transition is unique among TSNC regions and is the main source of ascending projections to SM (Yoshida, A. *et al.*, 1991; Ikeda, M. *et al.*, 2003). These data suggest that the caudal Vc underlies the sensory-discriminative aspects of ocular pain and modulation of ocular cells in more rostral regions via intersubnuclear connections. By contrast, the Vi/Vc transition appears to play a significant role in mediating ocular-specific reflexes (e.g., lacrimation, eye blink). Projections to SM, coupled with the finding that many Vi/Vc neurons display enhanced responsiveness after morphine, suggests that this region may be part of the neural circuit that recruits endogenous pain controls in response to craniofacial tissue injury. Since a high percentage of ocular cells at each region also respond to meningeal stimulation (Strassman, A. M. *et al.*, 1994; Burstein, R. *et al.*, 1998; Schepelmann, K. *et al.*, 1999), it is proposed that rostral and caudal portions of Vc mediate different aspects of headache as well as ocular pain.

5.32.5 Chronic Craniofacial Pain

Chronic pain involving craniofacial tissues is a significant public health concern and a recognized research priority for the National Institutes of Health (NIH; e.g., PA 03-173: *Neurobiology of Persistent Pain Mediated by the Trigeminal Nerve*). The classification, diagnosis, and management of

chronic craniofacial pain remain difficult since the mechanisms for many of these conditions are not well understood and animal models, though instructive, do not mimic the clinical state (Vos, B. P. *et al.*, 1994; Roveroni, R. C. *et al.*, 2001). Considerable progress has been in delineating the long-term changes in peripheral and central neural circuits that mediate pain sensation following tissue injury (Treede, R. D. *et al.*, 1992; Woolf, C. J. and Salter, M. W., 2000; Hunt, S. P. and Mantyh, P. W., 2001; Julius, D. and Basbaum, A. I., 2001; Lewin, G. R. *et al.*, 2004). Although similar cellular and molecular mechanisms may contribute to chronic pain due to Vn damage (Lavigne, G. *et al.*, 2005), many chronic craniofacial pain conditions such as TMD, migraine, or chronic daily headache and trigeminal neuralgia present with no overt signs of tissue injury. Indeed, it has long been appreciated that the correlation between tissue injury and magnitude of pain sensation may be weak (Wall, P. D., 1979). This has lead to proposals of emotional or neuropsychological (Tenenbaum, H. C. *et al.*, 2001; Korszun, A., 2002) and genetic factors as significant determinants of some forms of chronic craniofacial pain (TMD, Diatchenko, L. *et al.*, 2005; migraine, Wessman, M. *et al.*, 2004; trigeminal neuralgia, Duff, J. M., *et al.*, 1999; dry eye in Sjogren's syndrome, Takei, M. *et al.*, 2005). Chronic craniofacial pain can be broadly classified according to the pattern and origin of pain episodes: chronic/recurrent (TMD, migraine headache, trigeminal neuralgia), chronic/persistent (burning mouth, dry eye syndromes), and chronic deafferentation pain (postherpetic neuralgia, posttraumatic neuralgia, phantom tooth). The mechanisms that underlie these diverse conditions involve markedly different tissues and are likely quite heterogeneous. However, three features of many chronic craniofacial pain conditions are notable and provide evidence of commonality.

First, the prevalence of most chronic craniofacial pain conditions is higher in women than men (Dao, T. T. and LeResche, L., 2000; Macfarlane, T. V. *et al.*, 2002a). This is especially apparent for the chronic/recurrent conditions of TMD and migraine headache (LeResche, L., 1997; Rasmussen, B. K., 200l) and somewhat less so for trigeminal neuralgia (Kitt, C. A. *et al.*, 2000; Manzoni, G. C. and Torelli, P., 2005). Women also are more likely to develop burning mouth (Bergdahl, M. and Bergdahl, J., 1999; Grushka, M. *et al.*, 2003) and dry eye syndromes (Yazdani, C. *et al.*, 2001) and report greater sensory disturbances after Vn damage (Sandstedt, P. and Sorensen, S., 1995). Among TMD (Isselee, H. *et al.*, 2002; LeResche, L. *et al.*, 2003) and migraine patients (Rasmussen, B. K., 1993; MacGregor, E. A. and Hackshaw, A., 2004) pain severity and symptoms vary over the menstrual cycle suggesting a significant interaction with factors related to sex hormone status. Correspondingly, recent anatomical (Amandusson, A. *et al.*, 1996; Pajot, J. *et al.*, 2003; Bereiter, D. A. *et al.*, 2005a; 2005b; Puri, V. *et al.*, 2005) and electrophysiological evidence (Okamoto, K. *et al.*, 2003; Flake, N. M. *et al.*, 2005) from animal models support the notion that estrogen preferentially enhances the excitability of trigeminal neurons that contribute to craniofacial pain. Furthermore, within the TSNC, estrogen receptor-positive neurons are found almost exclusively within the superficial laminae of Vc and not in more rostral portions of the complex (Bereiter, D. A. *et al.*, 2005a) suggesting that this region plays a key role in differential processing of orofacial sensory information under different sex hormone conditions.

Second, spreading and referral of pain and sensitization evoked from outside the affected dermatomal region are common features of many chronic craniofacial pain conditions. Sensory disturbances occurring outside the affected region have been well documented in clinical studies of TMD (Maixner, W. *et al.*, 1998; Sarlani, E. and Greenspan, J. D., 2003; 2005), migraine (Burstein, R. *et al.*, 2000; Katsarava, Z., *et al.*, 2002; Goadsby, P. J., 2005), trigeminal neuralgia (Dubner, R. *et al.*, 1987; Nurmikko, T. J. and Eldridge, P. R., 2001; Devor, M. *et al.*, 2002), and burning mouth syndrome (Svensson, P. *et al.*, 1993; Ito, M. *et al.*, 2002). Patients with postherpetic neuralgia involving trigeminal dermatomes had lower thermal warm and cool thresholds, while those with infection of spinal dermatomes had elevated thresholds (Pappagallo, M. *et al.*, 2000) suggesting different underlying pathologies for neuropathic pain in trigeminal and spinal systems. Mechanical allodynia and increased temporal summation are consistent with the notion that central neural mechanisms maintain chronic craniofacial pain, while peripheral mechanisms are required mainly for initiation of the pain state.

Third, many chronic craniofacial pain conditions are accompanied by significant disturbances of the autonomic and/or endocrine systems. Chronic TMD patients display altered secretion of stress hormones (Jones, D. A. *et al.*, 1997; Korszun, A. *et al.*, 2002) and elevated levels of neuropeptides and proinflammatory cytokines that could affect blood flow to joints (Kopp, S., 2001). The relationship between vascular reactivity and migraine has long been considered a

critical variable (Janig, W., 2003; Goadsby, P. J., 2005), whereas stimulus-evoked oral mucosal blood flow is greater in patients with burning mouth syndrome (Heckmann, S. M. *et al.*, 2001). Evidence from animal models indicate that contributions from vagus nerve activity (Khasar, S. G. *et al.*, 2001) and adrenal medullary outflow (Green, P. G. *et al.*, 2001) have marked sex-related effects on cutaneous pain behavior. Although treatments to reduce sympathetically maintained pain generally have a poor outcome for posttraumatic trigeminal neuralgic patients (Gregg, J. M., 1990), the influence of the autonomic nervous system on other forms chronic craniofacial pain has not been adequately explored. It may be significant that brainstem regions critically involved in control of autonomic outflow also are densely stained for estrogen receptor-positive neurons (Shughrue, P. J. *et al.*, 1997; Simonian, S. X. *et al.*, 1998; Merchenthaler, I. *et al.*, 2004). Collectively, these features underscore the hypothesis that an interaction between sex hormone status and autonomic outflow occurs within the central nervous system to alter the expression of chronic craniofacial facial pain.

We recognize that chronic craniofacial pain is a complex problem with varying etiologies and possible contributions from genetic, neuropsychological, and neurobiological factors. However, regardless of the origin and relative contribution of these factors on pain circuits within the brain, a greater understanding of the unique organizational features of the trigeminal system may provide new perspectives and strategies to manage chronic craniofacial pain that would not otherwise be apparent from studies conducted only at the spinal level.

References

Aigner, M., Robert, Lukas J., Denk, M., Ziya-Ghazvini, F., Kaider, A., and Mayr, R. 2000. Somatotopic organization of primary afferent perikarya of the guinea-pig extraocular muscles in the trigeminal ganglion: a post-mortem DiI-tracing study. Exp. Eye Res. 70, 411–418.

Aimi, Y., Fujimura, M., Vincent, S. R., and Kimura, H. 1991. Localization of NADPH-diaphorase-containing neurons in sensory ganglia of the rat. J. Comp. Neurol. 306, 382–392.

Akazawa, C., Nakamura, Y., Sango, K., Horie, H., and Kohsaka, S. 2004. Distribution of the galectin-1 mRNA in the rat nervous system: its transient upregulation in rat facial motor neurons after facial nerve axotomy. Neuroscience 125, 171–178.

Albers, K. M., Perrone, T. N., Goodness, T. P., Jones, M. E., Green, M. A., and Davis, B. M. 1996. Cutaneous overexpression of NT-3 increases sensory and sympathetic neuron number and enhances touch dome and hair follicle innervation. J. Cell Biol. 134, 487–497.

Allen, G. V., Barbrick, B., and Esser, M. J. 1996. Trigeminal-parabrachial connections: possible pathway for nociception-induced cardiovascular reflex responses. Brain Res. 715, 125–135.

Altschuler, S. M., Bao, X., Bieger, D., Hopkins, D. A., and Miselis, R. R. 1989. Viscerotopic representation of the upper alimentary tract in the rat: sensory ganglia and nuclei of the solitary and spinal trigeminal tracts. J. Comp. Neurol. 283, 248–268.

Amandusson, A., Hermanson, O., and Blomqvist, A. 1996. Colocalization of oestrogen receptor immunoreactivity and preproenkephalin mRNA expression to neurons in the superficial laminae of the spinal and medullary dorsal horn of rats. Eur. J. Neurosci. 8, 2440–2445.

Ambalavanar, R. and Morris, R. 1992. The distribution of binding by isolectin I-B4 from *Griffonia simplicifolia* in the trigeminal ganglion and brainstem trigeminal nuclei in the rat. Neuroscience 47, 421–429.

Ambalavanar, R., Moritani, M., and Dessem, D. 2005. Trigeminal P2X(3) receptor expression differs from dorsal root ganglion and is modulated by deep tissue inflammation. Pain 117, 280–291.

Anggard, A., Lundberg, J. M., and Lundblad, L. 1983. Nasal autonomic innervation with special reference to peptidergic nerves. Eur. J. Respir. Dis. Suppl. 128, 143–149.

Anton, F. and Peppel, P. 1991. Central projections of trigeminal primary afferents innervating the nasal mucosa: a horseradish peroxidase study in the rat. Neuroscience 41, 617–628.

Arbab, M. A., Delgado, T., Wiklund, L., and Svendgaard, N. A. 1988. Brain stem terminations of the trigeminal and upper spinal ganglia innervation of the cerebrovascular system: WGA-HRP transganglionic study. J. Cereb. Blood Flow Metab. 8, 54–63.

Artinger, K. B., Fedtsova, N., Rhee, J. M., Bronner-Fraser, M., and Turner, E. 1998. Placodal origin of Brn-3-expressing cranial sensory neurons. J. Neurobiol. 36, 572–585.

Arvidsson, J. 1982. Somatotopic organization of vibrissae afferents in the trigeminal sensory nuclei of the rat studied by transganglionic transport of HRP. J. Comp. Neurol. 211, 84–92.

Arvidson, B. 1983. Influence of age on the development of cadmium-induced vascular lesions in rat sensory ganglia. Environ. Res. 32, 240–246.

Arvidsson, J. and Raappana, P. 1989. An HRP study of the central projections from primary sensory neurons innervating the rat masseter muscle. Brain Res. 480, 111–118.

Arvidsson, J., Pfaller, K., and Gmeiner, S. 1992. The ganglionic origins and central projections of primary sensory neurons innervating the upper and lower lips in the rat. Somatosensory Motor Res. 9, 199–209.

Bae, Y. C., Oh, J. M., Hwang, S. J., Shigenaga, Y., and Valtschanoff, J. G. 2004. Expression of vanilloid receptor TRPV1 in the rat trigeminal sensory nuclei. J. Comp. Neurol. 478, 62–71.

Baker, C. V., Stark, M. R., and Bronner-Fraser, M. 2002. Pax3-expressing trigeminal placode cells can localize to trunk neural crest sites but are committed to a cutaneous sensory neuron fate. Dev. Biol. 249, 219–236.

Barker, D. J. and Welker, W. I. 1969. Receptive fields of first-order somatic sensory neurons innervating rhinarium in coati and raccoon. Brain Res. 14, 367–386.

Basbaum, A. I. 1999. Distinct neurochemical features of acute and persistent pain. Proc. Natl. Acad. Sci. U. S. A. 96, 7739–7743.

Beckstead, R. M. and Norgren, R. 1979. An autoradiographic examination of the central distribution of the trigeminal, facial, glossopharyngeal, and vagal nerves in the monkey. J. Comp. Neurol. 184, 455–472.

Beitel, R. E. and Dubner, R. 1976. Response of unmyelinated (C) polymodal nociceptors to thermal stimuli applied to monkey's face. J. Neurophysiol. 39, 1160–1175.

Beitz, A. J. 1982. The organization of afferent projections to the midbrain periaqueductal gray of the rat. Neuroscience 7, 133–159.

Belmonte, C., Garcia-Hirschfeld, J., and Gallar, J. 1997. Neurobiology of ocular pain. Prog. Retin. Eye Res. 16, 117–156.

Benoliel, R., Eliav, E., and Tal, M. 2001. No sympathetic nerve sprouting in rat trigeminal ganglion following painful and non-painful infraorbital nerve neuropathy. Neurosci. Lett. 297, 151–154.

Bereiter, D. A. and Bereiter, D. F. 2000. Morphine and NMDA receptor antagonism reduce c-*fos* expression in spinal trigeminal nucleus produced by acute injury to the TMJ region. Pain 85, 65–77.

Bereiter, D. A., Cioffi, J. L., and Bereiter, D. F. 2005a. Oestrogen receptor-immunoreactive neurons in the trigeminal sensory system of male and cycling female rats. Arch. Oral. Biol. 50, 971–979.

Bereiter, D. A., Hathaway, C. B., and Benetti, A. P. 1994. Caudal portions of the spinal trigeminal complex are necessary for autonomic responses and display Fos-like immunoreactivity after corneal stimulation in the cat. Brain Res. 657, 73–82.

Bereiter, D. A., Hirata, H., and Hu, J. W. 2000. Trigeminal subnucleus caudalis: beyond homologies with the spinal dorsal horn. Pain 88, 221–224.

Bereiter, D. A., Okamoto, K., and Bereiter, D. F. 2005b. Effect of persistent monoarthritis of the temporomandibular joint region on acute mustard oil-induced excitation of trigeminal subnucleus caudalis neurons in male and female rats. Pain 117, 58–67.

Bereiter, D. A., Okamoto, K., Tashiro, A., and Hirata, H. 2005c. Endotoxin-induced uveitis causes long-term changes in trigeminal subnucleus caudalis neurons. J. Neurophysiol. 94, 3815–3825.

Bergdahl, M. and Bergdahl, J. 1999. Burning mouth syndrome: prevalence and associated factors. J. Oral Pathol. Med. 28, 350–354.

Beuerman, R. W. and Tanelian, D. L. 1979. Corneal pain evoked by thermal stimulation. Pain 7, I–l4.

Bleys, R. L., Groen, G. J., and Hommersom, R. F. 1996. Neural connections in and around the cavernous sinus in rat, with special reference to cerebrovascular innervation. J. Comp. Neurol. 369, 277–291.

Bohotin, C., Scholsem, M., Multon, S., Martin, D., Bohotin, V., and Schoenen, J. 2003. Vagus nerve stimulation in awake rats reduces formalin-induced nociceptive behaviour and fos-immunoreactivity in trigeminal nucleus caudalis. Pain 101, 3–12.

Boissonade, F. M., Sharkey, K. A., and Lucier, G. E. 1993. Trigeminal nuclear complex of the ferret: anatomical and immunohistochemical studies. J. Comp. Neurol. 329: 291–312.

Bongenhielm, U., Boissonade, F. M., Westermark, A., Robinson, P. P., and Fried, K. 1999. Sympathetic nerve sprouting fails to occur in the trigeminal ganglion after peripheral nerve injury in the rat. Pain 82, 283–288.

Bongenhielm, U., Nosrat, C. A., Nosrat, I., Eriksson, J., Fjell, J., and Fried, K. 2000. Expression of sodium channel SNS/PN3 and ankyrin(G) mRNAs in the trigeminal ganglion after inferior alveolar nerve injury in the rat. Exp. Neurol. 164, 384–395.

Bongenhielm, U., Yates, J. M., Fried, K., and Robinson, P. P. 1998. Sympathectomy does not affect the early ectopic discharge from myelinated fibres in ferret inferior alveolar nerve neuromas. Neurosci. Lett. 245, 89–92.

Bossut, D. F., Whitsel, E. A., and Maixner, W. 1992. A parametric analysis of the effects of cardiopulmonary vagal electrostimulation on the digastric reflex in cats. Brain Res. 579, 253–260.

Brannstrom, M. 1986. The hydrodynamic theory of dentinal pain: sensation in preparations, caries, and the dentinal crack syndrome. J. Endod. 12, 453–457.

Bruce, L. L., McHaffie, J. G., and Stein, B. E. 1987. The organization of trigeminotectal and trigeminothalamic neurons in rodents: a double-labeling study with fluorescent dyes. J. Comp. Neurol. 262, 315–330.

Bruenech, J. R. and Ruskell, G. L. 2001. Muscle spindles in extraocular muscles of human infants. Cells Tissues Organs 169, 388–394.

Bryant, B. and Silver, W. L. 2000. Chemesthesis: the Common Chemical Sense. In: Neurobiology of Taste and Smell, 2nd edn (*eds*. T. E. Finger, W. L. Silver, and D. Restrepo), pp. 73–100. Wiley-Liss.

Bullitt, E. 1990. Expression of c-fos-like protein as a marker for neuronal activity following noxious stimulation in the rat. J. Comp. Neurol. 296, 517–530.

Burstein, R., Yamamura, H., Malick, A., and Strassman, A. M. 1998. Chemical stimulation of the intracranial dura induces enhanced responses to facial stimulation in brain stem trigeminal neurons. J. Neurophysiol. 79, 964–982.

Burstein, R., Yarnitsky, D., Goor-Aryeh, I., Ransil, B. J., and Bajwa, Z. H. 2000. An association between migraine and cutaneous allodynia. Ann. Neurol. 47, 614–624.

Butler, P. J. and Jones, D. R. 1997. Physiology of diving of birds and mammals. Physiol. Rev. 77, 837–899.

Buzas, B. and Cox, B. M. 1997. Quantitative analysis of mu and delta opioid receptor gene expression in rat brain and peripheral ganglia using competitive polymerase chain reaction. Neuroscience 76, 479–489.

Byers, M. R. 1984. Dental sensory receptors. Int. Rev. Neurobiol. 25, 39–94.

Byers, M. R., Chudler, E. H., and Iadorola, M. J. 2000. Chronic tooth pulp inflammation causes transient and persistent expression of Fos in dynorphin-rich regions of rat brainstem. Brain Res. 861, 191–207.

Caous, C. A., de Sousa Buck, H., and Lindsey, C. J. 2001. Neuronal connections of the paratrigeminal nucleus: a topographic analysis of neurons projecting to bulbar, pontine and thalamic nuclei related to cardiovascular, respiratory and sensory functions. Autonomic Neurosci. 94, 14–24.

Capra, N. F. 1987. Localization and central projections of primary afferent neurons that innervate the temporomandibular joint in cats. Somatosensory Motor Res. 4, 201–213.

Catania, K. C. 1999. A nose that looks like a hand and acts like an eye: the unusual mechanosensory system of the star-nosed mole. J. Comp. Physiol. A 185, 367–372.

Catania, K. C. and Kaas, J. H. 1997. Somatosensory fovea in the star-nosed mole: behavioral use of the star in relation to innervation patterns and cortical representation. J. Comp. Neurol. 387, 215–233.

Catania, K. C. and Remple, M. S. 2002. Somatosensory cortex dominated by the representation of teeth in the naked mole-rat brain. Proc. Natl. Acad. Sci. U. S. A. 99, 5692–5697.

Cechetto, D. F., Standaert, D. S., and Saper, C. B. 1985. Spinal and trigeminal dorsal horn projections to the parabrachial nucleus in the rat. J. Comp. Neurol. 240, 153–162.

Chalazonitis, A., Kessler, J. A., Twardzik, D. R., and Morrison, R. S. 1992. Transforming growth factor alpha, but not epidermal growth factor, promotes the survival of sensory neurons *in vitro.* J. Neurosci. 12, 583–594.

Chandler, M. J., Zhang, J., Qin, C., and Foreman, R. D. 2002. Spinal inhibitory effects of cardiovascular inputs in monkeys:

neuronal processing in high cervical segments. J. Neurophysiol. 87, 1290–1302.
Chattipakorn, S. C., Light, A. R., Willcockson, H. H., Nahri, M., and Maixner, W. 1999. The effect of fentanyl on c-fos expression in the trigeminal brainstem complex produced by pulpal heat stimulation in the ferret. Pain 82, 207–215.
Cheng, S. B., Kuchiiwa, S., Kuchiiwa, T., and Nakagawa, S. 2000. Three novel pathways to the lacrimal glands of the cat: an investigation with cholera toxin B subunit as a retrograde tracer. Brain Res. 873, 160–164.
Chiang, C. Y., Hu, B., Hu, J. W., Dostrovsky, J. O., and Sessle, B. J. 2002. Central sensitization of nociceptive neurons in trigeminal subnucleus orlais depends on the integrity of subnucleus caudalis. J. Neurophysiol. 88, 256–264.
Chiang, C. Y., Hu, J. W., Dostrovsky, J. O., and Sessle, B. J. 1989. Changes in mechanoreceptive field properties of somatosensory brainstem neurons induced by stimulation of nucleus raphe magnus in cats. Brain Res. 485, 371–381.
Chiang, C. Y., Hu, J. W., and Sessle, B. J. 1994. Parabrachial area and nucleus raphe magnus-induced modulation of nociceptive and nonnociceptive trigeminal subnucleus caudalis neurons activated by cutaneous or deep inputs. J. Neurophysiol. 71, 2430–2445.
Cody, F. W., Lee, R. W., and Taylor, A. 1972. A functional analysis of the components of the mesencephalic nucleus of the fifth nerve in the cat. J. Physiol. 226, 249–261.
Collo, G., North, R. A., Kawashima, E., Merlo-Pich, E., Neidhart, S., Surprenant, A., and Buell, G. 1996. Cloning of P2X5 and P2X6 receptors and the distribution and properties of an extended family of ATP-gated ion channels. J. Neurosci. 16, 2495–2507.
Cometto-Muniz, J. E. and Cain, W. S. 1995. Relative sensitivity of the ocular trigeminal, nasal trigeminal and olfactory systems to airborne chemicals. Chem. Senses 20, 191–198.
Connor, J. M., Lauterborn, J. C., Yan, Q., Gall, C. M., and Varon, S. 1997. Distribution of brain-derived neurotrophic factor (BDNF) protein and mRNA in the normal adult rat CNS: evidence for anterograde axonal transport. J. Neurosci. 17, 2295–2313.
Contreras, R. J., Beckstead, R. M., and Norgren, R. 1982. The central projections of the trigeminal, facial, glossopharyngeal and vagus nerves: an autoradiographic study in the rat. J. Autonomic Nerv. Syst. 6, 303–322.
Cook, S. P., Vulchanova, L., Hargreaves, K. M., Elde, R., and McCleskey, E. W. 1997. Distinct ATP receptors on pain-sensing and stretch-sensing neurons. Nature 387, 505–508.
Craig, A. D. 2004. Distribution of trigeminothalamic and spinothalamic lamina I terminations in the macaque monkey. J. Comp. Neurol. 477, 119–148.
Craig, A. D. and Burton, H. 1981. Spinal and medullary lamina I projection to nucleus submedius in medial thalamus: a possible pain center. J. Neurophysiol. 45, 443–466.
Dado, R. J. and Giesler, G. J. 1990. Afferent input to nucleus submedius in rats: retrograde labeling of neurons in the spinal cord and caudal medulla. J. Neurosci. 10, 2672–2686.
Dallel, R., Duale, C., Luccarini, P., and Molat, J. L. 1999. Stimulus-function, wind-up and modulation by diffuse noxious inhibitory controls of responses of convergent neurons of the spinal trigeminal nucleus oralis. Eur. J. Neurosci. 11, 31–40.
Dallel, R., Luccarini, P., Molat, J. L., and Woda, A. 1996. Effects of systemic morphine on the activity of convergent neurons of spinal trigeminal nucleus oralis in the rat. Eur. J. Pharmacol. 314, 19–25.
Dallel, R., Raboisson, P., Woda, A., and Sessle, B. J. 1990. Properties of nociceptive and non-nociceptive neurons in trigeminal subnucleus oralis of the rat. Brain Res. 521, 95–106.
Dao, T. T. and LeResche, L. 2000. Gender differences in pain. J. Orofacial Pain 14, 169–184.
DaSilva, A. F., Becerra, L., Makris, N., Strassman, A. M., Gonzalez, R. G., Geatrakis, N., and Borsook, D. 2002. Somatotopic activation in the human trigeminal pain pathway. J. Neurosci. 22, 8183–8192.
Davis, K. D. and Dostrovsky, J. O. 1988. Effect of trigeminal subnucleus caudalis cold block on the cerebrovascular-evoked responses of rostral trigeminal complex neurons. Neurosci. Lett. 94, 303–308.
Davis, B. M., Albers, K. M., Seroogy, K. B., and Katz, D. M. 1994. Overexpression of nerve growth factor in transgenic mice induces novel sympathetic projections to primary sensory neurons. J. Comp. Neurol. 349, 464–474.
DeLeon, M., Covenas, R., Chadi, G., Narvaez, J. A., Fuxe, K., and Cintra, A. 1994. Subpopulations of primary sensory neurons show coexistence of neuropeptides and glucocorticoid receptors in the rat spinal and trigeminal ganglia. Brain Res. 636, 338–342.
Denny-Brown, D. and Yanagisawa, N. 1973. The function of the descending root of the fifth nerve. Brain 96, 783–814.
Devor, M., Amir, R., and Rappaport, Z. H. 2002. Pathophysiology of trigeminal neuralgia: the ignition hypothesis. Clin. J. Pain 18, 4–13.
Diatchenko, L., Slade, G. D., Nackley, A. G., Bhalang, K., Sigurdsson, A., Belfer, I., Goldman, D., Shabalina, S. A., Shagin, D., Max, M. B., Makarov, S. S., and Maixner, W. 2005. Genetic basis for individual variations in pain perception and the development of a chronic pain condition. Human Mol. Genet. 14, 135–143.
Dib-Hajj, S., Black, J. A., Felts, P., and Waxman, S. G. 1996. Down-regulation of transcripts for Na channel alpha-SNS in spinal sensory neurons following axotomy. Proc. Natl. Acad. Sci. U. S. A. 93, 14950–14954.
Ding, Y. Q., Kaneko, T., Nomura, S., and Mizuno, N. 1996. Immunohistochemical localization of μ-opioid receptors in the central nervous system of the rat. J. Comp. Neurol. 367, 375–402.
Dohrn, C. S., Mullett, M. A., Price, R. H., and Beitz, A. J. 1994. Distribution of nitric oxide synthase-immunoreactive interneurons in the spinal trigeminal nucleus. J. Comp. Neurol. 346, 449–460.
Drummond, P. D. 1992. The mechanism of facial sweating and cutaneous vascular responses to painful stimulation of the eye. Brain 115, 1417–1428.
Dubner, R. and Bennett, G. J. 1983. Spinal and trigeminal mechanisms of nociception. Annu. Rev. Neurosci. 6, 38l–418.
Dubner, R., Sharav, Y., Gracely, R. H., and Price, D. D. 1987. Idiopathic trigeminal neuralgia: sensory features and pain mechanisms. Pain 31, 23–33.
Duff, J. M., Spinner, R. J., Lindor, N. M., Dodick, D. W., and Atkinson, J. L. 1999. Familial trigeminal neuralgia and contralateral hemifacial spasm. Neurology 53, 216–218.
Edvinsson, L. and Uddman, R. 2005. Neurobiology in primary headaches. Brain Res. Brain Res. Rev 48, 438–456.
Elcock, C., Boissonade, F. M., and Robinson, P. P. 2001. Changes in neuropeptide expression in the trigeminal ganglion following inferior alveolar nerve section in the ferret. Neuroscience 102, 655–667.
Elkabes, S., Dreyfus, C. F., Schaar, D. G., and Black, I. B. 1994. Embryonic sensory development: local expression of neurotrophin-3 and target expression of nerve growth factor. J. Comp. Neurol. 341, 204–213.
Eriksson, J., Bongenhielm, U., Kidd, E., Matthews, B., and Fried, K. 1998. Distribution of P2X3 receptors in the rat trigeminal ganglion after inferior alveolar nerve injury. Neurosci. Lett. 254, 37–40.

Esteve, P. and Bovolenta, P. 1999. cSix4, a member of the six gene family of transcription factors, is expressed during placode and somite development. Mech. Dev. 85, 161–165.

Feil, K. and Herbert, H. 1995. Topographic organization of spinal and trigeminal somatosensory pathways to the rat parabrachial and Kolliker-Fuse nuclei. J. Comp. Neurol. 353, 506–528.

Feindel, W., Penfield, W., and McNaughton, F. 1960. The tentorial nerves and localization of intracranial pain in man. Neurology 10, 555–563.

Flake, N. M., Bonebreak, D. B., and Gold, M. S. 2005. Estrogen and inflammation increase the excitability of rat temporomandibular joint afferent neurons. J. Neurophysiol. 93, 1585–1597.

Fritschy, J. M. and Mohler, H. 1995. GABAA-receptor heterogeneity in the adult rat brain: differential regional and cellular distribution of seven major subunits. J. Comp. Neurol. 359, 154–194.

Gauriau, C. and Bernard, J. F. 2004. A comparative reappraisal of projections from the superficial laminae of the dorsal horn in the rat: the forebrain. J. Comp. Neurol. 468, 24–56.

Georgiades, P., Wood, J., and Brickell, P. M. 1998. Retinoid X receptor-gamma gene expression is developmentally regulated in the embryonic rodent peripheral nervous system. Anat. Embryol. (Berl.) 197, 477–484.

Ghilardi, J. R., Allen, C. J., Vigna, S. R., McVey, D. C., and Mantyh, P. W. 1992. Trigeminal and dorsal root ganglion neurons express CCK receptor binding sites in the rat, rabbit, and monkey: possible site of opiate-CCK analgesic interactions. J. Neurosci. 12, 4854–4866.

Ginestal, E. and Matute, C. 1993. Gamma-aminobutyric acid-immunoreactive neurons in the rat trigeminal nuclei. Histochemistry 99, 49–55.

Goadsby, P. J. 2005. Trigeminal autonomic cephalgias: fancy term or constructive change to the IHS classification? J. Neurol. Neurosurg. Psychiatry 76, 301–305.

Gobel, S. and Purvis, M. B. 1972. Anatomical studies of the organization of the spinal V nucleus: the deep bundles and the spinal V tract. Brain Res. 48, 27–44.

Goedert, M., Otten, U., Hunt, S. P., Bond, A., Chapman, D., Schlumpf, M., and Lichtensteiger, W. 1984. Biochemical and anatomical effects of antibodies against nerve growth factor on developing rat sensory ganglia. Proc. Natl. Acad. Sci. U S. A. 81, 1580–1584.

Goksor, E., Rosengren, L., and Wennergren, G. 2002. Bradycardic response during submersion in infant swimming. Acta Paediatr. 91, 307–312.

Gonzalez-Martinez, T., Germana, G. P., Monjil, D. F., Silos-Santiago, I., de Carlos, F., Germana, G., Cobo, J., and Vega, J. A. 2004. Absence of Meissner corpuscles in the digital pads of mice lacking functional TrkB. Brain Res. 1002, 120–128.

Green, P. G., Dahlqvist, S. R., Isenberg, W. M., Mao, F. J., and Levine, J. D. 2001. Role of adrenal medulla in development of sexual dimorphism in inflammation. Eur. J. Neurosci. 14, 1436–1444.

Greenwood, L. F. and Sessle, B. J. 1976. Inputs to trigeminal brain stem neurons from facial, oral, tooth pulp and pharyngolarygeal tissues: II. Role of trigeminal nucleus caudalis in modulating responses to innocuous and noxious stimuli. Brain Res. 117, 227–238.

Gregg, J. M. 1990. Studies of traumatic neuralgia in the maxillofacial region: symptom complexes and response to microsurgery. J. Oral Maxillofac. Surg. 48, 135–140; discussion 141.

Grushka, M., Epstein, J. B., and Gorsky, M. 2003. Burning mouth syndrome and other oral sensory disorders: a unifying hypthesis. Pain Res. Manag. 8, 133–135.

Guo, A., Vulchanova, L., Wang, J., Li, X, and Elde, R. 1999. Immunocytochemical localization of the vanilloid receptor 1 (VR1): relationship to neuropeptides, the P2X3 purinoceptor and IB4 binding sites. Eur. J. Neurosci. 11, 946–958.

Guy, N., Chalus, M., Dallel, R., and Voisin, D. L. 2005. Both oral and caudal parts of the spinal trigeminal nucleus project to the somatosensory thalamus in the rat. Eur. J. Neurosci. 21, 741–754.

Hallas, B. H. and Jacquin, M. F. 1990. Structure–function relationships in rat brain stem subnucleus interpolaris. IX. inputs from subnucleus caudalis. J. Neurophysiol. 64, 28–45.

Hansson, S. R., Mezey, E., and Hoffman, B. J. 1998. Ontogeny of vesicular monoamine transporter mRNAs VMAT1 and VMAT2. II. Expression in neural crest derivatives and their target sites in the rat. Brain Res. Dev. Brain Res. 110, 159–174.

Harding, A., Paxinos, G., and Halliday, G. 2004. The serotonin and tachykinin systems. In: Paxinos, G. (*ed.*), The Rat Nervous System, pp.1205–256, Elsevier.

Hayes, R. L., Price, D. D., Ruda, M. A., and Dubner, R. 1981. Neuronal activity in medullary dorsal horn of awake monkeys trained in a thermal discrimination task. II. Behavioral modulation of responses to thermal and mechanical stimuli. J. Neurophysiol. 46, 428–443.

Heckmann, S. M., Heckmann, J. G., Hilz, M. J., Popp, M., Marthol, H., Neundorfer, B., Henry, M. A., Johnson, L. R., Nousek-Goebl, N., and Westrum, L. E. 1996. Light microscopic localization of calcitonin gene-related peptide in the normal feline trigeminal system and following retrogasserian rhizotomy. J. Comp. Neurol. 365, 526–540.

Henry, M. A., Westrum, L. E., Bothwell, M., and Johnson, L. R. 1993. Nerve growth factor receptor (p75)-immunoreactivity in the normal adult feline trigeminal system and following retrogasserian rhizotomy. J. Comp. Neurol. 335, 425–436.

Hicar, M. D., Robinson, M. L., and Wu, L. C. 2002. Embryonic expression and regulation of the large zinc finger protein KRC. Genesis 33, 8–20.

Hildebrand, C., Fried, K., Tuisku, F., and Johansson, C. S. 1995. Teeth and tooth nerves. Prog. Neurobiol. 45, 165–222.

Hirata, H., Hu, J. W., and Bereiter, D. A. 1999. Responses of medullary dorsal horn neurons to corneal stimulation by CO_2 pulses in the rat. J. Neurophysiol. 82, 2092–2107.

Hirata, H., Okamoto, K., and Bereiter, D. A. 2003. $GABA_A$ receptor activation modulates corneal unit activity in rostral and caudal portions of trigeminal subnucleus caudalis. J. Neurophysiol. 90, 2837–2849.

Hirata, H., Okamoto, K., Tashiro, A., and Bereiter, D. A. 2004. A novel class of neurons at the trigeminal subnucleus interpolaris/caudalis transition region monitors ocular surface fluid status and modulates tear production. J. Neurosci. 24, 4224–4232.

Hirata, H., Takeshita, S., Hu, J. W., and Bereiter, D. A. 2000. Cornea–responsive medullary dorsal horn neurons: modulation by local opioid agonists and projections to thalamus and brainstem. J. Neurophysiol. 84, 1050–1061.

Hocevar, A., Tomsic, M., Praprotnik, S., Hojnik, M., Kveder, T., and Rozman, B. 2003. Parasympathetic nervous system dysfunction in primary Sjogren's syndrome. Ann. Rheum. Dis. 62, 702–704.

Hoffmann, K. D. and Matthews, M. A. 1990. Comparison of sympathetic neurons in orofacial and upper extremity nerves: implications for causalgia. J. Oral Maxillofac. Surg. 48, 720–726; discussion 727.

Holland, G. R. and Robinson, P. P. 1992. Axon populations in cat lingual and chorda tympani nerves. J. Dent. Res. 71, 1468–1472.

Hoyes, A. D. and Barber, P. 1976. Ultrastructure of the corneal nerves in the rat. Cell Tissue Res. 172, 133–144.

Hu, B., Chiang, C. Y., Hu, J. W., Dostrovsky, J. O., and Sessle, B. J. 2002. P2X receptors in trigeminal subnucleus

caudalis modulate central sensitization in trigeminal subnucleus oralis. J. Neurophysiol. 88, 1614–1624.
Hu, J. W. and Sessle, B. J. 1984. Comparison of responses of cutaneous nociceptive and nonnociceptive brain stem neurons in trigeminal subnucleus caudalis (medullary dorsal horn) and subnucleus oralis to natural and electrical stimulation of tooth pulp. J. Neurophysiol. 52, 39–53.
Huerta, M. F., Hashikawa, T., Gayoso, M. J., and Harting, J. K. 1985. The trigemino-olivary projection in the cat: contributions of individual subnuclei. J. Comp. Neurol. 241, 180–190.
Hu, J. W., Sun, K. Q., Vernon, H., and Sessle, B. J. 2005. Craniofacial inputs to upper cervical dorsal horn: implications for somatosensory information processing. Brain Res. 1044, 93–106.
Hunt, S. P. and Mantyh, P. W. 2001. The molecular dynamics of pain control. Nat. Rev. Neurosci. 2, 83–91.
Ichikawa, H. and Sugimoto, T. 2002. The difference of osteocalcin-immunoreactive neurons in the rat dorsal root and trigeminal ganglia: co-expression with nociceptive transducers and central projection. Brain Res. 958, 459–462.
Ichikawa, H., Deguchi, T., Nakago, T., Jacobowitz, D. M., and Sugimoto, T. 1994. Parvalbumin, calretinin and carbonic anhydrase in the trigeminal and spinal primary neurons of the rat. Brain Res. 655, 241–245.
Ichikawa, H., Itota, T., Torii, Y., Inoue, K., and Sugimoto, T. 1999. Osteocalcin-immunoreactive primary sensory neurons in the rat spinal and trigeminal nervous systems. Brain Res. 838, 205–209.
Ichikawa, H., Jacobowitz, D. M., and Sugimoto, T. 1993. Calretinin-immunoreactive neurons in the trigeminal and dorsal root ganglia of the rat. Brain Res. 617, 96–102.
Ichikawa, H., Jacobowitz, D. M., and Sugimoto, T. 1997. S100 protein-immunoreactive primary sensory neurons in the trigeminal and dorsal root ganglia of the rat. Brain Res. 748, 253–257.
Ikeda, M., Tanami, T., and Matsushita, M. 1984. Ascending and descending internuclear connections of the trigeminal sensory nuclei in the cat. A study with the retrograde and anterograde horseradish peroxidase technique. Neuroscience 12, 1243–1260.
Ikeda, T., Terayama, R., Jue, S., Sugiyo, S., Dubner, R., and Ren, K. 2003. Differential rostral projections of caudal brainstem neurons receiving trigeminal input after masseter inflammation. J. Comp. Neurol. 465, 220–233.
Isselee, H., Laat, A. D., Mot, B. D., and Lysens, R. 2002. Pressure-pain threshold variation in temporomandibular disorder myalgia over the course of the menstrual cycle. J. Orofac. Pain 16, 105–117.
Ito, M., Kurita, K., Ito, T., and Arao, M. 2002. Pain threshold and pain recovery after experimental stimulation in patients with burning mouth syndrome. Psychiatry Clin. Neurosci. 56, 161–168.
Izumi, H. 1999. Nervous control of blood flow in the orofacial region. Pharmacol. Ther. 81, 141–161.
Jacquin, M. F., Chiaia, N. L., Haring, J. H., and Rhoades, R. W. 1990. Intersubnuclear connections within the rat trigeminal brainstem complex. Somatosensory Motor Res. 7, 399–420.
Jacquin, M. F., Renehan, W. E., Mooney, R. D., and Rhoades, R. W. 1986. Structure–function relationships in rat medullary and cervical dorsal horns. I. Trigeminal primary afferents. J. Neurophysiol. 55, 1153–1186.
Jacquin, M. F., Semba, K., Egger, M. D., and Rhoades, R. W. 1983. Organization of HRP-labeled trigeminal mandibular primary afferent neurons in the rat. J. Comp. Neurol. 215, 397–420.
Jain, N., Qi, H. X., Catania, K. C., and Kaas, J. H. 2001. Anatomic correlates of the face and oral cavity representations in the somatosensory cortical area 3b of monkeys. J. Comp. Neurol. 429, 455–468.
Janig, W. 2003. Relationship between pain and autonomic phenomena in headache and other pain conditions. Cephalalgia 23, 43–48.
Jones, D. A., Rollman, G. B., and Brooke, R. I. 1997. The cortisol response to psychological stress in temporomandibular dysfunction. Pain 72, 171–182.
Julius, D. and Basbaum, A. I. 2001. Molecular mechanisms of nociception. Nature 413, 203–210.
Kai-Kai, M. A. 1989. Cytochemistry of the trigeminal and dorsal root ganglia and spinal cord of the rat. Comp. Biochem. Physiol. 93A, 183–193.
Kai-Kai, M. A. and Che, Y. M. 1995. Distribution of arginine-vasopressin in the trigeminal, dorsal root ganglia and spinal cord of the rat: depletion by capsaicin. Comp. Biochem. Physiol. A Physiol. 110, 71–78.
Kanjhan, R., Housley, G. D., Burton, L. D., Christie, D. L., Kippenberger, A., Thorne, P. R., Luo, L., and Ryan, A. F. 1999. Distribution of the P2X2 receptor subunit of the ATP-gated ion channels in the rat central nervous system. J. Comp. Neurol. 407, 11–32.
Katsarava, Z., Lehnerdt, G., Duda, B., Ellrich, J., Diener, H. C., and Kaube, H. 2002. Sensitization of trigeminal nociception specific for migraine but not pain of sinusitis. Neurology 59, 1450–1453.
Kawabata, A., Itoh, H., Kawao, N., Kuroda, R., Sekiguchi, F., Masuko, T., Iwata, K., and Ogawa, A. 2004. Activation of trigeminal nociceptive neurons by parotid PAR-2 activation in rats. Neuroreport 15, 1617–1621.
Keay, K. A., Feil, K., Gordan, B. D., Herbert, H., and Bandler, R. 1997. Spinal afferents to functionally distinct periaqueductal gray columns in the rat: an anterograde and retrograde tracing study. J. Comp. Neurol. 385, 207–229.
Kelleher, K. L., Matthaei, K. I., Leck, K. J., and Hendry, I. A. 1998. Developmental expression of messenger RNA levels of the alpha subunit of the GTP-binding protein, Gz, in the mouse nervous system. Brain Res. Dev Brain Res. 107, 247–253.
Kemppainen, P., Forster, C., and Handwerker, H. O. 2001. The importance of stimulus site and intensity in differences of pain-induced vascular reflexes in human orofacial regions. Pain 91, 331–338.
Kenshalo, D. R. 1960. Comparison of thermal sensitivity of the forehead, lip, conjunctiva and cornea. J. Appl. Physiol. 15, 987–991.
Kerr, F. W. L. 1961. Structural relation of trigeminal spinal tract to upper cervical roots and solitary nucleus in cat. Exp. Neurol. 4, 134–146.
Kerr, F. W. L. 1963. The divisional organization of afferent fibres of the trigeminal nerve. Brain 86, 721–732.
Khasar, S. G., Isenberg, W. M., Miao, F. J., Gear, R. W., Green, P. G., and Levine, J. D. 2001. Gender and gonadal hormone effects on vagal modulation of tonic nociception. J. Pain 2, 91–100.
Khasar, S. G., Miao, F. J., Janig, W., and Levine, J. D. 1998. Vagotomy-induced enhancement of mechanical hyperalgesia in the rat is sympathoadrenal-mediated. J. Neurosci. 15, 3043–3049.
Kido, M. A., Kiyoshima, T., Ibuki, T., Shimizu, S., Kondo, T., Terada, Y., and Tanaka, T. 1995. A topographical and ultrastructural study of sensory trigeminal nerve endings in the rat temporomandibular joint as demonstrated by anterograde transport of wheat germ agglutinin-horseradish peroxidase (WGA-HRP). J. Dental Res. 74, 1353–1359.
Kim, S. J., Lee, J. W., Chun, H. S., Joh, T. H., and Son, J. H. 1997. Monitoring catecholamine differentiation in the

embryonic brain and peripheral neurons using *E. coli* lacZ as a reporter gene. Mol. Cells 7, 394–398.
Kirchner, A., Birklein, F., Stefan, H., and Handwerker, H. O. 2000. Left vagus nerve stimulation suppresses experimentally induced pain. Neurology 55, 1167–1171.
Kitahama, K., Nagatsu, I., Geffard, M., and Maeda, T. 2000. Distribution of dopamine-immunoreactive fibers in the rat brainstem. J. Chem. Neuroanat. 18, 1–9.
Kitchener, P. D., Dziegielewska, K. M., Knott, G. W., Miller, J. M., Nawratil, P., Potter, A. E., and Saunders, N. R. Fetuin expression in the dorsal root ganglia and trigeminal ganglia of perinatal rats. Int. J. Dev. Neurosci. 15, 717–727.
Kitt, C. A., Gruber, K., Davis, M., Woolf, C. J., and Levine, J. D. 2000. Trigeminal neuralgia: opportunities for research and treatment. Pain 85, 3–7.
Klein, R., Smeyne, R. J., Wurst, W., Long, L. K., Auerbach, B. A., Joyner, A. L., and Barbacid, M. 1993. Targeted disruption of the trkB neurotrophin receptor gene results in nervous system lesions and neonatal death. Cell 75, 113–122.
Kopp, S. 2001. Neuroendocrine, immune, and local responses related to temporomandibular disorders. J. Orofacial Pain 15, 9–28.
Korszun, A. 2002. Facial pain, depression and stress-connections and directions. J. Oral Pathol. Med. 31, 615–619.
Korszun, A., Young, E. A., Singer, K., Carlson, N. E., Brown, M. B., and Crofford, L. 2002. Basal circadian cortisol secretion in women with temporomandibular disorders. J. Dent. Res. 81, 279–283.
Krout, K. E., Belzer, R. E., and Loewy, A. D. 2002. Brainstem projections to midline and intralaminar thalamic nuclei of the rat. J. Comp. Neurol. 448, 53–101.
Kruger, L. and Young, R. F. 1981. Specialized features of the trigeminal nerve and its central connections. In: The Cranial Nerves (*eds*. M. Samii and P. J. Jannetta), pp. 274–301. Springer-Verlag.
Kruger, L., Saporta, S., and Feldman, S. G. 1977. Axonal Transport Studies of the Sensory Trigeminal Complex. In: Pain in the Trigeminal Region (*eds*. D. J. Anderson and B. Matthews), pp. 191–201. Elsevier.
Kruger, L., Sternini, C., Brecha, N. C., and Mantyh, P. W. 1988. Distribution of calcitonin-gene-related peptide immunoreactivity in relation to the rat central somatosensory projection. J. Comp. Neurol. 273, 149–162.
Kumada, M., Dampney, R. A. L., and Reis, D. J. 1977. The trigeminal depressor response: a novel vasodepressor response originating from the trigeminal system. Brain Res. 119, 305–326.
Lavigne, G., Woda, A., Truelove, E., Ship, J. A., Dao, T., and Goulet, J. P. 2005. Mechanisms associated with unusual orofacial pain. J. Orofac. Pain 19, 9–21.
Lennartsson, B. 1979. Muscle spindles in the human anterior digastric muscle. Acta Odontol. Scand. 37, 329–333.
LeResche, L. 1997. Epidemiology of temporomandibular disorders: implications for the investigation of etiological factors. Crit. Rev. Oral Biol. Med. 8, 291–305.
LeResche, L., Mancl, L., Sherman, J. J., Gandara, B., and Dworkin, S. F. 2003. Changes in temporomandibular pain and other symptoms across the menstrual cycle. Pain 106, 253–261.
Levine, J. D., Collier, D. H., Basbaum, A. I., Moskowitz, M. A., and Helms, C. A. 1985. Hypothesis: the nervous system may contribute to the pathophysiology of rheumatoid arthritis. J. Rheumatol. 12, 406–411.
Levitt, P. and Moore, R. Y. 1979. Origin and organization of brainstem catecholamine innervation in the rat. J. Comp. Neurol. 186, 505–528.
Levy, D. and Strassman, A. M. 2002. Distinct sensitizing effects of the cAMP-PKA second messenger cascade on rat dural mechanonociceptors. J. Physiol. 538, 483–493.
Lewin, G. R., Lu, Y., and Park, T. J. 2004. A plethora of painful molecules. Curr. Opin. Neurobiol. 14, 443–449.
Li, Y. Q., Takada, M., Ohishi, H., Shinonaga, Y., and Mizuno, N. 1992. Trigeminal ganglion neurons which project by way of axon collaterals to both the caudal spinal trigeminal and the principal sensory trigeminal nuclei. Brain Res. 594, 155–159.
Linden, R. W. 1978. Properties of intraoral mechanoreceptors represented in the mesencephalic nucleus of the fifth nerve in the cat. J. Physiol. 279, 395–408.
Lipton, J. A., Ship, J. A., and Larach-Robinson, D. 1993. Estimated prevalence and distribution of reported orofacial pain in the United States. J. Am. Dent. Assoc. 124, 115–121.
Liu, Y., Broman, J., and Edvinsson, L. 2004. Central projections of sensory innervation of the rat superior sagittal sinus. Neuroscience 129, 431–437.
Lu, J., Hathaway, C. B., and Bereiter, D. A. 1993. Adrenalectomy enhances Fos-like immunoreactivity within the spinal trigeminal nucleus induced by noxious thermal stimulation of the cornea. Neuroscience 54, 809–818.
Ma, P. M. 1991. The barrelettes – architectonic vibrissal representations in the brainstem trigeminal complex of the mouse. I. Normal structural organization. J. Comp. Neurol. 309, 161–199.
Macfarlane, T. V., Blinkhorn, A. S., Davies, R. M., Kincey, J., and Worthington, H. V. 2002a. Association between female hormonal factors and oro-facial pain: study in the community. Pain 97, 5–10.
Macfarlane, T. V., Blinkhorn, A. S., Davies, R. M., Kincey, J., and Worthington, H. V. 2002b. Oro-facial pain in the community: prevalence and associated impact. Comm. Dent. Oral Epidemiol. 30, 52–60.
MacGregor, E. A. and Hackshaw, A. 2004. Prevalence of migraine on each day of the natural menstrual cycle. Neurology 63, 351–353.
Maixner, W., Fillingim, R., Sigurdsson, A., Kincaid, S., and Silva, S. 1998. Sensitivity of patients with temporomandibular disorders to experimentally evoked pain: evidence for altered temporal summation of pain. Pain 76, 71–81.
Maklad, A., Quinn, T., and Fritzsch, B. 2001. Intracranial distribution of the sympathetic system in mice: DiI tracing and immunocytochemical labeling. Anat. Rec. 263, 99–111.
Malick, A. and Burstein, R. 1998. Cells of origin of the trigeminohypothalamic tract in the rat. J. Comp. Neurol. 400, 125–144.
Manger, P. R., Woods, T. M., and Jones, E. G. 1995. Representation of the face and intraoral structures in area 3b of the squirrel monkey (*Saimiri sciureus*) somatosensory cortex, with special reference to the ipsilateral representation. J. Comp. Neurol. 362, 597–607.
Mantle-St, John, L. A. and Tracey, D. J. 1987. Somatosensory nuclei in the brainstem of the rat: independent projections to the thalamus and cerebellum. J. Comp. Neurol. 255, 259–271.
Mantyh, P. W. 1982. The ascending input to the midbrain periaqueductal gray of the primate. J. Comp. Neurol. 211, 50–64.
Mantyh, P. W., Allen, C. J., Rogers, S., DeMaster, E., Ghilardi, J. R., Mosconi, T., Kruger, L., Mannon, P. J., Taylor, I. L., and Vigna, S. R. 1994. Some sensory neurons express neuropeptide Y receptors: potential paracrine inhibition of primary afferent nociceptors following peripheral nerve injury. J. Neurosci. 14, 3958–3968.
Manzoni, G. C. and Torelli, P. 2005. Epidemiology of typical and atypical craniofacial neuralgias. Neurol. Sci. 26, S65–S67.
Marfurt, C. F. 1981. The somatotopic organization of the cat trigeminal ganglion as determined by the horseradish peroxidase technique. Anat. Rec. 201, 105–118.

Marfurt, C. F. and del Toro, D. R. 1987. Corneal sensory pathway in the rat: a horseradish peroxidase tracing study. J. Comp. Neurol. 261, 450–459.

Marfurt, C. F. and Echtenkamp, S. F. 1988. Central projections and trigeminal ganglion location of corneal afferent neurons in the monkey, *Macaca fascicularis*. J. Comp. Neurol. 272, 370–382.

Marfurt, C. F. and Rajchert, D. M. 1991. Trigeminal primary afferent projections to ''non-trigeminal'' areas of the rat central nervous system. J. Comp. Neurol. 303, 489–511.

Marfurt, C. F. and Turner, D. F. 1984. The central projections of tooth pulp afferent neurons in the rat as determined by the transganglionic transport of horseradish peroxidase. J. Comp. Neurol. 223, 535–547.

Margeta-Mitrovic, M., Mitrovic, I., Riley, R. C., Jan, L. Y., and Basbaum, A. I. 1999. Immunohistochemical localization of GABAB receptors in the rat central nervous system. J. Comp. Neurol. 405, 299–321.

Martin-Schild, S., Gerall, A. A., Kastin, A. J., and Zadina, J. E. 1999. Differential distribution of endomorphin 1- and endomorphin2-like immunoreactivies in the CNS of the rodent. J. Comp. Neurol. 405, 450–471.

Matthews, B. 1989. Autonomic mechanisms in oral sensations. Proc. Finn. Dent. Soc. 85, 365–373.

McLachlan, E. M., Janig, W., Devor, M., and Michaelis, M. 1993. Peripheral nerve injury triggers noradrenergic sprouting within dorsal root ganglia. Nature 363, 543–546.

McNeill, D. L., Chandler, M. J., Fu, Q. G., and Foreman, R. D. 1991. Projection of nodose ganglion cells to the rat upper cervical spinal cord in the rat. Brain Res. Bull. 27, 151–155.

Menetrey, D. and Basbaum, A. I. 1987. Spinal and trigeminal projections to the nucleus of the solitary tract: a possible substrate for somatovisceral and viscerovisceral reflex activation. J. Comp. Neurol. 255, 439–450.

Meng, I. D. and Bereiter, D. A. 1996. Differential distribution of Fos-like immunoreactivity in the spinal trigeminal nucleus after noxious and innocuous thermal and chemical stimulation of rat cornea. Neuroscience 72, 243–254.

Meng, I. D., Hu, J. W., and Bereiter, D. A. 1998. Differential effects of morphine on corneal-responsive neurons in rostral versus caudal regions of spinal trigeminal nucleus in the rat. J. Neurophysiol. 79, 2593–2602.

Meng, I. D., Hu, J. W., Benetti, A. P., and Bereiter, D. A. 1997. Encoding of corneal input in two distinct regions of the spinal trigeminal nucleus in the rat: cutaneous receptive field properties, responses to thermal and chemical stimulation, modulation by diffuse noxious inhibitory controls, and projections to the parabrachial area. J. Neurophysiol. 77, 43–56.

Merchenthaler, I., Lane, M. V., Numan, S., and Dellovade, T. L. 2004. Distribution of estrogen receptor a and b in the mouse central nervous system: *in vivo* autoradiographic and immunocytochemical analyses. J. Comp. Neurol. 473, 270–291.

Meunier, A., Latremoliere, A., Mauborgne, A., Bourgoin, S., Kayser, V., Cesselin, F., Hamon, M., and Pohl, M. 2005. Attenuation of pain-related behavior in a rat model of trigeminal neuropathic pain by viral-driven enkephalin overproduction in trigeminal ganglion neurons. Mol. Ther. 11, 608–616.

Meyer, R. A., Ringkamp, M., Campbell, J. N., and Raja, S. N. 2006. Peripheral Mechanisms of Cutaneous Nociception. In: Wall and Melzack's Textbook of Pain (*eds*. S. B. McMahon and M. Koltzenburg), pp. 3–34. Elsevier.

Moiseenkova, V., Bell, B., Motamedi, M., Wozniak, E., and Christensen, B. 2003. Wide-band spectral tuning of heat receptors in the pit organ of the copperhead snake (*Crotalinae*). Am. J. Physiol. Regul. Integr. Comp. Physiol. 284, R598–R606.

Molenaar, G. J. 1978. The sensory trigeminal system of a snake in the possession of infrared receptors. I. The sensory trigeminal nuclei. J. Comp. Neurol. 179, 123–135.

Molliver, D. C. and Snider, W. D. 1997. Nerve growth factor receptor TrkA is down-regulated during postnatal development by a subset of dorsal root ganglion neurons. J. Comp. Neurol. 381, 428–438.

Moore, C. I. 2004. Frequency-dependent processing in the vibrissa sensory system. J. Neurophysiol. 91, 2390–2399.

Mosconi, T., Snider, W. D., and Jacquin, M. F. 2001. Neurotrophin receptor expression in retrogradely labeled trigeminal nociceptors – comparisons with spinal nociceptors. Somatosens. Mot. Res. 18, 312–321.

Mukasa, T., Urase, K., Momoi, M. Y., Kimura, I., and Momoi, T. 1997. Specific expression of CPP32 in sensory neurons of mouse embryos and activation of CPP32 in the apoptosis induced by a withdrawal of NGF. Biochem. Biophys. Res. Commun. 231, 770–774.

Muller, L. J., Marfurt, C. F., Kruse, F., and Tervo, T. M. 2003. Corneal nerves: structure, contents and function. Exp. Eye Res. 76, 521–542.

Nakamura, K., Kaneko, T., Yamashita, Y., Hasegawa, H., Katoh, H., and Negishi, M. 2000. Immunohistochemical localization of prostaglandin EP3 receptor in the rat nervous system. J. Comp. Neurol. 421, 543–569.

Nakaya, Y., Kaneko, T., Shigemoto, R., Nakanishi, S., and Mizuno, N. 1994. Immunohistochemical localization of substance P receptor in the central nervous system of the adult rat. J. Comp. Neurol. 347, 249–274.

Nauta, H. J., Wehman, J. C., Koliatsos, V. E., Terrell, M. A., and Chung, K. 1999. Intraventricular infusion of nerve growth factor as the cause of sympathetic fiber sprouting in sensory ganglia. J. Neurosurg. 91, 447–453.

Ndiaye, A., Pinganaud, G., Buisseret-Delmas, C., Buisseret, P., and Vanderwerf, F. 2002. Organization of trigeminocollicular connections and their relations to the sensory innervation of the eyelids in the rat. J. Comp. Neurol. 448, 373–387.

Neuhuber, W. L. and Zenker, W. 1989. Central distribution of cervical primary afferents in the rat, with emphasis on proprioceptive projections to vestibular, perihypoglossal, and upper thoracic spinal nuclei. J. Comp. Neurol. 280, 231–253.

Nishimori, T., Sera, M., Suemune, S., Yoshida, A., Tsuru, K., Tsuiki, Y., Akisaka, T., Okamoto, T., Dateoka, Y., and Shigenaga, Y. 1986. The distribution of muscle primary afferents from the masseter nerve to the trigeminal sensory nuclei. Brain Res. 372, 375–381.

Noden, D. M. 1991. Vertebrate craniofacial development: the relation between ontogenetic process and morphological outcome. Brain Behav. Evol. 38, 190–225.

Nomura, S., Itoh, K., Sugimoto, T., Yasui, Y., Kamiya, H., and Mizuno, N. 1986. Mystacial vibrissae representation within the trigeminal sensory nuclei of the cat. J. Comp. Neurol. 253, 121–133.

Nurmikko, T. J. and Eldridge, P. R. 2001. Trigeminal neuralgia – pathophysiology, diagnosis and current treatment. Br. J. Anaesth. 87, 117–132.

Ohishi, H., Neki, A., and Mizuno, N. 1998. Distribution of a metabotropic glutamate receptor, mGluR2, in the central nervous system of the rat and mouse: an immunohistochemical study with a monoclonal antibody. Neurosci. Res. 30, 65–82.

Okabe, H., Okubo, T., Adachi, H., Ishikawa, T., and Ochi, Y. 1997. Immunohistochemical demonstration of cytokeratin in human embryonic neurons arising from placodes. Brain Dev. 19, 347–352.

Okamoto, K., Hirata, H., Takeshita, S., and Bereiter, D. A. 2003. Response properties of TMJ neurons in superficial laminae

at the spinomedullary junction of female rats vary over the estrous cycle. J. Neurophysiol. 89, 1467–1477.
Okuse, K., Chaplan, S. R., McMahon, S. B., Luo, Z. D., Calcutt, N. A., Scott, B. P., Akopian, A. N., and Wood, J. N. 1997. Regulation of expression of the sensory neuron-specific sodium channel SNS in inflammatory and neuropathic pain. Mol. Cell Neurosci. 10, 196–207.
Oliveras, J. L., Maixner, W., Dubner, R., Bushnell, M. C., Jr., Kenshalo, D. R., Duncan, G. H., Thomas, D. A., and Bates, R. 1986. The medullary dorsal horn: a target for the expression of opiate effects on the perceived intensity of noxious heat. J. Neurosci. 6, 3086–3093.
Olszewski, J. 1950. On the anatomical and functional organization of the trigeminal nucleus. J. Comp. Neurol. 92, 401–413.
Pajot, J., Ressot, C., Ngom, I., and Woda, A. 2003. Gonadectomy induces site-specific differences in nociception in rats. Pain 104, 367–373.
Panneton, W. M. 1991. Primary afferent projections from the upper respiratory tract in the muskrat. J. Comp. Neurol. 308, 51–65.
Panneton, W. M. and Burton, H. 1981. Corneal and periocular representation within the trigeminal sensory complex in the cat studied with transganglionic transport of horseradish peroxidase. J. Comp. Neurol. 199, 327–344.
Panneton, W. M. and Burton, H. 1985. Projections from the paratrigeminal nucleus and the medullary and spinal dorsal horns to the peribrachial area in the cat. Neuroscience 15, 779–797.
Panneton, W. M., Johnson, S. N., and Christensen, N. D. 1994. Trigeminal projections to the peribrachial region in the muskrat. Neuroscience 58, 605–625.
Pappagallo, M., Oaklander, A. L., Quatrano-Piacentini, A. L., Clark, M. R., and Raja, S. N. 2000. Heterogenous patterns of sensory dysfunction in postherpetic neuralgia suggest multiple pathophysiologic mechanisms. Anesthesiology 92, 691–698.
Penfield, W. and Rasmussen, T. 1950. The Cerebral Cortex of Man: a Clinical Study of Localization of Function. Macmillan.
Petersen, C. C. 2003. The barrel cortex – integrating molecular, cellular and systems physiology. Pflugers Arch. 447, 126–134.
Petralia, R. S., Yokotani, N., and Wenthold, R. J. 1994. Light and electron microscope distribution of the NMDA receptor subunit NMDAR1 in the rat nervous system using a selective anti-peptide antibody. J. Neurosci. 14, 667–696.
Pfaller, K. and Arvidsson, J. 1988. Central distribution of trigeminal and upper cervical primary afferents in the rat studied by anterograde transport of horseradish peroxidase conjugated to wheat germ agglutinin. J. Comp. Neurol. 268, 91–108.
Pfeiffer, B., Buse, E., Meyermann, R., and Hamprecht, B. 1995. Immunocytochemical localization of glycogen phosphorylase in primary sensory ganglia of the peripheral nervous system of the rat. Histochem. Cell Biol. 103, 69–74.
Pioro, E. P. and Cuello, A. C. 1990. Distribution of nerve growth factor receptor-like immunoreactivity in the adult rat central nervous system. Effect of colchicine and correlation with the cholinergic system – II. Brainstem, cerebellum and spinal cord. Neuroscience 34, 89–110.
Pirker, S., Schwarzer, C., Wieselthaler, A., Sieghart, W., and Sperk, G. 2000. GABA(A) receptors: immunocytochemical distribution of 13 subunits in the adult rat brain. Neuroscience 101, 815–850.
Potrebic, S., Ahn, A. H., Skinner, K., Fields, H. L., and Basbaum, A. I. 2003. Peptidergic nociceptors of both trigeminal and dorsal root ganglia express serotonin 1D receptors: implications for the selective antimigraine action of triptans. J. Neurosci. 23, 10988–10997.
Price, D. D. and Dubner, R. 1977. Neurones that subserve the sensori-discriminative aspects of pain. Pain 3, 307–338.
Price, D. D., Dubner, R., and Hu, J. W. 1976. Trigeminothalamic neurons in nucleus caudalis responsive to tactile, thermal, and nociceptive stimulation of monkey's face. J. Neurophysiol. 39, 936–953.
Price, D. D., Greenspan, J. D., and Dubner, R. 2003. Neurons involved in the exteroceptive function of pain. Pain 106, 215–219.
Proske, U., Gregory, J. E., and Iggo, A. 1998. Sensory receptors in monotremes. Phil. Trans. R. Soc. Lond. B Biol. Sci. 353, 1187–1198.
Puri, V., Cui, L., Liverman, C. S., Roby, K. F., Klein, R. M., Welch, K. M., and Berman, N. E. 2005. Ovarian steroids regulate neuropeptides in the trigeminal ganglion. Neuropeptides 39, 409–417.
Ramien, M., Roucco, I., Cuello, A. C., Louis, M. S., and Ribeiro-da-Silva, A. 2004. Parasympathetic nerve fibers invade the upper dermis following sensory denervation of the rat lower lip skin. J. Comp. Neurol. 469, 83–95.
Randich, A. and Gebhart, G. F. 1992. Vagal afferent modulation of nociception. Brain Res. Rev. 17, 77–99.
Remple, M. S., Henry, E. C., and Catania, K. C. 2003. Organization of somatosensory cortex in the laboratory rat (Rattus norvegicus): evidence for two lateral areas joined at the representation of the teeth. J. Comp. Neurol. 467, 105–118.
Renehan, W. E. and Jacquin, M. F. 1993. Anatomy of Central Nervous System Pathways Related to Head Pain. In: The Headaches (*eds*. J. Olesen, P. Tfelt-Hansen, and K. Welch), pp. 59–68. Raven.
Reuss, S. 1999. Trigeminal innervation of the mammalian pineal gland. Microsc. Res. Tech. 46, 305–309.
Rodrigo, J., Springall, D. R., Uttenthal, O., Bentura, M. L., Abadia-Molina, F., Riveros-Moreno, V., Martinez-Murillo, R., Polak, J. M., and Moncada, S. 1994. Localization of nitric oxide synthase in the adult rat brain. Phil. Trans. R. Soc. Lond. B Biol. Sci. 345, 175–221.
Rodrigo, J., Suburo, A. M., Bentura, M. L., Fernandez, T., Nakade, S., Mikoshiba, K., Martinez-Murillo, R., and Polak, J. M. 1993. Distribution of the inositol 1,4,5-trisphosphate receptor, P400, in adult rat brain. J. Comp. Neurol. 337, 493–517.
Roveroni, R. C., Prada, C. A., Cecilia, M., Veiga, F. A., and Tambeli, C. H. 2001. Development of a behavioral model of TMJ pain in rats: the TMJ formalin test. Pain 94, 185–191.
Rozsa, A. J. and Beuerman, R. W. 1982. Density and organization of free nerve endings in the corneal epithelium of the rabbit. Pain 14, 105–120.
Ruan, H. Z., Moules, E., and Burnstock, G. 2004. Changes in P2X3 purinoceptors in sensory ganglia of the mouse during embryonic and postnatal development. Histochem. Cell Biol. 122, 539–551.
Sandstedt, P. and Sorensen, S. 1995. Neurosensory disturbances of the trigeminal nerve: a long-term follow-up of traumatic injuries. J. Oral Maxillofac. Surg. 53, 498–505.
Sarlani, E. and Greenspan, J. D. 2003. Evidence for generalized hyperalgesia in temporomandibular disorders patients. Pain 102, 221–226.
Sarlani, E. and Greenspan, J. D. 2005. Why look in the brain for answers to temporomandibular disorder pain? Cells Tissues Organs 180, 69–75.
Sarlani, E., Schwartz, A. H., Greenspan, J. D., and Grace, E. G. 2003. Facial pain as first manifestation of lung cancer: a case of lung cancer-related cluster headache and a review of the literature. J. Orofac. Pain 17, 262–267.

Saxon, D. W. and Hopkins, D. A. 1998. Efferent and collateral organization of paratrigeminal nucleus projections: an anterograde and retrograde fluorescent tracer study in the rat. J. Comp. Neurol. 402, 93–110.

Schaller, B. 2004. Trigeminocardiac reflex. A clinical phenomenon or a new physiological entity? J. Neurol. 251, 658–665.

Schepelmann, K., Ebersberger, A., Pawlak, M., Oppmann, M., and Messlinger, K. 1999. Response properties of trigeminal brain stem neurons with input from dura mater encephali in the rat. Neuroscience 90, 543–554.

Scholz, J. and Woolf, C. J. 2002. Can we conquer pain? Nat. Neurosci. 5, 1062–1067.

Sessle, B. J. 2000. Acute and chronic craniofacial pain: brainstem mechanisms of nociceptive transmission and neuroplasticity, and their clinical correlates. Crit. Rev. Oral Biol. Med. 11, 57–91.

Sessle, B. J., Hu, J. W., Dubner, R., and Lucier, G. E. 1981. Functional properties of neurons in cat trigeminal subnucleus caudalis (medullary dorsal horn). II. Modulation of responses to noxious and nonnoxious stimuli by periaqueductal gray, nucleus raphe magnus, cerebral cortex, and afferent influences, and effect of naloxone. J Neurophysiol. 45, 193–207.

Shenker, N., Haigh, R., Roberts, E., Mapp, P., Harris, N., and Blake, D. 2003. A review of contralateral responses to a unilateral inflammatory lesion. Rheumatology 42, 1279–1286.

Shigenaga, Y., Chen, I. C., Suemune, S., Nishimori, T., Nasution, I. D., Yoshida, A., Sato, H., Okamoto, T., Sera, M., and Hosoi, M. 1986a. Oral and facial representation within the medullary and upper cervical dorsal horns in the cat. J. Comp. Neurol. 243, 388–408.

Shigenaga, Y., Nakatani, Z., Nishimori, T., Suemune, S., Kuroda, R., and Matano, S. 1983. The cells of origin of cat trigeminothalamic projections: especially in the caudal medulla. Brain Res. 277, 20l–222.

Shigenaga, Y., Okamoto, T., Nishimori, T., Suemune, S., Nasution, I. D., Chen, I. C., Tsuru, K., Yoshida, A., Tabuchi, K., Hosoi, M., and Tsuru, H. 1986b. Oral and facial representation in the trigeminal principal and rostral spinal nuclei of the cat. J. Comp. Neurol. 244, 1–18.

Shigenaga, Y., Sera, M., Nishimori, T., Suemune, S., Nishimura, M., Yoshida, A., and Tsuru, K. 1988. The central projection of masticatory afferent fibers to the trigeminal sensory nuclear complex and upper cervical spinal cord. J. Comp. Neurol. 268, 489–507.

Shigenaga, Y., Suemune, S., Nishimura, M., Nishimori, T., Sato, H., Ishidori, H., Yoshida, A., Tsuru, K., Tsuiki, Y., Dakeoka, Y., Nasution, I. D., and Hosoi, M. 1986c. Topographic representation of lower and upper teeth within the trigeminal sensory nuclei of adult cat as demonstrated by the transganglionic transport of horseradish peroxidase. J. Comp. Neurol. 251, 299–3l6.

Shughrue, P. J., Lane, M. V., and Merchenthaler, I. 1997. Comparative distribution of estrogen receptor-a and -b mRNA in the rat central nervous system. J. Comp. Neurol. 388, 507–525.

Silverman, J. D. and Kruger, L. 1985. Projections of the rat trigeminal sensory nuclear complex demonstrated by multiple fluorescent dye retrograde transport. Brain Res. 361, 383–388.

Simonian, S. X., Delaleu, B., Caraty, A., and Herbison, A. E. 1998. Estrogen receptor expression in brainstem noradrenergic neurons of the sheep. Neuroendocrinology 67, 392–402.

Sjoqvist, O. 1938. Studies on pain conduction in the trigeminal nerve. A contribution to the surgical treatment of facial pain. Acta Psychiat. Neurol. Scand. 1, 1–139.

Sobreviela, T., Clary, D. O., Reichardt, L. F., Brandabur, M. M., Kordower, J. H., and Mufson E. J. 1994. TrkA-immunoreactive profiles in the central nervous system: colocalization with neurons containing p75 nerve growth factor receptor, choline acetyltransferase, and serotonin. J. Comp. Neurol. 350, 587–611.

Son, J. H., Min, N., and Joh, T. H. 1996. Early ontogeny of catecholaminergic cell lineage in brain and peripheral neurons monitored by tyrosine hydroxylase-lacZ transgene. Brain Res. Mol. Brain Res. 36, 300–308.

Steinbusch, H. W. M. 1981. Distribution of serotonin-immunoreactivity in the central nervous system of the rat-cell bodies and terminals. Neuroscience 6, 557–618.

Stenholm, E., Bongenhielm, U., Ahlquist, M., and Fried, K. 2002. VRl- and VRL-l-like immunoreactivity in normal and injured trigeminal dental primary sensory neurons of the rat. Acta Odontol. Scand. 60, 72–79.

Strack, S., Wadzinski, B. E., and Ebner, F. F. 1996. Localization of the calcium/calmodulin-dependent protein phosphatase, calcineurin, in the hindbrain and spinal cord of the rat. J. Comp. Neurol. 375, 66–76.

Strassman, A. M. and Vos, B. P. 1993. Somatotopic and laminar organization of Fos-like immunoreactivity in the medullary and cervical dorsal horn induced by noxious facial stimulation in the rat. J. Comp. Neurol. 331, 495–516.

Strassman, A. M., Potrebic, S., and Maciewicz, R. J. 1994. Anatomical properties of brainstem trigeminal neurons that respond to electrical stimulation of dural blood vessels. J. Comp. Neurol. 346, 349–365.

Sugimoto, T., Fujiyoshi, Y., He, Y. F., Xiao, C., and Ichikawa, H. 1997a. Trigeminal primary projection to the rat brain stem sensory trigeminal nuclear complex and surrounding structures revealed by anterograde transport of cholera toxin B subunit-conjugated and *Bandeiraea simplicifolia* isolectin B4-conjugated horseradish peroxidase. Neurosci. Res. 28, 361–371.

Sugimoto, T., Fujiyoshi, Y., Xiao, C., He, Y. F., and Ichikawa, H. 1997b. Central projection of calcitonin gene-related peptide (CGRP)- and substance P (SP)-immunoreactive trigeminal primary neurons in the rat. J. Comp. Neurol. 378, 425–442.

Svensson, P., Bjerring, P., Arendt-Nielsen, L., and Kaaber, S. 1993. Sensory and pain thresholds to orofacial argon laser stimulation in patients with chronic burning mouth syndrome. Clin. J. Pain 9, 207–215.

Takemura, M., Nagase, Y., Yoshida, A., Yasuda, K., Kitamura, S., Shigenaga, Y., and Matano, S. 1993. The central projections of the monkey tooth pulp afferent neurons. Somatosens. Mot. Res. 10, 217–227.

Takemura, M., Sugimoto, T., and Sakai, A. 1987. Topographic organization of central terminal region of different sensory branches of the rat mandibular nerve. Exp. Neurol. 96, 540–557.

Takei, M., Shiraiwa, H., Azuma, T., Hayashi, Y., Seki, N., and Sawada, S. 2005. The possible etiopathogenic genes of Sjogren's syndrome. Autoimmun. Rev. 4, 479–484.

Tal, M. and Devor, M. 1992. Ectopic discharge in injured nerves: comparison of trigeminal and somatic afferents. Brain Res. 579, 148–151.

Talley, E. M., Rosen, D. I., Lee, A., Guyenet, P. G., and Lynch, K. R. 1996. Distribution of alpha 2A-adrenergic receptor-like immunoreactivity in the rat central nervous system. J. Comp. Neurol. 372, 111–134.

Tamura, S., Morikawa, Y., Miyajima, A., and Senba, E. 2003. Expression of oncostatin M receptor beta in a specific subset of nociceptive sensory neurons. Eur. J. Neurosci. 17, 2287–2298.

Tanimoto, T., Takeda, M., and Matsumoto, S. 2002. Suppressive effect of vagal afferents on cervical dorsal horn neurons responding to tooth pulp electrical stimulation in the rat. Exp. Brain Res. 145, 468–479.

Tashiro, T., Higo, S., and Matsuyama, T. 1984. Soma size comparison of the trigeminal ganglion cells giving rise to the ascending and descending tracts: a horseradish peroxidase study in the cat. Exp. Neurol. 84, 37–46.

Tatehata, T., Shiosaka, S., Wanaka, A., Rao, Z. R., and Tohyama, M. 1987. Immunocytochemical localization of the choline acetyltransferase containing neuron system in the rat lower brain stem. J. Hirnforsch. 28, 707–716.

Tenenbaum, H. C., Mock, D., Gordan, A. S., Goldberg, M. B., Grossi, M. L., Locker, D., and Davis, K. D. 2001. Sensory and affective components of orofacial pain: is it all in your brain? Crit. Rev. Oral Biol. Med. 12, 455–468.

Thackray, A. M. and Field, H. J. 1996. Differential effects of famciclovir and valaciclovir on the pathogenesis of herpes simplex virus in a murine infection model including reactivation from latency. J. Infect. Dis. 173, 291–299.

Thor, K. B., Blitz-Siebert, A., and Helke, C. J. 1992. Autoradiographic localization of 5HT1 binding sites in the medulla oblongata of the rat. Synapse 10, 185–205.

Toda, K., Ishii, N., and Nakamura, Y. 1997. Characteristics of mucosal nociceptors in the rat oral cavity: an in vitro study. Neurosci. Lett. 228, 95–98.

Treede, R. D., Meyer, R. A., Raja, S. N., and Campbell, J. N. 1992. Peripheral and central mechanisms of cutaneous hyperalgesia. Prog. Neurobiol. 38, 397–421.

Trowbridge, H. O., Franks, M., Korostoff, E., and Emling, R. 1980. Sensory response to thermal stimulation in human teeth. J. Endod. 6, 405–412.

Trulsson, M. and Johansson, R. S. 2002. Orofacial mechanoreceptors in humans: encoding characteristics and responses during natural orofacial behaviors. Behav. Brain Res. 135, 27–33.

Tsuzuki, K., Fukuoka, T., Sakagami, M., and Noguchi, K. 2003. Increase of preprotachykinin mRNA in the uninjured mandibular neurons after rat infraorbital nerve transection. Neurosci. Lett. 345, 57–60.

Tsuzuki, K., Kondo, E., Fukuoka, T., Yi, D., Tsujino, H., Sakagami, M., and Noguchi, K. 2001. Differential regulation of P2X(3) mRNA expression by peripheral nerve injury in intact and injured neurons in the rat sensory ganglia. Pain 91, 351–360.

Van Bijsterveld, O. P., Kruize, A. A., and Bleys, R. L. 2003. Central nervous system mechanisms in Sjogren's syndrome. Br. J. Ophthalmol. 87, 128–130.

Van Ham, J. J. and Yeo, C. H. 1992. Somatosensory trigeminal projections to the inferior olive, cerebellum and other precerebellar nuclei in rabbits. Eur. J. Neurosci. 4, 302–317.

Vass, Z., Shore, S. E., Nuttall, A. L., Jansco, G., Brechtelsbauer, P. B., and Miller, J. M. 1997. Trigeminal ganglion innervation of the cochlea – a retrograde transport study. Neuroscience 79, 605–615.

Veinante, P., Jacquin, M. F., and Deschenesm, M. 2000. Thalamic projections from the whisker-sensitive regions of the spinal trigeminal complex in the rat. J. Comp. Neurol. 420, 233–243.

Verge, V. M., Wiesenfeld-Hallin, Z., and Hokfelt, T. 1993. Cholecystokinin in mammalian primary sensory neurons and spinal cord: *in situ* hybridization studies in rat and monkey. Eur. J. Neurosci. 5, 240–250.

Villar, M. J., Cortes, R., Theodorsson, E., Wiesenfeld-Hallin, Z., Schalling, M., Fahrenkrug, J., Emson, P. C., and Hokfelt, T. 1989. Neuropeptide expression in rat dorsal root ganglion cells and spinal cord after peripheral nerve injury with special reference to galanin. Neuroscience 33, 587–604.

Vos, B. P., Strassman, A. M., and Maciewicz, R. J. 1994. Behavioral evidence of trigeminal neuropathic pain following chronic constriction injury to the rat's infraorbital nerve. J. Neurosci. 14, 2708–2723.

Wall, P. D. 1979. On the relation of injury to pain. Pain 6, 253–264.

Wanaka, A., Milbrandt, J., and Johnson, E. M., Jr. 1991. Expression of FGF receptor gene in rat development. Development 111, 455–468.

Wang, H., Rivero-Melian, C., Robertson, B., and Grant, G. 1994. Transganglionic transport and binding of the isolectin B4 from Griffonia simplicifolia I in rat primary sensory neurons. Neuroscience 62, 539–551.

Wasner, G., Backonja, M. M., and Baron, R. 1998. Traumatic neuralgias: complex regional pain syndromes (reflex sympathetic dystrophy and causalgia): clinical characteristics, pathophysiological mechanisms and therapy. Neurol. Clin. 16, 851–868.

Welker, C. 1971. Microelectrode delineation of fine grain somatotopic organization of (SmI) cerebral neocortex in albino rat. Brain Res. 26, 259–275.

Wessman, M., Kaunisto, M. A., Kallela, M., and Palotie, A. 2004. The molecular genetics of migraine. Ann. Med. 36, 462–473.

Westlund, K. N. and Craig, A. D. 1996. Association of spinal lamina I projections with brainstem catecholamine neurons in the monkey. Exp. Brain Res. 110, 151–162.

Whitehead, M. C., Ganchrow, J. R., Ganchrow, D., and Yao, B. 1999. Organization of geniculate and trigeminal ganglion cells innervating single fungiform taste papillae: a study with tetramethylrhodamine dextran amine labeling. Neuroscience 93, 931–941.

Wiberg, M., Westman, J., and Blomqvist, A. 1986. The projection to the mesencephalon from the sensory trigeminal nuclei. An anatomical study in the cat. Brain Res. 399, 51–68.

Wolf, E., Petersson, K., Petersson, A., and Nilner, M. 2001. Long-lasting orofacial pain – a study of 109 consecutive patients referred to a pain group. Swed. Dent. J. 25, 129–136.

Wood, J. N., Boorman, J. P., Okuse, K., and Baker, M. D. 2004. Voltage-gated sodium channels and pain pathways. J. Neurobiol. 61, 55–71.

Woolf, C. J. and Salter, M. W. 2000. Neuronal plasticity: increasing the gain in pain. Science 288, 1765–1768.

Xiang, Z., Bo, X., and Burnstock, G. 1998. Localization of ATP-gated P2X receptor immunoreactivity in rat sensory and sympathetic ganglia. Neurosci. Lett. 256, 105–108.

Yan, Q., Radeke, M. J., Matheson, C. R., Talvenheimo, J., Welcher, A. A., and Feinstein, S. C. 1997. Immunocytochemical localization of TrkB in the central nervous system of the adult rat. J. Comp. Neurol. 378, 135–157.

Yatim, N., Billig, I., Compoint, C., Buisseret, P., and Buisseret-Delmas, C. 1996. Trigeminocerebellar and trigemino-olivary projections in rats. Neurosci. Res. 25, 267–283.

Yazdani, C., McLaughlin, T., Smeeding, J. E., and Walt, J. 2001. Prevalence of treated dry eye disease in a managed care population. Clin. Ther. 23, 1672–1682.

Yoshida, A., Dostrovsky, J. O., Sessle, B. J., and Chiang, C. Y. 1991. Trigeminal projections to the nucleus submedius of the thalamus in the rat. J. Comp. Neurol. 307, 609–625.

Yoshimura, N., White, G., Weight, F. F., and de Groat, W. C. 1994. Patch-clamp recordings from subpopulations of autonomic and afferent neurons identified by axonal tracing techniques. J. Auton. Nerv. Syst. 49, 85–92.

Young, R. F. and King, R. B. 1973. Fiber spectrum of the trigeminal sensory root of the baboon determined by electron microscopy. J. Neurosurg. 38, 65–71.

Young, R. F. and Perryman, K. M. 1984. Pathways for orofacial pain sensation in the trigeminal brain-stem nuclear complex of the Macaque monkey. J. Neurosurg. 61, 563–568.

Zerari-Mailly, F., Buisseret-Delmas, P., and Nosjean, A. 2005. Trigemino-solitarii-facial pathway in rats. J. Comp. Neurol. 487, 176–189.

Zhang, X., Ji, R. R., Arvidsson, J., Lundberg, J. M., Bartfai, T., Bedecs, K., and Hokfelt, T. 1996. Expression of peptides, nitric

oxide synthase and NPY receptor in trigeminal and nodose ganglia after nerve lesions. Exp. Brain Res. 111, 393–404.

Further Reading

Arvidsson, J. and Rice, F. L. 1991. Central projections of primary sensory neurons innervating different parts of the vibrissae follicles and intervibrissal skin on the mystacial pad of the rat. J. Comp. Neurol. 309, 1–16.

Crockett, D. P., Wang, L., Zhang, R. X., and Egger, M. D. 1999. Distribution of the low-affinity neurotrophin receptor (p75) in the developing trigeminal brainstem complex in the rat. Anat. Rec. 254, 549–565.

Darian-Smith, I. 1973. The Trigeminal System. In: Handbook of Sensory Physiology, vol. 2 Somatosensory System (*ed*. A. Iggo), pp. 271–314. Springer.

Hummel, T. 2001. Oral mucosal blood flow in patients with burning mouth syndrome. Pain 90, 281–286.

Kawabata, A., Feil, K., Gordan, B. D., Herbert, H., and Bandler, R. 1997. Spinal afferents to functionally distinct periaqueductal gray columns in the rat: an anterograde and retrograde tracing study. J. Comp. Neurol. 385, 207–229.

Lima, D., Mendes-Ribeiro, J. A., and Combra, A. 1991. The spino-latero-reticular system of the rat: Projections from the superficial dorsal horn and structural characterization of marginal neurons involved. Neuroscience 45, 137–152.

Luo, P. and Dessem, D. 1995. Inputs from identified jaw-muscle spindle afferents to trigeminothalamic neurons in the rat: a double-labeling study using retrograde HRP and intracellular biotinamide. J. Comp. Neurol. 353, 50–66.

Panneton, W. M., Klein, B. G., and Jacquin, M. F. 1991. Trigeminal projections to contralateral dorsal horn originate in midline hairy skin. Somatosensory Motor Res. 8, 165–173.

Pedersen, J., Reddy, H., Funch-Jensen, P., Arendt-Nielsen, L., Gregersen, H., and Drewes, A. M. 2004. Differences between male and female responses to painful thermal and mechanical stimulation of the human esophagus. Dig. Dis. Sci. 49, 1065–1074.

Rasmussen, B. K. 1993. Migraine and tension-type headache in a general population: precipitating factors, female hormones, sleep pattern and relation to lifestyle. Pain 53, 65–72.

Rasmussen, B. K. 2001. Epidemiology of headache. Cephalalgia 21, 774–777.

Sessle, B. J. and Hu, J. W. 1981. Raphe-induced suppression of the jaw-opening reflex and single neurons in trigeminal subnucleus oralis, and influence of naloxone and subnucleus caudalis. Pain 10, 19–36.

Shigenaga, Y., Nishimura, M., Suemune, S., Nishimori, T., Doe, K., and Tsuru, H. 1989. Somatotopic organization of tooth pulp primary afferent neurons in the cat. Brain Res. 477, 66–89.

Wiberg, M., Westman, J., and Blomqvist, A. 1987. Somatosensory projection to the mesencephalon: an anatomical study in the monkey. J. Comp. Neurol. 264, 92–117.

Willis, W. D., Jr., Zhang, X., Honda, C. N., and Giesler, G. J., Jr. 2001. Projections from the marginal zone and deep dorsal horn to the ventrobasal nuclei of the primate thalamus. Pain 92, 267–276.

Yoshida, A., Dostrovsky, J. O., and Chiang, C. Y. 1992. The afferent and efferent connections of the nucleus submedius in the rat. J. Comp. Neurol. 324, 115–133.

5.33 Migraine – A Disorder Involving Trigeminal Brainstem Mechanisms

P J Goadsby, University of California, San Francisco, CA, USA

© 2008 Elsevier Inc. All rights reserved.

5.33.1	**Introduction**	461
5.33.2	**Migraine – Explaining the Clinical Features**	461
5.33.3	**Genetics of Migraine**	462
5.33.3.1	Genetic Epidemiology	462
5.33.3.2	Familial Hemiplegic Migraine	462
5.33.4	**Migraine Aura**	462
5.33.5	**Headache – Anatomy**	463
5.33.5.1	The Trigeminal Innervation of Pain-Producing Intracranial Structures	463
5.33.6	**Headache Physiology – Peripheral Connections**	463
5.33.6.1	Plasma Protein Extravasation	463
5.33.6.2	Sensitization and Migraine	463
5.33.6.3	Neuropeptide Studies	464
5.33.7	**Headache Physiology – Central Connections**	464
5.33.7.1	The Trigeminocervical Complex	464
5.33.7.2	Higher-Order Processing	466
5.33.7.2.1	Thalamus	466
5.33.7.2.2	Activation of modulatory regions	466
5.33.8	**Central Modulation of Trigeminal Pain**	466
5.33.8.1	Brain Imaging in Humans	466
5.33.8.2	Animal Experimental Studies of Sensory Modulation	467
5.33.8.3	Electrophysiology of Migraine in Humans	467
5.33.9	**What is Migraine?**	467
References		468

5.33.1 Introduction

Headache in general, and in particular migraine (Goadsby, P. J. *et al.*, 2002) and cluster headache (Goadsby, P. J., 2002), is better understood now than has been the case for the last four millennia (Lance, J. W. and Goadsby, P. J., 2005). Migraine is a common, disabling recurrent disorder of the central nervous system with a core manifestation involving activation, or the perception of activation, of trigeminal nociceptive afferents (Olesen, J. *et al.*, 2005). Here how studies of the anatomy and physiology of the pain-producing innervation of the dura mater and large cranial vessels, the trigeminovascular system, has contributed to our current understanding of one of the most common maladies of humans will be explored.

5.33.2 Migraine – Explaining the Clinical Features

Migraine is in essence a familial episodic disorder whose key marker is headache with certain associated features (Table 1). It is these features that give clues to its pathophysiology, and ultimately will provide insights leading to new treatments.

The essential elements to be considered are:

Genetics of migraine;

Physiological basis for the aura;

Anatomy of head pain, particularly that of the trigeminovascular system;

Physiology and pharmacology of activation of the peripheral branches of ophthalmic branch of the trigeminal nerve;

Table 1 International Headache Society features of migraine (Headache Classification Committee of the International Headache Society, 2004)

Repeated episodic headache (4–72 h) with the following features:	
Any two of:	Any one of:
unilateral	nausea/vomiting
throbbing	photophobia and phonophobia
worsened by movement	
moderate or severe	

Physiology and pharmacology of the trigeminal nucleus, in particular its caudal most part, the trigeminocervical complex (TCC);

Brainstem and diencephalic modulatory systems that influence trigeminal pain transmission and other sensory modality processing.

5.33.3 Genetics of Migraine

One of the most important aspects of the pathophysiology of migraine is the inherited nature of the disorder. It is clear from clinical practice that many patients have first-degree relatives who also suffer from migraine (Lance, J. W. and Goadsby, P. J., 2005). Transmission of migraine from parents to children has been reported as early as the seventeenth century, and numerous published studies have reported a positive family history.

5.33.3.1 Genetic Epidemiology

Studies of twin pairs are the classical method to investigate the relative importance of genetic and environmental factors. A Danish study included 1013 monozygotic and 1667 dizygotic twin pairs of the same gender, obtained from a population-based twin register. The pairwise concordance rate was significantly higher among monozygotic than dizygotic twin pairs ($P < 0.05$). Several studies have attempted to analyze the possible mode of inheritance in migraine families and conflicting results have been obtained. Both twin studies and population-based epidemiological surveys strongly suggest that migraine without aura is a multifactorial disorder, caused by a combination of genetic and environmental factors.

5.33.3.2 Familial Hemiplegic Migraine

In approximately 50% of the reported families, familial hemiplegic migraine (FHM) has been assigned to chromosome 19p13. Few clinical differences have been found between chromosome 19-linked and unlinked FHM families. Indeed, the clinical phenotype does not associate particularly with the known mutations. The most striking exception is cerebellar ataxia, which occurs in approximately 50% of the chromosome 19-linked, but in none of the unlinked families. Another less striking difference includes the fact that patients from chromosome 19-linked families are more likely to have attacks that can be triggered by minor head trauma or are that associated by coma.

The biological basis for the linkage to chromosome 19 is mutations (Ophoff, R. A. *et al.*, 1996) involving the $Ca_v2.1$ (P/Q) type voltage-gated calcium channel *CACNA1A* gene. Now known as FHM-I, this mutation is responsible for about 50% of identified families. Mutations in the *ATP1A2* gene have been identified to be responsible for about 20% of FHM families. Interestingly, the phenotype of some FHM-II involves epilepsy, while it has also been suggested that alternating hemiplegia of childhood can be due to *ATP1A2* mutations. The latter cases are most unusual for migraine. Most recently mutations in the neuronal voltage-gated sodium channel *SCN1A* have been identified as the cause of FHM-III, thus continuing the ionopathic theme.

Taken together, the known mutations suggest that migraine, or at least the neurological manifestations currently called the aura, are caused by an ionopathy. Linking the channel disturbance for the first time to the aura process has demonstrated that human mutations expressed in a knockin mouse produce a reduced threshold for cortical spreading depression (CSD), which has some profound implications for understanding that process.

5.33.4 Migraine Aura

Migraine aura is defined as a focal neurological disturbance manifest as visual, sensory, or motor symptoms (Headache Classification Committee of the International Headache Society, 2004). It is seen in about 30% of patients, and it is clearly neurally driven. The case for the aura being the human equivalent of the CSD of Leao has been

well made (Lauritzen, M., 1994). In humans, visual aura has been described as affecting the visual field, suggesting the visual cortex, and it starts at the center of the visual field and propagates to the periphery at a speed of 3 mm min^{-1}. This is very similar to spreading depression described in rabbits. Blood flow studies in patients have also shown that a focal hyperemia tends to precede the spreading oligemia, and again this is similar to what would be expected with spreading depression. After this passage of oligemia, the cerebrovascular response to hypercapnia in patients is blunted while autoregulation remains intact. Again this pattern is repeated with experimental spreading depression. Human observations have rendered the arguments reasonably sound that human aura has as its equivalent in animals in CSD. An area of controversy surrounds whether aura triggers the rest of the attack, and is indeed painful. Based on the available experimental and clinical data this author is not at all convinced that aura is painful *per se*, but this does not diminish its interest or the importance of understanding it. Indeed therapeutic developments may shed further light on these relationships, and studies are required to understand how in some patients aura is clearly not a sufficient trigger to pain.

5.33.5 Headache – Anatomy

5.33.5.1 The Trigeminal Innervation of Pain-Producing Intracranial Structures

Surrounding the large cerebral vessels, pial vessels, large venous sinuses, and dura mater is a plexus of largely unmyelinated fibers that arise from the ophthalmic division of the trigeminal ganglion and in the posterior fossa from the upper cervical dorsal roots. Trigeminal fibers innervating cerebral vessels arise from neurons in the trigeminal ganglion that contain substance P and calcitonin gene-related peptide (CGRP), both of which can be released when the trigeminal ganglion is stimulated either in humans or cats (Goadsby, P. J. *et al.*, 1988). Stimulation of the cranial vessels, such as the superior sagittal sinus (SSS), is certainly painful in humans (Wolff, H. G., 1948). Human dural nerves that innervate the cranial vessels largely consist of small diameter myelinated and unmyelinated fibers that almost certainly subserve a nociceptive function.

5.33.6 Headache Physiology – Peripheral Connections

5.33.6.1 Plasma Protein Extravasation

Moskowitz M. A. (1990) has provided a series of experiments to suggest that the pain of migraine may be a form of sterile neurogenic inflammation. Although this seems clinically implausible, the model system has been helpful in understanding some aspects of trigeminovascular physiology. Neurogenic plasma extravasation can be seen during electrical stimulation of the trigeminal ganglion in the rat. Plasma extravasation can be blocked by ergot alkaloids, indomethacin, acetylsalicylic acid, and the serotonin-5-$HT_{1B/1D}$ agonist, sumatriptan. The pharmacology of abortive antimigraine drugs has been reviewed in detail. In addition there are structural changes in the dura mater that are observed after trigeminal ganglion stimulation. These include mast cell degranulation and changes in postcapillary venules including platelet aggregation. While it is generally accepted that such changes, and particularly the initiation of a sterile inflammatory response, would cause pain, it is not clear whether this is sufficient of itself, or requires other stimulators, or promoters. Preclinical studies suggest that CSD may be a sufficient stimulus to activate trigeminal neurons, although this has been a controversial area.

Although plasma extravasation in the retina, which is blocked by sumatriptan, can be seen after trigeminal ganglion stimulation in experimental animals, no changes are seen with retinal angiography during acute attacks of migraine or cluster headache. A limitation of this study was the probable sampling of both retina and choroids elements in rats, given that choroidal vessels have fenestrated capillaries. Clearly, however, blockade of neurogenic plasma protein extravasation is not completely predictive of antimigraine efficacy in humans as evidenced by the failure in clinical trials of substance P, neurokinin-1 antagonists, specific plasma protein extravasation (PPE) blockers, CP122,288 and 4991w93, an endothelin antagonist, and a neurosteroid. The implications of these data have been recently reviewed (Peroutka, S. J., 2005).

5.33.6.2 Sensitization and Migraine

While it is highly doubtful that there is a significant sterile inflammatory response in the dura mater during migraine, it is clear that some form of sensitization takes

place during migraine, since allodynia is common. About two-thirds of patients complain of pain from non-noxious stimuli, allodynia (Selby, G. and Lance, J. W., 1960). A particularly interesting aspect is the demonstration of allodynia in the upper limbs ipsilateral and contralateral to the pain. This finding is consistent with at least third-order neuronal sensitization, such as sensitization of thalamic neurons, and firmly places the pathophysiology within the central nervous system. Sensitization in migraine may be peripheral with local release of inflammatory markers, which would certainly activate trigeminal nociceptors. More likely in migraine is a form of central sensitization, which may be classical central sensitization, or a form of disinhibitory sensitization with dysfunction of descending modulatory pathways (Knight, Y. E. *et al.*, 2002). Just as dihydroergotamine (DHE) can block trigeminovascular nociceptive transmission, probably at least by a local effect in the TCC, DHE can block central sensitization associated with dural stimulation by an inflammatory soup, as can cyclo-oxygenase block both sensitization and trigeminocervical transmission.

5.33.6.3 Neuropeptide Studies

Electrical stimulation of the trigeminal ganglion in both humans and cats leads to increases in extracerebral blood flow and local release of both CGRP and SP (Goadsby, P. J. *et al.*, 1988). In the cat trigeminal ganglion stimulation also increases cerebral blood flow by a pathway traversing the greater superficial petrosal branch of the facial nerve (Goadsby, P. J. and Duckworth, J. W., 1987) again releasing a powerful vasodilator peptide, vasoactive intestinal polypeptide (VIP; May, A. and Goadsby, P. J., 1999). Interestingly, the VIPergic innervation of the cerebral vessels is predominantly anterior rather than posterior, and this may contribute to this region's vulnerability to spreading depression, explaining why the aura is so very often seen to commence posteriorly. Stimulation of the more specifically vascular pain-producing superior sagittal sinus increases cerebral blood flow and jugular vein CGRP levels. Human evidence that CGRP is elevated in the headache phase of migraine (Goadsby, P. J. *et al.*, 1990), supporting the view that the trigeminovascular system may be activated in a protective role in these conditions. Moreover, nitric oxide (NO)-donor-triggered migraine, which is in essence typical migraine, also results in increases in CGRP that are blocked by sumatriptan, just as in spontaneous migraine (Goadsby, P. J. and Edvinsson, L., 1993). It is of interest in this regard that compounds that have not shown activity in migraine (Peroutka, S. J., 2005), notably the conformationally restricted analogue of sumatriptan, CP122,288, and the conformationally restricted analog of zolmitriptan, 4991w93, were both ineffective inhibitors of CGRP release after superior sagittal sinus in cats. The recent development of nonpeptide highly specific CGRP antagonists, and the announcement of proof-of-concept for a CGRP antagonist in acute migraine (Olesen, J. *et al.*, 2004), firmly establishes this as a novel and important new emerging principle for acute migraine. At the same time the lack of any effect of CGRP blockers on plasma protein extravasation, explains in some part why that model has proved inadequate at translation into human therapeutic approaches (Peroutka, S. J., 2005).

5.33.7 Headache Physiology – Central Connections

5.33.7.1 The Trigeminocervical Complex

Fos immunohistochemistry is a method for looking at activated cells by plotting the expression of Fos protein. After meningeal irritation with blood Fos expression is noted in the trigeminal nucleus caudalis, while after stimulation of the superior sagittal sinus Fos-like immunoreactivity is seen in the trigeminal nucleus caudalis and in the dorsal horn at the C_1 and C_2 levels in cats and monkey. These latter findings are in accord with similar data using 2-deoxyglucose measurements with superior sagittal sinus stimulation. Similarly, stimulation of a branch of C_2, the greater occipital nerve, increases metabolic activity in the same regions, i.e., trigeminal nucleus caudalis and $C_{1/2}$ dorsal horn, and fos expression can be elicited by injection of mustard oil into the occipital muscles. In experimental animals one can record directly from trigeminal neurons with both supratentorial trigeminal input and input from the greater occipital nerve, a branch of the C_2 dorsal root (Bartsch, T. and Goadsby, P. J., 2002). Stimulation of the greater occipital nerve for 5 min results in substantial increases in responses to supratentorial dural stimulation, which can last for over 1 h. Conversely, stimulation of the middle meningeal artery dura mater with the C-fiber irritant mustard oil sensitizes responses to occipital muscle stimulation. Taken together these data suggest convergence of cervical and ophthalmic inputs at the level of the second-order neuron. Moreover, stimulation of a lateralized

structure, the middle meningeal artery, produces Fos expression bilaterally in both cat and monkey brains. This group of neurons from the superficial laminas of trigeminal nucleus caudalis and $C_{1/2}$ dorsal horns should be regarded functionally as the TCC.

These data demonstrate that trigeminovascular nociceptive information comes by way of the most caudal cells. This concept provides an anatomical explanation for the referral of pain to the back of the head in migraine. Moreover, experimental pharmacological evidence suggests that some abortive antimigraine drugs, such as, ergot derivatives, acetylsalicylic acid, sumatriptan, eletriptan, naratriptan, rizatriptan, and zolmitriptan can have actions at these second-order neurons that reduce cell activity and suggest a further possible site for therapeutic intervention in migraine. This action can be dissected out to involve each of the 5-HT_{1B}, 5-HT_{1D}, and 5-HT_{1F} receptor subtypes, and are consistent with the localization of these receptors on peptidergic nociceptors. Interestingly, triptans also influence the CGRP promoter, and regulate CGRP secretion from neurons in culture, as well as perhaps require cell surface expression for their effect. Furthermore, the demonstration that some part of this action is postsynaptic with either 5-HT_{1B} or 5-HT_{1D} receptors located nonpresynatically offers a prospect of highly anatomically localized treatment options (Figure 1).

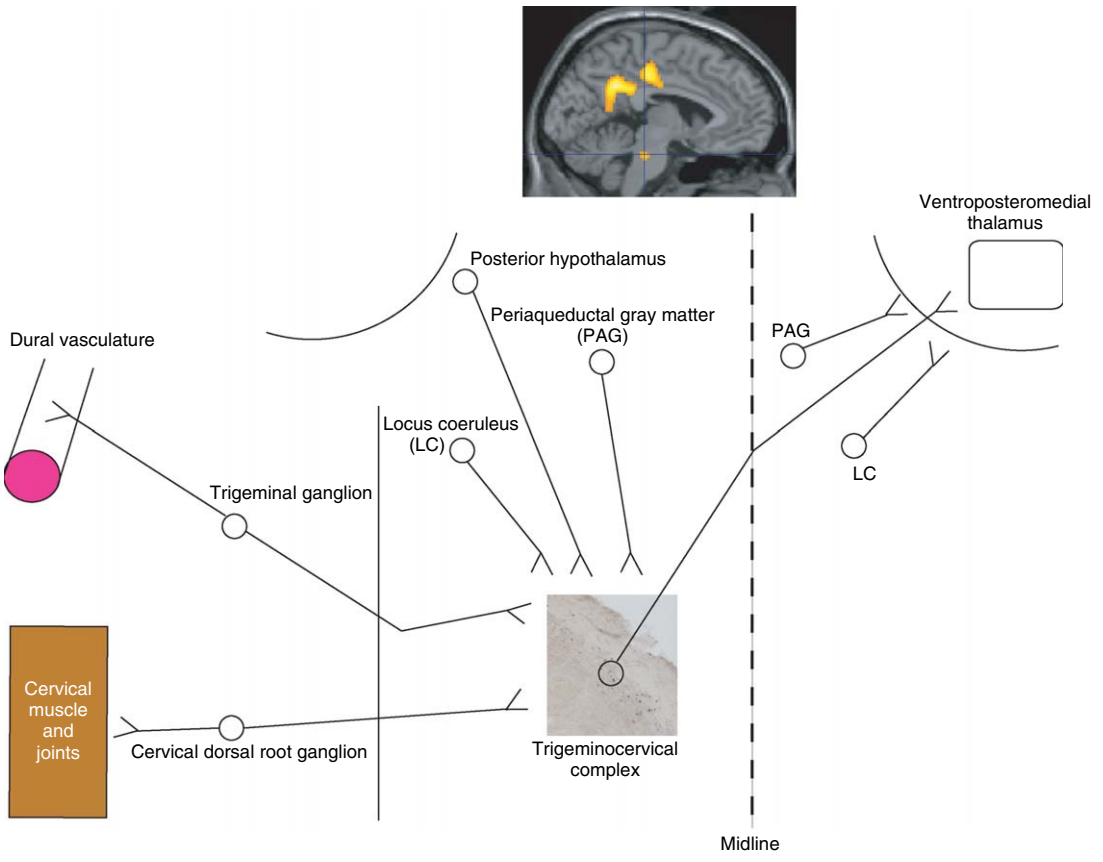

Figure 1 Illustration of the some elements of migraine biology. Patients inherit a dysfunction in brain control systems for pain and other afferent stimuli, which can be triggered and are in turn capable of activating the trigeminovascular system as the initiating event in a positive feedback of neurally driven vasodilatation. Nociceptive afferents from the cervical region terminate in the trigeminocervical complex (illustrated by Fos protein expression in the superficial laminas) and this accounts for the nontrigeminal distribution of pain in many patients. These afferents project to the thalamus, including ventroposteromedial thalamus, and are at least influenced by neurons in the posterior hypothalamic gray, the periaqueductal gray (PAG), and probably by neurons of the nucleus locus coeruleus in the pons. Functional brain imaging suggests that the brainstem, notably the pons as illustrated after Bahra, A., Matharu, M. S., Buchel, C., Frackowiak, R. S. J., and Goadsby, P. J. 2001. Brainstem activation specific to migraine headache. Lancet 357, 1016–1017, is a pivotal region in the migraine process.

Table 2 Neuroanatomical processing of vascular head pain

	Structure	*Comments*
Target innervation: Cranial vessels Dura mater	Ophthalmic branch of trigeminal nerve	
First	Trigeminal ganglion	Middle cranial fossa
Second	Trigeminal nucleus (quintothalamic tract)	Trigeminal nucleus caudalis and C_1/C_2 dorsal horns
Third	Thalamus	Ventrobasal complex Medial nucleus of posterior group Intralaminar complex
Modulatory	Midbrain Hypothalamus	Periaqueductal gray matter ?
Final	Cortex	Insulas Frontal cortex Anterior cingulate cortex Basal ganglia

5.33.7.2 Higher-Order Processing

Following transmission in the caudal brainstem and high cervical spinal cord information is relayed rostrally (Table 2).

5.33.7.2.1 Thalamus

Processing of vascular nociceptive signals in the thalamus occurs in the ventroposteromedial (VPM) thalamus, medial nucleus of the posterior complex, and in the intralaminar thalamus. It has been shown by application of capsaicin to the superior sagittal sinus that trigeminal projections with a high degree of nociceptive input are processed in neurons particularly in the ventroposteromedial thalamus and in its ventral periphery. These neurons in the VPM can be modulated by activation of gamma-aminobutyric acid $(GABA)_A$ inhibitory receptors, and perhaps of more direct clinical relevance by propranolol though a β_1-adrenoceptor mechanism (Shields, K. G. and Goadsby, P. J., 2005). Remarkably, triptans through $5\text{-}HT_{1B/1D}$ mechanisms can also inhibit VPM neurons locally, as demonstrated by microiontophoretic application, suggesting a hitherto unconsidered locus of action for triptans in acute migraine. Human imaging studies have confirmed activation of thalamus contralateral to pain in acute migraine (Bahra, A. *et al.*, 2001).

5.33.7.2.2 Activation of modulatory regions

Stimulation of nociceptive afferents by stimulation of the superior sagittal sinus in cats activates neurons in the ventrolateral periaqueductal gray matter (PAG). PAG activation in turn feeds back to the TCC with an inhibitory influence. PAG is clearly included in the area of activation seen in positron emission tomography (PET) studies in migraineurs. This typical negative feedback system will be further considered below as a possible mechanism for the symptomatic manifestations of migraine.

Another potentially modulatory region activated by stimulation of nociceptive trigeminovascular input is the posterior hypothalamic gray. This area is crucially involved in several primary headaches, notably cluster headache (Goadsby, P. J., 2002), Short-lasting unilateral neuralgiform headache attacks with conjunctival injection and tearing (SUNCT), paroxysmal hemicrania and hemicrania continua. Moreover, the clinical features of the premonitory phase, and other features of the disorder, suggest dopamine neuron involvement. Orexinergic neurons in the posterior hypothalamus can be both pro- and antinociceptive, offering a further possible region whose dysfunction might involve the perception of head pain.

5.33.8 Central Modulation of Trigeminal Pain

5.33.8.1 Brain Imaging in Humans

Functional brain imaging with PET has demonstrated activation of the dorsal midbrain, including the PAG, and in the dorsal pons, near the locus coeruleus, in studies during migraine without aura.

Dorsolateral pontine activation is seen with PET in spontaneous episodic and chronic migraine, and with nitrogylcerin-triggered attacks (Bahra, A. *et al.*, 2001; Afridi, S. *et al.*, 2005). These areas are active immediately after successful treatment of the headache but are not active interictally. The activation corresponds with the brain region that Raskin initially reported, and confirmed, to cause migrainelike headache when stimulated in patients with electrodes implanted for pain control. Similarly, excess iron in the PAG of patients with episodic and chronic migraine, and chronic migraine can develop after a bleed into a cavernoma in the region of the PAG, or with a lesion of the pons. What could dysfunction of these brain areas lead to?

5.33.8.2 Animal Experimental Studies of Sensory Modulation

It has been shown in experimental animals that stimulation of nucleus locus coeruleus, the main central noradrenergic nucleus, reduces cerebral blood flow in a frequency-dependent manner (Goadsby, P. J. *et al.*, 1982) through an α_2-adrenoceptor-linked mechanism. This reduction is maximal in the occipital cortex. While a 25% overall reduction in cerebral blood flow is seen, extracerebral vasodilatation occurs in parallel (Goadsby, P. J. *et al.*, 1982). In addition, the main serotonin-containing nucleus in the brainstem, the midbrain dorsal raphe nucleus, can increase cerebral blood flow when activated. Furthermore, stimulation of PAG will inhibit sagittal sinus-evoked trigeminal neuronal activity in cats, while blockade of P/Q-type voltage-gated Ca^{2+} channels in the PAG facilitates trigeminovascular nociceptive processing (Knight, Y. E. *et al.*, 2002) with the local GABAergic system in the PAG still intact.

5.33.8.3 Electrophysiology of Migraine in Humans

Studies of evoked potentials and event-related potentials provide some link between animal studies and human functional imaging. Authors have shown changes in neurophysiological measures of brain activation but there is much discussion as to how to interpret such changes (Schoenen, J. *et al.*, 2003). Perhaps the most reliable theme is that the migrainous brain does not habituate to signals in a normal way. Similarly, contingent negative variation (CNV), an event related potential, is abnormal in migraineurs compared to controls. Changes in CNV predict attacks and preventive therapies alter, normalize, such changes. Attempts to correlate clinical phenotypes with electrophysiological changes, may enhance further studies in this area.

5.33.9 What is Migraine?

Migraine is an inherited, episodic disorder involving sensory sensitivity. Patients complain of pain in the head that is throbbing, but there is no reliable relationship between vessel diameter and the pain, or its treatment. They complain of discomfort from normal lights and the unpleasantness of routine sounds. Some mention otherwise pleasant odors are unpleasant. The anatomical connections of, for example, the pain pathways are clear, the ophthalmic division of the trigeminal nerve subserves sensation within the cranium and explains why the top of the head is headache, and the maxillary division is facial pain. The convergence of cervical and trigeminal afferents explains why neck stiffness or pain is so common in primary headache. The genetics of channelopathies is opening up a plausible way to think about the episodic nature of migraine. However, where is the lesion, what is actually the pathology?

Migraine aura cannot be the trigger alone, there is no evidence at all after 4000 years that it occurs in more than 30% of migraine patients; aura can be experienced without pain at all, and is seen in the other primary headaches. Perhaps electrophysiological changes in the brain have been mislabeled as hyperexcitability whereas dyshabituation might be a simpler explanation. If migraine was basically an attentional problem with changes in cortical synchronization (Niebur, E. *et al.*, 2002), hypersynchronization, all its manifestations could be accounted for in a single over-arching pathophysiological hypothesis of a disturbance of subcortical sensory modulation systems. While it seems likely that the trigeminovascular system, and its cranial autonomic reflex connections, the trigeminal-autonomic reflex (May, A. and Goadsby, P. J., 1999), act as a feed-forward system to facilitate the acute attack, the fundamental problem in migraine is in the brain. Unraveling its basis will deliver great benefits to patients and considerable understanding of some very fundamental neurobiological processes.

Acknowledgment

The work of the author has been supported by the Migrane Trust.

References

Afridi, S., Matharu, M. S., Lee, L., Kaube, H., Friston, K. J., Frackowiak, R. S. J., and Goadsby, P. J. 2005. A PET study exploring the laterality of brainstem activation in migraine using glyceryl trinitrate. Brain 128, 932–939.

Bahra, A., Matharu, M. S., Buchel, C., Frackowiak, R. S. J., and Goadsby, P. J. 2001. Brainstem activation specific to migraine headache. Lancet 357, 1016–1017.

Bartsch, T. and Goadsby, P. J. 2002. Stimulation of the greater occipital nerve induces increased central excitability of dural afferent input. Brain 125, 1496–1509.

Goadsby, P. J. 2002. Pathophysiology of cluster headache: a trigeminal autonomic cephalgia. Lancet Neurol. 1, 37–43.

Goadsby, P. J. and Duckworth, J. W. 1987. Effect of stimulation of trigeminal ganglion on regional cerebral blood flow in cats. Am. J. Physiol. 253, R270–R274.

Goadsby, P. J. and Edvinsson, L. 1993. The trigeminovascular system and migraine: studies characterizing cerebrovascular and neuropeptide changes seen in humans and cats. Ann. Neurol. 33, 48–56.

Goadsby, P. J., Edvinsson, L., and Ekman, R. 1988. Release of vasoactive peptides in the extracerebral circulation of man and the cat during activation of the trigeminovascular system. Ann. Neurol. 23, 193–196.

Goadsby, P. J., Edvinsson, L., and Ekman, R. 1990. Vasoactive peptide release in the extracerebral circulation of humans during migraine headache. Ann. Neurol. 28, 183–187.

Goadsby, P. J., Lambert, G. A., and Lance, J. W. 1982. Differential effects on the internal and external carotid circulation of the monkey evoked by locus coeruleus stimulation. Brain Res. 249, 247–254.

Goadsby, P. J., Lipton, R. B., and Ferrari, M. D. 2002. Migraine – current understanding and treatment. New Engl. J. Med. 346, 257–270.

Headache Classification Committee of the International Headache Society. 2004. The International Classification of Headache Disorders (2nd edn.). Cephalalgia 24, 1–160.

Knight, Y. E., Bartsch, T., Kaube, H., and Goadsby, P. J. 2002. P/Q-type calcium channel blockade in the PAG facilitates trigeminal nociception: a functional genetic link for migraine? J. Neurosci. 22, 1–6.

Lance, J. W. and Goadsby, P. J. 2005. Mechanism and Management of Headache. Elsevier.

Lauritzen, M. 1994. Pathophysiology of the migraine aura. The spreading depression theory. Brain 117, 199–210.

May, A. and Goadsby, P. J. 1999. The trigeminovascular system in humans: pathophysiological implications for primary headache syndromes of the neural influences on the cerebral circulation. J. Cerebr. Blood Flow Metabol. 19, 115–127.

Moskowitz, M. A. 1990. Basic mechanisms in vascular headache. Neurolog. Clin. 8, 801–815.

Niebur, E., Hsiao, S. S., and Johnson, K. O. 2002. Synchrony: a neural mechanism for attentional selection? Curr. Opin. Neurobiol. 12, 190–194.

Olesen, J., Diener, H. C., Husstedt, I. W., Goadsby, P. J., Hall, D., Meier, U., Pollentier, S., and Lesko, L. M. 2004. Calcitonin gene-related peptide (CGRP) receptor antagonist BIBN4096BS is effective in the treatment of migraine attacks. New Engl. J. Med. 350, 1104–1110.

Olesen, J., Tfelt-Hansen, P., Ramadan, N., Goadsby, P. J., and Welch, K. M. A. 2005. The Headaches. Lippincott, Williams & Wilkins.

Ophoff, R. A., Terwindt, G. M., Vergouwe, M. N., van Eijk, R., Oefner, P. J., Hoffman, S. M. G., Lamerdin, J. E., Mohrenweiser, H. W., Bulman, D. E., Ferrari, M., Haan, J., Lindhout, D., van Ommen, G. J., Hofker, M. H., Ferrari, M. D., and Frants, R. R. 1996. Familial hemiplegic migraine and episodic ataxia type-2 are caused by mutations in the Ca^{2+} channel gene CACNL1A4. Cell 87, 543–552.

Peroutka, S. J. 2005. Neurogenic inflammation and migraine: implications for therapeutics. Mol. Intervent. 5, 306–313.

Schoenen, J., Ambrosini, A., Sandor, P. S., and Maertens de Noordhout, A. 2003. Evoked potentials and transcranial magnetic stimulation in migraine: published data and viewpoint on their pathophysiologic significance. Clin. Neurophysiol. 114, 955–972.

Selby, G. and Lance, J. W. 1960. Observations on 500 cases of migraine and allied vascular headache. J. Neurol. Neurosurg. Psychiatry 23, 23–32.

Shields, K. G. and Goadsby, P. J. 2005. Propranolol modulates trigeminovascular responses in thalamic ventroposteromedial nucleus: a role in migraine? Brain 128, 86–97.

Wolff, H. G. 1948. Headache and Other Head Pain. Oxford University Press.

5.34 Tooth Pain

M R Byers, University of Washington, Seattle WA, USA

© 2008 Elsevier Inc. All rights reserved.

5.34.1	Introduction	470
5.34.2	Dental Sensory Mechanisms	470
5.34.2.1	Normal Teeth/Acute Pain	470
5.34.2.2	Inflammatory Tooth Pain	472
5.34.2.3	Dental Neuropathic Pain	472
5.34.3	Tooth Pain: Diagnosis and Management	473
5.34.4	Conclusions	474
References		474

Glossary

ASIC receptors Acid-sensing ion channels that detect low pH, a typical condition of pulpitis.

atypical odontalgia A condition in which tooth pain derives from neuropathic or referred mechanisms. Tooth extractions or root canals do not relieve the pain.

BK receptors Activated by the inflammatory mediator, bradykinin.

convergence Many sensory afferents from multiple tissues project to individual central trigeminal neurons.

dentin Specialized, calcified, collagenous matrix that surrounds the pulp.

hot tooth An inflamed tooth that resists regional anesthesia and remains sensitive when neighboring teeth are numb.

hypersensitive dentin Sharp pain elicited from light touch to exposed dentin.

ionotropic receptors Activated by specific ligands causing ion flux through receptor pores.

mesencephalic trigeminal nucleus Location of cell bodies of primary sensory neurons that innervate stretch receptors in periodontal ligament, sutures, or mastication muscles.

metabotropic receptors Interaction with ligand activates G-protein intracellular signaling.

NK receptors Receptors for neurokinins such as substance P or neurokinin A.

nucleus caudalis Caudal region of spinal trigeminal subnuclei, specialized for processing, relaying and modulating orofacial pain.

odontalgia Tooth pain.

odontoblast Neural crest-derived cells that make dentin and regulate the pulp–dentin barrier.

P2 receptors Purinergic nucleotide receptors that respond to adenosine triphosphate (ATP).

periapex Region at base of root socket that surrounds the root apex, and includes periodontal ligament, neurovascular bundles and endings, and alveolar bone.

prepain The first sensation (tingling, vibration, or touch) elicited by electrical stimulation of teeth. It changes to sharp tooth pain at stronger levels of stimulation.

pulpitis Inflamed tooth pulp that can be healed locally (reversible), that can consume the pulp and spread into periapex (irreversible), or that can be undetected (silent) until it reaches the periapex.

receptive field Patch of tissue that activates a primary afferent or central neuron.

referred pain Pain that is felt at a different site from the neural activity that causes it.

Ruffini mechanoreceptors Complex stretch mechanoreceptors located in periodontal ligament.

Trk receptors Tyrosine kinase receptors that respond to neurotrophin factors.

TRP receptors Transient receptor potential channels (vanilloid receptor family) that are activated by capsaicin, heat, or low pH.

5.34.1 Introduction

Tooth pain is the most common type of orofacial pain (Lipton, J. *et al.*, 1993; Hargreaves, K. M., 2002). Dental nerve fibers branch centrally to activate many neurons in the trigeminal brainstem complex or extratrigeminal relay sites, and those central neurons also receive extensive convergent input from other orofacial tissues, making location of tooth pain difficult. However, most of the time our teeth do not hurt, and most dental neural activity is unperceived. The sensory functions of tooth nerves are presented here, along with unusual features of central processing, mechanisms, perception, diagnosis, and treatment of tooth pain, which can be sharp or dull, focused or diffuse, episodic or relentless, referred or neuropathic (for reviews see: Närhi, M. V. O. *et al.*, 1996; Olgart, L., 1996; Byers, M. R. and Närhi, M. V. O., 1999; Dionne, R. A. and Berthold, C. W., 2001; Byers, M. R. and Närhi, M. V. O., 2002; Hargreaves, K. M., 2002; Hu, J. W., 2004; Lavigne, G. *et al.*, 2004; Truelove, E., 2004; Sessle, B. J., 2005; Henry, M. A. and Hargreaves, K. M., 2007).

5.34.2 Dental Sensory Mechanisms

5.34.2.1 Normal Teeth/Acute Pain

A-fibers respond especially well to acute stimuli that move fluid in dentin (Brännström, M and Åström, A., 1972) and C-fibers respond to acute heat stimuli or pulp damage (Närhi, M. V. O. *et al.*, 1996; Närhi, M. V. O., 2005). Different factors affect axonal conduction in trigeminal nerves, ganglion, central tracts, and synaptic termination regions in the brainstem (Figure 1). Dental afferents project to low threshold mechanoreceptive, nociceptive-specific, and wide-dynamic-range central neurons, all of which receive a major input from other tissues, often from more than one trigeminal division (Sessle, B. J. *et al.*, 1986).

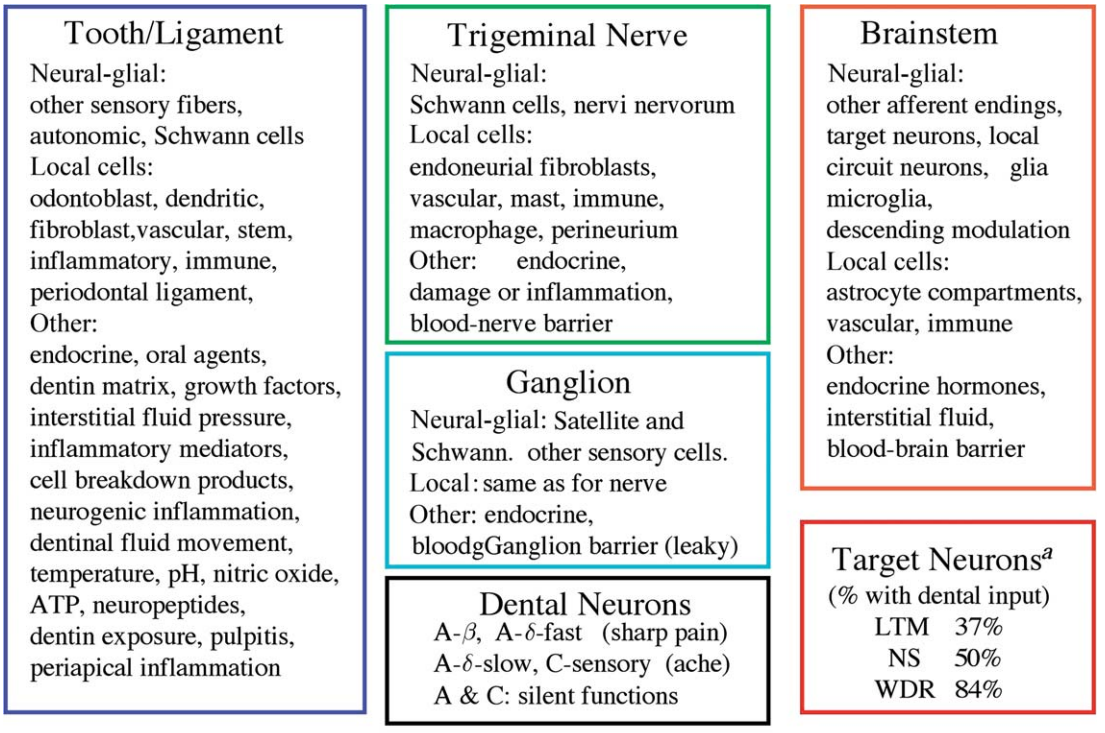

[a] Inputs from teeth were most common for WDR neurons in nucleus caudalis of cats (Sessle, B. J. *et al.*, 1986).

Figure 1 Interactions affecting dental neuronal function. ATP, adenosine triphosphate; LTM, low-threshold mechanoreceptor; NS, nociceptive specific; WDR, wide-dynamic neuron. Target Neurons: reprinted from Pain, 27, Sessele, B. J., Hu J. W., Amano, N., and Zhong, G., Convergence of cutaneous, tooth pulp, visceral, neck and muscle afferents onto nociceptive and non-nociceptive neurons in trigeminal subnucleus caudalis (medullary dorsal horn) and its implications for referred pain, 219–235, Copyright 1986, with permission from The International Association for the Study of Pain.

Most tooth pain perceptions are acute, and they derive from activation of neurons in nucleus caudalis, although rostral trigeminal nuclei are also involved, and there are other connection sites such as the paratrigeminal nucleus and reticular formation (Sessle, B. J., 2000; 2005).

Human studies show three kinds of evoked sensation from dental nerves: prepain, sharp pain, and dull ache. The first two depend on activation of fast A-β and A-δ-fibers and the latter involves polymodal capsaicin-sensitive slow A-δ and C-fibers (Närhi, M. V. O. *et al.*, 1996; Ikeda, H. *et al.*, 1997), some of which express neuropeptide receptors for autocrine modulation (Suzuki, H. *et al.*, 2002). Each of our teeth is innervated by many hundreds of highly branched trigeminal neurons, and the density of sensory nerve endings in coronal pulp and inner dentin is enormous (Figure 2). However, most intradental neural activity involves unperceived neural efferent functions or reflexes, such as vasodilatation by neuropeptides from sensory fibers that is counterbalanced by sympathetic-mediated vasoconstriction (Figure 3; Olgart, L. 1996; Fristad, I. *et al.*, 1997; Berggreen, E. and Heyeraas, K. J., 2000). Touch sensations during chewing come from Ruffini mechanoreceptors in the periodontal ligament outside the roots, while unconscious aspects of jaw reflexes involve intradental mechanoreceptive A-fibers and the periodontal endings of mesencephalic trigeminal neurons (Dong, W. K. *et al.*, 1993). Dental neurons can express a variety of ionotropic receptors (e.g., TRP-V1, TRP-V2, $P2X_3$, ASIC), metabotropic receptors (BK-1, BK-2, NK1-3, TrkA), ion channels, receptors for neuropeptides, neurotrophins, and opioid peptides that sensitize, inhibit, or modulate sensory neurons (Hu, J. W., 2004), and even immune regulators (Wadachi, R. and Hargreaves, K. M., 2006). The regulation of the pulpal milieu and the quality of tooth pain vary in relation to those activating and modulating systems.

Many dental nerve endings form close appositions with the odontoblasts (Figures 2(a) and 2(b)), while others end freely in pulp and dentin. Neuro-odontoblast interactions are not fully understood, and may involve odontoblast support for the free sensory endings, modulation of sensory activity, and/or specific sensory activity. The lack of synaptic contacts or gap

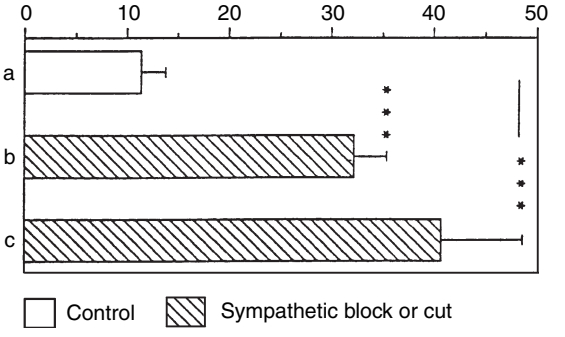

Figure 3 Laser Doppler demonstration of sensory nerve-mediated increased blood flow in rat incisor pulp after α-adrenergic block (b) or sympathectomy (c) compared to intact blood flow (a). All teeth received brief bipolar electrical stimulation of the intact tooth crown. Reproduced from Olgart, L. and Kerezoudis, N. P. 1994. Nerve–pulp interactions. Arch. Oral Biol. 39, 47S–54S, with permission.

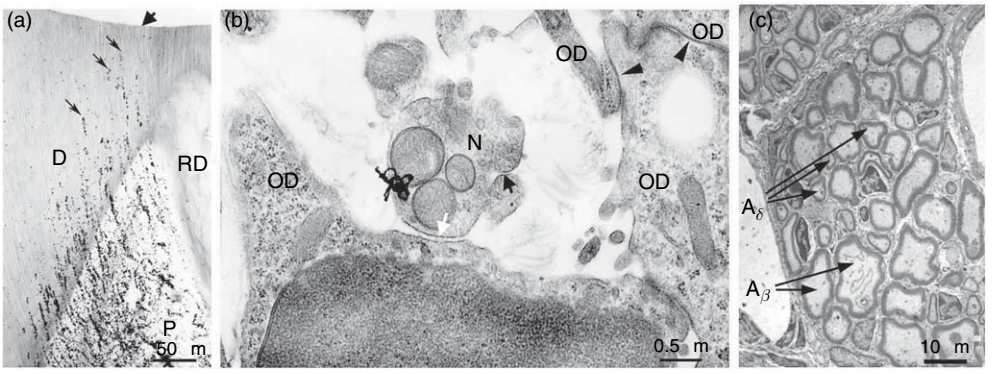

Figure 2 (a) Sensory endings in pulp (P) and dentin (D) (thin arrows) are shown by autoradiography of axonally transported ^{3}H-protein in adult rat molars. They avoid reparative dentin (RD) but come close to surface of tooth (wide arrow). Reprinted from Byers, M.R. 1984. Dental sensory receptors. Int. Rev. Neurobiol. 25, 39–94. (b) Electron microscopic autoradiography showed that transported ^{3}H-proteins (black coiled silver grain) are confined to sensory endings (N). Odontoblasts (OD) are connected by numerous gap junctions (arrowheads). A special apposition separates OD and N (white arrow). Reproduced from Byers, M. R. 1977. Fine structure of trigeminal receptors in rat molars. In: Pain in the Trigeminal Region (*eds*. D. J. Anderson and B. Matthews), pp. 13–24, with permission from Elsevier. (c) Mouse molar root nerves include A-β fibers that exceed 6 μm in diameter and several sizes of A-δ axons.

junctions between odontoblasts and nerves suggests a supportive role. However, demonstrations of neural-like ion channels (Guo, L. and Davidson, R. M., 1998) and TREK-1, a mechanosensitive potassium channel, in odontoblasts (Magloire, H. *et al.*, 2003) show that they are excitable and mechanosensitive. They also attract sensory nerves (Maurin, J. C. *et al.*, 2004) and express neurotrophin factors and receptors in developing, adult, and injured teeth (Fried, K. *et al.*, 2000; Woodnutt, D. A. *et al.*, 2000). It is still not clear whether odontoblast excitability directly affects tooth pain or just allows those cells to monitor dentinogenic requirements.

5.34.2.2 Inflammatory Tooth Pain

When pulp or periapex are inflamed, there are local cellular changes, nerve sprouting, peripheral and central sensitization, and neurochemical plasticity that alter the quality of tooth pain perceptions (Hargreaves, K. M., 2002; Hu, J. W., 2004). Many of the events in inflamed teeth are typical of any inflammation, but there are unusual nerve-sprouting reactions near the pulpitis, and those either subside if healing occurs, or they persist for months or years when lesions escape into the periapical region (Figures 4(a) and 4(b); Byers, M. R. and Närhi, M. V. O., 1999). Important changes occur in dental neuronal satellite cell glia (Figure 4(c)) when inflammation continues in teeth, such as expression of glial fibrillary acidic protein (Stephenson, J. L. and Byers, M. R., 1995). Specialized vascular reactions also occur (Olgart, L., 1996). Recording from individual fibers shows that there are expansions of receptive fields of the A-fiber afferents after 1–2 weeks of inflammation (Figure 5), that would further affect sensitization in the central neurons.

5.34.2.3 Dental Neuropathic Pain

Teeth are major players in referred orofacial pain, either as the source or the referral site, and that situation can lead to unnecessary multiple extractions. Teeth can also exhibit neuropathic symptoms such as hyperalgesia, allodynia, and spontaneous pain (Truelove, E., 2004; Lavigne, G. *et al.*, 2004). A principal mechanism for atypical odontalgia or dental neuropathic pain is the extensive convergence of inputs onto brainstem neurons from a wide area, often involving multiple trigeminal divisions and a variety of tissues (Sessle, B. J., 2000; 2005), and glial actions also affect pain quality (Xie, Y. F. *et al.*, 2006).

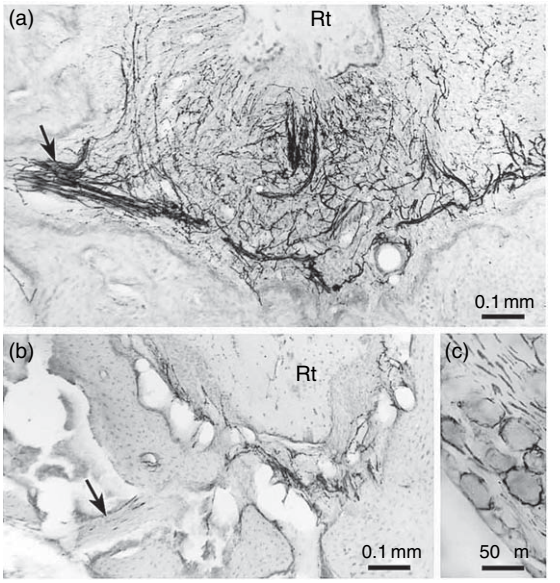

Figure 4 (a, b) Several weeks after tooth injury the lesion has destroyed the pulp and emerged from the root (Rt) into periapical tissue, where there is intense sprouting and immunoreactivity for calcitonin gene-related peptide (CGRP) nerve fibers compared to a normal molar (b). Arrows indicate sensory nerve in alveolar canal. (c) Satellite cells surrounding trigeminal cell bodies are shown by immunocytochemistry to express glial fibrillary acidic protein (black rings) after molar injury in adult rats. (a, b) Reproduced from Kimberly, C. L. and Byers, M. R. 1988. Inflammation of rat molar pulp and periodontium causes increased calcitonin gene-related peptide and axonal sprouting. Anat. Rec. 222, 289–300, with permission.

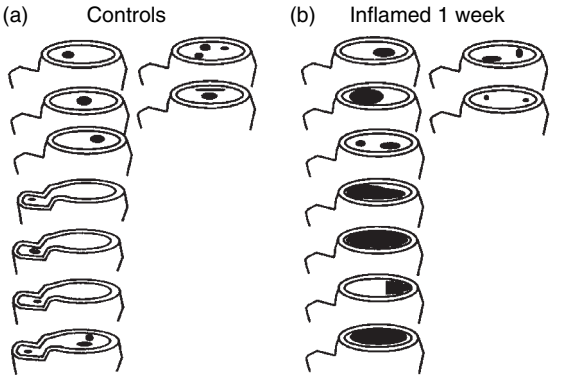

Figure 5 Receptive fields (black patches) for individual A-fibers were larger in dog teeth after 1 week of induced pulpitis compared to control teeth. Reproduced from Närhi, M. V. O., Yamamoto, H., and Ngassapa, D. 1996. Function of Intradental Nociceptors in Normal and Inflamed Teeth. In: Dentin/Pulp Complex (*eds*. M. Shimono, T. Maeda, H. Suda, and K. Takahashi), pp. 136–140. Quintessence Publishing Co, Inc., with permission.

5.34.3 Tooth Pain: Diagnosis and Management

Dentists routinely use evoked acute pain to diagnose tooth pathology, pulp vitality, and treatment (Bender, I. B., 2000). Dental procedures such as orthodontia or root canal treatment cause transient pain that usually decreases within a few days, as the local inflammation subsides, especially with nonsteroidal anti-inflammatory treatment (Dionne, R. A. and Berthold, C. W., 2001). However, pain can persist weeks, months, or years, especially in individuals who have had long-term tooth pain or other chronic pain (Bender, I. B., 2000; Truelove, E., 2004). Tooth pain can expand to a wide area, making it difficult to locate the pathology. Competition from a second pain source can narrow the site to just one tooth, at least for a few minutes to aid diagnosis (Figure 6). This diffuse noxious inhibition implies substantial changes in central physiology for the widely dispersed tooth pains

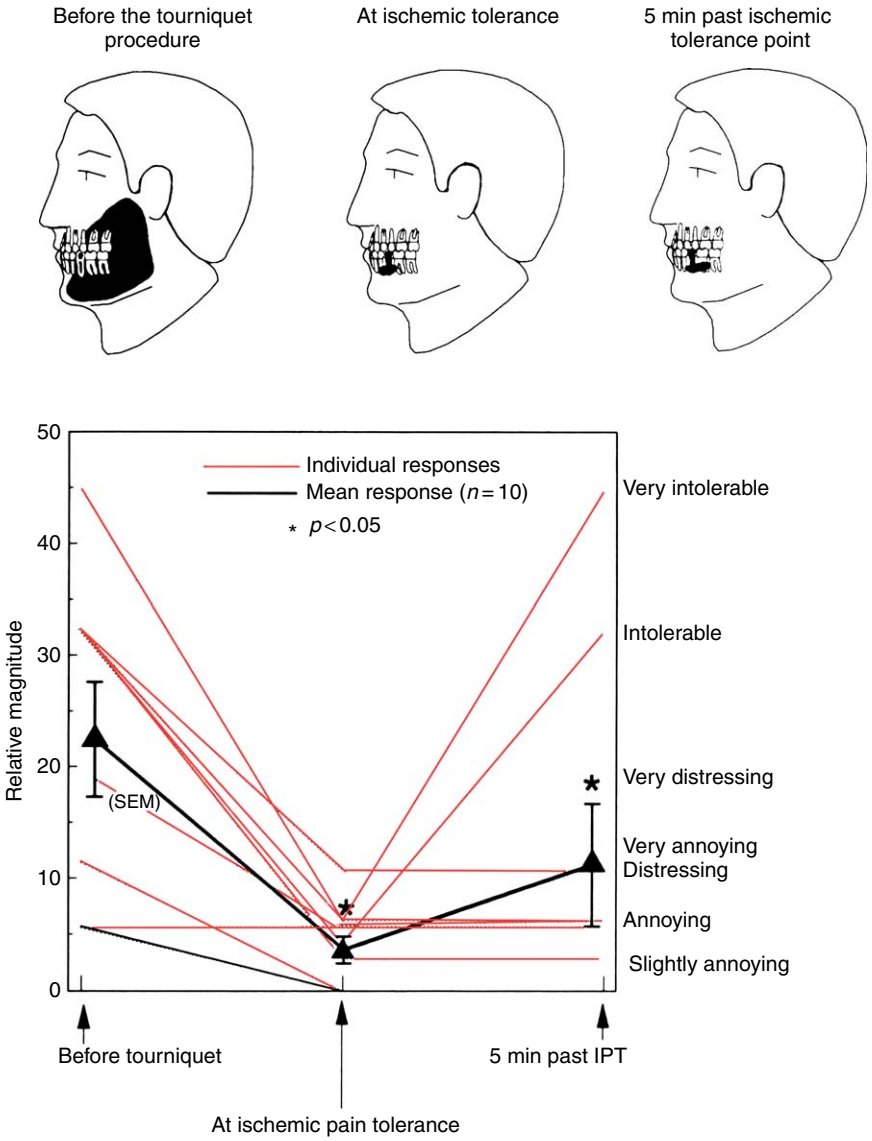

Figure 6 Prior to tourniquet-evoked arm pain, the area of dental pain was large. After maximal arm pain, the tooth pain area was reduced to an individual tooth. By 5 min later, the pain was still focused although the pain intensity (red lines) was returning to prestimulus levels. IPT, ischemic pain tolerance. Reprinted from Pain, 57, Sigurdsson, A. and Maxiner, W., Effects of experimental and clinical noxious counterirritants on pain perception, 265–275, Copyright 1994, with permission from The International Association for the Study of Pain.

(Sessle, B. J., 2005), though important changes in neural sodium channels occur in painful teeth (Renton, T. *et al.*, 2005; Henry, M. A. and Hargreaves, K. M., 2007) offering possible pharmacologic therapeutic targets.

5.34.4 Conclusions

Unusual features of tooth pain include: (1) difficulty locating the source of pain; (2) intense pain from stimulation of dentin; (3) hypersensitive dentin after loss of its protective enamel or periodontal covering, with concomitant pulpitis; (4) special neuro-pulpal interactions; (5) silent pulpal inflammation that only becomes painful when it invades periapical tissues; (6) the hot tooth problem, in which an inflamed painful tooth becomes difficult to anesthetize, even when the rest of the jaw is numb; and (7) referred pain. It is, perhaps, surprising that prolonged tooth pain is unusual, given the huge number of dental procedures every day that can cause tooth, nerve, or bone damage (i.e., dental implants that screw into the jaw, third molar extractions, delicate access for anesthetic injections to reach bone-encased nerves, root canals that remove pulp to eliminate infection). The keys to prevention of debilitating chronic tooth pain include avoiding nerve damage in the jaw, and removal of infected pulp (Bender, I. B., 2000; Hargreaves, K. M., 2002; Hu, J. W., 2004; Truelove, E., 2004; Sessle, B. J., 2005; Henry, M. A. and Hargreaves, K. M., 2007).

References

Bender, I. B. 2000. Pulp pain diagnosis – a review. J. Endodon. 26, 175–179.

Berggreen, E. and Heyeraas, K. J. 2000. Effect of the sensory neuropeptide antagonists h-CGRP (8-37) and SR 140.33 on pulpal and gingival blood flow in ferrets. Arch. Oral Biol. 45, 537–542.

Brännström, M and Åström, A. 1972. The hydrodynamics of dentine: its possible relationship to dentinal pain. Int. Dent. J. 22, 219–227.

Byers, M. R. 1978. Fine Structure of Trigeminal Receptors in Rat Molars. In: Pain in the Trigeminal Region (*eds*. D. J. Anderson and B. Matthews), pp. 13–24, Elsevier.

Byers, M. R. and Närhi, M. V. O. 1999. Dental injury models: experimental tools for understanding neuro-inflammatory interactions and polymodal nociceptor functions. Crit. Rev. Oral Biol. Med. 10, 4–39.

Byers, M. R. and Närhi, M. V. O. 2002. Nerve Supply of the Pulpodentin Complex and Responses to Injury. In: Seltzer and Bender's Dental Pulp (*eds*. K. M. Hargreaves and H. E. Goodis), pp. 151–179. Quintessence.

Dionne, R. A. and Berthold, C. W. 2001. Therapeutic uses of non-steroidal anti-inflammatory drugs in dentistry. Crit. Rev. Oral Biol. Med. 12, 315–330.

Dong, W. K., Shiwaku, T., Kawakami, Y., and Chudler, E. H. 1993. Static and dynamic responses of periodontal ligament mechanoreceptors and intradental mechanoreceptors. J. Neurophysiol. 69, 1567–1582.

Fried, K., Nosrat, C., Lillesaar, C., and Hildebrand, C. 2000. Molecular signaling and pulpal nerve development. Crit. Rev. Oral Biol. Med. 11, 318–332.

Fristad, I., Kvinnsland, I. H., Johnsson, R., and Heyeraas, K. J. 1997. Effect of intermittent long-lasting electrical tooth stimulation on pulpal blood flow and immunocompetent cells: a hemodynamic and immunohistochemical study in young rat molars. Exp. Neurol. 146, 230–239.

Guo, L. and Davidson, R. M. 1998. Potassium and chloride channels in freshly isolated odontoblasts. J. Dent. Res. 77, 341–350.

Hargreaves, K. M. 2002. Pain Mechanisms of the Pulpodentin Complex. In: Seltzer and Bender's Dental Pulp (*eds*. K. M. Hargreaves and H. E. Goodis), pp. 181–203. Quintessence.

Henry, M. A. and Hargreaves, K. M. 2007. Peripheral mechanisms of odontogenic pain. Dent. Clin. North Am. 51, 19–44.

Hu, J. W. 2004. Tooth Pulp. In: Clinical Oral Physiology (*eds*. T. S. Miles, B. Nauntofte, and P. Svensson), pp. 141–162. Quintessence.

Ikeda, H., Tokita, Y., and Suda, H. 1997. Capsaicin-sensitive A-delta fibers in cat tooth pulp. J. Dent. Res. 76, 1341–1349.

Kimberly, C. L. and Byers, M. R. 1988. Inflammation of rat molar pulp and periodontium causes increased calcitonin gene-related peptide and axonal sprouting. Anat. Rec. 222, 289–300.

Lavigne, G., Woda, A., Truelove, E., Ship, J. A., Dao, T., and Goulet, J. P. 2004. Mechanisms associated with unusual orofacial pain. J. Orofac. Pain 19, 9–21.

Lipton, J., Ship, J., and Larach-Robinson, D. 1993. Estimated prevalence and distribution of reported orofacial pain in the United States. J. Am. Dent. Assoc. 124, 115–121.

Magloire, H., Lesage, F., Couble, M. L., Lazdunski, M., and Bleicher, F. 2003. Expression and localization of TREK-1 K^+ channels in human odontoblasts. J. Dent. Res. 82, 542–545.

Maurin, J. C., Couble, M. L., Didier-Bazes, M., Brisson, C., Magloire, H., and Bleicher, F. 2004. Expression and localization of reelin in human odontoblasts. Matrix Biol. 23, 277–285.

Närhi, M. V. O., Yamamoto, H., and Ngassapa, D. 1996. Function of Intradental Nociceptors in Normal and Inflamed Teeth. In: Dentin/Pulp Complex (*eds*. M. Shimono, T. Maeda, H. Suda, and K. Takahashi), pp. 136–140. Quintessence.

Närhi, M. V. O. 2006. Nociceptors in the Dental Pulp. In: Pain Encyclopedia (*eds*. R. F. Schmidt and W. D. Willis), Springer.

Olgart, L. 1996. Neural control of pulpal blood flow. Crit. Rev. Oral Biol. Med. 7, 159–171.

Olgart, L. and Kerezoudis, N. P. 1994. Nerve–pulp interactions. Arch. Oral Biol. 39, 47S–54S.

Renton, T., Yiangou, Y., Plumpton, C., Tate, S., Bountra, C., and Anand, P. 2005. Sodium channel Nav1.8 immunoreactivity in painful human dental pulp. BMC Oral Health 5, 5.

Sessle, B. J. 2000. Acute and chronic craniofacial pain: brainstem mechanisms of nociceptive transmission and neuroplasticity, and their clinical correlates. Crit. Rev. Oral Biol. Med. 11, 57–91.

Sessle, B. J. 2005. Orofacial Pain. In: The Paths of Pain (*eds*. H. Merskey, J. D. Lowser, and R. Dubner), pp. 131–150. IASP Press.

Sessle, B. J., Hu, J. W., Amano, N., and Zhong, G. 1986. Convergence of cutaneous, tooth pulp, visceral, neck and muscle afferents onto nociceptive and non-nociceptive neurons in trigeminal subnucleus caudalis (medullary dorsal horn) and its implications for referred pain. Pain 27, 219–235.

Stephenson, J. L. and Byers, M. R. 1995. GFAP immunoreactivity in trigeminal ganglion satellite cells after tooth injury in rats. Exp. Neurol. 131, 11–22.

Sigurdsson, A. and Maixner, W. 1994. Effects of experimental and clinical noxious counterirritants on pain perception. Pain 57, 265–275.

Suzuki, H., Iwanaga, T., Yoshie, H., Li, J., Yamabe, K., Yanaihara, N., Langel, U., and Maeda, T. 2002. Expression of galanin receptor-1 (GALR1) in the rat trigeminal ganglia and molar teeth. Neurosci. Res. 42, 197–207.

Truelove, E. 2004. Management issues of neuropathic trigeminal pain from a dental perspective. J. Orofac. Pain 18, 374–380.

Wadachi, R. and Hargreaves, K. M. 2006. Trigeminal nociceptors express TLR-4 and CD-14; a mechanism for pain due to infection. J. Dent. Res. 85, 49–53.

Woodnutt, D. A., Wager-Miller, J., O'Neill, P. C., Bothwell, M., and Byers, M. R. 2000. Neurotrophin receptors and nerve growth factor are differentially expressed in adjacent nonneuronal cells of normal and injured tooth pulp. Cell Tissue Res. 299, 225–236.

Xie, Y. F., Zhang, S., Chiang, C. Y., Hu, J. W., Dostrovsky, J. O., and Sessle, B. J. 2006. Involvement of glia in central sensitization in trigeminal subnucleus cudalis (medullary dorsal horn). Brain Behav. Immun. (in press).

5.35 Ascending Pathways: Anatomy and Physiology

D Lima, Universidade do Porto, Porto, Portugal

© 2008 Elsevier Inc. All rights reserved.

5.35.1	**Introduction**	479
5.35.1.1	Defining Nociceptive Ascending Pathways	479
5.35.1.2	The Spinothalamic System	480
5.35.2	**Spinocervical Pathway**	481
5.35.2.1	Spinal Laminae of Origin and Sites of Termination	481
5.35.2.2	Structural Types of Neurons Involved	482
5.35.2.3	Spinal Location of Ascending Fibers	482
5.35.2.4	Response properties	482
5.35.2.5	Pathways Driven at the Target	483
5.35.3	**Spinobulbar Pathways**	483
5.35.3.1	Ventrolateral Reticular Formation	483
5.35.3.1.1	Spinal laminae of origin and sites of termination	483
5.35.3.1.2	Structural types of neurons involved	484
5.35.3.1.3	Spinal location of ascending fibers	485
5.35.3.1.4	Surface receptors	485
5.35.3.1.5	Neurotransmitters	485
5.35.3.1.6	Response properties	486
5.35.3.1.7	Pathways driven at the target	486
5.35.3.2	Dorsal Reticular Nucleus	487
5.35.3.2.1	Spinal laminae of origin and sites of termination	487
5.35.3.2.2	Structural types of neurons involved	488
5.35.3.2.3	Spinal location of ascending fibers	488
5.35.3.2.4	Surface receptors	488
5.35.3.2.5	Neurotransmitters	488
5.35.3.2.6	Response properties	488
5.35.3.2.7	Pathways driven at the target	489
5.35.3.3	Nucleus Tractus Solitarii	489
5.35.3.3.1	Spinal laminae of origin and sites of termination	489
5.35.3.3.2	Structural types of neurons involved	489
5.35.3.3.3	Spinal location of ascending fibers	491
5.35.3.3.4	Neurotransmitters	491
5.35.3.3.5	Response properties	491
5.35.3.3.6	Pathways driven at the target	491
5.35.3.4	Rostral Ventromedial Medulla	492
5.35.3.4.1	Spinal laminae of origin and sites of termination	492
5.35.3.4.2	Structural types of neurons involved	493
5.35.3.4.3	Spinal location of ascending fibers	493
5.35.3.4.4	Neurotransmitters	493
5.35.3.4.5	Response properties	493
5.35.3.4.6	Pathways driven at the target	493
5.35.4	**Spinopontine Pathways**	494
5.35.4.1	Parabrachial Nuclei	494
5.35.4.1.1	Spinal laminae of origin and sites of termination	494
5.35.4.1.2	Structural types of neurons involved	495
5.35.4.1.3	Spinal location of ascending fibers	495
5.35.4.1.4	Surface receptors	496

5.35.4.1.5	Neurotransmitters	496
5.35.4.1.6	Response properties	496
5.35.4.1.7	Pathways driven at the target	497
5.35.5	**Spinomesencephalic Pathways**	497
5.35.5.1	Periaqueductal Gray	497
5.35.5.1.1	Spinal laminae of origin and sites of termination	497
5.35.5.1.2	Structural types of neurons involved	500
5.35.5.1.3	Spinal location of ascending fibers	500
5.35.5.1.4	Surface receptors	500
5.35.5.1.5	Neurotransmitters	500
5.35.5.1.6	Response properties	500
5.35.5.1.7	Pathways driven at the target	501
5.35.6	**Spinodiencephalic Pathways**	501
5.35.6.1	Lateral Thalamus	502
5.35.6.1.1	Spinal laminae of origin and sites of termination	502
5.35.6.1.2	Structural types of neurons involved	504
5.35.6.1.3	Spinal location of ascending fibers	504
5.35.6.1.4	Surface receptors	505
5.35.6.1.5	Neurotransmitters	505
5.35.6.1.6	Response properties	505
5.35.6.1.7	Pathways driven at the target	507
5.35.6.2	Medial Thalamus	507
5.35.6.2.1	Spinal laminae of origin and sites of termination	507
5.35.6.2.2	Structural types of neurons involved	508
5.35.6.2.3	Spinal location of ascending fibers	509
5.35.6.2.4	Neurotransmitters	509
5.35.6.2.5	Response properties	509
5.35.6.2.6	Pathways driven at the target	509
5.35.6.3	Hypothalamus	510
5.35.6.3.1	Spinal laminae of origin and sites of termination	510
5.35.6.3.2	Spinal location of ascending fibers	511
5.35.6.3.3	Surface receptors	512
5.35.6.3.4	Response properties	512
5.35.6.3.5	Pathways driven at the target	512
5.35.7	**Spinothelencephalic Pathways**	512
5.35.7.1	Thelencephalic Targets of Spinal Ascending Fibers	512
5.35.7.2	Spinal Laminae of Origin	513
5.35.8	**Discussion**	514
5.35.8.1	Multiple Parallel Ascending Pathways	514
5.35.8.2	Spinal Neuronal Populations at the Origin of Nociceptive Ascending Pathways	516
5.35.8.3	Stimulus Discrimination	517
5.35.8.4	Nociceptive Ascending Pathways as Part of a Complex Nociceptive Integration System	517
References		518

Glossary

anterograde tracing Staining of axonal terminal arborizations with a substance (tracer) picked up by the neuronal soma and dendrites and transported through the axon up to its terminal structures.

antidromic activation Evoking neuronal spikes by electric activation of the axon terminal field.

antinociceptive action A neuronal effect that results in decrease of responses to pain

and inhibiton of neurons driven by nociceptive input.

ascending pathway Neuronal tract that conveys input from caudal to rostral areas along the spinal cord and brain.

contralateral pathway Pathway connecting gray matter regions (nuclei) located in opposite sides of the spinal cord or brain.

dendrites The branch units of a dendritic arbor.

dendritic arbor The receptive area of a neuron, organized from the perikarya as the ramifying branches of a tree.

dendritic spines Small protrusions of the dendritic surface that more often appear as a knob connected to the dendritic shaft by a short pedicle.

electrophysiological recording Recording of changes in the membrane potential or current in a neuron.

facilitatory loop Neuronal circuit playing a positive feedback action so that neuronal activity is enhanced.

fiber decussation Crossing of axons from one side to the other side of the spinal cord or the brain.

high-threshold neurons Neurons responsive solely to stimuli of high intensity (noxious).

ipsilateral pathway Pathway connecting gray matter regions (nuclei) located in the same side of the spinal cord or brain.

low-threshold neurons Neurons responsive solely to stimuli of low intensity (innocuous).

neuronal soma The central area of a neuron where the nucleus and most organelles are located.

neurotransmitters Molecules that functionally connect neurons at synapses by being delivered by the presynaptic element upon depolarization and acting upon ligand-gated receptors at the postsynaptic element.

nociresponsive Driven by the arrival of nociceptive input.

noxious stimulation Presentation of stimuli that represent a potential or effective aggression to a peripheral tissue.

pain inhibitory center Region in the central nervous system whose stimulation results in pain depression.

primary sensory neurons Neurons that convey input from the periphery to the central nervous system.

receptive field of a neuron The peripheral area whose stimulation elicits neuronal responses.

retrograde tracing Staining of the neuronal soma and dendritic arbors with a substance (tracer) picked up by the respective axonal boutons and transported back through the axon.

second-order neurons Neurons that transmit input from primary sensory neurons to higher order processing centers.

somatotopy Structural arrangement that correlates topographic organization at different sites, either at the periphery or in the central nervous system.

spinofugal transmission Input transmission away from the spinal cord.

target Area where the axon terminal arborization of a neuron is distributed.

transmitter receptors Plasma membrane molecules which, upon activation by a ligand (neurotransmitter), open ionic channels inducing alteration in the membrane potential.

wide dynamic-range neurons Neurons responsive to stimuli of graded intensities, from innocuous to noxious, but more intensively at the noxious range.

5.35.1 Introduction

5.35.1.1 Defining Nociceptive Ascending Pathways

Nociceptive information traveling from the periphery in primary sensory neurons is transmitted to second-order neurons located at the spinal cord and cranial sensory nuclei. From this first relay, various pathways distribute nociceptive input through higher processing centers so that pain is ultimately perceived in its multiple dimensions and adequate adaptive responses are generated. These ascending pathways are believed to terminate in the cortex with one or several relay stations in their way, although for most of the tracts, studies demonstrating that the intervening neurons are indeed serially connected from the spinal cord to the cortex are missing. The term 'nociceptive ascending pathways' is thus normally used in

a restricted sense, to designate the neuronal tracts that connect the spinal cord with supraspinal regions, each pathway being named from the brain area at which it terminates.

The nociceptive nature of a pathway is classically demonstrated by recording responses to noxious stimuli from spinal neurons antidromically activated from the target (Perl, E. R. and Whitlock, D. G. 1961; Dilly, P. N. *et al.*, 1968). More recently, detection of molecular markers of nociceptive activation (Hunt, S. P. *et al.*, 1987) in conjunction with retrograde tracing has been largely used. By revealing large populations of putative nociceptive neurons, such a procedure allows an easy characterization of the location and morphology of neurons projecting in each pathway, and is particularly valuable to uncover varying population activation patterns as a function of stimulation conditions (Lima, D., 1998).

The structural features that best describe a pathway are the topographic and morphofunctional characteristics of the spinal neurons involved and the area of termination of their axons. Studies addressing the morphology of spinal projecting neurons are particularly few and mainly related to lamina I. One of the reasons for the restricted use of this kind of evaluation is the lack of systematic models of classification of spinal neurons apart from laminae I (Gobel, S. 1978a; Lima, D. and Coimbra, A., 1983; 1986) and II (Gobel, S., 1978b). Recent studies, however, call our attention to the importance of neuronal morphology, in particular, dendritic geometry, in defining the signal-processing properties of neurons (Prescott, S. A. and De Koninck, Y. 2002; Szucs, P. *et al.*, 2003; Mainen, Z. F. and Sejnowski, T. J. 2006), which justify taking these aspects into account when addressing the anatamophysiology of a pathway.

The multitude of ascending nociceptive pathways, together with the subtleness of the anatomical and physiological features that separate them as to their origin at the spinal cord, makes it difficult to attribute a particular functional meaning to each one. A tentative way of unraveling the role of each pathway in nociceptive processing has been the elucidation of the connections established by the target.

5.35.1.2 The Spinothalamic System

The classical view of the ascending nociceptive system puts particular emphasis on the dual distribution of nociceptive input through a lateral pathway responsible for sharp, well-localized short lasting pain, and a medial pathway responsible for diffuse, poorly localized persisting pain (Figure 1). From the spinal cord, nociceptive input is conveyed both to the posterior lateral sensory nuclei of the thalamus, in the lateral or neospinothalamic pathway (Bowsher, D. 1957; Mehler, W. R. 1957; Willis, W. D. *et al.*, 1974; Giesler, G. J. *et al.*, 1976) and to medial thalamic nuclei, in the medial or paleospinothalamic pathway (Mehler, W. R. *et al.*, 1956; Bowsher, D. 1957; Mehler,

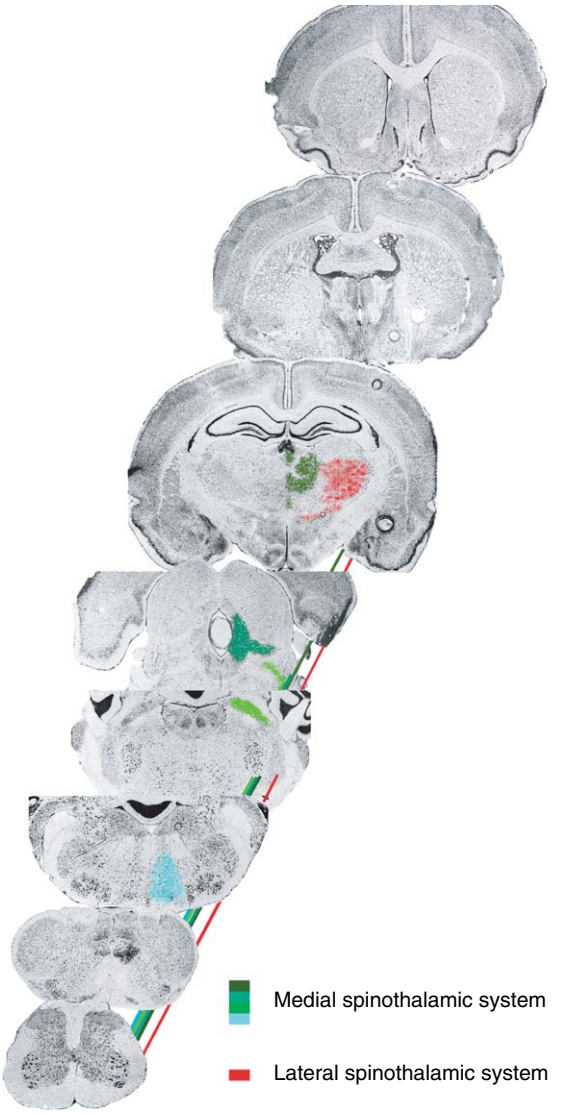

Figure 1 Diagrammatic representation of the areas of termination of the lateral spinothalamic pathway and the medial spinothalamic pathway, and the spinoreticular pathways that serve as relays in the medial spinothalamic system. Brain and spinal cord photomicrographs were adapted from Paxinos, G. and Watson, C. 1998. The Rat Brain in Stereotaxic Coordinates, 4th edn. Academic Press.

W. R. 1957; Giesler, G. J. *et al*., 1981b). While the first is monosynaptic, made up of spinal neurons projecting directly to the thalamus (Trevino, D. L. and Carstens, E. 1975; Willis, W. D. *et al*., 1979; Giesler, G. J. *et al*., 1979a), the second is either monosynaptic or polysynaptic with a variable number of relays along the brainstem (Johnson, F. H. 1954; Mehler, W. R. *et al*., 1956; Rossi, G. F. and Brodal, A. 1957; Bowsher, D. 1957; Carstens, E. and Trevino, D. L. 1978b; Willis, W. D. *et al*., 1979; Giesler, G. J. *et al*., 1979a).

The lateral spinothalamic pathway was proposed to be involved in the discriminative aspects of pain (Bowsher, D. 1957; Melzack, R. and Casey, K. L. 1968) based on early studies on the perception deficits resulting from lesions of lateral thalamic nuclei (Dejerine, J. and Roussy, G. 1906; Melzack, R. and Casey, K. L. 1968). This was later supported by studies showing that both spinal and thalamic neurons of the lateral spinothalamic pathway present small receptive fields (Giesler, G. J. *et al*., 1981b; Willis, W. D. 1988), are capable of encoding the extent of the stimulated area and the intensity of the stimulus(Kenshalo, D. R., Jr. *et al*., 1979; Peschanski, M. *et al*., 1980; Guilbaud, G. *et al*., 1985; Willis, W. D. 1988; Guilbaud, G. and Kayser, V. 1988), and terminate following a somatotopic pattern in the thalamus and cortex respectively (Whitsel, B. L. *et al*., 1978; Boivie, J. 1979). The medial spinothalamic pathway was claimed to deal with the affective and volitive aspects of pain (Bowsher, D. 1957; Melzack, R. and Casey, K. L. 1968) based on similar behavioral studies on human and experimental animals suffering from lesions of various brainstem or thalamic areas (Dejerine, J. and Roussy, G. 1906; Walker, A. E. 1942b; Hécaen, H. *et al*., 1949). This view was again supported by studies revealing that spinal and thalamic neurons of the medial pathway present large receptive fields, responses unrelated to stimulus intensity (Giesler, G. J. *et al*., 1981b; Guilbaud, G. *et al*., 1985) and no topographical arrangement of their axonal terminal arborizations in both the thalamus (Boivie, J. 1979) and cortex (Morison, R. S. and Dempsey, E. W. 1942; Jones, E. G. and Leavitt, R. Y. 1974).

In the last decades, the use of very sensitive electrophysiological and tracing techniques revealed a wide variety of brainstem loci capable of contributing as relays to the medial spinothalamic system (reviewed by (Lima, D., 1997), and uncovered ascending pathways that bypass the thalamus to terminate directly on telencephalic areas, including the cortex (Cliffer, K. D. *et al*., 1991). In this chapter, the various pathways involved in the spinofugal transmission of nociceptive input will be referred following a caudorostral sequence.

5.35.2 Spinocervical Pathway

The spinocervical pathway is one of the ascending putative nociceptive pathways uncovered the earliest, based on its capacity to activate cortical sensory areas (Catalano, J. V. and Lamarche, G., 1957; Mark, R. F. and Steiner, J., 1958) and on the finding that neurons of the lateral cervical nucleus (LCN) project to the ventrobasal complex of the thalamus (Ha, H. and Liu, C. N., 1966; Craig, A. D. and Burton, H., 1979; Baker, M. L. and Giesler, G. J., 1985; Giesler, G. J., *et al*., 1987). It has been claimed, however, to be mostly dedicated to the processing of tactile, hair movement input (Lundberg, A. and Oscarsson, O., 1961; Taub, A. and Bishop, P. O., 1965) and be mainly represented in carnivores (Flink, R. and Westman, J., 1986). The identification of a neuronal column continuing the lateral cervical nucleus caudally along the entire length of the cord (the lateral spinal nucleus), together with the finding that their neurons also send projections to the thalamus as well as to many other brain areas (see ahead), raised the possibility that the lateral cervical nucleus is part of a more extensive spinal neuronal aggregation lying within the dorsolateral fasciculus, which serves as a relay in various ascending nociceptive pathways. Nonetheless, differences in the morphology and response properties of lateral cervical and lateral spinal neurons (Giesler, G. J. *et al*., 1979b; Menétrey, D. *et al*., 1980) point to a specific role of the former in conveying ascending input to the lateral thalamus.

5.35.2.1 Spinal Laminae of Origin and Sites of Termination

Neurons projecting to the lateral cervical nucleus are mainly located in the ipsilateral spinal cord at lamina IV (Figure 2) (Bryan, R. N. *et al*., 1973; Craig, A. D., 1976; Brown, A. G. *et al*., 1976; Cervero, F. *et al*., 1977; Brown, A. G. *et al*., 1977; Craig, A. D., 1978; Brown, A. G. *et al*., 1980a; Baker, M. L. and Giesler, G. J., 1984), where they amount to 60% of the entire population, followed by lamina III (10%) (Brown, A. G. *et al*., 1980a). Scattered neurons are present in other laminae such as laminae I, V, VI, and VII (Craig, A. D., 1976; Craig, A. D., 1978; Brown, A. G. *et al*., 1980a;

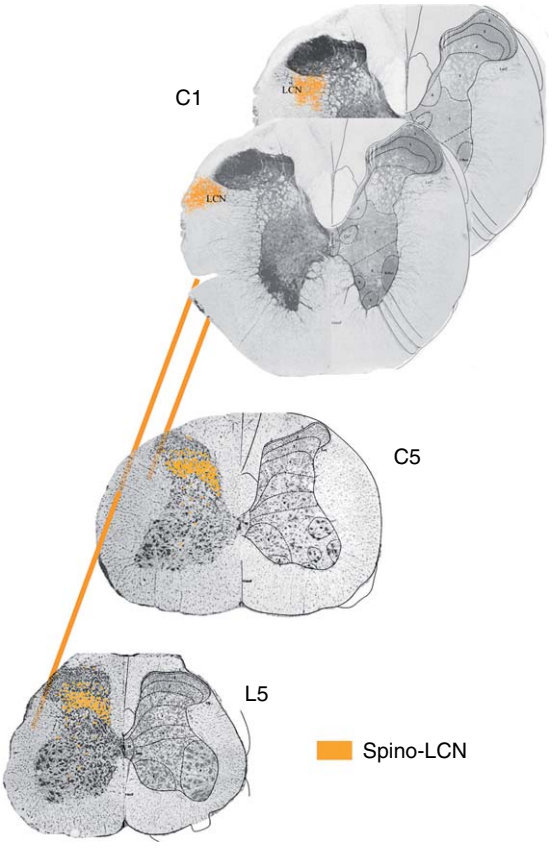

Figure 2 Diagram representing the spinal laminae of origin, ascendingb course in the spinal cord, and areas of termination of the spino-LCN pathway. Note the somatotopic arrangement of the axon terminal fields according to their rostrocaudal origin. (in this figure and figures 3, 7, 10, 12, 13, 15, 17, 19, 21 and 24, the left side is ipsilateral to the side of arrival of peripheral input) Brain and spinal cord photomicrographs were adapted from Paxinos, G. and Watson, C. 1998. The Rat Brain in Stereotaxic Coordinates, 4th edn. Academic Press.

Baker, M. L. and Giesler, G. J., 1984). Axonal terminals are somatotopically organized, fibers originated in caudal levels terminating in the dorsolateral aspect of the caudal portion of the lateral cervical nucleus, and fibers originated in rostral levels in the medial aspect of its rostral portion (Figure 2) (Svensson, B. A. *et al.*, 1985).

5.35.2.2 Structural Types of Neurons Involved

Neurons targeting the lateral cervical nucleus are commonly described as small-sized (10–20 μm) (Craig, A. D., 1978; Baker, M. L. and Giesler, G. J., 1984), but neurons with large round soma have also been observed in lamina IV (Craig, A. D., 1978). They present dorsally oriented dendrites (Brown, A. G. *et al.*, 1976; Jankowska, E. *et al.*, 1976; Brown, A. G. *et al.*, 1977; Craig, A. D., 1978; Brown, A. G. *et al.*, 1980b), which extend rostrocaudally for up to 2000 μm without penetrating lamina II (Brown, A. G. *et al.*, 1977; Brown, A. G. *et al.*, 1980b).

5.35.2.3 Spinal Location of Ascending Fibers

Spinal axons targeting the lateral cervical nucleus course ipsilaterally in the dorsal part of the lateral funiculus (Figure 2) (Brown, A. G. *et al.*, 1977; Baker, M. L. and Giesler, G. J., 1984; Giesler, G. J. *et al.*, 1988). According to Ha and Liu (Ha, H. and Liu, C. N., 1966), they are often collaterals of fibers coursing to more rostral levels.

5.35.2.4 Response properties

Nociceptive neurons at the origin of the spinocervical pathway present background activity in bursts (Brown, A. G. and Franz, D. N., 1969). They are activated by Aβ, Aδ, and C primary afferent fibers (Taub, A. and Bishop, P. O., 1965), A fibers exciting the entire neuronal population either alone (29%) or in convergence with C fibers (71%) (Brown, A. G. *et al.*, 1975). They belong in the low-threshold (LT), wide-dynamic range (WDR) and high-threshold (NS) classes (Brown, A. G. and Franz, D. N., 1969; Bryan, R. N. *et al.*, 1973; Bryan, R. N. *et al.*, 1974; Cervero, F. *et al.*, 1977; Downie, J. W. *et al.*, 1988). Neurons receiving high-threshold input were reported to make up between 60% and 86% of the entire projecting population (Cervero, F. *et al.*, 1977; Kajander, K. C. and Giesler, G. J., 1987). High-threshold input is generated either by pressure, pinch, heat, or cold (Brown, A. G. and Franz, D. N., 1969; Bryan, R. N. *et al.*, 1973; Bryan, R. N. *et al.*, 1974; Cervero, F. *et al.*, 1977; Downie, J. W. *et al.*, 1988), while low-threshold input is mainly originated in hair follicle afferent receptors (Brown, A. G. and Franz, D. N., 1969). Receptive fields are small and located in hairy as well as glabrous skin (Bryan, R. N. *et al.*, 1974; Kunze, W. A. A. *et al.*, 1987; Downie, J. W. *et al.*, 1988). They are organized somatotopically so that cells located more laterally have receptive fields in the dorsal surface of the body and cells located more medially in the ventral surface (Bryan, R. N. *et al.*, 1973; Bryan, R. N. *et al.*, 1974; Brown, A. G. *et al.*,

1980a). Inhibitory receptive fields were described adjacent to the excitatory receptive field (Brown, A. G. *et al.*, 1987; Short, A. D. *et al.*, 1990) or in the contralateral limb (Brown, A. G. and Franz, D. N., 1969). Natural stimuli causing neuronal inhibition include hair movement, pressure, and squeezing (Brown, A. G. and Franz, D. N., 1969; Brown, A. G. *et al.*, 1987; Short, A. D. *et al.*, 1990). Convergence of cutaneous and deep tissues input has been reported (Kniffki, K. D. *et al.*, 1977; Hamann, W. C. *et al.*, 1978; Harrison, P. J. and Jankowska, E., 1984). Only cells responsive to both hair movement and skin pressure were shown to receive group III and IV muscle afferent input (Hamann, W. C. *et al.* 1978). Muscle and joint primary afferent activation can also elicit neuronal inhibition (Hamann, W. C. *et al.* 1978; Harrison, P. J. and Jankowska, E. 1984).

5.35.2.5 Pathways Driven at the Target

Axons from neurons in the lateral cervical nucleus join the medial lemniscus contralaterally and terminate in the midbrain, the ventral posterial lateral nucleus (VPL), and the posterior complex (PO) of the thalamus (Ha, H. and Liu, C. N., 1966). In the midbrain, the lateral part of the periaqueductal gray (PAG) receives afferents from the lateral two-thirds of the lateral cervical nucleus (Mouton, L. J. and Holstege, G., 2000; Mouton, L. J. *et al.*, 2004). In the VPL, fibers ascending from the lateral cervical nucleus are topographically arranged so that those originated in its dorsolateral portion terminate in the VPL, *pars lateralis*, and those originated in its ventromedial portion terminate in the VPL, *pars medialis* (Craig, A. D. and Burton, H., 1979).

5.35.3 Spinobulbar Pathways

Most spinobulbar pathways were uncovered relatively recently and are not as thoroughly studied as the more rostrally terminating pathways such as the spinomesencephalic and the spinothalamic. With the exception of the rostral ventromedial medulla (RVM), the majority of the studies dealing with spinobulbar pathways were performed in the rat. An anecdotic study addressing the spinal pathways terminating in the caudal medulla of the pigeon (Galhardo, V. *et al.*, 2000), however, reveals remarkable similarities with the rat, pointing to a high degree of phylogenetic conservation.

5.35.3.1 Ventrolateral Reticular Formation

5.35.3.1.1 Spinal laminae of origin and sites of termination

Spinal cells projecting to the caudal ventrolateral reticular formation (VLM) are distributed through laminae I, II, IV–VII, VIII, X, and the lateral spinal nucleus (Figure 3) (Menétrey, D. *et al.*, 1983; Menétrey, D. *et al.*, 1984; Leah, J. *et al.*, 1988; Lima, D. *et al.*, 1991; Galhardo, V. *et al.*, 2000). Projections were first described to be mainly contralateral (Menétrey, D. *et al.*, 1983; Menétrey, D. *et al.*, 1984; Thies, R., 1985), but an important ipsilateral component was revealed by the use of more sensitive retrograde tracers (Menétrey, D. *et al.*, 1982; Lima, D. *et al.*, 1991; Menétrey, D. *et al.*, 1992b; Galhardo, V. *et al.*, 2000). There is, however, a large variability in the proportion of cells labeled in each spinal side, particularly with respect to cells located in the superficial dorsal horn. Both ipsilateral and contralateral predominance have been observed, in a few cases in the same animal at different rostrocaudal levels (Lima, D. *et al.*, 1991). The occurrence of subtle differences in the area of termination of each spinal side along the cord length was proposed as a tentative explanation, but experiments designed to clarify a putative somatotopic arrangement are missing.

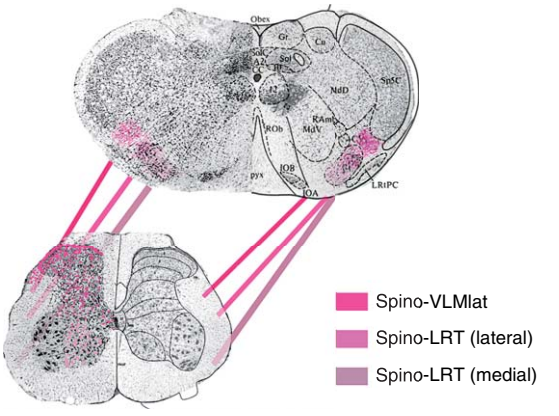

Figure 3 Diagram representing the spinal laminae of origin, ascending course in the spinal cord, and areas of termination of the spino-VLM pathway. Note the contribution of lamina II neurons. Brain and spinal cord photomicrographs were adapted from Paxinos, G. and Watson, C. 1998. The Rat Brain in Stereotaxic Coordinates, 4th edn. Academic Press.

Spino-VLM axons appear to give axonal collaterals to various sites within the brainstem (Thies, R., 1985), such as the parabrachial nuclei (PBN) and the PAG (Spike, R. C. *et al.*, 2003).

The use of discrete injections, which became possible with the advent of particularly sensitive tracing methods, clearly demonstrated that the spino-VLM system is composed of three pathways originating in three distinct spinal regions (Figure 3).

The pathway originating in the superficial dorsal horn (laminae I–III) and lateral spinal nucleus was observed in the rat (Lima, D. and Coimbra, A., 1991; Tavares, I. *et al.*, 1993), cat, and monkey (Craig, A. D., 1995) to terminate in the lateral-most portion of the VLM (VLMlat), in between the spinal trigeminal nucleus and the ventral tip of the lateral reticular nucleus (LRt). The pathways originating in the deep dorsal horn (laminae IV–VI) and intermediate/ventral horn (laminae VII and X) terminate, respectively, in the lateral half and the medial half of the LRt (Lima, D. *et al.*, 1991).

A curious aspect of the spino-VLMlat projection is the participation of a large amount of cells of the substantia gelatinosa, or lamina II (Figure 4) (Lima, D. *et al.*, 1991; Lima, D. and Coimbra, A., 1991), an area that was not shown to participate significantly in any other ascending pathway and is therefore usually taken as involved in nociceptive modulatory local or propriospinal circuits (see Chapter Spinal Cord Physiology of Nociception). Lamina II neurons project, together with neurons in lamina I and the lateral spinal nucleus, to the VLMlat (Figure 3), contributing to almost one-third of the entire spinal-VLMlat projection in the cervical enlargement, and to one-fifth in the lumbar enlargement.

(Lima, D. and Coimbra, A., 1991). There are still no clues on the physiological meaning of this unique lamina II projection to the VLMlat. Studies aimed at clarifying whether these cells participate in inhibitory circuits similar to those described in the superficial dorsal horn failed to reveal GABA content in these neurons (Tavares, I. and Lima, D., 2002).

5.35.3.1.2 Structural types of neurons involved

Lamina I neurons projecting in the spino-VLM pathway were characterized in the rat, based on the comparison of the structural features of neurons retrogradely labeled with CTb at various spinal cord levels in the three anatomical planes (Lima, D. *et al.*, 1991). In the rat, as in the pigeon (Galhardo, V. *et al.*, 2000), spino-VLM neurons belong in three (fusiform,

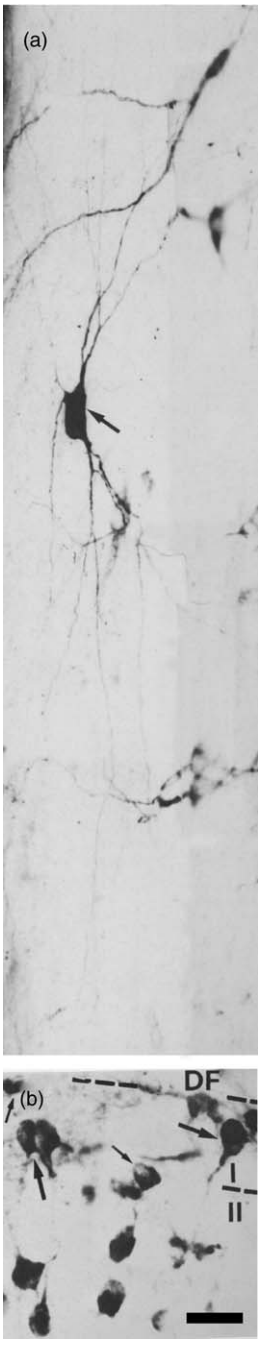

Figure 4 Superficial dorsal horn neurons labeled retrogradely with cholera toxin subunit B (CTb) from the VLMlat. (a) Lamina I neuron of the fusiform type, subtype B, in horizontal view. (b) Lamina I fusiform neurons and lamina II neurons in transverse view. Note the ventrally oriented dendrites of fusiform B neurons (large arrows in (b)). DF – Dorsal funiculus. Scale bar = 30 μm. Adapted from figure 3 of Lima, D., Mendes-Ribeiro, J. A., and Coimbra, A. 1991. The spino-latero-reticular system of the rat: projections from the superficial dorsal horn and structural characterization of marginal neurons involved. Neuroscience 45, 137–152.

pyramidal, and flattened) of the four structural neuronal groups present in lamina I. The majority (around 80%) are of the fusiform type, a neuronal group whose main characteristic is the strict longitudinal spiny dendritic arbor. Some fusiform neurons present a few dendrites oriented ventrally and penetrating the entire width of lamina II (Figure 4). These neurons, classified as fusiform B by Lima and Coimbra (Lima, D. and Coimbra, A., 1986), represent a large fraction of VLMlat-projecting fusiform cells (20%) when compared to the small contribution of this neuronal subtype (6%) to the entire lamina I fusiform neuronal population (Lima, D. and Coimbra, A., 1986). Curiously, fusiform B neurons could not be observed in other spinofugal pathways. This finding is particularly interesting in the light of the contribution of lamina II neurons to this pathway (Figure 4). It may indicate that neurons of the fusiform B subtype cooperate with lamina II neurons in transmitting to the VLMlat primary input arriving at lamina II. The remaining 20% VLM-projecting lamina I neurons belong to the flattened and pyramidal types in similar amounts. These two cell groups have in common long practically aspiny dendrites coursing horizontally, parallel to the dorsal surface of lamina I. Pyramidal neurons have, in addition, dendrites that ramify inside the white matter overlying lamina I.

VLM-projecting lamina II neurons present ovoid, rostrocaudally elongated dendritic arbors that extend as parasagittal sheets through the entire width of lamina II (Lima, D. and Coimbra, A., 1991), resembling the central and the limiting cells of Ramón y Cajal (Ramón y Cajal, S., 1909).

5.35.3.1.3 Spinal location of ascending fibers

According to the intense fiber staining occurring in the dorsolateral fasciculus after retrograde tracer injections in theVLMlat (Lima, D. *et al.*, 1991), VLM projections from laminae I–III course in the dorsal portion of the lateral funiculus (Figure 3), as is the case of the spinomesencephalic (McMahon, S. B. and Wall, P. D., 1985; Hylden, J. L. K. *et al.*, 1986b) and spinothalamic (Apkarian, A. V. *et al.*, 1985; Apkarian, A. V. and Hodge, C. J., 1989c) pathways.

5.35.3.1.4 Surface receptors

Large numbers of lamina I neurons projecting to the VLM express neurokinin I (NK1) (Figure 5) (Todd, A. J. *et al.*, 2000; Spike, R. C. *et al.*, 2003; Castro, A. R. *et al.*, 2006) and $GABA_B$ receptors (Castro, A. R. *et al.*, 2006), the co-localization of both being relatively frequent (Castro, A. R. *et al.*, 2006).

In addition, 90% of the large deep dorsal horn neurons with dendrites entering superficial laminae and exhibiting the NK1 receptor project to the VLM (Todd, A. J. *et al.*, 2000). Appositions of serotonin (5HT) and noradrenalin-containing axonal boutons upon VLM-projecting lamina I neurons are common (Tavares, I. *et al.*, 1996a; Polgar, E. *et al.*, 2002). Serotoninergic boutons establish symmetrical synaptic contacts and are more abundant upon neurons expressing the NK1 receptor (Polgar, E. *et al.*, 2002).

5.35.3.1.5 Neurotransmitters

As in most ascending pathways conveying nociceptive input, studies addressing the neurochemical content of

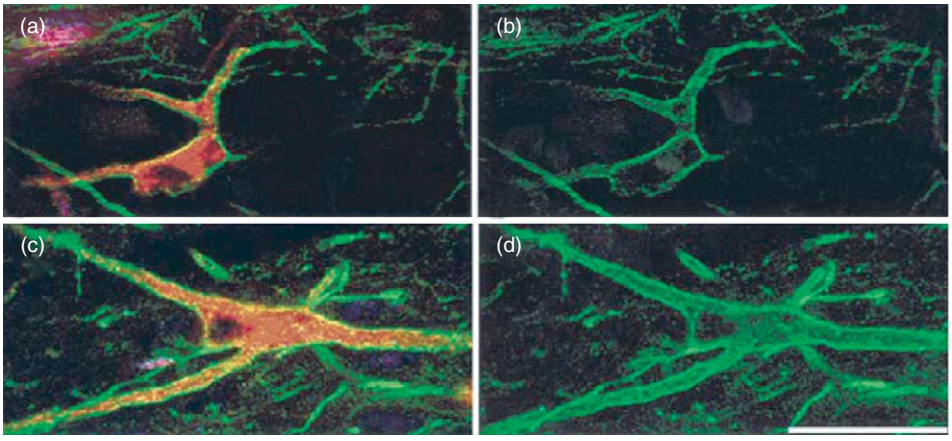

Figure 5 Flattened (a, b) and pyramidal (c, d) lamina I neurons, in horizontal view, retrogradely labeled with cholera toxin subunit B (CTb) from the VLM (red) and immunoreactive for the NK1 receptor (green). Scale bar = 50 μm. Adapted from figure 9 of Spike, R. C., Puskar, Z., Andrew, D., and Todd, A. J. 2003. A quantitative and morphological study of projection neurons in lamina I of the rat lumbar spinal cord. Eur. J. Neurosci. 18, 2433–2448.

the neurons of origin of the spino-VLM pathway have focused on neuropeptides. The exhaustive study of Leah and collaborators (Leah, J. *et al.*, 1988) revealed a relatively large amount of vasoactive intestinal peptide (VIP), bombesin, dynorphin, and substance P-immunoreactive VLM-projecting neurons in the lateral spinal nucleus. A few enkephalin immunoreactive neurons were observed in lamina X. Calbindin is present in particularly large numbers of lumbosacral cells projecting to the VLM-bilaterally, especially within lamina I and the lateral spinal nucleus, but also in lamina X (Menétrey, D. *et al.*, 1992b). Although fusiform neurons in lamina I (Lima, D. *et al.*, 1993) and neurons in lamina II (Todd, A. J. and Spike, R. C., 1993) are known to contain GABA, GABA-immunostaining of neurons retrogradely labeled from the VLM could not be observed (Tavares, I. and Lima, D., 2002).

5.35.3.1.6 Response properties

The response properties of neurons projecting to the ventrolateral reticular formation were studied in the rat (Menétrey, D. *et al.*, 1984) and cat (Thies, R., 1985). A high proportion of VLM-projecting neurons are spontaneously active (Menétrey, D. *et al.*, 1984; Thies, R., 1985). NS neurons make up about half of the entire population of VLM-projecting neurons (Menétrey, D. *et al.*, 1984; Thies, R., 1985). The remaining are either WDR or LT/proprioceptive neurons (Menétrey, D. *et al.*, 1984; Thies, R., 1985). They often present bilateral symmetrical receptive fields as well as cutaneous inhibitory receptive fields (Menétrey, D. *et al.*, 1984). Convergence of cutaneous, visceral, and muscle input is frequently observed (Thies, R., 1985). By monitoring noxious-evoked c-*fos* induction (Tavares, I. *et al.*, 1993), 10% to 20% of VLM-projecting neurons were shown to be activated by heat or mechanical stimulation in laminae I and IIo. In lamina IIi, neurons were activated in fewer numbers and only after thermal stimulation.

5.35.3.1.7 Pathways driven at the target

The VLM projects to several brain areas also receiving nociceptive input from the spinal cord and involved in pain control as well as cardiovascular, endocrine, or limbic functioning. Among these areas stand the RVM; the dorsal reticular nucleus (DRt); the A_5, A_6, and A_7 pontine noradrenergic groups (Tavares, I. *et al.*, 1996b); the hypothalamus (Calaresu, F. R. *et al.*, 1984; Malick, A. *et al.*, 2000); and the central nucleus of the amygdala (Zardettosmith, A. M. and Gray, T. S., 1995). Studies focused on the brainstem showed that the VLMlat is the VLM region that establishes connections with other supraspinal pain inhibitory centers (Tavares, I. *et al.*, 1996b; Cobos, A. *et al.*, 2003), pointing to a role of the superficial dorsal horn-VLMlat pathway in driving the potent descending inhibition that can be elicited upon stimulation of VLM (Gebhart, G. F. and Ossipov, M. H., 1986). At the RVM and the pontine A_5 noradrenergic group, terminal arborizations of VLM axons appose spinal-projecting neurons (Figure 6), indicating that pain control actions from those areas are indeed under the control of the VLM (Tavares, I. *et al.*, 1996b).

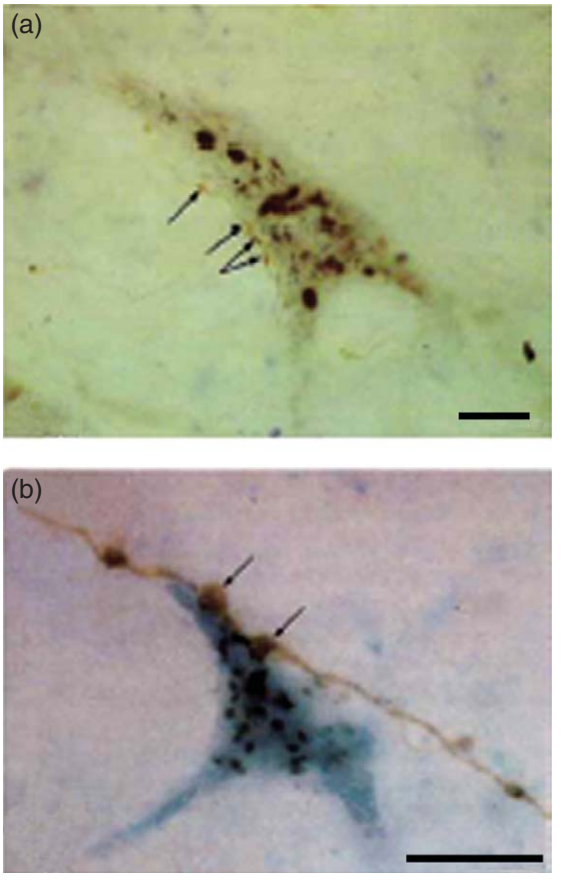

Figure 6 RVM (a) and A_5 (b) neurons retrogradely labeled with cholera toxin subunit B (CTb) from the spinal cord (brown granules) and receiving appositions (arrows) from axonal boutons anterogradely labeled with biotinilated dextran amine (BDA) from the VLM. Neuron in (b) is immunoreactive for dopamine-β-Hydroxylase (DBH; blue). Scale bar = 20 μm. (Adapted from figure 3 of Tavares, I., Lima, D., and Coimbra, A. 1996b. The ventrolateral medulla of the rat is connected with the spinal cord dorsal horn by an indirect descending pathway relayed in the A5 noradrenergic cell group. J. Comp. Neurol. 374, 84–95).

In the A_5, spinal-projecting neurons contacted by VLMlat fibers are noradrenergic (Figure 6) and postsynaptic in asymmetric, putative excitatory synaptic contacts (Tavares, I. *et al.*, 1996b). This was taken as suggestive that the spinal α_2 adrenoreceptor-mediated antinociceptive action triggered in the VLM is dependent on VLMlat activation and relayed in the A_5 group.

The VLM also sends direct descending projections to the spinal cord (Tavares, I. and Lima, D., 1994). Projections to both the superficial and deep dorsal horn originate in the VLMlat (Tavares, I. and Lima, D., 1994). Data from several studies indicate that noradrenaline is not used in the direct VLM-spinal pathway (Westlund, K. N. *et al.*, 1981; Westlund, K. N. *et al.*, 1983; Tavares, I. *et al.*, 1996b). VLMlat axons targeting lamina I make up a reciprocal closed VLM-spino-VLM loop which is entirely excitatory at the VLM level, and both excitatory and inhibitory at the spinal level (Tavares, I. *et al.*, 1998; Tavares, I. and Lima, D., 2002).

The cerebellar connections of the LRt (Cledenin, M. *et al.*, 1974; Parenti, R. *et al.*, 1996), together with the fact that, contrary to the VLMlat, the LRt does not contribute descending projections to the spinal cord dorsal horn (Tavares, I. and Lima, D., 1994), point to a role of the deep dorsal horn/ventral horn-LRt pathways in the control of motor activity in response to pain.

5.35.3.2 Dorsal Reticular Nucleus

5.35.3.2.1 Spinal laminae of origin and sites of termination

The medullary dorsal reticular nucleus (DRt) was first shown in the rat to be the site of termination of an important, mainly ipsilateral, pathway ascending from the spinal cord (Lima, D. and Coimbra, A., 1985; Lima, D., 1990; Villanueva, L. *et al.*, 1991). By the same time, neurons in the DRt were shown to be exclusively or preferentially activated by noxious stimuli from the skin and viscera (Villanueva, L. *et al.*, 1988). The spino-DRt pathway was later uncovered in other species such as the cat, monkey (Craig, A. D., 1995), and pigeon (Galhardo, V. *et al.*, 2000). It is constituted by a dorsal and ventral component differing in the area of termination within the DRt (Figure 7).

The dorsal pathway terminates at the dorsal-most portion of the DRt, immediately above the level of the central canal and surrounding the ventral border of the cuneate nucleus (Almeida, A. *et al.*, 1995; Almeida, A. *et al.*, 2000). It originates from the medial-most part of laminae I–III ipsilaterally, with a marked predominance of lamina I, and from lamina X, bilaterally (Figure 7) (Lima, D., 1990). The ventral pathway terminates ventrally to the area of termination of the dorsal pathway, within both sides of the DRt (Almeida, A. *et al.*, 1995; Almeida, A. *et al.*, 2000).

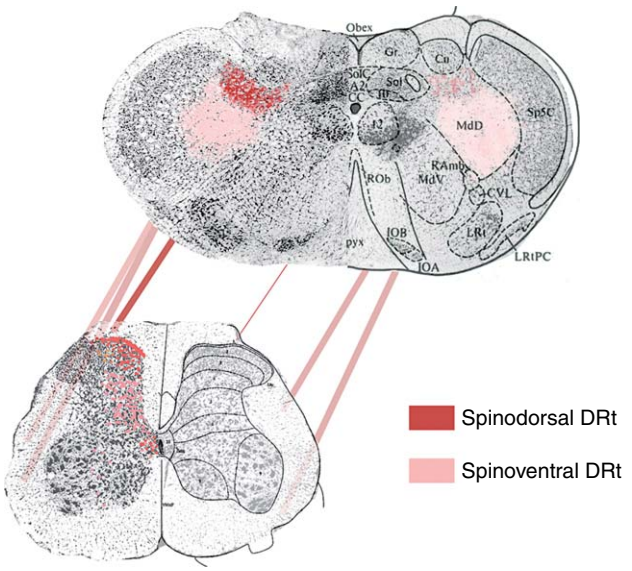

Figure 7 Diagram representing the spinal laminae of origin, ascending course in the spinal cord, and areas of termination of the spino-DRt pathway. Note the preferential medial location of dorsal horn neurons. Fibers of the spinodorsal DRt pathway course in the dorsal funiculus. Brain and spinal cord photomicrographs were adapted from Paxinos, G. and Watson, C. 1998. The Rat Brain in Stereotaxic Coordinates, 4th edn. Academic Press.

Its cells of origin prevail ipsilaterally in the medial portion of laminae IV–VI, with additional bilateral participation from laminae VII and X (Figure 7) (Lima, D., 1990). Interestingly, retrograde labeling from the superficial or deep dorsal horn demonstrated descending pathways arising, respectively, from the ipsilateral dorsal-most part of the DRt or from both sides of the ventral DRt (Tavares, I. and Lima, D., 1994). The DRt is thus part of two distinct reciprocal loops connecting its dorsal part with the superficial dorsal horn ipsilaterally, and ventral part with the deep dorsal horn bilaterally (Almeida, A. *et al.*, 1993; Almeida, A. *et al.*, 2000).

5.35.3.2.2 Structural types of neurons involved

Lamina I neurons projecting to the dorsal DRt were structurally characterized in the rat based on observations of neurons retrogradely filled with CTb in the three anatomical planes (Lima, D. and Coimbra, A., 1990). As to other spinal laminae, no data have been collected so far. In the rat, about 30% of lamina I neurons projecting to the DRt belong in the pyramidal and flattened types in similar amounts. The remaining 70% are of the multipolar type, a finding particularly curious taking into account that multipolar neurons were not seen to project in other ascending pathways. These cells are rather peculiar due to the typical lamina II crossing of the dendritic arbor, the bush pattern of the highly ramified proximal dendritic branches and the profusion and large variety of dendritic spines (Lima, D. and Coimbra, A., 1986). Another interesting feature of multipolar cells is their preferential location in the medial third of lamina I in the rat (Lima, D. and Coimbra, A., 1983; Lima, D. and Coimbra, A., 1986). The same structural types of lamina I neurons were seen to project to the DRt in the pigeon, although flattened and pyramidal neurons were relatively more abundant in this species (Galhardo, V. *et al.*, 2000).

5.35.3.2.3 Spinal location of ascending fibers

An interesting aspect of the spino-DRt pathway, apparently only shared with the spino-NTS pathway (Gamboa-Esteves, F. O. *et al.*, 2001c), is the course of their axons in the dorsal funiculus. This was first suggested by the dorsal orientation of axonal processes of lamina I neurons labeled retrogradely from the DRt and by comparing retrograde labeling rostrally and caudally to lesions of the dorsal funiculus (Lima, D., 1990). Retrograde labeling was completely abolished in ipsilateral laminae I–III and markedly diminished in the deep dorsal horn at segments caudal to the lesion. Anterograde tracing later revealed that numerous fibers are labeled in the dorsal funiculus after injections in superficial laminae, and in the dorsolateral fasciculus after injections in deep dorsal horn laminae (Almeida, A. *et al.*, 1995). Accordingly, injections in the dorsal funiculus resulted in DRt labeling restricted to its ipsilateral dorsal part, while injections in the dorsolateral fasciculus produced ipsilateral ventral DRt labeling (Almeida, A. *et al.*, 1995). These findings not only confirm a dual ascending tract for the dorsal and ventral DRt pathways, but also indicate that fiber decussation in the ventral pathway takes place near the segment of origin, as in most other pathways.

5.35.3.2.4 Surface receptors

A significant amount of lamina I neurons projecting to the DRt express the NK1 receptor alone (Todd, A. J. *et al.*, 2000; Castro, A. R. *et al.*, 2006) or together with the $GABA_B$ receptor (Castro, A. R. *et al.*, 2006). DRt-projecting neurons expressing only the $GABA_B$ receptor are, however, much more numerous (Castro, A. R. *et al.*, 2006). In laminae III–IV, about 20% of NK1-expressing neurons project to the DRt (Todd, A. J. *et al.*, 2000).

5.35.3.2.5 Neurotransmitters

So far, there are no studies addressing the possible neurotransmitters used in the spino-DRt pathway. Nevertheless, it is interesting to note that, although immunoreactions for GABA revealed immunostaining of lamina I neurons of the multipolar type, (Lima, D. *et al.*, 1993), even in the early 2000s, GABA could not be detected in projecting spinal neurons (Gamboa-Esteves, F. O. *et al.*, 2001b; Tavares, I. and Lima, D., 2002).

5.35.3.2.6 Response properties

The few data regarding the response characteristics of spino-DRt neurons rely on the induction of the c-*fos* proto-oncogene as a marker of activation of spinal neurons following noxious stimulation (Hunt, S. P. *et al.*, 1987). This kind of approach only permitted to conclude on the activation by various kinds of cutaneous and visceral noxious stimulation of DRt-projecting lamina I neurons of all the three structural groups involved, namely multipolar, flattened, and pyramidal (Almeida, A. and Lima, D., 1997). The rate of activation of DRt-projecting

lamina I neurons varied from 20% to 80% depending on the kind of stimulation applied and the neuronal cell group (Almeida, A. and Lima, D., 1997). In the deep dorsal horn, although high levels of c-*fos* expression were observed, the amount of activation of projecting neurons did not exceed 5%. Electrophysiological studies are absolutely needed to further characterize the response properties of spino-DRt neurons and to clarify the involvement of the deep dorsal horn in the transmission of nociceptive input to the DRt.

5.35.3.2.7 Pathways driven at the target

Projections from the DRt reach the parafascicular, ventromedial, and reunions thalamic nuclei (Figure 8) in the rat (Villanueva, L. *et al.*, 1998), which in turn are connected with telencephalic areas involved in emotional/affective and cognitive control. A putative spinoreticulothalamocortical projection relayed at the DRt has been proposed (Desbois, C. and Villanueva, L., 2001). Widespread projections to other brain targets of nociceptive ascending pathways have also been described. These include the VLM; the NTS; the rostral ventromedial medulla; the pontine noradrenergic cell groups A_5, A_6, and A_7 (PBN); the PAG; the posterior thalamus; the hypothalamus; the septal nuclei; the globus pallidus; and the amygdala (Figure 8) (Bernard, J. F. and Besson, J. M., 1990; Bernard, J. F. *et al.*, 1990; Villanueva, L. *et al.*, 1998; Leite-Almeida, H. *et al.*, 2006). Important projections to the orofacial motor nuclei (Bernard, J. F. *et al.*, 1990; Leite-Almeida, H. *et al.*, 2006) as well as to the deep cerebellar nuclei (Leite-Almeida, H. *et al.*, 2006) favor an important role in the organization of facial expressions and vocalization triggered by noxious stimulation.

The DRt also projects to the spinal cord superficial (Tavares, I. and Lima, D., 1994) and deep dorsal horn (Tavares, I. and Lima, D., 1994; Villanueva, L. *et al.*, 1995) as well as to the intermediate/ventral horn (Villanueva, L. *et al.*, 1995). DRt axons terminating in lamina I participate in a closed reciprocal spinodorsal DRt-spinal loop which, based on the asymmetric structure of synapses, is likely to be excitatory at both the spinal and medullary levels (Figure 9) (Almeida, A. *et al.*, 1993; Almeida, A. *et al.*, 2000; Lima, D. and Almeida, A., 2002). Nociceptive input arriving at the DRt is thus thought to drive a reverberating, lamina I centered pain facilitatory circuit, which is in accordance with the high proportion of c-*fos* activated spino-DRt neurons when compared to that of activated cells projecting to other targets (Lima, D., 1998). A ventral DRt-deep dorsal horn pain facilitatory loop is also likely to be established as indicated by the increased responsiveness of WDR deep dorsal horn neurons upon DRt stimulation (Dugast, C. *et al.*, 2003).

5.35.3.3 Nucleus Tractus Solitarii

5.35.3.3.1 Spinal laminae of origin and sites of termination

The spino-NTS pathway was demonstrated in the rat (Menétrey, D. and Basbaum, A. I., 1987; Leah, J. *et al.*, 1988; Esteves, F. *et al.*, 1993) and pigeon (Galhardo, V. *et al.*, 2000). It originates in laminae I, IV–VI, VII, X, and the lateral spinal nucleus, mainly contralaterally, but with an important ipsilateral component (Figure 10) (Esteves, F. *et al.*, 1993).

In the rat, the thoracic and sacral autonomic cell columns were also shown to participate (Menétrey, D. and Basbaum, A. I., 1987; Menétrey, D. and DePommery, J., 1991). In addition, an important contribution from the superficial laminae of the spinal trigeminal nucleus, *pars caudalis*, was revealed (Menétrey, D. and Basbaum, A. I., 1987). The spino-NTS pathway terminates in the caudal part of the NTS, the general visceral zone (Figure 10) (Loewy, A. D., 1990). Based on restricted retrograde tracer injections, cells projecting to the lateral subnucleus are fewer than those targeting the medial NTS, and do not include lamina I cells (Figure 10) (Esteves, F. *et al.*, 1993). Anterograde tracing confirmed this finding by showing that fibers originating in the superficial dorsal horn terminate bilaterally in the medial part of the commissural subnucleus, while fibers originating in the deep dorsal horn terminate ipsilaterally in the lateral subnucleus, with a few fibers distributed to the dorsomedial subnucleus (Gamboa-Esteves, F. O. *et al.*, 2001c).

5.35.3.3.2 Structural types of neurons involved

Again, studies referring to the structural characteristics of spino-NTS neurons only addressed lamina I. Similar to what was observed for the VLM, lamina I neurons projecting to the NTS belong in the fusiform, pyramidal, and flattened groups. However, contrary to the VLM, fusiform neurons contribute a small fraction. In spite of constituting half of the lamina I neuronal population (Lima, D. and Coimbra, A., 1983; Lima, D. and Coimbra, A., 1986), fusiform neurons amount only to 25% of NTS-projecting lamina I neurons, whereas flattened and pyramidal neurons make up

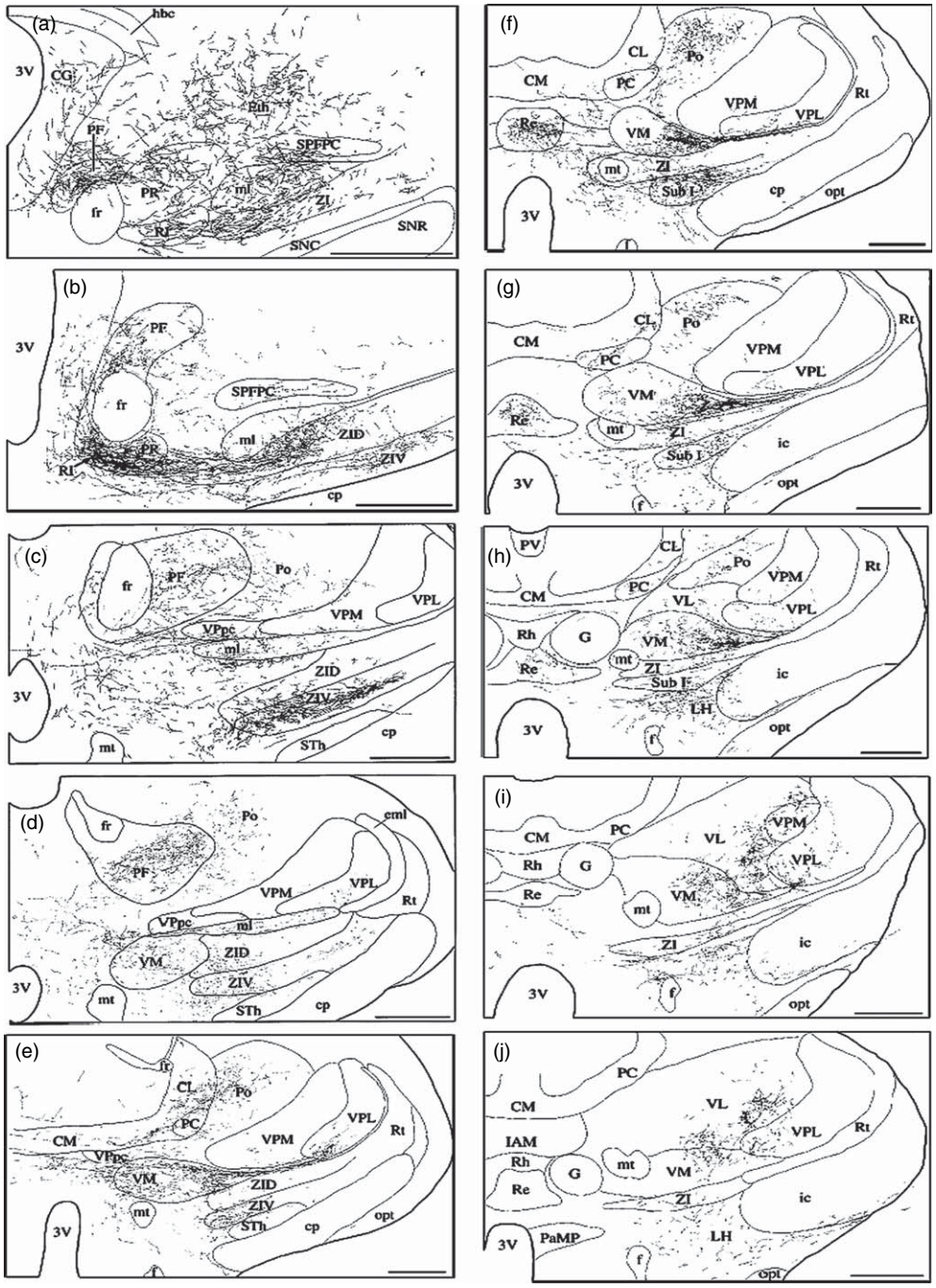

Figure 8 Distribution of DRt efferents anterogradely labeled with *phaseolus vulgaris* leucoagglutinin (PHA-L) in the diencephalon and telencephalon, in horizontal view. Adapted from figure 6 of Villanueva, L., Desbois, C., Le Bars, D., and Bernard, J. F. 1998. Organization of diencephalic projections from the medullary subnucleus reticularis dorsalis and the adjacent cuneate nucleus: a retrograde and anterograde tracer study in the rat. J. Comp. Neurol. 390, 133–160.

about 35–40% each. Similar relative amounts were observed in the pigeon, although pyramidal cells prevailed followed by flattened and fusiform cells (Galhardo, V. *et al.*, 2000). The abundant participation of flattened cells in the spino-NTS pathway deserves particular attention since it may be related to the specific role of this pathway in pain processing. Flattened cells make up 10% of the entire lamina I

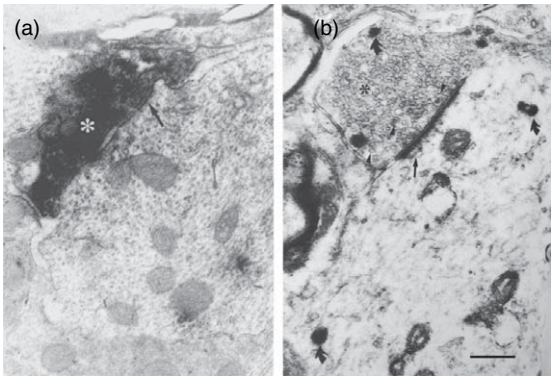

Figure 9 Anterogradely labeled axonal bouton (*) in the DRt (a) and superficial dorsal horn (b) establishing asymmetric synaptic contacts (arrows) upon retrogradely labeled dendrites after injecting cholera toxin subunit B (CTb) in the superficial dorsal horn (a) or horseradish peroxidase (HRP) in the dorsal DRt (b). In (b), tracer deposits are pointed by cuved arrows. Scale bar −0.3 μm (a) Adapted from figure 3 of Almeida, A., Tavares, I., and Lima, D. 2000. Reciprocal connections between the medullary dorsal reticular nucleus and the spinal dorsal horn in the rat. Eur. J. Pain. 4, 373–387. (b) Adapted from figure 3 of Almeida, A., Tavares, I., Lima, D., and Coimbra, A. 1993. Descending projections from the medullary dorsal reticular nucleus make synaptic contacts with spinal cord lamina I cells projecting to that nucleus: an electron microscopic tracer study in the rat. Neuroscience 55, 1093–1106.

neuronal population and participate in a similar proportion in the spino-VLM (Lima, D. *et al.*, 1991) and the spino-DRt (Lima, D. and Coimbra, A., 1990) pathways. Their relative amount in the NTS system is, however, particularly high surpassing the one observed in the lateral spinothalamic system (25–30% at the spinal enlargements).

5.35.3.3.3 Spinal location of ascending fibers

By comparing anterograde tracing produced by injections centered in the dorsal funiculus or the dorsolateral fasciculus with that obtained from superficial or deep dorsal horn laminae, it was concluded that fibers from lamina I neurons course in the dorsal funiculus and fibers from deep dorsal horn neurons in the dorsolateral fasciculus (Figure 10) (Gamboa-Esteves, F. O. *et al.*, 2001c).

5.35.3.3.4 Neurotransmitters

A small fraction of the neurons projecting to the NTS was found, in immunocytochemical studies, to contain dynorphin in lamina I, VIP in the lateral spinal nucleus, and bombesin in lamina X (Leah, J. *et al.*, 1988). Calbindin was immunodetected in spinal NTS-projecting neurons located mainly in lamina I (Figure 11) and the lateral spinal nucleus (Menétrey, D. *et al.*, 1992b; Gamboa-Esteves, F. O. *et al.*, 2001a), as well as in lamina I of the spinal trigeminal nucleus, *pars caudalis* (Menétrey, D. *et al.*, 1992a). In lamina I, about 40% of fusiform NTS-projecting neurons contain calbindin. Pyramidal and flattened neurons also exhibit calbindin (Figure 11), but in smaller fractions (Gamboa-Esteves, F. O. *et al.*, 2001a). Glutamate also occurs mainly in fusiform neurons followed by pyramidal neurons, and co-localizes extensively with calbindin (Gamboa-Esteves, F. O. *et al.*, 2001a). Nitric oxide synthase is present in fewer cells, almost all of them the fusiform type (Gamboa-Esteves, F. O. *et al.*, 2001a). Calbindin-immunoreactive NTS-projecting neurons are c-*fos* activated by visceral and cutaneous stimulation (Gamboa-Esteves, F. O. *et al.*, 2001b). Glutamate-positive and nitric oxide synthase-positive neurons are c-*fos* activated only by visceral stimulation (Gamboa-Esteves, F. O. *et al.*, 2001b). About 5% neurons of NTS-projecting neurons of the pyramidal group are immunoreactive for substance P (Gamboa-Esteves, F. O. *et al.*, 2001a).

5.35.3.3.5 Response properties

By the use of the c-*fos* approach, spino-NTS neurons located in lamina I were shown to be activated by cutaneous and visceral noxious stimulation (Menétrey, D. and DePommery, J., 1991; Lima, D. *et al.*, 1994; Gamboa-Esteves, F. O. *et al.*, 2001b). They belong in the three neuronal groups that participate in the pathway (Esteves, F. *et al.*, 1993) irrespective of the kind of cutaneous or visceral noxious stimulation employed (Lima, D. *et al.*, 1994). However, cells activated by visceral input prevail over those activated by cutaneous input, and neurochemical differences between cutaneous- and visceral-activated cells were found (Gamboa-Esteves, F. O. *et al.*, 2001b).

5.35.3.3.6 Pathways driven at the target

The caudal NTS projects to several brain areas involved in pain processing such as the caudal ventrolateral reticular formation (Cobos, A. *et al.*, 2003), the dorsal reticular nucleus (Almeida, A. *et al.*, 2002), the rostral ventromedial medulla (Sim, L. J. and Joseph, S. A., 1994), the PBN (Cechetto, D. F. *et al.*, 1985), the PAG (Bandler, R. and Tork, I., 1987; Herbert, H. and Saper, C. B., 1992), and the hypothalamus (Reis, L. C. *et al.*, 2000). The NTS is also connected with the medullary vasopressor (Agarwal, S. K. and Calaresu,

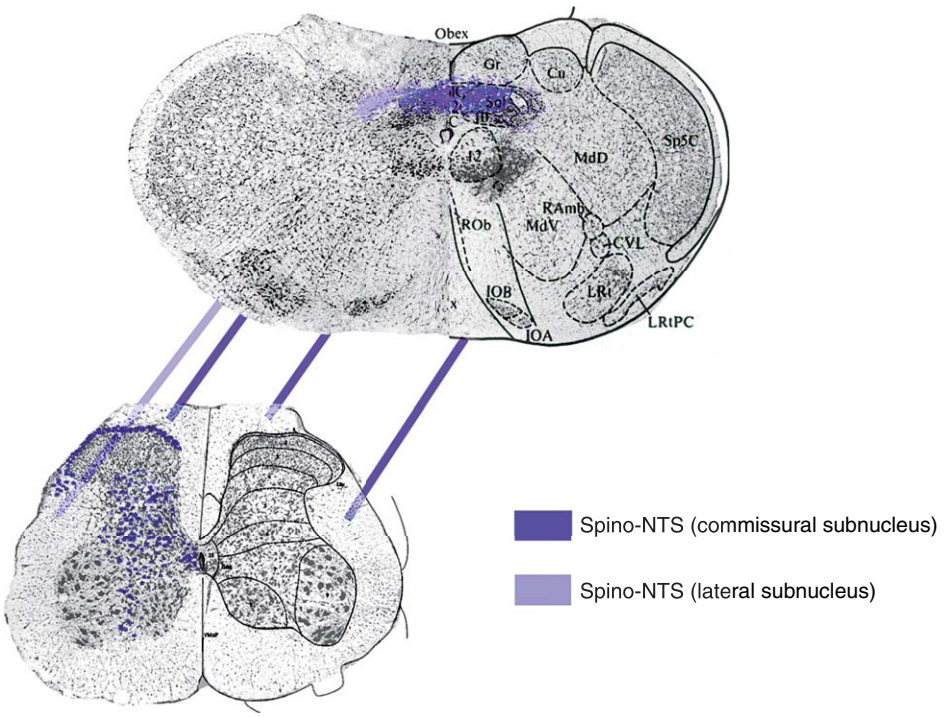

Figure 10 Diagram representing the spinal laminae of origin, ascending course in the spinal cord, and areas of termination of the spino-NTS pathway. Note the deep dorsal horn location of neurons terminating in the lateral subnucleus. Brain and spinal cord photomicrographs were adapted from Paxinos, G. and Watson, C. 1998. The Rat Brain in Stereotaxic Coordinates, 4th edn. Academic Press.

F. R., 1990) and vasodepressor (VLM) areas (Cobos, A. *et al.*, 2003). Although the NTS–VLM pathway is potentially involved in nociceptive/cardiovascular integration (Tavares, I. *et al.*, 1997), different VLM neurons are likely to mediate the antinociceptive and vasodepressive effects (Lima, D. *et al.*, 2001).

The caudal NTS also gives rise to projections descending directly to the spinal cord (Loewy, A. D. and Burton, H., 1978; Mtui, E. P. *et al.*, 1993; Tavares, I. and Lima, D., 1994). NTS fibers targeting the dorsal horn originate in the commissural subnucleus and terminate in superficial laminae (Tavares, I. and Lima, D., 1994).

5.35.3.4 Rostral Ventromedial Medulla

5.35.3.4.1 Spinal laminae of origin and sites of termination

Spinal cells projecting in the spino-RVM pathway predominate in laminae V, VII, VIII, and X (Figure 12) in the rat (Maunz, R. A. *et al.*, 1978; Kevetter, G. A. and Willis, W. D., 1982; Kevetter, G. A. *et al.*, 1982; Kevetter, G. A. and Willis, W. D., 1983; Chaouch, A. *et al.*, 1983; Peschanski, M. and Besson, J. M., 1984; Nahin, R. L. and Micevych, P. E., 1986; Nahin, R. L. *et al.*, 1986), cat (Abols, I. A. and Basbaum, A. I., 1981; Ammons, W. S., 1987), and monkey (Haber, L. H. *et al.*, 1982; Kevetter, G. A. *et al.*, 1982).

The pathway is mainly contralateral, although a large number of ipsilaterally and bilaterally projecting cells have also been reported (Figure 12) (Haber, L. H. *et al.*, 1982; Thies, R. and Foreman, R. D., 1983; Foreman, R. D. *et al.*, 1984; Ammons, W. S., 1987). Cells are distributed throughout the entire length of the spinal cord, but are much more numerous at the upper cervical level due to an important contribution of the ipsilateral ventral horn (Kevetter, G. A. and Willis, W. D., 1983). Scattered neurons were observed in lamina I (Foreman, R. D. *et al.*, 1984; Leah, J. *et al.*, 1988) and the lateral spinal nucleus in the rat (Leah, J. *et al.*, 1988). The axonal termination domain distributes through the nucleus reticularis gigantocellularis and the nucleus paragigantocellularis (Figure 12) (Bowsher, D. and Westman, J., 1970; Kerr, F. W. L., 1975; Peschanski, M. and Besson, J. M., 1984). In the cat and monkey, fibers originating in lamina I were seen to extend medially through the reticular formation to terminate in nucleus raphe magnus (Craig, A. D., 1995).

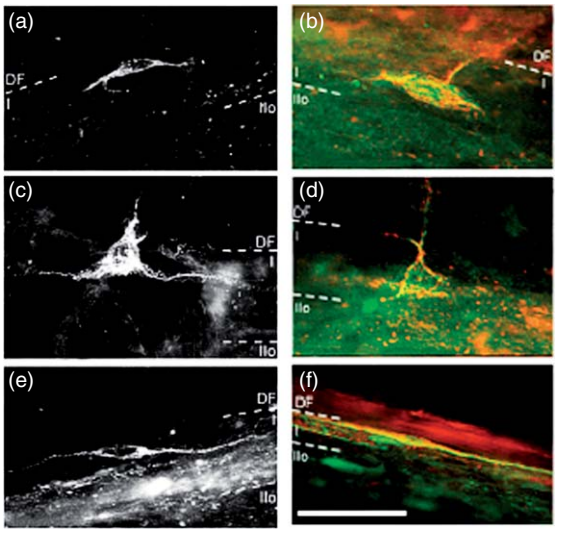

Figure 11 Lamina I neurons of the flattened (a, b), pyramidal (c, d), and fusiform (e, f) types retrogradely labeled with cholera toxin subunit B (CTb) from the NTS, in parasagittal view. In (b, d, and f), retrogradely labeled neurons present immunoreactivity for calbindin (green). Scale bar = 50 μm. (Adapted from figures 3 and 5 of Gamboa-Esteves, F. O., Kaye, J. C., McWilliam, P. N., Lima, D., and Batten, T. F. 2001a. Immunohistochemical profiles of spinal lamina I neurons retrogradely labelled from the nucleus tractus solitarii in rat suggest excitatory projections. Neuroscience 104, 523–538).

5.35.3.4.2 Structural types of neurons involved

Spino-RVM neurons located in lamina VII in the monkey were structurally relatively small as compared to spinothalamic neurons, with multipolar or, less frequently, fusiform or round perikarya and long dendrites across the lateromedial axis (Kevetter, G. A. *et al.*, 1982).

5.35.3.4.3 Spinal location of ascending fibers

Spino-RVM axons course in the contralateral ventrolateral quadrant in the spinal cord (Figure 12) and follow ventrolaterally in the caudal medulla oblongata before they turn medially to reach their sites of termination (Rossi, G. F. and Brodal, A., 1957; Anderson, F. D. and Berry, C. M., 1959; Mehler, W. R. *et al.*, 1960; Kerr, F. W. L., 1975; Nahin, R. L. *et al.*, 1986).

5.35.3.4.4 Neurotransmitters

Immunocytochemical staining for enkephalin was observed in spino-RVM neurons located in laminae VII and X (Nahin, R. L. and Micevych, P. E., 1986). Neurons in lamina X were also shown to contain cholecystokinin (CCK), somatostatin and, in fewer numbers, bombesin (Leah, J. *et al.*, 1988). In the lateral spinal nucleus, a relatively large neuronal population is immunoreactive to VIP, while bombesin and dynorphin are expressed in just a few neurons (Leah, J. *et al.*, 1988). Scarce somatostatin-immunoreactive neurons occur in lamina V (Leah, J. *et al.*, 1988).

5.35.3.4.5 Response properties

Spino-RVM neurons are excited by stimulation of Aδ and C fibers from the skin, muscles, and viscera (Maunz, R. A. *et al.*, 1978; Thies, R. and Foreman, R. D., 1983; Foreman, R. D. *et al.*, 1984; Ammons, W. S., 1987). Both noxious and innocuous stimulation are effective, but the majority of RVM-projecting neurons are nociceptive (Maunz, R. A. *et al.*, 1978; Haber, L. H. *et al.*, 1982; Thies, R. and Foreman, R. D., 1983; Foreman, R. D. *et al.*, 1984). Neurons responding only to cutaneous input belong in the LT, WDR, and NS classes (Fields, H. L. *et al.*, 1977). Receptive fields vary from limited (Fields, H. L., *et al.*, 1977) to large and complex, often including inhibitory regions (Fields, H. L. *et al.*, 1977; Maunz, R. A. *et al.*, 1978; Cervero, F. and Wolstencroft, J. H., 1984). Neurons responding to stimulation of deep structures are particularly numerous. They are mostly activated by deep noxious stimulation (Cervero, F. and Wolstencroft, J. H., 1984) and may receive convergent noxious or innocuous input from the skin (Fields, H. L. *et al.*, 1977; Cervero, F. and Wolstencroft, J. H., 1984). Neurons responsive to cutaneous, deep, and visceral noxious stimulation have also been reported (Foreman, R. D. *et al.*, 1984; Blair, R. W. *et al.*, 1984a, 1984b; Ammons, W. S., 1987). The majority of these cells belong in the high-threshold class, the remaining being WDR neurons (Thies, R. and Foreman, R. D., 1983; Foreman, R. D. *et al.*, 1984). Similar to pure somatic neurons, spinoreticular neurons with visceral input present either well-delimited or complex receptive fields, the latter including areas resulting in innocuous- or noxious-evoked inhibition (Thies, R. and Foreman, R. D., 1983; Foreman, R. D. *et al.*, 1984). Ten percent to 20% of the neurons projecting to the RVM also target the lateral thalamus (Haber, L. H. *et al.*, 1982; Foreman, R. D. *et al.*, 1984).

5.35.3.4.6 Pathways driven at the target

The RVM was shown to project to the medial thalamus, including the intralaminar complex (Giesler, G.

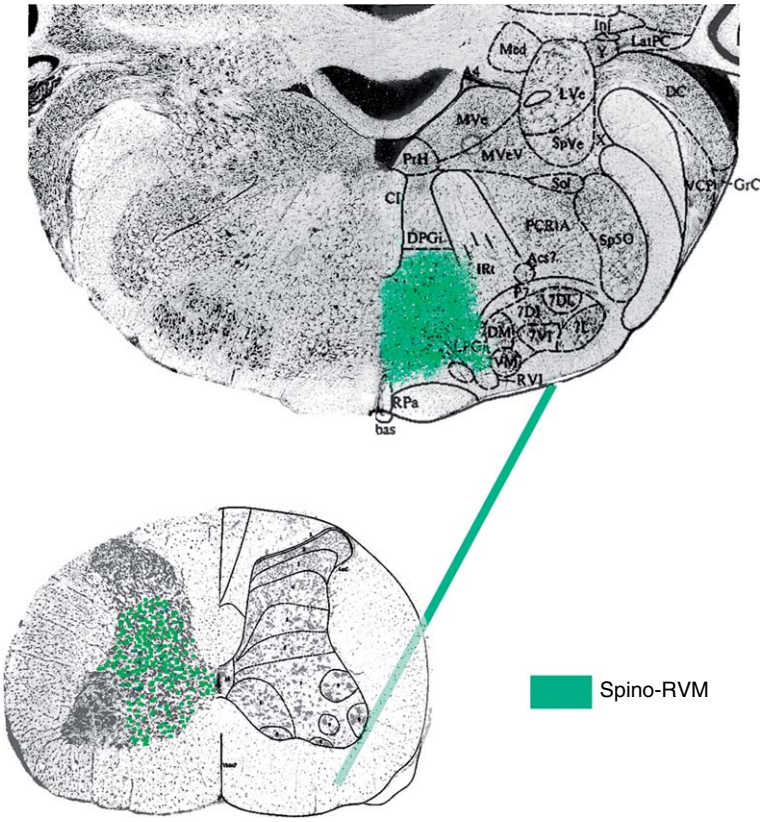

Figure 12 Diagram representing the spinal laminae of origin, ascending course in the spinal cord, and areas of termination of the spino-RVM pathway. Brain and spinal cord photomicrographs were adapted from Paxinos, G. and Watson, C. 1998. The Rat Brain in Stereotaxic Coordinates, 4th edn. Academic Press.

J. *et al*., 1981b; Peschanski, M. and Besson, J. M., 1984), and hence was proposed to function as a relay station in a spinoreticulothalamic pathway involved in motor responses to noxious stimulation. It is also at the origin of an important pain control descending pathway that terminates in the superficial and deep dorsal horn and includes pain inhibitory and facilitatory neurons (Fields, H. L. *et al*., 1995; Fields, H. L., 2000).

5.35.4 Spinopontine Pathways

The search for spinal fibers terminating in the brainstem (Craig, A. D., 1995), in particular in catecholaminergic nuclei (Westlund, K. N. and Craig, A. D., 1996), revealed various pontine spinal targets, which include the ventrolateral pons (A5), the locus coeruleus (A6), the subcoerulear region, the Kölliker–Fuse nucleus, and the PBN (Figure 13). These studies were, however, focused on lamina I ascending fibers, and, except for the PBN, such putative nociceptive pathways were not thoroughly investigated. This section will, therefore, deal only with the spino-PBN system.

5.35.4.1 Parabrachial Nuclei

5.35.4.1.1 Spinal laminae of origin and sites of termination

Injections centered in the PBN in both the rat (Cechetto, D. F. *et al*., 1985; Lima, D. and Coimbra, A., 1989; Hylden, J. L. *et al*., 1989; Menétrey, D. and DePommery, J., 1991; Traub, R. J. and Murphy, A., 2002) and cat (Panneton, W. M. and Burton, H., 1985; Hylden, J. L. K. *et al*., 1986a; 1986b) produce dense bilateral retrograde labeling in lamina I, mainly near the dorsal root entry zone, as well as in the lateral reticular portion of lamina V and laminae VIII and X (Figure 13). Additional labeling was observed in the intermediolateral column at thoracic levels, and in the parasympathetic column at sacral levels (Menétrey, D. and DePommery, J. 1991). Spino-PBN neurons with

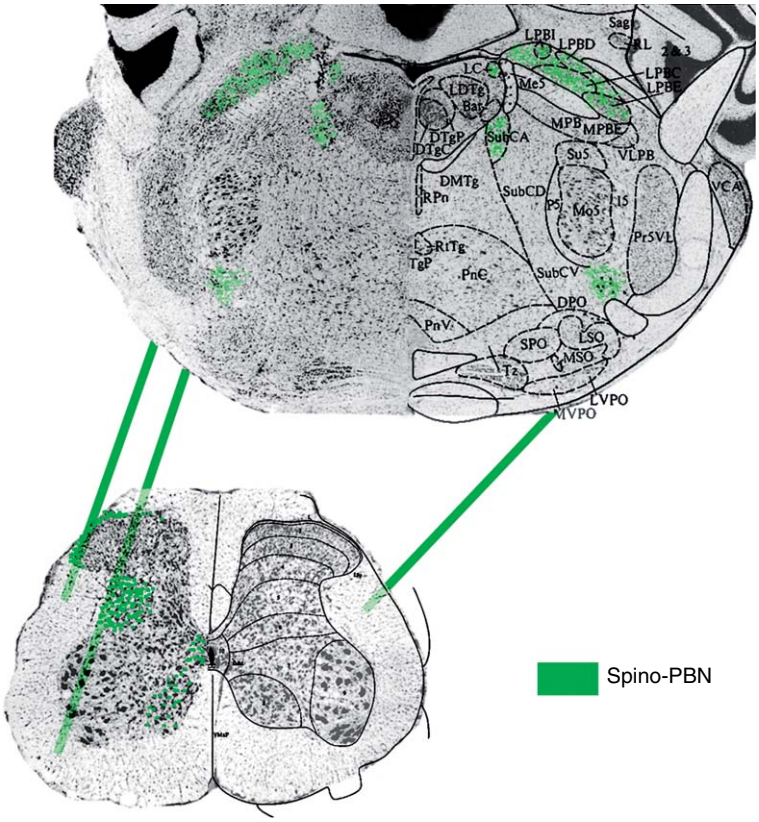

Figure 13 Diagram representing the spinal laminae of origin, ascending course in the spinal cord, and areas of termination of the spino-PBN pathway. Note the preferential lateral location of dorsal horn neurons. Spinal axonal termination areas in the locus coeruleus (LC), nucleus subcoeruleus (subCA) and the A_5 noradrenergic group are also represented. Brain and spinal cord photomicrographs were adapted from Paxinos, G. and Watson, C. 1998. The Rat Brain in Stereotaxic Coordinates, 4th edn. Academic Press.

axonal collaterals to the lateral thalamus were observed in all spinal areas with a marked prevalence in lamina I (Hylden, J. L. K. *et al.*, 1985; Hylden, J. L. *et al.*, 1989). A large percentage of spino-PBN neurons also project to the VLM (Spike, R. C. *et al.*, 2003).

The areas of termination of spinal fibers in the PBN are distributed bilaterally through the dorsal part of the lateral parabrachial nucleus, namely the dorsal, central, internal, and superior lateral subnuclei and the Kölliker–Fuse (Figure 13) (Cechetto, D. F. *et al.*, 1985; Blomqvist, A. *et al.*, 1989; Slugg, R. M. and Light, A. R., 1994). The medial and ventral lateral subnuclei are not targeted by spinal axons (Cechetto, D. F. *et al.*, 1985). No topographical arrangement has been disclosed (Blomqvist, A. *et al.*, 1989).

5.35.4.1.2 Structural types of neurons involved

Lamina I neurons labeled retrogradely in the rat following CTb injections centered in the PBN (although extending to the cuneiform nucleus) belonged in the fusiform (65–70%) and pyramidal (30–35%) groups (Lima, D. and Coimbra, A., 1989). In the cat, lamina I neurons antidromically activated from mesencephalic sites with similar location and intracellularly stained resembled fusiform neurons (Figure 14) both from the description of their longitudinally extended spiny dendritic arbors and from their camera lucida drawings (Hylden, J. L. K. *et al.*, 1986a; see Figure 5).

5.35.4.1.3 Spinal location of ascending fibers

In the cat, spino-PBN fibers course bilaterally in the dorsolateral fasciculus and ipsilaterally in the ventrolateral and ventral funiculi (Figure 13) (Hylden, J. L. K. *et al.*, 1986b; Hylden, J. L. *et al.*. 1989). Fibers originated in lamina I were shown to ascend through the dorsal aspect of the dorsolateral fasciculus (Hylden, J. L. K. *et al.*, 1986b). About one-fifth of

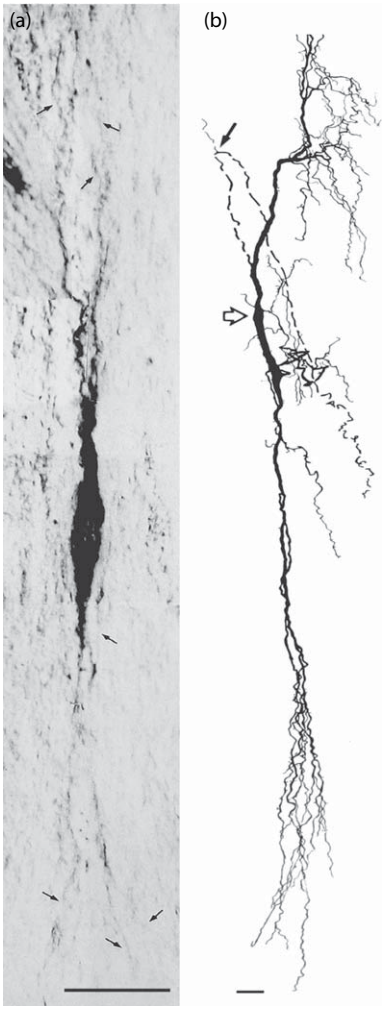

Figure 14 Lamina I PBN-projecting neurons retrogradely labeled with CTb (a) or intracellularly stained during antidromic activation (b), in horizontal (a) and parasagittal (b) views. In (a), arrows point to thin distal dendritic branches. In (b), the arrow points to the axon and the open arrow to the cell body. Scale bars = 30 μm. (a) Adapted from figure 4 of Lima, D. and Coimbra, A. 1989. Morphological types of spinomesencephalic neurons in the marginal zone (lamina I) of the rat spinal cord, as shown after retrograde labeling with cholera toxin subunit B. J. Comp. Neurol. 279, 327–339. (b) Adapted from figure 5 of Hylden, J. L. K., Hayashi, H., Dubner, R., and Bennett, G. J. 1986a. Physiology and morphology of the lamina I spinomesencephalic projections. J. Comp. Neurol. 247, 505–515).

lamina I neurons project bilaterally along the spinal cord (Hylden, J. L. K. *et al.*, 1986a).

5.35.4.1.4 Surface receptors

Most spino-PBN neurons located in lamina I express the NK1 receptor (Todd, A. J. *et al.*, 2000; Spike, R. C. *et al.*, 2003), and most lamina I neurons expressing the NK1 receptor and receiving synaptic contacts from TRPV1 immunoreactive primary afferent fibers project to the PBN (Hwang, S. J. *et al.*, 2003). Lamina I PBN-projecting Giant cells (lamina I cells three times larger than the remaining, amounting to about 5% in each lamina I structural group) (Lima, D. and Coimbra, A., 1983, 1986) of the pyramidal type were shown to lack the NK1 receptor and exhibit instead the glycine receptor-associated protein gephyrin (Puskar, Z. *et al.*, 2001). These cells are apposed by nitric oxide synthase and GABA-containing axonal boutons (Puskar, Z. *et al.*, 2001). In the deep dorsal horn, about 60% of NK1-immunoreacive neurons project to the PBN (Todd, A. J. *et al.*, 2000).

5.35.4.1.5 Neurotransmitters

Around half of the lamina I neuronal population projecting to the PBN immunostains for either dynorphin or enkephalin. Staining of sequential sections did not reveal co-localization of the two peptides (Standaert, D. *et al.*, 1986). According to Lima and colleagues (Lima, D. and Coimbra, A., 1989; Lima, D. *et al.*, 1993), lamina I enkephalinergic PBN-projecting cells should belong in the pyramidal group, whereas dynorphinergic cells could be either pyramidal or fusiform. Lumbosacral neurons projecting both ipsi- and contralaterally, mainly from lamina I and the lateral spinal nucleus, are immunoreactive for calbindin (Menétrey, D. *et al.*, 1992b).

5.35.4.1.6 Response properties

Neurons antidomically activated from the PBN in lamina I of the lumbar spinal cord of the rat (Bester, H. *et al.*, 2000) and cat (Hylden, J. L. K. *et al.*, 1985; Hylden, J. L. K. *et al.*, 1986a) belong mostly in the NS class (75–90%), the remaining being WDR neurons. They present extremely low spontaneous activity and small receptive fields, respond to stimulation of Aδ and C primary afferent fibers and conduct in the C–Aδ range (Hylden, J. L. K. *et al.*, 1986a; Bester, H. *et al.*, 2000). The large majority respond to both mechanical and heat-noxious stimulation and a few also to noxious cold stimulation. C-*fos* studies identified thoracolumbar spino-PBN neurons located preferentially in the superficial dorsal horn that were activated by visceral input (Menétrey, D. and DePommery, J., 1991; Traub, R. J. and Murphy, A., 2002). In whole-cell patch-clamp recordings, most lamina I neurons projecting to the PBN present a gap firing pattern, with a voltage-dependent delay in action potential firing, which was only shared by part

of the neurons projecting to the PAG and not by neurons that were not labeled from these two sites (Ruscheweyh, R. *et al.*, 2004).

5.35.4.1.7 Pathways driven at the target

By combining antidromic activation from the thalamus with orthodromic activation from the periphery, Bourgeais and coworkers (Bourgeais, L. *et al.*, 2001b) demonstrated that neurons in the parabrachial internal lateral nucleus responding exclusively, with sustained firing, to noxious stimulation of large receptive fields, project to the paracentral thalamic nucleus. This spino-PBN-paracentral thalamic pathway was claimed to be responsible for triggering the aversive reactions to pain at the prefrontal cortex. By the use of a similar approach as well as by anatomical tracing, a spino-PBN-amygdaloid pathway with relay neurons in the external pontine parabrachial area and terminating in the lateral capsular division of the central nucleus of the amygdala was demonstrated (Ma, W. and Peschanski, M., 1988; Bernard, J. F. and Besson, J. M., 1990). This pathway was confirmed by retrograde transneuronal tracing from the amygdala with pseudorabies virus, and found to originate mainly in lamina I neurons (Jasmin, L. *et al.*, 1997).

5.35.5 Spinomesencephalic Pathways

Spinomesencephalic pathways target a multitude of regions located close to each other, which include the PAG, the intercollicular nucleus, the superior colliculus, the cuneiform nuclei, the posterior and anterior pretectal nuclei, and the nucleus of Darkschewitsch (Wiberg, M. and Blomqvist, A., 1984; Björkeland, M. and Boivie, J., 1984; Yezierski, R. P., 1988). The PAG itself, the major target of spinofugal mesencephalic pathways, has its spinal afferents distributed through several areas, each one playing particular integrative roles (Yezierski, R. P., 1988). Most retrograde tracing studies that refer to the spino-PAG pathway are based on injections that encompass different areas of the PAG as well as part of the above referred neighbor regions. Since the PAG is the principal site of termination of the spinomesencephalic tract, this chapter, will focus on the spino-PAG pathway without separating the various mesencephalic targets, as a large number of studies addressing this ascending system do. However, it should be kept in mind that it comprises several parallel systems that are likely to deal with different aspects of pain processing.

5.35.5.1 Periaqueductal Gray

5.35.5.1.1 Spinal laminae of origin and sites of termination

Neurons of origin of the spino-PAG pathway are located in lamina I, the reticular region of laminae IV–V, laminae VI–VIII, lamina X, and the lateral spinal nucleus (Figure 15) in the rat (Menétrey, D. *et al.*, 1982; Beitz, A. J., 1982; Liu, R. P., 1983; Swett, J. E. *et al.*, 1985; Yezierski, R. P., 1988; Lima, D. and Coimbra, A., 1989; Yezierski, R. P. and Broton, J. G., 1991; Yezierski, R. P. and Mendez, C. M., 1991), cat (Wiberg, M. and Blomqvist, A., 1984; Yezierski, R. P., 1988), and monkey (Trevino, D. L., 1976; Mantyh, P. W., 1982; Wiberg, M. *et al.*, 1987; Yezierski, R. P., 1988; Zhang, D. *et al.*, 1990). In the cat, cells located in lamina I were found to account for the majority of spino-PAG neurons in the cervical and lumbar enlargements, but only to around 30% in the remaining spinal segments (Mouton, L. J. *et al.*, 2001). In the rat, an additional important projection, apparently exclusive of this pathway, originates from neurons located inside the white matter overlying lamina I, at the dorsal funiculus (Lima, D. and Coimbra, A., 1989).

Projections originated in the dorsal horn are mainly contralateral, especially from lamina I, the lateral spinal nucleus, and the dorsal funiculus (Trevino, D. L., 1976; Wiberg, M. *et al.*, 1987; Lima, D. and Coimbra, A., 1989), although a significant ipsilateral projection from lumbosacral spinal segments has been reported (Menétrey, D. *et al.*, 1992b). Projections originated in lamina X and the ventral horn are bilateral (Figure 15) (Trevino, D. L., 1976; Wiberg, M. *et al.*, 1987; Lima, D. and Coimbra, A., 1989). The upper cervical cord makes a major additional bilateral contribution both from the ventral horn and the lateral cervical nucleus (Yezierski, R. P. and Mendez, C. M., 1991; Mouton, L. J. and Holstege, G., 2000). Spino-PAG neurons were shown to leave axonal collaterals in the DRt, RVM, and locus coeruleus in the rat (McMahon, S. B. and Wall, P. D., 1985; Pechura, C. and Liu, R., 1986), and to collateralize a lot within the mesencephalon (Hylden, J. L. K. *et al.*, 1985; Yezierski, R. P. and Schwartz, R. H., 1986). Projections to both the mesencephalon and thalamus were reported in the rat (Harmann, P. A. *et al.*, 1988; Yezierski, R. P. and Mendez, C. M., 1991), cat (Hylden, J. L. K. *et al.*, 1986a; Yezierski, R. P. and Broton, J. G., 1991) and

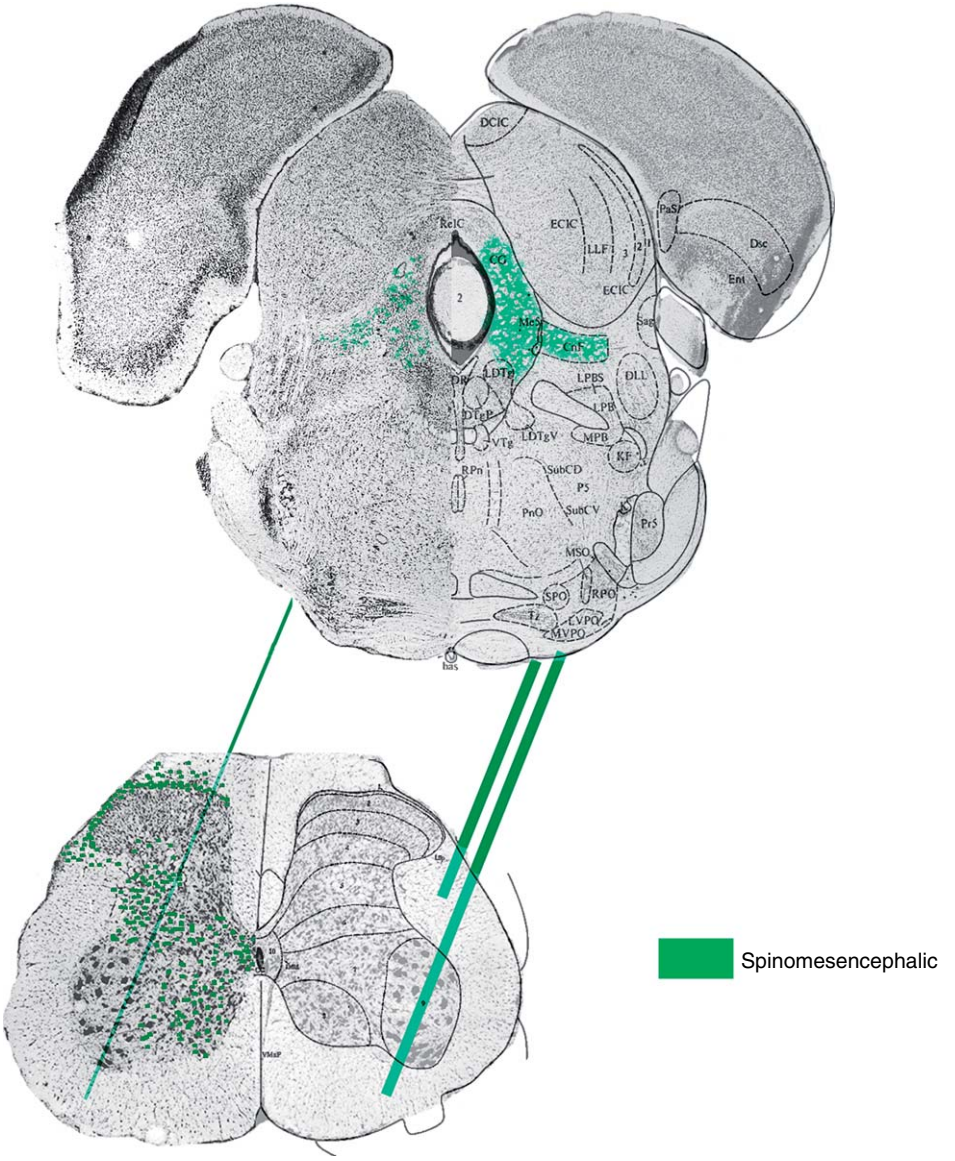

Figure 15 Diagram representing the spinal laminae of origin, ascending course in the spinal cord, and areas of termination of the spinomesencephalc pathway. (Only the caudal termination area is represented) Brain and spinal cord photomicrographs were adapted from Paxinos, G. and Watson, C. 1998. The Rat Brain in Stereotaxic Coordinates, 4th edn. Academic Press.

monkey (Price, D. D. *et al*., 1978; Yezierski, R. P. *et al*., 1987; Zhang, D. *et al*., 1990). Thalamic sites of termination are mainly located in the ventrobasal complex, but collateralization to the posterior complex and medial thalamic nuclei has also been observed (Yezierski, R. P. and Mendez, C. M., 1991).

The mesencephalic sites of termination of the fibers ascending from the spinal cord and the spinal trigeminal nucleus were depicted in the rat (Yezierski, R. P., 1988), cat (Wiberg, M. and Blomqvist, A., 1984; Björkeland, M. and Boivie, J., 1984; Wiberg, M. *et al*., 1987; Yezierski, R. P., 1988), and monkey (Kerr, F. W. L., 1975; Wiberg, M. *et al*., 1987; Yezierski, R. P., 1988). The termination pattern is very similar in the three species (Figure 15). With the exception of the nucleus of Darkschewitsch, terminal arborizations are sparse in the most rostral part of the mesencephalon (Yezierski, R. P., 1988; Lima, D. and Coimbra, A., 1989). Fibers are mainly distributed through the middle and caudal part of the PAG, nucleus cuneiformis,

deep and intermediate gray layers of the superior colliculus, and intercollicular nucleus (Wiberg, M. *et al*., 1987; Yezierski, R. P., 1988). In the caudal-most PAG of the monkey, but not in the rat and cat (Figure 16), spinal afferents contribute to two distinct dorsolateral and ventrolateral dense arborizations, while immediately rostrally, in the intercollicular region, they concentrate in a sole domain located laterally (Wiberg, M. *et al*., 1987; Yezierski, R. P., 1988), with additional labeling dorsally to the aqueduct (Yezierski, R. P., 1988).

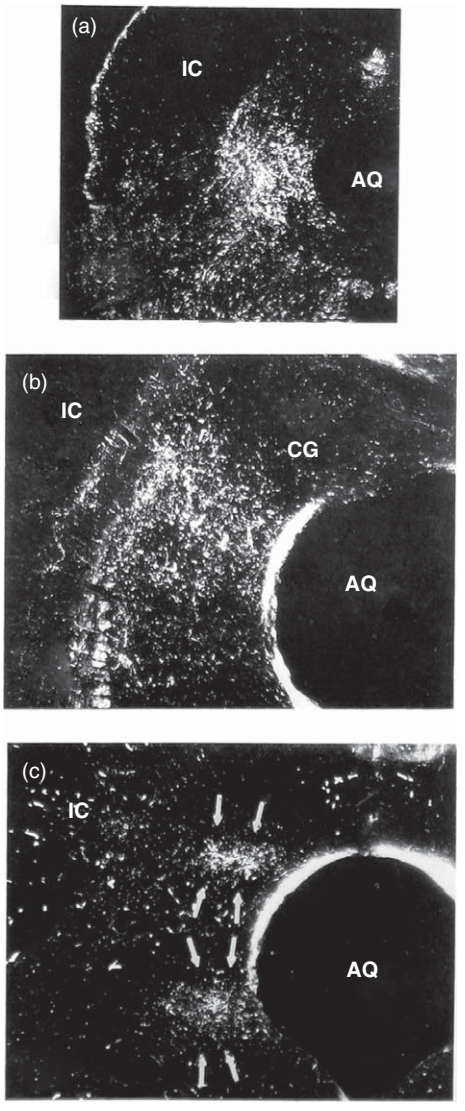

Figure 16 Anterograde labeling in the caudal midbrain following injection of wheat grem agglutinin–horseradish peroxidase (WGA-HRP) in the lumbosacral spinal cord of the rat (a), cat (b), and monkey (c). AQ, Cerebral aqueduct; CG , Periaqueductal gray; IC, Inferior colliculus. Adapted from figure 3 of Yezierski, R. P. 1988. Spinomesencephalic tract: projections from the lumbosacral spinal cord of the rat, cat, and monkey. J. Comp. Neurol. 267, 131–146.

This is an interesting finding in the light of data showing that the dorsolateral/lateral PAG is involved in aversive/defense behavior and vasopressor responses, and the vantrolateral PAG in immobility, positive reinforcing, and vasodepression (Lovick, T. A., 1993).

The possibility that the spino-PAG pathway is a composite of multiple pathways subserving the various functions in which the PAG is involved is supported by studies showing that different regions in the PAG receive afferents from distinct spinal neuronal populations (Keay, K. A. and Bandler, R., 1992; VanderHorst, V. G. J. M. *et al*., 1996; Mouton, L. J. and Holstege, G.., 2000). Neurons at spinal segments C1–C3 that project to the lateral part of the PAG are mainly located in lamina I, whereas those projecting to the ventrolateral part of the PAG prevail in laminae VII–VIII (Keay, K. A. and Bandler, R., 1992). In the lumbosacral spinal cord, neurons in medial lamina VII and lamina VIII terminate in the lateral part of the lateral PAG and adjacent tegmentum, whereas neurons distributed thoughout laminae I and V terminate diffusely in the dorsal and lateral PAG (VanderHorst, V. G. J. M. *et al*., 1996). In the cat, Mouton and Holstege (Mouton, L. J. and Holstege, G., 2000) described five distinct spinal neuronal groups based on their clustering pattern in the spinal cord and termination pattern in the PAG: (1) neurons located in laminae I and V along the entire length of the spinal cord and terminating in all parts of the intermediate and caudal PAG; (2) neurons located bilaterally in lateral laminae VI–VII and dorsolateral lamina VIII of segments C1–C3 and terminating in the ventrolateral and lateral part of the entire PAG and deep tectum; (3) neurons located in lamina X of the thoracic and upper lumbar cord and terminating in the ventrolateral and lateral PAG and deep tectum; (4) neurons located in medial laminae VI–VII of segments L5–S3 and terminating in the lateral and ventrolateral intermediate and caudal PAG; and (5) neurons located laterally in lamina I of segments L6–S2 and laminae V–VII and X of segments S1–S3 and terminating in the medial part of the ventrolateral intermediate and caudal PAG. According to electrophysiologcal studies using antidromic activation (Yezierski, R. P. and Schwartz, R. H., 1986), spinal cells projecting to the rostral-most part of the PAG are located more ventrally, in laminae V–VII, than those projecting to the intercollicular and caudal levels, to where lamina I neurons project.

5.35.5.1.2 Structural types of neurons involved

Spinomesencephalic neurons were characterized as to the size and shape of the soma both in the rat and cat (Menétrey, D. *et al.*, 1980; VanderHorst, V. G. J. M. *et al.*, 1996). Neurons in lamina I are smaller than in other laminae and present oval to fusiform soma in transverse view (VanderHorst, V. G. J. M. *et al.*, 1996). Neurons in the lateral spinal nucleus and lamina X present oval to fusiform soma of variable sizes. Deep dorsal horn and ventral horn neurons are large and multipolar (Menétrey, D. *et al.*, 1980; VanderHorst, V. G. J. M. *et al.*, 1996).

A detailed structural characterization was obtained for lamina I neurons retrogradely labeled with CTb in the rat (Lima, D. and Coimbra, A., 1989). Large numbers of fusiform and pyramidal neurons were shown to participate. However, all injections were directed to the ventrolateral caudal PAG and encompassed part of the PBN. Injections hitting mainly the PBN failed to stain as many pyramidal neurons as those targeting the ventrolateral PAG, while still labeling a relatively large number of fusiform neurons. Pyramidal neurons were therefore taken as projecting mainly to the ventrolateral PAG and fusiform neurons to the PBN (Lima, D. and Coimbra, A., 1989). Some fusiform neurons projecting to the PAG were shown to have myelinated axons and give off collaterals inside lamina I (Hylden, J. L. K. *et al.*, 1986a).

5.35.5.1.3 Spinal location of ascending fibers

Fibers of the spinomesencephalic pathway are classically considered to travel in the ventrolateral quadrant of the spinal white matter (Mehler, W. R. *et al.*, 1960; Kerr, F. W. L., 1975). More recent data using antidromic activation revealed that fibers arising from lamina I decussate near their level of origin and course in the dorsal part of the dorsolateral fasciculus (McMahon, S. B. and Wall, P. D., 1985; Hylden, J. L. K. *et al.*, 1986b).

5.35.5.1.4 Surface receptors

The majority of spino-PAG neurons in lamina I, but not in the deep dorsal horn, express the NK1 receptor (Todd, A. J. *et al.*, 2000). Their amounts are, however, smaller than those of neurons projecting to the VLM or the PBN (Spike, R. C. *et al.*, 2003).

5.35.5.1.5 Neurotransmitters

In the lateral spinal nucleus and lamina X, neurons containing various neuropeptides and projecting to a mesencephalic area centered in the PAG (but extending to the parabrachial nuclei) were observed (Leah, J. *et al.*, 1988). Neurons in the lateral spinal nucleus were immunoreactive for VIP, bombesin, and substance P, while those located in lamina X were immunoreactive for bombesin and enkephalin. A few VIP-immunoreactive neurons were located in lamina I. At lumbosacral spinal levels, calbindin immunoreactive PAG-projecting neurons were observed bilaterally in all spinal areas of origin of the pathway, with a particularly high concentration in lamina I and the lateral spinal nucleus (Menétrey, D. *et al.*, 1992b).

5.35.5.1.6 Response properties

The response properties of spinal neurons projecting to the PAG were recorded in the rat (Menétrey, D. *et al.*, 1980), cat (Yezierski, R. P. and Schwartz, R. H., 1986; Yezierski, R. P. and Broton, J. G., 1991), and monkey (Yezierski, R. P. *et al.*, 1987). PAG-projecting neurons belong in the LT, WDR, and NS classes. Both WDR and NS neurons respond to mechanical and heat stimuli at the noxious range. WDR neurons largely prevail over the other neuronal classes, representing about half of the population recorded. Many WDR cells were found to respond to both cutaneous and visceral/deep tissue stimulation (Yezierski, R. P. and Schwartz, R. H., 1986; Yezierski, R. P. *et al.*, 1987). In the rat, NS neurons are predominant in lamina I, WDR neurons are distributed through both lamina I and the deep dorsal horn, and LT cells prevail in the deep dorsal horn (Menétrey, D. *et al.*, 1980). In the cat and monkey, neurons are distributed evenly through the dorsal horn and around the central canal irrespective of the physiological class they belong to (Yezierski, R. P. and Schwartz, R. H., 1986; Yezierski, R. P. *et al.*, 1987).

C-*fos* studies (Clement, C. I. *et al.*, 2000; Keay, K. A. *et al.*, 2002) revealed neurons at the thoracic spinal cord that project to the rostral ventrolateral PAG to be activated by noxious visceral stimulation. Neurons at both the lumbosacral and upper cervical spinal cord and projecting to the caudal ventrolateral PAG were activated by hind limb muscle noxious stimulation. Lamina I neurons projecting to the caudal ventrolateral PAG at the lumbar enlargement and expressing c-*fos* following either mechanical, thermal, or chemical noxious stimulation of the skin or noxious stimulation of the urinary bladder belong in

both the fusiform and pyramidal groups (Lima, D. *et al*., 1992; Lima, D., 1998).

Most spino-PAG neurons, including those few cells projecting to both the PAG and the ventrobasal complex of the thalamus, present small excitatory receptive fields confined to a single limb (Yezierski, R. P. *et al*., 1987). However, neurons with extensive and complex receptive fields have also been observed, in particular in the upper cervical cord and in deep spinal laminae, including lamina X (Menétrey, D. *et al*., 1980; Yezierski, R. P. and Schwartz, R. H., 1986; Yezierski, R. P., 1990; Yezierski, R. P. and Broton, J. G., 1991). Both groups present complex inhibitory receptive fields and include NS and WDR neurons (Yezierski, R. P. and Schwartz, R. H., 1986; Yezierski, R. P. *et al*., 1987; Yezierski, R. P. and Broton, J. G., 1991).

Spino-PAG lamina I neurons have slow conducting velocities, at the Aδ range, while those in the deep dorsal horn and ventral horn conduct at the low A$_\beta$ range (Yezierski, R. P. *et al*., 1987). Neurons in the lateral spinal nucleus present particularly slow axons, which belong in the unmyelinated and thin myelinated classes (Menétrey, D. *et al*., 1980). A recent study using whole-cell patch-clamp in spinal slices showed that spino-PAG neurons present either gap-firing or burst-firing patterns, contrary to neurons that were not labeled from either the PAG or the PBN (Ruscheweyh, R. *et al*., 2004).

5.35.5.1.7 Pathways driven at the target

The spinomesencephalic pathway was first uncovered as a relay station of the medial spinothalamic tract. Early anatomical studies revealed a projection from the mesencephalon to the intralaminar nuclei of the thalamus (Bowsher, D., 1957). Later anterograde tracing studies confirmed this connection as well as important projections to the hypothalamus, striatum, and amygdala (Eberhart, J. A. *et al*., 1985; Meller, S. T. and Dennis, B. J., 1991). Discrete injections confined to different portions of the PAG in the rabbit showed that the ventral portion is the main source of afferent systems (Meller, S. T. and Dennis, B. J., 1991). Two distinct ascending systems were recognized: a periventricular system terminating in intralaminar and midline thalamic nuclei and along the hypothalamus, and a ventrolateral system terminating in the ventral tegmental area, ventral thalamus, zona incerta, amygdala, substantia innonimata, lateral preopric nucleus, diagonal band of Broca, and the lateral septal nucleus. This multitude of pathways is likely to reflect the morphofunctional complexity of the PAG and is taken as indicative of a PAG role in motor responses, escape/avoidance, aversive versus positive reinforcing, and neuroendocrine and autonomic responses to pain (Lovick, T. A., 1993).

A dense descending projection connects the ventrolateral portion of the caudal PAG with the ipsilateral nucleus raphe magnus (NRM) and adjacent reticular formation, locus coeruleus (LC), nucleus subcoeruleus, and the ventral reticular formation of the medulla (Meller, S. T. and Dennis, B. J., 1991). Sparse fibers originated in the dorsal PAG and superior colliculus also terminate in the locus coeruleus/subcoeruleus area (Cowie, R. J. and Holstege, G., 1992). Since PAG projections to the spinal cord are limited and restricted to laminae VII–VIII (Behbehani, M. M., 1995), the analgesic effects elicited from PAG stimulation are likely to be mediated by these PAG-pontine and PAG-medullary pathways (Lovick, T. A., 1993).

5.35.6 Spinodiencephalic Pathways

Of the pathways terminating in the diencephalon, the spinothalamic are by far those known for longer and therefore more thoroughly investigated. Although a large proportion of the studies dealing with the spinothalamic system address together the lateral and medial pathways, it turned clear from clinical (Dejerine, J. and Roussy, G., 1906; Walker, A. E., 1942a; Hécaen, H. *et al*., 1949), electrophysiological (Kenshalo, D. R., Jr. *et al*., 1979; Giesler, G. J. *et al*., 1981b), and anatomical (Boivie, J., 1979) studies that each pathway is engaged in particular aspects of nociceptive processing. The medial pathway has been implicated in arousal, motivational, affective, and motor responses to pain, and the lateral pathway in stimulus discrimination. Accordingly, in this chapter, the two pathways will be dealt with separately in spite of the difficulties raised by being often assessed as a whole, particularly in retrograde tracing studies. There are, nonetheless, common aspects that will be more thoroughly described in the context of the lateral spinothalamic pathway. Also, a relatively large percentage of spinothalamic neurons (around 15%) of various species and different spinal laminae projects to both the lateral and medial thalamus (Giesler, G. J. *et al*., 1981b; Kevetter, G. A. and Willis, W. D., 1983; Stevens, R. T. *et al*., 1989; Craig, A. D. *et al*., 1989). These neurons share, however, all the properties of lateral spinothalamic neurons

(Giesler, G. J. *et al*., 1981b) and are therefore considered as part of the lateral spinothalamic pathway.

5.35.6.1 Lateral Thalamus

The lateral spinothalamic pathway was the first nociceptive spinofugal pathway described (Edinger, L., 1890). Its identification, at the turning of the nineteenth century, was based on the observation in necropsia tissue from humans, of degenerating profiles at the lateral sensory thalamus after ventrolateral cordotomy that disrupted pain sensation (Quensel, F., 1898; Kohnstamm, O., 1900; Thiele, F. H. and Horsley, V., 1901; Collier, J. and Buzzard, E. F., 1903; Foerster, O. and Gagel, O., 1932; Clark, W. E. L., 1936). Only much later, with the advent of neurophysiology and tracing techniques, this pathway was revealed in detail. Nevertheless, early clinical studies (Dejerine, J. and Roussy, G., 1906; Melzack, R. and Casey, K. L., 1968) correlated the lateral spinothalamic pathway with the discriminative processing of nociceptive input.

5.35.6.1.1 Spinal laminae of origin and sites of termination

The lateral spinothalamic pathway takes origin on the contralateral spinal cord in laminae I, IV–VI, VII–VIII, X, and the lateral spinal nucleus (Figure 17) in the rat, cat, and monkey (Trevino, D. L. and Carstens, E., 1975; Carstens, E. and Trevino, D. L.,

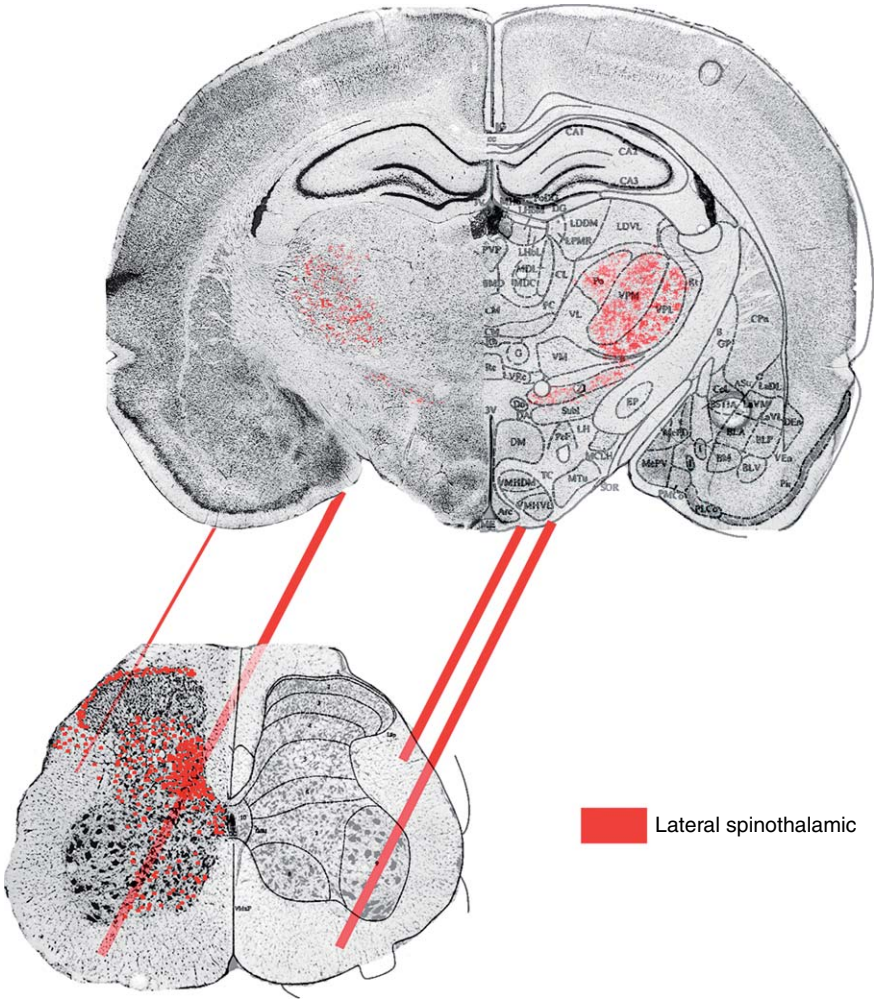

Figure 17 Diagram representing the spinal laminae of origin, ascending course in the spinal cord and areas of termination of the lateral spinothalamic pathway. Note the cluster appearance of axon termination in the VPL. Brain and spinal cord photomicrographs were adapted from Paxinos, G. and Watson, C. 1998. The Rat Brain in Stereotaxic Coordinates, 4th edn. Academic Press.

1978b; Willis, W. D. *et al*., 1979; Giesler, G. J. *et al*., 1979a; Berkley, K. J., 1980; Leah, J. *et al*., 1988; Lima.D. and Coimbra, A., 1988; Burstein, R. *et al*., 1990b).

In laminae I and IV, a somatotopic arrangement has been described, neurons receiving input from extensor surfaces being located more laterally than neurons receiving input from flexor surfaces (Willis, W. D. *et al*., 1974). The amount of spinothalamic neurons varies considerably along the rostrocaudal extent of the spinal cord due to additional intense labeling in particular areas at various spinal levels. This is the case of the deep dorsal horn contralaterally, and the intermediate/ventral horn, bilaterally, in spinal segments C1–C2 (Carstens, E. and Trevino, D. L., 1978a; Carstens, E. and Trevino, D. L., 1978b; Giesler, G. J. *et al*., 1979a; Lima.D. and Coimbra, A., 1988; Burstein, R. *et al*., 1990b), and the intermediate basilar nucleus of Cajal, contralaterally, in the rat (Giesler, G. J. *et al*., 1979a; Lima.D. and Coimbra, A., 1988; Burstein, R. *et al*., 1990b). Due to this regional variability, together with the fact that the multiple spinal groups projecting to the lateral thalamus also project to many other supraspinal targets, the erroneous assumption that thalamic projections from certain areas, such as lamina I, to the main lateral spinal target, the VPL, are not sufficiently relevant gained credit (Blomqvist, A. *et al*., 2000; Craig, A. D. *et al*., 2002; Klop, E. M. *et al*., 2004). However, although the relative participation of lamina I neurons is below 10% in the cat (Klop, E. M. *et al*., 2004) and rat (Burstein, R. *et al*., 1990b) when the spinal cord is considered as a whole, small relative amounts are only found in segments where additional labeling occurs in particular spinal groups, as is the case of the upper cervical and lumbar cord (Burstein, R. *et al*., 1990b). Notably, in the cervical enlargement of the rat, numbers of lamina I spinothalamic neurons equal those in the deep dorsal horn (Burstein, R. *et al*., 1990b). Moreover, many lamina I neurons in the contralateral spinal and medullary dorsal horn of the monkey project to the ventrobasal complex of the thalamus, amounting to one-third of the entire dorsal horn labeled population (Willis, W. D. *et al*., 2001).

Although the spinothalamic lateral pathway is classically considered to project contralaterally except for the ventral horn in segments C_1–C_2 (Trevino, D. L. and Carstens, E., 1975; Carstens, E. and Trevino, D. L., 1978a; Carstens, E. and Trevino, D. L., 1978b; Willis, W. D. *et al*., 1979; Giesler, G. J. *et al*., 1979a), the use of very sensitive tracers such as CTb disclosed an important ipsilateral component (Lima.D. and Coimbra, A., 1988). Ipsilateral neurons amounted to about half the neurons labeled in the contralateral side in the lateral spinal nucleus and the deep dorsal horn in almost all the spinal segments examined. In the ventral horn, ipsilateral neurons equalized in number contralateral neurons, except in the cervical enlargement, where they were more abundant. Only in lamina I and the intermediate basilar nucleus of Cajal, contralateral neurons largely surpassed ipsilateral neurons. The need of using a very sensitive tracing technique to reveal the ipsilateral neuronal population suggests that these neurons may actually be contralaterally projecting neurons that send axonal collaterals to the ipsilateral thalamus. However, there is evidence from ventral spinal lesions in primates that nociceptive input is also conveyed supraspinally in the ipsilateral anterolateral quadrant (Vierck, C. J. and Luck, M. M., 1979).

The areas of spinal axon arborization in the lateral thalamus (Figure 17) were thoroughly studied in primates, including the monkey (Mehler, W. R. *et al*., 1960; Bowsher, D., 1961; Mehler, W. R., 1966; Mehler, W. R., 1969; Kerr, F. W. L. and Lippman, H. H., 1974; Boivie, J., 1979; Berkley, K. J., 1980; Mantyh, P. W., 1983a; Apkarian, A. V. and Hodge, C. J., 1989a) and humans (Mehler, W. R., 1962; Mehler, W. R., 1974). In these species, as in the rat (Lund, R. D. and Webster, K. E., 1967; Mehler, W. R., 1969; Zemlan, F. P. *et al*., 1978; Peschanski, M. *et al*., 1983; Cliffer, K. D. *et al*., 1991), the VPL is the major recipient of spinal fibers. In the VPL, spinal afferents are somatotopically arranged in rostrocaudally oriented clusters so that axons arriving from the lumbosacral spinal cord terminate in the lateral part of the nucleus and axons from the cervical enlargement terminate in the medial part (Boivie, J., 1979; Mantyh, P. W., 1983a). Such a somatotopic arrangement supports the ability of the lateral spinothalamic pathway to process spatial discrimination. Other important lateral thalamic areas of spinal termination are the posterior complex (PO), the ventral posteroinferior nucleus (VPI) and the zona incerta (ZI) ((Mehler, W. R., 1974; Boivie, J., 1979; Apkarian, A. V. and Hodge, C. J., 1989a; Cliffer, K. D. *et al*., 1991). In the cat, fibers in the lateral spinothalamic pathway appear to be fewer and terminate in the ZI, the posterior complex, and in a shell area surrounding the VPL ventrolaterally (Boivie, J., 1971; Jones, E. G. and Burton, H., 1974; Berkley, K. J., 1980; Mantyh, P. W., 1983b; Craig, A. D. and Burton, H., 1985). Recently, Craig and colleagues claimed that a region located posteromedially to the VPL,

which they called VMpo, is the site of termination of the lamina I spinothalamic fibers (Craig, A. D. *et al.*, 1994, 2002; Blomqvist, A. *et al.*, 2000). However, besides the fact that the so-called VMpo was most probably included in the area of termination of spinal and trigeminal thalamic afferents described by Mehler (Mehler, W. R., 1966) in humans, numerous retrograde and anterograde studies have proved that lamina I neurons project to many other areas in the thalamus (references given earlier), including a study by Craig (Craig, A. D., 2003) using anterograde tracing with *phaseolus vulgaris* leucoagglutinin. Moreover, this assumption was based on the dense calbindin-staining observed in the VMpo, but neither is the calbindin-immunoreactive region restricted to the VMpo lying within the medial aspect of the ventral posterior medial nucleus (Graziano, A. and Jones, E. G., 2004), nor are calbindin-immonoreactive projecting cells exclusively located in lamina I (Menétrey, D. *et al.*, 1992b).

5.35.6.1.2 Structural types of neurons involved

Spinothalamic cells were shown, in retrograde labeling studies, to have cell bodies that vary in shape from roundish or flattened to polygonal (Willis, W. D. *et al.*, 1979). They are mainly small in lamina I and include cells with fusiform, pyriform, and triangular shapes in transverse view, beyond the classic Waldeyer cells. In deep dorsal horn as well as the ventral horn, they are medium to large sized and polygonal in shape. Similar data were obtained by Apkarian and Hodge (Apkarian, A. V. and Hodge, C. J., 1989d), although in this case, tracer injections included the medial thalamus. Spinothalamic cells intracellularly stained in laminae IV–VIII of the cat (Meyers, D. E. R. and Snow, P. J., 1982) and monkey (Surmeier, D. J. *et al.*, 1988) presented long dendritic branches that could reach the lateral funiculus, lamina I and lamina X. In the intermediomedial gray matter, spinothalamic cells presented spheroidal cell bodies and narrow dendrites (Milne, R. J. *et al.*, 1982). Around the central canal, neuropeptide-containing spinothalamic cells had oval cell bodies and dendrites oriented transversely, reaching the central canal medially (Leah, J. *et al.*, 1988).

Injections of CTb confined to the VPL in the rat revealed that VPL-projecting lamina I neurons belong in the pyramidal and flattened groups (Lima.D. and Coimbra, A., 1988). Pyramidal cells prevailed over flattened cells in the cervical and lumbar enlargements (70% and 77%, respectively), the reverse occurring at C1 and C2 (40%) (Lima.D. and Coimbra, A., 1988). In the cat (Zhang, E. T. *et al.*, 1996) and monkey (Zhang, E. T. and Craig, A. D., 1997), large tracer injections filling both the lateral and medial thalamus, resulted in labeling of fusiform neurons, beyond pyramidal and flattened neurons. Although the authors explained their labeling of fusiform neurons by putative species differences, fusiform neurons were most probably labeled from the medial thalamus (see further). It should be emphasized that, in the studies by Craig and co-workers (Zhang, E. T. *et al.*, 1996; Zhang, E. T. and Craig, A. D., 1997), flattened neurons were designated 'multipolar' due to their appearance in horizontal view, on which the authors based their observations. However, this designation is misleading and should be avoided since a neuronal group completely distinct in dendritic geometry and specializations was previously designated 'multipolar' in the rat (Lima, D. and Coimbra, A., 1986), and subsequently observed in the cat (Galhardo, V. and Lima, D., 1999), monkey (Lima, D. *et al.*, 2002), and pigeon (Galhardo, V. *et al.*, 2000) as well. When compared to flattened neurons, multipolar neurons have ventrally oriented rather than horizontal dendritic arbors and highly spiny rather than smooth dendritic branches. This kind of misuse of nomenclature already led some authors to disregard the occurrence of flattened neurons as an independent group in the cat and monkey, based on the results of retrograde labeling and immunostaining (Yu, X. H. *et al.*, 1999), despite the fact that flattened neurons were clearly identified in both species by the use of Golgi impregnation (Galhardo, V. and Lima, D., 1999; Lima, D. *et al.*, 2002).

5.35.6.1.3 Spinal location of ascending fibers

Axons of the lateral spinothalamic tract travel in the ventral, ventrolateral, and dorsolateral funiculi after decussating the spinal cord within a short distance from the cell body (Applebaum, A. E. *et al.*, 1975; Willis, W. D. *et al.*, 1979; Giesler, G. J. *et al.*, 1981a; Jones, M. W. *et al.*, 1985; Surmeier, D. J. *et al.*, 1988; Stevens, R. T. *et al.*, 1989; Apkarian, A. V. and Hodge, C. J., 1989a,b). Spinothalamic axons from lamina I cells were shown to project through the dorsolateral fasciculus in the cat (Apkarian, A. V. *et al.*, 1985; Stevens, R. T. *et al.*, 1989) and monkey (Apkarian, A. V. and Hodge, C. J., 1989a,b,c). Neurons located in the deep dorsal horn and ventral horn project through the ventrolateral fasciculus and ventral funiculus (Stevens, R. T. *et al.*, 1989; Apkarian, A. V. and Hodge, C. J., 1989b; Zhang, X. J. *et al.*, 2000). In the

ventrolateral quadrant of the spinal cord white matter, axons are arranged somatotopically so that those originating in more caudal levels are located dorsolaterally to the more rostral ones (Horrax, G., 1929; Foerster, O. and Gagel, O., 1932; Hyndman, O. R. and Van Epps, C., 1939; Walker, A. E., 1940; Applebaum, A. E. *et al.*, 1975). The termination sites of the dorsolateral and ventrolateral fibers are equally distributed in the lateral thalamus, except for VPI and the ZI whose spinal afferents course mainly in the dorsolateral fasciculus and the ventral spinal quadrant, respectively (Apkarian, A. V. and Hodge, C. J., 1989a).

5.35.6.1.4 Surface receptors

Enkephalin immunoreactive varicosities were shown to establish asymmetric synaptic contacts upon medullary and spinal neurons retrogradely labeled from large HRP injections centered in the lateral thalamus of the cat and monkey (Ruda, M. A. *et al.*, 1984). These neurons make up 30% of lamina I and 50% of lamina V labeled neurons. In transverse sections, neurons present bipolar configuration in lamina I (equivalent to flattened neurons of Lima, D. and Coimbra, A., 1986) and multipolar configuration in lamina V (Ruda, M. A. *et al.*, 1984). Spinothalamic neurons exhibiting immunostaining for the NMDA receptor (Zou, X. Y. *et al.*, 2000) and metabotropic glutamate receptor subtype 1 (mGluR1) (Millis, C. D. and Hulsebosch, C. E., 2002) have been described in studies. A study focused on lamina I neurons retrogradely labeled from large injections comprising both the lateral and medial thalamus revealed NK1 receptors in flattened (called 'multipolar' by the authors) and pyramidal neurons, the latter being relatively few, however (Yu, X. H. *et al.*, 1999). This was taken as supporting the nonnociceptive nature of pyramidal neurons, although large amounts of pyramidal neurons expressing the NK1 receptor were observed by other authors (Todd, A. J. *et al.*, 2002), and pyramidal neurons are c-*fos*-activated following various kinds of noxious stimulation (Lima, D., 1998).

5.35.6.1.5 Neurotransmitters

Most studies addressing the neurochemical nature of spinothalamic neurons looked for the presence of neuropeptides in the rat. Neuropeptide-containing lateral spinothalamic neurons were preferentially observed in the lateral spinal nucleus and around the central canal (including lamina X). Both VIP (Nahin, R. L., 1988) and bombesin (Leah, J. *et al.*, 1988) were observed in the lateral spinal nucleus at the lumbar cord. In lamina X, neurons immunoreactive for bombesin (Leah, J. *et al.*, 1988), CCK (Ju, G. *et al.*, 1987; Leah, J. *et al.*, 1988), and galanin (Ju, G. *et al.*, 1987) were described. Galanin and CCK were seen to co-localize in lamina X neurons projecting to the VPL (Ju, G. *et al.*, 1987). Neurons containing glutamate or glutaminase were described in the lateral trigeminothalamic system in areas where WDR and low-threshold neurons predominate (Magnusson, K. R. *et al.*, 1987). Calbindin was claimed to be present in the majority of lamina I spinothalamic neurons of all structural groups projecting to the thalamus (Craig, A. D. *et al.*, 2002), although anterograde tracing combined with immunocytochemical staining failed to reveal calbindin-immunostaining in lamina I axons terminating in the thalamus (Graziano, A. and Jones, E. G., 2004).

5.35.6.1.6 Response properties

Spinothalamic cells were shown to present background activity at variable firing rates depending on the species and their laminar location in the spinal cord. Only few lamina I cells present background activity (Craig, A. D. and Kniffki, K. D., 1985) in the cat as compared to lamina I cells in the monkey (Ferrington, D. G. *et al.*, 1987) and to laminae IV–V cells in both species (Giesler, G. J. *et al.*, 1981b; Ferrington, D. G. *et al.*, 1986). Most spinothalamic cells respond to stimulation of C primary afferent fibers (Chung, J. M. *et al.*, 1979), but many of them respond to volleys in Aδ and Aβ fibers of somatic nerves as well (Foreman, R. D. *et al.*, 1975; Beall, J. E. *et al.*, 1977; Chung, J. M. *et al.*, 1979). Spinothalamic cells also respond to Aδ and C-fiber volleys in visceral nerves (Foreman, R. D. and Weber, R. N., 1980; Blair, R. W. *et al.*, 1981; Foreman, R. D. *et al.*, 1981, 1984; Rucker, H. K. and Holloway, J. A., 1982; Ammons, W. S., 1987) and to group II, III, and IV muscle afferents (Foreman, R. D. *et al.*, 1979). Lateral spinothalamic neurons were found to be activated by mechanical and/or thermal noxious stimulation of the skin in the rat (Giesler, G. J. *et al.*, 1976), cat (Fox, R. E. *et al.*, 1980; Ferrington, D. G. *et al.*, 1986), and monkey (Willis, W. D. *et al.*, 1974, 1979; Applebaum, A. E. *et al.*, 1975; Price, D. D. *et al.*, 1978; Kenshalo, D. R., Jr. *et al.*, 1979; Giesler, G. J. *et al.*, 1981b; Surmeier, D. J. *et al.*, 1986a,b; Ferrington, D. G. *et al.*. 1987) as well as by noxious chemical stimulation (Simone, D. A. *et al.*, 1991) and low-threshold mechanical (Willis, W. D. *et al.*, 1974; Applebaum, A. E. *et al.*, 1975; Giesler, G. J. *et al.*, 1976; Price, D. D. *et al.*, 1978) cooling

(Dostrovsky, J. O. and Craig, A. D., 1996; Craig, A. D. *et al.*, 2001) and warming (Andrew, D. and Craig, A. D., 2001) stimulation. Nociceptive neurons belong in both the NS and WDR classes (Willis, W. D. *et al.*, 1974; Giesler, G. J. *et al.*, 1981b; Ferrington, D. G. *et al.*, 1986). NS neurons are equally distributed throughout laminae I and IV–V, while WDR neurons predominate in laminae IV–V (Willis, W. D. *et al.*, 1974) and neurons responsive to cooling are located in lamina I (Craig, A. D. *et al.*, 2001). Thermal-responsive neurons belonging in either the NS or the WDR neuronal classes were shown to be capable of encoding noxious heat intensity (Figure 18) irrespective of their location in lamina I or the deep dorsal horn (Kenshalo, D. R., Jr. *et al.*, 1979; Ferrington, D. G. *et al.*, 1986; Surmeier, D. J. *et al.*, 1986a, b).

Neurons with convergent input from the skin and viscera also contribute to the lateral spinothalamic pathway (Foreman, R. D. and Weber, R. N., 1980; Blair, R. W. *et al.*, 1981; Foreman, R. D. *et al.*, 1984; Ammons, W. S. *et al.*. 1984; Ammons, W. S., 1987; Al-Chaer, E. D. *et al.*, 1999; Chandler, M. J. *et al.*, 2000). Curiously, in lamina X, neurons of the postsynaptic dorsal column tract were shown to receive viscerosomatic input and reported to be more numerous than those of the spinothalamic tract (Al-Chaer, E. D. *et al.*, 1999; Dorsal Columns and Visceral Pain).These neurons belong in the WDR, NS, or high-threshold inhibitory classes, and present cutaneous receptive fields that occupy regions to which pain is frequently referred (Foreman, R. D. and Weber, R. N., 1980; Foreman, R. D. *et al.*, 1984; Ammons, W. S. *et al.*, 1984). Some of these neurons were shown to leave axonal collaterals in the medial medullary reticular formation (Foreman, R. D. *et al.*, 1984). Some spinothalamic neurons receive convergent input from the skin and deep tissues (Willis, W. D. *et al.*, 1974; Giesler, G. J. *et al.*, 1981b; Ferrington, D. G. *et al.*, 1986). These neurons are thought to have a proprioceptive function (Milne, R. J. *et al.*, 1982). They are mainly located in the lateral part of lamina V and intermediomedial gray matter (Stilling's nucleus) and respond to either weak or intense cutaneous stimulation (Willis, W. D. *et al.*, 1974).

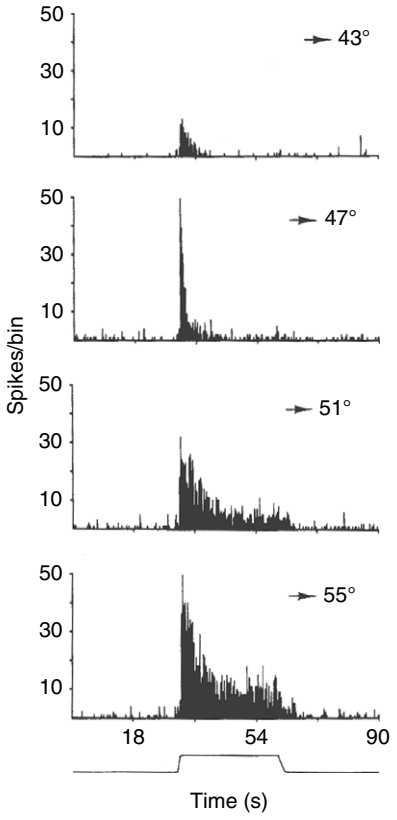

Figure 18 Responses of a lateral spinothalamic neuron to heat stimulation of increasing intensities. Adapted from figure 1 of Surmeier, D. J., Honda, C. N., and Willis, W. D. 1986a. Temporal features of the responses of primate spinothalamic neurons to noxious thermal stimulation of hairy and glabrous skin. J. Neurophysiol. 56, 351–369.

Lateral spinothalamic neurons normally present ipsilateral receptive fields that vary from very small (less than one digit) to moderate (the entire limb) (Willis, W. D. *et al.*, 1974; Giesler, G. J. *et al.*, 1981b), as well as additional inhibitory receptive fields (Gerhart, K. D. *et al.*, 1981; Giesler, G. J. *et al.*, 1981b; Ammons, W. S., 1987). In a few cells, convergent inhibitory cutaneous or visceral receptive fields were reported (Willis, W. D. *et al.*, 1974; Blair, R. W. *et al.*, 1981; Milne, R. J. *et al.*, 1982). Receptive fields tend to be smaller in high-threshold neurons and in lamina I neurons (Applebaum, A. E. *et al.*, 1975; Giesler, G. J. *et al.*, 1981b; Ferrington, D. G. *et al.*, 1987). The relatively small size of the receptive fields of lateral spinothalamic neurons favors a role in discriminating the size of the stimulated area (Giesler, G. J. *et al.*, 1981b).

C-*fos* induction after noxious cutaneous or visceral stimulation was observed in spinothalamic neurons in laminae I, III–VII, and X (Palecek, J. *et al.*, 2003). Curiously, neurons projecting in the postsynaptic dorsal column pathway were activated in similar proportions by the noxious cutaneous stimuli and in even higher proportions by the visceral stimuli (Palecek, J. *et al.*, 2003). In lamina I, both flattened and pyramidal neurons projecting to the

VPL were c-*fos*-activated following cutaneous mechanical, thermal, and chemical noxious stimulation, and, in smaller amounts, following visceral chemical stimulation (Lima, D. *et al.*, 1992; Lima, D., 1998).

5.35.6.1.7 Pathways driven at the target

The VPL is long-known for sending nociceptive input to the parietal somatosensory cortex (Burton, H. and Jones, E. G., 1976; Whitsel, B. L. *et al.*, 1978; Kenshalo, D. R., Jr. *et al.*, 1980). Combined anterograde tracing from the spinal cord and retrograde tracing from the somatosensory cortex in the monkey revealed that overlapping between spinal thalamic afferents and thalamic neurons projecting to cortical areas SI or SII occurs in the VPL, but also in the VPI and PO, the VPL being the area where the number of overlapping neurons is smaller (Stevens, R. T. *et al.*, 1993; Shi, T. and Apkarian, A. V., 1995). VPL afferents in cortical areas SI and SII are arranged in a somatotopic fashion (Burton, H. and Jones, E. G., 1976; Whitsel, B. L. *et al.*, 1978) so that the more posterior the thalamic source of afferents, the more posterior the cortical termination sites. Sparse cells in the lateral part of the VPL and the ventral part of the VPI target the cingulated cortex (Apkarian, A. V. and Shi, T., 1998).

The PO projects to the granular insular and retroinsular cortex in primates (Burton, H. and Jones, E. G., 1976) and was therefore proposed to be involved in nociceptive visceral processing (Cechetto, D. F. and Saper, C. B., 1987). PO neurons projecting to the anterior insula were seen to clearly overlap with spinothalamic axonal arborizations (Apkarian, A. V. and Shi, T., 1998). Neurons in the VPI also show insular projections, but with no overlapping. Moreover, neurons projecting to the insula do not overlap with neurons projecting to SI (Apkarian, A. V. and Shi, T., 1998).

5.35.6.2 Medial Thalamus

The medial spinothalamic pathway was described at the middle 1960s as an ascending nociceptive system especially devoted to the processing of the affective and motivational aspects of pain (Melzack, R. and Casey, K. L., 1968). While anatomical degeneration studies demonstrated the termination in medial thalamic nuclei of spinal axons ascending in the ventrolateral quadrant of the spinal cord (Bowsher, D., 1957, 1961; Mehler, W. R. *et al.*, 1960; Boivie, J., 1971), clinical studies revealed that, in patients with lesions centered in the medial thalamus, the painful poorly localized unpleasant feeling was abolished (Hécaen, H. *et al.*, 1949).

5.35.6.2.1 Spinal laminae of origin and sites of termination

Spinal neurons projecting to medial thalamic nuclei prevail in the contralateral intermediate and ventral gray matter (Figure 19) in the rat (Giesler, G. J. *et al.*, 1979a), cat (Carstens, E. and Trevino, D. L., 1978b), and monkey (Willis, W. D. *et al.*, 1979; Giesler, G. J. *et al.*, 1981b). In the cat, although a predominant location in laminae VII and VIII has been described by some authors (Carstens, E. and Trevino, D. L., 1978b; Comans, P. E. and Snow, P. J., 1981), others point to a laminar distribution similar to that observed for the lateral spinothalamic pathway, namely laminae I, IV–VI, and VII to X (Stevens, R. T. *et al.*, 1989; Craig, A. D. *et al.*, 1989). Lamina I was also shown to be the source of spinal afferents to the nucleus submedius in the cat and monkey (Craig, A. D. and Burton, H., 1981; Stevens, R. T. *et al.*, 1989) and to contribute to the spinal projections to the intralaminar complex in the monkey (Albe-Fessard, D. *et al.*, 1975; Ammons, W. S. *et al.*, 1985). In the rat, projections from laminae IV–VII were recently shown to target the central lateral nucleus, whereas the medial dorsal nucleus was found to be mainly innervated bilaterally by the lateral spinal nucleus and, to a lesser extent, by contralateral lamina I (Gauriau, C. and Bernard,J.F., 2004).

Spinal afferents ascending to the medial thalamus appear to be fewer than those reaching the lateral thalamus (Mehler, W. R. *et al.*, 1960; Apkarian, A. V. and Hodge, C. J., 1989a). They target similar medial thalamic regions in the rat (Lund, R. D. and Webster, K. E., 1967; Mehler, W. R., 1969; Zemlan, F. P. *et al.*, 1978; Cliffer, K. D. *et al.*, 1991), cat (Boivie, J., 1971; Berkley, K. J., 1980; Mantyh, P. W., 1983a; Craig, A. D. and Burton, H., 1985), monkey (Mehler, W. R. *et al.*, 1960; Boivie, J., 1979; Mantyh, P. W., 1983a; Apkarian, A. V. and Hodge, C. J., 1989a), and humans (Mehler, W. R., 1962; Mehler, W. R., 1974). These include the medial dorsal and paraventricular nuclei and the intralaminar complex, namely the central lateral, center median, paracentral, and parafascicular nuclei (Figure 19). In the monkey, the medial dorsal nucleus (except for its dorsomedial part) and the central lateral nucleus are the major sites of termination of spinal fibers (Apkarian, A. V. and Hodge, C. J., 1989a). The nucleus submedius is also a consistent site of spinal axon arborization in the cat (Boivie, J., 1971; Craig, A. D. and Burton, H., 1981; Mantyh, P.

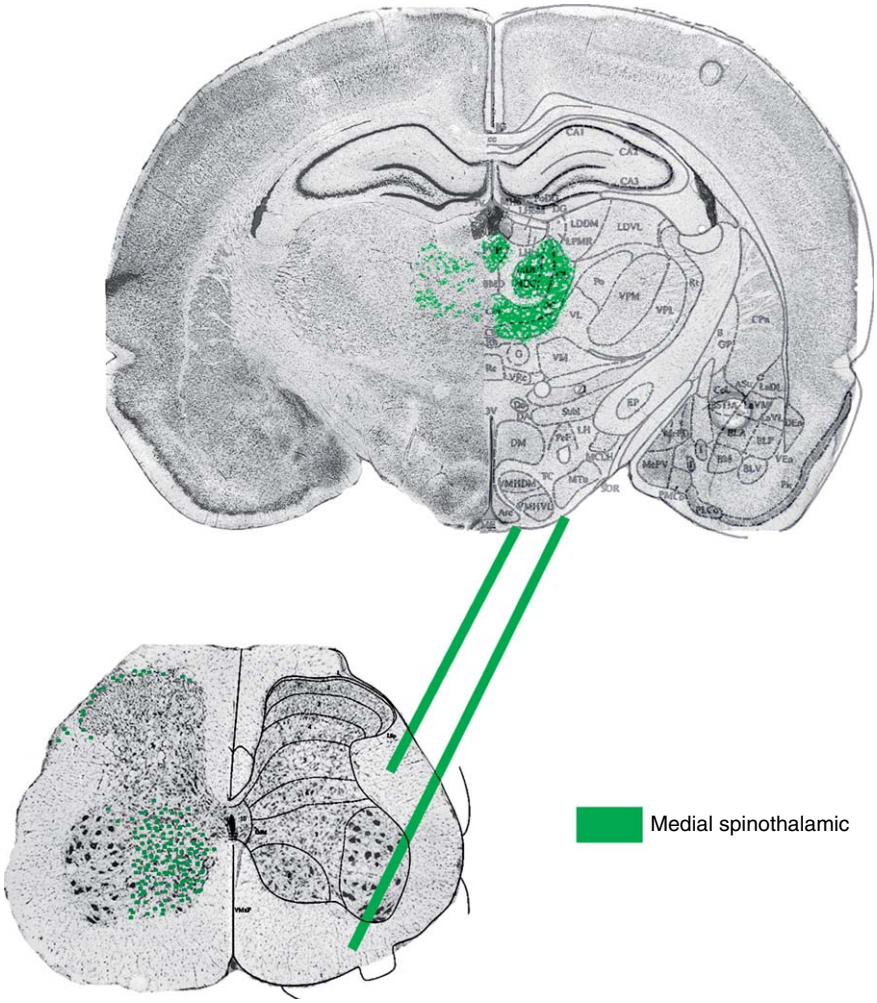

Figure 19 Diagram representing the spinal laminae of origin, ascending course in the spinal cord and areas of termination of the medial spinothalamic pathway. Brain and spinal cord photomicrographs were adapted from Paxinos, G. and Watson, C. 1998. The Rat Brain in Stereotaxic Coordinates, 4th edn. Academic Press.

W., 1983b; Craig, A. D. and Burton, H., 1985) and monkey (Boivie, J., 1979; Mantyh, P. W., 1983a; Apkarian, A. V. and Hodge, C. J., 1989a), but in relatively small amounts (Mantyh, P. W., 1983a; Apkarian, A. V. and Hodge, C. J., 1989a).

Contrary to the lateral thalamus, no somatotopic arrangement of spinal terminals could be detected in the intralaminar complex (Boivie, J., 1979), which agrees with electrophysiological studies (Giesler, G. J. *et al.*, 1981b; Guilbaud, G. *et al.*, 1985) as to the inadequacy of the medial spinothalamic system to process information related to stimulus discrimination. In the nucleus submedius, however, a somatotopic organization was described, with fibers from more rostral spinal levels terminating more rostrally in the nucleus (Craig, A. D. and Burton, H., 1985).

5.35.6.2.2 Structural types of neurons involved

Although there are no descriptions of the morphology of spinal neurons labeled from injections restricted to medial thalamic nuclei, data on laminae VI–X spinothalamic cells revealed medium to large-sized soma of polygonal or occasionally flattened configuration (Willis, W. D. *et al.*, 1979). Following injections filling both the lateral and medial thalamus in the cat and monkey (Zhang, E. T. *et al.*, 1996; Zhang, E. T. and Craig, A. D., 1997), lamina I neurons belonging in the fusiform, pyramidal, and flattened groups were labeled. As to pyramidal and flattened neurons, the possibility that labeled neurons picked up the tracer in the lateral thalamus can not be ruled out, since they were shown to project to the VPL in

the rat (Lima, D. and Coimbra, A., 1988). Fusiform neurons, however, most probably project to medial thalamic nuclei as they could not be labeled from the VPL in the rat (Lima, D. and Coimbra, A., 1988).

5.35.6.2.3 Spinal location of ascending fibers

Spinal axons targeting the medial thalamus were early shown to course in the ventral quadrant of the spinal cord (Mehler, W. R. *et al.*, 1960; Bowsher, D., 1961; Mehler, W. R., 1969). In the rat this appears to be the way taken by all spinothalamic axons (Giesler, G. J. *et al.*, 1981a), whereas in the monkey axons were shown to distribute through the lateral funiculus also (Giesler, G. J. *et al.*, 1981b; Apkarian, A. V. and Hodge, C. J., 1989a). Studies using anterograde tracing after lesioning either the contralateral spinal ventral quadrant or the contralateral dorsolateral fasciculus (Apkarian, A. V. and Hodge, C. J., 1989a) revealed that the termination pattern of fibers coursing in both pathways is similar except for the fibers targeting the dorsolateral region of the medial dorsal nucleus, which course mostly in the ventral quadrant. The ventral quadrant also contributes with particularly large amounts of fibers to the central lateral nucleus afferents, mainly in its more anterior portion.

5.35.6.2.4 Neurotransmitters

Enkephalin (Coffield, J. A. and Miletiæ, V., 1987; Nahin, R. L., 1988) and dynorphin (Nahin, R. L., 1988) were immunodetected in deep dorsal horn and intermediate gray spinal neurons projecting to the medial thalamus. Enkephalin-immunoreactive neurons amount to 10% of the entire spinothalamic population (Coffield, J. A. and Miletiæ, V., 1987). Spinothalamic lamina X neurons immunoreactive for CCK (Ju, G. *et al.*, 1987; Leah, J. *et al.*, 1988) and galanin (Ju, G. *et al.*, 1987) are likely to terminate in the parafascicular nucleus, which was shown to contain fibers immunoreactive to both neuropeptides (Ju, G. *et al.*, 1987).

5.35.6.2.5 Response properties

Neurons projecting to the medial thalamus respond, although weakly, to activation of A (α to δ) and C primary afferent fibers with sustained afterdischarges (Giesler, G. J. *et al.*, 1981b). Their background activity is practically nil. They conduct at relatively low velocities, which amount to about half those of lateral spinothalamic neurons (Giesler, G. J. *et al.*, 1981b). Most medial spinothalamic neurons belong in the NS class (around two-third vs. one-third in the lateral spinothalamic pathway). Some are WDR neurons and a few respond to deep tissue stimulation (Giesler, G. J. *et al.*, 1981b). They normally present very large, frequently complex, receptive fields that may encompass the entire surface of the body (Figure 20).

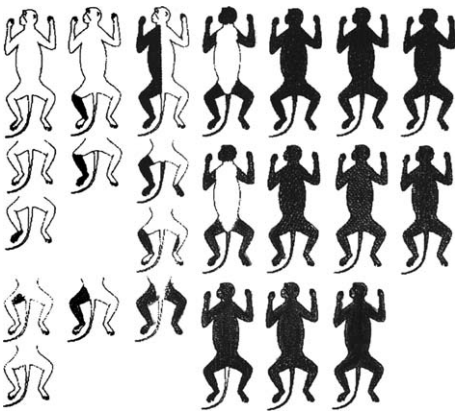

Figure 20 Receptive fields of spinal cells projecting to the medial thalamus in the monkey. Adapted from figure 3 of Giesler, G. J., Yezierski, R. P., Gerhart, K. D., and Willis, W. D. 1981b. Spinothalamic tract neurons that project to medial and/or lateral thalamic nuclei: evidence for a physiologically novel population of spinal cord neurons. J. Neurophysiol. 46, 1285–1308.

Inhibitory receptive fields are rare (Giesler, G. J. *et al.*, 1981b). Viscerosomatic convergence has been reported (Rucker, H. K. and Holloway, J. A., 1982).

5.35.6.2.6 Pathways driven at the target

Intralaminar nuclei, in particular the central lateral nucleus, project to widely distributed areas of the cerebral cortex, including sensorimotor areas, and to the basal ganglia (Jones, E. G. and Leavitt, R. Y., 1974). Ascending pathways terminating in the intralaminar nuclei have hence been proposed to be involved in motor and arousal nociceptive responses. Nociceptive pathways from the medial dorsal nucleus and the central lateral nucleus terminate, respectively, in the anterior cingulated cortex and frontal motor cortex (Wang, C. C. and Shyu, B. C., 2004). The posterior cingulated cortex also receives projections from restricted areas of both, the medial dorsal and the central lateral nuclei (Apkarian, A. V. and Shi, T., 1998). These connections are consonant with the role of the medial thalamic pathway in the emotional aspects of nociception (Wang, C. C. and Shyu, B. C., 2004). The medial dorsal nucleus and the nucleus submedius, which are similar in the response properties of their nociceptive neurons (Dostrovsky,

J. O. *et al.*, 1987), project to adjacent regions in the orbital cortex (Krettek, J. E. and Price, J. L., 1977; Craig, A. D. *et al.*, 1982; Yoshida, A. *et al.*, 1992).

5.35.6.3 Hypothalamus

5.35.6.3.1 Spinal laminae of origin and sites of termination

A direct spinohypothalamic pathway (Figure 21) was uncovered in the rat (Burstein, R. *et al.*, 1987; Burstein, R. *et al.*, 1990a; Burstein, R. *et al.*, 1990b; Menétrey, D. and DePommery, J., 1991) and cat (Katter, J. T. *et al.*, 1991) by the use of both electrophysiologic and tracing methods. It originates bilaterally, although with a slight contralateral prevalence, from the entire extent of the spinal cord (Figure 22) (Burstein, R. *et al.*, 1987, 1990a; 1990b) as well as from the spinal trigeminal nucleus, mainly the *pars caudalis* (Malick, A. and Burstein, R., 1998). Neurons in the deep dorsal horn make up the largest population of spinohypothalamic neurons, especially at upper cervical segments (around 50%), followed by the lateral spinal nucleus (around 30%), laminae I and X (around 10% each), and the intermediate ventral horn (Burstein, R. *et al.*, 1990a).

An additional contribution from the parasympathetic cell column was described in the rat (Burstein, R. *et al.*, 1990a; Menétrey, D. and DePommery, J., 1991). In the cat, the spinohypothalamic tract appears to be much smaller and to contain fewer lamina I

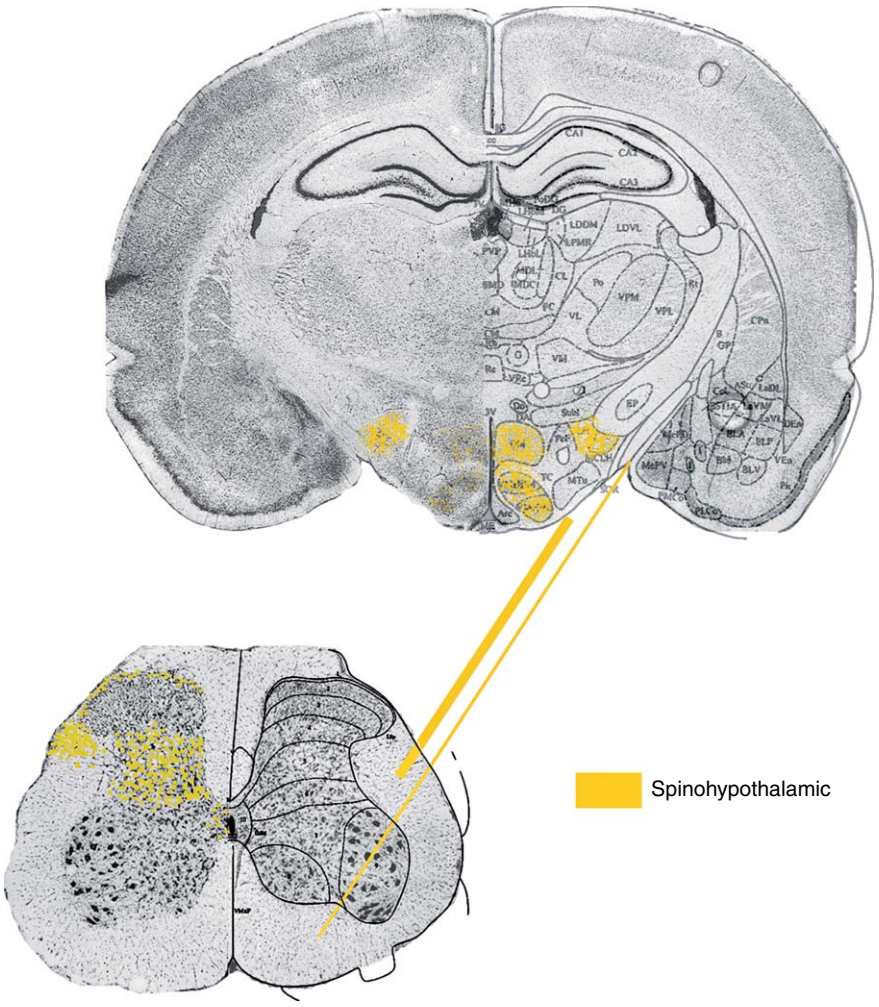

Figure 21 Diagram representing the spinal laminae of origin, ascending course in the spinal cord, and areas of termination of the spinohypothalamic pathway. Note that ipsilaterally terminating axons course contralaterally in the spinal cord. Brain and spinal cord photomicrographs were adapted from Paxinos, G. and Watson, C. 1998. The Rat Brain in Stereotaxic Coordinates, 4th edn. Academic Press.

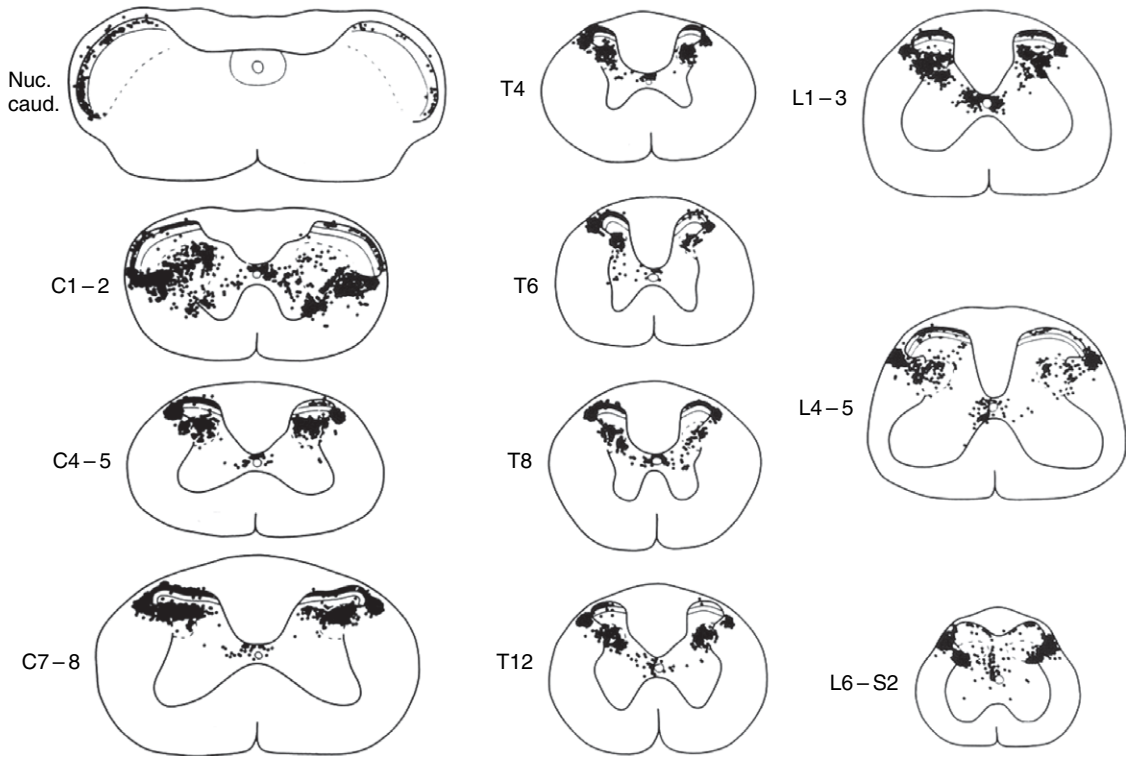

Figure 22 Distribution in the spinal cord and spinal trigeminal nucleus, *pars caudalis*, of neurons retrogradely labeled from injection of fluorogold encompassing the lateral and medial hypothalamus. (Adapted from figure 4 of Burstein, R., Cliffer, K. D., and Geisler, G. J. 1990b. Cells of origin of the spinohypothalamic tract in the rat. J. Comp. Neurol. 291, 329–344).

neurons than in the rat (Katter, J. T. *et al.*, 1991). No differences in spinal distribution were found between the medial and lateral hypothalamic pathways, except for the sacral parasympathetic nucleus, which appears to project mainly to medial nuclei (Burstein, R. *et al.*, 1990a). According to a recent study by Braz and coworkers (Braz, J. M. *et al.*, 2005) in which transgenic mice expressing a transneuronal tracer in a subset of nociceptors were used, nociceptive input conveyed by nonpeptidergic primary afferent neurons is relayed to lamina V neurons projecting to the ventromedial hypothalamus by spinal neurons located in the dorsal part of lamina II.

Consonant with retrograde and antidromic stimulation studies, terminal arborizations of spinal axons were shown to distribute massively through the lateral hypothalamus, although important labeling was also observed in the medial hypothalamus (Figure 21) (Burstein, R. *et al.*, 1987; Cliffer, K. D. *et al.*, 1991). In the lateral hypothalamus, fibers terminate bilaterally along its rostrocaudal extent, and throughout the course of the supraoptic decussation. In the medial hypothalamus, fibers terminate mainly contralaterally in the posterior and dorsal hypothalamic areas, the dorsomedial, paraventricular and suprachiasmatic nuclei, and the preoptic area (Cliffer, K. D. *et al.*, 1991). Anterograde tracer injections restricted to the superficial or deep dorsal horn confirmed that the latter contributes much more fibers to the spinohypothalamic pathway, the main areas of termination being the posterior hypothalamic area, the posterior part of the lateral hypothalamic area, and the ventral part of the paraventricular hypothalamic nucleus (Gauriau, C. and Bernard. J. F., 2004).

5.35.6.3.2 Spinal location of ascending fibers

A few studies based on degeneration following spinal lesions revealed the termination in the lateral (Anderson, F. D. and Berry, C. M., 1959; Ring, G. and Ganchrow, D., 1983) and medial (Kerr, F. W. L., 1975) hypothalamus of spinal fibers coursing in the ventral funiculus. However, electrophysiological studies using antidromic activation from the supraoptic decussation showed that only 5% of the spinohypothalamic axons course in the ventral funiculus (Burstein, R. *et al.*, 1991). The remaining travel through the lateral funiculus, mainly in the

dorsolateral fasciculus (57%), irrespective of their origin in the superficial or deep dorsal horn (Figure 21) (Burstein, R. *et al.*, 1991). Although spinal and trigeminal neurons project to the hypothalamus bilaterally, their axons ascend contralaterally in the spinal cord (Burstein, R. *et al.*, 1991) and brainstem (Kostarczyk, E. *et al.*, 1997). Those terminating ipsilaterally cross the midline within the supraoptic decussation (Burstein, R. *et al.*, 1991). Extensive collateralization along the entire brainstem has been reported (Kostarczyk, E. *et al.*, 1997).

5.35.6.3.3 Surface receptors

A particularly high number of spinal neurons projecting to the hypothalamus are apposed by profiles immunoreactive to nitric oxide synthase or to interferon-γ receptor in the lateral spinal nucleus (Kayalioglu, G. *et al.*, 1999).

5.35.6.3.4 Response properties

The majority of the neurons antidromically activated from the hypothalamus both in the spinal cord and the spinal trigeminal nucleus belong in the WDR and NS classes and also respond to noxious heat or cooling (Burstein, R. *et al.*, 1987, 1991; Malick, A. *et al.*, 2000; Zhang, X. J. *et al.*, 2002). Incremental responses to increasingly intense noxious heat stimulation were observed (Burstein, R. *et al.*, 1987). Low-threshold neurons make up 20% of the trigeminohypothalamic neurons (Malick, A. *et al.* 2000) and only 4% of the spinohypothalamic neurons (Burstein, R. *et al.*, 1991). The cutaneous receptive fields are particularly small indicating that this pathway may convey relatively precise information about the stimulated area (Burstein, R. *et al.*, 1991; Malick, A. *et al.*, 2000). About half of the spinohypothalamic neurons recorded in the thoracic spinal cord were activated by visceral distension with responses that increased with increasing stimulus intensities (Zhang, X. J. *et al.*, 2002). Eight percent of lumbar spinohypothalamic neurons respond to deep low-threshold input (Burstein, R. *et al.*, 1991).

5.35.6.3.5 Pathways driven at the target

Projections from the hypothalamus, namely the dorsomedial nucleus, descend through a dorsal pathway to the PAG, and through a ventral smaller pathway to the NTS (Thompson, R. H. *et al.*, 1996). According to c-*fos* studies (Snowball, R. K. *et al.*, 2000), neurons projecting to the ventrolateral PAG receive visceral input in the lateral hypothalamus, presumably in convergence with somatic input, and neurons projecting to the NTS are concentrated in the posterolateral hypothalamus and the paraventricular nucleus. Projections connecting the paraventricular nucleus with the ventrolateral medulla were also reported (Hardy, S. G. P., 2001).

5.35.7 Spinothelencephalic Pathways

During the last decade, evidence accumulated about the existence of ascending nociceptive pathways that connect the spinal cord directly with various telencephalic regions in the rat. Although data are mainly based on anatomic retrograde and anterograde tracing studies, both the location of the spinal cells of origin, the demonstration of cells responding to noxious stimulation in areas such as the amygdala (Miyagama, T. *et al.*, 1986), and a recent study using genetic-controlled transneuronal tracing initiated in IB4-positive putative nociceptive primary afferent fibers (Braz, J. M. *et al.*, 2005) suggest that some of these areas are spinal targets of nociceptive input.

The data on spinotelencephalic pathways collected till the early years of 2000 are still few and each study deals with several systems. Therefore, notwithstanding their probable functional individuality, they will be described together although tentatively grouped according to their putative functions.

5.35.7.1 Thelencephalic Targets of Spinal Ascending Fibers

Studies using very sensitive anterograde tracers, such as *phaseolus vulgaris* leucoagglutinin or dextran (Burstein, R. *et al.*, 1987; Cliffer, K. D. *et al.*, 1991; Gauriau, C. and Bernard J. F., 2004), revealed axonal terminal arborizations in various regions of the basal forebrain and cortex (Figure 23), which can be grouped as areas involved in motor control and areas of the limbic system.

The first group includes the globus pallidus, substantia nigra, and nucleus accumbens, in particular its medial part. A participation in the striatopallidal system as well as a role in innate motor patterns triggered by noxious stimuli has been proposed for the spinal–globus pallidus projection (Braz, J. M. *et al.*, 2005). Limbic spinal targets include nuclei of the septal complex, thought to be involved in motivation and emotion, but also in attention, arousal, learning, and memory (Burstein, R. *et al.*, 1987; Cliffer, K. D.

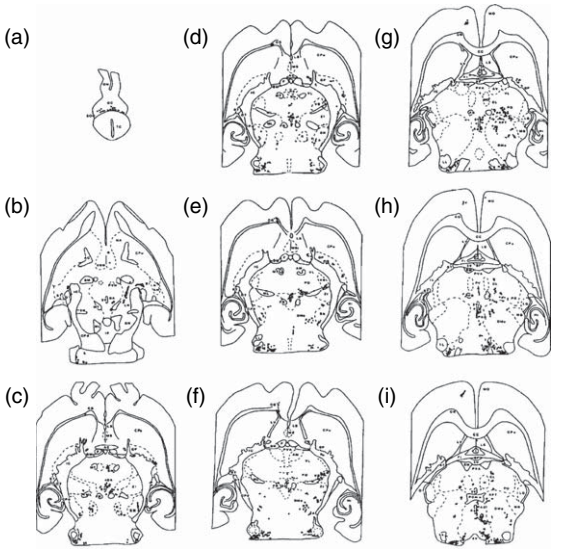

Figure 23 Distribution of spinal fibers labeled anterogradely with *phaseolus vulgaris* leucoagglutinin in the diencephalon and telencephalon, in horizontal view. Adapted from figure 3 of Cliffer, K. D., Burstein, R., and Giesler, G. J. 1991. Distributions of spinothalamic, spinohypothalamic, and spinotelencephalic fibers revealed by anterograde transport of PHA-L in rats. J. Neurosci. 11, 852–868.

et al., 1991). Positive and negative reinforcement associated with learning trials during nociceptive processing have been claimed to be accomplished by this pathway (Cliffer, K. D. *et al.*, 1991). The central nucleus of the amygdala together with what has been called the 'extended amygdala', namely the substantia innonimata and the Bed Nucleus of the stria terminalis, also receive direct projections from the spinal cord (Cliffer, K. D. *et al.*, 1991; Gauriau, C. and Bernard.J.F., 2004), as do the medial orbital and infralimbic cortices (Cliffer, K. D. *et al.*, 1991). Projections to the orbital cortex may affect autonomic, endocrine, and behavioral functions in relation to pain (Burstein, R. and Potrebic, S., 1993). The horizontal and vertical limbs of the diagonal band of Broca are also targeted by spinal axons (Burstein, R. *et al.*, 1987; Cliffer, K. D. *et al.*, 1991).

These direct spinotelencephalic projections appear to be paralleled by ascending polysynaptic pathways relaying not only in the brainstem, as is the case of the spinoparabrachialamygdaloid pathway (Ma, W. and Peschanski, M., 1988; Bernard, J. F. and Besson, J. M., 1990; Jasmin, L. *et al.*, 1997), but also within the telencephalon. Anterograde tracer injections in the central and basolateral anterior nuclei of the amygdala revealed projections from there to the substantia innonimata and stria terminalis as well as the posterior hypothalamus (Bourgeais, L. *et al.*, 2001a).

5.35.7.2 Spinal Laminae of Origin

Based on anterograde labeling from restricted injections in various spinal laminae, Gauriau and Bernard (Gauriau, C. and Bernard. J. F., 2004) concluded that cells of origin of spinopallidal fibers are located in the deep dorsal horn, laminae VII and X and, in smaller amounts, in the superficial dorsal horn (Table 1). Marked labeling was obtained in the lateral aspect of the globus pallidus from neurons located in lamina V, as revealed by transneuronal tracing with wheat germ agglutinin synthesized by IB4-positive primary afferents in mice (Braz, J. M. *et al.*, 2005).

Spinal fibers projecting to the nucleus accumbens and the septal nuclei have similar bilateral origins at the reticulated portion of the deep dorsal horn, the lateral spinal nucleus, and lamina X throughout the entire length of the spinal cord (Burstein, R. and Giesler, G. J., 1989). Deep dorsal horn neurons account to half of the entire projection population, followed by the lateral spinal nucleus, and lamina X (about 15% each). Neurons in lamina I and the intermediate/ventral horn are very few, but the first are slightly more numerous in the spinoseptal pathway (Table 1).

Spinal neurons projecting to the amygdala present similar laminar distribution (Menétrey, D. and DePommery, J., 1991; Burstein, R. and Potrebic, S., 1993). Neurons in the reticulated region of the deep dorsal horn also make up about half of the entire spinoamygdala population, but they are located in its dorsal portion in cervical segments and ventral portion in thoracolumbar segments. The lateral spinal nucleus contributes to 25% of the projection, lamina X to 13% (mainly at upper lumbar segments), and the intermediate and ventral horn to 10%, at upper cervical and lumbar segments (Table 1). Neurons in lamina V receiving primary afferent input through lamina II neurons activated by IB4-positive primary afferents also send projections to the amygdala, as well as to the bed nucleus of stria terminalis (Braz, J. M. *et al.*, 2005). A projection to the dorsal part of substantia innonimata from the superficial and deep dorsal horn, contralaterally, and from the lateral spinal nucleus, ipsilaterally, has been described (Gauriau, C. and Bernard. J.F., 2004).

Table 1 Relative participation of spinal cord laminae in the various nociceptive ascending pathways

	LSN	*I*	*II*	*III*	*IV*	*V*	*VI*	*VII*	*VIII*	*X*
LCN		■		■ (10%)	■ (60%)	■	■	■		
VLMlat	■	■	■	■						■
LRt					■	■	■	■	■	■
DRt dorsal		■ (Medial)	■ (Medial)	■ (Medial)						■
DRt ventral					■ (Medial)	■ (Medial)	■ (Medial)	■		■
NTS	■	■			■	■	■	■		■
RVM						■		■	■	■
PBN		■ (Lateral)				■ (Lateral)			■	■
PAG	■	■			■ (Lateral)	■ (Lateral)	■	■	■	■
Lateral thalamus	■	■			■	■	■	■	■	■
Medial thalamus	■	■						■	■	
Hypothalamus	■ (30%)	■ (10%)			■ (----------50%----------)					■ (10%)
N. Pallidus		■			■	■	■	■		■
N. Accumbens	■ (25%)				■ (----------50%----------)					■ (10%)
Septal nucleus	■ (15%)	■			■ (----------50%----------)					■ (15%)
Amygdala	■ (25%)					■ (-----50%-----)		■ (–10%–)	■	■ (10%)
Subst. inonimata					■	■	■			
Orbital cortex	■ (15%)					■ (-----62%-----)	■	■ (–13%–)	■	■ (10%)

Relative amounts refer to each pathway and do not allow comparisons between pathways. Whenever quantified, the relative contribution to each pathway is referred between brackets. LSN, lateral spinal nucleus; LCN, lateral cervical nucleus; VLMlat, caudal ventrolateral reticular formation, lateral portion; LRt, lateral reticular nucleus; DRt dorsal, dorsal reticular nucleus, dorsal portion; DRt ventral, dorsal reticular nucleus – ventral portion; NTS, nucleus tractus solitarii; RVM, rostral ventromedial medulla; PBN, parabrachial nuclei; PAG, periaqueductal gray; I–X, spinal laminae.

The orbital cortex receives its major spinal projections from the contralateral reticulated area of the deep dorsal horn (62%) at the cervical level or its ventromedial aspect at the thoracic and lumbar levels. The lateral spinal nucleus contributes to 15% of the projection, but mainly at lumbar segments, while the intermediate/ventral horn and lamina X contribute to 13% and 10%, respectively, both at the upper cervical and lower thoracic/upper lumbar segments (Table 1) (Burstein, R. and Potrebic, S., 1993).

5.35.8 Discussion

5.35.8.1 Multiple Parallel Ascending Pathways

The main feature that stands out is the multiplicity of the ascending nociceptive system in terms of the variety of supraspinal regions that are targeted (Figure 24). This has been interpreted as the anatomical substrate for the triggering of a multitude of responses to the noxious event, from autonomic and motor reactions to affective and cognitive behaviors. Nevertheless, it is curious to note that, contrary to what was thought in the middle of the twentieth century, nociceptive input does not necessarily arrive to high processing motor, affective, and cognitive centers in the thelencephalon through multisynaptic chains capable of filtering information at various successive levels, but can reach those areas through direct spinofugal pathways.

Another aspect that emerges is that multiple polysynaptic pathways seem to parallel monosynaptic connections between the spinal cord and each supraspinal target. So far, this organization pattern was demonstrated only for a few systems, such as the medial paracentral spinothalamic and the spinoamygdaloid

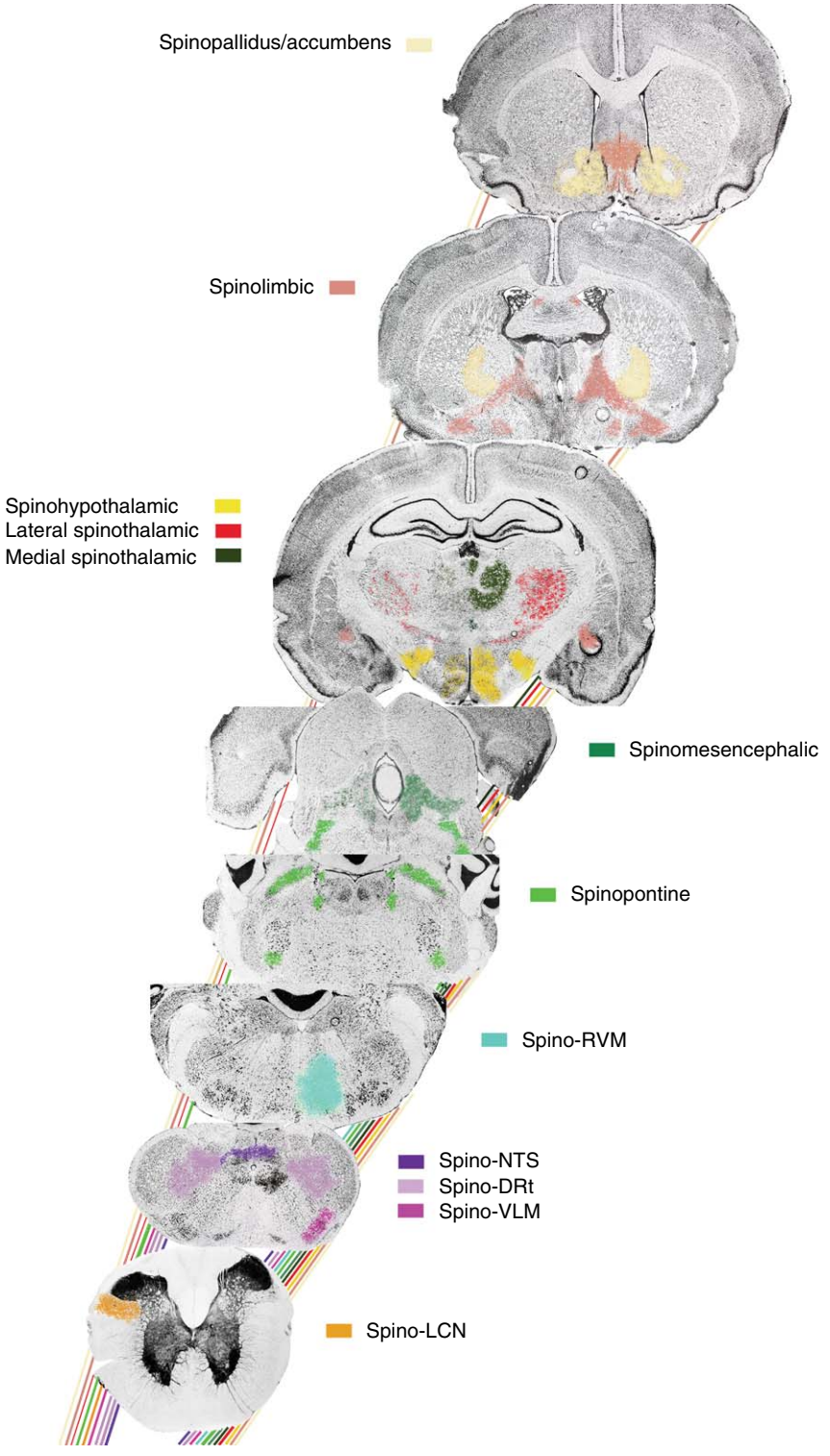

Figure 24 Diagram illustrating the termination areas of the various ascending nociceptive pathways. The laterality of the ascending tracts and termination fields with respect to the side of arrival of primary afferent input is represented, the left side being ipsilateral and the right side contralateral. Brain and spinal cord photomicrographs were adapted from Paxinos, G. and Watson, C. 1998. The Rat Brain in Stereotaxic Coordinates, 4th edn. Academic Press.

systems, served by a direct pathway and a disynaptic pathway with a relay in the PBN (Ma, W. and Peschanski, M., 1988; Bernard, J. F. and Besson, J. M., 1990; Jasmin, L. *et al.*, 1997). However, the fact that most spinal targets send projections to other brain areas that are also targeted by spinal fibers strongly suggests a similar architecture for most systems, with the participation of parallel monosynaptic and multisynaptic chains of different lengths. Such an arrangement may imply that the responses to the noxious event generated at each site evolve along time according to postarriving of noxious-evoked input generated in other pain-processing centers. Notwithstanding the extensive anatomical and electrophysiological data that are still needed to corroborate this hypothesis, it is worth to take it into consideration in future investigation.

5.35.8.2 Spinal Neuronal Populations at the Origin of Nociceptive Ascending Pathways

When facing such a variety of nociceptive ascending pathways, it is tempting to assume that they differ by either channeling different sensory modalities to brain regions specifically dedicated to their processing, or by the responses they induce to whatever stimulus through activation of a particular supraspinal region. For the first assumption to be correct, the spinal source of input should differ between different pathways. The overview of the ascending nociceptive system here presented clearly shows that this is not the case. On the contrary, if one compares the contribution of the various spinal laminae to each pathway (Table 1), the first emerging picture is that of a strong similarity, which favors the second assumption that the functional properties of a pathway depend on the functional engagement of its target. However, in spite of a large overlap, there are subtle dissimilarities between pathways consisting of a preponderance of some laminae over others or differences in the location of the projecting neurons in each lamina (Table 1). Also the electrophysiological response properties of spinal neurons participating in the various pathways overlap considerably (Table 2): all pathways including nociceptive specific, wide-dynamic-range and low-threshold neurons, as well as neurons responding to cutaneous, visceral, and deep noxious stimuli. Again, subtle differences are likely to occur about the proportion of neurons of each kind that take part in each pathway (Table 2). Differences between pathways over the amount of projecting neurons they involve have also been pointed out (Apkarian, A. V. and Hodge, C. J., 1989d; Burstein, R. *et al.*, 1990b; Mouton, L. J. and Holstege, G., 1998; Willis, W. D. *et al.*, 2001) but a complete picture of the quantitative variations is still hard to attain due to the use of tracers of variable sensitivity. As to the possibility that each pathway identity relies on a particular neurochemical architecture at the spinal relay, data are too scarce to allow any sort of considerations.

Table 2 Relative participation of low threshold (LT), wide-dynamic-range (WDR) and nociceptive specific (NS) spinal cord neurons in the various nociceptive ascending pathways

	LT	*WDR*	*NS*
LCN	Mainly hair movement	60–86%	
VLM	25%	25%	50%
NTS	+	The majority	
RVM	+	The majority	
PBN	−	+	+ (75–90% in lamina I)
PAG	+ (DDH)	50% (Lamina I + DDH	+ (lamina I)
Lateral thalamus	+	+	35%
Medial thalamus	+	+	70%
Hypothalamus	4%	The majority	

DDH, deep dorsal horn. Other abbreviations as in Table 1.

The difficulty in concealing this anatomofunctional organization with the well-known capacity of modality discrimination during acute physiological pain led some authors to ascribe discrimination capacity to a particular spinal region, leaving the remaining spinal cord with a secondary, largely unknown but eventually not important role in pain processing. The high concentration of nociceptive specific neurons in lamina I, together with the convergence of input of various nature and peripheral origin to this lamina and the easy separation of its structural neuronal groups (see Chapter Spinal Cord Physiology of Nociception) brought it into focus during the last decade. However, lamina I does not contribute to all spinofugal nociceptive pathways while participating similarly in many others (Table 1). Moreover, an appraisal of the participation of the various lamina I structural cell groups in a sample of nociceptive ascending pathways revealed

Table 3 Relative amounts of supraspinally projecting lamina I neurons

	Fusiform	*Flattened*	*Pyramidal*	*Multipolar*
VLM	80%	10%	10%	
DRt		10–30%	5–20%	60–85%
NTS	25%	40%	35%	
PBN	70%		30%	
PAG	30%		70%	
Thalamus VBC		25–30% (enlargements)	70–75% (enlargements)	

VBC, ventrobasal complex of the thalamus.

large superposition, although again slight differences as to their relative amount in each pathway and the specific involvement or noninvolvement of certain groups were detected (Table 3). What is noteworthy is that when taken together, the various electrophysiological studies on the response properties of lamina I neurons do not support a clear-cut structural–functional correlation based on stimulus-modality processing (see discussion in Galhardo, V. *et al*., 2000). The possibility that stimulus characterization at the central nervous system depends on a combinatory activation process rather than on the activation of specific channels should be addressed in the future.

As a working hypothesis, it could be postulated at this point that each pathway has particular characteristics that depend on both, the kind of input it transmits (defined by the relative contribution of the various spinal neurons) and the functional properties of the target. Ultimately, for each noxious event, ascending transmission of nociceptive input would be the result of the relative activation of the various pathways.

5.35.8.3 Stimulus Discrimination

A clear separation between the lateral and the medial spinothalamic nociceptive pathways as to the ability of the former to discriminate between stimulus location and intensity has been established, based mainly on the electrophysiological properties of neurons projecting in each pathway. Amongst the supporting data stand out the relatively small size of the receptive fields, the stimulus intensity-encoding capacity, and the somatotopic organization of the spinal, thalamic, and cortical neurons in the lateral pathway, as opposed to the medial pathway. It should be noted, however, that early studies pointed out that the medial spinothalamic system conveys spinal input either directly or through a brainstem relay, but spinal neurons projecting to brainstem regions connected to the medial thalamus do not necessarily share the same properties of the medial spinothalamic neurons. Receptive fields of spino-RVM and spino-PAG neurons vary from small, confined to a sole limb, to very large and complex. PBN-projecting spinal neurons were shown to present small receptive fields (Bester, H. *et al*., 2000), contrary to PBN neurons projecting to the paracentral nucleus of the thalamus, which have large receptive fields (Bourgeais, L. *et al*., 2001b). Also noteworthy in this respect is the fact that neurons in the RVM and PAG send axonal collaterals to the lateral thalamus, while neurons projecting through the lateral spinothalamic or the spinocervical pathways send collaterals to the medial thalamus. As a whole, the data suggest that, although the lateral spinothalamic pathway as well as the spinocervical and the spinohypothalamic pathways appear to be morphofuntionally organized to allow stimulus location and intensity discrimination, an extensive cross-talk between the various nociceptive ascending pathways is likely to take place.

5.35.8.4 Nociceptive Ascending Pathways as Part of a Complex Nociceptive Integration System

Although the ascending transmission system and the descending endogenous pain control system (see Chapter Descending Control Mechanisms) are normally dealt with separately, evidence has been accumulated to prove that they are both part of a sole nociceptive system buildup in such a way that information is treated at different brain levels in order to integrate nociception and various brain functions. The brain areas of termination of the ascending nociceptive pathways are those and the same from where pain-control actions are elicited upon local stimulation (Jones, S. L., 1992). These areas are intimately connected with each other, and

each of them with the spinal cord dorsal horn, in most cases through direct descending projections that very often participate in spino-brain-spinal reciprocal loops (Lima, D. *et al*., 1998). Descending pain-control actions appear to be triggered not only by arriving of nociceptive input, but also by the current state of processing of other functions carried out at those brain areas, as blood pressure variations at the caudal ventrolateral reticular formation (Tavares, I. and Lima, D., 2002).

The so-called ascending and descending systems are arranged as an intricate network of neuronal pathways that interchange information and dynamically control, through modulation of spinal dorsal horn activity, the level of activation of the perception and response centers. Pain perception and pain reactions are thus adapted to autonomic, affective, and cognitive states, which in turn are short- or long-term modified in response to the noxious event. The various nociceptive ascending pathways must not be viewed as static separate lines that allow the passage of nociceptive signals to distinct brain regions, but rather as an ensemble of spinal transmission neurons that tune pain perception and reactions according to peripheral and central conditions through a constant and dynamic interplay with the brain.

References

Abols, I. A. and Basbaum, A. I. 1981. Afferent connections of the rostral medulla of the cat: a neural-substrate for midbrain-medullary interactions in the modulation of pain. J. Comp. Neurol. 201, 285–297.

Agarwal, S. K. and Calaresu, F. R. 1990. Reciprocal connections between nucleus tractus solitarii and rostral ventrolateral medulla. Brain Res. 523, 305–308.

Al-Chaer, E. D., Feng, Y., and Willis, W. D. 1999. Comparative study of viscerosomatic input onto postsynaptic dorsal column and spinothalamic tract neurons in the primate. J. Neurophysiol. 82, 1876–1882.

Albe-Fessard, D., Boivie, J., Grant, G., and Levante, A. 1975. Labelling of cells in the medulla oblongata and the spinal cord of the monkey after injections of horseradish peroxidase in the thalamus. Neurosci. Lett. 1, 75–80.

Almeida, A. and Lima, D. 1997. Activation by cutaneous or visceral noxious stimulation of spinal neurons projecting to the medullary dorsal reticular nucleus in the rat: a *c-fos* study. Eur. J. Neurosci. 9, 686–695.

Almeida, A., Cobos, A., Tavares, A., and Lima, D. 2002. Brain afferents to the medullary dorsal reticular nucleus: a retrograde and anterograde tracing study in the rat. Eur. J. Neurosci. 16, 81–95.

Almeida, A., Tavares, I., and Lima, D. 1995. Projection sites of superficial or deep dorsal horn in the dorsal reticular nucleus. Neuroreport 6, 1245–1248.

Almeida, A., Tavares, I., and Lima, D. 2000. Reciprocal connections between the medullary dorsal reticular nucleus and the spinal dorsal horn in the rat. Eur. J. Pain. 4, 373–387.

Almeida, A., Tavares, I., Lima, D., and Coimbra, A. 1993. Descending projections from the medullary dorsal reticular nucleus make synaptic contacts with spinal cord lamina I cells projecting to that nucleus: an electron microscopic tracer study in the rat. Neuroscience 55, 1093–1106.

Ammons, W. S. 1987. Characteristics of spinoreticular and spinothalamic neurons with renal input. J. Neurophysiol. 50, 480–495.

Ammons, W. S., Blair, R. W., and Foreman, R. D. 1984. Responses of primate T1–T5 spinothalamic neurons to gallbladder distension. Am. J. Physiol. 247, R995–R1002.

Ammons, W. S., Girardot, M. N., and Foreman, R. D. 1985. T2–T5 spinothalamic neurons projecting to medial thalamus with viscerosomatic input. J. Neurophysiol. 54, 73–89.

Anderson, F. D. and Berry, C. M. 1959. Degeneration studies of long ascending fiber systems in the cat brain stem. J. Comp. Neurol. 111, 195–229.

Andrew, D. and Craig, A. D. 2001. Spinothalamic lamina I neurons selectively responsive to cutaneous warming in cats. J. Physiol. 537, 489–495.

Apkarian, A. V. and Hodge, C. J. 1989a. The primate spinothalamic pathways: III. Thalamic terminations of the dorsolateral and ventral spinothalamic pathways. J. Comp. Neurol. 288, 493–511.

Apkarian, A. V. and Hodge, C. J. 1989b. The primate spinothalamic pathways: II. The cells of origin of the dorsolateral and ventral spinothalamic pathways. J. Comp. Neurol. 288, 474–492.

Apkarian, A. V. and Hodge, C. J. 1989c. A dorsolateral spinothalamic tract in macaque monkey. Pain 37, 323–333.

Apkarian, A. V. and Hodge, C. J. 1989d. The primate spinothalamic pathways: I. A quantitative study of the cells of origin of the spinothalamic pathway. J. Comp. Neurol. 288, 447–473.

Apkarian, A. V. and Shi, T. 1998. Thalamocortical Connections of the Cingulate and Insula in Relation to Nociceptive Inputs to the Cortex. In: Pain Mechanisms and Management (*eds*. S. N. Ayrapetyan and A. V. Apkarian), pp. 212–220. IOS Press.

Apkarian, A. V., Stevens, R. T., and Hodge, C. J. 1985. Funicular location of ascending axons of lamina L cells in the cat spinal-cord. Brain Res. 334, 160–164.

Applebaum, A. E., Beall, J. E., Foreman, R. D., and Willis, W. D. 1975. Organization and receptive fields of primate spinothalamic tract neurons. J. Neurophysiol. 38, 572–586.

Baker, M. L. and Giesler, G. J. 1984. Anatomical studies of the spinocervical tract of the rat. Somatosens. Res. 2, 1–18.

Bandler, R. and Tork, I. 1987. Midbrain periaqueductal grey region in the cat has afferent and efferent connections with solitary tract nuclei. Neurosci. Lett. 74, 1–6.

Beall, J. E., Foreman, R. D., Willis, W. D., and Applebaum, A. E. 1977. Spinal cord potentials evoked by cutaneous afferents in the monkey. J. Neurophysiol. 40, 199–211.

Behbehani, M. M. 1995. Functional characteristics of the midbrain periaqueductal gray. Prog. Neurobiol. 46, 575–605.

Beitz, A. J. 1982. The organization of afferent-projections to the midbrain periaqueductal gray of the rat. Neuroscience 7, 133–159.

Berkley, K. J. 1980. Spatial relationships between the terminations of somatic sensory and motor pathways in the rostral brainstem of cats and monkeys. I. Ascending somatic sensory inputs to lateral diencephalon. J. Comp. Neurol. 193, 283–317.

Bernard, J. F. and Besson, J. M. 1990. The spino(trigemino)-pontoamygdaloid pathway: electrophysiological evidence for an involvement in pain processes. J. Neurophysiol. 63, 473–490.

Bernard, J. F., Villanueva, L., Carroué, J., and Le Bars, D. 1990. Efferent projections from the subnucleus reticularis dorsalis

(SRD): a *Phaseolus vulgaris* leucoagglutinin study in the rat. Neurosci. Lett. 116, 257–262.
Bester, H., Chapman, V., Besson, J. M., and Bernard, J. F. 2000. Physiological properties of the lamina I spinoparabrachial neurons in the rat. J. Neurophysiol. 83, 2239–2259.
Björkeland, M. and Boivie, J. 1984. The termination of spinomesencephalic fibers in cat. An experimental anatomical study. Anat. Embryol. 170, 265–277.
Blair, R. W., Ammons, W. S., and Foreman, R. D. 1984a. Responses of thoraric spinothalamic and spinoreticular cells to coronary artery occlusion. J. Neurophysiol. 51, 636–648.
Blair, R. W., Weber, R. N., and Foreman, R. D. 1981. Characteristics of primate spinothalamic tract neurons receiving viscerosomatic convergent inputs in the T3–T5 segments. J. Neurophysiol. 46, 797–811.
Blair, R. W., Weber, R. N., and Foreman, R. D. 1984b. Responses of thoracic spinoreticular and spinothalamic cells to intracardiac bradykinin. Am. J. Physiol. 246, H500–H507.
Blomqvist, A., Ma, W., and Berkley, K. J. 1989. Spinal input to the parabrachial nucleus in the cat. Brain Res. 480, 29–36.
Blomqvist, A., Zhang, E. T., and Craig, A. D. 2000. Cytoarchitectonic and immunohistochemical characterization of a specific pain and temperature relay, the posterior portion of the ventral medial nucleus, in the human thalamus. Brain 123, 601–619.
Boivie, J. 1971. The termination of the spinothalamic tract in the cat. An experimental study with silver degeneration methods. Exp. Brain Res. 12, 331–353.
Boivie, J. 1979. An anatomical reinvestigation of the termination of the spinothalamic tract in the monkey. J. Comp. Neurol. 186, 343–370.
Bourgeais, L., Gauriau, C., and Bernard, J. F. 2001a. Projections from the nociceptive area of the central nucleus of the amygdala to the forebrain: a PHA-L study in the rat. Eur. J. Neurosci. 14, 229–255.
Bourgeais, L., Monconduit, L., Villanueva, L., and Bernard, J. F. 2001b. Parabrachial internal lateral neurons convey nociceptive messages from the deep laminas of the dorsal horn to the intralaminar thalamus. J. Neurosci. 21, 2159–2165.
Bowsher, D. 1957. Termination of the central pain pathway in man: the conscious appreciation of pain. Brain 80, 606–622.
Bowsher, D. 1961. The termination of secondary somatosensory neurons within the thalamus of Macaca mulatta: an experimental degeneration study. J. Comp. Neurol. 117, 213–227.
Bowsher, D. and Westman, J. 1970. The gigantocellular reticular region and its spinal afferents: a light and electron microscopic study in the cat. J. Anat. 106, 23–36.
Braz, J. M., Nassar, M. A., Wood, J. N., and Basbaum, A. I. 2005. Parallel 'pain' pathways arise from subpopulations of primary afferent nociceptor. Neuron 47, 787–793.
Brown, A. G. and Franz, D. N. 1969. Responses of spinocervical tract neurones to natural stimulation of identified cutaneous receptors. Exp. Brain Res. 7, 231–249.
Brown, A. G., Fyffe, R. E., Noble, R., Rose, P. K., and Snow, P. J. 1980a. The density, distribution and topographical of spinocervical tract neurones in the cat. J. Physiol. 300, 409–428.
Brown, A. G., Hamann, W. C., and Martin, H. F. 1975. Effects of activity in non-myelinated afferent fibres on the spinocervical tract. Brain Res. 98, 243–259.
Brown, A. G., House, C. R., Rose, P. K., and Snow, P. J. 1976. The morphology of spinocervical tract neurones in the cat. J. Physiol. 260, 719–738.
Brown, A. G., Koerber, H. R., and Noble, R. 1987. An intracellular study of spinocervical tract cell responses to natural stimuli and single hair afferent fibres in cats. J. Physiol. 382, 331–354.
Brown, A. G., Rose, P. K., and Snow, P. J. 1977. The morphology of spinocervical tract neurones revealed by intracellular injection of horseradish peroxidase. J. Physiol. 270, 747–764.
Brown, A. G., Rose, P. K., and Snow, P. J. 1980b. Dendritic trees and cutaneous receptive fields of adjacent spinocervical tract neurones in the cat. J. Physiol. 300, 429–440.
Bryan, R. N., Coulter, J. D., and Willis, W. D. 1974. Cells of origin of the spinocervical tract in the monkey. Exp. Neurol. 42, 574–586.
Bryan, R. N., Trevino, D. L., Coulter, J. D., and Willis, W. D. 1973. Location and somatotopic organization of the cells of origin of the spino-cervical tract. Exp. Brain Res. 17, 177–189.
Burstein, R. and Giesler, G. J. 1989. Retrograde labeling of neurons in spinal cord that project directly to nucleus accumbens or the septal nuclei in the rat. Brain Res. 497, 149–154.
Burstein, R. and Potrebic, S. 1993. Retrograde labelling of neurons in the spinal cord that project directly to the amygdala or the orbital cortex in the rat. J. Comp. Neurol. 335, 469–485.
Burstein, R., Cliffer, K. D., and Giesler, G. J. Jr. 1987. Direct somatosensory projections from the spinal cord to the hypothalamus and telencephalon. J. Neurosci. 4159–4164.
Burstein, R., Cliffer, K. D., and Giesler, G. J. 1990a. Cells of origin of the spinohypothalamic tract in the rat. J. Comp. Neurol. 291, 329–344.
Burstein, R., Dado, R. J., Cliffer, K. D., and Giesler, G. J., Jr. 1991a. Physiological characterization of spinohypothalamic tract neurons in the lumbar enlargement of rats. J. Neurophysiol. 66, 261–284.
Burstein, R., Cliffer, K. D., and Geisler, G. J. 1990b. Cells of origin of the spinohypothalamic tract in the rat. J. Comp. Neurol. 291, 329–344.
Burton, H. and Jones, E. G. 1976. The posterior thalamic region and its cortical projection in new world and old world monkeys. J. Comp. Neurol. 168, 249–301.
Calaresu, F. R., Ciriello, J., Caverson, M. M., Chechetto, D. F., and Krukoff, T. L. 1984. Functional neuroanatomy of central pathways controlling the circulation. In: Hypertension and the brain (*eds*. G. P. Guthrie, Jr. and T. A. Kotchen), pp. 3–22. Futura Publishing.
Carstens, E. and Trevino, D. L. 1978a. Anatomical and physiological properties of ipsilaterally projecting spinothalamic neurons in the second cervical segment of the cat's spinal cord. J. Comp. Neurol. 182, 167–184.
Carstens, E. and Trevino, D. L. 1978b. Laminar origins of spinothalamic projections in the cat as determined by the retrograde transport of horseradish peroxidase. J. Comp. Neurol. 182, 151–166.
Castro, A. R., Morgado, C., Lima, D., and Tavares, I. 2006. Differential expression of NK1 and $GABA_B$ receptors in spinal neurons projecting to antinociceptive or pronociceptive medullary centers. Brain Res Bull. 69, 266–275.
Catalano, J. V. and Lamarche, G. 1957. Central pathway for cutaneous impulses in the cat. Am. J. Physiol. 189, 141–144.
Cechetto, D. F. and Saper, C. B. 1987. Evidence for a viscerotopic sensory representation in the cortex and thalamus in the rat. J. Comp. Neurol. 262, 27–45.
Cechetto, D. F., Standaert, D. G., and Saper, C. B. 1985. Spinal and trigeminal dorsal horn projections to the parabrachial nucleus in the rat. J. Comp. Neurol. 240, 153–160.
Cervero, F. and Wolstencroft, J. H. 1984. A positive feeedback loop between spinal cord nociceptive pathways and antinociceptive areas of the cat's brain stem. Pain 20, 125–138.
Cervero, F., Iggo, A., and Molony, V. 1977. Responses of spinocervical tract neurones to noxious stimulation of the skin. J. Physiol. 267, 537–558.

Chandler, M. J., Zhang, J., Qin, C., Yuan, Y., and Foreman, R. D. 2000. Intrapericardiac injections of algogenic chemicals excite primate C1-C2 spinothalamic tract neurons. Am. J. Physiol. Regul. Integr. Comp. Physiol. 279, R560–R568.

Chaouch, A., Menétrey, D., Binder, D., and Besson, J. M. 1983. Neurons at the origin of the component of the bulbopontine spinoreticular tract in the rat: an anatomical study using horseradish peroxidase retrograde transport. J. Comp. Neurol. 214, 309–320.

Chung, J. M., Kenshalo, D. R., Gerhart, K. D., and Willis, W. D. 1979. Excitation of primate spinothalamic neurons by cutaneous C-fiber volleys. J. Neurophysiol. 42, 1354–1369.

Clark, W. E. L. 1936. The termination of ascending tracts in the thalamus of the thalamus of the macaque monkey. J. Anat. 71, 7–40.

Cledenin, M., Ekerot, C. F., Oscarsson, O., and Rosén, I. 1974. The lateral reticular nucleus in the cat. II: Organization of component activated from bilateral ventral flexor reflex tract (bVFRT). Exp. Brain Res. 21, 487–500.

Clement, C. I., Keay, K. A., Podzebenko, K., Gordon, B. D., and Bandler, R. 2000. Spinal sources of noxious visceral and noxious deep somatic afferent drive onto the ventrolateral periaqueductal gray of the rat. J. Comp. Neurol. 425, 323–344.

Cliffer, K. D., Burstein, R., and Giesler, G. J. 1991. Distributions of spinothalamic, spinohypothalamic, and spinotelencephalic fibers revealed by anterograde transport of PHA-L in rats. J. Neurosci. 11, 852–868.

Cobos, A., Lima, D., Almeida, A., and Tavares, I. 2003. Brain afferents to the lateral caudal ventrolateral medulla: a retrograde and anterograde tracing study in the rat. Neuroscience 120, 485–498.

Coffield, J. A. and Miletiæ, V. 1987. Immunoreactive enkephalin is contained within some trigeminal and spinal neurons projecting to the rat medial thalamus. Brain Res. 425, 380–383.

Collier, J. and Buzzard, E. F. 1903. The degenerations resulting from lesions of posterior nerve roots and away from transverse lesions of the spinal cord in man. Brain 26, 559–591.

Comans, P. E. and Snow, P. J. 1981. Ascending projections to nucleus parafascicularis of the cat. Brain Res. 230, 337–341.

Cowie, R. J. and Holstege, G. 1992. Dorsal mesencephalic projections to pons, medulla, and spinal-cord in the cat - limbic and nonlimbic components. J. Comp. Neurol. 319, 536–559.

Craig, A. D. 1976. Spinocervical tract cells in cat and dog, labeled by the retrogade transport of horseradish peroxidase. Neurosci. Lett. 3, 173–177.

Craig, A. D. 1978. Spinal and medullary input tothe lateral cervical nucleus. J. Comp. Neurol. 181, 729–744.

Craig, A. D. 1995. Distribution of brainstem projections from spinal lamina I neurons in the cat and the monkey. J. Comp. Neurol. 361, 225–248.

Craig, A. D. 2003. Distribution of trigeminothalamic and spinothalamic lamina I, terminations in the cat. Somatosens. Mot. Res. 20, 209–222.

Craig, A. D. and Burton, H. 1979. The lateral cervical nucleus in the cat: anatomic organization of cervico-thalamic neurons. J. Comp. Neurol. 185, 329–346.

Craig, A. D. and Burton, H. 1981. Spinal and medullary lamina I projection to nucleus submedius in medial thalamus: a possible pain center. J. Neurophysiol. 45, 443–466.

Craig, A. D. and Burton, H. 1985. The distribution and topographical organization in the thalamus of antegradely-transported horseradish peroxidase after spinal injections in cat and raccoon. Exp. Brain Res. 58, 227–254.

Craig, A. D. and Kniffki, K. D. 1985. Spinothalamic lumbosacral lamina I cells responsive to skin and muscle stimulation in the cat. J. Physiol. 365, 197–221.

Craig, A. D., Bushnell, M. C., Zhang, E. T., and Blomqvist, A. 1994. A thalamic nucleus specif for pain and temperature sensation. Nature 372, 770–773.

Craig, A. D., Krout, K., and Andrew, D. 2001. Quantitative response characteristics of thermoreceptive and nociceptive lamina I spinothalamic neurons in the cat. J. Neurophysiol. 86, 1459–1480.

Craig, A. D., Linington, A. J., and Kniffki, K. D. 1989. Cells of origin of spinothalamic tract projections to the medial and lateral thalamus in the cat. J. Comp. Neurol. 289, 568–585.

Craig, A. D., Wiegand, S. J., and Price, J. L. 1982. The thalamo-cortical projection of the nucleus submedius in the cat. J. Comp. Neurol. 206, 28–48.

Craig, A. D., Zhang, E. T., and Blomqvist, A. 2002. Association of spinothalamic lamina I neurons and their ascending axons with calbindin-immunoreactivity in monkey and human. Pain 97, 105–115.

Dejerine, J. and Roussy, G. 1906. Le syndrome thalamique. Rev. Neurol. 14, 521–532.

Desbois, C. and Villanueva, L. 2001. The organization of lateral ventromedial thalamic connecions in the rat: a link for the distribution of nociceptive signals to widespread cortical regions. Neuroscience 102, 885–898.

Dilly, P. N., Wall, P. D., and Webster, K. E. 1968. Cells of origin of the spinothalamic tract in the cat and rat. Exp. Neurol. 21, 550–562.

Dostrovsky, J. O. and Craig, A. D. 1996. Cooling-specific spinothalamic neurons in the monkey. J. Neurophysiol. 76, 3656–3665.

Dostrovsky, J. O., Guilbaud, G., and Gautron, M. 1987. Nociceptive neurons in nucleus submedius of the arthritic rat. Pain 4, S263.

Downie, J. W., Ferrington, D. G., Sorkin, L. S., and Willis, W. D. 1988. The primate spinocervicothalamic pathway: responses of cells of the lateral cervical nucleus and spinocervical tract to innocuous and noxious stimuli. J. Neurophysiol. 59, 861–885.

Dugast, C., Almeida, A., and Lima, D. 2003. The medullary dorsal reticular nucleus enhances the responsiveness of spinal nociceptive neurons to peripheral stimulation in the rat. Eur. J. Neurosci. 18, 580–588.

Eberhart, J. A., Morrell, J. I., Krieger, M. S., and Pfaff, D. W. 1985. An autoradiographic study of projections ascending from the midbrain central gray, and from the region lateral to it, in the rat. J. Comp. Neurol. 241, 285–310.

Edinger, L. 1890. Einiges vom Verlauf der Gefuehlsbahnen im centralen Nervensysteme. Deut. Med. Woch. 16, 421–426.

Esteves, F., Lima, D., and Coimbra, A. 1993. Structural types of spinal cord marginal (lamina I) neurons projecting to the nucleus of the tractus solitarius in the rat. Somatosens. Mot. Res. 10, 203–216.

Ferrington, D. G., Sorkin, L. S., and Willis, W. D. 1986. Responses of spinothalamic tract cells in the cat cervical spinal cord to innocuous and graded noxious stimuli. Somatosens. Res 3, 339–358.

Ferrington, D. G., Sorkin, L. S., and Willis, W. D. 1987. Responses of spinothalamic tract cells in the superficial dorsal horn of the primate lumbar spinal cord. J. Physiol. 388, 681–703.

Fields, H. L. 2000. Pain modulation: expectation, opioid analgesia and virtual pain. Prog. Brain Res. 122, 245–253.

Fields, H. L., Clanton, C. H., and Anderson, S. D. 1977. Somatosensory properties of spinoreticular neurons in the cat. Brain Res. 120, 49–66.

Fields, H. L., Malick, A., and Burstein, R. 1995. Dorsal horn projection targets of On and OFF cells in the rostral ventromedial medulla. J. Neurophysiol. 1742–1759.

Flink, R. and Westman, J. 1986. Different neuron populations in the feline lateral cervical nucleus: A light and electron microscopic study with the retrograde axonal transport technique. J. Comp. Neurol. 250, 265–281.

Foerster, O. and Gagel, O. 1932. Die Vorderseitenstrangdurchschneidung beim Menschens. Eine klinisch-patho-physiologisch-anatomische Studie. Z. Ges. Neurol. Psychiat. 138, 1–92.

Foreman, R. D. and Weber, R. N. 1980. Responses from neurons of the primate spinothalamic tract to electrical stimulation of afferents from the cardiopulmonary region and somatic structures. Brain Res. 186, 463–468.

Foreman, R. D., Applebaum, A. E., Beall, J. E., Trevino, D. L., and Willis, W. D. 1975. Responses of primate spinothalamic tract neurons to electrical stimulation of hindlimb peripheral nerve. J. Neurophysiol. 38, 132–145.

Foreman, R. D., Blair, R. W., and Weber, R. N. 1984. Viscerosomatic convergence onto T2-T4 spinoreticular, spinoreticular-spinothalamic, and spinothalamic tract neurons in the cat. Exp. Neurol. 85, 597–619.

Foreman, R. D., Hancock, M. B., and Willis, W. D. 1981. Responses of spinothalamic tract cells in the thoracic spinal cord of the monkey to cutaneous and visceral inputs. Pain 11, 149–162.

Foreman, R. D., Kenshalo, D. R., Jr., Schmidt, R. F., and Willis, W. D. 1979. Field potentials and excitation of primate spinothalamic neurons in response to volleys in muscle afferents. J. Physiol. 286, 197–213.

Fox, R. E., Holloway, J. A., Iggo, A., and Mokha, S. S. 1980. Spinothalamic neurones in the cat: some electrophysiological obhservations. Brain Res. 182, 186–190.

Galhardo, V. and Lima, D. 1999. Structural characterization of marginal (Lamina I) spinal cord neurons in the cat: A Golgi Study. J. Comp. Neurol. 414, 315–333.

Galhardo, V., Lima, D., and Necker, R. 2000. Spinomedullary pathways in the pigeon (Columba livia): Differential involvement of lamina I cell. J. Comp. Neurol. 423, 631–645.

Gamboa-Esteves, F. O., Kaye, J. C., McWilliam, P. N., Lima, D., and Batten, T. F. 2001a. Immunohistochemical profiles of spinal lamina I neurons retrogradely labelled from the nucleus tractus solitarii in rat suggest excitatory projections. Neuroscience 104, 523–538.

Gamboa-Esteves, F. O., Lima, D., and Batten, T. F. C. 2001b. Neurochemistry of superficial spinal neurones projecting to nucleus of the solitary tract that express c-fos on chemical somatic and visceral nociceptive input in the rat. Metab. Brain Dis. 16, 151–164.

Gamboa-Esteves, F. O., Tavares, I., Almeida, A., Batten, T. F., McWilliam, P. N., and Lima, D. 2001c. Projection sites of superficial and deep spinal dorsal horn cells in the nucleus tractus solitarii of the rat. Brain Res. 921, 195–205.

Gauriau, C. and Bernard, J. F. 2004. A comparative reappraisal of projections from the superficial laminae of the dorsal horn in the rat: the forebrain. J. Comp. Neurol. 468, 24–56.

Gebhart, G. F. and Ossipov, M. H. 1986. Characterization of inhibition of the spinal nociceptive tail-flick reflex in the rat from the medullary lateral reticular nucleus. J. Neurosci. 6, 701–713.

Gerhart, K. D., Yezierski, R. P., Giesler, G. J., and Willis, W. D. 1981. Inhibitory receptive fields of primate spinothalamic tract cells. J. Neurophysiol. 46, 1309–1325.

Giesler, G. J. and Elde, R. P. 1985. Immunocytochemical studies of the peptidergic content of fibers and terminals within the lateral spinal and lateral cervical nuclei. J. Neurosci. 5, 833–1841.

Giesler, G. J., Björkeland, M., Xu, Q., and Grant, G. 1988. Organization of the spinocervicothalamic pathways in the rat. J. Comp. Neurol. 268, 223–233.

Giesler, G. J., Menétrey, D., and Basbaum, A. I. 1979a. Differential origins of spinothalamic tract projections to medial and lateral thalamus in the rat. J. Comp. Neurol. 184, 107–126.

Giesler, G. J., Menétrey, D., Guilbaud, G., and Besson, J. M. 1976. Lumbar cord neurons at the origin of the spinothalamic tract in the rat. Brain Res. 118, 320–324.

Giesler, G. J., Miller, L. R., Madsen, A. M., and Katter, J. T. 1987. Evidence for the existence of a lateral cervical nucleus in mice, guinea pigs and rabbits. J. Comp. Neurol. 263, 106–112.

Giesler, G. J., Spiel, H. R., and Willis, W. D. 1981a. Organization of spinothalamic tract axons within the rat spinal cord. J. Comp. Neurol. 195, 243–252.

Giesler, G. J., Urca, G., Cannon, J. T., and Liebeskind, J. C. 1979b. Response properties of neurons of the lateral cervical nucleus in the rat. J. Comp. Neurol. 186, 65–78.

Giesler, G. J., Yezierski, R. P., Gerhart, K. D., and Willis, W. D. 1981b. Spinothalamic tract neurons that project to medial and/or lateral thalamic nuclei: evidence for a physiologically novel population of spinal cord neurons. J. Neurophysiol. 46, 1285–1308.

Gobel, S. 1978a. Golgi studies of the neurons in layer I of the dorsal horn of the medulla (trigeminal nucleus caudalis). J. Comp. Neurol. 180, 375–394.

Gobel, S. 1978b. Golgi studies of the neurons in layer II of the dorsal horn of the medulla (trigeminal nucleus caudalis). J. Comp. Neurol. 180, 395–414.

Graziano, A. and Jones, E. G. 2004. Widespread thalamic terminations of fibers arising in the superficial medullary dorsal horn of monkeys and their relation to calbindin immunoreactivity. J. Neurosci. 24, 248–256.

Guilbaud, G. and Kayser, V. 1988. New evidence for the involvement of the rat ventrobasal thalamic complex in nociception: electrophysiological and neuropharmacological studies. 93–107.

Guilbaud, G., Peschanski, M., and Besson, J. M. 1985. Experimental Data Related to Nociception and Pain at the Supraspinal Level. In: Textbook of Pain (*eds*. P. D. Wall and R. Melzack), pp. 110–118. Churchill Livingston.

Ha, H. and Liu, C. N. 1966. Organization of the spino-cervico-thalamic system. J. Comp. Neurol. 127, 445–470.

Haber, L. H., Moore, B. D., and Willis, W. D. 1982. Electrophysiological response properties of spinoreticular neurons in the monkey. J. Comp. Neurol. 207, 75–84.

Hamann, W. C., Hong, S. K., Kniffki, K. D., and Schmidt, R. F. 1978. Projections of primary afferent fibres from muscle to neurones of the spinocervical tract of the cat. J. Physiol. 283, 369–378.

Hardy, S. G. P. 2001. Hypothalamic projections to cardiovascular centers of the medulla. Brain Res. 894, 233–240.

Harmann, P. A., Carlton, S. M., and Willis, W. D. 1988. Collaterals of spinothalamic tract cells to the periaqueductal gray: a fluorescent double-labelling study in the rat. Brain Res. 441, 87–97.

Harrison, P. J. and Jankowska, E. 1984. An intracellular study of descending and non-cutaneous afferent input to spinocervical tract neurones in the cat. J. Physiol. 356, 245–261.

Hécaen, H., Talairach, J., David, M., and Dell, M. B. 1949. Coagulations limitees du thalamus dans les algies du syndrome thalamique – resultats therapeutiques et physiologiques. Rev. Neurol. 81, 917–931.

Herbert, H. and Saper, C. B. 1992. Organization of medullary adrenergic and noradrenergic projections to the periaqueductal gray matter in the rat. J. Comp. Neurol. 315, 34–52.

Horrax, G. 1929. Experiences with cordotomy. Arch. Surg. 1140–1164.

Hunt, S. P., Pini, A., and Evan, G. 1987. Induction of c-fos-like protein in spinal cord neurons following sensory stimulation. Nature 328, 632–634.

Hwang, S. J., Burette, A., and Valtschanoff, J. G. 2003. VR1-positive primary afferents contact NK1-positive spinoparabrachial neurons. J. Comp. Neurol. 460, 255–265.

Hylden, J. L. K., Anton, F., and Nahin, R. L. 1989. Spinal lamina I projection neurons in the rat: collateral innervation of parabrachial area and thalamus. Neuroscience 28, 27–37.

Hylden, J. L. K., Hayashi, H., and Bennett, G. J. 1986b. Lamina I spinomesencephalic neurons in the cat ascend via the dorsolateral funiculi. Somatosens. Res. 4, 31–41.

Hylden, J. L. K., Hayashi, H., Bennett, G. J., and Dubner, R. 1985. Spinal lamina I neurons projecting to the parabrachial area of the cat midbrain. Brain Res. 336, 195–198.

Hylden, J. L. K., Hayashi, H., Dubner, R., and Bennett, G. J. 1986a. Physiology and morphology of the lamina I spinomesencephalic projections. J. Comp. Neurol. 247, 505–515.

Hyndman, O. R. and Van Epps, C. 1939. Possibility of differential section of the spinothalamic tract. A clinical and histological study. Arch. Surg. 38, 1036–1053.

Jankowska, E., Rastad, J., and Westman, J. 1976. Intracellular application of horseradish peroxidase and its light and electron microscopical appearance in spinocervical tract cells. Brain Res. 105, 557–562.

Jasmin, L., Burkey, A. R., Card, J. P., and Basbaum, A. I. 1997. Transneuronal labeling of a nociceptive pathway, the spino-(trigemino-) parabrachio-amygdaloid, in the rat. J. Neurosci. 17, 3751–3765.

Johnson, F. H. 1954. Experimental study of spino-reticular connections in the cat. Anat. Rec. 118, 316.

Jones, E. G. and Burton, H. 1974. Cytoarchitecture and somatic sensory connectivity of thalamic nuclei other than the ventrobasal complex in the cat. J. Comp. Neurol. 154, 395–432.

Jones, E. G. and Leavitt, R. Y. 1974. Retrograde axonal-transport and demonstration of nonspecific projections to cerebral-cortex and striatum from thalamic intralaminar nuclei in rat, cat and monkey. J. Comp. Neurol. 154, 349–377.

Jones, M. W., Hodge, C. J., Apkarian, A. V., and Stevens, R. T. 1985. A dorsolateral spinothalamic pathway in cat. Brain Res. 335, 188–193.

Jones, S. L. 1992. Descending Control of Nociception. In: The Initial Processing of Pain and its Descending Control: Spinal and Trigeminal Systems (*ed*. A. R. Light), pp. 203–295. Karger.

Ju, G., Melander, T., Ceccatelli, S., Hökfelt, T., and Frey, P. 1987. Immunohistochemical evidence for a spinothalamic pathway co-containing cholecystokinin- and galanin-like immunoreactivities in the rat. Neuroscience 20, 439–456.

Kajander, K. C. and Giesler, G. J. 1987. Responses of neurons in the lateral cervical nucleus of the cat to noxious cutaneous stimulation. J. Neurophysiol. 57, 1686–1704.

Katter, J. T., Burstein, R., and Giesler, G. J. 1991. The cells of origin of the spinohypothalamic tract in cats. J. Comp. Neurol. 303, 101–112.

Kayalioglu, G., Robertson, B., Kristensson, K., and Grant, G. 1999. Nitric oxide synthase and interferon-gamma receptor immunoreactivities in relation to ascending spinal pathways to thalamus, hypothalamus, and the periaqueductal grey in the rat. Somatosens. Mot. Res. 16, 280–290.

Keay, K. A. and Bandler, R. 1992. Anatomical evidence for segregated input from the upper cervical spinal-cord to functionally distinct regions of the periaqueductal gray region of the cat. Neurosci. Lett. 139, 143–148.

Keay, K. A., Clement, C. I., Matar, W. M., Heslop, D. J., Henderson, L. A., and Bandler, R. 2002. Noxious activation of spinal or vagal afferents evokes distinct patterns of fos-like immunoreactivity in the ventrolateral periaqueductal gray of unanaesthetised rats. Brain Res. 948, 122–130.

Kenshalo, D. R., Jr., Giesler, G. J., Leonard, R. B., and Willis, W. D. 1980. Responses of neurons in the primate ventral posterior lateral nucleus to noxious stimuli. J. Neurophysiol. 43, 1594–1614.

Kenshalo, D. R., Jr., Leonard, R. B., Chung, J. M., and Willis, W. D. 1979. Responses of primate spinothalamic neurons to graded and to repeated noxious heat stimuli. J. Neurophysiol. 42, 1370–1389.

Kerr, F. W. L. 1975. The ventral spinothalamic tract and other ascending systems of the ventral funiculus of the spinal cord. J. Comp. Neurol. 159, 335–356.

Kerr, F. W. L. and Lippman, H. H. 1974. The primate spinothalamic tract as demonstrated by anterolateral cordotomy and commissural myelotomy. Adv. Neurol. 4, 147–156.

Kevetter, G. A. and Willis, W. D. 1982. Spinothalamic cells in the rat lumbar cord with collaterals to the medullary reticular formation. Brain Res. 238, 181–185.

Kevetter, G. A. and Willis, W. D. 1983. Collaterals of spinothalamic cells in the rat. J. Comp. Neurol. 215, 453–464.

Kevetter, G. A., Haber, L. H., Yezierski, R. P., Chung, J. M., Martin, R. F., and Willis, W. D. 1982. Cells of origin of the spinoreticular tract in the monkey. J. Comp. Neurol. 207, 61–74.

Klop, E. M., Mouton, L. J., and Holstege, G. 2004. Less than 15% of the spinothalamic fibers originate from neurons in lamina I in cat. Neurosci. Lett. 360, 125–128.

Kniffki, K. D., Mense, S., and Schmidt, R. F. 1977. The spinocervical tract as a possible pathway for muscular nociception. J. Physiol. (Paris) 73, 359–366.

Kohnstamm, O. 1900. Ueber die Coordinationskerne des Hirnstammes und die absteigenden Spinalbahnen. Nach den Ergebnissen der combinierten Degenerationsmethode. Mschr. Psychiat. Neurol. 8, 261–293.

Kostarczyk, E., Zhang, X. J., and Giesler, G. J. 1997. Spinohypothalamic tract neurons in the cervical enlargement of rats: Locations of antidromically identified ascending axons and their collateral branches in the contralateral brain. J. Neurophysiol. 77, 435–451.

Krettek, J. E. and Price, J. L. 1977. The cortical projections of the mediodorsal nucleus and adjacent thalamic nuclei in the rat. J. Comp. Neurol. 171, 157–191.

Kunze, W. A. A., Wilson, P., and Snow, P. J. 1987. Response of lumbar spinocervical tract cells to natural and electrical stimulation of the hindlimb footpads in cats. Neurosci. Lett. 75, 253–258.

Leah, J., Menétrey, D., and De Pommery, J. 1988. Neuropeptides in long ascending spinal tract cells in the rat: evidence for parallel processing of ascending information. Neuroscience 24, 195–207.

Leite-Almeida, H., Valle-Fernandes, A., and Almeida, A. 2006. Brain projections from the medullary dorsal reticular nucleus: an anterograde and retrograde tracing study in the rat. Neuroscience 140, 577–595.

Lima, D. 1990. A spinomedullary projection terminating in the dorsal reticular nucleus of the rat. Neuroscience 34, 577–589.

Lima, D. 1997. Functional anatomy of spinofugal nociceptive pathways. Pain Rev. 4, 1–19.

Lima, D. 1998. Anatomical basis for the dynamic processing of nociceptive input. Eur. J. Pain. 2, 195–202.

Lima, D. and Almeida, A. 2002. The medullary dorsal reticular nucleus as a pronociceptive centre of the pain control system. Prog. Neurobiol. 66, 81–108.

Lima, D. and Coimbra, A. 1983. The neuronal population of the marginal zone (lamina I) of the rat spinal cord. A study based on reconstructions of serially sectioned cells. Anat. Embryol. 167, 273–288.

Lima, D. and Coimbra, A. 1985. Marginal neurons of the rat spinal cord at the origin of a spinobulboreticular projection. Neurosci. Lett. 22, S9.

Lima, D. and Coimbra, A. 1986. A Golgi study of the neuronal population of the marginal zone (lamina I) of the rat spinal cord. J. Comp. Neurol. 244, 53–71.

Lima, D. and Coimbra, A. 1988. The spinothalamic system of the rat: structural types of retrogradely labeled neurons in the marginal zone (lamina I). Neuroscience 27, 215–230.

Lima, D. and Coimbra, A. 1989. Morphological types of spinomesencephalic neurons in the marginal zone (lamina I) of the rat spinal cord, as shown after retrograde labeling with cholera toxin subunit B. J. Comp. Neurol. 279, 327–339.

Lima, D. and Coimbra, A. 1990. Structural types of marginal (Lamina I) neurones projecting to the dorsal reticular nucleus of the medulla oblongata. Neuroscience 34, 591–606.

Lima, D. and Coimbra, A. 1991. Neurons in the substantia gelatinosa rolandi (lamina II) project to the caudal ventrolateral reticular formation of the medulla oblongata in the rat. Neurosci. Lett. 132, 16–18.

Lima, D., Albino-Teixeira, A., and Tavares, I. 2001. The caudal medullary ventrolateral reticular formation in nociceptive-cardiovascular integration. An experimental study in the rat. Exp. Physiol. 87.2, 267–274.

Lima, D., Almeida, A., and Tavares, A. 1998. The endogenous pain control system: facilitating and inhibitory pathways. In: Pain Mechanisms and Management (*eds*. S. N. Ayrapetyan and A. V. Apkarian), pp. 192–210. IOS Press.

Lima, D., Avelino, A., and Coimbra, A. 1992. Differential participation of marginal cells in the transmission of nociceptive input to the thalamus and mesencephalon. Eur. J. Neurosci. Suppl. 5, 2057.

Lima, D., Avelino, A., and Coimbra, A. 1993. Morphological characterization of marginal (Lamina I) neurons immunoreactive for substance P, enkephalin, dynorphin and gamma-aminobutyric acid in the rat spinal cord. J. Chem. Neuroanat. 6, 43–52.

Lima, D., Castro, A. R., Castro-Lopes, J. M., and Galhardo, V. 2002. Differential expression of GABAB receptors in monkey lamina I neuronal types; a Golgi and immunocytochemical study. Society Neurosci Abst 258.4.

Lima, D., Esteves, F., and Coimbra, A. 1994. C-*fos* activation by Noxious Input of Spinal Neurons Projecting to the Nucleus of the Tractus Solitarius in the Rat. In: Proceedings of the 7th World Congress on Pain (*ed*. G. F. Gebhart), Vol. 2, pp. 423–434. IASP Press.

Lima, D., Mendes-Ribeiro, J. A., and Coimbra, A. 1991. The spino-latero-reticular system of the rat: projections from the superficial dorsal horn and structural characterization of marginal neurons involved. Neuroscience 45, 137–152.

Liu, R. P. 1983. Laminar origins of spinal projection to the periaqueductal gray of the rat. Brain Res. 264, 118–122.

Loewy, A. D. 1990. Central autonomic pathways. In: Central Regulation of Autonomic Functions (*eds*. A. D. Loewy and K. M. Spyer), pp. 88–103. Oxford University Press.

Loewy, A. D. and Burton, H. 1978. Nuclei of the solitary tract: Efferent projections to the lower brain stem and spinal cord of the cat. J. Comp. Neurol. 181, 421–450.

Lovick, T. A. 1993. Integrated activity of cardiovascular and pain integratory systems: Role in adaptive behaviour. Prog. Neurobiol. 40, 631–644.

Lund, R. D. and Webster, K. E. 1967. Thalamic afferents from the spinal cord and trigeminal nuclei. An experimental anatomical study in the rat. J. Comp. Neurol. 130, 313–328.

Lundberg, A. and Oscarsson, O. 1961. Three ascending spinal pathways in the dorsal part of the lateral funiculus. Acta. Physiol. Scand. 51, 1–16.

Ma, W. and Peschanski, M. 1988. Spinal and trigeminal projections to the parabrachial nucleus in the rat-electron-microscopic evidence of a spino-ponto-amygdalian somatosensory pathway. Somatosens. Res. 5, 247–257.

Magnusson, K. R., Magnusson, K. R., Clements, J. R., Larson, A. A., Madl, J. E., and Beitz, A. J. 1987. Localization of glutamate in trigeminothalamic projection neurons: a combined retrograde transport-immunohistochemical study. Somatosens. Res. 4, 177–190.

Mainen, Z. F. and Sejnowski, T. J. 2006. Influence of dendritic structure on firing pattern in model neocortical neurons. Nature 382, 363–366.

Malick, A. and Burstein, R. 1998. Cell of origin of the trigeminohypothalamic tract in the rat. J. Comp. Neurol. 400, 125–144.

Malick, A., Strassman, A. M., and Burstein, R. 2000. Trigeminohypothalamic and reticulohypothalamic tract in the upper cervical spinal cord and caudal medulla of the rat. J. Neurophysiol. 84, 2078–2112.

Mantyh, P. W. 1982. The ascending input to the midbrain periaqueductal gray of the primate. J. Comp. Neurol. 211, 50–64.

Mantyh, P. W. 1983a. The spinothalamic tract in the primate: a re-examination using wheatgerm agglutinin conjugated to horseradish peroxidase. Neuroscience 9, 847–862.

Mantyh, P. W. 1983b. The terminations of the spinothalamic tract in the cat. Neurosci. Lett. 38, 119–124.

Mark, R. F. and Steiner, J. 1958. Cortical projection of impulser in myelinated cutaneous afferent nerve fibres of the cat. J. Physiol. 142, 544–562.

Maunz, R. A., Pitts, N. G., and Peterson, B. W. 1978. Cat spinoreticular neurons: locations, responses and changes in responses during repetitive stimulation. Brain Res. 148, 365–379.

McMahon, S. B. and Wall, P. D. 1985. Electrophysiological mapping of brainstem projections of spinal cord lamina I cells in the rat. Brain Res. 19–26.

Mehler, W. R. 1957. The mammalian pain tract in phylogeny. Anat. Rec. 127, 332.

Mehler, W. R. 1962. The anatomy of the so-called 'pain tract' in man: an analysis of the course and distribution of the ascending fibers of the fasciculus anterolateralis. In: Basic Research in Paraplegia (*eds*. J. D. French and R. W. Porter), pp. 26–55. Thomas.

Mehler, W. R. 1966. Some observations on secondary ascending afferent systems in the central nervous system. In: Pain (*eds*. R. S. Knighton and P. R. Dumke), pp. 11–32. Little Brown.

Mehler, W. R. 1969. Some neurological species differences – a posteriori. Ann. NY Acad. Sci. 167, 424–468.

Mehler, W. R. 1974. Central pain and the spinothalamic tract. Adv. Neurol. 4, 127–146.

Mehler, W. R., Feferman, M. E., and Nauta, W. J. H. 1956. Ascending axon degeneration following anterolateral chordotomy in the monkey. Anat. Rec. 124, 332–333.

Mehler, W. R., Feferman, M. E., and Nauta, W. J. H. 1960. Ascending axon degeneration following anterolateral cordotomy. An experimental study in the monkey. Brain 83, 718–751.

Meller, S. T. and Dennis, B. J. 1991. Efferent projections of the periaqueductal gray in the rabbit. Neuroscience 40, 191–216.

Melzack, R. and Casey, K. L. 1968. Sensory, motivational and central control determinants of pain. pp. 423–443.

Menétrey, D. and Basbaum, A. I. 1987. Spinal and trigeminal projections to the nucleus of the solitary tract – a possible substrate for somatovisceral and viscerovisceral reflex activation. J. Comp. Neurol. 255, 439–450.

Menétrey, D. and DePommery, J. 1991. Origins of spinal ascending pathways that reach central areas involved in viscenoception and visceronociception in the rat. Eur. J. Neurosci. 3, 249–259.

Menétrey, D., Chaouch, A., and Besson, J. M. 1980. Location and properties of dorsal horn neurons at origin of spinoreticular tract in lumbar enlargement of the rat. J. Neurophysiol. 44, 862–877.

Menétrey, D., Chaouch, A., Binder, D., and Besson, J. M. 1982. The origin of the spinomesencephalic tract in the rat: an anatomical study using the retrograde transport of horseradish peroxidase. J. Comp. Neurol. 206, 193–207.

Menétrey, D., DePommery, J., Baimbridge, K. G., and Thomasset, M. 1992a. Calbindin-D28K (CaBP28k)-like immunoreactivity in ascending projections.1. Trigeminal nucleus caudalis and dorsal vagal complex projections. Eur. J. Neurosci. 4, 61–69.

Menétrey, D., DePommery, J., and Besson, J. M. 1984. Electrophysiological characteristics of lumbar spinal cord neurons backfired from lateral reticular nucleus in the rat. J. Neurophysiol. 52, 595–611.

Menétrey, D., DePommery, J., Thomasset, M., and Baimbridge, K. G. 1992b. Calbindin-D28K (CaBP28k)-like immunoreactivity in ascending projections. II. Spinal Projections to brain stem and mesencephalic areas. Eur. J. Neurosci. 4, 70–76.

Menétrey, D., Roudier, F., and Besson, J. M. 1983. Spinal neurons reaching the lateral reticular nucleus as studied in the rat by retrograde transport of horseradish peroxidase. J. Comp. Neurol. 220, 439–452.

Meyers, D. E. R. and Snow, P. J. 1982. The morphology of physiologically identified deep spinothalamic tract cells in the lumbar spinal cord of the cat. J. Physiol. 329, 373–388.

Millis, C. D. and Hulsebosch, C. E. 2002. Increased expression of metabotropic glutamate receptor subtype 1 on spinothalamic tract neurons following spinal cord injury in the rat. Neurosci. Lett. 319, 59–62.

Milne, R. J., Foreman, R. D., and Willis, W. D. 1982. Responses of primate spinothalamic neurons located in the sacral intermediomedical gray (Stilling's nucleus) to proprioceptive input from the tail. Brain Res. 234, 227–236.

Miyagawa, T., Ando, R., Sakurada, S., Sakurada, T., and Kisara, K. 1986. Effects of tooth pulp stimulation on single unit activity of the amygdala in cats. Nippon Yakurigaku Zasshi 88, 173–178.

Morison, R. S. and Dempsey, E. W. 1942. A study of thalamo-cortical relations. Am. J. Physiol. 135, 281–292.

Mouton, L. J. and Holstege, G. 1998. Three times as many lamina I neurons project to the periaqueductal gray than to the thalamus: a retrograde tracing study in the cat. Neurosci. Lett. 255, 107–110.

Mouton, L. J. and Holstege, G. 2000. Segmental and laminar organization of the spinal neurons projecting to the periaqueductal gray (PAG) in the cat suggests the existence of at least five separate clusters of Spino-PAG neurons. J. Comp. Neurol. 428, 389–410.

Mouton, L. J., Klop, E. M., and Holstege, G. 2001. Lamina I-periaqueductal gray (PAG) projections represent only a limited part of the total spinal and caudal medullary input to the PAG in the cat. Brain. Res. Bull. 54, 167–174.

Mouton, L. J., Klop, E. M., Broman, J., Zhang, M., and Holstege, G. 2004. Lateral cervical nucleus projections to periaqueductal gray matter in cat. J. Comp. Neurol. 471, 434–445.

Mtui, E. P., *et al.* 1993. Projections from the nucleus tractus solitarii to the spinal cord. J. Comp. Neurol. 337, 231–252.

Nahin, R. L. 1988. Immunocytochemical identification of long ascending, peptidergic lumbar spinal neurons terminating in either the medial or lateral thalamus in the rat. Brain Res. 443, 345–349.

Nahin, R. L. and Micevych, P. E. 1986. A long ascending pathway of enkephalin-like immunoreactive spinoreticular neurons in the rat. Neurosci. Lett. 65, 271–276.

Nahin, R. L., Madsen, A. M., and Giesler, G. J. 1986. Funicular location of the ascending axons of neurons adjacent to the spinal cord central canal in the rat. Brain Res. 384, 367–372.

Palecek, J., Paleckova, V., and Willis, W. D. 2003. Fos expression in spinothalamic and postsynaptic dorsal column neurons following noxious visceral and cutaneous stimuli. Pain 104, 249–257.

Panneton, W. M. and Burton, H. 1985. Projections from the paratrigeminal nucleus and the medullary and spinal dorsal horns to the peribrachial area in the cat. Neuroscience 15, 779–797.

Parenti, R., Cicirata, F., Panto, M. R., and Serapide, M. F. 1996. The projections of the lateral reticular nucleus to the deep cerebellar nuclei. An experimental analysis in the rat. Eur. J. Neurosci. 8, 2157–2167.

Paxinos, G. and Watson, C. 1998. The Rat Brain in Stereotaxic Coordinates, 4th ed. Academic Press.

Pechura, C. and Liu, R. 1986. Spinal neurons which project to the periaqueductal gray and the medullary reticular formation via axon collaterals: a double-label fluorescence study in the rat. Brain Res. 374, 357–361.

Perl, E. R. and Whitlock, D. G. 1961. Somatic stimuli exciting spinothalamic projections to thalamic neurons in cat and monkey. Exp. Neurol. 3, 256–296.

Peschanski, M. and Besson, J. M. 1984. A spino-reticulo-thalamic pathway in the rat: an anatomical study with reference to pain transmission. Neuroscience 12, 165–178.

Peschanski, M., Guilbaud, G., Gautron, M., and Besson, J. M. 1980. Encoding of noxious heat messages in neurons of the ventrobasal thalamic complex in the rat. Brain Res. 197, 401–413.

Peschanski, M., Mantyh, P. W., and Besson, J. M. 1983. Spinal afferents to the ventrobasal thalamic complex in the rat: an anatomical study using wheat-germ agglutinin conjugated to horseradish peroxidase. Brain Res. 278, 240–244.

Polgar, E., Puskár, Z., Watt, C., Matesz, C., and Todd, A. J. 2002. Selective innervation of lamina I projection neurones that possess the neurokinin 1 receptor by serotonin-containing axons in the rat spinal cord. Neuroscience 109, 799–809.

Prescott, S. A. and De Koninck, Y. 2002. Four cell types with distinctive membrane properties and morphologies in lamina I of the spinal dorsal horn of the adult rat. J. Physiol. 539, 817–836.

Price, D. D., Hayes, R. L., Rude, M., and Dubner, R. 1978. Spatial and temporal transformations of input to spinothalamic tract neurons and their relation to somatic sensations. J. Neurophysiol. 41, 933–947.

Puskar, Z., Polgar, E., and Todd, A. J. 2001. A population of large lamina I projection neurons with selective inhibitory input in rat spinal cord. Neuroscience 102, 167–176.

Quensel, F. 1898. Ein Fall von Sarcom der Dura spinalis. Beitrag zur Kenntnis der secundaeren Degenerationen nach Rueckenmarkscompression. Neurol. Zbl. 17, 482–493.

Ramón y Cajal, S. 1909. Histologie dusystème nerveux de l'homme et des vertébrés. Maloine.

Reis, L. C., Colombari, E., Canteras, N. S., and Cravo, S. L. 2000. Projections from nucleus tractus solitarii (NTS) and ventrolateral medulla (VLM) to paraventricular nucleus of the hypothalamus (PVH) and median preoptic nucleus (MnPO). Projections from nucleus tractus solitarii (NTS) and ventrolateral medulla (VLM) to paraventricular nucleus of the hypothalamus (PVH) and median preoptic nucleus (MnPO). FASEB J. 14, A66.

Ring, G. and Ganchrow, D. 1983. Projections of nucleus caudalis and spinal cord to brainstem and diencephalon in the hedgehog (*Erinaceus europaeus* and *Paraechinus aethiopicus*): A degeneration study. J. Comp. Neurol. 216, 132–151.

Rossi, G. F. and Brodal, A. 1957. Terminal distribution of spinoreticular fibers in the cat. Arch. Neurol. Psychiat. 78, 439–453.

Rucker, H. K. and Holloway, J. A. 1982. Viscerosomatic convergence onto spinothalamic tract neurons in the cat. Brain Res. 243, 155–157.

Ruda, M. A., Coffield, J., and Dubner, R. 1984. Demonstration of postsynaptic opioid modulation of thalamic projection neurons by the combined techniques of retrograde horseradish peroxidase and enkephalin immunocytochemistry. J. Neurosci. 4, 2117–2132.

Ruscheweyh, R., Ikeda, H., Heinke, B., and Sandkuhler, J. 2004. Distinctive membrane and discharge properties of rat spinal lamina I projection neurons in vitro. J. Physiol. 555, 527–543.

Shi, T. and Apkarian, A. V. 1995. Morphology of thalamocortical neurons projecting to the primary somatosensory cortex and their relationship to spinothalamic terminals in the squirrel monkey. J. Comp. Neurol. 361, 1–24.

Short, A. D., Brown, A. G., and Maxwell, D. J. 1990. Afferent inhibition and facilitation of transmission through the spinocervical tract in the anaesthetized cat. J. Physiol. 429, 511–528.

Sim, L. J. and Joseph, S. A. 1994. Efferent of the opiocortin-containing region of the commissural nucleus tractus solitarius. Peptides 15, 169–174.

Simone, D. A., Sorkin, L. S., Oh, U., Chung, J. M., Owens, C., LaMotte, R. H., and Willis, W. D. 1991. Neurogenic hyperalgesia: Central neural correlates in responses of spinothalamic tract neurons. J. Neurophysiol. 66, 228–246.

Slugg, R. M. and Light, A. R. 1994. Spinal cord and trigeminal projections to the pontine parabrachial region in the rat as demonstrated with phaseolus-vulgaris-leukoagglutinin. J. Comp. Neurol. 339, 49–61.

Snowball, R. K., Semenenko, F. M., and Lumb, B. M. 2000. Visceral inputs to neurons in the anterior hypothalamus including those that project to the periaqueductal gray: A functional anatomical and electrophysiological study. Neuroscience 99, 351–361.

Spike, R. C., Puskar, Z., Andrew, D., and Todd, A. J. 2003. A quantitative and morphological study of projection neurons in lamina I of the rat lumbar spinal cord. Eur. J. Neurosci. 18, 2433–2448.

Standaert, D., Watson, S., Houghten, R., and Saper, C. 1986. Opioid peptide immunoreactivity in spinal and trigeminal dorsal horn neurons projecting to the parabrachial nucleus in the rat. J. Neurosci. 6, 1220–1226.

Stevens, R. T., Hodge, C. J., and Apkarian, A. V. 1989. Medial, intralaminar and lateral terminations of lumbar spinothalamic tract neurons: a fluorescent double label study. Somatosens. Mot. Res. 6, 285–308.

Stevens, R. T., London, S. M., and Apkarian, A. V. 1993. Spinothalamocortical projections to the secondary somatosensory cortex (SII) in squirrel monkey. Brain Res. 631, 241–246.

Surmeier, D. J., Honda, C. N., and Willis, W. D. 1986a. Temporal features of the responses of primate spinothalamic neurons to noxious thermal stimulation of hairy and glabrous skin. J. Neurophysiol. 56, 351–369.

Surmeier, D. J., Honda, C. N., and Willis, W. D. 1986b. Responses of primate spinothalamic neurons to noxious thermal stimulation of glabrous and hairy skin. J. Neurophysiol. 56, 328–350.

Surmeier, D. J., Honda, C. N., and Willis, W. D. 1988. Natural grouping of primate spinothalamic neurons based on cutaneous stimulation. Physiological and anatomical features. J. Neurophysiol. 59, 833–860.

Svensson, B. A., Rastad, J., Westman, J., and Wiberg, M. 1985. Somatotopic termination of spinal afferents to the feline lateral cervical nucleus. Exp. Brain Res. 57, 576–584.

Swett, J. E., McMahon, S. B., and Wall, P. D. 1985. Long ascending projections to the midbrain from cells of lamina I and nucleus of the dorsolateral funiculus of the rat spinal cord. J. Comp. Neurol. 238, 401–416.

Szucs, P., Odeh, F., Szokol, K., and Antal, M. 2003. Neurons with distinctive firing patterns, morphology and distribution in lamina V-VII of the neonatal rat lumbar spinal cord. Eur. J. Neurosci. 17, 537–544.

Taub, A. and Bishop, P. O. 1965. The spinocervical tract: dorsal column linkage, conduction velocity, primary afferent spectrum. Exp. Neurol. 13, 1–21.

Tavares, I., Almeida, A., Albino-Teixeira, A., and Lima, D. 1997. Lesions of the caudal ventrolateral medulla block the hypertension-induced inhibition of noxious-evoked *c-fos* expression in the rat spinal cord. Eur. J. Pain 1, 149–160.

Tavares, I., Almeida, A., Esteves, F., Lima, D., and Coimbra, A. 1998. The caudal ventrolateral medullary reticular formation is reciprocally connected with the spinal cord. Society Neurosci Abst 24, 1132.

Tavares, I. and Lima, D. 1994. Descending projections from the caudal medulla oblongata to the superficial or deep dorsal horn of the rat spinal cord. Exp. Brain Res. 99, 455–463.

Tavares, I. and Lima, D. 2002. The caudal ventrolateral medulla as an important inhibitory modulator of pain transmission in the spinal cord. J. Pain. 3, 337–346.

Tavares, I., Lima, D., and Coimbra, A. 1993. Neurons in the superficial dorsal horn of the rat spinal cord projecting to the medullary ventrolateral reticular formation express *c-fos* after noxious stimulation of the skin. Brain Res. 623, 278–286.

Tavares, I., Lima, D., and Coimbra, A. 1996a. Catecholaminergic and serotonergic input to spinal dorsal horn neurons projecting to the caudal ventrolateral medulla of the rat. Abst 8th World Congress on Pain 448.

Tavares, I., Lima, D., and Coimbra, A. 1996b. The ventrolateral medulla of the rat is connected with the spinal cord dorsal horn by an indirect descending pathway relayed in the A5 noradrenergic cell group. J. Comp. Neurol. 374, 84–95.

Thiele, F. H. and Horsley, V. 1901. A study of the degenerations observed in the central nervous system in a case of fracture dislocation of the spine. Brain 24, 519–531.

Thies, R. 1985. Activation of lumbar spinoreticular neurons by stimulation of muscle, cutaneous and sympathetic afferents. Brain Res. 333, 151–155.

Thies, R. and Foreman, R. D. 1983. Inhibition and excitation of thoracic spinoreticular neurons by electrical stimulation of vagal afferent nerves. Exp. Neurol. 82, 1–16.

Thompson, R. H., Canteras, N. S., and Swanson, L. W. 1996. Organization of projections from the dorsomedial nucleus of the hypothalamus: A PHA-L study in the rat. J. Comp. Neurol. 376, 143–173.

Todd, A. J., McGill, M. M., and Shehad, S. A. S. 2000. Neurokinin 1 receptor expression by neurons in laminae I, III and IV of the rat spinal dorsal horn that project to the brainstem. Eur. J. Neurosci. 12, 689–700.

Todd, A. J., Puskar, Z., Spike, R. C., Hughes, C., Watt, C., and Forrest, L. 2002. Projection neurons in lamina I of rat spinal cord with the neurokinin 1 receptor are selectively innervated by substance p-containing afferents and respond to noxious stimulation. J. Neurosci. 22, 4103–4113.

Todd, A. J. and Spike, R. C. 1993. Localization of classical neurotransmitters and neuropeptides within neurons in

lamina I-III of the mammalian spinal dorsal horn. Prog. Neurobiol. 41, 609–645.
Traub, R. J. and Murphy, A. 2002. Colonic inflammation induces fos expression in the thoracolumbar spinal cord increasing activity in the spinoparabrachial pathway. Pain 95, 93–102.
Trevino, D. L. 1976. The Origin and Pojections of a Spinal Nociceptive and Thermoreceptive Pathway. In: Sensory Functions of the Skin in Primates, with Special Reference to Man (*ed*. Y. Zotterman), pp. 367–376. Pergamon Press.
Trevino, D. L. and Carstens, E. 1975. Confirmation of the location of spinothalamic neurons in the cat and monkey by the retrograde transport of horseradish peroxidase. Brain Res. 98, 177–182.
VanderHorst, V. G. J. M., Mouton, L. J., Blok, B. F. M., and Holstege, G. 1996. Distinct cell groups in the lumbosacral cord of the cat project to different areas in the periaqueductal gray. J. Comp. Neurol. 376, 361–385.
Vierck, C. J. and Luck, M. M. 1979. Loss and recovery of reactivity to noxious stimulation in monkeys with primary spinothalamic cordotomies, followed by secundary and tertiary lesions of other cord sectors. Brain 102, 233–248.
Villanueva, L., Bernard, J. F., and Le Bars, D. 1995. Distribution of spinal cord projections from the medullary subnucleus reticularis dorsalis and the adjacent cuneate nucleus: a *Phaseolus vulgaris*-leucoagglutinin study in the rat. J. Comp. Neurol. 352, 11–32.
Villanueva, L., Bouhassira, D., Bing, Z., and Le Bars, D. 1988. Convergence of heterotopic nociceptive information onto subnucleus reticularis dorsalis (SRD) neurons in the rat medulla. J. Neurophysiol. 60, 980–1009.
Villanueva, L., Bouhassira, D., Bing, Z., and Le Bars, D. 1991. Spinal afferent projections to subnucleus reticularis dorsalis in the rat. J. Neurophysiol. 60, 980–1009.
Villanueva, L., Desbois, C., Le Bars, D., and Bernard, J. F. 1998. Organization of diencephalic projections from the medullary subnucleus reticularis dorsalis and the adjacent cuneate nucleus: a retrograde and anterograde tracer study in the rat. J. Comp. Neurol. 390, 133–160.
Walker, A. E. 1940. The spinothalamic tract in man. Arch. Neurol. Psychiat. 43, 284–298.
Walker, A. E. 1942a. Relief of pain by mesencephalic tractotomy. Arch. Neurol. Psychiat. 48, 865–880.
Walker, A. E. 1942b. Somatotopic localization of spino thalamic and sensory trigeminal tracts in mesencephalon. Arch. Neurol. Psychiat. 48, 884–889.
Wang, C. C. and Shyu, B. C. 2004. Differential projections from the mediodorsal and centrolateral thalamic nuclei to the frontal cortex in rats. Brain Res. 995, 226–235.
Westlund, K. N. and Craig, A. D. 1996. Association of spinal lamina I projections with brainstem catecholamine neurons in the monkey. Exp. Brain Res. 110, 151–162.
Westlund, K. N., Bowker, R. M., Ziegler, M. G., and Coulter, J. D. 1983. Noradrenergic projections to the spinal cord of the rat. Brain Res. 263, 15–31.
Westlund, K. N., Bowker, R. M., Ziegler, M. G., and Dan, J. 1981. Origins of spinal noradrenergic pathways demonstrated by retrograde transport of antibody to dopamine-â-hydroxylase. Neurosci. Lett. 25, 243–249.
Whitsel, B. L., Rustioni, A., Dreyer, D. A., Loe, P. R., Allen, E. E., and Metz, C. B. 1978. Thalamic projections to S-1 in macaque monkey. J. Comp. Neurol. 178, 385–409.
Wiberg, M. and Blomqvist, A. 1984. The spinomesencephalic tract in the cat: its cells of origin and termination pattern as demonstrated by the intraaxonal transport method. Brain Res. 291, 1–18.
Wiberg, M., Westman, J., and Blomqvist, A. 1987. Somatosensory projection to the mesencephalon: an anatomical study in the monkey. J. Comp. Neurol. 264, 92–117.
Willis, W. D. 1988. Nociceptive neurons in the primate ventral posterior lateral (VPL) nucleus. In: Cellular Thalamic Mechanisms (*eds*. M. Bentivoglio and R. Spreafico), pp. 77–92. Elsevier.
Willis, W. D., Kenshalo, D. R., Jr., and Leonard, R. B. 1979. The cells of origin of the primate spinothalamic tract. J. Comp. Neurol. 188, 543–574.
Willis, W. D., Trevino, D. L., Coulter, J. D., and Maunz, R. A. 1974. Responses of primate spinothalamic tract neurons to natural stimulation of hindlimb. J. Neurophysiol. 37, 358–372.
Willis, W. D., Zhang, X., Honda, C. N., and Giesler, G. J. 2001. Projections from the marginal zone and deep dorsal horn to the ventrobasal nuclei of the primate thalamus. Pain 92, 267–276.
Yezierski, R. P. 1988. Spinomesencephalic tract: projections from the lumbosacral spinal cord of the rat, cat, and monkey. J. Comp. Neurol. 267, 131–146.
Yezierski, R. P. 1990. The effects of midbrain and medullary stimulation on spinomesencephalic tract cells in the cat. J. Neurophysiol. 63, 240–255.
Yezierski, R. P. and Broton, J. G. 1991. Functional properties of spinomesencephalic tract (SMT) cells in the upper cervical spinal cord of the cat. Pain 45, 187–196.
Yezierski, R. P. and Mendez, C. M. 1991. Spinal distribution and collateral projections of rat spinomesencephalic tract cells. Neuroscience 44, 113–130.
Yezierski, R. P. and Schwartz, R. H. 1986. Response and receptive-field properties of spinomesencephalic tract cells in the cat. J. Neurophysiol. 55, 76–96.
Yezierski, R. P., Sorkin, L. S., and Willis, W. D. 1987. Response properties of spinal neurons projecting to midbrain or midbrain-thalamus in the monkey. Brain Res. 437, 165–170.
Yoshida, A., Dostrovsky, J. O., and Chiang, C. Y. 1992. The afferent and efferent connections of the nucleus submedius in the rat. J. Comp. Neurol. 324, 115–133.
Yu, X. H., *et al.* 1999. NK-1 receptor immunoreactivity in distinct morphological types of lamina I neurons of the primate spinal cord. J. Neurosci. 19, 3545–3555.
Zardettosmith, A. M. and Gray, T. S. 1995. Catecholamine and NPY efferents from the ventrolateral medulla to the amygdala in the rat. Brain Res. Bull. 38, 253–260.
Zemlan, F. P., Leonard, C. M., Kow, L. M., and Plaff, D. W. 1978. Ascending tracts of the lateral columns of the rat spinal cord: a study using the silver impregnation and horseradish peroxidase techniques. Exp. Neurol. 62, 298–334.
Zhang, D., Carlton, S. M., Sorkin, L. S., and Willis, W. D. 1990. Collaterals of primate spinothalamic tract neurons to the periaqueductal gray. J. Comp. Neurol. 296, 277–290.
Zhang, E. T. and Craig, A. D. 1997. Morphology and distribution of spinothalamic lamina I neurons in the monkey. J. Neurosci. 17, 3274–3284.
Zhang, E. T., Han, Z. S., and Craig, A. D. 1996. Morphological classes of spinothalamic lamina I neurons in the cat. J. Comp. Neurol. 367, 537–549.
Zhang, X. J., Gokin, A. P., and Giesler, G. J. 2002. Responses of spinohypothalamic tract neurons in the thoracic spinal cord of rats to somatic stimuli and to graded distention of the bile duct. Somatosens. Mot. Res. 19, 5–17.
Zhang, X. J., Wenk, H. N., Honda, C. N., and Giesler, G. J. 2000. Locations of spinothalamic tract axons in cervical and thoracic spinal cord white matter in monkeys. J. Neurophysiol. 83, 2869–2880.
Zou, X. Y., Lin, Q., and Willis, W. D. 2000. Enhanced phosphorylation of NMDA receptor 1 subunits in spinal cord dorsal horn and spinothalamic tract neurons after intradermal injection of capsaicin in rats. J. Neurosci. 20, 6989–6997.

5.36 Dorsal Columns and Visceral Pain

W D Willis Jr. and K N Westlund, University of Texas Medical Branch, Galveston, TX, USA

© 2008 Elsevier Inc. All rights reserved.

5.36.1	**Clinical Evidence Concerning Spinal Cord Pathways That Signal Visceral Pain**	528
5.36.1.1	Spinothalamic Tract	528
5.36.1.1.1	Anterolateral cordotomy	528
5.36.1.1.2	Commissural myelotomy	529
5.36.1.2	Posterior Column	529
5.36.1.2.1	Hitchcock procedure (stereotactic C1 central myelotomy)	529
5.36.1.2.2	Limited midline myelotomy	529
5.36.2	**Basic Science Evidence Concerning Spinal Cord Pathways That Signal Visceral Pain**	530
5.36.2.1	Spinothalamic Tract	530
5.36.2.2	Spinoreticular, Spinoparabrachial, Spinoamygdalar, and Spinohypothalamic Tracts	531
5.36.2.3	Postsynaptic Dorsal Column Path	531
5.36.2.3.1	Historical evidence for a visceral projection in the dorsal column	531
5.36.2.3.2	Effects of interruption of the dorsal column or a lesion of dorsal column nuclei on responses of brainstem and thalamic neurons to noxious visceral stimuli	531
5.36.2.3.3	Effects of a dorsal column lesion on behavioral responses	533
5.36.2.3.4	Effects of a dorsal column lesion on the regional cerebral blood flow changes that result from colorectal distention in monkeys	534
5.36.2.3.5	Blockade of synaptic relay in sacral cord by morphine or 6-cyano-7-nitroquinoxaline-2,3-dione	534
5.36.2.3.6	Projections of the postsynaptic dorsal column pathway	536
5.36.2.3.7	Upregulation of NK1 receptors in PSDC neurons after colon inflammation	538
5.36.2.3.8	Fos expression in PSDC neurons after noxious visceral stimulation	538
5.36.3	**Descending Facilitation**	539
References		540

Glossary

activity box Apparatus used to determine the amount and time course of exploratory activity of an animal, such as a rat.

central neuropathic pain pain that develops following injury to the central nervous system.

CNQX 6-cyano-7-nitroquinoxaline-2,3-dione, a non-*N*-methyl-D-aspartic acid receptor antagonist.

kainic acid lesion damage produced by injection of kainic acid, a substance that produces excitotoxicity.

NMDA *N*-methyl-D-aspartic acid.

pain referral Projection of the source of pain to an area of the body distant to the actual area of injury.

paresthesias Unusual sensations, such as tingling or burning.

rhizotomy Transaction of one or more spinal roots.

viscerospecific responses Neuronal activity evoked by sensory input from a particular visceral organ.

5.36.1 Clinical Evidence Concerning Spinal Cord Pathways That Signal Visceral Pain

5.36.1.1 Spinothalamic Tract

5.36.1.1.1 Anterolateral cordotomy

It is well known that ascending pathways in the anterolateral quadrant of the human spinal cord transmit pain and temperature signals, since pain is relieved (at least temporarily) and thermal sense is lost over the appropriate part of the contralateral body following an anterolateral cordotomy (Spiller, W. G., 1905; Spiller, W. G. and Martin, E., 1912; Foerster, O. and Gagel, G., 1932; reviewed in Gybels, J. M. and Sweet, W. H., 1989). The signals are transmitted from one side of the body to the contralateral thalamus (Kenshalo, D. R. *et al.*, 1980; Chung, J. M. *et al.*, 1986; Bushnell, M. C. *et al.*, 1993; Lee, J. I. *et al.*, 1999; 2005) and from there to the appropriate regions of the cerebral cortex (see Casey, K. L. and Bushnell, M. C., 2000). It has been presumed that the pain signals are conveyed chiefly by the spinothalamic tract, which decussates at the spinal cord level (Mehler, W. R., 1962), although other pathways that accompany the spinothalamic tract are also likely to contribute. These include the spinoreticular, spinoparabrachial, spinohypothalamic, and other tracts (Willis, W. D. and Westlund, K. N.,1997; Willis, W. D. and Coggeshall, R. E., 2004). Innocuous thermal signals are attributed just to the spinothalamic tract.

Anterolateral cordotomy can relieve superficial and deep somatic pain, as well as visceral pain (and can block thermal sense), provided that the lesion is extensive enough (Gybels, J. M. and Sweet, W. H., 1989; Nathan, P. W. *et al.*, 2001). For complete pain relief on the contralateral side of the body, a cordotomy at an upper cervical level needs to extend from just posterior to the denticulate ligament, across the remainder of the lateral funiculus and well into the anterior funiculus (Figure 1(a); Nathan, P. W. *et al.*, 2001).

However, even after an initially successful cordotomy, pain relief may not persist more than a few months to a year or so, although in some cases the pain relief is of very long duration (Gybels, J. M. and Sweet, W. H., 1989). It is unclear why the pain can recur. Some suggestions are that other pathways now convey the pain signals, the disease advances (e.g., metastatic cancer may activate spinothalamic neurons whose axons were not interrupted by the cordotomy), or central neuropathic pain develops. Because of the recurrence of pain after a large proportion of cordotomies, neurosurgeons have tended to limit the use of this procedure to patients with pain from a terminal disease, usually cancer, or to abandon the procedure altogether in favor of pharmacotherapy.

Visceral pain can be relieved by cordotomy, provided that the lesion extends into the anterior funciculus medially to the spinal cord gray matter (Gybels, J. M. and Sweet, W. H., 1989). A unilateral cordotomy can be effective if the visceral pain is

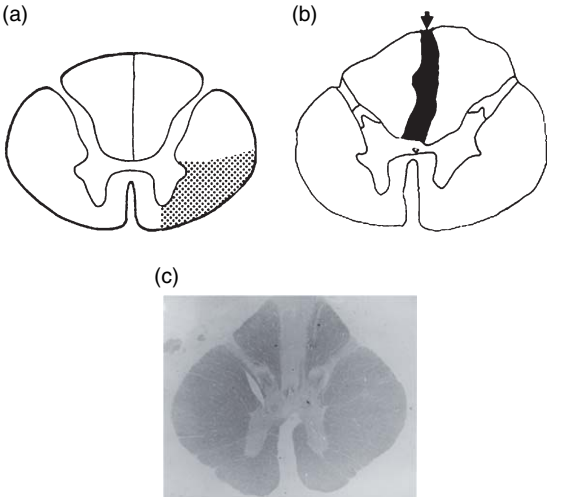

Figure 1 (a) Drawing of a cross section of the human spinal cord at the third cervical level. The dotted area shows the region that needs to be sectioned by a cordotomy in order to relieve contralateral pain completely. Note that the lesion must extend to a level that is posterior to the expected location of the denticulate ligament and anteromedially across the lateral funicuclus and into the anterior funiculus. (b) Drawing of a cross section of the human spinal cord at a mid-thoracic level showing the location of a limited midline myelotomy that was used to relieve completely the pain of colon cancer for the duration of the 3-month survival period. No opioid analgesics were required after a tapering-off period. (c) Photomicrograph of a cross section of the human spinal cord at the level of a limited midline myelotomy that was placed at a mid-thoracic level in a patient with a painful presacral sarcoma. The lesion (shown by the area of demyelination near the midline of the dorsal columns) eliminated the pain and the need for narcotics for the duration of the patient's survival time, which was 3 years postsurgery. (a) From Nathan, P. W., Smith, M., and Deacon, P. 2001. The crossing of the spinothalamic tract. Brain 124, 793–803. (b) From Hirshberg, R. M., Al-Chaer, E. D., Lawand, N. B., Westlund, K. N., and Willis, W. D. 1996. Is there a pathway in the posterior funiculus that signals visceral pain? Pain 47, 291–305.

restricted to one side. However, if the pain is bilateral, a bilateral cordotomy may be needed. Unfortunately, this can lead to undesired side effects, such as incontinence because of interruption of descending pathways that control bowel and bladder function. If the cordotomy is done at a high cervical level for pain originating from the upper part of the body, there is danger that the respiratory control pathways may be interrupted, leading to severe (potentially lethal) difficulty with breathing.

5.36.1.1.2 Commissural myelotomy

An alternative procedure called commissural myelotomy is directed at interrupting the axons of spinothalamic tract neurons of both sides as they cross the midline (Armour, D., 1927; Mansuy, L. *et al*., 1944; 1976; see Gybels, J. M. and Sweet, W. H., 1989). A lesion is made near the midline of the spinal cord and extending rostrocaudally for as many segments as needed to interrupt the appropriate projections. The lesion should be sufficiently deep to ensure that the crossing spinothalamic axons in the anterior white commissure are cut. Of course, the crossing axons of a number of tracts that accompany the spinothalamic tract, such as spinoreticular axons, are also interrupted, as are many axons in the posterior funiculi. According to the analysis of Dargent, M. *et al.* (1963), this procedure is apparently particularly effective for vaginal and visceral pain. Interestingly, commissural myelotomy often relieves clinical pain even if on testing there is no hypalgesia. Furthermore, pain and temperature sensation may be lost over a much greater extent of the body than could be predicted from the location and dimensions of the commissural myelotomy (Gybels, J. M. and Sweet, W. H., 1989). Based on evidence reviewed in the following, it now seems likely that the effect of a commissural myelotomy depends at least in part on the interruption of a visceral pain pathway that ascends in the posterior funiculi.

5.36.1.2 Posterior Column

5.36.1.2.1 Hitchcock procedure (stereotactic C1 central myelotomy)

Hitchcock developed a completely different approach to lesioning the spinal cord to relieve pain (Hitchcock, E., 1970; 1974; 1977; see also Papo, L. and Luongo, A., 1976; Eiras, J. *et al*., 1980; Schvarcz, J. R., 1977; 1978; Sourek, K., 1985). He placed a lesion in the central part of the upper cervical spinal cord using a stereotactic approach. The location of the lesion was sometimes determined by recordings of evoked potentials but more often by the sensory effects of electrical stimulation through the electrode and by the changes in the sensory examination produced by a lesion. Stimulation in the central cord at C1 at 50 Hz typically resulted in a burning sensation in the chest or abdomen (Hitchcock, E., 1970; see Gybels, J. M. and Sweet, W. H., 1989). A lesion in the same location produced a change in pinprick sensation, either a loss of the ability to distinguish sharp from blunt or loss of a sensation of pain in response to pinprick. The analgesia was bilateral. Cancer pain was relieved in most cases, and the relief persisted until death or for over 5 years. Some patients (20%) failed to have a sensory loss and also did not experience pain relief.

In the surgical series done by Schvarcz J. R. (1977; 1978), lesions were made at a depth of 5 mm from the posterior surface of the spinal cord, reaching the base of the posterior column. Electrical stimulation produced paresthesias in the feet, legs, or trunk (and also in the trigeminal distribution). Relief of cancer pain persisted in 78% of cases for at least 0.5–2 years (most of the patients died by this time). Other types of pain, including peripheral and central neuropathic pain, were relieved for 0.5–4 years. No neurological deficits were seen. Several other clinical studies reported similar results (Papo, L. and Luongo, A., 1976; Eiras, J. *et al*., 1980; Sourek, K., 1985).

5.36.1.2.2 Limited midline myelotomy

Instead of a lesion at an upper cervical level, Gildenberg P. L. and Hirshberg R. M. (1984) made a midline lesion at T10 in patients with pelvic cancer pain. The location was chosen to be just above the level of entrance of primary afferent fibers from the pelvic viscera into the spinal cord. The procedure was termed a limited midline myelotomy. Eight cases done by Hirshberg, using a mechanical probe, were described further and a postmortem specimen showing the spinal cord lesion in one patient was illustrated (Figure 1(b)) in Hirshberg R. M. *et al.* (1996). The lesion interrupted the medial parts of the posterior funiculi but did not appear to intrude into the central gray matter or anterior white commissure. The results of the lesions in the eight cases were generally quite favorable, with pain relief that lasted as long as the patients survived and with little or no need for strong analgesic drugs.

The chief of neurosurgery at our institution, Dr. H. J. W. Nauta, made lesions using a technique similar to that described by Hirshberg in a series of

patients who had pain from pelvic or other cancers. The results in each case were again generally favorable and the need for strong analgesics greatly reduced. In one case, a midline myelotomy was done in a patient with inflammatory bowel disease secondary to irradiation that had successfully eradicated a cervical cancer (Nauta, H. J. W. *et al.*, 1997; 2000). The patient had severe ongoing pain, and the pain intensified during bowel movements. As a consequence of the pain, the patient had lost a substantial fraction of her body weight, and it was judged that she would not survive much more weight loss. After midline myelotomy, this patient lived for almost 5 years with no further pelvic pain (although she did experience subdiaphragmatic pain because of peritonitis). She died from complications of diabetes.

In another of the cases reported by Nauta H. J. W. *et al.* (1997; 2000), pain was reduced from 10 to 2–3 on the visual analog scale, and narcotic medication was tapered from 30 mg of intravenously administered morphine per hour preoperatively to 5 mg per hour within 5 days postoperatively. Another patient had unbearable pain from a presacral sarcoma, despite several efforts to resect the tumor. A midline myelotomy was done in the area shown in Figure 1(c). The lesion resulted in dramatic pain relief for the remainder of the patient's life. He survived the surgery by 36 months, and for most of this time he did not require narcotic medication. In general, only in some cases were even minor and transient sensory side effects observed. Pelvic cancer pain was consistently reduced following midline myelotomy, and narcotic usage could be decreased on average by 83%.

Several other groups around the world have had similar experiences with midline myelotomies (Becker, R. *et al.*, 1999; Kim, Y. S. and Kwon, S. J., 2000; Filho, O. V. *et al.*, 2001; Hu, J. S. and Li, Y. J., 2002; Hwang, S. L. *et al.*, 2004), and the results have been reviewed by Becker, R. *et al.*, (2002).

5.36.2 Basic Science Evidence Concerning Spinal Cord Pathways That Signal Visceral Pain

5.36.2.1 Spinothalamic Tract

The spinothalamic tract conveys somatic but also some visceral nociceptive information to the thalamus (Figure 2(a)). Studies in which recordings were made from antidromically activated spinothalamic tract neurons have demonstrated that many of these

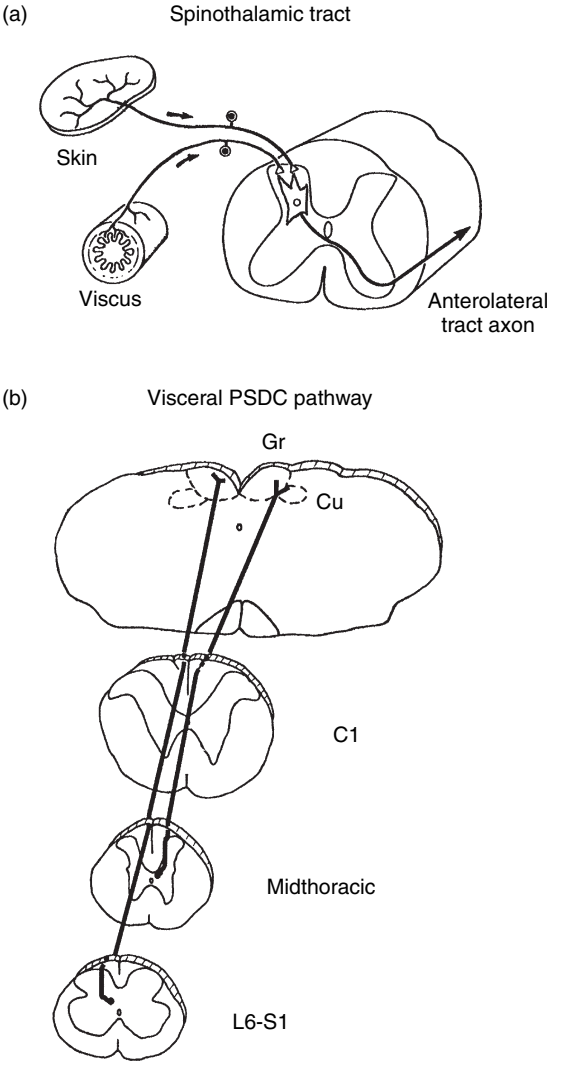

Figure 2 (a) Convergence of visceral and somatic afferent inputs on an anterolateral tract neuron. Such viscerosomatic convergence is thought to be responsible for referral of visceral pain to somatic structures. (b) Course followed by the axonal projections of postsynaptic dorsal column neurons found in the central region of the spinal cord gray matter at sacral and mid-thoracic levels. The anterograde tracer, phaseolus vulgaris leucoagglutinin (PHA-L), was injected and then several days later traced in axons of the dorsal column to the brainstem. The projection from the sacral cord ascended at the midline, whereas that from the mid-thoracic cord ascended more laterally, just ventral to the dorsal intermediate sulcus. Information about visceral nociception most likely travels with other sensory input to the thalamus in the medial lemniscus. Data from Wang, C. C., Willis, W. D., and Westlund, K. N. 1999. Ascending projections from the central, visceral processing region of the spinal cord: a PHA-L study in rats. J. Comp. Neurol. 415, 341–367; illustration from Willis, W. D., Al-Chaer, E. D., Quast M. J., and Westlund, K. N. 1999. A visceral pain pathway in the dorsal column of the spinal cord. Proc. Natl. Acad. Sci. U. S. A 96, 7675–7679.

cells can be activated (or in some instances inhibited) following stimulation of viscera. For example, Foreman and his group have shown that feline and primate spinothalamic tract cells can be excited by electrical stimulation of cardiopulmonary visceral afferent fibers, occlusion of a coronary artery, or injection of bradykinin into the coronary circulation (see review by Foreman, R. D., 1989). Similarly, spinothalamic tract cells have been shown to respond to electrical stimulation of the greater splanchnic nerve (Hancock, M. B. *et al.*, 1975; Foreman, R. D. *et al.*, 1981), distension of any of several hollow viscera, including the gall bladder (Ammons, W. S. *et al.*, 1984), kidney (Ammons, W. S., 1987), ureter (Ammons, W. S., 1989), urinary bladder (Milne, R. J. *et al.*, 1981), and colon (Al-Chaer, E. D. *et al.*, 1999) or noxious stimulation of the testicle (Milne, R. J. *et al.*, 1981). In general, spinothalamic tract and other neurons that are activated by visceral stimulation also respond to stimulation of somatic tissue. This convergence of visceral and somatic input onto spinal cord neurons, including nociceptive neurons that project to the brain, is thought to help account for the referral of visceral pain to the body wall in many clinical conditions (Figure 2(a); Head, H., 1893). Examples of the somatic receptive fields of viscero-sensitive spinothalamic cells that correspond to the distribution of pain referral are noted in Foreman (Foreman, R. D., 1989) and Milne (Milne, R. J. *et al.*, 1981). Only rarely can a spinal neuron be found that seems to respond to just visceral stimuli and not to somatic ones. However, when the search stimulus is colon distension, rather than antidromic activation from the lateral thalamus, viscerospecific responses can be recorded from cells located rostrally in the central lateral nucleus of the intralaminar complex of the thalamus (Ren, Y. *et al.*, 2006). This region has been shown to receive direct spinal innervation from lamina X neurons (Wang, C. C. *et al.*, 1999) and is rich in opiates (Sar, M. *et al.*, 1978). The spinothalamic projection from lamina X is situated at the medial-most edge of the spinothalamic tract and shifts laterally as it ascends with the spinothalamic tract.

5.36.2.2 Spinoreticular, Spinoparabrachial, Spinoamygdalar, and Spinohypothalamic Tracts

Several studies have demonstrated the effectiveness of visceral stimulation in exciting (or inhibiting) spinoreticular tract neurons (Blair, R. W. *et al.* 1984; Hobbs, S. F. *et al.*, 1990), spinoparabrachial and spinoamygdalar neurons (Menetrey, D. and De Pommery, J., 1991; Bernard, J. F. *et al.*, 1994), and spinohypothalamic tract neurons (Katter, J. T. *et al.*, 1996; Zhang, X. *et al.*, 2002). A cordotomy or a commissural myelotomy is likely to interrupt these pathways, and thus the relief of visceral pain by such lesions is likely to be at least partially explained by this, as well as by interruption of the spinothalamic tract.

5.36.2.3 Postsynaptic Dorsal Column Path

5.36.2.3.1 Historical evidence for a visceral projection in the dorsal column

Recordings from the human posterior funiculus have revealed the presence of visceral afferents that respond to distention of the urinary bladder (Puletti, F. and Blomqvist, A. J., 1967). Responses at various levels of the dorsal column-medial lemniscus pathway have also been reported in animal experiments following electrical stimulation of visceral nerves (Amassian, V. E., 1951; Aidar, O. *et al.*, 1952; Rigamonti, D. D. and Hancock, M. B., 1974; 1978).

5.36.2.3.2 Effects of interruption of the dorsal column or a lesion of dorsal column nuclei on responses of brainstem and thalamic neurons to noxious visceral stimuli

To determine if there is a visceral nociceptive pathway in the dorsal columns of experimental animals, recordings were made from viscero-responsive neurons in the ventral posterior lateral nucleus of the thalamus in rats before and after surgical interruption of either the dorsal columns bilaterally or the ipsilateral ventrolateral column, which contains the spinothalamic and associated nociceptive pathways (Al-Chaer, E. D. *et al.*, 1996a). The dorsal column lesion reduced the responses of the thalamic neurons to colorectal distension on average by about 80% (Figure 3(Ae), cf. upper and middle rows of records). The remaining response was eliminated by the lesion of the ventrolateral quadrant of the spinal cord (Figure 3(Ae), lower row of records). Responses to weak mechanical stimuli applied to the skin were abolished by the dorsal column lesion, whereas the responses to the strongest mechanical stimuli were affected only by the ventrolateral quadrant lesion (Figure 3(Ad)). Similar effects were seen when the noxious visceral stimulus was inflammation of the colon by intraluminal injection of mustard oil (not illustrated). The mustard oil produced a progressive

increase in the background activity of the viscerosensitive thalamic neurons. A dorsal column lesion was more effective in reducing the background activity than was a ventrolateral quadrant lesion.

Neurons in the rat ventral posterior lateral thalamic nucleus could also be found that responded to distention of the duodenum (Figure 3(Ba); Feng, Y. *et al.*, 1998). In these experiments, a lesion of the dorsal column placed at the midline failed to reduce the responses (Figure 3(Bb)). However, bilateral lesions just ventral to the dorsal intermediate sulcus at an upper cervical level were effective (Figure 3(Bc)).

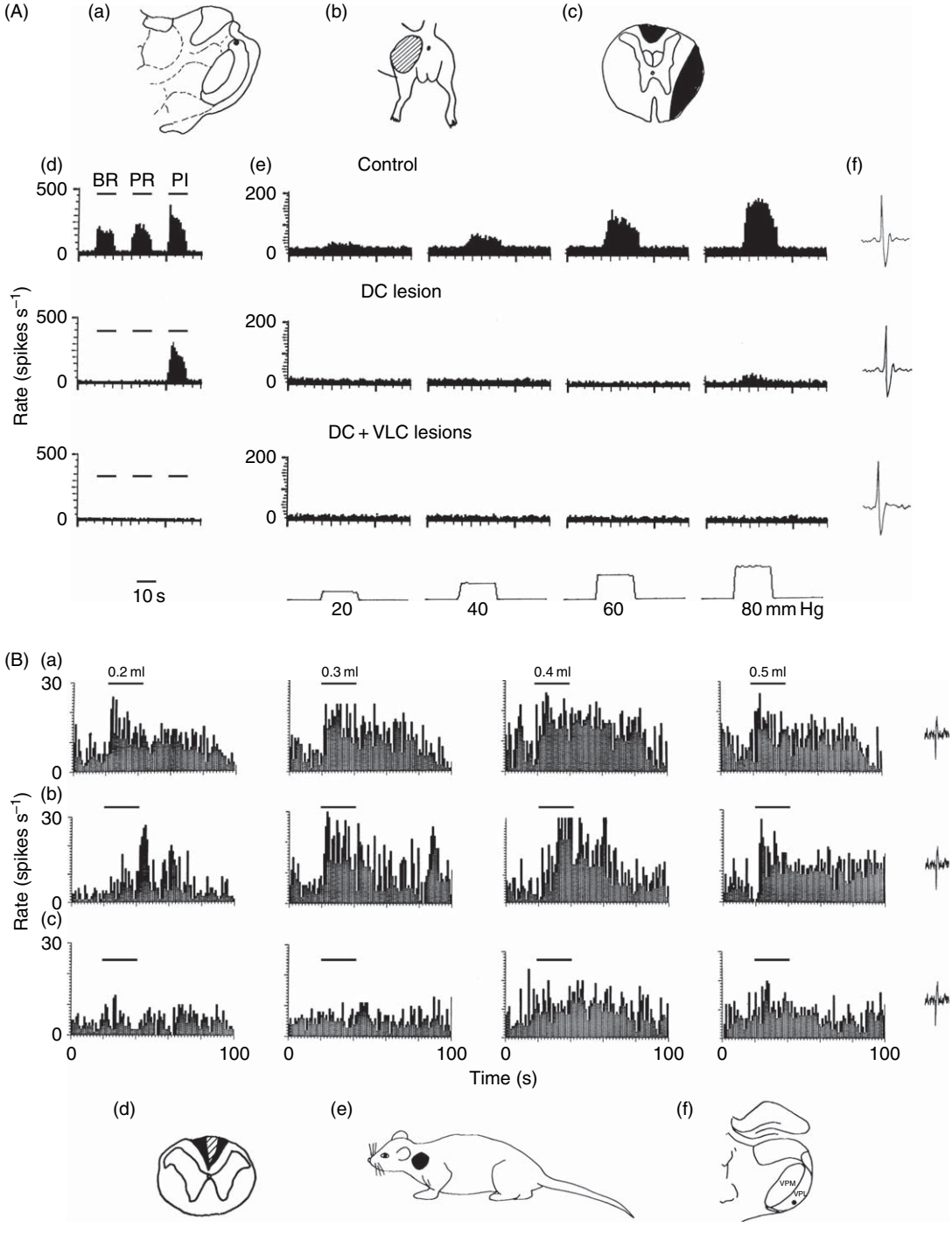

This shift in the location of the dorsal column lesion needed to interrupt nociceptive responses in the thalamus relates to the fact that the visceral input originated from an abdominal, rather than a pelvic organ (see Figure 2(b), discussion below, and Wang, C. C. *et al.*, 1999).

The off-midline part of the dorsal column pathway that carries visceral input from the thoracic level of the spinal cord was investigated in behavioral (see Figure 2(b) and discussion below) and electrophysiological studies after noxious chemical irritation of the pancreas (Houghton, A. K. *et al.*, 1997; 2001). Noxious stimulation of the pancreas by applications of bradykinin to its exposed surface in anesthetized rats resulted in excitation of neurons in the ventral posterior nucleus of the thalamus (Houghton, A. K. *et al.*, 2001). The mean firing rate of thalamic neurons was increased $412 \pm 120\%$ above baseline during the first 40 s after bradykinin application to the pancreas and was sustained for 3–6 min. Large dorsal column lesions effectively eliminated the increased responses of thalamic neurons to applications of bradykinin on the pancreas and baseline activity remained constant. Enhanced responses to skin pinch after pancreatic application of bradykinin dropped after a dorsal column lesion from 242% over baseline back to 100%. The effects of noxious stimulation of the pancreas with bradykinin involved a spinal synaptic relay rather than a vagal relay since thalamic activation was prevented by intrathecal administration of morphine. This action of morphine could be antagonized by naloxone.

Visceral responses can also be recorded from neurons in the ventral posterior lateral nucleus in monkeys (cf., Chandler, M. J. *et al.*, 1992; Brüggemann, J. *et al.*, 1994), as in rats. The effects of a dorsal column lesion on such responses in monkeys are consistent with those obtained in rats (Al-Chaer, E. D. *et al.*, 1998).

The thalamic responses to visceral input are relayed through the dorsal column nuclei. Visceral responses of neurons in the rat ventral posterior lateral thalamic nucleus could be reduced by small electrolytic or kainic acid lesions of the nucleus gracilis (Al-Chaer, E. D. *et al.*, 1997). Responses of cells in the nucleus gracilis have been recorded after noxious stimulation of either the colon or the pancreas (Al-Chaer, E. D. *et al.*, 1996b; 1997; Houghton, A. K. *et al.*, 2001).

5.36.2.3.3 Effects of a dorsal column lesion on behavioral responses

Changes observed in behavioral experiments were consistent with the electrophysiological findings. For example, when a rat is put into an unfamiliar plastic activity box, it moves freely around in the box until it adapts to this new environment. The movements can be tracked automatically by computer. Beams of ultraviolet light cross the plastic box, and whenever a beam is blocked by the animal, this is counted as a movement. Under normal conditions, the exploratory activity gradually decreases over about 45 min. However, if the animal experiences pain, for example, because of the presence of

Figure 3 (A) shows the effects of sequential lesions of the dorsal columns (DC) and of the ventrolateral column (VLC) on one side on the responses of a neuron in the rat ventral posterior thalamic nucleus to a graded series of mechanical and visceral stimuli. The filled circle in (a) shows the recording site; the hatched area in (b) the somatic receptive field, and the black areas on a drawing of a transverse section of the spinal cord in (c) the extent of the lesions. Responses to brushing the skin (BR), application of pressure to a fold of skin with an arterial clip (PR) and pinching the skin with a stronger arterial clip (PI) are seen in (d), before and after the lesions. The responses to colorectal distentions of 20, 40, 60, and 80 mmHg are shown in (e), before and after the lesions. The action potential of the thalamic neuron at different times during the experiment is illustrated in (f) to indicate the stability of the recording. (B) Shows the effects of lesions of the dorsal columns placed in the upper cervical spinal cord at the midline or bilaterally just ventral to the dorsal intermediate sulci on the responses of a neuron in the rat ventral posterior lateral nucleus. In (a), upper row of records, are shown the responses of the neuron to graded distensions of the duodenum. The volumes of fluid injected into a balloon at the end of a catheter inserted into the duodenum are indicated in ml. The middle row of records (b) was taken after a midline lesion was made in the dorsal columns. The lesion had no clear effect. The lower row of records (c) shows that bilateral lesions of the dorsal columns ventral to the dorsal intermediate sulci substantially reduced the responses. The action potential of the thalamic neuron at different times during the experiment is shown in (b) to indicate the stability of the recording. The midline lesion is indicated by the hatched area and the more laterally placed lesions by the black area in (d). The receptive field of the neuron is shown in (e) and the recording site in (f) (A) From Al-Chaer, E. D., Lawand, N. B., Westlund, K. N., and Willis, W. D. 1996a. Visceral nociceptive input into the ventral posterolateral nucleus of the thalamus: a new function for the dorsal column pathway. J. Neurophysiol. 76, 2661–2674. (B) From Feng, Y., Cui, M., Al-Chaer, E. D., and Willis, W. D. 1998. Epigastric antinociception by cervical dorsal column lesions in rats. Anesthesiology 89, 411–420.

allodynia or hyperalgesia, the exploratory activity decreases more rapidly.

Exploratory activity is also reduced in rats with pancreatitis (Houghton, A. K. *et al.*, 1997), and this reduction is counteracted following a lesion of the dorsal columns. Similarly, infusion of bradykinin into the common bile and pancreatic duct in rats results in a reduction in rearing behavior, and this vertical exploratory behavior is increased after a dorsal column lesion (Houghton, A. K. *et al.*, 2001). Since the pancreas is an intra-abdominal organ, rather than a pelvic organ, the dorsal column had to be interrupted bilaterally and it included the areas ventral to the dorsal intermediate sulci (see below and Wang, C. C. *et al.*, 1999).

Feng Y. *et al.* (1998) inserted a balloon into the duodenum through a catheter. Distention of the balloon resulted in contractions of the abdominal muscles that were graded in force depending on the amount of balloon distention. Interruption of the dorsal columns resulted in a reduction in these abdominal muscle contractions.

The role of the dorsal column versus that of the spinothalamic tract and associated pathways was tested by Palecek J. *et al.* (2002). Exploratory activity of rats was shown to be reduced following either an intradermal injection of capsaicin (Figure 4(a)) or by inflammation of the colon with mustard oil, coupled with a mild degree of colorectal distention (Figure 4(c)). The effects of a capsaicin injection on exploratory activity could be reversed by dorsal rhizotomies on the side of the injection or by a lesion of the ventrolateral column of the spinal cord on the side opposite to the injection, but not by a bilateral lesion of the dorsal column (Figure 4(b)). By contrast, the effects of colon inflammation and distention on exploratory activity were eliminated by a bilateral lesion of the dorsal columns, and this change persisted for at least 90 days (Figure 4(d)).

5.36.2.3.4 Effects of a dorsal column lesion on the regional cerebral blood flow changes that result from colorectal distention in monkeys

In each of four monkeys anesthetized with isoflurane, it was possible to survey the changes in regional cerebral blood flow that were produced by colorectal distention, using a 4.7 T magnet for functional magnetic resonance imaging (Willis, W. D. *et al.*, 1999). The images were averaged over a standard period of time with or without visceral distention. The intensity of the colorectal distention was to 80 mm of Hg, well into the noxious range. Images through a coronal section of the brain at the level of the posterior thalamus were compared, before and after surgery (Figure 5). In one animal, sham surgery was done over the dorsal column, but no lesion was made (Figure 5, left-most images). In the other three animals, the dorsal columns were interrupted at a mid-thoracic level. At various times after recovery from the surgery, the animals were re-anesthetized and fMRIs repeated at several intervals up to 4 months after the surgery. The sham surgery had no obvious effect on the regional cerebral blood flow produced by noxious colorectal distention. However, the lesion of the dorsal columns completely eliminated the blood flow changes in all three animals, and this effect of the lesion persisted for as long as the animals were followed (Figure 5).

5.36.2.3.5 Blockade of synaptic relay in sacral cord by morphine or 6-cyano-7-nitroquinoxaline-2,3-dione

The experiments described above indicate that the dorsal columns contain axons that signal visceral pain. However, a lesion of the dorsal columns interrupts not only the ascending branches of dorsal root ganglion cells that project to the dorsal column nuclei but also axons belonging to the postsynaptic dorsal column pathway (reviewed in Willis, W. D. and Coggeshall, R. E, 2004). An experiment was therefore designed to determine if noxious visceral signals are conveyed by the direct dorsal column projection or by postsynaptic dorsal column neurons (Al-Chaer, E. D. *et al.*, 1996b). The experimental arrangement is shown in Figure 6.

Recordings were made from the nucleus gracilis, rather than from the thalamus, to avoid the complication of visceral signals conveyed by the spinothalamic and accompanying pathways, as well as by the dorsal columns. The visceral stimulus was graded colorectal distention. The location of the part of the spinal cord that relayed the information to the medulla was restricted to the sacral segments by transecting the hypogastric nerves bilaterally. A microdialysis fiber was inserted across the sacral cord in order to introduce drugs into the dorsal horn that could block synaptic transmission but that would not interfere with direct nerve impulse transmission. The drugs included morphine and the non-*N*-methyl-D-aspartic acid (NMDA) glutamate receptor antagonist, 6-cyano-7-nitroquinoxaline-2,3-dione (CNQX). The prediction was that these drugs would prevent the responses of neurons of the gracile nucleus to

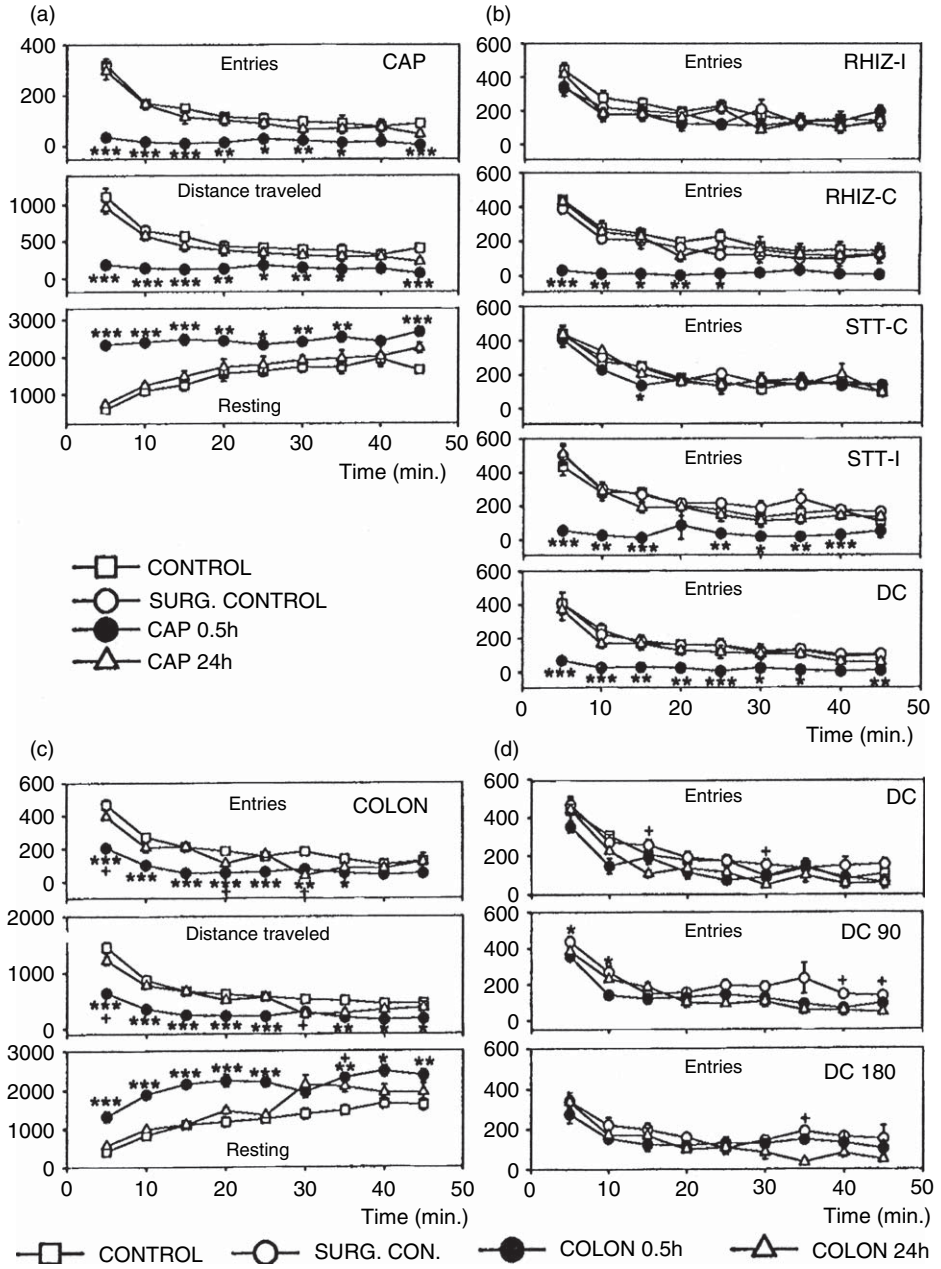

Figure 4 Time course of exploratory activity as monitored by a computer after introduction of rats into an activity box. The level of exploratory activity is determined by the number of interruptions of infrared light beams over a period of 45 min after the rat was placed in the activity box. The parameters included number of entries into a different zone, total distance traveled, and resting time. In (a) and (b), an intradermal injection of capsaicin was given, whereas in (c) and (d) mustard oil was injected into the colon and a latex balloon inserted and inflated to a pressure of 30 mmHg. At 30 min following either stimulus, exploratory activity was tested. Note that in (a), the capsaicin (CAP) injection resulted in a significant reduction in exploratory activity (and increased resting time). In (b), this was prevented by a prior extensive dorsal rhizotomy on the side ipsilateral to the injection (RHIZ-I), but was unaffected by a contralateral dorsal rhizotomy (RHIZ-C). A lesion that interrupted the spinothalamic tract contralateral to the injection (STT-C) also eliminated the reduction in exploratory activity following CAP, whereas an ipsilateral cordotomy (STT-I) had no effect; nor did a bilateral dorsal column (DC) lesion. In (c), colon inflammation and distention reduced the exploratory activity, and in (d) this change was eliminated by a dorsal column (DC) lesion. The effect lasted for 90 (DC 90) and 180 (DC 180) days. From Palecek, J., Paleckova, V., and Willis, W. D. 2002. The roles of pathways in the spinal cord lateral and dorsal funiculi in signaling nociceptive somatic and visceral stimuli in rats. Pain 96, 297–307.

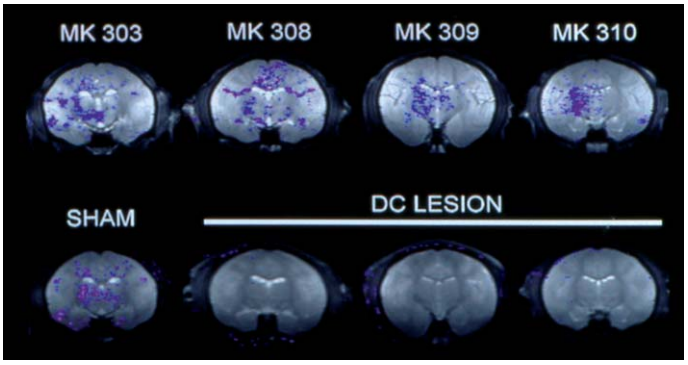

Figure 5 Functional magnetic resonance imaging showing the changes in regional cerebral blood flow in the brains of four different monkeys in coronal slices made at the level of the posterior thalamus. The blood flow changes were evoked by repeated colorectal distention to 80 mmHg under isoflurane anesthesia. The images in the upper row were made prior to surgery. Those in the lower row were from the same animals but after surgery. The animal whose images are shown at the left was subjected to sham surgery: the dorsal column was exposed at a mid-thoracic level, but no lesion was made. In the other three animals, the dorsal columns were interrupted at a mid-thoracic level. There was no obvious difference in regional blood flow changes in the animal with sham surgery, but the blood flow changes in the other animals were completely eliminated (previously unpublished data.).

colorectal distention if postsynaptic dorsal column neurons were responsible for the responses, but not if the direct dorsal column pathway were involved. This was important, since it was conceivable that noxious visceral signals could be transmitted to the dorsal column nuclei by unmyelinated, peptidergic branches of dorsal root ganglion neurons. Such fibers have been demonstrated, although the functions of these axons are still unknown (see Willis, W. D. and Coggeshall, R. E., 2004). The results of this experiment indicated that the postsynaptic dorsal column pathway is responsible for the visceral pain signals that ascend in the dorsal columns. Both morphine and CNQX blocked visceral nociceptive transmission from the colon to the gracile nucleus, and the effects of morphine were reversed by naloxone, indicating that the morphine acted on opiate receptors (Figure 7). The CNQX must have exerted its effect by blocking a critical synaptic relay that involves non-NMDA glutamate receptors.

5.36.2.3.6 Projections of the postsynaptic dorsal column pathway

The course of the ascending axons of postsynaptic dorsal column neurons in the sacral spinal cord was traced using the *Phaseolus vulgaris leukoagglutinin* (PHA-L) anterograde tracing technique and compared with the projections from postsynaptic dorsal column neurons in the mid-thoracic spinal cord (Wang, C. C. *et al.*, 1999). Injections of PHA-L were made into the central region of the spinal cord for several reasons. This area is known to receive visceral afferent input (Honda, C. N., 1985; Sugiura, Y. *et al.*, 1989), and recordings had been made in this region from a number of postsynaptic dorsal column neurons that responded to noxious visceral stimuli (Al Chaer, E. D. *et al.*, 1996a; 1996b). Many cells around the central canal have ascending projections in the dorsal columns that are labeled following injections of retrograde tracer into the dorsal column nuclei or the dorsal column itself (Hirshberg, R. M. *et al.*, 1996). The nociceptive visceral information is likely to be relayed from the dorsal column nuclei to the lateral thalamus by way of the medial lemnsicus.

However, recent observations indicate that many postsynaptic dorsal column neurons that are activated by noxious visceral stimuli are also located in the nucleus proprius of the spinal cord dorsal horn (Palecek, J. *et al.*, 2003b), presumably adjacent to postsynaptic dorsal column neurons that lack visceral input (Figure 8).

Postsynaptic dorsal column neurons in lamina X of the sacral cord were found to project their axons through the medial part of the fasciculi gracilis to the nuclei gracilis (Figure 2(b); Wang, C. C. *et al.*, 1999). Thus, the projections of these postsynaptic dorsal column cells are in exactly the position in the medial posterior columns that was targeted by the Hitchcock procedure (Hitchcock, E. 1970; 1974; 1977) and by limited midline myelotomy (see Hirshberg, R. M. *et al.*, 1996; Nauta, H. J. W. *et al.*, 1997; 2000). These axons would also be interrupted by a commissural myelotomy. However, axons that

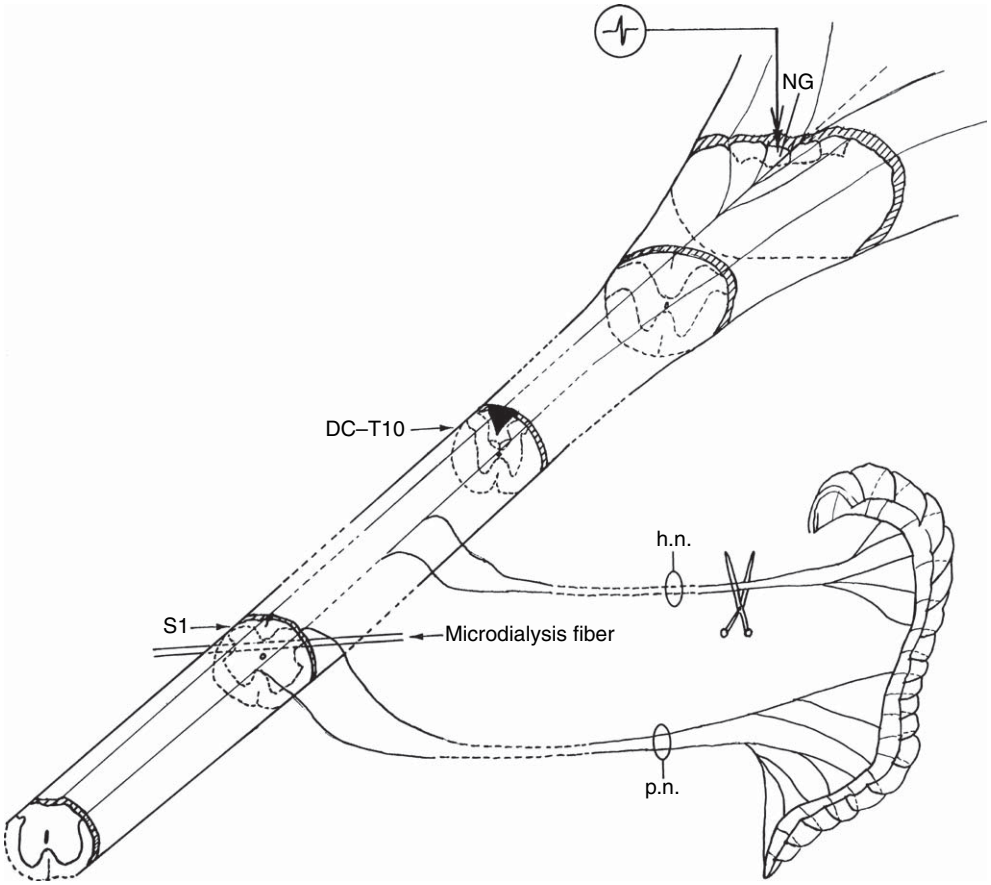

Figure 6 Drawing of the experimental arrangement. Recordings were made of the responses of neurons in the nucleus gracilis (NG, upper right) in response to colorectal distension. This avoided the problem that would have been encountered with thalamic recordings, since neurons of the ventral posterior lateral nucleus could be affected by either the dorsal column pathway or the spinothalamic tract. The input from the colon to the spinal cord was limited to just that traversing the pelvic nerve and ending in the sacral spinal cord. This was done by sectioning the hypogastric nerves prior to the experiment. A microdialysis fiber was placed across the spinal cord at S1 so that drugs that are likely to block synaptic transmission in the dorsal horn could be administered locally. Access to the dorsal column (DC) at T10 permitted a test of the effect of a dorsal column lesion. From Al-Chaer, E. D., Lawand, N. B., Westlund, K. N., and Willis, W. D. 1996a. Visceral nociceptive input into the ventral posterolateral nucleus of the thalamus: a new function for the dorsal column pathway. J. Neurophysiol. 76, 2661–2674.

ascend from postsynaptic dorsal column neurons in the mid-thoracic cord to the lateral part of the gracilis nucleus and the medial part of the cuneate nucleus do so near the dorsal intermediate septum (Figure 2(b); Wang, C. C. *et al*., 1999). Thus, there appears to be a viscerotopic organization of this visceral pathway similar to that of the somatosensory part of the postsynaptic dorsal column pathway (see Willis, W. D. and Coggeshall, R. E., 2004). The results of the studies of stimulation of internal organs of the abdomen described above by Houghton A. K. *et al.* (1997; 2001) and Feng Y. *et al.*(1998) are consistent with this observation. In these studies, distention or chemical irritation of abdominal viscera was used to activate neurons in the rat ventral posterior lateral nucleus. Lesions placed in the dorsal column at the midline failed to influence the responses. However, lesions lateral to the midline in the area of the dorsal intermediate septum were effective. Clinical studies from a group in Korea (Kim, Y. S. and Kwon, S. J., 2000) report favorable results in patients experiencing stomach cancer pain when lesions were made near the incoming thoracic dorsal root fibers rather than at the midline. This indicates that the viscerotopic organization is similar in humans and animals and that off-midline myelotomies will offer better relief of thoracic or upper abdominal visceral pain than do midline myelotomies.

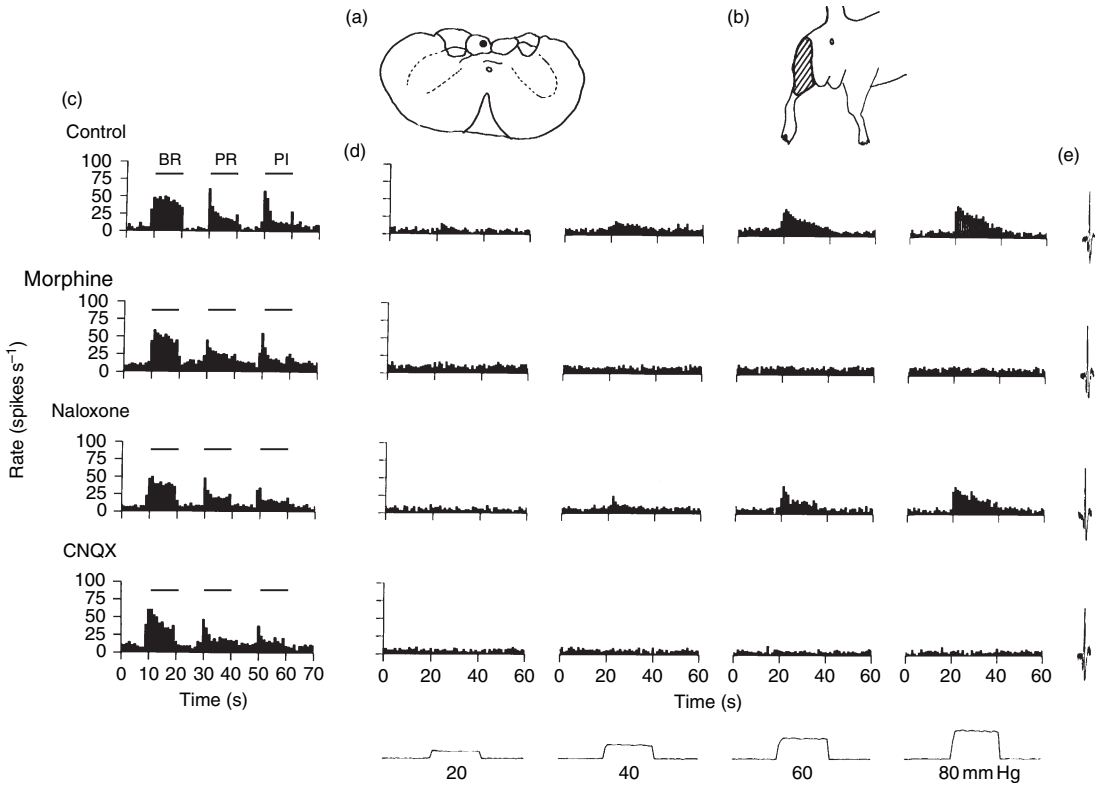

Figure 7 Effects of morphine and CNQX administered into the sacral cord by microdialysis on the responses of a neuron in the gracile nucleus to graded somatic and visceral stimuli. (a) Shows the recording site in the gracile nucleus. (b) Indicates the receptive field of the gracile neuron. In (c) are the responses of the gracile neuron to BR, PR, and PI stimuli applied to the cutaneous receptive field. (d) Shows the responses to graded colorectal distention to 20, 40, 60, and 80 mmHg. The upper row of recordings in (c) and (d) are the control responses taken before administration of drugs. The second row of recordings shows the effects of morphine given by microdialysis. There was little, if any, change in the responses to the somatic stimuli, but the responses to colorectal distention were eliminated. The third row of recordings shows that systemically administered naloxone counteracted the effects of morphine. The lowest row of recordings shows the effect of CNQX in blocking the responses to colorectal distention. In (e) are action potentials recorded at different times during the experiment to show the stability of the recordings. From Al-Chaer, E. D., Lawand, N. B., Westlund, K. N., and Willis, W. D. 1996b. Pelvic visceral input into the nucleus gracilis is largely mediated by the postsynaptic dorsal column pathway. J. Neurophysiol. 76, 2675–2690.

5.36.2.3.7 Upregulation of NK1 receptors in PSDC neurons after colon inflammation

The cells of origin of several nociceptive pathways that ascend from the spinal cord to the brain are known to contain neurokinin-1 (NK-1) receptors (Todd, A. J. *et al.*, 2000). These pathways include the spinothalamic and spinoreticular tracts. However, postsynaptic dorsal horn neurons do not contain NK-1 receptors under normal conditions, although an up-regulation of these receptors does occur in some of these neurons following visceral inflammation (Palecek, J.*et al.*, 2003a).

5.36.2.3.8 Fos expression in PSDC neurons after noxious visceral stimulation

A comparison was made of the numbers and locations of neurons belonging to the spinothalamic tract and to the postsynaptic dorsal column pathway that express Fos, the product of the immediate/early gene, c-fos, following either an intradermal injection of capsaicin or distention of the ureter (see Figure 8; Palecek, J. *et al.*, 2003b). The spinothalamic neurons were retrogradely labeled from the contralateral thalamus and the postsynaptic dorsal column neurons from the ipsilateral nucleus gracilis. Ureter distention was accomplished by tightening a ligature that had previously been placed around the ureter. The ureter was distended proximal to the site where the ligature blocked the flow of urine. Fos-labeled neurons were distributed over a considerable length of the spinal cord, from T11 to L6. This study confirmed that spinothalamic tract cells can be activated by a noxious visceral stimulus and that postsynaptic dorsal column neurons are also activated by such stimuli.

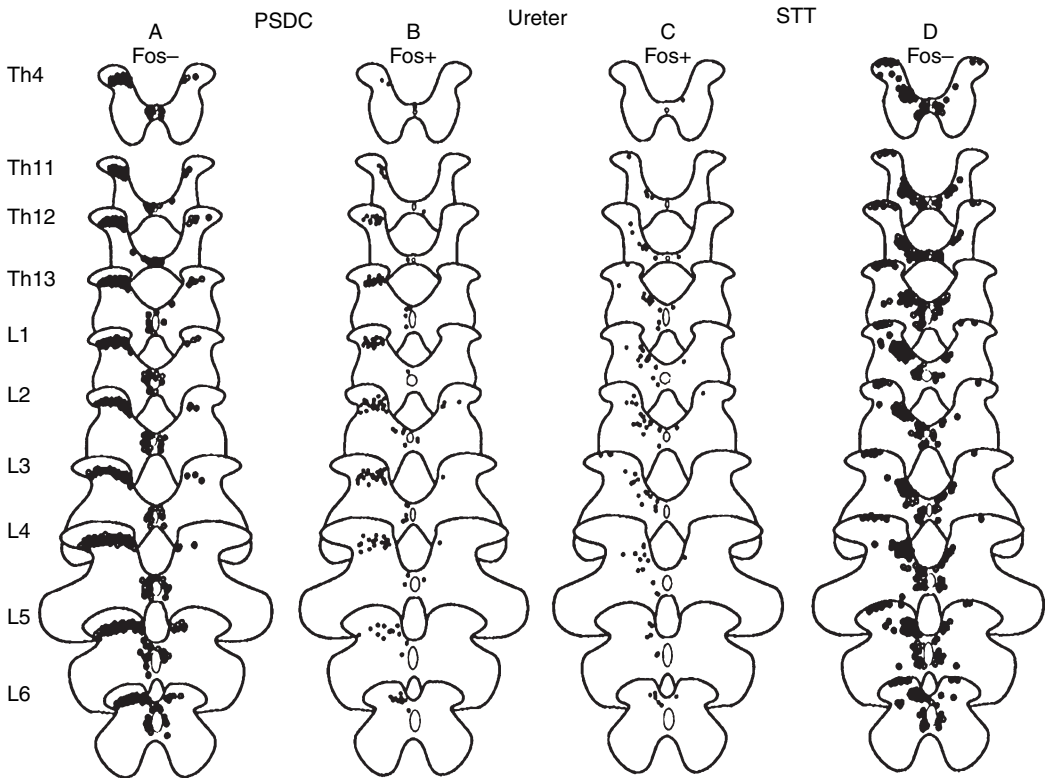

Figure 8 Effect of distention of the ureter in evoking expression of Fos protein in identified projection neurons in rats. Postsynaptic dorsal column neurons were labeled retrogradely following injection of a tracer into the nucleus gracilis (left-most column), and spinothalamic neurons were identified following injection of a different retrograde tracer into the ventral posterior lateral nucleus of the thalamus (right-most column). The middle columns show neurons identified by retrograde labeling that were also labeled for Fos protein following distention of the ureter. From Palecek, J., Paleckova, V., and Willis, W. D. 2003b. Fos expression in spinothalamic and postsynaptic dorsal column neurons following noxious visceral and cutaneous stimuli. Pain 104, 249–257.

5.36.3 Descending Facilitation

It has been shown that the responses of spinal cord neurons to visceral stimulation depend in large part on a spino-bulbo-spinal circuit (Cervero, F. and Wolstencroft, J. H., 1984; Tattersall, J. E. *et al.*, 1986; Zhuo, M. and Gebhart, G. F., 2002) that when activated facilitates visceral responses at the spinal cord level. Our anterograde tract tracing studies of the projections from lamina X demonstrate an ascending component that joins the medial edge of the spinothalamic tract (Wang, C. C. *et al.*, 1999). This ascending pathway has terminations in the nucleus raphe magnus, rostral ventromedial medulla, and medial reticular formation. This pathway is the only reported direct input to the nucleus raphe magnus from the spinal cord and is likely to be important for the activation of brainstem facilitatory neurons with axons that descend into the spinal cord to enhance the responses of spinal cord neurons to noxious visceral stimuli.

Palecek J. and Willis W. D. (2003) confirmed that a dorsal column lesion did not affect visceromotor reflex responses under normal conditions (cf., Ness, T. J. and Gebhart, G. F., 1988). However, the enhanced visceromotor responses to graded colorectal distention that followed colon inflammation with mustard oil were reduced or prevented by bilateral lesions of the dorsal columns. This suggests that the visceral reflex is enhanced because of activity induced by the colon inflammation and conveyed to the brainstem by way of the dorsal column. A lesion of the ventrolateral spinal cord eliminated the visceromotor reflex, presumably by interrupting a facilitatory pathway that descends from the brainstem and/or the ascending spinothalamic projection from lamina X.

It is our working hypothesis that interruption of the postsynaptic dorsal column pathway by a lesion placed

in the dorsal columns reduces visceral pain not only because such a lesion prevents visceral pain signals from reaching the thalamus by way of the dorsal column nuclei and medial lemniscus, but also because of a reduction of descending facilitation affecting visceral nociceptive neurons in the spinal cord, including post-synaptic dorsal column and spinothalamic tract neurons.

References

Aidar, O., Geohegan, W. A., and Ungewitter, L. H. 1952. Splanchnic afferent pathways in the central nervous system. J. Neurophysiol. 15, 131–138.

Al-Chaer, E. D., Feng, Y., and Willis, W. D. 1998. A role for the dorsal column in nociceptive visceral input into the thalamus of primates. J. Neurophysiol. 79, 3143–3150.

Al-Chaer, E. D., Feng, Y., and Willis, W. D. 1999. Comparative study of viscerosomatic input onto postsynaptic dorsal column and spinothalamic tract neurons in the primate. J. Neurophysiol. 82, 1876–1882.

Al-Chaer, E. D., Lawand, N. B., Westlund, K. N., and Willis, W. D. 1996a. Visceral nociceptive input into the ventral posterolateral nucleus of the thalamus: a new function for the dorsal column pathway. J. Neurophysiol. 76, 2661–2674.

Al-Chaer, E. D., Lawand, N. B., Westlund, K. N., and Willis, W. D. 1996b. Pelvic visceral input into the nucleus gracilis is largely mediated by the postsynaptic dorsal column pathway. J. Neurophysiol. 76, 2675–2690.

Al-Chaer, E. D., Westlund, K. N., and Willis, W. D. 1997. Nucleus gracilis: an integrator for visceral and somatic information. J. Neurophysiol. 78, 521–527.

Amassian, V. E. 1951. Fiber groups and spinal pathways of cortically represented visceral afferents. J. Neurophysiol. 14, 445–460.

Ammons, W. S. 1987. Characteristics of spinoreticular and spinothalamic neurons with renal input. J. Neurophysiol. 50, 480–495.

Ammons, W. S. 1989. Primate spinothalamic cell responses to ureteral occlusion. Brain Res. 496, 124–130.

Ammons, W. S., Blair, R. W., and Foreman, R. D. 1984. Responses of primate T1-T5 spinothalamic neurons to gallbladder distension. Am. J. Physiol. 247, R995–R1002.

Armour, D. 1927. Surgery of the spinal cord and its membranes. Lancet i, 691–697.

Becker, R., Gatscher, S., Sure, U., and Bertalanffy, H. 2002. The punctuate midline myelotomy concept for visceral cancer pain control- case report and review of the literature. Acta Neurochir. Suppl. 79, 77–78.

Becker, R., Sure, U., and Bertalanffy, H. 1999. Punctate midline myelotomy. A new approach in the management of visceral pain. Acta Neurochir. (Wien) 141, 881–883.

Bernard, J. F., Huang, G. F., and Besson, J. M. 1994. The parabrachial area: electrophysiological evidence for an involvement in visceral nociceptive processes. J. Neurophysiol. 71, 1646–1660.

Blair, R. W., Ammons, W. S., and Foreman, R. D. 1984. Responses of thoracic spinothalamic and spinoreticular cells to coronary artery occlusion. J. Neurophysiol. 51, 636–648.

Brüggemann, J., Shi, T., and Apkarian, A. V. 1994. Squirrel monkey lateral thalamus. II. Viscero-somatic convergent representation of urinary bladder, colon and esophagus. J. Neurosci. 14, 6796–6814.

Bushnell, M. C., Duncan, G. H., and Tremblay, N. 1993. Thalamic VPM nucleus in the behaving monkey. I. Multimodal and discriminative properties of thermosensitive neurons. J. Neurophysiol. 69, 739–752.

Casey, K. L. and Bushnell, M.C. (*eds.*) (2000) Pain Imaging. IASP Press.

Cervero, F. and Wolstencroft, J. H. 1984. A positive feedback loop between spinal cord nociceptive pathways and antinociceptive areas of the cat's brain stem. Pain 20, 125–138.

Chandler, M. J., Hobbs, S. F., Qing-Gong, Fu., Kenshalo, D. R., Blair, R. W., and Foreman, R. D. 1992. Responses of neurons in ventroposterolateral nucleus of primate thalamus to urinary bladder distension. Brain Res. 571, 26–34.

Chung, J. M., Lee, K. H., Surmeier, D. J., Sorkin, L. S., Kim, J., and Willis, W. D. 1986. Response characteristics of neurons in the ventral posterior lateral nucleus of the monkey thalamus. J. Neurophysiol. 56, 370–390.

Dargent, M., Mansuy, L., Cohen, J., and De Rougemont, J. 1963. Les problems poses par la douleur dans l'evolution des cancers gynécologiques. Lyon chirurg. 59, 62–83.

Eiras, J., Garcia, J., Gomez, J., Carvavilla, L. I., and Ucar, S. 1980. First results with extralemniscal myelotomy. Acta Neurochir. Suppl. 30, 377–381.

Feng, Y., Cui, M., Al-Chaer, E. D., and Willis, W. D. 1998. Epigastric antinociception by cervical dorsal column lesions in rats. Anesthesiology 89, 411–420.

Filho, O. V., Araujo, M. R., Florencio, R. S., Silva, M. A. C., and Silveira, M. T. 2001. CT-guided percutaneous punctuate midline myelotomy for the treatment of intractable visceral pain: a technical note. Stereotact. Funct. Neurosurg. 77, 177–182.

Foerster, O. and Gagel, G. 1932. Die Vorderseitenstrangdurchschneidung beim Menschen: Eine klinisch-pathophysioligisch-anatomische Studie. Z. Ges. Neurol. Psychiat. 138, 1–92.

Foreman, R. D. 1989. Organization of the spinothalamic tract as a relay for cardiopulmonary sympathetic afferent fiber activity. In: Progress in Sensory Physiology (*ed*. D. Ottoson), Vol. 9, pp. 1–51. Springer.

Foreman, R. D., Hancock, M. B., and Willis, W. D. 1981. Responses of spinothalamic tract cells in the thoracic spinal cord of the monkey to cutaneous and visceral inputs. Pain 11, 149–162.

Gildenberg, P. L. and Hirshberg, R. M. 1984. Limited myelotomy for the treatment of intractable cancer pain. J. Neurol. Neurosurg. Psychiat. 47, 94–96.

Gybels, J. M. and Sweet, W. H. 1989. Neurosurgical Treatment of Persistent Pain. Karger.

Hancock, M. B., Foreman, R. D., and Willis, W. D. 1975. Convergence of visceral and cutaneous input onto spinothalamic tract cells in the thoracic spinal cord of the cat. Exp. Neurol. 47, 240–248.

Head, H. 1893. On disturbances of sensation with especial reference to the pain of visceral disease. Brain 16, 1–132.

Hirshberg, R. M., Al-Chaer, E. D., Lawand, N. B., Westlund, K. N., and Willis, W. D. 1996. Is there a pathway in the posterior funiculus that signals visceral pain? Pain 47, 291–305.

Hitchcock, E. 1970. Stereotactic cervical myelotomy. J. Neurol. Neurosurg. Psychiat. 33, 224–230.

Hitchcock, E. 1974. Stereotactic myelotomy. Proc. R. Soc. Med. 67, 771–772.

Hitchcock, E. 1977. Stereotactic spinal surgery. Neurol. Surg. 433, 271–280.

Hobbs, S. F., Oh, U. T., Brennan, T. J., Chandler, M. J., Kim, K. S., and Foreman, R. D. 1990. Urinary bladder and hindlimb stimuli inhibit T1–T6 spinothalamic and spinoreticular cells. Am. J. Physiol. 258, R10–R20.

Honda, C. N. 1985. Visceral and somatic afferent convergence onto neurons near the central canal in the sacral spinal cord of the cat. J. Neurophysiol. 53, 1059–1078.

Houghton, A. K., Kadura, S., and Westlund, K. N. 1997. Dorsal column lesions reverse the reduction in homecage activity in rats with pancreatitis. NeuroReport 8, 3795–3800.

Houghton, A. K., Wang, C. C., and Westlund, K. N. 2001. Do nociceptive signals from the pancreas travel in the dorsal column? Pain 89, 207–220.

Hu, J. S. and Li, Y. J. 2002. Clinical application of midline myelotomy to treat visceral cancer pain. Natl. Med. J. China 82, 856–867 (in Chinese).

Hwang, S. L., Lin, C. L., Lieu, A. S., Kuo, T. H., Yu, K. L. K., Ou-Yang, F., Wang, S. N., Lee, K. T., and Howng, S. L. 2004. Punctate midline myelotomy for intractable visceral pain caused by hepatobiliary or pancreatic cancer. J. Pain Symptom Management 27, 79–84.

Katter, J. T., Dado, R. J., Kostarczyk, E., and Giesler, G. J. 1996. Spinothalamic and spinohypothalamic tract neurons in the sacral spinal cord of rats. II. Responses to cutaneous and visceral stimuli. J. Neurophysiol. 75, 2606–2628.

Kenshalo, D. R., Giesler, G. J., Leonard, R. B., and Willis, W. D. 1980. Responses of neurons in primate ventral posterior lateral nucleus to noxious stimuli. J. Neurophysiol. 43, 1594–1614.

Kim, Y. S. and Kwon, S. J. 2000. High thoracic midline dorsal column myelotomy for severe visceral pain due to advanced stomach cancer. Neurosurgery 46, 85–92.

Lee, J. I., Antezanna, D., Dougherty, P. M., and Lenz, F. A. 1999. Responses of neurons in the region of the thalamic somatosensory nucleus to mechanical and thermal stimuli graded into the painful range. J. Comp. Neurol. 410, 541–555.

Lee, J. I., Ohara, S., Dougherty, P. M., and Lenz, F. A. 2005. Pain and temperature encoding in the human thalamic somatic sensory nucleus (ventral caudal): inhibition-related bursting evoked by somatic stimuli. J. Neurophysiol. 94, 1676–1687.

Mansuy, L., Lecuire, J., and Acassat, L. 1944. Technique de la myélotomie commissurale postérieure. J. Chir. 60, 206–213.

Mansuy, L., Sindou, M., Fischer, G., and Brunon, J. 1976. La cortotomie spino-thalamique dans les douleurs cancéreuses. Résultats d'une série de 124 malades operas par abord direct postérieur. Neuro-chirurgie 22, 437–444.

Mehler, W. R. 1962. The anatomy of the so-called ''pain tract'' in man: analysis of the course and distribution of the ascending fibers of the fasciculus anterolateralis. In: Basic Research in Paraplegia (*eds*. J. D. French and R. W. Porter), pp. 26–55. Thomas.

Menetrey, D. and De Pommery, J. 1991. Origins of spinal ascending pathways that rech central areas involved in visceroception and visceronociception in the rat. Eur. J. Neurosci. 3, 249–259.

Milne, R. J., Foreman, R. D., Giesler, G. J., and Willis, W. D. 1981. Convergence of cutaneous and pelvic visceral nociceptive input onto primate spinothalamic neurons. Pain 11, 163–183.

Nathan, P. W., Smith, M., and Deacon, P. 2001. The crossing of the spinothalamic tract. Brain 124, 793–803.

Nauta, H. J. W., Hewitt, E., Westlund, K. N., and Willis, W. D. 1997. Surgical interruption of a midline dorsal column visceral pain pathway: case report and review of the literature. J. Neurosurg. 86, 538–542.

Nauta, H. J. W., Soukup, V. M., Fabian, R. H., Lin, J. H. T., Grady, J. J., Williams, C. G. A., Campbell, G. A., Westlund, K. N., and Willis, W. D. 2000. Punctate mid-line myelotomy for the relief of visceral cancer pain. J. Neurosurg. (Spine 1) 92, 125–130.

Ness, T. J. and Gebhart, G. F. 1988. Colorectal distention as a noxious visceral stimulus: physiologic and pharmacologic characterization of pseudoaffective reflexes in the rat. Brain Res. 450, 153–169.

Palecek, J. and Willis, W. D. 2003. The dorsal column pathway facilitates visceromotor responses to colorectal distention after colon inflammation in rats. Pain 104, 501–507.

Palecek, J., Paleckova, V., and Willis, W. D. 2002. The roles of pathways in the spinal cord lateral and dorsal funiculi in signaling nociceptive somatic and visceral stimuli in rats. Pain 96, 297–307.

Palecek, J., Paleckova, V., and Willis, W. D. 2003a. Postsynaptic dorsal column neurons express NK1 receptors following colon inflammation. Neuroscience 116, 565–572.

Palecek, J., Paleckova, V., and Willis, W. D. 2003b. Fos expression in spinothalamic and postsynaptic dorsal column neurons following noxious visceral and cutaneous stimuli. Pain 104, 249–257.

Papo, L. and Luongo, A. 1976. High cervical commissural myelotomy in the treatment of pain. J. Neurol. Neurosurg. Psychiat. 39, 705–710.

Puletti, F. and Blomqvist, A. J. 1967. Single neuron activity in posterior columns of the human spinal cord. J. Neurosurg. 27, 255–259.

Ren, Y., Lu, Y., Yang, H., and Westlund, K. N. Responses of neurons in central lateral thalamic nucleus to mechanical and chemical visceral stimulation in rats. APS Abstracts, American Pain Society, 2006.

Rigamonti, D. D. and Hancock, M. B. 1974. Analysis of field potentials elicited in the dorsal column nuclei by splanchnic nerve A-beta afferents. Brain Res. 77, 326–329.

Rigamonti, D. D. and Hancock, M. B. 1978. Viscerosomatic convergence in the dorsal column nuclei of the cat. Exp. Neurol. 61, 337–348.

Sar, M., Stumpf, W. E., Miller, R. J., Chang, K.-J., and Cuatrecasas, P. 1978. Immunohistochemical localization of enkephalin in rat brain and spinal cord. J Comp. Neurol. 182, 17–38.

Schvarcz, J. R. 1977. Functional exploration of the spinomedullary junction. Acta Neurochir. Suppl. 24, 179–185.

Schvarcz, J. R. 1978. Spinal cord stereotactic techniques re trigeminal nucleotomy and extralemniscal myelotomy. Appl. Neurophysiol. 41, 99–112.

Sourek, K. 1985. Central thermromyelo-coagulation for intractable chronic pain and opioid peptides. In: 8th International Congress of Neurological Surgery, Toronto, 1985, Abstract 221.

Spiller, W. G. 1905. The occasional clinical resemblance between caries of the vertebrae and lumbothoracic syringomyelia and the location within the spinal cord of the fibres for the sensations of pain and temperature. Univ. Pennsylvania Med. Bull. 18, 147–154.

Spiller, W. G. and Martin, E. 1912. The treatment of persistent pain of organic origin in the lower part of the body by division of the anterolateral column of the spinal cord. JAMA 58, 1489–1490.

Sugiura, Y., Terui, N., and Hossoya, Y. 1989. Difference in distribution of central terminals between visceral and somatic unmyelinated (C) primary afferent fibers. J. Neurophysiol. 62, 834–840.

Tattersall, J. E., Cervero, F., and Lumb, B. M. 1986. Effects of reversible spinalization on the visceral input to viscerosomatic neurons in the lower thoracic spinal cord of the cat. J. Neurophysiol. 56, 785–796.

Todd, A. J., McGill, M. M., and Shehab, S. A. 2000. Neurokinin 1 receptor expression by neurons in laminae I, III and IV of the rat spinal dorsal horn that project to the brainstem. Eur. J. Neurosci. 12, 689–700.

Wang, C. C., Willis, W. D., and Westlund, K. N. 1999. Ascending projections from the central, visceral processing region of the spinal cord: a PHHA-L study in rats. J. Comp. Neurol. 415, 341–367.

Willis, W. D. and Coggeshall, R. E. 2004. Sensory Mechanisms of the Spinal Cord, 3rd edn. Kluwer Academic/Plenum.

Willis, W. D. and Westlund, K. N. 1997. Neuroanatomy of the pain system and of the pathways that modulate pain. J. Clin. Neurophysiol. 14, 2–31.

Willis, W. D., Al-Chaer, E. D., Quast, M. J., and Westlund, K. N. 1999. A visceral pain pathway in the dorsal column of the spinal cord. Proc. Natl. Acad. Sci. U. S. A. 96, 7675–7679.

Zhang, X., Gokin, A. P., and Giesler, G. J. 2002. Responses of spinohypothalamic tract neurons in the thoracic spinal cord of rats to somatic stimuli and to graded distention of the bile duct. Somatosens. Mot. Res. 19, 5–17.

Zhuo, M. and Gebhart, G. F. 2002. Facilitation and attenuation of a visceral nociceptive reflex from the rostroventral medulla in the rat. Gastroenterology 122, 1007–1019.

5.37 Visceral Pain

G F Gebhart and K Bielefeldt, University of Pittsburgh, Pittsburgh, PA, USA

© 2008 Elsevier Inc. All rights reserved.

5.37.1	**Introduction**	543
5.37.2	**Visceral Sensation**	544
5.37.2.1	Organization of Visceral Sensory Innervation	545
5.37.2.2	Visceral Nociceptors and Sensory Endings	545
5.37.2.3	Chemical Character of Visceral Sensory Neurons	547
5.37.2.4	Central Organization of Visceral Pain	549
5.37.2.4.1	Vagus nerves	549
5.37.2.4.2	Spinal nerves	549
5.37.2.4.3	Spinal pathways and supraspinal terminations	550
5.37.3	**Functional Basis of Visceral Pain**	551
5.37.3.1	Visceral Mechanoreceptors and Mechano-Nociceptors	552
5.37.3.1.1	Afferent fiber recordings	552
5.37.3.1.2	Information acquired in vitro	553
5.37.3.1.3	Gene deletions, visceral pain, and mechanosensation	556
5.37.3.2	Sleeping (Silent) Nociceptors	557
5.37.3.3	Visceral Chemo-Nociception	558
5.37.4	**Visceral Hypersensitivity**	559
5.37.4.1	Sensitization and Excitability of Visceral Nociceptors	560
5.37.4.2	Central Sensitization	561
5.37.4.3	Central Modulation of Visceral Pain	563
5.37.5	**Summary**	564
References		565

Glossary

referred visceral pain Visceral pain is not generally felt at the source, but rather is perceived as arising from other tissues (skin and/or muscle) innervated by non-visceral nerves having input onto second-order spinal neurons that converges with input from visceral organs onto the same spinal neurons. Accordingly, visceral pain is commonly referred (or transferred, an older terminology) to non-visceral tissues.

nociceptor sensitization Sensitization of nociceptors reflects a change in their excitability expressed as an increase in response magnitude to a noxious intensity of stimulation accompanied by a reduction in threshold stimulus intensity required to activate the nociceptor.

visceral nociceptors Sensory endings in viscera which, when activated by an adequate stimulus (stretch/tension, ischemia, inflammatory mediators), commonly give rise to sensations of discomfort and pain.

visceral hypersensitivity Increased sensitivity or response to a visceral stimulus, which can arise from sensitization of visceral sensory endings (e.g., visceral mechanoreceptors), sensitization of central nervous system neurons receiving increased input from sensitized visceral sensory endings, or a combination of both. Clinically, visceral hypersensitivity is associated with discomfort or pain produced by normally non-pain-producing stimuli (e.g., ingestion of food, normal bladder fillling) and commonly includes increased sensitivity to probing in the areas of referred visceral sensation, which moreover are increased in size (area).

5.37.1 Introduction

Of all possible sources of pain within the body, pain arising from internal organs commonly generates the greatest autonomic and emotional responses. This is linked to several characteristics of visceral pain, the most apparent being that the source of pain is neither visible nor typically felt at the source. Visceral pain also is commonly diffuse in character and poorly localized. In addition, it is also referred (or transferred) to nonvisceral, somatic structures (like skin and muscle), and there is considerable overlap in areas of referred pain from adjacent organs. For example, sites of referral from thoracic and abdominal organs (esophagus, gallbladder, and heart) overlap, making it difficult for both physicians and patients to determine the source of pain. That diffuse substernal chest pain has high emotional valence is readily appreciated, given the potential significance of such pain. Similarly, pelvic genitourinary organs have overlapping patterns of referral with the distal colon. It is also characteristic of visceral pain that the areas of referred sensation increase in size and sensitivity in organ inflammation and disease. For example, repetitive episodes of angina lead to increased tenderness (hyperalgesia) of chest and shoulder skin and abdominal tenderness spreads and increases in area in interstitial cystitis and irritable bowel syndrome (IBS).

Distinct from cutaneous, muscle, or joint pain, tissue-damaging stimuli do not commonly produce pain when applied to the viscera. Tissue crushing, cutting, or burning stimuli applied to visceral tissue generally produce little conscious sensation and rarely produce pain. Instead, stretch of the smooth muscle layers of hollow organs (e.g., by distension), traction on the mesentery, ischemia, and inflammation are more reliably uncomfortable or pain-producing in viscera. The bases of the above attributes of visceral pain and unique features that distinguish visceral from nonvisceral pain are the focus of this chapter.

5.37.2 Visceral Sensation

The viscera are invested with a wide range of sensory receptors, although when activated in healthy organs they do not generally give rise to conscious sensation. This raises the issue of whether these neurons are afferent or sensory, which is considered below in Section 5.37.3. We are generally unaware of movement of air in and out of the lungs, blood flowing through vessels, beating of the heart, or food in the stomach despite the fact that sensory receptors in the bronchial tree, lungs, vessels, heart, esophagus, and stomach are activated by these events. Information from activation of visceral sensory neurons is faithfully transmitted to the central nervous system, but rarely is perceived. Rather, activation of most visceral sensory receptors plays important roles in the regulation and maintenance of many essential functions (e.g., respiration, blood flow, food digestion), which requires rapid feedback to adjust to changes in demand due to exertion, food intake or other activities. While autonomic functions associated with the visceral afferent innervation can influence affective and cognitive processes and are, in turn, influenced by affective and cognitive processes, most of the afferent input from the viscera never reaches consciousness.

Visceral events, of course, do lead to conscious sensations. Under physiological conditions, humans perceive a sense of fullness related to organs involved in food intake (i.e., stomach) or waste elimination (rectum and bladder). Aside from these sensations related to functions that trigger intentional changes in behavior, most consciously perceived input from the viscera carries negative connotations, such as nausea, palpitation, dyspnea, discomfort (e.g., overfilling, gas, bloating), and pain. Normally, visceral pain is infrequent, but in cases of functional gastrointestinal disorders (e.g., nonulcer dyspepsia, IBS (see Chapter Irritable Bowel Syndrome), noncardiac chest pain, functional abdominal pain syndrome), interstitial cystitis/painful bladder syndrome, inflammatory visceral disorders (e.g., pancreatitis, inflammatory bowel disease), neoplasias, etc., discomfort and pain are common, persistent, and typically difficult to treat.

The so-called functional visceral disorders are characterized by pain and discomfort and enhanced sensitivity to stimuli in the absence of a demonstrable organic cause (i.e., there are no apparent structural, biochemical, or inflammatory conditions to explain the symptoms). Such functional disorders constitute a significant socioeconomic burden worldwide; the estimated prevalence of abdominal pain syndromes can range widely for different specific syndromes, but prevalence rates typically range between 22% and 28% of the adult population (Halder, S. L. and Locke, G. R., 2007). Characteristically, these and other visceral disorders are characterized by hypersensitivity, meaning

that normally non-pain-producing visceral events are perceived as uncomfortable or painful, which is likely contributed to by both peripheral and central nervous system mechanisms.

5.37.2.1 Organization of Visceral Sensory Innervation

The viscera are unique among all tissues in the body. Each internal organ is innervated by two nerves, which share some functions, but are not physiologically redundant and include important functional distinctions. Anatomically, the visceral sensory innervation is physically associated with the sympathetic and parasympathetic divisions of the autonomic nervous system. Correspondingly, Langley J. N. (1921) termed visceral afferent fibers associated with sympathetic nerves afferent sympathetic fibers. This sometimes confusing nomenclature has been replaced by use of the name of the nerve (e.g., inferior cardiac, lumbar splanchnic, pelvic), which in addition avoids assigning putative function(s) to the visceral innervation. Given the physical association of the visceral innervation with the autonomic nervous system, visceral afferent fibers are thus contained in nerves that terminate in the spinal cord (spinal nerves) or in the brainstem (vagus nerves).

The bilateral vagus nerves are perhaps the most widely distributed nerves in the body. They innervate most internal organs, including all of the thoracic viscera (proximal esophagus, heart, bronchopulmonary system), most of the abdominal viscera (distal esophagus, stomach, small and proximal large intestines, liver, pancreas, etc.), and some of the pelvic viscera. The vagus nerves are mixed and contain both efferent and afferent axons, but most axons in the vagus nerves ($\geq$80%) are sensory (afferent) fibers and the remainder parasympathetic efferents. The nodose (primarily) and smaller, rostrally located jugular ganglia contain the cell bodies of vagal afferent fibers, most of which terminate bilaterally with some viscerotopic organization in the medullary brainstem nuclei of the solitary tract (NTS). Some vagal afferents, at least in nonhuman primates and rats, project to the upper cervical spinal cord (C1–2), where they may contribute to referred sensations and modulate nociceptive processing within the spinal cord (Foreman, R., 1999).

The cell bodies of spinal afferents innervating the viscera are located bilaterally in dorsal root ganglia (DRG) from the cervical to sacral spinal cord. As mentioned above, their axons travel with sympathetic efferent fibers (except for the pelvic nerves) and, thus, traverse pre- and paravertebral ganglia *en route* to the spinal cord (Figure 1). In prevertebral ganglia, some afferent axons give rise to collateral branches that synapse on intraganglionic neurons and influence organ function (e.g., motility, secretion).

5.37.2.2 Visceral Nociceptors and Sensory Endings

Because tissue-damaging crushing, cutting, or burning stimuli that generate pain from skin do not commonly produce pain when applied to the viscera, it was long argued that the viscera were not innervated, and when visceral innervation was established, it was argued that the viscera were insensate. It is now well established that stimuli adequate for activation of visceral nociceptors differ from those adequate for activation of cutaneous nociceptors. They include distension of hollow organs, traction on the mesentery, ischemia, and inflammation. For example, experimental hollow organ distension reproduces in patients the localization, intensity, and quality of sensations associated with their visceral disorder. Because distension of hollow organs, as well as traction on the mesentery, are mechanical events (stretch), it is assumed that many visceral nociceptors are mechanoreceptors with receptive endings in visceral smooth muscle layers or serosa where they transduce the mechanical energy of tension/stretch into electrical activity (nerve membrane depolarization, action potentials). There are chemo-nociceptors in epithelial and subepithelial layers of visceral organs, but they have not been studied as extensively as have mechanoreceptors and their receptive endings have not been identified as they have for some mechanoreceptors.

Virtually all visceral sensory neuron axons are slowly conducting, thinly myelinated Aδ- or unmyelinated C-fibers. Because mechanical events are common in most organs, visceral mechanosensation and endings in muscle layers of hollow organs that respond to tension/stretch have been the focus of most studies. Unfortunately, the morphology of spinal nerve peripheral terminals in organs is virtually unknown; they are assumed to be free without structural specialization. However, two morphologically distinct endings associated principally with vagal afferent endings have been described. Intraganglionic laminar endings (IGLEs), which have been shown to be mechanosensitive, and intramuscular arrays (IMAs) are located in the upper gastrointestinal tract (Zagorodnyuk, V. P. and

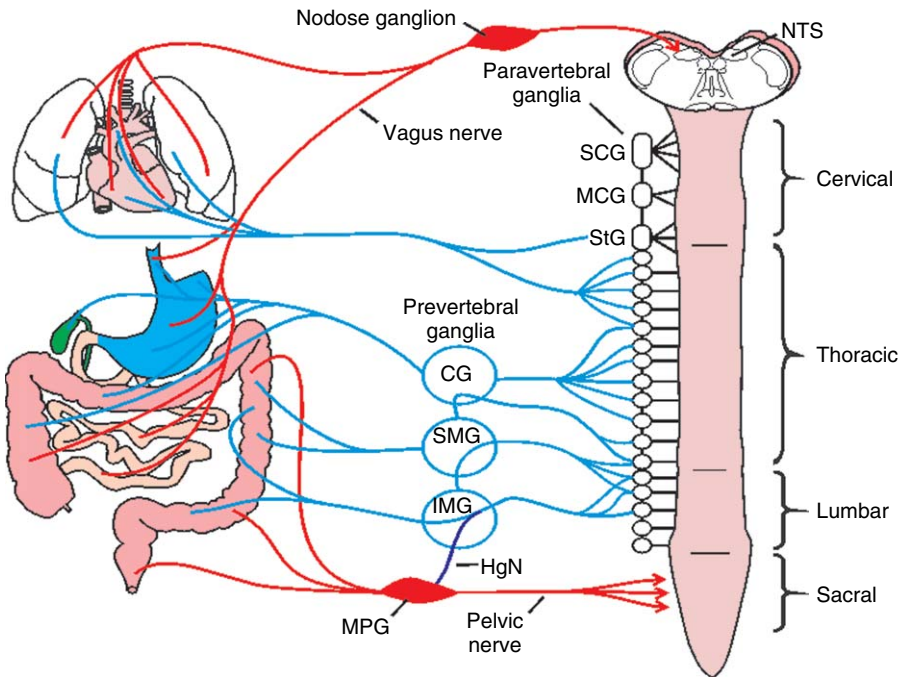

Figure 1 Cartoon illustrating innervation of the viscera. The vagus nerve innervates organs in the thoracic and abdominal cavities. Visceral afferent nerves that terminate in the spinal cord also innervate organs in the thoracic and abdominal cavities as well as those in the pelvic floor, including the genitalia (not shown). The cell bodies of vagal sensory neurons are contained in the nodose and jugular (not shown) ganglia with central terminations bilaterally in the nucleus tractus solitarii (NTS). The cell bodies of spinal visceral sensory neurons are contained in dorsal root ganglia interposed between the paravertebral ganglia (the sympathetic chain) and the spinal cord and are not illustrated in this cartoon. CG, coeliac ganglion; HgN, hypogastric nerve; IMG and SMG, inferior and superior mesenteric ganglia, respectively; MPG, major pelvic ganglion. SCG, superior cervical ganglia; MCG, middle cervical ganglia; StG, stellate cervical ganglia.

Brookes, S. J. H., 2000; Zagorodnyuk, V. P. *et al.*, 2003). As their name indicates, vagal IGLEs appear as branching endings surrounding neurons within a ganglion of the myenteric plexus (Phillips, R. J. and Powley, T. L., 2000; Powley, T. L. and Phillips, R. J., 2002). IGLEs associated with vagal afferent terminals are present throughout much of the gastrointestinal tract, but are most densely distributed in the esophagus, stomach, and duodenum (Wang, F. B. and Powley, T. L., 2000). Like IGLEs, IMAs are also thought to be mechanosensitive, but differ in morphology and distribution from IGLEs. IMAs are long arrays of terminals, typically running parallel with each other and parallel to the orientation of smooth muscle cells. They bridge between the parallel terminals within one of the muscle layers of an organ and form a lattice-like network. IMA distribution within the gastrointestinal tract is more restricted than that of IGLEs; IMAs associated with vagal afferent terminals are present in the stomach (cardia) and sphincters of the upper gastrointestinal tract and are uncommon in the intestines. Although terminal end organs have not been described for visceral spinal nerves, an IGLE-like low threshold, slowly adapting mechanoreceptor has been reported in the colonic and rectal innervation of the guinea-pig (Lynn, P. A. *et al.*, 2003).

Whether activation of either IGLEs or IMAs give rise to visceral pain is uncertain because it would appear, based on their essentially proximal and distal distribution within the gastrointestinal tract and low response threshold, that neither are particularly well suited to that function. Powley T. L. and Phillips R. J. (2002) have speculated that IGLEs detect rhythmic motor activity, which requires response to muscle/organ tension; IMAs also respond to muscle/organ stretch. However, the association of IMAs with sphincters, and because IGLEs and IMAs have heretofore been best described and characterized in association with vagal afferent endings, suggests a role for these mechanosensors in normal physiological processes (e.g., food intake, defecation) rather than nociception. Recent studies suggest that varicose branch points of spinal afferents within the serosa or deeper layers of the gastrointestinal tract

may correspond to fibers activated by high-intensity, noxious mechanical stimuli (Blackshaw, L. A. *et al.*, 2007).

5.37.2.3 Chemical Character of Visceral Sensory Neurons

During ontogeny, sensory neurons develop different phenotypes dependent on their differential sensitivity and exposure to growth factors. As mentioned above, essentially all visceral sensory neurons have unmyelinated or thinly myelinated axons. In DRG, this population of sensory neurons can be separated into two largely distinct groups based on the expression of growth factor receptors or other neurochemical markers (Molliver, D. C. *et al.*, 1997). Small-diameter peptide-containing DRG neurons express the high-affinity receptor for nerve growth factor trkA, the temperature-, proton-, and capsaicin-sensitive transient receptor potential vanilloid ion channel (TRPV)1 and the neuropeptides substance P and/or calcitonin gene-related peptide (CGRP). The second group of small-diameter DRG cells depends on glial cell line-derived neurotrophic factor (GDNF) during embryonic development, binds the plant lectin isolectin B4 (IB4) and releases neurotransmitters such as adenosine triphosphate (ATP) rather than peptides as transmitters. Immuno- histochemical studies have consistently shown that about 80% of visceral sensory neurons within the DRG are peptidergic and contain CGRP or substance P. Visceral sensory neurons in the placode-derived nodose ganglia, however, depend on different growth factors during development and show a different distribution of neurochemical markers. While the expression of neuropeptides CGRP and/or substance P is closely associated with the presence of TRPV1 channels in DRG neurons, this does not hold for nodose ganglion neurons; less than 10% express neuropeptides CGRP or substance P, whereas about 50% of nodose neurons exhibit TRPV1-like immunoreactivity.

In studies of cutaneous or muscle sensory neurons, expression of TRPV1, CGRP, or the presence of IB4 binding are often used as surrogate markers to classify neurons as nociceptive. As discussed below, 70–80% of mechanosensitive spinal afferents innervating abdominal or pelvic viscera are activated by innocuous intensities of stimulation (i.e., are low-threshold mechanosensors). Most studies of mechanosensitive vagal afferents, however, reveal an even more homogeneous response profile; high-threshold mechanosensitive fibers are rarely found. Thus, peptide expression is a poor predictor of physiological properties of visceral sensory neurons, arguing against the use of neurochemical content as a surrogate indicator of function.

Subsequent studies have established by immunohistochemistry, *in situ* hybridization, and/or current or voltage response to ligands applied directly to cell soma that some visceral sensory neurons also contain other peptides (e.g., vasoactive intestinal polypeptide, cholecystokinin) and express ligand-gated channels and receptors (e.g., different members of the family of transient receptor potential channels, including TRPV1, acid-sensing ion channels (ASICs), both ionotropic and metabotropic glutamate, purinergic, serotoninergic, γ-aminobutyric acid (GABA)-ergic, and opioid receptors). As information continues to accumulate, it is apparent that there is no marker at present that distinguishes visceral sensory neurons from nonvisceral sensory neurons or visceral nociceptors from nonnociceptors.

It could be argued that visceral sensory neuron terminals are generally exposed to a richer chemical milieu than other sensory neurons (and thus express a wider array of receptors and channels, although this has not been quantified). The environments in which visceral sensory endings reside include exposure to acids, digestive enzymes, hormones, nutrients, toxins (ingested or secreted by gut flora, for example), metabolites of xenobiotics, and bioactive chemicals released from nearby enteric nervous system neurons, sympathetic nerve terminals, epithelial cells like enterochromaffin cells in the gut, and urothelial cells in the urinary bladder and mast cells. Visceral sensory neurons have been shown to respond to products released in these environments, including protons, norepinephrine, serotonin, histamine, tryptase, ghrelin, cholecystokinin, and other gastric and duodenal secretions that initiate digestion and motility.

In the gastrointestinal tract, serotonin plays an especially important role as a signaling molecule. More than 90% of the body's serotonin is found within the intestine with most stored in secretory granules on the basolateral side of enteroendocrine cells. These enteroendocrine cells are specialized epithelial cells that can release into the lamina propria a variety of mediators, including serotonin, upon mechanical or chemical stimulation, which secondarily activate extrinsic and intrinsic sensory neurons. Interestingly, the number of enteroendocrine cells increases after intestinal inflammation and remains

elevated in patients with continuing complaints despite resolution of the inciting infection (Spiller, R. C. *et al.*, 2000), suggesting that serotonin release from enteroendocrine cells is important in the pathogenesis of functional bowel disorders.

An example illustrating the importance of luminal factors within the gastrointestinal tract is the interaction between the PAR_2 receptor and the pancreatic enzyme trypsin, which is especially relevant under pathologic conditions. The PAR_2 receptor is a member of the proteinase-activated receptor (PAR) family, a group of G-protein-coupled receptors characterized by a tethered peptide–ligand that is part of the molecule and can activate the receptor once cleaved from the molecule by specific proteases. The pancreatic protease trypsin is one of the endogenous proteases that cleaves the ligand and thus activates the receptor. Pancreatic acinar cells secrete precursor forms of proteolytic enzymes, such as trypsin, that require activation within the lumen of the small intestine. During pancreatitis, however, activated trypsin is also present in the pancreatic duct and parenchyma. Experimental infusion of trypsin into the pancreatic duct activates pancreatic sensory neurons, most of which express PAR_2 immunoreactivity, and triggers aversive behavior in animals. Selective experimental activation of PAR_2 receptors mimics this effect, suggesting an important role of PAR_2 in pain during acute pancreatitis (Hoogerwerf, W. A. *et al.*, 2001; 2004). Similarly, mouse colon sensory neurons contain immunoreactivity for the PAR_2 receptor and PAR_2 agonists depolarize those neurons and cause a sustained hyperexcitability (Ahmed, K. *et al.*, 2007). Relevant to IBS, biopsy samples from IBS patients release greater amounts of proteases than do samples from controls (Cenac, N. *et al.*, 2007). Supernatants from colonic biopsies of IBS patients produce visceral hypersensitivity when given intracolonically in control, but not PAR_2 knockout mice. Mast cells, which are closely associated with nerves in the human gastrointestinal mucosa (Stead, R. H. *et al.*, 1989), are also a source of tryptase as well as other potential mediators and modulators of visceral sensation (Bueno, L. *et al.*, 1997; Barbara, G. *et al.*, 2006). Mucosal biopsies from IBS patients contained mediators that increased activity in rat mesenteric afferents, an effect inhibited by histamine H_1 receptor blockade and serine protease inactivation (Barbara, G. *et al.*, 2007).

In the airway system, similarly specialized cells have been identified within the epithelium of the intrapulmonary bronchial tree. Based on their ultrastructural and neurochemical characteristics with large, dense core vesicles and neuropeptide expression, they are referred to as neuroendocrine cells or neuroendocrine bodies when clustered in small groups (Cutz, E., 1982). Histological studies combining immunohistochemistry, retrograde labeling, and/or vagotomy reveal a complex innervation with vagal and spinal afferents projecting to these cells or cell clusters, where nerve terminals branch with formation of varicosities at branch points (Adriaensen, D. I. *et al.*, 2003). Neuroepithelial bodies likely function as oxygen sensors within the airways as hypoxia inhibits potassium currents (Fu, X. W. *et al.*, 2000). However, acute allergic inflammation triggers depletion of peptides from airway neuroepithelial cells, suggesting a role in broader signaling under physiologic and pathophysiologic conditions (Dakhama, A. *et al.*, 2002).

While the expression of one or another receptor or ligand-gated channel of a particular subunit composition may be determined at some future time to identify all or a subset of visceral sensory neurons, one feature of visceral sensory neurons may distinguish them from nonvisceral counterparts, and that is cell size. Cutaneous nociceptors are on the whole associated with thinly myelinated and unmyelinated axons and it is generally the case that these nociceptors have small-diameter cell bodies (e.g., $\leq$15–20 μm). Virtually all visceral sensory neurons have thinly myelinated or unmyelinated axons, yet their cell bodies tend to be medium in size (e.g., $\geq$25 μm in diameter), at least those associated with the gastrointestinal tract and urinary bladder. This is of importance when nociceptors are studied and identified principally on the basis of cell diameter because visceral nociceptors are not generally contained in the population of small-diameter sensory neurons assumed to be nociceptors solely because of small diameter.

The foregoing addresses, at least indirectly, identification of and assignment of function of sensory neurons, including visceral sensory neurons, based on different properties of the cells: size (diameter), cell content (e.g., peptides), expression of one or another channel or receptor, dependence on exposure during development to different growth factors. Assignment of function based upon one or more of these properties is unfortunately relatively common in the literature, and is both confusing to nondiscriminating readers and misleading. It is not possible at present to assign function (e.g., nociceptor) to a sensory neuron based on any of the above properties. As discussed

below, nociceptors, including visceral nociceptors, are defined by response to an adequate stimulus, and even then assignment of function can be difficult, if not contentious, if the quality of the stimulus is uncertain, unknown or of limited physiologic relevance, such as punctate stimulation of viscera.

5.37.2.4 Central Organization of Visceral Pain

5.37.2.4.1 Vagus nerves

Although they extensively innervate the viscera, the vagus nerves are generally considered not to play a role in nociception. However, they may contribute to the complex sensory experience of visceral pain, which includes strong autonomic reactions, including nausea or dyspnea. Vagal afferents project to the bilaterally located nuclei of the solitary tract in the dorsal medulla, an important relay station for visceral input. Vagal input reaches more rostral brain structures involved in autonomic regulation, such as the hypothalamus, supraoptic nucleus, and – via the parabrachial nucleus and ventro-medial thalamus – the insular cortex, anterior cingulate cortex, and amygdala, regions that play a role the regulation of affective responses to different stimuli including pain.

5.37.2.4.2 Spinal nerves

Because vagotomy was found to be generally ineffective in relieving visceral pain, whereas spinal nerve transaction or destruction of sympathetic prevertebral ganglia often provided pain relief (at least for a limited period of time), the spinal visceral nerves (sympathetic afferents) were inferred to be the conveyors of nociceptive information from the organs to the spinal cord. Their termination in the spinal cord is noteworthy on several counts. Firstly, spinal visceral afferent fibers terminate in a pattern that largely overlaps with terminations of cutaneous nociceptors: superficial layers of the spinal dorsal horn, deeper in lamina V and dorsal to the central canal, an area often referred to as lamina X. Visceral afferent fibers also terminate within the interomediolateral cell column/sacral parasympathetic nucleus where afferent input influences efferent output back to the same as well as to other organs (Figure 2). Secondly, spinal visceral afferents represent less than 10%, and probably closer to 5%, of the total afferent input into the spinal cord from all tissues. In compensation for this relatively sparse input, the central projection of a single visceral afferent fiber bifurcates at its spinal segment of entry in the dorsal root into caudally and rostrally directed main branches that can extend in either the dorsal funiculus or Lissauer's tract for two or three spinal segments before penetrating the spinal dorsal horn. In addition, during their longitudinal journey these main branches give off multiple collateral branches into the spinal dorsal horn (superficial laminae and laminae V and X, including contralateral laminae V and X) where, moreover, their number of terminal swellings are greater than found on cutaneous C-fiber

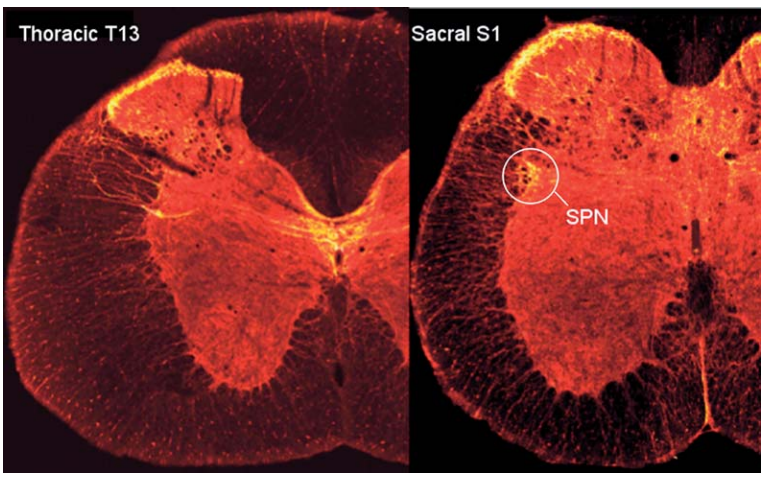

Figure 2 Distribution of visceral afferent terminals in the thoracic and sacral spinal cord. Photomicrographs illustrate internalization of the substance P receptor (yellow) in the superficial dorsal horn and area dorsal to the central canal in rat T13 and S1 spinal cord sections. Internalization of the substance P receptor was produced by distension of the colon in the rat (Honoré, P., Kamp, E. H., Rogers, S. D., Gebhart, G. F., and Mantyh, P. W. 2002. Activation of lamina I spinal cord neurons that express the substance p receptor in visceral nociception and hyperalgesia. J. Pain 3, 3–11). SPN, sacral parasympathetic nucleus.

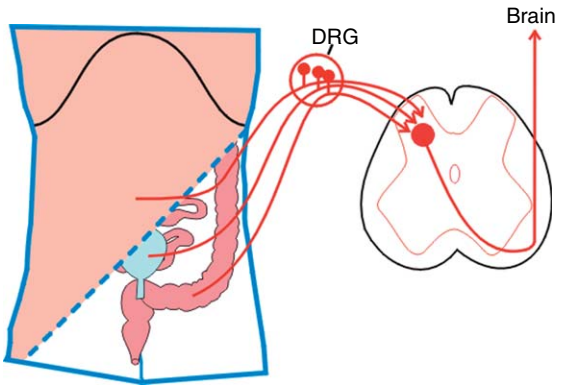

Figure 3 Illustration of viscerosomatic and visceroviscerel convergence of inputs onto a second-order spinal neuron. Illustrated is input from the abdominal skin, urinary bladder, and distal colon onto the same spinal neuron. Activation of the second-order neuron is illustrated here as being conveyed to the brain via the anterolateral ascending pathway; not illustrated is a postsynaptic dorsal column pathway, which also conveys visceral sensory information to the brain. DRG, dorsal root ganglion.

terminations within the spinal dorsal horn (which are typically limited to the spinal segment of entry). These anatomic characteristics of visceral afferent spinal terminations surely contribute to the diffuse nature of visceral pain and difficulty in localizing its source.

A final notable and defining characteristic of spinal visceral input that also contributes to poor localization is convergence. It is a feature of virtually all second-order spinal neurons upon which visceral afferent fibers terminate that convergent inputs from somatic and/or other visceral organs are also received. Typically, a single dorsal horn neuron that receives a visceral input (e.g., from colon) has a convergent cutaneous receptive field and also receives input from another viscus (e.g., urinary bladder, uterus) (Figure 3). Thus, viscerosomatic and visceroviscerel convergence upon second-order spinal neurons is the general rule (rather than the exception), and further compromises localization of visceral inputs.

5.37.2.4.3 Spinal pathways and supraspinal terminations

Spinal visceral afferent input is further transmitted rostrally and distributed widely in the brainstem (largely associated with reflex functions; e.g., micturition), hypothalamus, and thalamus and then to areas of the cerebral cortex where discriminative and affective components of visceral information assumes consciousness and triggers responses/behavior. Interestingly, thalamic and cortical neurons that receive a visceral input also exhibit viscerosomatic and visceroviscerel convergence (e.g., Apkarian, A. *et al.*, 1995) (Figure 4). The ascending pathways in spinal cord white matter that convey visceral information to the brain are contained principally in the anterolateral quadrants of the spinal cord and in the dorsal columns. Thus, there are spinomedullary, spinopontine, spinomesencephalic, spinohypothalamic, and spinothalamic tracts that ascend in the anterolateral quadrant of the spinal cord, predominantly contralateral to the side of input. The postsynaptic dorsal column paths are ipsilateral to the side of input and ascend to the nuclei gracilis and cuneatus in the medulla, where they cross and ascend to the contralateral ventrobasal thalamus (e.g., Palecek, J. *et al.*, 2002). In addition to these principal pathways that convey information to supraspinal sites, there are intraspinal propriospinal pathways that are less well understood and presumably have modulatory functions and another pathway from lamina I neurons to pontine parabrachial nuclei and thence to the amygdala, principally the central nucleus. This latter pathway is believed to specifically convey visceral information of a noxious character to the amygdala, which importantly is associated with anxiety and affective dimensions of pain (Phelps, E. A. and LeDoux, J, E., 2005).

Functional imaging studies have complemented and expanded our appreciation of the central representation of visceral inputs. Although the current spatial resolution of imaging methods has limited ability to study the initial processing of visceral input in the brainstem, reports to date suggest that cutaneous and visceral stimuli activate similar brain regions. Pain-induced anxiety, which tends to be more significant during visceral stimulation, is associated with stronger activation of the midbrain periaqueductal gray (PAG) (Dunckley, P. *et al.*, 2005). Similarly, activation of cortical structures does not show a pattern during visceral pain distinct from somatic pain, with the anterior cingulate cortex (ACC), the anterior insular cortex and – less consistently – the primary and secondary sensory cortices activated by both visceral and somatic pain (Hobson, A. R. and Aziz, Q., 2004). Despite the overall similarity between brain patterns of activation produced by cutaneous and visceral stimuli, subtle differences have emerged. Compared to noxious cutaneous stimulation, visceral pain tends to cause a stronger activation of the ACC and typically activates the

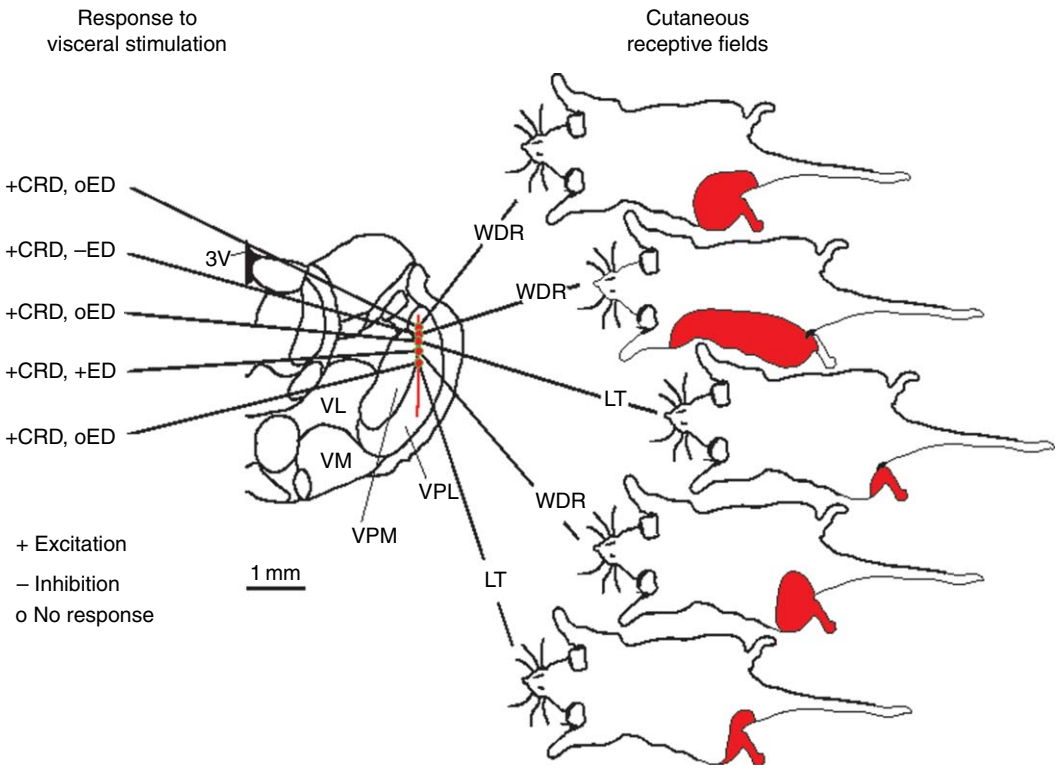

Figure 4 Illustration of viscerosomatic and viscerovisceral convergence onto neurons recorded in the rat thalamus. The vertical tract recording electrode through the ventral posteriolateral (VPL) thalamus illustrates, from top to bottom, cutaneous receptive fields on the right for five sequential thalamic neurons and responses of the same neurons to colorectal distension (CRD) and esophageal distension (ED) on the left. All neurons studied responded to both CRD and either innocuous cutaneous stimulation (identified as low threshold, LT) or both innocuous and noxious cutaneous stimulation (identified as wide dynamic range, WDR). Some neurons were also inhibited, excited or did not respond to ED. From Danzebrink R. M. and Gebhart G. F. (unpublished).

perigenual portion of the ACC, which has been linked to the generally stronger emotional reactions associated with visceral pain (Strigo, I. A. *et al.*, 2003). Interestingly, only the intensity and not the pattern of activation differs between perceived and unperceived (subliminal) visceral stimulus intensities (Sidhu, H. *et al.*, 2004).

5.37.3 Functional Basis of Visceral Pain

Nociceptors are defined by response to a noxious stimulus and their ability to encode suprathreshold stimulus intensities. Sherrington C. S. (1906) defined noxious stimuli as those that damage or threaten damage to skin, and this definition, which has been applied widely to all tissues, is problematic with respect to the viscera because tissue-damaging visceral insult is not reliably pain-producing. Instead, visceral stimuli that reliably generate sensations of discomfort or pain include, as stated previously, hollow organ overdistension, traction on the mesentery, organ ischemia, and organ inflammation, the latter two perhaps acting indirectly to alter the chemical milieu at an afferent receptive ending to increase neuron excitability to other stimuli. Accordingly, tension/stretch (produced by muscle contraction or organ distension, respectively) is an adequate acute noxious visceral stimulus at intensities (e.g., balloon pressures) above threshold for activation of visceral mechano-nociceptors. In experimental studies with humans, verbal reports or various scaling procedures identify distending pressures that are uncomfortable or painful. Concomitant recording of contractile phenomena allows differentiation between stretch (activation of receptor in parallel with muscle cells) and tension (activation of receptors in series with muscle cells). In nonhuman animal experiments, whether the intensity of visceral stimulation is noxious has to be inferred

from autonomic responses, which generally are produced at intensities of stimulation below the noxious threshold, or animal behavior. It is also noteworthy that innervation of the viscera, relative to skin, is sparse and thus spatial summation is important to activation of visceral mechanoreceptors and the production of discomfort or pain. Thus, in nonhuman animals it is necessary to use a distending balloon of sufficient length to produce a change in behavior that can be interpreted as aversive or painful. In the absence of behavioral evidence, the quality of mechanical stimulation is unknown and often difficult to establish as relevant to activation of mechano-nociceptors and visceral pain.

5.37.3.1 Visceral Mechanoreceptors and Mechano-Nociceptors

5.37.3.1.1 Afferent fiber recordings

Obviously, the stomach and temporary storage organs like the urinary bladder and distal colon/rectum experience periodic filling (and emptying), which distends these organs, commonly without generating either discomfort or pain. Mechanosensors in these organs are sensitive to and respond to filling within the physiological range, eventually leading, for example, to an urge to evacuate the bladder or bowel. Consistent with these sensations and functions produced by organ filling, most mechanosensitive afferent fibers contained in the nerves innervating these organs have low thresholds for response. The proportion of low-threshold mechanosensitive endings in spinal nerves innervating the stomach, esophagus, and gallbladder (splanchnic nerves) and the urinary bladder, uterus, and distal colon (pelvic nerves) is 70–80%, and this has been a generally consistent finding across species (cat, chicken, ferret, guinea-pig, mouse, opossum, and rat). The remaining 20–30% of afferent fibers have high thresholds for response, typically $\geq$30 mm Hg distending pressure, which corresponds very well to colon distending pressures in rats that produce behavior leading to avoidance of the stimulus. Because high-threshold mechanoreceptors in the viscera respond only to intensities of stimulation in the noxious range and encode the intensity of suprathreshold stimuli, they fulfill requirements as nociceptors and are considered to be mechano-nociceptors that signal acute visceral pain.

Unlike low-threshold cutaneous mechanoreceptors, which when activated give rise to sensation (e.g., movement of a hair follicle, movement of a cotton wisp across the skin), low-threshold visceral mechanoreceptors when activated within the physiological range of intensities generally produce no conscious sensation, but rather contribute to autonomic regulation of organ function. It has been suggested consequently that these receptors and associated axons are not sensory, but rather afferent. However, low-threshold visceral mechanoreceptors possess the uncommon attribute of continuing to respond, if not also to encode, stimulus intensity well into the noxious range. Thus, their activation at some (high) intensity of stimulation can lead to sensations perceived as uncomfortable or painful. The afferent–sensory function of visceral nerves was appreciated by Sherrington C. S. (1900), who commented that activation of visceral nerves rarely resulted in conscious sensations (i.e., an afferent function), but when sensation was produced it was typically pain (i.e., a sensory function). In all visceral nerves studied, including gastric vagal afferent fibers, low-threshold mechanosensitive afferents, when tested with high-intensity stimuli, respond vigorously and typically at a rate (frequency) greater than their high-threshold mechano-nociceptor counterparts (Figure 5). Clearly, as stimulus intensity increases, high-threshold mechano-nociceptors are also activated and it can be argued that uncomfortable or painful sensation arises from their activation. Their contribution is undeniable in acute visceral pain, but low-threshold mechanoreceptors (like their high-threshold counterparts) also possess the ability to be sensitized (see below and Figure 5), a quality commonly associated only with nociceptors. Accordingly, it is likely that both low- and high-threshold mechanoreceptors in hollow organs contribute to sensations of discomfort and pain in functional gastrointestinal (nonulcer dyspepsia, IBS) and urinary bladder (interstitial cystitis/painful bladder syndrome) disorders as well as in ischemia, inflammation, or neoplastic diseases associated with visceral pain. Consistent with this interpretation, psychophysical experiments in human volunteers have demonstrated that pharmacologic modulation of sensory function similarly shift thresholds for nonpainful and painful sensations (Vandenberghe, J. *et al.*, 2005).

There are two additional features of low- and high-threshold mechanosensitive endings in viscera that suggest their functions are not always or easily separable. First, both respond to either or both chemical and thermal stimuli in addition to mechanical stimulation (the usual experimental search stimulus). That is, they are polymodal and virtually all mechanosensitive endings when tested have been found to respond also to a

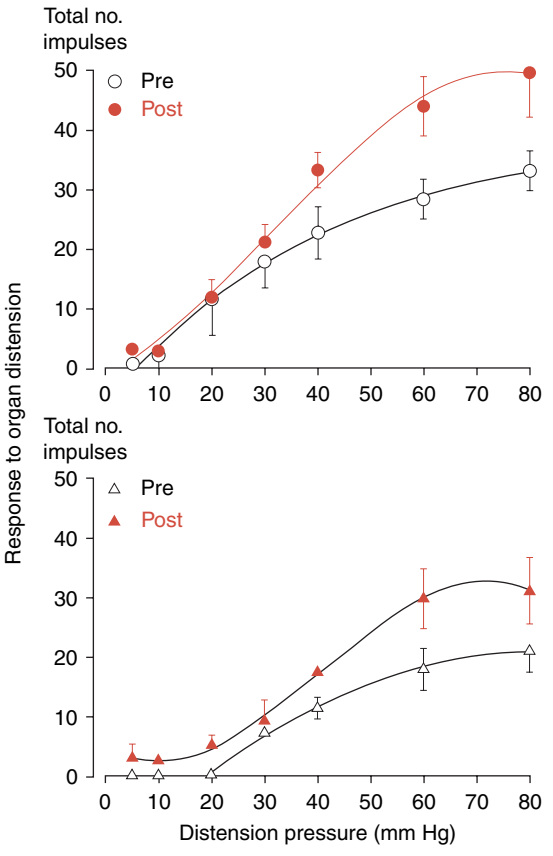

Figure 5 Stimulus–response functions for low-threshold (top) and high-threshold (bottom) mechanosensitive pelvic nerve fibers innervating the urinary bladder of the rat. Before bladder irritation, high-threshold fibers first responded at 30 mm Hg bladder distension and then encoded distending pressure throughout the range of pressures tested. In contrast, low-threshold fibers begin to respond at physiologic distending pressures, but also encoded distending pressures throughout the ranges of pressures tested. Note that response magnitude of low-threshold fibers is greater than for high-threshold fibers at all intensities of bladder distension. Note also that response magnitude increases significantly for both low- and high-threshold fibers after bladder irritation and response threshold for high-threshold fibers decreases significantly into the physiologic range (i.e., both low- and high-threshold mechanosensitive fibers sensitize). Reproduced from Su, X., Sengupta, J. N., and Gebhart, G. F. 1997. Effects of opioids on mechanosensitive pelvic nerve afferent fibers innervating the urinary bladder of the rat. J. Neurophysiol. 77, 1566–1580, used with permission from the American Physiological Society.

chemical and/or to a thermal stimulus. A considerable literature has established the sensitivity of visceral afferents in both the vagal and spinal innervations to chemical stimuli (principally hormones and putative mediators as well as nutrients that may act directly or indirectly through enteroendocrine cells). Whether such chemosensitive endings, typically studied in the mucosal surfaces of the gastrointestinal tract, are also mechano- or thermosensitive has not been systematically examined, although when examined mechanosensitivity is commonly noted. If specific and selective visceral chemosensors without mechanosensitivity exist, which is very likely the case, the argument that both low- and high-threshold polymodal mechanosensors can contribute to discomfort and pain is strengthened. Secondly, low- and high-threshold mechanoreceptors cannot be distinguished on the basis of fiber type (Aδ or C), size or content of cell soma, or pharmacologically (e.g., sensitivity to chemical or inflammatory mediators).

5.37.3.1.2 *Information acquired* in vitro

In addition to mechanoreceptor characteristics described above, in which afferent fibers were studied while distending intact hollow organs or occluding vessels, *in vitro* studies of visceral organs, typically opened and pinned flat in a dish with nerves attached, provide different information (Figure 6). For example, receptive endings in the organ can be readily localized by response to applied mechanical stimuli and the endings can be further isolated experimentally and subjected directly to chemical and thermal stimuli. Esophagus, stomach, small bowel, urinary bladder, uterus, ureter, testes, and colon–rectum all have been studied in this fashion. As above, mechanical search stimuli typically have been used and include brushing/stoking the mucosal surface of the organ to locate receptive endings functionally identified as mucosal, punctuate pressure to identify serosal receptors, and circumferential stretch of the organ to identify muscular stretch receptors. Single-fiber studies in all organs examined to date reveal typical patterns of activation, allowing inferential assignment of mucosal, muscular, and serosal receptive endings. Mucosal receptors respond only to stroking of the mucosal surface and not to stretch/tension, whereas muscular receptors respond to stretch/tension and not stroking the mucosal surface. Finally, only intense punctate stimuli activate serosal receptors. In some organs (e.g., stomach, urinary bladder, and colon) receptive endings that respond to both mucosal stroking and stretch/tension have been found (termed muscular–mucosal endings; Figure 6). It should be noted that these descriptors of receptive endings have not been histologically confirmed and are based solely on responses to mechanical stimuli. Nonetheless, use of *in vitro*

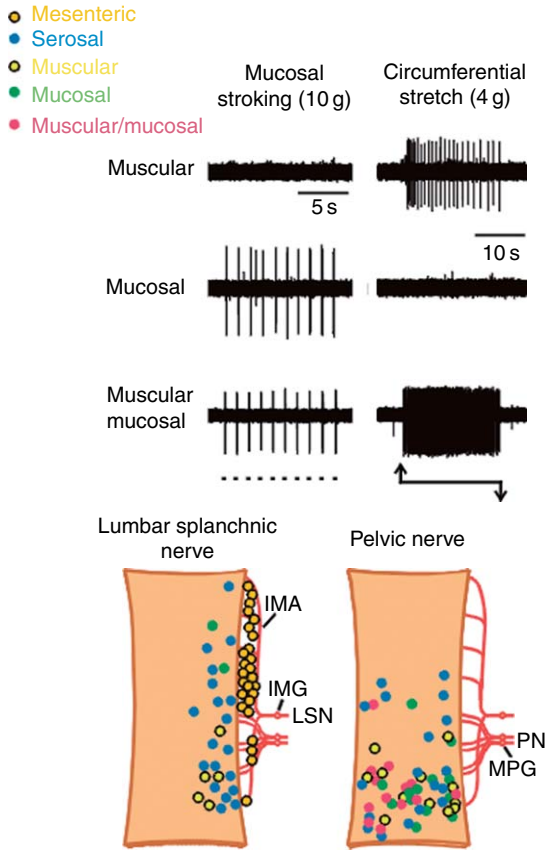

Figure 6 Responses of different types of the mechanosensitive endings innervating the mouse colon. Muscular receptors are illustrated topmost as responding to circumferential stretch of the colon but not stroking of the mucosal surface. Mucosal endings respond to mucosal stroking, but not to stretch, and muscle–mucosal fibers respond to both stroking of the mucosa and circumferential stretch. The application of strokes across the mucosal receptive ending and the duration of stretch are illustrated beneath the recordings. The distribution of receptive endings for the lumbar splanchnic nerve and pelvic nerve innervations of the mouse colon are illustrated bottommost, showing receptive endings located in the mesentery and serosa as well as those associated with muscle, mucosa and muscle-mucosa. IMA, inferior mesenteric artery; IMG, inferior mesenteric ganglion; LSN, lumbar splanchnic nerve; MPG, major pelvic ganglion; PN, pelvic nerve. Adapted from Brierley, S. M., Jones, R. C. W., III, Gebhart, G. F., and Blackshaw, L. A. 2004. Splanchnic and pelvic mechanosensory afferents signal different qualities of colonic stimuli in mice. Gastroenterology 127, 166–178.

organ–nerve preparations has confirmed many of the findings of earlier work and, importantly, has notably expanded our understanding of the contributions of mechanosensitive endings in viscera to presumed functions. For example, in addition to increasing recognition that the vagus nerves are involved in chemo-nociception (see below), there is also evidence for a role of vagal afferents in esophageal mechano-nociception (Yu, S. *et al.*, 2005). Nonnociceptive esophageal tension receptors exhibited saturable responses to esophageal distension, whereas nociceptive Aδ- and C-fiber esophageal vagal afferents discriminated noxious intensities of esophageal distension (and also responded to activators of TRPV1).

Significantly, studies of the two nerves innervating the same organ have been carried out for both the mouse colon and mouse urinary bladder. Although is has long been appreciated that the two nerves innervating an organ execute different functions, comparison of the properties of the two innervations provides new information that could, for example, inform development of therapeutic strategies. In a comparison between the lumbar splanchnic nerve and pelvic nerve innervations of the mouse colon (Brierley, S. M. *et al.*, 2004), most of the colonic receptive endings in the lumbar splanchnic nerve responded to blunt probing and were located along the mesenteric attachment and the serosa (Figure 6). In contrast, no pelvic nerve receptive endings were found in the mesenteric attachment and significantly more receptive endings responded to stretch than in the lumbar splanchnic nerve, including muscular–mucosal endings (which were not found in the lumbar splanchnic innervation). Analysis of response properties of the same receptive endings in the different innervations revealed further differences. Responses to the same intensities of stroking and stretch stimuli were significantly greater in pelvic nerve endings than in lumbar splanchnic counterparts. Overall, the pelvic nerve innervation of the mouse colon contained greater proportions of stretch/tension and mucosal receptors, which moreover generated greater magnitude responses, than the lumbar splanchnic innervation. Similarly, comparison of the lumbar splanchnic nerve and pelvic nerve innervations of the mouse urinary bladder reveals significant differences between the proportions and distribution of types of mechanosensitive receptive endings. As found for the colon, the distribution of lumbar splanchnic receptive endings in urinary bladder was more circumscribed than the distribution of pelvic nerve receptive endings, which again contained an ending (muscular–urothelial) not found in the lumbar splanchnic innervation.

A final means of study of visceral sensory neurons is to study cell soma using patch clamp methodology. These studies do not, of course, permit the type of

functional evaluation derived from single-fiber studies, and instead address aspects of mechanisms and changes in visceral neuron excitability, specifically the differential roles of voltage- or ligand-gated ion channels. Such studies have been carried out in rat stomach (vagal and splanchnic innervations), mouse intestine, mouse colon, rat colon, and rat urinary bladder (lumbar splanchnic and pelvic innervations). Because of low innervation density, the study of visceral sensory neurons requires the injection of retrograde labels into muscle layers of the organ of interest. The uptake and retrograde transport of the label into the soma allows identification of neurons projecting to the organ of interest. Consistent with results obtained *in vivo*, isolated visceral sensory neurons do not generate spontaneous activity. However, cells obtained from animals with experimentally induced inflammation show significant oscillation of the resting membrane potential, resulting in spontaneous action potential discharge, demonstrating an increase in excitability. This increase in excitability is associated with an increase in voltage-sensitive sodium currents, primarily a tetrodotoxin (TTX)-resistant sodium current, and a decrease in voltage-sensitive potassium currents, primarily the transient or A-type current (Yoshimura, N. and deGroat, W. C., 1999; Stewart, T. M. *et al.*, 2003; Dang, K. *et al.*, 2004; Beyak, M. J. and Vanner, S., 2005; Xu, G. *et al.*, 2006).

In addition to voltage-sensitive ion channels, the expression and properties of ligand-gated channels also changes in animal models of visceral pain. Ischemia is the most common cause of cardiac pain, experienced by millions of Americans suffering from coronary artery disease. Tissue acidosis due to accumulation of lactate can activate cardiac afferents and likely triggers ischemic pain. Perhaps consistent with the importance of ischemia as a trigger of visceral pain, a comparison between cardiac sensory neurons and randomly chosen neurons in the same DRG showed that a higher fraction of visceral sensory neurons express ASICs (Benson, C. J. *et al.*, 1999). Experimental injury, such as gastric ulceration, increases the current density of these acid-sensitive currents in visceral sensory neurons (Sugiura, T. *et al.*, 2005), demonstrating that sensitization does not only affect excitability (i.e., the generation of action potentials in response to a given stimulus), but also the signal transduction process (i.e., the depolarization triggered by a mechanical, chemical, or thermal stimulus). Based on the properties of proton-evoked currents, most visceral sensory neurons express different members of the ASIC family of ion channels as well as the vanilloid receptor TRPV1. The preferential expression of TRPV1 in small-diameter, presumably nociceptive neurons raised the question whether it may play a role in visceral pain. A high percentage (60–80%) of mouse and rat colon sensory neurons express TRPV1 (Robinson, D. R. *et al.*, 2004; Christianson, J. A. *et al.*, 2006) and TRPV1 is the principal detector in mouse colon of extracellular acidosis (Sugiura, T. *et al.*, 2007). Serotonin acutely alters TRPV1 function in colon sensory neurons, shifting the temperature-activation curve of this ion channel to normal body temperatures (Sugiura, T. *et al.*, 2004). About 90% of the body's serotonin is found within the gastrointestinal tract, primarily in enterochromaffin cells, and serotonin is released in high concentrations during mucosa stimulation. Studies of patients with functional bowel diseases, such as IBS, suggest changes in serotonin release and/or reuptake within the intestinal mucosa, raising the question whether modulation of TRPV1 function may contribute to the enhanced responses to physiologic stimuli seen in these patients. In addition to modulation by G-protein-coupled receptors, changes in TRPV1 expression have been examined under experimental and clinical conditions. Animal models of visceral inflammation as well as distinct human disorders from gastroesophageal reflux disease, painful bladder syndrome to rectal urgency are associated with increases in TRPV1 expression (e.g., Chan, C. L. H. *et al.*, 2003; Bhat, Y. and Bielefeldt, K., 2006; Mukerji, G. *et al.*, 2006).

Purines, which include ATP and its breakdown products, are released during cell injury and may thus play a role in nociception. Among the families of purinergic receptors, the ligand-gated P2X receptors have attracted special attention because of their role in visceral sensation. As described Chapter Urothelium as a Pain Organ, the bladder epithelium (urothelium) releases ATP during physiologic stimulation, such as stretch. Bladder sensory neurons express P2X receptors and respond to purinergic agonists (Yoshimura, N. *et al.*, 2003; Dang, K. *et al.*, 2005). Cystitis significantly increases the peak current triggered by purinergic agonists, consistent with a potential role of this signaling pathway in causing discomfort and increased micturition frequency, associated with bladder inflammation. Similarly, colon distension in the rat releases ATP in a stimulus-dependent manner, and the release of ATP is increased further after experimental induction of colon inflammation (Wynn, G. *et al.*, 2003; 2004).

Responses to colon distension in the colitis model were attenuated by a purinergic receptor antagonist, suggesting a role for ATP in colon mechanosensory transduction.

5.37.3.1.3 Gene deletions, visceral pain, and mechanosensation

The availability of mice with selected gene deletions (knockout mice) has provided the opportunity to examine the potential role of several molecules in visceral pain. To date, voltage-gated sodium channel ($Na_V1.8$), TRPV1, purinergic receptor (P2X), and ASIC knockout mice have been studied and each molecule has been found to contribute at least in part to responses to noxious visceral stimuli or of visceral mechanoreceptors. As mentioned above, the TTX-resistant sodium current is increased in neurons obtained from animals with gastrointestinal or bladder inflammation. In sensory neurons, TTX-resistant current is largely due to activation of the voltage-gated sodium channel $Na_V1.8$. Genetic deletion of this ion channel in mice is associated with a decrease in aversive behavior in response to intraperitoneal injection of acetic acid (Laird, J. M. *et al.*, 2002), supporting a potential role of $Na_V1.8$ in visceral pain. The pain behavior in this model is also likely contributed to by activation of nonvisceral afferents within the parietal peritoneum. More direct evidence was provided by other studies, one employing transient suppression of TTX-resistant sodium currents in bladder sensory neurons with antisense oligonucleotides, which abolished the increase in micturition frequency seen after acute bladder irritation (Yoshimura, N. *et al.*, 2001), and the other employing $Na_V1.8$ and $Na_V1.9$ knockout mice, which reported that neuron hyperexcitability produced by jejunitis was absent in $Na_V1.8$, but not $Na_V1.9$ knockout mice (Hillsley, K. *et al.*, 2006).

Genetic deletion of functional TRPV1 receptors also leads to changes in visceral function, suggesting a role of TRPV1 in visceral mechanosensation. TRPV1 knockout mice have a higher frequency of nonvoiding bladder contractions (Birder, A. L. *et al.*, 2001). Nerve recordings from mesenteric nerve bundles innervating the small bowel and colonic afferents within the pelvic nerve revealed blunted mechanosensation in TRPV1 knockout mice compared with wild-type controls (Rong, W. *et al.*, 2004; Jones, R. C. W. *et al.*, 2005). Deletion of TRPV1 also altered responses to inflammatory mediators, consistent with a potential role of this ion channel in peripheral sensitization (Jones, R. C. W. *et al.*, 2005). However, biophysical studies have not demonstrated a direct activation of TRPV1 by stretch. Thus, the channel likely alters cellular excitability and enhances responses to different stimulus modalities, including stretch.

As discussed separately in more detail (Chapter Urothelium as a Pain Organ), purinergic receptors play an important role in bladder function. Bladder filling triggers ATP release from urothelial cells, which activates bladder sensory neurons and may trigger reflex micturition. Consistent with this model, P2X3 knockout mice exhibit bladder hyporeflexia (Cockayne, D. A. *et al.*, 2000).

A more complex picture emerges from studies examining the role of different members of the ASIC family in visceral sensation. Genetic deletion of ASIC3 blunts responses to colorectal distension and mechanical stimulation of gastroesophageal afferents in mice, suggesting a role in visceral mechanosensation (Jones, R. C. W. *et al.*, 2005; Page, A. J. *et al.*, 2005). In contrast, deletion of ASIC1a increased mechanosensitivity of gastroesophageal and colonic afferents without affecting cutaneous afferents and deletion of ASIC2 blunted responses of gastroesophageal, but enhanced those of mesenteric afferents in the distal colon (Page, A. J. *et al.*, 2005). ASICs form heteromultimeric channels, leading to speculation that the subunit composition has significant effects on the mechanosensitive properties of visceral sensory neurons (Wemmie, J. *et al.*, 2006). Thus, genetic studies showed that – as is true for cutaneous pain – no single molecule explains the complex phenomenon of pain. Yet, some differences between cutaneous and visceral sensation has emerged, most notably the potential role of TRPV1 and P2X receptors in mechanosensation.

The foregoing studies focused on the initial events triggered by noxious visceral stimulation, namely signal transduction and cellular excitability in primary afferent neurons. Consistent with a role of substance P and neurokinin receptors in synaptic transmission of visceral afferent input within the spinal cord, genetic deletion of neurokinin receptor 1 blunted responses to intraperitoneal injection of acetic acid in mice (Laird, J. M. A. *et al.*, 2000). Despite these findings and preclinical studies with different neurokinin receptor blockers in rodent models of visceral pain, neurokinin antagonists do not appear to be effective when used to treat visceral pain in humans.

The genetic basis for visceral pain has also been addressed in humans. Considering the high

prevalence of functional gastrointestinal disorders in the general population and the expression of pain and discomfort as the primary symptoms, most studies have focused on IBS or nonulcer dyspepsia. As mentioned above, serotonin plays an important role in afferent signaling within the gastrointestinal tract. Mechanical or chemical stimuli can trigger serotonin release from enteroendocrine cells into the lamina propria, where high tissue concentrations activate terminals of both intrinsic and extrinsic primary afferent neurons within the vicinity. Reuptake of serotonin by the high-affinity transporter serotonin transporter (SERT) expressed by epithelial cells terminates this signal. This led to the hypothesis that differences in the properties of SERT may contribute to the pathogenesis of functional gastrointestinal disorders. Consistent with this assumption, deletion of SERT in mice triggers changes in bowel habits with alternating diarrhea and constipation, a common clinical manifestation in patients with IBS (Gershon, M. D. and Tack, J., 2007). Two allelic variants of the serotonin transporter have been identified in humans. These alleles have different kinetics of serotonin uptake, leading to the hypothesis that they may contribute to the pathogenesis of functional bowel disorders. While initially supported, several studies have failed to show a linkage between one of the alleles and IBS (Camilleri, M., 2004). Holtmann G. *et al.* (2004) examined the link between a G-protein β subunit and functional dyspepsia. Prior studies had shown that the expression of the two allelic forms of this molecule affected intracellular signaling in neurons and was linked to affective disorders. As was true for SERT, a subsequent study did not confirm the linkage reported in this initial observation (Andresen, V. *et al.*, 2006). These conflicting results likely reflect the fact that a complex trait, such as enhanced sensitivity to visceral stimulation, can typically not be explained by a single gene defect, but rather a complex interaction between multiple genetic and environmental factors. Thus, contributions of any single candidate gene to the variance of phenotypic expression will be limited, requiring very large studies to more conclusively address their role in the development of visceral pain syndromes.

5.37.3.2 Sleeping (Silent) Nociceptors

In the mid-1980s Schmidt and coworkers (Schmidt, R. F., 1996) characterized a novel nociceptor in the knee joint of the cat they dubbed silent or sleeping. These nociceptors could be activated by electrical stimulation, but not by the usual high-intensity mechanical stimuli tested. During the minutes and hours after experimental inflammation of the knee joint, however, these nociceptors became progressively sensitive to mechanical stimuli, including to nonnoxious movement of the joint, and developed spontaneous activity. It has subsequently been established that sleeping nociceptors do respond to mechanical stimulation in the absence of inflammation, but only at intensities that are potentially damaging to tissue, and hence they are not truly silent. Microneurographic studies suggest that between 15% and 20% of C-fiber nociceptors in human skin are of the sleeping variety (Torebjörk, H. E. *et al.*, 1996), and sleeping nociceptors also have been documented in the visceral innervation (Figure 7), although estimates of their number vary widely from ~30% to >80%. Studies of sleeping visceral nociceptors have focused principally on the pelvic nerve innervation of the rat or cat urinary bladder and colon. Whether the afferents studied were actually sleeping is uncertain, and it has to be appreciated that assignment to this category is typically based on the absence of a response to organ distension in the noxious range. Given the filling, storage, and emptying functions of the bladder and colon, which are supported by the high proportion (~70%) of pelvic nerve afferents with low thresholds for mechanical activation, that a similar large

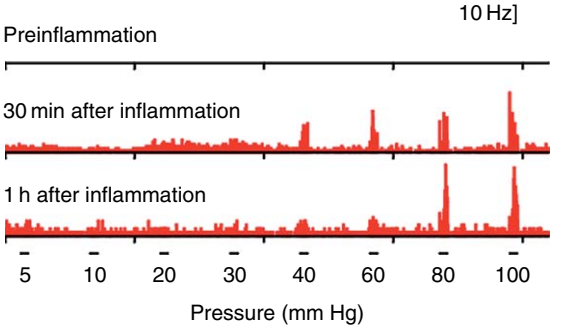

Figure 7 Illustration of a mechanically insensitive, silent (sleeping) visceral nociceptor. Responses to balloon distension of the colon (5–100 mm Hg, 20 s) are shown before experimental organ inflammation (the fiber did not respond to colon distension or bladder distension, not shown), 30 and 60 min after intracolonic instillation of zymosan. Spontaneous activity is apparent after colon inflammation as are responses to colon distension. Adapted from Coutinho, S., Su, X., Sengupta, J. N., and Gebhart, G. F. 2000. Role of Sensitized Pelvic Nerve Afferents from the Inflamed Rat Colon in The Maintenance of Visceral Hyperalgesia. In: Nervous System Plasticity and Chronic Pain, Progress in Brain Research (*eds*. J. Sandküher, B. Bromm, and G. F. Gebhart), Vol. 129, pp. 375–387. Elsevier.

proportion of pelvic nerve afferents are of the sleeping variety seems disproportionate. It is clear, however, that the proportion of sleeping nociceptors in the visceral innervation is greater than has been reported in skin, but the proportion and contributions of sleeping nociceptors to visceral pain states remains to be established. Some of these mechanically insensitive afferents may have been chemosensitive and would have responded to a chemical stimulus not tested. A potential role of chemical signaling is supported by recruitment of silent vagal gastric afferents after exposure to bile acids (Page, A. J. *et al.*, 2002).

5.37.3.3 Visceral Chemo-Nociception

Most studies of visceral afferents focus on mechanosensation, as mechanical stimuli can trigger reproducible responses without inducing tissue damage. However, visceral afferents are also exposed to potentially noxious chemical signals, such as acidity in the proximal gastrointestinal tract, and products that may accumulate during ischemia, such as lactate, protons, and bradykinin, and thus contribute to visceral discomfort and pain. Gastro-esophageal reflux disease (GERD, gastric acid reflux into the lower esophagus), myocardial ischemia, and lower airway irritation are all associated with discomfort and/or pain. Although experimental evidence obtained in animal studies is limited, both spinal and vagal afferents are involved in chemo-nociception.

Using the expression of the immediate early gene *c-fos* as a surrogate marker for neuronal activation after acid exposure of the stomach, noxious chemical stimuli activated vagal but not spinal pathways (Schuligoi, R. *et al.*, 1998). This is consistent with behavioral responses to intragastric acid administration, which were blunted after vagotomy (Lamb, K. *et al.*, 2003). In studies of mouse vagal gastro-esophageal afferent fibers, more than 50% of fibers that responded to circular tension also responded to bile acid (a component of gastric acid reflux into the esophagus); significantly, a population of mechanically insensitive (sleeping) afferents was activated by bile acid, suggesting the presence of specific chemosensors (which did to respond to other chemicals studied) (Page, A. J. *et al.*, 2002). Additional support for vagal involvement in chemo-nociception is provided by results showing that independent of the acute response to protons (glycocholic acid and hydrochloric acid), acid exposure enhanced subsequent responses of gastric vagal afferents to mechanical stimulation, suggesting a sensitizing interaction between different stimulus modalities (Kang, Y. *et al.*, 2004) (Figure 8).

Coronary artery occlusion in animals or myocardial ischemia in humans leads to the release and accumulation of a variety of substances in sinus blood (e.g., bradykinin, adenosine, serotonin, prostaglandins; see Meller, S. T. and Gebhart, G. F., 1992 for a review) that have been shown to activate cardiac afferent fibers in the spinal innervation. Experimental coronary artery occlusion also triggers a rapid decrease in myocardial pH, and both protons and lactic acid (which accumulates during tissue hypoxia) have been shown to activate ischemia-sensitive cardiac afferent fibers in the spinal splanchnic innervation (Pan, H. L. *et al.*, 1999). Many ischemia-sensitive cardiac (Pan, H. and Chen, S. R., 2002) and abdominal splanchnic afferents are also responsive to bradykinin, serotonin, and prostaglandins (see Longhurst, J. C., 1995 for review) as well as mechanical probing. As in other organs, myocardial ischemia has been reported to recruit mechanically insensitive (sleeping) cardiac splanchnic afferent fibers (Pan, H. and Chen, S. R., 2002).

In healthy subjects, the afferent innervation of the lower airways does not normally contribute to conscious sensations. However, dyspnea, chronic cough, and chronic obstructive pulmonary disease, in addition to inhalation of irritant chemicals, are associated with discomfort and/or pain, and it appears that the vagal afferent innervation plays a dominant role. As indicated previously, the cell bodies of vagal sensory fibers are contained in the nodose and smaller jugular ganglia, which are derived from placode and neural crest cells, respectively. Undem, B. J. and coworkers have provided evidence that the vagal ganglionic source of axons supplying the airways is associated with the neurochemical and physiological phenotype of the afferent fiber (Riccio, M. M. *et al.*, 1996). Nodose ganglion Aδ-fibers have low thresholds for mechanical activation, adapt rapidly to mechanical stimulation, and are not activated by capsaicin. In contrast, jugular ganglion Aδ-fibers have higher thresholds for mechanical activation, adapt slowly to mechanical stimulation, and are typically responsive to capsaicin. C-fibers associated with somata in both the nodose and jugular ganglia are also mechanically sensitive and also respond to capsaicin and bradykinin (Undem, B. J. *et al.*, 2004); in addition, C-fibers innervating the lung from the nodose ganglion express P2X receptors and respond to purinergic agonists (jugular C-fibers do not). Because proportions of these mechanically sensitive nodose and

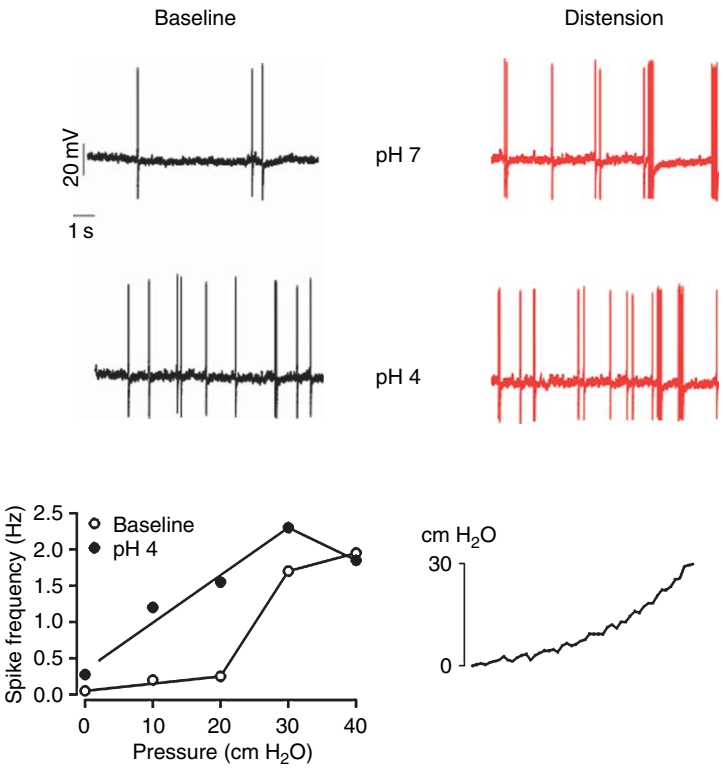

Figure 8 Intracellular recordings from a nodose ganglion neuron innervating the mouse stomach show low baseline activity (top left) and an increase (response) in activity (top right) during luminal distension (0–30 cm H_2O, 10 s, shown bottom right). When the luminal proton concentration was raised to pH 4, baseline activity and the response to distension increased. The stimulus response function for this neuron is summarized on the bottom left and demonstrates a significant shift to the left in the presence of an increase in luminal pH to 4. From Bielefeldt K. (unpublished).

jugular ganglia afferents are sensitive to acidic solutions and other algogenic chemical stimuli, they are considered to function as airway and lung nociceptors. In support, airway inflammation increases the mechanical sensitivity of the rapidly adapting population of vagal afferents and triggers an increase in the synthesis of neuropeptides substance P and CGRP (Undem, B. J. *et al.*, 2002).

5.37.4 Visceral Hypersensitivity

Like other tissues in the body, an increase in the excitability of sensory neurons innervating an organ can lead to exaggerated responses to applied stimuli, including intensities of stimulation in the physiologic range that normally do not lead to conscious sensation. Inflammation of visceral tissues, like inflammation of skin, muscle, or joints, typically increases visceral neuron excitability and raises normally unattended afferent input from the viscera to the level of consciousness in the form of discomfort and pain. By far, however, most persistent visceral pain conditions are characterized by hypersensitivity in the absence of inflammation or other cause. Accordingly, visceral hypersensitivity has been suggested to represent a biomarker for functional gastrointestinal and bladder disorders, which in the case of IBS can be experimentally established by balloon distension of the rectum. These functional disorders are relatively common, persistent, and generally inexplicable clinically. The characteristic discomfort and pain is often precipitated by ingestion of food, but also can be disassociated from events that logically would be expected to exacerbate symptoms. Typically, nonnoxious intensities of visceral stimulation (e.g., ingestion of food or beverage, low pressures of gastric or rectal distension, bladder filling) trigger painful sensations, which some have inappropriately and inaccurately termed visceral allodynia.

There is an association (~30%) between IBS and previous (and resolved) gastrointestinal infection, but antecedent or contemporaneous events that lead to development of functional disorders are otherwise unknown. Abuse in childhood, including sexual abuse, has been advanced as a contributing factor in development of functional disorders as have stress and anxiety, which are commonly reported by patients and can clearly exacerbate symptoms. Given that the cause of such disorders is unknown, there has been considerable attention paid to peripheral versus central nervous system contributions to initiation and maintenance of discomfort and pain in functional disorders. Both visceral sensory neuron excitability and sensitization and central nervous system dysregulation are considered below.

5.37.4.1 Sensitization and Excitability of Visceral Nociceptors

Sensitization is a defining characteristic of nociceptors first described by Perl for cutaneous nociceptors (see Perl, E., 1996 for an overview) and which has since been established for nociceptors innervating other tissues. Sensitization is an increase in response magnitude to suprathreshold stimuli and/or a decrease in response threshold; not uncommonly, both response magnitude increases and response threshold decreases (and spontaneous activity can develop) (see Figure 5 for examples of sensitization of responses of low- and high-threshold mechanosensitive pelvic nerve afferent fibers to bladder distension). Experimentally, sensitization is commonly produced following tissue inflammation or insult, and an extensive literature has identified mediators and mechanisms of inflammation-produced sensitization, principally in nonvisceral tissues (e.g., McMahon, S. B. *et al.*, 2006). Clinically, in functional disorders, sensitization of visceral sensory neurons is present in the absence of gross inflammation or tissue insult, but visceral sensory neurons can sensitize after exposure to noninjurious stimuli. For example, gastric vagal mechanosensitive afferents uniformly have low thresholds for response to balloon distension of the stomach, but also encode stimulus intensity into the noxious range. Response magnitude to gastric distension can be affected not only by intragastric instillation of acids or by gastric ulceration, but also by transient intragastric exposure to stimuli that do not injure the tissue (e.g., see Kang, Y. *et al.*, 2004). The significance of these findings is twofold. First, gastric vagal mechanoreceptors, which are generally considered not to contribute to visceral pain, do sensitize and significantly increase input into the central nervous system (nucleus of the solitary tract) which must have consequences, if not to interpretation or awareness of gastric sensation, then at least (or in addition) to efferent outflow to the stomach via the dorsal vagal motor nucleus. Second, that innocuous gastric stimuli can produce a time-limited sensitization of responses of gastric vagal mechanoreceptors reveals considerable neural plasticity, suggesting that normal visceral events can modulate visceral sensory neuron excitability even in healthy persons.

Because sensitization reveals an underlying change in neuron excitability, changes in neuron ion channels must be responsible for increases in response magnitude and decreases in response threshold, at least during the initial period of sensitization (see above and Gold, M. S., 2006). Experimental models of visceral hypersensitivity are associated with an increase in neuron input resistance and decrease in resting membrane potential. While the exact mechanisms have not been studied in visceral sensory neurons, changes in the expression and/or function of two pore domain potassium channels and hyperpolarization-activated I_H likely also contribute. In addition, both voltage-gated sodium (Na_V) and voltage-gated potassium (K_V) channels have been documented to change in visceral sensory neurons as predicted based on understanding of general biophysical principles. In experimental models of gastric ulceration, gastritis, ileitis, colitis, and cystitis, peak inward sodium currents significantly increase after visceral insult, and the increase is largely contributed to by the TTX-resistant component of the current (e.g., $Na_V1.8$), although precisely which sodium channel has not been established. In addition to changes in threshold, the sensitization is characterized by an increase in action potentially frequency during stimulation. Again voltage-sensitive sodium channels play an important role in this context. As already mentioned, current density increases, the voltage dependence of channel activation shifts and recovery from inactivation is accelerated, and all of these factors clearly facilitate repetitive firing. Conversely, the outward potassium current (the A type current) is reduced and the voltage dependence of activation shifts to more positive potentials in visceral sensory neurons after visceral insult, which is also consistent with an increase in neuron excitability.

5.37.4.2 Central Sensitization

In addition to increased responses and decreased response thresholds, sensitization of visceral nociceptors importantly leads to changes in excitability of central nervous system neurons upon which they terminate, a consequence termed central sensitization. Nociceptor sensitization and central sensitization are considered to underlie, respectively, the expression of primary and secondary hypersensitivity. The most readily apparent reflection of central sensitization in the clinical setting is expansion of the area of referred sensation, which is accompanied by tenderness to palpation (a reflection of peripheral sensitization). The spinal cord has been the principal focus of study with respect to central sensitization, but neurons in supraspinal sites also undergo changes in excitability and, as discussed below, supraspinal sites can contribute significantly to the maintenance of central sensitization and may play a critical role in the maintenance of chronic pain disorders, including functional visceral disorders.

The sensitization of central neurons, which has been studied extensively in the spinal cord, results from increased release of neuroactive substances (e.g., glutamate, neurokinins like substance P) from visceral sensory nerve terminals in the spinal cord and from second-order spinal interneurons upon which they may terminate. Because supraspinal sites are also engaged by persistent nociceptive input, another source of neuroactive substances (e.g., serotonin, norepinephrine, and GABA) is derived from projections to the spinal cord from the brainstem. Finally, nonneuronal glia become activated in persistent pain conditions, which has been widely documented in nonhuman animal somatic inflammatory models, and can contribute additional neuroactive substances (e.g., cytokines, chemokines) and modulators to the complex chemical milieu in spinal cord. Contributions from the latter sources (supraspinal sites and glia) likely become more important over time, and their influence may persist and contribute to altered sensations from the viscera in the absence of sustained visceral nociceptor sensitization (see below).

Changes within the spinal cord and brain stem areas of visceral input following experimental organ inflammation or noxious stimulation have been assessed by following expression of the immediate early gene, *c-fos*, upregulation of the neuronal isoform of nitric oxide synthase, and internalization of the receptor for substance P, the neurokinin 1 receptor. These experimental approaches show that organ insult causes an increase in the indicator studied as well as an anatomical expansion of indicator beyond the normal, resting range of visceral input to the spinal cord. Figure 9 illustrates this point for the

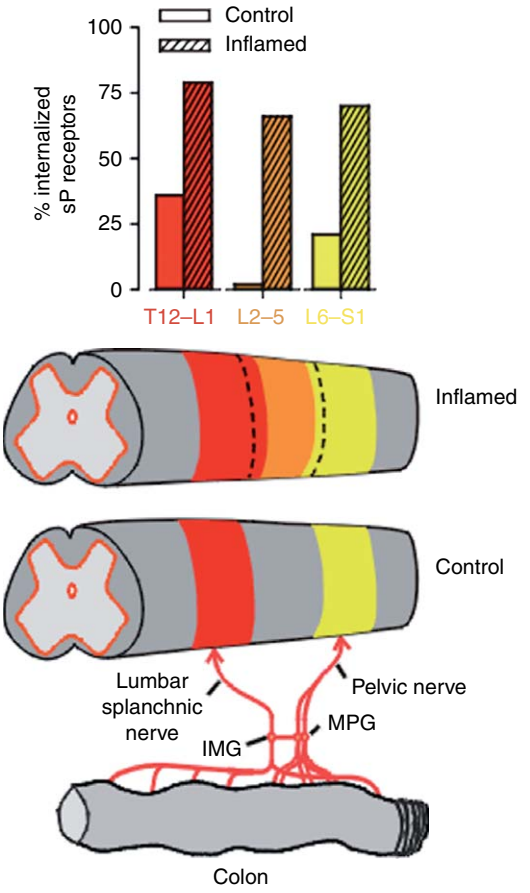

Figure 9 Internalization of substance P (sP) receptors by colon distension in the absence (control) and 3 h following intracolonic instillation of zymosan (inflamed). In the absence of colon insult (control), noxious colon distension (80 mm Hg, 20 s) leads to internalization of the sP receptor in superficial spinal laminae in an anatomically appropriate distribution (i.e., T12–L1 and L6–S1 spinal segments via the lumbar splanchnic nerve and pelvic nerve innervations of the rat colon – there is no receptor internalization in lumbar spinal segments 2–5). Three hours after intracolonic instillation of an inflamogen, zymosan (inflamed), a time at which responses to colon distension are significantly increased (i.e., colon hypersensitivity is present behaviorally), the amount of sP receptor internalized (quantified at top) is significantly increased and now includes L2–5. IMG, inferior mesenteric ganglia; MPG, major pelvic ganglion. Adapted from Honoré , P., Kamp, E. H., Rogers, S. D., Gebhart, G. F., and Mantyh, P. W. 2002. Activation of lamina I spinal cord neurons that express the substance p receptor in visceral nociception and hyperalgesia. J. Pain 3, 3–11.

spinal cord, showing that internalization of the substance P receptor produced by colon distension increases significantly after colon insult and, moreover, now includes an area of the spinal cord that showed no receptor internalization after colon distension in the absence of insult (Honoré, P. *et al.*, 2002). This representation of central sensitization occurred within hours after colonic insult, revealing that mechanosensitive colon afferents sensitize, sleeping afferents awaken, and the visceral innervation and second-order neurons upon which the afferents terminate are rapidly and easily modified (i.e., are highly plastic). Other studies in rats show rapid changes in supraspinal sites as well, suggesting their involvement in states of increased central excitability (e.g., Coutinho, S. *et al.*, 1998). Central sensitization also affects somatic and visceral inputs that converge on spinal neurons, as shown by reduced thresholds for hindpaw withdrawal after bladder or colon insult (Jaggar, S. I. *et al.*, 1999; Miranda, A. *et al.*, 2004; Lamb, K. *et al.*, 2006). Such data obtained in animals are consistent with results from human studies. For example, repetitive colorectal distension increases pain perception and the area of cutaneous pain referral in normals (Ness, T. J. *et al.*, 1990) as well as patients with functional bowel disease (Munakata, J. *et al.*, 1997). Similarly, infusion of 0.15 M hydrochloric acid into the distal esophagus not only reduces stimulus threshold in the distal esophagus, but also in the nonacid-exposed esophagus as well as on the chest wall area of referral within an hour after acid exposure (Sarkar, S. *et al.*, 2000; 2001), again revealing that central sensitization produced by a visceral input is also apparent in the area of somatic referral.

Another expression of central sensitization, which can reflect either spinal or supraspinal involvement, is sensitization that develops between organs with inputs onto spinal dorsal horn neurons within the same spinal segments, an expression of viscero-visceral convergence (e.g., urinary bladder and colon), or between organs that do not share patterns of spinal segmental overlap. The former are easy to understand anatomically, and while not rigorously studied in the human population, patients with functional bowel disorders often also complain about pelvic pain or symptoms consistent with interstitial cystitis (Whitehead, W. *et al.*, 2002). Conversely, many patients with interstitial cystitis also suffer from functional bowel disorders (Alagiri, M. *et al.*, 1997). In nonhuman animals, it has been established that colon inflammation triggers bladder hyperactivity (Pezzone, M. A. *et al.*, 2005) and, conversely, that cystitis produces colon hypersensitivity (Lamb, K. *et al.*, 2006; Winnard, K. P. *et al.*, 2006).

Animal and human studies have clearly established the contribution of supraspinal sites to sensitization to visceral input. In susceptible rodent strains, stress enhances behavioral responses to visceral distension (Coutinho, S. V. *et al.*, 2002; Bradesi, S. *et al.*, 2005). While multiple mechanisms may contribute to this modulation of visceral input, descending inhibitory or facilitatory pathways likely play a role (see below), as shown by the effects of electrical stimulation within the rostral ventromedial medulla on responses to noxious colorectal distension (Zhuo, M. and Gebhart, G. F., 2002) and of selective abolition of descending facilitatory influences in a model of rodent pancreatitis (Vera-Portocarrero, L. P. *et al.*, 2007). These reports are consistent with data obtained in human volunteers. Activation of descending inhibitory mechanisms through heterotopic stimulation blunted perception of rectal distension in healthy volunteers (Song, G. H. *et al.*, 2006). Conversely, uncomfortable visceral input triggered by acid infusion into the duodenum lowered the pain threshold to proximal esophageal stimulation (Hobson, A. R. *et al.*, 2004). These experiments also support a rapid involvement (minutes to hours) of supraspinal sites in central sensitization. Longer-term evidence of supraspinal contributions to central sensitization is provided by both clinical reports of esophageal or gastric hypersensitivity in patients with IBS (or somatic disorders like fibromyalgia) (Price, D. D. *et al.*, 2007a; 2007b; Sharma, A. and Aziz, Q., 2007) and by various manipulations limited to the neonatal period that lead either to visceral hypersensitivity or increased susceptibility to organ insult in adult animals. In rats, neonatal colon irritation (intracolonic mustard oil) or colon distension (Al Chaer, E. D. *et al.*, 2000), urinary bladder inflammation (intravesical zymosan, Randich, A. *et al.*, 2006), maternal separation (a stressor, Coutinho, S. V. *et al.*, 2002), or neonatal immune challenge with the bacterial endotoxin lipopolysaccharide (Spencer, S. J. *et al.*, 2007) are all associated with increased organ sensitivity in the adult animal. Because these experimental neonatal manipulations are not associated with adult organ inflammation, the adult visceral hypersensitivity in these models is considered to be maintained by central nervous system mechanisms, including dysregulation or reorganization (discussed in Section 5.37.4.3).

Mechanistically, both human and nonhuman animal studies have established an important role for peripheral, spinal (and supraspinal) *N*-methyl-D-aspartate (NMDA) receptors in central sensitization following visceral insult (e.g., McRoberts, J. A. *et al.*, 2001; Willert, R. P. *et al.*, 2004; see Woolf, C. J. and Thompson, S. W., 1991 for a general overview), although the relevant spinal neurons and signal transduction pathways in visceral sensory pathways are not revealed by these findings. The process of central sensitization is linked to long-term potentiation, which has been extensively studied in the hippocampus in relation to learning and memory, and in spinal cord exhibits similar characteristics that involve transcriptional and other events that lead to changes in excitability that can outlast the peripheral input. Although not focused on visceral inputs, these studies are based on features common to visceral nociceptive input: recordings from lamina I spinal dorsal horn neurons that project to the pontine parabrachial area and coactivation of substance P and NMDA receptors (Ikeda, H. *et al.*, 2003; 2006). Study of this population of spinal neurons, upon which visceral afferents likely terminate (along with nonvisceral nociceptive afferents), reveals synaptic plasticity dependent upon neuroactive substances contained and released from visceral afferent terminals in the spinal cord and a cellular process that likely contributes to induction of central sensitization.

5.37.4.3 Central Modulation of Visceral Pain

One consequence of peripheral events that lead to central sensitization is activation of endogenous pain modulatory systems and there is growing appreciation that visceral disorders characterized by persistent discomfort and pain reveal, at least in part, a dysregulated central nervous system. The concept that there exist endogenous mechanisms that modulate pain arose from studies showing that electrical stimulation or chemical activation (e.g., glutamate to activate cells or drugs like opioids acting at their cognate receptors) in the brainstem PAG produced powerful descending inhibitory effects on spinal nociceptive inputs. The initial focus of such studies was on inhibitory inputs descending from the brainstem and on modulation of noxious inputs. Presently, it is appreciated that descending influences require a relay in the rostral ventromedial medulla between the PAG and spinal cord, are not restricted to modulation of only noxious inputs, and importantly not limited to only inhibitory influences. Normally, descending modulation represents a balance between inhibitory and facilitatory influences, with inhibition typically dominant. Facilitatory influences, however, have been shown to predominate in some experimental conditions and have been hypothesized to contribute to maintenance of persistent pain states (Porreca, F. *et al.*, 2002; Gebhart, G. F., 2004). With respect to functional visceral disorders that persist in the absence of a defined pathobiology, and many of which are comorbidly expressed with other generalized disorders (e.g., fibromyalgia), the concept of a dysregulated modulatory system has gained both currency and experimental support.

Most nonhuman animal studies have examined nonvisceral pain, but several studies have confirmed for visceral inputs what has been more widely documented for nonvisceral inputs. Activation of brainstem sites (PAG and rostral ventromedial medulla) has been shown to facilitate visceromotor reflexes (Zhuo, M. and Gebhart, G. F., 2002) and spinal dorsal horn neuron responses (Zhuo, M. *et al.*, 2002) to noxious colon distension in the rat. Similarly, an experimental pancreatitis in rats has been shown to be maintained by facilitatory influences descending from the rostral ventromedial medulla (Vera-Portocarrero, L. P. *et al.*, 2007). These studies confirm that modulation of spinal nociceptive visceral transmission does not differ in character from modulation of nonvisceral inputs. Importantly, studies in humans suggest that facilitatory modulatory influences can contribute to persistent pain states, including visceral pain states. Such studies rely on interpretation of changes in patterns or intensity of brain imaging or on localization, wave form, and magnitude of event-related cortical potentials.

For example, Dimcevski G. *et al.* (2007) recently reported functional brain reorganization in chronic pancreatitis patients. They electrically stimulated at different sites from above the gastro-esophageal junction to the horizontal part of the duodenum and recorded event-related brain potentials from surface electrodes on the scalp and also assessed sensation. They found that neuronal sources in the insula were most consistently changed in chronic pancreatitis patients relative to healthy controls and concluded that reorganization in this part of the brain is a contributing mechanism to pain in chronic pancreatitis. This and other reports (e.g., Price, D. D. *et al.*, 2007a; 2007b) clearly reveal that central mechanisms are important to the maintenance of persistent visceral

pain conditions. Mechanisms by which the excitability of neurons in these or other brain areas might increase or decrease and be sustained are unknown. Stress and other external factors, as well as cognitive and emotional events, can contribute to activity in supraspinal sites and influence the interpretation of information arriving there from internal organs. The matrix of brain areas activated by painful visceral stimuli is similar to that seen during anticipation of such a painful stimulus, demonstrating the importance of cognitive influences (Yágüez, L. *et al.*, 2005). Stress activates the hypothalamic–pituitary–adrenal axis, resulting in the release of various neuroendocrine mediators. Studies in humans have demonstrated different neuroendocrine responses in patients with chronic visceral pain syndromes (Posserud, I. *et al.*, 2004). These mediators may directly or indirectly affect visceral sensory function (e.g., Taché, Y. *et al.*, 2004) and may function as targets for pharmacologic interventions.

5.37.5 Summary

(1) The principal conscious sensations that arise from the viscera are discomfort and pain. Typically, visceral pain is diffuse and difficult to localize, not distinctly felt at the source and instead referred to other tissues.

(2) Most experimental work in humans and nonhuman animals has utilized hollow organ distension, an adequate (in the Sherringtonian context) noxious visceral stimulus. Visceral inflammation and ischemia are also considered to be adequate stimuli, but they are more difficult to control experimentally and thus have been less widely used. It is generally held that pain cannot be produced from all viscera (e.g., the parenchyma of solid organs like the liver) or from organs that have only an afferent innervation (and not a sensory innervation), but new knowledge has expanded our understanding of visceral sensations and suggest that these and other issues of visceral insensitivity should be reevaluated.

(3) The innervation of the viscera is unique. Each organ is innervated by two nerves, either the vagus nerve and a spinal visceral nerve or a splanchnic nerve and the pelvic nerve, and the function(s) of each nerve differ. The route from the organ to the spinal cord of spinal visceral nerves involves transit of prevertebral ganglia, where axon collaterals of visceral nerves can influence organ function, as well as paravertebral ganglia. Vagal afferent fibers terminate centrally in the brainstem nucleus of the solitary tract.

(4) Cell bodies of the vagus nerves are contained in the nodose ganglia (primarily) and cell bodies of all other visceral nerves are contained in DRG. Generally, visceral sensory neuron cell bodies are larger in size than would be expected given that virtually all visceral sensory neurons have thinly myelinated or unmyelinated axons, which in the somatic realm are associated with small-diameter cell bodies.

(5) Spinal visceral nerves terminate in laminae I, II, V, and X, but importantly branch significantly within the spinal cord and extend both rostrally and caudally from the spinal segment of entry. Significantly, some terminations reach the contralateral side of the spinal cord.

(6) Most mechanoreceptors in viscera have low thresholds for response to stretch/tension (e.g., balloon distension), but a significant proportion ($\sim$20–30%) have high thresholds for response. The latter group fulfills criteria for nociceptors: their response threshold is in the noxious range (generally $\geq$30 mm Hg distending stimulus) and they encode stimulus intensity in the noxious range, but do not encode innocuous intensities of stimulation.

(7) Low-threshold visceral mechanoreceptors respond in the physiologic range, but in addition possess properties that suggest involvement in visceral discomfort and pain. Unlike low-threshold cutaneous mechanoreceptors, low-threshold visceral mechanoreceptors respond vigorously to noxious intensities of stimulation, continue to encode stimulus intensity into the noxious range, and sensitize (a defining characteristic of nociceptors). These properties are not unlike some low-threshold sensory neurons that innervate another deep tissue, muscle.

(8) Low-threshold visceral mechanoreceptors are normally and principally involved in afferent and reflex functions, but in conjunction with high-threshold visceral mechanoreceptors can contribute to intense acute visceral pain. In functional, inflammatory or ischemic visceral disorders, where sensitization develops and sleeping visceral nociceptors become active, we believe that all mechanosensitive visceral endings can contribute to uncomfortable and painful visceral sensation.

(9) Visceral sensory neurons sensitize and thereby contribute to central sensitization, a consequence of increased input to the central nervous system that is not limited only to the spinal cord. Tenderness to palpation and an increase in the area of referred sensation, respectively, mark peripheral and central sensitization.

(10) Functionally, visceral sensory neurons in the different innervations of the same organ are affected differently by sensitizing events. This perhaps should not be surprising given that the proportions and distributions of mechanosensitive endings of the two innervations differ significantly for the organs studied to date. This is a developing area of investigation that has the potential to lead to therapeutic strategies targeting a selective innervation of a viscus.

(11) Brainstem modulatory circuitry normally exerts an inhibitory influence on spinal pain transmission. Increased visceral input from sensitized receptors initiates processes of sensitization in both spinal and supraspinal sites, which can alter the balance between descending inhibitory and facilitatory influences on spinal pain transmission. In cases of long lasting visceral hypersensitivity (e.g., functional bowel disorders), the hypothesis that the hypersensitivity is maintained by supraspinal influences in the absence of sensitized visceral input is tenable.

References

Adriaensen, D. I., Brouns, I., Van Genechten, J., and Timmermans, J-P. 2003. Functional morphology of pulmonary neuroepithelial bodies: extremely complex airway receptors. Anat. Rec. 270, 25–40.

Ahmed, K., Amadesi, S., Bautista, F., Bunnett, N., and Vanner, S. J. 2007. Mechanisms of protease activated receptor 2 – evoked hyperexcitability of nociceptive neurons innervating the mouse colon. J. Physiol. 580, 977–991.

Alagiri, M., Chottiner, S., Ratner, V., Slade, D., and Hanno, P. M. 1997. Interstitial cystitis: unexplained associations with other chronic disease and pain syndromes. Urology 49, 52–57.

Al-Chaer, E. D., Kawasaki, M., and Pasricha, P. J. 2000. A new model of chronic visceral hypersensitivity in adult rats induced by colon irritation during postnatal development. Gastroenterology 119, 1276–1285.

Andresen, V., Camilleri, M., Kim, H. J., Stephens, D. A., Carlson, P. J., Talley, N. J., Saito, Y. A., Urrutia, R., and Zinsmeister, A. R. 2006. Is there an association between GN[beta]3-C825T genotype and lower functional gastrointestinal disorders? Gastroenterology 130, 1985–1994.

Apkarian, A., Bruggemann, J., Shi, T., and Airapetian, L. 1995. A Thalamic Model for True and Referred Visceral Pain. In: Visceral Pain, Progress in Pain Research and Management (*ed*. G. F. Gebhart), Vol. 5, pp. 217–259. IASP Press.

Barbara, G., Stanghellini, V., De Giorgio, R., and Corindaldesi, R. 2006. Functional gastrointestinal disorders and mast cells: implications for therapy. Neurogastroenterol. Motil. 18, 6–17.

Barbara, G., Wang, B., Stanghellini, V., De Giorgio, R., Cremon, C., Di Nardo, G., Trevisani, M., Campi, B., Geppetti, P., Tonini, M., Bunnett, N., Grundy, D., and Corinaldesi, R. 2007. Mast cell-dependent excitation of visceral-nociceptive sensory neurons in irritable bowel syndrome. Gastroenterology 132, 26–27.

Benson, C. J., Eckert, S. P., and McCleskey, E. W. 1999. Acid-evoked currents in cardiac sensory neurons: a possible mediator of myocardial ischemic sensation. Circ. Res. 84, 921–928.

Beyak, M. J. and Vanner, S. 2005. Inflammation-induced hyperexcitability of nociceptive gastrointestinal DRG neurones: the role of voltage-gated ion channels. Neurogastroenterol. Motil. 17, 175–186.

Bhat, Y. and Bielefeldt, K. 2006. Capsaicin receptor (TRPV1) and non-erosive reflux disease. Eur. J. Gastroenterol. Hepatol. 18, 263–270.

Birder, L. A., Kanai, A. J., de Groat, W. C., Kiss, S., Nealen, M. L., Burke, N. E., Dineley, K. E., Watkins, S., Reynolds, I. J., and Caterina, M. J. 2001. Vanilloid receptor expression suggests a sensory role for urinary bladder epithelial cells. Proc. Natl. Acad. Sci. U. S. A. 98, 13396–13401.

Blackshaw, L. A., Brookes, S. J. H., Grundy, D., and Schemann, M. 2007. Sensory transmission in the gastrointestinal tract. Neurogastrol. Motil. 19(Supp 1), 1–19.

Bradesi, S., Schwetz, I., and Ennes, H. S. 2005. Repeated exposure to water avoidance stress in rats: A new model for sustained visceral hyperalgesia. Am. J. Physiol. 289, G42–G53.

Brierley, S. M., Jones, R. C. W., III, Gebhart, G. F., and Blackshaw, L. A. 2004. Splanchnic and pelvic mechanosensory afferents signal different qualities of colonic stimuli in mice. Gastroenterology 127, 166–178.

Bueno, L., Floramonti, J., Delvaux, M., and Frexinos, J. 1997. Mediators and pharmacology of visceral sensitivity: from basic to clinical investigations. Gastroenterology 112, 1714–1743.

Camilleri, M. 2004. Is there a SERT-ain association with IBS? Gut 53, 1396–1399.

Cenac, N., Andrews, C. N., Holzhausen, M., Chapman, K., Cottrell, G., Andrade-Gordon, P., Steinhoff, M., Barbara, G., Beck, P., Bunnett, N. W., Sharkey, K., Ferraz, G. P., Shaffer, E., and Vergnolle, N. 2007. Role for protease activity in visceral pain in irritable bowel syndrome. J. Clin. Invest. 117, 636–647. doi:10.1172/JCI29255.

Chan, C. L. H., Facer, P., Davis, J. B., Smith, G. D., Egerton, J., Bountra, C., Williams, N. S., and Anand, P. 2003. Sensory fibres expressing capsaicin receptor TRPV1 in patients with rectal hypersensitivity and faecal urgency. Lancet 361, 385–391.

Christianson, J. A., Traub, R. J., and Davis, B. M. 2006. Differences in spinal distribution and neurochemical phenotype of colonic afferents in mouse and rat. J. Comp. Neurol. 494, 246–259.

Cockayne, D. A., Hamilton, S. G., Zhu, Q. M., Dunn, P. M., Zhong, Y., Novakovic, S., Malmberg, A. B., Cain, G., Berson, A., Kassotakis, L., Hedley, L., Lachnit, W. G., Burnstock, G., McMahon, S. B., and Ford, A. P. 2000. Urinary bladder hyporeflexia and reduced pain-related behaviour in p2x3-deficient mice. Nature 407, 1011–1015.

Coutinho, S. V., Plotsky, P. M., Sablad, M., Miller, J. C., Zhou, H., Bayati, A. I., McRoberts, J. A., and Mayer, E. A. 2002. Neonatal maternal separation alters stress-induced responses to viscerosomatic nociceptive stimuli in rat. Am. J. Physiol. 282, G307–G316.

Coutinho, S., Su, X., Sengupta, J. N., and Gebhart, G. F. 2000. Role of Sensitized Pelvic Nerve Afferents from the Inflamed Rat Colon in The Maintenance of Visceral Hyperalgesia. In: Nervous System Plasticity and Chronic Pain, Progress in Brain Research (*eds*. J. Sandküher, B. Bromm, and G. F. Gebhart), Vol. 129, pp. 375–387. Elsevier.

Coutinho, S., Urban, M. O., and Gebhart, G. F. 1998. Role of glutamate receptors and nitric oxide in the rostral ventromedial medulla in visceral hyperalgesia. Pain 78, 59–69.

Cutz, E. 1982. Neuroendocrine cells of the lung. An overview of morphologic characteristics and development. Exp. Lung Res. 3, 185–208.

Dakhama, A., Kanehiro, A., Makela, M. J., Loader, J. E., Larsen, G. L., and Gelfand, E. W. 2002. Regulation of airway hyperresponsiveness by calcitonin gene-related peptide in allergen sensitized and challenged mice. Am. J. Respir. Crit. Care Med. 165, 1137–1144.

Dang, K., Bielefeldt, K., and Gebhart, G. F. 2004. Gastric ulcers reduce A-type potassium currents in rat gastric sensory ganglion neurons. Am. J. Physiol. 286, G573–G579.

Dang, K., Bielefeldt, K., and Gebhart, G. F. 2005. Differential responses of bladder lumbosacral and thoracolumbar dorsal root ganglion neurons to purinergic agonists, protons, and capsaicin. J. Neurosci. 25, 3973–3984.

Dimcevski, G., Saber, A. K., Funch-Jensen, P., Le Pera, D., Valeriani, M., Arendt-Nielsen, L., and Drewes, A. 2007. Pain in chronic pancreatitis: the role of reorganization in the central nervous system. Gastroenterology 132, 1546–1556.

Dunckley, P., Wise, R. G., Fairhurst, M., Hobden, P., Aziz, Q., Chang, L., and Tracey, I. 2005. A comparison of visceral and somatic pain processing in the human brainstem using functional magnetic resonance imaging. J. Neurosci. 25, 7333–7341.

Foreman, R. 1999. Mechanisms of cardiac pain. Annu. Rev. Physiol. 61, 143–167.

Fu, X. W., Wang, D., Nurse, C. A., Dinauer, M. C., and Cutz, E. 2000. NADPH oxidase is an O_2 sensor in airway chemoreceptors: evidence from K^+ current modulation in wild-type and oxidase-deficient mice. Proc. Natl. Acad. Sci. U. S. A. 97, 4374–4379.

Gebhart, G. F. 2004. Descending modulation of pain. Neurosci. Biobehav. Rev. 27, 729–737.

Gershon, M. D. and Tack, J. 2007. The serotonin signaling system: from basic understanding to drug development for functional GI disorders. Gastroenterology 132, 397–414.

Gold, M. S. 2006. Ion Channels: Recent Advances and Clinical Applications. In: Proceedings of the 11th World Congress on Pain (*eds*. H. Flor, E. Kalso, and J. O. Dostrovsky) pp. 73–92. IASP Press.

Halder, S. L. and Locke, G. R., III. 2007. Epidemiology and Socioeconomic Impact of Visceral and Abdominal Pain Syndromes. In: Chronic Abdominal and Visceral Pain (*eds*. P. Pasricha, W. Willis, and G. F. Gebhart), pp. 11–16. Informa Healthcare.

Hillsley, K., Lin, J.-H., Stnaisz, A., Grundy, D., Aerssens, J., Peeters, P. J., Moechars, D., Coulie, B., and Stead, R. H. 2006. Dissecting the role of sodium currents in visceral sensory neurons in a model of chronic hyperexcitability using $Na_V1.8$ and $Na_V1.9$ null mice. J. Physiol. 576, 257–267.

Hobson, A. R. and Aziz, Q. 2004. Brain imaging and functional gastrointestinal disorders: has it helped our understanding. Gut 53, 1198–1206.

Hobson, A. R., Khan, R. W., Sarkar, S., Furlong, P. L., and Aziz, Q. 2004. Development of esophageal hypersensitivity following experimental duodenal acidification. Am. J. Gastroenterol. 99, 813–820.

Holtmann, G., Siffert, W., Haag, S., Mueller, N., Langkafel, M., Senf, W., Zotz, R., and Talley, N. J. 2004. G-protein 3 subunit 825 CC genotype is associated with unexplained (functional) dyspepsia. Gastroenterology 126, 971–979.

Honoré, P., Kamp, E. H., Rogers, S. D., Gebhart, G. F., and Mantyh, P. W. 2002. Activation of lamina I spinal cord neurons that express the substance p receptor in visceral nociception and hyperalgesia. J. Pain 3, 3–11.

Hoogerwerf, W. A., Shenoy, M., Winston, J., Xiao, S. Y., He, Z., and Pasricha, P. J. 2004. Trypsin mediates nociception via the proteinase-activated receptor 2: a potentially novel role in pancreatic pain. Gastroenterology 127, 883–891.

Hoogerwerf, W. A., Zou, L., Shenoy, M., Sun, D., Micci, M. A., Lee-Hellmich, H., Xiao, S. Y., Winston, J. H., and Pasricha, P. J. 2001. The proteinase-activated receptor 2 is involved in nociception. J. Neurosci. 21, 9036–9042.

Ikeda, H., Heinke, B., Ruscheweyh, R., and Sandkuhler, J. 2003. Synaptic plasticity in spinal lamina i projection neurons that mediate hyperalgesia. Science 299, 1237–1240.

Ikeda, H., Stark, J., Fischer, H., Wagner, M., Drdla, R., Jajer, T., and Sandkuhler, J. 2006. Synaptic amplifier of inflammatory pain in the spinal dorsal horn. Science 312, 1659–1662.

Jaggar, S. I., Scott, H. C., and Rice, A. S. 1999. Inflammation of the rat urinary bladder is associated with a referred thermal hyperalgesia which is nerve growth factor dependent. Br. J. Anaesth. 83, 442–448.

Jones, R. C. W., III, Xu, L., and Gebhart, G. F. 2005. The mechanosensitivity of mouse colon afferent fibers and their sensitization by inflammatory mediators require transient receptor potential vanilloid 1 and acid-sensing ion channel 3. J. Neurosci. 25, 10981–10989.

Kang, Y., Bielefeldt, K., and Gebhart, G. F. 2004. Sensitization of mechanosensitive gastric vagal afferent fibers in the rat by thermal and chemical stimuli and gastric ulcers. J. Neurophysiol. 91, 1981–1989.

Laird, J. M. A., Olivar, T., Roza, C., De Felipe, C., Hunt, S. P., and Cervero, F. 2000. Deficits in visceral pain and hyperalgesia of mice with a disruption of the tachykinin NK1 receptor gene. Neuroscience 98, 345–352.

Laird, J. M., Souslova, V., Wood, J. N., and Cervero, F. 2002. Deficits in visceral pain and referred hyperalgesia in Nav1.8 (SNS/PN3)-null mice. J. Neurosci. 22, 8352–8356.

Lamb, K., Kang, Y. M., Gebhart, G. F., and Bielefeldt, K. 2003. Gastric inflammation triggers hypersensitivity to acid in awake rats. Gastroenterology 125, 1410–1418.

Lamb, K., Zhong, F., Gebhart, G. F., and Bielefeldt, K. 2006. Experimental colitis in mice and sensitization of converging visceral and somatic afferent pathways. Am. J. Physiol. 290, G451–G457.

Langley, J. N. 1921. The Autonomic Nervous System. Heffer.

Longhurst, J. C. 1995. Chemosensitive Abdominal Visceral Afferents. In: Visceral Pain Research and Management (*ed*. G. F. Gebhart), Vol. 5, pp. 99–132. IASP Press.

Lynn, P. A., Olsson, C., Zagorodnyuk, V., Costa, M., and Brookes, S. J. H. 2003. Rectal intraganglionic laminar endings are transduction sites of extrinsic mechanoreceptors in the guinea pig rectum. Gastroenterology 125, 786–794.

McMahon, S. B., Bennett, D. L. H., and Bevan, S. 2006. Inflammatory Mediators and Modulators of Pain. In: Wall and Melzack's Textbook of Pain, 5th edn. (*eds*. S. B. McMahon and M. Koltzenburg), pp. 49–72. Elsevier.

McRoberts, J. A., Coutinho, S. V., Marvizon, J. C., Grady, E. F., Tognetto, M., Sengupta, J. N., Ennes, H. S., Chaban, V. V.,

Amadesi, S., Creminon, C., Lanthorn, T., Geppetti, P., Bunnett, N. W., and Mayer, E. A. 2001. Role of peripheral *N*-methyl-D-aspartate (NMDA) receptors in visceral nociception in rats. Gastroenterology 120, 1737–1748.

Meller, S. T. and Gebhart, G. F. 1992. A critical review of the afferent pathways and the potential chemical mediators involved in cardiac pain. Neuroscience 48, 501–524.

Miranda, A., Peles, S., Rudolph, C., Shaker, R., and Sengupta, J. N. 2004. Altered visceral sensation in response to somatic pain in the rat. Gastroenterology 126, 1082–1089.

Molliver, D. C., Wright, D. E., Leitner, M. L., Parsadanian, A. S., Doster, K., Wen, D., Yan, O., and Snider, W. D. 1997. Ib4-binding drg neurons switch from ngf to gdnf dependence in early postnatal life. Neuron 19, 849–861.

Mukerji, G., Yiangou, Y., Agarwal, S. K., and Anand, P. 2006. Transient receptor potential vanilloid receptor subtype 1 in painful bladder syndrome and its correlation with pain. J. Urol. 176, 797–801.

Munakata, J., Naliboff, B., Harraf, F., Kodner, A., Lembo, T., Chang, L., Silverman, D. H., and Mayer, E. A. 1997. Repetitive sigmoid stimulation induces rectal hyperalgesia in patients with irritable bowel syndrome. Gastroenterology 112, 55–63.

Ness, T. J., Metcalf, A. M., and Gebhart, G. F. 1990. A psychophysiological study in humans using phasic colonic distension as a noxious visceral stimulus. Pain 43, 377–386.

Page, A. J., Brierley, S. M., Martin, C. M., Price, M. P., Symonds, E., Butler, R., Wemmie, J. A., and Blackshaw, L. A. 2005. Different contributions of asic channels 1a, 2, and 3 in gastrointestinal mechanosensory function. Gut 54, 1408–1415.

Page, A. J., Martin, C. M., and Blackshaw, L. A. 2002. Vagal mechanoreceptors and chemoreceptors in mouse stomach and esophagus. J. Neurophysiol. 87, 2095–2103.

Palecek, J., Paleckova, V., and Willis, W. D. 2002. The roles of pathways in the spinal cord lateral and dorsal funiculi in signaling nociceptive somatic and visceral stimuli in rats. Pain 96, 297–307.

Pan, H. and Chen, S. R. 2002. Myocardial ischemia recruits mechanically insensitive cardiac sympathetic afferents in cats. J. Neurophysiol. 87, 660–668.

Pan, H. L., Longhurst, J. C., Eisenach, J. C., and Chen, S. R. 1999. Role of protons in activation of cardiac sympathetic C-fibre afferents during ischaemia in cats. J. Physiol. 518, 857–866.

Perl, E. 1996. Pain and the Discovery of Nociceptors. In: Neurobiology of Nociceptors (*eds*. C. Belmonte and F. Cervero), pp. 5–36. Oxford University Press.

Pezzone, M. A., Liang, R., and Fraser, M. O. 2005. A model of neural cross-talk and irritation in the pelvis: implications for the overlap of chronic pelvic pain disorders. Gastroenterology 128, 1953–1964.

Phelps, E. A. and LeDoux, J. E. 2005. Contributions of the amygdala to emotion processing: from animal models to human behavior. Neuron 48, 175–187.

Phillips, R. J. and Powley, T. L. 2000. Tension and stretch receptors in gastrointestinal smooth muscle: re-evaluating vagal mechanoreceptor electrophysiology. Brain Res. Rev. 34, 1–26.

Porreca, F., Ossipov, M. H., and Gebhart, G. F. 2002. Tonic descending facilitation as a mechanism of chronic pain. Trends Neurosci. 25, 319–325.

Posserud, I., Agerforz, P., Ekman, R., Bjornsson, E. S., Abrahamsson, H., and Simren, M. 2004. Altered visceral perceptual and neuroendocrine response in patients with irritable bowel syndrome during mental stress. Gut 53, 1102–1108.

Powley, T. L. and Phillips, R. J. 2002. Musings on the wanderer: what's new in our understanding of vago-vagal reflexes?: I. Morphology and topography of vagal afferents innervating the GI tract. Am. J. Physiol. 283, G1217–G1225.

Price, D. D., Craggs, J., Verne, N., Perlstein, W. M., and Robinson, M. E. 2007a. Placebo analgesia is accompanied by large reductions in pain-related brain activity in irritable bowel syndrome patients. Pain 127, 63–72.

Price, D. D., Robinson, M. E., and Verne, G. N. 2007b. Measuring Pain and Hyperalgesia in Persistent Pain Conditions with a Special Emphasis on Irritable Bowel Syndrome. In: Chronic Abdominal and Visceral Pain (*eds*. P. Pasricha, W. Willis, and G. F. Gebhart), pp. 127–140. Informa Healthcare.

Randich, A., Uzzell, T., DeBerry, J. J., and Ness, T. J. 2006. Neonatal urinary bladder inflammation produces adult bladder hypersensitivity. J. Pain 7, 469–479.

Ricco, M. M., Kummer, W., Biglari, B., Myers, A. C., and Undem, B. J. 1996. Interganglionic segregation of distinct vagal afferent fibre phenotypes in guinea-pig airways. J. Physiol 496, 521–530.

Robinson, D. R., McNaughton, P. A., Evans, M. L., and Hicks, G. A. 2004. Characterization of the primary spinal afferent innervation of the mouse colon using retrograde labelling. Neurogastroenterol. Motil. 16, 113–124.

Rong, W., Hillsley, K., Davis, J. B., Hicks, G., Winchester, W. J., and Grundy, D. 2004. Jejunal afferent nerve sensitivity in wild-type and TRPV1 knockout mice. J. Physiol. 560, 867–881.

Sarkar, S., Aziz, Q., Woolf, C. J., Hobson, A. R., and Thompson, D. G. 2000. Contribution of central sensitisation to the development of non-cardiac chest pain. Lancet 356, 1154–1159.

Sarkar, S., Hobson, A. R., Furlong, P. L., Woolf, C. J., Thompson, D. G., and Aziz, Q. 2001. Central neural mechanisms mediating human visceral hypersensitivity. Am. J. Physiol. 281, G1196–G1202.

Schmidt, R. F. 1996. The Articular Polymodal Nociceptor in Health and Disease. In: ThePolymodal Receptor: A Gateway to Pathological Pain, Progress in Brain Research (*eds*.T. Kumazawa, L. Kruger, and K. Mizumura), Vol. 113, pp. 53–81. Elsevier.

Schuligoi, R., Joci, M., Heinemann, A., Schoninkle, E., Pabst, M. A., and Holzer, P. 1998. Gastric acid-evoked c-fos messenger RNA expression in rat brainstem is signaled by capsaicin-resistant vagal afferents. Gastroenterology 115, 649–660.

Sharma, A. and Aziz, Q. 2007. Mechanisms of Visceral Sensitization in Humans. In: Chronic Abdominal and Visceral Pain (*eds*. P. Pasricha, W. Willis, and G. F. Gebhart), pp. 141–160. Informa Healthcare.

Sherrington, C. S. 1900. Cutaneous Sensations. In: Textbook of Physiology (*ed*. E. A. Schäffer), pp. 920–1001. Pentland.

Sherrington, C. S. 1906. The Integrative Action of the Nervous System. Scribner.

Sidhu, H., Kern, M., and Shaker, R. 2004. Absence of increasing cortical FMRI activity volume in response to increasing visceral stimulation in IBS patients. Am. J. Physiol. 287, G425–G435.

Song, G. H., Venkatraman, V., Ho, K. Y., Chee, M. W., Yeoh, K. G., and Wilder-Smith, C. H. 2006. Cortical effects of anticipation and endogenous modulation of visceral pain assessed by functional brain MRI in irritable bowel syndrome patients and healthy controls. Pain 126, 79–90.

Spencer, S. J., Hyland, N. P., Sharkey, K. A., and Pittman, Q. J. 2007. Neonatal immune challenge exacerbates experimental colitis in adult rats: potential role for TNF-α. Am. J. Physiol. 292, R308–R315.

Spiller, R. C., Jenkins, D., Thornley, J. P., Hebden, J. M., Wright, T., Skinner, M., and Neal, K. R. 2000. Increased rectal mucosal enteroendocrine cells, T lymphocytes and

increased gut permeability following acute campylobacter enteritis and in post-dysenteric irritable bowel syndrome. Gut 47, 804–811.
Stead, R. H., Dixon, M. F., Bramwell, N. H., Riddell, R. H., and Bienenstock, J. 1989. Mast cells are closely apposed to nerves in the human gastrointestinal mucosa. Gastroenterology 97, 575–585.
Stewart, T. M., Beyak, M. J., and Vanner, S. J. 2003. Ileitis modulates potassium and sodium currents in guinea pig dorsal root ganglia neurons. J. Physiol. 552, 797–807.
Strigo, I. A., Duncan, G. H., Boivin, M., and Bushnell, M. C. 2003. Differentiation of visceral and cutaneous pain in the human brain. J. Neurophysiol. 89, 3294–3303.
Su, X., Sengupta, J. N., and Gebhart, G. F. 1997. Effects of opioids on mechanosensitive pelvic nerve afferent fibers innervating the urinary bladder of the rat. J. Neurophysiol. 77, 1566–1580.
Sugiura, T., Bielefeldt, K., and Gebhart, G. F. 2004. TRPV1 function in mouse colon sensory neurons is enhanced by metabotropic 5-hydroxytryptamine receptor activation. J. Neurosci. 24, 9521–9530.
Sugiura, T., Bielefeldt, K., and Gebhart, G. F. 2007. Mouse colon sensory neurons detect extracellular acidosis via TRPV1. Am. J. Physiol. 292, C1768–C1774.
Sugiura, T., Dang, K., Lamb, K., Bielefeldt, K., and Gebhart, G. F. 2005. Acid-sensing properties in rat gastric sensory neurons from normal and ulcerated stomach. J. Neurosci. 25, 2617–2627.
Taché, Y., Martinez, V., Wang, L., and Million, M. 2004. CRF1 receptor signaling pathways are involved in stress-related alterations of colonic function and viscerosensitivity: implications for irritable bowel syndrome. Br. J. Pharmacol. 141, 1321–1330.
Torebjörk, H. E., Schmelz, M., and Handwerker, H. O. 1996. Functional Properties of Human Cutaneous Nociceptors and their Role in Pain and Hyperalgesia. In: Neurobiology of Nociceptors (*eds*. C. Belmonte and F. Cervero), pp. 349–369. Oxford University Press.
Undem, B. J., Carr, M. J., and Kollarik, M. 2002. Physiology and plasticity of putative cough fibres in the Guinea pig. Pulm. Pharmacol. Ther. 15, 217–219.
Undem, B. J., Chuaychoo, B., Lee, M. G, Weinreich, D., Myers, A. C., and Kollarik, M. 2004. Sybtypes of vagal afferent c-fibres in guinea-pig lungs. J. Physiol. 556, 905–917.
Vandenberghe, J., Vos, R., Persoons, P., Demyttenaere, K., Janssens, J., and Tack, J. 2005. Dyspeptic patients with visceral hypersensitivity: sensitisation of pain specific or multimodal pathways? Gut 54, 914–919.
Vera-Portocarrero, L. P., Yie, J., Kowal, J., Ossipov, M., King, T., and Porreca, F. 2006. Descending facilitation from the rostral ventromedial medulla maintains visceral pain in rats with experimental pancreatitis. Gastroenterology 130, 2155–2164.
Wang, F. B. and Powley, T. L. 2000. Topographic inventories of vagal afferents in gastrointestinal muscle. J. Comp. Neurol. 421, 302–324.
Wemmie, J., Price, M., and Welsh, M. 2006. Acid-sensing ion channels: advances, questions and therapeutic opportunities. Trends Neurosci. 29, 578–586.
Whitehead, W., Palsson, O., and Jones, K. 2002. Systematic review of the comorbidity of irritable bowel syndrome with other disorders: What are the causes and implications? Gastroenterology 122, 1140–1156.
Willert, R. P., Woolf, C. J., Hobson, A. R., Delaney, C., Thompson, D. G., and Aziz, Q. 2004. The development and maintenance of human visceral pain hypersensitivity is dependent on the *N*-methyl-D-aspartate receptor. Gastroenterology 126, 683–692.
Winnard, K. P., Dmitrieva, N., and Berkley, K. 2006. Cross-organ interactions between reproductive, gastrointestinal, and urinary tracts: modulation by estrous stage and involvement of the hypogastric nerve. Am. J. Physiol. 291, R1592–R1601.
Woolf, C. J. and Thompson, S. W. 1991. The induction and maintenance of central sensitization is dependent on *N*-methyl-D-aspartic acid receptor activation: implications for the treatment of post-injury pain hypersensitivity states. Pain 44, 293–299.
Wynn, G., Ma, B., Ruan, H. Z., and Burnstock, G. 2004. Purinergic component of mechanosensory transduction is increased in a rat model of colitis. Am. J. Physiol. 287, G647–G657.
Wynn, G., Rong, W., Xiang, Z., and Burnstock, G. 2003. Purinergic mechanisms contribute to mechanosensory transduction in the rat colorectum. Gastroenterology 25, 1398–1409.
Xu, G., Winston, J., Shenoy, M., Yin, H., and Pasricha, P. J. 2006. Enhanced excitability and suppression of A-type K^+ current of pancreas-specific afferent neurons in a rat model of chronic pancreatitis. Am. J. Physiol. 291, G424–G431.
Yágüez, L., Coen, S., Gregory, L. J., Amaro, E., Jr., Altman, C., Brammer, M. J., Bullmore, E. T., Williams, S. C. R., and Aziz, Q. 2005. Brain response to visceral aversive conditioning: a functional magnetic resonance imaging study. Gastroenterology 128, 1819–1829.
Yoshimura, N. and de Groat, W. C. 1999. Increased excitability of afferent neurons innervating rat urinary bladder after chronic bladder inflammation. J. Neurosci. 19, 4644–4653.
Yoshimura, N., Seki, S., Erickson, K. A., Erickson, V. L., Chancellor, M. B., and de Groat, W. C. 2003. Histological and electrical properties of rat dorsal root ganglion neurons innervating the lower urinary tract. J. Neurosci. 23, 4355–4361.
Yoshimura, N., Seki, S., Novakovic, S. D., Tzoumaka, E., Erickson, V. L., Erickson, K. A., Chancellor, M. B., and de Groat, W. C. 2001. The involvement of the tetrodotoxin-resistant sodium channel nav1.8 (pn3/sns) in a rat model of visceral pain. J. Neurosci. 21, 8690–8696.
Yu, S., Undem, B. J., and Kollarik, M. 2005. Vagal afferent nerves with nociceptive properties in guinea-pig oesophagus. J. Physiol. 563, 831–842.
Zagorodnyuk, V. P. and Brookes, S. J. H. 2000. Transduction sites of vagal mechanoreceptors in the guinea pig esophagus. J. Neurosci. 20, 6249–6255.
Zagorodnyuk, V. P., Chen, B. N., Costa, M., and Brookes, J. H. 2003. Mechanotransduction by intraganglionic laminar endings of vagal tension receptors in the guinea-pig oesophagus. J. Physiol. 553, 575–587.
Zhuo, M. and Gebhart, G. F. 2002. Facilitation and attenuation of a visceral nociceptive reflex from the rostroventral medulla in the rat. Gastroenterology 122, 1007–1019.
Zhuo, M., Sengupta, J. N., and Gebhart, G. F. 2002. Biphasic modulation of spinal visceral nociceptive transmission from the rostroventral medial medulla in the rat. J. Neurophysiol. 87, 2225–2236.

Further Reading

Berkley, K. J., Robbins, A., and Sato, Y. 1988. Afferent fibers supplying the uterus in the rat. J. Neurophysiol. 59, 142–163.
Brune, K. and Handwerker, H. O. (*eds.*) 2004. Hyperalgesia: Molecular Mechanisms and Clinical Implications, Progress in Pain Research and Management, Vol. 30. IASP Press.
Carr, M. J. and Undem, B. J. 2003. Bronchopulmonary afferent nerves. Respirology 8, 291–301.
Cervero, F. 1994. Sensory innervation of the viscera: peripheral basis of visceral pain. Physiol. Rev. 74, 95–138.

Francis, C. Y., Duffy, J. N., Whorwell, P. J., and Morris, J. 1997. High prevalence of irritable bowel syndrome in patients attending urological outpatient departments. Dig. Dis. Sci. 42, 404–407.

Gebhart, G. F. (*ed.*) 1995. Visceral Pain, Progress in Pain Research and Management, , Vol. 5. IASP Press.

Jänig, W. 2006. The Integrative Action of the Autonomic Nervous System. Cambridge University Press.

Kollarik, M. and Undem, B. J. 2002. Mechanisms of acid-induced activation of airway afferent nerve fibres in guinea-pig. J. Physiol. 543, 591–600.

Kollarik, M. and Undem, B. J. 2003. Activation of bronchopulmonary vagal afferent nerves with bradykinin, acid and vanilloid receptor agonists in wild-type and TRPV1$^{-/-}$ mice. J. Physiol. 555, 115–123.

Kreis, M. E., Jiang, W., Kirkup, A. J., and Grundy, D. 2002. Cosensitivity of vagal mucosal afferents to histamine and 5-HT in the rat jejunum. Am. J. Physiol. 283, G612–G617.

Linden, D. R., Chen, J.-X., Gershon, M. D., Sharkey, K. A., and Mawe, G. M. 2003. Serotonin availability is increased in mucosa of guinea pigs with TNBS-induced colitis. Am. J. Physiol. 285, G207–G216.

Ness, T. J. and Gebhart, G. F. 1990. Visceral pain: a review of experimental studies. Pain 41, 167–234.

Pan, H. L. and Longhurst, J. C. 1996. Ischaemia-sensitive sympathetic afferents innervating the gastrointestinal tract function as nociceptors in cats. J. Physiol. 492, 841–850.

Pasricha, P. J., Willis, W. D.,, and Gebhart, G. F. (*eds.*) 2007. Chronic Abdominal and Visceral Pain., Informa Healthcare.

Spiller, R. and Grundy, D. (*eds.*) 2004. Pathophysiology of the Enteric Nervous System., Blackwell Publishing.

5.38 Irritable Bowel Syndrome

S Bradesi and E A Mayer, University of California, Los Angeles, CA, USA

I Schwetz, Medical University, Graz, Austria

© 2008 Elsevier Inc. All rights reserved.

5.38.1	Introduction	571
5.38.2	Clinical Presentation and Epidemiology	571
5.38.3	The Bidirectional Brain–Gut Axis Model	572
5.38.4	Visceral Hypersensitivity	572
5.38.4.1	Peripheral Up-Regulation of Visceral Afferent Sensitivity	573
5.38.4.2	Spinal and Supraspinal Up-Regulation of Visceral Afferent Sensitivity	574
5.38.5	Treatment Options	575
5.38.6	Summary and Conclusions	575
References		575

5.38.1 Introduction

Recurrent abdominal pain or discomfort in the absence of detectable structural or biochemical abnormalities, associated with alterations in bowel habits, are the principal symptoms of irritable bowel syndrome (IBS) (Drossman, D. A. *et al.*, 2002). Due to the likely heterogeneity of the syndrome (Mayer, E. A. and Collins, S. M., 2002) and the lack of reliable organic markers, the development of a unifying, and generally agreed upon, hypothesis of the pathophysiology of IBS has remained an elusive goal. Many investigators in the field agree that an enhanced perception of physiologically occurring, or experimentally generated visceral events (visceral hypersensitivity) (Mayer, E. A. and Gebhart, G. F., 1994; see Vagal Afferent Neurons and Pain and Visceral Pain) in conjunction with alterations in gastrointestinal motility and secretory function, are key pathophysiological mechanisms underlying the cardinal clinical features of IBS. In contrast, many other alterations reported in IBS patients over the past decades, including altered mucus production and altered gastrointestinal motility, have turned out to be epiphenomena which are unlikely to be essential for symptom generation. Considerable evidence supports the role of psychosocial (Bennett, E. J. *et al.*, 1998; Collins, S. M., 2002) and physical (Gwee, K. A. *et al.*, 1996) (i.e., acute gastroenteric infections) stressors as central and peripheral triggers of first symptom onset or symptom exacerbation of long-standing IBS (Mayer, E. A. *et al.*, 2001), and an IBS hypothesis of hyperresponsiveness of central stress circuits has been proposed (Mayer, E. A. and Collins, S. M., 2002).

5.38.2 Clinical Presentation and Epidemiology

IBS is one of the most common and most thoroughly studied functional disorders of the gastrointestinal tract (Drossman, D. A. *et al.*, 2002). In additional to chronic abdominal pain, the clinical presentation of IBS typically also includes nonpainful abdominal discomfort (sensations of urgency, bloating, fullness, gas and constipation) (Lembo, T. J. and Fink, R. N., 2002) and visible abdominal distension. These gastrointestinal symptoms are frequently associated with extraintestinal symptoms such as fatigue, decreased energy level, impaired sleep, depression, and anxiety (Zimmerman, J., 2003). In the absence of generally agreed upon reliable biological markers, the diagnosis of IBS remains one based on the presence of the so-called symptom criteria (Thompson, W. G. *et al.*, 1999). The most widely accepted diagnostic criteria are the Rome II Criteria that evolved from the Rome I and the Manning criteria initially defined about a decade ago (Longstreth, G. F., 2005). Different IBS patient subtypes have been identified based on their bowel habit predominance and have been classified as: constipation, diarrhea, or alternating periods of both. In a large US sample, approximately 50% of IBS patients present alternating bowel habit (IBS-A),

30% diarrhea (IBS-D), and 20% constipation (IBS-C) (Tillisch, K. *et al.,* 2005).

Large population based studies in the US have found a prevalence of IBS of about 14% with a greater proportion of women affected (female-to-male ratio approximately 3:1 to 3:2). The socioeconomic consequences of IBS are considerable with a large impact on work productivity and absenteeism (Dean, B. B. *et al.,* 2005). In addition, a substantial reduction in health-related quality of life (HRQoL) has been observed in IBS patients with moderate to severe symptoms who are seen in a referral setting compared with healthy controls (Spiegel, B. M. *et al.,* 2004). Interestingly, bowel habit alterations contributed little to the HRQoL impairment in this study, while extraintestinal manifestations such as loss of energy, fatigue, and excessive worry were important determinants. The annual cost of IBS in the US has been estimated to be between $1.7 billion and $10 billion in direct medical cost (repetitive use of multiple healthcare resources) and $20 billion for indirect costs (work absenteeism and impaired productivity) representing a high socioeconomic burden on society (Inadomi, J. M. *et al.,* 2003).

While research over the past few years has provided significant advances in the understanding of IBS pathophysiology, the precise mechanism(s) underlying symptom generation remains incompletely understood, generating considerable controversy among investigators. As a result, the development of effective IBS therapies has been slow and disappointing (Bradesi, S. *et al.,* 2006). IBS pathophysiology is often viewed within the so-called biopsychosocial model in which altered physiology (gastrointestinal motility and secretion, enhanced perception of visceral stimuli (visceral hypersensitivity) and psychosocial factors interact and determine the clinical expression of IBS (Schwetz, I. *et al.,* 2004). From a biological perspective, IBS symptomatology can be viewed as the manifestation of alterations in the brain–gut axis, specifically as a dysregulation in the complex interplay between events occurring within the gut, the enteric nervous system, and the central nervous system (Mulak, A. and Bonaz, B., 2004).

5.38.3 The Bidirectional Brain–Gut Axis Model

Brain-gut interactions play a prominent role in the modulation of gut function in health and disease (Mayer, E. A. *et al.,* 2001; Taché, Y. *et al.,* 2001). Therefore, every conceptual model of IBS has to take into account that neither the central nervous system nor the gastrointestinal tract function in isolation, but that both systems interact with each other under normal conditions and particularly during perturbations of homeostasis. Afferent signals arising from the lumen of the gut are transmitted via various visceral afferent pathways (enteric, spinal, vagal) to the central nervous system. Homeostatic reflexes, which generate appropriate gut responses to physiological as well as pathological visceral stimuli, occur at the level of the enteric nervous system, the spinal cord, and pontomedullary nuclei and limbic regions. Vagal visceral afferent inputs may also play an important role in such diverse functions as modulation of emotion, pain sensitivity, satiety, and immune response (Jänig, W. and Habler, H.-J., 2000). Whereas the reflex circuits within the enteric nervous system in principle can regulate and synchronize all basic gastrointestinal functions (motility, secretion, blood flow), coordination of gut functions with the overall homeostatic state of the organism requires continuous communication between the central nervous system and the gastrointestinal tract (Mayer, E. A. and Collins, S. M., 2002). Descending cortico-limbic influences can set the gain and responsiveness of these reflexes, or impose distinct patterns of motor responses on lower circuits, should the overall condition of the body make it necessary. Such top-down override of local reflex function occurs during sleep, during the stress response, or during strong emotions such as fear and anger (Ito, M., 2002; Mayer, E. A., 2000a; Taché, Y. *et al.,* 2001; Welgan, P. *et al.,* 1988). While the great majority of homeostatic afferent input from the gut (as well as other viscera) to the central nervous system is not consciously perceived, there are both peripheral and central adaptive mechanisms which can result in enhanced perception and altered reflex responses to visceral stimuli (Mayer, E. A. and Gebhart, G. F., 1994).

5.38.4 Visceral Hypersensitivity

The initial clinical observations that led to the hypothesis that IBS patients exhibit visceral hypersensitivity include recurring abdominal pain, tenderness during palpation of the sigmoid colon during physical examination, and excessive pain during endoscopic evaluation of the sigmoid colon (Mayer, E. A. and Gebhart, G. F., 1994). Multiple human experimental studies using barostat-controlled balloon distension

paradigms have reported lowered colorectal perceptual thresholds, increased sensory ratings and viscerosomatic referral areas in IBS patients compared to healthy individuals (Bouin, M. *et al.,* 2002; Chang, L. *et al.,* 2000a; Mertz, H. *et al.,* 1995). Despite the uncertainty about the underlying mechanism(s), this kind of experimentally induced visceral hypersensitivity has been considered a pathophysiological hallmark of the disease. Within the framework of homeostatic afferents, the finding of chronic, conscious awareness of unpleasant visceral sensations, together with the presence of altered reflex regulation in the gut, could be explained by several different mechanisms, including the following: (1) a peripheral up-regulation of the sensitivity of visceral afferent pathways which may be related to alterations in the activity of various effector cells within the gut (enteric nerves, enterochromaffin cells, immune cells); (2) a spinal or brainstem alteration in the sensitivity to incoming visceral afferents which could be a consequence of primary peripheral or central inputs; or (3) a primary central amplification of perceptual and reflex responses to incoming visceral afferent signals. In addition, the frequent presence of compromised vital functions such as sleep, mood, sexual drive, and affect, suggest a possible involvement of other homeostatic mechanisms, such as tonic serotonergic pontomedullary systems (Mason, P., 2005). It remains to be determined if these various abnormalities occur in distinct subsets of patients, at different stages of the disorder, or if various combinations of them generate a heterogeneous patient population.

5.38.4.1 Peripheral Up-Regulation of Visceral Afferent Sensitivity

The concept that gut mucosal alterations may play a role in the pathophysiology of IBS has been prompted by several lines of clinical and preclinical evidence including: (1) alterations in the number of immune cells, particularly mast cells, within intestinal biopsies of patients meeting diagnostic criteria for IBS (Barbara, G. *et al.,* 2004; O'Sullivan, M. *et al.,* 2000; Weston, A. P. *et al.,* 1993), and the demonstration in rodent studies that mucosal mast cells play a prominent role of transducers within the brain–gut axis (Santos, J. *et al.,* 2005; Soderholm, J. D. *et al.,* 2002; Wilson, L. M. and Baldwin, A. L., 1999); (2) demonstration of visceral hypersensitivity in different animal models of gut immune system activation (Barbara, G. *et al.,* 1997; Barreau, F. *et al.,* 2004; La, J. H. *et al.,* 2003; Lamb, K. *et al.,* 2006); (3) preliminary evidence that supernatants from human mucosal biopsies (taken from IBS patients) have a unique effect on visceral afferent function in rodent bioassays (Barbara, G. *et al.,* 2005a; Barbara, G. *et al.,* 2005b); (4) the development of IBS-like symptoms in a small number of individuals following an episode of acute gastroenteritis (Gwee, K. A. *et al.,* 1998; Spiller, R. C., 2005) and in a subset of patients with inflammatory bowel disease (Bernstein, C. N. *et al.,* 1996); (5) evidence for alteration in the normal gut flora (including bacterial overgrowth) (Balsari, A. *et al.,* 1982; O'Leary, C. and Quigley, E. M., 2003; Swidsinski, A. *et al.,* 1999); and (6) therapeutic responses to treatment with antibiotics and probiotic treatments (Madden, J. A. and Hunter, J. O., 2002; Pimentel, M. *et al.,* 2000, 2003). Without discussing this large body of evidence supporting each of these points (Barbara, G. *et al.,* 2006; Crowell, M. D. *et al.,* 2005; Schwetz, I. *et al.,* 2003; Spiller, R. C., 2005), it is assumed, by many investigators focusing on peripheral etiologies of visceral hypersensitivity, that the mucosal immune activation plays some role in maintaining a chronic state of visceral afferent sensitization. Based on recent preclinical evidence, it is conceivable that transient peripheral sensitization may result in long-lasting up-regulation of spino-bulbo-spinal pain amplification mechanisms (Suzuki, R. *et al.,* 2005). While such peripheral mechanisms (in particular an increase in mucosal mast cells and intestinal enterochromaffin cells) may play an important role in a subset of IBS patients, or in the mediation of certain types of IBS symptoms, a series of observations argues against a simple relationship between peripheral mucosal events and IBS symptoms. For example, it has long been known that some patients in remission from inflammatory bowel disease, especially ulcerative colitis, report symptoms similar to those of IBS patients (Isgar, B. *et al.,* 1983; Simren, M. *et al.,* 2000). In contrast, inflammatory bowel disease patients (without associated IBS features) who have chronically recurring gut inflammation do not exhibit visceral hypersensitivity (Chang, L. *et al.,* 2000b) or enhanced central nervous system responses to visceral distension during periods of remission (Loennig-Baucke, V. *et al.,* 1989; Rao, S. S. C. *et al.,* 1987). In addition, clinical states characterized by chronic inflammation of the esophagus (gastroesophageal reflux disease) and stomach (*Helicobacter pylori* chronic gastritis) are also not associated with visceral mechanical hyperalgesia (Fass, R. *et al.,* 1998; Mertz, H. *et al.,* 1998). On the contrary, it has been reported that

Crohn's patients with isolated inflammation in the small bowel have elevated discomfort thresholds to controlled distension of the rectum (Bernstein, C. N. *et al.,* 1996), and that patients with ulcerative colitis do not show sensitization following repetitive noxious distension of the sigmoid colon (Chang, L. *et al.,* 2000b). Taken together, these data are consistent with the interpretation that chronic mucosal inflammatory changes in the esophagus, stomach, or colon by themselves do not necessarily result in mechanical visceral hypersensitivity. Chronic intestinal inflammation in inflammatory bowel disease seems to be associated with the activation of counterregulatory antinociceptive systems, inhibition of pain facilitatory pathways or both, resulting in a reduced perception of visceral afferent information (Chang, L. *et al.,* 2000b). One may speculate that genetic polymorphisms recently identified as being associated with greater pain sensitivity may be related to such compromised endogenous pain modulation systems (Diatchenko, L. *et al.,* 2005).

5.38.4.2 Spinal and Supraspinal Up-Regulation of Visceral Afferent Sensitivity

A growing body of literature supports the concept of an enhanced stress responsiveness playing a role in the development of IBS symptoms in a subset of patients (reviewed in Mayer, E. A., 2000b; Mayer, E. A. *et al.,* 2001). An individual's response to stress (perturbation of homeostasis) is generated by a central network comprised of integrative brain structures, referred to as the emotional motor system (EMS) (for a detailed review see Mayer, E. A., 2000b); Mayer, E. A. *et al.,* 2001). The main output systems of the EMS are ascending monoaminergic pathways, the autonomic nervous system, the hypothalamic–pituitary–adrenal axis and endogenous pain modulatory systems. The neuropeptide, corticotropin-releasing factor (CRF), plays a prominent role in integrating these various outputs in response to physical and psychological stressors (Bale, T. L., 2005).

The responsiveness of the EMS and its various output pathways is under partial genetic control (Pezawas, L. *et al.,* 2005) and is programmed by prenatal (Matthews, S. G., 2002) and postnatal (Ladd, C. O. *et al.,* 2000) aversive events and by certain types of pathological stress (Fuchs, E. and Fluegge, G., 1995). In humans, early (pre- and postnatal) life adverse experiences can lead to long-lasting stress hyperresponsiveness, which in turn has been associated with a wide range of health impairments in adult life (Whitehead, M. and Holland, P., 2003). Long-term consequences of early aversive events also include an increased vulnerability for stress-sensitive disorders such as IBS and posttraumatic stress disorder (Lowman, B. C. *et al.,* 1987). Stress hyperresponsiveness is related in part to permanent, stress-induced hypersecretion of CRF (Heim, C. *et al.,* 2000). A number of preclinical studies support the concept of centrally mediated alteration of visceral perception. Different stress paradigms were found to lead to enhanced visceral response to colonic distension (Bradesi, S. *et al.,* 2002; Gue, M. *et al.,* 1997; Schwetz, I. *et al.,* 2005), which can be mimicked or abolished by central administration of pharmacological agents. For example, central CRF injection was found to mimic the effect of stress on visceral sensitivity, whereas stress-induced visceral hyperalgesia may be reduced by central injection of a CRF receptor subtype 1 antagonist (Taché, Y. *et al.,* 2004). Similarly, a neurokinin-1 receptor antagonist injected into the spinal cord in stress-sensitized guinea pigs (Greenwood-Van Meerveld, B. *et al.,* 2003) or rats (Bradesi, S. *et al.,* 2005) abolished the stress-induced visceral hyperalgesia to colorectal distension. Together, the data available suggest the role of central stress circuits in the alteration of visceral nociceptive response in animal models for IBS. In contrast to the well-known analgesic response to severe acute stressors (stress-induced somatic analgesia), prolonged and milder stressors that are associated with anxiety-like states are commonly associated with hyperalgesic responses (Boccalon, S. *et al.,* 2006; Vendruscolo, L. F. *et al.,* 2004).

Suggestive evidence for an alteration in central pain modulation mechanisms in IBS patients comes from a series of functional brain-imaging studies. In response to rectal balloon distension, IBS patients have shown increased activation of subregions of the dorsal anterior cingulate cortex (ACC) (Naliboff, B. D. *et al.,* 2001b; Porreca, F. *et al.,* 2002; Verne, G. N. *et al.,* 2003), a brain region involved in attentional and emotional modulation of stimulus perception (Petrovic, P. and Ingvar, M., 2002). Dorsal ACC subregions provide input to subcortical endogenous pain inhibitory circuits (Petrovic, P. and Ingvar, M., 2002), as well as to subcortical pain facilitatory circuits (Zhuo, M. and Gebhart, G. F., 2002). The relative balance between these simultaneously activated pain modulation systems determines the overall modulation of perception (Porreca, F. *et al.,* 2002). Thus, the finding of greater dorsal ACC

activation by a visceral stimulus in IBS may be related to greater attention and possibly associated activation of pain facilitation circuits to a visceral stimulus in IBS. On the other hand, the lesser activation of the periaqueductal gray (PAG) reported in some studies (Naliboff, B. D. *et al.,* 2001b) is consistent with possible deficiencies in the cortical activation of endogenous pain inhibition systems. Several recent studies (Chang, L., 2005) provide further support for the hypothesis of altered endogenous pain modulation in IBS patients. In one study (Mayer, E. A. *et al.,* 2005), IBS patients were compared to patients with ulcerative colitis and with healthy control subjects. IBS patients showed consistently greater activation of limbic/paralimbic brain regions (amygdala, hypothalamus, ventral/rostral ACC, dorsomedial prefrontal cortex) suggestive of increased activation of arousal circuits by a visceral stimulus. In addition, the results showed activation in the ulcerative colitis and control subjects, but not in IBS patients, in the lateral prefrontal regions and a midbrain region including the PAG. A connectivity analysis using structural equation modeling supported these regions acting as part of a pain inhibition network that involves lateral and medial prefrontal influences on the PAG. Another study provided evidence for the abnormal activation of diffuse noxious inhibitory control systems in response to a noxious stimulus in IBS patients (Wilder-Smith, C. H. *et al.,* 2004).

Several lines of evidence indicate that patients with IBS and other functional disorders have hypervigilance for symptom relevant sensations (Berman, S. M. *et al.,* 2002). In a recent longitudinal study of IBS patients exposed to six sessions of rectal inflations over a 1-year period, regional cerebral blood flow to the inflations and anticipation of inflations using $H_2^{15}O$ positron emission tomography (PET) at the first and last session were evaluated (Naliboff, B. D. *et al.,* 2001a). Subjective ratings of the rectal inflations normalized over the course of the study consistent with decreased vigilance towards the visceral stimuli. Stable activation of the central pain matrix (including thalamus and insula) by the rectal stimulus was observed over the 12-month period, while activity in limbic, paralimbic ,and pontine regions decreased. An analysis examining the co-variation of these brain regions supported the hypothesis of changes in an arousal network including limbic, pontine, and cortical areas underlying the decreased perception seen over the multiple stimulation studies.

5.38.5 Treatment Options

Despite its high prevalence and considerable impact on patients' HRQoL, treatment options for IBS continue to be limited and there are few well designed studies to support the effectiveness of some of the most commonly used therapies (for review see Camilleri, M., 2004). Traditional treatment algorithms have primarily been aimed at peripheral targets and are largely symptom-based (e.g., laxatives, antidiarrheals, prokinetics). In addition, centrally targeted therapies include various forms of cognitive behavioral therapy (Hutton, J., 2005), low-dose tricyclic antidepressants (Drossman, D. A. *et al.,* 2003) and, in patients with co-morbid psychiatric conditions, full dose serotonin reuptake inhibitors (Creed, F. *et al.,* 2003). A series of compounds are currently in development, which is targeted at central circuits involved in stress responsiveness and pain modulation (Bradesi, S. *et al.,* 2006).

5.38.6 Summary and Conclusions

Despite its high prevalence, and considerable burden of illness, treatment of IBS remains unsatisfactory. However, considerable progress has been made to identify alterations at different levels of the brain–gut axis which may contribute to characteristic symptoms. In the absence of generally agreed upon animal models of the syndrome, functional brain-imaging techniques in well defined human patient populations has a high promise to identify central abnormalities related to altered stress responsiveness and associated pain modulation circuits. A number of novel treatment approaches aimed at these central abnormalities are currently under development.

References

Bale, T. L. 2005. Sensitivity to stress: Dysregulation of CRF pathways and disease development. Horm. Behav. 48, 1–10.

Balsari, A., Ceccarelli, A., Dubini, F., Fesce, E., and Poli, G. 1982. The fecal microbial population in the irritable bowel syndrome. Microbiologica 5, 185–194.

Barbara, G., Cremon, C., Riccardo, V., Elisabetta, C., Balestra, B., Di Nardo, G., De Giorgio, R., Stanghellini, V., Corinaldesi, R., and Tonini, M. 2005a. Colonic mucosal mast cell mediators from patients with irritable bowel syndrome excite enteric cholinergic motor neurons. Gastroenterology 128, A-58 (abstract).

Barbara, G., Stanghellini, V., De Giorgio, R., and Corinaldesi, R. 2006. Functional gastrointestinal disorders and mast cells: Implications for therapy. Neurogastroenterol. Motil. 18, 6–17.

Barbara, G., Stanghellini, V., De Giorgio, R., Cremon, C., Cottrell, G. S., Santini, D., Pasquinelli, G., Morselli-Labate, A. M., Grady, E. F., Bunnett, N. W., Collins, S. M., and Corinaldesi, R. 2004. Activated mast cells in proximity to colonic nerves correlate with abdominal pain in irritable bowel syndrome. Gastroenterology 126, 693–702.

Barbara, G., Vallance, B. A., and Collins, S. M. 1997. Persistent intestinal neuromuscular dysfunction after acute nematode infection in mice. Gastroenterology 113, 1224–1232.

Barbara, G., Wang, B., Grundy, D., Cremon, C., De Giorgio, R., Di Nardo, G., Trevisani, M., Campi, B., Geppetti, P., Tonini, M., Stanghellini, V., and Corinaldesi, R. 2005b. Mast cells are increased in the colonic mucosa of patients with irritable bowel syndrome and excite visceral sensory pathways. Gastroenterology 128, A-626 (abstract).

Barreau, F., Cartier, C., Ferrier, L., Fioramonti, J., and Bueno, L. 2004. Nerve growth factor mediates alterations of colonic sensitivity and mucosal barrier induced by neonatal stress in rats. Gastroenterology 127, 524–534.

Bennett, E. J., Tennant, C. C., Piesse, C., Badcock, C. A., and Kellow, J. E. 1998. Level of chronic life stress predicts clinical outcome in irritable bowel syndrome. Gut 43, 256–261.

Berman, S. M., Naliboff, B. D., Chang, L., FitzGerald, L., Antolin, T., Camplone, A., and Mayer, E. A. 2002. Enhanced preattentive central nervous system reactivity in irritable bowel syndrome. Am. J. Gastroenterol. 97, 2791–2797.

Bernstein, C. N., Niazi, N., Robert, M., Mertz, H., Kodner, A., Munakata, J., Naliboff, B., and Mayer, E. A. 1996. Rectal afferent function in patients with inflammatory and functional intestinal disorders. Pain 66, 151–161.

Boccalon, S., Scaggiante, B., and Perissin, L. 2006. Anxiety stress and nociceptive responses in mice. Life Sci. 78, 1225–1230.

Bouin, M., Plourde, V., Boivin, M., Riberdy, M., Lupien, F., Laganiere, M., Verrier, P., and Poitras, P. 2002. Rectal distension testing in patients with irritable bowel syndrome: Sensitivity, specificity, and predictive values of pain sensory thresholds. Gastroenterology 122, 1771–1777.

Bradesi, S., Eutamene, H., Garcia-Villar, R., Fioramonti, J., and Bueno, L. 2002. Acute and chronic stress differently affect visceral sensitivity to rectal distension in female rats. Neurogastroenterol. Motil. 14, 75–82.

Bradesi, S., Kokkotou, E., Song, B., Marvizon, J. C., Mittal, Y., McRoberts, J. A., Ennes, H. S., Pothoulakis, C., Ohning, G., and Mayer, E. A. 2005. Sustained visceral hyperalgesia following chronic psychological stress in rats involves up-regulation of spinal NK1 receptors. Gastroenterology 128, A-494 (abstract).

Bradesi, S., Tillisch, K., and Mayer, E. A. 2006. Emerging drugs for IBS. Expert Opin. Emerg. Drugs 11, 293–313.

Camilleri, M. 2004. Treating irritable bowel syndrome: overview, perspective and future therapies. Br. J. Pharmacol. 141, 1237–1248.

Chang, L. 2005. Brain responses to visceral and somatic stimuli in irritable bowel syndrome: A central nervous system disorder? Gastroenterol. Clin. North. Am. 34, 271–279.

Chang, L., Mayer, E. A., Johnson, T., FitzGerald, L., and Naliboff, B. 2000a. Differences in somatic perception in female patients with irritable bowel syndrome with and without fibromyalgia. Pain 84, 297–307.

Chang, L., Munakata, J., Mayer, E. A., Schmulson, M. J., Johnson, T. D., Bernstein, C. N., Saba, L., Naliboff, B., Anton, P. A., and Matin, K. 2000b. Perceptual responses in patients with inflammatory and functional bowel disease. Gut 47, 497–505.

Collins, S. M. 2002. A case for an immunological basis for irritable bowel syndrome. Gastroenterology 122, 2078–2080.

Creed, F., Fernandes, L., Guthrie, E., Palmer, S., Ratcliffe, J., Read, N., Rigby, C., Thompson, D., Tomenson, B. North of England IBS Research Group. 2003. The cost-effectiveness of psychotherapy and paroxetine for severe irritable bowel syndrome. Gastroenterology 124, 303–317.

Crowell, M. D., Harris, L., Jones, M. P., and Chang, L. 2005. New insights into the pathophysiology of irritable bowel syndrome: Implications for future treatments. Curr. Gastroenterol. Rep. 7, 272–279.

Dean, B. B., Aguilar, D., Barghout, V., Kahler, K. H., Frech, F., Groves, D., and Ofman, J. J. 2005. Impairment in work productivity and health-related quality of life in patients with IBS. Am. J. Manag. Care. 11, S17–S26.

Diatchenko, L., Slade, G. D., Nackley, A. G., Bhalang, K., Sigurdsson, A., Belfer, I., Goldman, D., Xu, K., Shabalina, S. A., Shagin, D., Max, M. B., Makarov, S. S., and Maixner, W. 2005. Genetic basis for individual variations in pain perception and the development of chronic pain condition. Hum. Mol. Gen. 14, 135–143.

Drossman, D. A., Camilleri, M., Mayer, E. A., and Whitehead, W. E. 2002. AGA technical review on irritable bowel syndrome. Gastroenterology 123, 2108–2131.

Drossman, D. A., Toner, B. B., Whitehead, W. E., Diamant, N. E., Dalton, C. B., Duncan, S., Emmott, S., Proffitt, V., Akman, D., Frusciante, K., Le, T., Meyer, K., Bradshaw, B., Mikula, K., Morris, C. B., Blackman, C. J., Hu, Y., Jia, H., Li, J. Z., Koch, G. G., and Bangdiwala, S. I. 2003. Cognitive-behavioral therapy versus education and desipramine versus placebo for moderate to severe functional bowel disorders. Gastroenterology 125, 19–31.

Fass, R., Naliboff, B., Higa, L., Johnson, C., Kodner, A., Munakata, J., Ngo, J., and Mayer, E. A. 1998. Differential effect of long-term esophageal acid exposure on mechanosensitivity and chemosensitivity in humans. Gastroenterology 115, 1363–1373.

Fuchs, E. and Fluegge, G. 1995. Modulation of binding sites for corticotropin-releasing hormone by chronic psychosocial stress. Psychoneuroendocrinology 20, 33–51.

Greenwood-Van Meerveld, B., Gibson, M. S., Johnson, A. C., Venkova, K., and Sutkowski-Markmann, D. 2003. NK1 receptor-mediated mechanisms regulate colonic hypersensitivity in the guinea pig. Pharmacol. Biochem. Behav. 74, 1005–1013.

Gue, M., Del Rio-Lacheze, C., Eutamene, H., Theodorou, V., Fioramonti, J., and Bueno, L. 1997. Stress-induced visceral hypersensitivity to rectal distension in rats: Role of CRF and mast cells. Neurogastroenterol. Motil. 9, 271–279.

Gwee, K. A., Collins, S. M., Marshall, J. S., Underwood, J. E., Moochala, S. M., and Read, N. W. 1998. Evidence of inflammatory pathogenesis in post-infectious irritable bowel syndrome. Gastroenterology 114, 758 (abstract).

Gwee, K. A., Graham, J. C., McKendrick, M. W., Collins, S. M., Marshall, J. S., Walters, S. J., and Read, N. W. 1996. Psychometric scores and persistence of irritable bowel after infectious diarrhoea. Lancet 347, 150–153.

Heim, C., Ehlert, U., and Hellhammer, D. H. 2000. The potential role of hypercortisolism in the pathophysiology of stress-related bodily disorders. Psychoneuroendocrinology 25, 1–35.

Hutton, J. 2005. Cognitive behaviour therapy for irritable bowel syndrome. Eur. J. Gastroenterol. Hepatol. 17, 11–14.

Inadomi, J. M., Fennerty, M. B., and Bjorkman, D. 2003. Systematic review: The economic impact of irritable bowel syndrome. Aliment. Pharmacol. Ther. 18, 671–682.

Isgar, B., Harman, M., Kaye, M. D., and Whorwhell, P. J. 1983. Symptoms of irritable bowel syndrome in ulcerative colitis in remission. Gut 24, 190–192.

Ito, M. 2002. Controller-regulator model of the central nervous system. J. Integr. Neurosci. 1, 129–143.

Jänig, W. and Habler, H.-J. 2000. Specificity in the Organization of the Autonomic Nervous System: A Basis for Precise

Neural Regulation of Homeostatic and Protective Body Functions. In: The Biological Basis for Mind Body Interactions (*ed*. E. A. Mayer and C. B. Saper), pp. 351–367. Elsevier Science.

La, J. H., Kim, T. W., Sung, T. S., Kang, J. W., Kim, H. J., and Yang, I. S. 2003. Visceral hypersensitivity and altered colonic motility after subsidence of inflammation in a rat model of colitis. World J. Gastroenterol. 9, 2791–2795.

Ladd, C. O., Huot, R. L., Thrivikraman, K. V., Nemeroff, C. B., Meaney, M. J., and Plotsky, P. 2000. Long-term Behavioral and Neuroendocrine Adaptations to Adverse Early Experience. In: The Biological Basis for Mind Body Interactions (*ed*. E. A. Mayer and C. B. Saper), pp. 81–103. Elsevier.

Lamb, K., Zhong, F., Gebhart, G. F., and Bielefeldt, K. 2006. Experimental colitis in mice and sensitization of converging visceral and somatic afferent pathways. Am. J. Physiol. Gastrointest. Liver Physiol. 290, G451–G457.

Lembo, T. J. and Fink, R. N. 2002. Clinical assessment of irritable bowel syndrome. J. Clin. Gastroenterol. 35, S31–S36.

Loennig-Baucke, V., Metcalf, A. M., and Shirazi, S. 1989. Anorectal manometry in active and quiescent ulcerative colitis. Am. J. Gastroenterol. 84, 892–897.

Longstreth, G. F. 2005. Definition and classification of irritable bowel syndrome: Current consensus and controversies. Gastroenterol. Clin. North. Am. 34, 173–187.

Lowman, B. C., Drossman, D. A., Cramer, E. M., and McKee, D. C. 1987. Recollection of childhood events in adults with irritable bowel syndrome. J. Clin. Gastroenterol. 9, 324–330.

Madden, J. A. and Hunter, J. O. 2002. A review of the role of the gut microflora in irritable bowel syndrome and the effects of probiotics. Br. J. Nutr. 88, S67–S72.

Mason, P. 2005. Deconstructing endogenous pain modulations. J. Neurophysiol. 94, 1659–1663.

Matthews, S. G. 2002. Early programming of the hypothalamo-pituitary-adrenal axis. Trends Endocrinol. Metab. 13, 373–380.

Mayer, E. A. 2000a. Spinal and supraspinal modulation of visceral sensation. Gut 47, iv69–iv72.

Mayer, E. A. 2000b. The neurobiology of stress and gastrointestinal disease. Gut 47, 861–869.

Mayer, E. A., Berman, S., Suyenobu, B., Labus, J., Mandelkern, M. A., Naliboff, B. D., and Chang, L. 2005. Differences in brain responses to visceral pain between patients with irritable bowel syndrome and ulcerative colitis. Pain 115, 398–409.

Mayer, E. A. and Collins, S. M. 2002. Evolving pathophysiologic models of functional gastrointestinal disorders. Gastroenterology 122, 2032–2048.

Mayer, E. A. and Gebhart, G. F. 1994. Basic and clinical aspects of visceral hyperalgesia. Gastroenterology 107, 271–293.

Mayer, E. A., Naliboff, B. D., Chang, L., and Coutinho, S. V. 2001. Stress and the gastrointestinal tract: V. Stress and irritable bowel syndrome. Am. J. Physiol. Gastrointest. Liver. Physiol. 280, G519–G524.

Mertz, H., Fullerton, S., Naliboff, B., and Mayer, E. A. 1998. Symptoms and visceral perception in severe functional and organic dyspepsia. Gut 42, 814–822.

Mertz, H., Naliboff, B., Munakata, J., Niazi, N., and Mayer, E. A. 1995. Altered rectal perception is a biological marker of patients with irritable bowel syndrome. Gastroenterology 109, 40–52.

Mulak, A. and Bonaz, B. 2004. Irritable bowel syndrome: A model of the brain-gut interactions. Med. Sci. Monit. 10, RA55–RA62.

Naliboff, B. D., Derbyshire, S. W. G., Berman, S. M., Mandelkern, M. A., Chang, L., Stains, J., and Mayer, E. A. 2001a. Assessing the stability of brain activation to visceral stimulation in IBS. Gastroenterology 120, A133 (abstract).

Naliboff, B. D., Derbyshire, S. W. G., Munakata, J., Berman, S., Mandelkern, M., Chang, L., and Mayer, E. A. 2001b. Cerebral activation in irritable bowel syndrome patients and control subjects during rectosigmoid stimulation. Psychosom. Med. 63, 365–375.

O'Leary, C. and Quigley, E. M. 2003. Small bowel bacterial overgrowth, celiac disease, and IBS: What are the real associations? Am. J. Gastroenterol. 98, 720–722.

O'Sullivan, M., Clayton, N., Breslin, N. P., Harman, I., Bountra, C., McLaren, A., and O'Morain, C. A. 2000. Increased mast cells in the irritable bowel syndrome. Neurogastroenterol. Motil. 12, 449–457.

Petrovic, P. and Ingvar, M. 2002. Imaging cognitive modulation of pain processing. Pain 95, 1–5.

Pezawas, L., Meyer-Lindenberg, A., Drabant, E. M., Verchinski, B. A., Munoz, K. E., Kolachana, B. S., Egan, M. F., Mattay, V. S., Hariri, A. R., and Weinberger, D. R. 2005. 5-HTTLPR polymorphism impacts human cingulate-amygdala interactions: A genetic susceptibility mechanism for depression. Nat. Neurosci. 8, 828–834.

Pimentel, M., Chow, E. J., and Lin, H. C. 2000. Eradication of small intestinal bacterial overgrowth reduces symptoms of irritable bowel syndrome. Am. J. Gastroenterol. 95, 3503–3506.

Pimentel, M., Chow, E. J., and Lin, H. C. 2003. Normalization of lactulose breath testing correlates with symptom improvement in irritable bowel syndrome. A double-blind, randomized, placebo-controlled study. Am. J. Gastroenterol. 98, 412–419.

Porreca, F., Ossipov, M. H., and Gebhart, G. F. 2002. Chronic pain and medullary descending facilitation. Trends Neurosci. 25, 319–325.

Rao, S. S. C., Read, N. W., Davison, P. A., Bannister, J. J., and Holdsworth, C. D. 1987. Anorectal sensitivity and responses to rectal distention in patients with ulcerative colitis. Gastroenterology 93, 1270–1275.

Santos, J., Guilarte, M., Alonso, C., and Malagelada, J. R. 2005. Pathogenesis of irritable bowel syndrome: The mast cell connection. Scand. J. Gastroenterol. 40, 129–140.

Schwetz, I., Bradesi, S., and Mayer, E. A. 2003. Current insights into the pathophysiology of irritable bowel syndrome. Curr. Gastroenterol. Rep. 5, 331–336.

Schwetz, I., Bradesi, S., and Mayer, E. A. 2004. The pathophysiology of irritable bowel syndrome. Minerva. Med. 95, 419–426.

Schwetz, I., McRoberts, J. A., Coutinho, S. V., Bradesi, S., Gale, G., Fanselow, M., Million, M., Ohning, G., Taché, Y., Plotsky, P. M., and Mayer, E. A. 2005. Corticotropin-releasing factor receptor 1 mediates acute and delayed stress-induced visceral hyperalgesia in maternally separated Long Evans rats. Am. J. Physiol. Gastrointest. Liver Physiol. 289, G704–G712.

Simren, M., Axelsson, J., Abrahamsson, H., Svedlund, J., and Bjsrnsson, E. S. 2000. Symptoms of irritable bowel syndrome in inflammatory bowel disease in remission and relationship to psychological factors. Gastroenterology 118, A702. (Abstract).

Soderholm, J. D., Yang, P. C., Ceponis, P., Vohra, A., Riddell, R., Sherman, P. M., and Perdue, M. H. 2002. Chronic stress induces mast cell-dependent bacterial adherence and initiates mucosal inflammation in rat intestine. Gastroenterology 123, 1099–1108.

Spiegel, B. M., Gralnek, I. M., Bolus, R., Chang, L., Dulai, G. S., Mayer, E. A., and Naliboff, B. 2004. Clinical determinants of health-related quality of life in patients with irritable bowel syndrome. Arch. Intern. Med. 164, 1773–1780.

Spiller, R. C. 2005. Irritable bowel syndrome. Br. Med. Bull. 72, 15–29.

Suzuki, R., Rahman, W., Rygh, L. J., Webber, M., Hunt, S. P., and Dickenson, A. H. 2005. Spinal-supraspinal serotonergic circuits regulating neuropathic pain and its treatment with gabapentin. Pain 117, 292–303.

Swidsinski, A., Khilkin, M., Ortner, M., Swidsinski, S., Wirth, J., Weber, J., Schlien, P., Lochs, H. 1999. Alteration of bacterial concentration in colonic biopsies from patients with irritable bowel syndrome (IBS). Gastroenterology 116, A-1. (Abstract).

Taché, Y., Martinez, V., Million, M., and Wang, L. 2001. Stress and the gastrointestinal tract III. Stress-related alterations of gut motor function: Role of brain corticotropin-releasing factor receptors. Am. J. Physiol. Gastrointest. Liver Physiol. 280, G173–G177.

Taché, Y., Martinez, V., Wang, L., and Million, M. 2004. CRF1 receptor signaling pathways are involved in stress-related alterations of colonic function and viscerosensitivity: implications for irritable bowel syndrome. Br. J. Pharmacol. 141, 1321–1330.

Thompson, W. G., Longstreth, G. F., Drossman, D. A., Heaton, K. W., Irvine, E. J., and Müller-Lissner, S. A. 1999. Functional bowel disorders and functional abdominal pain. Gut 45, II43–II47.

Tillisch, K., Labus, J. S., Naliboff, B. D., Bolus, R., Shetzline, M., Mayer, E. A., and Chang, L. 2005. Characterization of the alternating bowel habit subtype in patients with irritable bowel syndrome. Am. J. Gastroenterol. 100, 896–904.

Vendruscolo, L. F., Pamplona, F. A., and Takahashi, R. N. 2004. Strain and sex differences in the expression of nociceptive behavior and stress-induced analgesia in rats. Brain Res. 1030, 277–283.

Verne, G. N., Himes, N. C., Robinson, M. E., Gopinath, K. S., Briggs, R. W., Crosson, B., and Price, D. D. 2003. Central representation of visceral and cutaneous hypersensitivity in the irritable bowel syndrome. Pain 103, 99–110.

Welgan, P., Meshkinpour, H., and Beeler, M. 1988. Effect of anger on colon motor and myoelectric activity in irritable bowel syndrome. Gastroenterology 94, 1150–1156.

Weston, A. P., Biddle, W. L., Bhatia, P. S., and Miner, P. B. J. 1993. Terminal ileal mucosal mast cells in irritable bowel syndrome. Dig. Dis. Sci. 38, 1590–1595.

Whitehead, M. and Holland, P. 2003. What puts children of lone parents at a health disadvantage? Lancet 361, 271.

Wilder-Smith, C. H., Schindler, D., Lovblad, K., Redmond, S. M., and Nirkko, A. 2004. Brain functional magnetic resonance imaging of rectal pain and activation of endogenous inhibitory mechanisms in irritable bowel syndrome patient subgroups and healthy controls. Gut 53, 1595–1601.

Wilson, L. M. and Baldwin, A. L. 1999. Environmental stress causes mast cell degranulation, endothelial and epithelial changes, and edema in the rat intestinal mucosa. Microcirculation 6, 189–198.

Zhuo, M. and Gebhart, G. F. 2002. Facilitation and attenuation of a visceral nociceptive reflex from the rostroventral medulla in the rat. Gastroenterology 122, 1007–1019.

Zimmerman, J. 2003. Extraintestinal symptoms in irritable bowel syndrome and inflammatory bowel diseases: Nature, severity, and relationship to gastrointestinal symptoms. Dig. Dis. Sci. 48, 743–749.

5.39 Pain in Childbirth

U Wesselmann, The Johns Hopkins University School of Medicine, Baltimore, MD, USA

© 2008 Elsevier Inc. All rights reserved.

5.39.1	**Introduction**	579
5.39.2	**Physiological Aspects of Labor Pain**	580
5.39.2.1	Variables Associated with the Severity of Labor Pain	580
5.39.2.2	Treatment of Pain in Childbirth	581
5.39.2.2.1	Analgesia for Labor and Delivery	581
5.39.2.2.2	Nonpharmacological, complementary and alternative therapies for relief of pain in childbirth	582
5.39.3	**Pain during Pregnancy**	582
5.39.4	**Postpartum Pain**	582
5.39.5	**Future Aspects**	582
References		583

Glossary

dysmenorrhea Painful cramping of the lower abdomen occurring before or during menses primarily as a result of endogenous prostaglandins, often accompanied by other symptoms such as sweating, tachycardia, headaches, nausea, vomiting, diarrhea, and tremulousness.

dyspareunia Painful intercourse.

epidural analgesia Regional analgesia produced by injection of local anesthetic solution into the peridural space.

postpartum pain Pain after childbirth; the postpartum period starts immediately following childbirth but the length of the period is not well defined.

referred pain Pain perceived in a region different from the injured area during the time of injury.

stages of labor pain There are three stages of labor pain. Stage 1 begins with regular uterine contractions and ends with complete cervical dilatation at 10 cm. Stage 2 begins once the cervix has completely dilated and ends with delivery of the fetus. Stage 3 lasts from the delivery of the fetus until the delivery of the placenta.

5.39.1 Introduction

The experience of pain during childbirth is a complex, multidimensional response to sensory stimuli generated during labor and delivery. Pain in childbirth occurs in the context of an individual woman's physiology and psychology, as well as in the context of the sociology of the culture and the health care system and its providers surrounding her. For the majority of women in all societies and cultures, natural childbirth is likely to be one of the most painful events in their lifetime. Average pain scores for labor pain are exceeded only by those for causalgia in chronic-pain patients and amputation of a digit in acute-pain patients (Melzack, R., 1984). Different from other acute and chronic pain experiences, pain during childbirth is not associated with a pathological process. It is surprising that this physiological process associated with the most basic and fundamental life experience causes severe pain, and this has been the subject of many philosophic and religious debates. The International Association for the Study of Pain (IASP) defines pain as an unpleasant sensory and emotional experience associated with actual or potential tissue damage or described in terms of such damage (Merskey, H., 1979). Traditionally, different approaches to pain management of the pain in childbirth have addressed either the sensory or the affective dimension of

pain, while more recently a multidimensional approach has been advocated, addressing both dimensions of labor pain (Lowe, N. K., 2002; Melzack, R., 1984).

5.39.2 Physiological Aspects of Labor Pain

Compared to many other pain conditions, research on the neurophysiological mechanisms of pain in childbirth has been sparse, due to the difficulty of developing animal models that could be studied adequately using electrophysiological and neuroanatomical techniques. Studies examining the influence of pregnancy on somatosensory responses in animals and humans have shown hypoalgesia in late pregnancy prior to the onset of labor and this chance in nociceptive threshold is at least in part opioid-mediated (Bajaj, P. *et al.*, 2002; Jarvis, S. *et al.*, 1997). There are three distinct stages of labor pain related to uterine contractions, cervical stretching, and distension of the vaginal canal during fetal descend (for reviews see: McDonald, J. S., 2001; Rowlands, S. and Permezel, M., 1998). The first stage begins with regular uterine contractions and ends with complete cervical dilatation at 10 cm. Stage 1 has been further subdivided into an earlier latent phase and an ensuing active phase, which begins at about 3–4 cm of cervical dilatation and heralds a period of more rapid cervical dilation. Once the cervix has completely dilated, stage 2 of labor has begun. It ends with delivery of the fetus. Stage 3 of labor lasts from the delivery of the fetus until the delivery of the placenta. Pain during the first stage of labor (dilatation phase) is thought to be due to nociceptive stimuli arising from mechanical distension of the lower uterine segment and cervical dilatation. In addition, high-threshold mechanoreceptors in the myometrium may be activated in response to uterine contractions. Several chemical nociceptive mediators have been suggested, including bradykinines, leukotrienes, prostaglandins, serotonin, lactic acid, and Substance P. Pain of the first stage of labor is predominantly mediated by neural pathways involving the T10 to L1 spinal cord segments. Similar to other types of visceral pain, labor pain may present with referred pain to somatic structures in corresponding myotomes and dermatomes, including the abdominal wall, lumbosacral region, iliac crests, gluteal areas and thighs. Pain in the second and third stages of labor involves spinal cord segments S2 to S4, and is considered to be due to distension and traction on pelvic structures surrounding the vaginal vault and from distension of the pelvic floor and perineum. The mean intensity of pain in childbirth has been reported to be positively correlated with the intensity, duration, and frequency of uterine contractions and with the degree of cervical distension.

Pain associated with childbirth provokes a generalized stress response, which has widespread physiological and potentially adverse effects on the progress of labor and the well-being of the mother and the fetus (Brownridge, P., 1995; Beilin, Y., 2002). Respiratory effects include hyperventilation, which might lead to maternal hypocarbia and respiratory alkalosis, and rise in cardiac output, peripheral resistance, and blood pressure. Pain associated with uterine contraction results in stimulation of the release of stress-related hormones from the adrenal sympathetic axis and the hypophyseal–pituitary axis. Labor pain promotes maternal and fetal acidosis, which is due to a catecholamine-induced shift toward lipolytic metabolism, hyperventilation, physical exertion, starvation, and diminished buffering capacity secondary to respiratory alkalosis. While these effects may be largely innocuous during the course of uncomplicated labor, they present a great risk in the presence of certain medical and obstetric complications and in situations where fetal compromise already exists.

5.39.2.1 Variables Associated with the Severity of Labor Pain

There is a very high level of individual variability in the severity of labor pain and this has been correlated with several factors (Melzack, R., 1984; Brownridge, P., 1995). Primiparas and younger women report more pain than multiparas and older women. Women of higher socioeconomic status report less pain than women of lower socioeconomic status. In addition physical factors might play a role in increased pain ratings during labor, including increased fetal size and increased maternal body weight. Labor pain is influenced by maternal positions – women experience more pain when delivering in the horizontal position as compared to the upright position. Childbirth at night has been reported to be less painful than childbirth during the day. Women with a history of dysmenorrhea report higher pain levels during labor as compared to women, who do not have a history of menstrual pain. In contrast, a previous history of

nongynecological pain is correlated with decreased labor pain.

Severe fear of pain associated with childbirth occurs in 6–10% of parturients and is highly correlated to pain levels reported during the first stage of labor (for review see Saisto, T. and Halmesmäki, E., 2003). It is not an isolated variable, but associated with the woman's personal characteristics including general anxiety and fear of pain in general, low self-esteem, depression, dissatisfaction with her partnership, and lack of support. Fear of labor pain is strongly associated with fear of pain in general, independent of parity and is one of the most common reasons for requesting a cesarean section. Fear of childbirth has been reported to complicate about 20% of pregnancies in developed countries.

Although it is often assumed that culture and ethnicity have a significant influence on the intensity of labor pain, numerous studies have documented that there is no difference in self-report pain intensity ratings (see Lowe, N. K., 2002 for review). However, pain behavior is significantly influenced by culture and ethnicity, due to learned values and attitudes to the perception and expression of acute pain.

The environmental influences on pain perception have been explored in two prospective studies from Scandinavia comparing low-risk women delivering at birth centers and at standard obstetrical hospital-based units (Skibsted, L. and Lange, A. P., 1992; Waldenström, U. and Nilsson, C. A., 1994). These studies suggest that the environment provided may affect a woman's ability to cope with pain. While women delivering in birth centers reported significantly higher pain intensities than women delivering in hospital settings, there were no differences between the two groups with respect to satisfaction with the quality of the birth experience. These results emphasize the importance of differentiation between pain intensity and the attitude toward the pain experienced in labor and delivery.

It has been postulated that the memory for pain associated with disease, trauma, or surgical and medical procedures can be more damaging than its initial experience (Song, S.-O. and Carr, D. B., 1999). Although pain in childbirth is one of the most intense pains many women experience in their lifetime, childbirth is one of the most positive events of life for most women. Review of the literature on memory for labor pain shows that while memory of the events of childbirth is very accurate, the accuracy of recalled labor pain remains in question. Memories of labor pain can evoke intense negative reactions in a few women, but are more likely to give rise to positive consequences related to coping, self-efficacy and self-esteem (Niven, C. A. and Murphy-Black, T., 2000).

It is important to emphasize that labor pain, although being a very prominent aspect of childbirth, is just one aspect of the childbirth experience. A recent systematic review of the literature on pain and women's satisfaction with the experience of childbirth demonstrated that the influences of pain, pain relief, and intra-partum medical interventions on subsequent satisfaction are not as powerful as the personal expectations, the amount of support from caregivers, the quality of the caregiver-patient relationship, and involvement of decision making (Hodnett, E. D., 2002).

5.39.2.2 Treatment of Pain in Childbirth

5.39.2.2.1 Analgesia for Labor and Delivery

Analgesia for labor and delivery is now safer than ever and can be offered during all stages of labor, targeted to the individual needs and wishes of the pregnant woman, without compromising the safety of her or her unborn child (for reviews see Beilin, Y., 2002; Caton, D. *et al.*, 2002; Nystedt, A. *et al.*, 2004). Anesthesia related maternal mortality has decreased from 4.3 million live births during the years 1979–81 to 1.7 per million live births during the years 1988–90. The increased use of regional anesthesia techniques is partially responsible for this decrease in mortality. The most popular method for analgesia during labor and delivery is epidural analgesia using a combination of local anesthetics and opioids. Its popularity is related to its efficacy and safety. Drugs can be applied as continuous epidural infusions or as patient-controlled epidural analgesia. During the early stages of labor dilute solutions of local anesthetic can be used to achieve analgesia. As labor progresses, more concentrated solutions of local anesthetics can be used and opioids can be added. Typically the epidural catheter is inserted to maintain a low dermatomal level of analgesia for vaginal delivery (T10 to L1). If a cesarean section is required, the dermatomal level can be raised to T4. Combined spinal epidural techniques offer the advantage of a very rapid onset of analgesia with minimal motor block. The future of obstetric anesthesia lies in refining currently available drugs and techniques to make obstetric anesthesia even safer and more efficacious.

5.39.2.2.2 Nonpharmacological, complementary and alternative therapies for relief of pain in childbirth

Many nonpharmacological, complementary and alternative medicine methods exist to relieve labor pain (for reviews see Simkin, P. P. and O'Hara M., 2002; Smith, C. A. *et al.*, 2003; Cluett, E. R. *et al.*, 2004; Cyna, A. M. *et al.*, 2004; Huntley, A. L. *et al.*, 2004; Lee, H. and Ernst, E., 2004). These methods appeal to women and caregivers who are interested to reduce labor pain without creating potentially serious side-effects and high costs. In addition many women appreciate the simplicity of these approaches and the sense of control they gain from actively managing their pain. However, few of these therapies have been subjected to proper scientific study. Meta-analysis of randomized controlled trials has indicated that acupuncture and hypnosis may be beneficial for the management of pain in childbirth. There is evidence that water immersion during the first stage of labor reduces the use of analgesia and reported pain intensity, without adverse outcomes on labor duration, operative delivery, or neonatal outcomes. The effects of water immersion during the later stages of labor are not clear. No differences were observed for women receiving aromatherapy, music, or audio analgesia.

5.39.3 Pain during Pregnancy

While the focus of this review is on pain associated with childbirth, it is important to note that pain is also a significant issue during pregnancy (Stuge, B. *et al.*, 2003). Approximately 50% of women experience back pain and/or pelvic pain during their pregnancy, and in up to 15% of the cases the pain is rated as severe. Several hypotheses have been suggested to explain the etiology of this pain, including increased weight, decreased stability of the pelvic girdle due to hormonal changes and referred visceral pain mechanisms. The role of the hormone relaxin and pelvic pain in pregnancy is controversial. Physical therapy is often recommended for the prevention and treatment of these pregnancy-related pains, but the effects of these interventions have not been systematically studied and thus it is not clear if they are of any benefit to the pregnant women.

5.39.4 Postpartum Pain

While most of the discussion of adverse sequelae of labor and delivery has focused on urinary and fecal incontinence, there is now increasing awareness that pain associated with childbirth is not only related to the process of labor and delivery. Women report significant pains in many sites of the body after delivery, a phenomenon which has been defined as postpartum pain. Postpartum pains may include urogenital, pelvic, back and breast pains as well as headaches, persisting for months to years after labor and delivery (Audit Commission, 1997). It has been hypothesized that anesthetic techniques during labor and delivery and gonadal hormonal changes may play a role in the etiology of these pain complaints. Forty-nine percent of women report significant dyspareunia when resuming sexual intercourse after childbirth (Buhling, K. J. *et al.*, 2005). Women with a history of operative vaginal delivery have the highest prevalence of severe perineal pain when resuming sexual intercourse. The persistence of dyspareunia for longer than 6 months after delivery ranges from 3.4% to 14% based on mode of delivery. Treatment approaches for early intervention to prevent persistent perineal pain after childbirth have not been explored in detail. A meta-analysis assessing the effectiveness of topically applied anesthetics to the perineal region in the early postpartum period showed no compelling evidence of pain reduction (Hedayati, H. *et al.*, 2005). However, there has been no evaluation of the long-term effects of topically applied local anesthetics.

5.39.5 Future Aspects

Pain in childbirth is a complex, multidimensional experience. While the focus of this chapter is on the pain aspect of childbirth, it is important to keep in mind that pain is an important aspect, but not the only aspect of the childbirth experience. The acknowledgment of the existence of pain associated with labor and delivery and the recognition of the severity of this pain by the medical community over the last 50 years has resulted in a broad spectrum of pharmacological and nonpharmacological pain management options that can be offered to the parturient today. There have been tremendous advancements in the pharmacological treatment of pain in labor and delivery over the last 25 years, mainly due to

improved regional anesthesia techniques. The future of obstetric anesthesia lies in refining currently available drugs and techniques and in developing new drugs targeted at specific pathophysiological mechanisms to make obstetric anesthesia even safer and more efficacious. This will require translational research efforts ranging from basic science to clinical research. As a first step an animal model has recently been developed in the rat to study the neurophysiological and neuropharmacological mechanisms of pain associated with uterine cervical distension (Liu, B. *et al.*, 2005). Neuroanatomical studies of the sensory pathways from the uterine cervix have shown that P2X3-receptor-expressing sensory neurons might play a role during birthing and signal nociceptive information such as labor pain (Papka, R. E. *et al.*, 2005). Numerous nonpharmacological and alternative treatments are available for the treatment of pain in childbirth. While there is experience with some of those approaches already for centuries, many of these treatments have not been subjected to proper scientific study. Clinical studies assessing the effects of these interventions on pain in childbirth and on a woman's satisfaction with the childbirth experience, as well as studies assessing the effects on the safety for the pregnant woman and her child are urgently needed.

Acknowledgments

Ursula Wesselmann is supported by NIH grants DK57315 (NIDDK), DK066641 (NIDDK), and HD39699 (NICHD, Office of Research for Women's Health).

References

Audit Commission 1997. First Class Delivery: improving Maternity Services in England and Wales. Audit Commission.

Bajaj, P., Madsen, H., Moller, M., and Arendt-Nielsen, L. 2002. Antenatal women with or without pelvic pain can be characterized by generalized or segmental hypoalgesia in late pregnancy. J. Pain 3, 451–460.

Beilin, Y. 2002. Advances in labor analgesia. Mt. Sinai J. Med. 69, 38–44.

Brownridge, P. 1995. The nature and consequences of childbirth pain. Eur. J. Obstet. Gynecol. Reprod. Biol. 59 Suppl, S9–15.

Buhling, K. J., Schmidt, S., Robinson, J. N., Klapp, C., Siebert, G., and Dudenhausen, J. W. 2005. Rate of dyspareunia after delivery in primiparae according to mode of delivery. Eur. J. Obstet. Gynecol. Reprod. Biol.124, 42–46.

Caton, D., Corry, M. P., Frigoletto, F. D., Hopkins, D. P., Lieberman, E., Mayberry, L., Rooks, J. P., Rosenfield, A., Sakala, C., Simkin, P., and Young, D. 2002. The nature and management of labor pain: executive summary. Am. J. Obstet. Gynecol. 186, S1–15.

Cluett, E. R., Nikodem, V. C., McCandlish, R. E., and Burns, E. E. 2004. Immersion in water in pregnancy, labor and birth. Cochrane Database Syst. Rev. CD000111.

Cyna, A. M., McAuliffe, G. L., and Andrew, M. I. 2004. Hypnosis for pain relief in labor and childbirth: a systematic review. Br. J. Anaesth. 93, 505–511.

Hedayati, H., Parsons, J., and Crowther, C. A. 2005. Topically applied anaesthetics for treating perineal pain after childbirth. Cochrane Database Syst. Rev. CD004223.

Hodnett, E. D. 2002. Pain and women's satisfaction with the experience of childbirth: a systematic review. Am. J. Obstet. Gynecol. 186, S160–172.

Huntley, A. L., Coon, J. T., and Ernst, E. 2004. Complementary and alternative medicine for labor pain: a systematic review. Am. J. Obstet. Gynecol. 191, 36–44.

Jarvis, S., McLean, K. A., Chirnside, J., Deans, L. A., Calvert, S. K., Molony, V., and Lawrence, A. B. 1997. Opioid-mediated changes in nociceptive threshold during pregnancy and parturition in the sow. Pain 72, 153–159.

Lee, H. and Ernst, E. 2004. Acupuncture for labor pain management: A systematic review. Am. J. Obstet. Gynecol. 191, 1573–1579.

Liu, B., Eisenach, J. C., and Tong, C. 2005. Chronic estrogen sensitizes a subset of mechanosensitive afferents innervating the uterine cervix. J. Neurophysiol. 93, 2167–2173.

Lowe, N. K. 2002. The nature of labor pain. Am. J. Obstet. Gynecol. 186, S16–24.

McDonald, J. S. 2001. Pain of Childbirth. In: Bonica's Management of Pain, 3rd edn. (*ed*. J. D. Loeser), pp. 1388–1414. Lippincott Williams & Wilkins.

Melzack, R. 1984. The myth of painless childbirth (the John J. Bonica lecture). Pain 19, 321–337.

Merskey, H. 1979. Pain terms: a list with definitions and a note on usage. Recommended by the IASP Subcommittee on Taxonomy. Pain 6, 249–252.

Niven, C. A. and Murphy-Black, T. 2000. Memory for labor pain: a review of the literature. Birth 27, 244–253.

Nystedt, A., Edvardsson, D., and Willman, A. 2004. Epidural analgesia for pain relief in labor and childbirth – a review with a systematic approach. J. Clin. Nurs. 13, 455–466.

Papka, R. E., Hafemeister, J., and Storey-Workley, M. 2005. P2X receptors in the rat uterine cervix, lumbosacral dorsal root ganglia, and spinal cord during pregnancy. Cell Tissue Res. 321, 35–44.

Rowlands, S. and Permezel, M. 1998. Physiology of pain in labor. Baillieres Clin. Obstet. Gynaecol. 12, 347–362.

Saisto, T. and Halmesmaki, E. 2003. Fear of childbirth: a neglected dilemma. Acta Obstet. Gynecol. Scand. 82, 201–208.

Simkin, P. P. and O'Hara, M. 2002. Nonpharmacologic relief of pain during labor: systematic reviews of five methods. Am. J. Obstet. Gynecol. 186, S131–159.

Skibsted, L. and Lange, A. P. 1992. The need for pain relief in uncomplicated deliveries in an alternative birth center compared to an obstetric delivery ward. Pain 48, 183–186.

Smith, C. A., Collins, C. T., Cyna, A. M., and Crowther, C. A. 2003. Complementary and alternative therapies for pain management in labor. Cochrane Database Syst. Rev. CD003521.

Song, S-O. and Carr, D. B. 1999. Pain and memory. IASP Clin. Updates 7, 1–4.

Stuge, B., Hilde, G., and Vollestad, N. 2003. Physical therapy for pregnancy-related low back and pelvic pain: a systematic review. Acta Obstet. Gynecol. Scand. 82, 983–990.

Waldenström, U. and Nilsson, C. A. 1994. Experience of childbirth in birth center care. A randomized controlled study. Acta Obstet. Gynecol. Scand. 73, 547–554.

5.40 Urothelium as a Pain Organ

L A Birder, University of Pittsburgh School of Medicine, Pittsburgh, PA, USA

© 2008 Elsevier Inc. All rights reserved.

5.40.1	Urothelial Cells: Detectors of Mechanical, Chemical, and Thermal Stimuli	585
5.40.1.1	Sensor Molecules Expressed in Urothelium Which Could Contribute to Bladder Pain	585
5.40.1.2	Response to Stimuli: Transducer Function of Urothelial Cells	587
5.40.2	How Might Urothelial Cells Influence Pain Processes?	588
5.40.3	Potential Clinical Implications: Urothelial Receptors/Release Mechanisms as Targets for Drug Treatment	589
References		589

5.40.1 Urothelial Cells: Detectors of Mechanical, Chemical, and Thermal Stimuli

The urothelium is a specialized lining of the urinary tract, extending from the renal pelvis to the urethra. The urothelium is composed of at least three layers: a basal cell layer attached to a basement membrane, an intermediate layer, and a superficial apical layer with large hexagonal cells (diameters of 25–250 μm) which are also termed umbrella cells (Lewis, S. A., 2000; Apodaca, G., 2004). The umbrella cells, and, perhaps, intermediate cells may have projections to the basement membrane (Martin, B.F., 1972; Hicks M., 1975; Apodaca, G., 2004). Basal cells, which are thought to be precursors for other cell types, normally exhibit a low (3–6 months) turnover rate; however, accelerated proliferation can occur in pathology. For example, using a model (protamine sulfate) that selectively damages the umbrella cell layer has shown that the urothelium rapidly undergoes both functional and structural changes in order to restore the barrier following injury (Lavelle, J. *et al.*, 2002).

While the urothelium has been historically viewed primarily as a barrier, it is becoming increasingly appreciated as a responsive structure capable of detecting physiological and chemical stimuli, and releasing a number of signaling molecules. A number of investigators have described the release of diffusible mediators from the urothelium which could influence urinary bladder function (Ferguson, D.R. *et al.*, 1997; Hawthorn, M.H. *et al.*, 2000; Burnstock, G., 2001; Chess-Williams, R., 2002). There is now abundant evidence which indicates that urothelial cells display a number of properties similar to sensory neurons (nociceptors/mechanoreceptors) (see Table 1; Lewis, S. A. and Hanrahan, J. W., 1985; Birder, L. *et al.*, 1998; 2004; Smith, P. R. *et al.*, 1998; Birder, L. *et al.*, 2001; 2002a; 2002b; Chess-Williams, R., 2002; Beckel, J. *et al.*, 2004; Birder, L., *et al.*, 2004; Chess-Williams, R., 2004; Burnstock, G. and Knight, G. E., 2004; Murray, E. *et al.*, 2004; Tempest, H. V. *et al.*, 2004; Chopra, B. *et al.*, 2005; Birder, L. *et al.*, 2007) and that both types of cells use diverse signal transduction mechanisms to detect physiological stimuli.

5.40.1.1 Sensor Molecules Expressed in Urothelium Which Could Contribute to Bladder Pain

One example of a urothelial sensor molecule is the TRP channel, TRPV1, known to play a prominent role in nociception and in urinary bladder function (Szallasi, A., 2001). It is well established that painful sensations induced by capsaicin, the pungent substance in hot peppers, are caused by stimulation of TRPV1, an ion channel protein (Caterina, M. J. *et al.*, 1997; Caterina, M. J., 2001) which is activated by capsaicin as well as by moderate heat, protons, and lipid metabolites such as anandamide (endogenous ligand of both cannabinoid and vanilloid receptors). TRPV1 is expressed throughout the afferent limb of the micturition reflex pathway, Figure 1, including urinary bladder unmyelinated (C-fiber) nerves that detect bladder distension or the presence of irritant chemicals (Chancellor M. B. and de Groat, W. C., 1999). In the urinary bladder, TRPV1 is not only expressed by afferent nerves or myofibroblasts that form close contact with urothelial cells, but also by the urothelial cells themselves (Birder, L. *et al.*, 2001). Urothelial TRPV1 receptor expression correlates with the sensitivity to vanilloid compounds, as exogenous application of capsaicin or resiniferatoxin to cultured cells increases intracellular calcium and

Table 1 Examples of sensor molecules (i.e., receptors/ion channels) associated with neurons that have been identified in urothelial cells

Sensor function/stimuli	*Urothelial sensor molecules*	*Neuronal sensor molecules*
ATP	P2X/P2Y	P2X/P2Y
Capsaicin resiniferatoxin	TRPV1	TRPV1
Heat	TRPV1; TRPV2; TRPV4	TRPV1; TRPV2; TRPV3; TRPV4
Cold	TRPM8; TRPA1	TRPM8; TRPA1
H^+	TRPV1; ?	TRPV1; ASIC; DRASIC
Osmolarity	In part TRPV4	In part TRPV4
Bradykinin	B1; B2	B1; B2
Acetylcholine	Nicotinic/muscarinic	Nicotinic/muscarinic
Norepinephrine	α/β subtypes	α/β subtypes
Nerve growth factor	p75/trkA	p75/trkA
Mechanosensitivity	Amiloride sensitive Na^+ channels	Amiloride sensitive Na^+ channels

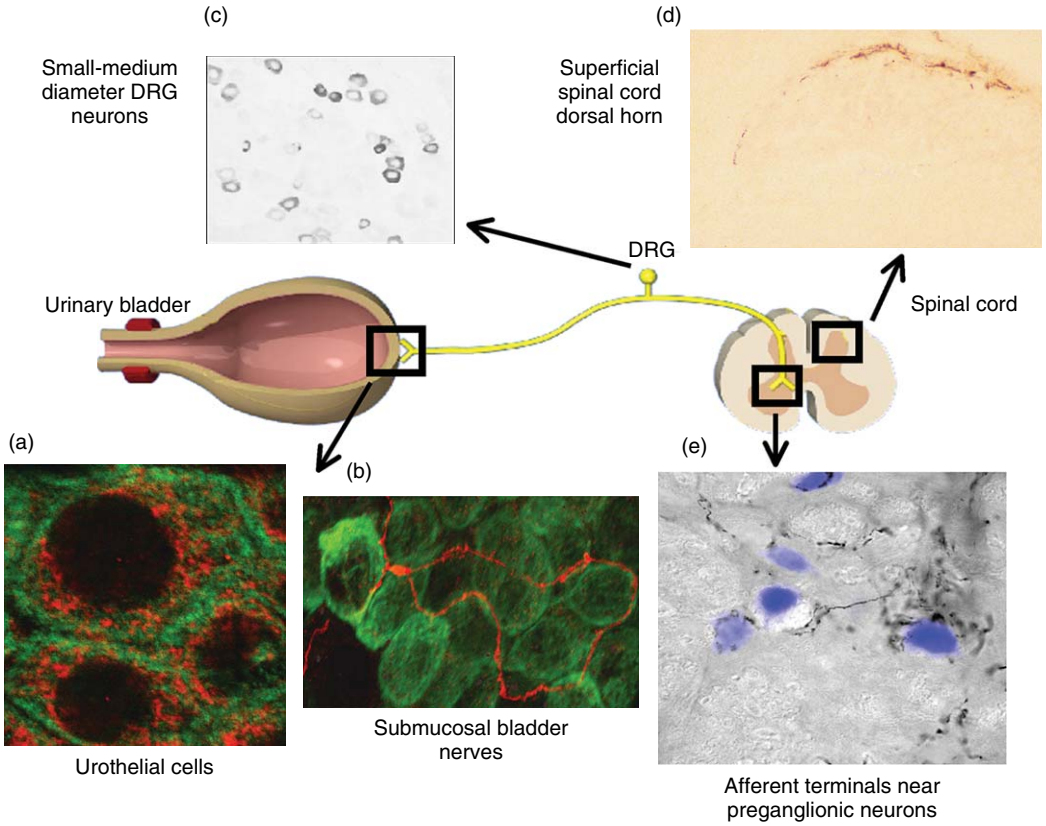

Figure 1 TRPV1 is expressed throughout the afferent limb of the micturition reflex pathway. TRPV1-immunoreactivity (cy-3, red) in basal epithelial cells (cyt 17, FITC green) (a); in nerve fibers (cy-3, red) located in close proximity to basal cells (FITC, green) (b) (punctate TRPV1 staining in urothelial cells was electronically subtracted to facilitate imaging of the TRPV1-immunoreactive nerve fiber); in small to medium diameter dorsal root ganglion (DRG) neurons (c); and in superficial regions of the spinal cord dorsal horn (d) (staining indicate TRPV1 nerve fibers). (e) TRPV1-positive afferent terminals (in black) are localized in close proximity to pre-ganglionic neurons (PGN neurons labeled by injection of a tracer dye, fast blue, into the major pelvic ganglion). Reproduced from Birder, L. A. 2005. More than just a barrier: Urothelium as a drug target for urinary bladder pain. Am. J. Physiol. Renal. Physiol. 289(3): F489–F495, used with permission from the American Physiological Society.

evokes transmitter (NO, nitric oxide; ATP, adenosine triphosphate) release (Birder, L. *et al.*, 2001; 2002a). In neurons, TRPV1 is thought to integrate/amplify the response to various stimuli playing an essential role in the development of inflammation-induced hyperalgesia (Ghuang, H. H. *et al.*, 2001; Holzer, P., 2004). Thus, it seems likely that urothelial TRPV1 might participate in a similar manner, in the detection of irritant stimuli following bladder inflammation or infection.

Anatomically normal, TRPV1-null mice exhibited a number of alterations in bladder urothelial cell function including a reduction of *in vitro*, stretch-evoked ATP release and membrane capacitance as well as a decrease in hypotonic-evoked ATP release (Birder, L. *et al.*, 2002a). These findings demonstrate that the functional significance of TRPV1 in the bladder extends beyond pain sensation to include participation in normal bladder function, and is essential for normal mechanically evoked purinergic signaling by the urothelium.

In addition to TRPV1, urothelial cells also express additional TRP channels, including TRPV2, TRPV4, TRPM8, and TRPA1. In contrast to TRPV1, TRPV2, and TRPV4, which are detectors of warm temperatures (TRPV4 can also be gated by hypotonic stimuli) (Liedtke, W. *et al.*, 2000; Alessandri-Haber, N. *et al.*, 2003; Chung, M. K. *et al.*, 2003), TRPM8 and TRPA1 have been shown to be activated by cold (25–28 °C) temperatures as well as by cooling agents (menthol, icilin) and are expressed in a subset of sensory neurons as well as in non-neural cells. This expression suggests that these cells express a range of thermoreceptors underlying both cold and heat stimuli (Stein, R. J. *et al.*, 2004). While the functional role of these thermosensitive channels in urothelium remains to be clarified, it seems likely that a primary role for these proteins may be to recognize noxious stimuli in the bladder. However, the diversity of stimuli which can activate these proteins suggests a much broader sensory and/or cellular role. For example, TRPM8 expression has been shown to be increased in some epithelia in malignant disorders (prostate tumors), suggesting a role in proliferating cells (Tsavaler, L. *et al.*, 2001). Thus, further studies are needed to fully elucidate the role of TRP channels in urothelium and their influence on bladder function.

Purinergic receptors, which are activated by ATP and related nucleotides, are known to play an important role in bladder function and chronic pain (Burnstock, G., 2001; North, R. A., 2004). Two families of purinergic receptors have been identified, P2X and P2Y, both of which are expressed in urothelial cells (Lee, H.Y. *et al.*, 2000; Birder, L. *et al.*, 2004; Tempest, H. V. *et al.*, 2004). Although the function of purinergic receptors in nonexcitable cells is less clear than in afferent neurons, the presence of such receptors may be associated with cell proliferation, apoptosis, secretion, and sensory transduction (Coutinho-Silva R. *et al.*, 2005; Greig, A. V. *et al.*, 2003). In the urinary bladder, recent studies have shown that urothelial-derived ATP release can act as a trigger for exocytosis, in part, via autocrine activation of urothelial purinergic (P2X; P2Y) receptors (Wang, E. C. *et al.*, 2005). This type of signaling may be similar to that in airway epithelium, where nucleotides released to the epithelial surface may act in a paracrine/autocrine manner to regulate ion transport and/or other functions via interactions with luminal epithelial purinergic receptors (Poulsen, A. N. *et al.*, 2005).

5.40.1.2 Response to Stimuli: Transducer Function of Urothelial Cells

Release of chemical mediators (NO, ATP, acetylcholine (ACh); substance P; prostaglandins (PG)) (Ferguson, D. R. *et al.*, 1997; Birder, L. *et al.*, 1998; Burnstock, G., 2001; Birder, L. *et al.*, 2003; Chess-Williams, R., 2004) from urothelial cells suggests that these cells exhibit specialized sensory and signaling properties that could allow reciprocal communication with neighboring urothelial cells as well as nerves or other cells (i.e., immune, myofibroblasts, inflammatory) in the bladder wall. Recent studies have shown that both afferent as well as autonomic axons are located in close proximity to the urothelium (Wayabayashi, Y. *et al.*, 1995; Birder, L. *et al.*, 2001). For example, peptide and TRPV1 immunoreactive nerve fibers have been found localized throughout the urinary bladder musculature and in a plexus beneath and extending into the urothelium. Confocal microscopy revealed that TRPV1 immunoreactive nerve fibers are in close association with basal urothelial cells such that their fluorescent signals overlapped within 0.5 μm optical sections. This type of communication suggests that these cells may be targets for transmitters released from bladder nerves or other cells, or that chemicals released by urothelial cells may also alter the excitability of bladder nerves.

Studies have demonstrated that ATP released from urothelium during bladder stretch could contribute to activation of bladder afferents.

That ATP released from urothelial cells during stretch can activate a population of suburothelial bladder afferents expressing $P2X_3$ receptors, signaling changes in bladder fullness and pain supports this idea (Ferguson, D. R. *et al.*, 1997; Burnstock, G., 2001). Accordingly, $P2X_3$ null mice exhibit a urinary bladder hyporeflexia, suggesting that this receptor and neural–epithelial interactions are essential for normal bladder function (Cockayne, D. A. *et al.*, 2000). This type of regulation may be similar to epithelial-dependent secretion of mediators in airway epithelial cells which is thought to modulate submucosal nerves and bronchial smooth muscle tone and may play an important role in inflammation (Homolya, L. *et al.*, 2000; Jallat-Daloz, I. *et al.*, 2001). Thus, it is possible that activation of bladder nerves and urothelial cells can modulate bladder function directly or indirectly via the release of chemical factors in the urothelial layer.

5.40.2 How Might Urothelial Cells Influence Pain Processes?

Recent evidence has demonstrated that urothelial cells exhibit plasticity whereby inflammation or injury can alter the expression and/or sensitivity of a number of urothelial-sensor molecules. Examples include changes in urothelial expression of various receptors including tyrosine kinase (trk), low-affinity nerve growth factor (p75), bradykinin, TRPV1, protease-activated receptors (PPARs), and purinergic receptor (P2X and P2Y) subtypes in animal models as well as in patients diagnosed with a number of bladder disorders including neurogenic bladder and interstitial cystitis (IC) – a chronic clinical disease characterized by urgency, frequency, and bladder pain upon filling (an innocuous stimulus) (Murray, E. *et al.*, 2004; North, R. A., 2004; Tempest, H. V. *et al.*, 2004; Chopra, B. *et al.*, 2005; Dattilio, A. and Vizzard, M. A., 2005). Such changes could contribute to pain and hypersensitivity exhibited in these painful syndromes. Because urothelial cells appear to exhibit sensory function, it is possible that plasticity in urothelial receptors is then linked with pain in various bladder syndromes.

Sensitization can be triggered by various mediators (ATP, NO, nerve growth factor (NGF), PGE_2) which may be released by both neuronal and non-neuronal cells (urothelial cells, fibroblasts, mast cells) located near the bladder luminal surface. An important component of the inflammatory response is ATP release from various cell types including urothelium, which can initiate painful sensations by exciting purinergic (P2X) receptors on sensory fibers (Cockayne, D. A. *et al.*, 2000; Burnstock, G., 2001). Recently, it has been shown in sensory neurons that ATP can potentiate the response of vanilloids by lowering the threshold for protons, capsaicin, and heat (Tominaga, M. *et al.*, 2001). This represents a novel mechanism by which large amounts of ATP released from damaged or sensitized cells in response to injury or inflammation may trigger the sensation of pain. These findings have clinical significance and suggest that alterations in afferents or epithelial cells in pelvic viscera may contribute to the sensory abnormalities in a number of pelvic disorders, such as IC, which is consistent with augmented release of ATP in urothelial cells from some patients with IC (Sun, Y. *et al.*, 2001). A comparable disease in cats is termed feline interstitial cystitis (FIC) (Buffington, C. A. *et al.*, 1999; 2001), which is also accompanied by alterations in stretch-evoked release of urothelially derived ATP (Birder, L. *et al.*, 2003).

Though the urothelium maintains a tight barrier to ion and solute flux, a number of factors such as tissue pH, mechanical or chemical trauma, or bacterial infection can modulate this barrier function of the urothelium (Hicks, M., 1975; Anderson, G. *et al.*, 2003). When this function is compromised during injury or inflammation, it can result in the passage of toxic substances into the underlying tissue (neural/muscle layers) resulting in urgency, frequency, and pain during bladder distension. For example, inflammation, injury (spinal cord transection), or IC, all of which increase endogenously generated levels of NO, increase permeability to water/urea in addition to producing ultrastructural changes in the apical layer (Lavelle, J. *et al.*, 2000; Apodaca, G. *et al.*, 2003). Although the mechanism is unknown, these findings may be similar to that in other epithelia where excess production of NO has been linked to changes in epithelial integrity (Han, X. *et al.*, 2004).

Disruption of epithelial integrity may also be due to substances such as antiproliferative factor (APF), which has been shown to be secreted by bladder epithelial cells from IC patients and can inhibit epithelial proliferation thereby adversely affecting barrier function (Keay, S. *et al.*, 1999; 2004).

5.40.3 Potential Clinical Implications: Urothelial Receptors/ Release Mechanisms as Targets for Drug Treatment

It is conceivable that the effectiveness of some agents currently used in the treatment of bladder disorders may involve urothelial receptors and/or release mechanisms. For example, intravesical instillation of vanilloids (capsaicin or resiniferatoxin) improves urodynamic parameters in patients with neurogenic detrusor overactivity and reduces bladder pain in patients with hypersensitivity disorders, presumably by desensitizing bladder nerves (Szallasi, A. and Fowler, C. J., 2002; Kim, J. H. *et al.*, 2003). This treatment could also target TRPV1 on urothelial cells, whereby a persistent activation might lead to receptor desensitization or depletion of urothelial transmitters. Recent studies have demonstrated that intradetrusor injection with botulinum neurotoxin type A (BoNTA) is an effective treatment for bladder hypersensitivity disorders including neurogenic detrusor overactivity (Harper, M. *et al.*, 2004; Reitz, A. and Schurch, B., 2004). Following injection, the toxin binds to bladder cholinergic nerve terminals and cleaves the protein, SNAP25, necessary for exocytosis and release of acetylcholine (Harper M. *et al.*, 2004). There is evidence the BoNTA can suppress the release of a number of mediators (acetylcholine, ATP, and neuropeptides) from both neural and non-neural cells (Morris, J. L. *et al.*, 2001). Suppression of neurotransmitter release from urothelium would serve to blunt afferent activity driven by urothelial-derived release of mediators in a number of lower urinary tract dysfunctions. These findings suggest that urothelial cells exhibit specialized sensory and signaling properties that could allow them to respond to their chemical and physical environments and to engage in reciprocal communication with neighboring urothelial cells as well as nerves within the bladder well. Taken together, pharmacologic interventions aimed at targeting urothelial receptor/ion channel expression or release mechanisms may provide a new strategy for the clinical management of bladder disorders.

Acknowledgments

This work was supported by grants to L.A.B. from the NIH (RO1 DK54824 and RO1 DK57284).

References

Alessandri-Haber, N., Yeh, J. J., Boyd, A. E., Parada, C. A., Chen, X., Reichling, D. B., and Levine, J. D. 2003. Hypotonicity induces TRPV4-mediated nociception in rat. Neuron 39, 497–511.

Anderson, G., Palermo, J., Schilling, J., Roth, R., Heuser, J., and Hultgren, S. 2003. Intracellular bacterial biofilm-like pods in urinary tract infections. Science 301, 105–107.

Apodaca, G. 2004. The uroepithelium: not just a passive barrier. Traffic 5, 1–12.

Apodaca, G., Kiss, S., Ruiz, W. G., Meyers, S., Zeidel, M. L., and Birder, L. 2003. Disruption of barrier epithelium function after spinal cord injury. Am. J. Physiol. 284, F966–F970.

Barrick, S. R., Lee, H., Meyers, S., Caterina, M. J., Kanai, A. J., Zeidel, M. L., Chopra, B., de Groat, W. C., and Birder, L. 2003 Expression and function of TRPV4 in urinary bladder urothelium. Soc. Neurosci. Abstr. 26, 608.6.

Beckel, J., Barrick, S. R., Keast, J.R., Meyers, S., Kanai, A. J., de Groat, W. C., Zeidel, M. L., and Birder, L. 2004. Expression and function of urothelial muscarinic receptors and interactions with bladder nerves. Soc. Neurosci. 26, 846.23.

Birder, L., Apodaca, G., de Groat, W. C., and Kanai, A. J. 1998. Adrenergic- and capsaicin-evoked nitric oxide release from urothelium and afferent nerves in urinary bladder. Am. J. Physiol. 275, F226–F229.

Birder, L., Kanai, A. J., de Groat, W. C., Kiss, S., Nealen, M. L., Burke, N. E., Dineley, K. E., Watkins, S., Reynolds, I. J., and Caterina, M. J. 2001. Vanilloid receptor expression suggests a sensory role for urinary bladder epithelial cells. Proc. Natl. Acad. Sci. U. S. A. 98, 13396–13401.

Birder, L., Kullmann, A., Lee, H., Barrick, S., de Groat, W., Kanai, A., and Caterina, M. 2007. Activation of Urothelial-TRPV4 by 4α-PDD contributes to altered bladder reflexes in the rat. JPET (in press).

Birder, L., Nakamura, Y., Kiss, S., Nealen, M. L., Barrick, S. R., Kanai, A. J., Wang, E., Ruiz, W. G., de Groat, W. C., Apodaca, G., Watkins, S., and Caterina, M. J. 2002a. Altered urinary bladder function in mice lacking the vanilloid receptor TRPV1. Nat. Neurosci. 5, 856–860.

Birder, L., Nealen, M. L., Kiss, S., de Groat, W. C., Caterina, M. J., Wang, E., Apodaca, G., and Kanai, A. J. 2002b. Beta-adrenoceptor agonists stimulate endothelial nitric oxide synthase in rat urinary bladder urothelial cells. J. Neurosci. 22, 8063–8070.

Birder, L., Barrick, S. R., Roppolo, J. R., Kanai, A. J., de Groat, W. C., Kiss, S., and Buffington, C. A. 2003. Feline interstitial cystitis results in mechanical hypersensitivity and altered ATP release from bladder urothelium. *American* J. Physiol. 285, F423–F429.

Birder, L., Ruan, H. Z., Chopra, B., Xiang, Z., Barrick, S. R., Buffington, C. A., Roppolo, J. R., Ford, A. P., de Groat, W. C., and Burnstock, G. 2004. Alterations in P2X and P2Y purinergic receptor expression in urinary bladder from normal cats and cats with interstitial cystitis. Am. J. Physiol. 287, F1084–F1091.

Buffington, C. A. 2001. Visceral pain in humans: lessons from animals. Curr. Pain Headache Rep. 5, 44–51.

Buffington, C. A., Chew, D. J., and Woodworth, B. E. 1999. Feline interstitial cystitis. J. Am. Vet. Med. Assoc. 215, 682–687.

Burnstock, G. 2001. Purine-mediated signalling in pain and visceral perception. Trends Pharmacol. Sci. 22, 182–188.

Burnstock, G. and Knight, G. E. 2004. Cellular distribution and functions of P2 receptor subtypes in different systems. Int. Rev. Cytol. 240, 301–304.

Caterina, M. J. 2001. The vanilloid receptor: a molecular gateway to the pain pathway. Ann. Rev. Neurosci. 24, 602–607.

Caterina, M. J., Schumacher, M. A., Tominaga, M., Rosen, T. A., Levine, J. D., and Julius, D. 1997. The capsaicin receptor: a heat activated ion channel in the pain pathway. Nature 389, 816–824.

Chancellor, M. B. and de Groat, W. C. 1999. Intravesical capsaicin and resiniferatoxin therapy: spicing up the ways to treat the overactive bladder. J. Urol. 162, 3–11.

Chess-Williams, R. 2002. Muscarinic receptors of the urinary bladder: detrusor, urothelial and prejunctional. Auton. Autacoid. Pharmacol. 22, 133–145.

Chess-Williams, R. 2004. Potential therapeutic targets for the treatment of detrusor overactivity. Expert Opin. Ther. Targets 8, 95–106.

Chopra, B., Barrick, S. R., Meyers, S., Beckel, J., Zeidel, M. L., Ford, A. P., de Groat, W. C., and Birder, L. A. 2005. Expression and function of bradykinin B1 and B2 receptors in normal and inflamed rat urinary bladder urothelium. J. Physiol. 562, 859–871.

Chung, M. K., Lee, H., and Caterina, M. J. 2003. Warm temperatures activate TRPV4 in mouse 308 keratinocytes. J. Biol. Chem. 278, 32037–32046.

Cockayne, D. A., Hamilton, S. G., Zhu, Q. M., Dunn, P. M., Zhong, Y., Novakovic, S., Malmberg, A. B., Cain, G., Berson, A., Kassotakis, L., Hedley, L., Lachnit, W. G., Burnstock, G., McMahon, S. B., and Ford, A. P. D. W. 2000. Urinary bladder hyporeflexia and reduced pain-related behaviour in P2X(3)-deficient mice. Nature 407, 1011–1015.

Coutinho-Silva, R., Stahl, L., Cheung, K. K., de Campos, N. E., de Oliveira Souza, C., Ojcius, D. M., and Burnstock, G. 2005. P2X and P2Y purinergic receptors on human intestinal epithelial carcinoma cells: effects of extracellular nucleotides on apoptosis and cell proliferation. Am. J. Physiol. 288, G1024–G1035.

Dattilio, A. and Vizzard, M. A. 2005. Up-regulation of protease activated receptors in bladder after cyclophosphamide induced cystitis and colocalization with capsaicin receptor (VR1) in bladder nerve fibers. J. Urol. 173, 635–639.

Ferguson, D. R., Kennedy, I., and Burton, T. J. 1997. ATP is released from rabbit urinary bladder epithelial cells by hydrostatic pressure changes – a possible sensory mechanism? J. Physiol. 505.2, 503–511.

Ghuang, H. H., Prescott, E. D., Kong, H., Shields, S., Jordt, S. E., Basbaum, A. I., Chao, M. V., and Julius, D. 2001. Bradykinin and nerve growth factor release the capsaicin receptor from PtdIns(4,5)P_2-mediated inhibition. Nature 411, 957–962.

Greig, A. V., Linge, C., Terenghi, G., McGrouther, D. A., and Burnstock, G. 2003. Purinergic receptors are part of a functional signaling system for proliferation and differentiation of human epidermal keratinocytes. J. Invest. Dermatol. 120, 1007–1015.

Han, X., Fink, M. P., Uchiyama, T., Yang, R., and Delude, R. L. 2004. Increased iNOS activity is essential for pulmonary epithelial tight junction dysfunction in endotoxemic mice. Am. J. Physiol. 286, L259–L267.

Harper, M., Fowler, C. J., and Dasgupta, P. 2004. Botulinum toxin and its applications in the lower urinary tract. BJU Int. 93, 702–706.

Hawthorn, M. H., Chapple, C. R., Cock, M., and Chess-Williams, R. 2000. Urothelium-derived inhibitory factor(s) influences on detrusor muscle contractility *in vitro*. Br. J. Pharmacol. 129, 416–419.

Hicks, M. 1975. The mammalian urinary bladder: an accommodating organ. Biol. Rev. 50, 215–246.

Holzer, P. 2004. TRPV1 and the gut: from a tasty receptor for a painful vanilloid to a key player in hyperalgesia. Eur. J. Pharmacol. 500, 231–241.

Homolya, L., Steinberg, T. H., and Boucher, R.. C. 2000. Cell to cell communication in response to mechanical stress via bilateral release of ATP and UTP in polarized epithelia. J. Cell Biol. 150, 1349–1360.

Jallat-Daloz, I., Cognard, J. L., Badet, J. M., and Regnard, J. 2001. Neural-epithelial cell interplay: *in vitro* evidence that vagal mediators increase PGE_2 production by human nasal epithelial cells. Allerg. Asthma Proc. 22, 17–23.

Keay, S., Warren, J. W., Zhang, C. O., Tu, L. M., Gordon, D. A., and Whitmore, K. E. 1999. Antiproliferative activity is present in bladder but not renal pelvic urine from interstitial cystitis patients. J. Urol. 162, 1487–1489.

Keay, S. K., Szekely, Z., Conrads, T. P., Veenstra, T. D., Barchi, J. J., Zhang, C. O., Koch, K. R., and Michejda, C. J. 2004. An antiproliferative factor from interstitial cystitis patients is a frizzled 8 protein-related sialoglycopeptide. Proc. Natl. Acad. Sci. U. S. A. 101, 11803–11808.

Kim, J. H., Rivas, D. A., Shenot, P. J., Green, B., Kennelly, M., Erickson, J. R., O'Leary, M., Yoshimura, N., and Chancellor, M. B. 2003. Intravesical resiniferatoxin for refractory detrusor hyperreflexia: a multicenter, blinded, randomized, placebo-controlled trial. J. Spinal Cord Med. 26, 358–363.

Lavelle, J., Meyers, S., Ramage, R., Bastacky, S., Doty, D., Apodaca, G., and Zeidel, M. L. 2002. Bladder permeability barrier: recovery from selective injury of surface epithelial cells. Am. J. Physiol. 283, F242–F253.

Lavelle, J., Meyers, S., Ruiz, W. G., Buffington, C. A., Zeidel, M. L., and Apodaca, G. 2000. Urothelial pathophysiological changes in feline interstitial cystitis: a human model. Am. J. Physiol. 278, F540–F553.

Lee, H. Y., Bardini, M., and Burnstock, G. 2000. Distribution of P2X receptors in the urinary bladder and the ureter of the rat. J. Urol. 163, 2002–2007.

Lewis, S. A. 2000. Everything you wanted to know about the bladder epithelium but were afraid to ask. Am. J. Physiol. 278, F867–F874.

Lewis, S. A. and Hanrahan, J. W. 1985. Apical and basolateral membrane ionic channels in rabbit urinary bladder epithelium. Pflugers Arch 405, S83–S88.

Liedtke, W., Choe, Y., Marti-Renom, M. A., Bell, A. M., Denis, C. S., and Sali, A. 2000. Vanilloid receptor-related osmotically activated channel (VR-OAC), a candidate vertebrate osmoreceptor. Cell 103, 525–535.

Martin, B. F. 1972. Cell replacement and differentiation in transitional epithelium: a histological and autoradiographic study of the guinea-pig bladder and ureter. J. Anat. 112, 433–455.

Morris, J. L., Jobling, P., and Gibbins, I. L. 2001. Differential inhibition by botulinum neurotoxin A of cotransmitters released from autonomic vasodilator neurons. Am. J. Physiol. 281, H2124–H2127.

Murray, E., Malley, S. E., Qiao, L. Y., Hu, V. Y., and Vizzard, M. A. 2004. Cyclophosphamide induced cystitis alters neurotrophin and receptor kinase expression in pelvic ganglia and bladder. J. Urol. 172, 2434–2439.

North, R. A. 2004. P2X3 receptors and peripheral pain mechanisms. J. Physiol. 554, 301–308.

Poulsen, A. N., Klausen, T. L., Pedersen, P. S., Willumsen, N. J., and Frederidsen, O. 2005. Regulation of ion transport via apical purinergic receptors in intact rabbit airway epithelium. Pflugers Arch. 450(4), 227–235.

Reitz, A. and Schurch, B. 2004. Intravesical therapy options for neurogenic detrusor overactivity. Spinal Cord 42, 267–272.

Smith, P. R., Mackler, S. A., Weiser, P. C., Brooker, D. R., Ahn, Y. J., Harte, B. J., McNulty, K. A., and Kleyman, T. R. 1998. Expression and localization of epithelial sodium channel in mammalian urinary bladder. Am. J. Physiol. 274, F91–F96.

Stein, R. J., Santos, S., Nagatomi, J., Hayashi, Y., Minnery, B. S., Xavier, M., Patel, A. S., Nelson, J. B., Futrell, W. J.,

Yoshimura, N., Chancellor, M. B., and deMiguel, F. 2004. Cool (TRPM8) and hot (TRPV1) receptors in the bladder and male genital tract. J. Urol. 172, 1175–1178.

Sun, Y., Keay, S., DeDeyne, P. G., and Chai, T. C. 2001. Augmented stretch activated adenosine triphosphate release from bladder uroepithelial cells in patients with interstitial cystitis. J. Urol. 166, 1951–1956.

Szallasi, A. 2001. Vanilloid receptor ligands: hopes and realities for the future. Drugs Aging 18, 561–573.

Szallasi, A. and Fowler, C. J. 2002. After a decade of intravesical vanilloid therapy: still more questions than answers. Lancet Neurol. 1, 167–172.

Tempest, H. V., Dixon, A. K., Turner, W. H., Elneil, S., Sellers, L. A., and Ferguson, D. R. 2004. P2X and P2Y receptor expression in human bladder urothelium and changes in interstitial cystitis. BJU Int. 93, 1344–1388.

Tominaga, M., Wada, M., and Masu, M. 2001. Potentiation of capsaicin receptor activation by metabotropic ATP receptors: a possible mechanism for ATP-evoked pain and hypersensitivity. Proc. Natl. Acad. Sci. USA 29, 820–825.

Tsavaler, L., Shapero, M. H., Morkowski, S., and Laus, R. 2001. TRP-p8, a novel prostate specific gene, is up regulated in prostate cancer and other malignancies and shares high homology with transient receptor potential calcium channel proteins. Cancer Res. 61, 3760–3769.

Wang, E. C., Lee, J. M., Ruiz, W. G., Balestreire, E. M., von Bodungen, M., Barrick, S., Cockayne, D. A., Birder, L. A., and Apodaca, G. 2005. ATP and purinergic-receptors dependent membrane traffic in bladder umbrella cells. J. Clin. Invert. 115, 2412–2422.

Wayabayashi, Y., Kojima, Y., Makiura, Y., Tomoyoshi, T., and Maeda, T. 1995. Acetylcholinesterase positive axons in the mucosa of urinary bladder of adult cats: retrograde tracing and degeneration studies. Histol. Histopathol. 10, 523–530.

5.41 The Brainstem and Nociceptive Modulation

M M Heinricher, Oregon Health & Science University, Portland, OR, USA

S L Ingram, Washington State University, Vancouver, WA, USA

© 2008 Elsevier Inc. All rights reserved.

5.41.1	**The Periaqueductal Gray–Rostral Ventromedial Medulla Pain-Modulating System**	594
5.41.1.1	Functional Characterization of the Periaqueductal Gray–Rostral Ventromedial Medulla Pain-Modulating System	594
5.41.1.2	Pain Modulation as Part of Adaptive Responses to Behavioral and Physiological Challenges	595
5.41.2	**The Periaqueductal Gray**	596
5.41.2.1	The Periaqueductal Gray and Facilitation of Nociception	597
5.41.2.2	Afferents to the Periaqueductal Gray	597
5.41.2.3	Efferents from the Periaqueductal Gray	598
5.41.2.4	Columnar Organization of the Periaqueductal Gray	598
5.41.2.5	Intrinsic Circuitry and Neurotransmitters in the Periaqueductal Gray	599
5.41.2.5.1	Endogenous opioids	599
5.41.2.5.2	Norepinephrine	603
5.41.2.5.3	Substance P	603
5.41.2.5.4	Cannabinoids	604
5.41.3	**The Rostral Ventromedial Medulla**	604
5.41.3.1	Connections of the Rostral Ventromedial Medulla	604
5.41.3.2	The Rostral Ventromedial Medulla and Facilitation of Nociception	604
5.41.3.3	The Neural Basis for Bidirectional Control from the Rostral Ventromedial Medulla: On- and Off- Cells	605
5.41.3.3.1	Physiological classification of rostral ventromedial medulla neurons based on reflex-related activity	605
5.41.3.3.2	Role of on- and off-cells in pain modulation	607
5.41.3.3.3	Role of neutral cells	608
5.41.3.4	Pharmacology of Nociceptive Modulation in the Rostral Ventromedial Medulla	609
5.41.3.4.1	Gamma-aminobutyric acid and glutamate: the off-cell pause and on-cell burst	609
5.41.3.4.2	Opioid actions in the rostral ventromedial medulla	610
5.41.3.4.3	Norepinephrine	611
5.41.3.4.4	Cannabinoids	612
5.41.3.4.5	Cholecystokinin	612
5.41.3.4.6	Neurotensin	612
5.41.3.4.7	Nociceptin/orphanin FQ	612
5.41.3.5	Physiological Activation of Nociceptive Modulatory Neurons in the Rostral Ventromedial Medulla	613
5.41.3.5.1	Response of RVM neurons to noxious stimulation: does pain inhibit pain?	613
5.41.3.5.2	Behavioral state control: anesthesia and sleep/waking cycle	613
5.41.3.5.3	Micturition	614
5.41.3.5.4	Environmental analgesia	614
5.41.4	**Conclusion**	615
References		616

Glossary

cyclooxygenase An enzyme–protein complex that catalyzes the production of prostaglandins from arachidonic acid. Cyclooxygenase activity is inhibited by nonsteroidal anti-inflammatory drugs, such as aspirin and ibuprofen.

GIRK G-protein-activated inwardly rectifying potassium channel. A potassium-selective channel that is gated by activated betagamma subunits of Gi/Go G proteins.

Kv channel Voltage-gated potassium channel.

12-lipoxygenase An enzyme that catalyzes the conversion of arachidonic acid to the hydroxyeicosenoic acid (12-HETE) structure.

NSAIDs Nonsteroidal anti-inflammatory drugs. Drugs that inhibit cyclooxygenases and the production of prostaglandins involved in the inflammatory response (e.g., aspirin, ibuprofen, naproxen).

phospholipase A_2 An enzyme that catalyes the formation of arachidonic acid from phospholipids.

5.41.1 The Periaqueductal Gray–Rostral Ventromedial Medulla Pain-Modulating System

The idea that there are well-defined central systems that selectively modulate nociception is usually traced to the demonstration that electrical stimulation in the periaqueductal gray (PAG) region of rats produced potent analgesia. This phenomenon came to be called stimulation-produced analgesia when subsequent work confirmed this finding using quantitative tests of nociception in animals, and when such stimulation was shown to produce clinical analgesia in humans. This was an important advance in documenting that the brain itself could regulate the processing of nociceptive information. Inspired by stimulation-produced analgesia, a significant research effort led to the definition of a brainstem pain modulatory network with critical links in the rostral ventromedial medulla (RVM) as well as the PAG (Figure 1). The antinociception resulting from stimulation in these structures is in large part due to regulation of nociceptive processing at the level of the spinal cord. The PAG–RVM system mediates the analgesic actions of opioids, and it is recruited by internal and environmental challenges. Accumulating evidence from neuroimaging studies supports a role for this system in top-down modulation of pain in humans, such as that produced by placebo or shifts in attention. An overview of descending control, including that mediated by the PAG–RVM system, is provided in Chapter Descending Control Mechanisms. The purpose of this chapter is to review the properties of pain-modulating neurons within the PAG and RVM, and to place this circuitry in a behavioral context.

5.41.1.1 Functional Characterization of the Periaqueductal Gray–Rostral Ventromedial Medulla Pain-Modulating System

The PAG is a cell-rich region surrounding the cerebral aqueduct in the midbrain. The RVM is defined functionally, rather than cytoarchitecturally, and includes the nucleus raphe magnus and adjacent reticular formation. Numerous behavioral studies have demonstrated that nonselective activation of neurons within the PAG or RVM produces a potent antinociception. Activation of PAG–RVM output neurons must mediate this antinociception, as direct excitation of either PAG or RVM neurons produces antinociception and inhibition of noxious-evoked activity of dorsal horn neurons, whereas inactivation of either the PAG or RVM does not. The PAG–RVM modulatory network is also an important substrate for opioid analgesia. Focal application of morphine or mu-opioid agonists at either site is sufficient to produce antinociception comparable to that resulting from systemic morphine administration (see Fields, H. L. *et al.*, 2005 or Heinricher, M. M. and Morgan, M. M., 1999 for reviews).

Along with the evidence that this system mediates the analgesic actions of exogenous and endogenous opioids, the fact that the net behavioral effect of nonselective experimental activation of the PAG or RVM is antinociception led to a general view of the PAG–RVM system as an analgesia system. This system is indeed activated by acute stress and opioid analgesics to inhibit spinal nociceptive processing. However, there is now increasing evidence that the system, especially the

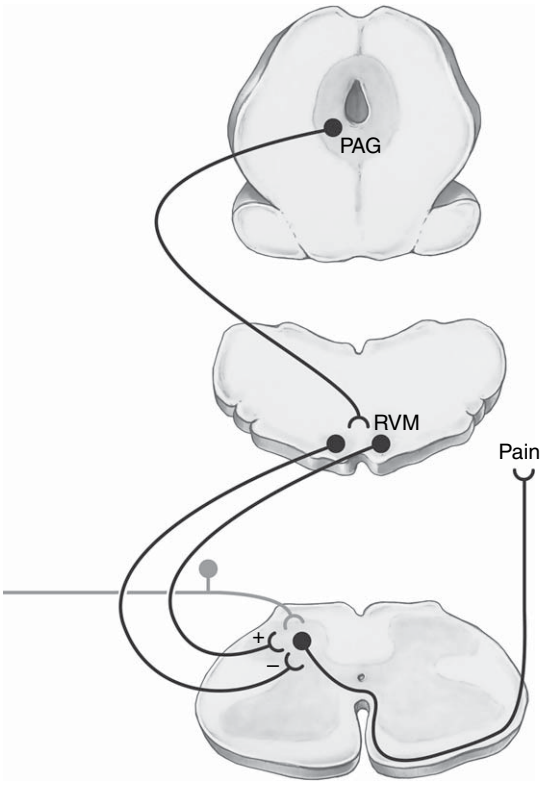

Figure 1 Functional organization of brainstem pain-modulating system with links in midbrain periaqueductal gray (PAG) and rostral ventromedial medulla (RVM). The PAG projects to the RVM. The RVM in turn regulates spinal nociceptive circuitry via a projection through the dorsolateral funiculus to the dorsal horn. This system exerts bidirectional control, and separate populations of RVM neurons mediate descending inhibition and descending facilitation. The PAG is reciprocally linked with forebrain structures including prefrontal cortex, amygdala, and hypothalamus. These substantial interconnections provide an anatomical substrate through which emotional and cognitive variables could influence nociception via the PAG–RVM system.

RVM, also facilitates nociception. The RVM has been implicated in hyperalgesia and allodynia associated with inflammation, nerve injury, acute opioid withdrawal, chronic opioid administration, and the sickness response (see Sections 5.41.2.1 and 5.41.3.2, also Porreca, F. *et al.*, 2002 and Heinricher, M. M. *et al.*, 2003 for recent reviews). The PAG–RVM circuit should therefore be viewed not specifically as an analgesia system, but more generally, as a pain-modulation system. From this perspective, the system has the potential for graded enhancement or inhibition of nociception under different conditions.

5.41.1.2 Pain Modulation as Part of Adaptive Responses to Behavioral and Physiological Challenges

One of the earliest hints that stimulation-produced analgesia was not an experimental curiosity was the demonstration of environmental or stress-induced analgesia. Stress-induced analgesia refers to the fact that any number of situations or experimental procedures that could be characterized as stressful induce behaviorally measurable, and in some cases quite potent, analgesia. For example, stress-induced analgesia can be produced by electric shock, forced swim, and centrifugal rotation as well as biologically relevant threat stimuli such as odors from stressed animals of the same species or exposure to a predator. Analgesia is also elicited as a conditioned response to cues that have been paired previously with noxious or aversive events. This analgesia can be opioid or nonopioid in nature and has been shown by a number of investigators to be mediated by the PAG–RVM system (Bodnar, R. J. *et al.*, 1980; Lewis, J. W. *et al.* 1980; Watkins, L. R. *et al.* 1982; Fanselow, M. S. 1986).

In addition to antinociception, electrical or chemical stimulation of the PAG also evokes autonomic changes commonly associated with cardiovascular aspects of defense, including hypertension (in anesthetized animals) and altered heart rate (Lovick, T. A., 1993; Bandler, R. *et al.*, 2000; Morgan, M. M. and Carrive, P., 2001). Patients in whom deep brain electrodes were implanted in the rostral midbrain/PAG region for relief of intractable pain often found the stimulation to be distinctly disquieting, with reports of a feeling of impending doom or a desire to flee when the stimulation was activated (Nashold, B. S. *et al.*, 1969). Consistent with these reports in humans, rats will work to terminate electrical stimulation in the dorsal PAG (Kiser, R. S. *et al.*, 1978). Moreover, stimulation-produced antinociception in rats is accompanied by species-specific defense behaviors, which include immobility and escape or attack (Bandler, R. and DePaulis, A., 1991; Fanselow, M. S. 1991; Morgan, M. M. and Carrive, P. 2001; Carrive, P. and Morgan, M. M. 2004).

Two factors contributed to the idea that antinociception is recruited as part of defense behaviors: the fact that antinociception is readily evoked by learned or innate danger signals and the observation that stress induces analgesia through activation of the PAG–RVM system. Pain behaviors must sometimes be inhibited in order to give higher precedence to more pressing needs such as escaping from an aggressor or avoiding detection by a predator. However, a more

general view of pain modulation has now developed. Pain inhibition is currently viewed as one component of a number of organized responses that allow an organism to prioritize nociceptive behaviors relative to other internal and external demands. In addition to antinociception, such responses typically include autonomic, endocrine, and motor elements. One example of such an organized defense response would be antinociception as part of preparation for fight or flight when confronted by a predator. Although the circuitry through which the PAG–RVM system is brought into play in response to threat remains to be fully elucidated, inputs from the amygdala and hypothalamus are likely to be critical (Helmstetter, F. J., 1992; Lovick, T. A., 1993; Lumb, B. M. *et al.*, 2002).

There is also evidence that the PAG–RVM system is engaged as part of the response to general immune challenge, as occurs with systemic bacterial infection. Thus, systemic administration of lipopolysaccharide (LPS), a well-accepted model for bacterial infection and sickness, results in changes in nociception mediated at least in part by the RVM (Watkins, L. R. *et al.*, 1994; Romanovsky, A. A. *et al.*, 1996). Just as antinociception is viewed as an adaptive response to external threat, hyperalgesia associated with sickness may promote recuperative behaviors and facilitate healing. As with the defense response to external threat, the system is engaged during sickness to prioritize processing of nociceptive information in accord with other physiological and behavioral goals.

It is likely that the PAG–RVM system also mediates the more subtle shifts in pain processing that occur in the absence of extreme challenge. For example, reflexes or other more highly organized behaviors evoked by noxious stimuli would be expected to interfere with feeding or other homeostatic behaviors. Nociceptive threshold is increased in hungry cats given access to food (Casey, K. L. and Morrow, T. J. 1988; 1989). Moreover, there appears to be an equilibrium between responding to noxious inputs and the need to maintain energy balance. Feeding is suppressed in favor of pain behaviors during the first phase of the formalin response, generally thought to represent a relatively intense sensation. By contrast, pain behaviors are reduced in favor of feeding during the second, less intense, phase of the formalin response (LaGraize, S. C. *et al.*, 2004a). Similarly, paw withdrawal to noxious heat is attenuated during micturition, presumably allowing complete emptying of the bladder without interruption by noxious-evoked movements (Baez, M. A. *et al.* 2005).

Distraction or more global variables such as positive or negative mood also alter pain (see Villemure, C. and Bushnell, M. C., 2002 for a review). Similarly, expectation that a particular manipulation will relieve pain can lead to inhibition of pain (Price, D. D. *et al.*, 1999). Understanding the neural mechanisms through which these and other higher psychological factors modulate pain has been challenging, as these variables are at best difficult to study in nonhuman subjects. Moreover, some modulation of pain perception undoubtedly occurs within thalamocortical circuits. However, imaging studies in humans have now demonstrated that the PAG is activated in placebo and distraction paradigms. There are also changes in activation of this system and associated structures when subjects anticipate pain, and in functional pain disorders (see Tracey, I., in press for a recent review). Studies of opioid-dependent placebo have been most compelling. Petrovic P. *et al.* (2002) found that a placebo procedure (infusion of an inactive vehicle in subjects who had been given the powerful opiate remifentanil in a separate trial) resulted in reduced pain reports and activation of the PAG. This region had previously been activated by the exogenous opiate, suggesting that the placebo manipulation recruited endogenous opioid circuitry within the PAG. Wager T. D. *et al.* (2004) saw similar activation of the anterior cingulate and PAG in a conditioned placebo paradigm. These two studies suggest that recruitment of the PAG contributes to the pain inhibition produced by placebo. Similar studies investigating the effects of attention on pain responses also suggest that activation of the PAG–RVM system contributes to pain suppression when attention is redirected from the noxious stimulus to inputs that have greater behavioral significance (Tracey, I. *et al.*, 2002; Valet, M. *et al.*, 2004). Although correlative, these imaging studies suggest that the PAG–RVM system plays a role in pain modulation produced by placebo, shifts in attention and presumably other cognitive and affective variables.

5.41.2 The Periaqueductal Gray

The PAG comprises heterogeneous cell populations surrounding the cerebral aqueduct. It extends rostrally from the pericoerulear area of the pons to the opening of the third ventricle. As described above, electrical stimulation or focal application of opioids in the PAG produces behaviorally measurable antinociception. However, in addition to pain modulation, it integrates a variety of complex functions, including

cardiovascular and other aspects of defense, general autonomic control, reproductive behaviors, and vocalization (Bandler, R. and Shipley, M. T., 1994).

5.41.2.1 The Periaqueductal Gray and Facilitation of Nociception

The idea that the PAG–RVM system exerts bidirectional control is now well accepted (Porreca, F. *et al.*, 2002; Heinricher, M. M. *et al.*, 2003). Although the focus of functional studies of descending facilitation has been primarily on the RVM (see below, Section 5.41.3.2), there is some evidence that the PAG also contributes to hyperalgesia under some conditions.

First, the PAG contributes to normal levels of responsiveness on the formalin test and to enhanced nociceptive behaviors after foot shock, suggesting a net facilitating output from this region in these paradigms (McLemore, S. *et al.*, 1999; Berrino, L. *et al.*, 2001). Dorsolateral PAG may be important in a generalized sensory sensitization induced by footshock (Crown, E. D. *et al.*, 2004), a facilitation that is recruited in parallel with the well-documented descending inhibition evoked by footshock. Second, focal application of capsaicin or bradykinin into the PAG has a pronociceptive effect (Burdin, T. A. *et al.*, 1992; McGaraughty, S. *et al.*, 2003). Third, prostaglandin release within the PAG apparently recruits descending facilitation, possibly under conditions of inflammation or systemic infection (Vanegas, H. and Tortorici, V. 2002). Thus, cyclooxygenase is constitutively expressed in PAG, and direct microinjection of cyclooxygenase inhibitors in this region reduces responding on cutaneous and visceral nociceptive tests. Moreover, direct application of prostaglandin E_2 in the PAG produces behavioral hyperalgesia and activates RVM neurons that facilitate nociception (Heinricher, M. M. *et al.*, 2004a). Taken together, these findings document the ability of the PAG to facilitate nociception. Consistent with this idea, a recent imaging study demonstrated that stimulation of an area of capsaicin-induced secondary hyperalgesia in human subjects was associated with activation of the PAG (Zambreanu, L. *et al.*, 2005).

5.41.2.2 Afferents to the Periaqueductal Gray

The PAG integrates information from all levels of the central nervous system. The spinal cord sends direct, somatotopically organized projections from the dorsal horn and the intermediate gray to the ventrolateral and lateral PAG (Menetrey, D. *et al.*, 1982; Yezierski, R. P. and Mendez, C. M. 1991). These afferents convey innocuous and noxious information from cutaneous, musculoskeletal, and visceral structures (Wiberg, M. *et al.*, 1987; Yezierski, R. P., 1988; Yezierski, R. P. and Mendez, C. M., 1991; Clement, C. I. *et al.*, 2000). Inputs from the lumbosacral cord arise from a number of regions, including those receiving afferents from pelvic and pudendal nerves (Vanderhorst, V. G. *et al.*, 1996). These latter afferents are proposed to provide important sensory information contributing to PAG functions in sexual behavior and micturition. Approximately half of the spinal input to the PAG is from the upper cervical spinal cord, but the significance of this cervical predominance has not been determined (Vanderhorst, V. G. *et al.*, 2002).

The most substantial afferent inputs to the PAG are from forebrain, including prefrontal and agranular insular cortices as well as the amygdala and hypothalamus (Bandler, R. and Shipley, M. T., 1994; An, X. *et al.*, 1998; Floyd, N. S. *et al.*, 2000). Connections from medial prefrontal cortex are part of a medial prefrontal network associated with visceromotor control through links with the hypothalamus (Ongur, D. and Price, J. L., 2000). Stimulation in the anterior cingulate has been reported by different laboratories to facilitate or suppress nociceptive responses (Hardy, S. G., 1985; Fuchs, P. N. *et al.*, 1996; Calejesan, A. A. *et al.*, 2000). Lesions of the anterior cingulate are generally agreed to reduce nociception in animal models (Pastoriza, L. N. *et al.*, 1996; Donahue, R. R. *et al.*, 2001; LaGraize, S. C. *et al.*, 2004b; in press), consistent with reports in human patients (Foltz, E. L. and Lowell, E. W. 1962; Davis, K. D. *et al.*, 1994; Talbot, J. D. *et al.*, 1995). However, the antinociceptive effect of lesions is presumably due to interference with cortical processing, rather than to activation of descending control. Effects of experimental manipulation of the ventrolateral orbital cortex (VLO) on nociception are similarly complex. Stimulation of the VLO has been reported by one group of investigators to facilitate nociception (Hutchison, W. D. *et al.*, 1996) and another to suppress nociception (Zhang, Y. Q. *et al.*, 1997). The antinociceptive effect of VLO stimulation was blocked by lesion of the PAG, indicating that the connections from this cortex to the PAG are relevant to nociceptive modulation (Zhang, Y. Q. *et al.*, 1997).

Hypothalamic afferents to the PAG are predominantly from the lateral hypothalamus and the anterior hypothalamus/medial preoptic area (MPO)

(Shipley, M. T. *et al.*, 1991; Semenenko, F. M. and Lumb, B. M. 1992; Behbehani, M. M. and Da Costa Gomez, T. M., 1996). At least some of the anterior hypothalamic neurons projecting to the PAG are nociceptive (Lumb, B. M. *et al.*, 2002; Parry, D. M. *et al.*, 2002). The MPO has important roles in autonomic regulation including thermoregulation and fever, as well as in sleep, mating, and maternal behaviors. Electrical stimulation of the MPO produces *c-fos* labeling throughout the PAG (Rizvi, T. A. *et al.*, 1996) and activates PAG–RVM output neurons (Semenenko, F. M. and Lumb, B. M., 1999). Direct application of prostaglandin E_2 in the MPO at low doses produces hyperalgesia that is likely mediated by the PAG–RVM system (Hosoi, M. *et al.*, 1997; Abe, M. *et al.*, 2001; Heinricher, M. M. *et al.*, 2004b).

The central nucleus of the amygdala has massive reciprocal connections with the PAG (Rizvi, T. A. *et al.*, 1991; da Costa Gomez, T. M. and Behbehani, M. M., 1995). The central nucleus receives inputs from the basolateral nucleus, which is a major target of cortical afferents to the amygdala. The central nucleus of the amygdala also receives nociceptive input from the spinal cord, both directly and indirectly via the parabrachial nucleus (Burstein, R. and Potrebic, S., 1993; Gauriau, C. and Bernard, J. F., 2004). PAG neurons respond to stimulation in the amygdala (da Costa Gomez, T. M. *et al.*, 1996), and both stimulation and injection of morphine into the amygdala result in antinociception that is dependent on activation of the descending pathway from PAG to RVM (Pavlovic, Z. W. *et al.*, 1996; Helmstetter, F. J. *et al.*, 1998; McGaraughty, S. and Heinricher, M. M., 2002; 2004).

Afferents to the PAG from the brainstem arise from the medulla, including the RVM. Other brainstem sources of inputs to the PAG include the nucleus tractus solitarius, adjacent nucleus cuneiformis, pontine reticular formation, and the locus coeruleus and other catecholaminergic nuclei (Beitz, A. J., 1982; Herbert, H. and Saper, C. B., 1992).

The strong input to the PAG from forebrain and hypothalamus provides an anatomical substrate through which emotional and cognitive variables could influence pain via the PAG. Information related to motivation and emotion thus converges with direct and indirect visceral and somatic afferent input in the PAG. This convergence is presumably important to pain modulation in allowing the organism to regulate nociceptive processing in accord with current needs and motivational state, particularly in response to environmental or internal challenge.

5.41.2.3 Efferents from the Periaqueductal Gray

The PAG has only a sparse projection to the spinal cord, but a dense projection to the RVM, which in turn projects to the dorsal horn via the dorsolateral funiculus. Inactivation of the RVM prevents the antinociceptive effects of PAG manipulations, indicating that the connection from the PAG to the RVM is the neuroanatomical basis for descending modulation of nociception by the PAG. PAG–RVM projection neurons express neuropeptides, excitatory amino acids, and serotonin. Functional studies implicate excitatory amino acids, serotonin, and endogenous opioids in recruitment of the RVM by the PAG to produce antinociception. A second relay through which the PAG is likely to influence spinal nociceptive processing is pontine catecholaminergic cell groups, as ultrastructural studies demonstrate that these neurons receive inputs from the ventrolateral PAG (see Fields, H. L. *et al.*, 2005 for a recent review).

5.41.2.4 Columnar Organization of the Periaqueductal Gray

Based on both connectivity and function, the PAG has been subdivided into rostrocaudaully oriented columns, designated as dorsomedial (or dorsal), dorsolateral, lateral, and ventrolateral (Carrive, P. and Morgan, M. M., 2004). These columns roughly correspond with subdivisions based on cytoarchitecture that were proposed previously by Beitz A. J. (1985) and Beitz A. J. and Shepard R. D. (1985). Cortical, hypothalamic, and spinal afferents show a preferential distribution to different columns, although there is substantial spread across columnar boundaries (Rizvi, T. A. *et al.*, 1992; An, X. *et al.*, 1998; Floyd, N. S. *et al.*, 2000). Projections to the RVM arise in the dorsomedial, lateral, and ventrolateral columns, but not the dorsolateral column (Abols, I. A. and Basbaum, A. I., 1981; Van Bockstaele, E. J. *et al.*, 1991).

Pain modulation is not constrained by columnar boundaries, and electrical stimulation or microinjection of mu-opioid agonists or neuroexcitant agents throughout the dorsoventral extent of the PAG produces analgesia, particularly at more caudal levels (Waters, A. J. and Lumb, B. M., 1997 Carrive, P. and Morgan, M. M., 2004; Morgan, M. M. and Clayton, C. C. 2005). Antinociception resulting from stimulation in the ventrolateral PAG must be mediated by an endogenous opioid connection, as it is blocked by naloxone. By contrast, the antinociception resulting from

electrical stimulation more dorsally is not mediated by endogenous opioids (Morgan, M. M. 1991).

Antinociception evoked by stimulation of the dorsal and lateral columns is often associated with escape-like behaviors or defensive posturing, hypertension, and tachycardia. By contrast, antinociception produced by stimulation of the ventrolateral PAG is often accompanied by immobility, bradycardia, and in anesthetized animals, hypotension (Depaulis, A. *et al.*, 1994; Morgan, M. M. and Carrive, P., 2001). These findings gave rise to the proposal that the lateral/dorsolateral columns function specifically in active coping, particularly when confronted with an external threat. By contrast, the ventrolateral column was hypothesized to be important in passive coping and recuperation, for example, in response to visceral pain or some other challenge that cannot be controlled or escaped (Keay, K. A. and Bandler, R., 2001).

Two aspects of this framework for PAG organization have been controversial. The first issue is the interpretation of immobility evoked by stimulation in the ventrolateral column. It is not possible to determine from lack of movement alone whether an animal should be viewed as engaging in recuperative behaviors or whether it is instead freezing, that is, exhibiting an active cryptic defense that reduces the likelihood of detection by a predator (Blanchard, R. J. *et al.* 1986; Fanselow, M. S., 1991; Bittencourt, A. S. *et al.*, 2004). The argument that immobility represents passive coping rather than a defensive response is based largely on observations that stimulation in the ventrolateral column in anesthetized animals produce hypotension (Keay, K. A. and Bandler, R., 2001). However, hypotension is not evoked by such stimulation in awake behaving animals (Morgan, M. M. and Carrive, P., 2001). Furthermore, hypotension may not imply a quiescence or recuperative state. For example, although the freezing in a conditioned fear paradigm is associated with hypertension (Carrive, P. 2000), defensive freezing to various threat stimuli can be associated with profound hypotension in various species of wild-trapped rodents (Hofer, M. A., 1970).

A second contentious issue is whether active offensive and escape behaviors should be associated specifically with the lateral/dorsolateral columns, whereas immobility is a function of the ventrolateral column. Immobility as well as escape can be evoked with stimulation of the lateral/dorsolateral columns. Notably, the current needed to induce immobility is lower than that required for active flight behaviors with stimulation in this column (Bittencourt, A. S. *et al.*, 2004). Conversely, bursts of running are often interspersed with periods of inactivity during antinociception evoked from the ventrolateral column (Vianna, D. M. *et al.*, 2001; Morgan, M. M. and Clayton, C. C., 2005). As in the lateral/dorsolateral columns, the current needed to elicit freezing with stimulation in the ventrolateral PAG is lower than that required to elicit jumping (Vianna, D. M. *et al.*, 2001). Moreover, although lesions of the ventrolateral PAG reduce freezing and release running behavior in response to threat (Walker, P. and Carrive, P., 2003, Farook, J. M. *et al.*, 2004), lesions of the dorsolateral PAG have no effect on either freezing or running evoked by exposure to a cat or to a context associated with footshock. In addition, changes in heart rate and activity in this paradigm are seen only when the animal is denied access to a safe hiding place (Dielenberg, R. A. *et al.*, 2004; Farook, J. M. *et al.*, 2004; Leman, S. *et al.*, 2003). Thus, neither active fight or flight behaviors nor immobility appears to be a specific output of a particular column.

These observations suggest that although the idea that the lateral/dorsolateral and ventral columns of the PAG represent centers for active and passive coping has had great heuristic value, a full understanding of the functional significance of the PAG columns is likely to require sophisticated analyses of the neural circuitry of these regions in relevant behavioral paradigms.

5.41.2.5 Intrinsic Circuitry and Neurotransmitters in the Periaqueductal Gray

5.41.2.5.1 Endogenous opioids

All three opioid receptors, mu (MOR), delta (DOR), and kappa (KOR) opioid receptors, are moderately to densely expressed in the PAG (Mansour, A. *et al.*, 1995; Gutstein H. B. *et al.*, 1998; Kalyuzhny, A. E. and Wessendorf, M. W., 1998). The PAG is also rich in endogenous opioids (Mansour, A. *et al.*, 1995). Enkephalin-like immunoreactivity is most dense in the ventrolateral PAG and enkephalin-containing terminals are found apposed to both gamma aminobutyric acid (GABA)ergic and non-GABAergic dendrites, including those of a small percentage of PAG–RVM neurons (Williams, F. G. and Beitz, A. J., 1990). Endomorphin-2 (Tyr-Pro-Phe-Phe-NH_2), an endogenous peptide with high selectivity for the MOR (Zadina, J. E. *et al.*, 1997), is concentrated in the PAG as well as the dorsal horn of the spinal cord (Schreff, M. *et al.*, 1998). Although the endomorphins have a high affinity for the MOR, it appears that these

peptides are only partial agonists for the MOR in the PAG (Narita, M. *et al.*, 2000). Another endogenous opioid found in the PAG is β-endorphin. Discrete populations of β-endorphin-containing neurons in the ventromedial hypothalamus project to the PAG and have been implicated in analgesia produced by electrical stimulation and stress (Millan, M. J., 2002).

MOR agonists produce potent antinociception when applied directly in the PAG (Heinricher, M. M. and Fields, H. L., 2003). The behavioral antinociception produced by these agents is mediated by activation of output neurons projecting to the RVM (Sandkühler, J. and Gebhart, G. F., 1984; Tortorici, V. and Morgan, M. M., 2002). However, as the direct postsynaptic action of MOR agonists on PAG neurons is hyperpolarization (Chieng, B. and Christie, M. J., 1994a; Osborne, P. B. *et al.*, 1996), activation of the output neurons must be via disinhibition. MOR agonists are thought to act presynaptically to block GABAergic inhibition of PAG output neurons. Consistent with this hypothesis, blockade of GABA transmission within the PAG by microinjection of a $GABA_A$ receptor antagonist produces antinociception (Moreau, J. L. and Fields, H. L., 1986; Depaulis, A. *et al.*, 1987). Also consistent with this hypothesis are observations that MOR1 is frequently expressed in GABAergic neurons within the PAG. However, a substantial subset of PAG–RVM projection neurons do express MOR1 (Kalyuzhny, A. E. and Wessendorf, M. W., 1998; Commons, K. G. *et al.*, 2000). These MOR1-positive neurons may target nociceptive facilitating neurons in the RVM (Vanegas, H. *et al.*, 1984; Cheng, Z. F. *et al.*, 1986; Morgan, M. M. *et al.*, 1992;). If so, these MOR1-positive output neurons would be involved in descending facilitation rather than descending inhibition.

Postsynaptic effects of MOR agonists on PAG neurons include hyperpolarization (via activation of a postsynaptic G-protein-activated inwardly rectifying potassium conductance, GIRK) and inhibition of calcium channels (Connor, M. and Christie, M. J., 1998) (Figure 2). MOR agonists also have presynaptic effects, inhibiting GABA and glutamate release from terminals within the ventrolateral PAG (Chieng, B. and Christie, M. J., 1994b; Vaughan, C. W. and Christie, M. J. 1997; Vaughan, C. W. *et al.*, 1997). Presynaptic inhibition of GABAergic neurotransmission is through activation of the arachidonic acid–

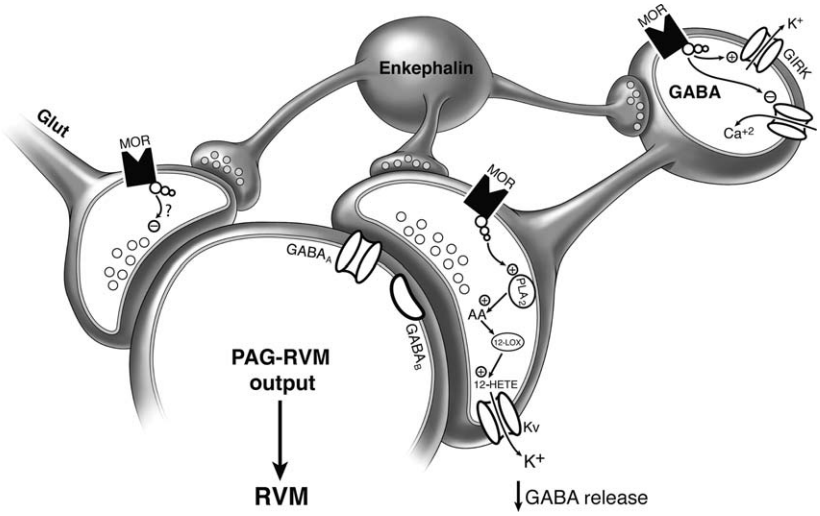

Figure 2 Cellular mechanisms of opioid action within the periaqueductal gray (PAG). Enkephalin-containing synapses are apposed to cell bodies as well as to GABA- and glutamate-containing terminals. The postsynaptic mu-uopoid receptor (MOR) activates G-protein-activated inwardly rectifying potassium channels (GIRKs) and inhibits voltage-gated Ca^{2+} channels to hyperpolarize cells and decrease cell activity. Presynaptic MORs inhibit both GABA and glutamate release on ventrolateral PAG neurons, and apparently use different signal transduction pathways in the terminals. MORs localized to GABA terminals are coupled to voltage-gated potassium channels via activation of the arachidonic acid/12-lipoxygenase (12-LOX) second messenger pathway. Hyperpolarization of the terminal decreases GABA release. The signal transduction pathway for MOR inhibition of glutamate release is currently unknown. MORs are found on GABA containing interneurons in the PAG, as well as on PAG output neurons projecting to the rostral ventromedial medulla (RVM). Activation of the descending antinociceptive pathway by opioids occurs via disinhibition. 12-HETE, 12-hydroxyeicosenoic acid; Kv, voltage-gated potassium; PLA_2, phospholipase A_2.

phospholipase A_2 second messenger pathway. Stimulation of this pathway results in activation of voltage-gated potassium channels (Kv channels) by metabolites of 12-lipoxygenase (Vaughan, C. W. and Christie, M. J., 1997; Vaughan, C. W. *et al.*, 1997). This pathway is independent of adenylyl cyclase, protein kinase A or protein kinase C activity (Vaughan, C. W. *et al.*, 1997). Further research is needed to determine the relevance of the various presynaptic versus postsynaptic opioid actions to the nociceptive modulatory function of the PAG. As already noted, there is good evidence that the behavioral antinociception produced by local application of MOR agonists involves activation of the PAG–RVM output neurons via disinhibition. Whether postsynaptic inhibition or the suppression of glutamatergic transmission plays a role in antinociception is unknown. However, at least in the PAG slice, the effect of presynaptic inhibition of GABAergic transmission apparently predominates, because bath application of the MOR agonist [D-Ala2, N-Met-Phe4, Gly-015] enkephalin (DAMGO) results in activation of neurons that are also directly hyperpolarized by the opioid (Chiou, L. C. and Huang, L. Y., 1999). Thus, under *in vitro* conditions, disinhibition has a relatively large impact, and the net effect of MOR agonist administration is neuronal activation. However, it is not known whether, or under what conditions, endogenous opioids are released to act simultaneously on presynaptic and postsynaptic receptors.

In general, activation of DOR and KORs in the PAG does not result in significant antinociception, at least in rats. A number of groups have found no analgesic effect of microinjection of DOR agonists in the PAG in rats (Bodnar, R. J. *et al.*, 1988; Smith, D. J. *et al.*, 1988; Ossipov, M. H. *et al.*, 1995), although there is one report that microinjection of the $delta_2$ agonist deltorphin into the PAG produces a modest increase in latency of the tail flick response (Rossi, G. C. *et al.*, 1994). KOR agonists are also ineffective in producing analgesia in the PAG (Fang, F. G. *et al.*, 1989). At the cellular level, DOR and KOR agonists have no effect on presynaptic GABA release and in rat do not activate postsynaptic potassium channels (Vaughan, C. W. and Christie, M. J., 1997). However, in mice, KOR agonists inhibit presynaptic GABA release in the PAG, and agonists of all three opioid receptor subtypes activate postsynaptic potassium channels (Vaughan, C. W. *et al.*, 2003). The functions of the three receptors may therefore be different in the two species, and it would obviously be of interest to test the behavioral effects of DOR- and KOR-selective agonists in the PAG in the mouse.

5.41.2.5.1.(i) Opioid/nonsteroidal anti-inflammatory drugs interactions Microinjections of nonsteroidal anti-inflammatory drugs (NSAIDs) into the PAG produce analgesia (Tortorici, V. and Vanegas, H., 1995). This antinociception is apparently mediated at least in part by an endogenous opioid peptide, as the analgesia produced by NSAIDs microinjected into the PAG and RVM is attenuated by the opioid antagonist naloxone (Vanegas, H. and Tortorici, V., 2002).

In addition to stimulating release of endogenous opioids, recent evidence at the cellular level suggests that NSAIDs may also augment the signaling pathway used by opiates, potentiating the actions of exogenous opioids (Figure 3). Coapplication of NSAIDs potentiates the inhibition of GABA release by the MOR partial agonist morphine, although NSAIDs have no effect on GABA release in the absence of morphine (Vaughan, C. W. *et al.*, 1997). NSAIDs primarily inhibit cyclooxygenases (COX-1 and COX-2), one of three types of enzymes (cyclooxygenases, 5-lipoxygenases, and 12-lipoxygenases) that metabolize arachidonic acid. One hypothesis proposed to explain the mechanism of increased analgesia with coapplication of opioids and NSAIDs is that blockade of COX-1 shunts arachidonic acid metabolism through the lipoxygenase pathways to increase the potency of opioid receptor agonists (Vaughan, C. W. *et al.*, 1997; Vaughan, C. W. 1998; Christie, M. J. *et al.*, 1999). The fact that inhibitors of 5-lipoxygenases also appear to potentiate the effects of opioid agonists in the PAG adds further weight to this proposal (Vaughan, C. W. *et al.*, 1997; Christie, M. J. *et al.*, 1999). These results are important in that the combined administration of NSAIDs and opiates may allow lower doses of morphine to be used to provide adequate analgesia while reducing the probability of the development of tolerance and side effects (such as respiratory depression) associated with high doses of opiates. Functional studies of NSAID/opioid interactions in the PAG would therefore be of great interest.

5.41.2.5.1.(ii) Opioid tolerance and dependence The PAG has been implicated in opioid tolerance as well as dependence. Opioid tolerance is the diminished responsiveness to the antinociceptive actions of opioids with chronic administration. Dependence refers to the occurrence of withdrawal signs and/or rebound responses upon removal of the opioid or

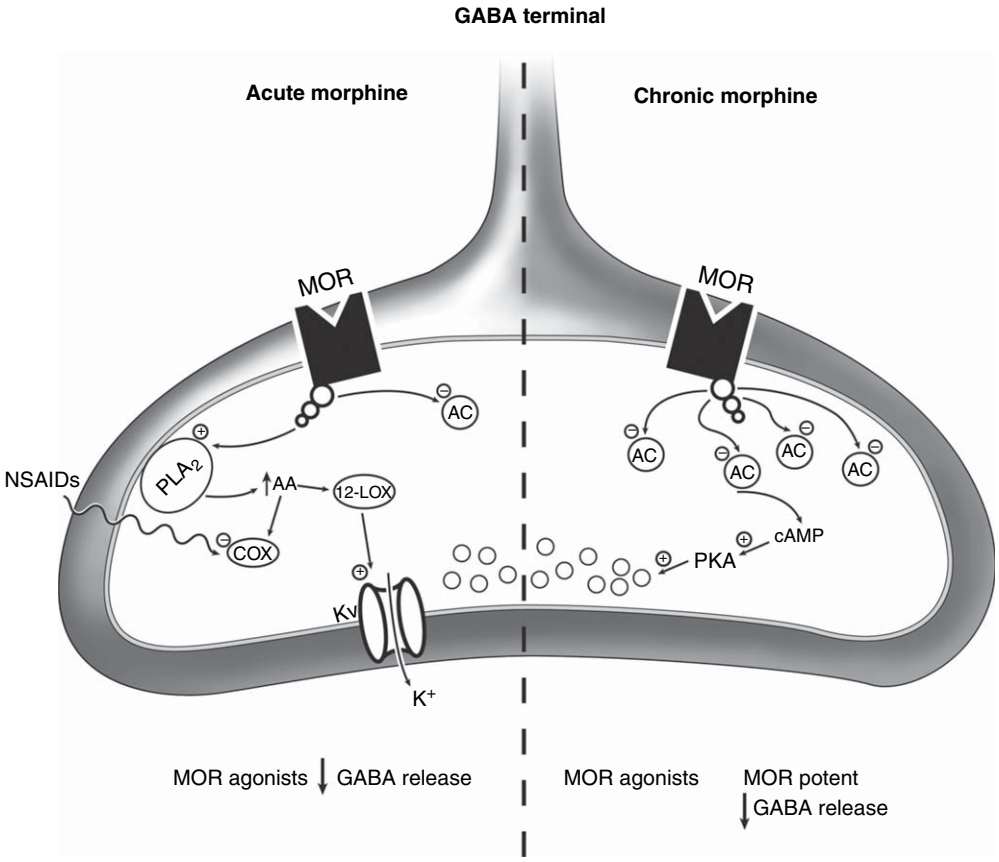

Figure 3 Mu-opioid receptor (MOR) coupling in presynaptic GABA terminals changes with chronic morphine administration. Acute administration of MOR agonists activates MORs coupled to phospholipase A_2 (PLA_2). Activation of PLA_2 increases production of arachidonic acid, which is further metabolized by 12-lipoxygenase (12-LOX). Lipoxygenase metabolites such as 12-HETE activate voltage-gated potassium channels (Kv channels) to hyperpolarize and decrease GABA release from the terminals. Nonsteroidal anti-inflammatory drugs (NSAIDs) potentiate this action of opioids by inhibiting cyclooxygenase (COX)-mediated arachidonic acid metabolism, thereby shunting arachidonic acid to the 12-LOX pathway. Activation of MORs presumably also acutely inhibits adenylyl cyclase (AC) activity in these terminals. Chronic morphine administration upregulates AC and protein kinase A (PKA) activity. After chronic, but not acute, opioid treatment, GABA release is enhanced by increased PKA activity. MOR agonists are more potent inhibitors of this PKA-dependent release, so that opioid removal or blockade of MORs by antagonists results in a rebound increase in GABA release. This increased GABA release may contribute to withdrawal behaviors mediated by the PAG.

administration of an opioid antagonist. Animals exhibit tolerance to the antinociceptive actions of MOR agonists when morphine or MOR agonists are applied directly in the PAG, especially in the caudal ventrolateral aspect (Morgan, M. M. *et al.*, 2005). This tolerance is not due to associative mechanisms, as continuous administration via an implanted pump leads to tolerance in the absence of cues associated with drug administration (Lane, D. A. *et al.*, 2004). The PAG is apparently critical for the development of antinociceptive tolerance when opioids are given systemically because animals chronically treated with morphine microinjected into the PAG display cross-tolerance with morphine given systemically (Jacquet, Y. F. and Lajtha, A., 1976; Siuciak, J. A. and Advokat, C., 1987). Moreover, blockade of PAG opioid receptors using local microinjection of the opioid antagonist naltrexone prevents the development of tolerance to systemically administered morphine (Lane, D. A. *et al.*, 2005). Although RVM neurons lose their responsiveness to PAG morphine administration in tolerant animals (Tortorici, V. *et al.*, 2001), tolerance does not develop as readily when morphine is microinjected into the RVM itself (Morgan, M. M. *et al.*, 2005), and blockade of the RVM does not interfere with the development of tolerance when morphine is applied directly in the PAG (Lane, D. A. *et al.*, 2005). In addition, animals do

not develop behavioral tolerance to direct activation of PAG output neurons that mediate antinociception, for example by microinjecting kainic acid (Morgan, M. M. *et al*., 2003). These latter two findings demonstrate that tolerance is not a result of adaptations downstream from the opioid-sensitive PAG neuron, and indicate that the search for molecular and cellular mechanisms of opioid tolerance should focus on these opioid-sensitive neurons.

The idea that the PAG has a role in opioid dependence derives primarily from observations that blockade of PAG opioid receptors produces a number of withdrawal signs in tolerant animals, and that chronic administration of morphine in the PAG leads to the development of dependence (Bozarth, M. A. 1994). In addition, precipitated withdrawal is associated with increased expression of *c-fos* throughout the PAG, especially in the ventrolateral and lateral aspects (Chieng, B. *et al*., 1995). A substantial number of neurons expressing *c-fos* after precipitated withdrawal are GABAergic (Chieng, B. *et al*., 2005), and neurons positive for *c-fos* do not project to the RVM (Bellchambers, C. E. *et al*., 1998). Thus, as was the case with tolerance, the locus for withdrawal signs in the PAG appears to be upstream from the output neuron projecting to the RVM.

Studies of the membrane properties of PAG neurons following chronic opioid treatment and withdrawal document a host of changes that could contribute to tolerance and/or dependence (Williams, J. T. *et al*., 2001; Bailey, C. P. and Connor, M., 2005). These studies have emphasized altered effects of opioids on GABAergic inhibition and potassium channels. Opioid tolerance is widely assumed to involve a functional uncoupling between opioid receptors and their effectors. The decreased ability of opioids to inhibit the firing of PAG neurons after chronic morphine treatment is consistent with this idea (Bagley E. E. *et al*., 2005; Chieng, B. and Christie, M. D., 1996). However, MOR activation of GIRK channels in PAG is not reduced in animals subjected to repeated intermittent morphine administration that is sufficient to induce antinociceptive tolerance (Ingram, S. L. *et al*., 2007), and the ability of MOR agonists to inhibit GABA release is potentiated rather than reduced in slices from animals treated with chronic morphine. These enhanced actions of MOR agonists are mediated by upregulation of the protein kinase A pathway (Ingram S. L. *et al*., 1998; Hack, S. P. *et al*., 2003). Moreover, recent findings demonstrate that induction of a GABA transporter-mediated cation current in opioid-sensitive neurons in the PAG may be the mechanism of the increased firing rate of these neurons during withdrawal (Bagley, E. E. *et al*., 2005). These latter observations would argue that uncoupling of MOR from pre- or postsynaptic effectors does not underlie antinociceptive tolerance in the PAG. Rather, compensatory mechanisms may mask an underlying increase in the coupling of presynaptic MOR to its effectors that is revealed upon removal of the opioid, leading to withdrawal behaviors. Further work will be needed to bridge the gap between the cellular and behavioral analyses of tolerance and dependence.

5.41.2.5.2 Norepinephrine

The PAG has reciprocal connections with pontomedullary catecholaminergic cell groups (Herbert, H. and Saper, C. B. 1992; Bajic, D. *et al*., 2001). Norepinephrine has multiple effects on PAG neurons that are mediated by α_1- and α_2-adrenergic receptors. Activation of α_1-receptors depolarizes all PAG neurons, whereas α_2-receptor activation hyperpolarizes all neurons, suggesting that both receptors are colocalized on PAG neurons (Vaughan, C. W. *et al*., 1996). However, most neurons preferentially display either a hyperpolarizing or depolarizing response to norepinephrine itself. Neurons in ventrolateral PAG were more likely to be depolarized (~85%), whereas lateral PAG neurons were split equally in exhibiting depolarizing and hyperpolarizing responses. The α_2-mediated hyperpolarization is due to activation of a potassium conductance while the α_1-mediated depolarization depends on inhibition of a potassium conductance and an unidentified norepinephrine-sensitive conductance (Pan, Z. Z. *et al*., 1994; Vaughan, C. W. *et al*., 1996).

The α_2-adrenoceptor agonist clonidine also suppresses GABAergic synaptic transmission, and this suppression is enhanced after chronic morphine treatment (Ingram, S. L. *et al*., 1998). This action of clonidine may be related to its ability to suppress many of the signs of the opioid withdrawal syndrome (Christie, M. J. *et al*., 1997).

5.41.2.5.3 Substance P

NK1 receptors are found in the PAG (Commons, K. G. and Valentino, R. J., 2002), and substance P activates both opioid-sensitive and opioid-insensitive neurons in this region (Ogawa, S. *et al*., 1992; Drew, G. M. *et al*., 2005). In primary afferents and the dorsal horn, substance P has long been associated with nociceptive transmission, and noxious stimulation also increases the release of substance P in the

PAG. This observation would suggest that substance P plays a role in nociceptive transmission in the PAG as in the dorsal horn. However, local morphine administration also increases substance P release in the PAG, and microinjection of exogenous substance P in this region produces significant antinociception (Xin, L. *et al.*, 1997; Rosen, A. *et al.*, 2004). The role of substance P in nociceptive transmission or modulation thus remains to be determined. Substance P has also been implicated in defensive behaviors and aggression, and it produces a conditioned place aversion when microinjected into the dorsolateral PAG (Aguiar, M. S. and Brandao, M. L., 1994). These results point to a more general role for this peptide in defense. Thus substance P may apparently influence a number of functions in the PAG, and functional studies using antagonists are needed to determine the role of endogenous substance P in nociceptive processing and modulation.

5.41.2.5.4 Cannabinoids

Cannabinoids have been used for centuries to provide pain relief (Walker, J. M. and Huang S. M., 2002a) but are of limited utility today because of the significant psychoactive side effects and illegal status in the United States. CB1 receptors are dense throughout the PAG (Herkenham, M. *et al.*, 1991; Tsou, K. *et al.*, 1998). Cannabinoids, like opioids, can mediate antinociception by activating the PAG–RVM descending pathway (see Iversen, L. and Chapman, V., 2002 and Walker, J. M. and Huang, S. M., 2002b for reviews). Endocannabinoids, like endogenous opioids, contribute to the antinociceptive effect of activating the PAG–RVM system (Walker, J. M. *et al.*, 1999; Hough, L. B. *et al.*, 2002), and endocannabinoids in the PAG were recently shown to contribute to stress-induced analgesia (Hohmann, A. G. *et al.*, 2005). Activation of CB1 receptors inhibits both GABA and glutamate release via presynaptic mechanisms. However, cannabinoids have negligible postsynaptic actions on PAG neurons (Vaughan, C. W. *et al.*, 2000).

5.41.3 The Rostral Ventromedial Medulla

5.41.3.1 Connections of the Rostral Ventromedial Medulla

The RVM can be viewed as the brainstem output from the PAG–RVM system, receiving a dense innervation from the PAG and projecting to the dorsal horn through the dorsolateral funiculus. Forebrain structures and the hypothalamus/MPO thus influence the RVM through the PAG, as well as by means of less dense connections directly to the RVM itself. In addition, RVM neurons are likely to receive spinothalamic inputs, either through direct connections to their widespread dendritic arbors or relayed via other brainstem regions such as nucleus reticularis gigantocellularis or the PAG (see Fields, H. L. *et al.*, 2005, for a review.)

In addition to a direct projection to the dorsal horn, the RVM can apparently influence spinal nociceptive processing via catecholamine cell groups in the pons, particularly the A7 cell group. Although there are no noradrenergic neurons within the RVM, antinociception produced by electrical or chemical stimulation in this region is frequently attenuated or blocked by intrathecal administration of noradrenergic antagonists (Hammond, D. L. and Yaksh, T. L., 1984; Proudfit, H. K., 1992). This indicates that part of the antinociceptive effect of RVM stimulation is relayed through one of the descending catecholaminergic pathways, most likely the A7 cell group in the mesopontine tegmentum. The RVM sends connections to the A7 region (Clark, F. M. and Proudfit, H. K., 1991), and these axons originate from a population of neurons distinct from that projecting to the dorsal horn (Buhler, A. V. *et al.*, 2004). This connection to A7 allows the RVM to engage spinally projecting noradrenergic neurons, which would parallel the direct projections from the RVM to the dorsal horn.

The primary outputs from the RVM are thus descending projections to the dorsal horn, both directly and via the mesopontine tegmentum. Ascending connections have also been demonstrated anatomically (Zagon, A. *et al.*, 1994; Hermann, D. M. *et al.*, 1996), but whether these rostral projections play a role in nociceptive modulation is unknown.

5.41.3.2 The Rostral Ventromedial Medulla and Facilitation of Nociception

Although the most robust effect of nonselective experimental activation of the RVM is antinociception, low-intensity electrical stimulation of the RVM and infusions of neuropeptides and *N*-methyl-D-aspartic acid (NMDA) in this region have been shown by various groups to facilitate nociceptive processing (Zhuo, M. and Gebhart, G. F., 1992; Urban, M. O. and Smith, D. J., 1993; Smith, D. J. *et al.*, 1997; Zhuo, M. and Gebhart, G. F., 1997; Kovelowski, C. J. *et al.*, 2000; Friedrich, A. E. and

Gebhart, G. F., 2003; Heinricher, M. M. and Neubert, M. J., 2004; Neubert, M. J. *et al.*, 2004). Inactivation studies demonstrate that hyperalgesia produced by electrical stimulation is not merely an experimental curiosity: lesions implicate the RVM in a variety of models of hyperalgesia and persistent pain, including sickness, acute opiate withdrawal, chronic opioid-induced hyperalgesia, Freund's adjuvant, and mustard oil inflammatory hyperalgesia, following noxious stimulation of a remote body part, and in neuropathic pain models (Kaplan, H. and Fields, H. L., 1991; Morgan, M. M. *et al.*, 1994; Watkins, L. R. *et al.*, 1994; Pertovaara, A. *et al.*, 1996; Ren, K. and Dubner, R., 1996; Urban, M. O. *et al.*, 1996; Mansikka, H. and Pertovaara, A., 1997; Wiertelak, E. P. *et al.*, 1997; Terayama, R. *et al.*, 2000; Porreca, F. *et al.*, 2001; Vanderah, T. W. *et al.*, 2001a; 2001b).

These inactivation studies clearly demonstrate a role for descending facilitation in a variety of enhanced pain states, including inflammation. Nevertheless, there is evidence for an increase in descending inhibition from the RVM during inflammation (Ren, K. and Dubner, R., 2002), with potentiation of the analgesic effectiveness of opioids in the RVM (Hurley, R. W. and Hammond, D. L., 2000; 2001). One intriguing possibility is that inflammation increases the number of RVM neurons expressing MOR (Zhang, L. *et al.*, 2004). Given both the clear demonstration that descending facilitation contributes to the hyperalgesia associated with inflammation and the apparently contradictory evidence for increased descending inhibition, an important question is whether different aspects of nociceptive transmission are differentially affected by inhibition and facilitation during inflammation (Vanegas, H., 2004; Vanegas, H. and Schaible, H.-G., 2004).

5.41.3.3 The Neural Basis for Bidirectional Control from the Rostral Ventromedial Medulla: On- and Off- Cells

5.41.3.3.1 Physiological classification of rostral ventromedial medulla neurons based on reflex-related activity

Initial electrophysiological approaches to the function of the RVM focused on the responses of RVM neurons to noxious stimulation (Anderson, S. D. *et al.*, 1977; Behbehani, M. M. and Pomeroy, S. L., 1978; Guilbaud, G. *et al.*, 1980; Heinricher, M. M. and Rosenfeld, J. P., 1985). In these experiments in deeply anesthetized animals, some neurons were excited, some inhibited, and some unresponsive. The emphasis of most investigators at that time was on the subset of neurons excited by noxious inputs, at least in part because of the idea that pain inhibits pain. However, the notion of recruitment of the pain-inhibiting output from the RVM by noxious stimulation was difficult to reconcile with the observation that noxious-evoked firing of these neurons was suppressed by opioids given in doses thought sufficient to produce analgesia (Anderson, S. D. *et al.*, 1977; Gebhart, G. F., 1982; Heinricher, M. M. and Rosenfeld, J. P., 1985). The on/off/neutral cell classification, introduced by Fields, H. L. *et al.* (1983a), was a significant advance in that it provided a defined framework for hypotheses relating RVM neuronal firing to the pain-modulating function of the region. This approach to RVM physiology was based on the recognition that pain-modulating neurons should discharge in relationship to variables implicated in pain modulation, rather than in response to noxious stimulation. Thus, pain-inhibiting neurons should be activated by analgesic drugs, and during periods of suppressed nociceptive responsiveness, such as that induced by intense stress. Conversely, firing of pain-facilitating neurons should be suppressed during analgesia, and enhanced during hyperalgesia (see Fields, H. M. and Heinricher, M. M., 1985 for an early discussion of the implications of the on/off/neutral cell classification).

In the on/off/neutral cell framework, RVM neurons are recorded in lightly anesthetized rats so that cell firing can be related to changes in nociceptive responding, as measured by spinal nocifensor reflexes. Off-cells are characterized by a cessation of firing during nociceptive reflexes (Figure 4). On-cells are defined by a burst of activity during nociceptive reflexes (Figure 4). Onset of the on-cell reflex-related burst and off-cell pause precede the reflex itself, as well as the thalamic response to the noxious stimulus (Hernandez, N. *et al.*, 1989). Because nociceptive reflexes are generally suppressed when RVM neurons are experimentally activated using electrical stimulation or glutamate microinjection, the fact that off-cell activity ceases abruptly just prior to the execution of nociceptive reflexes suggested that off-cells are the antinociceptive output neurons of the RVM, and that the pause in firing permits responses to occur. Conversely, because on-cells are active during the animal's response to a noxious stimulus, it seemed unlikely that they exert a significant inhibitory effect on nociception. Rather, the reflex-related burst suggested that these neurons have

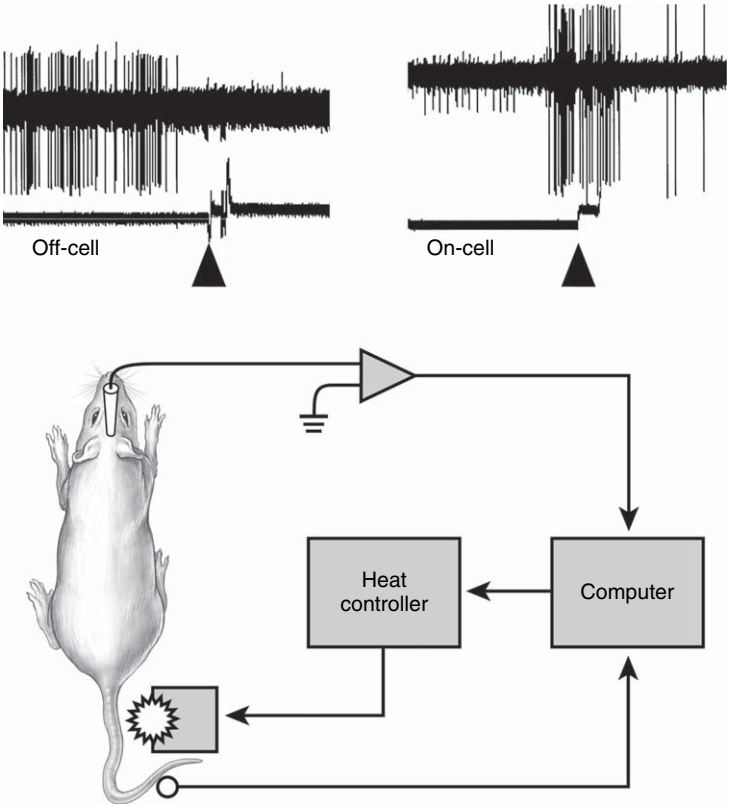

Figure 4 Two cell populations in the rostral ventromedial medulla (RVM), on- and off-cells, explain descending inhibition and facilitation from the RVM. Bottom: Experimental setup shows simultaneous brainstem recording and reflex testing. Top: Single oscilloscope sweeps show activity of a representative off- and on-cell during a tail heat trial. Upper trace is cell discharge, lower trace shows tail position, with arrowhead indicating tail movement. Heat is applied starting at the beginning of the trace. Each trace is 10 s.

a pronociceptive role. Both hypotheses have subsequently received ample confirmation in experiments using selective pharmacological manipulation of the different cell classes (see Section 5.41.3.3.2). At least some cells of both classes project to the dorsal horn (Fields, H. L. *et al.*, 1995).

The remaining cells in the RVM are classified as neutral cells because they show no change in activity associated with nociceptive reflexes. Whether neutral cells have a role in pain modulation remains to be determined (see Section 5.41.3.3.3).

Noxious pinch typically activates on-cells and suppresses off-cell firing. Cutaneous application of mustard oil, which produces an acute inflammation, evokes a strong activation of on-cells and suppresses off-cell firing, leaving neutral cells unaffected (Kincaid, W. *et al.*, in press). Occasional discrepancies between responses to heat and pinch are most likely explained by the fact that the heat-related classification is based on the reflex response evoked by a stimulus at just threshold intensity (Fields, H. L. *et al.*, 1983a; Jinks, S. L. *et al.*, 2004a), whereas pinch stimuli in work published to date have not been limited to withdrawal threshold in intensity, and have not been linked to a withdrawal reflex (Leung, C. G. and Mason, P., 1998; Ellrich, J. *et al.*, 2000; 2001).

On- and off-cell firing is not constant over time. In animals lightly anesthetized with barbiturates, on- and off-cells frequently show alternations between periods of silence and spontaneous discharge. Simultaneous recordings from pairs of on- and off-cells show that excitability within each class varies across the population, but that firing within each class is in phase. Consequently, a subset of either the on- or off-cell class is active at any given time (Barbaro, N. M. *et al.*, 1989), but the two populations are not active simultaneously. By contrast, serotonergic neurons (which can be considered a specific division of neutral cells (Gao, K. *et al.*, 1997; Mason, P., 1997; Gao, K. *et al.*, 1998)) display regular, more or less

constant activity. Nonserotonergic neutral cells vary in their firing, but are often continuously active for prolonged periods. If a withdrawal reflex is evoked when on-cells are in an active period, there is little or no discernible increase in firing (Barbaro N. M. *et al.*, 1986). Because on-cell firing apparently approaches this ceiling during active phases, definitive classification of a neuron as a neutral cell rather than an on-cell requires extensive characterization, with reflex trials delivered during periods of low spontaneous activity. Indeed, Barbaro N. M. *et al.* (1986) noted that earlier work from the Fields group had likely misclassified a number of on-cells as neutral cells.

On-, off-, and neutral cell classes can be identified in awake behaving animals (Oliveras, J. L. *et al.*, 1990; 1991a; 1991b; Leung, C. G. and Mason, P., 1999; Foo, H. and Mason, P., 2005). However, on-cells are more active during waking than sleep, firing in association with the animals' movements. Neurons of this class are also generally more responsive when animals are awake, and more easily activated by innocuous stimulation than when the animals are anesthetized or asleep. Off-cells are more active when the animal is sleeping, and are inhibited in association with movement in awake animals (Leung, C. G. and Mason, P., 1999; Foo, H. and Mason, P., 2005).

5.41.3.3.2 Role of on- and off-cells in pain modulation

Initial functional investigations revealed a number of correlations consistent with the idea that off-cells suppress, while on-cells facilitate, nociception. Both on- and off-cell classes respond to experimental manipulations of the PAG that produce behavioral analgesia (Vanegas, H. *et al.*, 1984; Hutchison, W. D. *et al.*, 1996; Tortorici, V. and Morgan, M. M., 2002). Withdrawal reflexes can generally be elicited at a lower threshold or with shorter latency if on-cells are active and off-cells inactive (Heinricher, M. M. *et al.*, 1989; Ramirez, F. and Vanegas, H., 1989; Bederson, J. B. *et al.*, 1990; Foo, H. and Mason, P., 2003). Antinociception produced by administration of morphine systemically or within the PAG is associated with a uniform activation of off-cells and inhibition of on-cells. Importantly, in animals in which opioid administration fails to produce behavioral analgesia, changes in cell firing are inconsistent. Thus, changes in on- and off-cell firing are related to antinociception rather than to opioid administration as such (Fields, H. L. *et al.*, 1983b; Cheng, Z. F. *et al.*, 1986.). Reduced nociceptive thresholds in acute opioid withdrawal and secondary hyperalgesia during noxious stimulation of a distant body region are correlated with on-cell activation (Bederson, J. B. *et al.*, 1990; Morgan, M. M. and Fields, H. L., 1994). On-cells also facilitate escape responses to intense noxious stimulation, and probably contribute to secondary hyperalgesia during acute inflammation (Jinks, S. L. *et al.*, 2004b; Kincaid, W. *et al.*, in press). Finally, on-cells have been implicated in hyperalgesia associated with the sickness response. Hyperalgesia produced by systemic administration of bacterial endotoxin is blocked by lesion of the RVM (Watkins, L. R. *et al.*, 1994; Wiertelak, E. P. *et al.*, 1997). Although on-cells have not been studied in animals challenged with endotoxin, these neurons are activated by direct administration of prostaglandin E_2 in the MPO (Heinricher, M. M. *et al.*, 2004b), which can be considered a model for central components of the sickness response (Oka, T. *et al.*, 1994; Hosoi, M. *et al.*, 1997).

The obvious limitation of these observations is that they are correlative. The RVM plays an important role in a number of functions other than pain modulation, and many neurons in this region are known to exhibit correlations with various physiological parameters including EEG, blood pressure, and body temperature. Causal inferences relating on- or off-cell discharge to altered nociceptive processing thus require selective experimental manipulation of each cell class as a whole, for example, by microinjection of drugs that differentially alter the firing of the different classes. If altered firing of a particular class leads to modified nociceptive responses, one can conclude that the observed change in cell activity mediated the resulting change in behavior.

A series of studies using the above approach of manipulating RVM circuitry directly have demonstrated that activation of off-cells is sufficient to produce analgesia, and required for the antinociceptive actions of systemically administered morphine (Heinricher, M. M. and Tortorici, V., 1994; Heinricher, M. M. *et al.*, 1994; 1997; 1999; 2001a; 2001b; Meng, I. D. and Johansen, J. P., 2004; Neubert, M. J. *et al.*, 2004; Meng, I. D. *et al.*, 2005). Similar approaches have recently been extended to testing the effects of off-cell activation. Such studies show that on-cells do not contribute significantly to nociceptive threshold under basal conditions as suppression of the reflex-related firing of on-cells does not by itself reduce responding (Heinricher, M. M. and McGaraughty, S., 1998; Meng, I. D. *et al.*, 2005). However, direct activation of on-cells has a pronociceptive effect: microinjection of neurotensin or cholecystokinin (CCK) at doses that activate on-cells

selectively produces thermal hyperalgesia (Heinricher, M. M. and Neubert, M. J., 2004; Neubert, M. J. *et al.*, 2004). Activation of on-cells by CCK likely contributes to nerve injury pain (Kovelowski, C. J. *et al.*, 2000; Porreca, F. *et al.*, 2001; Burgess, S. E. *et al.*, 2002). Microinjection of a CCK-2 receptor antagonist in the RVM also interferes with the paradoxical hyperalgesia associated with prolonged opioid administration (Xie, J. Y. *et al.* 2005), indicating that CCK-mediated activation of on-cells is also involved in this phenomenon. Viewed collectively, the above data provide strong evidence that off-cells suppress nociception, and that on-cells facilitate nociception. The balance of activity between the on- and off-cell populations therefore allows graded bidirectional control of nociceptive responding (Figure 5).

Functional studies demonstrate that the RVM exerts bidirectional control over visceral, as well as cutaneous, hyperalgesia (Coutinho, S. V. *et al.*, 1998). The behavioral response to colorectal distension is suppressed by microinjection of morphine in the RVM (Friedrich, A. E. and Gebhart, G. F., 2003), which is known to activate off-cells (Heinricher, M. M. *et al.*, 1994). Conversely, microinjection of CCK, at a dose that likely activates on-cells (Heinricher, M. M. and Neubert, M. J., 2004), enhances the behavioral response to colorectal distension (Friedrich, A. E. and Gebhart, G. F., 2003). Thus, on- and off-cells appear to modulate behavioral responses evoked by colorectal distension just as they modulate responses evoked by cutaneous heat. The lack of congruence between visceral inputs to RVM neurons and heat-evoked reflex-related responses of these neurons (Brink, T. S. and Mason, P., 2004) may be related to the inhibitory effect of colorectal distension on sensory processing of cutaneous stimuli (Bouhassira, D. *et al.*, 1994; 1998; Pertovaara, A. and Kalmari, J., 2002; Kalmari, J. and Pertovaara, A., 2004). More generally, a difference in on- and off-cell firing associated with cutaneous versus visceral noxious-evoked reflexes emphasizes the basic principle that the functions of RVM neurons must be inferred from their outputs (i.e., from the behavioral or physiological effect of selective manipulation of the difference cell classes), rather from inputs.

5.41.3.3.3 Role of neutral cells

All cells that are not classified as on- or off-cells are grouped together under the heading of neutral cells. Whether these neurons have any role in pain modulation has long been an important question. By definition, the firing of neutral cells is unchanged during behavioral responses to noxious stimulation, and neutral cell firing is also unaffected by MOR or DOR agonists, norepinephrine, neurotensin, or CCK, all of which alter firing of on- and/or off-cells and nociceptive behavior when applied in the RVM (Heinricher, M. M. *et al.*, 1994; 1988; Harasawa, I. *et al.*, 2000; Heinricher, M. M. *et al.*, 2001a; Neubert, M. J., *et al.*, 2004). KOR agonists depress the firing of some neutral cells, but the functional implications of this depression have not been explored (Meng, I. D. *et al.*, 2005). The differential pharmacology of neutral cells supports their categorization as distinct from on- and off-cells. Neutral cells, or subpopulations of neutral cells, might be involved in some other functions of the RVM, for example thermoregulation (Nakamura, K. *et al.*, 2002; Madden, C. J. and Morrison, S. F., 2003).

Despite the lack of direct evidence that neutral cells have a role in pain modulation, interest in this cell class remains high. This is in part because a subset of neutral cells contains serotonin (Potrebic, S. B. *et al.*, 1994; Mason, P., 2001), and serotonin is implicated in descending facilitation as well as descending inhibition of nociception (Le Bars, D., 1988; Calejesan, A. A. *et al.*, 2000; Suzuki, R. *et al.*, 2004). However, there is significant controversy as to

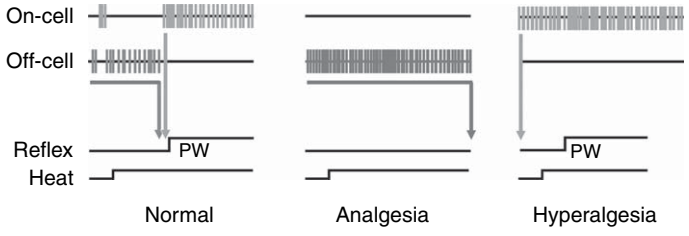

Figure 5 Balance of activity between on- and off-cell populations allows graded bidirectional control of nociceptive responding. *Left column, normal conditions*: Application of heat (arrow) to a rat's tail or paw evokes a paw withdrawal reflex. The off-cell pauses and on-cell becomes active just before the reflex occurs. *Middle column*, *analgesia*: Manipulations that cause off-cells to become continuously active also suppress on-cell firing and application of heat does not evoke a response. *Right column, hyperalgesia*: Reflexes occur with a shorter latency if heat is applied during a period when on-cells are activated (for example, as a consequence of a prior noxious stimulus).

the exact role of serotonergic neutral cells in pain modulation. Immunohistochemically identified serotonergic neurons express MOR, DOR, and KOR (Kalyuzhny, A. E. and Wessendorf, M. W., 1999; Wang, H. and Wessendorf, M.W., 1999; Marinelli, S. *et al.*, 2002). However, neutral cells, including putative serotonergic neutral cells, as a class do not respond to morphine or MOR agonists given systemically or microinjected into the RVM (Barbaro, N. M. *et al.*, 1986; Heinricher, M. M. *et al.*, 1994; Gao, K. *et al.*, 1998). Why neurons that express the MOR fail to respond to MOR agonists remains an important puzzle. A similar mismatch between *in vivo* functional data and immunohistochemical data arises with the neurotensin receptor. Some immunohistochemically identified serotonergic neurons express neurotensin receptor-like immunoreactivity (NT1-ir), and behavioral studies show that microinjection of high doses of neurotensin or a NT1 agonist produce antinociception (Smith, D. J. *et al.*, 1997; Neubert, M. J. *et al.*, 2004; Buhler, A. V. *et al.* 2005). However, physiologically identified neutral cells do not respond to neurotensin when microinjected into the RVM at a dose sufficient to produce behavioral antinociception (Neubert, M. J. *et al.*, 2004). Again, there is no obvious explanation for why neurons expressing the NT1 receptor show no change in firing following microinjection of neurotensin. Resolution of these discrepancies between immunohistochemical and electrophysiological findings will require immunohistochemical labeling of functionally identified neurons.

A second reason for continued interest in neutral cells is the report that the response properties of many neutral cells change to those of on- or off-cells over the course of hours during prolonged inflammation (Miki, K. *et al.*, 2002). A subset of neutral cells may therefore be involved in long-term facilitation or inhibition of nociception, or in other changes in behavior or physiology during inflammation. As discussed above however, the pharmacology of such cells would presumably differ from cells classified as on- or off-cells in the absence of inflammation.

5.41.3.4 Pharmacology of Nociceptive Modulation in the Rostral Ventromedial Medulla

Among the neuropeptides and neurotransmitters found in RVM neurons are serotonin, substance P, enkephalin, thyrotropin-releasing hormone, galanin, somatostatin, CCK, GABA, and acetylcholine (Bowker, R. M. *et al.*, 1983; Mantyh, P. W. and Hunt, S. P., 1984; Menetrey, D. and Basbaum, A. I., 1987; Millhorn, D. E. *et al.*, 1987a; 1987b; Bowker, R. M. and Abbott, L. C., 1988; Millhorn, D. E. *et al.*, 1989; Palkovits, M. and Horvath, S., 1994; Skinner, K. *et al.*, 1997). With the exception of serotonin (see above, Section 5.41.3.3.1), the relationship between physiological/functional class (on-, off-, and neutral cell classification) and expression of different neurotransmitters has yet to be examined.

5.41.3.4.1 Gamma-aminobutyric acid and glutamate: the off-cell pause and on-cell burst

One approach to identifying the neurotransmitter (s) mediating defined synaptic inputs is to attempt to block those inputs using iontophoretic application of neurotransmitter antagonists (Hicks, T. P., 1983). Iontophoresis of $GABA_A$ receptor antagonists selectively blocks the off-cell pause, demonstrating that this reflex-related inhibition of off-cell firing is mediated by GABA (Heinricher, M. M. *et al.*, 1991). Consistent with the idea that the off-cell pause removes descending inhibition and permits noxious information to be processed, microinjection of $GABA_A$ receptor antagonists in the RVM blocks the off-cell pause and produces behavioral antinociception (Drower, E. J. and Hammond, D. L., 1988; Heinricher, M. M. and Kaplan, H. J. 1991; Heinricher, M. M. and Tortorici, V., 1994; Gilbert, A. K. and Franklin, K. B., 2001). Interestingly, Nason M. W., Jr. and Mason P. (2004) recently suggested that the effect of RVM GABA receptor antagonism is selective for stimulation of the tail, with facilitation rather than inhibition of responses evoked by stimulation of the foot. However, this is difficult to reconcile with the antinociception observed by others using the hot plate and formalin tests, as both of these tests involve stimulation of the hindpaw (Gilbert, A. K. and Franklin, K. B., 2001). The source of GABAergic input to off-cells is unknown, but it is presumed to be the target of MOR agonists (see Section 5.41.3.4.2).

Although firing of both on-cells and neutral cells is inhibited by iontophoretically applied GABA, neither cell class displays significant disinhibition during iontophoresis of $GABA_A$ receptor antagonists. This observation implies that on-cells and neutral cells express GABA receptors, but that there is little ongoing GABAergic control of their firing, at least in the lightly anesthetized rat (Heinricher, M. M. *et al.*, 1991).

Iontophoretic application of excitatory amino acids excites all three classes of RVM neurons. However, antagonist studies specifically implicate excitatory amino acid transmitters in reflex-related activation of on-cells and opioid-induced activation of off-cells. Thus, iontophoretic application of the broad-spectrum excitatory amino acid antagonist kynurenate blocks the reflex-related on-cell burst, without affecting the activity of off-cells or neutral cells (Heinricher, M. M. and Roychowdhury, R., 1997). Kynurenate microinjected into the RVM at a dose that blocks on-cell activation does not result in increased withdrawal latency to noxious heat, indicating that the on-cell burst does not control nociceptive threshold, at least under normal conditions (Heinricher, M. M. and McGaraughty, S., 1998). However, it is possible that the firing of on-cells during and after the withdrawal modulates the magnitude or force of the reflex, or primes responses to subsequent stimuli (Ramirez, F. and Vanegas, H., 1989; Jinks, S. L. *et al.*, 2004b).

A second important role for excitatory amino acid transmission in the RVM is the recruitment of off-cells by opioids (Heinricher, M. M. *et al.*, 2001b). Disinhibition of off-cells leads to NMDA-mediated activation of these neurons, amplifying the effect of disinhibition (see the next Section 5.41.3.4.2).

5.41.3.4.2 Opioid actions in the rostral ventromedial medulla

All three opioid receptors, MOR, DOR, and KOR, are found in the RVM, although their expression is much less dense than in the PAG (Gutstein H. B. *et al.*, 1998; Kalyuzhny, A. E. *et al.*, 1996; Wang, H. and Wessendorf, M. W., 1999). The RVM, and specifically activation of off-cells, is required for the analgesic actions of systemically administered morphine (Dickenson, A. H. *et al.*, 1979; Azami, J. *et al.*, 1982; Mitchell, J. M. *et al.*, 1998; Heinricher, M. M. *et al.*, 2001a; 2001b; Gilbert, A. and Franklin, K., 2002). Like the PAG, the RVM supports MOR-mediated analgesia. Thus, direct local microinjection of morphine or MOR agonists in the RVM produces an antinociception equivalent to that produced by systemic morphine administration (Heinricher, M. M. and Morgan, M. M., 1999). Moreover, PAG and RVM interact in a synergistic fashion (Rossi, G. C. *et al.*, 1994). This is at least in part because exogenous opioid administration at one site recruits endogenous opioid mechanisms at the other. Thus, microinjection of morphine in the PAG apparently evokes release of endogenous opioids in the RVM (Kiefel, J. M. *et al.*, 1993; Pan, Z. Z. and Fields, H. L., 1996; Roychowdhury, S. M. and Fields, H. L., 1996) to produce its antinociceptive effect.

The local actions of MOR agonists within the RVM are well understood at both the cellular and circuit levels. On-cells are directly inhibited by MOR agonists. Neither neutral cells nor off-cells are directly sensitive to MOR agonists, but off-cells are activated indirectly, most likely via disinhibition (Figure 6). Microinjection of MOR agonists in the RVM suppresses on-cell firing and activates off-cells, resulting in behavioral antinociception (Heinricher, M. M. *et al.*, 1992; 1994). The activation of off-cells is required for the antinociceptive effect (Heinricher, M. M. *et al.*, 1997). Suppression of on-cell firing is not necessary for RVM-mediated analgesia (Heinricher, M. M. *et al.*, 1994; Neubert, M. J. *et al.*, 2004), although it likely contributes. Selective inhibition of on-cell firing reduces the force, although not the latency, of withdrawal to noxious heat (Heinricher, M. M. and McGaraughty, S., 1998; Jinks, S. L. *et al.*, 2004b).

Studies at the cellular level reveal that some neurons are inhibited directly by MOR agonists, whereas others are disinhibited via presynaptic inhibition of GABAergic transmission (Pan, Z. Z. *et al.*, 1990). These findings are thus consistent with the direct inhibition of on-cells and indirect activation of off-cells observed *in vivo*. RVM neurons studied *in vitro* are classified as secondary cells, which are directly

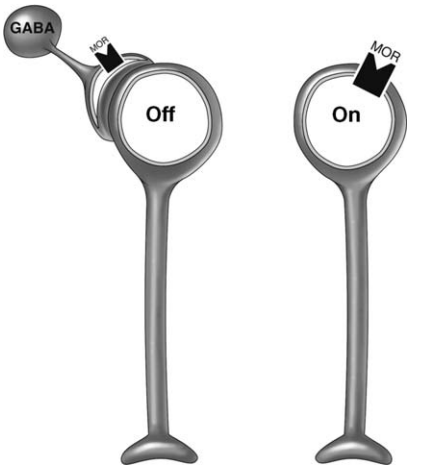

Figure 6 Disinhibition of off-cells, direct inhibition of on-cells mediates opioid analgesia. On-cells are inhibited, directly, by morphine and mu-opioid receptor (MOR) agonists. Off-cells are not inhibited by MOR agonists, but are activated, via disinhibition. MORs are thus presumed to be located on on-cells, and on gamma aminobutyric acid (GABA)ergic inputs to off-cells.

inhibited by MOR agonists, and primary cells, which are not. Primary cells do however receive opioid-sensitive GABAergic inputs, and are disinhibited by MOR agonists (Pan, Z. Z. *et al.*, 1990). Secondary cells presumably map to on-cells recorded *in vivo*, and primary cells to off-cells and neutral cells identified *in vivo*.

5.41.3.4.2.(i) Delta opioid receptor Like MOR agonists, DOR agonists, particularly $delta_2$ agonists, produce behavioral hypoalgesia when microinjected into the RVM. The effects of $delta_1$ agonists are less robust than those of $delta_2$ agonists (see Heinricher, M. M. and Fields, H. L., 2003 for review of the role of the DOR in pain modulation in the RVM). *In vitro*, the DOR agonists deltorphin and [D-Pen2, D-Pen5] enkephalin (DPDPE) elicit hyperpolarizing currents in a substantial minority of RVM neurons (Marinelli S. *et al.*, 2005). Some, but not all, of these neurons were also hyperpolarized by MOR agonists. It thus appears that a subset of DOR-sensitive RVM neurons falls into the secondary cell category. In experiments *in vivo*, microinjection of deltorphin into the RVM increases the latency and reduces the amplitude of the reflex-related on-cell burst, reduces the duration of the reflex-related off-cell pause, and evokes a small but statistically significant increase in tail flick latency (Harasawa, I. *et al.*, 2000).

Molecular, cellular, and behavioral approaches point to interactions between MOR- and DOR-mediated processes, but experiments designed to uncover such interactions within the RVM reveal that the effects of MOR and DOR agonists in the RVM are independent under basal conditions (Hurley, R. W. and Hammond, D. L. 2001; Kalra, A. *et al.*, 2001). However, there is a time-dependent recruitment of supraspinal DOR function in inflammation, so that DOR agonists microinjected into the RVM are more effective in animals subjected to long-lasting inflammation compared to noninflamed controls. MOR agonists are also more potent in these animals (Hurley, R. W. and Hammond, D. L., 2000; 2001). This increased opioid action may reflect an increase in the release of endogenous opioids acting at the DOR (Williams F. G. *et al.*, 1995) and/or translocation of DOR from the cytoplasm to the plasma membrane (Commons, K. G. *et al.*, 2001; Commons, K. G., 2003). Coexpression of MOR and DOR on individual RVM neurons may also play a role (Marinelli, S. *et al.*, 2005).

5.41.3.4.2.(ii) Kappa opioid receptor The role of the KOR in the pain-modulating functions of the RVM remains controversial. Electrophysiological studies in the RVM slice demonstrate pre- and post-synaptic effects of KOR agonists in the RVM. However, it is unclear whether neurons in which KOR agonists evoke an outward current are a separate population from those inhibited by MOR agonists (Pan, Z. Z. *et al.*, 1997; Ackley, M. A. *et al.*, 2001; Marinelli, S. *et al.*, 2002; Bie, B. and Pan, Z. Z., 2003). Microinjection of a KOR agonist into the RVM has been reported to either have no behavioral effect (Pan, Z. *et al.*, 2000; Meng, I. D. *et al.*, 2005) or to produce antinociception, depending on the nociceptive test as well as the sex of the animal (Tershner, S. A. *et al.*, 2000; Ackley, M. A. *et al.*, 2001). KOR agonists also block the antinociceptive effect of PAG microinjection of a MOR agonist or systemic morphine administration (Pan, Z. *et al.*, 2000; Bie, B. and Pan, Z. Z., 2003; Meng, I. D. *et al.*, 2005) as well as MOR-mediated conditioned hypoalgesia (Foo, H. and Helmstetter F. J., 2000). This antianalgesic effect of the KOR agonist is presumably due to a blockade of off-cell activation (Bie, B. and Pan, Z. Z., 2003; Meng, I. D *et al.*, 2005). KOR agonists can also block hyperalgesia when microinjected into the RVM, presumably via presynaptic blockade of excitatory inputs to on-cells (Ackley, M. A. *et al.*, 2001; Meng, I. D. *et al.*, 2005).

5.41.3.4.3 Norepinephrine

As with the KOR, norepinephrine likely influences both the nociceptive facilitating and inhibiting outputs from the RVM. Behavioral studies have reported that blockade of α_1-adrenergic receptors produces antinociception (Sagen, J. and Proudfit, H. K., 1981) and reduces hyperalgesia associated with acute opioid withdrawal (Bie, B. *et al.*, 2003). Agonists at the α_1 receptor produce hyperalgesia and conditioned place avoidance, and the increased nociception is dissociated from the negative affective state in these animals (Hirakawa, N. *et al.*, 2000).

Surprisingly, α_2 agonists have been reported to produce analgesia (Sagen, J. and Proudfit, H. K., 1985; Haws, C. W. *et al.*, 1990) as well as to block opioid analgesia (Bie, B. *et al.*, 2003) when microinjected into the RVM. The neural basis for these conflicting results is unclear, as electrophysiological studies are also inconsistent. *In vivo*, iontophoretically applied norepinephrine and α_2 agonists suppress the firing of on-cells, whilst α_1 agonists activate on-cells. Off-cells and neutral cells do not respond to

iontophoretically applied norepinephrine or adrenergic agents (Heinricher, M. M. *et al.*, 1988). By contrast, in experiments in the RVM slice, α_2 agonists hyperpolarize primary cells (presumably off-cells and/or neutral cells), and α_1 agonists activate all cells (Bie, B. *et al.*, 2003). The findings from the *in vivo* study are thus more consistent with an antinociceptive effect of α_2 receptor activation, whereas the studies in the slice are more consistent with the antiopioid action of these agents.

5.41.3.4.4 Cannabinoids

As noted above (Section 5.41.2.5.4), the PAG–RVM system is now recognized to mediate at least part of the antinociceptive effect of cannabinoids. The RVM is required for the antinociceptive action of systemically administered cannabinoid agonists (Meng, I. D. *et al.*, 1998), and microinjection of CB1 agonists into the RVM produces moderate antinociception (Martin, W. J. *et al.*, 1998; Monhemius, R. *et al.*, 2001; Meng, I. D. and Johansen, J. P., 2004). Off-cells display a measurable increase in activity after local infusion of a CB1 agonist in the RVM, and the reflex-related activity of on-cells is significantly reduced (Meng, I. D. and Johansen, J. P., 2004). Both of these effects are presumed to reflect a presynaptic action, as cannabinoids block excitatory and inhibitory synaptic currents, but have negligible postsynaptic effects in RVM (Vaughan C. W. *et al.*, 1999).

5.41.3.4.5 Cholecystokinin

Endogenous CCK has long been recognized to counter opioid analgesia and to contribute to enhanced nociception, particularly in neuropathic pain states (Stanfa, L. *et al.*, 1994; Wiesenfeld-Hallin, Z. *et al.*, 1999). In humans, CCK antagonism increases the analgesic actions of morphine and placebo (Price, D. D. *et al.*, 1985; Benedetti, F. and Amanzio, M., 1997; McCleane, G. J., 1998). CCK is found in the RVM (Skinner, K. *et al.*, 1997), and has both pronociceptive and antiopioid actions in this region. CCK in the RVM is implicated in the expression of allodynia and thermal hyperalgesia in the spinal nerve ligation model of nerve injury pain as well as in hyperalgesia associated with chronic morphine administration (Kovelowski, C. J. *et al.*, 2000; Xie, J. Y. *et al.*, 2005). Furthermore, focal application of relatively high doses of exogenous CCK in the RVM produces cutaneous and visceral hyperalgesia (Kovelowski, C. J. *et al.*, 2000; Friedrich, A. E. and Gebhart, G. F., 2003; Heinricher, M. M. and Neubert, M. J., 2004). Notably, CCK activates on-cells selectively when microinjected in a dose sufficient to produce behavioral hyperalgesia. This points to on-cells as critical mediators of CCK hyperalgesia in the RVM (Heinricher, M. M. and Neubert, M. J., 2004).

CCK also has antiopioid actions in the RVM, albeit through a different mechanism than that through which it produces hyperalgesia. Focal application of a low dose of CCK in the RVM attenuates both opioid activation of off-cells and opioid-induced antinociception without affecting baseline nociceptive responding or the activity of on-cells (Heinricher, M. M. *et al.*, 2001a). The signal transduction mechanisms that underlie this antiopioid action of CCK are unknown. In the hippocampus, CCK reduces opioid-induced disinhibition by increasing GABA release (Miller, K. K. *et al.*, 1997), raising the possibility that CCK acts presynaptically to block disinhibition of off-cells in the RVM.

5.41.3.4.6 Neurotensin

Like CCK, neurotensin has multiple effects in the RVM. Microinjection of this peptide within the RVM gives rise to a dose-related, bidirectional effect on nociceptive behaviors (tail flick, hot plate, and visceromotor responses to colorectal distension) and dorsal horn nociceptive neurons. Extremely low doses produce facilitation, whereas high doses produce antinociception. Intermediate doses are without effect (Urban, M. O. and Smith, D. J., 1993; Smith, D. J. *et al.*, 1997; Urban, M. O. and Gebhart, G. F., 1997; Urban, M. O. *et al.*, 1999; Neubert, M. J. *et al.*, 2004.). Behavioral hyperalgesia is mediated by selective activation of on-cells, whereas the hypoalgesia produced by higher doses is due to recruitment of off-cells. Neutral cells do not respond to neurotensin at any dose (Neubert, M. J. *et al.* 2004).

5.41.3.4.7 Nociceptin/orphanin FQ

The identification of an opioid-like receptor (ORL-1) that did not bind classical opioid peptides suggested that additional peptides might exist that could modulate nociception. However, despite its structural and functional similarities to the opioid receptors, activation of ORL-1 by its endogenous ligand, referred to as nociceptin or orphanin FQ (OFQ), does not produce antinociception when applied within the RVM. Rather nociceptin/OFQ potently inhibits all neurons in the RVM. As a consequence, focal application of nociception/OFQ in the RVM is effectively a functional lesion of the

region, and interferes with both antinociceptive and pronociceptive outputs (see Heinricher, M. M., in press for a review).

5.41.3.5 Physiological Activation of Nociceptive Modulatory Neurons in the Rostral Ventromedial Medulla

Given a pronociceptive role for on-cells and an antinociceptive role for off-cells, the obvious question that arises is how and when these two classes of neurons with opposing functions are recruited to modulate nociception. This question remains a significant challenge, in part because a number of factors likely to influence nociception via the RVM involve higher-order neural structures and psychological processes that are difficult to study in rodents, particularly under anesthesia. Nevertheless, we do have some information as to how and when RVM nociceptive modulatory neurons are recruited to modulate nociceptive processing.

5.41.3.5.1 Response of RVM neurons to noxious stimulation: does pain inhibit pain?

Noxious-evoked withdrawals are associated with a period of on-cell activation and off-cell inhibition that can last from less than a second to many minutes. This period, during which the balance between the on- and off-cell populations is shifted toward on-cell activation, is associated with heightened nociceptive responsiveness that can be blocked by lesion of the RVM (Heinricher, M. M. *et al.* 1989; Ramirez, F. and Vanegas, H., 1989; Morgan, J. L. and Fields, H. L., 1994; Foo, H. and Mason, P., 2003). Thus noxious stimulation *per se* recruits the RVM to facilitate nociception. This conclusion is consistent with the early suggestion of Cervero F. and Wolstencroft J. H. (1984) that the RVM is part of a short-term positive feedback loop activated by noxious stimulation. Such a positive feedback process presumably prepares the organism to respond more briskly or at a lower threshold to subsequent damaging inputs. This view of on-cells as part of a positive feedback loop is further supported by evidence that on-cells are activated by acute cutaneous inflammation, and that the RVM is necessary for secondary hyperalgesia in this paradigm (Urban, M. O. *et al.*, 1996; Kincaid, W. *et al.*, in press).

The evidence for positive feedback mediated by the RVM is plainly at odds with the long-standing idea that pain inhibits pain, which arose from observations of an apparent lack of pain observed in some patients subjected to intense trauma (Wall, P. D. 1979; Melzack, R. *et al.*, 1982) and the from the ability of footshock or other noxious stimuli to suppress animals' responses to other painful events (Maier, S. F., 1986). Several factors must be considered in addressing this issue. First, other brainstem pathways, such as that through the medullary subnucleus reticularis dorsalis (Le Bars, D., 2002), act in parallel with the output from the RVM. The net effect of a given noxious stimulus on spinal nociceptive processing and pain sensation will reflect the actions of these pathways as well as that of the RVM. In addition, higher-order processes, such as fear or stress, are likely to be significant when an animal is subjected to an experimental noxious stimulus, particularly one over which it has no control. Such higher influences will be most prominent in awake behaving animals, and may shift the balance in the RVM towards activation of off-cells rather than on-cells. Such a shift is presumably the basis for stress-induced analgesia or antinociception associated with fear conditioning (Bodnar, R. J. *et al.*, 1980; Fanselow, M. S. 1986; Helmstetter, F. J. and Tershner, S. A., 1994). Conditioned fear, for example, produces antinociception mediated by the amygdala and the RVM, and direct opioid activation of the amygdala activates RVM off-cells via the PAG (Helmstetter, F. J. and Landeira-Fernandez, J., 1990; Helmstetter, F. J., 1992; Helmstetter, F. J. and Bellgowan, P. S., 1993; Helmstetter, F. J. and Tershner, S. A., 1994; Helmstetter, F. J. *et al.*, 1998; McGaraughty, S. and Heinricher, M. M., 2002; 2004).

Thus, because of higher-order inputs to the RVM and the actions of other descending pathways, the behavioral response to a given noxious stimulus may be enhanced or suppressed in the presence of pain. Which behavioral outcome predominates will depend on the stimulus history, the environment in which the stimulus is applied and the behavioral state of the animal.

5.41.3.5.2 Behavioral state control: anesthesia and sleep/waking cycle

The influence of behavioral state variables on nociceptive processing at the first central relay in the dorsal horn (Hayes, R. L. *et al.*, 1981; Bushnell, M. C. *et al.*, 1984; Soja, P. J. *et al.*, 1999) suggests that pathways descending from the brain to the dorsal horn contribute to the influence of behavioral state on nociception. One possibility that has been considered is that RVM neurons might mediate effects of general anesthesia or sleep/waking on nociceptive processing.

Correlative data suggest that on- and/or off-cell firing could contribute to isoflurane-induced motor depression at lighter planes of anesthesia (Jinks, S. L. *et al.*, 2004a). However, firing of both on- and off-cells is depressed when isoflurane concentration is increased to levels above that required to suppress nocifensor reflexes (Leung, C. G. and Mason, P., 1995). These neurons are thus unlikely to mediate the effects of a anesthesia at a surgical plane on nociceptive withdrawals.

Analysis of the role of on- and off-cells in mediating changes in nociception across the sleep–waking cycle is impeded by lack of a clear understanding of how nociception changes with sleep/waking. In cats, Kshatri A. M. *et al.* (1998) demonstrated that the latency of the tail flick reflex was slightly increased during slow-wave sleep compared to waking, but substantially longer during paradoxical sleep. Consistent with this, noxious-evoked activity of trigeminal neurons is depressed during paradoxical sleep, but not slow-wave sleep, compared to waking (Cairns, B. E. *et al.*, 1995; 1996). By contrast, Mason P. *et al.* (2001) reported that paw withdrawals evoked by heat were enhanced during slow-wave sleep compared to waking, suggesting a disinhibition of nociception during slow-wave sleep. Parallel recording studies from this group demonstrated that off-cells were more active during slow-wave sleep and on-cells and neutral cells were less active compared to waking (Leung, C. G. and Mason, P., 1999). It is therefore unlikely that on- or off-cells mediated the enhanced nociception seen in their behavioral analysis. However, these authors noted that rats return to sleep more quickly following noxious stimulation if the stimulus is delivered when the rats are sleeping rather than awake. They suggested that this could point to a role for off-cells in controlling arousal. However, it is not clear that the duration of waking triggered by the noxious stimulus could be differentiated from the ongoing waking pattern in their analysis. It remains to be determined whether off-cells control arousal, or mediate the influence of arousal on nociception.

A further question is whether on- and off-cells contribute to the atonia of paradoxical sleep. This has not been tested directly. However, although stimulation throughout the length of the medial pontomedullary reticular formation can produce atonia in decerebrate rats (Hajnik, T. *et al.*, 2000), the most effective sites are generally dorsal to the area defined as the RVM. Moreover, microinjection of kainate or morphine in the RVM in intact behaving rats does not produce loss of motor tone, even though locomotor activity in an open field is reduced (Morgan, M. M. and Whitney, P. K., 2000). Finally, the firing of on- and off-cells does not vary between slow wave sleep and paradoxical sleep (Foo, H. and Mason, P., 2003). Taken together, these data indicate that on- and off-cells are unlikely to mediate atonia during paradoxical sleep.

5.41.3.5.3 Micturition

Baez M. A. *et al.* (2005) recently reported that paw withdrawal to noxious heat is attenuated during micturition, presumably preventing potential interruption of bladder emptying by noxious stimulus-evoked movements. Consistent with the idea that off-cells inhibit and on-cells facilitate nociception during micturition, many presumptive off-cells were active during urine expulsion, whereas presumptive on-cells were inhibited. However, these authors propose a somewhat broader role for RVM neurons, as electrical stimulation in the RVM and morphine microinjection in the PAG are known to suppress bladder contractions (Sugaya, K. *et al.*, 1998; Matsumoto, S. *et al.*, 2004). Baez M. A. *et al.* (2005) therefore suggested that off-cell activation suppresses voiding, possibly by depressing transmission of bladder afferent information.

5.41.3.5.4 Environmental analgesia

Decreases in pain responsiveness can be induced by a wide range of experimental procedures, including electrical shock, forced swim, and centrifugal rotation (Watkins, L. R and Mayer, D. J., 1982; Bodnar, R. J., 1986; Maier, S. F., 1986). Biologically relevant threat stimuli such as odors from stressed animals of the same species or exposure to a predator also induce antinociception (Fanselow, M. S., 1985; Lester, L. S. and Fanselow, M. S., 1985; Kavaliers, M. 1988; Lichtman, A. H. and Fanselow, M. S., 1990). Activation of endogenous pain-modulating systems can also enhance the analgesic effects of exogenous opioids. Thus, presentation of a stressful shock potentiates morphine-induced antinociception, an effect that increases as the intensity of stress is increased (Grau, J. W. *et al.*, 1981; Rosellini, R. A. *et al.*, 1994). The PAG–RVM system is implicated in at least some of these environmentally induced changes in nociceptive responsiveness. Most important, some forms of environmental analgesia can be attenuated by lesioning the RVM (Prieto, G. J. *et al.*, 1983; Watkins, L. R. *et al.*, 1983b). Moreover, administration of a stressful foot shock blocks both the

pause in firing that characterizes off-cells and the typical on-cell burst of activity (Friederich, M. W. and Walker, J. M., 1990). This indicates that footshock and possibly other stressors affect the activity of on- and off-cell classes in a manner consistent with their respective pronociceptive and antinociceptive roles.

Antinociception is also elicited as a conditioned response to previously neutral cues paired with noxious or aversive events (Fanselow, M. S., 1986). This latter phenomenon is termed conditioned antinociception, and has been widely adopted for experimental analysis of endogenous mechanisms involved in nociceptive modulation. In conditioned antinociception paradigms, antinociception is recruited in concert with other behaviors and autonomic adjustments as part of a defensive reaction (Williams, F. G. *et al.*, 1990; Fanselow, M. S., 1991; Harris, J. A. and Westbrook, R. F., 1995). Benzodiazepine receptor inverse agonists have anxiogenic or fear-promoting effects, and yield antinociception after either intracerebral or systemic administration (Rodgers, R. J. and Randall, J. I., 1988; Helmstetter, H. J. *et al.*, 1990; Fanselow, M. S. and Kim, J. J., 1992). Conversely, hypoalgesia is reduced by manipulations that would be expected to reduce fear, such as administration of anxiolytic agents (Fanselow, M. S. and Helmstetter, H. J., 1988).

The amygdala, a forebrain structure with a well-documented role in fear, stress and anxiety, is critical in organization of the fear-related processes described above (Davis, M., 1992a; 1992b). Notably, amygdala lesions attenuate freezing and analgesia in rats exposed to a cat, which is an innate fear stimulus for this species (Blanchard, D. C. and Blanchard, R. J., 1972; Fox, R. J. and Sorenson, C. A., 1994), and to intense, nonnoxious noise (Helmstetter, F. J. and Bellgowan, P. S., 1994; Bellgowan, P. S. and Helmstetter, F. J., 1996). Such lesions have no effect on baseline nociceptive responsiveness (Helmstetter, F. J. 1992; Fox, R. J. and Sorenson, C. A., 1994; Manning, B. H. and Mayer, D. J., 1995; Watkins, L. R. *et al.*, 1993).

Antinociception produced by fear-related processes organized in the amygdala is mediated by the PAG–RVM system. Thus, conditioned antinociception involves suppression of nociceptive processing at the level of the spinal cord (Harris, J. A. *et al.*, 1995), and is disrupted by lesions of the PAG or the RVM, or by infusion of an opiate antagonist into the PAG (Watkins, L. R. *et al.*, 1983a; 1983b; Kinscheck, I. B. *et al.*, 1984; Helmstetter, F. J. and Landeira-Fernandez, J., 1990; Helmstetter, F. J. and Tershner, S. A., 1994). The amygdala sends a sparse projection into the RVM region, raising the possibility that the amygdala could directly influence the RVM (Price, J. L. and Amaral, D. G., 1981; Hermann, D. M. *et al.*, 1997). However, the projection from the amygdala to the PAG is much more robust, and the PAG is thought to be a necessary relay in the antinociception associated with conditioned fear. Amygdala projections to the PAG arise from the central nucleus, and to a lesser extent the medial nucleus (Krettek, J. E. and Price, J. L., 1978; Rizvi, T. A. *et al.*, 1991; Canteras, N. S. *et al.*, 1995). Terminations from the central nucleus are concentrated in PAG regions that in turn send projections to the RVM (Rizvi, T. A. *et al.*, 1991). Activation of the central or basolateral nucleus of the amygdala alters the firing of PAG neurons, with approximately equal proportions of PAG neurons showing excitation and inhibition (Sandrew, B. B. and Poletti, C. E., 1984; da Costa Gomez, T. M.and Behbehani, M. M., 1995). Effects of basolateral stimulation are mediated primarily through the central nucleus (da Costa Gomez, T. M. *et al.*, 1996). Finally, microinjection of morphine in the basolateral nucleus of the amygdala activates off-cells and suppresses on-cell firing, and these changes in on- and off-cell activity are associated with behavioral antinociception (McGaraughty, S. and Heinricher, M. M., 2002). Taken together, the above findings indicate that one way in which the modulatory circuitry of the PAG–RVM circuitry is engaged physiologically is via activation of the amygdala by stimuli that induce fear.

5.41.4 Conclusion

The effort to understand the neural basis of nociceptive modulation by the PAG–RVM system highlights the importance of studying functionally identified neurons. The RVM can both facilitate and inhibit nociception. Furthermore, this region is also implicated in a number of functions other than nociceptive modulation, including reproductive behaviors, cardiovascular and respiratory control, sleep–waking and arousal, thermoregulation, and behavioral suppression. A meaningful analysis of how the RVM contributes to enhanced pain states therefore requires functional identification of the neurons under study, so that mechanisms contributing to nociceptive facilitation can be distinguished from those involved in nociceptive inhibition or other functions. The

on/off/neutral cell classification introduced over 20 years ago by Fields H. L. *et al.* (1983a) has been very productive. It has predicted the pharmacology of individual neurons (responses to opioids, norepinephrine, cannabinoids, neurotensin, and CCK) and allowed functional links between activation of on-cells and increased nociception, and between activation of off-cells and decreased nociception. Application of a similar analysis to the PAG, which is implicated in a host of functions from autonomic control to reproductive behavior and vocalization, would greatly advance our understanding of the neural circuitry of pain modulation in this region.

Numerous neurotransmitters and neuropeptides have been implicated in pain modulating functions of the PAG and RVM. Under what conditions are these substances released? Are they local or external to the PAG–RVM? Anatomical studies document substantial reciprocal connections between the PAG and limbic forebrain structures. Which of these connections are relevant to pain modulation, and under what conditions are they activated? These and similar questions must be addressed in order to meet the greater challenge of defining how and when this system is brought into play to enhance or inhibit pain.

Acknowledgments

MMH was supported by grants from NIDA (DA 05608) and NINDS (NS 40365), and S. L. I. by a NARSAD Young Investigator Award and a grant from NIDA (DA 015498).

References

Abe, M., Oka, T., Hori, T., and Takahashi, S. 2001. Prostanoids in the preoptic hypothalamus mediate systemic lipopolysaccharide-induced hyperalgesia in rats. Brain Res. 916, 41–49.

Abols, I. A. and Basbaum, A. I. 1981. Afferent connections of the rostral medulla of the cat: a neural substrate for midbrain-medullary interactions in the modulation of pain. J. Comp. Neurol. 201, 285–297.

Ackley, M. A., Hurley, R. W., Virnich, D. E., and Hammond, D. L. 2001. A cellular mechanism for the antinociceptive effect of a kappa opioid receptor agonist. Pain 91, 377–388.

Aguiar, M. S. and Brandao, M. L. 1994. Conditioned place aversion produced by microinjections of substance p into the periaqueductal gray of rats. Behav. Pharmacol. 5, 369–373.

An, X., Bandler, R., Ongur, D., and Price, J. L. 1998. Prefrontal cortical projections to longitudinal columns in the midbrain periaqueductal gray in macaque monkeys. J. Comp. Neurol. 401, 455–479.

Anderson, S. D., Basbaum, A. I., and Fields, H. L. 1977. Response of medullary raphe neurons to peripheral stimulation and to systemic opiates. Brain Res. 123, 363–368.

Azami, J., Llewelyn, M. B., and Roberts, M. H. 1982. The contribution of nucleus reticularis paragigantocellularis and nucleus raphe magnus to the analgesia produced by systemically administered morphine, investigated with the microinjection technique. Pain 12, 229–246.

Baez, M. A., Brink, T. S., and Mason, P. 2005. Roles for pain modulatory cells during micturition and continence. J. Neurosci. 25, 384–394.

Bagley, E. E., Chieng, B. C., Christie, M. J., and Connor, M. 2005. Opioid tolerance in periaqueductal gray neurons isolated from mice chronically treated with morphine. Br. J. Pharmacol. 146, 68–76

Bailey, C. P. and Connor, M. 2005. Opioids: cellular mechanisms of tolerance and physical dependence. Curr. Opin. Pharmacol. 5, 60–68.

Bajic, D., Van Bockstaele, E. J., and Proudfit, H. K. 2001. Ultrastructural analysis of ventrolateral periaqueductal gray projections to the a7 catecholamine cell group. Neuroscience 104, 181–197.

Bandler, R. and DePaulis, A. 1991. Midbrain Periaqueductal Gray Control of Defensive Behavior in Cat and Rat. In: Midbrain Periaqueductal Gray Matter (*eds*. A. DePaulis and R. Bandler), pp. 175–198. Plenum.

Bandler, R. and Shipley, M. T. 1994. Columnar organization in the midbrain periaqueductal gray: modules for emotional expression? Trends Neurosci. 17, 379–389.

Bandler, R., Keay, K. A., Floyd, N., and Price, J. 2000. Central circuits mediating patterned autonomic activity during active vs. passive emotional coping. Brain Res. Bull. 53, 95–104.

Barbaro, N. M., Heinricher, M. M., and Fields, H. L. 1986. Putative pain modulating neurons in the rostral ventral medulla: reflex-related activity predicts effects of morphine. Brain Res. 366, 203–210.

Barbaro, N. M., Heinricher, M. M., and Fields, H. L. 1989. Putative nociceptive modulatory neurons in the rostral ventromedial medulla of the rat display highly correlated firing patterns. Somatosens. Mot. Res. 6, 413–425.

Bederson, J. B., Fields, H. L., and Barbaro, N. M. 1990. Hyperalgesia during naloxone-precipitated withdrawal from morphine is associated with increased on-cell activity in the rostral ventromedial medulla. Somatosens. Mot. Res. 7, 185–203.

Behbehani, M. M. and Da Costa Gomez, T. M. 1996. Properties of a projection pathway from the medial preoptic nucleus to the midbrain periaqueductal gray of the rat and its role in the regulation of cardiovascular function. Brain Res. 740, 141–150.

Behbehani, M. M. and Pomeroy, S. L. 1978. Effect of morphine injected in periadueductal gray on the activity of single units in nucleus raphe magnus of the rat. Brain Res. 149, 266–269.

Beitz, A. J. 1982. The organization of afferent projections to the midbrain periaqueductal gray of the rat. Neuroscience 7, 133–159.

Beitz, A. J. 1985. The midbrain periaqueductal gray in the rat. I. Nuclear volume, cell number, density, orientation, and regional subdivisions. J. Comp. Neurol. 237, 445–459.

Beitz, A. J. and Shepard, R. D. 1985. The midbrain periaqueductal gray in the rat. Ii. A golgi analysis. J. Comp. Neurol. 237, 460–475.

Bellchambers, C. E., Chieng, B., Keay, K. A., and Christie, M. J. 1998. Swim-stress but not opioid withdrawal increases expression of c-fos immunoreactivity in rat periaqueductal

gray neurons which project to the rostral ventromedial medulla. Neuroscience 83, 517–524.
Bellgowan, P. S. and Helmstetter, F. J. 1996. Neural systems for the expression of hypoalgesia during nonassociative fear. Behav. Neurosci. 110, 727–736.
Benedetti, F. and Amanzio, M. 1997. The neurobiology of placebo analgesia: from endogenous opioids to cholecystokinin. Prog. Neurobiol. 52, 109–125.
Berrino, L., Oliva, P., Rossi, F., Palazzo, E., Nobili, B., and Maione, S. 2001. Interaction between metabotropic and NMDA glutamate receptors in the periaqueductal grey pain modulatory system. Naunyn Schmiedebergs Arch. Pharmacol. 364, 437–443.
Bie, B., Fields, H. L., Williams, J. T., and Pan, Z. Z. 2003. Roles of α_1- and α_2-adrenoceptors in the nucleus raphe magnus in opioid analgesia and opioid abstinence-induced hyperalgesia. J. Neurosci. 23, 7950–7957.
Bie, B. and Pan, Z. Z. 2003. Presynaptic mechanism for anti-analgesic and anti-hyperalgesic actions of kappa-opioid receptors. J. Neurosci. 23, 7262–7268.
Bittencourt, A. S., Carobrez, A. P., Zamprogno, L. P., Tufik, S., and Schenberg, L. C. 2004. Organization of single components of defensive behaviors within distinct columns of periaqueductal gray matter of the rat: role of *n*-methyl-D-aspartic acid glutamate receptors. Neuroscience 125, 71–89.
Blanchard, D. C. and Blanchard, R. J. 1972. Innate and conditioned reactions to threat in rats with amygdaloid lesions. J. Comp. Physiol. Psychol. 81, 281–290.
Blanchard, R. J., Flannelly, K. J., and Blanchard, D. C. 1986. Defensive behaviors of laboratory and wild *Rattus norvegicus*. J. Comp. Psychol. 100, 101–107.
Bodnar, R. J. 1986. Neuropharmacological and neuroendocrine substrates of stress-induced analgesia. Ann. N. Y. Acad. Sci. 467, 345–360.
Bodnar, R. J., Kelly, D. D., Brutus, M., and Glusman, M. 1980. Stress-induced analgesia: neural and hormonal determinants. Neurosci. Biobehav. Rev. 4, 87–100.
Bodnar, R. J., Williams, C. L., Lee, S. J., and Pasternak, G. W. 1988. Role of mu 1-opiate receptors in supraspinal opiate analgesia: a microinjection study. Brain Res. 447, 25–34.
Bouhassira, D., Chollet, R., Coffin, B., Lemann, M., Le Bars, D., Willer, J. C., and Jian, R. 1994. Inhibition of a somatic nociceptive reflex by gastric distention in humans. Gastroenterology 107, 985–992.
Bouhassira, D., Sabate, J. M., Coffin, B., Le Bars, D., Willer, J. C., and Jian, R. 1998. Effects of rectal distensions on nociceptive flexion reflexes in humans. Am. J. Physiol. 275, G410–417.
Bowker, R. M. and Abbott, L. C. 1988. The origins and trajectories of somatostatin reticulospinal neurons: a potential neurotransmitter candidate of the dorsal reticulospinal pathway. Brain Res. 447, 398–403.
Bowker, R. M., Westlund, K. N., Sullivan, M. C., Wilber, J. F., and Coulter, J. D. 1983. Descending serotonergic, peptidergic and cholinergic pathways from the raphe nuclei: a multiple transmitter complex. Brain Res. 288, 33–48.
Bozarth, M. A. 1994. Physical dependence produced by central morphine infusions: an anatomical mapping study. Neurosci. Biobehav. Rev. 18, 373–383.
Brink, T. S. and Mason, P. 2004. Role for raphe magnus neuronal responses in the behavioral reactions to colorectal distension. J. Neurophysiol. 92, 2302–2311.
Buhler, A. V., Choi, J., Proudfit, H. K., and Gebhart, G. F. 2005. Neurotensin activation of the NTR1 on spinally-projecting serotonergic neurons in the rostral ventromedial medulla is antinociceptive. Pain 114, 285–294.
Buhler, A. V., Proudfit, H. K., and Gebhart, G. F. 2004. Separate populations of neurons in the rostral ventromedial medulla project to the spinal cord and to the dorsolateral pons in the rat. Brain Res. 1016, 12–19.
Burdin, T. A., Graeff, F. G., and Pela, I. R. 1992. Opioid mediation of the antiaversive and hyperalgesic actions of bradykinin injected into the dorsal periaqueductal gray of the rat. Physiol. Behav. 52, 405–410.
Burgess, S. E., Gardell, L. R., Ossipov, M. H., Malan, T. P., Jr., Vanderah, T. W., Lai, J., and Porreca, F. 2002. Time-dependent descending facilitation from the rostral ventromedial medulla maintains, but does not initiate, neuropathic pain. J. Neurosci. 22, 5129–5136.
Burstein, R. and Potrebic, S. 1993. Retrograde labeling of neurons in the spinal cord that project directly to the amygdala or the orbital cortex in the rat. J. Comp. Neurol. 335, 469–485.
Bushnell, M. C., Duncan, G. H., Dubner, R., and He, L. F. 1984. Activity of trigeminothalamic neurons in medullary dorsal horn of awake monkeys trained in a thermal discrimination task. J. Neurophysiol. 52, 170–187.
Cairns, B. E., Fragoso, M. C., and Soja, P. J. 1995. Activity of rostral trigeminal sensory neurons in the cat during wakefulness and sleep. J. Neurophysiol. 73, 2486–2498.
Cairns, B. E., McErlane, S. A., Fragoso, M. C., Jia, W. G., and Soja, P. J. 1996. Spontaneous discharge and peripherally evoked orofacial responses of trigemino-thalamic tract neurons during wakefulness and sleep. J. Neurosci. 16, 8149–8159.
Calejesan, A. A., Kim, S. J., and Zhuo, M. 2000. Descending facilitatory modulation of a behavioral nociceptive response by stimulation in the adult rat anterior cingulate cortex. Eur. J. Pain 4, 83–96.
Canteras, N. S., Simerly, R. B., and Swanson, L. W. 1995. Organization of projections from the medial nucleus of the amygdala: a PHAL study in the rat. J. Comp. Neurol. 360, 213–245.
Carrive, P. 2000. Conditioned fear to environmental context: cardiovascular and behavioral components in the rat. Brain Res. 858, 440–445.
Carrive, P. and Morgan, M. M. 2004. Periaqueductal Gray. In: The Human Nervous System (*eds*. G. Paxinos and J. K. Mai), pp. 393–423. Elsevier.
Casey, K. L. and Morrow, T. J. 1988. Supraspinal nocifensive responses of cats: spinal cord pathways, monoamines, and modulation. J. Comp. Neurol. 270, 591–605.
Casey, K. L. and Morrow, T. J. 1989. Effect of medial bulboreticular and raphe nuclear lesions on the excitation and modulation of supraspinal nocifensive behaviors in the cat. Brain Res. 501, 150–161.
Cervero, F. and Wolstencroft, J. H. 1984. A positive feedback loop between spinal cord nociceptive pathways and antinociceptive areas of the cat's brain stem. Pain 20, 125–138.
Cheng, Z. F., Fields, H. L., and Heinricher, M. M. 1986. Morphine microinjected into the periaqueductal gray has differential effects on 3 classes of medullary neurons. Brain Res. 375, 57–65.
Chieng, B. and Christie, M. D. 1996. Local opioid withdrawal in rat single periaqueductal gray neurons *in vitro*. J. Neurosci. 16, 7128–7136.
Chieng, B. and Christie, M. J. 1994a. Hyperpolarization by opioids acting on mu-receptors of a sub-population of rat periaqueductal gray neurones *in vitro*. Br. J. Pharmacol. 113, 121–128.
Chieng, B. and Christie, M. J. 1994b. Inhibition by opioids acting on mu-receptors of gabaergic and glutamatergic postsynaptic potentials in single rat periaqueductal gray neurones in vitro. Br. J. Pharmacol. 113, 303–309.
Chieng, B. C., Hallberg, C., Nyberg, F. J., and Christie, M. J. 2005. Enhanced c-fos in periaqueductal grey gabaergic

neurons during opioid withdrawal. Neuroreport 16, 1279–1283.
Chieng, B., Keay, K. A., and Christie, M. J. 1995. Increased fos-like immunoreactivity in the periaqueductal gray of anaesthetised rats during opiate withdrawal. Neurosci. Lett. 183, 79–82.
Chiou, L. C. and Huang, L. Y. 1999. Mechanism underlying increased neuronal activity in the rat ventrolateral periaqueductal grey by a mu-opioid. J. Physiol. 518 (Pt 2), 551–559.
Christie, M. J., Vaughan, C. W., and Ingram, S. L. 1999. Opioids, NSAIDs and 5-lipoxygenase inhibitors act synergistically in brain via arachidonic acid metabolism. Inflamm. Res. 48, 1–4.
Christie, M. J., Williams, J. T., Osborne, P. B., and Bellchambers, C. E. 1997. Where is the locus in opioid withdrawal? Trends Pharmacol. Sci. 18, 134–140.
Clark, F. M. and Proudfit, H. K. 1991. Projections of neurons in the ventromedial medulla to pontine catecholamine cell groups involved in the modulation of nociception. Brain Res. 540, 105–115.
Clement, C. I., Keay, K. A., Podzebenko, K., Gordon, B. D., and Bandler, R. 2000. Spinal sources of noxious visceral and noxious deep somatic afferent drive onto the ventrolateral periaqueductal gray of the rat. J. Comp. Neurol. 425, 323–344.
Commons, K. G. 2003. Translocation of presynaptic delta opioid receptors in the ventrolateral periaqueductal gray after swim stress. J. Comp. Neurol. 464, 197–207.
Commons, K. G. and Valentino, R. J. 2002. Cellular basis for the effects of substance P in the periaqueductal gray and dorsal raphe nucleus. J. Comp. Neurol. 447, 82–97.
Commons, K. G., Aicher, S. A., Kow, L. M., and Pfaff, D. W. 2000. Presynaptic and postsynaptic relations of mu-opioid receptors to gamma-aminobutyric acid-immunoreactive and medullary-projecting periaqueductal gray neurons. J. Comp. Neurol. 419, 532–542.
Commons, K. G., Beck, S. G., Rudoy, C., and Van Bockstaele, E. J. 2001. Anatomical evidence for presynaptic modulation by the delta opioid receptor in the ventrolateral periaqueductal gray of the rat. J. Comp. Neurol. 430, 200–208.
Connor, M. and Christie, M. J. 1998. Modulation of Ca^{2+} channel currents of acutely dissociated rat periaqueductal grey neurons. J. Physiol. 509, 47–58.
Coutinho, S. V., Urban, M. O., and Gebhart, G. F. 1998. Role of glutamate receptors and nitric oxide in the rostral ventromedial medulla in visceral hyperalgesia. Pain 78, 59–69.
Crown, E. D., Grau, J. W., and Meagher, M. W. 2004. Pain in a balance: noxious events engage opposing processes that concurrently modulate nociceptive reactivity. Behav. Neurosci. 118, 1418–1426.
da Costa Gomez, T. M. and Behbehani, M. M. 1995. An electrophysiological characterization of the projection from the central nucleus of the amygdala to the periaqueductal gray of the rat: the role of opioid receptors. Brain Res. 689, 21–31.
da Costa Gomez, T. M., Chandler, S. D., and Behbehani, M. M. 1996. The role of the basolateral nucleus of the amygdala in the pathway between the amygdala and the midbrain periaqueductal gray in the rat. Neurosci. Lett. 214, 5–8.
Davis, M. 1992a. The Role of the Amygdala in Conditioned Fear. In: The Amygdala: Neurobiological Aspects of Emotion, Memory and Mental Dysfunction (*eds*. J. P. Aggleton), pp. 255–305. Wiley–Liss.
Davis, M. 1992b. The role of the amygdala in fear and anxiety. Annu. Rev. Neurosci. 15, 353–375.
Davis, K. D., Hutchison, W. D., Lozano, A. M., and Dostrovsky, J. O. 1994. Altered pain and temperature perception following cingulotomy and capsulotomy in a patient with schizoaffective disorder. Pain 59, 189–199.
Depaulis, A., Keay, K. A., and Bandler, R. 1994. Quiescence and hyporeactivity evoked by activation of cell bodies in the ventrolateral midbrain periaqueductal gray of the rat. Exp. Brain Res. 99, 75–83.
Depaulis, A., Morgan, M. M., and Liebeskind, J. C. 1987. Gabaergic modulation of the analgesic effects of morphine microinjected in the ventral periaqueductal gray matter of the rat. Brain Res. 436, 223–228.
Dickenson, A. H., Oliveras, J. L., and Besson, J. M. 1979. Role of the nucleus raphe magnus in opiate analgesia as studied by the microinjection technique in the rat. Brain Res. 170, 95–111.
Dielenberg, R. A., Leman, S., and Carrive, P. 2004. Effect of dorsal periaqueductal gray lesions on cardiovascular and behavioral responses to cat odor exposure in rats. Behav. Brain Res. 153, 487–496.
Donahue, R. R., LaGraize, S. C., and Fuchs, P. N. 2001. Electrolytic lesion of the anterior cingulate cortex decreases inflammatory, but not neuropathic nociceptive behavior in rats. Brain Res. 897, 131–138.
Drew, G. M., Mitchell, V. A., and Vaughan, C. W. 2005. Postsynaptic actions of substance P on rat periaqueductal grey neurons *in vitro*. Neuropharmacology 49, 587–595.
Drower, E. J. and Hammond, D. L. 1988. Gabaergic modulation of nociceptive threshold: effects of thip and bicuculline microinjected in the ventral medulla of the rat. Brain Res. 450, 316–324.
Ellrich, J., Ulucan, C., and Schnell, C. 2000. Are 'neutral cells' in the rostral ventro-medial medulla subtypes of on- and off-cells? Neurosci. Res. 38, 419–423.
Ellrich, J., Ulucan, C., and Schnell, C. 2001. Is the response pattern of on- and off-cells in the rostral ventromedial medulla to noxious stimulation independent of stimulation site? Exp. Brain Res. 136, 394–399.
Fang, F. G., Haws, C. M., Drasner, K., Williamson, A., and Fields, H. L. 1989. Opioid peptides (dago-enkephalin, dynorphin a (1–13), bam 22p) microinjected into the rat brainstem: comparison of their antinociceptive effect and their effect on neuronal firing in the rostral ventromedial medulla. Brain Res. 501, 116–128.
Fanselow, M. S. 1985. Odors released by stressed rats produce opioid analgesia in unstressed rats. Behav. Neurosci. 99, 589–592.
Fanselow, M. S. 1986. Conditioned fear-induced opiate analgesia: a competing motivational state theory of stress analgesia. Ann. N. Y. Acad. Sci. 467, 40–54.
Fanselow, M. S. 1991. The Midbrain Periaqueductal Gray as a Coordinator of Action in Response to Fear and Anxiety. In: The Midbrain Periaqueductal Gray Matter (*eds*. A. DePaulis and R. Bandler), pp. 151–173. Plenum.
Fanselow, M. S. and Helmstetter, F. J. 1988. Conditional analgesia, defensive freezing, and benzodiazepines. Behav. Neurosci. 102, 233–243.
Fanselow, M. S. and Kim, J. J. 1992. The benzodiazepine inverse agonist dmcm as an unconditional stimulus for fear-induced analgesia: implications for the role of $gaba_a$ receptors in fear-related behavior. Behav. Neurosci. 106, 336–344.
Farook, J. M., Wang, Q., Moochhala, S. M., Zhu, Z. Y., Lee, L., and Wong, P. T. 2004. Distinct regions of periaqueductal gray (PAG) are involved in freezing behavior in hooded pvg rats on the cat-freezing test apparatus. Neurosci. Lett. 354, 139–142.
Fields, H. L. and Heinricher, M. M. 1985. Anatomy and physiology of a nociceptive modulatory system. Philos. Trans. R. Soc. Lond. B. Biol. Sci. 308, 361–374.
Fields, H. L., Basbaum, A. I., and Heinricher, M. M. 2005. Central nervous system mechanisms of pain modulation. In: Wall and Melzack's textbook of pain, 5th ed. (*ed*. McMahon, S. and Koltzenburg, M. Elsevier.

Fields, H. L., Bry, J., Hentall, I., and Zorman, G. 1983a. The activity of neurons in the rostral medulla of the rat during withdrawal from noxious heat. J. Neurosci. 3, 2545–2552.
Fields, H. L., Malick, A., and Burstein, R. 1995. Dorsal horn projection targets of ON and OFF cells in the rostral ventromedial medulla. J. Neurophysiol. 74, 1742–1759.
Fields, H. L., Vanegas, H., Hentall, I. D., and Zorman, G. 1983b. Evidence that disinhibition of brain stem neurones contributes to morphine analgesia. Nature 306, 684–686.
Floyd, N. S., Price, J. L., Ferry, A. T., Keay, K. A., and Bandler, R. 2000. Orbitomedial prefrontal cortical projections to distinct longitudinal columns of the periaqueductal gray in the rat. J. Comp. Neurol. 422, 556–578.
Foltz, E. L. and Lowell, E. W. 1962. Pain ''relief'' by frontal cingulumotomy. J. Neurosurg. 19, 89–100.
Foo, H. and Helmstetter, F. J. 2000. Activation of kappa opioid receptors in the rostral ventromedial medulla blocks stress-induced antinociception. Neuroreport 11, 3349–3352.
Foo, H. and Mason, P. 2003. Discharge of raphe magnus ON and OFF cells is predictive of the motor facilitation evoked by repeated laser stimulation. J. Neurosci. 23, 1933–1940.
Foo, H. and Mason, P. 2005. Movement-related discharge of ventromedial medullary neurons. J. Neurophysiol. 93, 873–883.
Fox, R. J. and Sorenson, C. A. 1994. Bilateral lesions of the amygdala attenuate analgesia induced by diverse environmental challenges. Brain Res. 648, 215–221.
Friederich, M. W. and Walker, J. M. 1990. The effect of foot-shock on the noxious-evoked activity of neurons in the rostral ventral medulla. Brain Res. Bull. 24, 605–608.
Friedrich, A. E. and Gebhart, G. F. 2003. Modulation of visceral hyperalgesia by morphine and cholecystokinin from the rat rostroventral medial medulla. Pain 104, 93–101.
Fuchs, P. N., Balinsky, M., and Melzack, R. 1996. Electrical stimulation of the cingulum bundle and surrounding cortical tissue reduces formalin-test pain in the rat. Brain Res. 743, 116–123.
Gao, K., Chen, D. O., Genzen, J. R., and Mason, P. 1998. Activation of serotonergic neurons in the raphe magnus is not necessary for morphine analgesia. J. Neurosci. 18, 1860–1868.
Gao, K., Kim, Y. H., and Mason, P. 1997. Serotonergic pontomedullary neurons are not activated by antinociceptive stimulation in the periaqueductal gray. J. Neurosci. 17, 3285–3292.
Gauriau, C. and Bernard, J. F. 2004. A comparative reappraisal of projections from the superficial laminae of the dorsal horn in the rat: the forebrain. J. Comp. Neurol. 468, 24–56.
Gebhart, G. F. 1982. Opiate and opioid peptide effects on brain stem neurons: relevance to nociception and antinociceptive mechanisms. Pain 12, 93–140.
Gilbert, A. and Franklin, K. 2002. The role of descending fibers from the rostral ventromedial medulla in opioid analgesia in rats. Eur. J. Pharmacol. 449, 75.
Gilbert, A. K. and Franklin, K. B. 2001. GABAergic modulation of descending inhibitory systems from the rostral ventromedial medulla (RVM). Dose-response analysis of nociception and neurological deficits. Pain 90, 25–36.
Grau, J. W., Hyson, R. L., Maier, S. F., Madden, J. T., and Barchas, J. D. 1981. Long-term stress-induced analgesia and activation of the opiate system. Science 213, 1409–1411.
Guilbaud, G., Peschanski, M., Gautron, M., and Binder, D. 1980. Responses of neurons of the nucleus raphe magnus to noxious stimuli. Neurosci. Lett. 17, 149–154.
Gutstein, H. B., Mansour, A., Watson, S. J., Akil, H., and Fields, H. L. 1998. Mu and kappa opioid receptors in periaqueductal gray and rostral ventromedial medulla. Neuroreport 9, 1777–1781.
Hack, S. P., Vaughan, C. W., and Christie, M. J. 2003. Modulation of GABA release during morphine withdrawal in midbrain neurons *in vitro*. Neuropharmacology 45, 575–584.
Hajnik, T., Lai, Y. Y., and Siegel, J. M. 2000. Atonia-related regions in the rodent pons and medulla. J. Neurophysiol. 84, 1942–1948.
Hammond, D. L. and Yaksh, T. L. 1984. Antagonism of stimulation-produced antinociception by intrathecal administration of methysergide or phentolamine. Brain Res. 298, 329–337.
Harasawa, I., Fields, H. L., and Meng, I. D. 2000. Delta opioid receptor mediated actions in the rostral ventromedial medulla on tail flick latency and nociceptive modulatory neurons. Pain 85, 255–262.
Hardy, S. G. 1985. Analgesia elicited by prefrontal stimulation. Brain Res. 339, 281–284.
Harris, J. A. and Westbrook, R. F. 1995. Effects of benzodiazepine microinjection into the amygdala or periaqueductal gray on the expression of conditioned fear and hypoalgesia in rats. Behav. Neurosci. 109, 295–304.
Harris, J. A., Westbrook, R. F., Duffield, T. Q., and Bentivoglio, M. 1995. Fos expression in the spinal cord is suppressed in rats displaying conditioned hypoalgesia. Behav. Neurosci. 109, 320–328.
Haws, C. M., Heinricher, M. M., and Fields, H. L. 1990. Alpha-adrenergic receptor agonists, but not antagonists, alter the tail-flick latency when microinjected into the rostral ventromedial medulla of the lightly anesthetized rat. Brain Res. 533, 192–195.
Hayes, R. L., Dubner, R., and Hoffman, D. S. 1981. Neuronal activity in medullary dorsal horn of awake monkeys trained in a thermal discrimination task. Ii. Behavioral modulation of responses to thermal and mechanical stimuli. J. Neurophysiol. 46, 428–443.
Heinricher, M. M. 2005. Nociceptin/orphanin FQ: pain, stress and neural circuits. Life Sci. 77(25), 3127–3132.
Heinricher, M. M. and Fields, H. L. 2003. The Delta Opioid Receptor and Brain Pain-Modulating Circuits. In: The Delta Receptor: Molecular and Effect of Delta Opioid Compounds (*eds*. K. J. Chang, F. Porreca, and J. Woods), pp. 467–480. Marcel Dekker.
Heinricher, M. M. and Kaplan, H. J. 1991. GABA-mediated inhibition in rostral ventromedial medulla: role in nociceptive modulation in the lightly anesthetized rat. Pain 47, 105–113.
Heinricher, M. M. and McGaraughty, S. 1998. Analysis of excitatory amino acid transmission within the rostral ventromedial medulla: implications for circuitry. Pain 75, 247–255.
Heinricher, M. M. and Morgan, M. M. 1999. Supraspinal Mechanisms of Opioid Analgesia. In: Opioids and Pain Control (*ed*. C. Stein), pp. 46–69. Cambridge University Press.
Heinricher, M. M. and Neubert, M. J. 2004. Neural basis for the hyperalgesic action of cholecystokinin in the rostral ventromedial medulla. J. Neurophysiol. 92, 1982–1989.
Heinricher, M. M. and Rosenfeld, J. P. 1985. Microinjection of morphine into nucleus reticularis paragigantocellularis of the rat: suppression of noxious-evoked activity of nucleus raphe magnus neurons. Brain Res. 359, 388–391.
Heinricher, M. M. and Roychowdhury, S. 1997. Reflex-related activation of putative pain facilitating neurons in rostral ventromedial medulla (RVM) depends upon excitatory amino acid transmission. Neuroscience 78, 1159–1165.
Heinricher, M. M. and Tortorici, V. 1994. Interference with GABA transmission in the rostral ventromedial medulla: disinhibition of off-cells as a central mechanism in nociceptive modulation. Neuroscience 63, 533–546.
Heinricher, M. M., Barbaro, N. M., and Fields, H. L. 1989. Putative nociceptive modulating neurons in the rostral ventromedial medulla of the rat: firing of on- and off-cells is

related to nociceptive responsiveness. Somatosens. Mot. Res. 6, 427–439.
Heinricher, M. M., Haws, C. M., and Fields, H. L. 1988. Opposing Actions of Norepinephrine and Clonidine on Single Pain-Modulating Neurons in Rostral Ventromedial Medulla. In: Pain Research and Clinical Management (*eds*. R. Dubner, G. F. Gebhart, and M. R. Bond), pp. 590–594. Elsevier.
Heinricher, M. M., Haws, C. M., and Fields, H. L. 1991. Evidence for GABA-mediated control of putative nociceptive modulating neurons in the rostral ventromedial medulla: iontophoresis of bicuculline eliminates the off-cell pause. Somatosens. Mot. Res. 8, 215–22.
Heinricher, M. M., Martenson, M. E., and Neubert, M. J. 2004a. Prostaglandin E_2 in the midbrain periaqueductal gray produces hyperalgesia and activates pain-modulating circuitry in the rostral ventromedial medulla. Pain 110, 419–426.
Heinricher, M. M., McGaraughty, S., and Farr, D. A. 1999. The role of excitatory amino acid transmission within the rostral ventromedial medulla in the antinociceptive actions of systemically administered morphine. Pain 81, 57–65.
Heinricher, M. M., McGaraughty, S., and Grandy, D. K. 1997. Circuitry underlying antiopioid actions of orphanin FQ in the rostral ventromedial medulla. J. Neurophysiol. 78, 3351–3358.
Heinricher, M. M., McGaraughty, S., and Tortorici, V. 2001a. Circuitry underlying antiopioid actions of cholecystokinin within the rostral ventromedial medulla. J. Neurophysiol. 85, 280–286.
Heinricher, M. M., Morgan, M. M., and Fields, H. L. 1992. Direct and indirect actions of morphine on medullary neurons that modulate nociception. Neuroscience 48, 533–543.
Heinricher, M. M., Morgan, M. M., Tortorici, V., and Fields, H. L. 1994. Disinhibition of off-cells and antinociception produced by an opioid action within the rostral ventromedial medulla. Neuroscience 63, 279–288.
Heinricher, M. M., Neubert, M. J., Martenson, M. E., and Gonçalves, L. 2004b. Prostaglandin E_2 in the medial preoptic area produces hyperalgesia and activates pain-modulating circuitry in the rostral ventromedial medulla. Neuroscience 128, 389–398.
Heinricher, M. M., Pertovaara, A., and Ossipov, M. H. 2003. Descending Modulation after Injury. In: Progress in Pain Research and Management, Vol. 24 (*eds*. J. O. Dostrovsky, D. B. Carr, and M. Koltzenburg), pp. 251–260. IASP Press.
Heinricher, M. M., Schouten, J. C., and Jobst, E. E. 2001b. Activation of brainstem *n*-methyl-D-aspartate receptors is required for the analgesic actions of morphine given systemically. Pain 92, 129–138.
Helmstetter, F. J. 1992. The amygdala is essential for the expression of conditional hypoalgesia. Behav. Neurosci. 106, 518–528.
Helmstetter, F. J. and Bellgowan, P. S. 1993. Lesions of the amygdala block conditional hypoalgesia on the tail flick test. Brain Res. 612, 253–257.
Helmstetter, F. J. and Bellgowan, P. S. 1994. Hypoalgesia in response to sensitization during acute noise stress. Behav. Neurosci. 108, 177–185.
Helmstetter, F. J. and Landeira-Fernandez, J. 1990. Conditional hypoalgesia is attenuated by naltrexone applied to the periaqueductal gray. Brain Res. 537, 88–92.
Helmstetter, F. J. and Tershner, S. A. 1994. Lesions of the periaqueductal gray and rostral ventromedial medulla disrupt antinociceptive but not cardiovascular aversive conditional responses. J. Neurosci. 14, 7099–7108.
Helmstetter, F. J., Calcagnetti, D. J., and Fanselow, M. S. 1990. The beta-carboline dmcm produces hypoalgesia after central administration. Psychobiology 18, 293–297.
Helmstetter, F. J., Tershner, S. A., Poore, L. H., and Bellgowan, P. S. 1998. Antinociception following opioid stimulation of the basolateral amygdala is expressed through the periaqueductal gray and rostral ventromedial medulla. Brain Res. 779, 104–118.
Herbert, H. and Saper, C. B. 1992. Organization of medullary adrenergic and noradrenergic projections to the periaqueductal gray matter in the rat. J. Comp. Neurol. 315, 34–52.
Herkenham, M., Lynn, A. B., Johnson, M. R., Melvin, L. S., de Costa, B. R., and Rice, K. C. 1991. Characterization and localization of cannabinoid receptors in rat brain: a quantitative *in vitro* autoradiographic study. J. Neurosci. 11, 563–583.
Hermann, D. M., Luppi, P. H., Peyron, C., Hinckel, P., and Jouvet, M. 1996. Forebrain projections of the rostral nucleus raphe magnus shown by iontophoretic application of choleratoxin b in rats. Neurosci. Lett. 216, 151–154.
Hermann, D. M., Luppi, P. H., Peyron, C., Hinckel, P., and Jouvet, M. 1997. Afferent projections to the rat nuclei raphe magnus, raphe pallidus and reticularis gigantocellularis pars alpha demonstrated by iontophoretic application of choleratoxin (subunit b). J. Chem. Neuroanat. 13, 1–21.
Hernandez, N., Lopez, Y., and Vanegas, H. 1989. Medullary on- and off-cell responses precede both segmental and thalamic responses to tail heating. Pain 39, 221–230.
Hicks, T. P. 1983. Antagonism of synaptic transmission *in vivo*: contributions of microiontophoresis. Brain Behav. Evol. 22, 1–12.
Hirakawa, N., Tershner, S. A., Fields, H. L., and Manning, B. H. 2000. Bi-directional changes in affective state elicited by manipulation of medullary pain-modulatory circuitry. Neuroscience 100, 861–871.
Hofer, M. A. 1970. Cardiac and respiratory function during sudden prolonged immobility in wild rodents. Psychosom. Med. 32, 633–647.
Hohmann, A. G., Suplita, R. L., Bolton, N. M., Neely, M. H., Fegley, D., Mangieri, R., Krey, J. F., Walker, J. M., Holmes, P. V., Crystal, J. D., Duranti, A., Tontini, A., Mor, M., Tarzia, G., and Piomelli, D. 2005. An endocannabinoid mechanism for stress-induced analgesia. Nature 435, 1108–1112.
Hosoi, M., Oka, T., and Hori, T. 1997. Prostaglandin e receptor ep_3 subtype is involved in thermal hyperalgesia through its actions in the preoptic hypothalamus and the diagonal band of broca in rats. Pain 71, 303–311.
Hough, L. B., Nalwalk, J. W., Stadel, R., Timmerman, H., Leurs, R., Paria, B. C., Wang, X., and Dey, S. K. 2002. Inhibition of improgan antinociception by the cannabinoid $(cb)_1$ antagonist *n*- (piperidin-1-yl)-5- (4-chlorophenyl)-1- (2,4-dichlorophenyl)-4-methyl-1h-p yrazole-3-carboxamide (sr141716a): lack of obligatory role for endocannabinoids acting at cb (1) receptors. J. Pharmacol. Exp. Ther. 303, 314–322.
Hurley, R. W. and Hammond, D. L. 2000. The analgesic effects of supraspinal μ and δ opioid receptor agonists are potentiated during persistent inflammation. J. Neurosci. 20, 1249–1259.
Hurley, R. W. and Hammond, D. L. 2001. Contribution of endogenous enkephalins to the enhanced analgesic effects of supraspinal μ opioid receptor agonists after inflammatory injury. J. Neurosci 21, 2536–2545.
Hutchison, W. D., Harfa, L., and Dostrovsky, J. O. 1996. Ventrolateral orbital cortex and periaqueductal gray stimulation-induced effects on on- and off-cells in the rostral ventromedial medulla in the rat. Neuroscience 70, 391–407.
Ingram, S. L., Fossum, E., and Morgan, M. M. 2007. Behavioral and electrophysiological evidence for opioid tolerance in adolescent rats. Neuropsychopharmacology 32, 600–606.

Ingram, S. L., Vaughan, C. W., Bagley, E. E., Connor, M., and Christie, M. J. 1998. Enhanced opioid efficacy in opioid dependence is caused by an altered signal transduction pathway. J. Neurosci. 18, 10269–10276.

Iversen, L. and Chapman, V. 2002. Cannabinoids: a real prospect for pain relief? Curr. Opin. Pharmacol. 2, 50–55.

Jacquet, Y. F. and Lajtha, A. 1976. The periaqueductal gray: site of morphine analgesia and tolerance as shown by 2-way cross tolerance between systemic and intracerebral injections. Brain Res. 103, 501–513.

Jinks, S. L., Carstens, E., and Antognini, J. F. 2004a. Isoflurane differentially modulates medullary on and off neurons while suppressing hind-limb motor withdrawals. Anesthesiology 100, 1224–1234.

Jinks, S. L., Carstens, E., and Antognini, J. F. 2004b. Medullary on-cells facilitate multilimb movements elicited by intense noxious stimulation. Abstract Viewer/Itinerary Planner. Society for Neuroscience, Online, Program 296.297.

Kalmari, J. and Pertovaara, A. 2004. Colorectal distension-induced suppression of a nociceptive somatic reflex response in the rat: modulation by tissue injury or inflammation. Brain Res. 1018, 106–110.

Kalra, A., Urban, M. O., and Sluka, K. A. 2001. Blockade of opioid receptors in rostral ventral medulla prevents antihyperalgesia produced by transcutaneous electrical nerve stimulation (tens). J. Pharmacol. Exp. Ther. 298, 257–263.

Kalyuzhny, A. E. and Wessendorf, M. W. 1998. Relationship of μ- and δ-opioid receptors to GABAergic neurons in the central nervous system, including antinociceptive brainstem circuits. J. Comp. Neurol. 392, 528–547.

Kalyuzhny, A. E. and Wessendorf, M. W. 1999. Serotonergic and GABaergic neurons in the medial rostral ventral medulla express kappa-opioid receptor immunoreactivity. Neuroscience 90, 229–234.

Kalyuzhny, A. E., Arvidsson, U., Wu, W., and Wessendorf, M. W. 1996. M-opioid and δ-opioid receptors are expressed in brainstem antinociceptive circuits: studies using immunocytochemistry and retrograde tract-tracing. J. Neurosci. 16, 6490–6503.

Kaplan, H. and Fields, H. L. 1991. Hyperalgesia during acute opioid abstinence: evidence for a nociceptive facilitating function of the rostral ventromedial medulla. J. Neurosci. 11, 1433–1439.

Kavaliers, M. 1988. Brief exposure to a natural predator, the short-tailed weasel, induces benzodiazepine-sensitive analgesia in white-footed mice. Physiol. Behav. 43, 187–193.

Keay, K. A. and Bandler, R. 2001. Parallel circuits mediating distinct emotional coping reactions to different types of stress. Neurosci. Biobehav. Rev. 25, 669–678.

Kiefel, J. M., Rossi, G. C., and Bodnar, R. J. 1993. Medullary mu and delta opioid receptors modulate mesencephalic morphine analgesia in rats. Brain Res. 624, 151–161.

Kincaid, W., Neubert, M. J., Xu, M., Kim, C.-J., and Heinricher, M. M. 2006. Role for medullary pain facilitating neurons in secondary thermal hyperalgesia. J. Neurophysiol. 95, 33–41.

Kinscheck, I. B., Watkins, L. R., and Mayer, D. J. 1984. Fear is not critical to classically conditioned analgesia: the effects of periaqueductal gray lesions and administration of chlordiazepoxide. Brain Res. 298, 33–44.

Kiser, R. S., Lebovitz, R. M., and German, D. C. 1978. Anatomic and pharmacologic differences between two types of aversive midbrain stimulation. Brain Res. 155, 331–342.

Kovelowski, C. J., Ossipov, M. H., Sun, H., Lai, J., Malan, T. P., and Porreca, F. 2000. Supraspinal cholecystokinin may drive tonic descending facilitation mechanisms to maintain neuropathic pain in the rat. Pain 87, 265–273.

Krettek, J. E. and Price, J. L. 1978. Amygdaloid projections to subcortical structures within the basal forebrain and brainstem in the rat and cat. J. Comp. Neurol. 178, 225–254.

Kshatri, A. M., Baghdoyan, H. A., and Lydic, R. 1998. Cholinomimetics, but not morphine, increase antinociceptive behavior from pontine reticular regions regulating rapid-eye-movement sleep. Sleep 21, 677–685.

Lagraize, S. C., Borzan, J., Peng, Y. B., and Fuchs, P. N. 2006. Selective regulation of pain affect following activation of the opioid anterior cingulate cortex system. Exp. Neurol. 197(1), 22–30.

LaGraize, S. C., Borzan, J., Rinker, M. M., Kopp, J. L., and Fuchs, P. N. 2004a. Behavioral evidence for competing motivational drives of nociception and hunger. Neurosci. Lett. 372, 30–34.

LaGraize, S. C., Labuda, C. J., Rutledge, M. A., Jackson, R. L., and Fuchs, P. N. 2004b. Differential effect of anterior cingulate cortex lesion on mechanical hypersensitivity and escape/avoidance behavior in an animal model of neuropathic pain. Exp. Neurol. 188, 139–148.

Lane, D. A., Patel, P. A., and Morgan, M. M. 2005. Evidence for an intrinsic mechanism of antinociceptive tolerance within the ventrolateral periaqueductal gray of rats. Neuroscience 135, 227–234.

Lane, D. A., Tortorici, V., and Morgan, M. M. 2004. Behavioral and electrophysiological evidence for tolerance to continuous morphine administration into the ventrolateral periaqueductal gray. Neuroscience 125, 63–69.

Le Bars, D. 1988. Serotonin and Pain. In: Neuronal Serotonin (*eds*. N. N. Osborne and M. Hamon), pp. 171–226. Wiley.

Le Bars, D. 2002. The whole body receptive field of dorsal horn multireceptive neurones. Brain Res. Rev. 40, 29–44.

Leman, S., Dielenberg, R. A., and Carrive, P. 2003. Effect of dorsal periaqueductal gray lesion on cardiovascular and behavioural responses to contextual conditioned fear in rats. Behav. Brain Res. 143, 169–176.

Lester, L. S. and Fanselow, M. S. 1985. Exposure to a cat produces opioid analgesia in rats. Behav. Neurosci. 99, 756–759.

Leung, C. G. and Mason, P. 1995. Effects of isoflurane concentration on the activity of pontomedullary raphe and medial reticular neurons in the rat. Brain Res. 699, 71–82.

Leung, C. G. and Mason, P. 1998. Physiological survey of medullary raphe and magnocellular reticular neurons in the anesthetized rat. J. Neurophysiol. 80, 1630–1646.

Leung, C. G. and Mason, P. 1999. Physiological properties of raphe magnus neurons during sleep and waking. J. Neurophysiol. 81, 584–595.

Lewis, J. W., Cannon, J. T., and Liebeskind, J. C. 1980. Opioid and nonopioid mechanisms of stress analgesia. Science 208, 623–625.

Lichtman, A. H. and Fanselow, M. S. 1990. Cats produce analgesia in rats on the tail-flick test: naltrexone sensitivity is determined by the nociceptive test stimulus. Brain Res. 533, 91–94.

Lovick, T. A. 1993. Integrated activity of cardiovascular and pain regulatory systems: role in adaptive behavioural responses. Prog. Neurobiol. 40, 631–644.

Lumb, B. M., Parry, D. M., Semenenko, F. M., McMullan, S., and Simpson, D. A. 2002. C-nociceptor activation of hypothalamic neurones and the columnar organisation of their projections to the periaqueductal grey in the rat. Exp. Physiol. 87, 123–128.

Madden, C. J. and Morrison, S. F. 2003. Excitatory amino acid receptor activation in the raphe pallidus area mediates prostaglandin-evoked thermogenesis. Neuroscience 122, 5–15.

Maier, S. F. 1986. Stressor controllability and stress-induced analgesia. Ann. N. Y. Acad. Sci. 467, 55–72.

Manning, B. H. and Mayer, D. J. 1995. The central nucleus of the amygdala contributes to the production of morphine antinociception in the formalin test. Pain 63, 141–152.

Mansikka, H. and Pertovaara, A. 1997. Supraspinal influence on hindlimb withdrawal thresholds and mustard oil-induced secondary allodynia in rats. Brain Res. Bull. 42, 359–365.

Mansour, A., Fox, C. A., Akil, H., and Watson, S. J. 1995. Opioid-receptor mRNA expression in the rat CNS: anatomical and functional implications. Trends Neurosci. 18, 22–29.

Mantyh, P. W. and Hunt, S. P. 1984. Evidence for cholecystokinin-like immunoreactive neurons in the rat medulla oblongata which project to the spinal cord. Brain Res. 291, 49–54.

Marinelli, S., Connor, M., Schnell, S. A., Christie, M. J., Wessendorf, M. W., and Vaughan, C. W. 2005. Δ-opioid receptor-mediated actions on rostral ventromedial medulla neurons. Neuroscience 132, 239–244.

Marinelli, S., Vaughan, C. W., Schnell, S. A., Wessendorf, M. W., and Christie, M. J. 2002. Rostral ventromedial medulla neurons that project to the spinal cord express multiple opioid receptor phenotypes. J. Neurosci. 22, 10847–10855.

Martin, W. J., Tsou, K., and Walker, J. M. 1998. Cannabinoid receptor-mediated inhibition of the rat tail-flick reflex after microinjection into the rostral ventromedial medulla. Neurosci. Lett. 242, 33–36.

Mason, P. 1997. Physiological identification of pontomedullary serotonergic neurons in the rat. J. Neurophysiol. 77, 1087–1098.

Mason, P. 2001. Contributions of the medullary raphe and ventromedial reticular region to pain modulation and other homeostatic functions. Annu. Rev. Neurosci. 24, 737–777.

Mason, P., Escobedo, I., Burgin, C., Bergan, J., Lee, J. H., Last, E. J., and Holub, A. L. 2001. Nociceptive responsiveness during slow-wave sleep and waking in the rat. Sleep 24, 32–38.

Matsumoto, S., Levendusky, M. C., Longhurst, P. A., Levin, R. M., and Millington, W. R. 2004. Activation of mu opioid receptors in the ventrolateral periaqueductal gray inhibits reflex micturition in anesthetized rats. Neurosci. Lett. 363, 116–119.

McCleane, G. J. 1998. The cholecystokinin antagonist proglumide enhances the analgesic efficacy of morphine in humans with chronic benign pain. Anesth. Analg. 87, 1117–1120.

McGaraughty, S. and Heinricher, M. M. 2002. Microinjection of morphine into various amygdaloid nuclei differentially affects nociceptive responsiveness and RVM neuronal activity. Pain 96, 153–162.

McGaraughty, S. and Heinricher, M. M. 2004. Lesions of the periaqueductal gray disrupt input to the rostral ventromedial medulla following microinjections into the medial or basolateral nuclei of the amygdala. Brain Res. 1009, 223–227.

McGaraughty, S., Chu, K. L., Bitner, R. S., Martino, B., Kouhen, R. E., Han, P., Nikkel, A. L., Burgard, E. C., Faltynek, C. R., and Jarvis, M. F. 2003. Capsaicin infused into the PAG affects rat tail flick responses to noxious heat and alters neuronal firing in the RVM. J. Neurophysiol. 90, 2702–2710.

McLemore, S., Crown, E. D., Meagher, M. W., and Grau, J. W. 1999. Shock-induced hyperalgesia: Ii. Role of the dorsolateral periaqueductal gray. Behav. Neurosci. 113, 539–549.

Melzack, R., Wall, P. D., and Ty, T. C. 1982. Acute pain in an emergency clinic: latency of onset and descriptor patterns related to different injuries. Pain 14, 33–43.

Menetrey, D. and Basbaum, A. I. 1987. The distribution of substance p-, enkephalin- and dynorphin-immunoreactive neurons in the medulla of the rat and their contribution to bulbospinal pathways. Neuroscience 23, 173–187.

Menetrey, D., Chaouch, A., Binder, D., and Besson, J. M. 1982. The origin of the spinomesencephalic tract in the rat: an anatomical study using the retrograde transport of horseradish peroxidase. J. Comp. Neurol. 206, 193–207.

Meng, I. D. and Johansen, J. P. 2004. Antinociception and modulation of rostral ventromedial medulla neuronal activity by local microinfusion of a cannabinoid receptor agonist. Neuroscience 124, 685–693.

Meng, I. D., Johansen, J. P., Harasawa, I., and Fields, H. L. 2005. Kappa opioids inhibit physiologically identified medullary pain modulating neurons and reduce morphine antinociception. J. Neurophysiol. 93, 1138–1144.

Meng, I. D., Manning, B. H., Martin, W. J., and Fields, H. L. 1998. An analgesia circuit activated by cannabinoids. Nature 395, 381–383.

Miki, K., Zhou, Q. Q., Guo, W., Guan, Y., Terayama, R., Dubner, R., and Ren, K. 2002. Changes in gene expression and neuronal phenotype in brain stem pain modulatory circuitry after inflammation. J. Neurophysiol. 87, 750–760.

Millan, M. J. 2002. Descending control of pain. Prog. Neurobiol. 66, 355–474.

Miller, K. K., Hoffer, A., Svoboda, K. R., and Lupica, C. R. 1997. Cholecystokinin increases GABA release by inhibiting a resting K^+ conductance in hippocampal interneurons. J. Neurosci. 17, 4994–5003.

Millhorn, D. E., Hokfelt, T., Seroogy, K., Oertel, W., Verhofstad, A. A., and Wu, J. Y. 1987a. Immunohistochemical evidence for colocalization of gamma-aminobutyric acid and serotonin in neurons of the ventral medulla oblongata projecting to the spinal cord. Brain Res. 410, 179–185.

Millhorn, D. E., Hokfelt, T., Verhofstad, A. A., and Terenius, L. 1989. Individual cells in the raphe nuclei of the medulla oblongata in rat that contain immunoreactivities for both serotonin and enkephalin project to the spinal cord. Exp. Brain Res. 75, 536–542.

Millhorn, D. E., Seroogy, K., Hökfelt, T., Schmued, L. C., Terenius, L., Buchan, A., and Brown, J. C. 1987b. Neurons of the ventral medulla oblongata that contain both somatostatin and enkephalin immunoreactivities project to nucleus tractus solitarii and spinal cord. Brain Res. 424, 99–108.

Mitchell, J. M., Lowe, D., and Fields, H. L. 1998. The contribution of the rostral ventromedial medulla to the antinociceptive effects of systemic morphine in restrained and unrestrained rats. Neuroscience 87, 123–133.

Monhemius, R., Azami, J., Green, D. L., and Roberts, M. H. 2001. CB1 receptor mediated analgesia from the nucleus reticularis gigantocellularis pars alpha is activated in an animal model of neuropathic pain. Brain Res. 908, 67–74.

Moreau, J. L. and Fields, H. L. 1986. Evidence for GABA involvement in midbrain control of medullary neurons that modulate nociceptive transmission. Brain Res. 397, 37–46.

Morgan, M. M. 1991. Differences in Antinociception Evoked from Dorsal and Ventral Regions of the Caudal Periaqueductal Gray Matter. In: The Midbrain Periaqueductal Gray Matter (*eds*. A. DePaulis and R. Bandler), pp. 139–150. Plenum.

Morgan, M. M. and Carrive, P. 2001. Activation of the ventrolateral periaqueductal gray reduces locomotion but not mean arterial pressure in awake, freely moving rats. Neuroscience 102, 905–910.

Morgan, M. M. and Clayton, C. C. 2005. Defensive behaviors evoked from the ventrolateral periaqueductal gray of the rat: comparison of opioid and GABA disinhibition. Behav. Brain Res. 164, 61–66.

Morgan, M. M. and Fields, H. L. 1994. Pronounced changes in the activity of nociceptive modulatory neurons in the rostral ventromedial medulla in response to prolonged thermal noxious stimuli. J. Neurophysiol. 72, 1161–1170.

Morgan, M. M. and Whitney, P. K. 2000. Immobility accompanies the antinociception mediated by the rostral ventromedial medulla of the rat. Brain Res. 872, 276–281.

Morgan, M. M., Clayton, C. C., and Boyer-Quick, J. S. 2005. Differential susceptibility of the PAG and RVM to tolerance to the antinociceptive effect of morphine in the rat. Pain 113, 91–98.

Morgan, M. M., Clayton, C. C., and Lane, D. A. 2003. Behavioral evidence linking opioid-sensitive gabaergic neurons in the ventrolateral periaqueductal gray to morphine tolerance. Neuroscience 118, 227–232.

Morgan, M. M., Heinricher, M. M., and Fields, H. L. 1992. Circuitry linking opioid-sensitive nociceptive modulatory systems in periaqueductal gray and spinal cord with rostral ventromedial medulla. Neuroscience 47, 863–871.

Morgan, M. M., Heinricher, M. M., and Fields, H. L. 1994. Inhibition and facilitation of different nocifensor reflexes by spatially remote noxious stimuli. J. Neurophysiol. 72, 1152–1160.

Nakamura, K., Matsumura, K., Kaneko, T., Kobayashi, S., Katoh, H., and Negishi, M. 2002. The rostral raphe pallidus nucleus mediates pyrogenic transmission from the preoptic area. J. Neurosci. 22, 4600–4610.

Narita, M., Mizoguchi, H., Narita, M., Dun, N. J., Hwang, B. H., Endoh, T., Suzuki, T., Nagase, H., Suzuki, T., and Tseng, L. F. 2000. G protein activation by endomorphins in the mouse periaqueductal gray matter. J. Biomed. Sci. 7, 221–225.

Nashold, B. S., Wilson, W. P., and Slaughter, D. G. 1969. Sensations evoked by stimulation in the midbrain in man. J. Neurosurg. 30, 14–24.

Nason, M. W., Jr. and Mason, P. 2004. Modulation of sympathetic and somatomotor function by the ventromedial medulla. J. Neurophysiol. 92, 510–522.

Neubert, M. J., Kincaid, W., and Heinricher, M. M. 2004. Nociceptive facilitating neurons in the rostral ventromedial medulla. Pain 110, 158–165.

Ogawa, S., Kow, L. M., and Pfaff, D. W. 1992. Effects of lordosis-relevant neuropeptides on midbrain periaqueductal gray neuronal activity *in vitro*. Peptides 13, 965–975.

Oka, T., Aou, S., and Hori, T. 1994. Intracerebroventricular injection of prostaglandin E_2 induces thermal hyperalgesia in rats: the possible involvement of ep3 receptors. Brain Res. 663, 287–292.

Oliveras, J. L., Martin, G., and Montagne-Clavel, J. 1991a. Drastic changes of ventromedial medulla neuronal properties induced by barbiturate anesthesia. Ii. Modifications of the single-unit activity produced by brevital, a short-acting barbiturate in the awake, freely moving rat. Brain Res. 563, 251–260.

Oliveras, J. L., Martin, G., Montagne, J., and Vos, B. 1990. Single unit activity at ventromedial medulla level in the awake, freely moving rat: effects of noxious heat and light tactile stimuli onto convergent neurons. Brain Res. 506, 19–30.

Oliveras, J. L., Montagne-Clavel, J., and Martin, G. 1991b. Drastic changes of ventromedial medulla neuronal properties induced by barbiturate anesthesia. I. Comparison of the single-unit types in the same awake and pentobarbital-treated rats. Brain Res. 563, 241–250.

Ongur, D. and Price, J. L. 2000. The organization of networks within the orbital and medial prefrontal cortex of rats, monkeys and humans. Cereb Cortex 10, 206–219.

Osborne, P. B., Vaughan, C. W., Wilson, H. I., and Christie, M. J. 1996. Opioid inhibition of rat periaqueductal grey neurones with identified projections to rostral ventromedial medulla *in vitro*. J. Physiol. 490, 383–389.

Ossipov, M. H., Kovelowski, C. J., Nichols, M. L., Hruby, V. J., and Porreca, F. 1995. Characterization of supraspinal antinociceptive actions of opioid delta agonists in the rat. Pain 62, 287–293.

Palkovits, M. and Horvath, S. 1994. Galanin immunoreactive neurons in the medulla oblongata of rats. Acta Biol. Hung. 45, 399–417.

Pan, Z. Z. and Fields, H. L. 1996. Endogenous opioid-mediated inhibition of putative pain-modulating neurons in rat rostral ventromedial medulla. Neuroscience 74, 855–862.

Pan, Z. Z., Grudt, T. J., and Williams, J. T. 1994. Alpha 1-adrenoceptors in rat dorsal raphe neurons: regulation of two potassium conductances. J. Physiol. 478 Pt 3, 437–447.

Pan, Z., Hirakawa, N., and Fields, H. L. 2000. A cellular mechanism for the bidirectional pain-modulating actions of orphanin FQ/nociceptin. Neuron 26, 515–522.

Pan, Z. Z., Tershner, S. A., and Fields, H. L. 1997. Cellular mechanism for anti-analgesic action of agonists of the kappa- opioid receptor. Nature 389, 382–385.

Pan, Z. Z., Williams, J. T., and Osborne, P. B. 1990. Opioid actions on single nucleus raphe magnus neurons from rat and guinea-pig *in vitro*. J. Physiol. 427, 519–532.

Parry, D. M., Semenenko, F. M., Conley, R. K., and Lumb, B. M. 2002. Noxious somatic inputs to hypothalamic-midbrain projection neurones: a comparison of the columnar organisation of somatic and visceral inputs to the periaqueductal grey in the rat. Exp. Physiol. 87, 117–122.

Pastoriza, L. N., Morrow, T. J., and Casey, K. L. 1996. Medial frontal cortex lesions selectively attenuate the hot plate response: possible nocifensive apraxia in the rat. Pain 64, 11–17.

Pavlovic, Z. W., Cooper, M. L., and Bodnar, R. J. 1996. Opioid antagonists in the periaqueductal gray inhibit morphine and beta-endorphin analgesia elicited from the amygdala of rats. Brain Res. 741, 13–26.

Pertovaara, A. and Kalmari, J. 2002. Neuropathy reduces viscero-somatic inhibition via segmental mechanisms in rats. Neuroreport 13, 1047–1050.

Pertovaara, A., Wei, H., and Hamalainen, M. M. 1996. Lidocaine in the rostroventromedial medulla and the periaqueductal gray attenuates allodynia in neuropathic rats. Neurosci. Lett. 218, 127–130.

Petrovic, P., Kalso, E., Petersson, K. M., and Ingvar, M. 2002. Placebo and opioid analgesia – imaging a shared neuronal network. Science 295, 1737–1740.

Porreca, F., Burgess, S. E., Gardell, L. R., Vanderah, T. W., Malan, T. P., Jr., Ossipov, M. H., Lappi, D. A., and Lai, J. 2001. Inhibition of neuropathic pain by selective ablation of brainstem medullary cells expressing the μ-opioid receptor. J. Neurosci. 21, 5281–5288.

Porreca, F., Ossipov, M. H., and Gebhart, G. F. 2002. Chronic pain and medullary descending facilitation. Trends Neurosci. 25, 319–325.

Potrebic, S. B., Fields, H. L., and Mason, P. 1994. Serotonin immunoreactivity is contained in one physiological cell class in the rat rostral ventromedial medulla. J. Neurosci. 14, 1655–1665.

Price, J. L. and Amaral, D. G. 1981. An autoradiographic study of the projections of the central nucleus of the monkey amygdala. J. Neurosci. 1, 1242–1259.

Price, D. D., Milling, L. S., Kirsch, I., Duff, A., Montgomery, G. H., and Nicholls, S. S. 1999. An analysis of factors that contribute to the magnitude of placebo analgesia in an experimental paradigm. Pain 83, 147–156.

Price, D. D., von der Gruen, A., Miller, J., Rafii, A., and Price, C. 1985. Potentiation of systemic morphine analgesia in humans by proglumide, a cholecystokinin antagonist. Anesth. Analg. 64, 801–806.

Prieto, G. J., Cannon, J. T., and Liebeskind, J. C. 1983. N. Raphe magnus lesions disrupt stimulation-produced analgesia from ventral but not dorsal midbrain areas in the rat. Brain Res. 261, 53–57.

Proudfit, H. K. 1992. The Behavioural Pharmacology of the Noradrenergic System. In: Towards the Use of Noradrenergic Agonists for the Treatment of Pain (*eds*. J. M. Besson and G. Guilbaud), pp. 119–136. Elsevier.

Ramirez, F. and Vanegas, H. 1989. Tooth pulp stimulation advances both medullary off-cell pause and tail flick. Neurosci. Lett. 100, 153–156.

Ren, K. and Dubner, R. 1996. Enhanced descending modulation of nociception in rats with persistent hindpaw inflammation. J. Neurophysiol. 76, 3025–3037.

Ren, K. and Dubner, R. 2002. Descending modulation in persistent pain: an update. Pain 100, 1–6.

Rizvi, T. A., Ennis, M., Behbehani, M. M., and Shipley, M. T. 1991. Connections between the central nucleus of the amygdala and the midbrain periaqueductal gray: topography and reciprocity. J. Comp. Neurol. 303, 121–131.

Rizvi, T. A., Ennis, M., and Shipley, M. T. 1992. Reciprocal connections between the medial preoptic area and the midbrain periaqueductal gray in rat: a WGA-HRP and PHA-L study. J. Comp. Neurol. 315, 1–15.

Rizvi, T. A., Murphy, A. Z., Ennis, M., Behbehani, M. M., and Shipley, M. T. 1996. Medial preoptic area afferents to periaqueductal gray medullo-output neurons: a combined fos and tract tracing study. J. Neurosci. 16, 333–344.

Rodgers, R. J. and Randall, J. I. 1988. Environmentally Induced Analgesia: Situational Factors, Mechanisms and Significance. In: Endorphins, Opiates and Behavioral Processes. (*eds*. R. J. Rodgers and S. J. Cooper), pp. 107–144. Wiley.

Romanovsky, A. A., Kulchitsky, V. A., Akulich, N. V., Koulchitsky, S. V., Simons, C. T., Sessler, D. I., and Gourine, V. N. 1996. First and second phases of biphasic fever: two sequential stages of the sickness syndrome? Am. J. Physiol. 271, R244–253.

Rosellini, R. A., Abrahamsen, G. C., Stock, H. S., and Caldarone, B. J. 1994. Modulation of hypoalgesia by morphine and number of shock trials: covariation of a measure of context fear and hypoalgesia. Physiol. Behav. 56, 183–188.

Rosen, A., Zhang, Y. X., Lund, I., Lundeberg, T., and Yu, L. C. 2004. Substance p microinjected into the periaqueductal gray matter induces antinociception and is released following morphine administration. Brain Res. 1001, 87–94.

Rossi, G. C., Pasternak, G. W., and Bodnar, R. J. 1994. Mu and delta opioid synergy between the periaqueductal gray and the rostro-ventral medulla. Brain Res. 665, 85–93.

Roychowdhury, S. M. and Fields, H. L. 1996. Endogenous opioids acting at a medullary μ-opioid receptor contribute to the behavioral antinociception produced by GABA antagonism in the midbrain periaqueductal gray. Neuroscience 74, 863–872.

Sagen, J. and Proudfit, H. K. 1981. Hypoalgesia induced by blockade of noradrenergic projections to the raphe magnus: reversal by blockade of noradrenergic projections to the spinal cord. Brain Res. 223, 391–396.

Sagen, J. and Proudfit, H. K. 1985. Evidence for pain modulation by pre- and postsynaptic noradrenergic receptors in the medulla oblongata. Brain Res. 331, 285–293.

Sandkühler, J. and Gebhart, G. F. 1984. Relative contributions of the nucleus raphe magnus and adjacent medullary reticular formation to the inhibition by stimulation in the periaqueductal gray of a spinal nociceptive reflex in the pentobarbital-anesthetized rat. Brain Res. 305, 77–87.

Sandrew, B. B. and Poletti, C. E. 1984. Limbic influence on the periaqueductal gray: a single unit study in the awake squirrel monkey. Brain Res. 303, 77–86.

Schreff, M., Schulz, S., Wiborny, D., and Hollt, V. 1998. Immunofluorescent identification of endomorphin-2-containing nerve fibers and terminals in the rat brain and spinal cord. Neuroreport 9, 1031–1034.

Semenenko, F. M. and Lumb, B. M. 1992. Projections of anterior hypothalamic neurones to the dorsal and ventral periaqueductal grey in the rat. Brain Res. 582, 237–245.

Semenenko, F. M. and Lumb, B. M. 1999. Excitatory projections from the anterior hypothalamus to periaqueductal gray neurons that project to the medulla: a functional anatomical study. Neuroscience 94, 163–174.

Shipley, M. T., Ennis, M., Rizvi, T. A., and Behbehani, M. M. 1991. Topographical Specificity of Forebrain Inputs to the Midbrain Periaqueductal Gray: Evidence for Discrete Longitudinally Organized Input Columns. In: The Midbrain Periaqueductal Gray (*eds*. A. Depaulis and R. Bandler), pp. 417–448. Plenum.

Siuciak, J. A. and Advokat, C. 1987. Tolerance to morphine microinjections in the periaqueductal gray (PAG) induces tolerance to systemic, but not intrathecal morphine. Brain Res. 424, 311–319.

Skinner, K., Basbaum, A. I., and Fields, H. L. 1997. Cholecystokinin and enkephalin in brain stem pain modulating circuits. Neuroreport 8, 2995–2998.

Smith, D. J., Hawranko, A. A., Monroe, P. J., Gully, D., Urban, M. O., Craig, C. R., Smith, J. P., and Smith, D. L. 1997. Dose-dependent pain-facilitatory and -inhibitory actions of neurotensin are revealed by SR 48692, a nonpeptide neurotensin antagonist: influence on the antinociceptive effect of morphine. J. Pharmacol. Exp. Ther. 282, 899–908.

Smith, D. J., Perrotti, J. M., Crisp, T., Cabral, M. E., Long, J. T., and Scalzitti, J. M. 1988. The mu opiate receptor is responsible for descending pain inhibition originating in the periaqueductal gray region of the rat brain. Eur. J. Pharmacol. 156, 47–54.

Soja, P. J., Cairns, B. E., and Kristensen, M. P. 1999. Transmission through Ascending Trigeminal and Lumbar Sensory Pathways: Dependence on Behavioral State. In: Handbook of Behavioral State Control (*eds*. R. Lydic and H. A. Baghdoyan), pp. 521–544. CRC Press.

Stanfa, L., Dickenson, A., Xu, X. J., and Wiesenfeld-Hallin, Z. 1994. Cholecystokinin and morphine analgesia: variations on a theme. Trends Pharmacol. Sci. 15, 65–66.

Sugaya, K., Ogawa, Y., Hatano, T., Koyama, Y., Miyazato, T., and Oda, M. 1998. Evidence for involvement of the subcoeruleus nucleus and nucleus raphe magnus in urine storage and penile erection in decerebrate rats. J. Urol. 159, 2172–2176.

Suzuki, R., Rygh, L. J., and Dickenson, A. H. 2004. Bad news from the brain: descending 5-HT pathways that control spinal pain processing. Trends Pharmacol. Sci. 25, 613–617.

Talbot, J. D., Villemure, J. G., Bushnell, M. C., and Duncan, G. H. 1995. Evaluation of pain perception after anterior capsulotomy: a case report. Somatosens. Mot. Res. 12, 115–126.

Terayama, R., Guan, Y., Dubner, R., and Ren, K. 2000. Activity-induced plasticity in brain stem pain modulatory circuitry after inflammation. Neuroreport 11, 1915–1919.

Tershner, S. A., Mitchell, J. M., and Fields, H. L. 2000. Brainstem pain modulating circuitry is sexually dimorphic with respect to mu and kappa opioid receptor function. Pain 85, 153–159.

Tortorici, V. and Morgan, M. M. 2002. Comparison of morphine and kainic acid microinjections into identical PAG sites on the activity of RVM neurons. J. Neurophysiol. 88, 1707–1715.

Tortorici, V. and Vanegas, H. 1995. Anti-nociception induced by systemic or PAG-microinjected lysine–acetylsalicylate in rats. Effects on tail-flick related activity of medullary off- and on-cells. Eur. J. Neurosci. 7, 1857–1865.

Tortorici, V., Morgan, M. M., and Vanegas, H. 2001. Tolerance to repeated microinjection of morphine into the periaqueductal gray is associated with changes in the behavior of off- and on-cells in the rostral ventromedial medulla of rats. Pain 89, 237–244.

Tracey, I. 2005. Nociceptive processing in the human brain. Curr. Opin. Neurobiol. 15(4), 478–487.

Tracey, I., Ploghaus, A., Gati, J. S., Clare, S., Smith, S., Menon, R. S., and Matthews, P. M. 2002. Imaging attentional modulation of pain in the periaqueductal gray in humans. J. Neurosci. 22, 2748–2752.

Tsou, K., Brown, S., Sanudo-Pena, M. C., Mackie, K., and Walker, J. M. 1998. Immunohistochemical distribution of cannabinoid CB1 receptors in the rat central nervous system. Neuroscience 83, 393–411.

Urban, M. O. and Gebhart, G. F. 1997. Characterization of biphasic modulation of spinal nociceptive transmission by neurotensin in the rat rostral ventromedial medulla. J. Neurophysiol. 78, 1550–1562.

Urban, M. O. and Smith, D. J. 1993. Role of neurotensin in the nucleus raphe magnus in opioid-induced antinociception from the periaqueductal gray. J. Pharmacol. Exp. Ther. 265, 580–586.

Urban, M. O., Coutinho, S. V., and Gebhart, G. F. 1999. Biphasic modulation of visceral nociception by neurotensin in rat rostral ventromedial medulla. J. Pharmacol. Exp. Ther. 290, 207–213.

Urban, M. O., Jiang, M. C., and Gebhart, G. F. 1996. Participation of central descending nociceptive facilitatory systems in secondary hyperalgesia produced by mustard oil. Brain Res. 737, 83–91.

Valet, M., Sprenger, T., Boecker, H., Willoch, F., Rummeny, E., Conrad, B., Erhard, P., and Tolle, T. R. 2004. Distraction modulates connectivity of the cingulo-frontal cortex and the midbrain during pain – an FMRI analysis. Pain 109, 399–408.

Van Bockstaele, E. J., Aston-Jones, G., Pieribone, V. A., Ennis, M., and Shipley, M. T. 1991. Subregions of the periaqueductal gray topographically innervate the rostral ventral medulla in the rat. J. Comp. Neurol. 309, 305–327.

Vanderah, T. W., Ossipov, M. H., Lai, J., Malan, T. P., and Porreca, F. 2001a. Mechanisms of opioid-induced pain and antinociceptive tolerance: descending facilitation and spinal dynorphin. Pain 92, 5–9.

Vanderah, T. W., Suenaga, N. M., Ossipov, M. H., Malan, T. P., Jr., Lai, J., and Porreca, F. 2001b. Tonic descending facilitation from the rostral ventromedial medulla mediates opioid-induced abnormal pain and antinociceptive tolerance. J. Neurosci. 21, 279–286.

Vanderhorst, V. G., Mouton, L. J., Blok, B. F., and Holstege, G. 1996. Distinct cell groups in the lumbosacral cord of the cat project to different areas in the periaqueductal gray. J. Comp. Neurol. 376, 361–385.

Vanderhorst, V. G., Terasawa, E., and Ralston, H. J., 3rd 2002. Estrogen receptor-alpha immunoreactive neurons in the ventrolateral periaqueductal gray receive monosynaptic input from the lumbosacral cord in the rhesus monkey. J. Comp. Neurol. 443, 27–42.

Vanegas, H. 2004. To the descending pain-control system in rats, inflammation-induced primary and secondary hyperalgesia are two different things. Neurosci. Lett. 361, 225–228.

Vanegas, H. and Schaible, H.-G. 2004. Descending control of persistent pain: inhibitory or facilitatory? Brain Res. Rev. 46, 295–309.

Vanegas, H. and Tortorici, V. 2002. Opioidergic effects of nonopioid analgesics on the central nervous system. Cell. Mol. Neurobiol. 22, 655–661.

Vanegas, H., Barbaro, N. M., and Fields, H. L. 1984. Midbrain stimulation inhibits tail-flick only at currents sufficient to excite rostral medullary neurons. Brain Res. 321, 127–133.

Vaughan, C. W. 1998. Enhancement of opioid inhibition of GABAergic synaptic transmission by cyclo-oxygenase inhibitors in rat periaqueductal grey neurones. Br. J. Pharmacol. 123, 1479–1481.

Vaughan, C. W. and Christie, M. J. 1997. Presynaptic inhibitory action of opioids on synaptic transmission in the rat periaqueductal grey *in vitro*. J. Physiol. 498, 463–472.

Vaughan, C. W., Bagley, E. E., Drew, G. M., Schuller, A., Pintar, J. E., Hack, S. P., and Christie, M. J. 2003. Cellular actions of opioids on periaqueductal grey neurons from c57b16/j mice and mutant mice lacking mor-1. Br. J. Pharmacol. 139, 362–367.

Vaughan, C. W., Bandler, R., and Christie, M. J. 1996. Differential responses of lateral and ventrolateral rat periaqueductal grey neurones to noradrenaline *in vitro*. J. Physiol. 490, 373–381.

Vaughan, C. W., Connor, M., Bagley, E. E., and Christie, M. J. 2000. Actions of cannabinoids on membrane properties and synaptic transmission in rat periaqueductal gray neurons *in vitro*. Mol. Pharmacol. 57, 288–295.

Vaughan, C. W., Ingram, S. L., Connor, M. A., and Christie, M. J. 1997. How opioids inhibit GABA-mediated neurotransmission. Nature 390, 611–614.

Vaughan, C. W., McGregor, I. S., and Christie, M. J. 1999. Cannabinoid receptor activation inhibits GABAergic neurotransmission in rostral ventromedial medulla neurons *in vitro*. Br. J. Pharmacol. 127, 935–940.

Vianna, D. M., Graeff, F. G., Brandao, M. L., and Landeira-Fernandez, J. 2001. Defensive freezing evoked by electrical stimulation of the periaqueductal gray: comparison between dorsolateral and ventrolateral regions. Neuroreport 12, 4109–4112.

Villemure, C. and Bushnell, M. C. 2002. Cognitive modulation of pain: How do attention and emotion influence pain processing? Pain 95, 195–199.

Wager, T. D., Rilling, J. K., Smith, E. E., Sokolik, A., Casey, K. L., Davidson, R. J., Kosslyn, S. M., Rose, R. M., and Cohen, J. D. 2004. Placebo-induced changes in fMRI in the anticipation and experience of pain. Science 303, 1162–1167.

Walker, P. and Carrive, P. 2003. Role of ventrolateral periaqueductal gray neurons in the behavioral and cardiovascular responses to contextual conditioned fear and poststress recovery. Neuroscience 116, 897–912.

Walker, J. M. and Huang, S. M. 2002a. Cannabinoid analgesia. Pharmacol. Ther. 95, 127–135.

Walker, J. M. and Huang, S. M. 2002b. Endocannabinoids in pain modulation. Prostaglandins Leukot. Essent. Fatty Acids 66, 235–242.

Walker, J. M., Huang, S. M., Strangman, N. M., Tsou, K., and Sanudo-Pena, M. C. 1999. Pain modulation by release of the endogenous cannabinoid anandamide. Proc. Natl. Acad. Sci. U. S. A. 96, 12198–12203.

Wall, P. D. 1979. On the relation of injury to pain. Pain 6, 253–264.

Wang, H. and Wessendorf, M. W. 1999. Mu- and delta-opioid receptor mRNAs are expressed in spinally projecting serotonergic and nonserotonergic neurons of the rostral ventromedial medulla. J. Comp. Neurol. 404, 183–196.

Waters, A. J. and Lumb, B. M. 1997. Inhibitory effects evoked from both the lateral and ventrolateral periaqueductal grey are selective for the nociceptive responses of rat dorsal horn neurones. Brain Res. 752, 239–249.

Watkins, L. R. and Mayer, D. J. 1982. Organization of endogenous opiate and nonopiate pain control systems. Science 216, 1185–1192.

Watkins, L. R., Cobelli, D. A., and Mayer, D. J. 1982. Opiate vs non-opiate footshock induced analgesia (FSIA): descending and intraspinal components. Brain Res. 245, 97–106.

Watkins, L. R., Kinscheck, I. B., and Mayer, D. J. 1983a. The neural basis of footshock analgesia: the effect of periaqueductal gray lesions and decerebration. Brain Res. 276, 317–324.

Watkins, L. R., Wiertelak, E. P., Goehler, L. E., Mooney-Heiberger, K., Martinez, J., Furness, L., Smith, K. P., and Maier, S. F. 1994. Neurocircuitry of illness-induced hyperalgesia. Brain Res. 639, 283–299.

Watkins, L. R., Wiertelak, E. P., and Maier, S. F. 1993. The amygdala is necessary for the expression of conditioned but not unconditioned analgesia. Behav. Neurosci. 107, 402–405.

Watkins, L. R., Young, E. G., Kinscheck, I. B., and Mayer, D. J. 1983b. The neural basis of footshock analgesia: the role of specific ventral medullary nuclei. Brain Res. 276, 305–315.

Wiberg, M., Westman, J., and Blomqvist, A. 1987. Somatosensory projection to the mesencephalon: an anatomical study in the monkey. J. Comp. Neurol. 264, 92–117.

Wiertelak, E. P., Roemer, B., Maier, S. F., and Watkins, L. R. 1997. Comparison of the effects of nucleus tractus solitarius and ventral medial medulla lesions on illness-induced and subcutaneous formalin- induced hyperalgesias. Brain Res. 748, 143–150.

Wiesenfeld-Hallin, Z., de Arauja Lucas, G., Alster, P., Xu, X. J., and Hökfelt, T. 1999. Cholecystokinin/opioid interactions. Brain Res. 848, 78–89.

Williams, F. G. and Beitz, A. J. 1990. Ultrastructural morphometric analysis of GABA-immunoreactive terminals in the ventrocaudal periaqueductal grey: analysis of the relationship of GABA terminals and the $GABA_a$ receptor to periaqueductal grey-raphe magnus projection neurons. J. Neurocytol. 19, 686–696.

Williams, F. G., Mullet, M. A., and Beitz, A. J. 1995. Basal release of met-enkephalin and neurotensin in the ventrolateral periaqueductal gray matter of the rat: a microdialysis study of antinociceptive circuits. Brain Res. 690, 207–216.

Williams, J. L., Worland, P. D., and Smith, M. G. 1990. Defeat-induced hypoalgesia in the rat: effects of conditioned odors, naltrexone, and extinction. J. Exp. Psychol. Anim. Behav. Proc. 16, 345–357.

Williams, J. T., Christie, M. J., and Manzoni, O. 2001. Cellular and synaptic adaptations mediating opioid dependence. Physiol. Rev. 81, 299–343.

Xie, J. Y., Herman, D. S., Stiller, C. O., Gardell, L. R., Ossipov, M. H., Lai, J., Porreca, F., and Vanderah, T. W. 2005. Cholecystokinin in the rostral ventromedial medulla mediates opioid-induced hyperalgesia and antinociceptive tolerance. J. Neurosci. 25, 409–416.

Xin, L., Geller, E. B., Liu-Chen, L. Y., Chen, C., and Adler, M. W. 1997. Substance p release in the rat periaqueductal gray and preoptic anterior hypothalamus after noxious cold stimulation: effect of selective *mu* and *kappa* opioid agonists. J. Pharmacol. Exp. Ther. 282, 1055–1063.

Yezierski, R. P. 1988. Spinomesencephalic tract: projections from the lumbosacral spinal cord of the rat, cat, and monkey. J. Comp. Neurol. 267, 131–146.

Yezierski, R. P. and Mendez, C. M. 1991. Spinal distribution and collateral projections of rat spinomesencephalic tract cells. Neuroscience 44, 113–130.

Zadina, J. E., Hackler, L., Ge, L. J., and Kastin, A. J. 1997. A potent and selective endogenous agonist for the μ-opiate receptor. Nature 386, 499–502.

Zagon, A., Totterdell, S., and Jones, R. S. 1994. Direct projections from the ventrolateral medulla oblongata to the limbic forebrain: anterograde and retrograde tract-tracing studies in the rat. J. Comp. Neurol. 340, 445–468.

Zambreanu, L., Wise, R. G., Brooks, J. C., Iannetti, G. D., and Tracey, I. 2005. A role for the brainstem in central sensitisation in humans. Evidence from functional magnetic resonance imaging. Pain 114, 397–407.

Zhang, L., Sykes, K. T., and Hammond, D. L. 2004. Peripheral inflammation increases the proportion of spinally projecting neurons that express functional opioid receptors in the rostral ventromedial medulla (RVM). Abstract Viewer/ Itinerary Planner. Society for Neuroscience. Online, Program 297.294.

Zhang, Y. Q., Tang, J. S., Yuan, B., and Jia, H. 1997. Inhibitory effects of electrically evoked activation of ventrolateral orbital cortex on the tail-flick reflex are mediated by periaqueductal gray in rats. Pain 72, 127–135.

Zhuo, M. and Gebhart, G. F. 1992. Characterization of descending facilitation and inhibition of spinal nociceptive transmission from the nuclei reticularis gigantocellularis and gigantocellularis pars alpha in the rat. J. Neurophysiol. 67, 1599–1614.

Zhuo, M. and Gebhart, G. F. 1997. Biphasic modulation of spinal nociceptive transmission from the medullary raphe nuclei in the rat. J. Neurophysiol. 78, 746–758.

5.42 Emotional and Behavioral Significance of the Pain Signal and the Role of the Midbrain Periaqueductal Gray (PAG)

K Keay and R Bandler, University of Sydney, Sydney, NSW, Australia

© 2008 Elsevier Inc. All rights reserved.

5.42.1	**More than a Sensation?**	627
5.42.2	**Coping with Pain**	627
5.42.2.1	Active versus Passive Emotional Coping	627
5.42.2.2	Neural Representations of Active Emotional Coping	628
5.42.2.2.1	Dorsolateral periaqueductal gray	628
5.42.2.2.2	Lateral periaqueductal gray	630
5.42.2.3	Neural Representation of Passive Emotional Coping	630
5.42.2.3.1	Ventrolateral periaqueductal gray	630
5.42.2.4	Outputs Mediating Active and Passive Emotional Coping	630
5.42.2.4.1	Lateral periaqueductal gray and ventrolateral periaqueductal gray	630
5.42.2.4.2	Dorsolateral periaqueductal gray	630
5.42.3	**Conclusion**	633
References		633

5.42.1 More than a Sensation?

In a provocative article entitled *On the Relation of Injury to Pain*, Wall P. D. (1979) suggested that "... pain is better classified as an awareness of a need state than as a sensation; that it has more in common with the phenomena of hunger and thirst than it has with seeing and hearing ...." He also observed, somewhat anecdotally, that as pain changed from acute to chronic the emotional coping reaction also changed. Livingston W. K. (1998) in his posthumously published book *Pain and Suffering* stated a similar belief that "... pain is not strictly a physical sensation that can be defined simply by its anatomical and physiological substrates." Writing even earlier, Lewis T. (1942) observed that different emotional coping reactions were evoked by pain of different tissue origins, "... while painful sensations derived from the human skin are associated with brisk movements, with a rise of pulse rate and with a sense of invigoration ... painful sensations derived from deeper structures are associated often with quiescence, with slowing of the pulse, falling of the blood pressure, sweating and nausea." He went on to suggest that "... the difference in the quality of skin pain and of deep pain is so clear ... that it would perhaps seem unsafe to class both together under the one unqualified term pain and concluded that "... we should bear in mind the possibly serious fallacy of regarding both types (of pain) as represented in a common centre."

It is striking that these eminent researchers although starting from different perspectives arrive at a shared view, namely, that in addition to knowledge of the anatomy and physiology of its ascending sensory pathways, understanding how pain is localized in the brain also requires knowledge of the neurobiology of the emotional coping strategies triggered by different classes of pain.

5.42.2 Coping with Pain

5.42.2.1 Active versus Passive Emotional Coping

Animals (including humans) employ different strategies to cope with different classes of pain. Active emotional coping, which is characterized by engagement with the environment (i.e., fight or flight), is the usual response to escapable pain. Components of active coping include increased vigilance, hyperreactivity, increased somatomotor activity, and increased sympathetic activity. Passive emotional coping, is the antithesis of active coping. Instead of engagement with the environment, there is disengagement (e.g., conservation-withdrawal (Henry, J. P. and Stephens, P. M., 1977)). Components of passive coping include: decreased vigilance, hyporeactivity, quiescence, and falls in arterial pressure and heart rate. Passive

emotional coping is the usual response to inescapable pain, i.e., pain of deep origin (muscle, joint, viscera) or any persistent/chronic pain (Lewis, T., 1942; Wall, P. D., 1979; Bandler, R. *et al*., 2000; Keay, K. A. *et al*., 2001).

5.42.2.2 Neural Representations of Active Emotional Coping

Research carried out in rats, cats, and primates has identified longitudinally oriented, neuronal columns within the midbrain periaqueductal gray (PAG) as critical substrates integrating active or passive emotional coping. As seen in Figure 1 active emotional coping responses (i.e., a coordinated reaction of freezing, fight or flight, hypertension, tachycardia, and a nonopioid-mediated analgesia) are evoked when excitatory amino acids are microinjected into either the dorsolateral (dlPAG) or lateral (lPAG) column. (Bandler, R. and Shipley, M. T., 1994). Anatomical and functional studies suggest, however, different neural circuits and triggers are involved.

5.42.2.2.1 Dorsolateral periaqueductal gray

The dlPAG is distinguished from the lPAG by the presence (e.g., nitric oxide synthase (NOS), cholecystokinin (CCK), acetylcholine (ACh), Met-enkephalin) or absence (e.g., cytochrome oxidase and Gly-2 transporter) of specific neurochemicals (for a review, see Keay, K. A. and Bandler, R., 2004). Anatomically, major descending inputs to dlPAG originate from medial prefrontal cortical (PFC) fields and select medial hypothalamic nuclei, but there is a striking absence of ascending afferents arising from either brainstem or spinal cord (Figure 2). The predominance of forebrain, primarily cortical inputs, led to the suggestion that when triggered by psychological (cortical) stimuli, active coping is mediated by the dlPAG (Bandler, R. *et al*., 2000). Consistent with this suggestion, the potential threat signaled by the presence of a cat (sight and/or odor, but without physical contact) triggers active coping and a selective increase in immediate early gene (c-fos) expression in the dlPAG of the rat (Figure 2) (Canteras, N. S. and Goto, M., 1999).

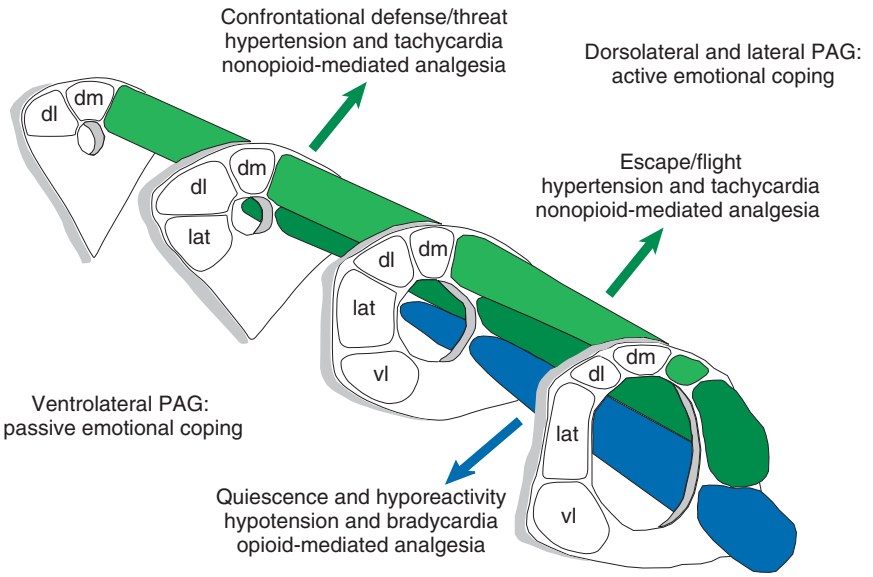

Figure 1 Schematic illustration of the dorsomedial (dm), dorsolateral (dl), lateral (lat), and ventrolateral (vl) neuronal columns within the periaqueductal gray (PAG). Injections of excitatory amino acids (EAA) within the dorsolateral and lateral PAG evoke active emotional coping strategies, whereas passive emotional coping strategies are evoked from the ventrolateral PAG. Specifically, EAA injections made within the dlPAG and lPAG columns evoke defensive reactions (confrontation, threat, escape, flight), hypertension, tachycardia, and a non-opioid-mediated analgesia. In contrast, EAA injections made within the vlPAG evoke cessation of spontaneous activity (quiescence), decreased responsiveness to the environment (hyporeactivity), hypotension, bradycardia, and an opioid-mediated analgesia. Adapted from Bandler, R. and Shipley, M. T. 1994. Columnar organization in the midbrain periaqueductal gray: modules for emotional expression? Trends Neurosci. 17, 379–389.

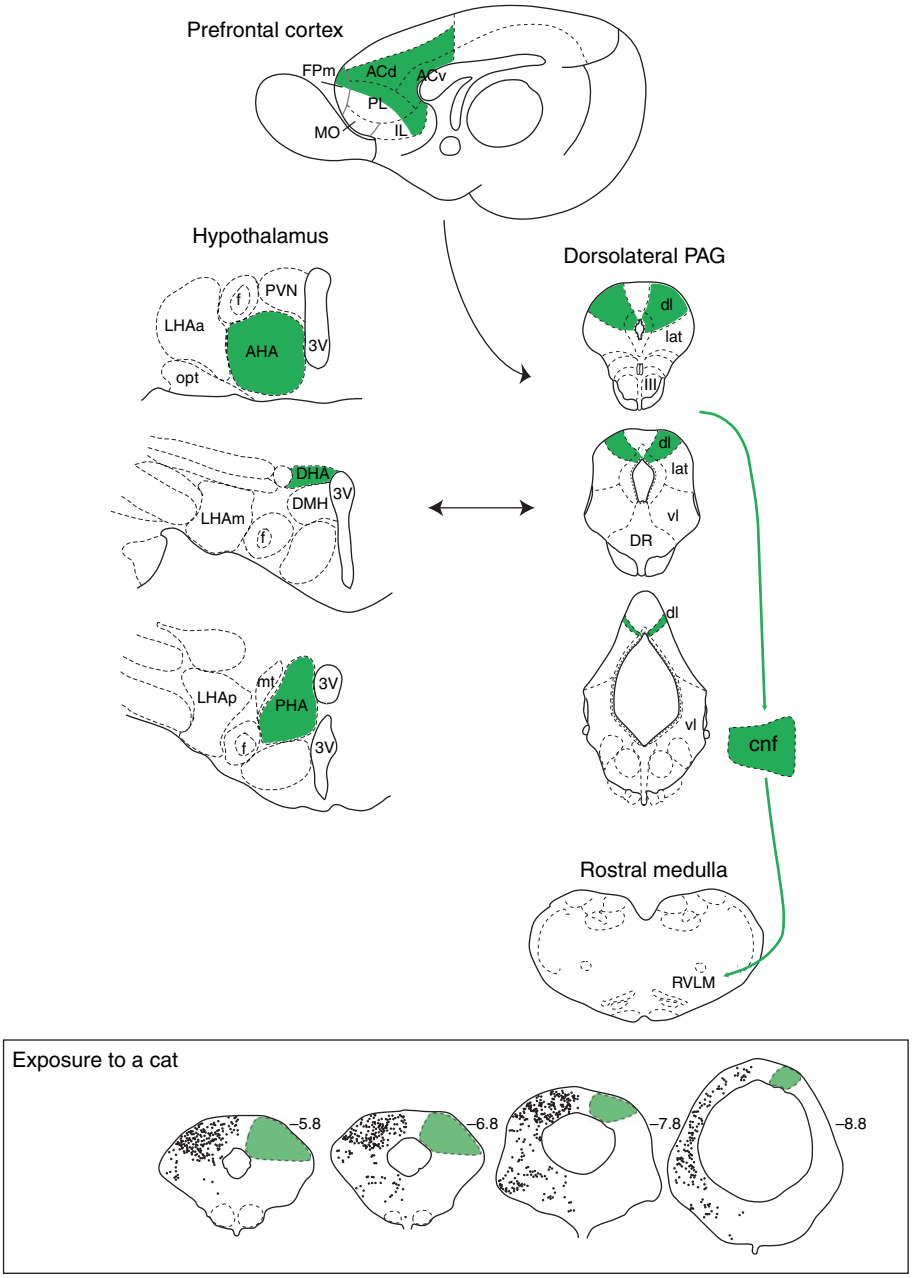

Figure 2 Schematic illustration of the major afferent and efferent projections of the dorsolateral periaqueductal gray (dlPAG). Major forebrain inputs to the dlPAG arise from dorsal, medial prefrontal cortical fields, and medial hypothalamic regions. The dlPAG does not project directly to the medulla, but can influence the rostral ventrolateral medulla via the cuneiform nucleus (cnf). The lower panel illustrates the pattern of neural activation (c-fos expression) evoked by a psychological stressor (exposure, without physical contact, of a rat to a cat), which evokes active emotional coping. The shaded area indicates the dorsolateral PAG column. RVLM, rostral ventrolateral medulla ACd, dorsal anterior cingulate cortex; ACv, ventral anterior cingulate cortex; AId, dorsal agranular insular cortex; AIp, posterior agranular insular cortex; DLO, dorsolateral orbital cortex; FPm, medial frontal pole; IL, infralimbic cortex; MO, medial orbital cortex; PL, prelimbic cortex; PRh, perirhinal cortex; VLOm, ventrolateral orbital cortex, medial part; VO, ventral orbital cortex AHA, anterior hypothalamic area; DHA, dorsal hypothalamic area; DMH, dorsomedial hypothalamic area; LHAa, lateral hypothalamic area, anterior; LHAm, lateral hypothalamic area, medial; LHAp, lateral hypothalamic area, posterior; PHA, posterior hypothalamic area; PVN, periventricular hypothalamic nucleus; f, fornix; mt, mamillothalmic tract; opt, optic tract; 3V, third ventricle; dl, dorsolateral PAG; lat, lateral PAG; vl, ventrolateral PAG, DR, dorsal raphe. Exposure to a cat: Adapted from Canteras, N. S. and Goto, M. 1999. Fos-like immunoreactivity in the periaqueductal gray of rats exposed to a natural predator. Neuroreport 10, 413–418.

5.42.2.2.2 Lateral periaqueductal gray

Although the boundary between the lPAG and dlPAG can be established on neurochemical grounds, the boundary between the lPAG and ventrolateral periaqueductal gray (vlPAG) rests on functional criteria (see Figure 1 and Section 5.42.2.3). Anatomically, the lPAG receives modest descending afferents of cortical and dorsal hypothalamic origins. However, in contrast to the dlPAG, the lPAG receives substantial and somatotopically organized ascending inputs from laminae I, II, IV, and V of the spinal cord, as well as the caudal, spinal trigeminal complex (Sp5) (Figure 3). The predominance of inputs arising from noci-responsive spinal and SpV regions suggests that active coping in response to physical stimuli (e.g., acute cutaneous pain) is mediated by the lPAG. In support of this hypothesis, brief applications of a noxious, cutaneous (thermal) stimulus evoked increased *Fos* expression within the lPAG, hypertension and active coping (Figure 3) (Keay, K. A. and Bandler, R. 1993; 2002).

5.42.2.3 Neural Representation of Passive Emotional Coping

Passive coping (i.e., a coordinated, conservation-withdrawal reaction of quiescence, hyporeactivity, hypotension, bradycardia, and an opioid-mediated analgesia) is evoked by microinjection of excitatory amino acids into the vlPAG column (Figure 1) (Bandler, R. and Shipley, M. T., 1994; Keay, K. A. and Bandler, R., 2001).

5.42.2.3.1 Ventrolateral periaqueductal gray

In common with the lPAG, substantial ascending inputs to the vlPAG originate from superficial and deep dorsal horn of spinal cord (and the transition zone between caudal and interpolar parts of Sp5, personal observations) (Keay, K. A. *et al.*, 1997). Double-label anatomical tracing studies indicate, however, that vlPAG and lPAG projections arise from distinct and separate populations of spinal neurons (Clement, C. I. *et al.*, 2000). Further, spino-vlPAG projections are not somatotopically organized (Keay, K. A. *et al.*, 1997). The vlPAG also receives substantial ascending inputs from nuclei of the solitary tract (NTS), as well as descending inputs from select orbital and insular cortical fields and the lateral hypothalamus (Figure 4). The convergence within the vlPAG of spinal, medullary, and forebrain afferents suggests that passive coping, whether evoked by physical or psychological stimuli, is mediated by the vlPAG. In support of this view, Fos expression is strongly evoked in the vlPAG when passive coping is triggered either (1) as a primary response to a deep or persistent noxious stimulus (see Figure 4) (Clement, C. I. *et al.*, 1996; Keay, K. A. *et al.*, 1997; 2001; Keay, K. A. and Bandler, R., 2002) or (2) in order to promote recovery and healing, as a delayed response to acute injury (for a discussion, see Wall, P. D., 1979; Keay, K. A. and Bandler, R., 2004).

5.42.2.4 Outputs Mediating Active and Passive Emotional Coping

5.42.2.4.1 Lateral periaqueductal gray and ventrolateral periaqueductal gray

Although they mediate distinct emotional coping strategies, the same ventromedial and ventrolateral medullary regions are projected upon by lPAG and vlPAG (see Figures 3 and 4) (Keay, K. A. and Bandler, R., 2001). Consistent with the opposing functional roles of lPAG and vlPAG, electrophysiological studies reveal opposite effects on medullary target neurons. For example, presympathetic rostral ventrolateral medulla (RVLM) vasopressor neurons are excited by lPAG stimulation, but inhibited by vlPAG stimulation (Verberne, A. J. and Boudier, H. R. S., 1991; Lovick, T. A., 1992a; 1992b; Verberne, A. and Guyenet, P., 1992). In contrast to shared descending targets, there exist distinct ascending projections to specific hypothalamic and midline and intralaminar thalamic fields (Floyd, N. S. *et al.*, 1996; 2000; Krout, K. E. and Loewy, A. D., 2000; Floyd, N. S. *et al.*, 2001).

5.42.2.4.2 Dorsolateral periaqueductal gray

Although it integrates an identical emotional coping strategy to the lPAG, the dlPAG has few direct medullary outputs. Its influence on the ventrolateral medulla is likely mediated indirectly, in part via a substantial projection to the cuneiform region (see Figure 2) (Redgrave, P. *et al.*, 1988; Mitchell, I. J. *et al.*, 1988a; 1988b). The dlPAG also projects to distinct thalamic and hypothalamic fields (Floyd, N. S. *et al.*, 1996; 2000; Krout, K. E. and Loewy, A. D., 2000; Floyd, N. S. *et al.*, 2001).

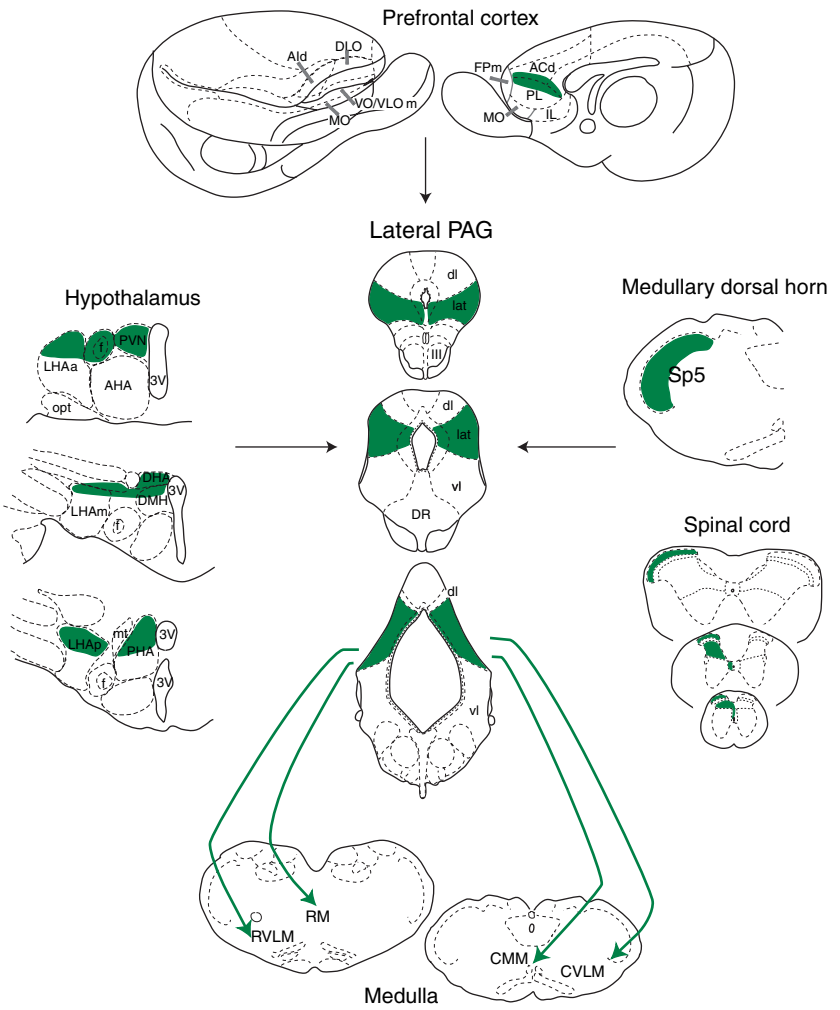

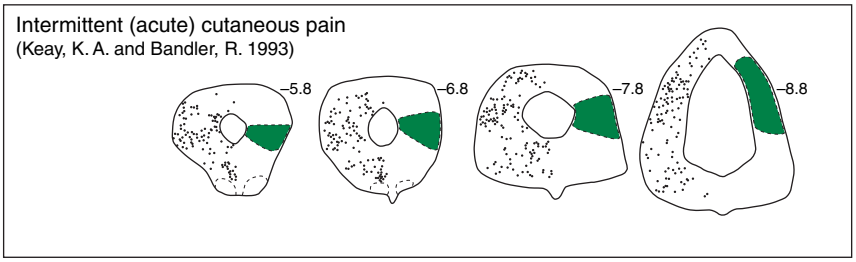

Figure 3 Schematic illustration of the major afferent and efferent projections of the lateral periaqueductal gray (lPAG). Major inputs to lPAG arise from spinal cord and the medullary dorsal horn (spinal trigeminal complex (SpV)). In addition, more modest inputs arise from a restricted part of medial prefrontal cortex as well as dorsal hypothalamic regions. The lPAG projects directly to both the rostral and caudal ventrolateral medulla (RVLM, CVLM), as well as the rostral and caudal ventromedial medulla (RM, CMM). The panel in the lower part of the figure shows the pattern of neural activation (c-fos expression) evoked by an acute cutaneous noxious stimulus (intermittent radiant heat), which evokes active emotional coping. The shaded area indicates the lPAG column. For abbreviations see caption to Figure 2.

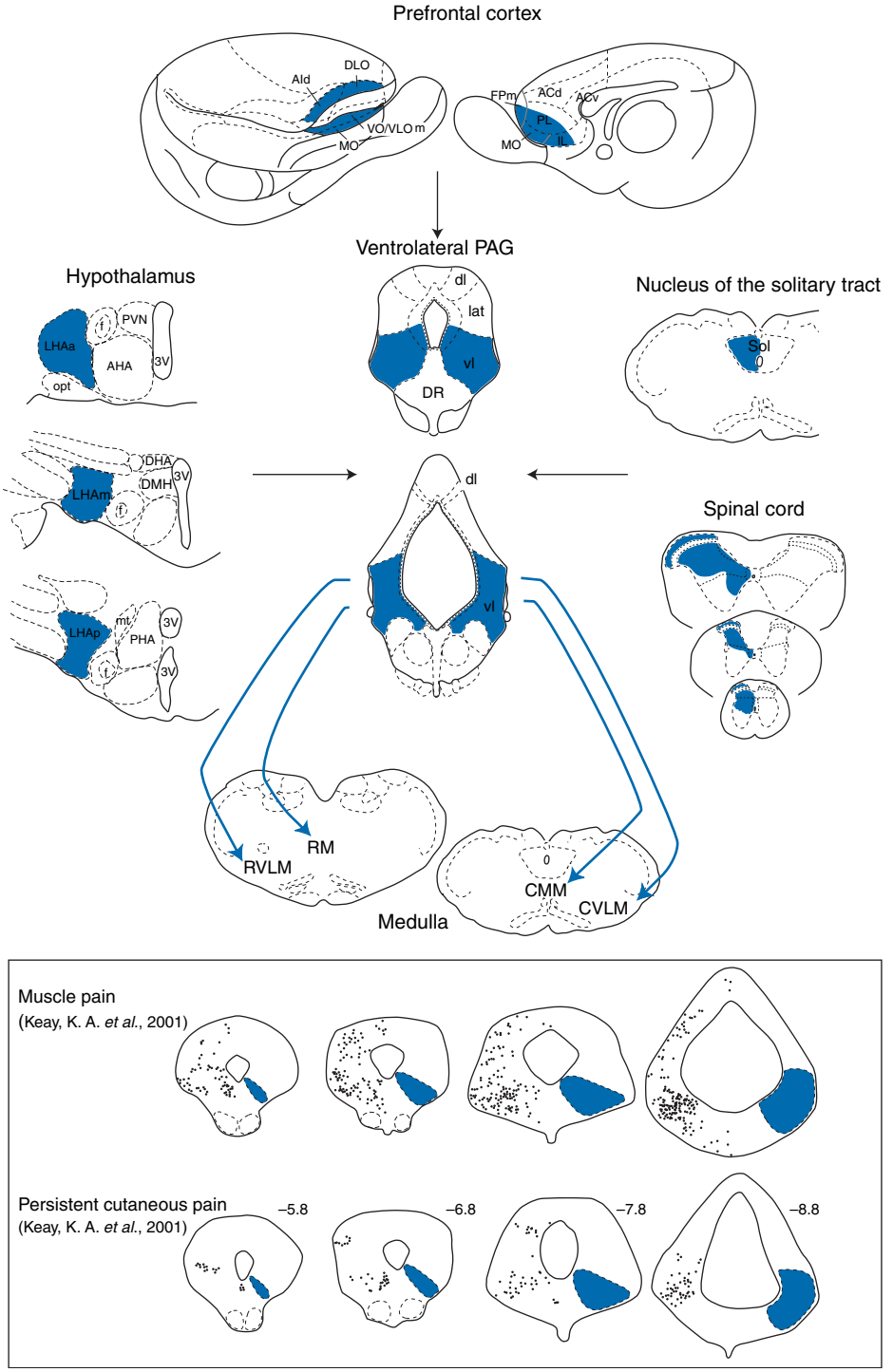

Figure 4 Schematic illustration of the major afferent and efferent projections of the ventrolateral periaqueductal gray (vlPAG). Major inputs to vlPAG arise from spinal cord and the nucleus of the solitary tract. In addition, significant inputs arise also from ventromedial prefrontal cortex and orbital/insular cortices. As well, substantial inputs arise from lateral hypothalamic fields. The vlPAG projects directly to both rostral and caudal ventrolateral medulla (RVLM, CVLM), as well as the rostral and caudal ventromedial medulla (RM, CMM). The panel in the lower part of the figure shows the patterns of neural activation (c-fos expression) evoked by an acute deep noxious stimulus (muscle pain: i.m. formalin) and a persistent cutaneous noxious stimulus (clip applied to dorsum of neck), each of which evoke passive emotional coping. The shaded area indicates the vlPAG column. For abbreviations see caption to Figure 2.

5.42.3 Conclusion

Animals (including humans) share the capacity to respond to escapable or inescapable pain with different emotional coping strategies. It has been established that the PAG is divisible into distinct longitudinal neuronal columns, which mediate distinct coping strategies (dlPAG/lPAG: active emotional coping; vlPAG: passive emotional coping). Further, each PAG column lies embedded within parallel, but distinct circuits, which extend rostrally to include specific PFC and hypothalamic regions (Bernard, J. F. and Bandler, J. F., 1998; Keay, K. A. and Bandler, R., 2001). On the output side, each PAG column projects either directly (lPAG/vlPAG) or indirectly (dlPAG) onto ventrolateral and ventromedial medullary regions containing (1) somatic and autonomic premotor neurons and (2) neurons mediating antinociception. A substantial body of evidence supports the view that the different PAG columns, and, their associated circuits, play critical roles in integrating the somatic, autonomic and antinociceptive components which characterize the distinct emotional coping reactions evoked by pain of different tissue origins and/or durations.

References

Bandler, R. and Shipley, M. T. 1994. Columnar organization in the midbrain periaqueductal gray: modules for emotional expression? Trends Neurosci. 17, 379–389.

Bandler, R., Keay, K. A., Floyd, N., and Price, J. 2000. Central circuits mediating patterned autonomic activity during active vs. passive emotional coping. Brain Res. Bull. 53, 95–104.

Bandler, R., Price, J. L., and Keay, K. A. 2000. Brain mediation of active and passive emotional coping. Progr. Brain Res. 122, 333–349.

Bernard, J. F. and Bandler, R. 1998. Parallel circuits for emotional coping behaviour: new pieces in the puzzle. J. Comp. Neurol. 401, 429–436.

Canteras, N. S. and Goto, M. 1999. Fos-like immunoreactivity in the periaqueductal gray of rats exposed to a natural predator. Neuroreport 10, 413–418.

Clement, C. I., Keay, K. A., Owler, B. K., and Bandler, R. 1996. Common patterns of increased and decreased fos expression in midbrain and pons evoked by noxious deep somatic and noxious visceral manipulations in the rat. J. Comp. Neurol. 366, 495–515.

Clement, C. I., Keay, K. A., Podzebenko, K., Gordon, B. D., and Bandler, R. 2000. Spinal sources of noxious visceral and noxious deep somatic afferent drive onto the ventrolateral periaqueductal gray of the rat. J. Comp. Neurol. 425, 323–344.

Floyd, N. S., Keay, K. A., and Bandler, R. 1996. A calbindin immunoreactive ''deep pain'' recipient thalamic nucleus in the rat. Neuroreport 7, 622–626.

Floyd, N. S., Price, J. L., Ferry, A. T., Keay, K. A., and Bandler, R. 2000. Orbitomedial prefrontal cortical projections to distinct longitudinal columns of the periaqueductal gray in the rat. J. Comp. Neurol. 422, 556–578.

Floyd, N. S., Price, J. L., Ferry, A. T., Keay, K. A., and Bandler, R. 2001. Orbitomedial prefrontal cortical projections to hypothalamus in the rat. J. Comp. Neurol. 432, 307–328.

Henry, J. P. and Stephens, P. M. 1977. Stress Health and the Social Environment: A Sociobiological Approach to Medicine. Springer.

Keay, K. A. and Bandler, R. 1993. Deep and superficial noxious stimulation increases fos-like immunoreactivity in different regions of the midbrain periaqueductal grey of the rat. Neurosci. Lett. 154, 23–26.

Keay, K. A. and Bandler, R. 2001. Parallel circuits mediating distinct emotional coping reactions to different types of stress. Neurosci. Biobehav. Rev. 25, 669–678.

Keay, K. A. and Bandler, R. 2002. Distinct central representations of inescapable and escapable pain: observations and speculation. Exp. Physiol. 87, 275–279.

Keay, K. A. and Bandler, R. 2004. Periaqueductal Gray. In: The Rat Nervous System, 3rd edn. (*ed*. G. Paxinos), pp. 243–257. Elsevier.

Keay, K. A., Clement, C. I., Depaulis, A., and Bandler, R. 2001. Different representations of inescapable noxious stimuli in the periaqueductal gray and upper cervical spinal cord of freely moving rats. Neurosci. Lett. 313, 17–20.

Keay, K. A., Clement, C. I., Owler, B., Depaulis, A., and Bandler, R. 1994. Convergence of deep somatic and visceral nociceptive information onto a discrete ventrolateral midbrain periaqueductal gray region. Neuroscience 61, 727–732.

Keay, K. A., Feil, K., Gordon, B. D., Herbert, H., and Bandler, R. 1997. Spinal afferents to functionally distinct periaqueductal gray columns in the rat: an anterograde and retrograde tracing study. J. Comp. Neurol. 385, 207–229.

Krout, K. E. and Loewy, A. D. 2000. Periaqueductal gray matter projections to midline and intralaminar thalamic nuclei of the rat. J. Comp. Neurol. 424, 111–141.

Lewis, T. 1942. Pain. MacMillan.

Livingston, W. K. 1998. Pain and Suffering. IASP Press.

Lovick, T. A. 1992a. Inhibitory modulation of the cardiovascular defence response by the ventrolateral periaqueductal grey matter in rats. Exp. Brain Res. 89, 133–139.

Lovick, T. A. 1992b. Midbrain influences on ventrolateral medullo-spinal neurones in the rat. Exp. Brain Res. 90, 147–152.

Mitchell, I. J., Dean, P., and Redgrave, P. 1988a. The projection from superior colliculus to cuneiform area in the rat. Ii. Defence-like responses to stimulation with glutamate in cuneiform nucleus and surrounding structures. Exp. Brain Res. 72, 626–639.

Mitchell, I. J., Redgrave, P., and Dean, P. 1988b. Plasticity of behavioural response to repeated injection of glutamate in cuneiform area of rat. Brain Res. 460, 394–397.

Redgrave, P., Dean, P., Mitchell, I. J., Odekunle, A., and Clark, A. 1988. The projection from superior colliculus to cuneiform area in the rat. I. Anatomical studies. Exp. Brain Res. 72, 611–625.

Verberne, A. and Guyenet, P. 1992. Midbrain central gray: influence on medullary sympathoexcitatory neurons and the baroreflex in rats. Am. J. Physiol. 263, R24–R33.

Verberne, A. J. and Boudier, H. R. S. 1991. Midbrain central grey: regional heamodynamic control and excitatory amino acidergic mechanisms. Brain Res. 550, 86–94.

Wall, P. D. 1979. On the relation of injury to pain. Pain 6, 253–264.

Further Reading

Bandler, R. and Keay, K. A. 1996. Columnar organization in the midbrain periaqueductal gray and the integration of emotional expression. Progr. Brain Res. 107, 285–300.

Keay, K. A., Clement, C. I., Matar, W. M., Heslop, D. J., Henderson, L. A., and Bandler, R. 1997. Noxious activation of spinal or vagal afferents evoked distinct patterns of fos-like immunoreactivity in the ventrolateral periaqueductal grey of unanaesthetised rats. Brain Res. 948, 122–130.

Lovick, T. and Bandler, R. 2005. The organization of the Midbrain Periaqueductal Grey and the Integration of Pain Behaviour. In: The Neurobiology of Pain (*eds*. S. Hunt and M. Koltzenburg), pp. 267–287. Oxford University Press.

5.43 The Thalamus and Nociceptive Processing

J O Dostrovsky, University of Toronto, Toronto, ON, Canada

A D Craig, Barrow Neurological Institute, Phoenix, AZ, USA

© 2008 Elsevier Inc. All rights reserved.

5.43.1	**Introduction**	635
5.43.2	**Comparative Anatomical Findings**	636
5.43.2.1	Thalamic Nuclei Receiving Direct Spinothalamic Tract Inputs	636
5.43.2.1.1	Ventroposterior nuclei	636
5.43.2.1.2	Posterior part of the ventromedial nucleus	637
5.43.2.1.3	Ventral lateral nucleus	638
5.43.2.1.4	Parafascicular nucleus	638
5.43.2.1.5	Medial dorsal nucleus	638
5.43.2.1.6	Central lateral nucleus	638
5.43.2.1.7	Nucleus submedius	639
5.43.2.2	Indirect Nociceptive Pathways to the Thalamus	639
5.43.3	**Comparative Physiological Findings**	639
5.43.3.1	Ventroposterior Nuclei	640
5.43.3.2	Ventroposterior Inferior Nucleus	641
5.43.3.3	Posterior Thalamus and Posterior Part of the Ventromedial Nucleus	641
5.43.3.4	Intralaminar Nuclei	643
5.43.3.5	Medial Dorsal Nucleus	643
5.43.4	**Direct Physiological Evidence in Humans**	644
5.43.4.1	Nociceptive Neurons	645
5.43.4.2	Innocuous Cooling-Responsive Neurons	645
5.43.4.3	Stimulation-Induced Pain and Temperature Sensations	646
5.43.5	**The Thalamus and Central Neuropathic Pain**	647
5.43.5.1	Physiological Observations in Central Pain Patients	647
5.43.5.2	Thalamic Bursting Activity	648
5.43.5.3	Effects of Thalamic Lesions on Pain	648
5.43.5.4	The Thalamic Pain Syndrome	649
5.43.6	**Pharmacology**	649
References		650

5.43.1 Introduction

The thalamus has been recognized to play a very important role in the higher-level processing of nociceptive inputs ever since the clinical observations by Dejerine J. and Roussy G. (1906) and Head H. and Holmes G. (1911) of pain resulting from strokes affecting the lateral thalamus. Modern-day anatomical and electrophysiological techniques have provided a wealth of information regarding the processing of nociceptive information at the thalamic level.

The concept that medial thalamus is involved in the affective/motivational aspect of pain and the lateral thalamus in the sensory/discriminative aspect of pain originated with the comprehensive analysis of 23 thalamic pain patients by Head and Holmes, and it was emphasized particularly by Melzack R. and Casey K. L. (1968). For many years, the available anatomical and physiological evidence suggested that these functions be ascribed to indirect spinoreticulothalamic (paleospinothalamic) input to medial thalamus and direct (neospinothalamic) spinothalamic tract (STT)-mediated input to somatosensory lateral thalamus, which was most prominent in humans. However, the recent evidence summarized below indicates that lamina I STT input to distinct portions of medial and lateral thalamus can be directly associated with these functions.

This chapter will review the major findings relating to the anatomy, physiology, and pharmacology of thalamus with respect to understanding its role in the mediation of acute and chronic pain. The chapter will start with an overview of thalamic anatomy and the termination sites of ascending somatosensory pathways focusing on the STT in the primate. Then the physiological findings in animals will be summarized, followed by discussions of findings in humans and a summary of thalamic pharmacology.

5.43.2 Comparative Anatomical Findings

In contrast to spinal cord, there are significant species differences in the anatomy of the pathways and the nuclei mediating nociception at the thalamic level. This chapter will focus on findings from primates including humans and will commence with a description of the thalamic termination sites of ascending pathways involved in the transmission of nociceptive information. The major pathway involved in the relay of nociceptive and thermoreceptive information is the STT and the functionally equivalent component of the trigeminothalamic tract (TTT) that originates in the medullary dorsal horn (subnucleus caudalis of the trigeminal spinal tract nucleus, also termed the medullary dorsal horn). Although the STT is frequently described as a single tract, this chapter will describe separately the terminations of its two components, the lateral and the ventral. The lateral STT originates largely from lamina I of the superficial dorsal horn and contains many neurons responding specifically to noxious stimuli and innocuous thermoreceptive neurons. In contrast, the ventral STT originates largely from neurons in deeper layers, most of which respond to innocuous tactile and proprioceptive inputs in addition to nociceptive inputs (Craig, A. D. and Dostrovsky, J. O., 1999; Craig, A. D., 2003).

5.43.2.1 Thalamic Nuclei Receiving Direct Spinothalamic Tract Inputs

There are six major regions of termination of the STT and TTT within the primate thalamus: the ventroposterior nucleus (VP), the posterior portion of the ventromedial nucleus (VMpo), the ventrolateral nucleus (VL), the central lateral nucleus (CL), the parafascicular nucleus (Pf), and the ventrocaudal portion of the medial dorsal nucleus (MDvc) (Mehler, W. R., 1969; Boivie, J., 1979; Berkley, K. J., 1980; Craig, A. D., 2003; 2004). Each of these is described in more detail below.

5.43.2.1.1 Ventroposterior nuclei

The VP that comprises the ventroposterior lateral (VPL) and ventroposterior medial (VPM) nuclei receives its major ascending afferent input from the medial lemniscus and is the main relay nucleus for tactile and kinesthetic information. This nucleus is also frequently termed the ventrobasal complex and in the human, the ventrocaudal nucleus (Vc) (Hassler, R., 1959; Mehler, W. R., 1966; Jones, E. G., 1990). However, it is well established that the STT and TTT also have terminations in this region. The STT terminations in VP form clusters (also referred to as archipelago), which are especially dense along its caudal border with the posterior group and pulvinar and along its rostral border with the VL and near the laminae that occur within VP (Stepniewska, I. *et al.*, 2003). The terminations are roughly in register with the detailed somatotopic organization of the low-threshold mechanoreceptive (LTM) lemniscal terminations and thalamocortical neurons, with craniofacial inputs to VPM, arm/forelimb inputs to medial VPL, and leg/hindlimb inputs to lateral VPL. Some of the STT axons terminating in VP also send a collateral into the CL (Applebaum, A. E. *et al.*, 1979; Giesler, G. J. Jr. *et al.*, 1981).

The main source of STT and TTT terminations in VP is from the neurons in the deep dorsal horn (laminae IV and V) as shown in Figure 1(b). Interestingly, these terminations appear directed to VP neurons that are immunopositive for calbindin in contrast to the lemniscal afferents from the dorsal column nuclei (DCN) and principal trigeminal nucleus, which terminate in the vicinity of neurons that are immunopositive for parvalbumin (Rausell, E. and Jones, E. G., 1991). Furthermore, the calbindin-immunopositive neurons project to the superficial layers of cortex, whereas the parvalbumin neurons project to the middle layers (Gingold, S. I. *et al.*, 1991; Rausell, E. and Jones, E. G., 1991). Another difference between spinothalamic and lemniscal terminations is that the latter but not the former form triadic synapses with GABAergic presynaptic dendrites (Ralston, H. J., III and Ralston, D. D., 1994). These differences suggest that the spinothalamic nociceptive inputs are processed differently than the innocuous mechanoreceptive inputs in VP.

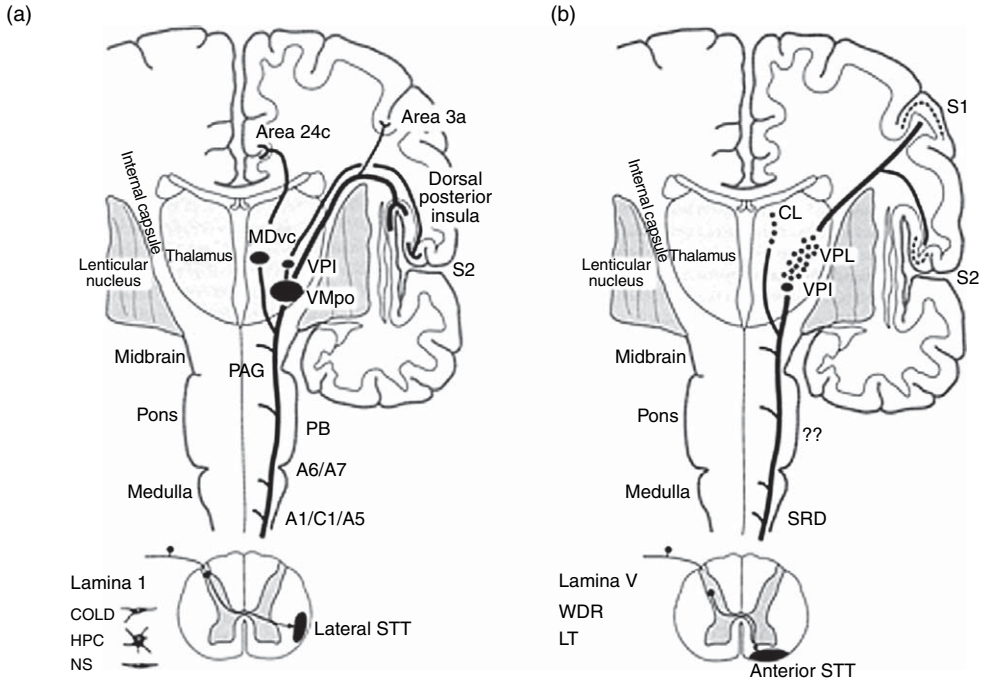

Figure 1 A schematic summary diagram of the ascending projections from the spinal cord to the thalamus and on to the cortex. (a) The lateral spinothalamic tract arising from nociceptive (HPC and NS) and innocuous thermoreceptive (COLD) neurons in lamina I. The major thalamic termination sites are in the posterior part of the ventromedial nucleus (VMpo), ventroposterior inferior nucleus (VPI), and the ventrocaudal part of the medial dorsal nucleus (MDvc). Also shown are the brainstem terminations in the ventrolateral medulla (A1/C1/A5), the dorsolateral pons (A6/A7), the parabrachial nucleus (PB), the periaqueductal gray (PAG), and the cortical projections of the thalamic sites receiving the lamina I inputs. (b) The ascending projections of lamina IV–V cells, primarily wide dynamic range (WDR) neurons and low-threshold mechanoreceptive (LTM) neurons, via the ventral spinothalamic tract (STT) to the VPI, ventroposterior lateral nucleus (VPL), ventrolateral nucleus (VL), and central lateral nucleus (CL). Terminations also occur in the brainstem in the subnucleus reticularis dorsalis (SRD) and other sites, probably including the reticular core. Adapted with permission from Craig, A. D. and Dostrovsky, J.O. 1999. Medulla to Thalamus. In: Textbook of Pain (*eds*. P. D. Wall and R. Melzack), pp. 183–214. Churchill-Livingstone.

Immediately ventral to VPL and VPM lies the ventroposterior inferior nucleus (VPI; roughly equivalent to the parvicellular part of the ventrocaudal nucleus (Vcpc) in humans). Curiously, this nucleus receives STT and TTT inputs from neurons located not only in laminae IV and V but also in lamina I, as well as from vestibular afferents (Ralston, H. J., III and Ralston, D. D., 1992). The VPI projects to secondary somatosensory cortex (SII) and retroinsular (vestibular) cortex (Friedman, D. P. and Murray, E. A., 1986; Stevens, R. T. *et al*., 1993).

Species differences. In the rat, there are STT and TTT terminations throughout VP (Mehler, W. R., 1969; Peschanski, M., 1984), which originate from both superficial and deep layers of the dorsal horn. In contrast, in the cat, the STT and TTT terminate along the ventral aspect of VPL (and VPI and the basal part of the ventromedial nucleus (VMb)) and there are almost no terminals within VP (Berkley, K. J., 1980; Craig, A. D. and Burton, H., 1985).

5.43.2.1.2 Posterior part of the ventromedial nucleus

Recent studies in the monkey have revealed that there is a very prominent and dense projection from STT and TTT neurons in lamina I to a region that has been termed the posterior ventromedial nucleus (VMpo), which lies immediately posterior and inferior to VP and is contiguous rostrally with the VMb (Craig, A. D., 2004). Of particular interest and importance are the findings that the STT and TTT terminations are topographically organized (Craig, A. D., 2003; 2004) and that the VMpo neurons project in a topographic manner to the dorsal posterior insula, a region that is consistently activated by thermal and nociceptive stimuli. The VMpo is the

major projection target of the lamina I neurons in the primate, which comprise its almost exclusive ascending sensory input (Figure 1(a)). The trigeminal inputs terminate anteriorly and lumbar inputs most posteriorly. This anteroposterior topographic arrangement contrasts with the mediolateral topography of the VP.

The dense lamina I STT and TTT terminations in VMpo are clearly delineated with the use of immunohistochemical labeling for calbindin. A region of calbindin-positive terminal labeling has been observed in a comparable location in the human thalamus (Blomqvist, A. *et al.*, 2000) and corresponds with the area of dense STT terminations observed in thalamus following cordotomies performed to alleviate pain (Mehler, W. R., 1966). This region can also be delineated in monkeys and humans based on its different cytoarchitecture. Electron microscopy has revealed that the glutamatergic STT and TTT terminations form triadic synapses with the VMpo relay cell dendrites and GABAergic presynaptic dendrites (Beggs, J. *et al.*, 2003). This is similar to the termination of lemniscal afferents in VP but contrasts with the STT terminations in VP. The triadic contacts are believed to provide high synaptic security and temporal fidelity. VMpo was not specifically identified in earlier anatomical studies, but the region was included in the caudal VP (Mehler, W. R., 1966), the Vc portae (Hassler, R., 1970), and the posterior complex (Po) (Jones, E. G., 1990).

Species differences. In the cat, there is a sparse lamina I terminal field in the ventral VMb, and this may constitute a primordial homologue of the primate VMpo. In support of this notion is the fact that lesions to this part of VMb in the cat disrupt discriminative thermal sensation (Norrsell, U. and Craig, A. D., 1999) and that it projects to insular cortex (Clasca, F. *et al.*, 1997). A homologous region does not appear to exist in the rat.

5.43.2.1.3 Ventral lateral nucleus

Moderately dense STT terminations are observed extending rostrally from VP into caudal VL in cats and monkeys that overlap with inputs from the cerebellum (Berkley, K. J., 1980; Stepniewska, I. *et al.*, 2003). These inputs probably originate from neurons in the deep dorsal horn and ventral horn (laminae V and VII). VL projects to the motor cortex (Jones, E. G., 1985), and this STT component is most likely related with sensorimotor integration rather than nociception.

5.43.2.1.4 Parafascicular nucleus

The centré median (CM) and Pf regions are frequently cited as playing a major role in nociception. However, there is only a weak STT projection to Pf that originates from lamina I and V cells, and more recent anatomical studies fail to confirm earlier reports of STT terminations in CM. The Pf and CM nuclei appear to be involved in motor-related processing as their main connections are with the basal ganglia, substantia nigra, and motor cortex (Jones, E. G., 1985; Royce, G. J. *et al.*, 1989; Sadikot, A. F. *et al.*, 1992).

5.43.2.1.5 Medial dorsal nucleus

Recent studies in the monkey reveal moderately dense STT and TTT projections to the MDvc. The terminals are topographically organized along an anteroposterior axis, with trigeminal input located most posteriorly. The cells of origin of this projection are in lamina I of the spinal and medullary dorsal horn (Ganchrow, D., 1978; Craig, A. D., 2004). Cells in MDvc project to area 24c in the cortex at the fundus of the anterior cingulate sulcus (limbic motor cortex), rather than to the orbitofrontal and prefrontal cortex where the remainder of medial dorsal nucleus (MD) projects (Ray, J. P. and Price, J. L., 1993; Craig, A. D., 2003). It is likely that this region of MD plays an important role in mediating the affective/motivational aspect of pain. There appears to be no homologous region in the cat or rat (see Section 5.43.2.1.7).

5.43.2.1.6 Central lateral nucleus

Dense STT terminations are observed in the caudal part of CL and in some other portions of the nucleus. The cells of origin are located in laminae V and VII (Applebaum, A. E. *et al.*, 1979; Giesler, G. J., Jr. *et al.*, 1981; Craig, A. D., Jr. *et al.*, 1989). Projections from different regions of the spinal cord terminate in different cell clusters but do not appear to be topographically organized (Craig, A. D. and Burton, H., 1985). This nucleus also receives projections from the cerebellum, tectum, substantia nigra, and globus pallidus. Most of the neurons in this region project to the basal ganglia, but there are also projections to the superficial and deep layers of posterior parietal and motor cortices (Jones, E. G., 1985; Royce, G. J. *et al.*, 1989). The function of the STT input to this nucleus is unknown, but one can speculate that it may be involved in motor set, attention, and orientation. Similar STT terminations have been observed in cats, rats, and other vertebrates.

5.43.2.1.7 *Nucleus submedius*

In the cat, there are dense and topographically organized terminations of the TTT and STT arising from spinal and medullary dorsal horn lamina I neurons in the medial thalamic nucleus submedius (Sm). Although Sm originates developmentally from the pronucleus of MD, it projects to the ventrolateral orbital cortex rather than to the cingulate cortex and thus constitutes a major phylogenetic difference from the lamina I projection to MDvc in the primate (Craig, A. D., Jr. *et al.*, 1982; Coffield, J. A. *et al.*, 1992). In the cat, the spinal input to the anterior cingulate relays in the ventral VP (Musil, S. Y. and Olson, C. R., 1988; Yasui, Y. *et al.*, 1988) and also indirectly by way of the parabrachial nucleus (PB) (Devinsky, O. *et al.*, 1995). In the rat, input to Sm originates primarily from trigeminal cells at the junction of the caudalis and interpolaris subnuclei of the trigeminal spinal tract nucleus and from trigeminal and cervical lamina I cells, as well as other cells in the spinal cord (Dado, R. J. and Giesler, G. J., Jr., 1990; Yoshida, A. *et al.*, 1992).

5.43.2.2 Indirect Nociceptive Pathways to the Thalamus

In addition to the STT, there are several polysynaptic pathways that may be involved in relaying nociceptive signals to the thalamus. First, the postsynaptic dorsal column pathway comprises dorsal horn neurons located primarily in laminae IV–VI and X whose axons ascend ipsilaterally in the superficial dorsolateral funiculus and deep dorsal columns and terminate in the ventral and rostral portions of the DCN (gracile and cuneate nuclei). These portions of the DCN have projections to motor-related regions of the brainstem rather than to VP (Brodal, A., 1982; Willis, W. D., 1985; Berkley, K. J. *et al.*, 1986). Although most of the neurons in this pathway respond only to nonnoxious cutaneous mechanical stimuli, some respond also to noxious stimuli. Some of the nociceptive neurons in this pathway convey visceral activity in the rat and possibly also in the primate (Al-Chaer, E. D. *et al.*, 1998; see also Villanueva, L. and Nathan, P., 2000). However, functional imaging studies of visceral pain in humans reveal a pattern of activation that does not appear consistent with the hypothesis that this pathway is important for visceral pain in humans (e.g., Strigo, I. A. *et al.*, 2003). Second, the spinocervicothalamic tract comprises dorsal horn neurons whose axons ascend ipsilaterally in the dorsolateral funiculus and terminate in the lateral cervical nucleus that is located at the level of C1-2 just lateral to the superficial dorsal horn (Boivie, J., 1983). The neurons of the lateral cervical nucleus project to the contralateral VP via the medial lemniscus. This pathway is prominent in the cat and raccoon but very small in the primate. Some of the neurons in this pathway respond to nociceptive stimuli although most respond only to innocuous stimuli (Kajander, K. C. and Giesler, G. J., Jr., 1987; Downie, J. W. *et al.*, 1988). Third, evidence obtained in the rat indicates that spinal input to a dorsal reticular region in the caudal medulla is relayed by way of a portion of the ventromedial nucleus to layer 1 of widespread regions of the frontal cortex (Desbois, C. *et al.*, 1999; Desbois, C. and Villanueva, L., 2001). This region also has a descending projection to the deep dorsal horn of the spinal cord. Modulation of activity, such as those associated with alerting responses, is suggested as a potential function, but whether this pathway exists in primates and humans is unknown. Fourth, a spinoreticulothalamic pathway (paleospinothalamic tract) was hypothesized long ago to accommodate clinical observations made in patients with thalamic pain syndrome (see below). Modern evidence indicates that spinal terminations in the brainstem reticular formation do not overlap with the locations of cells that project to thalamus, except within the PB (Blomqvist, A. and Berkley, K. J., 1992). The PB receives contralateral spinal input and ipsilateral trigeminal input that originates mainly from lamina I but also from lamina V cells. There is only a crude topography, and although there is considerable anatomical overlap with ascending homeostatic afferent input from the nucleus of the solitary tract, evidence in the rat indicates that nociceptive neurons are mainly modality selective (Bernard, J. F. and Besson, J. M., 1990). In primates, PB projects mainly to VMb in the thalamus, as well as to hypothalamus and amygdala, but in rats, it projects more broadly within medial thalamus and to various cortical regions associated with autonomic control.

5.43.3 Comparative Physiological Findings

The previous section described the pathways and thalamic termination sites of spinal and trigeminal neurons that include nociceptive neurons. On this basis, one would expect to find neurons in the

thalamic termination sites that would also respond to noxious inputs, and this is particularly the case for the regions receiving inputs from lamina I. There have indeed been many reports of nociceptive neurons in lateral, posterior, and medial areas of the thalamus. However, it should be kept in mind that the existence of neurons responding to noxious stimuli in a given region of thalamus does not necessarily signify that the region is involved in mediating the sensations of pain that would be expected to be elicited by noxious stimuli giving rise to the noxious responses. For example, the responses could be related to arousal, attentional, and motor consequences of the noxious stimulus. The following section will summarize the physiological findings reported for each of the main thalamic regions receiving nociceptive inputs.

5.43.3.1 Ventroposterior Nuclei

As mentioned earlier, the VPL and VPM are the main thalamic targets for innocuous tactile information ascending via the medial lemniscus from the DCN and principal trigeminal nucleus. It is thus not surprising that most of the neurons in this region respond exclusively to innocuous low-threshold mechanical cutaneous inputs. These neurons are organized in a high-resolution somatotopic fashion and project primarily to areas 3b and 1 of primary somatosensory (SI) cortex. There is an anterior and dorsally located shell that contains neurons responding to deep, muscle and joint afferent inputs, and this proprioceptive information is relayed to areas 3a and 2 of SI cortex (Kaas, J. H. *et al*., 1984; Jones, E. G., 1990).

It is generally considered that VP is the main relay nucleus for nociceptive inputs involved in mediating the sensory aspects of pain (localization and intensity discrimination) (Melzack, R. and Casey, K. L., 1968; Willis, W. D., 1985), since it receives STT inputs (primates and rodents, but not carnivores) and projects to the somatotopically organized SI cortex. Indeed, there have been many reports of nociceptive neurons within VP in the primate and rodent. In the monkey, about 10% of the neurons are nociceptive and most of these are of the wide dynamic range (WDR – responding to both LTM inputs and nociceptive inputs) type (Figure 2) (Willis, W. D., 1985; Apkarian, A. V. and Shi, T., 1994; Willis, W. D. and Westlund, K. N., 1997). They usually have moderately large receptive fields (e.g., more than half of the face or arm), and these are organized in a crude somatotopic manner roughly corresponding to the somatotopy of the intermingled LTM neurons (Willis, W. D. and Westlund, K. N., 1997). In the monkey, these neurons are concentrated in the posterior part of VP and near the major fiber laminae, consistent with the predominant location of the terminations of the STT and TTT axons of lamina V neurons (Applebaum, A. E. *et al*., 1979; Boivie, J., 1979; Kenshalo, D. R., Jr. *et al*., 1980; Casey, K. L. and Morrow, T. J., 1983; Gingold, S. I. *et al*., 1991; Bushnell, M. C. *et al*., 1993). Anatomical studies have provided evidence suggesting that the nociceptive neurons project to areas 3b and 1 of SI cortex. Interestingly, these studies suggest that the cortical terminations of these nociceptive neurons are in the most superficial layers of cortex in contrast to the VP LTM neurons whose axons terminate in the middle layer of cortex (Rausell, E. *et al*., 1992; Shi, T. *et al*., 1993), indicating a possible modulatory role for these nociceptive inputs. Electrophysiological studies have confirmed that some of these WDR neurons within VP can be antidromically activated from areas 3b and 1 of SI (Kenshalo, D. R., Jr. *et al*., 1980). Curiously, visceral noxious stimuli activate not only VP WDR neurons but also LTM neurons and do not appear to be somatotopically organized (Chandler, M. J. *et al*., 1992; Al-Chaer, E. D. *et al*., 1998).

Species differences: In the rat, nociceptive-specific (NS) and WDR nociceptive cells have been reported throughout VP intermixed in a roughly topographic manner with the LTM neurons (Guilbaud, G. *et al*., 1980). The receptive fields of these nociceptive neurons are generally quite large and often bilateral. Some receive convergent visceral input. In rats with experimentally induced arthritis or neuropathies, increased numbers of WDR VP cells that project to the sensorimotor cortex have been reported (Guilbaud, G. *et al*., 1990). In contrast to the primate and rodent, in the cat, there are virtually no nociceptive cells within VP proper. However, NS and WDR nociceptive neurons in this species can be found in the dorsal and ventral aspects of VP, the ventral aspect of VMb and VPI. These are the regions where STT and TTT terminations occur (see above). The nociceptive neurons within this shell-like region are organized in a crude mediolateral topographic pattern in parallel (but not in register) with the somatotopy of the adjacent VP. A portion of these neurons receive convergent input from skin, muscle, viscera, tooth pulp, or cranial vasculature (Davis, K. D. and Dostrovsky, J. O., 1988; Bruggemann, J. *et al*., 1994). Some of these neurons have been shown to project to area 3a of SI, SII, and/or anterior cingulate cortex (Yasui, Y. *et al*., 1988; Craig, A. D. and Dostrovsky, J. O., 2001).

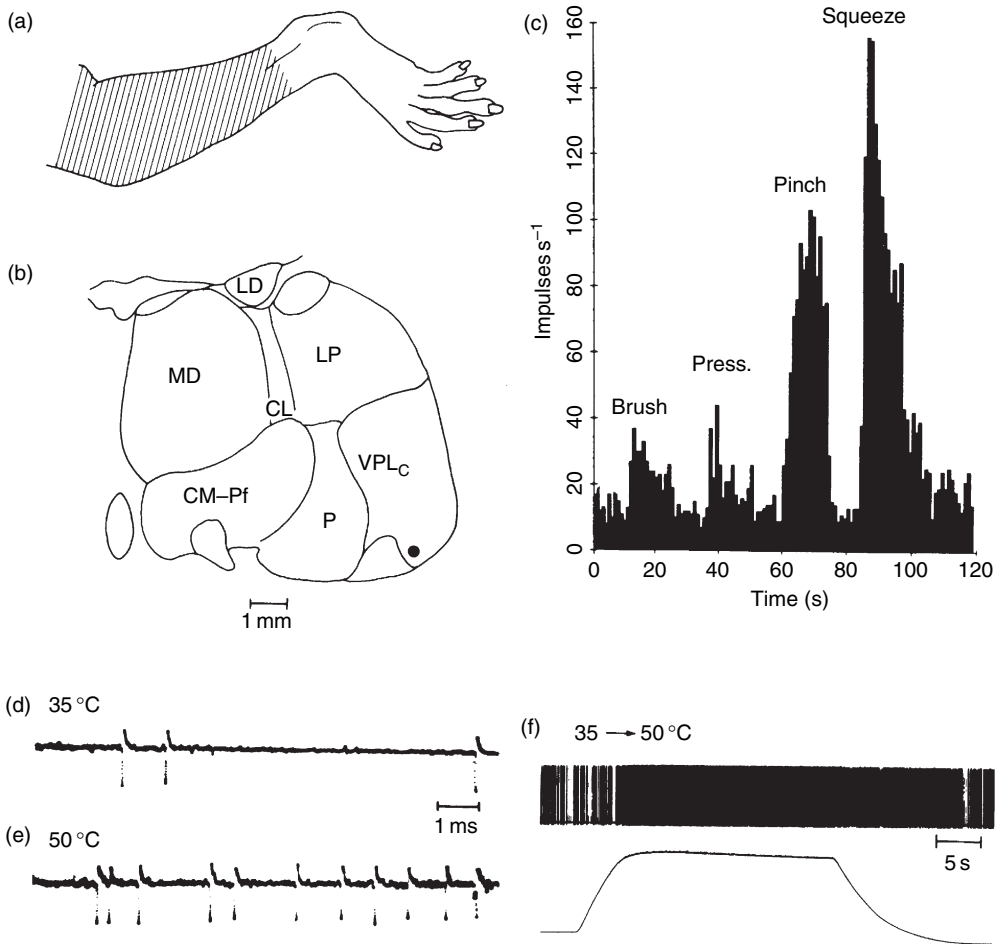

Figure 2 Example of responses of a wide-dynamic-range (WDR) neuron in ventroposterior nuclei (VP). The receptive field on the leg is shown in (a). The location of the recording site in VPLc (VP) is indicated in (b). The histogram (c) shows the responses to graded intensities of mechanical stimulation. This neuron also responded to noxious thermal stimulation (d, e, and f). Modified with kind permission from Kenshalo, D. R., Jr., Giesler, G. J., Jr., Leonard, R. B., and Willis, W. D. 1980. Responses of neurons in primate ventral posterior lateral nucleus to noxious stimuli. J. Neurophysiol. 43, 1594–1614.

5.43.3.2 Ventroposterior Inferior Nucleus

The neurons in the region located immediately inferior (ventral) to VPL and VPM (VPI) project to SII (Krubitzer, L. *et al.*, 1995) and to retroinsular (vestibular) cortex. Some of the neurons in this region are excited by nociceptive inputs (Figure 3). These WDR and NS neurons are arranged in a topographic representation within this region in the monkey (Apkarian, A. V. and Shi, T., 1994).

5.43.3.3 Posterior Thalamus and Posterior Part of the Ventromedial Nucleus

The posterior thalamus has frequently been implicated in pain processing and has been shown in various species to contain nociceptive neurons (Albe-Fessard, D. *et al.*, 1985; Willis, W. D., 1985; Willis, W. D., Jr., 1997). Although it was formerly regarded as undifferentiated, more detailed and recent observations in monkeys and humans have described a distinct nucleus that has been termed VMpo. The VMpo has been shown to be the recipient of a major projection from lamina I STT and TTT neurons. In accordance with its lamina I inputs, it has been shown to contain NS and thermoreceptive neurons (Craig, A. D. *et al.*, 1994). Their responses are similar to those of lamina I STT and TTT neurons, and they have small receptive fields that are topographically organized in a rostrocaudal axis, in correspondence with the topographically organized terminations of the afferent inputs (Figure 4).

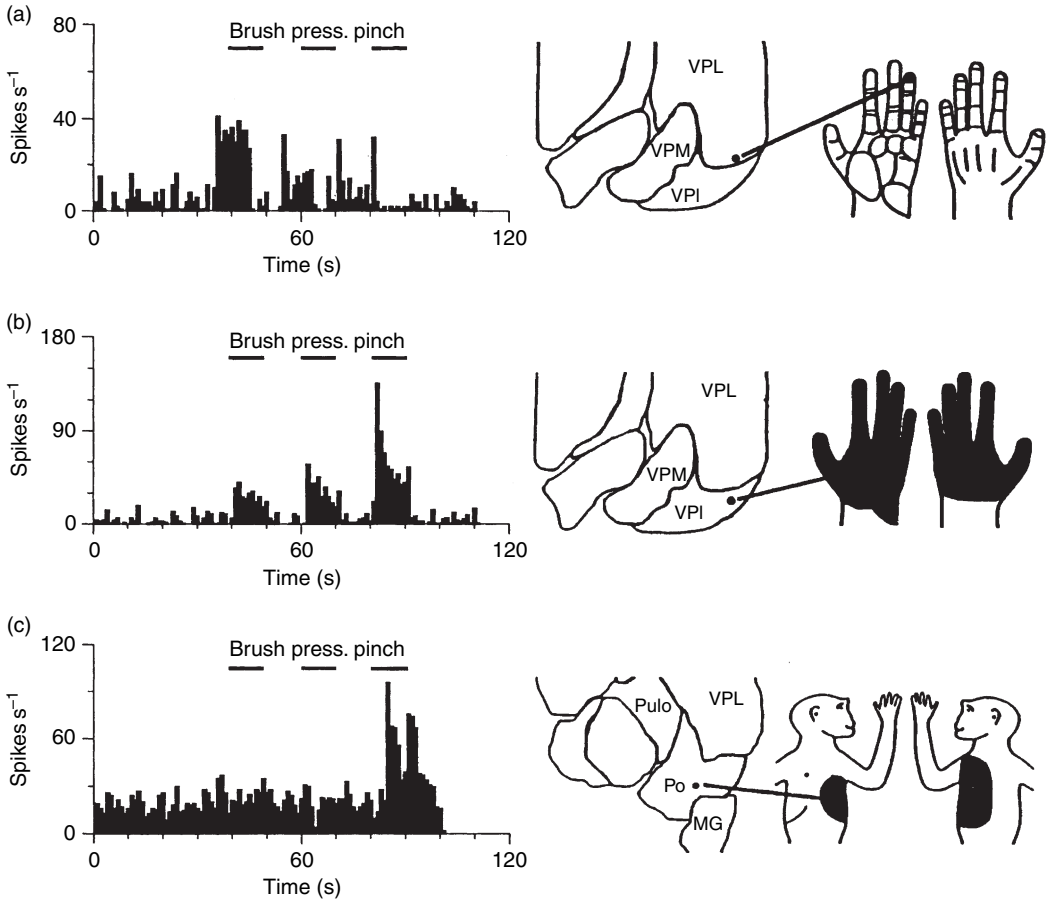

Figure 3 Example of responses of nociceptive neurons in ventroposterior inferior nucleus (VPI) and posterior complex (Po). Reproduced with kind permission from Apkarian, A. V. and Shi, T. 1994. Squirrel monkey lateral thalamus. I. Somatic nociresponsive neurons and their relation to spinothalamic terminals. J. Neurosci. 14, 6779–6795.

Neuronal recordings in awake monkeys in the presumed VMpo (originally assumed to be in VPM but subsequently re-interpreted from the original histology to be in VMpo (Craig, unpublished observations) revealed strong correlation between the neuronal activity and the behavioral detection of noxious and innocuous thermal stimuli applied to the face. Furthermore, lidocaine-induced block of activity in this region reduced the monkey's behavioral responses to these stimuli (Bushnell, M. C. *et al.*, 1993; Duncan, G. H. *et al.*, 1993).

Further support for the critical role of VMpo in relaying nociceptive and thermoreceptive information for perception of pain and temperature is the finding that it has a strong and topographic projection to the dorsal margin of the posterior insula (Craig, A. D., 2003), where preliminary fMRI observations in monkeys show strong activation with noxious stimuli (Craig, A. D., 2002). Furthermore, human imaging studies have consistently found this region of insular cortex to be activated by noxious and thermal stimuli. This rostrocaudally organized topography is distinct from the mediolateral topography observed in SII and in the adjacent parietal operculum (Disbrow, E. *et al.*, 2000). There is also a minor projection from VMpo to area 3a of SI cortex.

Species differences. In the cat and rat where there is no clearly differentiated nociceptive and thermoreceptive relay site in the Po, there are nevertheless nociceptive neurons, but they tend to have very large receptive fields and are not arranged in a clear somatotopic fashion (Poggio, G. F. and Mountcastle, V. B., 1960; Carstens, E. and Yokota, T., 1980). This region does receive some lamina I inputs in the cat. In the rat, there is convergent STT input from laminae I and V to the posterior triangular nucleus, which projects to the region of SII and to the amygdala. It is possible that in the rat, nociceptive inputs also arise

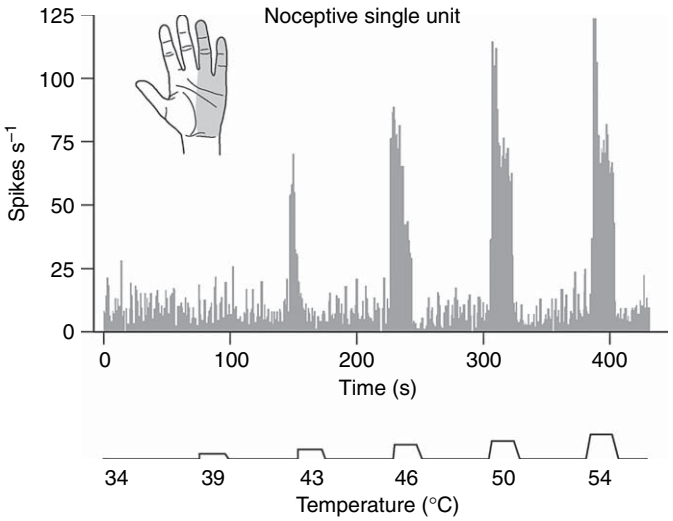

Figure 4 Example of the responses of a posterior part of the ventromedial (VMpo) nociceptive neuron. The histogram shows the graded responses of a single nociceptive-specific neuron to noxious heat pulses applied with a thermode applied to the receptive field on the contralateral ulnar hand. Adapted with kind permission from Craig, A. D., Bushnell, M. C., Zhang, E. -T., and Blomqvist, A. 1994. A thalamic nucleus specific for pain and temperature sensation. Nature 372, 770–773.

via a descending corticothalamic route (Diamond, M. E. *et al.*, 1992; Berkley, K. J. *et al.*, 1993). Furthermore, there is no direct projection to the portion of insular cortex homologous to that targeted by VMpo in the primate. The part of Po dorsal to VP in the cat, where some nociceptive neurons have been reported (Hutchison, W. D. *et al.*, 1992; Bruggemann, J. *et al.*, 1994), projects to area 5a (Jones, E. G., 1985). Nevertheless, in both the cat and the rat, there exists a narrow region along the ventral aspect of VMb that contains nociceptive and viscerоceptive neurons and projects to the insular cortex adjacent to the gustatory cortex (Yasui, Y. *et al.*, 1991; Clasca, F. *et al.*, 1997; Norrsell, U. and Craig, A. D., 1999).

5.43.3.4 Intralaminar Nuclei

As described earlier, several regions in medial thalamus receive direct inputs from the spinal cord and the trigeminal nucleus, but there are also indirect inputs to these regions from the brainstem, and in particular from the PB.

Neurons responding to noxious electrical, mechanical, or heat stimuli have been recorded throughout the intralaminar thalamus, in particular in CL and CM–Pf. Most of these recordings have been obtained in anesthetized rats and cats although some recordings have been performed in monkeys (Albe-Fessard, D. *et al.*, 1985; Bushnell, M. C. *et al.*, 1993; Bruggemann, J. *et al.*, 1994). Most of the nociceptive neurons in this region have large receptive fields that can be bilateral. Studies employing graded natural stimuli have revealed that some of the cells can code for stimulus intensity. Although natural stimulation was used in only some studies, cells with graded responses to noxious heat have been observed. In particular, a study in the awake monkey by Bushnell M. C. and Duncan G. H. (1989) reported the existence of nociceptive neurons in the CM–Pf and CL region that responded in a graded fashion to noxious thermal stimuli applied to the face (Figure 5). It is possible that the responses of at least some of these neurons may be related to attention and arousal rather than to perception of pain. It is interesting that many intralaminar neurons have been shown to respond to eye movements (Schlag, J. and Schlag-Rey, M., 1986), which is consistent with the termination of ascending inputs from the cerebellum and the superior colliculus. Indeed, it has been proposed that this region plays a role in gaze orientation (Jones, E. G., 1985).

5.43.3.5 Medial Dorsal Nucleus

As mentioned earlier, Craig and colleagues have recently described a direct lamina I input to the MDvc in the monkey. A particular interesting feature of this projection is that the MDvc contains neurons that project to the anterior cingulate cortex (Craig, A. D. and Zhang, E.-T., 1996), a region

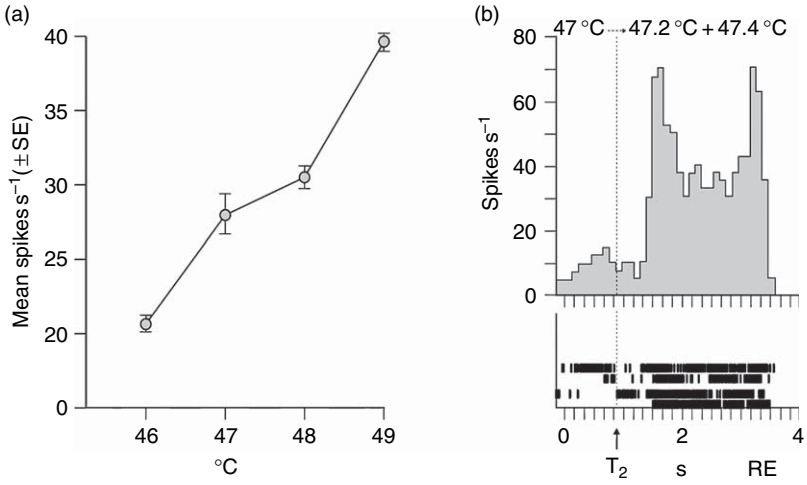

Figure 5 Responses of a neuron in posteromedial thalamus of an awake monkey to noxious thermal stimuli to the face. (a) The mean firing rate to increasing temperatures. (b) A peristimulus histogram with associated dot raster display showing increased firing when the temperature increased from 47 °C to 47.2 °C or 47.4 °C. In this particular example, the monkey did not respond until the end of the trial (RE button release). Adapted with kind permission from Bushnell, M. C. and Duncan, G. H. 1989. Sensory and affective aspects of pain perception: is medial thalamus restricted to emotional issues. Exp. Brain Res. 78, 415–418.

frequently implicated in pain. There is only very limited information regarding the properties of the neurons in MDvc; however, preliminary studies in anesthetized monkeys indicate that it contains a discrete group of NS neurons with large, sometimes bilateral receptive fields (Craig, A. D., 2003). Furthermore, this study reports that their spontaneous firing can be inhibited by innocuous thermal (cool, warm) stimuli. This phenomenon could provide an explanation for the well-known cold-induced inhibition of pain and the thermal grill illusion of pain (see below). It is possible that some of the recordings of nociceptive neurons in medial thalamus in the study of Bushnell M. C. and Duncan G. H. (1989) mentioned above may also have included neurons located in MDvc.

Species differences. Whereas in the monkey (and presumably the human), the STT and the TTT project to MDvc, in the cat and the rat, there is a projection that originates mainly in lamina I to the developmentally related Sm. Several studies have reported the existence of NS neurons in Sm in the rat (Dostrovsky, J. O. and Guilbaud, G., 1988; Coffield, J. A. and Miletic, V., 1993; Kawakita, K. *et al.*, 1993). Receptive fields are generally quite large and some have inputs from deep tissues. In the Freund's adjuvant-induced arthritic rat, many Sm cells were found to respond to joint movements, which are normally not effective in activating the Sm neurons (Dostrovsky, J. O. and Guilbaud, G., 1988). Various studies in the rat that have examined the effects of lesioning or electrically and chemically induced excitation of Sm have provided evidence for a role of Sm and its cortical target VLO in the activation of descending antinociceptive pathways by way of the periaqueductal gray (PAG) (Roberts, V. J. and Dong, W. K., 1994; Zhang, S. *et al.*, 1998). Although it has been shown in the cat that there is also a projection from innocuous thermoreceptive cool lamina I STT neurons in addition to the NS neurons (Craig, A. D. and Dostrovsky, J. O., 2001), neurons excited by cooling stimuli have not been found. It is possible, however, that inputs from these neurons may provide a basis for the cold-induced inhibition of nociceptive processing, similar to MDvc of the primate (Ericson, A. C. *et al.*, 1996).

5.43.4 Direct Physiological Evidence in Humans

Functional stereotactic surgery for the treatment of chronic pain or tremor provides a unique opportunity to record and stimulate in the thalamus of awake patients. There have been several studies that have provided information of interest in terms of furthering our understanding of the role of thalamus in pain and these are described below.

5.43.4.1 Nociceptive Neurons

Lenz and colleagues have searched for neurons in VP (often termed Vc in humans) and the immediately adjacent posterior and inferior region of thalamus. Although most of the neurons in Vc respond only to nonnoxious mechanical stimulation of the skin (LTM neurons), they reported that some neurons also had an increased response to noxious mechanical stimuli and some responded weakly to noxious or innocuous thermal stimuli in addition to innocuous tactile stimuli (i.e., WDR neurons) (for review, see Lenz, F. A. and Dougherty, P. M., 1997; Lee J. *et al.*, 1999). These WDR neurons were primarily located in the posteroinferior portion of VP. In the adjoining posteroinferior area, which includes VMpo (Blomqvist, A. *et al.*, 2000), they found NS neurons that responded to noxious heat but no LTM neurons (Lenz, F. A. *et al.*, 1993a). Although nociceptive neurons have frequently been reported in medial thalamus of anesthetized animals, there have only been a few old reports of neurons responding to noxious stimuli in awake human medial thalamus. It is difficult to evaluate these old reports since few details were provided and more recent studies have not been able to confirm the findings (Lenz, F. A. *et al.*, 1997). However, there have been very few opportunities to record from neurons in medial thalamus, and the number of neurons that can be tested with noxious stimuli in the awake patient is limited, and this may account for the lack of definitive evidence.

5.43.4.2 Innocuous Cooling-Responsive Neurons

Neurons responding selectively to innocuous cooling of the skin have been found in the human thalamic region located medial and posteroinferior to VP, which likely corresponds to VMpo (Davis, K. D. *et al.*, 1999). These neurons had discrete receptive fields on the contralateral body and responses similar to those of lamina I spinal and trigeminal neurons (Figure 6(a)). This finding is consistent with the findings in animals, where cooling-specific neurons have only been found

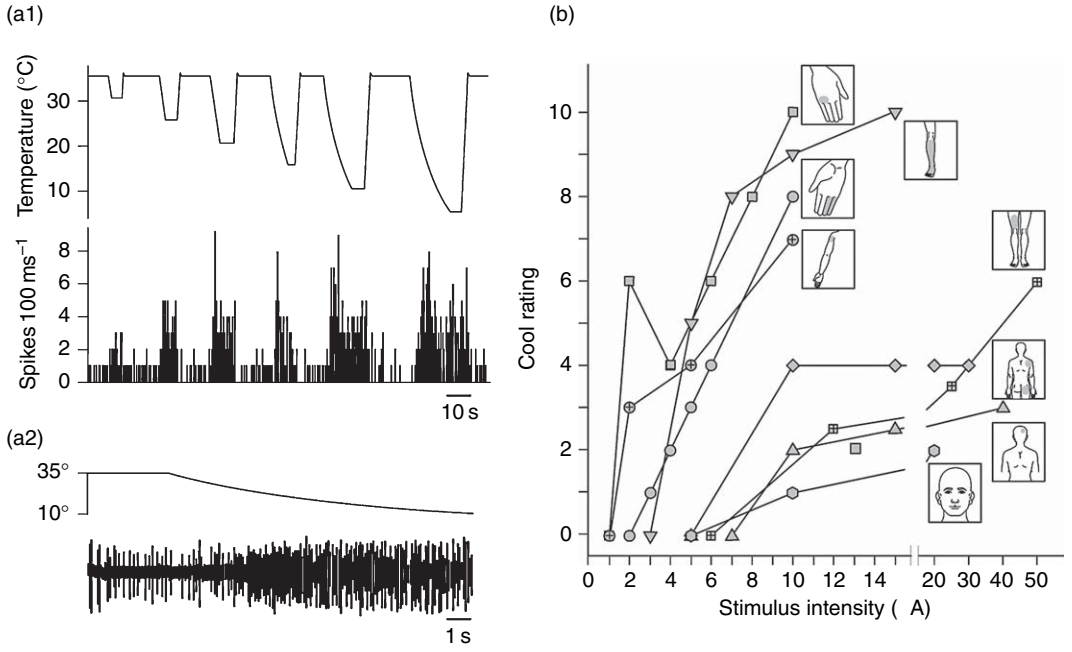

Figure 6 (a1) Recording from a single neuron in the presumed posterior ventromedial nucleus (VMpo) region in an awake patient showing responses to cooling stimuli applied to receptive field on the fifth digit. The top trace shows the temperature of the thermode with increasing cooling steps. The bottom trace is a histogram of the neuronal firing showing graded responses to the increasing cooling steps. (a2) Segment of raw trace of neuronal recording from (a1) showing response to first part of a cooling step. (b) Thalamic stimulation evoked cool sensations. Verbal ratings (0–10 scale) of the innocuous cool sensations evoked by threshold and suprathreshold intensities of thalamic microstimulation obtained in eight patients. Figurines adjacent to each line depict the location of the thalamic stimulation-evoked sensation at threshold. Reprinted with kind permission from Davis, K. D., Lozano, R. M., Manduch, M., Tasker, R. R., Kiss, Z. H., and Dostrovsky, J. O. 1999. Thalamic relay site for cold perception in humans. J. Neurophysiol. 81, 1970–1973.

in the cat medial VPM and in the monkey VMpo. Animal studies have also shown that cooling-specific neurons are found only in lamina I of the trigeminal medullary dorsal horn (nucleus caudalis) and spinal dorsal horn. Thus, the existence of cooling-specific neurons in the human VMpo is consistent with the evidence cited above that this region receives a major input from lamina I neurons. The close association of pain and temperature further supports an important role of VMpo in the relay of pain signals in the human.

5.43.4.3 Stimulation-Induced Pain and Temperature Sensations

The electrophysiological studies in human patients during stereotactic surgery provide a unique opportunity to determine the sensations evoked by electrical stimulation within the brain, since these are performed with the patient awake. As might be expected, electrical stimulation (1 s trains of 100–300 Hz) within VP and adjacent regions of the thalamus usually evokes innocuous paresthesia. These sensations, which can be elicited by low stimulus intensities (e.g., 2 μA), are perceived as originating from a small region of the contralateral side of the body (Figure 7). The projected fields are usually in register with the receptive fields of the neurons recorded at the stimulation site. Increasing the intensity of stimulation results in an increase in the perceived intensity of sensation and usually also with an increase in the projected field size, but although the sensation can be very

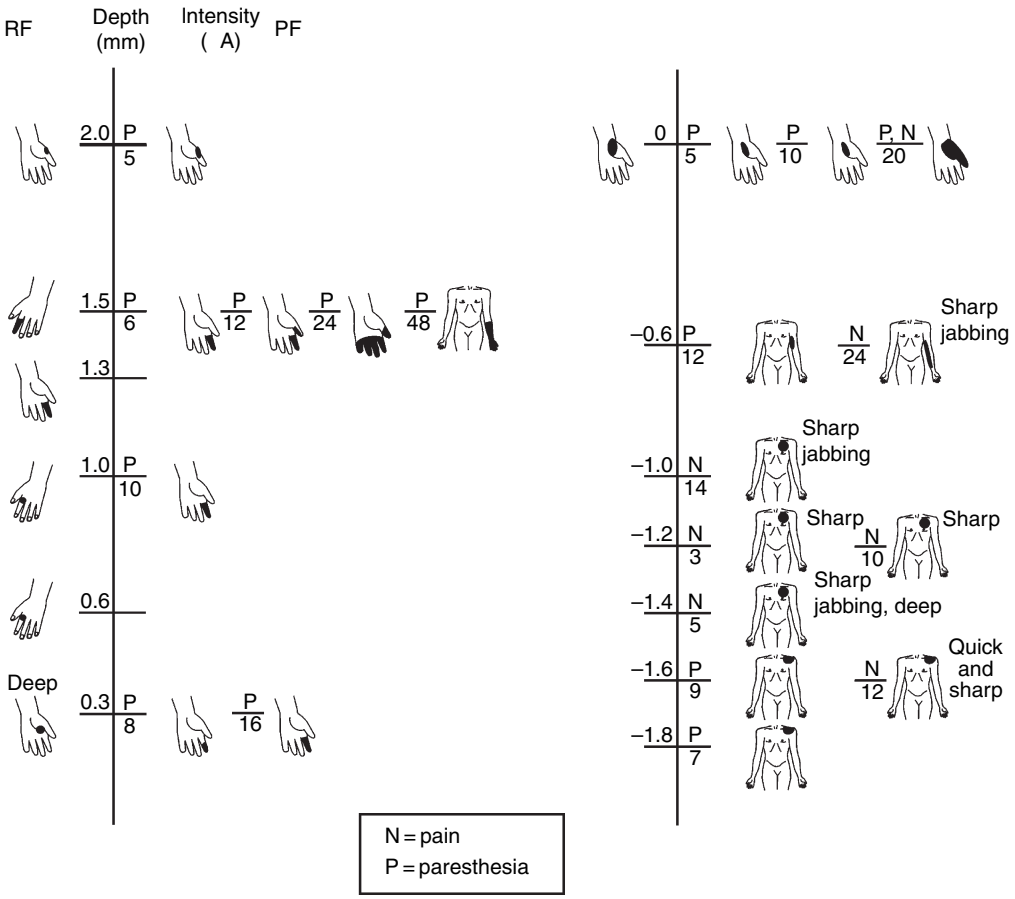

Figure 7 Stimulation-evoked pain in a chronic pain patient (causalgia left arm). The diagram shows a reconstruction of an electrode track through the ventrocaudal nucleus and on into the posteroinferior region, showing the locations of the receptive fields (RF) of the low-threshold mechanoreceptive neurons recorded at sites along the electrode track on the left of the vertical line and the projected fields (PF) induced by stimulation on the right side. The electrode track has been broken down into two contiguous segments. Depths of recordings are indicated in millimeters to the left of the line at each recording/stimulation site. While the electrode was in ventrocaudal nucleus (Vc), as evidenced by the low-threshold mechanoreceptive fields, stimulation induced nonpainful paresthesia (P). However, at the bottom of the Vc (0) and at deeper sites, stimulation induced painful sensations (N).

intense, it is not usually reported as painful. Nevertheless, stimulation at some sites in some patients is reported as eliciting a distinct painful and/or temperature sensation even at the threshold for sensation (Hassler, R. and Riechert, T., 1959; Halliday, A. M. and Logue, V., 1972; Tasker, R. R., 1984; Lenz, F. A. *et al*., 1993b; Davis, K. D. *et al*., 1996; Dostrovsky, J. O. *et al*., 2000). These sites are generally located near the posterior–inferior border of VP and extend several millimeters posterior, inferior, and medial to it (Figure 7). The incidence of sites where pain and/or thermal sensations can be evoked is much higher in the posteroinferior region than within VP (except in poststroke pain patients – see below). The sensations are always on the contralateral side of the body and can arise from a small region. The sensations are reported as being quite natural in contrast to the paresthesia (tingling or shock-like) sensations evoked within VP. There have been reports of cases where thalamic stimulation evoked pain arising from deep or visceral sites although these are rare (Lenz, F. A. *et al*., 1994; Davis, K. D. *et al*., 1995). Interestingly, Lenz and colleagues found that microstimulation within VP at sites where WDR neurons responding to noxious mechanical stimuli were found rarely elicited pain or temperature sensations, whereas at the sites in the region posteroinferior to VP where stimulation evoked pain, there was a high likelihood of finding nociceptive neurons (Lenz, F. A. and Dougherty, P. M., 1997). It seems likely that the sites in the region posteroinferior to VP where stimulation evokes pain and temperature are close to or in VMpo. It is also notable that at the sites where neurons responding selectively to cooling stimuli were found, microstimulation evoked cooling sensations arising from the same area of skin where the receptive fields of the neurons were located (Figure 6(b)). Increasing the stimulus intensity at such sites increased the intensity of the cold sensation (i.e., it felt colder).

There have been few studies of the effects of stimulation in medial thalamus. A few studies reported that stimulation in the posterior aspect of medial thalamus can evoke pain (Sano, K., 1979; Jeanmonod, D. *et al*., 1994). However, in most cases the stimuli were delivered from large-tipped electrodes and the sensations were only elicited at high current intensities, so current spread (e.g., to the STT) is an issue. Several more recent studies have failed to replicate these findings.

5.43.5 The Thalamus and Central Neuropathic Pain

5.43.5.1 Physiological Observations in Central Pain Patients

There have been many studies that have demonstrated the marked plasticity of the brain and in particular the alterations in neuronal properties and somatotopic organization at all levels of the somatosensory system subsequent to peripheral or central damage to the ascending pathways (Wall, J. T. *et al*., 2002). Although much less is known about the plasticity of the pain system, especially at the thalamic and cortical levels, it is reasonable to expect that marked changes will occur following damage to ascending nociceptive pathways. Indeed, there have been several animal studies that examined the effects of STT damage on thalamic physiology (Weng, H. R. *et al*., 2000; 2003). Studies in patients who have sustained deafferentation due, for example, to amputation or spinal cord injury provide evidence for plasticity (Lenz, F. A. *et al*., 1994; Davis, K. D. *et al*., 1998). For example, there is evidence suggesting expansion of the representation of intact regions into deafferented regions of VP thalamus. Micro-stimulation in such regions was found to evoke sensations arising from the phantom limb in amputees or to the deafferented body region in spinal injury patients (Lenz, F. A. *et al*., 1994; Davis, K. D. *et al*., 1998). Although these stimuli usually resulted in nonpainful paresthesia rather than pain, these types of changes may be involved in the development of chronic pain in these types of patients. Of particular interest have been the findings of two studies that found changes in the stimulation-evoked sensations in poststroke pain and some other types of chronic central pain patients. The incidence of stimulation sites in VP where stimulation evoked sensations in such patients was markedly elevated (Lenz, F. A. *et al*., 1998; Dostrovsky, J. O. *et al*., 2000). In addition, there was an increase in the number of sites in the posteroinferior region where pain sensations were evoked and a decrease in sites where innocuous thermal stimuli were evoked (Figure 8). These findings provide further evidence suggesting that there have been alterations in the thalamic and cortical processing of somatosensory inputs leading to increased perception of pain. It is interesting, however, that deep brain stimulation within thalamus (Siegfried, J., 1987; Kupers, R. C. and Gybels, J. M., 1993) can alleviate the pain in some of these chronic pain patients, possibly by disrupting the pathological patterns and balance of activity in these regions.

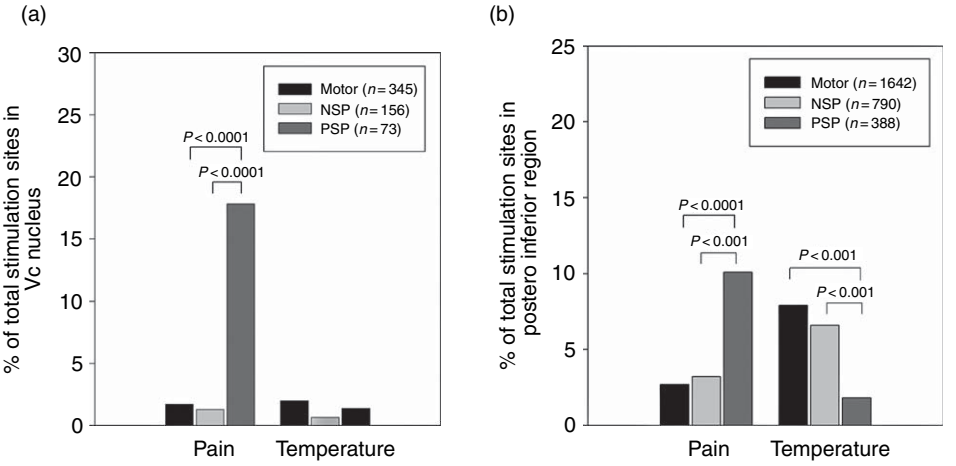

Figure 8 Bar graphs showing the incidence of sites in the ventrocaudal nucleus (a) and the posteroinferior region (b) where stimulation evoked sensations of pain or innocuous temperature in movement disorder patients (Motor), chronic nonpoststroke pain patients (NSP), and poststroke pain patients (PSP). Reprinted with kind permission from Dostrovsky, J. O., Manduch, M., Davis, K. D., Tasker, R. R., Lozano, A. M. 2000. Thalamic Stimulation-Evoked Pain and Temperature Sites in Pain and Non-pain Patients. In: Proceedings of the 9th World Congress on Pain (*eds*. M. Devor, M. C. Rowbotham, and Z. Wiesenfeld-Hallin), pp. 419–425. IASP Press.

5.43.5.2 Thalamic Bursting Activity

Thalamic neurons switch to a bursting mode when they are hyperpolarized. This bursting activity is generated by activation of low-threshold T-type calcium channels that give rise to a calcium spike and a burst of sodium channel-generated action potentials (so-called LTS bursting). This bursting activity is generally only observed during sleep. However, recordings in medial and lateral thalamus of chronic pain patients during the awake state revealed the existence of neurons firing in typical calcium spike-mediated bursts (Lenz, F. A. *et al*., 1989; Jeanmonod, D. *et al*., 1993; Lenz, F. A. *et al*., 1994). It was proposed that this activity may be related to the patients' chronic pain and in fact may mediate the spontaneous pain in these patients (Lenz, F. A. and Dougherty, P. M., 1997; Llinas, R. R. *et al*., 1999). However, similar LTS firing in similar regions of thalamus can also be observed in patients without pain and thus is not specific to pain (Jeanmonod, D. *et al*., 1996; Radhakrishnan, V. *et al*., 1999). More recently, Llinas R. R. *et al*. (1999) have proposed that LTS bursting in thalamus may be the cause of many different neurological diseases including chronic pain and have termed this condition thalamic dysrhythmia. Nevertheless, the role of LTS bursting in chronic central pain remains unclear.

It has been proposed that central neuropathic pain may be mediated by reduced GABAergic inhibition in the thalamus (Roberts, V. J. and Dong, W. K., 1994). Studies in the primate have found that following chronic cervical rhizotomy there is a downregulation of thalamic $GABA_A$ receptors (Rausell, E. *et al*., 1992), providing some support for this suggestion. On the other hand, several positron emission tomography (PET) studies have obtained evidence suggesting that chronic neuropathic pain is associated with decreased blood flow, suggesting decreased activity (Apkarian, A. V. *et al*., 2005).

5.43.5.3 Effects of Thalamic Lesions on Pain

There have been many studies since the original pioneering studies of Dejerine and Roussy and Head and Holmes which have documented that strokes affecting the lateral thalamus can lead to central pain (poststroke pain and thalamic pain syndrome) (Pagni, C. A., 1998). In addition, infarcts and lesions that involve the posteroinferior region can also result in analgesia and thermanesthesia (Head, H. and Holmes, G., 1911; Hassler, R. and Riechert, T., 1959; Hassler, R., 1970; Tasker, R. R., 1984). Lesions have been purposefully made in medial thalamus of chronic pain patients for relief of their pain (Gybels, J. M. and Sweet, W. H., 1989). However, such procedures are rarely undertaken at the present time as most neurosurgeons do not believe that they are effective. It is possible, however, that in some of

the reported successes the lesions may have included MDvc and/or VMpo (Jeanmonod, D. *et al.*, 1994; Lenz, F. A. and Dougherty, P. M., 1997). Interestingly, lesions in medial thalamus that spare the lateral thalamus and STT do not appear to cause central pain (Bogousslavsky, J. *et al.*, 1988).

5.43.5.4 The Thalamic Pain Syndrome

The poststroke central (thalamic) pain (CPSP) syndrome was first recognized by Dejerine and Roussy, and it has been comprehensively analyzed clinically by Head H. and Holmes G. (1911), Riddoch G. and Critchley Mc. D. (1937), Schott B. *et al.* (1986), Boivie J. (1994), Pagni C. A. (1998), and others. The first patients had lesions confined to the thalamus, and so the syndrome was first called thalamic pain. However, patients with central pain have lesions that interrupt the ascending lateral STT – lamina I – spinothalamocortical pathway by way of VMpo to the dorsal posterior insula at any level (Schmahmann, J. D. and Leifer, D., 1992; Pagni, C. A., 1998; Craig, A. D., 2003). Such lesions produce loss of pain and temperature sensation, but in about half of such cases, this disruption results, immediately or after a variable delay, in the paradoxical appearance of ongoing pain in the deafferented region. Head and Holmes inferred that this meant that pain sensation occurred in the thalamus, but we now know that the thalamus serves mainly as a relay for activity ascending to the cortex. This syndrome likely results from disruption of the interactions at cortical and subcortical levels between components of the pain processing network. One such interaction is the inhibition caused by cooling on pain, and it has been suggested that interruption of this interaction could cause central pain by disinhibition (Craig, A. D., 1998). The suggestion is based on similarities with the thermal grill illusion of pain, in which reduced activity in cooling-specific lamina I STT neurons can unmask the cold-activated burning pain elicited by polymodal nociceptive lamina I STT neurons (HPC) in the anterior cingulate cortex. A study of thermal sensation in a central pain patient directly supports that hypothesis (Morin, C. *et al.*, 2002). A recent imaging study of a central pain patient suggested that the posterolateral thalamic lesion did not involve VMpo but that conclusion was incompatible with the patient's loss of thermal sensation (cf. Craig, A. D. *et al.*, 2000; Montes, C. *et al.*, 2005). The indirect ascending nociceptive input to the medial thalamus by way of the PB may also play a role in central pain.

5.43.6 Pharmacology

The pharmacology of thalamic nociceptive neurons has not been extensively studied. However, it is reasonable to assume that they share many common features with those of other thalamic neurons about which much more is known. The two most important transmitters are glutamate and GABA (McCormick, D. A., 1992; Steriade, M. *et al.*, 1997; Sherman, S. M. and Guillery, R. W., 2001). Glutamate is released by the ascending axons of medial lemniscal and STT and TTT pathways to excite thalamocortical neurons. The released glutamate acts at both NMDA and non-NMDA (AMPA and/or kainate) ionotropic glutamate receptors. In the cat and primate, there are also many interneurons within the thalamus and these also receive glutamatergic inputs from these afferents that activate in addition to the ionotropic receptors and metabotropic glutamate receptors (Jones, E. G., 1985; Magnusson, K. R. *et al.*, 1987; Ericson, A. C. *et al.*, 1995; Blomqvist, A. *et al.*, 1996; Sherman, S. M. and Guillery, R. W., 2001). The thalamocortical neurons also receive a massive glutamatergic projection from layer 6 of the cortex, which activates both ionotropic and metabotropic receptors (Rustioni, A. *et al.*, 1983; Jones, E. G., 1987; Deschenes, M. and Hu, B., 1990; Eaton, S. A. and Salt, T. E., 1990; 1996; Salt, T. E. and Eaton, S. A., 1996). The thalamocortical neurons release glutamate at their cortical terminals (Kharazia, V. N. and Weinberg, R. J., 1994; Pirot, S. *et al.*, 1994).

GABA is the major inhibitory neurotransmitter in the thalamus, and the major source of these inputs is from the thalamic reticular nucleus (TRN). The TRN GABAergic neurons are topographically organized and receive excitatory inputs from collaterals of thalamocortical and corticothalamic neurons. In cats and primates, but not rats, there are also GABAergic interneurons within the thalamus (Houser, C. R. *et al.*, 1980; Rustioni, A. *et al.*, 1983; Jones, E. G., 1985; Steriade, M. *et al.*, 1997). The TRN produces both short- and long-latency inhibitory responses; the short-latency IPSPs are mediated by $GABA_A$ receptors, whereas the long-latency responses are mediated by the $GABA_B$ metabotropic receptors (Lee, S. M. *et al.*, 1994). Interestingly, activation of presynaptic glutamate metabotropic receptors reduces the release of GABA from the TRN receptors (Salt, T. E. and Eaton, S. A., 1995). Most of the studies of thalamic GABAergic

mechanisms have involved nonnociceptive neurons; however, studies in Pf have shown that thalamic nociceptive neurons receive inhibitory inputs from the TRN and are inhibited by GABA (Reyes-Vazquez, C. and Dafny, N., 1983; Jia, H. *et al.*, 2004), and microinjection of the $GABA_A$ antagonist bicuculline or agonist muscimol into Sm enhanced or depressed, respectively, the antinociception induced by the prior microinjection of morphine into the rat Sm (Jia, H. *et al.*, 2004). There is also recent evidence for modulation of $GABA_B$ receptors in VP and Po by noxious inputs (inflammation) (Ferreira-Gomes, J. *et al.*, 2004).

The thalamic relay neurons as well as the TRN and inhibitory interneurons also receive projections from serotoninergic neurons in the dorsal raphe nucleus, and norardrenergic and cholinergic neurons in the peribrachial region (see reviews by McCormick, D. A., 1992; Steriade, M. *et al.*, 1997). Their role in nociception is, however, unclear. There have been recent studies in the rat that have demonstrated an involvement of serotoninergic mechanisms in modulation of transmission through the Sm, and these may play a role in a pain modulatory system proposed to relay in Sm (Xiao, D. Q. *et al.*, 2005). There is also evidence that 5HT modulates nociceptive processing in the rat Pf (Harte, S. E. *et al.*, 2005). Several neuropeptides have also been identified in thalamic afferents and neurons. For example, tachykinins, cholecystokinin, and enkephalins have been identified in spinothalamic fibers ending in the rat and human thalamus and are presumably coreleased with glutamate, but their function is not known (Coffield, J. A. and Miletic, V., 1987; Gall, C. *et al.*, 1987; Hirai, T. and Jones, E. G., 1989; Battaglia, G. *et al.*, 1992; Nishiyama, K. *et al.*, 1995).

It is usually assumed that the analgesia produced by opiates results from an action at the spinal and brainstem levels. However, there is increasing evidence for a role of opioids also at thalamic and cortical levels, and thus, a direct depressant effect of opioids on thalamic and cortical nociceptive neurons may contribute to the opioid-induced analgesia. Opioid receptors and enkephalinergic terminals have been identified in the thalamus (Mansour, A. *et al.*, 1987; Miletic, V. and Coffield, J. A., 1988). Systemic morphine inhibits thalamic nociceptive neurons (e.g., Benoist, J. M. *et al.*, 1983), but this does not prove that effect is due to an action at the thalamic level. However, there have been studies that have shown that local application of opioid agents can depress the responses of thalamic nociceptive neurons (He, L. F. *et al.*, 1991; Coffield, J. A. and Miletic, V., 1993) and produce antinociception when microinjected into Sm (Yang, Z. J. *et al.*, 2002). Furthermore, the use of radiolabeled μ-opioid agonists with PET has shown high opiate receptor levels in the human thalamus (see review in Apkarian, A. V. *et al.*, 2005), and evidence for their involvement in endogenous pain modulation.

References

Al-Chaer, E. D., Feng, Y., and Willis, W. D. 1998. A role for the dorsal column in nociceptive visceral input into the thalamus of primates. J. Neurophysiol. 79, 3143–3150.

Albe-Fessard, D., Berkley, K. J., Kruger, L., Ralston, H. J., III, and Willis, W. D., Jr. 1985. Diencephalic mechanisms of pain sensation. Brain Res. 356, 217–296.

Apkarian, A. V. and Shi, T. 1994. Squirrel monkey lateral thalamus. I. Somatic nociresponsive neurons and their relation to spinothalamic terminals. J. Neurosci. 14, 6779–6795.

Apkarian, A. V., Bushnell, M. C., Treede, R. D., and Zubieta, J. K. 2005. Human brain mechanisms of pain perception and regulation in health and disease. Eur. J. Pain 9, 463–484.

Applebaum, A. E., Leonard, R. B., Kenshalo, D. R., Jr., Martin, R. F., and Willis, W. D. 1979. Nuclei in which functionally identified spinothalamic tract neurons terminate. J. Comp. Neurol. 188, 575–585.

Battaglia, G., Spreafico, R., and Rustioni, A. 1992. Substance P innervation of the rat and cat thalamus. I. Distribution and relation to ascending spinal pathways. J. Comp. Neurol. 315, 457–472.

Beggs, J., Jordan, S., Ericson, A. C., Blomqvist, A., and Craig, A. D. 2003. Synaptology of trigemino- and spinothalamic lamina I terminations in the posterior ventral medial nucleus of the macaque. J. Comp. Neurol. 459, 334–354.

Benoist, J. M., Kayser, V., Gautron, M., and Guilbaud, G. 1983. Low dose of morphine strongly depresses responses of specific nociceptive neurones in the ventrobasal complex of the rat. Pain 15, 333–344.

Berkley, K. J. 1980. Spatial relationships between the terminations of somatic sensory and motor pathways in the rostral brainstem of cats and monkeys. I. Ascending somatic sensory inputs to lateral diencephalon. J. Comp. Neurol. 193, 283–317.

Berkley, K. J., Budell, R. J., Blomqvist, A., and Bull, M. 1986. Output systems of the dorsal column nuclei in the cat. Brain Res. Bull. 11, 199–225.

Berkley, K. J., Guilbaud, G., Benoist, J. M., and Gautron, M. 1993. Responses of neurons in and near the thalamic ventrobasal complex of the rat to stimulation of uterus, cervix, vagina, colon, and skin. J. Neurophysiol. 69, 557–568.

Bernard, J. F. and Besson, J. M. 1990. The spino(trigemino)pontoamygdaloid pathway: electrophysiological evidence for an involvement in pain processes. J. Neurophysiol. 63, 473–490.

Blomqvist, A. and Berkley, K. J. 1992. A re-examination of the spino-reticulo-diencephalic pathway in the cat. Brain Res. 579, 17–31.

Blomqvist, A., Ericson, A. C., Craig, A. D., and Broman, J. 1996. Evidence for glutamate as a neurotransmitter in spinothalamic tract terminals in the posterior region of owl monkeys. Exp. Brain Res. 108, 33–44.

Blomqvist, A., Zhang, E. T., and Craig, A. D. 2000. Cytoarchitectonic and immunohistochemical characterization of a specific pain and temperature relay, the posterior portion of the ventral medial nucleus, in the human thalamus. Brain 123 (Pt 3), 601–619.

Bogousslavsky, J., Regli, F., and Uske, A. 1988. Thalamic infarcts: clinical syndromes, etiology, and prognosis. Neurology 38, 837–848.

Boivie, J. 1979. An anatomical reinvestigation of the termination of the spinothalamic tract in the monkey. J. Comp. Neurol. 186, 343–370.

Boivie, J. 1983. Anatomic and Physiologic Features of the Spino-cervico-thalamic Pathway. In: Somatosensory Integration in the Thalamus (*eds*. G. Macchi, A. Rustioni, and R. Spreafico), pp. 63–106. Elsevier.

Boivie, J. 1994. Central Pain. In: Texbook of Pain (*ed*. P. D. Wall), pp. 871–902. Churchill Livingstone.

Brodal, A. 1982. Neurological Anatomy. Oxford.

Bruggemann, J., Vahle-Hinz, C., and Kniffki, K. D. 1994. Projections from the pelvic nerve to the periphery of the cat's thalamic ventral posterolateral nucleus and adjacent regions of the posterior complex. J. Neurophysiol. 72, 2237–2245.

Bushnell, M. C. and Duncan, G. H. 1989. Sensory and affective aspects of pain perception: is medial thalamus restricted to emotional issues. Exp. Brain Res. 78, 415–418.

Bushnell, M. C., Duncan, G. H., and Tremblay, N. 1993. Thalamic VPM nucleus in the behaving monkey. I. Multimodal and discriminative properties of thermosensitive neurons. J. Neurophysiol. 69, 739–752.

Carstens, E. and Yokota, T. 1980. Viscerosomatic convergence and responses to intestinal distension of neurons at the junction of midbrain and posterior thalamus in the cat. Exp. Neurol. 70, 392–402.

Casey, K. L. and Morrow, T. J. 1983. Ventral posterior thalamic neurons differentially responsive to noxious stimulation of the awake monkey. Science 221, 675–677.

Chandler, M. J., Hobbs, S. F., Fu, Q. G., Kenshalo, D. R., Jr., Blair, R. W., and Foreman, R. D. 1992. Responses of neurons in ventroposterolateral nucleus of primate thalamus to urinary bladder distension. Brain Res. 571, 26–34.

Clasca, F., Llamas, A., and Reinoso-Suarez, F. 1997. Insular cortex and neighboring fields in the cat: a redefinition based on cortical microarchitecture and connections with the thalamus. J. Comp. Neurol. 384, 456–482.

Coffield, J. A. and Miletic, V. 1987. Immunoreactive enkephalin is contained within some trigeminal and spinal neurons projecting to the rat medial thalamus. Brain Res. 425, 380–383.

Coffield, J. A. and Miletic, V. 1993. Responses of rat nucleus submedius neurons to enkephalins applied with micropressure. Brain Res. 630, 252–261.

Coffield, J. A., Bowen, K. K., and Miletic, V. 1992. Retrograde tracing of projections between the nucleus submedius, the ventrolateral orbital cortex, and the midbrain in the rat. J. Comp. Neurol. 321, 488–499.

Craig, A. D. 1998. A new version of the thalamic disinhibition hypothesis of central pain. Pain Forum 7, 1–14.

Craig, A. D. 2002. New and Old Thoughts on the Mechanisms of Pain Following Spinal Cord Injury. In: Spinal Cord Injury Pain: Assessment, Mechanisms, and Treatment (*eds*. R. P. Yezierski and K. J. Burchiel), pp. 237–261. IASP Press.

Craig, A. D. 2003. Pain mechanisms: labeled lines versus convergence in central processing. Annu. Rev. Neurosci. 26, 1–30.

Craig, A. D. 2004. Distribution of trigeminothalamic and spinothalamic lamina I terminations in the macaque monkey. J. Comp. Neurol. 477, 119–148.

Craig, A. D. and Burton, H. 1985. The distribution and topographical organization in the thalamus of anterogradely-transported horseradish peroxidase after spinal injections in cat and raccoon. Exp. Brain Res. 58, 227–254.

Craig, A. D., Chen, K., Bandy, D., and Reiman, E. M. 2000. Thermosensory activation of insular cortex. Nat. Neurosci. 3, 184–190.

Craig, A. D. and Dostrovsky, J. O. 1999. Medulla to Thalamus. In: Textbook of Pain (*eds*. P. D. Wall and R. Melzack), pp. 183–214. Churchill-Livingstone.

Craig, A. D. and Dostrovsky, J. O. 2001. Differential projections of thermoreceptive and nociceptive lamina I trigeminothalamic and spinothalamic neurons in the cat. J. Neurophysiol. 86, 856–870.

Craig, A. D. and Zhang, E.-T. 1996 Anterior cingulate projection from MDvc (a lamina I spinothalamic target in the medial thalamus of the monkey). Soc. Neurosci. Abstr. 22, 111.

Craig, A. D., Bushnell, M. C., Zhang, E.-T., and Blomqvist A. 1994. A thalamic nucleus specific for pain and temperature sensation. Nature 372, 770–773.

Craig, A. D., Jr., Linington, A. J., and Kniffki, K. D. 1989. Cells of origin of spinothalamic tract projections to the medial and lateral thalamus in the cat. J. Comp. Neurol. 289, 568–585.

Craig, A. D., Jr., Wiegand, S. J., and Price, J. L. 1982. The thalamo-cortical projection of the nucleus submedius in the cat. J. Comp. Neurol. 206, 28–48.

Dado, R. J. and Giesler, G. J., Jr. 1990. Afferent input to nucleus submedius in rats: retrograde labeling of neurons in the spinal cord and caudal medulla. J. Neurosci. 10, 2672–2686.

Davis, K. D. and Dostrovsky, J. O. 1988. Responses of feline trigeminal spinal tract nucleus neurons to stimulation of the middle meningeal artery and sagittal sinus. J. Neurophysiol. 59, 648–666.

Davis, K. D., Kiss, Z. H. T., Luo, L., Tasker, R. R., Lozano, A. M., and Dostrovsky, J. O. 1998. Phantom sensations generated by thalamic microstimulation. Nature 391, 385–387.

Davis, K. D., Kiss, Z. H. T., Tasker, R. R., and Dostrovsky, J. O. 1996. Thalamic stimulation-evoked sensations in chronic pain patients and in nonpain (movement disorder) patients. J. Neurophysiol. 75, 1026–1037.

Davis, K. D., Lozano, R. M., Manduch, M., Tasker, R. R., Kiss, Z. H., and Dostrovsky, J. O. 1999. Thalamic relay site for cold perception in humans. J. Neurophysiol. 81, 1970–1973.

Davis, K. D., Tasker, R. R., Kiss, Z. H., Hutchison, W. D., and Dostrovsky, J. O. 1995. Visceral pain evoked by thalamic microstimulation in humans. Neuroreport 6, 369–374.

Dejerine, J. and Roussy, G. 1906. La syndrome thalamique. Rev. Neurol. 14, 521–532.

Desbois, C. and Villanueva, L. 2001. The organization of lateral ventromedial thalamic connections in the rat: a link for the distribution of nociceptive signals to widespread cortical regions. Neuroscience 102, 885–898.

Desbois, C., Le, B. D., and Villanueva, L. 1999. Organization of cortical projections to the medullary subnucleus reticularis dorsalis: a retrograde and anterograde tracing study in the rat. J. Comp. Neurol. 410, 178–196.

Deschenes, M. and Hu, B. 1990. Electrophysiology and pharmacology of the corticothalamic input to lateral thalamic nuclei: an intracellular study in the cat. Eur. J. Neurosci. 2, 140–152.

Devinsky, O., Morrell, M. J., and Vogt, B. A. 1995. Contributions of anterior cingulate cortex to behaviour. Brain 118(Pt 1), 279–306.

Diamond, M. E., Armstrong-James, M., Budway, M. J., and Ebner, F. F. 1992. Somatic sensory responses in the rostral

sector of the posterior group (POm) and in the ventral posterior medial nucleus (VPM) of the rat thalamus: dependence on the barrel field cortex. J. Comp. Neurol. 319, 66–84.

Disbrow, E., Roberts, T., and Krubitzer, L. 2000. Somatotopic organization of cortical fields in the lateral sulcus of Homo sapiens: evidence for SII and PV. J. Comp. Neurol. 418, 1–21.

Dostrovsky, J. O. and Guilbaud, G. 1988. Noxious stimuli excite neurons in nucleus submedius of the normal and arthritic rat. Brain Res. 460, 269–280.

Dostrovsky, J. O., Manduch, M., Davis, K. D., Tasker, R. R., and Lozano, A. M. 2000. Thalamic Stimulation-Evoked Pain and Temperature Sites in Pain and Non-Pain Patients. In: Proceedings of the 9th World Congress on Pain (*eds*. M. Devor, M. C. Rowbotham, and Z. Wiesenfeld-Hallin), pp. 419–425. IASP Press.

Downie, J. W., Ferrington, D. G., Sorkin, L. S., and Willis, W. D., Jr. 1988. The primate spinocervicothalamic pathway: responses of cells of the lateral cervical nucleus and spinocervical tract to innocuous and noxious stimuli. J. Neurophysiol. 59, 861–885.

Duncan, G. H., Bushnell, M. C., Oliveras, J. L., Bastrash, N., and Tremblay, N. 1993. Thalamic VPM nucleus in the behaving monkey. III. Effects of reversible inactivation by lidocaine on thermal and mechanical discrimination. J. Neurophysiol. 70, 2086–2096.

Eaton, S. A. and Salt, T. E. 1990. Thalamic NMDA receptors and nociceptive sensory synaptic transmission. Neurosci. Lett. 110, 297–302.

Eaton, S. A. and Salt, T. E. 1996. Role of *N*-methyl-D-aspartate and metabotropic glutamate receptors in corticothalamic excitatory postsynaptic potentials *in vivo*. Neuroscience 73, 1–5.

Ericson, A. C., Blomqvist, A., Craig, A. D., Ottersen, O. P., and Broman, J. 1995. Evidence for glutamate as neurotransmitter in trigemino-and spinothalamic tract terminals in the nucleus submedius of cats. Eur. J. Neurosci. 7, 305–317.

Ericson, A. C., Blomqvist, A., Krout, K., and Craig, A. D. 1996. Fine structural organization of spinothalamic and trigeminothalamic lamina I terminations in the nucleus submedius of the cat. J. Comp. Neurol. 371, 497–512.

Ferreira-Gomes, J., Neto, F. L., and Castro-Lopes, J. M. 2004. Differential expression of GABA(B(1b)) receptor mRNA in the thalamus of normal and monoarthritic animals. Biochem. Pharmacol. 68, 1603–1611.

Friedman, D. P. and Murray, E. A. 1986. Thalamic connectivity of the second somatosensory area and neighboring somatosensory fields of the lateral sulcus of the macaque. J. Comp. Neurol. 252, 348–373.

Gall, C., Lauterborn, J., Burks, D., and Seroogy, K. 1987. Co-localization of enkephalin and cholecystokinin in discrete areas of rat brain. Brain Res. 403, 403–408.

Ganchrow, D. 1978. Intratrigeminal and thalamic projections of nucleus caudalis in the squirrel monkey (*Saimiri sciureus*): a degeneration and autoradiographic study. J. Comp. Neurol. 178, 281–312.

Giesler, G. J., Jr., Yezierski, R. P., Gerhart, K. D., and Willis, W. D. 1981. Spinothalamic tract neurons that project to medial and/or lateral thalamic nuclei: evidence for a physiologically novel population of spinal cord neurons. J. Neurophysiol. 46, 1285–1308.

Gingold, S. I., Greenspan, J. D., and Apkarian, A. V. 1991. Anatomic evidence of nociceptive inputs to primary somatosensory cortex: relationship between spinothalamic terminals and thalamocortical cells in squirrel monkeys. J. Comp. Neurol. 308, 467–490.

Guilbaud, G., Benoist, J. M., Jazat, F., and Gautron, M. 1990. Neuronal responsiveness in the ventrobasal thalamic complex of rats with an experimental peripheral mononeuropathy. J. Neurophysiol. 64, 1537–1554.

Guilbaud, G., Peschanski, M., Gautron, M., and Binder, D. 1980. Neurones responding to noxious stimulation in VB complex and caudal adjacent regions in the thalamus of the rat. Pain 8, 303–318.

Gybels, J. M. and Sweet, W. H. 1989. Neurosurgical Treatment of Persistent Pain. Physiological and Pathological Mechanisms of Human Pain. Pain and Headache, Vol. 11. Karger.

Halliday, A. M. and Logue, V. 1972. Painful Sensations Evoked by Electrical Stimulation in the Thalamus. In: Neurophysiology Studied in Man (*ed*. G. G. Somjen), pp. 221–230. Excerpts Medica.

Harte, S. E., Kender, R. G., and Borszcz, G. S. 2005. Activation of 5-HT1A and 5-HT7 receptors in the parafascicular nucleus suppresses the affective reaction of rats to noxious stimulation. Pain 113, 405–415.

Hassler, R. 1959. Architechtronic Organization of the Thalamic Nuclei. In: An Introduction to Stereotaxis with an Atlas of the Human Brain (*eds*. G. Schaltenbrand and P. Bailey), pp. 142–180. Thieme.

Hassler, R. 1970. Dichotomy of Facial Pain Conduction in the Diencephalon. In: Trigeminal Neuralgia (*eds*. R. Hassler and A. E. Walker), pp. 123–138. Sanders.

Hassler, R. and Riechert, T. 1959. Klinische und anatomische Befunde bei stereotaktischen Schmerzoperationen im thalamus. Arch. Psychiatr. 200, 93–122.

He, L. F., Dong, W. Q., and Wang, M. Z. 1991. Effects of iontophoretic etorphine and naloxone, and electroacupuncture on nociceptive responses from thalamic neurones in rabbits. Pain 44, 89–95.

Head, H. and Holmes, G. 1911. Sensory disturbances from cerebral lesions. Brain 34, 102–254.

Hirai, T. and Jones, E. G. 1989. A new parcellation of the human thalamus on the basis of histochemical staining. Brain Res. Brain Res. Rev. 14, 1–34.

Houser, C. R., Vaughn, J. E., Barber, R. P., and Roberts, E. 1980. GABA neurons are the major cell type of the nucleus reticularis thalami. Brain Res. 200, 341–354.

Hutchison, W. D., Luhn, M. A., and Schmidt, R. F. 1992. Knee joint input into the peripheral region of the ventral posterior lateral nucleus of cat thalamus. J. Neurophysiol. 67, 1092–1104.

Jeanmonod, D., Magnin, M., and Morel, A. 1993. Thalamus and neurogenic pain: physiological, anatomical and clinical data. Neuroreport 4, 475–478.

Jeanmonod, D., Magnin, M., and Morel, A. 1994. A thalamic concept of neurogenic pain. Proc. 7th Cong. Pain 2, 767–787.

Jeanmonod, D., Magnin, M., and Morel, A. 1996. Low-threshold calcium spike bursts in the human thalamus. Common physiopathology for sensory, motor and limbic positive symptoms. Brain 119(Pt 2), 363–375.

Jia, H., Xie, Y. F., Xiao, D. Q., and Tang, J. S. 2004. Involvement of GABAergic modulation of the nucleus submedius (Sm) morphine-induced antinociception. Pain 108, 28–35.

Jones, E. G. 1985. The Thalamus. Plenum.

Jones, E. G. 1987. Immunocytochemical Studies on Thalamic Afferent Transmitters. In: Thalamus and Pain (*eds*. J. M. Besson, G. Guilbaud, and M. Peschanski), pp. 83–109. Excerpta Medica.

Jones, E. G. 1990. Correlation and revised nomenclature of ventral nuclei in the thalamus of human and monkey. Stereotact. Funct. Neurosurg. 54–55, 1–20.

Kaas, J. H., Nelson, R. J., Sur, M., Dykes, R. W., and Merzenich, M. M. 1984. The somatotopic organization of the ventroposterior thalamus of the squirrel monkey, *Saimiri sciureus*. J. Comp. Neurol. 226, 111–140.

Kajander, K. C. and Giesler, G. J., Jr. 1987. Responses of neurons in the lateral cervical nucleus of the cat to noxious cutaneous stimulation. J. Neurophysiol. 57, 1686–1704.

Kawakita, K., Dostrovsky, J. O., Tang, J. S., and Chiang, C. Y. 1993. Responses of neurons in the rat thalamic nucleus submedius to cutaneous, muscle and visceral nociceptive stimuli. Pain 55, 327–338.

Kenshalo, D. R., Jr., Giesler, G. J., Jr., Leonard, R. B., and Willis, W. D. 1980. Responses of neurons in primate ventral posterior lateral nucleus to noxious stimuli. J. Neurophysiol. 43, 1594–1614.

Kharazia, V. N. and Weinberg, R. J. 1994. Glutamate in thalamic fibers terminating in layer IV of primary sensory cortex. J. Neurosci. 14, 6021–6032.

Krubitzer, L., Clarey, J., Tweedale, R., Elston, G., and Calford, M. 1995. A redefinition of somatosensory areas in the lateral sulcus of macaque monkeys. J. Neurosci. 15, 3821–3839.

Kupers, R. C. and Gybels, J. M. 1993. Electrical stimulation of the ventroposterolateral thalamic nucleus (VPL) reduces mechanical allodynia in a rat model of neuropathic pain. Neurosci. Lett. 150, 95–98.

Lee, J., Dougherty, P. M., Antezana, D., and Lenz, F. A. 1999. Responses of neurons in the region of human thalamic principal somatic sensory nucleus to mechanical and thermal stimuli graded into the painful range. J. Comp. Neurol. 410, 541–555.

Lee, S. M., Friedberg, M. H., and Ebner, F. F. 1994. The role of GABA-mediated inhibition in the rat ventral posterior medial thalamus. II. Differential effects of GABAA and GABAB receptor antagonists on responses of VPM neurons. J. Neurophysiol. 71, 1716–1726.

Lenz, F. A. and Dougherty, P. M. 1997. Pain Processing in the Human Thalamus. In: Thalamus, Volume II, Experimental and Clincal Aspects (*eds*. M. Steriade, E. G. Jones, and D. McCormick), pp. 617–651. Elsevier.

Lenz, F. A., Gracely, R. H., Baker, F. H., Richardson, R. T., and Dougherty, P. M. 1998. Reorganization of sensory modalities evoked by microstimulation in region of the thalamic principal sensory nucleus in patients with pain due to nervous system injury. J. Comp. Neurol. 399, 125–138.

Lenz, F. A., Kwan, H. C., Dostrovsky, J. O., and Tasker, R. R. 1989. Characteristics of the bursting pattern of action potentials that occurs in the thalamus of patients with central pain. Brain Res. 496, 357–360.

Lenz, F. A., Kwan, H. C., Martin, R., Tasker, R., Richardson, R. T., and Dostrovsky, J. O. 1994. Characteristics of somatotopic organization and spontaneous neuronal activity in the region of the thalamic principal sensory nucleus in patients with spinal cord transection. J. Neurophysiol. 72, 1570–1587.

Lenz, F. A., Seike, M., Lin, Y. C., Baker, F. H., Rowland, L. H., Gracely, R. H., and Richardson, R. T. 1993a. Neurons in the area of human thalamic nucleus ventralis caudalis respond to painful heat stimuli. Brain Res. 623, 235–240.

Lenz, F. A., Seike, M., Richardson, R. T., Lin, Y. C., Baker, F. H., Khoja, I., Jaeger, C. J., and Gracely, R. H. 1993b. Thermal and pain sensations evoked by microstimulation in the area of human ventrocaudal nucleus. J. Neurophysiol. 70, 200–212.

Llinas, R. R., Ribary, U., Jeanmonod, D., Kronberg, E., and Mitra, P. P. 1999. Thalamocortical dysrhythmia: a neurological and neuropsychiatric syndrome characterized by magnetoencephalography. Proc. Natl. Acad. Sci. U. S. A. 96, 15222–15227.

Magnusson, K. R., Clements, J. R., Larson, A. A., Madl, J. E., and Beitz, A. J. 1987. Localization of glutamate in trigeminothalamic projection neurons: a combined retrograde transport-immunohistochemical study. Somatosens. Res. 4, 177–190.

Mansour, A., Khachaturian, H., Lewis, M. E., Akil, H., and Watson, S. J. 1987. Autoradiographic differentiation of mu, delta, and kappa opioid receptors in the rat forebrain and midbrain. J. Neurosci. 7, 2445–2464.

McCormick, D. A. 1992. Neurotransmitter actions in the thalamus and cerebral cortex and their role in neuromodulation of thalamocortical activity. Prog. Neurobiol. 39, 337–388.

Mehler, W. R. 1966. The posterior thalamic region in man. Confin. Neurol. 27, 18–29.

Mehler, W. R. 1969. Some neurological species differences – a posteriori. Ann. N. Y. Acad. Sci. 167, 424–468.

Melzack, R. and Casey, K. L. 1968. Sensory, Motivational, and Central Control Determinants of Pain. In: The Skin Senses (*ed*. D. R. Kenshalo), pp. 423–443. Thomas.

Miletic, V. and Coffield, J. A. 1988. Enkephalin-like immunoreactivity in the nucleus submedius of the cat and rat thalamus. Somatosens. Res. 5, 325–334.

Morin, C., Bushnell, M. C., Luskin, M. B., and Craig, A. D. 2002. Disruption of thermal perception in a multiple sclerosis patient with central pain. Clin. J. Pain 18, 191–195.

Montes, C., Magnin, M., Maarrow, J., Frot, M., Convers, P., Mauguiére, F., and Garcia-Larrea, L. 2005. Thalamic thermo-algesic transimission: ventral posterior (VP) complex versus VMpo in the light of a thalamic in farct with central pain. Pain 113, 223–232.

Musil, S. Y. and Olson, C. R. 1988. Organization of cortical and subcortical projections to anterior cingulate cortex in the cat. J. Comp. Neurol. 272, 203–218.

Nishiyama, K., Kwak, S., Murayama, S., and Kanazawa, I. 1995. Substance P is a possible neurotransmitter in the rat spinothalamic tract. Neurosci. Res. 21, 261–266.

Norrsell, U. and Craig, A. D. 1999. Behavioral thermosensitivity after lesions of thalamic target areas of a thermosensory spinothalamic pathway in the cat. J. Neurophysiol. 82, 611–625.

Pagni, C. A. 1998. Central Pain: A Neurosurgical Challenge. Edizioni Minerva Medica.

Peschanski, M. 1984. Trigeminal afferents to the diencephalon in the rat. Neuroscience 12, 465–487.

Pirot, S., Jay, T. M., Glowinski, J., and Thierry, A. M. 1994. Anatomical and electrophysiological evidence for an excitatory amino acid pathway from the thalamic mediodorsal nucleus to the prefrontal cortex in the rat. Eur. J. Neurosci. 6, 1225–1234.

Poggio, G. F. and Mountcastle, V. B. 1960. A study of the functional contributions of the lemniscal and spinothalamic systems to somatic sensibility. Bull. Johns Hopkins Hosp. 106, 266–316.

Radhakrishnan, V., Tsoukatos, J., Davis, K. D., Tasker, R. R., Lozano, A. M., and Dostrovsky, J. O. 1999. A comparison of the burst activity of lateral thalamic neurons in chronic pain and non-pain patients. Pain 80, 567–575.

Ralston, H. J., III and Ralston, D. D. 1992. The primate dorsal spinothalamic tract: evidence for a specific termination in the posterior nuclei (Po/SG) of the thalamus. Pain 48, 107–118.

Ralston, H. J., III, and Ralston, D. D. 1994. Medial lemniscal and spinal projections to the macaque thalamus: an electron microscopic study of differing GABAergic circuitry serving thalamic somatosensory mechanisms. J. Neurosci. 14, 2485–2502.

Rausell, E. and Jones, E. G. 1991. Histochemical and immunocytochemical compartments of the thalamic VPM nucleus in monkeys and their relationship to the representational map. J. Neurosci. 11, 210–225.

Rausell, E., Bae, C. S., Vinuela, A., Huntley, G. W., and Jones, E. G. 1992. Calbindin and parvalbumin cells in monkey VPL thalamic nucleus: distribution, laminar cortical projections, and relations to spinothalamic terminations. J. Neurosci. 12, 4088–4111.

Ray, J. P. and Price, J. L. 1993. The organization of projections from the mediodorsal nucleus of the thalamus to orbital and medial prefrontal cortex in macaque monkeys. J. Comp. Neurol. 337, 1–31.

Reyes-Vazquez, C. and Dafny, N. 1983. Microiontophoretically applied THIP effects upon nociceptive responses of neurons in medial thalamus. Appl. Neurophysiol. 46, 254–260.

Riddoch, G. and Critchley, Mc.D. 1937. La physiopatholgie de la douleru d'oriinge centrale. Rev. Neurol. 68, 77–104.

Roberts, V. J. and Dong, W. K. 1994. The effect of thalamic nucleus submedius lesions on nociceptive responding in rats. Pain 57, 341–349.

Royce, G. J., Bromley, S., Gracco, C., and Beckstead, R. M. 1989. Thalamocortical connections of the rostral intralaminar nuclei: an autoradiographic analysis in the cat. J. Comp. Neurol. 288, 555–582.

Rustioni, A., Schmechel, D. E., Spreafico, R., Cheema, S., and Cuenod, M. 1983. Excitatory and Inhibitory Amino Acid Putative Neurotransmitters in the Ventralis Posterior Complex: An Autoradiographic and Immunocytochemical Study in Rats and Cats. In: Somatosensory Integration in the Thalamus (*eds*. G. Machhi, A. Rustioni, and R. Spreafico), pp. 365–383. Elsevier.

Sadikot, A. F., Parent, A., and François, C. 1992. Efferent connections of the centromedian and parafascicular thalamic nuclei in the squirrel monkey: a PHA-L study of subcortical projections. J. Comp. Neurol. 315, 137–159.

Salt, T. E. and Eaton, S. A. 1995. Distinct presynaptic metabotropic receptors for L-AP4 and CCG1 on GABAergic terminals: pharmacological evidence using novel alpha-methyl derivative mGluR antagonists, MAP4 and MCCG, in the rat thalamus in vivo. Neuroscience 65, 5–13.

Salt, T. E. and Eaton, S. A. 1996. Functions of ionotropic and metabotropic glutamate receptors in sensory transmission in the mammalian thalamus. Prog. Neurobiol. 48, 55–72.

Sano, K. 1979. Stereotaxic Thalamolaminotomy and Posteromedial Hypothalamotomy for the Relief of Intractable Pain. In: Advances in Pain Research and Therapy (*eds*. J. J. Bonica and V. Ventafridda), pp. 475–485. Raven Press.

Schlag, J. and Schlag-Rey, M. 1986. Role of the central thalamus in gaze control. Prog. Brain Res. 64, 191–201.

Schmahmann, J. D. and Leifer, D. 1992. Parietal pseudothalamic pain syndrome. Clinical features and anatomic correlates. Arch. Neurol. 49, 1032–1037.

Schott, B., Laurent, B., and Mauguiere, F. 1986. Les douleurs thalamiques. Etude critique de 43 case. Rev. Neurol. 142, 308–315.

Sherman, S. M. and Guillery, R. W. 2001. Exploring the Thalamus. Academic Press.

Shi, T., Stevens, R. T., Tessier, J., and Apkarian, A. V. 1993. Spinothalamocortical inputs nonpreferentially innervate the superficial and deep cortical layers of SI. Neurosci. Lett. 160, 209–213.

Siegfried, J. 1987. Stimulation of Thalamic Nuclei in Human: Sensory and Therapeutical Aspects. In: Thalamus and Pain (*eds*. J.-M. Besson, G. Guilbaud, and M. Peschanski), pp. 271–278. Excerpta Medica.

Stepniewska, I., Sakai, S. T., Qi, H. X., and Kaas, J. H. 2003. Somatosensory input to the ventrolateral thalamic region in the macaque monkey: potential substrate for parkinsonian tremor. J. Comp. Neurol. 455, 378–395.

Steriade, M., Jones, E. G., and McCormick, D. A. 1997. Thalamus. Elsevier Science.

Stevens, R. T., London, S. M., and Apkarian, A. V. 1993. Spinothalamocortical projections to the secondary somatosensory cortex (SII) in squirrel monkey. Brain Res. 631, 241–246.

Strigo, I. A., Duncan, G. H., Boivin, M., and Bushnell, M. C. 2003. Differentiation of visceral and cutaneous pain in the human brain. J. Neurophysiol. 89, 3294–3303.

Tasker, R. R. 1984. Stereotaxic Surgery. In: Textbook of Pain (*eds*. P. D. Wall and R. Melzack), pp. 639–655. Churchill Livingstone.

Villanueva, L. and Nathan, P. 2000. Multiple Pain Pathways. In: Proceedings of the 9th World Congress on Pain (*eds*. M. Devor, M. C. Rowbotham, and Z. Wiesenfeld-Hallin), pp. 371–376. IASP Press.

Wall, J. T., Xu, J., and Wang, X. 2002. Human brain plasticity: an emerging view of the multiple substrates and mechanisms that cause cortical changes and related sensory dysfunctions after injuries of sensory inputs from the body. Brain Res. Brain Res. Rev. 39, 181–215.

Weng, H. R., Lee, J. I., Lenz, F. A., Schwartz, A., Vierck, C., Rowland, L., and Dougherty, P. M. 2000. Functional plasticity in primate somatosensory thalamus following chronic lesion of the ventral lateral spinal cord. Neuroscience 101, 393–401.

Weng, H. R., Lenz, F. A., Vierck, C., and Dougherty, P. M. 2003. Physiological changes in primate somatosensory thalamus induced by deafferentation are dependent on the spinal funiculi that are sectioned and time following injury. Neuroscience 116, 1149–1160.

Willis, W. D. 1985. The Pain System. Karger.

Willis, W. D., Jr. 1997. Nociceptive Functions of Thalamic Neurons. In: Thalamus, Volume II, Experimental and Clinical Aspects (*eds*. M. Steriade, E. G. Jones, and D. A. McCormick), pp. 373–424. Elsevier Science Ltd.

Willis, W. D. and Westlund, K. N. 1997. Neuroanatomy of the pain system and of the pathways that modulate pain. J. Clin. Neurophysiol. 14, 2–31.

Xiao, D. Q., Zhu, J. X., Tang, J. S., and Jia, H. 2005. 5-hydroxytryptamine 1A (5-HT1A) but not 5-HT3 receptor is involved in mediating the nucleus submedius 5-HT-evoked antinociception in the rat. Brain Res. 1046, 38–44.

Yang, Z. J., Tang, J. S., and Jia, H. 2002. Morphine microinjections into the rat nucleus submedius depress nociceptive behavior in the formalin test. Neurosci. Lett. 328, 141–144.

Yasui, Y., Breder, C. D., Saper, C. B., and Cechetto, D. F. 1991. Autonomic responses and efferent pathways from the insular cortex in the rat. J. Comp. Neurol. 303, 355–374.

Yasui, Y., Itoh, K., Kamiya, H., Ino, T., and Mizuno, N. 1988. Cingulate gyrus of the cat receives projection fibers from the thalamic region ventral to the ventral border of the ventrobasal complex. J. Comp. Neurol. 274, 91–100.

Yoshida, A., Dostrovsky, J. O., and Chiang, C. Y. 1992. The afferent and efferent connections of the nucleus submedius in the rat. J. Comp. Neurol. 324, 115–133.

Zhang, S., Tang, J. S., Yuan, B., and Jia, H. 1998. Inhibitory effects of glutamate-induced activation of thalamic nucleus submedius are mediated by ventrolateral orbital cortex and periaqueductal gray in rats. Eur. J. Pain 2, 153–163.

5.44 Psychophysics of Sensations Evoked by Stimulation of the Human Central Nervous System

S Ohara, C A Bagley, H C Lawson, and F A Lenz, Johns Hopkins Hospital, Baltimore, MD, USA

© 2008 Elsevier Inc. All rights reserved.

5.44.1	Introduction	656
5.44.2	The Spinothalamic Tract	656
5.44.3	The Dorsal Column Pathway	657
5.44.4	Thalamic Nuclei	657
5.44.4.1	Lateral Thalamic Nuclei	657
5.44.4.2	Medial and Intralaminar Thalamic Nuclei	663
5.44.5	Cortex	663
5.44.5.1	Parasylvian Cortex and Pain Memory	663
5.44.6	Conclusions	665
References		665

Glossary

dorsal columns A pathway carrying axons of fibers in the peripheral nerve through the posterior aspect of the spinal cord to the dorsal column nucleus at the posterior aspect of the medulla where they synapse and ascend through the medial lemnisus to the principal nucleus of thalamus. Classically, this pathway transmits low-threshold muscle and cutaneous afferents but recent studies demonstrate that afferents transmitting nociceptive, thermal, or visceral inputs are also transmitted.

nociceptive specific (NS) neurons Neurons responding only to stimuli which are noxious or painful.

wide dynamic range (WDR) neurons Neurons responding to stimuli across the intensive continuum into the painful or noxious range.

projected field in the somatosensory system A part of the body at which a sensation is evoked in response to stimulation of the central nervous system.

receptive field In the somatosensory system: skin region, stimulation of which can influence the discharge of the neuron under study

somatic sensory nuclear group of the thalamus Nuclei receiving input from the dorsal column nuclei, the spino- or the trigeminothalamic tract by either a direct or a transsynaptic route. Summary term for the specific somatosensory nuclei of the thalamus. Most commonly used taxonomy is for monkey thalamus: VPL (ventroposterolateral), VPM (ventroposteromedial), VPI (ventroposteroinferior) corresponding to humans: Vc (ventrocaudal, both medial and lateral). Adjacent, both posterior medial, to VPM ventral medial posterior (VMpo), a putative pain and temperature signaling nucleus may be located (Craig, A. D. *et al.*, 1994, cf. Willis, W. D., Jr. *et al.*, 2001, Graziano, A. and Jones, E. G., 2004; Lenz, F. A. *et al.*, 2004). VMpo may be located medial to ventral caudal portae (Vcpor), while intralaminar nuclei mostly a thin layer of neurons located medial to Vim, Vc, and Vcpor (see Figure 1(a)).

spinothalamic tract (STT) The pain and temperature signaling pathway from neurons in the spinal dorsal horn to the lateral and anterolateral funiculi of the spinal cord and the brainstem to the lateral, posterior, medial, and intralaminar nuclei of thalamus.

spinothalamocortical pathways Cortical areas which receive input from thalamic nuclei that themselves receive STT input. These thalamocortical connections include those from Vc to primary somatosensory and secondary somatosensory cortex, from Vcpor, Vcpc, and VMpo to parietal opercular, insular, and retroinsular cortex, and finally from the medial dorsal nucleus to anterior cingulate cortex.

sylvian fissure Also called lateral sulcus, the sylvian fissure separates the temporal lobe from the frontal and parietal lobes (see Figure 6, left – middle and lower levels). The insula is a cortical surface, which is located deep to the lateral fissure and parallel to the cortical surface on coronal and axial sections (Figure 6, middle and right). The frontal, parietal, and temporal opercula are folds of cortex that extend over the insula and meet each other over the insula. The sulcus between the frontal–parietal opercula and the temporal operculum is the sylvian fissure.

Talairach coordinates Initially developed for a specific stereotactic frame; based on one single brain; frequently used as common coordinate system; *x*: left–right, *y*: anterior–posterior, *z*: superior–inferior; the reference point (0, 0, 0) is the anterior commissure (Talairach, J. and Tournoux, P., 1988).

thalamus A subcortical gray matter structure characterized by reciprocal connections with the cortical mantle and by inputs from the periphery and nuclei of the brain, such as the pallidum.

5.44.1 Introduction

The dorsal column pathway and the spinothalamic tract (STT) are the two main somatosensory spinal tracts afferent to the thalamus. The dorsal column pathway is formed by the axons of low-threshold mechanoreceptors with cell bodies in the dorsal root ganglion. These axons terminate to the principal somatic sensory nucleus of the thalamus (human ventral caudal or Vc, monkey ventral posterior or VP) (Jones, E. G. *et al.*, 1982; Kaas, J. H. *et al.*, 1984; Lenz, F. A. *et al.*, 1988; Willis, W. D. and Coggeshall, R. E., 1991). The dorsal columns do contain a postsynaptic pain pathway signaling noxious visceral stimuli, which terminates in the Vc (Uddenberg, N., 1968; Rustioni, A. *et al.*, 1979; Willis, W. D., *et al.*, 1991; Al Chaer, E. D. *et al.*, 1996b). The STT is a pain pathway that originates from the spinal dorsal horn, and ascends in the anterolateral quadrant of the spinal cord before terminating in the thalamus (Willis, W. D., Jr. *et al.*, 2001). Stimulation of these thalamic nuclei in man reveals the psychophysical dimensions of these pathways which is the subject of this chapter.

5.44.2 The Spinothalamic Tract

Many neurons in the STT are characterized by their response to noxious or painful stimuli. Some of these respond to the somatic stimuli across the intensive continuum into the noxious range (WDR – wide dynamic range). These cells arise from both superficial (lamina I) and deep laminae of the dorsal horn (laminae IV–V) (Kumazawa, T. and Perl, E. R., 1978; Willis, W. D., 1985; Ferrington, D. G. *et al.*, 1987). Some neurons in the superficial dorsal horn respond only to different stimuli including noxious stimuli (nociceptive specific (NS) cells), cold (Kumazawa, T. and Perl, E. R., 1978; Willis, W. D., 1985; Ferrington, D. G. *et al.*, 1987; Craig, A. D. *et al.*, 1994), injection of histamine (itch – Andrew, D. and Craig, A. D., 2001; Craig, A. D., 2003b), or visceral stimuli (Craig, A. D., 2003a). The deep and superficial laminae of the dorsal horn project to the brain, respectively, through the ventral lateral (ventral STT) and the dorsal lateral spinal funiculi (dorsal STT) (Apkarian, A. V. and Hodge, C. J., 1989; Cusick, C. G. *et al.*, 1989; Ralston, H. J. and Ralston, D. D., 1992; Craig, A. D., 1998, 2003b; Price, D. D. *et al.*, 2003).

The population of neurons in the superficial dorsal horn responding only to noxious stimuli has led to the description of the STT as a structure signaling only pain – a labeled line (Perl, E. R., 1984; Willis, W. D., 1985). A recent version of this hypothesis suggests that the STT is a series of labeled lines for cool and itch, as well as pain that jointly reflect the internal state of the body (interoception) (Craig, A. D., 2003a; 2003b). In this view, pain is the emotion produced by disequilibrium of the internal state. An alternate view is that pain is signaled by WDR neurons which transmit a

graded signal, the strength of which might be decoded in the brain to identify the presence of a painful stimulus (Price, D. D. and Dubner, R., 1977; Willis, W. D., 1985; Price, D. D. *et al.*, 2003). This chapter examines recent evidence from stimulation of the human central nervous system as they impact these hypotheses.

One approach to identifying the pain pathway has been to stimulate the cord during cordotomy using paired-pulse stimulus parameters that selectively activate the axons arising in the superficial or deep laminae (Mayer, D. J. *et al.*, 1975). This interpulse threshold was more consistent with that of cells in the deep than the superficial dorsal horn (Price, D. D. and Mayer, D. J., 1975). The results suggest that the sensory aspect of pain is signaled through the axons in ventral STT which originate from the WDR neurons in the deep dorsal horn (Price, D. D. and Dubner, R., 1977; Dubner, R. *et al.*, 1989).

5.44.3 The Dorsal Column Pathway

The dorsal column pathway is formed by the axons of low-threshold mechanoreceptors that project through the dorsal column nuclei and medial lemniscus to the region of the principle somatic sensory nucleus (ventral caudal, Vc) (Jones, E. G. *et al.*, 1982; Kaas, J. H. *et al.*, 1984; Lenz, F. A. *et al.*, 1988; Willis, W. D. *et al.*, 1991). As shown in Figure 1 receptive fields are quite constant within a particular parasagittal plane in Vc. From medial to lateral planes, the sequence of neuronal cutaneous receptive fields progresses from intraoral through face, thumb, fingers (radial to ulnar), and arm to leg. Proximal parts of the limbs are represented dorsal to the corresponding digits (Lenz, F. A. *et al.*, 1988).

Substantial evidence demonstrates that the dorsal columns do contain a postsynaptic pain pathway signaling noxious visceral stimuli, rather than noxious somatic stimuli, which terminates in the VP (Uddenberg, N., 1968; Rustioni, A. *et al.*, 1979; Willis, W. D. *et al.*, 1991; Al Chaer, E. D. *et al.*, 1996b). This postsynaptic pathway has been demonstrated by infusion of neurotransmitter agonists/antagonists into the dorsal horn, which alters the response of neurons in the dorsal column nuclei to visceral stimuli. Furthermore, lesions of rat nucleus gracilis diminish the response of neurons in VP to visceral as well as cutaneous stimuli (Al-Chaer, E. D. *et al.*, 1997).

The cells of origin of this pathway are located just dorsal to the central canal, as demonstrated by antidromic invasion from nucleus gracilis (Al Chaer, E. D. *et al.*, 1996a), and by retrograde and anterograde tracer studies (Christensen, M. D. *et al.*, 1996). Retrograde tracer studies depositing marker in the nucleus gracilis (Christensen, M. D. *et al.*, 1996) label cell bodies of origin of the pathway in the medial base of the dorsal horn just above the central canal. Injection of tracer into this area resulted in fiber labeling of the dorsal column midline and in the medial aspect of the nucleus gracilis. Fibers originating in the thoracic cord terminate in the lateral part of nucleus gracilis and adjacent to the medial parts of nucleus cuneatus (Wang, C. C. *et al.*, 1999; Willis, W. D. *et al.*, 1999). Along with the STT, a major terminus of the postsynaptic dorsal horn pathway is the lateral thalamus.

5.44.4 Thalamic Nuclei

5.44.4.1 Lateral Thalamic Nuclei

The human principal sensory nucleus (Vc) (Hassler, R., 1959) is divided into a core area (equivalent to monkey VP, see Olszewski, J., 1952; Hirai, T. and Jones, E. G., 1989), posterior, and inferior regions. These two regions are defined relative to the most posterior and inferior cell with a response to nonpainful, cutaneous stimuli (cell 57 in Figure 1(b)). In the core, the majority of cells respond to innocuous, mechanical, and cutaneous stimulation. This latter area corresponds to the posterior and inferior subnuclei of Vc, which are ventral caudal portae (Vcpor), ventral caudal parvocellular nucleus (Vcpc) (Mehler, W. R., 1966), the posterior nucleus, and the magnocellular medial geniculate (Mehler, W. R., 1962; Mehler, W. R., 1966; Lenz, F. A. *et al.*, 1993b) (see Vc and Vcpor in sagittal section in Figure 1(a)). Studies of patients at autopsy following lesions of the STT show terminations in all this nuclei (Bowsher, D., 1957; Mehler, W. R., 1966; Mehler, W. R., 1969). This area includes the ventral medial nucleus – posterior part (VMpo), which may receive STT inputs and may signal pain and temperature (Craig, A. D. *et al.*, 1994; Blomqvist, A. *et al.*, 2000; cf. Willis, W. D., Jr. *et al.*, 2001; Graziano, A. *et al.*, 2004). The physiology recapitulates this anatomy.

Cells in Vc responding to painful and thermal stimuli are of several types, including WDR and NS cells responding to painful thermal and mechanical stimuli (see figure 2 in Lee, J.-I. *et al.*, 1999). Figure 2(a) demonstrates the response of a single neuron with WDR properties to a painful 45 °C

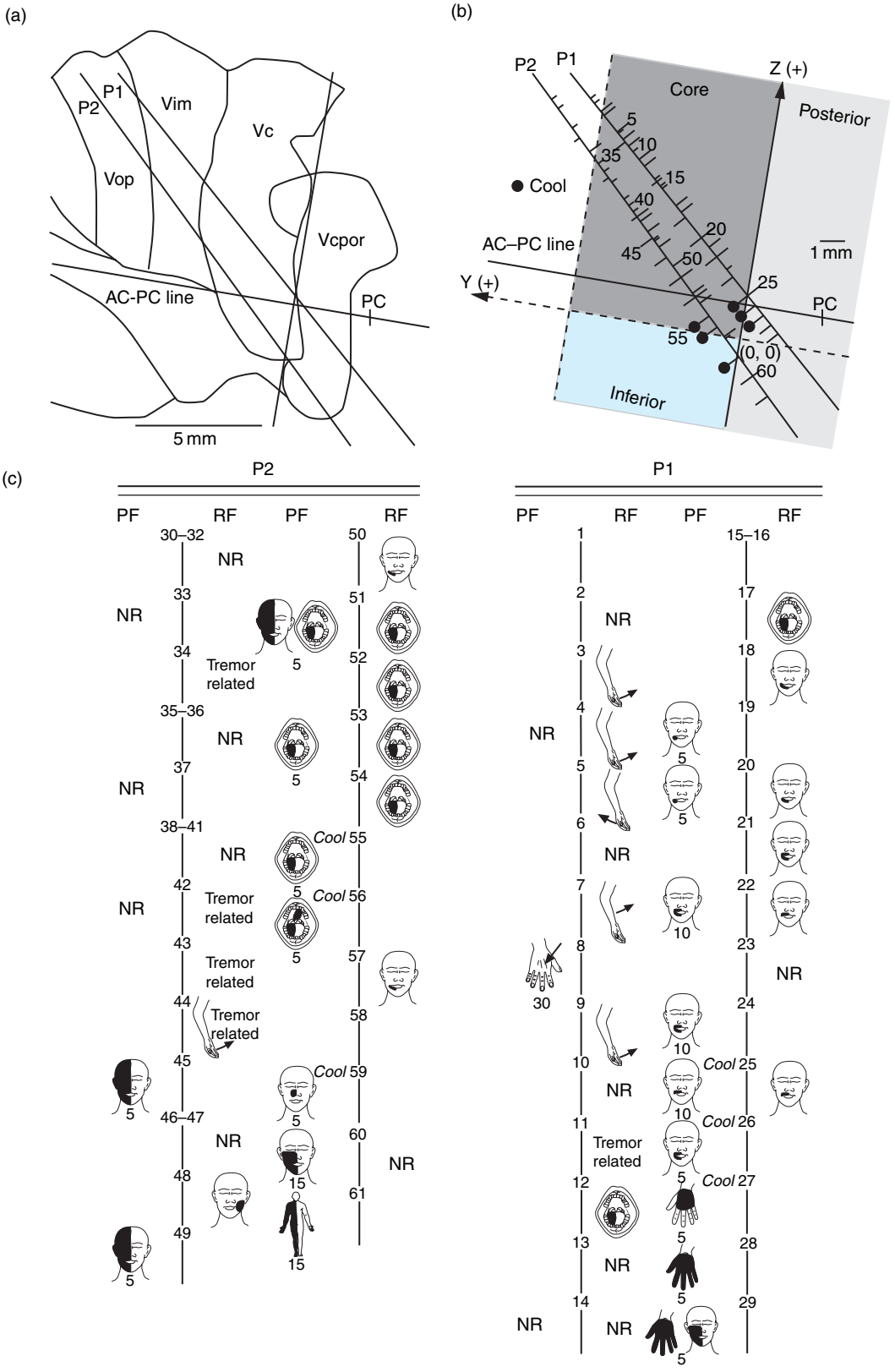
(a)
P1
P2
Vim
Vc
Vop
Vcpor
AC-PC line
PC
5 mm
(b)
P2
P1
Z (+)
Core
Posterior
5
10
35
15
Cool
40
20
AC–PC line
45
50
1 mm
25
Y (+)
PC
55
(0, 0)
60
Inferior
(c)
P2
P1
PF
RF
PF
RF
30–32
NR
33
NR
34
Tremor related
35–36
NR
37
NR
38–41
NR
42
NR
Tremor related
43
Tremor related
44
Tremor related
45
46–47
NR
48
49
50
51
52
53
54
Cool 55
Cool 56
57
58
Cool 59
60
NR
61
5
15
1
2
NR
3
4
NR
5
6
NR
7
8
30
9
10
NR
11
Tremor related
12
13
NR
14
NR
15–16
17
18
19
20
21
22
23
NR
24
Cool 25
Cool 26
Cool 27
28
29
10

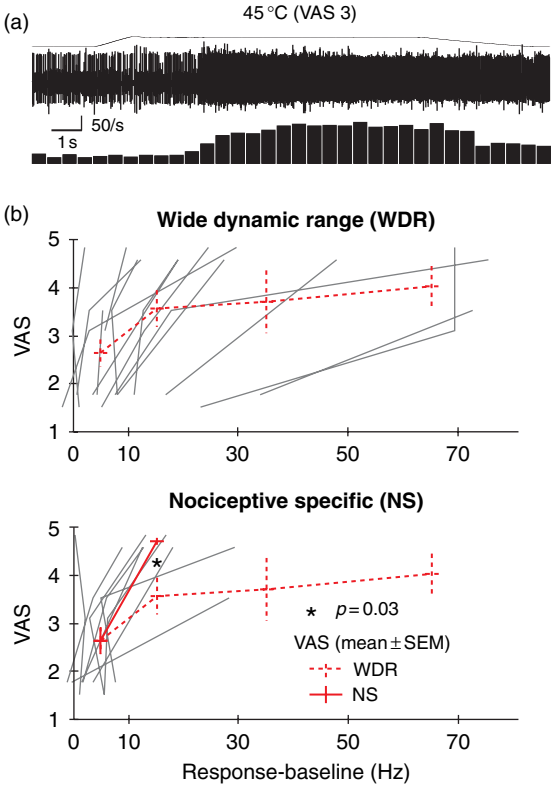

Figure 2 Activity of neurons in the region of Vc (ventrocaudal) responding to painful thermal stimuli. The response to nonpainful and painful heat/mechanical stimuli applied within the receptive field (RF) (Lenz, F. A. *et al.*, 1994b; Lee, J.-I. *et al.*, 1999) is compared with the visual analog scale of intensity (VAS) evoked by the same stimulus. (a) The response of a cell wide dynamic range (WDR) to painful heat. (b) VAS and firing rates for the response to painful stimuli are plotted for nociceptive (NS) cells which respond only to painful stimuli and WDR neurons, which respond in a graded fashion to nonpainful and painful stimuli. Average and one standard deviation scores by decade to 20 Hz and by 30 Hz steps from 20 to 80 Hz were compared by Mann–Whitney *U* test. Reprinted from Lenz F. A., Ohara, S., Gracely, R. H., Dougherty, P. M., and Patel, S. H. 2004. Pain encoding in the human forebrain: binary and analog exteroceptive channels. J. Neurosci. 24, 6540-6544 with permission ©2004 by the Society for Neuroscience).

stimulus. Responses to painful stimuli were characterized by the mean firing rate during painful stimulation, recorded through the microelectrode (Figure 2(b), *x*-axis), and by visual analog scale of intensity (VAS) ratings of microstimulation-evoked pain (*y*-axis). Some low-threshold cells respond to nonpainful mechanical and cold stimuli (Figure 2) (Lenz, F. A. *et al.*, 1993a; Lenz, F. A. and Dougherty, P. M., 1998; Lee, J.-I. *et al.*, 1999). Cells in the core and posterior region respond only to noxious heat stimuli (Lenz, F. A. *et al.*, 1993a; 2004) and to noxious cold stimuli (Davis, K. D. *et al.*, 1999).

Nociceptive cells in Vc appear to signal pain based on temporary lesioning and stimulation studies. Blockade of the activity in this region by injection of local anesthetic into monkey VP, corresponding to human Vc (Hirai, T. *et al.*, 1989), significantly interferes with the monkey's ability to discriminate temperature in both the innocuous and noxious range (Duncan, G. H. *et al.*, 1993). Stimulation within Vc and the regions posterior and inferior to it can evoke the sensations of pain (Hassler, R. and Reichert, T., 1959; Willis, W. D., 1985; Dostrovsky, J. O. *et al.*, 1991; Lenz, F. A. *et al.*, 1993b) and temperature (Lenz, F. A. *et al.*, 1993b; Davis, *et al.*, 1999).

The largest study of stimulation-evoked pain and temperature responses examined results of threshold microstimulation of the region of Vc in 124 thalami (116 patients), as summarized in Figure 3. The location of pain and temperature responses is defined relative to the posterior and inferior borders of the principal somatic sensory nucleus (Vc). Warm sensations were evoked more frequently in the posterior region (5.7%) than in the core (2.3%). Otherwise the proportions were not significantly different for cool or pain sensations between the core or the posterior region or both (cool 2.5%, 2.2%; pain 2.8%, 4.1%).

Figure 1 Map of receptive and projected fields for trajectories in the regions of the Vc (ventrocaudal) in a single patient (number 193.97). (a) Positions of the trajectories relative to nuclear boundaries as predicted radiologically from the position of the anterior commissure–posterior commissure (AC–PC) line. The AC–PC line is indicated by the horizontal line in the panel; the trajectories are shown by the two oblique lines. The positions of nuclei are inferred from the AC–PC line and therefore are only an approximate indicator of nuclear location. Scale as indicated. Abbreviations defined in the text. (b) Location of the cells, stimulation sites, and trajectories (P1 and P2) relative to the AC–PC line (a solid line) and the ventral border of the core of Vc (a dotted line). The locations of stimulation sites are indicated by ticks to the left of the trajectory; the locations of the cells are indicated by ticks to the right of the trajectory. Cells with receptive fields (RFs) are indicated by long ticks; those without are indicated by short ticks. The cold sensation evoked is indicated by filled circles at the end of the tick to the left of the trajectory. Scale is as indicated. Each site where a cell was recorded or stimulation was carried out or both is indicated by the same number in (b) and (c). The core of Vc and the regions posterior and inferior are as labelled. (c) P1 and P2 show the site number, PF, and RF for that site. The threshold (in microamperes) is indicated below the PF diagram. Reprinted from Ohara S. and Lenz F. A. (2003) Medial lateral extent of thermal and pain sensations evoked by microstimulation in somatic sensory nuclei of human thalamus. J. Neurophysiol. 90, 2367-2377, used with permission from the American physiological society.

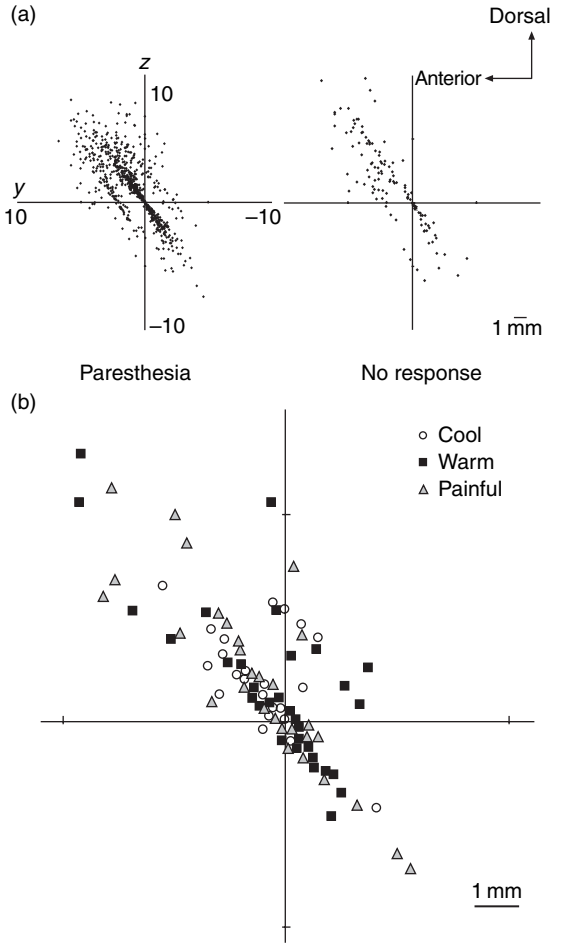

Figure 3 Locations of sites where microstimulation evoked paresthesias (a, left), no response (NR) (a, right), and thermal and pain sensations (b). Site location is shown relative to the posterior and inferior borders of the core of Vc. Note that thermal and pain sensations were evoked both in the core and posterior regions of Vc. Paresthesic sites are most dense where NR sites are least dense over the core and the posterior regions. Scale as indicated. Reprinted from Ohara S. and Lenz F. A. 2003. Medial lateral extent of thermal and pain sensations evoked by microstimulation in somatic sensory nuclei of human thalamus. J. Neurophysiol. 90, 2367-2377, used with permission from the American Physiological Society.

Warm sensations were evoked more frequently in the lateral plane (10.8%) than in the medial planes of the posterior region (3.9%) but no other significant medial lateral differences for any sensation were found in the core or posterior region or overall.

These results are in contrast to previous studies reporting a larger proportion of thermal/pain sites were evoked in the posterior and inferior regions (Lenz, F. A. *et al.*, 1993b; Davis, K. D. *et al.*, 1996). These latter studies took the anterior commissure–posterior commissure line (ACPC) as the floor of Vc, contrary to atlas and physiologic maps (Schaltenbrand, G. and Bailey, P., 1959; Lenz, F. A. *et al.*, 1988). This recent study suggests that sites where thermal or pain sensations are evoked are located both within and posterior, inferior, and medial to Vc. If the proportion of such sites is larger in posterior and inferior regions, then those sites must be very close to the borders of the core.

Patterned stimulation at sites in the region of Vc, an STT terminal region, evokes sensations consistent with one of two pathways – one binary (pain+) and the other analog (pain−/+) (Figure 3). Specifically, current was applied at five frequencies (10, 20, 38, 100, and 200 Hz) in bursts of 4, 7, 20, 50, and 100 pulses in an ascending staircase protocol, the type of protocol commonly used in studies of pain (Gracely, R. H. *et al.*, 1988; Yarnitsky, D. and Sprecher, E., 1994), including our studies (Greenspan, J. D. *et al.*, 2004). Stimulation at pain+ sites evoked a constant high level of pain over large, often cutaneous, projected fields (PFs). These sites were characterized both by descriptors, which did not change along the staircase, or by more intense stimulation-evoked pain than that evoked at the pain−/+ sites (Figure 4). These results suggest that pain+ sites participate in a binary, exteroceptive, labeled line which signals the presence of a painful external stimulus.

The thalamic stimulation thresholds for nonpainful and painful sensations are not significantly different (Lenz, F. A. *et al.*, 1993b; Ohara, S. *et al.*, 2003) suggesting that pain−/+ sites did not result from activation of the system transmitting nonpainful sensations (largely medial lemniscal) before that transmitting painful sensations (largely STT) (Willis, W. D., 1985). In addition, the equivalence of current, pulse, and frequency thresholds for pain at both types of sites predicts that the neural elements, that is, possibly WDR and NS cells, should be activated together if they were found at the same site. At such sites, analog pain+ responses would be predicted to occur because the combination of binary plus analog neural elements at a site will have analog properties, given the assumption of linearity. However, analog pain+ sites were not observed. For all these reasons, it is plausible that our observations may be the result of selective activation of two functionally distinct pathways.

Figure 2(a) demonstrates the mean firing rate minus baseline (Figure 2(b), x-axis) for the response of multiple single WDR and NS neurons to painful stimuli versus VAS score (Figure 2(b), y-axis). There

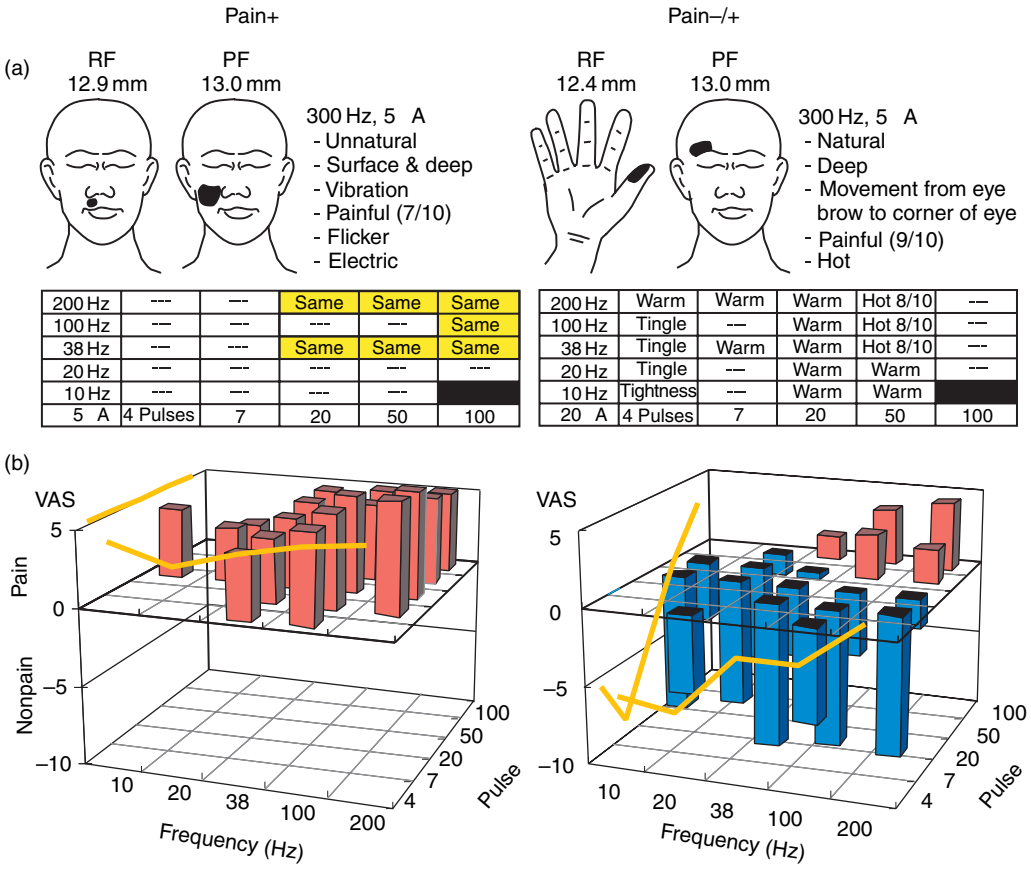

Figure 4 Pain+ and pain−/+ stimulation sites. Sensations evoked by threshold microstimulation were characterized by the PF and by descriptors from a validated questionnaire, and by a visual analog scale of intensity (VAS) (Lenz, F. A. *et al.*, 1993b; 1998a; Lenz, F. A. and Byl, N. N. 1999). (a, left) Site where stimulation at 300 Hz and 5 μA produced pain in the PF shown in the figurine and of the quality as described. Pain identical to that evoked by 300 Hz was evoked at most sites with trains ≥20 pulses and frequencies ≥200 Hz (yellow rectangle, see text). (a, right) Site where tightness was evoked in the first column at 10 Hz and then tingle at 20, 38, and 100 Hz. At 200 Hz and thereafter, warm was evoked at each step in the staircase, excepting 7 pulses – 10, 20, 100 Hz, until 50 pulses – 38 Hz. At this step and further up, the staircase painful heat was evoked. (b) Average VAS ratings across all pain+ and pain−/+ sites. Ratings were taken in response to pulse and frequency pairs ascending the staircase. The yellow lines along the outside surfaces of the 3D displays indicate the average VAS ratings across all sites by frequency and number of pulses. Reprinted from Lenz F. A., Ohara, S., Gracely, R. H., Dougherty, P. M., and Patel, S. H. 2004. Pain encoding in the human forebrain: binary and analog exteroceptive channels. J. Neurosci. 24, 6540-6544, with permission (©2004; by the Society for Neuroscience).

was a significantly steeper initial rise in VAS scores for the neurons that only responded to painful stimuli (NS neurons), than for WDR neurons. The steep initial rise of VAS with the firing rate of NS versus WDR neurons (Figure 2(b)) is consistent with the shorter dynamic range of thalamic NS cells (Apkarian, A. V. and Shi, T., 1994), and with the binary response to stimulation at pain+ sites (Figure 2(b)).

We suggest that the first pathway is characterized as a binary pain response signaling the presence/absence of painful stimuli, consistent with an alerting/alarm function (Becker, D. E. *et al.*, 1993; Zaslansky, R. *et al.*, 1995). The second pathway may be an analog route in which activity is graded with intensity of the painful stimulus, consistent with STT neurons, which encode the properties of external stimuli (Willis, W. D., 1985; Price, D. D. *et al.*, 2003). Itch was rarely evoked and never in isolation. Emotion descriptors (e.g., nauseating, cruel, suffocating) were uncommonly endorsed at either pain+ and pain−/+ sites (cf. Lenz, F. A. *et al.*, 1995). Therefore, both painful responses to stimulation were described in terms usually applied to external stimuli (exteroception) rather than to internal or emotional phenomena

(interoception). Exteroreceptive sensations can be associated with a strong affective dimension.

Pain with a strong unpleasant or affective component can be evoked by stimulation of the lateral thalamus in the region of Vc. These sensations have the character of memories of a previously experienced pain, unlike the pain sensations evoked by thalamic sensation which are not related to previous experience (see above) or a diffuse unpleasant sensation of the type evoked by stimulation of the medial thalamus (see below). In the first case, stimulation in Vcpc (Figure 5) evoked chest pain with an affective dimension in the case of a patient with coronary artery disease which had been effectively treated by balloon angioplasty (Lenz, F. A. *et al.*, 1994a).

Microstimulation at site 49 (Figure 5) evoked an unnatural, painful (visual analog scale – 4.6/10), mechanical sensation in the flank and an unnatural nonpainful electrical sensation involving the left arm and leg. At sites 51 and 53 (Figure 5) microstimulation evoked a sensation described by the patient as "heart pain," which was "like what I took nitroglycerin for" except that "it starts and stops suddenly." It was not accompanied by dyspnea, diaphoresis, or after effects. The PF involved the precordium and left side of the chest from the sternum in the midline to the anterior axillary line. Microstimulation at site 51 also evoked a sensation of nonpainful surface, tingling in the left leg, which coincided with the stimulation-associated angina.

Characteristics of the patient's stimulation-associated angina and usual angina were measured by using a questionnaire. The same descriptors for stimulation-associated angina were chosen intraoperatively during stimulation at both sites 51 and 53 (Figure 5) including: natural, deep, painful (visual analog scale – 10/10), squeezing, frightful, fatiguing, and identical to her angina. The questionnaire was administered three times over several months postoperatively to describe the patient's usual angina. The following descriptors were chosen: natural (3/3 administrations), deep (3/3), painful (3/3), squeezing (3/3), frightful (2/3), suffocating (2/3), and fatiguing (2/3). Her usual angina involved the left side of the chest, arm, and neck and was associated with a surface (3/3), nonpainful (3/3), and tingling (3/3) in the left arm and hand. This coincidence of descriptors is unlikely to occur at random ($p < 10^{-6}$, combinatorial analysis).

Similar emotional responses, including crying in response to thalamic stimulation in the same region, have been reported in the case of atypical chest pain, dysparunia, and the pain of childbirth (Davis, K. D.

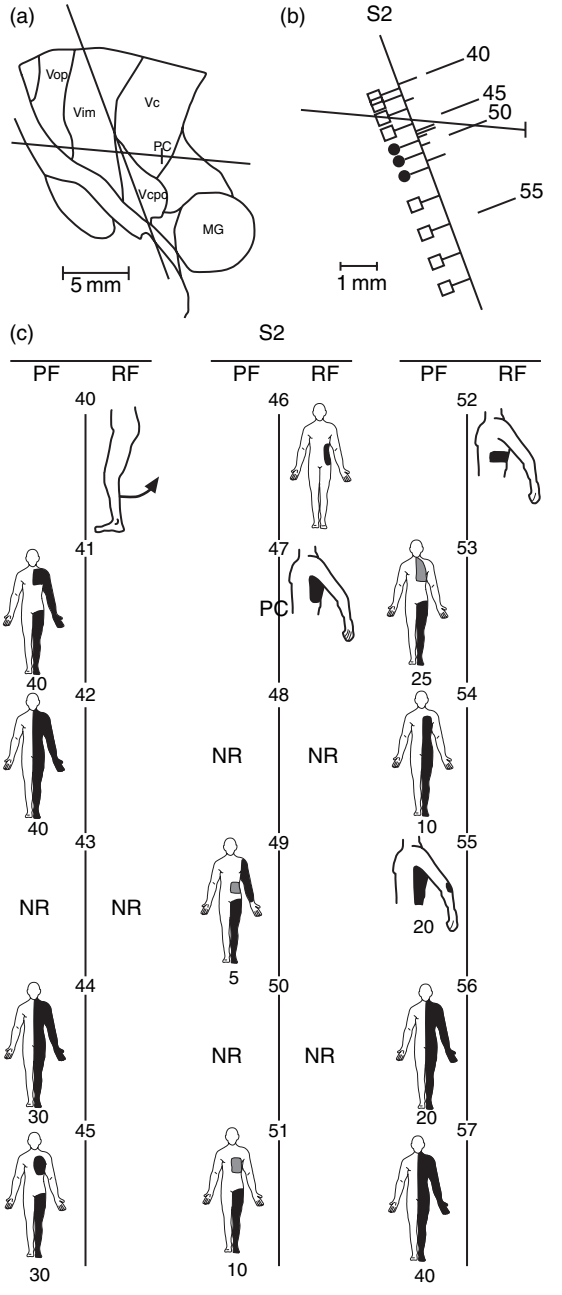

Figure 5 (a) Thalamic map of a patient with a history of angina pectoris successfully treated with coronary artery balloon angioplasty. (b) Dark circular balloons on ticks to the right of the line indicate sites (sites 49, 51, 53) where thalamic microstimulation evoked painful sensations in PFs indicated by stippling in the figurines (c). Open square balloons in (b) indicate sites where nonpainful, tingling sensations were evoked. All abbreviations and other conventions are as in the legend to Figure 1. Reproduced from Lenz F. A., Gracely, R. H., Hope, E. J., Baker, F. H., Rowland, L. H., Dougherty, P. M., and Richardson, R. T. 1994a. The sensation of angina can be evoked by stimulation of the human thalamus. Pain 59, 119-125, with permission from Elsevier.

et al., 1995; Lenz, F. A. *et al.*, 1995). Clinical criteria including a battery of cardiac tests (enzymes, EKGs, stress test) ruled out angina of cardiac origin in both these patients. Explorations in 50 patients without a history of angina found that stimulation-associated angina was not evoked at any of the 19 stimulation sites with PFs on the chest wall. PFs were located on the left chest wall at three sites and the right chest wall at 16. At one of these 19 sites an unnatural, sharp, mechanical, painful, and vibration was described in response to stimulation but emotional descriptors were not endorsed.

Preoperative pain was clearly of cardiac origin in the patient with angina (Lenz, F. A. *et al.*, 1994a), but clearly not of cardiac origin in the patient with panic disorder. The association of stimulation-associated angina and the affective dimension was not unexpected (Lenz, F. A. *et al.*, 1994a) as angina is often associated with a strong affective dimension, unlike other chest pains (Matthews, M. B., 1985; Braunwald, E., 1988; Procacci, P. and Zoppi, M., 1989; Pasternak, R. C. *et al.*, 1992). Stimulation-evoked sharp chest pain occurred without an affective dimension in a retrospective analysis of patients without prior experience of spontaneous chest pain with a strong affective dimension. Therefore, it is possible that in the case, stimulation-associated chest pain included an affective dimension as a result of conditioning by the prior experience of spontaneous chest pain with a strong affective dimension. In retrospect, the affective dimension of stimulation-associated angina might arise by similar conditioning.

5.44.4.2 Medial and Intralaminar Thalamic Nuclei

The medial and intralaminar nuclei also play a role in signaling pain sensations. Medial to Vc, the most dense STT terminal pattern is found in the intralaminar nucleus centralis lateralis (Mehler, W. R., 1962; 1969), while a much less dense termination is found in other interlaminar nuclei central medial, parafascicularis (Mehler, W. R., 1962), and the medial dorsal nucleus (Mehler, W. R., 1969). Nociceptive neurons have been identified in an area that apparently corresponds to the human central median nucleus (Ishijima, B. *et al.*, 1975; Tsubokawa, T. and Moriyasu, N., 1975; Rinaldi, P. C. *et al.*, 1991).

Milliampere-current-level stimulation at sites probably located in the parafascicular, limitans, and central medial (parvocellular part) nuclei was reported to evoke a diffuse, burning pain, or sometimes to exacerbate the patient's ongoing pain (Sano, K., 1979). This pain was evoked in projected fields as large as the whole body or hemibody. Stimulation at sites, possibly the medial dorsal and periventricular nuclei evoked a generalized unpleasant sensation, not localized to a particular body part (Sano, K., 1979). Both responses may be consistent with the STT pathway or a multisynaptic pathway traversing the reticular formation (Willis, W. D., 1985).

5.44.5 Cortex

Functional imaging studies of the response to the application of painful stimuli (Jones, A. K. *et al.*, 1991; Talbot, J. D. *et al.*, 1991; Casey, K. L. *et al.*, 1994; Craig, A. D. *et al.*, 1996; Andrew, D. *et al.*, 2001) have identified three cortical areas with metabolic activation: primary somatosensory, parasylvian, and cingulate cortex. These cortical areas all receive input arising from nociceptors as demonstrated by cortical potentials evoked by cutaneous application of a laser (laser-evoked potentials – LEP) (Ohara, S. *et al.*, 2004b), which selectively activates nociceptors (Bromm, B. *et al.*, 1984). Pain-related responses to stimulation have been identified in relation to the parasylvian cortex.

5.44.5.1 Parasylvian Cortex and Pain Memory

Parasylvian cortex receives input from the nuclei around, and subnuclei within Vc (Van Buren, J. M. and Borke, R. C., 1972) such as Vcpc, Vcpor, and putative VMpo. Parasylvian receives nociceptive input as evidenced by the presence of neurons responding to noxious stimuli (Robinson, C. J. and Burton, H., 1980; Dong, W. K. *et al.*, 1989; 1994) and of LEP generators (Lenz, F. A. *et al.*, 1998c; Vogel, H. *et al.*, 2003; Ohara, S. *et al.*, 2004b). The LEP generator is anterior to primary auditory cortex, adjacent to the S2 (secondary somatosensory cortex) generator for vibratory SEPs (somatosensory-evoked potentials) (Hamalainen, H. *et al.*, 1990; Ohara, S. *et al.*, 2004b). Source modeling suggests that the LEP generator is in the dorsal insula–parietal operculum (Figure 6) (Lenz, F. A. *et al.*, 1998b; Vogel, H. *et al.*, 2003), different from the location of the local generator for the P3 event-related potentials in the temporal base (Lenz, F. A. *et al.*, 1998b). Differences between the locations of the late component of the LEP, the P2 wave, and the P3 suggest that the LEP P2 is not a P3-

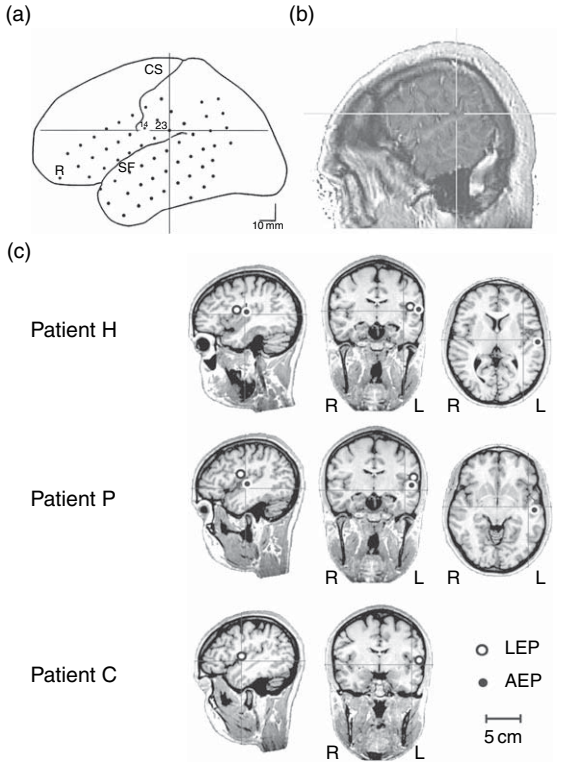

Figure 6 Verification of subdural grid electrode position in head model for dipole source analysis. Positions of all subdural grid electrodes were determined in a postoperative CT scan. These positions were entered into a spherical head model for dipole source analysis, from which they were projected back into a preoperative magnetic resonance imaging (MRI) of this patient's brain (patient H). (a) Intraoperative sketch shows the sylvian fissure with frontotemporal grid electrode 23 near the end of the fissure, and electrode 14 just posterior of the central sulcus. (b) Location of electrode 23 was projected from brain electromagnetic source analysis software (BESA) head coordinates into the preoperative MRI, showing excellent coincidence of the different coordinate systems used in this study. A similar correlation was found for electrode 14 and the central sulcus. (c) Projection of dipole source locations for LEP (○) and auditory – evoked potentials (AEP) (●). The projection was performed in Talairach space of a standard brain MRI. Left to right, panels show sagittal, coronal, and axial sections in patients H, P, and C, top to bottom. The LEP source was located above the sylvian fissure, and the AEP was located further posterior and below the fissure. The axial slice was aligned to pass through Heschl's gyrus (AEP generator) to illustrate the relative location of the source of the AEP (available only in patients H and P). Reprinted from Vogel H., Port, J. D., Lenz, F. A., Solaiyappan, M., Krauss, G., and Treede, R. D. 2003. Dipole source analysis of laser-evoked subdural potentials recorded from parasylvian cortex in humans. J. Neurophysiol. 89, 3051–3060, used with permission the American Physiological Society.

like wave, signaling the alertness evoked by painful stimuli (Zaslansky, R. *et al.*, 1995; Lenz, F. A. *et al.*, 1998b). Rather, it is likely that the LEP P2 is primarily related to the sensation of pain (Ohara, S. *et al.*, 2004a).

The pain-related function of this area is consistent with decreased pain discrimination and tolerance with lesions of the parietal operculum and insula, respectively (Greenspan, J. D. *et al.*, 1999). Studies in which LEPs were recorded through depth electrodes implanted in S2 and insula did not show a phase reversal in the parietal operculum, that is, S2 (Frot, M. *et al.*, 1999). Stimulation through electrodes placed in the posterior, superior insula produced pains described as burning, stinging, electrical, and disabling sensations (Ostrowsky, K. *et al.*, 2002). In a earlier series, stimulation of the exposed insula during awake craniotomies ($n = 5$) produced pain uncommonly but did produce nausea, tastes, somatic sensations in the epigastric area, and rising sensations in the epigastric and umbilical areas (Penfield, W. and Jasper, H. 1954). Thus there is evidence from human stimulation studies that insula, possibly the posterior–superior portion, is involved in pain-related processes.

Pain with a strong, vivid, affective dimension evoked by stimulation of the region of Vc may be related activation of its parasylvian cortical projection zone (see Section 5.44.4.1) (Locke, S. *et al.*, 1961; Mehler, W. R., 1962; Van Buren, J. M. and Borke, R. C., 1972). These vivid memories are similar to those evoked by stimulation around the lateral sulcus in patients with epilepsy (Halgren, E. *et al.*, 1978; Gloor, P. *et al.*, 1982b; Gloor, P., 1990). These memories may be related to cortical activation rather than medial temporal structures as they are not fully formed memories like those described here (Halgren, E. *et al.*, 1978; Gloor, P. *et al.*, 1982a). Furthermore, fully formed memories can be evoked after removal of mesial temporal structures (Moriarity, J. L. *et al.*, 2001). Therefore, pain with a strong affective dimension in response to thalamic stimulation results might be related to the activation of limbic and associated cortical structures (Lenz, F. A. *et al.*, 1995). The role of the medial temporal lobe might be transiently involved in the formation of these memories, before being located in cortex, independent of medial temporal lobe structures (Mishkin, M., 1979; Friedman, D. P. *et al.*, 1986; Zola-Morgan, S. and Squire, L. R., 1990).

Painful stimuli sometimes lead to long-term changes in pain processing, as well as to signaling

the presence of the stimulus. This appears to be the situation in the case of stimulation sites in and posterior to Vc, where stimulation can evoke complex, fully formed, pain in patients with angina or atypical chest pain. These memories seem to be due to long term changes in forebrain function, that is, conditioning, since memories of this type have not been reported in response to STT stimulation.

S2 and insular cortical areas involved in pain processing also satisfy criteria for areas involved in memory through corticolimbic connections (Mishkin, M., 1979). In monkeys, a nociceptive submodality selective area has been found within S2 (Dong, W. K. *et al*., 1994; Willis, W. D., Jr. *et al.,* 2001). S2 cortex projects to insular areas that project to amygdala (Friedman, D. P. *et al*., 1986). S2 and insular cortex have bilateral primary noxious sensory input (Chatrian, G. E. *et al*., 1975), and cells in these areas responding to noxious stimuli have bilateral representation (Dong, W. K. *et al*., 1994) and project to the medial temporal lobe (Chatrian, G. E. *et al*., 1975; Dong, W. K. *et al*., 1989). Parasylvian cortical areas receive input from nociceptive subnuclei within Vc, and from nuclei nearby (see Lateral Thalamic Nuclei) and so may be involved in memory for pain (Burton, H., 1986). This proposal is consistent with Mishkin's hypothesis of somatic sensory memory mediated through corticolimbic connections (Mishkin, M., 1979).

5.44.6 Conclusions

These stimulation results are consistent with those of functional imaging studies that have identified brain regions activated in a binary fashion by the application of a very specific, painful stimulus, while further increases in stimulus intensity do not produce increased activation. These brain regions may also mediate the long-term relationship of some intense pains to the strong affective dimension, which accompanies them. This relationship may also explain the affective dimension of chronic pain, which results from an intensely painful experience. These complex experiences of pain are not evoked by stimulation of the STT, again suggesting that these memories of pain involve conditioning of forebrain structures, rather than simple activation by a painful stimulus.

Acknowledgments

This work is supported by the National Institutes of Health – National Institute of Neurological Disorders and Stroke (NS38493 and NS40059 to F. A. L.).

References

Al Chaer, E. D., Lawand, N. B., Westlund, K. N., and Willis, W. D. 1996a. Pelvic visceral input into the nucleus gracilis is largely mediated by the postsynaptic dorsal column pathway. J. Neurophysiol. 76, 2675–2690.

Al Chaer, E. D., Lawand, N. B., Westlund, K. N., and Willis, W. D. 1996b. Visceral nociceptive input into the ventral posterolateral nucleus of the thalamus: a new function for the dorsal column pathway. J. Neurophysiol. 76, 2661–2674.

Al-Chaer, E. D., Westlund, K. N., and Willis, W. D. 1997. Nucleus gracilis: an integrator for visceral and somatic information. J. Neurophysiol. 78, 521–527.

Andrew, D. and Craig, A. D. 2001. Spinothalamic lamina I neurons selectively sensitive to histamine: a central neural pathway for itch. Nat. Neurosci. 4, 72–77.

Apkarian, A. V. and Hodge, C. J. 1989. Primate spinothalamic pathways. II. The cells of origin of the dorsolateral and ventral spinothalamic pathways. J. Comp. Neurol. 288, 474–492.

Apkarian, A. V. and Shi, T. 1994. Squirrel monkey lateral thalamus. I. Somatic nociresponsive neurons and their relation to spinothalamic terminals. J. Neurosci. 14, 6779–6795.

Becker, D. E., Yingling, C. D., and Fein, G. 1993. Identification of pain, intensity, and P300 components in the pain evoked potential. Electroencephalogr. Clin. Neurophysiol. 88, 290–301.

Blomqvist, A., Zhang, E. T., and Craig, A. D. 2000. Cytoarchitectonic and immunohistochemical characterization of a specific pain and temperature relay, the posterior portion of the ventral medial nucleus, in the human thalamus. Brain 123(Pt 3), 601–619.

Bowsher, D. 1957. Termination of the central pain pathway in man: the conscious appreciation of pain. Brain 80, 606–620.

Braunwald, E. 1988. The History. In: Heart Disease: A Textbook of Cardiovascular Medicine (*ed*. E. Braunwald), pp. 1–12. W. B. Saunders.

Bromm, B. and Treede, R. D. 1984. Nerve fibre discharges, cerebral potentials and sensations induced by CO_2 laser stimulation. Hum. Neurobiol. 3, 33–40.

Burton, H. 1986 Second Somatosensory Cortex and Related Areas. In: Cerebral Cortex, Sensory–Motor Areas and Aspects of Cortical Connectivity, (*eds*. E. G. Jones and A. Peters), Vol. 5. pp. 31–98. Plenum .

Casey, K. L., Minoshima, S., Berger, K. L., Koeppe, R. A., Morrow, T. J., and Frey, K. A. 1994. Positron emission tomographic analysis of cerebral structures activated specifically by repetitive noxious heat stimuli. J. Neurophysiol. 71, 802–807.

Chatrian, G. E., Canfield, R. C., Knauss, T. A., and Eegt, E. L. 1975. Cerebral responses to electrical tooth pulp stimulation in man. An objective correlate of acute experimental pain. Neurology 25, 745–757.

Christensen, M. D., Willis, W. D., and Westlund, K. N. 1996. Anatomical evidence for cells of origin of a postsynaptic dorsal column visceral pathway: sacral spinal cord cells innervating the medial nucleus gracilis. Society For Neuroscience Abstract 22, 109.

Craig, A. D. 1998. A new version of the thalamic disinhibition hypothesis of central pain. Pain Focus 7, 1–14.

Craig, A. D. 2003a. A new view of pain as a homeostatic emotion. Trends Neurosci. 26, 303–307.

Craig, A. D. 2003b. Pain mechanisms: labeled lines versus convergence in central processing. Annu. Rev. Neurosci. 26, 1–30.

Craig, A. D., Bushnell, M. C., Zhang, E. T., and Blomqvist, A. 1994. A thalamic nucleus specific for pain and temperature sensation. Nature 372, 770–773.

Craig, A. D., Reiman, E. M., Evans, A., and Bushnell, M. C. 1996. Functional imaging of an illusion of pain. Nature 384, 258–260.

Cusick, C. G., Wall, J. T., Felleman, D. J., and Kaas, J. H. 1989. Somatotopic organization of the lateral sulcus of owl monkeys: area 3b, S-II, and a ventral somatosensory area. J. Comp. Neurol. 282, 169–190

Davis, K. D., Kiss, Z. H. T., Tasker, R. R., and Dostrovsky, J. O. 1996. Thalamic stimulation-evoked sensations in chronic pain patients and nonpain (movement disorder) patients. J. Neurophysiol. 75, 1026–1037.

Davis, K. D., Lozano, A. M., Manduch, M., Tasker, R. R., Kiss, Z. H. T., and Dostovsky, J. O. 1999. Thalamic relay site for cold perception in humans. J. Neurophysiol. 81, 1970–1973.

Davis, K. D., Tasker, R. R., Kiss, Z. H. T., Hutchison, W. D., and Dostrovsky, J. O. 1995. Visceral pain evoked by thalamic microstimulation in humans. Neuroreport 6, 369–374.

Dong, W. K., Chudler, E. H., Sugiyama, K., Roberts, V. J., and Hayashi, T. 1994. Somatosensory, multisensory, and task-related neurons in cortical area 7b (PF) of unanesthetized monkeys. J. Neurophysiol. 72, 542–564.

Dong, W. K., Salonen, L. D., Kawakami, Y., Shiwaku, T., Kaukoranta, E. M., and Martin, R. F. 1989. Nociceptive responses of trigeminal neurons in SII-7b cortex of awake monkeys. Brain Res. 484, 314–324.

Dostrovsky, J. O., Wells, F. E. B., and Tasker, R. R. 1991. Pain Evoked by Stimulation in Human Thalamus. In: International Symposium on Processing Nociceptive Information (*ed*. Y. Sjigenaga), pp. 115–120. Elsevier.

Dubner, R., Kenshalo, D. R., Jr., Maixner, W., Bushnell, M. C., and Oliveras, J. L. 1989. The correlation of monkey medullary dorsal horn neuronal activity and the perceived intensity of noxious heat stimuli. J. Neurophysiol. 62, 450–457

Duncan, G. H., Bushnell, M. C., Oliveras, J. L., Bastrash, N., and Tremblay, N. 1993. Thalamic VPM nucleus in the behaving monkey. III. Effects of reversible inactivation by lidocaine on thermal and mechanical discrimination. J. Neurophysiol. 70, 2086–2096.

Ferrington, D. G., Sorkin, L. S., and Willis, W. D. 1987. Responses of spinothalamic tract cells in the superficial dorsal horn of the primate lumbar spinal cord. J. Physiol. (Lond.) 388, 681–703.

Friedman, D. P., Murray, E. A., O'Neill, J. B., and Mishkin, M. 1986. Cortical connections of the somatosensory fields of the lateral sulcus of macaques: evidence for a corticolimbic pathway for touch. J. Comp. Neurol. 252, 323–347.

Frot, M. and Mauguiere, F. 1999. Timing and spatial distribution of somatosensory responses recorded in the upper bank of the sylvian fissure (SII area) in humans. Cereb. Cortex 9, 854–863.

Gloor, P. 1990. Experiential phenomena of temporal lobe epilepsy: facts and hypotheses. Brain 113, 1673–1694.

Gloor, P., Olivier, A., Quesney, L. F., Andermann, F., and Horowitz, S. 1982a. The role of the limbic system in experiential phenomena of temporal lobe epilepsy. Ann. Neurol. 12, 129–144.

Gloor, P., Olivier, A., Quesney, L. F., Andermann, F., and Horowitz, S. 1982b. The role of the limbic system in experiential phenomena of temporal lobe epilepsy. Ann. Neurol. 12, 129–144.

Gracely, R. H., Lota, L., Walter, D. J., and Dubner, R. 1988. A multiple random staircase method of psychophysical pain assessment. Pain 32, 55–63.

Graziano, A. and Jones, E. G. 2004. Widespread thalamic terminations of fibers arising in the superficial medullary dorsal horn of monkeys and their relation to calbindin immunoreactivity. J. Neurosci. 24, 248–256.

Greenspan, J. D., Lee, R. R., and Lenz, F. A. 1999. Pain sensitivity alterations as a function of lesion location in the parasylvian cortex. Pain 81, 273–282.

Greenspan, J. D., Ohara, S., Sarlani, E., and Lenz, F. A. 2004. Allodynia in patients with post-stroke central pain (CPSP) studied by statistical quantitative sensory testing within individuals. Pain 109, 357–366.

Halgren, E., Walter, R. D., Cherlow, D. G., and Crandall, P. H. 1978. Mental phenomena evoked by electrical stimulation of the human hippocampal formation and amygdala. Brain 101, 83–117.

Hamalainen, H., Kekoni, J., Sams, M., Reinikainen, K., and Naatanen, R. 1990. Human somatosensory evoked potentials to mechanical pulses and vibration: contributions of SI and SII somatosensory cortices to P50 and P100 components. Electroencephalogr. Clin. Neurophysiol. 75, 13–21.

Hassler, R. 1959. Anatomy of the Thalamus. In: Introduction to Stereotaxis with an Atlas of the Human Brain (*eds*. G. Schaltenbrandand and P. Bailey), pp. 230–290. Thieme.

Hassler, R. and Reichert, T. 1959 Klinische und anatomische Befunde bei stereotaktischen Schmerzoperationen im Thalamus. Arch. Psychiat. Nerverkr. 200, 93–122.

Hirai, T. and Jones, E. G. 1989. A new parcellation of the human thalamus on the basis of histochemical staining. Brain Res. Rev. 14, 1–34.

Ishijima, B., Yoshimasu, N., Fukushima, T., Hori, T., Sekino, H., and Sano, K. 1975. Nociceptive neurons in the human thalamus. Confin. Neurol. 37, 99–106.

Jones, A. K., Brown, W. D., Friston, K. J., Qi, L. Y., and Frackowiak, R. S. 1991. Cortical and subcortical localization of response to pain in man using positron emission tomography. Proc. R. Soc. Lond. B Biol. Sci. 244, 39–44.

Jones, E. G., Friedman, D. P., and Hendry, S. H. 1982. Thalamic basis of place- and modality-specific columns in monkey somatosensory cortex: a correlative anatomical and physiological study. J. Neurophysiol. 48, 545–568.

Kaas, J. H., Nelson, R. J., Sur, M., Dykes, R. W., and Merzenich, M. M. 1984 The somatotopic organization of the ventroposterior thalamus of the squirrel monkey, *Saimiri sciureus*. J. Comp. Neurol. 226, 111–140.

Kumazawa, T. and Perl, E. R. 1978. Excitation of marginal and substantia gelatinosa neurons in the primate spinal cord: indications of their place in dorsal horn functional organization. J. Comp. Neurol. 177, 417–434

Lee, J.-I., Antezanna, D., Dougherty, P. M., and Lenz, F. A. 1999. Responses of neurons in the region of the thalamic somatosensory nucleus to mechanical and thermal stimuli graded into the painful range. J. Comp. Neurol. 410, 541–555

Lenz, F. A. and Byl, N. N. 1999. Reorganization in the cutaneous core of the human thalamic principal somatic sensory nucleus (ventral caudal) in patients with dystonia. J. Neurophysiol. 82, 3204–3212.

Lenz, F. A. and Dougherty, P. M. 1998. Cells in the human principal thalamic sensory nucleus (ventralis caudalis – Vc) respond to innocuous mechanical and cool stimuli. J. Neurophysiol. 79, 2227–2230.

Lenz, F. A., Dostrovsky, J. O., Tasker, R. R., Yamashiro, K., Kwan, H. C., and Murphy, J. T. 1988. Single-unit analysis of the human ventral thalamic nuclear group: somatosensory responses. J. Neurophysiol. 59, 299–316.

Lenz, F. A., Gracely, R. H., Baker, F. H., Richardson, R. T., and Dougherty, P. M. 1998a. Reorganization of sensory modalities evoked by stimulation in the region of the principal sensory nucleus (ventral caudal – Vc) in patients with pain secondary to neural injury. J. Comp. Neurol. 399, 125–138.

Lenz, F. A., Gracely, R. H., Hope, E. J., Baker, F. H., Rowland, L. H., Dougherty, P. M., and Richardson, R. T. 1994a. The sensation of angina can be evoked by stimulation of the human thalamus. Pain 59, 119–125.

Lenz, F. A., Gracely, R. H., Romanoski, A. J., Hope, E. J., Rowland, L. H., and Dougherty, P. M. 1995. Stimulation in the human somatosensory thalamus can reproduce both the affective and sensory dimensions of previously experienced pain. Nat. Med. 1, 910–913.

Lenz, F. A., Gracely, R. H., Rowland, L. H., and Dougherty, P. M. 1994b. A population of cells in the human thalamic principal sensory nucleus respond to painful mechanical stimuli. Neurosci. Lett. 180, 46–50.

Lenz, F. A., Ohara, S., Gracely, R. H., Dougherty, P. M., and Patel, S. H. 2004. Pain encoding in the human forebrain: binary and analog exteroceptive channels. J. Neurosci. 24, 6540–6544.

Lenz, F. A., Rios, M., Chau, D., Krauss, G. L., Zirh, T. A., and Lesser, R. P. 1998b. Painful stimuli evoke potentials recorded from the parasylvian cortex in humans. J. Neurophysiol. 80, 2077–2088.

Lenz, F. A., Rios, M. R., Zirh, T. A., Krauss, G., and Lesser, R. P. 1998c. Painful stimuli evoke potentials recorded over the human anterior cingulate gyrus. J. Neurophysiol. 79, 2231–2234.

Lenz, F. A., Seike, M., Lin, Y. C., Baker, F. H., Rowland, L. H., Gracely, R. H., and Richardson, R. T. 1993a. Neurons in the area of human thalamic nucleus ventralis caudalis respond to painful heat stimuli. Brain Res. 623, 235–240.

Lenz, F. A., Seike, M., Richardson, R. T., Lin, Y. C., Baker, F. H., Khoja, I., Jaeger, C. J., and Gracely, R. H. 1993b. Thermal and pain sensations evoked by microstimulation in the area of human ventrocaudal nucleus. J. Neurophysiol. 70, 200–212.

Locke, S., Angevine, J. B., and Marin, O. S. M. 1961. Projection of magnocellular medial geniculate nucleus in man. Anat. Rec. 139, 249–250.

Matthews, M. B. 1985. Clinical Diagnosis. In: Angina Pectoris (*ed*. D. G. Julian), pp. 62–83. Churchill Livingstone.

Mayer, D. J., Price, D. D., and Becker, D. P. 1975. Neurophysiological characterization of the anterolateral spinal cord neurons contributing to pain perception in man. Pain 1, 51–58.

Mehler, W. R. 1962. The Anatomy of the So-Called ''Pain Tract'' in Man: An Analysis of the Course and Distribution of the Ascending Fibers of the Fasciculus Anterolateralis. In: Basic Research in Paraplegia (*eds*. J. D. French and R. W. Porter), pp. 26–55. Thomas.

Mehler, W. R. 1966. The posterior thalamic region in man. Confin. Neurol. 27, 18–29.

Mehler, W. R. 1969. Some neurological species differences – a posteriori. Ann. N. Y. Acad. Sci. 167, 424–468.

Mishkin, M. 1979. Analogous neural models for tactual and visual learning. Neuropsychologia 17, 139–151.

Moriarity, J. L., Boatman, D., Krauss, G. L., Storm, P. B., and Lenz, F. A. 2001 Human ''memories'' can be evoked by stimulation of the lateral temporal cortex after ipsilateral medial temporal lobe resection. J. Neurol. Neurosurg. Psychiatry 71, 549–551.

Ohara, S. and Lenz, F. A. 2003. Medial lateral extent of thermal and pain sensations evoked by microstimulation in somatic sensory nuclei of human thalamus. J. Neurophysiol. 90, 2367–2377.

Ohara, S., Crone, N. E., Weiss, N., Treede, R. D., and Lenz, F. A. 2004a. Amplitudes of laser evoked potential recorded from primary somatosensory, parasylvian and medial frontal cortex are graded with stimulus intensity. Pain 110, 318–328.

Ohara, S., Crone, N. E., Weiss, N., Treede, R. D., and Lenz, F. A. 2004b. Cutaneous painful laser stimuli evoke responses recorded directly from primary somatosensory cortex in awake humans. J. Neurophysiol. 91, 2734–2746.

Olszewski, J. 1952. The Thalamus of *Maccaca mulatta*. Karger.

Ostrowsky, K., Magnin, M., Ryvlin, P., Isnard, J., Guenot, M., and Mauguiere, F. 2002. Representation of pain and somatic sensation in the human insula: a study of responses to direct electrical cortical stimulation. Cereb. Cortex 12, 376–385.

Pasternak, R. C., Braunwald, E., and Sobel, B. E. 1992 Acute Myocardial Infarction. In: Cardiac Disease (*ed*. E. Braunwald), pp. 1200–1291. W. B. Saunders.

Penfield, W. and Jasper, H. 1954. Epilepsy and the Functional Anatomy of the Human Brain. Little Brown.

Perl, E. R. 1984 Pain and Nociception. In: The Nervous System: Sensory Processes, Part 2 (*eds*. J. M. Brookhart, V. B. Mountcastle, I. Darian-Smith, and S. R. Geiger), pp. 915–975. American Physiological Society.

Price, D. D. and Dubner, R. 1977. Neurons that subserve the sensory-discriminative aspects of pain. Pain 3, 307–338.

Price, D. D., Greenspan, J. D., and Dubner, R. 2003. Neurons involved in the exteroceptive function of pain. Pain 106, 215–219.

Price, D. D. and Mayer, D. J. 1975. Neurophysiological characterization of the anterolateral quadrant neurons subserving pain in *M. mulatta*. Pain 1, 59–72.

Procacci, P. and Zoppi, M. 1989. Heart Pain. In: Textbook of Pain (*eds*. P. D. Wall and R. Melzack), pp. 410–419. Churchill Livingstone.

Ralston, H. J. and Ralston, D. D. 1992. The primate dorsal spinothalamic tract: evidence for a specific termination in the posterior nuclei [Po/SG] of the thalamus. Pain 48, 107–118.

Rinaldi, P. C., Young, R. F., Albe-Fessard, D. G., and Chodakiewitz, J. 1991. Spontaneous neuronal hyperactivity in the medial and intralaminar thalamic nuclei in patients with deafferentation pain. J. Neurosurg. 74, 415–421.

Robinson, C. J. and Burton, H. 1980. Somatic submodality distribution within the second somatosensory (SII), 7b, retroinsular, postauditory, and granular insular cortical areas of M. fascicularis. J. Comp. Neurol. 192, 93–108.

Rustioni, A., Hayes, N. L., and O'Neill, S. 1979. Dorsal column nuclei and ascending spinal afferents in macaques. Brain 102, 95–125.

Sano, K. 1979. Stereotaxic Thalamolaminotomy and Posteromedial Hypothalamotomy for the Relief of Intractable Pain. In: Advances in Pain Research and Therapy (*eds*. J. J. Bonica and V. Ventrafridda) Vol. 2, pp. 475–485. Raven Press.

Schaltenbrand, G. and Bailey, P. 1959. Introduction to Stereotaxis with an Atlas of the Human Brain. Thieme.

Talairach, J. and Tournoux, P. 1988. Co-Planar Stereotaxic Atlas of the Human Brain, 3D Proportional System: An Approach to Cerebral Imaging. Georg Thieme Verlag.

Talbot, J. D., Marrett, S., Evans, A. C., Meyer, E., Bushnell, M. C., and Duncan, G. H. 1991. Multiple representations of pain in human cerebral cortex. Science 251, 1355–1358.

Tsubokawa, T. and Moriyasu, N. 1975. Follow-up results of centre median thalamotomy for relief of intractable pain. A method of evaluating the effectiveness during operation. Confin. Neurol. 37, 280–284.

Uddenberg, N. 1968. Functional organization of long, second-order afferents in the dorsal funiculus. Exp. Brain Res. 4, 377–382.

Van Buren, J. M. and Borke, R. C. 1972. Variations and Connections of the Human Thalamus. Springer.

Vogel, H., Port, J. D., Lenz, F. A., Solaiyappan, M., Krauss, G., and Treede, R. D. 2003. Dipole source analysis of laser-evoked subdural potentials recorded from parasylvian cortex in humans. J. Neurophysiol. 89, 3051–3060.

Wang, C. C., Willis, W. D., and Westlund, K. N. 1999. Ascending projections from the area around the spinal cord central canal: a *Phaseolus vulgaris* leucoagglutinin study in rats. J. Comp. Neurol. 415, 341–367.

Willis, W. D. 1985 The Pain System. Karger.

Willis, W. D., Al Chaer, E. D., Quast, M. J., and Westlund, K. N. 1999. A visceral pain pathway in the dorsal column of the spinal cord. Proc. Natl. Acad. Sci. U. S. A. 96, 7675–7679.

Willis, W. D. and Coggeshall, R. E. 1991. Sensory Mechanisms of the Spinal Cord. Plenum.

Willis, W. D., Jr., Zhang, X., Honda, C. N., and Giesler, G. J., Jr. 2001. Projections from the marginal zone and deep dorsal horn to the ventrobasal nuclei of the primate thalamus. Pain 92, 267–276.

Yarnitsky, D. and Sprecher, E. 1994. Thermal testing: normative data and repeatability for various test algorithms. J. Neurol. Sci. 125, 39–45.

Zaslansky, R., Sprecher, E., Tenke, C. E., Hemli, J. A., and Yarnitsky, D. 1995. The P300 in pain evoked potentials. Pain 66, 39–49.

Zola-Morgan, S. and Squire, L. R. 1990. The primate hippocampal formation: evidence for a time-limited role in memory storage. Science 250, 288–290.

5.45 Nociceptive Processing in the Cerebral Cortex

R D Treede, Ruprecht-Karls-University Heidelberg, Heidelberg, Germany

A V Apkarian, Northwestern University, Chicago, IL, USA

© 2008 Elsevier Inc. All rights reserved.

5.45.1	**Introduction**	670
5.45.2	**Methods to Study Nociceptive Processing in the Human Cerebral Cortex**	671
5.45.3	**Cortical Regions that are Part of the Nociceptive System**	673
5.45.3.1	The Primary Somatosensory Cortex	673
5.45.3.2	Parasylvian Cortex: the Operculo-Insular Region	674
5.45.3.2.1	The secondary somatosensory cortex (SII)	675
5.45.3.2.2	The frontal operculum	675
5.45.3.2.3	The insula	676
5.45.3.3	The Posterior Parietal Cortex	676
5.45.3.4	The Cingulate Cortex	677
5.45.3.5	The Prefrontal Cortex	678
5.45.4	**Functional Roles of Cortical Nociceptive Signal Processing**	678
5.45.4.1	Location and Quality of Phasic Pain	678
5.45.4.2	The Time Domain	680
5.45.4.3	Attention and Distraction Effects on Pain-Evoked Cortical Activity	680
5.45.4.4	Anticipation and Expectation	681
5.45.4.5	Empathy	681
5.45.5	**Pain Modulation**	681
5.45.5.1	Psychological Modulation of Pain	681
5.45.5.1.1	Hypnosis and pain-evoked cortical activity	681
5.45.5.1.2	Mood and emotional states and pain-evoked cortical activity	682
5.45.5.1.3	Placebo and pain-evoked cortical activity	682
5.45.5.2	Pharmacological Modulation of Pain	682
5.45.5.2.1	Opiates	682
5.45.5.2.2	Dopamine	683
5.45.5.2.3	Estrogen	683
5.45.6	**Overview Regarding the Role of the Cortex in Acute Pain Perception**	683
5.45.7	**Clinical Applications**	684
5.45.8	**Chronic Pain**	684
5.45.8.1	Studying Brain Activity in Chronic Pain with Nonspecific Painful Stimuli	684
5.45.8.2	Clinical Pain Conditions Studied by Stimulation and the Role of the Cortex	685
5.45.8.2.1	Migraine	686
5.45.8.2.2	Cluster headache	686
5.45.8.2.3	Cardiac pain	686
5.45.8.2.4	Irritable bowel syndrome	686
5.45.8.3	Spontaneous Pain as a Confound in Assessing Brain Activity	687
5.45.8.4	Functional Magnetic Resonance Imaging of Spontaneous Pain	689
5.45.8.5	Neuropathic Pain	689
5.45.8.6	Low Back Pain and Fibromyalgia	690
5.45.8.7	Overview Regarding the Role of the Cortex in Chronic Pain Perception	690
5.45.9	**Conclusions and Outlook**	691
References		691

Glossary

ACC anterior cingulate cortex (n.b.: some authors use this as a summary term for ACC and MCC)
CBP Chronic back pain
CRPS Complex regional pain syndrome
EEG Electro-encephalography
fMRI Functional magnetic resonance imaging
IBS Irritable bowel syndrome
IC Insular cortex
MCC mid-cingulate cortex (n.b.: some authors call this region the posterior part of ACC)
MEG Magneto-encephalography
MRS Magnetic resonance spectroscopy
OIC Operculo-insular cortex, consisting of insular cortex plus the frontal, parietal and temporal operculum.
PAG Periaqueductal grey
PET Positron emission tomography
PFC prefrontal cortex
PHN Postherpetic neuralgia
SI Primary somatosensory cortex
SII Secondary soamtosensory cortex
SCI Spinal cord injury
SPECT Single photon emission computed tomography
Th Thalamus

5.45.1 Introduction

Conscious perception of external stimuli requires encoding by sensory organs, processing within the respective sensory system, and activation of the appropriate sensory cortical areas. Based on a small case series of infra- and supratentorial brain lesions, Head H. and Holmes G. (1911) postulated that the sensation of pain is an exception to this rule and that its conscious perception occurs in the essential organ of the thalamus. In spite of evidence to the contrary from clinical reports (Marshall, J., 1951; Biemond, A., 1956), evoked potentials in humans (Spreng, M. and Ichioka, M., 1964; Duclaux, R. *et al.*, 1974; Carmon, A. *et al.*, 1976; Chen, A. C. N. *et al.*, 1979; Bromm, B. and Treede, R. D., 1984), single unit recordings in animals (Lamour, Y. *et al.*, 1982; Kenshalo, D. R. and Isensee, O., 1983), neuroanatomical tracing (Gingold, S. I. *et al.*, 1991), and some early PET studies (Buchsbaum, M. S. *et al.*, 1984), it was maintained for a long time that the cortical representation of pain is a *quantité négligable*.

This situation changed, when the modern neuroimaging techniques of positron emission tomography (PET) and later functional magnetic resonance imaging (fMRI) demonstrated systematic metabolic and perfusion changes in a large number of cortical areas following painful stimuli (Talbot, J. D. *et al.*, 1991; Jones, A. K. P. *et al.*, 1991a; Apkarian, A. V. *et al.*, 1992; Davis, K. D. *et al.*, 1995). These findings were supported by invasive and noninvasive electrophysiological studies in humans, using magnetoencephalography (MEG), electroencephalography (EEG), subdural recordings directly from the surface of the brain, and depth recordings during stereotactic procedures (for a systematic review see Apkarian, A. V. *et al.*, 2005).

Meanwhile it has been recognized that painful stimuli activate a vast network of cortical areas, including the primary and secondary somatosensory cortex (SI, SII), the insula, posterior parietal cortex, anterior and mid-cingulate cortex, and parts of the prefrontal cortex (PFC; Figure 1). These areas are involved in the generation of painful percepts as well as in the descending control of pain (for review see Kenshalo, D. R. and Willis, W. D., 1991; Treede, R. D. *et al.*, 1999; Price, D. D., 2000; Apkarian, A. V. *et al.*, 2005). Most of these areas are also involved in other sensory, emotional, cognitive, motor or autonomic functions. Hence, the nociceptive system converges with other systems for the generation of the conscious percept of pain. In that sense, the nociceptive system is not different from the visual system, for example. But it is still an open question, to what extent any cortical regions can be considered as nociceptive specific.

In this chapter we will briefly review the methods used to assess nociceptive processing in the human brain, present connectivity and functional properties of each of the principal cortical regions of the nociceptive system, and summarize the roles of the cerebral cortex in various aspects of pain perception and pain modulation.

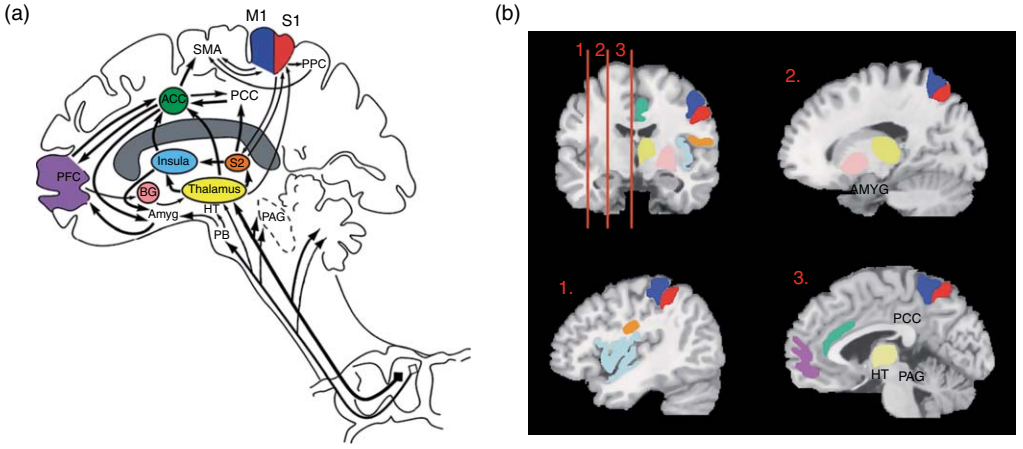

Figure 1 Cortical regions involved in pain perception, their interconnectivity and ascending pathways. Locations of brain regions involved in pain perception are color coded in a schematic drawing and in an example magnetic resonance image (MRI). (a) Schematic diagram shows the regions, their interconnectivity, and afferent pathways. (b) The areas corresponding to those shown in the schematic are shown in an anatomical MRI, on a coronal slice and three sagittal slices as indicated on the coronal slice: primary and secondary somatosensory cortices (S1, S2, red and orange), anterior and mid-cingulate cortex (ACC, green), insula (blue), thalamus (yellow), prefrontal cortex (PFC, purple), primary and supplementary motor cortex (M1 and SMA), posterior parietal cortex (PPC), posterior cingulate cortex (PCC), basal ganglia (BG, pink), hypothalamus (HT), amygdala (AMYG), parabrachial nuclei (PB), and periaqueductal gray (PAG). Reproduced from Apkarian, A. V., Bushnell, C., Treede, R. D., and Zubieta, J. K. 2005. Human brain mechanisms of pain perception and regulation in health and disease. Eur. J. Pain 9, 463–484.

5.45.2 Methods to Study Nociceptive Processing in the Human Cerebral Cortex

Table 1 summarizes properties of the different brain imaging techniques that have been used to define the nociceptive network in the human brain. The most direct approach to learn about the functions of cortical neurons is direct intracellular or extracellular recording of their electrical activity during sensory stimulation and in different contexts. This technique is mostly restricted to animal studies (Kenshalo, D. R. and Isensee, O., 1983; Dong, W. K. *et al.*, 1994) and has rarely been possible in humans (Hutchison, W. D. *et al.*, 1999). Field potentials within the brain invert their polarity, when an electrode track passes through or close to their generator source. This technique has been used in the course of presurgical epilepsy diagnostics (Frot, M. and Mauguière, F., 1999), but since the electrode tracks are related to the clinical indications, only few parts of the brain have been sampled that way. Presurgical epilepsy diagnostics using subdural electrode grids samples a much larger part of the brain surface, and dipole source analysis can be used to estimate the depths of the generators below the grids (Vogel, H. *et al.*, 2003). All of these invasive recordings in the human brain need to be interpreted with caution, because the cortical pathology that provided the indication for the procedure (e.g., epilepsy, tumors) may have altered nociceptive signal processing.

EEG and MEG are noninvasive techniques for the direct assessment of electrical activity in the brain. Mathematical algorithms are available to estimate the location of the generators within the brain from the signals recorded at the surface of the head with an accuracy of about 10 mm (Scherg, M., 1992; Pascual-Marqui, R. D. *et al.*, 1994; Hari, R. and Forss, N., 1999). EEG and MEG techniques provide accurate timing information. As a result, both methods have been used mainly to identify the arrival of information to various cortical regions (stimulus-evoked potentials). Spontaneous fluctuations in EEG and MEG would provide a view of the interactions between cortical areas. However, the application of the latter to painful states has remained minimal (Chen, A. C. N., 1993; Ohara, S. *et al.*, 2006). MEG detects brain magnetic activity, a signal that is proportional and orthogonal to the local electrical activity. Depending on the orientation of a local generator source and the gyral geometry of the brain region, evoked potentials in different brain areas may be better detected by MEG or EEG. The main weakness of EEG and MEG methods is their limited spatial resolution (on the order of 1 cm for both methods).

PET, single photon emission-computed tomography (SPECT), and fMRI measure brain activity

Table 1 Brain mapping techniques, their properties, and application in pain studies

Method	*Energy source*	*Spatial resolution (mm)*	*Temporal resolution (s)*	*Constraints*	*Output measured*	*Application in pain studies*
EEG/MEG	Intrinsic electricity	10	0.001	Lack of unique localization	Electrophysiology of brain events	Increasing in use, mainly for detecting temporal sequences
fMRI	Radio waves, magnetic fields	4–5	4–10	Immobilization, loud, cooperation	Relative cerebral blood flow	Most used, mainly for localizing brain activity
MRS	Radio waves, magnetic fields	10	10–100	Immobilization, loud	Relative chemical concentrations	Recently used, for detecting long term changes in brain chemistry
Nuclear (PET/ SPECT)	Radiation	5–10	60–1000	Radiation limits, immobilization	Physiology, neurochemistry, absolute values	Decreasing in use, becoming limited to neurochemistry
Brain imaging techniques available but rarely or not yet used in pain studies						
Single or multiunit electrophysiology	Intrinsic electricity	0.01–1	0.001	Invasive, direct access to brain	Electrophysiology	
Near infrared spectroscopy and imaging	Infrared light	0.05	0.05	Immobilization, surface > depth, limited field of view	Relative cerebral blood flow	
Transcranial magnetic/ electric stimulation	Magnetic/ electric fields	10	0.01	Risk of seizures, immobilization, loud	Electrophysiology, conduction times	
Structural MRI	Radio waves, magnetic fields	1	N/A	Immobilization, loud	Structure, vasculature, white matter	
Postmortem	N/A	0.001	N/A	Postmortem	Microarchitecture, chemoarchitecture	

EEG, electroencephalography; MEG, magnetoencephalography; fMRI, functional magnetic resonance imaging; MRS, magnetic resonance spectroscopy; PET, positron emission tomography; SPECT, single photon emission-computed tomography; N/A, not applicable.

indirectly by imaging changes in blood flow, blood oxygenation, or local metabolic changes (Peyron, R. *et al.*, 2000; Davis, K. D., 2003). All three methods can provide similar spatial resolution, although PET and fMRI methodologies are now far more advanced than SPECT. The statistical models and experimental designs available for PET and fMRI are robust and very rich. Therefore, these two techniques are currently most extensively used for detecting brain circuitry underlying many cognitive states, including pain. The temporal resolution of PET and SPECT is in the order of tens of seconds, while for fMRI it is shorter. PET and SPECT provide the additional opportunity for examining *in vivo* biochemistry and pharmacology by imaging the distributions of specific neurotransmitters or receptors. Recent MRI methods, like magnetic resonance spectroscopy (MRS), have also provided the ability to examine brain biochemistry. This approach is developing rapidly and has the potential to become a major method in the near future for studying brain chemistry. In addition, voxel based morphometry allows to image structural changes related to disease states (May, A. *et al.*, 1999).

5.45.3 Cortical Regions that are Part of the Nociceptive System

5.45.3.1 The Primary Somatosensory Cortex

The primary somatosensory cortex (SI) is located in the anterior part of the parietal lobe, where it constitutes the postcentral gyrus. It consists of Brodmann areas 1, 2, 3a, and 3b (Figure 2(a)). Areas 3b and 1 receive cutaneous tactile input, areas 3a and 2 proprioceptive input.

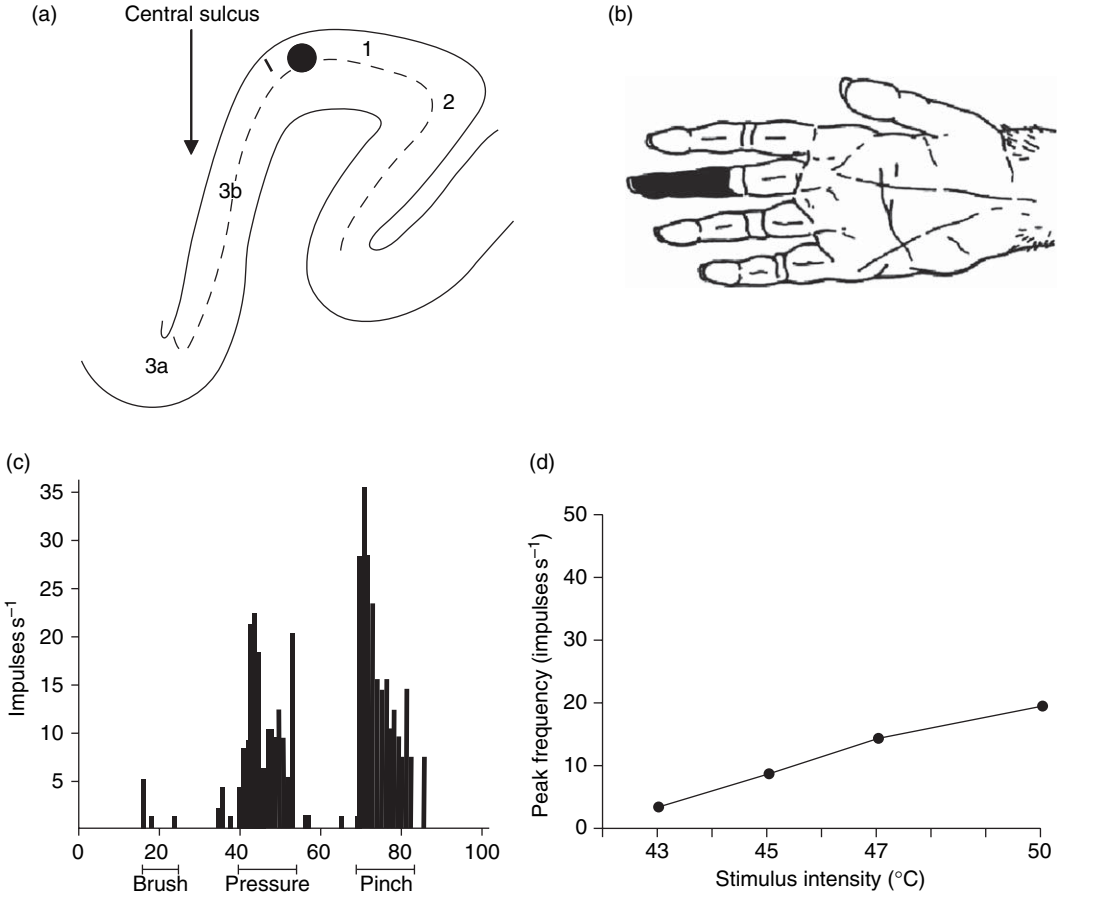

Figure 2 Nociceptive specific neuron in the primary somatosensory cortex (SI). (a) Left: SI consists of Brodmann areas 1, 2, 3a, and 3b in the postcentral gyrus. Black dot: location of the recorded neuron. (b) The small receptive field is consistent with a role in spatial discrimination. (c) Stimulus response function to painful mechanical stimuli. (d) Stimulus response function to painful heat stimuli. Modified from Kenshalo, D. R., Iwata, K., Sholas, M., and Thomas, D. A. 2000. Response properties and organization of nociceptive neurons in area 1 of monkey primary somatosensory cortex. J. Neurophysiol. 84, 719–729.

Nociceptive input to monkey SI was demonstrated anatomically. SI receives direct spinothalamocortical input from the ventrobasal nuclei, in particular the ventro-posterolateral (VPL) nucleus (Gingold, S. I. *et al.*, 1991). Nociceptive neurons in SI are found in clusters, raising the possibility that SI may contain nociceptive specific columns (Lamour, Y. *et al.*, 1983). Since evidence for nociceptive neurons in the most superficial cortical layers is lacking, this hypothesis has not yet been confirmed. Nociceptive neurons are rare in monkey SI and have mainly been found in area 1 (Kenshalo, D. R. *et al.*, 2000), whereas optical imaging techniques have also suggested nociceptive input to area 3a (Tommerdahl, M. *et al.*, 1996). Thus, nociceptive signal processing within SI may be spatially distinct from tactile signal processing that is primarily directed to area 3b. There is also some EEG and MEG evidence in humans that nociceptive areas may be situated more medially within SI than tactile areas with the same receptive fields, suggesting that nociceptive and tactile signal processing may occur in different subareas of SI (Ploner, M. *et al.* 2000; Schlereth, T. *et al.*, 2003). Nociceptive input to human SI has been confirmed by subdural recordings (Kanda, M. *et al.*, 2000; Ohara, S. *et al.*, 2004). About 75% of the PET and fMRI studies reported activation of SI (Bushnell, M. C. *et al.*, 1999; Apkarian, A. V. *et al.*, 2005).

Nociceptive neurons in SI have small receptive fields (Figure 2(b)) that are somatotopically arranged, and hence are ideally suited to code for the location of nociceptive stimuli (Kenshalo, D. R. and Isensee, O., 1983). Somatotopy of nociceptive processing in the human SI has been confirmed by EEG and PET studies (Tarkka, I. M. and Treede, R. D., 1993; Andersson, J. L. R. *et al.*, 1997). Action potential discharges of nociceptive SI neurons in monkey are modulated by the intensity of both mechanical and heat stimuli (Figures 2(c) and 2(d)) and their discharges correlate with detection speed (Kenshalo, D. R. *et al.*, 1988). These findings suggest that nociceptive SI neurons are involved in the coding of pain intensity. This conclusion has been confirmed by a PET study of hypnotic modulation of perceived pain intensity that also modulated perfusion of SI (Hofbauer, R. K. *et al.*, 2001) and by correlation analysis (Timmermann, L. *et al.*, 2001).

5.45.3.2 Parasylvian Cortex: the Operculo-Insular Region

The parasylvian cortex has a complicated macroscopic structure and only some of its cytoarchitectonic areas have been charted in detail (Eickhoff, S. B. *et al.*, 2006). In lateral views of the brain, the Sylvian fissure runs above the temporal lobe and separates it from the parietal and frontal lobes above the fissure. Hidden deep inside the Sylvian fissure lies a further lobe of the brain: the insula (Figure 3(a)). The insula is covered by the

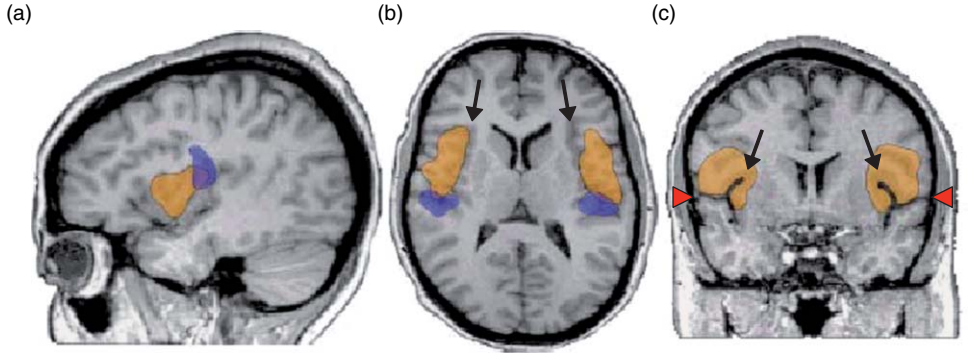

Figure 3 Nociceptive regions in parasylvian cortex. (a) Sagittal section shows the insula as a triangular region deep inside the Sylvian fissure. (b) Transaxial section illustrates the secondary somatosensory cortex (SII) as identified by tactile stimuli (blue) and regions responsive to nociceptive stimulation (orange) that extend further rostrally and medially. (c) Coronal section shows that the temporal operculum covers the insula below the Sylvian fissure, and frontal and parietal opercula cover the insula above the fissure. Frontal and parietal opercula consist of an outer part on the convexity of the brain, a horizontal part above the Sylvian Fissure, and an inner vertical part facing the insula across its circular sulcus. Arrowheads: Sylvian fissure (lateral sulcus). Arrows: circular sulcus of the insula. Modified from Treede, R. D., Baumgärtner, U., and Lenz, F. A. 2007. Nociceptive Processing in the Secondary Somatosensory Cortex. In: Encyclopedia of Pain (*eds*. R. F. Schmidt and W. D. Willis), pp. 1376–1379. Springer.

temporal, parietal and frontal opercula. Coronal sections reveal that the parasylvian cortex consists of the insula itself, the inner vertical surface of the opercula, the horizontal banks of the Sylvian fissure, and most laterally the outer surface of the convexity of the brain (Figure 3(c)).

The majority of human imaging studies showed consistent activation of the parasylvian cortex during painful stimulation, and this activation overlapped only partly with that by tactile stimuli (Treede, R. D. *et al.*, 2007). Lesions in parasylvian cortex cause deficits in pain perception (Greenspan, J. D. *et al.*, 1999), and intracortical electrical stimulation of this region is painful (Ostrowsky, K. *et al.*, 2002). Thus, this region is a good candidate to contain some nociceptive specific cortical areas, if they exist.

About 75% of the PET and fMRI studies reported activation of the SII region, and 94% found activation of the insula (Treede, R. D. *et al.*, 2000; Apkarian, A. V. *et al.*, 2005). But due to the curvature and oblique course of the Sylvian fissure (Özcan, M. *et al.*, 2005), activated areas are often misallocated, even across major sulci. Whereas the operculo-insular cortex in the parasylvian region has been recognized as one of the most important nociceptive cortical areas, its precise anatomical and functional organization has yet to be determined. In particular it is not yet known, whether insula and operculum subserve distinct functions or form one uniform area.

5.45.3.2.1 The secondary somatosensory cortex (SII)

The secondary somatosensory cortex is located in the superior bank of the Sylvian fissure, where it makes up a major part of the parietal operculum (Figures 1(b), 3(b), and 3(c)). Nociceptive input to monkey SII was demonstrated anatomically. SII receives direct spino-thalamo-cortical input from the ventrobasal nuclei, in particular the ventro-postero-inferior nucleus VPI (Stevens, R. T. *et al.*, 1993). Nociceptive input to human SII has been confirmed by subdural recordings (Lenz, F. A. *et al.*, 1998a).

Single neuron recordings in SII have largely focused on the tactile representation (Robinson, C. J. and Burton, H. 1980; Fitzgerald, P. J. *et al.*, 2006). The SII region contains multiple somatotopic representations of the body, suggesting the existence of several subregions (Disbrow, E. *et al.*, 2000, Fitzgerald, P. J. *et al.*, 2004). Although most neurons in SII have contralateral receptive fields, this is the first part of the somatosensory system with a sizable proportion of bilateral receptive fields. Hence, most imaging and electrophysiological studies in humans have shown a bilateral response to unilateral stimulation, with a contralateral preponderance. Functionally, SII is considered to play a role in tactile object recognition and memory (Seitz, R. J. *et al.*, 1991).

Evoked potential recordings in humans following brief laser heat stimuli showed that SII was activated simultaneously with or even earlier than SI (Ploner, M. *et al.*, 1999; Schlereth, T. *et al.*, 2003). Combined anterograde and retrograde tracer studies in monkey (Apkarian, A. V. and Shi, T., 1994) support the concept that nociceptive input reaches SII more directly than tactile input. Hence, SII has been supposed to be important for the recognition of painful stimuli as such.

In contrast to the abundance of evidence for nociceptive activation of the SII region from human studies, there are few single neuron recordings in this area showing specific nociceptive responses (Treede, R. D. *et al.*, 2000). In monkey, some convergence with visual input encoding the approach of a sharp object to the face has raised the possibility of a representation of threat. These neurons, however, were not in SII proper but in area 7b which is adjacent to SII in monkey but not in humans (Dong, W. K. *et al.*, 1994). These neurons are now considered to be part of the posterior parietal cortex (see below). Since neurons in all studies on SII were searched using mechanical skin stimulation, it is possible that these studies missed nociceptive specific neurons, because many primary nociceptive afferents are mechanically insensitive (Treede, R. D. *et al.*, 1998). Thus, an intriguing possibility is that tactile and nociceptive inputs are represented in different areas within the SII region.

5.45.3.2.2 The frontal operculum

Dipole source analysis of laser-evoked potentials (LEPs) in healthy volunteers, and subdural and depth recordings in patients undergoing epilepsy surgery have identified an area in the inner vertical surface of the frontal operculum (Figure 4(a)) that was activated by painful heat stimuli with a shorter latency (about 150 ms) than any other cortical area (Tarkka, I. M. and Treede, R. D., 1993; Valeriani, M. *et al.*, 1996; Ploner, M. *et al.*, 1999; Frot, M. and Mauguière, F., 2003; Schlereth, T. *et al.*, 2003; Vogel, H. *et al.*, 2003). This area anterior of the tactile SII area has a different somatotopic orientation (face: anterior, foot: posterior) than SII itself (face: lateral, foot: medial; Vogel, H. *et al.*, 2003). The thalamic source of nociceptive input to this region is not yet

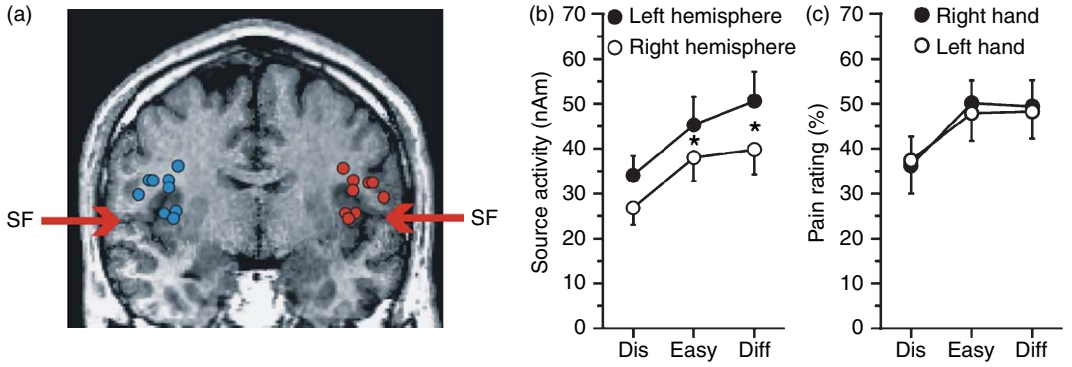

Figure 4 Nociceptive input to the frontal operculum. (a) Projection of dipole source locations for the first component of laser-evoked potentials (LEPs) onto a coronal magnetic resonance image slice at Talairach y = −6 mm. The distribution around the roof of the circular insular sulcus, ranging from the inner vertical face of the frontal operculum to the adjacent dorsal insula matches the projection area of the nociceptive thalamic nucleus VMpo. (b) Task effects and interhemispheric differences. (c) The hemispheric asymmetry of opercular activation (left hemisphere > right hemisphere) was not reflected or caused by different visual analog score pain ratings between both hands. Dis, distraction task; Easy, easy spatial and intensity discrimination tasks; diff, difficult discrimination tasks. ANOVA:* $P < 0.05$. Modified from Schlereth, T., Baumgärtner, U., Magerl, W., Stoeter, P., and Treede, R. D. 2003. Left-hemisphere dominance in early nociceptive processing in the human parasylvian cortex. Neuroimage 20, 441–454.

clear: it may be VPI like for the posteriorly adjacent SII, or it may be VMpo like for the medially adjacent dorsal insula. Somatotopy in the frontal operculum would be consistent with that of a VMpo projection target (Craig, A. D., 1995). Nociceptive input to the frontal operculum in humans has been confirmed by subdural and depth recordings (Lenz, F. A. *et al.*, 1998a; Frot, M. *et al.*, 1999). Responses in this area are modulated during spatial and intensity discrimination tasks and show a left-hemisphere dominance (Figures 4(b) and 4(c)).

5.45.3.2.3 The insula

The insula is located deep inside the Sylvian fissure, where it can be visualized as a triangular shape in sagittal sections (Figure 3(a)). It often contains two long sulci in its posterior part and three short sulci rostrally. Several functional subdivisions of the insula have been suggested (Dieterich, M. *et al.*, 2003; Schweinhardt, P. *et al.*, 2006), but there is no consensus yet. Parts of the insula subserve varied functions in the somatosensory, vestibular, gustatory and autonomic nervous system, which led to the suggestion that this region serves for a central representation of the internal state of the body (Craig, A. D., 2002). This concept is consistent with the interoceptive aspects of nociception.

Another source of nociceptive input into the parasylvian cortex is the posterior inferior part of the ventrobasal nucleus (Lenz, F. A. *et al.*, 1993), a region designated as VMpo by some authors (Craig, A. D. *et al.*, 1994). VMpo projects to the dorsal insula and the adjacent frontal operculum. Nociceptive input to the insula in humans has been confirmed by depth recordings (Frot, M. *et al.*, 2003). The somatotopic representation of pain in the dorsal insula in monkey (face: anterior, foot: posterior) is orthogonal to that in SII (face: lateral, foot: medial; Baumgärtner, U. *et al.*, 2006b). Direct electrical stimulation of the insula is painful with a strong affective component (Ostrowsky, K. *et al.*, 2002).

5.45.3.3 The Posterior Parietal Cortex

The posterior parietal cortex is located adjacent and posterior to SI. It comprises Brodmann areas 5 and 7 (Figure 5(c)). Nociceptive input to this region is suggested by studies in monkey that reported short-latency responses to nociceptive stimuli in area 7b; the same neurons also responded to visual stimuli of sharp objects directed at their receptive field (Dong, W. K. *et al.*, 1994). In the tactile system, this region is part of a dorsally directed stream involved in stimulus location, convergence with visual information and the generation of spatial information for motor control. Nociceptive input to this region in humans has not yet been explored with subdural recordings, but there is some evidence from EEG

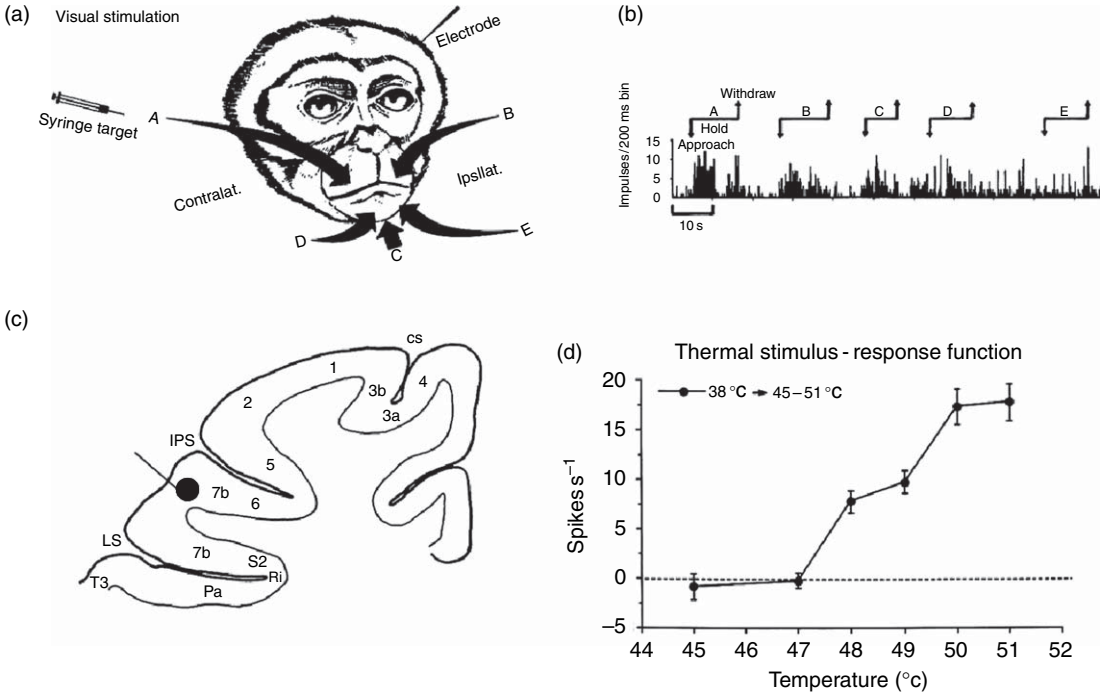

Figure 5 Nociceptive neuron in posterior parietal cortex (Area 7b threat neuron). (a) Bilateral receptive field in the orofacial region; seeing a syringe approach the receptive field was also an adequate stimulus. (b) Responses to the stimuli shown in (a). (c) Location of the recorded neuron on a coronal section that passes through both the central sulcus (CS) and the Sylvian fissure (LS: lateral sulcus). (d) Stimulus response function to painful heat stimuli. IPS, Intraparietal sulcus. Modified from Dong, W. K., Chudler, E. H., Sugiyama, K., Roberts, V. J., and Hayashi, T. 1994. Somatosensory, multisensory, and task-related neurons in cortical area 7b (PF) of unanesthetized monkeys. J. Neurophysiol. 72, 542–564.

and MEG studies in humans that nociceptive stimuli activate parietal lobe posterior of SI (Schlereth, T. *et al.*, 2003; Forss, N. *et al.*, 2005). Few fMRI studies have assessed this region (Kulkarni, B. *et al.*, 2005; Schmahl, C. *et al.*, 2006).

5.45.3.4 The Cingulate Cortex

The cingulate cortex is located above the corpus callosum and around its anterior knee (Figure 6). The anterior cingulate cortex (ACC) comprises Brodmann areas 24 and 32, whereas the posterior cingulate cortex (PCC) contains areas 23 and 31 (Vogt, B. A. *et al.*, 1995). ACC receives nociceptive thalamocortical input from the mediodorsal (MD) and parafascicular (Pf) nuclei (Vogt, B. A. *et al.*, 1979). ACC has been further subdivided into mid-cingulate cortex, which is associated with response selection and motor efferent functions, and ACC proper that is related to emotion and autonomic efferent functions (Vogt, B. A., 2005). Nociceptive input to human cingulate cortex has been confirmed by subdural recordings and by intracortical recordings (Lenz, F. A. *et al.*, 1998b; Hutchison, W. D. *et al.*, 1999). About 87% of the PET and fMRI studies reported activation of the cingulate cortex (Apkarian, A. V. *et al.*, 2005), but no region of the cingulate cortex is considered to be nociceptive specific (Vogt, B. A., 2005).

Nociceptive neurons in ACC have large or even whole-body receptive fields (Figure 7, Sikes, R. W. and Vogt, B. A., 1992; Yamamura, H. *et al.*, 1996). For this reason it is unlikely that they contribute to the sensory dimension of pain. Monkey ACC neurons activate during pain avoidance behavior, reflecting anticipation, and response selection (Koyama, T. *et al.*, 1998; 2001). The cingulate cortex is supposed to participate in the affective-motivational dimension of pain. This conclusion has been confirmed by a PET study of hypnotic modulation of perceived pain affect that also modulated perfusion of ACC (Hofbauer, R. K. *et al.*, 2001) and by correlation analysis (Tölle, T. R. *et al.*, 1999).

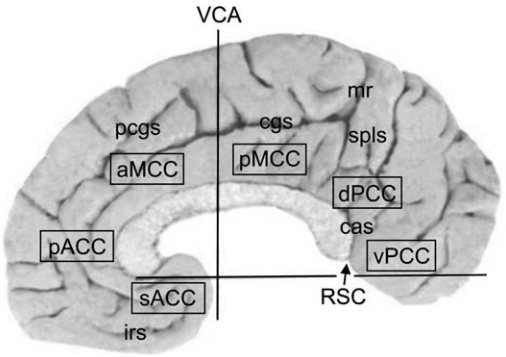

Figure 6 Distribution of cingulate cortex regions and subregions. Region borders are marked with arrows. Cross-hair shows vertical plane at the anterior commissure (VCA) and the anterior–posterior commissural line. A functional overview, derived from the analysis of a large volume of literature illustrates general regional function. aMCC, anterior mid-cingulate cortex; cas, callosal sulcus; cgs, cingulate sulcus; dPCC, dorsal posterior cingulate cortex; irs, inferior rostral sulcus; mr, marginal ramus of cgs; pACC, pregenual anterior cingulate cortex; pcgs, paracingulate sulcus; pMCC, posterior mid-cingulate cortex; RSC, retrosplenial cortex; sACC, subgenual anterior cingulate cortex; spls, splenial sulci; vPCC, ventral posterior cingulate cortex. Reproduced from Vogt, B. A. 2005. Pain and emotion interactions in subregions of the cingulate gyrus. Nat. Rev. Neurosci. 6, 533–544.

5.45.3.5 The Prefrontal Cortex

The PFC (including Brodmann areas 9, 10, 46) comprises the major part of the frontal lobe and is located anterior of the motor cortical areas. There is no evidence that it would receive a direct nociceptive thalamo-cortical input, but the PFC receives cortico-cortical input from the cingulate gyrus that may convey nociceptive information. About 55% of the PET and fMRI studies reported activation of the PRC in healthy subjects, and 81% of the studies in chronic pain patients (Apkarian, A. V. *et al.*, 2005). The PRC is assumed to participate in the cognitive-evaluative dimension of pain and in endogenous pain control (Lorenz, J. *et al.*, 2003; Schmahl, C. *et al.*, 2006).

5.45.4 Functional Roles of Cortical Nociceptive Signal Processing

Pain perception has been conceived to consist of sensory-discriminative, affective-motivational and cognitive-evaluative dimensions (Melzack, R. and Casey, K. L. 1968). The sensory-discriminative dimension includes intensity discrimination, pain qualities, stimulus localization and timing discrimination; this dimension is traditionally thought to involve lateral thalamic nuclei and the somatosensory cortices SI and SII. The affective-motivational dimension includes perception of the negative hedonic quality of pain, autonomic nervous system manifestations of emotions, and motivated behavioral responses; this dimension is traditionally thought to involve medial thalamic nuclei and the limbic cortices ACC and MCC. The insula has an intermediate position in that concept, receiving input from lateral thalamus but projecting into the limbic system. The cognitive-evaluative dimension includes interaction with previous experience, cognitive influence on perceived pain intensity and an overall evaluation of its salience; this dimension is traditionally thought to involve the PRC. Numerous neuroimaging studies have assessed various experimental paradigms derived from several psychological concepts that do not easily fit into the traditional three dimensions of pain. Therefore, we here report imaging evidence for involvement of cortical areas in specific functions instead of the dimensions of pain.

5.45.4.1 Location and Quality of Phasic Pain

Neuroimaging studies have examined brain regions activated by many types of painful stimulation, including noxious heat and cold, muscle stimulation using electric shock or hypertonic saline, topical and intradermal capsaicin, colonic distention, rectal distension, gastric distension, esophageal distension, ischemia, cutaneous electric shock, ascorbic acid, laser heat, as well as an illusion of pain evoked by combinations of innocuous temperatures (Apkarian, A. V. *et al.*, 2005; Bushnell, M. C. and Apkarian, A. V., 2005). Despite the differences in sensation, emotion and behavioral responses provoked by these different types of pain, individuals can easily identify each as being painful. Thus, there appears to be a common construct of pain with an underlying network of brain activity in the areas described above. Nevertheless, despite the similarities in pain experiences and similarities in neural activation patterns, each pain experience is unique. Subjects can usually differentiate noxious heat from noxious cold from noxious pressure. This ability to differentiate pains is particularly puzzling, since there is ubiquitous convergence of information from cutaneous, visceral and muscle tissue throughout the

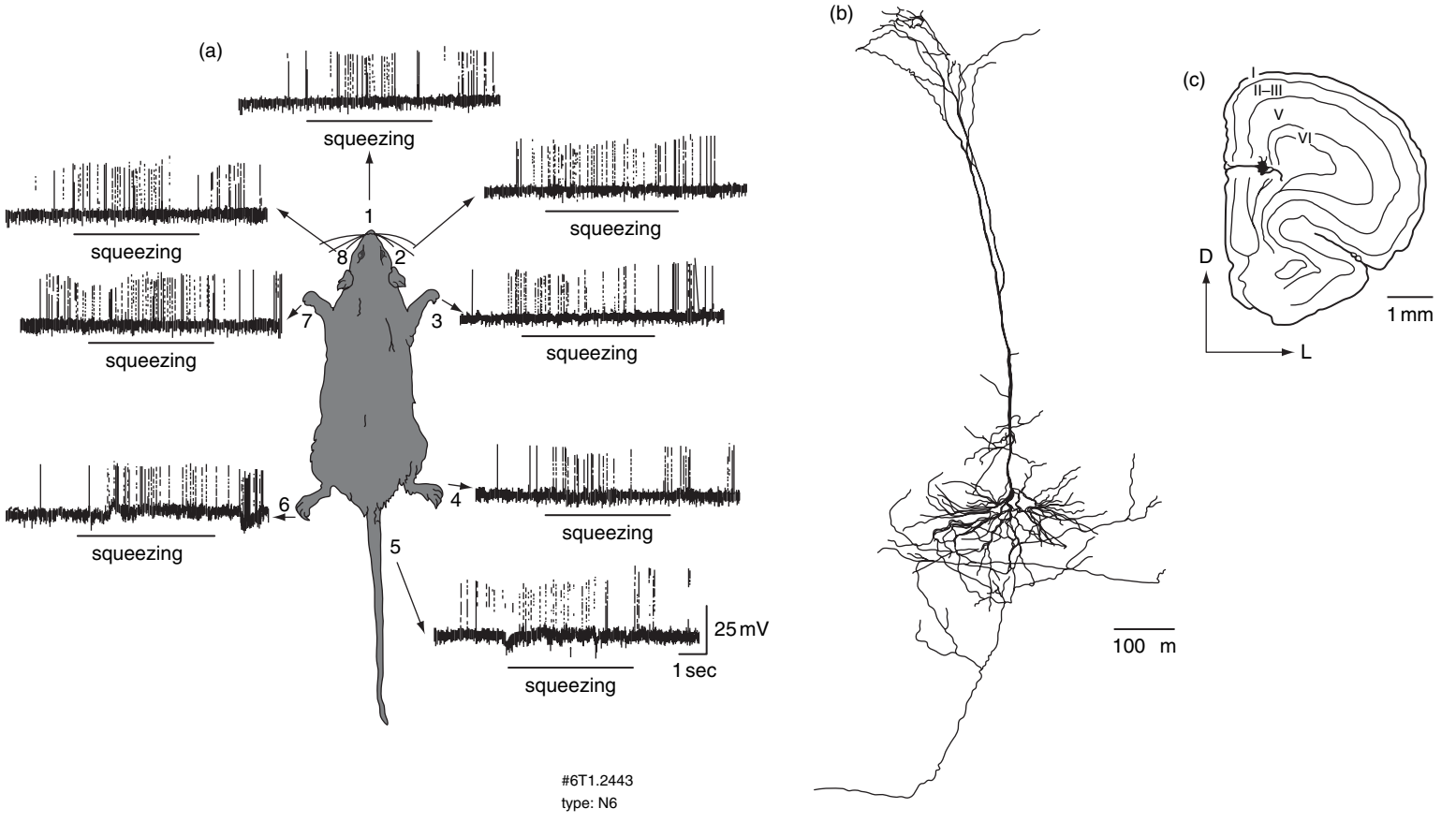

Figure 7 Nociceptive neuron in the anterior cingulate gyrus. (a) Responses to painful mechanical stimuli show a whole-body receptive field for this neuron. (b) Intracellular dye injection reveals a lamina V pyramidal neuron. (c) Location of the recorded neuron in the rat cingulate cortex. Reproduced from Yamamura, H., Iwata, K., Tsuboi, Y., Toda, K., Kitajima, K., Shimizu, N., Nomura, H., Hibiya, J., Fujita, S. and Sumino, R. 1996. Morphological and electrophysiological properties of ACCx nociceptive neurons in rats. Brain Res. 735, 83–92.

afferent nociceptive system (Willis, W. D. and Coggeshall, R. E., 2004). The convergence and the similarities in brain regions activated by different types of pain are consistent with phenomena such as referred pain, but cannot explain either the ability to identify the origin of pain or with contrasting behavioral reactions to cutaneous and visceral pain (withdrawal versus quiescence).

There is evidence from single neuron recordings, MEG, PET, and fMRI that neural activity in SI cortex could underlie the identification of the locus of cutaneous pain. Kenshalo and colleagues (Kenshalo, D. R. *et al.*, 1988; Kenshalo, D. R. and Isensee, O., 1983) showed that SI nociceptive neurons have discrete receptive fields, so that different neurons respond to painful stimulation in different skin areas. Correspondingly, EEG, PET, and fMRI studies have shown a topographic organization of nociceptive responses in SI cortex similar to the organization of tactile responses, i.e., a medio-lateral organization of foot, hand, face, and intra-abdominal areas (Tarkka, I. M. and Treede, R. D., 1993; Andersson, J. L. R. *et al.*, 1997; DaSilva, A. F. M. *et al.*, 2002; Strigo, I. A. *et al.*, 2003; Vogel, H. *et al.*, 2003). Most imaging studies find little somatotopic organization of pain in other cortical areas (Tarkka, I. M. and Treede, R. D., 1993; Xu, X. P. *et al.*, 1997), thus suggesting that responses in SI cortex may be most important for pain localization. More recently, a somatotopic organization has also been documented for operculo-insular cortex (Vogel, H. *et al.*, 2003; Baumgärtner, U. *et al.*, 2006a). A left hemisphere dominance has been reported for the sensory dimension of pain (Schlereth, T. *et al.*, 2003), whereas right hemisphere dominance was observed for the affective dimension (Pauli, P. *et al.*, 1999; Brooks, J. C. W. *et al.*, 2002).

Strigo I. A. and colleagues (2003) directly compared brain activations produced by esophageal distension and cutaneous heat on the chest that were matched for pain intensity. They found that the two qualitatively different pains produced different primary loci of activation with insula, SI, motor and prefrontal cortices. Such local differences in responses within the nociceptive network might subserve our ability to distinguish visceral and cutaneous pain as well as the differential emotional, autonomic, and motor responses associated with these different sensations.

5.45.4.2 The Time Domain

Most information about the temporal sequence of pain-evoked brain activation comes from EEG or MEG studies. The dual pain sensation elicited by a single brief painful stimulus that is due to the different conduction times in nociceptive A- and C-fibers (about 1 s difference) is reflected in two sequential brain activations in EEG and MEG recordings from SI, SII, and MCC (Bromm, B. *et al.*, 1983; Bragard, D. *et al.*, 1996; Magerl, W. *et al.*, 1999; Opsommer, E. *et al.*, 2001; Iannetti, G. D. *et al.*, 2003). EEG mapping studies (Kunde, V. and Treede, R. D., 1993; Miyazaki, M. *et al.*, 1994), source analysis (Tarkka, I. M. and Treede, R. D., 1993; Valeriani, M. *et al.*, 1996; Ploner, M. *et al.*, 1999), and intracranial recordings (Lenz, F. A. *et al.*, 1998a; Frot, M. *et al.*, 1999) show that the earliest pain-induced brain activity originates in the vicinity of SII. In contrast, tactile stimuli activate this region only after processing in the primary somatosensory cortex (Ploner, M. *et al.*, 2000). The adjacent dorsal insula is activated slightly but significantly later than the operculum (Frot, M. and Mauguière, F., 2003). These observations support the suggestion derived from anatomical studies that the SII region and adjacent insula are primary receiving areas for nociceptive input to the brain (Apkarian, A. V. and Shi, T., 1994; Craig, A. D., 2002).

5.45.4.3 Attention and Distraction Effects on Pain-Evoked Cortical Activity

Early human brain imaging studies examining the effects of attention and distraction show modulation of pain-evoked activity in a number of cortical regions, including sensory and limbic structures, as well as prefrontal areas (Bushnell, M. C. *et al.*, 1999; Longe, S. E. *et al.*, 2001; Bantick, S. J. *et al.*, 2002; Schlereth, T. *et al.*, 2003). These results generally show reduced activations in sensory regions of the cortex and some increased activity in more frontal regions, suggesting that attentional modulation is mediated through the latter structures resulting in reduced sensory processing, where the attentional distraction is usually reported resulting in reduced perceived magnitude of pain. A more recent study extends these notions by showing that during distraction there is a functional interaction between pregenual ACC and frontal cortex exerting a top-down modulation on periaqueductal gray (PAG) and thalamus to in turn reduce activity in cortical sensory regions and correspondingly decrease perception of pain (Petrovic, P. *et al.*, 2000; Tracey, I. *et al.*, 2002; Valet, M. *et al.*, 2004). Given that ACC is implicated in attentional modulation as well as pain perception, a distraction study indicates that some portions of the

pregenual ACC region are decreased with distraction while others are increased, consistent with these two different functions (Frankenstein, U. N. *et al.*, 2001).

5.45.4.4 Anticipation and Expectation

Anticipation or expectation of pain can activate many of the cortical areas related to perception of pain in the absence of a physical pain stimulus (Ploghaus, A. *et al.*, 1999; Hsieh, J. C. *et al.*, 1999b; Sawamoto, N. *et al.*, 2000; Porro, C. A. *et al.*, 2002). Two studies have attempted to identify the circuitry for modulation of pain by expectation. In one study MCC, caudate nucleus, cerebellum, and nucleus cuneiformis were modulated by systematic manipulation of pain intensity expectation by two different cues (Keltner, J. R. *et al.*, 2006), whereas pain intensity itself modulated somatosensory cortex, insula, and rostral ACC. In the second study expectancy was modulated by a placebo procedure, resulting mainly in modulation including MCC, PRC, cerebellum, pons, and parahippocampal gyrus (Kong, J. *et al.*, 2006). The latter study is complicated by the fact that the procedure is a combination of manipulation of expectancy and placebo acupuncture treatment. Generally, there remains a strong need for systematic studies to identify brain elements that modulate pain responses due to expectation.

5.45.4.5 Empathy

A provocative study opened the field regarding the interaction between pain and empathy, where the authors defined empathy as the ability to have an experience of another's pain. Using this definition and comparing brain activity for experiencing pain or knowing that their loved one, present in the same room, was experiencing the same pain, the authors showed many cortical regions similarly activated for both conditions, especially bilateral operculo-insular cortex and MCC (Singer, T. *et al.*, 2004). These results were interpreted as evidence for the affective component of pain being active in both empathy and pain, and thus concluded that empathy for pain involves the affective component, but not the sensory component, of pain. The study induced a flurry of activity in attempting to understand the relationship between empathy and pain. Multiple groups have replicated the main finding and proposed different underlying mechanisms (Morrison, I. *et al.*, 2004; Botvinick, M. *et al.*, 2005; Jackson, P. L. *et al.*, 2005), with multiple studies showing that at least MCC activity reflects the pain experienced by others and that multiple cortical areas involved in sensory processing of pain are also activated.

The overall notion that empathy involves assessment of the pain experienced by others – pain mirroring – was tested directly in subjects with alexithymia, a cognitive and emotional deficit leading to difficulty in identifying one's own emotional state and also other people's emotional state. The study showed in fact reduced activity in PRC and MCC during a pain empathy condition in this patient population (Moriguchi, Y. *et al.*, 2006). Even though these results are internally consistent, their interpretation remains problematic. Simple introspection casts doubt on the notion that empathy means actually experiencing another person's pain. Instead, what is called empathy may be the assessment of the magnitude of negative emotion that the other person may be experiencing, i.e., a cognitive function of interpersonal communication. According to that concept, empathy may be defined as a complex form of psychological inference that enables us to understand the personal experience of another person through cognitive/evaluative and affective processes. A study in patients with congenital insensitivity to pain (Danziger, N. *et al.*, 2006) reported a deficit in rating pain-inducing events, but normal inference of pain from facial expressions (empathy), indicating that empathy for pain does not require an intact pain percept.

5.45.5 Pain Modulation

5.45.5.1 Psychological Modulation of Pain

The psychological modulation of pain has been observed very early on and studied in the clinical and laboratory settings (Beydoun, A. *et al.*, 1993; Villemure, C. and Bushnell, M. C., 2002). Modern brain imaging techniques now provide powerful tools with which mechanisms of these modulations can be documented and dissected. Given that these are cognitive/attentional modulations their effects should be observed at the cortical level.

5.45.5.1.1 Hypnosis and pain-evoked cortical activity

Hypnosis can alter pain perception. It has been used to differentially modulate sensory and affective dimensions of pain and thus distinguish the cortical regions involved in these dimensions. Such studies indicate that SI activity is preferentially modulated

when the hypnotic instructions are directed to the intensity of pain, while MCC activity is preferentially modulated when hypnosis is directed to the unpleasantness of pain (Rainville, P. *et al.*, 1997, Hofbauer, R. K. *et al.*, 2001). Brain activity for hypnotically induced pain perception seem to be different from activity for imagined pain in sensory, limbic, and prefrontal activation patterns (Derbyshire, S. W. *et al.*, 2004). The sensory and limbic cortical activations for hypnotically induced and stimulation-induced pain seem relatively similar, the only region that may be differentiating them seems to be the medial PRC (Raij, T. T. *et al.*, 2005).

5.45.5.1.2 Mood and emotional states and pain-evoked cortical activity

Studies show that experimental procedures that improve mood generally reduce pain, while those that have a negative effect on mood increase pain (Zelman, D. C. *et al.*, 1991; Marchand, S. and Arsenault, P., 2002). One study showed that looking at fearful faces increased their level of anxiety and discomfort, which also resulted in enhanced esophageal stimulation-evoked activity in limbic regions like ACC and insula (Phillips, M. L. *et al.*, 2003).

5.45.5.1.3 Placebo and pain-evoked cortical activity

Placebo is a potent modulator of pain; it afflicts all clinical studies of pain pharmacology. Placebo effects have also been seen in depression and in Parkinson's disease and recent brain imaging studies show a robust brain and subcortical reward circuitry's involvement in these (Lidstone, S. C. and Stoessl, A. J., 2007). The first neurochemical evidence for opiate involvement of placebo was demonstrated about 30 years ago by showing that placebo analgesia can be blocked by naloxone (Levine, J. D. *et al.*, 1978). Consistent with this notion, changes in endogenous opiate release are shown to be involved in placebo-induced analgesia, where PRC (medial and lateral) as well as insula and ventral striatum seem to be involved, where high placebo responders increased opiate release in ventral striatum was positively correlated with pain ratings (Zubieta, J. K. *et al.*, 2005). Results generally consistent with this brain response pattern have been demonstrated by a number of other groups (Wager, T. D. *et al.*, 2004; Benedetti, F. *et al.*, 2005; Kong, J. *et al.*, 2006); the medial prefrontal/rostral ACC responses for placebo seem to recruit PAG and amygdala (Bingel, U. *et al.*, 2006); and involvement of PAG in placebo-induced analgesia is observed in the above studies as well, which links opiate descending modulation with prefrontal cortical control of placebo analgesia. The correspondence between placebo analgesia and reward was directly studied and the results show a strong correspondence between brain regions involved in each (Petrovic, P. *et al.*, 2005).

5.45.5.2 Pharmacological Modulation of Pain

A league table of analgesic efficacy has been generated based on pain-related evoked potentials (Scharein, E. and Bromm, B., 1998). Since these studies used electrical stimuli that circumvent peripheral nociceptive transduction mechanisms, this table reflects central rather than peripheral analgesic actions, as evidenced, e.g., by the higher efficacy of the antidepressant imipramine than the nonsteroidal anti-inflammatory drug (NSAID) acetylsalicylic acid. Since dipole source analysis has not been applied in these EEG studies, possible cortical sites of actions were not differentiated. Combining fMRI and pharmacology promises to provide that type of information (Tracey, I., 2001; Borsook, D. *et al.*, 2006). In addition, PET techniques can be used for direct tracing of cortical distribution of a given drug, when it has been labeled with the positron emitting ^{11}C isotope.

5.45.5.2.1 Opiates

There is a vast literature regarding opiate-mediated descending modulation through the PAG and a similarly large literature on its effects on inhibitory interneurons in the spinal cord. At the cortical level, it has been noted that opiate receptors are present in many parts of the nociceptive system, with high specific binding in ACC, insula, and frontal operculum, and with moderate specific binding in MCC, SII, and SI (Jones, A. K. P. *et al.*, 1991b; Baumgärtner, U. *et al.*, 2006a).

Recent studies of opiate-mediated responses in the brain have used two approaches, examination of metabolic function in response to pharmacological agents and direct measurement of opiate receptor binding potential. Exogenous administration of μ-opioid receptor agonist drugs show dose-dependent increased metabolic activity in regions rich with μ-opioid receptors, which in the cortex are mainly localized to PRC and ACC (Firestone, L. L. *et al.*, 1996; Schlaepfer, T. E. *et al.*, 1998; Wagner, K. J. *et al.*, 2001). Also, μ-opioid agonist fentanyl on brain responses to painful stimuli

have been explored, showing that most cortical responses to pain are reduced or eliminated, confirming analgesic effects of the opiate (Casey, K. L. *et al.*, 2000; Petrovic, P. *et al.*, 2002). Changes in endogenous opioid system is studied using a selective μ-opioid radiotracer, showing activation of opiate neurotransmission in rostral ACC, PRC, and insula during a tonic muscle pain (Zubieta, J. K. *et al.*, 2001).

5.45.5.2.2 Dopamine

Dopamine is best known for its role in motor, motivation, and pleasure control. There is accumulating evidence to suggest that dopamine acting at the level of the basal ganglia may also be involved in pain modulation. Human brain imaging studies document increased pain sensitivity to be associated with lower levels of endogenous dopamine (Pertovaara, A. *et al.*, 2004; Martikainen, I. K. *et al.*, 2005; Scott, D. J. *et al.*, 2006); and sustained experimental pain results in release of dopamine in the basal ganglia (Scott, D. J. *et al.*, 2006), and indicate an interaction between opiate activity and dopamine where alfentanil administration results in decreased mechanical pain and decreased release of dopamine in the basal ganglia (Hagelberg, N. *et al.*, 2002). Moreover, abnormal levels of dopamine in the basal ganglia have been associated with chronic pain in burning mouth syndrome and atypical facial pain (Jaaskelainen, S. K. *et al.*, 2001; Hagelberg, N. *et al.*, 2003a; 2003b), and perhaps in fibromyalgia (Wood, P. B. *et al.*, 2007). Patients with restless legs syndrome display a pronounced mechanical hyperalgesia to pinprick stimuli that is slowly reversed by dopaminergic agonists (Stiasny-Kolster, K. *et al.*, 2004), but this action is probably mediated by extrastriatal dopamine receptors.

5.45.5.2.3 Estrogen

Gender is one of the most important determinants of human health. Women far outnumber men in susceptibility to many autoimmune disorders, fibromyalgia, and chronic pain, differences in physiological responses to stress may potentially be an important risk factor for these disorders as physiologic responses to stress seem to differ according to gender, with phase of menstrual cycle, menopausal status and with pregnancy (Kajantie, E. and Phillips, D. I., 2006). Consistent with this idea recent fMRI study shows that brain activity in premenopausal women as studied for negative valence/high arousal in contrast to neutral visual stimuli show differences when the task is performed during early follicular menstrual cycle phase compared to late follicular/mid-cycle; with greater activity found during early follicular phase in amygdala, hypothalamus, hippocampus, orbital frontal cortex, and ACC, suggesting that estrogen may attenuate arousal in women through cortical-subcortical control of hypothalamic–pituitary–adrenal circuitry (Goldstein, J. M. *et al.*, 2005). There is also growing evidence of gender differences in the anatomy of the brain, its connectivity, and in cognitive abilities (Hampson, E., 2002; Becker, J. B. *et al.*, 2005). Multiple studies have documented that threshold and tolerance for pain is lower for women (Wiesenfeld-Hallin, Z., 2005; Rolke, R. *et al.*, 2006; Wilson, J. F., 2006).

Gender differences in cortical activity for acute pain has been observed in early studies (Paulson, P. E. *et al.*, 1998). The association of sex hormones with pain perception and pain memory was studied by Zubieta J. K. and colleagues (Zubieta, J. K. *et al.*, 2002; Smith, Y. R. *et al.*, 2006). They scanned healthy women during their early follicular phase when estrogen levels are low and then repeated the scan during that same phase in another month after they had worn for a week an estrogen-releasing skin patch which increased their estrogen to levels normally seen in the menstrual cycle. These studies showed that more μ-opioid receptors were available in the presence of high estrogen levels, and women reported less pain in response to acute painful stimuli than when their estrogen levels were low. Moreover, estrogen-associated variations in the activity of μ-opioid neurotransmission correlated with individual ratings of the sensory and affective perceptions of pain and the subsequent recall of that experience. These data demonstrate a significant role of estrogen in modulating endogenous opioid neurotransmission and associated psychophysical responses to an acute pain stressor in humans. Approximately similar results have been reported by another group (De Leeuw, R. *et al.*, 2006).

5.45.6 Overview Regarding the Role of the Cortex in Acute Pain Perception

The above sections describe the contribution of modern imaging studies to our understanding of the involvement of the cortex in pain perception. Cortical activity is demonstrated to possess properties necessary for involvement in pain perception, like somatotopic representation of painful stimuli,

correlation with stimulus intensity, modulation with attention, modulation with expectation and other psychological variables, and distinct brain regions showing differential activity for sensory and affective dimensions of pain, as well as attenuation of responses with analgesic drugs (Apkarian, A. V. *et al.*, 2005). Thus, human brain imaging studies have asserted the role of the cortex in acute pain.

However, because imaging studies identify brain responses in a correlative manner, they may all reflect secondary processes. Perception of pain automatically directs attention to the source of pain, results in autonomic responses, motor reflexes to escape from the pain, and other emotional and cognitive responses that undoubtedly are at least partially mediated through cortical processes. Therefore, the role of the cortex in pain perception in contrast to its activity as a consequence of these secondary responses remains unclear and needs to be properly addressed in future studies (Apkarian, A. V., 2004).

In fact, unpublished data from Apkarian's laboratory suggest that a large proportion of the brain network activated with acute pain may be responses that are commonly involved in general magnitude estimation for any sensory modality, and as a result are not specific for nociception (abstract Society for Neuroscience 2006), suggesting that the majority of cortical activity for acute pain are instead sensory, cognitive, emotional, and attentional responses to nociceptive inputs. Careful clinical and neuropsychological examination of patients with small brain lesions, combined with high-resolution structural and neuropharmacological neuroimaging in the same patients, will be needed to address the question what brain structures are necessary for acute pain perception. Anatomical tracing studies and single unit recordings should address the question, to what extent nociceptive specific neurons exist in these brain structures. For most parts of the nociceptive cortical network, as illustrated above, it is likely that they participate only partly in pain perception, by providing certain feature extraction functions, but they also participate in other functions in different contexts.

5.45.7 Clinical Applications

It should be emphasized that although the subjective phenomenon of being in pain can be considered an emergent phenomenon of cortical activity (Treede, R. D., 2001), there is currently no measure of brain activity that would objectively show whether or not a person is in pain. Therefore, neither EEG/MEG nor imaging with fMRI or PET can be used to verify the presence of ongoing spontaneous pain.

EEG and MEG recordings of evoked potentials, however, are sensitive enough to verify whether the ascending nociceptive pathways are intact in a given individual patient (Bromm, B. and Lorenz, J., 1998; Treede, R. D. *et al.*, 2003; Cruccu, G. *et al.*, 2004). A prerequisite for this use of EEG and MEG technology is a phasic adequate stimulus for nociceptor activation. Radiant heat pulses of a few milliseconds duration, as generated by infrared lasers, have been validated for this purpose (Plaghki, L. and Mouraux, A., 2003), and LEPs can thus be used to verify the presence of negative sensory signs of nociception (hypoalgesia).

Neither fMRI nor PET are sensitive enough to allow clinical assessment of nociceptive pathways in individual cases, since so far no activation paradigm has been developed that would reliably induce a particular cortical activation pattern in each and every healthy subject. Thus, negative findings with these techniques are inconclusive.

For the study of pathological nociceptive processing at the group level, however, fMRI and PET techniques are extremely powerful. These techniques have broadened our understanding of the pathophysiology of conditions with decreased pain perception such as afferent pathway lesions or borderline personality disorder, and conditions with increased pain perception such as neuropathic pain or fibromyalgia (Gracely, R. H. *et al.*, 2004; Maihöfner, C. *et al.*, 2005; Garcia-Larrea, L. *et al.*, 2006; Schmahl, C. *et al.*, 2006; Schweinhardt, P. *et al.*, 2006). In addition, PET allows direct estimation of pharmacological and biochemical processes in the brain, such as alterations in dopamine or opioid receptor availability (Hagelberg, N. *et al.*, 2003a; Willoch, F. *et al.*, 2004).

5.45.8 Chronic Pain

5.45.8.1 Studying Brain Activity in Chronic Pain with Nonspecific Painful Stimuli

Chronic pain might result from cortical processing of chronic nociceptive spinothalamic input according to the same mechanisms as in acute pain, or there might be specific changes in cortical processing of nociceptive input in patients with chronic pain. Such changes

could then either be a causal factor for or a consequence of the chronicity of the pain condition.

A recent meta-analysis in fact shows that across some 100 studies one can establish statistically significant differences in incidence of different brain areas activated by experimental painful stimuli between acute and chronic pain conditions: PRC shows a stronger activation in chronic pain patients, whereas other nociceptive cortical areas and the thalamus show a weaker response (Table 2). A simple interpretation of these findings would be that nociceptive signal processing for experimental painful stimuli in chronic pain patients involves a reduced sensory discriminative component and an increased affective-motivational or cognitive-evaluational component. That interpretation would also be consistent with the stronger affective component of clinical pain as compared to experimental pain (Chen, A. C. N. and Treede, R. D., 1985). But there are further implications: Is the result a consequence of some trivial confounds or does it signify changes in the physiology of pain? One could construct a long list of confounds that may underlie the observation, from attentional shifts, to coping mechanisms, to effects of drug use, and heightened anxiety and depression.

The standard approach for studying brain activity for acute pain is to induce pain by a mechanical or thermal stimulus and determine brain regions modulated with the stimulus period and even with the various intensities used. Therefore, it is natural to carry the same technology to the clinical arena and apply it to chronic pain patients. As an example, we discuss one study which attempted to identify brain activity in complex regional pain syndrome (CRPS) patients using fMRI (Apkarian, A. V. *et al.*, 2001a; 2001b).

The design of the study was to examine brain activity for thermal stimuli applied to the body part where CRPS pain was present, and compare brain responses to this stimulus between CRPS and healthy subjects. Moreover, as the pain in CRPS patients with sympathetically maintained pain (SMP) may be modulated by a sympathetic block, it was reasoned that one could decrease the patients' ongoing pain and then re-examine brain activity responses to the same stimulus. The study was done in a small group of patients and this by itself is an important weakness. The main observation was that thermal stimuli in CRPS evoked more prefrontal cortical activity than usually seen in healthy subjects, and this was reversed (became more similar in pattern to normal subjects' brain activity to thermal stimuli) following sympathetic blocks. The introduction of sympathetic blocks necessitated the use of the same procedure in healthy subjects as well, where its effects were minimal. The study also observed that when a placebo block resulted in decreased pain perception then the cortical response pattern changed similarly to that of effective blocks. These results show that brain activity may be distinct between CRPS and healthy subjects for thermal stimuli.

5.45.8.2 Clinical Pain Conditions Studied by Stimulation and the Role of the Cortex

A direct approach to studying clinical pain states is to provoke it and examine brain activity. This is doable by drugs in headaches and in cardiac pain. As a result there is growing literature in both fields. There is also now good evidence that migraine with aura is accompanied with decreased blood flow and decreased activity in the occipital cortex, and migraine with or

Table 2 Frequency of brain areas active during pain in normal subjects as compared to patients with clinical pain conditions

	ACC	*SI*	*SII*	*IC*	*Th*	*PFC*
Pain in normal subjects in 68 studies	47/54 (87%)	39/52 (75%)	38/51 (75%)	45/48 (94%)	28/35 (80%)	23/42 (55%)
Clinical pain conditions in 30 studies	13/29 (45%)	7/25 (28%)	5/25 (20%)	15/26 (58%)	16/27 (59%)	21/26 (81%)
Comparison between pain in normal subjects and in clinical conditions	$P < 0.001$	$P < 0.001$	$P < 0.001$	$P < 0.001$	$P = 0.095$	$P = 0.038$

Incidence values are based on positron emission tomography, single photon emission-computed tomography, and functional magnetic resonance imaging studies. For details see Apkarian *et al.*, 2005. P values are based on Fisher's exact statistics contrasting incidence for each area. ACC, anterior cingulate cortex; IC, insular cortex; PFC, prefrontal cortex; SI, primary somatosensory cortex; SII, secondary somatosensory cortex; Th, thalamus.

without aura is associated with increased cortical thickness in visual cortical regions involved in motion detection (Granziera, C. *et al.*, 2006).

5.45.8.2.1 Migraine

Migraine attacks are characterized by unilateral severe headache often accompanied by nausea, phonophobia and photophobia. Activation of the trigeminovascular system is thought to be responsible for the pain itself, and cortical spreading depression (CSD) seems to underlie the aura symptoms. This view has been greatly advanced and substantiated by brain imaging studies. fMRI studies show CSD-typical cerebrovascular changes in the cortex of migraineurs while experiencing a visual aura (Hadjikhani, N. *et al.*, 2001). The subsequent decrease in fMRI signal is temporally correlated with the scotoma that follows the scintillations. These fMRI signal changes develop first in the extrastriate cortex, contralateral to the visual changes. It then slowly migrated towards more anterior regions of the visual cortex, representing peripheral visual fields, in agreement with the progressive movement of the scintillations and scotoma from the centre of vision towards the periphery. A recent study that analyzed visually triggered attacks showed hyperemia in the occipital cortex, independently of whether the headache was preceded by visual symptoms (Cao, Y. *et al.*, 1999). An alternative view considers migraine aura and headache as parallel rather than sequential processes, and proposes that the primary cause of migraine headache is an episodic dysfunction in brainstem nuclei that are involved in the central control of nociception (Goadsby, P. J. *et al.*, 2002).

5.45.8.2.2 Cluster headache

The pathophysiology of cluster headache is thought to involve multiple brain regions. Brain imaging studies imply that the associated excruciatingly severe unilateral pain is likely mediated by activation of the first (ophthalmic) division of the trigeminal nerve, while the autonomic symptoms are due to activation of the cranial parasympathetic out-flow from the VIIth cranial nerve. The circadian rhythmicity of cluster headache has led to the concept of a central origin for its initiation (Strittmatter, M. *et al.*, 1996).

Using PET in cluster headache patients, significant activations ascribable to the acute cluster headache were observed in the ipsilateral hypothalamic gray matter and in multiple cortical areas including cingulate and PRC. When compared to the headache-free state only hypothalamic activity was distinct (May, A. *et al.*, 2000). This highly significant activation was not seen in cluster headache patients out of the bout when compared to the patients experiencing an acute cluster headache attack. In contrast to migraine, no brainstem activation was found during the acute attack compared to the resting state. Newer MRS results further substantiate this idea by showing reduced metabolites within the hypothalamus of cluster headache patients in contrast to healthy or migraine headache controls (Wang, S. J. *et al.*, 2006). These data suggest that while primary headaches such as migraine and cluster headache may share a common pain pathway, the trigeminovascular innervation, and activate similar cortical regions, the underlying pathogenesis may be quite different.

5.45.8.2.3 Cardiac pain

Cardiac pain and its variants have been studied by brain imaging using various drugs that bring about these symptoms (Rosen, S. D. *et al.*, 1996; 2002). In patients with myocardial ischemia the perception of angina is associated with activity in the hypothalamus, PAG, thalami, rostral ACC, and bilateral PRC. In patients with silent myocardial ischemia it seems that the silence is not due to impaired afferent signaling, but rather it is associated with a failure of transmission of signals from the thalamus to the frontal cortex. In contrast, in patients with syndrome X, a condition of chest pain with ischemiclike stress electrocardiography but entirely normal coronary angiogram, activity in the right anterior insula distinguished these patients from patients with known coronary disease. These patients appear to have a deficit in central pain habituation (Valeriani, M. *et al.*, 2005). Overall, these studies imply that difference between different cardiac pain conditions are due to central processing, e.g., syndrome X is interpreted as a cortical pain syndrome, a top-down process, in contrast with the bottom-up generation of a pain percept caused by myocardial ischemia in coronary artery disease.

5.45.8.2.4 Irritable bowel syndrome

Irritable bowel syndrome (IBS) is a disorder of abdominal pain or discomfort associated with bowel dysfunction. Hypersensitivity to visceral, but not somatic, stimuli has been demonstrated in IBS. A number of groups have examined brain activity in this condition mainly by monitoring responses to

painful and nonpainful rectal distensions, as well as responses to the anticipation of painful distensions. Two studies are interesting since both show in normal subjects a significant positive correlation between cingulate cortex activity and subjective rating of rectal distension pain, and in both studies this relationship completely disappears in IBS patients (Silverman, D. H. *et al.*, 1997; Mertz, H. *et al.*, 2000). IBS is more prevalent in women than in men. Brain imaging studies have now shown gender differences in brain activity in IBS (Berman, S. M. *et al.*, 2000; Naliboff *et al.*, 2001; Berman, S. M. *et al.*, 2002b; Nakai, A. *et al.*, 2003). There are large differences between the studies, making their synthesis difficult (see Ringel, Y., 2006).

More recent studies show a hint for sensitization in IBS patients because subliminal and supraliminal distensions of rectal distension seem to indicate small differences between IBS and healthy controls in the total cortical volume activated or in regional activity as a function of distention volume (Andresen, V. *et al.*, 2005; Lawal, A. *et al.*, 2006). A study of IBS in contrast to healthy subjects examined thermal and visceral hyperalgesia and related brain activity (Verne, G. N. *et al.*, 2003). This seems the only study where besides pain intensity and unpleasantness measures, the authors also document fear and anxiety and show that all are rated higher by IBS for both heat and rectal distention, and not surprisingly these increased sensations and emotions give rise to larger cortical activations in IBS. The latter is most likely a reflection of a perceptual magnitude mismatch between the groups and says little as to the IBS cortical activity abnormalities. Such mismatches at least for fear and anxiety most likely are common in the majority of studies of IBS. One assumes that the simple introduction of a rectal balloon in IBS would result in increased anxiety, which undoubtedly effects cortical activity to visceral and somatic pain, yet its specific contribution has remained unexplored.

In a more elegant study the authors use perception-related ratings during rectal distention to evoke either urge to defecate or pain, and compared brain activity related to the ratings between IBS patients and healthy subjects. (Kwan, C. L. *et al.*, 2005). The approach is similar to the technique used in mapping brain activity for spontaneous pain in chronic back pain (CBP) and in postherpetic neuralgia (PHN; Baliki, M. N. *et al.*, 2006; Geha, P. Y. *et al.*, 2007). The results show large differences between the two groups contrasted, with far more extensive brain activations in the healthy subjects. The results are complicated by the fact that the authors do not take into consideration the influence of spontaneous pain. Still, this is perhaps one of the best-controlled IBS studies, and indicates distinct cortical areas involved in the urge and pain perceptions in each group.

There is now evidence that serotonin (5-HT) may be involved in IBS. One study (Nakai, A. *et al.*, 2003) examined serotonin synthesis in the brain and indicated greater brain regional serotonin synthesis in female IBS. There is also evidence that alosetron, a 5-HT_3 receptor antagonist, is clinically effective in treating some subtypes of IBS. Berman S. M. *et al.* (2002a) examined brain activity in a large population of IBS, before and after a randomized, placebo-controlled, 3-week use of alosetron. Treatment improved IBS symptoms and regional cerebral blood flow in brain regions rich with 5-HT_3 receptor and involved in emotional and aversive functions: amygdala, ventral striatum, and dorsal pons, implying that the therapeutic effects are due to central actions and not peripheral. Thus, generally the IBS studies show that brain responses are different to rectal stimuli in patients, and that these central events may be critical to IBS.

5.45.8.3 Spontaneous Pain as a Confound in Assessing Brain Activity

A person who has lived for years in the presence of pain, must have developed some coping mechanisms that aid in pursuing other everyday life interests in spite of the presence of the pain. How does this impact the brain? Can one consider the patient in chronic pain as composed of a brain-signaling pain together with a brain undertaking other tasks as in healthy subjects? Or, does the presence of ongoing pain interact and impact other processes as well? Certainly our cognitive and anatomic studies suggest that the latter is more likely. We have now direct evidence of the modulation that ongoing pain imposes on brain activity in general.

A recent study reported brain activity for spontaneous pain in PHN patients before and after topical lidocaine treatment (Geha, P. Y. *et al.*, 2007). The PHN patients were imaged before, after 6-hours and 2-weeks treatment with lidocaine. Behaviorally and based on questionnaires most participants showed a modest but significant decrease in their ongoing pain. The patients were scanned while they were either rating their ongoing pain or rating a visual bar that varied in time in a pattern that mimicked their ratings of pain (Figure 8). Thus, the

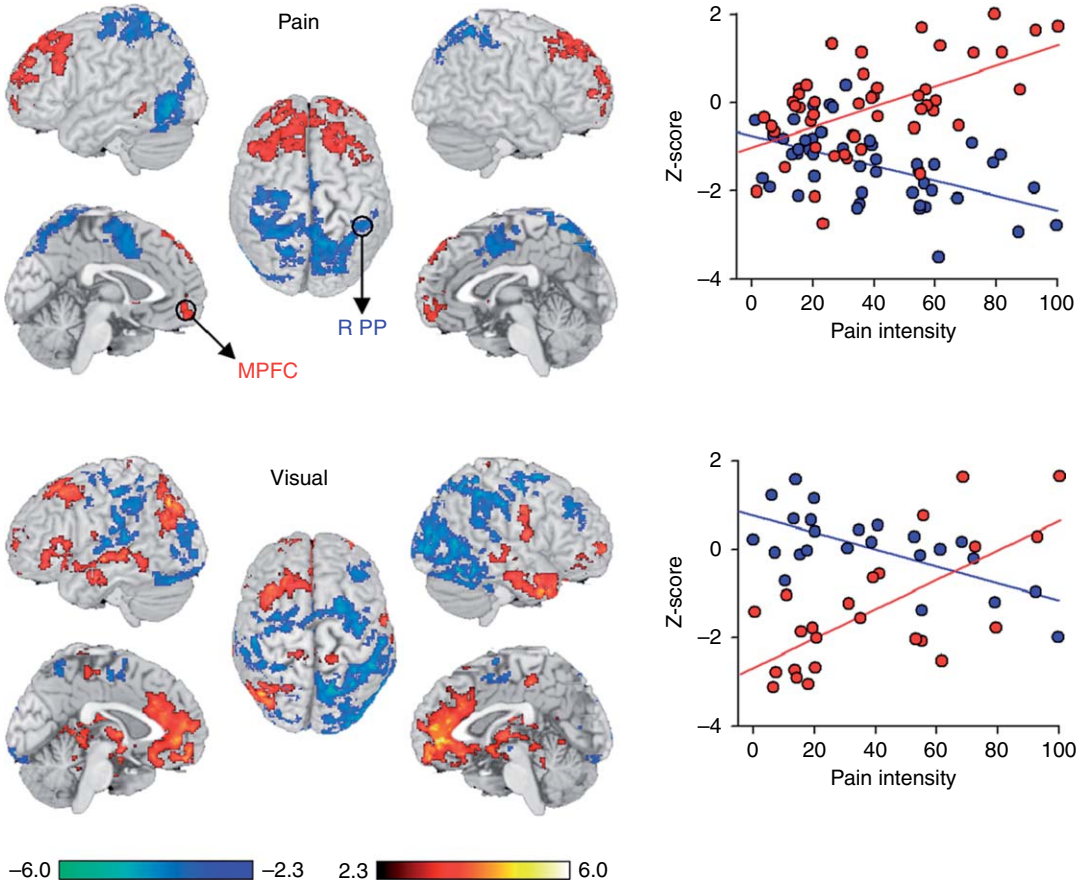

Figure 8 Intensity of ongoing pain changes brain activity and thus cognitive processing. Eleven postherpetic neuralgia patients were studied by functional magnetic resonance imaging (fMRI) once before and twice after lidocaine application on the painful skin. In all sessions, patients performed two different tasks: in the Pain task they continuously rated the fluctuations of their spontaneous pain, and brain activity related to this was identified using methods. In the Visual task they rated fluctuations of a bar varying in time, brain activity was determined with the same approach as for the pain task. The relationship between brain activity and intensity of ongoing pain was determined by using a covariate analysis, where for each fMRI scan its related pain intensity was used to determine the effect of this parameter on brain responses. Across-subject and across all scans average variation of brain activity is displayed for both tasks in the left. Red are brain regions that are positively correlated and blue regions that are negatively correlated with intensity of ongoing pain (normalized to z-values). The right scatter-grams show this effect for two brain regions (right posterior parietal cortex, R PP, $x = 33$ $y = -45$ $z = 50$; and medial prefrontal cortex, MPFC, $x = 9$ $y = 50$ $z = -40$, as respectively circled). Each dot represents a single patient's activity at a single time. Top scatter-gram is for Pain task; bottom for Visual task, red symbols and regression line are for MPFC; blue for R PP. MPFC exhibited significant positive correlations with pain intensity for pain ($r = 0.49$, $P < 0.05$) and visual ($r = 58$, $P < 0.01$) task, while R PP showed negative correlation for pain ($r = -0.48$, $P < 0.05$) and visual ($r = -0.64$, $P < 0.01$) task. Brain areas that show increased correlation with ongoing pain are interpreted as a functional compensation for the decreased attentional resources. Reproduced from Geha, P. Y., Baliki, M. N., Chialvo, D. R., Harden, R. N., Paice, J. A., and Apkarian, A. V. 2007. Brain activity for spontaneous pain of postherpetic neuralgia and its modulation by lidocaine patch therapy. Pain 128, 88–100.

latter is a control task that captures motor and cognitive parts of the task but, of course, it does not reflect the pain. Brain activity for both tasks was increasing from first to third session. This observation is similar to earlier reports that decrease in clinical pain in many cases results in increased brain activity. In this case, however, the internal control was also changing in a manner parallel to the pain condition, hinting that the effects of decreased pain was modulating more than just pain-related circuitry.

To identify the role of spontaneous pain on brain activity in general, a correlation analysis was done for both tasks with mean spontaneous pain. Figure 8 shows the influence of pain intensity on across-sessions averaged brain activity for both tasks.

The resultant map is generally similar for both tasks: activity in medial and lateral prefrontal regions was positively correlated, while posterior parietal attentional areas were negatively correlated with mean pain intensity. This result shows that brain activity for both tasks is influenced by the level of spontaneous pain, implying that pain intensity influences task performance in general. This is in line with previous studies showing that ongoing pain may interfere with cognitive functions (Lorenz, J. *et al.*, 1997).

This result reinforces the need for correcting brain activity by a control condition performed at the same pain level that is the necessity of subtracting the visual task from spontaneous pain rating task, at each treatment session. For both tasks, the fact that posterior parietal cortical activity was negatively correlated with mean ongoing pain suggests that the attentional abilities of patients are directly related to the intensity of their pain, which would in turn impact their abilities in performing anything that would demand concentration.

Moreover, multiple prefrontal regions were positively correlated to the mean pain, suggesting that the patients' brain regions underlying higher cognitive functions become more active as the pain intensity increases. The exact cognitive implications for these brain activity patterns remain unclear. In contrast, the finding indicates that the intensity of spontaneous pain impacts brain activity for any task that the subject attempts to perform, enhancing some aspects and inhibiting others. Therefore, the decreased brain activity reported for pain tasks in many clinical pain conditions (Peyron, R. *et al.*, 2000; Derbyshire, S. W., 2003; Apkarian, A. V. *et al.*, 2005; Kupers, R. and Kehlet, H., 2006) is most likely a reflection of the presence of the spontaneous pain, and is not specific to the task being investigated.

The fact that pain intensity seems to modulate brain activity in general has another powerful consequence. It suggests that simply studying brain activity, in tasks unrelated to pain, one should be able to identify the presence of pain and study its effects on sensory/cognitive/motor/attentional processing, an exciting prospect that remains to be pursued.

5.45.8.4 Functional Magnetic Resonance Imaging of Spontaneous Pain

Spontaneous pain is highly prevalent in clinical pain conditions, and is usually the primary drive for patients seeking medical care. Thus, understanding its related brain circuitry is both scientifically and therapeutically imperative. Cortical responses to standard mechanical or thermal stimulation are of limited value for understanding these clinical pain conditions. Spontaneous pain fluctuates unpredictably in the time scale of seconds to minutes, and these fluctuations have characteristic properties that differentiate between different chronic pain conditions such as PHN and CBP (Foss, J. M. *et al.*, 2006). This variability (specific fractal dimension) can also be observed in fMRI signals when such patients rate their spontaneous pain. Therefore, this technique was applied to study brain activity in CBP (Baliki, M. N. *et al.*, 2006) and PHN patients (Geha, P. Y. *et al.*, 2007) in relation to their subjective report of fluctuations of spontaneous pain.

The combination of relating brain activity to spontaneous pain and correcting for confounds by subtracting brain activity for visual bar lengths, provides a robust approach with which clinical pain may be studied directly. Note that in this case the brain activity is related to exactly the event that the patient complains about. With this approach, in CBP patients (Baliki, M. N. *et al.*, 2006) it was shown that the brain regions activated when the pain was increasing correspond to brain regions seen for acute pain in normal subjects. In contrast, for time periods when the pain was high and sustained, the brain activity was mainly limited to medial PRC, a region usually not activated for acute pain. The resultant brain activity was strongly correlated to the patients' reported pain intensity at the time of the scan, specifically with medial prefrontal activity. Also, the duration or chronicity of the pain was captured in the insular activity, a region activated only during increases in spontaneous pain. Thus, two fundamental properties of CBP its intensity and duration were directly reflected in the brain activity identified in these patients. By applying a thermal painful stimulus in the same patients (as well as in healthy subjects) the same study showed that brain regions reflecting the stimulus intensity were not related to that reflecting the intensity of spontaneous pain. In turn, the brain region that reflected spontaneous pain intensity was only activated for the latter and did not reflect thermal painful stimulus intensity. Therefore, at least in the patient group studied spontaneous pain involved a different brain activity pattern than acute pain.

5.45.8.5 Neuropathic Pain

Patients with neuropathic pain show decreased responses in the thalamus to experimental painful

stimuli (Peyron, R. *et al.*, 2000). A MRS study showed a decrease in the level of *N*-acetyl-aspartate, a neuronal marker, in the thalami of patients with chronic neuropathic pain after spinal cord injury (SCI), when compared to patients with SCI but without pain (Pattany, P. M. *et al.*, 2002). Thus, neurochemical brain imaging provides evidence for the occurrence of long-term changes in the brain chemistry and morphology of chronic neuropathic pain patients. Thalamic activity in neuropathic patients was also reported to increase after pain relief (Hsieh, J. C. *et al.*, 1995), and to be significantly negatively correlated with the duration of the condition in CRPS patients (Fukumoto, M. *et al.*, 1999). Thus, the reduced activation of the thalamus may also be an altered functional state rather than an irreversible degeneration. Neuropathic pain patients in addition show a reduced availability of opioid receptor binding sites (Maarrawi, J. *et al.*, 2007). This reduction was symmetric in peripheral neuropathic pain, suggesting a possible release of endogenous opioids, but lateralized to the hemisphere contralateral to the pain in central pain patients, consistent with a loss of receptors (Jones, A. K. P. *et al.*, 2004, Willoch, F. *et al.*, 2004).

Brain activity differences between healthy subjects and patients in activation paradigms are difficult to interpret since they do not distinguish between brain activity specifically related to the clinical condition and abnormalities in sensory processing secondarily associated with the clinical state. Particularly in neuropathic pain, the accompanying sensory deficit may be reflected in the imaging results and not the pain. Reduced relevance of the acute stimulus to subjects who are already in pain may also account for much of the decreased regional brain activity in neuropathic pain. To overcome such nonspecific brain activity differences one needs to compare brain activity for stimuli where perceptual evaluation has been equated between patients and normal healthy subjects.

Three studies (Hsieh, J. C. *et al.*, 1995; 1999a; Apkarian, A. V. *et al.*, 2001b) have looked at the regions of the brain modulated by relief of chronic neuropathic pain: CRPS, peripheral neuropathy, and trigeminal neuropathy. Two of these studies show that the PRC activity is decreased, and all three studies report decreased rostral ACC activity, after successful pain relief. It is to be noted that in addition to those regions some areas were also less activated with pain relief such as the insula (Hsieh, J. C. *et al.*, 1995) and the anterior limbic thalamus (Hsieh, J. C. *et al.*, 1999a), whereas others were more activated after pain relief like the medial PRC (Hsieh, J. C. *et al.*, 1999a). This heterogeneity is not surprising because pattern of brain activity may be specific to each neuropathic pain condition.

5.45.8.6 Low Back Pain and Fibromyalgia

As mentioned above, brain activity of healthy subjects and patients with increased pain sensitivity should be compared in such a way that perceived intensity has been matched across the two groups. A recent study used such a design and showed generally heightened brain activity for painful stimuli of equivalent perceptual intensity both in fibromyalgia and CBP patients as compared to healthy subjects (Gracely, R. H. *et al.*, 2002; Giesecke, T. *et al.*, 2004). Morphometric and neurochemical brain imaging studies provide evidence for the occurrence of long-term changes in the brain chemistry and morphology of chronic pain patients. The level of *N*-acetyl-aspartate, a neuronal marker, was decreased in the medial and lateral PRC of CBP patients compared to an age- and gender-matched control group (Grachev, I. D. *et al.*, 2000). A morphometric study in chronic pain showed also a decrease in gray matter density in the dorsolateral PRC and the thalamus of CBP patients when compared to matched controls (Apkarian, A. V. *et al.*, 2004). Furthermore, these long-term chemical and morphological changes are significantly correlated with different characteristics of pain such as pain duration (Apkarian, A. V. *et al.*, 2004), pain intensity (Pattany, P. M. *et al.*, 2002; Grachev, I. D. *et al.*, 2002; Apkarian, A. V. *et al.*, 2004), and sensory-affective components (Grachev, I. D. *et al.*, 2002). The morphometric and neurochemical studies imply an active role of the central nervous system in chronic pain, suggesting that supraspinal reorganization may be critical for chronic pain.

5.45.8.7 Overview Regarding the Role of the Cortex in Chronic Pain Perception

In spite of a plethora of data there remains a host of uncertainties about their significance. Overall, the clinical brain imaging studies indicate reduced information transmission through the thalamus to the cortex, and increased activity in PFC, mostly in medial PFC coupled with atrophy in dorsolateral PFC. The number of studies remain very small and hence our confidence as to the reproducibility of these changes remain minimal. Still, the observations

regarding cortical and thalamic activity changes in chronic pain are in general consistent with the notion that chronic pain conditions preferentially engage brain areas involved in cognition/emotion and decreases activity in regions involved in sensory evaluation of nociceptive inputs.

Evidence has been presented that brain activity, chemistry, and morphology may be reorganized in chronic pain conditions. Does this evidence imply that there is supraspinal reorganization, above and beyond what is established in the periphery and spinal cord? That is, even if we establish a brain pattern of activity for some chronic pain condition, does this reflect some unique contribution of the brain to this state or is it simply a reflection of lower level reorganization? The answer is not straightforward. However, only by answering such questions will brain imaging be able to provide new information to the myriad mechanisms described for peripheral and spinal cord reorganization in chronic pain.

5.45.9 Conclusions and Outlook

The study of nociceptive processing in the cerebral cortex has come a long way. In contrast to earlier assumptions, the classical somatosensory cortex areas are not the only ones activated by painful stimuli. In addition, limbic areas such as the anterior and midcingulate cortex and the insula have also been recognized as part of the nociceptive network, and more recently also cognitive areas in the PRC. Limbic areas are usually considered to mediate emotional processes, but they are also involved in autonomic and motor functions. In this way, progress in understanding the cortical nociceptive network mirrors that in understanding the subcortical networks, which also include many connections to autonomic and motor nuclei as well as hypothalamus, cerebellum, and basal ganglia. Images of brain activation by painful stimuli leave the impression that at least half of the brain participates in processing nociceptive information. At other times, many of the same areas participate in visual, motor, emotional, cognitive, or other signal processing. In that sense, our current understanding of the nociceptive network in the brain is consistent with our current understanding of how the brain uses distributed processing for its many functions. It is not clear, however, to what extent any part of the cerebral cortex is specific for nociception. The best candidate region for such a function lies in the parasylvian cortex, in the vicinity of SII and the dorsal insula. In chronic pain, nociceptive processing in the cerebral cortex is partly preserved and partly altered, in particular with respect to PRC functions. This reorganization may be a neuroplastic response to the chronicity of pain, it may reflect activation of antinociceptive processes, or it may even represent a predisposing factor for the development of chronic pain. The methods available for the study of nociceptive processing in the brain allow to address many of these open questions in the near future, and this part of pain research is bound to remain a very productive one.

References

Andersson, J. L. R., Lilja, A., Hartvig, P., Långström, B., Gordh, T., Handwerker, H., and Torebjörk, E. 1997. Somatotopic organization along the central sulcus, for pain localization in humans, as revealed by positron emission tomography. Exp. Brain Res. 117, 192–199.

Andresen, V., Bach, D. R., Poellinger, A., Tsrouya, C., Stroh, A., Foerschler, A., Georgiewa, P., Zimmer, C., and Monnikes, H. 2005. Brain activation responses to subliminal or supraliminal rectal stimuli and to auditory stimuli in irritable bowel syndrome. Neurogastroenterol. Motil. 17, 827–837.

Apkarian, A. V. 2004. Cortical pathophysiology of chronic pain. Novartis Found. Symp. 261, 239–245.

Apkarian, A. V. and Shi, T. 1994. Squirrel monkey lateral thalamus. I. Somatic nociresponsive neurons and their relation to spinothalamic terminals. J. Neurosci. 14, 6779–6795.

Apkarian, A. V., Bushnell, C., Treede, R. D., and Zubieta, J. K. 2005. Human brain mechanisms of pain perception and regulation in health and disease. Eur. J. Pain 9, 463–484.

Apkarian, A. V., Grachev, I. D., and Krauss, B. R. 2001a. Imaging brain pathophysiology of chronic CRPS pain. In: Complex Regional Pain Syndrome (*eds*. R. Harden, W. Janig, and J. C. Baron), pp. 209–227. IASP Press.

Apkarian, A. V., Sosa, Y., Sonty, S., Levy, R. E., Harden, R., Parrish, T., and Gitelman, D. 2004. Chronic back pain is associated with decreased prefrontal and thalamic gray matter density. J. Neurosci. 24, 10410–10415.

Apkarian, A. V., Stea, R. A., Manglos, S. H., Szeverenyi, N. M., King, R. B., and Thomas, F. D. 1992. Persistent pain inhibits contralateral somatosensory cortical activity in humans. Neurosci. Lett. 140, 141–147.

Apkarian, A. V., Thomas, P. S., Krauss, B. R., and Szeverenyi, N. M. 2001b. Prefrontal cortical hyperactivity in patients with sympathetically mediated chronic pain. Neurosci. Lett. 311, 193–197.

Baliki, M. N., Chialvo, D. R., Geha, P. Y., Levy, R. M., Harden, R. N., Parrish, T. B., and Apkarian, A. V. 2006. Chronic pain and the emotional brain: specific brain activity associated with spontaneous fluctuations of intensity of chronic back pain. J. Neurosci. 26, 12165–12173.

Bantick, S. J., Wise, R. G., Ploghaus, A., Clare, S., Smith, S. M., and Tracey, I. 2002. Imaging how attention modulates pain in humans using functional MRI. Brain 125, 310–319.

Baumgärtner, U., Buchholz, H. G., Bellosevich, A., Magerl, W., Siessmeier, T., Rolke, R., Höhnemann, S., Piel, M., Rösch, F., Wester, H. J., Henriksen, G., Stoeter, P., Bartenstein, P., Treede, R. D., and Schreckenberger, M. 2006a. High opiate receptor binding potential in the human lateral pain system. Neuroimage 30, 692–699.

Baumgärtner, U., Tiede, W., Treede, R. D., and Craig, A. D. 2006b. Laser-evoked potentials are graded and somatotopically organized anteroposteriorly in the operculoinsular cortex of anesthetized monkeys. J. Neurophysiol. 96, 2802–2808.

Becker, J. B., Arnold, A. P., Berkley, K. J., Blaustein, J. D., Eckel, L. A., Hampson, E., Herman, J. P., Marts, S., Sadee, W., Steiner, M., Taylor, J., and Young, E. 2005. Strategies and methods for research on sex differences in brain and behavior. Endocrinology 146, 1650–1673.

Benedetti, F., Mayberg, H. S., Wager, T. D., Stohler, C. S., and Zubieta, J. K. 2005. Neurobiological mechanisms of the placebo effect. J. Neurosci. 25, 10390–10402.

Berman, S. M., Chang, L., Suyenobu, B., Derbyshire, S. W., Stains, J., Fitzgerald, L., Mandelkern, M., Hamm, L., Vogt, B., Naliboff, B. D., and Mayer, E. A. 2002a. Condition-specific deactivation of brain regions by 5-HT3 receptor antagonist Alosetron. Gastroenterology 123, 969–977.

Berman, S., Munakata, J., Naliboff, B. D., Chang, L., Mandelkern, M., Silverman, D., Kovalik, E., and Mayer, E. A. 2000. Gender differences in regional brain response to visceral pressure in IBS patients. Eur. J. Pain 4, 157–172.

Berman, S. M., Naliboff, B. D., Chang, L., Fitzgerald, L., Antolin, T., Camplone, A., and Mayer, E. A. 2002b. Enhanced preattentive central nervous system reactivity in irritable bowel syndrome. Am. J. Gastroenterol. 97, 2791–2797.

Beydoun, A., Morrow, T. J., Shen, J. F., and Casey, K. L. 1993. Variability of laser-evoked potentials: attention, arousal and lateralized differences. Electroencephalogr. Clin. Neurophysiol. 88, 173–181.

Bingel, U., Lorenz, J., Schoell, E., Weiller, C., and Büchel, C. 2006. Mechanisms of placebo analgesia: rACC recruitment of a subcortical antinociceptive network. Pain 120, 8–15.

Borsook, D., Becerra, L., and Hargreaves, R. 2006. A role for fMRI in optimizing CNS drug development. Nat. Rev. Drug Discov. 5, 411–424.

Biemond, A. 1956. The conduction of pain above the level of the thalamus opticus. Arch. Neurol. Psychiat. 75, 231–244.

Botvinick, M., Jha, A. P., Bylsma, L. M., Fabian, S. A., Solomon, P. E., and Prkachin, K. M. 2005. Viewing facial expressions of pain engages cortical areas involved in the direct experience of pain. Neuroimage 25, 312–319.

Bragard, D., Chen, A. C. N., and Plaghki, L. 1996. Direct isolation of ultra-late (C-fibre) evoked brain potentials by CO2 laser stimulation of tiny cutaneous surface areas in man. Neurosci. Lett. 209, 81–84.

Bromm, B. and Lorenz, J. 1998. Neurophysiological evaluation of pain. Electroenceph. Clin. Neurophysiol. 107, 227–253.

Bromm, B. and Treede, R. D. 1984. Nerve fibre discharges, cerebral potentials and sensations induced by CO_2 laser stimulation. Human Neurobiol. 3, 33–40.

Bromm, B., Neitzel, H., Tecklenburg, A., and Treede, R. D. 1983. Evoked cerebral potential correlates of C-fibre activity in man. Neurosci. Lett. 43, 109–114.

Brooks, J. C. W., Nurmikko, T. J., Bimson, W. E., Singh, K. D., and Roberts, N. 2002. fMRI of thermal pain: effects of stimulus laterality and attention. Neuroimage 15, 293–301.

Buchsbaum, M. S., Kessler, R., King, A., Johnson, J., and Cappelletti, J. 1984. Simultaneous cerebral glucography with positron emission tomography and topographic electroencephalography. Prog. Brain Res. 62, 263–269.

Bushnell, M. C. and Apkarian, A. V. 2005. Representation of Pain in the Brains. In: Wall and Melzack's Textbook of Pain, Chapter 6, 5th Edition (*eds*. S. B. McMahon and M. Koltzenburg), pp. 107–124. Elsevier.

Bushnell, M. C., Duncan, G. H., Hofbauer, R. K., Ha, B., Chen, J. I., and Carrier, B. 1999. Pain perception: is there a role for primary somatosensory cortex? Proc. Natl. Acad. Sci. U. S. A. 96, 7705–7709.

Cao, Y., Welch, K. M. A., Aurora, S., and Vikingstad, E. M. 1999. Functional MRI-BOLD of visually triggered headache in patients with migraine. Arch. Neurol. 56, 548–554.

Carmon, A., Mor, J., and Goldberg, J. 1976. Evoked cerebral responses to noxious thermal stimuli in humans. Exp. Brain Res. 25, 103–107.

Casey, K. L., Svensson, P., Morrow, T. J., Raz, J., Jone, C., and Minoshima, S. 2000. Selective opiate modulation of nociceptive processing in the human brain. J. Neurophysiol. 84, 525–533.

Chen, A. C. N. 1993. Human brain measures of clinical pain: a review. I. Topographic mappings. Pain 54, 115–132.

Chen, A. C. N. and Treede, R. D. 1985. The McGill pain questionnaire in the assessment of phasic and tonic experimental pain: behavioral evaluation of the 'pain inhibiting pain' effect. Pain 22, 67–69.

Chen, A. C. N., Chapman, C. R., and Harkins, S. W. 1979. Brain evoked potentials are functional correlates of induced pain in man. Pain 6, 365–374.

Craig, A. D. 1995. Supraspinal Projections of Lamina I Neurons. In: Forebrain Areas Involved in Pain Processing (*eds*. J. M. Besson, G. Guilbaud, and H. Ollat), pp. 13–25. John Libbey Eurotext.

Craig, A. D. 2002. How do you feel? Interoception: the sense of the physiological condition of the body. Nat. Rev. 3, 655–666.

Craig, A. D., Bushnell, M. C., Zhang, E. T., and Blomqvist, A. 1994. A thalamic nucleus specific for pain and temperature sensation. Nature 372, 770–773.

Cruccu, G., Anand, P., Attal, N., Garcia-Larrea, L., Haanpää, M., Jørum, E., Serra, J., and Jensen, T. S. 2004. EFNS guidelines on neuropathic pain assessment. Eur. J. Neurol. 11, 153–162.

DaSilva, A. F. M., Becerra, L., Makris, N., Strassman, A. M., Gonzalez, R. G., Geatrakis, N., and Borsook, D. 2002. Somatotopic activation in the human trigeminal pain pathway. J. Neurosci. 22, 8183–8192.

Danziger, N., Prkachin, K. M., and Willer, J. C. 2006. Is pain the price of empathy? The perception of others' pain in patients with congenital insensitivity to pain. Brain 129, 2494–2507.

Davis, K. D. 2003. Neurophysiological and anatomical considerations in functional imaging of pain. Pain 105, 1–3.

Davis, K. D., Wood, M. L., Crawley, A. P., and Mikulis, D. J. 1995. fMRI of human somatosensory and cingulated cortex during painful electrical nerve stimulation. Neuroreport 7, 321–325.

De Leeuw, R., Albuquerque, R. J., Andersen, A. H., and Carlson, C. R. 2006. Influence of estrogen on brain activation during stimulation with painful heat. J. Oral Maxillofac. Surg. 64, 158–166.

Derbyshire, S. W. 2003. A systematic review of neuroimaging data during visceral stimulation. Am. J. Gastroenterol. 98, 12–20.

Derbyshire, S. W., Whalley, M. G., Stenger, V. A., and Oakley, D. A. 2004. Cerebral activation during hypnotically induced and imagined pain. Neuroimage 23, 392–401.

Dieterich, M., Bense, S., Lutz, S., Drzezga, A., Stephan, T., Bartenstein, P., and Brandt, T. 2003. Dominance for vestibular cortical function in the non-dominant hemisphere. Cereb. Cortex 13, 994–1007.

Disbrow, E., Roberts, T., and Krubitzer, L. 2000. Somatotopic organization of cortical fields in the lateral sulcus of homo sapiens: evidence for SII and PV. J. Comp. Neurol. 418, 1–21.

Dong, W. K., Chudler, E. H., Sugiyama, K., Roberts, V. J., and Hayashi, T. 1994. Somatosensory, multisensory, and task-related neurons in cortical area 7b (PF) of unanesthetized monkeys. J. Neurophysiol. 72, 542–564.

Duclaux, R., Franzen, O., Chatt, A. B., Kenshalo, D. R., and Stowell, H. 1974. Responses recorded from human scalp evoked by cutaneous thermal stimulation. Brain Res. 78, 279–290.

Eickhoff, S. B., Schleicher, A., Zilles, K., and Amunts, K. 2006. The human parietal operculum. I. Cytoarchitectonic mapping of subdivisions. Cereb. Cortex 16, 254–267.

Firestone, L. L., Gyulai, F., Mintun, M., Adler, L. J., Urso, K., and Winter, P. M. 1996. Human brain activity response to fentanyl imaged by positron emission tomography. Anesth. Analg. 82, 1247–1251.

Fitzgerald, P. J., Lane, J. W., Thakur, P. H., and Hsiao, S. S. 2004. Receptive field properties of the macaque second somatosensory cortex: evidence for multiple functional representations. J. Neurosci. 24, 11193–11204.

Fitzgerald, P. J., Lane, J. W., Thakur, P. H., and Hsiao, S. S. 2006. Receptive field (RF) properties of the macaque second somatosensory cortex: RF size, shape, and somatotopic organization. J. Neurosci. 26, 6485–6495.

Foss, J. M., Apkarian, A. V., and Chialvo, D. R. 2006. Dynamics of pain: fractal dimension of temporal variability of spontaneous pain differentiates between pain States. J. Neurophysiol. 95, 730–736.

Forss, N., Raij, T. T., Seppa, M., and Hari, R. 2005. Common cortical network for first and second pain. Neuroimage 24, 132–142.

Frankenstein, U. N., Richter, W., McIntyre, M. C., and Remy, F. 2001. Distraction modulates anterior cingulate gyrus activations during the cold pressor test. Neuroimage 14, 827–836.

Frot, M. and Mauguière, F. 1999. Operculo-insular responses to nociceptive skin stimulation in humans (A review). Neurophysiol. Clin. 29, 401–410.

Frot, M. and Mauguière, F. 2003. Dual representation of pain in the operculo-insular cortex in humans. Brain 126, 438–450.

Frot, M., Rambaud, L., Guénot, M., and Mauguière, F. 1999. Intracortical recordings of early pain-related CO2-laser evoked potentials in the human second somatosensory (SII) area. Clin. Neurophysiol. 110, 133–145.

Fukumoto, M., Ushida, T., Zinchuk, V. S., Yamamoto, H., and Yoshida, S. 1999. Contralateral thalamic perfusion in patients with reflex sympathetic dystrophy syndrome. Lancet 354, 1790–1791.

Garcia-Larrea, L., Maarrawi, J., Peyron, R., Costes, N., Mertens, P., Magnin, M., and Laurent, B. 2006. On the relation between sensory deafferentation, pain and thalamic activity in Wallenberg's syndrome: a PET-scan study before and after motor cortex stimulation. Eur. J. Pain 10, 677–688.

Geha, P. Y., Baliki, M. N., Chialvo, D. R., Harden, R. N., Paice, J. A., and Apkarian, A. V. 2007. Brain activity for spontaneous pain of postherpetic neuralgia and its modulation by lidocaine patch therapy. Pain 128, 88–100.

Giesecke, T., Gracely, R. H., Grant, M. A., Nachemson, A., Petzke, F., Williams, D. A., and Clauw, D. J. 2004. Evidence of augmented central pain processing in idiopathic chronic low back pain. Arthritis Rheum. 50, 613–623.

Gingold, S. I., Greenspan, J. D., and Apkarian, A. V. 1991. Anatomic evidence of nociceptive inputs to primary somatosensory cortex: relationship between spinothalamic terminals and thalamocortical cells in squirrel monkeys. J. Comp. Neurol. 308, 467–490.

Goadsby, P. J., Lipton, R. B., and Ferrari, M. D. 2002. Migraine – current understanding and treatment. N. Engl. J. Med. 346, 257–270.

Goldstein, J. M., Jerram, M., Poldrack, R., Ahern, T., Kennedy, D. N., Seidman, L. J., and Makris, N. 2005. Hormonal cycle modulates arousal circuitry in women using functional magnetic resonance imaging. J. Neurosci. 25, 9309–9316.

Gracely, R. H., Geisser, M. E., Giesecke, T., Grant, M. A., Petzke, F., Williams, D. A., and Clauw, D. J. 2004. Pain catastrophizing and neural responses to pain among persons with fibromyalgia. Brain 127, 835–843.

Gracely, R. H., Petzke, F., Wolf, J. M., and Clauw, D. J. 2002. Functional magnetic resonance imaging evidence of augmented pain processing in fibromyalgia. Arthritis Rheum. 46, 1333–1343.

Grachev, I. D., Fredrickson, B. E., and Apkarian, A. V. 2000. Abnormal brain chemistry in chronic back pain: an *in vivo* proton magnetic resonance spectroscopy study. Pain 89, 7–18.

Grachev, I. D., Fredrickson, B. E., and Apkarian, A. V. 2002. Brain chemistry reflects dual states of pain and anxiety in chronic low back pain. J. Neural Transm. 109, 1309–1334.

Granziera, C., DaSilva, A. F., Snyder, J., Tuch, D. S., and Hadjikhani, N. 2006. Anatomical alterations of the visual motion processing network in migraine with and without aura. PLoS Med. 3, e402.

Greenspan, J. D., Lee, R. R., and Lenz, F. A. 1999. Pain sensitivity alterations as a function of lesion location in the parasylvian cortex. Pain 81, 273–282.

Hadjikhani, N., Sanchez, d. R., Wu, O., Schwartz, D., Bakker, D., Fischl, B., Kwong, K. K., Cutrer, F. M., Rosen, B. R., Tootell, R. B., Sorensen, A. G., and Moskowitz, M. A. 2001. Mechanisms of migraine aura revealed by functional MRI in human visual cortex. Proc. Natl. Acad. Sci. U. S. A. 98, 4687–4692.

Hagelberg, N., Forssell, H., Aalto, S., Rinne, J. O., Scheinin, H., Taiminen, T., Nagren, K., Eskola, O., and Jaaskelainen, S. K. 2003a. Altered dopamine D2 receptor binding in atypical facial pain. Pain 106, 43–48.

Hagelberg, N., Forssell, H., Rinne, J. O., Scheinin, H., Taiminen, T., Aalto, S., Luutonen, S., Nagren, K., and Jaaskelainen, S. 2003b. Striatal dopamine D1 and D2 receptors in burning mouth syndrome. Pain 101, 149–154.

Hagelberg, N., Kajander, J. K., Nagren, K., Hinkka, S., Hietala, J., and Scheinin, H. 2002. Mu-receptor agonism with alfentanil increases striatal dopamine D2 receptor binding in man. Synapse 45, 25–30.

Hampson, E. 2002. Sex Differences in Human Brain and Cognition: the Influence of Sex Steroids in Early and Adult Life. In: Behavioral endocrinology, 2nd edn. (*eds*. J. B. Becker, S. M. Breedlove, D. Crews, and M. M. McCarthy) pp. 579–628. MIT Press.

Hari, R. and Forss, N. 1999. Magnetoencephalography in the study of human somatosensory cortical processing. Phil. Trans. R. Soc. Lond. B 354, 1145–1154.

Head, H. and Holmes, G. 1911. Sensory disturbances from cerebral lesions. Brain 34, 102–254.

Hofbauer, R. K., Rainville, P., Duncan, G. H., and Bushnell, M. C. 2001. Cortical representation of the sensory dimension of pain. J. Neurophysiol. 86, 402–411.

Hsieh, J. C., Belfrage, M., Stoneelander, S., Hansson, P., and Ingvar, M. 1995. Central representation of chronic ongoing neuropathic pain studied by positron emission tomography. Pain 63, 225–236.

Hsieh, J. C., Meyerson, B. A., and Ingvar, M. 1999a. PET study on central processing of pain in trigeminal neuropathy. Eur. J. Pain 3, 51–65.

Hsieh, J. C., Stone-Elander, S., and Ingvar, M. 1999b. Anticipatory coping of pain expressed in the human anterior

cingulate cortex: a positron emission tomography study. Neurosci. Lett. 262, 61–64.
Hutchison, W. D., Davis, K. D., Lozano, A. M., Tasker, R. R., and Dostrovsky, J. O. 1999. Pain-related neurons in the human cingulate cortex. Nature Neurosci. 2, 403–405.
Iannetti, G. D., Truini, A., Romaniello, A., Galeotti, F., Rizzo, C., Manfredi, M., and Cruccu, G. 2003. Evidence of a specific spinal pathway for the sense of warmth in humans. J. Neurophysiol. 89, 562–570.
Jaaskelainen, S. K., Rinne, J. O., Forssell, H., Tenovuo, O., Kaasinen, V., Sonninen, P., and Bergman, J. 2001. Role of the dopaminergic system in chronic pain – a fluorodopa-PET study. Pain 90, 257–260.
Jackson, P. L., Meltzoff, A. N., and Decety, J. 2005. How do we perceive the pain of others? A window into the neural processes involved in empathy. Neuroimage 24, 771–779.
Jones, A. K. P., Brown, W. D., Friston, K. J., Qi, L. Y., and Frackowiak, R. S. J. 1991a. Cortical and subcortical localization of response to pain in man using positron emission tomography. Proc. R. Soc. Lond. B 244, 39–44.
Jones, A. K. P., Qi, L. Y., Fujirawa, T., Luthra, S. K., Ashburner, J., Bloomfield, P., Cunningham, V. J., Itoh, M., Fukuda, H., and Jones, T. 1991b. *In vivo* distribution of opioid receptors in man in relation to the cortical projections of the medial and lateral pain systems measured with positron emission tomography. Neurosci. Lett. 126, 25–28.
Jones, A. K. P., Watabe, H., Cunningham, V. J., and Jones, T. 2004. Cerebral decreases in opioid receptor binding in patients with central neuropathic pain measured by [^{11}C]diprenorphine binding and PET. Eur. J. Pain 8, 479–485.
Kajantie, E. and Phillips, D. I. 2006. The effects of sex and hormonal status on the physiological response to acute psychosocial stress. Psychoneuroendocrinology 31, 151–178.
Kanda, M., Nagamine, T., Ikeda, A., Ohara, S., Kunieda, T., Fujiwara, N., Yazawa, S., Sawamoto, N., Matsumoto, R., Taki, W., and Shibasaki, H. 2000. Primary somatosensory cortex is actively involved in pain processing in human. Brain Res. 853, 282–289.
Keltner, J. R., Furst, A., Fan, C., Redfern, R., Inglis, B., and Fields, H. L. 2006. Isolating the modulatory effect of expectation on pain transmission: a functional magnetic resonance imaging study. J. Neurosci. 26, 4437–4443.
Kenshalo, D. R. and Isensee, O. 1983. Responses of primate SI cortical neurons to noxious stimuli. J. Neurophysiol. 50, 1479–1496.
Kenshalo, D. R. and Willis, W. D. 1991. The Role of the Cerebral Cortex in Pain Sensation. In: Cerebral Cortex, Vol. 9 (*ed*. A. Peters), pp. 153–212. Plenum Press.
Kenshalo, D. R., Chudler, E. H., Anton, F., and Dubner, R. 1988. SI nociceptive neurons participate in the encoding process by which monkeys perceive the intensity of noxious thermal stimulation. Brain Res. 454, 378–382.
Kenshalo, D. R., Iwata, K., Sholas, M., and Thomas, D. A. 2000. Response properties and organization of nociceptive neurons in area 1 of monkey primary somatosensory cortex. J. Neurophysiol. 84, 719–729.
Kong, J., Gollub, R. L., Rosman, I. S., Webb, J. M., Vangel, M. G., Kirsch, I., and Kaptchuk, T. J. 2006. Brain activity associated with expectancy-enhanced placebo analgesia as measured by functional magnetic resonance imaging. J. Neurosci. 26, 381–388.
Koyama, T., Kato, K., Tanaka, Y. Z., and Mikami, A. 2001. Anterior cingulate activity during pain-avoidance and reward tasks in monkeys. Neurosci. Res. 39, 421–430.
Koyama, T., Tanaka, Y. Z., and Mikami, A. 1998. Nociceptive neurons in the macaque anterior cingulate activate during anticipation of pain. Neuroreport 9, 2663–2667.
Kunde, V. and Treede, R. D. 1993. Topography of middle-latency somatosensory evoked potentials following painful laser stimuli and non-painful electrical stimuli. Electroenceph. Clin. Neurophysiol. 88, 280–289.
Kulkarni, B., Bentley, D. E., Elliott, R., Youell, P., Watson, A., Derbyshire, S. W., Frackowiak, R. S., Friston, K. J., and Jones, A. K. 2005. Attention to pain localization and unpleasantness discriminates the functions of the medial and lateral pain systems. Eur. J. Neurosci. 21, 3133–3142.
Kupers, R. and Kehlet, H. 2006. Brain imaging of clinical pain states: a critical review and strategies for future studies. Lancet Neurol. 5, 1033–1044.
Kwan, C. L., Diamant, N. E., Pope, G., Mikula, K., Mikulis, D. J., and Davis, K. D. 2005. Abnormal forebrain activity in functional bowel disorder patients with chronic pain. Neurology 65, 1268–1277.
Lamour, Y., Guilbaud, G., and Willer, J. C. 1983. Rat somatosensory (Sml) cortex: II. Laminar and columnar organization of noxious and non-noxious inputs. Exp. Brain Res. 49, 46–54.
Lamour, Y., Willer, J. C., and Guilbaud, G. 1982. Neuronal responses to noxious stimulation in rat somatosensory cortex. Neurosci. Lett. 29, 35–40.
Lawal, A., Kern, M., Sidhu, H., Hofmann, C., and Shaker, R. 2006. Novel evidence for hypersensitivity of visceral sensory neural circuitry in irritable bowel syndrome patients. Gastroenterology 130, 26–33.
Lenz, F. A., Rios, M., Chau, D., Krauss, G. L., Zirh, T. A., and Lesser, R. P. 1998a. Painful stimuli evoke potentials recorded from the parasylvian cortex in humans. J. Neurophysiol. 80, 2077–2088.
Lenz, F. A., Seike, M., Richardson, R. T., Lin, Y. C., Baker, F. H., Khoja, I., Jaeger, C. J., and Gracely, R. H. 1993. Thermal and pain sensations evoked by microstimulation in the area of human ventrocaudal nucleus. J. Neurophysiol. 70, 200–212.
Lenz, F. A., Rios, M., Zirh, A., Chau, D., Krauss, G., and Lesser, R. P. 1998b. Painful stimuli evoke potentials recorded over the human anterior cingulate gyrus. J. Neurophysiol. 79, 2231–2234.
Levine, J. D., Gordon, N. C., and Fields, H. L. 1978. The mechanism of placebo analgesia. Lancet 2, 654–657.
Lidstone, S. C. and Stoessl, A. J. 2007. Understanding the placebo effect: contributions from neuroimaging. Mol. Imaging Biol. 9, 176–185.
Longe, S. E., Wise, R., Bantick, S., Lloyd, D., Johansen-Berg, H., McGlone, F., and Tracey, I. 2001. Counter-stimulatory effects on pain perception and processing are significantly altered by attention: an fMRI study. Neuroreport 12, 2021–2025.
Lorenz, J., Beck, H., and Bromm, B. 1997. Cognitive performance, mood and experimental pain before and during morphine-induced analgesia in patients with chronic non-malignant pain. Pain 73, 369–375.
Lorenz, J., Minoshima, S., and Casey, K. L. 2003. Keeping pain out of mind: the role of the dorsolateral prefrontal cortex in pain modulation. Brain 126, 1079–1091.
Maarrawi, J., Peyron, R., Mertens, P., Costes, N., Magnin, M., Sindou, M., Laurent, B., and Garcia-Larrea, L. 2007. Differential brain opioid receptor availability in central and peripheral neuropathic pain. Pain 127, 183–194.
Magerl, W., Ali, Z., Ellrich, J., Meyer, R. A., and Treede, R. D. 1999. C- and Ad-fiber components of heat-evoked cerebral potentials in healthy human subjects. Pain 82, 127–137.
Maihöfner, C., Forster, C., Birklein, F., Neundörfer, B., and Handwerker, H. O. 2005. Brain processing during

mechanical hyperalgesia in complex regional pain syndrome: a functional MRI study. Pain 114, 93–103.
Marchand, S. and Arsenault, P. 2002. Odors modulate pain perception: a gender-specific effect. Physiol. Behav. 76, 251–256.
Martikainen, I. K., Hagelberg, N., Mansikka, H., Hietala, J., Nagren, K., Scheinin, H., and Pertovaara, A. 2005. Association of striatal dopamine D2/D3 receptor binding potential with pain but not tactile sensitivity or placebo analgesia. Neurosci. Lett. 376, 149–153.
Marshall, J. 1951. Sensory disturbances in cortical wounds with special reference to pain. J. Neurol. Neurosurg. Psychiatry 14, 187–204.
May, A., Ashburner, J., Büchel, C., McGonigle, D. J., Friston, K. J., Frackowiak, R. S., and Goadsby, P. J. 1999. Correlation between structural and functional changes in brain in an idiopathic headache syndrome. Nat. Med. 5, 836–838.
May, A., Bahra, A., Buchel, C., Frackowiak, R. S., and Goadsby, P. J. 2000. PET and MRA findings in cluster headache and MRA in experimental pain. Neurology 55, 1328–1335.
Melzack, R. and Casey, K. L. 1968. Sensory, Motivational, and Central Control Determinants of Pain. A New Conceptual Model. In: The Skin Senses. (*eds*. D. R Kenshalo and C. Charles), pp. 423–443. Thomas.
Mertz, H., Morgan, V., Tanner, G., Pickens, D., Price, R., Shyr, Y., and Kessler, R. 2000. Regional cerebral activation in irritable bowel syndrome and control subjects with painful and nonpainful rectal distention. Gastroenterology 118, 842–848.
Miyazaki, M., Shibasaki, H., Kanda, M., Xu, X., Shindo, K., Honda, M., Ikeda, A., Nagamine, T., Kaji, R., and Kimura, J. 1994. Generator mechanism of pain-related evoked potentials following CO2 laser stimulation of the hand: scalp topography and effect of predictive warning signal. J. Clin. Neurophysiol. 11, 242–254.
Moriguchi, Y., Decety, J., Ohnishi, T., Maeda, M., Mori, T., Nemoto, K., Matsuda, H., and Komaki, G. 2006. Empathy and judging other's pain: an fMRI study of alexithymia. Cereb. Cortex doi: 10.1093/cercor/bh1130.
Morrison, I., Lloyd, D., di Pellegrino, G., and Roberts, N. 2004. Vicarious responses to pain in anterior cingulate cortex: is empathy a multisensory issue? Cogn. Affect. Behav. Neurosci. 4, 270–278.
Nakai, A., Kumakura, Y., Boivin, M., Rosa, P., Diksic, M., D'Souza, D., and Kersey, K. 2003. Sex differences of brain serotonin synthesis in patients with irritable bowel syndrome using a [^{11}C]methyl-l-tryptophan, positron emission tomography and statistical parametric mapping. Can. J. Gastroenterol. 17, 191–196.
Özcan, M., Baumgärtner, U., Vucurevic, G., Stoeter, P., and Treede, R. D. 2005. Spatial resolution of fMRI in the human parasylvian cortex: comparison of somatosensory and auditory activation. Neuroimage 25, 877–887.
Ohara, S., Crone, N. E., Weiss, N., and Lenz, F. A. 2006. Analysis of synchrony demonstrates 'pain networks' defined by rapidly switching, task-specific, functional connectivity between pain-related cortical structures. Pain 123, 244–253.
Ohara, S., Crone, N. E., Weiss, N., Treede, R. D., and Lenz, F. A. 2004. Cutaneous painful laser stimuli evoke responses recorded directly from primary somatosensory cortex in awake humans. J. Neurophysiol. 91, 2734–2746.
Opsommer, E., Weiss, T., Plaghki, L., and Miltner, W. H. R. 2001. Dipole analysis of ultralate (C-fibres) evoked potentials after laser stimulation of tiny cutaneous surface areas in humans. Neurosci. Lett. 298, 41–44.
Ostrowsky, K., Magnin, M., Ryvlin, P., Isnard, J., Guenot, M., and Mauguière, F. 2002. Representation of pain and somatic sensation in the human insula: a study of responses to direct electrical cortical stimulation. Cereb. Cortex 12, 376–385.
Pascual-Marqui, R. D., Michel, C. M., and Lehmann, D. 1994. Low resolution electromagnetic tomography: a new method for localizing electrical activity in the brain. Int. J. Psychophysiol. 18, 49–65.
Pattany, P. M., Yezierski, R. P., Widerstrom-Noga, E. G., Bowen, B. C., Martinez-Arizala, A., Garcia, B. R., and Quencer, R. M. 2002. Proton magnetic resonance spectroscopy of the thalamus in patients with chronic neuropathic pain after spinal cord injury. AJNR Am. J. Neuroradiol. 23, 901–905.
Pauli, P., Wiedemann, G., and Nickola, M. 1999. Pain sensitivity, cerebral laterality, and negative affect. Pain 80, 359–364.
Paulson, P. E., Minoshima, S., Morrow, T. J., and Casey, K. L. 1998. Gender differences in pain perception and patterns of cerebral activation during noxious heat stimulation in humans. Pain 76, 223–229.
Pertovaara, A., Martikainen, I. K., Hagelberg, N., Mansikka, H., Nagren, K., Hietala, J., and Scheinin, H. 2004. Striatal dopamine D2/D3 receptor availability correlates with individual response characteristics to pain. Eur. J. Neurosci. 20, 1587–1592.
Petrovic, P., Dietrich, T., Fransson, P., Andersson, J., Carlsson, K., and Ingvar, M. 2005. Placebo in emotional processing-induced expectations of anxiety relief activate a generalized modulatory network. Neuron 46, 957–969.
Petrovic, P., Kalso, E., Petersson, K. M., and Ingvar, M. 2002. Placebo and opioid analgesia- imaging a shared neuronal network. Science 295, 1737–1740.
Petrovic, P., Petersson, K. M., Ghatan, P. H., Stone-Elander, S., and Ingvar, M. 2000. Pain-related cerebral activation is altered by a distracting cognitive task. Pain 85, 19–30.
Peyron, R., Laurent, B., and García-Larrea, L. 2000. Functional imaging of brain responses to pain. A review and meta-analysis 2000. Neurophysiol. Clin. 30, 263–288.
Phillips, M. L., Gregory, L. J., Cullen, S., Cohen, S., Ng, V., Andrew, C., Giampietro, V., Bullmore, E., Zelaya, F., Amaro, E., Thompson, D. G., Hobson, A. R., Williams, S. C., Brammer, M., and Aziz, Q. 2003. The effect of negative emotional context on neural and behavioural responses to oesophageal stimulation. Brain 126, 669–684.
Plaghki, L. and Mouraux, A. 2003. How do we selectively activate skin nociceptors with a high power infrared laser? Physiology and biophysics of laser stimulation. Neurophysiol. Clin. 33, 269–277.
Ploghaus, A., Tracey, I., Gati, J. S., Clare, S., Menon, R. S., Matthews, P. M., and Rawlins, J. N. 1999. Dissociating pain from its anticipation in the human brain. Science 284, 1979–1981.
Ploner, M., Schmitz, F., Freund, H. J., and Schnitzler, A. 1999. Parallel activation of primary and secondary somatosensory cortices in human pain processing. J. Neurophysiol. 81, 3100–3104.
Ploner, M., Schmitz, F., Freund, H. J., and Schnitzler, A. 2000. Differential organization of touch and pain in human primary somatosensory cortex. J. Neurophysiol. 83, 1770–1776.
Porro, C. A., Baraldi, P., Pagnoni, G., Serafini, M., Facchin, P., Maieron, M., and Nichelli, P. 2002. Does anticipation of pain affect cortical nociceptive systems? J. Neurosci. 22, 3206–3214.
Price, D. D. 2000. Psychological and neural mechanisms of the affective dimension of pain. Science 288, 1769–1772.
Raij, T. T., Numminen, J., Narvanen, S., Hiltunen, J., and Hari, R. 2005. Brain correlates of subjective reality of physically and

psychologically induced pain. Proc. Natl. Acad. Sci. U. S. A. 102, 2147–2151.
Rainville, P., Duncan, G. H., Price, D. D., Carrier, B., and Bushnell, M. C. 1997. Pain affect encoded in human anterior cingulate but not somatosensory cortex. Science 277, 968–971.
Ringel, Y. 2006. New directions in brain imaging research in functional gastrointestinal disorders. Dig. Dis. 24, 278–285.
Robinson, C. J. and Burton, H. 1980. Somatic submodality distribution within the second somatosensory (SII), 7b, retroinsular, postauditory, and granular insular cortical areas of M. fascicularis. J. Comp. Neurol. 192, 93–108.
Rolke, R., Baron, R., Maier, C., Tölle, T. R., Treede, R. D., Beyer, A., Binder, A., Birbaumer, N., Birklein, F., Botefur, I. C., Braune, S., Flor, H., Huge, V., Klug, R., Landwehrmeyer, G. B., Magerl, W., Maihofner, C., Rolko, C., Schaub, C., Scherens, A., Sprenger, T., Valet, M., and Wasserka, B. 2006. Quantitative sensory testing in the German Research Network on Neuropathic Pain (DFNS): standardized protocol and reference values. Pain 123, 231–243.
Rosen, S. D., Paulesu, E., Nihoyannopoulos, P., Tousoulis, D., Frackowiak, R. S., Frith, C. D., Jones, T., and Camici, P. G. 1996. Silent ischemia as a central problem: regional brain activation compared in silent and painful myocardial ischemia. Ann. Intern. Med. 124, 939–949.
Rosen, S. D., Paulesu, E., Wise, R. J., and Camici, P. G. 2002. Central neural contribution to the perception of chest pain in cardiac syndrome X. Heart 87, 513–519.
Sawamoto, N., Honda, M., Okada, T., Hanakawa, T., Kanda, M., Fukuyama, H., Konishi, J., and Shibasaki, H. 2000. Expectation of pain enhances responses to nonpainful somatosensory stimulation in the anterior cingulate cortex and parietal operculum/posterior insula: an event-related functional magnetic resonance imaging study. J. Neurosci. 20, 7438–7445.
Scharein, E. and Bromm, B. 1998. The intracutaneous pain model in the assessment of analgesic efficacy. Pain Rev. 5, 216–246.
Scherg, M. 1992. Functional imaging and localization of electromagnetic brain activity. Brain Topogr. 5, 103–111.
Schlaepfer, T. E., Strain, E. C., Greenberg, B. D., Preston, K. L., Lancaster, E., Bigelow, G. E., Barta, P. E., and Pearlson, G. D. 1998. Site of opioid action in the human brain: mu and kappa agonists' subjective and cerebral blood flow effects. Am. J. Psychiatry 155, 470–473.
Schlereth, T., Baumgärtner, U., Magerl, W., Stoeter, P., and Treede, R. D. 2003. Left-hemisphere dominance in early nociceptive processing in the human parasylvian cortex. Neuroimage 20, 441–454.
Schmahl, C., Bohus, M., Esposito, F., Treede, R. D., Di Salle, F., Greffrath, W., Ludaescher, P., Jochims, A., Lieb, K., Scheffler, K., Hennig, J., and Seifritz, E. 2006. Neural correlates of antinociception in borderline personality disorder. Arch. Gen. Psychiatry 63, 659–667.
Schweinhardt, P., Glynn, C., Brooks, J., McQuay, H., Jack, T., Chessell, I., Bountra, C., and Tracey, I. 2006. An fMRI study of cerebral processing of brush-evoked allodynia in neuropathic pain patients. Neuroimage 32, 256–265.
Scott, D. J., Heitzeg, M. M., Koeppe, R. A., Stohler, C. S., and Zubieta, J. K. 2006. Variations in the human pain stress experience mediated by ventral and dorsal basal ganglia dopamine activity. J. Neurosci. 26, 10789–10795.
Seitz, R. J., Roland, P. E., Bohm, C., Greitz, T., and Stone-Elander, S. 1991. Somatosensory discrimination of shape: tactile exploration and cerebral activation. Eur. J. Neurosci. 3, 481–492.
Sikes, R. W. and Vogt, B. A. 1992. Nociceptive neurons in area 24 of rabbit cingulate cortex. J. Neurophysiol. 68, 1720–1732.
Silverman, D. H., Munakata, J. A., Ennes, H., Mandelkern, M. A., Hoh, C. K., and Mayer, E. A. 1997. Regional cerebral activity in normal and pathological perception of visceral pain. Gastroenterology 112, 64–72.
Singer, T., Seymour, B., O'Doherty, J., Kaube, H., Dolan, R. J., and Frith, C. D. 2004. Empathy for pain involves the affective but not sensory components of pain. Science 303, 1157–1162.
Smith, Y. R., Stohler, C. S., Nichols, T. E., Bueller, J. A., Koeppe, R. A., and Zubieta, J. K. 2006. Pronociceptive and antinociceptive effects of estradiol through endogenous opioid neurotransmission in women. J. Neurosci. 26, 5777–5785.
Spreng, M. and Ichioka, M. 1964. Langsame Rindenpotentiale bei Schmerzreizung am Menschen. Pflügers Arch. 279, 121–132.
Stevens, R. T., London, S. M., and Apkarian, A. V. 1993. Spinothalamocortical projections to the secondary somatosensory cortex (SII) in squirrel monkey. Brain Res. 631, 241–246.
Stiasny-Kolster, K., Magerl, W., Oertel, W. H., Möller, J. C., and Treede, R. D. 2004. Static mechanical hyperalgesia without dynamic tactile allodynia in patients with restless legs syndrome. Brain 127, 773–782.
Strigo, I. A., Duncan, G. H., Boivin, M., and Bushnell, M. C. 2003. Differentiation of visceral and cutaneous pain in the human brain. J. Neurophysiol. 89, 3294–3303.
Strittmatter, M., Hamann, G. F., Grauer, M., Fischer, C., Blaes, F., Hoffmann, K. H., and Schimrigk, K. 1996. Altered activity of the sympathetic nervous system and changes in the balance of hypophyseal, pituitary and adrenal hormones in patients with cluster headache. Neuroreport 7, 1229–1234.
Talbot, J. D., Marrett, S., Evans, A. C., Meyer, E., Bushnell, M. C., and Duncan, G. H. 1991. Multiple representations of pain in human cerebral cortex. Science 251, 1355–1358.
Tarkka, I. M. and Treede, R. D. 1993. Equivalent electrical source analysis of pain-related somatosensory evoked potentials elicited by a CO_2 laser. J. Clin. Neurophysiol. 10, 513–519.
Timmermann, L., Ploner, M., Haucke, K., Schmitz, F., Baltissen, R., and Schnitzler, A. 2001. Differential coding of pain intensity in the human primary and secondary somatosensory cortex. J. Neurophysiol. 86, 1499–1503.
Tölle, T. R., Kaufmann, T., Siessmeier, T., Lautenbacher, S., Berthele, A., Munz, F., Zieglgänsberger, W., Willoch, F., Schwaiger, M., Conrad, B., and Bartenstein, P. 1999. Region-specific encoding of sensory and affective components of pain in the human brain: a positron emission tomography correlation analysis. Ann. Neurol. 45, 40–47.
Tommerdahl, M., Delemos, K. A., Vierck, C. J., Favorov, O. V., and Whitsel, B. L. 1996. Anterior parietal cortical response to tactile and skin-heating stimuli applied to the same skin site. J. Neurophysiol. 75, 2662–2670.
Tracey, I. 2001. Prospects for human pharmacological functional magnetic resonance imaging (phMRI). J. Clin. Pharmacol. Suppl. 21S–28S.
Tracey, I., Ploghaus, A., Gati, J. S., Clare, S., Smith, S., Menon, R. S., and Matthews, P. M. 2002. Imaging attentional modulation of pain in the periaqueductal gray in humans. J. Neurosci. 22, 2748–2752.
Treede, R. D. 2001. Neural Basis of Pain. In: International Encyclopedia of the Social & Behavioral Sciences (*eds*. N. J. Smelser and P. B. Baltes), pp. 11000–11005. Elsevier.

Treede, R. D., Apkarian, A. V., Bromm, B., Greenspan, J. D., and Lenz, F. A. 2000. Cortical representation of pain: functional characterization of nociceptive areas near the lateral sulcus. Pain 87, 113–119.

Treede, R. D., Baumgärtner, U., and Lenz, F. A. 2007. Nociceptive Processing in the Secondary Somatosensory Cortex. In: Encyclopedia of Pain (*eds*. R. F. Schmidt and W. D. Willis), pp. 1376–1379. Springer.

Treede, R. D., Kenshalo, D. R., Gracely, R. H., and Jones, A. K. P. 1999. The cortical representation of pain. Pain 79, 105–111.

Treede, R. D., Meyer, R. A., and Campbell, J. N. 1998. Myelinated mechanically insensitive afferents from monkey hairy skin: heat response properties. J. Neurophysiol. 80, 1082–1093.

Treede, R. D., Lorenz, J., and Baumgärtner, U. 2003. Clinical usefulness of laser-evoked potentials. Neurophysiol. Clin. 33, 303–314.

Valeriani, M., Rambaud, L., and Mauguière, F. 1996. Scalp topography and dipolar source modelling of potentials evoked by CO_2 laser stimulation of the hand. Electroenceph. Clin. Neurophysiol. 100, 343–353.

Valeriani, M., Sestito, A., Le Pera, D., De Armas, L., Infusino, F., Maiese, T., Sgueglia, G. A., Tonali, P. A., Crea, F., Restuccia, D., and Lanza, G. A. 2005. Abnormal cortical pain processing in patients with cardiac syndrome X. Eur. Heart J. 26, 975–982.

Valet, M., Sprenger, T., Boecker, H., Willoch, F., Rummeny, E., Conrad, B., Erhard, P., and Tölle, T. R. 2004. Distraction modulates connectivity of the cingulo-frontal cortex and the midbrain during pain – an fMRI analysis. Pain 109, 399–408.

Verne, G. N., Himes, N. C., Robinson, M. E., Gopinath, K. S., Briggs, R. W., Crosson, B., and Price, D. D. 2003. Central representation of visceral and cutaneous hypersensitivity in the irritable bowel syndrome. Pain 103, 99–110.

Villemure, C. and Bushnell, M. C. 2002. Cognitive modulation of pain: how do attention and emotion influence pain processing? Pain 95, 195–199.

Vogel, H., Port, J. D., Lenz, F. A., Solaiyappan, M., Krauss, G., and Treede, R. D. 2003. Dipole source analysis of laser-evoked subdural potentials recorded from parasylvian cortex in humans. J. Neurophysiol. 89, 3051–3060.

Vogt, B. A. 2005. Pain and emotion interactions in subregions of the cingulate gyrus. Nat. Rev. Neurosci. 6, 533–544.

Vogt, B. A., Nimchinsky, E. A., Vogt, L. J., and Hof, P. R. 1995. Human cingulate cortex: surface features, flat maps, and cytoarchitecture. J. Comp. Neurol. 359, 490–506.

Vogt, B. A., Rosene, D. L., and Pandya, D. N. 1979. Thalamic and cortical afferents differentiate anterior from posterior cingulate cortex in the monkey. Science 204, 205–207.

Wager, T. D., Rilling, J. K., Smith, E. E., Sokolik, A., Casey, K. L., Davidson, R. J., Kosslyn, S. M., Rose, R. M., and Cohen, J. D. 2004. Placebo-induced changes in fMRI in the anticipation and experience of pain. Science 303, 1162–1167.

Wagner, K. J., Willoch, F., Kochs, E. F., Siessmeier, T., Tölle, T. R., Schwaiger, M., and Bartenstein, P. 2001. Dose-dependent regional cerebral blood flow changes during remifentanil infusion in humans: a positron emission tomography study. Anesthesiology 94, 732–739.

Wang, S. J., Lirng, J. F., Fuh, J. L., and Chen, J. J. 2006. Reduction in hypothalamic 1H-MRS metabolite ratios in patients with cluster headache. J. Neurol. Neurosurg. Psychiatry 77, 622–625.

Wiesenfeld-Hallin, Z. 2005. Sex differences in pain perception. Gend. Med. 2, 137–145.

Willis, W. D. and Coggeshall, R. E. 2004. Sensory Mechanisms of the Spinal Cord: Primary Afferent Neurons and the Spinal Dorsal Horn, Vol. 1. Kluwer Academic/ Plenum Publishers.

Willoch, F., Schindler, F., Wester, H. E., Empl, M., Straube, A., Schwaiger, M., Conrad, B., and Tölle, T. R. 2004. Central poststroke pain and reduced opioid receptor binding within pain processing circuitries: a [C-11]diprenorphine PET study. Pain 108, 213–220.

Wilson, J. F. 2006. The pain divide between men and women. Ann. Intern. Med 144, 461–464.

Wood, P. B., Patterson, J. C., Sunderland, J. J., Tainter, K. H., Glabus, M. F., and Lilien, D. L. 2007. Reduced presynaptic dopamine activity in fibromyalgia syndrome demonstrated with positron emission tomography: a pilot study. J. Pain 8, 51–58.

Yamamura, H., Iwata, K., Tsuboi, Y., Toda, K., Kitajima, K., Shimizu, N., Nomura, H., Hibiya, J., Fujita, S., and Sumino, R. 1996. Morphological and electrophysiological properties of ACCx nociceptive neurons in rats. Brain Res. 735, 83–92.

Xu, X. P., Fukuyama, H., Yazawa, S., Mima, T., Hanakawa, T., Magata, Y., Kanda, M., Fujiwara, N., Shindo, K., Nagamine, T., and Shibasaki, H. 1997. Functional localization of pain perception in the human brain studied by PET. Neuroreport 8, 555–559.

Zelman, D. C., Howland, E. W., Nichols, S. N., and Cleeland, C. S. 1991. The effects of induced mood on laboratory pain. Pain 46, 105–111.

Zubieta, J. K., Smith, Y. R., Bueller, J. A., Xu, Y., Kilbourn, M. R., Jewett, D. M., Meyer, C. R., Koeppe, R. A., and Stohler, C. S. 2001. Regional mu opioid receptor regulation of sensory and affective dimensions of pain. Science 293, 311–315.

Zubieta, J. K., Bueller, J. A., Jackson, L. R., Scott, D. J., Xu, Y., Koeppe, R. A., Nichols, T. E., and Stohler, C. S. 2005. Placebo effects mediated by endogenous opioid activity on μ-opioid receptors. J. Neurosci. 25, 7754–7762.

Zubieta, J. K., Smith, Y. R., Bueller, J. A., Xu, Y., Kilbourn, M. R., Jewett, D. M., Meyer, C. R., Koeppe, R. A., and Stohler, C. S. 2002. μ-Opioid receptor-mediated antinociceptive responses differ in men and women. J. Neurosci. 22, 5100–5107.

5.46 Phantom Limb Pain

H Flor, Central Institute of Mental Health, Mannheim, Germany

© 2008 Elsevier Inc. All rights reserved.

5.46.1	Definition	699
5.46.2	Peripheral Mechanisms of Phantom Limb Pain	700
5.46.3	Central Factors	701
5.46.3.1	The Spinal Cord	701
5.46.3.2	Supraspinal Changes	702
5.46.4	Implications for the Treatment and Prevention of Phantom Limb Pain	703
5.46.5	Future Developments	704
References		704

Glossary

cortical reorganization Changes in the maps of the primary sensory or motor areas of the cortex related to injury or stimulation. Cortical representations can increase or decrease in size or they can shift to other locations on the sensory or motor map.

central sensitization Short- or long-term changes in the excitability of central neurons and their synaptic strength that lead to an enhanced or altered processing of peripheral sensory input resulting in hypersensibility.

neuroma When a limb is severed, a terminal swelling or endbulb is formed with axonal sprouting occurring. In the case of an amputation this sprouting and endbulb formation lead to neuroma, a tangled mass that is formed when the axons cannot reconnect or can only partially reconnect as is the case in partial lesions. These neuroma generate abnormal activity that is called ectopic because it does not originate from the nerve endings.

nonpainful phantom limbs and nonpainful phantom sensations These phenomena refer to the continued presence of the limb (corporeal awareness of the limb) and nonpainful sensations such as tingling or pressure sensations.

nonpainful residual limb sensations The residual limb can also have nonpainful sensations such as tingling or cramping sensations that can be distinguished from phantom sensation as well as from painful sensation.

phantom limb pain or phantom pain Pain in a body part that is no longer present. It may be related to a certain position or movement of the phantom and may be elicited or exacerbated by a range of physical (e.g., changes in weather or pressure on the residual limb) and psychological factors (e.g., emotional stress). It seems to be more intense in the distal portions of the phantom and may have a number of different qualities such as stabbing, throbbing, burning, or cramping. Phantom limb pain is often confused with pain in the area adjacent to the amputated body part.

postamputation pain Pain at the site of the wound that must be distinguished from pain in the residual limb and phantom limb pain that may all co-occur in the early phase after amputation.

preamputation pain Pain that occurred in the amputated body part before the amputation. It may be related to the incidence, type, and severity of phantom limb pain in the phase following the amputation.

residual limb pain or stump pain Pain in the body part adjacent to the amputation. It is usually positively correlated with phantom limb pain.

5.46.1 Definition

The amputation of a body part is often followed by the sensation that the deafferented body part is still present. These sensations may include not only the feeling of the continued presence of the limb but also nonpainful and painful phantom sensations such as the feeling of a specific position, shape, or movement of the missing limb, feelings of warmth or cold, itching, tingling or electric sensations, and other paresthesias.

Phantom limb pain (or phantom pain) is pain in the body part that is no longer present. This occurs to some degree in 50–80% of all amputees (Nikolajsen, L. and Jensen, T. S., 2006). Phantom limb pain may be related to a certain position or movement of the phantom and may be elicited or exacerbated by a range of physical (e.g., changes in weather or pressure on the residual limb) and psychological factors (e.g., emotional stress). It seems to be more intense in the distal portions of the phantom and may have a number of different qualities such as stabbing, throbbing, burning, or cramping (Hill, A., 1999). Phantom limb pain belongs to the neuropathic pain syndromes and is assumed to be related to damage to the axons of peripheral neurons with secondary changes induced in central neurons. Phantom body pain may also occur following spinal cord injury. Phantom limb pain is infrequent if the amputation occurred at a very young age. However, older children exhibit as high an incidence of phantom limb pain as adults. Although phantom sensations seem to occur occasionally in congenital amputees (i.e., those born without a limb), phantom limb pain seems to be very rare under these circumstances (Flor, H., 2002). The long-term course of phantom limb pain is unclear. While some authors report a slight decline in pain prevalence over the course of several years, others have described high prevalence rates also in long-term amputees. Both peripheral and central factors have been discussed as determinants of phantom limb pain. Psychological factors do not seem to be a primary cause, but they may well affect the course and the severity of the pain (Sherman, R. A., 1997). The general view today is that multiple changes along the neuraxis contribute to the experience of phantom limb pain.

5.46.2 Peripheral Mechanisms of Phantom Limb Pain

Peripheral changes that give rise to nociceptive input from the residual limb have been viewed as an important determinant of phantom limb pain. This is supported by the moderately high correlation between pain in the residual limb (stump) and phantom limb pain. Ectopic discharge from stump neuromas has been postulated as a potential source of such nociceptive input (Devor, M., 2006). When peripheral nerves are cut or injured, terminal swelling and regenerative sprouting of the injured axon end occur. In this process, neuromas form in the residual limb. The disorganized endings of C fibers and demyelinated A fibers in neuromas have increased excitability and often show spontaneous impulse activity (ectopic discharge). Mechanical, chemical, and thermal stimulation may further exacerbate this ectopic discharge. The increased excitability of injured nerves that results in ectopic discharge seems to result from upregulation or novel expression, and altered trafficking, of molecules that are responsible for neuronal excitability, such as voltage-sensitive sodium channels (Devor, M., 2006). In addition, abnormal connections between injured axons, such as ephapses, may contribute to the spontaneous ectopic activity. Phantom limb pain is often present very soon after amputation before a palpable, swollen neuroma could have formed. However, ectopic discharge also appears rapidly, apparently originating at first in swollen endbulbs at the cut axon end rather than in outgrowing sprouts.

Local anesthesia of the stump does not eliminate phantom limb pain in all amputees (Birbaumer, N. *et al.*, 1997). This fact motivated a search for other potential sources of ectopic input from the periphery. An additional site of ectopic discharge is the dorsal root ganglion (DRG). Ectopia originating in the DRG can summate with ectopia originating from neuromas in the stump. Indeed, processes such as cross-excitation can lead to the depolarization and activation of neighboring neurons, significantly amplifying the overall ectopic barrage (Devor, M., 2006). In experimental preparations and in humans it was found that anesthetic block of neuromas eliminates spontaneous and stimulation-induced nerve activity related to the stump, but not ectopic activity potentially originating in the DRG (Nystrom, B. and Hagbarth, K. E., 1981). Interestingly, there is evidence for genetic factors in the predisposition to develop ectopic neuroma, DRG discharge, and neuropathic pain. For example, Devor M. *et al.* (2005) presented evidence for the presence of several genes that predisposes to the pain behavior that follows peripheral neurectomy in rodents. This neuroma model of neuropathic pain has been considered to be a valid animal surrogate of phantom limb pain in humans.

Elevated sympathetic discharge, as well as increased levels of circulating epinephrine, can trigger and exacerbate ectopic neuronal activity from neuromas (Devor, M., 2006). In addition to such sympathetic–sensory coupling at the level of the neuroma, sympathetic–sensory coupling also occurs at the level of the DRG. This may account for the frequent exacerbation of phantom pain at times of emotional distress. Additional factors such as temperature, oxygenation level, and local inflammation

in neuromas and associated DRGs may also play a role. The sympathetic maintenance of phantom limb pain in some patients is supported by evidence that systemic adrenergic blocking agents, and targeted chemical or surgical blockade of sympathetic nerves and ganglia, sometimes reduce phantom limb pain. Likewise, injections of epinephrine into stump neuromas have been shown to increase phantom limb pain and paresthesias in some amputees. Although sympathetically maintained pain does not necessarily covary with regional sympathetic abnormalities, in some patients, sympathetic dysregulation in the residual limb is apparent. Reduced near-surface blood flow to a limb has been implicated as a predictive physiological correlate of burning phantom limb pain. Correspondingly, onset and intensity of cramping and squeezing descriptions of phantom pain have been related to muscle tension in the residual limb. This relationship seems not to hold for any other descriptors of phantom pain. In addition, lower skin temperature in the residual limb in amputees with phantom limb pain and phantom sensation and a close relationship between phantom limb sensation and skin conductance responses in the residual limb can be viewed as evidence of a sympathetic-efferent somatic-afferent mechanism (for review see Sherman, R. A., 1997).

5.46.3 Central Factors

5.46.3.1 The Spinal Cord

Anecdotal evidence in human amputees first suggested that spinal mechanisms may play a role in phantom limb pain. For example, during spinal anesthesia, phantom pains have been reported to reoccur in patients who were pain-free at the time of the procedure. Experimental data in human amputees are lacking, but increasing amounts of evidence based on animal models of nerve injury are becoming available.

Increased activity in peripheral nociceptors leads to an enduring change in the synaptic responsiveness of neurons in the dorsal horn of the spinal cord, a process called central sensitization (Woolf, C. J. and Salter, M., 2006). Central sensitization is also triggered by nerve injury such as occurs during amputation. For example, spinal changes associated with nerve injury include increased firing of the dorsal horn neurons, structural changes at the central endings of the primary sensory neurons, and reduced inhibitory processes. Inhibitory GABAergic and glycinergic interneurons in the spinal cord may actually be destroyed by rapid ectopic discharge or other effects of axotomy, contributing to a hyperexcitable spinal cord (Scholz, J. and Woolf, C., 2006). Changes have also been noted in ascending projection neurons. The cascade of biological events that take place in the spinal cord after peripheral nerve damage may trigger abnormal firing of spinal origin. Part of this sensitization is due to facilitation of the response of *N*-methyl-D-aspartic acid (NMDA) receptors to the primary afferent neurotransmitter glutamate (Sandkühler, J., 2000). A remarkable effect of the spinal changes evoked by nerve injury is that low-threshold afferents may become functionally connected to ascending spinal projection neurons that carry nociceptive information. When this happens, normally innocuous A-fiber input from the periphery, ectopic input as well as input from residual intact low-threshold afferents, may contribute to phantom pain sensation.

A number of additional central nervous system (CNS) processes are thought to contribute to the hyperexcitability of spinal cord circuitry following major nerve damage. For example, there may be downregulation of opioid receptors, both on primary afferent endings and on intrinsic spinal neurons. This is expected to add to disinhibition due to the reduction of GABA and glycine activity. In addition, cholycystokinin, an endogenous inhibitor of the opiate receptor, is upregulated in injured tissue (for review see Woolf, C. J. and Salter, M., 2006). Another interesting example of changed gene expression after axotomy is the appearance of the neuropeptide substance P in low-threshold Aβ neurons. Substance P is normally expressed only by Aδ and C afferents, most of which are nociceptors. The injury-triggered expression of substance P by Aβ fibers may render them more like nociceptors. For example, it may permit ectopic or normal activity in Aβ fibers to trigger and maintain central sensitization. Changes such as these in gene expression in injured afferents (and in some postsynaptic spinal neurons), which result in a change in their functioning (i.e., their phenotype), are referred to as phenotypic switch. Recent work based on gene chip technology indicates that hundreds of genes are up- or downregulated in DRG and spinal neurons following peripheral nerve injury.

Following peripheral nerve injury, degeneration of central projection axon occurs. Massive deafferentation is observed when dorsal roots are injured, or avulsed from the spinal cord. Deafferentation may act

hand-in-hand with the central effects of peripheral denervation to bring about the changes that contribute to spinal hyperexcitability. A mechanism that may be of special relevance to phantom phenomena is the invasion of regions of the spinal cord functionally vacated from injured afferents. For example, in the neuroma model in rats and cats, there is an expansion of receptive fields on skin adjacent to the denervated part of the limb, and a shift of activity from these adjacent areas into regions of the spinal cord that previously served the part of the limb that was functionally deafferented by the nerve lesion (Devor, M. and Wall, P. D., 1978). Such reorganization of the spinal map of the limb, which is probably due to unmasking of previously silent connections, is reflected in brainstem and cortical remapping also.

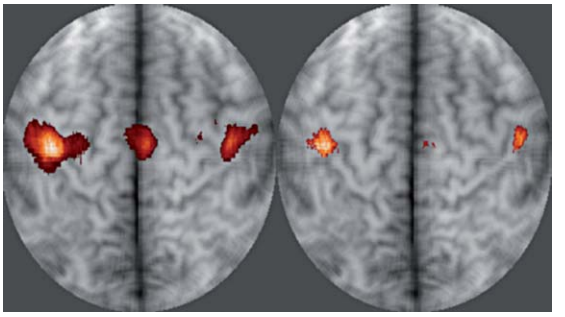

Figure 1 The representation of lip movements in amputees with phantom limb pain (left) and without phantom limb pain (right) in primary somatosensory cortex based on functional magnetic resonance imaging. Note that the amputees with phantom limb pain activate both the cortical hand and the mouth representation whereas the amputees without phantom limb pain activate only the cortical mouth representation.

5.46.3.2 Supraspinal Changes

Supraspinal changes related to phantom limb pain involve the brain stem, the thalamus, and the cerebral cortex (for review see Flor, H. *et al.*, 2006). New insights into phantom limb pain have come from studies demonstrating changes in the functional and structural architecture of primary somatosensory cortex subsequent to amputation and deafferentation in adult monkeys. In these studies, the amputation of digits in an adult owl monkey led to an invasion of adjacent areas into the representation zone of the deafferented fingers. Several imaging studies (for review see Flor, H., 2002) have reported that upper extremity amputees actually show a shift of the mouth into the hand representation in primary somatosensory and motor cortex (Figure 1). Flor H. *et al.* (1995) provided evidence that these cortical changes are less related to referred sensations but rather have a close association with phantom limb pain. The larger the shift of the mouth representation into the zone that formerly represented the amputated hand and arm the larger the phantom limb pain. These cortical changes could be reversed by the elimination of peripheral input from the amputation stump using brachial plexus anesthesia. Peripheral anesthesia completely eliminated cortical reorganization and phantom limb pain in half of the amputees that were studied. In the remaining half, both cortical reorganization and phantom limb pain remained unchanged (Birbaumer, N. *et al.*, 1997). This result suggests that in some amputees, cortical reorganization and phantom limb pain may be maintained by peripheral input whereas in others central, potentially intracortical changes might be more important.

It is so far not known to what extent spinal changes contribute to these supraspinal alterations. It was shown that axonal sprouting in the cortex underlies the reorganizational changes observed in amputated monkeys (Florence, S. L. *et al.*, 1998). Thalamic stimulation and recordings in human amputees have revealed that reorganizational changes may also occur at the thalamic level and are closely related to the perception of phantom limbs and phantom limb pain (Davis, K. D. *et al.*, 1998). Studies in animals have shown that these changes may be relayed from the spinal and brain stem level; however, changes on the subcortical levels may also originate in the cortex, which has strong efferent connections to the thalamus and lower structures.

Sometimes pain in the phantom is similar to the pain that existed in the limb prior to amputation. The likelihood of this ranges from 10% to 79% in different reports and depends on the type and time of assessment (see Katz, J. and Melzack, R., 1990). The type and time of assessment and potential errors in retrospective reports are important determinants of the incidence of these pain memories. It has been proposed that pain memories established prior to the amputation are powerful elicitors of phantom limb pain (Katz, J. and Melzack, R., 1990; Flor, H., 2002). Pain memories may be implicit and not readily accessible to conscious recollection. The term implicit pain memory refers to central changes related to nociceptive input that lead to subsequent altered processing of the somatosensory system and do not require changes

in conscious processing of the pain experience (Flor, H., 2002). In patients with chronic back pain it was shown that increasing chronicity is correlated with an increase in the representation zone of the back in primary somatosensory cortex, and it was also reported that the experience of acute pain alters the map in primary somatosensory cortex. These data suggest that long-lasting noxious input may lead to long-term changes at the central and especially at the cortical level. It has long been known that the primary somatosensory cortex is involved in the processing of pain and that it may be important for the sensory-discriminative aspects of the pain experience. There have also been reports that phantom limb pain was abolished after the surgical removal of portions of the primary somatosensory cortex and that stimulation of somatosensory cortex evoked phantom limb pain. If a somatosensory pain memory has been established with an important neural correlate in spinal and supraspinal structures, such as in primary somatosensory cortex, subsequent deafferentation and an invasion of the amputation zone by neighboring input may preferentially activate cortical neurons coding for pain. Since the cortical area coding input from the periphery seems to stay assigned to the original zone of input, the activation in the cortical zone representing the amputated limb is referred to this limb and the activation is interpreted as phantom sensation and phantom limb pain. It is likely that not only the areas involved in sensory-discriminative aspects of pain reorganize but also that those areas that mediate affective–motivational aspects of pain such as the insula and the anterior cingulate cortex undergo plastic changes that contribute to the experience of phantom pain. A prospective study (Larbig *et al.,* unpublished data) showed that the best predictor of phantom limb pain 12 months after an amputation is chronic pain before the amputation thus supporting the pain memory hypothesis. However, these authors tested a sample that did not include traumatic amputees but mainly amputees with long-standing prior pain problems. Further research is needed to better clarify these relationships.

5.46.4 Implications for the Treatment and Prevention of Phantom Limb Pain

Several studies, including large surveys of amputees, have shown that most treatments for phantom limb pain are ineffective and fail to consider the mechanisms underlying the production of the pain (Sindrup, S. H. and Jensen, T. S., 1999). Most studies are uncontrolled short-term assessments of small samples of phantom limb pain patients. The maximum benefit reported from a host of treatments such as local anesthesia, sympathectomy, dorsal root entry zone lesions, cordotomy and rhizotomy, neurostimulation methods, or pharmacological interventions such as anticonvulsants, barbiturates, antidepressants, neuroleptics, and muscle relaxants seems to be around 30%. This does not exceed the placebo effect reported in other studies. Controlled studies have been performed for opioids, calcitonin, ketamine, dextromethorphan, and gabapentin (see Nikolajsen, L. and Jensen, T. S., 2006), all of which were found to effectively reduce phantom limb pain. Mechanism-based treatments are rare but have been shown to be effective in a few small but mostly uncontrolled studies. Lidocaine was found to reduce phantom limb pain of patients with neuromas in two small-sample controlled studies. Biofeedback treatments resulting in vasodilatation of the residual limb or decreased muscle tension in the residual limb help to reduce phantom limb pain and seem promising in patients where peripheral factors contribute to the pain (Flor, H., 2002).

Based on the findings from neuroelectric and neuromagnetic source imaging, changes in cortical reorganization might influence phantom limb pain. Animal work on stimulation-induced plasticity would suggest that extensive behaviorally relevant stimulation of a body part leads to the expansion of its representation zone. It was shown that intensive use of a myoelectric prosthesis was positively correlated with both reduced phantom limb pain and reduced cortical reorganization. When cortical reorganization was partialled out, the relationship between prosthesis use and reduced phantom limb pain was no longer significant suggesting that cortical reorganization mediates this relationship. An alternative approach in patients where prosthesis use is not viable is the application of behaviorally relevant stimulation. A 2-week training that consisted of a discrimination training of electric stimuli to the stump for 2 h per day led to significant improvements in phantom limb pain and a significant reversal of cortical reorganization (Flor, H. *et al.*, 2001). A control group of patients who received standard medical treatment and general psychological counseling in this time period did not show similar changes in cortical reorganization and phantom limb pain. The basic idea of the

treatment was to provide input into the amputation zone and thus undo the reorganizational changes that occurred subsequent to the amputation. Mirror treatment (where a mirror is used to trick the brain into perceiving movement of the phantom when the intact limb is moved) might be effective but has so far only been tested in an anecdotal manner.

Preemptive analgesia refers to the attempt to prevent chronic pain by early intervention before acute pain occurs, for example, before and during surgery. Based on the data on sensitization of spinal neurons by afferent barrage it has been suggested that general anesthesia should be complemented by peripheral anesthesia thus preventing peripheral nociceptive input from reaching the spinal cord and higher centers. However, preemptive analgesia that included both general and spinal anesthesia has not consistently been efficacious in preventing the onset of phantom limb pain (for review see Nikolajsen, L. and Jensen, T. S., 2006). A preexisting pain memory that has already led to central and especially cortical changes would not necessarily be affected by a short-term elimination of afferent barrage. Thus, it is possible that peripheral analgesia would eliminate new but not preexisting central changes in the perioperative phase. In addition, a short-term blockade is not sufficient to prevent discharges from severed peripheral nerves to reach the CNS. The perioperative use of NMDA receptor antagonists or GABA agonists might therefore be useful.

5.46.5 Future Developments

Both peripheral and central factors and their interaction need to be examined more closely in animal models of amputation-related pain and in human amputees. The role of spinal mechanisms has so far not been sufficiently elucidated. The detection of genes relevant for the development of phantom pain-like behaviors in animal is an important step and may aid in the identification of predisposing factors for phantom limb pain as well as in the development of new interventions. The development of more powerful treatments for phantom limb pain needs controlled treatment outcome, prospective and double-blind placebo-controlled outcome research. Only then effective evidence-based interventions will be available.

Acknowledgment

The preparation of this article was supported by a grant from the Deutsche Forschungsgemeinschaft (FL 156/29).

References

Birbaumer, N., Lutzenberger, W., Montoya, P., Larbig, W., Unertl, K., Töpfner, S., and Flor, H. 1997. Effects of regional anesthesia on phantom limb pain are mirrored in changes in cortical reorganization. J. Neurosci. 17, 5503–5508.

Davis, K. D., Kiss, Z. H. T., Luo, L., Tasker, R. R., Lozano, A. M., and Dostrovsky, J. O. 1998. Phantom sensations generated by thalamic microstimulation. Nature 391, 385–387.

Devor, M. 2006. Response of Nerves to Injury in Relation to Neuropathic Pain. In: Melzack and Wall's Textbook of Pain, 5th edn. (*eds*. S. McMahon and M. Koltzenburg), pp. 905–927. Churchill-Livingstone.

Devor, M. and Wall, P. D. 1978. Reorganization of the spinal cord sensory map after peripheral nerve injury. Nature 276, 76.

Devor, M., del Canho, S., and Raber, P. 2005. Heritability of symptoms in the neuroma model of neuropathic pain: replication and complementation analysis. Pain 116, 294–301.

Flor, H. 2002. Phantom limb pain: characteristics, aetiology and treatment. Lancet Neurology 3, 182–189.

Flor, H., Denke, C., Schaefer, M., and Grüsser, S. 2001. Sensory discrimination training alters both cortical reorganization and phantom limb pain. Lancet 357, 1763–1764.

Flor, H., Elbert, T., Knecht, S., Wienbruch, C., Pantev, C., Birbaumer, N., and Taub, E. 1995. Phantom limb pain as a perceptual correlate of cortical reorganization following arm amputation. Nature 357, 482–484.

Flor, H, Nikolajsen, L, and Jensen, T. 2006. Neuroplastic changes in phantom limbs and phantom limb pain. Nat. Neurosci. Rev. 1, 813–881.

Florence, S. L., Taub, H. B., and Kaas, J. H. 1998. Large-scale sprouting of cortical connections after peripheral injury in adult macaque monkeys. Science 282, 1117–1120.

Hill, A. 1999. Phantom limb pain: a review of the literature on attributes and potential mechanisms. J. Pain Sympt. Manage 17, 125–142.

Jensen, T. S. and Nikolajsen, L. 2000. Pre-emptive analgesia in postamputation pain: an update. Prog. Brain Res. 129, 493–503.

Katz, J. and Melzack, R. 1990. Pain 'memories' in phantom limbs: review and clinical observations. Pain 43, 319–336.

Nikolajsen, L. and Jensen, T. S. 2006. Phantom Limb and Other Postamputation Phenomena. In: Wall and Melzacks Textbook of Pain, 5th edn. (*eds*. M. Koltzenburg and S. McMahon), pp. 961–971. Churchill-Livingstone.

Nystrom, B. and Hagbarth, K. E. 1981. Microelectrode recordings from transsected nerves in amputees with phantom limb pain. Neurosci. Lett. 27, 211–216.

Sandkühler, J. 2000. Learning and memory in pain pathways. Pain 88, 113–118.

Sherman R. A. (*ed*.) 1997. Phantom Limb Pain. Plenum.

Sindrup, S. H. and Jensen, T. S. 1999. Efficacy of pharmacological treatments of neuropathic pain: an update and effect related to mechanism of drug action. Pain 83, 389–400.

Scholz, J. and Woolf, C. 2006. Neuropathic Pain: A Neurodegenerative Disease. In: Proceedings of the 11th

World Congress on Pain (*eds*. H. Flor, E. Kalso. and J. Dostrovsky), pp. 373–384. IASP Press.
Woolf, C. J. and Salter, M. 2006. Plasticity and Pain: Role of the Dorsal Horn. In: Melzack and Wall's Textbook of Pain, 5th edn. (*eds*. S. McMahon and M. Koltzenburg), pp. 91–105. Churchill-Livingstone.

Further Reading

Abraham, R. B., Marouani, N., and Weinbroum, A. A. 2003. Dextromethorphan mitigates phantom pain in cancer amputees. Ann. Surg. Oncol. 10, 268–274.
Appenzeller, O. and Bicknell, J. M. 1969. Effects of nervous system lesion on phantom experience in amputees. Neurology 19, 141–146.
Bone, M., Critchley, P., and Buggy, D. J. 2002. Gabapentin in postamputation phantom limb pain: a randomized, double-blind, placebo-controlled, cross-over study. Reg. Anesth. Pain Med. 27, 481–486.
Chabal, C., Jacobson, L., Russell, L. C., and Burchiel, K. J. 1989. Pain responses to perineuromal injection of normal saline, gallamine, and lidocaine in humans. Pain 36, 321–325.
Chabal, C., Jacobson, L., Russell, L. C., and Burchiel, K. J. 1992. Pain response to perineuromal injection of normal saline, epinephrine, and lidocaine in humans. Pain 49, 9–12.
Cronholm, B. 1951. Phantom limbs in amputees. A study of changes in the integration of centripetal impulses with special reference to referred sensations. Acta. Psychiatr. Neurol. Scand. Suppl. 72, 1–310.
Devor, M. and Govrin-Lippman, R. 1993. Angelides K. Na+ channels immunolocalization in peripheral mammalian axons and changes following nerve injury and neuroma formation. J. Neurosci. 13, 1976–1992.
Devor, M. and Raber, P. 1990. Heritability of symptoms in an experimental model of neuropathic pain. Pain 42, 51–67.
Devor, M., Jänig, W., and Michaelis, M. 1994. Modulation of activity in dorsal root ganglion neurones by sympathetic activation in nerve-injured rats. J. Neurophysiol. 71, 38–47.
Ehde, D. M., Czerniecki, J. M., Smith, D. G., Campbell, K. M., Edwards, W. T., *et al.* 2000. Chronic phantom sensations, phantom pain, residual limb pain, and other regional pain after lower limb amputation. Arch. Phys. Med. Rehab. 8, 1039–1044.
Ephraim, P. L., Wegener, S. T., Mackenzie, E. J., Dillingham, T. R., and Pezzin, L. E. 2005. Phantom pain, residual limb pain, and back pain in amputees: results of a national survey. Arch. Phys. Med. Rehabil. 86, 1910–1919.
Ergenzinger, E. R., Glasier, M. M., Hahm, J. O., and Pons, T. P. 1998. Cortically induced thalamic plasticity in the primate somatosensory system. Nat. Neurosci. 1, 226–229.
Flor, H., Braun, C., Elbert, T., and Birbaumer, N. 1997. Extensive reorganization of primary somatosensory cortex in chronic back pain patients. Neurosci. Lett. 224, 5–8.
Flor, H., Elbert, T., Mühlnickel, W., Pantev, C., Wienbruch, C., and Taub, E. 1998. Cortical reorganization and phantom phenomena in congenital and traumatic upper-extremity amputees. Exp. Brain Res. 119, 205–212.
Florence, S. L. and Kaas, J. H. 1995. Large-scale reorganization at multiple levels of the somatosensory pathway following therapeutic amputation of the hand in monkey. J. Neurosci. 15, 8083–8095.
Grüsser, S., Winter, C., Mühlnickel, W., Denke, C., Karl, A., Villringer, K., and Flor, H. 2001. The relationship of perceptual phenomena and cortical reorganization in upper extremity amputees. Neuroscience 102, 263–272.
Huse, E., Larbig, W., Flor, H., and Birbaumer, N. 2001. The effect of opioids on phantom limb pain and cortical reorganization. Pain 90, 47–55.
Jaeger, H. and Maier, C. 1992. Calcitonin in phantom limb pain: a double-blind study. Pain 48, 21–27.
Jensen, T. S., Krebs, B., Nielsen, J., and Rasmussen, P. 1985. Immediate and long-term phantom limb pain in amputees: incidence, clinical characteristics and relationship to preamputation pain. Pain 21, 267–278.
Jensen, T. S., Krebs, B., Nielsen, J., and Rasmussen, P. 2000. Immediate and long-term phantom limb pain in amputees: Incidence, clinical characteristics and relationship to pre-amputation of somatosensory and motor cortex after peripheral nerve or spinal cord injury in primates. Prog. Brain Res. 128, 173–179.
Katz, J. 1992. Pychophysical correlates of phantom limb experience. J. Neurol. Neurosurg. Psychiatry 55, 811–821.
Katz, J. and Melzack, R. A. 1991. Auricular transcutaneous electrical nerve stimulation (TENS) reduces phantom limb pain. J. Pain Sympt. Manage 6, 77–83.
Karl, A., Birbaumer, N., Lutzenberger, W., Cohen, L. G., and Flor, H. 2001. Reorganization of motor and somatosensory cortex in upper extremity amputees with phantom limb pain. J. Neurosci. 21, 3609–3618.
Kooijman, C. M., Dijkstra, P. U., Geertzen, J. H. B., Elzinga, A., and van der Schans, C. P. 2000. Phantom pain and phantom sensations in upper limb amputees: an epidemiological study. Pain 87, 33–41.
Krane, E. J. and Heller, L. B. 1995. The prevalence of phantom sensation and pain in pediatric amputees. J. Pain Sympt. Manage 10, 21–29.
Lotze, M., Grodd, W., Birbaumer, N., Erb, M., Huse, E., Larbig, W., and Flor, H. 1999. Does use of a myoelectric prosthesis prevent cortical reorganization and phantom limb pain? Nat. Neurosci. 2, 501–502.
Mackenzie, N. 1983. Phantom limb pain during spinal anaesthesia. Recurrence in amputees. Anaesthesia 38, 886–887.
MacLachlan, M., McDonald, D., and Waloch, J. 2004. Mirror treatment of lower limb phantom pain: a case study. Disabil. Rehabil. 26, 901–904.
Nathan, P. W. 1983. Pain and the sympathetic system. J. Auton. Nerv. Syst. 7, 363–370.
Nikolajsen, L. and Jensen, T. S. 2001. Phantom limb pain. Br. J. Anaesth. 87, 107–116.
Nikolajsen, L., Gottrup, H., Kristensen, A. G., and Jensen, T. S. 2000. Memantine (a *N*-methyl-D-aspartate receptor antagonist) in the treatment of neuropathic pain after amputation or surgery: a randomized, double-blinded, cross-over study. Anesth. Analg. 91, 960–966.
Nikolajsen, L., Hansen, C. L., Nielsen, J., Keller, J., Arendt-Nielsen, L., *et al.*, 1996. The effect of ketamine on phantom limb pain: a central neuropathic disorder maintained by peripheral input. Pain 67, 69–77.
Nikolajsen, L., Ilkjaer, S., Christensen, J. H., Kroner, K., and Jensen, T. S. 1997a. Randomised trials of epidural bupivacaine and morphine in prevention of stump and phantom pain in lower-limb amputation. Lancet 350, 1353–1357.
Nikolajsen, L., Ilkjaer, S., and Jensen, T. S. 2000. Relationship between mechanical sensitivity and post-amputation pain: a perspective study. Eur. J. Pain 4, 327–334.
Nikolajsen, L., Ilkjaer, S., Kroner, K., Christensen, J. H., and Jensen, T. S. 1997b. The influence of preamputation pain on postamputation stump and phantom pain. Pain 72, 393–405.
Ramachandran, V. S., Rogers-Ramachandran, D. C., and Stewart, M. 1992. Perceptual correlates of massive cortical reorganization. Science 258, 1159–1160.

Sherman, R. A. 1989. Stump and phantom limb pain. Neurol. Clin. 7, 249–264.
Sherman, R. A. and Sherman, C. J. 1983. Prevalence and characteristics of chronic phantom limb pain. Results of a trial survey. Am. J. Phys. Med. 62, 227–238.
Soros, P., Knecht, S., Bantel, C., Imai, T., Wusten, R., *et al.* 2000. Functional reorganization of the human primary somatosensory cortex after acute pain demonstrated by magnetoencephalography. Neurosci. Lett. 298, 195–198.
Wei, F. and Zhuo, M. 2001. Potentiation of sensory responses in the anterior cingulate cortex following digit amputation in the anaesthetised rat. J. Physiol. 532, 823–833.
Wiech, K., Preissl, H., Kiefer, T., Töpfner, S., Pauli, P., *et al.* 2001. Prevention of phantom limb pain and cortical reorganization in the early phase after amputation in humans. Soc. Neurosci. Abstr. 28, 163.
Wilkins, K. L., McGrath, P. J., Finley, G. A., and Katz, J. 1998. Phantom limb sensations and phantom limb pain in child and adolescent amputees. Pain 78, 7–12.

5.47 Human Insular Recording and Stimulation

F Mauguière, Lyon I University and INSERM U879, Bron, France

M Frot, INSERM U879, Bron France

J Isnard, Lyon I University and INSERM U879, Bron, France

© 2008 Elsevier Inc. All rights reserved.

5.47.1	**Anatomy, Connections, and Physiology of the Insula in Primates**	708
5.47.1.1	The Insula as the Fifth Lobe of the Brain	708
5.47.1.2	The Insula as a Node in a Distributed Cortical Network	709
5.47.1.3	The Insula as a Polymodal Area	710
5.47.1.4	The Insula as Part of the Mirror-Neuron System	710
5.47.2	**Rational, Ethical Limitations and Procedure of Insular Recording and Stimulations in Humans**	710
5.47.2.1	Recording and Stimulation of the Human Insula Are Justified only in the Context of Presurgical Evaluation of Epilepsy	710
5.47.2.2	Depth Intracortical Electrodes Are Needed to Explore the Insula	711
5.47.2.3	The Number of Electrodes Is Limited by Ethical Issues	711
5.47.2.4	The Site of Electrode Implantation Is Guided by Diagnostic Purposes	711
5.47.2.5	Only Data Recorded in Nonepileptogenic Cortex are Physiologically Relevant	711
5.47.3	**Insular Recordings of Pain Evoked Responses in Humans**	711
5.47.3.1	The Laser Stimulus	711
5.47.3.2	Cortical Surface Recordings (Electrocorticography)	712
5.47.3.3	Intracortical S2 Recordings	712
5.47.3.4	Intracortical Insular Recordings	712
5.47.3.5	Topographic Specificity of Insular Laser-Evoked Potentials	714
5.47.3.6	Interhemispheric Transmission of S2 and Insular Laser-Evoked Potentials	714
5.47.4	**Insular Stimulation**	714
5.47.4.1	The Challenge of Insular Stimulation	714
5.47.4.2	Pain Evoked by Insular Stimulation	715
5.47.4.3	Anatomical Location of the Insular Pain Area	715
References		715

Glossary

cytoarchitectony (cytoarchitectonic) Anatomical method based on microscopic observation of brain slices used to delineate cortical areas according to the organization of the different types of gray matter cells (neurons). This technique permits the drawing of cytoarchitectonic maps of the cortex, of which the most widely used is that of Korbinian Brodmann, first described in 1909, which counts 52 distinct areas in the human brain. The thickness of two different types of cortical cells layers (granule and pyramidal cells) and the number of layers are the two main parameters used for cytoarchitectonic mapping. Granule cells are over-represented in primary sensory (visual, auditory, and somatosensory) cortical areas (granular cortex), while large pyramidal cells are characteristic of the primary motor cortex (agranular cortex).

deep-brain stimulation Technique involving stimulating the brain with electric current pulses of low intensity using depth electrodes implanted through the skull. In humans, this technique can be used for therapeutic or diagnostic purposes. High-frequency continuous (or chronic) deep-brain stimulation is used as a treatment in various neurological diseases, e.g., Parkinson's disease. For diagnosis purposes, single pulses or trains of pulses are used mostly in presurgical assessment

of patients with drug-resistant focal epileptic seizures in order to map the seizure focus (or epileptogenic zone) and the functional areas surrounding the focus. Chronically implanted electrodes are painless; they also permit the recording of ongoing brain activity and evoked potentials.

discharge (epileptic discharge, after-discharge) Abnormal electroencephalographic (EEG) activity with abrupt onset and termination lasting at least several seconds seen during an epileptic seizure; discharges can be recorded either by scalp or by depth electrodes. They can occur spontaneously or be triggered by deep-brain stimulation and then named after-discharges.

electroencephalography (EEG) The record of electrical activity of the brain taken by means of electrodes placed on the surface of the scalp. First applied to study the activity of the human brain by Hans Berger in 1924, this noninvasive technique is still used routinely for the diagnosis of epilepsy.

evoked potentials (EPs) Brain electric response (wave or complex of waves) elicited by and time-locked to a physiological or nonphysiological stimulus, the timing of which can be reliably assessed, e.g., a short duration. Laser beam applied to the skin surface. Because of their low voltage most of EPs are not evident from the ongoing electroencephalographic (EEG) activity after a single stimulation. Repeated stimulations and computer summation techniques are thus needed for their detection. The number of single responses to be summated is a function of the signal-to-noise ratio (ratio between the EP and ongoing EEG activity voltages); this number is higher for scalp than for depth intracerebral recordings.

somatotopy (somatotopic) Representation maps of peripheral skin areas and joints in the somatosensory cortex that were first described in the human brain by Wilder Penfield using electric stimulation of parietal cortex. The even existence of such maps demonstrates that granule cells receiving inputs from the same peripheral areas are grouped together in the somatosensory cortex. Microelectrode recordings in mammalian brain including monkeys have shown that separate somatotopic maps of the peripheral skin and joint receptors can be drawn in the somatosensory cortical areas.

somatosensory areas (S1, S2) Cortical areas containing a full somatotopic map of the contralateral body half that have been identified in mammals and human brain by means of electric cortical stimulation, evoked potentials, brain imaging (functional magnetic resonance imaging), and unit or multiple cell responses. The human primary sensory area (S1) is located in the postcentral parietal gyrus and the second somatosensory area (S2) is located in the upper bank of the sylvian fissure (parietal operculum).

stereotaxy (stereotactic) The stereotactic space first described by Jean Talairach is a three-dimensional representation of the human brain in which each point in the brain can be located according to its coordinates (*x*, *y*, and *z*) in a Cartesian space. The space is defined by the intersection of the mid-sagittal plane and the plane perpendicular to mid-sagittal plane passing through the anterior and posterior commissure of the brain (AC–PC). Using depth electrodes implanted perpendicular to the mid-sagittal plane, any given recording or stimulation site can be localized by its stereotactic coordinates.

5.47.1 Anatomy, Connections, and Physiology of the Insula in Primates

5.47.1.1 The Insula as the Fifth Lobe of the Brain

In an article published in 1896 that was devoted to the comparative anatomy of the insula Clark T. E. (1896) quoted 39 synonyms used in anatomical literature to name the fifth lobe of the brain buried in the lateral sulcus and covered by the opercular parts of the frontal, parietal, and temporal lobes, among which the term insula, first proposed by Reil in 1804, has prevailed. Due to its anatomical situation in depth of brain lateral fissure (see Figure 1 and Tanriover, N. *et al.*, 2004), and its cytoarchitectonic organization the insula has long be considered by anatomists as a rather isolated lobe of the brain mostly devoted to the processing of body and visceral sensation including gustation, pain, and other emotions, as well as to visceromotor and autonomic control. In primates including humans, the insula shows a caudorostral sequence of three distinct cytoarchitectonic areas namely; (1) a large area of granular cortex, at its upper and posterior part, whose structure is very similar to that of the second

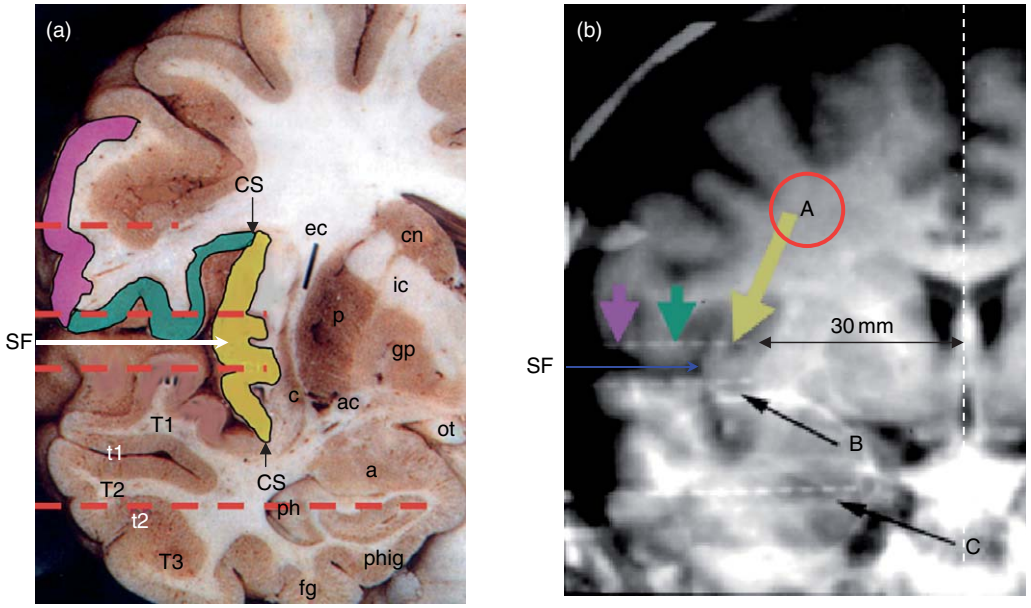

Figure 1 Anatomy of the human insular lobe (frontal slices). A) Anatomical fontal brain section showing the deep location of the insula (in yellow) in the sylvian fissure (SF, white arrow), which separates the frontal and parietal lobes (above) from the temporal lobe (below). The second somatosensory area (S2 in green), which occupies the superior bank of the SF, has common borders with the lower part of the primary somatosensory area (S1 in purple), and the insula. The circular sulcus (CS) separates the insula from the parietal operculum S2 and the first temporal gyrus (T1). The dashed red lines indicates the trajectory of depth electrodes used for insular, parietal, and temporal lobes recordings in patients with epilepsy of the temporal lobe and perisylvian cortex (see Isnard, J. *et al*., 2004). See also Figure 4 for sagittal view of the insula. B) Magnetic resonance imaging (MRI) slice showing the projection of the recording electrodes implanted horizontally perpendicular to the midline sagittal plane (dashed vertical white line). Recording contacts appears as small white segments along the electrodes trajectory. The deepest contacts of electrodes A and B are located in the insular cortex. The depths coordinates (x) of each contact is calculated from the midline sagittal plane in the human brain stereotactic space of Talairach. The x coordinates of insular recording sites vary from 27 mm to 36 mm from midline. Electrode A (red circle) contacts explore from depth to surface: the insula (yellow arrow), the S2 area (green arrow; $38 < x < 46$ mm) and the lower part of the S1 area (purple arrow; $48 < x < 63$ mm). Electrode B contacts explore the insula and the first temporal gyrus (T1 in Figure 1A). Electrode C contacts explore the second temporal gyrus (T2 in Figure 1B) and hippocampus. a, amygdala; ac, anterior commissure; c, claustrum; CS, circular sulcus; cn, caudate nucleus; ec, external capsule; fg, fusiform grus; gp, globus pallidus; ic, internal capsule; ot, optic tract; phig, parahippocamplal gyrus; SF, sylvian fissure; T1, first temporal gyrus; t1, first temporal sulcus; T2, second temporal gyrus; t2, second temporal sulcus; T3, third temporal gyrus.

somatosensory (S2) cortical area, which is involved mostly in the processing of somatosensory and pain sensation; (2) a transitional dysgranular field localized in its anterosuperior part involved in gustation and visceral sensation; and (3) an anteroventral agranular field, which is in continuity with the temporal pole and olfactory proisocortex, and related to olfactory and autonomic functions (see Tanriover, N. *et al*., 2004 for a review).

5.47.1.2 The Insula as a Node in a Distributed Cortical Network

The insula is characterized by anatomical borders that are defined by a limiting sulcus (the circuminsular fissure) but also by fuzzy cytoarchitectonic borders with neighboring cortical areas and by a dense network of corticocortical connections with adjacent or more distant cortical areas. Therefore its function cannot be sketched as an isolated functional center, as suggested by the term insula. A complete description of insular connections is given in the review by Augustine J. R. (1996) showing that the insula is connected to the limbic areas, amygdalar nucleus, basal ganglia, and all of the cortical lobes, except the occipital lobe. Several attempts have been made to identify functional networks in which the insula could play the role of a functional node. Among these networks the perisylvian–insular, the temporo–limbic–insular and the mesial–orbitofrontal–insular

networks (Mesulam, M. M. and Mufson, E. J., 1982) deserve the attention of pain physiologists because they are involved in pain localization and intensity encoding, as well as in emotional and behavioral reaction to pain.

5.47.1.3 The Insula as a Polymodal Area

The question of insular physiology has been addressed by studies using neuroimaging, evoked potentials (EPs), and direct stimulation in humans as well microelectrode studies in monkeys (Augustine, J. R., 1996). These studies have confirmed that the insula is involved in somatosensory and pain sensation as assessed by numerous functional imaging studies in humans (see Peyron, R. *et al.*, 2002 for a review), as well as by the somatosensory and pain-evoked response recordings and direct electric stimulations of the insular cortex that are detailed below in this chapter. However, the insula also proved to be a highly organized lobe with multiple specific functions other than pain including in particular:

Visceral sensation, visceromotor control.

Cardiovascular function as demonstrated by insular stimulation in epileptic patients that produces changes in heart rate or blood pressure in 50% of cases (Oppenheimer, S. M. *et al.*, 1992), thus leading to suspect a role of insular discharges in cardiac arrhythmias causing sudden death during epileptic seizures.

Gustation as assessed first by the stimulation studies of Penfield W. and Faulk M. E. (1955) and further confirmed by neuroimaging studies and microelectrode recordings of insular neurons in monkeys. These physiological findings are consistent with the altered taste perception observed in patients with insular lesions.

Audition and language, in particular allocation of auditory attention, tuning in to novel auditory stimuli, temporal, and phonological processing of auditory stimuli. Furthermore several studies suggest that both right and left insulas are involved in the control of speech production.

5.47.1.4 The Insula as Part of the Mirror-Neuron System

Some recent studies suggest that the insular lobe could belong to the mirror-neuron system that characterizes regions of the brain that are able to respond when the subject performs an action and when the subject observes another individual doing a similar action (see Rizzolatti, G. and Craighero, L., 2004 for a review). The concept also refers to regions of the brain that are able to encode for a sensation (or emotion) perceived by the subject and to respond to the observation of others experiencing that sensation (or emotion). In the human insula, the regions involved in visceral sensation or visceromotor responses are also responding to faces expressing disgust (Krolak-Salmon, P. *et al.*, 2003). Similarly the human insula respond to both pain perception and empathy for others' pain (Jackson, P. L. *et al.*, 2005).

5.47.2 Rational, Ethical Limitations and Procedure of Insular Recording and Stimulations in Humans

5.47.2.1 Recording and Stimulation of the Human Insula Are Justified only in the Context of Presurgical Evaluation of Epilepsy

In humans, electrical stimulation of the cortex, as well as invasive intracranial recordings of the cerebral activity, including surface recordings using electrodes placed on the cortex (electrocorticography) and depth recordings using electrodes implanted directly in the cortex (stereotactic electroencephalography or SEEG), aims at localizing the area that produces focal epileptic seizures. This area, referred to as the epileptogenic zone (EZ; Rosenow, F. and Luders, H. O., 2001), is that which is surgically removed to obtain seizure freedom in patients whose epilepsy cannot be controlled by conventional drug treatment. Ethically such recordings are justified only when the EZ cannot be localized noninvasively either by scalp recordings or neuroimaging techniques. In this context, invasive explorations aim mostly at recording spontaneous seizures. They are also used to perform a functional mapping of the cortex located in, or in the vicinity of, the EZ, in order to predict the functional consequences of the surgical treatment, which consists of removing the EZ cortex. This procedure, named cortectomy, is possible provided that the EZ is not located in an eloquent area involved in essential cortical functions such as language, memory, motor control, and vision. Both the recording of responses evoked by sensory stimulations and direct electrical stimulation of the cortex are commonly used to achieve this functional mapping in epilepsy surgery centers around the world. This context obviously entails some limitations in the use of depth cortical

recordings and stimulation in studies of human brain physiology.

5.47.2.2 Depth Intracortical Electrodes Are Needed to Explore the Insula

Due to its deep location in the lateral fissure the insula can be explored either by electrocorticography during surgery in patients whose frontoparietal or temporal operculum has been removed by a previous cortectomy, as was the case in the few patients first explored in Montreal by Penfield W. and Faulk M. E. (1955), or by depth SEEG electrodes implanted perpendicular to the mid-sagittal plane through the opercular cortex (Figure 1). These electrodes usually have five to ten contacts, each of 2 mm in length separated by 1.5 mm and can be left in place chronically up to 15 days (Isnard, J. *et al.*, 2000; 2004). Only the deepest contacts of such electrodes reach the insular cortex while the superficial ones explore the frontoparietal or temporal opercular cortex. Therefore, concerning somatosensory responsive areas located close to the lateral fissure, it must be checked on individual brain magnetic resonance imaging (MRI) whether contacts are located in the suprasylvian external parietal cortex (area S1), in the parietal operculum cortex (area S2), or in the insula. Oblique electrodes trajectories can also been used to explore the insula, thus increasing the number of contacts located in the insular cortex.

5.47.2.3 The Number of Electrodes Is Limited by Ethical Issues

Only the minimal number of electrodes that are useful to diagnosis can be implanted. Consequently the spatial resolution of the mapping in each individual is low, and pooling interindividual data is necessary to draw topographic functional maps of the human insula based on depth electrode data.

5.47.2.4 The Site of Electrode Implantation Is Guided by Diagnostic Purposes

Implantation sites are guided by the hypothesis issued from noninvasive investigations concerning the most probable EZ location. Furthermore the trajectory of electrode tracts is restricted by the anatomy of blood vessels that are particularly dense in the lateral fissure. Therefore, some parts of the insula are rarely or never explored.

5.47.2.5 Only Data Recorded in Nonepileptogenic Cortex are Physiologically Relevant

Data from cortical recordings or stimulations can be considered as reflecting the normal physiology of the brain on the condition that they have been obtained in cortical areas that are not involved in the epileptogenic process and do not show increased excitability to peripheral inputs or local electric fields produced by stimulation. Two criteria are commonly used to check this, which are first the absence of insular epileptic discharge in the insula during spontaneous seizures and, second, the absence of sustained afterdischarge after electrical stimulation of the insular cortex.

5.47.3 Insular Recordings of Pain Evoked Responses in Humans

In what follows we will describe responses to pain and nonpainful cutaneous stimuli because the same contact in the insula most often detects both types of responses. Moreover pain intensity rating is subjective and corresponds to various levels of stimulus intensity between subjects. In complement to insular responses we will also describe responses recorded in the second somatosensory (S2) area (Figure 1), which is located in the superior bank of the lateral fissure, because it has a blurred anatomical border with the granular insular cortex and is also involved in building up pain sensation.

5.47.3.1 The Laser Stimulus

Most of the studies on pain-EPs in normal subjects and patients use a laser beam (mostly CO_2) applied on the skin surface as a stimulus. The laser beam is known to stimulate the endings of small diameters fibers and mostly those of A delta fibers. When the power output is fixed, the amount of thermal energy delivered depends on the duration of the pulse, which is in the order of a few milliseconds and, thus, permits an accurate timing for the analysis of the electrophysiologic response. The energy density of the laser beam is expressed in milli-Joules per mm^2 of skin surface ($mJ\ mm^{-2}$). Threshold values for pain show large interindividual variations between 30 and 40 $mJ\ mm^{-2}$ using a CO_2 laser beam. In most studies, the sensation perceived by the subject is that of sharp pinprick, without poststimulus pain, considered as

characteristic of the sensations produced by the stimulation of A delta fibers. Although they are able to rate it on a visual analog scale of pain (usually at 4–7 on a 10 level scale), the subjects do not identify this sensation as a pain comparable to what they might have experienced in the past. Indeed no natural pain is provoked by selective activation of the A delta fibers, and this must be kept in mind when using laser stimulation in pain studies. In particular, the laser stimulus can be considered as adequate to assess the intensity coding of a pain stimulus, but is suboptimal for studying of the emotional reaction to pain.

5.47.3.2 Cortical Surface Recordings (Electrocorticography)

Lenz F. A. *et al.* (1998) were the first to record cortical surface recordings by means of a subdural grid of electrodes placed on the surface of the parietal operculum with CO_2-laser-evoked potentials (LEPs) peaking between 160 and 340 ms after the stimulus. The spatial distribution of this response over the cortical surface of the perisylvian cortex was considered as compatible with generators located in the parietal operculum and/or in the insular cortices. However subdural electrodes placed over the sylvian area do not allow direct recording neither in the deep aspect of the frontoparietal opercular cortex nor in the insula.

5.47.3.3 Intracortical S2 Recordings

In humans, LEPs at stimulus intensities below and above pain threshold are recorded in the suprasylvian opercular cortex corresponding to the human S2 area (Frot, M. *et al.*, 2001). These responses are not picked up in the other areas most often explored in presurgical assessment of epilepsy including the amygdala, hippocampus, and orbitofrontal cortex. They show a biphasic negative–positive waveform peaking at 137 ± 13 ms (N140) and 172 ± 11 ms (P170), respectively, after stimulation of opposite hand (Figure 2). Similar responses are equally recorded in the homologous cortex, ipsilateral to the painful stimulus with a delay of 10–17 ms. The LEP voltage in S2 shows a significant increase as soon as the stimulus intensity reaches the sensory threshold as well as between sensory and pain thresholds while it rapidly reaches a plateau for intensities above pain threshold (Frot, M. *et al.*, 2007; Figure 3).

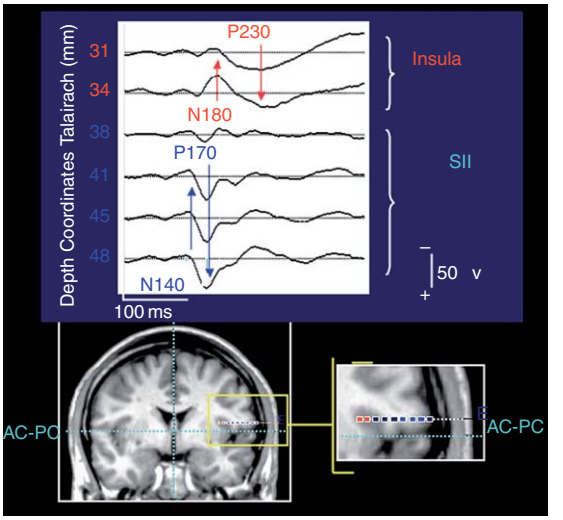

Figure 2 Pain laser-evoked potentials (LEPs) to skin laser stimulation of the dorsum of the hand. The lower part of the figure shows frontal magnetic resonance imaging slices of the right insula with projection of the contacts of a recording electrode exploring the insula (red) and S2 (blue). The vertical dashed blue line represent the midline sagittal plane, and the horizontal dashed blue line the anterior commissure–posterior commissure (AC–PC) horizontal plane used for stereotactic implantation of depth electrodes. Evoked potentials illustrated in the upper part of the figure are obtained by averaging responses to repeated stimulations of the left hand by a CO_2 laser beam. Figures along the vertical axis are the depth coordinates (x) in mm from midline of each recording contact. Note that distinct responses are obtained in both areas, which are separated by a delay of 50 ms.

5.47.3.4 Intracortical Insular Recordings

LEPs contralateral to stimulation recorded in the insular cortex itself (Frot, M. and Mauguière, F., 2003) consist in a N180 negative response (mean latency: 180 ± 16.5 ms) followed by a P230 positivity (mean latency: 226 ± 16 ms; Figure 2). As for S2, insular LEPs ipsilateral to stimulation peak 10–17 ms later than contralateral ones. LEP amplitudes increase between sensory and pain threshold intensities but, contrary to what is observed in S2, continue to increase significantly at intensities over the pain threshold (Figure 3).

The reason for the delay of ~ 50 ms (50 ± 16 ms between S2 N140 and insular N180 peaking latencies) observed between S2 and insular pain responses remains questionable. It is too long for a monosynaptic transmission from S2 to the insula, the two areas being interconnected through direct projections. Alternatively, knowing that both S2 and the insula

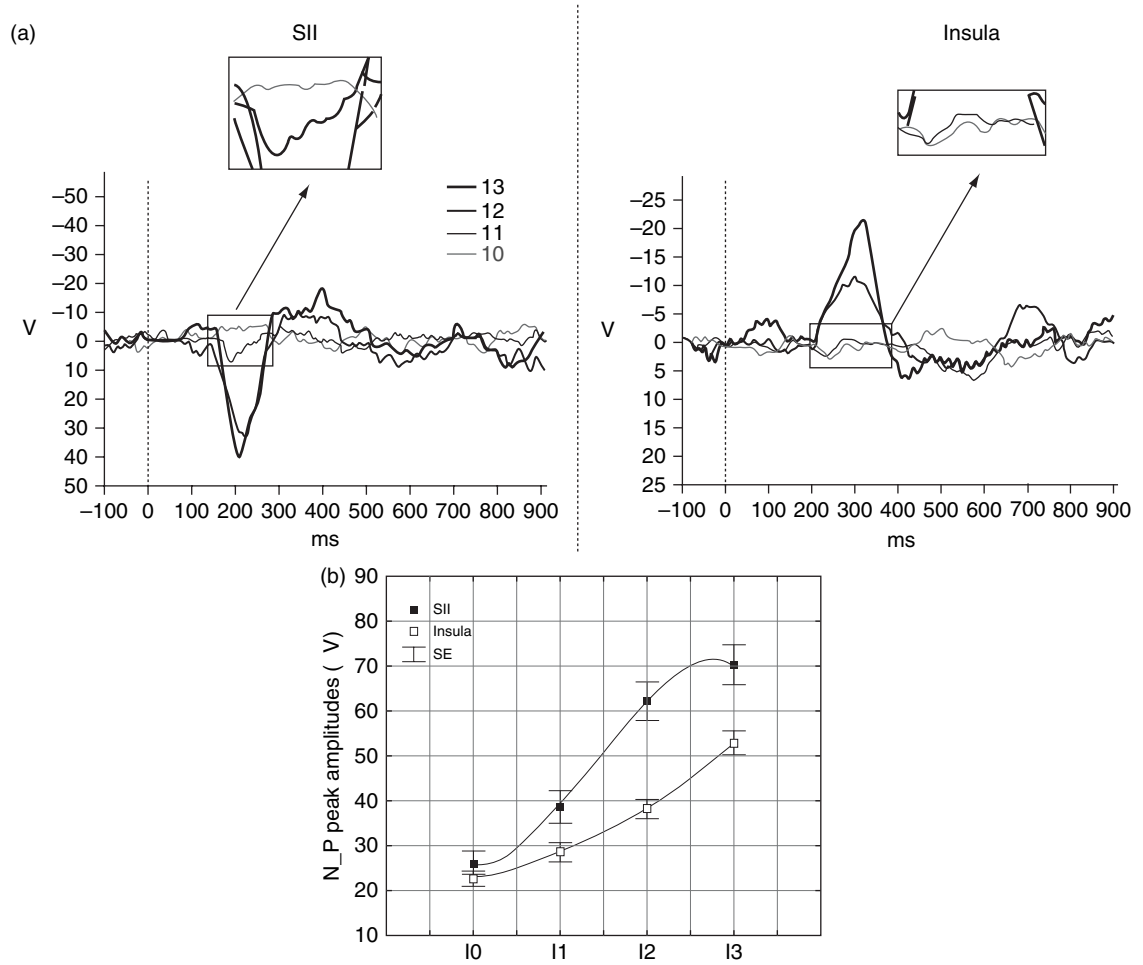

Figure 3 Effects of stimulus intensity on laser-evoked potential (LEP) amplitude in S2 and insula. A) LEP traces in S2 and insula to four different stimulus intensities are superimposed. CO_2 Laser pulses were applied at four different intensities in each subject. The power output being fixed, the amount of thermal energy delivered depends on the duration of the pulse. Pulse duration is set up according to subjects' subjective reports, rated on a visual analog scale (VAS) with an anchor point corresponding to the pain threshold. The printed scales consist of 10-cm horizontal lines where the left extreme is labeled no sensation and the right extreme maximal pain, and an anchored level 4 was at pain threshold (Lickert-type scale). The different stimuli and related subjective sensation are as follows: I0: below sensory threshold (pulse duration: 5–15 ms, mean energy density: 7 mJ mm^{-2}, no sensation); I1: above sensory threshold (pulse duration: 15–45 ms, mean energy density: 19 mJ mm^{-2}, producing a detectable nonpainful sensation reported for more than 90% of stimulations; For one-third of patients this sensation is a warmth sensation and for the others two-thirds a slight nonpainful pinprick sensation; VAS: 1.6 ± 1.09); I2: pain threshold (pulse duration: 25–80 ms, mean energy density: 33 mJ mm^{-2}, producing a pricking sensation, like a hair pulling or a drop of hot boiling water on the skin; VAS: 3.9 ± 1.46); I3: 20% above pain threshold (pulse duration: 35–110 ms, mean energy density: 46 mJ mm^{-2}, producing a pricking sensation described as clearly painful; VAS: 5.4 ± 1.6). In S2, a significant increase of the LEP is observed as soon as the stimulus intensity reaches the sensory threshold (between I0 and I1, $P < 0.001$), as well as between sensory and pain thresholds (I1 to I2, $P < 0.001$) while amplitudes rapidly reach a plateau for intensities above pain threshold (no significant amplitude difference between I2 and I3). In the insula, no significant amplitude increase is observed for low-stimulation intensities between I0 and I1, LEP amplitudes also increase between sensory and pain threshold intensities ($P < 0.05$ between I1 and I2) and continue to increase significantly at higher intensities over pain threshold ($P < 0.001$ between I2 and I3). B) Insula and S2 LEPs peaking amplitudes as a function of stimulus intensity. In these polynomial regression curves of the stimulus–response functions S2 LEPs amplitudes show a S-shaped profile with increasing stimulus intensities that reaches a plateau above pain threshold, while insular LEP amplitudes show an exponential profile. Laser stimuli above pain threshold trigger a maximal response in S2 and a pain level-related response in the insula (Modified from Frot, M., Magnin, M., Mauguière, F., and Garcia-Larrea, L. 2007. Human SII and posterior insula differently encode thermal laser stimuli. Cereb. Cortex 17, 610–620).

receive direct projections from the thalamus (see for a review Augustine, J. R., 1996) the explanation could be that the latter are triggered via thalamocortical fibers with a slower conduction than that of thalamic projections to the S2 area. To our knowledge, however, no electrophysiological demonstration of this hypothesis is hitherto available. A third hypothesis could be that the suprasylvian cortex and the insula are activated by inputs conveyed by peripheral fibers with different conduction velocities. Some studies have estimated the A delta conduction velocity in a large range of 7–20 m s^{-1} suggesting the existence of different A delta fiber subpopulations, with different conduction velocities. One can hypothesize that these different subpopulations of peripheral fibers could project in distinct cortical regions. However, to our knowledge, no electrophysiological study has been devoted to the identification of separate subpopulations of fibers with different conduction velocities in the spinothalamic tract or thalamocortical projections.

5.47.3.5 Topographic Specificity of Insular Laser-Evoked Potentials

Due to the anatomical proximity between the S2 area and the granular part of the insula the question arises whether insular responses might reflect the diffusion of S2 LEPs with a polarity reversal across the sylvian fissure, which is almost virtual in that region. The fact that when two contacts, or more, explore the insular cortex there is an amplitude increase from surface to depth of the N180–P230 response suggests that this is not so (see Frot, M. and Mauguière, F. 2003 for a complete discussion). However, the absolute proof that the N180–P230 is generated in the insular cortex would be its polarity reversal between the surface and the depth of the insular gray matter; unfortunately usual stereotactic recordings in patients do not have enough spatial resolution (2 mm interval between two neighboring contacts of 1.5 mm) to assess the distribution of potentials perpendicular to the cortical surface.

5.47.3.6 Interhemispheric Transmission of S2 and Insular Laser-Evoked Potentials

Insular and S2 responses to pain are bilateral; ipsilateral potentials peaking with a delay of 10–20 ms after contralateral ones. This delay is compatible with the interhemispheric transmission time through fibers of the corpus callosum as estimated by numerous studies (e.g., 15 ms between primary visual areas); it is in the same range as that measured between ipsi- and contralateral S2 magnetic fields evoked by electrical stimulation of the median nerve. The possibility remains, however, that responses ipsilateral to the stimulus could be triggered via ipsilateral thalamic fibers with slower conduction velocities. Only intracortical recordings of S2 or insular EPs to ipsilateral stimuli in patients with a lesion of the homologous areas in the opposite hemisphere could address this question directly.

5.47.4 Insular Stimulation

5.47.4.1 The Challenge of Insular Stimulation

In humans, it has long been a challenge to stimulate the insular cortex. Thus, only a few studies have reported nonnociceptive somesthetic symptoms, cardiovascular effects as well as visceromotor and viscerosensitive sensations consecutive to direct electrical stimulation of the insular cortex. Truly painful responses have not been reported during stimulation of any area of the cerebral cortex in humans by Penfield W. and Faulk M. E. (1955), who extensively stimulated the surface of all cortical areas of the human brain, including the insula, using surface electrodes. However, they did not explore the posterior part of the insula where electric stimulation evokes painful sensations.

Electric stimulations are produced by a current-regulated neurostimulator designed for a safe diagnostic stimulation of the human brain. Square pulses of current are applied between two adjacent contacts (bipolar stimulation) at a frequency of 50 Hz, pulse duration of 0.5 ms, train duration of 5 s, and intensity of 0.8–6.0 mA. These parameters are used to avoid any tissue injury (charge density per square pulse $<55\ \mu C\ cm^{-2}$; Gordon, B. *et al.*, 1990). This stimulation paradigm ensures a good spatial specificity with respect to the desired structures to be stimulated. The study of current densities in the cortex for bipolar stimulation with a 10-mA stimulating current shows that the peak current density occurs in the region immediately beneath the bipolar electrodes (0.05 A cm^{-2}) and declines rapidly to 0.02 A cm^{-2} 0.5 cm away, and that the current density decreases in relation to the square of the distance into the cortex. In S1, S2, and the insula, the minimal stimulation intensity necessary to elicit a clinical response is 1.6–1.9 mA (Mazzola, L. *et al.*, 2006). With these stimuli there is virtually no current spread out of the stimulation current dipole as defined by the distance of 5.5 mm

between the outer and inner limits of the superficial and deep-stimulating contacts, respectively (Ostrowsky, K. *et al*., 2002). Moreover it has been demonstrated that no significant cerebral blood flow change occurs at the site of cortical stimulation, or in its close vicinity, in the absence of epileptic after discharge.

5.47.4.2 Pain Evoked by Insular Stimulation

Painful sensations in response to direct electric stimulation of the insula have been reported by Ostrowsky K. *et al*. (2000; 2002) and more recently by Mazzola L. *et al*. (2006). Qualities of the evoked pain are described as burning, stinging, disabling sensation, or electrical shock. Pain intensity varies from mild to intolerable but is not related to stimulation intensity. Pain disappears as soon as the stimulation is interrupted in most cases except a few where an intense pain is followed by a sore feeling that can last up to 1 min after the end of the stimulation. It is located contralateral to the stimulation site or bilaterally when midline parts of the body are involved, and affects large areas of the body (e.g., face, upper limb, whole half of the body), suggesting that receptive fields for pain in the insular cortex are more extended that somatosensory fields in the SI and SII cortex (Mazzola, L. *et al*., 2006).

5.47.4.3 Anatomical Location of the Insular Pain Area

The area where pain can be elicited by direct electric stimulation occupies the posterosuperior part of the insular lobe (Figure 4). Surface electrodes cannot reach this area unless the lower precentral motor and postcentral somatosensory cortex be removed. This is the most probable reason why early electrocorticographic studies using that type of electrodes failed to produce pain by cortical stimulation in humans. Because only a few contacts can be placed in the insula of a given individual during stereotactic exploration of the brain with depth electrodes it is uncertain whether a pain somatopic representation of the body, comparable to that demonstrated in the primary somatosensory cortex (S1), does exist in the pain insular area. Moreover due to the large skin extent of pains evoked by insular stimulation that the somatotopic pain representation is likely to be much more fuzzy, with overlapping receptive fields, in the insular pain area than in S1 or S2 somatosensory areas.

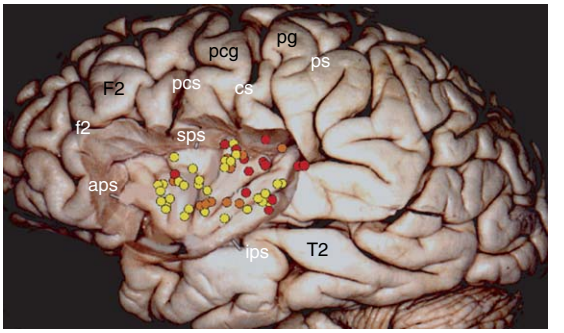

Figure 4 Pain insular area. The locations of stimulation sites in a population of patients are plotted on a sagittal view of the insula exposed by removal of the supra and infrasylvian cortex according to the type of somatosensory sensation reported by the subjects. Red dots: pain, Orange dots: nonpainful warm sensation, yellow dots: nonpainful paresthesias. Note that most of pain sensations are evoked by stimulation the posterior part of the insula situated behind the tip of the central sulcus (cs), while nonpainful responses are obtained over a larger and more anterior surface of the insular lobe. Aps, anterior peri-insular sulcus; cs, central sulcus; F2, second frontal gyrus; f2, second frontal sulcus; ips, inferior peri-insular sulcus; pcg, precentral gyrus; pg, postcentral gyrus; ps, parietal sulcus; sps, superior peri-insular sulcus; T2, second temporal gyrus.

References

Augustine, J. R. 1996. Circuitry and functional aspects of the insular lobe in primates including humans. Brain Res. Rev. 22, 229–244.

Clark, T. E. 1896. The comparative anatomy of the insula. J. Comp. Neurol. 6, 59–100.

Frot, M. and Mauguière, F. 2003. Dual representation of pain in the operculo-insular cortex in humans. Brain 126, 438–450.

Frot, M., Garcia-Larrea, L., Guénot, M., and Mauguière, F. 2001. Responses of the supra-sylvian (SII) cortex in humans to painful and innocuous stimuli. A study using intra-cerebral recordings. Pain 94, 65–73.

Frot, M., Magnin, M., Mauguière, F., and Garcia-Larrea, L. 2007. Human SII and posterior insula differently encode thermal laser stimuli. Cereb. Cortex 17, 610–620.

Gordon, B., Lesser, R. P., Rance, N. E., Hart, J., Jr., Webber, R., Uematsu, S., and Fisher, R. S. 1990. Parameters for direct cortical electrical stimulation in the human: histopathologic confirmation. Electroencephalogr. Clin. Neurophysiol. 75, 371–377.

Isnard, J., Guénot, M., Ostrowsky, K., Sindou, M., and Mauguière, F. 2000. The role of the insular cortex in temporal lobe epilepsy. Ann. Neurol. 48, 614–623.

Isnard, J., Guénot, M., Sindou, M., and Mauguière, F. 2004. Clinical manifestations of insular lobe epileptic discharges: a stereo-electroencephalographic study. Epilepsia 45, 1079–1790.

Jackson, P. L., Meltzoff, A. N., and Decety, J. 2005. How do we perceive the pain of the others? A window into the neural processes involved in empathy. Neuroimage 24, 771–779.

Krolak-Salmon, P., Henaff, M. A., Isnard, J., Tallon-Baudry, C., Guénot, M., Vighetto, A., Bertrand, O., and Mauguière, F. 2003. An attention modulated response to disgust in human ventral anterior insula. Ann. Neurol. 53, 446–453.

Lenz, F. A., Rios, M., Chau, D., Krauss, G. L., Zirh, T. A., and Lesser, R. P. 1998. Painful stimuli evoke potentials recorded from the parasylvian cortex in humans. J. Neurophysiol. 80, 2077–2088.

Mazzola, L., Isnard, J., and Mauguière, F. 2006. Somatosensory and pain responses to stimulation of the second somatosensory area (SII) in humans. A comparison with SI and insular responses. Cereb. Cortex 16, 960–968.

Mesulam, M. M. and Mufson, E. J. 1982. Insula of the old world monkey. I. Architectonics in the insulo orbito-temporal component of the paralimbic brain. J. Comp. Neurol. 212, 1–22.

Oppenheimer, S. M., Gelb, A., Girvin, J. P., and Hachinski, V. C. 1992. Cardio-vascular effects of human insular cortex stimulation. Neurology 42, 1727–1732.

Ostrowsky, K., Isnard, J., Ryvlin, P., Guenot, M., Fischer, C., and Mauguière, F. 2000. Functional mapping of the insular cortex: clinical implication in temporal lobe epilepsy. Epilepsia 41, 681–686.

Ostrowsky, K., Magnin, M., Ryvlin, P., Isnard, J., Guénot, M., and Mauguière, F. 2002. Representation of pain and somatic sensation in the human insula: a study of responses to direct electrical cortical stimulation. Cereb. Cortex 12, 376–385.

Penfield, W. and Faulk, M. E. 1955. The insula. Further observations on its function. Brain 78, 445–470.

Peyron, R., Frot, M., Schneider, F., Garcia-Larrea, L., Mertens, P., Barral, F. G., Sindou, M., Laurent, B., and Mauguière, F. 2002. Role of operculo-insular cortices in human pain processing. Converging evidence from PET, fMRI, dipole modeling and intra-cerebral recordings of evoked potentials. Neuroimage 17, 1336–1346.

Rizzolatti, G. and Craighero, L. 2004. The mirror-neuron system. Ann. Rev. Neurosci. 27, 169–192.

Rosenow, F. and Luders, H. O. 2001. Presurgical evaluation of epilepsy. Brain 124, 1683–1700.

Tanriover, N., Rhoton, A. L., Kawashima, M., Ulm, A. J., and Yasuda, A. 2004. Microsurgical anatomy of the insula and the sylvian fissure. J. Neurosurg. 100, 891–922.

Relevant Websites

http://imaging.mrc-cbu.cam.ac.uk – CBU Imaging
http://en.wikipedia.org

5.48 The Rostral Agranular Insular Cortex

L Jasmin, Neurosurgery and Gene Therapeutics Research Institute, Los Angeles, CA, USA

P T Ohara, University of California, San Francisco, CA, USA

© 2008 Elsevier Inc. All rights reserved.

5.48.1	What Is the Rostral Agranular Insular Cortex?	717
5.48.2	Function of the Rostral Agranular Insular Cortex	717
5.48.3	Anatomical Location	717
5.48.4	Neurochemical Signature	718
5.48.5	Connections of the Rostral Agranular Insular Cortex	718
5.48.6	Behavioral Studies	719
5.48.7	Relationship with Adjacent Cortical Regions	719
5.48.8	Overview in the Rat	720
5.48.9	From Rats to Humans	720
5.48.10	Perspective	721
References		721

Glossary

amygdala A group of neurons that is part of the limbic system. The amygdala is involved in many aspects of behavior such as memory, emotion, and motivation.

immunocytochemical staining A method that uses antibodies to identify and locate specific cellular components, such as neurotransmitters.

medial frontal, infralimbic, and cingulate cortices Different parts of the cerebral cortex that have been shown to be involved in different aspects of processing painful information.

nociception The perception of a stimulus that is potentially injurious to one's body.

nucleus accumbens A part of the limbic system involved in reward and addiction.

thalamus A part of the brain located at the center that processes sensory and motor information and sends the resulting information to the cerebral cortex.

5.48.1 What Is the Rostral Agranular Insular Cortex?

The rostral agranular insular cortex (RAIC) is a small area of the cerebral cortex located on the lateral aspect of the rat's cerebral hemisphere. The RAIC can be distinguished in terms of its location, cellular architecture, neurochemistry, and connectivity. Functionally, the RAIC is involved in processing pain information and, depending on which cells are activated, can act through connections with other brain areas to reduce or increase pain responses. The RAIC therefore is one of a limited number of cortical regions involved in the perception and response to pain.

5.48.2 Function of the Rostral Agranular Insular Cortex

Many parts of the cerebral cortex do not have precisely defined functions and usually do not have precisely defined borders. Until recently, the RAIC was one such region, but a picture indicating that the RAIC is involved in the behavioral responses to nociceptive (painful) stimuli is beginning to emerge from animal and human studies.

5.48.3 Anatomical Location

In the rat, the RAIC occupies a small area of the lateral aspect of cerebral cortex just above a groove,

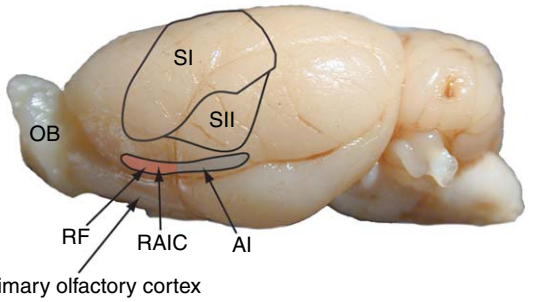

Figure 1 Lateral view of the rat brain. The rhinal fissure (RF) is seen as a prominent groove starting near the ventral anterior cortex and extending toward the posterior cortex. The agranular insular cortex is a thin strip of cortex lying just above (dorsal to) the RF and the rostral part (RAIC) is indicated in red. The approximate location of the primary somatosensory cortex (SI) and the secondary somatosensory cortex (SII) are indicated for reference. OB, olfactory bulb.

which is one of the few surface features of the rat cortex, called the rhinal fissure (Figure 1) (Paxinos, G., 1995). Agranular cortex is defined by the absence of a layer 4 that gives the cortex a less granular appearance than the adjacent areas. The region was described by Krettek J. E. and Price J. L. (1977) as a strip of agranular cortex located immediately above the rhinal fissure and bounded dorsally by granular cortex. Rostrally, the agranular cortex was further subdivided into a ventral and a dorsal agranular region. This description was later modified (Cechetto, D. F. and Saper, C. B., 1987) to include a dysgranular field between the agranular and granular cortices. The dysgranular field had a layer 4 that was intermediate in prominence between the fully developed layer 4 of the granular cortex and the absent layer 4 of the agranular cortex. Later studies all distinguish agranular, dysgranular, and granular fields although the precise boundaries, particularly between the dorsal agranular and dysgranular fields, were delineated differently.

5.48.4 Neurochemical Signature

Although classically cortical regions are defined by cytoarchitecture and location, modern neuroanatomical techniques have refined our understanding of cortical organization based on connections and neurochemical profile. The RAIC has been shown to be distinguished from surrounding regions by a distinct pattern of immunocytochemical staining (Figure 2) (Ohara, P. T. *et al.*, 2003). The first feature is a concentration of neurons in layer 5 of the RAIC that express the $GABA_B$ receptor (Jasmin, L. *et al.*, 2003), which is one of several types of receptors activated by the inhibitory neurotransmitter, gamma-aminobutyric acid (GABA). Similar concentrations of $GABA_B$ receptor-bearing neurons are also found in the insular cortex posterior to the RAIC and in a few other brain regions but are less concentrated in the remainder of the cortex. The neurons in layer 5 of the RAIC that express the $GABA_B$ receptor are large pyramidal projection neurons that have axons that leave the cortex and innervate other brain regions. This finding suggests that the neurons in the RAIC that have $GABA_B$ receptors play a specific role in how the RAIC communicates with other brain areas. A second notable feature of the RAIC is the concentration of nerve fibers containing the neurotransmitter dopamine. In the rat, there is only sparse dopamine innervation throughout most of the cortex dopamine fibers that are found in high concentration in then infralimbic cortex and in the RAIC (Figure 2). These dopamine fibers originate in a region of the brainstem called the ventral tegmental area (VTA) and probably are involved in determining the overall level of activity of the RAIC rather than conveying specific sensory information.

5.48.5 Connections of the Rostral Agranular Insular Cortex

The specific connections of a cortical region also help define the boundaries and give insight into the functions of the region. The RAIC shares the general pattern of connection common to most regions of cortex receiving its major subcortical afferents from the thalamus, having reciprocal connection with other cortical regions, and projecting to a number of subcortical sites (Jasmin, L. *et al.*, 2004). The picture that emerges from an analysis of the projections is that the RAIC plays a role in pain mechanisms. The inputs from the thalamus are from the nuclei that convey sensory information from the body. However, this input is not from thalamic nuclei that subserve the fine-detailed discriminative aspect of sensation (i.e., those that project to the primary somatosensory cortex), rather the input is from nuclei located in the midline of the thalamus that are generally associated with emotional or affective aspects of pain. The principal cortical connection of the RAIC is with areas such as the medial frontal, infralimbic, and cingulate cortices, which have long been known to

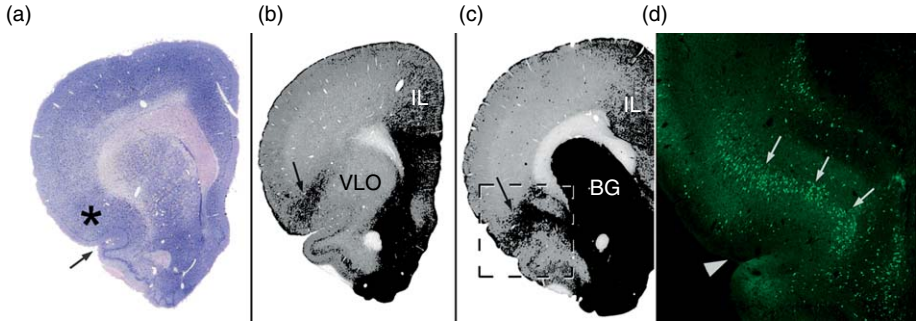

Figure 2 Coronal sections through the left anterior rat brain showing some of the characteristic features of the RAIC. (a) A section stained with a Nissl stain to show the general appearance and location of the RAIC. The rhinal fissure is indicated by the arrow and the asterisk indicates the location of the RAIC. (b, c) Sections stained immunocytochemically to show the location of fibers containing the neurotransmitter, dopamine. The contrast has been digitally enhanced to show the dopamine more clearly. The arrow indicates the region of dopamine staining that corresponds to the location of the RAIC. Intense staining is also present in the infralimbic cortex (IL), which is also a pain-related area, and in the basal ganglia (BG), which is a motor-related site. The ventrolateral orbital cortex (VLO), a site also associated with pain behavior, shows no dopamine staining. (d) A higher magnification of the boxed region indicated in (c). This section is stained to show the location of neurons that express the $GABA_B$ receptor (green-colored structures) in cortical layer 5. The arrowhead indicated the location of the rhinal fissure.

be associated with pain responses. The RAIC projects to a number of subcortical sites including the lateral hypothalamus, dorsal raphe, periaqueductal gray matter, pericerulear region, rostroventral medulla, and parabrachial nuclei – all of which play a role in pain inhibition mechanisms. Significant to the probable function of the RAIC are projections to the amygdala and the nucleus accumbens. These projections include a large component originating in the cells in layer 5 that express the $GABA_B$ receptor described above. The amygdala is known to be involved in several aspects of behavior including fear, anxiety, and attention (Williams, M. A. *et al.*, 2005).

5.48.6 Behavioral Studies

In addition to the connectional studies, there are a number of behavioral studies that give insight into the function of the RAIC. Direct injections of compounds into the RAIC have shown that morphine injection, increasing dopamine levels, and increasing GABA levels all result in behavioral antinociception. Because increasing GABA in the RAIC results in antinociception and the action of GABA is to inhibit neuronal activity, it suggests that activity in the RAIC is pronociceptive. Additional pharmacological experiments suggest that the neurons that express the $GABA_A$ and those that express the $GABA_B$ receptor change pain thresholds through different pathways. These antinociceptive effects mediated by cells that possess $GABA_A$ receptors occur through projections to the brainstem and activation of descending pain inhibitory systems. However, as noted above, the RAIC is characterized by an abundance of cells that have $GABA_B$ receptors. The changes in pain behavior mediated by the $GABA_B$ receptor-bearing neurons point to projections to the amygdala playing a key role. The proposal that the activity in the RAIC leads to increased pain was tested by inhibiting $GABA_A$ receptor-bearing neurons and at the same time activating $GABA_B$ receptor-bearing neurons. This experiment resulted in an increase in pain behavior (Jasmin, L. *et al.*, 2003). These studies highlight two important issues. First, changes in activity of the RAIC can result in both increases and decreases in pain response and the overall effect of the RAIC results from a balance of pro- and antinociceptive activity. Second, the RAIC probably changes pain behavior both by activating descending inhibitory circuits and by changing activity in the amygdala and other cortical area to change the emotional/affective response to painful stimuli.

5.48.7 Relationship with Adjacent Cortical Regions

The location and small size of the RAIC makes it difficult to unequivocally isolate it from surrounding regions. The agranular insular cortex has been most associated with visceral and gustatory responses, and

a number of studies on cells in the region have indicated that they respond to visceral input. These functions, however, seem more related to the more posterior regions of the agranular cortex or the dysgranular cortex immediately above the RAIC. Immediately anterior to the RAIC is the ventrolateral orbital cortex (VLO). This region of cortex in the rat is also associated with pain responses (Xie, Y. F. *et al.*, 2004). As with all parts of the cerebral cortex, it is often difficult to define a clear boundary between any two regions. For this, and other technical reasons such as diffusion of drugs when injected into a specific site, it is possible that some studies previously carried out on the VLO may have encroached upon the RAIC and vice versa. There are both similarities and differences between the VLO and the RAIC. Morphine injected into the VLO and RAIC both produce antinociception, but the application of drugs that inhibit GABA has no effect in the RAIC but do have antinociceptive effects in the VLO. There is less dopamine innervation of VLO, and although the VLO contains $GABA_B$ receptor-bearing cells, they are not as numerous as in the RAIC (Ohara, P. T. *et al.*, 2003). Whether the VLO and RAIC are really separate entities with specific, separate functions related to pain or whether both regions are parts of a larger forebrain nociceptive system is not clear.

5.48.8 Overview in the Rat

The major connections of the RAIC are with areas that have established roles in nociceptive information processing and behavior responses to nociceptive stimuli. RAIC projections to other cortical areas and subcortical sites such as the amygdala are likely to participate in the sensorimotor integration of nociceptive processing, while the hypothalamus and brainstem projections are most likely to contribute to descending pain inhibitory control.

5.48.9 From Rats to Humans

The agranular insular cortex is found in other mammals including cats, monkeys, and primates including humans (Augustine, J. R., 1996; Mesulam, M.-M., 2000). In primates, the divisions of the insular cortex are the same as in rats and the RAIC occupies an area immediately noticeable, that is, dorsal to the primary olfactory cortex.

The advent of high-resolution functional imaging has resulted in the availability of data relating to cortical function that has previously been difficult to obtain from animal studies (Figure 3). Specifically, it is possible to relate verbal descriptions and emotional responses to painful stimuli to specific cortical sites. In humans, imaging techniques and direct recording of field potentials show that painful stimuli activate the insular cortex (Coghill, R. C. *et al.*, 1994; Brooks, J. C. *et al.*, 2005). It has been possible to distinguish between activation of the anterior and of the posterior region of the agranular cortex located in the insular region (Strigo, I. A. *et al.*, 2003). The anterior insula, which might be considered most equivalent to the RAIC, is activated when a strong emotional response is associated with the nociceptive stimulus. The posterior insula and the adjacent parietal cortex, in turn, are activated by all nociceptive stimuli, independently of their emotional content. These differences in function between the anterior and the posterior insula are explained by their neural connectivity. Notably, ascending nociceptive afferents from the spinal cord and brainstem directly activate the posterior insula

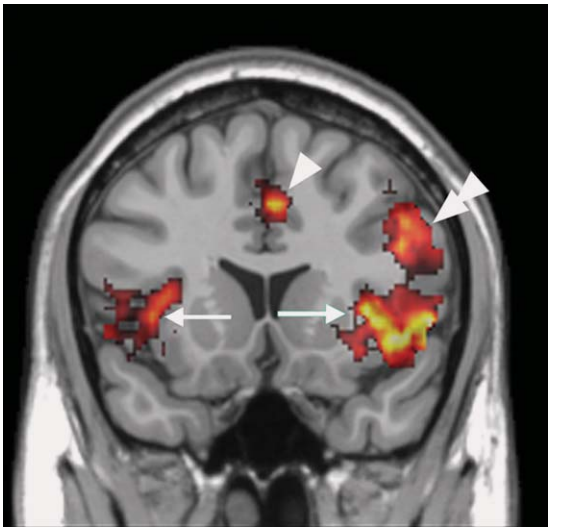

Figure 3 A functional magnetic resonance imaging blood oxygen level-dependent (fMRI BOLD) image averaged from nine normal healthy subjects who received a painful stimulus to the back. Note that the insular cortex is activated (arrows, red and yellow areas) on both sides of the cortex although more prominently on the left side. This bilateral activation of the insular region can be contrasted with the unilateral activation of other cortical regions such as the cingulate cortex (arrowhead) and dorsolateral prefrontal cortex (double arrowhead). Why the activation is lateralized in these latter areas in not known but is a common occurrence. Photo courtesy of Dr. Vania Apkarian, Northwestern University.

only. Accordingly, direct electrical stimulation of the posterior insula results in the generation of thermal sensations (Ostrowsky, K. *et al.*, 2002), and lesions of the posterior insula, and not the anterior insula, affect recognition of nociceptive heat (Greenspan, J. D. *et al.*, 1999). On the other hand, the anterior insula is implicated in the emotional awareness that occurs when a nociceptive stimuli endangers the self (Craig, A. D., 2002).

One aspect of function that has emerged from human studies and not fully explored in animal experiments is that in some cases activation of the anterior insula is lateralized. For example, air hunger activates mostly the right side (Banzett, R. B. *et al.*, 2000), and from this and other results, the right insular cortex has been assigned a greater role in the consciousness of the external world as well as interest in novelty (Manes, F. *et al.*, 1999). The left insula is more implicated in the regulation of cardiovascular function (Phillips, M. L. *et al.*, 2003).

5.48.10 Perspective

Our understating of cortical functioning, particularly with respect to pain, must be considered rudimentary. Although we refer to the RAIC as a distinct entity with a specific function in the rat, we need to remain aware of the close relationship it has with adjacent areas serving visceral functions and nearby regions such as the VLO involved in nociceptive processing. The most complete understanding of the RAIC will only come about when we understand how it is integrated into the other cortical and subcortical sites that appear to form a pain matrix. We also need to understand the relationship between the RAIC in the rat and the agranular insular cortex in the human. Although there are clear parallels between the two areas in terms of cytoarchitecture and function, it is not clear that they are strictly equivalent areas and our understanding of pain mechanisms in general will have to take into account such species-specific similarities and/or differences.

References

Augustine, J. R. 1996. Circuitry and functional aspects of the insular lobe in primates including humans. Brain Res. Brain Res. Rev. 22, 229–244.

Banzett, R. B., Mulnier, H. E., Murphy, K., Rosen, S. D., Wise, R. J., and Adams, L. 2000. Breathlessness in humans activates insular cortex. Neuroreport 11, 2117–2120.

Brooks, J. C., Zambreanu, L., Godinez, A., Craig, A. D., and Tracey, I. 2005. Somatotopic organisation of the human insula to painful heat studied with high resolution functional imaging. Neuroimage 27, 201–209.

Cechetto, D. F. and Saper, C. B. 1987. Evidence for a viscerotopic sensory representation in the cortex and thalamus in the rat. J. Comp. Neurol. 262, 27–45.

Coghill, R. C., Talbot, J. D., Evans, A. C., Meyer, E., Gjedde, A., Bushnell, M. C., and Duncan, G. H. 1994. Distributed processing of pain and vibration by the human brain. J. Neurosci. 14, 4095–4108.

Craig, A. D. 2002. How do you feel? Interoception: the sense of the physiological condition of the body. Nat. Rev. Neurosci. 3, 655–666.

Greenspan, J. D., Lee, R. R., and Lenz, F. A. 1999. Pain sensitivity alterations as a function of lesion location in the parasylvian cortex. Pain 81, 273–282.

Jasmin, L., Burkey, A. R., Granato, A., and Ohara, P. T. 2004. Rostral agranular insular cortex and pain areas of the central nervous system: a tract-tracing study in the rat. J. Comp. Neurol. 468, 425–440.

Jasmin, L., Rabkin, S. D., Granato, A., Boudah, A., and Ohara, P. T. 2003. Analgesia and hyperalgesia from GABA-mediated modulation of the cerebral cortex. Nature 424, 316–320.

Krettek, J. E. and Price, J. L. 1977. The cortical projections of the medio-dorsal nucleus and adjacent thalamic nuclei in the rat. J. Comp. Neurol. 171, 157–192.

Manes, F., Paradiso, S., Springer, J. A., Lamberty, G., and Robinson, R. G. 1999. Neglect after right insular cortex infarction. Stroke 30, 946–948.

Mesulam, M.-M. 2000. Principles of Behavioral and Cognitive Neurology. Oxford University Press.

Ohara, P. T., Granato, A., Moallem, T. M., Wang, B. R., Tillet, Y., and Jasmin, L. 2003. Dopaminergic input to GABAergic neurons in the rostral agranular insular cortex of the rat. J. Neurocytol. 32, 131–141.

Ostrowsky, K., Magnin, M., Ryvlin, P., Isnard, J., Guenot, M., and Mauguiere, F. 2002. Representation of pain and somatic sensation in the human insula: a study of responses to direct electrical cortical stimulation. Cereb. Cortex 12, 376–385.

Paxinos, G. (*ed.*) 1995. The Rat Nervous System. Academic Press.

Phillips, M. L., Gregory, L. J., Cullen, S., Coen, S., Ng, V., Andrew, C., Giampietro, V., Bullmore, E., Zelaya, F., Amaro, E., Thompson, D. G., Hobson, A. R., Williams, S. C., Brammer, M., and Aziz, Q. 2003. The effect of negative emotional context on neural and behavioural responses to oesophageal stimulation. Brain 126, 669–684.

Strigo, I. A., Duncan, G. H., Boivin, M., and Bushnell, M. C. 2003. Differentiation of visceral and cutaneous pain in the human brain. J. Neurophysiol. 89, 3294–3303.

Williams, M. A., McGlone, F., Abbott, D. F., and Mattingley, J. B. 2005. Differential amygdala responses to happy and fearful facial expressions depend on selective attention. Neuroimage 24, 417–425.

Xie, Y. F., Wang, J., Huo, F. Q., Jia, H., and Tang, J. S. 2004. Mu but not delta and kappa opioid receptor involvement in ventrolateral orbital cortex opioid-evoked antinociception in formalin test rats. Neuroscience 126, 717–726.

Further Reading

Allen, G. V., Saper, C. B., Hurley, K. M., and Cechetto, D. F. 1991. Organization of visceral and limbic connections in the insular cortex of the rat. J. Comp. Neurol. 311, 1–16.

Altier, N. and Stewart, J. 1998. Dopamine receptor antagonists in the nucleus accumbens attenuate analgesia induced by

ventral tegmental area substance P or morphine and by nucleus accumbens amphetamine. J. Pharmacol. Exp. Ther. 285, 208–215.

Altier, N. and Stewart, J. 1999. The role of dopamine in the nucleus accumbens in analgesia. Life Sci. 65, 2269–2287.

Clasca, F., Llamas, A., and Reinoso-Suarez, F. 1997. Insular cortex and neighboring fields in the cat: a redefinition based on cortical microarchitecture and connections with the thalamus. J. Comp. Neurol. 384, 456–482.

Clasca, F., Llamas, A., and Reinoso-Suarez, F. 2000. Cortical connections of the insular and adjacent parieto-temporal fields in the cat. Cereb.. Cortex 10, 371–399.

Dupont, S., Bouilleret, V., Hasboun, D., Semah, F., and Baulac, M. 2003. Functional anatomy of the insula: new insights from imaging. Surg. Radiol. Anat. 25, 113–119.

Gear, R. W., Aley, K. O., and Levine, J. D. 1999. Pain-induced analgesia mediated by mesolimbic reward circuits. J. Neurosci. 19, 7175–7181.

van Groen, T., Kadish, I., and Wyss, J. M. 1999. Efferent connections of the anteromedial nucleus of the thalamus of the rat. Brain Res. Brain Res. Rev. 30, 1–26.

Hof, P. R., Mufson, E. J., and Morrison, J. H. 1995. Human orbitofrontal cortex: cytoarchitecture and quantitative immunohistochemical parcellation. J. Comp. Neurol. 359, 48–68.

Kawaguchi, Y. and Kondo, S. 2002. Parvalbumin, somatostatin and cholecystokinin as chemical markers for specific GABAergic interneuron types in the rat frontal cortex. J. Neurocytol. 31, 277–287.

Kawaguchi, Y. and Kubota, Y. 1998. Neurochemical features and synaptic connections of large physiologically-identified GABAergic cells in the rat frontal cortex. Neuroscience 85, 677–701.

Kawaguchi, Y. and Shindou, T. 1998. Noradrenergic excitation and inhibition of GABAergic cell types in rat frontal cortex. J. Neurosci. 18, 6963–6976.

Li, Y., Li, J. J., and Yu, L. C. 2002. Anti-nociceptive effect of neuropeptide Y in the nucleus accumbens of rats: an involvement of opioid receptors in the effect. Brain Res. 940, 69–78.

Li, N., Lundeberg, T., and Yu, L. C. 2001. Involvement of CGRP and CGRP1 receptor in nociception in the nucleus accumbens of rats. Brain Res. 901, 161–166.

Margeta-Mitrovic, M., Mitrovic, I., Riley, R. C., Jan, L. Y., and Basbaum, A. I. 1999. Immunohistochemical localization of GABA(B) receptors in the rat central nervous system. J. Comp. Neurol. 405, 299–321.

Meyer, S., Strittmatter, M., Fischer, C., Georg, T., and Schmitz, B. 2004. Lateralization in autonomic dysfunction in ischemic stroke involving the insular cortex. Neuroreport 15, 357–361.

Ray, J. P. and Price, J. L. 1992. The organization of the thalamocortical connections of the mediodorsal thalamic nucleus in the rat, related to the ventral forebrain-prefrontal cortex topography. J. Comp. Neurol. 323, 167–197.

Schmidt, B. L., Tambeli, C. H., Barletta, J., Luo, L., Green, P., Levine, J. D., and Gear, R. W. 2002. Altered nucleus accumbens circuitry mediates pain-induced antinociception in morphine-tolerant rats. J. Neurosci. 22, 6773–6780.

Schmidt, B. L., Tambeli, C. H., Gear, R. W., and Levine, J. D. 2001. Nicotine withdrawal hyperalgesia and opioid-mediated analgesia depend on nicotine receptors in nucleus accumbens. Neuroscience 106, 129–136.

Sengupta, J. N., Snider, A., Su, X., and Gebhart, G. F. 1999. Effects of kappa opioids in the inflamed rat colon. Pain 79, 175–185.

Suhara, T., Yasuno, F., Sudo, Y., Yamamoto, M., Inoue, M., Okubo, Y., and Suzuki, K. 2001. Dopamine D2 receptors in the insular cortex and the personality trait of novelty seeking. Neuroimage 13, 891–895.

Tambeli, C. H., Parada, C. A., Levine, J. D., and Gear, R. W. 2002. Inhibition of tonic spinal glutamatergic activity induces antinociception in the rat. Eur. J. Neurosci. 16, 1547–1553.

5.49 Descending Control Mechanisms

K Ren and R Dubner, University of Maryland, Baltimore, MD, USA

© 2008 Elsevier Inc. All rights reserved.

5.49.1	**Introduction**	724
5.49.2	**Organization of Descending Pathways**	725
5.49.2.1	Key Structures and Pathways	725
5.49.2.1.1	Midbrain PAG matter	725
5.49.2.1.2	PAG–RVM–spinal dorsal horn circuitry	726
5.49.2.1.3	Dorsolateral pontomesencephalic tegmentum	727
5.49.2.1.4	Caudal medulla	728
5.49.2.1.5	Forebrain sites	729
5.49.2.1.6	Summary	730
5.49.2.2	Neurotransmitters	730
5.49.2.2.1	Endogenous opioids and related peptides	730
5.49.2.2.2	Monoamines	732
5.49.2.2.3	Amino acids	734
5.49.2.2.4	Others	735
5.49.2.2.5	Summary	737
5.49.2.3	Neuronal Activity in Descending Pathways	738
5.49.2.3.1	Pain modulatory neurons	738
5.49.2.3.2	Descending influence on dorsal horn neurons	739
5.49.2.4	Multiplicity of Descending Control	740
5.49.3	**Plasticity of Descending Pathways**	740
5.49.3.1	Descending Modulation in Persistent Pain	741
5.49.3.1.1	Responses of descending pathways to injury	741
5.49.3.1.2	Descending inhibition in persistent pain	741
5.49.3.1.3	Descending facilitation in persistent pain	742
5.49.3.1.4	Descending facilitation versus inhibition	743
5.49.3.2	Dynamics of Descending Pain Modulation	743
5.49.3.2.1	Time-dependent shift in descending control	743
5.49.3.2.2	Phenotypic changes in pain modulatory neurons	745
5.49.3.2.3	Involvement of excitatory amino acids and receptors	746
5.49.3.2.4	Molecular mechanisms of activity-dependent plasticity in descending pathways	746
5.49.3.2.5	Changes in sensitivity to opioids	747
5.49.3.2.6	Aging-related alteration in descending pain modulation	747
5.49.3.3	Significance of Altered Descending Modulation in Persistent Pain	747
5.49.4	**Therapeutic Implications: Activating Descending Pathways**	748
5.49.4.1	Electrical Stimulation	748
5.49.4.1.1	Brain stimulation	748
5.49.4.1.2	Spinal cord stimulation	748
5.49.4.1.3	Vagal stimulation	748
5.49.4.1.4	Transcutaneous electrical nerve stimulation	748
5.49.4.2	Pharmacological Approaches	748
5.49.4.2.1	Opioids	748
5.49.4.2.2	Alpha 2 adrenoceptor agonists	749
5.49.4.3	Peripheral Stimulation	749
5.49.4.3.1	Diffuse noxious inhibitory controls	749
5.49.4.3.2	Acupuncture	749
5.49.4.4	Psychological Factors	749

5.49.4.4.1	Stress	749
5.49.4.4.2	Placebo	749
5.49.5	**Concluding Remarks**	749
References		749

5.49.1 Introduction

Pain is a sensory process that reflects the level and intensity of noxious stimulus on one hand but is also closely controlled or modulated by the central nervous system (CNS). In fact, the intensity of the perceived pain is not necessarily proportional to the amount of stimulus under different conditions (Figure 1). Although psychological factors contribute to the variability of pain, the most important underlying mechanisms responsible for the variant pains are the existence of the endogenous pain modulatory systems, in which brainstem descending pathways play a fundamental role (Fields, H. L. and Basbaum, A. I., 1999; Millan, M. J., 2002). These pathways provide the neural mechanisms by which attentional, motivational, and cognitive variables filter ascending sensory information.

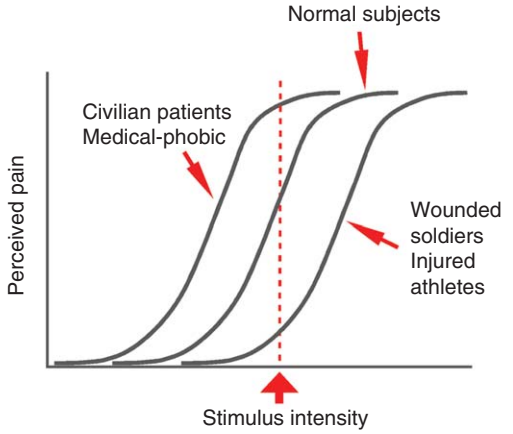

Figure 1 The variant pains. In this illustrative diagram, the intensity of the perceived pain is plotted against the stimulus intensity. The stimulus-response function curve of the normal subjects is located in the middle. For wounded soldiers and injured athletes, the curve may be shifted to the right and for civilian patients and medical-phobic, the curve may be shifted to the left. The shift of the curve is translated as changes in the sensation of pain. At certain stimulus intensity (arrow-dashed line), the civilian population may feel more pain and the wounded soldiers show less pain, when compared to the normal subjects. The endogenous pain modulatory system contributes to the variability of pain under different conditions. Adapted from Cervero, F. and Laird, J. M. 1996. Mechanisms of touch-evoked pain (allodynia): a new model. Pain 68, 13–23.

Our knowledge of the descending pain modulatory systems spans at least four decades. In 1965, Wall and Melzack in their gate control theory of pain questioned the concept of an invariant relationship between stimulus and sensation and a fixed, direct-line connection from the skin to the brain. They proposed that central signals arising from the brain could influence afferent input at the earliest synaptic levels of the somesthetic system, the spinal dorsal horn (Melzack, R. and Wall, P. D., 1965). Evidence supporting the concept was available even earlier when Hagbarth and colleagues (Hagbarth K. E. and Kerr, D. I., 1954; Hernandez-Peon, R. and Hagbarth, K. E., 1955) showed that sensory transmission through spinal cord and trigeminal sensory nuclei was influenced by descending fibers from the cerebral cortex. The gate control hypothesis placed this evidence within the framework of a theory of how pain modulation could account, in part, for the variant relationship between noxious stimuli and the sensations they produced. The first evidence to support endogenous pain control came from the study of Reynolds (Reynolds, D. V., 1969) who demonstrated that focal brain stimulation of the midbrain periaqueductal gray (PAG) produced sufficient analgesia to allow surgery in rats without the use of chemical anesthetics. Liebeskind and colleagues quickly confirmed this finding and concluded that stimulation of the PAG activated a normal function of the brain: pain inhibition (Mayer, D. J. *et al.*, 1971; Mayer, D. J. and Liebeskind, J. C., 1974). Later evidence indicates that pain modulation is not limited to inhibition. Descending pathways also facilitate pain transmission at the spinal level (Ren, K. *et al.*, 2000; Millan, M. J., 2002; Gebhart, G. F., 2004). Most recently, studies have been moved to address the role of pain modulatory circuitry in persistent, or chronic pain conditions. New lines of evidence suggest that the descending pathways exhibit dramatic plasticity and multiplicity and are actively involved in the development of persistent pain after tissue or nerve injury (Porreca, F. *et al.*, 2002; Ren, K. and Dubner, R., 2002; Gebhart, G. F., 2004; Vanegas, H. and Schaible, H.-G., 2004).

5.49.2 Organization of Descending Pathways

There are multiple brain sites and pathways that are involved in descending pain modulation, ranging from the cerebral cortex to caudal medulla (Fields, H. L. and Basbaum, A. I., 1978; 1999; Gebhart, G. F., 1988; Oliveras, J. L. and Besson, J. M., 1988; Sandkuhler, J., 1996; Willis, W. D. and Westlund, K. N., 1997; Millan, M. J., 2002) (Figure 2). To date, the most well characterized endogenous pain modulatory pathway involves a circuitry linking the midbrain PAG, rostral ventromedial medulla (RVM), and the spinal cord. The second important source of descending pain control is from the dorsolateral pontomesencephalic tegmentum (DLPT), which includes the cuneiform nucleus in the midbrain ventrolateral to PAG and locus coeruleus/subcoeruleus (LC/SC) together with other neighboring noradrenaline cell groups (Fields, H. L. and Basbaum, A. I., 1999). In the caudal medulla, ventrolateral medulla (CVLM) including lateral reticular nucleus (LRN), the subnucleus reticularis dorsalis (SRD), and the nucleus tractus solitarius (NTS) have been identified to play a role in descending pain control. Additionally, hypothalamus and other forebrain sites also participate in descending pain modulation.

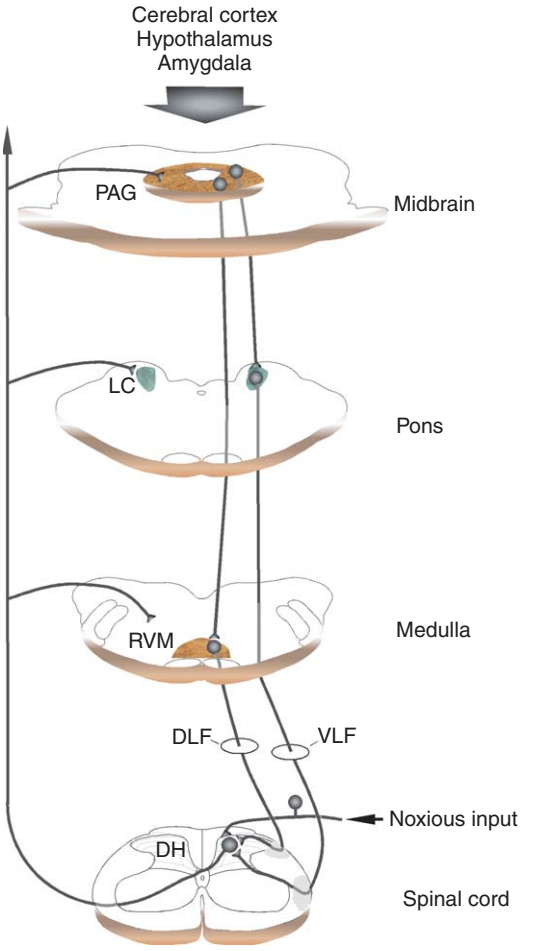

Figure 2 Two major brainstem descending pathways involved in pain modulation. The PAG in the midbrain has efferent projection to the rostral ventromedial medulla (RVM) and locus coeruleus (LC). The RVM and LC directly project to the spinal dorsal horn (DH) where nociceptive input is initially processed. The descending input from the RVM and LC travels in the dorsolateral (DLF) and ventrolateral funiculus (VLF) and modulates spinal pain transmission (only postsynaptic modulation of dorsal horn projection neuron is shown). Supraspinal projecting neurons also issue collaterals to reach pain modulatory structures and the PAG also receives input from forebrain structures including cerebral cortex, hypothalamus, and amygdala. See text for details of other key structures and pathways related to descending pain control. The drawings of brain tissue sections are adapted from Paxinos, G. and Watson, C. 2005. The Rat Brain in Stereotaxic Coordinates, 5th edn. Academic Press.

5.49.2.1 Key Structures and Pathways

5.49.2.1.1 Midbrain PAG matter

PAG neurons are organized in longitudinal columns that function to integrate behavioral responses to noxious and stressful stimuli (Bandler, R. and Shipley, M. T., 1994; Cameron, A. A. *et al.*, 1995a; 1995b). The dorsal raphe nucleus ventromedial to the cerebral aqueduct and the cuneiform nucleus lateral to the ventrolateral PAG are also considered a functional entity with PAG for descending pain control (Jensen, T. S. and Gabhart, G. F., 1988; Fields, H. L. and Basbaum, A. I., 1999). The anatomical studies implicate the importance of the midbrain PAG in descending pain modulation. Ascending fibers from the spinal cord including axons of lamina I neurons terminate in the PAG (Menetrey, D. *et al.*, 1982; Hylden, J. L. K. *et al.*, 1986; Azkue, J. J. *et al.*, 1998). Afferent input from the cerebral cortex, hypothalamus, the cuneiform nucleus, caudal brainstem nuclei such as nucleus raphe magnus (NRM), also enters PAG (Beitz, A. J., 1982b). The PAG provides major input to most areas that are involved in endogenous pain control, including RVM, LC/SC, A5, pontine parabrachial nuclei (PB), NTS, hypothalamus and amygdala (Jensen, T. S. and Gabhart, G. F., 1988; Fields, H. L. and Basbaum, A. I., 1999). The PAG

also is a site for regulation of other homeostatic functions (Gauriau, C. and Bernard, J. F., 2002). For instance, PAG neurons are activated by cardiovascular input (Murphy, A. Z. *et al.*, 1995). Somatovisceral interaction may occur in distinct organized columns of neurons in the PAG.

Animal studies have demonstrated that electrical stimulation of PAG produces profound antinociception, or analgesia (Reynolds, D. V., 1969; Mayer, D. J. *et al.*, 1971, Mayer, D. J. and Liebeskind, J. C., 1974; Fardin, V. *et al.*, 1984a). The stimulation-produced analgesia was not due to a generalized sensory and motor deficit. The animals could move and were responsive to audiovisual stimuli during stimulation, while the responses to noxious stimuli were absent. Stimulation of PAG also selectively inhibits responses of dorsal horn and trigeminal sensory neurons to noxious stimulus (Sessle, B. J. *et al.*, 1981; Dostrovsky, J. O. *et al.*, 1983; Gebhart, G. F., 1988). The stimulus-produced analgesia has been successfully observed in humans with chronic intractable pain. Electrical stimulation of the midbrain periaqueductal and hypothalamus periventricular areas produces long-standing analgesia from very brief periods of stimulation. With implanted electrodes in the brain, some patients can self-stimulate for 10–15 min, two to three times per day for adequate pain control (Kumar, K. *et al.*, 1997). It has been observed in patients who have had failure of the implanted stimulation system, that the actual return of pain to its original pre-stimulation level takes 10 days to 2 weeks (Kumar, K. *et al.*, 1997). This would indicate that activation of the endogenous pain control system has a long-lasting effect.

5.49.2.1.2 PAG–RVM–spinal dorsal horn circuitry

Convergent lines of evidence indicate that PAG stimulation-produced analgesia is relayed through other brainstem nuclei. The RVM has been identified as the premier relay station between the PAG and spinal dorsal horn. The RVM is termed for collective structures that are functionally involved in descending pain modulation, mainly consisting of the midline nucleus raphe magnus (NRM) and the adjacent gigantocellular reticular nucleus, alpha part (GiA). Anatomically, the raphe pallidus nucleus (Rpa) and a portion of the medial lateral paragigantocellular nucleus (LPGi) also are located in this region (Zagon, A., 1995; Paxinos, G. and Watson, C., 2005). Extensive evidence supports the critical involvement of the PAG–RVM–spinal dorsal horn pathway in descending pain control.

In the rat, suppression of NRM neurotransmission by either lesions, local anesthesia, or microinjection of the *N*-methyl-D-aspartate (NMDA) receptor antagonist reverses the spinal inhibition of nocifensive behavior produced by activation of PAG neurons (Behbehani, M. M. and Fields, H. L., 1979; Aimone, L. D. and Gebhart, G. F., 1986). Lidocaine block of the NRM blocks PAG stimulation-produced inhibition of spinal nociceptive neurons in cat (Gebhart, G. F. *et al.*, 1983).

RVM does not receive direct input from the spinal cord, although indirect spinal input can reach RVM through the adjacent Gi (Basbaum, A. I. and Fields, H. L., 1984; Fields, H. L. and Basbaum, A. I., 1999). The major source of input to the RVM is from the PAG and cuneiformis nucleus (Fardin, V. *et al.*, 1984b; Fields, H. L. and Basbaum, A. I., 1999). The ventrolateral cell column of PAG projects to NRM and the dorsolateral PAG region projects to the GiA (Cameron, A. A., *et al.*, 1995b). However, Van Bockstaele E. J. *et al.* (1991) show that injections of tracers into the dorsal PAG resulted in anterograde labeling in the NRM.

Electrical stimulation and microinjection of an opioid receptor agonist into the PAG activate NRM neurons that project to the spinal cord (Behbehani, M. M. and Pomeroy, S. L.,1978; Fields, H. L. and Anderson, S. D., 1978). The excitation of NRM neurons by injection of glutamate into the PAG is associated with an increase in nociceptive response threshold (Behbehani, M. M. and Fields, H. L., 1979).

The RVM has major projections to the spinal cord. Neurons of all subregions of RVM, NRM, GiA, and LPGi send axons to the spinal cord via the dorsolateral funiculus (DLF) (Basbaum, A. I. and Fields, H. L., 1979; 1984). The densest terminal fields of RVM descending fibers are in superficial and deep dorsal horn where nociceptive information is processed.

Activation of RVM neurons produces antinociception. In the cat, electrical stimulation of NRM completely suppresses the behavioral responses to noxious pinch of the skin and modifies the jaw-opening reflex threshold to tooth pulp stimulation (Oliveras, J. L. *et al.*, 1975). Electrical stimulation of NRM or opioid microinjection inhibits activity of dorsal horn nociceptive neurons (Fields, H. L. and Anderson, S. D., 1978; Dickenson, A. H. *et al.*, 1979; Jones, S. L. and Light, A. R., 1990).

The DLF mediates descending modulation of dorsal horn substantia gelatinosa neurons (Cervero, F. *et al.*, 1979). Spinal DLF lesions block antinociception produced by brainstem stimulation (Basbaum, A. I. *et al.*, 1977).

Thus, although studies suggest that some PAG neurons project directly to the spinal cord and spinal trigeminal nucleus (Mantyh, P. W. and Peschanski, M., 1982; Mantyh, P. W., 1983; Skirboll, L. *et al.*, 1983; Li, Y. Q. *et al.*, 1993), the RVM relay is necessary for the analgesic effect of PAG. Whether PAG can modulate dorsal horn sensory transmission through a direct pathway to the spinal cord still needs to be determined.

5.49.2.1.3 Dorsolateral pontomesencephalic tegmentum

In addition to the PAG–RVM–dorsal horn circuitry, the components of the DLPT constitute separate parallel descending pathways responsible for pain modulation (Dubner, R. and Bennett, G. J., 1983; Gebhart, G. F., 1988; Fields, H. L. and Basbaum, A. I., 1999). One member of the DLPT, the cuneiform nucleus, is located in the midbrain lateral reticular formation neighboring ventrolateral PAG and shares anatomical and physiological similarities with PAG related to descending pain modulation. Electrical stimulation of the midbrain lateral reticular formation produces powerful inhibition of dorsal horn nociceptive neurons in cats (Carstens, E. *et al.*, 1980). The other members of the DLPT consist of LC/SC, A7 cell group, PB and Kölliker-Fuse nuclei. The critical role of these pontine noradrenaline cell groups in descending control has been established.

5.49.2.1.3.(i) The PAG–LC/SC–spinal pathway

The LC in the dorsal pontine is the major noradrenergic nucleus originally designated the A6 cell group by Dahlström A. and Fuxe K. (1964). The SC is located immediately ventral to the LC and assigned to the A7 noradrenaline cell group by Westlund K. N. *et al.* (1983). Since the two structures are relatively small and the spinal projecting fibers from the LC are mainly from the ventral part, electrical stimulation will affect both nuclei (Jones, S. L., 1991). The following studies provide evidence that the LC/SC–spinal pathway represents an additional source of descending pain modulation.

The LC/SC neurons project to the spinal cord. Initially, bulbospinal noradrenergic fibers are thought to originate from the A1 cell group in the caudal medulla (Dahlström, A. and Fuxe, K., 1964). Using combined dopamine–beta-hydroxylase immunohistochemistry and retrograde tracing, Westlund K. N. *et al.* (1983) demonstrated that brainstem descending noradrenergic fibers are exclusively from the pontine noradrenergic cell groups. In the rat, the LC and SC provide major descending noradrenergic axons to the spinal cord. These findings form the anatomical basis for a role of the LC/SC in descending control. One concern on the spinal projection of LC/SC neurons is that they apparently terminate most heavily in laminae VII, VIII, and IX of the ventral horn. The termination of LC fibers is moderate in the deep dorsal horn and relatively sparse in the superficial dorsal horn (Clark, F. M. and Proudfit, H. K., 1991). However, there appears to be a substrain difference in LC/SC descending projection related to the commercial sources. More lamina I terminations are from the LC in rats raised in Harlan Sprague-Dawley while the SC of Sasco source provides more lamina I projection (Fritschy, J. M. and Grzanna, R., 1990; Sluka, K. A. and Westlund, K. N., 1992; Willis, W. D. *et al.*, 1995; Proudfit, H. K., 2002).

LC/SC stimulation produces inhibition of dorsal horn nociceptive neurons in rats and cats (Mokha, S. S. *et al.*, 1986; Jones, S. L. and Gebhart, G. F., 1986; Jones, S. L., 1991). Selective spinal lesions indicate that the effect of LC/SC is mediated by the ventrolateral funiculus (VLF) (Jones, S. L., 1991), whereas the NRM stimulation-produced inhibition is conveyed via the DLF (Basbaum, A. I. *et al.*, 1977).

Unlike the PAG, the effect of LC on spinal nociceptive transmission is not mediated through RVM since local anesthesia of NRM does not block LC stimulation-produced inhibition of dorsal horn neurons (Jones, S. L., 1991).

Intrathecal yohimbine, an alpha 2 adrenoceptor antagonist, blocks the LC stimulation-produced inhibition of nociceptive reflex in rats (Gebhart, G. F., 1988).

The LC/SC may also relay the effect of PAG since they receive PAG input. In monkey, dense projection to the LC is identified from the PAG (Mantyh, P. W., 1983). In rat, the dorsolateral PAG cell column innervates LC/SC (Cameron, A. A. *et al.*, 1995b), although another study suggests that PAG does not have major projections to the LC proper (Ennis, M. *et al.*, 1991).

5.49.2.1.3.(ii) Other noradrenaline cell groups in the DLPT participating in descending modulation

5.49.2.1.3.(ii).(a) A7 cell column The A7 cell group spans rostrocaudally the caudal midbrain and

rostral pons in the rat (Paxinos, G. and Watson, C., 2005). The rostral tip of the A7 group can be seen at the same transverse plane as the cuneiform nucleus and PAG. In the pons, the A7 is located medial to the dorsal part of the ventrolateral principal sensory trigeminal nucleus and ventral to the supratrigeminal and Kölliker-Fuse nuclei. The caudal A7 cells end before the appearance of the LC. The A7 cells also provide dense projection to the spinal cord (Westlund, K. N. *et al.*, 1983). This cell group may play a unique role in the descending circuitry. The A7 group has reciprocal connections with RVM and may mediate some effect of RVM on spinal nociceptive transmission (Fields, H. L. and Basbaum, A. I., 1999; Buhler, A. V. *et al.*, 2004).

5.49.2.1.3.(ii).(b) Parabrachial nucleus The PB consists of several distinct subnuclei located in the dorsolateral pons and belongs to the pontine cell groups that give rise to noradrenergic terminals in the spinal cord (Westlund, K. N. *et al.*, 1983). The PB has been demonstrated as an important relay station in pain pathways. Spinal and subnucleus caudalis lamina I nociceptive neurons project to PB (Hylden, J. L. K. *et al.*, 1989; Bester, H. *et al.*, 2000). PAG neurons project to the PB in the rat (Krout, K. E. *et al.*, 1998). The PB has further connections with the amygdala (Bernard, J. F. *et al.*, 1993) and the hypothalamus (Bester, H. *et al.*, 1997), and sends descending projections to the spinal and medullary dorsal horn (Yoshida, A. *et al.*, 1997). The activation of the PB descending pathway modulates spinal and trigeminal nociceptive transmission (Girardot, M. N. *et al.*, 1987; Chiang, C. Y. *et al.*, 1994; Willis, W. D. and Westlund, K. N., 1997).

5.49.2.1.3.(ii).(c) The Kölliker-Fuse nucleus The Kölliker-Fuse nucleus is immediately dorsal to the A7 cell group (Paxinos, G. and Watson, C., 2005) and is the major source of spinopetal noradrenergic fibers in the cat (Stevens, R. T. *et al.*, 1982). The Kölliker-Fuse nucleus is more developed in humans than in other animal species (Lavezzi, A. M. *et al.*, 2004). Young R. F. *et al.* (1992) show that chronic stimulation of the Kölliker-Fuse nucleus region can relieve intractable pain in patients and the effect is comparable to that of PAG/periventricular stimulation.

5.49.2.1.3.(ii).(d) A5 cell column The A5 cell group spans the ventrolateral pontine tegmentum at the mid-pon level to the rostral ventrolateral medulla (RVLM) in the rat. This cell group shares many similarities with other noradrenergic cell groups in the DLPT such as spinal projection (Westlund, K. N. *et al.*, 1983; Clark, F. M. and Proudfit, H. K., 1993) and extensive connections with other pain modulatory nuclei including PAG and CVLM (Cameron, A. A. *et al.*, 1995b; Tavares, I. and Lima, D., 2002). Stimulation of the A5 produces inhibition of the nociceptive tail flick reflex in rats and the effect is mediated through spinal opioid and alpha adrenoceptors (Burnett, A. and Gebhart, G. F., 1991). Since A5 has been primarily considered as an important site for cardiovascular regulation, this cell group may play a role in somatoautonomic integration.

5.49.2.1.4 Caudal medulla

Several structures in the caudal medulla have emerged as important players in endogenous pain control. As these sites overlap with those critical in visceral and cardiovascular functions, the caudal medulla provides a point of convergence to facilitate interactions between somatosensory and autonomic regulation.

5.49.2.1.4.(i) Caudal ventrolateral medulla Anatomically, the CVLM is not a clearly defined structure, the center of which is about 2 mm ventral to the dorsal surface of the medulla and medial to the ventral pole of the spinal trigeminal nucleus in the rat. Rostrocaudally, the CVLM is within the most caudal segment of the medulla starting from approximately 0.5 mm rostral to the calamus scriptorius (Aicher, S. A. *et al.*, 1996). This region is also referred as the lateral reticular formation and includes the A1 catecholamine cell group. The poorly defined ventromedial border of lamina V of the trigeminal subnucleus caudalis may fall into the territory of the CVLM, or vice versa. It has been consistently observed that a variety of noxious stimuli, including noxious heating of the hindpaw, peritoneal inflammation, urinary bladder inflammation, deep muscle irritation or inflammation, all induce Fos protein expression in the CVLM (see Ren, K., 2002).

5.49.2.1.4.(i).(a) Lateral reticular nucleus The LRN is a large nucleus located bilaterally in the ventrolateral medullary reticular formation. It receives input from a variety of structures including PAG and NRM and projects to the spinal cord (Janss, A. J. and Gebhart, G. F., 1987; Lee, H. S. and Mihailoff, G. A., 1999). Electrical or chemical stimulation of the LRN produces inhibition of

the nociceptive reflex and spinal dorsal horn unit responses to noxious stimuli. The LRN-produced descending inhibition is partially mediated by bilateral DLF and spinal alpha 2 adrenergic and serotonin receptors (Janss, A. J. and Gebhart, G. F., 1987; 1988).

5.49.2.1.4.(i).(b) Lateral CVLM The CVLMlat, a small area of the medullary reticular formation between the ventral pole of the spinal trigeminal nucleus and LRN, has recently been proposed to have a major role in descending pain inhibition (Tavares, I. and Lima, D., 2002). The CVLMlat has reciprocal connections with spinal lamina I neurons and output to the A5 cell group and RVM. These indirect spinopetal pathways from the CVLMlat via A5 and RVM may mediate noradrenergic and serotonergic antinociception produced by CVLM activation. Neurons in this region are reciprocally connected to the RVM and activated after orofacial tissue injury (Sugiyo, S. *et al.*, 2005). A group of reticulohypothalamic tract neurons in the CVLM may overlap with the CVLMlat (Malick, A. *et al.*, 2000). Most of these neurons respond to both innocuous and noxious stimulation of the head but only to noxious stimulation of extracephalic regions. Their response properties suggest that they participate in pain modulation.

5.49.2.1.4.(ii) Subnucleus reticularis dorsalis The SRD includes a group of neurons distributed in the dorsal medullary reticular formation medial to the trigeminal subnucleus caudalis (also called medullary reticular nucleus, dorsal part, MdD) (Paxinos, G. and Watson, C., 2005). The SRD contributes to the spinoreticular–thalamic pathway by receiving nociceptive information from the spinal dorsal horn and relays it to the thalamus (Villaneuva, L., *et al.* 1998). The diffuse noxious inhibitory control (DNIC), proposed by Le Bars and colleagues, is mediated via the SRD and independent of the RVM-spinal pathway (Bouhassira, D. *et al.*, 1992; 1993). The SRD is also proposed as a pronociceptive center (Lima, D. and Almeida, A., 2002).

5.49.2.1.4.(iii) Nucleus tractus solitarius The NTS is a key structure in somatovisceral processing, since this nucleus receives somatic and visceral input and has extensive efferent connections with other nuclei (Randich, A. and Maixner, W., 1984; Ren, K. *et al.*, 1990). Notably, PAG neurons project to NTS (Cameron, A. A. *et al.*, 1995b). Activation of NTS neurons produces descending pain inhibition and the vagal afferent modulation of nociception is mediated through NTS (Randich, A. and Gebhart, G. F., 1992). The function of NTS supports somatovisceral and somatoautonomic interactions.

5.49.2.1.5 Forebrain sites

A number of forebrain structures provide descending input to brainstem nuclei, particularly the PAG (Beitz, A. J., 1982b).

5.49.2.1.5.(i) Hypothalamus The subregions of the hypothalamus provide the largest descending input to the PAG (Beitz, A. J., 1982b). The periventricular gray (PVG) of the hypothalamus is the rostral extension of PAG and rich in opioids. Axons of PVG neurons can reach the spinal cord (Jensen, T. S. and Gabhart, G. F., 1988; Van den Pol, A. N. and Collins, W .F., 1994). Stimulation of PVG can produce effective pain relief in patients (Kumar, K. *et al.*, 1997). The lateral hyphthalamus (LH) has reciprocal connections with the PAG and NRM (Aimone, L. D. *et al.*, 1988; Cameron, A. A. *et al.*, 1995a; 1995b). Inhibition of spinal nociceptive transmission from the LH requires a bulbar relay in the NRM (Aimone, L. D. *et al.*, 1988).

5.49.2.1.5.(ii) Amygdala The ascending nociceptive input reaches the amygdala through a relay in the PB (Gauriau, C. and Bernard, J. F., 2002). The amygdala has reciprocal connections with PAG (Rizvi, T. A. *et al.*, 1991). Activation of amygdala neurons produces analgesia that is mediated through PAG (see Fields, H. L. and Basbaum, A. I., 1999). The dorsal PAG interacts with the amygdala to affect fear and anxiety and the amygdala is an important site for interrelating sensory and affective dimensions of pain (Behbehani, M. M., 1995; Price, D. D., 2002).

5.49.2.1.5.(iii) Cerebral cortex Recent brain imaging studies have generated a wealth of information on activation of the cortical areas during pain processing. It also shows that the cerebral cortex is not only the end point of the pain pathway, but also a source of descending input that contributes to the fine-tuning of pain threshold and modulation of the emotional aspect of pain (Jasmin, L. *et al.*, 2003b; Petrovic, P. *et al.*, 2004). One interesting pathway involves the anterior cingulate cortex (ACC) and amygdala in pain modulation. The ACC–amygdala pathway may modulate pain-related stress and aversive responses, as well as pain-related fear memory (Gao, Y. J. *et al.*, 2004; Petrovic, P. *et al.*,

2004; Tang, J. *et al.*, 2005). Transcranial magnetic stimulation of the dorsolateral prefrontal cortex increased human pain tolerance level (Graff-Guerrero, A. *et al.*, 2005).

5.49.2.1.6 Summary

It is clear from the above overview that the pivotal anatomical substrates for descending pain control are located within the brainstem. In addition to the midbrain PAG, a number of important sites are in the medulla. The medulla oblongata is classically termed the vital center for life with its critical involvement in cardiovascular and respiratory controls. Since pain is arguably one of the most important body functions for survival, it is not surprising that the structures that are vital for pain modulation are also located in the medulla to facilitate interactions between somatosensory and autonomic regulation. The interplay of the descending system with visceral (NTS-PB), cardiovascular (CVLM, A5, PAG), respiratory (Kölliker-Fuse nucleus), micturation (RVM, pons), arousal (A6), and emotional (amygdala, ACC) regulation is extensive and serves to enhance survival (Randich, A. and Maixner, W., 1984; Randich, A. and Gebhart, G. F., 1992; Murphy, A. Z. *et al.*, 1995; Mason, P., 2001).

5.49.2.2 Neurotransmitters

A plethora of transmitters (also see Chapter Pharmacological Modulation of Pain) have been shown to be involved in descending pain control (Duggan, A. W., 1985; Fields, H. L. *et al.*, 1991; Millan M. J., 2002). The most studied and established candidates include endogenous opioid peptides, noradrenaline, and serotonin (5-HT). All these transmitters participate in inhibition and facilitation of pain transmission through their respective receptor subtypes. The major neurotransmitters that are implicated in descending pain control are briefly discussed below.

5.49.2.2.1 Endogenous opioids and related peptides

5.49.2.2.1.(i) Opioid peptides

Tsou K. and Jang C. S. (1964) discovered that the most sensitive sites for the analgesic action of morphine were located in the PAG and the adjacent hypothalamic periventricular area. These early findings suggested that opiate drugs like morphine acted by binding to a receptor in the brain and that there likely were endogenous ligands or chemical mediators whose actions were mimicked by opiates. Opiate binding sites in the brain were subsequently demonstrated in early 1970s by radioligand binding assays (Pert, C. B. and Snyder, S. H., 1973; Simon, E. J. *et al.*, 1973; Terenius, L., 1973) and the first endogenous opioid peptides enkephalins were identified soon after (Hughes, J. *et al.*, 1975). To date, four classes of opioid peptides have been found in the brain: endorphins, enkephalins, dynorphins, and endomorphins (Hughes, J. *et al.*, 1975; Li, C. H. and Chung, D., 1976; Goldstein, A. *et al.*, 1979; Zadina, J. E. *et al.*, 1997). Martin W. R. *et al.* (1976) first proposed the existence of three subtypes of opioid receptors based on three different syndromes produced by congeners of morphine. All three opioid receptors, μ (MOP), δ (DOP), and κ (KOP), have now been cloned (Evans, C. J. *et al.*, 1992; Kieffer, B. L. *et al.*, 1992; Chen, Y. *et al.*, 1993; Meng, F. *et al.*, 1993). The endogenous opioid peptides and their respective precursors, amino acid sequence, and preferred receptor subtypes are summarized in Table 1. Recent studies also indicate the existence of alternative splicing (Pan, L. *et al.*, 2005), subtypes of the mu, delta, and kappa receptors (Fowler, C. J. and Fraser, G. L., 1994;

Table 1 Endogenous opioid peptides involved in pain modulation

Precursor	*Name*	*Amino acid sequence*	*Receptor*
POMC (pro-opiomelanocortin)	β-Endorphin	Tyr-Gly-Gly-Phe-Met-Thr-Ser-Glu-(human) Lys-Ser-Gln-Thr-Pro-Leu-Val-Thr-Leu-Phe-Lys-Asn-Ala-Ile-Ile-Lys-Asn-Ala-Tyr-Lys-Lys-Gly-Glu-OH	$\mu \geq \delta$
Proenkephalin	Leu-enkephalin	Tyr-Gly-Gly-Phe-Leu-OH	$\delta \geq \mu$
Proenkephalin	Met-enkephalin	Tyr-Gly-Gly-Phe-Met-OH	$\delta \geq \mu$
Prodynorphin	Dynorphin A	Tyr-Gly-Gly-Phe-Leu-Arg-Arg-Ile-Arg-Pro-Lys-Leu-Lys-Trp-Asp-Asn-Gln-OH	κ
Unidenitified	Endomorphin-1	Tyr-Pro-Trp-Phe-NH_2	μ
Unidenitified	Endomorphin-2	Tyr-Pro-Phe-Phe-NH_2	μ

Zaki, P. A. *et al.*, 1996; Pasternak, G. W., 2001), and opioid receptor gene polymorphism (Ikeda, K. *et al.*, 2005). The functional significance of the further molecular diversity of opioid receptor subtypes in descending pain control is poorly understood.

The endogenous opioids and their receptors are distributed in structures involved in descending pain control at all levels including the amygdala, hypothalamus, PAG, DLPT, RVM, and spinal cord (Basbaum, A. I. and Fields, H. L., 1984; Ruda, M. A., 1988; Mansour, A. *et al.*, 1995; Fields, H. L. and Basbaum, A. I., 1999; Wang, H. and Wessendorf, M. W., 2002). Notably, beta-endorphin terminals from hypothalamus descend along the borders of the third ventricle and reach PAG, DLPT, and NRM (Finley, J. C. *et al.*, 1981; Jensen, T. S. and Gabhart, G. F., 1988). Rostral ventromedial medulla neurons express multiple opioid receptor phenotypes (Marinelli, S. *et al.*, 2002). In the RVM, spinally projecting serotonergic and nonserotonergic neurons express mu- and delta-opioid receptor mRNAs (Wang, H. and Wessendorf, M. W., 1999). Enkephalinergic axons in the spinal cord synapse with thalamic projection neurons (Ruda, M. A., 1982), providing postsynaptic modulation of ascending nociceptive information.

Microinjection of morphine into the PAG produces behavioral analgesia (Camarata, P. J. and Yaksh, T. L., 1985). Brain stimulation-produced analgesia can be reversed by naloxone, an opioid receptor antagonist (Akil, H. *et al.*, 1976). Behavioral analgesia produced by an opioid receptor agonist is related to the inhibition of spinal nociceptive neurons (Yaksh, T. L., 1978). However, the effect of opioid agonists on dorsal horn nociceptive neurons is more variable and can be both inhibitory and facilitatory (Gebhart, G. F., 1982; Stamford, J. A., 1995). This paradox is likely related to the sampling limitation during single unit recording and cautions on predicting behavioral outcome from activity of single neurons. Using Fos immunoreactivity to study a population of activated neurons simultaneously, opioids produce behavioral analgesia that is correlated to an inhibition of dorsal horn neuronal activation as indicated by a reduction of noxious stimulus-induced Fos immunoreactivity (Gogas, K. R. *et al.*, 1991). Is the endogenoous opioid system tonically active? The findings from opioid receptor knockout mice suggest a low endogenous opioid tone with each receptor subtype contributing differentially to the modulation of transient pain (Matthes, H. W. *et al.*, 1996; Sora, I. *et al.*, 1997; Gaveriaux-Ruff, C. and Kieffer, B. L., 2002).

Although there is no question that opioids produce potent pain inhibition through their respective receptors at all levels of the descending circuitry, the role of spinopetal opioidergic fibers in mediating descending modulation from supraspinal sites has yet to be convincingly demonstrated. Intrathecal administration of the opioid receptor antagonists in rats has been shown to reverse or attenuate analgesia produced by intracerebroventricular morphine (Gogas, K. R. *et al.*, 1996), intra-PAG injection of beta-endorphin (Tseng, L. F. and Tang, R., 1990), electrical stimulation of the RVM (Zorman, G. *et al.*, 1982; Lu, Y. *et al.*, 2004), or the hypothalamic arcuate nucleus (Wang, Q. *et al.*, 1990). However, the contribution of intrinsic opioidergic interneurons in the spinal dorsal horn to supraspinal-produced analgesia cannot be ruled out. In the cat, opioid peptides intrinsic to the spinal cord play a major role in inhibition of spinal nociceptive transmission (Duggan, A. W., 1985).

5.49.2.2.1.(ii) Orphanin FQ, nocistatin, and neuropeptideFF Orphanin FQ, or nociceptin, is a heptadecapeptide that was identified as the endogenous ligand for the orphan-opioid-receptor-like 1 (ORL-1, now nociceptin/orphanin FQ peptide receptor, NOP) receptor (Meunier, J. C. *et al.*, 1995; Reinscheid, R. K. *et al.*, 1995). Genetically, Orphanin FQ and NOP belong to the same family with the opioids and their receptors and they share homology with dynorphin A and the kappa opioid receptor, respectively. However, orphanin FQ does not interact with three classical opioid receptors, largely due to the replacement of the first tyrosine residue by phenylalanine. Most studies show that orphanin FQ produces analgesia at the spinal level and both pro- and anti-nociception supraspinally (Meunier, J. C., 1997; Henderson, G. and McKnight, A. T., 1997). However, intrathecal low dose of orphanin FQ also produces allodynia (Yamamoto, T. *et al.*, 1999). Orphanin FQ can suppress both pain facilitatory and inhibitory neurons in the RVM, which may explain its dual effects on pain processing under different conditions (Pan, Z. Z. *et al.*, 2000; Vaughan, C. W. *et al.*, 2001; Heinricher, M. M., 2005).

Nocistatin is liberated from the same orphanin FQ precursor protein, proorphanin, after posttranslational cleavage but binds to a receptor distinct from NOP (Okuda-Ashitaka, E. *et al.*, 1998). Nocistatin opposes action of orphanin FQ, and can be considered a functional antagonist of orphanin FQ

(Yamamoto, T. *et al.*, 1999; Millan, M. J., 2002). Proorphanin also yields another heptadecapeptide, orphanin FQ2, which may participate in pain inhibition (Rossi, G. C. *et al.*, 1998).

The octapeptide neuropeptideFF (NPFF, Phe-Leu-Phe-Gln-Pro-Gln-Arg-Phe-NH_2) is originally isolated from the bovine brain and found to possess anti-morphine property (Yang, H. Y. *et al.*, 1985). NPFF fibers project to the PAG from hypothalamus and to the RVM from the NTS (Aarnisalo, A. A. and Panula, P., 1995). In the spinal cord, NPFF-immunoreactive cell bodies and terminals are localized to laminae I–IV and X and DLF, but a supraspinal origin of NPFF was not found (Kivipelto, L. and Panula, P., 1991). Available evidence indicates that NPFF produces antinociception at the spinal level and pronociception (anti-opioid) at the supraspinal level (Millan, M. J., 2002; Mollereau, C. *et al.*, 2005).

5.49.2.2.2 Monoamines

It is now well established that descending monoaminergic fibers mediate descending modulation from the supraspinal sites (Yaksh, T. L., 1979; Basbaum, A. I. and Fields, H. L., 1984; Gebhart, G. F., 1988; Tjolsen, A. *et al.*, 1991; Hung, K. C. *et al.*, 2003). The major pathways involve noradrenergic fibers from the DLPT and serotonergic fibers from the NRM, the major nucleus of RVM. The two pathways can be co-activated and may act synergistically to participate in descending pain modulation (Gebhart, G. F., 1988; Sawynok, J., 1989; Danzebrink, R. M. and Gebhart, G. F., 1991).

5.49.2.2.2.(i) Noradrenaline Intrathecal administration of the alpha 2-adrenoceptor antagonist yohimbine, but not the nonselective opioid receptor antagonist naloxone and alpha 1 adrenoceptor antagonist prazosin, attenuates descending inhibition of nocifensive tail flick reflex produced by focal stimulation of the LC/SC region (Jones, S. L., 1991). The PAG-produced inhibition of dorsal horn neurons is reduced by microdialysis of alpha 2 adrenoceptor antagonists idazoxan and yohimbine into the dorsal horn (Peng, Y. B. *et al.*, 1996). Selective depletion of spinal noradrenaline by intrathecal DSP4 attenuates morphine analgesia (Zhong, F. X. *et al.*, 1985). These results clearly indicate a role of spinopetal noradrenergic fibers in descending modulation since there are no noradrenaline-producing cell bodies in the spinal cord (Swanson, L. W. and Hartman, B. K., 1975). Consistently, depletion of spinal NA by 6-hydroxydopamine decreases and intrathecal NA elevates the nociceptive threshold (Reddy, S. V. *et al.*, 1980). Opioid analgesia is enhanced in norepinephrine transporter knockout mice and the effect is blocked by yohimbine (Bohn, L. M. *et al.*, 2000). Intrathecal administration of the adrenoceptor antagonists produces a decrease in nociceptive threshold in the rat, suggesting that the descending noradrenergic system is tonically active (Sagen, J. and Proudfit, H. K., 1984). The antinociceptive effect of NA in the spinal cord does not appear to require GABAergic, glycinergic, opioidergic, and serotonergic activity (Reddy, S. V. *et al.*, 1980), and may involve both pre- and postsynaptic mechanisms (Sonohata, M. *et al.*, 2004). *In vivo* whole-cell patch-clamp recordings from rat substantia gelatinosa neurons show that NA reduces EPSC and suppresses action potentials evoked by a noxious stimulus, an effect that is blocked by antagonism of alpha 2, but not alpha 1, adrenoceptors (Sonohata, M. *et al.*, 2004).

Studies using transgenic mice, such as D79N mice with a point mutation of the alpha 2A adrenoceptors, have examined the subtypes of spinal alpha 2 adrenoceptors involved in descending inhibition. Most studies support a role for the alpha 2A subtype in spinal analgesia (Hunter, J. C. *et al.*, 1997; Lakhlani, P. P. *et al.*, 1997; Stone, L. S. *et al.*, 1997; Kingery, W. S. *et al.*, 2000; Malmberg, A. B. *et al.*, 2001; Mansikka, H. *et al.*, 2004; Ozdogan, U. K. *et al.*, 2004). However, alpha 2C adrenoceptor-bearing terminals synapse with NK-1 projection cells in the rat dorsal horn (Olave, M. J. and Maxwell, D. J., 2003), suggesting a role in postsynaptic modulation. The alpha 2C adrenoceptors have been shown to be involved in spinal analgesia and adrenergic–opioid synergy (Fairbanks, C. A. *et al.*, 2002; Lahdesmaki, J. *et al.*, 2003). The alpha 2B adrenoceptors may play an important role in the pontine noradrenergic nuclei involved in analgesic action of nitrous oxide (Sawamura, S. *et al.*, 2000).

After peripheral nerve injury, there is a decrease in alpha 2A mRNA and protein immunoreactivity in the spinal cord of the rat (Stone, L. S. *et al.*, 1999; Leiphart, J. W. *et al.*, 2003); these findings suggesting a reduced noradrenergic transmission in these rats. However, there is also an increased descending noradrenergic innervation to the spinal dorsal horn after nerve injury, possibly serving to enhance inhibition (Ma, W. and Eisenach, J. C., 2003). Interestingly, pain hypersensitivity after nerve injury develops similarly in the wild-type mice and those with mutation of alpha 2A, 2B, or 2C adrenoceptors, suggesting that

the net inhibitory tone is not affected by loss of alpha 2 adrenoceptors (Malmberg, A. B. *et al.*, 2001). It is worth noting that, different from previous observations in normal rats (Sagen, J. and Proudfit, H. K., 1984), the baseline nociceptive threshold is not affected in mice with mutation of either of the three alpha 2 subtypes (Malmberg, A. B. *et al.*, 2001), suggesting that compensatory mechanisms may have developed in the mutant mice to balance the loss of tonic noradrenergic inhibition.

In contrast to a predominant inhibitory role of the alpha 2 adrenoceptors, the alpha 1 adrenoceptor may be involved in descending pain facilitation (Holden, J. E. *et al.*, 1999; Nuseir, K. and Proudfit, H. K., 2000; Hedo, G. and Lopez-Garcia, J. A., 2001; Holden, J. E. and Naleway, E., 2001) and supraspinal pronociceptive action (Kingery, W. S. *et al.*, 2002). Intracellular recordings from adult rat spinal slice support the opposing actions of NA on substantia gelatinosa neurons. Noradrenaline induces hyperpolarization or increased spontaneous excitatory postsynaptic potentials in subpopulations of dorsal horn neurons, which is selectively blocked by alpha 2 (yohimbine) and alpha 1 (prazosin) adrenoceptor antagonists, respectively (North, R. A. and Yoshimura, M., 1984).

5.49.2.2.2.(ii) Serotonin There is dense serotonergic innervation in the spinal dorsal horn (Ruda, M. A. *et al.*, 1982; Ruda, M. A., 1988), which is almost exclusively derived from supraspinal sources (LaMotte, C. C., 1988; Fields, H. L. *et al.*, 1991; Mason, P., 2001; Millan, M. J., 2002). The NRM is the major structure that issues descending serotonergic fibers to the spinal cord (Bowker, R. M. *et al.*, 1988), although not all descending axons from the NRM are serotonergic (Jones, S. L. and Light, A. R., 1992; Wang, H. and Wessendorf, M. W., 1999). Descending inhibition produced by focal electrical stimulation in the PAG or NRM is mediated in part by descending serotonergic pathways acting on spinal serotonergic receptors. Microinjection of morphine into the PAG and stimulation of NRM evokes the release of serotonin from spinal cord (Yaksh, T. L. and Tyce, G. M., 1979; Rivot, J. P. *et al.*, 1982). Intrathecal methysergide, a nonselective 5-HT receptor antagonist, increases the intensity of stimulation in the PAG and the NRM for inhibition of the nocifensive tail flick reflex while naloxone has no effect (Gebhart, G. F., 1988). The role of the descending serotonergic pathway in descending pain inhibition is well established (Fields, H. L. and Basbaum, A. I., 1978; Basbaum, A. I. and Fields, H. L., 1984).

It has become clear that descending serotonergic fibers also participate in facilitation of nociception (Zhuo, M. and Gebhart, G. F., 1991; Millan, M. J., 2002; Suzuki, R. *et al.*, 2002b; 2004b) The nociceptive facilitation triggered by low intensity vagal afferent stimulation involves descending serotonergic pathways (Ren, K. *et al.*, 1991). Although spinal application of 5-HT generally produces an analgesic effect, excitation of dorsal horn neurons by serotonergic agonists is also reported (Todd, A. J. and Millar, J., 1984; Zhang, Y. *et al.*, 2001). In the spinal slice preparation, serotonin can recruit silent glutamatergic synapses in the superficial dorsal horn and enhance synaptic transmission (Li, P. and Zhuo, M., 1998). This result supports a facilitatory role of descending serotonergic fibers in spinal plasticity in response to injury. Indeed, intrathecal administration of methysergide has been shown to attenuate neuropathic pain in the rat (Pertovaara, A. *et al.*, 2001). In carrageenan-inflamed rats, the facilitation of dorsal horn neuronal responses to noxious stimuli by agonists of 5-HT_{1A} and 5-HT_{1B} receptors is further enhanced (Zhang, Y. *et al.*, 2001). Blockade of spinal 5-HT_3 receptors reduces tissue injury-induced persistent pain (Zeitz, K. P. *et al.*, 2002).

At least 12 different subtypes of 5-HT receptors may be involved in pain modulation (Hoyer, D. *et al.*, 1994; Millan, M. J., 2002). However, their roles in descending pain control have only been evaluated in a few subtypes including 5-HT_{1A}, 5-HT_{1B}, 5-HT_{2A}, 5-HT_3, and 5-HT_4 receptors (Millan, M. J., 2002). Recent studies have identified a pronociceptive role of the 5-HT_3 subtype (Suzuki, R. *et al.*, 2002b; Zeitz, K. P. *et al.*, 2002). A number of studies have indicated a facilitatory role of the 5-HT_{1A} receptor while others pointed to an opposite effect (Millan, M. J., 2002). The equivocal literature on the role of 5-HT receptors in pain modulation suggests sophisticated differential involvement of the 5-HT receptor subtypes in pain modulation and transmission. Moreover, different experimental conditions including the chosen endpoints, stimulation modality, anesthetic state, and *in vivo* versus *in vitro* preparations are also confounding factors.

Despite a well-documented contribution of the descending serotonergic pathway to pain modulation, the specific role of RVM serotonergic neurons in the operation of descending circuitry is not understood. Stimulation of the PAG that produces analgesia does not excite RVM serotonergic neurons (Gao, K. *et al.*, 1997). Thus, these cells may not mediate the signal from PAG, at least not directly.

Stimulation of NRM that induces antinociception does not release 5-HT in the spinal cord, although further increasing the stimulation intensity results in 5-HT release (Sorkin, L. S. *et al.*, 1993). These results are consistent with earlier findings that both serotonergic and nonserotonergic pathways contribute to descending inhibition (Rivot, J. P. *et al.*, 1980). Careful analysis of the characteristics of RVM serotonergic neurons revealed that their levels of activity depend on the conscious state (Mason, P., 2001). Serotonergic cells exhibit the highest level of discharge during waking when nociceptive threshold is relatively high compared to the sleep state. One hypothesis is that the descending serotonergic modulation of pain transmission is state dependent and closely related to alterations in serotonergic tone.

5.49.2.2.2.(iii) Dopamine Similar to noradrenaline and serotonin, spinal dopamine is virtually exclusively of supraspinal origin, mainly from the hypothalamus (see Millan, M. J., 2002). The dopamine receptor consists of D_1 and D_2 subtypes and they both have been localized in the spinal cord including the dorsal horn. The D_1 receptor may support opioid analgesia from PAG activation (Flores, J. A. *et al.*, 2004) and the activity of the D_2 subtype may oppose opioid analgesia (King, M. A. *et al.*, 2001). The contribution of the descending dopaminergic pathway to modulation of spinal nociceptive transmission remains to be determined.

5.49.2.2.3 Amino acids

Excitatory and inhibitory amino acid neurotransmitters are widely distributed in the pain modulatory circuitry including the PAG, DLPT, RVM, and spinal cord. They clearly participate in the process of descending pain control through actions on their respective receptors.

5.49.2.2.3.(i) Glutamate Activation of supraspinal glutamate synapses is associated with antinociception. Glutamate-containing neurons are observed in the PAG of the cat (Barbaresi, P. *et al.*, 1997). Stimulation-produced analgesia from the PAG is mediated by excitatory amino acid receptors in the RVM (Aimone, L. D. and Gebhart, G. F., 1986; van Praag, H. and Frenk, H., 1990; Spinella, M. *et al.*, 1996). Stimulation of the cuneiform nucleus excites about 50% of NRM neurons, an effect blocked by an excitatory amino acid antagonist (Richter, R. C. and Behbehani, M. M., 1991). However, microinjection of glutamate into the discrete brainstem sites including some sites in the PAG can also induce pain-like behavior via activation of NMDA receptors (Jensen, T. S. and Yaksh, T. L., 1992). Thus, the glutamatergic transmission within the pain modulatory circuitry is also capable of bidirectional pain modulation.

Glutamate receptors consist of ionotropic and metabotropic (mGluR) subfamilies. The former includes NMDA, alpha-amino-3-hydroxy-5-methyl-4-isoxazole propionic acid (AMPA), and kainate (KA) receptor subtypes, and the eight subtypes of metabotropic glutamate receptors (mGluR's) are subdivided into three groups. Studies on the role of specific glutamate subtypes in descending pain control are still in the preliminary stage. In the PAG, group I mGluR may be involved in pain inhibition involving an interaction with NMDA receptors (Maione, S. *et al.*, 1998; Berrino, L. *et al.*, 2001). In the RVM, activation of group II mGluR produces descending inhibition of the nociceptive tail flick reflex (Kim, S. J. *et al.*, 2002). Activation of AMPA and NMDA receptors contributes to plasticity in the RVM in response to tissue injury (Urban, M. O. and Gebhart, G. F., 1999; Ren, K. and Dubner, R., 2002).

Unlike noradrenaline and serotonin, primary afferent fibers are rich in glutamate (Battaglia, G. and Rustioni, A., 1988). At the spinal level, glutamate receptors play a major role in the development of persistent pain. It is difficult to isolate the effect of descending glutamatergic input from that of primary afferent origin. Limited information is available on the anatomy of descending glutamatergic pathways. One study shows that descending pathways from the DLPT nuclei contain glutamatergic fibers (Liu, R. H. *et al.*, 1995). However, whether they contribute to descending pain modulation is unclear.

5.49.2.2.3.(ii) Gamma-aminobutyric acid and glycine In general, gamma-aminobutyric acid (GABA) and glycine are used by inhibitory interneurons. In the PAG, GABAergic terminals are abundant (Reichling, D. B. and Basbaum, A. I., 1990). Blocking GABA receptors in the ventral PAG enhances morphine-produced analgesia in this region, consistent with the view that GABAergic neurons inhibit PAG output neurons involved in descending inhibition (Depaulis, A. *et al.*, 1987). GABAergic terminals from the PAG descend to the RVM (Reichling, D. B. and Basbaum, A. I., 1990).

RVM GABA-containing neurons and GABAergic terminals of PAG neurons both synapse with spinally projecting RVM neurons (Cho, H. J. and Basbaum, A. I., 1991). Inhibition of GABAergic transmission in the RVM leads to disinhibition of pain inhibitory activity. Apparently, the GABA system may set up the tone of descending inhibition and help to maintain an adequate level of pain sensitivity, which is essential to normal body function. Direct GABAergic innervation of the spinal dorsal horn by fibers descending from the RVM has been described (Antal, M. *et al.*, 1996). However, confounded by the presence of abundant intrinsic GABAergic neurons in the spinal cord, the role of descending GABAergic fibers in descending control is unclear.

Alterations of GABAergic activity may result in either an increase or decrease in pain sensitivity. In the insular cortex of the rat, increasing and decreasing GABA transmission produces analgesia and hyperalgesia, respectively (Jasmin, L. *et al.*, 2003b). Thus, GABAergic activity in this region appears to facilitate cortical output related to descending inhibition, which is in contrast to PAG and RVM. In the RVM, the $GABA_B$ agonist baclofen produces antinociception at low dose (0.1–1.0 ng) and hyperalgesia at high dose (30–150 ng) (Thomas, D. A. *et al.*, 1995; Hammond, D. L. *et al.*, 1998). Intrathecal methysergide antagonizes the baclofen-produced antinociception, suggesting that analgesia is related to disinhibition of bulbospinal serotonergic neurons (Hammond, D. L. *et al.*, 1998). GABAergic neurons in the DLPT also exert bidirectional pain modulation by providing tonic inhibition of two populations of noradrenergic neurons in the A7 group (Nuseir, K. and Proudfit, H. K., 2000).

Stimulation of the PAG and NRM results in release of glycine in the spinal dorsal horn and inhibition of nociceptive neuronal activity (Sorkin, L. S. *et al.*, 1993; Cui, M. *et al.*, 1999). Iontophoresis of glycine and GABA receptor agonists suppresses responses of primate spinothalamic tract neurons to noxious stimuli (Lin, Q. *et al.*, 1999). Clearly, disinhibition of glycinergic and GABAergic neurotransmission constitutes a mechanism of central sensitization and persistent pain (Cronin, J. N. *et al.*, 2004; Zeilhofer, H. U., 2005), although to what extent the descending control intervenes in this process needs to be specifically addressed. Glycine may contribute to the development of hyperalgesia via an intriguing way. As a required co-agonist for NMDA receptor activation, glycine released from inhibitory interneurons in the superficial dorsal horn can escape the synaptic cleft and access and facilitate nearby NMDA receptors through spillover (Ahmadi, S. *et al.*, 2003).

5.49.2.2.4 Others

A number of additional neurotransmitters also participate in descending pain control, although their roles are studied less extensively and a large portion of the study has focused on the different segmental levels. Some key observations are discussed below.

5.49.2.2.4.(i) Cannabinoids Endocannabinoids (endogenous marijuana-like compounds) include anandamide and 2-arachidonylglycerol, which act on two subclasses of cannabinoid receptors, CB_1 and CB_2 (Cravatt, B. F. and Lichtman, A. H., 2004; Hohmann, A. G. *et al.*, 2005). The CB1 receptors are localized in the CNS including important structures of descending pain control (Tsou, K. *et al.*, 1998). Endogenous cannabinoids produce analgesia via mechanisms apparently different from those of endogenous opioids, although they may act in similar neural circuitry involving the PAG and RVM (Walker, J. M. and Huang, S. M., 2002). Stress induces endocannabinoids in the PAG associated with analgesia that can be reversed by CB1 receptor blockade in the region (Hohmann, A. G. *et al.*, 2005). In CB_1-mutant mice, the stress-induced analgesia is selectively affected, leaving the opioid analgesia unaffected (Valverde, O. *et al.*, 2000). The analgesic effect of cannabinoids requires the RVM circuitry and cannabinoids modulate activity of RVM pain modulating neurons (Meng, I. D. *et al.*, 1998). Although generally considered to be localized peripherally, increasing evidence indicates that the CB_2 receptor in the spinal cord plays a role in the persistent pain process (Zhang, J. *et al.*, 2003).

5.49.2.2.4.(ii) Brain-derived neurotrophic factor In the adult mammalian brain, brain-derived neurotrophic factor (BDNF) facilitates excitatory synaptic transmission and long-term synaptic plasticity. Studies have shown that exogenously applied BDNF into the PAG produces analgesia in rats (Siuciak, J. A. *et al.*, 1995; Frank, L. *et al.*, 1997). Overexpression of BDNF in the spinal cord alleviates neuropathic pain (Cejas, P. J. *et al.*, 2000; Eaton, M. J. *et al.*, 2002). The analgesic effect of exogenous BDNF may be attributed to a downregulation of TrkB after a large dose of the BDNF treatment (Frank, L. *et al.*, 1997; Chen, H. and Weber, A. J., 2004). If BDNF is microinjected into the RVM at a dose within the

physiological range (10–100 fmol), pain facilitation occurs (Guo, W. *et al.*, 2006). BDNF-containing neurons in the PAG project to and release BDNF in the RVM. Intra-RVM sequestration of BDNF by TrkB–IgG fusion protein or anti-BDNF antibody and knockdown of TrkB by RNAi attenuates pain after inflammation (Guo, W. *et al.*, 2006). The effect of BDNF in the RVM is dependent on the activation of NMDA receptors. BDNF induces tyrosine phosphorylation of the NMDA receptor NR2A subunit via a signal transduction cascade that involves IP3, PKC, and Src (Guo, W. *et al.*, 2006). Thus, supraspinal BDNF–TrkB signaling contributes to net descending pain facilitation through a mechanism involving NMDA receptor activity.

5.49.2.2.4.(iii) Substance P Although substance P is a major neurotransmitter released from primary afferents at the spinal level, it is also widely distributed in supraspinal structures involved in descending pain control (Beitz, A. J., 1982a). A group of PAG neurons containing both substance P and cholecystokinin (CCK) projects to the spinal cord (Skirboll, L. *et al.*, 1983). However, the function of this descending pathway is unclear. A significant population of PAG neurons possesses neurokinin 1 (NK1) receptors, the primary binding site for substance P, and many NK1-positive PAG neurons also contain glutamate and to a lesser extent, enkephalin (Commons, K. G. and Valentino, R. J., 2002). This raises the possibility that activation of NK1 in the PAG may be upstream to glutamatergic activation and affect activity of the descending circuitry. Both pro- and antinociceptive properties have been attributed to the NK1 receptor. Holden J. E. *et al.* (2002) show that antinociception from lateral hypothalamic stimulation is mediated by NK1 receptors in the A7 cell group in rats. Suzuki R. *et al.* (2002b) demonstrate that excitation of spinal NK1-bearing projection neurons results in input to the RVM, which triggers descending pain facilitation.

5.49.2.2.4.(iv) Neurotensin Microdialysis of morphine into the ventromedial PAG induces neurotensin release (Stiller, C. O. *et al.*, 1997). The neurotensinergic input from the PAG to the RVM has been described (Beitz, A. J., 1982c). Neurotensin is involved in bidirectional descending modulation from the RVM. Microinjection of low dose (30 fmol) of neurotensin into the RVM produces hyperalgesia and facilitation of dorsal horn neuronal responses to noxious stimuli and high doses of neurotensin (0.3–3 nmol) produces antinociception (Urban, M. O. *et al.*, 1996; Urban, M. O. and Gebhart, G. F., 1997). Activation of the NT_1 receptor on spinally projecting serotonergic neurons in the RVM produces antinociception through release of serotonin in the spinal dorsal horn (Buhler, A. V. *et al.*, 2005).

5.49.2.2.4.(v) Cholecystokinin Dense immunoreactive cholecystokinin (CCK) terminals are localized to PAG and RVM neurons (Skinner, K. *et al.*, 1997). However, CCK-containing neurons in the PAG do not appear to project to the NRM (Beitz, A. J. *et al.*, 1983). Most studies agree that CCK acts as an anti-opioid peptide through CCK_2 (CCK_B) receptors (Han, J. S., 1995; Fields, H. L. and Basbaum, A. I., 1999; Veraksits, A. *et al.*, 2003). Cholecystokinin in the RVM mediates opioid-induced hyperalgesia and antinociceptive tolerance (Xie, J. Y. *et al.*, 2005). Intra-RVM pretreatment with a selective CCK_2, but not CCK_1 (CCK_A), receptor antagonist significantly potentiates the antihyperalgesic effect of morphine in a model of visceral nociception (Friedrich, A. E. and Gebhart, G. F., 2003). Supraspinal CCK may drive tonic descending facilitation mechanisms to maintain neuropathic pain in the rat (Kovelowski, C. J. *et al.*, 2000). The cellular mechanisms of the pronociceptive and anti-opioid actions of CCK involve an action on pain modulatory neurons in the RVM (Heinricher, M. M. *et al.*, 2001; Heinricher, M. M. and Neubert, M. J., 2004).

5.49.2.2.4.(vi) Acetylcholine The DLPT nuclei and RVM regions have been found to send descending cholinergic fibers to the spinal cord (Bowker, R. M. *et al.*, 1983; Jones, B. E. *et al.*, 1986). The cholinergic pedunculopontine tegmental nucleus (PPTg) in the DLPT, immediately ventral to the cuneiform nucleus, has attracted attention. The PPTg is one of the two most sensitive sites for intracranial nicotine-produced antinociception (Iwamoto, E. T., 1991). Neurons in the PPTg are responsive to noxious tail pinch (Carlson, J. D. *et al.*, 2004). Microinjection of nicotine into the NRM, the other sensitive site for the effect of nicotine, produces antinociception (Iwamoto, E. T., 1991). Intra-NRM ABT-594, a cholinergic channel modulator, produces analgesia, presumably through an action on alpha 4-containing nicotinic acetylcholine receptors coexpressed by serotonergic neurons (Bitner, R. S. *et al.*, 1998). The dorsal raphe nucleus is also a potential site for nicotinic analgesia (Cucchiaro, G. *et al.*, 2005). Spinal cholinergic receptors contribute to descending inhibition from the Gi/GiA region, although it is unclear

whether the source of acetylcholine transmitters is supraspinal (Zhuo, M. and Gebhart, G. F., 1990). At the spinal level, acetylcholine tonically modulate serotonergic transmission (Cordero-Erausquin, M. and Changeux, J. P., 2001) and both inhibitory and excitatory neurons are responsive to nicotinic stimulation (Cordero-Erausquin, M. *et al.*, 2004).

5.49.2.2.4.(vii) Histamine Central histamine is mainly derived from the tuberomammilllary nucleus of the hypothalamus and histaminergic terminals are found in the PAG, LC, RVM, and spinal cord (Millan, M. J., 2002). Among four classes of histamine receptors ($H_{1–4}$), $H_{1–3}$ receptors have been localized to the CNS but their roles in descending pain control are unclear. Activation of central H_1 receptor induces behavioral hyperalgesia in mice involving the phospholipase C–protein kinase C pathway (Galeotti, N. *et al.*, 2004). Intracerebroventricular injection of H_3 agonist is hyperalgesic in rodents (Malmberg-Aiello, P. *et al.*, 1994). However, activation of spinal histamine H_3 receptors inhibits mechanical nociception (Cannon, K. E. *et al.*, 2003). It is clear that the effects of histamine-related agents may be mediated through nonhistamine receptors. A histamine-derived compound, improgan, produces analgesia exclusively through the supraspinal circuitry involving PAG and RVM through unknown receptor mechanisms (Hough, L. B. *et al.*, 1997; Nalwalk, J. W. *et al.*, 2004).

5.49.2.2.4.(viii) Prostaglandin Recent observations suggest a role of centrally produced prostaglandins in descending pain modulation. Microinjection of prostaglandin E2 into the medial preoptic region and PAG regulates pain modulatory neurons in the RVM, the effects including activation of ON cells and suppression of OFF cells, and produces thermal hyperalgesia (Heinricher, M. M. *et al.*, 2004a; 2004b). These findings support the emerging view that the CNS glia-inflammatory cytokine network, in association with the cyclooxygenase 2-prostaglandin cascade, is involved in the development of hyperalgesia after tissue and nerve injury (Samad, T. A. *et al.*, 2001; Watkins, L. R. *et al.*, 2003). Such pathways may increase descending facilitation from the RVM circuitry and produce pain and hyperalgesia.

5.49.2.2.4.(ix) Orexins (hypocretin) The novel neuropeptides orexin A and B are selectively synthesized in the lateral and posterior hypothalamus and originally identified as a regulator of feeding behavior (Sakurai, T. *et al.*, 1998). A number of studies have suggested a role of orexin in descending pain modulation. Hypothalamic descending axons containing orexin innervate all levels of the spinal cord including superficial dorsal horn (van den Pol, A. N., 1999). Orexin A-like immunoreactive fibers in the spinal cord are mostly confined to axon terminals containing dense-cored vesicles and mainly forming asymmetric synapses (Guan, J. L. *et al.*, 2003). Initial analysis indicates that orexin-B modulates superficial dorsal horn neurons in the rat spinal cord. Orexin-B increases spontaneous inhibitory postsynaptic currents in the majority of dorsal horn neurons and also produces excitatory effects on a smaller population of dorsal horn neurons (Grudt, T. J. *et al.*, 2002). Orexins produces analgesia through central but not peripheral mechanisms and do not appear to involve the endogenous opioids (Mobarakeh, J. I. *et al.*, 2005). Activation of spinal orexin-A receptor produces antiallodynic effect in the rat with carrageenan-induced inflammation (Yamamoto, T. *et al.*, 2003). In the prepro-orexin (precursor of orexins) knockout mice, the baseline pain threshold is not altered but the knockout mice exhibit enhanced hyperalgesia after inflammation and reduced stress-induced analgesia (Watanabe, S. *et al.*, 2005). These results suggest that hypothalamic orexins and related descending pathways are activated by persistent pain and stress to produce pain inhibition.

5.49.2.2.5 Summary

The bulbospinal noradrenergic and serotonergic pathways are the most established systems with regard to descending pain modulation. The roles of other neurotransmitters and receptors in descending pain control are mainly documented at the segmental levels. The interactions between these transmitters and receptors, including receptor subtypes, are extremely extensive and sophisticated (see Chapter Pharmacological Modulation of Pain) (Millan, M. J., 2002), although their contributions are discussed individually here. A striking feature of the involvement of neurochemicals in descending pain control is that almost every substance has been shown to be involved in both inhibitory and facilitatory pain control, either through actions at the different receptor subtypes, different levels of the neuraxis, or different concentrations; and that the same transmitter may produce opposite modulatory effects at different, or even the same, segmental levels. This factor contributes to some conflicting results in this area and seriously complicates the interpretation of the

findings derived from genetic approaches that involve manipulation of specific receptor(s) at the systemic level.

5.49.2.3 Neuronal Activity in Descending Pathways

5.49.2.3.1 Pain modulatory neurons

By comparing neuronal activity to the occurrence of nociceptive reflexes in lightly anesthetized rats, Fields H. L. *et al.* (1983a) identified three classes of neurons in the RVM. One type of cell typically shows a burst of activity immediately prior to the onset of the tail flick from a noxious thermal stimulus, thus named an ON cell. Another type of cell exhibits a pause in activity just before the tail flick and is called an OFF cell. The activity of the third class of cell, NEUTRAL cell, exhibits no clear relationship to nociceptive reflexes in response to transient stimuli. The firing profiles of ON and OFF cells suggest that they are pain modulatory neurons since their activity is correlated with facilitation and inhibition of nocifensive behaviors, respectively. In fact, both RVM ON and OFF cells project to the spinal cord, particularly laminae I, II, and V of the dorsal horn (Fields, H. L. *et al.*, 1995), and are modulated by PAG stimulation and opioids (Vanegas, H. *et al.*, 1984; Fields, H. L. *et al.*, 1983b; Fields, H. L. *et al.*, 1991). Although less studied, ON and OFF cells are also found elsewhere involved in pain modulation, including the PAG (Heinricher, M. M. *et al.*, 1987), cuneiformis nucleus, PB (Haws, C. M. *et al.*, 1989) and nucleus submedius of the thalamus (Fu, J. J. *et al.*, 2002). It should be clarified that OFF-cell activity may not be solely responsible for suppressing nocifensive withdrawals. In the unanesthetized rat during slow wave sleep, animals are able to execute withdrawal from noxious stimulation when OFF cell continues to fire (Leung, C. G. and Mason, P., 1999). Simultaneous recordings from spinal and RVM neurons show that ON- and OFF-cell firing reflects well input from the spinal dorsal horn, suggesting a role in gating ascending nociceptive information (Hernandez, N. *et al.*, 1989; Hernandez, N. and Vanegas, H., 2001). In addition to regulation of nocifensive responses, ON- and OFF-cell activity may also play a role in integrating cardiovascular, visceral, and somatosensory input (Thurston, C. L. and Randich, A., 1995) and regulating homeostatic functions (Mason, P., 2001).

In vitro recordings from medullary slices identified two distinct cell types in the NRM, primary and secondary cells (Pan, Z. Z. *et al.*, 1990). Primary cells exhibit large GABA-mediated synaptic potentials and are insensitive to opioids, while secondary cells have little or no GABAergic input and are hyperpolarized by opioids. Primary and secondary are likely corresponding to OFF and ON cells, respectively, based on their pharmacological characteristics, such that local iontophoretic of morphine directly inhibits ON cells but does not affect OFF cells (Fields, H. L. and Basbaum, A. I., 1999). Excitatory amino acid transmission is involved in modulating both ON and OFF cell activity (Heinricher, M. M. *et al.*, 1999), which is in line with the evidence that both primary and secondary cell types receive excitatory amino acid input. Models have been proposed to understand the functional significance of neuronal activity within the RVM circuitry. In the disinhibition model, opioids directly inhibit ON cells (corresponding to secondary cells) and release the GABAergic inhibition of OFF cells (corresponding to primary cells), resulting in pain inhibition (Fields, H. L. and Basbaum, A. I., 1999). RVM neurons are also subject to modulation by noradrenergic input (Hammond, D. L. *et al.*, 1980), which mainly originated from the DLPT nuclei (Tanaka, M. *et al.*, 1996; Meng, X. W. *et al.*, 1997). Opposite to the spinal cord, activation of alpha 2 adrenoceptors hyperpolarizes primary cells and attenuates opioid analgesia, and activation of alpha 1 adrenoceptors depolarizes primary cells and enhances analgesia (Bie, B. *et al.*, 2003).

The finding of ON and OFF cells provides a cellular mechanism for bidirectional descending pain control and favors our understanding of variability of pain (Fields, H. L., 1988). It should be emphasized that the descending facilitation parallels inhibition and is an active process. The enhanced nociceptive responsiveness in morphine-dependent rats after treatment with opioid receptor antagonists is accompanied by an increased RVM ON-cell firing (Bederson, J. B. *et al.*, 1990). In spite of a well-documented RVM–spinal serotonergic projection in descending pain control, Gao K. and Mason P. (2000) found that serotonergic RVM cells that respond to noxious tail heat are not ON or OFF cells. The transmitters released by axon terminals of RVM ON and OFF cells in the spinal cord remain to be verified.

Pan Z. Z. *et al.* (1997) show that activation of the kappa-receptor hyperpolarizes primary cells that are disinhibited through the inhibition of secondary cells by mu-opioid receptors. Thus, mu- and kappa-opioid receptors may produce opposing actions on RVM pain modulatory neurons. This kappa effect reverses the analgesic effect of mu-opioids (Bie, B. and Pan, Z. Z.,

2003). Activation of the kappa-opioid receptor in the RVM has also been shown to produce antinociception in a test modality-dependent manner. Microinjection of a kappa-receptor agonist U69593 into the RVM increased withdrawal latency of paw, but not the tail, to noxious thermal stimulus (Ackley, M. A. *et al.*, 2001). The opioid withdrawal-induced hyperalgesia is attenuated by intra-RVM kappa-agonist (Bie, B. and Pan, Z. Z., 2003). The cellular mechanisms of these differential actions of the kappa-opioid on RVM neurons and behavioral nociception are unclear and appear to involve a presynaptic inhibition of glutamatergic input to pain modulatory neurons (Ackley, M. A. *et al.*, 2001; Bie, B. and Pan, Z. Z., 2003) (also see Chapter The Brainstem and Nociceptive Modulation).

5.49.2.3.2 Descending influence on dorsal horn neurons

5.49.2.3.2.(i) Tonic effect Wall P. D. (1967) originally observed that blocking impulses descending from the brainstem induced an increased activity of laminae IV/V dorsal horn neurons in the cat. In contrast, the response of lamina VI neurons to movement was mainly reduced. This suggests a tonic brainstem descending inhibition on cutaneous sensory processing in the dorsal horn and a facilitatory control over proprioceptive activity. The tonic inhibition of dorsal horn neurons is confirmed by later studies (Besson, J. M. *et al.*, 1975; Cervero, F. *et al.*, 1976; Dickhaus, H. *et al.*, 1985; Ren, K. and Dubner, R., 1996).

It is worth noting that if a portion of the descending pathways is blocked or only NRM is anesthetized, dorsal horn nociceptive neurons do not show an increased activity (Cervero, F. *et al.*, 1979; Gebhart, G. F. *et al.*, 1983). Apparently, tonic suppression of dorsal horn activity is implemented by multiple descending pathways or supraspinal sites; and the loss of inhibition from one pathway can be compensated by others.

The findings of Wall also reveal the plastic nature of dorsal horn neurons. In lamina IV, many low threshold neurons became wide dynamic range neurons; and in lamina V, the receptive fields of nociceptive neurons were expanded during the spinal cord block. Collins J. G. and Ren K. (1987) showed that, after a low dose of pentobarbital in the intact awake cat, dorsal horn neurons (originally only responsive to noxious stimuli) became responsive to low-intensity stimuli, that is, the wide dynamic range response profile is unmasked. This effect is likely due to a release of inhibitory systems that regulate spinal dorsal horn activity, consistent with Wall's hypothesis (Wall, P. D., 1967).

5.49.2.3.2.(ii) Inhibitory effect Descending input produces inhibition of dorsal horn neurons through multiple synaptic mechanisms (Light, A. R. *et al.*, 1986; Zhang, D. X. *et al.*, 1991; Fields, H. L. and Basbaum, A. I., 1999). As spinal serotonin and noradrenaline are almost exclusively of supraspinal origin, they provide postsynaptic control of spinal neurons. Westlund K. N. *et al.* (1990) demonstrated that spinothalamic neurons in primate receive direct catecholaminergic innervation. Stimulation of the NRM produces direct postsynaptic inhibition of spinothalamic tract neurons (Giesler, G. J. Jr. *et al.*, 1981). Descending input can also modulate secondary order neurons indirectly through action on interneurons. NRM and spinal stimulation increases glycine and GABA release into the spinal cord, suggesting activation of inhibitory interneurons (Sorkin, L. S. *et al.*, 1993; Cui, J. G. *et al.*, 1997). Since changes in activity of interneurons can lead to changes in presynaptic inhibition related to primary afferent depolarization, primary afferent fibers are also indirectly modulated by descending input (Martin, R. F. *et al.*, 1979).

5.49.2.3.2.(iii) Facilitatory effect Supraspinal structures also exert facilitatory influences on spinal nociceptive transmission. Tattersall J. E. *et al.* (1986) report that 44% of neurons recorded from the lower thoracic spinal cord of the cat show reduced response to visceral stimulation after reversible spinalization, suggesting that they are under descending excitatory control. Excitation and inhibition of dorsal horn neurons are produced by stimulation of the DLF of the spinal cord (Dubuisson, D. and Wall, P. D., 1979; McMahon, S. B. and Wall, P. D., 1988), NRM (Dubuisson, D. and Wall, P. D., 1980), and Gi (Haber, L. H. *et al.*, 1980). Even microinjection of morphine into the NRM produces facilitation of C-fiber responses of some dorsal horn nociceptive neurons (Le Bars, D. *et al.*, 1980). Although in most cases, it is unclear whether facilitation occurs on inhibitory interneurons, excitation of which may result in subsequent inhibition, Haber L. H. *et al.* (1980) demonstrate the Gi stimulation-produced excitation of primate spinothalamic tract neurons, indicating descending facilitation of nociceptive transmission. Several studies suggest a spinal–brainstem loop in the modulation of spinal pain processing. The activity of this loop involves descending inhibition or facilitation of dorsal horn neurons (Cervero, F.

and Wolstencroft, J. H., 1984; McMahon, S. B. and Wall, P. D., 1988; Suzuki, R. *et al.*, 2002b). Spinal 5-HT_3 receptors mediate descending facilitation of deep dorsal horn neurons, which involves a circuitry consisting of ascending NK1-expressing neurons in the superficial dorsal horn and descending fibers from RVM (Suzuki, R. *et al.*, 2002b).

5.49.2.4 Multiplicity of Descending Control

The bidirectional descending modulation of nociception has now been appreciated. It appears that some sites in the rostral medulla play an essential role in this balanced descending modulation. Depending on the intensities used and the specific site, stimulation of the Gi and RVM regions produces facilitation (5–25 μA) and inhibition (50–200 μA) of nocifensive reflexes and dorsal horn nociceptive neurons (Zhuo, M. and Gebhart, G. F., 1992; 1997). RVM neurons may exert bidirectional control of nociception through descending serotonergic pathways (Zhuo, M. and Gebhart, G. F., 1991) as well as via the A7 catecholamine cell group. Enkephalin-containing neurons in the RVM project to the A7 cell group and microinjection of morphine in the A7 cell group produces facilitation and inhibition of spinal nociception mediated by alpha 1- and alpha 2-adrenoceptors (Holden, J. E. *et al.*, 1999). The other site that is involved in descending facilitation is the subnucleus reticularid dorsalis (SRD) of the caudal medulla (Lima, D. and Almeida, A., 2002). Lesioning the SRD depresses nociceptive responses to acute and inflammatory pain, whereas stimulation produces pain facilitation. The SRD-mediated facilitation requires a reciprocal disynaptic putative excitatory circuit that links the SRD and the spinal dorsal horn. It is interesting that both facilitatory and inhibitory pathways can be triggered by activation of visceral afferents. Under certain circumstances, vagal afferent stimulation at relative low intensities produces facilitation of the nociceptive tail flick reflex as well as dorsal horn nociceptive neuronal activity (Randich, A. and Gebhart, G. F., 1992). The neural relays involved in vagal afferent-produced facilitation and inhibition also include sites within the RVM. Thus, spinal nociceptive processing is subject to bidirectional control from supraspinal sites so that the intensity of perceived pain can be fine-tuned by descending pathways.

In general, when biphasic pain modulation is observed at the same site, facilitation is produced by electrical stimulation given at lesser intensities or receptor agents administered at lower doses and inhibition is found at higher intensities of stimulation or larger doses of the receptor agents, with few exceptions (Thomas, D. A. *et al.*, 1995; Hammond, D. L. *et al.*, 1998). This may explain why descending facilitation was not recognized in many earlier reports because the facilitation might often be masked by more intense electrical stimulation or higher drug doses used to produce net descending inhibition. It remains to be explained how and why a manipulation at the same site by varying stimulation intensities would produce opposing effects on nociceptive transmission. Pain modulating neurons of different modalities intermingle with each other within the RVM and the membrane properties of ON and OFF cells are very similar (Zagon, A. *et al.*, 1997). One can only speculate that the net effect of excitation of brainstem nuclei is related to differential activation of subsets of neurons with different connections and different combinations of neurotransmitter receptors. In the case of BDNF, brain microinjection at a dose within the normal range, determined by measuring its concentration *in vivo*, produces nociceptive facilitation (Guo, W. *et al.*, 2006), but higher doses lead to antinociception (Siuciak, J. A. *et al.*, 1995; Frank, L. *et al.*, 1997; Guo, W. *et al.*, 2006). This suggests that activation of BDNFergic transmission at the physiological level results in facilitation and inhibition produced by larger doses may result from the recruitment of excessive synapses that are not normally active simultaneously. We should also be aware that supraspinal descending influences might exert differential effects on motor reflex and dorsal horn neuronal activity that are used by most animal studies as the endpoints (Willer, J. C. *et al.*, 1979). Future studies should validate pain facilitation and inhibition by including the affective component of pain and not merely measure reflex behaviors (Vierck, C. J. Jr. *et al.*, 2004; Neubert, J. K. *et al.*, 2005).

5.49.3 Plasticity of Descending Pathways

To be able to feel pain is a normal and essential function for living. Pain warns the body against injury and illness so that responses will be undertaken to protect the body. Normally, pain goes away when the damage is resolved and tissues are healed, and will not be long-lasting. However, chronic pain develops under a variety of conditions even without the

presence of injury, and the suffering from excessive persistent pain has been a major health problem. Most earlier studies on the descending pain control mechanisms have focused on responses to acute or transient noxious stimuli, which has built up the fundamentals for our understanding of the system. Recent studies have turned attention to chronic pain conditions and examined the effects of pain that last for hours, days, or longer, following tissue damage or nerve injury. Persistent pain conditions are associated with prolonged functional changes in the nervous system, evidenced by the development of dorsal horn hyperexcitability, or activity-dependent plasticity, also commonly referred to as central sensitization. Evidence has accumulated to indicate that descending pathways also exhibit plasticity that contributes to altered pain processing after injury (Porreca, F. *et al.*, 2002; Ren, K. and Dubner, R., 2002; Vanegas, H. and Schaible, H.-G., 2004).

5.49.3.1 Descending Modulation in Persistent Pain

5.49.3.1.1 Responses of descending pathways to injury

In the rat inflammation model, intraplantar injection of carrageenan induces inflammation and hyperalgesia that is associated with an increased Fos protein expression, a marker of neuronal activation, in the PB and LC/SC (Bellavance, L. L. and Beitz, A. J., 1996; Buritova, J. *et al.*, 1998; Tsuruoka, M. *et al.*, 2003). In adjuvant-induced inflammation and the sciatic nerve ligation model, there is a selective increase in proneurotensin mRNA expression in the PAG (Williams, F. G. and Beitz, A. J., 1993). In contrast, veratridine-induced GABA release is decreased in the PAG after hind paw inflammation (Renno, W. M. and Beitz, A. J., 1999). Orofacial inflammation activates the coeruleotrigeminal antinociceptive pathway (Matsutani, K. *et al.*, 2003) and hind paw inflammation induces an increase in NA levels in the spinal dorsal horn, suggesting activation of descending noradrenergic pathways (Tsuruoka, M. *et al.*, 1999).

In rats receiving chronic constriction injury of the sciatic nerve (the CCI model), in addition to the sensory structures of the cortex and thalamus, changes in brain neural activity are observed in a variety of regions involved in descending control including the hypothalamic arcuate nucleus and central gray matter, LC, PB, and Gi (Mao, J. *et al.*, 1993). The activation of GiA-mediated descending pain inhibition is shown in rats with partial sciatic nerve ligation (Azami, J. *et al.*, 2001). In the CCI model, there is an upregulation of spinal CB_1 receptors and an increased antihyperalgesic and antiallodynic effect of Win 55,212-2, a CB receptor agonist (Lim, G. *et al.*, 2003), although it is unclear whether descending input contributes to this enhanced pain inhibition.

Intraplantar injection of formalin has been used extensively as a model of prolonged chemical nociception. In rats receiving formalin injection, there is an increase in noradrenaline and serotonin concentrations in the spinal dorsal horn. Intrathecal pretreatment with yohimbine, an alpha 2 adrenoceptor antagonist, and methysergide, a 5-HT receptor antagonist, significantly enhanced nocifensive behavior (Omote, K. *et al.*, 1998). These results suggest activation of descending monoaminergic pathways by formalin. In the PAG, formalin injection leads to a decrease in GABA release (Maione, S. *et al.*, 1999). A decreased GABAergic tone in the PAG presumably will disinhibit PAG neurons and result in activation of opioid interneurons in the RVM, leading to increased descending inhibition.

In humans with secondary hyperalgesia after heat/capsaicine sensitization, the PAG and the cuneiform nucleus activation is observed using whole-brain functional magnetic resonance imaging (Zambreanu, L. *et al.*, 2005). These multiple lines of evidence indicate that, not only can stimulation of pain modulatory circuitry attenuate hyperalgesia and dorsal horn neuronal hyperexcitability after inflammation and nerve injury (Morgan, M. M. *et al.*, 1991; Sotgui, M. L., 1993), descending pathways are also activated under persistent pain conditions.

5.49.3.1.2 Descending inhibition in persistent pain

There is now considerable evidence that inflammatory injury induces an enhanced net descending inhibition at sites of primary hyperalgesia (Ren, K. and Dubner, R., 2002). In cats with knee joint inflammation, descending inhibition is greater in neurons with input from the inflamed knee as revealed by reversible spinalization with a cold block and DNIC-induced inhibition (Schaible H. G. *et al.*, 1991; Danziger, N. *et al.*, 1999; 2001). Similar phenomenon is observed in rats with adjuvant-induced hind paw inflammation. Local anesthetic block of the thoracic spinal cord leads to an increased activity of dorsal horn nociceptive neurons that is greater in inflamed than that in noninflamed rats (Ren, K. and Dubner, R.,

1996). Studies using Fos protein expression as a marker of neuronal activation have reached a similar conclusion. There are more inflammation-induced Fos-expressing neurons in the spinal dorsal horn in spinally transected or DLF-lesioned rats, when compared to sham-operated inflamed rats (Ren, K. and Dubner, R., 2002). Kauppila P. *et al.* (1998) show that thermal but not mechanical nociceptive responses are further enhanced in hind paw-inflamed and spinal nerve-ligated rats after spinalization at the midthoracic level. Furthermore, behavioral hyperalgesia is intensified in rats with lesions of the dorsal lateral quadrant of the spinal cord after inflammation or formalin injection (Abbott, F. V. *et al.*, 1996; Ren, K. and Dubner, R., 1996). These studies reveal the net descending inhibitory effects after tissue injury. The enhanced descending net inhibition serves to dampen injury-induced dorsal horn hyperexcitability and hyperalgesia.

The source of the enhanced inhibition can be traced back to brainstem structures. Local anesthesia of the RVM results in a further increase in dorsal horn nociceptive neuronal activity in hind paw-inflamed rats (Ren, K. and Dubner, R., 1996). Focal lesions of the RVM and LC are followed by an increase in spinal Fos expression and hyperalgesia after inflammation (Tsuruoka, M. and Willis, W. D., 1996; Wei, F. *et al.*, 1999). When lidocaine was microinjected into the NRM in adjuvant-inflamed rats, increases in activity were observed in over 75% of the spinal dorsal horn neurons (Ren, K. and Dubner, R., 1996). Interestingly, there appears to be laminar selectivity in the effect of RVM serotoninergic and LC noradrenergic descending pathways. The descending serotoninergic and noradrenergic pathways differentially suppress the responses of spinal neurons, including spinoparabrachial neurons, in the deep and superficial dorsal horn, respectively (Ren, K. *et al.*, 2000). It appears that both RVM and LC descending pathways are major sources of enhanced net inhibition in inflamed animals.

5.49.3.1.3 Descending facilitation in persistent pain

Descending input also exerts a facilitatory effect following injury. Emerging evidence indicates that descending facilitation not only parallels inhibition but also can be a driving force for the development of persistent pain (Porreca, F. *et al.*, 2002; see Figure 3). The selective destruction of the Gi with a soma-selective neurotoxin, ibotenic acid, leads to an attenuation of hyperalgesia and a reduction of

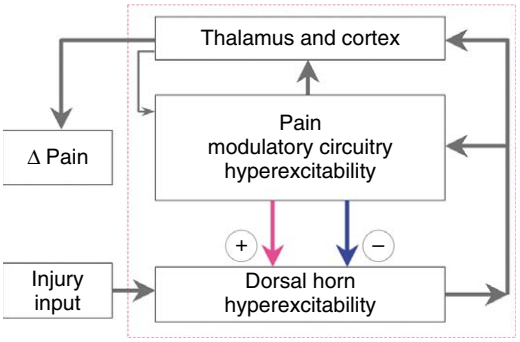

Figure 3 Diagram illustrating descending pain facilitation and inhibition in persistent pain. An enhanced primary afferent input after injury may lead to dorsal horn hyperexcitability and produce dynamic changes in excitability within brain stem pain modulatory circuitry. The net effect of descending modulation depends on a balance between inhibitory (−) and facilitatory (+) input to the spinal cord. An increase in descending net facilitatory modulation may lead to the development of persistent pain. Adapted from Ren, K., Zhuo, M., and Willis, W. D. 2000. Multiplicity and Plasticity of Descending Modulation of Nociception: Implications for Persistent Pain. In: Proceedings of the 9th World Congress on Pain (*eds*. M. Devor, M. C. Rowbotham, and Z. Wiesenfeld-Hallin), pp. 387–400. IASP Press.

inflammation-induced spinal Fos expression (Wei, F. *et al.*, 1999). The descending facilitatory effect may also originate from the medullary SRD (Lima, D. and Almeida, A., 2002) and other brain sites such as the anterior cingulate cortex (Calejesan, A. A. *et al.*, 2000).

Descending facilitation significantly contributes to the deveolpment of certain types of persistent pain, particularly those associated with secondary hyperalgesia or nerve injury. Spinalization blocks mustard oil-produced secondary allodynia and hyperexcitability of dorsal horn neurons (Mansikka, H. and Pertovaara, A., 1997). RVM lesions prevent formalin-induced nocifensive behavior (Wiertelak, E. P. *et al.*, 1997) and inhibit secondary hyperalgesia produced by topical application of mustard oil (Urban, M. O. and Gebhart, G. F., 1999). Masseter muscle inflammation produces mechanical hyperalgesia of the overlying skin that is blocked by RVM lesions, and likely includes secondary hyperalgesia of the skin and primary hyperalgesia of the muscle (Sugiyo, S. *et al.*, 2005). The same phenomenon occurs in models of neuropathic pain. Suzuki R. *et al.* (2004a) show that descending facilitatory control of mechanically evoked responses is enhanced in dorsal horn neurones after nerve injury. Local anesthesia of the PAG or RVM attenuates allodynia in rats receiving

ligation of the two spinal nerves (Pertovaara, A. *et al.*, 1996; Kovelowski, C. J. *et al.*, 2000). The tactile allodynia and cold hypersensitivity after nerve injury depends upon activation of bulbospinal descending facilitatory pathways (Ossipov, M. H. *et al.*, 2000; Urban, M. O. *et al.*, 2003). Microinjection of the CCK_2 receptor antagonist L365,260 into the RVM reverses tactile allodynia and thermal hyperalgesia after L5/L6 spinal nerve ligation and intra-RVM CCK-8 produces allodynia and hyperalgesia (Kovelowski, C. J. *et al.*, 2000). These findings indicate that CCK may drive descending facilitation to maintain neuropathic pain in rats, which is consistent with the anti-opioid action of CCK in RVM. In nerve-injured rats, lesions of the DLF, local anesthetic block of the RVM, and lesions of RVM mu-opioid receptor expressing cells do not prevent the onset, but reverse the later maintenance of tactile and thermal hypersensitivity (Porreca, F. *et al.*, 2001; Burgess, S. E. *et al.*, 2002). These observations point to an ascending–descending loop that is activated in response to prolonged stimulation to facilitate spinal nociceptive processing. The ascending dorsal column pathways likely contribute to this pain facilitatory circuitry in neuropathic pain models (Miki, K. *et al.*, 2000). There is no evidence of activation of the dorsal column pathway in models of inflammatory primary and secondary hyperalgesia.

5.49.3.1.4 Descending facilitation versus inhibition

Clearly, descending modulation of persistent pain involves both inhibition and facilitation. Although there may exist selective circuitry that is responsible for multiple phases of modulation, it is rather surprising that the facilitatory sites in the rostral medulla generally overlap with the sites that also produce inhibition. The inhibition and facilitation may also share some synaptic mechanisms with subtle difference in sensitivity. Although many of the above cited studies have concluded that the hyperalgesia is dependent completely on facilitatory influences from the brainstem, it should be noted that the same effects could be produced by a reduction in descending inhibition leading to a dominance of descending facilitation. The serotonin concentration in the NRM is reduced in mice with diabetic neuropathy and sciatic nerve ligation, which is associated with a reduced opioid analgesia (Sounvoravong, S. *et al.*, 2004). Thus, neuropathic hyperalgesia may be dependent on a net descending facilitatory effect wherein a simultaneous descending inhibition is dominated by the facilitation. After tissue or nerve injury, there is an increase in synaptic strength for both descending inhibition and facilitation. Both facilitatory and inhibitory circuitry may be activated by ascending input after injury (Herrero, J. F. and Cervero, F., 1996; Gozariu, M. *et al.*, 1998). There is an increase in ON- and OFF-cell activity after inflammation (Miki, K. *et al.*, 2002). Thus, the balance between synaptic excitation and inhibition under different conditions appears important. The Gi plays a role in descending facilitation of nociceptive transmission after transient noxious stimuli (Zhuo, M. and Gebhart, G. F., 1992). Lesions of the Gi produce an attenuation of hyperalgesia and spinal Fos expression after inflammation (Wei, F. *et al.*, 1999). However, combined Gi and NRM lesions reverse the opposite Gi or NRM lesion-induced effects. It is possible that severe persistent pain may be enhanced when the facilitatory network overrides the inhibition. In cases of neuropathic pain and secondary hyperalgesia, descending facilitation provides a driving force for the maintenance of persistent pain (also see Chapter Neuropathic Pain: Basic Mechanisms (Animal)).

5.49.3.2 Dynamics of Descending Pain Modulation

5.49.3.2.1 Time-dependent shift in descending control

There is a gradual build-up of descending inhibition in the early phase of tissue inflammation (Schaible, H. G. *et al.*, 1991; Ren, K. and Dubner, R., 1996; Hurley, R. W. and Hammond, D. L., 2000). The difference in inflammation-induced Fos expression between transected and sham controls is clear at 3 days but not apparent shortly (2 h) after inflammation (Ren, K. and Ruda, M. A., 1996). In early stages of inflammation, the dynamic response is similar in both the spinally intact and transected rats, suggesting that descending inhibitory inputs play less of a role in the early response to peripheral inflammation. In contrast, at 3 days after inflammation, descending inhibition is enhanced to counteract continuous noxious input. The results from electrophysiological studies also suggest a progressive enhancement of descending inhibition of dorsal horn neurons during the development of inflammation (Schaible, H. G. *et al.*, 1991). An effect of Freund's adjuvant on the contralateral spinal cord may also be subject to the inhibitory control of descending inputs as suggested by a clear contralateral increase in Fos-positive cells

in transected rats after inflammation (Ren, K. and Ruda, M. A., 1996). Williams F. G. and Beitz A. J. (1993) demonstrate that after peripheral inflammation or nerve injury, the increase in neurotensin mRNA expression was confined to the ventromedial PAG and the dorsal raphe nucleus initially and spreads to the structures neighboring the PAG including the cuneiform nucleus and the PPTg as the injury persists. The enhanced descending inhibition in inflamed animals has been shown to subside in the late stage at 2 weeks (Guan, Y. *et al.*, 2003). In the ankle monoarthritis rat model, tonic descending inhibition of convergent neurons with input from the inflamed ankle was enhanced during the acute stage (1–2 d) and then decreased in the chronic stage (3–4 weeks) of monoarthritis (Danziger, N. *et al.*, 1999; 2001).

The dynamic changes in descending inhibition after inflammation can be examined over time by monitoring antinocifensive responses in lightly anesthetized rats during RVM stimulation (Figure 4). Terayama R. *et al.* (2000) directly compared the potency of descending inhibition during the development of inflammation in the lightly anesthetized rat preparation. Following a unilateral hind paw inflammation, the stimulus-response function (S-R) curve for the inflamed paw was initially shifted to the right of the noninflamed paw at 3 h and then gradually shifted to the left and reached the maximal potency at 24 h after inflammation (Figure 4(b)). These findings indicate that inflammation induces dramatic changes in the excitability of RVM pain-modulating circuitry. Early (up to 3 h) in the development of inflammation there is an increased descending facilitation also shown by Urban M. O. and Gebhart G. F. (1999), which reduces the net effect of the inhibition. Over time, the level of descending inhibition increases, or descending facilitation decreases, leading to a net enhancement of antinocifensive behavior. Direct stimulation of the DLF that bypasses brainstem synaptic mechanisms does not produce a change in excitability, indicating that the changes are due to supraspinal mechanisms at the level of the RVM or higher.

Thus the activity of descending pathways exhibits considerable plasticity. Brainstem descending pathways become progressively more involved in suppressing incoming nociceptive signals in primary hyperalgesic zones following inflammation. Injury-related, persistent primary afferent input is most likely responsible for triggering this ascending–descending feedback circuit.

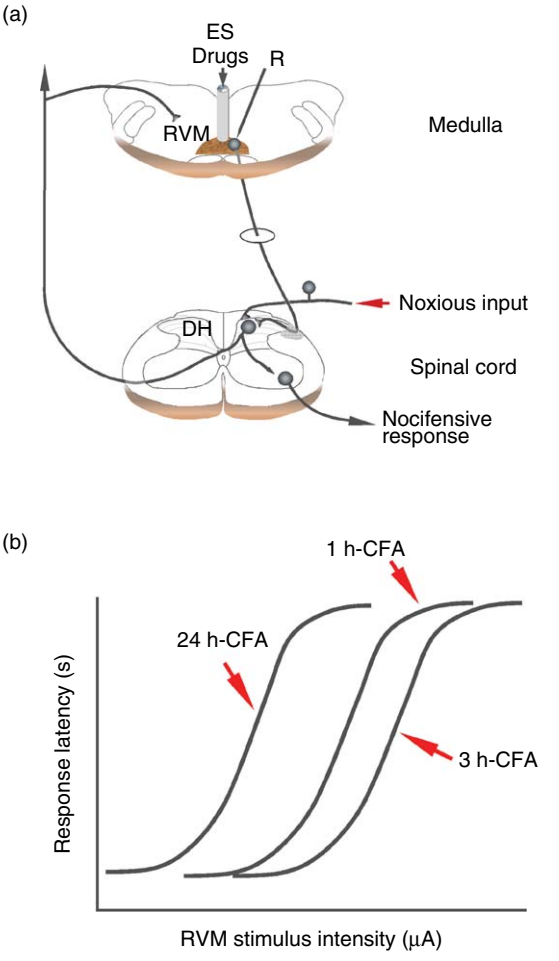

Figure 4 Time- and stimulus intensity-dependent changes in RVM electrical stimulation-produced suppression of nocifensive responses. (a) Schematic representation of the experimental setup. In lightly anesthetized animals, nocifensive responses such as paw withdrawal can be evoked by noxious stimulus. Electrical stimulation (ES) or drugs can be delivered through a guide cannula placed in the RVM. Neuronal activity can be recorded (R) in this preparation (see Figure 5). (b) The nocifensive response latency is plotted against the RVM ES intensity. The stimulus-response function (S-R) curve illustrates intensity-dependent inhibition of nocifensive responses, as indicated by an increase in response latency. Animals were inflamed with complete Freund's adjuvant (CFA), an inflammatory agent. The S-R curve at 1 h post-CFA is located in the middle. At 3 h post-CFA, the curve shifted to the right, suggesting a decrease in descending inhibition at this time. At 24 h post-CFA, the S-R curve shifted to the left, suggesting an enhanced descending inhibition. These results demonstrate dynamic changes in descending pain control during the development of inflammatory hyperalgesia. Adapted from Terayama, R., Guan, Y., Dubner, R., and Ren, K. 2000. Activity-induced plasticity in brain stem pain modulatory circuitry after inflammation. Neuroreport 11, 1915–1919.

5.49.3.2.2 Phenotypic changes in pain modulatory neurons

The time-dependent plasticity in descending pain modulatory circuitry involves changes in the response profiles of RVM neurons. Montagne-Clavel J. and Oliveras J. L. (1994) have shown changes in RVM neuronal properties after inflammation in the awake, freely moving rat, which suggests an increase in the population of neurons involved in pain modulatory activity. Using paw withdrawal as a behavioral correlate to assess the relationship between nocifensive behavior and RVM neural activity, ON-, OFF-, and NEUTRAL-like cells can be identified (Miki, K. *et al.*, 2002). Interestingly, some NEUTRAL-like cells change their response profile and can be reclassified as ON- or OFF-like cells through continuous recordings during the development of inflammation (Figure 5). These findings suggest that NEUTRAL cells have potential to become involved in pain modulation after injury. Another study by Schnell C. *et al.* (2002) shows that rat RVM neurons may display different properties depending on the site of peripheral stimulation. A NEUTRAL cell responds in an ON or OFF fashion to stimuli applied to the craniofacial region, although it is nonresponsive to noxious stimulation of the tail.

The switch in the response profile of RVM neurons correlates with the temporal changes in excitability in the RVM after inflammation. This phenotypic change of RVM neurons is verified in a population study that shows a significant increase in the percentage of ON- and OFF-like cells, and a decrease in the NEUTRAL-like cell population 24 h after inflammation as compared to control animals (Miki, K. *et al.*, 2002). The studies of RVM neurons support the view that enhanced descending modulation after inflammation involves both facilitation and inhibition since there are changes in the responses of both ON and OFF cells (Miki, K. *et al.*, 2002; de Novellis, V. *et al.*, 2005). After inflammation, there is a greater increase in ON-like cell responses before the onset of paw withdrawal as compared to that in naïve controls. ON-cell activity is associated with facilitation of nocifensive behavior (Fields, H. L. and Basbaum, A. I., 1999). In contrast, OFF-like cell responses are reduced after inflammation indicated

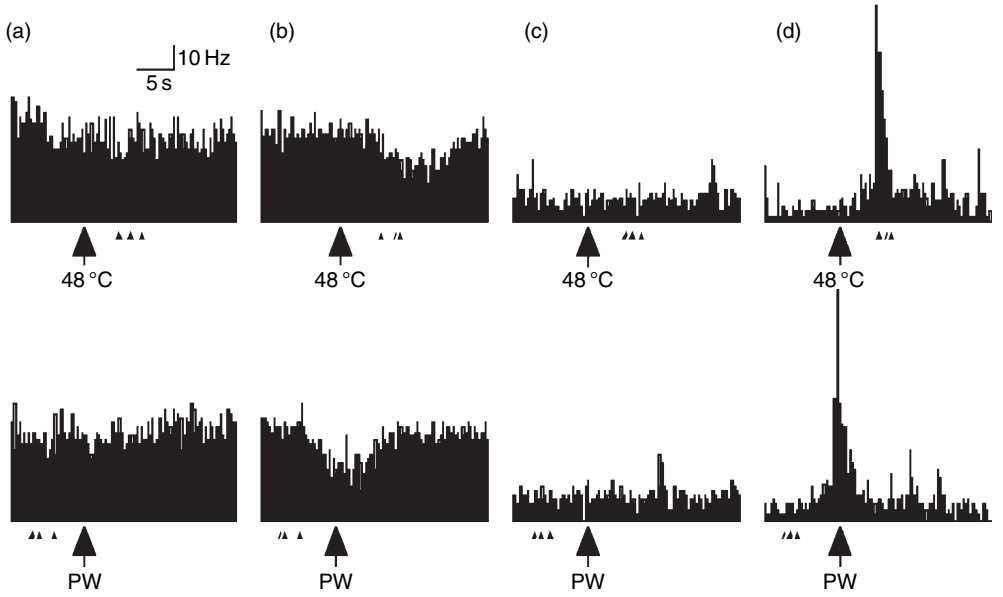

Figure 5 Examples of phenotypic changes of RVM neurons following inflammation. (a) Neutral-like cell, 9 h post-CFA. (b) Panels illustrate that at 14.5 h post-CFA, the same neuron shown in A exhibited a reduction of activity immediately before the paw withdrawal, characteristic of an OFF-like cell. (c) Neutral-like cell, 2 h post-CFA. (d) The same cell shown in (c) became an ON-like cell at 5.5 h post-CFA when the cell showed a burst of activity immediately before the paw withdrawal. All histograms were averaged from three repeated trials (200 ms bin width). The histograms are time-locked to the thermal stimuli (upper row) or the onset of paw withdrawal (lower row), respectively. Small arrowheads indicate the onset of paw withdrawal s (upper row) or onset of thermal stimuli (48 °C, lower row) for individual trials, respectively. Note that the changes in neuronal activity are best correlated with the paw withdrawal response. Adapted from Miki, K., Zhou, Q. Q., Guo, W., Guan, Y., Terayama, R., Dubner, R., and Ren, K. 2002. Changes in gene expression and neuronal phenotype in brain stem pain modulatory circuitry after inflammation. J. Neurophysiol. 87, 750–760.

by a less reduction in neuronal activity after the noxious stimulus, and a lack of a complete pause. The pause in OFF-cell activity is associated with disinhibition; the lack of the pause and the less reduction in neuronal activity suggest an increased inhibition of nocifensive behavior.

5.49.3.2.3 Involvement of excitatory amino acids and receptors

What are the cellular mechanisms that underlie these changes? Excitatory amino acids (EAAs) have been shown to mediate descending modulation in response to transient noxious stimulation and early inflammation (Urban, M. O. and Gebhart, G. F., 1999; Heinricher, M. M. *et al.*, 1999), and they are involved in the development of RVM excitability associated with inflammatory hyperalgesia (Terayama, R. *et al.*, 2000; Guan, Y. *et al.*, 2002; Miki, K. *et al.*, 2002). Microinjection of NMDA into the RVM produces effects that are dependent upon the postinflammatory time period. At 3 h post inflammation, low doses of NMDA produce facilitation of the response to noxious heat of the inflamed hind paw and the noninflamed hind paw and tail, supporting findings that descending facilitatory effects are NMDA receptor dependent and occur early after inflammation (Urban, M. O. and Gebhart, G. F., 1999). Higher doses of NMDA at 3 h post inflammation only produce inhibition. At 24 h post inflammation, NMDA produces only inhibition. All of these effects are blocked by administration of NMDA receptor antagonists. AMPA, a selective AMPA receptor agonist, produces dose- and time-dependent inhibition that is significantly greater at 24 h compared to that at 3 h post inflammation. There is a leftward shift of the dose-response curves of NMDA- and AMPA-produced inhibition at 24 h post inflammation as compared to 3 h. The leftward shift of the dose-response curves of EAA receptor agonists parallels the time-dependent enhancement of net descending inhibition produced by RVM electrical stimulation, which is also attenuated by NMDA receptor antagonists (Terayama, R. *et al.*, 2000). These results suggest that the enhanced EAA neurotransmission contributes to the time-dependent functional changes in descending modulation.

5.49.3.2.4 Molecular mechanisms of activity-dependent plasticity in descending pathways

Correlate changes in gene transcription and protein translation have been found in the descending circuitry after injury. Williams F. G. and Beitz A. J. (1993) show that adjuvant-induced hindpaw inflammation increased neurotensin mRNA expression in the PAG and the lateral tegmental nuclei, from which neurotensinergic neurons project to the RVM. The increased sensitivity of EAA receptors in the descending circuitry during the development of inflammatory hyperalgesia is related to transcriptional and translational modulation of the receptors (Ren, K. and Dubner, R., 2002). Examination of the mRNA expression of the NR1, NR2A, and NR2B subunits of the NMDA receptor in the RVM reveals an upregulation that parallels the time course of the RVM excitability changes. This is accompanied by an increase in NMDA receptor protein. Protein phosphorylation is a major mechanism for regulation of receptor function. The native NMDA receptor is likely a tetramer that consists of two NR1 and two NR2 subunits. Phosphorylation of multiple sites in the cytoplasmic C-termini of the NR1 and NR2 subunits, including tyrosine, serine, and threonine residues, is known to modulate NMDA receptor activity and affect synaptic transmission. There was an increase in NR2A, but not NR2B, tyrosine phosphorylation in the RVM after inflammation (Guo, W. *et al.*, 2006). In contrast, inflammation induces an increase in NR2B, but not NR2A subunit tyrosine phosphorylation in the spinal cord. A time-dependent increase in NR1 serine phosphorylation has also been identified in the RVM after inflammation.

There is also an increase in the AMPA receptor GluR1 subunit levels in the RVM post inflammation (Guan, Y. *et al.*, 2003). AMPA receptor subunits (GluR1–4) exist in the two flip and flop isoforms that differentially affect the desensitization properties of the receptor. Reverse transcription polymerase chain reaction analysis indicates that inflammation induces a significant upregulation of mRNAs encoding the GluR1-flip (5–24 h post inflammation), GluR2-flip (24 h post inflammation) and GluR2-flop (24 h post inflammation) isoforms in the RVM, whereas the levels of GluR1-1 flop mRNAs do not exhibit significant changes (Guan, Y. *et al.*, 2003). GluR1 serine 831 phosphoprotein levels are also increased as early as 30 min after inflammation. The increase in GluR1 phosphorylation depends on primary afferent input and interestingly, is blocked by NMDA receptor antagonists, suggesting an NMDA receptor-mediated modification of AMPA receptor function in the RVM circuitry.

These findings indicate that EAA receptors in the RVM undergo selective transcriptional, translational, and posttranslational modulation following inflammation. The activity-induced plasticity in descending circuitry complements the hyperexcitability in ascending pain transmission pathways (Dubner, R. and Ruda, M. A., 1992). The increased neuronal barrage at the spinal level activates spinal projection neurons that then activate glutamatergic, opioidergic, and presumably GABAergic neurons at the brainstem level leading to a similar but not necessarily identical form of neuronal plasticity.

5.49.3.2.5 Changes in sensitivity to opioids

5.49.3.2.5.(i) Increased analgesic potency Rats with inflammatory hyperalgesia exhibit an increased sensitivity to opioid analgesics (Neil, A. *et al.*, 1986). Typically, there is a leftward shift of the dose-response curve for opioids from the inflamed hyperalgesic paw when compared to the noninflamed paw (Hylden, J. L. K. *et al.*, 1991). Kayser V. *et al.* (1991) suggest that this increased opioid sensitivity in inflamed animals is related to a peripheral mechanism as it is significantly attenuated after local injections of very low doses (0.5–1 μg) of naloxone. Ossipov M. H. *et al.* (1995) demonstrate that the increased morphine analgesic potency is mediated through delta opioid receptors. This delta-mediated effect may require mu-opioid receptor-induced trafficking of delta-receptors to neuronal membranes (Morinville, A. *et al.*, 2003). The increased opioid sensitivity after inflammation may also be explained by changes in central pain modulating pathways. Hurley R. W. and Hammond D. L. (2000; 2001) demonstrate enhancement and plasticity of the descending inhibitory effects of mu and delta 2 opioid receptor agonists microinjected into the RVM during the development and maintenance of inflammatory hyperalgesia.

5.49.3.2.5.(ii) Opioid tolerance and hyperalgesia Hyperalgesia may occur after long exposure to opioids as opioid tolerance develops (Mao, J., 2002). The underlying mechanisms may involve activity of the pain modulatory circuitry. Morphine-tolerant rats exhibit an increased glutamate synaptic transmission in RVM neurons (Bie, B. and Pan, Z. Z., 2005). Chronic morphine treatment induces delta receptor-mediated synaptic inhibition in PAG neurons that is not seen in the untreated mice (Hack, S. P. *et al.*, 2005). The activation of descending pain facilitatory pathways from the RVM and an increase in CCK activity may contribute to hyperalgesia after prolonged morphine exposure (Ossipov, M. H. *et al.*, 2005).

5.49.3.2.6 Aging-related alteration in descending pain modulation

Iwata K. *et al.* (2002) have reported age-related plasticity in descending pathways in rats. It is found that, in aged rats, there is an increased dorsal horn nociceptive neuronal activity and nocifensive behavior associated with a significant loss of serotonergic and noradrenergic fibers in the spinal dorsal horn. These results suggest a reduced descending inhibition with advancing age. Human studies concur that the DNIC, a form of endogenous pain inhibition, is reduced in the older adults (Edwards, R. R. *et al.*, 2003).

5.49.3.3 Significance of Altered Descending Modulation in Persistent Pain

Descending pathways modulate the intensity of perceived pain under normal conditions and persistent pain as a result of injury. The activity-dependent plasticity within the pain modulatory circuitry is a normal function of the brain and presumably is activated to protect the organism from further environmental injury. The dynamic changes in descending modulation after inflammation and primary hyperalgesia and allodynia are protective. The early facilitation may function to enhance nocifensive escape behavior whereas the dominant late inhibition may provide a mechanism by which movement of the injured site is suppressed or reduced to aid in healing and recuperation. Gebhart G. F. (2004) proposes that the need to escape from a predator requires enhanced control of pain and thus more descending inhibition, which is supported by opioid and nonopioid mechanisms of stress-induced analgesia seen in animals (Hayes, R. L. *et al.*, 1978). However, the significance of the enhanced descending facilitation found at sites of secondary hyperalgesia and after nerve injury is unclear. Gebhart G. F. (2004) hypothesizes that descending facilitation is necessary to maintain hyperalgesia as the tissue heals and to protect the injured tissue from further insult. The enhanced descending pain modulation clearly includes shifts in the balance between inhibitory and facilitatory components. Present evidence suggests that there is a different balance in neural networks receiving input from zones of secondary hyperalgesia where there is

no primary injury. The balance toward facilitatory influences appears to be maintained for longer periods. Activation of these sites would lead to an enhancement of movement behavior that could also be protective.

Injury to neural tissues will also upset the balance between facilitation and inhibition. The dynamic plasticity of descending pathways after peripheral nerve injury leading to neuropathic pain may render the system vulnerable and lead to pathological consequences. In this situation, the initiation of hyperalgesia is not dependent upon descending facilitation, whereas the maintenance of the hyperalgesia for long periods of time is dependent on such descending facilitation. Nerve injury may activate a descending nociceptive system that normally is protective but can become a source of persistent pain after pathology in the nervous system.

5.49.4 Therapeutic Implications: Activating Descending Pathways

The mechanisms underlying various clinical approaches for analgesia and pain control involve activation of descending pathways. One important area of research is to find efficient and selective ways to activate endogenous descending pathways for pain control.

5.49.4.1 Electrical Stimulation

Electrical stimulation has been applied to the all levels of the nervous system to produce analgesia or pain attenuation. Presumably, this approach activates endogenous pain control including the descending pathways to the spinal cord. However, the underlying mechanisms for the stimulation-produced analgesia, particularly the selectivity of the stimulation against certain types of chronic pain in humans, remain to be elucidated.

5.49.4.1.1 Brain stimulation

Stimulation-produced analgesia has been confirmed in humans (Kumar, K. *et al.*, 1997; Wallace, B. A. *et al.*, 2004). For pain control, the most commonly used sites for deep brain stimulation have been the periventricular gray and PAG regions, which is consistent with findings in animal studies that these areas are involved in opioid analgesia and descending pain inhibition. Practically, this approach is only considered on patients suffering from intractable pain refractory to other treatments.

5.49.4.1.2 Spinal cord stimulation

Effective pain control can be achieved by direct spinal cord stimulation (SCS) through an implanted stimulator in the epidural space (Shealy, C. N. *et al.*, 1967; Janfaza, D. R. *et al.*, 1998). In theory, spinal stimulation can bypass brainstem circuitry to directly activate descending fibers or antidromically excite collaterals of ascending fibers that indirectly inhibit projection neurons, leading to inhibition of pain transmission at the spinal level. However, the mechanisms of SCS-produced pain relief are more complex (Meyerson, B. A. and Linderoth, B., 2000). One interesting aspect is that SCS is selectively effective against neuropathic pain and hyperalgesia, leaving normal nociceptive threshold unaffected (Meyerson, B. A. and Linderoth, B., 2000).

5.49.4.1.3 Vagal stimulation

Animal studies have provided evidence that stimulation of vagal afferent fibers produces antinociception, although low intensity may facilitate pain (Randich, A. and Gebhart, G. F., 1992). Taking advantage of the approved vagal stimulation approach for epilepsy, the effect of vagal stimulation on pain has been confirmed in humans (Kirchner, A. *et al.*, 2000; Ness, T. J. *et al.*, 2000). Vagal stimulation may offer another alternative method for activating the body's pain control system.

5.49.4.1.4 Transcutaneous electrical nerve stimulation

Peripheral stimulation can be applied through transcutaneous electrical nerve stimulation (TENS), an alternative modality for pain relief (Shealy, C. N., 2003). Although the results have been controversial, the clinical efficacy of this approach has been demonstrated by many studies. The effect of TENS is likely produced through modulation of the intrinsic spinal pain processing and release of endogenous opioids (Sluka, K. A. and Walsh, D., 2003).

5.49.4.2 Pharmacological Approaches

5.49.4.2.1 Opioids

Opioid agents have been used extensively for analgesia. Even applied peripherally, a central action involving activation of the endogenous pain control system is required for the analgesic effect of the opioids. The opioids are potent and efficacious

analgesics. However, their side effects have limited their use in chronic pain conditions.

5.49.4.2.2 Alpha 2 adrenoceptor agonists

Extensive documentation of the role of descending noradrenergic pathways in pain inhibition provides the bases for the use of α_2 adrenoceptor agonists for analgesic purpose. Epidural clonidine for cancer pain is the approved application (Kamibayashi, T. and Maze, M., 2000). The use of the α_2 agonist can reduce the dose of fentanyl because of their synergistic action. Intrathecal clonidine has been shown to improve the effect of SCS (Schechtmann, G. *et al.*, 2004).

5.49.4.3 Peripheral Stimulation

5.49.4.3.1 Diffuse noxious inhibitory controls

Heterotopic noxious stimulation produces analgesia in humans (Reinert, A. *et al.*, 2000), which can be understood by the DNIC hypothesis proposed by Le Bars and colleagues (Le Bars, D. *et al.*, 1979a; 1979b). DNIC provides a rationale for understanding counterirritation-produced hypoalgesia and help in the design of nonpharmacological approaches for pain relief (see Chapter Diffuse Noxious Inhibitory Controls (DNIC)). Additionally, non-noxious manipulations also provide pain relief (Simkin, P. P. and O′Hara, M., 2002), presumably through modulation of pain processing by interfering stimuli.

5.49.4.3.2 Acupuncture

Acupuncture and moxibustion have been used for pain relief for thousands of years. The analgesic effect of acupuncture is related to the recruitment of endogenous opioids (Han, J. S., 2004; Zhang, R. X. *et al.*, 2004) and pain modulatory circuitry (Ma, F. *et al.*, 2004). Since a typical needling during the acupuncture treatment does not induce pain in humans, the mechanisms of acupuncture analgesia are likely different from that of DNIC.

5.49.4.4 Psychological Factors

5.49.4.4.1 Stress

Analgesia can be produced by stress through both opioid and nonopioid mechanisms (Hayes, R. L. *et al.*, 1978; Watkins, L. R. and Mayer, D. J., 1982). Stress activates the PAG–RVM pathway, which apparently is a mechanism of stress-induced antinociception (Bellchambers, C. E. *et al.*, 1998). Fear conditioning induces antinociception involving the amygdala, PAG, and RVM (Helmstetter, F. J. and Tershner, S. A., 1994). The relative painless state in the injured athlete or the wounded soldiers may be explained by stress-induced pain control related to a particular setting.

5.49.4.4.2 Placebo

Placebo analgesia may be mediated by endogenous opioids (Levine, J. D. *et al.*, 1978; Benedetti, F. and Amanzio, M., 1997). The imaging studies show that the neural substrate related to placebo effect on pain lies in the prefrontal and dorsal anterior cingulate cortex (Lieberman, M. D. *et al.*, 2004). It appears that expectation is a factor for triggering the placebo response (see Chapter The Placebo Effect) (Benedetti, F. *et al.*, 2003).

5.49.5 Concluding Remarks

Tremendous progress has been made in the past four decades on descending pain control mechanisms. In addition to well-established descending pain inhibition, the demonstration of descending pain facilitation provides a more complete picture of the body's endogenous pain modulatory system. The simultaneous descending excitatory and inhibitory inputs contribute to a balance between perception and suppression of noxious events. We now appreciate that the pain modulatory system undergoes dramatic changes after injury. There is a concurrent activation of brainstem descending inhibitory and facilitatory pathways and the interaction between these pathways will dictate, or affect, the development of neuronal hyperexcitability and behavioral hyperalgesia. The dynamic plasticity of descending pathways may sometimes render the system vulnerable and lead to pathological consequences. The imbalance between these modulatory pathways may be one mechanism underlying variability in acute and chronic pain conditions. For patients suffering from deep pains such as temporomandibular disorders, fibromyalgia, and low back pain, the diffuse nature and amplification of persistent pain, in part, may be the result of a net increase in endogenous facilitation.

References

Aarnisalo, A. A. and Panula, P. 1995. Neuropeptide FF-containing efferent projections from the medial hypothalamus of rat: a *Phaseolus vulgaris* leucoagglutinin study. Neuroscience 65, 175–192.

Abbott, F. V., Hong, Y., and Franklin, K. B. 1996. The effect of lesions of the dorsolateral funiculus on formalin pain and morphine analgesia: a dose–response analysis. Pain 65, 17–23.

Ackley, M. A., Hurley, R. W., Virnich, D. E., and Hammond, D. L. 2001. A cellular mechanism for the antinociceptive effect of a kappa opioid receptor agonist. Pain 91, 377–388.

Ahmadi, S., Muth-Selbach, U., Lauterbach, A., Lipfert, P., Neuhuber, W. L., and Zeilhofer, H. U. 2003. Facilitation of spinal NMDA receptor currents by spillover of synaptically released glycine. Science 300, 2094–2097.

Aicher, S. A., Saravay, R. H., Cravo, S., Jeske, I., Morrison, S. F., Reis, D. J., and Milner, T. A. 1996. Monosynaptic projections from the nucleus tractus solitarii to C1 adrenergic neurons in the rostral ventrolateral medulla: comparison with input from the caudal ventrolateral medulla. J. Comp. Neurol. 373, 62–75.

Aimone, L. D. and Gebhart, G. F. 1986. Stimulation-produced spinal inhibition from the midbrain in the rat is mediated by an excitatory amino acid neurotransmitter in the medial medulla. J. Neurosci. 6, 1803–1813.

Aimone, L. D., Bauer, C. A., and Gebhart, G. F. 1988. Brainstem relays mediating stimulation-produced antinociception from the lateral hypothalamus in the rat. J. Neurosci. 8, 2652–2663.

Akil, H., Mayer, D. J., and Liebeskind, J. C. 1976. Antagonism of stimulation-produced analgesia by naloxone, a narcotic antagonist. Science 191, 961–962.

Antal, M., Petko, M., Polgar, E., Heizmann, C. W., and Storm-Mathisen, J. 1996. Direct evidence of an extensive GABAergic innervation of the spinal dorsal horn by fibres descending from the rostral ventromedial medulla. Neuroscience 73, 509–518.

Azami, J., Green, D. L., Roberts, M. H., and Monhemius, R. 2001. The behavioural importance of dynamically activated descending inhibition from the nucleus reticularis gigantocellularis pars alpha. Pain 92, 53–62.

Azkue, J. J., Mateos, J. M., Elezgarai, I., Benitez, R., Lazaro, E., Streit, P., and Grandes, P. 1998. Glutamate-like immunoreactivity in ascending spinofugal afferents to the rat periaqueductal grey. Brain Res. 790, 74–81.

Bandler, R. and Shipley, M. T. 1994. Columnar organization in the midbrain periaqueductal gray: modules for emotional expression? Trends Neurosci. 17, 379–389.

Barbaresi, P., Gazzanelli, G., and Malatesta, M. 1997. Glutamate-positive neurons and terminals in the cat periaqueductal gray matter (PAG): a light and electron microscopic immunocytochemical study. J. Comp. Neurol. 383, 381–396.

Basbaum, A. I. and Fields, H. L. 1979. The origin of descending pathways in the dorsolateral funiculus of the spinal cord of the cat and rat: further studies on the anatomy of pain modulation. J. Comp. Neurol. 187, 513–531.

Basbaum, A. I. and Fields, H. L. 1984. Endogenous pain control systems: brainstem spinal pathways and endorphin circuitry. Annu. Rev. Neurosci. 7, 309–338.

Basbaum, A. I., Marley, N. J., O′Keefe, J., and Clanton, C. H. 1977. Reversal of morphine and stimulus-produced analgesia by subtotal spinal cord lesions. Pain 3, 43–56.

Battaglia, G. and Rustioni, A. 1988. Coexistence of glutamate and substance P in dorsal root ganglion neurons of the rat and monkey. J. Comp. Neurol. 277, 302–312.

Bederson, J. B., Fields, H. L., and Barbaro, N. M. 1990. Hyperalgesia following naloxone-precipitated withdrawal from morphine is associated with increased on-cell activity in the rostral ventromedial medulla. Somatosens. Motor Res. 7, 185–203.

Behbehani, M. M. 1995. Functional characteristics of the midbrain periaqueductal gray. Prog. Neurobiol. 46, 575–605.

Behbehani, M. M. and Fields, H. L. 1979. Evidence that an excitatory connection between the periaqueductal gray and nucleus raphe magnus mediates stimulation produced analgesia. Brain Res. 170, 85–93.

Behbehani, M. M. and Pomeroy, S. L. 1978. Effect of morphine injected in periaqueductal gray on the activity of single units in nucleus raphe magnus of the rat. Brain Res. 149, 266–269.

Beitz, A. J. 1982a. The nuclei of origin of brain stem enkephalin and substance P projections to the rodent nucleus raphe magnus. Neuroscience 7, 2753–2768.

Beitz, A. J. 1982b. The organization of afferent projections to the midbrain periaqueductal gray of the rat. Neuroscience 7, 133–159.

Beitz, A. J. 1982c. The sites of origin brain stem neurotensin and serotonin projections to the rodent nucleus raphe magnus. J. Neurosci. 2, 829–842.

Beitz, A. J., Shepard, R. D., and Wells, W. E. 1983. The periaqueductal gray-raphe magnus projection contains somatostatin, neurotensin and serotonin but not cholecystokinin. Brain Res. 261, 132–137.

Bellavance, L. L. and Beitz, A. J. 1996. Altered c-fos expression in the parabrachial nucleus in a rodent model of CFA-induced peripheral inflammation. J. Comp. Neurol. 366, 431–447.

Bellchambers, C. E., Chieng, B., Keay, K. A., and Christie, M. J. 1998. Swim-stress but not opioid withdrawal increases expression of c-fos immunoreactivity in rat periaqueductal gray neurons which project to the rostral ventromedial medulla. Neuroscience 83, 517–524.

Benedetti, F. and Amanzio, M. 1997. The neurobiology of placebo analgesia: from endogenous opioids to cholecystokinin. Prog. Neurobiol. 52, 109–125.

Benedetti, F., Pollo, A., Lopiano, L., Lanotte, M., Vighetti, S., and Rainero, I. 2003. Conscious expectation and unconscious conditioning in analgesic, motor, and hormonal placebo/nocebo responses. J. Neurosci. 23, 4315–4323.

Bernard, J. F., Alden, M., and Besson, J-M. 1993. The organization of the efferent projections from the pontine parabrachial area to the amygdaloid complex: a Phaseolus vulgaris leucoagglutinin (PHA-L) study in the rat. J. Comp. Neurol. 329, 201–229.

Berrino, L., Oliva, P., Rossi, F., Palazzo, E., Nobili, B., and Maione, S. 2001. Interaction between metabotropic and NMDA glutamate receptors in the periaqueductal grey pain modulatory system. Naunyn Schmiedebergs Arch. Pharmacol. 364, 437–443.

Besson, J. M., Guilbaud, G., and Le Bars, D. 1975. Descending inhibitory influences exerted by the brain stem upon the activities of dorsal horn lamina V cells induced by intra-arterial injection of bradykinin into the limbs. J. Physiol. 248725–739.

Bester, H., Besson, J.-M., and Bernard, J. F. 1997. Organization of efferent projections from the parabrachial area to the hypothalamus: a Phaseolus vulgaris-leucoagglutinin study in the rat. J. Comp. Neurol 383, 245–281.

Bester, H., Chapman, V., Besson, J-M., and Bernard, J. F. 2000. Physiological properties of the lamina I spinoparabrachial neurons in the rat. J. Neurophysiol. 83, 2239–2259.

Bie, B. and Pan, Z. Z. 2003. Presynaptic mechanism for anti-analgesic and anti-hyperalgesic actions of kappa-opioid receptors. J. Neurosci. 23, 7262–7268.

Bie, B. and Pan, Z. Z. 2005. Increased glutamate synaptic transmission in the nucleus raphe magnus neurons from morphine-tolerant rats. Mol. Pain. 1, 7.

Bie, B., Fields, H. L., Williams, J. T., and Pan, Z. Z. 2003. Roles of alpha1- and alpha2-adrenoceptors in the nucleus raphe magnus in opioid analgesia and opioid abstinence-induced hyperalgesia. J. Neurosci. 23, 7950–7957.

Bitner, R. S., Nikkel, A. L., Curzon, P., Arneric, S. P., Bannon, A. W., and Decker, M. W. 1998. Role of the nucleus raphe magnus in antinociception produced by ABT-594: immediate early gene responses possibly linked to neuronal nicotinic acetylcholine receptors on serotonergic neurons. J. Neurosci. 18, 5426–5432.

Bohn, L. M., Xu, F., Gainetdinov, R. R., and Caron, M. G. 2000. Potentiated opioid analgesia in norepinephrine transporter knock-out mice. J. Neurosci. 20, 9040–9045.

Bouhassira, D., Chitour, D., Villanueva, L., and Le Bars, D. 1993. Morphine and diffuse noxious inhibitory controls in the rat: effects of lesions of the rostral ventromedial medulla. Eur. J. Pharmacol. 232, 207–215.

Bouhassira, D., Villanueva, L., Bing, Z., and Le Bars, D. 1992. Involvement of the subnucleus reticularis dorsalis in diffuse noxious inhibitory controls in the rat. Brain Res. 595, 353–357.

Bowker, R. M., Abbott, L. C., and Dilts, R. P. 1988. Peptidergic neurons in the nucleus raphe magnus and the nucleus gigantocellularis: their distributions, interrelationships, and projections to the spinal cord. Prog. Brain Res. 77, 95–127.

Bowker, R. M., Westlund, K. N., Sullivan, M. C., Wilber, J. F., and Coulter, J. D. 1983. Descending serotonergic, peptidergic and cholinergic pathways from the raphe nuclei: a multiple transmitter complex. Brain Res. 288, 33–48.

Buhler, A. V., Proudfit, H. K., and Gebhart, G. F. 2004. Separate populations of neurons in the rostral ventromedial medulla project to the spinal cord and to the dorsolateral pons in the rat. Brain Res. 1016, 12–19.

Buhler, A. V., Choi, J., Proudfit, H. K., and Gebhart, G. F. 2005. Neurotensin activation of the NTR1 on spinally-projecting serotonergic neurons in the rostral ventromedial medulla is antinociceptive. Pain 114, 285–294.

Burgess, S. E., Gardell, L. R., Ossipov, M. H., Malan, T. P., Jr., Vanderah, T. W., Lai, J., and Porreca, F. 2002. Time-dependent descending facilitation from the rostral ventromedial medulla maintains, but does not initiate, neuropathic pain. J. Neurosci. 22, 5129–5136.

Buritova, J., Besson, J. M., and Bernard, J. F. 1998. Involvement of the spinoparabrachial pathway in inflammatory nociceptive processes: a c-Fos protein study in the awake rat. J. Comp. Neurol. 397, 10–28.

Burnett, A. and Gebhart, G. F. 1991. Characterization of descending modulation of nociception from the A5 cell group. Brain Res. 546, 271–281.

Camarata, P. J. and Yaksh, T. L. 1985. Characterization of the spinal adrenergic receptors mediating the spinal effects produced by the microinjection of morphine into the periaqueductal gray. Brain Res. 336, 133–142.

Cameron, A. A., Khan, I. A., Westlund, K. N., and Willis, W. D. 1995b. The efferent projections of the periaqueductal gray in the rat: a Phaseolus vulgaris-leucoagglutinin study. II. Descending projections. J. Comp. Neurol. 351, 585–601.

Cameron, A. A., Khan, I. A., Westlund, K. N., Cliffer, K. D., and Willis, W. D. 1995a. The efferent projections of the periaqueductal gray in the rat: a Phaseolus vulgaris-leucoagglutinin study. I. Ascending projections. J. Comp. Neurol. 351, 568–584.

Calejesan, A. A., Kim, S. J., and Zhuo, M. 2000. Descending facilitatory modulation of a behavioral nociceptive response by stimulation in the adult rat anterior cingulate cortex. Eur. J. Pain 4, 83–96.

Cannon, K. E., Nalwalk, J. W., Stadel, R., Ge, P., Lawson, D., Silos-Santiago, I., and Hough, L. B. 2003. Activation of spinal histamine H3 receptors inhibits mechanical nociception. Eur. J. Pharmacol. 2003 470, 139–147.

Carlson, J. D., Iacono, R. P., and Maeda, G. 2004. Nociceptive excited and inhibited neurons within the pedunculopontine tegmental nucleus and cuneiform nucleus. Brain Res. 1013, 182–187.

Carstens, E., Klumpp, D., and Zimmermann, M. 1980. Differential inhibitory effects of medial and lateral midbrain stimulation on spinal neuronal discharges to noxious skin heating in the cat. J Neurophysiol. 43, 332–342.

Cejas, P. J., Martinez, M., Karmally, S., McKillop, M., McKillop, J., Plunkett, J. A., Oudega, M., and Eaton, M. J. 2000. Lumbar transplant of neurons genetically modified to secrete brain-derived neurotrophic factor attenuates allodynia and hyperalgesia after sciatic nerve constriction. Pain 86, 195–210.

Cervero, F. and Laird, J. M. 1996. Mechanisms of touch-evoked pain (allodynia): a new model. Pain 68, 13–23.

Cervero, F. and Wolstencroft, J. H. 1984. A positive feedback loop between spinal cord nociceptive pathways and antinociceptive areas of the cat's brain stem. Pain 20, 125–138.

Cervero, F., Iggo, A., and Ogawa, H. 1976. Nociceptor-driven dorsal horn neurones in the lumbar spinal cord of the cat. Pain 2, 5–24.

Cervero, F., Molony, V., and Iggo, A. 1979. Supraspinal linkage of substantia gelatinosa neurones: effects of descending impulses. Brain Res. 175, 351–355.

Chen, H. and Weber, A. J. 2004. Brain-derived neurotrophic factor reduces TrkB protein and mRNA in the normal retina and following optic nerve crush in adult rats. Brain Res. 1011, 99–106.

Chen, Y., Mestek, A., Liu, J., Hurley, J. A., and Yu, L. 1993. Molecular cloning and functional expression of a mu-opioid receptor from rat brain. Mol. Pharmacol. 44, 8–12.

Chiang, C. Y., Hu, J. W., and Sessle, B. J. 1994. Parabrachial area and nucleus raphe magnus-induced modulation of nociceptive and nonnociceptive trigeminal subnucleus caudalis neurons activated by cutaneous or deep inputs. J. Neurophysiol. 71, 2430–2445.

Cho, H. J. and Basbaum, A. I. 1991. GABAergic circuitry in the rostral ventral medulla of the rat and its relationship to descending antinociceptive controls. J. Comp. Neurol. 303, 316–328.

Clark, F. M. and Proudfit, H. K. 1991. The projection of locus coeruleus neurons to the spinal cord in the rat determined by anterograde tracing combined with immunocytochemistry. Brain Res. 538, 231–245.

Clark, F. M. and Proudfit, H. K. 1993. The projections of noradrenergic neurons in the A5 catecholamine cell group to the spinal cord in the rat: anatomical evidence that A5 neurons modulate nociception. Brain Res. 616, 200–210.

Collins, J. G. and Ren, K. 1987. WDR response profiles of spinal dorsal horn neurons may be unmasked by barbiturate anesthesia. Pain 28, 369–378.

Commons, K. G. and Valentino, R. J. 2002. Cellular basis for the effects of substance P in the periaqueductal gray and dorsal raphe nucleus. J. Comp. Neurol. 447, 82–97.

Cordero-Erausquin, M. and Changeux, J. P. 2001. Tonic nicotinic modulation of serotoninergic transmission in the spinal cord. Proc. Natl. Acad. Sci. U. S. A. 98, 2803–2807.

Cordero-Erausquin, M., Pons, S., Faure, P., and Changeux, J. P. 2004. Nicotine differentially activates inhibitory and excitatory neurons in the dorsal spinal cord. Pain 109, 308–318.

Cravatt, B. F. and Lichtman, A. H. 2004. The endogenous cannabinoid system and its role in nociceptive behavior. J Neurobiol. 61, 149–160.

Cronin, J. N., Bradbury, E. J., and Lidierth, M. 2004. Laminar distribution of GABAA- and glycine-receptor mediated tonic inhibition in the dorsal horn of the rat lumbar spinal cord: effects of picrotoxin and strychnine on expression of Fos-like immunoreactivity. Pain 112, 156–163.

Cucchiaro, G., Chaijale, N., and Commons, K. G. 2005. The dorsal raphe nucleus as a site of action of the antinociceptive and behavioral effects of the alpha4 nicotinic receptor agonist epibatidine. J. Pharmacol. Exp. Ther. 313, 389–394.

Cui, J. G., O'Connor, W. T., Ungerstedt, U., Linderoth, B., and Meyerson, B. A. 1997. Spinal cord stimulation attenuates augmented dorsal horn release of excitatory amino acids in mononeuropathy via a GABAergic mechanism. Pain 73, 87–95.

Cui, M., Feng, Y., McAdoo, D. J., and Willis, W. D. 1999. Periaqueductal gray stimulation-induced inhibition of nociceptive dorsal horn neurons in rats is associated with the release of norepinephrine, serotonin, and amino acids. J. Pharmacol. Exp. Ther. 289, 868–876.

Dahlström, A. and Fuxe, K. 1964. Evidence for the existence of monoamine-containing neurons in the central nervous system. I. Demonstration of monoamines in the cell bodies of brain stem neurons. Acta Physiol. Scand. 62(Suppl 232), 1–55.

Danzebrink, R. M. and Gebhart, G. F. 1991. Intrathecal coadministration of clonidine with serotonin receptor agonists produces supra-additive visceral antinociception in the rat. Brain Res. 555, 35–42.

Danziger, N., Weil-Fugazza, J., Le Bars, D., and Bouhassira, D. 1999. Alteration of descending modulation of nociception during the course of monoarthritis in the rat. J. Neurosci. 19, 2394–2400.

Danziger, N., Weil-Fugazza, J., Le Bars, D., and Bouhassira, D. 2001. Stage-dependent changes in the modulation of spinal nociceptive neuronal activity during the course of inflammation. Eur J Neurosci. 13, 230–240.

de Novellis, V., Mariani, L., Palazzo, E., Vita, D., Marabese, I., Scafuro, M., Rossi, F., and Maione, S. 2005. Periaqueductal grey CB1 cannabinoid and metabotropic glutamate subtype 5 receptors modulate changes in rostral ventromedial medulla neuronal activities induced by subcutaneous formalin in the rat. Neuroscience 134, 269–281.

Depaulis, A., Morgan, M. M., and Liebeskind, J. C. 1987. GABAergic modulation of the analgesic effects of morphine microinjected in the ventral periaqueductal gray matter of the rat. Brain Res. 436, 223–228.

Dickenson, A. H., Oliveras, J. L., and Besson, J. M. 1979. Role of the nucleus raphe magnus in opiate analgesia as studied by the microinjection technique in the rat. Brain Res. 170, 95–111.

Dickhaus, H., Pauser, G., and Zimmermann, M. 1985. Tonic descending inhibition affects intensity coding of nociceptive responses of spinal dorsal horn neurones in the cat. Pain 23, 145–158.

Dostrovsky, J. O., Shah, Y., and Gray, B. G. 1983. Descending inhibitory influences from periaqueductal gray, nucleus raphe magnus, and adjacent reticular formation. II. Effects on medullary dorsal horn nociceptive and nonnociceptive neurons. J. Neurophysiol. 49, 948–960.

Dubner, R. and Bennett, G. J. 1983. Spinal and trigeminal mechanisms of nociception. Annu. Rev. Neurosci. 6, 381–418.

Dubner, R. and Ruda, M. A. 1992. Activity-dependent neuronal plasticity following tissue injury and inflammation. Trends Neurosci. 15, 96–103.

Dubuisson, D. and Wall, P. D. 1979. Medullary raphe influences on units in laminae 1 and 2 of cat spinal cord. J. Physiol. (Lond) 300, 33P.

Dubuisson, D. and Wall, P. D. 1980. Descending influences on receptive fields and activity of single units recorded in laminae 1,2 and 3 of cat spinal cord. Brain Res. 199, 283–298.

Duggan, A. W. 1985. Pharmacology of descending control systems. Phil. Trans. R. Soc. Lond. B 308, 375–391.

Eaton, M. J., Blits, B., Ruitenberg, M. J., Verhaagen, J., and Oudega, M. 2002. Amelioration of chronic neuropathic pain after partial nerve injury by adeno-associated viral (AAV) vector-mediated over-expression of BDNF in the rat spinal cord. Gene Ther. 9, 1387–1395.

Edwards, R. R., Fillingim, R. B., and Ness, T. J. 2003. Age-related differences in endogenous pain modulation: a comparison of diffuse noxious inhibitory controls in healthy older and younger adults. Pain 101, 155–165.

Ennis, M., Behbehani, M., Shipley, M. T., Van Bockstaele, E. J., and Aston-Jones, G. 1991. Projections from the periaqueductal gray to the rostromedial pericoerulear region and nucleus locus coeruleus: anatomic and physiologic studies. J. Comp. Neurol. 306, 480–494.

Evans, C. J., Keith, D. E., Jr., Morrison, H., Magendzo, K., and Edwards, R. H. 1992. Cloning of a delta opioid receptor by functional expression. Science 258, 1952–1955.

Fairbanks, C. A., Stone, L. S., Kitto, K. F., Nguyen, H. O., Posthumus, I. J., and Wilcox, G. L. 2002. alpha(2C)-Adrenergic receptors mediate spinal analgesia and adrenergic-opioid synergy. J. Pharmacol. Exp. Ther. 300, 282–290.

Fardin, V., Oliveras, J. L., and Besson, J. M. 1984a. A reinvestigation of the analgesic effects induced by stimulation of the periaqueductal gray matter in the rat. II. Differential characteristics of the analgesia induced by ventral and dorsal PAG stimulation. Brain Res. 306, 125–139.

Fardin, V., Oliveras, J. L., and Besson, J. M. 1984b. Projections from the periaqueductal gray matter to the B3 cellular area (nucleus raphe magnus and nucleus reticularis paragigantocellularis) as revealed by the retrograde transport of horseradish peroxidase in the rat. J. Comp. Neurol. 223, 483–500.

Fields, H. L. 1988. Sources of variability in the sensation of pain. Pain 33, 195–200.

Fields, H. L. and Anderson, S. D. 1978. Evidence that raphe-spinal neurons mediate opiate and midbrain stimulation-produced analgesias. Pain 5, 333–349.

Fields, H. L. and Basbaum, A. I. 1978. Brainstem control of spinal pain-transmission neurons. Annu. Rev. Physiol. 40, 217–248.

Fields, H. L. and Basbaum, A. I. 1999. Central Nervous System Mechanisms of Pain Modulation. In: Textbook of Pain (*eds*. P. D. Wall and R. Melzack R) pp. 309–329. London: Churchill Livingstone.

Fields, H. L., Heinricher, M. M., and Mason, P. 1991. Neurotransmitters in nociceptive modulatory circuits. Annu. Rev. Neurosci. 14, 219–245.

Fields, H. L., Bry, J., Hentall, I., and Zorman, G. 1983a. The activity of neurons in the rostral medulla of the rat during withdrawal from noxious heat. J. Neurosci. 3, 2545–2552.

Fields, H. L., Malick, A., and Burstein, R. 1995. Dorsal horn projection targets of ON and OFF cells in the rostral ventromedial medulla. J. Neurophysiol. 74, 1742–1759.

Fields, H. L., Vanegas, H., Hentall, I. D., and Zorman, G. 1983b. Evidence that disinhibition of brain stem neurones contributes to morphine analgesia. Nature 306, 684–686.

Finley, J. C., Lindstrom, P., and Petrusz, P. 1981. Immunocytochemical localization of beta-endorphin-containing neurons in the rat brain. Neuroendocrinology 33, 28–42.

Flores, J. A., El Banoua, F., Galan-Rodriguez, B., and Fernandez-Espejo, E. 2004. Opiate anti-nociception is attenuated following lesion of large dopamine neurons of the periaqueductal grey: critical role for D1 (not D2) dopamine receptors. Pain 110, 205–214.

Fowler, C. J. and Fraser, G. L. 1994. Mu-, delta-, kappa-opioid receptors and their subtypes. A critical review with emphasis

on radioligand binding experiments. Neurochem. Int. 24, 401–426.
Frank, L., Wiegand, S. J., Siuciak, J. A., Lindsay, R. M., and Rudge, J. S. 1997. Effects of BDNF infusion on the regulation of TrkB protein and message in adult rat brain. Exp. Neurol. 145, 62–70.
Friedrich, A. E. and Gebhart, G. F. 2003. Modulation of visceral hyperalgesia by morphine and cholecystokinin from the rat rostroventral medial medulla. Pain 104, 93–101.
Fritschy, J. M. and Grzanna, R. 1990. Demonstration of two separate descending noradrenergic pathways to the rat spinal cord: evidence for an intragriseal trajectory of locus coeruleus axons in the superficial layers of the dorsal horn. J. Comp. Neurol. 291, 553–582.
Fu, J. J., Tang, J. S., Yuan, B., and Jia, H. 2002. Response of neurons in the thalamic nucleus submedius (Sm) to noxious stimulation and electrophysiological identification of on- and off-cells in rats. Pain 99, 243–251.
Galeotti, N., Malmberg-Aiello, P., Bartolini, A., Schunack, W., and Ghelardini, C. 2004. H1-receptor stimulation induces hyperalgesia through activation of the phospholipase C-PKC pathway. Neuropharmacology 47, 295–303.
Gao, K. and Mason, P. 2000. Serotonergic Raphe magnus cells that respond to noxious tail heat are not ON or OFF cells. J. Neurophysiol. 84, 1719–1725.
Gao, K., Kim, Y. H., and Mason, P. 1997. SEROTONERGIC pontomedullary neurons are not activated by antinociceptive stimulation in the periaqueductal gray. J. Neurosci. 17, 3285–3292.
Gao, Y. J., Ren, W. H., Zhang, Y. Q., and Zhao, Z. Q. 2004. Contributions of the anterior cingulate cortex and amygdala to pain- and fear-conditioned place avoidance in rats. Pain 110, 343–353.
Gauriau, C. and Bernard, J. F. 2002. Pain pathways and parabrachial circuits in the rat. Exp. Physiol. 87, 251–258.
Gaveriaux-Ruff, C. and Kieffer, B. L. 2002. Opioid receptor genes inactivated in mice: the highlights. Neuropeptides 36, 62–71.
Gebhart, G. F. 1982. Opiate and opioid peptide effects on brain stem neurons: relevance to nociception and antinociceptive mechanisms. Pain 12, 93–140.
Gebhart, G. F. 1988. Descending Inhibition of Nociceptive Transmission. In: Basic Mechanisms of Headache (*eds*. J. Olesen and L. Edvinsson), pp. 202–212. Elsevier.
Gebhart, G. F. 2004. Descending modulation of pain. Neurosci. Biobehav. Rev. 27, 729–737.
Gebhart, G. F., Sandkuhler, J., Thalhammer, J. G., and Zimmermann, M. 1983. Inhibition of spinal nociceptive information by stimulation in midbrain of the cat is blocked by lidocaine microinjected in nucleus raphe magnus and medullary reticular formation. J. Neurophysiol. 50, 1446–1459.
Giesler, G. J., Jr., Gerhart, K. D., Yezierski, R. P., Wilcox, T. K., and Willis, W. D. 1981. Postsynaptic inhibition of primate spinothalamic neurons by stimulation in nucleus raphe magnus. Brain Res. 204, 184–188.
Girardot, M. N., Brennan, T. J., Martindale, M. E., and Foreman, R. D. 1987. Effects of stimulating the subcoeruleus-parabrachial region on the non-noxious and noxious responses of T1–T5 spinothalamic tract neurons in the primate. Brain Res. 409, 19–30.
Gogas, K. R., Presley, R. W., Levine, J. D., and Basbaum, A. I. 1991. The antinociceptive action of supraspinal opioids results from an increase in descending inhibitory control: correlation of nociceptive behavior and c-fos expression. Neuroscience 42, 617–628.
Gogas, K. R., Cho, H. J., Botchkina, G. I., Levine, J. D., and Basbaum, A. I. 1996. Inhibition of noxious stimulus-evoked pain behaviors and neuronal fos-like immunoreactivity in the spinal cord of the rat by supraspinal morphine. Pain 65, 9–15.
Goldstein, A., Tachibana, S., Lowney, L. I., Hunkapiller, M., and Hood, L. 1979. Dynorphin-(1–13), an extraordinarily potent opioid peptide. Proc. Natl. Acad. Sci. U. S. A. 76, 6666–6670.
Gozariu, M., Bouhassira, D., Willer, J. C., and Le Bars, D. 1998. The influence of temporal summation on a C-fibre reflex in the rat: effects of lesions in the rostral ventromedial medulla (RVM). Brain Res. 792, 168–172.
Graff-Guerrero, A., Gonzalez-Olvera, J., Fresan, A., Gomez-Martin, D., Carlos Mendez-Nunez, J., and Pellicer, F. 2005. Repetitive transcranial magnetic stimulation of dorsolateral prefrontal cortex increases tolerance to human experimental pain. Brain Res. Cogn. Brain Res. May 31; (Epub ahead of print).
Grudt, T. J., van den Pol, A. N., and Perl, E. R. 2002. Hypocretin-2 (orexin-B) modulation of superficial dorsal horn activity in rat. J. Physiol. 538(Pt 2), 517–525.
Guan, J. L., Wang, Q. P., and Shioda, S. 2003. Immunoelectron microscopic examination of orexin-like immunoreactive fibers in the dorsal horn of the rat spinal cord. Brain Res. 987, 86–92.
Guan, Y., Terayama, R., Dubner, R., and Ren, K. 2002. Plasticity in excitatory amino acid receptor-mediated descending pain modulation after inflammation. J. Pharmacol. Exp. Ther. 300, 513–520.
Guan, Y., Guo, W., Zou, S-P., Dubner, R., and Ren, K. 2003. Inflammation–induced upregulation of AMPA receptor subunit expression in brain stem pain modulatory circuitry. Pain 104, 401–413.
Guo, W., Robbins, M. T., Wei, F., Zou, S., Dubner, R., and Ren, K. 2006. Supraspinal brain-derived neurotrophic factor signaling: a novel mechanism for descending pain facilitation. J. Neurosci. 26, 126–137.
Haber, L. H., Martin, R. F., Chung, J. M., and Willis, W. D. 1980. Inhibition and excitation of primate spinothalamic tract neurons by stimulation in region of nucleus reticularis gigantocellularis. J. Neurophysiol. 43, 1578–1593.
Hack, S. P., Bagley, E. E., Chieng, B. C., and Christie, M. J. 2005. Induction of delta-opioid receptor function in the midbrain after chronic morphine treatment. J. Neurosci. 25, 3192–3198.
Hagbarth, K. E. and Kerr, D. I. 1954. Central influences on spinal afferent conduction. J. Neurophysiol. 17, 295–307.
Hammond, D. L., Levy, R. A., and Proudfit, H. K. 1980. Hypoalgesia following microinjection of noradrenergic antagonists in the nucleus raphe magnus. Pain 9, 85–101.
Hammond, D. L., Nelson, V., and Thomas, D. A. 1998. Intrathecal methysergide antagonizes the antinociception, but not the hyperalgesia produced by microinjection of baclofen in the ventromedial medulla of the rat. Neurosci. Lett. 244, 93–96.
Han, J. S. 1995. Cholecystokinin octapeptide (CCK-8): a negative feedback control mechanism for opioid analgesia. Prog. Brain Res. 105, 263–271.
Han, J. S. 2004. Acupuncture and endorphins. Neurosci. Lett. 361, 258–261.
Haws, C. M., Williamson, A. M., and Fields, H. L. 1989. Putative nociceptive modulatory neurons in the dorsolateral pontomesencephalic reticular formation. Brain Res. 483, 272–282.
Hayes, R. L., Bennett, G. J., Newlon, P. G., and Mayer, D. J. 1978. Behavioral and physiological studies of non-narcotic analgesia in the rat elicited by certain environmental stimuli. Brain Res. 155, 69–90.
Hedo, G. and Lopez-Garcia, J. A. 2001. Alpha-1A adrenoceptors modulate potentiation of spinal nociceptive pathways in the rat spinal cord *in vitro*. Neuropharmacology 41, 862–869.
Heinricher, M. M. 2005. Nociceptin/orphanin FQ: pain, stress and neural circuits. Life Sci. 77, 3127–3132.

Heinricher, M. M., Cheng, Z. F., and Fields, H. L. 1987. Evidence for two classes of nociceptive modulating neurons in the periaqueductal gray. J. Neurosci. 7, 271–278.

Heinricher, M. M., Martenson, M. E., and Neubert, M. J. 2004a. Prostaglandin E2 in the midbrain periaqueductal gray produces hyperalgesia and activates pain-modulating circuitry in the rostral ventromedial medulla. Pain 110, 419–426.

Heinricher, M. M., McGaraughty, S., and Farr, D. A. 1999. The role of excitatory amino acid transmission within the rostral ventromedial medulla in the antinociceptive actions of systemically administered morphine. Pain 81, 57–65.

Heinricher, M. M., McGaraughty, S., and Tortorici, V. 2001. Circuitry underlying antiopioid actions of cholecystokinin within the rostral ventromedial medulla. J. Neurophysiol. 85, 280–286.

Heinricher, M. M. and Neubert, M. J. 2004. Neural basis for the hyperalgesic action of cholecystokinin in the rostral ventromedial medulla. J. Neurophysiol. 92, 1982–1989.

Heinricher, M. M., Neubert, M. J., Martenson, M. E., and Goncalves, L. 2004b. Prostaglandin E2 in the medial preoptic area produces hyperalgesia and activates pain-modulating circuitry in the rostral ventromedial medulla. Neuroscience 128, 389–398.

Helmstetter, F. J. and Tershner, S. A. 1994. Lesions of the periaqueductal gray and rostral ventromedial medulla disrupt antinociceptive but not cardiovascular aversive conditional responses. J. Neurosci. 14, 7099–7108.

Henderson, G. and McKnight, A. T. 1997. The orphan opioid receptor and its endogenous ligand–nociceptin/orphanin FQ. Trends Pharmacol. Sci. 18, 293–300.

Hernandez, N. and Vanegas, H. 2001. Encoding of noxious stimulus intensity by putative pain modulating neurons in the rostral ventromedial medulla and by simultaneously recorded nociceptive neurons in the spinal dorsal horn of rats. Pain 91, 307–315.

Hernandez, N., Lopez, Y., and Vanegas, H. 1989. Medullary on- and off-cell responses precede both segmental and thalamic responses to tail heating. Pain 39, 221–230.

Hernandez-Peon, R. and Hagbarth, K. E. 1955. Interaction between afferent and cortically induced reticular responses. J. Neurophysiol. 18, 44–55.

Herrero, J. F. and Cervero, F. 1996. Supraspinal influences on the facilitation of rat nociceptive reflexes induced by carrageenan monoarthritis. Neurosci. Lett. 209, 21–24.

Hohmann, A. G., Suplita, R. L., Bolton, N. M., Neely, M. H., Fegley, D., Mangieri, R., Krey, J. F., Walker, J. M., Holmes, P. V., Crystal, J. D., Duranti, A., Tontini, A., Mor, M., Tarzia, G., and Piomelli, D. 2005. An endocannabinoid mechanism for stress-induced analgesia. Nature 435, 1108–1112.

Holden, J. E. and Naleway, E. 2001. Microinjection of carbachol in the lateral hypothalamus produces opposing actions on nociception mediated by alpha(1)- and alpha(2)-adrenoceptors. Brain Res. 911, 27–36.

Holden, J. E., Schwartz, E. J., and Proudfit, H. K. 1999. Microinjection of morphine in the A7 catecholamine cell group produces opposing effects on nociception that are mediated by alpha1- and alpha2-adrenoceptors. Neuroscience 91, 979–990.

Holden, J. E., Van Poppel, A. Y., and Thomas, S. 2002. Antinociception from lateral hypothalamic stimulation may be mediated by NK(1) receptors in the A7 catecholamine cell group in rat. Brain Res. 953, 195–204.

Hough, L. B., Nalwalk, J. W., Li, B. Y., Leurs, R., Menge, W. M., Timmerman, H., Carlile, M. E., Cioffi, C., and Wentland, M. 1997. Novel qualitative structure-activity relationships for the antinociceptive actions of H2 antagonists, H3 antagonists and derivatives. J. Pharmacol. Exp. Ther. 283, 1534–1543.

Hoyer, D., Clarke, D. E., Fozard, J. R., Hartig, P. R., Martin, G. R., Mylecharane, E. J., Saxena, P. R., and Humphrey, P. P. 1994. International Union of Pharmacology classification of receptors for 5-hydroxytryptamine (Serotonin). Pharmacol. Rev. 46, 157–203.

Hughes, J., Smith, T. W., Kosterlitz, H. W., Fothergill, L. A., Morgan, B. A., and Morris, H. R. 1975. Identification of two related pentapeptides from the brain with potent opiate agonist activity. Nature 258, 577–580.

Hung, K. C., Wu, H. E., Mizoguchi, H., Leitermann, R., and Tseng, L. F. 2003. Intrathecal treatment with 6-hydroxydopamine or 5,7-dihydroxytryptamine blocks the antinociception induced by endomorphin-1 and endomorphin-2 given intracerebroventricularly in the mouse. J. Pharmacol. Sci. 93, 299–306.

Hunter, J. C., Fontana, D. J., Hedley, L. R., Jasper, J. R., Lewis, R., Link, R. E., Secchi, R., Sutton, J., and Eglen, R. M. 1997. Assessment of the role of alpha2-adrenoceptor subtypes in the antinociceptive, sedative and hypothermic action of dexmedetomidine in transgenic mice. Br. J. Pharmacol. 122, 1339–1344.

Hurley, R. W. and Hammond, D. L. 2000. The analgesic effects of supraspinal mu and delta opioid receptor agonists are potentiated during persistent inflammation. J. Neurosci. 20, 1249–1259.

Hurley, R. W. and Hammond, D. L. 2001. Contribution of endogenous enkephalins to the enhanced analgesic effects of supraspinal mu opioid receptor agonists after inflammatory injury. J. Neurosci. 21, 2536–2545.

Hylden, J. L. K., Anton, F., and Nahin, R. L. 1989. Spinal lamina I projection neurons in the rat: collateral innervation of parabrachial area and thalamus. Neuroscience 28, 27–37.

Hylden, J. L. K., Hayashi, H., Dubner, R., and Bennett, G. J. 1986. Physiology and morphology of the lamina I spinomesencephalic projection. J. Comp. Neurol. 247, 505–515.

Hylden, J. L. K., Thomas, D. A., Iadarola, M. J., and Dubner, R. 1991. Spinal opioid analgesic effects are enhanced in a model of unilateral inflammation/hyperalgesia: possible involvement of noradrenergic mechanisms. Eur. J. Pharmacol. 194, 135–143.

Ikeda, K., Ide, S., Han, W., Hayashida, M., Uhl, G. R., and Sora, I. 2005. How individual sensitivity to opiates can be predicted by gene analyses. Trends Pharmacol. Sci. 26, 311–317.

Iwamoto, E. T. 1991. Characterization of the antinociception induced by nicotine in the pedunculopontine tegmental nucleus and the nucleus raphe magnus. J. Pharmacol. Exp. Ther. 257, 120–133.

Iwata, K., Fukuoka, T., Kondo, E., Tsuboi, Y., Tashiro, A., Noguchi, K., Masuda, Y., Morimoto, T., and Kanda, K. 2002. Plastic changes in nociceptive transmission of the rat spinal cord with advancing age. J. Neurophysiol. 87, 1086–1093.

Janfaza, D. R., Michna, E., Pisini, J. V., and Ross, E. L. 1998. Bedside implantation of a trial spinal cord stimulator for intractable anginal pain. Anesth. Analg. 87, 1242–1244.

Janss, A. J. and Gebhart, G. F. 1987. Spinal monoaminergic receptors mediate the antinociception produced by glutamate in the medullary lateral reticular nucleus. J. Neurosci. 7, 2862–2873.

Janss, A. J. and Gebhart, G. F. 1988. Quantitative characterization and spinal pathway mediating inhibition of spinal nociceptive transmission from the lateral reticular nucleus in the rat. J. Neurophysiol. 59, 226–47.

Jasmin, L., Rabkin, S. D., Granato, A., Boudah, A., and Ohara, P. T. 2003b. Analgesia and hyperalgesia from GABA-

mediated modulation of the cerebral cortex. Nature 424, 316–320.
Jensen, T. S. and Gabhart, G. F. 1988. General anatomy of antinociceptive systems. In: Basic mechanisms of headache (*eds*. J. Olesen and L. Edvinsson L), pp. 189–200. Elsevier.
Jensen, T. S. and Yaksh, T. L. 1992. Brainstem excitatory amino acid receptors in nociception: microinjection mapping and pharmacological characterization of glutamate-sensitive sites in the brainstem associated with algogenic behavior. Neuroscience 46, 535–547.
Jones, S. L. 1991. Descending noradrenergic influences on pain. Prog. Brain Res. 88, 381–394.
Jones, S. L. and Light, A. R. 1990. Electrical stimulation in the medullary nucleus raphe magnus inhibits noxious heat-evoked fos protein-like immunoreactivity in the rat lumbar spinal cord. Brain Res. 530, 335–338.
Jones, S. L. and Gebhart, G. F. 1986. Quantitative characterization of ceruleospinal inhibition of nociceptive transmission in the rat. J. Neurophysiol. 56, 1397–1410.
Jones, S. L. and Light, A. R. 1992. Serotoninergic medullary raphespinal projection to the lumbar spinal cord in the rat: a retrograde immunohistochemical study. J. Comp. Neurol. 322, 599–610.
Jones, B. E., Pare, M., and Beaudet, A. 1986. Retrograde labeling of neurons in the brain stem following injections of [3H]choline into the rat spinal cord. Neuroscience 18, 901–916.
Kamibayashi, T. and Maze, M. 2000. Clinical uses of alpha2 - adrenergic agonists. Anesthesiology 93, 1345–1349.
Kauppila, T., Kontinen, V. K., and Pertovaara, A. 1998. Influence of spinalilzation on spinal withdrawal reflex responses varies depending on the submodality of the test stimulus and the experimental pathophysiological condition in the rat. Brain Res. 797, 234–242.
Kayser, V., Chen, Y. L., and Guilbaud, G. 1991. Behavioural evidence for a peripheral component in the enhanced antinociceptive effect of a low dose of systemic morphine in carragenin-induced hyperalgesic rats. Brain Res. 560, 237–244.
Kieffer, B. L., Befort, K., Gaveriaux-Ruff, C., and Hirth, C. G. 1992. The delta-opioid receptor: isolation of a cDNA by expression cloning and pharmacological characterization. Proc. Natl. Acad. Sci. U. S. A. 89, 12048–12052.
Kim, S. J., Calejesan, A. A., and Zhuo, M. 2002. Activation of brainstem metabotropic glutamate receptors inhibits spinal nociception in adult rats. Pharmacol. Biochem. Behav. 73, 429–437.
King, M. A., Bradshaw, S., Chang, A. H., Pintar, J. E., and Pasternak, G. W. 2001. Potentiation of opioid analgesia in dopamine2 receptor knock-out mice: evidence for a tonically active anti-opioid system. J. Neurosci. 21, 7788–7792.
Kingery, W. S., Guo, T. Z., Davies, M. F., Limbird, L., and Maze, M. 2000. The alpha(2A) adrenoceptor and the sympathetic postganglionic neuron contribute to the development of neuropathic heat hyperalgesia in mice. Pain 85, 345–358.
Kingery, W. S., Agashe, G. S., Guo, T. Z., Sawamura, S., Davies, M. F., Clark, J. D., Kobilka, B. K., and Maze, M. 2002. Isoflurane and nociception: spinal alpha2A adrenoceptors mediate antinociception while supraspinal alpha1 adrenoceptors mediate pronociception. Anesthesiology 96, 367–374.
Kirchner, A., Birklein, F., Stefan, H., and Handwerker, H. O. 2000. Left vagus nerve stimulation suppresses experimentally induced pain. Neurology 55, 1167–1171.
Kivipelto, L. and Panula, P. 1991. Origin and distribution of neuropeptide-FF-like immunoreactivity in the spinal cord of rats. J. Comp. Neurol. 307, 107–119.
Kovelowski, C. J., Ossipov, M. H., Sun, H., Lai, J., Malan, T. P., and Porreca, F. 2000. Supraspinal cholecystokinin may drive tonic descending facilitation mechanisms to maintain neuropathic pain in the rat. Pain 87, 265–273.
Krout, K. E., Jansen, A. S., and Loewy, A. D. 1998. Periaqueductal gray matter projection to the parabrachial nucleus in rat. J. Comp. Neurol. 401, 437–454.
Kumar, K., Toth, C., and Nath, R. K. 1997. Deep brain stimulation for intractable pain: a 15-year experience. Neurosurgery. 40, 736–746, Discussion 746–747.
Lahdesmaki, J., Scheinin, M., Pertovaara, A., and Mansikka, H. 2003. The alpha2A-adrenoceptor subtype is not involved in inflammatory hyperalgesia or morphine-induced antinociception. Eur. J. Pharmacol. 468, 183–189.
Lakhlani, P. P., MacMillan, L. B., Guo, T. Z., McCool, B. A., Lovinger, D. M., Maze, M., and Limbird, L. E. 1997. Substitution of a mutant alpha2a-adrenergic receptor via ''hit and run'' gene targeting reveals the role of this subtype in sedative, analgesic, and anesthetic-sparing responses *in vivo*. Proc. Natl. Acad. Sci. U. S. A. 94, 9950–9955.
LaMotte, C. C. 1988. Lamina X of primate spinal cord: distribution of five neuropeptides and serotonin. Neuroscience 25, 639–658.
Lavezzi, A. M., Ottaviani, G., Rossi, L., and Matturri, L. 2004. Cytoarchitectural organization of the parabrachial/Kolliker-Fuse complex in man. Brain Dev. 26, 316–320.
Le Bars, D., Dickenson, A. H., and Besson, J. M. 1980. Microinjection of morphine within nucleus raphe magnus and dorsal horn neurone activities related to nociception in the rat. Brain Res. 189, 467–481.
Le Bars, D., Dickenson, A. H., and Besson, J. M. 1979a. Diffuse noxious inhibitory controls (DNIC). I. Effects on dorsal horn convergent neurones in the rat. Pain 6, 283–304.
Le Bars, D., Dickenson, A. H., and Besson, J. M. 1979b. Diffuse noxious inhibitory controls (DNIC). II. Lack of effect on non-convergent neurones, supraspinal involvement and theoretical implications. Pain 6, 305–327.
Lee, H. S. and Mihailoff, G. A. 1999. Fluorescent double-label study of lateral reticular nucleus projections to the spinal cord and periaqueductal gray in the rat. Anat. Rec. 256, 91–98.
Leiphart, J. W., Dills, C. V., and Levy, R. M. 2003. Decreased spinal alpha2a- and alpha2c-adrenergic receptor subtype mRNA in a rat model of neuropathic pain. Neurosci. Lett. 349, 5–8.
Leung, C. G. and Mason, P. 1999. Physiological properties of raphe magnus neurons during sleep and waking. J. Neurophysiol. 81, 584–595.
Levine, J. D., Gordon, N. C., and Fields, H. L. 1978. The mechanism of placebo analgesia. Lancet. 2, 654–657.
Li, C. H. and Chung, D. 1976. Isolation and structure of an untriakontapeptide with opiate activity from camel pituitary glands. Proc. Natl. Acad. Sci. U. S. A. 73, 1145–1148.
Li, Y. Q., Takada, M., Matsuzaki, S., Shinonaga, Y., and Mizuno, N. 1993. Identification of periaqueductal gray and dorsal raphe nucleus neurons projecting to both the trigeminal sensory complex and forebrain structures: a fluorescent retrograde double-labeling study in the rat. Brain Res. 623, 267–277.
Li, P. and Zhuo, M. 1998. Silent glutamatergic synapses and nociception in mammalian spinal cord. Nature 393, 695–698.
Lieberman, M. D., Jarcho, J. M., Berman, S., Naliboff, B. D., Suyenobu, B. Y., Mandelkern, M., and Mayer, E. A. 2004. The neural correlates of placebo effects: a disruption account. Neuroimage 22, 447–455.
Light, A. R., Casale, E. J., and Menetrey, D. M. 1986. The effects of focal stimulation in nucleus raphe magnus and periaqueductal gray on intracellularly recorded neurons in spinal laminae I and II. J. Neurophysiol 56, 555–571.

Lim, G., Sung, B., Ji, R. R., and Mao, J. 2003. Upregulation of spinal cannabinoid-1-receptors following nerve injury enhances the effects of Win 55,212-2 on neuropathic pain behaviors in rats. Pain 105, 275–283.

Lima, D. and Almeida, A. 2002. The medullary dorsal reticular nucleus as a pronociceptive centre of the pain control system. Prog. Neurobiol. 66, 81–108.

Lin, Q., Wu, J., Peng, Y. B., Cui, M., and Willis, W. D. 1999. Inhibition of primate spinothalamic tract neurons by spinal glycine and GABA is modulated by guanosine 3′,5′-cyclic monophosphate. J. Neurophysiol. 81, 1095–1103.

Liu, R. H., Fung, S. J., Reddy, V. K., and Barnes, C. D. 1995. Localization of glutamatergic neurons in the dorsolateral pontine tegmentum projecting to the spinal cord of the cat with a proposed role of glutamate on lumbar motoneuron activity. Neuroscience 64, 193–208.

Lu, Y., Sweitzer, S. M., Laurito, C. E., and Yeomans, D. C. 2004. Differential opioid inhibition of C- and A delta- fiber mediated thermonociception after stimulation of the nucleus raphe magnus. Anesth. Analg. 98, 414–419.

Ma, F., Xie, H., Dong, Z. Q., Wang, Y. Q., and Wu, G. C. 2004. Effects of electroacupuncture on orphanin FQ immunoreactivity and preproorphanin FQ mRNA in nucleus of raphe magnus in the neuropathic pain rats. Brain Res. Bull. 63, 509–513.

Ma, W. and Eisenach, J. C. 2003. Chronic constriction injury of sciatic nerve induces the up-regulation of descending inhibitory noradrenergic innervation to the lumbar dorsal horn of mice. Brain Res. 970, 110–118.

Maione, S., Marabese, I., Leyva, J., Palazzo, E., de Novellis, V., and Rossi, F. 1998. Characterisation of mGluRs which modulate nociception in the PAG of the mouse. Neuropharmacology 37, 1475–1483.

Maione, S., Marabese, I., Oliva, P., de Novellis, V., Stella, L., Rossi, F., Filippelli, A., and Rossi, F. 1999. Periaqueductal gray matter glutamate and GABA decrease following subcutaneous formalin injection in rat. Neuroreport 10, 1403–1407.

Malick, A., Strassman, A. M., and Burstein, R. 2000. Trigeminohypothalamic and reticulohypothalamic tract neurons in the upper cervical spinal cord and caudal medulla of the rat. J. Neurophysiol. 84, 2078–2112.

Malmberg, A. B., Hedley, L. R., Jasper, J. R., Hunter, J. C., and Basbaum, A. I. 2001. Contribution of alpha(2) receptor subtypes to nerve injury-induced pain and its regulation by dexmedetomidine. Br. J. Pharmacol. 132, 1827–1836.

Malmberg-Aiello, P., Lamberti, C., Ghelardini, C., Giotti, A., and Bartolini, A. 1994. Role of histamine in rodent antinociception. Br. J. Pharmacol. 111, 1269–1279.

Mansikka, H. and Pertovaara, A. 1997. Supraspinal influence on hindlimb withdrawal thresholds and mustard oil-induced secondary allodynia in rats. Brain Res. Bull. 42, 359–365.

Mansikka, H., Lahdesmaki, J., Scheinin, M., and Pertovaara, A. 2004. Alpha(2A) adrenoceptors contribute to feedback inhibition of capsaicin-induced hyperalgesia. Anesthesiology 101, 185–190.

Mansour, A., Fox, C. A., Akil, H., and Watson, S. J. 1995. Opioid-receptor mRNA expression in the rat CNS: anatomical and functional implications. Trends Neurosci. 18, 22–29.

Mantyh, P. W. 1983. Connections of midbrain periaqueductal gray in the monkey. II. Descending efferent projections. J. Neurophysiol. 49, 582–594.

Mantyh, P. W. and Peschanski, M. 1982. Spinal projections from the periaqueductal grey and dorsal raphe in the rat, cat and monkey. Neuroscience 7, 2769–2776.

Mao, J. 2002. Opioid-induced abnormal pain sensitivity: implications in clinical opioid therapy. Pain 100, 213–217.

Mao, J., Mayer, D. J., and Price, D. D. 1993. Patterns of increased brain activity indicative of pain in a rat model of peripheral mononeuropathy. J. Neurosci. 13, 2689–2702.

Marinelli, S., Vaughan, C. W., Schnell, S. A., Wessendorf, M. W., and Christie, M. J. 2002. Rostral ventromedial medulla neurons that project to the spinal cord express multiple opioid receptor phenotypes. J. Neurosci. 22, 10847–10855.

Martin, R. F., Haber, L. H., and Willis, W. D. 1979. Primary afferent depolarization of identified cutaneous fibers following stimulation in medial brain stem. J. Neurophysiol. 42, 779–790.

Martin, W. R., Eades, C. G., Thompson, J. A., Huppler, R. E., and Gilbert, P. E. 1976. The effects of morphine- and nalorphine- like drugs in the nondependent and morphine-dependent chronic spinal dog. J. Pharmacol. Exp. Ther. 197, 517–532.

Mason, P. 2001. Contributions of the medullary raphe and ventromedial reticular region to pain modulation and other homeostatic functions. Annu. Rev. Neurosci. 24, 737–777.

Matsutani, K., Tsuruoka, M., Shinya, A., Furuya, R, Kawawa, T., and Inoue, T. 2003. Coeruleotrigeminal suppression of nociceptive sensorimotor function during inflammation in the craniofacial region of the rat. Brain Res. Bull. 61, 73–80.

Matthes, H. W., Maldonado, R., Simonin, F., Valverde, O., Slowe, S., Kitchen, I., Befort, K., Dierich, A., Le Meur, M., Dolle, P., Tzavara, E., Hanoune, J., Roques, B. P., and Kieffer, B. L. 1996. Loss of morphine-induced analgesia, reward effect and withdrawal symptoms in mice lacking the mu-opioid-receptor gene. Nature 383, 819–823.

Mayer, D. J. and Liebeskind, J. C. 1974. Pain reduction by focal electrical stimulation of the brain: an anatomical and behavioral analysis. Brain Res. 68, 73–93.

Mayer, D. J., Wolfle, T. L., Akil, H., Carder, B., and Liebeskind, J. C. 1971. Analgesia from electrical stimulation in the brainstem of the rat. Science 174, 1351–1354.

McMahon, S. B. and Wall, P. D. 1988. Descending excitation and inhibition of spinal cord lamina I projection neurons. J. Neurophysiol. 59, 1204–1219.

Melzack, R. and Wall, P. D. 1965. Pain mechanisms: a new theory. Science 150, 971–979.

Menetrey, D., Chaouch, A., Binder, D., and Besson, J. M. 1982. The origin of the spinomesencephalic tract in the rat: an anatomical study using the retrograde transport of horseradish peroxidase. J. Comp. Neurol. 206, 193–207.

Meng, F., Xie, G. X., Thompson, R. C., Mansour, A., Goldstein, A., Watson, S. J., and Akil, H. 1993. Cloning and pharmacological characterization of a rat kappa opioid receptor. Proc. Natl. Acad. Sci. U. S. A. 90, 9954–9958.

Meng, I. D., Manning, B. H., Martin, W. J., and Fields, H. L. 1998. An analgesia circuit activated by cannabinoids. Nature 395, 381–383.

Meng, X. W., Budra, B., Skinner, K., Ohara, P. T., and Fields, H. L. 1997. Noradrenergic input to nociceptive modulatory neurons in the rat rostral ventromedial medulla. J. Comp. Neurol. 377, 381–391.

Meyerson, B. A. and Linderoth, B. 2000. Mechanisms of spinal cord stimulation in neuropathic pain. Neurol. Res. 22, 285–292.

Meunier, J. C. 1997. Nociceptin/orphanin FQ and the opioid receptor-like ORL1 receptor. Eur. J. Pharmacol. 340, 1–15.

Meunier, J. C., Mollereau, C., Toll, L., Suaudeau, C., Moisand, C., Alvinerie, P., Butour, J. L., Guillemot, J. C., Ferrara, P., Monsarrat, B., Mazarguil, H., Vassart, G., Parmentier, M., and Costentin, J. 1995. Isolation and structure of the endogenous agonist of opioid receptor-like ORL1 receptor. Nature 377, 532–535.

Miki, K., Zhou, Q. Q., Guo, W., Guan, Y., Terayama, R., Dubner, R., and Ren, K. 2002. Changes in gene expression and neuronal phenotype in brain stem pain

modulatory circuitry after inflammation. J. Neurophysiol. 87, 750–760.
Miki, K., Iwata, K., Tsuboi, Y., Morimoto, T., Kondo, E., Dai, Y., Ren, K., and Noguchi, K. 2000. Dorsal column-thalamic pathway is involved in thalamic hyperexcitability following peripheral nerve injury: a lesion study in rats with experimental mononeuropathy. Pain 85, 263–271.
Millan, M. J. 2002. Descending control of pain. Prog. Neurobiol. 66, 355–474.
Mobarakeh, J. I., Takahashi, K., Sakurada, S., Nishino, S., Watanabe, H., Kato, M., and Yanai, K. 2005. Enhanced antinociception by intracerebroventricularly and intrathecally-administered orexin A and B (hypocretin-1 and -2) in mice. Peptides 26, 767–777.
Mokha, S. S., McMillan, J. A., and Iggo, A. 1986. Pathways mediating descending control of spinal nociceptive transmission from the nuclei locus coeruleus (LC) and raphe magnus (NRM) in the cat. Exp. Brain Res. 61, 597–606.
Mollereau, C., Roumy, M., and Zajac, J. M. 2005. Opioid-modulating peptides: mechanisms of action. Curr. Top Med Chem. 5, 341–355.
Montagne-Clavel, J. and Oliveras, J. L. 1994. Are ventromedial medulla neuronal properties modified by chronic peripheral inflammation? A single-unit study in the awake, freely moving polyarthritic rat. Brain Res. 657, 92–104.
Morgan, M. M., Gold, M. S., Liebeskind, J. C., and Stein, C. 1991. Periaqueductal gray stimulation produces a spinally mediated, opioid antinociception for the inflamed hindpaw of the rat. Brain Res. 545, 17–23.
Morinville, A., Cahill, C. M., Esdaile, M. J., Aibak, H., Collier, B., Kieffer, B. L., and Beaudet, A. 2003. Regulation of delta-opioid receptor trafficking via mu-opioid receptor stimulation: evidence from mu-opioid receptor knock-out mice. J. Neurosci. 23, 4888–4898.
Murphy, A. Z., Ennis, M., Rizvi, T. A., Behbehani, M. M., and Shipley M, T. 1995. Fos expression induced by changes in arterial pressure is localized in distinct, longitudinally organized columns of neurons in the rat midbrain periaqueductal gray. J. Comp. Neurol. 360, 286–300.
Nalwalk, J. W., Svokos, K., Taraschenko, O., Leurs, R., Timmerman, H., and Hough, L. B. 2004. Activation of brain stem nuclei by improgan, a non-opioid analgesic. Brain Res. 1021, 248–255.
Neil, A., Kayser, V., Gacel, G., Besson, J-M., and Guilbaud, G. 1986. Opioid receptor types and antinociceptive activity in chronic inflammation: both kappa and mu opiate agonistic effects are enhanced in arthritic rats. Eur. J. Pharmacol. 130, 203–208.
Ness, T. J., Fillingim, R. B., Randich, A., Backensto, E. M., and Faught, E. 2000. Low intensity vagal nerve stimulation lowers human thermal pain thresholds. Pain 86, 81–85.
Neubert, J. K., Widmer, C. G., Malphurs, W., Rossi, H. L., Vierck, C. J., Jr., and Caudle, R. M. 2005. Use of a novel thermal operant behavioral assay for characterization of orofacial pain sensitivity. Pain 116, 386–395.
North, R. A. and Yoshimura, M. 1984. The actions of noradrenaline on neurones of the rat substantia gelatinosa *in vitro*. J. Physiol. 349, 43–55.
Nuseir, K. and Proudfit, H. K. 2000. Bidirectional modulation of nociception by GABA neurons in the dorsolateral pontine tegmentum that tonically inhibit spinally projecting noradrenergic A7 neurons. Neuroscience 96, 773–783.
Okuda-Ashitaka, E., Minami, T., Tachibana, S., Yoshihara, Y., Nishiuchi, Y., Kimura, T., and Ito, S. 1998. Nocistatin, a peptide that blocks nociceptin action in pain transmission. Nature 392, 286–289.
Olave, M. J. and Maxwell, D. J. 2003. Neurokinin-1 projection cells in the rat dorsal horn receive synaptic contacts from axons that possess alpha2C-adrenergic receptors. J. Neurosci. 23, 6837–6846.
Oliveras, J. L. and Besson, J. M. 1988. Stimulation-produced analgesia in animals: behavioural investigations. Prog. Brain Res. 77, 141–157.
Oliveras, J. L., Redjemi, F., Guilbaud, G., and Besson, J. M. 1975. Analgesia induced by electrical stimulation of the inferior centralis nucleus of the raphe in the cat. Pain 1, 139–145.
Omote, K., Kawamata, T., Kawamata, M., and Namiki, A. 1998. Formalin-induced nociception activates a monoaminergic descending inhibitory system. Brain Res. 814, 194–198.
Ossipov, M. H., Kovelowski, C. J., and Porreca, F. 1995. The increase in morphine antinociceptive potency produced by carrageenan-induced hindpaw inflammation is blocked by naltrindole, a selective delta-opioid antagonist. Neurosci. Lett. 184, 173–176.
Ossipov, M. H., Lai, J., Malan, T. P., Jr., and Porreca, F. 2000. Spinal and supraspinal mechanisms of neuropathic pain. Ann. N. Y. Acad. Sci. U. S. A. 909, 12–24.
Ossipov, M. H., Lai, J., King, T., Vanderah, T. W., and Porreca, F. 2005. Underlying mechanisms of pronociceptive consequences of prolonged morphine exposure. Biopolymers. 80, 319–324.
Ozdogan, U. K., Lahdesmaki, J., Mansikka, H., and Scheinin, M. 2004. Loss of amitriptyline analgesia in alpha 2A-adrenoceptor deficient mice. Eur. J. Pharmacol. 485, 193–196.
Pan, L., Xu, J., Yu, R., Xu, M. M., Pan, Y. X., and Pasternak, G. W. 2005. Identification and characterization of six new alternatively spliced variants of the human mu opioid receptor gene, Oprm. Neuroscience 133, 209–220.
Pan, Z. Z., Hirakawa, N., and Fields, H. L. 2000. A cellular mechanism for the bidirectional pain-modulating actions of orphanin FQ/nociceptin. Neuron 26, 515–522.
Pan, Z. Z., Tershner, S. A., and Fields, H. L. 1997. Cellular mechanism for anti-analgesic action of agonists of the kappa-opioid receptor. Nature 389, 382–385.
Pan, Z. Z., Williams, J. T., and Osborne, P. B. 1990. Opioid actions on single nucleus raphe magnus neurons from rat and guinea-pig *in vitro*. J. Physiol. 427, 519–532.
Pasternak, G. W. 2001. Incomplete cross tolerance and multiple mu opioid peptide receptors. Trends Pharmacol. Sci. 22, 67–70.
Paxinos, G. and Watson, C. 2005. The Rat Brain in Stereotaxic Coordinates, 5th edn. Academic Press.
Peng, Y. B., Lin, Q., and Willis, W. D. 1996. Involvement of alpha-2 adrenoceptors in the periaqueductal gray-induced inhibition of dorsal horn cell activity in rats. J. Pharmacol. Exp. Ther. 278, 125–135.
Pert, C. B. and Snyder, S. H. 1973. Opiate receptor: demonstration in nervous tissue. Science 179, 1011–1014.
Pertovaara, A., Keski-Vakkuri, U., Kalmari, J., Wei, H., and Panula, P. 2001. Response properties of neurons in the rostroventromedial medulla of neuropathic rats: attempted modulation of responses by [1DMe]NPYF, a neuropeptide FF analogue. Neuroscience 105, 457–68.
Pertovaara, A., Wei, H., and Hamalainen, M. M. 1996. Lidocaine in the rostroventromedial medulla and the periaqueductal gray attenuates allodynia in neuropathic rats. Neurosci. Lett. 218, 127–130.
Petrovic, P., Carlsson, K., Petersson, K. M., Hansson, P., and Ingvar, M. 2004. Context-dependent deactivation of the amygdala during pain. J. Cogn. Neurosci. 16, 1289–1301.
Porreca, F., Ossipov, M. H., and Gebhart, G. F. 2002. Chronic pain and medullary descending facilitation. Trends Neurosci. 25, 319–325.

Porreca, F., Burgess, S. E., Gardell, L. R., Vanderah, T. W., Malan, T. P., Jr., Ossipov, M. H., Lappi, D. A., and Lai, J. 2001. Inhibition of neuropathic pain by selective ablation of brainstem medullary cells expressing the micro-opioid receptor. J. Neurosci. 21, 5281–5288.

Price, D. D. 2002. Central neural mechanisms that interrelate sensory and affective dimensions of pain. Mol. Interv. 2, 392–403.

Proudfit, H. K. 2002. The challenge of defining brainstem pain modulation circuits. J. Pain 3, 350–354.

Randich, A. and Gebhart, G. F. 1992. Vagal afferent modulation of nociception. Brain Res. Rev 17, 77–99.

Randich, A. and Maixner, W. 1984. Interactions between cardiovascular and pain regulatory systems. Neurosci. Biobehav. Rev. 8, 343–367.

Reddy, S. V., Maderdrut, J. L., and Yaksh, T. L. 1980. Spinal cord pharmacology of adrenergic agonist-mediated antinociception. J. Pharmacol. Exp. Ther. 213, 525–533.

Reichling, D. B. and Basbaum, A. I. 1990. Contribution of brainstem GABAergic circuitry to descending antinociceptive controls: II. Electron microscopic immunocytochemical evidence of GABAergic control over the projection from the periaqueductal gray to the nucleus raphe magnus in the rat. J. Comp. Neurol. 302, 378–393.

Reinert, A., Treede, R., and Bromm, B. 2000. The pain inhibiting pain effect: an electrophysiological study in humans. Brain Res. 862, 103–110.

Reinscheid, R. K., Nothacker, H. P., Bourson, A., Ardati, A., Henningsen, R. A., Bunzow, J. R., Grandy, D. K., Langen, H., Monsma, F. J., Jr., and Civelli, O. 1995. Orphanin FQ: a neuropeptide that activates an opioidlike G protein-coupled receptor. Science 270, 792–794.

Ren, K. 2002. The medulla oblongata: the vital center for descending modulation. J. Pain 3, 355–357.

Ren, K. and Ruda, M. A. 1996. Descending modulation of Fos expression after persistent peripheral inflammation. Neuroreport 7, 2186–2190.

Ren, K. and Dubner, R. 1996. Enhanced descending modulation of nociception in rats with persistent hindpaw inflammation. J. Neurophysiol. 76, 3025–3037.

Ren, K. and Dubner, R. 2002. Descending modulation in presistent pain: an update. Pain 100, 1–6.

Ren, K., Randich, A., and Gebhart, G. F. 1990. Modulation of spinal nociceptive transmission from nuclei tractus solitarii: a relay for effects of vagal afferent stimulation. J. Neurophysiol. 63, 971–986.

Ren, K., Randich, A., and Gebhart, G. F. 1991. Spinal serotonergic and kappa opioid receptors mediate facilitation of the tail flick reflex produced by vagal afferent stimulation. Pain 45, 321–329.

Ren, K., Zhuo, M., and Willis, W. D. 2000. Multiplicity and Plasticity of Descending Modulation of Nociception: Implications for Persistent Pain. In: Proceedings of the 9th World Congress on Pain (*eds*. M. Devor, M. C. Rowbotham, and Z. Wiesenfeld-Hallin), pp. 387–400. IASP Press.

Renno, W. M. and Beitz, A. J. 1999. Peripheral inflammation is associated with decreased veratridine-induced release of GABA in the rat ventrocaudal periaqueductal gray: microdialysis study. J. Neurol. Sci. 163, 105–110.

Reynolds, D. V. 1969. Surgery in the rat during electrical analgesia induced by focal brain stimulation. Science 164, 444–445.

Richter, R. C. and Behbehani, M. M. 1991. Evidence for glutamic acid as a possible neurotransmitter between the mesencephalic nucleus cuneiformis and the medullary nucleus raphe magnus in the lightly anesthetized rat. Brain Res. 544, 279–286.

Rivot, J. P., Chaouch, A., and Besson, J. M. 1980. Nucleus raphe magnus modulation of response of rat dorsal horn neurons to unmyelinated fiber inputs: partial involvement of serotonergic pathways. J. Neurophysiol. 44, 1039–1057.

Rivot, J. P., Chiang, C. Y., and Besson, J. M. 1982. Increase of serotonin metabolism within the dorsal horn of the spinal cord during nucleus raphe magnus stimulation, as revealed by *in vivo* electrochemical detection. Brain Res. 238, 117–126.

Rizvi, T. A., Ennis, M., Behbehani, M. M., and Shipley, M. T. 1991. Connections between the central nucleus of the amygdala and the midbrain periaqueductal gray: topography and reciprocity. J. Comp. Neurol. 303, 121–131.

Rossi, G. C., Mathis, J. P., and Pasternak, G. W. 1998. Analgesic activity of orphanin FQ2, murine prepro-orphanin FQ141–157 in mice. Neuroreport 9, 1165–1168.

Ruda, M. A. 1982. Opiates and pain pathways: demonstration of enkephalin synapses on dorsal horn projection neurons. Science 215, 1523–1525.

Ruda, M. A. 1988. Spinal dorsal horn circuitry involved in the brain stem control of nociception. Prog. Brain Res. 77, 129–140.

Ruda, M. A., Coffield, J., and Steinbusch, H. W. 1982. Immunocytochemical analysis of serotonergic axons in laminae I and II of the lumbar spinal cord of the cat. J. Neurosci. 2, 1660–1671.

Sagen, J. and Proudfit, H. K. 1984. Effect of intrathecally administered noradrenergic antagonists on nociception in the rat. Brain Res. 310, 295–301.

Sakurai, T., Amemiya, A., Ishii, M., Matsuzaki, I., Chemelli, R. M., Tanaka, H., Williams, S. C., Richardson, J. A., Kozlowski, G. P., Wilson, S., Arch, J. R., Buckingham, R. E., Haynes, A. C., Carr, S. A., Annan, R. S., McNulty, D. E., Liu, W. S., Terrett, J. A., Elshourbagy, N. A., Bergsma, D. J., and Yanagisawa, M. 1998. Orexins and orexin receptors: a family of hypothalamic neuropeptides and G protein-coupled receptors that regulate feeding behavior. Cell 92, 573–585.

Samad, T. A., Moore, K. A., Sapirstein, A., Billet, S., Allchorne, A., Poole, S., Bonventre, J. V., and Woolf, C. J. 2001. Interleukin-1beta-mediated induction of Cox-2 in the CNS contributes to inflammatory pain hypersensitivity. Nature 410, 471–475.

Sandkuhler, J. 1996. The organization and function of endogenous antinociceptive systems. Prog. Neurobiol. 50, 49–81.

Sawamura, S., Kingery, W. S., Davies, M. F., Agashe, G. S., Clark, J. D., Kobilka, B. K., Hashimoto, T., and Maze, M. 2000. Antinociceptive action of nitrous oxide is mediated by stimulation of noradrenergic neurons in the brainstem and activation of [alpha]2B adrenoceptors. J. Neurosci. 20, 9242–9251.

Sawynok, J. 1989. The 1988 Merck Frosst Award. The role of ascending and descending noradrenergic and serotonergic pathways in opioid and non-opioid antinociception as revealed by lesion studies. Can. J. Physiol. Pharmacol. 67, 975–988.

Schaible, H. G., Neugebauer, V., Cervero, F., and Schmidt, R. F. 1991. Changes in tonic descending inhibition of spinal neurons with articular input during the development of acute arthritis in the cat. J. Neurophysiol. 66, 1021–1032.

Schechtmann, G., Wallin, J., Meyerson, B. A., and Linderoth, B. 2004. Intrathecal clonidine potentiates suppression of tactile hypersensitivity by spinal cord stimulation in a model of neuropathy. Anesth. Analg. 99, 135–139.

Schnell, C., Ulucan, C., and Ellrich, J. 2002. Atypical on-, off- and neutral cells in the rostral ventromedial medulla oblongata in rat. Exp. Brain Res. 145, 64–75.

Sessle, B. J., Hu, J. W., Dubner, R., and Lucier, G. E. 1981. Functional properties of neurons in cat trigeminal subnucleus caudalis (medullary dorsal horn). II. Modulation

of responses to noxious and nonnoxious stimuli by periaqueductal gray, nucleus raphe magnus, cerebral cortex, and afferent influences, and effect of naloxone. J. Neurophysiol. 45, 193–207.

Shealy, C. N. 2003. Transcutaneous electrical nerve stimulation: the treatment of choice for pain and depression. J. Altern. Complement. Med. 9, 619–623.

Shealy, C. N., Mortimer, J. T., and Reswick, J. B. 1967. Electrical inhibition of pain by stimulation of the dorsal columns: preliminary clinical report. Anesth. Analg. 46, 489–491.

Simkin, P. P. and O'hara, M. 2002. Nonpharmacologic relief of pain during labor: systematic reviews of five methods. Am. J. Obstet. Gynecol. 186, S131–159.

Simon, E. J., Hiller, J. M., and Edelman, I. 1973. Stereospecific binding of the potent narcotic analgesic (3H) Etorphine to rat-brain homogenate. Proc. Natl. Acad. Sci. U. S. A. 70, 1947–1949.

Siuciak, J. A., Wong, V., Pearsall, D., Wiegand, S. J., and Lindsay, R. M. 1995. BDNF produces analgesia in the formalin test and modifies neuropeptide levels in rat brain and spinal cord areas associated with nociception. Eur. J. Neurosci. 7, 663–670.

Skinner, K., Basbaum, A. I., and Fields, H. L. 1997. Cholecystokinin and enkephalin in brain stem pain modulating circuits. Neuroreport 8, 2995–2998.

Skirboll, L., Hokfelt, T., Dockray, G., Rehfeld, J., Brownstein, M., and Cuello, A. C. 1983. Evidence for periaqueductal cholecystokinin-substance P neurons projecting to the spinal cord. J. Neurosci. 3, 1151–1157.

Sluka, K. A. and Walsh, D. 2003. Transcutaneous electrical nerve stimulation: basic science mechanisms and clinical effectiveness. J. Pain 4, 109–121.

Sluka, K. A. and Westlund, K. N. 1992. Spinal projections of the locus coeruleus and the nucleus subcoeruleus in the Harlan and the Sasco Sprague-Dawley rat. Brain Res. 579, 67–73.

Sonohata, M., Furue, H., Katafuchi, T., Yasaka, T., Doi, A., Kumamoto, E., and Yoshimura, M. 2004. Actions of noradrenaline on substantia gelatinosa neurones in the rat spinal cord revealed by *in vivo* patch recording. J. Physiol. 555(Pt 2), 515–526.

Sora, I., Takahashi, N., Funada, M., Ujike, H., Revay, R. S., Donovan, D. M., Miner, L. L., and Uhl, G. R. 1997. Opiate receptor knockout mice define mu receptor roles in endogenous nociceptive responses and morphine-induced analgesia. Proc. Natl. Acad. Sci. U. S. A. 94, 1544–1549.

Sorkin, L. S., McAdoo, D. J., and Willis, W. D. 1993. Raphe magnus stimulation-induced antinociception in the cat is associated with release of amino acids as well as serotonin in the lumbar dorsal horn. Brain Res. 618, 95–108.

Sotgui, M. L. 1993. Descending influence on dorsal horn neuronal hyperactivity in a rat model of neuropathic pain. Neuroreport. 4, 21–24.

Sounvoravong, S., Nakashima, M. N., Wada, M., and Nakashima, K. 2004. Decrease in serotonin concentration in raphe magnus nucleus and attenuation of morphine analgesia in two mice models of neuropathic pain. Eur. J. Pharmacol. 484, 217–223.

Spinella, M., Cooper, M. L., and Bodnar, R. J. 1996. Excitatory amino acid antagonists in the rostral ventromedial medulla inhibit mesencephalic morphine analgesia in rats. Pain 64, 545–552.

Stamford, J. A. 1995. Descending control of pain. Br. J. Anaesth. 75, 217–227.

Stevens, R. T., Hodge, C. J., Jr., and Apkarian, A. V. 1982. Kolliker-Fuse nucleus: the principal source of pontine catecholaminergic cells projecting to the lumbar spinal cord of cat. Brain Res. 239, 589–594.

Stiller, C. O., Gustafsson, H., Fried, K., and Brodin, E. 1997. Opioid-induced release of neurotensin in the periaqueductal gray matter of freely moving rats. Brain Res. 774, 149–158.

Stone, L. S., MacMillan, L. B., Kitto, K. F., Limbird, L. E., and Wilcox, G. L. 1997. The alpha2a adrenergic receptor subtype mediates spinal analgesia evoked by alpha2 agonists and is necessary for spinal adrenergic-opioid synergy. J. Neurosci. 17, 7157–7165.

Stone, L. S., Vulchanova, L., Riedl, M. S., Wang, J., Williams, F. G., Wilcox, G. L., and Elde, R. 1999. Effects of peripheral nerve injury on alpha-2A and alpha-2C adrenergic receptor immunoreactivity in the rat spinal cord. Neuroscience 93, 1399–1407.

Sugiyo, S., Takemura, M., Dubner, R., and Ren, K. 2005. Trigeminal transition zone-rostral ventromedial medulla connections and facilitation of orofacial hyperalgesia after masseter inflammation in rats. J. Comp. Neurol. (in press).

Suzuki, R., Rahman, W., Hunt, S. P., and Dickenson, A. H. 2004a. Descending facilitatory control of mechanically evoked responses is enhanced in deep dorsal horn neurones following peripheral nerve injury. Brain Res. 1019, 68–76.

Suzuki, R., Rygh, L. J., and Dickenson, A. H. 2004b. Bad news from the brain: descending 5-HT pathways that control spinal pain processing. Trends Pharmacol. Sci. 25, 613–617.

Suzuki, R., Green, G. M., Millan, M. J., and Dickenson, A. H. 2002a. Electrophysiologic characterization of the antinociceptive actions of S18616, a novel and potent alpha 2-adrenoceptor agonist, after acute and persistent pain states. J. Pain 3, 234–243.

Suzuki, R., Morcuende, S., Webber, M., Hunt, S. P., and Dickenson, A. H. 2002b. Superficial NK1-expressing neurons control spinal excitability through activation of descending pathways. Nat. Neurosci. 5, 1319–1326.

Swanson, L. W. and Hartman, B. K. 1975. The central adrenergic system. An immunofluorescence study of the location of cell bodies and their efferent connections in the rat utilizing dopamine-beta-hydroxylase as a marker. J. Comp. Neurol. 163, 467–505.

Tanaka, M., Matsumoto, Y., Murakami, T., Hisa, Y., and Ibata, Y. 1996. The origins of catecholaminergic innervation in the rostral ventromedial medulla oblongata of the rat. Neurosci. Lett. 207, 53–56.

Tang, J., Ko, S., Ding, H. K., Qiu, C. S., Calejesan, A. A., and Zhuo, M. 2005. Pavlovian fear memory induced by activation in the anterior cingulate cortex. Mol. Pain 1, 6.

Tavares, I. and Lima, D. 2002. The caudal ventrolateral medulla as an important inhibitory modulator of pain transmission at the spinal cord. J. Pain 3, 337–346.

Terayama, R., Guan, Y., Dubner, R., and Ren, K. 2000. Activity-induced plasticity in brain stem pain modulatory circuitry after inflammation. Neuroreport 11, 1915–1919.

Terenius, L. 1973. Stereospecific interaction between narcotic analgesics and a synaptic plasm a membrane fraction of rat cerebral cortex. Acta Pharmacol. Toxicol. (Copenh). 32, 317–320.

Tattersall, J. E., Cervero, F., and Lumb, B. M. 1986. Effects of reversible spinalization on the visceral input to viscerosomatic neurons in the lower thoracic spinal cord of the cat. J. Neurophysiol. 56, 785–796.

Thomas, D. A., McGowan, M. K., and Hammond, D. L. 1995. Microinjection of baclofen in the ventromedial medulla of rats: antinociception at low doses and hyperalgesia at high doses. J Pharmacol. Exp. Ther. 275, 274–284.

Thurston, C. L. and Randich, A. 1995. Responses of on and off cells in the rostral ventral medulla to stimulation of vagal afferents and changes in mean arterial blood pressure in intact and cardiopulmonary deafferented rats. Pain 62, 19–38.

Tjolsen, A., Berge, O. G., and Hole, K. 1991. Lesions of bulbospinal serotonergic or noradrenergic pathways reduce nociception as measured by the formalin test. Acta Physiol. Scand. 142, 229–236.

Todd, A. J. and Millar, J. 1984. Antagonism of 5-hydroxytryptamine-evoked excitation in the superficial dorsal horn of the cat spinal cord by methysergide. Neurosci Lett. 48, 167–170.

Tseng, L. F. and Tang, R. 1990. Different mechanisms mediate beta-endorphin- and morphine-induced inhibition of the tail-flick response in rats. J. Pharmacol. Exp. Ther. 252, 546–551.

Tsou, K. and Jang, C. S. 1964. Studies on the site of analgesic action of morphine by intracerebral microinjections. Sci. Sin. 13, 1099–1109.

Tsou, K., Brown, S., Sanudo-Pena, M. C., Mackie, K., and Walker, J. M. 1998. Immunohistochemical distribution of cannabinoid CB1 receptors in the rat central nervous system. Neuroscience 83, 393–411.

Tsuruoka, M. and Willis, W. D. 1996. Bilateral lesions in the area of the nucleus locus coeruleus affect the development of hyperalgesia during carrageenan-induced inflammation. Brain Res. 726, 233–236.

Tsuruoka, M., Hitoto, T., Hiruma, Y., and Matsui, Y. 1999. Neurochemical evidence for inflammation-induced activation of the coeruleospinal modulation system in the rat. Brain Res. 821, 236–240.

Tsuruoka, M., Arai, Y. C., Nomura, H., Matsutani, K., and Willis, W. D. 2003. Unilateral hindpaw inflammation induces bilateral activation of the locus coeruleus and the nucleus subcoeruleus in the rat. Brain Res. Bull. 61, 117–123.

Urban, M. O. and Gebhart, G. F. 1997. Characterization of biphasic modulation of spinal nociceptive transmission by neurotensin in the rat rostral ventromedial medulla. J. Neurophysiol. 78, 1550–1562.

Urban, M. O. and Gebhart, G. F. 1999. Supraspinal contributions to hyperalgesia. Proc Natl Acad Sci USA 96, 7687–7692.

Urban, M. O., Jiang, M. C., and Gebhart, G. F. 1996. Participation of central descending nociceptive facilitatory system in secondary hyperalgesia produced by mustard oil. Brain Res. 737, 83–91.

Urban, M. O., Hama, A. T., Bradbury, M., Anderson, J., Varney, M. A., and Bristow, L. 2003. Role of metabotropic glutamate receptor subtype 5 (mGluR5) in the maintenance of cold hypersensitivity following a peripheral mononeuropathy in the rat. Neuropharmacology 44, 983–993.

Valverde, O., Ledent, C., Beslot, F., Parmentier, M., and Roques, B. P. 2000. Reduction of stress-induced analgesia but not of exogenous opioid effects in mice lacking CB1 receptors. Eur. J. Neurosci. 12, 533–539.

Van Bockstaele, E. J., Aston-Jones, G., Pieribone, V. A., Ennis, M., and Shipley, M. T. 1991. Subregions of the periaqueductal gray topographically innervate the rostral ventral medulla in the rat. J. Comp. Neurol. 309, 305–327.

Van den Pol, A. N. 1999. Hypothalamic hypocretin (orexin): robust innervation of the spinal cord. J. Neurosci. 19, 3171–3182.

Van den Pol, A. N. and Collins, W. F. 1994. Paraventriculospinal tract as a model for axon injury: spinal cord. J. Comp. Neurol. 349, 244–258.

Vanegas, H. and Schaible, H-G. 2004. Descending control of persistent pain: inhibitory or facilitatory? Brain Res. Rev. 46, 295–309.

Vanegas, H., Barbaro, N. M., and Fields, H. L. 1984. Midbrain stimulation inhibits tail-flick only at currents sufficient to excite rostral medullary neurons. Brain Res. 321, 127–133.

van Praag, H. and Frenk, H. 1990. The role of glutamate in opiate descending inhibition of nociceptive spinal reflexes. Brain Res. 524, 101–105.

Vaughan, C. W., Connor, M., Jennings, E. A., Marinelli, S., Allen, R. G., and Christie, M. J. 2001. Actions of nociceptin/orphanin FQ and other prepronociceptin products on rat rostral ventromedial medulla neurons *in vitro*. J. Physiol. 534(Pt 3), 849–859.

Veraksits, A., Runkorg, K., Kurrikoff, K., Raud, S., Abramov, U., Matsui, T., Bourin, M., Koks, S., and Vasar, E. 2003. Altered pain sensitivity and morphine-induced anti-nociception in mice lacking CCK2 receptors. Psychopharmacology (Berl). 166, 168–175.

Vierck, C. J., Jr., Kline, R., 4th, and Wiley, R. G. 2004. Comparison of operant escape and innate reflex responses to nociceptive skin temperatures produced by heat and cold stimulation of rats. Behav. Neurosci. 118, 627–635.

Walker, J. M. and Huang, S. M. 2002. Endocannabinoids in pain modulation. Prostaglandins Leukot. Essent. Fatty Acids. 66, 235–242.

Wall, P. D. 1967. The laminar organization of dorsal horn and effects of descending impulses. J. Physiol. 188, 403–423.

Wallace, B. A., Ashkan, K., and Benabid, A. L. 2004. Deep brain stimulation for the treatment of chronic, intractable pain. Neurosurg. Clin. N. Am. 15, 343–357, vii.

Wang, H. and Wessendorf, M. W. 1999. Mu- and delta-opioid receptor mRNAs are expressed in spinally projecting serotonergic and nonserotonergic neurons of the rostral ventromedial medulla. J. Comp. Neurol. 404, 183–96.

Wang, H. and Wessendorf, M. W. 2002. Mu- and delta-opioid receptor mRNAs are expressed in periaqueductal gray neurons projecting to the rostral ventromedial medulla. Neuroscience 109, 619–634.

Wang, Q., Mao, L. M., Shi, Y. S, and Han, J. S. 1990. Lumbar intrathecal administration of naloxone antagonizes analgesia produced by electrical stimulation of the hypothalamic arcuate nucleus in pentobarbital-anesthetized rats. Neuropharmacology 29, 1123–1129.

Watanabe, S., Kuwaki, T., Yanagisawa, M., Fukuda, Y., and Shimoyama, M. 2005. Persistent pain and stress activate pain-inhibitory orexin pathways. Neuroreport 16, 5–8.

Watkins, L. R. and Mayer, D. J. 1982. Organization of endogenous opiate and nonopiate pain control systems. Science 216, 1185–1192.

Watkins, L. R., Milligan, E. D., and Maier, S. F. 2003. Glial proinflammatory cytokines mediate exaggerated pain states: implications for clinical pain. Adv. Exp. Med. Biol. 521, 1–21.

Wei, F., Dubner, R., and Ren, K. 1999. Nucleus reticularis gigantocellularis and nucleus raphe magnus in the brain stem exert opposite effects on behavioral hyperalgesia and spinal Fos protein expression after peripheral inflammation. Pain 80, 127–141.

Westlund, K. N., Bowker, R. M., Ziegler, M. G., and Coulter, J. D. 1983. Noradrenergic projections to the spinal cord of the rat. Brain Res. 263, 15–31.

Westlund, K. N., Carlton, S. M., Zhang, D., and Willis, W. D. 1990. Direct catecholaminergic innervation of primate spinothalamic tract neurons. J. Comp. Neurol. 299, 178–86.

Wiertelak, E. P., Roemer, B., Maier, S. F., and Watkins, L. R. 1997. Comparison of the effects of nucleus tractus solitarius and ventral medial medulla lesions on illness-induced and subcutaneous formalin-induced hyperalgesias. Brain Res. 748, 143–150.

Willer, J. C., Boureau, F., and Albe-Fessard, D. 1979. Supraspinal influences on nociceptive flexion reflex and pain sensation in man. Brain Res. 179, 61–68.

Williams, F. G. and Beitz, A. J. 1993. Chronic pain increases brainstem proneurotensin/neuromedin-N mRNA expression:

a hybridization-histochemical and immunohistochemical study using three different rat models for chronic nociception. Brain Res. 611, 87–102.
Willis, W. D. and Westlund, K. N. 1997. Neuroanatomy of the pain system and of the pathways that modulate pain. J. Clin. Neurophysiol. 14, 2–31.
Willis, W. D., Westlund, K. N., and Carlton, S. M. 1995. Pain, In: The Rat Nervous System, 2nd edn. (*ed*. G. Paxinos), pp. 725–750. Academic Press.
Xie, J. Y., Herman, D. S., Stiller, C. O., Gardell, L. R., Ossipov, M. H., Lai, J., Porreca, F., and Vanderah, T. W. 2005. Cholecystokinin in the rostral ventromedial medulla mediates opioid-induced hyperalgesia and antinociceptive tolerance. J. Neurosci. 25, 409–416.
Yaksh, T. L. 1978. Opiate receptors for behavioral analgesia resemble those related to the depression of spinal nociceptive neurons. Science 199, 1231–1233.
Yaksh, T. L. 1979. Direct evidence that spinal serotonin and noradrenaline terminals mediate the spinal antinociceptive effects of morphine in the periaqueductal gray. Brain Res. 160, 180–185.
Yaksh, T. L. and Tyce, G. M. 1979. Microinjection of morphine into the periaqueductal gray evokes the release of serotonin from spinal cord. Brain Res. 1979 171, 176–181.
Yamamoto, T., Saito, O., Shono, K., and Hirasawa, S. 2003. Activation of spinal orexin-1 receptor produces anti-allodynic effect in the rat carrageenan test. Eur. J. Pharmacol. 481, 175–180.
Yamamoto, T., Nozaki-Taguchi, N, Sakashita, Y., and Kimura, S. 1999. Nociceptin/orphanin FQ: role in nociceptive information processing. Prog. Neurobiol. 57, 527–535.
Yang, H. Y., Fratta, W., Majane, E. A., and Costa, E. 1985. Isolation, sequencing, synthesis, and pharmacological characterization of two brain neuropeptides that modulate the action of morphine. Proc. Natl. Acad. Sci. U. S. A. 82, 7757–7761.
Yoshida, A., Chen, K., Moritani, M., Yabuta, N. H., Nagase, Y., Takemura, M., and Shigenaga, Y. 1997. Organization of the descending projections from the parabrachial nucleus to the trigeminal sensory nuclear complex and spinal dorsal horn in the rat. J. Comp. Neurol. 383, 94–111.
Young, R. F., Tronnier, V., and Rinaldi, P. C. 1992. Chronic stimulation of the Kolliker-Fuse nucleus region for relief of intractable pain in humans. J. Neurosurg. 76, 979–985.
Zadina, J. E., Hackler, L., Ge, L. J., and Kastin, A. J. 1997. A potent and selective endogenous agonist for the mu-opiate receptor. Nature 386, 499–502.
Zagon, A. 1995. Internal connections in the rostral ventromedial medulla of the rat. J. Auton. Nerv. Syst. 53, 43–56.
Zagon, A., Meng, X., and Fields, H. L. 1997. Intrinsic membrane characteristics distinguish two subsets of nociceptive modulatory neurons in rat RVM. J. Neurophysiol. 78, 2848–2858.
Zaki, P. A., Bilsky, E. J., Vanderah, T. W., Lai, J., Evans, C. J., and Porreca, F. 1996. Opioid receptor types and subtypes: the delta receptor as a model. Annu. Rev. Pharmacol. Toxicol. 36, 379–401.
Zambreanu, L., Wise, R. G., Brooks, J. C., Iannetti, G. D., and Tracey, I. 2005. A role for the brainstem in central sensitisation in humans. Evidence from functional magnetic resonance imaging. Pain 114, 397–407.
Zeilhofer, H. U. 2005. The glycinergic control of spinal pain processing. Cell. Mol. Life Sci. 2005 Jun 17 (Epub ahead of print).
Zeitz, K. P., Guy, N., Malmberg, A. B., Dirajlal, S., Martin, W. J., Sun, L., Bonhaus, D. W., Stucky, C. L., Julius, D., and Basbaum, A. I. 2002. The 5-HT3 subtype of serotonin receptor contributes to nociceptive processing via a novel subset of myelinated and unmyelinated nociceptors. J. Neurosci. 22, 1010–1019.
Zhang, D. X., Owens, C. M., and Willis, W. D. 1991. Two forms of inhibition of spinothalamic tract neurons produced by stimulation of the periaqueductal gray and the cerebral cortex. J. Neurophysiol. 65, 1567–1579.
Zhang, Y., Yang, Z., Gao, X., and Wu, G. 2001. The role of 5-hydroxytryptamine1A and 5-hydroxytryptamine1B receptors in modulating spinal nociceptive transmission in normal and carrageenan-injected rats. Pain 92, 201–211.
Zhang, J., Hoffert, C., Vu, H. K., Groblewski, T., Ahmad, S., and O′Donnell, D. 2003. Induction of CB2 receptor expression in the rat spinal cord of neuropathic but not inflammatory chronic pain models. Eur. J. Neurosci. 17, 2750–2754.
Zhang, R. X., Lao, L., Wang, L., Liu, B., Wang, X., Ren, K., and Berman, B. M. 2004. Involvement of opioid receptors in electroacupuncture-produced anti-hyperalgesia in rats with peripheral inflammation. Brain Res. 1020, 12–17.
Zhong, F. X., Ji, X. Q., and Tsou, K. 1985. Intrathecal DSP4 selectively depletes spinal noradrenaline and attenuates morphine analgesia. Eur. J. Pharmacol. 116, 327–330.
Zhuo, M. and Gebhart, G. F. 1990. Spinal cholinergic and monoaminergic receptors mediate descending inhibition from the nuclei reticularis gigantocellularis and gigantocellularis pars alpha in the rat. Brain Res. 535, 67–78.
Zhuo, M. and Gebhart, G. F. 1991. Spinal serotonin receptors mediate descending facilitation of a nociceptive reflex from the nuclei reticularis gigantocellularis and gigantocellularis pars alpha in the rat. Brain Res. 550, 35–48.
Zhuo, M. and Gebhart, G. F. 1992. Characterization of descending facilitation and inhibition of spinal nociceptive transmission from the nuclei reticularis gigantocellularis and pars alpha in the rat. J. Neurophysiol. 67, 1599–1614.
Zhuo, M. and Gebhart, G. F. 1997. Biphasic modulation of spinal nociceptive transmission from the medullary raphe nuclei in the rat. J. Neurophysiol. 78, 746–758.
Zorman, G., Belcher, G., Adams, J. E., and Fields, H. L. 1982. Lumbar intrathecal naloxone blocks analgesia produced by microstimulation of the ventromedial medulla in the rat. Brain Res. 236, 77–84.

Further Reading

Calejesan, A. A., Ch′ang, M. H., and Zhuo, M. 1998. Spinal serotonergic receptors mediate facilitation of a nociceptive reflex by subcutaneous formalin injection into the hindpaw in rats. Brain Res. 798, 46–54.
Dubner, R. and Ren, K. 1999. Endogenous mechanisms of sensory modulation. Pain Suppl. 6, S45–53.
Guan, Y., Guo, W., Robbins, M. T., Dubner, R., and Ren, K, 2004. Changes in AMPA receptor phosphorylation in the rostral ventromedial medulla after inflammatory hyperalgesia. Neurosci. Lett. 366, 201–205.
Janss, A. J., Cox, B. F., Brody, M. J., and Gebhart, G. F. 1987. Dissociation of antinociceptive from cardiovascular effects of stimulation in the lateral reticular nucleus in the rat. Brain Res. 405, 140–149.
Jasmin, L., Boudah, A., and Ohara, P. T. 2003a. Long-term effects of decreased noradrenergic central nervous system

innervation on pain behavior and opioid antinociception. J. Comp. Neurol. 460, 38–55.
Mason, P. 1997. Central mechanisms of pain modulation. Curr. Op. Neurobiol. 9, 436–441.
Rahman, W., Suzuki, R., Rygh, L. J., and Dickenson, A. H. 2004. Descending serotonergic facilitation mediated through rat spinal 5HT3 receptors is unaltered following carrageenan inflammation. Neurosci. Lett. 361, 229–231.
Vaccarino, A. L. and Chorney, D. A. 1994. Descending modulation of central neural plasticity in the formalin pain test. Brain Res. 666, 104–108.
Villanueva, L., Desbois, C., Le Bars, D., and Bernard, J. F. 1998. Organization of diencephalic projections from the medullary subnucleus reticularis dorsalis and the adjacent cuneate nucleus: a retrograde and anterograde tracer study in the rat. J. Comp. Neurol. 390, 133–160.
Wei, F., Ren, K., and Dubner, R. 1998. Inflammation-induced Fos protein expression in the rat spinal cord is enhanced following dorsolateral or ventrolateral funiculus lesions. Brain Res. 782, 136–141.
Woolf, C. J. and Salter, M. W. 2000. Neuronal plasticity: increasing the gain in pain. Science 288, 1765–1768.

5.50 Diffuse Noxious Inhibitory Controls (DNIC)

D Le Bars, INSERM U-713, Paris, France

J C Willer, INSERM U-731, Paris, France

© 2008 Elsevier Inc. All rights reserved.

5.50.1	Introduction	764
5.50.2	A Spinally Mediated Process	764
5.50.3	A Spinally Mediated Process Involving Supraspinal Structures	768
5.50.4	A Model in the Rat	769
5.50.5	The Role of Wide-Dynamic-Range Neurons	769
5.50.6	Summary and Conclusions	772
References		772

Glossary

allodynia Pain caused by stimuli that would not normally cause pain (i.e., non-noxious stimuli).

basic somesthetic activity Description of the ongoing activity in somatosensory pathways in the absence of any deliberate stimuli but including stimuli provided by the environment.

blink reflex Exteroceptive reflex of the orbicularis oculi muscles usually evoked by stimuli such as a mechanical tap on the glabella or by electrical currents delivered to the skin in the periorbital region.

Brown-Séquard syndrome Patient with a hemisection of the spinal cord of traumatic origin.

bulbospinal control A neural control mechanism originating in the brainstem and projecting to the spinal cord.

dermatome Area of skin innervated by nerves from a given segment of the spinal cord.

descending inhibition Inhibition of spinal cord function produced by pathways originating in the brain.

diffuse noxious inhibitory controls (DNICs) Neural controls triggered by noxious stimulation of widespread areas of the body which exert an inhibitory influence on wide-dynamic-range (WDR) neurons.

electromyography (EMG) All electrophysiological methods for exploring the physiology and pathophysiology of peripheral nerves and muscles.

excitatory receptive field Area of the body (surface or interior) which when stimulated will produce excitation of a given neuron.

hemianalgesia Loss of pain sensation from one half of the body.

heterotopic Part of the body remote from the area of interest (e.g., the excitatory receptive field of a neuron).

Hoffmann reflex (H reflex) Monosynaptic reflex from the calf muscles elicited by electrical stimulation of the sciatic nerve.

inhibitory receptive field Area of the body (surface or interior) which when stimulated will produce inhibitory effects on the activity of a given neuron.

jaw-opening reflex Exteroceptive reflex produced by stimulation of facial or intraoral afferents and involving activation of jaw opening muscles (e.g., the digastric) and/or inhibition of activity in jaw closing muscles (e.g., the masseter).

jerk reflex Myotatic monosynaptic reflex usually elicited by a percussion of a muscle's tendon using a reflex testing hammer.

Lasègue's maneuver Elevation of a lower limb in an extended position on a patient lying on a bed. This technique explores the Lasègue's sign which is the painful limitation of the angle of elevation in cases of radicular compression of the sciatic nerve.

microelectrophoretic application Application of a substance in its ionic form from a microelectrode by the application of electrical current.

monoarthritis Inflammation of a single joint.

mononeuropathy A disturbance of function or pathological changes in a single nerve.

nociceptive stimulus Stimulus that activates nociceptive afferents (which could be a noxious stimulus or an electrical stimulus).

noxious stimulus Stimulus that causes or threatens to cause tissue damage.

polyarthritis Inflammation of several joints.

propriospinal mechanism Neural mechanism mediated entirely within the spinal cord.

R_{III} reflex Electromyographic response elicited by electrical painful stimulation of the (purely cutaneous) sural or ulnar nerve by recording from the biceps femoris (lower limb) or biceps brachialis (upper limb), respectively. So-named because it involves activation of group III (Aδ) afferents.
subnucleus reticularis dorsalis (SRD) Brainstem nucleus located ventral to the cuneate nucleus, between trigeminal nucleus caudalis and the nucleus of the solitary tract.
supraspinal mechanism Neural mechanism that involves structures above the spinal cord.
tetraplegic Patient with a complete transection of traumatic origin at a high level of the spinal cord thus affecting all four limbs.
transcutaneous electrical nerve stimulation (TENS) Technique for inducing analgesia/hypoalgesia by electrically stimulating peripheral nerves through the skin (i.e., with electrodes placed on the skin).
trigeminal nucleus caudalis Most caudal part of the trigeminal sensory nuclear complex (or of the trigeminal spinal nucleus); also sometimes called the medullary dorsal horn.
ventrolateral quadrant Part of the spinal cord where spinoreticular and spinothalamic fibers travel.
Wallenberg's syndrome Patient with a unilateral lesion of the retro-olivary part of the brainstem resulting from the ischemia of a posterior cerebellar artery.
wide-dynamic-range (WDR) neurons Neurons of the dorsal horn activated by both noxious and non-noxious stimuli.

5.50.1 Introduction

Painful stimuli can diminish or even mask pain elicited by stimulation of a remote (extrasegmental) part of the body (see references in Melzack, R., 1989; Le Bars, D. and Willer, J. C., 2002). This phenomenon has been known since ancient times as illustrated by the Hippocrates' aphorism: "If a patient be subject to two pains arising in different parts of the body simultaneously, the stronger blunts the other." Numerous popular therapeutic methods for the alleviation of pain – some used spontaneously by patients – take advantage of this common clinical observation. It is often referred to as counter-irritation or counter-stimulation. In Kabylia, for example, healers treat rheumatic pain by placing a red-hot scythe close to the abdomen of the patient and then vibrating it at a frequency of about 3 Hz, in order to create a series of acute burning-type painful sensations.

A working hypothesis was developed that some of the neurons involved in the transmission of nociceptive signals might be inhibited by nociceptive stimulation of peripheral territories outside their own excitatory receptive fields. Such a hypothesis was found to be correct at as early a stage in the processing of nociceptive signals as the spinal cord. This phenomenon was termed diffuse noxious inhibitory control (DNIC). Since these spinal neurons are involved in mediating both pain and nociceptive reflexes, DNIC can be studied at three related endpoints: spinal neuronal activities, reflexes, and sensations. The first two are accessible in animals while the last two can be studied in human beings (Figure 1).

5.50.2 A Spinally Mediated Process

Combined psychophysical measurements and recordings of nociceptive reflexes in man have shown that the spinal cord is involved in the phenomenon of pain inhibiting pain (Willer, J. C. *et al.*, 1984). Electrical stimulation of the sural nerve at the ankle simultaneously induces a nociceptive reflex in a knee flexor muscle (the R_{III} reflex) and a pinprick type of painful sensation in the territory of the nerve (Willer, J. C., 1977). Both the reflex and the sensation have strong relationships with the stimulus intensities – with the thresholds for both parameters being practically identical.

One line of study involved recording these parameters (i.e., the reflex and pain) before, during, and after the application of heterotopic conditioning stimuli such as the immersion of a hand in a thermoregulated water bath at various temperatures (Figure 2, upper panels). When the temperature of the bath was lower than 45 °C, the immersion of the

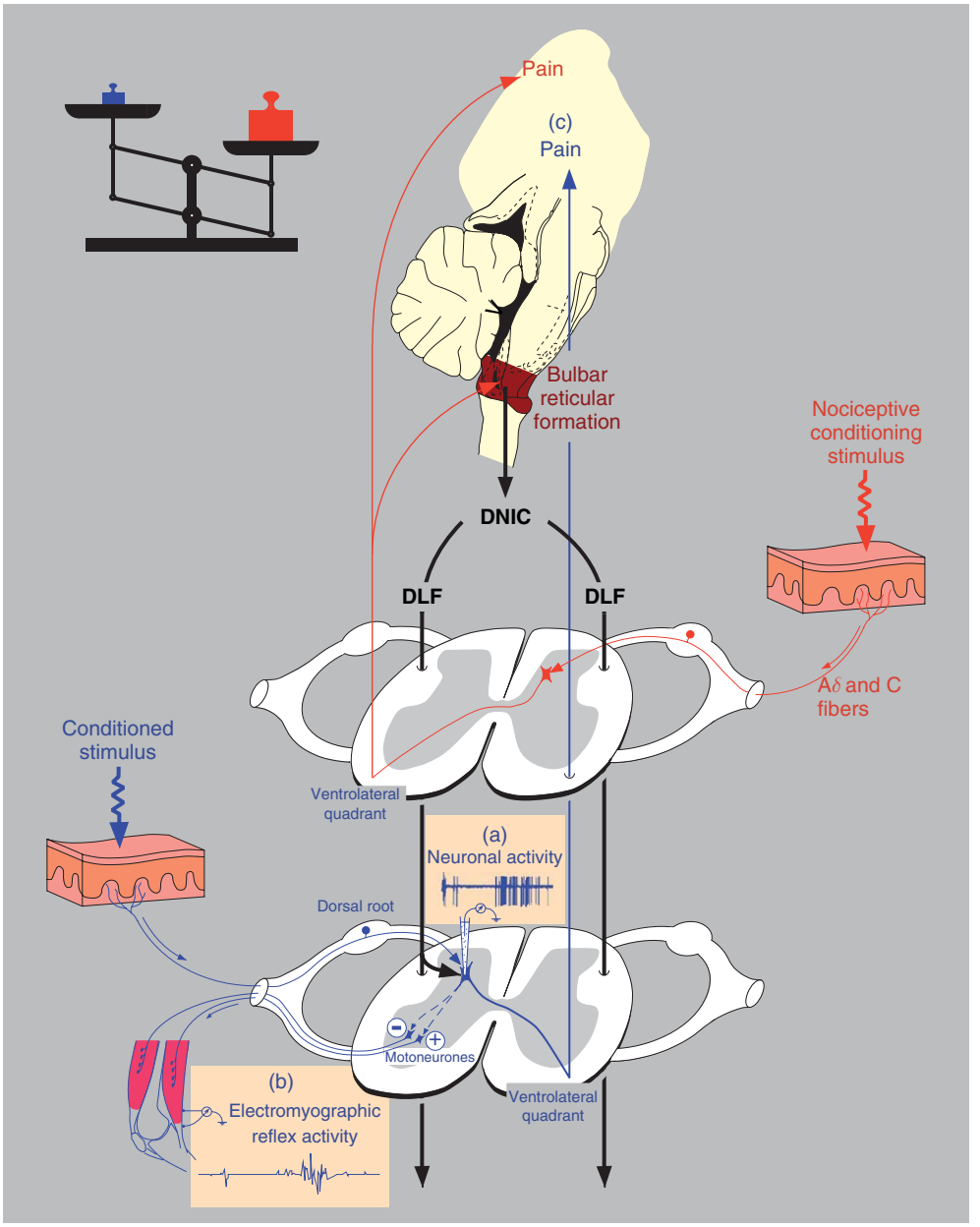

Figure 1 Nociceptive signals activate dorsal horn neurons, which in turn transfer the information to the brain to elicit pain and to spinal interneurons (broken blue line) to elicit somatic and vegetative reflexes. The effects on motoneurons through polysynaptic pathways trigger a movement that moves the stimulated area away from the stimulus. This movement results from both excitatory (e.g., contraction of flexor muscles) and inhibitory mechanisms – the latter affecting antagonist muscles. In animals, one can record from neurons (a) and from muscles (b) but the sensation (c) cannot be assessed. In man, on the other hand, one cannot record from neurons but it is possible to monitor both the sensation and the reflex activities. In an experimental paradigm designed for the study of pain inhibiting pain phenomena, one requires a conditioned stimulus (here in blue) with the corresponding endpoints (a, b, or c) and a conditioning stimulus (here in red). A painful focus activates dorsal horn neurons that send an excitatory signal through the ventrolateral quadrant toward higher centers, including the lower brainstem. This signal activates DNICs, which will inhibit WDR neurons through the dorsolateral funiculi (DLF). With two painful foci, the resulting sensation will depend on the balance of the nociceptive information elicited from the two sources. The power of such nociceptive information depends on the three dimensions of any nociceptive stimulus, namely strength, duration, and area. In an experimental situation designed to observe inhibitions of the response to the conditioned stimulus, the beam of the balance should tilt in favor of the conditioning stimulus. This is illustrated in Figure 2 where the response to a 20 ms duration series of electrical pulses is inhibited by the stimulation of the hand for 2 min.

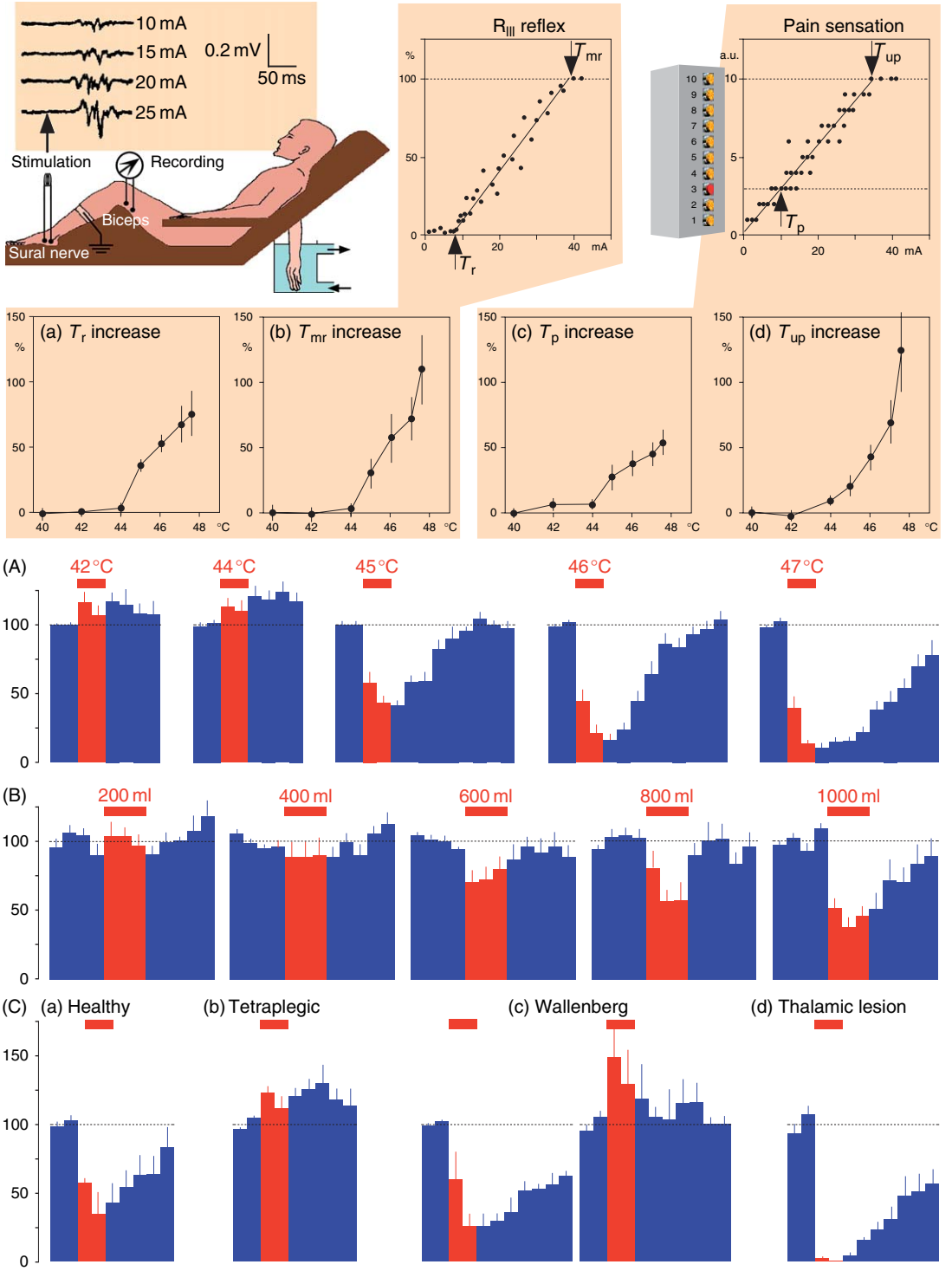
10 mA
15 mA
20 mA
25 mA
0.2 mV
50 ms
Stimulation
Recording
Biceps
Sural nerve
R_{III} reflex
T_{mr}
T_r
Pain sensation
T_{up}
T_p
a.u.
(a) T_r increase
(b) T_{mr} increase
(c) T_p increase
(d) T_{up} increase
(A)
42 °C
44 °C
45 °C
46 °C
47 °C
(B)
200 ml
400 ml
600 ml
800 ml
1000 ml
(C)
(a) Healthy
(b) Tetraplegic
(c) Wallenberg
(d) Thalamic lesion

hand did not elicit any change in the stimulus–response relationships. By contrast, temperatures between 45 and 47.5 °C caused the stimulus–response curves to shift to the right as a direct function of the temperature. Similar effects were observed when other painful procedures were applied as conditioning stimuli (e.g., cold, pressure, exercise under ischemia, high-intensity transcutaneous electrical nerve stimulation) (Willer, J. C. *et al*., 1984; 1989; Danziger, N. *et al*., 1998; France, C. R. and Suchowiecki, S., 1999; Sandrini, G. *et al*., 2000).

The temporal evolution of these phenomena can be studied by applying a heterotopic conditioning stimulus while the sural nerve is stimulated at a constant intensity (Figure 2, lower panels). This procedure revealed aftereffects of long duration. For example, a 2 min immersion of the hand in a 47 °C water bath completely abolished the R_{III} reflex and it took more than 9 min to achieve a full recovery (Figure 2(A)). Very similar effects were produced by visceral stimulation (gastric or rectal distension) in healthy volunteers (Bouhassira, D. *et al*., 1994; 1998). During gastric distension for example (Figure 2(B)), the inhibitory effects increased with the volume of distension and the resultant sensation. As with the inhibitions elicited by stimulation of somatic structures, these visceral-evoked inhibitions were correlated to the intensity of the conditioning stimuli. However, they could be triggered by stimuli which were unpleasant but not quite painful (Figure 2(C)). When they become clearly painful, the duration of the inhibitory effects outlasted the duration of the distension by several minutes.

Clinical pains can also activate this type of inhibition. Thus, in patients suffering from sciatic pain due to a herniated disk, a Lasègue's maneuver of the affected leg, which elicits a typical radicular pain, also blocks the R_{III} reflex, both in the affected and

Figure 2 (Upper panels) Experimental setup for recording the nociceptive R_{III} flexion reflex from the biceps femoris muscle in the lower limb using surface electrodes. The reflex is evoked by electrical stimulation of the ipsilateral sural nerve. The insert shows typical examples of electromyographic (EMG) responses elicited by increasing stimulus intensities (from top to bottom). The subjective sensation was estimated by the subject on a 10-level scale (box with switches shown in insert), with the pain threshold being defined as level 3. Examples of stimulus–response curves for the nociceptive reflex and subjective reports of sensations produced by a wide range of stimulation intensities applied randomly are shown on the left and right graphs, respectively. Note the close correlations between (1) the reflex threshold (T_r) and the pain threshold (T_p) around 10 mA; and (2) the stimulus intensities producing maximal responses, that is, the threshold of the maximal reflex recruitment (T_{mr}) versus the threshold of unbearable pain (T_{up}). Such recruitment curves were built before and during a 2 min period of immersion of the right hand in a thermoregulated water bath. No effects were seen at lower temperatures but a shift of the curves to the right was elicited when the temperature reached painful levels (45 °C and above). The shift applied to the reflex (a, b) and sensation (c, d) thresholds. (Lower panels) The temporal evolution of the reflex can be monitored by employing repeated, constant, stimulation of the sural nerve (1.2 times threshold every 6 s). The individual R_{III} reflex is expressed in terms of the percentages of the mean value recorded during a control period. Each vertical bar represents the mean of ten responses recorded during 1 min. Graphs show pooled data from several subjects. (A) Effects of immersion of the hand. The nonpainful temperature (42 and 44 °C, left) did not modify the reflex. By contrast, the painful temperatures (45, 46, and 47 °C) depressed the reflex during and after the period of conditioning. The extent of these depressions was temperature dependent. Note the long duration (around 10 min) of the inhibitory posteffects following the application of the highest temperature (47 °C, right). (B) Effects of visceral stimulation. Gastric distension by means of a balloon introduced into the proximal part of the stomach was applied for a 3 min period. The inflation of the balloon in volumes of 200 or 400 ml did not modify the R_{III} reflex, whereas volumes of 600, 800, and 1000 ml produced inhibitions correlated to the volume of distension. The 600 and 800 ml distensions were unpleasant while the 1000 ml volume was clearly painful. (C) Effects of nociceptive electrical stimuli (20–25 mA) applied to the upper limb of healthy volunteers or patients with lesions of the spinal cord or the brain. (a) In healthy volunteers; (b) in tetraplegic patients, the conditioning stimulus did not inhibit the R_{III} reflex; (c) in patients with a Wallenberg syndrome (unilateral lesion of the retro-olivary part of the brainstem) the conditioning stimuli did or did not inhibit the R_{III} reflex depending on whether it was applied to the normal hand (ipsilateral to the brain lesion) or the analgesic hand (contralateral to the brain lesion); and (d) in patients with thalamic lesions, the conditioning stimulation applied to the analgesic hand (contralateral to the brain lesion) did produce inhibition of the R_{III} reflex. (Upper panels) Adapted from Willer, J. C., Roby, A., and Le Bars, D. 1984. Psychophysical and electrophysiological approaches to the pain relieving effect of heterotopic nociceptive stimuli. Brain 107, 1095–1112. (A) Adapted from Willer, J. C., De Broucker, T., and Le Bars, D. 1989. Encoding of nociceptive thermal stimuli by diffuse noxious inhibitory controls in humans. J. Neurophysiol. 62, 1028–1038. (B) Adapted from Bouhassira, D., Chollet, R., Coffin, B., *et al.* 1994. Inhibition of a somatic nociceptive reflex by gastric distention in humans. Gastroenterology 107, 985–992. (C) Adapted from Roby-Brami, A., Bussel, B., Willer, J. C., and Le Bars, D. 1987. An electrophysiological investigation into the pain-relieving effects of heterotopic nociceptive stimuli: probable involvement of a supraspinal loop. Brain 110, 1497–1508; and De Broucker, T., Cesaro, P., Willer, J. C., Le Bars, D. 1990. Diffuse noxious inhibitory controls (DNIC) in man: involvement of the spino-reticular tract. Brain 113, 1223–1234.

in the nonaffected leg (Willer, J. C. *et al.*, 1987). When the Lasègue's maneuver is performed on the healthy limb, it is painless and has no effect on the reflex. In patients suffering from neuropathic pain, the R_{III} reflex is inhibited when pain is triggered by pressure ('static allodynia'), but not when it is triggered by light brushing ('dynamic allodynia') (Bouhassira, D. *et al.*, 2003). Interestingly, it is generally agreed that the former is due to the activation of nociceptive processes via Aδ- and C-fibers, while the latter is due to the activation of Aβ-fibers.

In summary, a painful conditioning stimulus can depress both a preexisting pain and its associated nociceptive reflex at the first spinal relays for the transmission of nociceptive information. Interestingly, nociceptive brainstem reflexes such as the blink or jaw-opening reflexes are also inhibited by remote painful stimulation (Pantaleo, T. *et al.*, 1988; Maillou, P. and Cadden, S. W., 1997; Ellrich, J. and Treede, R. D., 1998). By contrast, nonnociceptive reflexes such as jerk or Hoffmann reflexes remain unaffected during such procedures. One must stress here that there has to be an obvious imbalance between the conditioned and the conditioning stimuli for a clear depressive effect to be seen. For instance, in the examples shown in Figure 2, the conditioned stimuli were short (20 ms) trains of electrical shocks, whereas the conditioning stimuli were applied over time periods of several seconds to large areas of the body. Clearly, spatiotemporal summation is required to elicit visible inhibitory effects because of the reciprocal nature of the phenomenon triggered by two remote painful foci. A balance, the beam of which tips (or does not tip) in favor of one or other pain, could symbolize the net result of such a reciprocal process (Figure 1, upper left). Of course, clinical situations are always much more complicated than these experimental situations which are deliberately designed to simplify the problem under analysis. More particularly, it seems likely that the existence of multiple painful foci would produce very complicated interactions between excitatory and inhibitory processes.

5.50.3 A Spinally Mediated Process Involving Supraspinal Structures

Are the inhibitory mechanisms described above due to propriospinal mechanisms or do they involve supraspinal structures? To answer this question, the effects on the R_{III} reflex in the right leg, of nociceptive conditioning stimuli applied to the fourth and fifth fingers of the left hand were compared in normal subjects and tetraplegic patients with lesions of traumatic origin at the cervical-5–7 level (Roby-Brami, A. *et al.*, 1987). In the normal subjects (Figure 2(Ca)), the painful conditioning stimuli strongly depressed both the R_{III} reflex and the associated pain. By contrast, in the tetraplegic patients, nociceptive stimulation of the same territories, which, being in the cervical-8 and thoracic-1 dermatomes, were clinically unaffected by the spinal lesion, and did not produce any depression of the R_{III} reflex (Figure 2(Cb)). One can therefore conclude that the inhibitory effects triggered by heterotopic nociceptive stimuli are sustained by a loop that includes supraspinal structures.

In order to identify, or at least localize, these supraspinal structures, observations were made on patients with cerebral lesions causing contralateral hemianalgesia (De Broucker, T. *et al.*, 1990). These were patients with either a lesion of the retro-olivary part of the medulla (Wallenberg's syndrome, Figure 2(Cc)) or a unilateral thalamic lesion (Figure 2(Cd)). In the former group, no inhibitions were observed when the (not felt) nociceptive conditioning stimulus was applied to the affected side of the body, contralateral to the brain lesion. If this stimulus was applied to the normal side, ipsilateral to the brain lesion, it was felt as painful and triggered inhibitory effects very similar to those seen in normal subjects. By contrast, in the patients with a thalamic lesion, the R_{III} reflex was strongly depressed, as in normal subjects, by the nociceptive conditioning stimulus applied to the affected side (which was not felt as painful). Thalamic structures and consequently spinothalamic pathways, are therefore not involved in DNIC, whereas brainstem – probably reticular – structures seem to play a key role in these phenomena. These observations also demonstrate unambiguously that such phenomena can be elicited in the absence of a painful sensation, provided the nociceptive nature of the information reaches some brain structures. This suggests that the observed phenomenon does not result from a competition between the two attentional foci that the conditioned and the conditioning pain represent in the healthy volunteers. This is an important observation as it is known that the perception of pain is sensitive to attentional processes (Bushnell, M. C. *et al.*, 1985; Willer, J. C. *et al.*, 1979).

An exceptional case was also reported in a patient with a Brown-Séquard syndrome due to a hemisection

of the spinal cord (left side, T6 level) produced by a knife-stab in the back (Bouhassira, D. *et al*., 1993). The R_{III} reflexes elicited by stimulation of cutaneous afferents in the ulnar and sural nerves were studied in the upper and lower limbs by recording from the biceps brachialis and biceps femoris muscles, respectively. For each limb, the R_{III} reflex was elicited regularly before, during, and after periods of nociceptive electrical conditioning stimulation applied successively to the other three limbs. Inhibitions of around 90% followed by strong poststimulus effects were observed in all situations except that (1) no inhibition could be obtained when the conditioning stimuli were applied to the lower right limb (contralateral to the spinal lesion), and (2) the R_{III} reflex in the lower left limb was completely insensitive to any of the conditioning stimuli. These results strongly suggest that in human beings (1) the ascending part of the loop subserving DNIC is completely crossed at the spinal level, and (2) the descending part is confined to the white matter ipsilateral to the limb being tested.

5.50.4 A Model in the Rat

Another nociceptive reflex – this time recorded in the anaesthetized rat – is the C-fiber reflex which can be elicited by electrical stimulation of the sural nerve and recorded from the biceps femoris muscle. This reflex can be strongly inhibited by both mechanical and thermal noxious heterotopic stimuli applied to the muzzle, a paw or the tail, and by colorectal distension. These inhibitory effects on the C-fiber reflex did not occur in spinal animals, or ipsilateral to a rostral unilateral lesion of the dorsolateral funiculus (DLF). Such observations are consistent with several reports showing the inhibition of reflexes or the increase of nociceptive thresholds elicited by heterotopic noxious conditioning. For example, the reflex discharge in the common peroneal nerve following electrical stimulation of the sural nerve in the rat was inhibited by pinching the muzzle or tail; the gastrocnemius medialis reflex evoked by sural nerve stimulation in the decerebrate rabbit was inhibited by electrical stimulation of the contralateral common peroneal or of the ipsi- or contralateral median nerves; the digastric reflex evoked by tooth pulp stimulation in the cat was inhibited by toe pinch, percutaneous electrical stimulation of a limb or electrical stimulation of the saphenous nerve. In behavioral experiments, intraperitoneal or cutaneous injections of an irritant agent or noxious heat all produce an increase in nociceptive thresholds in distant somatic structures, notably the tail (e.g., tail flick test) and paws (e.g., paw withdrawal test). (See references in Le Bars, D. *et al*., 2001.)

5.50.5 The Role of Wide-Dynamic-Range Neurons

In several species (rat, mouse, cat, and probably monkey), most WDR and some nociceptive-specific neurons are strongly inhibited by a noxious stimulus applied outside their excitatory receptive fields. Such effects do not appear to be somatotopically organized but apply to the whole body. Figure 3 shows examples of recordings from lumbar WDR neurons in the rat. The activities of these neurons – whether elicited by pinching their receptive field or by applying an excitatory amino acid to their membranes – were strongly inhibited by noxious mechanical (pinch of the muzzle, the contralateral hindpaw or the tail) or thermal stimuli (immersion of the tail in a 52 °C water bath) (Figure 3(A)). These examples illustrate the whole body inhibitory receptive fields of WDR neurons as recorded in intact rats. Interestingly, such inhibitory controls are exacerbated during clinical pains, for example, when an animal suffers from monoarthritis, polyarthritis or a peripheral mononeuropathy (Danziger, N. *et al*., 2000; 2001).

These properties of dorsal horn neurons were observed at the level of various segments of the spinal cord and in both nucleus caudalis and nucleus oralis of the trigeminal system – thus suggesting a general organization. In keeping with the human studies shown in Figure 2, there is a clear relationship between the intensity of the conditioning stimulus and the strength of the resultant DNIC. With strong stimuli, the inhibitory effects are powerful and followed by long-lasting poststimulus effects, which can persist for several minutes. In some cases, the inhibitory effects can involve a complete abolition of activity for a long period of time following removal of the conditioning stimuli ('switch off') and the activity can be restored to preconditioning levels by further manipulations of the excitatory receptive field ('switch on') (Cadden, S. W., 1993). (See references in Le Bars, D., 2002.)

With regard to the viscera, some differences should be noted: visceral stimuli, for example, distension of the colon or urinary bladder, generally produce inhibitions with slower rates of onset and recovery but

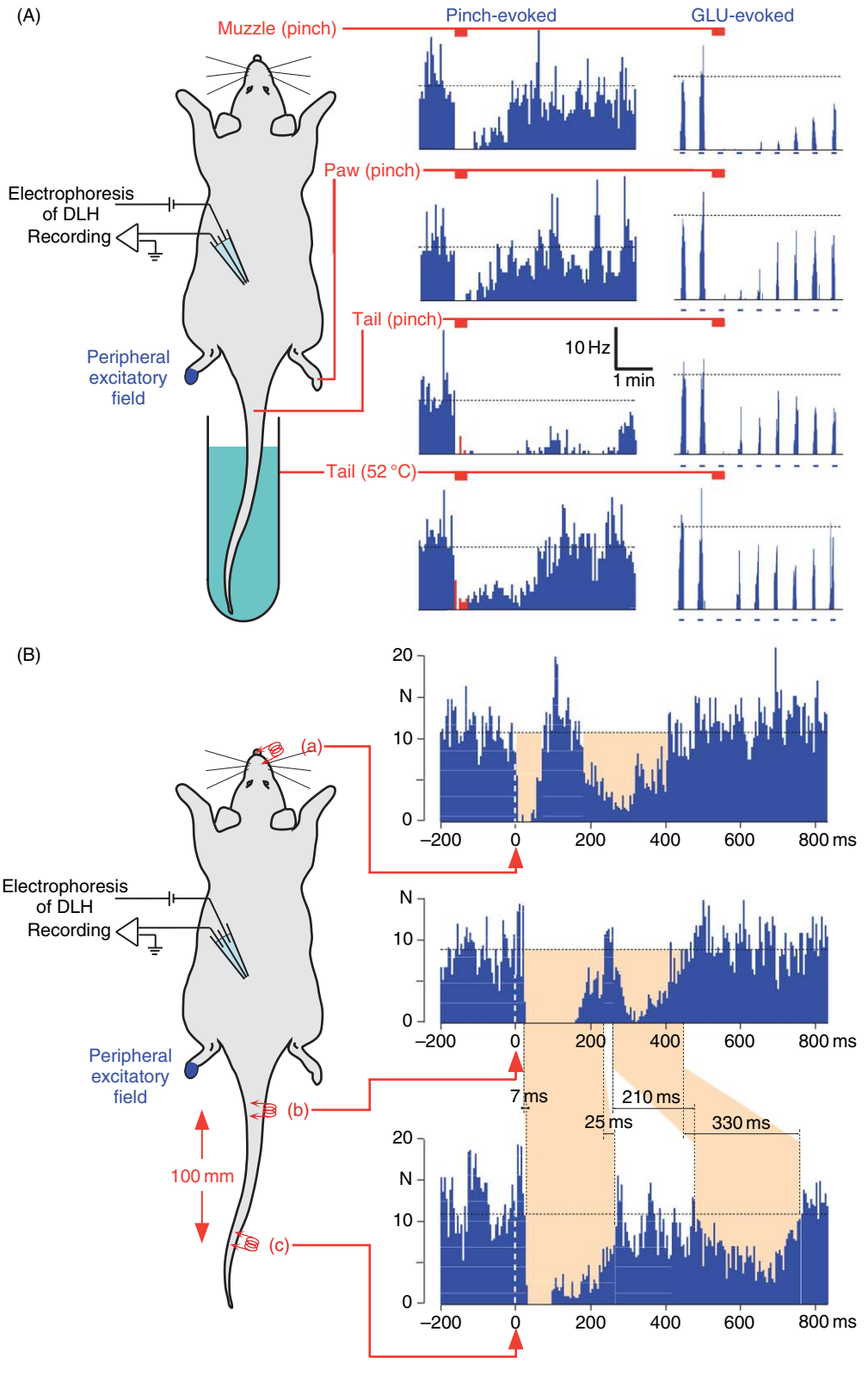
(A)
Muzzle (pinch)
Pinch-evoked
GLU-evoked
Paw (pinch)
Electrophoresis
of DLH
Recording
Tail (pinch)
10 Hz
1 min
Peripheral
excitatory
field
Tail (52 °C)
(B)
20
N
10
0
–200
0
200
400
600
800 ms
(a)
Electrophoresis
of DLH
Recording
Peripheral
excitatory
field
(b)
100 mm
(c)
7 ms
25 ms
210 ms
330 ms

starting at intensities below a painful level (Cadden, S. W. and Morrison, J. F. B., 1991). It was proposed that these differences might have reflected different amounts and patterns of activity in the relevant primary afferent fibers rather than being due to different central neural mechanisms. Again, this is consistent with human studies (e.g., Figure 2(B)).

In any case, these data suggest that DNICs are triggered specifically by the activation of peripheral nociceptors whose signals are carried by Aδ- and C-fibers. In order to investigate further the types of peripheral fiber involved in DNIC, use was made of the facts that (1) trigeminal and spinal dorsal horn neurons respond with relatively steady discharges to the microelectrophoretic application of excitatory amino acids; and (2) DNICs act by a final postsynaptic inhibitory mechanism involving hyperpolarization of the neuronal membrane. It was found that when trigeminal WDR neurons were directly excited by the microelectrophoretic application of glutamate, the percutaneous application of single square-wave, electrical stimuli to the tail always induced a biphasic depression of the resultant activity. Both the early and late components of this inhibition occurred with shorter latencies when the base rather than the tip of the tail was stimulated. Such differences in latency were used to estimate the mean conduction velocities of the peripheral fibers triggering the inhibitions: the means were found to be 7.3 and 0.7 m s^{-1}, which fall into the Aδ- and C-fiber ranges, respectively. Such biphasic inhibitions could be elicited from any part of the body and recorded from any WDR neurons. Figure 3(B) shows a recording from a lumbar WDR neuron with an excitatory receptive field located on the extremity of the ipsilateral hind paw: two components of inhibition were induced by the activation of Aδ and C-fibers, respectively, when a single 2 ms duration shock of 10 mA was applied to the muzzle, the base or the tip of the tail.

DNICs are not observed in anesthetized or decerebrate animals in which the spinal cord has been sectioned. It is therefore obvious that the mechanisms underlying DNICs are not confined to the spinal cord and that supraspinal structures must be involved. Such a system is therefore completely different from segmental inhibitory systems, which work both in intact and in spinal animals, and can be triggered by the activation of low-threshold afferents. DNICs are also very different from the propriospinal inhibitory processes that can be triggered by noxious inputs. It should also be noted that DNIC are blocked by increasing the anesthetic regimen (Jinks, S. L. *et al.*, 2003).

The ascending and descending limbs of this loop travel through the ventrolateral and dorsolateral funiculi, respectively. Since thalamic lesions do not affect DNICs, it has been proposed that they result from a physiological activation of some of the brainstem structures that produce descending inhibition

Figure 3 (A) Example of inhibitions of a spinal WDR neuron elicited by noxious heterotopic stimuli. Recordings were made in the lumbar dorsal horn from a WDR neuron with a receptive field located on the ipsilateral hind paw. The neuron was activated either by a sustained pinch of its receptive field or by regular (once a minute) microelectrophoretic applications of the excitatory amino acid, glutamate (GLU, 20 nA, horizontal bars). Conditioning stimuli were pinch of the muzzle, the contralateral hind paw or the tail, and immersion of the tail in a 52 °C water bath (from top to bottom, respectively). Note that all these conditioning stimuli virtually blocked both the pinch-evoked and the DLH-induced firing. In the latter case, the inhibitions remained for several minutes in most cases, suggesting that WDR neurons were hyperpolarized for a long time following the conditioning stimulation. (B) Example of heterotopic activation of Aδ- and C-fibers triggering inhibitions in a spinal WDR neuron. Left: Schematic representation of the experimental design. Recordings were made in the lumbar dorsal horn from a WDR neuron with a receptive field located on the ipsilateral hind paw. The continuous microelectrophoretic application of the excitatory amino acid, DL-homocysteic acid (DLH) induced a steady discharge from the neuron under study. The repetitive application of individual percutaneous electrical stimuli of adequate intensities to the contralateral muzzle (a), the base (b), or the tip (c) of the tail induced biphasic depressions of the neuronal activity. Right: Peristimulus histograms (bin width 5 ms) prepared during the continuous microelectrophoretic application (15 nA) of DLH onto the membrane of the neuron. The broken white lines show the timing of percutaneous electrical stimulation (10 mA; 2 ms duration; 0.66 Hz; 200 ms delay; 100 sweeps). The broken black line represents the mean firing calculated during the prestimulation control period (−200 to 0 ms). Two waves of inhibition can be seen. They occurred earlier when the base of the tail (b) was stimulated instead of the tip (c). The time gaps are shown as yellow areas between the histograms, for both inhibitory components. The gap was 7 and 25 ms for the beginning and the end of the first component; it was 150 and 290 ms for the beginning and the end of the second component. Knowing that the distance between b and c was 100 mm, one can easily calculate the conduction velocities of fibers that elicited the first and second components: 4–14 m s^{-1} and 0.3–0.7 m s^{-1} respectively. These fibers therefore belong to the Aδ- and C- groups, respectively. (A) Adapted from Villanueva, L., Cadden, S. W., and Le Bars, D. 1984. Evidence that diffuse noxious inhibitory controls (DNIC) are mediated by a final post-synaptic inhibitory mechanism. Brain Res. 298, 67–74.

(see Chapter 5.49). Surprisingly, DNICs were not modified by lesions of the following structures: the periaqueductal gray (PAG), cuneiform nucleus, parabrachial area, locus coeruleus/subcoeruleus, rostral ventromedial medulla (RVM). By contrast, lesions of subnucleus reticularis dorsalis (SRD) in the caudal medulla strongly reduced DNICs. The SRD is located ventral to the cuneate nucleus, between trigeminal nucleus caudalis and the nucleus of the solitary tract and contains neurons with characteristics that suggest they have a key role in processing specifically nociceptive information (Villanueva, L. *et al*., 1996). Indeed, they are preferentially or exclusively activated by nociceptive stimuli from a whole-body receptive field; they encode the intensity of cutaneous and visceral stimulation within noxious ranges; and they are activated exclusively by activity in Aδ- or Aδ- and C-peripheral fibers. In addition, they send descending projections through the dorsolateral funiculus that terminate in the dorsal horn at all levels of the spinal cord. The fact that the supraspinal loop sustaining DNICs is confined to the most caudal part of the medulla was confirmed in a series of experiments where the potency of DNIC was tested in animals with complete transections at different levels of the brainstem.

5.50.6 Summary and Conclusions

There is a body of evidence, based on both human and animal experiments, which strongly suggests that the phenomenon of 'pain inhibiting pain' is sustained by a well-defined neurological substratum based on a spino-reticulo-spinal loop. DNICs are in fact a very special and generalized case of lateral inhibition and it is very likely that they subserve a related function. Although lateral inhibition is sometimes thought of in terms of creating illusions, such phenomena play an important role in other senses (see Chapters 1.01 and 3.30). It is very probable that DNICs, as revealed by the empiric observation that pain inhibits pain, also play an important role in pain processing, probably by focusing the pain network onto a particular part of the body. The DNIC system could be understood as a filter allowing the extraction by the brain of a clear signal of pain from a basic somesthetic activity provided by dorsal horn WDR neurons (see Chapter 5.25). If these statements are correct, then defocusing should alleviate the unpleasantness of pain. Interestingly, the reference analgesic drug, morphine, blocks DNICs in both man and animals (Le Bars, D. *et al*., 1992).

Many sources of descending inhibition from the brain that modulate the spinal transmission of nociceptive information have been described in animals (see Chapters 5.41 and 5.49). To date, the only descending inhibitory mechanisms that have been described in man are DNICs.

References

Bouhassira, D., Chollet, R., Coffin, B., Lemann, M., Le Bars, D., Willer, J. C., and Jian, R. 1994. Inhibition of a somatic nociceptive reflex by gastric distention in humans. Gastroenterology 107, 985–992.

Bouhassira, D., Danziger, N., Guirimand, F., and Attal, N. 2003. Comparison of the pain suppressive effects of clinical and experimental painful conditioning stimuli. Brain. 126, 1068–1078.

Bouhassira, D, Le Bars, D., Bolgert, F., Laplane, D., and Willer, J. C. 1993. Diffuse noxious inhibitory controls (DNIC) in man. A neurophysiological investigation of a patient with a form of Brown-Séquard syndrome. Ann. Neurol. 34, 536–543.

Bouhassira, D., Sabate, J. M., Coffin, B., Le Bars, D., Willer, J. C., and Jian, R. 1998. Effects of rectal distensions on nociceptive flexion reflexes in humans. Am. J. Physiol. 275, G410–G417.

Bushnell, M. C., Duncan, G. H., Dubner, R., Jones, R. L., and Maixner, W. 1985. Attentional influences on noxious and innocuous cutaneous heat detection in humans and monkeys. J. Neurosci. 5, 1103–1110.

Cadden, S. W. 1993. The ability of inhibitory controls to 'switch-off' activity in dorsal horn convergent neurones in the rat. Brain Res. 628, 65–71.

Cadden, S. W. and Morrison, J. F. B. 1991. Effects of visceral distension on the activities of neurones receiving cutaneous inputs in the rat lumbar dorsal horn; comparison with effects of remote noxious somatic stimuli. Brain Res. 558, 63–74.

Danziger, N., Gautron, M., Le Bars, D., and Bouhassira, D. 2001. Activation of diffuse noxious inhibitory controls (DNIC) in rats with an experimental peripheral mononeuropathy. Pain 91, 287–296.

Danziger, N., Rozenberg, S., Bourgeois, P., Charpentier, G., and Willer, J. C. 1998. Depressive effects of segmental and heterotopic application of transcutaneous electrical nerve stimulation and piezo-electric current on lower limb nociceptive flexion reflex in human subjects. Arch. Phys. Med. Rehabil. 79, 191–200.

Danziger, N., Le Bars, D., and Bouhassira, D. 2000. Diffuse Noxious Inhibitory Controls and Arthritis in the Rat. In: Pain and Neuroimmune Interactions (*eds*. N. E. Saadé, A. V. Apkarian, and S. J. Jabbur), pp. 69–78. Kluwer Academic Press.

De Broucker, T., Cesaro, P., Willer, J. C., and Le Bars, D. 1990. Diffuse noxious inhibitory controls (DNIC) in man: involvement of the spino-reticular tract. Brain 113, 1223–1234.

Ellrich, J. and Treede, R. D. 1998. Characterization of blink reflex interneurons by activation of diffuse noxious inhibitory controls in man. Brain Res. 803, 161–168.

France, C. R. and Suchowiecki, S. 1999. A comparison of diffuse noxious inhibitory controls in men and women. Pain 81, 77–84.

Jinks, S. L., Antognini, J. F., and Carstens, E. 2003. Isoflurane depresses diffuse noxious inhibitory controls in rats between

0.8 and 1.2 minimum alveolar anesthetic concentration. Anesth. Analg. 97, 111–116.

Le Bars, D. 2002. The whole body receptive field of dorsal horn multireceptive neurones. Brain Res. Rev. 40, 29–44.

Le Bars, D. and Willer, J. C. 2002. Pain Modulation Triggered by High-Intensity Stimulation: Implication for Acupuncture Analgesia. In: Acupuncture: Is there a Physiological Basis? (*eds*. P. Li, A. Sato, and J. Campbell), International Congress Serie 1238, pp. 11–29. Elsevier.

Le Bars, D., De Broucker, T., and Willer, J. C. 1992. Morphine blocks pain inhibitory controls in humans. Pain 48, 13–20.

Le Bars, D., Gozariu, M., and Cadden, S. W. 2001. Animal models of nociception. Pharmacol. Rev. 53, 597–652.

Maillou, P. and Cadden, S. W. 1997. Effects of remote deep somatic noxious stimuli on a jaw reflex in man. Arch. Oral. Biol. 42, 323–327.

Melzack, R. 1989. Folk Medicine and the Sensory Modulation of Pain. In: Textbook of Pain (*eds*. P. D. Wall and R. Melzack), pp. 897–905. Churchill Livingstone.

Pantaleo, T., Duranti, R., and Bellini, F. 1988. Effects of heterotopic ischemic pain on muscular pain threshold and blink reflex in humans. Neurosci. Lett. 85, 56–60.

Roby-Brami, A, Bussel, B., Willer, J. C., and Le Bars, D. 1987. An electrophysiological investigation into the pain-relieving effects of heterotopic nociceptive stimuli: probable involvement of a supraspinal loop. Brain 110, 1497–1508.

Sandrini, G., Milanov, I., Malaguti, S., Nigrelli, M. P., Moglia, A., and Nappi, G. 2000. Effects of hypnosis on diffuse noxious inhibitory controls. Physiol. Behav. 69, 295–300.

Villanueva, L., Bouhassira, D., and Le Bars, D. 1996. The medullary subnucleus reticularis dorsalis (SRD) as a key link in both the transmission and modulation of pain signals. Pain 67, 231–240.

Villanueva, L., Cadden, S. W., and Le Bars, D. 1984. Evidence that diffuse noxious inhibitory controls (DNIC) are mediated by a final post-synaptic inhibitory mechanism. Brain Res. 298, 67–74.

Willer, J. C. 1977. Comparative study of perceived pain and nociceptive flexion reflex in man. Pain 3, 69–80.

Willer, J. C., Boureau, F., and Albe-Fessard, D. 1979. Supraspinal influences on nociceptive flexion reflex and pain sensation in man. Brain Res. 179, 61–68.

Willer, J. C., De Broucker, T., and Le Bars, D. 1989. Encoding of nociceptive thermal stimuli by diffuse noxious inhibitory controls in humans. J. Neurophysiol. 62, 1028–1038.

Willer, J. C., Roby, A., and Le Bars, D. 1984. Psychophysical and electrophysiological approaches to the pain relieving effect of heterotopic nociceptive stimuli. Brain 107, 1095–1112.

Willer, J. C., Barranquero, A., Kahn, M. F., and Salliere, D. 1987. Pain in sciatica depresses lower limb cutaneous reflexes to sural nerve stimulation. J. Neurol. Neurosurg. Psych. 50, 1–5.

5.51 Fibromyalgia

R Staud, University of Florida, Gainesville, FL, USA

© 2008 Elsevier Inc. All rights reserved.

5.51.1	Introduction	775
5.51.2	Pathogenesis of Fibromyalgia	776
5.51.3	Muscle Nociception	776
5.51.4	Triggering Events for Fibromyalgia	776
5.51.5	Abnormal Response to Stressors	776
5.51.6	Posttraumatic Stress Disorder and Fibromyalgia	777
5.51.7	Fibromyalgia and Affective Spectrum Disorders	777
5.51.8	Central Sensitization in Fibromyalgia	777
5.51.9	Temporal Summation of Second Pain (Wind-Up)	777
5.51.10	Abnormal Wind-Up of Fibromyalgia Patients	778
5.51.11	Wind-Up Measures as Predictors of Clinical Pain Intensity in Fibromyalgia Patients	778
5.51.12	Fibromyalgia and Other Chronic Pain Conditions	778
5.51.13	Myofascial Pain Syndrome	778
5.51.14	Trigger Points	778
5.51.15	Relationship between Myofascial Pain and Fibromyalgia	779
5.51.16	Inflammatory Connective Tissue Diseases	779
5.51.17	Treatment of Fibromyalgia	779
5.51.18	Prognosis of Fibromyalgia	780
5.51.19	Conclusions	780
References		780

Glossary

chronic pain Pain for more than 3 months.

central sensitization Increased sensitivity to painful stimuli due to functional changes of the central nervous system (neuroplasticity).

peripheral sensitization Increased sensitivity to painful stimuli due to decreased thresholds of primary nociceptive afferents.

tender point (TP) Nine paired body areas at tendon insertion points of the neck, chest, buttocks, as well as all upper and lower extremities as defined by the 1990 American College of Rheumatology. TPs represent areas of mechanical allodynia (pain threshold $\leq 4\,\mathrm{kg\,cm^{-2}}$). Eleven or more TPs as well as chronic widespread pain are required to fulfill fibromyalgia criteria.

trigger point (TrP) Painful muscle areas that show increased muscle tension (taut bands), a twitch response to palpation, and referred pain.

wind-up Central pain mechanisms that depend on *N*-methyl-D-aspartate and substance P receptor mechanisms.

5.51.1 Introduction

Chronic nonmalignant pain is very frequent in the general population (Croft, P. *et al.*, 1993). Fibromyalgia (FM) represents the combination of chronic widespread pain with mechanical allodynia and disproportionably affects women (ratio women:men 9:1). Like many other syndromes, FM has no single specific feature but is a symptom complex of self-reported or elicited findings. In 1990, the American College of Rheumatology (ACR) published diagnostic criteria for FM which include chronic widespread pain (>3 months) and mechanical tenderness in at least 11 out of 18 tender points (TP; Wolfe, F. *et al.*, 1990). Most

TP sites are located at tendon insertion areas and have shown few detectable tissue abnormalities. Besides musculoskeletal pain and mechanical tenderness most FM patients also complain of insomnia, fatigue, and distress. In addition FM coaggregates with major mood disorders (Raphael, K. G. *et al.*, 2004).

5.51.2 Pathogenesis of Fibromyalgia

FM can be characterized as a pain amplification syndrome of patients who often display widespread hyperalgesia and allodynia to mechanical, thermal, and chemical stimuli. However, the hypersensitivity of FM patients is not limited to pain, but also includes light, sound, and smell. The cause for this heightened sensitivity is unknown, but central nervous system (CNS) sensory processing abnormalities have been reported in several studies (Desmeules, J. A. *et al.*, 2003; Staud, R., 2004). Most of these studies found evidence of central sensitization of dorsal horn neurons of the spinal cord and the brain including those that are related to pain. The pathogenesis of central sensitization in FM is unclear but may be related to prior stressors, including infections and traumas. Because most FM patients relate their pain to deep tissues, particularly muscles, these structures may play an important role in the initiation and maintenance of central sensitization and pain. No consistent tissue abnormalities have been reported in FM patients that would explain persistent pain. However, focal muscle areas, like trigger points (TrPs), may play an important role for FM pain because little nociceptive input from peripheral tissues is required for the maintenance of central sensitization (Bengtsson, M. *et al.*, 1989).

5.51.3 Muscle Nociception

Nociceptive input from muscle may be particularly relevant for FM pain. Muscle pain travels in myelinated A-delta fibers (group III) and in unmyelinated type C fibers (group IV). Pain receptors are mostly located at free nerve endings which are concentrated around small arterioles and capillaries between the muscle fibers. The cell bodies for these nerves are found in the dorsal root ganglion and synapse in lamina I and IV–V of the dorsal horn of the spinal cord. Activation of peripheral nociceptors leads to a release of neurotransmitters in the spinal cord, mostly substance P and calcitonin gene-related peptide (CGRP). There is also a retrograde migration of substance P from cell bodies which is then released in the region of the free nerve endings. This retrograde flow can sensitize tissues and increase their responsiveness to less intense stimuli. Muscle nociceptors are activated by mechanical stimuli (stretching or pressure), bradykinin, serotonin, and potassium ions, but are not activated by normal muscle movements or even increased muscle tension. Sensory input from muscle, as opposed to skin, is a much more potent effector of central sensitization and this may be particularly relevant for FM (Wall, P. D. and Woolf, C. J., 1984).

5.51.4 Triggering Events for Fibromyalgia

The onset of FM has frequently been associated with certain triggers or stressors include physical trauma, infections, emotional distress, endocrine disorders, and immune activation (Greenfield, S. *et al.*, 1992; Middleton, G. D. *et al.*, 1994; Waylonis, G. W. and Perkins, R. H., 1994). These stressors have been associated with the degree of pain, disability, life interference, and affective distress of FM patients (Turk, D. C. *et al.*, 1996). Strong evidence for trauma as a trigger of FM symptoms comes from studies of patients with acute injuries who developed chronic widespread pain at much higher rates than controls (Al Allaf, A. W. *et al.*, 2002; Buskila, D. and Neumann, L., 2002). Additional evidence for such an association include postinjury reported sleep abnormalities (Berglund, A. *et al.*, 2001), local injury sites as a source of chronic distant regional pain (Arendt-Nielsen, L. and Svensson, P., 2001), and recent evidence of injury-related CNS neuroplasticity in FM (Carli, G., 2000). Further prospective studies, however, are needed to confirm these associations and to identify the mechanisms that are relevant for posttraumatic FM pain (White, K. P. *et al.*, 2000).

5.51.5 Abnormal Response to Stressors

The biological response to stressors appears predictable in animals and humans. Particularly, events that are perceived as inescapable or unavoidable, or which appear unpredictable, evoke the strongest adverse biological responses (Gold, P. W. *et al.*, 1988a;

1988b; Chrousos, G. P. and Gold, P. W., 1992; Viau, V. *et al.*, 1993; Sapolsky, R. M. *et al.*, 2000). This may explain why victims of trauma appear to develop much higher rates of FM than persons with self-inflicted injuries (Greenfield, S. *et al.*, 1992). In addition, early life stressors can have a permanent and profound impact on subsequent biological responses to stress in animals and humans. Studies in rodents have demonstrated that exposure to multiple stressors including trauma or separation in the neonatal period can lead to permanent changes in the biological response to stress (Sapolsky, R. M., 1996; McNamara, R. K. *et al.*, 2002). This permanent effect of early stressors could explain the higher than expected incidence of traumatic childhood events in individuals who later develop chronic pain (Anderberg, U. M. *et al.*, 2000; Bailey, B. E. *et al.*, 2003).

5.51.6 Posttraumatic Stress Disorder and Fibromyalgia

Posttraumatic stress disorder (PTSD) often occurs after a significant traumatic event and is characterized by behavioral, emotional, functional, and physiological symptoms. Relevant traumatic events related to PTSD are usually perceived as threatening one's life or physical integrity and can lead to emotional responses including horror, helplessness, or intense fear. The psychological symptoms of PTSD include re-experience of the traumatic event, avoidance, and increased arousal. It has been shown that the experience of trauma is associated with increased somatic and physical complaints, including pain (Beckham, J. C. *et al.*, 1997; 1998). More than 50% of patients with FM suffer from PTSD in the USA and Israel (Sherman, J. J. *et al.*, 2000; Cohen, H. *et al.*, 2002). Compared to the prevalence of PTSD in the general population (6%), FM patients show greatly increased rates similar to Vietnam veterans and victims of natural disasters (Shore, J. H. *et al.*, 1986; Green, M. M. *et al.*, 1993). Not surprisingly, the incidence of FM is also increased in patients with PTSD (21%) and often associated with increased pain ratings, more distress, and higher functional impairment (Amir, M. *et al.*, 1997). As with several other disorders, however, it is unclear whether PTSD is the cause or consequence for FM.

5.51.7 Fibromyalgia and Affective Spectrum Disorders

Several studies have reported that FM is comorbid with major depressive disorder (MDD; Arnold, L. M. *et al.*, 2000; White, K. P. *et al.*, 2002). In addition, anxiety is very prevalent in patients with FM (Thieme, K. *et al.*, 2004). The outcome of a recent large family study of FM probands was consistent with the hypothesis that FM and MDD are characterized by shared, genetically mediated risk factors (Raphael, K. G. *et al.*, 2004). Although the findings of this study should not be interpreted that MDD and FM represent different forms of the same syndrome, they strongly suggest that FM and MDD share important CNS mechanisms.

5.51.8 Central Sensitization in Fibromyalgia

Whereas peripheral sensitization is related to changes of primary nociceptive afferent properties, central sensitization requires functional changes in the CNS (neuroplasticity). Behaviorally, centrally sensitized patients, like FM sufferers report abnormal or heightened pain sensitivity with spreading of hypersensitivity to uninjured sites and the generation of pain by low threshold mechanoreceptors that are normally silent in pain processing (Torebjork, H. E. *et al.*, 1992). Thus, tissue injury may not only cause pain but also an expansion of dorsal horn receptive fields and central sensitization.

5.51.9 Temporal Summation of Second Pain (Wind-Up)

In 1965, Mendell and Wall described for the first time, that repetitive C-fiber stimulation can result in a progressive increase of electrical discharges from second-order neurons in the spinal cord (Mendell, L. M. and Wall, P. D., 1965). This important mechanism of pain amplification in the dorsal horn neurons of the spinal cord is related to temporal summation of second pain or wind-up (WU) and has been used in FM patients for the evaluation of central sensitization (Staud, R. *et al.*, 2001). This technique reveals sensitivity to input from unmyelinated (C) afferents and the status of the *N*-methyl-D-aspartate (NMDA) receptor systems that are implicated in a

variety of chronic pain conditions. Temporal summation depends upon activation of NMDA transmitter systems by C nociceptors, and chronic central pain states like FM can result from excessive temporal summation of pain (Staud, R. and Smitherman, M. L., 2002).

5.51.10 Abnormal Wind-Up of Fibromyalgia Patients

Several recent studies have demonstrated psychophysical evidence that input to central nociceptive pathways is abnormally processed in patients with FM (Staud, R. and Domingo, M., 2001a; 2001b; Staud, R. *et al.*, 2001; Vierck, C. J. *et al.*, 2001; Price, D. D. *et al.*, 2002; Staud, R., 2002). When WU pain is evoked both in normal controls and FM patients, the perceived magnitude of the experimental stimuli (heat, cold, pressure, electricity) is greater for FM patients compared to controls, as is the amount of temporal summation within a series of stimuli. Following a series of stimuli, after-sensations are greater in magnitude, last longer, and are more frequently painful in FM subjects. These results indicate both augmentation and prolonged decay of nociceptive input in FM patients and provide convincing evidence for the presence of central sensitization.

5.51.11 Wind-Up Measures as Predictors of Clinical Pain Intensity in Fibromyalgia Patients

The important role of central pain mechanisms, like WU, for FM patients is also supported by their ability to predict clinical pain intensity. Thermal WU ratings correlate with clinical pain intensity (Pearson's $r = 0.529$), thus emphasizing the important role of these pain mechanisms for FM. In addition, statistical prediction models that includes TP count, pain-related negative affect, and WU ratings have been shown to account for nearly 50% of the variance in FM clinical pain intensity (Staud, R. *et al.*, 2003; 2004).

5.51.12 Fibromyalgia and Other Chronic Pain Conditions

Many systemic illnesses can also present with diffuse pain similar to FM, including polymyalgia rheumatica (Gowin, K. M., 2000), rheumatoid arthritis, Sjogren's syndrome, inflammatory myopathies (Sultan, S. M. *et al.*, 2002), systemic lupus erythematosus (Tench, C. *et al.*, 2002), multiple sclerosis, and joint hypermobility syndrome (Nef, W. and Gerber, N. J., 1998). Furthermore, several infectious diseases including hepatitis C, Lyme disease, coxsackie B infection, HIV, and parvovirus infection, frequently result in chronic pain states (Barkhuizen, A., 2002). Although the majority of FM patients report the insidious onset of pain and fatigue, approximately half of all patients describe the start of chronic pain after a traumatic or infectious event.

5.51.13 Myofascial Pain Syndrome

Myofascial pain or regional musculoskeletal pain is one of the most common pain syndromes encountered in clinical practice. Myofascial pain represents the most common cause of chronic pain, including neck and shoulder pain, tension headaches, and lower back pain (Granges, G. and Littlejohn, G., 1993; Fricton, J. R., 1994; Macfarlane, G. J. *et al.*, 1996; Borg-Stein, J. and Simons, D. G., 2002). The term myofascial pain was introduced in the early 1950s by Janet Travell. She also defined the term myofascial TrP and demonstrated with David Simons that individual muscles have specific nondermatomal patterns of TrP pain referral (Simons, D. G. *et al.*, 1999). In 1983, both authors first described the clinical picture and pathophysiology of a new syndrome which they named myofascial pain syndrome (MPS; Long, S. P. and Kephart, W., 1998; Simons, D. G. *et al.*, 1999). MPS has been defined as a chronic pain syndrome accompanied by TrPs in one or more muscles or groups of muscles. Similar to FM, it is more frequently found in women compared to men. Besides the presence of TrPs and referred pain, MPS is frequently associated with limitation of movement, weakness, and autonomic dysfunction (Long, S. P. and Kephart, W., 1998) similar to FM.

5.51.14 Trigger Points

TrPs represent areas of local mechanical hyperalgesia that can be found in MPS and several chronic pain conditions, including FM, osteoarthritis, and rheumatoid arthritis. They are defined as specific areas of hyperirritability in muscle, but can also be detected in ligaments, tendons, periosteum, scar tissue, or skin (Han, S. C. and Harrison, P., 1997; Simons, D. G. *et al.*,

1999). TrPs are located in palpable taut bands and produce local and referred pain, which is specific for the particular muscle. When TrPs are mechanically stimulated, so-called taut bands within a muscle, rather than the entire muscle, will contract (Chu, J., 1998). They are often associated with a local muscle twitch response, which can easily be elicited by needling or palpation of the TrP (Chu, J., 1998; 1999). Latent TrPs are similar to active TrPs, but they are not associated with spontaneous pain and no referral of pain occurs. However, latent TrPs are painful when palpated.

5.51.15 Relationship between Myofascial Pain and Fibromyalgia

Approximately 70% of patients with FM have TrPs (Granges, G. and Littlejohn, G., 1993). A TP is considered to be different from a TrP because of the absence of referred pain, local twitch response, and a taut band in the muscle. The distinction between TPs and TrPs requires careful physical examination. TrPs are frequently located in areas of muscular TPs of patients with FM (Wolfe, F. *et al*., 1992; Borg-Stein, J. and Stein, J., 1996) suggesting that some muscular TPs in patients with FM may actually be TrPs (Inanici, F. *et al*., 1999). The presence of TrPs in most if not all FM patients represents evidence for local muscle abnormalities in this chronic musculoskeletal pain syndrome. Although it is unclear if TrPs are the cause or effect of muscle injury, they represent abnormally contracted muscle fibers. This muscle contraction can lead to accumulation of histamine, serotonin, tachykinins, and prostaglandins, which may result in the activation of local nociceptors. Prolonged muscle contractions may also result in local hypoxemia and energy depletion (Simons, D. G. *et al*., 1999).

5.51.16 Inflammatory Connective Tissue Diseases

Many patients (up to 25%) with chronic arthritis have also wide-spread pain similar to FM. These patients may also present with symptoms of chronic fatigue, impaired memory and concentration, and mood abnormalities. Most of these patients, however, will have findings suggestive of inflammation, including joint pain/swelling, rashes, muscle weakness, as well as laboratory abnormalities, like elevated erythrocyte sedimentation rate (ESR), C-reactive protein (CRP), anemia, autoantibodies (rheumatoid factor, cyclic citrullinated peptide antibodies, anti-nuclear antibodies (ANA)), etc.

5.51.17 Treatment of Fibromyalgia

Treatment of patients with chronic widespread pain like FM needs to be individually tailored to each patient's needs. This includes the assessment of biopsychosocial abnormalities which are readily detectable in most FM patients. Importantly the identification of pain generators is essential for an effective treatment plan. Thus patients with arthritis, particularly osteoarthritis of the spine will benefit from muscle relaxants, physical therapy, and massage. In addition, these patients may respond well to therapy with cyclo-oxygenase (COX) inhibitors. Identification and treatment of mood abnormalities is crucial because affective spectrum disorders seem to share important mechanisms with FM.

Pharmacotherapy for FM has been most successful with antidepressant, muscle relaxant, or anticonvulsant drugs. These drugs affect the release of various neurochemicals (e.g., serotonin, norepinephrine, substance P) that have a broad range of activities in the brain and spinal cord, including modulation of pain sensation and tolerance. None of these drugs, however, is currently approved by the US Food and Drug Administration for the treatment of FM.

Most FM patients will respond to low-dose tricyclic medications, such as amitriptyline and cyclobenzaprine, as well as cardiovascular exercise, cognitive behavioral therapy (CBT), patient education, or a combination of these for the management of FM. Also tramadol, selective serotonin reuptake inhibitors (SSRI), selective norepinephrine re-uptake inhibitors (SNRI), and anticonvulsants have been found to be moderately effective. There is some evidence for the efficacy of strength training exercise, acupuncture, hypnotherapy, biofeedback, massage, and warm water baths. However, many commonly used FM therapies like guaifenesine have been found to be ineffective.

The efficacy of FM patients to manage their pain seems to correlate with their functional status. Brain imaging and psychological profiles have identified at least three FM subgroups, that is, patients who are highly dysfunctional, interpersonally distressed, or are effective copers (Giesecke, T. *et al*., 2003). Such

studies provide an explanation why some treatments seem to be differentially effective in individual patients. Thus optimal FM management will require a combination of pharmacological and nonpharmacological therapies with patients and healthcare professionals working as a team.

5.51.18 Prognosis of Fibromyalgia

FM can be mild or disabling, but often has substantial emotional and social consequences. About 50% of all patients have difficulty with or are unable to perform routine daily activities. Estimates of patients who have had to stop working or change jobs range from 30% to 40%. Patients with FM suffer job losses and social abandonment more often than people with other conditions that cause pain and fatigue. Although FM symptoms seem to remain stable, several long-term studies indicate that physical function and pain worsen over time (Forseth, K. O. *et al.*, 1999; Baumgartner, E., 2002). Significant life stressors often result in a poor outcome, including diminished capacity to work, poor self-efficacy, increased pain sensations, disturbed sleep, fatigue, and depression. A recent study reported increased mortality in patients with widespread pain compared to those without chronic pain (McBeth, J. *et al.*, 2003). Although this study did not specifically evaluate FM, these findings may be relevant for FM patients. The higher mortality was mostly associated with malignancies, although the cause for this association is currently unknown.

5.51.19 Conclusions

The pathogenesis of FM pain is currently unknown, but up to 50% of the variance can be explained by central sensitization and distress. However, additional mechanisms like tonic peripheral nociceptive input may play an important role for the initiation and maintenance of the increased pain sensitivity of FM patients. FM, like many other chronic pain syndromes, is treatable, and remission can occur in many patients who actively participate in effective disease management programs. New treatment strategies, however, may benefit from interventions that improve peripheral and central pain sensitization as well as the affective disorders of FM patients.

References

Al Allaf, A. W., Dunbar, K. L., Hallum, N. S., Nosratzadeh, B., Templeton, K. D., and Pullar, T. 2002. A case-control study examining the role of physical trauma in the onset of fibromyalgia syndrome. Rheumatology 41, 450–453.

Amir, M., Kaplan, Z., Neumann, L., Sharabani, R., Shani, N., and Buskila, D. 1997. Posttraumatic stress disorder, tenderness and fibromyalgia. J. Psychosom. Res. 42, 607–613.

Anderberg, U. M., Marteinsdottir, I., Theorell, T., and von Knorring, L. 2000. The impact of life events in female patients with fibromyalgia and in female healthy controls. Eur. Psychiatry 15, 295–301.

Arendt-Nielsen, L. and Svensson, P. 2001. Referred muscle pain: basic and clinical findings. Clin. J. Pain 17, 11–19.

Arnold, L. M., Keck, P. E., Jr., and Welge, J. A. 2000. Antidepressant treatment of fibromyalgia: a meta-analysis and review. Psychosomatics 41, 104–113.

Bailey, B. E., Freedenfeld, R. N., Kiser, R. S., and Gatchel, R. J. 2003. Lifetime physical and sexual abuse in chronic pain patients: psychosocial correlates and treatment outcomes. Disabil. Rehabil. 25, 331–342.

Barkhuizen, A. 2002. Rational and targeted pharmacologic treatment of fibromyalgia. Rheum. Dis. Clin. North Am. 28, 261–290.

Baumgartner, E., Finckh, A., Cedraschi, C., and Vischer, T. L. 2002. A six year prospective study of a cohort of patients with fibromyalgia. Ann. Rheum. Dis. 61, 644–645.

Beckham, J. C., Crawford, A. L., Feldman, M. E., Kirby, A. C., Hertzberg, M. A., Davidson, J. R., and Moore, S. D. 1997. Chronic posttraumatic stress disorder and chronic pain in Vietnam combat veterans. J. Psychosom. Res. 43, 379–389.

Beckham, J. C., Moore, S. D., Feldman, M. E., Hertzberg, M. A., Kirby, A. C., and Fairbank, J. A. 1998. Health status, somatization, and severity of posttraumatic stress disorder in Vietnam combat veterans with posttraumatic stress disorder. Am. J. Psychiatry 155, 1565–1569.

Bengtsson, M., Bengtsson, A., and Jorfeldt, L. 1989. Diagnostic epidural opioid blockade in primary fibromyalgia at rest and during exercise. Pain 39, 171–180.

Berglund, A., Alfredsson, L., Jensen, I., Cassidy, J. D., and Nygren, A. 2001. The association between exposure to a rear-end collision and future health complaints. J. Clin. Epidemiol. 54, 851–856.

Borg-Stein, J. and Simons, D. G. 2002. Myofascial pain. Arch. Phys. Med. Rehabil. 83, S40–S47.

Borg-Stein, J. and Stein, J. 1996. Trigger points and tender points: one and the same? Does injection treatment help? Rheum. Dis. Clin. North Am. 22, 305–322.

Buskila, D. and Neumann, L. 2002. The development of widespread pain after injuries. J. Musculoskel. Pain 10, 261–267.

Carli, G. 2000. Neuroplasticity and clinical pain. Prog. Brain Res. 129, 325–330.

Chrousos, G. P. and Gold, P. W. 1992. The concepts of stress and stress system disorders. Overview of physical and behavioral homeostasis. JAMA 267, 1244–1252.

Chu, J. 1998. Twitch response in myofascial trigger points. J. Musculoskel. Pain 6, 99–116.

Chu, J. 1999. Twitch-obtaining intramuscular stimulation: observations in the management of radiculopathic chronic low back pain. J. Musculosket. Pain 7, 131–146.

Cohen, H., Neumann, L., Haiman, Y., Matar, M. A., Press, J., and Buskila, D. 2002. Prevalence of post-traumatic stress disorder in fibromyalgia patients: overlapping syndromes or post-traumatic fibromyalgia syndrome? Semin. Arthritis Rheum. 32, 38–50.

Croft, P., Rigby, A. S., Boswell, R., Schollum, J., and Silman, A. 1993. The prevalence of chronic widespread pain in the general population. J. Rheumatol. 20, 710–713.

Desmeules, J. A., Cedraschi, C., Rapiti, E., Baumgartner, E., Finckh, A., Cohen, P., Dayer, P., and Vischer, T. L. 2003. Neurophysiologic evidence for a central sensitization in patients with fibromyalgia. Arthritis Rheum. 48, 1420–1429.

Forseth, K. O., Forre, O., and Gran, J. T. 1999. A 5.5 year prospective study of self-reported musculoskeletal pain and of fibromyalgia in a female population: significance and natural history. Clin. Rheumatol. 18, 114–121.

Fricton, J. R. 1994. Myofascial pain. Clin. Rheumatol. 8, 857–880.

Giesecke, T., Williams, D. A., Harris, R. E., Cupps, T. R., Tian, X., Tian, T. X., Gracely, R. H., and Clauw, D. J. 2003. Subgrouping of fibromyalgia patients on the basis of pressure-pain thresholds and psychological factors. Arthritis Rheum. 48, 2916–2922.

Gold, P. W., Goodwin, F. K., and Chrousos, G. P. 1988a. Clinical and biochemical manifestations of depression. Relation to the neurobiology of stress (1). N. Engl. J. Med. 319, 348–353.

Gold, P. W., Goodwin, F. K., and Chrousos, G. P. 1988b. Clinical and biochemical manifestations of depression. Relation to the neurobiology of stress (2). N. Engl. J. Med. 319, 413–420.

Gowin, K. M. 2000. Diffuse pain syndromes in the elderly. Rheum. Dis. Clin. North Am. 26, 673–682.

Granges, G. and Littlejohn, G. 1993. Prevalence of myofascial pain syndrome in fibromyalgia syndrome and regional pain syndrome: a comparative study. J. Musculoskel. Pain 1, 19–35.

Green, M. M., McFarlane, A. C., Hunter, C. E., and Griggs, W. M. 1993. Undiagnosed post-traumatic stress disorder following motor vehicle accidents. Med. J. Aust. 159, 529–534.

Greenfield, S., Fitzcharles, M. A., and Esdaile, J. M. 1992. Reactive fibromyalgia syndrome. Arthritis Rheum. 35, 678–681.

Han, S. C. and Harrison, P. 1997. Myofascial pain syndrome and trigger-point management. Reg. Anesth. 22, 89–101.

Inanici, F., Yunus, M. B., and Aldag, J. C. 1999. Clinical features and psychologic factors in regional soft tissue pain: comparison with fibromyalgia syndrome. J. Musculoskelet. Pain 7, 293–301.

Long, S. P. and Kephart, W. 1998. Myofascial Pain Syndrome. In: The Management of Pain (*eds*. M. A. Ashburn and L. J. Rice), pp. 299–321. Churchill Livingstone.

Macfarlane, G. J., Thomas, E., Papageorgiou, A. C., Schollum, J., Croft, P. R., and Silman, A. J. 1996. The natural history of chronic pain in the community: a better prognosis than in the clinic? J. Rheumatol. 23, 1617–1620.

McBeth, J., Silman, A. J., and Macfarlane, G. J. 2003. Association of widespread body pain with an increased risk of cancer and reduced cancer survival: a prospective, population-based study. Arthritis Rheum. 48, 1686–1692.

McNamara, R. K., Huot, R. L., Lenox, R. H., and Plotsky, P. M. 2002. Postnatal maternal separation elevates the expression of the postsynaptic protein kinase c substrate rc3, but not presynaptic GAP-43, in the developing rat hippocampus. Dev. Neurosci. 24, 485–494.

Mendell, L. M. and Wall, P. D. 1965. Responses of single dorsal cord cells to peripheral cutaneous unmyelinated fibres. Nature 206, 97–99.

Middleton, G. D., McFarlin, J. E., and Lipsky, P. E. 1994. The prevalence and clinical impact of fibromyalgia in systemic lupus erythematosus. Arthritis Rheum. 37, 1181–1188.

Nef, W. and Gerber, N. J. 1998. Hypermobility syndrome. When too much activity causes pain. Schweiz. Med. Wochenschr. 128, 302–310.

Price, D. D., Staud, R., Robinson, M. E., Mauderli, A. P., Cannon, R. L., and Vierck, C. J. 2002. Enhanced temporal summation of second pain and its central modulation in fibromyalgia patients. Pain 99, 49–59.

Raphael, K. G., Janal, M. N., Nayak, S., Schwartz, J. E., and Gallagher, R. M. 2004. Familial aggregation of depression in fibromyalgia: a community-based test of alternate hypotheses. Pain 110, 449–460.

Sapolsky, R. M. 1996. Why stress is bad for your brain. Science 273, 749–750.

Sapolsky, R. M., Romero, L. M., and Munck, A. U. 2000. How do glucocorticoids influence stress responses? Integrating permissive, suppressive, stimulatory, and preparative actions. Endocr. Rev. 21, 55–89.

Sherman, J. J., Turk, D. C., and Okifuji, A. 2000. Prevalence and impact of posttraumatic stress disorder-like symptoms on patients with fibromyalgia syndrome. Clin. J. Pain 16, 127–134.

Shore, J. H., Tatum, E. L., and Vollmer, W. M. 1986. Psychiatric reactions to disaster: the Mount St. Helens experience. Am. J. Psychiatry 143, 590–595.

Simons, D. G., Travell, J. G., Simons, L. S., and Cummings, B. D. 1999. Myofascial Pain and Dysfunction: The Trigger Point Manual. Upper Half of the Body. 2nd edn. Lippincott Williams & Wilkins.

Staud, R. 2002. Evidence of involvement of central neural mechanisms in generating fibromyalgia pain. Curr. Rheumatol. Rep. 4, 299–305.

Staud, R. 2004. New evidence for central sensitization in patients with fibromyalgia. Curr. Rheumatol. Rep. 6, 259.

Staud, R. and Domingo, M. 2001a. Evidence for abnormal pain processing in fibromyalgia syndrome. Pain Med. 2, 208–215.

Staud, R. and Domingo, M. 2001b. New insights into the pathogenesis of fibromyalgia syndrome. Med. Aspects Hum. Sex. 1, 51–57.

Staud, R. and Smitherman, M. L. 2002. Peripheral and central sensitization in fibromyalgia: pathogenetic role. Curr. Pain Headache Rep. 6, 259–266.

Staud, R., Price, D. D., Robinson, M. E., and Vierck, C. J. 2004. Body pain area and pain-related negative affect predict clinical pain intensity in patients with fibromyalgia. J. Pain 5, 338–343.

Staud, R., Robinson, M. E., Vierck, C. J., Cannon, R. L., Mauderli, A. P., and Price, D. D. 2003. Ratings of experimental pain and pain-related negative affect predict clinical pain in patients with fibromyalgia syndrome. Pain 105, 215–222.

Staud, R., Vierck, C. J., Cannon, R. L., Mauderli, A. P., and Price, D. D. 2001. Abnormal sensitization and temporal summation of second pain (wind-up) in patients with fibromyalgia syndrome. Pain 91, 165–175.

Sultan, S. M., Ioannou, Y., Moss, K., and Isenberg, D. A. 2002. Outcome in patients with idiopathic inflammatory myositis: morbidity and mortality. Rheumatology (Oxf.) 41, 22–26.

Tench, C., Bentley, D., Vleck, V., McCurdie, I., White, P., and D'Cruz, D. 2002. Aerobic fitness, fatigue, and physical disability in systemic lupus erythematosus. J. Rheumatol. 29, 474–481.

Thieme, K., Turk, D. C., and Flor, H. 2004. Comorbid depression and anxiety in fibromyalgia syndrome: relationship to somatic and psychosocial variables. Psychosom. Med. 66, 837–844.

Torebjork, H. E., Lundberg, L. E., and LaMotte, R. H. 1992. Central changes in processing of mechanoreceptive input in capsaicin-induced secondary hyperalgesia in humans. J. Physiol. 448, 765–780.

Turk, D. C., Okifuji, A., Starz, T. W., and Sinclair, J. D. 1996. Effects of type of symptom onset on psychological distress and disability in fibromyalgia syndrome patients. Pain 68, 423–430.

Viau, V., Sharma, S., Plotsky, P. M., and Meaney, M. J. 1993. Increased plasma ACTH responses to stress in nonhandled compared with handled rats require basal levels of

corticosterone and are associated with increased levels of ACTH secretagogues in the median eminence. J. Neurosci. 13, 1097–1105.

Vierck, C. J., Staud, R., Price, D. D., Cannon, R. L., Mauderli, A. P., and Martin, A. D. 2001. The effect of maximal exercise on temporal summation of second pain (wind-up) in patients with fibromyalgia syndrome. J. Pain 2, 334–344.

Wall, P. D. and Woolf, C. J. 1984. Muscle but not cutaneous C-afferent input produces prolonged increases in the excitability of the flexion reflex in the rat. J. Physiol. Lond. 356, 443–458.

Waylonis, G. W. and Perkins, R. H. 1994. Post-traumatic fibromyalgia. A long-term follow-up. Am. J. Phys. Med. Rehabil. 73, 403–412.

White, K. P., Harth, M., Speechley, M., and Ostbye, T. 2000. A general population study of fibromyalgia tender points in noninstitutionalized adults with chronic widespread pain. J. Rheumatol. 27, 2677–2682.

White, K. P., Nielson, W. R., Harth, M., Ostbye, T., and Speechley, M. 2002. Chronic widespread musculoskeletal pain with or without fibromyalgia: psychological distress in a representative community adult sample. J. Rheumatol. 29, 588–594.

Wolfe, F., Simons, D. G., Fricton, J. R., Bennett, R. M., Goldenberg, D. L., Gerwin, R., Hathaway, D., McCain, G. A., Russell, I. J., and Sanders, H. O. 1992. The fibromyalgia and myofascial pain syndromes: a preliminary study of tender points and trigger points in persons with fibromyalgia, myofascial pain syndrome and no disease. J. Rheumatol. 19, 944–951.

Wolfe, F., Smythe, H. A., Yunus, M. B., Bennett, R. M., Bombardier, C., Goldenberg, D. L., Tugwell, P., Campbell, S. M., Abeles, M., and Clark, P. 1990. The American College of Rheumatology 1990 criteria for the classification of fibromyalgia. Report of the Multicenter Criteria Committee. Arthritis Rheum. 33, 160–172.

5.52 Pain Perception – Nociception during Sleep

G J Lavigne, Université de Montréal, Montreal, QC, Canada

K Okura, Tokushima Graduate School, Tokushima, Japan

M T Smith, John Hopkins Medical School, Baltimore, MD, USA

© 2008 Elsevier Inc. All rights reserved.

5.52.1	**Pain in Relation to Sleep**	784
5.52.1.1	Definition, Epidemiology, and Relevance	784
5.52.1.2	Cognitive Disturbances	785
5.52.1.3	Sleep Fragmentation and Deprivation	785
5.52.1.4	Circadian Variation in Pain Perception	786
5.52.2	**Perception of Pain during Sleep: Nociception or Sleep Arousal**	786
5.52.2.1	Nociception – Pain Perception during Sleep	786
5.52.2.2	Sleep Arousal: Brain and Autonomic Activation	789
5.52.3	**Circular Relation between Pain and Poor Sleep and Putative Consequence on Health Cost**	790
References		791

Glossary

alpha EEG wave intrusion The intrusion of fast-frequency electroencephalographic (EEG) alpha (7.5–11 Hz) activity into slow wave sleep (SWS) or into deep sleep (stages 3 and 4). SWS is dominated by large and slow EEG waves of delta type (0.5–4.0 or 0.75–4.5 Hz); it also characterizes sleep stages 3 and 4. SWS is not a specific biological marker of pain during sleep.

sleep awakening (major arousal) A sudden increase in EEG and heart rate frequency with a rise in muscle tone that lasts more than 10 or 15 s. Subject is not usually aware of external influences. An excessive number of major arousals during sleep is frequently followed by a complaint of unrefreshing sleep and cognitive impairment the following day.

cyclic alternating pattern Repetition of micro-arousals every 20–60 s as a sentinel that allows for a reset of physiological functions (e.g., heart rate, respiration, muscle tone) or prepares the body for an appropriate response in relation to potential disrupting events.

micro-arousal A sudden increase, during sleep, in EEG activity and heart rate frequency under a cardiac sympathetic dominance with a possible rise in muscle tone. It should last more than 3 s but less than 10 or 15 s depending on scoring method. A sleeping subject is normally unaware of this physiological activity; it tends to be repeated 8–15 times per hour of sleep.

nociception The receiving and transmitting of noxious sensory signals from the periphery to the central nervous system.

pain An unpleasant and sensory, cognitive, and emotional experience normally associated or not with tissue damage, which usually requires a minimal level of consciousness for expression.

pain threshold The lowest experimental stimulation perceived as being painful by a conscious subject in 50% of the trials.

sleep A natural physiological and behavioral state usually characterized by a partial isolation from the environment except when an unpleasant or potentially harmful or life-threatening event is present.

sleep stage A division of the specific sleep period into sleep stages (St): light sleep (St 1 or 2), deep sleep (St 3 and 4) are both described as non-REM sleep, and the REM or paradoxical sleep. Most body movements occur in light non-REM sleep (periodic limb movement, sleep bruxism). Sleep apnea (cessation of breathing for more than 10 s) is dominant in deep sleep and in REM sleep. REM behavior disorder (RBD) is characterized by sudden movement in REM sleep that is normally associated with muscle hypotonia (behaviorally described as motor paralysis).

sleep fragmentation Interruption of any sleep stage by isolated or repetitive events such as sleep stage shifts (deeper to lighter), micro-arousals, frank awakenings, with or without low duration of deep St 3 and 4 sleep and possible alpha EEG wave intrusion. As a result, sleep continuity may be impaired and poor sleep quality (e.g., unrefreshing) is frequently reported upon awakening.

5.52.1 Pain in Relation to Sleep

5.52.1.1 Definition, Epidemiology, and Relevance

Pain is a sensation that usually requires a certain level of consciousness before it is interpreted as an unpleasant sensory experience. Most persistent pain states can trigger complaints of poor sleep quality. Poor sleep quality is reported in 50–90% of patients with the following chronic pain conditions: arthritis, cervical and orofacial pain, low back pain, cancer pain, fibromyalgia. (Atkinson, J. H. *et al.*, 1988; Dao, T. T. T. *et al.*, 1994; Morin, C. M. *et al.*, 1998; Smith, M. T. *et al.*, 2000; Dauvilliers, Y. and Touchon, J., 2001; Riley, J. L. III *et al.* 2001; Roizenblatt, S. *et al.*, 2001; McCracken, L. M. and Iverson, G. L., 2002). Sleep quality is also impaired in the presence of other medical conditions of which pain is a common symptom, including: headaches, irritable bowel syndrome, spinal cord injury, and metastatic breast cancer (Cohen, M. *et al.*, 2000; Menefee, L. A. *et al.*, 2000; Moldofsky, H., 2001; Widerstrom-Noga, E. G. *et al.*, 2001; Rains, J. C. and Penzien, D. B., 2002; Koopman, C. *et al.*, 2002; Okifuji, A. and Turk, D. C., 2002; Lavigne, G. J. *et al.*, 2005). According to a recent survey from the National Sleep Foundation (USA), up to 20% of the adult population reports that their sleep is disrupted by somatic discomfort and pain.

The interaction between pain and poor sleep is supported by cohort and case control studies. Patients with orofacial pain are 3.7 more times at risk of reporting poor sleep (Macfarlane, T. V. and Worthington, H. V., 2004). In a survey done in the USA with 1506 community women and men aged between 55 and 84, it was found that bodily pain was associated with a risk for complaints of insomnia (e.g., difficulty falling asleep, middle of the night/early morning awakenings, or nonrestorative sleep). Odds ratios for insomnia among those reporting bodily pain were estimated to be between 1.88 and 2.68 (Foley, D. *et al.*, 2004). It has also been reported that the prevalence of insomnia is 2 times higher in Canadian chronic pain patients in comparison to the general population without pain (Sutton, D. A. *et al.*, 2001; Moldofsky, H., 2001). A cross-sectional study done in Hungary with over 12 643 adults showed that insomnia-related complaints were 3 times higher in chronic pain patients than in nonpain subjects (Novak, M. *et al.*, 2004). Finally, the concomitance of sleep disorders and pain may modify the subjective sensation related to sleep quality (e.g., refreshing) since 50% of insomnia patients with pain reported that pain interfered with daily activities (Novak, M. *et al.*, 2004). Moreover, in the presence of bodily pain there is an increase (OR of 1.73) in self-reports of daytime sleepiness (Foley, D. *et al.*, 2004) a topic further described in the next section.

In explorations of the interaction between high pain intensity and poor sleep, it is important to consider that chronic pain is frequently concomitant with anxiety, fatigue, mood disturbance, depression, and poor physical fitness (Menefee, L. A. *et al.*, 2000b; Riley, III. J. L. *et al.*, 2001; Smith, M. T. *et al.*, 2000; McCraken, L. M. and Iverson, G. L. 2002b; Nicassio, P. M. *et al.*, 2002; Sayar, K. *et al.*, 2002; Yatani, H. *et al.*, 2002). For example, fatigue is frequently reported in chronic pain patients and can explain 6.5% of the variability between pain intensity and complaints of poor sleep. Depression may further explain up to 40% of this variability. The presence of frank sleep apnea, a major risk for fatigue and daytime sleepiness, seems to be relatively low in chronic pain patients, as reported in a recent review (Dauvilliers, Y. and Touchon, J. 2001; Donald, F. *et al.*, 1996). However, the cumulative effect of poor sleep over a given night and possibly over several nights also needs to be considered. While it is recognized that daytime sleepiness may result from long interruptions of respiration (more than 10 s is defined as sleep apnea), less information is available on the cumulative consequence of several briefer hypoxic events, which may alter cognitive function and brain metabolism (Bonnet, M. H. 1985; Wesenten, N. J. *et al.*, 1999; Stepanski, E. J., 2002; Martin, S. E. *et al* 1996; Van Dogen, H. P. *et al.*, 2003; Gozal, D. and O'Brien, L. M., 2004). Recent work in fibromyalgia, for instance, suggests the possibility of a high rate of sleep-related upper airway resistance syndrome that

when reversed by continuous positive airway pressure therapy, may improve daytime function (Gold, A. R. *et al.*, 2004). The impact of the above-mentioned variables on pain and sleep interaction and their reversal by continuous positive airway pressure (CPAP) needs to be further assessed in controlled and blind studies.

5.52.1.2 Cognitive Disturbances

Very few studies have investigated the effect of pain on cognitive functions such as memory and attention. Three studies using chronic musculoskeletal pain and fibromyalgia patients suggest a causative association (Kewman, D. G. *et al.*, 1991; Landro, N. I. *et al.*, 1997; Côté, K. A. and Moldofsky, H., 1997). The impact of cognitive deficits and their potential aggravation by disturbed sleep needs to be further studied. The potential impact of several classes of pain medication (e.g., opioids, anticonvulsants, muscle relaxants, antidepressants) on sleep and daytime alertness is also a particularly important line of research with real-life consequences ranging from sleep-related industrial accidents to impaired driving ability (George, C .F. P., 2003; Chapman, S., 2001). A recent experimental study done in normal volunteers showed that a one night infusion of morphine during sleep time can alter sleep quality by reducing deep-sleep duration and increasing sleep stage 2 duration (Shaw, I. R., *et al.*, 2005). Evidence-based data on long-term use of morphine on sleep homeostasis are missing.

5.52.1.3 Sleep Fragmentation and Deprivation

Sleep fragmentation is usually characterized by a rapid shift from a deeper sleep stage to a lighter one or by an increase in the number of brief arousals up to longer awakenings during the night (see Glossary for definitions). The number of body movements and respiratory disturbance events, which are often associated with arousals, seems to have an additive effect on daytime functioning over the following day or days. Sleep deprivation is a more general term that either characterizes the absence or very short duration of a given sleep stage and/or the near absence or reduction of sleep as tested by experimental manipulations. As recently demonstrated, measures of the impact of chronic sleep loss fall into a clear hierarchy: mood measures being more sensitive than cognitive tasks, which are in turn more sensitive than performance of motor tasks (Bonnet, M. H., 2005).

The increase in sleep fragmentation in normal subjects or in patients with sleep apnea seems to be clearly associated with a reduction in next-day performance, sleepiness, and impaired alertness (Bonnet, M. H., 1985; Wesenten, N. J. *et al.*, 1999; Stepanski, E. J., 2002; Martin, S. E. *et al.*, 1996; Van Dogen, H. P. *et al.*, 2003). A minimum of 5–6 h of sleep seems to be the threshold below which daytime performance is altered and, interestingly, several days are required before a return to baseline levels (Van Dogen, H. P. *et al.*, 2003). There is still no definitive evidence indicating that lack of deep sleep (St 3 and 4) or of slow wave EEG activity (SWA) increases pain sensitivity, although some animal and human experimental studies suggest such a link (see review from Kundermann, B. *et al.*, 2004a; Kundermann, B. and Lautenbacher, S., 2007). To our knowledge only one study has compared deep-sleep deprivation with other sleep stages or total sleep deprivation (Onen, A. H. *et al.*, 2001). Moreover, the absence of deep sleep is a feature of all chronic-pain conditions (Okura, K. *et al.*, 2004).

Before summarizing the studies on sleep deprivation and changes in pain perception, it is important to reiterate that study design and data analysis need to control for: (1) the differences between groups for age, since after 40 years of age, slow wave density, a dominant feature of deep sleep, tends to decline; (2) presence of respiratory disturbances during sleep, since patients with fibromyalgia who complain of daytime hypersomnolence tend to present with more micro-arousals, a higher number of short respiratory disturbances and longer oxygen desaturation periods than matched normal controls, an effect reversed by CPAP (Sergi, M. *et al.*, 1999; Gold, A. R. *et al.*, 2004); (3) the concomitant effect of fatigue, mood depression, anxiety, poor lifestyle habits, etc., as described above. In addition to the above issues, it is also important to note that the literature of sleep deprivation and pain is generally limited by experimental studies done with small sample sizes and a lack of adequate control groups.

Several studies have been conducted in normal subjects to assess the effect of deep-sleep deprivation on next-day pain perception. The disruption of sleep stage 4 or SWS by sound was associated with an increase in muscle tenderness and a reduction in pain threshold (mechanical pressure) the next morning, but this effect was less dominant when studies controlled for concomitant influences of fatigue (Moldofsky, H. and Scarisbrick, P., 1976; Lentz, M. J. *et al.*, 1999; Older, S. A. *et al.*, 1998). Negative findings have been reported by others (Drewes, A. M. *et al.*, 1997; Kundermann, B.

et al., 2004a; Older, S. A. *et al.*, 1998; Arima, T. *et al.*, 2001; Smith, M. T., *et al.*, 2007). Surprisingly, when normal subjects were deprived of SWA sleep, REM sleep or total sleep duration, no change in thermal pain threshold was noted during any of the sleep interruptions (Onen, A. H. *et al.*, 2001). In this study, however, total sleep deprivation slightly reduced mechanical pain tolerance scores (8%) and in the period after sleep recovery, a significant rebound effect was noted, such that mechanical pain tolerance was 15% higher. A recent study done in normal volunteers showed that two nights of total sleep deprivation reduced both heat and cold pain thresholds, but had no effect on warmth and cold detection threshold; results suggested that change in pain threshold was not specific to alterations in somatosensory function (Kundermann, B. *et al.*, 2004b). Kundermann and colleagues also suggested, in a comprehensive review, that the role of stress and changes in endogenous serotonin and opioid activity can also play an important role in arousal and changes in pain perception (Kundermann, B. *et al.*, 2004a).

It is important to clarify that experimental sleep deprivation, which has been induced in the above studies, is an extreme manipulation that may be different from the natural ongoing sleep disruption experienced by chronic pain patients. As described above, fragmentation or deprivation, not necessarily limited to St 3 and 4, seems to alter cognitive function and memory consolidation; all sleep stages seem to be equally important for the preservation and maintenance of daytime functions (Stickgold, R. *et al.*, 2000; Mednick, S. *et al.*, 2003; Gais, S. *et al.*, 2000).

5.52.1.4 Circadian Variation in Pain Perception

Surprisingly, most studies using normal nonpain subjects without mood alteration have failed to demonstrate a clear circadian variation in experimental pain threshold or pain intensity reports over a 24 h schedule or when comparing evening and morning data (Rogers, E. J. and Vilkin, B. 1978; Strian, F. *et al.*, 1989; Koltyn, K. F. *et al.*, 1999; Lavigne, G. J. *et al.*, 2000; Bentley, A. J. *et al.*, 2003; Lavigne, G. J. *et al.*, 2004). In patients with chronic pain, however, symptom presentation often has a typical circadian pattern. Arthritic pain is often worse in the morning, while pain levels related to fibromyalgia, myofascial orofacial pain, and some headache conditions are typically higher in the afternoon (Bellamy, N. *et al.*, 1991; Reilly, P. A. and Littlejohn, G. O., 1993; Dao, T. T. T. *et al.*, 1994). Furthermore, not all pain conditions involve pain that directly interferes with sleep; in patients with torticolis, pain is rapidly reduced by adopting the supine posture (Lobbezoo, F. *et al.*, 1996; Bentley, A. J., 2007).

5.52.2 Perception of Pain during Sleep: Nociception or Sleep Arousal

5.52.2.1 Nociception – Pain Perception during Sleep

While awake, tactile and thermal sensory input of sufficient intensity can activate A delta, A beta, and C sensory fibres projecting to the thalamus and several cortical areas (Bromm, B. and Lorenz, J. 1998; Coghill, R.C. *et al.*, 1994; Le Pera, D. *et al.*, 2000; Peyron, R. *et al.*, 2000). The long duration of painful hypertonic saline infusions seems to activate A delta and C afferent fibers that in the wake state reach the thalamus, amygdale, and other cortical areas associated with pain processing (Le Pera, D. *et al.*, 2000; Zubieta, J. K. *et al.*, 2001). During sleep, however, a putative gating process of somatosensory inputs is thought to prevent awakening resulting from irrelevant input or non-life-threatening events. Several studies suggest that sleep-preserving sensory gating mechanisms are likely to be located at the upper brain stem area (see Figure 1) in the so-called reticular activating system (Pompeiano, O. and Swett, J. E. 1963; Hernandez-Peon, R. *et al.*, 1965; Soja, P. J. *et al.*, 2001; Soja, P. J., 2007; Nofzinger, E. and Derbyshire, S. W. G., 2007). However, the balance between wakefulness system(s) and sleep-promoting neuronal network(s) in relation to sensory discrimination and pain during sleep is poorly understood and requires further investigation.

Regarding sensory perception during sleep, it is crucial to discriminate between studies made using sound and those using tactile stimulations. The results of sound studies have made it apparent that acoustic stimulation triggers more sleep arousals and awakenings in non-REM light sleep stages (St 1 and 2) than in deep sleep (St 3 and 4) or in REM sleep (Rechstaffen, A. and Kales, A., 1968; Carley, D. W. *et al.*, 1997; Kato, T. *et al.*, 2004). Sound is a different sensory modality from pain: its main function with respect to sleep is to alert the individual to wake up (alarm clock) or to parental duties (a baby's cry). Tactile stimulation, however, is more likely to be interpreted as a touch to the body, which may or may not enforce the awakening process and is likely to be interpreted differently than sound by a sleeping

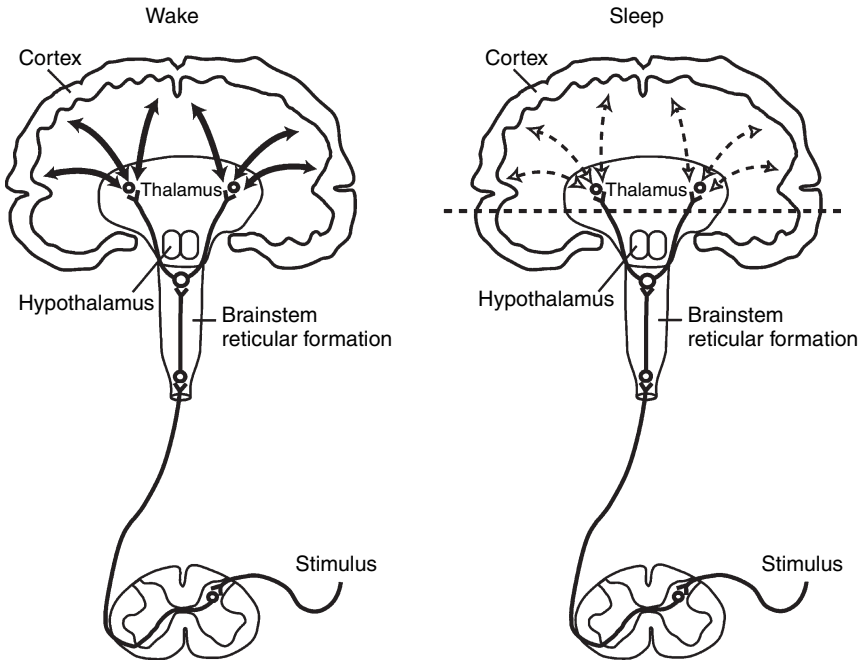

Figure 1 During wake state, there is a free flow in neuronal activity from spinal cord or/and brainstem to and from thalamus and cortical networks. During sleep, a gating mechanism seems to isolate the upper brain from most incoming inputs originating at somatosensory level. However, some circuits, for example, auditory processing, remain fully active. The exact anatomical site of the separation (see dashed line) between spinal and brainstem networks and thalamo-cortical pathways remain to be demonstrated.

brain (Velluti, R. A. *et al.*, 2000; Kato, T. *et al.*, 2004; Soja, P. J. *et al.*, 2001) Moreover, during sleep the term nociception is probably more accurate to describe the process of potentially harmful inputs, interpreted in conscious and awake subjects as pain (Bromm, B. and Lorenz, J., 1998; Lavigne, G. J. *et al.*, 2000).

Studies done in the 1960s, using tactile-cutaneous sensory stimulations during wake/sleep states, are a rich source of information (Pompeiano, O. and Swett, J. E., 1963; Hernandez-Peon, R. *et al.*, 1965) It was suggested that a filtering mechanism is active during synchronized or non-REM sleep at the first relay of neurons in the brainstem mesencephalic-reticular formation and in the trigeminal sensory nucleus. More recent work lends further support to the concept that sleep involves a selective isolation from the external milieu. Recordings of ascending spinoreticular and trigemino-thalamic tract neurons show that a gating mechanism seems to be present during sleep when brief sensory or pain stimulations are applied to the skin of the animal. Furthermore, the neurons behaved differently across sleep stages, that is, during non REM or REM sleep: air puff activated trigemino-thalamic tract neurons during REM sleep whereas neuronal activity following tooth pulp stimulation was suppressed (Cairns, B. E. *et al.*, 1996; Soja, P. J. *et al.*, 2001). It was further suggested that the serotoninergic and nonserotoninergic brainstem raphe magnus cells are involved to an important extent in the sensory modulation of pain inputs (Foo, H. and Mason, P., 2003). Interestingly, recording of thalamic cells in one human has confirmed previous animal findings suggesting that thalamic neurons discharge differently during states of waking and sleeping. It was observed that the discharge of thalamic neurons was in a tonic mode while the patient was awake and in a bursting mode when the patient was in light sleep; nevertheless none of these cells had a clear sensory receptive field in the periphery (Tsoukatos, J. *et al.*, 1997). These findings are similar to those from animal studies showing that thalamic neurons are under a global inhibition during sleep while cortical neurons, by contrast, are highly active (Steriade, M. and Timofeev, I., 2003). The exact location of the mechanism(s) supporting the somatosensory dissociation during sleep remains under investigation (see Figure 1). The balance between mechanisms that maintain vigilance or promote sleep continuity, however, seems to be state-dependent and related to the modulation of neuronal networks at the level of the reticular activating system.

The initiation of an awakening and conscious reaction during sleep may be secondary to a decrease in the sensory gating in sleep resulting in the recovery of the free flow between ascending and descending brainstem, thalamus and cortical activities (Siegel, J., 2004; Skinner, R. D. *et al.*, 2004). In other words, it is as if the reptilian brain maintains basic survival function during sleep, and interaction with thalamo-cortical networks depends on the nature (sound, touch, and harmful stimulus), magnitude, and duration of the stimulation. Obviously, this hypothesis needs to be supported by further evidence.

A recent paper summarizing the evidence on brain activation during sleep provides relevant information (Peigneux, P. *et al.*, 2003). During light sleep, pontine tegmentum and thalamus are deactivated while mesencephalic regions remain active. In deep sleep, all three structures are relatively deactivated while activity is largely maintained at the cortical temporal and insular lobe levels. Paradoxically, all the above structures are activated during REM sleep, although a strong dissociation is present: there is no peripheral efferent activity (e.g., the motor cortex does not trigger a movement except in the presence of sleep pathology: the REM behaviour disorder). There is little evidence strongly supporting a clear-cut gating of sensory information at the lower brain level, to prevent awakening from irrelevant sensory inputs. However, the role of the amygdala and the hypothalamus is discussed in the interpretation of sensory gating outside the higher thalamocortical levels (Morrison, A. R. *et al.*, 2000; Lee, R. S. *et al.*, 2001). A review of behavioral animal and human studies is also useful for a better understanding of the modulation of sensory inputs during sleep.

The interaction between the pain system and vigilance versus sleep is further supported by a cat study using the classical tail flick sensory motor reflex (Kshatri, A. M. *et al.*, 1998). It was suggested that the gating of sensory inputs during sleep depends on the integrity of the cholinergic system at the medial pontine–reticular level. This work also clearly showed, in comparison to the wake state and in the absence of any medication, that the reflex latency was 3 times longer in non-REM sleep (quiet sleep in animal) and 5 times longer in REM sleep. This finding again supports the concept of higher responsiveness to brief sensory inputs during non-REM in comparison to REM sleep. However, another cat study revealed that under tonic sensory nociceptive influences (formalin injection in the foot) the animals tended to remain awake with delayed sleep onset for the first 2 days, and a reduction in duration of deep sleep (St 3 and 4 in humans) and REM sleep stages (Carli, G. *et al.*, 1987) Interestingly, after 2 days, the animals recovered, exhibiting total sleep time and deep sleep of longer duration; a typical pattern seen after sleep deprivation (Onen, A. H. *et al.*, 2001; Kundermann, B. *et al.*, 2004a). Another sleep and pain study in rats, using the experimental adjuvant arthritis model in both hind paws, also showed fragmentation of the typical sleep and wake pattern (Landis, C. A. *et al.*, 1988). The number of brief sleep periods was increased over the circadian rhythm; total sleep time and deep sleep duration were also shorter in rats with arthritis. The above-mentioned animal studies suggest that a sleeping brain is not completely isolated from the external milieu and that pain-nociception can activate networks related to vigilance and body protection. This activation appears to be related to the type (phasic versus tonic, intensity, etc.) and duration of the painful stimuli (Velluti R. A. *et al.*, 2000; Soja, P. J. *et al.*, 2001; Kato, T. *et al.*, 2004; Lavigne, G. J. *et al.*, 2004).

In humans, the perception of pain during sleep also depends on the duration and type of stimulus used; brief sensory nerve-related or mild duration thermal or long duration chemical or mechanical stimulations initiate different types of responses that need to be interpreted accordingly. In a study using the spinal motor responses, following brief stimulation of the leg sural nerve to evoke a flexion reflex, it was noted that the reflex latency was prolonged during sleep in comparison to wake state (Sandrini, G. *et al.*, 2001). In parallel, the threshold was 60% higher in non-REM and 200% higher in REM sleep than during wake state. This study supports the above-mentioned animal findings, suggesting that during sleep lower brain neurons modulate pain inputs in such a way that a hypoalgesic response seems to be present. In contrast, when sensory processing from periphery to cortex was estimated with extremely brief (<60 ms) sensory-laser or electrical evoked responses to pain, the somatosensory cortically evoked potential completely disappeared during light sleep (Bedyoun, A. *et al.*, 1993; Wang, X. *et al.*, 2003). This absence of somatosensory evoked potentials during sleep stands in contrast to similarly present auditory stimuli in which evoked potentials are largely preserved during sleep. Sound appears to play a more sensitive role in preserving bodily integrity during sleep than tactile-somatosensory input (Kato, T. *et al.*, 2004). Alternatively, in collaboration

with the Italian Milano sleep group, we found that longer (6–12 s) moderate heat pain stimulation (46 °C) applied over the upper arm can evoke a clear sleep behavioral response: nearly twice the number of micro-arousals (see Glossary for definition) in light non-REM sleep compared to deep or REM sleep (Lavigne,G. J. *et al.*, 2000). These results were confirmed by another group that found that higher thermal pain temperatures were required to elicit arousal during deep sleep and REM in comparison to light sleep. These temperatures were closer to waking pain tolerance levels instead of pain threshold level (Bentley, A. J. *et al.*, 2003). More recently, with the objective of challenging sensory pain processing across sleep stages, we used a hypertonic saline infusion in the arm muscle to mimic longer clinical pain episodes (>100 s). A similar procedure has been used by others during sleep (Drewes, A. M. *et al.*, 1997). Interestingly, we found that micro-arousal responses were also more dominant in light sleep in comparison to deep and REM sleep, and a clear and dominant sleep awakening response was present with an equipotent response rate in all sleep stages (Lavigne, G. J. *et al.*, 2004).

This evidence suggests that when a painful stimulus or a clinical pain episode lasts long enough, the protective mechanism that maintains sleep continuity (the gating barrier to irrelevant input) is released and a clear behavioral response may occur with a potential return to consciousness. Recent clinical evidence for impaired somatosensory gating during sleep in chronic pain conditions has been suggested by findings of decreased sleep spindle activity in chronic low back pain and fibromyalgia patients (Harman, K. *et al.*, 2002; Landis, C. A. *et al.*, 2004). Thus it can be hypothesized that brief sensory stimuli, such as electrical or thermal pain, are too brief to be processed by a sleeping brain as potentially harmful, whereas longer-lasting or tonic painful stimuli akin to clinical pain states are more likely to elicit a full-blown arousal response.

5.52.2.2 Sleep Arousal: Brain and Autonomic Activation

The above arousal and awakening responses observed with thermal and deep muscle infusion are not only restricted to a cortical activation as seen on electroencephalogram. They are also associated with a clear increase in heart rate and a change in respiration that is frequently interrupted with the onset of the pain stimulation (Lavigne, G. J. *et al.*, 2000; Lavigne, G. J. *et al.*, 2001; Bentley, A. J. *et al.*, 2003; Lavigne, G. J. *et al.*, 2004). It is interesting to note that the so-called fast alpha EEG intrusion, which for a long time was believed to be a marker of pain in relation to sleep, is not considered to provide the sole explanation for poor sleep in pain patients (Moldofsky, H., 2001; Mahowald, M. L. and Mahowald M. W., 2000; Roizenblat, S. *et al.*, 2001; Rains, J. C. and Penzien, D. B., 2003). More recent thinking conceptualizes pain as a disruptor of sleep homeostasis that may increase sleep arousal instability, described as an augmentation in the normal cyclical alternating pattern in which brain and cardiac activation tends to recur in clusters (Staedt, J. *et al.*, 1993; Moldofsky, H., 2001; Roizenblatt, S. *et al.*, 2001; Parrino, L., Zucconi, M. and Terzano, M. G., 2007).

Cardiac activation during sleep is used as an indirect estimate of sympathetic (e.g., accelerator) and parasympathetic (decelerator or brake) balance during wake and sleep states. During wake state, a sympathetic dominance predominates, maintaining a high level of vigilance. Sympathetic-cardiac dominance is also present during REM sleep, a state with high cortical and cardiac activity but with a behavioral muscle paralysis. Conversely, during non-REM sleep, parasympathetic-cardiac activity is dominant and this may provide a recuperative function since there is an inverse coupling: a low sympathetic dominance is inversely coupled with a high degree of SWA in each consecutive non-REM to REM cycle (Brandenberger, G. *et al.*, 2001). Interestingly, in insomnia and fibromyalgia patients, a sympathetic dominance persists across NREM sleep cycles at levels similar to wake and REM sleep states (Bonnet, M. H. and Arand D. L., 1998; Martínez-Lavín, M. *et al.*, 1998). It has been hypothesized that enhanced sympathetic activity during sleep may over-facilitate arousal mechanisms and cyclical patterns of brain activation. However, this hypothesis was not supported in a study of medication-free women suffering from fibromyalgia in comparison to women with efficient sleep and no pain (McMillan, D. *et al.*, 2004). By contrast, when patients with chronic fibromyalgia (widespread pain) and pain (low back, etc.) presenting with poor sleep efficiency were matched for age and gender to normal sleepers, we found (see Figure 2) that the normal parasympathetic and sympathetic balance was lost in both pain groups during non-REM sleep with an inverse coupling of SWA, that is, a lower density of SWA was observed during consecutive sleep stages compared to control

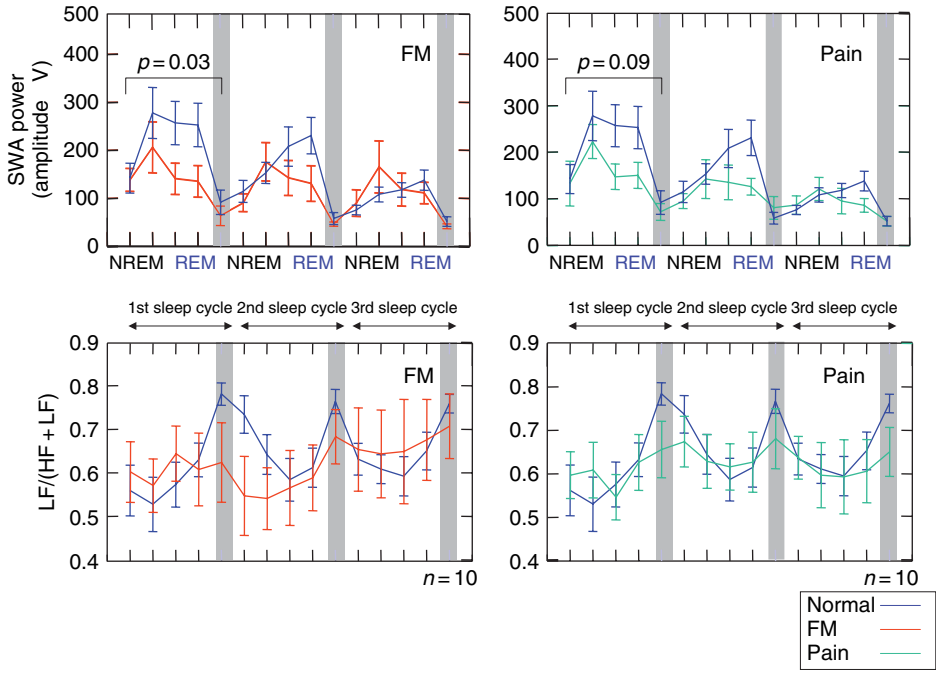

Figure 2 Dynamics of SWA and HRV over three consecutive sleep cycles. In normal subjects, SWA shows an inverse coupling with sympathetic activity (low-frequency divided by high-frequency plus low-frequency. One of the heart rate variability: HRV). During non-REM sleep, SWA was high when the sympathetic cardiac activity was low, and, conversely, SWA was low when HRV was high in REM sleep. In comparison to normal subjects, fibromyalgia (FM) chronic widespread pain patients showed a significant reduction in SWA for the first sleep cycle only (*t*-test: $p = 0.03$). Chronic pain patients (PAIN) also presented a similar trend in SWA, but not statistically significant (*t*-test: $p = 0.09$). PAIN patients did not show a rise in sympathetic activity during REM sleep ($p =$ NS: repeated ANOVA); FM patients showed a trend toward no rise in REM sleep.

subjects (Okura, K. *et al.*, 2005). Furthermore, like previous studies of men with fibromyalgia in a wake state, our preliminary analysis suggests that men maintain a high sympathetic activity across all sleep stages (Cohen, H. *et al.*, 2001). Women, however, do not show the usual rise in sympathetic activity during REM sleep. Our data differ from those of (Martinez-Lavin, M., *et al.*, 1998) since we separated data into consecutive non-REM and REM cycles. Caution is needed when interpreting the above-mentioned observations since parasympathetic and sympathetic balance tends to be altered with age and acute stress in relation to sleep (Brandenberger, G. *et al.*, 2003; Hall, M. *et al.*, 2004).

5.52.3 Circular Relation between Pain and Poor Sleep and Putative Consequence on Health Cost

The initiation of pain (e.g., acute post-op or trauma) usually precedes or coincides with the onset of poor sleep in close to 53–89% of patients (Morin, C. M. *et al.*, 1998; Smith, M. T. *et al.*, 2000; Riley, J. L., III *et al.*, 2001). In other words, in retrospective accounts, sleep disturbance is generally not considered a major problem for many patients until an injury is experienced; then pain and sleep become salient interacting issues. Intensive, time-series diary studies using multilevel modeling statistical techniques consistently show that over time, a day with intense pain is frequently followed by a poor sleep quality and subsequent ratings of poor sleep are in turn linked to next-day increases in clinical pain. This circular relationship, also described as a vicious circle, has been observed in patients with fibromyalgia, severe skin burns, and rheumatoid arthritis (Affleck, G. *et al.*, 1996; Raymond, I. *et al.*, 2001; Stone, A. A. *et al.*, 1997; Nicassio, P. M. *et al.*, 2002; Lavigne, G. J. *et al.*, 2005). As has been mentioned above, the influences of fatigue, mood alteration, other sleep disorders (such as sleep apnea or periodic limb movement), and medication use have not been well controlled for in these studies.

No direct data, to our knowledge, reports on the cost of pain and its interaction with poor sleep. However, an extensive study done in a Canadian

population (125 574 respondents) estimated that for every four patients seen by a family physician, three will report chronic pain (Meana, M. *et al*., 2004). When the potential cognitive disruption of pain medications is considered together with the rates at which analgesic, antidepressant, codeine, and hypnotics medications are used (3–4 times more often by women with chronic pain), it becomes apparent that the reduced ability of chronic pain patients with poor sleep to perform daily tasks is a societal burden (Meana, M. *et al*., 2004b). Moreover, given the aging population and the high prevalence of chronic pain (reported by over 50% of elderly of both genders), it is clear that health managers have a major challenge in planning service use (Harstall, C. and Ospina, M., 2003; Meana, M. *et al*., 2004).

The economic cost of chronic pain can probably be estimated in the order of billion dollars from headaches to pelvic pain; obviously specific estimation needs to be done. The large range of costs, for various pain symptoms and syndromes, reflects a lack of reliable information, although it is clear that chronic pain conditions are extremely costly (Latham, J. and Davis B. D., 1994). To date, an approximate estimate of the additional burden that poor sleep places on chronic pain costs can be only derived from cost studies of insomnia, which have yielded estimates ranging from 77 to 92 billion dollars (Stoller, M. K., 1994). If we agree that the suggested prevalence of chronic pain in adult population stands at 11% (Harstall, C. and Ospina, M., 2003) and that insomnia (defined as difficulties in sleep onset or in maintaining sleep and/or perception of nonrestorative sleep) is reported conservatively at a similar prevalence (Martin, S. A. *et al*., 2004) we can extrapolate, based on the assumption that one chronic pain patient in two will report similar insomnia complaints, that the overall direct cost is probably over 1 billion dollars. Indirect costs arising from as sick leave, hospitalization, and vehicular accident also need to be estimated, as has been done for other sleep disorders (Barbé, F. *et al*., 1998; George, C. F. P., 2003).

There is an obvious need for prospective and systematic studies of pain and economics that will estimate cost of health care, corrected for concomitant conditions such as aging, diabetes, obesity, cardiovascular problems, sleep disorders, depression, and anxiety (Lavigne, G. and Manzini, C., 2007). Moreover, indirect cost of absenteeism, low working performance, accident, reduced familial activities and risk of divorce also need to be factored into estimates of the cost of pain in relation to poor sleep.

References

Affleck, G., Urrows, S., and Tennen, H. 1996. Sequential daily relations of sleep, pain intensity, and attention to pain among women with fibromyalgia. Pain 68, 363–368.

Arima, T., Arendt-Nielsen, L., and Svensson, P. 2001. Effect of jaw muscle pain and soreness evoked by capsaicin before sleep on orofacial motor activity during sleep. J. Orofac. Pain 15(3), 245–256.

Atkinson, J. H., Ancoli-Israel, S., and Slater, M. A. 1988. Subjective sleep disturbance in chronic back pain. Clin. J. Pain 4, 225–232.

Barbé, F., Pericas, J., Munoz, A., Findley, L., Anto, J. M., and Agusti, A. G. N. 1998. Automobile accidents in patients with sleep apnea syndrome. Am. J. Respir. Crit. Care Med. 158, 18–22.

Bedyoun, A., Morrow, T. J., and Shen, J. 1993. Variability of laser-evoked potentials: attention, arousal and laterizes differences. Electroenceph Clin Neurophysiol 88, 173–181.

Bentley, A. J. 2007. Pain Perception during Sleep and Circadian Influences: The Experimental Evidence. In: *Sleep and Pain (eds*. G. Lavigne, B. J. Sessle, M. Choinière, P. J. Soja), pp. 123–136. IASP Press..

Bellamy, N., Sothern, R. B., and Campbell, J. 1991. Circadian rhythm in pain, stiffness, and manual dexterity in rheumatoid arthritis: relation between discomfort and disability. Annals. Rheum Dis 50, 243–248.

Bentley, A. J., Newton, S., and Zio, C. D. 2003. Sensitivity of sleep stages to painful thermal stimuli. J. Sleep Res. 12, 143–147.

Bonnet, M. H. 2005. Acute Sleep Deprivation. In: Principles and Practice Sleep of Medicine (*eds*. M. H. Kryger, T. Roth, W. C. Dement), 5, pp. 51–66. Elsevier Saunders.

Bonnet, M. H. 1985. Effect of sleep disruption on sleep, performance, and mood. Sleep 8(1), 11–19.

Bonnet, M. H. and Arand, D. L 1998. Heart rate variability in insomniacs and matched normal sleepers. Psychosom. Med. 60, 610–615.

Brandenberger, G., Ehrhart, J., Piquard, F., and Simon, C. 2001. Inverse coupling between ultradian oscillations in delta wave activity and heart rate variability during sleep. Clin. Neurophysiol. 112, 992–996.

Brandenberger, G., Viola, A. U., Ehrhart, J., Charloux, A., Geny, B., Piquard, F., and Simon, C. 2003. Age related changes in cardiac autonomic control during sleep. J. Sleep Res. 12, 173–180.

Bromm, B. and Lorenz, J. 1998. Neurophysiological evaluation of pain. Electroenceph. Clin. Neurophysiol. 107, 227–253.

Cairns, B. E., McErlane, S. A., and Fragoso, M. C. 1996. Spontaneous discharge and peripherally evoked orofacial responses of trigemino-thalamic tract neurons during wakefulness and sleep. J. Neurosci. 16, 8149–8159.

Carley, D. W., Applebaum, R., Basner, R. C., Onal, E., and Lopata, M. 1997. Respiratory and arousal responses to acoustic stimulation. Chest 112(6), 1567–1571.

Carli, G., Montesano, A., Rapezzi, S., and Paluffi, G. 1987. Differential effects of persistent nociceptive stimulation on sleep stages. Behav. Brain Res. 26, 89–98.

Chapman, S. 2001. The effects of opioids on driving ability in patients with chronic pain. APS Bull. 11, 5–9.

Coghill, R. C., Talbot, J. D., Evans, A. C., Meyer, E., Gjedde, A., Bushnell, M. C., and Duncan, G. H. 1994. Distributed processing of pain and vibration by the human brain. J. Neurosci. 14, 4095–4108.

Cohen, M., Menefee, L. A., and Doghramji, K. 2000. Sleep in chronic pain: problems and treatments. Int. Rev. Psychiat 12, 115–126.

Cohen, H., Neumann, L., Alhosshle, A., Kotler, A., Abu-Shakra, M., and Buskila, D. 2001. Abnormal sympathovagal balance in men with fibromyalgia. J. Rheumatol. 28, 581–589.

Côté, K. A and Moldofsky, H. 1997. Sleep, daytime symptoms, and cognitive performance in patients with fibromyalgia. J. Rheumatol. 24, 2014–2023.

Dao, T. T. T., Lund, J. P., and Lavigne, G. J. 1994. Comparison of pain and quality of life in bruxers and patients with myofascial pain of the masticatory muscles. Orofac. Pain. 8, 350–356.

Dauvilliers, Y. and Touchon, J. 2001. Le sommeil du fibromyalgique: revue des données cliniques et polygraphiques. Neurophysiol. Clin. 2001 31, 18–33.

Donald, F., Esdaile, J. M., Kimoff, J. R., and Fitzcharles, M. A. 1996. Musculoskeletal complaints and fibromyalgia in patients attending a respiratory sleep disorders clinic. J. Rheumatol. 23(9), 1612–1616.

Drewes, A. M., Nielsen, K. M., and Arendt-Nielsen, L. 1997. The effect of cutaneous and deep pain on the electroencephalogram during sleep – An experimental study. Sleep 20, 623–640.

Foley, D., Ancoli-Israel, S., Britz, P., and Walsh, J. 2004. Sleep disturbances and chronic disease in older adults: results of the 2003 National Sleep Foundation Sleep in America Survey. J. Psychosom. Res. 56(5), 497–502.

Foo, H. and Mason, P. 2003. Brainstem modulation of pain during sleep and waking. Sleep Med. Rev. 7, 145–154.

Gais, S., Plihal, W., and Wagner, U. 2000. Early sleep triggers memory for early visual discrimination skills. Nature Neurosci 3, 1335–1339.

George, C. F. P. 2003. Driving simulators in clinical practice. Sleep Med. Rev. 7, 311–320.

Gold, A. R., Dipalo, F., Gold, M. S., and Broderick, J. 2004. Inspiratory airflow dynamics during sleep in women with fibromyalgia. Sleep 27(3), 459–466.

Gozal, D. and O'Brien, L. M. 2004. Snoring and obstructive sleep apnoea in children: why should we treat? Paediatr. Respir. Rev. 5 (Suppl A), S371–S376.

Hall, M., Vasko, R., Buysse, D., Ombao, H., Chen, Q., Cashmere, J. D., Kupper, D., and Thayer, J. F. 2004. Acute stress affects heart rate variability during sleep. Psychosomatic Med 66, 56–62.

Harstall, C. and Ospina, M. 2003. How prevalent is chronic pain. Pain Clin. Update 11(2), 1–4.

Harman, K., Pivik, R. T., D'Eon, J. L., Wilson, K. G., Swenson, J. R., and Matsunaga, L. 2002. Sleep in depressed and nondepressed participants with chronic low back Pain: electroencephalographic and behavior findings. Sleep 25(7), 775–783.

Hernandez-Peon, R., O'Flaherty, J. J., and Mazzuchelli-O'Flaherty, A. L. 1965. Modifications of tactile evoked potentials at the spinal trigeminal sensory nucleus during wakefulness and sleep. Experimental Neurol. 13, 40–57.

Kato, T., Guitard, F., Rompré, P. H., Lund, J. P., Montplaisir, J. Y., and Lavigne, G. J. 2004. Experimentally induced arousals during sleep: a cross-modality matching paradigm. 2004. J. Sleep Res. 13, 1–10.

Kewman, D. G., Vaishampayan, N., and Zald, D. 1991. Cognitive impairment in musculoskeletal pain patients. Int'l. J. Psychiat. Med. 21, 253–262.

Koltyn, K. F., Focht, B. C., and Ancker, J. M. 1999. Experimentally induced pain perception in men and women in the morning and evening. Int. J. Neurosci. 98, 1–11.

Koopman, C., Nouriani, B., and Erickson, V. E. 2002. Sleep disturbances in women with metastatic breast cancer. Breast Journal 6, 362–370.

Kshatri, A. M., Baghdoyan, H. A., and Lydic, R. 1998. Cholinomimetics, but not morphine, increase antinociceptive behavior from pontine reticular regions regulating rapid eye movement sleep. Sleep 21(7), 677–685.

Kundermann, B. and Lautenbacher, S. 2007. Effects of Impaired Sleep Quality and Sleep Deprivation on Diurnal Pain Perception. In: *Sleep and Pain (eds*. C. Lavigne, B. J. Sessle, M. Choinière, P. J. Soja), Seattle IASP Press.

Kundermann, B., Krieg, J. C., Schreiber, W., and Lautenbacher, S. 2004a. The effect of sleep deprivation on pain. Pain Res. Manage. 39(1), 25–32.

Kundermann, B., Spernal, J., Huber, M. T., Krieg, J. C., and Lautenbacher, S. 2004b. Sleep deprivation affects thermal pain thresholds but not somato-sensory thresholds in healthy volunteers. Psychosomatic. Med. 66, 932–937.

Landis, C. A., Robinson, C. R., and Levine, J. D. 1988. Sleep fragmentation in the arthritic rat. Pain 34, 93–99.

Landis, C. A., Lentz, M. J., Rothermel, J., Buchwald, D., and Shaver, J. L. 2004. Decreased sleep spindles and spindle activity in midlife women with fibromyalgia and pain. Sleep 27(4), 741–750.

Landro, N. I., Stiles, T. C., and Sletvold, H. 1997. Memory functioning in patients with primary fibromyalgia and major depression and healthy controls. J. Psychosom Res. 42, 297–306.

Latham, J. and Davis, B. D. 1994. The socioeconomic impact of chronic pain. Disabil. Rehabil. 16(1), 39–44.

Lavigne, G. J. and Manzini, C. 2007. Pain and Poor Sleep: Impact on Public Health. In: *The Public Health Impact of Sleep Disorders (eds*. S. R. Pandi-Perumal and D. Leger), pp. 193–208.

Lavigne, G. J., Brousseau, M., Kato, T., Mayer, P., Manzini, C., Guitard, F., and Montplaisir, J. Y. 2004. Experimental pain perception remains equally active over all sleep stages. Pain 110, 646–655.

Lavigne, G. J., McMillan, D., and Zucconi, M. 2005. Pain and Sleep. In: principles and practice sleep of medicine (*eds*. M. H. Kryger, T. Roth, W. C. Dement), Vol. 106, pp. 1246–1255. Elsevier Saunders.

Lavigne, G. J., Zucconi, M., and Castronovo, C. 2000. Sleep arousal response to experimental thermal stimulation during sleep in human subjects free of pain and sleep problems. Pain 84, 283–290.

Lavigne, G. J., Zucconi, M., Castronovo, C., Manzini, C., Veglia, F., Smirne, S., and Ferini-Strambi, L. 2001. Heart rate changes during sleep in response to experimental thermal (nociceptive) stimulations in healthy subjects. Clin. Neurophysiol. 112, 532–535.

Lee, R. S., Steffenson, S. C., and Henriksen, S. J. 2001. Discharge profiles of ventral tegmental area GABA neurons during movement, anesthesia, and the sleep-wake cycle. J. Neurosci. 21(5), 1757–1766.

Lentz, M. J., Landis, C. A., and Rothermel, J. 1999. Effects of selective slow wave sleep disruption on musculoskeletal pain and fatigue in middle aged women. J. Rheumatol. 26, 1586–1592.

Le Pera, D., Svensson, P., Valeriani, M., Watanabe, I., Arendt-Nielsen, L., and Chen, A. C. 2000. Long-lasting effect evoked by tonic muscle pain on parietal EEG activity in humans. Clin. Neurophysiol. 111(12), 2130–2137.

Lobbezoo, F., Thu Thon, M., and Montplaisir, J. 1996. Relationship between sleep, neck muscle activity, and pain in cervical dystonia. Can. J. Neurol. Sci. 23, 285–290.

Macfarlane, T. V. and Worthington, H. V. 2004. Association between orofacial pain and other symptoms: a population based study. Oral. Biosci and Med. 1, 45–54.

Mahowald, M. L. and Mahowald, M. W. 2000. Nighttime sleep and daytime functioning (sleepiness and fatigue) in less well-defined chronic rheumatic diseases with particular reference

to the 'alpha-delta NREM sleep anomaly'. Sleep Med. 1, 195–207.
Martin, S. A., Aikens, J. E., and Chervin, R. D. 2004. Toward cost-effectiveness analysis in the diagnosis and treatment of insomnia. S. Med. Rev. 8(1), 63–72.
Martin, S. E., Engleman, M. H., Deary, I. J., and Douglas, N. J. 1996. The effect of sleep fragmentation on daytime function. Am. J. Respir. Crit. Care Med. 153, 1328–1332.
Martínez-Lavín, M., Hermosillo, A. G., and Rosas, M. 1998. Circadian studies of autonomic nervous balance in patients with fibromyalgia: a heart rate variability analysis. Arthri. Rheum. 41, 1966–1971.
McCracken, L. M. and Iverson, G. L. 2002. Disrupted sleep patterns and daily functioning in patients with chronic pain. Pain Res. Manage. 7, 75–79.
McMillan, D., Landis, C., Lentz, M., Shaver, J., Heitkemper, M., Rothermel, J., Blunden, P., and Buchwald, D. 2004. Hearth rate variability during sleep in women with fibromyalgia. Sleep. 27, A324 (abstract Suppl.).
Meana, M., Cho, R., and DesMeules, M. 2004. Chronic pain: the extra burden on Canadian women. BMC Women's Health 4 (Suppl 1), S17.
Mednick, S., Nakayama, K., and Stickgold, R. 2003. Sleep dependent learning: a nap is as good as a night. Nature Neurosci. 6, 697–698.
Menefee, L. A., Cohen, M., and Anderson, W. R. 2000. Sleep disturbance and nonmalignant chronic pain: a comprehensive review of the literature. Pain Med 1, 156–172.
Moldofsky, H. 2001. Sleep and pain: clinical review. Sleep Med. Rev. 5, 387–398.
Moldofsky, H. and Scarisbrick, P. 1976. Induction of neurasthenic musculoskeletal pain syndrome by selective sleep stage deprivation. Psychosom. Med. 38, 35–44.
Morin, C. M., Gibson, D., and Wade, J. 1998. Self-reported sleep and mood disturbance in chronic pain patients. Clin. J. Pain. 14, 311–314.
Morrison, A. R., Sanford, L. D., and Ross, R. J. 2000. The amygdale: A critical modulator of sensory influence on sleep. Biol. Signals Recept. 9, 283–296.
Nicassio, P. M., Moxham, E. G., and Schuman, C. E. 2002. The contribution of pain, reported sleep quality, and depressive symptoms to fatigue in fibromyalgia. Pain. 100, 271–279.
Nofzinger, E. A. and Derbyshire, S. W. G. 2007. Pain Imaging in Relation to Sleep. In: *Sleep and Pain (eds*. G. Lavigne, B. J. Sessle, M. Choinière, P. J. Soja), pp. 153–173. IASP Press.
Novak, M., Mucsi, I., Shapiro, C. M., Rethelyi, J., and Kopp, M. S. 2004. Increased Utilization of health services by insomniacs – an epidemiological perspective. J. Psychosom. Res. 56, 527–536.
Okifuji, A. and Turk, D. C. 2002. Stress and psychophysiological dysregulation in patients with fibromyalgia syndrome. Appl. Psychophysiol. Biofeed 27(2), 129–141.
Okura, K., Lavigne, G. J., Montplaisir, J. Y., Rompré, P. H., Huynh, N., and Lafranchi, P. 2005. Slow wave activity and heart rate variation are less dominant in fibromyalgia and chronic pain patients than in controls. Sleep 28, 0894.
Okura, K., Rompré, S., Manzini, C., Rompré, P. H., Huynh, N., Montplaisir, J. Y., and Lavigne, G. J. 2004. Sleep duration and quality in chronic pain patients in comparison to the sleep of fibromyalgia, insomnia, RLS and control subjects. Sleep. 27: (abstract Suppl.) A329 No. 736.
Older, S. A., Battafarano, D. F., and Danning, C. L. 1998. The effects of delta wave sleep interruption on pain thresholds and fibromyalgia like symptoms in healthy subjects; correlations with insulin like growth factor 1. J. Rheum. 25, 1180–1186.
Onen, A. H., Alloui, A., and Gross, A. 2001. The effects of total sleep deprivation, selective sleep interruption and sleep recovery on pain tolerance thresholds in healthy subjects. J. Sleep Res. 10, 35–42.
Parrino, L., Zucconi, M., and Terzano, M. G. Sleep Fragmentation and Arousal in the Pain Patient. In: Sleep and Pain (*eds* G. Lavigne, B. J. Sessle, M. Choinière, P. J. Soja,) pp. 213–231. IASP Press.
Peigneux, P., Laureys, S., Cleeremans, A., and Maquet, P. 2003. Cerebral Correlates of Memory Consolidation during Human Sleep : Contribution of Functional Neuroimaging. In: Sleep and Brain Plasticity. (*eds*. P. Maquet, C. Smith, R. Stickgold), Chap. 11,209–224.
Peyron, R., Laurent, B., and Garcia-Larrea, L. 2000. Functionnal imaging of brain responses to pain. A review and meta-analysis. Neurophysiol. Clin. 30, 263–288.
Pompeiano, O. and Swett, J. E. 1963. Actions of grated cutaneous and muscular afferent volleys on brain stem units in the decerebrate, cerebellectomized cat. Arch. Ital. Biol. 101, 552–583.
Rains, J. C. and Penzien, D. B. 2002. Chronic headache and sleep disturbance. Curr. Pain Headache Rep. 6, 498–504.
Rains, J. C. and Penzien, D. B. 2003. Sleep and chronic pain challenges to the αEEG sleep pattern as a pain specific sleep anormaly. J. Psychosom. Res. 54, 77–83.
Raymond, I., Nielsen, T. A., and Lavigne, G. J. 2001. Quality of sleep and its daily relationship to pain intensity in hospitalized adult burn patients. Pain 92, 381–388.
Rechtschaffen, A. and Kales, A. 1968. A manual of standardized terminology, techniques and scoring techniques for sleep stages of human subjects. Brain Res. Inst., University of California.
Reilly, P. A. and Littlejohn, G. O. 1993. Diurnal variation in the symptoms and signs of the fibromyalgia syndrome (FS). J. Musculoskel. Pain 1, 237–243.
Riley, III, J. L., Benson, M. B., and Gremillion, H. A. 2001. Sleep disturbances in orofacial pain patients: pain-related or emotional distress? J. Craniomandib. Pract. 19, 106–113.
Rogers, E. J. and Vilkin, B. 1978. Diurnal variation in sensory and pain thresholds correlated with mood states. J. Clin. Psychiat. 39(5), 431–438.
Roizenblatt, S., Moldofsky, H., and Benedito-Silva, A. A. 2001. Alpha sleep characteristics in fibromyalgia. Arthritis. Rheum. 44, 222–230.
Sandrini, G., Milanov, I., and Rossi, B. 2001. Effects of sleep on spinal nociceptive reflexes in humans. Sleep 24, 13–17.
Sayar, K., Arikan, M., and Yontem, T. 2002. Sleep quality in chronic pain patients. Can. J. Psychiatry. 47, 844–848.
Sergi, M., Rizzi, M., Braghiroli, A., Puttini, P. S., Greco, M., Cazzola, M., and Andreoli, A. 1999. Periodic breathing during sleep in patients affected by fibromyalgia syndrome. Eur. Respir. J. 14, 203–208.
Shaw, I. R., Lavigne, G., Mayer, P., and Choinière, M. 2005. Acute intravenous administration of morphine perturbs sleep architecture in healthy pain-free young adults: a preliminary study. Sleep. 28(6), 677–682.
Siegel, J. 2004. Brain mechanisms that control sleep and waking. Naturwissens Chaften 91, 355–365.
Skinner, R. D., Homma, Y., and Garcia-Rill, E. 2004. Arousal mechanisms related to posture and locomotion. 2. Ascending modulation. Prog. Brain Res. 143, 291–298.
Smith, M. T. and Haythornthwaite, J. A. 2007. Cognitive-Behavioral Treatment for Insomnia and Pain. In: *Sleep and Pain (eds*. G. Lavigne, B. J. Sessle, M. Choinière, P. J. Soja), pp. 439–457. IASP Press.
Smith, M. T., Perlis, M. L., and Smith, M. S. 2000. Sleep quality and presleep arousal in chronic pain. J. Behav. Med. 23, 1–13.
Soja, P. J. 2007. Modulation of Prethalamic Sensory Inflow during sleep versus Wakefulness. In: *Sleep and Pain (eds*. G. Lavigne, B. J. Sessle, M. Choinière, P. J. Soja), pp. 45–76. IASP Press.

Soja, P. J., Pang, W., Taepavarapruk, N., and McErlane, S. A. 2001. Spontaneous spike activity of spinoreticular tract neurons during sleep and wakefulness. Sleep 24, 18–25.
Staedt, J., Windt, H., and Hajak, G. 1993. Cluster arousal analysis in chronic pain- disturbed sleep. J. Sleep Res. 2, 134–137.
Stepanski, E. J. 2002. The effect of sleep fragmentation on daytime function. Sleep 25(3), 268–276.
Steriade, M. and Timofeev, I. 2003. Neuronal Plasticity during Sleep Oscillations in Corticothalamic Systems. In: Sleep and Brain Plasticity (*eds*. P. Maquet, C. Smith, and R. Stickgold), Chap. 14,270–291.
Stickgold, R., James, L. T., and Hobson, J. A. 2000. Visual discrimination learning requires sleep after training. Nature Neurosci. 3(12), 1237–1238.
Stoller, M. K. 1994. Economic effects of insomnia. Clini. Ther. 16(5), 873–897.
Stone, A. A., Brokerick, J. E., Porter, L. S., and Kaell, A. T. 1997. The experience of rheumatoid arthritis pain and fatigue: examining momentary reports and correlates over one week. Arthritis. Care Res. 10(3), 185–193.
Strian, F., Lautenbacher, S., and Galfe, G. 1989. Diurnal variations in pain perception and thermal sensitivity. Pain 36, 125–131.
Sutton, D. A., Moldofsky, H., and Badley, E. M. 2001. Insomnia and health problems in Canadians. Sleep 24, 665–670.
Tsoukatos, J., Kiss, Z. H. T., Davis, K. D., Tasker, R. R., and Dostrovsky, J. O. 1997. Patterns of neuronal firing in the human lateral thalamus during sleep and wakefulness. Exp. Brain Res. 113, 273–282.
Van Dongen, H. P., Maislin, P., Mullington, J. M., and Dinges, D. F. 2003. The cumulative cost of additional wakefulness: dose–response effects on neurobehavioral functions and sleep physiology from chronic sleep restriction and total sleep deprivation. Sleep 26(2), 117–126.
Velluti, R. A., Pena, J. L., and Pedemonte, M. 2000. Reciprocal actions between sensory signals and sleep. Biol. Signals Recept. 9, 297–308.
Wang, X., Inui, K., Qiu, Y., Hoshiyama, M., Tran, T. D., and Kakigi, R. 2003. Effects of sleep on pain related somato sensory evoked potentials in humans. Neurosci. Res. 45, 53–57.
Wesenten, N. J., Balkin, T. J., and Belenky, G. 1999. Does sleep fragmentation impact recuperation? A review and reanalysis. J. Sleep Res. 8, 237–245.
Widerstrom-Noga, E. G., Felipe-Cuervo, E., and Yezierski, R. P. 2001. Chronic pain after spinal injury: interference with sleep and daily activities. Arch. Phys. Med. Rehabil. 82, 1571–1577.
Yatani, H., Studts, J., and Cordova, M. 2002. Comparison of sleep quality and clinical and psychologic characteristics in patients with temporomandibular disorders. J. Orofac. Pain 16, 221–228.
Zubieta, J. K., Smith, Y. R., Bueller, J. A., Xu, Y., Kilbourn, M. R., Jewett, D. M., Meyer, C. R., Koeppe, R. A., and Stohler, C. S. 2001. Regional Mu opioid receptor regulation of sensory and affective dimensions of pain. Science 293, 311–315.

Relevant Website

http://www.sleepfoundation.org – National Sleep Foundation.

5.53 Pharmacological Modulation of Pain

A Dray, AstraZeneca Research and Development, Montreal, PQ, Canada

© 2008 Elsevier Inc. All rights reserved.

5.53.1	Introduction	795
5.53.2	G-Protein-Coupled Receptors	796
5.53.3	Opioids and Their Receptors	796
5.53.4	Kinins and Their Receptors	798
5.53.5	Protease-Activated Receptors	799
5.53.6	Cannabinoids and Their Receptors	799
5.53.7	Mrg-Related GPCR and Their Ligands	801
5.53.8	Prostanoids and Receptors	801
5.53.9	Cytokines, Chemokines, and Their Receptors	802
5.53.10	Adrenoceptors	803
5.53.11	Glutamate Regulation and Glutamate Receptors	804
5.53.12	Gamma-Aminobutyric Acid Receptors	805
5.53.13	Ion Channels	805
5.53.13.1	Ligand-Gated Channels	805
5.53.14	Purinergic Receptors	806
5.53.14.1	P2X Receptors	806
5.53.14.2	Acid-Sensing Channels	807
5.53.15	Sodium Channels	807
5.53.16	Calcium Channels	808
5.53.17	Neurotrophins and Their Receptors	809
5.53.18	Kinases	810
5.53.19	Botulinum Toxin	810
5.53.20	Nitric Oxide	811
5.53.21	Summary and Conclusions	811
References		811

5.53.1 Introduction

Chronic pain is a complex integration of sensory, affective, and cognitive processes encompassing a variety of clinical conditions that have been generalized as nociceptive (rheumatoid and osteoarthritis (OA)), neuropathic (postdiabetic neuropathy, posttraumatic neuralgia), or etiologically mixed (low back pain, cancer pain; for references see Merskey, H. *et al*., 2005; Campbell, J. N. *et al*., 2006). Pain conditions are etiologically diverse and there is limited understanding of clinical pain mechanisms and of environmental and social factors that aggravate pain such as stress and anxiety. In addition, it has been difficult to provide a unifying linkage of pain symptoms with the cellular mechanistic processes underlying these symptoms that would rationalize chronic pain therapy. The complexity of chronic pain is further reflected in the diversity of molecular targets considered to drive pain processes. Furthermore there is the evolving view that the pharmacology of pain may alter with time-dependent expression of targets, in the initiation versus the maintenance phases of pain, and that target expression is state-dependent (related to relative activity of the pain process or pathway). Thus poor understanding of pain pharmacology has seriously hampered the introduction of new drugs as there have been few drugs introduced with a new mechanism of action within living memory.

A recent step to building rational pain therapy has embraced a mechanism-based approach guided by advances in pain pharmacology. Thus major symptoms such as hyperalgesia, allodynia, and spontaneous pain have been linked with some of the identifiable, and often overlapping, neural cellular processes. The key processes are considered to be sensitization (reduced threshold for stimulation of pain pathways), hyperexcitability (amplification or

prolongation of nerve discharges in pain pathways), and spontaneous nerve activity (ectopic and/or spontaneous discharges in pain pathways). These processes or mechanisms are driven by molecular changes that provide the targets for pharmacological characterization and analgesia intervention (summarized in Figure 1). It is important to remember that for the most part these neural mechanisms and their molecular drivers have been explored in animal models and rarely consolidated to the same degree in human studies.

There have been a number of excellent reviews of pain mechanisms and molecules (Hunt, S. P. and Mantyh, P., 2001; Scholz, J. and Woolf, C. J., 2002; Watkins, L. R. and Maier, S., 2002) in the peripheral nervous system and central nervous system (CNS). Causative factors for pain are inflammatory mediators, factors released and made in response to nerve injury, phenotypic changes in neural pathways as well as supporting glial cells, structural modifications including nerve sprouting (sympathetic and sensory fibers), nerve rewiring (sensory and CNS fibers), and neurodegeneration of specific neurons in the CNS resulting in a hyperexcitable nervous system. Specific molecular interactions that drive the aforementioned excitability changes may differ according to the specific injury and consequent chemical environments that are created. The molecular interactions involve all major families of regulatory proteins (G-protein-coupled receptors (GPCRs), ion channels, regulatory enzymes, neurotrophins, kinases), offering an abundance of analgesic targets and therapeutic opportunities. The pharmacology of these targets is evolving and is dependent on the availability of reliable chemical and biopharmaceutical tools.

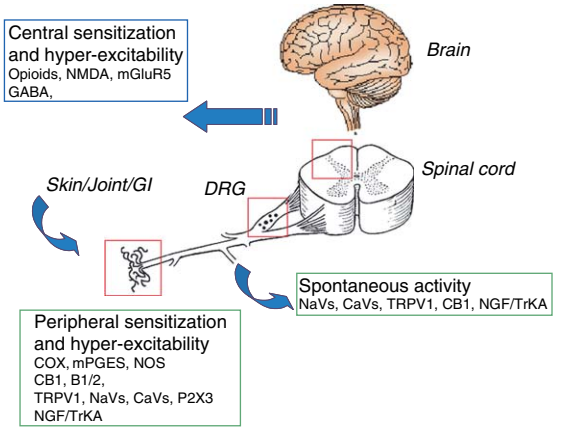

Figure 1 Mechanistic processes in chronic pain and key molecular drivers.

In this chapter I have selected from the emerging pharmacology of pain molecular approaches (summarized in Table 1) that will provide direction for future pain treatments.

5.53.2 G-Protein-Coupled Receptors

GPCRs have been a relatively tractable family of drug targets in a number of therapeutic arenas. A variety of GPCRs are involved in regulating neural excitability in pain pathways, often through the action of a variety of inflammatory mediators. These mediators act peripherally or centrally, via an equally large variety of specific membrane receptors (Scholz, J. and Woolf, C. J., 2002). In general, GPCRs signal via the production of second messengers (cyclic adenosine monophosphate (cAMP), cyclic guanosine monophosphate (cGMP), diacylglycerol (DAG), phospholipase C (PLC)) coupled with intracellular protein kinases and phosphatases (protein kinase A, several isotypes of protein kinase C (PKC)) which in their turn, phosphorylate and dephosphorylate specific cellular proteins including ligand- (e.g., TRPV1) and voltage-gated membrane ion channels (e.g., NaV1.8) which are important in regulating nerve excitability.

5.53.3 Opioids and Their Receptors

Opioids, and morphine in particular, are among the most effective pain medications. They act at peripheral, spinal, and supraspinal sites through a variety of opioid receptors (μ-, δ-, and κ-opioid receptors). These receptors are considered to be targets for an endogenous opioid system that has been extensively reviewed (Yaksh, T. L., 1997). μ-Opioid receptor activation commonly causes a variety of well-documented, target-related, CNS side effects including sedation, dysphoria, respiratory depression, and constipation. Thus there has been a vigorous attempt to exploit the peripheral antinociceptive actions of opioids as a means of avoiding CNS side effects. In support of this approach, sensory neurons express and transport opioid receptors to both the central and peripheral terminals. At central terminals, opioids reduce transmitter release from primary afferent nociceptors, thus blocking synaptic transmission while in the periphery opioid receptor activation directly hyperpolarize sensory neurons and attenuate nerve sensitization or hyperexcitability induced by inflammation or injury (Hurley, R. W. and Hammond, D. L., 2000; Sawynok, J., 2003).

Table 1 Pharmacological modulators of pain and emerging mechanisms of action and clinical indications.

Molecular Target	*Pharmacological tools*		*Analgesia mechanism and targeted tissue*	*Pain indications*
	Agonist	*Antagonist*		
μ-Opioid receptors	Morphine, fentanyl	Naloxone, naltrexone	Agonist: reduced peripheral and CNS excitability	Acute and chronic pain states
δ-Opioid receptor	Enkephalin, DPDPE, SNC80	Naltrindole	Agonist: Modulation of CNS pathways	Nociceptive and inflammatory
B1 receptor	Des Arg9 bradykinin	des Arg10, HOE-140; SSR240612, NVP-SAA 164	Antagonist: inflammatory tissue: pain pathway: PNS, CNS	Nociceptive and inflammatory
B2 receptor	Bradykinin	Icatibant, bradyzide	Antagonist: inflammatory tissue: pain pathway: PNS, CNS	Nociceptive and inflammatory
PAR2	Proteases	Unknown	Antagonist: PNS	Nociceptive and inflammatory
CB1	THC, anandamide, 2-arachidonylglycerol, palmitoylethanolamide, WIN55, 212-2, ajulemic acid	SR141716A (rimonabant), SR147778,	Agonist: Pain pathways PNS and CNS	Nociceptive and neuropathic
CB2	THC, anandamide, 2-arachidonylglycerol, palmitoylethanolamide, WIN55, 212-2, ajulemic acid, GW405833, HU-308, AM 1241	SR144428	Agonist: Pain pathways PNS and CNS	Nociceptive and neuropathic
SNSR	BAM8-22, γ2-MSH	Unknown	Antagonist: PNS	Nociceptive
COX-1 constitutive		Ibuprofen, naproxene	Inhibition of PG synthesis	Nociceptive and inflammatory
COX-2 induced		Ibuprofen, naproxene, celecoxib, rofecoxib	Inhibition of PG synthesis in PNS and CNS	Nociceptive and inflammatory
mPGES		Unknown	Inhibition of PG synthesis in PNS and CNS	Nociceptive and inflammatory
IL-1β	IL-1β	Unknown	Antibody versus ligand	Nociceptive and neuropathic
TNF-α	TNF-α	Anti-TNF, etanercept, adalimumab	Antibody versus ligand	Nociceptive and neuropathic
α-2	Clonidine, dexmedetomidine		Inhibition of neuroexcitability in PNS and CNS	Nociceptive and neuropathic
iGluR	Glutamate, kainate, AMPA, NMDA	LY293558, GV196771, ifenprodil, CP-101, 606	Antagonist: CNS pathways	Nociceptive and neuropathic
mGluR (5)	Glutamate	MPEP, SIB1757	Antagonist: CNS pathways	Nociceptive and neuropathic
$GABA_A$	Muscimol	Bicuculline	Agonist: reduced CNS excitability	Nociceptive and neuropathic
$GABA_B$	Baclofen	CGP35348	Agonist: reduced CNS excitability	Nociceptive and neuropathic
TRPV1	Capsaicin	Capsazepine, DD161515, SB705498	Antagonist: PNS excitability	Nociceptive and neuropathic
TRPA1	Cinnamaldehyde	Unknown	Antagonist: PNS	Neuropathic

(*Continued*)

Table 1 (Continued)

Molecular Target	*Pharmacological tools*		*Analgesia mechanism and targeted tissue*	*Pain indications*
	Agonist	*Antagonist*		
TRPM1	Menthol, icilin	Unknown	Antagonist: PNS	Neuropathic
P2X3	ATP, α, β-methy ATP	A-3174919	Antagonist: PNS	Nociceptive
P2X4	ATP	TNP-ATP	Antagonist: CNS	Neuropathic
P2X7	ATP	Unknown	Antagonist: CNS and PNS excitability	Nociceptive and neuropathic
ASIC1-3	Low pH	A-317567	Antagonist: PNS	Nociceptive
NaV1.3, NaV1.8, NaV1.7, NaV1.9		Lidocaine, mexiletine, lamotrigine	Blocker: PNS excitability	Nociceptive and neuropathic
CaV2.2		SNX-111, NMED-160	Blockers: PNS and CNS excitability	Nociceptive and neuropathic
CaV3.2		Ethosuximide	Blocker: PNS	Neuropathic
NGF	NGF	ALE0540, PD90780, RN624 (mAb)	Antiligand: PNS excitability	Nociceptive and neuropathic
P38-kinase	ATP	SB203580, CNI-14930	Blocker: PNS and CNS excitability	Nociceptive and neuropathic
iNOS		L-NAME, GW27415	Blocker: PNS and CNS excitability	Nociceptive and neuropathic

AMPA, α-amino-3-hydroxy-5-methyl-4-isoxazolepropionic acid; ATP, adenosine triphosphate; B, bradykinin; CaV, voltage-gated calcium channels; CB, cannabinoid; CNS, central nervous system; COX, cyclo-oxygenase; DPDPE, [D-Pen2,D-Pen5]-enkephalin; GABA, gamma-aminobutyric acid; iNOS, inducible nitric oxide synthase; L-NAME, L-N-nitro-L-arginine methyl ester; mGluR, metabotropic glutamate receptor; MPEP, 2-methyl-6-(phenylethynyl)-pyridine; mPGES, microsomal-associated prostaglandin E synthase; NaV, voltage-gated sodium channel; NGF, nerve growth factor; NMDA, *N*-methyl-D-aspartic acid; PAR, protease-activated receptor; PG, prostaglandin; PNS, peripheral nervous system; SNSR, sensory neuron specific receptor; THC, tetrahydrocannabinol; mAb, monoclonal antibody; TNP-ATP, 2′,3′-*O*-(2,4,6-trinitrophenyl) adenosine 5′-triphosphate.

In addition peripherally mediated opioid analgesia may be enhanced because μ-opioid receptor expression is increased by inflammation and nerve injury (Stein, C. *et al.*, 2003). This is also accompanied by a peripheral increase in the expression of opioids peptides. Novel opioids such as [8-(3,3-diphenyl-propyl)-4-oxo-1-phenyl-1,3,8-triazaspiro[4.5]dec-3-yl]-acetic acid (DiPOA) and the antidiarrheal drug loperamide, whose distribution is peripherally restricted, have shown efficacy in a number of post-operative, inflammatory, and neuropathic pain models (Whiteside, G. T. *et al.*, 2005a; Shidoda, K. *et al.*, 2006).

The pharmacology and analgesic efficacy of δ-opioid receptors (DOR) have also been explored since there is a potential for analgesic efficacy without the confounding side effects of other opioid (μ and κ) receptor therapies. A variety of studies have supported the concept that δ-selective ligands produce analgesia without notable sedation, respiratory depression, or inhibition of gastrointestinal motility. These studies have used genetic methods ranging from the knockdown of receptors to deletion of the DOR gene as well as pharmacological tools such as selective peptides and nonpeptide agonists ([D-Pen2,D-Pen5]-enkephalin (DPDPE), SNC80, AM-390) and antagonists (e.g., naltrindole; see Dray, A., 1999 for references).

δ Ligands may provide less analgesic efficacy than morphine but their effectiveness appears to depend on the pain stimulus, the type of injury, and the influence of their neurochemical environment. Thus, systemically administered δ ligands have low analgesic efficacy in acute pain models but show robust analgesia efficacy in a variety of chronic pain conditions accompanies by inflammation (Cahill, C. M. *et al.*, 2001). Enhanced activity has been attributed to stimulus-induced trafficking of DOR from the cytoplasm to nerve membranes in CNS neurons (Cahill, C. M. *et al.*, 2001). Activity and environment-dependent receptor trafficking also appears as an important regulatory mechanism in sensory neurons (Bao, L. *et al.*, 2003) but further studies are required to understand the significance of this in clinical pain and analgesia.

5.53.4 Kinins and Their Receptors

Bradykinin is an important peptidic mediator of inflammatory pain causing nociceptor activation and sensitization via constitutively expressed bradykinin B2

receptors (BK2) on peripheral nociceptors (Dray, A., 1997). It also stimulates the production and release of prostaglandin (PGs) cytokines and nitric oxide (NO). The abundant metabolite of bradykinin, des Arg9 bradykinin (kallidin), activates BK1 receptors which also occur constitutively, but in low abundance, in the periphery (Dray, A. and Perkins, M. N., 1993; Wotherspoon, G. and Winter, J., 2000) and in the primate CNS (Shughrue, P. J. *et al.*, 2003). Both receptors are coupled to similar transduction mechanism including G-αi and G-αq causing stimulation of DAG, PLC, and the release of intracellular calcium.

BK2 receptors are considered to undergo desensitization following prolonged kinin exposure, whereas BK1 receptors do not desensitize rapidly and thus may promote more prolonged pain and inflammation. In keeping with this, BK1 receptors are dramatically unregulated in many tissues, including sensory neurons (Levy, D. and Zochodne, D. W., 2000) and spinal cord (Fox, A. *et al.*, 2003; Ferreira, J. *et al.*, 2005), following tissue or ultraviolet injury (Eisenbarth, H. *et al.*, 2004) or traumatic nerve injury and by mediators such as interleukin (IL)-1β or the neurotrophin glial cell line-derived neurotrophic factor (GDNF; Fox, A. *et al.*, 2003; Valleni, V. *et al.*, 2004). These kinins cause a cascade of secondary changes, including prostanoid production, phosphorylation of signaling proteins such as PKC, and the sensitization of sensory transducers such as the TRPV1 receptor (Marceau, F. *et al.*, 1998). These events are linked with heat and mechanical hyperalgesia (Liang, Y. F. *et al.*, 2001; Fox, A. *et al.*, 2003).

There is an abundance of evidence supporting the analgesic potential of BK2 receptor antagonists (Stewart, J. M., 2004). For example, BK2 antagonists (icatibant [HOE-140], bradyzide) and BK1 antagonist (des Arg10 HOE-140; SSR240612) produce robust antihyperalgesic effects in a variety of animal models of inflammatory hyperalgesia (Burgess, G. M. *et al.*, 2000; Fox, A. *et al.*, 2003, Gougat, J. *et al.*, 2004) as well as in models of nerve injury-induced hyperalgesia (Gabra, B. H. and Sirois, P., 2003). In keeping with this deletion of the BK receptor genes reduces immune cell chemotaxis, spinal sensitization, as well as heat and mechanical allodynia following traumatic and diabetic nerve lesions (Pesquero, J. B. *et al.*, 2000; Ferreira, J. *et al.*, 2005; Gabra, B. H. *et al.*, 2005). To strengthen the translation of BK1 receptor therapy to humans, transgenic mice expressing human BK1 receptors, show robust inflammatory pain that was attenuated by the oral administration of the human-selective BK1 antagonist NVP-SAA 164 (Fox, A. *et al.*, 2005).

Kinin antagonists have not been extensively evaluated in clinical pain although they inhibit other kinin-mediated changes in humans, for example, cancer, allergy, and vasodilatation. However, recent clinical study using a single dose intra-articular joint administration of Icatibant (Flechtenmacher, J. *et al.*, 2004) produced long-lasting (up to 1 week) relief of movement-related pain in patients suffering from OA. This study highlights a strong proof of principle for BK2 involvement in OA and that localized monotherapy with a selective antagonist can produce significant pain relief.

5.53.5 Protease-Activated Receptors

Several proteases, from circulating inflammatory cells and vascular epithelium, cleave a variety of protease-activated receptors (PARs) that are associated with sensory neurons (Vergnolle, N. *et al.*, 2003). PAR2 in particular has been highlighted as a regulator of sensory nerve excitability and plays an important role in inflammatory hyperalgesia. Thus PAR2 agonists contribute to neurogenic inflammation through the stimulation of peripheral substance P and calcitonin gene-related peptide (CGRP) release and to spinal hyperexcitability via release of these neuropeptides in the spinal cord. PAR2 receptor activation directly increases dorsal root ganglion (DRG) excitability and sensitizes TRPV1 receptors via a PKC mechanism (Amadesi, S. *et al.*, 2004); thus contributing to inflammation-induced hyperalgesia. In keeping with this, deletion of the *TRPVR1* gene or pretreatment with the TRPV1 antagonist capsazepine, abolished PAR2-induced thermal hyperalgesia, suggesting that TRPV1 is required for PAR2-induced hyperalgesia. PAR1 is also coexpressed on peptide-containing DRGs, and although PAR1 agonists induce neurogenic inflammation they do not sensitize TRPV1 receptors, nor do they induce hyperalgesia. Overall these data suggest that PAR2 antagonists would have antihyperalgesic activity (Mantyh, P. W. and Yaksh, T. L., 2001)

5.53.6 Cannabinoids and Their Receptors

Two major cannabinoid receptor subtypes, CB1 and CB2 are associated with pain modulation and have received much attention in recent years (reviewed by Fox, A. and Bevan, S., 2005). These receptors are

widely distributed in the nervous system but CB1 receptors are located in greatest abundance in the CNS and on peripheral sensory neurons. CB2 receptors have been found mainly in peripheral tissues including immune tissues and keratinocytes (Hohmann, A. G. and Herkenham, M., 1999; Rice, A. S. C. *et al.*, 2002) but more recently on some sensory and CNS cells. Several fatty acids, for example, anandamide, 2-arachidonylglycerol, and palmitoylethanolamide, have been identified as endogenous ligands for these receptors and are termed endocannabinoids. They are released from postsynaptic nerve terminals to modulate postsynaptic excitability and transmitter release at presynaptic elements via Gi/Go-coupled activity. Specific antagonists such as SR141716A and SR147778 for CB1 and SR144428 for CB2 have been used to characterize receptor functions.

For the most part CB1 receptors are located on neurons where activation causes attenuation of presynaptic N-calcium channel activity and inhibition of transmitter release (Kreitzer, A. C. and Regeher, W. G., 2002). In contrast, activation of neuroglia (astrocytes, microglia) is accompanied by *de novo* expression of both CB1 and CB2 and increased release of endocannabinoids (Stella, N. 2004). Specifically CB2 receptors are expressed in spinal microglia following peripheral nerve lesions but not by peripheral inflammation (Zhang, J. M. *et al.*, 2003). The significance of this is presently unclear although prolonged CB receptor activation has been associated with increased expression of neuroprotective modulators such as brain-derived neurotrophic factor (BDNF; Marsicano, G. *et al.*, 2003).

Both CB1 and CB2 receptor types have been shown to have a key role in the modulation of nociceptors. Although CB1 effects have been best characterized, the mechanism and sites of action are incompletely understood. It is likely that an interplay of several CB1-driven systems occurs during acute or chronic pain. Brainstem structures appear to be important. For example, CB1-induced local activation of the periaqueductal gray (PAG; by stress-induced release of endocannabinoids) has been suggested to be involved in aversive responses and acute stress-induced analgesia (Finn, D. P. *et al.*, 2004; Hohmann, A. G. *et al.*, 2005). This was blocked by SR141716A (rimonabant, the CB1 antagonist) but not by naltrexone (μ-opioid antagonist). Paradoxically, recent data suggest that deletion of the CB1 receptor in mice is associated with a greater vulnerability to stress (Fride, E. *et al.*, 2005). Finally CB1-induced analgesia has been proposed to be driven by activation of descending inhibitory mechanisms. In keeping with this, block of the descending noradrenergic systems (Gutierrez, T. *et al.*, 2003) has been proposed to account, in part, for CB1-induced antinociception.

Several studies have now shown that CB2 agonists modulation acute pain, for example, AM1241 and GW405833 (incision model) (LaBuda, C. J. *et al.*, 2005) while GW405833 has been reported to exhibit efficacy in neuropathic and inflammatory pain models (Valenzano, K. J. *et al.*, 2005). Interestingly another CB2 agonist, JWH-133 shows antihyperalgesia as well as anti-inflammatory activity (Elmes, S. J. R. *et al.*, 2005). The effects of CB2 agonists appear not to be due to the release of endogenous opioids as actions were unaffected by naltrexone (Whiteside, G. T. *et al.*, 2005b).

Several clinical studies have supported the use of cannabinoids, such as tetrahydrocannabinol (THC), to reduce pain. However this action is commonly accompanied by adverse effect such as euphoria, dizziness, and sedation (Campbell, F. A. *et al.*, 2001; Wade, D. T. *et al.*, 2003; Svenden, K. B. *et al.*, 2004). The reduction of CNS side effects has been approached through targeting peripheral CB receptors, since both CB1 and CB2 receptor activation produce antinociception. In support of this approach, the systemic administration of WIN55,212-2, a nonselective CB agonist, attenuated inflammatory hyperalgesia and this action was reversed by peripheral (intraplantar) but not spinal administration of a CB1 antagonist (Fox, A. and Bevan, S., 2005). Moreover a peripherally restricted CB1 agonist (e.g., NVP-001, personal communication) was shown to reduced inflammatory hyperalgesia by directly reducing nociceptor excitability (Richardson, J. D. *et al.*, 1998). Finally, CT-3 (ajulemic acid) a nonspecific CB1 and CB2 agonist, with limited CNS availability produced analgesia in a number of inflammatory and neuropathic pain models (Burstein, S. H. *et al.*, 2004; Dyson, A. *et al.*, 2005) as well as in human neuropathic pain, at doses which cause minimal CNS side effects (Karst, M. *et al.*, 2003). The mechanism of action of CT-3 appears to involve mainly CB1 receptors and a number of other indirect actions including activation of peroxisome proliferator-activated receptor (PPAR)-γ receptors and inhibition of inflammatory cell activity and mediator release (Liu, J. *et al.*, 2003).

Selective CB2 ligands (HU-308, AM-1241, and GW405833) as well as nonselective compounds (HU-210 and CP55940) have shown antinociceptive effects in a variety of inflammatory and neuropathic

pain models (Malan, T. P. *et al.*, 2003, Valenzano, K. J. *et al.*, 2005). These effects are still present in CB1-knockout (KO) mice, absent in CB2-KO animals, can be revered by CB2 antagonist such as SR144528, and occur without major CNS side effects (sedation, catalepsy, or motor impairments). It is unclear how these effects are produced since CB2 receptors have not been found on sensory neurons (Sokal, D. M. *et al.*, 2003). Rather an indirect effect via immune cell modulation and the naloxone-reversible release of β-endorphin from keratinocytes has been proposed (Ibrahim, M. M. *et al.*, 2005). In contrast, a number of reports have suggested that CB2 agonists, for example, JWH-133, may reduce C-fiber excitability directly (Ross, R. A. *et al.*, 2001; Sagar, D. R. *et al.*, 2005). There is also a possibility that CB2 agonists cause antinociception via the CNS as CB2 receptors are expressed in spinal microglia after nerve injury (Zhang, J. M. *et al.*, 2003), and CB2 activation may modulate microglial activity (Water, L. *et al.*, 2003). Indeed the direct spinal administration of JWH-133 attenuated mechanical allodynia (Sagar, D. R. *et al.*, 2005). Clearly greater understanding is still required with respect to the mechanisms of CB2-mediated analgesia.

Other approaches to address the role of endogenous cannabinoid systems in pain and analgesia have targeted fatty acid amide hydrolysis (FAAH), the major degradation pathway for endogenous cannabinoids (Cravatt, B. F. and Lichtman, A. H., 2004). Thus in mice lacking this enzyme (Cravatt, B. J. *et al.*, 2001), or treatment of naïve mice with a novel FAAH inhibitor such as OL135 (Lichtman, A. H. *et al.*, 2004), increases the analgesic efficacy of anandamide and significantly elevated brain anandamide levels were measured. In addition, OL135 increased pain threshold in acute pain models, decreased the mechanical allodynia of neuropathic pain, and decreased thermal hyperalgesia in models of persistent pain (Chang, L. *et al.*, 2006). Surprisingly a CB2 rather than CB1 antagonist attenuated the effect of OL135 in the persistent pain models and its effects appeared to be mediated by a naloxone-reversible mechanism. In this latter respect several reports have indicated analgesic synergy, between μ-opioid and CB receptors. Thus combinations of these agonist have been shown to provide pain reduction with minimal side effects in acute pain models (Cichewicz, D. L. and McCarthy, E. A., 2003). However, it is still unclear whether such synergy can be exploited in chronic pain treatment.

5.53.7 Mrg-Related GPCR and Their Ligands

The mas-related gene (Mrg) family is a large family of GPCRs which vary in numbers depending on species, are rather exclusively expressed in subsets of small sensory neurons (Dong, X. *et al.*, 2001), and may be co-localized with markers for nociceptive neurons such as TRPV1 (Lembo, P. M. C. *et al.*, 2002). Selective manipulations of individual Mrgs have provided exquisite markers for subsets of small sensory neurons showing selective epidermal and spinal innervation, suggesting a close anatomical and functional relationship (Zylka, M. J. *et al.*, 2005).

Focus on the human mrgX subfamily (six genes in humans), also called sensory neuron-specific receptors (SNSR), has revealed a complex pharmacology. The endogenous ligand for SNSR is unconfirmed, but several mammalian peptide ligands have been identified with high affinity for this receptor. These peptides include bovine adrenal medullary peptide 22 (BAM22), and its fragment BAM8-22 derived from the endogenous opioid precursor pro-enkephalin A, as well as two unrelated peptides γ2-melanocytostimulating hormone (MSH) and CT-γ2-MSH. Apart from BAM22, these substances do not activate opioid receptors, rather they increase peripheral and spinal excitability to potentiate thermal and mechanical nociception (Grazzini, E. *et al.*, 2004). This suggests that the same gene products can facilitate as well as inhibit sensory neurons and that an SNSR antagonist should be sought to inhibit hyperalgesia. Although these data strongly support a role for SNSRs in the modulation of pain, the endogenous ligand for this receptor has not been confirmed and there is little direct evidence linking SNSRs in the etiology of acute or chronic pain.

5.53.8 Prostanoids and Receptors

A variety of prostanoid cyclo-oxygenase (COX) enzyme products (PGE_2, PGD_2, $PGF_{2\alpha}$, thromboxane, PGI_2) occur during inflammation but PGE_2 is considered to be the major contributor to inflammatory pain. Thus blocking the major synthetic enzymes, COX-1 (constitutive) and COX-2 (inducible), or inhibition of prostanoid receptors continue to be important approaches for reducing inflammatory pain (Flower, R. J., 2003). Experience with selective inhibitors of COX-2 (celecoxib, rofecoxib) shows

improved gastrointestinal tract safety but little improvement in analgesic efficacy. A relatively infrequent though increased cardiovascular risk (coronary constriction) has been observed with some COX inhibitors. The mechanism is not understood but has led to Vioxx (rofecoxib) being withdrawn from therapy and considerable clinical debate about the safety of future approaches to COX inhibition.

An alternative approach for the clinical improvement of COX inhibitors has been to combine COX inhibition with NO donation (CINOD). Such molecules (NO-naproxene, NO-ibuprofen) have been claimed to show improved efficacy and safety over the parent nonsteroidal anti-inflammatory drugs (NSAIDs) due to actions (improved side effects and efficacy) of cleaved NO (Fiorucci, S. *et al.*, 2001).

Recently a splice variants of COX-1 has been identified, COX-3 (Chandrasekharan, N. V. *et al.*, 2002). However it has low enzymic capability and its distribution and low abundance in the CNS and in periphery does not make this a compelling target for analgesia. However several NSAIDs (acetaminophen, diclofenac, phenacetin) show low efficacy but some degree of selectivity for COX-3. Overall however the analgesic efficacy of acetaminophen is poorly correlated with COX inhibition. Interestingly endogenous acetaminophen metabolism produces a conjugated arachidonic acid derivative (AM404) that shows cannabinoidlike analgesia properties (Hogestatt, E. D. *et al.*, 2005; Ottani, A. *et al.*, 2006). Furthermore gene deletion studies suggested that COX-3 inhibition may be linked with the antipyretic and analgesia properties of NSAIDs. Clearly further studies are needed to link this enzyme to inflammatory pain pathophysiology.

Another route of inhibiting PGE_2 synthesis is via the blockade of PGE synthase (PGES), a major route of conversion of PGH_2 to PGE_2. Two isoforms of the enzyme have been identified, membrane or microsomal-associated PGES (mPGES-1) and a cytosolic enzyme (cPGES/p23) which are linked with COX-2- and COX-1-dependent PGE_2 production, respectively (Jakobsson, P. J. *et al.*, 1999; Claveau, D. *et al.*, 2003). Both isoforms are upregulated by inflammatory mediators and gene deletion studies in mice indicate an important role for mPGES in acute and chronic inflammation and inflammatory pain (Trebino, C. E. *et al.*, 2003).

Apart from prominent roles in regulating peripheral excitability during inflammatory pain, COX-1 (glia) and COX-2 (ventral horn cells) are constitutively present in spinal cord and are increased by inflammation, peripheral nerve injury, or by administration of cytokines, leading to increased production of spinal PGE_2. In keeping with this, several NSAIDs have been shown to reduce inflammatory hyperalgesia via inhibition of spinal COX activity (Yaksh, T. L. *et al.*, 2001). Several mechanisms have been proposed for the PGE_2-induced increase in spinal excitability. Prominent are the contribution of EP1 receptors and spinal release of glutamate. Recently however the spinal effects of PGE_2 have been linked with a glycine receptor. Thus deletion of the GlyR3α subunit gene, reduced pain sensitivity caused by PGE_2 administration or inflammation (Harvey, R. J. *et al.*, 2004).

Finally, PGE_2 exerts its effects via a variety of EP receptors (EP1, 2, 3 4) present both in peripheral sensory neurons and in the spinal cord. Activation of these receptors produces a complexity of effects, ranging from Ca^{2+} influx to cAMP activation or inhibition. In the periphery, sensitization by PGE_2 as been shown to be cAMP mediated causing the enhancement of tetrodotoxin-resistant (TTX-r) sodium currents in nociceptors via channel phosphorylation (England, S. *et al.*, 1996; Gold, M. S. *et al.*, 1998). However in the spinal cord, excitability was enhanced by EP1 receptors but reduced by an EP3α agonist (ONO-AE-248) suggesting further complexity in the prostanoid regulation of pain mechanisms (Bar, K. J. *et al.*, 2004).

5.53.9 Cytokines, Chemokines, and Their Receptors

Cytokines are produced by a variety of immune cells as well as brain neuroglial cells in response to injury and inflammation. They are powerful mediators of hyperalgesia (see Abbadie, C., 2005).

Probably the most characterized are IL-1β and tumor necrosis factor (TNF)-α that act via specific receptors on sensory neurons. Their effects can be attenuated by receptor antagonists (IL-1-r) that sequester the ligand as well as by neutralizing antibodies. Indeed the TNF antibody, etanercept, has been developed for the treatment of chronic inflammation and the presence of TNF-α has been correlated with a number of painful inflammatory clinical conditions (Lindenlaub, T. and Sommer, C., 2003). Cytokines induce hyperalgesia by a number of direct and indirect actions. Thus IL-1β activates nociceptors directly and produces heat sensitization via intracellular kinase activation, but it may also

cause indirect nociceptor sensitization via the production of kinins and prostanoids (Sommer, C. and Kress, M., 2004). TNF-α also activates sensory neurons directly via TNFR1 and TNFR2 receptors, (Pollock, J. *et al.*, 2002; Ohtori, S. *et al.*, 2004) and initiates a cascade of inflammatory reactions through the production of IL-1, IL-6, and IL-8. It is significant that direct TNF-α application in the periphery induces neuropathic pain behavior that is blocked by ibuprofen and celecoxib (Schafers, M. *et al.*, 2004), while nerve ligation causes increased TNF-α in damaged as well as adjacent undamaged axons (Schafers, M. *et al.*, 2003a). Interestingly anti-TNF-α treatment with TNF antibody, adalimumab, produced a prolonged reduction of pain symptoms in OA (Grunke, M. and Schulze-Koops, H., 2006).

There appears to be a complex interplay between cytokines, and it should be noted that like other mediators of pain not all should be considered as detrimental. Thus IL-6 has been associated with potential beneficial effects after nerve injury including protection against cell death and the promotion of growth. However there is also compelling evidence of a strong association with this cytokine in several human pain conditions including herniated lumbar disc pain and pain caused by failed back surgery (De Jongh, R. F. *et al.*, 2003).

A variety of studies have demonstrated an important role for spinal inflammatory and neuroimmune processes triggered by peripheral inflammation and nerve injuries. These processes involve the regulation of a variety of receptors, channels, and enzymes with patterns that are likely to differentiate one pain state from another (Honore, P. *et al.*, 2000). In addition, activation of spinal neuroglial cells (microglia, astrocytes, satellite cells) stimulates a cascade of secondary excitability changes (Watkins, L. R. and Maier, S., 2002). Neuroglia make close-junctional connections with other cells, providing a means of spreading excitability changes beyond the boundaries of spinal segmental input. Neuroglia also secrete a number of mediators such NO, neurotrophins, IL-1β, TNF-α, free radicals, and glutamate. In addition, neuroglial mediators may contribute to spinal excitability by causing dysfunction or degeneration of inhibitory spinal neurons (Moore, A. K. *et al.*, 2002). In keeping with an important role for neuroglial mediators, treatments with anti-inflammatory agents or modulators of neuroglial activity such as propentofylline and minocycline inhibit glial activation and the release of glial products with reduced behavioral signs of hyperexcitability (Watkins, L. R. and Maier, S., 2002; Raghavendra, V. *et al.*, 2003).

Chemokines are important peripheral and central mediators of inflammation. The major chemokines and their respective receptors are macrophage-derived chemokine (MDC)/CCR4, regulated upon activation, normal T-cell expressed, and secreted (RANTES)/CCR5, fractalkine/CX3CR1, and SDF-1α/CXCR4. Receptors are located on leukocytes, on central neurons, sensory neurons, and neuroglial cells (Watkins, L. R. and Maier, S., 2002). Apart from their major chemoattractant effects, chemokines contribute directly to inflammatory hyperalgesia through G-protein-coupled activation and sensitization of sensory neurons (Oh, S. B. *et al.*, 2001). Block of CX3CR1 by a fractalkine receptor-neutralizing antibody induces antiallodynic effects in models of peripheral nerve inflammation (Milligan, E. D. *et al.*, 2005b). However some chemokines appear beneficial. Thus gene therapy (AV-333) has been used to increase IL-10 production through the delivery of viral and nonviral vectors by acute spinal intrathecal delivery. This experimental treatment has been shown to reverse mechanical allodynia in the chronic constriction injury (CCI) model of neuropathic pain (Milligan, E. D. *et al.*, 2005a).

5.53.10 Adrenoceptors

A number of chronic pain disorders termed sympathetically maintained pain have highlighted the importance of the release of sympathetic transmitters (epinephrine or norepinephrine) from sympathetic varicosities and the involvement of adrenergic receptors in pain etiology. For example following peripheral nerve injury sprouting of sympathetic nerve endings occurs at several sites. Thus sympathetic/sensory coupling at the level of the DRG (Zhang, J. M. *et al.*, 2004), at the site of injury (neuroma), and in the periphery (Shinder, V. *et al.*, 1999) have been demonstrated. In keeping with this some neuropathic pain symptoms have been attenuated by sympathetic blocks or surgical sympathectomy.

Other studies have shown the expression of α1- and α2-adrenoceptors on sensory neurons or postganglionic sympathetic terminals (Sato, J. and Perl, E. R., 1991; Tracey, D. J. *et al.*, 1995; Lee, D. H. *et al.*, 1999) after nerve injuries. Under these conditions sensory neurons can be directly activated by the endogenous release of sympathetic transmitters (via

α1 receptors) or in the clinic by intradermal injection of norepinephrine (Ali, Z. *et al*., 2000).

On the other hand, transdermal applications of the α2-agonist, clonidine via transdermal patches or creams, has proven efficacious in a variety of neuropathic pain conditions (Byas-Smith, M. G. *et al*.,1995). Since clonidine has been shown to decrease the excitability of small sensory neurons from nerve injured animals (Ma, W. *et al*., 2005) the antinociceptive efficacy of clonidine is considered to be due to α2 receptor-coupled inhibition. Clonidine and other α2-agonists such as dexmedetomidine have also been used systemically to inhibit of sensory transmission in the spinal cord by block of pre- and postsynaptic membrane excitability. Unfortunately sedation and hypotension are major target-related side effects of these compounds. Great efforts have been made to identify ligands with improved α2-receptor subtype selectivity, to avoid side effects, but thus far this has not been particularly successful.

5.53.11 Glutamate Regulation and Glutamate Receptors

Glutamate is the major excitatory neurotransmitter in the CNS with important regulatory roles for pain transmission. However there is also considerable evidence that it plays a role in pain processing in the periphery (Carlton, S. M. *et al*., 1995; Bahave, G., *et al*., 2001). Glutamate acts through receptor-coupled ligand-gated ion channels (α-amino-3-hydroxy-5-methyl-4-isoxazolepropionic acid (AMPA)/kinate receptors: iGluRs) and GPCR-coupled receptors (metabotropic glutamate receptors (mGluRs)). Injections of glutamate or metabolically stable receptor-selective agonists such as *N*-methyl-D-aspartic acid (NMDA), AMPA, and kainate, cause a reduction in thermal and mechanical thresholds for pain, while application of iGluR and mGluR antagonists attenuate pain in acute models (Zhou *et al*.,1996; Bhave, G., *et al*., 2001).

Building upon this has been significant progress in development of a glutamate antagonist optimized for clinic testing. For example, the AMPA-kinate receptor antagonist, LY293558 has been shown to have efficacy in models of neuropathic pain (Blackburn-Munro, G. *et al*., 2004) and to reduce capsaicin-induced pain in human volunteers as well as clinical dental pain with minimal side effects (Sang, C. N. *et al*., 1998).

There has been a great deal of information linking NMDA receptors in central sensitization and CNS excitability during chronic pain and repetitive stimulation of pain pathways. Indeed NMDA antagonists show robust attenuation of pain behaviors but provoke a number of side effects (sedation, confusion, and motor incoordination) and thus have an insufficient therapeutic window. There has been a refocus on more specific NMDA-receptor subtype blockers (NR1 and NR2) directed toward the glycine modulatory site to avoid side effects. This site actively modulates the NMDA channel only during the sustained stimulation of the receptor, which is considered to occur during chronic pain. Selective NR1-Gly antagonists have been claimed to reduce pain with reduced side effects (Danysz, W. and Parsons, C. G., 1998; Quartaroli, M. *et al*., 2001). However clinical experience has not yet confirmed this. GV196771 did not show efficacy against clinical pain, possible due to inadequate penetration into the CNS (Wallace, M. S. *et al*., 2002).

Alternative initiatives have targeted other NMDA receptor subtypes such as the NR2B receptor, which has a specific distribution in sensory pathways. Blockade of this receptor has also been claimed to produce antinociception (ifenprodil, CP-101,606) with reduced side effects (Taniguchi, K. *et al*., 1997). This concept has yet to be evaluated in the clinic.

Metabotropic glutamate receptors, particularly mGluR1 and mGluR5, have been reported to play a key role in sustaining heightened central excitability in chronic pain with minimal involvement in acute nociception. Thus spinal administration of selective agonists such as dihydroxy phenyl glycine produced allodynia, while mGluR5 was shown to be significantly overexpressed in some, but not all, chronic pain models (Hudson, L. J. *et al*., 2002). Furthermore antisense-oligonucleotide and antibody treatments, directed at these receptors, reduce chronic inflammatory and neuropathic pain behaviors (Fundytus, M. E. *et al*., 2002). In keeping with these observations, the mGluR5-selective antagonists 2-methyl-6-(phenylethynyl)-pyridine (MPEP) did not reduce acute physiological pain responses but reduced heat hyperalgesia and allodynia in models of inflammatory and neuropathic pain (Walker, K. *et al*., 2001; Hudson, L. J. *et al*., 2002; Urban, M. O. *et al*., 2003).

Peripheral mGluR5 receptors have also been claimed to modulate pain (Jang, J. H. *et al*., 2004). Thus local administration of mGluR5 (MPEP, SIB1757) have been effective in reducing pain behavior (Dogrul, A. *et al*., 2000; Zhu, C. Z. *et al*., 2004) suggesting a potential for using peripheral mGlu5 antagonists in pain therapy.

Metabotropic group II receptors (mGluR2 and mGluR3) also modulate pain transmission. The mGluR2 is located in sensory neurons and presynaptic nerve terminals whereas mGluR3 is found all over the brain. MGluR3 can be selectively increased in the spinal dorsal horn neurons after peripheral ultraviolet injury (Boxall, S. J. *et al.*, 1998). mGluR2/3 receptor activation appears necessary to reduce nerve terminal excitability and modulate pain transmission since treatment with L-acetyl-carnitine reduced inflammatory hyperalgesia and mechanical allodynia and increased the expression of mGlur2/3. The effect of L-acetyl-carnitine were attenuated by LY379268, a mGlu2/3 antagonist (Chiechio, S. *et al.*, 2002).

5.53.12 Gamma-Aminobutyric Acid Receptors

Gamma-aminobutyric acid (GABA) receptors are emerging as important regulators of pain, particularly in the spinal cord as they are abundantly expressed both on spinal afferent nerve terminals and spinal neurons. Activation of both subtypes of GABA receptor by muscimol ($GABA_A$ agonist) or baclofen ($GABA_B$ agonist) reduced pain behavior. In contrast, $GABA_A$ (bicuculline) and $GABA_B$ (CGP35348) antagonists cause pain when injected into the spinal intrathecal space (Malan, T. P. *et al.*, 2002). Loss of GABA (Ibuki, T. *et al.*, 1997) and impaired GABA-mediated inhibition through loss of spinal interneurons has been demonstrated in models of neuropathic pain (Moor, A. K., *et al.*, 2002).

Improvement of GABA synthesis through promotion of its synthetic enzyme, glutamic acid decarboxylase (GAD), has been achieved by gene transfer of a GAD promoter (in herpes simplex virus vector) via peripheral injection. This was taken up into sensory neurons and transported to DRGs to reduce spinal excitability, as well as mechanical and thermal allodynia caused by nerve injury (Hao, S. *et al.*, 2005).

Other important changes in ionic regulation have been highlighted to occur in chronic pain which indirectly affects GABA- and glycine-mediated inhibition and excitability in the spinal cord. In particular changes in transmembrane ion transporters have been associated with modulation of primary afferent excitability and related to neuropathic pain disorders. Thus the chloride transporter NKCC1, localized in primary sensory neurons, is responsible for maintaining the high chloride ion gradient in afferent terminals. This allows the outflow of chloride ions associated with the primary afferent depolarization (PAD) and presynaptic inhibition, following $GABA_A$ receptor activation of afferent terminals. Deletion of the NKCC1 gene induced touch-evoked pain caused by light stroking. This was shown to be due to increased nerve terminal excitability caused by a reduced capability to generate presynaptic inhibition (Laird, J. M. A. *et al.*, 2004).

On the other hand increasing the expression of this cotransporter or increasing its efficacy through AMPA mediated Ca/CaM-kinase II phosphorylation has been postulated (Cervero, F. *et al.*, 2003) to increase PAD sufficient to reach the firing threshold of the nerve terminal. This mechanism may also contribute to spinal sensitization following nerve injury and may indeed generate antidromic action potentials triggering a dorsal root reflex or the ectopic discharges in sensory nerves which cause, or contribute to spontaneous pain.

Spinal sensitization that occurs following peripheral nerve injury may also arise by other mechanisms of spinal disinhibition. This has been hypothesized to involve the reduced expression of the potassium-chloride exporter KCC2, seen only in superficial spinal lamina 1 neurons after injury. In addition, knockdown of KCC2 with antisense or block of this transporter with ((dihydronindenyl)oxy) alkanoic acid (DIOA) causes a similar shift in the transmembrane ionic gradient in spinal lamina 1 neurons and a consequent behavioral hyperalgesia resembling that seen after nerve injury (Coull, J. A. M. *et al.*, 2003). In addition, normal spinal inhibitory currents, mediated by GABA and glycine interneurons, are reversed in the absence of KCC2, so that the effects of GABA become predominant excitatory, due to the outward, rather than inward, flow of chloride ions. The emerging view suggests that a variety of changes in ionic regulation occur during chronic pain. This adds complexity to the puzzle of pain but opportunity for intervention. It will be important to learn how these disinhibitory mechanisms contribute in different chronic pain conditions and whether they are critical for pain initiation as well as its maintenance.

5.53.13 Ion Channels

5.53.13.1 Ligand-Gated Channels

Transient receptor potential (TRP) channels form a large family of sensory transducers involved in cellular calcium regulation. Many are localized to

mammalian sensory nerves and are involved in the transduction of temperature and chemical signals that result in pain. The TRPV family has received considerable attention and is considered a good targeted for developing analgesics (Krause, J. E. *et al.*, 2005). TRPV1, originally called the vanilloid receptor because of its selective activation by capsaicin and pungent vanilloids, has the properties of a noxious heat transducer. The effects of capsaicin on sensory neurons are complex, involving activation through ligand-operated cation channels, and the extracellular influx as well as the intracellular increase in calcium ions. Calcium-induced stimulation of phosphatase such as cacineurin then reduces excitability via inactivation voltage-gated calcium (CaV) channels as well as rapid CaV2.2 internalization (Wu, Z. Z. *et al.*, 2005). This mechanism explains the transient and reversible analgesia effects of capsaicin either on peripheral or spinal afferent nerve terminals. TRP channel regulation of heat transduction is complex as animals with deleted *TRPV1* and *TRPV2* genes appear to have normal heat sensitivity (Woodbury, J. *et al.*, 2004) whereas gene deletion of *TRPV1* prevented inflammatory heat hyperalgesia (Caterina, M. J. *et al.*, 2000).

The TRPV1 receptor has assumed an increasingly prominent role in regulating sensory neuronal excitability in inflammatory pain. A variety of inflammatory agents including protons, bradykinin, adenosine triphosphate (ATP), PGE2, 12-lipoxygenase products, PAR2, anandamide, and nerve growth factor (NGF) indirectly sensitize TRPV1, or regulate its expression, to cause thermal hyperalgesia. A common mechanism appears to be GPCR-coupled stimulation of PLC, the formation of intermediates inositol triphosphate (IP3) and DAG and the activation and mobilization of PKC (Vellani, V. *et al.*, 2001) which can phosphorylate the TRPV1 receptor.

Earlier analgesia strategies, targeting TRPV1, were focused on capsaicin-like agonists that induced functional inactivation of sensory fibers by causing reversible subepidermal degeneration. This has been successfully translated into the clinic with the introduction of a number of topical capsaicin therapies for inflammatory pain. Currently there is a focus on TRPV1 channel blockers or selective antagonists against the TRPV1 receptor (Garcia-Martiez, C. *et al.*, 2002). Supporting these approaches, competitive (AMG-9810, personal communication) and noncompetitive vanilloid receptor-1 (VR1) antagonists (DD161515; Sachez-Baez, F. *et al.*, 2002) block chemical and thermal pain sensitivity, heralding the emergence of a novel therapy. Indeed recent clinical studies in human volunteers have shown that oral SB705498 attenuated capsaicin and ultraviolet C (UVC)-induced pain and hyperalgesia (Chizh, B. *et al.*, 2006).

Other TRP channels (TRPV3, TRPV4, TRPA1) have been suggested to be involved in transduction. Thus TRPA1 (ANKTM1) is colocalized with TRPV1, is activated by capsaicin and mustard oil but can also be sensitized by inflammatory mediators including bradykinin to produce cold-induced burning pain (Bandell, M. *et al.*, 2004). In addition TRPV1 can oligomerize with other TRP family members including TRPV3. TRPV3 is also a heat transducer that it sensitive in the physiological temperature range and responds to noxious heat, but is insensitive to capsaicin. This is found in keratinocytes and appears to be upregulated in inflammatory pain conditions. It is unclear how activity of TRPV3 leads to nociceptor activation. So far there are few chemical tools to help characterize the functions of these TRP receptors and support their value as analgesia targets.

5.53.14 Purinergic Receptors

5.53.14.1 P2X Receptors

The unique localization of the P2X3 receptor to small sensory fibers has highlighted its importance in pain. Large amounts of the endogenous ligand, ATP are released after tissue injury and during inflammatory injuries while both ATP and a stable analogue α,β-Me ATP, induce pain and are pronociceptive when administered intradermally in human volunteers.

In chronic inflammatory pain, P2X3-mediated excitability is enhanced while reduction of P2X3 receptors, by antisense oligonucleotide administrations, reduced inflammatory hyperalgesia as well as that evoked by α,β-Me ATP (Honore, P. *et al.*, 2002). In keeping with this a number of antagonists including 2′,3′-*O*-(2,4,6-trinitrophenyl) adenosine 5′-triphosphate (TNP-ATP), pyridoxal-phosphate-6-azophenyl-2′,4′-disulfonate (PPADS), and suramin, reduce pain behavior. More selective, and druglike, antagonists such as A-3174919 reduced pain in a number of acute and chronic pain models supporting the possibility for future analgesia therapy (Jarvis, M. F. *et al.*, 2002).

It should be noted that a number of other purinergic receptor subtypes, for example, P2X4 and P2X7, have also been suggested to modulate pain

through altered central excitability and the release of neuroglial-cell products. Thus activated microglial, astrocytes, and satellite cells release a variety of inflammatory mediators including IL-1β, TNF-α, prostanoids, and NO upon ATP stimulation. Indeed increased expression of P2X4 has been shown to occur in spinal microglial after peripheral nerve lesions and this was related to painful mechanical allodynia. This behavior was blocked by spinal administrations of the selective P2X4 antagonist TNP-ATP (Tsuda, M. *et al.*, 2003). Remarkably spinal administration of activated microglia reproduced TNP-ATP sensitive mechanical allodynia in naïve animals.

Increased P2X7 expression has been found in peripheral macrophages following inflammation but this receptor is also expression in spinal neurons and microglia following peripheral nerve injury (Deuchars, S. A. *et al.*, 2001). In keeping with an important role in chronic pain both microglia and P2X7 receptors are upregulated in human chronic pain patients while deletion of the P2X7 receptor gene produced a complete absence of mechanical and thermal pain in mice (Chessell, I. P. *et al.*, 2005).

It is worth noting that other nucleotide-gated ion channels have also been shown to be important for regulating peripheral excitability. Thus the sodium/potassium repolarizing pacemaker current, Ih, which is activated during membrane hyperpolarization is important for generation of rhythmic and spontaneous action potentials in sensory neurons following nerve injury. Ih currents are controlled by cyclic nucleotides (cAMP and cGMP) via a family (HCN1–4 channels) of ligand-gated ion channels that are constitutively expressed in sensory nerves and differentially distributed after crush or inflammatory nerve injuries (Chaplan, S. R. *et al.*, 2003; Yao, H. *et al.*, 2003). Nerve injury has been shown to enhance the Ih and this can be blocked with ZD7288 which also prevents repetitive firing in damaged sensory neurons and reverses touch hypersensitivity in neuropathic pain models (Chaplan, S. R. *et al.*, 2003). This approach clearly has great potential for addressing peripheral excitability in neuropathic pain disorders.

5.53.14.2 Acid-Sensing Channels

Proton production is increased in inflammation and is likely to be involved in inflammatory hyperalgesia and in the sensation of muscle aching and discomfort due to the hypoxia/anoxia of muscle exercise. Indeed direct activation of nociceptors accounts for the sharp stinging pain produced by intradermal injections of acidic solutions and low extracellular pH enhancing the effects of other inflammatory mediators (Krishtal, O., 2003; Mamet, J. *et al.*, 2003).

Exogenously administered acidic solutions produce a rapid but transient increase in membrane cation permeability as well as a more prolonged permeability increase in sensory neurons. This can give rise to sustained nerve activation as well as an enhanced mechanosensitivity. The mechanism of proton-induced activation of sensory neurons underlying pain has not been fully elucidated, but appears to be driven by a number of acid-sensing ion channel (ASICs) particularly ASIC1 and ASIC3 (also called DRASIC). ASIC3 has been shown to have a strong antinociceptive phenotype following deletion of this gene in KO mice (Sluka, K. A. *et al.*, 2003).

A novel blocker (A-317567) of peripheral ASIC1, ASIC2, and ASIC3 channels has been described (Dube, G. R. *et al.*, 2005). This produces antihyperalgesia in models of inflammatory and postoperative pain but there have been no reports of therapeutic advances with more selective inhibitors.

5.53.15 Sodium Channels

Voltage-gated sodium channels are characterized by their primary structure and sensitivity to tetrodotoxin (TTX). A variety of TTX sensitive (NaV1.1, Nav1.2, NaV1.6, and Nav1.7) and TTX insensitive (Nav1.8, NaV1.9) channels are involved in regulating sensory neural excitability (Matzner, O. and Devor, M., 1994; Eglen, R. M. *et al.*, 1999). Changes in the expression, trafficking, and redistribution of NaVs, following inflammation or nerve injury is considered to account for the abnormal firing (ectopic generators) of afferent nerves (Devor, M., 2005). However channel redistribution appears complex as most channels appear to be downregulated in DRGs after nerve injury whereas, for example, NaV1.8 is redistributed along small axons. It has also been important to recognize that channel expression and nerve excitability are changed dramatically in uninjured axons that are closely apposed to injury (Gold, M. S. *et al.*, 2003).

The TTX-R sodium channel, NaV1.8, is uniquely expressed in all sensory neurons (IB4 positive and NGF sensitive) and appears to be an important contributor in the generation of abnormal excitability in sensory axons. Thus knockdown of NaV1.8 produces a marked reduction in abnormal pain responsiveness in pain models (Lai, J. *et al.*, 2003).

Inflammation also causes the overexpression of NaV1.7 in several types of sensory neurons in models of inflammatory pain (Gould, H. J. *et al.*, 2004) and in inflamed human tooth pulp. Interestingly NaV1.7 overexpression can be prevented by pretreatment with COX-1 and COX-2 inhibitors (ibuprofen, NS-398).

The clinical utility of nonselective sodium channel blockade in pain treatment has been well established with the use of local anesthetics such as lidocaine. Clinical experience has confirmed that local block of abnormally active afferents reduces secondary pain in established neuropathic pain conditions (Gracely, R. *et al.*, 1992). Interestingly this can be achieved at lower concentrations than are required for block of conduction in quiescent fibers highlighting a potential therapeutic advantage for selective fiber block (Devor, M. *et al.*, 1992). The basis of this is due to the state-dependent increase in the affinity of channel blockers for ion channel proteins (Devor, M., 2005). An additional utility of lidocaine is that intravenous administration has been reported to produce long-lasting pain relief both in animal models (Araujo, M. C. *et al.*, 2003) and in intractable neuropathic pain (Kastrup, J. *et al.*, 1987). The major disadvantages of nonselective sodium channel blockers are cardiotoxicity and CNS sedation and confusion produced by NaV1.5 and NaV1.2 channel block, respectively. Thus great activity is currently focused on discovering novel but selective sodium channel blockers.

In this regard novel activity-dependent sodium channel blockers (e.g., NW-1029) have been shown to reduce excitability of peripheral nerves and cause antihyperalgesia in models of inflammatory and neuropathic pain (Veneroni, O. *et al.*, 2003). Overall however, channel blockers still appear insufficiently selective to avoid cardiac and CNS side effects.

An alternative approach to selectively regulate ion channels is to block the trafficking of channels to the nerve membrane. For example the functioning of NaV1.8 may be reduced by preventing its interaction with p-11, an annexin II-related protein that tethers the channel to the nerve membrane (Okuse, K. *et al.*, 2002). In addition, channel-associated cell surface glycoproteins such as contactin may be involved in concentrating specific channel subtypes, e.g., NaV1.8 and NaV1.9 (IB4 positive) but not NaV1.6 and NaV1.7 (IB4 negative) in DRG nerve membranes, with an associated increased in current density (Rush, A. M. *et al.*, 2005). Although these approaches are attractive it is unclear whether they will impact on nerve excitability associated with specific pain etiology.

NaV1.3 is another ion channel that is dramatically regulated after injury. This channel has been found abundantly in fetal but not in adult tissue. However NaV1.3 is dramatically upregulated in adult sensory neurons and spinal cord following peripheral and CNS injury (Hains, B. C. *et al.*, 2004). The expression of NaV1.3 has been suggested to make an important contribution to the sustained and high-frequency firing found in injured afferents related to neuropathic pain (Cummins, T. R. and Waxman, S. G., 1997; Kim, C. H. *et al.*, 2002). Further it has been proposed that NaV1.3 expression may not be directly related to neural injury as it was not correlated with activating transcription factor (ATF)-3 expression, a neuronal cell death marker (Lindia, J. A. *et al.*, 2005), but caused by a deficiency of growth factor. In this respect, GDNF administration reduced NaV1.3 expression and attenuated neuropathic pain behavior (Boucher, T. J. *et al.*, 2000). In contrast, antisense treatments that significantly reduced sensory neuronal NaV1.3 expression in the spared nerve injury (SNI) model of neuropathic pain did not attenuate nerve injury-induced allodynia (mechanical or cold; Lindia, J. A. *et al.*, 2005) whereas this was reduced by the nonselective channel blockers mexiletine and lamotrigine.

5.53.16 Calcium Channels

A variety of calcium channels (CaV) have been identified and characterized. Several have been shown to be prominently involved in pain regulation (Yaksh, T. L., 2006). The N-type calcium channel CaV2.2 is an important regulator of nerve terminal excitability and neurotransmitter release. It has been well established that there is complex chemical regulation of N-channels, particularly through GPCR signaling. For example, N-channel activity is attenuated by analgesic drugs such as opioids, with a resultant modulation of sensory transmitter release, e.g., substance P, CGRP, and glutamate, at both spinal and at peripheral sensory nerve terminals. N-channel trafficking may also be affected by GPCRs. For example, activation of the orphanin FQ receptor (ORL) by nociceptin causes channel internalization and downregulation of calcium entry (Altier, C. *et al.*, 2005).

Of additional importance is the fact that deletion of the N-channel gene reduces inflammatory and neuropathic pain (Kim, C. *et al.*, 2001; Saegusa, H. *et al.*, 2001). Moreover selective blockers such as ziconotide,

(a naturally occurring conopeptide) and verapamil have been used to characterize channel activity while ziconitide (SNX-111, Prialt) has been used experimentally and clinically by intrathecal administration, to show utility for pain relief (Xiao, W. H. and Bennett, G. J., 1995; Snutch, T. P., 2005). Building on this concept, small molecule CaV2.2 channel blockers with oral availability are now reported to have been developed, e.g., NMED-160, showing efficacy in chronic pain models (Snutch, T. P., 2005).

While it is believed that blockers of CaV2.2 exert their major analgesic effects via the spinal cord, peripheral actions are also possible. Thus N-channels expression also occurs in peripheral terminals and has been shown to increase following axotomy (Baccei, M. L. and Kocsis, J. D., 2000). This suggests that peripheral N-channels can be targeted for neuropathic pain treatments; thus avoiding potential CNS side effects such as sedation.

Low-voltage-activated T channels (CaV3.1, CaV3.2, and CaV3.3) also appear important for pain transmission and as targets for pain therapy. Thus they are expressed in superficial laminas of the spinal cord and in DRG neurons (for references see Altier, C. and Zamponi, G. W., 2004; Yaksh, T. L., 2006). T-channels appear unaffected in DRGs after axotomy (Baccei, M. L. and Kocsis, J. D., 2000) but may play a more prominent role in regulating spinal excitability and spinal sensitization following repetitive C-fiber stimulation (Ikeda, H. *et al.*, 2003). Moreover nerve injury-induced hyper-responsiveness was blocked by the T-channel blocker ethosuximide (Matthews, E. A. and Dickenson, A. H., 2001) which also attenuated mechanical allodynia in animal models of vincristine- and paclitaxel-induced neuropathic pain (Flatters, S. J. and Bennett, G. J., 2004).

Finally a strongly validated approach for neuropathic pain has targeted the $\alpha 2,\delta 1$ calcium channel subunit, the substrate for the antiallodynic drugs, gabapentin and pregabalin. This subunit is important for channel assembly, is expressed in small DRGs and in spinal neurons, and its overexpression has been associated with allodynia in a number of specific pain models (Luo, Z. D. *et al.*, 2002).

5.53.17 Neurotrophins and Their Receptors

The neurotrophins represent an important family of regulatory proteins essential for sensory nerve development, survival, and determination of chemical phenotype including excitability (Sah, D. W. H. *et al.*, 2003; Zweifel, L. S. *et al.*, 2005). Several neurotrophins have been identified including NGF, brain-derived growth factor (BDNF) and neurotrophins (NT) 3, neurotrophin 4/5. Each neurotrophin binds with high affinity to receptor tyrosine kinases (Trk): NGF to TrkA, BDNF and NT4/5 to TrkB, and NT3 to TrkC. NT3 also binds with TrkA and TrkB. Mature neurotrophins also bind to a structurally distinct receptor p75 which affects neuronal development through downstream signaling. Neurotrophins arise from proneurotrophin precursors following extracellular cleavage by metalloproteinases and plasmin. It should be observed that proneurotrophins also signal through the p75 receptor and may produce opposite effects from neurotrophins, e.g., apoptosis rather than cell survival (Lu, B. *et al.*, 2005).

NGF has been most studies with respect to inflammatory hyperalgesia as its production is unregulated by inflammation in macrophages, fibroblasts, and Schwann cells. NGF has emerged as a key regulator of sensory neuron excitability and as an important mediator of injury-induced nociceptive and neuropathic pain (Ro, L. S. *et al.*, 1999; Theodosiou, M. *et al.*, 1999; Hefti, F. F. *et al.*, 2005). NGF acts via TrkA and p75 to activate a number of kinase pathways (e.g., p38 kinase; Ji, R. R. *et al.*, 2002) leading to altered gene transcription and the increased synthesis of sensory neuropeptides (substance P, CGRP), ion channels (TRPV1, NaV1.8, ASIC3; Fjell, J. *et al.*, 1999; Ji, R. R. *et al.*, 2002; Mamet, J. *et al.*, 2003), membrane receptors such as bradykinin and P2X3 (Petersen, M. *et al.*, 1998; Ramer, M. S. *et al.*, 2001), and structural molecules including neurofilament and channel anchoring proteins such as the annexin light chain p11 (Okuse, K. *et al.*, 2002).

Increased expression and release of NGF have been demonstration in several painful conditions in animal models (e.g., ultraviolet injury, surgical injury; Oddiah, D. *et al.*, 1998; Miller, L. J. *et al.*, 2002) and in human conditions including arthritis, cystitis, prostitis, and headache (Aloe, L. *et al.*, 1992; Halliday, D. A. *et al.*, 1998; Sarchielli, P. *et al.*, 2001). Administration of exogenous NGF induces thermal and mechanical hyperalgesia in animals and humans (Andreev, N. *et al.*, 1995; Apfel, S. C., 2002), which is considered to be due in part to mast cell degranulation and by directly increasing sensory neuronal excitability (Sah, D. W. H. *et al.*, 2003).

Few small molecule NGF antagonists are available but ALE0540, which inhibits the binding of

NGF to TrkA and p75, and PD90780 which inhibits NGF binding to p75, have been proposed to have efficacy in chronic pain models (Owolabi, J. B. *et al.*, 1999; Colquhoun, A. *et al.*, 2004). In contrast, the use of TrkA-immunoglobulin G (IgG) and NGF monoclonal antisera have confirmed the importance of NGF in pain. Thus anti-NGF treatment have provided positive behavioral and biochemical readouts in several models of chronic nociceptive (including visceral) and neuropathic pain (Obata, K. *et al.*, 2004; Hefti, F. F. *et al.*, 2005; Sevcik, M. A. *et al.*, 2005; Shelton, D. L. *et al.*, 2005). These studies have also indicted a lack of effect on acute nociceptive processing or on sympathetic nerves whose phenotype is also regulated by NGF.

The importance of NGF has also received clinical confirmations since RN624, a humanized anti-NGF monoclonal antibody (mAb), has been reported to be efficacious in reducing pain and improved mobility in OA (Lane, N. *et al.*, 2005). Anti-NGF mAb therapy appears as an attractive therapeutic approach with the potential for long-lasting pain treatment, similar in efficacy to morphine, without necessarily compromising physiological nociception.

NGF also induces the synthesis of another neurotrophin, BDNF, from peptide-containing sensory neurons. BDNF also accumulates in sensory neurons following painful nerve injury (see Sah, D. W. H. *et al.*, 2003). Release of BDNF in the spinal dorsal horn increasing spinal excitability and pain sensitization via TrkB receptors. This initiates a variety of effects, including direct neural excitation, activation of a signaling cascade via the phosphorylation of NMDA receptors, and an altered regulation of the neural chloride transporter that contributes to pain hypersensitivity (Coull, J. A. M. *et al.*, 2005).

In keeping with these observations, spinal BDNF administration induces thermal and mechanical allodynia whereas anti-BNDF neutralization or TrkB IgG administration reduces inflammation or nerve injury-mediated hypersensitivity pain in a number of animal models (Kerr, B. J. *et al.*, 1999; Theodosiou, M. *et al.*, 1999; Deng, Y. S. *et al.*, 2000).

Finally glial cell-line-derived neurotrophic factor, GDNF represents an extensive family of ligands and membrane receptor complexes which have an important role in regulating peripheral and central neural phenotypes. GDNF-related ligands include neurturin and artemin, which act via the complex RET Trk receptor and co-receptors GFRα1, GFRα2, GFRα3, and GFRα4.

Although there appears not to be a specific role in inflammation, GDNF has been shown to have neuroprotective and restorative properties in a number of neurodegenerative and neuropathic pain states (Sah, D. W. H. *et al.*, 2003). Specifically GDNF treatment has been shown to restore peripheral sensory neuron function, including peptide and ion channel expression patterns, following painful peripheral nerve injury accompanied by an attenuation of pain behaviors. Unfortunately clinical observations using GDNF have shown unacceptable side effects such as weight loss and allodynia, which has discouraged therapeutic developments (Nutt, J. G. *et al.*, 2003).

5.53.18 Kinases

As mentioned earlier inflammatory mediators also activate a number of protein kinases in sensory neurons and in the spinal cord. These include PKA, PKC, and mitogen-activated protein kinases (MAPK) considered to be important downstream regulators of excitability through altering gene transcription and posttranslational modification of target proteins (Woolf, C. J. and Salter, M. W., 2000). There are several types of MAPKs including extracellular signal-regulated kinases (ERK), cJUN, N-terminal kinase (JNK), and p38 kinase that are considered as targets for inflammatory pain. For example, several inhibitors of p38 kinase (e.g., SB203580, CNI-14930) posses anti-inflammatory as well as antihyperalgesic properties in a variety of animal models (Schafers *et al.*, 2003b).

5.53.19 Botulinum Toxin

Another approach to pain modulation has been the use of botulinum toxins (BoTNs). This family of neurotoxins has been traditionally used as an experimental tool to study muscle nerve interactions. Recently BoTN-A has been approved for clinical use to induce muscle relaxation. The mechanism of action of BoTN is related to inhibition of transmitter release from motor fibers through proteolytic cleavage of a number of synaptosomal regulatory proteins (SNARE, syntaxin, SNAP-25, synaptobrevin). More recent studies also indicated potential for inhibition of neuropeptide transmitter release from small afferent neurons (Welch, M. J. *et al.*, 2000; Mense, S., 2004). In keeping with this BoTN has been shown to provide long-lasting pain relief following administration into human osteoarthritic

joints and improve bladder dysfunction in overactive bladder patients. This was correlated with loss of both P2X3 and VR1 receptors in the bladder (Apostolidis, A. *et al.*, 2005).

5.53.20 Nitric Oxide

NO induces a delayed burning pain upon intradermal injection (Holthusen, H. and Arndt, J. O., 1994) and NO donors have been postulated to activate cerebral sensory fibers directly, causing release of the sensory vasodilator CGRP (Wei, P. *et al.*, 1992). Indeed NO has been suggested to contribute to migraine and other types of head pain (Olesen, J. *et al.*, 1994) and there is an abundance of evidence linking NO in the etiology of a number of chronic pain conditions (Millan, M. J., 1999).

Peripheral nerve injury and inflammation increases the expression of NO in sensory neurons and causes the upregulation of the nitric oxide synthase (NOS) isozymes neuronal NOS (nNOS) and inducible NOS (iNOS) in the spinal cord (Gordh, T. *et al.*, 1998) as a result of axonal neurodegeneration, neuroglial cell activation and inflammation (Levy, D. *et al.*, 2001). In keeping with these observations, treatment with nonspecific NOS inhibitors such as L-N-nitro-L-arginine methyl ester (L-NAME) has been shown to prevent or reduce pain hypersensitivity (Meller, S. T. *et al.*, 1992; Hao, J. X. and Xu, X. J., 1996; Handy, R. L. and Moore, P. K., 1998). Indeed particular interest has been devoted to producing selective blockers of iNOS, to avoid side effects associated with nonspecific block of nNOS and endothelial NOS (eNOS). Recently GW27415, a selective iNOS inhibitor has been shown to partially reduce Freund's complete adjuvant (FCA)-induced inflammatory pain as well the hypersensitivity associated with the CCI neuropathy model. This action was most likely to have been caused via a peripheral mechanism as no iNOS expression was detectable in sensory ganglia or spinal cord (Alba, J. D. *et al.*, 2006).

5.53.21 Summary and Conclusions

Pharmacological understanding of pain is the foundation on which new and effective therapies for pain can emerge. Great advances have been made with greater availability of improved chemical and biological tools. This has fueled greater understanding of the mechanistic and molecular substrates of pain, derived for the most part from our studies of animal models (see Figure 1). The complexity and heterogeneity of chronic pain states will clearly remain an enormously challenging area for future research. There is still a great need for human data showing the regulated expression of pain molecules and clinical data that provides more rapid evaluation of emerging pharmacological concepts. This will allow the most valuable targets to be selected for analgesia development in the clinic.

Clearly the improvements in our pharmacological understand of pain has also provided an abundance of opportunities for developing analgesics. Among the most comprehensively studied molecules in chronic pain are inflammatory mediators and their key receptors. These include PGE2/EP1, bradykinin/BK1 and BK2, ATP/P2X3, cytokines/ IL-1β, chemokines/ CCr2 and neurotrophins/NGF/TrkA that sensitize and increase excitability in peripheral and central pain pathways. Many of these mediators act through GPCRs and there appears to be some convergence of mechanisms with changes in expression and regulation of ion channel. Key channels for pain are either ligand gated, for example, TRPV1, P2X3, P2X4, P2X7, or voltage gated, for example, NaV1.8, NaV1.7, NaV1.3, CaV2.2.

A variety of additional cellular process including protein phosphorylation of membrane receptors and channels via key kinases, for example, MAPK, as well as complex phenotype change regulated by neurotrophins require further understanding. In addition, the emerging importance of neuroglia and their pharmacology needs exploration and consolidation.

Finally despite the great advances in pain pharmacology, many pain molecules remain poorly validated as good targets for analgesia. Stronger clinical translation is highly likely with the progression of pharmacological opportunities into humans.

References

Abbadie, C. 2005. Chemokines, chemokine receptors and pain. Trends Immunol. 26, 529–534.

Alba, J. D., Clayton, N. M., Collins, S. D., Colthup, P., Chessell, I., and Knowles, R. G. 2006. GW274150, a novel and highly selective inhibitor of the inducible isoform of nitric oxide synthase (iNOS), shows analgesic effects in rat models of inflammatory and neuropathic pain. Pain 120, 170–181.

Ali, Z., Raja, S. N., Wesselmann, U., Fuchs, P. N., Meyer, R. A., and Campbell, J. N. 2000. Intradermal injection of norepinephrine evokes pain in patients with sympathetically maintained pain. Pain 88, 161–168.

Aloe, L., Tuveri, M. A., Carcassi, U., and Levi-Montalcini, R. 1992. Nerve growth factor in the synovial fluid of patients with chronic arthritis. Arthritis Rheum. 35, 3351–3355.

Altier, C. and Zamponi, G. W. 2004. Targeting Ca channels to treat pain: T type versus N-type. Trends Pharmacol. Sci. 26, 465–470.

Altier, C., Khosravani, H., Evans, R. M. Hameed, S., Peloquin, J. B., Vartian, B. A., Chen, L., Beedle, A. M., Ferguson, S. S., Mezghrani, A., Dubel, S. J., Bourinet, E., McRory, J. E., and Zamponi, G. W. 2005. ORL-1 receptor mediated internalization of N-type calcium channels. Nature Neurosci. 9, 31–40.

Amadesi, S., Nie, J., Vergnolle, N., Cottrell, G. S., Grady, E. F., Trevisani, M., Manni, C., Geppetti, P., McRoberts, J. A., Ennes, H., Davis, J. B., Mayer, E. A., and Bunnett, N. W. 2004. Protease-activated receptor 2 sensitizes the capsaicin receptor transient receptor potential vanilloid receptor 1 to induce hyperalgesia. J. Neurosci. 24, 4300–4312.

Andreev, N., Dimitrieva, N., Kolzenburg, M., and McMahon, S. B. 1995. peripheral administration of nerve growth factor in the adult rat produces a thermal hyperalgesia that requires the presence of sympathetic post-ganglionic neurones. Pain 63, 109–115.

Apfel, S. C. 2002. Nerve growth factor for the treatment of diabetic neuropathy: what went wrong, what went right, and what does the future hold? Int. Rev. Neurobiol. 50, 393–413.

Apostolidis, A., Popat, R., Yiangou, Y., Cockyne, D., Ford, A. B. D. W., Davis, J. B., Dasgupta, P., Fowler, C. J., and Anand, P. 2005. Decreased sensory receptors P2X (3) and TRPV1 in suburothelial nerve fibers following intradetrusor injection of botulinum toxin for human detrusor overactivity. J. Urol. 174, 977–982.

Araujo, M. C., Sinnott, C. J., and Strichartz, G. R. 2003. Multiple phases of relief from experimental mechanical allodynia by systemic lidocaine: responses to early and late infusions. Pain 103, 21–29.

Baccei, M. L. and Kocsis, J. D. 2000. Voltage gated calcium currents in axotomized rat cutaneous afferent neurons. spinal dorsal horn of rats. Eur. J. Neurosci. 419, 1336–1342.

Bandell, M., Story, G. M., Hwang, S. W., Viswanath, V., Eid, S. R., Petrus, M. J., Earley, T. J., and Pataapouian, A. 2004. Noxious cold ion channel TRPA1 is activated by pungent compounds and bradykinin. Neuron 41, 849–853.

Bao, L., Jin, S. X., Zhang, C., Wang, L. H., Xu, Z. Z., Zhang, F. X., Wang, L. C., Ning, F. S., Cai, H. J., Guan, J. S., Xiao, H. S., Xu, Z. Q., He, C., Hokfelt, T., Zhou, Z., and Zhang, X. 2003. Activation of delta opioid receptors induces receptor induces receptor insertion and neuropeptide secretion. Neuron 37, 121–133.

Bar, K. J., Natura, G., Telleria-Diaz, A., Tascher, P., Vogel, R., Vasques, E., Schaible, H. G., and Ebersberger, A. 2004. Changes in the effect of spinal prostaglandin E2 during inflammation: prostaglandin E9EP1-EP4) receptors in spinal nociceptive processing of input from the normal and inflamed knee joint. J. Neurosci. 24, 642–651.

Bhave, G. and Gereau, R. W. 2004. Posttranslational mechanisms of peripheral sensitization. J. Neurobiol. 6188–6106.

Bhave, G., Karim, F., Carlton, S. M., and Gereau, R. W. 2001. Peripheral group I metabotropic glutamate receptors modulate nociception in mice. Nat. Neurosci. 4, 417–423.

Blackburn-Munro, G., Bomholt, S. F., and Erichsen, H. K. 2004. Behavioural effects of the novel AMPA/GluR5 selective receptor antagonist NS1209 after systemic administration in animal models of experimental pain. Neuropharmacology 47, 351–362.

Boucher, T. J., Okuse, K., Bennett, D. L., Munson, J. B., Wood, J. N., and McMahon, S. B. 2000. Potent analgesic effects of GDNF in neuropathic pain states. Science 290, 124–127.

Boxall, S. J., Berthele, A., Laurie, D. J., Sommer, B., Zieglgansberger, W., Urban, L., and Tolle, T. R. 1998. Enhanced expression of metabotropic glutamate receptor 3 messenger RNA in the rat spinal cord during ultraviolet irradiation induced peripheral inflammation. Neuroscience 82, 591–602.

Burgess, G. M., Perkins, M. N., Rang, H. P., Campbell, E. A., Browen, M. C., McIntyre, P., Urban, L., Dziadulewicz, E. K., Ritchie, T. J., Hallet, A., Snell, C. R., Wrigglesworth, R., Lee, W., Davis, C., Phagoo, S. B., Davis, A. J., Phillips, E., Drake, G. S., Hughes, G. A., Dunstan, A., and Bloomfield, G. C. 2000. Bradyzide, a potent nonpeptide B2 bradykinin receptors antagonist with long lasting oral activity in animal models of inflammatory hyperalgesia. Br. J. Pharmacol. 129, 77–86.

Burstein, S. H., Karst, M., Schneider, U., and Zurier, R. B. 2004. Ajulemic acid: a novel cannabinoid produces analgesia without a ''high''. Life Sci. 75, 1513–1522.

Byas-Smith, M. G., Max, M. B., Muir, J., and Kingman, A. 1995. Transdermal clonidine compared to placebo in painful diabetic neuropathy using a two-stage 'enriched enrollment' design. Pain 60, 267–274.

Cahill, C. M., Morinville, A., Lee, M. C., Vincent, J. P., Collier, B., and Beaudet, A. 2001. Prolonged morphine treatment targets delta opioid receptors to neuronal plasma membranes and enhances delta-mediated antinociception. J. Neurosci. 21, 7598–7607.

Campbell, F. A., Tramer, M. R., Carroll, D., Reynolds, D. J., Moore, R. A., and McQuay, H. J. 2001. Are cannabinoids an effective and safe treatment option in the management of pain? A quantitative systematic review. BMJ 323, 13–16.

Campbell, J. N., Basbaum, A. I., Dray, A., Dubner, R., Dworkin, R. H., and Sang, C. N. (*eds.*) 2006. Emerging Strategies for the Treatment of Neuropathic Pain. IASP Press.

Carlton, S. M., Hargett, G. L., and Coggeshall, R. E. 1995. Localization and activation of glutamate receptors in unmyelinated axons of rat glabrous skin. Neurosci. Lett. 197, 25–28.

Caterina, M. J., Leffer, A., Malmberg, A. B., Martin, W. J., Trafton, J., Petersen-Zeitz, K. R., Koltzenburg, M., Basbaum, A. I., and Julius, D. 2000. Impaired nociception and pain sensation I mice lacking the capsaicin receptor. Science 288, 306–313.

Cervero, F., Laird, J. M. A., and Garcia-Nicas, E. 2003. Secondary hyperalgesia and presynaptic inhibition: an update. Eur. J. Pharmacol. 7, 345–351.

Chandrasekharan, N. V., Dai, H., Roos, K. L. T., Evanson, N. K., Tomsik, J., Elton, T. S., and Simmons, D. L. 2002. COX-3, a cyclooxygenase-1 variant inhibited by acetaminophen and other analgesic/antipyretic drugs: cloning, structure, and expression. Proc. Natl. Acad. Sci. U. S. A. 99, 13926–13931.

Chang, L., Luo, L., Palmer, J. A., Sutton, S., Wilson, S. J., Barbier, A. J., Breitenbucher, J. G., Chaplan, S. R., and Webb, M. 2006. Inhibition of fatty acid amide hydrolase produces analgesia by multiple mechanisms. Br. J. Pharmacol. 148, 102–113.

Chaplan, S. R., Guo, H. Q., Lee, D. H., Luo, L., Liu, C., Kuei, C., Velumian, A. A. L., Butler, M. P., Brown, S. M., and Dubin, A. E. 2003. Neuronal hyperpolarization-activated pacemaker channels drive neuropathic pain. J. Neurosci. 23, 1169–1178.

Chessell, I. P., Hatcher, J. P., Bountra, C., Michel, A. D., Hughes, J. P., Green, P., Egerton, J., Murfin, M., Richardson, J., Peck, W. L., Grahames, C. B., Casula, M. A., Yiangou, Y., Birch, R., Anand, P., and Buell, G. N. 2005. Disruption of the P2x7 purinoceptor gene abolishes chronic inflammatory and neuropathic pain. Pain 114, 386–396.

Chiechio, S., Caricasole, A., Barletta, E., Storto, M., Catania, M. V., Copani, A., Vertechy, M., Nicolai, R., Calvani, M., Melchiorri, D., and Nicoletti, F. 2002. L-Acetylcarnitine induces analgesia by selectively

up-regulating mGlu2 metabotropic glutamate receptors. Mol. Pharmacol. 61, 989–996.
Chizh, B., Napolitano, A., O'Donnell, M., Wang, J., Brooke, A., Lai, R., Aylott, M., Bullman, J., Gray, E., Williams, P., and Appleby, J. 2006. The TRPV1 antagonist SB705498 attenuates TRPV1 receptor-mediated activity and inhibits inflammatory hyperalgesia in humans: results from a Phase 1 study. Am. Pain Soc. 765.
Cichewicz, D. L. and McCarthy, E. A. 2003. Antinociceptive synergy between delta9 tetrahydrocannabinol and opioids after oral administration J. Pharmacol. Exp. Ther. 304, 1010–1015.
Claveau, D., Sirinyan, M., Guay, J., Gordon, R., Chan, C. C., Bureau, Y., Riendeau, D., and Mancini, J. A. 2003. Microsomal prostaglandin synthase-1 is a major terminal synthase that is selectively up-regulated during cyclooxygenase-2-dependent prostaglandin E2 production in the rat adjuvant-arthritis model. J. Immunol. 170, 4738–4744.
Colquhoun, A., Lawrance, G. M., Shamovsky, I. L., Riopelle, R. J., and Ross, G. M. 2004. Differential activity of the nerve growth factor (NGF) antagonist PD90780 [7-benzoylamino)-4,9-dihydro-4methyl-8-oxo-pyrazolo-[5,1-b]-quinazoline-2-carboxylic acid] suggest altered NGF-p75NTR interactions in the presence of TrkA. J. Pharmacol. Exp. Ther. 310, 505–511.
Coull, J. A. M., Boudreau, R., Bachand, K., Prescott, S. A., Nault, F., Sik, A., de Konink, P., and de Konink, Y. 2003. Trans-synaptic shift in ionic gradient in spinal lamina 1 neurons as a mechanism of neuropathic pain. Nature 424, 938–942.
Cravatt, B. F. and Lichtman, A. H. 2004. The endogenous cannabinoid system and its role in nociceptive behavior. J. Neurobiol. 61, 149–160.
Cravatt, B. J., Demarest, K., Patricelli, M. P., Bracey, M. H., Giang, D. K., Martin, B. R., and Lichtman, A. H. 2001. Supersensitivity to anandamide and enhanced endogenous cannabinoid signaling in mice lacking fatty acid amide hydrolyse. Proc. Natl. Acad. Sci. U. S. A. 98, 9371–9376.
Cummins, T. R. and Waxman, S. G. 1997. Downregulation of tetrodotoxin-resistant sodium currents and upregulation of a rapidly repriming tetrodotozin-sensitive sodium current in small spinal sensory neurons after nerve injury. J. Neurosci. 17, 3503–3514.
Danysz, W. and Parsons, C. G. 1998. GlycineB recognition site of NMDA receptors and its antagonists. Amino Acids 14, 205–206.
De Jongh, R. F., Vissers, K., Meert, T. F., Booij, L. H. D. J., de Deyne, C. S., and Heylen, R. J. 2003. The role of interleukin-6 in nociception and pain. Anaesth. Analg. 96, 1096–1103.
Deng, Y. S., Zhong, J. H., and Zhou, X. F. 2000. Effects of endogenous neurotrophin on sympathetic sprouting in the dorsal root ganglia and allodynia following spinal nerve injury. Exp. Neurol. 164, 344–350.
Devor, M. 2005. Sodium channels and mechanisms of neuropathic pain. J. Pain 7, S3–S12.
Devor, M., Wall, P. D., and Catalan, N. 1992. Systemic lidocaine silences ectopic neuroma and DRG discharges without blocking nerve conduction. Pain 48, 261–268.
Deuchars, S. A., Atkinson, L., Brooke, R. E., Musa, H., Milligan, C. J., Batten, T. F. C., Buckley, N. J., Parson, S. H., and Deuchars, J. 2001. Neuronal P2X7 receptors are targeted to presynaptic terminals in the central and peripheral nervous systems. J. Neurosci. 21, 7143–7152.
Dogrul, A., Ossipov, M. H., Lai, J., Malan, T. P., and Porecca, F. 2000. Peripheral and spinal antihyperalgesic activity of SIB-1757, a metabotropic glutamate receptor (mGluR5) antagonist, in experimental neuropathic pain in rats. Neurosci. Lett. 292, 115–118.
Dong, X., Han, S., Zylka, M. J., Simon, M. I., and Anderson, D. J. 2001. A diverse family of GPCRs expressed in specific subsets of nociceptive sensory neurons. Cell 106, 619–632.
Dray, A. 1997. Kinins and their receptors in hyperalgesia. Can. J. Pharmacol. 75, 704–712.
Dray, A. 1999. Alternatives to mu-Opioid Analgesics: delta-Opioid and Galanin-Receptor Selective Compounds. In: Progress in Pain research and Management (*eds*. E. Kalso, H. J. McQuay, and Z. Wiesenfeld-Hallin), pp. 269–280. IASP Press.
Dray, A. and Perkins, M. N. 1993. Bradykinin and inflammatory pain. Trends Neurosci. 16, 99–104.
Dube, G. R., Lehto, S. G., Breese, N. M., Baker, S. J., Wang, X., Matulenko, M. A., Honore, P., Stewart, A. O., Moreland, R. B., and Brioni, J. D. 2005. Electrophysiological and *in vivo* characterization of A-317567, a novel blocker of acid sensing ion channels. Pain 117, 88–96.
Dyson, A., Peacock, M., Chen, A., Courade, J. P., Yaqoob, M., Groark, A., Brain, C., Loong, Y., and Fox, A. 2005. Antihyperalgesic properties of the cannabinoid CT-3 in chronic neuropathic and inflammatory pain states in the rat. Pain 116, 129–137.
Eglen, R. M., Hunter, J. C., and Dray, A. 1999. Ions in the fire: recent ion-channel research and approaches to pain therapy. Trends Pharmacol. Sci. 8, 337–342.
Eisenbarth, H., Rukwied, R., Petersen, M., and Schmelz, M. 2004. Sensitization to bradykinin B1 and B2 receptor activation in UV-B irradiated human skin. Pain 110, 197–204.
Elmes, S. J. R., Winyard, L. A., Medhurst, L. A., Clayton, S. J., Wilson, N. M., Kendall, A. W., and Chapman, V. 2005. Activation of CB1 and CB2 receptors attenuates the induction and maintenance of inflammatory pain in the rat. Pain 118, 327–335.
England, S., Bevan, S., and Dougherty, R. J. 1996. PGE2 modulate the tetrodotoxin-resistant sodium current in neonatal dorsal root ganglion neurons via the cyclic AMP-protein kinase A cascade. J. Physiol. 495, 429–440.
Ferreira, J., Beirith, A., Mori, M. A. S., Araujo, R. C., Bader, M., Pesqero, J. B., and Calixto, J. B. 2005. Reduced nerve injury induced neuropathic pain in kinin B1 receptor knock-out mice. J. Neurosci. 25, 2405–2412.
Fiorucci, S., Antonelli, E., Burgand, J. L., and Morelli, A. 2001. Nitric-oxide releasing NSAIDs: a review of their current status. Drug Saf. 24, 801–811.
Finn, D. P., Jhaveri, M. D., Beckett, S. R., Kendall, D. A., Marsden, C. A., and Chapman, V. 2004. Cannabinoids modulate ultrasound-induced aversive responses in rats. Psychopharmacology 172, 41–51.
Flatters, S. J. and Bennett, G. J. 2004. Ethosuximaide reverses paclitaxel and vincristine-induced painful peripheral neuropathy. Pain 109, 150–161.
Flechtenmacher, J., Talke, M., Veith, D., Heil, K., Gebauer, A., and Schoenharting, M. 2004. Icatibant induces pain relief in patients with osteoarthritis of the knee. 9th World Cong. Osteoarthritis Res. Soc. Intl. 12, Abst. P332.
Fjell, J., Cummings, T. R., Fried, K., Black, J. A., and Waxman, S. G. 1999. *In vivo* NGF deprivation reduces SNS expression and TTX-R sodium currents in IB4-negative DRG neurons. J Neurophysiol. 81, 803–810.
Flower, R. J. 2003. The development of COX2 inhibitors. Nat. Rev. 2, 179–191.
Fox, A. and Bevan, S. 2005. Therapeutic potential of cannabinoid receptor agonists as analgesic agents. Exp. Opin. Invest. Drugs 14, 695–703.
Fox, A., Kaur, S., Li, B., Panasar, M., Saha, U., Davis, C., Dragoni, I., Colley, S., Ritchie, T., Bevan, S., Burgess, G., and McIntyre, P. 2005. Antihyperalgesic activity of a novel nonpeptide bradykinin B1 receptor antagonist in transgenic mice expressing the human B1 receptor. Br. J. Pharmacol. 144, 889–899.

Fox, A., Wotherspoon, G., McNair, K., Hudson, L., Patel, S., Gentry, C., and Winter, L. 2003. Regulation and function of spinal and peripheral neuronal B(1) bradykinin receptors in inflammatory mechanical hyperalgesia. Pain 104, 683–691.

Fride, E., Suris, R., Weidenfeld, J., and Mechoulam, R. 2005. Differential response to acute and repeated stress in cannabinoid cB1 receptor knockout newborn and adult mice. Behav. Pharmacol. 16, 431–440.

Fundytus, M. E., Osborne, M. G., Henry, J. L., Coderre, T. J., and Dray, A. 2002. Antisense oligonucleotide knockdown of mGluR(1) alleviates hyperalgesia and allodynia associated with chronic inflammation. Pharmacol. Biochem. Behav. 73, 401–410.

Gabra, B. H. and Sirois, P. 2003. Beneficial effects of chronic treatment with the selective bradykinin B1 receptor antagonists, R-715 and R-953, in attenuating streptozotocin-diabetic thermal hyperalgesia. Peptides 24, 1131–1139.

Gabra, B. H., Merino, V. F., Bader, M., Pasquero, J. B., and Sirois, P. 2005. Absence of diabetic hyperalgesa in bradykinin B1 receptor-knockout mice. Reg. Pept. 127, 245–248.

Garcia-Martiez, C., Humet, M., Planells-Casas, R., Gomis, A., Capri, M., Viaa, F., de la Pena, E., Sachez-Baez, F., Carbonell, T., de Felipe, C., Perez-Paya, E., Belmote, C., Messeguer, A., and Ferrer-Motiel, A. 2002. Attenuation of thermal nociception and hyperalgesia by VR1 blockers. Proc. Natl. Acad. Sci. U. S. A. 99, 2374–2379.

Gold, M. S., Levine, J. D., and Correa, M. 1998. Modulation of TTX-R INa by PKC and PKA and their role in PGE2-induced sensitization of rat sensory neurons *in vitro*. J. Neurosci. 18, 10345–10355.

Gold, M. S., Weinreich, D., Kim, C. S., Wang, R., Treanor, J., Porecca, F., and Lai, J. 2003. Redistribution of Na(V) 1.8 in uninjured axons enables neuropathic pain. J. Neurosci. 23, 158–166.

Gordh, T., Sharma, H. S., Alm, P., and Westman, J. 1998. Spinal nerve lesion induces upregulation of neuronal nitric oxide synthase in the spinal cord. An immunohistochemical investigation in the rat. Amino Acids 14, 105–112.

Gougat, J., Ferrari, B., Sarran, L., Planchenault, C., Poncelet, M., Maruani, J., Alonso, R., Cudennec, A., Croci, T., Guagnini, F., Urban-Szabo, K., Martinolle, J. P., Soubrié, P., Finance, O., and Le Fur, G. 2004. SSR240612 [(2*R*)-2-[((3*R*)-3-(1,3-benzodioxol-5-yl)-3-[[(6-methoxy-2-naphthyl)sulfonyl]amino]propanoyl)amino]-3-(4-[[2*R*,6*S*)-2,6-dimethylpiperidinyl]methyl]phenyl)-*N*-isopropyl-*N*-methylpropanamide hydrochloride], a new nonpeptide antagonist of the bradykinin B_1 receptor: biochemical and pharmacological characterization. J. Pharmacol. Exp. Ther. 309, 661–669.

Gould, H. J., England, J. D., Soignier, R. D., Nolan, P., Minor, L. D., Liu, Z. P., Levinson, S. R., and Paul, D. 2004. Ibuprofen block changes in NaV1.7 and 1.8 sodium channels associated with complete Freund's adjuvant-induced inflammation in rat. J. Pain 5, 270–280.

Gracely, R., Lynch, S., and Bennett, G. 1992. Painful neuropathy: altered central processing, maintained dynamically by peripheral input. Pain 51, 175–194.

Grazzini, E., Puma, C., Roy, M. O., Yu, X. H., O'Donnell, D., Schmidt, R., Dautry, S., Ducharme, J., Perkins, M., Panetta, R., Laird, J. M. A., Ahmad, S., and Lembo, P. M. 2004. Sensory neuron-specific receptor activation elicits central and peripheral nociceptive effects in rats. Proc. Nat. Acad. Sci. U. S. A. 101, 7171–7180.

Grunke, M. and Schulze-Koops, H. 2006. Successful treatment of inflammatory knee osteoarthritis with tumour necrosis factor blockade. Annu. Rheum. Dis. 65, 555–556.

Gutierrez, T., Nackley, A. G., Neely, M. H., Freeman, K. G., Edwards, G. L., and Hohmann, A. G. 2003. Effects of neurotoxic destruction of descending noradrenergic pathways on cannabinoid antinociception in models of acute and tonic nociception. Brain Res. 987, 176–185.

Hains, B. C., Saab, C. Y., Klein, J. P., Craner, M. J., and Waxman, S. G. 2004. Altered sodium channel expression in second-order spinal sensory neurons contributes to pain after peripheral nerve injury. J. Neurosci. 24, 4832–4839.

Halliday, D. A., Zettler, C., Rush, R. A., Scicchitano, R., and McNeil, J. D. 1998. Elevated growth factor levels in the synovial fluid of patients with inflammatory joint disease. Neurochem. Res. 23, 919–922.

Handy, R. L. and Moore, P. K. 1998. A comparison of the effects of L-NAME, 7NI and l-NIL on carrageenan induced hindpaw edema and NOS activity. Br. J. Pharmacol. 12, 1119–1126.

Hao, J. X. and Xu, X. J. 1996. Treatment of a chronic allodynia-like response in spinally injured rats: effects of systemically administered nitric oxide synthase inhibitors. Pain 66, 313–319.

Hao, S., Mata, M., Wolfe, D., Glorioso, J. C., and Fink, D. J. 2005. Gene transfer of glutamic acid decarboxylase reduces neuropathic pain. Ann. Neurol. 57, 914–918.

Harvey, R. J., Depner, U. B., Wassle, H., Ahmadi, S., Heidl, C., Reinold, H., Smart, T. G., Harvey, K., Schultz, B., Abo-Salem, O. M., Zimmer, A., Poisbeau, P., Welzl, H., Wolfer, D. P., Betz, H., Zeilhofer, H. U., and Muller, U. 2004. GlyRα3: an essential target for spinal PGE2-mediated inflammatory pain sensitization. Science 304, 884–887.

Hefti, F. F., Rosenthal, A., Walicka, P. A., Wyatt, S., Vergara, G., Shelton, D. L., and Davis, A. M. 2005. Novel class of pain drug based on antagonism of NGF. Trends Pharmacol. Sci. 27, 85–91.

Hogestatt, E. D., Jonsson, B. A. G., Ermund, A., Andersson, D. A., Bjork, H., Alexander, J. P., Cravatt, B. J., Basbaum, A. I., and Zygmunt, P. M. 2005. Conversion of acetaminophen to bioactive N-acylphenolamine AM4040 via fatty acid amide hydrolase-dependent arachidonic acid conjugation in the nervous system. J. Biol. Chem. 280, 31405–31412.

Hohmann, A. G. and Herkenham, M. 1999. Cannabinoid receptors undergo axonal flow in sensory nerves. Neuroscience 92, 1171–1175.

Hohmann, A. G., Suplita, R. L., Bolton, N. M., Neely, M. H., Fegley, D., Mangieri, R., Krey, J. F., Walker, J. M., Holmes, P. V., Crystal, J. D., Duranti, A., Tonini, A., Mor, M., Tarzia, G., and Piomelli, D. 2005. An endocannabinoid mechanism for stress-induced analgesia. Nature 435, 1108–1112.

Holthusen, H. and Arndt, J. O. 1994. Nitric oxide evokes pain in humans on intracutaneous injection. Neurosci. Letts. 165, 71–74.

Honore, P., Kage, K., Mikusa, J., Watt, A. T., Johnston, J. F., Wyatt, J. R., Faltynek, C. R., Jarvis, M. F., and Lynch, K. 2002. Analgesic profile of intrathecal P2X(3) antisense oligonucleotide treatment in chronic inflammatory and neuropathic pain states in rats. Pain 99, 11–19.

Honore, P., Rogers, S. D., Schwei, M. J., Salak-Johnson, J. L., Luger, N. M., Sabino, M. C., Clohisy, D. R., and Mantyh, P. W. 2000. Murine models of inflammatory, neuropathic and cancer pan each generate a unique set of neurochemical changes in the spinal cord and sensory neurons. J. Neurosci. 98, 585–598.

Hudson, L. J., Bevan, S., McNair, K., Gentry, C., Fox, A., Kuhn, R., and Winter, J. 2002. Metabotropic glutamate receptor 5 upregulation in A-fibers after spinal nerve injury: 2-Methyl-6-(phenylethynyl)-pyridine (MPEP) reverses the induced thermal hyperalgesia. J. Neurosci. 22, 2660–2668.

Hunt, S. P. and Mantyh, P. 2001. The molecular dynamics of pain control. Nat. Rev. 2, 83–91.

Hurley, R. W. and Hammond, D. L. 2000. The analgesic effects of supraspinal mu and delta opioid receptor agonists are potentiated during persistent inflammation J. Neurosci. 20, 1249–1259.

Ibrahim, M. M., Porreca, F., Lai, J., Albrecht, P. J., Rise, F. L., Khodorova, A., Davar, G., Makriyannis, A., Vanderah, T. W., Mata, H. P., and Malan, T. P. 2005. CB2 cannabinoid receptor activation produces antinociception by stimulating peripheral release of endogenous opioids. Proc. Natl. Acad. Sci. U. S. A. 102, 3093–3098.

Ibuki, T., Hama, A. T., Wang, X. T., Pappas, G. D., and Sagen, J. 1997. Loss of GABA-immunoreactivity in the spinal dorsal horn of rats with peripheral nerve injury and promotion of recovery by adrenal medullary grafts. Neuroscience 76, 845–858.

Ikeda, H., Heinke, B., Ruscheweyh, R., and Sandkuhler, J. 2003. Synaptic plasticity in spinal lamina 1 projection neurons that mediate hyperalgesia. Science 299, 1237–1240.

Jakobsson, P. J., Thoen, S., Morgenstern, R., and Samuelsson, B. 1999. Identification of human prostaglandin E synthase: a microsomal, glutathione-dependent, inducible enzyme, constituting a potential novel drug target. Proc. Natl. Acad. Sci. U. S. A. 96, 7220–7225.

Jang, J. H., Kim, D. W., Sang Nam, T., Se Paik, K., and Leem, J. W. 2004. Peripheral glutamate receptors contribute to mechanical hyperalgesia in a neuropathic pain model of the rat. Neuroscience 128, 169–176.

Jarvis, M. F., Burgard, E. C., McGaraughty, S., Honore, P., Lynch, K., Brennan, T. J., Subieta, A., van Biesen, T., Cartmell, J., Bianchi, B., Niforatos, W., Kage, K., Yu, H. X., Mikusa, J., Wismer, C. T., Zhu, C. Z., Chu, K., Lee, C. H., Stewart, A. O., Polakowski, J., Cox, B. F., Kowaluk, E., Williams, M., Sullivan, J., and Faltynek, C. 2002. A-3174919, a novel potent and selective non nucleotide antagonist of P2X(3) and P2X(2/3) receptors, reduces chronic inflammatory and neuropathic pain in the rat. Proc. Natl. Acad. Sci. U. S. A. 99, 17179–17184.

Ji, R. R., Samad, T. A., Jin, S. X., Schmoll, R., and Woolf, C. J. 2002. P38 MAPK activation by NGF in primary sensory neurons after inflammation increases TRPV1 levels and maintains heat hyperalgesia. Neuron 36, 57–68.

Karst, M., Salim, K., Burstein, S., Conrad, I., Hoy, L., and Schneider, U. 2003. Analgesic effect of the synthetic cannabinoid CT-3 on chronic neuropathic pain. JAMA 290, 1757–1762.

Kastrup, J., Petersen, P., Dejgard, A., and Angelo, F. R. 1987. Intravenous lidocaine infusion – a new treatment of chronic painful diabetic neuropathy. Pain 28, 69–75.

Kerr, B. J., Bradbury, E. J., Bennett, D. L., Trivedi, P. M., Dassan, P., French, J., Shelton, D. B., McMahon, S. B., and Thompson, S. W. 1999. Brain derived neurotrophic factor modulates nociceptive sensory neurone input and NMDA-evoked responses in the rat spinal cord. J. Neurosci. 19, 5136–5149.

Kim, C., Jun, K., Lee, T., Kim, S. S., *et al.*, 2001. Altered nociceptive responses in mice deficient in the α1B subunit of the voltage dependent calcium channel. Mol. Cell Neurosci. 18, 235–245.

Kim, C. H., Oh, Y., Chung, J. M., and Chung, K. 2002. Changes in three subtypes of tetrodotoxin sensitive sodium channel expression in the axotomized dorsal root ganglion in the rat. Neurosci. Letts. 323, 125–128.

Krause, J. E., Chenard, B. L., and Cortright, D. N. 2005. Transient receptor potential ion channels for the discovery of pain therapeutics Curr. Opin. Inv. Drugs 6, 48–57.

Kreitzer, A. C. and Regeher, W. G. 2002. Retrograde signaling by endocannabinoids. Curr. Opin. Neurobiol. 12, 324–330.

Krishtal, O. 2003. The ASICs: signaling molecules? Modulators? TINS 26, 477–483.

LaBuda, C. J., Koblish, M., and Little, P. J. 2005. Cannabinoid CB2 receptor agonist activity in the hindpaw incision model of postoperative pain. Eur. J. Pharmacol. 527, 172–175.

Lai, J., Hunter, J. C., and Porreca, F. 2003. The role of voltage-gated sodium channels in neuropathic pain. Curr. Opin. Neurobiol. 13, 291–297.

Laird, J. M. A., García-Nicas, E., Delpire, E. J., and Cervero, F. 2004. Presynaptic inhibition and spinal pain processing in mice: a possible role of the NKCC1 cation-chloride co-transporter in hyperalgesia. Neurosci. Letts. 361, 200–203.

Lane, N., Webster, L., Shiao-Ping, L., Gray, M., Hefti, F., and Walicke, P. 2005. RN624 (Anti-NGF) improves pain and function in subjects with moderate knee osteoarthritis: a phase I study. Arthritis Rheumat. 52, S461.

Lee, D. H., Liu, X., Kim, H. T., Chung, K., and Chung, J. M. 1999. Receptor subtype mediating the adrenergic sensitivity of pain behavior and ectopic discharges in neuropathic Lewis rats. J. Neurophysiol. 81, 2226–2233.

Lembo, P. M. C., Grazzini, E., Groblewski, T., O'Donnell, D., Roy, M. O., Zhang, J., Hoffert, C., Cao, J., Schmidt, R., Pelletier, M., Labarre, M., Gosselin, M., Fortin, Y., Banville, D., Shen, S. H., Strom, P., Payza, K., Dray, A., Walker, P., and Ahmad, S. 2002. Proenkephalin A gene products activate a new family of sensory neuron-specific GPCRs. Nat. Neurosci. 5, 201–209.

Levy, D. and Zochodne, D. W. 2000. Increased mRNA expression of the B1 and B2 bradykinin receptors and antinociceptive effects of their antagonists in an animal model of neuropathic pain. Pain 86, 265–271.

Levy, D., Kubes, P., and Zachodne, D. W. 2001. Delayed peripheral nerve degeneration, regeneration and pain in mice lacking inducible nitric oxide synthase. J. Neuropathol. Exp. Neurol. 60, 411–421.

Liang, Y. F., Haake, B., and Reeh, P. W. 2001. Sustained sensitization and recruitment of rat cutaneous nociceptors by bradykinin and a novel theory of its excitatory action. J. Physiol. 532, 229–239.

Lichtman, A. H., Leung, D., Shelton, C. C., Saghatelian, A., Hardouin, C., Boger, D. L., Cravatt, B. J. 2004. Reversible inhibitors of fatty acid amide hydrolase that promote analgesia: evidence for an unprecedented combination of potency and selectivity. J. Pharmacol. Exp. Ther. 311, 441–448.

Lindenlaub, T. and Sommer, C. 2003. Cytokines in sural nerve biopsies from inflammatory and non-inflammatory neuropathies. Acta Neuropathol. 105, 593–602.

Lindia, J. A., Kohler, M. G., Martin, W. J., and Abbadie, C. 2005. Relationship between sodium channel Nav1.3 expression and neuropathic pain behavior in rats. Pain 117, 145–153.

Liu, J., Li, H., Bursten, S. H., Zurier, R. B., and Chen, J. D. 2003. Activation and binding of peroxisomal proliferator-activated receptor gamma by synthetic cannabinoid ajulemic acid. Mol. Pharmacol. 63, 983–992.

Lu, B., Pang, P. T., and Woo, N. H. 2005. The Yin and Yang of neurotrophin action. Nat. Rev. Neurosci. 6, 603–614.

Luo, Z. D., Calcutt, N. A., Higuera, E. S., Valder, C. R., Song, Y. H., Svensson, C. I., and Myers, R. R. 2002. Injury type-specific calcium channel alpha (2) delta-1 subunit up-regulation in rat neuropathic pain models correlates with antiallodynic effects of gabapentin. J. Pharmacol. Exp. Ther. 303, 1199–1205.

Ma, W., Zhang, Y., Bantel, C., and Eisenach, J. C. 2005. Medium and large injured dorsal root ganglion cells increase TRPV-1, accompanied by increased alpha2C-adrenoceptor co-expression and functional inhibition by clonidine. Pain 113, 386–394.

Malan, T. P., Ibrahim, M. M., Lai, J., Vanderah, T. W., Makriyannis, A., and Porreca, F. 2003. CB2 cannabinoid

receptor agonists: pain relief without psychoactive effects?. Curr. Opin. Pharmacol. 3, 62–67.
Malan, T. P., Mata, H. P., and Porreca, F. 2002. Spinal GABA(A) and GABA(B) receptor pharmacology in a rat model of neuropathic pain. Anesthesiology 96, 1161–1167.
Mamet, J., Lazdunski, M., and Voilley, N. 2003. How nerve growth factor drives physiological and inflammatory expression of acid-sensing ion channels 3 in sensory neurons. J. Biol. Chem. 278, 48907–48913.
Mantyh, P. W. and Yaksh, T. L. 2001. Sensory neurons are PARtial to pain. Nat. Med. 7, 772–773.
Marceau, F., Hess, J. F., and Bachvarov, D. R. 1998. The B1 receptors for kinins. Pharmacol. Rev. 50, 357–386.
Marsicano, G., Goodenough, S., Monory, K., Hermann, H., Eder, M., Cannich, A., Azad, S. C., Cascio, M., Ortega Gutierrez, S., Van der Stelt, M., Lopez-Rodriguez, M. L., Casanova, E., Schutz, G., Zieglgansberger, W., Di Marzo, V., Behl, C., and Lutz, B. 2003. CB1 cannabinoid receptors and on demand defense against excitotoxicity. Science 302, 84–88.
Matthews, E. A. and Dickenson, A. H. 2001. Effects of spinally delivered N- and P-type voltage dependent calcium channel antagonists on dorsal horn neuronal responses in a rat model of neuropathy. Eur. J. Pharmacol. 415, 141–149.
Matzner, O. and Devor, M. 1994. Hyperexcitability at sites of nerve injury depends on voltage sensitive – sodium channels. J. Neurophysiol. 72, 349–359.
Meller, S. T., Pechman, P. S., Gebhart, G. F., and Maves, T. J. 1992. Nitric oxide mediates the thermal hyperalgesia produced in a model of neuropathic pain in the rat. Neuroscience 50, 7–10.
Mense, S. 2004. Neurobiological basis for the use of botulinum toxin in pain therapy. J. Neurol. 251, S11–S17.
Merskey, H., Loeser, J.D., and Dubner, R. (*eds.*) 2005. The Paths of Pain: 1975–2005. IASP Press.
Millan, M. J. 1999. The induction of pain: an integrative review. Prog. Neurobiol. 57, 1–164.
Miller, L. J., Fischer, K. A., Goralnick, S. J., Litt, M., Burleson, J. A., Albertsen, P., and Kreutzer, D. L. 2002. Nerve growth factor and chronic prostatis/chronic pelvic pain syndrome. Urology 59, 603–608.
Milligan, E., Zapata, V., Schoeniger, D., Chacur, M., Green, P., Poole, S., Martin, D., Maier, S. F., and Watkins, L. R. 2005b. An initial investigation of spinal mechanisms underlying pain enhancement induced by fractalkine, a neuronally released chemokine. Eur. J. Neurosci. 22, 2775–2782.
Milligan, E. D., Langer, S. J., Sloane, E. M., He, L., Wieseler-Frank, J., O'Connor, K., Martin, D., Forsayeth, J. R., Maier, S. F., Johnson, K., Chavez, R. A., Leinwand, L. A., and Watkins, L. R. 2005a. Controlling pathological pain by adenovirally driven spinal production of the anti-inflammatory cytokine, interleukin-10. Eur. J. Neurosci. 21, 2136–2148.
Moore, A. K., Kohno, T., Karchewski, L. A., Scholz, J., Baba, H., and Woolf, C. J. 2002. Partial peripheral nerve injury promotes a selective loss of GABAergic inhibition in the superficial dorsal horn of the spinal cord. J. Neurosci. 22, 6724–6731.
Nutt, J. G., Burchiel, K. J., Comella, C. L., Jankovic, J., Lang, A. E., Laws, E. R., Jr., Lozano, A. M., Penn, R. D., Simpson, R. K., Jr., Stacy, M., and Wooten, G. F. ICV GDNF Study Group. 2003. Implanted intracerebroventricular. Glial cell line-derived neurotrophic factor. Randomized, double-blind trial of glial cell line-derived neurotrophic factor (GDNF) in PD. Neurology 60, 69–73.
Obata, K., Yamanaka, H., Kobayashi, K., Dai, Y., Mizushima, T., Katsura, H., Fukuoka, T., Tokunaga, A., and Noguchi, K. 2004. Role of mitogen-activated protein kinase activation in injured and intact primary afferent neurons for mechanical and heat hypersensitivity after spinal nerve ligation. J. Neurosci. 24, 10211–10222.
Oddiah, D., Anand, P., McMahon, S. B., and Rattray, M. 1998. Rapid increase of NGF, BDNF and NT3 mRNAs in inflamed bladder. Neuroreport 9, 603–608.
Oh, S. B., Tran, P. B., Gillard, S. E., Hurley, R. W., Hammond, D. L., and Miller, R. J. 2001. Chemokines and glycoprotein 120 produce pain hypersensitivity by directly exciting primary nociceptive neurons. J. Neurosci. 21, 5027–5035.
Ohtori, S., Takahashi, K., Moriya, H., and Myers, R. R. 2004. TNF-alpha and TNF-alpha receptor type 1 upregulation in glia and neurons after peripheral nerve injury: studies in murine DRG and spinal cord. Spine 29, 1082–1088.
Okuse, K., Malik-Hall, M., Baker, M. D., Poon, W. Y., Kong, H., Chao, M. V., and Wood, J. N. 2002. Annexin II light chain regulates sensory neurone-specific sodium channel expression. Nature 417, 653–656.
Olesen, J., Thomsen, L. L., and Iversen, H. 1994. Nitric oxide is a key molecule in migraine and other vascular headaches. Trend Pharmacol. Sci. 15, 149–153.
Ottani, A., Leone, S., Sandrini, M., Ferrari, A., and Bertolinin, A. 2006. The analgesic activity of paracetamol is prevented by the blockade of cannabinoid CB1 receptors. Eur. J. Pharmacol. 531, 280–281.
Owolabi, J. B., Rizkalla, G., Tehim, A., Ross, G. M., Riopelle, R. J., Kamboj, R., Ossipov, M., Bian, D., Wegert, S., Porreca, F., and Lee, DK. 1999. Characterization of antiallodynic actions ALE-0540, a novel nerve growth factor receptor antagonist, in the rat. J. Pharmacol. Exp. Ther. 289, 1271–1276.
Pesquero, J. B., Araujo, R. C., Heppenstall, P. A., Stucjy, C. L., Silva, J. A., Walther, T., Oliveira, S. M., Pasquero, J. L., Paiva, A. C. M., Calixto, J. B., Lewin, G. R., and Bader, M. 2000. Hypoalgesia and altered inflammatory responses in mice lacking kinin B1 receptors. Proc. Natl. Acad. Sci. U. S. A. 97, 8140–8145.
Petersen, M., Segond von Bachet, G., Heppelmann, B., and Kolzenburg, M. 1998. Nerve growth factor regulates the expression of bradykinin binding sites on adult sensory neurons via the neurotrophin p75. Neuroscience 83, 161–169.
Pollock, J., McFarlane, S. M., Connell, M. C., Zehavi, U., Vandenabeele, P., MacEwan, D. J., and Scott, R. H. 2002. TNF-alpha receptors simultaneously activate Ca^{2+} mobilisation and stress kinases in cultured sensory neurons. Neuropharmacology 42, 93–106.
Quartaroli, M., Fasdelli, N., Bettelini, L., Maraia, G., and Corsi, M. 2001. GV196771A, an NMDA receptor/glycine site antagonist, attenuates mechanical allodynia in neuropathic rats and reduces tolerance induced by morphine in mice. Eur. J. Pharmacol. 430, 219–227.
Raghavendra, V., Tanga, F., Rutkowski, M. D., and DeLeo, J. A. 2003. Anti-hyperalgesic and morphine-sparing actions pf propentofylline following peripheral nerve injury in rats: mechanistic implications of spinal glia and proinflammatory cytokines. Pain 104, 655–664.
Ramer, M. S., Bradbury, E. J., and McMahon, S. B. 2001. Nerve growth factor induces P2X(3) expression in sensory neurons. J. Neurochem. 77, 864–875.
Rice, A. S. C., Farquhar-Smith, W. P., and Nagy, I. 2002. Endocannabinoids and pain: spinal and peripheral analgesia in inflammation and neuropathy. Prostaglandins Leukot. Essent. Fatty Acids 66, 243–256.
Richardson, J. D., Kilo, S., and Hargreaves, K. M. 1998. Cannabinoids reduce hyperalgesia and inflammation via interactions with peripheral CB1 receptors. Pain 75, 111–119.
Ro, L. S., Chen, S. T., Tang, L. M., and Jacobs, J. M. 1999. Effect of NGF and anti-NGF on neuropathic pain in rats following chronic constriction injury of the sciatic nerve. 79, 265–274.

Ross, R. A., Coutts, A. A., McFarlane, S. M., Anavi-Goffer, S., Irving, A. J., Pertwee, R. G., MacEwan, D. J., and Scott, R. H. 2001. Actions of cannabinoid receptor ligands on rat cultured sensory neurones: implications of antinociception. Neuropharmacology 40, 221–232.

Rush, A. M., Craner, M. J., Kageyama, T., Dib-Haj, S. D., and Waxman, S. G. 2005. Contactin regulates the current density and axonal expression of tetrodotoxin-resistant but not tetrodotoxin- sensitive sodium channels in DRG neurons. Eur. J. Neurosci. 22, 39–49.

Sachez-Baez, F., Carbonell, T., de Felipe, C., Perez-Paya, E., Belmote, C., Messeguer, A. and Ferrer-Motiel, A. 2002. Attenuation of thermal nociception and hyperalgesia by VR1 blockers. Proc. Natl. Acad. Sci. U. S. A. 99, 2374–2379.

Saegusa, H., Kurihara, T., Zong, S., Kazuno, A., Matsuda, Y., Nonaka, T., Han, W., Toriyama, H., and Tanabe, T. 2001. Suppression of inflammation and neuropathic pain symptoms in mice lacking the N-type Ca^{2+} channel. EMBO J. 20, 2349–2356.

Sagar, D. R., Kelly, S., Millns, P. J., O'Shaugnessey, C. T., Kendall, D. A., and Chapman, V. 2005. Inhibitory effects of CB1 and CB2 receptor agonist on responses of DRG neurons and dorsal horn neurons in neuropathic rats. Eur. J. Neurosci. 22, 371–379.

Sah, D. W. H., Ossipov, M. H., and Porreca, F. 2003. Neurotrophic factors as novel therapeutics for neuropathic pain. Nat. Rev. Drug Disc. 2, 460–472.

Sang, C. N., Hostetter, M. P., Gracely, R. H., Chappell, A. S., Schoepp, D. D., Lee, G., Whitcup, S., Caruso, R., and Max, M. B. 1998. AMPA/kainate antagonist LY293558 reduces capsaicin-evoked hyperalgesia but not pain in normal skin in humans. Anesthesiology 89, 1060–1067.

Sarchielli, P., Alberti, A., Floridi, A., and Gallai, V. 2001. Levels of nerve growth factor in cerebrospinal fluid of chronic headache patients. Neurology 57, 132–134.

Sato, J. and Perl, E. R. 1991. Adrenergic excitation of cutaneous pain receptors induced by peripheral nerve injury. Science 251, 1608–1610.

Sawynok, J. 2003. Topical and peripherally acting analgesics. Pharmacol. Rev. 55, 1–20.

Schafers, M., Marziniak, M., Sorkin, L. S., Yaksh, T. L., and Sommer, C. 2004. Cyclooxygenase inhibition in nerve-injury and TNF-induced hyperalgesia in the rat. Exp. Neurol. 185, 160–168.

Schafers, M., Sorkin, L. S., Geis, C., and Shubayev, V. I. 2003a. Spinal ligation induces transient upregulation of tumor necrosis factor receptors 1 and 2 in injured and adjacent uninjured dorsal root ganglia of rat. Neurosci. Letts. 347, 179–182.

Schafers, M., Svensson, C. I., Sommer, C., and Sorkin, L. S. 2003b. Tumor necrosis factor-alpha induces mechanical allodynia after spinal nerve ligation by activation of p38 MAPK in primary sensory neurons. J. Neurosci. 23, 2517–2521.

Scholz, J. and Woolf, C. J. 2002. Can we conquer pain? Nature Neurosci. 5, 1062–1065.

Sevcik, M. A., Ghilardi, J. R., Peters, C. M., Lindsay, T. H., Halvorson, K. G., Jonas, BM, Kubota, K., Kuskowski, M. A., Boustany, L., Shelton, D. L., and Mantyh, P. W. 2005. Anti-NGF therapy profoundly reduces bone cancer pain and the accompanying increase in markers for peripheral and central sensitisation. Pain 115, 128–141.

Shelton, D. L., Zeller, J., Ho, W. H., Pons, J., and Rosenthal, A. 2005. Nerve growth factor mediates hyperalgesia and cachexia in auto-immune arthritis. Pain 116, 8–16.

Shidoda, K., Hruby, V. J., and Porecca, F. 2006. Antihyperalgesic effects of loperamide in a model of rat neuropathic pain are mediated by peripheral δ-opioid receptors. Neurosci Letts. 411, 143–146.

Shinder, V., Govrin-Lippmann, R., Cohen, S., Belenky, M., Ilin, P., Fried, K., Wilkinson, H. A., and Devor, M. 1999. Structural basis of sympathetic-sensory coupling in rat and human dorsal root ganglia following peripheral nerve injury. J. Neurocytol. 28, 743–761.

Shughrue, P. J., Ky, B., and Austin, C. P. 2003. Localization of B1 bradykinin receptors mRNA in the primate brain and spinal cord: an *in situ* hybridization study. J. Comp. Neurol. 46, 372–384.

Sluka, K. A., Price, M. P., Breese, N. M., Stucky, C. L., Wemmie, J. A., and Welsh, M. J. 2003. Chronic hyperalgesia induced by repeated acid injections in muscle is abolished by loss of ASIC3, but not ASIC1. Pain 106, 229–239.

Snutch, T. P. 2005. Targeting chronic and neuropathic pain: the N-type calcium channel comes of age. NeuroRx. 2, 662–670.

Sokal, D. M., Elmes, S. J. R., Kendall, D. A., and Chapman, V. 2003. Intraplantar injection of anandamide inhibits mechanically-evoked responses of spinal neurons via activation of Cb2 receptors in anaesthetized rats. Neuropharmacology 45, 404–411.

Sommer, C. and Kress, M. 2004. Recent findings on how proinflammatory cytokines cause pain: peripheral mechanisms in inflammatory and neuropathic hyperalgesia. Neurosci. Letts. 361, 184–187.

Stein, C., Schafer, M., and Machelska, H. 2003. Attacking pain at its source: new perspectives on opioids. Nature Med. 9, 1003–1008.

Stella, N. 2004. Cannabinoid signaling in glial cells. Glia 48, 267–277.

Stewart, J. M. 2004. Bradykinin antagonists: discovery and development. Peptides 25, 527–732.

Svenden, K. B., Jensen, T. S., and Bach, F. W. 2004. Does the cannabinoid dronabilon reduce central pain in multiple sclerosis? Randomized double blind placebo controlled crossover trial. BMJ 329, 253.

Taniguchi, K., Shinjo, K., Mizutani, M., Shimada, K., Ishikawa, T., Menniti, F., and Nagahisa, A. 1997. Antinociceptive actions of CP-101,606, an NMDA receptor NR2B subunit antagonist. Br. J. Pharmacol. 12, 809–812.

Theodosiou, M., Rush, R. A., Zhou, X. F., Hu, D., Walker, J. S., and Tracey, D. J. 1999. Hyperalgesia due to nerve damage: role of nerve growth factor. Pain 81, 245–255.

Tracey, D. J., Cunningham, J. E., and Romm, M. A. 1995. Peripheral hyperalgesia in experimental neuropathy: mediation by alpha 2-adrenoreceptors on post-ganglionic sympathetic terminals. Pain 60, 317–327.

Trebino, C. E., Stock, J. L., Gibbons, C. P., Naiman, B. M., Wachtmann, T. S., Umland, J. P., Pandher, K., Lapointe, J. M., Saha, S., Roach, M. L., Carter, D., Thomas, N. A., Durtschi, B. A., McNeish, J. D., Hambor, J. E. Jakobsson, P. J., Carty, T. J., Perez, J. R. and Audoly, L. P. 2003. Impaired inflammatory and pain responses in mice lacking an inducible prostaglandin E synthase. Proc. Natl. Acad. Sci. U. S. A. 100, 9044–9049.

Tsuda, M., Shigemoto-Mogami, Y., Koizumi, S., Mizokoshi, A., Kohsaka, S., Salter, M. W., and Inoue, K. 2003. P2X4 receptors induced in spinal microglia gate tactile allodynia after nerve injury. Nature 424, 778–783.

Urban, M. O., Hama, A. T., Bradbury, M., Anderson, J., Varney, M. A., and Bristow, L. 2003. Role of metabotropic glutamate receptor subtype 5 (mGluR5) in the maintenance of cold hypersensitivity following a peripheral mononeuropathy in the rat. Neuropharmacology 44, 983–993.

Valenzano, K. J., Tafesse, L., Lee, G., Harrison, J. E., Bulet, J. M., Gottshall, S. L., Mark, L., Pearson, M. S., Miller, W., Shan, S., Rabadi, L., Rotshteyn, Y., Chaffer, S. M.,

Turchin, P. I., Elsmore, D. A., Toth, M., Koetzner, L., and Whiteside, G. T. 2005. Pharmacological and pharmacokinetic characterization of the cannabinoid receptor 2 agonist GW405833, utilizing rodent models of acute and chronic pain, anxiety, ataxia and catalepsy. Neuropharmacology 48, 658–672.

Vellani, V., Mappleback, S., Moriondo, A., Davis, J. B., and McNaughton, P. A. 2001. Protein kinase C activation gating of the vanilloid receptor VR1 by capsaicin, protons, heat and anandamide. J. Physiol. 534, 813–825.

Valleni, V., Zachrisson, O., and McNaughton, P. A. 2004. Functional bradykinin B1 receptors are expressed in nociceptive neurons and are upregulated by the neurotrophin GDNF. J. Physiol. 560, 391–401.

Veneroni, O., Maj, R., Calbresi, M., Faravelli, L., Farielo, R. G., and Salvati, P. 2003. Anti-allodynic effect of NW-1029, a novel Na channel blocker, in experimental animal models of inflammatory and neuropathic pain. Pain 102, 17–25.

Vergnolle, N., Ferazzini, M., D'Andrea, M. R., Buddenkotte, J., and Steinhoff, M. 2003. Proteinase-activated receptors: novel signals for peripheral nerves. Trends Neurosci. 26, 496–500.

Wade, D. T., Robson, P., House, H., Makela, P., Aram, J. A. 2003. Preliminary controlled study to determine whether whole-plant cannabis extracts can improve intractable neurogenic symptoms. Clin. Rehabil. 17, 21–29.

Walker, K., Bowes, M., Panesar, M., Davis, A., Gentry, C., Kesingland, A., Gasparini, F., Spooren, W., Stoehr, N., Pagano, A., Flor, P. J., Vranesic, I., Lingenhoehl, K., Johnson, E. C., Varney, M., Urban, L., and Kuhn, R. 2001. Metabotropic glutamate receptor subtype 5 (mGlu5) and nociceptive function. I. Selective blockade of mGlu5 receptors in models of acute, persistent and chronic pain. Neuropharmacology 40, 1–9.

Wallace, M. S., Rowbotham, M. C., Katz, N. P., Dworkin, R. H., Dotson, R. M., Galer, B. S., Rauck, R. L., Backonja, M. M., Quessy, S. N., and Meisner, P. D. 2002. A randomized, double blind, placebo-controlled trial of a glycine antagonist in neuropathic pain. Neurology 59, 1694–1700.

Water, L., Franklin, A., Witting, A., Wade, C., Xie, Y., Kunos, G., Mackie, K., and Stella, N. 2003. Nonpsychotropic cannabinoid receptors regulate microglial cell migration. J. Neurosci. 23, 1398–1405.

Watkins, L. R. and Maier, S. 2002. Beyond neurons: evidence that immune and glial cells contribute to pathological pain states. Physiol. Rev. 82, 981–1011.

Wei, P., Moskowitz, M. A., Boccalini, P., and Kontos, H. A. 1992. Calcitonin gene-related peptide mediates nitroglycerin and sodium nitroprusside-induced vasodilatation in feline cerebral arterioles. Circulation Res. 70, 1313–1319.

Welch, M. J., Purkiss, J. R., and Foster, K. A. 2000. Sensitivity of embryonic rat dorsal root ganglia neurons to *Clostridium botulinum* neurotoxins. Toxicon 38, 245–258.

Whiteside, G. T., Boulet, J. M., and Walker, K. 2005a. The role of central and peripheral mu opioid receptors in inflammatory pain and edema: a study using morphine and DiPOA ([8-(3,3-diphenyl-propyl)-4-oxo-1-phenyl-1,3,8-triaza-spiro[4.5]dec-3-yl]-acetic acid). J. Pharmacol. Exp. Ther. 314, 1234–1240.

Whiteside, G. T., Gottshall, S., Boulet, J. M., Chaffer, S. M., Harrison, J. E., Pearson, J. E., Turchin, P. I., Mark, L., Garrison, A. E., and Valenzano, K. J. 2005b. A role for cannabinoid receptors, but not endogenous opioids in the antinociceptive activity of the CB(2) selective agonist GW405833. Eur. J. Pharmacol. 528, 65–72.

Woodbury, J., Zwick, M., Wang, S., Lawson, J. J., Caterina, M. J., Koltzenbury, M., Albers, K. M., Koerber, H. R., and Davis, B. M. 2004. Nociceptors Lacking TRPV1 and TRPV2 Have Normal Heat Responses. J. Neurosci. 24, 6410–6415.

Woolf, C. J. and Salter, M. W. 2000. Neuronal plasticity: increasing the gain in pain. Science 288, 1765–1769.

Wotherspoon, G. and Winter, J. 2000. Bradykinin B1 receptor is constitutively expressed in the rat sensory nervous system. Neurosci. Letts. 294, 175–178.

Wu, Z. Z., Chen, S. R., and Pan, H. L. 2005. Transient receptor potential vanilloid type 1 activation down-regulates voltage-gated calcium channels through calcium dependent calcineurin in sensory neurons. J. Biol. Chem. 280, 18142–18151.

Yaksh, T. L. 1997. Pharmacology and mechanisms of opioid analgesic activity. Acta Anaesth. Scand. 41, 94–111.

Yaksh, T. L. 2006. Calcium channels as therapeutic targets in neuropathic pain. J. Pain 7, S13–S30.

Yaksh, T. L., Dirig, D. M., Conway, C. M., Svensson, C., Luo, Z. D., and Isakson, P. C. 2001. The acute hyperalgesic action of non-steroidal, anti-inflammatory drugs and release of spinal prostaglandin E2 is mediated by the inhibition of constitutive spinal cyclooxygenase-2 (COX-2) but not COX-1. J. Neurosci. 21, 5847–5853.

Yao, H., Donnelly, D. F., Ma, C., and LaMotte, R. H. 2003. Upregulation of the hyperpolarization-activation cation current after chronic compression of the dorsal root ganglion. J. Neurosci. 23, 2069–2074.

Xiao, W. H. and Bennett, G. J. 1995. Synthetic omega-conopeptides applied to the site of nerve injury suppress neuropathic pains in rats. J. Pharmacol. Exp. Ther. 274, 666–672.

Zhang, J. M., Li, H., and Munir, M. A. 2004. Decreasing sympathetic sprouting in pathological sympathetic ganglia: a new mechanism for treating neuropathic pain using lidocaine. Pain 109, 143–149.

Zhang, J. M., Hoffert, C., Vu, K., Groblewski, T., Ahmad, S., and O'Donnell, D. 2003. Induction of CB2 receptor expression in the rat spinal cord of neuropathic but not inflammatory chronic pain models. Eur. J. Neurosci. 17, 2750–2754.

Zhu, C. Z., Wilson, S. G., Mikusa, J. P., Wismer, C. T., Gauvin, D. M., Lynch, J. J., 3rd., Wade, C. L., Decker, M. W., and Honore, P. 2004. Assessing the role of metabotropic glutamate receptor 5 in multiple nociceptive modalities. Eur. J. Pharmacol. 506, 107–118.

Zweifel, L. S., Kuruvilla, R., and Ginty, D. D. 2005. Functions and mechanisms of retrograde neurotrophin signaling. Nat. Rev. Neurosci. 6, 615–625.

Zylka, M. J., Rise, F. L., and Anderson, D. J. 2005. Topographically distinct epidermal nociceptive circuits revealed by axonal tracers targeted to Mrgprd. Neuron 45, 17–25.

Further Reading

Abdulla, F. A. and Smith, P. A. 2001. Axotomy- and autotomy-induced changes in the excitability of rat dorsal root ganglion neurons. Am. J. Physiol. 85, 630–643.

Cahill, C. M., Morinville, A., Hoffert, C., O'Donnell, D., and Beaudet, A. 2003. Up-regulation and trafficking of delta opioid receptor in a model of chronic inflammation: implications for pain control. Pain 101, 199–208.

Davis, K. D., Treede, R. D., Raja, S. N., Meyer, R. A., and Campbell, J. N. 1991. Topical application of clonidine relieves hyperalgesia in patients with sympathetically maintained pain. Pain 47, 309–317.

Dray, A. 1994. Tasting the inflammatory soup: the role of peripheral neurones. Pain Rev. 1, 153–171.

Ferreira, J., Campos, M. M., Pesquero, J. B., Araujo, R. C., Bader, M., and Calixto, J. B. 2001. Evidence for the participation of kinins in Freund's adjuvant induced inflammatory and nociceptive responses in kinin B1 and B2 knockout mice. Neuropharmacology 41, 1006–1012.

Hao, S., Mta, M., and Goins, W. 2003. Transgene-mediated enkephaline release enhances the effect of morphine and evades tolerance to produce a sustained antiallodynic effect. Pain 102, 135–142.

Kim, S. F., Huri, D. A., and Snyder, S. H. 2005. Inducible nitric oxide synthase binds, N-nitrosylates and activates cyclooxygenase-2. Science 310, 1966–1970.

Kress, M., Izydorcyk, I., and Kuhn, A. 2001. N- and L-but not P/Q-type calcium channels contribute to neuropeptide release from rat skin *in vitro*. Neuroreport 12, 867–870.

Ossovskaya, V. S. and Bunnett, N. W. 2003. Protease-activated receptors: contribution to physiology and disease. J. Physiol. 552, 589–601.

5.54 Forebrain Opiates

J-K Zubieta, University of Michigan, Ann Arbor, MI, USA

© 2008 Elsevier Inc. All rights reserved.

5.54.1	Introduction	821
5.54.2	Endogenous Opioid Mechanisms in the Regulation of Pain	821
5.54.2.1	μ-Opioid-Receptor-Mediated Pain Processing	821
5.54.2.2	κ-Opioid-Receptor-Mediated Processing	824
5.54.2.3	δ-Opioid-Receptor-Mediated Processing	825
5.54.2.4	Opioid Receptor-like (ORL-1, NOP Receptor)-Mediated Processing	826
References		827

5.54.1 Introduction

The initial studies on the neurobiology of pain and the discovery and understanding of the endogenous opioid systems have been historically intrinsically linked. In the 1960s, early research by Liebeskind and coworkers (Mayer, D. J. *et al.*, 1971) demonstrated that the electrical stimulation of the ventral periaqueductal and periventricular gray produced profound analgesia, an effect that was independently observed by Reynolds D. V. (1969). During the same time, Tsou K. and Jang C. S. (1964) observed similar analgesic effects when morphine was microinjected into these locations. As a consequence, and before opioid receptors or their ligands had been isolated, Mayer D. J. *et al.* (1971) proposed that electrical stimulation induced analgesia by activating neural substrates that are involved in the blockage of pain and that were related to the analgesic action of morphine. These observations were followed by the subsequent use of electrical stimulation of the posterior aspect of the paraventricular nucleus of the thalamus for the treatment of pain (Richardson, D. E. and Akil, H., 1977a; 1977b). In 1973, Snyder and Pert published the first manuscript demonstrating the existence of opioid receptors (Pert, C. B. and Snyder, S. H., 1973), a development that was paralleled by the work of Eric Simon (Simon, E. J. *et al.*, 1973) and Lars Terenius (Terenius, L., 1973). These initial findings were followed by the identification of met- and leu-enkephalin (Hughes, J. *et al.*, 1975), β-endorphin (Li, C. H. *et al.*, 1976; Loh, H. H. *et al.*, 1976), and the dynorphin peptides (Goldstein, A. *et al.*, 1979). The 1990s saw the cloning of the opioid receptors delta (δ) (Evans, C. J. *et al.*, 1992; Kieffer, B. L. *et al.*, 1992), mu (μ) (Chen, Y. *et al.*, 1993; Thompson, R. C. *et al.*, 1993), and kappa (κ) (Li, S. *et al.*, 1993; Meng, F. *et al.*, 1993). These are seven transmembrane domain G-protein-coupled receptors inhibiting adenyl cyclase and modulating calcium and potassium conductance.

5.54.2 Endogenous Opioid Mechanisms in the Regulation of Pain

5.54.2.1 μ-Opioid-Receptor-Mediated Pain Processing

This chapter will cover the regulation of pain by supraspinal opioid systems. Investigation of these mechanisms has been most extensive for those pertaining to the μ-opioid receptor, as this is the site of action of opiate analgesics and the receptor most consistently associated with pain suppression. Knockout animals devoid of these receptors display shorter latencies in the tail flick and hot plate tests, thought to involve spinal and supraspinal mechanisms, respectively, as well as a lack of morphine effects (Sora, I. *et al.*, 1997). Its endogenous ligands include β-endorphin, derived from the peptide precursor proopiomelanocortin (POMC), the recently described endomorphins 1 and 2, and in some circuits, the enkephalins (cleaved from the larger preproenkephalin precursor). POMC-containing neurons are located in the arcuate nucleus of the hypothalamus and periarcuate regions of the medial-basal hypothalamus, with a smaller group localized in the nucleus of the tractus solitarius of the medulla. Projections are extensive to the periventricular thalamus, septum, and amygdala, dorsally descending to the periaqueductal gray (PAG), midline

raphe, and reticular formation, and laterally to the anterior and lateral hypothalamus. Lighter innervation is observed in the medial portion of the nucleus accumbens and olfactory cortex (Khachaturian, H. *et al.*, 1985). Animals devoid of a functioning POMC gene show a lack of naloxone-reversible analgesia induced by mild swim stress, but greater nonopioid (naloxone nonreversible) analgesic effects and normal effects of morphine. These data demonstrated the involvement of β-endorphin in stress-induced analgesic responses, while also highlighting the presence of alternate mechanisms not mediated by β-endorphin and μ-opioid receptors (Rubinstein, M. *et al.*, 1996).

In contrast to the narrow localization of POMC-containing cells, enkephalinergic cells and projections are widely distributed, forming both local circuits and long projections, with similar distributions for met- and leu-enkephalin, albeit with a higher level of met-enkephalin in all regions. The highest concentrations of terminals with these peptides are encountered in the globus pallidus and central and lateral amygdala nuclei. Globus pallidus and ventral pallidal projections form part of the enkephalinergic striatopallidal pathway, with cell bodies arising primarily in the nucleus accumbens and to a lesser extent in the ventromedial hypothalamus. Cell bodies containing preproenkephalin are also encountered in the olfactory bulb, septal nuclei, bed nucleus of the stria terminalis, throughout the basal ganglia and in the cortex. Terminal densities are moderate to dense in the cingulate, piriform, and entorhinal cortex, anterior and periventricular thalamus, and preoptic hypothalamus (the latter from both local projections and terminals arising from the amygdala and periamygdalar area). Both cell bodies and rich local projections are encountered in the PAG, raphe, locus coeruleus, nucleus ambiguus, and nucleus of the solitary tract (Petrusz, P. *et al.*, 1985). Enkephalin-deficient mice display large increases in the concentration of μ-opioid receptors in the globus pallidus, central nucleus of the amygdala, bed nucleus of the stria terminalis and substantia innominata, preoptic, medial and lateral hypothalamus, medial thalamus, PAG, raphe, nucleus ambiguus, and nucleus of the tractus solitarius, suggesting substantial enkephalinergic activity on μ-opioid receptors in these regions, with compensatory upregulation in the knockouts (Brady, L. S. *et al.*, 1999). Enkephalin-deficient mice display reductions in supraspinal analgesic responses as measured with the hot-plate test and rapid nocifensive responses in the formalin assay, but unaltered spinal analgesic responses (tail-flick test) and stress-induced analgesia (Konig, M. *et al.*, 1996).

Last, the most recently identified family of opioid peptides, the endomorphins 1 and 2, and in a manner similar to that for β-endorphin, is synthesized in the brain only in hypothalamic cells (periventricular, arcuate, and ventromedial and dorsomedial nuclei), and project to pain-processing regions of the brainstem and pons (trigeminal tract, parabrachial nucleus, nucleus of the tractus solitarious, PAG, and locus coeruleus) as well as to midline thalamic nuclei and the amygdala. Besides the hypothalamic cell bodies, the only other known areas containing endomorphin-positive cell bodies include the nucleus of the tractus solitarius and the dorsal root ganglia. Consistent with its actions at μ-opioid receptors, intracerebroventricular administration of endomorphins induces profound analgesia that may be dissociated from the rewarding properties associated with μ-opioid receptor agonists (Zadina, J. E., 2002).

Initial studies on the role of supraspinal μ-opioid-receptor-mediated antinociception focused on the role of the PAG and its connections with the rostroventral medulla (RVM). These are regions that, together with the dorsolateral pontine tegmentum, control nociceptive transmission via projections through the spinal cord dorsolateral funiculus to the dorsal horn laminae (Fields, H. L. and Basbaum, A. I., 1978). Much of the focus during the following decades was then dedicated to the understanding of the mechanisms underlying this modulation. Both pain facilitatory and inhibitory cells have been described at the level of the RVM (Moreau, J. L. and Fields, H. L., 1986; Heinricher, M. M. *et al.*, 1987; Urban, M. O. and Smith, D. J., 1994; Zhuo, M. and Gebhart, G. E., 1997). μ-Opioid receptors, through the activation of enkephalinergic neurotransmission and GABA interneurons in the PAG and RVM (al-Rodhan, N. *et al.*, 1990), increase the activity of inhibitory (off) cells reducing pain transmission. The administration of μ-opioid receptor agonists systemically, or directly into the PAG or RVM, increases the activity of these off cells, with blockade of the activation of these neurons preventing morphine's antinociceptive effects (Heinricher, M. M. *et al.*, 1999). Not surprisingly, in view of these results, the possible role of μ-opioid neurotransmission beyond the PAG, RVM, and descending pathways into the spinal cord (e.g., supraspinal mechanisms) was thought to be less critical and mostly regarded as secondary to the analgesia mediated primarily by brainstem and spinal cord regions.

Nevertheless, examination of the distribution of μ-opioid receptors, mRNA in the rodent (Mansour,

A. *et al.*, 1995) and *in vivo* μ-opioid receptor availability in the human brain (Frost, J. *et al.*, 1985) demonstrate a broad distribution of these sites in telencephalic areas. Administration of μ-opioid receptor agonists increases the blood flow of brain regions rich in μ-opioid receptors (cingulate, prefrontal, temporal and insular cortices, thalamus, hypothalamus, basal ganglia, amygdala, and brainstem) (Adler, L. J. *et al.*, 1997; Schlaepfer, T. *et al.*, 1998; Casey, K. *et al.*, 2000; Wagner, K. J. *et al.*, 2001), and reduces pain-induced activation in the thalamus (Casey, K. *et al.*, 2000). Some of these areas, such as thalamic and hypothalamic nuclei, the central nucleus of the amygdala, the agranular insular cortex and lateral orbitofrontal cortex, have been associated with the suppression of pain behavior in animal models (Mayer, D. J. and Liebeskind, J. C., 1974; Yaksh, T. L. and Rudy, T. A., 1978; Bodnar, R. J. *et al.*, 1980; Coffield, J. A. *et al.*, 1992; Burkey, A. R. *et al.*, 1996; Manning, B., 1998; Manning, B. and Franklin, K., 1998; Harte, S. *et al.*, 2000; Manning, B. H. *et al.*, 2001). However, the inhibition of pain signaling elicited by the activation of μ-opioid receptors in these supraspinal regions is thought to take place through their connections with the PAG, since inactivation of the PAG or the administration of opioid antagonists in this area abolishes the analgesic response. In turn, PAG-induced analgesia is blocked by μ-opioid receptor antagonists microinjected in the RVM, then reducing nociceptive transmission from the spinal cord (Kiefel, J. M. *et al.*, 1993; Roychowdhury, S. M. and Fields, H. L., 1996).

In view of the critical role of the PAG and RVM on μ-opioid-receptor-mediated antinociception, perhaps the question to be answered regarding the involvement of opioid systems in supraspinal nuclei is their respective role in the experience of pain as a complex phenomenon. Opioid neurotransmission is activated in humans during clinical pain, or experimental pain of some duration, as evidenced by enhancements in pain ratings after the administration of naloxone, a nonselective opioid receptor antagonist (Levine, J. *et al.*, 1978). Conversely, experimental pain of relatively short duration (e.g., <10 min) does not elicit an apparent activation of opioid neurotransmission, evidenced by a lack of increases in pain ratings after naloxone administration (Grevert, P., and Goldstein, A., 1977). These findings are similar to those observed in response to nonpainful stressors, whereby prolonged or unpredictable stimuli activate opioid neurotransmission, leading to the term stress-induced analgesia (Madden, J. T. *et al.*, 1977; Watkins, L. and Mayer, D., 1982). It is therefore possible that the progressive engagement of supraspinal μ-opioid mechanisms may be of greater importance for the control of noxious stimuli as it progresses from a relatively simple sensory experience to one that requires the assessment of its significance and an appropriate response by the organism.

Two studies have examined the activity of μ-receptor-mediated opioid neurotransmission in humans during the experience of pain. Both studies employed the μ-opioid-receptor-selective radiotracer [^{11}C]carfentanil and positron emission tomography. Bencherif B. *et al.* (2002) utilized the capsaicin model of experimental pain, while in Zubieta J. K. *et al.* (2001), jaw muscle pain was induced by the intramuscular infusion of hypertonic saline. The former, in a smaller sample, showed evidence of activation of μ-opioid-receptor-mediated neurotransmission in the thalamus. In the latter, engagement of this neurotransmitter system was observed in a number of brain areas, including the PAG, dorsal and rostral anterior cingulate, dorsolateral prefrontal cortex, anterior and posterior insular cortex, medial and lateral thalamus, hypothalamus, ventral basal ganglia, and amygdala. Invariably, the relationship between μ-opioid activation and subjective ratings of pain was in the negative direction (the larger the activation the lower the pain ratings), with sensory or pain affect elements being modulated by different regions. Some of these regions had been previously implicated in opioid-mediated suppression of nociceptive responses in animal models (e.g., PAG, thalamus, hypothalamus, amygdala, and to a lesser extent areas of the insular cortex), as noted above. Conversely, while pain-induced increases in synaptic activity of the prefrontal cortex (Baron, R. *et al.*, 1999; Lorenz, J. *et al.*, 2002) and dorsal anterior cingulate cortex (Rainville, P. *et al.*, 1997) had been described and associated with hyperalgesia and pain affect, respectively, the involvement of the endogenous opioid system on these processes had not been previously explored. Similarly, the ventral basal ganglia (nucleus accumbens, ventral pallidum) have been typically associated with either responses to natural rewards or drugs of abuse, stress, or, as is more recently postulated, with salient stimuli irrespective of its valence (Horvitz, J., 2000). These data then appear to indicate that, besides its traditional role in the modulation of descending inhibitory pathways into the PAG and RVM, supraspinal μ-opioid receptors are additionally involved in the local

processing of complex assessments of the pain experience. In this regard, μ-opioid receptors appear implicated in regulating emotional responses, as examined in knockout rodents devoid of these receptors. These animals display an enhancement of anxiety-like responses in the elevated arm maze (Filliol, D. *et al.*, 2000) and deficits in attachment behavior (Moles, A. *et al.*, 2004). Proenkephalin knockouts also show a lack of conditioned place aversion to naloxone (Skoubis, P. D. *et al.*, 2005), increased aggressive behavior to an intruder and anxiety-like behavior in the open arm maze, as well as alterations in supraspinal but not spinal pain processing (Konig, M. *et al.*, 1996), additionally involving this neurotransmitter system in emotional behavioral responses.

Work in humans has also shown that in the case of some of the brain regions in which μ-opioid systems become active during pain (e.g., rostral anterior cingulate, dorsolateral prefrontal cortex, nucleus accumbens, and insular cortex), cognitive expectations associated with the administration of a placebo with expected analgesic properties are also capable of activating this neurotransmitter system to mediate the placebo analgesic effect (Benedetti, F. *et al.*, 2005; Zubieta, J. K. *et al.*, 2005).

A relatively less explored area in the understanding of μ-opioid receptor modulation of pain is the additional influences of age and gonadal steroids (e.g., sex effects). In rodents, age-associated declines in μ-opioid receptor concentrations have been reported (Piva, F. *et al.*, 1987). However, humans demonstrate opposite effects, with increases in most brain regions shown in postmortem material (Gross-Isseroff, R. *et al.*, 1990; Gabilondo, A. *et al.*, 1995) and in neuroimaging studies (Zubieta, J. K. *et al.*, 1999), albeit the psychophysical correlates of these changes in receptor concentrations have not been determined. In human subjects, women further demonstrate declines in μ-opioid receptor levels after menopause (Zubieta, J. K. *et al.*, 1999). In this regard, trophic effects of estradiol have been shown at the level of μ-opioid receptor levels and their mRNA, POMC content, and β-endorphin release in animal models (Hammer, R. P. and Bridges, R. S., 1987; Dondi, D. *et al.*, 1992; Quinones-Jenab, V. *et al.*, 1997; Eckersell, C. *et al.*, 1998). The clinical implications of these effects have not been well developed, albeit sex differences have been observed in the effects of μ-opioid receptor agonists, including their side effects and cardiovascular parameters, which appear to be more prominently affected in women (Zacny, J. P., 2001; Fillingim, R. B. and Gear, R. W., 2004). A less prominent activation of μ-opioid-receptor-mediated neurotransmission, as measured with neuroimaging techniques, has been shown in women studied under conditions of low estradiol, low progesterone during an experimental pain challenge (Zubieta, J. K. *et al.*, 2002). This effect, observed in the thalamus, amygdala, and nucleus accumbens, was reversed after selectively increasing estradiol plasma levels, which also increased μ-opioid receptor concentrations in these regions (Smith, Y. R. *et al.*, 2006). These data then suggest an active regulation of μ-opioid-receptor-mediated mechanisms by gonadal steroids.

5.54.2.2 κ-Opioid-Receptor-Mediated Processing

The prodynorphin-derived peptides, which present the highest affinity and colocalization with κ-opioid receptors, consist of extended forms of leu-enkephalin coded by a different gene and mRNA. These peptides include dynorphin A, B, and neoendorphins α and β (Goldstein, A. *et al.*, 1979). Their involvement in pain regulatory mechanisms has been controversial, as both anti- and pronociceptive responses have been described in response to κ-agonists depending on the brain regions studied. Similarly to β-endorphin and endomorphin systems, there is a dense accumulation of dynorphin-containing cells in the multiple regions of the hypothalamus, forming both local circuits and longer projections, particularly to the amygdala and descending to brainstem, pontine, and medullary/spinal regions (e.g., PAG, but also substantia nigra). However, and closer to the distribution of the enkephalin peptides, cell bodies are also encountered in limbic areas of the cortex, such as the anterior cingulate, orbitofrontal, insular, periamygdaloid, and entorhinal cortex, in the basal ganglia (caudate, putamen, globus pallidus), nucleus accumbens, amygdala, particularly in its central nucleus, PAG, raphe nuclei, locus coeruleus, nucleus ambiguus, and nucleus of the solitary tract. Long pathways have been described from the striatum to the substantia nigra and ventral pallidum, as well as from the amygdala to brainstem and pons regions. Minimal innervation of the thalamus has been observed, which is confined to midline and intralaminar nuclei (Fallon, J. and Ciofi, P., 1990). Mice devoid of the dynorphin gene show an upregulation of κ-receptors in the nucleus accumbens shell and core, hypothalamus, amygdala, and substantia

nigra, consistent with their high level of dynorphin innervation, and suggesting an active role of this peptide in the modulation of the κ-receptors in these brain regions (Clarke, S. *et al.*, 2003).

Intrathecal administration of κ-opioid agonists or their microinjection in the RVM has been shown to result in antinociceptive responses in various rat models (Harada, Y. *et al.*, 1995; Ackley, M. A. *et al.*, 2001), albeit modest, and typically requiring high doses. These effects have also been demonstrated to be sex dimorphic, with female rats demonstrating a more profound analgesic effect than the males in the tail-flick test (Tershner, S. A. *et al.*, 2000). In κ-receptor knockout animals, female but not male rats demonstrate decreased withdrawal latencies in the tail-immersion test, compared to wild-type animals (Martin, M. *et al.*, 2003). Consistent with these findings, one study has shown a preferential antinociceptive effect of opiates with κ-opioid activity in women, with respect to men, after surgical extraction of the third molar (Gear, R. *et al.*, 1996).

κ-Opioid agonists, however, have also been shown to antagonize morphine analgesia, by the hyperpolarization of pain-inhibitory cells activated by μ-opioid receptors in the RVM (Pan, Z. Z. *et al.*, 1997; Meng, I. D. *et al.*, 2005). Therefore pronociceptive, antianalgesic effects of κ-opioids may exist simultaneously with antinociceptive activity, depending on the brain regions involved or the existing level of μ-opioid receptor activity. Opposing effects of μ- and κ-receptors have also been shown at the level of the medial thalamus, whereby microinjection of μ-agonists increased, and κ-agonists reduced, the thresholds for pain-induced vocalization and motor responses in male rodents (Carr, K. D. and Bak, T. H., 1988). Dynorphin also appears to be involved in the maintenance of hyperalgesia and persistent pain, with only spinal mechanisms having been investigated at this time (Wang, Z. *et al.*, 2001).

Dynorphin and κ-opioid agonists further antagonize dopamine release in the basal ganglia (Zhang, Y. *et al.*, 2004), whether induced by μ-opioid receptor agonists, psychostimulants, or stressors, by the inhibition of dopamine (DA) cells in the ventral tegmental area and substantia nigra or possibly indirectly through the regulation of DA reuptake at the level of the nucleus accumbens (Thompson, A. C. *et al.*, 2000; Margolis, E. B. *et al.*, 2003; McLaughlin, J. P. *et al.*, 2003; Narita, M. *et al.*, 2005). Dopaminergic mechanisms, typically associated with responses to drugs of abuse and more generally to salient stimuli regardless of its valence, have been found dysregulated in chronic pain patients, albeit the clinical consequences of these alterations are presently unknown (Hagelberg, N. *et al.*, 2004).

5.54.2.3 δ-Opioid-Receptor-Mediated Processing

The enkephalins are thought to be the endogenous ligand for the δ-opioid receptor, in addition to acting on μ-opioid receptors, as noted above. Their distribution was described in this chapter under Section 5.54.2.1. Knockout mice devoid of the enkephalin gene display increases in the regional concentration of μ- and δ-opioid receptors (Brady, L. S. *et al.*, 1999), suggesting an effect of this peptide in both receptor systems. In the case of the δ-receptor, these increases were observed in the caudate–putamen, nucleus accumbens core and shell, ventral pallidum, globus pallidus, the central nucleus of the amygdala, preoptic area, and lateral hypothalamus. Microinjection of δ-receptor agonists in the PAG and medullary reticular formation has been shown to induce antinociception (Jensen, T. S. and Yaksh, T. L., 1986). Their intracerebroventricular administration has also been shown to have antinociceptive properties in tests of spinal and supraspinal nociceptive mechanisms in wild-type and μ-opioid-receptor-deficient mice (Porreca, F. *et al.*, 1984; Vaught, J. L. *et al.*, 1988; Ossipov, M. H. *et al.*, 1995). Rodent, primate, and human δ-opioid receptors are uniformly distributed throughout the cortex, diffusely in the striatum, and moderately to densely in the nucleus accumbens, ventral pallidum, hippocampus, amygdala, medial thalamus, hypothalamus, PAG, and raphe nuclei. Low concentrations are observed in lateral thalamic nuclei and the cerebellum (Lewis, M. E. *et al.*, 1981; 1983; Moskowitz, A. S. and Goodman, R. R., 1985; Smith, J. S. *et al.*, 1999; Cahill, C. M. *et al.*, 2001b). This distribution, which emphasizes a limbic and paralimbic organization as well as its relationship with pain circuitry, has suggested the involvement of this receptor and neurotransmitter system in emotional and stress regulation in addition to antinociceptive mechanisms. Regarding the latter, δ-opioid-receptor-agonist-induced analgesia and respiratory depression has been shown either reduced (Matthes, H. W. *et al.*, 1998) or in some cases abolished (Scherrer, G. *et al.*, 2004), depending on the assays employed, in animals devoid of μ-opioid receptors. These results then suggested the presence of functional interactions between μ- and δ-opioid-receptor types. Conversely, δ-opioid

stress-induced analgesia after forced swim stress was found maintained in μ-opioid receptor knockout mice. These data supported a lack of interactions between μ- and δ-opioid receptors when endogenous opioid transmission was activated by a stressor, as opposed to exogenously administered agonists. However, and in the same studies, two phases of the stress-induced analgesia were observed, one early response mediated by δ-opioid receptors, and a later response that was abolished in the μ-opioid receptor knockouts and unaffected by δ-opioid receptor antagonists (LaBuda, C. J. *et al.*, 2000).

Utilizing single, double, and triple knockouts for μ-, κ-, and δ-opioid receptors Martin M. *et al.* (2003) have suggested that δ-opioid receptors, together with μ-opioid receptors, were involved in mechanical nociception and some, but not other phases of inflammatory pain. Besides their independent functions, interactions between μ- and δ-receptors have also been demonstrated at various levels. Treatment with μ-opioid agonists has been shown to increase the concentration of membrane-bound δ-receptors in the spinal cord by increasing their trafficking from intracellular sites, an effect that was abolished in μ-opioid receptor knockout animals (Cahill, C. M. *et al.*, 2001a; Morinville, A. *et al.*, 2003). Furthermore, interacting complexes of μ- and δ-receptors (heterodimers) have been demonstrated in spinal cord and neuroblastoma cell lines, as well as synergistic interactions in analgesic effects between the two receptor types (Gomes, I. *et al.*, 2004).

Regarding other possible effects of δ-opioid neurotransmission, stressors have been shown to decrease the concentration of δ-opioid receptors in limbic areas of the rat (Fadda, P. *et al.*, 1991) and increase that of enkephalin mRNA in the ventral medulla (Mansi, J. A. *et al.*, 2000) and hypothalamus (Helmreich, D. L. *et al.*, 1999; Dumont, E. C. *et al.*, 2000), confirming their involvement in the modulation of the stress response, albeit not in its neuroendocrine components, at least in primates (Williams, K. L. *et al.*, 2003). Antidepressant-like effects have also been demonstrated in animal models of depression, suggesting the participation of this system in complex behavioral functions (Jutkiewicz, E. M. *et al.*, 2003; Torregrossa, M. M. *et al.*, 2004).

5.54.2.4 Opioid Receptor-like (ORL-1, NOP Receptor)-Mediated Processing

The opioid receptor-like (ORL1) receptor (now denominated NOP) is the most recently identified opioid receptor, with high homology with other opioid receptors, but does not bind to traditional opioid peptides. It is present in high concentrations in the septum, diagonal band of Broca, hypothalamus (preoptic, arcuate, paraventricular, ventromedial), hippocampus, medial amygdala, substantia nigra, locus coeruleus, raphe nuclei, PAG, as well as in the dorsal and ventral horns of the spinal cord and in the trigeminal nucleus. It is also moderately concentrated in the thalamus, cortex (olfactory, cingulate, claustrum, and frontoparietal areas), the shell of the nucleus accumbens, and islets of Calleja. Low levels are observed in the caudate–putamen, core of the nucleus accumbens, and cerebellum (Mollereau, C. *et al.*, 1994). The 17-amino acid peptide orphanin FQ/nociceptin (OFQ/N), the endogenous ligand for this receptor, was subsequently isolated. It presented high homology with opioid peptide transmitters, particularly dynorphin (Meunier, J. C. *et al.*, 1995; Reinscheid, R. K. *et al.*, 1995). This peptide is synthesized as part of a larger precursor, preproOFQ/N, with a distribution largely overlapping with that of the NOP receptor in the rat brain (Mollereau, C. *et al.*, 1996; Darland, T. *et al.*, 1998). Like opioid agonists, OFQ/N inhibits adenylate cyclase and calcium channels, and induces an inhibitory effect on postsynaptic neurons by opening potassium channels and hyperpolarization (Hawes, B. E. *et al.*, 2000; Moran, T. D. *et al.*, 2000). This inhibitory effect has been invoked in explaining the often-times contradictory effects of generalized routes of OFQ/N peptide administration (e.g., intracerebroventricular) (Darland, T. *et al.*, 1998). For example, initial reports described increases in pain behavior (Meunier, J. C. *et al.*, 1995; Reinscheid, R. K. *et al.*, 1995), no effect on pain responses (Mogil, J. S. *et al.*, 1996a; 1996b; Tian, J. H. *et al.*, 1997), or even hyperalgesia (Rossi, G. C. *et al.*, 1996; 1997), and a reversal of the analgesic actions of morphine and endogenous opioid peptides (Mogil, J. S. *et al.*, 1996a; 1996b). It is thought that these effects depend on the populations of cells being inhibited, as OFQ/N can hyperpolarize neurons that both facilitate and inhibit pain signal transmission at the level of the RVM (Heinricher, M. M. *et al.*, 1997), as well as most of the neuronal populations rich in the NOP receptor (e.g., hypothalamus, medulla, hippocampus, amygdala, ventral tegmental area, locus coeruleus, and PAG) (see Heinricher, M. M., 2003 for a recent review). Using data acquired by the microinjection of OFQ/N in the RVM, Heinricher M. M. *et al.* (1997) proposed that the behavioral effects of this peptide depend on the state of activity of the output neurons affected by the peptide. Under conditions of stimulation (opioid withdrawal,

stress, and opioid agonist effects) the effects of OFQ/N would oppose the state of activation in the relevant circuits, inducing an opposing effect, with additional influencing variables, such as sex or genotype, also suggested to influence its effects (Mogil, J. S. and Pasternak, G. W., 2001; Flores, C. A. *et al*., 2003). On the other hand, and during basal states, OFQ/N effects would be minimal (Heinricher, M. M. *et al*., 1997). Consistent with these findings, OFQ/N enhanced stress-induced ACTH production at the level of the pituitary and plasma corticosterone, an effect that in this case was also observed to a lesser extent in nonstressed animals (Devine, D. P. *et al*., 2001). Knockout rodents devoid of either OFQ/N or NOP receptors do not appear to have significant changes in nociceptive responses or changes in opiate analgesia under nonstimulated conditions (Nishi, M. *et al*., 1997; Koster, A. *et al*., 1999; Kest, B. *et al*., 2001; Mamiya, T. *et al*., 2001). In a neuropathic pain model, NOP mRNA expression increased in pain regulatory circuitry (raphe magnus, PAG, and RVM), albeit the behavioral consequences of these increases have not been explored (Ma, F. *et al*., 2005).

References

Ackley, M. A., Hurley, R. W., Virnich, D. E., and Hammond, D. L. 2001. A cellular mechanism for the antinociceptive effect of a kappa opioid receptor agonist. Pain 91, 377–388.

Adler, L. J., Gyulai, F. E., Diehl, D. J., Mintun, M. A., Winter, P. M., and Firestone, L. L. 1997. Regional brain activity changes associated with fentanyl analgesia elucidated by positron emission tomography. Anesth. Analg. 8, 4120–126.

Baron, R., Baron, Y., Disbrow, E., and Roberts, T. P. 1999. Brain processing of capsaicin-induced secondary hyperalgesia: a functional MRI study. Neurology 53, 548–557.

Bencherif, B., Fuchs, P. N., Sheth, R., Dannals, R. F., Campbell, J. N., and Frost, J. J. 2002. Pain activation of human supraspinal opioid pathways as demonstrated by [^{11}C]-carfentanil and positron emission tomography (PET). Pain 99, 589–598.

Benedetti, F., Mayberg, H. S., Wager, T. D., Stohler, C. S., and Zubieta, J. K. 2005. Neurobiological mechanisms of the placebo effect. J. Neurosci. 25, 10390–10402.

Bodnar, R. J., Kelly, D. D., Brutus, M., and Glusman, M. 1980. Stress-induced analgesia: neural and hormonal determinants. Neurosci. Biobehav. Rev. 4, 87–100.

Brady, L. S., Herkenham, M., Rothman, R. B., Partilla, J. S., Konig, M., Zimmer, A. M., and Zimmer, A. 1999. Region-specific up-regulation of opioid receptor binding in enkephalin knockout mice. Brain Res. Mol. Brain Res. 68, 193–197.

Burkey, A. R., Carstens, E., Wenniger, J. J., Tang, J., and Jasmin, L. 1996. An opioidergic cortical antinociception triggering site in the agranular insular cortex of the rat that contributes to morphine antinociception. J. Neurosci. 16, 6612–6623.

Cahill, C. M., Morinville, A., Lee, M. C., Vincent, J. P., Collier, B., and Beaudet, A. 2001a. Prolonged morphine treatment targets delta opioid receptors to neuronal plasma membranes and enhances delta-mediated antinociception. J. Neurosci. 21, 7598–7607.

Cahill, C. M., McClellan, K. A., Morinville, A., Hoffert, C., Hubatsch, D., O'Donnell, D., and Beaudet, A. 2001b. Immunohistochemical distribution of delta opioid receptors in the rat central nervous system: evidence for somatodendritic labeling and antigen-specific cellular compartmentalization. J. Comp. Neurol. 440, 65–84.

Carr, K. D. and Bak, T. H. 1988. Medial thalamic injection of opioid agonists: mu-agonist increases while kappa-agonist decreases stimulus thresholds for pain and reward. Brain Res. 441, 173–184.

Casey, K., Svensson, P., Morrow, T., Raz, J., Jone, C., and Minoshima, S. 2000. Selective opiate modulation of nociceptive processing in the human brain. J. Neurophysiol. 84, 525–533.

Chen, Y., Mestek, A., Liu, J., Hurley, J. A., and Yu, L. 1993. Molecular cloning and functional expression of a mu-opioid receptor from rat brain. Mol. Pharmacol. 44, 8–12.

Clarke, S., Zimmer, A., Zimmer, A. M., Hill, R. G., and Kitchen, I. 2003. Region selective up-regulation of micro-, delta- and kappa-opioid receptors but not opioid receptor-like 1 receptors in the brains of enkephalin and dynorphin knockout mice. Neuroscience 122, 479–489.

Coffield, J. A., Bowen, K. K., and Miletic, V. 1992. Retrograde tracing of projections between the nucleus submedius, the ventrolateral orbital cortex, and the midbrain in the rat. J. Comp. Neurol. 321, 488–499.

Darland, T., Heinricher, M. M., and Grandy, D. K. 1998. Orphanin FQ/nociceptin: a role in pain and analgesia, but so much more. Trends Neurosci. 21, 215–221.

Devine, D. P., Watson, S. J., and Akil, H. 2001. Nociceptin/orphanin FQ regulates neuroendocrine function of the limbic–hypothalamic–pituitary–adrenal axis. Neuroscience 102, 541–553.

Dondi, D., Limonta, P., Maggi, R., and Piva, F. 1992. Effects of ovarian hormones on brain opioid binding sites in castrated female rats. Am. J. Physiol. 263, E507–E511.

Dumont, E. C., Kinkead, R., Trottier, J. F., Gosselin, I., and Drolet, G. 2000. Effect of chronic psychogenic stress exposure on enkephalin neuronal activity and expression in the rat hypothalamic paraventricular nucleus. J. Neurochem. 75, 2200–2211.

Eckersell, C., Popper, P., and Micevych, P. 1998. Estrogen-induced alteration of μ-opioid receptor immunoreactivity in the medial preoptic nucleus and medial amygdala. J. Neurosci. 18, 3967–3976.

Evans, C. J., Keith, D. E., Jr., Morrison, H., Magendzo, K., and Edwards, R. H. 1992. Cloning of a delta opioid receptor by functional expression. Science 258, 1952–1955.

Fadda, P., Tortorella, A., and Fratta, W. 1991. Sleep deprivation decreases mu and delta opioid receptor binding in the rat limbic system. Neurosci. Lett. 129, 315–317.

Fallon, J. and Ciofi, P. 1990. Dynorphin Containing Neurons. In: Handbook of Chemical Neuroanatomy (*eds*. A. Björklund, T. Hökfelt, and M. Kuhar), pp. 1–130. Elsevier.

Fields, H. L. and Basbaum, A. I. 1978. Brainstem control of spinal pain-transmission neurons. Annu. Rev. Physiol. 40, 217–248.

Fillingim, R. B. and Gear, R. W. 2004. Sex differences in opioid analgesia: clinical and experimental findings. Eur. J. Pain 8, 413–425.

Filliol, D., Ghozland, S., Chluba, J., Martin, M., Matthes, H., Simonin, F., Befort, K., Gaveriaux-Ruff, C., Dierich, A., Le, M. M., Valverde, O., Maldonado, R., and Kieffer, B. 2000. Mice deficient for delta- and mu-opioid receptors exhibit

opposing alterations of emotional responses. Nat. Genet. 25, 195–200.
Flores, C. A., Shughrue, P., Petersen, S. L., and Mokha, S. S. 2003. Sex-related differences in the distribution of opioid receptor-like 1 receptor mRNA and colocalization with estrogen receptor mRNA in neurons of the spinal trigeminal nucleus caudalis in the rat. Neuroscience 118, 769–778.
Frost, J., Wagner, H. J., Dannals, R., Ravert, H., Links, J., Wilson, A., Burns, H., Wong, D., McPherson, R., and Rosenbaum, A., *et al.* 1985. Imaging opiate receptors in the human brain by positron tomography. J. Comput. Assist. Tomogr. 9, 231–236.
Gabilondo, A., Meana, J., and Garcia-Sevilla, J. 1995. Increased density of mu-opioid receptors in the postmortem brain of suicide victims. Brain Res. 682, 245–250.
Gear, R., Miaskowski, C., Gordon, N., Paul, S., Heller, P., and Levine, J. 1996. Kappa-opioids produce significantly greater analgesia in women than in men. Nat. Med. 2, 1248–1250.
Goldstein, A., Tachibana, S., Lowney, L. I., Hunkapiller, M., and Hood, L. 1979. Dynorphin-(1–13), an extraordinarily potent opioid peptide. Proc. Natl. Acad. Sci. U. S. A. 76, 6666–6670.
Gomes, I., Gupta, A., Filipovska, J., Szeto, H. H., Pintar, J. E., and Devi, L. A. 2004. A role for heterodimerization of mu and delta opiate receptors in enhancing morphine analgesia. Proc. Natl. Acad. Sci. U. S. A. 101, 5135–5139.
Grevert, P. and Goldstein, A. 1977. Effects of naloxone on experimentally induced ischemic pain and on mood in human subjects. Proc. Natl. Acad. Sci. U. S. A. 74, 1291–1294.
Gross-Isseroff, R., Dillon, K., Israeli, M., and Biegon, A. 1990. Regionally selective increases in mu opioid receptor density in the brains of suicide victims. Brain Res. 530, 312–316.
Hagelberg, N., Jaaskelainen, S. K., Martikainen, I. K., Mansikka, H, Forssell, H., Scheinin, H., Hietala, J., and Pertovaara, A. 2004. Striatal dopamine D2 receptors in modulation of pain in humans: a review. Eur. J. Pharmacol. 500, 187–192.
Hammer, R. P., Jr. and Bridges, R. S. 1987. Preoptic area opioids and opiate receptors increase during pregnancy and decrease during lactation. Brain Res. 420, 48–56.
Harada, Y., Nishioka, K., Kitahata, L. M., Nakatani, K., and Collins, J. G. 1995. Contrasting actions of intrathecal U50,488H, morphine, or [D-Pen2, D-Pen5] enkephalin or intravenous U50,488H on the visceromotor response to colorectal distension in the rat. Anesthesiology 83, 336–343.
Harte, S., Lagman, A., and Borszcz, G. 2000. Antinociceptive effects of morphine injected into the nucleus parafascicularis thalami of the rat. Brain Res. 874, 78–86.
Hawes, B. E., Graziano, M. P., and Lambert, D. G. 2000. Cellular actions of nociceptin: transduction mechanisms. Peptides 21, 961–967.
Heinricher, M. M. 2003. Orphanin FQ/nociceptin: from neural circuitry to behavior. Life Sci. 73, 813–822.
Heinricher, M. M., Cheng, Z. F., and Fields, H. L. 1987. Evidence for two classes of nociceptive modulating neurons in the periaqueductal gray. J. Neurosci. 7, 271–278.
Heinricher, M. M., McGaraughty, S., and Grandy, D. K. 1997. Circuitry underlying antiopioid actions of orphanin FQ in the rostral ventromedial medulla. J. Neurophysiol. 78, 3351–3358.
Heinricher, M. M., McGaraughty, S., and Farr, D. A. 1999. The role of excitatory amino acid transmission within the rostral ventromedial medulla in the antinociceptive actions of systemically administered morphine. Pain 81, 57–65.
Helmreich, D. L., Watkins, L. R., Deak, T., Maier, S. F., Akil, H., and Watson, S. J. 1999. The effect of stressor controllability on stress-induced neuropeptide mRNA expression within the paraventricular nucleus of the hypothalamus. J. Neuroendocrinol. 11, 121–128.
Horvitz, J. 2000. Mesolimbic and nigrostriatal dopamine responses to salient non-rewarding stimuli. Neuroscience 96, 651–656.
Hughes, J., Smith, T. W., Kosterlitz, H. W., Fothergill, L. A., Morgan, B. A., and Morris, H. R. 1975. Identification of two related pentapeptides from the brain with potent opiate agonist activity. Nature 258, 577–580.
Jensen, T. S. and Yaksh, T. L. 1986. Comparison of the antinociceptive action of mu and delta opioid receptor ligands in the periaqueductal gray matter, medial and paramedial ventral medulla in the rat as studied by the microinjection technique. Brain Res. 372, 301–312.
Jutkiewicz, E. M., Rice, K. C., Woods, J. H., and Winsauer, P. J. 2003. Effects of the delta-opioid receptor agonist SNC80 on learning relative to its antidepressant-like effects in rats. Behav. Pharmacol. 14, 509–516.
Kest, B., Hopkins, E., Palmese, C. A., Chen, Z. P., Mogil, J. S., and Pintar, J. E. 2001. Morphine tolerance and dependence in nociceptin/orphanin FQ transgenic knock-out mice. Neuroscience 104, 217–222.
Khachaturian, H., Lewis, M. E., Tsou, K., and Watson, S. J. 1985. Beta-Endorphin, Alpha-MSH, ACTH, and Related Peptides. In: Handbook of Chemical Neuroanatomy (*eds*. A. Bjorklundand and T. Hokfelt), pp. 216–272. Elsevier Science.
Kiefel, J. M., Rossi, G. C., and Bodnar, R. J. 1993. Medullary mu and delta opioid receptors modulate mesencephalic morphine analgesia in rats. Brain Res. 624, 151–161.
Kieffer, B. L., Befort, K., Gaveriaux-Ruff, C., and Hirth, C. G. 1992. The delta-opioid receptor: isolation of a cDNA by expression cloning and pharmacological characterization. Proc. Natl. Acad. Sci. U. S. A. 89, 12048–12052.
Konig, M., Zimmer, A. M., Steiner, H., Holmes, P. V., Crawley, J. N., Brownstein, M. J, and Zimmer, A. 1996. Pain responses, anxiety and aggression in mice deficient in pre-proenkephalin. Nature 383, 535–538.
Koster, A., Montkowski, A., Schulz, S., Stube, E. M., Knaudt, K., Jenck, F., Moreau, J. L., Nothacker, H. P., Civelli, O., and Reinscheid, R. K. 1999. Targeted disruption of the orphanin FQ/nociceptin gene increases stress susceptibility and impairs stress adaptation in mice. Proc. Natl. Acad. Sci. U. S. A. 96, 10444–10449.
LaBuda, C. J., Sora, I., Uhl, G. R., and Fuchs, P. N. 2000. Stress-induced analgesia in mu-opioid receptor knockout mice reveals normal function of the delta-opioid receptor system. Brain Res. 869, 1–5.
Levine, J., Gordon, N., Jones, R., and Fields, H. 1978. The narcotic antagonist naloxone enhances clinical pain. Nature 272, 826–827.
Lewis, M. E., Pert, A., Pert, C. B., and Herkenham, M. 1983. Opiate receptor localization in rat cerebral cortex. J. Comp. Neurol. 216, 339–358.
Lewis, M. E., Mishkin, M., Bragin, E., Brown, R. M., Pert, C. B., and Pert, A. 1981. Opiate receptor gradients in monkey cerebral cortex: correspondence with sensory processing hierarchies. Science 211, 1166–1169.
Li, C. H., Lemaire, S., Yamashiro, D., and Doneen, B. A. 1976. The synthesis and opiate activity of beta-endorphin. Biochem. Biophys. Res. Commun. 71, 19–25.
Li, S., Zhu, J., Chen, C., Chen, Y. W., Deriel, J. K., Ashby, B., and Liu-Chen, L. Y. 1993. Molecular cloning and expression of a rat kappa opioid receptor. Biochem. J. 295(Pt 3), 629–633.
Loh, H. H., Tseng, L. F., Wei, E., and Li, C. H. 1976. Beta-endorphin is a potent analgesic agent. Proc. Natl. Acad. Sci. U. S. A. 73, 2895–2898.
Lorenz, J., Cross, D., Minoshima, S., Morrow, T., Paulson, P., and Casey, K. 2002. A unique representation of heat allodynia in the human brain. Neuron 35, 383–393.

Ma, F., Xie, H., Dong, Z. Q., Wang, Y. Q., and Wu, G. C. 2005. Expression of ORL1 mRNA in some brain nuclei in neuropathic pain rats. Brain Res. 1043, 214–217.

Madden, J. T., Akil, H., Patrick, R., and Barchas, J. 1977. Stress-induced parallel changes in central opioid levels and pain responsiveness in the rat. Nature 265, 358–360.

Mamiya, T., Noda, Y., Ren, X., Nagai, T., Takeshima, H., Ukai, M., and Nabeshima, T. 2001. Morphine tolerance and dependence in the nociceptin receptor knockout mice. J. Neural. Transm. 108, 1349–1361.

Manning, B. 1998. A lateralized deficit in morphine antinociception after unilateral inactivation of the central amygdala. J. Neurosci. 18, 9453–9470.

Manning, B. and Franklin, K. 1998. Morphine analgesia in the formalin test: reversal by microinjection of quaternary naloxone into the posterior hypothalamic area or periaqueductal gray. Behav. Brain Res. 92, 97–102.

Manning, B. H., Merin, N. M., Meng, I. D., and Amaral, D. G. 2001. Reduction in opioid- and cannabinoid-induced antinociception in rhesus monkeys after bilateral lesions of the amygdaloid complex. J. Neurosci. 21, 8238–8246.

Mansi, J. A., Laforest, S., and Drolet, G. 2000. Effect of stress exposure on the activation pattern of enkephalin-containing perikarya in the rat ventral medulla. J. Neurochem. 74, 2568–2575.

Mansour, A., Fox, C. A., Akil, H., and Watson, S. J. 1995. Opioid-receptor mRNA expression in the rats CNS: anatomical and functional implications. Trends Neurosci. 18, 22–29.

Margolis, E. B., Hjelmstad, G. O., Bonci, A., and Fields, H. L. 2003. Kappa-opioid agonists directly inhibit midbrain dopaminergic neurons. J. Neurosci. 23, 9981–9986.

Martin, M., Matifas, A., Maldonado, R., and Kieffer, B. L. 2003. Acute antinociceptive responses in single and combinatorial opioid receptor knockout mice: distinct mu, delta and kappa tones. Eur. J. Neurosci. 17, 701–708.

Matthes, H. W., Smadja, C., Valverde, O., Vonesch, J. L., Foutz, A. S., Boudinot, E., Denavit-Saubie, M., Severini, C., Negri, L., Roques, B. P., Maldonado, R., and Kieffer, B. L. 1998. Activity of the delta-opioid receptor is partially reduced, whereas activity of the kappa-receptor is maintained in mice lacking the mu-receptor. J. Neurosci. 18, 7285–7295.

Mayer, D. J. and Liebeskind, J. C. 1974. Pain reduction by focal electrical stimulation of the brain: an anatomical and behavioral analysis. Brain Res. 68, 73–93.

Mayer, D. J., Wolfle, T. L., Akil, H., Carder, B., and Liebeskind, J. C. 1971. Analgesia from electrical stimulation in the brainstem of the rat. Science 174, 1351–1354.

McLaughlin, J. P., Marton-Popovici, M., and Chavkin, C. 2003. Kappa opioid receptor antagonism and prodynorphin gene disruption block stress-induced behavioral responses. J. Neurosci. 23, 5674–5683.

Meng, I. D., Johansen, J. P., Harasawa, I., and Fields, H. L. 2005. Kappa opioids inhibit physiologically identified medullary pain modulating neurons and reduce morphine antinociception. J. Neurophysiol. 93, 1138–1144.

Meng, F., Xie, G. X., Thompson, R. C., Mansour, A., Goldstein, A., Watson, S. J., and Akil, H. 1993. Cloning and pharmacological characterization of a rat kappa opioid receptor. Proc. Natl. Acad. Sci. U. S. A. 90, 9954–9958.

Meunier, J. C., Mollereau, C., Toll, L., Suaudeau, C., Moisand, C., Alvinerie, P., Butour, J. L., Guillemot, J. C., Ferrara, P., and Monsarrat, B., *et al.* 1995. Isolation and structure of the endogenous agonist of opioid receptor-like ORL1 receptor. Nature 377, 532–535.

Mogil, J. S. and Pasternak, G. W. 2001. The molecular and behavioral pharmacology of the orphanin FQ/nociceptin peptide and receptor family. Pharmacol. Rev. 53, 381–415.

Mogil, J. S., Grisel, J. E., Reinscheid, R. K., Civelli, O., Belknap, J. K., and Grandy, D. K. 1996a. Orphanin FQ is a functional anti-opioid peptide. Neuroscience 75, 333–337.

Mogil, J. S., Grisel, J. E., Zhangs, G., Belknap, J. K., and Grandy, D. K. 1996b. Functional antagonism of mu-, delta- and kappa-opioid antinociception by orphanin FQ. Neurosci. Lett. 214, 131–134.

Moles, A., Kieffer, B. L., and D'Amato, F. R. 2004. Deficit in attachment behavior in mice lacking the mu-opioid receptor gene. Science 304, 1983–1986.

Mollereau, C., Parmentier, M., Mailleux, P., Butour, J. L., Moisand, C., Chalon, P., Caput, D., Vassart, G., and Meunier, J. C. 1994. ORL1, a novel member of the opioid receptor family. Cloning, functional expression and localization. FEBS Lett. 341, 33–38.

Mollereau, C., Simons, M. J., Soularue, P., Liners, F., Vassart, G., Meunier, J. C., and Parmentier, M. 1996. Structure, tissue distribution, and chromosomal localization of the prepronociceptin gene. Proc. Natl. Acad. Sci. U. S. A. 93, 8666–8670.

Moran, T. D., Abdulla, F. A., and Smith, P. A. 2000. Cellular neurophysiological actions of nociceptin/orphanin FQ. Peptides 21, 969–976.

Moreau, J. L. and Fields, H. L. 1986. Evidence for GABA involvement in midbrain control of medullary neurons that modulate nociceptive transmission. Brain Res. 397, 37–46.

Morinville, A., Cahill, C. M., Esdaile, M. J., Aibak, H., Collier, B., Kieffer, B. L., and Beaudet, A. 2003. Regulation of delta-opioid receptor trafficking via mu-opioid receptor stimulation: evidence from mu-opioid receptor knock-out mice. J. Neurosci. 23, 4888–4898.

Moskowitz, A. S. and Goodman, R. R. 1985. Autoradiographic analysis of mu1, mu2, and delta opioid binding in the central nervous system of C57BL/6BY and CXBK (opioid receptor-deficient) mice. Brain Res. 360, 108–116.

Narita, M., Kishimoto, Y., Ise, Y., Yajima, Y., Misawa, K., and Suzuki, T. 2005. Direct evidence for the involvement of the mesolimbic kappa-opioid system in the morphine-induced rewarding effect under an inflammatory pain-like state. Neuropsychopharmacology 30, 111–118.

Nishi, M., Houtani, T., Noda, Y., Mamiya, T., Sato, K., Doi, T., Kuno, J., Takeshima, H., Nukada, T., Nabeshima, T., Yamashita, T., Noda, T., and Sugimoto, T. 1997. Unrestrained nociceptive response and disregulation of hearing ability in mice lacking the nociceptin/orphaninFQ receptor. Embo. J. 16, 1858–1864.

Ossipov, M. H., Kovelowski, C. J., Nichols, M. L., Hruby, V. J., and Porreca, F. 1995. Characterization of supraspinal antinociceptive actions of opioid delta agonists in the rat. Pain 62, 287–293.

Pan, Z. Z., Tershner, S. A., and Fields, H. L. 1997. Cellular mechanism for anti-analgesic action of agonists of the kappa-opioid receptor. Nature 389, 382–385.

Pert, C. B. and Snyder, S. H. 1973. Opiate receptor: demonstration in nervous tissue. Science 179, 1011–1014.

Petrusz, P., Merchenthaler, I., and Maderdrut, J. 1985. Distribution of Enkephalin-Containing Neurons in the Central Nervous System. In: Handbook of Chemical Neuroanatomy (*eds*. A. Björklundand and T. Hökfelt), pp. 273–334. Elsevier.

Piva, F., Maggi, R., Limonta, P., Dondi, D., and Martini, L. 1987. Decrease of mu opioid receptors in the brain and in the hypothalamus of the aged male rat. Life Sci. 40, 391–398.

Porreca, F., Mosberg, H. I., Hurst, R., Hruby, V. J., and Burks, T. F. 1984. Roles of mu, delta and kappa opioid receptors in spinal and supraspinal mediation of gastrointestinal transit effects and hot-plate analgesia in the mouse. J. Pharmacol. Exp. Ther. 230, 341–348.

Quinones-Jenab, V., Jenab, S., Ogawa, S., Inturrisi, C., and Pfaff, D. W. 1997. Estrogen regulation of mu-opioid receptor

mRNA in the forebrain of female rats. Brain Res. Mol. Brain Res. 47, 134–138.
Rainville, P., Duncan, G., Price, D., Carrier, B., and Bushnell, M. 1997. Pain affect encoded in human anterior cingulate but not somatosensory cortex. Science 277, 968–971.
Reinscheid, R. K., Nothacker, H. P., Bourson, A., Ardati, A., Henningsen, R. A., Bunzow, J. R., Grandy, D. K., Langen, H., Monsma, F. J., Jr, and Civelli, O. 1995. Orphanin FQ: a neuropeptide that activates an opioidlike G protein-coupled receptor. Science 270, 792–794.
Reynolds, D. V. 1969. Surgery in the rat during electrical analgesia induced by focal brain stimulation. Science 164, 444–445.
Richardson, D. E. and Akil, H. 1977a. Pain reduction by electrical brain stimulation in man. Part 1: Acute administration in periaqueductal and periventricular sites. J. Neurosurg. 47, 178–183.
Richardson, D. E. and Akil, H. 1977b. Pain reduction by electrical brain stimulation in man. Part 2: Chronic self-administration in the periventricular gray matter. J Neurosurg. 47, 184–194.
al-Rodhan, N., Chipkin, R., and Yaksh, T. L. 1990. The antinociceptive effects of SCH-32615, a neutral endopeptidase (enkephalinase) inhibitor, microinjected into the periaqueductal, ventral medulla and amygdala. Brain Res. 520, 123–130.
Rossi, G. C., Leventhal, L., Bolan, E., and Pasternak, G. W. 1997. Pharmacological characterization of orphanin FQ/nociceptin and its fragments. J. Pharmacol. Exp. Ther. 282, 858–865.
Rossi, G. C., Leventhal, L., and Pasternak, G. W. 1996. Naloxone sensitive orphanin FQ-induced analgesia in mice. Eur. J. Pharmacol. 311, R7–R8.
Roychowdhury, S. M. and Fields, H. L. 1996. Endogenous opioids acting at a medullary mu-opioid receptor contribute to the behavioral antinociception produced by GABA antagonism in the midbrain periaqueductal gray. Neuroscience 74, 863–872.
Rubinstein, M., Mogil, J. S., Japon, M., Chan, E. C., Allen, R. G., and Low, M. J. 1996. Absence of opioid stress-induced analgesia in mice lacking β-endorphin by site directed mutagenesis. Proc. Natl. Acad. Sci. U. S. A. 93, 3995–4000.
Scherrer, G., Befort, K., Contet, C., Becker, J., Matifas, A., and Kieffer, B. L. 2004. The delta agonists DPDPE and deltorphin II recruit predominantly mu receptors to produce thermal analgesia: a parallel study of mu, delta and combinatorial opioid receptor knockout mice. Eur. J. Neurosci. 19, 2239–2248.
Schlaepfer, T., Strain, E., Greenberg, B., Preston, K., Lancaster, E., Bigelow, G., Barta, P., and Pearlson, G 1998. Site of opioid action in the human brain: mu and kappa agonists' subjective and cerebral blood flow effects. Am. J. Psychiatry. 155, 470–473.
Simon, E. J., Hiller, J. M., and Edelman, I. 1973. Stereospecific binding of the potent narcotic analgesic (3H) Etorphine to rat-brain homogenate. Proc. Natl. Acad. Sci. U. S. A. 70, 1947–1949.
Skoubis, P. D., Lam, H. A., Shoblock, J., Narayanan, S., and Maidment, N. T. 2005. Endogenous enkephalins, not endorphins, modulate basal hedonic state in mice. Eur. J. Neurosci. 21, 1379–1384.
Smith, Y. R., Stohler, C. S., Nichols, T. E., Bueller, J. A., Koeppe, R. A., and Zubieta, J. K. 2006. Pronociceptive and antinociceptive effects of estradiol through endogenous opioid neurotransmission in women. J. Neurosci. 26, 5777–5785.
Smith, J. S., Zubieta, J. K., Price, J. C., Flesher, J. E., Madar, I., Lever, J. R., Kinter, C. M., Dannals, R. F., and Frost, J. J. 1999. Quantification of delta-opioid receptors in human brain with N1′-([^{11}C]methyl) naltrindole and positron emission tomography. J. Cereb. Blood Flow Metab. 19, 956–966.
Sora, I., Takahashi, N., Funada, M., Ujike, H., Revay, R. S., Donovan, D. M., Miner, L. L., and Uhl, G. R. 1997. Opiate receptor knockout mice define μ receptor roles in endogenous nociceptive responses and morphine-induced analgesia. Proc. Natl. Acad. Sci. U. S. A. 94, 1544–1549.
Terenius, L. 1973. Characteristics of the ''receptor'' for narcotic analgesics in synaptic plasma membrane fraction from rat brain. Acta Pharmacol. Toxicol. (Copenh) 33, 377–384.
Tershner, S. A., Mitchell, J. M., and Fields, H. L. 2000. Brainstem pain modulating circuitry is sexually dimorphic with respect to mu and kappa opioid receptor function. Pain 85, 153–159.
Thompson, R. C., Mansour, A., Akil, H., and Watson, S. J. 1993. Cloning and pharmacological characterization of a rat mu opioid receptor. Neuron 11, 903–913.
Thompson, A. C., Zapata, A., Justice, J. B., Jr., Vaughan, R. A., Sharpe, L. G., and Shippenberg, T. S. 2000. Kappa-opioid receptor activation modifies dopamine uptake in the nucleus accumbens and opposes the effects of cocaine. J. Neurosci. 20, 9333–9340.
Tian, J. H., Xu, W., Fang, Y., Mogil, J. S., Grisel, J. E., Grandy, D. K., and Han, J. S. 1997. Bidirectional modulatory effect of orphanin FQ on morphine-induced analgesia: antagonism in brain and potentiation in spinal cord of the rat. Br. J. Pharmacol. 120, 676–680.
Torregrossa, M. M., Isgor, C., Folk, J. E., Rice, K. C., Watson, S. J., and Woods, J. H. 2004. The delta-opioid receptor agonist (+)BW373U86 regulates BDNF mRNA expression in rats. Neuropsychopharmacology 29, 649–659.
Tsou, K. and Jang, C. S. 1964. Studies on the site of analgesic action of morphine by intracerebral micro-injection. Sci. Sin. 13, 1099–1109.
Urban, M. O. and Smith, D. J. 1994. Nuclei within the rostral ventromedial medulla mediating morphine antinociception from the periaqueductal gray. Brain Res. 652, 9–16.
Vaught, J. L., Mathiasen, J. R., and Raffa, R. B. 1988. Examination of the involvement of supraspinal and spinal mu and delta opioid receptors in analgesia using the mu receptor deficient CXBK mouse. J. Pharmacol. Exp. Ther. 245, 13–16.
Wang, Z., Gardell, L. R., Ossipov, M. H., Vanderah, T. W., Brennan, M. B., Hochgeschwender, U., Hruby, V. J., Malan, T. P., Jr., Lai, J., and Porreca, F. 2001. Pronociceptive actions of dynorphin maintain chronic neuropathic pain. J. Neurosci. 21, 1779–1786.
Wagner, K. J., Willoch, F., Kochs, E. F., Siessmeier, T., Tolle, T. R., Schwaiger, M., and Bartenstein, P. 2001. Dose-dependent regional cerebral blood flow changes during remifentanil infusion in humans: a positron emission tomography study. Anesthesiology 94, 732–739.
Watkins, L. and Mayer, D. 1982. Organization of endogenous opiate and nonopiate pain control systems. Science 216, 1185–1192.
Williams, K. L., Ko, M. C., Rice, K. C., and Woods, J. H. 2003. Effect of opioid receptor antagonists on hypothalamic–pituitary–adrenal activity in rhesus monkeys. Psychoneuroendocrinology 28, 513–528.
Yaksh, T. L. and Rudy, T. A. 1978. Narcotic analgestics: CNS sites and mechanisms of action as revealed by intracerebral injection techniques. Pain 4, 299–359.
Zacny, J. P. 2001. Morphine responses in humans: a retrospective analysis of sex differences. Drug Alcohol Depend. 63, 23–28.
Zadina, J. E. 2002. Isolation and distribution of endomorphins in the central nervous system. Jpn. J. Pharmacol. 89, 203–208.
Zhang, Y., Butelman, E. R., Schlussman, S. D., Ho, A., and Kreek, M. J. 2004. Effect of the endogenous kappa opioid agonist dynorphin A(1–17) on cocaine-evoked increases in

striatal dopamine levels and cocaine-induced place preference in C57BL/6J mice. Psychopharmacology (Berl) 172, 422–429.

Zhuo, M. and Gebhart, G. F. 1997. Biphasic modulation of spinal nociceptive transmission from the medullary raphe nuclei in the rat. J. Neurophysiol. 78, 746–758.

Zubieta, J. K., Dannals, R., and Frost, J. 1999. Gender and age influences on human brain mu opioid receptor binding measured by PET. Am. J. Psychiatry. 156, 842–848.

Zubieta, J. K., Bueller, J. A., Jackson, L. R., Scott, D. J., Xu, Y., Koeppe, R. A., Nichols, T. E., and Stohler, C. S. 2005. Placebo effects mediated by endogenous opioid activity on mu-opioid receptors. J. Neurosci. 25, 7754–7762.

Zubieta, J. K., Smith, Y. R., Bueller, J. A., Xu, Y., Kilbourn, M. R., Jewett, D. M., Meyer, C. R., Koeppe, R. A., and Stohler, C. S. 2002. mu-Opioid receptor-mediated antinociceptive responses differ in men and women. J. Neurosci. 22, 5100–5107.

Zubieta, J. K., Smith, Y., Bueller, J., Xu, Y., Kilbourn, M., Meyer, C., Koeppe, R., and Stohler, C. 2001. Regional mu opioid receptor regulation of sensory and affective dimensions of pain. Science 293, 311–315.

5.55 Neuropathic Pain: Basic Mechanisms (Animal)

M H Ossipov and F Porreca, University of Arizona, Tucson, AZ, USA

Published by Elsevier Inc.

5.55.1	**Introduction**	833
5.55.2	**Injury-Induced Sensitization of Peripheral Nerves and Neuropathic Pain**	834
5.55.2.1	Role of Peripheral Nerve Degeneration in Neuropathic Pain	835
5.55.2.2	Role of Nerve Growth Factor in Immediate Pronociceptive Function	836
5.55.2.3	Nerve Growth Factor May Mediate Posttranslational Pronociceptive Functions	836
5.55.2.4	Sodium Channels and Enhanced Peripheral Nerve Activity	837
5.55.2.5	Role of Calcium Channels	839
5.55.3	**Enhanced Afferent Discharges Lead to Central Sensitization in the Spinal Cord**	840
5.55.4	**Excitatory Transmitters Promote Central Sensitization**	841
5.55.5	**Descending Facilitation Promotes Enhanced Pain**	842
5.55.5.1	Role of the Rostralventromedial Medulla in Descending Facilitation of Pain	842
5.55.5.2	The ON Cells of the Rostralventromedial Medulla Promote Pain Through Descending Facilitation	843
5.55.5.3	Cholecystokinin in the Rostralventromedial Medulla May Mediate Pain Facilitation	844
5.55.6	**Second-Order Projection Neurons Expressing NK1 Receptors May Result in Activation of Descending Pain Facilitation**	844
5.55.7	**Descending Facilitation Maintains a Sensitized Spinal Cord: Upregulation of Spinal Dynorphin and Enhanced Release of Primary Afferent Transmitters**	845
5.55.7.1	Descending Facilitation Maintains a Sensitized Spinal Cord: Upregulation of Spinal Dynorphin and Enhanced Release of Primary Afferent Transmitters	846
5.55.7.2	Descending Facilitation Maintains a Sensitized Spinal Cord: Serotonergic Contributions	846
5.55.8	**Summary**	847
References		848

5.55.1 Introduction

Neuropathic pain is defined by the International Association for the Study of Pain (IASP) as "pain initiated or caused by a primary lesion or dysfunction in the nervous system". Although this definition functions well as a guide for the clinical assessment of neuropathic pain, a definitive categorization of neuropathic pain is difficult because there are many descriptions of the pain syndrome. Neuropathic pain may arise from an actual injury to a peripheral nerve or it may arise in the absence of any obvious nerve damage (e.g., trigeminal neuralgia and complex regional pain syndrome (CRPS), type I). Disease processes, such as diabetic neuropathy, postherpetic neuralgia resulting from varicella zoster infection (shingles), and complications from AIDS also may cause neuropathic pain, as may alterations in peripheral nerve function induced by chemotherapeutic regimens. Neuropathic pain may include spontaneous, or stimulus-independent, pain that has been described as shooting, burning, lancinating, prickling, and electrical. Evoked, or stimulus-dependent, neuropathic pain includes allodynia, defined by IASP as "pain due to a stimulus which does not normally provoke pain." These stimuli may be nonnoxious heat, light touch, or even a puff of cool air. Moreover, mechanical allodynia may be static, as evoked by a light touch, or dynamic, as evoked by a light brush of the skin. Hyperalgesia is identified when a stimulus that normally produces a nociceptive responses produces an exaggerated responses. The different forms through which neuropathic pain manifests suggest that differing mechanisms are likely to mediate the different features of the condition. The numerous features of neuropathic pain can complicate an accurate clinical diagnosis. For this reason, efforts have emphasized the development of highly specific questionnaires emphasizing a unique set of symptoms that can aid clinical diagnosis with relatively little effort. Features that appear to be most often related to neuropathic pain include tingling

or numbness, pain evoked by heat or cold, and especially, a sensation of heat or a burning-like quality is associated with the neuropathic pain state (Krause, S. J. and Backonja, M. M., 2003; Backonja, M. M. and Stacey, B., 2004; Bennett, M. I. *et al.*, 2007). More recently, a questionnaire identified at DN4 was designed to assess the presence of pain combined with parasthesias or dysesthesias (Bouhassira, D. *et al.*, 2005).

5.55.2 Injury-Induced Sensitization of Peripheral Nerves and Neuropathic Pain

There are several factors common to the neuropathic pain state, regardless of the etiology that may initiate the condition. It has been repeatedly demonstrated that peripheral nerve injury is associated with a heightened sensitivity of nerves to sensory stimuli, a phenomenon that has been termed peripheral sensitization. Importantly, peripheral sensitization is not restricted to the injured nerve fibers, but also includes adjacent, uninjured (but abnormal) nerves. Injured nerves may form a tangled mass of connective tissue termed a neuroma with distally sprouting regenerating axons. Physical manipulation of the neuroma elicits sensations ranging from minor dysesthesias to intense pain. Electrophysiologic studies showed that both myelinated and unmyelinated fibers in neuromas show a basal spontaneous activity as well as enhanced discharges provoked by touch or movement, indicating that the neuroma may serve as an ectopic generator of action potentials. In addition, cell bodies of the dorsal root ganglia (DRG) may also generate ectopic discharges, thus producing spontaneous hyperesthesias and pain as well as enhanced sensitivity to stimuli. Traumatic injury of the rat sciatic nerve produced by loose ligatures, the chronic constriction injury or CCI model, resulted in spontaneous discharges generated from the DRG. In this study, discharges were recorded from 15% to 35% of myelinated and 3% of unmyelinated fibers (Kajander, K. C. *et al.*, 1992). Electrophysiological recordings performed on sciatic nerve bundles after CCI also demonstrated spontaneous and evoked ectopic discharges from the region of injury (Tal, M. and Bennett, G. J., 1994). Surprisingly, these spontaneous discharges of DRG neurons occurred from cells of both injured as well as intact nerves (Michaelis, M. *et al.*, 1996). Additionally, electrophysiologic studies showed spinal nerve transection enhanced the spontaneous activity of nerve fibers in adjacent, uninjured nerve roots and in peripheral nerves (Ali, Z. *et al.*, 1999; Wu, G., *et al.*, 2001). Such studies raised the question of relative contributions of enhanced excitability from injured and uninjured fibers in eliciting neuropathic pain. Yoon Y. W. *et al.* (1996) used a model of neuropathic pain in which the L5 spinal nerve was injured (the spinal nerve ligation or SNL model, Kim, S. H. and Chung, J. M., 1992) and showed that the behavioral signs of pain were abolished by dorsal rhizotomy or bupivacaine applied to the injured spinal nerves emphasizing the importance of afferent drive. Moreover, dorsal rhizotomy or bupivacaine at L4 and L5 also abolished behavioral signs of mechanical and cold allodynia, but not signs of ongoing pain (Yoon, Y. W. *et al.*, 1996). The contribution of uninjured nerves, or uninjured adjacent fibers, to neuropathic pain has been debated. In an insightful study, Belzberg and coworkers (Li, Y. *et al.*, 2000) used the SNL model and found that the behavioral signs of experimental neuropathic pain produced by ligation of the L5 spinal nerve were not abolished by rhizotomy at L5, but rather were abolished by rhizotomy at L4. These findings suggested a prominent role for uninjured but abnormal adjacent nerve fibers following nerve injury and were consistent with the suggested importance of uninjured, but abnormal, L4 afferents; these fibers show significant redistribution of sodium channels such as $Na_V1.8$ following L5 injury (Lai, J. *et al.*, 2002) and this may reflect a mechanism which drives neuropathic pain (see below). It has also been suggested that sensitization of uninjured peripheral nerves may result, in part, from ephaptic excitation caused by the close proximity of injured and noninjured nerves within the nerve trunks or in the DRG (Devor, M. and Wall, P. D., 1990; Attal, N. and Bouhassira, D., 1999). Sensitization of peripheral nerves may mediate SNL-induced thermal hyperalgesia, but may not mediate tactile allodynia. Unlike tactile allodynia, thermal hyperalgesia was abolished by the intravenous infusion of the quaternary lidocaine analogs QX-314 and QX-222, which do not cross the blood–brain barrier (Chen, Q. *et al.*, 2004). In contrast, both tactile and thermal parameters of enhanced pain were abolished by systemic lidocaine, or microinjection of lidocaine or QX-222 into the rostralventromedial medulla (RVM) (Chen, Q. *et al.*, 2004). These observations emphasize the contribution of a central mechanism (addressed below) which may act in addition to peripheral mechanisms to elicit neuropathic pain states.

5.55.2.1 Role of Peripheral Nerve Degeneration in Neuropathic Pain

Degeneration of peripheral nerves provokes the release of proinflammatory cytokines such as interleukins and tumor necrosis factor (TNF), and neurotrophic factors in the region of the target tissue. The initial reaction is followed by macrophage infiltration that further mediate proinflammatory signals. This accumulation of proinflammatory substances may sensitize adjacent nerve terminals of uninjured fibers. Myelinated peripheral nerve fibers undergoing Wallerian degeneration elicit the release of several pronociceptive factors in the target tissue and cytokines along the peripheral nerve, thereby sensitizing the adjacent nerve endings of uninjured nerve fibers, and exciting and potentially producing an ectopic focus in the uninjured adjacent C fibers (Li, Y. *et al.*, 2000). Wallerian degeneration of the injured, spontaneously active myelinated fibers may excite unmyelinated fibers through the comingling of injured and uninjured nerves that occurs within the Remak bundles of the sciatic nerve trunk (Wu, G. *et al.*, 2001; 2002). Furthermore, Wallerian degeneration associated with injured nerves causes alterations in the Schwann cells that provoke them to release proinflammatory mediators, including glutamate as well as nerve growth factor (NGF) (Shamash, S. *et al.*, 2002; MacInnis, B. L. and Campenot, R. B., 2005). Within the nerve trunk, these substances may diffuse to adjacent uninjured nerve fibers and enhance sensitivity such that an ectopic locus may develop. Release of proinflammatory mediators including NGF in the peripheral terminal fields that include uninjured neurons may sensitize these fibers to ensuing stimulation, thus producing peripheral sensitization. It has been shown that nerve injury causes significant elevations in NGF and its mRNA in Schwann cells, macrophages, and fibroblasts at the site of injury (Shamash, S. *et al.*, 2002; MacInnis, B. L. and Campenot, R. B., 2005). Treatment of cultured fibroblasts or keratinocytes with inflammatory mediators, including histamine and interleukin-1 also provoke upregulation of NGF (Kanda, N. and Watanabe, S., 2003). Moreover, NGF promotes degranulation of mast cells, which release inflammatory mediators and thereby promotes peripheral sensitization of nociceptors as well as further release of NGF (Lewin, G. R. *et al.*, 1994; Stempelj, M. and Ferjan, I., 2005). Denervation of the skin due to degeneration of peripheral nerves produce regions that are insensate surrounded by regions of increased sensitivity to noxious stimuli perhaps as a consequence of upregulation of NGF by keratinocytes (Taherzadeh, O. *et al.*, 2003). Increased NGF production promotes sprouting of peripheral nerve terminals into the region into the boundary between the denervated region and that with normal innervation (Rajan, B. *et al.*, 2003). Collateral sprouting of peripheral axons together with the pronociceptive actions of peripheral NGF can promote nociceptive hypersensitivity in the region immediately surrounding the zone of denervation (Griffin, J. W., 2006).

Other growth factors, such as those in the glial-cell-line-derived neutrotropic factor (GDNF) family including GDNF and artemin, may play a significant role in expression of neuropathic pain. NGF and GDNF family members may act at peripheral nociceptive primary afferents, leading to enhancement of sensitivity to noxious inputs (Zwick, M. *et al.*, 2002; Elitt, C. M. *et al.*, 2006; Griffin, J. W., 2006; Malin, S. A. *et al.*, 2006). Injury-induced upregulation of growth factors such as NGF results in a situation where intact, uninjured nociceptive C fibers expressing the trkA receptor are exposed to a surplus of NGF and may become overtrophed in response to nerve injury (Griffin, J. W., 2006). In these fibers, NGF would promote nociceptive transmission through phosphorylation of TRPV1 ion channels, as well as posttranslational mechanisms that include upregulation of ion channels, redistribution of $Na_V1.8$ and increased synthesis of substance P and CGRP (Boucher, T. J. *et al.*, 2000; Boucher, T. J. and McMahon, S. B., 2001; Griffin, J. W., 2006). In contrast, the axons of the injured peripheral fibers, which include C fiber nociceptors as well as some myelinated sensory fibers, are not able to traffic target-derived growth factors to the cell body. These peripheral nerves may be considered to be undertrophed (Griffin, J. W., 2006) and can demonstrate increased expression of tetrodotoxin (TTX)-sensitive (TTX-S) sodium channels and enhanced spontaneous activity, adaptations which may underlie such painful conditions as postamputation pain and neuropathic pain associated with mastectomy and thoracotomy scars (Griffin, J. W., 2006). This hypothesis was tested by providing support with exogenous trophic factors including GDNF and artemin. Administration of exogenous GDNF normalized expression of sodium channels and the reversed the behavioral signs of neuropathic pain (Boucher, T. J. *et al.*, 2000; Boucher, T. J. and McMahon, S. B., 2001; Wang, R. *et al.*, 2003). In addition, exogenous GDNF delivered by the intrathecal route also abolished electrophysiologic

signs of enhanced firing, ectopic discharges, and normalized sodium channel currents in injured peripheral nerves (Boucher, T. J. *et al.*, 2000; Boucher, T. J. and McMahon, S. B., 2001) as well as multiple biochemical markers in the DRG (Wang, R. *et al.*, 2003). Systemic treatment with artemin to rats with SNL also normalized the expression of biochemical markers of neuropathy, including the expression and redistribution of $Na_V1.8$ and abolished signs of neuropathic pain (Gardell *et al.*, 2003b). The pronociceptive role of neurotrophic factors is discussed below.

5.55.2.2 Role of Nerve Growth Factor in Immediate Pronociceptive Function

NGF binds preferentially to the high-affinity tyrosine kinase receptor subtype trkA and to the low-affinity, nonselective neurotrophin receptor p75 (Sah, D. W. *et al.*, 2005a; 2005b). The neuronal distribution of the trkA receptor indicates a substantial role of NGF in nociceptive processes, since trkA is found almost exclusively on small-diameter unmyelinated peptidergic DRG neurons (Sah, D. W. *et al.*, 2003). Double-labeling studies indicate that 92% of trkA-expressing DRG neurons also express CGRP and substance P, whereas it is present on about 20% of myelinated DRG neurons (Bennett, D. L. *et al.*, 2000; Averill, S. *et al.*, 2004). Investigations performed with a skin–nerve preparation showed that NGF increased mechanical hyperalgesia mediated by thin myelinated fibers and thermal hyperalgesia mediated by unmyelinated nociceptors (Stucky, C. L. *et al.*, 2002). Electrophysiologic studies revealed that endogenous NGF regulates the sensitivity of unmyelinated nociceptors to chemical and thermal stimuli (Bennett, D. L. *et al.*, 1998). Sensitization to heat stimulus or to capsaicin application is induced rapidly by NGF (Shu, X. and Mendell, L. M., 2001). Within 10 min of exposure to NGF, there is a rapid potentiation of capsaicin-evoked ion currents in cultured DRG neurons gated by TRPV1 (Shu, X. and Mendell, L. M., 2001). Activation of the trkA receptor by NGF leads to, among other events, phosphorylation of TRPV1, in part through the signaling cascades associated with PKA, PKC, MEK, and the MAP kinases (Shu, X. and Mendell, L. M., 1999; 2001). Moreover, NGF increases nociceptor activity by a rapid facilitation of sodium currents and suppression of an outward potassium current. Behavioral hyperalgesia is evoked by NGF administered systemically or into the endoneurium of a peripheral nerve (Ruiz, G. *et al.*, 2004; Ruiz, G. and Banos, J. E., 2005). Clinical studies also showed that exogenous NGF produced long-lasting mechanical allodynia and hyperalgesia and mild-to-moderate myalgia (Apfel, S. C., 2000; Svensson, P. *et al.*, 2003). Conversely, manipulations that block NGF activity alleviate signs of hyperalgesia. Blockade of NGF activity with the trkA–IgG fusion protein, that antagonist ALE-540 or with antiserum to NGF abolished mechanical and thermal hyperalgesia in animal models of inflammation, incision, or nerve injury (Owolabi J. B. *et al.*, 1999; Banik, R. K. *et al.*, 2005). More recently, intrathecal injection of antibody to NGF blocked behavioral signs of cold allodynia after nerve ligation (Obata, K. *et al.*, 2005). In addition, anti-NGF given by intrathecal injection or local application onto the L4 spinal nerve abolished signs of thermal and mechanical hyperalgesia in rats with peripheral nerve injury (Obata, K. *et al.*, 2004; 2006). The prominent role of NGF in the expression of chronic pain states has led a number of pharmaceutical companies, including Pfizer/Rinat, Amgen, and PainCeptor Pharma to initiate drug discovery and development efforts targeting NGF or trkA (Shelton, D. L. *et al.*, 2005; Hefti, F. F. *et al.*, 2006). Drug development approaches include sequestering or binding NGF so that it does not interact with the trkA receptor, trkA receptor antagonists, or disruption of the signaling pathways linked to trkA receptor activation (Hefti, F. F. *et al.*, 2006).

5.55.2.3 Nerve Growth Factor May Mediate Posttranslational Pronociceptive Functions

In addition to its immediate actions in the periphery, NGF can also initiate long-lasting posttranscriptional changes in peripheral nerves to promote and sustain an enhanced pain state. When NGF binds to the trkA receptor at the peripheral terminal, it is rapidly internalized and the phosphorylated trkA–NGF complex is accumulated in signaling endosomes that are transported to the DRG, where it triggers the activation of several intracellular signaling cascades, including expression of the MAP kinases, ERK, and p38 (Ji, R. R. *et al.*, 2002; McMahon, S. B. and Cafferty, W. B., 2004). Inflammation or exogenous NGF administered spinally causes phosphorylation of p38 in nociceptors in the DRG, but not the dorsal horn, along with a substantial upregulation of TRPV1 in the DRG (Ji, R. R. *et al.*, 2002; McMahon, S. B. and Cafferty, W. B., 2004; Malik-Hall, M. *et al.*, 2005). Moreover, there is evidence that the TRPV1 receptor is preferentially trafficked to the peripheral terminals of the nociceptors, where it can contribute to

peripheral sensitization and hyperalgesia (Ji, R. R. *et al.*, 2002). Furthermore, hyperalgesia may also be maintained by the increased expression of peptidic neurotransmitters specific to primary afferent nociceptors. The exposure of DRG cultures to NGF produced 15- to 60-fold increases in mRNA for substance P and CGRP in trkA-expressing cells, and increased capsaicin-evoked release of CGRP or substance P from cultured trigeminal neurons and from central terminals of primary afferent nociceptors in spinal cord sections (McMahon, S. B. and Cafferty, W. B., 2004; Puntambekar, P. *et al.*, 2005). Animals with diabetic or chemotherapy-induced neuropathy treated with NGF showed abnormally elevated levels of substance P and CGRP protein and mRNA (Tomlinson, D. R. *et al.*, 1997). These functional consequences of NGF expression, including stimulation of BDNF production, may enable transition from peripheral to central sensitization after injury, resulting in chronic pain (Sah, D. W. *et al.*, 2003; McMahon, S. B., *et al.*, 2005; Sah, D. W. *et al.*, 2005a; 2005b). Moreover, retrogradely transported NGF promotes the upregulation of ion channels that promote activation of peripheral nerves and enhances nociceptive transmission. For example, hyperalgesia is also maintained by NGF-mediated upregulation of ASIC3 and upregulation and redistribution of $Na_V1.8$ on primary afferent nociceptors (McMahon, S. B. and Jones, N. G., 2004). Importantly, it was shown that peripheral nerve injury is associated with enhanced retrograde transport of NGF to the cell bodies of spared, or uninjured adjacent, peripheral nerves, thus promoting pronociceptive transcriptional changes in these nerves as well. For example, ligation of the L5 spinal nerve increased the expression of p75NTR in the DRG that was abolished by spinal administration of anti-NGF (Obata, K. *et al.*, 2006). Moreover, the application of anti-NGF onto the L4 spinal nerve after ligation of the L5 spinal nerve blocked the injury-induced upregulation of p75NTR (Obata, K. *et al.*, 2006). The spinal injection of the NGF/TrkA antagonist K252a blocked injury-induced thermal and cold hyperalgesia and the upregulation of phosphorylated trkA, p38, and of TRPV1 and TRPA1 in L4 DRG (Obata, K. *et al.*, 2006).

5.55.2.4 Sodium Channels and Enhanced Peripheral Nerve Activity

Because of their critical role in the generation of action potentials and neuronal excitation, the increased abnormal spontaneous and ectopic discharges of injured peripheral nerves are related to increased activity of voltage-gated sodium channels (VGSCs) (Lai, J. *et al.*, 2002; 2003). The VGSCs have been linked to excitability of primary afferent nociceptors and may mediate sensitized pain states (Lai, J. *et al.*, 2003). Peripheral nerve injury is also associated with changes in the expression and distribution of isoforms of the VGSCs (Novakovic, S. D. *et al.*, 2001). Three sodium channels merit special consideration.

The TTX-S sodium channel $Na_V1.3$ is fast-activating channel normally present in brain tissue but scarce in the DRG. However, peripheral nerve injury results in a substantial expression this channel in peripheral nerves, and it is believed that this novel expression may be partly responsible for the enhanced excitability of the primary afferents (Waxman, S. G. *et al.*, 1999; Lai, J. *et al.*, 2003). However, although its biophysical properties favor generation of spontaneous discharges, a causal relationship between expression of $Na_V1.3$ in the DRG and neuronal discharges has not been established. It had been hypothesized that upregulation of $Na_V1.3$ in peripheral nerves might mediate neuropathic pain as intrathecal treatment with GDNF abolished behavioral signs of enhanced pain, injury-induced enhanced peripheral neuronal excitability, and the upregulation of $Na_V1.3$ (Boucher, T. J. *et al.*, 2000). Other studies, however, showed that intrathecal GDNF normalized many changes observed in the DRG following peripheral nerve injury (Wang, R. *et al.*, 2003) making specific conclusions about $Na_V1.3$ difficult. Observations that knockdown of $Na_V1.3$ by antisense treatment abolished both the enhanced neuronal activity and behavioral signs of neuropathic pain in nerve-injured rats seemed to support this hypothesis (Hains, B. C. *et al.*, 2004). However, more recent evidence has clearly shown that this channel may not be relevant to enhanced pain after nerve injury. Studies employing two different conditional mutant mice lines, one with knockout of $Na_V1.3$ in nociceptors and another with global knockout of $Na_V1.3$ throughout the nervous system, showed that behavioral signs of neuropathic pain developed normally in both mutant lines after peripheral nerve injury (Nassar, M. A. *et al.*, 2006). Knockout of $Na_V1.3$ also did not alter responses to acute nociceptive stimuli or to inflammation (Nassar, M. A. *et al.*, 2006). Accordingly, it is believed that the $Na_V1.3$ channel is neither sufficient nor necessary for the expression of neuropathic pain (Nassar, M. A. *et al.*, 2006).

The TTX-insensitive sodium channel $Na_V1.8$ exhibits properties consistent with a role in neuropathic pain (Sangameswaran, L. *et al.*, 1997; Lai, J. *et al.*, 2002). It is expressed primarily in small-diameter,

unmyelinated peripheral nerve fibers (C fibers) and in other cells in the DRG, and is not found in other peripheral or central neurons or nonneuronal tissue (Sangameswaran, L. *et al.*, 1997; Akopian, A. N. *et al.*, 1999). Studies employing mutant mice lacking the $Na_V1.8$ channel or antisense knockdown techniques have shown that this channel is not essential for resting membrane potentials, neuronal excitation thresholds, or basal nociceptive thresholds (Akopian, A. N. *et al.*, 1999; Renganathan, M., *et al.*, 2001; Lai, J. *et al.*, 2003). In contrast, knockdown of $Na_V1.8$ in rats with SNL reversed behavioral signs of neuropathic pain (Porreca, F. *et al.*, 2000; Lai, J. *et al.*, 2003), which is consistent with the ability of $Na_V1.8$ to enable DRG neurons to fire repetitively after stimulation (Akopian, A. N. *et al.*, 1999; Renganathan, M., *et al.*, 2001). There is evidence that suggests that behavioral neuropathic pain may be partly mediated through an abnormal redistribution of $Na_V1.8$ after nerve injury (Lai, J. *et al.*, 2003). Recent investigations found that the μO-conotoxin MrVIB produced a selective block of the $Na_V1.8$ current (Ekberg, J. *et al.*, 2006). Intrathecal injections of MrVIB produced dose-dependent attenuation of tactile allodynia and thermal hyperalgesia in rats with peripheral nerve injury, leading to the conclusion that blockade of $Na_V1.8$ may provide one therapeutic avenue for the alleviation of neuropathic pain (Ekberg, J. *et al.*, 2006).

Interestingly, immunological and electrophysiological studies showed that SNL resulted in a downregulation of $Na_V1.8$ protein or conductance in the DRG of injured neurons but upregulation in adjacent, uninjured unmyelinated, and myelinated DRG neurons (Porreca, F. *et al.*, 1998; Gold, M. S. *et al.*, 2003). This redistribution of $Na_V1.8$ after SNL was blocked by antisense knockdown techniques (Gold, M. S. *et al.*, 2003; Lai, J. *et al.*, 2003). The injury-induced changes in immunoreactivity of $Na_V1.8$ was correlated with an increase in tetrodotoxin-resistant (TTX-R) compound action potential at C fiber conduction velocity along with a minor contribution at A fiber conduction velocity, suggesting a functional reorganization of $Na_V1.8$ along unmyelinated fibers and in some myelinated fibers (Gold, M. S. *et al.*, 2003). Antisense-mediated knockdown of $Na_V1.8$ immunoreactivity and TTX-R current in these uninjured axons correlates with the reversal of both mechanical and thermal hypersensitivity, suggesting that this reorganization of $Na_V1.8$ activity along the uninjured axons may be necessary for expression of neuropathic pain in the injured rat (Gold, M. S. *et al.*, 2003; Lai, J. *et al.*, 2003). A redistribution of $Na_V1.8$ along the injured sciatic nerve has been also observed in the chronic constriction injury model of neuropathic pain, and $Na_V1.8$ immunoreactivity is evident in peripheral nerve tissues from patients with chronic neuropathic pain (Novakovic, S. D. *et al.*, 1998; Coward, K. *et al.*, 2000). Immunohistochemical studies of human tooth pulp obtained from painful and nonpainful teeth demonstrated that fine unmyelinated nerve fibers expressed $Na_V1.8$ (Renton, T. *et al.*, 2005). In addition, there was an increased expression of $Na_V1.8$ in nerve fibers obtained from painful teeth (Renton, T. *et al.*, 2005).

$Na_V1.7$, a TTX-S VGSC is found predominantly in small-diameter sensory DRG neurons and in sympathetic nerves and plays a prominent role in enhanced pain states (Wood, J. N. *et al.*, 2004b). Recent investigations confirm that this channel mediates the intense burning pain associated with familial erythermalgia. Primary erythermalgia is a rare, autosomal-dominant condition that manifests itself by intermittent bouts of swelling of the feet or hands, intense burning pain, and erythemia (Yang, Y. *et al.*, 2004). The syndrome may be provoked by warmth or exercise and is refractory to therapeutic interventions (Yang, Y. *et al.*, 2004). It was found that individuals afflicted with erythromelalgia expressed a T to A transversion mutation in the gene *SCN9A*, which codes the alpha-subunit of the $Na_V1.7$ sodium channel (Yang, Y. *et al.*, 2004). These mutations of the $Na_V1.7$ sodium channel were found to promote abnormal activity of small-diameter nociceptors, which would be consistent with a small-fiber neuropathy (Drenth, J. P. *et al.*, 2005). Electrophysiologic studies demonstrated that the mutated channel produced a hyperpolarizing shift in activation, slowed deactivation of the channel and markedly increased the ramp current, with the net effect being a marked hyperexcitation of the cells (Dib-Hajj, S. D. *et al.*, 2005). The $Na_V1.7$ sodium channel is upregulated after carrageenan-induced inflammation, and genetically modified mice with knockdown of the $Na_V1.7$ channel of sensory neurons showed an attenuated inflammation-induced hyperalgesia (Wood, J. N. *et al.*, 2004a). More recently, voltage clamp studies performed on transfected mouse DRG cells showed that the human mutations lowered the thresholds for generation of action potentials and repetitive firing, thus provoking high-frequency firing of nociceptive small-diameter sensory neurons in the DRG (Dib-Hajj, S. D. *et al.*, 2005). It is now believed that enhanced sensitivity of this sodium channel may exacerbate activation of the TRPV1 channels, thus driving nociceptor hyperexcitability.

More recent studies were undertaken with patients with the autosomal dominant spontaneous pain condition, paroxysmal extreme pain disorder (PEPD), which manifests as paroxysmal episodes of burning pain in ocular, mandibular, and rectal regions. Mutational analysis of SCN9A obtained from individuals with PEPD and unafflicted family members revealed that the mutation was associated with enhanced $Na_V1.7$ current activity (Fertleman, C. R. *et al.*, 2006). Although primary erythermalgia and PEPD are due to mutations of *SCN9A*, these familial disorders are considered allelic variants that are clinically and mechanistically distinct, related to the specific effects of the mutations on the sodium channel activity (Fertleman, C. R. *et al.*, 2006). On the other side of the spectrum, individuals with one of three distinct nonsense mutations of *SCN9A* show a loss of function of the $Na_V1.7$ channel activity show a marked insensitivity to pain (Cox, J. J. *et al.*, 2006). This sodium channel appears to be critical to nociceptive processing, both acutely and in chronic pain states (Cox, J. J. *et al.*, 2006; Fertleman, C. R. *et al.*, 2006). In spite of the evidence pointing to a prominent role of voltage-gated sodium channels in nociception and enhanced pain due to nerve injury, therapeutic interventions based on blockade of the sodium channels have, to this point, been disappointing. A large multicenter clinical investigation that was recently concluded showed that lamotrigine, which is a nonselective sodium channel blocker, failed to produce changes that were different from placebo in patients with diabetic neuropathy (Vinik, A. I. *et al.*, 2007). A multicenter clinical investigation with oxcarbazepine for diabetic neuropathy suggested that this nonselective sodium channel blocker produced a moderate effect that may be clinically meaningful (Dogra, S. *et al.*, 2005). Though currently unclear, one conclusion is that sodium channel blockers may not be suitable for routine use against neuropathic pain, but may be appropriate for responsive subgroups of neuropathic pain patients (Sindrup, S. H. and Jensen, T. S., 2007). One such example may be patients with postherpetic neuralgia mediated by irritable nociceptors (Sindrup, S. H. and Jensen, T. S., 2007).

5.55.2.5 Role of Calcium Channels

Calcium channels also are critical elements that modulate neuronal excitation (Snutch, T. P. *et al.*, 2001). The N-type calcium channel, which is blocked by omega-conotoxin, has been identified in DRG neurons (Nowycky, M. C. *et al.*, 1985; McCleskey, E. W. *et al.*, 1987). This channel is predominant on nerve terminals of primary afferent terminals in the superficial lamina of the spinal dorsal horn and participates in nociceptive transmission since it is critical to depolarization-coupled release of neurotransmitters, including substance P, CGRP, and glutamate, from these terminals (Santicioli, P. *et al.*, 1992). It was suggested that nerve injury results in either increased frequency of opening of the N-type calcium channel, or an increase in the population (see Snutch, T. P. *et al.*, 2001; Snutch T. P., 2005, for reviews). Blocking the activity of the N-type calcium channel with the omega-conotoxin–GVIA abolished enhanced electrically evoked responses of dorsal horn neurons as well as windup and post-discharge phenomena in nerve-injured rats, which is consistent with inhibition of signs of enhanced pain (Matthews, E. A. and Dickenson, A. H., 2001b). The spinal administration of a novel N-type calcium channel blocker ziconitide produced antinociception in uninjured rats and abolished tactile and thermal hyperesthesias in those with peripheral nerve injuries (Scott, D. A. *et al.*, 2002; Wang, Y. X. *et al.*, 2000a; 2000b). Recent clinical trials with ziconotide (PRIALT) provide strong evidence that blockade of the N-type calcium channel may provide a significant clinical benefit in the management of severe, refractory pain, such as deafferentation pain or pain due to cancer or neuropathies associated with HIV/AIDS and postherpetic neuralgia (Wang, Y. X., *et al.*, 2000a; 2000b; Miljanich, G. P., 2004; Prommer, E. E., 2005).

The T-type calcium channel is present in DRG neurons and on second-order neurons of the dorsal horn of the spinal cord (Talley, E. M. *et al.*, 1999; see Hildebrand, M. E. and Snutch, T. P., 2006, for a review). Activation of the NK1 receptor and of the T-type voltage-gated calcium channels (VGCCs) acts synergistically with activation of the NMDA/calcium channel complex to facilitate firing of the NK1-expressing cells of lamina I, thus promoting central sensitization (Ikeda, H. *et al.*, 2003). This observation is consistent with observations that blockade of the T-type VGCC produced dose-dependent reversal of behavioral signs of neuropathic pain in rats with peripheral nerve injury (Dogrul, A. *et al.*, 2003). Moreover, pharmacologic blockade of T-type VGCCs also diminished electrophysiologic signs of postsynaptic sensitization indicated by windup and after-discharges in nerve-injured rats (Matthews, E. A. and Dickenson, A. H., 2001a). The role of this VGCC in pain modulation makes the T-type calcium channel an attractive target for drug development. Although several compounds are

under preclinical investigation as T-type channel blockers, no clinical data exist with which to gauge their clinical utility against neuropathic pain (Hildebrand, M. E. and Snutch, T. P., 2006).

5.55.3 Enhanced Afferent Discharges Lead to Central Sensitization in the Spinal Cord

The pronociceptive changes that occur in peripheral afferent fibers after nerve injury promote enhanced activity of these fibers, and this afferent drive is thought to result in hyperalgesia and allodynia (Amir, R. *et al.*, 2002). However, although although onset of neuropathic pain is consistent with the initiation of the increased afferent discharges, the enhanced activity of peripheral fibers diminishes fairly rapidly, whereas the behavioral signs of enhanced pain persist long after the initial insult, indicating that mechanisms which sustain neuropathic pain may differ from those which initiate such pain (Liu, C. N. *et al.*, 2001; Ossipov, M. H. *et al.*, 2005; Sun, Q. *et al.*, 2005). There is general agreement that these behavioral manifestations of enhanced pain are mediated in large part by an enhanced responsiveness of the spinal cord to sensory inputs, or central sensitization, which may be both initiated, and in part, sustained by the primary afferent barrage. Sensitization of second-order neurons of the spinal dorsal horn has been illustrated experimentally by the phenomena of windup. Windup is characterized by progressively increasing responses of spinal dorsal horn neurons in response to repetitive electrical stimulation of C fibers (Mendell, L. M., 1966; Woolf, C. J., 1996). Windup is relatively short term in duration and occurs only in response to stimulation of C fibers, and, in the uninjured state, not of A-beta fibers, and is nociceptive specific (Woolf, C. J., 1996; Ji, R. R. *et al.*, 2003; Ji, R. R. and Strichartz, G., 2004). Conditioning stimuli in the form of electrically evoked trains of C fiber activity has been found to produce long-term responsiveness of dorsal horn units to additional stimuli, a profile that appears similar to long-term potentiation (LTP) (Woolf, C. J., 1996; Ji, R. R. *et al.*, 2003; Ji, R. R. and Strichartz, G., 2004). Although these dorsal horn neurons are unreactive to A-beta fiber inputs in the resting state, they become sensitized through repetitive C fiber stimulation which can render them excitable by A-beta fiber inputs, and this may represent a mechanism which contributes to touch-evoked allodynia (Woolf, C. J., 1996; Ji, R. R. *et al.*, 2003; Ji, R. R. and Strichartz, G., 2004).

The state of central sensitization is generally characterized by electrophysiologic parameters that include a reduction in sensory thresholds, increased responsiveness of second-order neurons to afferent inputs along with after-discharges, and expansion of the receptive field along with recruitment of afferent fibers that are not normally nociceptive (Cook, A. J. *et al.*, 1987). Behaviorally, a reduction in sensory threshold is demonstrated by the significantly reduced withdrawal latencies to noxious thermal stimuli or reduced thresholds to noxious mechanical stimuli (Woolf, C. J. and Thompson, S. W., 1991; Hedo, G. *et al.*, 1999). In addition, light tactile stimuli that do not elicit behavioral responses in normal animals produce nocifensive behaviors in the sensitized state (Woolf, C. J. and Thompson, S. W., 1991; Hedo, G. *et al.*, 1999; Ossipov, M. H. and Porreca, F., 2005). For example, sensitization induced by the intradermal injection of capsaicin reduced pain thresholds to noxious heat and elicited allodynia to light brush in human volunteers (Simone, D. A. *et al.*, 1989). Similarly, intradermal injection of capsaicin reduced the stimulus threshold required to elicit responses of the spinothalamic tract (STT) neurons to light brush and also increased the response intensity of these second-order neurons (Simone, D. A. *et al.*, 1991). Peripheral nerve injury was shown to increase the spontaneous activity of dorsal horn neurons and to enhance the responses of these neurons to noxious heat or light touch applied to the injured hindpaw (Suzuki, R. and Dickenson, A., 2005a; 2005b). Moreover, nerve injury also provoked pronounced after-discharges and significantly enlarged the receptive field of dorsal horn neurons in response to noxious heat or pinch (Suzuki, R. *et al.*, 2004a; Suzuki, R. and Dickenson, A., 2005a; 2005b). Peripheral nerve injury also caused a shift to the left of the stimulus–response function of wide dynamic range (WDR) neurons in response to tactile, but not thermal, stimuli (Kauppila, T. *et al.*, 1998; Pertovaara, A. *et al.*, 2001).

In addition to electrophysiologic means, immunohistochemical detection of the proto-oncogene product FOS in the spinal cord has been widely employed as an indicator for neurons that are activated by noxious inputs, and its enhanced expression in the spinal dorsal horn is suggestive of sensitization (Hunt, S. P. *et al.*, 1987; Shortland, P. and Molander, C., 1998). Peripheral nerve injury produced significant increases in noxious and touch-evoked FOS expression in the superficial and intermediate laminae of the spinal dorsal horn (Catheline, G. *et al.*, 1999; Vera-Portocarrero, L. P. *et al.*, 2006; Zhang, E. T. *et al.*, 2007). Electrical stimulation at A-beta fiber intensity or application of light

touch evoked FOS expression, but only after nerve injury or inflammation (Ma, Q. P. and Woolf, C. J., 1996; Shortland, P. and Molander, C., 1998; Nomura, H. *et al.*, 2002). Recently, gentle stroking of the hindpaw, which did not evoke FOS expression in normal rats, but caused significant increases in FOS expression after nerve injury (Catheline, G. *et al.*, 1999; Zhang, E. T. *et al.*, 2007). The enhanced expression of FOS was found in the superficial and deep laminae of the spinal dorsal horn (Zhang, E. T. *et al.*, 2007). Together, these studies indicate that peripheral nerve injury can promote a state of sensitization of spinal dorsal horn neurons.

5.55.4 Excitatory Transmitters Promote Central Sensitization

Sensitization of the spinal cord elicited by enhanced peripheral afferent inputs results in part from the recruitment of subthreshold stimuli to evoke a neuronal response that is related to increased release of excitatory neurotransmitters form the primary afferent terminals (Li, Q. J. and Lu, G. W., 1989; Li, J. *et al.*, 1999). Microdialysis studies demonstrated the release of glutamate and aspartate from primary afferents in response to the capsaicin injected intradermally in the plantar aspect of the hindpaw of the rat or electrical stimulation of the sciatic nerve at C fiber intensity (Paleckova, V. *et al.*, 1992; Sluka, K. A. and Willis, W. D., 1998). Similarly, behavioral hypersensitivity and central sensitization due to peripheral nerve injury or inflammation are associated with increased evoked release of glutamate and aspartate from primary afferent terminals (Paleckova, V. *et al.*, 1992; Kawamata, M. and Omote, K., 1996; Sluka, K. A. and Willis, W. D., 1998; Kawamata, M. and Omote, K., 1999). Spontaneous and stimulus-evoked release of substance P and CGRP from primary afferent terminals is increased after peripheral nerve injury (Paleckova, V. *et al.*, 1992; Sluka, K. A. and Willis, W. D., 1998; Wallin, J. and Schott, E., 2002; Gardell, L. R. *et al.*, 2003a; 2003b). Increased release of excitatory neurotransmitters, including glutamate, substance P, and CGRP is believed to contribute to central sensitization and to hyperalgesia. For example, CGRP release after intradermal capsaicin increased WDR activity in the dorsal horn in response to brush or pinch (Sun, R. Q. *et al.*, 2003; Sun, R. Q. *et al.*, 2004).

The existence of excitatory NMDA autoreceptors on central terminals of primary afferents has been described (Liu, H. *et al.*, 1997). Nociception and release of substance P and glutamate from primary afferent terminals evoked by spinal NMDA was abolished by capsaicin, indicating that presynaptic NMDA receptors provoke further release of excitatory transmitters (Liu, H. *et al.*, 1997). Glutamate may also act at presynaptic metabotropic receptors to promote sensitization (Ohishi, H. *et al.*, 1995). Prostacyclin and PGE2 enhanced capsaicin-evoked release of substance P and CGRP through presynaptic excitation (Southall, M. D. *et al.*, 1998; Southall, M. D. and Vasko, M. R., 2001; Southall, M. D. *et al.*, 2002). These observations are consistent with the fact that central sensitization elicited by C fiber stimulation or inflammation was blocked by NMDA antagonists (Woolf, C. J. and Salter, M. W., 2000).

A measure indicative of the level of primary afferent drive into the spinal dorsal horn is the determination of internalization of the NK1 receptor on second-order neurons that are activated by substance P released from primary afferent nociceptors (Allen, B. J. *et al.*, 1999; Honore, P. *et al.*, 1999). Under nonsensitized conditions, noxious stimulation, such as electrical stimulation at C fiber intensity, subcutaneous capsaicin or noxious heat or pinch, will evoke rapid internalization of the NK1 receptor almost exclusively in the outer lamina of the spinal cord (Allen, B. J. *et al.*, 1999; Honore, P. *et al.*, 1999). Moreover, nonnoxious stimulation does not evoke internalization of NK1. However, when sensitization occurs due to inflammation or peripheral nerve injury, there is a marked enhancement of noxious-induced NK1 internalization, and NK1 internalization is found in the deeper laminae of the spinal cord as well (Allen, B. J. *et al.*, 1999; Honore, P. *et al.*, 1999). In addition, nonnoxious stimuli such as light brush also evoke NK1 internalization in the intermediate and deep laminae of the spinal dorsal horn (Allen, B. J. *et al.*, 1999; Honore, P. *et al.*, 1999; Khasabov, S. G. *et al.*, 2002). Critically, electrical stimulation at A-beta fiber intensity does not elicit NK1 internalization after nerve injury, indicating that the effect produced by light brush is not a direct result of large-diameter fiber stimulation, but is likely to be secondary to other mechanisms driving sensitization (Allen, B. J. *et al.*, 1999; Khasabov, S. G. *et al.*, 2002). NK1 internalization observed in the deeper laminae may be due in part to diffusion of substance P to NK1 receptors on sensitized deep lamina neurons, or partly due to the small number of direct synaptic contacts between C fibers and deep lamina neurons (Allen, B. J. *et al.*, 1999; Khasabov, S. G. *et al.*, 2002).

Recent studies demonstrated that the postsynaptic second-order neurons of the spinal dorsal horn

express message for the bradykinin B2 receptor (Wang, H. B. *et al.*, 2005). Patch-clamp studies showed that activation of the B2 receptor produces a dose-dependent potentiation of AMPA and NMDA currents in dorsal horn neurons. Excitation of the B2 receptor mediates increased frequency and amplitude of AMPA-mediated excitatory postsynaptic potentials, whereas B2 antagonists abolished electrophysiologic signs of central sensitization in dorsal horn neurons (Wang, H. B. *et al.*, 2005). These studies suggest that spinal bradykinin B2 receptors represent an important postsynaptic mechanism in promoting central sensitization and enhanced pain through the potentiation of glutaminergic synaptic transmission (Wang, H. B. *et al.*, 2005). While the importance of bradykinin receptors in enhancing pain, including chronic neuropathic pain (see below) seem clear, the mechanism by which the receptors are activated is not known.

5.55.5 Descending Facilitation Promotes Enhanced Pain

The existence of a pronociceptive pain facilitatory system projecting from the RVM has been well established (see Porreca, F. *et al.*, 2002; Heinricher, M. M. *et al.*, 2003; Ossipov, M. H. and Porreca, F., 2005 for reviews). It has been demonstrated that the microinjection of lidocaine into the RVM abolished behavioral signs of enhanced pain after nerve injury or inflammation, and abolished the sensitization of spinal WDR neurons to mustard oil induced inflammation (Mansikka, H. and Pertovaara, A., 1997; Burgess, S. E. *et al.*, 2002; Pertovaara, A. and Almeida, A., 2006). Lesions of the descending projections from the RVM in the dorsolateral funiculus also abolished behavioral hypersensitivity after inflammation or nerve injury (Wei, F. *et al.*, 1998; 1999; Ossipov, M. H. *et al.*, 2000; Burgess, S. E. *et al.*, 2002). Finally, it was found that selective ablation of RVM neurons that express the mu-opioid receptor, and which may label cells which contribute to descending facilitation, also abolished behavioral signs of sensitization and the enhanced capsaicin-evoked release of CGRP (Burgess, S. E. *et al.*, 2002; Gardell, L. R. *et al.*, 2003a; 2003b; Porreca, F. *et al.*, 2002). Importantly, disruption of descending facilitation abolished behavioral hypersensitization during later, but not initial, phases after nerve injury, indicating that it is essential to the maintenance of a sensitized state (Burgess, S. E. *et al.*, 2002; Porreca, F. *et al.*, 2002; Gardell, L. R. *et al.*, 2003a; 2003b). Most recently, it was shown that activation of descending facilitation from the RVM was subsequent to stimulation of NK1-expressing lamina I postsynaptic cells and increased the neuronal responses of WDR neurons of the deeper laminae of the dorsal horn after nerve injury or inflammation (Suzuki, R. *et al.*, 2002; 2004a; Rahman, W. *et al.*, 2004; 2006). Spinal ondansetron blocked the sensitization of these WDR neurons, which is consistent with a descending serotonergic facilitatory pathway from the RVM (Suzuki, R. *et al.*, 2002; Rahman, W. *et al.*, 2004; Suzuki, R. *et al.*, 2004a; Rahman, W. *et al.*, 2006).

5.55.5.1 Role of the Rostralventromedial Medulla in Descending Facilitation of Pain

The RVM and surrounding tissue has long been recognized as a region critical to nociceptive processing and receives inputs from ascending nociceptive pathways as well as from descending pain modulatory sites. The RVM is considered to be the final common relay for descending inhibition of nociceptive inputs. More recently, this region has also been demonstrated to mediate a significant descending pain facilitatory system as well (Fields, H. L. and Basbaum, A. I., 1999; Porreca, F. *et al.*, 2002; Heinricher, M. M. *et al.*, 2003; Ossipov, M. H. and Porreca, F., 2005). Stimulation of this region, either through electrical stimulating electrodes or through the microinjection of glutamate or neurotensin, resulted in biphasic effects on behavioral and electrophysiologic responses to noxious stimuli (Zhuo, M. and Gebhart, G. F., 1997; Fields, H. L. and Basbaum, A. I., 1999). Whereas high levels of stimulation inhibited nociceptive responses, lower levels of stimulation facilitated the same responses (Zhuo, M. and Gebhart, G. F., 1997; Urban, M. O. *et al.*, 1999). Similarly, microinjection of the neurotensin antagonist SR48692 into the RVM also produced a biphasic effect on nociceptive responses. Taken together, these observations indicate that the RVM is capable of mediating both pain inhibitory functions, which are likely to predominate under basal conditions, and facilitation of pain, which would predominate under conditions of enhanced pain (Ossipov, M. H. *et al.*, 2001). Pharmacologic manipulations that attenuate RVM activity also block enhanced nociception. For example, thermal hyperalgesia induced by naloxone-precipitated withdrawal or by previous prolonged exposure to a nociceptive stimulus can be blocked by the

microinjection of lidocaine into the RVM (Kaplan, H. and Fields, H. L., 1991; Morgan, M. M. and Heinricher, M. M., 1992). It is likely that activation of these pronociceptive circuits in the RVM in response to persistent or prolonged noxious inputs leads to a facilitation of more pain (Porreca, F. *et al.*, 2002). Tail withdrawal responses to noxious thermal or mechanical stimuli can be facilitated by the subcutaneous injection of formalin into a hindpaw, and this effect can be reversed by local infusion of the hydrophilic lidocaine derivative QX-314 injected at the site of formalin (Calejesan, A. A. *et al.*, 1998). It is currently understood that descending pain facilitatory systems arising from the RVM are likely mediated through spinopetal serotonergic projections that enhance nociceptive inputs at the level of the spinal cord. The relationship among noxious inputs, the RVM, and descending serotonergic projections to chronic pain states is described in greater detail below.

5.55.5.2 The ON Cells of the Rostralventromedial Medulla Promote Pain Through Descending Facilitation

Neuronal populations within the RVM have been described as ON cells, OFF cells and neutral cells based upon electrophysiologic responses to noxious heat applied to the tail of lightly anesthetized rats (Fields, H. L., 2000; Ossipov, M. H. *et al.*, 2001; Neubert, M. J. *et al.*, 2004). By definition, the OFF cells are tonically active and pause in firing immediately before a withdrawal response from a noxious thermal stimulus, whereas the ON cells accelerate firing immediately before the nociceptive reflex occurs (Fields, H. L. and Heinricher, M. M., 1985; Neubert, M. J. *et al.*, 2004). As the name implies, the activity of the neutral cells does not correlate with nociceptive inputs. Characterization of the neurons of the RVM were initially determined in lightly anesthetized rat preparations, and it was found that tail flick latency was longer during periods of increased OFF cell activity and shorter when the ON cells were active. The considerable body of evidence collected subsequent to these studies confirmed the role of these neurons in the modulation of nociception and extended the findings to other models of acute and enhanced pain. It is now generally accepted that the activity of OFF cells correlates with inhibition of nociceptive inputs and of behavioral nocifensive responses to nociception. In the presence of opioids, OFF cells continue firing after a noxious stimulus is applied and inhibit electrophysiologic and behavioral parameters of nociception through descending inhibition from the RVM (Fields, H. L. and Heinricher, M. M., 1985; Neubert, M. J. *et al.*, 2004). In contrast, the electrophysiologically determined response characteristics of the ON cells are consistent with a pronociceptive function, and it is believed that these neurons serve as the source of descending facilitation from the RVM (Fields, H. L. and Heinricher, M. M., 1985; Heinricher, M. M. *et al.*, 2003; Neubert, M. J. *et al.*, 2004). Accordingly, manipulations that promote nociceptive responsiveness also increase ON cell activity, which is consistent with pain facilitation.

The enhanced behavioral responses to noxious stimuli elicited during naloxone-precipitated withdrawal from morphine correlates with increased spontaneous activity of the RVM ON cells, and both behavioral hyperalgesia and enhanced on cell activity are abolished by lidocaine microinjected into the RVM (Bederson, J. B. *et al.*, 1990; Kaplan, H. and Fields, H. L., 1991). Prolonged application of a noxious thermal stimulus increased ON cell activity and facilitated behavioral nociceptive responses, and both the electrophysiologic and behavioral responses were abolished by microinjection of lidocaine into the RVM (Kaplan, H. and Fields, H. L., 1991; Morgan, M. M. and Fields, H. L., 1994). Electrophysiologic monitoring of RVM neurons demonstrated that the microinjection of either cholecystokinin (CCK) or neurotensin at doses that selectively activated on cells produced facilitated behavioral responses to nociceptive stimuli in lightly anesthetized rats (Heinricher, M. M. and Neubert, M. J., 2004; Neubert, M. J. *et al.*, 2004). Application of mustard oil to the skin of the rat produced increased firing of ON cells and thermal hyperalgesia that were both blocked by NMDA antagonist application into the RVM (Kincaid, W. *et al.*, 2006; Xu, M. *et al.*, 2007). It was also shown that inflammation induces an upregulation of NMDA receptors on the ON cells, along with increased phosphorylation of AMPA receptors, thus enhancing ON cell activity and facilitating nociceptive responses (Guan, Y. *et al.*, 2003; 2004). Finally, recent studies showed that inflammation results in upregulation of BDNF, which facilitates ON cell firing through an NMDA-dependent mechanism (Guo, W. *et al.*, 2006). Most recently, it was discovered that capsaicin injected into a hindpaw or iontophoretic application of Sar^{9},$Met(O_2)^{11}$-substance P into the RVM enhanced ON cell activity and potentiated the responses of ON cells to iontophoretic NMDA (Budai, D. *et al.*, 2007). Conversely,

iontophoretic administration of an NK1 antagonist into the RVM abolished the enhanced responses of ON cells (Budai, D. *et al.*, 2007). Taken together, these studies indicate that ON cells promote nociception, and that enhanced ON cell activity underlies hyperalgesia associated with chronic pain states. In addition, it is suggested that substance P in the RVM may modulate enhanced ON cell activity, and consequently, enhanced pain states.

In light of these observations, it has been proposed that neuropathic pain due to peripheral nerve injury may be initially mediated through enhanced afferent activity, but that the enhanced discharges lead to a sensitized spinal cord and neuroplastic changes culminating in an enhancement of descending facilitation mediated through ON cells of the RVM (Heinricher, M. M. *et al.*, 2003; Ossipov, M. H. *et al.*, 2005; Ossipov, M. H. and Porreca, F., 2006). Considerable electrophysiologic evidence exists to indicate that the population of RVM neurons that express the mu-opioid receptor, or a subset of these cells, are likely to drive descending facilitation (Heinricher, M. M. *et al.*, 1994; Neubert, M. J. *et al.*, 2004). Based on this evidence, presumptive pain facilitatory neurons of the RVM were selectively ablated by using the mu-opioid receptor as a portal of entry into these cells for dermorphin conjugated with the cytotoxin saporin (Porreca, F. *et al.*, 2001; Burgess, S. E. *et al.*, 2002; Vera-Portocarrero, L. P. *et al.*, 2006). With this technique, when the agonist binds to the receptor, internalization occurs, bringing the conjugated agonist and saporin complex into the cell body, where saporin is released and leads to inhibition of ribosome activity, thus causing cell death within 2–3 weeks (Mantyh, P. W. *et al.*, 1997). Selective ablation of pain facilitatory neurons of the RVM by microinjection of the dermorphin–saporin conjugate either 7 days prior to SNL or once tactile and thermal hyperesthesias were well established, respectively, prevented and reversed the behavioral signs of neuropathic pain (Porreca, F. *et al.*, 2001; Burgess, S. E. *et al.*, 2002). Importantly, these behavioral signs of neuropathic pain were abolished 1 week after SNL, and not earlier. Similarly, physical disruption of descending facilitatory tracts from the RVM or microinjection of lidocaine at different time points after SNL produced similar results (Porreca, F. *et al.*, 2001; Burgess, S. E. *et al.*, 2002). Enhanced expression of FOS in the spinal cord is indicative of sensitization. Recently, it was shown that SNL enhanced both the intensity and laminar distribution of FOS evoked by noxious stimuli to include the intermediate laminae of the dorsal horn and promoted novel expression of FOS in response to light brush (Vera-Portocarrero, L. P. *et al.*, 2006; Zhang, E. T. *et al.*, 2007). Microinjection of dermorphin–saporin conjugate into the RVM abolished enhanced FOS expression due to SNL (Vera-Portocarrero, L. P. *et al.*, 2006). These observations indicate that the maintenance phase of the neuropathic pain state is dependent on the certain neuroplastic changes that result in activation of a tonic descending pain facilitation from the RVM, whereas the earlier initiation phase is independent of descending systems.

5.55.5.3 Cholecystokinin in the Rostralventromedial Medulla May Mediate Pain Facilitation

It was recently shown that CCK opposes the antinociceptive activity of morphine by attenuating the morphine-induced activation of OFF cells, which constitute part of the descending inhibition of nociceptive inputs (Heinricher, M. M. *et al.*, 2001; Heinricher, M. M. and Neubert, M. J., 2004). The microinjection of CCK into the RVM produces enhancement of responses to light tactile or noxious thermal stimuli similar to that observed after SNL (Kovelowski, C. J. *et al.*, 2000; Xie, J. Y. *et al.*, 2005). Moreover, the microinjection of CCK2 antagonists into the RVM attenuated behavioral signs of neuropathic pain in rats with SNL (Kovelowski, C. J. *et al.*, 2000; Xie, J. Y. *et al.*, 2005). The behavioral hyperesthesias and hyperalgesia elicited by RVM CCK were abolished by dorsolateral funiculus (DLF) lesions or microinjection of L365,260 (Kovelowski, C. J. *et al.*, 2000; Xie, J. Y. *et al.*, 2005). In addition to its activities in inhibiting morphine-induced activation of OFF cells, it was also recently demonstrated that CCK provokes a direct and selective activation of ON cells of the RVM and that this activation is directly related to the production of hyperalgesia (Heinricher, M. M. and Neubert, M. J., 2004).

5.55.6 Second-Order Projection Neurons Expressing NK1 Receptors May Result in Activation of Descending Pain Facilitation

Converging evidence strongly indicates that central sensitization and hypersensitivity to sensory stimuli is dependent predominantly on the long-term sensitization of the lamina I cells that express the NK1

receptor (Ikeda, H. *et al.*, 2003). Electrophysiologic studies have revealed that approximately 75% of the neurons of lamina I are nociceptive specific, and the remainder are either WDR neurons or polymodal nociceptors that also respond to noxious cold (Suzuki, R. and Dickenson, A. H., 2005a; 2005b). Approximately one-half of the lamina I neurons express the NK1 receptor and project to supraspinal sites that process nociception, including the parabrachial region and the thalamus (Suzuki, R. and Dickenson, A. H., 2005a; 2005b). Recent studies showed that selective ablation of lamina I neurons that express the NK1 receptor abolish behavioral signs of neuropathic pain in rats with SNL (Nichols, M. L. *et al.*, 1999; Honore, P. *et al.*, 1999; Suzuki, R. *et al.*, 2002). In these studies, ablation was performed by spinal injection of substance P conjugated to saporin. Internalization of the NK1 receptor stimulated by substance P introduced the conjugate into the cell body, where saporin interfered with protein synthesis, causing eventual death of the cell (Honore, P. *et al.*, 1999; Nichols, M. L. *et al.*, 1999). Electrophysiologic studies indicated that signs of spinal sensitization induced by intraplantar capsaicin or peripheral inflammation were abolished by selective ablation of the NK1-expressing neurons of lamina I (Khasabov, S. G. *et al.*, 2002; 2005). Additional electrophysiologic studies demonstrated that SNL-induced enhancement of neuronal responses to noxious thermal stimuli or light brush, neuronal after-discharge, and enlargement of the receptive field were abolished in rats with SNL and in which NK1-expressing spinal neurons were selectively ablated with spinal injections of substance P conjugated to saporin (Suzuki, R. *et al.*, 2004a; 2004b; Suzuki, R. and Dickenson, A. H., 2005a; 2005b). Moreover, evoked expression of FOS in the RVM and in neurons in the deep laminae of the spinal cord was also abolished by selective ablation of NK1-expressing neurons of lamina I (Suzuki, R. *et al.*, 2002; Suzuki, R. and Dickenson, A. H., 2005a; 2005b). Based on these observations, especially the critical finding that the projection neurons of the superficial lamina of the spinal cord appear to promote sensitization of dorsal horn neurons in the deep lamina through an indirect mechanism, led to the hypothesis that injury-induced enhanced noxious inputs are transmitted to supraspinal sites, leading to the activation of a pronociceptive descending pain facilitatory system that maintains the state of spinal sensitization and maintains the neuropathic pain state.

5.55.7 Descending Facilitation Maintains a Sensitized Spinal Cord: Upregulation of Spinal Dynorphin and Enhanced Release of Primary Afferent Transmitters

The enhancement of descending facilitation from the RVM is believed to lead to neuroplastic changes in the spinal cord that favor a sensitized state and enhanced nociceptive inputs. A number of studies have demonstrated that enhanced descending facilitation elicited by peripheral nerve injury is associated with an upregulation of spinal dynorphin content and enhanced release of excitatory neurotransmitters from primary afferent neurons. Based on these observations, we formulated the hypothesis that neuropathic pain is initially driven by enhanced primary afferent the ectopic discharge but is then maintained in large part through descending facilitation and upregulation of spinal dynorphin (Lai, J. *et al.*, 2001; Porreca, F. *et al.*, 2002; Ossipov, M. H. and Porreca, F., 2006). Dynorphin upregulation occurs in the same postsynaptic lamina I cells that also express FOS in response to sensitization (Ji, R. R., 2004; Kawasaki, Y. *et al.*, 2004). Elevated levels of spinal dynorphin enhance capsaicin-evoked release of CGRP and substance P from primary afferent terminals and of PGE2, presumably from postsynaptic cells, which further enhances the release of excitatory amino acids from afferent terminals (Gardell, L. R. *et al.*, 2003a; 2003b; Koetzner, L. *et al.*, 2004). Sequestration of dynorphin with antiserum or surgical and neurochemical manipulations that blocked the upregulation of spinal dynorphin also abolished enhanced transmitter release and behavioral neuropathic pain (Burgess, S. E. *et al.*, 2002; Porreca, F. *et al.*, 2002; Gardell, L. R. *et al.*, 2003a; 2003b).

It is well established that elevated levels of spinal dynorphin and its fragments have a prominent pronociceptive role in chronic pain states (Lai, J. *et al.*, 2001). The spinal injection of antiserum to dynorphin did not abolish behavioral signs of neuropathic pain in mice with SNL when administered 2 days after the injury, but was effective 10 days after SNL (Wang, Z. *et al.*, 2001; Gardell, L. R. *et al.*, 2004). Moreover, knockout mice that do not express dynorphin still develop behavioral signs of neuropathic pain after SNL, but these signs resolve within 1 week (Wang, Z. *et al.*, 2001; Gardell, L. R. *et al.*, 2004). The dynorphin-dependent maintenance phase is dependent on descending

facilitation form the RVM. Surgical and pharmacologic manipulations that disrupt descending facilitation abolish both dynorphin upregulation and the maintenance, but not the initiation, of behavioral signs of neuropathic pain. Rats with SNL and either lesions of the DLF or selective ablation of facilitatory RVM neurons after microinjection of the dermorphin–saporin conjugate did not show an upregulation of spinal dynorphin levels and the behavioral signs of neuropathic pain resolved over the time course during which dynorphin upregulation would be expected after SNL (Burgess, S. E. *et al.*, 2002; Gardell, L. R. *et al.*, 2003a). Thus, in the absence of elevated spinal dynorphin, neuropathic pain is not maintained.

Elevated levels of spinal dynorphin promote the release of transmitters from primary afferent terminals, thereby enhancing nociceptive input. The time course and profile of the effect of spinal dynorphin on capsaicin-evoked release of CGRP from primary afferent terminals correlates closely with the behavioral studies. Addition of antiserum to dynorphin abolishes the enhanced capsaicin-evoked release of CGRP 10 days after SNL, but not 2 days after SNL (Burgess, S. E. *et al.*, 2002; Gardell, L. R. *et al.*, 2003a). Disruption of descending facilitation by microinjection of dermorphin–saporin conjugate into the RVM or by lesioning the DLF also abolishes SNL-induced enhancement of capsaicin-evoked release of CGRP (Burgess, S. E. *et al.*, 2002; Gardell, L. R. *et al.*, 2003a). The significance of this line of investigation requires additional examination, however.

5.55.7.1 Descending Facilitation Maintains a Sensitized Spinal Cord: Upregulation of Spinal Dynorphin and Enhanced Release of Primary Afferent Transmitters

The mechanism through which dynorphin may exert a pronociceptive function in the spinal cord is not fully understood. It was once suggested that dynorphin may act at the glycine coagonist site to potentiate the effect of glutamate at the NMDA receptor (Zhang, L. *et al.*, 1997). However, other studies provided evidence that dynorphin could inhibit opening of ion channels mediated by the NMDA receptor (Chen, L. and Huang, L. Y., 1998). Bakalkin and coworkers suggested that dynorphin could promote the formation of pores through the cell membrane, allowing the leakage of sodium and calcium ions, thus sensitizing neurons in this fashion, but this mechanism was not explicitly demonstrated (Hugonin, L. *et al.*, 2006). The mechanism by which dynorphin may promote nociception has recently been suggested to be mediated through bradykinin receptors (Lai, J. *et al.*, 2006). Bradykinin B1 and B2 receptors are present on nerve terminals of primary afferent fibers (Botticelli, L. J. *et al.*, 1981; Cloutier, F. *et al.*, 2002), and are in close proximity to interneurons that express dynorphin (Botticelli, L. J. *et al.*, 1981). Moreover, the B1 and B2 receptors are upregulated after SNL (Lai, J. *et al.*, 2006). A pronociceptive role of these receptors is indicated since intrathecal administration of bradykinin produced behavioral signs of hyperalgesia (Wang, H. B. *et al.*, 2005). Behavioral signs of enhanced pain after nerve injury were attenuated in B1 or B2 knockout mice (Ferreira, J. *et al.*, 2002; Wang, H. B. *et al.*, 2005). Curiously, although the bradykinin receptors are present in the spinal cord, there is little evidence of bradykinin synthesis within the spinal cord, suggesting the either bradykinin must diffuse from the circulatory system to act at the receptors, or there may be another endogenous ligand (Lai, J. *et al.*, 2006). It was shown that dynorphin induced a transient increase in calcium conductance in embryonic DRG cells that was blocked by B2 antagonists (Lai, J. *et al.*, 2006). Dynorphin-induced calcium currents were also blocked by B1 or B2 antagonists in transfected cells expressing these receptors (Lai, J. *et al.*, 2006). In the same study, it was shown that dynorphin demonstrated specific binding to the B1 and B2 receptors (Lai, J. *et al.*, 2006). Finally, antagonists of the B1 or B2 receptors given intrathecally produced dose-dependent attenuation of behavioral parameters indicative of neuropathic pain in rats with SNL, but only at the time points when spinal dynorphin was elevated (Lai, J. *et al.*, 2006). The antagonists were without effect during the dynorphin-independent early phase of nerve injury. Taken together, these studies indicate that dynorphin may mediate its pronociceptive enhancement of neuropathic pain through actions at the bradykinin receptors. The activity of dynorphin at bradykinin receptors could underlie the sensitization of dorsal horn neurons as described above (Wang, H. B. *et al.*, 2005).

5.55.7.2 Descending Facilitation Maintains a Sensitized Spinal Cord: Serotonergic Contributions

More recent studies suggest that descending serotonergic projections from the RVM may promote spinal sensitization through an action at the 5-HT_3 receptor. The 5-HT_3 receptor facilitates release or transmitter from nerve terminals through a ligand-gated Ca^{2+} channel (Miquel, M. C. *et al.*,

2002; Zeitz, K. P. *et al.*, 2002). This receptor is predominant in the superficial laminae of the spinal dorsal horn (Doucet, E. *et al.*, 2000; Miquel, M. C. *et al.*, 2002). Of this population, the major portion, approximately 85%, are found on primary afferent nerve terminals and the remainder at postsynaptic sites (Doucet, E. *et al.*, 2000; Miquel, M. C. *et al.*, 2002). Electrophysiologic studies indicated that primary afferent nerves that express the 5-HT_3 receptor on their terminals include C fiber nociceptors and myelinated A-delta nociceptors sensitive to mechanical stimuli (Zeitz, K. P. *et al.*, 2002). This distribution is consistent with the modulation of mechanical-evoked nociceptive signals, and the 5-HT_3 receptor has been shown to facilitate nociceptive transmission at the level of the spinal cord (Zeitz, K. P. *et al.*, 2002). Double-labeling studies in the nucleus raphe magnus (NRM) detected a population of serotonergic neurons that express FOS in response to noxious stimulation, suggesting the existence of a pronociceptive serotonergic projection from the RVM (Suzuki, R. *et al.*, 2002). Moreover, it was found that serotonergic terminals from the RVM are juxtaposed with cell bodies in the intermediate laminae of the dorsal horn, some of which also express the NK1 receptor (Todd, A. J. *et al.*, 2000; Todd, A. J., 2002). Antagonists of the 5-HT_3 receptor or depletion of serotonin from the spinal cord abolished the enhanced responses of dorsal horn neurons to mechanical stimulation in rats with SNL (Rahman, W. *et al.*, 2006). The 5-HT_3 antagonist ondansetron abolished behavioral signs of neuropathic pain and electrophysiologic parameters indicative of sensitization of superficial and deep dorsal horn neurons in rats with SNL (Suzuki, R. *et al.*, 2004a; 2004b). The effects of ondansetron were blocked by disrupting enhanced RVM activity through the ablation of NK1-expressing dorsal horn neurons with substance P–saporin conjugate, indicating that the 5-HT_3 receptors were activated by a descending serotonergic pain facilitatory system from the RVM (Suzuki, R.*et al.*, 2004a; 2004b).

Collectively, these observations paint a picture suggesting that neuropathic pain states are maintained, at least in part, by increased sensitivity of primary afferent neurons to noxious stimuli. In addition, it is hypothesized that persistent nociceptive inputs elicits supraspinal neuroplastic changes that results in the activation of a tonic descending facilitation of nociceptive inputs, which is mediated by an upregulation of spinal dynorphin content. Thus, increased spinal dynorphin serves to promote excitatory transmitter release, which in turn promotes the maintenance of the tonic descending facilitatory system, thus perpetuating a chronic pain state. The existence of a pronociceptive spinal–supraspinal loop that maintains a sensitized spinal cord may also provide a mechanism through which tactile hyperesthesia might be mediated.

5.55.8 Summary

Tremendous progress in our understanding of mechanisms that initiate and maintain neuropathic pain has been made over the past two decades. Importantly, such increased understanding has led to programs aimed at the development of novel therapeutics for neuropathic pain. It has been well appreciated that peripheral nerve injury produces increased activity of the injured and adjacent uninjured peripheral nerve fibers. This enhanced activity, or peripheral sensitization, is maintained in part by increased or relocation of ion channels that promote axonal firing. Programs are in place in the pharmaceutical industry to develop subtype selective sodium channel blockers that may diminish enhance activities of injured or adjacent nerves. Increase in pronociceptive mediators, including cytokines, chemokines, and growth factors have been noted in multiple experimental models of neuropathic pain. The enhanced primary afferent activity leads to a state of sensitization of the spinal cord neurons, such that they are more responsive to sensory inputs. Approaches aimed at decreasing sensitization of nociceptors through anti-NGF strategies, or through the administration of exogenous growth factors of the GDNF family, are either in development or under consideration by the pharmaceutical industry. Enhanced activity of sensitized nociceptors can increase ascending sensory inputs to supraspinal centers and neuroplastic changes that help maintain a sensitized state. One prominent change is increased availability of CCK in the RVM and enhanced descending facilitation of pain from this region. The enhanced pain facilitation leads to further changes in the spinal cord, notably upregulation of spinal dynorphin to pathological levels. Dynorphin, along with pronociceptive transmitters such as PGEs and glutamate, enhance the release of excitatory transmitters from primary afferent terminals. The result is a net increase in nociceptive inputs that help perpetuate this pronociceptive spinal/supraspinal/spinal pain facilitatory loop. Such knowledge underlies efforts to development of N-type calcium channel

blockers. Understanding the changes that occur at each of these nodes in this cycle could lead to means through which this self-perpetuating chain of events may be broken, thus abolishing the mechanisms that perpetuate chronic pain. The accelerating understanding of pain regulatory systems advanced by the discovery of underlying mechanisms driving enhanced abnormal pain will be continuously validated by clinical trials of drugs with novel mechanisms of action. Critically, new mechanisms of action will be tested clinically with the expectation that improved therapy can be provided to patients.

References

Akopian, A. N., Souslova, V., England, S., Okuse, K., Ogata, N., Ure, J., Smith, A., Kerr, B. J., McMahon, S. B., Boyce, S., Hill, R., Stanfa, L. C., Dickenson, A. H., and Wood, J. N. 1999. The tetrodotoxin-resistant sodium channel SNS has a specialized function in pain pathways. Nat. Neurosci. 2, 541–548.

Ali, Z., Ringkamp, M., Hartke, T. V., Chien, H. F., Flavahan, N. A., Campbell, J. N., and Meyer, R. A. 1999. Uninjured C-fiber nociceptors develop spontaneous activity and alpha-adrenergic sensitivity following L6 spinal nerve ligation in monkey. J. Neurophysiol. 81, 455–466.

Allen, B. J., Li, J., Menning, P. M., Rogers, S. D., Ghilardi, J., Mantyh, P. W., and Simone, D. A. 1999. Primary afferent fibers that contribute to increased substance P receptor internalization in the spinal cord after injury. J. Neurophysiol. 81, 1379–1390.

Amir, R., Michaelis, M., and Devor, M. 2002. Burst discharge in primary sensory neurons: triggered by subthreshold oscillations, maintained by depolarizing afterpotentials. J. Neurosci. 22, 1187–1198.

Apfel, S. C. 2000. Neurotrophic factors and pain. Clin. J. Pain 16, 7–11.

Attal, N. and Bouhassira, D. 1999. Mechanisms of pain in peripheral neuropathy. Acta Neurol. Scand. Suppl. 173, 12–24.

Averill, S., Michael, G. J., Shortland, P. J., Leavesley, R. C., King, V. R., Bradbury, E. J., McMahon, S. B., and Priestley, J. V. 2004. NGF and GDNF ameliorate the increase in ATF3 expression which occurs in dorsal root ganglion cells in response to peripheral nerve injury. Eur. J. Neurosci. 19, 1437–1445.

Backonja, M. M. and Stacey, B. 2004. Neuropathic pain symptoms relative to overall pain rating. J. Pain 5, 491–497.

Banik, R. K., Subieta, A. R., Wu, C., and Brennan, T. J. 2005. Increased nerve growth factor after rat plantar incision contributes to guarding behavior and heat hyperalgesia. Pain 117, 68–76.

Bederson, J. B., Fields, H. L., and Barbaro, N. M. 1990. Hyperalgesia during naloxone-precipitated withdrawal from morphine is associated with increased on-cell activity in the rostral ventromedial medulla. Somatosens. Mot. Res. 7, 185–203.

Bennett, M. I., Attal, N., Backonja, M. M., Baron, R., Bouhassira, D., Freynhagen, R., Scholz, J., Tolle, T. R., Wittchen, H. U., and Jensen, T. S. 2007. Using screening tools to identify neuropathic pain. Pain 127, 199–203.

Bennett, D. L., Boucher, T. J., Armanini, M. P., Poulsen, K. T., Michael, G. J., Priestley, J. V., Phillips, H. S., McMahon, S. B., and Shelton, D. L. 2000. The glial cell line-derived neurotrophic factor family receptor components are differentially regulated within sensory neurons after nerve injury. J. Neurosci. 20, 427–437.

Bennett, D. L., Koltzenburg, M., Priestley, J. V., Shelton, D. L., and McMahon, S. B. 1998. Endogenous nerve growth factor regulates the sensitivity of nociceptors in the adult rat. Eur. J. Neurosci. 10, 1282–1291.

Botticelli, L. J., Cox, B. M., and Goldstein, A. 1981. Immunoreactive dynorphin in mammalian spinal cord and dorsal root ganglia. Proc. Natl. Acad. Sci. U. S. A. 78, 7783–7786.

Boucher, T. J. and McMahon, S. B. 2001. Neurotrophic factors and neuropathic pain. Curr. Opin. Pharmacol. 1, 66–72.

Boucher, T. J., Okuse, K., Bennett, D. L., Munson, J. B., Wood, J. N., and McMahon, S. B. 2000. Potent analgesic effects of GDNF in neuropathic pain states. Science 290, 124–127.

Bouhassira, D., Attal, N., Alchaar, H., Boureau, F., Brochet, B., Bruxelle, J., Cunin, G., Fermanian, J., Ginies, P., Grun-Overdyking, A., Jafari-Schluep, H., Lanteri-Minet, M., Laurent, B., Mick, G., Serrie, A., Valade, D., and Vicaut, E. 2005. Comparison of pain syndromes associated with nervous or somatic lesions and development of a new neuropathic pain diagnostic questionnaire (DN4). Pain 114, 29–36.

Budai, D., Khasabov, S. G., Mantyh, P. W., and Simone, D. A. 2007. NK-1 receptors modulate the excitability of ON cells in the rostral ventromedial medulla. J. Neurophysiol. 97, 1388–1395.

Burgess, S. E., Gardell, L. R., Ossipov, M. H., Malan, T. P., Jr., Vanderah, T. W., Lai, J., and Porreca, F. 2002. Time-dependent descending facilitation from the rostral ventromedial medulla maintains, but does not initiate, neuropathic pain. J. Neurosci. 22, 5129–5136.

Calejesan, A. A., Ch'ang, M. H., and Zhuo, M. 1998. Spinal serotonergic receptors mediate facilitation of a nociceptive reflex by subcutaneous formalin injection into the hindpaw in rats. Brain Res. 798, 46–54.

Catheline, G., Le Guen, S., Honore, P., and Besson, J. M. 1999. Are there long-term changes in the basal or evoked Fos expression in the dorsal horn of the spinal cord of the mononeuropathic rat? Pain 80, 347–357.

Chen, Q. and Huang, L. Y. 1998. Dynorphin block of *N*-methyl-D-aspartate channels increases with the peptide length. J. Pharmacol. Exp. Them. 284, 824–831.

Chen, Q., King, T., Vanderah, T. W., Ossipov, M. H., Malan, T. P., Jr., Lai, J., and Porreca, F. 2004. Differential blockade of nerve injury-induced thermal and tractile hypersensitivity by systemically adminstered brain-penetrating and peripherally restricted local anesthetics. J. Pain 5, 281–289.

Cloutier, F., de Sousa Buck, H., Ongali, B., and Couture, R. 2002. Pharmacologic and autoradiographic evidence for an up-regulation of kinin B2 receptors in the spinal cord of spontaneously hypertensive rats. Br. J. Pharmacol. 135, 1641–1654.

Cook, A. J., Woolf, C. J., Wall, P. D., and McMahon, S. B. 1987. Dynamic receptive field plasticity in rat spinal cord dorsal horn following C-primary afferent input. Nature 325, 151–153.

Coward, K., Plumpton, C., Facer, P., Birch, R., Carlstedt, T., Tate, S., Bountra, C., and Anand, P. 2000. Immunolocalization of SNS/PN3 and NaN/SNS2 sodium channels in human pain states. Pain 85, 41–50.

Cox, J. J., Reimann, F., Nicholas, A. K., Thornton, G., Roberts, E., Springell, K., Karbani, G., Jafri, H., Mannan, J., Raashid, Y., Al-Gazali, L., Hamamy, H., Valente, E. M., Gorman, S., Williams, R., McHale, D. P., Wood, J. N., Gribble, F. M., and Woods, C. G. 2006. An SCN9A

channelopathy causes congenital inability to experience pain. Nature 444, 894–898.
Devor, M. and Wall, P. D. 1990. Cross-excitation in dorsal root ganglia of nerve-injured and intact rats. J. Neurophysiol. 64, 1733–1746.
Dib-Hajj, S. D., Rush, A. M., Cummins, T. R., Hisama, F. M., Novella, S., Tyrrell, L., Marshall, L., and Waxman, S. G. 2005. Gain-of-function mutation in Nav1.7 in familial erythromelalgia induces bursting of sensory neurons. Brain 128, 1847–1854.
Dogra, S., Beydoun, S., Mazzola, J., Hopwood, M., and Wan, Y. 2005. Oxcarbazepine in painful diabetic neuropathy: a randomized, placebo-controlled study. Eur. J. Pain 9, 543–554.
Dogrul, A., Gardell, L. R., Ossipov, M. H., Tulunay, F. C., Lai, J., and Porreca, F. 2003. Reversal of experimental neuropathic pain by T-type calcium channel blockers. Pain 105, 159–168.
Doucet, E., Miquel, M. C., Nosjean, A., Verge, D., Hamon, M., and Emerit, M. B. 2000. Immunolabeling of the rat central nervous system with antibodies partially selective of the short form of the 5-HT_3 receptor. Neuroscience 95, 881–892.
Drenth, J. P., Te Morsche, R. H., Guillet, G., Taieb, A., Kirby, R. L., and Jansen, J. B. 2005. SCN9A mutations define primary erythromelalgia as a neuropathic disorder of voltage gated sodium channels. J. Invest. Dermatol. 124, 1333–1338.
Ekberg, J., Jayamanne, A., Vaughan, C. W., Aslan, S., Thomas, L., Mould, J., Drinkwater, R., Baker, M. D., Abrahamsen, B., Wood, J. N., Adams, D. J., Christie, M. J., and Lewis, R. J. 2006. muO-conotoxin MrVIB selectively blocks Nav1.8 sensory neuron specific sodium channels and chronic pain behavior without motor deficits. Proc. Natl. Acad. Sci. U. S. A. 103, 17030–17035.
Elitt, C. M., McIlwrath, S. L., Lawson, J. J., Malin, S. A., Molliver, D. C., Cornuet, P. K., Koerber, H. R., Davis, B. M., and Albers, K. M. 2006. Artemin overexpression in skin enhances expression of TRPV1 and TRPA1 in cutaneous sensory neurons and leads to behavioral sensitivity to heat and cold. J. Neurosci. 26, 8578–8587.
Ferreira, J., Campos, M. M., Araujo, R., Bader, M., Pesquero, J. B., and Calixto, J. B. 2002. The use of kinin B-1 and B-2 receptor knockout mice and selective antagonists to characterize the nociceptive responses caused by kinins at the spinal level. Neuropharmacology 43, 1188–1197.
Fertleman, C. R., Baker, M. D., Parker, K. A., Moffatt, S., Elmslie, F. V., Abrahamsen, B., Ostman, J., Klugbauer, N., Wood, J. N., Gardiner, R. M., and Rees, M. 2006. SCN9A mutations in paroxysmal extreme pain disorder: allelic variants underlie distinct channel defects and phenotypes. Neuron 52, 767–774.
Fields, H. L. 2000. Pain modulation: expectation, opioid analgesia and virtual pain. Prog. Brain Res. 122, 245–253.
Fields, H. L. and Basbaum, A. I. 1999. Central Nervous System Mechanisms of Pain Modulation. In: Textbook of Pain (*eds*. P. D. Wall and R. Melzack), pp. 309–329. Churchill Livingstone.
Fields, H. L. and Heinricher, M. M. 1985. Anatomy and physiology of a nociceptive modulatory system. Philos. Trans. R. Soc. Lond. B Biol. Sci. 308, 361–374.
Gardell, L. R., Ibrahim, M., Wang, R., Wang, Z., Ossipov, M. H., Malan, T. P., Porreca, F., and Lai, J. 2004. Mouse strains that lack spinal dynorphin upregulation after peripheral nerve injury do not develop neuropathic pain. Neuroscience 123, 43–52.
Gardell, L. R., Vanderah, T. W., Gardell, S. E., Wang, R., Ossipov, M. H., Lai, J., and Porreca, F. 2003a. Enhanced evoked excitatory transmitter release in experimental neuropathy requires descending facilitation. J. Neurosci. 23, 8370–8379.
Gardell, L. R., Wang, R., Ehrenfels, C., Ossipov, M. H., Rossomando, A. J., Miller, S., Buckley, C., Cai, A. K., Tse, A., Foley, S. F., Gong, B., Walus, L., Carmillo, P., Worley, D., Huang, C., Engber, T., Pepinsky, B., Cate, R. L., Vanderah, T. W., Lai, J., Sah, D. W., and Porreca, F. 2003b. Multiple actions of systemic artemin in experimental neuropathy. Nat. Med. 9, 1383–1389.
Gold, M. S., Weinreich, D., Kim, C. S., Wang, R., Treanor, J., Porreca, F., and Lai, J. 2003. Redistribution of Na(V)1.8 in uninjured axons enables neuropathic pain. J. Neurosci. 23, 158–166.
Griffin, J. W. 2006. The Roles of Growth Factors in Painful Length-Dependent Axonal Neuropathies. In: Emerging Strategies for the Treatment of Neuropathic Pain (*eds*. J. N. Campbell *et al.*), pp. 271–290. IASP Press.
Guan, Y., Guo, W., Robbins, M. T., Dubner, R., and Ren, K. 2004. Changes in AMPA receptor phosphorylation in the rostral ventromedial medulla after inflammatory hyperalgesia in rats. Neurosci. Lett. 366, 201–205.
Guan, Y., Guo, W., Zou, S. P., Dubner, R., and Ren, K. 2003. Inflammation-induced upregulation of AMPA receptor subunit expression in brain stem pain modulatory circuitry. Pain 104, 401–413.
Guo, W., Robbins, M. T., Wei, F., Zou, S., Dubner, R., and Ren, K. 2006. Supraspinal brain-derived neurotrophic factor signaling: a novel mechanism for descending pain facilitation. J. Neurosci. 26, 126–137.
Hains, B. C., Saab, C. Y., Klein, J. P., Craner, M. J., and Waxman, S. G. 2004. Altered sodium channel expression in second-order spinal sensory neurons contributes to pain after peripheral nerve injury. J. Neurosci. 24, 4832–4839.
Hedo, G., Laird, J. M., and Lopez-Garcia, J. A. 1999. Time-course of spinal sensitization following carrageenan-induced inflammation in the young rat: a comparative electrophysiological and behavioural study *in vitro* and *in vivo*. Neuroscience 92, 309–318.
Hefti, F. F., Rosenthal, A., Walicke, P. A., Wyatt, S., Vergara, G., Shelton, D. L., and Davies, A. M. 2006. Novel class of pain drugs based on antagonism of NGF. Trends Pharmacol. Sci. 27, 85–91.
Heinricher, M. M. and Neubert, M. J. 2004. Neural basis for the hyperalgesic action of cholecystokinin in the rostral ventromedial medulla. J. Neurophysiol. 92, 1982–1989.
Heinricher, M. M., McGaraughty, S., and Tortorici, V. 2001. Circuitry underlying antiopioid actions of cholecystokinin within the rostral ventromedial medulla. J. Neurophysiol. 85, 280–286.
Heinricher, M. M., Morgan, M. M., Tortorici, V., and Fields, H. L. 1994. Disinhibition of off-cells and antinociception produced by an opioid action within the rostral ventromedial medulla. Neuroscience 63, 279–288.
Heinricher, M. M., Pertovaara, A., and Ossipov, M. H. 2003. Descending Modulation After Injury. In: Proceedings of the 10th World Congress on Pain (*eds*. D. O. Dostrovsky, D. B. Carr, and M. Koltzenburg), pp. 251–260. IASP Press.
Hildebrand, M. E. and Snutch, T. P. 2006. Contributions of T-type calcium channels to the pathophysiology of pain signaling. Drug Discov. Today: Dis. Mech. 3, 335–341.
Honore, P., Menning, P. M., Rogers, S. D., Nichols, M. L., Basbaum, A. I., Besson, J. M., and Mantyh, P. W. 1999. Spinal substance P receptor expression and internalization in acute, short-term, and long-term inflammatory pain states. J. Neurosci. 19, 7670–7678.
Hugonin, L., Vukojevic, V., Bakalkin, G., and Graslund, A. 2006. Membrane leakage induced by dynorphins. FEBS Lett. 580, 3201–3205.
Hunt, S. P., Pini, A., and Evan, G. 1987. Induction of c-fos-like protein in spinal cord neurons following sensory stimulation. Nature 328, 632–634.
Ikeda, H., Heinke, B., Ruscheweyh, R., and Sandkuhler, J. 2003. Synaptic plasticity in spinal lamina I projection neurons that mediate hyperalgesia. Science 299, 1237–1240.

Ji, R. R. 2004. Peripheral and central mechanisms of inflammatory pain, with emphasis on MAP kinases. Curr. Drug Targets Inflamm. Allergy 3, 299–303.

Ji, R. R. and Strichartz, G. 2004. Cell signaling and the genesis of neuropathic pain. Sci. STKE, 252 reE14.

Ji, R. R., Befort, K., Brenner, G. J., and Woolf, C. J. 2002. ERK MAP kinase activation in superficial spinal cord neurons induces prodynorphin and NK-1 upregulation and contributes to persistent inflammatory pain hypersensitivity. J. Neurosci. 22, 478–485.

Ji, R. R., Kohno, T., Moore, K. A., and Woolf, C. J. 2003. Central sensitization and LTP: do pain and memory share similar mechanisms? Trends Neurosci. 26, 696–705.

Ji, R. R., Samad, T. A., Jin, S. X., Schmoll, R., and Woolf, C. J. 2002. p38 MAPK activation by NGF in primary sensory neurons after inflammation increases TRPV1 levels and maintains heat hyperalgesia. Neuron 36, 57–68.

Kajander, K. C., Wakisaka, S., and Bennett, G. J. 1992. Spontaneous discharge originates in the dorsal root ganglion at the onset of a painful peripheral neuropathy in the rat. Neurosci. Lett. 138, 225–228.

Kanda, N. and Watanabe, S. 2003. Histamine enhances the production of nerve growth factor in human keratinocytes. J. Invest. Dermatol. 121, 570–577.

Kaplan, H. and Fields, H. L. 1991. Hyperalgesia during acute opioid abstinence: evidence for a nociceptive facilitating function of the rostral ventromedial medulla. J. Neurosci. 11, 1433–1439.

Kauppila, T., Kontinen, V. K., and Pertovaara, A. 1998. Influence of spinalization on spinal withdrawal reflex responses varies depending on the submodality of the test stimulus and the experimental pathophysiological condition in the rat. Brain Res. 797, 234–242.

Kawamata, M. and Omote, K. 1996. Involvement of increased excitatory amino acids and intracellular Ca^{2+} concentration in the spinal dorsal horn in an animal model of neuropathic pain. Pain 68, 85–96.

Kawamata, T. and Omote, K. 1999. Activation of spinal *N*-methyl-D-aspartate receptors stimulates a nitric oxide/cyclic guanosine 3,5-monophosphate/glutamate release cascade in nociceptive signaling. Anesthesiology 91, 1415–1424.

Kawasaki, Y., Kohno, T., Zhuang, Z. Y., Brenner, G. J., Wang, H., Van Der Meer, C., Befort, K., Woolf, C. J., and Ji, R. R. 2004. Ionotropic and metabotropic receptors, protein kinase A, protein kinase C, and Src contribute to C-fiber-induced ERK activation and cAMP response element-binding protein phosphorylation in dorsal horn neurons, leading to central sensitization. J. Neurosci. 24, 8310–8321.

Khasabov, S. G., Rogers, S. D., Ghilardi, J. R., Peters, C. M., Mantyh, P. W., and Simone, D. A. 2002. Spinal neurons that possess the substance P receptor are required for the development of central sensitization. J. Neurosci. 22, 9086–9098.

Khasabov, S. G., Ghilardi, J. R., Mantyh, P. W., and Simone, D. A. 2005. Spinal neurons that express NK-1 receptors modulate descending controls that project through the dorsolateral funiculus. J. Neurophysiol. 93, 998–1006.

Kincaid, W., Neubert, M. J., Xu, M., Kim, C. J., and Heinricher, M. M. 2006. Role for medullary pain facilitating neurons in secondary thermal hyperalgesia. J. Neurophysiol. 95, 33–41.

Kim, S. H. and Chung, J. M. 1992. An experimental model for peripheral neuropathy produced by segmental spinal nerve ligation in the rat. Pain 50, 355–363.

Koetzner, L., Hua, X. Y., Lai, J., Porreca, F., and Yaksh, T. 2004. Nonopioid actions of intrathecal dynorphin evoke spinal excitatory amino acid and prostaglandin E2 release mediated by cyclooxygenase-1 and -2. J. Neurosci. 24, 1451–1458.

Kovelowski, C. J., Ossipov, M. H., Sun, H., Lai, J., Malan, T. P., and Porreca, F. 2000. Supraspinal cholecystokinin may drive tonic descending facilitation mechanisms to maintain neuropathic pain in the rat. Pain 87, 265–273.

Krause, S. J. and Backonja, M. M. 2003. Development of a neuropathic pain questionnaire. Clin. J. Pain 19, 306–314.

Lai, J., Gold, M. S., Kim, C. S., Bian, D., Ossipov, M. H., Hunter, J. C., and Porreca, F. 2002. Inhibition of neuropathic pain by decreased expression of the tetrodotoxin-resistant sodium channel, NaV1.8. Pain 95, 143–152.

Lai, J., Hunter, J. C., and Porreca, F. 2003. The role of voltage-gated sodium channels in neuropathic pain. Curr. Opin. Neurobiol. 13, 291–297.

Lai, J., Luo, M. C., Chen, Q., Ma, S., Gardell, L. R., Ossipov, M. H., and Porreca, F. 2006. Dynorphin A activates bradykinin receptors to maintain neuropathic pain. Nat. Neurosci. 9, 1534–1540.

Lai, J., Ossipov, M. H., Vanderah, T. W., Malan, T. P., Jr., and Porreca, F. 2001. Neuropathic pain: the paradox of dynorphin. Mol. Interv. 1, 160–167.

Lewin, G. R., Rueff, A., and Mendell, L. M. 1994. Peripheral and central mechanisms of NGF-induced hyperalgesia. Eur. J. Neurosci. 6, 1903–1912.

Li, Q. J. and Lu, G. W. 1989. The property of peripheral input of projection neurons in the spinal cord dorsal horn. Sci. China B 32, 1224–1232.

Li, Y., Dorsi, M. J., Meyer, R. A., and Belzberg, A. J. 2000. Mechanical hyperalgesia after an L5 spinal nerve lesion in the rat is not dependent on input from injured nerve fibers. Pain 85, 493–502.

Li, J., Simone, D. A., and Larson, A. A. 1999. Windup leads to characteristics of central sensitization. Pain 79, 75–82.

Liu, H., Mantyh, P. W., and Basbaum, A. I. 1997. NMDA-receptor regulation of substance P release from primary afferent nociceptors. Nature 386, 721–724.

Liu, C. N., Raber, P., Ziv-Sefer, S., and Devor, M. 2001. Hyperexcitability in sensory neurons of rats selected for high versus low neuropathic pain phenotype. Neuroscience 105, 265–275.

Ma, Q. P. and Woolf, C. J. 1996. Basal and touch-evoked fos-like immunoreactivity during experimental inflammation in the rat. Pain 67, 307–316.

MacInnis, B. L. and Campenot, R. B. 2005. Regulation of Wallerian degeneration and nerve growth factor withdrawal-induced pruning of axons of sympathetic neurons by the proteasome and the MEK/Erk pathway. Mol.Cell Neurosci. 28, 430–439.

Malik-Hall, M., Dina, O. A., and Levine, J. D. 2005. Primary afferent nociceptor mechanisms mediating NGF-induced mechanical hyperalgesia. Eur. J. Neurosci. 21, 3387–3394.

Malin, S. A., Molliver, D. C., Koerber, H. R., Cornuet, P., Frye, R., Albers, K. M., and Davis, B. M. 2006. Glial cell line-derived neurotrophic factor family members sensitize nociceptors *in vitro* and produce thermal hyperalgesia *in vivo*. J. Neurosci. 26, 8588–8599.

Mansikka, H. and Pertovaara, A. 1997. Supraspinal influence on hindlimb withdrawal thresholds and mustard oil-induced secondary allodynia in rats. Brain Res. Bull. 42, 359–365.

Mantyh, P. W., Rogers, S. D., Honore, P., Allen, B. J., Ghilardi, J. R., Li, J., Daughters, R. S., Lappi, D. A., Wiley, R. G., and Simone, D. A. 1997. Inhibition of hyperalgesia by ablation of lamina I spinal neurons expressing the substance P receptor. Science 278, 275–279.

Matthews, E. A. and Dickenson, A. H. 2001a. Effects of ethosuximide, a T-type Ca(2+) channel blocker, on dorsal horn neuronal responses in rats. Eur. J. Pharmacol. 415, 141–149.

Matthews, E. A. and Dickenson, A. H. 2001b. Effects of spinally delivered N- and P-type voltage-dependent calcium channel

antagonists on dorsal horn neuronal responses in a rat model of neuropathy. Pain 92, 235–246.
McCleskey, E. W., Fox, A. P., Feldman, D. H., Cruz, L. J., Olivera, B. M., Tsien, R. W., and Yoshikami, D. 1987. Omega-conotoxin: direct and persistent blockade of specific types of calcium channels in neurons but not muscle. Proc. Natl. Acad. Sci. U. S. A. 84, 4327–4331.
McMahon, S. B. and Cafferty, W. B. 2004. Neurotrophic influences on neuropathic pain. Novartis Found. Symp. 261, 68–92.
McMahon, S. B. and Jones, N. G. 2004. Plasticity of pain signaling: role of neurotrophic factors exemplified by acid-induced pain. J. Neurobiol. 61, 72–87.
McMahon, S. B., Cafferty, W. B., and Marchand, F. 2005. Immune and glial cell factors as pain mediators and modulators. Exp. Neurol. 192, 444–462.
Mendell, L. M. 1966. Physiological properties of unmyelinated fiber projection to the spinal cord. Exp. Neurol. 16, 316–332.
Michaelis, M., Devor, M., and Janig, W. 1996. Sympathetic modulation of activity in rat dorsal root ganglion neurons changes over time following peripheral nerve injury. J. Neurophysiol. 76, 753–763.
Miljanich, G. P. 2004. Ziconotide: neuronal calcium channel blocker for treating severe chronic pain. Curr. Med. Chem. 11, 3029–3040.
Miquel, M. C., Emerit, M. B., Nosjean, A., Simon, A., Rumajogee, P., Brisorgueil, M. J., Doucet, E., Hamon, M., and Verge, D. 2002. Differential subcellular localization of the 5-HT_3-As receptor subunit in the rat central nervous system. Eur. J. Neurosci. 15, 449–457.
Morgan, M. M. and Fields, H. L. 1994. Pronounced changes in the activity of nociceptive modulatory neurons in the rostral ventromedial medulla in response to prolonged thermal noxious stimuli. J. Neurophysiol. 72, 1161–1170.
Morgan, M. M. and Heinricher, M. M. 1992. Activity of neurons in the rostral medulla of the halothane-anesthetized rat during withdrawal from noxious heat. Brain Res. 582, 154–158.
Nassar, M. A., Baker, M. D., Levato, A., Ingram, R., Mallucci, G., McMahon, S. B., and Wood, J. N. 2006. Nerve injury induces robust allodynia and ectopic discharges in Nav1.3 null mutant mice. Mol. Pain 2, 33.
Neubert, M. J., Kincaid, W., and Heinricher, M. M. 2004. Nociceptive facilitating neurons in the rostral ventromedial medulla. Pain 110, 158–165.
Nichols, M. L., Allen, B. J., Rogers, S. D., Ghilardi, J. R., Honore, P., Luger, N. M., Finke, M. P., Li, J., Lappi, D. A., Simone, D. A., and Mantyh, P. W. 1999. Transmission of chronic nociception by spinal neurons expressing the substance P receptor. Science 286, 1558–1561.
Nomura, H., Ogawa, A., Tashiro, A., Morimoto, T., Hu, J. W., and Iwata, K. 2002. Induction of Fos protein-like immunoreactivity in the trigeminal spinal nucleus caudalis and upper cervical cord following noxious and non-noxious mechanical stimulation of the whisker pad of the rat with an inferior alveolar nerve transection. Pain 95, 225–238.
Novakovic, S. D., Eglen, R. M., and Hunter, J. C. 2001. Regulation of Na^+ channel distribution in the nervous system. Trends Neurosci. 24, 473–478.
Novakovic, S. D., Tzoumaka, E., McGivern, J. G., Haraguchi, M., Sangameswaran, L., Gogas, K. R., Eglen, R. M., and Hunter, J. C. 1998. Distribution of the tetrodotoxin-resistant sodium channel PN3 in rat sensory neurons in normal and neuropathic conditions. J. Neurosci. 18, 2174–2187.
Nowycky, M. C., Fox, A. P., and Tsien, R. W. 1985. Three types of neuronal calcium channel with different calcium agonist sensitivity. Nature 316, 440–443.
Obata, K., Katsura, H., Mizushima, T., Yamanaka, H., Kobayashi, K., Dai, Y., Fukuoka, T., Tokunaga, A., Tominaga, M., and Noguchi, K. 2005. TRPA1 induced in sensory neurons contributes to cold hyperalgesia after inflammation and nerve injury. J. Clin. Invest. 115, 2393–2401.
Obata, K., Katsura, H., Sakurai, J., Kobayashi, K., Yamanaka, H., Dai, Y., Fukuoka, T., and Noguchi, K. 2006. Suppression of the p75 neurotrophin receptor in uninjured sensory neurons reduces neuropathic pain after nerve injury. J. Neurosci. 26, 11974–11986.
Obata, K., Yamanaka, H., Kobayashi, K., Dai, Y., Mizushima, T., Katsura, H., Fukuoka, T., Tokunaga, A., and Noguchi, K. 2004. Role of mitogen-activated protein kinase activation in injured and intact primary afferent neurons for mechanical and heat hypersensitivity after spinal nerve ligation. J. Neurosci. 24, 10211–10222.
Ohishi, H., Nomura, S., Ding, Y. Q., Shigemoto, R., Wada, E., Kinoshita, A., Li, J. L., Neki, A., Nakanishi, S., and Mizuno, N. 1995. Presynaptic localization of a metabotropic glutamate receptor, mGluR7, in the primary afferent neurons: an immunohistochemical study in the rat. Neurosci. Lett. 202, 85–88.
Ossipov, M. H. and Porreca, F. 2005. Endogenous Pain Modulation: Descending Excitatory Systems. In: Handbook of Clinical Neurology (*eds*. F. Cervero and T. S. Jensen), pp. 211–238. Elsevier.
Ossipov, M. H. and Porreca, F. 2006. Role of Descending Facilitation in Neuropathic Pain States. In: Emerging Strategies for the Treatment of Neuropathic Pain (*eds*. J. N. Campbell *et al.*), pp. 211–238. IASP Press.
Ossipov, M. H., Hong Sun, T., Malan, P., Jr., Lai, J., and Porreca, F. 2000. Mediation of spinal nerve injury induced tactile allodynia by descending facilitatory pathways in the dorsolateral funiculus in rats. Neurosci. Lett. 290, 129–132.
Ossipov, M. H., Lai, J., Malan, T. P., Jr., Vanderah, T. W., and Porreca, F. 2001. Tonic Descending Facilitation as a Mechanism of Neuropathic Pain. In: Neuropatic Pain: Pathophysiology and Treatment (*eds*. P. T. Hansson *et al.*), pp. 107–124. IASP Press.
Ossipov, M. H., Lai, J., and Porreca, F. 2005. Mechanisms of Experimental Neuropathic Pain: Integration from Animal Models. In: Wall and Melzack's Textbook of Pain (*eds*. S. B. McMahon and M. Koltzenburg), pp. 929–946. Elsevier.
Owolabi, J. B., Rizkalla, G., Tehim, A., Ross, G. M., Riopelle, R. J., Kamboj, R., Ossipov, M., Bian, D., Wegert, S., Porreca, F., and Lee, D. K. 1999. Characterization of antiallodynic actions of ALE-0540, a novel nerve growth factor receptor antagonist, in the rat. J. Pharmacol. Exp. Ther. 289, 1271–1276.
Paleckova, V., Palecek, J., McAdoo, D. J., and Willis, W. D. 1992. The non-NMDA antagonist CNQX prevents release of amino acids into the rat spinal cord dorsal horn evoked by sciatic nerve stimulation. Neurosci. Lett. 148, 19–22.
Pertovaara, A. and Almeida, A. 2006. Endogenous Pain Modulation: Descending Inhibitory Systems. In: Handbook of Clinical Neurology (*eds*. F. Cervero and T. S. Jensen), pp. 179–192. Elsevier.
Pertovaara, A., Wei, H., Kalmari, J., and Ruotsalainen, M. 2001. Pain behavior and response properties of spinal dorsal horn neurons following experimental diabetic neuropathy in the rat: modulation by nitecapone, a COMT inhibitor with antioxidant properties. Exp. Neurol. 167, 425–434.
Porreca, F., Burgess, S. E., Gardell, L. R., Vanderah, T. W., Malan, T. P., Jr., Ossipov, M. H., Lappi, D. A., and Lai, J. 2001. Inhibition of neuropathic pain by selective ablation of brainstem medullary cells expressing the mu-opioid receptor. J. Neurosci. 21, 5281–5288.
Porreca, F., Ossipov, M. H., and Gebhart, G. F. 2002. Chronic pain and medullary descending facilitation. Trends Neurosci. 25, 319–325.

Porreca, F., Ossipov, M. H., Lai, J., Wegert, S., Bian, D., Rogers, S., Mantyh, P., Novakovich, S., and Hunter, J. C. 2000. Blockade of Diabetic, Chemotherapeutic, and NGF-Induced Pain by Antisense Knockdown of PN3/SNS, a TTX-Resistant Sodium Channel. In: Proceedings of the 9th World Congress on Pain (*eds*. M. Devor, M. C. Rowbotham, and Z. Wiesenfeld-Hallin), pp. 273–285. IASP Press.

Porreca, F., Tang, Q. B., Bian, D., Riedl, M., Elde, R., and Lai, J. 1998. Spinal opioid mu receptor expression in lumbar spinal cord of rats following nerve injury. Brain Res. 795, 197–203.

Prommer, E. E. 2005. Ziconotide: can we use it in palliative care? Am. J. Hosp. Palliat. Med. 22, 369–374.

Puntambekar, P., Mukherjea, D., Jajoo, S., and Ramkumar, V. 2005. Essential role of Rac1/NADPH oxidase in nerve growth factor induction of TRPV1 expression. J. Neurochem. 95, 1689–1703.

Rahman, W., Suzuki, R., Rygh, L. J., and Dickenson, A. H. 2004. Descending serotonergic facilitation mediated through rat spinal $5HT_3$ receptors is unaltered following carrageenan inflammation. Neurosci. Lett. 361, 229–231.

Rahman, W., Suzuki, R., Webber, M., Hunt, S. P., and Dickenson, A. H. 2006. Depletion of endogenous spinal 5-HT attenuates the behavioural hypersensitivity to mechanical and cooling stimuli induced by spinal nerve ligation. Pain 123, 264–274.

Rajan, B., Polydefkis, M., Hauer, P., Griffin, J. W., and McArthur, J. C. 2003. Epidermal reinnervation after intracutaneous axotomy in man. J. Comp. Neurol. 457, 24–36.

Renganathan, M., Cummins, T. R., and Waxman, S. G. 2001. Contribution of Na(v)1.8 sodium channels to action potential electrogenesis in DRG neurons. J. Neurophysiol. 86, 629–640.

Renton, T., Yiangou, Y., Plumpton, C., Tate, S., Bountra, C., and Anand, P. 2005. Sodium channel Nav1.8 immunoreactivity in painful human dental pulp. BMC Oral Health 5, 5.

Ruiz, G. and Banos, J. E. 2005. The effect of endoneurial nerve growth factor on calcitonin gene-related peptide expression in primary sensory neurons. Brain Res. 1042, 44–52.

Ruiz, G., Ceballos, D., and Banos, J. E. 2004. Behavioral and histological effects of endoneurial administration of nerve growth factor: possible implications in neuropathic pain. Brain Res. 1011, 1–6.

Sah, D. W., Ossipov, M. H., and Porreca, F. 2003. Neurotrophic factors as novel therapeutics for neuropathic pain. Nat. Rev. Drug Discov. 2, 460–472.

Sah, D. W., Ossipov, M. H., Rossomando, A., Silvian, L., and Porreca, F. 2005a. New approaches for the treatment of pain: the GDNF family of neurotrophic growth factors. Curr. Top. Med. Chem. 5, 577–583.

Sah, D. W., Porreca, F., and Ossipov, M. H. 2006. Modulation of Neurotrophic Growth Factors as a Therapeutic Strategy for Neuropathic Pain. Drug Dev. Res. 67, 389–403.

Sangameswaran, L., Fish, L. M., Koch, B. D., Rabert, D. K., Delgado, S. G., Ilnicka, M., Jakeman, L. B., Novakovic, S., Wong, K., Sze, P., Tzoumaka, E., Stewart, G. R., Herman, R. C., Chan, H., Eglen, R. M., and Hunter, J. C. 1997. A novel tetrodotoxin-sensitive, voltage-gated sodium channel expressed in rat and human dorsal root ganglia. J. Biol. Chem. 272, 14805–14809.

Santicioli, P., Del, B. E., Tramontana, M., Geppetti, P., and Maggi, C. A. 1992. Release of calcitonin gene-related peptide like-immunoreactivity induced by electrical field stimulation from rat spinal afferents is mediated by conotoxin-sensitive calcium channels. Neurosci. Lett. 136, 161–164.

Scott, D. A., Wright, C. E., and Angus, J. A. 2002. Actions of intrathecal omega-conotoxins CVID, GVIA, MVIIA, and morphine in acute and neuropathic pain in the rat. Eur. J. Pharmacol. 451, 279–286.

Shamash, S., Reichert, F., and Rotshenker, S. 2002. The cytokine network of Wallerian degeneration: tumor necrosis factor-alpha, interleukin-1alpha, and interleukin-1beta. J. Neurosci. 22, 3052–3060.

Shelton, D. L., Zeller, J., Ho, W. H., Pons, J., and Rosenthal, A. 2005. Nerve growth factor mediates hyperalgesia and cachexia in auto-immune arthritis. Pain 116, 8–16.

Shortland, P. and Molander, C. 1998. The time-course of abeta-evoked c-fos expression in neurons of the dorsal horn and gracile nucleus after peripheral nerve injury. Brain Res. 810, 288–293.

Shu, X. Q. and Mendell, L. M. 1999. Neurotrophins and hyperalgesia. Proc. Natl. Acad. Sci. U. S. A. 96, 7693–7696.

Shu, X. and Mendell, L. M. 2001. Acute sensitization by NGF of the response of small-diameter sensory neurons to capsaicin. J. Neurophysiol. 86, 2931–2938.

Simone, D. A., Baumann, T. K., and LaMotte, R. H. 1989. Dose-dependent pain and mechanical hyperalgesia in humans after intradermal injection of capsaicin. Pain 38, 99–107.

Simone, D. A., Sorkin, L. S., Oh, U., Chung, J. M., Owens, C., LaMotte, R. H., and Willis, W. D. 1991. Neurogenic hyperalgesia: central neural correlates in responses of spinothalamic tract neurons. J. Neurophysiol. 66, 228–246.

Sindrup, S. H. and Jensen, T. S. 2007. Are sodium channel blockers useless in peripheral neuropathic pain? Pain 128, 6–7.

Sluka, K. A. and Willis, W. D. 1998. Increased spinal release of excitatory amino acids following intradermal injection of capsaicin is reduced by a protein kinase G inhibitor. Brain Res. 798, 281–286.

Snutch, T. P. 2005. Targeting chronic and neuropathic pain: the N-type calcium channel comes of age. NeuroRx 2, 662–670.

Snutch, T. P., Sutton, K. G., and Zamponi, G. W. 2001. Voltage-dependent calcium channels – beyond dihydropyridine antagonists. Curr. Opin. Pharmacol. 1, 11–16.

Southall, M. D. and Vasko, M. R. 2001. Prostaglandin receptor subtypes, EP3C and EP4, mediate the prostaglandin E2-induced cAMP production and sensitization of sensory neurons. J. Biol. Chem. 276, 16083–16091.

Southall, M. D., Bolyard, L. A., and Vasko, M. R. 2002. Twenty-four hour exposure to prostaglandin downregulates prostanoid receptor binding but does not alter PGE(2)-mediated sensitization of rat sensory neurons. Pain 96, 285–296.

Southall, M. D., Michael, R. L., and Vasko, M. R. 1998. Intrathecal NSAIDS attenuate inflammation-induced neuropeptide release from rat spinal cord slices. Pain 78, 39–48.

Stempelj, M. and Ferjan, I. 2005. Signaling pathway in nerve growth factor induced histamine release from rat mast cells. Inflamm. Res. 54, 344–349.

Stucky, C. L., Shin, J. B., and Lewin, G. R. 2002. Neurotrophin-4: a survival factor for adult sensory neurons. Curr. Biol. 12, 1401–1404.

Sun, R.-Q., Lawand, N. B., Lin, Q., and Willis, W. D. 2004. Role of calcitonin gene-related peptide in the sensitization of dorsal horn neurons to mechanical stimulation after intradermal injection of capsaicin. J. Neurophysiol. 92, 320–326.

Sun, R. Q., Lawand, N. B., and Willis, W. D. 2003. The role of calcitonin gene-related peptide (CGRP) in the generation and maintenance of mechanical allodynia and hyperalgesia in rats after intradermal injection of capsaicin. Pain 104, 201–208.

Sun, Q., Tu, H., Xing, G. G., Han, J. S., and Wan, Y. 2005. Ectopic discharges from injured nerve fibers are highly correlated with tactile allodynia only in early, but not late, stage in rats with spinal nerve ligation. Exp. Neurol. 191, 128–136.

Suzuki, R. and Dickenson, A. 2005a. Spinal and supraspinal contributions to central sensitization in peripheral neuropathy. Neurosignals 14, 175–181.

Suzuki, R. and Dickenson, A. H. 2005b. Differential pharmacological modulation of the spontaneous stimulus-independent activity in the rat spinal cord following peripheral nerve injury. Exp. Neurol. 198, 72–80.

Suzuki, R., Morcuende, S., Webber, M., Hunt, S. P., and Dickenson, A. H. 2002. Superficial NK1-expressing neurons control spinal excitability through activation of descending pathways. Nat. Neurosci. 5, 1319–1326.

Suzuki, R., Rahman, W., Hunt, S. P., and Dickenson, A. H. 2004a. Descending facilitatory control of mechanically evoked responses is enhanced in deep dorsal horn neurones following peripheral nerve injury. Brain Res. 1019, 68–76.

Suzuki, R., Rygh, L. J., and Dickenson, A. H. 2004b. Bad news from the brain: descending 5-HT pathways that control spinal pain processing. Trends Pharmacol. Sci. 25, 613–617.

Svensson, P., Cairns, B. E., Wang, K., and Arendt-Nielsen, L. 2003. Injection of nerve growth factor into human masseter muscle evokes long-lasting mechanical allodynia and hyperalgesia. Pain 104, 241–247.

Tal, M. and Bennett, G. J. 1994. Extra-territorial pain in rats with a peripheral mononeuropathy: mechano-hyperalgesia and mechano-allodynia in the territory of an uninjured nerve. Pain 57, 375–382.

Talley, E. M., Cribbs, L. L., Lee, J. H., Daud, A., Perez-Reyes, E., and Bayliss, D. A. 1999. Differential distribution of three members of a gene family encoding low voltage-activated (T-type) calcium channels. J. Neurosci. 19, 1895–1911.

Taherzadeh, O., Otto, W. R., Anand, U., Nanchahal, J., and Anand, P. 2003. Influence of human skin injury on regeneration of sensory neurons. Cell Tissue Res. 312, 275–280.

Todd, A. J. 2002. Anatomy of primary afferents and projection neurones in the rat spinal dorsal horn with particular emphasis on substance P and the neurokinin 1 receptor. Exp. Physiol. 87, 245–249.

Todd, A. J., McGill, M. M., and Shehab, S. A. 2000. Neurokinin 1 receptor expression by neurons in laminae I, III and IV of the rat spinal dorsal horn that project to the brainstem. Eur. J. Neurosci. 12, 689–700.

Tomlinson, D. R., Fernyhough, P., and Diemel, L. T. 1997. Role of neurotrophins in diabetic neuropathy and treatment with nerve growth factors. Diabetes 46(Suppl. 2), 43–49.

Urban, M. O., Coutinho, S. V., and Gebhart, G. F. 1999. Biphasic modulation of visceral nociception by neurotensin in rat rostral ventromedial medulla. J. Pharmacol. Exp. Ther. 290, 207–213.

Vera-Portocarrero, L. P., Zhang, E. T., Ossipov, M. H., Xie, J. Y., King, T., Lai, J., and Porreca, F. 2006. Descending facilitation from the rostral ventromedial medulla maintains nerve injury-induced central sensitization. Neuroscience 140, 1311–1320.

Vinik, A. I., Tuchman, M., Safirstein, B., Corder, C., Kirby, L., Wilks, K., Quessy, S., Blum, D., Grainger, J., White, J., and Silver, M. 2007. Lamotrigine for treatment of pain associated with diabetic neuropathy: results of two randomized, double-blind, placebo-controlled studies. Pain 128, 169–179.

Wallin, J. and Schott, E. 2002. Substance P release in the spinal dorsal horn following peripheral nerve injury. Neuropeptides 36, 252–256.

Wang, Y. X., Gao, D., Pettus, M., Phillips, C., and Bowersox, S. S. 2000a. Interactions of intrathecally administered ziconotide, a selective blocker of neuronal N-type voltage-sensitive calcium channels, with morphine on nociception in rats. Pain 84, 271–281.

Wang, Z., Gardell, L. R., Ossipov, M. H., Vanderah, T. W., Brennan, M. B., Hochgeschwender, U., Hruby, V. J., Malan, T. P., Jr., Lai, J., and Porreca, F. 2001. Pronociceptive actions of dynorphin maintain chronic neuropathic pain. J. Neurosci. 21, 1779–1786.

Wang, R., Guo, W., Ossipov, M. H., Vanderah, T. W., Porreca, F., and Lai, J. 2003. Glial cell line-derived neurotrophic factor normalizes neurochemical changes in injured dorsal root ganglion neurons and prevents the expression of experimental neuropathic pain. Neuroscience 121, 815–824.

Wang, H. B., Kohno, T., Amaya, F., Brenner, G. J., Ito, N., Allchorne, A., Ji, R. R., and Woolf, C. J. 2005. Bradykinin produces pain hypersensitivity by potentiating spinal cord glutamatergic synaptic transmission. J. Neuroscience. 25, 7986–7992.

Wang, Y. X., Pettus, M., Gao, D., Phillips, C., and Scott Bowersox, S. 2000b. Effects of intrathecal administration of ziconotide, a selective neuronal N-type calcium channel blocker, on mechanical allodynia and heat hyperalgesia in a rat model of postoperative pain. Pain 84, 151–158.

Waxman, S. G., Cummins, T. R., Dib-Hajj, S., Fjell, J., and Black, J. A. 1999. Sodium channels, excitability of primary sensory neurons, and the molecular basis of pain. Muscle Nerve 22, 1177–1187.

Wei, F., Dubner, R., and Ren, K. 1999. Dorsolateral funiculus-lesions unmask inhibitory or disfacilitatory mechanisms which modulate the effects of innocuous mechanical stimulation on spinal Fos expression after inflammation. Brain Res. 820, 112–116.

Wei, F., Ren, K., and Dubner, R. 1998. Inflammation-induced Fos protein expression in the rat spinal cord is enhanced following dorsolateral or ventrolateral funiculus lesions. Brain Res. 782, 136–141.

Wood, J. N., Abrahamsen, B., Baker, M. D., Boorman, J. D., Donier, E., Drew, L. J., Nassar, M. A., Okuse, K., Seereeram, A., Stirling, C. L., and Zhao, J. 2004a. Ion channel activities implicated in pathological pain. Novartis Found Symp. 261, 32–40.

Wood, J. N., Boorman, J. P., Okuse, K., and Baker, M. D. 2004b. Voltage-gated sodium channels and pain pathways. J Neurobiol. 61, 55–71.

Woolf, C. J. 1996. Windup and central sensitization are not equivalent. Pain 66, 105–108.

Woolf, C. J. and Salter, M. W. 2000. Neuronal plasticity: increasing the gain in pain. Science 288, 1765–1769.

Woolf, C. J. and Thompson, S. W. 1991. The induction and maintenance of central sensitization is dependent on *N*-methyl-D-aspartic acid receptor activation; implications for the treatment of post-injury pain hypersensitivity states. Pain 44, 293–299.

Wu, G., Ringkamp, M., Hartke, T. V., Murinson, B. B., Campbell, J. N., Griffin, J. W., and Meyer, R. A. 2001. Early onset of spontaneous activity in uninjured C-fiber nociceptors after injury to neighboring nerve fibers. J. Neurosci. 21, RC140.

Wu, G., Ringkamp, M., Murinson, B. B., Pogatzki, E. M., Hartke, T. V., Weerahandi, H. M., Campbell, J. N., Griffin, J. W., and Meyer, R. A. 2002. Degeneration of myelinated efferent fibers induces spontaneous activity in uninjured C-fiber afferents. J. Neurosci. 22, 7746–7753.

Xie, J. Y., Herman, D. S., Stiller, C. O., Gardell, L. R., Ossipov, M. H., Lai, J., Porreca, F., and Vanderah, T. W. 2005. Cholecystokinin in the rostral ventromedial medulla mediates opioid-induced hyperalgesia and antinociceptive tolerance. J. Neurosci. 25, 409–416.

Xu, M., Kim, C. J., Neubert, M. J., and Heinricher, M. M. 2007. NMDA receptor-mediated activation of medullary pro-nociceptive neurons is required for secondary thermal hyperalgesia. Pain 127, 253–262.

Yang, Y., Wang, Y., Li, S., Xu, Z., Li, H., Ma, L., Fan, J., Bu, D., Liu, B., Fan, Z., Wu, G., Jin, J., Ding, B., Zhu, X., and Shen, Y. 2004. Mutations in SCN9A, encoding a sodium channel alpha subunit, in patients with primary erythromelalgia. J. Med. Genet. 41, 171–174.

Yoon, Y. W., Na, H. S., and Chung, J. M. 1996. Contributions of injured and intact afferents to neuropathic pain in an experimental rat model. Pain 64, 27–36.

Zeitz, K. P., Guy, N., Malmberg, A. B., Dirajlal, S., Martin, W. J., Sun, L., Bonhaus, D. W., Stucky, C. L., Julius, D., and Basbaum, A. I. 2002. The 5-HT_3 subtype of serotonin receptor contributes to nociceptive processing via a novel subset of myelinated and unmyelinated nociceptors. J. Neurosci. 22, 1010–1019.

Zhang, E. T., Ossipov, M. H., Zhang, D. Q., Lai, J., and Porreca, F. 2007. Nerve injury-induced tactile allodynia is present in the absence of FOS labeling in retrogradely labeled post-synaptic dorsal column neurons. Pain, 128, 143–154.

Zhang, L., Peoples, R. W., Oz, M., Harvey-White, J., Weight, F. F., and Brauneis, U. 1997. Potentiation of NMDA receptor-mediated responses by dynorphin at low extracellular glycine concentrations. J. Neurophysiol. 78, 582–590.

Zhuo, M. and Gebhart, G. F. 1997. Biphasic modulation of spinal nociceptive transmission from the medullary raphe nuclei in the rat. J. Neurophysiol. 78, 746–758.

Zwick, M., Davis, B. M., Woodbury, C. J., Burkett, J. N., Koerber, H. R., Simpson, J. F., and Albers, K. M. 2002. Glial cell line-derived neurotrophic factor is a survival factor for isolectin B4-positive, but not vanilloid receptor 1-positive, neurons in the mouse. J Neurosci. 22, 4057–4065.

Further Reading

Ali, Z., Meyer, R. A., and Campbell, J. N. 1996. Secondary hyperalgesia to mechanical but not heat stimuli following a capsaicin injection in hairy skin. Pain 68, 401–411.

Backonja, M. M. and Krause, S. J. 2003. Neuropathic pain questionnaire – short form. Clin. J. Pain 19, 315–316.

Chapman, V., Suzuki, R., and Dickenson, A. H. 1998. Electrophysiological characterization of spinal neuronal response properties in anaesthetized rats after ligation of spinal nerves L5–L6. J. Physiol. 507(Pt 3), 881–894.

Cunha, F. Q., Teixeira, M. M., and Ferreira, S. H. 1999. Pharmacological modulation of secondary mediator systems – cyclic AMP and cyclic GMP – on inflammatory hyperalgesia. Br. J. Pharmacol. 127, 671–678.

Eschenfelder, S., Habler, H. J., and Janig, W. 2000. Dorsal root section elicits signs of neuropathic pain rather than reversing them in rats with L5 spinal nerve injury. Pain 87, 213–219.

Han, H. C., Lee, D. H., and Chung, J. M. 2000. Characteristics of ectopic discharges in a rat neuropathic pain model. Pain 84, 253–261.

Hunt, S. P. and Mantyh, P. W. 2001. The molecular dynamics of pain control. Nat. Rev. Neurosci. 2, 83–91.

Ikeda, H., Stark, J., Fischer, H., Wagner, M., Drdla, R., Jager, T., and Sandkuhler, J. 2006. Synaptic amplifier of inflammatory pain in the spinal dorsal horn. Science 312, 1659–1662.

Ji, R. R. 2004. Mitogen-activated protein kinases as potential targets for pain killers. Curr. Opin. Invest. Drug. 5, 71–75.

Li, W. P., Xian, C., Rush, R. A., and Zhou, X. F. 1999b. Upregulation of brain-derived neurotrophic factor and neuropeptide Y in the dorsal ascending sensory pathway following sciatic nerve injury in rat. Neurosci. Lett. 260, 49–52.

Ma, W., Peschanski, M., and Ralston, H. J.3. 1987. The differential synaptic organization of the spinal and lemniscal projections to the ventrobasal complex of the rat thalamus. Evidence for convergence of the two systems upon single thalamic neurons. Neuroscience 22, 925–934.

Malmberg, A. B. and Yaksh, T. L. 1993. Spinal nitric oxide synthesis inhibition blocks NMDA-induced thermal hyperalgesia and produces antinociception in the formalin test in rats. Pain 54, 291–300.

Malmberg, A. B. and Yaksh, T. L. 1995. Cyclooxygenase inhibition and the spinal release of prostaglandin E2 and amino acids evoked by paw formalin injection: a microdialysis study in unanesthetized rats. J. Neurosci. 15, 2768–2776.

Malmberg, A. B., Chen, C., Tonegawa, S., and Basbaum, A. I. 1997. Preserved acute pain and reduced neuropathic pain in mice lacking PKCgamma (see comments). Science 278, 279–283.

Malmberg, A. B., Hamberger, A., and Hedner, T. 1995. Effects of prostaglandin E2 and capsaicin on behavior and cerebrospinal fluid amino acid concentrations of unanesthetized rats: a microdialysis study. J. Neurochem. 65, 2185–2193.

Mayer, D. J., Mao, J., Holt, J., and Price, D. D. 1999. Cellular mechanisms of neuropathic pain, morphine tolerance, and their interactions. Proc. Natl. Acad. Sci. U. S. A. 96, 7731–7736.

Miki, K., Fukuoka, T., Tokunaga, A., and Noguchi, K. 1998. Calcitonin gene-related peptide increase in the rat spinal dorsal horn and dorsal column nucleus following peripheral nerve injury: up-regulation in a subpopulation of primary afferent sensory neurons. Neuroscience 82, 1243–1252.

Miki, K., Iwata, K., Tsuboi, Y., Morimoto, T., Kondo, E., Dai, Y., Ren, K., and Noguchi, K. 2000. Dorsal column–thalamic pathway is involved in thalamic hyperexcitability following peripheral nerve injury: a lesion study in rats with experimental mononeuropathy. Pain 85, 263–271.

Minami, T., Nishihara, I., Ito, S., Sakamoto, K., Hyodo, M., and Hayaishi, O. 1995. Nitric oxide mediates allodynia induced by intrathecal administration of prostaglandin E2 or prostaglandin F2 alpha in conscious mice. Pain 61, 285–290.

Minami, T., Nishihara, I., Uda, R., Ito, S., Hyodo, M. and Hayaishi, O., 1994. Involvement of glutamate receptors in allodynia induced by prostaglandins E2 and F2 alpha injected into conscious mice. Pain 57, 225–231.

Noguchi, K., Kawai, Y., Fukuoka, T., Senba, E., and Miki, K. 1995. Substance P induced by peripheral nerve injury in primary afferent sensory neurons and its effect on dorsal column nucleus neurons. J. Neurosci. 15, 7633–7643.

Ossipov, M. H. and Porreca, F. 2005. Descending Modulation of Pain. In: The Paths of Pain (*eds*. H. Merskey, J. D. Loeser, and R. Dubner). pp. 117–130. IASP Press.

Ossipov, M. H. and Porreca, F. 2007. Neuropathic Pain: Basic Mechanisms (Animal). In: Handbook of the Senses (*eds*. A. I. Basbaum, C. Bushnell, and D. Julius). Elsevier, in press.

Ossipov, M. H., Zhang, E. T., Carvajal, C., Gardell, L., Quirion, R., Dumont, Y., Lai, J., and Porreca, F. 2002. Selective mediation of nerve injury-induced tactile hypersensitivity by neuropeptide Y. J. Neurosci. 22, 9858–9867.

Seybold, V. S., McCarson, K. E., Mermelstein, P. G., Groth, R. D., and Abrahams, L. G. 2003. Calcitonin gene-related peptide regulates expression of neurokinin1 receptors by rat spinal neurons. J. Neurosci. 23, 1816–1824.

Sun, H., Ren, K., Zhong, C. M., Ossipov, M. H., Malan, T. P., Lai, J., and Porreca, F. 2001. Nerve injury-induced tactile allodynia is mediated via ascending spinal dorsal column projections. Pain 90, 105–111.

Sun, R. Q., Tu, Y. J., Lawand, N. B., Yan, J. Y., Lin, Q., and Willis, W. D. 2004. Calcitonin gene-related peptide receptor activation produces pka- and pkc-dependent mechanical hyperalgesia and central sensitization. J. Neurophysiol. 92, 2859–2866.

Suzuki, R. and Dickenson, A. H. 2000. Neuropathic pain: nerves bursting with excitement. Neuroreport 11, 17–21.
Suzuki, R., Kontinen, V. K., Matthews, E., Williams, E., and Dickenson, A. H. 2000. Enlargement of the receptive field size to low intensity mechanical stimulation in the rat spinal nerve ligation model of neuropathy. Exp. Neurol. 163, 408–413.
Vetter, G., Geisslinger, G., and Tegeder, I. 2001. Release of glutamate, nitric oxide and prostaglandin E2 and metabolic activity in the spinal cord of rats following peripheral nociceptive stimulation. Pain 92, 213–218.
Willis, W. D. and Coggeshall, R. E. 2004. Sensory Mechanisms of the Spinal Cord, Vol. 1, Primary Afferent Neurons and the Spinal Dorsal Horn, 3rd edn. Kluwer Academic/Plenum Publishers.
Willis, W. D., Jr. 2001. Role of neurotransmitters in sensitization of pain responses. Ann. N. Y. Acad. Sci. 933, 142–156.
Woolf, C. J. 1996. Phenotypic modification of primary sensory neurons: the role of nerve growth factor in the production of persistent pain. Philos. Trans. R. Soc. Lond. B Biol. Sci. 351, 441–448.

Relevant Website

www.iasp-pain.org – International Association for the Study of Pain.

5.56 Animal Models and Neuropathic Pain

I Decosterd and T Berta, University of Lausanne, Lausanne, Switzerland

© 2008 Elsevier Inc. All rights reserved.

5.56.1	Introduction	857
5.56.2	Animal Models of Neuropathic Pain	857
5.56.2.1	Models of Central Neuropathic Pain: Spinal Cord Injuries	858
5.56.2.2	Models of Peripheral Neuropathic Pain: Injury to Roots, Dorsal Root Ganglia, and Spinal Nerves	859
5.56.2.3	Models of Peripheral Neuropathic Pain: Injury to Peripheral Nerves	859
5.56.2.4	Models of Peripheral Neuropathic Pain: Distal Nerve Branch Injuries	860
5.56.2.5	Nontraumatic Models of Neuropathic Pain	861
5.56.3	Behavioral Assessment of Neuropathic Pain in Animal Models: Spontaneous Pain, Stimulus-Evoked Pain, and Stimulus-Induced Pain	861
5.56.4	Conclusions	862
References		862

Glossary

allodynia Pain due to a stimulus which does not normally provoke pain.

autotomy Self amputation by animal that severs its own appendages (usually distal phalanges).

hyperalgesia An increased response to a stimulus which is normally painful.

neuropathic pain Pain initiated or caused by a primary lesion or dysfunction in the nervous system.

neuropathy A disturbance of function or pathological change in a nerve.

spontaneous pain Pain without an evident stimulus.

stimulus-evoked pain pain evoked by a mechanical/thermal/chemical stimulus.

Wallerian degeneration The degeneration of a nerve fiber induces by injury or disease, characterized by segmentation of the myelin and resulting in atrophy and destruction of the axon.

5.56.1 Introduction

Animal models in pain research offer great promise for both the identification of pain mechanisms, and the investigation of possible therapeutic applications. Our understanding of neuropathic pain (NP) has progressed during last few decades and although animal models have provided important information, in humans a clear pattern of the mechanisms responsible for its generation and maintenance is still unclear. Therefore, it is essential to put forward advanced animal models based, on the investigation of specific mechanisms, as well as refining the way in which the data is interpreted. Moreover, it is clear that the quest of a unique and universal animal model of all symptoms in patients ignores the complexity of the mechanisms involved. Therefore, it is important to select the best model for each specific research interest or a combination of appropriate but distinct models. In this chapter we will argue for the most frequently used animal models of NP, compare their advantages and disadvantages, and summarize the behavioral characterization.

5.56.2 Animal Models of Neuropathic Pain

At present, animal models of NP cover various etiologies and are related to symptoms leading to an extensive picture of clinical NP manifestations. The majority of animal models of NP involve traumatic

injuries to peripheral nerves, nerve roots, or spinal cord by transection, ligation, or compression (Figure 1). Other experimental models are related to direct or indirect nerve inflammation, ischemia, drug toxicity, or systemic metabolic disorders. Each animal model has been characterized by precise behavioral-based evaluations using different modalities of sensory stimulus. Many temporal and spatial profiles of molecular, physiological, and structural changes occurring during the development of NP have been investigated and most of the rodent models are compatible with actual electrophysiological measurements, functional imaging techniques, as well as genomic and proteomic screenings.

5.56.2.1 Models of Central Neuropathic Pain: Spinal Cord Injuries

Partial or complete spinal cord injuries result in loss of function in varying degrees below the level of injury, and are often associated with central NP pain syndromes (Christensen, M. D. and Hulsebosch, C. E., 1997a; Siddall, P. J. and Loeser, J. D., 2001). This type of injury involves functional and structural changes, partial loss of normal descending pathway, and hyperexcitability of dorsal horn neurons (Woolf, C. J., 1983; Woolf, C. J. and Fitzgerald, M., 1983; Hulsebosch, C. E., 2002). Spinal cord transection, contusion, compression, and chemical toxicity induce all at-level or below-level signs of pain hypersensitivity (Vierck, C. J. *et al.*, 1999; Sjolund, B. H., 2002; Rosenzweig, E. S. and McDonald, J. W., 2004). In the hemisection model (Christensen, M. D. *et al.*, 1996), a lateral spinal hemisection is performed at T13 level. After a period of motor dysfunction, ipsilateral to the injury, rats display persistent stimulus-evoked hypersensitivity of the four limbs associated with vocalization. This model was successfully used to observe molecular and structural reorganization of the spinal cord in NP (Christensen, M. D. and Hulsebosch, C. E., 1997b; Bennett, A. D. *et al.*, 2000; Hains, B. C. *et al.*, 2003b). The anterolateral cordotomy model (Vierck, C. J. and Light, A. R., 1999) consists in an unilateral injury of the anterolateral column at the T9–T11 spinal segments. The injury is associated with overgrooming and signs of allodynia/hyperalgesia. The model has been adapted

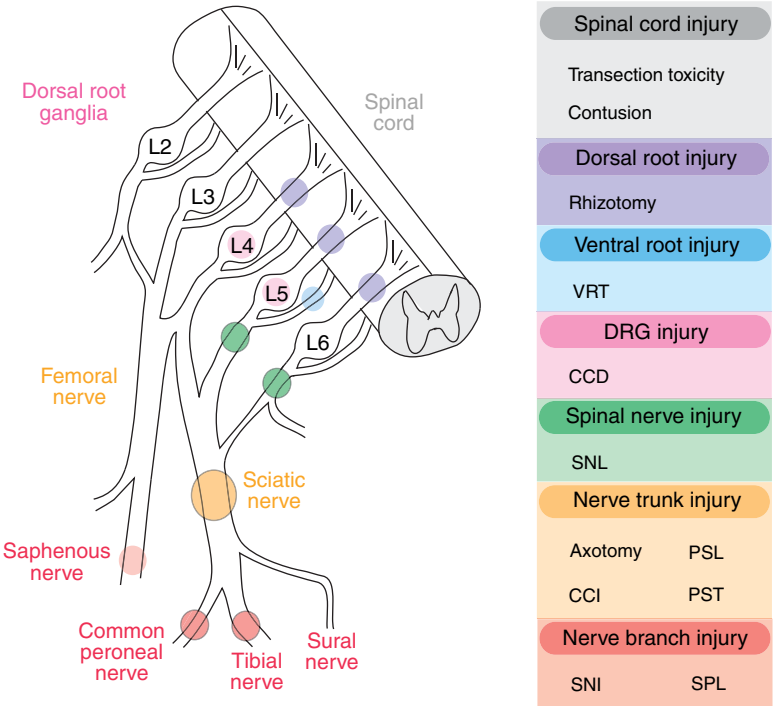

Figure 1 Anatomy of the rat lumbar plexus and the location of the different injuries used to create the different neuropathic pain models. VRT, ventral root transection; CCD, chronic compression of dorsal root ganglia; SNL, spinal nerve ligation; CCI, chronic constriction injury; PSL, partial sciatic ligation; PST, partial sciatic nerve transection; SNI, spared nerve injury (tibial and c. peroneal nerves are injured, sural nerve is intact); SPL, saphenous nerve partial ligation (30–50% of the saphenous is transected).

to primates and much information has been acquired on thalamus circuitry in NP (Weng, H.-R. *et al.*, 2000). The model of spinal cord contusion (Gruner, J. A., 1992; Siddall, P. *et al.*, 1995) is produced by an impact injury on the spinal cord at the level of T12/L1 using a weight dropped with a standard impact device (MASCIS, Multi-Center Animal Spinal Cord Injury Study). The incidence of pain hypersensitivity is correlated to the extent of the injury (Hulsebosch, C. E. *et al.*, 2000; Mills, C. D. *et al.*, 2001; Gwak, Y. S. *et al.*, 2004) and evidence of hyperexcitability of dorsal horn neurons and regulation of voltage-gated sodium channels have been shown (Hains, B. C. *et al.*, 2003a). Squeezing the spinal cord is the basis of the compression injury model (Fehlings, M. G. and Nashmi, R., 1995). A 35- or 50-g clip compression is placed on the dura mater at the juncture of T12 and T13 spinal segments and leads to microvasculature disruption, ischemia, and progressive axonal injury associated with the development of tactile allodynia (Bruce, J. C. *et al.*, 2002). Other central models of NP use toxic substances. The photochemically induced lesion of the spinal cord (Hao, J. X. *et al.*, 1991) is produced by the intravenous injection of erythrosine B (a photosensitizing dye) immediately followed by irradiation with an argon laser beam at T13 level. This procedure results in an ischemic lesion of thoracic spinal cord by occlusion of spinal cord vessels and produces a particularly severe mechanical and cold allodynia-like behavior in skin territories innervated by the rostral border of the injury (Hao, J. X. *et al.*, 1991; 1992). Excitotoxic spinal cord injury (ESCI) is directly mediated by the intraspinal injection at levels ranging from T10 to L4 of quisqualic acid (QUIS), an α-amino-3-hydroxy-5-methylisoxazole-4-propionic acid (AMPA) metabotropic receptor agonist (Yezierski, R. P. *et al.*, 1993; 1998). This model offers the considerable advantage of avoiding surgical laminectomy, and although less representative of a clinical pathology, it induces sustained NP-like symptoms related to a precise mechanism. The QUIS model leads to a gradual and specific loss of neurons associated to NP-like behaviors and the extension of the injury and the intensity of changes are dependent on the depth and volume of the QUIS injections.

5.56.2.2 Models of Peripheral Neuropathic Pain: Injury to Roots, Dorsal Root Ganglia, and Spinal Nerves

Surgical procedures on selective root, dorsal root ganglia, and spinal nerves allows direct access to sensory and motor fibers and a clear segmental location of injured and noninjured primary afferents. Spontaneous and stimulus-evoked pain are sustained by different mechanisms such as deafferentation, ectopic activities in dorsal root ganglion (DRG), and spinal cord neurons, Wallerian degeneration of the peripheral axons and central reorganization (Eschenfelder, S. *et al.*, 2000; Li, Y. *et al.*, 2000). For dorsal and ventral root rhizotomies, typically at L5 level, the root is ligated and transected 3–4 mm proximal to the DRG (Colburn, R. W. *et al.*, 1999; Li, L. *et al.*, 2002). The ventral root transection model provides an additional feature to investigate NP, in the sense that lesion of a motor nerve induces alteration of pain sensitivity (Li, L. *et al.*, 2002; Sheth, R. N. *et al.*, 2002). Robust mechanical and cold allodynia-like behaviors have been documented (Sheen, K. and Chung, J. M., 1993), whereas loose ligation of L4–L6 dorsal roots produces only mechanical allodynia (Tabo, E. *et al.*, 1999). The chronic compression of dorsal root ganglia (CCD), proposed as a model of lower back pain/disc herniation, consists of the placement of a fine stainless-steel rod into the L5/L4 intervertebral foramen (Hu, S. J. and Xing, J. L., 1998). Heat hyperalgesia and a tactile allodynia are the resulting behaviors encountered in this model (Zhang, J. M. *et al.*, 1999; Ma, C. and LaMotte, R. H., 2005). The widely used spinal nerve ligation (SNL), where L5/L6 spinal nerve are tightly ligated (Kim, S. H. and Chung, J. M., 1992), produces robust and consistent sympathetic-dependent NP-related behaviors including indirect signs of spontaneous pain, heat hyperalgesia, mechanical allodynia/hyperalgesia, and cold allodynia (Choi, Y. *et al.*, 1994). This type of damage has also been applied successfully to mice and primates (Choi, Y. *et al.*, 1994; Ali, Z. *et al.*, 1999; Mogil, J. S. *et al.*, 1999). The additional and considerable advantage of SNL is the possibility to distinguish injured (L5/L6) and noninjured (L4) DRG and spinal segments.

5.56.2.3 Models of Peripheral Neuropathic Pain: Injury to Peripheral Nerves

The first models of NP used complete transection of major peripheral nerve. Wall and co-workers produce an entire denervation of the distal hindlimb, damaging the sciatic and saphenous nerves, to model anesthesia dolorosa, a type of NP referred to denervated zone without any sensory input from that area. Nerves were transected at midthigh level and the proximal stump was either tightly ligated or encapsulated into a

polyethylene tube (Wall, P. D. *et al.*, 1979a; 1979b). The total sciatic transection prevents stimulus-evoked assessment of the hindlimb but self-mutilation (autotomy) was the major feature of the experimental anesthesia dolorosa mode. Degrees of autotomy have been defined according to the extension of self-mutilation in the hindpaw and are used to evaluate the progression of the neuropathy. The subsequent chronic constriction injury (CCI) model, four catgut ligations loosely placed around the sciatic nerve (Bennett, G. J. and Xie, Y. K., 1988) or the partial sciatic ligation (PSL) model, ligation of one-third to one-half of the sciatic nerve in rats (Seltzer, Z. *et al.*, 1990) or mice (Malmberg, A. B. and Basbaum, A. I., 1998), allow sensory testing in the hindpaw (Figure 2). Moderate autotomy, guarding, and excessive grooming of the injured limb were noticed as well as thermal/mechanical hyperalgesia- and allodynia-like behavior were recorded (Bennett, G. J., 1993). Alternative to the CCI models include application of fixed-diameter polyethylene cuffs around the sciatic nerve, favoring a standardization of the loose, but constrictive ligatures in CCI (Mosconi, T. and Kruger, L., 1996). Another valuable alternative is the partial sciatic nerve transection (PST) model where half of the diameter of the sciatic nerve is only transected, avoiding inflammation caused by suture material with PSL. Chronic constriction of the trigeminal nerve (infraorbital nerve CCI, ION–CCI) was designed by Vos B. P. *et al.* (1994) as a model of trigeminal pain. ION–CCI model elicits excessive grooming of the face, mechanical allodynia, and thermal hyperalgesia (Imamura, Y. *et al.*, 1997). Sensory assessment of the animal face is difficult; however, the recent introduction of an automated thermal behavioral assay should provide valuable characterizations of orofacial pain models (Neubert, J. K. *et al.*, 2005).

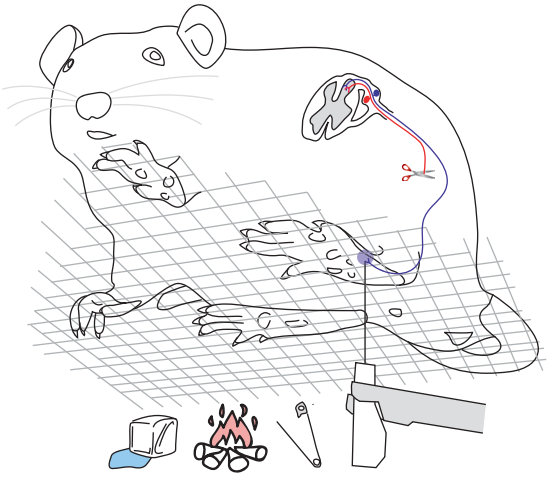

Figure 2 In many experimental models of neuropathic pain (NP), stimulus-evoked pain sensitivity is assessed in the plantar side of the hindpaw with various stimuli, usually in the territory of spared or regenerated afferents.

5.56.2.4 Models of Peripheral Neuropathic Pain: Distal Nerve Branch Injuries

Injuries to distal nerves branches offer the advantage that they can be anatomically defined, helping the standardization of surgical procedures. The spared nerve injury (SNI) in rats and mice is based on the ligation and transection of the tibial and common peroneal nerves leaving the sural nerve intact (Decosterd, I. and Woolf, C. J., 2000; Bourquin, A. F. *et al.*, 2006). This model results in early, robust, and intense mechanical allodynia/hyperalgesia and cold allodynia in the territory of the sural nerve (Figure 3). It offers the advantage of sparing an almost sensory nerve in combination with a clear separation of injured and noninjured axons distal to the injury. SNI has also been adapted to neonatal animals (Howard, R. F. *et al.*, 2005) and variants of the model have been described in rats and mice (Lee, B. H. *et al.*, 2000; Shields, S. D. *et al.*, 2003). Recently, the saphenous nerve partial ligation (SPL) model (30–50% of the saphenous nerve, a branch of the femoral nerve that innervates the medial part of the paw, is tightly ligated) leads to the development of NP-related symptoms (Walczak, J. S. *et al.*, 2005). The relevance in this model is that the injury of an exclusively sensory nerve is easily transferable for investigations with skin–nerve preparations (Reeh, P. W., 1986). Injury to peripheral branches has also been

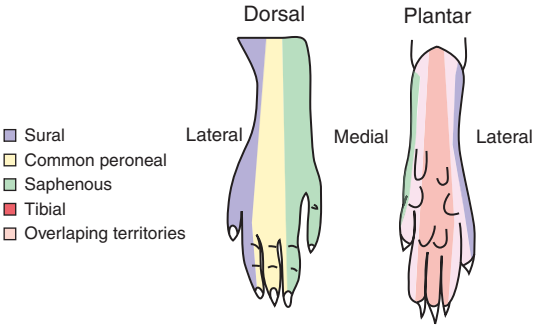

Figure 3 Areas of the dorsal and plantar paw innervated by the sciatic and femoral nerves in the rat. Some overlap between territories may occur (pink).

applied to the trigeminal nerve to study orofacial pain and similar to the SNI model, transection of a branch of the trigeminal nerve (infra-alveolar nerve) leads to hypersensitivity in the whisker pad area, which is innervated by a spared nerve (ION) (Tsuboi, Y. *et al.*, 2004).

5.56.2.5 Nontraumatic Models of Neuropathic Pain

Vincristine, taxol, and cisplatin may lead to peripheral neuropathy and NP in cancer patients. Models based on these substances have been created with different features of NP-related symptoms, usually in a dose-dependent manner (de Koning, P. *et al.*, 1987; Cavaletti, G. *et al.*, 1995; Aley, K. O. *et al.*, 1996; Authier, N. *et al.*, 2000; Mimura, Y. *et al.*, 2000; Nozaki-Taguchi, N. *et al.*, 2001). Diabetes is a major cause of painful neuropathy in humans. The diabetic model was induced by intraperitoneal injections of streptozotocin (STZ), which leads to pancreatic islet destruction and chronic hyperglycemia (Courteix, C. *et al.*, 1993; 1994). NP symptoms such as hyperalgesia- and allodynia-like behavior appear 2 weeks after. STZ produces functional, biochemical, and structural abnormalities in the sciatic nerve similar to those seen in human diabetic neuropathy (Sima, A. A. and Sugimoto, K., 1999). Prolonged ischemia of the hindpaw was proposed as a surrogate to complex regional pain syndrome (CRPS) type I (Coderre, T. J. *et al.*, 2004). After 8 h and lasting for 4 weeks, mechanical hyperalgesia and bilateral mechanical/thermal allodynia was observed along with excessive shaking and licking of hindpaws (Coderre, T. J. *et al.*, 2004). Axonal damage is combined with inflammation and nerve inflammatory models, without direct nerve injury were developed by wrapping the sciatic nerve with cellulose-containing inflammatory reagents such as carrageenan or complete Freund's adjuvant (CFA) (Eliav, E. *et al.*, 1999). In these cases, the course of pain hypersensitivity is very short (2–5 days only).

5.56.3 Behavioral Assessment of Neuropathic Pain in Animal Models: Spontaneous Pain, Stimulus-Evoked Pain, and Stimulus-Induced Pain

Tests based on pain sensitivity consider the type of injury, the remaining capacity of withdrawal reflexes (e.g., when neuromuscular defect is caused by the nerve injury), plus the localization, the intensity, and the time course of symptoms. NP in humans is characterized by modification of basal pain sensitivity with ongoing/spontaneous pain, and stimulus-evoked hyper- or hyposensitivity (Woolf, C. J. and Decosterd, I., 1999). Spontaneous pain appears independently of any external stimulus and cannot be assessed directly in animals. Only indirect physiological or behavioral surrogates of spontaneous pain are measurable: spontaneous discharges in sensory neurons, autotomy, posture (e.g., guarding behavior) movements (e.g., brisk paw flinches), or changes in general behavior (e.g., grooming, sleep patterns, vocalization, exploratory behavior) (Mogil, J. S. and Crager, S. E., 2004). All raised substantial issues that have meant laboratories favoring the recording of stimulus-evoked pain.

Stimulus-evoked pain is elicited by distinct stimuli like touch, pinprick, or temperature (heat or cold). Change in the threshold of response and/or quality of response are generally used as outcomes of allodynia/hyperalgesia-like behavior.

Mechanical allodynia-like behavior is usually measured by using a series of calibrated monofilaments of logarithmic incremental force (von Frey hairs) (Bennett, G. J., 2001). Monofilaments are applied in various territories of the animal's body, and positive responses are recorded when the application induces a withdrawal, movement, or vocalization. The evaluation of nociceptive threshold in sensible regions is the result of different procedures, such as the up–down method of Dixon (Chaplan, S. R. *et al.*, 1994). Cold allodynia-like behavior is assessed by placing an acetone drop on the area of interest, the acetone drop quickly evaporates eliciting a cold sensation (Choi, Y. *et al.*, 1994). Frequency of response to multiple applications as well as the type and duration of response have been used to score cold allodynia. Another method for measuring response to cold is the use of a cooled metal floor, usually at noxious low temperatures, thus evaluating cold hyperalgesia (Bennett, G. J. and Xie, Y. K., 1988; Choi, Y. *et al.*, 1994). Thermal hyperalgesia-like behavior is typically evaluated by measuring the latency and duration of reaction toward a heat noxious stimulus induced by a radial infrared beam (Hargreaves, K. *et al.*, 1988). Mechanical hyperalgesia-like behavior is evoked by a pinprick test, using a safety pin stimulus that provokes, in a normal animal, a small brisk withdrawal reflex, while abnormal responses are evoked in experimental NP rats. A large duration of withdrawal

and paw guarding/shaking/licking follows the stimulus (Tal, M. and Bennett, G. J., 1994).

Stimulus-induced pain refers to the capacity of external stimuli not only to directly evoke pain, but also to alter sensory processing such as to generate a state of pain hypersensitivity that outlast the primary stimuli. In animals, stimulus-evoked pain after capsaicin, inflammation, or nerve crush (Bennett, G. J. and Xie, Y. K., 1988; Choi, Y. *et al.*, 1994; Ma, Q. P. and Woolf, C. J., 1996; Kim, H. T. *et al.*, 2001; Decosterd, I. *et al.*, 2002) has been investigated after repeated low-threshold mechanical stimuli and further measurement of mechanical sensitivity is carried out using von Frey hairs. In this case, stimulus-induced pain has therefore been termed progressive tactile hypersensitivity.

Internal and external factors influence behavioral outcomes. These include: experimenter, genetic background, and gender of the animals, food, sawdust, noise, transportation, and so on (Chesler, E. J. *et al.*, 2002). Harmonized environments, as well as studies conducted by an investigator unaware of the treatment applied, facilitate this standardization of behavioral assessment.

5.56.4 Conclusions

Many factors need to be considered in any particular model such as the location, form, extension and evolution of the injury. At present, animal models of NP display unique and indispensable features and they are:

1. representative of a clinical entity or a fundamental mechanism;
2. ease in performance and reproducibility from investigator to investigator and laboratory to laboratory;
3. related to a development of symptoms consistent with clinical NP;
4. allowing well-characterized measure of pain sensitivity by behavioral assessments;
5. presenting robust alterations of nociceptive thresholds; and
6. compatible with reproducible pharmacological response.

Future challenges remain open for the development of new animal models as well as methods of measurement that include for instance measuring devices independent of the experimenter (Neubert, J. K. *et al.*, 2005). Pain symptoms are not equivalent to pain mechanisms, but they may reflect them. Similarly, all outcome measures in experimental models are not equivalent. A sophisticated approach using multiple models (Decosterd, I. *et al.*, 2004) is then required in order to correlate information obtained in experimental models with clinical syndromes of NP. Although all models of NP have weak points in modeling only partially human NP and the impossibility to have direct behavioral measurement of spontaneous pain, we believe that current and future models of NP will strengthen our knowledge of the underlying mechanisms and favor the development of new treatment strategies for this currently intractable form of pain.

References

Aley, K. O., Reichling, D. B., and Levine, J. D. 1996. Vincristine hyperalgesia in the rat: a model of painful vincristine neuropathy in humans. Neuroscience 73, 259–265.

Ali, Z., Ringkamp, M., Hartke, T. V., Chien, H. F., Flavahan, N. A., Campbell, J. N., and Meyer, R. A. 1999. Uninjured C-fiber nociceptors develop spontaneous activity and alpha-adrenergic sensitivity following L6 spinal nerve ligation in monkey. J. Neurophysiol. 81, 455–466.

Authier, N., Fialip, J., Eschalier, A., and Coudore, F. 2000. Assessment of allodynia and hyperalgesia after cisplatin administration to rats. Neurosci. Lett. 291, 73–76.

Bennett, G. J. 1993. An animal model of neuropathic pain: a review. Muscle Nerve 16, 1040–1048.

Bennett, G. J. 2001. Animal Models of Pain. In: Methods in Pain Research (*ed*. L. Kruger), pp. 67–91. CRC Press LLC.

Bennett, G. J. and Xie, Y. K. 1988. A peripheral mononeuropathy in rat that produces disorders of pain sensation like those seen in man. Pain 33, 87–107.

Bennett, A. D., Everhart, A. W., and Hulsebosch, C. E. 2000. Intrathecal administration of an NMDA or a non-NMDA receptor antagonist reduces mechanical but not thermal allodynia in a rodent model of chronic central pain after spinal cord injury. Brain Res. 859, 72–82.

Bourquin, A. F., Suveger, M., Pertin, M., Gilliard, N., Sardy, S., Davison, A. C., Spahn, D. R., and Decosterd, I. 2006. Assessment and analysis of mechanical allodynia- like behavior induced by spared nerve injury (SNI) in the mouse. Pain 122, 14.el–14. e14.

Bruce, J. C., Oatway, M. A., and Weaver, L. C. 2002. Chronic pain after clip-compression injury of the rat spinal cord. Exp. Neurol. 178, 33–48.

Cavaletti, G., Tredici, G., Braga, M., and Tazzari, S. 1995. Experimental peripheral neuropathy induced in adult rats by repeated intraperitoneal administration of taxol. Exp. Neurol. 133, 64–72.

Chaplan, S. R., Bach, F. W., Pogrel, J. W., Chung, J. M., and Yaksh, T. L. 1994. Quantitative assessment of tactile allodynia in the rat paw. J. Neurosci. Methods 53, 55–63.

Chesler, E. J., Wilson, S. G., Lariviere, W. R., Rodriguez-Zas, S. L., and Mogil, J. S. 2002. Influences of laboratory environment on behavior. Nat. Neurosci. 5, 1101–1102.

Choi, Y., Yoon, Y. W., Na, H. S., Kim, S. H., and Chung, J. M. 1994. Behavioral signs of ongoing pain and cold allodynia in a rat model of neuropathic pain. Pain 59, 369–376.

Christensen, M. D. and Hulsebosch, C. E. 1997a. Chronic central pain after spinal cord injury. J. Neurotrauma 14, 517–537.

Christensen, M. D. and Hulsebosch, C. E. 1997b. Spinal cord injury and anti-NGF treatment results in changes in CGRP density and distribution in the dorsal horn in the rat. Exp. Neurol. 147, 463–475.

Christensen, M. D., Everhart, A. W., Pickelman, J. T., and Hulsebosch, C. E. 1996. Mechanical and thermal allodynia in chronic central pain following spinal cord injury. Pain 68, 97–107.

Coderre, T. J., Xanthos, D. N., Francis, L., and Bennett, G. J. 2004. Chronic post-ischemia pain (CPIP): a novel animal model of complex regional pain syndrome-Type I (CRPS-I; reflex sympathetic dystrophy) produced by prolonged hindpaw ischemia and reperfusion in the rat. Pain 112, 94–105.

Colburn, R. W., Rickman, A. J., and DeLeo, J. A. 1999. The effect of site and type of nerve injury on spinal glial activation and neuropathic pain behavior. Exp. Neurol. 157, 289–304.

Courteix, C., Bardin, M., Chantelauze, C., Lavarenne, J., and Eschalier, A. 1994. Study of the sensitivity of the diabetes-induced pain model in rats to a range of analgesics. Pain 57, 153–160.

Courteix, C., Eschalier, A., and Lavarenne, J. 1993. Streptozocin-induced diabetic rats: behavioural evidence for a model of chronic pain. Pain 53, 81–88.

Decosterd, I. and Woolf, C. J. 2000. Spared nerve injury: an animal model of persistent peripheral neuropathic pain. Pain 87, 149–158.

Decosterd, I., Allchorne, A., and Woolf, C. J. 2002. Progressive tactile hypersensitivity after a peripheral nerve crush: non-noxious mechanical stimulus-induced neuropathic pain. Pain 100, 155–162.

Decosterd, I., Allchorne, A., and Woolf, C. J. 2004. Differential analgesic sensitivity of two distinct neuropathic pain models. Anesth. Analg. 99, 457–463.

Eliav, E., Herzberg, U., Ruda, M. A., and Bennett, G. J. 1999. Neuropathic pain from an experimental neuritis of the rat sciatic nerve. Pain 83, 169–182.

Eschenfelder, S., Habler, H. J., and Janig, W. 2000. Dorsal root section elicits signs of neuropathic pain rather than reversing them in rats with L5 spinal nerve injury. Pain 87, 213–219.

Fehlings, M. G. and Nashmi, R. 1995. Assessment of axonal dysfunction in an *in vitro* model of acute compressive injury to adult rat spinal cord axons. Brain Res. 677, 291–299.

Gruner, J. A. 1992. A monitored contusion model of spinal cord injury in the rat. J. Neurotrauma 9, 123–126.

Gwak, Y. S., Hains, B. C., Johnson, K. M., and Hulsebosch, C. E. 2004. Effect of age at time of spinal cord injury on behavioral outcomes in rat. J. Neurotrauma 21, 983–993.

Hains, B. C., Klein, J. P., Saab, C. Y., Craner, M. J., Black, J. A., and Waxman, S. G. 2003a. Upregulation of sodium channel Nav1.3 and functional involvement in neuronal hyperexcitability associated with central neuropathic pain after spinal cord injury. J. Neurosci. 23, 8881–8892.

Hains, B. C., Willis, W. D., and Hulsebosch, C. E. 2003b. Serotonin receptors 5-HT1A and 5-HT3 reduce hyperexcitability of dorsal horn neurons after chronic spinal cord hemisection injury in rat. Exp. Brain Res. 149, 174–186.

Hao, J. X., Xu, X. J., Aldskogius, H., Seiger, A., and Wiesenfeld-Hallin, Z. 1991. Allodynia-like effects in rat after ischaemic spinal cord injury photochemically induced by laser irradiation. Pain 45, 175–185.

Hao, J. X., Xu, X. J., Aldskogius, H., Seiger, A., and Wiesenfeld-Hallin, Z. 1992. Photochemically induced transient spinal ischemia induces behavioral hypersensitivity to mechanical and cold stimuli, but not to noxious-heat stimuli, in the rat. Exp. Neurol. 118, 187–194.

Hargreaves, K., Dubner, R., Brown, F., Flores, C., and Joris, J. 1988. A new and sensitive method for measuring thermal nociception in cutaneous hyperalgesia. Pain 32, 77–88.

Howard, R. F., Walker, S. M., Mota, P. M., and Fitzgerald, M. 2005. The ontogeny of neuropathic pain: postnatal onset of mechanical allodynia in rat spared nerve injury (SNI) and chronic constriction injury (CCI) models. Pain 115, 382–389.

Hu, S. J. and Xing, J. L. 1998. An experimental model for chronic compression of dorsal root ganglion produced by intervertebral foramen stenosis in the rat. Pain 77, 15–23.

Hulsebosch, C. E. 2002. Recent advances in pathophysiology and treatment of spinal cord injury. Adv. Physiol. Educ. 26, 238–255.

Hulsebosch, C. E., Xu, G. Y., Perez-Polo, J. R., Westlund, K. N., Taylor, C. P., and McAdoo, D. J. 2000. Rodent model of chronic central pain after spinal cord contusion injury and effects of gabapentin. J. Neurotrauma 17, 1205–1217.

Imamura, Y., Kawamoto, H., and Nakanishi, O. 1997. Characterization of heat-hyperalgesia in an experimental trigeminal neuropathy in rats. Exp. Brain Res. 116, 97–103.

Kim, S. H. and Chung, J. M. 1992. An experimental model for peripheral neuropathy produced by segmental spinal nerve ligation in the rat. Pain 50, 355–363.

Kim, H. T., Park, S. K., Lee, S. E., Chung, J. M., and Lee, D. H. 2001. Non-noxious A fiber afferent input enhances capsaicin-induced mechanical hyperalgesia in the rat. Pain 94, 169–175.

de Koning, P., Neijt, J. P., Jennekens, F. G., and Gispen, W. H. 1987. Evaluation of cis-diamminedichloroplatinum (II) (cisplatin) neurotoxicity in rats. Toxicol. Appl. Pharmacol. 89, 81–87.

Lee, B. H., Won, R., Baik, E. J., Lee, S. H., and Moon, C. H. 2000. An animal model of neuropathic pain employing injury to the sciatic nerve branches. Neuroreport 11, 657–661.

Li, Y., Dorsi, M. J., Meyer, R. A., and Belzberg, A. J. 2000. Mechanical hyperalgesia after an L5 spinal nerve lesion in the rat is not dependent on input from injured nerve fibers. Pain 85, 493–502.

Li, L., Xian, C. J., Zhong, J. H., and Zhou, X. F. 2002. Effect of lumbar 5 ventral root transection on pain behaviors: a novel rat model for neuropathic pain without axotomy of primary sensory neurons. Exp. Neurol. 175, 23–34.

Ma, C. and LaMotte, R. H. 2005. Enhanced excitability of dissociated primary sensory neurons after chronic compression of the dorsal root ganglion in the rat. Pain 113, 106–112.

Ma, Q. P. and Woolf, C. J. 1996. Progressive tactile hypersensitivity: an inflammation-induced incremental increase in the excitability of the spinal cord. Pain 67, 97–106.

Malmberg, A. B. and Basbaum, A. I. 1998. Partial sciatic nerve injury in the mouse as a model of neuropathic pain: behavioral and neuroanatomical correlates. Pain 76, 215–222.

Mills, C. D., Hains, B. C., Johnson, K. M., and Hulsebosch, C. E. 2001. Strain and model differences in behavioral outcomes after spinal cord injury in rat. J. Neurotrauma 18, 743–756.

Mimura, Y., Kato, H., Eguchi, K., and Ogawa, T. 2000. Schedule dependency of paclitaxel-induced neuropathy in mice: a morphological study. Neurotoxicology 21, 513–520.

Mogil, J. S. and Crager, S. E. 2004. What should we be measuring in behavioral studies of chronic pain in animals? Pain 112, 12–15.

Mogil, J. S., Wilson, S. G., Bon, K., Lee, S. E., Chung, K., Raber, P., Pieper, J. O., Hain, H. S., Belknap, J. K., Hubert, L., Elmer, G. I., Chung, J. M., and Devor, M. 1999. Heritability of nociception I: responses of 11 inbred mouse strains on 12 measures of nociception. Pain 80, 67–82.

Mosconi, T. and Kruger, L. 1996. Fixed-diameter polyethylene cuffs applied to the rat sciatic nerve induce a painful neuropathy: ultrastructural morphometric analysis of axonal alterations. Pain 64, 37–57.

Neubert, J. K., Widmer, C. G., Malphurs, W., Rossi, H. L., Vierck, C. J., and Caudle, R. M. 2005. Use of a novel thermal operant behavioral assay for characterization of orofacial pain sensitivity. Pain 116, 386–395.

Nozaki-Taguchi, N., Chaplan, S. R., Higuera, E. S., Ajakwe, R. C., and Yaksh, T. L. 2001. Vincristine-induced allodynia in the rat. Pain 93, 69–76.

Reeh, P. W. 1986. Sensory receptors in mammalian skin in an *in vitro* preparation. Neurosci. Lett. 66, 141–146.

Rosenzweig, E. S. and McDonald, J. W. 2004. Rodent models for treatment of spinal cord injury: research trends and progress toward useful repair. Curr. Opin. Neurol. 17, 121–131.

Seltzer, Z., Dubner, R., and Shir, Y. 1990. A novel behavioral model of neuropathic pain disorders produced in rats by partial sciatic nerve injury. Pain 43, 205–218.

Sheen, K. and Chung, J. M. 1993. Signs of neuropathic pain depend on signals from injured nerve fibers in a rat model. Brain Res. 610, 62–68.

Sheth, R. N., Dorsi, M. J., Li, Y., Murinson, B. B., Belzberg, A. J., Griffin, J. W., and Meyer, R. A. 2002. Mechanical hyperalgesia after an L5 ventral rhizotomy or an L5 ganglionectomy in the rat. Pain 96, 63–72.

Shields, S. D., Eckert, W. A., and Basbaum, A. I. 2003. Spared nerve injury model of neuropathic pain in the mouse: a behavioral and anatomic analysis. J. Pain 4, 465–470.

Siddall, P. J. and Loeser, J. D. 2001. Pain following spinal cord injury. Spinal Cord 39, 63–73.

Siddall, P., Xu, C. L., and Cousins, M. 1995. Allodynia following traumatic spinal cord injury in the rat. Neuroreport 6, 1241–1244.

Sima, A. A. and Sugimoto, K. 1999. Experimental diabetic neuropathy: an update. Diabetologia 42, 773–788.

Sjolund, B. H. 2002. Pain and rehabilitation after spinal cord injury: the case of sensory spasticity? Brain Res. Rev. 40, 250–256.

Tabo, E., Jinks, S. L., Eisele, J. H., Jr., and Carstens, E. 1999. Behavioral manifestations of neuropathic pain and mechanical allodynia, and changes in spinal dorsal horn neurons, following L4–L6 dorsal root constriction in rats. Pain 80, 503–520.

Tal, M. and Bennett, G. J. 1994. Extra-territorial pain in rats with a peripheral mononeuropathy: mechano-hyperalgesia and mechano-allodynia in the territory of an uninjured nerve. Pain 57, 375–382.

Tsuboi, Y., Takeda, M., Tanimoto, T., Ikeda, M., Matsumoto, S., Kitagawa, J., Teramoto, K., Simizu, K., Yamazaki, Y., Shima, A., Ren, K., and Iwata, K. 2004. Alteration of the second branch of the trigeminal nerve activity following inferior alveolar nerve transection in rats. Pain 111, 323–334.

Vierck, C. J. and Light, A. R. 1999. Effects of combined hemotoxic and anterolateral spinal lesions on nociceptive sensitvity. Pain 83, 447–457.

Vierck, C. J., Siddall, P., and Yezierski, R. P. 2000. Pain following spinal cord injury: animal models and mechanistic studies. Pain 89, 1–5.

Vos, B. P., Strassman, A. M., and Maciewicz, R. J. 1994. Behavioral evidence of trigeminal neuropathic pain following chronic constriction injury to the rat's infraorbital nerve. J. Neurosci. 14, 2708–2723.

Walczak, J. S., Pichette, V., Leblond, F., Desbiens, K., and Beaulieu, P. 2005. Behavioral, pharmacological and molecular characterization of the saphenous nerve partial ligation: a new model of neuropathic pain. Neuroscience 132, 1093–1102.

Wall, P. D., Devor, M., Inbal, R., Scadding, J. W., Schonfeld, D., Seltzer, Z., and Tomkiewicz, M. M. 1979a. Autotomy following peripheral nerve lesions: experimental anaesthesia dolorosa. Pain 7, 103–111.

Wall, P. D., Scadding, J. W., and Tomkiewicz, M. M. 1979b. The production and prevention of experimental anesthesia dolorosa. Pain 6, 175–182.

Weng, H.-R, Lee, J. I., Lenz, F. A., Schwartz, A., Vierck, C., Rowland, L., and Dougherty, P. M. 2000. Functional plasticity in primate somatosensory thalamus following chronic lesion of the ventral lateral spinal cord. Neuroscience 101, 393–401.

Woolf, C. J. 1983. Evidence for a central component of post-injury pain hypersensitivity. Nature 306, 686–688.

Woolf, C. J. and Decosterd, I. 1999. Implications of recent advances in the understanding of pain pathophysiology for the assessment of pain in patients. Pain Suppl. 6, S141–S147.

Woolf, C. J. and Fitzgerald, M. 1983. The properties of neurones recorded in the superficial dorsal horn of the rat spinal cord. J. Comp. Neurol. 221, 313–328.

Yezierski, R. P., Liu, S., Ruenes, G. L., Kajander, K. J., and Brewer, K. L. 1998. Excitotoxic spinal cord injury: behavioral and morphological characteristics of a central pain model. Pain 75, 141–155.

Yezierski, R. P., Santana, M., Park, S. H., and Madsen, P. W. 1993. Neuronal degeneration and spinal cavitation following intraspinal injections of quisqualic acid in the rat. J. Neurotrauma 10, 445–456.

Zhang, J. M., Song, X. J., and LaMotte, R. H. 1999. Enhanced excitability of sensory neurons in rats with cutaneous hyperalgesia produced by chronic compression of the dorsal root ganglion. J. Neurophysiol. 82, 3359–3366.

5.57 Neuropathic Pain: Clinical

R Baron, Christian-Albrechts-Universität Kiel, Kiel, Germany

© 2008 Elsevier Inc. All rights reserved.

5.57.1	**Definition of Neuropathic Pain**	866
5.57.2	**Epidemiology of Neuropathic Pain**	866
5.57.3	**Classification**	866
5.57.3.1	Disease/Anatomy-Based Classification	866
5.57.3.1.1	Painful peripheral (focal, multifocal, generalized) neuropathies	867
5.57.3.1.2	Central pain syndromes	871
5.57.3.1.3	Complex painful neuropathic disorders	872
5.57.3.1.4	Mixed pain syndromes	873
5.57.3.2	Mechanism-Based Classification	873
5.57.4	**Signs and Symptoms in Neuropathic Pain**	874
5.57.5	**Pathophysiological Mechanisms in Neuropathic Pain**	876
5.57.5.1	Peripheral Sensitization of Primary Afferent Nociceptors	876
5.57.5.2	Central Sensitization	878
5.57.5.3	Central Disinhibition and Fascilitation	879
5.57.5.4	Inflammation and Neuropathic Pain	880
5.57.6	**Pathophysiological Mechanisms in Patients in Relation to Their Somatosensory Profile**	880
5.57.6.1	Peripheral Sensitization of Primary Afferent Neurons in Patients	880
5.57.6.2	Sensitization to Catecholamines in Patients	882
5.57.6.3	Central Sensitization in Patients	884
5.57.6.4	Central Disinhibition Leading to Cold Hyperalgesia	885
5.57.6.5	Deafferentation: Hyperactivity of Central Pain Transmission Neurons	885
5.57.6.6	Inflammation in Patients	886
5.57.7	**Diagnostic Tools for Neuropathic Pain**	886
5.57.7.1	Questionnaires	887
5.57.7.2	Bedside Assessment of Neuropathic Pain	887
5.57.7.3	Apparative Assessment of Somatosensory Phenotypes	889
5.57.7.4	Skin Biopsies	889
5.57.7.5	Microneurography	891
5.57.7.6	Indirect Test of Afferent Unmyelinated Fiber Function	891
5.57.7.7	Imaging Techniques	892
5.57.7.8	Do We Have Diagnostic Tool to Dissect Individual Mechanisms in Neuropathic Pain?	892
5.57.8	**Therapy**	893
5.57.8.1	Antidepressants	894
5.57.8.2	Anticonvulsants (Ca Channel Modulators)	894
5.57.8.3	Anticonvulsants (Na Channel Blockers)	895
5.57.8.4	Tramadol and Opioid Analgesics	895
5.57.8.5	Topical Medications	895
5.57.8.5.1	Topical capsaicin	895
5.57.8.5.2	Topical lidocaine	895
5.57.8.6	*N*-Methyl-D-Aspartic Acid Receptor Antagonists	895
5.57.8.7	Cannabinoids	895
5.57.8.8	Treatment Guideline	896
References		897

Glossary

CRPS Complex regional pain syndrome.
DRG Dorsal root ganglion, spinal ganglion.
MEG Magnetic encephalography.
NCF Nucleus cuneiformis.
PAG Periaqueductal gray.
PET Positron emission tomography.
TRP Ion channels of transient receptor potential family.
TNF Tumor necrosis factor.
QST Quantitative sensory testing.

5.57.1 Definition of Neuropathic Pain

The current NeuPSIG (Neuropathic pain special interest group of the International Association for the Study of Pain) taxonomy of chronic pain, defines neuropathic pain as a "Pain arising as a direct consequence of a lesion or disease affecting the somatosensory system." The term 'disease' refers to identifiable disease processes such as inflammatory, autoimmune conditions, or channelopathies, while lesions refer to macro- or microscopically identifiable damage. The restriction to the somatosensory system is necessary, because diseases and lesions of other parts of the nervous system may cause nociceptive pain. For example, lesions or diseases of the motor system may lead to spasticity or rigidity, and thus may indirectly cause muscle pain. The latter pain conditions are now explicitly excluded from the condition neuropathic pain. Where possible, neuropathic pain should be qualified as being of peripheral or central origin in terms of the location of the lesion or disease process. This distinction is important, as lesions or diseases of the central nervous system (CNS) and peripheral nervous system (PNS) are distinct in terms of clinical manifestations and underlying pathophysiology.

5.57.2 Epidemiology of Neuropathic Pain

Chronic neuropathic pain is common in clinical practice, greatly impairs the quality of life of patients and is a major economical health problem. Estimates of point prevalence for neuropathic pain in the general population are as high as 5% (Daousi, C. *et al.*, 2004), a quarter of them suffering from severe intensity (McDermott, A. M. *et al.*, 2006). Moreover, a recent prospective cross-sectional survey in more than 12 000 chronic pain patients with both nociceptive and neuropathic pain types who were referred to pain specialists in Germany (Freynhagen, R. *et al.*, 2005/2006) revealed that already 13% of these patients suffer from the two classical neuropathic disorders, postherpetic neuralgia (PHN) and painful diabetic neuropathy and 40% of all patients at least have a neuropathic component to their discomfort (especially patients with chronic back pain and radiculopathy). In neuropathic patients pain therapy was already performed for 2–4 years, one-third of the patients mentioned three or more doctor visits for pain therapy in the past month and 8–20% already applied for pension (Table 1).

Comorbidities such as poor sleep, depressed mood, and anxiety are common in neuropathic pain and have a significant impact on the global pain experience. The German survey revealed that about 60% of neuropathic patients were moderate or severely depressed compared with 25% in the nociceptive patient group. Optimal sleep quality was only scored by 27% of the neuropathic patients and in 49% of the nociceptive pain patients, respectively.

5.57.3 Classification

5.57.3.1 Disease/Anatomy-Based Classification

It is common clinical practice to classify neuropathic pain according to the underlying etiology of the disorder and the anatomical location of the specific lesion (Jensen, T. S. and Baron, R., 2003). The majority of patients fall into four broad classes (Table 2): painful peripheral neuropathies (focal, multifocal, or generalized, e.g., traumatic, ischemic, inflammatory, toxic, metabolic, and hereditary), central pain syndromes (e.g., stroke, multiple sclerosis (MS), and spinal cord injury (SCI)), complex painful neuropathic disorders (complex regional pain syndromes, CRPSs) and mixed pain syndromes (combination of

Table 1 Sociodemographic and clinical characteristics in patients with postherpetic neuralgia (PHN) and diabetic painful neuropathy (DPN) (%)

	PHN	*DPN*
Number of patients	498	1144
Male	199 (40.0)	596 (52.1)
Female	299 (60.0)	548 (47.9)
Age (years)		
Mean	60.6	61.7
SD ±	15.4	13.2
Duration of pain treatment (months)		
Mean	24	52
SD ±	41	63
No. of doctor visits for pain during the past 4 weeks		
One visit	188 (37.8)	348 (30.4)
Two visits	135 (27.1)	339 (29.6)
Three or more	132 (26.5)	348 (30.4)
Ongoing psychotherapy	8 (1.6)	34 (3.0)
Intended/submitted pension application	42 (8.2)	221 (19.3)
Pain intensity on VAS during the past 4 weeks		
Mild	154 (30.9)	492 (43.0)
Moderate	239 (48.0)	424 (37.1)
Severe	105 (21.1)	228 (19.9)
VAS worst pain (mean)	7.4	6.3
VAS average pain (mean)	5.5	4.9

VAS, visual analogue scale.

nociceptive and neuropathic pain, e.g., chronic low back pain with radiculopathy).

The anatomical distribution pattern of the affected nerves provides valuable differential diagnostic clues as to possible underlying causes. Therefore, painful peripheral neuropathies are grouped into symmetrical generalized polyneuropathies, disease affecting many nerves simultaneously and into asymmetrical neuropathies with a focal or multifocal distribution or processes affecting the brachial or lumbosacral plexuses.

One important subgroup of painful polyneuropathies is characterized by a predominant or in some cases even isolated affection of small afferent fibers, i.e., unmyelinated C fibers and small myelinated Aδ fibers. In many cases, autonomic efferent small fiber systems are also affected. Several different etiologies may lead to small-fiber polyneuropathies (see below), up to 20% of cases, however, are of unknown cause. It is important to realize that conventional electrophysiological techniques like nerve conduction study (NCS), sensory-evoked potential (SEP), etc., only assess the function of myelinated peripheral axonal systems, the affection of small fibers are missed. Therefore, especially in small-fiber neuropathies alternative diagnostic procedures have to be used (see below).

5.57.3.1.1 Painful peripheral (focal, multifocal, generalized) neuropathies

Although most of the different neuropathic pain syndromes are common and well known to the pain specialists, there are certain entity-specific features that should be mentioned in detail (See also Table 3):

5.57.3.1.1.(i) Diabetic neuropathy

- High prevalence
- Several types of polyneuropathies, most prevalent symmetrical distally, sensory predominant neuropathy
- Numbness and paresthesias (sometimes burning quality) are common
- Sometimes spontaneous, deep, aching pain, and lightning pain
- Severe sensory neuropathy in diabetes may lead to painless perforating foot ulcers often associated with autonomic neuropathy
- Patients without pain tend to have areflexia with distal sensory loss particularly involving joint position sense
- Patients with severe burning pain and hyperesthesia tend to have sensory loss with a relative preservation of position sense and intact reflexes and often have accompanying autonomic neuropathy

Table 2 Disease-/anatomy-based classification of painful peripheral neuropathies

Painful peripheral neuropathies
- Focal, multifocal
  - Phantom pain, stump pain, nerve transection pain (partial or complete)
  - Neuroma (posttraumatic or postoperative)
  - Posttraumatic neuralgia
  - Entrapment syndromes
  - Mastectomy
  - Postthoracotomy
  - Morton's neuralgia
  - Painful scars
  - Herpes zoster and postherpetic neuralgia
  - Diabetic mononeuropathy, diabetic amyotrophy
  - Ischemic neuropathy
  - Borreliosis
  - Connective tissue disease (vasculitis)
  - Neuralgic amyotrophy
  - Peripheral nerve tumors
  - Radiation plexopathy
  - Plexus neuritis (idiopathic or hereditary)
  - Trigeminal or glossopharyngeal neuralgia
  - Vascular compression syndromes

Generalized (polyneuropathies)
- Metabolic or nutritional
  - Diabetic, often 'Burning feet syndrome'
  - Alcoholic
  - Amyloid
  - Hypothyroidism
  - Beri beri, pellagra
- Drugs
  - Antiretrovirals, cisplatin, disulfiram, ethambutol, isoniazid, nitrofurantoin, thalidomid, thiouracil, vincristine, chloramphenicol, metronidazole, taxoids, gold
- Toxins
  - Acrylamide, arsenic, clioquinol, dinitrophenol, ethylene oxide, pentachlorophenol, thallium
- Hereditary
  - Amyloid neuropathy
  - Fabry's disease
  - Charcot–Marie–Tooth disease type 5, type 2B
  - Hereditary sensory and autonomic neuropathy (HSAN) type 1, type 1B
- Malignant
  - Carcinomatous (paraneoplastic), myeloma
- Infective or postinfective, immune
  - Acute or inflammatory polyradiculoneuropathy (Guillain–Barré syndrome), borreliosis, HIV
- Other polyneuropathies
  - Erythromelalgia
  - Idiopathic small-fiber neuropathy
  - Trench foot (cold injury)

Central pain syndromes
- Vascular lesions in the brain (especially brainstem and thalamus) and spinal cord
  - Infarct
  - Hemorrhage
  - Vascular malformation
- Multiple sclerosis
- Traumatic spinal cord injury including iatrogenic cordotomy
- Traumatic brain injury
- Syringomyelia and syringobulbia
- Tumors
- Abscesses
- Inflammatory diseases other than multiple sclerosis; myelitis caused by viruses, syphilis
- Epilepsy
- Parkinson's disease

(*Continued*)

Table 2 (Continued)

Complex painful neuropathic disorders
Complex regional pain syndromes type I and II (reflex sympathetic dystrophy, causalgia)
Mixed pain syndromes
Chronic low back pain with radiculopathy
Cancer pain with malignant plexus invasion
Complex regional pain syndromes

Table 3 Special clinical features that are relevant for specific diagnoses

Special feature	*Possible diagnosis*
Cold allodynia	Traumatic nerve injury
	Trench foot syndrome
	Complex regional pain syndrome
	Oxaliplatin-induced polyneuropathy
	Central poststroke pain
Deep somatic allodynia	Complex regional pain syndrome
SMP	Complex regional pain syndrome, acute herpes
Isolated small-fiber affection	Diabetic polyneuropathy
	Amyloid polyneuropathy
	Fabry's disease
	Hereditary polyneuropathy
	Idiopathic small-fiber polyneuropathy
Painful polyneuropathy in several family members	Amyloid polyneuropathy,
	Fabry's disease
	Charcot–Marie–Tooth disease type 5, type 2B
	Hereditary sensory, autonomic polyneuropathy (HSAN) type 1, 1B

SMP, sympathetically maintained pain.

- Small sensory and autonomic fibers are involved early in diabetic neuropathy as well as in impaired glucose tolerance (IGT)
- Abnormal epidermal C fiber density is highly correlated with warm detection threshold (QST)
- Regeneration capacity of cutaneous C fibers (experimental challenge with topical capsaicin) is reduced
- Hyperglycemia in diabetic patients may itself be an important factor for acute exacerbations of pain
- Up 40% of patients with a so-called burning feet syndrome have a small-fiber neuropathy and many already demonstrate an IGT indicative of early diabetes

5.57.3.1.1.(ii) Alcoholic neuropathy

- Incidence of neuropathy in chronic alcoholism about 10%
- Paresthesias, burning pain, and tenderness of the feet
- Painful symptoms not related to the severity of somatosensory deficit
- Sensorimotor small- and large-fiber neuropathy
- Sometimes early small-fiber deficit

5.57.3.1.1.(iii) Amyloid neuropathy

- Predominant painful small fiber neuropathy in both inherited and sporadic forms
- Predominant distal sensory loss of pain and thermal sensations, often autonomic involvement
- Severe pain usually of a deep aching quality, sometimes shooting pains

5.57.3.1.1.(iv) Fabry's disease (angiokeratoma corporis diffusum)

- Lipid (glycosphingolipid) storage disorder, sex-linked recessive
- Heterozygous carrier females occasionally develop symptoms later in life
- Deficiency of α-galactosidase A lead to accumulation of glycosphingolipid (globotriaosylceramide) in tissues

- Painful small-fiber neuropathy early and presenting clinical feature
- Boys or young men present with tenderness of the feet and severe spontaneous burning pain in the legs
- Stroke in young adults due endothelial vasculopathy, about 5% of young male patients with cryptogenic stroke have Fabry's disease
- Extraneural manifestations: cutaneous telangiectasia, cardiac, renal, pulmonary failure
- Patients with preserved renal function involves exclusively small myelinated and unmyelinated fibers
- Normal results of nerve conduction studies
- Normal results of large-fiber quantitation by sural nerve biopsy

5.57.3.1.1.(v) Idiopathic small-fiber neuropathy

- Predominant or isolated loss of small fibers involving somatic and autonomic neurons
- Often elderly patients
- 40% of patients with a so-called burning feet syndrome have a small-fiber neuropathy suffering from burning sensation, dysesthesia and paresthesias in the feet, lancinating pains, and minimal or no distal weakness
- Abnormalities of epidermal skin innervation (skin biopsies)
- Normal results of nerve conduction studies
- Normal results of large-fiber quantitation by sural nerve biopsy

5.57.3.1.1.(vi) Human immunodeficiency virus- and highly active antiretroviral therapy–associated neuropathy

- Incidence about 15–30% in the human immunodeficiency virus (HIV) population
- Painful sensory polyneuropathy
- Distal painful paresthesias, spontaneous pain, evoked shock-like pain, and mechanical allodynia with symmetric stocking-like distribution associated with autonomic neuropathy
- Neuropathy is due to a combination of the virus itself and antiretroviral drugs (nucleoside analogue reverse transcriptase inhibitors, highly active antiretroviral therapy (HAART))
- Clinically, these two neuropathies are indistinguishable
- Nerve pathology in the painful sensory polyneuropathy includes axonal atrophy and endoneurial capillary thickening

5.57.3.1.1.(vii) Erythromelalgia (erythermalgia)

- Rare condition characterized by painful, red, hot extremities
- Acquired form sometimes associated with polycythemia rubra vera
- Rare hereditary form caused by a genetic defect of the sodium channel $Na_v1.7$
- Symptoms are aggravated by heat
- Immediate pain relief by cooling the affected limb
- Feet affected in more than 80%, hands in 25%
- Underlying small fiber neuropathy in some cases

5.57.3.1.1.(viii) Acute herpes zoster and postherpetic neuralgia

- Acute zoster: neurocutaneous disease with unilateral efflorescences within one or few dermatomes
- Reactivation of varicella zoster virus, which resides in latent form in sensory trigeminal and dorsal root ganglia following primary infection as varicella
- Preherpetic neuralgia (pain before cutaneous symptoms of acute zoster) of some days
- Every dermatome may be affected, thoracic 54%, especially Th5–10 (15%), trigeminal 20%, especially first branch (13%)
- PHN: chronic pain syndrome for more than 3 months after healing of acute zoster lesions
- Incidence of pain 9–15% after 1 month, 2–5% of all age groups after 1 year
- Main risk factor for PHN is age
- Spontaneous burning pain, stimulus-evoked pain, and shooting pains possible

5.57.3.1.1.(ix) Phantom limb pain

- Phantom limb: amputation of an extremity or other body part or transection of a peripheral nerve leads almost in all cases to a sensation of the missing or denervated limb
- Phantom limb pain: pain in the missing body part, up to 80% of patients, mainly after extremity amputation, cramp-like severe pain in distal phantom, sometime painful phantom movements
- Stump pain: the amputation stump itself shows mechanical allodynia especially close to the skin flap scar or near tender neuromas
- Telescoping: seemingly shrinking phantom
- Aggravation of both painful and nonpainful phantom sensations by external stimuli (noxious or

innocuous mechanical stimuli at the stump, sometimes at face or remote ipsilateral body parts)

- Aggravation of both painful and nonpainful phantom sensation by internal stimuli (micturition, yawning) or emotional stimuli
- Main reasons for amputations in times of peace: peripheral vascular disease (60%), half of the patients also suffer from additional diabetes mellitus, accidents (20%), rare causes like tumor, arterial thrombosis, and osteomyelitis (20%)
- Pathophysiological mechanisms: it seems obvious that the phantom limb image with its complex perceptual, emotional and cognitive qualities involves interaction of some cerebral structures. This, however, may not preclude the notion that neuronal mechanisms at a much lower level of the CNS or even within the severed peripheral nerves may furnish the brain with the information necessary for creating the phantom.

5.57.3.1.2 Central pain syndromes

Central pain is defined as chronic pain following a lesion or disease of the CNS. The cause of pain is a primary process within the CNS. All lesions that cause central pain affect the somatosensory pathways. They may be located at any level of the neuraxis. Thus lesions at the first synapse in the dorsal horn of the spinal cord or trigeminal nuclei, along the ascending pathways through the spinal cord (Figure 1) and brainstem, in the thalamus, in the subcortical white matter, and in the cerebral cortex have all been reported (Leijon, G. *et al.*, 1989).

The most common are cerebrovascular lesions, MS, and traumatic spinal cord injuries (SCIs). In these diseases the incidences are around 8%, 28%, and 40%, respectively (Siddall, P. J. *et al.*, 2003). In stroke, there is a particularly high prevalence among patients with brainstem and thalamic lesions, whereas there is no difference in the prevalence after ischemic and hemorrhagic events. In patients with thalamic infarction only patients with lesions that includes the ventroposterior region, which receives a particularly dense spinothalamic projection develop central pain. In MS it has not been possible to determine the location of the lesions that cause central pain, but clinical observations indicate that many of them are located in the spinal cord.

In stroke the pain is most frequently a hemipain (75%). In MS it affects one or both sides more often in the legs (87%) than in the upper extremities (31%). Trigeminal neuralgia, caused by a lesion in the brain stem, occurs in 5% of all MS patients. In all conditions, there is a large variation in the quality of central pain.

Often central pain develops with a latency of weeks or month after the inciting event. The most frequent clinical characteristics are spontaneous burning pain, shooting pain and evoked pain within the affected body part. Allodynia to touch or light pressure as well as to heat or cold are common. Many internal and external events influence central pain,

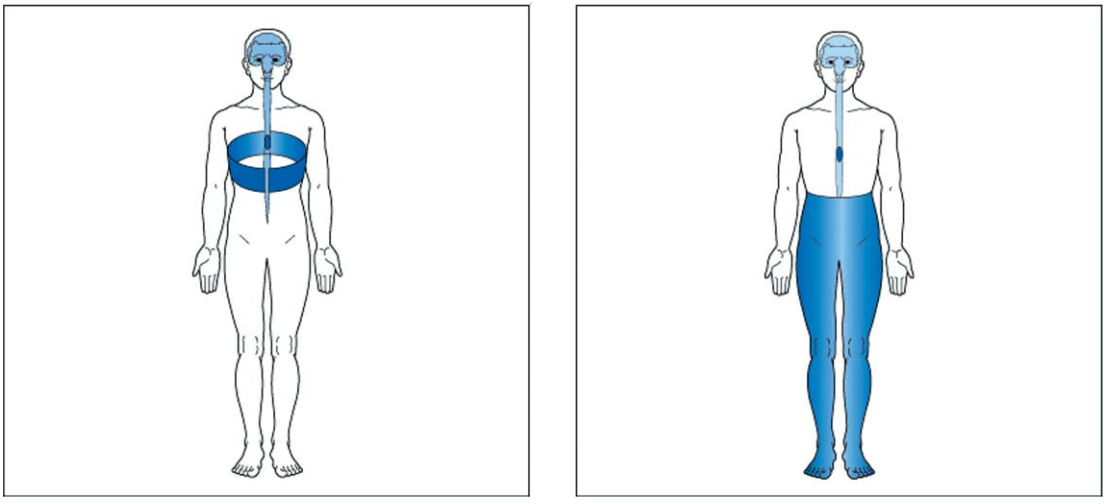

Figure 1 Different pains in spinal cord injury patients. (a) Typical pattern of below-level neuropathic pain following spinal cord injury (SCI) at T7. The dark shading represents the distribution of pain. (b) Typical pattern of at-level neuropathic pain following SCI at T7. The dark shading represents the distribution of pain. Adapted from Siddall, P. 2006. Pain Following Spinal Gord Injury. In: Walland Melzack's Textbook of Pain, 5th edn. (*eds.* McMahan, S. B. and Koltzenburg, M.), pp. 1043–1056. Elsevier.

such as cutaneous stimuli, body movements, visceral stimuli, emotions, and changes in mood.

In order to diagnose central pain it is necessary to ensure that the patient has a CNS disorder by a detailed history and a neurological examination, computed tomography (CT), magnetic resonance imaging (MRI), cerebrospinal fluid analysis, or electrophysiological techniques (in particular QST to assess spinothalamic function). It is necessary to exclude painful peripheral neuropathy as a cause. Polyneuropathy is not uncommon in, for instance stroke patients, a group with a high incidence of diabetes.

The pathophysiological mechanisms of central pain are unclear. An affection of the spinothalamocortical pathways seems to be crucial for the development of central pain, whereas isolated lesions of the lemniscal system are never associated with pain. Thus, the pain is always correlated with sensory disturbances, dominated by abnormalities in the sensibility to temperature and pain. Decreased sensibility to touch, vibration, and joint movements may be present, but is often less pronounced. It is hypothesized that central pain occurs only in patients who have lesions of the spinothalamocortical pathways. Lesioning of the spinothalamic tract leads to a loss of input to normal pain-modulating systems in particular in thalamic neurons. This loss may creates neuronal signs of hyperexcitability. Furthermore, infarction of the dorsolateral thalamus may lead to neuronal disinhibition in medial thalamic nuclei. Incomplete SCI may be associated with sensitization of spinal dorsal horn neurons.

5.57.3.1.2.(i) Spinal cord injury pain

- Prevalence of pain about 65% (Siddall, P. J. *et al.*, 2003)
- Four types of pain (Figure 1):

1. Nociceptive pain (musculoskeletal, spastic, visceral)
2. Neuropathic pain above level (secondary to nerve lesions: compressive mononeuropathies, CRPS)
3. Neuropathic pain at level (segmental, circumferential band-like distribution: nerve root compression, syringomyelia, spinal cord trauma, or ischemia)
4. Neuropathic pain below level (below the level of the spinal cord lesion perceived diffusely in anesthetic regions: spinal cord trauma, or ischemia)

- Musculoskeletal nociceptive pain is the most common (58%)
- At-level neuropathic pain 42%, sharp, shooting, electric, burning, and stabbing pain located in a region of sensory disturbance
- Below-level neuropathic pain 34%, develops months and even years following initial injury, spontaneous and/or evoked pain diffusely caudal to the level of SCI, burning, aching, stabbing, or electric shocks, often with hyperalgesia
- Fluctuation with mood, activity, infections
- Triggered by sudden noises, jarring movements
- Both complete and partial injuries may be associated with the diffuse, burning pain
- Incomplete injuries often show allodynia due to sparing of lemniscal tracts conveying touch sensations
- Mainly not painful phantom sensation present in 90%

5.57.3.1.3 Complex painful neuropathic disorders

In addition to the classical neuropathic syndromes like painful diabetic neuropathy, PHN, or phantom limb pain there are certain chronic painful conditions that share many clinical characteristics. These syndromes were formerly called reflex sympathetic dystrophy, M. Sudeck or causalgia and are now classified under the umbrella term CRPSs. CRPS are painful disorders that may develop as a disproportionate consequence of trauma typically affecting the limbs (Janig, W. and Baron, R., 2003; Baron, R. and Janig, W., 2004). CRPS type I usually develops after minor trauma with a small or no obvious nerve lesion at an extremity (e.g., bone fracture, sprains, bruises or skin lesions, surgeries). CRPS type II develops after trauma with a mostly large nerve lesion. The patients often report a burning spontaneous pain felt in the distal part of the affected extremity. Stimulus-evoked pains are a striking clinical feature; they include mechanical and thermal allodynia and/or hyperalgesia. These sensory abnormalities are most pronounced distally, and have no consistent spatial relationship to individual nerve territories or to the site of the inciting lesion. Typically, pain can be elicited by movement of and pressure on the joints (deep somatic allodynia), even if these are not directly affected by the inciting lesion.

Unlike other classical neuropathic pain syndromes CRPS show additional nonsensory features like signs of autonomic dysfunction (abnormal

regulation of blood flow and sweating), edema of skin and subcutaneous tissues, active and passive movement disorders, and trophic changes of skin, appendages of skin and subcutaneous tissues. Especially for the acute phase, there is accumulating evidence that inflammatory processes might be involved. Thus, it is likely that nociceptive as well as neuropathic mechanisms are responsible for pain generation in CRPS, which would then fit into the classification if a mixed pain syndrome (see below).

5.57.3.1.4 *Mixed pain syndromes*

There is agreement that both nociceptive and neuropathic processes contribute to many chronic pain syndromes and that these different mechanisms may explain the qualitatively different symptoms and signs that patients experience. In particular, patients with chronic low back pain, cancer pain, and CRPS seem to fit into this theoretical construct (Baron, R. and Binder, A., 2004).

In chronic low back pain, the nociceptive component stems from activation of intact nociceptors that innervate ligaments, small joints, muscle, and tendons. The neuropathic pain component is caused by mechanical compression of the nerve root or by action of inflammatory mediators originating from the degenerative disc on the nerve root. Cytokines and chemokines have been implicated in the chemical pathomechanism of radicular pain. Increased levels of tumor necrosis factor alpha (TNF-α), interleukin (IL)-1, IL-6, and granulocyte-macrophage colony stimulating factor (GM-CSF) have been detected in herniated disc tissue compared with normal, nondegenerated disc tissue. TNF-α applied to nerve roots reproduces the pathologic changes observed with nerve root exposure to nucleus pulposus extracts. Finally, in an animal model of radiculopathy induced by intervertebral disc material, inhibitors of TNF-α reversed the radicular pathology. So far it is unclear whether these mediators are capable of activating intact nerve root fibers even without any mechanical compression or if the combination of mechanical nerve damage and cytokine attack is the important prerequisite.

5.57.3.2 Mechanism-Based Classification

As described above neuropathic pain represents heterogeneous conditions, which neither can be explained by one single etiology or disease nor by a specific anatomical lesion, i.e., a disease- and anatomy-based classification is often insufficient. First, despite obvious differences in etiology, many of these conditions share common clinical phenomena; for example, touch-evoked pain in PHN and painful diabetic neuropathy. Conversely, different signs and symptoms can be present in the same disease; for example, pain paroxysms and stimulus-evoked abnormalities in PHN. Second, classification on the basis of anatomical location also has its shortcomings, as neuroplastic changes following nervous system lesions often give rise to sensory and pain distributions that do not respect nerve, root, segmental or cortical territories. Third, and most importantly, decades of rather discouraging systematic research on chronic pain therapy have revealed that a disease based strategy is of no or little help to these patients and their pain.

These observations have raised the question of whether an entirely different strategy, in which pain is analyzed on the basis of underlying mechanisms (Jensen, T. S. and Baron, R., 2003), could provide an alternative approach for examining and classifying patients, with the ultimate aim of obtaining a better treatment outcome (Woolf, C. W. *et al.*, 1998; Dworkin, R. H. *et al.*, 2003). Our increasing understanding of the mechanisms that underlie chronic pain, together with the discovery of new molecular therapy targets, has strengthened the demand for alternative concepts.

One theoretical possibility to identify pain mechanisms in patients is to assess differences in the somatosensory phenotype as precisely as possible. These specific patterns of signs and symptoms could be compared with the knowledge derived from animal experiments where the association of signs and symptoms and underlying mechanisms has been elucidated. This concept has led to the development of a symptom-oriented diagnostic approach to neuropathic pain conditions that supplements the etiology-based classification scheme, which recognizes the fact that neuropathic pains are usually a composite of several pain symptoms. A symptom-oriented approach does not negate the fact that distinct neuropathies present differently clinically, and that some neuropathic disease states may predispose to certain constellations of pain symptoms (e.g., touch-evoked pain in PHN). The rationale of this approach recognizes several principles:

- Clinically distinct pain symptoms such as ongoing stimulus-independent pain may be caused by similar, if not identical, neural mechanisms, even if the underlying neuropathies differ. For example,

nociceptive afferents that develop ongoing activity after axon injury could mediate ongoing pain regardless of the precipitating or sustaining neuropathic cause.

- More than one pain mechanism is usually present in an individual patient.
- Some symptoms, such as mechanical hypersensitivity, can be explained by several distinct neural mechanisms that may even coexist in an individual patient.

As said, a symptom-based approach to painful neuropathies can be useful for dissecting the underlying neural mechanisms, and this knowledge may eventually be harnessed for the development of novel analgesic drugs that differentially target these mechanisms. A very promising but still hypothetical approach is summarized in Table 5.

5.57.4 Signs and Symptoms in Neuropathic Pain

Pain associated with nerve injury has several clinical characteristics (Baron, R., 2006) (Tables 4 and 6). If a mixed peripheral nerve with a cutaneous branch or a central somatosensory pathway are involved, there is almost always an area of abnormal sensation and the patient's maximum pain is coextensive with or within an area of sensory deficit. This is a key diagnostic feature for neuropathic pain. The sensory deficit is usually to noxious and thermal stimuli, indicating damage to small-diameter afferent fibers.

Beside these negative somatosensory signs (deficit in function), which are bothering but not painful also positive signs are characteristic for neuropathic conditions. Paresthesias (ant crawling, tingling) are not painful. Painful positive signs are spontaneous (not stimulus-induced) ongoing pain and spontaneous shooting, electric schock-like sensations. Many patients with peripheral neuropathic pain also have evoked types of pain (stimulus-induced pain, hypersensitivity), which are characterized by several sensory abnormalities. They may be adjacent to or intermingled with skin areas of sensory deficit. Most often, patients report mechanical hypersensitivity followed by hypersensitivity to heat and cold. Two types of hypersensitivity can be distinguished. First, allodynia is defined as pain in response to a nonnociceptive stimulus. In case of mechanical allodynia even gentle mechanical stimuli such that even slight bending of hairs may evoke severe pain. Second, hyperalgesia is defined as an increased pain sensitivity to a nociceptive stimulus. Another evoked feature is summation, which is the progressive worsening of pain evoked by slow repetitive stimulation with mildly noxious stimuli, for example, pinprick. A small percentage of patients with peripheral nerve injury have a nearly pure hypersensitive syndrome in which no sensory deficit is demonstrable.

The quality of the reported sensation may also be a clue; neuropathic pain commonly has a burning and/or shooting quality with unusual tingling, crawling or electrical sensations (dysesthesiae).

Although all these characteristics are neither universally present in, nor absolutely diagnostic of

Table 4 Symptoms and signs of neuropathic pain

	Peripheral neuropathic pain	*Postherpetic neuralgia*	*Complex regional pain syndrome*
Ongoing pain	100%	100%	100%
Brush-evoked pain (dynamic mechanical allodynia)	36%	60%	60%
Pinprick hyperalgesia	38%	37%	Present
Static allodynia	35%	52%	Present
Deep somatic allodynia	None	None	90%
Heat allodynia	29%	29%	30%
Cold allodynia	46%	21%	30%
Edema	Low	Low	50%
Trophic changes	Present	Scars	90%
Sympathetically maintained pain	Low	Low	90% (early)

Source: Data from Pappagallo M. *et al*. (2000) and unpublished data from Peters and Nurmikko (for a group of patients with mixed peripheral neuropathic pain) and Baron (for complex regional pain syndrome). Adapted from Scadding, J. W. and Koltzenburg, M. 2006. Painful peripheral neuropathies. In: Wall and Melzack's Textbook of Pain. 5th edition. (eds. S. B. McMahon and M. Koltzenburg), pp. 973-1000. Elsevier.

Table 5 Proposed model for the relationship between neuropathic pain machanism and clinical symptoms and signs, and possible targets for the rapeutic interventions

Symptom	*Neuronal processes, mechanisms*	*Targets*	*Optimal compounds*	*Available*
Spontaneous pain (shooting)	Peripheral nociceptor hyperexcitability			
	Ectopic impulse generation, oscillations in DRG	Na channels	Selective Na channel blocker	Lidocaine, carbamazepine, oxcarbazepine, lamotrigine, TCA
Spontaneous pain (ongoing)	Peripheral nociceptor sensitization			
	Inflammation within nerves Cytokine-release	Cytokines	Cytokine antagonists Cyclooxygenase blocker	TNF-α antagonists NSAIDS?
Heat hyperalgesia	Reduced activation threshold to: Heat	TRPV1 receptor	TRPV1 receptor antagonists	Capsaicin cream
Cold hyperalgesia	Cold	TRPM8 receptor	TRPM8 receptor antagonists	Menthol?
Static mechanical hyperalgesia	Mechanical stimuli	ASCI receptor?	ASCI receptor antagonists	?
	Noradrenaline	α receptor	α receptor antagonists	Phentolamine, sympathetic block, TCA
SMP	Histamine	H1 receptor	H1 receptor antagonists	TCA
	Central dorsal horn hyperexcitability			
	Central sensitization on spinal level Ongoing C Input induces increased synaptic transmission	Presynaptic: μ receptors Ca channels($\alpha 2$–δ)	 μ receptor agonists Ca channel blocker, $\alpha 2$-δ ligands	 Opioids Gabapentin, pregabalin
	Amplification of C fiber input			
Dynamic mechanical hyperalgesia	Gating of Aβ fiber input (mechanical dynamic hyperalgesia)	Postsynaptic: NMDA receptors NK1 receptors NA channels Intracellular cascads	 NMDA receptor antagonists NK1 receptor antagonists Selective Na channel blocker Mitogen activated protein kinase mediators	 For example, ketamine, dextromethorphan ? For example, carbamazepine ?
	Gating of Aδ fiber input (mechanical punctate hyperalgesia)			
	Central spinal disinhibition, Aδ cold fiber function $\downarrow$	?	?	?
Punctate mechanical hyperalgesia	Intraspinal inhibitory interneurons $\downarrow$ (Functional, degeneration)			
	GABA-ergic Opioidergic	GABA-B receptors μ receptors	GABA-B agonists μ receptor agonists	Baclofen Opioids
	Changes of supraspinal descending modulation			
	Inibitory control (noradrenaline, 5-HT) $\downarrow$	$\alpha 2$ receptors Serotonine receptors	$\alpha 2$ receptor agonists NA/5-HT reuptake blocker	Clonidine TCA, venlafaxine, duloxetine
	Faciliatory control $\uparrow$	?	?	?

5-HT, 5-hydroxytryptamine (serotonin); ASIC, acid-sensing ion channel; GABA, γ-aminobutyric acid; MAPK, mitogen-activated protein kinase; NK1, neurokinin 1; NMDA, N-methyl-D-aspartate; NSAIDS, nonsteroidal anti-inflammatory drugs; SMP, sympathetically maintained pain; TCA, tricyclic antidepressants; TNF-α, tumor necrosis factor-α.
Adapted from Baron R. 2006. Machanism of disease: neuropathic pain – a clinical perspective. Nat. Clin. Pract. Neurol. 2, 95–106.

neuropathic pain, when they are present the diagnosis of neuropathic pain is likely (Table 4).

5.57.5 Pathophysiological Mechanisms in Neuropathic Pain

Most of the present pathophysiological ideas are derived from experimental work with animal models for neuropathic pain (Figure 2). This work has delineated a series of partially independent pathophysiological mechanisms presumed to be responsible for different types of neuropathic pain and different somatosensory abnormalities (Baron, R., 2006).

5.57.5.1 Peripheral Sensitization of Primary Afferent Nociceptors

Pain sensations are normally elicited by activity in unmyelinated (C) and thinly myelinated (Aδ) primary afferent neurons. After peripheral nerve lesion these neurons acquire an abnormal sensitization, i.e., an increased responsiveness of primary nociceptors to stimulation of their receptive field. The characteristic features of sensitized nociceptors are: pathological spontaneous discharge, a lowered activation threshold for thermal and mechanical stimuli, and an enhanced discharge to suprathreshold stimulation (hyperalgesia).

A large number of dramatic molecular and cellular changes at the level of the primary afferent nociceptor that are triggered by the nerve lesion underlie these pathological changes.

Nerve injury is matched by increased expression of messenger RNA for voltage gated sodium channels in primary afferent neurons. Two voltage-gated sodium channel genes ($Na_v1.8$ and $Na_v1.9$) are expressed selectively in nociceptive primary afferent neurons and an embryonic channel ($Na_v1.3$) is also upregulated in damaged peripheral nerves and associated with increased electrical excitability and spontaneous activity in neuropathic pain states. The accumulation of sodium channels at sites of ectopic impulse generation (sodium channel clusters) may be responsible for lowering of action potential threshold (Omana-Zapata, I. *et al.*, 1997). There is evidence that small primary afferent fibers may acquire a unique sodium channel expression profile after nerve lesion (e.g., a specific relation of up- and downregulation of channel proteins), which makes them an interesting target (Wood, J. N. *et al.*, 2004).

After peripheral nerve damage the accumulation of sodium channel clusters does not only occur at the site of the nerve lesion but also far proximally within the intact dorsal root ganglion (DRG). In the DRG a reciprocation between a phasically activating voltage-dependent, tetrodotoxin (TTX)-sensitive sodium conductance and a passive, voltage-independent potassium leak generates characteristic membrane potential oscillations. Ectopic firing is triggered when the amplitude of oscillation sinusoids reaches threshold (Amir, R. *et al.*, 2002). Pathological membrane properties within the DRG that occur after nerve lesion are of particular therapeutic interest as the DRG is spared of the blood brain barrier and might be easily accessible for systemic therapies (Jacobs, J. M. *et al.*, 1976). In addition to sodium currents, impaired potassium conductances in myelinated fibers were demonstrated in experimental diabetes and may underlie hyperexcitability in these fibers.

Damage to peripheral primary nociceptors also induces upregulation of a variety of receptor

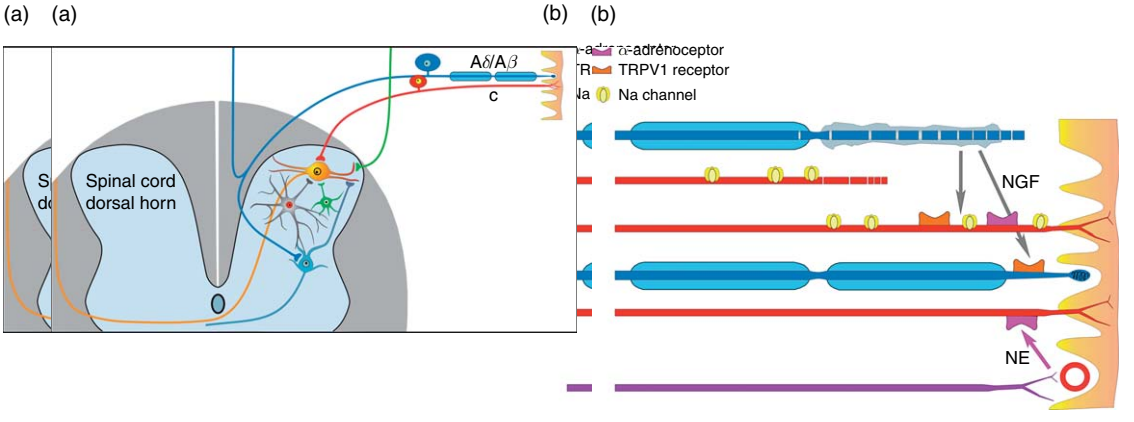

Figure 2 (continued)

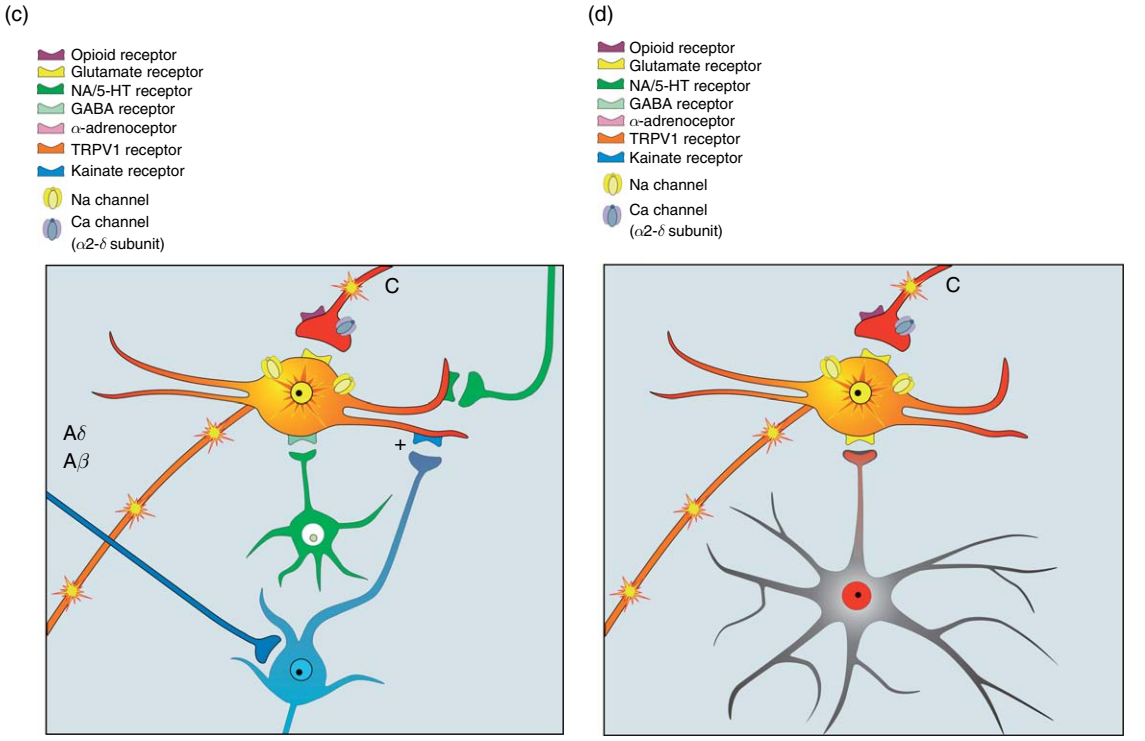

Figure 2 Mechanisms of peripheral sensitization and central sensitization in neuropathic pain. (a) Primary afferent pathways and their connections in the spinal cord dorsal horn. Nociceptive C fibers (red) terminate at spinothalamic projection neurons in upper laminae (orange neuron) whereas nonnociceptive myelinated A fibers project to deeper laminae. The second-order projection neuron is of wide dynamic range (WDR) type, that is, it receives direct synaptic input from nociceptive terminals and also multisynaptic input from myelinated A fibers (nonnoxions information, blue neuron system). γ-aminobutyric acid (GABA)-releasing interneurons (green neuron) normally exert inhibitory synaptic input on the WDR neuron. Furthermore, descending modulatory systems synapse at the WDR neuron (green descending terminal). Spinal cord glia cells (gray cell) also communicate with WDR neuron. (b) Peripheral changes at primary afferent neurons after partial nerve lesion leading to peripheral sensitization. Some axons are damaged and degenerate (upper two axons), whereas others (lower two axons) are still intact and connected with the peripheral end organ (skin). The lesion triggers the expression of sodium channels on damaged neurons. Furthermore, products such as nerve growth factor, which are associated with Wallerian degeneration, are released in the vicinity of spared fibers (arrows), triggering channel and receptor expression (sodium channels, TRPV1 receptors, adrenoceptors) on uninjured fibers. (c) Spontaneous activity in C nociceptors induces secondary changes in the central sensory processing, leading to spinal cord hyperexcitability (central sensitization of second-order WDR neurons indicated by star in orange neuron). This causes input from mechanoreceptive A fibers (light touch and punctate stimuli; blue neuron system) to be perceived as pain (dynamic and punctate mechanical allodynia; '+' indicates gating at synapse via AMPA/KA (α-amino-3-hydroxy-5-methyl-4-isoxazole propionic acid and kainate) receptors). Several presynaptic (opioid receptors, calcium channels) and postsynaptic molecular structures (glutamate receptors, NA (adrenceptors), 5-HT (serotonin) receptors, GABA receptors, sodium channels) are involved in central sensitization. Inhibitory interneurons and descending modulatory control systems (green neurons) are dysfunctional after nerve lesions, leading to disinhibition or facilitation of spinal cord dorsal horn neurons and to further central sensitization. (d) Peripheral nerve injury activates spinal cord nonneural glia cells (gray cell), which further enhances excitability in WDR neurons by releasing cytokines and glutamate. Adapted from Baron, R. 2006. Mechanisms of disease: neuropathic pain – a clinical perspective. Nat. Clin. Pract. Neurol. 2, 95–106.

proteins at the membrane some of them only marginally expressed under physiological conditions. Vanilloid receptors (TRPV1) are located predominantly on nociceptive afferent fibers and can be activated by the ingredient of hot chilli pepper (capsaicin). Physiologically, this receptor senses noxious heat (>43 °C) (Catarina, M. J. *et al.*, 2000). Accordingly, TRPV1-deficient knockout (KO) mice have obvious deficits in chemical and thermal heat nociception but normal reactions to noxious mechanical and to noxious cold stimuli.

After partial nerve injury and in streptozotocin-induced diabetic rats the lesion triggers a TRPV1 downregulation on many damaged afferents but a novel expression of TRPV1 on uninjured C and A fibers (Figure 2(b)) (Hudson, L. J. *et al.*, 2001; Hong, S. and Wiley, J. W., 2005) which is likely involved in the development C nociceptor sensitization and the associated symptom of heat hyperalgesia. Recent studies also provides evidence for a an upregulation of TRPV1 in medium and large injured dorsal root ganglion cells (Ma, W. *et al.*, 2005). However, TRPV1 does not appear to be the only transduction mechanism for heat sensitization after nerve injury. After partial sciatic nerve ligation, wild-type and TRPV1-null mice exhibited comparable persistent enhancement of mechanical and thermal nociceptive responses (Catarina, M. J. *et al.*, 2000). In this context, a recent study examined strain differences in the normal sensitivity to noxious heat in mice. These differences reflect differential responsiveness of primary afferent thermal nociceptors to heat stimuli due to a genetic variance in CGRP expression and sensitivity (Mogil, J. S. *et al.*, 2005).

In taxol-induced small-fiber painful polyneuropathy TRPV4 which is normally activated by heat of more than 30 °C seems to play a crucial role in producing taxol-induced mechanical hyperalgesia (Alessandri-Haber, N. *et al.*, 2004).

Investigations into temperature-sensitive excitatory ion channels also identified several cold-sensing ion channels in peripheral neurons. The cold- and menthol-sensitive TRP channel (TRPM8) is activated within the range of 8–28 °C (Patapoutian, A. *et al.*, 2003) and sensitized by menthol. This receptor is expressed in around 10% of all afferent ganglion neurons of rats, primarily within small-diameter cells (McKemy, D. D. *et al.*, 2002). TRPA1 is activated at lower temperatures and its exogenous ligand is cinnamaldehyde, a constituent of cinnamon oil, mustard oil, and horseradish. Peripheral nerve lesions have been shown to upregulate the expression of the latter cold-sensing ion channels in DRG cells of rats that developed cold allodynia (Obata, K. *et al.*, 2005). Therefore, upregulation or gating of these channels after injury may lead to the peripheral sensitization of cold-sensitive C nociceptors, resulting in the sensory phenomenon of cold hyperalgesia.

Besides these temperature-sensitive receptors experimental nerve injury also triggers the expression of functional α_1 or α_2 adrenoceptors on cutaneous afferent fibers, these neurons develop adrenergic sensitivity (Figure 2(b)). I.v. epinephrine or physiological noradrenaline release after stimulation of sympathetic efferents that have regenerated into the neuroma can excite afferent nociceptors. After section and reanastomosis of peripheral nerves, electrical stimulation of the sympathetic trunk at physiological stimulus frequencies activates regenerated C nociceptors through an α_1 adrenoceptor mechanism (Habler, H. J. *et al.*, 1987). Furthermore, sympathetic activity can sensitize identified intact nociceptors following damage to the nerve in which they run via an α_2 adrenoceptor mechanism (Sato, J. and Perl, E. R., 1991). The concept of a pathological coupling between sympathetic postganglionic fibers and afferent neurons via noradrenaline forms the conceptual framework for the therapeutic application of sympathetic blocks in certain pain syndromes, e.g., CRPS (Price, D. D. *et al.*, 1998; Baron, R. *et al.*, 1999b).

There is increasing evidence that also uninjured fibers running in a partially lesioned nerve may take part in pain signaling (Wasner, G. *et al.*, 2005). Uninjured fibers comingle with degenerating fibers in the same nerves. Products associated with Wallerian degeneration released in the vicinity of spared fibers (e.g., nerve growth factor (NGF)) may be the trigger for channel and receptor expression and may alter the properties of uninjured afferents (Hudson, L. J. *et al.*, 2001; Wu, G. *et al.*, 2001). Expression of sodium channels, TRPV1 receptors, adrenoreceptors and an increase of TNF-α sensitivity has been shown to play a role in uninjured fibers adjacent to lesioned axons.

5.57.5.2 Central Sensitization

As a consequence of peripheral nociceptor hyperactivity also dramatic secondary changes in the spinal cord dorsal horn occur. Peripheral nerve injury leads to an increase in the general excitability of nociceptive and multireceptive spinal cord neurons (multiple synaptic input from C as well as A fibers, wide dynamic range neurons). This phenomenon is called central sensitization and is defined as an increased responsiveness of nociceptive neurons in the CNS to their normal afferent input. Central sensitization is manifested by at least three different modes:

1. increase of neuronal activity to noxious stimuli,
2. expansion of size of neuronal receptive fields, and
3. spread of spinal hyperexcitability to other segments.

Central sensitization is initiated and maintained by activity in pathologically sensitized C fibers, which sensitize second-order spinal cord dorsal horn neurons by releasing glutamate acting on *N*-methyl-D-aspartic acid (NMDA) receptors and the neuropeptide substance P. Furthermore, central neuronal voltage-gated N-calcium channels located at the presynaptic sites on terminals of primary afferent nociceptors are involved in central sensitization by facilitation of the release of glutamate and substance P. This channel is overexpressed after peripheral nerve lesion and in rats with streptozotocin-induced diabetes (Luo, Z. D. *et al.*, 2001). As a consequence of peripheral nerve lesion the dorsal horn neurons abnormally express $HNa_v1.3$ (Hains, B. C. *et al.*, 2004) also enhancing central sensitization. Several intracellular cascades contribute to central sensitization, in particular the mitogen-activated protein kinase (MAPK) system (Ji, R. R. and Woolf, C. J., 2001). If central sensitization is established, normally innocuous tactile stimuli become capable of activating spinal cord pain signalling neurons via Aδ and Aβ low-threshold mechanoreceptors (Tal, M. and Bennett, G. J., 1994). By this mechanism, light innocuous mechanical stimuli to the skin induces pain, i.e., punctuate and dynamic mechanical allodynia. Besides these dramatic changes in the spinal cord, sensitized neurons were also found in the thalamus and primary somatosensory cortex after partial peripheral nerve injury (Guilbaud, G. *et al.*, 1992).

There is increasing evidence that neuropathic pain is in part mediated by an interaction of non-neural spinal cord glia and nociceptive neurons (Figure 2(d)). In experimental pain states in animals, astrocytes and microglia are activated by neuronal signals including substance P, glutamate, and fractalkine (Wieseler-Frank, J. *et al.*, 2005). Activation of glia by these substances in turn leads to the release of mediators that then act on other glia and also on central nociceptive neurons. These include proinflammatory cytokines and most likely also other neuroexcitatory compounds like glutamate. By this interaction central sensitization is augmented. While traditional therapies for pathological pain have focused on neuronal targets, glia might be new therapeutic targets.

Some patients with neuropathic pain, in particular patients with CRPS characteristically report 'extraterritorial' and/or 'mirror-' image pain. The pain is experienced not only in the area of trauma but also in neighboring healthy tissues. In cases of mirror-image pain, the pain is perceived from the healthy, corresponding part on the opposite side of the body. New data suggest that communication of activated astrocytes via gap junctions may mediate such spread of pain.

5.57.5.3 Central Disinhibition and Fascilitation

Physiologically dorsal horn neurons receive a strong intraspinal inhibitory control by gamma-aminobutyric acid (GABA)-ergic interneurons. Partial peripheral nerve injury may promote a selective apoptotic loss of these GABA-ergic inhibitory neurons in the superficial dorsal horn of the spinal cord (Moore, K. A. *et al.*, 2002), a mechanism which would further increases central sensitization. Furthermore, there is a novel mechanism of disinhibition following peripheral nerve injury. This mechanism involves a trans-synaptic reduction in the expression of the potassium chloride exporter KCC2 in lamina I nociceptive neurons. This induces a consequent disruption of the anion homeostasis in these dorsal horn neurons. The resulting shift in the transmembrane anion gradient caused normally inhibitory anionic synaptic currents to be excitatory. Due to this mechanism the release of GABA from normally inhibitory interneurons now exerts an excitatory action on lamina I neurons via $GABA_A$ receptors (Coull, J. A. *et al.*, 2003). The changes in lamina I neurons is induced by brain-derived neurotrophic factor (BDNF) released from activated spinal cord glia (Coull, J. A. *et al.*, 2005).

Dorsal horn neurons receive a powerful descending modulating control from supraspinal brainstem centers (inhibitory as well as faciliatory) (Vanegas, H. and Schaible, H. G., 2004) (Figures 2(a) and 2(c)). It was hypothesized that a loss of function in descending inhibitory serotonergic and noradrenergic pathway contributes to central sensitization and pain chronicity. This idea nicely explained the efficacy of serotonin and noradrenaline reuptake blocking antidepressants in neuropathic pain. However, in animals, mechanical allodynia after peripheral nerve injury was dependent upon tonic activation of descending pathways that facilitate pain transmission indicating that structures in the mesencephalic reticular formation – possibly the nucleus cuneiformis (NCF) and the periaqueductal gray (PAG) – are involved in central sensitization in neuropathic pain (Ossipov, M. H. *et al.*, 2000). Interestingly, exactly the same brainstem structures were shown to be active in humans with allodynia using advanced functional MRI (fMRI) techniques

(Zambreanu, L. *et al.*, 2005). Because in most animal pain models descending facilitation and inhibition are triggered simultaneously, it will be important to elucidate why inhibition predominates in some neuronal pools and facilitation in others.

5.57.5.4 Inflammation and Neuropathic Pain

The connective tissue sheath of peripheral nerves is innervated by sensory fibers, the nervi nervorum, which enter the sheath with the nutrient blood vessels. Some of these fine diameter primary afferents are nociceptors (Zochodne, D. W., 1993). Nervi nervorum are a potential source of pain in diseases of peripheral nerve especially in those conditions with an inflammatory component.

A different mechanism involves the production of inflammatory mediators at the site of nerve injury (local inflammation) that might be a critical factor in the cascade of events leading to neuropathic pain. Activated macrophages infiltrating from endoneurial blood vessels have been demonstrated in experimentally injured nerves (Sommer, C. and Myers, R. R., 1996) and also the dorsal root ganglia after nerve transection (Lu, X. and Richardson, P. M., 1993). Proinflammatory cytokines and in particular TNF-α released by activated macrophages can induce ectopic activity in injured but also in adjacent uninjured primary afferent nociceptors at the lesion site (Sorkin, L. S. *et al.*, 1997) and thus is a potential cause of pain and hyperalgesia (Sommer, C. *et al.*, 1998; Wagner, R. *et al.*, 1998; Sommer, C., 2003; Marchand, F. *et al.*, 2005).

5.57.6 Pathophysiological Mechanisms in Patients in Relation to Their Somatosensory Profile

Although we have achieved enormous progress in the understanding of pathophysiological mechanisms generating neuropathic pain the most important question is whether it is possible to translate these concepts into the clinical situation. In the following section the findings of the correlation of mechanisms and somatosensory abnormalities in animal experiments will be matched by observations in human experimental and clinical pain conditions.

In order to get more insight into the puzzle of neuropathic pain and even solve the therapeutic dilemma this type of translational research should be fostered in the future. The solution of the problem neuropathic pain can only be unraveled in the human experiment, that is, in patients that really feel all components of this complex sensation of neuropathic pain.

5.57.6.1 Peripheral Sensitization of Primary Afferent Neurons in Patients

Microneurographic single-fiber recordings support the idea of peripheral sensitzation of primary afferent neurons in patients with painful nerve lesions by demonstrating abnormal activity and reduced thresholds in cutaneous afferents. Abnormal ectopic activity of myelinated mechanosensitive fibers were found in traumatic nerve lesions, entrapment neuropathies, or radiculopathies (Figure 3). Because the ectopic nerve activity correlated in intensity and time course to the perceived paresthesias it is likely that pathological activity in A fibers is the underlying mechanism of positive nonpainful sensations.

Recordings from transected nerves in awake human amputees with phantom limb pain have demonstrated spontaneous ectopic activity as well as barrages of action potential firing in afferent A and C fibers projecting into the neuroma (Nystrom, B. and Hagbarth, K. E., 1981). Ectopic excitation occurred at multiple sites in damaged sensory neurons. Ongoing activity and mechanical sensitivity were recorded proximal to the nerve neuroma. Following local anesthetic blockade of the nerve distal to the recording site, impulses evoked by mechanical stimulation of the neuroma were abolished, but ongoing activity at the recording site continued, suggesting that this residual activity arose from the DRGs. As these patients suffered from spontaneous burning pain and electric shock-like sensations it is very likely that these symptoms are associated with ectopic firing in primary afferent C fibers.

In few patients with characteristic burning pain and heat hyperalgesia microneurographic recordings have provided evidence for sensitized C nociceptors. In patients with erythromelalgia nociceptors displayed ongoing activity, which is normally not observed in nociceptors, and there was a sensitization of mechanically insensitive afferents to nonpainful tactile stimuli. These abnormalities were only present in nociceptive fibers, but not of the sympathetic unmyelinated fibers, as an indicator of a neuropathic process (Figure 4) (Orstavik, K. *et al.*, 2003). In the

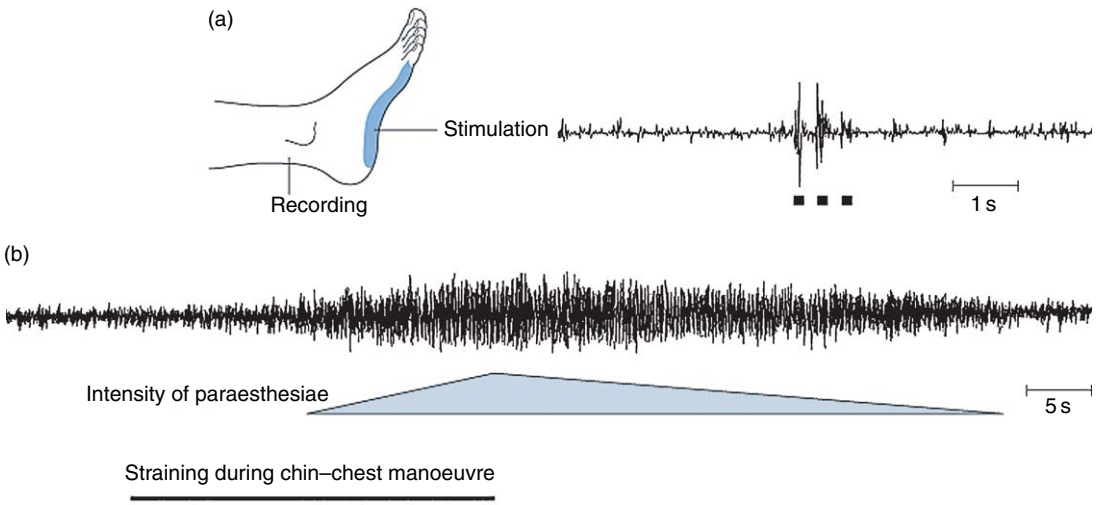

Figure 3 Microneurographic multiunit recording from the sural nerve in a patient with a compression of the S1 spinal root by a herniated disc. (a) Excitation of mechanosensitive units in the receptive field by tactile stimulation (bars). (b) Straining and chin–chest maneuver-provoked paresthesiae and an ectopic discharge of afferent fibers originating from the compressed root. Adapted from Nordin, M., Nyström, B., Wallin, U., and Hagbarth, K. E. 1984. Ectopic sensory discharges and paresthesiae in patients with disorders of peripheral nerve, dorsal roots and dorsal columns. Pain 20, 231–245. Elsevier Ltd.

autosomal dominantly inherited form of erythromelalgia a mutation in SCN9A was found, a gene that encodes the $Na_v1.7$ sodium channel, leading to an altered firing pattern in afferent neurons (Dib-Hajj, S. D. *et al.*, 2005). Hence, erythromelalgia is the first channelopathy associated with chronic pain.

Several clinical observations also support the concept of sensitized nociceptors in PHN patients. About 30% of patients with PHN do not show any loss of sensory function in the affected extremity indicating that in these particular group of patients loss of neurons is minimal or absent. Accordingly, thermal sensory thresholds in their region of greatest pain are either normal or even decreased (heat hyperalgesia) by up to 2–4 °C (Rowbotham, M. C. and Fields H. L., 1996; Pappagallo, M. *et al.*, 2000). The decrease of heat pain perception thresholds is a well-known phenomenon of peripheral nociceptor sensitization. Using skin punch biopsy, it was shown that thermal sensitivity is directly correlated with density of cutaneous innervation in the area of most severe pain (Rowbotham, M. C. *et al.*, 1996). Moreover, in PHN patients with heat hyperalgesia acute topical application of the vanilloid compound capsaicin (TRPV1 agonist), enhances pain, a sign that is indicative of an increased capsaicin sensitivity of nociceptors in the affected skin area and has been attributed to a sensitization of nociceptors as the driving element in some patients (Petersen, K. L. *et al.*, 2000). Furthermore, in a similar group of PHN patients cutaneous iontophoresis of histamine evoked a burning pain sensation whereas only itch was elicited in normal skin. Again, this phenomenon indicates that nociceptive neurons in the affected skin are abnormally sensitive to histamine (Baron, R. *et al.*, 2001) probably due to expression of a novel receptor pattern.

These observations suggest that spontaneous burning pain and heat hyperalgesia at least in part are associated with sensitization of primary afferent C fibers to TRPV1 agonists and histamine or with an altered firing pattern in these fibers due to abnormal sodium channels.

Cutaneous hypersensitivity to cold, i.e., cold hyperalgesia, is particularly prominent in patients with posttraumatic neuralgias, some small-fiber polyneuropathies and chronic CRPS. Another condition of acute cold intolerance occurs after systemic injection of the cancer chemotherapeutic agent oxaliplatin, which is associated with paresthesiae and painful hypersensitivity aggravated by cold. Psychophysical studies of human volunteers using the topical menthol model suggest that sensitization of cold-sensitive nociceptors can produce cold hyperalgesia in normal volunteers (Wasner, G. *et al.*, 2004). Peripheral sensitization also appears to occur in acute oxaliplatin-induced peripheral neuropathy (Lehky, T. J. *et al.*, 2004). Therefore, it is likely that cold hyperalgesia in some patients is induced by sensitization of primary afferent cold-sensitive nociceptors.

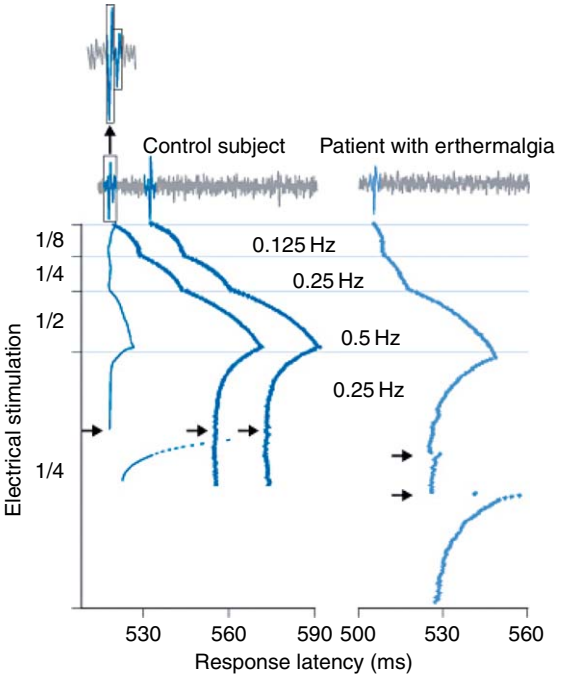

Figure 4 Microneurographic C fiber recordings from the peroneal nerve of a normal volunteer (left) and a patient suffering from erythromelalgia (right). The first trace shows the original nerve signal. The subsequent recordings are a falling leaf display in which each action potential is symbolized by a series of dots. Each row of dots represents the latency, at different electrical stimulation frequencies of the fiber, of its receptive field in the skin. Simultaneous recording of three afferent C fibers in a control subject shows two units with activity-dependent latency increases at low-frequency stimulation, and one unit that displays latency increases when excitation frequency increases to 1 impulse per 2 s. These biophysical features are characteristic for mechanically insensitive and mechanically sensitive nociceptive C fibers, respectively. Stimulation of the receptive field with a 750-mN von Frey hair (arrow) excited only the mechanosensitive C nociceptor, as evidenced by a strong latency shift to electrical stimulation. Mechanically insensitive afferents are not activated by this stimulus. The right panel shows a C fiber recording from a patient with erythromelalgia. The unit had the biophysical properties of a mechanically insensitive C fiber but responded reproducibly to mechanical stimulation (arrows). This is consistent with the hypothesis that mechanically insensitive afferents become sensitized in erythromelalgia. An alternative explanation would be that mechanically sensitive nociceptors start to display a different pattern of activity-dependent latency slowing in this disease. Adapted from Orstavik, K., Weidner, C., Schmidt, R., Schmelz, M., Hilliges, M., Jorum, E., Handwerker, H. and Torebjork, E. 2003. Pathological C-fibres in patients with a chronic painful condition. Brain 126, 567–578. Copyright 2003 Oxford University Press.

5.57.6.2 Sensitization to Catecholamines in Patients

Several clinical observations support the idea that nociceptors acquire a sensitivity to catecholamines that permits an abnormal excitation by either noradrenaline or by circulating catecholamines. This chemical sensitization makes the nociceptors susceptible for noradrenaline released from efferent sympathetic fibers in the periphery. The consecutive pathological sympathetic–afferent coupling forms the conceptual framework for sympathetically maintained pain states.

Noradrenergic sensitivity has been described in several human neuropathies and suggests that the ongoing pain can be caused or maintained by the sympathetic nervous system in selected patients: In amputees, perineuromal administration of physiological doses of norepinephrine induces intense pain as compared with saline injections (Raja, S. N. *et al.*, 1998). Intraoperative stimulation of the sympathetic chain induces an increase of spontaneous pain in patients with causalgia (CRPS II) but not in patients with hyperhidrosis. In PHN, application of norepinephrine into a symptomatic skin area increased spontaneous pain and dynamic mechanical hyperalgesia (Choi, B. and Rowbotham, M. C., 1997). In CRPS II and posttraumatic neuralgias, intracutaneous norepinephrine rekindles pain and hyperalgesia that had been relieved by sympathetic blockade. Also intradermal norepenephrine, in physiologically relevant doses, was demonstrated to evoke greater pain in the affected regions of patients with sympathetically maintained pain (SMP) than in the contralateral unaffected limb, and in control subjects (Ali, Z. *et al.*, 2000). Because noradrenaline-induced pain occurs during a differential blockade of myelinated fibers, unmyelinated fibers appear to signal sympathetically maintained pain (Torebjork, E. *et al.*, 1995).

We performed a study in patients with CRPS I using physiological stimuli of the sympathetic nervous system (Baron, R. *et al.*, 2002). Cutaneous sympathetic vasoconstrictor outflow to the painful extremity was experimentally activated to the highest possible physiological degree by whole body cooling. During the thermal challenge the affected extremity was clamped to 35 °C in order to avoid thermal effects at the nociceptor level. The intensity as well as area of spontaneous pain and mechanical allodynia (dynamic and punctate) increased significantly in patients that had been classified as having SMP by positive sympathetic blocks but not in SIP

patients (Figure 5). The experimental setup used in the latter study selectively alters sympathetic cutaneous vasoconstrictor activity without influencing other sympathetic systems innervating the extremities, i.e., piloarrector, sudomotor, and muscle vasoconstrictor neurons. Therefore, the interaction of sympathetic and afferent neurons measured here is likely to be located within the skin as

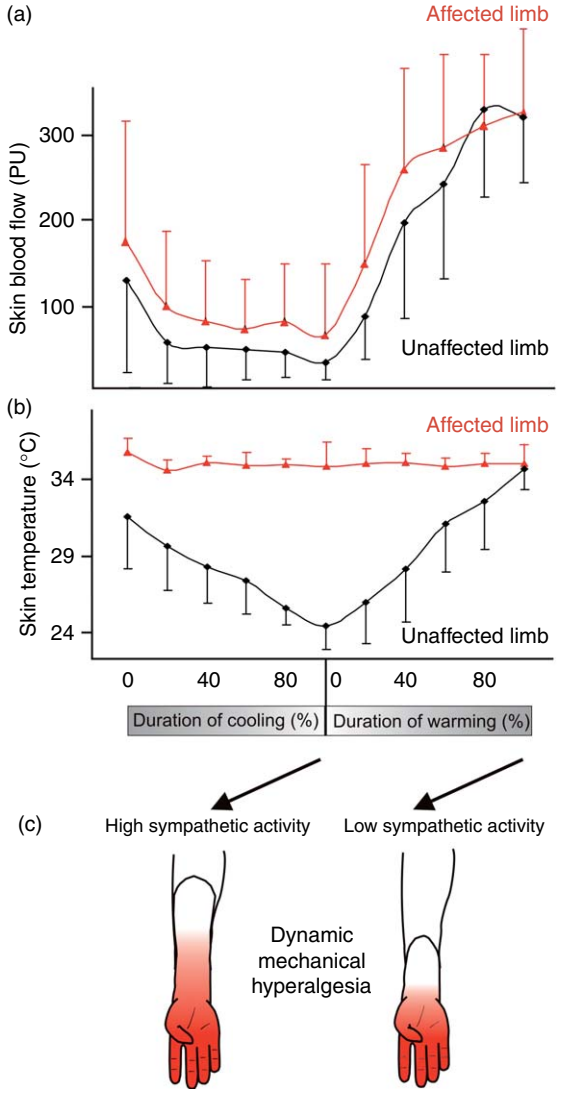

Figure 5 Experimental modulation of cutaneous sympathetic vasoconstrictor neurons by physiological thermoregulatory reflex stimuli in 13 complex regional pain syndrome (CRPS) patients. With the help of a thermal suit, whole-body cooling and warming was performed to alter sympathetic skin nerve activity. The subjects were lying in a suit supplied by tubes, in which running water of 12 °C and 50 °C, respectively (inflow temperature) was used to cool or warm the whole body. By these means sympathetic activity can be switched on and off. (a) High sympathetic vasoconstrictor activity during cooling induces considerable drop in skin blood flow on the affected and unaffected extremity (laser Doppler flowmetry). Measurements were taken at 5-min intervals (mean ± SD). (b) On the unaffected side, a secondary decrease of skin temperature was documented. On the affected side, the forearm temperature was clamped at 35 °C by a feedback-controlled heat lamp to exclude temperature effects on the sensory receptor level. Measurements were taken at 5-min intervals (mean ± SD). (c) Effect of cutaneous sympathetic vasoconstrictor activity on dynamic mechanical hyperalgesia in one CRPS patient with sympathetically maintained pain (SMP). Activation of sympathetic neurons (during cooling) leads to a considerable increase of the area of dynamic mechanical hyperalgesia. From Baron, R., Schattschneider, J., Binder, A., Siebrecht, D. and Wasner, G. 2002. Relation between sympathetic vasoconstrictor activity and pain and hyperalgesia in complex regional pain syndromes: a case–control study. Lancet 359, 1655–1660, with permission.

predicted by the pain-enhancing effect of intracutaneous norepinephrine injections (Ali, Z. *et al.*, 2000). Interestingly, the relief of spontaneous pain after sympathetic blockade was more pronounced than changes in spontaneous pain that could be induced experimentally by sympathetic activation. One explanation for this discrepancy might be that a complete sympathetic block affects all sympathetic outflow channels projecting to the affected extremity. It is very likely that in addition to a coupling in the skin, a sympathetic–afferent interaction may also occur in other tissues, in particular in the deep somatic domain such as bone, muscle, or joints. Supporting this view, especially these structures are extremely painful in some cases with CRPS (Baron, R. and Wasner, G., 2001). Furthermore, there may be patients who are characterized by a selective or predominant sympathetic–afferent interaction in deep somatic tissues sparing the skin (Wasner, G. *et al.*, 1999). In summary, it is likely that sympathetically maintained pain is a consequence of an adrenergic sensitization of C nociceptors.

5.57.6.3 Central Sensitization in Patients

One hallmark of central sensitization of spinal cord neurons in animals is that activity in A fiber mechanoreceptors is allowed to gain access to the nociceptive system and induces pain. These phenomena are called mechanical allodynia or hyperalgesia.

Mechanical hypersensitivity is a common phenomenon in neuropathic pain states in patients. There are several lines of evidence that also in patients central mechanisms contribute to these sensory phenomena. Two distinct types have been described in patients, dynamic mechanical and pinprick mechanical hypersensitivity.

There is consensus that dynamic mechanical allodynia is signaled out of the skin by afferent mechanoreceptors with large myelinated axons that normally encode nonpainful tactile stimuli:

1. Reaction time measurements show dynamic mechanical allodynia in patients to be signaled by afferents with conduction velocities appropriate for large myelinated axons (Lindblom, U. and Verrillo, R. T., 1979; Campbell, J. N. *et al.*, 1988),
2. transcutaneous or intraneural stimulation of nerves innervating the allodynic skin can evoke pain at stimulus intensities which only produce tactile sensations in healthy skin (Gracely, R. H. *et al.*, 1992; Price, D. D. *et al.*, 1992), and
3. using differential nerve blocks dynamic allodynia is abolished at time points when tactile sensations is lost, but other modalities remain unaffected (Campbell, J. N. *et al.*, 1988; Ochoa, J. L. and Yarnitsky, D., 1993).

Therefore, patients with dynamic mechanical allodynia would be expected to have central sensitization as their underlying mechanism.

Hyperalgesia to pinprick stimuli, typically elicited by probing of the skin with a stiff von Frey hair is distinct from dynamic mechanical allodynia because of its different spatial and temporal profile and the fact that it is signaled by nonsensitized, heat-insensitive, Aδ nociceptors.

Notably, in many neuropathic pain patients the mechanically sensitive skin area expands widely into the secondary zone, i.e., the area not affected by the primary nerve lesion, which is also indicative for CNS mechanisms involved. Furthermore, the area of secondary mechanical hypersensitivity is a dynamic phenomenon. In PHN patients with signs of peripheral nociceptor sensitization (heat hyperalgesia, see above) cutaneous capsaicin application into the primary skin area leads to an increase of the allodynic zone into previously nonallodynic and nonpainful skin that had normal sensory function and cutaneous innervation. These observations support the hypothesis that allodynia in a subgroup of PHN patients is a form of chronic secondary hyperalgesia dynamically maintained by input from intact and possibly sensitized ('irritable') primary afferent nociceptors to a sensitized CNS (Fields, H. L. *et al.*, 1998; Petersen, K. L. *et al.*, 2000). Because central sensitization involves the NMDA receptor, the fact that the NMDA receptor antagonist ketamine relieves some neuropathic pain disorders further supports the concept of central sensitization.

Besides these dramatic changes in the spinal cord, there is now evidence that higher centers of the neuraxis demonstrate an increased excitability as well as fundamental changes in the somatosensory representation. Magnetic encephalography (MEG), positron emission tomography (PET), and fMRI studies revealed cortical changes in patients with phantom limb pain, CRPS, and central pain syndromes (Flor, H. *et al.*, 1995; Willoch, F. *et al.*, 2000; Pleger, B. *et al.*, 2004; Willoch, F. *et al.*, 2004; Maihofner, C. *et al.*, 2005a) as well as experimental pain models (Baron, R. *et al.*, 1999a; Baron, R. *et al.*,

2000). Interestingly, these changes correlated with the intensity of the perceived pain and disappeared after successful treatment of the pain (Maihofner, C. *et al.*, 2004; Pleger, B. *et al.*, 2005).

5.57.6.4 Central Disinhibition Leading to Cold Hyperalgesia

Cutaneous hypersensitivity to cold, i.e., cold hyperalgesia is particularly prominent in patients with posttraumatic neuralgias, some polyneuropathies, and chronic CRPS. Some observations in neuropathic pain patients point to central disinhibition as the underlying mechanism in a subgroup of patients.

Cold stimuli are usually transmitted centrally by cold-sensitive Aδ fibers, whereas cold pain is conveyed via nociceptive cold-sensitive C fibers. In patients with polyneuropathies a disproportionate loss of Aδ axons and relative sparing of C fibers have been described (Ochoa, J. L. and Yarnitsky, D., 1994). These patients suffer from the so-called triple cold syndrome (CCC syndrome): cold hypoesthesia in combination with cold hyperalgesia and a cold skin. A selective damage of cold-sensitive Aδ fibers leads to a lack of inhibition (disinhibition) on C nociceptors transmission normally exerted by concomitant activation of myelinated cold Aδ fibers. This mechanism of a central interaction between cold specific afferents and nociceptors would nicely explain the combination of cold hyperalgesia and cold hypoesthesia in the above patients. Furthermore, it is suggested to play a crucial role in central pain syndromes after infarction of the dorsolateral thalamus with cold hyperalgesia and paradoxical heat sensation. In these patients the lesion in the lateral thalamus might disinhibit the nociceptive system projecting through the medial thalamus.

Recently, direct evidence was provided for the central disinhibhition theory of cold hyperalgesia in an experimental pain model in humans. Selective A fiber block induces the symptom combination of cold hyperalgesia and cold hypoesthesia and therefore mimics the situation in polyneuropathy patients with A fiber degeneration. With fMRI the disinhibition of the medial nociceptive system (medial thalamus, anterior cingulate cortex (ACC), and frontal cortices) could be demonstrated.

Thus, a loss of peripheral A fiber function disinhibits the nociceptive system centrally leading to cold hyperalgesia.

This is an entirely different mechanism as compared with the peripheral sensitization process of cold-sensitive C nociceptors described above leading to the same somatosensory phenomenon, cold hyperalgesia.

5.57.6.5 Deafferentation: Hyperactivity of Central Pain Transmission Neurons

The above data convincingly support a role for sensitization mechanisms in the peripheral as well as the CNS in the generation of neuropathic pain. However, in some patients there is a profound cutaneous deafferentation of the painful area. Up to 60% of PHN patients show considerable signs of neuronal degeneration and loss of sensory function within the affected tissues. Interestingly, some of these patients still suffer from severe dynamic mechanical allodynia although the function of nociceptors is diminished or absent in the same skin area (Wasner, G. *et al.*, 2005).

Punch skin biopsies and the anti-PGP 9.5 antibody, a panaxonal marker, were used in PHN patients and zoster patients without pain to quantify sensory nerve endings in the affected skin and compared the numbers with the homologous contralateral site (Rowbotham, M. C. et al., 1996; Oaklander, A.L., 1998; Oaklander, A.L., 2001). A severe loss could be demonstated on the affected side (20% as compared with the controls). Neurite loss was more prominent in the epidermis than in the dermis. Furthermore, the PHN group also had lost half of the neurites in the contralateral epidermis whereas distant areas where unaffected. However, these contralateral changes could not be observed with QST or axon reflex measurements (Baron, R. and Saguer, M., 1994).

Functional studies support the concept of degeneration of cutaneous C nociceptors. By using these C fiber axon reflex reactions it is possible to objectively assess cutaneous C fiber function in the human skin. In some patients the histamine evoked axon reflex vasodilatation and flare size were impaired or abolished in skin regions with intense dynamic allodynia (Baron, R. and Saguer, M., 1993). Similarly, during capsaicin stimulation, a subgroup did not experience worsening of pain (Petersen, K. L. *et al.*, 2000). Using quantitative sensory testing (QST) some chronic PHN patients have extremely high thermal thresholds in areas with marked dynamic allodynia (Nurmikko, T. and Bowsher, D., 1990; Nurmikko, T. *et al.*, 1994; Choi, B. and Rowbotham, M. C.,

1997). Thus, there is a subset of PHN patients with pain and loss of cutaneous C nociceptor function.

Assuming that the DRG cells and the central afferent connections are lost in such patients, their pain must be the result of intrinsic CNS changes. In animal studies, following complete primary afferent loss of a spinal segment, many dorsal horn cells begin to fire spontaneously at high frequencies (Lombard, M. C. and Larabi, Y., 1983; Fields, H. L. *et al.*, 1998). There is some evidence that a similar process may underlie the pain that follows extensive denervating injuries in human. Recordings of spinal neuron activity in a pain patient whose dorsal roots were injured by trauma to the cauda equina revealed high-frequency regular and paroxysmal bursting discharges (Loeser, J. D. *et al.*, 1967). That patient complained of spontaneous burning pain in a skin region that was anesthetic by the lesion (anesthesia dolorosa). Thus, extensive degeneration of primary afferents associated with severe somatosensory deficits points to an increased excitability of deafferented central neurons as underlying mechanism.

5.57.6.6 Inflammation in Patients

In patients with inflammatory demyelinating neuropathies such as acute Guillain–Barré syndrome or vasculitic neuropathies deep proximal aching pain in addition to paroxysmal types of pains is a characteristic phenomenon. Accordingly, COX2 was found to be upregulated in nerve biopsy specimens from patients with chronic inflammatory demyelinating neuropathy and an increased expression of proinflammatory cytokines have been demonstrated in peripheral nerves of most vasculitic neuropathies (Lindenlaub, T. and Sommer, C., 2003). About 15–50% of AIDS patients suffer from distal predominantly sensory neuropathy, which very often is painful. In sarcoidosis, painful small-fiber neuropathy may be present in a subgroup of patients. In the fluid of artificially produced skin blisters significantly higher levels of IL-6 and TNF-α were observed in CRPS-affected extremities as compared with the uninvolved extremity. In CRPS patients with hyperalgesia higher levels of the soluble TNF-α receptor type I were found (Maihofner, C., *et al.*, 2005b). Accordingly, a significant increases in IL-1β and IL-6, but not TNF-α was demonstrated in the CSF of individuals afflicted with CRPS as compared with controls (Alexander, G. M. *et al.*, 2005).

Acute zoster is accompanied by intense inflammation along the affected peripheral nerve that typically resolves in several weeks. However, a small subgroup of patients with PHN has inflammatory infiltrates throughout the affected peripheral nerve, DRG, and dorsal root (Watson, C. P. *et al.*, 1991). Moreover, Gilden D. H. *et al.* (1991) have described a subpopulation of PHN patients with evidence of continuing low-level viral expression whose pain responds to antiviral agents. Thus continuing VZV expression could produce sensitization and activity in primary afferents secondary to inflammation.

5.57.7 Diagnostic Tools for Neuropathic Pain

Modern research into the mechanisms of neuropathic pain clearly revealed that the nerve lesion leads to dramatic changes in the PNS and CNS that makes it distinct from other chronic pain types in which the nociceptive system is intact (chronic nociceptive pain, e.g., osteoarthritis). Furthermore, neuropathic pain states require different therapeutic approaches, e.g., anticonvulsants, that are not effective in nociceptive pain. To make the situation even more complex, many chronic pain states are characterized by a combination of both the pain types. Best examples for the so-called mixed pain syndromes are chronic radicular back pain, tumor pain, or CRPS.

For the clinician, it is, therefore, of utmost importance to have valid diagnostic tools that differentiate neuropathic from nociceptive pain or estimate the neuropathic pain component in mixed pain syndromes.

The easiest approach to this would be to use somatosensory symptoms assessed by questionnaires or history questions or simple signs testable at the bedside that are characteristic for neuropathic pain.

However, a recent study on this issue raised several caveats (Rasmussen, P. V. *et al.*, 2004): This study prospectively looked at symptoms and signs in 214 patients with suspected chronic neuropathic pain that were *a priori* classified by pain experts as having the so-called definite, possible or unlikely neuropathic pain. Pain symptoms including pain descriptors were recorded and sensory tests including repetitive pinprick stimulation, examination for cold-evoked pain by an acetone drop and brush-evoked pain were carried out in the maximal pain area and in a control area in order to determine if symptoms and signs cluster differentially in groups of patients with increasing evidence of neuropathic pain. Several symptoms (touch- or cold-provoked pain) and signs

(brush-evoked allodynia) were more prominent in patients with definite or possible neuropathic pain; however, there was considerable overlap with the clinical presentation of patients with unlikely neuropathic pain. Even worse, the used pain descriptors could not at all distinguish between the three clinical categories.

5.57.7.1 Questionnaires

Other approaches to find easy screening tools for neuropathic pain gave more promising results: a clinician-administered 10-item questionnaire (DN4) consists of sensory descriptors (seven items) as well as signs related to bedside sensory examination (three items) (Bouhassira, D. *et al.*, 2004). The interview questions address the quality of the pain (burning, painful cold, and electric shocks) and associated symptoms (tingling, pins and needles, numbness, and itching). The examination consists of the assessment of hypoesthesia to touch, prick and allodynia to brush. This questionnaire was validated in a prospective study of 160 patients presenting with pain of nociceptive and neuropathic origin and showed 86.0% of correctly identified patients (sensitivity 82.9%, specificity 89.9%).

A different approach to distinguish neuropathic from nonneuropathic pain uses a patient-based questionnaire with nine questions without the need of examinations by the physician (PainDetect) (Freynhagen, R. *et al.*, 2006). The questionnaire consists of slightly different sensory descriptors (seven items, burning pain, tingling or prickling (electricity), sensitivity to touch (clothes, blanket), pain caused by light pressure (e.g., with finger), shooting pain or electric shock-like pain, occasional painful cold or heat (e.g., bath tub), and numbness), the question whether the pain is spatially radiating and a questions addressing the individual pain pattern. In the latter, the patients have to choose one of four graphically illustrated pain patters (permanent pain with a light variability, stable permanent pain with paroxysmal pain attacks, paroxysmal pain attacks with no permanent pain, and pain attacks with fluctuating permanent pain in between). This questionnaire was validated in 392 patients recruited at 10 highly specialized pain centers with either pain of pure predominant neuropathic origin ($n = 167$, e.g., PHN, painful polyneuropathies, and nerve trauma) or pure or predominant nociceptive origin ($n = 225$, e.g., ostheoathritis, mechanical low back pain, and inflammatory arthropathies). Patients were diagnosed according to the results of two independent pain specialists who determined the predominant pain type (neuropathic versus nociceptive) by means of clinical experience as well as neurological examination, electrophysiologic, or imaging techniques. This questionnaire showed a correct classification rate of 82.5% with a sensitivity of 80.8% and a specificity 84.7%.

5.57.7.2 Bedside Assessment of Neuropathic Pain

Patients with neuropathic pain demonstrate a variety of distinct sensory symptoms and signs that can coexist in combinations (see above). Therefore, the sensory bedside examination should include the following qualities: touch, pinprick, pressure, cold, heat, vibration, temporal summation, and after sensations (Bouhassira, D. *et al.*, 2004; Cruccu, G. *et al.*, 2004, definition in Table 6). To assess either a loss (negative) or a gain of somatosensory function (positive sensory signs) the responses can be graded as normal, decreased or increased. The stimulus-evoked (positive) pain types are classified as hyperalgesic or allodynic, and according to the dynamic or static character of the stimulus (Rasmussen, P. V. *et al.*, 2004).

Touch can be assessed by gently applying cotton wool to the skin, pinprick sensation by the response to sharp pinprick stimuli, deep pain by gentle pressure on muscle and joints, and cold and heat sensation by measuring the response to a thermal stimulus, for example, thermorollers kept at 20 or 45 °C. Cold sensation can also be assessed by the response to acetone spray. Vibration can be assessed by a tuning fork placed at strategic points (interphalangeal joints, etc.). Abnormal temporal summation is the clinical equivalent to increasing neuronal activity following repetitive C fiber stimulation >0.3 Hz. This windup-like pain can be produced by mechanical and thermal stimuli. After-sensations – the persistence of pain long after termination of a painful stimulus – is another characteristic feature of neuropathic pain, which is closely related to a coexistent dynamic or static hyperalgesia. When present, allodynia or hyperalgesia can be quantified by measuring intensity and area. At present, it is generally agreed that assessment should be carried out in the area of maximal pain using the contralateral area as control. However, contralateral segmental changes following a unilateral nerve or root lesion cannot be excluded, so an examination at mirror sites may not necessarily represent a true control site.

Table 6 Definition and assessment of negative and positive sensory symptoms or signs in neuropathic pain

Symptom/sign	*Definition*	*Assessment Bedside exam*	*Expected pathological response*
Negative signs and symptoms			
Hypoesthesia	Reduced sensation to nonpainful stimuli	Touch skin with painters brush, cotton swab, or gauze	Reduced perception, numbness
Pall hypoesthesia	Reduced sensation to vibration	Apply tuning fork on bone or joint	Reduced perception threshold
Hypoalgesia	Reduced sensation to painful stimuli	Prick skin with single pin stimulus	Reduced perception, numbness
Thermhypoesthesia	Reduced sensation to cold/warm stimuli	Contact skin with objects of 10 °C (metal roller, glass with water, coolants like acetone) Contact skin with objects of 45 °C (metal roller, glass with water)	Reduced perception
Spontaneous sensations/pain			
Paraesthesia	Nonpainful ongoing sensation (ant crawling)	Grade intensity (0–10) Area in cm^2	–
Paroxysmal pain	Shooting electrical attacks for seconds	Number per time Grade intensity (0–10) Threshold for evocation	–
Superficial pain	Painful ongoing sensation often of burning quality	Grade intensity (0–10) Area in cm^2	–
Evoked pain			
Mechanical dynamic allodynia	Normally nonpainful light moving stimuli on skin evoke pain	Stroking skin with painters brush, cotton swab, or gauze	Sharp burning superficial pain Present in the primary affected zone but spread beyond into unaffected skin areas (secondary zone)
Mechanical static allodynia	Normally nonpainful gentle static pressure stimuli at skin evoke pain	Manual gentle mechanical pressure at the skin	Dull pain Present in the area of affected (damaged or sensitized) primary afferent nerve endings (primary zone)
Mechanical punctuate, pinprick hyperalgesia	Normally not painful/slightly stinging stimuli evoke pain	Manual pricking the skin with a safety pin, sharp stick, or stiff von Frey hair	Sharp superficial pain Present in the primary affected zone but spread beyond into unaffected skin areas (secondary zone)
Temporal summation	Repetitive application of identical single noxious stimuli is perceived as increasing pain sensation (windup like pain)	Pricking skin with safety pin at interval <3 s for 30 s	Sharp superficial pain of increasing intensity
Cold allodynia hyperalgesia	Normally nonpainful/slightly painful cold stimuli evoke pain	Contact skin with objects of 20 °C (metal roller, glass with water, coolants like acetone) Control: contact skin with objects of skin temperature	Painful often burning temperature sensation Present in the area of affected (damaged or sensitized) primary afferent nerve endings (primary zone)
Heat allodynia hyperalgesia	Normally nonpainful/slightly painful heat stimuli evoke pain	Contact skin with objects of 40 °C (metal roller, glass with water)	Painful burning temperature sensation

(*Continued*)

Table 6 (Continued)

Symptom/sign	*Definition*	*Assessment Bedside exam*	*Expected pathological response*
		Control: contact skin with objects of skin temperature	Present in the area of affected (damaged or sensitized) primary afferent nerve endings (primary zone)
Mechanical deep somatic allodynia	Normally nonpainful pressure on deep somatic tissues evoke pain	Manual light pressure at joints or muscle	Deep pain at joints or muscles

It is important to realized the spatial distribution of abnormal sensations. In neuropathic conditions, the distinction between primary and secondary area corresponds to the tissue supplied by damaged nerves and the area outside this innervation territory. Mechanical hypersensitivity often expands into the secondary area.

In Table 6 several sensory signs that can be found in peripheral neuropathies are defined and the appropriate tests to assess these signs clinically are summarized.

5.57.7.3 Apparative Assessment of Somatosensory Phenotypes

It is important to realize that conventional electrophysiological techniques like NCS, SEP, etc., only assess the function of myelinated peripheral axonal systems, the affection of small fibers including nociceptors are missed. Similarly, SEP measures the conduction in the lemniscal system (dorsal columns) and not the spinothalamic tract, which conveys noxious information. Therefore, alternative diagnostic procedures have to be used to analyze nociceptive fibers and tracts in the peripheral or CNS, especially to diagnose small fiber neuropathies and central pain states that are associated with a isolated damage to central nociceptive systems.

A sophisticated neurophysiologic technique to test both systems in the PNS and the CNS is QST, which uses standardized mechanical and thermal stimuli (graded von Frey hairs, several pinprick stimuli, pressure algometers, quantitative thermotesting, etc.). Another advantage of QST is that it assesses a loss of function (minus signs) as well as a gain of function (positive signs). For example Allodynia or hyperalgesia, can be quantified by measuring intensity, threshold for elicitation, duration, and area.

A standardized protocol for QST was recently proposed by the nationwide German Network on Neuropathic Pain (Rolke R. *et al.*, 2006) including 13 parameters of sensory testing procedures for the analysis of the exact somatosensory phenotype of neuropathic pain patients (Figure 6). To evaluate plus or minus signs in patients, an age- and gender-matched database for absolute and relative QST reference data was established for healthy human subjects. Until now this nationwide multicenter trial comprises complete sensory profiles of 180 healthy human subjects and more than 1500 neuropathic pain patients of a variety of entities. Thermal detection and pain thresholds including a test for the presence of paradoxical heat sensations, mechanical detection thresholds to von Frey filaments and a 64-Hz tuning fork, mechanical pain thresholds to pinprick stimuli and blunt pressure, stimulus/response functions for pinprick and dynamic mechanical allodynia (pain to light touch), and pain summation (windup ratio) using repetitive pinprick stimulation are determined. Data of healthy human subjects were analyzed for the influence of body side and region, age, and gender. For most variables pathological values of positive and negative signs can be detected on the basis of reference data.

5.57.7.4 Skin Biopsies

The advent of skin biopsy as a diagnostic and investigative tool has changed the diagnostic picture in neuropathic pain; skin biopsies can be done at several sites to establish a spatial profile of nerve fiber involvement, and can be repeated over time. They have generally met good patient acceptance in neuropathies, and even in allodynic states like PHN. They can be used to assess epidermal nerve fibers, predominantly C fiber nociceptors, sympathetic fibers innervating the cutaneous sweat glands, and myelinated Aβ and Aδ fibers in the dermis.

Immunostaining of skin punch biopsies for the panaxonal marker protein gene product 9.5 (PGP9.5), a neuronal ubiquitin hydrolase is believed to identify axons of all categories of nerve fibers. In a

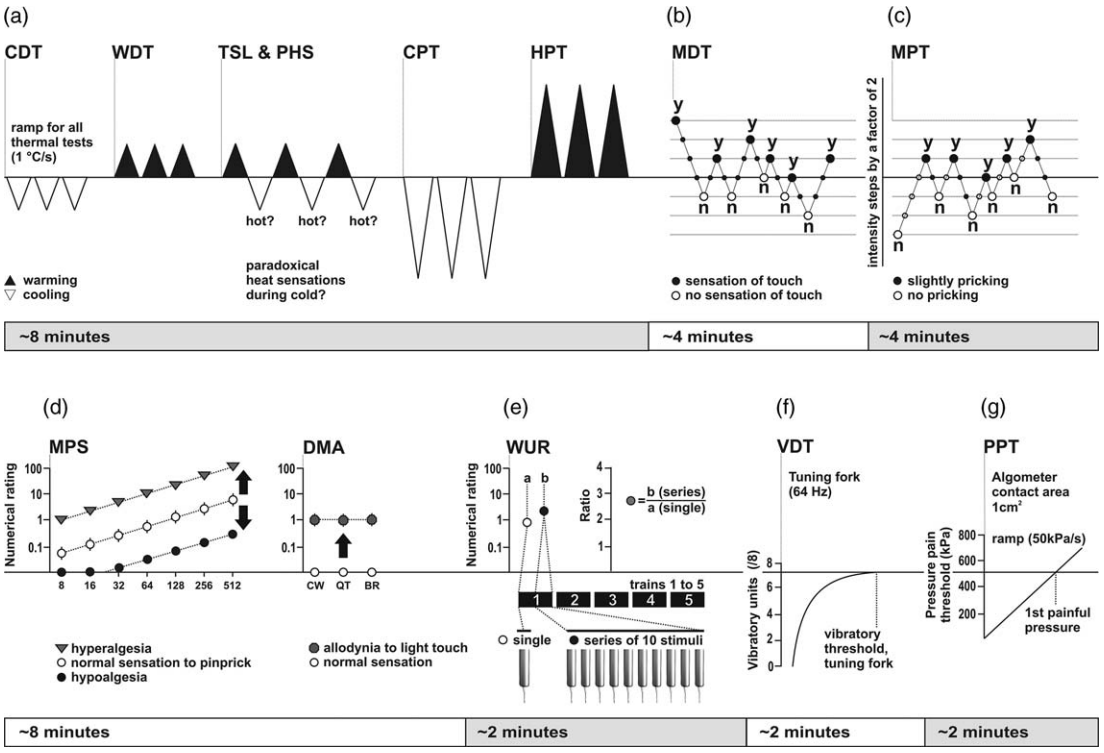

Figure 6 Quantitative sensory testing (QST) – a battery of sensory tests: figure of methods. The standardized QST protocol assesses 13 variables in seven test procedures (a–g). All procedures are presented including a time frame for testing over one area. (a) (thermal testing; CDT, cold detection threshold; WDT, warm detection threshold; TSL, thermal sensory limen for alternating warm and cold stimuli; PHS, number of paradoxical heat sensations during the TSL procedure; CPT, cold pain threshold; HPT, heat pain threshold) comprises detection and pain thresholds for cold, warm, or hot stimuli (C and Aδ fiber mediated). (b) (MDT, mechanical detection threshold) tests for Aβ fiber function using von Frey filaments. (c) (MPT, mechanical pain threshold) tests for Aδ-fiber-mediated hyper- or hypoalgesia to pinprick stimuli. (d) (stimulus/response functions: MPS for pinprick stimuli, and ALL for dynamic mechanical allodynia) assesses again Aδ-mediated sensitivity to sharp stimuli (pinprick), and also Aβ-fiber-mediated sensitivity to stroking light touch (CW, cotton wisp; QT, cotton wool tip; BR, brush). (e) (WUR, windup ratio) compares the verbal ratings within five trains of a single pinprick stimulus (*a*) with a series (*b*) of 10 repetitive pinprick stimuli to calculate WUR as the ratio: *b*/*a*. (f) (VDT, vibration detection threshold) tests again for Aβ fiber function using a Rydel–Seiffer 64-Hz tuning fork. (g) (PPT, pressure pain threshold) is the only test for deep pain sensitivity, most probably mediated by muscle C and Aδ fibers.

variety of neuropathies affecting small caliber nerve fibers, denervation has been documented to occur in a length-dependent manner. These include diabetes mellitus, HIV-associated sensory neuropathy (Polydefkis, M. *et al*., 2002), Fabry's disease (Scott, L. J. *et al*., 1999), restless legs syndrome, and idiopathic small-fiber sensory neuropathies (Holland, N. R. *et al*., 1997).

Punch skin biopsies have more recently been used as a serial measure, to examine changes in epidermal innervation over time, or after therapeutic interventions in various neuropathic conditions. For example, epidermal reinnervation occured concomitant with symptomatic improvement in sensory neuropathy (Nodera, H. *et al*., 2003), and impressive increases in epidermal, dermal, and sweat gland innervation densities have been documented with improvement in neuropathic status spontaneously or after therapies (Hart, A. M. *et al*., 2002).

Cutaneous innervation is usually reduced in PHN skin compared to mirror-image skin when assessed with PGP (Rowbotham, M. C. *et al*., 1996; Oaklander, A.L. *et al*., 1998; Petersen, K. L. *et al*., 2000) (Figure 7). However, a significant proportion of PHN subjects have similar fiber densities in both PHN and mirror-image skin, suggesting that the symptoms of pain and sensory dysfunction is not due to a mere loss in overall innervation density (Rowbotham, M. C. *et al*., 1996; Petersen, K. L. *et al*., 2000). Oaklander demonstrated that the average cutaneous fiber density was lower in subjects with established PHN than in those who had recovered without PHN after herpes zoster.

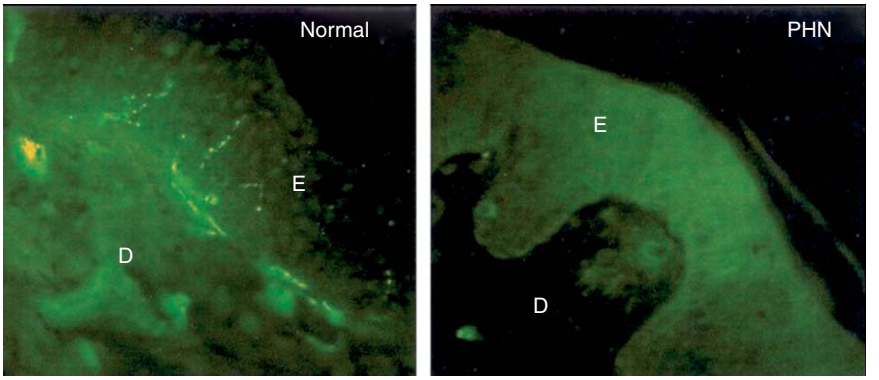

Figure 7 Representative skin biopsy samples from a postherpetic neuralgia (PHN) patient. PGP 9.5 immunofluorescence in normal and mirror-image painful PHN skin. The patient suffered from spontaneous pain and allodynia, but had a marked loss of thermal sensation (heat pain threshold elevated by 7.3 °C). D, dermis; E, epidermis. (Reprinted from Rowbotham, M. C., Yosipovitch, G., Connolly, M.K., Finlay, D., Forde, G. and Fields, H. L. 1996. Cutaneous innervation density in the allodynic form of postherpetic neuralgia. Neurobiol. Dis. 3, 205–214. Copyright 1996 Academic Press.)

Furthermore, mirror-image skin had lower fiber densities than distant control skin in subjects with established PHN (Oaklander, A.L. *et al.*, 1998).

5.57.7.5 Microneurography

Microneurography has been used to assess functional abnormalities in single small fibers. This technique makes it possible to subgroup C nociceptors in healthy controls into a variety of physiologically different classes. The technique requires huge technical skills from the researcher and is very time consuming.

Regarding pathological states it has been possible to identify spontaneously active C fibers in patients e.g., with erythromelalgia (Orstavik, K. *et al.*, 2003) (Figure 4). However, the results about abnormal firing patterns in diabetic neuropathy patients obtained so far have not been conclusive (Handwerker, personal communication). One major problem has been that normal aging changes the functional properties of C afferents dramatically. As the patient populations are generally older, normative data from a cohort of healthy older subjects have to be obtained. Furthermore, as recordings are performed from single afferent C fibers and not from whole nerves it is not possible to obtain reliable quantitative data about fiber numbers.

5.57.7.6 Indirect Test of Afferent Unmyelinated Fiber Function

The function of afferent unmyelinated fibers in the skin can be objectively assessed by using the efferent effector component of C fibers as indirect means (Baron, R. and Saguer, M., 1993; Schuller, T. B. *et al.*, 2000). Studies of the axon reflex vasodilatation (neurogenic flare) using visual inspection (Figure 8), thermography, or laser Doppler flowmetry in response to a chemical stimulus that activates cutaneous C fibers (histamine, capsaicin) are commonly used. While independent of patient cooperation, a major drawback of this technique is the dependence on a variety of other factors that affect the effector response.

Figure 8 Histamine flares in a patient with severe postherpetic neuralgia in the right segment Th6. Histamine iontophoresis was performed within the allodynic transitional zone at the cranial border of the affected and adjacent segment and on the contralateral corresponding site. The formerly affected dermatome is characterized by heavy scar tissue, whereas the allodynic area shows no scars or secondary pigmentation. Note the difference in flare size (ipsilateral 260 mm^2, contralateral 2060 mm^2) indicating an impairment of nociceptive C fiber function in the allodynic region. Adapted from Baron, R. and Saguer, M. 1993. Copyright 1993 Oxford University Press.

5.57.7.7 Imaging Techniques

A new MRI technique, MR neurography makes it possible to identify small patches of inflammation in peripheral nerves. This might be of value in inflammatory neuropathies, acute zoster, or schwannoma and neuroma detection (Haanpaa, M. *et al.*, 1998; Bendszus, M. *et al.*, 2004) (Figure 9). More patients with visable lesions associated with acute herpes zoster still had pain after 3 months. No data are available to demonstrate changes that occur in chronic PHN. MRI can also identify changes in peripheral nerves and secondary neurogenic alterations in skeletal muscle (Koltzenburg, M. and Bendszus, M., 2004). Prolongation of the T2 relaxation time and gadolinium enhancement of denervated muscle develop in parallel with the development of pathological spontaneous activity on EMG that is a feature of axonal damage. Axonal nerve lesions cause a hyperintense signal on T2-weighted MRI of the affected nerve at and distal to the lesion site, which correlates with Wallerian degeneration and nerve edema. While the MRI changes do not distinguish between painful and painless nerve lesions, they supplement the differential diagnosis of peripheral nerve disease. Furthermore, diffusion tensor imaging technique is capable of detecting degeneration of fibers in the dorsal columns in severe peripheral neuropathies.

5.57.7.8 Do We Have Diagnostic Tool to Dissect Individual Mechanisms in Neuropathic Pain?

The modern theoretical concept of a mechanism-based therapy uses the assumption that a specific symptom predicts a specific underlying mechanism. It should be possible for a clinician to identify a particular mechanism by assessing a specific sensory symptom. There are, however, some important caveats with such an approach. Recent clinical experimental studies indicate that it is not appropriate to link one single symptom with exactly one mechanism. It was shown that one specific symptom may be generated by several entire different underlying pathophysiological mechanisms. It became clear that only a specific symptom constellation, a symptom profile, i.e., a combination of negative and positive sensory phenomena, might be able to predict the mechanisms and not just one single symptom. In order to translate these ideas into the clinical framework of neuropathic pain the most important approach is to characterize the somatosensory phenotype of the patients as precisely as possible.

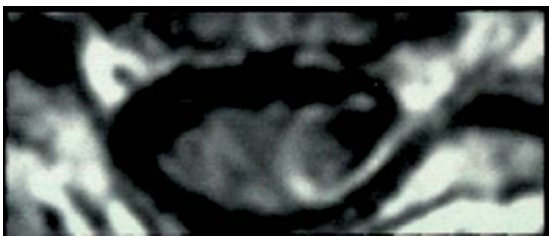

Figure 9 Magnetic resonance image of a patient with acute herpes zoster. Spinal cord in the cervical affected region. Note the contrast enhancement in the dorsal root, dorsal horn of the spinal cord, and lesser also in the ventral root. The patients was severely affected with pain and motor weakness at the left arm (T1 image with contrast medium). Photo courtesy of Prof. Dr. T. Tölle, Munich.

For example, standardized QST methods described above can nicely distinguish between phenotypic subtypes of PHN patients with distinct sensory symptom constellations that are likely correlated with different underlying mechanisms (sensitization type, deafferentation type, see above). Distinct pathophysiological changes in the excitability of peripheral and central neurons are likely involved in pain generation (for details, see Figure 10).

As attractive a subtype classification based on the nociceptor function and evoked pain types might be it should be emphasized that not all PHN patients fit exactly into one category or the other. It rather seems to be a continuum. Furthermore, in a large group of PHN patients many heterogeneous patterns of sensory dysfunction were detected (Pappagallo, M. *et al.*, 2000). Accordingly, detailed testing of sensory function, chemical stimulation, and cutaneous innervation in one PHN patient clearly showed areas of relative preservation in close vicinity to impaired thermal sensation, both within the affected dermatome (Petersen, K. L. *et al.*, 2000). Furthermore, the sensory patterns showed a variation over the time course of PHN. However, by classification of PHN patients due to sensory perception thresholds within the most painful skin area it is possible to detect the predominant individual sensory profile and the most likely underlying pain-generating mechanism.

Another caveat addressing the predictive value of QST measurements for therapy was recently revealed by two independent studies. It was hypothesized that topically applied lidocaine that is believed to act on ectopic discharges in nociceptive fibers would be in particular beneficial for patients with sensitized peripheral nociceptors as compared with patients with a loss of dermal nociceptors. In contrast to the hypothesis, however, skin biopsies, QST, histamine test as well nerve conduction studies could not identify

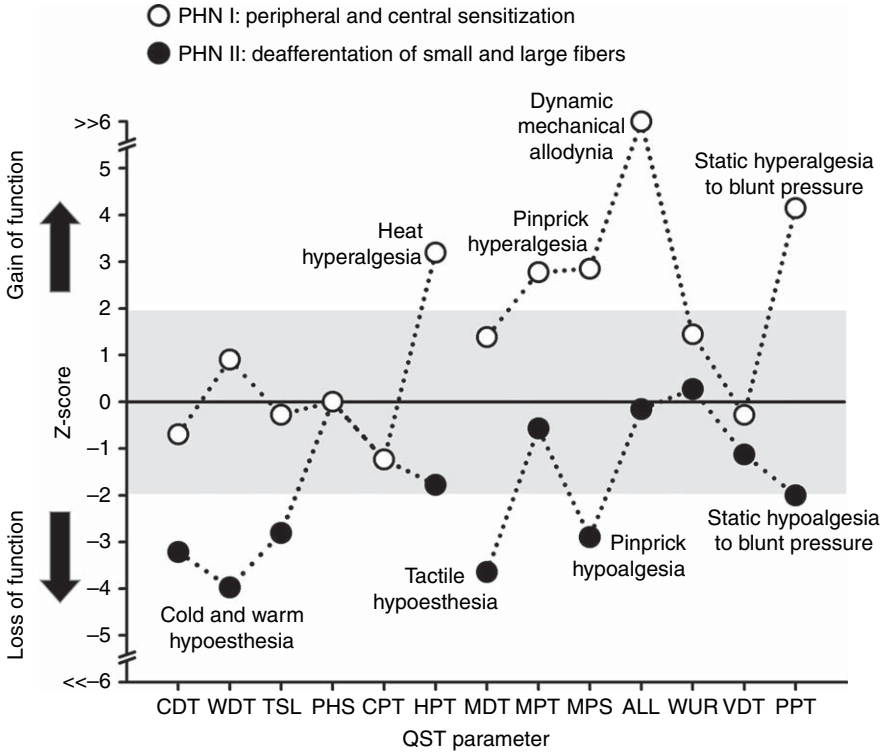

Figure 10 *Z*-score sensory profiles of two patients suffering from postherpetic neuralgia (PHN). Patient PHN I (open circles) presents the Quantitative sensory testing (QST) profile of a 70-year-old woman suffering from PHN for 8 years. Ongoing pain was 80 on a 0 to 100 numerical rating scale. The profile shows a predominant gain of sensory function in terms of heat pain hyperalgesia (HPT), pinprick mechanical hyperalgesia (MPS), dynamic mechanical allodynia (ALL), and static hyperalgesia to blunt pressure (PPT) outside the 95% confidence interval of the distribution of healthy subjects (=gray zone). This profile is consistent with a combination of peripheral and central sensitization. Patient PHN II (filled circles) shows the QST profile of a 71-year-old woman with pain for 8 months. Ongoing pain was 70 on a 0 to 100 numerical rating scale. The QST profile shows predominant loss of sensory function. Note the cold (CDT), warm detection thresholds (WDT), thermal sensory limen (TSL), heat pain thresholds (HPT), tactile detection thresholds (MDT), and mechanical pain thresholds to pinprick stimuli (MPT) outside the normal range as presented by the gray zone. This profile is consistent with a combined small- and large-fiber sensory deafferentation. *Z*-score: Numbers of standard deviations between patient data and group-specific mean value. Adapted from Rolke, R., Baron, R., Maire, C., Tölle, T. R., Treede, R. D., Binder, A., Birbaumer, N., Birklein, F., Bötefür, C. I., Braune, S., Flor, H., Huge, V., Klug, R., Landwchrmeyer, G. B., Magerl, W., Maihöfer, G., Rolko, C., Scherens, A., Sprenger, T., Valet, M., and Wasserka, B. 2006. Quantitative Sensory testing in the German Research Network on Neuropathic Pain (DFNS): standardized protocol and reference values. Pain 123, 231–243.

lidocaine responders in painful neuropathies (Herrmann, D. N. *et al.*, 2006) and PHN (Wasner, G. *et al.*, 2005). Alternatively, it might be possible that surviving A fibers in C-nociceptor-deprived skin may express sodium channels, develop ectopic firing and might therefore be the target for lidocaine.

5.57.8 Therapy

The number of trials for peripheral neuropathic pain has expanded greatly in the past few years. These have been summarized in several recent meta-analyses that are referred to in the following (Baron, R. and Wasner, G., 2006;; McQuay H. *et al.*, 1995; McQuay, H. J. *et al.*, 1996; Sindrup, S. H. and Jensen, T. S., 1999; Dworkin, R. H. *et al.*, 2003; Finnerup, N. B. *et al.*, 2005; Siddall, P. J. and Middleton, J. W., 2005). For central neuropathic pain there are limited data. The treatments discussed below have all been demonstrated to provide statistically significant and clinically meaningful treatment benefits compared with placebo in multiple randomized controlled trials (Table 7).

Nonmedical treatments, i.e., interventional procedures, neurostimulation techniques, neurosurgical destructive techniques, psychological therapy as well as physiotherapy and occupational therapy are not the focus of this review.

Table 7 Pharmacological therapy of neuropathic pain syndromes

Compound	*Evidence*
Antidepressants	
Amitriptyline	PHN ⇑⇑, PNP ⇑⇑, PTN ⇑, STR ⇑
Venlafaxine	PNP ⇑⇑
Duloxetine	PNP ⇑⇑
Anticonvulsants (Na channel)	
Carbamazepine	PNP ⇑, TGN ⇑⇑
Oxcarbazepine	PNP ⇑
Lamotrigine	HIV ⇑, PNP ⇑, STR ⇑
Anticonvulsants (Ca channel)	
Gabapentin	PHN ⇑⇑, PNP ⇑⇑, HIV ⇑, CRPS ⇑, PHAN ⇑, SCI ⇑, MIX ⇑, CANC ⇑
Pregabalin	PHN ⇑⇑, PNP ⇑⇑, SCI ⇑
Tramadol	PHN ⇑, PNP ⇑⇑
Long-acting strong opioids	
Morphine	PHN ⇑, PHAN ⇑
Oxycodone	PHN ⇑, PNP ⇑⇑
Cannabinoids	MS ⇑⇑, PA ⇔, MIX ⇑
Topical therapy	
Capsaicin cream	PHN ⇑, PNP ⇑, PTN ⇑
Lidocaine patch	PHN ⇑⇑, MIX ⇑

CANC, neuropathic cancer pain; CRPS, complex regional pain syndrome; HIV, HIV neuropathy; MIX, mixed neuropathic pain cohort; MS, central neuropathic associated with MS (multiple sclerosis); PA, central neuropathic pain after plexus avulsion; PHAN, phantom pain; PHN, postherpetic neuralgia; PNP, polyneuropathy (mainly diabetic); PTN, posttraumatic neuralgia; SCI, spinal cord injury; STR, poststroke pain; TGN, trigeminal neuralgia.
Levels of evidence: ⇑⇑, several randomized clinical trials (RCTs) or meta-analyses; ⇑, at least 1 RCT; ⇔, unclear.

5.57.8.1 Antidepressants

The effectiveness of tricyclic antidepressants (TCAs) in neuropathic pain may account for their broad range of pharmacological actions. These compounds are inhibitors of the reuptake of monoaminergic transmitters. They are believed to potentiate the effects of biogenic amines in CNS pain-modulating pathways. In addition, they block voltage dependent sodium channels and α adrenergic receptors.

Venlafaxine and duloxetine that blocks both serotonin and norepinephrine reuptake (serotonin noradrenaline reuptake inhibitors (SNRI)) were efficacious in diabetic painful neuropathy (DPN). In a comparison of venlafaxine and imipramine in patients with painful polyneuropathy, both antidepressants demonstrated superior pain relief compared with placebo but did not differ from each other.

Selective serotonin reuptake inhibitors (SSRI) have fewer adverse effects and are generally better tolerated than TCAs. However, they did not show convincing efficacy in neuropathic pain states.

5.57.8.2 Anticonvulsants (Ca Channel Modulators)

There are extensive clinical trials of gabapentin for chronic neuropathic pain. These studies examined patients with PHN, DPN, mixed neuropathic pain syndromes, phantom limb pain, Guillain–Barré syndrome, and acute and chronic pain from SCI. Improvements in sleep, mood, and quality of life were also demonstrated. Pregabalin, the successor drug of gabapentin was shown to be efficacious in PHN, DPN, and SCI. There is growing evidence supporting the mechanism of action on the $\alpha 2\delta$ subunit of neuronal calcium channels partly located at the presynaptic spinal terminals of primary afferent nociceptors. One advantage over gabapentin is its superior bioavailability, which makes it easier to use without the need of long titration periods. Gabapentin and pregabalin are generally well tolerated, safe, have no drug interactions, and no negative impact on cardiac function. This advantages makes them a suitable option especially for the elderly, a population very often suffering from several comorbidities that need multiple drug therapies.

5.57.8.3 Anticonvulsants (Na Channel Blockers)

For lamotrigine there is evidence of efficacy for HIV sensory neuropathy, DPN, and central poststroke pain. Carbamazepine is very effective in trigeminal neuralgia. However, the strength of evidence is much lower for the benefit of these drugs in other types of neuropathic pain. Oxcarbazepine which has fewer side effects and drug–drug interactions than carbamazepine was shown to be effective in painful diabetic neuropathy (Dogra, S. *et al.*, 2005).

5.57.8.4 Tramadol and Opioid Analgesics

Tramadol is a norepinephrine and serotonin reuptake inhibitor with a major metabolite that is a μ opioid agonist. Sustained efficacy for several weeks has been demonstrated for oral tramadol in PHN, DPN, and in patients with painful polyneuropathy of various causes.

Strong opioids are clearly effective in postoperative, inflammatory, and cancer pain. However, the use of narcotic analgesics for patients with chronic neuropathic pain was highly controversial, even among experts in the field of pain management. However, to date several positive trials of oral strong opioid analgesics in various neuropathic pain entities have been published. In an interesting three-period crossover study comparing treatment with opioid analgesics, TCAs, and placebo in patients with PHN, controlled-release morphine provided statistically significant benefits for pain and sleep but not for physical function and mood. In that trial, patients preferred treatment with opioid analgesics compared with TCAs and placebo despite a greater incidence of adverse effects and more dropouts during opioid treatment (Raja, S. N. *et al.*, 2002). Our experience is that many patients with pain due to central and peripheral nerve injury can be successfully and safely treated on a chronic basis with stable doses of narcotic analgesics. However, the use of opioids requires caution in patients with a history of chemical dependence or pulmonary disease. We recommend using long-acting opioid analgesics (e.g., sustained release preparation or transdermal applications) when alternative approaches to treatment have failed.

5.57.8.5 Topical Medications

5.57.8.5.1 Topical capsaicin

Capsaicin is an agonist of the vanilloid receptor (TRPV1) that is present on the sensitive terminals of primary nociceptive afferents. On initial application, it has an excitatory action and produces burning pain and hyperalgesia, but with repeated or prolonged application it inactivates the receptive terminals of nociceptors. Therefore, this approach is reasonable for those patients whose pain is maintained by anatomically intact sensitized nociceptors. Capsaicin has been reported to reduce the pain of PHN and DPN.

5.57.8.5.2 Topical lidocaine

A second topical medication for neuropathic pain is local anesthetics. Local anesthetics block voltage-dependent sodium channels. Although the site of action of membrane-stabilizing drugs for relief of pain has not been proven in patients, *in vitro* studies have shown that ectopic impulses generated by damaged primary afferent nociceptors are abolished by concentrations of local anesthetics much lower than that required for blocking normal axonal conduction. Studies report pain relief with topically applied special formulations of local anesthetic (lidocaine patches (5%)) in PHN and other neuropathies.

5.57.8.6 *N*-Methyl-D-Aspartic Acid Receptor Antagonists

These drugs block excitatory glutamate receptors in the CNS that are thought to be responsible for the increased central excitability (central sensitization) following noxious stimuli. Clinically available substances with NMDA receptor blocking properties include ketamine, dextromethorphane, memantine, and amantadine. Studies of small cohorts have generally confirmed the analgesic effects of ketamine in patients suffering from PHN. However, studies with oral NMDA antagonists formulations (e.g., dextromethorphane) showed positive results in DPN but the drug was without beneficial effect in PHN.

5.57.8.7 Cannabinoids

Cannabinoid receptors type 1 (CB1) have been demonstrated in upper laminae of the spinal dorsal horn intimately concerned with the processing of nociceptive information as well as on the cell bodies of primary afferent neurons. Relief of central pain was found with the oral tetrahydocannabinol dronabinol in MS patients and in plexus avulsion pain

although in the latter the primary outcome measure defined in the hypothesis was failed. Cannabinoids were also effective in mixed peripheral neuropathic pain.

5.57.8.8 Treatment Guideline

In the previous section a variety of treatment regimens were reviewed that have shown to be effective. In summary, the relevant medical management of neuropathic pain consists of five main classes of oral medication (serotonin-/norepinephrine-modulating antidepressants, Na blocker anticonvulsants, Ca modulator anticonvulsants, tramadol, and opioids) and two categories of topical medications mainly for patients with cutaneous allodynia and hyperalgesia (capsaicin and local anesthetics).

A useful way to compare the efficacy of different treatments is the consultation of systematic reviews to determine the best available drugs (Sindrup, S. H. and Jensen, T. S., 1999; 2000; Dworkin, R. H. and Schmader, K. E., 2003). Up to now, more than 110 randomized controlled trials for the medical treatment of neuropathic pain have been published. In this respect, the measure: "Numbers needed to treat (NNT)" has been a useful measure. Numbers needed to treat is: the number of patients needed to treat with a certain drug to obtain one patient with a defined degree of pain relief. This method permit a comparison between different drugs and diseases and it allows generation of large numbers in order to provide reliable information about efficacy. Usually the NNT for more than 50% pain relief is used because it is easily understood and seems in many cases to be a relevant clinical effect. However, the methodological complexity of pooling data from small crossover and large parallel group trials and methodological shortcomings of some trials in a systematic review, remain as limitations.

In Figure 11 the NNT values of drugs for treatment of neuropathic pain is shown in relation to the number of patient that have been treated with each of the drug to get a sense of the validity of the different trials.

Because more than one mechanism is at work in most patients, a combination of two or more analgesic agents to cover multiple types of mechanisms will generally produce greater pain relief and fewer side effects. Therefore, in most patients, a stepwise proceeding with a successive monotherapy is not appropriate. Early combinations of two or three compounds out of different classes is the general practical approach. In fact, in a controlled four-period crossover trial, combined gabapentin and morphine achieved better analgesia at lower doses of each drug than either as a single agent, with constipation, sedation, and dry mouth as the most frequent adverse effects.

Drug-related adverse effects are common in the treatment of neuropathic pain, not only because of the specific medications used but also because many patients with this condition are older, take other medications, and have comorbid illnesses. Therefore, the drugs of first choice has to be judged on the basis of these data.

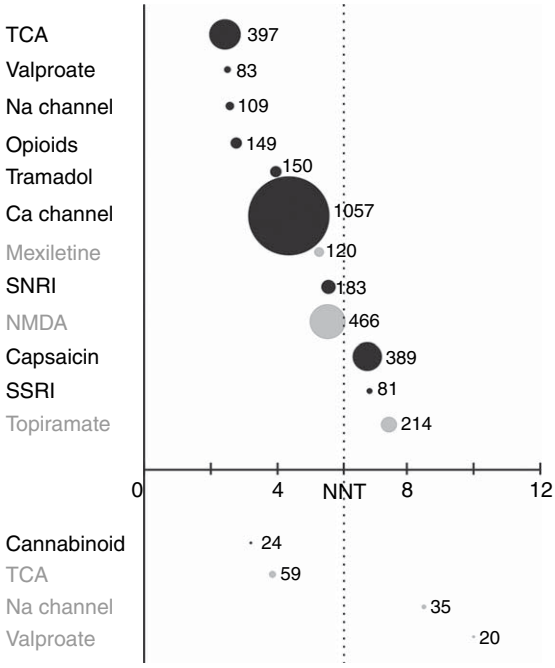

Figure 11 Numbers needed to treat in peripheral and central neuropathic pain. Combined numbers needed to treat (NNT) to obtain one patient with more than 50% pain relief in (a) peripheral neuropathic pain (painful polyneuropathy, postherpetic neuralgia, and peripheral nerve injury pain) and (b) central pain (central poststroke pain, pain following spinal cord injury and multiple sclerosis). SNRI, serotonin noradrenaline reuptake inhibitors; SSRI, selective serotonin reuptake inhibitor. Circle size and related numbers indicate number of patients who have received active treatment. Gray circle: at least half of conducted trials showed no significant effect. Right to Dotted line: clinical relevance should be questioned. (After Finnerup, N. B., Otto, M., McQuay, H. J., Jensen, T. S., Sindrup, S. H. 2005. Algorithm for neuropathic pain treatment: an evidence based proposal. Pain 118, 289–305.)

There are several exceptions from the above general treatment recommendations that should be emphasized: First, treatment guidelines for trigeminal neuralgia are distinct and include carbamazepine and baclofen. Second, the pharmacological therapy may be similar in CRPS, although controlled trials of first-line medications are lacking. However, it is very likely that antiinflammatory strategies in particular in the acute phase might be helpful. Third, although chronic neuropathic back pain (i.e., cervical and lumbar radiculopathic pain) is probably the most prevalent pain syndrome to which neuropathic mechanisms contribute, there are no accepted diagnostic criteria for identifying this neuropathic component. It is likely that a combination of neuropathic, skeletal, and myofascial mechanisms account for this type of pain in many patients.

Acknowledgments

This work was supported by the Deutsche Forschungsgemeinschaft (DFG Ba 1921/1-2), the German Ministry of Research and Education within the German Research Network on Neuropathic Pain (BMBF, 01EM01/04), and an unrestricted educational grant of Pfizer (Germany).

References

Alessandri-Haber, N., Dina, O. A., Yeh, J. J., Parada, C. A., Reichling, D. B., and Levine, J. D. 2004. Transient receptor potential vanilloid 4 is essential in chemotherapy-induced neuropathic pain in the rat. J. Neurosci. 24, 4444–4452.

Alexander, G. M., van Rijn, M. A., van Hilten, J. J., Perreault, M. J., and Schwartzman, R. J. 2005. Changes in cerebrospinal fluid levels of pro-inflammatory cytokines in CRPS. Pain 116, 213–219.

Ali, Z., Raja, S. N., Wesselmann, U., Fuchs, P., Meyer, R. A., and Campbell, J. N. 2000. Intradermal injection of norepinephrine evokes pain in patients with sympathetically maintained pain. Pain 88, 161–168.

Amir, R., Liu, C. N., Kocsis, J. D., and Devor, M. 2002. Oscillatory mechanism in primary sensory neurones. Brain 125, 421–435.

Baron, R. 2006. Mechanisms of disease: neuropathic pain – a clinical perspective. Nat. Clin. Pract. Neurol. 2, 95–106.

Baron, R. and Binder, A. 2004. How neuropathic is sciatica? The mixed pain concept. Orthopade 33, 568–575.

Baron, R. and Janig, W. 2004. Complex regional pain syndromes – how do we escape the diagnostic trap? Lancet 364, 1739–1741.

Baron, R. and Saguer, M. 1993. Postherpetic neuralgia. Are C-nociceptors involved in signalling and maintenance of tactile allodynia? Brain 116, 1477–1496.

Baron, R. and Saguer, M. 1994. Axon-reflex reactions in affected and homologous contralateral skin after unilateral peripheral injury of thoracic segmental nerves in humans. Neurosci. Lett. 165, 97–100.

Baron, R. and Wasner, G. 2001. Complex regional pain syndromes. Curr. Pain Headache Rep. 5, 114–123.

Baron, R. and Wasner, G. 2006. Prevention and treatment of postherpetic neuralgia. Lancet 367, 186–188.

Baron, R., Baron, Y., Disbrow, E., and Roberts, T. P. L. 1999a. Brain processing of capsaicin-induced secondary hyperalgesia: a functional MRI study. Neurology 53, 548–557.

Baron, R., Baron, Y., Disbrow, E., and Roberts, T. P. L. 2000. Activation of the somatosensory cortex during Aβ-fiber mediated hyperalgesia – a MSI study. Brain Res. 871, 75–82.

Baron, R., Levine, J. D., and Fields, H. L. 1999b. Causalgia and reflex sympathetic dystrophy: does the sympathetic nervous system contribute to the generation of pain? Muscle Nerve 22, 678–695.

Baron, R., Schattschneider, J., Binder, A., Siebrecht, D., and Wasner, G. 2002. Relation between sympathetic vasoconstrictor activity and pain and hyperalgesia in complex regional pain syndromes: a case–control study. Lancet 359, 1655–1660.

Baron, R., Schwarz, K., Kleinert, A., Schattschneider, J., and Wasner, G. 2001. Histamine-induced itch converts into pain in neuropathic hyperalgesia. Neuroreport 12, 3475–3478.

Bendszus, M., Wessig, C., Solymosi, L., Reiners, K., and Koltzenburg, M. 2004. MRI of peripheral nerve degeneration and regeneration: correlation with electrophysiology and histology. Exp. Neurol. 188, 171–177.

Bouhassira, D., Attal, N., Fermanian, J., Alchaar, H., Gautron, M., Masquelier, E., Rostaing, S., Lanteri-Minet, M., Collin, E., Grisart, J., and Boureau, F. 2004. Development and validation of the neuropathic pain symptom inventory. Pain 108, 248–257.

Campbell, J. N., Raja, S. N., Meyer, R. A., and Mackinnon, S. E. 1988. Myelinated afferents signal the hyperalgesia associated with nerve injury. Pain 32, 89–94.

Catarina, M. J., Leffler, A., Malmberg, A. B., Martin, W. J., Trafton, J., Petersen-Zeitz, K. R., Koltzenburg, M., Basbaum, A. I., and Julius, D. 2000. Impaired nociception and pain sensation in mice lacking the capsaicin receptor. Science 288, 306–313.

Choi, B. and Rowbotham, M. C. 1997. Effect of adrenergic receptor activation on post-herpetic neuralgia pain and sensory disturbances. Pain 69, 55–63.

Coull, J. A., Beggs, S., Boudreau, D., Boivin, D., Tsuda, M., Inoue, K., Gravel, C., Salter, M. W., and De Koninck, Y. 2005. BDNF from microglia causes the shift in neuronal anion gradient underlying neuropathic pain. Nature 438, 1017–1021.

Coull, J. A., Boudreau, D., Bachand, K., Prescott, S. A., Nault, F., Sik, A., De Koninck, P., and De Koninck, Y. 2003. Trans-synaptic shift in anion gradient in spinal lamina I neurons as a mechanism of neuropathic pain. Nature 424, 938–942.

Cruccu, G., Anand, P., Attal, N., Garcia-Larrea, L., Haanpaa, M., Jorum, E., Serra, J., and Jensen, T. S. 2004. EFNS guidelines on neuropathic pain assessment. Eur. J. Neurol. 11, 153–162.

Daousi, C., MacFarlane, I. A., Woodward, A., Nurmikko, T. J., Bundred, P. E., and Benbow, S. J. 2004. Chronic painful peripheral neuropathy in an urban community: a controlled comparison of people with and without diabetes. Diabet. Med. 21, 976–982.

Dib-Hajj, S. D., Rush, A. M., Cummins, T. R., Hisama, F. M., Novella, S., Tyrrell, L., Marshall, L., and Waxman, S. G. 2005. Gain-of-function mutation in Nav1.7 erythromelalgia induces bursting of sensory neurons. Brain.128, 1847–1854.

Dogra, S., Beydoun, S., Mazzola, J., Hopwood, M., and Wan, Y. 2005. Oxcarbazepine in painful diabetic neuropathy: a

randomized, placebo-controlled study. Eur. J. Pain 9, 543–554.
Dworkin, R. H. and Schmader, K. E. 2003. Treatment and prevention of postherpetic neuralgia. Clin. Infect. Dis. 36, 877–882.
Dworkin, R. H., Backonja, M., Rowbotham, M. C., Allen, R. R., Argoff, C. R., Bennett, G. J., Bushnell, M. C., Farrar, J. T., Galer, B. S., Haythornthwaite, J. A., Hewitt, D. J., Loeser, J. D., Max, M. B., Saltarelli, M., Schmader, K. E., Stein, C., Thompson, D., Turk, D. C., Wallace, M. S., Watkins, L. R., and Weinstein, S. M. 2003. Advances in neuropathic pain: diagnosis, mechanisms, and treatment recommendations. Arch. Neurol. 60, 1524–1534.
Fields, H. L., Rowbotham, M., and Baron, R. 1998. Postherpetic neuralgia: irritable nociceptors and deafferentation. Neurobiol. Dis. 5, 209–227.
Finnerup, N. B., Otto, M., McQuay, H. J., Jensen, T. S., and Sindrup, S. H. 2005. Algorithm for neuropathic pain treatment: an evidence based proposal. Pain 118, 289–305.
Flor, H., Elbert, T., Knecht, S., Wienbruch, C., Pantev, C., Birbaumer, N., Larbig, W., and Taub, E. 1995. Phantom-limb pain as a perceptual correlate of cortical reorganization following arm amputation. Nature 375, 482–484.
Freynhagen, R., Tölle, T. R., and Baron, R. 2005. painDETECT – ein Palmtop-basiertes Verfahren für Versorgungsforschung, Qualitätsmanagement und Screening bei chronischen Schmerzen. Akt. Neurol 54, P641.
Gilden, D. H., Dueland, A. N., Cohrs, R., Martin, J. R., Kleinschmidt-DeMasters, B. K., and Mahalingam, R. 1991. Preherpetic neuralgia. Neurology 41, 1215–1218.
Gracely, R. H., Lynch, S. A., and Bennett, G. J. 1992. Painful neuropathy: altered central processing maintained dynamically by peripheral input (published erratum appears in Pain (1993, Feb.) 52(2), 251–253) (see comments). Pain 51, 175–194.
Guilbaud, G., Benoist, J. M., Levante, A., Gautron, M., and Willer, J. C. 1992. Primary somatosensory cortex in rats with pain-related behaviours due to a peripheral mononeuropathy after moderate ligation of one sciatic nerve: neuronal responsivity to somatic stimulation. Exp. Brain Res. 92, 227–245.
Haanpaa, M., Dastidar, P., Weinberg, A., Levin, M., Miettinen, A., Lapinlampi, A., Laippala, P., and Nurmikko, T. 1998. CSF and MRI findings in patients with acute herpes zoster. Neurology 51, 1405–1411.
Habler, H. J., Janig, W., and Koltzenburg, M. 1987. Activation of unmyelinated afferents in chronically lesioned nerves by adrenaline and excitation of sympathetic efferents in the cat. Neurosci. Lett. 82, 35–40.
Hains, B. C., Saab, C. Y., Klein, J. P., Craner, M. J., and Waxman, S. G. 2004. Altered sodium channel expression in second-order spinal sensory neurons contributes to pain after peripheral nerve injury. J. Neurosci. 24, 4832–4839.
Hart, A. M., Wiberg, M., Youle, M., and Terenghi, G. 2002. Systemic acetyl-L-carnitine eliminates sensory neuronal loss after peripheral axotomy: a new clinical approach in the management of peripheral nerve trauma. Exp. Brain Res. 145, 182–189.
Herrmann, D. N., Pannoni, V., Barbano, R. L., Pennella-Vaughan, J., and Dworkin, R. H. 2006. Skin biopsy and quantitative sensory testing do not predict response to lidocaine patch in painful neuropathies. Muscle Nerve 33, 42–48.
Holland, N. R., Stocks, A., Hauer, P., Cornblath, D. R., Griffin, J. W., and McArthur, J. C. 1997. Intraepidermal nerve fiber density in patients with painful sensory neuropathy. Neurology 48, 708–711.
Hong, S. and Wiley, J. W. 2005. Early painful diabetic neuropathy is associated with differential changes in the expression and function of vanilloid receptor 1. J. Biol. Chem. 280, 618–627.
Hudson, L. J., Bevan, S., Wotherspoon, G., Gentry, C., Fox, A., and Winter, J. 2001. VR1 protein expression increases in undamaged DRG neurons after partial nerve injury. Eur. J. Neurosci. 13, 2105–2114.
Jacobs, J. M., Macfarlane, R. M., and Cavanagh, J. B. 1976. Vascular leakage in the dorsal root ganglia of the rat, studied with horseradish peroxidase. J. Neurol. Sci. 29, 95–107.
Janig, W. and Baron, R. 2003. Complex regional pain syndrome: mystery explained? Lancet Neurol. 2, 687–697.
Jensen, T. S. and Baron, R. 2003. Translation of symptoms and signs into mechanisms in neuropathic pain. Pain 102, 1–8.
Ji, R. R. and Woolf, C. J. 2001. Neuronal plasticity and signal transduction in nociceptive neurons: implications for the initiation and maintenance of pathological pain. Neurobiol. Dis. 8, 1–10.
Koltzenburg, M. and Bendszus, M. 2004. Imaging of peripheral nerve lesions. Curr. Opin. Neurol. 17, 621–626.
Lehky, T. J., Leonard, G. D., Wilson, R. H., Grem, J. L., and Floeter, M. K. 2004. Oxaliplatin-induced neurotoxicity: acute hyperexcitability and chronic neuropathy. Muscle Nerve 29, 387–392.
Leijon, G., Boivie, J., and Johansson, I. 1989. Central post-stroke pain – neurological symptoms and pain characteristics. Pain 36, 13–25.
Lindblom, U. and Verrillo, R. T. 1979. Sensory functions in chronic neuralgia. J. Neurol. Neurosurg. Psychiatr. 42, 422–435.
Lindenlaub, T. and Sommer, C. 2003. Cytokines in sural nerve biopsies from inflammatory and non-inflammatory neuropathies. Acta Neuropathol. (Berl.) 105, 593–602.
Loeser, J. D., Ward, A. A., and White, L. E. 1967. Chronic deafferentation of human spinal cord neurons. J. Neurosurg. 29, 48–50.
Lombard, M. C. and Larabi, Y. 1983. Electrophysiological Study of Cervical Dorsal Horn Cells in Partially Deafferented Rats. In: Advances in Pain Research and Therapy (*ed*. J. J. Bonica), pp. 147–154. Raven Press.
Lu, X. and Richardson, P. M. 1993. Responses of macrophages in rat dorsal root ganglia following peripheral nerve injury. J. Neurocytol. 22, 334–341.
Luo, Z. D., Chaplan, S. R., Higuera, E. S., Sorkin, L. S., Stauderman, K. A., Williams, M. E., and Yaksh, T. L. 2001. Upregulation of dorsal root ganglion (alpha)2(delta) calcium channel subunit and its correlation with allodynia in spinal nerve-injured rats. J. Neurosci. 21, 1868–1875.
Ma, W., Zhang, Y., Bantel, C., and Eisenach, J. C. 2005. Medium and large injured dorsal root ganglion cells increase TRPV-1, accompanied by increased alpha2C-adrenoceptor co-expression and functional inhibition by clonidine. Pain 113, 386–394.
Maihofner, C., Forster, C., Birklein, F., Neundorfer, B., and Handwerker, H. O. 2005a. Brain processing during mechanical hyperalgesia in complex regional pain syndrome: a functional MRI study. Pain 114, 93–103.
Maihofner, C., Handwerker, H. O., Neundorfer, B., and Birklein, F. 2004. Cortical reorganization during recovery from complex regional pain syndrome. Neurology 63, 693–701.
Maihofner, C., Handwerker, H. O., Neundorfer, B., and Birklein, F. 2005b. Mechanical hyperalgesia in complex regional pain syndrome: a role for TNF-alpha? Neurology 65, 311–313.
Marchand, F., Perretti, M., and McMahon, S. B. 2005. Role of the immune system in chronic pain. Nat. Rev. Neurosci. 6, 521–532.
McDermott, A. M., Toelle, T. R., Rowbotham, D. J., Schaefer, C. P., and Dukes, E. M. 2006. The burden of

neuropathic pain: results from a cross-sectional survey. Eur. J. Pain 10, 127–135.
McKemy, D. D., Neuhausser, W. M., and Julius, D. 2002. Identification of a cold receptor reveals a general role for TRP channels in thermosensation. Nature 416, 52–58.
McQuay, H., Carroll, D., Jadad, A. R., Wiffen, P., and Moore, A. 1995. Anticonvulsant drugs for management of pain: a systematic review [see comments]. BMJ 311, 1047–1052.
McQuay, H. J., Tramer, M., Nye, B. A., Carroll, D., Wiffen, P. J., and Moore, R. A. 1996. A systematic review of antidepressants in neuropathic pain. Pain 68, 217–227.
Mogil, J. S., Miermeister, F., Seifert, F., Strasburg, K., Zimmermann, K., Reinold, H., Austin, J. S., Bernardini, N., Chesler, E. J., Hofmann, H. A., Hordo, C., Messlinger, K., Nemmani, K. V., Rankin, A. L., Ritchie, J., Siegling, A., Smith, S. B., Sotocinal, S., Vater, A., Lehto, S. G., Klussmann, S., Quirion, R., Michaelis, M., Devor, M., and Reeh, P. W. 2005. Variable sensitivity to noxious heat is mediated by differential expression of the CGRP gene. Proc. Natl. Acad. Sci. U. S. A. 102, 12938–12943.
Moore, K. A., Kohno, T., Karchewski, L. A., Scholz, J., Baba, H., and Woolf, C. J. 2002. Partial peripheral nerve injury promotes a selective loss of GABAergic inhibition in the superficial dorsal horn of the spinal cord. J. Neurosci. 22, 6724–6731.
Nodera, H., Barbano, R. L., Henderson, D., and Herrmann, D. N. 2003. Epidermal reinnervation concomitant with symptomatic improvement in a sensory neuropathy. Muscle Nerve 27, 507–509.
Nordin, M, Nyström, B., Wallin, U., and Hagbarth, K. E. 1984. Ectopic sensory discharges and paresthesiae in patients with disorders of peripheral nerve, dorsal roots and dorsal columns. Pain 20, 231–245.
Nurmikko, T. and Bowsher, D. 1990. Somatosensory findings in postherpetic neuralgia. J. Neurol. Neurosurg. Psychiatr. 53, 135–141.
Nurmikko, T., Wells, C., and Bowsher, D. 1994. Sensory Dysfunction in Postherpetic Neuralgia. In: Touch, Temperature, and Pain in Health and Disease: Mechanisms and Assessments, Vol. 3 (*eds*. J. Boivie, P. Hansson, and U. Lindblom), pp. 133–141. IASP Press.
Nystrom, B. and Hagbarth, K. E. 1981. Microelectrode recordings from transected nerves in amputees with phantom limb pain. Neurosci. Lett. 27, 211–216.
Oaklander, A. L. 1998. Unilateral postherpetic neuralgia is associated with bilateral sensory neuron damage. Neurology 44, 789–795.
Oaklander, A. L. 2001. The density of remaining nerve endings in human skin with and without postherpetic neuralgia after shingles. Pain 92, 139–145.
Oaklander, A. L., Romans, K., Horasek, S., Stocks, A., Hauer, P., and Meyer, R. A. 1998. Unilateral postherpetic neuralgia is associated with bilateral sensory neuron damage. Ann. Neurol. 44, 789–795.
Obata, K., Katsura, H., Mizushima, T., Yamanaka, H., Kobayashi, K., Dai, Y., Fukuoka, T., Tokunaga, A., Tominaga, M., and Noguchi, K. 2005. TRPA1 induced in sensory neurons contributes to cold hyperalgesia after inflammation and nerve injury. J. Clin. Invest. 115, 2393–2401.
Ochoa, J. L. and Yarnitsky, D. 1993. Mechanical hyperalgesias in neuropathic pain patients: dynamic and static subtypes. Ann. Neurol. 33, 465–472.
Ochoa, J. L. and Yarnitsky, D. 1994. The triple cold syndrome. Cold hyperalgesia, cold hypoaesthesia and cold skin in peripheral nerve disease. Brain 117, 185–197.
Omana-Zapata, I., Khabbaz, M. A., Hunter, J. C., Clarke, D. E., and Bley, K. R. 1997. Tetrodotoxin inhibits neuropathic ectopic activity in neuromas, dorsal root ganglia and dorsal horn neurons. Pain 72, 41–49.
Orstavik, K., Weidner, C., Schmidt, R., Schmelz, M., Hilliges, M., Jorum, E., Handwerker, H., and Torebjork, E. 2003. Pathological C-fibres in patients with a chronic painful condition. Brain 126, 567–578.
Ossipov, M. H., Lai, J., Malan, T. P., Jr., and Porreca, F. 2000. Spinal and supraspinal mechanisms of neuropathic pain. Ann. N. Y. Acad. Sci. 909, 12–24.
Pappagallo, M., Oaklander, A. L., Quatrano-Piacentini, A. L., Clark, M. R., and Raja, S. N. 2000. Heterogenous patterns of sensory dysfunction in postherpetic neuralgia suggest multiple pathophysiologic mechanisms. Anesthesiology 92, 691–698.
Patapoutian, A., Peier, A. M., Story, G. M., and Viswanath, V. 2003. ThermoTRP channels and beyond: mechanisms of temperature sensation. Nat. Rev. Neurosci. 4, 529–539.
Petersen, K. L., Fields, H. L., Brennum, J., Sandroni, P., and Rowbotham, M. C. 2000. Capsaicin evoked pain and allodynia in post-herpetic neuralgia. Pain 88, 125–133.
Pleger, B., Tegenthoff, M., Ragert, P., Forster, A. F., Dinse, H. R., Schwenkreis, P., Nicolas, V., and Maier, C. 2005. Sensorimotor retuning [corrected] in complex regional pain syndrome parallels pain reduction. Ann. Neurol. 57, 425–429.
Pleger, B., Tegenthoff, M., Schwenkreis, P., Janssen, F., Ragert, P., Dinse, H. R., Volker, B., Zenz, M., and Maier, C. 2004. Mean sustained pain levels are linked to hemispherical side-to-side differences of primary somatosensory cortex in the complex regional pain syndrome I. Exp. Brain Res. 155, 115–119.
Polydefkis, M., Yiannoutsos, C. T., Cohen, B. A., Hollander, H., Schifitto, G., Clifford, D. B., Simpson, D. M., Katzenstein, D., Shriver, S., Hauer, P., Brown, A., Haidich, A. B., Moo, L., and McArthur, J. C. 2002. Reduced intraepidermal nerve fiber density in HIV-associated sensory neuropathy. Neurology 58, 115–119.
Price, D. D., Long, S., and Huitt, C. 1992. Sensory testing of pathophysiological mechanisms of pain in patients with reflex sympathetic dystrophy [see comments]. Pain 49, 163–173.
Price, D. D., Long, S., Wilsey, B., and Rafii, A. 1998. Analysis of peak magnitude and duration of analgesia produced by local anesthetics injected into sympathetic ganglia of complex regional pain syndrome patients. Clin. J. Pain 14, 216–226.
Raja, S. N., Abatzis, V., and Frank, S. M. 1998. Role of a-adrenoceptors in neuroma pain in amputees. Anesthesiology 89, A1083.
Raja, S. N., Haythornthwaite, J. A., Pappagallo, M., Clark, M. R., Travison, T. G., Sabeen, S., Royall, R. M., and Max, M. B. 2002. Opioids versus antidepressants in postherpetic neuralgia: a randomized, placebo-controlled trial. Neurology 59, 1015–1021.
Rasmussen, P. V., Sindrup, S. H., Jensen, T. S., and Bach, F. W. 2004. Symptoms and signs in patients with suspected neuropathic pain. Pain 110, 461–469.
Rolke, R., Baron, R., Maire, C., Tölle, T. R., Treede, R. D., Binder, A., Birbaumer, N., Birklein, F., Bötefür, C. I., Braune, S., Flor, H., Huge, V., Klug, R., Landwchrmeyer, G. B., Magerl, W., Maihöfner, G., Rolko, C., Scherens, A., Sprenger, T., Valet, M., and Wasserka, B. 2006. Quantitative sensory testing in the German Research Network on Neuropathic Pain (DFNS): standardized protocol and reference values. Pain 123, 231–243.
Rowbotham, M. C. and Fields, H. L. 1996. The relationship of pain, allodynia and thermal sensation in post-herpetic neuralgia. Brain 119, 347–354.
Rowbotham, M. C., Yosipovitch, G., Connolly, M. K., Finlay, D., Forde, G., and Fields, H. L. 1996. Cutaneous innervation density in the allodynic form of postherpetic neuralgia. Neurobiol. Dis. 3, 205–214.

Sato, J. and Perl, E. R. 1991. Adrenergic excitation of cutaneous pain receptors induced by peripheral nerve injury. Science 251, 1608–1610.

Scadding, J. W. and Koltzenburg, M. 2006. Painful peripheral neuropathies. In: Wall and Melzack's Textbook of Pain. 5th edition. (*eds*. S. B. McMahon and M. Koltzenburg), pp. 973–1000. Elsevier.

Schuller, T. B., Hermann, K., and Baron, R. 2000. Quantitative assessment and correlation of sympathetic, parasympathetic, and afferent small fiber function in peripheral neuropathy. J. Neurol. 247, 267–272.

Scott, L. J., Griffin, J. W., Luciano, C., Barton, N. W., Banerjee, T., Crawford, T., McArthur, J. C., Tournay, A., and Schiffmann, R. 1999. Quantitative analysis of epidermal innervation in Fabry disease. Neurology 52, 1249–1254.

Siddall, P. J. and Middleton, J. W. 2005. A proposed algorithm for the management of pain following spinal cord injury. Spinal Cord. 44, 67–77.

Siddall, P. J., McClelland, J. M., Rutkowski, S. B., and Cousins, M. J. 2003. A longitudinal study of the prevalence and characteristics of pain in the first 5 years following spinal cord injury. Pain 103, 249–257.

Sindrup, S. H. and Jensen, T. S. 1999. Efficacy of pharmacological treatments of neuropathic pain: an update and effect related to mechanism of drug action. Pain 83, 389–400.

Sindrup, S. H. and Jensen, T. S. 2000. Pharmacologic treatment of pain in polyneuropathy. Neurology 55, 915–920.

Sommer, C. 2003. Painful neuropathies. Curr. Opin. Neurol. 16, 623–628.

Sommer, C. and Myers, R. R. 1996. Vascular pathology in CCI neuropathy: a quantitative temporal study. Exp. Neurol. 141, 113–119.

Sommer, C., Marziniak, M., and Myers, R. R. 1998. The effect of thalidomide treatment on vascular pathology and hyperalgesia caused by chronic constriction injury. Pain 74, 83–91.

Sorkin, L. S., Xiao, W.-H., Wagner, R., and Myers, R. R. 1997. Tumor necrosis factor-alpha induces ectopic activity in nociceptive primary afferent fibres. Neuroscience 81, 255–262.

Tal, M. and Bennett, G. J. 1994. Extra-territorial pain in rats with a peripheral mononeuropathy: mechano-hyperalgesia and mechano-allodynia in the territory of an uninjured nerve. Pain 57, 375–382.

Torebjork, E., Wahren, L., Wallin, G., Hallin, R., and Koltzenburg, M. 1995. Noradrenaline-evoked pain in neuralgia (see comments). Pain 63, 11–20.

Vanegas, H. and Schaible, H. G. 2004. Descending control of persistent pain: inhibitory or facilitatory? Brain Res. Brain Res. Rev. 46, 295–309.

Wagner, R., Janjigian, M., and Myers, R. R. 1998. Anti-inflammatory interleukin-10 therapy in CCI neuropathy decreases thermal hyperalgesia, macrophage recruitment, and endoneurial TNF-alpha expression. Pain 74, 35–42.

Wasner, G., Heckmann, K., Maier, C., and Baron, R. 1999. Vascular abnormalities in acute reflex sympathetic dystrophy (CRPS I) – complete inhibition of sympathetic nerve activity with recovery. Arch. Neurol. 56, 613–620.

Wasner, G., Kleinert, A., Binder, A., Schattschneider, J., and Baron, R. 2005. Postherpetic neuralgia: topical lidocaine is effective in nociceptor-deprived skin. J. Neurol. 252, 677–686.

Wasner, G., Schattschneider, J., Binder, A., and Baron, R. 2004. Topical menthol – a human model for cold pain by activation and sensitization of C nociceptors. Brain. 127, 1159–1171.

Watson, C. P., Deck, J. H., Morshead, C., Van der Kooy, D., and Evans, R. J. 1991. Post-herpetic neuralgia: further post-mortem studies of cases with and without pain. Pain 44, 105–117.

Wieseler-Frank, J., Maier, S. F., and Watkins, L. R. 2005. Immune-to-brain communication dynamically modulates pain: physiological and pathological consequences. Brain Behav. Immun. 19, 104–111.

Willoch, F., Rosen, G., Tolle, T. R., Oye, I., Wester, H. J., Berner, N., Schwaiger, M., and Bartenstein, P. 2000. Phantom limb pain in the human brain: unraveling neural circuitries of phantom limb sensations using positron emission tomography. Ann. Neurol. 48, 842–849.

Willoch, F., Schindler, F., Wester, H. J., Empl, M., Straube, A., Schwaiger, M., Conrad, B., and Tolle, T. R. 2004. Central poststroke pain and reduced opioid receptor binding within pain processing circuitries: a [11C]diprenorphine PET study. Pain 108, 213–220.

Wood, J. N., Boorman, J. P., Okuse, K., and Baker, M. D. 2004. Voltage-gated sodium channels and pain pathways. J. Neurobiol. 61, 55–71.

Woolf, C. J., Bennett, G. J., Doherty, M., Dubner, R., Kidd, B., Koltzenburg, M., Lipton, R., Loeser, J. D., Payne, R., and Torebjork, E. 1998. Towards a mechanism-based classification of pain? Pain 77, 227–229.

Wu, G., Ringkamp, M., Hartke, T. V., Murinson, B. B., Campbell, J. N., Griffin, J. W., and Meyer, R. A. 2001. Early onset of spontaneous activity in uninjured C-fiber nociceptors after injury to neighboring nerve fibers. J. Neurosci. 21, RC140.

Zambreanu, L., Wise, R. G., Brooks, J. C., Iannetti, G. D., and Tracey, I. 2005. A role for the brainstem in central sensitisation in humans. Evidence from functional magnetic resonance imaging. Pain 114, 397–407.

Zochodne, D. W. 1993. Epineurial peptides: a role in neuropathic pain? Can. J. Neurol. Sci. 20, 69–72.

5.58 Neurogenic Inflammation in Complex Regional Pain Syndrome (CRPS)

F Birklein, University of Mainz, Mainz, Germany

M Schmelz, University of Heidelberg, Mannheim, Germany

© 2008 Elsevier Inc. All rights reserved.

5.58.1	**Principles and Mechanisms of Neurogenic Inflammation – Basic Research**	901
5.58.1.1	Concept of Neurogenic Inflammation	901
5.58.1.2	Neuronal Basis of Neurogenic Inflammation	902
5.58.1.3	Humoral Interactions between Neurons and Inflammatory Cells	902
5.58.2	**Animal Models of Neuropathic Pain, Which Focus on Neurogenic Inflammation**	902
5.58.2.1	Bone Fracture Model for Complex Regional Pain Syndrome I	902
5.58.2.2	Nerve Transection Model for Complex Regional Pain Syndrome II	903
5.58.3	**Clinical Symptoms Suggesting Neurogenic Inflammation in Complex Regional Pain Syndrome**	903
5.58.3.1	Pain and Hyperalgesia	904
5.58.3.2	The Increase of Skin Perfusion and Temperature	904
5.58.3.3	Hyperhidrosis	904
5.58.3.4	Limb Edema	905
5.58.3.5	Trophic Changes	905
5.58.4	**Clinical Investigations Proving Neurogenic Inflammation in Complex Regional Pain Syndrome**	905
5.58.4.1	Experimental Studies	905
5.58.4.2	Treatment Studies	906
References		907

Glossary

ACE Angiotensin-converting enzyme.
CGRP Calcitonin gene-related peptide is the most potent vasodilator neuropeptide released from primary afferent nociceptors.
C-nociceptors Free nerve endings with high activation thresholds.
dermal microdialysis Single hollow semipermeable fibers are inserted into the skin.
laser Doppler Monochromatic light is directed to the skin. The frequency shift of the backscattered is proportional to skin perfusion.
NEP Neutral endopeptidase.
NGF Nerve growth factor.
NK1-R Substance P receptors.
polymorphism Common genetic variability.
QSART Quantitative measurement of peripheral axon reflex sweating.
SP Substance P binds to NK1 receptors at venoles and mediates plasma protein extravasation.
TNF-α Tumor necrosis factor-alpha.
TST Sweating induced by body heating – thermoregulatory sweating.

5.58.1 Principles and Mechanisms of Neurogenic Inflammation – Basic Research

5.58.1.1 Concept of Neurogenic Inflammation

It has been more than 100 years since Bayliss W. M. (1901) described antidromic vasodilation following electrical stimulation of centrally cut dorsal roots. Meanwhile it has become clear that retrogradely conducted action potentials invade the arborizations of the primary afferent neurons (axon reflex) and release neuropeptides from their terminals (Szolcsanyi, J., 1996). The acute effects of neuropeptide release in rodent skin are vasodilation and protein extravasation, the combination of which has

been termed neurogenic inflammation. Pivotal neuropeptides in the induction of neurogenic inflammation comprise calcitonin gene-related peptide (CGRP) for vasodilation and substance P (SP) for the induction of protein extravasation (Holzer, P., 1998).

5.58.1.2 Neuronal Basis of Neurogenic Inflammation

Chemical, thermal, and electrical stimulation has been widely used to elicit neurogenic inflammation. As a result of previous studies, mechanoinsensitive, but heat and chemosensitive C-nociceptors have been found responsible for the neurogenic vasodilation in pig (Lynn, B. *et al.*, 1996) and human skin (Schmelz, M. *et al.*, 2000), whereas in rodent, skin polymodal nociceptors play a crucial role (Gee, M. D. *et al.*, 1997).

A few approaches so far have tried to directly measure neuropeptide release in the skin, for example, *ex vivo* analysis by superfusion of excised rat skin (Kilo, S. *et al.*, 1997; Kress, M. *et al.*, 1999). In most studies, neurogenic vasodilation and protein extravasation have been used to functionally assess nociceptor activation. Vasodilation has been measured by laser Doppler techniques and infrared thermography. Assessment of protein extravasation requires more invasive techniques, for example, extravasation of albumin bound dyes like Evans blue, which can be photometrically quantified *ex vivo*. Recent advances in dermal microdialysis have opened new possibilities by allowing *in vivo* measurement of local mediator concentrations, including protein extravasation (Sauerstein, K. *et al.*, 2000).

5.58.1.3 Humoral Interactions between Neurons and Inflammatory Cells

In addition to the classical features of neurogenic inflammation, that is, vasodilation and protein extravasation, neuropeptides also directly interact with inflammatory cells. Primary afferent nociceptors release a variety of neuropeptides like neurokinin A, neurokinin B, somatostatin, corticotropin-releasing hormone (CRH), pituitary adenylate cyclase-activating polypeptide (PACAP), vasoactive intestinal peptide (VIP), galanin, and endomorphins (Steinhoff, M. *et al.*, 2003). A summary of important activating (Figure 1(a)) and inhibitory interactions (Figure 1(b)) between nociceptive nerve endings, tissue cells, and inflammatory cells is shown below. As an example, nerve growth factor (NGF) derived from keratinocytes and mast cells sensitizes nociceptors and also increases expression of mast cell tryptase and histamine (Groneberg, D. A. *et al.*, 2005) in mast cells. Histamine and tryptase activate nociceptive terminals via H1 and proteinase-activated receptors (PAR2) and release SP from the terminals (Steinhoff, M. *et al.*, 2000). SP via activation of NK1 receptors on the mast cells (van der Kleij, H. P. *et al.*, 2003) increases expression of histamine and tumor necrosis factor-alpha (TNF-α) (Ansel, J. C. *et al.*, 1993; Cocchiara, R. *et al.*, 1999), which in return sensitizes nociceptive terminals via activation of the TNF receptor.

5.58.2 Animal Models of Neuropathic Pain, Which Focus on Neurogenic Inflammation

Different animal models have been used to study the nature of neuropathic pain. Unfortunately, most studies focused on mechanisms and symptoms of pain but did not look at symptoms that characterize neurogenic inflammation after nerve lesion. Nevertheless, these pain models indicate that cytokines (TNF-α and NGF) were upregulated in the injured nerve (Herzberg, U. *et al.*, 1997a; 1997b; Schafers, M. *et al.*, 2002) and that neutralizing TNF-α reduces pain behavior (Sommer, C. *et al.*, 2001). It is the merit of Wade Kingery and his group that these shortcomings were meanwhile eliminated.

5.58.2.1 Bone Fracture Model for Complex Regional Pain Syndrome I

Most cases of complex regional pain syndrome (CRPS) I develop after bone fractures, e.g. to the wrist or the calf. Therefore, the most interesting animal model may be a controlled fracture of a large extremity bone. Very recently, skin temperature increase, edema, plasma protein extravasation (PPE), osteoporosis at the metaphysal parts of bones, and hyperalgesia-like behavior over weeks were observed in a rat model of tibial fracture (Guo, T. Z. *et al.*, 2004). As indicated above, these are signs of neurogenic inflammation, which can also be found in acute CRPS after bone fracture. These signs were even pronounced if the limbs of the rats were immobilized – as it is a common treatment in most human fractures. Supporting the neurogenic inflammation hypothesis of these symptoms, skin temperature difference, edema, and pain behavior can be reversed by NK1 antagonism (Kingery, W. S. *et al.*, 2003).

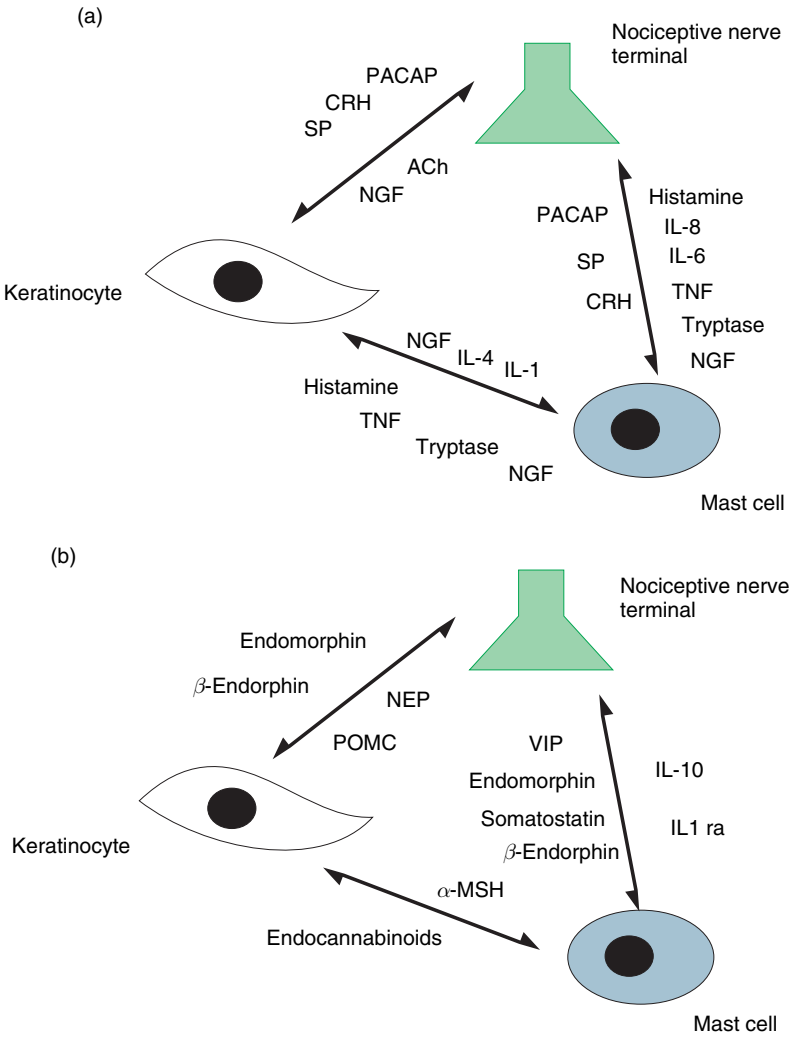

Figure 1 (a) Excitatory and (b) inhibitory neuroimmune interactions at peripheral nociceptors.

5.58.2.2 Nerve Transection Model for Complex Regional Pain Syndrome II

The sciatic nerve transection model was introduced as a surrogate for CRPS II. Soon after transection of the sciatic nerve, similar to the fracture model, rats develop increased skin temperature, paw edema, regional osteoporosis, and hyperalgesia-like behavior. Thus, symptoms after nerve transection also resemble acute CRPS. In this model, different treatments were tested. Steroids were able to reverse inflammatory symptoms (Kingery, W. S. *et al.*, 2001a; 2001b), and as described in the bone fracture model, NK1 antagonism was also effective (Kingery, W. S. *et al.*, 2003).

Taken together, both the bone fracture and the sciatic nerve transection model corroborates that many of the peripheral symptoms in acute posttraumatic CRPS may be due to C-fiber-mediated neurogenic inflammation.

5.58.3 Clinical Symptoms Suggesting Neurogenic Inflammation in Complex Regional Pain Syndrome

In general, neurogenic inflammation in CRPS can only assumed only if there has been an adequate limb trauma and if the initial clinical presentation corresponds to the primarily warm CRPS subtype (Veldman, P. H. J. M. *et al.*, 1993). In CRPS cases after minor trauma, which often start with a cold extremity (primarily cold), neurogenic inflammation

may not be present. Corresponding to the animal models, CRPS I and CRPS II could not be distinguished without detailed neurological investigation. CRPS II can be diagnosed when there is obvious evidence of peripheral nerve lesion – clinically (sensory loss, muscle weakness, and reflex loss) or neurophysiologically (nerve conduction and electromyography) (Harden, N. and Bruehl, S., 2004). However, these peripheral nerve lesions must involve either major nerves or skin nerves to be clinically recognized. Nerve lacerations (from broken bones) or stretches (from joint distraction) are usually unrecognizable. Injuries to small distal nerve branches, especially to purely sensory branches that innervate skin or bone, may not cause weakness or loss of reflexes, and thus go undetected in most clinical settings (Oaklander, A. L. and Birklein, F., 2004). For instance, a seemingly minor knee sprain can trigger CRPS if it is evaluated by knee arthroscopy, a well-documented cause of painful damage to the infrapatellar branch of the saphenous nerve (Mochida, H. and Kikuchi, S., 1995). Seemingly trivial medical procedures such as routine venipuncture can cause CRPS-inducing nerve damage to forearm nerves (Horowitz, S. H., 2001). Thus, we will not continue the traditional but often virtual differentiation between CRPS I and II in this chapter.

5.58.3.1 Pain and Hyperalgesia

In CRPS, pain and hyperalgesia are the most distressing symptoms. Since the initial trauma for CRPS usually does not include a complete nerve lesion, there are no serious reasons to doubt that pain and hyperalgesia result, at least partially, from activation of peripheral nociceptors. If these nociceptors are sensitized, they might be spontaneously active causing pain at rest (Orstavik, K. *et al.*, 2003) or they might respond more vigorously to physiological stimuli causing pain, for example, while moving a joint (Schaible, H. G. *et al.*, 2002). Nociceptor sensitization might furthermore drive spinal sensitization, which reinforces mechanical hyperalgesia. Since neurogenic inflammation, for example, the release of neuropeptides from nociceptors, is inevitably linked to nociceptor activation (even subthreshold for pain might be enough; Magerl, W. *et al.*, 1990), we regard pain and hyperalgesia as the one clinical symptom pointing to neurogenic inflammation in CRPS. In a study of 145 patients with untreated CRPS (Birklein, F. *et al.*, 2000), 75% reported pain even when the limb was completely at rest, but nearly all patients reported worsening of pain under certain circumstances – clinically indicating hyperalgesia. The most powerful stimulus that increased pain was joint movement. Accordingly, quantitative sensory testing revealed that on the affected skin there is a moderate decrease (about 4°C) of heat pain thresholds (Tahmoush, A. J. *et al.*, 2000). Heat pain sensitization of skin nociceptors is regarded as a clinical sign for peripheral sensitization (Baron, R., 2000). Even more obvious was the decrease of mechanical pain thresholds on the affected side. Our group investigated 40 CRPS patients and regularly found the presence of hyperalgesia to brief mechanical impact stimuli (Sieweke, N. *et al.*, 1999).

5.58.3.2 The Increase of Skin Perfusion and Temperature

In posttraumatic CRPS, skin temperature is increased usually during the first 6 months of the disease. The maximum skin temperature difference might be up to 10 °C (Birklein, F. *et al.*, 1997a; 1997b) Accordingly, skin color in this stage is reddish and the skin appears hyperemic. Only with disease chronification, skin temperature decreases on the affected side, the skin becomes bluish and appears thin and shiny (Birklein, F. *et al.*, 1998).

5.58.3.3 Hyperhidrosis

In 50% of the patients with CRPS, increased sweating can be clinically observed (Birklein, F. *et al.*, 1997a; 1997b); Two tests were used to localize sudomotor dysfunction along the neuraxis: thermoregulatory sweating test (TST) activates central thermoreceptors in the ventral hypothalamus (Jänig, W., 1990) and quantitative sudomotor axon reflex test (QSART) tests purely the peripheral sudomotor axon reflex (Low, P. A. *et al.*, 1983). In acute CRPS both TST and QSART are increased pointing to sudomotor dysfunction in the peripheral nervous system. From basic experiments we know that the capacity of sweat glands increases with increasing skin temperature (Sato, K. *et al.*, 1993) and that the neuropeptide CGRP, which might be responsible for increased skin temperature and perfusion, itself enhances sweat gland activity (Kumazawa, K. *et al.*, 1994).

5.58.3.4 Limb Edema

Edema is the most striking clinical sign in CRPS. During acute stages 81% of patients have visible edema on the affected limb (Birklein, F. *et al.*, 2000). The edema is pronounced at backs of hands or feet. After exercise or during the course of a day, when repeated nociceptor activation has occurred, edema increases. Only if CRPS persists longer and becomes chronic, edema dwindles (Birklein, F. *et al.*, 1999).

5.58.3.5 Trophic Changes

Trophic changes can be found in more than 50% of patients. Increased hair and nail growth appears several days after the onset of symptoms (Birklein, F. *et al.*, 2000). The well-known periarticular patchy osteoporosis, which can bee seen on X-ray pictures, belongs to the same group of symptoms (Maresca, V., 1985). This osteoporosis is a so-called high-turnover osteoporosis with increased osteoclastic activity (Leitha, T. *et al.*, 1996). Interestingly, TNF-α and SP (Goto, T. *et al.*, 1998) activate osteoclasts, and CGRP promotes hair growth (Hagner, S. *et al.*, 2002).

5.58.4 Clinical Investigations Proving Neurogenic Inflammation in Complex Regional Pain Syndrome

5.58.4.1 Experimental Studies

Many clinical symptoms of acute CRPS resemble inflammation: pain, edema, increased skin temperature, and blood flow. Inflammation in the classical sense with positive blood markers has not been proven, but any inflammation has a neurogenic component (Brain, S. D. and Williams, T. J., 1988). Peripheral trauma, in particular if it is accompanied by partial peripheral nerve lesion, causes a rapid release of cytokines like NGF (Herzberg, U. *et al.*, 1997a; 1997b) and TNF-α (Grellner, W., 2002). Both cytokines are able to activate and sensitize primary afferents, locally at the injury site or proximally in the respective nerve trunk. Recently, increased TNF-α has been shown in CRPS skin by analysis of suction blister fluids (Huygen, F. J. *et al.*, 2002). Our own group was able to demonstrate increased TNF-α in plasma samples of two different independent CRPS patients groups (Maihofner, C. *et al.*, 2005). Increase of TNF-α was correlated to mechanical hyperalgesia, a clinical surrogate for nociceptive sensitization.

Cytokines also increase the neuropeptide content of primary afferent neurons (Opree, A. and Kress, M., 2000). Activation of sensitized primary afferents then causes an increased release of neuropeptides into the affected body region (SP and CGRP). Chronic release of neuropeptides might be responsible for the above-mentioned CRPS symptoms. In addition, central neuropeptide release facilitates nociceptive sensitization. In analogy to migraine studies, we therefore measured CGRP in serum samples from patients with acute CRPS. CGRP was significantly increased, in particular when clinical inflammatory signs were present and when there was evidence for trauma-related nerve lesion (Birklein, F. *et al.*, 2001). In order to verify that increased CGRP indeed comes from primary nociceptive afferents, neurogenic inflammation was elicited directly in the skin by transcutaneous electrical stimulation via intradermal microdialysis capillaries. We first investigated the flare by using laser Doppler scanning on the affected and the unaffected side in our CRPS patients. Neurogenic flare was significantly more intense in patients, surprisingly on both sides – the affected and the clinically unaffected one (Leis, S. *et al.*, 2004). Another characteristic of neurogenic inflammation in rodents is SP-mediated PPE. In healthy humans, C fibers usually contain too less SP to induce PPE. In CRPS, however, significant PPE could be shown in almost all patients investigated. In contrast to the flare response, this increased PPE was limited to the affected side (Weber, M. *et al.*, 2001). These results suggested two possible pathomechanisms leading to facilitated neurogenic inflammation in CRPS – either increased release, hampered inactivation of neuropeptides, or both. In order to further unravel these mechanisms, we perfused SP in ascending concentrations through dermal microdialysis fibers in CRPS patients and controls. We found SP to be significantly more effective at inducing PPE in CRPS patients. Similar to the increased flare response, this increased responsiveness to SP was present on both the affected and the unaffected limbs (Leis, S. *et al.*, 2003) (Figure 2).

To summarize, in this series of experiments we found a trauma-related upregulation of neuropeptide release from primary afferent on the affected side and in addition an impaired inactivation of neuropeptides on both sides, possibly as a predisposing factor. Neuropeptide action in human tissue is terminated by degradation of peptidases. The most familiar peptidase, which cleaves SP and CGRP, is the angiotensin-converting enzyme (ACE). A previous

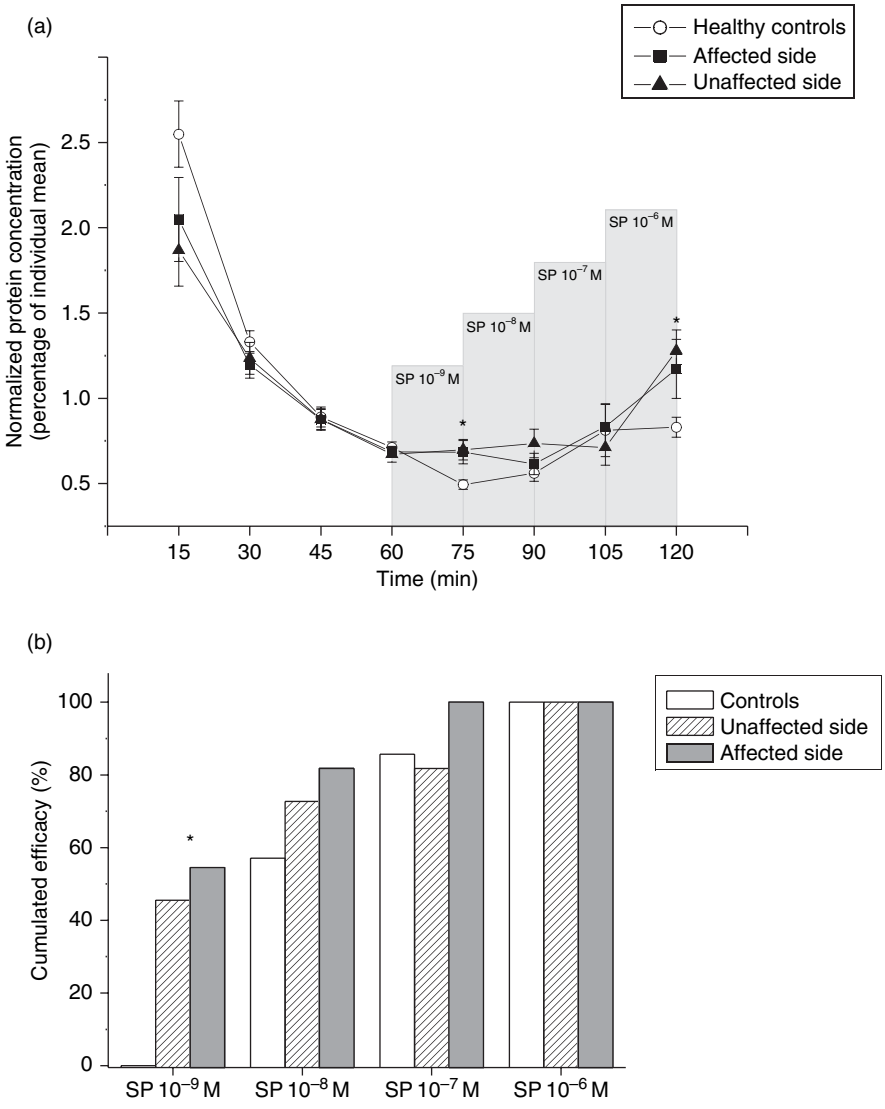

Figure 2 Substance P (SP) induced significantly increased protein extravasation in complex regional pain syndrome (CRPS) patients on the ipsilateral affected side (circles) and the contralateral unaffected side (triangles) as compared to healthy controls (squares). Significant differences at SP 10^{-9} M (receptor-dependent) and SP 10^{-6} M (receptor-independent) are marked. Results with intermediate SP concentrations might be false-negative due to SP receptor internalization.

report of an insertion/deletion (I/D) polymorphism in intron 16 within the ACE gene implicated an increased risk to develop CRPS I associated with the D allele (Kimura, T. *et al.*, 2000). However, in a linkage study in CRPS families, we failed to show any cosegregation of this polymorphism and the CRPS phenotype (Hühne, K. *et al.*, 2004). Therefore, we will focus on other enzymes that are involved in neuropeptide degradation. One promising example is the neutral endopeptidase (NEP). Blocking the NEP facilitates neurogenic inflammation in a way, which resembles the findings on the unaffected side in CRPS patients (Krämer, H. H. *et al.*, 2005).

5.58.4.2 Treatment Studies

Another indication for neurogenic inflammation in warm posttraumatic CRPS cases is the effectiveness of anti-inflammatory treatment with steroids, which is based on small, but controlled studies (Christensen, K. *et al.*, 1982). Cortisone has multiple effects in

CRPS – it inhibits the production of inflammatory mediators, reduces the transcription rate in dorsal root ganglia cells, and thereby reduces neuropeptide content of sensory neurons (Kingery, W. S. *et al*., 2001a; 2001b). Furthermore, it even facilitates the degradation of neuropeptides (Nadel, J. A., 1992) and inhibits ectopic impulse generation after nerve trauma by stabilizing nerve membranes. Thus, steroids may prevent the development of facilitated neurogenic inflammation and of neuropathic pain in warm CRPS.

References

Ansel, J. C., Brown, J. R., Payan, D. G., and Brown, M. A. 1993. Substance P selectively activates TNF-alpha gene expression in murine mast cells. J. Immunol. 150, 4478–4485.

Baron, R. 2000. Peripheral neuropathic pain: from mechanisms to symptoms. Clin. J. Pain 16, 12–20.

Bayliss, W. M. 1901. On the origin from the spinal cord of the vasodilator fibres of the hindlimb, and on the nature of these fibers. J. Physiol. (Lond.) 32, 1025–1043.

Birklein, F., Riedl, B., Claus, D., and Neundörfer, B. 1998. Pattern of autonomic dysfunction in time course of complex regional pain syndrome. Clin. Auton. Res. 8, 79–85.

Birklein, F., Riedl, B., Griessinger, N., and Neundörfer, B. 1999. Komplexes regionales schmerzsyndrom. Klinik und autonome störungen während akuter und chronischer krankheitsstadien. Nervenarzt 70, 335–341.

Birklein, F., Riedl, B., Handwerker, H. O., and Neundörfer, B. 1997a. Störung der thermoregulatorischen Hautdurchblutung bei sympathischer Reflexdystrophie. Akt. Neurol. 24, 61–66.

Birklein, F., Riedl, B., Sieweke, N., Weber, M., and Neundorfer, B. 2000. Neurological findings in complex regional pain syndromes – analysis of 145 cases. Acta Neurol. Scand. 101, 262–269.

Birklein, F., Schmelz, M., Schifter, S., and Weber, M. 2001. The important role of neuropeptides in complex regional pain syndrome. Neurology 57, 2179–2184.

Birklein, F., Sittl, R., Spitzer, A., Claus, D., Neundörfer, B., and Handwerker, H. O. 1997b. Sudomotor function in sympathetic reflex dystrophy. Pain 69, 49–54.

Brain, S. D. and Williams, T. J. 1988. Substance P regulates the vasodilator activity of calcitonin gene-related peptide. Nature 335, 73–75.

Christensen, K., Jensen, E. M., and Noer, I. 1982. The reflex sympathetic dystrophy syndrome response to treatment with systemic corticosteroids. Acta Chir. Scand. 148, 653–655.

Cocchiara, R., Lampiasi, N., Albeggiani, G., Bongiovanni, A., Azzolina, A., and Geraci, D. 1999. Mast cell production of TNF-alpha induced by substance P evidence for a modulatory role of substance P-antagonists. J. Neuroimmunol. 101, 128–136.

Gee, M. D., Lynn, B., and Cotsell, B. 1997. The relationship between cutaneous C fibre type and antidromic vasodilatation in the rabbit and the rat. J. Physiol. (Lond.) 503, 31–44.

Goto, T., Yamaza, T., Kido, M. A., and Tanaka, T. 1998. Light- and electron-microscopic study of the distribution of axons containing substance P and the localization of neurokinin-1 receptor in bone. Cell Tissue Res. 293, 87–93.

Grellner, W. 2002. Time-dependent immunohistochemical detection of proinflammatory cytokines (IL-1beta, IL-6, TNF-alpha) in human skin wounds. Forensic Sci. Int. 130, 90–96.

Groneberg, D. A., Serowka, F., Peckenschneider, N., Artuc, M., Grutzkau, A., Fischer, A., Henz, B. M., and Welker, P. 2005. Gene expression and regulation of nerve growth factor in atopic dermatitis mast cells and the human mast cell line-1. J. Neuroimmunol. 161, 87–92.

Guo, T. Z., Offley, S. C., Boyd, E. A., Jacobs, C. R., and Kingery, W. S. 2004. Substance P signaling contributes to the vascular and nociceptive abnormalities observed in a tibial fracture rat model of complex regional pain syndrome type I. Pain 108, 95–107.

Hagner, S., Haberberger, R. V., Overkamp, D., Hoffmann, R., Voigt, K. H., and McGregor, G. P. 2002. Expression and distribution of calcitonin receptor-like receptor in human hairy skin. Peptides 23, 109–116.

Harden, N. and Bruehl, S. 2004. Diagnostic Criteria: The Statistical Derivation of Four Criterion Factors. In: CRPS: Current Diagnosis and Therapy (*eds*. P. R. Wilson, M. Stanton-Hicks, and R. N. Harden), pp. 45–58. IASP Press.

Herzberg, U., Eliav, E., Dorsey, J. M., Gracely, R. H., and Kopin, I. J. 1997a. NGF involvement in pain induced by chronic constriction injury of the rat sciatic nerve. Neuroreport 8, 1613–1618.

Herzberg, U., Eliav, E., Dorsey, J. M., Gracely, R. H., and Kopin, I. J. 1997b. NGF involvement in pain induced by chronic constriction injury of the rat sciatic nerve. Neuroreport 8, 1613–1618.

Holzer, P. 1998. Neurogenic vasodilatation and plasma leakage in the skin. Gen. Pharmacol. 30, 5–11.

Horowitz, S. H. 2001. Venipuncture-induced neuropathic pain: the clinical syndrome, with comparisons to experimental nerve injury models. Pain 94, 225–229.

Hühne, K., Leis, S., Schmelz, M., Rautenstrauss, B., and Birklein, F. 2004. A polymorphic locus in the intron 16 of the human angiotensin-converting enzyme (ACE) gene is not correlated with complex regional pain syndrome I (CRPS I). Eur. J. Pain 8, 221–225.

Huygen, F. J., De Bruijn, A. G., De Bruin, M. T., Groeneweg, J. G., Klein, J., and Zijistra, F. J. 2002. Evidence for local inflammation in complex regional pain syndrome type 1. Mediators Inflamm. 11, 47–51.

Jänig, W. 1990. Functions of the Sympathetic Innervation of the Skin. In: Central Regulation of Autonomic Functions (*eds*. A. D. Loewy and K. M. Spyer), pp. 334–348. Oxford University Press.

Kilo, S., Harding-Rose, C., Hargreaves, K. M., and Flores, C. M. 1997. Peripheral CGRP release as a marker for neurogenic inflammation: a model system for the study of neuropeptide secretion in rat paw skin. Pain 73, 201–207.

Kimura, T., Komatsu, T., Hosada, R., Nishiwaki, K., and Shimada, Y. 2000. Angiotensin-Converting Enzyme Gene Polymorphism in Patients with Neuropathic Pain. In: Proceedings of the 9th World Congress in Pain (*eds*. M. Devor, M. Rowbotham, and Z. Wiesenfeld-Hallin), pp. 471–476. IASP Press.

Kingery, W. S., Davies, M. F., and Clark, J. D. 2003. A substance P receptor (NK1) antagonist can reverse vascular and nociceptive abnormalities in a rat model of complex regional pain syndrome type II. Pain 104, 75–84.

Kingery, W. S., Guo, T., Agashe, G. S., Davies, M. F., Clark, J. D., and Maze, M. 2001a. Glucocorticoid inhibition of neuropathic limb edema and cutaneous neurogenic extravasation. Brain Res. 913, 140–148.

Kingery, W. S., Guo, T., Agashe, G. S., Davies, M. F., Clark, J. D., and Maze, M. 2001b. Glucocorticoid inhibition of neuropathic limb edema and cutaneous neurogenic extravasation. Brain Res. 913, 140–148.

van der Kleij, H. P., Ma, D., Redegeld, F. A., Kraneveld, A. D., Nijkamp, F. P., and Bienenstock, J. 2003. Functional expression of neurokinin 1 receptors on mast cells

induced by IL-4 and stem cell factor. J. Immunol. 171, 2074–2079.

Krämer, H. H., Schmidt, K., Leis, S., Schmelz, M., Sommer, C., and Birklein, F. 2005. Inhibition of neutral endopeptidase (NEP) facilitates neurogenic inflammation. Exp. Neurol. 195(1), 179–184.

Kress, M., Guthmann, C., Averbeck, B., and Reeh, P. W. 1999. Calcitonin gene-related peptide and prostaglandin E2 but not substance P release induced by antidromic nerve stimulation from rat skin, *in vitro*. Neuroscience 89, 303–310.

Kumazawa, K., Sobue, G., Mitsuma, T., and Ogawa, T. 1994. Modulatory effects of calcitonin gene-related peptide and substance P on human cholinergic sweat secretion. Clin. Auton. Res. 4, 319–322.

Leis, S., Weber, M., Isselmann, A., Schmelz, M., and Birklein, F. 2003. Substance-P-induced protein extravasation is bilaterally increased in complex regional pain syndrome. Exp. Neurol. 183, 197–204.

Leis, S., Weber, M., Schmelz, M., and Birklein, F. 2004. Facilitated neurogenic inflammation in unaffected limbs of patients with complex regional pain syndrome. Neurosci. Lett. 359, 163–166.

Leitha, T., Staudenherz, A., Korpan, M., and Fialka, V. 1996. Pattern recognition in five-phase bone scintigraphy: diagnostic patterns of reflex sympathetic dystrophy in adults. Eur. J. Nucl. Med. 23, 256–262.

Low, P. A., Caskey, P. E., Tuck, R. R., Fealey, R. D., and Dyck, P. J. 1983. Quantitative sudomotor axon reflex test in normal and neuropathic subjects. Ann. Neurol. 14, 573–580.

Lynn, B., Schutterle, S., and Pierau, F. K. 1996. The vasodilator component of neurogenic inflammation is caused by a special subclass of heat-sensitive nociceptors in the skin of the pig. J. Physiol. (Lond.) 494, 587–593.

Magerl, W., Geldner, G., and Handwerker, H. O. 1990. Pain and vascular reflexes elicited by prolonged noxious mechano-stimulation. Pain 43, 219–225.

Maihofner, C., Handwerker, H. O., Neundorfer, B., and Birklein, F. 2005. Mechanical hyperalgesia in complex-regional pain syndrome: a role for tnf-alpha. Neurology 65(2), 311–313.

Maresca, V. 1985. Human calcitonin in the management of osteoporosis: a multicentre study. J. Int. Med. Res. 13, 311–316.

Mochida, H. and Kikuchi, S. 1995. Injury to infrapatellar branch of saphenous nerve in arthroscopic knee surgery. Clin. Orthop. Relat. Res. 88–94.

Nadel, J. A. 1992. Neurogenic inflammation in airways and its modulation by peptidases. Ann. N. Y. Acad. Sci. 664, 408–414.

Oaklander, A. L. and Birklein, F. 2004. Peripheral Somatosensory Abnormalities – Pathology and Pathophysiology. In: CRPS: Current Diagnosis and Therapy (*eds*. P. R. Wilson, M. Stanton-Hicks, and R. N. Harden), pp. 59–79. IASP Press.

Opree, A. and Kress, M. 2000. Involvement of the proinflammatory cytokines tumor necrosis factor-alpha, IL-1 beta, and IL-6 but not IL-8 in the development of heat hyperalgesia: effects on heat-evoked calcitonin gene-related peptide release from rat skin. J. Neurosci. 20, 6289–6293.

Orstavik, K., Weidner, C., Schmidt, R., Schmelz, M., Hilliges, M., Jorum, E., Handwerker, H., and Torebjork, E. 2003. Pathological C-fibres in patients with a chronic painful condition. Brain 126, 567–578.

Sato, K., Ohtsuyama, M., and Sato, F. 1993. Normal and Abnormal Eccrine Sweat Gland Function. In: Clinical Autonomic Disorders (*ed*. P. A. Low), pp. 93–104, Little, Brown.

Sauerstein, K., Klede, M., Hilliges, M., and Schmelz, M. 2000. Electrically evoked neuropeptide release and neurogenic inflammation differ between rat and human skin. J. Physiol. 529, 803–810.

Schafers, M., Geis, C., Brors, D., Yaksh, T. L., and Sommer, C. 2002. Anterograde transport of tumor necrosis factor-alpha in the intact and injured rat sciatic nerve. J. Neurosci. 22, 536–545.

Schaible, H. G., Ebersberger, A., and von Banchet, G. S. 2002. Mechanisms of pain in arthritis. Ann. N. Y. Acad. Sci. 966, 343–354.

Schmelz, M., Michael, K., Weidner, C., Schmidt, R., Torebjörk, H. E., and Handwerker, H. O. 2000. Which nerve fibers mediate the axon reflex flare in human skin? Neuroreport 11, 645–648.

Sieweke, N., Birklein, F., Riedl, B., Neundorfer, B., and Handwerker, H. O. 1999. Patterns of hyperalgesia in complex regional pain syndrome. Pain 80, 171–177.

Sommer, C., Lindenlaub, T., Teuteberg, P., Schafers, M., Hartung, T., and Toyka, K. V. 2001. Anti-TNF-neutralizing antibodies reduce pain-related behavior in two different mouse models of painful mononeuropathy. Brain Res. 913, 86–89.

Steinhoff, M., Stander, S., Seeliger, S., Ansel, J. C., Schmelz, M., and Luger, T. 2003. Modern aspects of cutaneous neurogenic inflammation. Arch. Dermatol. 139, 1479–1488.

Steinhoff, M., Vergnolle, N., Young, S. H., Tognetto, M., Amadesi, S., Ennes, H. S., Trevisani, M., Hollenberg, M. D., Wallace, J. L., Caughey, G. H., Mitchell, S. E., Williams, L. M., Geppetti, P., Mayer, E. A., and Bunnett, N. W. 2000. Agonists of proteinase-activated receptor 2 induce inflammation by a neurogenic mechanism. Nat. Med. 6, 151–158.

Szolcsanyi, J. 1996. Capsaicin-sensitive sensory nerve terminals with local and systemic efferent functions: facts and scopes of an unorthodox neuroregulatory mechanism. Prog. Brain Res. 113, 343–359.

Tahmoush, A. J., Schwartzman, R. J., Hopp, J. L., and Grothusen, J. R. 2000. Quantitative sensory studies in complex regional pain syndrome type 1/RSD. Clin. J. Pain 16, 340–344.

Veldman, P. H. J. M., Reynen, H. M., Arntz, I. E., and Goris, R. J. A. 1993. Signs and symptoms of reflex sympathetic dystrophy: prospective study of 829 patients. Lancet 342, 1012–1016.

Weber, M., Birklein, F., Neundorfer, B., and Schmelz, M. 2001. Facilitated neurogenic inflammation in complex regional pain syndrome. Pain 91, 251–257.

5.59 Complex Regional Pain Syndromes

R Baron, Christian-Albrechts-Universität Kiel, Kiel, Germany

© 2008 Elsevier Inc. All rights reserved.

5.59.1	**Introduction**	909
5.59.2	**Complex Regional Pain Syndrome Type I (Reflex Sympathetic Dystrophy)**	909
5.59.3	**Complex Regional Pain Syndrome Type II (Causalgia)**	910
5.59.4	**Important Issues that Are Unique in Complex Regional Pain Syndrome**	910
5.59.4.1	Motor Abnormalities	910
5.59.4.2	Inflammatory Processes	910
5.59.4.2.1	Immune cell-mediated inflammation and cytokine release	911
5.59.4.2.2	Neurogenic inflammation and nociceptor sensitization	911
5.59.4.2.3	Autoimmune etiology	911
5.59.4.3	Sensitization to Adrenergic Stimuli – Sympathetically Maintained Pain	912
5.59.5	**Future Research, Diagnostic Classification, and Therapeutic Strategies**	912
5.59.5.1	Integration of the Clinics and Basic Research	912
5.59.5.2	The Long Path Approaching the Central Nervous System	912
5.59.5.3	A Possible Link between Inflammation and the Sympathetic Nervous System	913
5.59.5.4	Do the Genes Predispose for Complex Regional Pain Syndrome?	913
5.59.5.5	The Future Need for Diagnostic Procedures	913
5.59.5.5.1	Validation of clinical diagnostic criteria	913
5.59.5.5.2	Tests which aid the diagnosis of complex regional pain syndrome	915
References		915

Glossary

CRPS Complex regional pain syndrome.
DRG Dorsal root ganglion, spinal ganglion.
MEG Magnetic encephalography.
PET Positron emission tomography.
QST Quantitative sensory testing.
TNF Tumor necrosis factor.

5.59.1 Introduction

The term complex regional pain syndrome (CRPS) describes a variety of painful conditions following injury, which appears regionally with a distal predominance of abnormal findings. The symptoms exceed in both magnitude and duration the expected clinical course of the inciting event and often result in significant impairment of motor function. The disorder shows a variable progression over time. These chronic pain syndromes comprise different additional clinical features including spontaneous pain, allodynia, hyperalgesia, edema, autonomic abnormalities, and trophic signs. In CRPS type I (reflex sympathetic dystrophy) minor injuries or fractures of a limb precede the onset of symptoms. CRPS type II (causalgia) develops after injury to a major peripheral nerve (Baron, R. *et al.*, 2002a; Janig, W. and Baron, R., 2003; Baron, R., 2004).

5.59.2 Complex Regional Pain Syndrome Type I (Reflex Sympathetic Dystrophy)

The most common precipitating event is a trauma affecting the distal part of an extremity (65%), especially fractures, postsurgical conditions, contusions, and strain or sprain. Less common occasions are central nervous system (CNS) lesions like spinal cord injuries and cerebrovascular accidents as well as cardiac ischemia (Wasner, G. *et al.*, 2003).

CRPS I patients develop asymmetrical distal extremity pain and edema without presenting an overt nerve lesion. These patients often report a burning spontaneous pain felt in the distal part of the affected extremity. Characteristically, the pain is disproportionate in intensity to the inciting event. The pain usually increases when the extremity is in a dependent position. Stimulus-evoked pains are a striking clinical feature. These sensory abnormalities often appear early, are most pronounced distally, and have no consistent spatial relationship to individual nerve territories or to the site of the inciting lesion. Typically, pain can be elicited by movement of and pressure on the joints (deep somatic allodynia), even if these are not directly affected by the inciting lesion.

Autonomic abnormalities include swelling and changes of sweating and skin blood flow. In the acute stages of CRPS I, the affected limb is often warmer than the contralateral limb. Sweating abnormalities, either hypohidrosis or, more frequently, hyperhidrosis are present in nearly all CRPS I patients. The acute distal swelling of the affected limb depends very critically on aggravating stimuli. Since it diminishes after sympathetic blocks, it is likely that it is maintained by sympathetic activity.

Trophic changes such as abnormal nail growth, increased or decreased hair growth, fibrosis, thin glossy skin, and osteoporosis may be present, particularly in chronic stages. Restrictions of passive movement are often present in long-standing cases and may be related to both functional motor disturbances and trophic changes of joints and tendons.

Weakness of all muscles of the affected distal extremity is often present. Small accurate movements are characteristically impaired. Nerve conduction and electromyography studies are normal, except in patients in very chronic and advanced stages. About half of the patients have a postural or action tremor representing an increased physiological tremor. In about 10% of the cases, dystonia of the affected hand or foot develops.

5.59.3 Complex Regional Pain Syndrome Type II (Causalgia)

The symptoms of CRPS II are similar to those of CRPS I. The only exception is that a lesion of peripheral nerve structures and subsequent focal deficits are mandatory for the diagnosis. The symptoms and signs spread beyond the innervation territory of the injured peripheral nerve and often occur remote from the site of injury but a restriction to the territory is not in conflict with the current definition.

5.59.4 Important Issues that Are Unique in Complex Regional Pain Syndrome

5.59.4.1 Motor Abnormalities

About 50% of the patients with CRPS show motor abnormalities (Deuschl, G. *et al.*, 1991; Bhatia, K. P. *et al.*, 1993). It is unlikely that these motor changes are related to a peripheral process (e.g., influence of the sympathetic nervous system on neuromuscular transmission and/or contractility of skeletal muscle). These somatomotor changes are more likely generated by central changes of activity in the motoneurons. With kinematic analysis of target reaching as well as grip force analysis to quantitatively assess motor deficits in CRPS patients (Schattschneider, J. *et al.*, 2001) abnormalities in the cerebral motor processing were revealed. A pathological sensorimotor integration located in the parietal cortex may induce an abnormal central programming and processing of motor tasks. Interestingly, the motor performance is also slightly impaired on the contralateral unaffected side (Ribbers, G. M. *et al.*, 2002). According to this view, a neglect-like syndrome was clinically described to be involved in the disuse of the extremity (Galer, B. S. *et al.*, 1995). Recent controlled studies also support an incongruence between central motor output and sensory input as underlying mechanism in CRPS. Using the method of mirror visual feedback, the visual input from a moving unaffected limb to the brain was able to reestablish the pain-free relationship between sensory feedback and motor execution. After 6 weeks of therapy, pain and function were improved as compared with the control group (McCabe, C. S. *et al.*, 2003; Moseley, G. L., 2004). Furthermore, a sustained inhibition of the motor cortex was found in CRPS patients on the contralateral as well as ipsilateral hemisphere (Juottonen, K. *et al.*, 2002; Schwenkreis, P. *et al.*, 2003).

5.59.4.2 Inflammatory Processes

Some of the clinical features of CRPS particularly in its early phase, that is, calor, dolor, rubor, functio lesae, and swelling suggest that the pathological extremity is exhibiting an excessive inflammatory

process (Leitha, T. *et al.*, 1996; van der Laan, L. and Goris, R. J., 1997; Calder, J. S. *et al.*, 1998). The idea of an inflammatory processes, in particular in the deep somatic tissues including bones, goes back to Sudeck who believed that this syndrome is an inflammatory bone atrophy ("entzündliche Knochenatrophie") (Sudeck, P., 1902; 1931). There are now several lines of evidence supporting this view.

5.59.4.2.1 Immune cell-mediated inflammation and cytokine release

Several studies in CRPS patients address the question to what extend an immune cell-mediated inflammation is involved. Skin biopsies in these patients showed a striking increase in the number of Langerhans cells that can release immune cell chemoattractants and proinflammatory cytokines (Calder, J. S. *et al.*, 1998). In accordance, in the fluid of artificially produced skin blisters significantly higher levels of IL-6 and tumor necrosis factor alpha (TNF-α) as well as tryptase (a measure of mast cell activity) were observed in the involved extremity as compared with the uninvolved extremity (Huygen, F. J. *et al.*, 2001; 2002). In CRPS patients with hyperalgesia, higher levels of the soluble TNF-α receptor type I were found (Maihofner, C. *et al.*, 2005b). Accordingly, a significant increases in IL-1β and IL-6, but not TNF-α was demonstrated in the cerebrospinal fluid (CSF) of individuals afflicted with CRPS as compared with controls (Alexander, G. M. *et al.*, 2005).

In this context, it is of particular interest that cutaneous denervation can cause rapid activation and proliferation of Langerhans cells that continues until reinnervation occurs. Thus, one might speculate that such cell proliferation may reflect also a functional denervation of cutaneous sympathetic outflow that occurs in CRPS (Wasner, G. *et al.*, 1999; 2001).

The patchy osteoporosis which is found in more advanced CRPS cases may also be consistent with a regional inflammatory process in deep somatic tissues. Both IL-1 and IL-6 cause proliferation and activation of osteoclasts and suppress the activity of osteoblasts.

Changes in hair growth can also be created by proinflammatory cytokines. TNF and IL-1 directly inhibit hair growth. Keratocyte-derived TNF and IL-6 cause retarded hair growth, signs of fibrosis, and in turn immune infiltration of the dermis, all present in CRPS patients.

5.59.4.2.2 Neurogenic inflammation and nociceptor sensitization

Because infection has so far not been shown to account for the inflammatory reactions in CRPS an exaggerated neurogenic inflammation has been proposed. Axon reflex vasodilatation was significantly increased on the affected side as measured with laser Doppler flowmetry after electrical C-fiber stimulation. Accordingly, systemic CGRP levels were found to be increased in acute CRPS but not in chronic stages (Birklein, F. *et al.*, 2001). Also, increased axon reflex sweating could be explained by release of CGRP from nociceptive terminals during nociceptor sensitization that act on peripheral sweat glands (Birklein, F. *et al.*, 2001).

In acute untreated CRPS I patients axon reflex activation was elicited by strong transcutaneous electrical stimulation of peptidergic unmyelinated afferents via intradermal microdialysis capillaries. Protein extravasation that was simultaneously assessed by the microdialysis system was only provoked on the affected extremity as compared with the normal side. The time course of electrically induced protein extravasation in the patients resembled the one observed following application of exogenous substance P (SP) (Weber, M. *et al.*, 2001).

Plasma extravasation could also be demonstrated with other experimental techniques: Bone scintigraphy demonstrated periarticular tracer uptake in acute CRPS (Leitha, T. *et al.*, 1996) and analysis of joint fluid and synovial biopsies in CRPS patients have shown an increase in protein concentration and synovial hypervascularity (Renier, J. C. *et al.*, 1983). Furthermore, synovial effusion is enhanced in affected joints as measured with magnetic resonance imaging (MRI) (Graif, M. *et al.*, 1998). Scintigraphic investigations with radiolabeled immunoglobulins show extensive plasma extravasation (Oyen, W. J. *et al.*, 1993).

5.59.4.2.3 Autoimmune etiology

There are several studies focusing at an autoimmune response in patients with CRPS. Autoantibodies against rat sympathetic neurons were detected in 40% of CRPS patients, whereas only 5% of other neuropathy patients showed these autoantibodies (Blaes, F. *et al.*, 2004). Immunoreactivity to *Campylobacter* was found in many early CRPS patients in particular associated with minimal trauma indicating a postinfectious autoimmune basis in some patients (Goebel, A. *et al.*, 2005).

5.59.4.3 Sensitization to Adrenergic Stimuli – Sympathetically Maintained Pain

After nerve lesion in animal experiments (Baron, R. *et al.*, 1999), afferent nociceptive and nonnociceptive neurons undergo dramatic functional and anatomical changes including upregulating of α-adrenoceptors. Noradrenaline released by the sympathetic nerve fibers may activate and/or sensitize the afferent neurons. This sympathetic–afferent coupling forms the theoretical basis for the clinical phenomenon of sympathetically maintained pain (SMP). The interaction may occur at the lesion site, along the lesioned nerve or even in the dorsal root ganglion (DRG).

Clinical studies in CRPS support the idea that nociceptors may develop catecholamine sensitivity (Baron, R. *et al.*, 1999): intraoperative stimulation of the sympathetic chain induces an increase of spontaneous pain in patients with causalgia (CRPS II) but not in patients with hyperhidrosis. In CRPS II, intracutaneous application of norepinephrine into a symptomatic area rekindles spontaneous pain and dynamic mechanical hyperalgesia that had been relieved by sympathetic blockade, supporting the idea that noradrenergic sensitivity of human nociceptors is present after partial nerve lesion. Also intradermal NE, in physiologically relevant doses, was demonstrated to evoke greater pain in the affected regions of patients with SMP, than in the contralateral unaffected limb, and in control subjects (Ali, Z. *et al.*, 2000).

We performed a study in patients with CRPS I using physiological stimuli of the sympathetic nervous system (Baron, R. *et al.*, 2002b). Cutaneous sympathetic vasoconstrictor outflow to the painful extremity was experimentally activated to the highest possible physiological degree by whole body cooling. The intensity as well as area of spontaneous pain and mechanical hyperalgesia (dynamic and punctate) increased significantly in patients that had been classified as having SMP by positive sympathetic blocks but not in sympathetically independent pain (SIP) patients. It is very likely that in addition to a coupling in the skin, a sympathetic–afferent interaction may also occur in other tissues, in particular in the deep somatic domain such as bone, muscle, or joints. Supporting this view, especially these structures are extremely painful in some cases with CRPS (Baron, R. and Wasner, G., 2001). Furthermore, there may be patients who are characterized by a selective or predominant sympathetic–afferent interaction in deep somatic tissues sparing the skin (Wasner, G. *et al.*, 1999).

5.59.5 Future Research, Diagnostic Classification, and Therapeutic Strategies

5.59.5.1 Integration of the Clinics and Basic Research

Recently a new animal model for CRPS I was introduced (Coderre, T. J. *et al.*, 2004). The clinical observation that signs of tissue inflammation and ischemia are present in many CRPS I patients led to the hypothesis that CRPS I might depend on an ischemia–reperfusion injury, which may at least in part induce the classical CRPS symptomatology. Consequently, an animal pain model was established that utilizes prolonged hindlimb ischemia for 3 h, followed by reperfusion, which produces a chronic postischemia pain syndrome. The reproducibility of this model awaits further confirmation.

In the future an integrative research approach on animal and human models combined with clinical research on patients who suffer from CRPS is a necessity if we are to unravel the mechanisms operating in CRPS and if we are to find the organising pathophysiological principles that orchestrate the different changes. It is essential that research on animal and human models and clinical investigations of CRPS should be closely aligned.

5.59.5.2 The Long Path Approaching the Central Nervous System

In recent years, research concentrated on investigation of peripheral mechanisms underlying the symptoms of CRPS. We are just now at a turning point recognising that important parts of the CRPS pathophysiology are obviously located within the CNS.

There is much evidence that the changed somatosensory perceptions observed in CRPS patients are likely due to changes in the central representation in the thalamus and cortex (Maleki, J. *et al.*, 2000). Positron emission tomography (PET) studies demonstrated adaptive changes in the thalamus during the course of the disease (Fukumoto, M. *et al.*, 1999). Furthermore, recent magnetic encephalography (MEG) and functional MRI (fMRI) studies revealed a shortened distance between little finger and thumb representations in the primary somatosensory (S1) cortex on the painful side (Maihofner, C. *et al.*, 2003; Pleger, B. *et al.*, 2004; Maihofner, C. *et al.*, 2005a). The MEG SI responses were increased on the

affected side, indicating processes of central sensitization (Juottonen, K. *et al.*, 2002). fMRI studies indicate that prefrontal cortical networks are involved in SMP in CRPS patients. Furthermore, in one CRPS patient a traumatic cerebral contusion of the left temporal lobe resolved the symptoms (Shibata, M. *et al.*, 1999; Apkarian, A. V. *et al.*, 2001).

We do not know the extent to which these central changes depend on continuous nociceptive input from the affected extremity; however, it has been shown that these generalized sensory changes may disappear after successful treatment of the pain (Maihofner, C. *et al.*, 2004; Pleger, B. *et al.*, 2005). In the future, we will fully understand that CRPS is a neurological disease affecting several functional systems that are closely integrated. This will include centers for the processing of cognitive and affective information.

5.59.5.3 A Possible Link between Inflammation and the Sympathetic Nervous System

In some patients sympatholytic procedures can ameliorate pain as well as inflammation and edema. Accordingly, animal studies have demonstrated that the sympathetic nervous system can influence the intensity of an inflammatory process (Levine, J. D. *et al.*, 1985; Jänig, W. *et al.*, 1996; Miao, F. J. *et al.*, 1996a; 1996b; Perl, E. R., 1996). The question arises whether the sympathetic nervous system might be involved in the inflammatory process in CRPS and whether it might interact with immune cells.

Under normal conditions, catecholamines act via β2-adrenoceptors on immune cells to inhibit the production and release of proinflammatory cytokines. These cells do not express α-adrenoceptors under basal conditions. However, the situation can dramatically change in chronic inflammation. Now, immune cells downregulate their expression of β2-adrenoceptors and upregulate their expression of α1-adrenoceptors over time (Gazda, L. S. *et al.*, 2001). In contrast to β2-adrenoceptors, α1-adrenoceptors stimulate the production and release of proinflammatory cytokines. If α1-adrenoceptors were to become expressed by the resident and/or recruited immune or immunocompetent cells of the affected CRPS extremity, then sympathetic activation would be predicted to cause pain and other inflammatory signs via cytokine release.

Summarizing the hypothetical ideas described above Figure 1 illustrates the possible interactions between sympathetic fibers, afferent fibers, blood vessels, and nonneural cells related to the immune system (e.g., macrophages) leading theoretically to the inflammatory changes observed in CRPS patients.

5.59.5.4 Do the Genes Predispose for Complex Regional Pain Syndrome?

One of the unsolved features in human pain diseases is the fact that only a minority of patients develop chronic pain after identical inciting events. Similarly, in certain nerve lesion animal models, differences in pain susceptibility were found to be due genetic factors (Mogil, J. S. *et al.*, 1999). To address this question in CRPS patients, gene technology has been used to characterize the genetic pattern of patients at risk to develop CRPS (Mailis, A. and Wade, J., 1994; 2001). In a cohort of 52 CRPS patients, class I and II major histocompatibility antigens were typed. The frequency of HLA-DQ1 was found to be significantly increased compared with control frequencies (Kemler, M. A. *et al.*, 1999). In patients with CRPS who progressed towards multifocal or generalized tonic dystonia an association with HLA-DR13 was reported (van Hilten, J. J. *et al.*, 2000). Furthermore, a different locus, centromeric in HLA-class I, was found to be associated with spontaneous development of CRPS, suggesting an interaction between trauma severity and genetic factors that describe CRPS susceptibility (van de Beek, W. J. *et al.*, 2003).

5.59.5.5 The Future Need for Diagnostic Procedures

To design experiments in CRPS patients, it is important to define the population as precisely as possible. An exact diagnostic classification of the study cohort is essential to perform clinical treatment trials on a homogeneous group.

5.59.5.5.1 Validation of clinical diagnostic criteria

The definition of standardized diagnostic criteria for CRPS in 1995 was a major advance (Stanton-Hicks, M. *et al.*, 1995). However, these criteria were derived based upon the consensus opinion of a small group of expert clinicians. While this was an appropriate first step it is important to continuously improve the criteria, i.e., to validate and, if necessary, modify these initial consensus-based criteria based upon results of systematic validation research. The CRPS diagnostic criteria were adequately sensitive (i.e., rarely miss a case of actual CRPS). However, both internal and external

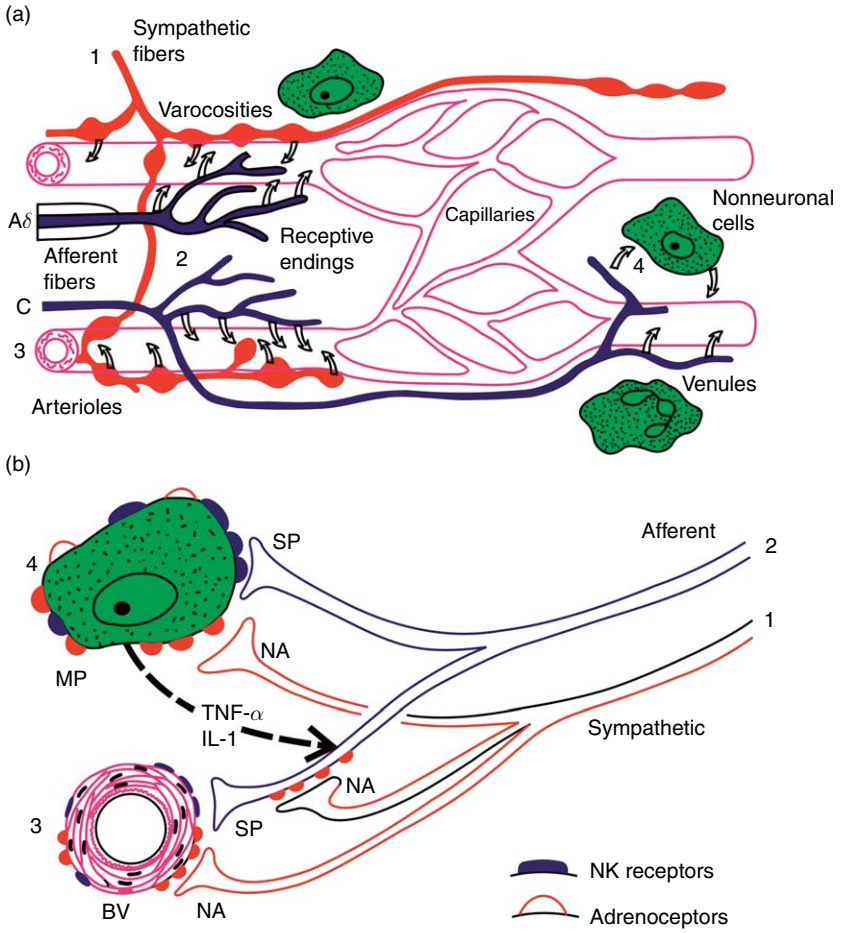

Figure 1 (a) The micromilieu of nociceptors. The microenvironment of primary afferents is thought to affect the properties of the receptive endings of myelinated (A) and unmyelinated (C) afferent fibers. This has been particularly documented for inflammatory processes, but one may speculate that pathological changes in the direct surroundings of primary afferents may contribute to other pain states as well. The vascular bed consists of arterioles (directly innervated by sympathetic and afferent fibers), capillaries (not innervated and not influenced by nerve fibers), and venules (not directly innervated but influenced by nerve fibers). The micromilieu depends on several interacting components: Neural activity in postganglionic noradrenergic fibers (1) supplying blood vessels (3, BV) causes release of noradrenaline (NA) and possibly other substances and vasoconstriction. Excitation of primary afferents (Aδ and C fibers) (2) causes vasodilation in precapillary arterioles and plasma extravasation in postcapillary venules (C fibers only) by the release of substance P (SP) and other vasoactive compounds (e.g., calcitonin gene-related peptide, CGRP). Some of these effects may be mediated by nonneuronal cells such as mast cells and macrophages (4). Other factors that affect the control of the microcirculation are the myogenic properties of arterioles (3) and more global environmental influences such as a change of the temperature and the metabolic state of the tissue. (b) Hypothetical relation between sympathetic noradrenergic nerve fibers (1), peptidergic afferent nerve fibers (2), blood vessels (3), and macrophages (4). The activated and sensitized afferent nerve fibers activate macrophages (MP) possibly via SP release. The immune cells start to release cytokines, such as tumor necrosis factor alpha (TNF-α) and interleukin-1 (IL-1), which further activate afferent fibers. SP (and CGRP) released from the afferent nerve fibers reacts with neurokinin 1 (NK1) receptors in the blood vessels (arteriolar vasodilation, venular plasma extravasation, neurogenic inflammation). The sympathetic nerve fibers interact with this system on three levels: (1) via adrenoceptors (mainly α) on the blood vessels (vasoconstriction); (2) via adrenoceptors (mainly β) on macrophages (further release of cytokines), and (3) via adrenoceptors (mainly α) on afferents (further sensitization of these fibers.) Adapted from Janig, W. and Baron, R. 2003. Complex regional pain syndrome: mystery explained? Lancet Neurol. 2, 687–697.

validation research suggests that CRPS was overdiagnosed (Bruehl, S. *et al.*, 1999; Harden, R. N. *et al.*, 1999). For example, an external validation of the International Association for the Study of Pain (IASP) criteria in 117 patients with CRPS and 43 patients with neuropathic pain without CRPS etiology demonstrated a sensitivity of 0.98 and a specificity of 0.36. The inclusion of a category motor and trophic signs and symptoms, for

Table 1 Revised diagnostic criteria for CRPS

A. Continuing pain, which is disproportionate to any inciting event
B. Categories of clinical signs/symptoms
1. Positive sensory abnormalities
2. Vascular abnormalities
Vasodilation
Vasoconstriction
Skin temperature asymmetries
Skin color changes
3. Edema, sweating abnormalities
Swelling
Hyperhidrosis
Hypohidrosis
4. Motor, trophic changes
Motor weakness
Tremor
Dystonia
Coordination deficits
Nail, hair changes
Skin atrophy
Joint stiffness
Soft tissue
Interpretation
Clinical use
≥1 Symptoms in ≥3 of the categories AND ≥1 signs at time of evaluation in ≥2 of the categories
Sensitivity = 0.85, specificity = 0.60
Research use
≥1 Symptoms in each of the categories each AND ≥1 signs at the time of evaluation in ≥2 of the categories each
Sensitivity = 0.70, specificity = 0.96

CRPS, complex regional pain syndrome.

example, improves specificity considerably without losing sensitivity (Bruehl, S. *et al*., 2002).

Based on this validation research a novel diagnostic algorithm was recently proposed (Table 1, Baron, R. and Janig, W., 2004; Burton, A. W. *et al*., 2005). In addition to the improved clinical categories, it became clear to distinguish between criteria for clinical use and a classification for research purposes. For the clinician and in particular for the patients, it is important to have a high sensitivity value combined with a fair specificity (e.g., 0.85 vs. 0.60, Table 1). For research purposes, however, it is much more important to have a high specificity in order to perform studies in a precisely diagnosed population (e.g., 0.7 vs. 0.96, Table 1).

5.59.5.5.2 Tests which aid the diagnosis of complex regional pain syndrome

Several diagnostic procedures have been evaluated in recent years (Table 2). New techniques to assess specific signs objectively are in the experimental testing phase. Cortical reorganization underlying somatosensory and motor abnormalities can be visualized using MEG and fMRI. Video-assisted kinematic analysis and tremor analysis is used to quantify and qualify motor abnormalities like weakness, coordination deficits and tremor. The acute inflammatory component of the disorder, in particular the role of specific inflammatory mediators, are explored using microdialysis techniques and analysing the content of suction blister fluid. These and other investigations will pave the way for a quantitative and objective analysis of these abnormalities. Furthermore, genetic patterns of patients at risk to develop CRPS have already been revealed and more genes determining the susceptible patient are to come.

Table 2 Diagnostic tests in CRPS

	Sensitivity	*Specificity*
Plain radiograph (only chronic stages)	73	57
Bone scan (only acute stages)	97	86
Quantitative sensory testing (QST)	High	Low
Temperature differences (during sympathetic stimulation)	76	93
MRI (skin, joint, etc.)	91	17

CRPS, complex regional pain syndrome; MRI, magnetic resonance imaging.

In summary, we have to stimulate researchers from various fields to unravel the diagnostic puzzle of the CRPS mystery using an interdisciplinary research approach.

Acknowledgments

This work was supported by the Deutsche Forschungsgemeinschaft (DFG Ba 1921/1-2), the German Ministry of Research and Education within the German Research Network on Neuropathic Pain (BMBF, 01EM01/04) and an unrestricted educational grant of Pfizer (Germany).

References

Alexander, G. M., van Rijn, M. A., van Hilten, J. J., Perreault, M. J., and Schwartzman, R. J. 2005. Changes in cerebrospinal fluid levels of pro-inflammatory cytokines in CRPS. Pain 116, 213–219.

Ali, Z., Raja, S. N., Wesselmann, U., Fuchs, P., Meyer, R. A., and Campbell, J. N. 2000. Intradermal injection of norepinephrine

evokes pain in patients with sympathetically maintained pain. Pain 88, 161–168.
Apkarian, A. V., Thomas, P. S., Krauss, B. R., and Szeverenyi, N. M. 2001. Prefrontal cortical hyperactivity in patients with sympathetically mediated chronic pain. Neurosci. Lett. 311, 193–197.
Baron, R. 2004. Mechanistic and clinical aspects of complex regional pain syndrome (CRPS). Novartis Found. Symp. 261, 220–233; discussion 233–238, 256–261.
Baron, R. and Janig, W. 2004. Complex regional pain syndromes – how do we escape the diagnostic trap? Lancet 364, 1739–1741.
Baron, R. and Wasner, G. 2001. Complex regional pain syndromes. Curr. Pain Headache Rep. 5, 114–123.
Baron, R., Fields, H. L., Janig, W., Kitt, C., and Levine, J. D. 2002a. National Institutes of Health Workshop: reflex sympathetic dystrophy/complex regional pain syndromes – state-of-the-science. Anesth. Analg. 95, 1812–1816.
Baron, R., Levine, J. D., and Fields, H. L. 1999. Causalgia and reflex sympathetic dystrophy: Does the sympathetic nervous system contribute to the generation of pain? Muscle Nerve 22, 678–695.
Baron, R., Schattschneider, J., Binder, A., Siebrecht, D., and Wasner, G. 2002b. Relation between sympathetic vasoconstrictor activity and pain and hyperalgesia in complex regional pain syndromes: a case–control study. Lancet 359, 1655–1660.
Bhatia, K. P., Bhatt, M. H., and Marsden, C. D. 1993. The causalgia–dystonia syndrome. Brain 116, 843–851.
Birklein, F., Schmelz, M., Schifter, S., and Weber, M. 2001. The important role of neuropeptides in complex regional pain syndrome. Neurology 57, 2179–2184.
Blaes, F., Schmitz, K., Tschernatsch, M., Kaps, M., Krasenbrink, I., Hempelmann, G., and Brau, M. E. 2004. Autoimmune etiology of complex regional pain syndrome (M. Sudeck). Neurology 63, 1734–1736.
Bruehl, S., Harden, R. N., Galer, B. S., Saltz, S., Backonja, M., and Stanton-Hicks, M. 2002. Complex regional pain syndrome: are there distinct subtypes and sequential stages of the syndrome? Pain 95, 119–124.
Bruehl, S., Harden, R. N., Galer, B. S., Saltz, S., Bertram, M., Backonja, M., Gayles, R., Rudin, N., Bhugra, M. K., and Stanton-Hicks, M. 1999. External validation of IASP diagnostic criteria for Complex Regional Pain Syndrome and proposed research diagnostic criteria. Pain 81, 147–154.
Burton, A. W., Bruehl, S., and Harden, R. N. 2005. Current diagnosis and therapy of complex regional pain syndrome: refining diagnostic criteria and therapeutic options. Expert Rev. Neurother. 5, 643–651.
Calder, J. S., Holten, I., and McAllister, R. M. 1998. Evidence for immune system involvement in reflex sympathetic dystrophy. J. Hand Surg. [Br.] 23, 147–150.
Coderre, T. J., Xanthos, D. N., Francis, L., and Bennett, G. J. 2004. Chronic post-ischemia pain (CPIP): a novel animal model of complex regional pain syndrome – Type I (CRPS-I; reflex sympathetic dystrophy) produced by prolonged hindpaw ischemia and reperfusion in the rat. Pain 112, 94–105.
Deuschl, G., Blumberg, H., and Lücking, C. H. 1991. Tremor in reflex sympathetic dystrophy. Arch. Neurol. 48, 1247–1252.
Fukumoto, M., Ushida, T., Zinchuk, V. S., Yamamoto, H., and Yoshida, S. 1999. Contralateral thalamic perfusion in patients with reflex sympathetic dystrophy syndrome. Lancet 354, 1790–1791.
Galer, B. S., Butler, S., and Jensen, M. P. 1995. Case reports and hypothesis: a neglect-like syndrome may be responsible for the motor disturbance in reflex sympathetic dystrophy (Complex Regional Pain Syndrome – 1). J. Pain Symptom Manage. 10, 385–391.
Gazda, L. S., Milligan, E. D., Hansen, M. K., Twining, C. M., Poulos, N. M., Chacur, M., O'Connor, K. A., Armstrong, C., Maier, S. F., Watkins, L. R., and Myers, R. R. 2001. Sciatic inflammatory neuritis (SIN): behavioral allodynia is paralleled by peri-sciatic proinflammatory cytokine and superoxide production. J. Peripher. Nerv. Syst. 6, 111–129.
Goebel, A., Vogel, H., Caneris, O., Bajwa, Z., Clover, L., Roewer, N., Schedel, R., Karch, H., Sprotte, G., and Vincent, A. 2005. Immune responses to *Campylobacter* and serum autoantibodies in patients with complex regional pain syndrome. J. Neuroimmunol. 162, 184–189.
Graif, M., Schweitzer, M. E., Marks, B., Matteucci, T., and Mandel, S. 1998. Synovial effusion in reflex sympathetic dystrophy: an additional sign for diagnosis and staging. Skeletal Radiol. 27, 262–265.
Harden, R. N., Bruehl, S., Galer, B. S., Saltz, S., Bertram, M., Backonja, M., Gayles, R., Rudin, N., Bhugra, M. K., and Stanton-Hicks, M. 1999. Complex regional pain syndrome: are the IASP diagnostic criteria valid and sufficiently comprehensive? Pain 83, 211–219.
Huygen, F. J., De Bruijn, A. G., De Bruin, M. T., Groeneweg, J. G., Klein, J., and Zijistra, F. J. 2002. Evidence for local inflammation in complex regional pain syndrome type 1. Mediators Inflamm. 11, 47–51.
Huygen, F. J., de Bruijn, A. G., Klein, J., and Zijlstra, F. J. 2001. Neuroimmune alterations in the complex regional pain syndrome. Eur. J. Pharmacol. 429, 101–113.
Janig, W. and Baron, R. 2003. Complex regional pain syndrome: mystery explained? Lancet Neurol. 2, 687–697.
Jänig, W., Levine, J. D., and Michaelis, M. 1996. Interactions of sympathetic and primary afferent neurons following nerve injury and tissue trauma. Prog. Brain Res. 113, 161–184.
Juottonen, K., Gockel, M., Silen, T., Hurri, H., Hari, R., and Forss, N. 2002. Altered central sensorimotor processing in patients with complex regional pain syndrome. Pain 98, 315–323.
Kemler, M. A., van de Vusse, A. C., van den Berg-Loonen, E. M., Barendse, G. A., van Kleef, M., and Weber, W. E. 1999. HLA-DQ1 associated with reflex sympathetic dystrophy. Neurology 53, 1350–1351.
Leitha, T., Korpan, M., Staudenherz, A., Wunderbaldinger, P., and Fialka, V. 1996. Five phase bone scintigraphy supports the pathophysiological concept of a subclinical inflammatory process in reflex sympathetic dystrophy. Q. J. Nucl. Med. 40, 188–193.
Levine, J. D., Dardick, S. J., Basbaum, A. I., and Scipio, E. 1985. Reflex neurogenic inflammation. I. Contribution of the peripheral nervous system to spatially remote inflammatory responses that follow injury. J. Neurosci. 5, 1380–1386.
Maihofner, C., Forster, C., Birklein, F., Neundorfer, B., and Handwerker, H. O. 2005a. Brain processing during mechanical hyperalgesia in complex regional pain syndrome: a functional MRI study. Pain 114, 93–103.
Maihofner, C., Handwerker, H. O., Neundorfer, B., and Birklein, F. 2003. Patterns of cortical reorganization in complex regional pain syndrome. Neurology 61, 1707–1715.
Maihofner, C., Handwerker, H. O., Neundorfer, B., and Birklein, F. 2004. Cortical reorganization during recovery from complex regional pain syndrome. Neurology 63, 693–701.
Maihofner, C., Handwerker, H. O., Neundorfer, B., and Birklein, F. 2005b. Mechanical hyperalgesia in complex regional pain syndrome: a role for TNF-alpha? Neurology 65, 311–313.
Mailis, A. and Wade, J. 1994. Profile of Caucasian women with possible genetic predisposition to reflex sympathetic dystrophy: a pilot study. Clin. J. Pain 10, 210–217.
Mailis, A. and Wade, J. 2001. Genetic Considerations in CRPS. In: Complex Regional Pain Syndrome (*eds*. R. N. Harden, R. Baron, and W. Jänig), Vol. 22, pp. 227–238. IASP Press.

Maleki, J., LeBel, A. A., Bennett, G. J., and Schwartzman, R. J. 2000. Patterns of spread in complex regional pain syndrome, type I (reflex sympathetic dystrophy). Pain 88, 259–266.

McCabe, C. S., Haigh, R. C., Ring, E. F., Halligan, P. W., Wall, P. D., and Blake, D. R. 2003. A controlled pilot study of the utility of mirror visual feedback in the treatment of complex regional pain syndrome (type 1). Rheumatology (Oxford) 42, 97–101.

Miao, F. J., Green, P. G., Coderre, T. J., Janig, W., and Levine, J. D. 1996a. Sympathetic-dependence in bradykinin-induced synovial plasma extravasation is dose-related. Neurosci. Lett. 205, 165–168.

Miao, F. J., Janig, W., Green, P. G., and Levine, J. D. 1996b. Inhibition of bradykinin-induced synovial plasma extravasation produced by intrathecal nicotine is mediated by the hypothalamopituitary adrenal axis. J. Neurophysiol. 76, 2813–2821.

Mogil, J. S., Wilson, S. G., Bon, K., Lee, S. E., Chung, K., Raber, P., Pieper, J. O., Hain, H. S., Belknap, J. K., Hubert, L., Elmer, G. I., Chung, J. M., and Devor, M. 1999. Heritability of nociception I: responses of 11 inbred mouse strains on 12 measures of nociception. Pain 80, 67–82.

Moseley, G. L. 2004. Graded motor imagery is effective for long-standing complex regional pain syndrome: a randomised controlled trial. Pain 108, 192–198.

Oyen, W. J., Arntz, I. E., Claessens, R. M., Van der Meer, J. W., Corstens, F. H., and Goris, R. J. 1993. Reflex sympathetic dystrophy of the hand: an excessive inflammatory response? Pain 55, 151–157.

Perl, E. R. 1996. Cutaneous polymodal receptors: characteristics and plasticity. Prog. Brain Res. 113, 21–37.

Pleger, B., Tegenthoff, M., Ragert, P., Forster, A. F., Dinse, H. R., Schwenkreis, P., Nicolas, V., and Maier, C. 2005. Sensorimotor retuning [corrected] in complex regional pain syndrome parallels pain reduction. Ann. Neurol. 57, 425–429.

Pleger, B., Tegenthoff, M., Schwenkreis, P., Janssen, F., Ragert, P., Dinse, H. R., Volker, B., Zenz, M., and Maier, C. 2004. Mean sustained pain levels are linked to hemispherical side-to-side differences of primary somatosensory cortex in the complex regional pain syndrome I. Exp. Brain Res. 155, 115–119.

Renier, J. C., Arlet, J., Bregeon, C., Basle, M., Seret, P., Acquaviva, P., Schiano, A., Serratrice, G., Amor, B., May, V., Delcambre, B., D'Eshoughes, J. R., Vincent, G., Ducastelle, F., and Pawlotsky, Y. 1983. The joint in algodystrophy. Joint fluid, synovium, cartilage. Rev. Rhum. Mal. Osteoartic. 50, 255–260.

Ribbers, G. M., Mulder, T., Geurts, A. C., and den Otter, R. A. 2002. Reflex sympathetic dystrophy of the left hand and motor impairments of the unaffected right hand: impaired central motor processing? Arch. Phys. Med. Rehabil. 83, 81–85.

Schattschneider, J., Wenzelburger, R., Deuschl, G., and Baron, R. 2001. Kinematic Analysis of the Upper Extremity in CRPS. In: Complex Regional Pain Syndrome, Vol. 22 (*eds*. R. N. Harden, R. Baron, and W. Jänig), pp. 119–128. IASP Press.

Schwenkreis, P., Janssen, F., Rommel, O., Pleger, B., Volker, B., Hosbach, I., Dertwinkel, R., Maier, C., and Tegenthoff, M. 2003. Bilateral motor cortex disinhibition in complex regional pain syndrome (CRPS) type I of the hand. Neurology 61, 515–519.

Shibata, M., Nakao, K., Galer, B. S., Shimizu, T., Taniguchi, H., and Uchida, T. 1999. A case of reflex sympathetic dystrophy (complex regional pain syndrome, type I) resolved by cerebral contusion. Pain 79, 313–315.

Stanton-Hicks, M., Janig, W., Hassenbusch, S., Haddox, J. D., Boas, R., and Wilson, P. 1995. Reflex sympathetic dystrophy: changing concepts and taxonomy. Pain 63, 127–133.

Sudeck, P. 1902. Über die akute (trophoneurotische) Knochenatrophie nach Entzündungen und Traumen der Extremitäten. Deut. Med. Wschr. 28, 336–342.

Sudeck, P. 1931. Die trophische Extremitätenstörung durch periphere (infektiöse und traumatische) Reize. Deutsch. Zeitschr. Chirurg. 234, 596–612.

van de Beek, W. J., Roep, B. O., van der Slik, A. R., Giphart, M. J., and van Hilten, B. J. 2003. Susceptibility loci for complex regional pain syndrome. Pain 103, 93–97.

van der Laan, L. and Goris, R. J. 1997. Reflex sympathetic dystrophy. An exaggerated regional inflammatory response? Hand Clin. 13, 373–385.

van Hilten, J. J., van de Beek, W. J., and Roep, B. O. 2000. Multifocal or generalized tonic dystonia of complex regional pain syndrome: a distinct clinical entity associated with HLA-DR13. Ann. Neurol. 48, 113–116.

Wasner, G., Heckmann, K., Maier, C., and Baron, R. 1999. Vascular abnormalities in acute reflex sympathetic dystrophy (CRPS I) – complete inhibition of sympathetic nerve activity with recovery. Arch. Neurol. 56, 613–620.

Wasner, G., Schattschneider, J., Binder, A., and Baron, R. 2003. Complex regional pain syndrome – diagnostic, mechanisms, CNS involvement and therapy. Spinal Cord 41, 61–75.

Wasner, G., Schattschneider, J., Heckmann, K., Maier, C., and Baron, R. 2001. Vascular abnormalities in reflex sympathetic dystrophy (CRPS I): mechanisms and diagnostic value. Brain 124, 587–599.

Weber, M., Birklein, F., Neundorfer, B., and Schmelz, M. 2001. Facilitated neurogenic inflammation in complex regional pain syndrome. Pain 91, 251–257.

5.60 Poststroke Pain

T S Jensen and N B Finnerup, Aarhus University Hospital, Aarhus, Denmark

© 2008 Elsevier Inc. All rights reserved.

5.60.1	**Introduction**	919
5.60.2	**Characteristics of Central Pain After Stroke**	919
5.60.2.1	Symptoms in Central Pain	920
5.60.2.2	Sensory Abnormalities	920
5.60.3	**Epidemiology of Poststroke Pain**	921
5.60.4	**Mechanisms of Pain**	922
5.60.5	**Treatment**	923
5.60.5.1	Antidepressants	923
5.60.5.2	Sodium Channel Blockers	923
5.60.5.3	Opioids	923
5.60.5.4	Gabapentin	924
5.60.5.5	GABA Agonists	924
5.60.5.6	Treatment Option	924
References		924

Glossary

allodynia Pain due to a stimulus that does not normally provoke pain.

central pain Pain initiated or caused by a primary lesion or dysfunction in the central nervous system.

hyperalgesia An increased response to a stimulus that is normally painful.

5.60.1 Introduction

Central poststroke pain (PSP) is defined as pain directly caused by a cerebrovascular lesion, regardless of the anatomical location within the central nervous system (CNS).

Neuropathic pain has mainly been discussed in the context of peripheral neuropathic pain, that is, conditions where the injury or the dysfunction is located within the peripheral nervous system (Jensen, T. S. *et al.*, 2001b). Typical examples of diseases affecting the peripheral nervous system giving rise to pain are painful polyneuropathies, such as diabetic neuropathy and toxic neuropathies, postherpetic neuralgia, trigemenial neuralgia, and nerve injuries. Although probably less common and more complex in nature, central neuropathic pain conditions share some of the same phenomena seen in peripheral neuropathic pain, that is, sensory loss in part of the territory with pain, the paradoxical presence of lost sensibility, and hypersensitivity to one or several submodalities of pain (Tasker, R. R. *et al.*, 1991; Schott, G. D., 1995; Bowsher, D. *et al.*, 1998; Boivie, J., 1999). This chapter will briefly review central neuropathic pain after stroke: its underlying mechanisms, clinical picture, and management.

5.60.2 Characteristics of Central Pain After Stroke

Despite the heterogeneity in etiology and anatomical location, neuropathic pains share certain characteristics (Boivie, J., 1999; Woolf, C. J. and Mannion, R. J., 1999; Jensen, T. S. *et al.*, 2001b; Dworkin, R. H. *et al.*, 2003):

- Pain located in a neuroanatomically defined area with partial or complete sensory loss.

- Ongoing pain (stimulus independent).
- Evoked types of pain (stimulus dependent).
- Hypersensitivity.

These symptoms and signs may occur in various combinations but do not necessarily have to be present altogether at the same time and in all patients affected by the same disease. There are no universally accepted criteria for PSP, but the following seem to be minimal criteria:

- A confirmed cerebrovascular accident.
- Development of pain after stroke.
- Sensory abnormality (hypo- or hypersensitivity to temperature or pinprick) in a body area corresponding to the CNS region damaged by the stroke.
- Pain located within the body area of sensory abnormality.

5.60.2.1 Symptoms in Central Pain

As for peripheral neuropathic pain, central pains are characterized by the presence of spontaneous types of pain and various types of evoked pains (Boivie, J., 1999; Jensen, T. S. *et al.*, 2001b).

Ongoing pains. These pains are spontaneous and may be continuous or paroxysmal. The character differs, but they can be shooting, shock-like, aching, cramping, crushing, smarting, burning, etc. No specific pain character has been associated with PSP (Boivie, J., 1999).

Evoked pains. The stimulus-evoked pains are classified according to the type of stimulus that provokes them. Several types of evoked pains can be present; the most prominent types in PSP are mechanical and thermal.

In some patients ongoing pain is dominating, in others evoked pain. Some patients have several of these phenomena, others only one type of hyperalgesia. For example, in some patients with neuropathy, cold allodynia may be the only abnormality present. Therefore, a number of different stimuli have to be used to document or exclude abnormality. The evoked pains are usually brief, lasting only for the duration of stimulation, but sometimes they can persist even after cessation of stimulation causing aftersensations (see below), which can last for minutes, hours, or perhaps days. In such cases, the distinction between evoked and spontaneous pain can be difficult. Both evoked and spontaneous pains may be confined to deep structures.

5.60.2.2 Sensory Abnormalities

Sensory disturbances are key phenomena in patients with PSP and a variety of disturbances may be present.

Sensory deficit and pain. An essential part of neuropathic pain is a loss (partial or complete) of afferent sensory function. In some patients the sensory deficit may be gross, in others subtle and difficult to detect with bedside methods, but quantitative testing can usually disclose minor changes. The sensory loss may involve all sensory abnormalities, but a loss of spinothalamic functions (cold, warmth, and pinprick) appears to be crucial, and there is now some evidence to indicate that spinothalamic loss is a necessary, albeit not sufficient, requirement for the development and maintenance of pain (Andersen, G. *et al.*, 1995; Vestergaard, K. *et al.*, 1995). In the study by Andersen G. *et al.* (1995), decreased sensibility to all types of stimuli was seen in the same proportion of patients, regardless of the presence of pain. It can occasionally be difficult to document sensory loss because of the additional presence of hypersensitivity phenomena in the same area.

Sensory hypersensitivity and pain. Another characteristic of PSP is the paradoxical presence of hyperphenomena in the painful area. These hyperphenomena may be present as hypersensitivity, allodynia, or dysesthesia to one or several sensory modalities (touch, pinprick, cold, or warmth). Allodynia or hypersensitivity has mainly been noted as a cutaneous phenomenon, but it was originally suggested that allodynia could also be present in deep structures as a hyperalgesia to pressure (Vestergaard, K. *et al.*, 1995). Consistent with this observation, Bowsher D. *et al.* (1998) noted movement-induced allodynia in 9 of 73 patients, and in another study, 22% of 92 patients with central pain had movement-induced pain (Bowsher, D., 1996). A dissociation of cutaneous and deep sensibility has been noted in three case reports (Mailis, A. and Bennett, G. J., 2002). In the study by Andersen G. *et al.* (1995), cold allodynia/dysesthesia was present in 88% of PSP patients but only in 3% of stroke patients with nonpainful sensory abnormalities. Similarly, 75% had touch-evoked allodynia or dysesthesia while none in the group without pain had these abnormalities. In the study by Bowsher D. *et al.* (1998), 59% of the patients had allodynia mostly seen as a mechanical allodynia. Abnormal temperature and pain sensibility are the most consistent abnormalities in PSP. In two studies, it was found that 81%

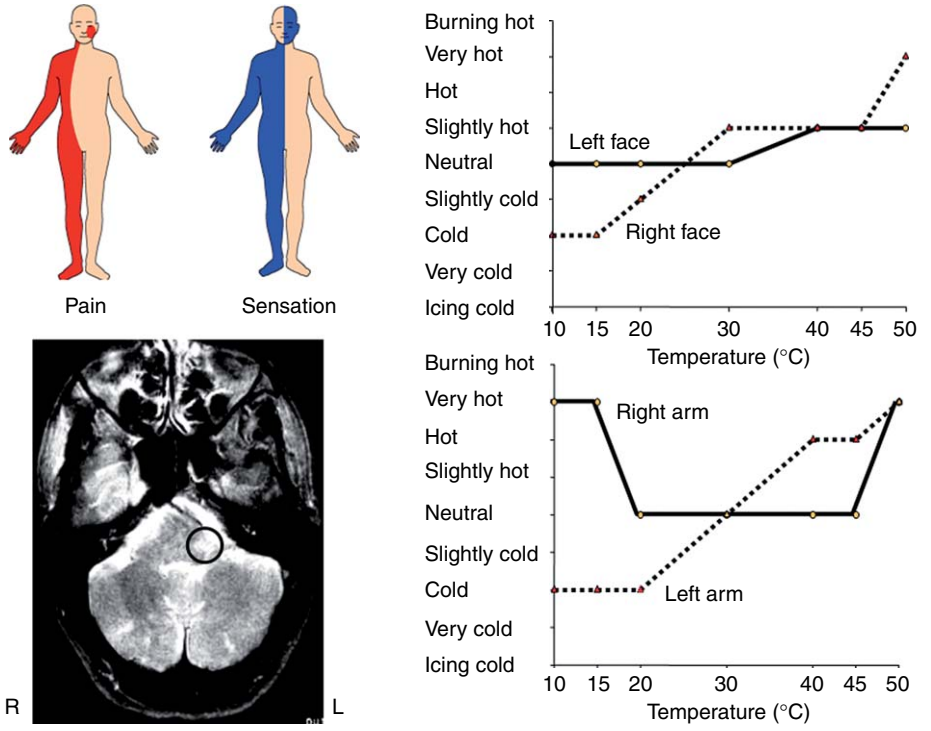

Figure 1 A case presenting a 75-year-old patient with lateral medullary infarction and central pain. At the age of 68, he experienced short-lasting vertigo. At the age of 72, he had a left brain infarction with left facial and right hemibody ongoing pain and burning pain evoked by touch. The magnetic resonance imaging (MRI) scan shows a left lateral medullary infarction. Stimulus–response functions of cold and warm stimuli in the patient using a thermotester showing decreased thermal sensation on the left side of the face and paradoxical sensitivity to cold on the left side of the body.

had reduced sensibility to temperature (Boivie, J., 1989; Andersen, G. *et al.*, 1995). In some studies, on the other hand, sensation to touch is only reduced in a smaller proportion of patients (Boivie, J., 1989).

Based on the observation that thermal sensation is also disturbed in a large proportion of stroke patients with no pain, it has been concluded that loss of spinothalamic function mediating thermal stimuli is a necessary, but probably not a sufficient condition for the development of PSP (Jensen, T. S. and Lenz, F. A., 1995). In addition to the sensory deficit, some patients may have a paradoxical sensitivity to cold and heat so that cold is perceived as hot and vice versa. An example of a patient with a lateral medullary infarction and such a sensory pattern is shown in Figure 1.

5.60.3 Epidemiology of Poststroke Pain

There is limited information on the frequency of PSP. A prospective study found that 8.4% of 191 unselected consecutive stroke patients developed PSP within the first year after stroke (Andersen, G. *et al.*, 1995). In an unpublished study from the UK, the frequency of PSP was found to be 11% in a group of stroke patients aged 80 years and above (Bowsher, D., personal communication).

In 63 patients with lateral medullary infarction, 16 (25%) developed central pain within 6 months after stroke. There was a significant relationship between the degree of sensory loss and the development of pain, suggesting to the authors that pain is a result of a lesion of the neospinothalamic system, which causes a denervation sensitivity of the paleospinothalamic system. In patients with sensory disturbances, the frequency of pain is much higher: thus 44% in one series (MacGowan, D. J. *et al.*, 1997) and 18% in another series (Andersen, G. *et al.*, 1995).

Stroke lesion. Both infarcts and hemorrhages may cause PSP (Andersen, G. *et al.*, 1995; Bowsher, D. *et al.*, 1998; Kim, J. S., 2003). Based on the fact that ischemic lesions are 7–8 times more frequent than are hemorrhages, infarction is the most common cause for PSP. Lesions are known to occur at any level of

the spinothalamic pathways and its cortical projection. Previous studies using computed tomography (CT) imaging show that the lesion involves the thalamus in one-fourth to one-third of cases (Bogousslavsky, J. *et al.*, 1988; Leijon, G. *et al.*, 1989; Andersen, G. *et al.*, 1995). In one study of PSP, more than 60% of patients had a lesion of the ventroposterior thalamic nucleus demonstrated by magnetic resonance imaging (MRI) (Bowsher, D. *et al.*, 1998). In a series of 63 patients with lateral medullary infarctions, it was found that 16 patients (25%) developed a PSP within 6 months after their stroke (MacGowan, D. J. *et al.*, 1997). In another series of 55 patients with medullary infarctions, 24 patients had sensory complaints from the face (Kim, J. S. and Choi-Kwon, S., 1999).

5.60.4 Mechanisms of Pain

The pathophysiological mechanisms underlying peripheral neuropathic pain have been reviewed extensively in recent years (Besson, J. M., 1999; Woolf, C. J. and Salter, M. W., 2000; Koltzenburg, M. and Scadding, J., 2001; Jensen, T. S. *et al.*, 2001a; Bolay, H. and Moskowitz, M. A., 2002).

Evidence from a large number of studies indicates that neuronal hyperexcitability, either at the level of the peripheral receptor or centrally, plays a key role in generating pain after nerve injury. The mechanisms responsible for central pain after stroke are much less clear. The combination of symptoms and signs is compatible with a general sensitization of second- or third-order neurons in the CNS that have lost part of their normal patterned input and are substituted by a changed afferent influx. In fact, sensitization is today considered to be an essential phenomenon behind persistent neuropathic pains (Woolf, C. J. and Salter, M. W., 2000; Woolf, C. J. and Max, M. B., 2001; Dworkin, R. H. *et al.*, 2003; Jensen, T. S. and Baron, R., 2003).

Patients with central pain display ongoing spontaneous pain and abnormally evoked pain with hypersensitivity to noxious and nonnoxious stimuli in the painful area. These findings suggest that hypersensitive pools of cells are present in the nervous system and that they probably are involved in generating pain (Tasker, R. R. *et al.*, 1991; Jensen, T. S. and Lenz, F. A., 1995; Schott, G. D., 1995). Several hypotheses have been forwarded. The most important ones are summarized briefly below:

Spinothalamic tract lesion. Sensory examination and more elaborative quantitative sensory analysis show that patients with PSP have abnormal temperature and pain sensitivity, but normal epicritic sensibility (touch, vibration, and pressure). In addition, it is well known that dorsolateral infarctions of the lower medulla and cordotomies, two conditions characterized by loss of spinothalamic but preservation of lemniscal pathways, cause central pain (Boivie, J. *et al.*, 1989; Vestergaard, K. *et al.*, 1995; Nathan, P. W. *et al.*, 2001).

Subsequent studies have indicated that while a spinothalamic tract lesion and its cortical projection is necessary for the development of pain, it is not sufficient for the development of central pain (Jensen, T. S. and Lenz, F. A., 1995) since similar somatosensory disturbances may occur in stroke patients without pain (Andersen, G. *et al.*, 1995; Vestergaard, K. *et al.*, 1995).

Lemniscal disinhibition. In their original description Head H. and Holmes G. (1911) suggested that injury to the lateral part of thalamus sets free a medial thalamic center and the result is allodynia to all types of stimuli. A consequence of this theory is that sensory modalities such as touch, vibration, and pressure conveyed by the lemniscal system exert a control over pain and temperature, so that sensory deficit in discrimination causes spontaneous pain and allodynia.

Loss of normal cold inhibition. On the basis of experimental studies in animals and in humans, Craig A. D. (2000) has suggested that central pain is due to loss of a normal inhibitory effect exerted by cool-signaling pathways from lamina I projecting to the thalamus and insula. According to this hypothesis, a lesion of the lateral cool projection system disinhibits the medial system of heat–pinch–cold neurons passing from lamina I to the medial part of the thalamus. This disinhibition then results in the release of cold allodynia and burning and ongoing pain (Craig, A. D. and Bushnell, M. C., 1994; Craig, A. D., 2000). Disruption of thermosensory integrations leads to a disinhibition of noxious responding thalamocortical neurons and a sensation of burning pain (Craig, A. D., 2000). The hypothesis and the processing of cold proposed by Craig has been criticized by Willis W. D. Jr. *et al.* (2002), and more recently, Greenspan J. D. *et al.* (2004) suggested, based on studies in 13 patients with PSP, that cold allodynia is not caused by loss of normal cold pathway but is rather due to input via an intact cold pathway driving nociceptive neurons in the thalamus. So it is still unclear whether and to what

extent an intact cold pathway plays a role for the cold allodynia seen in stroke patients.

Thalamus and PSP. In all instances of PSP, the thalamus is thought to play a role for the pain. The most critical parts of the thalamus are the ventroposterior part, the medial intralaminar nuclei, and the reticular nucleus, but the exact mechanisms of central pain are still unclear. Based on clinical and experimental observations, it has been suggested that the development of PSP may be related to an imbalance in the activity of the spinothalamic and reticulothalamic systems so that if the former is damaged, as for example in medullary infarction, this may result in pain from non-noxious stimuli via the reticulothalamic pathway (Tasker, R. R. *et al.*, 1991; MacGowan, D. J. *et al.*, 1997).

5.60.5 Treatment

There is limited amount of data on pharmacological treatment of PSP and no evidence to support treatment of the individual patient based on symptoms and signs. Pharmacological agents used to treat PSP share the ability to interfere with some of the processes involved in neuronal hyperexcitability either by decreasing excitatory or by increasing inhibitory transmission, thereby exerting a neuronal depressant effect.

5.60.5.1 Antidepressants

Tricyclic antidepressants inhibit the presynaptic reuptake of noradrenaline and serotonin and interfere with *N*-methyl-D-aspartate (NMDA) receptors and sodium channels (Sindrup, S. H. *et al.*, 2005). Amitriptyline 75 mg day^{-1} effectively relieved PSP (Leijon, G. and Boivie, J., 1989). The pain-relieving effect correlated with total plasma concentration, with a plasma concentration of amitriptyline and its metabolite nortriptyline exceeding the 300 nmol l^{-1} necessary for pain relief. Amitriptyline administered from the first day after a stroke and thereafter for 1 year in 39 stroke patients did not prevent PSP and allodynia (Lampl, C. *et al.*, 2002). Seven patients developed PSP (three receiving amitriptyline and four receiving placebo), and a large sample size is needed to exclude a type II error. Tricyclic antidepressants cannot be used in patients with heart failure, cardiac conduction disturbances, and epilepsy, and side effects including dry mouth, sweating, and sedation may limit their use. Recently, serotonin noradrenaline reuptake inhibitors with a better side-effect profile have been shown to relieve peripheral neuropathic pain, but these antidepressants are not yet studied in central pain conditions. Selective serotonin reuptake inhibitors are less effective in relieving neuropathic pain (Sindrup, S. H. *et al.*, 2005), and citalopram was found not to relieve PSP (Vestergaard, K. *et al.*, 1996).

5.60.5.2 Sodium Channel Blockers

In peripheral neuropathic pain, increased and abnormal sodium channels are known to be a source of neuronal hyperexcitability (Waxman, S. G. *et al.*, 2000). A role for such sodium channels and neuronal hyperexcitability in central pain in humans is supported by randomized controlled trials using sodium channel blockers. In 16 patients with central pain (six with PSP), lidocaine 5 mg kg^{-1} given intravenously over 30 min alleviated spontaneous ongoing pain, brush-induced allodynia, and mechanical hyperalgesia (Attal, N. *et al.*, 2000). This effect in central pain may be related to suppression of ectopic discharges from hyperexcitable central neurons. This is supported by a recent experimental study demonstrating increased expression of abnormal sodium channels functionally linked to neuronal hyperexcitability and central pain behaviors on second-order dorsal horn neurons close to a spinal cord lesion (Hains, B. C. *et al.*, 2003).

Along this line, the sodium channel blocker lamotrigine, at a relatively low dosage of 200 mg day^{-1}, reduced ongoing pain with a mean reduction of 30% and cold allodynia in PSP patients (Vestergaard, K. *et al.*, 2001). Lamotrigine was generally well tolerated. Side effects associated with the use of lamotrigine include dizziness, nausea, headache, and fatigue. Rash and potentially life-threatening hypersensitivity reactions are rare but potential risks, and slow dose escalation is recommended to minimize these risks. Carbamazepine 800 mg day^{-1} showed a statistically nonsignificant trend toward a pain-relieving effect in PSP (Leijon, G. and Boivie, J., 1989).

5.60.5.3 Opioids

Opioids seem to effectively relieve peripheral neuropathic pain with an effect size in line with tricyclic antidepressants and gabapentin/pregabalin (Finnerup, N. B. *et al.*, 2005) but seem to be less effective in PSP, although a subgroup of patients may respond well to opioids (Attal, N. *et al.*, 2002; Rowbotham, M. C. *et al.*, 2003).

5.60.5.4 Gabapentin

Gabapentin, which binds to the $\alpha_2\delta$ subunits of the voltage-dependent calcium channels, has not been studied in PSP but has been found to relieve spinal cord injury pain (Levendoglu, F. *et al.*, 2004), and given its tolerability, it is a treatment option in PSP.

5.60.5.5 GABA Agonists

Increasing γ-aminobutyric acid (GABA)-mediated inhibition using intravenous propofol is reported to relieve central pain including PSP (Canavero, S. and Bonicalzi, V., 2004), but propofol is very sedating and oral GABA agonists have not proven effective in neuropathic pain.

5.60.5.6 Treatment Option

Based on a few randomized controlled trials, an evidence-based treatment algorithm for PSP is not possible, but lamotrigine, gabapentin, tricyclic antidepressants, or serotonin noradrenaline reuptake inhibitors may be suggested as first choice.

Acknowledgments

This paper is in part based on support from Karen Elise Jensen Foundation, Danish Medical Research Council (grant no. 22-04-0561), and the Elsass Foundation.

References

Andersen, G., Vestergaard, K., Ingeman, N. M., and Jensen, T. S. 1995. Incidence of central post-stroke pain. Pain 61, 187–193.

Attal, N., Gaude, V., Brasseur, L., Dupuy, M., Guirimand, F., Parker, F., and Bouhassira, D. 2000. Intravenous lidocaine in central pain: a double-blind, placebo-controlled, psychophysical study. Neurology 54, 564–574.

Attal, N., Guirimand, F., Brasseur, L., Gaude, V., Chauvin, M., and Bouhassira, D. 2002. Effects of IV morphine in central pain: a randomized placebo-controlled study. Neurology 58, 554–563.

Besson, J. M. 1999. The neurobiology of pain. Lancet 353, 1610–1615.

Bogousslavsky, J., Regli, F., and Uske, A. 1988. Thalamic infarcts: clinical syndromes, etiology, and prognosis. Neurology 38, 837–848.

Boivie, J. 1989. On central pain and central pain mechanisms. Pain 38, 121–122.

Boivie, J. 1999. Central Pain. In: Textbook of Pain (*eds*. P. D. Wall and R. Melzack), pp. 879–914. Churchill Livingstone.

Boivie, J., Leijon, G., and Johansson, I. 1989. Central post-stroke pain – a study of the mechanisms through analyses of the sensory abnormalities. Pain 37, 173–185.

Bolay, H. and Moskowitz, M. A. 2002. Mechanisms of pain modulation in chronic syndromes. Neurology 59, S2–S7.

Bowsher, D. 1996. Central pain: clinical and physiological characteristics. J. Neurol. Neurosurg. Psychiatry 61, 62–69.

Bowsher, D., Leijon, G., and Thuomas, K. A. 1998. Central poststroke pain: correlation of MRI with clinical pain characteristics and sensory abnormalities. Neurology 51, 1352–1358.

Canavero, S. and Bonicalzi, V. 2004. Intravenous subhypnotic propofol in central pain: a double-blind, placebo-controlled, crossover study. Clin. Neuropharmacol. 27, 182–186.

Craig, A. D. 2000. The Functional Anatomy of Lamina I and Its Role in Post-Stroke Central Pain. In: Progress in Brain Research (*eds*. J. Sandkuhler, B. Bromm, and G. F. Gebhart), pp. 137–151. Elsevier Science.

Craig, A. D. and Bushnell, M. C. 1994. The thermal grill illusion: unmasking the burn of cold pain. Science 265, 252–255.

Dworkin, R. H., Backonja, M., Rowbotham, M. C., Allen, R. R., Argoff, C. R., Bennett, G. J., Bushnell, M. C., Farrar, J. T., Galer, B. S., Haythornthwaite, J. A., Hewitt, D. J., Loeser, J. D., Max, M. B., Saltarelli, M., Schmader, K. E., Stein, C., Thompson, D., Turk, D. C., Wallace, M. S., Watkins, L. R., and Weinstein, S. M. 2003. Advances in neuropathic pain: diagnosis, mechanisms, and treatment recommendations. Arch. Neurol. 60, 1524–1534.

Finnerup, N. B., Otto, M., McQuay, H. J., Jensen, T. S., and Sindrup, S. H. 2005. Algorithm for neuropathic pain treatment: an evidence based proposal. Pain 118, 289–305.

Greenspan, J. D., Ohara, S., Sarlani, E., and Lenz, F. A. 2004. Allodynia in patients with post-stroke central pain (CPSP) studied by statistical quantitative sensory testing within individuals. Pain 109, 357–366.

Hains, B. C., Klein, J. P., Saab, C. Y., Craner, M. J., Black, J. A., and Waxman, S. G. 2003. Upregulation of sodium channel Nav1.3 and functional involvement in neuronal hyperexcitability associated with central neuropathic pain after spinal cord injury. J. Neurosci. 23, 8881–8892.

Head, H. and Holmes, G. 1911. Sensory disturbances from cerebral lesions. Brain 34, 102–254.

Jensen, T. S. and Baron, R. 2003. Translation of symptoms and signs into mechanisms in neuropathic pain. Pain 102, 1–8.

Jensen, T. S. and Lenz, F. A. 1995. Central post-stroke pain: a challenge for the scientist and the clinician [editorial]. Pain 61, 161–164.

Jensen, T. S., Gottrup, H., Kasch, H., Nikolajsen, L., Terkelsen, A. J., and Witting, N. 2001a. Has basic research contributed to chronic pain treatment? Acta Anaesthesiol. Scand. 45, 1128–1135.

Jensen, T. S., Gottrup, H., Sindrup, S. H., and Bach, F. W. 2001b. The clinical picture of neuropathic pain. Eur. J. Pharmacol. 429, 1–11.

Kim, J. S. 2003. Central post-stroke pain or paresthesia in lenticulocapsular hemorrhages. Neurology 61, 679–682.

Kim, J. S. and Choi-Kwon, S. 1999. Sensory sequelae of medullary infarction, differences between lateral and medial medullary syndrome. Stroke 30, 2697–2703.

Koltzenburg, M. and Scadding, J. 2001. Neuropathic pain. Curr. Opin. Neurol. 14, 641–647.

Lampl, C., Yazdi, K., and Roper, C. 2002. Amitriptyline in the prophylaxis of central poststroke pain. Preliminary results of 39 patients in a placebo-controlled, long-term study. Stroke 33, 3030–3032.

Leijon, G. and Boivie, J. 1989. Central post-stroke pain – a controlled trial of amitriptyline and carbamazepine. Pain 36, 27–36.

Leijon, G., Boivie, J., and Johansson, I. 1989. Central post-stroke pain – neurological symptoms and pain characteristics. Pain 36, 13–25.

Levendoglu, F., Ogun, C. O., Ozerbil, O., Ogun, T. C., and Ugurlu, H. 2004. Gabapentin is a first line drug for the treatment of neuropathic pain in spinal cord injury. Spine 29, 743–751.

MacGowan, D. J., Janal, M. N., Clark, W. C., Wharton, R. N., Lazar, R. M., Sacco, R. L., and Mohr, J. P. 1997. Central poststroke pain and Wallenberg's lateral medullary infarction: frequency, character, and determinants in 63 patients. Neurology 49, 120–125.

Mailis, A. and Bennett, G. J. 2002. Dissociation between cutaneous and deep sensibility in central post-stroke pain (CPSP). Pain 98, 331–334.

Nathan, P. W., Smith, M., and Deacon, P. 2001. The crossing of the spinothalamic tract. Brain 124, 793–803.

Rowbotham, M. C., Twilling, L., Davies, P. S., Reisner, L., Taylor, K., and Mohr, D. 2003. Oral opioid therapy for chronic peripheral and central neuropathic pain. N. Engl. J. Med. 348, 1223–1232.

Schott, G. D. 1995. From thalamic syndrome to central poststroke pain. J. Neurol. Neurosurg. Psychiatry 61, 560–564.

Sindrup, S. H., Otto, M., Finnerup, N. B., and Jensen, T. S. 2005. Antidepressants in the treatment of neuropathic pain. Basic Clin. Pharmacol. Toxicol. 96, 399–409.

Tasker, R. R., de Corvallho, G., and Dostrovsky, J. O. 1991. The History of Central Pain Syndromes, with Observations Concerning Pathophysiology and Treatment. In: Pain and Central Nervous System Disease: The Central Pain Syndromes (*ed*. K. L. Casey), pp. 31–58. Raven Press.

Vestergaard, K., Andersen, G., Gottrup, H., Kristensen, B. T., and Jensen, T. S. 2001. Lamotrigine for central poststroke pain: a randomized controlled trial. Neurology 56, 184–190.

Vestergaard, K., Andersen, G., and Jensen, T. S. 1996. Treatment of central post-stroke pain with a selective serotonin reuptake inhibitor. Clin. J. Pain 3(Suppl. 5), 169.

Vestergaard, K., Nielsen, J., Andersen, G., Ingeman-Nielsen, M., Arendt-Nielsen, L., and Jensen, T. S. 1995. Sensory abnormalities in consecutive, unselected patients with central post-stroke pain. Pain 61, 177–186.

Waxman, S. G., Cummins, T. R., Dib-Hajj, S. D., and Black, J. A. 2000. Voltage-gated sodium channels and the molecular pathogenesis of pain: a review. J. Rehabil. Res. Dev. 37, 517–528.

Willis, W. D., Jr., Zhang, X., Honda, C. N., and Giesler, G. J., Jr. 2002. A critical review of the role of the proposed VMpo nucleus in pain. J. Pain 3, 79–94.

Woolf, C. J. and Mannion, R. J. 1999. Neuropathic pain: aetiology, symptoms, mechanisms, and management. Lancet 353, 1959–1964.

Woolf, C. J. and Max, M. B. 2001. Mechanism-based pain diagnosis: issues for analgesic drug development. Anesthesiology 95, 241–249.

Woolf, C. J. and Salter, M. W. 2000. Neuronal plasticity: increasing the gain in pain. Science 288, 1765–1769.

Further Reading

Loeser, J. D., Max, M. B., Saltarelli, M., Schmader, K. E., Stein, C., Thompson, D., Turk, D. C., Wallace, M. S., Watkins, L. R., and Weinstein, S. M. 2003. Advances in neuropathic pain: diagnosis, mechanisms, and treatment recommendations. Arch. Neurol. 60, 1524–1534.

5.61 Psychophysics of Pain

R H Gracely, University of Michigan Health System, VAMC, Ann Arbor, MI, USA

E Eliav, UMDNJ-New Jersey Dental School, Newark, NJ, USA

Published by Elsevier Inc.

5.61.1	**Measuring the Single Dimension of Pain in the Laboratory and in the Clinic**	927
5.61.1.1	Measuring Pain in the Laboratory	928
5.61.1.2	Measuring Pain in the Clinic	931
5.61.1.2.1	Quantitative sensory testing methods	932
5.61.1.2.2	Quantitative sensory testing signatures of pathological conditions	933
5.61.1.2.3	Clinical studies	933
5.61.1.3	Suprathreshold Pain Sensation	935
5.61.1.3.1	Advantages of multiple category items	937
5.61.1.3.2	Bounded continuous scales: the visual analog scale	938
5.61.1.3.3	Unbounded scales: ratio-scaling methods	939
5.61.1.4	The Different Goals of Traditional and Pain Psychophysics	940
5.61.1.4.1	Adapting psychophysical methods to pain assessment	940
5.61.1.5	Using Experimental Stimulation as an Anchor for Experimental and Clinical Pain Assessment	941
5.61.1.6	Other Suprathreshold Scaling Techniques: Discrimination and Single-Stimulus, Single-Response Designs in General	941
5.61.1.6.1	Discrimination	941
5.61.1.6.2	Sensory decision theory applications to pain assessment	942
5.61.1.6.3	Pragmatic problems with a fixed set of stimulus intensities	943
5.61.1.6.4	Utility of interactive adaptive methods	943
5.61.1.6.5	Stimulus integration: double-stimulus, single response methods	946
5.61.2	**Pain as Dual Variables of Intensity and Unpleasantness**	947
5.61.2.1	Psychophysical Studies of Feeling States: Hedonics	947
5.61.2.2	Validity of Hedonic Scales	948
5.61.2.3	Validity of Scales of Pain Unpleasantness	948
5.61.2.4	The Concept of Affective Gain	949
5.61.3	**Multidimensional Pain Assessment**	950
5.61.3.1	The Need for Scaling Multiple Pain Dimensions	950
5.61.3.2	Issues Concerning Multidimensional Scaling	954
5.61.4	**Conclusion**	956
References		956

5.61.1 Measuring the Single Dimension of Pain in the Laboratory and in the Clinic

To the layman, the pain threshold is often synonymous with the concept of pain sensitivity. It is used to describe individual differences, such as, "she has a high pain threshold." In pain research, the threshold describes a distinction between sensory qualities of nonpainful and painful. As the magnitude of a noxious stimulus is increased, the pain threshold marks the transition from the absence of pain sensation to the presence of pain sensation, and is quantified as the amount of stimulus intensity needed to evoke a painful sensation.

In the clinic, gross changes in pain threshold can be assessed in a qualitative way by administering a standard stimulus (e.g., safety pin, manual palpation) and by asking if the evoked sensation is painful (e.g., "does this hurt?"). More precise, quantitative methods increase the intensity of the stimulus until the evoked sensation is described as painful. The amount

of stimulus intensity at this point, or the average from a number of trials, is the pain threshold. Clinical examples of this method are the determination of the pain pressure threshold (PPT) to blunt pressure by mechanical or electrical dolorimeters for syndromes such as temporomandibular disorders or fibromyalgia (Petzke, F. *et al.*, 2003a; 2003b).

5.61.1.1 Measuring Pain in the Laboratory

In the laboratory, the pain threshold is determined by more extensive psychophysical procedures that are designed to control for a number of biases that may influence threshold assessments. These share a number of common features. They present a series of stimuli of varying intensity in a random sequence, or increasing from a randomly varied starting point. Subjects judge and rate the sensations evoked by each stimulus, and the different paradigms are designed to collect fresh judgments of the evoked sensations while minimizing extraneous information about stimulus intensity. They assume that the threshold is not succinct, but rather spans a range of stimulation in which painfulness is uncertain.

These laboratory methods include the classical Method of Limits, which uses alternating ascending and descending series of continuous or discrete stimuli, and the Method of Constant Stimuli that presents discrete stimuli of varying intensities that span the range from certain judgments of nonpainful to certain judgments of painful. Figure 1(a) shows an example of the method of limits. This method is usually modified for pain evaluation by using only ascending series to avoid the possibility of unacceptably painful stimulation at the beginning of a descending series. Biases are controlled by varying the starting point or step size, and traditionally in studies of nonpainful stimulation, the use of ascending and descending series to control for directional errors such as anticipation, of indicating the presence of pain before the sensation becomes painful, and errors of habituation, of continuing to use the nonpainful responses after the stimulus has become painful (Engen, T., 1971a). Figure 1(b) shows a histogram of a sequence of random stimuli that span the gray area between certain responding and an example of a probability function generated by this procedure. In addition to these classical methods, Figure 1(c) shows the logic of signal detection theory or sensory decision theory (SDT) evaluation, which can be conceptualized in sensory detection as a 2×2 table of the four possibilities of whether a particular stimulus value was delivered on a trial (versus delivery of nothing, termed a blank stimulus) and whether a sensation was detected or not. The common SDT terms for the four possibilities are a hit (correctly identifying a delivered stimulus), a correct rejection (correctly indicating that no stimulus was given) and the two errors of a miss (not identifying a stimulus when it was given), and a false alarm, indicating that a stimulus was given when it was not. The reader can appreciate that this 2×2 table is common in statistics, where the correct responses are referred to as accepting or rejecting the null hypothesis, and the errors are referred to as the α or type I error (labeling an effect as present when it is not, corresponding to a false alarm), and β or type II error (labeling something as absent when it is present, corresponding to a miss). Probably the most self-explanatory labels for the four outcomes are true positive, true negative, false-positive, and false-negative. While the classical methods consider the concept of a threshold to be fuzzy, and therefore best described by a mean or probability, SDT extends the concept to include two variables. One is a measure of sensitivity of the system, directly analogous to a statistic such as t or Z, which can be thought of as a distance between determinations of no detection and detection (or no pain and pain) divided by the variability of these judgments. The second refers to the labeling behavior, and is directly related to the α level (such as $p < 0.05$) arbitrarily set by an experimenter in statistics. It describes the willingness to use specific responses, and it can be liberal or conservative. As in statistics, this behavior divides the gray area of indecision into two types of error. For a given sensitivity, changing this behavior decreases one error only at the expense of increasing the other. For example, adapting a liberal criterion and calling uncertain sensations painful increases the false alarm error (or α, type I, or false-positive) while decreasing the miss error (or β, type II, or false-negative).

One of the first applications of SDT was to assess the performance of radar operators (Swets, J. A., 1964). In this context, the sensitivity parameter d' describes the overall sensitivity of the system, which includes the visual acuity of the human operator and the physical capabilities of the radar receiver. The response criterion parameter is set by the operator and in this case determined by the demand

characteristics. During wartime, operators must adapt a liberal criterion to label any suspicious blip as an enemy plane. This vigilant strategy minimizes the misses at the expense of increased false alarms. Other situations such as capital punishment must adapt the opposite conservative criterion, to be as sure as possible of a hit, minimizing false alarms at the expense of increased misses.

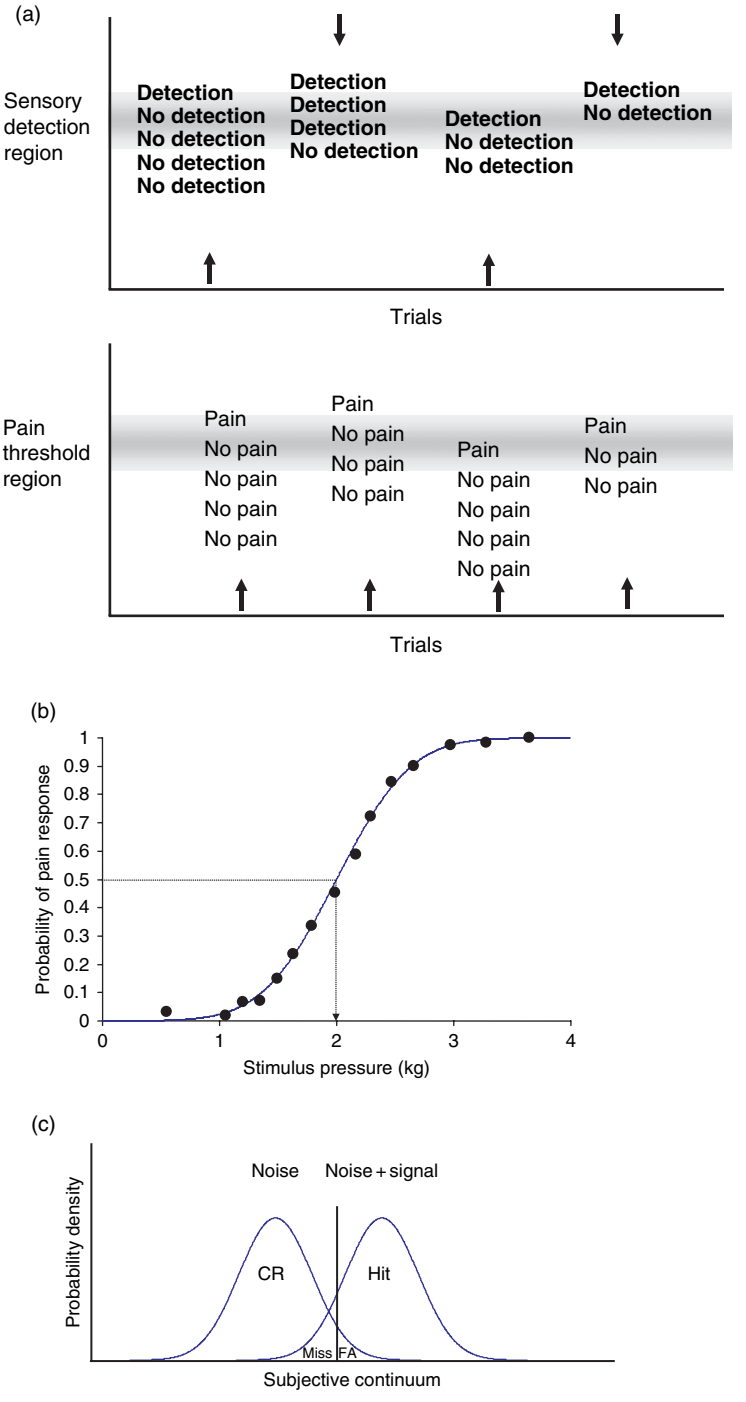

Figure 1 (Continued)

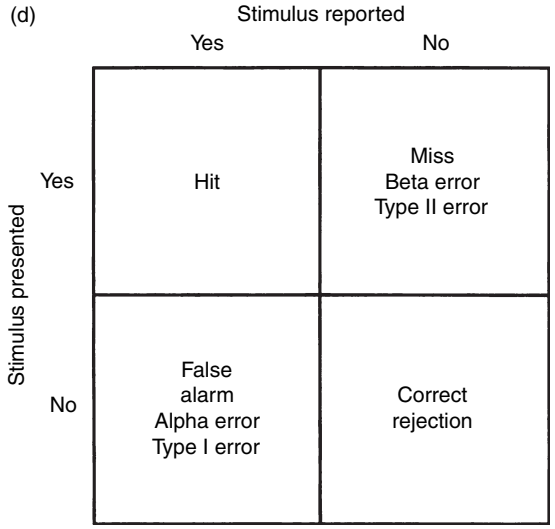

Figure 1 (a) The method of limits. Stimulus intensity is increased in successive discrete presentations on trial 1 until a positive response (yes) is made. Intensity is decreased on trial 2 until a negative response (no) is made. Several trials are run with varied initial starting intensities. The threshold is defined as the mean of the response transitions for each trial. A common modification of the method of limits to measure pain threshold delivers only ascending series to avoid excessively painful stimulation. (b and c) The method of constant stimuli. (b) Shows a range of stimulus intensities about the threshold that are presented in random sequence. (c) Shows the probability of a positive response over stimulus intensity. The result typically is an ogive shape (cumulative normal distribution) and the threshold is defined as the stimulus intensity corresponding to a specific response probability (in this case 0.5). This method emphasizes that the transition between no sensation, nonpainful sensation, and pain sensation shown in (a) is not distinct and varies over trials. (c and d) The logic of signal detection theory (SDT). (c) Shows the sensory distributions of a blank stimulus and an actual stimulus. Because of noise in the system, these distributions overlap. (d) Shows the four possibilities of signal presence and response choice. (d) This table is analyzed in terms of discrimination sensitivity and the relative frequency of the errors of false alarms or misses.

SDT methods are easily implemented by including the presentation of blank stimuli to determine the rate of false-positive errors. In addition to SDT, the robust method of two alternative forced choice (2ALFC) controls the labeling behavior rather than assessing it, while providing a measure of sensitivity similar to that provided by SDT. The 2ALFC is implemented by presenting two stimuli at the same time in different places (e.g., left and right hands) and asking which was the true stimulus or which had the greater sensation. The same method can also be used by applying two stimuli to the same (or different) place at different times and asking whether the first or second stimulus period contained the stimulus or had a greater sensation.

There are a number of issues that have been raised about the pain threshold, which assesses pain sensitivity only at the very bottom of the pain range. One issue is whether SDT methods are superior to the classical procedures. This is also an issue for suprathreshold scaling and this issue is presented below in the suprathreshold context. SDT methods usually require more trials than conventional procedures, which may be problematic if these trials are painful. Another issue is whether the pain threshold predicts suprathreshold sensitivity. Figure 2 shows that the answer is "not always." In the clinical condition of

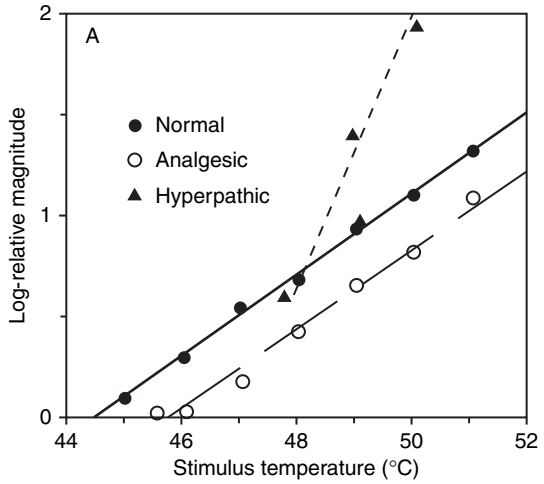

Figure 2 Pain thresholds may not indicate suprathreshold sensitivity. The triangles show the type of function that could be obtained in the clinical condition of hyperpathia in which the threshold is raised and suprathreshold sensitivity is increased.

hyperpathia, an elevated pain threshold (decreased pain sensitivity) is combined with significant suprathreshold sensitivity. Increasing the intensity of the stimulus does not evoke a sensation at usual levels and an explosive experience of pain at higher levels. In cases in which the pain threshold is predictive of suprathreshold sensitivity, an issue is whether it is more or less sensitive, and more or less responsive to pain interventions.

Another issue is the presence of prepain sensation. In studies of nonpainful modalities, the sensation is either not present or present, as shown in Figure 1(c). In pain studies, there are usually three alternatives: nothing, nonpainful sensation, and painful sensation. This leads to some operational difficulties with methods such as SDT, and changes detection tasks (with the control provided by blank stimulation) to rating tasks described below.

5.61.1.2 Measuring Pain in the Clinic

The requirements of clinical and laboratory assessments are usually quite different. Because of the limitations of time, the need to test multiple areas with multiple modalities, and the gross nature of many clinical abnormalities, clinical methods are necessarily brief and thus devoid of the protection against bias contained in the classical and more modern methods. This may not be an important issue in specific situations, but can significantly influence the outcome, especially when the comparisons are between individuals.

These issues of clinical versus laboratory methods were addressed in a recent study by Petzke F. *et al.* (2003a) that compared the influence of psychological distress on clinical and laboratory measures of the PPT in fibromyalgia. This study compared the methods described above. The qualitative clinical method is the manual tender point count, which applies a standard stimulus (4 kg of thumb pressure) to nine bilateral pairs of defined tender points defined by the American College Rheumatology (1990). The tenderness part of the diagnosis of fibromyalgia is satisfied if the standard stimulus evokes pain in at least 11 of the 18 tender point sites. The reader can appreciate that patients with fibromyalgia know about these points and criteria, and know what to say if they want to satisfy this aspect of the diagnosis.

The quantitative clinical measure used a standard commercial dolorimeter at the same 18 tender point sites, slowly increasing the pressure of a 1 cm diameter probe until the sensation is reported to be painful. The laboratory procedure used the multiple random staircase (MRS) method (see below) that uses a computerized interactive logic to determine the PTT and also pain sensitivity at more intense levels between pain threshold and tolerance (Petzke, F. *et al.*, 2003b).

Since one theory of tenderness in fibromyalgia is that it is the extreme tail of a normal distribution of tenderness, Petzke F. *et al.* (2003a) composed a group of 76 subjects that included both healthy controls and patients with fibromyalgia with a normally distributed range of PPTs determined by a dolorimeter. Table 1 shows the association of the different measures of pressure pain sensitivity with measures of psychological distress. The manual tender point count is significantly associated (23%) with distress, the more quantitative clinical dolorimeter is significantly but less associated (15% at tender points, 12% at thumb) with distress, while the random psychophysical method applied to the thumb is insignificantly associated with distress (4%).

Table 1 Results of regression analysis[a]

	R^2	*B*	*SE*	*Significance*
MTPC	0.23	0.24	0.06	0.001
DM-PT	0.15	−0.02	0.009	0.008
DM-THU	0.12	−0.08	0.033	0.019
RAN	0.04	0.59	0.42	0.169

[a]*R*-square, regression coefficient *B*, standard error of *B*, significance , for four dependent measures of tenderness measures with distress (GSI) as independent variable. MTPC is the manual tender point count, defined as the number of 18 predefined sites at which 4 kg of manual thumb pressure evokes pain. DM-PT is the mean of dolorimeter measures of the pain pressure threshold obtained at the 18 tender point sites. DM-THU is the dolorimeter-derived pain pressure threshold obtained at the left thumbnail. RAN is the pressure pain sensitivity at the left thumbnail determined by the multiple random staircase method. Adapted from Petzke, F., Gracely, R. H., Park, K. M., Ambrose, K., and Clauw, D. J. 2003b. What do tender points measure? Influence of distress on 4 measures of tenderness. J. Rheumatol. 30, 567–574.

5.61.1.2.1 Quantitative sensory testing methods

The influence of distress may be less of an issue in other clinical situations. In cases in which multiple determinations are made in a single individual and compared between sites, trait characteristics of individual response styles may cancel out. In addition, in many cases the abnormalities that are the target of the evaluations are so dramatic that they can be accurately assessed by a variety of methods. Indeed, simple threshold measures form the core of a set of procedures referred to as quantitative sensory testing (QST). After a considerable history in which clinicians applied pinpricks to patients in the clinic and psychologists applied electrical or thermal stimuli to healthy students in the laboratory, QST bridged the gap, applying an increasing number of stimulus methods and modalities to patients with a variety of pain complaints. The section below briefly summarizes these methods, and provides a few examples of studies in which pain psychophysical threshold procedures have elucidated mechanisms and aided diagnosis. It focuses on the pain in pain psychophysics.

The goal of sensory assessment is to obtain information from the neural system, which may help in diagnosis and treatment of disorders in the nervous system itself and in surrounding tissue. Traditionally, this examination included the response to a brush, a cotton swab, a warm or a cold object, and a pinprick (Hansson, P., 2002). QST extends these methods.

For clinical applications, the methods can be organized into a protocol that is applied routinely to all patients. Determination of an abnormality can be made on the basis of comparison to a set of standard control values, although comparison to a contralateral unaffected site in the same patient may be the best approach when available (Kemler, M. A. *et al.*, 2000).

Common stimulus modalities used to assess the function of specific nerve fibers are:

1. Touch, electrical, and vibratory stimuli for the evaluation of the function of the thickly myelinated Aβ fibers.
2. Cold detection threshold for the assessment of thinly myelinated Aδ fibers.
3. Heat detection threshold for the assessment of thin unmyelinated C-fibers.

Touch and vibration sensitivity is usually determined by the detection and pain thresholds to both calibrated monofilaments and a vibrating probe. Four different thermal parameters (thresholds to warm and cold stimuli, heat pain, and cold pain) are typically assessed by Peltier element-based thermal stimulators. The cold pain threshold is a specific test for cold allodynia, a common finding in conditions involving nerve injury. Altered heat pain thresholds can reflect either the function of myelinated Aδ fibers or unmyelinated C-fibers, depending on the rate, location, and sequence of stimulation (Collins, W. R. *et al.*, 1960; Price, D. D. *et al.*, 1989; Andersen, O. K. *et al.*, 1995; Koltzenburg, M., 1997).

Tests of the area of abnormality assess the threshold for sensory detection, and usually a higher threshold for pain. In some cases both may be altered, or the sensory detection threshold may be absent, and stimulation evokes only pain. The profile of altered sensory and pain thresholds across mechanical and thermal modalities provides information about the type of nerve abnormality, and can be supplemented by additional tests that examine pain processing at levels above the pain threshold (Hansson, P., 2002). Since it is important to ascertain whether the distribution of sensory abnormalities match the damaged nerve's dermatome, the borders of sensory dysfunction area should be carefully determined using the different modalities. The finding of extraterritorial pain that extends beyond the border of a dermatome is discussed below.

The response to electrical stimulation is usually not included in standard QST assessments, and several studies have found conflicting and inconsistent results using electrical tests (Hagberg, C. *et al.*, 1990; Vecchiet, L. *et al.*, 1991; Bendtsen, L. *et al.*, 1997). However, recent studies demonstrate a number of unique features of electrical stimulation. Unlike the other methods, which naturally stimulate nerve receptors, electrical stimuli may bypass the receptor to stimulate the axon of the primary afferent. Due to this property, electrical stimulation does not show the same temporal profile of sensitization, suppression, or fatigue as found in natural stimulation of receptors. In addition, at the threshold for detection, electrical stimuli exclusively activate the thickly myelinated Aβ fibers. Thus, a comparison of the detection threshold to both mechanical and electrical stimuli can provide a differential method that isolates receptor and postreceptor processes of Aβ fibers. Changes in both or in only electrical detection indicate a postreceptor process, while changes in only the results of mechanical stimulation indicate a receptor process. Thus, altered electrical sensitivity alone indicates a postreceptor process in large myelinated fibers. A single electrical test can identify a number of central processes, including spinal sensitization resulting in Aβ-mediated allodynia, and inflammatory processes that include the nerve in passage. One

problem with electrical sensory assessment is interpatient variability. This inconsistency can be reduced by expressing the electrical detection thresholds as the ratio between the pathological and the contralateral side, that is, the healthy side used as a control for the pathological side (Kemler, M. A. *et al.*, 2000).

The results of QST methods help distinguish between nociceptive and neuropathic pain, which differ significantly in etiology, mechanism, and effective treatment. Nociceptive pain is the normal condition in which actual or impending tissue damage is sensed by the receptor organs, nociceptors, resulting in a range of normal pain conditions that may be treated with conventional (e.g., NSAID, opioids) analgesics. Neuropathic pain describes a special condition in which the sensing neural apparatus is damaged, leading to a variety of pain sensations with unnatural characteristics of quality and distribution. Neuropathic pain can be particularly difficult to treat, and successful agents include drugs such as anticonvulsants that modify neural function.

5.61.1.2.2 Quantitative sensory testing signatures of pathological conditions

Mechanical nerve damage or total nerve transection is characterized by myelinated and unmyelinated nerve fiber hyposensitivity reflected in elevated detection thresholds to heat, electrical, and mechanical stimulation (Dao, T. T. and Mellor, A., 1998). Partial damage may be followed by either hypo- or hypersensitivity accompanied by ongoing neuropathic pain (Benoliel, R. *et al.*, 2001; 2002).

In contrast to the neuropathic process of mechanical nerve damage, specific nociceptive processes may provide a different, identifiable sensory signature. For example, early perineural inflammation produces short-lasting large myelinated nerve fiber hypersensitivity that results in reduced detection to electrical and mechanical stimuli. This increased detection sensitivity has been demonstrated in clinical studies and in animal spinal nerve models (Eliav, E. and Gracely, R. H., 1998; Eliav, E. *et al.*, 1999; Chacur, M. *et al.*, 2001; Eliav, E. *et al.*, 2001; 2003) and reproduced in a model of inflammatory trigeminal nerve neuropathy (Benoliel, R. *et al.*, 2002).

Although the mechanisms are not clear, muscle-induced pain may result in the opposite effect, that is, reduced large nerve fiber sensitivity reflected by elevated electrical or mechanical detection thresholds (Stohler, C. S. *et al.*, 2001; Eliav, E. *et al.*, 2003). In the orofacial region, there is both experimental and clinical evidence for this effect. Following injection of hypertonic saline to the masseter muscle, mechanical stimuli applied into the overlying skin induced significant increases in the verbal rating score (Svensson, P. *et al.*, 1998), and lowered pain thresholds to this type of stimulation have been found in patients with orofacial myofascial pain (Svensson, P. *et al.*, 1998; 2001).

Both neuropathic and intense nociceptive pain can initiate and maintain a condition of spinal central sensitization (CS). CS is characterized by spontaneous pain and evoked pain abnormalities that can cross dermatomes. One striking abnormality is dynamic mechanical allodynia, pain to light brushing of the skin. Theoretically, this can be mediated by either sensitized pain fibers or a functional change in large-diameter Aβ fibers that usually only mediate the sense of touch. Mechanical stimulation cannot distinguish between these alternatives, but recent evidence shows that a ratio between the electrical pain and the detection threshold of <2.0 may indicate altered central nervous system processing of Aβ fiber input (Sang, C. N. *et al.*, 2003). This result is strong evidence of altered central pain modulation and CS.

Combining the above procedures into one methodological approach provides a clinical decision-making tool that facilitates diagnosis and choice of treatment. The following section illustrates how these tests have helped identify the underlying mechanisms of three painful syndromes.

5.61.1.2.3 Clinical studies

5.61.1.2.3.(i) Burning mouth syndrome Burning mouth syndrome (BMS) is a putative centrally mediated pain that is poorly understood and treated. BMS is diagnosed only when the burning sensation is not associated with a local or systemic pathology. In contrast, burning mouth symptoms (BMST) is diagnosed in the presence of a known etiology for the altered sensation. BMS is an intraoral disorder most prevalent in postmenopausal women (Grushka, M., 1987; Grushka, M. *et al.*, 2002), characterized by a burning mucosal pain without major visible physical signs. Altered taste sensations have long been associated with BMS and nearly 70% of the patients complain of accompanying dysguesia (altered taste sensation) (Ship, J. A. *et al.*, 1995). Conventional QST in BMS patients identified defects in pain tolerance, altered chemosensory function, increased pain threshold to laser stimulation, and hypoesthesia of large and small nerves (Grushka, M. and Sessle, B., 1988; Grushka, M. and Sessle, B. J., 1991; Mott, A. E. *et al.*, 1993; Formaker, B. K. and Frank, M. E., 2000). Accumulating evidence suggests that BMS involves

central and peripheral nervous system pathologies induced by the damage to the taste system at the level of the chorda tympani nerve. This damage results in reduced trigeminal inhibition that in turn leads to an intensified response to oral irritants and eventually to oral phantom pain (i.e., BMS) (Grushka, M. *et al.*, 2003).

Recent studies of BMS show how electrical tests can enhance a QST examination. Electrical stimulation of the tongue can provoke two different sensations; one is described as itch (tingling) and the other as an electrical taste (Bujas, Z. *et al.*, 1979; Lindemann, B., 1996). The electrical taste threshold in the tongue is easily recognized as a sensation usually described as a battery-like or sour taste. The taste sensation is assumed to be conducted via the chorda tympani nerve and the itch sensation via the lingual nerve. Thus electrical detection thresholds of the anterior two thirds of the tongue likely evaluate the role of chorda tympani and lingual nerve function in BMS.

Eliav E. *et al.* (2007) found no difference between electrical taste and electrical detection thresholds among 23 BMS patients, 14 BMS patients, or 10 asymptomatic controls at extraoral nerve mental and infraorbital control sites. In the control and BMST patients, the ratio between the electrical taste and the itch sensation on the tongue was <0.7, while this ratio was significantly higher (1.4) in the BMS patients. This result is consistent with the hypothesis that BMS is an oral phantom-type pain induced by damage to the taste system (Grushka, M. *et al.*, 2003), and suggests that the electrical taste and itch ratio may be a useful diagnostic test for BMS.

5.61.1.2.3.(ii) Painful temporomandibular disorder Painful temporomandibular disorder (TMD) can be due to arthralgia in the temporomandibular joint or from processes in nearby muscle. Eliav E. *et al.* (2003) classified a cohort of patients as suffering from joint arthralgia ($n = 44$) or myalgia ($n = 28$). Electrical thresholds for Aβ fibers and heat thresholds for C-fibers were assessed in these patients and in 33 healthy control subjects. These tests were performed bilaterally in three trigeminal nerve sites: the auriculotemporal nerve territory, the buccal nerve territory, and the mental nerve territory.

Electrical detection threshold ratios were calculated by dividing the affected side by the control side; thus reduced ratios indicate hypersensitivity of the affected side. In control patients, ratios obtained at all sites did not vary significantly from the expected value of one. In arthralgia patients, the mean ratio obtained for the auriculotemporal nerve territory (0.63) was significantly lower than the ratio for the mental nerve (1.02) and buccal nerve (0.96) territories in patients and lower than the auriculotemporal nerve ratios in myalgia (1.27) and control subjects (1.00). In the myalgia group, the electrical detection threshold ratios in the auriculotemporal nerve territory were significantly elevated compared to the auriculotemporal nerve ratios in control subjects. There were no significant differences between and within the groups for electrical detection threshold ratios in the buccal and the mental nerve territories, and for the heat detection thresholds in all tested sites. Following arthrocentesis (fluid draining) delivered to 10 arthralgia patients, mean electrical detection threshold ratios in the auriculotemporal nerve territory were significantly elevated from 0.64 to 0.99, indicating resolution of the hypersensitivity. Thus, electrical stimulation distinguished between joint and muscle-related facial pain, and monitored the time course of the joint pain.

5.61.1.2.3.(iii) Sinusitis Sinusitis can be classified as acute (<1 month) or chronic (>3 months). The transition from acute to chronic likely involves a shift from acute inflammation to more persistent mechanisms that may involve nerve damage, changes that should be detectable by QST. In a pilot study by Eliav and coworkers (personal communication), neurosensory function was evaluated in seven patients and eight control subjects by measuring the electrical detection threshold for large myelinated nerve fibers and heat detection thresholds for the assessment of thinly myelinated nerve fibers. The sensory tests were conducted in the region of the infraorbital, supraorbital, and mental nerve distributions. Nine acute and five chronic sinusitis were diagnosed. Acute sinusitis was associated with bilateral large myelinated nerve hypersensitivity (to electrical stimulation) compared to healthy controls with no significant change in the unmyelinated nerve fiber detection threshold (to heat). Chronic sinusitis resulted in a large myelinated fiber hyposensitivity and a thin myelinated fiber bilateral hyposensitivity compared to healthy controls. These preliminary results suggest that QST may distinguish between an early inflammatory neuritis and a chronic condition likely accompanied by nerve damage.

5.61.1.2.3.(iv) Malignancy The ability of electrical stimulation to detect inflammation along the course of the nerve has also been applied to the

detection of malignancy. Eliav E. *et al.* (2002) assessed the sensitivity of Aβ primary afferents to weak electrical currents applied bilaterally to regions innervated by three peripheral branches of the trigeminal nerve. For dermatomes containing lesions, ratios of electrical detection thresholds (affected/unaffected side) were <0.8 in 12 patients. Biopsy showed that the lesions in 10 of these 12 patients were malignant. No malignancy was found in the remaining 11 patients. These results suggest that Aβ primary afferent hypersensitivity is observed to occur in nerves exposed to early soft tissue oral malignancies, and that a simple electrical test may provide a nonivasive and inexpensive method of early detection.

5.61.1.3 Suprathreshold Pain Sensation

Although the pain threshold is very useful in QST examinations, in some cases it may be necessary to assess pain sensitivity at higher, suprathreshold levels. As shown in Figure 2, in conditions such as hyperpathia the pain threshold may not predict suprathreshold sensitivity. In this case the psychophysical function rotates; decreased sensitivity at threshold levels is accompanied by increased sensitivity at suprathreshold levels. In addition, suprathreshold pain stimulation is important for goals outside of QST testing in which the painful stimulus is designed to simulate some aspects of spontaneous pain. In the clinical situation, threshold-level pain sensations are less relevant and the focus is on treatment of intense acute pain following injury or medical procedures, and the management of relentless chronic pain.

The psychophysical scaling techniques used to evaluate suprathreshold sensations are reviewed in a number of sources (Torgerson, W. S., 1958; Bock, R. D. and Jones, L. V., 1968; Engen, T., 1971b; Anderson, N. H. *et al.*, 1974; Marks, L. E., 1974; Stevens, S. S., 1975; Gescheider, G. A., 1985; Falmagne, J. C., 1986; Bolanowski, S. J. and Gescheider, G. A., 1991; Atkinson, R. C. *et al.*, 1998). In terms of the task performed by the subjects, these methods can be divided into three classes: discrete numerical or verbal category scales, bounded or confined continuous-measure equivalents of bounded scales such as the 10 cm visual analog scale (VAS), and unbounded scales such as the well-known method of magnitude estimation (using any number).

These methods also differ in analysis, with some common rating tasks analyzed by distinctly different procedures. For example, discrete numerical or verbal category scales can be analyzed by considering the distances between categories to be psychologically equal (formally titled as the method of equal appearing intervals (Engen, E., 1971b). Many pain studies have used discrete category scales such as the 0–10 numerical scale (Brennum, J. *et al.*, 1992), the four-point category scales of pain (none, mild, moderate, severe) or pain relief (none, some, lots, complete) (Gracely, R. H. and Naliboff, B. D., 1996). The most widely used McGill Pain Questionnaire (MPQ) (Melzack, R., 1975) is usually analyzed by assigning integer ranks to each category subscale.

The actual category values can be determined by the response behavior of the subjects as they use the scale. Thurstone L. I. (1959) developed a number of methods that use this approach, in which the spacing of two categories is inversely related to the extent that they are confused, such as the relative proportion that each response is used to describe the same stimulus intensity. The method of successive categories (Thurstone, L. I., 1959; Engen, E., 1971b) is applied to category scaling data and a related analysis is used for the simpler task of paired comparisons, in which subjects are presented a series of stimulus pairs and they indicate which of the pair is more intense. Thurstone analyses are rarely applied to pain assessment (LaMotte, R. H. and Campbell, J. N., 1978), but could be applied to many more studies currently using the method of equal appearing intervals to analyze categorical data. A comparison of the two methods can actually be performed post hoc, either validating the assumption of equal intervals or providing an alternative that more closely resembles the values of the category responses.

Methods that use response distributions can also be applied to clinical pain ratings, when the underlying stimulus intensities are not known. An example is Rasch analysis, which has been applied to the assessment of low back pain. The results can be used for item weighting or for item selection during further scale development (McArthur, D. J. *et al.*, 1991).

A third class of methods also determine the appropriate value for each category response. However, in contrast to the Thurstone methods of determining these values simultaneous with scaling, these methods quantify category values in a separate procedure. The scales can be used for both experimental and clinical pain assessment. A notable example of this approach is the MPQ. The 2–6 items within each of the 20 subscales were quantified during the development of the scale (Melzack, R. and Torgerson, W. S., 1971). One of

the most sophisticated examples of determining category scale values was performed by Tursky B. (1976), who requantified some of the MPQ items using a ratio-scaling paradigm advocated by Stevens S. S. (1975). The details of this method are described in Section 5.61.1.3.3.

Once category values are quantified, the issue is how these categories should be used to measure pain. Categorical scales can be presented in ordered sequences as a simple checklist such as the MPQ, or be placed at the appropriate locations on a spatial continuum to form a graphic rating scale (Heft, M. W. and Parker, S. R., 1984; Gracely, R. H., 1991). This continuum can be some type of VAS discussed below (Lembo, A. *et al.*, 2000). Figure 3 shows an example of an alternative format in which descriptors are placed at the appropriate locations along a higher-resolution numerical category scale. This type of scale is useful in situations in which the subjects cannot mark a line, such as in neuroimaging experiments or in telephone assessments.

A novel method presents the categories in random order and subjects rate experimental or clinical pain magnitude by choosing a category from the randomized list (Gracely, R. H. *et al.*, 1978a). This method is unique since it forces category choices based on the semantic content of the item rather than on its spatial location in a list. This method has two prominent advantages. First, basing choices on the meaning of a word or phrase may help subjects distinguish between different dimensions of pain experience (see below). Second, choices from a randomized list may be free of the rating biases associated with choosing responses from a bounded scale. These biases relate to the subject's tendency to spread repeated responses evenly over a category scale. This tendency results in scale responses that are influenced by the distribution of delivered stimulus intensities, including range, spacing, and frequency of presentation (Parducci, A., 1974). Varying these parameters distorts the resultant scale. Methodological improvements may reduce the effects of these distortions, such as iterative scaling techniques that systematically eliminate distortions (Pollack, I., 1965), and the use of open-ended scales described below (Stevens, S. S., 1975). The randomized descriptor method is likely the best improvement, since it eliminates the scaling space that forms the basis for the response spreading. The disadvantages of the random method is that resolution is limited to the number of categories (in contrast to a graphic rating scale) and that the task may be more difficult than scaling with an ordered set of categories.

Figure 3 Box scale of pain intensity. This scale combines a spatial range of verbal descriptors previously quantified and position on a logarithmic scale adjacent to a 0–20 category numerical category scale. Subjects use the descriptor space to determine an appropriate amount of intensity and to then choose the nearest numbered box to express this magnitude of pain intensity. This method increases the resolution beyond the number of descriptors, allows for semantic gaps such as mild to moderate, adds additional scaling space at the top, is used also for a scale of unpleasantness, does not require a motor response, and can be used for applications such as telephone surveys.

Although an undistorted scale is desirable for pain measurement, applied studies of pain may be more concerned with how these response behaviors adversely affect the evaluation of changes in pain sensitivity such as the effect of analgesic interventions. In this situation, the tendency to produce a uniform response distribution tends to diminish the response to a real pain treatment effect, reducing assay sensitivity. This is one of several normalizing effects; others include regression to the mean and the physiological

effect termed the law of initial values, together forming a group of effects informally called floor-ceiling effects. For example, study using a 0–6 category scale showed a reduced response range immediately after a pain-reducing intervention, which quickly spread to the previous response distribution, diminishing the effect. In contrast, a randomized verbal descriptor scale, with no spatial response range, showed a persistent reduction (Gracely, R. H. *et al.*, 1984).

5.61.1.3.1 Advantages of multiple category items

In contrast to scaling methods that average a large number of ratings, many clinical pain scales are based on a single score or only a few scores. One advantage of verbal categories is that they describe different magnitudes of similar or different pain dimensions, and a scale can consist of a number of items. Both the long (Melzack, R., 1975) and the short (Melzack, R., 1987) forms of the MPQ take advantage of this property. The use of composite scores from a number of items decreases the influence of random scaling errors. For example, the reliability and homogeneity of the overall score of the descriptor differential scale (DDS) is greater than the mean score obtained from each individual item (Gracely, R. H. and Kwilosz, D. M., 1988). This improvement obtained from the use of multiple items at a single testing time is similar to the improvement noted with repeated use of single items; averages of multiple responses to a single-item pain diary are superior to single responses or to the mean of only a few responses (Jensen, M. P. and McFarland, C. A., 1993). Multiple measures delivered at the same time must use different items, a requirement naturally filled by the use of verbal categories. The DDS uses this approach by presenting 12 quantified descriptors and instructing subjects to rate if their clinical pain is equal to that implied descriptors, or how much less or greater on a +10 to −10 scale. The DDS has been administered to patients in acute or chronic pain in several studies, revealing adequate reliability, internal consistency, validity, and sensitivity (Hargreaves, K. M. *et al.*, 1986; Kwilosz, D. M. *et al.*, 1986; Gracely, R. H. and Kwilosz, D. M., 1988; Doctor, J. N. *et al.*, 1995).

In these applications, the different categories must describe different amounts or aspects of pain, but do not have to be quantified. Quantifying these verbal categories provides additional advantages. Comparisons between the pattern of item responses and the previously determined descriptor values provide a measure of scaling consistency. The DDS shows high consistency that improves from the first to the second administration (Gracely, R. H. and Kwilosz, D. M., 1988). These consistency measures can be used at screening, or over the course of a study to identify subjects who obviously are not attending to the scaling task. Eliminating these subjects may improve psychometric properties and increase the sensitivity of an analgesic assay.

The use of multiple, quantified items also allows the construction of alternative forms, each with different descriptor items, that are theoretically equivalent. Kwilosz D. M. *et al.* (1984) validated such forms and used them to evaluate the accuracy of memory of acute postsurgical pain over a 1-week period. The use of alternative forms is critical in such studies. Without alternative forms, memory for pain cannot be distinguished from an alternative explanation, that it represents only the memory of a previous pain rating.

Finally, the methods used to quantify verbal categories can provide information about the stability of the meanings attached to the words, and the consistency for these meanings over the general population. The exact procedures used for the quantification are described in Section 5.61.1.3.3. The overall approach uses methods that reduce bias. Each subject uses two independent methods to rate the words and the comparison of these methods provides a check of internal consistency. The similarity of these scales validates both the methods and the general concept that verbal descriptors, with no physical metric of their own, can be rated as reliably as physical stimuli. After scales produced by different response methods are shown to be similar, they are combined into an overall scale of magnitude. Figure 4 shows an example of these separate and combined scales for descriptors of pain intensity (Gracely, R. H. *et al.*, 1978a).

In addition to these measures of internal consistency, comparisons among individuals evaluate common usage. The Gracely R. H. *et al.* (1978a) quantification of pain sensory intensity descriptors found evidence for common usage, expressed as objectivity. Mean individual reliabilities were 0.96 over 1 week, and the mean of correlations between each individual's scale and mean scale from the remaining subjects in a group were also 0.96. The equivalence of these correlations indicates very high objectivity; an individual's quantification of the verbal descriptors was predicted equally well by that individual or by a group norm. This objectivity indicated general agreement about the ordering and spacing of English words describing magnitudes of sensory

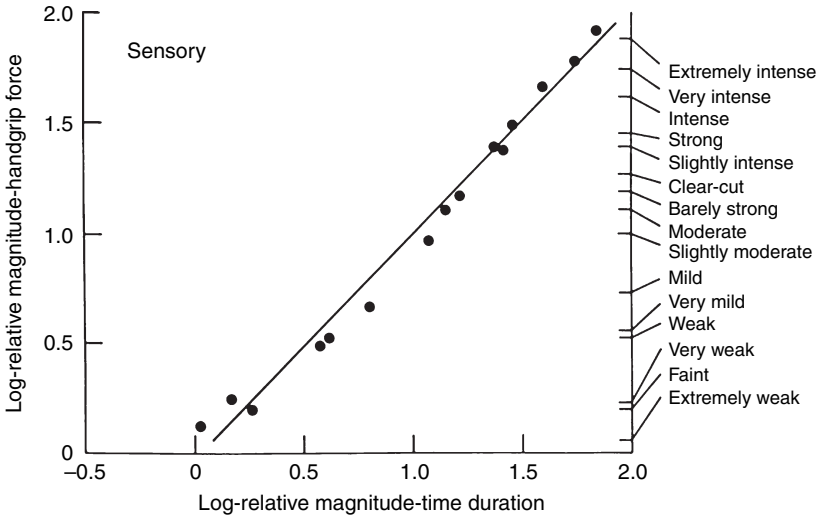

Figure 4 Relative magnitude of sensory intensity verbal descriptors derived from cross-modality matching to handgrip force (ordinate) and to time duration (abscissa). Each point is the geometric mean of 80 responses of 40 subjects to a single descriptor. The mean of the two magnitudes for each descriptor is shown on the right vertical axis. From Gracely, R. H., McGrath, P. A., and Dubner, R 1978a. Ratio scales of sensory and affective verbal pain descriptors. Pain 5, 5–18.

intensity, validating the use of a group normative scale. The results of these pain-related investigations were in general agreement with previous psychological studies of semantic meaning. For example, the adverbs very and slightly, when used to modify adjectives of pain magnitude (Gracely, R. H. and Dubner, R., 1987) or pain unpleasantness (Walther, D. J. and Gracely, R. H., 1986), appear to serve as multiplicative modifiers independent of the adjective modified (e.g., pain, distressing, unpleasantness). This property was described by Cliff N. (1959) and the constants found in that study using a Thurstone analysis of paired comparisons (1.30 for very, 0.55 for slightly) are in general agreement with those found with ratio-scaling procedures (1.44 for very, 0.42 for slightly; Gracely, R. H. and Dubner, R., 1987).

5.61.1.3.2 Bounded continuous scales: the visual analog scale

The VAS is likely the most widely used pain measurement tool. As shown in Figure 5, the VAS is usually a 10-cm line labeled at the ends with descriptors such as no pain and worst pain imaginable. Subjects indicate pain magnitude by marking the line, and a ruler is used to quantify the measurement on a 0- to 100-mm scale. Variations include vertical or horizontal alignments, placing descriptors along the scale, scales of different lengths, use of mechanical devices, and presentation on a computer or small

Figure 5 A typical visual analog scale (VAS). A horizontal 10-cm line is labeled with extremes of no pain and pain as bad as it could be. Subjects indicate pain magnitude by a mark on the line. Other formats use vertical orientations, plastic slide rules, presentations on a computer screen or handheld PDA, with different or more numerous verbal labels.

personal digital assistant (PDS) device (Jensen, M. P. *et al.*, 1986; Price, D. D., 1988; Jamison, R. N. *et al.*, 2002).

The popularity of the VAS is due to its ease of use and evidence to support the reliability and validity of this method. It has become a standard in clinical pharmacology, a field long dominated by the consistent use of four-point categorical scales of pain intensity and pain relief. The continuous nature of the VAS provides a 0–100 response resolution, limited by the observer's discriminative capacity rather than by the scale. It also allows for increased independence of multiple responses in designs requiring repeated measures, since subjects cannot remember previous responses as well as with category scales.

Other bounded continuous scales have been applied to pain assessment, usually requiring some form of apparatus. These include squeezing a handgrip dynamometer (Gracely, R. H. *et al.*, 1978b) using

a finger span device (Cooper, B. Y. *et al.*, 1986), a mechanical slide rule (Price, D. D., 1988), a slider along the back of a meter stick (McGrath, P. A. *et al.*, 1983), and a VAS presented on a PDA (Jamison, R. N. *et al.*, 2002).

Since the VAS and similar scales are bounded, representing a confined response space, they should be vulnerable to the same spatial rating biases demonstrated with category scales. They should be sensitive to stimulus range, spacing, and frequency of presentation. Subjects may spread out their responses after an analgesic intervention, reducing sensitivity. A few studies have addressed these biases and limitations of the VAS (Fernandez, E. *et al.*, 1991; Yarnitsky, D. *et al.*, 1996), but generally these effects have not been investigated in any detail.

5.61.1.3.3 Unbounded scales: ratio-scaling methods

Ratio scales are defined as having both a true zero point and a defined interval, corresponding to physical scales such as length and mass. In contrast, interval scales have a defined unit but no true zero point (Fahrenheit temperature scale). Other scales are classified as ordinal, ranks with no information about distances between values, as finishing first, second, and third in a race. The use of numbers to connote identity without order, such a sport jersey numbers, is referred to as nominal. These distinctions were emphasized by the late Stevens S. S. (1975), who promoted the use of ratio scales and developed a set of methods to produce scales with ratio properties (Engen, E., 1971b; Carterette, E. C. and Friedman, M. P., 1974; Marks, L. E., 1974; Stevens, S. S., 1975; Gescheider, G. A., 1985; Falmagne, J. C., 1986; Bolanowski, S. J. and Gescheider, G. A., 1991).

The ratio-scaling methods advocated by Stevens used instructions to rate stimulus-evoked sensations in a proportional or ratio manner. In the most commonly used ratio method of magnitude estimation, subjects used any number to rate the sensations produced by a series of stimuli. The instructions emphasized ratios or proportions, such as if a subsequent stimulus-evoked sensation felt twice as intense as a previous sensation, it should be rated by a number twice that used to describe the previous sensation. Ratio scaling avoided the biases of a bounded scale described above by offering an unlimited response continuum. This is literally true for measures such as magnitude estimation (number choice) and time duration, and virtually true for brightness (13 log unit range). Other ratio responses, which can be any adjustable continuum, may be relatively unbounded in practice but ultimately bounded due to physical (handgrip force) or safety (loudness) limitations (Gracely, R. H. and Naliboff, B. D., 1996).

The use of responses other than magnitude estimation is referred to as cross-modality matching, which describes the general case in which any adjustable response is used to match responses to any controllable stimulus modality. Magnitude estimation itself can be thought of cross-modality matching to number use.

The characteristic feature of the ratio-scaling methods advocated by Stevens S. S. (1975) is that the relationship between a particular response and a stimulus modality is described by a power function of the form $R = S^n$ in which R is the response, S the stimulus, and n the power function exponent (ignoring additive constants). This function is expressed conveniently in a logarithmic plot ($\log R = n + \log S$) since this format is linear and the exponent is equal to the slope of the function. The value of this slope, or exponent, is related to both the stimulus and the response modalities. Each modality is associated with its own specific exponent, and the theoretical exponent is the ratio of the response-specific exponent divided by the stimulus-specific exponent. Since the exponent for the very common response modality of magnitude estimation is 1, the theoretical exponent for any stimulus modality assessed by magnitude estimation would be equal to the reciprocal of the exponent of the psychophysical function, since the function exponent is equal to the response exponent (1) divided by the stimulus exponent.

The theoretical value computed from the modality-specific exponents will likely not be exactly the same since the empirical exponent is influenced by a number of other factors, including the influence of regression bias, which is a tendency to contract the response continuum, resulting in an empirical exponent always less than the theoretical exponent computed from the ratio of the response and stimulus-specific exponents. Other factors may also influence the empirical exponent. Although the open-ended nature of ratio-scaling methods such as magnitude estimation have been shown to reduce biases due to stimulus range, frequency, and spacing, there is considerable evidence that power function exponents can be influenced by factors such as stimulus range (Poulton, E. C., 1979), although the variation can be viewed as the factor that actually

determines the modality-specific exponent (Teghtsoonian, R., 1971).

Ratio-scaling methods have been applied to experimental pain assessment, with resulting power function exponents of 1.0 for radiant heat, 2.1–2.2 for contact heat, and 1.8 for electrical skin stimulation (Hardy, J. D. *et al.*, 1952; Tursky, B., 1974; Gracely, R. H., 1977; Price, D. D., 1988). However, theses applications provide examples of how experimental parameters may influence the size of the exponent. For example, the stimulus range is usually restricted in pain studies to avoid excessively high levels of pain. This restriction will tend to increase the value of the exponent. Similarly, constriction of the response scale, such as using a bounded VAS scale, will usually lower the exponent by about 50%. These lowered exponents are termed virtual exponents, since they reflect both the exponent of the underlying unrestrained continuum and the compressive effect of limiting the response range (Stevens, S. S., 1975). Price and coworkers (Price, D. D. *et al.*, 1983; Price, D. D., 1988) obtained exponents for VAS measures of thermal pain intensity (2.1–2.2) that were similar to those found with line production. However, the compressive effect should have resulted in a VAS exponent that was reduced to approximately one-half of that observed for line production. Price D. D. *et al.* (1983) posit that this lack of reduced exponent was due to specific instruction to subjects, to the use of the longer (15 versus 10 cm) scales, and experience with the range of stimuli. According to the investigators, this training essentially converts the bounded VAS to a line production response. Whatever the mechanism, the results of Price D. D. *et al.* (1983) serve as an excellent example of how the power function exponent may be manipulated by subject instructions. This is a critical issue when exponents are compared across studies that differ in instructions and scale formats.

5.61.1.4 The Different Goals of Traditional and Pain Psychophysics

Traditional Steven's psychophysics and other scaling methods have been concerned primarily with the shape of the function relating sensory magnitude to stimulus intensity. Steven's ratio-scaling methods focus on the magnitude of the slope (in log coordinates), which describes the rate-perceived intensity increases with a given increase in stimulus intensity. Most studies using these methods focus on the variation of slope with different stimulus modalities or response procedures. In addition, the function derived from ratio-scaling methods is compared to the functions obtained with different methods such as category scales in an effort to find the true function relating stimulus intensity to the magnitude of evoked sensation.

In contrast to the research focus of traditional psychophysical studies, pain psychophysics is necessarily concerned with the absolute level of sensation, addressing questions such as, "does this group experience greater pain than this group?" or "does this treatment reduce pain magnitude in comparison to a sham treatment?"

Since psychophysical methods generally focus on the shape and slope of the psychophysical function, they usually provide little information about the height of the function. In certain methods this height has little meaning. In the common use of a free modulus in ratio scaling, subjects choose their own personal unit of measurement, which arbitrarily determines the height of the psychophysical function. In another option in ratio scaling, the initial stimulus is described by a fixed response value (modulus) such as 10. The use of a modulus equalizes the units among subjects, eliminating differences in absolute magnitude between these subjects.

The emphasis on the shape of the function pervades much of the psychophysical literature, including comparisons of the different functions generated by bounded category scales and unbounded ratio-scaling procedures. Because of this emphasis on height rather than slope, much of this literature may have little applied utility to pain evaluation.

5.61.1.4.1 Adapting psychophysical methods to pain assessment

To provide absolute measurement useful for pain assessment, scales must be anchored to a subjective standard. Bounded scales include a degree of anchoring. In the bounded VAS scale, the possible range of pain from threshold to worst imaginable is represented by a short line. Thus a mark of 3 cm on a 10-cm scale represents a moderate amount of pain, a mark of 5 cm represents greater pain, and a mark of 6.7 cm represents more intense pain. Numerical category scales represent the range of possible pain magnitude in a similar response continuum. Verbal categories also present a limited response range; however, the use of verbal categories further defines

subjective standards along the scale. In a sense, verbal categories provide the anchoring of a response space in a manner similar to VAS and numerical categories, and in addition add a second anchoring system defined by the meanings of the words along the category. Subjects could conceivably use only one of these systems; they could use the meaning of the words irrespective of the number or spacing of the categories or alternatively treat the scale as a numerical scale without attending to the meaning of the words. Studies of the relative contribution of these two sources of subjective standard suggest that subjects use both sources of information in making judgments. Shifting the position of quantified descriptors from an arithmetic to a logarithmic spacing changes the scale, but not enough to suggest that subjects are only attending to word values (Gracely, unpublished observations). One feature of randomized scales discussed above is that this ambiguity is reduced, since information provided by spatial location in a list is purposefully omitted.

The anchoring provided by the limited range of bounded scales is absent in conventional ratio scaling, but can be included in several ways. In one approach, a subjective standard is used in conjunction with a modulus. Hilgard, in a study of hypnotic modification of cold pressor pain, instructed subjects to use the modulus 10 to describe a critical level of pain, one that "they would very much wish to terminate" (Hildard, E. R., 1975). In a second approach, subjects rate both pain stimuli and intermingled verbal stimuli that anchor responses, such as moderate or intense, like childbirth or headache, or pain severe enough to require medication. This second paradigm simultaneously scales the stimuli, the subjective standards, and anchors the pain responses (Gracely, R. H. and Wolskee, P. J., 1983).

A third approach uses verbal categories quantified by ratio methods. This method combines the anchoring provided by category scales with the advantages of ratio scaling, for example, permitting inferences such as, "this drug reduced pain by 36%." In this method the subjective anchors are quantified in a session separate from scaling pain sensations. The descriptors are used directly to measure pain sensations, effectively anchoring each judgment to a subjective standard. The second and third approaches are functionally similar, each with specific advantages. Pain scaling with the third, descriptor method, is efficient, with each response providing a subjective anchor. However, choosing specific descriptors forces each response into a discrete category. This method is also vulnerable to poor response behaviors, such as perseverance or use of a limited number of descriptors. Although longer, the use of the second approach that collects ratio-scaled responses to both pain and verbal stimuli may provide greater resolution and eliminate problems with the second approach.

5.61.1.5 Using Experimental Stimulation as an Anchor for Experimental and Clinical Pain Assessment

This approach uses evoked sensations as a standard anchor. Rather than match pain to a category or response space, pain is matched to pain evoked by methods such as contact heat, or matched to the intensity of a nonpainful stimulus such as the brightness of a light (Duncan, G. H. *et al.*, 1988). Another approach for clinical pain assessment anchors judgments by using the same pain rating scale to rate both clinical and experimental pain sensations (Gracely, R. H., 1979; Heft, M. W. *et al.*, 1980). The validity of these methods is dependent on little variance in experimental pain sensitivity across the population. Heat pain approaches this ideal. Other stimuli such as electrical tooth pulp stimuli are extremely variable. However, even in the case of heat there is considerable variation due to genetic (Kim, H. *et al.*, 2004; Mogil, J. S. *et al.*, 2005) and other factors. At this point it appears that the validity of an absolute pain scale must rely on the face validity of the meaning of words within a language and other scale properties such as number use and anchoring in a response space such as the VAS.

5.61.1.6 Other Suprathreshold Scaling Techniques: Discrimination and Single-Stimulus, Single-Response Designs in General

5.61.1.6.1 Discrimination

SDT evaluation of painful stimulation was presented in Section 5.61.1. Although usually used to assess detection, the applications to pain measurement have modified the procedure to assess category ratings of suprathreshold painful stimulation. In the usual detection paradigm, binary responses (detected, not detected) are made to random sequences of two stimulus conditions (present, blank). These stimulus and response pairs form a 2×2 table, with each of the four cells representing the outcomes (hit, miss, false alarm, and correct

rejection) used in the analysis. The analysis of detection examines the proportion of positive and negative responses to the presentations of a stimulus and blank stimulus, that is, between a stimulus pair and a response pair. The suprathreshold modification uses this set of stimuli and responses, and in addition, many more 2×2 tables formed from possible pairs of two stimuli and two category responses. In these cases, the lesser stimulus serves as a blank in the analysis, and the lesser response serves as a not detected. Among all of the stimulus and response possibilities, this analysis can be performed on any 2×2 table with sufficient responses in all four cells, that is, an adequate number of hits, misses, false alarms, and misses. Widely separated stimuli and response categories will usually not meet these criteria because of insufficient false alarms or misses.

The differences between direct scaling and SDT scaling are primarily in the analysis. A subject may not perceive any difference; both methods require category responses to randomly presented stimulus intensities. Each method presents multiple blocks of stimuli that vary in the number of stimuli, stimulus repetitions, and response categories. The two methods are actually similar in many respects. Direct scaling and SDT can be described as single-stimulus, single-response (SSSR) methods (Gracely, R. H. and Naliboff, B. D., 1996). All SSSR designs provide a mean response to each stimulus, and a measure of stimulus discrimination. It is clear that a mean response can be determined from any of the methods. Similarly, the evaluation of discrimination is not limited to the traditional SDT method of using a small number of stimulus intensities (e.g., four) and a large number of response categories (e.g., 12–14). A nonparametric pain-rating paradigm developed by Richard Coppola (Buchsbaum, M. S. *et al.*, 1981) uses the opposite approach; 4 responses categories are available to describe 31 stimulus intensities.

Discrimination can also be computed from the standard direct scaling paradigm in which any number of response formats are used to describe five to seven stimulus intensities presented two to four times each. The discrimination between any two stimulus pairs can be computed by parametric or nonparametric tests such as the *t*-test or the Mann–Whitney *U* test. This measure is similar to d'; both represent the ratio of difference in means of distributions and the variability of these distributions. All of the data can be used to compute overall discrimination by a parametric or nonparametric one-way analysis of variance with the stimuli as the factors and the repetitions as pseudosubjects. The resultant statistic is related to discrimination; high slopes and/or small standard errors around each stimulus will produce a large value of the statistic (e.g., *F*), while low slopes and/or large standard errors will result in small values of the statistic. This method has been applied to a study of the effect of naloxone (Gracely, R. H. *et al.*, 1987) on pain evoked by electrical tooth pulp stimulation using an analysis of variance and the *F* statistic, and to taste discrimination using the interclass correlation coefficient (ICC) as the measure of discrimination (Weiffenbach, J. M. *et al.*, 1986).

5.61.1.6.2 Sensory decision theory applications to pain assessment

A person suffering from acute or chronic pain lives with a burden that is difficult to understand unless it has been experienced. The burden is augmented by the fact that pain has no physical correlate; it is only defined and communicated by self-report. Mistrust of such reports adds to the burden of having pain; patients must fight for credibility as well as relief. Even in the laboratory, in which the level of a painful stimulus can be controlled, measures of pain are based on subjective reports. Although conventional psychophysical methods control for many biases, there is general agreement that any measure of pain can be clouded by extraneous factors that augment or reduce reported pain.

SDT was introduced to pain assessment as means of solving this problem, of separating out extraneous factors from a measure of actual pain. The method was used in studies examining the influence of placebo, nitrous oxide, the minor tranquilizer diazepam, the narcotic analgesic morphine, acupuncture, and transcutaneous electrical nerve stimulation (TENS) (Feather, B. W. *et al.*, 1972; Chapman, C. R. and Feather, B. W., 1973; Chapman, C. R. *et al.*, 1973; Clark, W. C. and Yang, Y. C., 1974; Chapman, C. R. *et al.*, 1975; Chapman, C. R. *et al.*, 1976; Yang, J. C. *et al.*, 1979). Subjects in these studies used category scales to rate the pain evoked by either electrical stimulation of the tooth pulp or heat applied to the skin. These investigations assumed that discriminative sensitivity, assessed by parameters such as d', represented true pain sensitivity, and a change in this parameter after an analgesic intervention would represent actual analgesia. Similarly, the response criterion parameter was assumed to represent response bias, and a change in only this parameter would represent a nonphysiological effect in which subjects changed the labels to describe the evoked pain sensation without any real

physiological change in this sensation. The results of these initial studies were consistent with this interpretation. Administration of placebo resulted in only a shift in the response criterion without a change in d', while the active interventions reduced d' with variable effects on the response criterion.

These results focused attention on the issues of pain measurement and generated additional studies and a lively dialog between proponents of the SDT method and critics who questioned the interpretation of the SDT variables in terms of pain sensitivity and labeling bias (Chapman, C. R., 1977; Rollman, G. B., 1977; Clark, W. C. and Yang, Y. C., 1983; Coppola, R. and Gracely, R. H., 1983). This focus identified at least three theoretical issues that potentially limit the interpretation of SDT parameters for pain evaluation (Gracely, R. H. and Naliboff, B. D., 1996). First, discriminability among sensations is not equivalent to sensory magnitude (Rollman, G. B., 1977; Coppola, R. and Gracely, R. H., 1983). It is also influenced by variability in the afferent system from receptor to brain, and cognitive variability in choosing labels to describe evoked sensations. Second, discriminability between sensations could be based on sensory qualities unrelated to pain magnitude (Gracely, R. H., 1994) such as radiation or temporal characteristics. Third, a change in the response criterion may represent analgesia. Pain is defined as a feeling of hurt with both sensory and affective components. An analgesic intervention that reduces the affective, unpleasant aspect of a pain sensation could conceivably result in a change in the response criterion without a change in the discriminability of the stimulus-evoked sensations.

The extent to which these theoretical limitations apply in practice is not known. At present, these issues can be considered to be working hypotheses to be addressed by further studies. Additional issues include the role of prepain sensation in the determination of sensitivity, and the negative influence of pain unpleasantness on discrimination of painful or nonpainful sensations. Until disproved, it may be best to assume that the influence of extraneous biases cannot be eliminated by analytical method but rather controlled as in other psychophysical experiments, through careful experimental designs that consider the many factors that can influence response behavior.

5.61.1.6.3 Pragmatic problems with a fixed set of stimulus intensities

Both direct scaling and SDT methods deliver a predetermined set of fixed stimulus values in a randomized sequence. These methods are easily applied to the evaluation of nonpainful stimuli, but become problematic when evaluating pain. Care must be taken to avoid delivering unacceptable stimulation to any person. This unacceptable level varies between healthy control subjects. One method simply limits the maximum stimulus to a value that is tolerated by the most sensitive subject. A problem with this approach is that the least sensitive individuals will not experience the same level of subjective pain as experienced by the more sensitive individuals. Another problem is that in studies of analgesia, an active drug may be identified by the effects on stimulus range; a wide range before the intervention may be contracted afterward, providing a clue that an active treatment had been administered. In addition, insensitive subjects may show no effect, since the stimuli evoked minimal pain sensations before the intervention.

These effects are observed in a group of homogenous subjects and pronounced in comparisons between normal and hypersensitive groups. The obvious solution to this problem is to determine ranges of tolerable stimulation for each individual and compute separate stimulus sets for each individual. This can be done once or possibly a second time after an analgesic intervention. This method has implications for the analysis. Rather than use parametric t-tests or analyses of variance, the analysis must use multivariate or regression methods to evaluate both the response and the subject-specific stimulus intensity associated with the response.

Direct scaling and SDT methods share another common feature. Both procedures were developed prior to laboratory computers and performed using pencil and paper methodology. Adaptations to computer administration simply automated the paper and pencil process.

5.61.1.6.4 Utility of interactive adaptive methods

A relatively recent set of procedures solves the problems with fixed stimulus sets by using interactive, computerized paradigms. These adaptive methods extend a concept developed by Cornsweet T. N. (1962), in which the stimulus series is based on the behavior of the subject. In its simplest form, this method is a tracking task in which a response of painful would lower the intensity of the next presented stimulus while a response of not painful would increase the intensity of the next presented stimulus. However, since the next stimulus is always response-

contingent, subjects, or even pigeons in the case of Cornsweet T. N. (1962), can become aware of the staircase rule and adapt simple strategies to reduce the painful stimulus (humans) or maximize positive reward (pigeons). Cornsweet's innovation minimized the contingency between the response and the change in the stimulus intensity by using two different and independent tracking paradigms and randomly alternating between them. This method of double random staircases was used in conjunction with a light detection task to demonstrate dark adaptation curves in the pigeon (Cornsweet, T. N., 1962). This method formed the basis for the method of MRS scaling of pain sensation. The MRS expanded on the double random staircase method in three ways. First, it increased the number of independent staircases, with the initial application using six staircases. Second, rather than assess only detection, the method was expanded to evaluate both detection-level and suprathreshold pain sensations. Third, the paradigm took advantage of computerization to become more interactive, with a dynamically changing amount of stimulus step size to match the method's performance to the discriminative ability of the subject.

Each staircase in the MRS is associated with a response interval between two categories or between two alternatives of a continuous rating scale (e.g., 20.5 mm on a 0- to 100-mm VAS scale). On each trial, a staircase is randomly chosen and stimulus intensity is delivered to the subject. The response determines the new stimulus intensity to be delivered the next time that particular staircase is again chosen. Different decision rules are possible; in the simplest, any response above the associated stimulus level reduces the intensity of the next delivered stimulus, while any response below the associated level increases the intensity of the next delivered stimulus. The amount the stimulus changes, the step size, is a dynamic variable particular to each staircase. It is usually large in the beginning and reduces if the direction of the response change (increase or decrease) changes too frequently (e.g., a very large step size that would administer either nonpainful or very painful stimuli). It can increase if the direction of the response change is the same over a large number of trials (e.g., an increment that is so small that the staircase never becomes painful).

The MRS method solves the problem of choosing appropriate stimulus ranges for each subject since it adjusts the range automatically. The initial stimulus values can be either set low for all staircases or set near the appropriate value by using the results of a simple ascending series. The method has a number of additional potential advantages (Gracely, R. H., 1988; Gracely, R. H., *et al.*, 1988). The results of the independent staircases can be compared to assess reliable scaling performance. Poor subject ability or compliance results in random walks for each staircase, while consistent responding produces characteristic response patterns. The method expresses the results in units of stimulus intensity, permitting simple comparisons across subjects or time. Figure 6 shows that the method can tract sensitivity over small intervals of time, demonstrating analgesia to fast-acting agents such as nitrous oxide or narcotic analgesics. Most importantly, the method results in a similar subjective range of pain in each subject regardless of individual pain sensitivities. This reduces confounds in which more sensitive subjects experience greater subjective levels of pain. In studies of pain control interventions, subjects experience the same level of pain before and after the intervention (i.e., after an efficacious analgesic the computer increases the stimulus intensities to evoke the previously experienced pain level). This minimizes biases associated with analgesic-induced reduction of the range

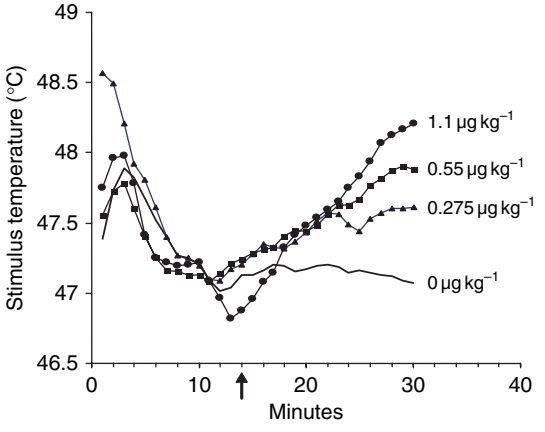

Figure 6 Fentanyl analgesia. The figure shows the effect of dose of the opioid fentanyl for the staircases titrated between moderate and intense. The double-random staircases titrated at this interval were combined into one mean staircase to show the results of four groups ($n = 16$ each). Stimulus intensity is shown on the ordinate, and time before, during, and after a 2-min double-blind intravenous infusion administered at 10 min (arrow) is shown on the abscissa. Subjects received either placebo, shown by solid line, or 0.275, 0.55, or 1.1 µg kg^{-1}fentanyl shown respectively by the triangles, squares, and circles. Fentanyl significantly increased staircase temperatures, indicating analgesia. Both rate of onset and final temperature were dose-related.

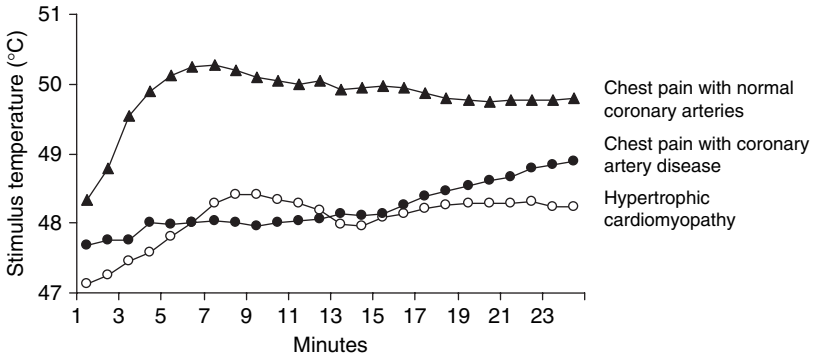

Figure 7 Multiple random staircase evaluation of thermal cutaneous pain sensitivity in cardiac patients. Threshold and suprathreshold values determined over a 34-min period are plotted for patients with chest pain and normal coronary arteries (triangles), hypertrophic cardiomyopathy (open circles), or coronary artery disease (closed circles). Stimulus temperatures required to produce these three subjective levels of pain sensation are plotted against time. These temperature differences indicate decreased cutaneous pain sensitivity in the chest pain, normal coronary artery group, suggesting that their chest pain does not result from a generalized pain sensitivity. Adapted from Cannon, R. C., Quyyumi, A. A., Schenke, W. H., Fananapazir, L., Tucker, E. E., Gaughan, A. M., Gracely, R. H., Cattan, E. L., and Epstein, S. 1990. Abnormal Cardiac Sensitivity in Patients with Chest Pain and Normal Coronary Arteries. J. Am. Coll. Cardiol. 16, 1359–1366.

of pain sensations that plagues methods that used fixed sets of stimulus intensities. Figure 7 suggests that the reductions of biases is also useful for the determination of stable values that can be compared among different groups. This figure shows the comparison of cutaneous pain sensitivity of patients suffering from angina pain, suggesting that patients with coronary artery disease are generally more sensitive than patients with pain but no evidence of coronary pathology (Cannon, R. C. *et al.*, 1990).

The last advantage is an ethical one; studies of analgesia at high stimulus intensities are achieved with less pain using the MRS method. For a simplistic example, that is, to study the analgesic effect at 10 kg of pressure, a conventional method delivers 10 kg, and an analgesic reduces the response to what would be evoked by 8 kg before the analgesic was administered. With the MRS, 8 kg is administered, which evokes a specific response. After the analgesic, the computer raises the pressure to 10 kg to evoke the same response. With the conventional method, the evaluation of the analgesic effect at 10 kg requires the subjects to experience the pain evoked by 10 kg. With the MRS method, the subjects only experience the pain produced by 8 kg of pressure.

The main principle of adaptive methods is that the intensity of stimulation delivered to the subjects is adjusted based on the subject's ratings of the sensations evoked by the stimulation. In addition to the staircase algorithm described above, which bases response change primarily on the immediate response history, an alternative method that computes probabilities from past responses provides a current best estimate of the stimulus–response function (Duncan, G. H. *et al.*, 1992). This method provides an excellent estimate of unvarying sensitivity, since all responses are used in the computation. However, these methods may not be optimal for the assessment of pain sensitivity that naturally varies, or is reduced by an analgesic intervention. In their present form, each of these procedures may be ideal for different purposes: the staircase algorithm for tracking changing pain sensitivity and the probability algorithm for evaluating unchanging sensitivity. However, the algorithm of each can be altered to approach the characteristic of the other. The sensitivity of probability methods to varying pain sensitivity can be increased by decreasing the time interval used for the computation of probabilities, while the use of a dynamic increment in staircase paradigms provides an influence of response history.

SSSR designs share common features and provide (1) information about the mean response applied to a stimulus and (2) the ability to discriminate stimulus-evoked sensations. The limitations of these parameters have been discussed above in Sensory Decision Theory Applications to Pain Assessment. The first parameter is a measure of perceived pain magnitude, influenced by a subject's response criterion. The second parameter is a measure of the intensity of the pain sensation, noise in the neural afferent system, and, most importantly, general

cognitive ability in consistently choosing the same labels to describe the same sensory magnitude. Neither is a pure measure of pain magnitude.

5.61.1.6.5 Stimulus integration: double-stimulus, single response methods

In contrast to SSSR methods in which subjects make a single response to a single stimulus, another family of methods presents two or more stimuli and collects a single response. Usually two stimuli are delivered, which could be termed a double-stimulus, single-response (DSSR) design. In the usual case, a pair of stimuli is administered on each trial and the subject chooses a single response to describe some integrated impression of the two stimuli. The analysis produces an independent scale for each stimulus set. The statistical interaction between these two scales can be used to assess both individual and group scaling performance. This evaluation of performance is a unique feature of these methods. Rather than passively collect responses to stimuli and accept the resultant scale, these procedures treat the processes as an experiment that either fails or succeeds. If successful, the separate scales are accepted. A negative outcome indicates a failure in one or more of the three operations involved in the task: scaling, integrating, or choosing a response. Two different methods have been used, differing primarily in the analysis. Functional measurement treats the responses as interval-level data and performs a parametric analysis. Conjoint measurement assumes only ordinal properties in the responses, and performs a nonparametric analysis.

This description and the term DSSR are oversimplified. In most applications to pain measurement, a subject provides a single response to two stimuli using a specified integrating operation such as averaging. The subjects could also be asked to respond to ratios, subtract or summate the sensations evoked by the two different stimuli. In other applications, two attributes of a single stimulus, rather than two separate stimuli, are assessed. In this case the integration is implicit. For example, subjects may rate the heaviness of weights varying independently in size and mass, and the analysis assesses the separate influence of mass and size without specific instructions. Applications to painful stimuli could vary both intensity and another attribute such as stimulation site, area, or stimulus duration. The design is not limited to two stimulus sets or two attributes. Subjects may integrate any number of delivered stimuli or stimulus attributes.

The literature on these DSSR methods includes a few studies that integrated pain sensations. One of the first presented all possible pairs of two identical sets of four electrocutaneous stimuli varying from 1 to 4 mA (Jones, B., 1980). Responses to the average painfulness of these stimuli were analyzed by functional measurement. A two-way analysis of variance (ANOVA) validated the method by showing two main effects and no interaction. Algom D. *et al.*, (1986) varied this design by asking subjects to integrate sensations evoked by painful and, aversive but not painful, stimuli. Subjects rated overall aversiveness of all possible pairs of six electrical stimuli and six loud auditory stimuli. Gracely R. H. and Wolskee P. J. (1983) extended the generality of this method for pain assessment (1983) by asking subjects to integrate the magnitude of pain sensations with the magnitude implied by a verbal descriptor. Subjects matched handgrip force to the average intensity of pain sensations produced by all possible pairs of five electrical tooth pulp stimuli and five verbal descriptors (weak, mild, moderate, strong, and intense). A functional measurement ANOVA analysis showed significant main effects for the tooth pulp and the verbal stimuli and a nonsignificant interaction, validating the method. This integration of somatic and verbal stimuli was replicated by Heft M. W. and Parker S. R. (1984) using electrical skin stimulation and a conjoint measurement analysis.

To summarize evaluation of a single pain dimension, SSSR methods that deliver single stimulus and collect a single response on each of multiple trials contain similar information regardless of how the response is analyzed. The responses contain information about the mean value of the stimulus and about the variability in response to the same stimulus and between different stimulus intensities. These are the most common methods for the evaluation of suprathreshold pain sensation. Measures of discrimination and response magnitude do not provide pure measures of analgesia, but are influenced by other factors such as cognitive ability and variable response criterion. These factors cannot be isolated by a SSSR method, but rather must be controlled by careful experimental design. Preliminary results with other procedures such as DSSR methods, however, may be capable of providing more information than SSSR methods, although the capabilities and limitations of these methods have not been examined in detail. Measures such as performance in DSSR designs or sensitivity measures in SDT designs may be considered as measures of performance, which may be

independent of pain or provide a behavioral measure of pain. Measures in which subjects judge intensity or some other aspect of a sensation must rely on the reduction of biases through adequate experimental control, and the anchoring of judgments to a standard. Choice of anchoring method may be based in part on which method has greater face validity: a mark on a VAS scale, a numerical category scale on a scale of 1 to 10 or 20, or the use of language and the commonalities inherent in language.

5.61.2 Pain as Dual Variables of Intensity and Unpleasantness

Pain is usually treated as a single dimension of intensity, such as heaviness. However, the history of pain literature emphasizes a second dimension. Aristotle and Plato described pain as a "passion of the soul," and contemporary science has used terms such as the reaction component, unpleasantness, discomfort, distress, affective, or evaluative.

5.61.2.1 Psychophysical Studies of Feeling States: Hedonics

Pain shares this feeling state with other sensory systems. Modalities involved with maintaining homeostatic equilibrium such as temperature and the chemical senses of taste and olfaction possess two distinct dimensions. The first is a dimension of sensory intensity that is shared with all other senses and that has been the focus of the discussion of pain measurement above. The second is a feeling state that for most homeostatic modalities can be either pleasant or unpleasant. Together, these bivalent feeling states have been described as hedonic. Generally, departures from homeostatic neutrality result in an unpleasant hedonic for sensations consistent with that departure; warm water is unpleasant if one is overheated, that is, hyperthermic. Sensations associated with the restoration of homeostatic are usually pleasant. Cool objects, air, or water feel pleasant when overheated. Thus, sensations of sensory intensity can be associated with either pleasant or unpleasant feelings; these sensations are characterized by bivalent hedonics. Hedonic ratings of sugar solutions are initially pleasant with increasing concentrations, then decline and become unpleasant at very high concentrations. Extreme temperatures are unpleasant, while more moderate departures from thermal neutrality can be pleasant. In addition to this bivalent nature, the examples above indicate that the sign and magnitude of the hedonic depends on the internal state. Hunger shifts the hedonic function for sugar solutions so that the formerly moderately pleasant concentrations become more pleasant, and formerly unpleasant concentrations become pleasant (Mower, G. *et al.*, 1977). Satiety has the opposite effect. After overeating at a buffet table, even favorite deserts lose their appeal. Similarly, thermal pleasantness or unpleasantness depends on core temperature. Water of a specific temperature can feel either pleasant or unpleasant, depending if one is hypothermic or hyperthermic (Mower, G., 1976).

In contrast to these bivalent hedonics, a number of sensations appear to be associated with only unpleasant feelings. Vertigo, nausea, and tinnitus do not usually have a positive counterpart, and of course pain is a prime example of an unpleasant sensation. This group of sensations can be characterized as having a univalent hedonic; they are unpleasant throughout the range of sensory intensity.

Although pain does not parallel the homeostatic regulatory functions of hunger, thirst, or temperature regulation, it does serve to protect the integrity of the organism by both avoiding or minimizing injurious stimulation, and once injured, to promote behaviors that maximize recuperation.

While the distinction between the sensory intensity and the hedonic dimension is readily apparent for modalities that can feel either good or bad, this distinction is less obvious for modalities such as pain that have only a univalent hedonic. Pain unpleasantness increases with intensity, and the intertwined nature may make it difficult to distinguish between these dimensions. VAS or cross-modality scales have used different sets of instructions with mixed results. Extensive instructions have been sufficient to facilitate the distinction between intensity and unpleasantness (Price, D. D., 1988), while instructions to cross-modality match or use magnitude estimation to rate unpleasantness appeared to result in scales only of the salient dimension of sensory intensity (Gracely, R. H. and Naliboff, B. D., 1996).

One tactic to avoid the influence of variable instructions is to build in the instruction by using verbal categories. The most popular example of using language to facilitate the discrimination of unpleasantness and other qualitative dimensions was initiated by Melzack R. and Torgerson W. S. (1971), who quantified a list of words compiled by Dallenbach K. M. (1939). In this study, the verbal stimuli were first sorted into discrete categories of qualitative meaning. For each category, the values of

the words within the category were computed using a Thurstone L. I. (1959) scaling analysis of stimulus rankings. The results of this study provided the core of the subsequent MPQ, which is undoubtedly the most widely used multidimensional pain assessment instrument (Melzack, R., 1975). This questionnaire and a short version are described more fully in The Need for Scaling Multiple Pain Dimensions.

Tursky B. (1976) applied Steven's ratio-scaling methods to a subset of the MPQ words. The selection of the specific words reduced the large number of categories of the Melzack and Torgerson study and the subsequent MPQ to a few dimensions common to all of pain experience. Gracely R. H. *et al.* (1978a; 1979) refined Tursky's methods by reducing the number of words further to describe two dimensions of sensory intensity and unpleasantness, and by omitting ambiguous descriptors (e.g., severe) to satisfy the criterion that the sensory intensity class could be used to described the intensity of any sensation. Initial studies demonstrated reliability and scaling consistency (Gracely, R. H., 1978a; 1978b) and subsequent studies evaluated the modulation of experimentally evoked pain sensations evoked by analgesic interventions.

5.61.2.2 Validity of Hedonic Scales

Development of separate scales to assess sensory intensity and hedonic tone does not ensure that such scales will actually assess these dimensions. It is conceivable that, regardless of the scale used, subjects may literally or figuratively take off their glasses and use the spatial properties of the scale to make responses. These responses may be made to the most salient dimension, perhaps the dimension of sensory intensity for a study assessing responses to experimental stimulation in healthy subjects and the dimension of unpleasantness for patients rating the magnitude of persistent chronic pain. This possibility must always be considered when a study finds that scales of sensory intensity and unpleasantness yield essentially the same result. Does such a finding indicate that the scales are indeed the same, or that they fail to discriminate between these dimensions?

Studies of hedonic scales establish validity in two ways. First, validity is assumed if the scales of sensory intensity and unpleasantness result in different psychophysical functions. The finding of similar functions does not invalidate the scales since the functions could be similar; thus similar scales are ambiguous for purposes of demonstrating validity. A related issue is that separate scales of intensity and hedonics should be physically similar, such as category scales or labeled VAS scales. Using different formats introduces method variance such that a finding of different psychophysical functions could represent the different scale formats and not the different subjective dimensions.

The second line of evidence for validity is that sensory and hedonic ratings are altered appropriately by interventions targeted at one or the other dimension. In the examples of temperature and taste described above, the validity of the scales is supported if manipulations that alter homeostasis alter hedonic ratings without changing ratings of sensory intensity.

Both types of evidence have been found for nonpainful modalities such as temperature, taste, and olfaction. The hedonic functions are different than ratings of sensory intensity, and are shifted by changes in internal state by manipulation of core temperature or hunger (Mower, G., 1976; Mower, G. *et al.*, 1977).

5.61.2.3 Validity of Scales of Pain Unpleasantness

Similar types of evidence have also been shown for ratings of painful stimulation. Evidence for different functions is shown in Figure 8, which summarizes the results of studies that assessed pain sensations evoked by electrical stimulation by choosing quantified descriptors of sensory intensity or unpleasantness. The result was significantly different functions. In contrast, instructions to use cross-modality matching to rate either dimensions resulted in the same function that was coincident with the verbal descriptor function of sensory intensity. This result suggests that the instructions alone were not sufficient to discriminate between these dimensions, and subjects rated the salient dimension of sensory intensity regardless of instructions to rate either sensory intensity or unpleasantness.

The second line of evidence for the validity of scales of pain unpleasantness, differential and appropriate response to an intervention, has been demonstrated in a study in which different groups of healthy controls used randomized lists of verbal descriptors to rate either the intensity or the unpleasantness of sensations evoked by electrocutaneous stimuli before and after the intravenous

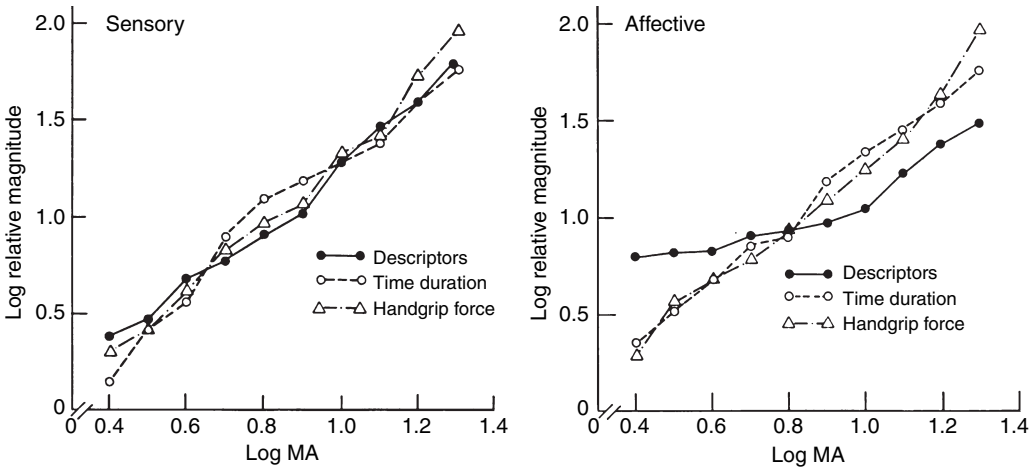

Figure 8 Verbal descriptor and cross-modality matching functions for sensory intensity and affective/unpleasantness responses. Log relative magnitude is plotted against stimulus intensity in log milliamperes. The *left graph* shows psychophysical functions derived from choosing sensory descriptors from a random list and from cross-modality matching time duration and handgrip force to the intensity of the pain sensations evoked by the stimuli. The *right graph* shows psychophysical functions derived from choosing unpleasantness descriptors from random lists and from cross-modality matching of time duration and handgrip force to the unpleasantness of the stimulus-evoked sensations. Each point is the mean of 4 observations from each of 16 subjects. All of the functions are similar except for the unpleasantness descriptor responses.

administration of the minor tranquilizer diazepam. Unpleasantness responses were reduced following diazepam while sensory intensity responses were not altered (Gracely, R. H. *et al.*, 1978b). Subsequent studies have demonstrated different functions for sensory intensity and unpleasantness (Greenspan, J. D. *et al.*, 2003) and differential effects following administration of the opioid fentanyl (Gracely, R. H. *et al.*, 1979), hypnosis (Malone, M. D., 1989; Rainville, P. *et al.*, 1997; Hofbauer, R. K. *et al.*, 2001), conditioning (Wunsh, A. *et al* 2003), and different experimental pain modalities (Rainville, P. *et al.*, 1992; Strigo, I. A. *et al.*, 2002; Dunckley, P. *et al.*, 2005). Tasks such as attending to either the localization or the unpleasantness of evoked pain have shown differential activation of lateral and medial structures, respectively (Bentley, D. E. *et al.*, 2004; Kulkarni, B. *et al.*, 2005).

5.61.2.4 The Concept of Affective Gain

Recent studies of supraspinal structures involved in sensory discrimination and unpleasantness may ultimately provide support for models of pain unpleasantness that posit an affective system that depends both on sensory input and what can be simply considered as the gain of the affective processing system (Gracely, R. H., 1992a; Price, D. D. and Harkins, S. W. 1992). Affective gain can be expressed as the amount of unpleasantness associated with a specific sensory pain intensity. Interventions that reduce the amount of unpleasantness without altering sensory intensity can be considered to reduce affective gain, while interventions that reduce both sensory intensity and unpleasantness equally can be considered to reduce only sensory input. In this case affective gain has not been changed, only the input to the affective gain system.

One result of this affective gain system is that in studies in which clinical pain varies or experimental pain is varied, there is an expected correlation between sensory intensity and unpleasantness. This correlation has led to the suggestion that the concepts of sensory intensity and unpleasantness are not independent and should be simply combined into a measure of overall pain magnitude (Gracely, R. H., 1992b). However, the affective gain, which has been expressed as the ratio of unpleasantness to sensory intensity ratings, is relatively independent of sensory intensity and a meaningful variable that has been specifically altered by pharmacological and cognitive interventions (Gracely, R. H. *et al.*, 1978b; Gracely, R. H., 1979; Malone, M. D. *et al.*, 1989; Rainville, P. *et al.*, 1997; Wunsh, A. *et al.*, 2003; Bentley, D. E. *et al.*, 2004; Kulkarni, B. *et al.*, 2005) and it varies widely over the type of experimental or clinical pain (Price, D. D. *et al.*, 1987; Rainville, P. *et al.*, 1992).

It is interesting to note that interventions can reduce only the affective gain in both pain modalities (e.g., hypnosis) and nonpainful modalities (core temperature, satiety) such as taste or temperature. This selective attenuation of affect may be only one of the few options available for intractable pain syndromes such as poststroke pain that currently are not adequately managed by available treatments. The aversive aspect of pain is not a unitary construct and includes multiple levels of distress. The term unpleasantness has been used to refer to the immediate disagreeable nature of pain that prompts withdrawal and other avoidance and escape behaviors. This conceptualization is similar to the homeostatic feelings of hunger, thirst, and hypo- or hyperthermia; all are negative feeling states that prompt behaviors that reduce the negative feeling. They are present in both animals and man. In addition to this immediate feeling state of unpleasantness, pain is also associated with an emotional or affective state that includes cognitive appraisals (thought) and described in terms of distress, hopelessness, and despair (Gracely, R. H., 1992a; Price, D. D. and Harkins S. W., 1992). Implicit in this view is an emotional state resulting from thoughts about both the present and the future consequences. While the presence of this level in animals is at least debatable, it is clear that the human ability to think about the future contributes to this secondary level of pain affect. In addition to these levels is a tertiary level that is not specific to pain (Gracely, R. H., 1992a). It is shared by all medical conditions and results from the presence of a condition, interaction with the health care system, and general concern about the present and future.

In addition to the hedonic and affective dimensions, pain varies in locus and spatial extent, and in sensory quality. Pain can be experienced in mechanical terms of pulling, squeezing, pressing, and tearing. It can be sharp or dull, deep or superficial, and localized or diffuse. Pain can burn, throb, or ache. Pain can be localized to one constant site, or spread or move. The following section describes methods that extend the measurement of pain sensation and unpleasantness to consider all secondary levels of pain affect and all of these sensory dimensions.

5.61.3 Multidimensional Pain Assessment

Sensations can be described by four attributes: location, duration, intensity, and quality. Pain can be localized and its presence or absence simply noted. Location and duration are recognized as important aspects of the pain experience, and while they are not always easily quantifiable, they are at least conceptually straightforward. In most situations, pain is treated as a single dimension of sensory intensity, although there is increasing recognition of the need to also assess pain unpleasantness. A number of approaches have extended the evaluation of pain to include all of the qualitative dimensions, affective dimensions, and in some cases the reaction to pain, including emotions, cognitions, behaviors, and neural and autonomic responses.

5.61.3.1 The Need for Scaling Multiple Pain Dimensions

The utility of extending pain measurement beyond a single dimension depends on the incremental value of the increased information in terms of diagnosis, choice of treatment, evaluation of treatment efficacy, or investigation of underlying mechanisms. In the case in which multiple pain qualities are assessed, multidimensional pain scales that determined the mixture of pain qualities present, similar to a color mixture for house paint, must demonstrate incremental utility over the assignment of a single dimension, or in the case of paint, a primary color such as blue, red, or yellow (Gracely, R. H. and Naliboff, B. D., 1996).

Clark W.C. *et al.* (1989)distinguish between restrictive and nonrestrictive measurement. Restricted measurement systems determine the number of dimensions *a priori*, while nonrestrictive systems discover the number and type of dimensions for a particular type of subject and pain condition. Naliboff points out that this distinction becomes blurred as results of these methods accumulate (Gracely, R. H. and Naliboff, B. D., 1996), "In actuality this differentiation in approach is not so clear since the objective of even 'unrestrictive' methods is to discover the real pain dimensions and therefore lead to restrictive measurement. Conversely, the system of sensory and affective dimensions was at least in part 'discovered' through empirical categorizing of reports."

Multidimensional scaling can be applied to any scale of pain intensity, and, similar to quantified category scales described above, can be used to evaluate verbal response items independent of pain experience. The most popular and widely used multidimensional pain instrument is the MPQ. The MPQ presents 20 categories of verbal descriptors with 2 to 6 descriptors per category for a total of 78

Sensory

1.	2.	3.	4.	5.
Flickering	Jumping	Pricking	Sharp	Pinching
Quivering	Flashing	Boring	Cutting	Pressing
Pulsing	Shooting	Drilling	Lacerating	Gnawing
Throbbing		Stabbing		Cramping
Beating		Lancinating		Crushing
Pounding				

6.	7.	8.	9.	10.
Tugging	Hot	Tingling	Dull	Tender
Pulling	Burning	Itchy	Sore	Taut
Wrenching	Scalding	Smarting	Hurting	Rasping
	Searing	Stinging	Aching	Splitting
			Heavy	

Affective

11.	12.	13.	14.	15.
Tiring	Sickening	Fearful	Punishing	Wretched
Exhausting	Suffocating	Frightful	Grueling	Blinding
		Terrifying	Cruel	
			Vicious	
			Killing	

Evaluative **Miscellaneous**

16.	17.	18.	19.	20.
Annoying	Spreading	Tight	Cool	Nagging
Troublesome	Radiating	Numb	Cold	Nauseating
Miserable	Penetrating	Drawing	Freezing	Agonizing
Intense	Piercing	Squeezing		Dreadful
Unbearable		Tearing		Torturing

Figure 9 Pain descriptors from the McGill Pain Questionnaire (MPQ). The 20 word sets are grouped into 4 major classes; 1–10 are sensory descriptors, 11–15 are affective descriptors, 16 is evaluative, and 17–20 are miscellaneous. Descriptors are ordered within each set based on increasing intensity of the particular pain quality. (McGill Pain Questionnaire, copyright, Ronald Melzack, 1975.)

pain-related descriptors (Figure 9). The MPQ is based on the pioneering study of Melzack R. and Togerson W. S. (1971), which used physician and nonphysician groups that classified a list of 102 pain descriptors in terms of similarity of pain quality. The words were grouped into three general classes of sensory words describing pain in terms of temporal, spacial, pressure, and thermal features, affective words describing tension, fear, and autonomic qualities, and evaluative words describing the general intensity of the pain experience. The result included 16 subclasses. In the second step, the words of each subclass where scaled for intensity. Ultimately, four additional miscellaneous categories were added for descriptors that were not adequately described by the three general categories. In theory, a patient's pain can be described by a profile of the 20 subclasses although in practice the results of the MPQ are usually expressed by the three general dimensions (sensory, affective, and evaluative) by summing the scores of the respective subclasses.

One psychometric property of the MPQ scoring system is that a general score such as the sensory class, or the overall score, can be obtained by either relatively high scores on a few subclasses or lower scores on a larger number of subclasses. This system equates a low-intensity pain with many qualities with a higher-intensity pain described by one or only a few qualities. Scaling verbosity, the tendency to choose many categories, inflates the scores. The subsequent short form of the MPQ avoids these issues by requiring a rating response to each verbal item from a subset of the MPQ items (Melzack, R., 1987).

Responses from the two forms of the MPQ and other multidimensional pain scales can be analyzed by several methods, including factor analysis, ideal

type analysis, and individual differences scaling (INDSCAL) (Gracely, R. H. and Naliboff, B. D., 1996). The factor analytic methods refine items into separate dimensions with maximal attainable internal consistency. These methods have been used to confirm 3D MPQ, and also in studies that aim to identify the true number of relevant pain dimensions (Melzack, R. and Katz, J., 1992; Holroyd, K. A. *et al.*, 1992).

However, there is an important distinction between studies that use factor analysis to analyze items in a questionnaire (the items are presented as stimuli and rated) and studies that use factor analysis to evaluate patients' actual use of a questionnaire. The analysis of items is a standard psychometric technique that indicates the number and homogeneity of the subscales in an instrument. Like the MPQ, the result is similar items grouped together by semantic similarity. In contrast, factor analysis of patient responses evaluates associative similarity (Torgerson, W. S. *et al.* 1988; Gracely, R. H., 1992b; Gracely, R. H. and Naliboff, B. D., 1996). These identify symptoms that coalesce in specific pain syndromes such as deep and throbbing or superficial and burning. They identify the constellation of symptoms found with the particular pain disorders present in the population using the scale. As Torgerson (private communication) has pointed out using a food analogy, factor analysis of items groups butter and margarine together and bread and cake together, but a factor analysis of responses to such a food scale would provide associate similarities, such as grouping bread and butter.

When factor analysis is used appropriately, the item analyses can also eliminate important information in the combinations of correlated items into a scale. For example, measures of both height and weight could be highly correlated in a sample of subjects and it might seem reasonable to combine these into an overall scale of body size. However, a consideration of the difference between the two yields potentially medically important information about conditions of overweight or underweight that would be missed by combining the similar items of height and weight into a single scale (Gracely, R. H., 1992b; Gracely, R. H. and Naliboff, B. D., 1996). Attempts to combine the correlated pain dimensions of intensity and unpleasantness into a single scale are similarly problematic because important information, the amount of unpleasantness associated with a particular pain intensity (affective gain), is lost in the process (Gracely, R. H., 1992b).

In addition to these issues, Naliboff notes that almost all factor analytic studies are based on the data collected at a single point in time and thus do not evaluate temporal properties of pain dimensions (Gracely, R. H. and Naliboff, B. D., 1996). Circadian and hormonal rhythms, pain interventions, behavioral patterns, and fluctuations in specific disease symptoms may alter the compositions of the multidimensional experience of pain that as yet is not captured by these instruments.

The subclass structure of the MPQ assumes that each descriptor represents a magnitude of a specific quality, for example that flickering, throbbing, and pounding represent different degrees of temporal variation. Torgerson and coworkers developed an alternative approach in which a descriptor could represent different amounts of various qualities (Torgerson, W. S. *et al.*, 1988). A specific descriptor could represent a pure quality, but this approach assumes that many of the pure qualities are not represented by a single word. These specific qualities were referred to as ideal types.

Torgerson's method required subjects to scale each descriptor by both its similarity to a set of ideal types and a quantitative dimension of magnitude, a study of 17 stimuli (16 from the original Melzack–Torgerson set), and identified four ideal types: bright, slow/rhythmic, thermal, and vibratory-arrhythmic. Figure 10 shows the results of studies using either sensory or affective descriptors, each in relation to three ideal types (Torgerson, W. S., 1988). Torgerson W. S. *et al.* (1988) used overlapping subsets of the original Melzack and Torgerson descriptors and ultimately derived 19 ideal types. Pain qualities as well as an overall quantitative pain intensity scale were obtained. The results generally confirmed the sensory intensity dimension of the MPQ organization with some refinement such as dividing the punctuate pressure MPQ class into separate dimensions of pricking, stabbing and drilling, boring, acknowledging the rotational character of the latter group. Words that closely matched the sensory ideal types include sharp, tugging, and pounding, and close affective types words included frightful, sickening, and cruel. Figure 11 shows the two pain descriptors closest to each of the 19 ideal types. Use of these descriptors to assess low back pain found an association between sensory qualities and diagnosis, and between the affective qualities and the psychological distress (BenDebba, M. *et al.*, 1993).

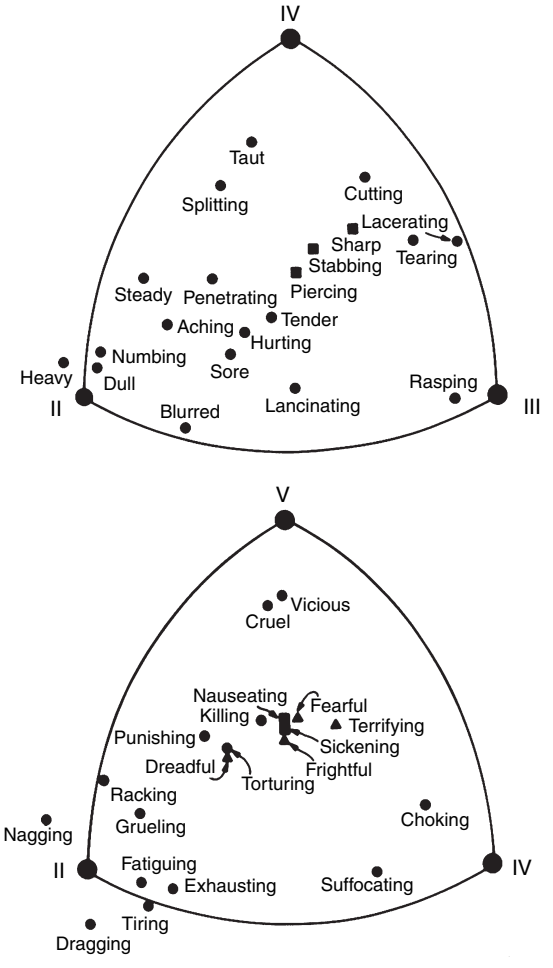

Figure 10 Surface plots illustrating the ideal type structures obtained from a set of sensory (*top*) and affective (*bottom*) words. The numbers at the vertices of the hyperspherical triangle correspond to three of the ideal types identified in each analysis. A total of four ideal types were identified for the sensory words and five for the affective words. From Torgerson, W. S., BenDebba, M., and Mason, K. J. 1988. Varieties of Pain. In: Proceedings of the Vth World Congress on Pain (*eds*. R. Dubner, G. R. Gebhart. and M. R. Bond), p. 368. Elsevier.

A third major approach to scaling multidimensional pain descriptors uses software developed to scale any type of multidimensional modality. Clark and coworkers use INDSCAL procedures combined with preference mapping (PREMAP) to define a multidimensional pain coordinate system and to place a particular judgment within this system. These software programs use judgments of proximity (sameness) to identify the number and type of dimensions inherent in the responses. As with other techniques, the meaning of the dimensions must be inferred from the configuration of the results, especially at the poles of the dimension. The PREMAP model aids in this process by having judges rate each stimuli on bipolar property scales, which are used to help interpret the meaning of the dimensions from the INDSCL analysis. This combination of INDSCAL/PREMAP method also provides a measure of the importance of each dimension to individual subjects.

Clark and coworkers have applied the INDSCAL/PREMAP method to judgments of pain descriptors, clinical pain ratings, and experimental pain stimuli. In the study of pain descriptors, 9 descriptors (mild pain, annoying, cramping, sickening, miserable, burning, unbearable pain, intense pain, and shooting) were presented to subjects in all 36 possible pairs and subjects judged the similarity of each pair of descriptors. The INDSCAL/PREMAP analysis resulted in three dimensions. Clark W. C. *et al.* (1989) labeled these three dimensions as evaluative, aversive, and somatosensory, although Syrjala K. (1989) raises issues about this interpretation. The evaluative dimension includes both pain magnitude and affective qualities. The aversive dimension also contains descriptors of pain magnitude combined with affective descriptor of sickening and shooting. The somatosensory dimension described two qualities related to depth and temporal qualities of pain.

Clark W. C. *et al.* (1989) also collected ratings from a group of patients with cancer and a control group. Interestingly, the cancer group found the affective descriptors to be less important than did the control group. Analysis of the importance of the affective variation within the patient group revealed variability in the importance of the affective descriptors, suggesting the possibility that those who found the affective dimensions to be important might be responding to interventions targeting affect such as antianxiety agents, while those assigning more importance to the somatosensory dimension might be more responsive to analgesics.

The INDSCAL/PREMAP method has also been used to assess the perceptual dimensions of pain evoked by experimental stimulation (Figure 12). Janal M. N. *et al.* (1991; 1993)delivered electrocutaneous and thermal stimuli in pairs and subjects rated the similarity of the pairs. The software identified a robust dimension of intensity and additional stimulus-specific dimensions: a frequency dimension for the electrical stimuli and a warm–hot dimension for the thermal stimuli. The intensity dimension for the

I. Sensory domain

1. Sharp Cutting	2. Boring Drilling	3. Stabbing Pricking	4. Dull Numbing	5. Rasping Tearing
6. Taut Splitting	7. Tugging Pulling	8. Squeezing Crushing	9. Hot Burning	10. Flickering Quivering
11. Pounding Throbbing	12. Itching Tickling	13. Radiating Spreading	14. Flashing Shocking	

II. Affective domain

15. Frightful Fearful	16. Dragging Fatiguing	17. Sickening Nauseating	18. Choking Suffocating	19. Cruel Vicious

Figure 11 Two pain descriptors closest to each of the 19 ideal types identified by Torgerson *et al*. From Torgerson, W. S., BenDebba, M., and Mason, K. J. 1988. Varieties of Pain. In: Proceedings of the Vth World Congress on Pain (*eds*. R. Dubner, G. R. Gebhart. and M. R. Bond), p. 368. Elsevier.

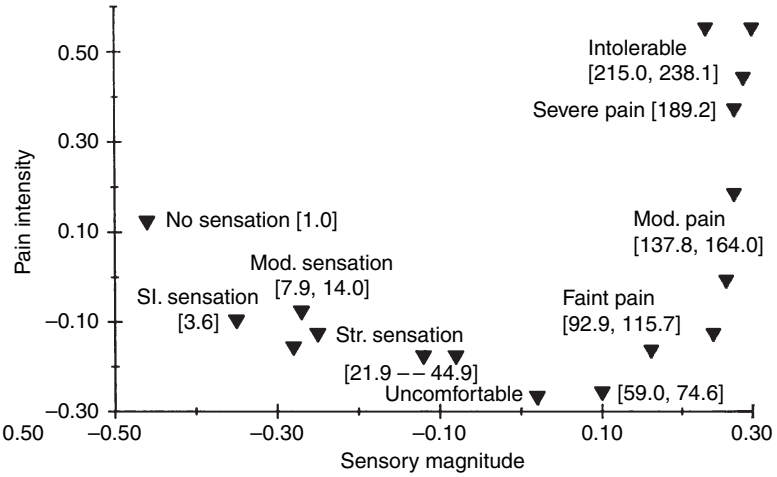

Figure 12 Sensory magnitude versus pain intensity dimensions from individual differences scaling (INDSCAL) analysis of electrocutaneous stimuli. Category labels for each stimulus are determined from the mean response from a method of limits procedure. Numbers in brackets refer to the mean power (mW) of the stimulus. Note that the stimuli labeled no sensation to faint pain order well on the abscissa (sensory magnitude dimension). Higher intensities are clustered together on the sensory magnitude dimension but separate out on the pain intensity dimension (the ordinate) from faint pain to intolerable. From Janal, M. N., Clark, W. C., and Carroll, J. D. 1991. Multidimensional scaling of painful and innocuous electrocutaneous stimuli: reliability and individual differences. Percept. Psychophys. 50, 108–116.

electrical stimuli distinguished between nonpainful and painful electrical stimulation. Together, these results suggest that this scaling approach scales the common dimension of intensity present for all stimuli and in addition produces separate scales specific to the unique characteristics of each stimulus modality.

5.61.3.2 Issues Concerning Multidimensional Scaling

The complex methods of multidimensional scaling have been shown to provide a sensitive assessment of common and stimulus-specific pain dimensions. When is this extra effort warranted? Naliboff

(Gracely, R. H. and Naliboff, B. D., 1996) identified four criteria: increase in reliability or accuracy, diagnostic sensitivity, improved evaluation of psychological and other variables that lead to improved treatment, and increasing basic knowledge of pain mechanisms.

There is at present little empirical evidence that the extra dimensions provided by these measures increase either reliability or accuracy. In most cases, the extra dimensions describe how different stimulus modalities are different, and add little to the dimensions common to all stimuli that are already adequately described by simple measures of pain intensity or possibly dual scales of pain intensity and unpleasantness. However, in certain instances, the distinction between different qualities may be important to describe pain changes in this quality (efficacy of nerve block, spontaneous change in pain qualities).

The use of these methods to determine pain quality as an aid to diagnosis has immediate face appeal. Current diagnostic decision making is based in large part on qualitative dimensions. Although these methods are promising, there are little data linking the outcome of these scales with diagnostic pain groupings. Studies have discriminated between heterogeneous groups such as back pain or headache. However, there is no evidence that these approaches provide any increase in utility over simple diagnostic tests and simple scales of one or two pain dimensions. Such evidence would have to be substantial, satisfying standard psychometric criteria for reliability, cross-validation in different setting, sensitivity, specificity, and predictive utility in relation to prevalence (Anastasi, A., 1968). If utility is demonstrated by these methods, it is likely to be in specific situations. One of the best examples of a more difficult discrimination aided by these methods is the study by Grushka M. and Sessle B. J. (1984)in which the MPQ distinguished a tooth with a reversibly inflamed pulp and a tooth in which the pulp inflammation was irreversible based on verbal pain reports.

Multidimensional analysis of pain ratings have also been proposed as a way to assess broader issues of psychological functioning in pain patients. Clark and coworkers have even suggested that questions such as "Is this patient really in pain or merely depressed?" can be addressed by an analysis of "What are the patient's coordinates in the multidimensional global pain space and which dimensions are most relevant for him?" The extension of this view is that treatment would follow from an analysis of an individual multidimensional diagnosis. A patient rating clinical pain high on a somatosensory burning dimension would receive a different medication than one with a similar pathophysiology but a greater score on a somatosensory tingling dimension or an affective dimension. To date there is no empirical support for the validity of using pain reports in this manner or for the assumption that assessment of subjective pain quality offers a more accurate and useful assessment of psychological functioning than more traditional mood or personality instruments.

Improved quantification of a patient's pain report might also increase health providers' ability to communicate, express empathy, and enlist cooperation from a suffering patient. Patients often complain that their pain report is misunderstood or dismissed by providers and perhaps a better common language could help this process. This may be especially relevant for changes in pain over the course of treatment and adjustment of pharmacological interventions. A potential difficulty with the current approach to multidimensional scaling is that the dimensions are often difficult for even the researcher to interpret. Application to the clinical setting requires translation into language with face validity for both clinicians and patients. This application of multidimensional assessment reinforces the need to examine pain as a dynamic process and to validate the ability of any multidimensional framework to monitor pain as it changes with time and treatment. In addition, the multidimensional analytical techniques applied to pain have to date emphasized the discovery and validation of painfulness dimensions, and not analytical tools for assessing pain in a clinical situation over time.

Perhaps the most promising area for application of multidimensional pain assessment is in basic research on neurophysiology and neuroanatomy of pain. There has been and will continue to be rapid growth in techniques for the study of ongoing central nervous system (CNS) processes such as functional brain imaging and CNS stimulation and recording techniques. Better quantification of a subject's subjective experience along with multiple dimensions may allow for specificity in the psychological domain corresponding to specific neurophysiological processes. For example, Lenz F. A. *et al.* (1993; 1994) have found that electrical stimulation of the thalamus in patients undergoing stereotactic neurosurgery evokes sensations that can be referred to distinct body locations. When these locations coincide with the locus of a chronic pain syndrome, the quality of the evoked pain is similar to

the quality of the pain experienced chronically by the patient. Evoked sensations located at other locations either were not painful or did not resemble the patient's clinical pain. These studies rely heavily on valid multidimensional pain assessment. In this case, the investigators used a tree-branching questionnaire that efficiently evaluated pain quality in an intraoperative environment.

5.61.4 Conclusion

Pain is in part a sensory experience that can be assessed by the methods used to evaluate other sensory modalities. While the concept of pain threshold is well known and often used to imply pain sensitivity, adequate evaluation of pain sensitivity must include the range of pain from threshold to tolerable suprathreshold intensities. While many traditional psychophysical methods focus on the relation between different stimulus intensities, pain measures strive to provide absolute pain assessment that facilitates evaluation of slow-acting analgesics or comparing pain levels between groups. Pain also varies greatly in quality, and in temporal and spatial characteristics. New measures employing multidimensional scaling and other novel methods continue to address these dimensions. Finally, similar to some modalities, pain motivates behaviors of avoidance, escape, guarding, and recuperation. It is immediately unpleasant and commands attention. If pain persists, it is associated with both plastic changes in the nervous systems and secondary affective components associated with cognitions of distress and despair. Assessment of sensory function provides an important part of the evaluation, and the application of psychophysical methods continues to increase the understanding of pain mechanisms and provide diagnostic information in individual patients. This realm of pain assessment provides necessary information, but no single approach is completely sufficient. In the clinic, measures of pain sensation and unpleasantness must be supplemented by measures from other branches of psychology and medicine, including cognitive style, personality, mood, beliefs, and function.

References

Algom, D., Raphaeli, N., and Cohen-Raz, L. 1986. Integration of noxious stimulation across separate somatosensory communications systems: a functional theory of pain. J. Exp. Psychol. Hum. Percept. Perform. 12, 92–102.

Anastasi, A. 1968. Psychological Testing, 3rd ed. Macmillan.

Anderson, N. H. 1974. Algebraic Models in Perception. In Handbook of Perception, Vol. 2 (*eds*. E. C. Carterette and M. P. Friedman), pp. 251–298. Academic Press.

Andersen, O. K., Gracely, R. H., and Arendt-Nielsen, L. 1995. Facilitation of the human nociceptive reflex by stimulation of A beta-fibres in a secondary hyperalgesic area sustained by nociceptive input from the primary hyperalgesic area. Acta Physiol. Scand. 155, 87–97.

Atkinson, R. C., Herrnstein, R. J., Lindzey, G., and Luce, R. D. 1998. Stevens Handbook of Experimental Psychology. 2nd ed., Vol. 1, Perception and Motivation. Vol. 1. John Wiley and Sons.

BenDebba, M., Torgerson, W. S., and Long, D. M. 1993. Measurement of affective and sensory qualities of back pain. *Paper presented at the 7th World Congress on Pain, Paris, France.*

Bendtsen, L., Jensen, R. A., and Olesen, J. 1997. Decreased pain threshold and tolerance in patients with chronic tension headache. Ugeskr. Laeg. 159, 4521–4525.

Benoliel, R., Eliav, E., and Iadarola, M. J. 2001. Neuropeptide Y in trigeminal ganglion following chronic constriction injury of the rat infraorbital nerve: is there correlation to somatosensory parameters? Pain 91, 111–121.

Benoliel, R., Wilensky, A., Tal, M., and Eliav, E. 2002. Application of a pro-inflammatory agent to the orbital portion of the rat infraorbital nerve induces changes indicative of ongoing trigeminal pain. Pain 99, 567–578.

Bentley, D. E., Watson, A., Treede, R. D., Barrett, G., Youell, P. D., Kulkarni, B., and Jones, A. K. 2004. Differential effects on the laser evoked potential of selectively attending to pain localisation versus pain unpleasantness. Clin. Neurophysiol. 115, 1846–1856.

Bock, R. D. and Jones, L. V. 1968. The Measurement and Prediction of Judgment and Choice. Holden-Day.

Bolanowski, S. J. and Gescheider, G. A. 1991. Ratio Scaling of Psychological Magnitude. Lawrence Erlbaum Associates, Inc.

Brennum, J., Arendt-Nielsen, L., Secher, N. H., Jensen, T. S., and Bjerring, P. 1992. Quantitative sensory examination during epidural anesthesia in man: effects of lidocaine. Pain 51, 27–34.

Buchsbaum, M. S., Davis, G. C., Copopola, R., and Naber, D. 1981. Opiate pharmacology and individual differences. I. Psychophysical pain measurements. Pain 10, 357–366.

Bujas, Z., Frank, M., and Pfaffmann, C. 1979. Neural effects of electrical taste stimuli. Sens. Processes. 3, 353–365.

Cannon, R. C., Quyyumi, A. A., Schenke, W. H., Fananapazir, L., Tucker, E. E., Gaughan, A. M., Gracely, R. H., Cattan, E. L., and Epstein, S. 1990. Abnormal Cardiac Sensitivity in Patients with Chest Pain and Normal Coronary Arteries. J. Am. Coll. Cardiol. 16, 1359–1366.

Carterette, E. C. and Friedman, M. P. 1974. Handbook of Perception, Vol. 2. Academic Press.

Chacur, M., Milligan, E. D., Gazda, L. S., Armstrong, C., Wang, H., Tracey, K. J., Maier, S. F., and Watkins, L. R. 2001. A new model of sciatic inflammatory neuritis (SIN): induction of unilateral and bilateral mechanical allodynia following acute unilateral peri-sciatic immune activation in rats. Pain 94, 231–244.

Chapman, C. R. 1977. Sensory decision theory methods in pain research: a reply to Rollman. Pain 3, 295–305.

Chapman, C. R. and Feather, B. W. 1973. Effects of diazepam on human pain tolerance and sensitivity. Psychosom. Med. 35, 330–340.

Chapman, C. R., Gehrig, J. D., and Wilson, M. E. 1975. Acupuncture compared with 33 percent nitrous oxide for dental analgesia: a sensory decision theory evaluation. Anesthesiology 42, 532–537.

Chapman, C. R., Murphy, T. M., and Butler, S. H. 1973. Analgesic strength of 33 percent nitrous oxide: a signal detection evaluation. Science 179, 1246–1248.

Chapman, C. R., Wilson, M. E., and Gehrig, J. D. 1976. Comparative effects of acupuncture and transcutaneous stimulation on the perception of painful dental stimuli. Pain 2, 265–283.

Clark, W. C. and Yang, J. C. 1974. Acupunctural analgesia? Evaluation by signal detection theory. Science 184, 1096–1098.

Clark, W. C. and Yang, J. C. 1983. Applications of Sensory Decision Theory to Problems in Laboratory and Clinical Pain. In: Pain Measurement and Assessment (*ed*. R. Melzack), pp. 15–25. Raven Press.

Clark, W. C., Janal, M. N., and Carroll, J. D. 1989. Multidimensional Pain Requires Multidimensional Scaling. In: Issues in Pain Measurement (*eds*. C. R. Chapman and J. D. Loeser), p. 285. Raven Press.

Cliff, N. 1959. Adverbs as multipliers. Psychol. Rev. 66, 27–44.

Collins, W. R. Jr., Nulsen, F. E., and Randt, C. T. 1960. Relation of peripheral nerve fiber size and sensation in man. Arch. Neurol. 3, 381–385.

Cooper, B. Y., Vierck, C. J, Jr, and Yeomans, D. C. 1986. Selective reduction of second pain sensation by systemic morphine in humans. Pain 24, 93–116.

Coppola, R. and Gracely, R. H. 1983. Where is the noise in SDT pain assessment? Pain 17, 257–266.

Cornsweet, T. N. 1962. The staircase-method in psychophysics. Am. J. Psychol. 75, 485–491.

Dallenbach, K. M. 1939. Pain: history and present status. Am. J. Psychol. 52, 331–347.

Dao, T. T. and Mellor, A. 1998. Sensory disturbances associated with implant surgery. Int. J. Prosthodont. 11, 462–469.

Doctor, J. N., Slater, M. A., and Atkinson, J. H. 1995. The descriptor differential scale of pain intensity: an evaluation of item & scale properties. Pain 61, 251–260.

Duncan, G. H., Feine, J. S., Bushnell, M. C., and Boyer, M. 1988. Use of Magnitude Matching for Measuring Group Differences in Pain Perception. In: Proceedings of the Vth World Congress on Pain (*eds*. R. Dubner, G. R. Gebhart, and M. R. Bond), pp. 383–390. Elsevier.

Duncan, G. H., Miron, D., and Parker, S. R. 1992. Yet another adaptive scheme for tracking threshold. *Meeting of the International Society for Psychophysics*, July, Stockholm, July.

Dunckley, P., Wise, R. G., Aziz, Q., Painter, D., Brooks, J., Tracey, I., and Chang, L. 2005. Cortical processing of visceral and somatic stimulation: differentiating pain intensity from unpleasantness. Neuroscience 133, 533–542.

Eliav, E. and Gracely, R. H. 1998. Sensory changes in the territory of the lingual and inferior alveolar nerves following lower third molar extraction. Pain 77, 191–199.

Eliav, E., Benoliel, R., and Tal, M. 2001. Inflammation with no axonal damage of the rat saphenous nerve trunk induces ectopic discharge and mechanosensitivity in myelinated axons. Neurosci. Lett. 311, 49–52.

Eliav, E., Herzberg, U., Ruda, M. A., and Bennett, G. J. 1999. Neuropathic pain from an experimental neuritis of the rat sciatic nerve. Pain 83, 169–182.

Eliav, E., Kamran, B., Gracely, R. H., and Benoliel, R. 2007. Evidence for chorda Tympani Dysfunction in Buring Mouth Syndrome patients. J. Orofacial. Pain 138, 628–633.

Eliav, E., Teich, S., Benoliel, R., Nahlieli, O., Lewkowicz, A. A., Baruchin, A., and Gracely, R. H. 2002. Large myelinated nerve fiber hypersensitivity in oral malignancy. Oral Surg. Oral Med. Oral Pathol. Oral Radiol. Endod. 94, 45–50.

Eliav, E., Teich, S., Nitzan, D., El Raziq, D. A., Nahlieli, O., Tal, M., Gracely, R. H., and Benoliel, R. 2003. Facial arthralgia and myalgia: can they be differentiated by trigeminal sensory assessment? Pain 104, 481–490.

Engen, T. 1971a. Psychophysics I. Discrimination and Detection. In: Experimental Psychology 3rd ed.,. (*eds*. J. W. Kling and L. A. Riggs), 3rd ed., p. 11. Holt.

Engen, T. 1971b. Psychophysics II. Scaling Methods. In: Experimental Psychology 3rd ed.,. (*eds*. J. W. Kling and L. A. Riggs), 3rd ed., p. 47. Holt.

Falmagne, J. C. 1986. Psychophysical measurement and theory. In: Handbook of Perception and Human Performance, Vol. 1, Sensory Processes and Perception (*eds*. K. R. Boff, L. Kaufman, and J. P. Thomas), John Wiley & Sons.

Feather, B. W., Chapman, C. R., and Fisher, S. B. 1972. The effect of placebo on the perception of painful radiant heat stimuli. Psychosoma. Med. 34, 290–294.

Fernandez, E., Nygren, T. E., and Thorn, B. E. 1991. An ''open-transformed scale'' for correcting ceiling effects and enhancing retest reliability: the example of pain. Percept. Psychophys. 49, 572–578.

Formaker, B. K. and Frank, M. E. 2000. Taste function in patients with oral burning. Chem. Senses 25, 575–581.

Gescheider, G. A. 1985. Psychophysics: Method, Theory, and Application. Lawrence Erlbaum Associates, Inc.

Gracely, R. H. 1977. Pain psychophysics. Doctoral dissertation, Department of Psychology, Brown University.

Gracely, R. H. 1979. Psychophysical Assessment of Human Pain. In: Advances in pain research and therapy, Vol. 3 (*eds*. J. J. Bonica, J. C. Liebeskind, and D. G. Able-Fessard), pp. 805–824. Raven Press.

Gracely, R. H. 1988. Multiple Random Staircase Assessment of Thermal Pain Perception. In: Proceedings of the Fifth World Congress on Pain (*eds*. R. Dubner, M. Bond, and G. Gebhart), p. 391. Elsevier.

Gracely, R. H. 1991. Experimental Pain Models. In: Advances in Pain Research and Therapy. Vol. 18, The Design of Analgesic Clinical Trials, (*eds*. M. Max, R. Portenoy, and E. Laska), p. 33, Raven Press.

Gracely, R. H. 1992a. Affective dimensions of pain: how many and how measured? APS J. 71, 243–247.

Gracely, R. H. 1992b. Evaluation of multidimensional pain scales. Pain 48, 297–300.

Gracely, R. H. 1994. Methods of Testing Pain Mechanisms in Normal Man. In: Textbook of Pain, 3rd edition. (*eds*. P. D. Wall and R. Melzack), p. 315. Churchill Livingstone.

Gracely, R. H. and Dubner, R. 1987. Reliability and validity of verbal descriptor scales of painfulness. Pain 29, 175–185.

Gracely, R. H. and Kwilosz, D. M. 1988. The descriptor differential scale: applying psychophysical principles to clinical pain assessment. Pain 35, 279–288.

Gracely, R. H. and Naliboff, B. D. 1996. Measurement of Pain Sensation. In: Handbook of Perception and Cognition: Somatosensory Systems (*ed*. L. Kruger), p. 243. Raven Press.

Gracely, R. H. and Wolskee, P. J. 1983. Semantic functional measurement of pain: integrating perception and language. Pain 15, 389–398.

Gracely, R. H., Deeter, W. R., Wolskee, P. J., and Dubner, R. 1987. Does naloxone alter experimental pain perception? Soc. Neurosci. Abstr. 6, 246.

Gracely, R. H., Dubner, R., and McGrath, P. A. 1979. Narcotic analgesia: fentanyl reduces the intensity but not the unpleasantness of painful tooth pulp stimulation. Science 203, 1261–1263.

Gracely, R. H., Lota, L., Walther, D. J., and Dubner, R. 1988. A multiple random staircase method of psychophysical pain assessment. Pain 32, 55–63.

Gracely, R. H., McGrath, P. A., and Dubner, R 1978a. Ratio scales of sensory and affective verbal pain descriptors. Pain 5, 5–18.

Gracely, R. H., McGrath, P., and Dubner, R. 1978b. Validity and sensitivity of ratio scales of sensory and affective verbal pain descriptors: manipulation of affect by diazepam. Pain 5, 19–29.

Gracely, R. H., Taylor, F., Schilling, R. M., and Wolskee, P. J. 1984. The effect of a simulated analgesic on verbal descriptor and category responses to thermal pain. Pain Suppl. 2, 173.

Greenspan, J. D., Roy, E. A., Caldwell, P. A., and Farooq, N. S. 2003. Thermosensory intensity and affect throughout the perceptible range. Somatosens. Mot. Res. 20, 19–26.

Grushka, M. 1987. Clinical features of burning mouth syndrome. Oral Surg. Oral Med. Oral Pathol. 63, 30–36.

Grushka, M. and Sessle, B. J. 1984. Applicability of the McGill Pain Questionnaire to the differentiation of 'toothache' pain. Pain 19, 49–57.

Grushka, M. and Sessle, B. 1988. Taste dysfunction in burning mouth syndrome. Gerodontics 4, 256–258.

Grushka, M. and Sessle, B. J. 1991. Burning mouth syndrome. Dent. Clin. North Am. 35, 171–184.

Grushka, M., Epstein, J. B., and Gorsky, M. 2002. Burning mouth syndrome. Am. Fam. Physician 65, 615–620.

Grushka, M., Epstein, J. B., and Gorsky, M. 2003. Burning mouth syndrome and other oral sensory disorders: a unifying hypothesis. Pain Res. Manag. 8, 133–135.

Hagberg, C., Hellsing, G., and Hagberg, M. 1990. Perception of cutaneous electrical stimulation in patients with cranioman-dibular disorders. J. Craniomandib. Disord. 4, 120–125.

Hansson, P. 2002. Neuropathic pain: clinical characteristics and diagnostic workup. Eur. J. Pain 6(Suppl), A47–A50.

Hardy, J. D., Wolff, H. G., and Goodell, H. S. 1952. Pain Sensations and Reactions. Hafner.

Hargreaves, K. M., Dionne, R. A., Meuller, G. P., Goldstein, D. S., and Dubner, R. 1986. Naloxone, fentanyl and diazepam modify plasma beta-endorphin levels during surgery. Clin. Pharmacol. Ther. 40, 165–171.

Heft, M. W. and Parker, S. R. 1984. An experimental basis for revising the graphic rating scale. Pain 19, 153–161.

Heft, M. W., Gracely, R. H., Dubner, R., and McGrath, P. A. 1980. A validation model for verbal descriptor scaling of human clinical pain. Pain 9, 363–373.

Hildgard, E. R. 1975. The alleviation of pain by hypnosis. Pain 1, 213–231.

Hofbauer, R. K., Rainville, P., Duncan, G. H., and Bushnell, M. C. 2001. Cortical representation of the sensory dimension of pain. J. Neurophysiol. 86, 402–411.

Holroyd, K. A., Holm, F. J., Keefe, F. J., Turner, J. A., Bradley, L. A., Murphy, W. D., Johnson, P., Anderson, K., Hinkle, A. L., and O'Malley, W. B. 1992. A multi-center evaluation of the McGill Pain Questionnaire: results from more than 1700 chronic pain patients. Pain 48, 297–300.

Jamison, R. N., Gracely, R. H., Raymond, S. A., Levine, J. G., Marino, B., Hermann, T. J., Daly, M., Fram, D., and Katz, N. P. 2002. Comparative study of electronic vs. paper VAS ratings: a randomized, crossover trial using healthy volunteers. Pain 99, 341–347.

Janal, M. N., Clark, W. C., and Carroll, J. D. 1991. Multidimensional scaling of painful and innocuous electrocutaneous stimuli: reliability and individual differences. Percept. Psychophys. 50, 108–116.

Janal, M. N., Clark, W. C., and Carroll, J. D. 1993. Multidimensional scaling of painful electrocutaneous stimulation: INDSCAL dimensions, signal detection theory indices, and the McGill Pain Questionnaire. Somatosens. Mot. Res. 10, 31–39.

Jensen, M. P. and McFarland, C. A. 1993. Increasing the reliability and validity of pain intensity measurement in chronic pain patients. Pain 55, 195–203.

Jensen, M. P., Koroly, P., and Braver, S. 1986. The measurement of clinical pain intensity: a comparison of six methods. Pain 27, 117–126.

Jones, B. 1980. Algebraic models for integration of painful and nonpainful electric shocks. Percept. Psychophys. 28, 572–576.

Kemler, M. A., Schouten, H. J., and Gracely, R. H. 2000. Diagnosing sensory abnormalities with either normal values or values from contralateral skin: comparison of two approaches in complex regional pain syndrome I. Anesthesiology 93, 718–727.

Kim, H., Neubert, J. K., San Miguel, A., Xu, K., Krishnaraju, R. K., Iadarola, M. J., Goldman, D., and Dionne, R. A. 2004. Genetic influence on variability in human acute experimental pain sensitivity associated with gender, ethnicity and psychological temperament. Pain 109, 488–496.

Koltzenburg, M., Stucky, C. L., and Lewin, G. R. 1997. Receptive properties of mouse sensory neurons innervating hairy skin. J. Neurophysiol. 78, 1841–1850.

Kulkarni, B., Bentley, D. E., Elliott, R., Youell, P., Watson, A., Derbyshire, S. W. G., Frackowiak, R. S. J., Friston, K. J., and Jones, A. K. P. 2005. Attention to pain localization and unpleasantness discriminates the functions of the medial and lateral pain systems. Eur. J. Neurosci. 21, 3133–3142.

Kwilosz, D. M., Gracely, R. H., and Torgerson, W. S. 1984. Memory for post-surgical dental pain. Pain Suppl. 2, 426.

Kwilosz, D. M., Schmidt, E. A., and Gracely, R. H. 1986. Assessment of clinical pain: cross-validation of parallel forms of the descriptor differential scale. Am. Pain Soc. Abstr. 6, 81.

LaMotte, R. H. and Campbell, J. N. 1978. Comparison of responses of warm and nociceptive C-fiber afferents in monkey with human judgments of thermal pain. J. Neurophysiol. 41, 509–528.

Lembo, A., Naliboff, B., Matin, K., Munakata, J., Parker, R., Gracely, R. H., and Mayer, E. A. 2000. Irritable bowel syndrome patients show altered sensitivity to exogenous opioids. Pain 87, 137–147.

Lenz, F. A., Gracely, R. H., Hope, E. J., Baker, F. H., Rowland, L. H., Dougherty, P. M., and Richardson, R. T. 1994. The sensation of angina pectoris can be evoked by stimulation of the human thalamus. Pain 59, 119–125.

Lenz, F. A., Seike, M., Richardson, R. T., Lin, Y. C., Baker, F. H., Khoja, I., Yeager, C. J., and Gracely, R. H. 1993. Thermal and pain sensations evoked by microstimulation in the area of human ventrocaudal nucleus (Vc). J. Neurophysiol. 70, 200–212.

Lindemann, B. 1996. Taste reception. Physiol. Rev. 76, 718–766.

Malone, M. D., Kurtz, R. M., and Strube, M. J. 1989. The effects of hypnotic suggestion on pain report. Am. J. Clin. Hypn. 31, 221–230.

Marks, L. E. 1974. Sensory Processes: The New Psychophysics. Academic Press.

McArthur, D. L., Cohen, M. J., and Schandler, S. L. 1991. Rash analysis of functional assessment scales: and example using pain behaviors. Arch. Phys. Med. Rehabil. 72, 296–304.

McGrath, P. A., Gracely, R. H., Dubner, R., and Heft, M. W. 1983. Non-pain and pain sensations evoked by tooth pulp stimulation. Pain 15, 377–388.

Melzack, R. 1975. The McGill Pain Questionnaire: major properties and scoring methods. Pain 1, 277–299.

Melzack, R. 1987. The short-form McGill Pain Questionnaire. Pain 30, 191–197.

Melzack, R. and Katz, J. 1992. The McGill Pain Questionnaire: Appraisal and Current Status. In: Handbook of Pain Assessment (*eds*. D. C. Turk and R. Melzack), p. 152. Guilford Press.

Melzack, R. and Torgerson, W. S. 1971. On the language of pain. Anesthesiology 34, 50–59.

Mogil, J. S., Miermeister, F., Seifert, F., Strasburg, K., Zimmermann, K., Reinold, H., Austin, J. S., Bernardini, N., Chesler, E. J., Hofmann, H. A., Hordo, C., Messlinger, K., Nemmani, K. V., Rankin, A. L., Ritchie, J., Siegling, A.,

Smith, S. B., Sotocinal, S., Vater, A., Lehto, S. G., Klussmann, S., Quirion, R., Michaelis, M., Devor, M., and Reeh, P. W. 2005. Variable sensitivity to noxious heat is mediated by differential expression of the CGRP gene. Proc. Natl. Acad. Sci. U. S. A. 102, 12938–12943.
Mower, G. 1976. Perceived intensity of peripheral thermal stimuli is independent of internal body temperature. J. Comp. Physiol. Psychol. 90, 1152–1155.
Mower, G., Mair, R., and Engen, T. 1977. Influence of internal factors on the perception of olfactory and gustatory stimuli. In: The Chemical Senses and Nutrition. (*eds*. M. R. Hare and O. Maller), Academic Press.
Mott, A. E., Grushka, M., and Sessle, B. J. 1993. Diagnosis and management of taste disorders and burning mouth syndrome. Dent. Clin. North Am. 37, 33–71.
Parducci, A. 1974. Contextual Effects: A Range-Frequency Analysis. In: Handbook of Perception, Vol. 2 (*eds*. E. C. Carterette and M. P. Friedman), p. 127. Academic Press.
Petzke, F., Clauw, D. J., Ambrose, K., Khine, A., and Gracely, R. H. 2003a. Increased pain sensitivity in fibromyalgia: effects of stimulus type and mode of presentation. Pain 105, 403–413.
Petzke, F., Gracely, R. H., Park, K. M., Ambrose, K., and Clauw, D. J. 2003b. What do tender points measure? Influence of distress on 4 measures of tenderness. J. Rheumatol. 30, 567–574.
Pollack, I. 1965. Iterative techniques for unbiased rating scales. Q. J. Exp. Psychol. 17, 139–148.
Price, D. D. 1988. Psychological and Neural Mechanisms of Pain., Raven Press.
Price, D. D. and Harkins, S. W. 1992. The affective-motivational dimension of pain: a two stage model. APS J. 1, 229–239.
Price, D. D., Harkins, S. W., and Baker, C. 1987. Sensory-affective relationships among different types of clinical and experimental pain. Pain 28, 297–307.
Price, D. D., McGrath, P. A., Rafii, A., and Buckingham, B. 1983. The validation of visual analogue scales as ratio scale measures in for chronic and experimental pain. Pain 17, 45–56.
Price, D. D., McHaffie, J. G., and Larson, M. A. 1989. Spatial summation of heat-induced pain: influence of stimulus area and spatial separation of stimuli on perceived pain sensation intensity and unpleasantness. J. Neurophysiol. 62, 1270–1279.
Poulton, E. C. 1979. Models for biases in judging sensory magnitude. Psychol. Bull. 86, 777–803.
Rainville, P., Duncan, G. H., Price, D. D., Carrier, B., and Bushnell, M. C. 1997. Pain affect encoded in human anterior cingulated but not somatosensory cortex. Science 277, 968–971.
Rainville, P., Feine, J. S., Bushnell, M. C., and Duncan, G. H. 1992. A psychophysical comparison of sensory and affective responses to four modalities of experimental pain. Somatosens. Mot. Res. 9, 265–277.
Rollman, G. B. 1977. Signal detection theory measurement of pain: a review and critique. Pain 3, 187–211.
Sang, C. N., Max, M. B., and Gracely, R. H. 2003. Stability and reliability of detection thresholds for human A-Beta and A-delta sensory afferents determined by cutaneous electrical stimulation. J. Pain Symptom Manage. 25, 64–73.
Ship, J. A., Grushka, M., Lipton, J. A., Mott, A. E., Sessle, B. J., and Dionne, R. A. 1995. Burning mouth syndrome: an update. J. Am. Dent. Assoc. 126, 842–853.
Stevens, S. S. 1975. Psychophysics: Introduction to its Perceptual, Neural and Social Prospects. Wiley.
Stohler, C. S., Kowlski, C. J., and Lund, J. P. 2001. Muscle pain inhibits cutaneous touch perception. Pain 92, 327–333.
Strigo, I. A., Bushnell, M. C., Boivin, M., and Duncan, G. H. 2002. Psychophysical analysis of visceral and cutaneous pain in human subjects. Pain 97, 235–246.
Svensson, P., Graven-Nielsen, T., and Arendt-Nielsen, L. 1998. Mechanical hyperesthesia of human facial skin induced by tonic painful stimulation of jaw muscles. Pain 74, 93–100.
Svensson, P., List, T., and Hector, G. 2001. Analysis of stimulus-evoked pain in patients with myofascial temporomandibular pain disorders. Pain 92, 399–409.
Swets, J. A. 1964. Signal detection and recognition by human observers, Wiley.
Syrjala, K. 1989. Multidimensional Versus Unidimensional Scaling: Little To Debate, Much To Determine. In: Issues in Pain Measurement (*eds*. C. R. Chapman and J. D. Loeser), p. 327. Raven Press.
Teghtsoonian, R. 1971. On the exponents in Stevens' law and the constant in Ekman's law. Psychol. Rev. 78, 71–80.
Thurstone, L. I. 1959. The measurement of values. University of Chicago Press.
Torgerson, W. S. 1958. Theory and Methods of Scaling. John Wiley and Sons.
Torgerson, W. S., BenDebba, M., and Mason, K. J. 1988. Varieties of Pain. In: Proceedings of the Vth World Congress on Pain (*eds*. R. Dubner, G. R. Gebhart. and M. R. Bond), p. 368. Elsevier.
Tursky, B. 1974. Physical physiological and psychological factors that affect pain reaction to electric shock. Psychophysiology 11, 95–112.
Tursky, B. 1976. The Development of a Pain Perception Profile: A Psychophysical Approach. In: Pain: New Perspectives in Therapy and Research (*eds*. M. Weisenberg and B. Tursky), p. 171. Plenum Press.
Vecchiet, L., Giamberardino, M. A., and Saggini, R. 1991. Myofascial pain syndromes: clinical and pathophysiological aspects. Clin. J. Pain 7 (Suppl), 1, S16–S22.
Walther, D. J. and Gracely, R. H. 1986. Ratio scales of pleasantness and unpleasantness affective descriptors. Am. Pain Soc. Abstr, 6, 34.
Weiffenbach, J. M., Cowart, B. J., and Baum, B. J. 1986. Taste intensity perception in aging. J. Gerontol. 41, 460–468.
Wunsch, A., Philippopt, P, and Plaghki, L. 2003. Affective associative leaning modifies the sensory perception of nociceptive stimuli without participant' awareness. Pain 102, 27–38.
Yang, J. C., Clark, W. C., Ngai, S. H., Berkowitz, B. A., and Spector, S. 1979. Analgesic action and pharmaco-kinetics of morphine and diazepam in man: an evaluation by sensory decision theory. Anesthesiology 51, 495–502.
Yarnitsky, D., Sprecher, E., Zaslansky, R., and Hemli, J. A. 1996. Multiple session experimental pain measurement. Pain. 67, 327–333.

Further Reading

ACR: Report of the Multicenter Criteria Committee. 1990. 1990 classification criteria of fibromyalgia from the American College of Rheumatology. Union Med. Can. 119, 272.
Gracely, R. H. 1985. Pain psychophysics. In: Advances in Behavioral Medicine Vol. 1 (*ed*. S. Manuk), JAI Press.
Price, D. D., Bush, F. M., Long, S., and Harkins, S. W. 1994. A comparison of pain measurement characteristics of mechanical and simple numerical rating scales. Pain 56, 217–226.
Rainville, P., Carrier, B., Hofbauer, R. K., Bushnell, M. C., and Duncan, G. H. 1999. Dissociation of sensory and affective dimensions of pain using hypnotic modulation. Pain 82, 159–171.
Warren, R. M. and Warren, R. P. 1963. A critique of SS Stevens' ''new psychophysics'' Percept. Mot. Skills 16, 797–810.

5.62 Consciousness and Pain

M Devor, Hebrew University of Jerusalem, Jerusalem, Israel

© 2008 Elsevier Inc. All rights reserved.

5.62.1	Introduction	961
5.62.2	Definitions	962
5.62.3	Pain and the Neurobiology of Consciousness	962
5.62.4	Pain versus Nociception	964
5.62.5	Neural Correlates of Pain Perception	964
5.62.5.1	Central Nervous System Activation	964
5.62.5.2	Central Nervous System Lesions	965
5.62.5.3	Central Nervous System Stimulation	965
5.62.6	Contents of Consciousness versus Its Presence	966
5.62.6.1	Contents	966
5.62.6.2	Pain and Loss of Consciousness	966
5.62.7	Conclusion	967
References		967

Glossary

the hard problem Mechanism or algorithm that accounts for the emergence of conscious experience and willed action from neural activity. The expression was coined by Chalmers D. (1995).

locked in Neurological condition, usually due to severe brain injury, in which an individual is awake and alert but completely paralyzed and unable to express himself with words or movement.

MPTA (mesopontine tegmental anesthesia area) Restricted location in the reticular formation bordering the brainstem mesencephalon and pons at which microinjection of minute quantities of pentobarbital, and other $GABA_A$-receptor active drugs, induces a brief period of general anesthesia.

nocifensive response Adaptive behavioral responses intended to avoid, minimize, or escape from noxious, tissue-threatening stimuli. Examples are the flexor reflex as well as more complex escape, distress vocalization, and avoidance behaviors. The term nocifensive does not necessarily imply a reasoned, intentional response.

stress-induced analgesia The observation that stressful events such as electrical shock or forced cold-water swim may be followed by a period of reduced pain sensitivity.

5.62.1 Introduction

Pain is a sensory and emotional experience, a mental state (Merskey, H., 1986). As such, it cannot be properly addressed without reference to the conscious brain. Analysis of skin receptors, spinal pathways, and other substrates of pain without considering the resulting conscious experience is analysis of nociception, not pain *per se* (see below). The hard problem of how neural activity gives rise to conscious experience and willed action is probably intractable as a subject of philosophical analysis (McGinn, C., 1999). However, despite alleged semantic proofs to the contrary, it should ultimately be amenable to solution using neurobiological tools. Just as life is now understood without reference to supernatural vital spirits, the proposition that consciousness is a bodiless ghost temporarily resident in the gray matter is implausible. It is too obviously subject to conventional neurobiological variables such as circadian

rhythmicity, pharmacological modifiers of membrane excitability and synaptic action, blood glucose levels, and so forth. Consciousness is a product of neural activity; there is nothing spooky about it (Searle, J. R., 1992). And while new principles might have to emerge before we fully understand it, they will be natural ones that play out within the cranial vault.

At present we do not know whether the hard problem is hard because of intrinsic complexity (like decoding the genome) or hard only because nobody has yet had the flash of insight necessary to see the essence of the problem and its simple solution. Think of a puzzle many of us faced as kids where six toothpicks were laid on the table and we were challenged to use them to construct four equilateral triangles. You can spend a lifetime working on this one, or solve it in a second by raising the toothpicks off the plane of the table to form a pyramid. Knowledge that the problem has a solution can help keep you from giving up, but it does not provide hints as to how to proceed, nor does it let you know in which of these two senses the problem is hard.

5.62.2 Definitions

Like alert awareness in general, the experience of pain is a causal consequence of neural activity in the brain – the execution of a neural algorithm. Unfortunately, we do not have the foggiest idea of how this algorithm operates, nor can we even conceive of an algorithm whose output would constitute pain experience. This is the reason that current attempts to define consciousness are basically futile. The numerous definitions that have been proposed are not definitions at all, but either metaphors (spotlight, stage, narrator, multiple drafts, etc.) or semantic restatements (e.g., alertness, subjective experience, self). Imagine some large-headed extraterrestrial arriving on earth and delivering the pain algorithm in the form of compiled code ready to run on a Pentium IV. He assures us that the computer is now conscious and experiences pain given an appropriate input signal. But would we have any way of knowing if this was in fact so unless he were willing to explain the principle in a way we could grasp? The red flashing icon that hurts would clearly prove nothing . . . you don't need a large head to make a computer do that. The computer analogy itself may be flawed . . . perhaps an entirely different sort of physical architecture is required to implement the algorithm.

The erstwhile conscious Pentium is not unlike humans who become locked in due to central nervous system (CNS) damage and are unable to feel, move, or communicate. However, reports of locked-in patients who found a way to make themselves understood (e.g., by an eye-blink code) leave no doubt that one can be fully awake and aware despite having no way of letting others know (Bauby, J.-D., 1997). Pain is subjective, inaccessible to others, not in its essence but because we do not yet know how to assess it objectively. This may change as noninvasive brain imaging technologies improve. It is important to realize that our inability to conceive of an algorithm that generates awareness in no way undermines the fact that such an algorithm is running in my brain right now, and in yours. To insist that research on the biology of consciousness must begin with a definition is misguided. It stymies research on the subject unnecessarily, before it has begun. The definition is the algorithm; it is the endpoint of the research, not the starting point. But where to begin?

5.62.3 Pain and the Neurobiology of Consciousness

Although they are private, first-person experiences, we can usually detect whether a person or an animal is conscious or unconscious, or in pain, by simple observations of behavior. This is enough to provide operational definitions for research. True, there may be gray areas (and deceit), but the problem is minor as long as one avoids subtle distinctions and sticks to major effects (see below). Thus, even without knowing the computation that generates conscious experience, practical experiments should be able to uncover some of its general characteristics. For example, it might be possible to learn whether the computation is carried out in a distributed manner or focally, and if focally, in what part of the brain. Beyond that, simply engaging in relevant biological research holds out the prospect that the imagination might be primed, increasing the likelihood of an intuitive leap taking place. Six toothpicks a pyramid makes.

Pain is a favorable point of entry into the neurobiology of consciousness for several reasons. First among them is its immediacy. In the visual system, extensive computation is required to extract meaning from contrasts falling on the retina. Is it a cloud

passing by or a rhinoceros charging? Only after this image analysis is completed does the visual scene become a useful object of attention. We do not have conscious access to the intermediate stages of visual image analysis just as we are not aware of the detailed command sequences sent spinally by our motor cortex, or the workings of our autonomic nervous system. The system delivers to a conscious brain the end product of the analysis, a meaningful visual scene, smooth gait, or a feeling of wellness. Output of the analysis is input to the consciousness algorithm. Injury to image analysis or motor sequencing functions of the brain may be crippling, but they cause blindness and spasticity, not obtunded consciousness or coma. Essential meaning in the pain system is an answer to the question: "Is it good for me or bad for me?" But unlike in vision, this information is available without extensive signal processing. Entry into the circuitry of consciousness via the pain system probably takes place within a synapse or two of the dorsal horn. A painful stimulus captures attention like no other.

A second advantageous feature of the pain system is the variable relation between provoking stimuli and the resulting percept. Photons of 450 nm invariably evoke blue, but 48 °C heat pulses do not necessarily evoke pain. The stimulus-color response function adjusts somewhat to environmental contingencies (e.g., color constancy despite variable illumination), but not nearly so robustly as the stimulus-pain response function. For example, at times of danger, pain normally evoked by an intense noxious stimulus, for example, an injury, may be completely suppressed (Melzack, R. *et al.*, 1982). It is generally presumed that this stress-induced analgesia evolved to increase the likelihood of successful fight or flight. Intense pain captures attention, occupying cerebral resources and degrading performance in other spheres. In an existential emergency, performance is critical; the wound can wait. In effect, the pain system disconnects the signal analysis (nociception) from the percept (pain). How is this done?

Most data suggest that the disconnect between injury and pain is executed primarily in the spinal cord. This is unlike color constancy, which is a cortical function. Disconnect reflects, at least in part, the operation of a specific neural circuit with a nodal point in the midbrain periaqueductal gray (PAG) and a variety of defined efferent effector pathways that employ known neurotransmitters, including bioamines and endogenous opiates (Fields, H. L. and Basbaum, A. I., 1999). The intrinsic descending pain control system(s), or something like it, is probably also engaged in other situations of noxious stimulus-pain disconnect such as the placebo effect, distracted attention, and hypnosis (Rainville, P. *et al.*, 1997; Benedetti, F. *et al.*, 1999). Appreciation of behavioral context (danger, anticipation, belief, and distraction) is a complex, multisensory, cortical function to be sure, but the actual pain disconnect appears to be carried out in the spinal cord or brainstem. Situations in which defined stimulus configurations yield alternative percepts, for example, ambiguous figures like the Necker cube, are fascinating grist for consciousness research. But in the pain system some of the actual neural pathways that implement flip-flop between alternative percepts (viz pain or no pain to a fixed noxious stimulus) have been worked out. For example, under some circumstances pharmacological blockade of enkephalinergic synapses can block the effect of placebos (Benedetti, F. *et al.*, 1999; Skoubis, P. D. *et al.*, 2005). We are talking here about the neural circuitry of belief and anticipation.

A third salient feature of the pain system is that a qualitative, emotional vector is an essential feature of the sensory experience. Authorities on pain psychophysics insist that people can assign a separate value to pain intensity and pain unpleasantness (Rainville, P. *et al.*, 1997). Moreover, drugs and lesions are said to be capable of dissociating between the two: "It hurts just as much as before, but it no longer bothers me" (i.e., no longer causes suffering). This is reflected in extensive involvement of the limbic system in functional brain imaging activations as well as in neuroanatomical connectivity (Peyron, R. *et al.*, 2000). A surprisingly large fraction of the human brain, including extensive regions of the frontal neocortex, appears to be devoted to limbic functions. Affect is undoubtedly an essential, if enigmatic, part of the circuitry of consciousness.

Finally, assuming a willingness to grant that animals, mammals at least, have mental states and neural mechanisms homologous to those that subserve conscious experience in man, the analysis of pain in animals offers a useful experimental shortcut. Present a red triangle to a monkey and it undoubtedly has a corresponding visual percept. To be certain, however (the beast may be daydreaming), and to know that both color and shape information were perceived, it is usually necessary to train the monkey beforehand in order to get an informative behavioral response. In the pain system behavioral responses that mark pain perception, nocifensive

responses, are built in, at least partly circumventing the need for extensive operant conditioning. Such responses include reflexes as well as complex escape behavior, distress vocalization, avoidance, and other such nonreflexive nocifensive behaviors. Granted, inferences about conscious perception in animals will always include an element of uncertainty. But progress can be made by taking as a given that mental states are present, and then later verifying in humans conclusions derived about biological mechanisms.

5.62.4 Pain versus Nociception

Nocifensive responses and avoidance learning could indicate the presence of perceived pain, or they could reflect automatic machine-like reactions of a nonconscious zombie (Woolf, C. J., 1984; Giacino, J. T. *et al.*, 2002; Kobylarz, E. J. and Schiff, N. D., 2004). Since Sherrington C. S. (1904) pain researchers have been trained to use the term nociception rather than pain when there is uncertainty that a conscious percept accompanies the nocifensive response. Nociception may occur when a person is unconscious, but by definition, pain cannot (Merskey, H., 1986). It is not obvious why conscious registration of noxious stimuli (i.e., pain) needs to occur at all. However, under normal circumstances nocifensive responses and pain experience go hand in hand. More than that, the pain system goes out of its way to ensure that noxious stimuli overcome distraction, and even arouse the individual from sleep and sedation. The experience of pain must have survival benefits that unconsciousness nociception cannot provide, perhaps in the realm of optimizing performance, learning, or empathy.

Investigators of other senses have not adopted a mnemonic equivalent to the pain–nociception dichotomy, but this distinction is not unique to pain. The monkey who responded to the red triangle could be machine-like, without awareness, like the door-opener mechanism in a supermarket. Monotonous visual or auditory impressions often do not register in awareness during routine tasks like driving. A particularly striking example is sensory processing during sleep. We toss and turn during sleep, unconscious, but continuously monitor the edge of the bed, and almost never fall out. Complex behavior does not necessarily require attention. And yet, despite periods on autopilot, most of the time we are aware and act with intent.

5.62.5 Neural Correlates of Pain Perception

5.62.5.1 Central Nervous System Activation

A noxious stimulus applied to the paw of an animal activates a large number of neurons in the spinal cord, many of which send ascending axons to the brain. A small minority, cells located in the most superficial layers of the dorsal horn, are nociceptive-selective in their responses. Most, however, have a wide dynamic range (WDR), and respond to weak as well as strong cutaneous stimuli. Still others show WDR responses combined with input from proprioceptive and visceral afferents (multireceptive neurons). The nociceptive-selective neurons have attracted the most attention, with some investigators insisting that their projections alone define the brain's pain-processing network (Craig, A. D., 2003). However, there is no rational basis for denying a role for the WDR and multireceptive neurons. These could well deliver a specific pain signal after extraction from the multiplexed mix (Price, D. D. *et al.*, 2003).

The spinal cord and corresponding brainstem trigeminal areas are sufficient alone to sustain simple nocifensive responses, and they play an important role in the early stages of pain processing. But it is a safe bet that the algorithm of conscious pain perception does not run in the spinal cord on the grounds that paraplegics are fully conscious, and may even report pain in their (phantom) legs. Pain happens supraspinally. Microelectrode recordings in animals and noninvasive functional imaging in humans show excitations in many brain areas following pain-provoking stimulation of the skin and internal organs (Peyron, R. *et al.*, 2000). These include structures that are well-known parts of the somatosensory system, such as the ventrobasal thalamus and the primary (S1) and secondary (S2) somatosensory cortices, as well as areas not classically thought of as somatosensory processors, such as the cerebellar cortex and the corpus striatum. Curiously, the classical somatosensory cortex (S1, S2) tends to show less robust and reliable activations than limbic cortical areas such as the anterior cingulate cortex (ACC), the insula, and parts of the frontal lobe. Noxious stimulation of different organs, skin versus viscera for example, reveals different if overlapping patterns of cortical activation appropriate to the different feels evoked (Rainville, P. *et al.*, 1997; Strigo, I. A. *et al.*, 2003). It is likely that

intensity, affect, localization, and other aspects of sensory quality are processed as a mosaic, in distinct brain areas. But this does not necessarily mean that perception is a mosaic. The various outputs of cortical processing may be bound in a central location.

5.62.5.2 Central Nervous System Lesions

Lesions in the primary visual cortex cause perceptual blindness although some visual performance persists based on subcortical and extrastriate pathways (blindsight, Poppel, E. *et al.*, 1973). In contrast, no cerebral area has been discovered in which lesions reliably produce analgesia or provide relief from ongoing pathophysiological pain. Even in the occasional case report of stroke or surgery relieving a preexisting chronic pain, pain typically returns. Indeed, cortical lesions frequently trigger chronic pain (Boivie, J. *et al.*, 1989; Gybels, J. M. and Sweet, W. H., 1990).

Large right parietal lesions can evoke a state of mind (anosognosia) where the individual denies that a body part belongs to him or her despite the obvious visual evidence to the contrary ("Whose leg is it that you put into my bed!"). The leg is no longer an integral part of the body schema, the inverse, as it were, of an amputation phantom. Nonetheless, pain is registered when the leg is pinched; only the source of the pain is denied. Prolonged anoxia, for example, in drowning victims, can cause still more extensive cortical lesions destroying essentially all of the cerebral cortex. If the patient survives, he or she may be left in a persistent vegetative state (PVS). In PVS the patient is eyes-open awake (with retained sleep–wake cycles), but largely unresponsive, and with massive loss of cognitive function and self-initiated movement. However, he or she typically continues to show appropriate, adaptive nocifensive responses, for example, to pinch stimuli (Plum, F. and Posner, J. B., 1980; Kinney, H. C. and Samuels, M. A., 1994; Kobylarz, E. J. and Schiff, N. D., 2004). With no possibility of communicating, reasonable people can differ over whether the patient has any residual conscious pain experience. Some authorities are sufficiently confident that pain is absent in PVS that once the decision is made to permit ending life, they see it as ethically acceptable to withdraw feeding and end life by slow starvation, rather than by painless injection.

The unexpected preservation of pain response following cortical lesions in S1, S2, and beyond can be interpreted in a number of ways: redundancy of cortical areas that support pain perception, a distributed architecture, or functional organization that is entirely different from the other senses. A final possibility, bordering on heresy, is that fundamental pain perception might not require the cerebral cortex (Dover, M., 2007).

5.62.5.3 Central Nervous System Stimulation

Expectations based on vision are violated even more dramatically in trials of direct cortical excitation. If pain function is multiply represented (redundant) focal lesions might not produce analgesia, but focal stimulation should nonetheless evoke pain. In fact, it has remained a mystery since the classic experiments of Penfield W. and Rasmussen T. (1955) why pain is rarely if ever evoked by stimulation of the cortical convexity (also see Libet, B., 1973), while visual, auditory, and (nonpainful) somatosensory percepts readily are. It may be argued that the relevant structures are buried in the midsagittal (cingulate gyrus) or Sylvian sulci (insula), or that unlike the other senses, multiple cortical areas must be activated simultaneously. However, it is very rare for epileptic seizures to include auras that are painful even though the underlying cortical discharge is frequently widespread and includes these buried cortices. Recent observations of pain evoked in a small number of epilepsy patients by depth electrodes on the insular cortex is a potential exception (Mazzola, L. *et al.*, 2006), but this needs detailed presentation and replication.

If not for the deeply held conviction that conscious perception is a high cortical function, the foregoing observations might have led to the tentative conclusion that the neural computations that generate pain experience do not, in fact, occur in or require the cortex. In contrast to the cortex, pain is readily evoked by focal (microelectrode) stimulation in areas of the thalamus and brainstem (Dostrovsky, J. O., 2000). Of course, this may simply reflect activation of ascending pathways, as for nerve or spinal cord stimulation. On the other hand, it might mean that the algorithm of pain experience runs subcortically. If this were the case, cortical (like cerebellar) activations evoked by noxious stimuli could reflect the contribution of noxious signals to functions such as memory formation, arousal, or the generation of motor sequences, rather than pain perception. Alternatively, the cortex could contribute qualitative detail to the pain percept such as precise localization and dynamics, which are not required for the raw feel

of pain. Indeed, given the high prevalence of chronic poststroke pain (Boivie, J. *et al.*, 1989), it is even possible that overall, cortical activity modulates pain by means of inhibitory control of subcortical circuitry.

5.62.6 Contents of Consciousness versus Its Presence

5.62.6.1 Contents

Much research on the neural correlates of perceptual states focuses on the contents of ongoing narrative. For example, an investigator may ask whether cerebral activation (or synchronization) in response to a fixed stimulus configuration changes when the resulting percept changes (e.g., at state transitions of ambiguous figures). In the realm of pain, many studies have shown that certain cortical activations in response to fixed noxious stimuli change when the resulting percept changes, say as a result of hypnotic suggestion or placebo/expectation (Rainville, P. *et al.*, 1999; Wager, T. D. *et al.*, 2004; Raij, T. T. *et al.*, 2005). An optimistic inference is that the altered neural activity correlates with the pain percept because it actually constitutes the pain percept. An alternative possibility, however, is that the change in the percept and in the underlying neural activity both occur subcortically, with the change in the cortex only secondary reflecting the fundamental subcortical change.

5.62.6.2 Pain and Loss of Consciousness

Compared to contents (states) of consciousness, much less research is done on the transition from consciousness to unconsciousness. By unconscious, I refer to the absence of consciousness, as in coma, not subconscious material that may be inaccessible. This more basic transition may sound mundane, but it is probably a more practical entry point into the underlying neural circuitry. Without question the most potent modality of pain suppression is general anesthesia. Shortly after adequate numbers of anesthetic molecules are inhaled or injected systemically, the most extreme of noxious stimuli can be delivered with no pain sensation at all. It might be argued that this is not analgesia at all as sensory experience is eliminated globally. Of course one might equally say that with loss of consciousness, analgesia is present, and that it is accompanied by blindness, deafness, and anosmia. Aspects of unconscious nociception may persist during anesthesia, such as cardiovascular and some spinal reflex response. Moreover, neurons at many levels of the neuraxis, from spinal cord to cerebral cortex, continue to respond to sensory input. This includes cortical responses to noxious and nonnoxious somatosensory stimuli. Indeed, nearly all of classical cortical neurophysiology was carried out in anesthetized animals. One could even make the case that consciousness is the thing that is lost by the action of general anesthetics. The mechanism of action of anesthetics is therefore of substantial interest with respect to pain – a unique experimental lead.

How do anesthetics obtund consciousness? The most widely held theory is that anesthetic agents distributed by the circulatory system directly access neurons throughout the CNS where they bind to membrane receptors and suppress either electrical excitability or synaptic action. For example, the anesthetic ketamine suppresses glutamatergic excitation while barbiturates such as pentobarbital enhance GABAergic inhibition. By this model, CNS suppression is global, quenched as if by a wet blanket. Anesthetics, however, can also act in a very different way. Microinjection of minute quantities of pentobarbital into a highly localized region of the mesopontine tegmentum, a region termed the mesopontine tegmental anesthesia area (MPTA), can induce all of the indicators of lost consciousness, assessed behaviorally and by electroencephalography. The same dose injected anywhere else in the brain has minimal or no effects (Devor, M. and Zalkind, V., 2001).

The discovery of the MPTA as a nodal site capable of switching the brain rapidly between alertness and unconsciousness is of considerable interest. Among other things, it indicates that neural circuitry exists that is capable of accessing and switching off pain perception, motor control, and consciousness. The difference between the wet blanket hypothesis and the MPTA circuit hypothesis is not in the molecular agents and receptors involved but in the system architecture. Tracing the connectivity of MPTA neurons provides a practical experimental avenue into the neural circuitry of pain as a conscious experience (Sukhotinsky, I. *et al.*, 2005; 2007). Are motor suppression, analgesia, and cognitive collapse inseparable consequences of loss of consciousness, or are these independent functions with independent circuitries that just happen to merge in the MPTA? Does loss of consciousness from fainting (syncope), concussion, and coma also involve MPTA circuitry?

Such questions have ceased to be topics for armchair speculation and can now be investigated using conventional neurobiological tools.

5.62.7 Conclusion

Pain is neither a noxious stimulus nor an adaptive nocifensive response. It is a mental state, a sensory and emotional percept experienced by a conscious brain by virtue of the operation of a neural algorithm, which is, in principle, knowable. Adaptive nocifensive responses and avoidance learning may occur in the absence of consciousness, but pain experience cannot. The pain system offers many advantages for the experimental discovery and analysis of the neural circuitry that subserves conscious perception.

References

Bauby, J.-D. 1997. The Diving Bell and the Butterfly: A Memoir of Life in Death, p. 131. Knopf.

Benedetti, F., Arduino, C., and Amanzio, M. 1999. Somatotopic activation of opioid systems by target-directed expectations of analgesia. J. Neurosci. 19, 3639–3648.

Boivie, J., Leijon, G., and Johansson, I. 1989. Central post-stroke pain – a study of the mechanisms through analysis of the sensory abnormalities. Pain 37, 173–185.

Chalmers, D. 1995. Facing up to the problem of consciousness. J. Consciousness Studies 2, 200–219.

Craig, A. D. 2003. Pain mechanisms: labeled lines versus convergence in central processing. Annu. Rev. Neurosci. 26, 1–30.

Devor, M. 2007. Pain, cortex, and consciousness. Behav. Brain. Sci. 30, 89–90.

Devor, M. and Zalkind, V. 2001. Reversible analgesia, atonia, and loss of consciousness on bilateral intracerebral microinjection of pentobarbital. Pain 94, 101–112.

Dostrovsky, J. O. 2000. Role of thalamus in pain. Prog. Brain Res. 129, 245–257.

Fields, H. L. and Basbaum, A. I. 1999. Central Nervous System Mechanisms of Pain Modulation. In: Textbook of Pain (*eds*. P. D. Wall and R. Melzack), pp. 309–329. Churchill Livingstone.

Giacino, J. T., Ashwal, S., Childs, N., Cranford, R., Jennett, B., Katz, D. I., Kelly, J. P., Rosenberg, J. H., Whyte, J., Zafonte, R. D., and Zasler, N. D. 2002. The minimally conscious state: definition and diagnostic criteria. Neurology 58, 349–353.

Gybels, J. M. and Sweet, W. H. 1990. Neurosurgical Treatment of Persistent Pain, p. 441. Karger.

Kinney, H. C. and Samuels, M. A. 1994. Neuropathology of the persistent vegetative state, a review. J. Neuropath. Exp. Neurol. 53, 548–558.

Kobylarz, E. J. and Schiff, N. D. 2004. Functional imaging of severely brain-injured patients: progress, challenges, and limitations. Arch. Neurol. 61, 1357–1360.

Libet, B. 1973. Electrical Stimulation of Cortex in Human Subjects, and Conscious Sensory Aspects. In: Handbook of Sensory Physiology, (*ed.* A. Iggo), Vol. II, pp. 743–790. Springer.

Mazzola, L., Isnard, J., and Mauguiere, F. 2006. Somatosensory and pain responses to stimulation of the second somatosensory area (SII) in humans. A comparison with SI and insular responses. Cereb. Cort. 16, 960–968.

McGinn, C. 1999. Can We Solve the Mind-Body Problem? In: The Nature of Consciousness: Philosophical Debates (*eds*. N. Block, O. Flanagan, and G. Guzeldere), pp. 529–542. MIT Press.

Melzack, R., Wall, P. D., and Ty, T. C. 1982. Acute pain in an emergency clinic: latency of onset and descriptor patterns related to different injuries. Pain 14, 33–43.

Merskey, H. 1986. Pain terms: a current list with definitions and notes on usage. Pain Suppl. 3, S215–S221.

Penfield, W. and Rasmussen, T. 1955. The Cerebral Cortex of Man. Macmillan.

Peyron, R., Laurent, B., and Garcia-Larrea, L. 2000. Functional imaging of brain responses to pain: a review and meta-analysis. Neurophysiol. Clin. 2000, 263–288.

Plum, F. and Posner, J. B. 1980. The Diagnosis of Stupor and Coma. Davis.

Poppel, E., Held, R., and Frost, D. 1973. Residual visual function after brain wounds involving the central visual pathways in man. Nature 243, 295–296.

Price, D. D., Greenspan, J. D., and Dubner, R. 2003. Neurons involved in the exteroceptive function of pain. Pain 106, 215–219.

Raij, T. T., Numminen, J., Narvanen, S., Hiltunen, J., and Hari, R. 2005. Brain correlates of subjective reality of physically and psychologically induced pain. Proc. Natl. Acad. Sci. U. S. A. 102, 2147–2151.

Rainville, P., Carrier, B., Hofbauer, R. K., Bushnell, M. C., and Duncan, G. H. 1999. Dissociation of sensory and affective dimensions of pain using hypnotic modulation. Pain 82, 159–171.

Rainville, P., Duncan, G. H., Price, D. D., Carrier, B., and Bushnell, M. C. 1997. Pain affect encoded in human anterior cingulate but not somatosensory cortex. Science 277, 968–971.

Searle, J. R. 1992. The Rediscovery of the Mind, p. 320. MIT Press.

Sherrington, C. S. 1904. Qualitative difference of spinal reflex corresponding with qualitative difference of cutaneous stimulus. J. Physiol. (Lond.) 30, 39–46.

Skoubis, P. D., Lam, H. A., Shoblock, J., Narayanan, S., and Maidment, N. T. 2005. Endogenous enkephalins, not endorphins, modulate basal hedonic state in mice. Eur. J. Neurosci. 21, 1379–1384.

Strigo, I. A., Duncan, G. H., Boivin, M., and Bushnell, M. C. 2003. Differentiation of visceral and cutaneous pain in the human brain. J. Neurophysiol. 89, 3294–3303.

Sukhotinsky, I., Hopkins, D. A., Lu, J., Saper, C. and Devor, M. 2005. Movement suppression during anesthesia: neural projections from the mesopontine tegmentum to areas involved in motor control. J. Comp. Neurol. 489, 425–448.

Sukhotinsky, I., Zalkind, V., Lu, J., Hopkins, D. A., Saper, C. B., and Devor, M. 2007. Neural pathways associated with loss of consciousness caused by intracerebral microinjection of $GABA_A$-active anesthetics. Eur. J. Neurosci. 25, 1417–1436.

Wager, T. D., Rilling, J. K., Smith, E. E., Sokolik, A., Casey, K. L., Davidson, R. J., Kosslyn, S. M., Rose, R. M., and Cohen, J. D. 2004. Placebo-induced changes in fMRI in the anticipation and experience of pain. Science 303, 1162–1167.

Woolf, C. J. 1984. Long term alterations in the excitability of the flexion reflex produced by peripheral tissue injury in the chronic decerebrate rat. Pain 18, 325–343.

5.63 Assessing Pain in Animals

S W G Derbyshire, University of Birmingham, Birmingham, UK

© 2008 Elsevier Inc. All rights reserved.

5.63.1	Introduction	969
5.63.2	The Biology of Pain	969
5.63.3	Animal Biology	970
5.63.4	The Psychology of Pain, the Psychology of Humans and the Psychology of Animals	971
5.63.5	Conclusion	972
References		973

Glossary

anthropomorphism The tendency to attribute human motivations, characteristics, or other attributes to nonhuman things including inanimate objects, the weather and, especially, animals.

cortex The outer layer of an organ. Thus, cerebral cortex: the layers of nerve cells at the outer part of the brain.

nociception The biological response to a noxious stimulus or other stimulus that threatens tissue damage if prolonged.

pain The subjective experience that often, but not always, accompanies nociception in socially conscious beings.

representational memory Memories of a particular event or thing with explicit representational content that can be consciously accessed.

5.63.1 Introduction

There are few living creatures that cannot respond to a noxious stimulus such as a pinch or a burning flame. Strike a match next to the humble *Drosophila* (fruit fly) larvae, for example, and it will bend and roll away (Goodman, M. B., 2003). Responses such as these are dependent upon specialized sensory neurons that preferentially respond to stimuli with the potential to cause tissue damage. These sensory neurons can be found in most animals, including fishes (Sneddon, L. U. *et al.*, 2003a; 2003b), as well as human beings and larvae. Clearly, then, all of these creatures have the apparatus to detect and respond to potentially dangerous stimulation, but can they all be said to feel pain?

If we define pain as the response to noxious stimulation then the answer must be yes, the larvae, fishes, and human being all feel pain. This definition, however, would also mean that a thermostat feels pain because it responds to excessive heat by changing its internal state. Similarly, even rocks must feel pain as they respond to excessive force by shattering. Such a definition seems much too permissive, but it is also flawed because it leads to a tautological understanding of pain. Pain is defined in terms of a stimulus that is deemed to be painful because it elicits the pain response. To put that more simply, pain is defined as pain (Derbyshire, S. W. G., 1999a). To escape from this tautology, a deeper examination of both the biology and the psychology of pain is required. Understanding the minimal necessary biology for pain will enable us to eliminate those animals that lack that biology from being able to experience pain. Similarly, understanding the psychological structure of pain will enable us to eliminate those animals that lack that structure from being able to experience pain.

5.63.2 The Biology of Pain

Modern imaging techniques have allowed unprecedented access to the workings of the brain and over the past decade a series of researchers have examined brain responses during pain experience (e.g., Craig,

A. D. *et al.*, 1996; Rosen, S. D. *et al.*, 1996; Coghill, R. C. *et al.*, 2003; Derbyshire, S. W. G. *et al.*, 2004). These studies have not identified a single center responsible for pain processing but have instead revealed a network or matrix of brain areas (see reviews by Treede, R. D. *et al.*, 1999; Derbyshire, S. W. G., 2000; Peyron, R. *et al.*, 2000; Vogt, B. A. *et al.*, 2003). This matrix includes subcortical structures, such as the thalamus, as well as cortical regions widely believed to be responsible for the higher processes of thought and feeling (Baars, B. J. *et al.*, 2003). The major areas of the cortex now demonstrated to be involved in pain processing include the anterior cingulate cortex, insular cortex, primary and secondary somatosensory cortices, and the prefrontal cortex (Treede, R. D. *et al.*, 1999; Derbyshire, S. W. G. 2000; Peyron, R. *et al.*, 2000; Vogt, B. A. *et al.*, 2003).

Evidence for the direct generation of pain by the cortex comes from an imaging study involving the so-called thermal grill illusion (Craig, A. D. *et al.*, 1996). The thermal grill illusion is the experience of a cold burn produced by interleaving bars that are cool (20 °C) and warm (40 °C) onto the palm of the hand. Instead of experiencing interleaved warmth and coolness, which is the actual stimulus being applied to the hand, the subject will report a feeling of pain that is similar to a cold burn. Explanation for this paradox rests upon the fact that the mammalian nervous system is generally designed to process warmth and coolness separately. Detection of coolness is suggested to proceed via the inhibition or deactivation of an intense cold pathway combined with the activation of a cool channel to produce the experience of coolness. The warm bars, however, act to inhibit the cool channel resulting in a net flow of information through the intense cold channel and the paradoxical experience of a burning cold (Casey, K. L., 1996). The nervous system is tricked, so to speak, into the experience of a burning cold pain sensation, and this trick results in the activation of anterior cingulate cortex and insular cortex. Thus, this activation of the cortex is directly associated with an experience of pain in the absence of an actual noxious stimulus.

In our laboratory, we have completed a study that also provides evidence for the direct involvement of the cortex in the generation of pain experience (Derbyshire, S. W. G. *et al.*, 2004). Eight subjects were selected for their ability to be hypnotized and to experience pain in the absence of any stimulation via hypnotic suggestion. Images of brain activation were recorded when actual noxious stimulation was provided to the subjects and when the pain was suggested in the absence of any stimulation. We demonstrated significant changes during this hypnotically induced pain experience within the anterior cingulate, insular, prefrontal, and parietal cortices. These findings compare well with the activation patterns during pain from an actual noxious source and provide direct experimental evidence in humans linking specific cortical activity with the immediate generation of a pain experience.

Thus, imaging studies demonstrate that the cortex is necessary for pain experience and, as rocks and thermostats do not have a cortex, they are excluded from the world of pain. The same is also true of fruit fly larvae. Other animals, however, are much more likely to share with humans the necessary biology for pain experience.

5.63.3 Animal Biology

In terms of gross anatomy and surface features, human cortex shares many features with the higher primates including the presence of neural structures widely associated with the pain neuromatrix. These similarities have facilitated the investigation of animal nociceptive systems with application to the human species (Vogt, B. A. *et al.*, 1987; Apkarian, A. V. and Hodge, C. J., 1989). At the same time, differences across species include how much the brain, and its constituent parts, weigh; the appearance of the individual cells in various brain regions; the destinations of axons from these cells; and the extent to which brain cells respond electrically when the sense organs are experimentally activated or when the animal is behaving. A review of each of these areas for all animals would be obviously vast and beyond the scope of this chapter (see Dehaene, S. *et al.*, 2005 for extensive comparison of humans and primates). For the purposes of expediency, I will focus only upon the higher primates and will consider only the comparative size and cytoarchitecture of the frontal cortex, which is often activated during pain and is more broadly involved in higher-cognitive abilities including the organization of mental contents that control creative thinking and language, and the artistic expression and planning of future actions (Damasio, A. R., 1985).

Human frontal cortex ranges in size from 239 to 330 cm^3, the range in the great apes is from 50 cm^3 (in a chimpanzee) to 112 cm^3 (in an orangutan) (Semendeferi, K. *et al.*, 2002). Within area 10 of the dorsolateral prefrontal cortex, the right human hemisphere has an estimated 254 million neurons, while

the great apes have less than one-third of that amount (Semendeferi, K. *et al.*, 2001). Although human area 10 has more neurons, it is less densely packed than in the apes such that the supragranular layers (layers II and III) stand out more in the human brain compared to apes. Consequently, humans have more space available for extrinsic and intrinsic connections, which may indicate increased communication within and between area 10 and other higher-order association cortices. The relative volume of white matter underlying prefrontal association cortices is also larger in humans than in apes, compatible with the idea that neural connectivity is increased in the human brain (Zhang, K. and Sejnowski, T. J., 2000).

We cannot replace psychological investigations by the examination of brain tissue (Walker, S. F., 1983; Derbyshire, S. W. G., 2000), but if the assumption that mental states reflect brain activation is to be taken seriously, then it is clear that the physical structure of animal brains must be taken into account when considering mental activity in animals. The similarities in structure between the brains of apes and humans suggest some commonality of function, but the differences in size, connectivity, and cytoarchitecture equally suggest important diversion of function. Until the relationship between the structure of the brain and function is fully realized, it will remain unclear what the differences in neural biology between humans and animals mean in terms of perception and experience, but further examination of the similarities in experience can proceed via comparative investigation of the psychology of animals and humans.

5.63.4 The Psychology of Pain, the Psychology of Humans and the Psychology of Animals

To avoid the tautological use of the term pain, we need some sort of definition of what pain is. In the absence of a definition, pain is ascribed when there are pain behaviors or pain stimuli or, more simply, pain is present when there is pain. The circularity arises because the description of behaviors that follow noxious insult and the psychological description of pain experience are at two different levels: the link between them is at the heart of the problem of understanding animal suffering or other types of animal experience (Nagel, T., 1974).

To escape the inherent tautology of describing pain as the result of painful stimuli, pain is generally defined as a sort of amalgam of cognition, sensation, and affective processes, commonly described under the rubric of the biopsychosocial model of pain (Waddell, G., 1987). Pain is no longer regarded as merely a physical sensation of noxious stimulus and disease, but is seen as a conscious experience that includes mental, emotional, and sensory mechanisms. This understanding is reflected in the current International Association for the Study of Pain (IASP) definition of pain as "an unpleasant sensory and emotional experience associated with actual or potential tissue damage, or described in terms of such damage" (Merskey, H., 1991).

By this definition, pain is a high-level process that makes no sense in the absence of sentience; pain accompanies injury in minds that are capable of subjectivity or consciousness. Without consciousness, there can be the response to noxious stimulation, technically referred to as nociception, but there cannot be pain. Thus, to understand how pain experience in particular becomes possible, it is necessary to understand the origin and course of development of conscious experience in general.

I suggest that the origin of human subjectivity lies within development. Before an infant can think about objects or events, or experience sensations and emotion, elements of thought must have their own independent existence in the infant's mind. This is something that is achieved via continued brain development in conjunction with discoveries made in action and in patterns of mutual adjustment and interactions with the infant's caregiver. For example, an important step toward subjectivity is the development of representational memory, allowing responses to learned information as well as material directly available. Representational memory begins to emerge as the frontal cortex develops between 2 and 4 months of age. From this point on, there is the possibility of tagging in memory, or labeling as a something, all the objects, emotions, and sensations that appear or are felt. When a primary caregiver points to a spot on the body and asks, "does that hurt?" she is providing content and enabling an internal discrimination. This type of interaction provides for content and symbols allowing the infant to locate and anchor emotions and sensations and to arrive at a particular state of being within her own mind. Although pain experience is clearly individual, it is created by a process that extends beyond the individual. If pain were an entirely private affair, no words would be able to express it because no external frame of reference would be comparable and therefore

adequate to express the sensation. Pain is not like this because clearly human beings do express their painful experiences and these expressions have meaning that allow for diagnosis and treatment. In so far as human beings live in a community of thinking, feeling, talking beings, the privacy of experience is broken down and externalized for further analysis. As we are able to externalize our inner world, so we are able to reflect upon that world and become self-aware or self-conscious. Thus, the contents of our inner world come to mean something to us only in so far as they mean something to others, and the realization of that meaning occurs through a developmental process that is social as well as natural (Derbyshire, S. W. G., 1999b; Malik, K., 2000).

The evidence for this type of self-awareness within the animal world is limited and controversial (Heyes, C. M., 1993; Vauclair, J., 1997). There is some evidence of potentially reflective consciousness from behaviors such as giving of alarm calls and the use of deception, but any awareness or insight that these behaviors may indicate is heavily circumscribed and does not generalize. There is no evidence that the awareness, however defined or understood, provides any transformative impact within the individual animal or group. A chimpanzee, for example, behaves today in the same way as a chimpanzee did 100 000 years ago. When chimps forage for food, they do not ask themselves why or consider better alternatives any more than does a beaver consider better ways of building dams. When swallows fly south in the winter, they do not ask why it is hotter in Africa or what would happen if they flew further south or whether they could stay by creating warmth in the north. Humans do ask these kinds of questions and do engage in behavior that transforms their circumstances. We are not trapped inside a purely personal, solipsistic view of the world. We have a conscious insight that makes pain and all other experiences possible.

Pain is much more than working nociceptors connected to a brain. When we feel pain, it is an experience we have spent a good portion of our psychological development learning to recognize. This feeling is not given directly by our brain, but is made through repeated experience, categorization, memory, and reconnection. This development is obviously dependent upon the presence of a sufficiently developed neural system, the human brain, but the content of that experience is dependent upon elements that lie outside the human brain. Animals do not have a human brain and do not share in the psychological development of humans. Animal pain is therefore dependent upon a false equivalence of both biology and psychology and can be rejected.

5.63.5 Conclusion

The fact that some animal behaviors are specific to noxious stimulation and are particular defensive reactions driven by homologous neuronal centers is a long way from demonstrating pain experience. In their report on fishes, Sneddon L. U. *et al.* (2003a) concede that what a fish feels "is possibly nothing like the experience of humans" but is nevertheless "no less important in terms of biology or ethics" than human pain. This is similar to the argument of Beckoff M. (2002) who has suggested, "even though the experience of pain might not be the same across species, individuals of different species can still suffer their own type or version of pain."

It is not obvious why, if the experience is nothing like our experience, it still retains the same moral dimension and should still be called pain. Equally, there is no description of what the pain experience is like for the animals, beyond it being nothing like the human experience but still being important. What is perhaps being argued is that while animals are incapable of a broad awareness they are capable of experiencing something like pain or a narrow awareness. Whereas human awareness is a general phenomenon, carried along with every experience we have, from hitting ourselves with a hammer to enjoying a sunny day, that of the animals might be piecemeal with the individual pieces, including pain, available whole and fully formed.

What remains unexplained is how the animal can be aware of that particular piece of experience. As discussed, humans use symbolic labeling to differentiate pain, red, and so forth, and it is through this public process of externalizing our thoughts and feelings that those thoughts and feelings come to have meaning to us (Malik, K., 2000). We become conscious (Hobson, P., 2002).

As a subjective experience, pain is one of the many exceptional properties of human existence. Belief in the exceptional properties of human beings, however, is not currently popular. John Gray, professor of European thought at the London School of Economics, for example, has coined the phrase Homo rapiens to describe the human race, which he presents as no better than bacteria (Gray, J., 2002). Although certainly an extreme view, Gray is not alone in comparing humanity to bacteria (Fernandez-

Armesto, F., 2004), or in suggesting the planet would do well to rid itself of our existence (Preston, P., 1993).

Even though many will likely reject the extreme antihumanism of Gray and others, far fewer will reject the notion that animals are ultimately quite similar to us. Almost every day, we are presented with new revelations about how animals are more like us than we ever imagined. A selection of news headlines includes: "How animals kiss and make up"; "Male birds punish unfaithful females"; "Dogs experience stress at Christmas"; "Capuchin monkeys demand equal rights"; "Scientists prove fish intelligence"; "Birds going through divorce proceedings"; "Bees can think say scientists"; "Chimpanzees are cultured creatures"; "Psychic' parrot expected to ruffle scientific feathers"; and, "They're in love. They're gay. They're penguins."

While this kind of anthropomorphism can seem harmless and is often amusing, the ultimate effect is similar to that of the frank antihumanists: to denigrate human abilities (Schwab, A., 2003; Guldberg, H., 2004). The sheer staggering scale and richness of human culture are unlike anything in any other species. The development of medicine, industry, transportation, communication, clean water, a stable food supply, warm habitats, and so on, are the discernible signs of culture and progress that are evidently absent from the nonhuman world.

This does not mean we should ignore issues of animal welfare, but it does mean that any discussion of animal welfare is a human debate and is fundamentally about what it means to be human (Engelhardt, T. H., 2001; Derbyshire, S. W. G., 2002). The self-reflective ability of humans, which encapsulates feelings and experience and which made tangible material and cultural progress possible, has moral and political consequences. Humans are free agents, within the limits of any given political system, and organize their behavior according to rights and customs that they create, which includes weighing and judging the life of humans or animals (Engelhardt, T. H., 2001).

Human beings take a central moral position, not via some act of special pleading, but as a function of their exceptional and special abilities (Engelhardt, T. H., 2001). We have an unavoidable moral centrality that places us into a position of authority over animals and at liberty to do with our own animals whatever we wish. Arguably, where the aim is one of frank malevolence, the agents involved have rejected morality itself and are acting in an antisocial manner worthy of sanction. It is probably appropriate to distinguish between practices aimed at cruelty and those motivated by a scientific, educational, or cultural practice. Such distinction will lead to a condemnation of some animal uses but will not count against those that are part of sport, consumption, or research (Engelhardt, T. H., 2001).

For researchers involved in understanding pain, there is a simple message. The use of animals has application to human welfare because of the similarities between the nociceptive system of animals and humans. There is the real possibility of discovering new ways of preventing noxious transmission, and the processing of noxious information, in humans through the use of animal models. At the same time, the use of animals is morally acceptable, because animals precisely lack the insight and conscious appreciation that makes pain, moral agency, and personhood possible.

References

Apkarian, A. V. and Hodge, C. J. 1989. Primate spinothalamic pathways. III. Thalamic terminations of the dorsolateral and ventral spinothalamic pathways. J. Comp. Neurol. 288, 493–511.

Baars, B. J., Ramsoy, T. Z., and Laureys, S. 2003. Brain, conscious experience and the observing self. Trends Neurosci. 26, 671–675.

Beckoff, M. 2002. Animal reflections. Nature 419, 255.

Casey, K. L. 1996. Resolving a paradox of pain. Nature 384, 217–218.

Coghill, R. C., McHaffie, J. G., and Yen, Y. F. 2003. Neural correlates of interindividual differences in the subjective experience of pain. Proc. Natl. Sci. U. S. A. 100, 8538–8542.

Craig, A. D., Reiman, E. M., Evans, A., and Bushnell, M. C. 1996. Functional imaging of an illusion of pain. Nature 384, 258–260.

Dehaene, S., Duhamel, J.-R, Hauser, M. D., and Rizzolatti, G. 2005. From Monkey Brain to Human Brain. Bradford Books.

Damasio, A. R. 1985. The Frontal Lobes. In: Clinical Neuropsychology (*eds*. K. Heilman and E. Valenstein), pp. 339–375. Oxford University Press.

Derbyshire, S. W. G. 1999a. The IASP definition captures the essence of pain experience. Pain Forum 8, 106–109.

Derbyshire, S. W. G. 1999b. Locating the beginnings of pain. Bioethics 13, 1–31.

Derbyshire, S. W. G. 2000. Exploring the pain "neuromatrix." Curr Rev. Pain 6, 467–477.

Derbyshire, S. W. G. 2002. Why Animal Rights Are Wrong. In: Animal Experiments: Good or Bad? (*ed*. E. Lee), pp. 37–55. Hodder & Stoughton.

Derbyshire, S. W. G., Whalley, M. G., Stenger, V. A., and Oakley, D. A. 2004. Cerebral activation during hypnotically induced and imagined pain. NeuroImage 23, 392–401.

Engelhardt, T. H. 2001. Animals: Their Right to be Used. In: Why Animal Experimentation Matters: The Use of Animals in Medical Research (*eds*. E. F. Paul and J. Paul), pp. 175–195. Transaction Publishers.

Fernandez-Armesto, F. 2004. So You Think You're Human? Oxford University Press.
Goodman, M. B. 2003. Sensation is painless. Trends Neurosci. 26, 643–645.
Gray, J. 2002. Straw Dogs: Thoughts on Humans and Other Animals. Granta Press.
Guldberg, H. 2004. Why humans are superior to apes. Spiked-online (http://www.spiked-online.co.uk/Articles/0000000CA40E.htm).
Heyes, C. M. 1993. Anecdotes, trapping and triangulating: do animals attribute mental states? Anim. Behav. 46, 177–188.
Hobson, P. 2002. The Cradle of Thought: Exploring the Origins of Thinking. Macmillan Press.
Malik, K. 2000. Man, Beast and Zombie. Weidenfeld and Nicholson.
Merskey, H. 1991. The definition of pain. Eur. Psychiatry 6, 153–159.
Nagel, T. 1974. What is it like to be a bat? Philos. Rev. 83, 435–450.
Peyron, R., Laurent, B., and Garcia-Larrea, L. 2000. Functional imaging of brain responses to pain. A review and meta-analysis. Neurophysiol. Clin. 30, 263–288.
Preston, P. 1993. The Hot Zone. Anchor Publications.
Rosen, S. D., Paulesu, E., Nihoyannopoulos, P., Tousoulis, D., Frackowiak, R. S. J., Frith, C. D., Jones, T., and Camici, P. G. 1996. Silent ischemia as a central problem: regional brain activation compared in silent and painful myocardial ischemia. Ann. Intern. Med. 124, 939–949.
Schwab, A. 2003. Hook, Line and Thinker: Angling and Ethics. Merlin Unwin Books.
Semendeferi, K., Armstrong, E., Schleicher, A., Zilles, K., and Van Hoesen, G. W. 2001. Prefrontal cortex in humans and apes: a comparative study of area 10. Am. J. Phys. Anthropol. 114, 224–241.
Semendeferi, K., Lu, A., Schenker, N., and Damasio, H. 2002. Humans and great apes share a large frontal cortex. Nat. Neurosci. 5, 272–276.
Sneddon, L. U., Braithwaite, V. A., and Gentle, M. J. 2003a. Do fishes have nociceptors? Evidence for the evolution of a vertebrate sensory system. Proc. R. Soc. Lond. B 270, 1115–1121.
Sneddon, L. U., Braithwaite, V. A., and Gentle, M. J. 2003b. Novel object test: examining nociception and fear in the rainbow trout. J. Pain 4, 431–440.
Treede, R. D., Kenshalo, D. R., Gracely, R. H., and Jones, A. K. P., 1999. The cortical representation of pain. Pain 79, 105–111.
Vauclair, J. 1997. Mental states in animals: cognitive ethology. Trends Cogn. Sci. 1, 35–39.
Vogt, B. A., Berger, G. R., and Derbyshire, S. W. G. 2003. Structural and functional dichotomy of human midcingulate cortex. Eur. J. Neurosci. 18. 3134–3144.
Vogt, B. A., Pandya, D. N., and Rosene, D. L. 1987. Cingulate cortex of the rhesus monkey. 1. Cyto-architecture and thalamic afferents. J. Comp. Neurol. 262, 256–270.
Waddell, G. 1987. A new clinical model for the treatment of low-back pain. Spine 12, 632–644.
Walker, S. F. 1983. Animal Thought. Routledge & Kegan Paul, International Library of Psychology Series.
Zhang, K. and Sejnowski, T. J. 2000. A universal scaling law between gray matter and white matter of cerebral cortex. Proc. Natl. Acad. Sci. U. S. A. 97, 5621–5626.

5.64 Psychological Modulation of Pain

D D Price, A Hirsh, and M E Robinson, University of Florida, Gainesville, FL, USA

© 2008 Elsevier Inc. All rights reserved.

5.64.1	**Overview of Pain**	976
5.64.1.1	Overview of Stages/Dimensions of Pain	976
5.64.1.1.1	Psychological stages of pain processing	976
5.64.1.1.2	Factors contributing to pain unpleasantness	976
5.64.1.2	Overview of Neurophysiological Processing of Pain	978
5.64.1.2.1	Ascending nervous system pathways for pain	978
5.64.1.2.2	Brain pathways and regions interrelating sensory and affective dimensions of pain	979
5.64.1.2.3	The pivotal role of the anterior cingulate cortex (ACC) in pain affect	979
5.64.2	**Modulation of Pain Sensation and Pain Affect by Attention and Distraction**	980
5.64.2.1	Psychophysical Studies of Effects of Attention and Distraction on Pain	980
5.64.2.1.1	Studies of basic distraction effects on pain	981
5.64.2.1.2	Studies of cross-modal attention effect on pain	981
5.64.2.1.3	Studies of spatial attention effects on pain	981
5.64.2.1.4	Studies of intra-modal attention effects on pain	981
5.64.2.1.5	Other accounts of pain modulation by attentional and cognitive processes	981
5.64.2.2	Separating the Influence of Attention and Emotions	982
5.64.2.3	Neurophysiological Studies of Effects of Attention on Pain Processing, Including Brain Imaging and Electrophysiological Studies	983
5.64.2.3.1	Effect of attention on pain-related activity in the dorsal horn	983
5.64.2.3.2	Effect of attention and distraction on pain-evoked activity in the brain	983
5.64.3	**Nonplacebo Effects of Expectation and Meaning**	984
5.64.3.1	Effects on Pain Intensity	984
5.64.3.2	Effects on the Affective Dimension of Experimental Pain	985
5.64.3.3	The Influence of Expectancy on the Immediate Unpleasantness of Clinical Pain	985
5.64.4	**Factors That Contribute to the Magnitude of Placebo Analgesia**	986
5.64.4.1	The Magnitudes of Placebo Analgesia and the General Contexts That Influence Them	987
5.64.4.2	Analyses of Factors That Contribute to the Magnitude of Placebo Analgesia	987
5.64.4.2.1	External factors that contribute to placebo analgesia	988
5.64.4.2.2	Experienced factors that contribute to placebo analgesia	989
5.64.4.2.3	Predicting placebo analgesia	990
5.64.4.3	Placebo Analgesia As an Emotional Response	990
5.64.4.3.1	Do placebo effects result from changes in emotional states?	991
5.64.4.3.2	Future directions	992
5.64.5	**Modulation of Pain Intensity and Pain Unpleasantness by Emotions**	992
5.64.5.1	Negative Emotions As a Constituent of Pain	992
5.64.5.1.1	Pain definitions	992
5.64.5.1.2	Is pain an emotion?	992
5.64.5.2	Effects of Emotion on Pain: Experimental Studies	993
5.64.5.2.1	The experience of pain-related emotions	993
5.64.5.2.2	Pain anticipation and pain-related fear/anxiety	995
5.64.5.2.3	Emotions unrelated to pain	996
5.64.5.2.4	Emotion or attention?	997
5.64.5.3	Effects of Emotions on Pain: Clinical Studies	997
5.64.6	**Summary and Conclusions**	998
References		998

5.64.1 Overview of Pain

5.64.1.1 Overview of Stages/Dimensions of Pain

5.64.1.1.1 Psychological stages of pain processing

As a preliminary foundation for these discussions, this chapter begins with very general and somewhat simplified psychological and neurophysiological overviews of pain processing mechanisms. As a starting point for discussion, one can think of pain modulatory mechanisms as those that can intervene in the pathways outlined in Figures 1 and 2. Pain contains both sensory and emotional dimensions and is often accompanied by desires to terminate, reduce, or escape its presence (Buytendyck, F. J. J., 1961; Melzack, R. and Casey, K. L., 1968). By definition, pain is unpleasant and contains emotional feelings. This is largely due to the fact that the sensory qualities of physical pain dispose us to feel unpleasantness in most contexts. Thus, sensory qualities associated with pain are usually unpleasant for the same reasons that nausea and air hunger are perceived as unpleasant, as indicated by the path from nociceptive sensations to unpleasantness in Figure 1. In addition, there are parallel contributions to pain unpleasantness because the meaning of these sensory qualities is shaped by context and by a person's ongoing anticipations and attitudes. These contextual and cognitive factors are partly the result of the fact that pain often occurs within a situation that is threatening, such as during physical trauma or disease. Part of the affective dimension of pain is the moment-by-moment unpleasantness of pain, comprised of emotional feelings that pertain to the present or short-term future, such as annoyance, fear, or distress. Pain-unpleasantness is often though not always closely linked to both the intensity and unique qualities of the painful sensation. Another component of pain affect, secondary pain affect, includes emotional feelings directed toward long term implications of having pain (e.g., suffering), as shown in Figure 1 by the path extending from pain unpleasantness to secondary pain affect.

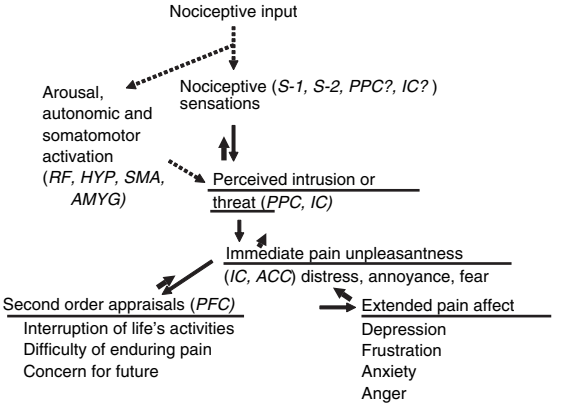

Figure 1 Schematic used to illustrate interactions between pain sensation, pain unpleasantness, and secondary pain affect (solid arrows). Neural structures likely to have a role in these dimensions are shown by abbreviations in adjacent parentheses and their full names are given in the legend of Figure 2. Dashed arrows indicate nociceptive or endogenous physiological factors that influence pain sensation and unpleasantness. From Price, D. D. and Bushnell, M. C. (*eds*.) 2004. Psychological Methods of Pain Control: Basic Science and Clinical Perspectives, pp. 322. IASP Press.

5.64.1.1.2 Factors contributing to pain unpleasantness

Multiple factors contribute to pain unpleasantness. Several sensory attributes of pain dispose unpleasant emotional feelings. The foremost among these is that sensations of pain are often, though not necessarily, more intense than other types of somatic sensations. Similar to other sensory modalities, it is commonly accepted that perceived intensity is a salient factor that contributes to the unpleasantness of pain. It may be the reason that very bright lights and loud sounds are sometimes metaphorically referred to as "painful". Qualities of sensations evoked by tissue damaging stimuli or stimuli that would produce tissue damage if maintained dispose us to perceive pain as invasive and intrusive for both the body and consciousness (Buytendyck, F. J. J., 1961; Price, D. D., 1999; 2000). Both neural and psychological processes related to sensory qualities of pain can be conceived as important causal links in the production of pain-related emotional disturbance. The persistence of these sensory qualities over time enhances unpleasantness. Thus, there exists a serial interaction between pain sensation intensity and pain unpleasantness.

Nociceptive, exteroceptive (e.g., sight, sound), and interoceptive sensory processes (e.g., startle, increased visceral responses) may provide parallel contributions to pain affect (Price, D. D., 1999). Pain itself can be conceptualized as both an exteroceptive and interoceptive phenomenon depending on the type of tissue that is stimulated and/or the types of sensory qualities that are present during pain. Consistent with Damasio's (Damasio, A., 1994) neurological view of emotion mechanisms, pain unpleasantness reflects the

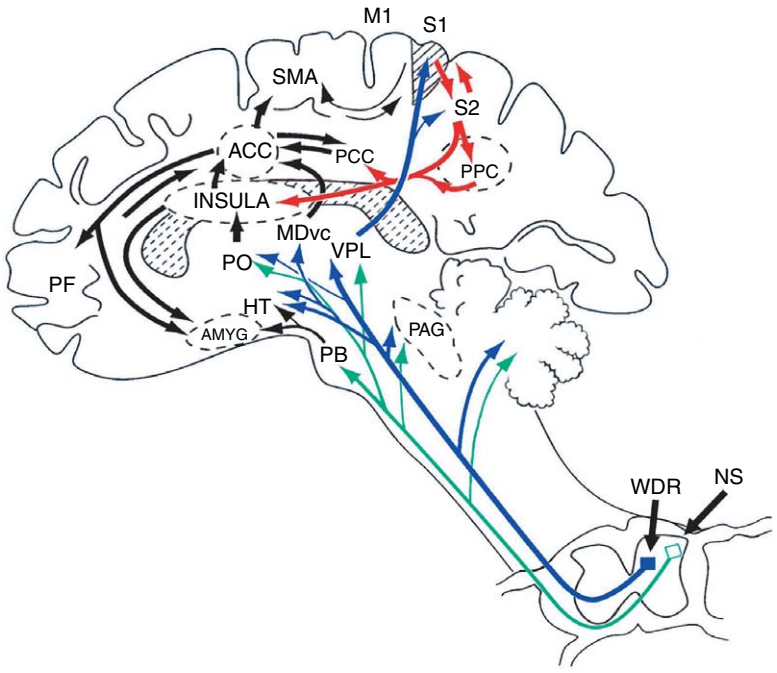

Figure 2 Schematic of ascending pathways, subcortical structures, and cerebral cortical structures involved in processing pain. PAG, periaqueductal gray; PB, parabrachial nucleus of the dorsolateral pons; VMpo, ventromedial part of the posterior nuclear complex; MDvc, ventrocaudal part of the medial dorsal nucleus; VPL, ventroposterior lateral nucleus; ACC, anterior cingulate cortex; PCC, posterior cingulate cortex; HY, hypothalamus; S-1 and S-2, first and second somatosensory cortical areas; PPC, posterior parietal complex; SMA, supplementary motor area; AMYG, amygdala; PF, prefrontal cortex. From Price, D. D. and Bushnell, M. C. (*eds.*) 2004. Pschological Methods of Pain Control: Basic Science and Clinical Perspectives, 322 pp. IASP Press.

contribution of several sources, including pain sensory qualities, arousal, visceral, and somatomotor responses. Thus, these psychophysiological sources of input, in combination with appraisal of the context in which they occur, give rise to a feeling of what is happening to the body and self, often but not necessarily accompanied by specific thoughts. This felt meaning derives largely from the experience of the body and constitutes the immediate unpleasantness of pain. For Damasio, "the essence of feeling an emotion is the experience of such changes in juxtaposition to the mental images that initiated the cycle" (Damasio, A., 1994, p. 145). In the case of pain, the mental image is that of a physically intrusive and qualitatively unique somatic perception.

Psychophysical studies demonstrate that pain sensation and pain unpleasantness represent two distinct dimensions of pain that demonstrate reliably different relationships to nociceptive stimulus intensity and are separately influenced by various psychological factors. Pain unpleasantness can be selectively influenced by emotions, changes in meaning of the pain, and factors related to the predictability, controllability, and duration of pain (Buytendyck, F. J. J., 1961; Melzack, R. and Casey, K. L., 1968). Pain unpleasantness also often leads to and sustains pain-related emotions that are based on cognitive appraisals that are more reflective than is pain unpleasantness. We term these latter pain-related emotional feelings as secondary pain affect. Unlike pain unpleasantness, secondary pain affect is based on more elaborate reflection related to that which one remembers or imagines. This involves meanings such as perceived interference with one's life, difficulties of enduring pain over time, and the implications for the future (Buytendyck F. J. J., 1961; Price, D. D., 1999). Pain is often experienced not only as a threat to the present state of one's body, comfort, or activity, but also to one's future well being and life in general. The perceived implications that present pain-related distress or annoyance holds for future well being and functioning support the link between pain unpleasantness and secondary pain affect, as illustrated in Figure 1. Studies of pain patients show the distinction between immediate pain unpleasantness and secondary pain affect and their sequential interactions.

5.64.1.2 Overview of Neurophysiological Processing of Pain

The stages of pain processing just described are also related to our present understanding of the neurophysiology of pain. Underlying neural mechanisms of sensory as well as primary and secondary affective dimensions of pain include multiple ascending spinal pathways to the brain and both parallel and serial processing in the brain. The neural representation associated with the experience of pain is likely to be related to a distributed network of brain structures that participate in the different dimensions of pain, such as identification of unique sensory qualities and their intensity, response selection, arousal, emotional feelings, and finally emotional expression and motivation. This network of brain circuitry is itself controlled by inhibitory and facilitatory interactions within the brain, as well as descending inhibitory and facilitatory control within brain-to-spinal cord pathways (Basbaum, A. I. and Fields, H. L., 1984; Price, D. D., 2000; Rainville, P. *et al.*, 1997). Thus, pain can be enhanced or reduced by interactions that take place at any one of several points in the schematics in Figures 1 and 2. A major pathway for pain modulation, known since the 1970s, is that of a brainstem-to-spinal cord pathway that utilizes endogenous opioids (Figure 3).

5.64.1.2.1 Ascending nervous system pathways for pain

The principle ascending pathways for pain (Figure 2) originate in specialized receptors in body tissues, called nociceptors. These receptors are specialized to respond to stimuli to tissues that either cause damage or would cause damage if they were maintained for a sufficient length of time. Nociceptors are connected to primary afferent neuron axons that synapse onto dorsal horn neurons (Figure 2). The dorsal horn of the spinal cord receives somatosensory information from most of the body, and the dorsal horn of the medulla oblongata receives input from the orofacial area via the trigeminal nerve. There are different classes of primary nociceptive afferent neurons that innervate different types of tissues, such as skin, muscle, joints, and viscera. Dorsal horn neurons that receive primary nociceptive neuron input are at the origin of ascending pathways to the brain that have different functional roles in pain processing. Two types of dorsal horn sensory projection neurons include nociceptive-specific neurons (NS) that respond predominantly to nociceptive stimuli and wide-dynamic-range (WDR) neurons that respond differentially to gentle and nociceptive stimulation. Both WDR and NS neurons project in the spinothalamic tract, the main somatosensory pathway for pain. The spinothalamic tract projects to the ventro-posterior-lateral thalamic nucleus (VPL), some medial thalamic nuclei, and nuclei just posterior and inferior to VPL. VPL (and VPM in the case of the trigeminal system) projects to the somatosensory cortices (S1 and S2), whereas medial and posterior thalamic nuclei mainly project to limbic cortical areas (Figure 2). The pathway to VPL/VPM is critical for sensory qualities of pain and appreciation of its perceived sensory intensity. In addition to this major pathway, there are pathways that proceed from the dorsal horn directly to reticular formation nuclei of the medulla and midbrain and to the hypothalamus. There also is a pathway that ascends to the amygdala by way of a synapse in the pons (Bernard, J. F. *et al.*, 1996). These various target structures are involved in pain because they participate in such functions as arousal and diffuse cortical activation (reticular formation nuclei), body regulation (hypothalamus), and affective states such as fear (amygdala). The central nucleus of the amygdala has been strongly implicated in fear, emotional memory, and behavior, and autonomic and somatomotor responses to threatening stimuli (Bernard, J. F. *et al.*, 1996). Various hypothalamic nuclei have also been implicated in these functions. Based largely on their central targets, all ascending pathways described above are likely to participate in the affective dimension of pain. Thus, some pathways directly activate cortical and subcortical limbic structures and the pathway to VPL/VPM and somatosensory cortex

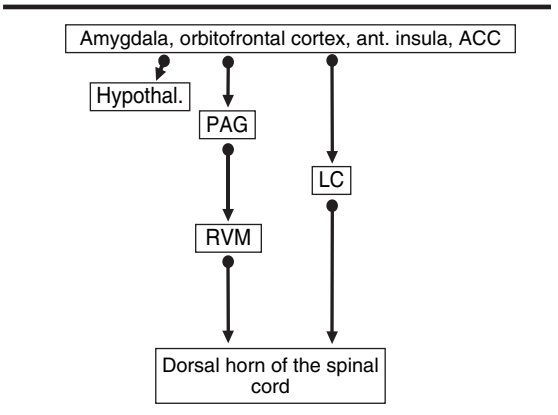

Figure 3 Schematic used to illustrate pathways and mechanisms that modulate pain. From Price, D. D. and Bushnell, M. C. (*eds.*) 2004. Pschological Methods of Pain Control: Basic Science and Clinical Perspectives, pp. 322. IASP Press.

activates these same limbic structures through a ventrally directed route, as shown in Figure 2. This latter pathway reflects the serial interaction between pain sensory qualities and intensity and pain unpleasantness. Thus, direct and indirect activation of emotion-related limbic structures is consistent with the pathways shown in the schematic of Figure 1. Emotions related to pain are a consequence of sensations related to pain (i.e., serial interrelationships) as well as other psychophysiological and contextual factors (i.e., parallel interrelationships). Some aspects of pain-related emotions may occur automatically as a result of direct input to subcortical limbic areas such as the amygdala, a structure implicated in fear.

5.64.1.2.2 Brain pathways and regions interrelating sensory and affective dimensions of pain

Once impulses in ascending pathways from the dorsal horn reach different targets within the brain, both serial and parallel circuitry is activated. The serial interconnections are established by the pathway to VPL and to somatosensory cortices that is anatomically interconnected with a ventrally directed corticolimbic pathway that integrates somatosensory input with other sensory modalities such as vision and audition and with learning and memory (Friedman, D. P. *et al.*, 1986). This pathway proceeds from primary and secondary somatosensory cortices to posterior parietal cortical areas and to insular cortex (IC) and from the latter to subcortical limbic structures (e.g., amygdala, perirhinal cortex, and hippocampus). This corticolimbic pathway may be critical for pain affect (Friedman, D. P. *et al.*, 1986). This serial corticolimbic somatosensory pathway ultimately converges on the same limbic and subcortical structures that may be more directly accessed by other ascending spinal pathways. The latter reflect parallel processing. This dual convergence may be related to a mechanism whereby multiple neural sources, including somatosensory cortices S1 and S2, contribute to pain affect and reflects both parallel and serial processing. This corticolimbic serial pathway directly implies that somatosensory cortices contribute to pain affect. This implication is consistent with psychophysical studies in which pain unpleasantness was shown to be the result of pain sensation intensity and with studies showing deficits in both pain sensation and pain unpleasantness as a result of somatosensory cortical lesions (see references in Price, D. D., 1999; 2000).

5.64.1.2.3 The pivotal role of the anterior cingulate cortex (ACC) in pain affect

As shown in Figure 2, ACC receives inputs from multiple sources, including thalamus, insular cortex, posterior cingulate cortex (PCC), and prefrontal cortex. Convergence of these inputs at the level of ACC would be consistent with a mechanism in which somatic perceptual and cognitive features of pain would be integrated with attentional and rudimentary emotion mechanisms. Based on neurological evidence, the ACC may have a complex pivotal role in interrelating attentional and evaluative functions with that of establishing emotional valence and response priorities (Devinsky, O. *et al.*, 1995). Response priorities would be closely related to premotor functions that are integrally related to motivation and emotions and may be associated with immediate efforts to cope with, escape, or avoid the pain and pain-evoking situation. For example, the projection of ACC to the supplementary premotor area may reflect the motor side of an overall affective-motivational dimension of pain. In this view, cortical areas controlling sensory, attentional, pre-motor, and affective functions of pain are part of a distributed network that has serial and parallel connections. This network has implications for psychological modulation of pain because each of these connections represents a stage of pain processing that can, in principle, be modified by psychological factors.

Response priorities change over an extended period of time. Pain unpleasantness endured over time engages prefrontal cortical areas involved in reflection and rumination over the future implications of a persistent pain condition. The ACC may serve this function by coordinating somatosensory features of pain with prefrontal cerebral mechanisms involved in attaching significance and long term implications to pain, a function associated with secondary pain affect (Apkarian, A. V. *et al.* 2001; Devinsky, O. *et al.*, 1995; Price, D. D., 1999; Verne, G. N. *et al.*, 2003). Thus, ACC may be a region that coordinates inputs from parietal areas involved in perception of bodily threat with frontal cortical areas involved in plans and response priorities for pain-related behavior. Both functions would help explain observations on patients with prefrontal lobotomy and patients with pain asymbolia as a result of insular cortical lesions (Price, D. D., 1999). The former have deficits in spontaneous concern or rumination about their pain but can experience the immediate threat of pain once it is brought to their attention. In contrast, asymbolia patients appear incapable of perceiving the threat of

nociceptive stimuli under any circumstances. The role of medial prefrontal cortical areas in secondary pain affect is also supported by recent brain imaging studies. These studies show increased prefrontal neural activity in clinical pain patients likely to have high levels of secondary pain affect (Apkarian, A. V. *et al.* 2001; Verne, G. N. *et al.*, 2003).

5.64.2 Modulation of Pain Sensation and Pain Affect by Attention and Distraction

There are neural circuits that provide top-down modulation of the pain experience. Central neural mechanisms associated with such phenomena as placebo/nocebo, hypnotic suggestion, attention, distraction, and even ongoing emotions are now thought to modulate pain by decreasing or increasing neural activity within many central neural structures, including the dorsal horn (Figure 3). This modulation includes endogenous pain-inhibitory and pain-facilitatory pathways that descend to spinal dorsal horn, the origin of ascending spinal pathways for pain (Basbaum, A. I. and Fields, H. L., 1978). Recent brain imaging studies have begun to reveal the cortical areas involved in pain modulation (Hofbauer, R. K. *et al.*, 2001; Koeppe, R. A. and Stohler, C. S., 2001; Petrovic, P. *et al.*, 2001, Rainville, P. *et al.*, 1997).

The modulation of pain by endogenous cortical and subcortical networks is consistent with other types of brain imaging experiments that show that anticipation of pain activates cortical nociceptive regions to some extent, though to a lesser degree than pain itself. Thus, the cortical networks shown in Figure 2 may be directly influenced by cognitive factors. These are likely to include not only anticipation of the presence of pain, but also anticipation of its reduction, as in the case of placebo or hypnotic analgesia. The modulatory mechanisms are likely to be diverse, extending from those which are confined only to neural interactions within the brain to those involving activation of brain-to-spinal cord circuits long known to potently reduce or enhance pain, as represented in Figure 3 (Basbaum, A. I. and Fields, H. L., 1978).

5.64.2.1 Psychophysical Studies of Effects of Attention and Distraction on Pain

Attentional manipulation can be achieved in numerous ways; however, distraction is the most general attentional manipulation for pain modification. An interesting stimulus can be presented to an individual, or the individual can engage in an attention-demanding task. Unfortunately, in addition to attention, other variables are often affected by these techniques. For example, mood and/or arousal may change in response to an interesting stimulus (e.g., music), and alteration of these states may contribute to changes in pain experience. Furthermore, simple distraction tasks often lack a measure of attentional state. This is problematic, as some individuals may attend to music during presentation of noxious stimuli, whereas others may focus only on the pain. In the case of attention-demanding tasks, some individuals who are particularly adept at performing the task (e.g., mental arithmetic) may devote much less attention to it than those who are less skilled.

A psychophysical paradigm with two balanced conditions provides a more controlled alteration of attentional state. An example is that of the cross-modality attention paradigm in which stimuli from two sensory modalities are presented simultaneously, and the participant must perform tasks that require attention to one modality. Attentional status is measured via task performance. These paradigms permit the control of level of arousal and vigilance, because the same stimuli are presented on all trials, task difficulty is equivalent between the two modalities, and only direction of attention is altered.

One variant of the balanced-condition psychophysical approach is the intra-modal spatial attention paradigm. In this paradigm, concurrent identical stimuli are presented to different receptive fields – or different body regions for somatosensory stimuli – and tasks are performed that require attention to one or the other location. Although used extensively with visual and auditory systems (Corbetta, M. and Shulman, G. L., 2002; Hikosaka, O. *et al.*, 1996), when applied to the pain system, this paradigm may engage diffuse noxious inhibitory controls (DNIC), a pain modulatory system evoked by simultaneous presentation of two noxious stimuli, that could alter pain perception (Le Bars, D. *et al.*, 1979a; 1979b; Price, D. D. and McHaffie, J. G., 1988). Consequently, this paradigm makes it difficult to distinguish changes in pain perception due to shifts of spatial attention from those due to other pain modulatory networks.

Finally, a balanced-condition psychophysical paradigm can require shifts of attention to different dimensions of the same stimulus within a single stimulus modality. For example, one can attend to the shape, color, texture, or motion of a visual stimulus.

Similarly, the quality of a painful stimulus – the burning, stinging, or aching sensations – can be the focus of attention. The unpleasantness of the sensation can also be attended to. Such manipulations can alter both the pain experience and pain-evoked neural activity.

5.64.2.1.1 Studies of basic distraction effects on pain

Many studies have compared experimental pain ratings in the presence and absence of a distracter (Bentsen, B. *et al.*, 1999; Hodes, R. L. *et al.*, 1990; Janssen, S. A. and Arntz, A., 1996; Johnson, M. H. and Petrie, S. M., 1997). Although not perfectly consistent, the vast majority of results indicate lower pain ratings during distraction. However, as noted above, caution is in order when attributing this pain modulation to directed attention, since uncontrolled other factors such as vigilance, mood, and anxiety, could contribute to the overall modulatory effect.

5.64.2.1.2 Studies of cross-modal attention effect on pain

Other studies have employed cross-modality psychophysical paradigms to specifically examine the modulatory effects of directed attention. For example, Miron (Miron, D. *et al.*, 1989) had participants detect changes in intensity of heat pain and visual stimuli. As expected, the speed and accuracy of detection of changes in stimuli were decreased when attention was directed to another stimulus modality. Their results further confirmed that pain stimuli were more effective in commanding attention than other stimuli. Subsequent results from the same investigators suggest that cross-modality attention may exert greater effects on the sensory dimension of pain than the unpleasantness dimension (Bushnell, M. C. *et al.*, 1999; Villemure, C. *et al.*, 2003). A limitation of all these studies is their focus on the sensory features of the stimulus. Requiring a study participant to attend to the emotional aspects of a stimulus might alter the affective more than the sensory component of pain.

5.64.2.1.3 Studies of spatial attention effects on pain

In a spatial attention paradigm, Bushnell M. C. *et al.* (1985) found that detection of changes to a heat stimulus applied to each side of the face was more rapid when these changes occurred on the side to which attention was directed. These results also demonstrated the modulatory effects of spatial attention on perceived intensity of noxious stimuli, as stimuli changes occurring outside a subject's attentional focus were less accurately detected. Furthermore, this study suggests that mechanisms of directed spatial attention involve areas of the nervous system that display a fine somatotopic organization of nociceptive information. The perceptual effects of spatial attention to pain are consistent with those of other sensory modalities and are critical for an organism's orientation to important features of the environment (Posner, M. E., 1980).

5.64.2.1.4 Studies of intra-modal attention effects on pain

In addition to focussing attention on different stimulus modalities and spatial locations, attention can also be directed to different features or dimensions of a stimulus. Several clinical and experimental studies have demonstrated decreased pain intensity and unpleasantness by directing subject attention to the sensory characteristics of pain (e.g., the burning, pricking, or aching sensation). A study of burn patients undergoing dressing changes found that those who focus on the sensory aspects of their pain report less pain than those distracted by music (Haythornthwaite, J. A. *et al.*, 2001). Another study of health-anxious chronic pain patients observed less anxiety and discomfort when attentional focus was directed only to the physical sensations of their pain (Hadjistavropoulos, H. D. *et al.*, 2000).

5.64.2.1.5 Other accounts of pain modulation by attentional and cognitive processes

An alternative account of attentional processing has been provided by Wegner D. M. (1994). He proposed the provocative theory of ironic processing, which has been applied to a number of cognitive processes (e.g., mood control, thought suppression) and has received some attention in the pain literature. This theory posits two cognitive mechanisms (the consciously controlled operating system and the automatic monitoring system) for achieving a desired mental state. The operating system searches for mental contents consistent with this state, whereas the monitoring system searches for mental contents inconsistent with this state. When the monitoring system locates such material, this material is brought into consciousness and thus activates the operating system. According to ironic processing theory, the operating system is compromised when mental capacity is reduced (e.g., because of pain, fatigue, stress), thereby permitting the undesired thoughts to enter

consciousness. A rebound effect then occurs where the undesired thoughts are more frequent than if they had not been initially suppressed (see Wenzlaff, R. M. and Wegner, D. M., 2000 for a review). As applied to pain, this theory holds that directed attention to pain would result in less pain compared to intentional distraction. Furthermore, pain suppression is suggested to have less antinociceptive effects than pain distraction. There is some evidence in the literature supporting both these hypotheses (e.g., Cioffi, D. and Holloway, J., 1993; Haythronthwaite, J. A. *et al.*, 2001).

What is to be made of the seemingly competing hypotheses of attentional modulation of pain and the divergent evidence that provides support for both these hypotheses? It may be that the antinociceptive effects of directed attention toward or away from pain is dependent upon the intensity of the pain and the cognitive and emotional state of the individual. For example, in situations of moderate pain intensity, where a patient is likely to be able to achieve/experience pain reduction, focused attention towards the pain may prove beneficial, à la ironic processing theory. How may this occur? Suppose a particular patient holds a moderate expectation for reduction in pain (due to some pharmacological agent, behavioral strategy, etc.) and a high desire for pain relief. Upon experiencing a small amount of pain relief – which the patient is able to perceive due to his/her focused attention on pain – some period of time following the treatment, the patient begins to notice that the treatment is working and, thus, expects further pain reduction. As a result of the experienced pain relief, the patient is also likely to be less fearful or anxious, and consequently reduces his/her desire for pain relief. As discussed more thoroughly below in the section on placebo, these changes in expectation (increase) and desire (decrease) can have powerful effects on the emotional state of the individual and, consequently, on the pain experience itself. In this manner, Wegner's contention that directed attention toward pain results in decreased pain is supported, although due to different mechanisms than outlined in his theory of ironic processing. Conversely, it may be the case that during episodes of extreme pain, directed attention away from the pain is the favored approach. During extreme pain, it is often the case that the patient has an intense desire for pain relief and a concomitant low expectation of achieving this relief. As this cognitive state is likely to produce intense negative emotions, which will be further reinforced by directed attention toward the pain and the experience of little pain reduction, it is likely that distraction techniques will prove most beneficial. Even in cases of moderate pain, if the patient has low expectations and high desire for pain relief (thus resulting in negative emotions), that individual may respond more favorably to a distraction technique than a pain-focused one. These are interesting and testable predictions, and they highlight the interaction between pain, cognition, and emotions. Other variables may also play an important role in these processes, as described below in the discussion of sex differences and pain-related attention.

In a laboratory cold-pressor paradigm, Keogh E. *et al.* (2000) found that for males, but not females, directed attention toward the pain sensation resulted in reports of less pain compared to a pain avoidance attentional condition. As a possible explanation for the seemingly paradoxical finding that men experience less pain by attending to it, the instructions required participants to concentrate on the sensations experienced during the task, and this sensory focussing may have reduced the painfulness of the situation. Thus, it appears that the use of attention-based strategies for pain reduction may be more effective for men than women.

5.64.2.2 Separating the Influence of Attention and Emotions

The attitude and emotional state of an individual can influence his/her perception of experimental and clinical pain (De Wied, M. and Verbaten, M. N., 2001; Marchand, S. and Arsenault, P., 2002; Meagher, *et al.*, 2001a; Schanberg, L.E. *et al.*, 2000; Weisenberg, M. *et al.*, 1998; Zelman, D. C. *et al.*, 1991). Unfortunately, pleasant stimuli used in laboratory studies to improve mood and reduce pain perception typically alter both attentional state and mood, thus confounding their effects. However, a recent study by Villemure C. *et al.* (2003) demonstrated that the effects of emotion and attention can be separated, and that these variables differentially alter pain intensity and pain-related unpleasantness. Using a cross-modality attention task, they showed that attending to the odor rather than heat pain reduced pain sensation intensity but did not alter pain-related unpleasantness, mood, or anxiety. In contrast, mood, anxiety level, and pain unpleasantness, but not pain intensity, were altered by odor valence. As compared to pleasant odor, unpleasant odor increased pain unpleasantness, negative mood, and anxiety. Their

results further suggest that the selective modulation of pain affect is a function of emotional changes, which were elicited by differences in odor valence.

5.64.2.3 Neurophysiological Studies of Effects of Attention on Pain Processing, Including Brain Imaging and Electrophysiological Studies

5.64.2.3.1 Effect of attention on pain-related activity in the dorsal horn

The attentional modulatory effects described above relate to studies of neural modulation of nociceptive transmission. Thus, dorsal horn sensory projection neurons, including WDR and NS neurons, undergo inhibition and facilitation from pathways that descend from the brain to the spinal cord (Figure 3). The stimulus-evoked impulse responses and the receptive field areas of these neurons can increase or decrease as a result of activity in various descending pathways under different behavioral conditions.

Descending modulatory influences and the behavioral conditions with which they are associated have been shown in experiments in awake trained monkeys (Hayes, R. L. *et al.*, 1981; Hoffman, D. S. *et al.*, 1981). These studies showed that responses of trigeminothalamic WDR and NS neurons of the medullary dorsal horn could be modified by different attentional sets and conditions of stimulus relevance. Nociceptive stimulus temperatures (45–49°) applied to the monkeys' face evoked impulse discharges in these neurons that were an increasing function of stimulus temperature. However, these neuronal impulse responses increased during a task in which the monkey discriminated a small temperature shift in the nociceptive range (a relevant attentional set) and decreased when they performed a similarly demanding visual discrimination task (an irrelevant attentional set). These opposing effects predict that the perceived intensity of pain should increase during thermal as compared to visual discrimination. A psychophysical study by Miron D. *et al.* (1989) confirmed this prediction.

The impulse frequencies elicited in WDR and NS trigeminothalamic neurons by the same range of nociceptive temperatures (45–49°) also can be modified by attentional factors related to anticipation. Impulse frequencies of these neurons were higher when a warning light preceded nociceptive stimuli as opposed to when these stimuli occurred unexpectedly. Thus, the magnitudes of the stimulus–response relationships are under dynamic modulatory control and may play as direct a role in determining pain perception as do the peripheral stimulus events themselves. The dorsal horn is part of a network involved in shaping pain perception, a network that includes the first synapse in ascending pathways for pain. This type of modulation had been anticipated by existing theories of pain (e.g., the gate control theory), but these studies were the first to demonstrate this principle in a behavioral context.

5.64.2.3.2 Effect of attention and distraction on pain-evoked activity in the brain

This type of study was extended by a similarly designed study of effects of attentional state on isolated nociceptive neurons in the thalamus (Bushnell, M. C. *et al.*, 1984; Bushnell, M. C. and Duncan, G. H., 1989). Similar to studies of trigeminothalamic neurons just described, tasks that directed a monkey's attention to a painful stimulus enhanced responses of medial thalamic neurons to nociceptive temperature stimuli applied to the monkeys' face, shown in Figure 4.

Imaging studies of the effects of attention and distraction in humans likewise show modulation of pain-evoked activity in the thalamus and several cortical regions, such as the primary somatosensory cortex (S1), anterior cingulate cortex (ACC), and insular cortex (IC) (Bantick, S. J. *et al.*, 2002; Brooks, J. C. *et al.*, 2002; Bushnell, M. C. *et al.*, 1999; Hoffman, H. G. *et al.*, 2004; Seminowicz, D. A. *et al.*, 2004; Valet, M. *et al.*, 2004). In one study, several pain-related brain regions were more activated during a pain-attention condition compared to a distraction condition (Peyron, R. *et al.*, 1999). In a similar study, Bushnell M. C. *et al.* (1999) showed the greatest attentional modulation of pain-evoked activity in S1 cortex, perhaps because subject attention was directed toward a sensory feature of the stimulus. Reciprocally, the primary auditory cortex was more activated when attention was directed to the auditory stimulus and not the painful stimulus, demonstrating the generality of attentional modulation across sensory modalities. Other regions, including the periaqueductal gray matter (PAG), ACC, and orbitofrontal cortex, may also be involved in the modulatory circuitry related to attention, as they have been shown to be activated during pain-distraction tasks (Petrovic, P. *et al.*, 2000; Tracey, I. *et al.*, 2002).

Results of EEG and MEG studies suggest that attentional modulation of pain likely involves both early sensory processing in S2-IC (Legrain, V. *et al.*,

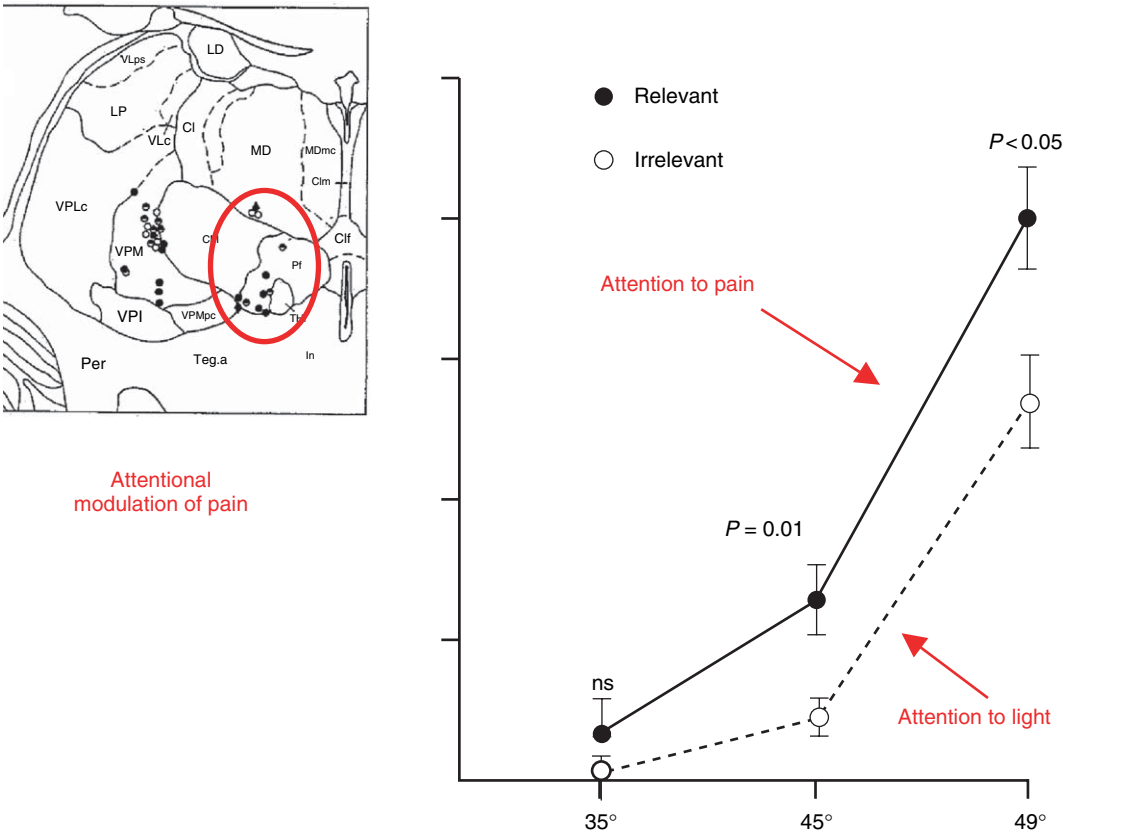

Figure 4 Stimulus–response functions showing single neuron responses in the medial thalamus (location shown in inset) during thermal stimuli of 35, 45, and 47 °C presented by a 1 cm^2 thermode on the maxillary facial area of a monkey. The solid line shows the responses when the monkey was required to attend to the thermal stimuli, and the dashed line shows responses to the same temperatures when the monkey was required to attend to a visual stimulus. Adapted from Bushnell, M. C and Duncan, G. H. 1989. Sensory and affective aspects of pain perception: Is medial thalamus restricted to emotional issues? Exp. Brain Res. 78, 415–418.

2002; Nakamura, Y. *et al.*, 2002) and later processing in ACC (Dowman, R., 2004; Garcia-Larrea, L. *et al.*, 1997; Siedenberg, R. and Treede, R. D., 1996). Changes in pain perception associated with attentional state appear to be due in part to changes in cortical processing and in part to a decrease in ascending afferent input from the spinal cord through activation of descending noxious inhibitory controls (DNIC).

5.64.3 Nonplacebo Effects of Expectation and Meaning

5.64.3.1 Effects on Pain Intensity

Studies attempting to modify either experimental or clinical pain intensity by manipulations designed to change expectancy show either weak or negligible effects, as indicated in a meta-analysis by Fernandez and Turk (Fernandez, E and Turk, D. C., 1989). Interestingly, 10 of 12 studies in their analysis showed that expectancy manipulations were least effective in reducing pain compared to other psychological strategies. A limitation of nearly all these studies, however, is that the independent variable is a manipulation or instruction designed to persuade participants to develop a positive expectation rather than a measure of expectation itself. Therefore, whereas the weight of all of these studies indicates weak or negligible effects of expectancy *manipulations* on pain intensity, it is not at all clear that direct effects of actual expectations have such weak effects. In fact, data published after Fernandez and Turk's (Fernandez, E and Turk, D. C., 1989) meta-analysis indicate that experiential manipulations of expectancy

have stronger effects than verbal manipulations of expectancy (Montgomery, G. H. and Kirsch, I., 1997; Voudouris, N. J. *et al.*, 1990).

5.64.3.2 Effects on the Affective Dimension of Experimental Pain

Studies of experimental pain wherein expectations can be directly manipulated provide the strongest evidence that desires and expectations are integral components of pain experience. Price D. D. *et al.* (1980) conducted a psychophysical analysis of experiential factors that influence the affective but not sensory discriminative dimension of heat pain. Trained participants made cross-modality matching judgments of both pain sensation intensity and unpleasantness. Non-noxious and noxious skin temperature stimuli were randomly interspersed during each experimental session. Changes in expectation of receiving painful stimulation were induced by preceding one-half of all the noxious stimuli by a warning signal. Results indicated that noxious temperatures were experienced as less unpleasant when preceded by a warning signal. In contrast, pain sensation magnitudes were unaffected by the warning signal. Moreover, the selective lowering of pain unpleasantness by the warning signal was greatest at the lowest end of the noxious temperature range (i.e. 45 °C) and was minimal at the highest end of the stimulus range (i.e., 51 °C). These data suggest that subjects prefer knowing that the next stimulus will be painful as compared to being surprised. Not knowing if the next stimulus will be painful is likely to produce anxiety; however, advanced warning has little effect if the intensity of stimulation is sufficiently high.

This interpretation of the anti-anxiety effects of a warning signal is supported by other experiments that reduce anxiety associated with experimental pain. Gracely *et al.* (1976) demonstrated that 5 mg diazepam significantly reduced affective descriptor responses to painful shock without altering sensory descriptor responses. Consistent with the Price D. D. *et al.* (1980) study, the reductions were greatest for low-intensity noxious stimuli. Another study by Gracely R. H. (1979) found a similar pattern for saline placebo administration. The results of all of these studies can be parsimoniously explained as a selective lowering of pain unpleasantness by reduction in anxiety. Part of pain unpleasantness is the anxiety associated with anticipating and receiving a noxious stimulus. Anxiety represents a state of wanting to avoid negative consequences combined with an experienced uncertainty of avoiding them (Barrell, J. J. *et al.*, 1985; Price, D. D. *et al.*, 1985). Regardless of how anxiety reduction is achieved, the result is that of selectively reducing pain unpleasantness, with the largest effects occurring for mildly painful intensities.

Expectations about the qualitative nature of pain sensations have also been shown to selectively influence pain affect. Johnson J. E. (1973) found that subjects who received a description of the painful sensations produced by forearm ischemia had lower levels of distress compared to subjects who only received a description of the procedure. Similar to Price D. D. *et al.* (1980), pain sensation intensities were unaffected by this difference in description. Thus, it appears that different kinds of expectations, either about the time of occurrence of pain or the types of sensations that will occur, can alter experienced unpleasantness without changing the intensity of experimentally induced painful sensation.

In summary, based on studies of experimental pain, it is apparent that expectations about different aspects of pain and about the contextual conditions in which pain is present influence pain differently. Expectations about when the pain will occur and what it means once it does occur may have relatively selective effects on the unpleasantness or immediate emotional disturbance associated with pain. Expectations about pain sensation intensity itself appear to have a modest influence on perceived pain intensity. Finally, manipulations designed to produce a positive expectation appear to have the weakest effect on pain intensity, although it is difficult to reach a definitive conclusion about this possibility because of the questionable pain measures used among most available studies.

5.64.3.3 The Influence of Expectancy on the Immediate Unpleasantness of Clinical Pain

The factors of desire for relief and expectation would intuitively have a greater influence on pain-related affect in the case of clinical pain, because the implications of having clinical pain are likely to be perceived as more open-ended and threatening than experimental pain. Unfortunately, few attempts have been made to directly assess the role of expectancy in clinical pain. Nevertheless, such a role is strongly supported by at least indirect evidence largely consistent with the idea that anxiety is a significant component of clinical pain affect. One study compared affective ratings of clinical pain in patients

whose pain is associated with a serious threat to health (cancer pain) to those of patients whose pain is of a less threatening nature (labor pain) (Price, D. D. *et al*., 1987). Comparisons were also made between women in labor whose focus was primarily on the birth of their child versus those who focused mainly on pain or on avoiding pain. In cancer pain patients, unpleasantness ratings were higher than sensory ratings, whereas the reverse was true for labor pain patients. Furthermore, patients who focused primarily on having the baby rated the unpleasantness of their pain as approximately one-half that of patients who focused primarily on pain or avoiding pain (Figure 5(a)); this difference occurred for each stage of labor. In contrast, no significant differences in pain sensation intensity ratings occurred between patients with these two orientations at any stage of labor (Figure 5(b)).

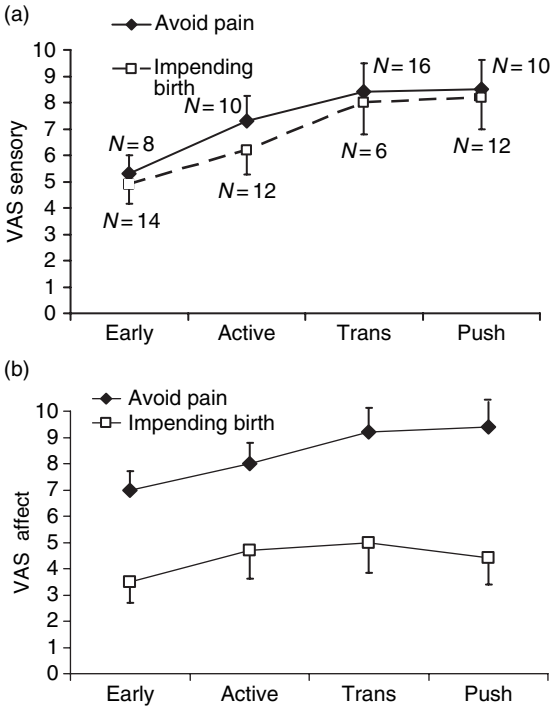

Figure 5 Mean sensory and affective VAS ratings of two groups of labor patients at various stages of labor. (a) Mean sensory ratings of the women who focused mainly on pain or avoiding pain (black diamonds) were very similar to women who focused mainly on the impending birth of the child. (b) Mean unpleasantness ratings of women focused on the impending birth were approximately half that of women who focused on pain or avoiding pain. Adapted from Price, D. D., Harkins, S. W., and Baker, C. 1987. Sensory-affective relationships among different types of clinical and experimental pain. Pain 28(3), 291–299.

The combination of all these results indirectly indicates that a person's goals, desires, and expectations about outcomes strongly influence emotional feelings associated with clinical pain. The influence of these factors is most apparent when divergent psychological orientations exist within a clinical pain condition. Thus, the unpleasantness generated by the immediate implications of cancer pain, including the reminder that pain sensation is a signal for the presence of disease, appears to add to that which is directly related to the pain sensations. One of the implications of having labor pain, on the other hand, is that birth of a baby is imminent. The positive emotional consequence of this implication appears to offset to some degree the unpleasantness of labor pain. This interpretation is further supported by the much greater degree of labor pain unpleasantness among women who focus on avoiding pain compared to those who focus on the birth of the baby. Part of what constitutes pain unpleasantness is the immediate implication of the pain condition. The implication, in turn, is related to a goal, desire, and an expectation associated with that goal.

Results from the studies of experimental pain described above indicate the existence of pharmacological and psychological manipulations that can selectively, and sometimes powerfully, reduce the immediate unpleasantness of pain. Some of these manipulations can be quite simple, such as stimulus duration or the presence or absence of a warning signal. Others are more complex and relate to restructuring the meanings associated with pain (e.g., some hypnotic suggestions). Manipulations that enhance pain unpleasantness also exist. The identification of experimental manipulations that selectively modify affective components of pain is critical for developing experimental strategies for identifying neurons, central pathways, and brain regions that are uniquely involved in the immediate affective dimension of pain.

5.64.4 Factors That Contribute to the Magnitude of Placebo Analgesia

For decades, placebo responses were mainly conceptualized as resulting from inert physical agents. Within the last few years, explanations of placebo responses have shifted from emphasis on environmental factors to human meanings and perceptions. We explore the roles of both external and experienced factors in producing placebo analgesia as well

as the relationships between them (see Chapter The Placebo Effect for placebo vignette).

5.64.4.1 The Magnitudes of Placebo Analgesia and the General Contexts That Influence Them

Although this study raised considerable controversy, the effect of placebo treatment was compared to a natural history condition in a recent meta-analysis of 29 studies (Hrobjartsson, A. and Gøtzsche, P. C., 2001). The effect size of placebo analgesia, measured as Cohen's d (pooled standardized mean difference), was 0.27, reflecting a small effect that is possibly clinically significant. Hrobjartsson and Gøtzsche suggested that the small placebo analgesia effect could be the result of confounding variables such as response bias, since pain reflects a subjective state. Interestingly, the large majority of the studies (24 of 29) included in the meta-analysis used a clinical trial design in which placebo administration served as the control condition. Verbal suggestions for analgesia are typically avoided in such studies and the only reference to placebo is made in the consent form in which patients are informed of the possibility of receiving an inert and/or ineffective agent. In most nonresearch clinical settings or in experimental studies of placebo analgesia mechanisms, however, positive suggestions or conditioning with effective agents are likely to enhance placebo analgesia, as will be discussed below. Therefore, patients are more likely to expect to receive a pain relieving medication in studies containing positive verbal suggestions in comparison to most clinical studies.

To determine whether placebo effect size is systematically influenced by the two contexts just described, two contrasting meta-analyses were conducted (Vase, L. *et al.*, 2002). In the first, twenty-three studies in which placebo treatments were used as a control condition were included, the majority of which were also included in the meta-analysis by Hrobjartsson and Gøtzsche. Most of these were clinical studies that tested an active drug or treatment. In the second, fourteen studies that were about placebo analgesic mechanisms were included. The mean effect size was 0.15 in the first meta-analysis of twenty-three studies, even smaller than Hrobjartsson and Gøtzsche's finding of 0.27. However, the mean effect size was 0.95 in the fourteen studies of placebo mechanisms, where strong suggestions for pain relief were typically given. Overall, these meta-analyses indicate that although the magnitude of placebo analgesia effects is highly variable, one of the potent factors influencing the placebo effect may be whether overt verbal suggestions are given for pain relief. The effect size of placebo analgesia in the studies where placebo analgesia was induced via either conditioning alone or suggestion alone was 0.83 and 0.85, respectively. However, the magnitude of placebo analgesia was 1.45 (almost twice as high as either factor alone) in the studies where the placebo analgesia effect was induced via a combination of conditioning and suggestion. Thus, it appears that the effect of external manipulations such as conditioning and suggestion are additive, implying that the placebo analgesia effect may be related to how the placebo agent is perceived, regardless of the exact external factors that lead to that perception.

5.64.4.2 Analyses of Factors That Contribute to the Magnitude of Placebo Analgesia

Given the variability in placebo analgesic effects and the systematic influence of the presence or absence of factors such as previous experience with effective treatments and verbal suggestions, an emerging goal of placebo analgesia research is to identify factors that contribute to the perceived efficacy of a therapeutic intervention. The contribution of placebo analgesia to the effectiveness of analgesic drugs was tested in a clinical study using hidden and open injections of traditional painkillers such as buprenorphine (Colloca, L. *et al.*, 2004). The patients needed less medication for analgesia when a doctor administrated open injections of painkilling agents with verbal suggestions for pain relief, than when a hidden machine administrated the painkilling agents. Presumably, the difference in analgesic response between open and hidden injections directly reflects the placebo analgesia effect. The difference between open and hidden injections could be eliminated by hidden injections of naloxone in a subsequent experimental study, demonstrating that part of the response variability to analgesic drugs can be attributed to opioid-mediated placebo analgesic effects. It may be particularly useful to explore exactly how subjects experience open injections versus hidden injections in order to clarify the mediating and moderating factors in placebo analgesia. As discussed below, such an approach is beginning to be applied to placebo analgesic research in general.

5.64.4.2.1 External factors that contribute to placebo analgesia

5.64.4.2.1.(i) Conditioning Previous experiences with pain, the analgesic remedy, and the setting are likely to influence perception of pain treatments. Some investigators propose the idea that placebo effects are based on Pavlovian conditioning. When a patient receives an agent (unconditioned stimulus) that leads to analgesia (unconditioned response), contextual cues such as the medical setting, the white coat, or the pill/syringe (conditioned stimuli) may be associated with pain relief (Wickramasekera, I. A., 1985). These contextual factors, which represent the conditioned stimuli, elicit pain relief in the absence of active agents. Cross-over studies have supported this hypothesis; the magnitude of placebo analgesia follows the graded doses of the active drug when placebo is given as the second drug (Laska, E. and Sunshine, A., 1973). Voudouris N. J. *et al.* (1985; 1989; 1990) conducted the first studies to investigate the contribution of conditioning with a design that included a repeated baseline control condition. Subjects were tested in three sessions: (1) pretest, where a noxious electrical stimulus was applied to determine the subjects' threshold, (2) manipulation, where an inert cream was applied to the skin and the stimulus was surreptitiously reduced to provide an experience of the cream's analgesic effect, and (3) posttest, where the analgesic cream was applied and the original intensity stimulus was delivered to the same area of the skin. Compared to a group given the cream with no conditioning, the conditioning group showed significant pain reduction by the placebo cream. This suggests that a previous pairing of reduced stimulus intensity with an inert cream can result in large analgesic effects.

With subjects undergoing ischemic arm pain, the contribution of conditioning also has been tested (Amanzio, M. and Benedetti, F., 1999). On the first day, subjects were tested during a no-treatment session. On the second and third day, a group of 14 subjects was conditioned with the opioid agent morphine and another group (14 subjects) was conditioned with the nonopioid agent ketorolac. On the fourth day, both groups received open injections of saline and were told that the agent was an antibiotic to test effects of conditioning alone without any effect of overt placebo suggestion. Conditioning in both the morphine and ketorolac groups produced moderate and statistically reliable placebo effects. When the open injection secretly contained naloxone in a subsequent morphine-conditioned group, the placebo effect could be completely prevented. In contrast, the placebo effect was not antagonized by naloxone if ketorolac was used as the conditioning stimulus. Thus, the placebo analgesia effect induced by opioid conditioning (morphine) was mediated by endogenous opioids, whereas the placebo analgesia effect induced by nonopioid conditioning (ketorolac) was not mediated by endogenous opioids.

5.64.4.2.1.(ii) Suggestion Expectation and belief in future pain relief can be induced by nonverbal and verbal suggestions, and expectations of caregivers can be transferred to patients. For example, the influence of nonverbal suggestions was indirectly tested in a study where the clinician knew that one group of patients would receive placebo whereas the other group would receive placebo as well as the active analgesic agent fentanyl (Gracely, R. H. *et al.*, 1985). The placebo analgesia effect was significantly higher in the second group, indicating that even without intentional or verbal communication, simply the clinician's belief that a patient may receive a powerful painkiller influences the magnitude of placebo analgesia. Several studies have investigated the influence of verbal suggestions for pain relief.

The same paradigm of ischemic tourniquet pain tolerance was used to test whether suggestion in itself was enough to produce placebo analgesia (Amanzio, M. and Benedetti, F., 1999). After the first day's no-treatment session, on the second day, patients were given an open injection of saline and told that the agent was a powerful painkiller. A small but statistically reliable placebo effect was produced by this placebo treatment. When the experiment was repeated with an open injection of naloxone instead of an open injection of saline on the second day, the placebo analgesia effect was entirely eliminated, indicating that suggestion induces a placebo analgesia effect that is mediated by endogenous opioids. Recent studies have shown that both direct and indirect suggestions for pain relief lead to placebo analgesia of large magnitudes (Pollo, A. *et al.*, 2001; Price, D. D. *et al.*, 1999; Vase, L. *et al.*, 2002). Additionally, several studies have shown that verbal suggestions can lead to reduction of pain in highly specific areas of the body and that these specific placebo effects may be mediated by endogenous opioids (Benedetti, F. *et al.*, 1999; De Pascalis, V. *et al.*, 2002; Montgomery, G. H. and Kirsch, I., 1996; Price, D. D. *et al.*, 1999).

The majority of the studies presented so far have shown that conditioning in itself or suggestion in itself may lead to placebo analgesia. However, in

most studies and especially in most clinical settings, previous exposure to analgesic agents and verbal suggestions for pain relief combine to produce placebo analgesia. The combination of morphine conditioning and verbal suggestions for inducing placebo analgesia was also examined in the study by Amanzio M. and Benedetti F. (1999). The magnitude of this placebo analgesia effect was approximately twice the size of the placebo effect induced via either conditioning or suggestion alone. Interestingly, this large placebo effect could be completely prevented by naloxone. Thus, even though conditioning and suggestion may make separate contributions to placebo analgesia effects, they are likely to both activate a common opioid analgesia network. A recent study suggests that conditioning and suggestion both influence conscious phenomena (e.g., pain) through expectations, whereas conditioning without conscious expectations can influence unconscious physiological processes such as cardiovascular responses and hormonal secretions (Benedetti, F. *et al.*, 2003).

5.64.4.2.2 Experienced factors that contribute to placebo analgesia

Patients are likely to perceive external factors such as conditioning and suggestion in different ways. Therefore, it is important to examine how these environmental factors and factors within the human experience relate to each other during placebo analgesia.

5.64.4.2.2.(i) Expectancy In pain studies, expectancy (the experienced likelihood of an outcome or an expected effect) can be measured by asking people about the level of pain they expect to experience. One of the first studies to directly measure and manipulate expected pain levels used a design in which subjects were conditioned with reduced stimulus intensity (cutaneous electrophoresis) in the presence of an inert cream (Montgomery, G. and Kirsch, I., 1997), similar to studies by Voudouris N. J. and co-workers (Voudouris, N. J. *et al.*, 1985; 1989; 1990). Subjects rated expected pain levels immediately after the conditioning trials. Pain ratings were noticeably reduced by the conditioning procedure in a group of subjects that did not know about the stimulus manipulation (i.e., the placebo analgesic effect). However, regression analyses showed that expected pain levels mainly accounted for this effect. Thus, expectancy accounted for 49% of the variance in post manipulation pain ratings. Furthermore, when another group of subjects was informed about the experimental design and learned that the cream was inert, their expected pain levels did not differ from expected pain levels during the baseline condition and the placebo analgesia effect disappeared. Thus, although conditioning can lead to placebo analgesia, it appears to be mediated by conscious expectations.

Using a similar paradigm, the extent to which expectations of pain relief can be graded and related to specific areas of the body was further tested (Price, D. D. *et al.*, 1999). In this study three 'strengths' of placebo cream were applied to the subjects forearm and external manipulations were performed to perpetuate the belief that cream A was a strong analgesic, cream B a weak analgesic, and cream C a control agent on three adjacent areas of the arm. Conditioning was accomplished by surreptitiously lowering the heat stimuli in areas A (large reduction) and B (small reduction) but not C (no reduction), after the creams were applied. Following these manipulation trials, subjects were asked to rate their expected pain levels for the next series of trials. The conditioning trials led to graded levels of expectancy for the three creams C, B, and A (of successively less intense pain). When identical stimulus intensities were applied during the postmanipulation trials, subjects rated pains in areas C, B, and A as progressively less intense, demonstrating a graded placebo effect. In this study, expected pain levels accounted for between 25% and 36% of the variance in postmanipulation pain ratings. These results provide further evidence for the somatotopic specificity of the placebo analgesic effect, given that these placebo effects were induced on three immediately adjacent areas of the arm.

5.64.4.2.2.(ii) Desire for pain reduction While expectancy appears to be an important psychological mediator of placebo analgesia, it is unlikely to work alone. Since motivation is known to influence perception, desire (the experiential dimension of wanting something to happen or wanting to avoid something happening) is also likely to be involved in placebo analgesia. In the study just described, the subjects' level of desire for pain reduction also was manipulated (Price, D. D. *et al.*, 1999). In one group, presenting them the prospect of receiving a large number of painful stimuli successfully increased their desire for pain relief. In a second group, informing them that only a few stimuli would be presented decreased desire. Interestingly, ratings of desire for

pain relief were not significantly associated with the magnitudes of placebo analgesia. One possible reason for this lack of association may be because pain was induced via brief heat stimuli in this experimental setting. Desire for pain relief may be more of a factor in clinical pain where the pain is threatening or has an uncertain duration, therefore likely inducing fear or anxiety. Consequently, it is important to investigate the contribution of expectations and desire for pain relief in more clinically relevant settings.

5.64.4.2.2.(iii) Memory of pain This same study also showed that distorted memory of recent pain also contributes to the placebo effect (Price, D. D. *et al.*, 1999). The placebo analgesia effect was assessed in two ways, on concurrent ratings of pain obtained immediately after the stimuli were applied and on retrospective ratings of pain obtained approximately two minutes after the stimuli were applied. Based on retrospective ratings, the magnitude of placebo analgesic effects was three to four times greater than the effect based on concurrent ratings. The main reason for this difference was that subjects remembered their baseline pain intensity as being much larger than it actually was. Similar to placebo analgesia effects based on concurrent ratings, the placebo effects based on remembered ratings were strongly correlated with expected pain intensities ($R = 0.5$–0.6). In fact, there was a stronger correlation between expected pain and remembered pain than between expected pain and actual pain. Consequently, it is important to measure placebo analgesia effects with concurrent ratings since it may be distorted by remembered pain. Moreover, since remembered pain and expected pain are closely related, these factors appear to interact. These effects of distorted memory on placebo analgesia have been replicated (De Pascalis, V. *et al.*, 2002).

5.64.4.2.3 Predicting placebo analgesia

Two similarly designed studies further explain how factors within and external to human experience may relate in placebo analgesia (Vase, L. *et al.*, 2003; Verne, G. N. *et al.*, 2003). In both studies, patients diagnosed with Irritable Bowl Syndrome (IBS) were exposed to rectal distention via a balloon barostat (a type of visceral stimulation that simulates their clinical pain) and tested under natural history, rectal placebo and rectal lidocaine conditions. Both pain intensity and unpleasantness were rated immediately after each stimulus. In the first study, a standard clinical trial was conducted where the patients were given an informed consent form stating that they "may receive an active pain reducing medication or an inert placebo agent" (Verne, G. N. *et al.*, 2003). The rectal lidocaine had a significant pain relieving effect compared to rectal placebo ($p < 0.001$), and the rectal placebo had a significant pain relieving effect compared to the natural history condition (Figure 6, left panel). Based on meta-analyses discussed earlier, the second study added a suggestion to the placebo condition and lidocaine condition (Vase, L. *et al.*, 2003). Patients of the second study were told at the beginning of each treatment condition that "the agent you have just been given is known to significantly reduce pain in some patients" (rectal placebo, rectal lidocaine). A much larger placebo analgesic effect was found in the second study. In fact, the magnitude of placebo analgesia was so high that there was no longer a significant difference between the magnitude of rectal lidocaine and rectal placebo (Figure 6, right panel). Therefore, these two studies indicate that it is possible to increase the magnitude of placebo analgesia to a level that matches an active agent by adding an overt suggestion for pain relief.

Patients were asked to rate their expected pain level and desire for pain relief immediately after the agent was administered (before the onset of its effects) in both studies. In the second study, the combination of expected pain levels and desire for pain relief accounted for 77% of the variance in post placebo pain ratings (see Table 1); however, expected pain levels have accounted for between 25% to 49% of the variance in post placebo pain ratings in previous studies. Therefore, it is possible that the combination of expected pain level and desire for pain relief accounts for a greater amount of the variance in post placebo pain ratings than either factor alone. Nevertheless, although the interaction between expected pain level and desire for pain relief seems to have contributed, the majority of the contribution came from the expected pain level (Table 1). Interestingly, the combination of expected pain level and desire for pain relief accounted for 81% of the variance in pain ratings during the rectal lidocaine condition. These findings further support the conclusion that placebo factors make strong contributions to the efficacy of active treatments.

5.64.4.3 Placebo Analgesia As an Emotional Response

More recently, the role of emotion in placebo analgesia has been examined in a number of studies.

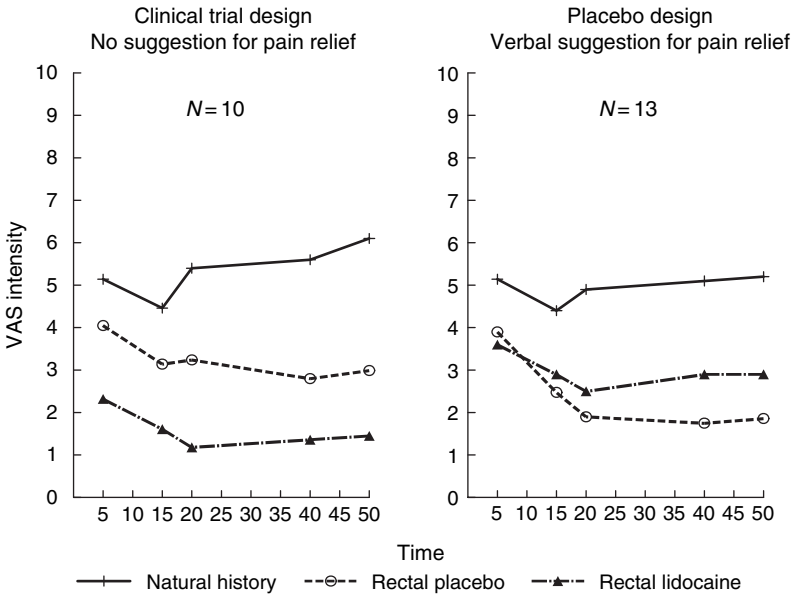

Figure 6 Comparisons of natural history, rectal placebo and rectal lidocaine scores on visceral pain intensity ratings (VAS) during a 50 min session within a clinical trial design, where no suggestions for pain relief are given (left) and within a placebo design with verbal suggestions for pain relief (right). From Vase, L., Robinson, M. E, Verne, G. N, and Price, D. D. 2003. The contribution of suggestion, expectancy and desire to placebo effect in irritable bowl syndrome patients. Pain 105, 17–25.

Table 1 The contribution of expectancy and desire to rectal placebo analgesia

Model	*R^2 change*	*F*	*P*
Expectancy[a] + desire	0.64	9.1	0.006
Expectancy X desire	0.12	5.0	0.05
Total model	0.77	10.2	0.003

[a]Denotes significant beta weight.
From Vase, L., Robinson, M. E, Verne, G. N, and Price, D. D. 2003. The contribution of suggestion, expectancy and desire to placebo effect in irritable bowl syndrome patients. Pain 105, 17–25.

Interactions between desire and expectation account for magnitudes of positive and negative feelings during hypothetical emotional situations and emotional feelings during actual events (Price, D. D. and Barrell, J. J., 2000). These same interactions also can account for direction and strength of choices during instances of decision making (Price, D. D. *et al.*, 2001). Placebo analgesia may be added to the list of phenomena that are associated with the desire-expectation model in showing that interactions between desire for relief and expected pain levels account for large and significant amounts of the variance in the placebo response.

5.64.4.3.1 Do placebo effects result from changes in emotional states?

Placebo effects also may change over time as a consequence of changes in emotional states. Similar to the studies on IBS patients described above, 26 IBS patients were exposed to rectal distension under natural history, rectal placebo, and rectal lidocaine conditions and ratings were obtained of expected pain, desire for pain relief, anxiety, and actual pain during each experimental condition (Vase, L. *et al.*, 2005). In this study, however, ratings of expected pain levels, desire for pain relief, and anxiety were obtained at two time points, at the onset of placebo administration (early) and midway through the 40 min observation period (late). Ratings of these three factors decreased from early to late time points as did pain ratings within the placebo condition. Decreases in these three factors across natural history versus placebo conditions accounted for 11% (not significant) of the variance in placebo responses (pain in natural history minus pain in placebo condition) at the onset of placebo administration and for 58% (significant at $P < 0.001$) of the variance in placebo responses in the late period of observation. These results suggest that the placebo effect can increase over time as a function of decreases in expected pain levels, desire for relief, and negative

emotions such as anxiety. These findings support the view that placebo effects may be at least partly mediated by changes in emotional states. Equally interesting is that similar results occurred for the lidocaine condition, providing further evidence that placebo effects and the factors that evoke them are embedded in active treatments.

Placebo treatments can initiate a more positive or less negative emotional state for a patient. It is possible that the placebo analgesia effect can at least partly result from decreases in negative emotions or increases in positive emotions. This possibility is supported in part by the studies just described and also by a study, which shows that pain, unpleasantness, and pain intensity may be reduced by evoking positive emotions or increased by evoking negative emotions (Chretien, P. and Rainville, P., 2004). Since this study was not about placebo effects, it provides an independent line of evidence that emotional feelings modulate pain. If placebo manipulations alter pain, they may do so by altering emotional states. Alternatively, it is possible that desire and expectation are merely factors that are common to both placebo mechanisms and emotions. In a recent study, it was found that low desire for pain relief decreased pain intensity and unpleasantness, whereas a high desire for pain relief increased pain unpleasantness but not pain intensity, suggesting that a decrease in desire may actually lower pain intensity (Chretien, P. and Rainville, P., 2004). These results are consistent with placebo studies described above (Vase, L. *et al.*, 2003; Verne, G. N. *et al.*, 2003).

5.64.4.3.2 Future directions

Whereas past explanations of placebo analgesia focused mainly on environmental factors and classical conditioning models, modern explanations focus more on human meanings, conscious expectations, and emotions as mediators or moderators of this phenomenon. This shift in emphasis is exciting because it suggests that the placebo analgesic response can be understood as a mind-body interaction and as a phenomenon of human consciousness, which has parallels within pain-regulating areas of the brain. Thus, future studies that combine brain imaging with analyses of dimensions of human experience should provide important neuroscientific and psychological insights into the mechanisms of placebo effects, with both significant scientific benefits and consequent improvements in the care of patients with pain.

5.64.5 Modulation of Pain Intensity and Pain Unpleasantness by Emotions

Emotions are closely related to pain in several ways. The notion of pain-related suffering corresponds to the experience of strong negative emotion associated with pain. Emotions also share a number of features with pain, including output viscero-motor responses and several experiential dimensions. In addition to co-occurring with pain, increasing evidence suggests that emotions play an important role in pain modulation. This may reflect the overlap between pain and emotion-related neurophysiological processes. This section begins with a brief discussion of emotions and follows with a consideration of the effects of emotion on experimental and clinical pain.

5.64.5.1 Negative Emotions As a Constituent of Pain

5.64.5.1.1 Pain definitions

The International Association for the Study of Pain (IASP) defines pain as "an unpleasant sensory and emotional experience associated with actual or potential tissue damage, or described in terms of such damage" (Merskey, H. and Spear, F. G., 1967). A slightly different definition is offered by Price D. D. (1999) in which pain is "a somatic perception containing (1) a bodily sensation with qualities like those reported during tissue damaging stimulation, (2) an experienced threat associated with this sensation, and (3) a feeling of unpleasantness or other negative emotions based on this experienced threat" (p. 1–2). In both definitions, negative emotions are a component of the pain experience. Price's (1999) stages of pain processing described earlier also highlight the relationship between pain and emotions.

5.64.5.1.2 Is pain an emotion?

The components of emotion theories also relate to pain processes. Perhaps the primary difference between pain and emotion is that pain requires the presence of "a bodily sensation with qualities like those reported during tissue damaging stimulation" (Price, D. D., 1999; p. 1). Pain sensations then can be regarded as a specific inducer of a primitive emotional response, which is consistent with theoretical accounts of emotion systems as closely related to evolutionary processes (e.g., Izard, C. E., 1993; Plutchik, R., 1980). The prototypical "pain face" has been documented and can be differentiated from

facial expressions of the basic emotions of fear, anger, and sadness (reviewed in Williams, A. C., 2002). Patterns of autonomic responses to nociceptive stimuli well documented in animals (Sato, A. *et al.*, 1997) may contribute to pain-related emotional responses as well as subjective feelings of unpleasantness (e.g. Fillingim, R. B. *et al.*, 1998; Rainville, P. *et al.*, 1999). The stages of pain processing described earlier include primary and secondary affective stages (Price, D. D., 1999), where the first corresponds to the basic experience of a threat, or the fear of tissue damage, and may include self-perception of autonomic and motor responses triggered automatically. The second stage reflects secondary evaluative processes consistent with modern views on the role of cognitive evaluative processes in emotions. This is also consistent with the experiential model in which emotional experiences are related to goals, desires, and expectations. A study by Price D. D. *et al.* (1980) indicated that this experiential model of emotions is predictive of variations in pain unpleasantness, but not pain intensity, which is consistent with the view that pain-related affective processes are emotional responses to pain sensations.

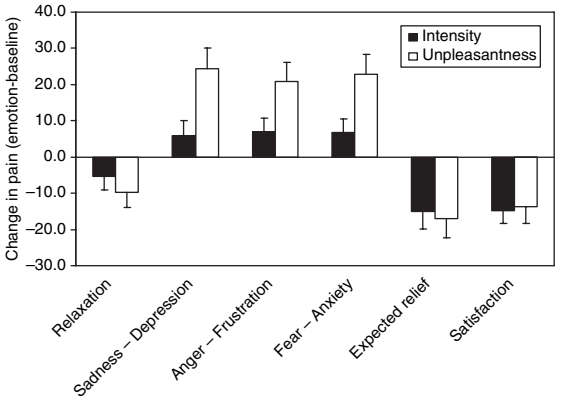

Figure 7 Changes in pain intensity and pain unpleasantness produced by 1 min immersions of the hand in hot water, from a baseline control condition and following the hypnotic induction of emotions. Significant increases in pain ($p < 0.05$) are found in response to negative emotions relative to the baseline ($y = 0$) and relaxation condition, with larger effects observed in pain unpleasantness than pain intensity. Decreases in pain were less pronounced and ns. in response to positive emotion induction. Adapted from Rainville, P. 2004. Pain and Emotions. In: Psychological Methods of Pain Control: Basic Science and Clinical Perspectives (*eds.* D. D. Price and M. C. Bushnell), pp. 117–141. IASP Press.

5.64.5.2 Effects of Emotion on Pain: Experimental Studies

In order to determine the effects of emotion on pain, one must first distinguish between emotions related to pain from emotions that co-occur with pain but are otherwise unrelated to pain. Emotions that are related to pain constitute secondary affective responses to pain. Emotions that are not related to pain may be considered distracters and/or they may produce brain-body responses that increase or decrease pain.

5.64.5.2.1 The experience of pain-related emotions

Hypnosis is one experimental paradigm that has been used to test the effect of pain-related emotions on pain. In a series of studies conducted by Rainville (reviewed in Rainville, P., 2004), positive and negative emotions were hypnotically induced in subjects undergoing an experimental pain task. Compared to baseline and hypnotic relaxation conditions, ratings of pain intensity and unpleasantness decreased in positive emotions conditions and increased in negative emotions conditions (Figure 7) (Huynh Bao, Q. V. and Rainville, P., 2002). Although affecting both pain intensity and unpleasantness, pain-related negative emotions primarily increased pain unpleasantness (Figure 7).

In a subsequent study examining the effects of anger and sadness, hypnotic suggestions for these emotions were associated with significant increases in desire to avoid and/or escape pain during the experimental task and reductions in expectations of avoiding and/or escaping pain (Figure 8(a)). Ratings of negative valence and arousal increased significantly in both negative emotion conditions, and subject ratings of their feeling of being in control (dominance) decreased significantly only in the sadness condition. In both negative emotion conditions, pain intensity and unpleasantness increased significantly, with pain unpleasantness showing a larger change (Figure 8(b)). Importantly, changes in pain unpleasantness, and pain intensity to a lesser degree, were predicted by changes in emotions (Table 2). The associations with pain unpleasantness remained significant after controlling for changes in pain intensity. However, after accounting for changes in pain unpleasantness, the associations with pain intensity were reduced to almost zero, save expectation that contributed some unique variance to changes in pain intensity. In a recent study, however, Chretien and Rainville (Chretien, P. and Rainville, P., 2004) found

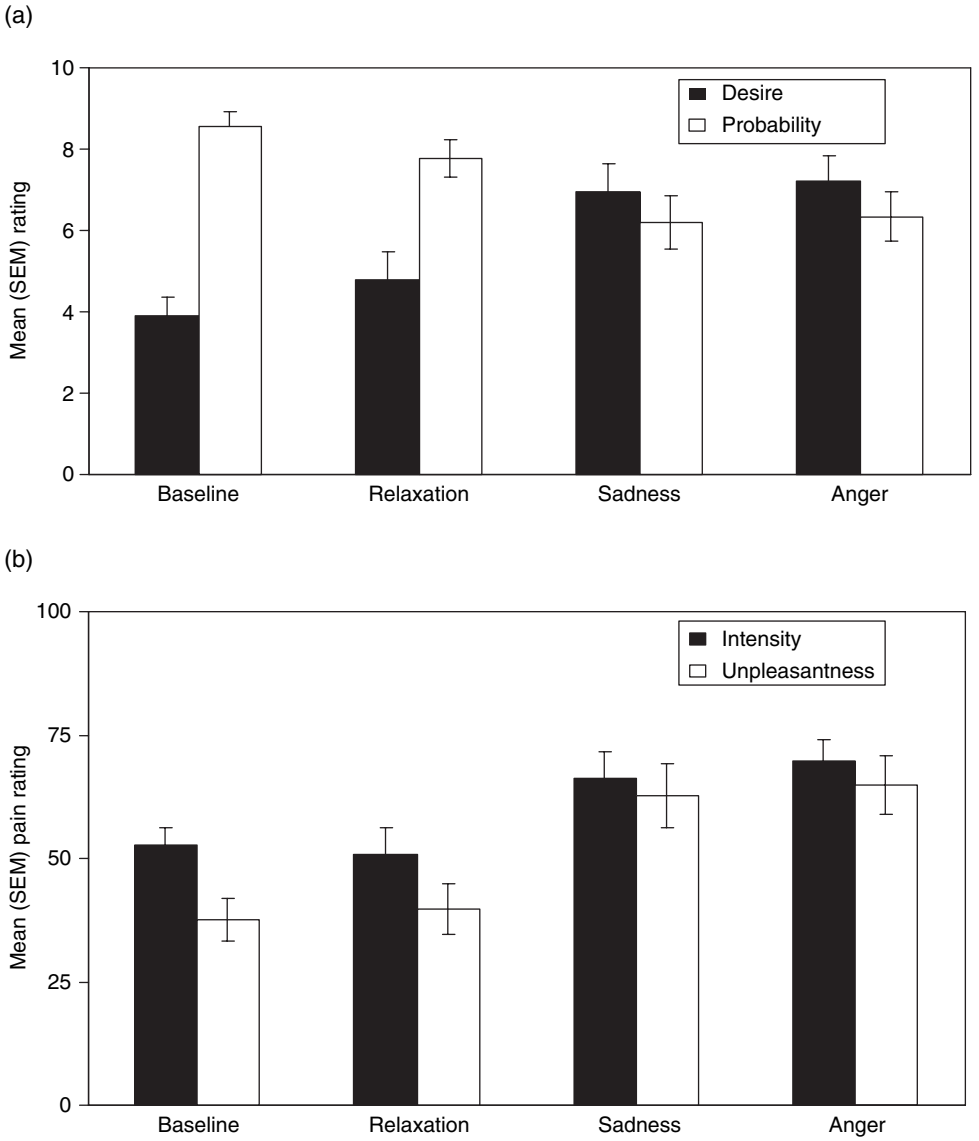

Figure 8 Effects of hypnotic relaxation and hypnotic induction of anger and sadness on subjective desires and expectations to avoid/escape pain (a) and on the pain intensity and unpleasantness produced by 1-min immersion of the hand in hot water (b). Desire increased and expectation decreased in the negative emotion conditions ($p < 0.05$). As a result, pain unpleasantness, and to a lesser extent, pain intensity increased in both conditions ($p < 0.05$). Figure adapted from Rainville, P. 2004. Pain and Emotions. In: Psychological Methods of Pain Control: Basic Science and Clinical Perspectives (*eds.* D. D. Price and M. C. Bushnell), pp. 117–141. IASP Press.

that the specific, hypnotic manipulation of desire to avoid/escape pain does produce a significant change in pain unpleasantness, independent of changes in pain intensity and expectation.

The previous study also included autonomic measures and found changes in heart rate to the experimental heat pain stimuli. Significant increases in heart rate were observed during negative emotions compared to baseline and control conditions, and this increase was positively associated with changes in pain and emotional experience (Table 3). After controlling for changes in pain intensity and felt arousal, changes in pain unpleasantness remained positively correlated with changes in cardiac responses. Conversely, cardiac responses were not significantly correlated with pain intensity after controlling for pain unpleasantness, and were only slightly correlated with pain intensity after controlling for

Table 2 Correlation coefficients between changes in pain intensity and unpleasantness, and changes in several emotional dimensions

Pearson-R	*Pain intensity*	*Pain unpleasantness*	*Partial intensity*	*Partial unpleasantness*
Desire	0.74***	0.83***	0.16	0.56***
Expectation	−0.36**	−0.65***	0.43*	−0.68***
Valence	0.65***	0.76***	0.04	0.52***
Felt arousal	0.52***	0.67***	−0.09	0.50***
Dominance	−0.47***	−0.53***	−0.05	−0.29*

*, $p < 0.05$; **, $p < 0.01$; ***, $p < 0.001$.
From Rainville, P. 2004. Pain and Emotions. In: Psychological Methods of Pain control: Basic Science and Clinical Perspectives (*eds.* D. D. Price and M. C. Bushnell), pp. 117–141. IASP Press.

Table 3 Correlation between changes in pain-evoked cardiac responses and changes in pain- and emotion-related dimensions

Pearson-R	*Modulation of RR changes*	*Residual (-INT)*	*Residual (-UNP)*	*Residual (-arousal)*
Pain intensity	−0.48***		+0.02	−0.27*
Pain unpleasantness	−0.59***	−0.38**		−0.35**
Desire to avoid-escape	−0.47***	−0.19	+0.03	−0.26
Expectation to avoid-escape	+0.44***	+0.33	+0.10	+0.16
Valence	−0.37**	−0.09	+0.14	−0.13
Felt arousal	−0.55***	−0.40**	−0.27*	
Dominance	+0.30*	+0.10	−0.01	+0.10

*, $p < 0.05$; **, $p < 0.01$; ***, $p < 0.001$.
From Rainville, P. 2004. Pain and Emotions. In: Psychological Methods of Pain control: Basic Science and Clinical Perspectives (*eds.* D. D. Price and M. C. Bushnell), pp. 117–141. IASP Press.

arousal. As would be expected, changes in felt arousal were positively associated with cardiac responses; however, this association was attenuated when changes in pain unpleasantness were controlled. This suggests that feelings of arousal and pain unpleasantness are closely related.

Figure 9 summarizes the findings of these studies examining the effect of pain-related emotions on pain. In this model, the nociceptive stimulus contributes to pain intensity, which then contributes to pain unpleasantness (Price, D. D., 1999; 2000; Rainville, P. *et al.*, 1999). The nociceptive stimulus also elicits autonomic responses and somatic feedback, and these factors influence felt arousal and pain unpleasantness. Pain-related desire and expectation contribute to modulate pain. Desire to avoid or escape pain primarily affects pain unpleasantness, independent of pain intensity (Table 2). Alternatively, expectation appears to have a modulatory affect on both pain intensity and unpleasantness, which is consistent with the placebo literature discussed previously. Furthermore, pain-related autonomic activity may be enhanced or diminished by descending neurophysiological mechanisms that are responsive to modulation of pain unpleasantness. When considered in their entirety, these results indicate that pain-related negative emotions have the primary effect of increasing pain unpleasantness and to a lesser degree pain intensity.

5.64.5.2.2 Pain anticipation and pain-related fear/anxiety

Other experimental studies have taken different approaches to examine the effects of emotions on pain perception. One phenomenon that has received particular attention is pain anticipation and the associated negative emotions. In addition to producing increased vigilance and attention towards future painful stimulation, anticipation of pain may also produce fearful responses and anxiety associated with the expectation of potential harm.

The effects of pain-related anxiety, fear, and fear-avoidance have been examined in clinical contexts as well as in animal studies. Meagher and Grau have

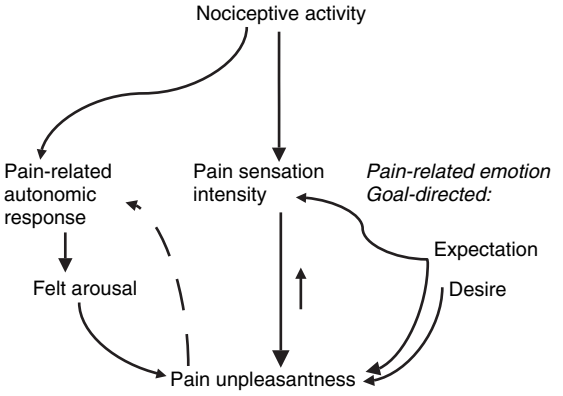

Figure 9 Pain-related emotions are suggested as affecting pain experience in several ways. Goal-directed desires appear to mainly influence pain unpleasantness, whereas goal-directed expectations affect both sensation intensity and pain unpleasantness. Physiological activity associated with autonomic activity that contributes to felt arousal. Adapted from Rainville, P. 2004. Pain and Emotions. In: Psychological Methods of Pain Control: Basic Science and Clinical Perspectives (*eds.* D. D. Price and M. C. Bushnell), pp. 117–141. IASP Press.

attempted to bridge the gap between these paradigms in a series of studies. Mild electric shocks in rats have been shown to produce hyperalgesia, whereas higher intensity stimuli typically results in stress-induced analgesia (e.g. Meagher, M. W. *et al.*, 2001b). In two human studies by Rhudy and Meagher (2000; 2001), pain threshold was increased in an anxiety condition and decreased in a fear condition, which they argued was consistent with the animal literature demonstrating anxiety-related hyperalgesia and fear-related analgesia. A subsequent study, however, found pain reductions in all conditions (Rhudy, J. L. and Meagher, M. W., 2003). Further complicating matters, the specific emotion experienced and its physiological features played important roles in pain modulation and these effects were influenced by gender. The mixed results of these and another study (Rhudy, J. L. and Meagher, M. W., 2003) highlight the importance of individual differences in the effect of the experimental manipulation and the effect of the emotion experienced on pain. A further complication arises when one considers attentional effects. The emotion-induction stimuli used in these studies, being distinct from the pain stimulus used to assess pain perception, might have competed with the less intense target pain stimulus for the subject's attentional resources. This possibility cannot be excluded based on the design of these studies.

Anticipation of pain is also suggested to be an important factor in pain modulation. Consistent with the previous discussion of the differential effects of pain-related and pain-unrelated emotions, Dougher M. J. *et al.* (1987) observed increased pain sensitivity in response to pain-specific, compared to non-specific, anxiety. Pain expectancies may also serve as a mediator of the effects of pain catastrophizing and depression on experimental pain in normals, as suggested recently by Sullivan M. J. *et al.* (2001a; 2001b). Interestingly, in this study expected mood was a stronger predictor of pain rating than expected pain, suggesting that the anticipation of an emotional response may contribute significantly to pain modulation.

5.64.5.2.3 Emotions unrelated to pain

Several experimental methods have been employed to induce emotions unrelated to pain in order to further examine the effect of emotional modulation on pain perception. Meagher M. W. *et al.* (2001b) found that presenting subjects with pictures that display fear and disgust before they underwent a cold-pressor test reduced threshold of pain intensity and unpleasantness; the fear stimuli also reduced pain tolerance. Conversely, erotic pictures increased pain intensity and unpleasantness threshold in men, but not women. A positive, graded increase in pain tolerance was observed with increases in the pleasantness of pictures presented during a cold-pressor test, whereas negative pictures that displayed pain-related images decreased pain tolerance (De Wied, M. and Verbaten, M. N., 2001). This is consistent with the distinction between pain-related and pain-unrelated emotions, pain-related emotions being generally associated with increased pain.

Reading positive and negative affectively valenced statements (Velten, E., 1968) has also been observed to increase and decrease experimental pain tolerance, respectively (Zelman, D. C. *et al.*, 1991). Willoughby S. G. *et al.* (2002), using this method, found decreases in pain tolerance related to pain catastrophizing in a depressed mood induction condition. Induction of positive affect via films has also been shown to reduce ratings of experimental pain (Weisenberg, M. *et al.*, 1998; Zillmann, D. *et al.*, 1996). Likewise, emotionally valenced music can exert pain modulatory effects (Roy, M. *et al.*, 2003; Whipple, B. and Glynn, N. J. 1992). Results of the studies by Roy and co-workers suggest that that the effects of emotions/moods are specific to pain processing and not merely due to non-specific distracting effects.

Sweet taste (Lewkowski, M. D. *et al.*, 2003) and pleasant odors (Marchand, S. and Arsenault, P., 2002) have also been shown to reduce experimental pain; however, the effect was only present in those with low arterial blood pressure in the study on taste and in women in the study on odors. Although providing further confirmation for the effects of positive and negative mood on pain perception, these findings highlight the importance of individual differences in these effects.

Studies using a cognitive-stress paradigm also demonstrate the effects of emotional modulation on pain perception and further highlight the importance of sex of the subject in this context. The cognitive stress of the stroop color-word task increased pain associated with capsaicin injection in women compared to men in one study (Logan, H. *et al.*, 2001). In this study, men showed a stronger correlation between pain increases and *physiological* indices of arousal, whereas women showed a stronger correlation between pain increases and *subjective* measures of arousal. This suggests that the effects of emotion-related physiological and subjective arousal on pain modulation may vary by sex. This study did not assess the specific emotion elicited during the cognitive task; however, a similar study found induced anger to be associated with increases in pain tolerance (Janssen, S. A. *et al.*, 2001).

5.64.5.2.4 Emotion or attention?

Emotion-induction stimuli naturally attract attention and consequently may compete with pain for attentional resources. This potential confound has long been recognized in the literature (e.g., Gardner, W. L. and Licklider, J. C., 1959; Gardner, W. L. *et al.*, 1960). As discussed earlier in section II.B. on attention, Villemure C. *et al.* (2003) demonstrated the pain modulatory effects of mood independent of attention. Although perhaps explaining the pain reduction induced by positive emotions in some instances, distraction does not account for increased pain ratings associated with negative emotions (e.g., Meagher, M. W. *et al.*, 2001b). Furthermore, attention usually exerts its effects on pain intensity and unpleasantness (e.g., Miron, D. *et al.*, 1989), whereas emotions – both pain-related and pain-unrelated – have a larger impact on pain unpleasantness (e.g., Huynh Bao, Q. V. and Rainville, P., 2002; 2003; Roy, M. *et al.*, 2003; Villemure, C. *et al.*, 2003). Specifically, negative emotions may increase pain unpleasantness by heightening an individual's awareness of his/her viscero-somatic responses independent of pain intensity. This would be consistent with studies showing negative emotions to be associated with increased self-focus and attention to somatic signals (Mor, N. and Winquist, J., 2002; also see Salovey, P., 1992).

5.64.5.3 Effects of Emotions on Pain: Clinical Studies

Clinical studies of the effects of emotions on pain have largely focused on specific emotions or emotion disorders. These studies have not extensively investigated the effects of arousal, valence, or specific experiential dimensions of emotions. Depression and anxiety have received the most attention in this literature (see the reviews by Robinson, M. E. and Riley, J. L., 1998; Keefe, F. J. *et al.*, 2001; Huyser, B. A. and Parker, J. C., 1999; Fernandez, E. and Milburn, T. W., 1994; Fernandez, E. and Turk, D. C., 1995), and a large-scale study by the World Health Organization found that patients with chronic pain have higher rates of depressive and anxious disorders (Gureje, O. *et al.*, 1998). Comorbid negative mood in patients with pain has been observed to be a significant negative predictor of treatment outcome in several domains, including spine surgery (Junge, A. *et al.*, 1995; Riley, J. L. *et al.*, 1995), multidisciplinary treatment programs (Swimmer, G. *et al.*, 1992) and conservative therapies (Gerke, D. C. *et al.*, 1989). Negative emotions may also serve as a mediator in the pain, impairment, and disability nexus, as suggested by Banks S. M. and Kerns R. D. (1996) and demonstrated by Holzberg and colleagues (1996). A number of investigations have demonstrated that the chronicity of injury and related pain is predicted by measures of negative mood. In particular, a strong association has been observed in chronic pain patients between pain unpleasantness and feelings of depression, anxiety, frustration, fear, and anger (Wade, J. B. *et al.*, 1990; 1996). Patient care cost and health care utilization have also been associated with negative mood in chronic pain patients (Engel, C. C. *et al.*, 1996). As a whole, this literature suggests that negative emotions are extremely prevalent in patients with pain and are predictive of a number of key variables, including treatment efficacy and health care costs.

One theory on the nature of the relationship between pain and negative emotions is that the experience of negative emotion increases or maintains

the report of chronic pain through some sensory process such as enhanced sensitivity to pain. By this account, the physiological perception of pain is modulated by one's emotions and cognitions, with depression and pain modulated by a similar process in the periaqueductal gray area of the dorsal horn. There is some evidence in the clinical literature for this contention, such as the study by Salovey P. and Birnbaum D. (1989) that found induction of negative mood to be associated with increased reports of aches and pains; however, this literature is thin and inconclusive.

Cognitive evaluations of the meaning of pain are an important component of the pain-emotion nexus. This is demonstrated in a study in which cancer patients who believed their pain to be due to the cancer reported more pain than patients who did not possess these beliefs. Pain-related emotions may mediate this effect. Other cognitive processes, such as attributional style (Love, A. W., 1988) and negative self-image (Holzberg, A. D. *et al.*, 1993), have been implicated in the relationship between pain and emotions. The constructs of pain catastrophizing and fear of pain have received considerable recent empirical attention and have been demonstrated to contribute to pain severity and distress in various patients (Crombez, G. *et al.*, 1999; Eccleston, C. *et al.*, 2001; Sullivan, M. J. *et al.*, 2001; Vlaeyen, J. W. and Linton, S. J., 2000); these effects may be mediated by increased attention to pain and/or changes in emotions. In fact, pain catastrophizing, fear, and other pain-related negative emotions, are consistently strong predictors of pain-related disability.

The effects of anger on pain also appear to depend on several factors, particularly the object of anger. Okifuji A. *et al.* (1999) found a positive relationship between pain severity and both anger directed at oneself and overall anger experienced. Depression and anger shared a similar relationship. In a recent review of this literature, Greenwood K. A. *et al.* (2003) found that gender, hostility, and anger management style, contribute to the effect of anger on pain. Interactions between these factors are complex (e.g., Burns, J. W. *et al.*, 1996) and beyond the scope of this discussion; however, anger remains of topic of increased interest in the pain literature.

In summary, negative emotions generally increase clinical pain, particularly pain unpleasantness, and are consistent predictors of pain behaviors and disability. Although the mechanisms by which emotions modulate clinical pain have not yet been entirely elucidated, the object of emotions appears to play a critical role. Emotions that are pain-related or directed toward the self appear to have the most deleterious effect.

5.64.6 Summary and Conclusions

This chapter has illustrated the potent modulating effects of psychological factors on pain. The evidence of these influences includes experimental studies that manipulate psychological factors such as mood, expectation, and desire for pain relief. Further evidence is provided by clinical studies that show strong predictive relationships between mood and pain, mood and disability, and placebo/expectancy manipulations and pain. Clearly, there is much overlap between different psychological mechanisms of pain modulation. For example, desires for relief and expectations are integral factors in placebo analgesia, yet they also play important roles in emotional influences on pain (Figure 9). Placebo analgesic mechanisms may well reflect modulation of pain by changes in emotions. On the other hand, attention and emotions have at least partly separate influences on pain. The neurophysiological basis of these psychological factors are partially understood, but much more work needs to be done to fully understand the basic mechanisms. Furthermore, the relationships and interactions of psychological factors to more traditional physiological and drug effects are also poorly understood and ripe for further study.

References

Amanzio, M. and Benedetti, F. 1999. Neuropharmacological dissection of placebo analgesia: expectation activated opioid systems versus conditioning-activated specific subsystems. J. Neurosci. 19. 484–494.

Apkarian, A. V., Thomas, P. S., Krauss, B. R., and Szeverenyi, N. M. 2001. Prefrontal cortical hyperactivity in patients with sympathetically mediated pain. Neurosci. Lett. 311(3), 193–197.

Banks, S. M. and Kerns, R. D. 1996. Explaining high rates of depression in chronic pain: a diathesis-stress framework. Psychol. Bull. 119, 96–110.

Bantick, S. J., Wise, R. G., Ploghaus, A., Clare, S., Smith, S. M., and Tracey, I. 2002. Imaging how attention modulates pain in humans using functional MRI. Brain 125, 310–319.

Barrell, J. J., Medieros, D., Barrell, J. E., and Price, D. D. 1985. Anxiety: an obstacle to performance. J. Hum. Psychol. 25, 106–122.

Basbaum, A. I. and Fields, H. L. 1978; Endogenous pain control mechanisms: review and hypothesis. Ann. Neurol. 4, 451–462.

Basbaum, A. I. and Fields, H. L. 1984. Endogenous pain control systems: brainstem spinal pathways and endorphin circuitry. Annu. Rev. Neurosci. 7, 309–338.

Beecher, H. K. 1959. Measurement of Subjective Responses: Quantitative effects of Drugs. Oxford University Press.

Benedetti, F., Arduino, C., and Amanzio, M. 1999. Somatotopic activation of opioid systems by target-directed expectations of analgesia. J. Neurosci. 19, 3639–3648.

Benedetti, F., Pollo, A., Lopiano, L., Lanotte, M., Vighetti, S., and Rainero, I. 2003. Conscious expectation and unconscious conditioning in analgesic, motor, and hormonal placebo/nocebo responses. J. Neurosci. 23, 4315–23.

Bentsen, B., Svensson, P., and Wenzel, A. 1999. The effect of a new type of video glasses on the perceived intensity of pain and unpleasantness evoked by a cold pressor test. Anesth. Prog. 46, 113–117.

Bernard, J. F., Bester, H., and Besson, J. M. 1996. Involvement of the spino-parabrachial amygdaloid and hypothalamic pathways in the autonomic and affective emotional aspects of pain. Prog. Brain Res. 107, 243–255.

Brooks, J. C., Nurmikko, T. J., Bimson, W. E., Singh, K. D., and Roberts, N. 2002. fMRI of thermal pain: effects of stimulus laterality and attention. Neuroimage 15, 293–301.

Burns, J. W., Johnson, B. J., Mahoney, N., Devine, J., and Pawl, R. 1996. Anger management style, hostility and spouse responses: gender differences in predictors of adjustment among chronic pain patients. Pain 64, 445–453.

Bushnell, M. C. and Duncan, G. H. 1989. Sensory and affective aspects of pain perception: Is medial thalamus restricted to emotional issues? Exp. Brain Res. 78, 415–418.

Bushnell, M. C., Duncan, G. H., Dubner, R., and He, L. F. 1984. Activity of trigeminothalamic neurons in medullary dorsal horn of awake monkeys trained in a thermal discrimination task. J. Neurophysiol. 52, 170–187.

Bushnell, M. C., Duncan, G. H., Dubner, R., Jones, R. L., and Maixner, W. 1985. Attentional influences on noxious and innocuous cutaneous heat detection in humans and monkeys. J. Neurosci. 5, 1103–1110.

Bushnell, M. C., Duncan, G. H., Hofbauer, R. K., Ha, B., Chen, J., and Carrier, B. 1999. Pain perception: is there a role for primary somatosensory cortex? Proc. Natl. Acad. Sci. USA 96, 7705–7709.

Buytendyck, F. J. J. 1961. Pain, Hutchinson.

Chretien, P. and Rainville, P. 2004. Desire for relief affects pain perception and autonomic nociceptive responses. J. Pain 3, 255.

Cioffi, D. and Holloway, 1993. J. Delayed costs of suppressed pain. J. Pers. Soc. Psychol. 64, 274–282.

Colloca, L., Lopiano, L., Lanotte, M., and Benedetti, F. 2004. Overt versus covert treatment for pain, anxiety, and Parkinson's disease. Lancet Neurol. 3, 679–684.

Corbetta, M. and Shulman, G. L. 2002. Control of goal-directed and stimulus-driven attention in the brain. Nat. Rev. Neurosci. 3, 201–215.

Crombez, G., Vlaeyen, J. W., Heuts, P. H., and Lysens, R. 1999. Pain-related fear is more disabling than pain itself: evidence on the role of pain-related fear in chronic back pain disability. Pain 80, 329–339.

Damasio, A. 1994. Descartes Error, Avon Books.

De Pascalis, V., Chiaradia, C., and Carotenuto, E. 2002. The contribution of suggestibility and expectation to placebo analgesia phenomenon in an experimental setting. Pain 96, 393–402.

Devinsky, O., Morrell, M. J., and Vogt, B. A. 1995. Contributions of anterior cingulate cortex to behavior. Brain 118(Pt 1), 279–306.

De Wied, M. and Verbaten, M. N. 2001. Affective pictures processing, attention, and pain tolerance. Pain 90, 163–172.

Dougher, M. J., Goldstein, D., and Leight, K. A. 1987. Induced anxiety and pain. J. Anxiety Disord. 1, 259–264.

Dowman, R. 2004. Distraction produces an increase in pain-evoked anterior cingulate activity. Psychophysiology 41, 613–624.

Eccleston, C., Crombez, G., Aldrich, S., and Stannard, C. 2001. Worry and chronic pain patients: a description and analysis of individual differences. Eur. J. Pain 5, 309–318.

Engel, C. C., von Korff, M., and Katon, W. J. 1996. Back pain in primary care: predictors of high health-care costs. Pain 65, 197–204.

Fernandez, E. and Milburn, T. W. 1994. Sensory and affective predictors of overall pain and emotions associated with affective pain. Clin. J. Pain 10, 3–9.

Fernandez, E. and Turk, D. C. 1989. The utility of cognitive coping strategies for altering pain perception: a meta-analysis. Pain 38, 123–135.

Fernandez, E. and Turk, D. C. 1995. The scope and significance of anger in the experience of chronic pain. Pain 61, 165–175.

Fillingim, R. B., Maixner, W., Bunting, S., and Silva, S. 1998. Resting blood pressure and thermal pain responses among females: effects on pain unpleasantness but not pain intensity. Int. J. Psychophysiol. 30, 313–318.

Friedman, D. P., Murray, E. A., and O'Neill, J. R. 1986. Cortical connections of the somatosensory fields of the lateral sulcus of macaques: evidence for a corticolimbic pathway for touch. J. Comp. Neurol. 252(3), 323–347.

Garcia-Larrea, L., Peyron, R., Laurent, B., and Mauguiere, F. 1997. Association and dissociation between laser-evoked potentials and pain perception. Neuroreport 8, 3785–3789.

Gardner, W. L. and Licklider, J. C. 1959. Auditory analgesia in dental operations. J. Am. Dent. Assoc. 59, 1144–1149.

Gardner, W. L., Licklider, J. C., and Weisz, A. Z. 1960. Suppression of pain by sound. Science 132, 32–33.

Gerke, D. C., Richards, L. C., and Goss, A. N. 1989. Discriminant function analysis of clinical and psychological variables in temporomandibular joint pain dysfunction. Aust. Dent. J. 34, 44–48.

Gracely, R. H. 1979. Psychophysical Assessment of Human Pain. In: Advances in Pain Research and Therapy (*eds*. J. J. Bonica, J. C. Liebeskind, and D. G. Albe-Fessard), Vol. 3, pp. 781–790. Raven Press.

Gracely, R. H., Dubner, R., Deeter, W. D., and Wolskee, P. J. 1985. Clinicians' expectations influence placebo analgesia. Lancet 5, 43.

Gracely, R. H., McGrath, P., and Dubner, R. 1976. Validity and sensitivity of ratio scales of sensory and affective verbal pain descriptors: manipulation of affect by diazepam. Pain 2, 19–29.

Greenwood, K. A., Thurston, R., Rumble, M., Waters, S. J., and Keefe, F. J. 2003. Anger and persistent pain: current status and future directions. Pain 103, 1–5.

Gureje, O., Von Korff, M., Simon, G., and Gater, R. 1998. Persistent pain and well-being: a world health organization study in primary care. JAMA 280, 147–151.

Hadjistavropoulos, H. D., Hadjistavropoulos, T., and Quine, A. 2000. Health anxiety moderates the effects of distraction versus attention to pain. Behav. Res. Ther. 38, 425–438.

Hayes, R. L., Dubner, R., and Hoffman, D. S. 1981. Neuronal activity in medullary dorsal horn of awake monkeys trained in a thermal discrimination task. II. Behavioral modulation of responses to thermal and mechanical stimuli. J. Neurophysiol. 46, 428–443.

Haythronthwaite, J. A., Lawrence, J. W., and Fauerbach, J. A. 2001. Brief cognitive interventions for burn pain. Ann. Behav. Med. 23, 42–49.

Hikosaka, O., Miyauchi, S., and Shimojo, S. 1996. Orienting a spatial attention – its reflexive, compensatory, and voluntary mechanisms. Brain Res. Cogn. Brain Res. 5, 1–9.

Hodes, R. L., Howland, E. W., Lightfoot, N., and Cleeland, C. S. 1990. The effects of distraction on responses to cold pressor pain. Pain 41, 109–114.

Hofbauer, R. K., Rainville, P., Duncan, G. H., and Bushnell, M. C. 2001. Cognitive modulation of pain sensation alters activity in human cerebral cortex. Neurophysiol. 86(1), 402–411.

Hoffman, D. S., Dubner, R., Hayes, R. L., and Medlin, T. P. 1981. Neuronal activity in medullary dorsal horn of awake monkeys trained in a thermal discrimination task. I. Responses to innocuous and noxious thermal stimuli. J. Neurophysiol. 46, 409–427.

Hoffman, H. G., Richards, T. L., Coda, B., Bills, A. R., Blough, D., Richards, A. L., and Sharar, S. R. 2004. Modulation of thermal pain-related brain activity with virtual reality: evidence from fMRI. Neuroreport 15, 1245–1248.

Holzberg, A. D., Robinson, M. E., and Geisser, M. E. 1993. The relationship of cognitive distortion to depression in chronic pain: the role of ambiguity and desirability in self-ratings. Clin. J. Pain 9, 202–206.

Holzberg, A. D., Robinson, M. E., Geisser, M. E., and Gremillion, H. A. 1996. The effects of depression and chronic pain on psychosocial and physical functioning. Clin. J. Pain 12, 118–125.

Huynh Bao, Q. V and Rainville, P. 2002. Emotional modulation of experimental pain under hypnosis. International Association for Dental Research Abstracts.

Huynh Bao, Q. V. and Rainville, P. 2003. Modulation of experimental pain by emotion induced using hypnosis. Pain Res. Manag. (Suppl 8), 35B.

Huyser, B. A. and Parker, J. C. 1999. Negative affect and pain in arthritis. Rheum. Dis. Clin. North. Am. 25, 105–121.

Izard, C. E. 1993. Four systems for emotion activation: cognitive and noncognitive processes. Psychol. Rev. 100, 68–90.

Janssen, S. A. and Arntz, A. 1996. Anxiety and pain: attentional and endorphinergic influences. Pain 66, 145–150.

Janssen, S. A., Spinhoven, P., and Brosschot, J. F. 2001. Experimentally induced anger, cardiovascular reactivity, and pain sensitivity. J. Psychosom. Res. 51, 479–485.

Johnson, J. E. 1973. Effects of accurate expectations about sensations on the sensory and distress components of pain. J. Pers. Soc. Psychol. 27, 261–275.

Johnson, M. H. and Petrie, S. M. 1997. The effects of distraction on exercise and cold pressor tolerance for chronic low back pain sufferers. Pain 69, 43–48.

Junge, A., Dvorak, J., and Ahrens, S. 1995. Predictors of bad and good outcomes of lumbar disc surgery. A prospective clinical study with recommendations for screening to avoid bad outcomes. Spine 20, 460–468.

Keefe, F. J., Lumley, M., Anderson, T., Lynch, T., and Carson, K. L. 2001. Pain and emotion: new research directions. J. Clin. Psychol. 57, 587–607.

Keogh, E., Hatton, K., and Ellery, D. 2000. Avoidance versus focused attention and the perception of pain: differential effects for men and women. Pain 85, 225–230.

Koeppe, R. A. and Stohler, C. S. 2001. Regional mu opioid receptor regulation of sensory and affective dimensions of pain. Science 293(5528), 311–315.

Laska, E., and Sunshine, A. 1973. Anticipation of analgesia. A placebo effect. Headache 13(1), 1–11.

Le Bars, D., Dickenson, A. H., and Besson, J. M. 1979a. Diffuse noxious inhibitory controls (DNIC). I. Effects on dorsal horn convergent neurones in the rat. Pain 6, 283–304.

Le Bars, D., Dickenson, A. H., and Besson, J. M. 1979b. Diffuse noxious inhibitory controls (DNIC). II. Lack of effect on non-convergent neurones, supraspinal involvement and theoretical implications. Pain 6, 305–327.

Legrain, V., Guerit, J. M., Bruyer, R., and Plaghki, L. 2002. Attentional modulation of the nociceptive processing into the human brain: selective spatial attention, probability of stimulus occurrence, and target detection effects on laser evoked potentials. Pain 99, 21–39.

Lewkowski, M. D., Ditto, B., Roussos, M., and Young, S. N. 2003. Sweet taste and blood pressure-related analgesia. Pain 106, 181–186.

Logan, H., Lutgendorf, S., Rainville, P., Sheffield, D., Iverson, K., and Lubaroff, D. 2001. Effects of Stress and Relaxation on capsaicin-induced pain. J. Pain. 2, 160–170.

Love, A. W. 1988. Attributional style of depressed chronic low back patients. J. Clin. Psychol. 44, 317–321.

Marchand, S. and Arsenault, P. 2002. Odors modulate pain perception: a gender-specific effect. Physiol Behav 76, 251–256.

Meagher, M. W., Arnau, R. C., and Rhudy, J. L. 2001a. Pain and emotion: effects of affective picture modulation. Psychosom. Med. 63, 79–90.

Meagher, M. W., Ferguson, A. R., Crown, E. D., McLemore, S., King, T. E., Sieve, A. N., and Grau, J. W. 2001b. Shock-induced hyperalgesia. IV. Generality. J. Exp. Psychol. Anim. Behav. Process. 27, 219–238.

Melzack, R. and Casey, K. L. 1968. Sensory, Motivational, and Central Control Determinants of Pain. In: The Skin Senses (*ed*. D. Kenshalo), pp. 423–443. CC Thomas.

Merskey, H. and Spear, F. G. 1967. The concept of pain. J. Psychosom. Res. 11, 59–67.

Miron, D., Duncan, G. H., and Bushnell, M. C. 1989. Effects of attention on the intensity and unpleasantness of thermal pain. Pain 39, 345–352.

Montgomery, G. H. and Kirsch, I. 1996. Mechanisms of placebo pain reduction: an empirical investigation. Psychol. Sci. 7, 174–176.

Montgomery, G. and Kirsch, I. 1997. Classical conditioning and the placebo effect. Pain 72, 107–113.

Mor, N. and Winquist, J. 2002. Self-focused attention and negative affect: a meta-analysis. Psych. Bull. 128, 638–662.

Nakamura, Y., Paur, R., Zimmermann, R., and Bromm, B. 2002. Attentional modulation of human pain processing in the secondary somatosensory cortex: a magnetoencephalographic study. Neurosci. Lett. 328, 29–32.

Okifuji, A., Turk, D. C., and Curran, S. L. 1999. Anger in chronic pain: investigations of anger targets and intensity. J. Psychosom. Res. 47, 1–12.

Petrovic, P., Kalso, E., Petersson, K. M., and Ingvar, M. 2001. Placebo and opioid analgesia–imaging a shared neuronal network. Science 295(5560), 1737–1740.

Petrovic, P., Petersson, K. M., Ghatan, P. H., Stone-Elander, S., and Ingvar, M. 2000. Pain-related cerebral activation is altered by a distracting cognitive task. Pain 85, 19–30.

Peyron, R., Garcia-Larrea, L., Gregoire, M. C., Costes, N., Convers, P., Lavenne, F., Mauguire, F., Michel, D., and Laurent, B. 1999. Haemodynamic brain responses to acute pain in humans: sensory and attentional networks. Brain 122, 1765–1780.

Plutchik, R. 1980. A General Psychoevolutionary Theory of Emotion. In: Emotion: Theory, Research, and Experience, Vol. 1. Theories of Emotion (*eds*. R. Plutchik and H. Kellerman), pp. 3–33. Academic Press.

Pollo, A., Amanzio, M., Arslanian, A., Casadio, C., Maggi, G., and Benedetti, F. 2001. Response expectancies in placebo analgesia and their clinical relevance. Pain 93, 77–84.

Posner, M. E. 1980. Orienting of attention. Quart. J. Exp. Psychol. 32, 3–25.

Price, D. D. 1999. Psychological Mechanisms of Pain and Analgesia. IASP Press.

Price, D. D. 2000. Psychological and neural mechanisms of the affective dimension of pain. Science 288, 1769–1772.

Price, D. D. and Barrell, J. J. 2000. Mechanisms of analgesia produced by hypnosis and placebo suggestions. Prog. Brain Res. 122, 255–71.

Price, D. D. and Bushnell, M. C. (eds.) 2004. Psychological Methods of Pain Control: Basic Science and Clinical Perspectives pp. 322. IASP Press.

Price, D. D. and McHaffie, J. G. 1988. Effects of heterotopic conditioning stimuli on first and second pain: a psychophysical evaluation in humans. Pain 34, 245–252.

Price, D. D., Barrell, J. E., and Barrell, J. J. 1985. A quantitative-experiential analysis of human emotions. Motiv. Emot. 9, 19–38.

Price, D. D., Barrell, J. J., and Gracely, R. H. 1980. A psychophysical analysis of experimential factors that selectively influence the affective dimension of pain. Pain 8, 137–149.

Price, D. D., Harkins, S. W., and Baker, C. 1987. Sensory-affective relationships among different types of clinical and experimental pain. Pain 28(3), 291–299.

Price, D. D., Milling, L. S., Kirsch, I., Duff, A., Montgomery, G. H., and Nicholls, S. S. 1999. An analysis of factors that contribute to the magnitude of placebo analgesia in an experimental paradigm. Pain 83, 147–156.

Price, D. D., Riley, J., and Barrell, J. J. 2001. Are lived choices based on emotional processes? Cogn. Emot. 15(3), 365–379.

Rainville, P. 2004. Pain and Emotions. In: Psychological Methods of Pain Control: Basic Science and Clinical Perspectives (*eds*. D. D. Price and M. C. Bushnell), pp. 117–141. IASP Press.

Rainville, P., Carrier, B., Hofbauer, R. K., Bushnell, M. C., and Duncan, G. H. 1999. Dissociation of pain sensory and affective dimensions using hypnotic modulation. Pain 82, 159–171.

Rainville, P., Duncan, G. H., Price, D. D., Carrier, B., and Bushnell, M. C. 1997. Pain affect encoded in human anterior cingulate but not somatosensory cortex. Science 277, 968–971.

Rhudy, J. L. and Meagher, M. W. 2000. Fear and anxiety: divergent effects on human pain thresholds. Pain 84, 65–75.

Rhudy, J. L. and Meagher, M. W. 2001. Noise stress and human pain thresholds: divergent effects in men and women. J. Pain 2, 57–64.

Rhudy, J. L. and Meagher, M. W. 2003. Negative affect: effects on an evaluative measure of human pain. Pain 104, 617–626.

Riley, J. L., Robinson, M. E., Geisser, M. E., Wittmer, V. T., and Graham-Smith, A. 1995. Relationship between MMPI-2 cluster profiles and surgical outcome in low-back pain patients. J. Spinal Disord. 8, 213–219.

Robinson, M. E. and Riley, J. L. 1998. Negative Emotion in Pain. In: Psychosocial Factors in Pain (*eds*. R. Gatchel and D. Turk), pp. 221–243. Guilford Press.

Roy, M., Peretz, I., and Rainville, P. 2003. Effects of emotion induced by music on experimental pain. Pain Res. Manag. (suppl 8), 33B.

Salovey, P. 1992. Mood-induced self-focused attention. J. Pers. Soc. Psychol. 62, 699–707.

Salovey, P. and Birnbaum, D. 1989. Influence of mood on health-relevant cognitions. J. Pers. Soc. Psychol. 57, 539–551.

Sato, A., Sato, Y., and Schmidt, R. F. 1997. The Impact of Somatosensoty Input on Autonomic Functions.In Reviews of Physiology Biochemistry and Pharmacology (*eds*. M. P. Blaustein, H. Grunicke, D. P. Konstanz, G. Schultz, and M. Schweiger) Vol. 130, pp. 119–134. Springer-Verlag.

Schanberg, L. E., Sandstrom, M. J., Starr, K., Gil, K. M., Lefebvre, J. C., Keefe, F. J., Affleck, G., and Tennen, H. 2000. The relationship of daily mood and stressful events to symptoms in juvenile rheumatic disease. Arthritis Care Res. 13, 33–41.

Seminowicz, D. A., Mikulis, D. J., and Davis, K. D. 2004. Cognitive modulation of pain-related brain responses depends on behavioral strategy. Pain 112, 48–58.

Siedenberg, R. and Treede, R. D. 1996. Laser-evoked potentials: exogenous and endogenous components. Electroencephalogr. Clin. Neurophysiol. 100, 240–249.

Sullivan, M. J., Rodgers, W. M., and Kirsch, I. 2001a. Catastrophizing, depression and expectancies for pain and emotional distress. Pain 91, 147–154.

Sullivan, M. J., Thorn, B., Haythornthwaite, J. A., Keefe, F., Martin, M., Bradley, L. A., and Lefebvre, J. C. 2001b. Theoretical perspectives on the relation between catastrophizing and pain. Clin. J. Pain 17, 52–64.

Swimmer, G., Robinson, M., and Geisser, M. 1992. The relationship of MMPI cluster type, pain coping strategy, and treatment outcome. Clin. J. Pain 8, 131–137.

Tracey, I., Ploghaus, A., Gati, J. S., Clare, S., Smith, S., Menon, R. S., and Matthews, P. M. 2002. Imaging attentional modulation of pain in the periaqueductal gray in humans. J. Neurosci. 22, 2748–2752.

Valet, M., Sprenger, T., Boecker, H., Wiloch, F., Rummeny, E., Conrad, B., Erhard, P., and Tolle, T. R. 2004. Distraction modulates connectivity of the cingulo-frontal cortex and the midbrain during pain – an fMRI analysis. Pain 109, 399–408.

Vase, L., Riley, J. L., and Price, D. D. 2002. A comparison of placebo effects in clinical analgesic trials versus studies of placebo analgesia. Pain 99, 443–452.

Vase, L., Robinson, M. E., Verne, G. N., and Price, D. D. 2003. The contribution of suggestion, expectancy and desire to placebo effect in irritable bowl syndrome patients. Pain 105, 17–25.

Vase, L., Robinson, M. E., Verne, G. N., and Price, D. D. 2005. Increased placebo analgesia over time in irritable bowel syndrome (IBS) patients is associated with desire and expectation but not endogenous opioid mechanisms. Pain 115(3), 338–347.

Velten, E. 1968. A laboratory task for induction of mood states. Behav. Res. Ther. 6, 473–482.

Verne, G. N., Robinson, M. E., Vase, L., and Price, D. D. 2003. Reversal of visceral and cutaneous hyperalgesia by local rectal anesthesia in irritable bowl syndrome (IBS) patients. Pain 105, 223–230.

Villemure, C., Slotnick, B. M., and Bushnell, M. C. 2003. Effects of odors on pain perception: deciphering the roles of emotion and attention. Pain 106, 101–108.

Vlaeyen, J. W. and Linton, S. J. 2000. Fear-avoidance and its consequences in chronic musculoskeletal pain: a state of the art. Pain 85, 317–332.

Voudouris, N. J., Peck, C. L., and Coleman, G. 1985. Conditioned placebo responses. J. Pers. Soc. Psychol. 48, 47–53.

Voudouris, N. J., Peck, C. L., and Colemann, G. 1998. Conditioned response models of placebo phenomena: further support. Pain 38, 109–116.

Voudouris, N. J., Peck, C. L., and Coleman, G. 1989. Conditioned response models of placebo phenomena: further support. Pain 38(1), 109–116.

Voudouris, N. J., Peck, C. L., and Coleman, G. 1990. The role of conditioning and verbal expectancy in the placebo response. Pain 43, 121–128.

Wade, J. B., Dougherty, L. M., Archer, R., and Price, D. D. 1996. Assessing the stages of pain processing: a multivariate analytical approach. Pain 68, 157–167.

Wade, J. B., Price, D. D., Hamer, R. M., Schwartz, S. M., and Hart, R. P. 1990. An emotional component analysis of chronic pain. Pain 40, 303–310.

Wegner, D. M. 1994. Ironic processes of mental control. Psychol. Rev. 101, 34–52.

Weisenberg, M., Raz, T., and Hener, T. 1998. The influence of film-induced mood on pain perception. Pain 76, 365–375.

Wenzlaff, R. M. and Wegner, D. M. 2000. Thought Suppression. In: Annual Review of Psychology (*ed*. S. T. Fiske), Vol. 51, pp. 51–91. Annual Reviews.

Whipple, B. and Glynn, N. J. 1992. Quantification of the effects of listening to music as a noninvasive method of pain control. Sch. Inq. Nurs. Pract. 6, 43–58.

Wickramasekera, I. A. 1985. Conditioned Response Model of the Placebo Effect: Predictions of the Model. In: Placebo: Theory, Research and Mechanisms (*eds*. L. White, B. Tursky, and G. E. Schwartz), pp. 255–287. Guilford Press.

Williams, A. C. 2002. Facial expression of pain: an evolutionary account. Behav. Brain Sci. 25, 439–55.

Willoughby, S. G., Hailey, B. J., Mulkana, S., and Rowe, J. 2002. The effect of laboratory-induced depressed mood state on responses to pain. Behav. Med. 28, 23–31.

Zelman, D. C., Howland, E. W., Nichols, S. N., and Cleeland, C. S. 1991. The effects of induced mood on laboratory pain. Pain 46, 105–111.

Zillmann, D., de Wied, M., King-Jablonski, C., and Jenzowsky, S. 1996. Drama-induced affect and pain sensitivity. Psychosom. Med. 58, 333–341.

Further Reading

Hrojartsson, A. and Gøtzsche, P. C. 2001. Is the placebo effect powerless? An analysis of clinical trials comparing placebo with no- treatment. N. Engl. J. Med. 344, 1594–1602.

Verne, G. N., Himes, N. C., Robinson, M. E., Gopinath, K. S., Briggs, R. W., Crosson, B., and Price, D. D. 2003. Central representation of visceral and cutaneous hypersensitivity in the irritable bowel syndrome. Pain 103, 99–110.

5.65 The Placebo Effect

F Benedetti, University of Turin Medical School, Turin, Italy

© 2008 Elsevier Inc. All rights reserved.

5.65.1	Top-Down Modulation of Pain	1003
5.65.2	Methodological Aspects	1003
5.65.3	Psychological Explanations	1004
5.65.4	Physiological Mechanisms	1005
5.65.5	The Nocebo Effect	1006
5.65.6	Clinical Implications	1007
References		1007

Glossary

immunosuppressive Adjective that indicates an inhibitory action on the immune system.

μ-opioid receptor Subtype of opioid receptors that bind μ-agonist drugs, such as morphine.

naloxone Antagonist drug of opioids.

natural history Spontaneous time course of a symptom, e.g., pain.

nocebo It has the opposite meaning of placebo, which indicates that a symptom may also increase after suggestions of increase.

Parkinson's disease Motor disorder characterized by three typical symptoms: rest tremor, muscle rigidity, and bradykinesia (reduction of movement velocity).

Pavlovian conditioning Conditioning according to Pavlov, in which the temporal contiguity between a neutral (conditioned) and an unconditioned stimulus leads to a conditioned response.

proglumide Antagonist drug of cholecystokinin.

subthalamic nucleus Nucleus located under the thalamus, which represents a major target of the surgical treatment of Parkinson's disease.

sumatriptan Agonist drug of serotonin 5-HT1 receptors that is used in the treatment of migraine.

5.65.1 Top-Down Modulation of Pain

The input coming from a damaged tissue and traveling along the pain pathways up to the brain is not always experienced in the same way. A complex modulation occurs at the supraspinal level and may either increase or decrease the global experience of pain (see chapter 5.65). Many psychological factors, for example, attention, emotions, mood, stress, expectation, anticipation, distraction, anxiety, depression, and fear, all modulate the global experience of pain, although the underlying mechanisms are poorly understood. In recent times, the placebo effect, particularly placebo analgesia, has emerged as an interesting model to understand the psychological and physiological mechanisms through which this intricate top-down modulation occurs. Of course, the understanding of the placebo effect can only explain some of these factors, such as expectation and anticipation. Nonetheless, its investigation has yielded new insights into the biological mechanisms that link a complex mental activity to different body functions. This chapter is a brief overview of what we know today about the neural mechanisms underlying the placebo effect. It will appear clear that this complex phenomenon can give us important information on the intricate mechanisms that link mind, brain, and body.

5.65.2 Methodological Aspects

The investigation of the placebo effect is full of pitfalls and drawbacks since, in order to identify a real psychobiological placebo response, several other phenomena have to be ruled out. In fact, the placebo itself is not always the cause of the effect that is observed (Colloca, L. and Benedetti, F., 2005). For

example, most painful conditions show a spontaneous temporal variation that is known as natural history. If subjects take a placebo just before their discomfort starts decreasing, they may believe that the placebo is effective, although that decrease would have occurred anyway. Clearly, this is not a placebo effect but a spontaneous remission that leads to a misinterpretation of the cause–effect relationship. Another example is regression to the mean, a statistical phenomenon assuming that individuals tend to receive their initial clinical assessment when their pain is near its greatest intensity, and that their pain level is likely to be lower when they return for a second pain assessment. In this case also, the improvement cannot be attributed to any intervention they might have undergone. A further source of confusion is represented by the fact that a particular type of error made by the patient, a false positive error, may explain the placebo effect in some circumstances. This phenomenon is based on signal detection theory, and is due to the occurrence of errors in the detection of ambiguous signals. It also happens that a co-intervention actually is responsible for the reduction of a symptom, such as the analgesic effect following the mechanical insertion of a needle to inject an inert solution. All these examples show that, although an improvement may occur after the administration of a placebo, the placebo is not necessarily the cause of the effect that is observed. Since all these phenomena are sometimes difficult to identify, the mechanisms of the placebo response must be investigated under strictly controlled experimental conditions (Vase, L. *et al.*, 2002; Colloca, L. and Benedetti, F., 2005). For example, in order to rule out spontaneous remission, a group taking the placebo is compared to a group receiving no treatment, the latter giving information on the natural course of the symptom. The difference between the placebo group and the no-treatment group represents the real psychobiological placebo response.

5.65.3 Psychological Explanations

The placebo effect involves both cognitive factors and conditioning mechanisms. The deceptive administration of a placebo treatment can lead the subjects to believe that the treatment is effective, so that anticipation and expectation of analgesia lead to a placebo analgesic response. Some studies show that different verbal instructions lead to different expectations and thus to different responses, and this plays a fundamental role in the placebo effect (Amanzio, M., and Benedetti, F., 1999; Benedetti, F. *et al.*, 1999b; Price, D. D. *et al.*, 1999). The context around a therapy may act not only through expectation and conscious anticipatory processes. In fact, there are some lines of evidence indicating that the placebo response is sometimes a conditioned response due to repeated associations between a conditioned stimulus (e.g., shape and color of aspirin pills) and an unconditioned stimulus (the active substance of aspirin) (Amanzio, M., and Benedetti, F., F., 1999; Siegel, S., 2002; Benedetti, F. *et al.*, 2003). In this case, it is the context itself that is the conditioned stimulus. However, even by considering a typical conditioning procedure, it has been shown that a conditioned placebo analgesic response can result from conditioning but is actually mediated by expectation. In other words, conditioning would lead to the expectation that a given event will follow another event, and this occurs on the basis of the information that the conditioned stimulus provides about the unconditioned stimulus (Benedetti, F. *et al.*, 2003).

There is experimental evidence that some physiological functions are affected by placebos through anticipatory conscious processes whereas some other functions undergo an unconscious mechanism of conditioning (Benedetti, F. *et al.*, 2003). For example, verbally induced expectations of either analgesia or hyperalgesia antagonize completely the effects of a conditioning procedure in experimentally induced pain. By contrast, verbally induced expectations of either increase or decrease of growth hormone and cortisol do not have any effect on the secretion of these hormones. However, if a preconditioning is performed with sumatriptan, a 5-$HT_{1B/1D}$ agonist that stimulates growth hormone and inhibits cortisol secretion, a significant increase of growth hormone and decrease of cortisol plasma concentrations can be found after placebo administration, even though opposite verbal suggestions are given. These findings suggest that placebo responses are mediated by conditioning when unconscious physiological functions, like hormonal secretion, are involved, whereas they are mediated by expectation when conscious physiological processes, like pain, come into play. Thus the placebo effect seems to be a phenomenon which can be learned either consciously or unconsciously, depending on the system that is involved (e.g., pain or hormone secretion).

5.65.4 Physiological Mechanisms

The complex cascade of events that may occur after placebo administration is shown in Figure 1. Several studies show that placebo-induced analgesia is antagonized by the opioid antagonist, naloxone, thus suggesting mediation by endogenous opioids (Levine, J. D. *et al.*, 1978; Amanzio, M., and Benedetti, F., 1999; Benedetti, F. *et al.*, 1999b). The cholecystokinin (CCK) antagonist, proglumide, has been found to enhance the placebo analgesic effect (Benedetti, F. *et al.*, 1995), which indicates that CCK has an inhibitory role in placebo-induced analgesia. The placebo analgesic responses are thus the result of the balance between endogenous opioids and endogenous CCK.

Placebo analgesia is not always mediated by endogenous opioids. In fact, if the placebo response is induced by means of strong expectation cues, it can be blocked by naloxone. Conversely, if the placebo response is induced by means of prior conditioning with a nonopioid drug, like ketorolac, it is naloxone-insensitive (Amanzio, M., and Benedetti, F., 1999). Today we know that specific placebo analgesic responses can be obtained in different parts of the body, and that these responses are naloxone-reversible (Benedetti, F. *et al.*, 1999b), which suggests that the placebo-activated endogenous opioid systems have a somatotopic organization.

The investigation of placebo analgesia by means of positron emission tomography found that similar

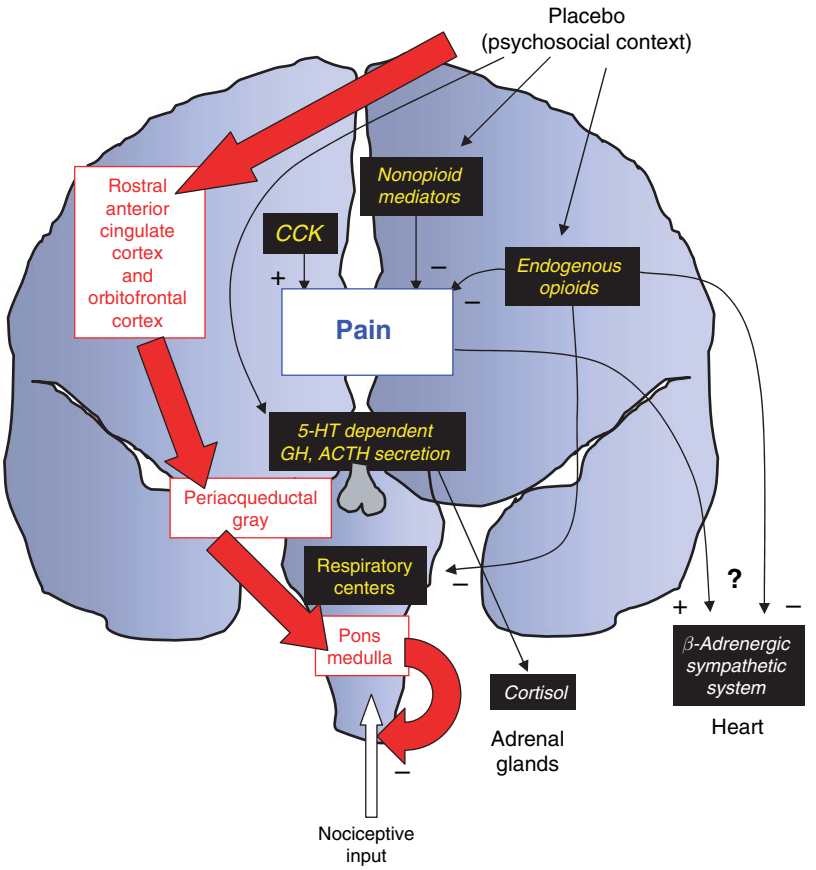

Figure 1 Events that might occur in placebo-induced analgesia. Nociceptive input may be inhibited by a descending network that involves the rostral anterior cingulate cortex, the orbitofrontal cortex, the periaqueductal gray, and the pons/medulla. Endogenous opioids might inhibit pain through this descending network and/or other mechanisms. The endogenous opioids also inhibit the respiratory centers. The β-adrenergic sympathetic system is also inhibited during placebo analgesia, although the mechanism is not known (either reduction of the pain itself or direct action of endogenous opioids). Nonopioid mechanisms are also involved. Cholecystokinin (CCK) counteracts the effects of the endogenous opioids thus reducing the placebo analgesic response. Placebo can also act on serotonin-dependent hormone secretion, mimicking the effect of the analgesic drug sumatriptan. 5-HT, serotonin; ACTH, adrenocorticotropic hormone; GH, growth hormone.

regions of the brain are affected by both a placebo and a narcotic drug, which indicates a related mechanism in placebo-induced and opioid-induced analgesia (Petrovic, P. *et al.*, 2002). In fact, the administration of a placebo induced the activation of the rostral anterior cingulate cortex (rACC) and the orbitofrontal cortex (OrbC). Moreover, there was a significant covariation in activity between the rACC and the lower pons/medulla corresponding to the rostral ventromedial medulla (RVM), and a subsignificant covariation between the rACC and the periaqueductal gray (PAG), thus suggesting that a descending rACC/PAG/RVM pain-modulating circuit is involved in placebo-induced analgesia. It is worth remembering that ACC and PAG are rich with opioid receptors, thus confirming the pharmacological studies with naloxone described above. By using functional magnetic resonance imaging to analyze the brain regions that are involved in placebo analgesia, another study showed that the activity of different regions involved in pain transmission, such as the thalamus, the anterior insula (aINS), and the caudal rACC, was decreased by a placebo treatment, which indicates a reduction of nociceptive transmission along the pain pathways (Wager, T. D. *et al.*, 2004). Furthermore, during the anticipatory phase of the placebo analgesic response, an activation of the dorsolateral prefrontal cortex (DLPFC), OrbC, superior parietal cortex (SPC), PAG, and other frontal regions occurs, suggesting the activation of a cognitive-evaluative network just before the placebo response. A recent attempt to identify the regions where endogenous opioids are released has been performed by using *in vivo* receptor binding techniques (Zubieta, J. K., 2005). A placebo-induced activation of μ-opioid receptors has also been found in different brain regions, such as the pregenual rostral anterior cingulate, DLPFC, INS, and the nucleus accumbens, which confirms once again the pharmacological blockade of placebo analgesia by opioid antagonists.

Placebo-activated endogenous opioids have also been shown to induce respiratory depression (Benedetti, F. *et al.*, 1999a), indicating that they act not only on pain mechanisms, but also on the respiratory centers. Also β-adrenergic sympathetic activity is reduced in placebo analgesia, and this might be due to either pain reduction itself or a direct action of placebo-activated endogenous opioids (Pollo, A. *et al.*, 2003). Some nonopioid mechanisms, such as the serotonin 5-$HT_{1B/1D}$ receptors, have also been investigated. For example, placebo-induced increase of growth hormone secretion and decrease of cortisol secretion have been described after pharmacological preconditioning with the serotonin agonist sumatriptan (Benedetti, F. *et al.*, 2003).

The placebo response is not limited to pain and analgesia, but it also occurs in many other conditions. The integration of the understanding of the placebo mechanisms in the field of pain and in other diseases is crucial and essential to identify similarities and differences that might help us appreciate the complexity of the placebo effect better. For example, as described above, placebo-induced hormonal responses can be obtained after repeated administrations of a hormone-stimulating drug (Benedetti, F. *et al.*, 2003), so can placebo-induced immunosuppressive responses after repeated administrations of an immunosuppressive drug (Goebel, M. U. *et al.*, 2002), which suggests a mechanism of Pavlovian conditioning in the endocrine and immune systems. Parkinson's disease has also been used as an interesting model to understand the neurobiological mechanisms of the placebo response, which might help understand placebo analgesia better. It has been shown that placebo administration in patients with Parkinson's disease activates endogenous dopamine in the striatum (de la Fuente-Fernandez, R. *et al.*, 2001) and modifies the pattern of activity of the neurons in the subthalamic nucleus (Benedetti, F. *et al.*, 2004). The placebo-induced release of dopamine might represent a mechanism of reward, whereby dopamine release by expectation of reward (in this case the expectation of clinical benefit) could represent a common biochemical substrate in many conditions, including pain.

5.65.5 The Nocebo Effect

The nocebo effect, or response, is a placebo effect in the opposite direction. In fact, expectation of pain increase may induce a hyperalgesic effect. In this case, anticipatory anxiety may play a fundamental role. In one study, negative expectations were induced by injecting an inert substance (saline solution) along with the instructions that pain was going to increase in a few minutes (Benedetti, F. *et al.*, 1997). As a consequence of this procedure, a pain increase was observed, and this increase was blocked by the CCK antagonist, proglumide. This indicates that expectation-induced hyperalgesia is mediated, at least in part, by CCK. These effects of proglumide

are not antagonized by naloxone, thus endogenous opioids are not involved. Since CCK plays a role in anxiety and negative expectations themselves are anxiogenic, proglumide is likely to act on a CCK-dependent increase of anxiety during the verbally induced negative expectations. Although, mainly due to ethical constraints, the nocebo effect has not been investigated in detail as has been done for the placebo effect, it shows the powerful effect of the top-down modulation of pain. In other words, cognitive and emotional factors can modulate pain perception in opposite directions.

5.65.6 Clinical Implications

One of the best evidences that suggest the important role of expectations and the top-down modulation of pain and analgesia is the decreased effectiveness of hidden therapies. In fact, it is possible to eliminate the placebo (psychosocial) component and to analyze the pharmacodynamic effects of an analgesic treatment, free of any psychological contamination. To eliminate the patient's expectations, the patient is made completely unaware that a medical therapy is being carried out. To do this, drugs are administered through hidden infusions by computer-controlled machines. The crucial point here is that the patients do not know that any analgesic is being injected, so that they do not expect anything. In postoperative pain, it was found that a hidden injection of different painkillers, in which the patients do not expect any outcome, is significantly less effective than an open one, in which the patients know that a pain reduction will occur (Colloca, L. *et al.*, 2004).

The difference between the open and hidden administration represents the placebo component, and underscores the importance of the placebo response in clinical practice. In fact, it basically shows that the specific effect of a treatment and the placebo response are additive. Since no placebo is given, the difference between an open and hidden injection cannot be called a placebo effect. Nevertheless it strongly indicates the important role of the psychosocial component of a therapy and the importance of the patient's perception that a therapy is being received. This new approach to the identification of the placebo effect might also have an important impact on the design of clinical trials (Colloca, L. and Benedetti, F., 2005; Finniss, D. G. and Benedetti, F., 2005).

References

Amanzio, M. and Benedetti, F. 1999. Neuropharmacological dissection of placebo analgesia: expectation-activated opioid systems versus conditioning-activated specific sub-systems. J. Neurosci. 19, 484–494.

Benedetti, F., Amanzio, M., Baldi, S., Casadio, C., and Maggi, G. 1999a. Inducing placebo respiratory depressant responses in humans via opioid receptors. Eur. J. Neurosci. 11, 625–631.

Benedetti, F., Amanzio, M., Casadio, C., Oliaro, A., and Maggi, G. 1997. Blockade of nocebo hyperalgesia by the cholecystokinin antagonist proglumide. Pain 71, 135–140.

Benedetti, F., Amanzio, M., and Maggi, G. 1995. Potentiation of placebo analgesia by proglumide. Lancet 346, 1231.

Benedetti, F., Arduino, C., and Amanzio, M. 1999b. Somatotopic activation of opioid systems by target-directed expectations of analgesia. J. Neurosci. 19, 3639–3648.

Benedetti, F., Colloca, L., Torre, E., Lanotte, M., Melcarne, A., Pesare, M., Bergamasco, B., and Lopiano, L. 2004. Placebo-responsive Parkinson patients show decreased activity in single neurons of subthalamic nucleus. Nat. Neurosci. 7, 587–588.

Benedetti, F., Pollo, A., Lopiano, L., Lanotte, M., Vighetti, S., and Rainero, I. 2003. Conscious expectation and unconscious conditioning in analgesic; motor and hormonal placebo/nocebo responses. J. Neurosci. 23, 4315–4323.

Colloca, L. and Benedetti, F. 2005. Placebos and painkillers: is mind as real as matter? Nat. Rev. Neurosci. 6, 545–552.

Colloca, L., Lopiano, L., Lanotte, M., and Benedetti, F. 2004. Overt versus covert treatment for pain, anxiety and Parkinson's disease. Lancet Neurol. 3, 679–684.

de la Fuente-Fernandez, R., Ruth, T. J., Sossi, V., Schulzer, M., Calne, D. B., and Stoessl, A. J. 2001. Expectation and dopamine release: mechanism of the placebo effect in Parkinson's disease. Science 293, 1164–1166.

Finniss, D. G. and Benedetti, F. 2005. Mechanisms of the placebo response and their impact on clinical trails and clinical practice. Pain 114, 3–6.

Goebel, M. U., Trebst, A. E., Steiner, J., Xie, Y. F., Exton, M. S., Frede, S., Canbay, A. E., Michel, M. C., Heemann, U., and Schedlowski, M. 2002. Behavioral conditioning of immunosuppression is possible in humans. FASEB J. 16, 1869–1873.

Levine, J. D., Gordon, N. C., and Fields, H. L. 1978. The mechanisms of placebo analgesia. Lancet 2, 654–657.

Petrovic, P., Kalso, E., Petersson, K. M., and Ingvar, M. 2002. Placebo and opioid analgesia – imaging a shared neuronal network. Science 295, 1737–1740.

Pollo, A., Vighetti, S., Rainero, I., and Benedetti, F. 2003. Placebo analgesia and the heart. Pain 102, 125–133.

Price, D. D., Milling, L. S., Kirsch, I., Duff, A., Montgomery, G. H., and Nicholls, S. S. 1999. An analysis of factors that contribute to the magnitude of placebo analgesia in an experimental paradigm. Pain 83, 147–156.

Siegel, S. 2002. Explanatory Mechanisms for Placebo Effects: Pavlovian Conditioning. In: The Science of the Placebo: Toward an Interdisciplinary Research Agenda (*eds*. H. A. Guess, A. Kleinman, J. W. Kusek, and L. W. Engel), pp. 133–157. BMJ Books.

Vase, L., Riley, J. L., and Price, D. D. 2002. A comparison of placebo effects in clinical analgesic trials versus studies of placebo analgesia. Pain 99, 443–452.

Wager, T. D., Rilling, J. K., Smith, E. E., Sokolik, A., Casey, K. L., Davidson, R. J., Kosslyn, S. M., Rose, R. M., and Cohen, J. D. 2004. Placebo-induced changes in fMRI in the anticipation and experience of pain. Science 303, 1162–1166.

Zubieta, J. K., Bueller, J. A., Jackson, L. R., Scott, D. J., Xu, Y., Koeppe, R. A., Nichols, T. E., and Stohler, C. S. 2005. Placebo effects mediated by endogenous. J. Neurosci. 25, 7754–7762.

5.66 Hypnotic Analgesia

P Rainville, Université de Montréal, Montreal, QC, Canada

I Marc, Université Laval, Quebec City, QC, Canada

© 2008 Elsevier Inc. All rights reserved.

5.66.1	Introduction	1009
5.66.2	Hypnosis Affects Consciousness-Related Brain Mechanisms	1010
5.66.3	Hypnotic Analgesia in the Brain	1011
5.66.4	Somatic Consequences of Hypnotic Analgesia	1012
5.66.5	Clinical Applications of Hypnotic Analgesia	1013
5.66.6	Conclusion	1014
References		1015

Glossary

affective dimension of pain The feelings of unpleasantness and/or other negative emotions associated with the sensory experience of pain. This dimension of the pain experience encompasses both the basic emotional and the motivational responses produced by the actual or potential threat associated with pain.

Automaticity Behavioral responses and changes in perception and subjective experience produced without a feeling voluntary control (self-agency), that is, changes induced by hypnotic suggestions may be felt passively, as if they were induced by an external cause/agent.

hypnotic state The coordinated changes in activity within networks of brain regions involved in the regulation of consciousness (vigilance, attention, and self-monitoring), associated with self-experienced increases in mental relaxation, mental absorption, and feelings of automaticity, and typically (although not necessarily) induced by suggestions.

hypnotic suggestion Suggestion given during a context of hypnosis for an experience to occur or a behavior to be carried out.

nociceptive processes Biological responses induced by actual or potential tissue damage and normally (although not always) associated with the experience of pain in humans.

nociceptive withdrawal reflex (RIII reflex) The RIII reflex is a spinally mediated multisynaptic cutaneous reflex involving the flexion of the stimulated limb and the extension of the opposite limb. It can be induced experimentally by a transcutaneous electrical stimulation of the sural nerve at the level of the ankle and measured by the amplitude of the electromyographic response of the ipsilateral bicep femoris (flexor of the leg).

positron emission tomography (PET) A nuclear medical imaging technique where a radioactive tracer is injected into the blood circulation of a living organism. Applied to brain imaging, this technique allows for the measurement of the distribution of blood flow or the availability of various receptors in the brain. In functional brain imaging studies, this technique is used to test the changes in local brain activity in various experimental conditions.

self-monitoring Processes by which intentions, actions, and somatic activity are registered by the brain and mind. This process is central to the representation of self and is thought to be altered during hypnosis.

somatosensory-evoked potential Changes in regional electrical activity of the cerebral cortex in response to acute somatosensory stimuli and typically measured using surface electroencephalography.

5.66.1 Introduction

Scientific conceptions of hypnosis can be traced back to the end of the eighteenth century, when the pseudoscientific theory of Franz Anton Mesmer on *Animal Magnetism* (Bouleur, Jt., 1998) was formally examined by a Royal Commission ordered by King Louis XVI and chaired by Benjamin Franklin (Salas, C. and Salas, D., 1996; Laurence, J. R., 2002). Although the commissioners noted that the interventions (i.e., magnetization) used by Mesmer did produce dramatic responses in some patients (including analgesia), they concluded that the subjects' imagination was the main mediating mechanisms activated under the power of suggestion. This explanation based on the subject's imaginative resources is consistent with most contemporary theories of hypnosis.

Modern theories of hypnosis are based on complementary psychosocial, cognitive, and neurobiological interpretations (Fromm, E. and Nash, M. R., 1992). Experimental research has provided objective evidence that hypnotic interventions have robust, and in many cases specific, physiological effects. Furthermore, recent brain imaging methods have provided insight into the mechanisms underlying hypnotic states and into the specific responses to various types of hypnotic suggestions, including those aimed at reducing pain. Those advances are paralleled by well-controlled clinical studies, providing conclusive evidence on the efficacy of hypnosis in the control of pain.

5.66.2 Hypnosis Affects Consciousness-Related Brain Mechanisms

At the core of hypnosis is a social interaction where a hypnotist gives suggestions to another person, thus leading some authors to explain hypnosis-related effects primarily as suggestion-induced changes in expectancy (Kirsch, I. and Lynn, S. R., 1995). Hypnosis may also be defined as basic changes in subjective experience typically induced by standard hypnosis induction procedures and sometimes described as a hypnotic state or an altered state of consciousness. As those changes may be self-induced (e.g., in autohypnosis or some forms of meditation), an explanation strictly based on social interactions and suggestions may be limited. The analysis of experiential changes associated with the induction of hypnotic states has revealed increases in mental ease and absorption, followed by reductions in self-monitoring and orientation, which in turn lead to feelings of automaticity (Price, D. D., 1996; Rainville, P. and Price, D. D., 2004). Increases in absorption (e.g., concentration and fascination) are consistent with the central role of attention processes in hypnotic responsiveness (Tellegen, A. and Atkinson, G., 1974; Nadon, R. *et al.*, 1987; Radtke, H. L. and Stam, H. J., 1991; Balthazard, C. G., and Woody, E. Z., 1992; Crawford, H. J., 1994). However, the subjective increase in automaticity has been identified as the classical suggestion effect characterizing hypnosis (Weitzenhoffer, A. M., 1980). This sense of automaticity may also relate to dissociative processes posited to explain the dual streams of consciousness reported by some subjects during hypnosis (Hilgard, E. R., 1992).

In agreement with the involvement of basic consciousness-related processes, increases in mental ease and absorption are associated with the changes in activity within brain networks underlying the regulation of vigilance and attention, including brainstem and medial thalamic nuclei, the anterior cingulate cortex, and the prefrontal and posterior parietal cortices (Maquet, P. *et al.*, 1999; Rainville, P. *et al.*, 1999b; 2002). Those findings are consistent with increases in rhythmic electroencephalographic activity within the theta frequency band, associated with attention and mental imagery (Sabourin, M. E. *et al.*, 1991; Crawford, H. J., 1994; Ray, W. J., 1997). Neurophysiological effects have been suggested to reduce the reciprocal inhibition between competing mental representations and processes, thereby facilitating the consideration of alternative experiences and allowing for a reinterpretation of sensory inputs during hypnosis (Rainville, P. and Price, D. D., 2004). In addition, feelings of automaticity relative to movement produced in response to hypnotic suggestions have been suggested to reflect a disruption of the coordinated activity of brain systems underlying the production and monitoring of self-generated actions within the frontoparietal cortices, thus leading to an altered sense of self-agency (Blakemore, S. J. and Frith, C., 2003; Blakemore, S. J., *et al.*, 2003). Generalizing those findings to the generation and regulation of mental images and thoughts, this suggests that hypnosis-related changes in perceptual and cognitive processes are felt as automatic because of the alteration in self-monitoring processes or the disruption in the communication

between brain systems involved in the production of the perceptual–cognitive–behavioral changes and those involved in self-monitoring of those changes (also see Woody, E. and Szechtman, H., 2000; Rainville, P. and Price, D. D., 2004; Raz, A. *et al.*, 2005; Egner, T. *et al.*, 2005). These basic changes provide the background state upon which suggestions are given to further modulate specific perceptual processes such as those involved in pain.

5.66.3 Hypnotic Analgesia in the Brain

There are a number of psychophysiological studies providing convincing evidence that hypnotic suggestions to modulate pain perception affect nociceptive processes in the central nervous system (CNS) (Arendt-Nielsen, L. *et al.*, 1990; Zachariae, R. and Bjerring, P., 1994; Crawford, H. J. *et al.*, 1998; De Pascalis, V. *et al.*, 1999; 2001). New evidence based on modern functional brain imaging methods has further demonstrated that the hypnotic modulation of pain affects responses within pain-related brain network. In normal conditions, brain responses to acute experimental pain tests involve the activation of primary and secondary somatosensory cortical areas, the insular cortex, and the anterior cingulate cortex (Apkarian, A. V. *et al.*, 2005). In a positron emission tomography (PET) experiment (Hofbauer, R. K. *et al.*, 2001), hypnotic suggestions were given to modulate the sensory intensity of pain before subjects immersed their hand in painfully hot water. In those conditions, the subjects' ratings of pain intensity confirmed the expected effects on pain experiences (Figure 1). Brain activity measured by PET further demonstrated significant changes in the amplitude of the responses within the primary somatosensory cortex, consistent with a role of this area in the perception of pain sensory intensity. In an earlier PET study using the same experimental model (immersion of the hand in hot water) (Rainville, P. *et al.*, 1997), hypnotic suggestions were given to modulate specifically the affective dimension of pain experience. In those conditions, the subjects reported changes in pain unpleasantness, but not pain intensity, and brain responses were modulated within the anterior cingulate cortex, but not the somatosensory cortex (Rainville, P. *et al.*, 1997). Furthermore, activity within the anterior cingulate cortex was found to correlate significantly with subjective reports of pain

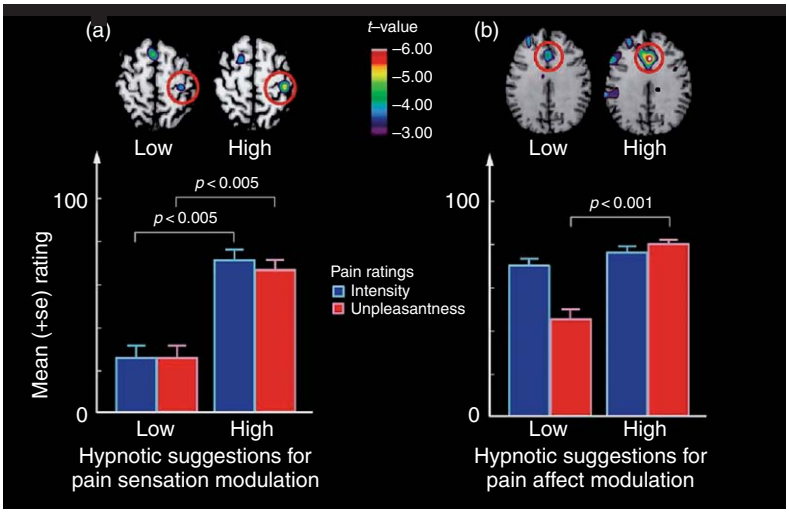

Figure 1 (a) Modulation of pain intensity and S1 activity. (b) Modulation of pain unpleasantness and anterior cingulate cortex activity. Horizontal slices of the brain are shown in conditions of decreased and increased pain intensity (a) and unpleasantness (b). Bar graph represent ratings of pain intensity and pain unpleasantness obtained in those conditions and demonstrate the significant modulation of both pain intensity and unpleasantness in the sensation-modulation experiment (a) and the significant modulation of pain unpleasantness only in the affect-modulation experiment (b). Reproduced from Rainville, P. 2002. Brain mechanisms of pain affect and pain modulation. Curr. Opin. Neurobiol. 12, 195–204.

unpleasantness, consistent with a contribution of this area to the affective dimension of pain. These studies

1. confirmed the efficacy of hypnosis to modulate pain-related brain responses,
2. demonstrated a functional segregation of brain activity associated more specifically with the sensory or affective dimensions of pain, and
3. provide further evidence supporting the specificity of hypnosis-related effects as a function of the precise content of the suggestions.

Importantly, such anatomofunctional specificity of the effects of hypnotic suggestions on perceptual processes has been observed in both the auditory modality (Szechtman, H. *et al.*, 1998) and in the visual modality (Kosslyn, S. M. *et al.*, 2000). This implies that the effect of hypnotic suggestions does not simply reflect a nonspecific response but involve the precise top-down modulation of targeted sensory–perceptual or affective–emotional processes. In the specific case of pain, this process may involve descending modulatory mechanisms affecting lower-level nociceptive activity in the CNS.

In addition to changes specifically found in pain-related areas, suggestions also produce widespread increases in lateral and medial prefrontal cortices including the dorsal aspect of the medial prefrontal cortex, as well as in parietal cortices (Rainville, P. *et al.*, 1999b; Faymonville, M. E. *et al.*, 2000). Interestingly, the activation found in the frontal and parietal cortices in response to hypnotic suggestions for pain modulation is consistent with the observations of the activation of the medial prefrontal cortex during hypnotic auditory hallucination (Szechtman, H. *et al.*, 1998), and of the lateral parietal cortex during hypnotically induced delusion of movement (Blakemore, S. J. *et al.*, 2003), as discussed above. In the case of pain modulation, those changes may also reflect the activation of modulatory circuits that affect pain-related areas directly through corticocortical connections or indirectly through descending projections affecting thalamic or brainstem nuclei. The medial prefrontal cortex, including the more dorsal and rostral parts of the anterior cingulate cortex may interact with other cortical and subcortical structures of the cerebral network involved in pain perception, including the insular cortices, the pain-related cingulate area, right prefrontal cortices, striatum, thalamus, and brainstem. Coactivation of the brainstem with the medial prefrontal cortex may further reflect the activation of descending mechanisms involved in the regulation of ascending spinothalamic nociceptive pathways (Faymonville, M. E. *et al.*, 2003). In addition to their contribution to the regulation of ascending pathways, descending modulatory processes are likely to influence the reflex nociceptive responses generally observed in the periphery.

5.66.4 Somatic Consequences of Hypnotic Analgesia

Descending mechanisms have played a central role in the conceptualization of pain modulation over the past 40 years (Melzack, R. and Wall, P. D., 1965; Melzack, R. and Casey, K. L., 1968). In relation to descending inhibitory mechanism, there are abundant research reports examining the effects of hypnotic analgesia on peripheral physiological responses to acute pain stimuli. One of the most interesting effects reported in that literature is the effect of hypnotic analgesia on the nociceptive withdrawal reflex (the RIII reflex). Various experimental conditions involving pain modulation by conditioning stimuli, contextual factors, and psychological variables have demonstrated a robust modulation of the RIII reflex (Willer, J. C. *et al.*, 1979; 1981; Sandrini, G. *et al.*, 2005). The modulation of pain by hypnotic suggestion has been shown to affect the amplitude of the RIII reflex, consistent with the involvement of descending modulatory processes during hypnotic analgesia (Kiernan, B. D. *et al.*, 1995; Sandrini, G. *et al.*, 2005). However, a subsequent study also showed that some subjects demonstrated an increase in the RIII response during effective hypnotic analgesia as reflected in increased pain threshold and reduced cortical response (somatosensory-evoked potential), suggesting that the activation of descending modulatory processes during hypnotic analgesia may present considerable interindividual variability (Danziger, N. *et al.*, 1998).

In addition to studies examining the RIII response, several reports have demonstrated that hypnotic analgesia affects autonomic response. Those include studies showing reduced cardiovascular response and pain ratings evoked by experimental ischemia (Lenox, J. R., 1970) and the cold pressor test (Hilgard, E. R.*et al.*, 1974; Hilgard, E. R. and Hilgard, J. R., 1994), and reduced cutaneous and cardiac sympathetic responses evoked by painful electric shocks (De Pascalis, V. *et al.*, 2001). In addition, a study

examining the effect of hypnotic suggestions focusing on the affective dimension of pain has found changes in heart rate responses correlated with changes in ratings of pain unpleasantness (Rainville, P. *et al.*, 1999a). Importantly, those effects were independent from changes in ratings of pain intensity, further supporting the distinction between pain sensation and pain affect and the stronger functional relation between autonomic responses and affective responses.

Taken together, studies on the modulation of motor and autonomic responses to noxious stimuli imply that the central neurophysiological mechanisms engaged during hypnotic analgesia modulate low-level brainstem and spinal systems responsible for the regulation of acute somatic responses to nociceptive stimuli. Combined with the studies demonstrating changes in pain-related brain activity, this strongly supports the specificity of hypnosis-related effects for the control of pain, providing a convincing demonstration that hypnotic analgesia can modulate both central and peripheral pain-related responses. This experimental demonstration of the neurophysiological mechanisms underlying hypnotic analgesia argues strongly in favor of the application of hypnosis for the control pain.

5.66.5 Clinical Applications of Hypnotic Analgesia

The increasing number of sophisticated neurophysiologic studies on hypnosis and pain has largely contributed to the renewed interest in hypnosis within healthcare settings. Consistent with the validation of hypnotic analgesia in experimental studies, nonpharmacological approaches including hypnosis have been strongly recommended in the management of pain. Among psychological strategies, there is accumulating evidence suggesting that hypnotic interventions are helpful for the management of acute procedural pain and anxiety. Chronic pain may also benefit from hypnosis interventions that must be integrated to the psychological, social, and environmental context.

Since the meta-analysis of Montgomery G. H. *et al.* (2000), which has focused on hypnotic analgesia in both clinical and experimental settings, some new randomized clinical trials have further documented the effectiveness of hypnosis in reducing pain and anxiety in various conditions. A more recent review of the literature has focused on randomized clinical trials to assess the efficacy of hypnotic interventions (Patterson, D. R. and Jensen, M. P., 2003). Authors have concluded that hypnosis has a reliable and significant impact on acute procedural as well as chronic pain conditions in adults. Evidence is also presented supporting the successful application of hypnosis in children to decrease pain and distress during needle-related procedures. Nevertheless, authors recommend that more high quality studies have to be conducted to specify the scope and limits of hypnotic interventions. Furthermore, they underline that reviews on hypnosis effectiveness are limited by the heterogeneity of the type of hypnotic interventions, emphasizing the importance of a more detailed description of the specific suggestions used (Patterson, D. R., 2004; Jensen, M. P. and Patterson, D. R., 2005). This also appears to be critical in view of the specificity of the effects of different types of hypnotic suggestions as described above for suggestions focusing on sensory or affective dimensions of the pain experience.

To illustrate the potential benefit of hypnotic analgesia, some clinical studies provide particularly convincing evidence. (Note: the readers should refer to Medline or Cochrane Review sites for an extensive search of clinical trials on hypnosis; here we describe a few original reports to illustrate the potential efficacy of hypnosis in a clinical setting.) The potential benefits of hypnosis in patients receiving conscious sedation for plastic surgery have been demonstrated in a randomized clinical trial ($n = 60$) (Faymonville, M. E. *et al.*, 1997). In this study, hypnosis did not only provide better perioperative pain and anxiety relief, but also decreased medication used and improved patient's satisfaction and surgical conditions as compared with conventional stress-reducing strategies support. In another randomized clinical trial ($n = 241$), the effects of structured attention and self-hypnotic relaxation on pain and anxiety during percutaneous vascular and renal procedures in radiology were compared to standard care (Lang, E. V. *et al.*, 2000). The hypnotic intervention was performed during the surgery with suggestions for relaxation, eye closing, deep breathing, sensation of floating, and finally suggestion to self-generate imagery and focus on a safe and pleasant experience. As pain increased with the procedure time in the standard care and attention groups, it remained stable or decreased slightly in the hypnosis group even if the patients in the hypnosis group had requested less intravenous analgesia during the procedure. Mean anxiety scores also decreased during the procedure

in the hypnosis group, while it remained stable in the structured attention group and increased in the standard care group. Finally, hypnosis improved hemodynamic stability significantly during the procedure consistent with the notion that the improvement in subjective reports of pain and negative emotions are accompanied by beneficial impact on peripheral responses to the noxious stimuli (here the surgical procedure). These results are highly consistent with the experimental studies reported above showing that the improvements in pain reports reflect a reduction in pain-related brain responses and are paralleled by an attenuation of peripheral responses as a consequence of active inhibitory processes acting on low-level nociceptive processes in the brain and spinal cord.

The benefits of hypnotic intervention on procedural pain and distress have also been demonstrated in children (Woodgate, R. L. and Degner, L. F., 2003; Wild, M. R. and Espie, C. A., 2004; Richardson, J. *et al.*, 2006). In a recently published randomized clinical study in children with cancer ($n = 45$), Liossi and co-workers have illustrated the benefit of teaching self-hypnosis to children undergoing repeated lumbar punctures by comparing the effects of a local anesthetic plus self-hypnosis, to the effects of a local anesthetic or a local anesthetic plus attention. In addition to showing hypnosis-related pain relief, this study also demonstrated a decrease in the child's anticipatory anxiety before the procedure (Liossi, C. *et al.*, 2006). Repeated invasive procedures such as cystourethrography are also painful and frightening for young children. Forty-four children (age range: 4–15 years) who were scheduled for at least the second VCUG were randomized to receive hypnosis ($n = 21$) or routine care with support ($n = 23$) while undergoing the procedure (Butler, L. D. *et al.*, 2005). Hypnosis was found to be beneficial for children, because it may decrease distress, improve the collaboration of patients, and facilitate the procedure. However, as children are often receiving light sedation and analgesia in addition to local anesthetic, more studies have to be conducted to determine the specific contribution of hypnosis in pain and anxiety management strategies and, more critically, the potential interaction between multiple interventions.

Another clinical application for hypnosis is labor pain. A recent Cochrane review on complementary and alternative therapies for pain management in labor concluded that women who were taught self-hypnosis (five clinical trials for a total of 749 women) had decreased requirements for pharmacological analgesia including epidural analgesia and were more satisfied with their pain management in labor compared with controls (Smith, C. A. *et al.*, 2006). In a preliminary study, Marc I. *et al.* (2007) also suggested that hypnosis significantly reduces the need for analgesic/sedative medication without increasing pain or distress in patients undergoing a first-trimerter surgical abortion. These effects further validate the use of hypnosis as an effective means to complement or replace the standard pharmacological approaches without reducing the quality of care, and sometimes by improving it.

There are several other conditions in which hypnosis may provide an advantageous approach to treat pain. In recent years, considerable work has been done by several teams on the use of hypnotic intervention in the treatment of mind–body dysfunction especially when stress and anxiety are involved. For example, irritable bowel syndrome is a functional gastrointestinal disorder characterized by chronic abdominal pain and altered bowel habits in the absence of any organic cause. Hypnosis as part of a structured intervention has been found to improve the status of all major symptoms in this condition (Gonsalkorale, W. M. and Whorwell, P. J., 2005). However, as is the case of many uncontrolled clinical studies, the use of hypnosis is associated with significant improvement but the specific contribution of hypnosis-related phenomena remains unclear. Of course, from a practical clinical perspective, the available evidence may be sufficient for the integration of hypnosis to clinical interventions, especially given the fact that adverse effects are unlikely to occur when hypnosis is proposed as an adjunct to standard care. Nevertheless, additional randomized controlled trials must be performed to extend the available evidence on the efficacy of hypnotic analgesia for the relief of acute pain and chronic pain condition (Stewart, J. H., 2005).

5.66.6 Conclusion

The effects of hypnosis and analgesic suggestions on brain activity are highly consistent with a modification of sensory and affective processes underlying the experience of pain. The available evidence clearly demonstrates the specificity of the effects on pain-related physiological processes both in the CNS and in the periphery. Hypnosis may also be used to improve relief during painful procedures and may

be integrated to the arsenal of strategies to relieve chronic pain conditions, especially if stress and anxiety are involved. Although many questions on the neurobiological mechanisms underlying hypnosis-related effects remain to be answered, the available evidence strongly supports the instrumental use of hypnosis to study conscious perceptual processes and the clinical use of hypnosis to reduce pain and suffering.

References

Apkarian, A. V., Bushnell, M. C., Treede, R. D., and Zubieta, J. K. 2005. Human brain mechanisms of pain perception and regulation in health and disease. Eur. J. Pain 9, 463–484.

Arendt-Nielsen, L., Zachariae, R., and Bjerring, P. 1990. Quantitative evaluation of hypnotically suggested hyperaesthesia and analgesia by painful laser stimulation. Pain 42, 243–251.

Balthazard, C. G. and Woody, E. Z. 1992. The spectral analysis of hypnotic performance with respect to ''absorption''. Int. J. Clin. Exp. Hypn. 40, 21–43.

Blakemore, S. J. and Frith, C. 2003. Self-awareness and action. Curr. Opin. Neurobiol. 13, 219–224.

Blakemore, S. J., Oakley, D. A., and Frith, C. D. 2003. Delusions of alien control in the normal brain. Neuropsychologia 41, 1058–1067.

Bouleur, Jt. 1998. Mesmerism: The Discovery of Animal Magnetism (1779). A new translation. Holmes Publishing Group.

Butler, L. D., Symons, B. K., Henderson, S. L., Shortliffe, L. D., and Spiegel, D. 2005. Hypnosis reduces distress and duration of an invasive medical procedure for children. Pediatrics 115, e77–e85.

Crawford, H. J. 1994. Brain dynamics and hypnosis: attentional and disattentional processes. Int. J. Clin. Exp. Hypn. 42, 204–232.

Crawford, H. J., Knebel, T., Kaplan, L., Vendemia, J. M. C., Xie, M., Jamison, S., and Pribram, K. H. 1998. Hypnotic analgesia. 1. Somatosensory event-related potential changes to noxious stimuli. 2. Transfer learning to reduce chronic low back pain. Int. J. Clin. Exp. Hypn. 46, 92–132.

Danziger, N., Fournier, E., Bouhassira, D., Michaud, D., De Broucker, T., Santarcangelo, E., Carli, G., Chertock, L., and Willer, J. C. 1998. Different strategies of modulation can be operative during hypnotic analgesia: a neurophysiological study. Pain 75, 85–92.

De Pascalis, V., Magurano, M. R., and Bellusci, A. 1999. Pain perception, somatosensory event-related potentials and skin conductance responses to painful stimuli in high, mid, and low hypnotizable subjects: effects of differential pain reduction strategies. Pain 83, 499–508.

De Pascalis, V., Magurano, M. R., Bellusci, A., and Chen, A. C. 2001. Somatosensory event-related potential and autonomic activity to varying pain reduction cognitive strategies in hypnosis. Clin. Neurophysiol. 112, 1475–1485.

Egner, T., Jamieson, G., and Gruzelier, J. 2005. Hypnosis decouples cognitive control from conflict monitoring processes of the frontal lobe. Neuroimage 27, 969–978.

Faymonville, M. E., Laureys, S., Degueldre, C., Delfiore, G., Luxen, A., Franck, G., Lamy, M., and Maquet, P. 2000. Neural mechanisms of antinociceptive effects of hypnosis. Anesthesiology 92, 1257–1267.

Faymonville, M. E., Mambourg, P. H., Joris, J., Vrijens, B., Fissette, J., Albert, A., and Lamy, M. 1997. Psychological approaches during conscious sedation. Hypnosis versus stress reducing strategies: a prospective randomized study. Pain 73, 361–367.

Faymonville, M. E., Roediger, L., Del Fiore, G., Delgueldre, C., Phillips, C., Lamy, M., Luxen, A., Maquet, P., and Laureys, S. 2003. Increased cerebral functional connectivity underlying the antinociceptive effects of hypnosis. Brain Res. Cogn. Brain Res. 17, 255–262.

Fromm, E. and Nash, M. R. 1992. Contemporary Hypnosis Research Guilford Press.

Gonsalkorale, W. M. and Whorwell, P. J. 2005. Hypnotherapy in the treatment of irritable bowel syndrome. Eur. J. Gastroenterol. Hepatol. 17, 15–20.

Hilgard, E. R. 1992. Dissociation and Theories of Hypnosis. In: Contemporary Hypnosis Research (*eds*. E. Fromm and M. R. Nash), pp. 69–101. Guilford Press.

Hilgard, E. R. and Hilgard, J. R. 1994. Hypnosis in the Relief of Pain, revised edn. Brunner/Mazel.

Hilgard, E. R., Morgan, A. H., Lange, A. F., Lenox, J. R., MacDonald, H., Marshall, G. D., and Sachs, L. B. 1974. Heart rate changes in pain and hypnosis. Psychophysiology 11, 69–702.

Hofbauer, R. K., Rainville, P., Duncan, G. H., and Bushnell, M. C. 2001. Cortical representation of the sensory dimension of pain. J. Neurophysiol. 86, 402–411.

Jensen, M. P. and Patterson, D. R. 2005. Control conditions in hypnotic-analgesia clinical trials: challenges and recommendations. Int. J. Clin. Exp. Hypn. 53, 170–197.

Kiernan, B. D., Dane, J. R., Philips, L. H., and Price, D. D. 1995. Hypnotic analgesia reduces R-III nociceptive reflex: further evidence concerning the multifactorial nature of hypnotic analgesia. Pain 60, 39–47.

Kirsch, I. and Lynn, S. J. 1995. The altered state of hypnosis: changes in the theoretical landscape. Am. Psychol. 50, 846–858.

Kosslyn, S. M., Thompson, W. L., Costantini-Ferrando, M. F., Alpert, N. M., and Spiegel, D. 2000. Hypnotic visual illusion alters color processing in the brain. Am. J. Psychiatry 157, 1279–1284.

Lang, E. V., Benotsch, E. G., Fick, L. J., Lutgendorf, S., Berbaum, M. L., Berbaum, K. S., Logan, H., and Spiegel, D. 2000. Adjunctive non-pharmacological analgesia for invasive medical procedures: a randomized trial. Lancet 355, 1486–1490.

Laurence, J. R. 2002. 1784. Int. J. Clin. Exp. Hypn. 50, 309–319.

Lenox, J. R. 1970. Effect of hypnotic analgesia on verbal report and cardiovascular responses to ischemic pain. J. Abnormal Psychol. 75, 199–206.

Liossi, C., White, P., and Hatira, P. 2006. Randomized clinical trial of local anesthetic versus a combination of local anesthetic with self-hypnosis in the management of pediatric procedure-related pain. Health Psychol. 25, 307–315.

Maquet, P., Faymonville, M. E., Degueldre, C., Delfiore, G., Franck, G., Luxen, A., and Lamy, M. 1999. Functional neuroanatomy of hypnotic state. Biol. Psychiatry 45, 327–333.

Marc, I., Rainville, P., Verreault, R., Vaillancourt, L., Masse, B., and Dodin, S. 2007. The use of hypnosis to improve pain management during voluntary interruption of pregnancy: an open randomized preliminary study. Contraception 75, 52–58.

Melzack, R. and Casey, K. L. 1968. Sensory, Motivational, and Central Control Determinants of Pain: A New Conceptual Model. In: The Skin Senses (*ed*. D. Kenshalo), pp. 423–443. Thomas.

Melzack, R. and Wall, P. D. 1965. Pain mechanisms: a new theory. Science 150, 971–978.

Montgomery, G. H., DuHamel, K. N., and Redd, W. H. 2000. A meta-analysis of hypnotically induced analgesia: how effective is hypnosis? Int. J. Clin. Exp. Hypn. 48, 138–153.

Nadon, R., Laurence, J. R., and Perry, C. 1987. Multiple predictors of hypnotic susceptibility. J. Pers. Soc. Psychol. 53, 948–960.

Patterson, D. R. 2004. Treating pain with hypnosis. Curr. Dir. Psychol. Sci. 13, 252–255.

Patterson, D. R. and Jensen, M. P. 2003. Hypnosis and clinical pain. Psychol. Bull. 129, 495–521.

Price, D. D. 1996. Hypnotic Analgesia: Psychological and Neural Mechanisms. In: Hypnosis and Suggestions in the Treatment of pain (*ed*. J. Barber), pp. 67–84. Norton.

Radtke, H. L. and Stam, H. J. 1991. The relationship between absorption, openness to experience, anhedonia, and susceptibility. Int. J. Clin. Exp. Hypn. 39, 39–56.

Rainville, P. 2002. Brain mechanisms of pain affect and pain modulation. Curr. Opin. Neurobiol. 12, 195–204.

Rainville, P. and Price, D. D. 2004. The Neurophenomenology of Hypnosis and Hypnotic Analgesia. In: Psychological Methods of Pain Control: Basic Science and Clinical Perspectives (*eds*. D. D. Price and M. C. Bushnell), Vol. 29, pp. 235–267. IASP Press.

Rainville, P., Carrier, B., Hofbauer, R. K., Bushnell, M. C., and Duncan, G. H. 1999a. Dissociation of pain sensory and affective dimensions using hypnotic modulation. Pain 82, 159–171.

Rainville, P., Duncan, G. H., Price, D. D., Carrier, B., and Bushnell, M. C. 1997. Pain affect encoded in human anterior cingulate but not somatosensory cortex. Science 277, 968–971.

Rainville, P., Hofbauer, R. K., Bushnell, M. C., Duncan, G. H., and Price, D. D. 2002. Hypnosis modulates activity in brain structures involved in the regulation of consciousness. J. Cogn. Neurosci. 14, 887–901.

Rainville, P., Hofbauer, R. K., Paus, T., Duncan, G. H., Bushnell, M. C., and Price, D. D. 1999b. Cerebral mechanisms of hypnotic induction and suggestion. J. Cogn. Neurosci. 11, 110–125.

Ray, W. J. 1997. EEG concomitants of hypnotic susceptibility. Int. J. Clin. Exp. Hypn. 45, 301–313.

Raz, A., Fan, J., and Posner, M. I. 2005. Hypnotic suggestion reduces conflict in the human brain. Proc. Natl. Acad. Sci. U. S. A. 102, 9978–9983.

Richardson, J., Smith, J. E., McCall, G., and Pilkington, K. 2006. Hypnosis for procedure-related pain and distress in pediatric cancer patients: a systematic review of effectiveness and methodology related to hypnosis interventions. J. Pain Symptom Manage. 31, 70–84.

Sabourin, M. E., Cutcomb, S. D., Crawford, H. J., and Pribram, K. 1991. EEG correlates of hypnotic susceptibility and hypnotic trance: spectral analysis and coherence. Int. J. Psychophysiol. 10, 125–142.

Salas, C. and Salas, D. 1996. The first scientific investigation of the paranormal ever conducted: testing the claims of Mesmerism, Commissioned by King Louis XVI, Designed conducted and written by Benjamin Franklin, Antoine Lavoisier & Others. Translated from ''Rapport des Comissaires chargés par le Roi de l'Examen du Magnétirme animal. Imprimé par Ordre du Roi No 4 à Paris de l'Imprimerie Royale (1784)''. Introduction by Shermer, M. Skeptic 4, 66–83.

Sandrini, G., Serrao, M., Rossi, P., Romaniello, A., Cruccu, G., and Willer, J. C. 2005. The lower limb flexion reflex in humans. Prog. Neurobiol. 77, 353–395.

Smith, C. A., Collins, C. T, Cyna, A. M., and Crowther, C. A. 2006. Complementary and alternative therapies for pain management in labour. Cochrane Database Syst. Rev. CD003521.

Stewart, J. H. 2005. Hypnosis in contemporary medicine. Mayo Clin. Proc. 80, 511–524.

Szechtman, H., Woody, E., Bowers, K. S, and Nahmias, C. 1998. Where the imaginal appears real: a positron emission tomography study of auditory hallucinations. Proc. Natl. Sci. U. S. A. 95, 1956–1960.

Tellegen, A. and Atkinson, G. 1974. Openness to absorbing and self-altering experiences (''absorption''), a trait related to hypnotic susceptibility. J. Abnorm. Psychol. 83, 268–277.

Weitzenhoffer, A. M. 1980. Hypnotic susceptibility revisited. Am. J. Clin. Hypn. 22, 130–146.

Wild, M. R. and Espie, C. A. 2004. The efficacy of hypnosis in the reduction of procedural pain and distress in pediatric oncology: a systematic review. J. Dev. Behav. Pediatr. 25, 207–213.

Willer, J. C., Boureau, F., and Albe-Fessard, D. 1979. Supraspinal influences on nociceptive flexion reflex and pain sensation in man. Brain Res. 179, 61–68.

Willer, J. C., Dehen, H., and Cambier, J. 1981. Stress-induced analgesia in humans: endogenous opioids and naloxone-reversible depression of pain reflexes. Science 212, 689–691.

Woodgate, R. L. and Degner, L. F. 2003. Expectations and beliefs about children's cancer symptoms: perspectives of children with cancer and their families. Oncol. Nurs. Forum 30, 479–491.

Woody, E. and Szechtman, H. 2000. Hypnotic hallucinations: towards a biology of epistemology. Contemp. Hypn. 17, 4–14.

Zachariae, R. and Bjerring, P. 1994. Laser-induced pain-related brain potentials and sensory pain ratings in high and low hypnotizable subjects during hypnotic suggestions of relaxation, dissociated imagery, focused analgesia, and placebo. Int. J. Clin. Exp. Hypn. 42, 56–80.

6.01 Cutaneous Mechanisms of Tactile Perception: Morphological and Chemical Organization of the Innervation to the Skin

F L Rice and P J Albrecht, Albany Medical College, Albany, NY, USA

© 2008 Elsevier Inc. All rights reserved.

6.01.1	**Overview of Tactile Perception**	3
6.01.1.1	Tactile Perception Depends upon Stimulus Detection and Predictability	4
6.01.1.2	The Skin is a Sense Organ as Well as a Protective Barrier	4
6.01.1.2.1	Primary sensory neurons	4
6.01.1.2.2	Sensory endings	5
6.01.1.3	Functional Classifications of Cutaneous Sensory Neurons	5
6.01.1.3.1	Basic categories	5
6.01.1.3.2	Cross category correlations	8
6.01.1.4	Multineuronal Activation and Tactile Perception	8
6.01.1.4.1	Adequate or preferred stimulus	8
6.01.1.4.2	Complex multineuronal integration	9
6.01.1.5	Stimulus Transduction by Sensory Endings	9
6.01.2	**Organization of Innervation Among Structurally Complex Tactile Organs**	9
6.01.2.1	Complex Tactile Organs with Multiple Types of Innervation	10
6.01.2.1.1	Vibrissa follicle sinus complexes	10
6.01.2.1.2	Guard hair follicles	10
6.01.2.1.3	Glabrous fingertip skin	11
6.01.2.1.4	Patterned vasculature	14
6.01.2.2	Morphological Variations Among Specific Types of Mechanoreceptive Endings	14
6.01.2.2.1	Merkel endings	14
6.01.2.2.2	Lanceolate endings and Meissner corpuscles	15
6.01.2.2.3	Pacinian and Golgi–Mazzoni corpuscles	17
6.01.2.2.4	Ruffini corpuscles	18
6.01.2.2.5	Free nerve endings	18
6.01.2.3	Interspecies Differences in Vibrissa Follicle–Sinus Complexes and Glabrous Fingertip Innervation	20
6.01.2.3.1	Rat and cat follicle–sinus complex	20
6.01.2.3.2	Raccoon glabrous fingertips	20
6.01.3	**Molecular Basis of Tactile Sensation**	21
6.01.3.1	Transient Receptor Potential Superfamily	21
6.01.3.2	Degenerin/Epithelial Sodium Channel Superfamily	21
6.01.3.3	Purinergic Receptors	22
6.01.3.4	Ca^{2+} Ion Channels	22
6.01.3.5	Other Molecules	22
6.01.4	**Peripheral Mechanisms of Sensory Integration**	23
6.01.4.1	Multimolecular Properties of Cutaneous Sensory Neurons	23
6.01.4.1.1	Meissner corpuscle innervation	23
6.01.4.1.2	Dorsal root ganglion neurons	24
6.01.4.2	Potential Role of Merkel Cells and Terminal Glia in Sensory Transduction and Integration	24
6.01.4.3	Sensory Transduction and Integration Among Epidermal Keratinocytes	24
6.01.5	**Summary**	26
References		27

Glossary

Aβ fiber Typically the largest-caliber, myelinated axons of sensory neurons that supply innervation to the skin and other tissues. They are typically low-threshold mechanoreceptors. Note: A different nomenclature using a Roman numeral system is often used in referring to axons of sensory neurons that supply skeletal muscle.

Aδ fiber Typically the smaller-caliber, myelinated axons of sensory neurons that supply innervation to the skin and other tissues. Although typically regarded as nociceptors, different types may have high- or low-threshold responses to different types of stimuli (mechanical, chemical, or thermal). Note: A different nomenclature using a Roman numeral system is often used in referring to axons of sensory neurons that supply skeletal muscle.

C fiber An unmyelinated axon of a sensory neuron that supplies the skin and other tissues. They are also very thin caliber, less than 1.5 μm in diameter. Although typically regarded as high-threshold nociceptors, different types may have high- or low-threshold responses to different types of stimuli (mechanical, chemical, or thermal). Note: A different nomenclature using a Roman numeral system is often used in referring to axons of sensory neurons that supply skeletal muscle.

chemoreceptor A sensory ending that responds optimally to chemical stimulation. The term may also refer to the entire sensory neurons whose ending have this property.

cranial root ganglion A swelling in cranial nerves which is located close to the brain stem cord and contains the cell bodies of primary sensory neurons whose axons are contained within cranial nerves. These nerves supply the skin and skeletal muscles of the entire body except for that of the face and oral and nasal cavities.

cutaneous innervation The nerve supply to the skin including the blood vessels and sweat glands of the skin. This consists of sensory components that detect various types of environmental stimuli, and autonomic motor components that cause changes in the diameter of arteries and arterioles and the secretion of sweat from sweat glands.

dermal papillae Cone-like dermal extensions that protrude in the epidermis or base of hair follicles.

Dorsal root ganglion A swelling in spinal nerves which is located close to the spinal cord and contains the cell bodies of primary sensory neurons whose axons are contained within spinal nerves. These nerves supply the skin and skeletal muscles of the entire body except for that of the face and oral and nasal cavities.

epidermis The outer layer of the skin that is composed primarily of several layers of compact keratinocytes. The deepest layer, stratum basalis, contains melanocytes and, in glabrous skin, may contain Merkel cells. Cells of the immune system – Langerhans/dendritic cells – are scattered among the keratinocytes.

free nerve ending The endings of axons in a target organ that typically resemble thin threads. They lack a unique morphology and accompanying structures composed of terminal glia or other accessory cells.

glabrous skin A special type of smooth skin that has a thick epidermis, often penetrated by dermal papillae, and lacks hair follicles. It is typically located on the ventral surfaces of the hands and feet.

high threshold Requiring strong stimulation to generate an action potential.

low threshold Able to generate action potentials in response to very faint stimulation.

mechanoreceptor A sensory ending that responds optimally to mechanical stimulation. The term may also refer to the entire sensory neurons whose ending has this property.

Meissner corpuscles Compact stacks of alternating layers of terminal glial cells and endings of Aβ and C fibers. Located in many dermal papillae of glabrous skin. Implicated as low-threshold mechanoreceptors that respond optimally to low-frequency (flutter) vibrations.

Merkel cell A specialized cell located in the deepest layer of the epidermis or the outermost layer of hair follicles that is in contact with sensory endings of Aβ fibers that are implicated in responding to gentle sustained compression of the skin or deflection of hairs.

Merkel endings or disks Flattened terminals of some types of low-threshold Aβ fiber mechnoreceptors that are juxtaposed to Merkel cells. Implicated as low-threshold, slowly adapting mechanoreceptors that have a prolonged response to sustained compression of the skin or deflection of hairs.

modality A particular physical property of a stimulus that can generate activity in sensory neurons.
myelin Layers of membrane that is formed by some Schwann cells wrapping around some types of axons (myelinated axons). In nerves, a Schwann cell will make a myelin sheath only around a segment of one axon.
nerve fiber An old anatomical term for an axon in a nerve. The term was originally used in reference to filamentous components within nerves before it was known that they were the axons of nerve cells.
neurons Nerve cells.
nociceptor A sensory ending that responds optimally to stimuli (mechanical, chemical, thermal, or mixed, i.e., polymodal) that elicit a perception of pain or pain-related behavioral response. The term may also refer to the entire sensory neurons whose ending has this property.
Pacinian Corpuscles Large-caliber unbranched sensory endings that are embedded in a large bulbous laminated structure composed of flattened terminal glia. The ending is supplied by a large-caliber Aβ fiber that is a low-threshold rapidly adapting mechanoreceptor that responds optimally to high-frequency vibrations.
pilo-neural complex A combination of several types of sensory endings that form an ensemble around hair follicles at about the mid-level of the hair shaft. Typically the ensemble consists of a palisade of blade-like lanceolate endings supplied by Aβ fibers, and a mix of circumferentially oriented endings supplied by Aβ and C fibers.
primary sensory neurons Special types of nerve cells that lack dendrites and that are activated by environmental stimulation instead of by synaptic input from other nerve cells. They have a single process that bifurcates into an axon. One end of the axon extends through spinal or cranial nerves to terminate as a specialized structures in the skin that respond to environmental stimuli. The other end extends through connectors to the spinal cord or brain stem (dorsal roots or cranial roots) to synapse on nerve cells in the central nervous system.
rapidly adapting neurons Nerve cells that briefly produce action potentials in response to sustained stimulation, typically at the onset and/or cessation of the stimulus.
Schwann cells A type of cell that encases axons within nerves. Each Schwann cell encases a short segment of the axon. The entire lengths of all axons in a nerve are encased by many consecutive Schwann cells.
slowly adapting neurons Nerve cells that have a prolonged production of action potentials in response to a sustained stimulation, although this activity may eventually cease after several milliseconds.
terminal glial cell A type of Schwann cell that forms an association with the endings of Aβ fibers that terminate in the dermis, skeletal muscle, tendons, joint capsules, and the wall of organs.
thermoreceptor A sensory ending that responds optimally to heat exchange. The term may also refer to the entire sensory neurons whose ending has this property.
unmyelinated axons Axons that are encased in Schwann cells that do not form myelin sheaths. Typically, segments of several unmyelinated axons are embedded in the surface of a single, non-myelinating Schwann cell.

6.01.1 Overview of Tactile Perception

A hungry seal glides beneath the ice searching for food in the darkened water. Despite the vigorous stimulation of his whiskers (vibrissae) caused by the rushing water and the presence of natural water currents, the seal detects a miniscule turbulence and in a split second recognizes that it is the wake of a fish and tracks it to his prey. This is a task that the seal can accomplish several minutes after the wake was generated by using only tactile input through its facial vibrissae (Dehnhardt, G. *et al.*, 2001; Schulte-Pelkum, N. *et al.*, 2007). A concert pianist performs a Beethoven concerto at lightening speed. Independently, all 10 of her fingers deftly detect the right keys and exert the appropriate pressure to convey the nuance of the composition to perfection. The complexity of the task has become so second nature that she is only conscious of the musical experience,

not the minute details that her fingertips are extracting from their contact with the piano keys. The joy that she brings to others is both fulfilling and is her means of earning a living.

This chapter will consider how the skin and its innervation in mammals are structurally and chemically organized to extract an extraordinary variety and range of physical features from the environment in order to provide a basis for the brain to formulate tactile perception. First, we will consider some basic principles of sensory perception and traditional functional classifications of cutaneous sensory innervation. Second, we will consider how several varieties of cutaneous innervation are integrated with microanatomical specializations to form highly sensitive and complex tactile organs, particularly vibrissa follicle–sinus complexes and glabrous fingertip skin. Third, we will briefly consider some of the known molecular mechanisms related to the detection of tactile stimulation. Finally, we will consider how the molecular complexity of individual sensory endings, local interactions between multiple sensory endings, and local interactions with non-neuronal components may result not only in sensory detection, but importantly also sensory integration beginning directly in the skin before sensory input reaches the central nervous system (CNS).

6.01.1.1 Tactile Perception Depends upon Stimulus Detection and Predictability

The fundamental principle underlying sensory systems is that every animal needs to establish a metabolic equilibrium that enables it to survive and procreate. In order to establish a survival equilibrium, an animal must be able to detect changes in its environment (stimuli) and generate appropriate reactions (responses) to those changes. In order for this to succeed, these processes must be consistent and predictable. This inherent stimulus–response capacity is present in all living animals, from single-celled animals such as amoebas to relatively simple multicellular animals like jellyfish to complex multicellular animals like mammals. In complex multicellular animals, the collective survival of individual cells requires differentiation into specialized superceding and collaborating systems (e.g., digestive, respiratory, cardiovascular). The nervous system is designed to coordinate the collective survival strategy but the fundamental principle remains the same: the need to consistently and predictably detect stimuli and generate survival responses. An important part of this strategy is to monitor not only the external environment, but also the internal environment. Both must be coordinated and interpreted in the context of each other, that is., the homeostasis of the animal in relation to its external environment.

6.01.1.2 The Skin is a Sense Organ as Well as a Protective Barrier

As a protective barrier, skin forms the largest interface with the external environment. As such, it is also the largest sense organ of the body. Importantly, any natural environmental interaction with the skin or its hairs, either by direct physical contact with an object or even minute air currents, typically involves more than one type of stimulus. These tactile stimuli can be a combination of mechanical force, heat exchange, or chemical interactions (Gardner, E. and Martin, J., 2000). Each type of stimulus can have a wide range of intensities and features such as sustained or fluctuating contact with the skin surface, deflection of a hair in a particular direction, loss or gain of heat, and irritating or soothing tissue reactions.

6.01.1.2.1 Primary sensory neurons

Cutaneous innervation is supplied by a structurally unique types of neurons – primary sensory neurons – that lack dendrites and synaptic contacts typical of all other types of neurons in the nervous system (Gardner, E. *et al.*, 2000). Primary sensory neurons bridge the gap between the peripheral skin, which is impacted by the external environment, and the CNS (brain, brainstem, and spinal cord) where these impacts are ultimately interpreted as tactile perception. The ability to perceive and integrate all types of cutaneous tactile stimuli (mechanical, thermal, and chemical) in parallel is the basis of normal tactile perception, attributable to the fact that no natural environmental interaction with the skin involves only a single type of cutaneous stimulation. Moreover, the sensory neuron innervation to the skin also assesses the intrinsic status of the organ, including internal mechanical activity such as vibration and tension caused by blood flow, and distortion of the skin caused by contractions of the musculature and movements of joints.

In keeping track of the location where a stimulus impinges on the body surface, the skin is organized into bilaterally symmetrical paired strips (referred to as dermatomes) that consecutively cover the entire body surface (Gardner, E. *et al.*, 2000). Each pair of

dermatomes has their stimulation detected by thousands of primary sensory neurons whose cell bodies are contained within consecutive pairs of dorsal root ganglia (DRG) and cranial nerve ganglia. These ganglia are located immediately lateral to each side of the spinal cord and the brainstem. As is discussed below, many functional types of primary sensory neurons have been categorized based on their capacity to respond to different physical properties of cutaneous stimuli. Since the primary sensory neurons are the first of many neurons involved in somatosensory processing, they are also referred to as first-order neurons responding to cutaneous stimuli. In bridging the gap between the skin and the CNS, each primary sensory neuron has a single process – an axon – that bifurcates, with one branch extending the length of a nerve to terminate in the skin, and the other branch extending through a dorsal or cranial root to enter, respectively, the spinal cord or brainstem and synapse on second-order neurons. Each second-order neuron receives converging inputs from several first-order neurons, thereby beginning the process of integrating the entire range of activity generated by cutaneous stimulation.

6.01.1.2.2 Sensory endings

Within the skin, the tip of the axon forms a sensory ending that is restricted to and responds to stimulation of a skin location referred to as a receptive field (Gardner, E. *et al.*, 2000). The receptive field may be a patch of skin or one or more hair follicles. In turn, each location in the skin is supplied by numerous neurons having different functional types of sensory endings (Figures 1 and 2). The size of the receptive field for a particular primary sensory neuron varies depending on the type of sensory ending and the location on the body surface. Performance of tactile tasks that require a high degree of spatial resolution, such as detecting the serrated edge of a coin, is accomplished by a high innervation density in which the skin territory is supplied by a large number of sensory neurons whose individual endings have small receptive fields. Each territory within the dermatome receives endings from a specific set of primary sensory neurons, and the neurons that supply adjacent sites within the dermatome terminate in adjacent second-order neurons. Thus, the body surface is mapped into the circuitry of the CNS to predictably keep track of each site of stimulation on the skin.

6.01.1.3 Functional Classifications of Cutaneous Sensory Neurons

6.01.1.3.1 Basic categories

The ability to discern different types and features of cutaneous stimuli at specific locations within the skin is due to the fact that each site is innervated by several functional types of sensory neurons. Different functional types have been traditionally classified according to three basic electrophysiological criteria: the rate at which the axon conducts action potentials, the type of stimulus (modality) that optimally generates an action potential, and the rate that the neuron adapts and no longer responds to a sustained stimulus (Brown, A. G. and Iggo, A., 1967; Gardner, E. *et al.*, 2000).

6.01.1.3.1.(i) Conduction rate Cutaneous sensory neurons are generally classified by having axons designated as Aβ, Aδ, or C fibers. Aβ fibers have the fastest conductance ($\sim$35–75 m s^{-1}) due to the fact that they have the largest caliber and the thickest myelin sheath. Aδ fibers are significantly slower ($\sim$5–30 m s^{-1}), having a much thinner caliber and thinner myelin sheath. C fibers are by far the slowest ($\sim$0.5–2 m s^{-1}), having the thinnest caliber and being unmyelinated.

6.01.1.3.1.(ii) Stimulus modality Modality generally refers to the type of physical energy that is converted to electrochemical activity in sensory neurons. However, the term is also used in the context of the related stimulus perception. Cutaneous sensory neurons are fundamentally restricted to responding to mechanical force, heat exchange, and chemical reactions. Low- and high-threshold mechanoreceptors are sensory neurons that are optimally activated by relatively mild or strong mechanical stimuli, respectively (Brown, A. G. and Iggo, A., 1967; Burgess, P. R. and Perl, E. R., 1967; Koerber, H. R. and Mandell, L. M., 1992). Mechanoreceptors have been further classified based upon whether the optimal activity is dependent upon the rate of application, duration, and direction of the stimulus with respect to the skin surface or hair. Warm or cold thermoreceptors respond to particular temperatures or changes in temperatures as a function of heat exchange to or from the skin (Iggo, A., 1964; Brown, A. G. and Iggo, A., 1967; Dhaka, A. *et al.*, 2006; Caterina, M. J., 2007). The heat exchange will depend upon the relative temperature and mass of the stimulus to the relative

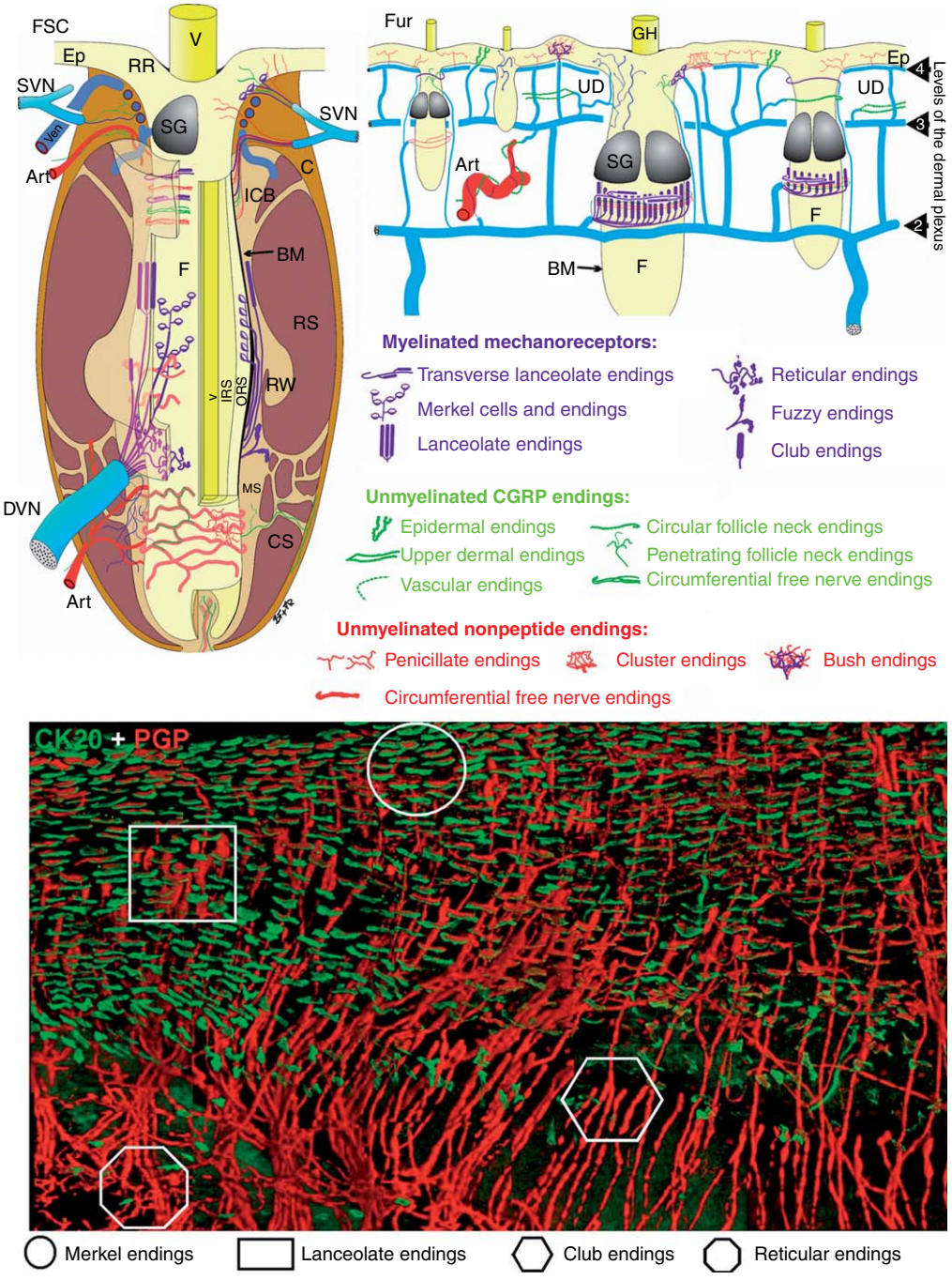

Figure 1 Top: Schematics of the structure and innervation of vibrissa follicle–sinus complexes (FSCs) and intervibrissa fur in mice and rats. Adapted from Funfschilling, U., Ng, Y. G., Zang, K., Miyazaki, J., Reichardt, L. F., and Rice, F. L. 2004. TrkC kinase expression in distinct subsets of cutaneous trigeminal innervation and nonneuronal cells. J. Comp. Neurol. 480, 392–414. Types of innervation are indicated by the color-coded symbols. Bottom: Confocal montage of double-labeled immunofluorescence images compiled from around the perimeter of whole-mount rat vibrissa follicle as seen from the interior where the vibrissa was located. Reproduced with permission from Dr. Satomi Ebara. All of the innervation is labeled by anti-PGP9.5 (red). Merkel cells are labeled by anticytokeratin 20 (green). Examples of different types of endings are shown in white contours. For additional details, see Fundin, B. T. *et al.* (1997b); Rice, F. L. *et al.* (1997); Ebara, S. *et al.* (2002); and Fünfschilling, U. *et al.* (2004). Art, arteriole; BM, basement membrane; C, collagen capsule; CS, cavernous sinus; DVN, deep vibrissa nerve; EP, epidermis; F, Follicle; GH, Guard hair; ICB; inner conical body; IRS, inner root sheath; MS, mesenchymal sheath; ORS, outer root sheath; RR, rete ridge; RS, ringsinus; RW, ring wulst; SG, sebaceous gland; SVN, superficial-vibrissa nerve; Tr, trabeculae; UP, upper dermis, V, vibrissa; VF, vibrissa follicle.

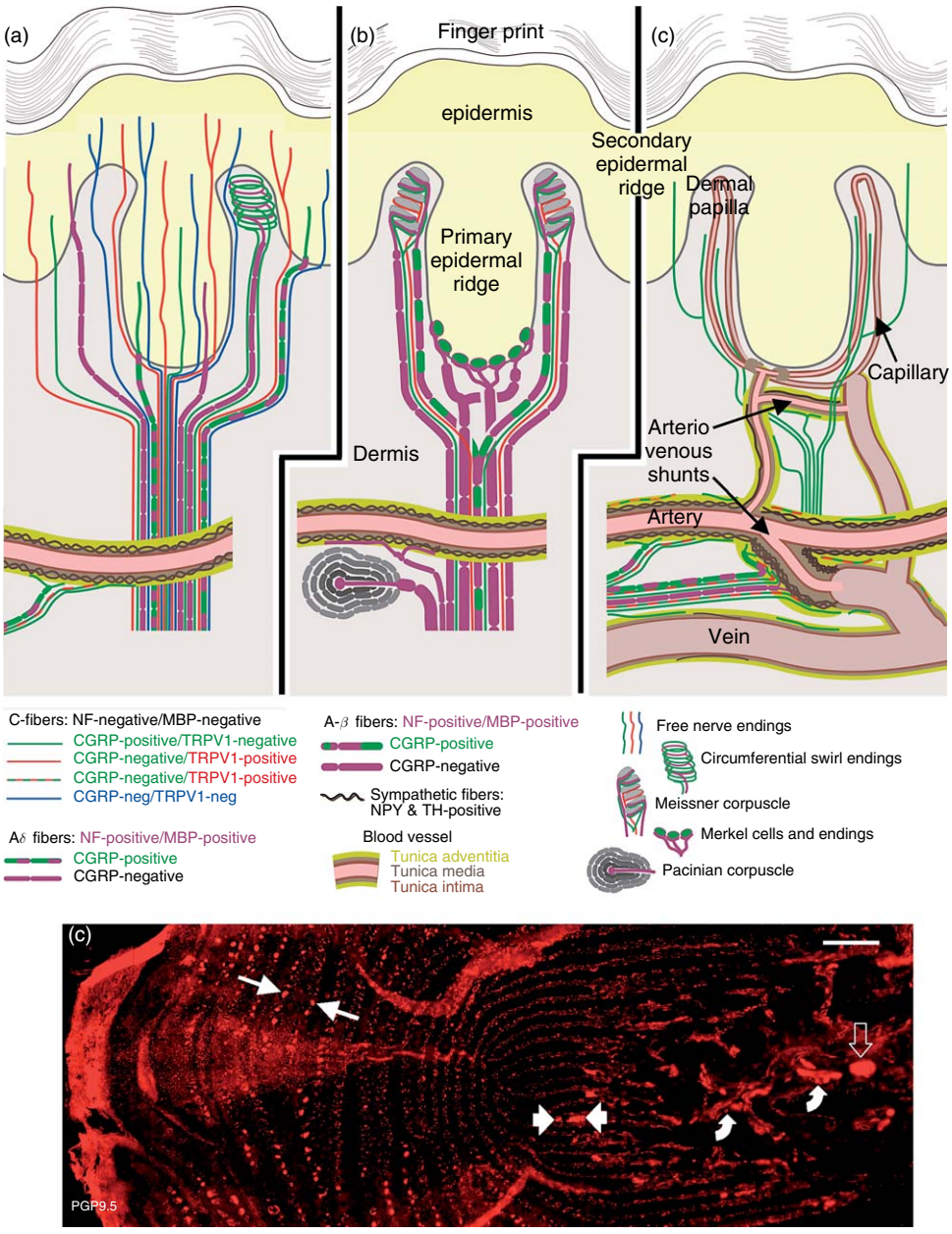

Figure 2 Schematics (a–c) and digital image montage (d) of the structure and innervation of the glabrous fingertip skin from Old World monkeys. Panels (a–c): Schematics representing the skin as seen in a cross section through a fingerprint ridge. Panel (a) represents only the Aδ- and the C-fiber innervation to the epidermis, the dermal papillae, and to a branch of a digital artery. Panel (b) represents only the Aβ fiber innervation and a nonpeptidergic Aδ-fiber innervation to a branch of the digital artery. Panel (c) represents the organization of the vasculature and its affiliated innervation. The superimposition of panels (a)–(c) would represent the total innervation and vasculature to such a site in glabrous digital skin. Types of innervation are indicated in the schematics below (a) and (b). (c) Anti-protein–gene product (PGP) immunofluorescence labeling and mapping of innervation in a 14 μm-thick section of the distal volar pad of the index finger. The section is cut parallel to the skin surface along the long axis of the finger and passes obliquely through the distal tip to the left. The central part of the section shows a transition to the dermal layer to the right. Rows of Meissner corpuscles (thin arrows) outline the pattern of the fingerprints. The pair of thin arrows shows two corpuscles that flank the same primary epidermal ridge. Broad arrows indicate Merkel endings sectioned parallel to the base of a primary epidermal ridge. The open arrow indicates a Pacinian corpuscle that is located among innervated arteries (curved arrows) deep in the dermis. Scale bar = 100 μm. Adapted from Paré M. *et al.* (2002; 2007).

temperature and mass of the skin. Chemoreceptors optimally respond to chemical substances and have been subdivided based upon relative responses to substances such as acids, plant extracts such as capsaicin or menthol, and/or other molecules endogenous to the skin such as glutamate and adenosine triphosphate (ATP) (Bessou, P. and Perl, E. R., 1969; Iggo, A., 1984; Owsianik, G. *et al.*, 2006). These responses will also be relative to the chemical status of the skin.

Another modality classification of primary sensory neurons is based on whether the stimulus evokes activity that is noxious to the point of being perceived as painful. These neurons are referred to as nociceptors and pain is regarded as a modality even though the activity is related to force, heat exchange, or chemical reactions that have the potential to, or actually do, cause tissue damage (Perl, E. R., 1980). As such, classifications of nociceptors are further subdivided into mechanical nociceptors, thermal nociceptors, chemonociceptors, or polymodal nociceptors (Burgess, P. R. and Perl, E. R., 1967; Perl, E. R., 1968; Bessou, P. and Perl, E. R., 1969; Cohen, R. H. and Perl, E. R., 1988; Koerber, H. R. and Mandell, L. M., 1992; Perl, E. R., 1996; Tominaga, M. and Caterina, M. J., 2004).

The existence of a perception that tissue is at risk or damaged presupposes that there must be an ongoing assessment of tissue conditions that fall within a range that are deemed viable. Although ongoing fluctuations of physical activity within the range of healthy tissue homeostasis need not be perceived consciously (and indeed would be distracting), nonetheless there are obviously sensory neurons that are perceiving these fluctuations and regulating responses to maintain this homeostasis. Such neurons detecting this unperceived modality have been referred to as metaboreceptors (Light, A. R. and Perl, E. R., 2003; Molliver, D. C. *et al.*, 2005). Although primarily regarded in relation to sensing muscle metabolism, metaboreceptors presumably would innervate and monitor all tissues including the skin. Indeed, it is quite likely that such metaboreceptors are constantly detecting stressful activity, which elicits subconscious corrective responses before conditions surpass a threshold perceived as painful. As is discussed below, a large population of neurons have chemical properties and experimentally assessed electrophysiological properties that are characterized as nociceptive, despite the fact that acute pain normally occurs on relatively rare occasions. Thus, it might be argued that all of these nociceptive neurons are metaboreceptors and that pain is the consciously perceived activity at the extreme of a continuum that is mostly involved in the unperceived regulation of homeostasis (Craig, A. D., 2003a; 2003b; Light, A. R. and Perl, E. R., 2003).

6.01.1.3.1.(iii) Adaptation Sensory neurons are classified as slowly adapting (SA) if they have a prolonged generation of action potentials in response to a sustained optimal stimulus, or as rapidly adapting (RA) if the generation of action potentials quickly ceases (Gardner, E. *et al.*, 2000). In the latter case, there is typically a brief response both when the stimulus begins and when it is removed. SA neurons are regarded as optimal for discriminating sustained events such as compression of the skin, and RA are optimal for transient events such as vibrations in the skin. Neurons may also be further classified based upon regular or irregular patterns of action potentials (e.g., SA type I, SA type II).

6.01.1.3.2 Cross category correlations

In general, primary sensory neurons that are low-threshold mechanoreceptors have Aβ fibers (Brown, A. G. and Iggo, A., 1967). Neurons that are high-threshold mechanoreceptors, thermoreceptors, chemoreceptors, nociceptors and metaboreceptors generally have either Aδ or C fibers (Burgess, P. R. and Perl, E. R., 1967; Bessou, P. and Perl, E. R., 1969; Kumazawa, T. and Perl, E. R., 1977). However, there are numerous exceptions to these generalities. At least some Aδ and C fibers were classified as low-threshold mechanoreceptors even among the earliest electrophysiological studies (Iggo, A., 1960; Bessou, P. *et al.*, 1971; Light, A. R. and Perl, E. R., 2003; Cole, J. *et al.*, 2006), but their existence has typically been overlooked in the emphasis on the relationship of most of these fibers to pain and thermal sensation. Moreover, some Aβ fiber, low-threshold mechanoreceptors have been shown to have biochemical properties implicated in thermal, chemical, and noxious stimulus transduction (Rice, F. L. *et al.*, 1997; Paré, M. *et al.*, 2001). The potential functional contributions of these properties have barely been investigated.

6.01.1.4 Multineuronal Activation and Tactile Perception

6.01.1.4.1 Adequate or preferred stimulus

Importantly, a long-known aspect of sensory ending physiology that is often unappreciated in

oversimplifying the classifications noted above is that the test parameters investigated are by necessity limited under experimental conditions. Thus, the experimentally determined electrophysiological assessments do not necessarily represent the complete, or perhaps even true, functional capability of a particular sensory neuron in response to natural environmental interactions (Bessou, P. and Perl, E. R., 1969). Therefore, the optimal stimulus that activates a sensory neuron under experimental conditions has rightly been referred to as the adequate or preferred stimulus in recognizing that other stimuli can also activate the neuron at least to a lesser degree (Gardner, E. and Martin, J., 2000). Consequently, electrophysiological studies have always shown a wide range of response properties that, for purposes of simplification, have been somewhat arbitrarily grouped into different classes (Gibson, J. M. and Welker, W. I., 1983a; 1983b). However, *in vivo*, any stimulus applied to the skin surface likely generates different levels of activity across several different types of sensory neurons (Connor, C. E. *et al.*, 1990; Khalsa, P. S. *et al.*, 1998; LaMotte, R. H. *et al.*, 1998; Friedman, R. M. *et al.*, 2002; Bensmaia, S. J. *et al.*, 2005; Leung, Y. Y. *et al.*, 2005; Leiser, S. C. and Moxon, K. A., 2007). Importantly, axons known to terminate in cutaneous locations have frequently been encountered that elicited no change in activity in relation to tested stimuli, indicating that their preferred stimulus may involve several combinations of different stimuli that may occur only under natural conditions (Brown, A. G. and Iggo, A., 1967; Burgess, P. R. and Perl, E. R., 1967).

6.01.1.4.2 Complex multineuronal integration

While making such classifications serves a useful purpose, it is important to recognize that the total pattern of all of the sensory neurons – not only that of the neurons optimally activated – contribute to the brain's formulation of a tactile perception. Regardless of the obvious complexity of this process, it is clear that the various physical properties of a natural cutaneous stimulation are differentially extracted across several types of neurons and then the input is reintegrated centrally to formulate a tactile perception. Indeed, the formulation of a tactile perception likely includes not only an assessment of those sensory neurons that are activated to varying degrees, but also the assessment of those neurons that have not been activated (Gardner, E. and Martin, J., 2000). In addition to the activity of cutaneous innervation during tactile tasks, activity in muscle- and joint-related sensory endings generated by exploratory movement also contributes to tactile perception.

6.01.1.5 Stimulus Transduction by Sensory Endings

Once sensory stimuli have sufficiently activated a sensory neuron, the outcome is an action potential that is electrochemically similar to that in any other neuron, although the shape of the axon potential may differ across fiber types (Dijouhri, L. *et al.*, 1998; Koerber, H. R., and Woodbury, C. J. 2002. As in any other neuron, the generation of an action potential depends upon sufficiently depolarizing the membrane to a threshold level at a site located at the beginning of the axon (Gardner, E. and Martin, J., 2000). In a typical neuron, the impulse-generating zone is located where the axon is attached to the cell body (the axon hillock). The threshold depolarization is achieved at this site through the spatiotemporal integration of excitatory and inhibitory graded responses generated by numerous synapses on the dendrites and the cell body. In general, the excitatory synaptic mechanisms open sodium channels to permit depolarization, whereas inhibitory synaptic mechanisms cause a countering hyperpolarization by activating potassium channels. In a primary sensory neuron, the impulse-generating zone is at the transition between the sensory ending and the beginning of the axon, and the threshold depolarization is achieved by activating ion channels in the sensory ending. Thus, the specific stimulus detection property of primary sensory neurons is dependent on the location (local tissue environment), structure, and chemistry of its sensory ending.

6.01.2 Organization of Innervation Among Structurally Complex Tactile Organs

Among large multicellular animals, especially mammals, the orofacial area and distal limbs are best positioned to interact with tactile environments. Thus, these areas have a particularly high innervation density and a wide variety of sensory endings. Moreover, important tactile sites also have intricate non-neuronal tissue specializations that likely enhance the impact of the various physical components of a stimulus. Two exceptional examples of these combined features are: (1) the presence of

patterned arrays of long tactile vibrissae and their associated follicle–sinus complexes (FSC) on the hairy-skin snouts of most mammalian quadrupeds (Figure 1) and (2) the presence of patterned epidermal ridges (fingerprints) on fingertip glabrous skin (Figure 2) especially in bipedal primates. In both examples, the different types of sensory endings are strategically located among specific microanatomical features (Cauna, N., 1954; Rice, F. L. *et al.*, 1997; Ebara, S. *et al.*, 2002; Paré, M. *et al.*, 2002).

6.01.2.1 Complex Tactile Organs with Multiple Types of Innervation

6.01.2.1.1 Vibrissa follicle sinus complexes

Each FSC consists of a large follicle core (an epidermal invagination), which is encased within dermal derivatives consisting of a thin mesenchymal sheath and an encapsulated blood sinus (Figures 1 and 3). The epidermis is thickened at the mouth of the follicle (rete ridge collar). The mesenchymal sheath expands at the upper end of the sinus (inner conical body, ICB), anchors a ring of tissue at the mid-level of the sinus (ringwulst), and exudes tissue strands (trabeculae) that fan out to the connective tissue capsule at the deep end of the sinus. The upper portion of the blood sinus – referred to as the ring sinus – has an open lumen in which the ringwulst is suspended, while the lower portion – referred to as the cavernous sinus – is laced with trabeculae. The base of each follicle is penetrated by a dermal papilla.

The FSC receives innervation via a deep vibrissal nerve (DVN) that penetrates the deep aspect of the sinus capsule and via several smaller superficial vibrissal nerves (SVN) that penetrate the superficial aspect. Each type of nerve supplies sensory endings to separate deep and superficial portions as though the FSC consisted of two distinct functional entities. Importantly, each type of nerve supplies more than one type of Aβ fiber whose particular morphologically distinct ending has a unique site of termination within the FSC microanatomy (Rice, F. L. *et al.*, 1997; Ebara, S. *et al.*, 2002). A unique morphological type of Aβ fiber ending is affiliated with each aspect of the FSC microanatomy. Furthermore, each nerve supplies several chemically distinct types of Aδ and C fibers, and many of these terminate at the same locations as the Aβ fiber endings.

Taken together, the specific distributions of sensory ending types among distinct microanatomical locations indicates that any perturbation of the vibrissa will generate a variety of mechanical forces at each location and would, therefore, differentially activate all the types of innervation terminating at these locations (Gibson, J. M. and Welker, W. I., 1983a; 1983b; Szwed, M. *et al.*, 2003; Leiser, S. C. and Moxon, K. A., 2007). Slight differences in the perturbations of the vibrissa would differentially alter the mechanical forces at each location, and thus the pattern of activity among all the sets of innervation. In general, the Aβ fibers supplied by the DVN have been implicated in detecting various movements of the vibrissa with respect to the interior structure of the FSC. The Aβ fibers supplied by SVN have been implicated in detecting movement of the vibrissa with respect to the mouth of the follicle and the movement of the entire FSC with respect to the skin surface caused by contraction of papillary muscles. Reflecting these potential different functions, SVN and DVN that supply the same FSC have been shown to have different patterns of terminations in the brainstem (Arvidsson, J. and Rice, F. L., 1991).

The vibrissae and their FSCs are also organized into predictable rows and numbers. Each row of follicles is paralleled by a dedicated fascicle of the trigeminal nerve. Based upon the organization of this macroanatomy and innervation, any encounter with a vibrissa-perturbing stimulus will generate differential patterns of activity among the innervation to all the follicles depending upon the size, shape, orientation, direction, velocity, texture, duration, and intensity of the stimulus (Mehta, S. B. and Kleinfeld, D., 2004; Kleinfeld, D. *et al.*, 2006; Mehta, S. B. *et al.*, 2007).

6.01.2.1.2 Guard hair follicles

Although less elaborate than FSCs, the much smaller hair follicles over the rest of the body also have associated with them different types of sensory endings that respond to various stimulations of hairs, consisting of sustained or transient displacements with or without preferential orientations (Brown, A. G. and Iggo, A., 1967). Although all follicles receive some innervation (Figure 1), the follicles of the larger body hairs – referred to as guard hairs – can have several varieties of endings in two locations (Figures 4(a)–4(c)): (1) at the mouth and the neck of the follicle, and (2) below the sebaceous gland. The latter site has an integrated array of endings referred to as the piloneural complex.

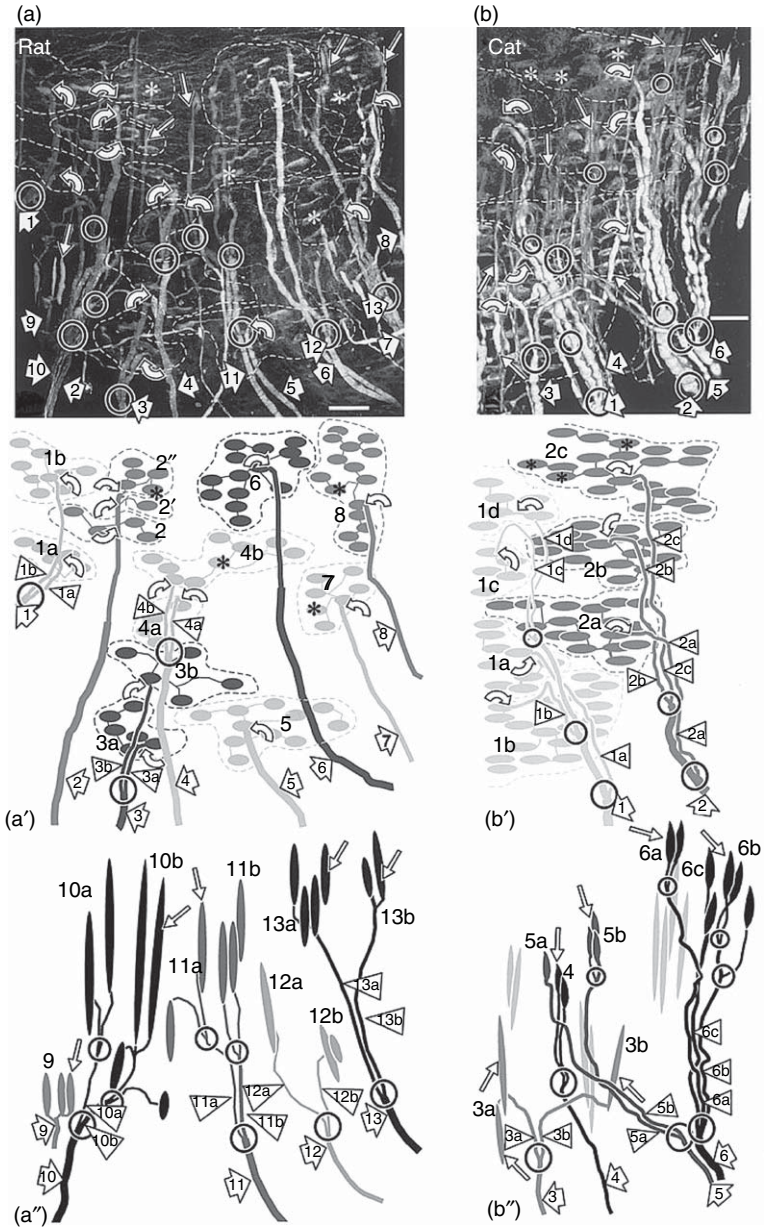

Figure 3 Comparison of the Merkel and lanceolate innervation at the level of the ring sinus in the rat (panels (a), (a′), and (a″)) and the cat (panels (b), (b′), and (b″)) as seen in confocal images of 100 μm-thick longitudinal sections that graze the surface of the vibrissa follicles. (a,b) Confocal images of anti-PGP9.5 labeling. Aβ fibers supplying Merkel endings (asterisks) and lanceolate endings (thin arrows) are indicated by the broad numbered arrows. Reconstructions of the Merkel arbors are shown in panels (a′) and (b′) and lanceolate arbors in panels (a″) and (b″). Curved arrows indicate where the distal ends of the Merkel Aβ fibers (broad numbered arrows) or their branches cross the basement membrane of the follicle to form terminal arbors enclosed by dashed lines. Larger circles indicate the first branch point. Successive branch points are indicated by successively smaller circles. Scale bars = 50 μm in (a) and 25 μm in (b). Reproduced from Ebara, S., Kumamoto, K., Matsuura, T., Mazurkiewicz, J. E., and Rice, F. L. 2002. Similarities and differences in the innervation of mystacial vibrissal follicle–sinus complexes in the rat and cat: a confocal microscopic study. J. Comp. Neurol. 449, 103–119.

6.01.2.1.3 Glabrous fingertip skin

In the glabrous fingertips of primates, the elevated fingerprints at the skin surface overlie especially thick primary epidermal ridges (Figures 2 and 5) (Cauna, N., 1954; Paré, M. *et al.*, 2002). The grooves between the fingerprints overlie relatively thinner

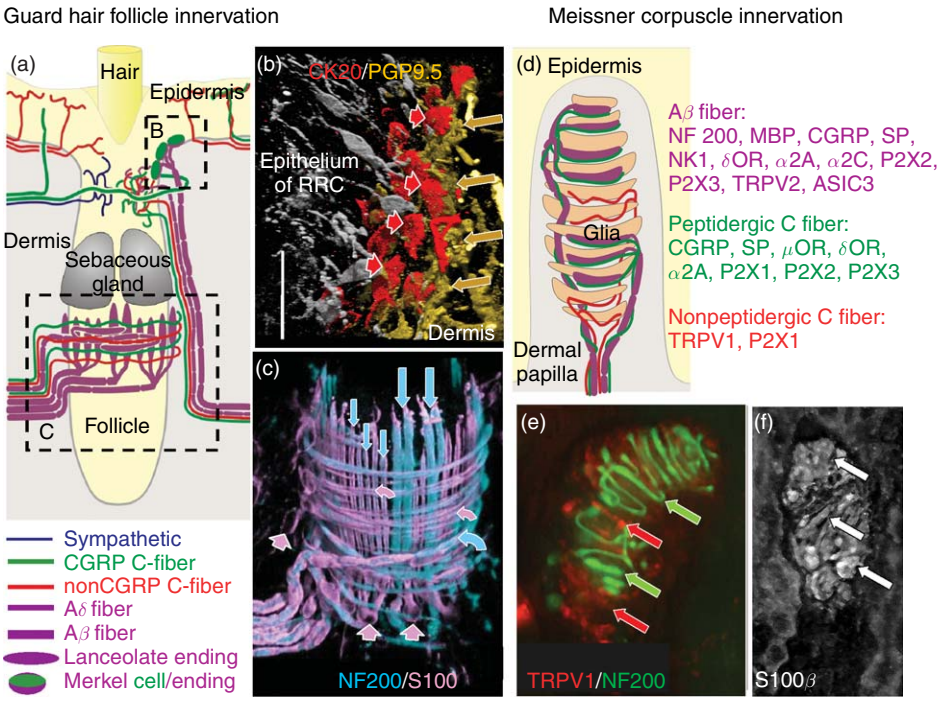

Figure 4 Schematic illustrations of mixed Aβ-fiber and C-fiber innervation to guard hair follicles (panels (a)–(c)) and Meissner corpuscles (panels (d)–(f)) accompanied by immunofluorescence images. (a) Enlargement from fur schematic in Figure 1 (see key in Figure 1). Broken line rectangles indicate sites of confocal images in panels (b) (Merkel rete ridge) and (c) (piloneural complex). (b) Confocal image of the epidermal rete ridge at the mouth of a cat hair follicle as seen in a 100 μm-thick section perpendicular to the skin surface. Reproduced with permission from Dr. Satomi Ebara. Merkel cells are labeled with anticytokeratin 20 (red) and Merkel endings with anti-PGP9.5 (gold). Each Merkel cell can be contacted by an ending from more than one Aβ fiber, and each Aβ fiber can form an ending on more than one Merkel cell. (c) Confocal image of a piloneural complex in a cat showing Aβ fiber endings (blue arrows) labeled with an antibody against 200 kDa neurofilament protein (blue) and terminal glial cells and their processes (pink arrows) labeled with anti-S100 (pink). Reproduced with permission from Dr. Satomi Ebara. Some Aβ fibers terminate as a palisade of longitudinally oriented lanceolate endings (narrow arrows). The fibers may terminate as one or two large endings (larger arrows) or multiple small endings (small arrows). Other Aβ fibers terminate as circumferentially oriented lanceolate endings (blue curved arrows). Terminal glial cells have multiple processes that line the lanceolate endings. Circumferentially oriented C-fiber terminals lack NF200 but are lined by terminal glial processes (pink curved arrows). Individual terminal glia can contact endings from more than one Aβ fiber. (d) Schematic of the innervation and immunolabeling characteristics of Meissner corpuscles in primate glabrous skin. Immunochemical properties of each type of innervation are shown to the right. Adapted from Paré, M., Elde, R., Mazurkiewicz, J. E., Smith, A. M., and Rice, F. L. 2001. The Meissner corpuscle revised: a multiafferented mechanoreceptor with nociceptor immunochemical properties. J. Neurosci. 21, 7236–7246. (e) Double immunolabeling reveals that Aβ fiber endings (green) terminate in strata alternating with TRPV1 expressing C fibers (red). (f) Terminal glia within the Meissner corpuscles express S100.

secondary epidermal ridges. Along the juncture between the parallel primary and secondary ridges, regularly and closely spaced dermal papillae protrude under epidermal invaginations and are slightly angled toward the elevated fingerprint (Bolanowski, S. J., Jr. and Pawson, L., 2003). Analogous to the nerve fascicles dedicated to each row of vibrissae, small nerves fascicles run in the dermis deep and parallel to the primary epidermal ridges. At regular intervals, smaller nerves ascend toward and branch to each side of the primary epidermal ridge (Figure 2). Thus, a functional unit analogous to a vibrissa follicle would be a skin sector parallel to the long axis of the primary ridge and spanning between the adjacent secondary ridges (Figure 2) (Cauna, N., 1956; Khalsa, P. S. *et al.*, 1998; LaMotte, R. H. *et al.*, 1998; Paré, M. *et al.*, 2002). However, unlike the spatial segregation of individual FSC, there is a gradually shifting overlap in the innervation along the primary ridge and to a lesser degree between adjacent primary ridges. As in the FSC, different types and combinations of Aβ, Aδ, and C fibers terminate at strategic locations in this microanatomical organization (Figure 2). Thus, the

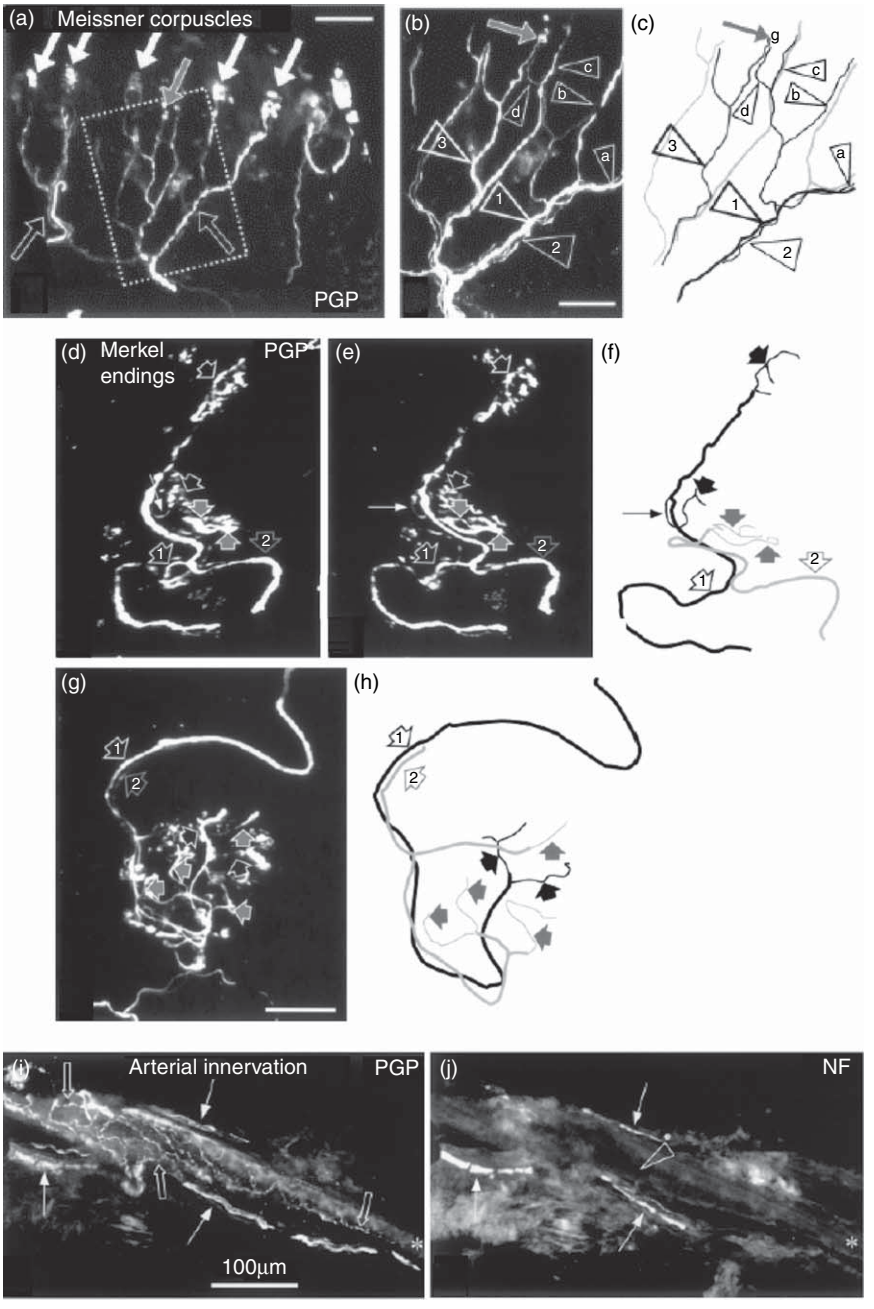

Figure 5 Immunofluorescence images and arbor reconstructions of Meissner, Merkel, and arterial innervation in monkey glabrous hand skin. (a–c) Confocal images and reconstructions of individual arbors in 100 μm-thick sections demonstrating that Meissner corpuscles can be innervated by more than one Aβ fiber, some of which innervate just one corpuscle, and others multiple corpuscles. (d–h) Confocal images and reconstructions of individual arbors in 100 μm-thick sections demonstrating that some Aβ fibers terminate on a discreet cluster of Merkel cells in one locale, whereas others give rise to *en passant* branches that terminate on Merkel cells in disparate locales. (I–j) Double-labeled immunofluorescence reveals that spindle-shaped structures typically interpreted as Ruffini corpuscles are arterial profiles that are innervated by a mix of neurofilament-negative C fibers and neurofilament-positive Aδ fibers. Reproduced from Paré, M., Smith, A. M., and Rice, F. L. 2002. Distribution and terminal arborizations of cutaneous mechanoreceptors in the glabrous finger pads of the monkey. J. Comp. Neurol. 445, 347–359.

fingertip anatomy and innervation are organized so that any contact with the fingerprints will generate differential patterns of activity across the entire ensemble of sensory endings enabling a detailed discrimination of the stimulus (Connor, C. E. and Johnson, K. O., 1992; Khalsa, P. S. *et al.*, 1998; LaMotte, R. H. *et al.*, 1998; Bensmaia, S. J. *et al.*, 2005; Leung, Y. Y. *et al.*, 2005).

6.01.2.1.4 Patterned vasculature

Importantly, the anatomical patterns of the vibrissa pads (Figure 1) and fingerprints (Figure 2) are paralleled by an equally elaborate vascular pattern (Fundin, B. T. *et al.*, 1997b; Paré, M. *et al.*, 2002). Although most vascular research has focused on the sympathetic innervation, vasculature also has an elaborate sensory innervation consisting of several different chemically distinct types of Aδ and C fibers. This sensory innervation preferentially terminates at strategic anatomical locations. Thus, the sensory innervation of the vasculature likely has a somatotopic organization that is as equally detailed as the rest of the skin. In the glabrous skin of primates and carnivores, one type of sensory ending – Pacinian corpuscles – supplied by Aβ fibers is commonly located in close affiliation with arteries in the dermis (Figures 2 and 7) (Rice, F. L. and Rasmusson, D. D., 2000; Paré, M. *et al.*, 2002). Pacinian corpuscles are typically regarded as tactile, low-threshold mechanoreceptors; however, both they and some of the Aδ and/or C fibers are likely assessing mechanically generated activity in the blood vessels, such as tension caused by blood pressure and vibrations caused by blood flow (Tuttle, R. S. and McCleary, M., 1975; Freeman, B. and Rowe, M., 1981). Conceivably, this innervation may function in a subconscious realm by monitoring the vasculature, as well as in the conscious realm when a vibratory stimulus is applied to the skin or the vasculature is distorted by mechanical displacement of the skin.

6.01.2.2 Morphological Variations Among Specific Types of Mechanoreceptive Endings

Both the FSC (as well as common hair follicles) and the glabrous skin contain the most common and widely distributed, morphologically distinct types of sensory endings (Iggo, A. and Andres, K. H., 1982). These endings had been detected by using reduced silver techniques in the late nineteenth century, long before physiological functional differences were detected. Variations of these types specific to other species and locations have been demonstrated. Although particular functions are commonly associated with particular types of endings, most of these associations are circumstantial despite numerous attempts to establish direct correlations.

6.01.2.2.1 Merkel endings

The tips of many Aβ fibers in both hairy and glabrous skin branch near the basement membrane of the epidermis. The branches penetrate the basement membrane to terminate as flattened disks juxtaposed to chemically distinct Merkel cells. Merkel cells are located next to the basement membrane among the deepest cells in the epidermis (lamina basalis) or the outermost cells of vibrissa follicles (outer root sheath) (Andres, K. H., 1966a; 1966b; Patrizi, G. and Munger, B. L., 1966; Iggo, A. and Muir, A. R., 1969). In the primate glabrous fingertips, Merkel cells and endings are located at the base of the primary epidermal ridges (Figures 2 and 5(d)–5(h)). In hairy skin, they are located at slightly thickened epidermal pads (Haarschibe), at the mouth of many hair follicles (Figure 4(a)), or at thickened epidermal spots (touch domes) between hairs. In the vibrissa FSC, SVN contain Aβ fibers that terminate on Merkel cells in the rete ridge collar (Figure 1), while DVN contain Aβ fibers that terminate on Merkel cells in the outer root sheath only at the level of the ring sinus (Figures 1 and 3(a′) and 3(b′)).

Physiologically, Merkel endings are purportedly SA, low-threshold mechanoreceptors that respond to skin compression or hair deflection for a fairly sustained duration (Iggo, A. and Muir, A. R., 1969; Gottschaldt, K. M. *et al.*, 1973). They are regarded as SA type I receptors that have a regularly spaced discharge rate, which increases in proportion to the intensity of the stimulus. Endings with this type of physiology typically have relatively small skin-surface receptive fields or are limited to a single vibrissa usually with a preferred direction of deflection. As such, Merkel endings have been implicated in high-resolution object discrimination (Connor, C. E. *et al.*, 1990; Friedman, R. M. *et al.*, 2002; Bensmaia, S. J. *et al.*, 2005).

Interestingly, detailed morphological assessments of individual Aβ fibers that terminate as Merkel endings have revealed a variety of terminal branch patterns (Rice, F. L. *et al.*, 1997; Ebara, S. *et al.*, 2002), which suggests that Merkel fibers might account for a variety of physiological response

properties (Gottschaldt, K. M. *et al.*, 1972; 1973; Gibson, J. M. and Welker, W. I., 1983a; 1983b). Both at the ring sinus level of the vibrissa follicles (Figure 3(a′)) and at the base of primary epidermal ridges in glabrous skin (Figures 5(d)–5(h)), some Aβ fibers terminate as several short branches, with each branch terminating directly on a single Merkel cell. The Merkel cells individually supplied by these short branches are located within a small, tightly circumscribed contiguous territory. This pattern of termination would be consistent with a regular discharge rate in response to a sustained stimulus. However, some Aβ fibers end with just a few relatively long branches that each contact several cells in succession over an extended territory. Moreover, in both types of terminal patterns, some Aβ fibers branch only at their tip whereas others can have several branches that arise *en passant* from different nodes along the length of the fiber (Figures 3(b′) and 5(g)–5(h)). In the latter case, the Merkel cells innervated by each *en passant* branch in FSC are located in adjacent territories along the length of the follicle. Both the terminations by branches on several Merkel cells in succession as well as the *en passant* branching patterns would indicate that such endings could generate complex patterns of activity that would be more consistent with irregular discharge rates classified as SA type II fibers.

Interesting differences also occur between Merkel endings that terminate along the length of the follicles in FSCs and those that terminate at the mouth of vibrissa and other hair follicles. Among the former, the Merkel disks contact the Merkel cells on the surface facing away from the basement membrane, whereas the latter contact the surface facing toward the basement membrane (Andres, K. H., 1966a; Patrizi, G. and Munger, B. L., 1966; Iggo, A. and Muir, A. R., 1969). The functional significance of these different arrangements is unknown. Among terminations along the length of the follicles, each Merkel cell is contacted by a single disk from a single Aβ fiber, albeit that fiber contacts several Merkel cells (Figures 3(a′) and 3(b′)) (Ebara, S. *et al.*, 2002). Moreover, a branch from one Aβ fiber never appears to cross over a branch from another fiber. Thus, each of these Aβ fibers innervates multiple Merkel cells located in segregated, nonoverlapping territories.

In contrast, single Merkel cells located in the epidermis at the mouth of follicles and epidermal touch domes have been shown to be innervated by more than one disk arising from more than one Aβ fiber (Figure 4(b)) (Ebara, S., personal communication). Additionally, branches from one fiber can cross over a branch from another fiber (Rice, F. L. *et al.*, 1997). Thus, the Merkel innervation at the mouth of hairs appears to be an overlapping system. Importantly, the activation of Merkel endings by mechanical stimuli was once thought to be limited to mechanisms intrinsic to the endings. However, recent data indicates that Merkel cells may be directly involved in initiating or mediating the transduction of mechanical sensory stimuli (Cahusac, P. M. *et al.*, 2005; Cahusac, P. M. and Senok, S. S., 2006; Lucarz, A. and Brand, G., 2007). Therefore, the anatomical arrangement of the Merkel innervation at the mouth of hairs may enable peripheral sensory stimuli integration at the level of the initial sensory transduction.

6.01.2.2.2 Lanceolate endings and Meissner corpuscles

Many Aβ fibers terminate as either lanceolate endings associated with vibrissae and guard hair follicles (Figures 1, 3, 4(a) and 4(c), and 6) (Fundin, B. T. *et al.*, 1997a; Rice, F. L. *et al.*, 1997) or Meissner corpuscles in the dermal papillae of glabrous skin (Figures 2, 4(d)–4(f), and 5(a)–5(c)) (Paré, M. *et al.*, 2001; 2002).

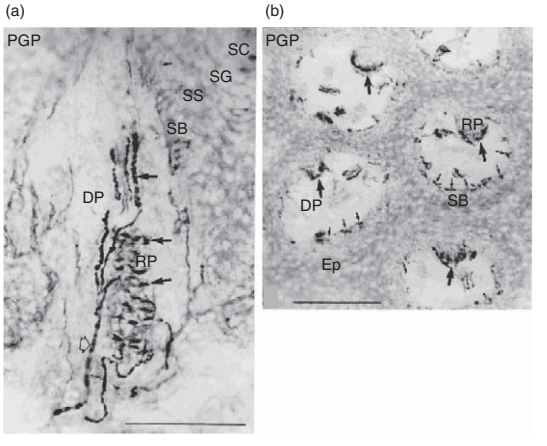

Figure 6 Merkel innervation in dermal papillae (DP) underlying epidermal domes in the glabrous digital skin of the raccoon. Panel (a) is cut perpendicular to the skin surface and panel (b) parallel to the surface. Merkel innervation (larger arrows) that is oriented and looks like a Meissner corpuscle as seen in panel (a) actually terminate in epidermal rete pegs. (RP) that protrude into the dermal papillae from the epidermis. Reproduced from Rice, F. L. and Rasmusson, D. D., 2000. Innervation of the digit on the forepaw of the raccoon. J.Comp. Neurol. 417, 467-490.

Lanceolate and Meissner Aβ fibers consistently have a slightly smaller caliber than those that terminate as Merkel endings and should have a slightly slower conduction velocity. Even though the endings are utterly different morphologically, they are being discussed together because they share many common properties (Figure 4). Conceivably, both are derivatives of the same type of sensory neurons whose endings only differ because of the locations that are available to innervate in the different types of skin. Both types of endings terminate in the dermis but are closely affiliated with the basement membrane of the epidermis or hair follicles, which are epidermal derivatives. Both types of endings are also affiliated with terminal glial cells, which are Schwann cell derivatives (Cauna, N. and Ross, L. L., 1960; Andres, K. H., 1966b; Patrizi, G. and Munger, B. L., 1966; Takahashi-Iwanaga, H. and Shimoda, H., 2003). Electrophysiological studies indicate that both types of endings are likely RA, low-threshold mechanoreceptors (Gottschaldt, K. M. *et al.*, 1973; Connor, C. E. and Johnson, K. O., 1992).

6.01.2.2.2.(i) Lanceolate endings Lanceolate endings are elongated flattened blade-like structures that are typically oriented parallel to the long axis of the vibrissa or hair follicles (Figures 1, 3(a″), and 3(b″), and 4(a)–4(c)). An Aβ fiber may terminate as a single ending or multiple endings arrayed like the tines of a fork. As seen in cross section by electron microscopy, the flat surface of each ending is lined by a terminal glial lamella, and the sharp edges have a fringe of cytoplasmic blebs lined with the basement membrane (Andres, K. H., 1966b; Patrizi, G. and Munger, B. L., 1966). The endings are slightly angled so that the blebs of one edge are embedded in densely packed collagen bundles in the basement membrane while the other edge is embedded in more loosely packed collagen bundles in the surrounding dermis. It has been assumed that these embedded edges would be subject to shear forces caused by hair deflection and are the likely sites of mechanically driven depolarization.

As seen in association with guard hair follicles, numerous lanceolate endings are arrayed side-by-side, forming a palisade around the perimeter of the follicle at a level just below the sebaceous gland (Figures 4(a) and 4(c)) (Biemesderfer, D. *et al.*, 1978; Rice, F. L. *et al.*, 1997). Smaller hair follicles can sometimes have just a few endings. In most cases, the palisade is formed by lanceolate endings supplied by multiple Aβ fibers that include a mix of those forming several relatively short endings and those with only one or two slightly longer endings. The endings from each fiber terminate adjacent to each other so that each fiber supplies a unique sector around the perimeter of the follicle. Serial reconstructions in thick sections indicate that some of the Aβ fibers may terminate exclusively on one follicle while others may branch fairly proximally and innervate multiple follicles (Mosconi, T. M. and Rice, F. L., 1991). Thus, a single follicle may activate some Aβ fibers exclusively, but activate other fibers in collaboration with other follicles. This arrangement may account for the fact that some Aβ fibers have been detected that respond transiently to single hair deflections with a preferred orientation, while others can be transiently activated by multiple hair deflections with little or no directional preference (Brown, A. G. and Iggo, A., 1967). Importantly, this arrangement indicates that hair follicles can be part of a punctate, single follicle system and a relatively diffuse, overlapping multifollicle system.

The palisades of lanceolate endings are actually part of a more extensive combination of endings referred to as the piloneural complex (Figures 5(a) and 5(c)). Slightly centrifugal to the palisades of lanceolate endings are usually circumferentially oriented free nerve endings (FNE) supplied by at least two different types of C fibers: a peptidergic type containing the neuropeptides, calcitonin gene-related peptide (CGRP) and substance P (SP), and a non-peptidergic type, which lacks these neuropeptides (Fundin, B. T. *et al.*, 1997a; Rice, F. L. *et al.*, 1997). In addition, some smaller-caliber Aβ fibers can each contribute multiple circumferentially oriented lanceolate-like endings that appear to arise *en passant* along the trajectory of the axon (Mosconi, T. M. *et al.*, 1993; Rice, F. L. *et al.*, 1997). The function of the C fiber innervation at this location is unknown, but the *en passant* lanceolate ending presumably would be a low-threshold mechanoreceptor that would lack any directional preference.

The longitudinally oriented lanceolate endings in the FSC are supplied by DVN and are much larger than those innervating guard hairs (Figures 3(a″) and 3(b″)). They are located in the mesenchymal sheath at the ring sinus level of FSC, at about the same level of the Merkel endings. Some of these Aβ fibers also terminate as a few longer branches, while others terminate as many shorter branches, but each fiber appears only to supply endings to one FSC (Arvidsson, J. and Rice, F. L., 1991). The circumferentially oriented components of piloneural complexes around guard hair follicles appear to be

displaced to the level of the ICB in FSC and are supplied by SVN.

6.01.2.2.2.(ii) Meissner corpuscles Like the piloneural complexes, Meissner corpuscles are supplied by multiple Aβ fibers, as well as at least two types of C fibers (Figures 4(d)–4(f)) (Cauna, N., 1956; Hilliges, M. *et al.*, 1996; Paré, M. *et al.*, 2001; 2002). The Aβ fibers terminate as stacks of multiple disks alternating with terminal Schwann cells. Within each corpuscle, zones of terminal disks from the Aβ fibers alternate with intervening zones supplied by nonpeptidergic C fibers. A second set of peptidergic C fibers (containing CGRP and SP) are intimately associated with the Aβ fiber terminals. The potential functional significance of this arrangement is discussed below. These endings have been implicated in optimally responding to low-frequency flutter vibration such as that caused by the mechanical friction stimulus generated when skin is rubbed against an object (Mountcastle, V. B. *et al.*, 1967; Connor, C. E. *et al.*, 1990; Friedman, R. M. *et al.*, 2002; Bensmaia, S. J. *et al.*, 2005). This is consistent with the fact that in fingertips they are located in closely spaced dermal papillae that protrude under the epidermis on each side of the primary epidermal ridges that underlie the raised fingerprint. This anatomical arrangement likely enhances the mechanical friction stimuli associated with contacting a surface. The corpuscles are purportedly anchored to the basement membrane of the enveloping epidermis by thin connective tissue strands, heightening their ability to detect even the slightest mechanical deformations of the skin surface (Cauna, N. and Ross, L. L., 1960; Takahashi-Iwanaga, H. and Shimoda, H., 2003).

Given their location on each side of the fingerprint, Meissners corpuscle are presumably impacted particularly by mechanical force transverse to the fingerprint, consistent with the fact that Meissner corpuscle activation often has a preferred directional component (Friedman, R. M. *et al.*, 2002). Because they are best activated by a moving stimulus (or movement of the skin over a static object) their individual resolving power is relatively poor compared to that of Merkel endings. As is the case with the lanceolate endings in the piloneural complexes, some Aβ fibers appear to innervate only one Meissner corpuscle, while the same corpuscle is also supplied by other fibers that innervate multiple corpuscles (Figures 5(a)–5(c)) (Paré, M. *et al.*, 2002). Thus, each corpuscle appears to participate in both punctate, nonoverlapping receptive systems and more diffuse, overlapping receptive systems.

6.01.2.2.3 Pacinian and Golgi–Mazzoni corpuscles

Particularly large-caliber Aβ fibers terminate within large, onion-like corpuscles composed of multiple, fairly loose concentric layers of Schwann cell lamellae enclosed within a dense outer capsule. They are located in the dermis well below the epidermis in both the hairy and the glabrous digital skin of primates and carnivores. In most cases, referred to as Pacinian corpuscles (Figures 7(b), 7(d), and 7(f)), the Aβ fiber terminates in the core as a single large-caliber blunt ending with a knob at the tip (Winkelmann, R. K. and Osment, L. S., 1956; Rice, F. L. and Rasmusson, D. D., 2000; Paré, M. *et al.*, 2002). In other cases, referred

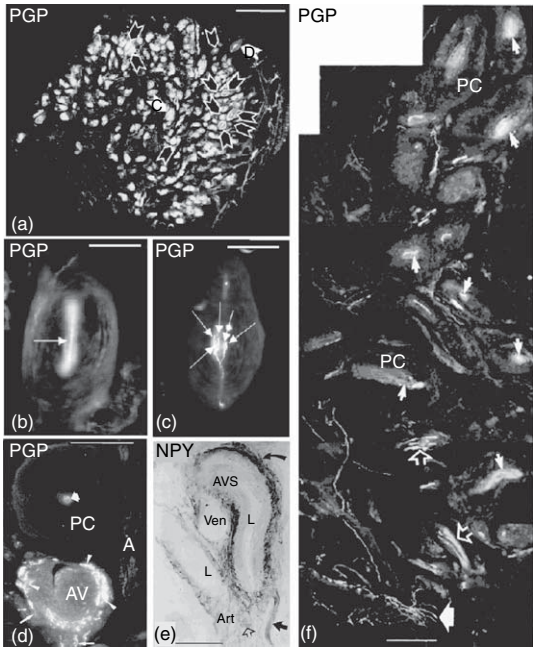

Figure 7 Immunofluorescence images of Pacinian and Golgi–Mazzoni corpuscles. (a) Monkey glabrous fingertip skin, (b) Pacinian, and (c) Golgi–Mazzoni corpuscles are located deep in the dermis (white chevrons in a) among sweat glands (black chevrons). (d,e) As seen here in the raccoon glabrous skin, Pacinian corpuscles are often closely affiliated with branches of digital arteries and arteriovenous shunts. The arteries and shunts have extensive calcitonin gene-related peptide (CGRP)-positive sensory innervation (d) and neuropeptide Y (NPY)-positive sympathetic innervation (e). (f) Numerous Pacinian corpuscles are packed against the base of the claws in the raccoon. Reproduced from Paré M. *et al.* (2002) and Rice F. L. and Rasmusson D. D. (2001).

to as Golgi–Mazzoni corpuscles, the axon terminates as several thin elongated parallel processes (Figure 7(c)). In both circumstances, the innermost Schwann cell next to the ending is anatomically and immunochemically distinct (Pawson, L. *et al.*, 2000). Experimentally, Pacinian corpuscles have been isolated from intestinal mesenteries and have been shown electrophysiologically to be low-threshold RA endings that entrain to high-frequency vibrations (Bolanowski, S. J., Jr., 1984; Bolanowski, S. J., Jr. and Zwislocki, J. J., 1984a; 1984b; Vallbo, A. B. and Johansson, R. S., 1984; Connor, C. E. and Johnson, K. O., 1992; Guclu, B. *et al.*, 2006). Whether the Golgi–Mazzoni corpuscles have a substantially different physiology is unknown. The entrainment of the Pacinian corpuscles begins at the upper end of the lower frequencies where purported Meissner corpuscles are no longer capable of maintaining their entrainments (Bensmaia, S. J. *et al.*, 2005; Leung, Y. Y. *et al.*, 2005). Thus, these two sets of endings complement each other to span a continuous range of low- to high-frequency vibration detection (Mountcastle, V. B. *et al.*, 1967; LaMotte, R. H. and Mountcastle, V. B., 1975).

Although they have a relatively high density in the fingertips, Pacinian corpuscles are very sparse compared to other endings. Their deep disposition in the dermis is consistent with the fact that they have very large receptive fields and no directional sensitivity (Connor, C. E. and Johnson, K. O., 1992). Interestingly, they are invariably in close juxtaposition to arteries (Figure 7(d)), especially arteriovenous shunts suggesting that their vibratory-detecting RA properties may respond to changes in blood flow, which would likely generate different frequencies of vibration in the arterial walls (Tuttle, R. S. and McCleary, M., 1975; Freeman, B. and Rowe, M., 1981). Pacinian corpuscles are also differentially concentrated around joints and the attachments of claws to distal phalanges (Rice, F. L. and Rasmusson, D. D., 2000) (Figure 7(f)). Both locations involve rigid tissues that would vibrate during joint movement or the scrapping of claws against objects.

Although the capsule lamellae were thought to transmit physical vibratory displacements to the sensory ending, recent intricate investigations using interference optics failed to find transmitted displacement even after indentations of the capsule well in excess of physiological relevance (Pawson, L. and Bolanowski, S. J., Jr., 2002; Guclu, B. *et al.*, 2006). This is consistent with the observation that barely detectable vibratory displacements of the skin surface can elicit activity within the Pacinian corpuscles deep in the dermis. However, the integrity of the capsule has been shown to be essential for their vibration-detecting properties, suggesting that the corpuscles are akin to a hydraulic system where incompressible fluid between the lamellae may be the force-transmitting medium, or the capsule lamellae participate in an electro chemical transducing mechanism.

6.01.2.2.4 Ruffini corpuscles

Spindle-shaped Ruffini corpuscles have long been regarded as one of the major types of innervation in the skin and have been thought to account for SA type II fibers responding particularly to stretch of the skin. Although such corpuscles have been definitively identified in the hairy paw skin of cats, both by electron microscopy (Chambers, M. R. *et al.*, 1972) and recent immunochemical techniques (Kumamoto, K. and Ebara, S., personal communication), no definitive Ruffini corpuscles have been demonstrated in recent investigations of the glabrous digital skin of raccoons, monkeys, or humans where SA type II fibers have been detected physiologically (Rice, F. L. and Rasmusson, D. D., 2000; Paré, M. *et al.*, 2002; 2003). As noted earlier, the identified SA type II fibers may actually be innervating diffuse patterns of Merkel cells. These recent studies have demonstrated that the spindle-shaped structures, interpreted as Ruffini corpuscles based on earlier reduced silver studies, are likely well-innervated segments of blood vessels (Figures 5(i) and 5(j)). Blood vessels have been shown to receive not only sympathetic innervation but also at least two types of peptidergic C fibers (Figure 7(e)) and at least one type of Aδ fiber. Conceivably these Aδ fibers may be mechanoreceptors that detect the tension in the blood vessel walls caused by blood pressure. As such, stretch of the skin might also affect the blood vessels and additionally activate these Aδ fiber endings.

6.01.2.2.5 Free nerve endings

Neither Aδ nor C fibers have been shown to terminate as endings with distinct anatomical specializations (Kruger, L. *et al.*, 1981; Mosconi, T. M. *et al.*, 1993; Kruger, L., 1996) nor have their terminations been regarded as being associated with specialized non-neuronal cells. Instead they all appear to terminate as more or less branched, nondescript endings referred to as FNE. Prior to the advent of more recent immunochemical techniques, the Aδ

and C fibers were rarely detected with the best available techniques, which were variants of reduced silver staining. As such, prior to the late 1980s, Aδ and C fibers were primarily thought to terminate diffusely in the dermis, although a few EM studies had detected them at least as far as the epidermal basement membrane but rarely into the epidermis. Thus, the epidermis was long thought to be mostly devoid of innervation. However, later immunochemical studies with antibodies against SP and CGRP revealed many terminals affiliated not only with the dermal blood vessels but also in the epidermis (Figure 8(a)) (Kruger, L., 1988; Kruger, L. *et al.*, 1989). Following the development of antibodies against a cytoplasmic enzyme, protein–gene product 9.5 (PGP9.5), which is especially concentrated in neuronal cytoplasm, far more nerve endings were revealed in the epidermis (Wang, L. *et al.*, 1990; Kennedy, W. R. and Wendelschafer-Crabb, G., 1993; Rice, F. L. *et al.*, 1993; Rice, F. L. and Rasmusson, D. D., 2000; Paré, M. *et al.*, 2007). It has now been well established that Aδ and C fibers terminate as FNE most extensively in the epidermis and in the tunica adventitia of blood vessels. These fibers also terminate in sweat glands and, as mentioned above, at many sites around hair and vibrissa follicles, as well as in Meissner corpuscles (Figures 1 and 2).

Most Aδ and C fibers are thought to mediate high-threshold mechanoreception, thermoreception, chemoreception, and nociception (Burgess, P. R. and Perl, E. R., 1967; Bessou, P. and Perl, E. R., 1969; Bessou, P. *et al.*, 1971; Koerber, H. R. and Mandell, L. M., 1992; Koerber, H. R. and Woodbury, C. J., 2002). At least some of these fibers, especially terminating in proximal hairy skin, are low-threshold mechanoreceptors (Brown, A. G. and Iggo, A., 1967; Koerber, H. R. and Woodbury, C. J., 2002). Aδ fibers are reportedly the source of D-hair low-threshold mechanoreceptors that are exquisitely sensitive to light contact with multiple hairs without a specific orientation (Koltzenburg, M. *et al.*, 1997). Recent evidence also indicates that low-threshold mechanoreceptors may be among C fiber innervation at the neck of hair follicles (Liu, Q., *et al.*, 2007). Thin-fiber low-threshold mechanoreceptors may also be

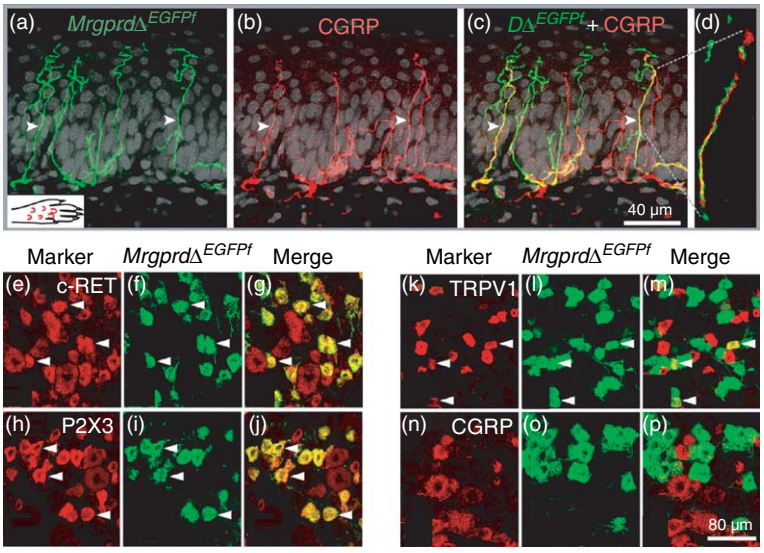

Figure 8 Mrgprd is expressed exclusively in C fibers that terminate in the epidermis and almost entirely lack calcitonin gene-related peptide (CGRP). (a–d) Green fluorescent protein expression driven from the gene locus for Mrgprd reveals that neurons expressing this G protein-coupled receptor (GPCR) supply C-fiber innervation that terminates exclusively in the epidermis and ascends through deep to superficial levels. Double labeling with anti-CGRP reveals that nearly all of the Mrgprd endings lack CGRP. CGRP-positive endings are generally located in the deep half of the epidermis and can be occasionally closely affiliated with a Mrgprd-positive ending (panel d). (e–p) Other immunochemical characteristics of Mrgprd-positive neurons in dorsal root ganglia. Many, but not all Mrgprd neurons express receptors (c-Ret) for the family of glial-derived neurotropic factors and vice versa, as well as P_2X_3. Nearly all Mrgprd neurons are TRPV1 or CGRP negative, are positive but a small proportion are positive. (Reproduced from Zylka, M.J., Rice, F.L., Anderson, D.J. 2005. Topographically distinct epidermal nociceptive circuits revealed by axonal tracers targeted to Mrgprd. Neuron 45, 17–25..

terminating at cutaneous arteries and arteriovenous shunts (Paré, M. *et al.*, 2002; Light, A. R. and Perl, E. R., 2003; Paré, M. *et al.*, 2003).

6.01.2.3 Interspecies Differences in Vibrissa Follicle–Sinus Complexes and Glabrous Fingertip Innervation

6.01.2.3.1 Rat and cat follicle–sinus complex

Although most mammalian quadrupeds have elaborate arrays of orofacial tactile vibrissae that serve the same fundamental purpose, different species use them in different environments that have different requirements (Ebara, S. *et al.*, 2002; Funfschilling, U. *et al.*, 2004; Marshall, C. D. *et al.*, 2006). For example, many species use their vibrissae in terrestrial environments, whereas others use them in aquatic environments. Although the vibrissae and their follicles differ in size, usually in proportion to body size, the basic elaborate structure of vibrissa FSC is similar among most species, including the fundamental types and locations of the innervation. In addition to Merkel and lanceolate endings described above, the FSC also have other unique types of Aβ fiber endings. These include club endings located in the mesenchymal sheath at the attachment of the ringwulst, and reticular and spiny endings located in the mesenchymal sheath at the level of the cavernous sinus. Various hypotheses have been proposed (some discussed above) regarding the function of the specific types of Aβ fiber endings; however, none have been proven (Zucker, E. and Welker, W. I., 1969; Gottschaldt, K. M. *et al.*, 1972; 1973; Lichtenstein, S. H. *et al.*, 1990; Rice, F. L. *et al.*, 1997; Szwed, M. *et al.*, 2003).

Although the basic structure and innervation are mostly the same across species, numerous interspecies differences exist in the proportions and ending branch patterns, indicating that these slight anatomical variations may be uniquely suited for the functional demands of the particular species. For example, in comparing the FSC of rats and cats, only the innervation that terminates as club endings appears to be identical, all of the other innervation terminations are different. Particularly, the ICB is densely innervated in rat FSC and includes a mix of C fiber endings and circumferentially oriented lanceolate endings supplied by Aβ fibers, whereas in the cat, the ICB is sparsely innervated only by C fibers. Merkel-related Aβ fibers at the level of the ring sinus in the rat primarily branch only at their tips to supply a local cluster of Merkel cells, whereas those in the cat branch *en passant* to supply several large contiguous territories of Merkel cells (Figures 3(a′) and 3(b′)). Presumably these differences are due to the fact that rats explore their environment by rapidly whisking their vibrissae to locate static objects (such as grain). In these animals, the ICB is located at the fulcrum where the entire FSC are rapidly rocked back and forth by the action of papillary muscles. The small terminal arbors of the Merkel endings may provide relatively high resolution for object discrimination. In contrast, cats explore their environment by protracting their vibrissae to a relatively fixed position in order to detect moving objects (such as mice). Therefore, they may lack the need for detecting rapid movement of their vibrissae, and their Merkel endings may be designed to detect more dynamic positional properties than object discrimination. As such, rats and cats presumably would have quite different vibrissal tactile perceptions.

6.01.2.3.2 Raccoon glabrous fingertips

Although raccoons have excellent tactile dexterity with their hands, the organization of their glabrous skin and its innervation is quite different than that in monkeys and humans (Figures 2 and 4–6). Instead of having fingerprints, raccoons have small, densely packed epidermal domes that each overlie a cone-shaped dermal papilla. Both raccoons and primates have Merkel innervation at the deepest epidermal locations, i.e., at the base of the epidermal domes in raccoons and at the base of the primary epidermal ridges in primates. Both species also have Pacinian corpuscles deep in the dermis. However, raccoons completely lack Meissner corpuscles. Instead, they have a second type of Merkel configuration where Aβ fibers innervate Merkel cells located in epidermal rete pegs that bulge into the sides of the dermal papillae. Moreover, raccoons also have small corpuscular endings located at the base of the epidermal domes. Although raccoons have Aβ fibers with SA and RA characteristics like those in primates, it is not known whether the unique Merkel endings on the rete pegs have SA characteristics like those typically attributed to Merkel endings in other locations, or if they have RA characteristics like those of Meissner corpuscles. Taken altogether, these examples demonstrate that different species (e.g., cat, rat, raccoon, primate) fulfill their tactile perception needs through slightly different anatomical arrangements of similar structures and innervation.

6.01.3 Molecular Basis of Tactile Sensation

The activation of sensory endings is dependent upon where they terminate, their morphology, and their chemistry. As well, tactile stimulus specificity is dependent upon the mechanisms that generate the sensory ending depolarization. Considerable research has been devoted to determining the molecular mechanisms involved in the transduction of physical stimuli into primary sensory neuron action potentials. For example, in the visual and olfactory senses, many of these transduction mechanisms have been determined, and the molecular mechanisms involved in initiating the generation of cutaneous tactile perceptions (thermal, mechanical, and chemical) are slowly being unraveled. However, particularly for mechanosensory (touch) transduction, the mechanisms are still largely unknown, although they likely involve the direct gating of ion channels (Sukharev, S. and Corey, D. P., 2004). Genetic studies in *Drosophila* and *Caenorhabditis elegans* have led to the identification of mammalian protein families that contribute directly, or indirectly, to the transduction of tactile stimulus energy to primary afferent fibers. Identified signaling protein families implicated in sensory stimuli transduction to primary afferents include the transient receptor potential (TRP) channels, the brain sodium channels/acid-sensing ion channels (BNaC/ASIC), purinergic (P_2Y, P_2X) receptors, and several others (Gillespie, P. G. and Walker, R. G., 2001; Sukharev, S. and Corey, D. P., 2004; Lumpkin, E. A. and Caterina, M. J., 2007).

6.01.3.1 Transient Receptor Potential Superfamily

The TRP ion channel superfamily encompasses a large group of cationic channels with varied structure, physiological regulation, and function that have been implicated in thermal, mechanical, and chemical sensory stimuli transduction (Gillespie, P. G. and Walker, R. G., 2001; Lumpkin, E. A. and Caterina, M. J., 2007). In particular, the TRPV1 (vanilloid family-1) channel has been implicated in thermal (hot; >43 °C) and chemical (e.g., pH, capsaicin) responsiveness, TRPM8 (melastatin-8) in thermal (cold; <25 °C) and chemical (e.g., menthol) responsiveness, and the TRPA1 (ankyrin family-1) has been implicated in thermal (noxious cold), chemical (e.g., wasabi, garlic), and mechanical (hair cells) responsiveness. TRPC1 (canonical-1) has been shown to be a membrane-stretch-activated channel, which is expressed in primary sensory neurons, and could likely mediate mechanical displacement forces impinging upon the neuronal membrane (Gillespie, P. G. and Walker, R. G., 2001; Sukharev, S. and Corey, D. P., 2004; Lin, S. Y. and Corey, D. P., 2005; Hardie, R. C., 2007; Lumpkin, E. A. and Caterina, M. J., 2007).

6.01.3.2 Degenerin/Epithelial Sodium Channel Superfamily

The BNaC/ASICs are members of the degenerin (DEG)/epithelial sodium channel (ENaC) superfamily of identified amiloride-sensitive, nonvoltage-regulated Na^+ channels with specific pore forming and transmembrane spanning region structure (Gillespie, P. G. and Walker, R. G., 2001; Sukharev, S. and Corey, D. P., 2004; Lumpkin, E. A. and Caterina, M. J., 2007). DEGs were identified in the *C. elegans* and were shown to be part of putative mechanosensitive channels in touch-responsive neurons. The structurally related mammalian ENaCs are responsible for sodium and fluid reabsorption across membranes of the kidney, lung, and colon, and have also been found in baroreceptors and somatic touch receptors where they are implicated in mechanosensation (Gillespie, P. G. and Walker, R. G., 2001; Sukharev, S. and Corey, D. P., 2004; Lumpkin, E. A. and Caterina, M. J., 2007). Specifically, the β and γ ENaC subunits, as well as the related protein, stomatin, have all been shown to be expressed within the lanceolate endings of the FSC, and β and γ ENaC subunits have been shown in Merkel and Meissner structures in rat footpad (Drummond, H. A. *et al.*, 2000; Fricke, B. *et al.*, 2000; Price, M. P. *et al.*, 2000; Garcia-Anoveros, J. *et al.*, 2001). By expression cloning, additional vertebrate homologs were discovered and initial screens detected expression primarily in mammalian brain (BNaC). Subsequent investigation demonstrated that BNaCs were sensitive to extracellular proton concentration (pH), opening under acidic conditions, thereby giving rise to the current naming scheme of ASIC (Gillespie, P. G. and Walker, R. G., 2001; Sukharev, S. and Corey, D. P., 2004; Lumpkin, E. A. and Caterina, M. J., 2007). As tissue acidosis is a hallmark of damage, several ASIC have been identified in small-caliber primary sensory neurons, presumptive Aδ and C fiber polymodal nociceptors, as well as Aδ and C fiber

innervation to dermal vasculature (Garcia-Anoveros, J. *et al.*, 2001; Molliver, D. C. *et al.*, 2005) where these channels may function in chemosensation. As well, BNaC1α (ASIC2a) is expressed within large-caliber Aβ-fiber mechanosensitive sensory endings and has been implicated as an essential molecule mediating mechanical stimulus transduction (Price, M. P. *et al.*, 2000; Garcia-Anoveros, J. *et al.*, 2001). Additionally, stomatin, an integral membrane protein shown to have high sequence homology with an adapter protein (MEC-2) identified as an essential part of the *C. elegans* mechanosensitive touch receptor, was shown to be expressed by mammalian sensory neurons (Mannsfeldt, A. G. *et al.*, 1999). Recently, it was demonstrated that null mutation of a stomatin-like protein (SLP3) eliminated mechanoreceptive responses in a substantial proportion of all types of low-threshold mechanoreceptive neurons, but left the remaining proportions functionally intact (Wetzel, C. *et al.*, 2007). This suggests that there may be subsets of functional mechanoreceptors that utilize additional molecular mechanisms. Additionally, SLP3 was shown to directly interact with ASIC2a, ASIC2b, and ASIC3 (Wetzel, C. *et al.*, 2007), further implying that these ion channels and adapter protein may function as part of a mammalian mechanoreceptor.

6.01.3.3 Purinergic Receptors

ATP is recognized as a potent co-neurotransmitter and cell-signaling intermediate, and mediates a myriad of physiological effects through two distinct receptor families (Lazarowski, E. R. *et al.*, 2003; Cockayne, D. A. *et al.*, 2005). The ATP-binding purinergic family of receptors fall into two broad classes: (1) the P_2Y family are G protein-coupled receptors (GPCRs) and generate second-messenger signaling molecules and lipid intermediates to modulate cell physiology and (2) the P_2X receptors are ion channels and directly affect cell physiology. A very wide array of signaling pathways active in the nervous, immune, endocrine, cardiovasculature, gastrointestinal, musculoskeletal, and reproductive systems utilize ATP, related ligands, and the purinergic receptor family to mediate homeostasis and response (Cockayne, D. A. *et al.*, 2005). Mechanosensitive receptive systems (hearing, vestibular sense, and touch) are largely thought to depend upon membrane-bound ion channels that are responsive to membrane deformation from mechanical forces (Sukharev, S. and Corey, D. P., 2004). In the cutaneous sensory system, expression of P_2X_2, P_2X_3, and $P_2X_{2/3}$ receptors has been found in small-caliber primary sensory neurons. These have been shown to be regulators of mechanical hyperalgesia following nerve injury, implying a role in mechanical stimulus transduction, at least following injury (Lazarowski, E. R. *et al.*, 2003; Cockayne, D. A. *et al.*, 2005). Additionally, the P_2Y_1 GPCR has been proposed to mediate mechanotransduction of light, non-noxious touch and has been shown to be expressed in large-caliber primary sensory neurons (Nakamura, F. and Strittmatter, S. M., 1996; Price, M. P. *et al.*, 2000). These results, taken with the ample literature demonstrating varied release of ATP following membrane distortions, implies a direct role of purinergic receptors (ionic and/or metabotropic) in mechanical stimulus transduction to primary afferent sensory neurons.

6.01.3.4 Ca^{2+} Ion Channels

The D-hair mechanosensitive receptor has been described as having the lowest mechanical threshold and the most dynamic sensitivity of all mechanoreceptors. Electrophysiological characterization and immunostaining of hairy skin have determined that these receptors are an Aδ medium-sized fiber, which appear to terminate as circumferentially oriented free endings around body hair follicles. Recently, a T-type Ca^{2+} ion channel, $Ca_v3.2$, was identified as a specific protein lost in $NT4^{-/-}$ mice, which do not develop the D-hair receptors. The precise location of expression and function of this channel, or the related $Ca_v3.3$, in mediating the D-hair response are currently unknown. Importantly though, these data indicate that a calcium-specific ion channel may also play a role in mechanotransduction (Shin, J. B. *et al.*, 2003).

6.01.3.5 Other Molecules

Several additional members of varied protein families are expressed within primary sensory neurons and are known to mediate or modulate important sensory functions, particularly aspects of nociception and the affective component pain. Nociception (the physiological transduction of noxious stimuli) and pain perception (the affective unpleasantness of nociceptive activation) are now known to be modulated by peripherally (as well as

centrally) acting opioids, cannabinoids, and endothelins, among others (Sawynok, J., 2003; Roosterman, D. *et al.*, 2006). For example, specific opioid receptors are found on primary sensory endings, endothelin-1 receptor A (ET-A) receptors are found in peripheral axons, and cannabinoid receptor-1 (CB-1) receptors are expressed in dorsal root ganglion (DRG) neurons (Pomonis, J. D. *et al.*, 2001; Mitrirattanakul, S. *et al.*, 2006; Roosterman, D. *et al.*, 2006). Activation of these receptors by peripherally acting ligands alters nociceptive input and pain perception (Sawynok, J., 2003). Pain is a ubiquitous sensory modality, in that pain can be brought about within each of the anatomically distinct sensory modalities. That is to say, we can detect nociceptive inputs and experience pain perceptions within each of our basic senses: sight, smell, taste, hearing, touching, and some would add even in a conscious sense, as with emotional pain. The potential roles that these pain-associated molecular families play in mediating aspects of tactile sensory transduction are unknown. However, recent evidence suggests that even large-caliber Aβ fibers associated with mechanical stimuli perception express several of these family members (Paré, M. *et al.*, 2001), and clinically, several painful neuropathic and neuropathy conditions are associated with a loss of the small-caliber C fibers, which are traditionally believed to carry nociceptive information (Petersen, K. L. *et al.*, 2002; Albrecht, P. J. *et al.*, 2006; Paré, M. *et al.*, 2007). Therefore, attributing pain, or possibly even nociception and nociceptive pathways, to any one distinct subclass of sensory neuron (i.e., small-caliber Aδ and C fibers) would appear to be a rather limited explanation of how noxious tactile stimuli are transduced and perceived as painful.

6.01.4 Peripheral Mechanisms of Sensory Integration

Rather than simplifying the link between the function and the morphology of specific types of sensory endings, the use of molecular techniques such as immunocytochemistry and null or gain of function mutations has indicated that most, if not all, sensory endings are multimodal and are potentially capable of transducing and integrating different types of stimuli. Indeed, it appears that the molecular mix of expression of various receptor/ligand systems within sensory endings determines the various response properties of that particular ending, and furthermore, the expression mixes are not static, but are likely modifiable in response to various tactile stimuli. Moreover, there is increasing evidence that nonneuronal cells such as Merkel cells, terminal glia, and epidermal keratinocytes may be sensory transducing and integrating structures that actively collaborate with the sensory endings. As well, there is evidence that some sensory endings may be directly interacting with each other in the skin.

6.01.4.1 Multimolecular Properties of Cutaneous Sensory Neurons

6.01.4.1.1 Meissner corpuscle innervation

As was described above, Meissner corpuscles in monkey glabrous fingertip skin are supplied by a mixture of branched and unbranched Aβ fibers and at least two types of C fibers (Figures 2 and 4(d)). Multiple immunolabeling combinations have revealed that these Aβ fibers, implicated as low-threshold RA mechanoreceptors, contain likely not only mechanically responsive ion channels, but also numerous other ion channels, receptors, and transmitters that have been implicated in thermal, chemical, and nociceptive transduction (Paré, M. *et al.*, 2001). These include receptors implicated both in excitatory and inhibitory mechanisms. Not only do these Aβ fiber endings contain CGRP and SP, which have been implicated in inflammatory pain mechanisms, but they also are closely associated with peptidergic C fibers and express receptors for those neuropeptides. The peptidergic C fibers also express a wide array of inhibitory and excitatory ion channels and receptors. These observations suggest that both the Aβ and peptidergic C fibers may respond to, and integrate, several varieties of stimuli, and also that the peptidergic C fibers may directly interact with the Aβ fiber endings. Anatomically, the combination of Aβ and peptidergic C fiber endings is located in segregated strata within the corpuscle, which alternate with segregated stratified terminations of a second type of C fiber that lacks neuropeptides but does express TRPV1. Furthermore, additional molecules implicated in sensory stimulus transduction are present on the terminal glia distributed in the endings. Taken together these observations indicate that Meissner corpuscles are highly complex multimodal sensory transducing and integrating structures whose known mechanoreceptive properties might be modulated by the thermal and chemical environment of skin.

6.01.4.1.2 Dorsal root ganglion neurons

The wide range of molecular properties detected by immunocytochemistry on sensory endings is consistent with the wide range of molecular properties seen in the primary sensory neuronal cell bodies in the ganglia. Although it remains extremely difficult to directly correlate particular neurons to the specific types and terminations of their endings (see Koerber, H. R. and Woodbury, C. J., 2002), numerous studies using immunolabeling of peptides and proteins, as well as assessments of mRNAs, reveal that each neuron expresses multiple channels and receptors indicating that they are all multimodal to varying degrees. This is consistent with the fact that most sensory neurons have long been known to respond to a lesser degree to stimuli other than those electrophysiologically defined as the preferred response and that appropriate combinations of stimuli had not been found to activate many sensory neurons.

Attempts at determining which molecules are consistently expressed together on the same neurons have demonstrated some common combinations. For example, a population of DRG neurons that only give rise to C fibers that terminate in the epidermis was found to specifically express a Mas1-related GPCR (Figure 8) (Zylka, M. J. *et al.*, 2005). These neurons consistently coexpressed a specific purinergic receptor (P_2X_3) and a glutamate receptor (mGluR5), but usually lack CGRP, TRPV1, and opioid receptors. In contrast, neurons that express CGRP typically coexpress SP and opioid receptors but lack purinergic receptors (Ju, G. *et al.*, 1987; Vulchanova, L. *et al.*, 1997; Olson, T. H. *et al.*, 1998; Stone, L. S. *et al.*, 1998; Guo, A. *et al.*, 1999; Koizumi, S. *et al.*, 2004; Zylka, M. J. *et al.*, 2005; Kwan, K. Y. *et al.*, 2006). However, small proportions of neurons have exceptions to these generalities. For instance, as previously noted, all the DRG neurons in mice express stomatin-like proteins implicated in mechanosensory transduction, including smaller-size neurons mostly implicated as the source of C-fiber thermoreceptors or nociceptors (Wetzel, C. *et al.*, 2007).

6.01.4.2 Potential Role of Merkel Cells and Terminal Glia in Sensory Transduction and Integration

Like Meissner corpuscles, the piloneural complexes affiliated with hair follicles may also be functionally multimodal, with the possibility that the circumferentially oriented C fiber endings interact with the Aβ fiber lanceolate endings, which themselves may have multimodal molecular properties (Rice, F. L. *et al.*, 1997; Takahashi-Iwanaga, H. and Habara, Y., 2004; Takahashi-Iwanaga, H., 2005). Importantly, within the piloneural complex, individual terminal glial cells can have processes that contact multiple lanceolate endings, including endings from two different Aβ fibers. As mentioned above, individual Merkel cells located at the mouth of hair follicles also can contact endings from more than one Aβ fiber (Ebara, personal communication). This indicates that these non-neuronal cells may not only be involved in sensory transduction, but also be coordinating activity across multiple low-threshold mechanoreceptive endings.

Electron microscopy of terminal glia and Merkel cells has revealed inclusion bodies and vesicles suggestive of some form of vesicular release (Andres, K. H., 1966b; Patrizi, G. and Munger, B. L., 1966; Iggo, A. and Muir, A. R., 1969; Iggo, A. and Andres, K. H., 1982). Immunochemical analyses are increasingly revealing that many molecules implicated in neural transmission are expressed in these accessory cells. For example, Merkel cells have been shown to express synaptophysin, neuropeptides, calcium regulatory proteins, glutamate, and tyrosine hydroxylase, as well as mechanically responsive ASICs and TRP channels (Fundin, B. T. *et al.*, 1997b; Rice, F. L. *et al.*, 1997; Price, M. P. *et al.*, 2000; Garcia-Anoveros, J. *et al.*, 2001; Tachibana, T. *et al.*, 2001; Ichikawa, H. and Sugimoto, T., 2003; Lucarz, A. and Brand, G., 2007). This indicates that the Merkel cells may likely respond to several types of physical stimuli and potentially release neurotransmitters or neuromodulators that could activate or modify the activity of Merkel endings. Terminal glial cells associated with lanceolate endings have been shown to generate Ca^{2+} signals in response to mechanical stimuli and exposure to ATP. These signals have been shown to propagate among lamellae of other terminal glia that form a network among the lanceolate endings.

6.01.4.3 Sensory Transduction and Integration Among Epidermal Keratinocytes

Although C- and Aδ-fiber FNE are not regarded as having associated non-neuronal cells (unlike Aβ fiber terminals), evidence is quickly accumulating that indicates that the FNE-innervated tissues are intimately involved in sensory processing. The majority of cutaneous FNE terminate within the epidermis or within the dermis associated with sensory structures

(e.g., hair follicles, Meissner corpuscles) or blood vessels. FNE within the epidermis terminate amongst a dense field of keratinocytes, and although direct communication junctions or synaptic contacts have not been observed between keratinocytes and primary sensory neuron endings, ultrastructural studies have shown direct membrane–membrane apposition (Wang, L. *et al.*, 1990). As well, epidermal keratinocytes have been shown to express several neural signaling mediators that can directly impact sensory endings (Khodorova, A. *et al.*, 2003; Ibrahim, M. M. *et al.*, 2005; Lumpkin, E. A. and Caterina, M. J., 2007). However, epidermal keratinocyte expression of neurotransmitter systems (e.g., adrenergic, cholinergic) and other neuromodulators (e.g., neuropeptides, cytokines, and. endocrine mediators) has largely been regarded as pertaining to the functions of the epidermis related to keratinization, barrier homeostasis (wound healing), and immunologic surveillance. More recently though, as current research continues to demonstrate that epidermal keratinocytes express and release an increasingly wide range of neuromediators, the potential functional roles that keratinocytes play in tactile sensory transduction are becoming appreciated.

For example, keratinocytes have been shown to express and to secrete the vasoconstrictive peptide, endothelin-1 (ET-1) (Yohn, J. J. *et al.*, 1993), which can bind to ET-A receptors and generate an algesic (pain-producing) response (Gokin, A. P. *et al.*, 2001; Zhou, Q. L. *et al.*, 2001). Presumably, these effects are mediated through direct receptor activation on Aδ or C fiber afferents, which have been shown to express the ET-A receptor (Pomonis, J. D. *et al.*, 2001). Keratinocytes within the deepest layer of live epidermis (stratum basalis) also express the ET-A receptor, but the function of this receptor on keratinocytes has largely been attributed to keratinocyte mitosis. However, ET-1 activation of a second ET-1 receptor, endothelin-1 receptor B (ET-B), can generate an analgesic (pain-alleviating) effect. The analgesic mechanism mediated via ET-B does not occur by direct stimulation of primary afferents, as the expression of ET-B is not found in DRG neurons. Instead, ET-B receptors are expressed among the upper live stratum of epidermal keratinocytes (Figure 9(b)), and continued investigation revealed that upon ET-B activation these keratinocytes released the endogenous opioid β-endorphin (Khodorova, A. *et al.*, 2003). Peptidergic epidermal FNE express opioid receptors and an associated inhibitory G-protein-coupled, inwardly rectifying potassium channel (GIRK2). Thus, an analgesic mechanism was established whereby stimulation of ET-B receptors on keratinocytes leads to the release of β-endorphin, which acts upon the peptidergic FNEs to inhibit the generation of action potentials via the opening of GIRK2 channels, thereby producing analgesia.

Since a mechanism involved in sensory stimuli integration and transduction is implicated for the ET-B receptor, it seems plausible that a role of the ET-A receptor in keratinocytes is also somehow involved with sensory transduction (in addition to mitosis). Likewise, the cannabinoid receptor-2 (CB-2) has been identified in the upper live stratum of epidermal keratinocytes, and specific agonists of the CB-2 receptor also activate the keratinocyte-derived β-endorphin-mediated analgesic mechanism (Ibrahim, M. M. *et al.*, 2005) (Figure 9(a)). Together, these examples of epidermal-derived mechanisms demonstrate the ability of keratinocytes to modulate sensory transduction. Additionally, there is ample indirect evidence to further substantiate a role of epidermal keratinocytes in sensory stimulus transduction and integration.

As noted above, nonpeptidergic endings in the epidermis have been shown to express purinergic receptors, and keratinocytes also express several purinergic receptors. These keratinocytes have been shown to express and release ATP after various stimulations, which further indicates that a direct signaling role from keratinocytes to primary sensory neurons likely exists, as well as a keratinocyte autocrine/paracrine signaling loop. For example, keratinocytes are known to respond to contact with specific amine-containing chemical irritants or direct mechanical stimulation via the release of ATP (Mizumoto, N. *et al.*, 2003; Koizumi, S. *et al.*, 2004). Thus, keratinocyte-mediated ATP release may facilitate the activation of FNE via P_2X receptors.

Epidermal keratinocytes have been shown to express TRPV1, TRPV3, and TRPV4 receptors each of which is known to respond to preferential ranges of physiologically relevant thermal stimuli (Peier, A. M. *et al.*, 2002; Chung, M. K. *et al.*, 2004). The TRPV1 receptor responds to noxious heat and is also expressed on FNE. The TRPV3 and TRPV4 receptors respond to non-noxious warmth and are more difficult to detect in sensory neurons. Furthermore, although dissociated sensory neurons can be activated directly by hot and cold thermal challenges, responses to warm temperatures are observed only when skin and nerve connectivity are

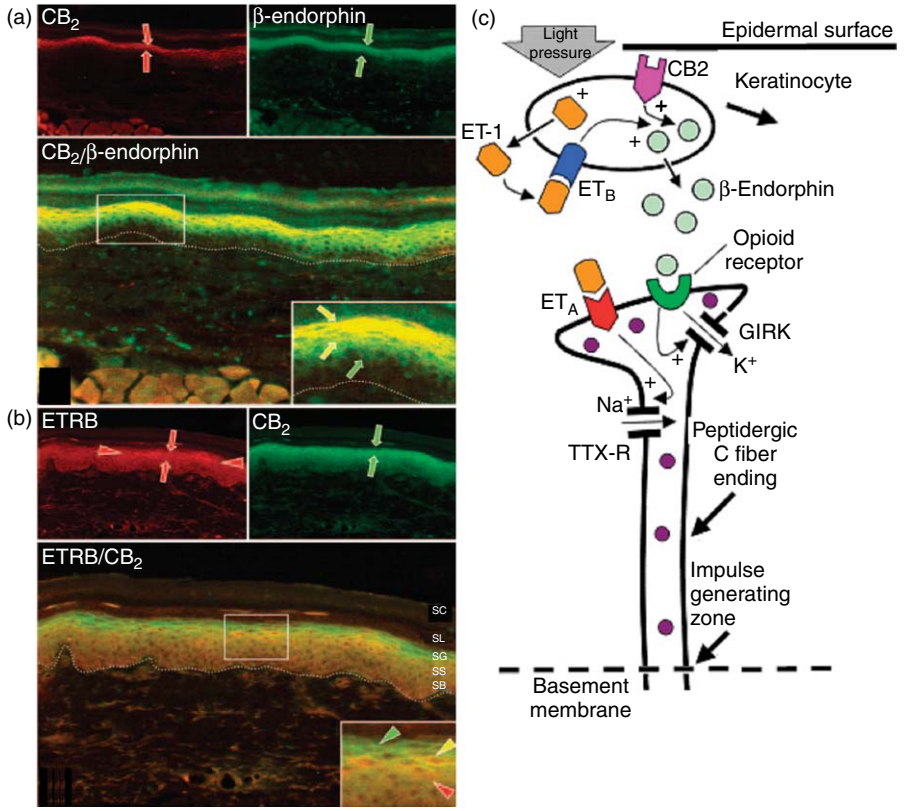

Figure 9 The keratinocytes of the epidermis can exert an analgesic effect. (a,b) Double-labeled immunofluorescence reveals that the upper stratum of keratinocytes coexpresses the endothelin receptor B (ETB) and CB2 receptors along with β-endorphin. (c) As shown schematically, ETB and CB2 activation results in an analgesic effect by releasing β-endorphin, which in turn inhibits peptidergic epidermal endings by binding to μ-opioid receptors that open GIRK2 channels.

maintained (Peier, A. M. *et al.*, 2002). Therefore, the ability to detect warmth as a tactile perception most likely involves a keratinocyte-mediated mechanism. Furthermore, expression of ENaC subunits has been demonstrated in epidermal keratinocytes (Roudier-Pujol, C. *et al.*, 1996). These sodium channels were first identified based upon their structural similarity to known mechanosensitive proteins from other species (described above), and although not directly demonstrated as yet, also imply that keratinocytes have an ability to directly respond to mechanical stimuli. How the responses of keratinocytes to these various tactile stimuli impact sensory transduction and integration is still unknown.

Interestingly, the distribution of various ligands and receptors within the epidermal keratinocytes is differentially stratified. Likewise, peptidergic endings have been shown to terminate preferentially in the deeper portion of the epidermis whereas non-peptidergic endings have been shown to terminate closer to the upper live strata (Zylka, M. J. *et al.*, 2005). Taken together, these recent discoveries strongly implicate the epidermis as a sensory transducing and integrating structure involving both excitatory and inhibitory mechanisms that in turn regulate the activity of the cutaneous sensory innervation (Figure 9(c)).

6.01.5 Summary

Skin, and particularly specialized sensory receptive structures such as vibrissa follicles and glabrous fingertips, has the capacity to rapidly detect a wide variety and range of tactile stimuli, including thermal, mechanical, and chemical. The sensitivity of these receptive functions is virtually inconceivable, and the generation of tactile perceptions is generally taken for granted. Despite over a century of research, the mechanisms responsible for these exquisite sensory capabilities are still largely unproven. Skin receives abundant primary afferent (sensory)

innervation. Cutaneous nerve anatomical and electrophysiological studies have detected a wide variety of ending types, distributions, and functions, and have determined that sensory endings are specialized to extract certain physical properties from complex cutaneous stimuli. After extracting these properties through discreet types of sensory neurons, these parallel inputs are hypothesized to recombine within the CNS circuitry to form the complex patterns of neuronal activity, which are interpreted as tactile perception. However, even the earliest electrophysiological studies recognized that among the discreet neuron populations, there were a range of sensory stimuli combinations and permutations, such that attempts to classify particular types of endings were somewhat arbitrary. It was also recognized that the preferred or optimal stimulus was based on the limitations of experimentally testable stimuli and that many sensory neurons had other less optimal stimulus response properties and still others had no detectable response.

More recent studies are demonstrating that the organization and function of cutaneous innervation has a far greater variety than was previously detected and that considerable sensory integration may be taking place within the skin and sensory endings, before inputs converge within the CNS. It is now appreciated that:

1. All sensory neurons have complex chemical properties consisting of multiple receptors and ion channels that can collectively respond to different types of physical stimulus properties. The sensory neuron properties can involve both inhibition and excitation of the sensory ending. As such, these receptors and ion channels could be regarded as the combination of synaptic inputs on typical neurons. Thus, the activation of a sensory ending under natural conditions would be due to the spatial and temporal summation of inputs from a variety of combinations.
2. Endings of a particular type (e.g., Merkel endings) may have different terminal branch patterns in the skin, which could result in different varieties of response patterns to a comparable stimulus.
3. Several varieties of sensory endings arising from Aβ, Aδ, and/or C fibers can be organized into complex ensembles such as Meissner corpuscles or piloneural complexes. These endings may function in concert with each other or interact with each other to provide an integrated output. Moreover, a single ensemble may be supplied by Aβ fibers that innervate only that ensemble and other Aβ fibers that innervate multiple ensembles.
4. Sensory transduction may be a combination of direct action of a stimulus on a sensory fiber ending and/or by indirect action mediated through accessory cells such as Merkel cells, terminal glia, or epidermal keratinocytes. The accessory cells may regulate the response property of the associated sensory ending or coordinate activity across multiple endings, and furthermore, the accessory cells, especially epidermal keratinocytes, may be primary sensory stimuli transducing and integrating structures. Peripheral mechanisms of complex sensory transduction and integration would provide an even greater variety of input to the CNS on which to construct particularly detailed tactile perceptions.

References

Albrecht, P. J., Hines, S., Eisenberg, E., Pud, D., Finlay, D. R., Connolly, M. K., Paré, M., Davar, G., and Rice, F. L. 2006. Pathologic alterations of cutaneous innervation and vasculature in affected limbs from patients with complex regional pain syndrome. Pain 120, 244–266.

Andres, K. H. 1966a. On the fine structure of Merkel's tactile apparatus in the sinus hair. Naturwissenschaften 53, 706.

Andres, K. H. 1966b. On the microstructure of receptors on sinus hair. Z. Zellforsch. Mikrosk. Anat. 75, 339–365.

Arvidsson, J. and Rice, F. L. 1991. Central projections of primary sensory neurons innervating different parts of the vibrissae follicles and intervibrissal skin on the mystacial pad of the rat. J. Comp. Neurol. 309, 1–16.

Bensmaia, S. J., Leung, Y. Y., Hsiao, S. S., and Johnson, K. O. 2005. Vibratory adaptation of cutaneous mechanoreceptive afferents. J. Neurophysiol. 94, 3023–3036.

Bessou, P. and Perl, E. R. 1969. Response of cutaneous sensory units with unmyelinated fibers to noxious stimuli. J. Neurophysiol. 32, 1025–1043.

Bessou, P., Burgess, P. R., Perl, E. R., and Taylor, C. B. 1971. Dynamic properties of mechanoreceptors with unmyelinated (C) fibers. J. Neurophysiol. 34, 116–131.

Biemesderfer, D., Munger, B. L., Binck, J., and Dubner, R. 1978. The pilo–Ruffini complex: a non-sinus hair and associated slowly-adapting mechanoreceptor in primate facial skin. Brain Res. 142, 197–222.

Bolanowski, S. J., Jr. 1984. Intensity and frequency characteristics of Pacinian corpuscles. III. Effects of tetrodotoxin on transduction process. J. Neurophysiol. 51, 831–839.

Bolanowski, S. J., Jr and Pawson, L. 2003. Organization of Meissner corpuscles in the glabrous skin of monkey and cat. Somatosens. Mot. Res. 20, 223–231.

Bolanowski, S. J., Jr. and Zwislocki, J. J. 1984a. Intensity and frequency characteristics of Pacinian corpuscles. I. Action potentials. J. Neurophysiol. 51, 793–811.

Bolanowski, S. J., Jr. and Zwislocki, J. J. 1984b. Intensity and frequency characteristics of Pacinian corpuscles. II. Receptor potentials. J. Neurophysiol. 51, 812–830.

Brown, A. G. and Iggo, A. 1967. A quantitative study of cutaneous receptors and afferent fibres in the cat and rabbit. J. Physiol. 193, 707–733.

Burgess, P. R. and Perl, E. R. 1967. Myelinated afferent fibres responding specifically to noxious stimulation of the skin. J. Physiol. 190, 541–562.

Cahusac, P. M. and Senok, S. S. 2006. Metabotropic glutamate receptor antagonists selectively enhance responses of slowly adapting type I mechanoreceptors. Synapse 59, 235–242.

Cahusac, P. M., Senok, S. S., Hitchcock, I. S., Genever, P. G., and Baumann, K. I. 2005. Are unconventional NMDA receptors involved in slowly adapting type I mechanoreceptor responses? Neuroscience 133, 763–773.

Caterina, M. J. 2007. Transient receptor potential ion channels as participants in thermosensation and thermoregulation. Am. J. Physiol. Regul. Integr. Comp. Physiol. 292, R64–R76.

Cauna, N. 1954. Nature and functions of the papillary ridges of the digital skin. Anat. Rec. 119, 449–468.

Cauna, N. 1956. Nerve supply and nerve endings in Meissner's corpuscles. Am. J. Anat. 29, 315–350.

Cauna, N. and Ross, L. L. 1960. The fine structure of Meissner's touch corpuscles of human fingers. J. Biophys. Biochem. Cytol. 8, 467–482.

Chambers, M. R., Andres, K. H., von Duering, M., and Iggo, A. 1972. The structure and function of the slowly adapting type II mechanoreceptor in hairy skin. Q. J. Exp. Physiol. Cogn. Med. Sci. 57, 417–445.

Chung, M. K., Lee, H., Mizuno, A., Suzuki, M., and Caterina, M. J. 2004. TRPV3 and TRPV4 mediate warmth-evoked currents in primary mouse keratinocytes. J. Biol. Chem. 279, 21569–21575.

Cockayne, D. A., Dunn, P. M., Zhong, Y., Rong, W., Hamilton, S. G., Knight, G. E., Ruan, H. Z., Ma, B., Yip, P., Nunn, P., McMahon, S. B., Burnstock, G., and Ford, A. P. 2005. P_2X_2 knockout mice and P_2X_2/P_2X_3 double knockout mice reveal a role for the P_2X_2 receptor subunit in mediating multiple sensory effects of ATP. J. Physiol. 567, 621–639.

Cohen, R. H. and Perl, E. R. 1988. Chemical factors in the sensitization of cutaneous nociceptors. Prog. Brain Res. 74, 201–206.

Cole, J., Bushnell, M. C., McGlone, F., Elam, M., Lamarre, Y., Vallbo, A., and Olausson, H. 2006. Unmyelinated tactile afferents underpin detection of low-force monofilaments. Muscle Nerve 34, 105–107.

Connor, C. E. and Johnson, K. O. 1992. Neural coding of tactile texture: comparison of spatial and temporal mechanisms for roughness perception. J. Neurosci. 12, 3414–3426.

Connor, C. E., Hsiao, S. S., Phillips, J. R., and Johnson, K. O. 1990. Tactile roughness: neural codes that account for psychophysical magnitude estimates. J. Neurosci. 10, 3823–3836.

Craig, A. D. 2003a. Interoception: the sense of the physiological condition of the body. Curr. Opin. Neurobiol. 13, 500–505.

Craig, A. D. 2003b. A new view of pain as a homeostatic emotion. Trends Neurosci. 26, 303–307.

Dehnhardt, G., Mauck, B., Hanke, W., and Bleckmann, H. 2001. Hydrodynamic trail-following in harbor seals (*Phoca vitulina*). Science 293, 102–104.

Dhaka, A., Viswanath, V., and Patapoutian, A. 2006. TRP ion channels and temperature sensation. Annu. Rev. Neurosci. 29, 135–161.

Djourhi, L., Bleazard, K., and Lawson, S. N. 1998. Association of somatic action potential shape with sensory receptive properties in guinea pig dorsal root ganglion neurons. J. Physiol. (Lond). 513, 857–872.

Drummond, H. A., Abboud, F. M., and Welsh, M. J. 2000. Localization of beta and gamma subunits of ENaC in sensory nerve endings in the rat foot pad. Brain Res. 894, 1–12.

Ebara, S., Kumamoto, K., Matsuura, T., Mazurkiewicz, J. E., and Rice, F. L. 2002. Similarities and differences in the innervation of mystacial vibrissal follicle–sinus complexes in the rat and cat: a confocal microscopic study. J. Comp. Neurol. 449, 103–119.

Freeman, B. and Rowe, M. 1981. The effect of sympathetic nerve stimulation on responses of cutaneous Pacinian corpuscles in the cat. Neurosci. Lett. 22, 145–150.

Fricke, B., Lints, R., Stewart, G., Drummond, H., Dodt, G., Driscoll, M., and von During, M. 2000. Epithelial Na^+ channels and stomatin are expressed in rat trigeminal mechanosensory neurons. Cell Tissue Res. 299, 327–334.

Friedman, R. M., Khalsa, P. S., Greenquist, K. W., and LaMotte, R. H. 2002. Neural coding of the location and direction of a moving object by a spatially distributed population of mechanoreceptors. J. Neurosci. 22, 9556–9566.

Fundin, B. T., Arvidsson, J., Aldskogius, H., Johansson, O., Rice, S. N., and Rice, F. L. 1997a. A comprehensive immunofluorescence and lectin binding analysis of intervibrissal fur innervation in the mystacial pad of the rat. J. Comp. Neurol. 385, 185–206.

Fundin, B. T., Pfaller, K., and Rice, F. L. 1997b. Different distributions of the sensory and autonomic innervation among the microvasculature of the rat mystacial pad. J. Comp. Neurol. 389, 545–568.

Funfschilling, U., Ng, Y. G., Zang, K., Miyazaki, J., Reichardt, L. F., and Rice, F. L. 2004. TrkC kinase expression in distinct subsets of cutaneous trigeminal innervation and nonneuronal cells. J. Comp. Neurol. 480, 392–414.

Garcia-Anoveros, J., Samad, T. A., Zuvela-Jelaska, L., Woolf, C. J., and Corey, D. P. 2001. Transport and localization of the DEG/ENaC ion channel BNaC1alpha to peripheral mechanosensory terminals of dorsal root ganglia neurons. J. Neurosci. 21, 2678–2686.

Gardner, E. and Martin, J. 2000. Coding of Sensory Information. In: Principles of Neuroscience, 4th edn. (*eds*. E. Kandel, J. Schwartz, and T. Jessell), pp. 411–429. McGraw-Hill.

Gardner, E., Martin, J., and Jessell, T. 2000. The Bodily Senses. In: Principles of Neuroscience, 4th edn. (*eds*. E. Kandel, J. Schwartz, and T. Jessell), pp. 430–450. McGraw-Hill.

Gibson, J. M. and Welker, W. I. 1983a. Quantitative studies of stimulus coding in first-order vibrissa afferents of rats. 2. Adaptation and coding of stimulus parameters. Somatosens. Res. 1, 95–117.

Gibson, J. M. and Welker, W. I. 1983b. Quantitative studies of stimulus coding in first-order vibrissa afferents of rats. 1. Receptive field properties and threshold distributions. Somatosens. Res. 1, 51–67.

Gillespie, P. G. and Walker, R. G. 2001. Molecular basis of mechanosensory transduction. Nature 413, 194–202.

Gokin, A. P., Fareed, M. U., Pan, H. L., Hans, G., Strichartz, G. R., and Davar, G. 2001. Local injection of endothelin-1 produces pain-like behavior and excitation of nociceptors in rats. J. Neurosci. 21, 5358–5366.

Gottschaldt, K. M., Iggo, A., and Young, D. W. 1972. Electrophysiology of the afferent innervation of sinus hairs, including vibrissae, of the cat. J. Physiol. 222, 60P–61P.

Gottschaldt, K. M., Iggo, A., and Young, D. W. 1973. Functional characteristics of mechanoreceptors in sinus hair follicles of the cat. J. Physiol. 235, 287–315.

Guclu, B., Schepis, E. A., Yelke, S., Yucesoy, C. A., and Bolanowski, S. J. 2006. Ovoid geometry of the Pacinian corpuscle is not the determining factor for mechanical excitation. Somatosens. Mot. Res. 23, 119–126.

Guo, A., Vulchanova, L., Wang, J., Li, X., and Elde, R. 1999. Immunocytochemical localization of the vanilloid receptor 1

(VR1): relationship to neuropeptides, the P_2X_3 purinoceptor and IB4 binding sites. Eur. J. Neurosci. 11, 946–958.
Hardie, R. C. 2007. TRP channels and lipids: from Drosophila to mammalian physiology. J. Physiol. 578, 9–24.
Hilliges, M., Astback, J., Wang, L., Arvidson, K., and Johansson, O. 1996. Protein gene product 9.5-immunoreactive nerves and cells in human oral mucosa. Anat. Rec. 245, 621–632.
Ibrahim, M. M., Porreca, F., Lai, J., Albrecht, P. J., Rice, F. L., Khodorova, A., Davar, G., Makriyannis, A., Vanderah, T. W., Mata, H. P., and Malan, T. P., Jr. 2005. CB2 cannabinoid receptor activation produces antinociception by stimulating peripheral release of endogenous opioids. Proc. Natl. Acad. Sci. U. S. A. 102, 3093–3098.
Ichikawa, H. and Sugimoto, T. 2003. Calcium-binding protein-immunoreactive innervation of the rat vibrissa. Brain Res. 970, 226–231.
Iggo, A. 1960. Cutaneous mechanoreceptors with afferent C fibres. J. Physiol. 152, 337–353.
Iggo, A. 1964. Temperature discrimination in the skin. Nature 204, 481–483.
Iggo, A. 1984. Cutaneous receptors and their sensory functions. J. Hand Surg. [Br.] 9, 7–10.
Iggo, A. and Andres, K. H. 1982. Morphology of cutaneous receptors. Annu. Rev. Neurosci. 5, 1–31.
Iggo, A. and Muir, A. R. 1969. The structure and function of a slowly adapting touch corpuscle in hairy skin. J. Physiol. 200, 763–796.
Ju, G., Hokfelt, T., Brodin, E., Fahrenkrug, J., Fischer, J. A., Frey, P., Elde, R. P., and Brown, J. C. 1987. Primary sensory neurons of the rat showing calcitonin gene-related peptide immunoreactivity and their relation to substance P-, somatostatin-, galanin-, vasoactive intestinal polypeptide- and cholecystokinin-immunoreactive ganglion cells. Cell Tissue Res. 247, 417–431.
Kennedy, W. R. and Wendelschafer-Crabb, G. 1993. The innervation of human epidermis. J. Neurol. Sci. 115, 184–190.
Khalsa, P. S., Friedman, R. M., Srinivasan, M. A., and Lamotte, R. H. 1998. Encoding of shape and orientation of objects indented into the monkey fingerpad by populations of slowly and rapidly adapting mechanoreceptors. J. Neurophysiol. 79, 3238–3251.
Khodorova, A., Navarro, B., Jouaville, L. S., Murphy, J. E., Rice, F. L., Mazurkiewicz, J. E., Long-Woodward, D., Stoffel, M., Strichartz, G. R., Yukhananov, R., and Davar, G. 2003. Endothelin-B receptor activation triggers an endogenous analgesic cascade at sites of peripheral injury. Nat. Med. 9, 1055–1061.
Kleinfeld, D., Ahissar, E., and Diamond, M. E. 2006. Active sensation: insights from the rodent vibrissa sensorimotor system. Curr. Opin. Neurobiol. 16, 435–444.
Koerber, H. R. and Mandell, L. M. 1992. Functional Heterogeneity of Dorsal root ganglion Cells. In: Sensory Neurons: Diverity, Development and Plasticity, pp. 77–96, Oxford University Press.
Koerber, H. R. and Woodbury, C. J. 2002. Comprehensive phenotyping of sensory neurons using an exvivo somatosensory system. Physiol. Behav. 77, 589–594.
Koizumi, S., Fujishita, K., Inoue, K., Shigemoto-Mogami, Y., Tsuda, M., and Inoue, K. 2004. Ca^{2+} waves in keratinocytes are transmitted to sensory neurons: the involvement of extracellular ATP and P_2Y_2 receptor activation. Biochem. J. 380, 329–338.
Koltzenburg, M., Stucky, C. L., and Lewin, G. R. 1997. Receptive properties of mouse sensory neurons innervating hairy skin. J. Neurophysiol. 78, 1841–1850.
Kruger, L. 1988. Morphological features of thin sensory afferent fibers: a new interpretation of 'nociceptor' function. Prog. Brain Res. 74, 253–257.
Kruger, L. 1996. The functional morphology of thin sensory axons: some principles and problems. Prog. Brain Res. 113, 255–272.
Kruger, L., Perl, E. R., and Sedivec, M. J. 1981. Fine structure of myelinated mechanical nociceptor endings in cat hairy skin. J. Comp. Neurol. 198, 137–154.
Kruger, L., Silverman, J. D., Mantyh, P. W., Sternini, C., and Brecha, N. C. 1989. Peripheral patterns of calcitonin-gene-related peptide general somatic sensory innervation: cutaneous and deep terminations. J. Comp. Neurol. 280, 291–302.
Kumazawa, T. and Perl, E. R. 1977. Primate cutaneous sensory units with unmyelinated (C) afferent fibers. J. Neurophysiol. 40, 1325–1338.
Kwan, K. Y., Allchorne, A. J., Vollrath, M. A., Christensen, A. P., Zhang, D. S., Woolf, C. J., and Corey, D. P. 2006. TRPA1 contributes to cold, mechanical, and chemical nociception but is not essential for hair-cell transduction. Neuron 50, 277–289.
LaMotte, R. H. and Mountcastle, V. B. 1975. Capacities of humans and monkeys to discriminate vibratory stimuli of different frequency and amplitude: a correlation between neural events and psychological measurements. J. Neurophysiol. 38, 539–559.
LaMotte, R. H., Friedman, R. M., Lu, C., Khalsa, P. S., and Srinivasan, M. A. 1998. Raised object on a planar surface stroked across the fingerpad: responses of cutaneous mechanoreceptors to shape and orientation. J. Neurophysiol. 80, 2446–2466.
Lazarowski, E. R., Boucher, R. C., and Harden, T. K. 2003. Mechanisms of release of nucleotides and integration of their action as P_2X- and P_2Y-receptor activating molecules. Mol. Pharmacol. 64, 785–795.
Leiser, S. C. and Moxon, K. A. 2007. Responses of trigeminal ganglion neurons during natural whisking behaviors in the awake rat. Neuron 53, 117–133.
Leung, Y. Y., Bensmaia, S. J., Hsiao, S. S., and Johnson, K. O. 2005. Time-course of vibratory adaptation and recovery in cutaneous mechanoreceptive afferents. J. Neurophysiol. 94, 3037–3045.
Lichtenstein, S. H., Carvell, G. E., and Simons, D. J. 1990. Responses of rat trigeminal ganglion neurons to movements of vibrissae in different directions. Somatosens. Mot. Res. 7, 47–65.
Light, A. R. and Perl, E. R. 2003. Unmyelinated afferent fibers are not only for pain anymore. J. Comp. Neurol. 461, 137–139.
Lin, S. Y. and Corey, D. P. 2005. TRP channels in mechanosensation. Curr. Opin. Neurobiol. 15, 350–357.
Liu, Q., Vrontou, S., Rice, F. L., Zylka, M. J., Dong, X., and Anderson, D. J. 2007. Molecular genetic visualization of a rare subset of unmyelinated sensory neurons that may detect gentle touch. Nat. Neurosci. (Epub ahead of print).
Lucarz, A. and Brand, G. 2007. Current considerations about Merkel cells. Eur. J. Cell. Biol. 5, 243–251.
Lumpkin, E. A. and Caterina, M. J. 2007. Mechanisms of sensory transduction in the skin. Nature 445, 858–865.
Mannsfeldt, A. G., Carroll, P., Stucky, C. L., and Lewin, G. R. 1999. Stomatin, a MEC-2 like protein, is expressed by mammalian sensory neurons. Mol. Cell. Neurosci. 13, 391–404.
Marshall, C. D., Amin, H., Kovacs, K. M., and Lydersen, C. 2006. Microstructure and innervation of the mystacial vibrissal follicle–sinus complex in bearded seals, *Erignathus barbatus* (Pinnipedia: Phocidae). Anat. Rec. A Discov. Mol. Cell Evol. Biol. 288, 13–25.

Mehta, S. B. and Kleinfeld, D. 2004. Frisking the whiskers: patterned sensory input in the rat vibrissa system. Neuron 41, 181–184.

Mehta, S. B., Whitmer, D., Figueroa, R., Williams, B. A., and Kleinfeld, D. 2007. Active spatial perception in the vibrissa scanning sensorimotor system. PLoS Biol. 5, e15.

Mitrirattanakul, S., Ramakul, N., Guerrero, A. V., Matsuka, Y., Ono, T., Iwase, H., Mackie, K., Faull, K. F., and Spigelman, I. 2006. Site-specific increases in peripheral cannabinoid receptors and their endogenous ligands in a model of neuropathic pain. Pain 126, 102–114.

Mizumoto, N., Mummert, M. E., Shalhevet, D., and Takashima, A. 2003. Keratinocyte ATP release assay for testing skin-irritating potentials of structurally diverse chemicals. J. Invest. Dermatol. 121, 1066–1072.

Molliver, D. C., Immke, D. C., Fierro, L., Paré, M., Rice, F. L., and McCleskey, E. W. 2005. ASIC3, an acid-sensing ion channel, is expressed in metaboreceptive sensory neurons. Mol. Pain 1, 35.

Mosconi, T. M. and Rice, F. L. 1991. Sensory innervation of the mystacial pad fur of the ferret. Neurosci. Lett. 121, 199–202.

Mosconi, T. M., Rice, F. L., and Song, M. J. 1993. Sensory innervation in the inner conical body of the vibrissal follicle–sinus complex of the rat. J. Comp. Neurol. 328, 232–251.

Mountcastle, V. B., Talbot, W. H., Darian-Smith, I., and Kornhuber, H. H. 1967. Neural basis of the sense of flutter-vibration. Science 155, 597–600.

Nakamura, F. and Strittmatter, S. M. 1996. P2Y1 purinergic receptors in sensory neurons: contribution to touch-induced impulse generation. Proc. Natl. Acad. Sci. U. S. A. 93, 10465–10470.

Olson, T. H., Riedl, M. S., Vulchanova, L., Ortiz-Gonzalez, X. R., and Elde, R. 1998. An acid sensing ion channel (ASIC) localizes to small primary afferent neurons in rats. Neuroreport 9, 1109–1113.

Owsianik, G., D'Hoedt, D., Voets, T., and Nilius, B. 2006. Structure–function relationship of the TRP channel superfamily. Rev. Physiol. Biochem. Pharmacol. 156, 61–90.

Paré, M., Albrecht, P. J., Noto, C. J., Bodkin, N. L., Pittenger, G. L., Schreyer, D. J., Tigno, X. T., Hansen, B. C., and Rice, F. L. 2007. Differential hypertrophy and atrophy among all types of cutaneous innervation in the glabrous skin of the monkey hand during aging and naturally occurring type 2 diabetes. J. Comp. Neurol. 501, 543–567.

Paré, M., Behets, C., and Cornu, O. 2003. Paucity of presumptive Ruffini corpuscles in the index finger pad of humans. J. Comp. Neurol. 456, 260–266.

Paré, M., Elde, R., Mazurkiewicz, J. E., Smith, A. M., and Rice, F. L. 2001. The Meissner corpuscle revised: a multiafferented mechanoreceptor with nociceptor immunochemical properties. J. Neurosci. 21, 7236–7246.

Paré, M., Smith, A. M., and Rice, F. L. 2002. Distribution and terminal arborizations of cutaneous mechanoreceptors in the glabrous finger pads of the monkey. J. Comp. Neurol. 445, 347–359.

Patrizi, G. and Munger, B. L. 1966. The ultrastructure and innervation of rat vibrissae. J. Comp. Neurol. 126, 423–435.

Pawson, L. and Bolanowski, S. J. 2002. Voltage-gated sodium channels are present on both the neural and capsular structures of Pacinian corpuscles. Somatosens. Mot. Res. 19, 231–237.

Pawson, L., Slepecky, N. B., and Bolanowski, S. J. 2000. Immunocytochemical identification of proteins within the Pacinian corpuscle. Somatosens. Mot. Res. 17, 159–170.

Peier, A. M., Reeve, A. J., Andersson, D. A., Moqrich, A., Earley, T. J., Hergarden, A. C., Story, G. M., Colley, S., Hogenesch, J. B., McIntyre, P., Bevan, S., and Patapoutian, A. 2002. A heat-sensitive TRP channel expressed in keratinocytes. Science 296, 2046–2049.

Perl, E. R. 1968. Myelinated afferent fibres innervating the primate skin and their response to noxious stimuli. J. Physiol. 197, 593–615.

Perl, E. R. 1980. Afferent basis of nociception and pain: evidence from the characteristics of sensory receptors and their projections to the spinal dorsal horn. Res. Publ. Assoc. Res. Nerv. Ment. Dis. 58, 19–45.

Perl, E. R. 1996. Cutaneous polymodal receptors: characteristics and plasticity. Prog. Brain Res. 113, 21–37.

Petersen, K. L., Rice, F. L., Suess, F., Berro, M., and Rowbotham, M. C. 2002. Relief of post-herpetic neuralgia by surgical removal of painful skin. Pain 98, 119–126.

Pomonis, J. D., Rogers, S. D., Peters, C. M., Ghilardi, J. R., and Mantyh, P. W. 2001. Expression and localization of endothelin receptors: implications for the involvement of peripheral glia in nociception. J. Neurosci. 21, 999–1006.

Price, M. P., Lewin, G. R., McIlwrath, S. L., Cheng, C., Xie, J., Heppenstall, P. A., Stucky, C. L., Mannsfeldt, A. G., Brennan, T. J., Drummond, H. A., Qiao, J., Benson, C. J., Tarr, D. E., Hrstka, R. F., Yang, B., Williamson, R. A., and Welsh, M. J. 2000. The mammalian sodium channel BNC1 is required for normal touch sensation. Nature 407, 1007–1011.

Rice, F. L. and Rasmusson, D. D. 2000. Innervation of the digit on the forepaw of the raccoon. J. Comp. Neurol. 417, 467–490.

Rice, F. L., Fundin, B. T., Arvidsson, J., Aldskogius, H., and Johansson, O. 1997. Comprehensive immunofluorescence and lectin binding analysis of vibrissal follicle sinus complex innervation in the mystacial pad of the rat. J. Comp. Neurol. 385, 149–184.

Rice, F. L., Kinnman, E., Aldskogius, H., Johansson, O., and Arvidsson, J. 1993. The innervation of the mystacial pad of the rat as revealed by PGP 9.5 immunofluorescence. J. Comp. Neurol. 337, 366–385.

Roosterman, D., Goerge, T., Schneider, S. W., Bunnett, N. W., and Steinhoff, M. 2006. Neuronal control of skin function: the skin as a neuroimmunoendocrine organ. Physiol. Rev. 86, 1309–1379.

Roudier-Pujol, C., Rochat, A., Escoubet, B., Eugene, E., Barrandon, Y., Bonvalet, J. P., and Farman, N. 1996. Differential expression of epithelial sodium channel subunit mRNAs in rat skin. J. Cell Sci. 109 (Pt 2), 379–385.

Sawynok, J. 2003. Topical and peripherally acting analgesics. Pharmacol. Rev. 55, 1–20.

Schulte-Pelkum, N., Wieskotten, S., Hanke, W., Dehnhardt, G., and Mauck, B. 2007. Tracking of biogenic hydrodynamic trails in harbour seals (*Phoca vitulina*). J. Exp. Biol. 210, 781–787.

Shin, J. B., Martinez-Salgado, C., Heppenstall, P. A., and Lewin, G. R. 2003. A T-type calcium channel required for normal function of a mammalian mechanoreceptor. Nat. Neurosci. 6, 724–730.

Stone, L. S., Broberger, C., Vulchanova, L., Wilcox, G. L., Hokfelt, T., Riedl, M. S., and Elde, R. 1998. Differential distribution of alpha2A and alpha2C adrenergic receptor immunoreactivity in the rat spinal cord. J. Neurosci. 18, 5928–5937.

Sukharev, S. and Corey, D. P. 2004. Mechanosensitive channels: multiplicity of families and gating paradigms. Sci. STKE 2004, re4.

Szwed, M., Bagdasarian, K., and Ahissar, E. 2003. Encoding of vibrissal active touch. Neuron 40, 621–630.

Tachibana, T., Endoh, M., and Nawa, T. 2001. Immunohistochemical expression of G protein alpha-subunit isoforms in rat and monkey Merkel cell–neurite complexes. Histochem. Cell Biol. 116, 205–213.

Takahashi-Iwanaga, H. 2005. Calcium signaling in terminal Schwann cells associated with lanceolate sensory endings in rat vibrissae. Ital. J. Anat. Embryol. 110, 19–24.

Takahashi-Iwanaga, H. and Habara, Y. 2004. Oscillatory calcium responses mediated by P2Y2 purinergic receptors in terminal Schwann cells of longitudinal lanceolate endings isolated from rat vibrissae. J. Comp. Neurol. 475, 416–425.

Takahashi-Iwanaga, H. and Shimoda, H. 2003. The three-dimensional microanatomy of Meissner corpuscles in monkey palmar skin. J. Neurocytol. 32, 363–371.

Tominaga, M. and Caterina, M. J. 2004. Thermosensation and pain. J. Neurobiol. 61, 3–12.

Tuttle, R. S. and McCleary, M. 1975. Mesenteric baroreceptors. Am. J. Physiol. 229, 1514–1519.

Vallbo, A. B. and Johansson, R. S. 1984. Properties of cutaneous mechanoreceptors in the human hand related to touch sensation. Hum. Neurobiol. 3, 3–14.

Vulchanova, L., Riedl, M. S., Shuster, S. J., Buell, G., Surprenant, A., North, R. A., and Elde, R. 1997. Immunohistochemical study of the P_2X_2 and P_2X_3 receptor subunits in rat and monkey sensory neurons and their central terminals. Neuropharmacology 36, 1229–1242.

Wang, L., Hilliges, M., Jernberg, T., Wiegleb-Edstrom, D., and Johansson, O. 1990. Protein gene product 9.5-immunoreactive nerve fibres and cells in human skin. Cell Tissue Res. 261, 25–33.

Wetzel, C., Hu, J., Riethmacher, D., Benckendorff, A., Harder, L., Eilers, A., Moshourab, R., Kozlenkov, A., Labuz, D., Caspani, O., Erdmann, B., Machelska, H., Heppenstall, P. A., and Lewin, G. R. 2007. A stomatin-domain protein essential for touch sensation in the mouse. Nature 445, 206–209.

Winkelmann, R. K. and Osment, L. S. 1956. The Vater–Pacinian corpuscle in the skin of the human finger tip. AMA Arch. Derm. 73, 116–122.

Yohn, J. J., Morelli, J. G., Walchak, S. J., Rundell, K. B., Norris, D. A., and Zamora, M. R. 1993. Cultured human keratinocytes synthesize and secrete endothelin-1. J. Invest. Dermatol. 100, 23–26.

Zhou, Q. L., Strichartz, G., and Davar, G. 2001. Endothelin-1 activates ET(A) receptors to increase intracellular calcium in model sensory neurons. Neuroreport 12, 3853–3857.

Zucker, E. and Welker, W. I. 1969. Coding of somatic sensory input by vibrissae neurons in the rat's trigeminal ganglion. Brain Res. 12, 138–156.

Zylka, M. J., Rice, F. L., and Anderson, D. J. 2005. Topographically distinct epidermal nociceptive circuits revealed by axonal tracers targeted to Mrgprd. Neuron 45, 17–25.

6.02 Merkel Cells

Z Halata and K I Baumann, University of Hamburg, Hamburg, Germany

M Grim, Charles University, Praha, Czech Republic

© 2008 Elsevier Inc. All rights reserved.

6.02.1	Localization and Ultrastructure of Merkel Nerve Endings	33
6.02.2	Merkel Nerve Endings in Mammalian Glabrous Skin	34
6.02.3	Merkel Nerve Endings in Mammalian Hairy Skin	34
6.02.4	Merkel Nerve Endings in Sinus Hairs of Mammals	34
6.02.5	Merkel Nerve Endings in the Mucosa of Mammals	35
6.02.6	Merkel-Like Cells with Suggested Neuroendocrine Function	36
6.02.7	Merkel Cell Carcinoma	36
6.02.8	Developmental Origin of Merkel Cells	36
6.02.9	Mechanoreceptor Function of Merkel Cells	36
References		37

Glossary

APUD Amine precursor uptake and decarboxylation.

CGRP Calcitonin gene related peptide.

CK Cytokeratin.

6.02.1 Localization and Ultrastructure of Merkel Nerve Endings

Merkel cells are usually associated with nerve endings located in the skin and some parts of the mucosa in all vertebrates. They function as mechanoreceptors and are found in mammalian epidermis as well as the epithelium of ectoderm-derived mucosa (Merkel, F., 1875; Iggo, A. and Muir, A. R., 1969; Halata, Z. *et al.*, 2003). However, in birds they are located in the superficial layer of the dermis (Saxod, R., 1978). Occasionally, dermal Merkel cells are also found in mammals especially in man (Mahrle, G. and Orfanos, C. E., 1974).

Light microscopically, Merkel cells can be best seen using their characteristic immunohistochemical staining for cytokeratins CK8, CK18, and CK20 (Moll, R. *et al.*, 1984; 1995). In addition, Merkel cells show immunoreactivity to neuron-specific enolase, chromogranin, vasoactive intestinal polypeptide, met-enkephalin, serotonin, substance P, calcitonin gene-related peptide (CGRP), somatostatin, calcitonin protein gene product 9.5, and bombesin (Hartschuh, W. *et al.*, 1979; Hartschuh, W. and Weihe, E., 1988; Cheng Chew, S. B. and Leung, P. Y., 1991; English, K. B. *et al.*, 1992).

Electron microscopically, Merkel cells (Figure 1) can be identified by their characteristic disk-shape, large lobulated nuclei and close contact with nerve terminals. Merkel cells bear spike-like protrusions that interdigitate with the surrounding keratinocytes and are attached by desmosomes. The cytoplasm contains

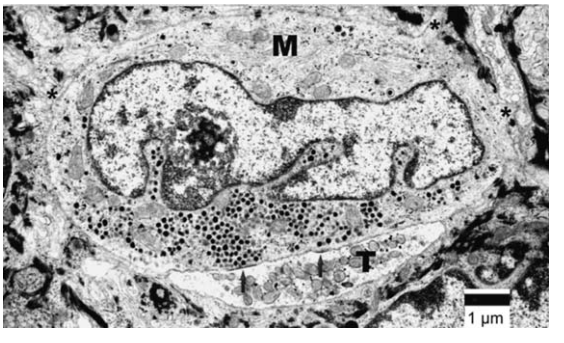

Figure 1 Ultrathin section from the planum nasale of a domestic cat. The typical Merkel nerve ending consists of a Merkel cell (M) with characteristic finger-like protrusions (*) and a discoid nerve terminal (T) containing a large number of mitochondria. Synapse-like contacts between Merkel cells and nerve terminal are marked by arrows. The cytoplasm of the Merkel cell facing the nerve terminal is packed with dense-core granules.

intermediate cytokeratin filaments and many large (50–110 nm) dense-core granules, particularly accumulated near the junction with the nerve fiber (Iggo, A. and Muir, A. R., 1969). The cytoplasmic membrane forms areas of synaptic membrane specialization with the membrane of an axonal terminal (Iggo, A. and Findlater, G. S., 1984). The nerve terminal is packed with mitochondria and optically clear vesicles.

6.02.2 Merkel Nerve Endings in Mammalian Glabrous Skin

Merkel cells in the mammalian glabrous skin are always in the basal layer of the epidermis (Figures 1 and 2). Pegged skin has solid epidermal pegs of different size anchoring the epidermis in the dermis containing blood sinus separating the epithelial pegs. Typical examples are the pig snout and planum nasale of mole and cat. Clusters of up to 40 Merkel cells are found in the basal layer of the epidermis at the base of these pegs. All Merkel cells are in synaptic contact with discoid terminals of branches of one myelinated axon (3–5 µm), losing the myelin sheath on entering the epidermis. In ridged skin (typically found in the tips of fingers and toes of primates and marsupials) clusters of up to 10 Merkel nerve endings are found at the base of the epidermal ridges near the ducts of sweat glands (Halata, Z., 1975).

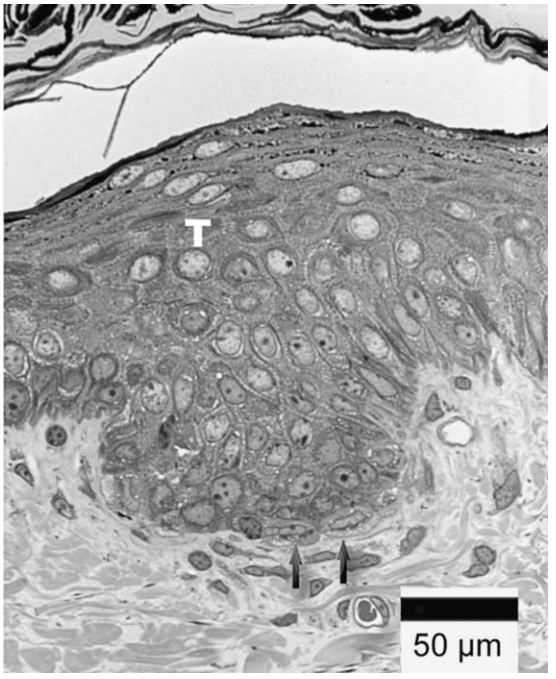

Figure 2 Semithin section of a touch dome (T) from the eyelid of a rhesus monkey. Merkel cells in the basal layer of the rete peg are marked by arrows.

6.02.3 Merkel Nerve Endings in Mammalian Hairy Skin

In hair follicles of velus hairs and guard hairs, Merkel nerve endings are found at the thickening of the follicle – the so-called bulge region – below the sebaccous gland. This part of the hair follicle does not change its form during the hair cycle and the bulge region is also a stem cell niche of the epidermis (Oshima, H. *et al.*, 2001).

Between hair follicles of the hairy skin, the epidermis forms epithelial pegs of different size and density, often referred to as touch dome (Haarscheibe; Figure 2). These are basically similar to the epithelial pegs in glabrous skin (see above), containing up to 150 Merkel nerve endings (Figure 3) supplied by one trunk nerve fiber.

6.02.4 Merkel Nerve Endings in Sinus Hairs of Mammals

Specialized large hairs (vibrissae, whiskers, or sinus hairs) are found in all mammals apart from man, arranged in groups especially in the face and

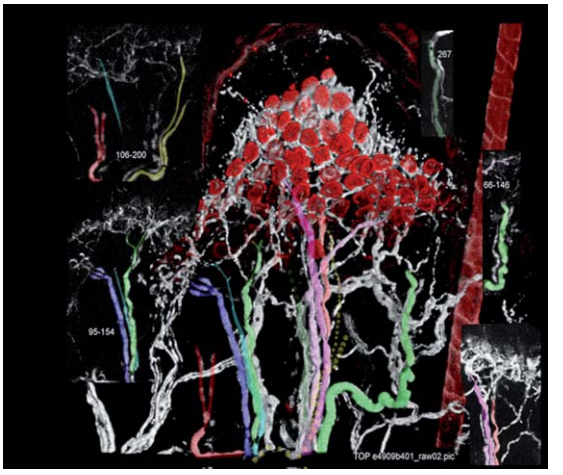

Figure 3 Touch dome from the interdigital skin of the cat paw reconstructed from confocal microscopic images. The trunk nerve fiber branches below the level of this figure into several preterminal nerve fibers (marked in different colors) before branching further into terminal nerve fibers, each making contact with 5–10 Merkel cells. In this touch dome a total of 137 Merkel cells (red) were counted. Figure kindly provided by Dr. Satomi Ebara, Kyoto, Japan.

innervated by the trigeminal nerve. They are large hair follicles embedded in blood sinus with strong sturdy hairs. Fibers of mimic muscles are inserted into the capsule of the blood sinus. The hair follicles are richly innervated with free nerve endings and a variety of different mechanoreceptors especially Merkel nerve endings. Sinus hairs of land mammals contain up to 2000 Merkel cells (Gottschaldt, K.-M. *et al.*, 1973; Ebara, S. *et al.*, 2002) while marine mammals can have up to 20 000 Merkel cells in one follicle (Dehnhardt, G. *et al.*, 2003). They have large cortical representations in somatotopically organized barrels (Woolsey, T. A. and van der Loos, H., 1970).

Merkel cells are located in the basal layer of the epithelium of the hair follicle in the thickened part below the sebaceous gland arranged like scales in a pine cone, oblique to the basal lamina (glassy membrane) sending cytoplasmic processes of about 3 µm through the glassy membrane. This area is surrounded by the ring sinus. All Merkel cells are in contact with discoid nerve terminals on the opposite side (Figure 4). The part of Merkel cells facing nerve terminals contains the typical dense-core (osmiophilic) granules. The myelinated axons (diameter about 5 µm) lose their myelin sheath and Schwann cells on penetrating the basal lamina, branching intensively supplying up to 50 Merkel cells (Ebara, S. *et al.*, 2002). Other Merkel nerve endings are found in the epidermis close to the penetration of the hair shaft in the rete pegs of the epidermis similar to the description above.

Figure 4 Ultrathin longitudinal section through the thickened portion below the sebaceous gland of a sinus hair from the upper lip of a rhesus monkey. Merkel cells (M) and nerve terminals (T) are arranged obliquely to the glassy membrane (*) like scales of a pine cone. The Merkel cell is always facing the glassy membrane. A lanceolate nerve terminal (L) in close contact with the glassy membrane is seen on the outer side.

6.02.5 Merkel Nerve Endings in the Mucosa of Mammals

In mucosa derived from the ectoderm (mouth, lips, and anal canal), Merkel cells can be found in many mammalian species. In the mouth, the so-called surrounding mucosa is not cornified and covers the surface of lips, cheeks, and the soft palate forming epithelial pegs containing numerous Merkel nerve endings at their base. Masticatory mucosa with cornified epithelium covering the hard palate and forming the surface of the gingiva has to withstand heavy mechanical loads during chewing of food. The basal layer of the epithelium forms rete ridges or rete pegs containing many Merkel nerve endings in the basal layer with identical structure as found in glabrous skin (Figure 5; Halata, Z. and Baumann, K. I., 1999). In contrast, the specialized mucosa covering the surface of the tongue with typically structured papillae and gustatory organs is free of Merkel nerve endings.

In the mucosa of the anal canal, Merkel nerve endings can be found in nonkeratinized and keratinized parts. In the nonkeratinized part, the epithelium is a flat stratified epithelium with rete pegs. In basal

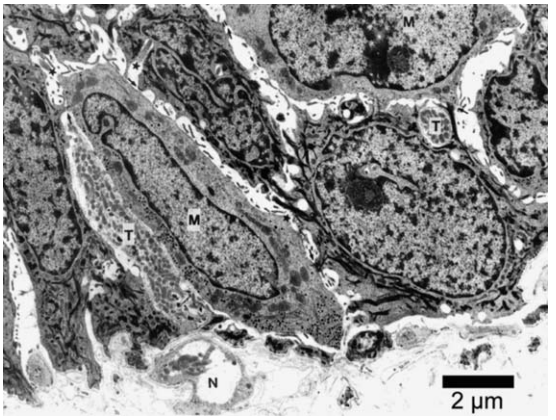

Figure 5 Ultrathin cross section through the papilla incisive of a rhesus monkey. Merkel cells (M) with cytoplasmic protrusions (*) and desmosomal contacts (arrows) with epithelial cells of the basal epithelial layer. Nerve terminals (T) from the afferent axon (N) covered by a Schwann cell.

parts of rete pegs typical Merkel nerve endings are present. Also the keratinized part shows rete pegs with numerous Merkel nerve endings (Rettig, T. and Halata, Z., 1990).

6.02.6 Merkel-Like Cells with Suggested Neuroendocrine Function

Structurally, Merkel cells resemble cells of the diffuse endocrine system found mainly in the epithelium of the gut and bronchial mucosa. Various substances were found in the osmiophilic granules of Merkel cells (see above), resulting in the classification of Merkel cells as part of the family of the amine precursor uptake and decarboxylation (APUD) system (Pearse, A. G. E., 1968; Fujita, T., 1977). These cells are believed to release neurotransmitters with paracrine function. Also in those areas where Merkel cells are usually found, pale oval cells with dense-core granules are occasionally found in the basal layer of the epidermis or mucosa of ectodermal origin. But these cells lack any contact with nerve terminals. In contrast to normal Merkel cells, these cells have oval nuclei with many nuclear pores. So far there is no evidence for exocytosis of substances from Merkel cells to support the assumption of a paracrine (Fujita, T., 1977) or neuroendocrine role (Boot, P. M. *et al.*, 1992), leaving the question about the functional role of those substances in the dense-core granules of Merkel cells widely open.

6.02.7 Merkel Cell Carcinoma

In a highly malignant type of skin tumor, cells were found with osmiophilic granules and positive immunohistochemical reaction with neuron-specific enolase (Tang, C. K. and Toker, C., 1978; Johannessen, J. V. and Gould, V. E., 1980). It is widely assumed that these tumors originate from Merkel cells, giving rise to the name Merkel cell carcinoma. However, direct evidence for this assumption is still lacking (Gould, V. E. *et al.*, 1985; Moll, R. *et al.*, 1992). Another assumption is that this tumor may originate from dermal neuroendocrine cells (Hoefler, H. *et al.*, 1985).

6.02.8 Developmental Origin of Merkel Cells

There has been a long controversy about the developmental lineage of Merkel cells. One view is that Merkel cells arise from a common ectodermal stem cell (English, K. B., 1974; Moll, I. *et al.*, 1986). This hypothesis is mainly supported by the finding of low molecular cytokeratin (CK8, CK18, and CK20) in Merkel cells of mammals (Moll, R. *et al.*, 1984; Moll, I. *et al.*, 1995; Kim, D. K. and Holbrook, K. A., 1995). In contrast, several studies suggested that they originate from the neural crest and migrate into the mammalian epidermis during the embryonic period (Hashimoto, K., 1972; Breathnach, A. S., 1978). Using the chick/quail marking system, it was shown that avian Merkel cells do not develop from ectodermal or mesodermal cells, but that they originate from the neural crest (Grim, M. and Halata, Z., 2000). In mammals, Szeder V. *et al.* (2003) examined Wnt1-cre/R26R double transgenic mice in which Merkel cells like all neural crest-derived cells are marked by the reporter gene LacZ. Thus, there is now unambiguous evidence for a neural crest origin of avian and mammalian Merkel cells.

6.02.9 Mechanoreceptor Function of Merkel Cells

Merkel's original description of touch corpuscles clearly described these complexes as mechanoreceptors (Merkel, F., 1875). They respond to punctate pressure on the skin (Iggo, A. and Muir, A. R., 1969) or bending of whiskers with long-lasting spike trains

(Gottschaldt, K.-M. *et al*., 1973). In all locations, the Merkel cells are positioned between the direction of the physiological mechanical stimulus and the nerve terminal. The surface of Merkel cells is equipped with protoplasmic protrusions anchoring between keratinocytes (Halata, Z. *et al*., 2003), which has led to comparisons with inner ear hair cells (Iggo, A. and Findlater, G. S., 1984; Baumann, K. I. *et al*., 1990) where bending of the hairs opens mechanically gated ion channels resulting in depolarization, increase of free intracellular calcium, and transmitter release (Crawford, A. C. *et al*., 1991).

There have been long controversies, whether the mechanoelectric transduction process occurs in the Merkel cell or whether the Merkel cell only directs the mechanical stimulus toward the nerve terminal. Unfortunately, the location of these receptors makes direct electrophysiological recordings with microelectrodes impossible. The slowly adapting responses of these receptors and the characteristic impulse pattern of action potentials with rather irregular interspike intervals were interpreted as an indication of a synaptic link (Iggo, A. and Muir, A. R., 1969; Horch, K. W. *et al*., 1974).

Various potential neurotransmitters were found in the dense-core granules of Merkel cells (Hartschuh, W. *et al*., 1979; Hartschuh, W. and Weihe, E., 1988; Cheng Chew, S. B. and Leung, P. Y., 1991; English, K. B. *et al*., 1992). However, attempts to impair transmission with the respective receptor blockers failed to show clear effects on receptor responses (Gottschaldt, K.-M. and Vahle-Hinz, C., 1982). Using calcium indicator dyes, increases of intracellular calcium concentration in Merkel cells during mechanical stimulation have been observed consistently in different species and locations (Chan, E. *et al*., 1996; Tazaki, M. and Suzuki, T., 1998). In spite of mechanical stimulation, no such increases are seen if the extracellular fluid is calcium free or amiloride (known to block mechanosensitive ion channels; Hamill, O. P. *et al*., 1992) is added to the solution (Halata, Z. *et al*., 2003). Further studies revealed the existence of voltage-gated calcium channels and presynaptic proteins in Merkel cells (Yamashita, Y. *et al*., 1992; Chan, E. *et al*., 1996; Haeberle, H. *et al*., 2004). Thus, mechanical stimulation causes an influx of calcium into Merkel cells, which in turn appears to trigger further release of calcium from intracellular stores (Calcium-induced calcium release; Senok, S. S. and Baumann, K. I., 1997). It has long been established that increase in free calcium is a requirement for synaptic transmitter release.

Recent experimental evidence suggests that glutamatergic transmission occurs at Merkel cell receptors although the specific type of glutamate receptor involved is still unclear (Fagan, B. M. and Cahusac, P. M. B., 2001; Hitchcock, I. S. *et al*., 2004; Haeberle, H. *et al*., 2004; Cahusac, P. M. B. *et al*., 2005). This synaptic transmission is probably essential for the slowly adapting responses during maintained mechanical stimuli (Ogawa, H., 1996; Senok, S. S. and Baumann, K. I., 1997).

References

Baumann, K. I., Hamann, W., and Leung, M. S. 1990. Acute affects of neomycin on slowly adapting typeI and typeII cutaneous mechanoreceptors in the anaesthetized cat and rat. J. Physiol. 425, 527–544.

Boot, P. M., Rowden, G., and Walsh, N. 1992. The distribution of Merkel cells in human fetal and adult skin. Am. J. Dermatopathol. 14, 391–396.

Breathnach, A. S. 1978. Development and differentiation of dermal cells in man. J. Invest. Dermatol. 71, 2–8.

Cahusac, P. M. B., Senok, S. S., Hitchcock, I. S., Genever, P. G., and Baumann, K. I. 2005. Are unconventional NMDA receptors involved in slowly adapting type I mechanoreceptor responses? Neuroscience 133, 763–773.

Chan, E., Yung, W. H., and Baumann, K. I. 1996. Cytoplasmic Ca2+ concentrations in intact Merkel cells of an isolated, functioning rat sinus hair preparation. Exp. Brain Res. 108, 357–366.

Cheng Chew, S. B. and Leung, P. Y. 1991. Immunocytochemical evidence of a met-enkephalin-like substance in the dense-core granules of mouse Merkel cells. Cell Tissue Res. 265, 611–614.

Crawford, A. C., Evan, M. G., and Fettiplace, R. 1991. The actions of calcium on the mechano-electrical transducer current of turtle hair cells. J. Physiol. 434, 389–398.

Dehnhardt, G., Mauck, B., and Hyvaerinen, H. 2003. The Functional Significance of the Vibrissal System of Marine Mammals. In: The Merkel cell (*eds*. K. I. Baumann, Z. Halata, and I. Moll), pp. 127–135. Springer.

Ebara, S., Kumamoto, K., Matsura, T., Mazurkiewicz, J. E., and Rice, F. L. 2002. Similarities and differences in the innervation of mystacial vibrissal follicle-sinus complexes in the rat and cat: a confocal microscopic study. J. Comp. Neurol. 449, 103–119.

English, K. B. 1974. Cell types in cutaneous type I mechanoreceptors (Haarscheiben) and their alterations with injury. Am. J. Anat. 141, 105–126.

English, K. B., Wang, Z. Z., Stayner, N., Stensaas, L. J., Martin, H., and Tuckett, R. P. 1992. Serotonin-like immunoreactivity in Merkel cells and their afferent neurons in touch domes from the hairy skin of rats. Anat. Rec. 232, 112–120.

Fagan, B. M. and Cahusac, P. M. B. 2001. Evidence for glutamate receptor mediated transmission at mechanoreceptors in the skin. Neuroreport 12, 341–347.

Fujita, T. 1977. Concept of paraneurons. Arch. Histol. Jap. 40(Suppl.), 1–12.

Gottschaldt, K.-M. and Vahle-Hinz, C. 1982. Evidence against transmitter function of met-enkephalin and chemosynaptic

impulse generation in ''Merkel cell'' mechanoreceptors. Exp. Brain Res. 45, 459–463.
Gottschaldt, K.-M., Iggo, A., and Young, D. W. 1973. Functional characteristics of mechanoreceptors in sinus hair follicles of the cat. J. Physiol. 235, 287–315.
Gould, V. E., Moll, R., Moll, I., Lee, I., and Franke, W. W. 1985. Biology of disease. Neuroendocrine (Merkel) cells of the skin: hyperplasias, dysplasias, and neoplasms. Lab. Invest. 52, 334–353.
Grim, M. and Halata, Z. 2000. Developmental origin of avian Merkel cells. Anat. Embryol. 202, 401–410.
Haeberle, H., Fujiwara, M., Chuang, J., Medina, M. M., Panditrao, M. V., Bechstedt, S., Howard, J., and Lumpkin, E. A. 2004. Molecular profiling reveals synaptic release machinery in Merkel cells. Proc. Natl. Acad. Sci. U. S. A. 101, 14503–14508.
Halata, Z. 1975. The mechanoreceptors of the mammalian skin. Ultrastructure and morphological classification. Adv. Anat. Embryol. Cell Biol. 50, 1–77.
Halata, Z. and Baumann, K. I. 1999. Sensory nerve endings in the hard palate and papilla incisiva of the rhesus monkey. Anat. Embryol. 199, 427–437.
Halata, Z., Grim, M., and Baumann, K. I. 2003. Friedrich Sigmund Merkel and his ''Merkel cell'', morphology, development, and physiology: review and new results. Anat. Rec. 271A, 225–239.
Hamill, O. P., Lane, J. W., and McBride, D. W. 1992. Amiloride - a molecular probe for mechanosensitive channels. TiPS. 13, 373–376.
Hartschuh, W. and Weihe, E. 1988. Multiple messenger candidates and marker substances in the mammalian Merkel cell-axon complex: a light and electron microscopic immunohistochemical study. In: Progress in Brain Research 74 (*eds*. W. Hamann and A. Iggo), pp. 181–187. Elsevier.
Hartschuh, W., Weihe, E., Buechler, M., Helmstaedter, V., Feurle, G. E., and Forssmann, W. G. 1979. Met-enkephalin-like immunoreactivity in Merkel cells. Cell Tissue Res. 201, 343–348.
Hashimoto, K. 1972. The ultrastructure of the skin of human embryos. X. Merkel tactile cells in the finger and nail. J. Anat. 111, 99–120.
Hitchcock, I. S., Genever, P. G., and Cahusac, P. M. 2004. Essential components for a glutamatergic synapse between Merkel cell and nerve terminal in rats. Neurosci.Lett. 362, 196–199.
Hoefler, H., Kerl, H., Lackinger, E., Helleis, G., and Denk, H. 1985. The intermediate filament cytoskeleton of cutaneous neuroendocrine carcinoma (Merkel cell tumour). Immunohistochemical and biochemical analyses. Virchows Arch. A 406, 339–350.
Horch, K. W., Whitehorn, D., and Burgess, P. R. 1974. Impulse generation in type I cutaneous mechanoreceptors. J Neurophysiol. 37, 267–281.
Iggo, A. and Findlater, G. S. 1984. A review of Merkel cell mechanisms. In: Sensory Receptor Mechanisms (*eds*. W. Hamann and A. Iggo), pp. 117–131. World Scientific Publ. Co.
Iggo, A. and Muir, A. R. 1969. The structure and function of a slowly adapting touch corpuscle in hairy skin. J. Physiol. 200, 763–796.
Johannessen, J. V. and Gould, V. E. 1980. Neuroendocrine skin carcinoma associated with calcitonin production: a Merkel cell carcinoma? Hum. Pathol. 11, 586–588.
Kim, D. K. and Holbrook, K. A. 1995. The appearance, density, and distribution of Merkel cells in human embryonic and fetal skin: their relation to sweat gland and hair follicle development. J. Invest. Dermatol. 104, 411–416.
Mahrle, G. and Orfanos, C. E. 1974. Merkel cells as human cutaneous neuroreceptor cells. Their presence in dermal neural corpuscles and in the external hair root sheath of human adult skin. Arch. Derm. Forsch. 251, 19–26.
Merkel, F. 1875. Tastzellen and Tastkoerperchen bei den Hausthieren und beim Menschen. Arch. Mikr. Anat. 11, 636–652.
Moll, I., Kuhn, C., and Moll, R. 1995. Cytokeratin 20 is a general marker of cutaneous Merkel cells while certain neuronal proteins are absent. J. Invest. Dermatol. 104, 910–915.
Moll, R., Lowe, A., Laufer, J., and Franke, W. W. 1992. Cytokeratin 20 in human carcinomas. A new histodiagnostic marker detected by monoclonal antibodies. Am. J. Pathol. 140, 427–447.
Moll, R., Moll, I., and Franke, W. W. 1984. Identification of Merkel cells in human skin by specific cytokeratin antibodies: changes of cell density and distribution in fetal and adult plantar epidermis. Differentiation 28, 136–154.
Moll, I., Moll, R., and Franke, W. W. 1986. Formation of epidermal and dermal Merkel cells during human fetal skin development. J. Invest. Dermatol. 87, 779–787.
Ogawa, H. 1996. The Merkel cell as a possible mechanoreceptor cell. Prog. Neurobiol. 49, 317–334.
Oshima, H., Rochat, A., Kedzia, C., Kobayashi, K., and Barrandon, Y. 2001. Morphogenesis and renewal of hair follicles from adult multipotent stem cells. Cell 104, 233–245.
Pearse, A. G. E. 1968. Common cytochemical and ultrastructural characteristics of cells producing polypeptide hormones (the APUD series) and their relevance to thyroid and ultimobranchial C cells and calcitonin. Proc. Royal. Soc. London (B) 170, 71–80.
Rettig, T. and Halata, Z. 1990. Structure of the sensory innervation of the anal canal in the pig. A light- and electron-microscopical study. Acta. Anat. 137, 189–201.
Saxod, R. 1978. Development of cutaneous sensory receptors in birds. In: Handbook of Sensory Physiology. Development of Sensory Systems (*ed*. M. Jacobson), pp. 337–417. Springer.
Senok, S. S. and Baumann, K. I. 1997. Functional evidence for calcium-induced calcium release in isolated rat vibrissal Merkel cell mechanoreceptors. J. Physiol. 500, 29–37.
Szeder, V., Grim, M., Halata, Z., and Sieber-Blum, M. 2003. Neural crest origin of mammalian Merkel cells. Dev. Biol. 253, 258–263.
Tang, C. K. and Toker, C. 1978. Trabecular carcinoma of the skin: an ultrastructural study. Cancer 42, 2311–2321.
Tazaki, M. and Suzuki, T. 1998. Calcium inflow of hamster Merkel cells in response to hyposomatic stimulation indicate a stretch activated ion channel. Neurosci. Lett. 243, 69–72.
Woolsey, T. A. and van der Loos, H. 1970. The structural organisation of layer IV in the somatosensory region (SI) of mouse cerebral cortex. Brain Res. 17, 205–242.
Yamashita, Y., Akaike, N., Wakamori, M., Ikeda, I., and Ogawa, H. 1992. Voltage-dependent currents in isolated single Merkel cells of rats. J. Physiol. 450, 143–162.

Further Reading

Moll, I., Lane, A. T., Franke, W. W., and Moll, R. 1990. Intraepidermal formation of Merkel cells in xenografts of human fetal skin. J. Invest. Dermatol. 94, 359–364.

6.03 Physiological Responses of Sensory Afferents in Glabrous and Hairy Skin of Humans and Monkeys

A W Goodwin and H E Wheat, University of Melbourne, Parkville, Vic, Australia

© 2008 Elsevier Inc. All rights reserved.

6.03.1	**Introduction**	39
6.03.2	**Glabrous Skin**	40
6.03.2.1	Receptors	40
6.03.2.2	Classification of Innervating Fibers	40
6.03.2.3	Afferent Responses to Ramps and Vibration	41
6.03.2.4	Activation of Cutaneous Afferents during Manipulation	42
6.03.2.5	Spatial Resolution of Single Afferents	42
6.03.2.6	Interpreting Resolution of Single Afferents	43
6.03.2.7	Responses to the Shape of an Object	44
6.03.2.8	Responses to Contact Force	44
6.03.2.9	Position in the Receptive Field	45
6.03.2.10	Signaling Must Be Viewed in Terms of Population Responses	45
6.03.2.11	More Realistic Population Responses	48
6.03.2.12	Measures of Stimulus Parameters	49
6.03.2.13	Complex Geometry of the Fingers	50
6.03.3	**Hairy Skin**	50
6.03.3.1	Classification of Innervating Fibers	51
6.03.3.2	Responses to Stroking	51
6.03.3.3	Proprioception	52
References		52

6.03.1 Introduction

The human body is covered by skin which, together with the special senses, forms our interface with the environment. Most of the body is covered by hairy skin but the palms of the hands and the soles of the feet are covered by glabrous skin, which does not have hairs. Sensation from both types of skin is mediated by a large number of specialized sensory receptors. These fall into three major categories, namely thermoreceptors, nociceptors, and mechanoreceptors. Thermoreceptors in the hand inform us of the temperature or thermal properties of objects we handle (a cold windowpane or a bath of warm water) whereas thermoreceptors in hairy skin play a crucial role in temperature regulation. Nociceptors alert us to stimuli that cause, or potentially cause, tissue damage and are critical to our survival. Thermoreceptors and nociceptors are covered in separate chapters of this encyclopedia.

Cutaneous mechanoreceptors, which respond to low-threshold or non-noxious mechanical stimuli, provide us with information about our environment; the complexity, richness, and importance of this information in our daily lives is often underestimated. In hairy skin, the sensory functions of whisker systems in navigation for animals like rodents and seals have long been appreciated. More recently, the role of hairy skin receptors in affective aspects of touch has been revealed.

The significance of glabrous skin to humans is far greater than suggested by the fact that it forms only a small proportion of human skin. This is because glabrous skin, which covers the front surface of the hand, is engaged in the myriad manipulations that are central to human existence. There are countless examples of hand function ranging from common everyday tasks, such as lifting a glass of water, shelling a pea, or peeling an orange, to complex contemporary tasks such as performing a liver transplant or driving a car. Such tasks are dependent on information from the cutaneous mechanoreceptors.

In this chapter we will first discuss, in some detail, neural signals from the glabrous skin of the hand.

Only primates have hands and therefore much of the data related to glabrous cutaneous mechanoreceptors were gathered in humans or monkeys. We will then discuss, more briefly, neural signals from hairy skin. Data on primate hairy skin mechanoreceptors is not extensive and much of our knowledge of these receptor properties stems from work done in other animals that have hairy skin, particularly for the complex signals in the whisker system, which is covered elsewhere.

6.03.2 Glabrous Skin

6.03.2.1 Receptors

Human glabrous skin (Figure 1) contains four classes of mechanoreceptors which vary in their structural complexity and in their location in the skin (Halata, Z., 1975). Meissner corpuscles and Pacinian corpuscles are mechanically complex, comprising repeating layers of fluid bounded by connective tissue or nerve terminals, resulting in a mechanical filter interposed between the stimulus and the mechanosensitive nerve terminals. Ruffini endings and Merkel complexes are simpler in that the mechanosensitive nerve terminals are not surrounded by a laminated filter. Meissner corpuscles in the uppermost part of the dermis and Merkel complexes at the epidermal–dermal junction are relatively close to the surface of the skin. Ruffini endings located in the mid part of the dermis and Pacinian corpuscles locate deep in the dermis, or subcutaneously, are further from the surface than Merkel or Ruffini endings.

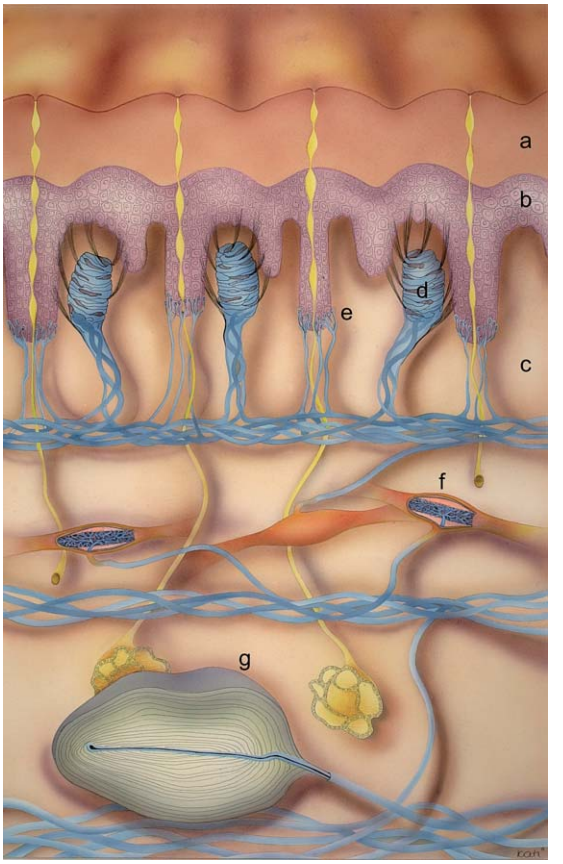

Figure 1 A cross-section through glabrous skin. Fingerprint patterns reflect the wavelike structure of the dermis (c), the epidermis (b), and the covering keratin (a). Peripheral nerve fibers, shown in blue, innervate four types of mechanoreceptors: the Meissner corpuscles (d), the Merkel endings (e), the Ruffini organs (f), and the Pacinian corpuscles (g). Reproduced with permission from Ian Darian-Smith.

6.03.2.2 Classification of Innervating Fibers

The mechanoreceptors are innervated by large myelinated axons belonging to the Aβ group. They range in diameter from 7–14 μm and have conduction velocities in the range of 15–60 m s^{-1} (Vallbo, A. B. and Johansson, R. S., 1984; Brink, E. E. and Mackel, R. G., 1993). These primary afferent axons, which are part of the sensory component of peripheral nerves, have cell bodies in the dorsal root ganglia; their proximal terminals enter the spinal cord via the dorsal roots. The anatomical relationship between primary afferent axons and mechanoreceptors differs for different receptors. For axons terminating on Merkel complexes, a single axon typically innervates several Merkel complexes (Pare, M. *et al.*, 2002). Similarly, many Meissner corpuscles may be innervated by the same axon, and a single Meissner corpuscle may be innervated by more than one axon (Quilliam, T. A., 1978). This contrasts with Pacinian corpuscles, each of which is supplied by a single unbranched axon (Quilliam, T. A., 1978). Ruffini ending have been studied mainly in hairy skin or structures like the joints, where the evidence is that each ending is innervated by a single axon and a single axon may innervate a number of endings (Iggo, A. and Andres, K. H., 1982).

Primary afferent fibers innervating glabrous skin fall into four classes which are easily defined by the afferents' responses to indenting probes. Rigorous classification requires machine-controlled probes but even simple hand-held probes allow unambiguous classification (Vallbo, A. B. and Johansson, R. S., 1984).

For two of the classes, afferents respond when the probe is pressing into or lifting out of the skin, the dynamic component, and also when indentation of the probe is maintained without change, the static component. These are termed slowly adapting (SA) afferents. For one class of SA afferents the receptive fields are spatially confined; there is a central small area, of the order of square millimeters, where thresholds are low, surrounded by an area where thresholds rise rapidly (Figure 2). These are termed SA type I (SAI) afferents. For the second group, the SA type II (SAII) afferents, thresholds rise more slowly with distance from the receptive field center so that the receptive fields are less confined and larger than those of SAI afferents. An additional property of SAII afferents is that they respond well to lateral stretch of the skin, for example when two points of skin on either side of the receptive field are pulled away from each other.

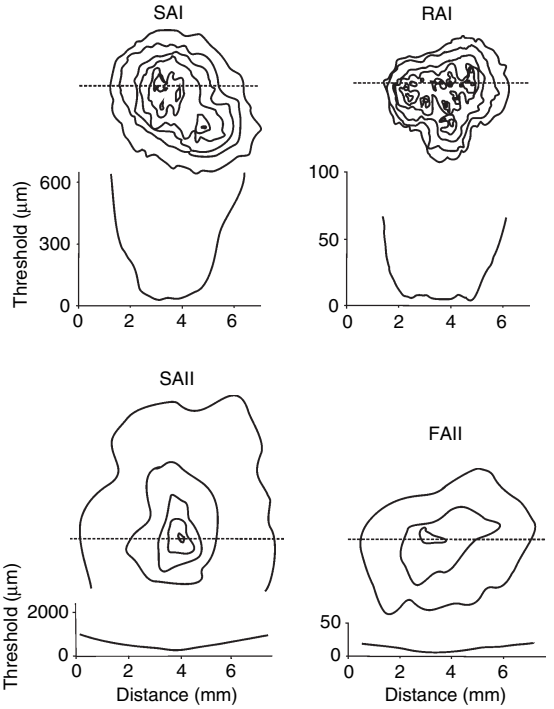

Figure 2 Receptive field structure for the four classes of mechanoreceptive afferents innervating glabrous skin. For each class, the lower figure shows threshold as a function of distance along a line through the receptive field center. The upper figures are contour plots showing thresholds along both dimensions of the receptive field. SA, slowly adapting; FA, rapidly adapting (adapted from Johansson, R. S. 1976. Receptive field sensitivity profile of mechanosensitive units innervating the glabrous skin of the human hand. Brain Res. 104, 330–334).

Fibers in the remaining two classes respond only to the dynamic component of probe indentation and are referred to as fast adapting (FA) afferents. Again, one class has relatively small and confined receptive fields whereas the other has larger more diffuse receptive fields. These are termed FA type I (FAI) and FA type II (FAII) afferents, respectively.

There is evidence, both direct and indirect, that SAI and FAI afferents terminate on the more superficial Merkel complexes and Meissner corpuscles, respectively, while SAII and FAII afferents innervate the deeper Ruffini endings and Pacinian corpuscles, respectively (Vallbo, A. B. and Johansson, R. S., 1984).

Monkey glabrous skin is similar in structure to human glabrous skin. It contains Merkel endings, Meissner corpuscles, and Pacinian corpuscles and the properties of monkey SAI, FAI, and FAII afferents are similar to those in humans. A major difference is that monkey glabrous skin does not appear to contain Ruffini endings and no SAII afferents have been reported (Pare, M. *et al.*, 2002).

Innervation density is not uniform over the hand (Johansson, R. S. and Vallbo, A. B., 1979). For SAI and FAI afferents, the density increases in a distal direction reaching a peak in the fingertips of about 0.7 and 1.4 afferents mm^{-2}, respectively. The proximal–distal gradient is less pronounced for SAII and FAII afferents which have lower densities than the type I afferents (0.09 and 0.22 mm^{-2}, respectively).

6.03.2.3 Afferent Responses to Ramps and Vibration

By using a machine to control the indentation of a probe, it is possible to specify either the force of indentation or the displacement of the probe. In addition, the temporal waveform of the indentation can be varied.

Trapezoids are a commonly used temporal waveform because they allow independent variation of the static component of indentation (the height of the trapezoid) and the dynamic component (the slope of the trapezoid) corresponding to the velocity of indentation. SAI afferents, which respond principally to the depth of indentation, have a range of threshold amplitudes (depths); the least sensitive fibers have thresholds about 10 times those of the most sensitive fibers (Knibestol, M., 1975). FAI afferent responses depend on both the depth and the velocity of indentation; depth threshold varies from 0.05 to 1.65 mm and velocity thresholds range from 0.4 to 39.3 mm s^{-1} (Knibestol, M., 1973). Response

thresholds for FAII afferents also depend on both the depth and velocity of indentation (Knibestol, M., 1973).

An effective way of studying FAI and FAII responses is to use sinusoidally vibrating probes, which clearly show the difference in their adaptation characteristics (Talbot, W. H. *et al.*, 1968). FAI afferents respond best (have minimum thresholds) for vibratory frequencies around 30 Hz. In contrast, thresholds of FAII afferents are minimum at frequencies around 300 Hz. The layered structure of Meissner and Pacinian corpuscles forms a mechanical filter which accounts, at least in part, for the dynamic characteristics of the FA afferent responses. There may also be a component of adaptation in the neural transduction process (French, A. S., 1992).

6.03.2.4 Activation of Cutaneous Afferents during Manipulation

Responses of the primary afferents to simple, but precisely controlled, indenting probes have provided invaluable information about the fundamental nature of the transduction process (Leung, Y. Y. *et al.*, 2005). However, such experiments do not provide a ready appreciation of the rich and complex information signaled to the central nervous system by those afferents when we manipulate the range of objects encountered daily.

Any form of manipulation requires motor output and it results in sensory input from a range of sources including cutaneous mechanoreceptors. There are various degrees of sensorimotor interaction depending on the nature of the task. In some tasks the sensory component dominates. For example, when determining the roughness of a piece of sandpaper, the purpose is to extract sensory information and the relatively simple role of the motor system is to engage the cutaneous mechanoreceptors with the surface being explored. Most manipulations are of a more complex nature. As an example, when picking an apple, the precise hand movements required rely on sensory information about parameters such as the size and shape of the apple. During such a task, the sensory input is used in two ways. First, in conscious perception; we are aware of factors such as the texture of the apple and its degree of slipperiness. Second, the sensory information is used by the motor control system either in a feedback manner, to optimize the hand movements, or to update memory, which can be used in a feedforward manner for similar tasks in the future. (Witney, A. G. *et al.*, 2004)

In general, input to the brain is multisensory. In the case of picking an apple, visual and proprioceptive information is obviously involved. What is easily overlooked is the importance of the cutaneous mechanoreceptors in such tasks. There are many pointers to their crucial role. For many finely controlled hand movements, such as doing up a button in the dark, visual input is absent and we rely entirely on cutaneous mechanoreceptive input and proprioception. Also, it is well established that blocking the cutaneous afferents with local anesthetic severely compromises complex manipulations or makes them impossible (Monzee, J. *et al.*, 2003).

What parameters of the object being manipulated, or of the manipulation itself, are potentially signaled to the central nervous system by the cutaneous mechanoreceptors? Candidates include: the local shape of the object, the position of contact on the skin, the texture of the surface, the contact force (which is three-dimensional and includes forces normal to the skin and forces tangential to the skin), the compliance or softness of the object, the coefficient of friction, and slip during the manipulation.

In order to characterize the information relayed by the cutaneous afferents during manipulation, it is necessary to use stimuli that are more complex than simple indenting probes. Stimuli that can be directly related to naturally occurring stimuli are particularly informative.

6.03.2.5 Spatial Resolution of Single Afferents

Single indenting probes provide limited information on the spatial resolving capacity of the four classes of cutaneous mechanoreceptive afferents. A more direct measure of spatial resolution can be obtained by stepping square-edged gratings of alternating grooves and ridges across the receptive fields of primary afferent fibers. The resulting afferent responses are modulated by the position of the stimulus in the receptive field (Phillips, J. R. and Johnson, K. O., 1981). Gap width is the principal determinant of response and modulation decreases as the spatial period of the grating decreases (Figure 3). Measured in this way, acuity is greatest for SAI afferents, which can resolve gap widths of around 1 mm. Acuity for FAI afferents is considerably less.

Measuring resolution with an indenting grating, with no lateral movement, is appropriate in the context of hand movements where there is no lateral motion between the skin and the surface, such as

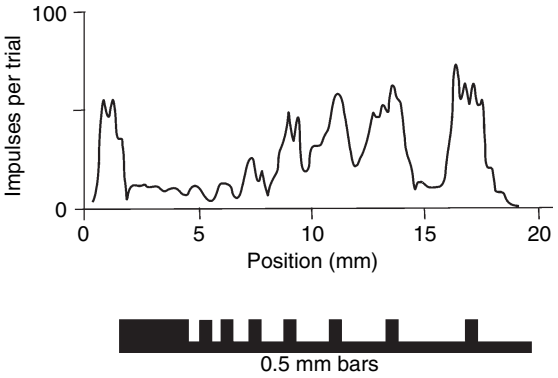

Figure 3 Responses of a single slowly adapting type I (SAI) afferent to a grating indenting the skin. The grating, with an incrementing spatial period (lower figure), was stepped across the receptive field between indentations. Upper curve shows response as a function of the position of the grating in the receptive field (adapted from Phillips, J. R. and Johnson, K. O. 1981. Tactile spatial resolution. II. Neural representation of bars, edges, and gratings in monkey primary afferents. J. Neurophysiol. 46, 1192–1203).

grasping an object with a rough surface. For manipulations where there is lateral motion, a more suitable stimulus comprises patterned surfaces scanned over the receptive field. There have been many such studies with a range of patterned surfaces including gratings of alternating grooves and ridges, raised dots analogous to Braille, and embossed letters (Goodwin, A. W. and Morley, J. W., 1987; Phillips, J. R. *et al.*, 1990; Blake, D. T. *et al.*, 1997; Yoshioka, T. *et al.*, 2001). Such stimuli are considerably more complex than an indenting stimulus and comprise both spatial and temporal components. All four afferent types respond in some way to patterned surfaces scanned across the skin. FAI and SAI afferents both respond vigorously (Figure 4), and the variation in response of single afferents is correlated with the perceived roughness of the surfaces. This relationship is more consistent for the SAI than the FAI afferents.

6.03.2.6 Interpreting Resolution of Single Afferents

Is the spatial resolution of a single afferent a meaningful concept? Consider the task of touching a grating of alternating grooves and ridges using a single vertical contact without lateral motion of the finger. Clearly information about the spatial properties of the grating is contained in the combined activity of the entire array of cutaneous afferents activated. Thus, any analysis of the spatial properties of a stimulus relayed by the mechanoreceptors necessitates a population analysis, even if only of an implicit nature. Figure 3 depicts the responses of a single SAI afferent when the grating shown is stepped across the afferent's receptive field. The direct way of interpreting this curve is as a receptive field profile, which shows the responses of a single fiber to a stimulus applied at increasing distances from the receptive field center. But the curve can also be

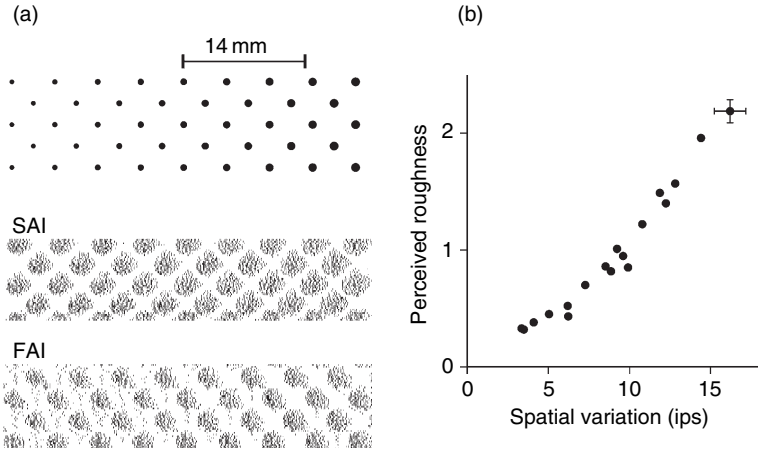

Figure 4 Responses to a pattern of dots, with incrementing spatial period, swept across the fingerpad. (a) Impulse patterns in a single fast adapting type I (FAI) afferent (bottom) and a single slow adapting type I (SAI) afferent (middle) are isomorphic with the dot pattern in the stimulus (top). (b) Human perception of roughness correlates with a measure, spatial variation, extracted from the SAI impulse patterns (adapted from Blake, D. T., Hsiao, S. S., and Johnson, K. O. 1997. Neural coding mechanisms in tactile pattern recognition: the relative contributions of slowly and rapidly adapting mechanoreceptors to perceived roughness. J. Neurosci. 17, 7480–7489).

viewed as the profile of responses across a population of afferents with receptive field centers located at increasing distances from center of the stimulus contact point. This interpretation of the data is necessary for any postulates about the nature of spatial information relayed to the brain. As will be discussed in a later section, there are many inherent simplifying assumptions in such an interpretation that are not valid.

A similar argument applies to interpreting responses to surfaces scanned across the skin. A common approach has been to generate spatial event plots, such as those illustrated in Figure 4 where the pattern of dots was swept across the receptive field of a single SAI afferent and a single FAI afferent. For each successive sweep, the stimulus is shifted, at right angles to the direction of scanning motion, by a small amount so that eventually the entire pattern is scanned over the receptive field center. The two-dimensional spatial event plots show the occurrence of action potentials in a single afferent. Each plot can by interpreted directly as the response of a single afferent to the stimulus located in a variety of different positions in its receptive field. But this is not as useful as the alternative view that the plot shows the responses of a two-dimensional population of afferents transmitting the spatial pattern of the surface to the brain. Again the simplifying assumptions about the population are potentially problematic.

6.03.2.7 Responses to the Shape of an Object

When stepping square-edged stimuli across the receptive fields of SAI afferents, it was observed that responses were more vigorous when an edge was located at the receptive field center than when a flat part of the object was located there (left part of Figure 3). The enhanced edge response suggests that the cutaneous afferents have the capacity to transmit information about the local shape of handled objects. This has been studied directly in experiments in which objects with defined and controlled local shapes were indented into or scanned across the skin.

A number of simple shapes have been used effectively to characterize tactile sensation. The local shape of an object (the shape at a particular point on the object) can be described by two orthogonal curvatures at that point. A sphere is perhaps the simplest shape; the curvature is the same in both orthogonal directions and is the same all over the object. Thus, a sphere can be described by a single parameter; either its radius or, more conveniently, its curvature, which is the reciprocal of the radius. A toroidal surface is defined by two orthogonal curvatures which are different, but each is constant over the entire surface. A cylinder is a special case of a toroid in which the curvature in one direction is zero (infinite radius) and the curvature in the orthogonal direction is nonzero and constant. Because such surfaces are simple to characterize mathematically and are easily manufactured, they have been used extensively to examine cutaneous mechanoreceptor responses.

Figure 5(a) shows the responses of a single SAI afferent when spheres of different curvature were indented into a monkey's fingerpad, contacting the afferent's receptive field center (Goodwin, A. W. *et al.*, 1995). The monotonic relationship confirms that SAI afferents are signaling information about the local shape of the object. Little information about shape was evident in the responses of FAI afferents. Similar results were obtained with sinusoidally shaped surfaces (Srinivasan, M. A. and LaMotte, R. H., 1987) and toroids (Khalsa, P. S. *et al.*, 1998).

For an indenting object, the nature of the contact is equivalent to that occurring when an object is grasped. To simulate the type of contact that occurs when an object is actively explored by the hand, which results in tangential motion between the skin and the object, simple surfaces such as toroids were scanned across the afferent's receptive field (LaMotte, R. H. *et al.*, 1998). Here too it is clear that SAI afferents are responsive to the shape of the object while FAI afferent responses are less shape sensitive.

Experiments in humans, using indenting spheres, show that with contact forces comparable in magnitude to those used in everyday manipulations, afferents innervating glabrous skin all over the distal segment of the finger are activated (Jenmalm, P. *et al.*, 2003). Responses of SAI, FAI, and SAII afferents are influenced by the curvature of the stimulus.

6.03.2.8 Responses to Contact Force

When grasping and manipulating an object, the cutaneous mechanoreceptors are activated by the contact forces exerted on the skin. Commonly, experimenters resolve the forces into two components and deal with them separately. The first component, the grip force, is normal to the skin surface. The second component, the load force, is tangential to the skin surface and may be at any angle in the tangential

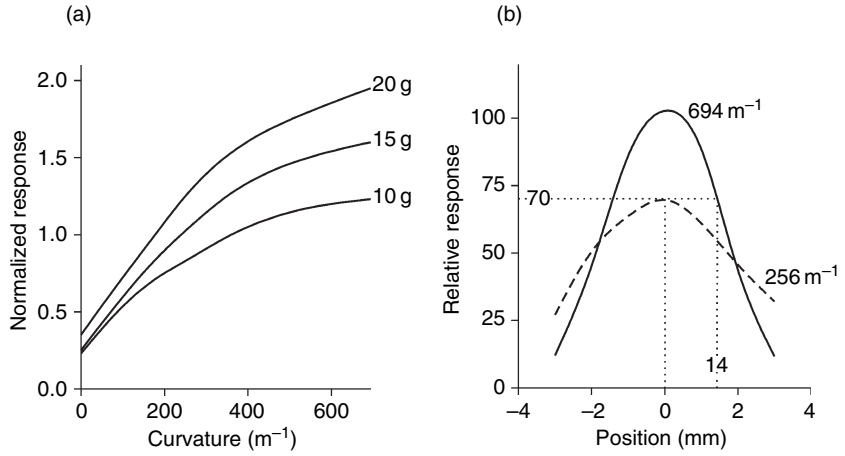

Figure 5 Responses of a single slow adapting type I (SAI) afferent to spheres indented in the receptive field. (a) Response increased with increasing curvature of the sphere and increased when contact force increased from 10 to 15 to 20 g. (b) Response as a function of position in the receptive field for a sphere of curvature 694 m^{-1} compared with that for a sphere of curvature 256 m^{-1}. Dotted lines demonstrate the ambiguity of a response of 70 imp s^{-1} (adapted from Goodwin, A. W., Browning, A. S., and Wheat, H. E. 1995. Representation of curved surfaces in responses of mechanoreceptive afferent fibers innervating the monkey's fingerpad. J. Neurosci. 15, 798–810).

plane. It has been known for some time that increasing the depth of indentation of a punctuate probe, which increases the force normal to the skin, results in an increase in responses of SAI and FAI afferents (Vega-Bermudez, F. and Johnson, K. O., 1999). The effect of controlled normal force on a single SAI afferent's responses is illustrated in Figure 5(a).

There are few studies of afferent responses to tangential or load forces. In the human it has been shown that responses of SAI, FAI, and SAII afferents are modulated by the direction of the tangential force (Birznieks, I. *et al.*, 2001). The alternative, and equivalent, interpretation is that all three afferent types are modulated by the three-dimensional force vectors.

6.03.2.9 Position in the Receptive Field

Machine-controlled punctuate probes lend themselves to field studies in which afferent responses can be measured when the probe is presented at a range of different positions in the receptive field. For the SAI illustrated in Figure 5(b), the solid line shows the receptive field mapped using a probe with a spherical tip of curvature 694 m^{-1} (radius 1.4 mm). There is a single point of maximum sensitivity, when the probe is located at the receptive field center, and responses decrease progressively as the probe is located further and further from the center. A similar profile holds for FAI afferents (Wheat, H. E. *et al.*, 1995). For SAII and FAII afferents, the receptive field profiles show a more gradual decrease in response with distance (Figure 2). Using finer probes (0.4 mm diameter) the receptive fields of SAI and FAI afferents show multiple points of high sensitivity within the central plateau region (Figure 2), suggesting that multiple mechanoreceptors converge on the single primary afferent fiber, which is consistent with their structure described above.

A crucial point is that the receptive field is not uniform, but rather is characterized by a profile of varying sensitivity or responsiveness. Moreover, the profile is stimulus dependent. When the receptive field of the SAI afferent in Figure 5(b) is mapped (broken line) with a more gently curved sphere of curvature 256 m^{-1} (radius 3.9 mm), the receptive field profile changes and is lower in amplitude and broader in width than the profile mapped with the more curved sphere.

For stimuli that are scanned across the skin, the equivalent to the receptive field map is the spatial event plot.

6.03.2.10 Signaling Must Be Viewed in Terms of Population Responses

Responses of single primary afferent fibers change when any one of several stimulus parameters change. Thus, it is not possible to determine the details of the stimulus from the response of a single afferent. For example, in Figure 5(b), the SAI afferent response of 70 imp s^{-1} could result from either a sphere of

curvature 256 m^{-1} located at position 0, or a sphere of curvature 694 m^{-1} located at position 1.4 mm (or even −1.4 mm). Such ambiguities are resolved in the responses of populations of neurons, which have the capacity to relay, with precision, multiple parameters of the stimulus.

Consider the simple task of grasping a sphere with the fingertips (comparable to grasping an apple). Psychophysics experiments have shown that the cutaneous mechanoreceptors in the fingertips convey to the brain high resolution and independent information about the shape or curvature of the sphere, the contact or grip force used, and the position of the contact on the skin (Goodwin, A. W. *et al.*, 1991; Wheat, H. E. *et al.*, 1995; Wheat, H. E. *et al.*, 2004). Humans can make accurate judgments about each of these parameters and the feedback is important for motor control.

Ideally, characterizing the population response requires that activity in each of the afferents of the population are recorded simultaneously, but technical limitations preclude this currently. A compromise approach is to synthesize an approximation to the population response as follows.

In Figure 5(b) a sphere of curvature 694 m^{-1} was indented into the receptive field of an SAI afferent at locations along a line through the receptive field center. This curve shows the effect of one parameter of the stimulus, the position of contact, on the response of the fiber. As explained above, this curve can be interpreted as an ideal one-dimensional population response. By indenting the probe at points over the two-dimensional receptive field, the two-dimensional receptive field profile, or ideal population response, can be obtained as shown in Figure 6(a). This shows the responses of a two-dimensional population of fibers with the sphere contacting the skin at a position arbitrarily defined as $x = 0$ and $y = 0$. If the position of contact on the skin changes, then the whole population response shifts a corresponding amount as illustrated in Figure 6(c) for a shift of 1 mm.

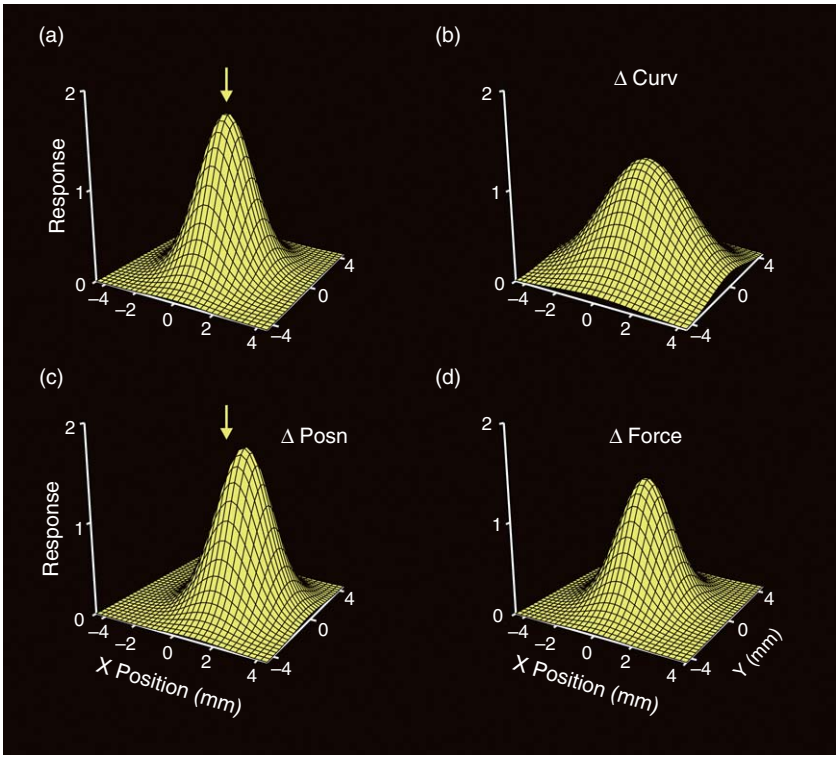

Figure 6 Ideal population responses for slowly adapting type I (SAI) afferents responding to spheres indented in the receptive field. (a) A sphere with curvature 694 m^{-1} indented at position $x = 0$, $y = 0$ on the skin. (b) Effect of changing the stimulus shape to a curvature of 256 m^{-1}. (c) Shifting the stimulus by 1 mm results in the population response shifting by 1 mm (compare responses to fixed arrows). (d) A reduction in contact force scales the entire response correspondingly. Compare responses in (b), (c), and (d) with response in (a) (adapted from Goodwin, A. W. and Wheat, H. E. 1999. Effects of nonuniform fiber sensitivity, innervation geometry, and noise on information relayed by a population of slowly adapting type I primary afferents from the fingerpad. J. Neurosci. 19, 8057–8070).

How do changes in a second stimulus parameter, the curvature of the sphere, affect the SAI afferent responses? The one-dimensional receptive field profile of the single SAI afferent for a less curved sphere, curvature 256 m^{-1}, is shown in Figure 5(b) and the two-dimensional profile for this sphere is shown in Figure 6(b). For the less curved sphere, the profile is reduced in height and is broader.

A third stimulus parameter is the contact force or grip force. For a sphere of any particular curvature, applied at any particular point in the receptive field, the response of a single SAI afferent increases with an increase in contact force (Figure 5(a)). In terms of the idealized population response in Figure 6(a), decreasing contact force decreases the response at all points as shown in Figure 6(d).

From inspection of the population response in Figure 6 it is evident how all three parameters of the stimulus are represented. The shape or curvature of the sphere is represented in the shape of the population response profile, the contact position is represented by the spatial location of the profile, and the contact force affects the overall scaling of the response. It is also apparent that the value of all three parameters can be extracted, without ambiguity, from the single population response.

In a similar way, the orientation of a cylinder indented into the skin can be seen in the ideal SAI population responses, constructed from two-dimensional receptive field profiles, depicted in Figure 7(a).

An analogous approach has been used for shaped objects scanned across the receptive field. With this mode of stimulation the relative motion between the skin and the object is equivalent to that when humans move their hands over objects during exploration or manipulation. The equivalent of the

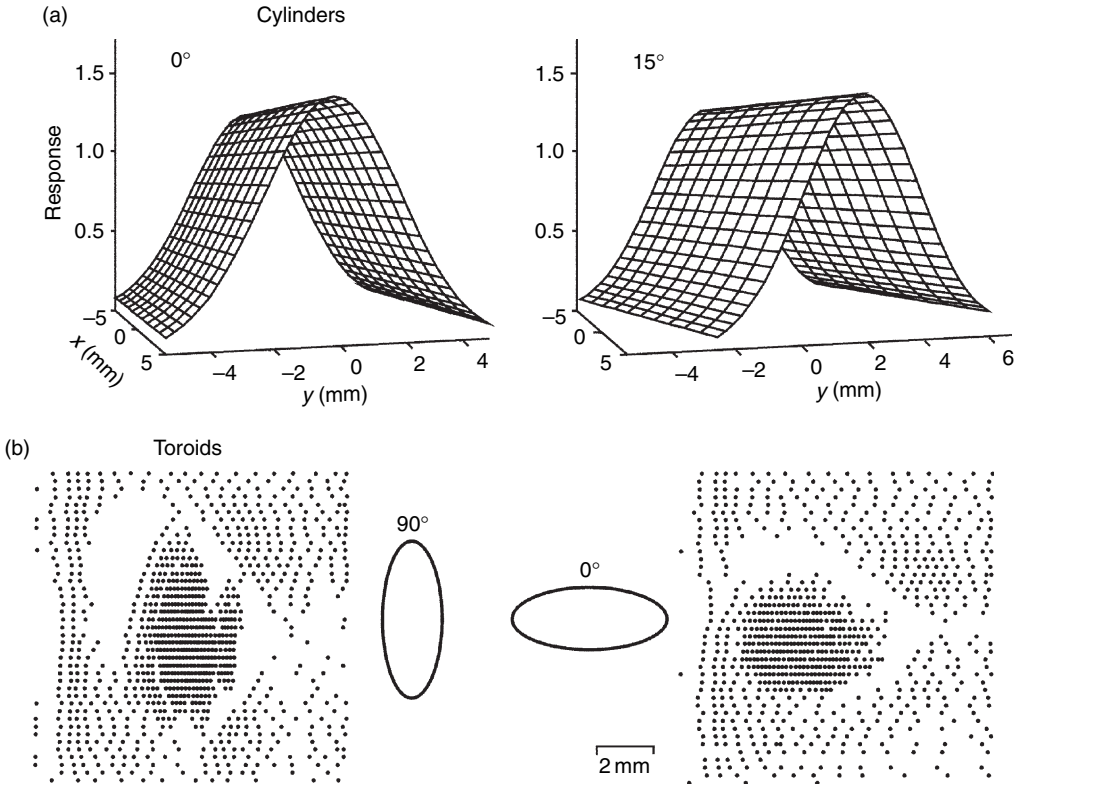

Figure 7 Ideal population responses of slowly adapting type I (SAI) afferents in a monkey's fingerpad. (a) Two-dimensional receptive field profiles reveal the orientation of a cylinder indented into the fingerpad. The cylinder, with a curvature of 172 m^{-1}, was oriented at 0° or 15°. Modified from Dodson M. J., Goodwin A. W., Browning A. S., and Gehring H. M. 1998. Peripheral neural mechanisms determining the orientation of cylinders grasped by the digits. J. Neurosci. 18, 521–530. (b) Spatial event plots show the orientation of a toroid scanned over the fingerpad. The 1 × 5 mm toroid was oriented at 90° or 0° (redrawn from LaMotte, R. H., Friedman, R. M., Lu, C., Khalsa, P. S., and Srinivasan, M. A. 1998. Raised object on a planar surface stroked across the fingerpad: responses of cutaneous mechanoreceptors to shape and orientation. J. Neurophysiol. 80, 2446–2466).

two-dimensional receptive field profile for indenting objects is the two-dimensional spatial event plot for scanned objects, which can also be viewed as an ideal population response. Shaped objects used have included spheres, toroids, and sinusoidal steps (LaMotte, R. H. and Srinivasan, M. A., 1987; LaMotte, R. H. *et al.*, 1998; Friedman, R. M. *et al.*, 2002). In Figure 7(b) the orientation of scanned toroids is reflected in the orientation of the spatial event plots.

6.03.2.11 More Realistic Population Responses

Real population responses are affected by a number of factors that are not apparent in the ideal reconstructions illustrated above. These factors have a significant impact, particularly when quantifying stimulus representation and resolution.

The ideal reconstructions are based on the implicit assumption that all afferents in the population have the same stimulus-response characteristics and, in particular, all have the same sensitivity or responsiveness. However, it is known that this is not the case; for example, the responsiveness of SAI afferent sensitivities vary over a 10-fold range (Knibestol, M., 1975; Goodwin, A. W. *et al.*, 1995). Variation in sensitivity results in distortion of the ideal profiles as illustrated in Figure 8. The broken line shows the ideal population response to a sphere of curvature 256 m^{-1}. Two more realistic population responses, where the constituent afferents have varying sensitivities, are shown by the solid lines; the sensitivities have a distribution matching the experimentally measured distribution. The profiles for the two more realistic populations differ from the ideal profile and differ from each other. In the case of stimuli scanned across the skin, there would be an equivalent distortion of the spatial event plots and the isomorphism between the plots and the stimulus apparent in Figure 4 would be reduced.

The second inherent assumption in most representations of ideal population responses is infinite innervation density, which is obviously not the case. For example, the profiles and dot plots in Figure 7 are sampled by a grid of a finite number of afferents. Estimates of the SAI and FAI afferent densities at the fingertip are 0.7 and 1.4 afferents mm^{-2}, which corresponds to a spacing between afferent receptive field centers of 1.2 and 0.85 mm, respectively (Johansson, R. S. and Vallbo, A. B., 1979; Darian-Smith, I. and Kenins, P., 1980).

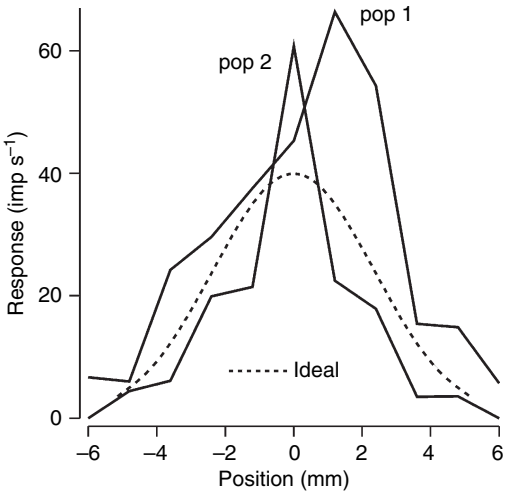

Figure 8 Variation in sensitivity distorts the slowly adapting type I (SAI) afferent population response to a sphere contacting the skin. Broken line shows an ideal population, where all afferents have the same sensitivity. Solid lines show two more realistic and different populations, where afferent sensitivities vary (redrawn from Goodwin, A. W. and Wheat, H. E. 1999. Effects of nonuniform fiber sensitivity, innervation geometry, and noise on information relayed by a population of slowly adapting type I primary afferents from the fingerpad. J. Neurosci. 19, 8057–8070).

Considering the spatial scale of the population response (of the order of millimeters to tens of millimeters) the consequences of receptive field spacing of this magnitude cannot be ignored. There are three additional complicating factors pertaining to innervation density. First, the estimates are derived from a single study in humans, backed up by a single study in monkeys, and are based on a number of assumptions and thus may be imprecise. Second, the pattern of innervation is not known and it may not be uniform. Third, during aging, and as a result of common diseases such as peripheral neuropathies, some primary afferents degenerate and this reduces the sampling density, perhaps unevenly. In Figure 9, estimates are shown for the effect of afferent density or receptive field spacing on the resolution of position in a population of SAI afferents.

A third assumption in ideal population reconstructions is that the neurons are free from noise. It is assumed that if the same stimulus is applied several times, then any particular neuron will respond identically each time. In fact, all neurons have some degree of variability or noise. In general, the

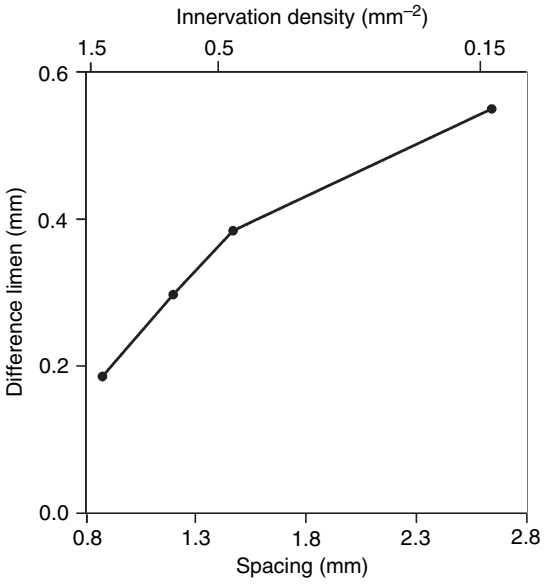

Figure 9 Decreasing innervation density results in decreasing resolution of position in the slowly adapting type I (SAI) population response, indicated by an increase in the difference limen for position. As density decreases, the spacing between receptive field centers increases (adapted from Goodwin, A. W. and Wheat, H. E. 1999. Effects of nonuniform fiber sensitivity, innervation geometry, and noise on information relayed by a population of slowly adapting type I primary afferents from the fingerpad. J. Neurosci. 19, 8057–8070).

primary afferents themselves have only a low level of noise (Jenmalm, P. *et al.*, 2003), but the central neurons processing the population responses have considerable noise (Lee, D. *et al.*, 1998). Such noise distorts the population responses. Multiple applications of the same stimulus will result in a range of different population responses; equivalently, there will be some uncertainty in the population response expected from a particular stimulus. In terms of human perception, this is one of the factors leading to the well-documented variability in discrimination (Galanter, E., 1984).

To redress the considerable limitations of ideal population responses, it is necessary to reconstruct more realistic population responses (Goodwin, A. W. and Wheat, H. E., 2004). Such reconstruction must take into account the inherent characteristics of the population including: varying sensitivity, pattern and density of innervation, and neural noise. A variety of mathematical and statistical approaches have been used. Computer simulations are relatively simple and particularly effective for exploring how the various population parameters affect the population response.

6.03.2.12 Measures of Stimulus Parameters

It may be possible to see how the various stimulus parameters are represented if the population responses are essentially isomorphic with the stimulus as in Figure 7 but, as explained above, in real populations the isomorphism is distorted. Even for isomorphic representations, any further quantitative analysis requires that some measure of the stimulus parameter is extracted from the population response. For example, any rigorous comparison with human behavior, or any tests of hypotheses about neural coding mechanisms, require quantitative measures of stimulus representations, including their resolution.

From Figure 6 it is evident that when the position of an object in contact with the skin shifts, there is a corresponding shift in the population response. But can this lead to a quantitative measure of object position, and how precise is such a measure given the distortions produced by the population parameters? To answer such questions it is necessary to hypothesize potential neural measures of the stimulus parameters. For example, one hypothesis for a measure of the position of contact of the stimulus on the skin is the centroid of the population response. Note in Figure 8 that the location of the peak of the population response is not a robust measure because it is highly susceptible to error from sensitivity variation, noise, and sampling. In contrast, the impact of these factors on the centroid are minimized by averaging.

By comparing proposed parameter representations with measured human behavior it is possible to reject hypotheses that result in a mismatch (Blake, D. T. *et al.*, 1997; Friedman, R. M. *et al.*, 2002). As an illustration, the correspondence between human roughness perception and a measure of roughness representation in the SAI afferents, spatial variation, is shown in Figure 4(b). The same correspondence does not hold for the FAI population.

When measures of stimulus representation are extracted from ideal populations, whether derived from receptive field profiles for contacting stimuli or spatial event plots for scanned stimuli, they do not take into account the significant differences in real populations. For this, simulations of more

realistic population responses are needed (Goodwin, A. W. and Wheat, H. E., 1999).

6.03.2.13 Complex Geometry of the Fingers

Glabrous skin is not a flat sheet. Moreover, the stresses and strains in skin are dependent on the characteristics of the underlying tissues, including bone. Consider the fingertips, which are the parts of the hand most commonly engaged in precise manipulations (Christel, M., 1993). The curvature of the fingertip varies, being relatively flat on the fingerpad and being highly curved on the distal and lateral parts. Bone, forming the distal phalanx, is incompressible and the subcutaneous tissues between the bone and the skin are nonuniform. Also, the skin is more mobile on the pad than it is close to tethering points such as the interphalangeal joints or creases. Finally, when comparing behavior or afferent responses in humans and monkeys, the difference in scale (Figure 10) must be considered.

There are two ways in which the geometry of the hand or fingers affects the responses of the cutaneous mechanoreceptors. At the simpler level, the nonuniform mechanics may result in quantitative differences in stimulus–response characteristics of identical mechanoreceptors located at different parts of the finger or hand, even when the stimulus is applied to the receptive field center in all cases. Less obviously, the curved fingers mean that during manipulation a large number of mechanoreceptors remote from the stimulus are active and convey information to the brain about the stimulus parameters. If grasping an object results in contact at the central part of the fingerpad, it is obvious that mechanoreceptors in the vicinity of the contact region on the fingerpad will be active. What is not so obvious, but true, is that mechanoreceptors all over the fingertip, including the curved lateral and distal portions may be active (Bisley, J. W. *et al.*, 2000). One approach to capture this wide-spread activity is to reconstruct the population response by applying the stimulus to a single common point on the fingertip while recording, in a number of experiments, from afferents innervating all parts of the fingertip (Khalsa, P. S. *et al.*, 1998; Birznieks, I. *et al.*, 2001). There are advantages and disadvantages to this approach.

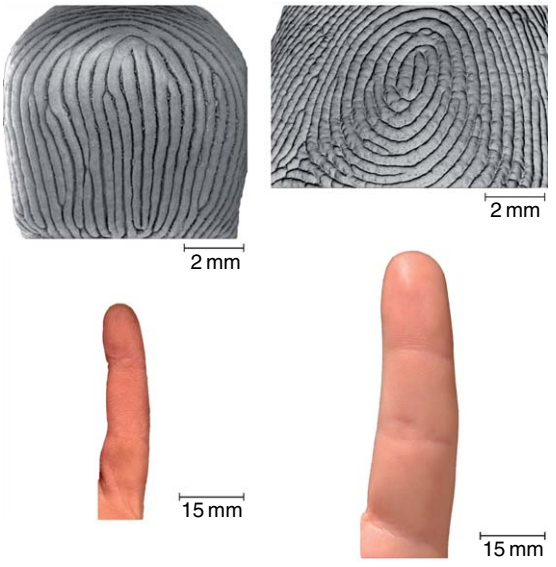

Figure 10 Comparison of monkey (left panel) and human (right panel) fingers. Whole index fingers (bottom) show the relative sizes of typical monkey and human fingers; there is of course considerable variation amongst individuals. Scanning electron micrographs (top) show fingerprint patterns. All our monkeys had the same linear proximal–distal pattern; humans have highly variable and unique patterns.

6.03.3 Hairy Skin

Although hairy skin is more extensive than glabrous skin, much less is known about the properties of its mechanoreceptors and their afferents than is the case for glabrous skin. There are a number of reasons for this. First, not all hairy skin is the same. Even in humans, receptive field properties of afferents innervating the arm differ from those of afferents innervating the dorsum of the hand or the face (Johansson, R. S. *et al.*, 1988; Edin, B. B. and Abbs, J. H., 1991; Vallbo, A. B. *et al.*, 1995). Second, much of the research on hairy skin has been performed on nonprimate species which are likely to have further differences from humans. An obvious example is the whisker system, which is highly developed in rodents, seals, and other mammals but is of little importance to humans (Zucker, E. and Welker, W. I., 1969; Dehnhardt, G. *et al.*, 1998). Third, stimuli used in hairy skin studies have usually been handheld and not well controlled. Fourth, unlike the obvious role played by glabrous skin mechanoreceptors during grasp and manipulation, the functional role of mechanoreceptors in human hairy skin appears to be more diffuse and is yet to be fully characterized.

6.03.3.1 Classification of Innervating Fibers

Mechanoreceptors in hairy skin may be located in hair follicles or in the skin between hairs. Large myelinated afferent fibers innervating these mechanoreceptors have been classified into five groups in numerous mammals, including humans (Burgess, P. R. *et al.*, 1968; Iggo, A. and Andres, K. H., 1982; Vallbo, A. B. *et al.*, 1995).

Two of the five classes of myelinated afferents are slowly adapting (Vallbo, A. B. *et al.*, 1995). SAI afferents innervate Merkel cells located in touch domes (Figure 11; Reinisch, C. M. and Tschachler, E., 2005).

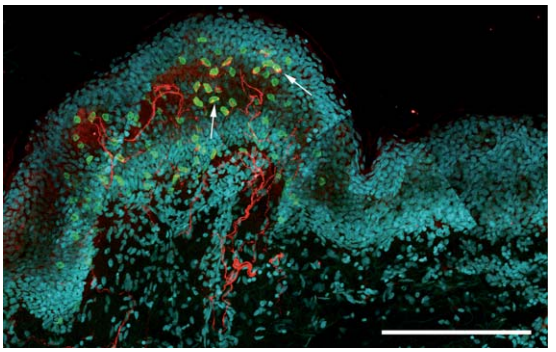

Figure 11 A touch dome in human hairy skin. Arrows mark contact zones between neurofilament (NF) positive nerve fibers and Merkel cells. Nuclei were counterstained with Hoechst. Scale bar = 200 μm (Reinisch, C. M. and Tschachler, E. 2005. The touch dome in human skin is supplied by different types of nerve fibers. Ann. Neurol. 58, 88–95).

Typically, SAI receptive fields contain a number of regions of high sensitivity (Figure 12(a)) indicating that each afferent innervates a cluster of Merkel cells, analogous to the innervation of SAI afferents in glabrous skin. SAII afferents innervate Ruffini organs and, as in glabrous skin, their receptive fields usually have a single zone of maximum responsivity.

Of the three rapidly adapting classes (Vallbo, A. B. *et al.*, 1995), the Pacinian units are similar to Pacinian afferents in glabrous skin with a single zone of maximum sensitivity in their receptive fields; they respond to taps on the skin remote from the receptive field center. The remaining two classes of rapidly adapting units have no counterpart in glabrous skin. These are the hair units innervating follicles, and the field units innervating skin between hairs. Hair units can often be activated by deflection of single hairs but they usually innervate many follicles, resulting in large receptive fields. Field units (Figure 12(b)) have large receptive fields with a number of zones of high sensitivity.

Hairy skin is also innervated by unmyelinated low-threshold mechanoreceptive afferents which, in humans, appear to mediate the emotional aspects of touch (Olausson, H. *et al.*, 2002).

6.03.3.2 Responses to Stroking

An effective method of activating hairy skin mechanoreceptors in a controlled way is by using a

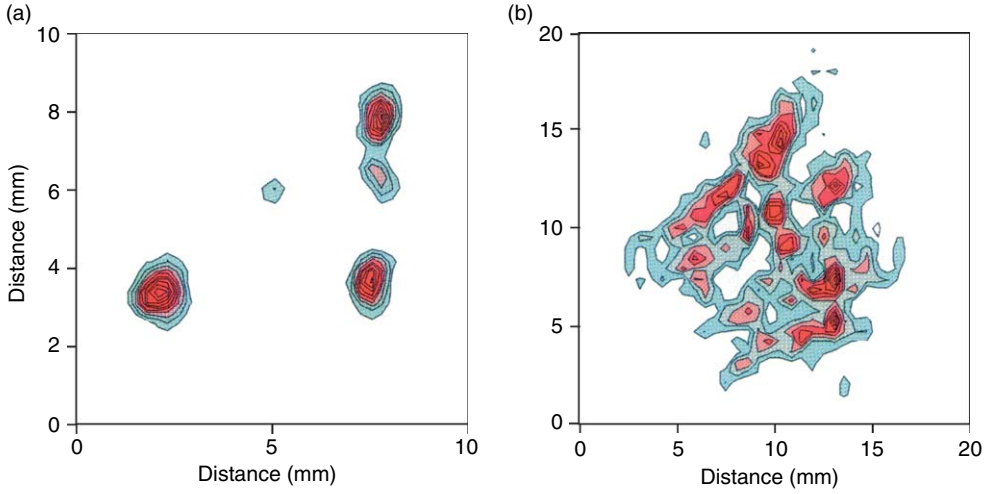

Figure 12 Color-coded contour plots showing two-dimensional receptive field structure for human hairy skin units. Sensitivity is graded from zero (white) to maximum (red). (a) A slowly adapting type I (SAI) afferent with a small number of confined regions of sensitivity. (b) A field unit with a large receptive field and multiple zones of sensitivity (redrawn from Vallbo, A. B., Olausson, H., Wessberg, J., and Kakuda, N. 1995. Receptive field characteristics of tactile units with myelinated afferents in hairy skin of human subjects. J. Physiol. 483, 783–795).

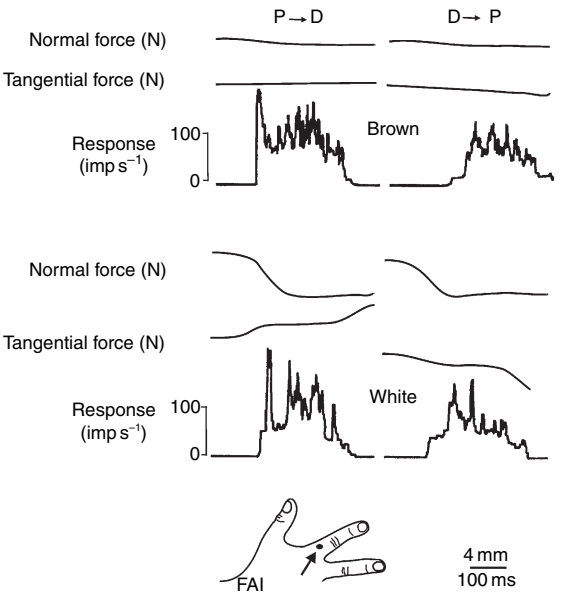

Figure 13 Responses of a fast-adapting unit in hairy skin to controlled brushing. The white brush resulted in higher forces than the brown brush. Stroking was in the proximal–distal direction on the left and in the distal–proximal direction on the right (adapted from Edin, B. B., Essick, G. K., Trulsson, M., and Olsson, K. Å. 1995. Receptor encoding of moving tactile stimuli in humans. I. Temporal pattern of discharge of individual low-threshold mechanoreceptors. J. Neurosci. 15, 830–847).

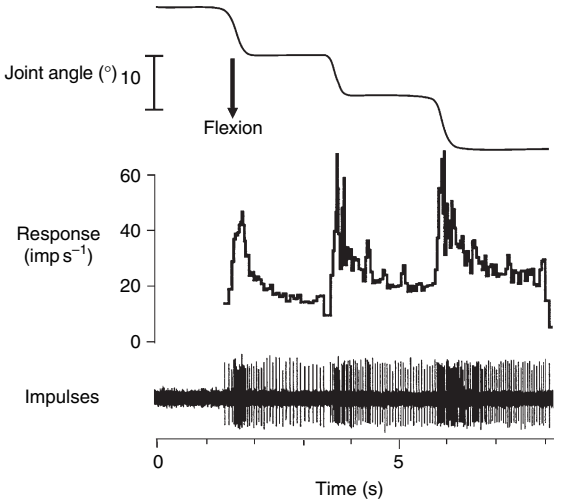

Figure 14 Responses of a slowly adapting type II (SAII) unit located in the hairy skin on the metacarpophalangeal joint of the index finger. Increasing flexion of the joint (top trace) resulted in an increased dynamic and static response of the unit (middle trace and bottom impulses) (adapted from Edin, B. B. and Abbs, J .H. 1991. Finger movement responses of cutaneous mechanoreceptors in the dorsal skin of the human hand. J. Neurophysiol. 65, 657–670).

mechanically driven brush. In some ways this simulates the natural contact that humans, and particularly other animals, make with the environment.

When human forearm skin is brushed, responses of both slowly and rapidly adapting units are modulated by the force, the velocity and the direction of brushing (Edin, B. B. *et al.*, 1995; Essick, G. K. and Edin, B. B., 1995). These responses (Figure 13) can explain the human ability to locate stimuli on the skin, determine their direction of movement, and discriminate the forces and velocities of movement.

6.03.3.3 Proprioception

Relatively recently it has become clear that mechanoreceptors in hairy skin are well situated for signaling the angles and movements of joints. Their role in proprioception for the hand contributes to primates' capacities to manipulate objects. At other joints, such as the knee, they are thought to play a key role in the control of posture and movement.

Whenever a joint moves, hairy skin for considerable distances around the joint are stretched or relaxed and the resultant stresses and strains activate the mechanoreceptors. For the finger joints (Figure 14), the hairy skin receptors provide graded information about joint angle (Edin, B. B. and Abbs, J. H., 1991). Electrical stimulation of these afferents, or stretching the skin on the dorsum of the hand in a controlled way, leads to the illusion of finger joint movement (Collins, D. F. and Prochazka, A., 1996). Similarly, afferents from hairy skin near the knee respond to knee position and movement (Edin, B. B., 2001), and stretching the skin around the knee or elbow leads to illusions of movement of those joints (Collins, D. F. *et al.*, 2005).

It is still to be determined how proprioceptive information from cutaneous and muscle spindle afferents are combined or what their relative importance is.

References

Birznieks, I., Jenmalm, P., Goodwin, A. W., and Johansson, R. S. 2001. Encoding of direction of fingertip forces by human tactile afferents. J. Neurosci. 21, 8222–8237.

Bisley, J. W., Goodwin, A. W., and Wheat, H. E. 2000. Slowly adapting type I afferents from the sides and end of the finger respond to stimuli on the center of the fingerpad. J. Neurophysiol. 84, 57–64.

Blake, D. T., Hsiao, S. S., and Johnson, K. O. 1997. Neural coding mechanisms in tactile pattern recognition: the relative contributions of slowly and rapidly adapting mechanoreceptors to perceived roughness. J. Neurosci. 17, 7480–7489.

Brink, E. E. and Mackel, R. G. 1993. Time course of action potentials recorded from single human afferents. Brain 116, 415–432.

Burgess, P. R., Petit, D., and Warren, R. M. 1968. Receptor types in cat hairy skin supplied by myelinated fibers. J. Neurophysiol. 31, 833–848.

Christel, M. 1993. Grasping Techniques and Hand Preferences in Hominoidea. In: *Hands of Primates (eds*. H. Preuschoft and D. J. Chivers), pp. 91–108. Springer.

Collins, D. F. and Prochazka, A. 1996. Movement illusions evoked by ensemble cutaneous input from the dorsum of the human hand. J. Physiol. 496, 857–871.

Collins, D. F., Refshauge, K. M., Todd, G., and Gandevia, S. C. 2005. Cutaneous receptors contribute to kinesthesia at the index finger, elbow, and knee. J. Neurophysiol. 94, 1699–1706.

Darian-Smith, I. and Kenins, P. 1980. Innervation density of mechanoreceptive fibres supplying glabrous skin of the monkey's index finger. J. Physiol. 309, 147–155.

Dehnhardt, G., Mauck, B., and Bleckmann, H. 1998. Seal whiskers detect water movements. Nature 394, 235–236.

Dodson, M. J., Goodwin, A. W., Browning, A. S., and Gehring, H. M. 1998. Peripheral neural mechanisms determining the orientation of cylinders grasped by the digits. J. Neurosci. 18, 521–530.

Edin, B. B. 2001. Cutaneous afferents provide information about knee joint movements in humans. J. Physiol. 531, 289–297.

Edin, B. B. and Abbs, J. H. 1991. Finger movement responses of cutaneous mechanoreceptors in the dorsal skin of the human hand. J. Neurophysiol. 65, 657–670.

Edin, B. B., Essick, G. K., Trulsson, M., and Olsson, K.Å. 1995. Receptor encoding of moving tactile stimuli in humans. I. Temporal pattern of discharge of individual low-threshold mechanoreceptors. J. Neurosci. 15, 830–847.

Essick, G. K. and Edin, B. B. 1995. Receptor encoding of moving tactile stimuli in humans. II. The mean response of individual low-threshold mechanoreceptors to motion across the receptive field. J. Neurosci. 15, 848–864.

French, A. S. 1992. Mechanotransduction. Annu. Rev. Physiol. 54, 135–152.

Friedman, R. M., Khalsa, P. S., Greenquist, K. W., and LaMotte, R. H. 2002. Neural coding of the location and direction of a moving object by a spatially distributed population of mechanoreceptors. J. Neurosci. 22, 9556–9566.

Galanter, E. 1984. Detection and Discrimination of Environmental Change. In: Handbook of Physiology – The Nervous System, Volume III (*eds*. J. M. Brookhart, V. B. Mountcastle, and I. Darian-Smith), pp. 103–121. American Physiological Society.

Goodwin, A. W. and Morley, J. W. 1987. Sinusoidal movement of a grating across the monkey's fingerpad: representation of grating and movement features in afferent fiber responses. J. Neurosci. 7, 2168–2180.

Goodwin, A. W. and Wheat, H. E. 1999. Effects of nonuniform fiber sensitivity, innervation geometry, and noise on information relayed by a population of slowly adapting type I primary afferents from the fingerpad. J. Neurosci. 19, 8057–8070.

Goodwin, A. W. and Wheat, H. E. 2004. Sensory signals in neural populations underlying tactile perception and manipulation. Annu. Rev. Neurosci. 27, 53–77.

Goodwin, A. W., John, K. T., and Marceglia, A. H. 1991. Tactile discrimination of curvature by humans using only cutaneous information from the fingerpads. Exp. Brain Res. 86, 663–672.

Goodwin, A. W., Browning, A. S., and Wheat, H. E. 1995. Representation of curved surfaces in responses of mechanoreceptive afferent fibers innervating the monkey's fingerpad. J. Neurosci. 15, 798–810.

Halata, Z. 1975. The mechanoreceptors of the mammalian skin. Ultrastructure and morphological classification. Adv. Anatomy Embryol. Cell Biol. 50, 1–77.

Iggo, A. and Andres, K. H. 1982. Morphology of cutaneous receptors. Annu. Rev. Neurosci. 5, 1–31.

Jenmalm, P., Birznieks, I., Goodwin, A. W., and Johansson, R. S. 2003. Influence of object shape on responses of human tactile afferents under conditions characteristic of manipulation. Eur. J. Neurosci. 18, 164–176.

Johansson, R. S. 1976. Receptive field sensitivity profile of mechanosensitive units innervating the glabrous skin of the human hand. Brain Res. 104, 330–334.

Johansson, R. S. and Vallbo, A. B. 1979. Tactile sensibility in the human hand: relative and absolute densities of four types of mechanoreceptive units in glabrous skin. J. Physiol. 286, 283–300.

Johansson, R. S., Trulsson, M., Olsson, K. A., and Westberg, K. G. 1988. Mechanoreceptor activity from the human face and oral mucosa. Exp. Brain Res. 72, 204–208.

Khalsa, P. S., Friedman, R. M., Srinivasan, M. A., and LaMotte, R. H. 1998. Encoding of shape and orientation of objects indented into the monkey fingerpad by populations of slowly and rapidly adapting mechanoreceptors. J. Neurophysiol. 79, 3238–3251.

Knibestol, M. 1973. Stimulus–response functions of rapidly adapting mechanoreceptors in the human glabrous skin area. J. Physiol. 232, 427–452.

Knibestol, M. 1975. Stimulus–response functions of slowly adapting mechanoreceptors in the human glabrous skin area. J. Physiol. 245, 63–80.

LaMotte, R. H. and Srinivasan, M. A. 1987. Tactile discrimination of shape: responses of slowly adapting mechanoreceptive afferents to a step stroked across the monkey fingerpad. J. Neurosci. 7, 1655–1671.

LaMotte, R. H., Friedman, R. M., Lu, C., Khalsa, P. S., and Srinivasan, M. A. 1998. Raised object on a planar surface stroked across the fingerpad: responses of cutaneous mechanoreceptors to shape and orientation. J. Neurophysiol. 80, 2446–2466.

Lee, D., Port, N. L., Kruse, W., and Georgopoulos, A. P. 1998. Variability and correlated noise in the discharge of neurons in motor and parietal areas of the primate cortex. J. Neurosci. 18, 1161–1170.

Leung, Y. Y., Bensmaia, S. J., Hsiao, S. S., and Johnson, K. O. 2005. Time-course of vibratory adaptation and recovery in cutaneous mechanoreceptive afferents. J. Neurophysiol. 94, 3037–3045.

Monzee, J., Lamarre, Y., and Smith, A. M. 2003. The effects of digital anesthesia on force control using a precision grip. J. Neurophysiol. 89, 672–683.

Olausson, H., Lamarre, Y., Backlund, H., Morin, C., Wallin, B. G., Starck, G., Ekholm, S., Strigo, I., Worsley, K., Vallbo, A. B., and Bushnell, M. C. 2002. Unmyelinated tactile afferents signal touch and project to insular cortex. Nat. Neurosci. 5, 900–904.

Pare, M., Smith, A. M., and Rice, F. L. 2002. Distribution and terminal arborizations of cutaneous mechanoreceptors in the glabrous finger pads of the monkey. J. Comp. Neurol. 445, 347–359.

Phillips, J. R. and Johnson, K. O. 1981. Tactile spatial resolution. II. Neural representation of bars, edges, and gratings in monkey primary afferents. J. Neurophysiol. 46, 1192–1203.

Phillips, J. R., Johansson, R. S., and Johnson, K. O. 1990. Representation of Braille characters in human nerve fibres. Exp. Brain Res. 81, 589–592.

Quilliam, T. A. 1978. The Structure of Finger Print Skin. In: *Active Touch – the Mechanism of Recongnition of Objects by Manipulation: a Multidiciplinary Approach (ed*. G. Gordon), pp. 1–18. Pergamon.

Reinisch, C. M. and Tschachler, E. 2005. The touch dome in human skin is supplied by different types of nerve fibers. Ann. Neurol. 58, 88–95.

Srinivasan, M. A. and LaMotte, R. H. 1987. Tactile discrimination of shape: responses of slowly and rapidly adapting mechanoreceptive afferents to a step indented into the monkey fingerpad. J. Neurosci. 7, 1682–1697.

Talbot, W. H., Darian-Smith, I., Kornhuber, H. H., and Mountcastle, V. B. 1968. The sense of flutter-vibration: comparison of the human capacity with response patterns of mechanoreceptive afferents from the monkey hand. J. Neurophysiol. 31, 301–334.

Vallbo, A. B. and Johansson, R. S. 1984. Properties of cutaneous mechanoreceptors in the human hand related to touch sensation. Human Neurobiol. 3, 3–14.

Vallbo, A. B., Olausson, H., Wessberg, J., and Kakuda, N. 1995. Receptive field characteristics of tactile units with myelinated afferents in hairy skin of human subjects. J. Physiol. 483, 783–795.

Vega-Bermudez, F. and Johnson, K. O. 1999. SA1 and RA receptive fields, response variability, and population responses mapped with a probe array. J. Neurophysiol. 81, 2701–2710.

Wheat, H. E., Goodwin, A. W., and Browning, A. S. 1995. Tactile resolution: peripheral neural mechanisms underlying the human capacity to determine positions of objects contacting the fingerpad. J. Neurosci. 15, 5582–5595.

Wheat, H. E., Salo, L. M., and Goodwin, A. W. 2004. Human ability to scale and discriminate forces typical of those occurring during grasp and manipulation. J. Neurosci. 24, 3394–3401.

Witney, A. G., Wing, A., Thonnard, J. L., and Smith, A. M. 2004. The cutaneous contribution to adaptive precision grip. Trends Neurosci. 27, 637–643.

Yoshioka, T., Gibb, B., Dorsch, A. K., Hsiao, S. S., and Johnson, K. O. 2001. Neural coding mechanisms underlying perceived roughness of finely textured surfaces. J. Neurosci. 21, 6905–6916.

Zucker, E. and Welker, W. I. 1969. Coding of somatic sensory input by vibrissae neurons in the rat's trigeminal ganglion. Brain Res. 12, 138–156.

6.04 Coding of Object Shape and Texture

S S Hsiao and S Bensmaia, The Johns Hopkins University, Baltimore, MD, USA

© 2008 Elsevier Inc. All rights reserved.

6.04.1	**Introduction**	55
6.04.2	**Peripheral Coding of 2D Shape and Texture**	56
6.04.2.1	Coding of 2D Shape	56
6.04.2.2	Coding of Surface Texture	57
6.04.2.2.1	Roughness/smoothness	57
6.04.2.2.2	Hardness/softness	59
6.04.2.2.3	Stickiness/slipperiness	59
6.04.3	**Coding of 3D Size and Shape**	59
6.04.3.1	Psychophysical Studies of 3D Size and Shape	59
6.04.3.2	Cortical Neurophysiological Studies of 3D Shape	60
6.04.3.2.1	Ascending pathways	60
6.04.3.2.2	Primary somatosensory cortex	61
6.04.3.2.3	Areas 5 and 7 (tactile dorsal pathway)	62
6.04.3.2.4	Second somatosensory cortex (tactile ventral pathway)	62
6.04.4	**Conclusion**	63
References		64

Glossary

adaptation The change in firing rate to a constant stimulus. Rapidly adapting neurons produce action potential only during the onset or offset of the stimulus. Slowly adapting neurons show a slow decline in firing rate during the sustained portion of the stimulus.

cutaneous Of or relating to the skin. The term cutaneous is typically used to refer to low-threshold mechanoreceptive afferents and their central connections.

isomorphic representation An one-to-one mapping between the spatial configuration of the stimulus and its neural representation.

kernels A set of mathematical functions that map one feature space into another.

mechanoreception The process of converting a deformation of the skin into neural signals. Cutaneous receptors have mechanoreceptive channels.

neural representation Spatial or temporal activity in a population of neurons that carries the information about a specific aspect of a stimulus or behavior.

proprioception The perception of the location and movement of body parts. For example, proprioception underlies the ability to perceive the conformation of the hands.

stress/strain Stress denotes a force per unit area; strain is the change in length per total length.

6.04.1 Introduction

Although object shape perception has been studied extensively in both vision and touch, the neural mechanisms underlying this ability have remained elusive. In vision, object recognition is based on inferring the 3D structure of objects from 2D images that originate from the retinas. These images flow centrally where they are combined and processed by neurons along the visual ventral stream to ultimately activate neurons in the inferotemporal (IT) cortex that are tuned to complex shapes such as faces. The problem of 3D shape processing in vision is difficult. First the visual system must segment images into

figure and ground. Then the 3D shape of the object must be inferred from disparity and image cues represented in the two 2D images. The problems that the tactile system faces in object perception are different. In touch, the hand has direct access to local 2D features from cutaneous signals at places where the skin contact the object and information about its global shape from proprioceptive signals that specify where those points of contact lie in 3D space. Tactile shape perception thus seems to rely on central mechanisms that integrate cutaneous inputs from the finger pads with proprioceptive inputs to produce central representations of objects. In both touch and vision, object perception is the product of matching transformed neural inputs against previously stored representations.

Recognizing objects with our hands is effortless, does not require visual input and is based on our ability to integrate information about the shape (e.g., sphere, cube), size (e.g., golf ball, basketball), and texture (e.g., tennis ball, baseball) to form a coherent representation. These features are processed independently and contribute to our ability to tactually identify objects. Object recognition begins with the activation of mechanoreceptive and proprioceptive afferents that innervate the skin, joints, and muscles of the hand and arm. A number of psychophysical and neurophysiological studies carried out over the past 30 years or so have led to an understanding of the organization of the peripheral afferent inputs and the roles they play in form and texture perception (for a detailed review, see Johnson, K. O., 2001). However, little is known about how and where these inputs are integrated in the central nervous system for object perception:

1. What are the central pathways and circuits that transform the peripheral inputs into the representations upon which perception is based?
2. What algorithms are used at each step of processing to represent objects and textures?
3. How is this transformed representation matched against previously stored representations?

In this chapter we first discuss the psychophysics and neurophysiology of 2D form and texture perception and review studies showing how form and texture are represented and coded in the responses of the peripheral afferents. We then discuss the central pathways of form and texture perception and review the current literature about how peripheral inputs are integrated in cortex to represent 2D shape and 3D objects.

6.04.2 Peripheral Coding of 2D Shape and Texture

6.04.2.1 Coding of 2D Shape

The processing of 2D spatial patterns presented to a single finger pad has been the focus of numerous psychophysical and neurophysiological studies (for a review, see Hsiao, S. S., *et al.*, 2003). These studies suggest that the somatosensory system, like the visual system, has two separate streams for processing spatial information. The slowly adapting type 1 (SA1) system is responsible for processing information related to texture and form, and the rapidly adapting (RA) system is responsible for processing information related to local movement on the skin (Johnson, K. O., 2001). Evidence that the SA1 system, which receives its inputs from Merkel cells, is responsible for 2D spatial form comes from studies showing that these afferents densely innervate the glabrous skin of the hand (about 100 afferent fibers per cm^2 at the fingertip in man and monkey) (Johansson, R. S. and Vallbo, A. B., 1979; Darian-Smith, I. and Kenins, P., 1980) and have small receptive fields (about 2–3 mm in diameter) and, because of their high sensitivity to skin strain (Phillips, J. R. and Johnson, K. O., 1981b; Sripati, A. P. *et al.*, 2006a), these afferents resolve the fine spatial details of patterned stimuli (down to about 0.5 mm) (Phillips, J. R. and Johnson, K. O., 1981a). Further, SA1 afferents have linear responses to skin indentations over a wide range (Blake, D. T. *et al.*, 1997b; Vega-Bermudez, F. and Johnson, K. O., 1999; Johnson, K. O. *et al.*, 2000), and are highly sensitive to local curvature and edges indented into the skin (LaMotte, R. H. and Srinivasan, M. A., 1996; Blake, D. T. *et al.*, 1997b; Goodwin, A. W. *et al.*, 1997; Wheat, H. E. and Goodwin, A. W., 2001). The responses of these afferents to spatial stimuli is only minimally affected by changes in scanning velocity (Hsiao, S. S. *et al.*, 1996; DiCarlo, J. J. and Johnson, K. O., 1999).

An example of the response of an SA1 afferent to scanned embossed letters is shown in Figure 1. The figure shows that the initial representation of 2D form in the SA1 population response is a crisp isomorphic neural image (i.e., has the same shape as the stimulus) that is minimally affected by changes in contact force or velocity. Evidence from neural coding studies show that this system underlies the ability of humans to recognize fine spatial patterns (Johnson, K. O. and Phillips, J. R., 1981; Vega-Bermudez, F. *et al.*, 1991). The SA1 system is the tactile processing system for 2D patterns and is analogous to the parvocellular pathway in vision (Hsiao, S. S., 1998).

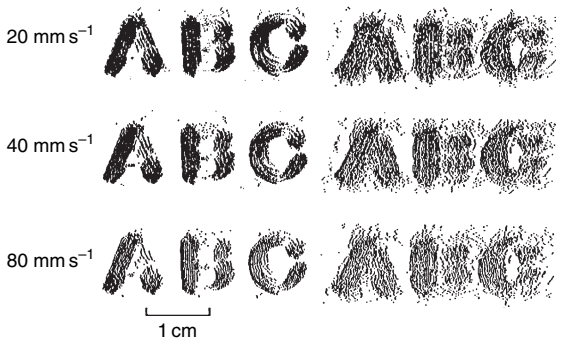

Figure 1 Responses of typical slowly adapting type 1 (SA1) (left) and rapidly adapting (RA) peripheral afferents to scanned embossed letters (8.0 mm high) at three scanning velocities. The figure shows that the SA1 afferents provide a crisp isomorphic representation of spatial patterns to the central nervous system.

The RA system, which receives its inputs from Meissner corpuscles also innervates the skin densely (about 150 afferents per cm^2 in man and monkey) (Johansson, R. S. and Vallbo, A. B., 1979; Darian-Smith, I. and Kenins, P., 1980). This system also sends to the central nervous system an isomorphic representation of spatial stimuli (Figure 1). However, the images are less crisp and evidence suggests that it only provides a crude sense of spatial form (Johnson, K. O. and Hsiao, S. S., 1992). In fact, recent studies have suggested that the RA system can actually interfere with fine form processing (Bensmaia, S. J. *et al.*, 2006). This system is thought to be responsible for the perception of low-frequency vibrations (called flutter) and the perception of tactile motion. RA afferents have intermediate spatial acuity, respond well to movement across the skin (Gardner, E. P. and Palmer, C. I., 1990) and are responsible for signaling microslips that occur when lifting objects (Johansson, R. S. and Westling, G., 1987; Westling, G. and Johansson, R. S., 1987; Srinivasan, M. A. *et al.*, 1990). The RA system is the tactile motion system and is analogous to the magnocellular system in vision (Hsiao, S. S., 1998).

The ability of the peripheral SA1 afferents to resolve the spatial details of stimuli comes from their high sensitivity to mechanical strain. Stimuli that are indented into the skin produce patterns of stresses and strains in the subcutaneous tissues beneath the surface of the skin that activate mechanoreceptive channels in the receptor endings of the afferent fibers. Continuum mechanics models (Phillips, J. R. and Johnson, K. O., 1981b; Johnson, K. O. and Hsiao, S. S., 1992; Sripati, A. *et al.*, 2006a) have shown that when a stimulus is indented into the skin the stresses are greatest at the edges where there is less tissue over which forces exerted at the skin surface can be distributed. Under the stimulus edges, then, the SA1 firing rates are much higher, which leads to an enhancement of the peripheral representation of features such as edges and corners. In contrast, RA afferents show little to no enhanced responses to edges (Sripati, A. *et al.*, 2006a). (see Chapter Physiological Responses of Sensory Afferents in Glabrous and Hairy Skin of Humans and Monkeys for a detailed discussion of the responses of the peripheral afferents to stimuli of varying curvature.)

6.04.2.2 Coding of Surface Texture

Like size and shape, information about surface texture plays a major role in tactile object recognition (e.g., baseball vs. an orange) and can be important when manipulating objects. For example, a ball made of foam is manipulated very differently than a ball made of steel. Multidimensional scaling studies show that texture perception is multidimensional and includes three main dimensions, namely, roughness/smoothness, hardness/softness, stickiness/slipperiness, and possibly a fourth dimension of warmth/coolness (Hollins, M. *et al.*, 1993; 2000; Bensmaia, S. J. and Hollins, M., 2005). Below, we discuss the neural coding mechanisms of the three main dimensions of texture.

6.04.2.2.1 Roughness/smoothness

By far the most widely studied aspect of texture is the sense of roughness. The subjective sense of roughness (and smoothness) varies along a single dimension and is not readily predicted by the surface properties. Psychophysical studies report that roughness increases linearly with particle size for sandpapers (Ekman, G. *et al.*, 1965) and increases with spatial period and groove width for gratings (Chapman, C. E. *et al.*, 2002). In studies using embossed dot patterns it has been shown that perceived roughness has an inverted U-shaped function with spatial period (increasing as dot spacing increases from 1.0 to 3.2 mm and decreasing as dot spacing increases to 6.2 mm), decreasing as dot diameter increases (from 0.5 to 1.0 mm) and increasing as dot height increases (from 280 to 620 μm) (Connor, C. E. *et al.*, 1990; Blake, D. T. *et al.*, 1997a).

In a series of studies pairing human psychophysics with macaque neurophysiology (see Johnson, K. O. *et al.*, 2002 for a review), Johnson, Hsiao and co-workers set out to establish the peripheral neural code underlying roughness perception (Connor, C. E. *et al.*, 1990;

Connor, C. E. and Johnson, K. O., 1992; Blake, D. T. *et al.*, 1997a; Yoshioka, T. *et al.*, 2001). Their approach consisted of devising and testing a set of hypotheses linking the activity in populations of peripheral afferent fibers evoked by a wide range of textured surfaces (embossed dot patterns, see above) to estimates of perceived roughness obtained from human subjects. These estimates, obtained for a variety of dot patterns, were plotted against predictions derived from each putative neural code. A hypothesis was eliminated if it failed to show a consistent relationship between the roughness estimates and the putative neural code. They rejected all neural codes based on:

1. the mean firing rate elicited by any of the mechanoreceptive afferents fibers;
2. all codes based on temporal variability in the firing of a given population of mechanoreceptive afferent fibers; and
3. all codes based on the firing of RA and Pacinian (PC) afferents.

The only remaining code that stood up against the entire battery of stimuli was one based on a measure of the spatial variation in firing rates among SA1 afferents (Figure 2). According to this hypothesis, there are populations of neurons in the central nervous system whose receptive fields comprise excitatory and inhibitory subregions, spaced about 2.0 mm apart, which is approximately the distance between two primary afferent spacings. Johnson, Hsiao, and co-workers showed that, as textured patterns like the ones shown in Figure 2 are scanned across the finger pad; populations of neurons with these kinds of receptive fields compute a measure of spatial variation in firing rate that closely matches the psychophysical data (Figure 2). For example, Connor C. E. *et al.* (1990) showed that closely spaced dots which equally excite the excitatory and inhibitory subregions produces low firing rates. Similarly, widely spaced dots also produced low firing rates because neurons were only rarely excited by the dots. Dots with intermediate spacings produced the highest firing rates and correspondingly elicited high subjective roughness magnitude estimates. The correlation between the psychophysics and the spatial variation measure in this study was about 0.98. Similar correlations between this neural measure and human psychophysics were found for patterns composed of fine textures (Yoshioka, T. *et al.*, 2001), patterns that varied in dot diameter (Blake, D. T. *et al.*, 1997a), and patterns that systematically altered the spatial and temporal (variation in firing rate

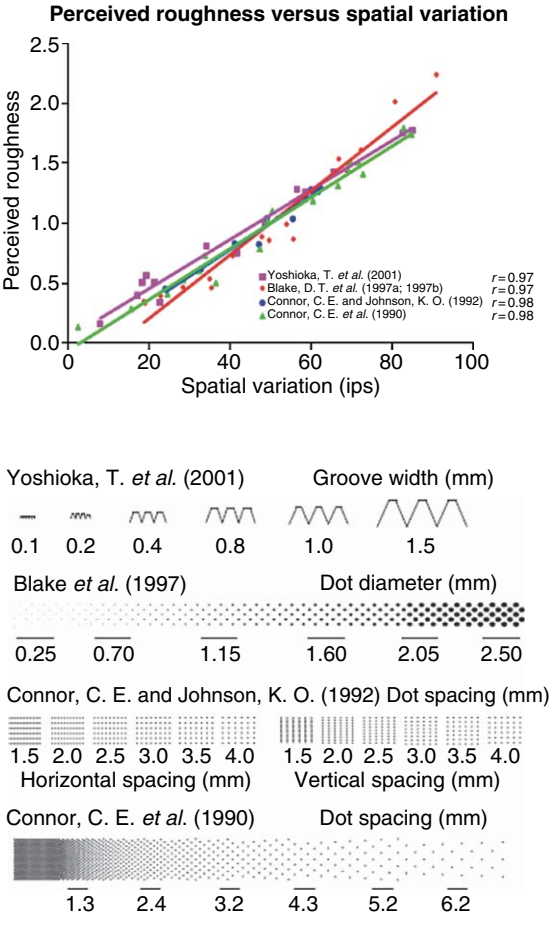

Figure 2 Summary of four neural coding studies of roughness perception. In all the four studies, human subjects performed roughness magnitude estimates of the surfaces shown at the bottom. These same surfaces were used as stimuli in neurophysiological experiments of the peripheral afferents of macaque monkeys. All neural codes that were tested were rejected except for a measure of spatial variation of firing in slowly adapting type 1 (SA1) afferents. The results are shown at the top where perceived roughness is plotted against the spatial variation measure. The plot shows that there is a consistent relationship between the neural measure and perceived roughness. The plot also shows that there is a linear relationship between perception and the neural code upon which it is based.

across time) variation in the afferent discharge (Connor, C. E. and Johnson, K. O., 1992). In all cases, roughness perception was linearly related to the SA1 spatial variation measure.

The predicted receptive field structures are exactly like the measured receptive fields of a subset neurons in area 3b (DiCarlo, J. J. *et al.*, 1998; DiCarlo, J. J. and Johnson, K. O., 1999; 2000) suggesting that roughness is derived from the mean firing rate of neurons in primary somatosensory cortex (SI).

Hollins and co-workers studied fine textures with spatial periods below about 200 μm and found that roughness for these fine surfaces correlates well with vibratory intensity and hypothesized that PC afferents may play a role in roughness perception for very fine surfaces (Hollins, M. *et al.*, 2001; 2002; Bensmaia, S. J. and Hollins, M., 2003; 2005).

6.04.2.2.2 Hardness/softness

Hardness/softness is the subjective continuum associated with the compliance of an object. Softness perception has been shown to rely primarily on cutaneous cues: eliminating kinesthetic information has no effect on subjects' ability to discriminate softness (Srinivasan, M. A. and LaMotte, R. H., 1995). As the hand is pressed against a compliant object, it conforms to the contour of the skin in proportion to the contact force. The compliance (and the softness) of the object appears to be signaled by the rate of growth of the area over which the skin contacts the object as the contact force increases, as well as the increase in the reaction force exerted by the object on the skin across the contact area. Softness perception likely relies on signals from SA1 afferents (Srinivasan, M. A. and LaMotte, R. H., 1996).

6.04.2.2.3 Stickiness/slipperiness

Stickiness/slipperiness is the sensory continuum associated with the friction between skin and surface. Indeed, magnitude estimates of stickiness have been shown to closely match the measured kinetic friction between skin and surface, that is, the ratio between the force exerted normal to the surface to that exerted parallel to the plane of the surface (Smith, A. M. and Scott, S. H., 1996). Furthermore, when judging stickiness, subjects do not substantially vary the normal forces they apply on the surface, but the applied tangential forces tend to vary across surfaces, suggesting that tangential forces are intimately linked with the perception of stickiness. The neural basis for stickiness is not known.

6.04.3 Coding of 3D Size and Shape

6.04.3.1 Psychophysical Studies of 3D Size and Shape

In the absence of visual input, tactile object recognition using a single hand is highly accurate and improves as the number of digits used to contact objects increases (Davidson, P. W., 1972; Kappers, A. M. L. and Koenderink, J. J., 1996). Interestingly, accuracy seems to decrease if two hands are used (Kappers, A. M. L. and Koenderink, J. J., 1996). Klatzky R. L. *et al.* (1985) showed that blindfolded subjects perform with an accuracy of 96% and a mean response time of less than 5 s when asked to identify 100 common objects. Further, Lederman S. J. and Klatzky R. L. (1993) showed that, when subjects explore objects, they use stereotypical movement patterns, which they call exploratory procedures (EPs). Among the eight kinds of EPs, two are critical for extracting information concerning object shape. The first, called enclosure, involves dynamic molding of the palm and/or fingers to the contours of the object. The second, called contour following, involves tracing the edges of objects with the fingers. Both procedures require that information about hand position (i.e., proprioception) be combined with tactile information from the skin (i.e., mechanoreception). In a similar study, Loo C. K. *et al.* (1983) showed that purely cutaneous information was sufficient for the discrimination of small objects but proprioceptive information is needed for the discrimination of large objects. Large objects are recognized more effectively when touched from the back (which is the natural way we grasp an object) than when touched from the front (Newell, F. N. *et al.*, 2001). Voisin J. *et al.* (2002a; 2002b) showed that the discrimination of an angle requires both cutaneous and proprioceptive input. Furthermore, Davidson P. W. (1972) showed that subjects are less successful at identifying 3D curved surfaces when tracing them with a single finger than when they contact surfaces simultaneously with multiple fingers.

Relatively, little is known about how information is integrated across fingers or even across finger pads of the same digit. Some psychophysical studies suggest that interactions between fingers are minimal. Loomis J. M. *et al.* (1991) tested the ability of human subjects to identify objects either visually or by touch and found that while performance improved considerably when the size of the visual field was doubled (simulating touching a surface with two fingers), subjects showed little improvement in performance when two, rather than one, fingers were used to explore the complex 3D patterns. Similarly, Craig J. C. (1985) reported that patterns presented to a single finger pad are identified more accurately and rapidly than when the same patterns are divided in half and presented to separate fingers on the same hand. In contrast, psychophysical evidence suggests that there are considerable interactions when tactile information is presented to multiple digits on the same and opposite hands. Evans P. M. *et al.* (1992) showed that

performance in identifying a spatial pattern is high when identical stimuli are presented to two fingers and low if a conflicting stimulus is presented to an adjacent finger even when subjects are told to ignore stimulation of the adjacent finger. The effect occurs regardless of whether the two fingers are adjacent or nonadjacent but does not occur if the patterns are presented to opposite hands. Pont S. C. *et al.* (1999) tested the ability of subjects to detect curvature using static and dynamic touch and found that discrimination using multiple fingers is better than discrimination using a single finger.

Proprioceptive input provides information about the location of the digits in space and information about hand conformation. A simple demonstration of the importance between hand conformation and cutaneous perception is the Aristotle illusion. In this illusion, a continuous edge feels like a single edge when the two fingers are next to each other but feels like two separate edges (with different orientations) when touched with the fingers crossed (Benedetti, F., 1985; Craig, J. C., 2003). Other studies have demonstrated that hand conformation affects motion perception. Rinker M. A. and Craig J. C. (1994) found that the perception of stimuli presented to a single finger pad is dramatically affected by hand conformation. In their study, subjects were asked to report the direction of stimuli moving across the thumb while a non-target-moving stimulus was presented to the index finger. They showed that when the hand is placed flat, stimuli moving in the opposite directions on the index finger interfere with perception on the thumb. However, if the hand conformation is changed such that the index finger and thumb are opposed (precision grip configuration used when grasping objects), then the identical motion on the index finger that interfered with direction perception now improves performance. The perception of shape can also be affected by the orientation of the hand. Oldfield S. R. and Phillips J. R. (1983) showed that the perception of letters changed when subjects pronated or supinated their hand. Thus an embossed lower case "d" pressed into the skin changes to a lower case "b" as the wrist is rotated. The most plausible explanation for these findings is that perception from the finger pads is not based simply on the perception of local features but rather is based on cutaneous features in the context of hand conformation and orientation.

Recently, Berryman L. J. *et al.* (2006) showed that the perception of object size is dependent on both proprioceptive and mechanoreceptive input. They showed that the perceived size of an object is based on the spread of the digits at initial contact. Further, they showed that size perception is independent of contact force and contact area and somehow takes into account the textural properties of objects. Thus, the softness of an object does not affect its perceived size.

6.04.3.2 Cortical Neurophysiological Studies of 3D Shape

6.04.3.2.1 Ascending pathways

As shown in Figure 3, there are two principal pathways that carry somatosensory information from the

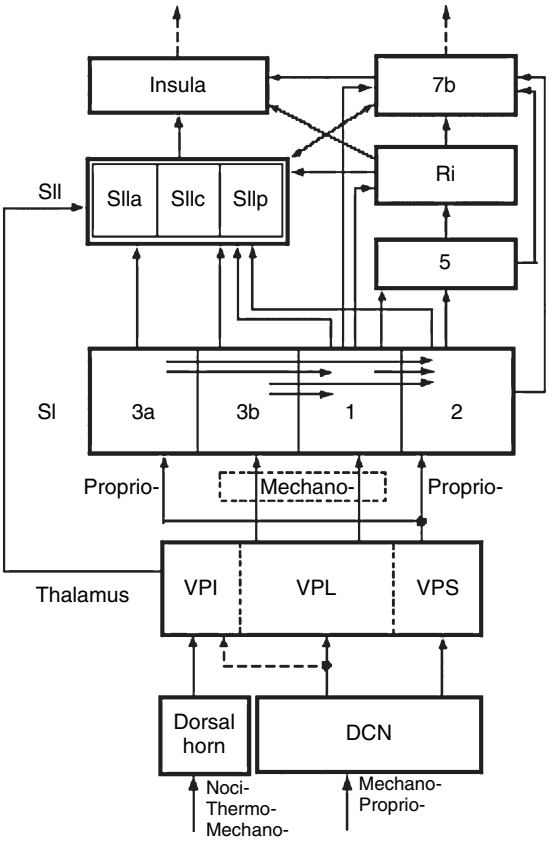

Figure 3 Functional organization of the somatosensory system. The pathway underlying form and texture processing starts with mechanoreceptive and proprioceptive afferents, which project to the dorsal column nuclei (DCN). These neurons then send their projections to the ventrobasal complex of the thalamus that has three subnuclei. The pathway then progresses to areas 3a, 3b, 1 and 2 of primary somatosensory cortex (SI) and then to the anterior, central, and posterior fields of the second somatosensory cortex (SII). The pathway for form and texture processing after SII cortex is largely unknown. VPI, ventroposterior lateral nucleus.

periphery to the cortex. One pathway, called the spinothalamic tract, carries information about nociception, temperature, and itch and does not play a role in object perception. The other pathway, called the dorsal column medial lemniscal pathway, carries information from the large diameter afferent fibers and is the critical pathway for conveying information from cutaneous and proprioceptive afferents. The information from mechanoreceptive and proprioceptive inputs remains segregated along this pathway.

6.04.3.2.2 Primary somatosensory cortex

The first cortical processing stage for somatosensory information is SI cortex, which consists of four areas (Kaas, J. H. *et al.*, 1979): Area 3a receives inputs from the shell region of the ventrobasal (VB) complex of the thalamus and neurons in this area respond to joint position (Burchfiel, J. L. and Duffy, F. H., 1972; Jones, E. G. and Porter, R., 1980; Friedman, D. P. and Jones, E. G., 1981) (Figure 3). Area 3b receives inputs from the core region of VB and 3b neurons tend to have slowly adapting RA responses with small receptive fields composed of excitatory and inhibitory subregions (Bankman, I. N. *et al.*, 1990; Hsiao, S. S. *et al.*, 1996; DiCarlo, J. J. *et al.*, 1998; Sripati, A. P. *et al.*, 2006b). Animals with lesions of area 3b show severe deficits in practically all aspects of tactile perception including form, texture, and shape perception (Randolph, M. and Semmes, J., 1974; Semmes, J. and Turner, B. H., 1977). Area 1 also receives cutaneous inputs from VB; however, the projection to area 1 is less dense than to 3b, and area 1 also receives projections from area 3b (Jones, E. G. and Powell, T. P. S., 1969). Neurons in area 1 have larger receptive fields than those in area 3b (Iwamura, Y. *et al.*, 1993), tend to have both slowly adapting and RA responses (Sur, M., 1980), and respond well to motion (Gardner, E. P., 1984). Lesions of area 1 are less devastating than lesions of area 3b, with animals showing mild but specific deficits in making rough–smooth and hard–soft discriminations (i.e., texture discriminations) (Randolph, M. and Semmes, J., 1974).

Area 2 receives both deep and cutaneous inputs from VB; neurons in this area have more complex responses than neurons in the other three areas of SI (Iwamura, Y. *et al.*, 1985). Besides receiving inputs from VB, area 2 also receives inputs from areas 3a, 3b, and 1, making it a prime candidate for being the initial processing stage for 3D shape processing (Pons, T. P. and Kaas, J. H., 1985; Porter, L. L. and Izraeli, R., 1993). Animals with lesions of area 2 are unable to discriminate gross object features (i.e., to judge objects as concave or convex, or square or diamond) (Randolph, M. and Semmes, J., 1974). Neurophysiological studies of area 2 provide strong evidence that this region is involved in 3D form perception (Iwamura, Y. and Tanaka, M., 1978; Gardner, E. P. and Costanzo, R. M., 1981; Koch, K. W. and Fuster, J. M., 1989; Debowy, D. J. *et al.*, 2001). Iwamura Y. and Tanaka M. (1978) reported that a large fraction of the neurons responded to simultaneous manipulation of the joints and punctate stimuli, and that some neurons appeared to be tuned to specific textures or shapes. They showed, for example, that some neurons in area 2 responded selectively to balls or cylinders but not to edges.

Several studies show that neurons in area 3b show selective responses to particular features of spatial stimuli (DiCarlo, J. J. *et al.*, 1998; DiCarlo, J. J. and Johnson, K. O, 1999; 2002; Sripati, A. P. *et al.*, 2006b). These studies report that neurons in area 3b have receptive fields composed of a central excitatory region with one or more inhibitory regions surrounding the excitatory region. The onset of the inhibitory subregion lags the excitatory input suggesting that it is of cortical origin. These excitatory and inhibitory subregions become fully elaborated approximately 20 ms following stimulus onset. Both of these regions are then rapidly followed by a larger replacing inhibition that lasts approximately 60 ms following stimulus onset. The regions of excitation and inhibition explain why neurons in 3b show feature selectivity. Peripheral neurons, which have mainly simple excitatory receptive fields, do not show orientation selectivity (Hsiao, S. S. *et al.*, 2002), however, a large fraction (70%) of the neurons in area 3b have asymmetric receptive field and consequently show orientation-tuned responses. One way of viewing these neurons is to think of them as spatiotemporal filters that are selective to particular features of the stimuli. These studies support the notion that area 3b lies at an intermediate step along a pathway where 2D spatial form is transformed from the isomorphic responses shown in Figure 1 to an altered representation that underlies perception of spatial form and the perception of roughness (DiCarlo, J. J. *et al.*, 1998; Chapman, C. E. *et al.*, 2002). The role of the replacing inhibition is to insure that the neurons are relatively insensitive to changes in scanning velocity. That is, the spatial response properties of the neuron are rapidly inhibited by the replacing inhibition thus limiting the degree of temporal smear that occurs with scanning.

Neurons in area 1 which receives inputs from both the thalamus and from area 3b appear to have larger but similar receptive field structures as area 3b neurons, although the responses are not as linear.

6.04.3.2.3 Areas 5 and 7 (tactile dorsal pathway)

Two principal processing streams diverge from SI cortex (Figure 3). One processing stream is directed caudally from SI to areas 5 and 7. Animals with lesions of areas 2 and 5 were unable to perform a wide range of form discrimination tasks. However, if area 2 is spared, animals show only a mild deficits in their ability to perform tactile discrimination tasks (Murray, E. A. and Mishkin, M., 1984). Similarly, animals with lesions of area 7 show only mild deficits in form discrimination (Semmes, J. and Turner, B. H., 1977). These results suggest that areas 5 and 7 are not involved in representing object shape. However, Sakata H. and Iwamura Y. (1978) reported that neurons located in the anterior bank of the intraparietal sulcus (area AIP), which is near the border between areas 2 and 5, exhibited shape-tuned responses: some neurons responded to rectangular blocks or straight edges but not to cylinders, whereas other neurons responded selectively to cylindrical bottles or apples. More recently, Koch K. W. and Fuster J. M. (1989) reported that neurons in areas 2 and 5 responded similarly to object shapes. One hypothesis is that areas 5 and 7 are involved in the perception of the immediate extrapersonal space and are responsible for representing the location of the body in space, for guidance of the body and hand, and for directing the attentional focus to targets in that space (Mountcastle, V. B. *et al.*, 1975; Sakata, H. and Iwamura, Y., 1978; Gardner, E. P. *et al.*, 2007a; 2007b). Further, neurons in these areas may play a role in matching hand grips with the characteristics of objects, since accurate positioning of the finger pads on an object surface is a prerequisite for subsequent handling and manipulation (Jeannerod, M. *et al.*, 1995). (See the chapter by Gardner, E. P., 1984 for further details on the roles of areas 5 and 7 in haptic processing.)

6.04.3.2.4 Second somatosensory cortex (tactile ventral pathway)

The other processing stream is directed ventrally toward the second somatosensory cortex (SII) and the insula and is concerned with object form perception (Murray, E. A. and Mishkin, M., 1984; Pons, T. P. *et al.*, 1992; Disbrow, E. *et al.*, 2001) and maybe closely linked with motor functions (Hinkley, L. B. *et al.*, 2007). Although SII also receives a direct projection from VB, several lines of evidence suggest that SII lies at a higher processing stage than SI cortex. First, lesions of SI cortex render neurons in SII silent (Pons, T. P. *et al.*, 1992). Second, while neurons in area 3b of SI cortex have small receptive fields restricted to single digits, neurons in SII tend to have larger receptive fields that often encompass multiple digits or the entire hand, with many neurons having bilateral receptive fields (Robinson, C. J. and Burton, H., 1980b; Hsiao, S. S. *et al.*, 1993; Fitzgerald, P. J. *et al.*, 2006). Third, 90% of the neurons in SII are affected by the attentive state of the animal (Hsiao, S. S. and Vega-Bermudez, F., 2002). Fourth, SII cortex, like SI cortex, is important for object and texture processing since animals with ablations of SII are unable to perform tactile tasks involving form and texture discriminations (Ridley, R. M. and Ettlinger, G., 1978; Murray, E. A. and Mishkin, M., 1984). Finally, neural responses in SII to scanned letters are significantly more complex and less isomorphic than are the responses of neurons in area 3b (Hsiao, S. S. *et al.*, 2003).

The functional organization of SII cortex is not well understood. Early reports suggested that it was composed of two areas (Robinson, C. J and Burton, H., 1980a; Burton, H. *et al.*, 1995; Krubitzer, L. A. *et al.*, 1995). Recent studies, however, suggest that it is composed of at least three fields (Fitzgerald, P. J. *et al.*, 2004) and possibly more in humans (Eickhoff, S. B. *et al.*, 2006). Fitzgerald P. J. *et al.* (2004) found that in monkeys, neurons in the anterior and posterior fields of SII cortex respond best to both proprioceptive and cutaneous input, whereas neurons in the central field respond primarily to cutaneous input. One possibility is that different tactile functions are distributed among the three fields and that different aspects of object shape are represented in each of the three fields. Another possibility is that SII cortex is more closely related to cognitive processing within the somatosensory system, which could explain why over 90% of the neurons in SII are affected by the animal's focus of attention (Hsiao, S. S. *et al.*, 1993; Jiang, W. *et al.*, 1997; Steinmetz, P. N. *et al.*, 2000; Meftah, E. M. *et al.*, 2002; Keysers, C. *et al.*, 2004).

Hsiao and co-workers (Hsiao, S. S *et al.*, 2002; Fitzgerald, P. J. *et al.*, 2006) have demonstrated that a large fraction of neurons in the somatosensory cortex show orientation tuning and that the representation of orientation is elaborated as one proceeds from SI to SII cortex. While neurons in the periphery do not show orientation tuning, about 70% of the neurons in area 3b and about 30% of the neurons in

the three areas of SII show tuned responses. In both SI and SII, the orientation tuning properties of the neurons (aspect ratio and bandwidth) are similar to those found in the visual system (Fitzgerald, P. J. *et al.*, 2006) suggesting that these neurons are involved in form processing. Neurons in SII have receptive fields that range from simple receptive fields, confined to a single finger pad, to large and complex receptive fields, comprising combinations of finger pads and exhibiting tuned, untuned excitatory, and untuned inhibitory pads (Fitzgerald, P. J. *et al.*, 2006). Furthermore, the tuning of individual neurons is highly similar across pads (Figure 4). In further studies, they report that many neurons in SII have positionally invariant responses to bars placed anywhere in the finger pad (Thakur, P. H. *et al.*, 2006).

The results from these studies suggest that neurons in SII cortex are ideally suited for coding features of large objects that span multiple finger pads. One hypothesis is that these receptive fields represent processing kernels that underlie the representation of 3D objects. Orientation-tuned pads may be responsible for detecting edges or corners of patterns and untuned excitatory pads for detecting the flat part of objects.

A working hypothesis for 3D object perception, supported by neural imaging studies (Roland, P. E. *et al.*, 1988; Seitz, R. J. *et al.*, 1991), is that surface features are extracted by neurons in areas 3b and 1, and primitives for object shape and size are extracted by neurons in area 2 (Bodegard, A. *et al.*, 2001; Ostry, D. J. and Romo, R., 2001). The processing then proceeds to the three areas that make up SII cortex, where the primitives are combined to form more elaborate representations of objects. Little is known about where the processing proceeds beyond SII. Candidate areas include AIP, supramarginal gyrus (Bodegard, A. *et al.*, 2001), and possibly visual areas like IT cortex (Sadato, N. *et al.*, 1996; Zangaladze, A. *et al.*, 1999; Merabet, L. *et al.*, 2004).

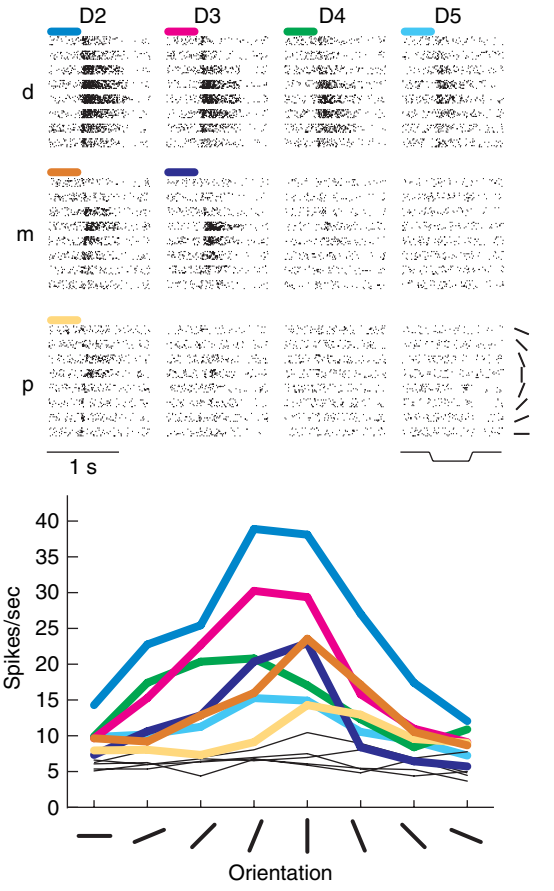

Figure 4 Receptive field of a neuron in SII cortex that has six orientation-tuned pads. D2, D3, D4, and D5 stand for the index, middle, ring, and pinky; d, m, and p stand for the distal, middle, and proximal finger pads. Each raster shows the occurrence of action potentials from an oriented bar indented into the finger pad at eight orientations (legend for the orientations is to the right of the raster for D5p. The bottom graph shows the tuning curves for all 12 pads. Adapted from Fitzgerald, P. J., Lane, J. W., Thakur, P. H., and Hsiao, S. S. 2006. Receptive field (RF) properties of the macaque second somatosensory cortex: RF size, shape, and somatotopic organization. J. Neurosci. 26, 6485–6495.

6.04.4 Conclusion

While much is known about the peripheral afferent systems that underlie somatic sensation, little is known about how information from those systems leads to perception. Emerging evidence suggests that the pathway for object perception progresses from area 3b to area 2 and then to SII cortex, where cutaneous inputs are combined in a stagewise manner with proprioceptive inputs to form representations of the 3D structure of objects. The pathway for texture processing is less clear. Clearly, spatial processing by the SA1 afferents plays the major role in roughness and hardness perception; however, the peripheral representation of stickiness has not been established. Evidence also suggests that areas 3b, 1, and possibly SII also play a major role in texture perception. Further studies are needed to investigate how objects are represented in cortex beyond SII cortex.

References

Bankman, I. N., Johnson, K. O., and Hsiao, S. S. 1990. Neural image transformation in the somatosensory system of the monkey: comparison of neurophysiological observations with responses in a neural network model. Cold Spring Harb. Symp. Quant. Biol. 55, 611–620.

Benedetti, F. 1985. Processing of tactile spatial information with crossed fingers. J. Exp. Psychol. Hum. Percept. Perform. 11, 517–525.

Bensmaia, S. J. and Hollins, M. 2003. The vibrations of texture. Somatosens. Mot. Res. 20, 33–43.

Bensmaia, S. J. and Hollins, M. 2005. Pacinian representations of fine surface texture. Percept. Psychophys. 67, 842–854.

Bensmaia, S. J., Craig, J. C., and Johnson, K. O. 2006. Temporal factors in tactile spatial acuity: evidence for RA interference in fine spatial processing. J. Neurophysiol. 95, 1783–1791.

Berryman, L. J., Yau, J. M., and Hsiao, S. S. 2006. Representation of object size in the somatosensory system. J. Neurophysiol. 96, 27–39.

Blake, D. T., Hsiao, S. S., and Johnson, K. O. 1997a. Neural coding mechanisms in tactile pattern recognition: the relative contributions of slowly and rapidly adapting mechanoreceptors to perceived roughness. J. Neurosci. 17, 7480–7489.

Blake, D. T., Johnson, K. O., and Hsiao, S. S. 1997b. Monkey cutaneous SAI and RA responses to raised and depressed scanned patterns: effects of width, height, orientation, and a raised surround. J. Neurophysiol. 78, 2503–2517.

Bodegard, A., Geyer, S., Grefkes, C., Zilles, K., and Roland, P. E. 2001. Hierarchical processing of tactile shape in the human brain. Neuron 31, 317–328.

Burchfiel, J. L and Duffy, F. H. 1972. Muscle afferent input to single cells in primate somatosensory cortex. Brain Res. 45, 241–246.

Burton, H., Fabri, M., and Alloway, K. D. 1995. Cortical areas within the lateral sulcus connected to cutaneous representations in areas 3b and 1: a revised interpretation of the second somatosensory area in macaque monkeys. J. Comp. Neurol. 355, 539–562.

Chapman, C. E., Tremblay, F., Jiang, W., Belingard, L., and Meftah, E. M. 2002. Central neural mechanisms contributing to the perception of tactile roughness. Behav. Brain Res. 135, 225–233.

Connor, C. E. and Johnson, K. O. 1992. Neural coding of tactile texture: comparisons of spatial and temporal mechanisms for roughness perception. J. Neurosci. 12, 3414–3426.

Connor, C. E., Hsiao, S. S., Phillips, J. R., and Johnson, K. O. 1990. Tactile roughness: neural codes that account for psychophysical magnitude estimates. J. Neurosci. 10, 3823–3836.

Craig, J. C. 1985. Attending to two fingers: two hands are better than one. Percept. Psychophys. 38, 496–511.

Craig, J. C. 2003. The effect of hand position and pattern motion on temporal order judgments. Percept. Psychophys. 65, 779–788.

Darian-Smith, I. and Kenins, P. 1980. Innervation density of mechanoreceptive fibers supplying glabrous skin of the monkey's index finger. J. Physiol. 309, 147–155.

Davidson, P. W. 1972. Haptic judgments of curvature by blind and sighted humans. J. Exp. Psychol. 93, 43–55.

Debowy, D. J., Ghosh, S., Ro, J. Y., and Gardner, E. P. 2001. Comparison of neuronal firing rates in somatosensory and posterior parietal cortex during prehension. Exp. Brain Res. 137, 269–291.

DiCarlo, J. J. and Johnson, K. O. 1999. Velocity invariance of receptive field structure in somatosensory cortical area 3b of the alert monkey. J. Neurosci. 19, 401–419.

DiCarlo, J. J. and Johnson, K. O. 2000. Spatial and temporal structure of receptive fields in primate somatosensory area 3b: effects of stimulus scanning direction and orientation. J. Neurosci. 20, 495–510.

DiCarlo, J. J. and Johnson, K. O. 2002. Receptive field structure in cortical area 3b of the alert monkey. Behav. Brain Res. 135, 167–178.

DiCarlo, J. J., Johnson, K. O., and Hsiao, S. S. 1998. Structure of receptive fields in area 3b of primary somatosensory cortex in the alert monkey. J. Neurosci. 18, 2626–2645.

Disbrow, E., Roberts, T., Poeppel, D., and Krubitzer, L. 2001. Evidence for interhemispheric processing of inputs from the hands in human S2 and PV. J. Neurophysiol. 85, 2236–2244.

Eickhoff, S. B., Schleicher, A., Zilles, K., and Amunts, K. 2006. The human parietal operculum. I. Cytoarchitectonic mapping of subdivisions. Cereb. Cortex 16, 254–267.

Ekman, G., Hosman, J., and Lindstrom, B. 1965. Roughness, smoothness and preference: a study of quantitative relations in individual subjects. J. Exp. Psychol. 70, 18–26.

Evans, P. M., Craig, J. C., and Rinker, M. A. 1992. Perceptual processing of adjacent and nonadjacent tactile nontargets. Percept. Psychophys. 52, 571–581.

Fitzgerald, P. J., Lane, J. W., Thakur, P. H., and Hsiao, S. S. 2004. Receptive field properties of the macaque second somatosensory cortex: evidence for multiple functional representations. J. Neurosci. 24, 11193–11204.

Fitzgerald, P. J., Lane, J. W., Thakur, P. H., and Hsiao, S. S. 2006. Receptive field (RF) properties of the macaque second somatosensory cortex: RF size, shape, and somatotopic organization. J. Neurosci. 26, 6485–6495.

Friedman, D. P. and Jones, E. G. 1981. Thalamic input to areas 3a and 2 in monkeys. J. Neurophysiol. 45, 59–85.

Gardner, E. P. 1984. Cortical Neuronal Mechanisms Underlying the Perception of Motion Across the Skin. In: Somatosensory Mechanisms (*eds*. C. von Euler, O. Franzén, U. Lindblom, and D. Ottoson), pp. 93–112. Macmillan Press.

Gardner, E. P. and Costanzo, R. M. 1981. Properties of kinesthetic neurons in somatosensory cortex of awake monkeys. Brain Res. 214, 301–319.

Gardner, E. P. and Palmer, C. I. 1990. Simulation of motion on the skin. III. Mechanisms used by rapidly adapting cutaneous mechanoreceptors in the primate hand for spatiotemporal resolution and two-point discrimination. J. Neurophysiol. 63, 841–859.

Gardner, E. P., Babu, K. S., Reitzen, S. D., Ghosh, S., Brown, A. S., Chen, J., Hall, A. L., Herzlinger, M. D., Kohlenstein, J. B., and Ro, J. Y. 2007a. Neurophysiology of prehension. I. Posterior parietal cortex and object-oriented hand behaviors. J. Neurophysiol. 97, 387–406.

Gardner, E. P., Ro, J. Y., Babu, K. S., and Ghosh, S. 2007b. Neurophysiology of prehension. II. Response diversity in primary somatosensory (S-I) and motor (M-I) cortices. J. Neurophysiol. 97, 1656–1670.

Goodwin, A. W., Macefield, V. G., and Bisley, J. W. 1997. Encoding of object curvature by tactile afferents from human fingers. J. Neurophysiol. 78, 2881–2888.

Hinkley, L. B., Krubitzer, L., Nagarajan, S., and Disbrow, E. A. 2007. Sensorimotor integration in S2, PV, and the parietal rostroventral areas of the human Sylvian fissure. J. Neurophysiol. 97, 1288–1297.

Hollins, M., Bensmaïa, S. J., Karlof, K., and Young, F. 2000. Individual differences in perceptual space for tactile textures: evidence from multidimensional scaling. Percept. Psychophys. 62, 1534–1544.

Hollins, M., Bensmaia, S. J., and Roy, E. A. 2002. Vibrotaction and texture perception. Behav. Brain Res. 135, 51–56.

Hollins, M., Bensmaia, S. J., and Washburn, S. 2001. Vibrotactile adaptation impairs discrimination of fine, but not coarse, textures. Somatosens. Mot. Res. 18, 253–262.
Hollins, M., Faldowski, R., Rao, S., and Young, F. 1993. Perceptual dimensions of tactile surface texture: a multidimensional-scaling analysis. Percept. Psychophys. 54, 697–705.
Hsiao, S. S. 1998. Similarities between Touch and Vision. In: Neural Aspects of Tactile Sensation (*ed*. J. W. Morley), pp. 131–165. Elsevier.
Hsiao, S. S. and Vega-Bermudez, F. 2002. Attention in the Somatosensory System. In: The Somatosensory System: Deciphering the Brain's Own Body Image (*ed*. R. J. Nelson), pp. 197–217. CRC Press.
Hsiao, S. S., Johnson, K. O., Twombly, I. A., and DiCarlo, J. J. 1996. Form Processing and Attention Effects in the Somatosensory System. In: Somesthesis and the Neurobiology of the Somatosensory Cortex (*eds*. O. Franzén, R. S. Johansson, and L. Terenius), pp. 229–247. Birkhäuser.
Hsiao, S. S., Johnson, K. O., and Yoshioka, T. 2003. Processing of Tactile Information in the Primate Brain. In: Comprehensive Handbook of Psychology, Vol. 3, Biological Psychology (*eds*. M. Gallagher and R. J. Nelson), pp. 211–236. Wiley.
Hsiao, S. S., Lane, J. W., and Fitzgerald, P. 2002. Representation of orientation in the somatosensory system. Behav. Brain Res. 135, 93–103.
Hsiao, S. S., O'Shaughnessy, D. M., and Johnson, K. O. 1993. Effects of selective attention of spatial form processing in monkey primary and secondary somatosensory cortex. J. Neurophysiol. 70, 444–447.
Iwamura, Y. and Tanaka, M. 1978. Postcentral neurons in hand region of area 2: their possible role in the form discrimination of tactile objects. Brain Res. 150, 662–666.
Iwamura, Y., Tanaka, M., Sakamoto, M., and Hikosaka, O. 1985. Comparison of the Hand and Finger Representation in Areas 3, 1, and 2 of the Monkey Somatosensory Cortex. In: Development, Organization, and Processing in Somatosensory Pathways (*eds*. M. J. Rowe and W. D. Willis), pp. 239–245. Alan R. Liss.
Iwamura, Y., Tanaka, M., Sakamoto, M., and Hikosaka, O. 1993. Rostrocaudal gradients in the neuronal receptive field complexity in the finger region of the alert monkey's postcentral gyrus. Exp. Brain Res. 92, 360–368.
Jeannerod, M., Arbib, M. A., Rizzolatti, G., and Sakata, H. 1995. Grasping objects: the cortical mechanisms of visuomotor transformation [review]. Trends Neurosci. 18, 314–320.
Jiang, W., Tremblay, F., and Chapman, C. E. 1997. Neuronal encoding of texture changes in the primary and the secondary somatosensory cortical areas of monkeys during passive texture discrimination. J. Neurophysiol. 77, 1656–1662.
Johansson, R. S. and Vallbo, Å. B. 1979. Tactile sensibility in the human hand: relative and absolute densities of four types of mechanoreceptive units in glabrous skin. J. Physiol. 286, 283–300.
Johansson, R. S. and Westling, G. 1987. Signals in tactile afferents from the fingers eliciting adaptive motor responses during precision grip. Exp. Brain Res. 66, 141–154.
Johnson, K. O. 2001. The roles and functions of cutaneous mechanoreceptors. Curr. Opin. Neurobiol. 11, 455–461.
Johnson, K. O. and Hsiao, S. S. 1992. Neural mechanisms of tactual form and texture perception. Annu. Rev. Neurosci. 15, 227–250.
Johnson, K. O. and Phillips, J. R. 1981. Tactile spatial resolution. I. Two-point discrimination, gap detection, grating resolution, and letter recognition. J. Neurophysiol. 46, 1177–1191.
Johnson, K. O., Hsiao, S. S., and Yoshioka, T. 2002. Neural coding and the basic law of psychophysics. Neuroscientist 8, 111–121.
Johnson, K. O., Yoshioka, T., and Vega-Bermudez, F. 2000. Tactile functions of mechanoreceptive afferents innervating the hand. J. Clin. Neurophysiol. 17, 539–558.
Jones, E. G. and Porter, R. 1980. What is area 3a? Brain Res. Brain Res. Rev. 2, 1–43.
Jones, E. G. and Powell, T. P. S. 1969. Connexions of the somatic sensory cortex of the rhesus monkey. II. Contralateral cortical connexions. Brain 92, 717–730.
Kaas, J. H., Nelson, R. J., Sur, M., Lin, C. S., and Merzenich, M. M. 1979. Multiple representations of the body within the primary somatosensory cortex of primates. Science 204, 521–523.
Kappers, A. M. L. and Koenderink, J. J. 1996. Haptic unilateral and bilateral discrimination of curved surfaces. Perception 25, 739–749.
Keysers, C., Wicker, B., Gazzola, V., Anton, J. L., Fogassi, L., and Gallese, V. 2004. A touching sight; SII/PV activation during the observation and experience of touch. Neuron 42, 335–346.
Klatzky, R. L., Lederman, S. J., and Metzger, V. A. 1985. Identifying objects by touch: an ''expert system''. Percept. Psychophys. 37, 299–302.
Koch, K. W. and Fuster, J. M. 1989. Unit activity in monkey parietal cortex related to haptic perception and temporary memory. Exp. Brain Res. 76, 292–306.
Krubitzer, L. A., Clarey, J., Tweedale, R., Elston, G., and Calford, M. B. 1995. A redefinition of somatosensory areas in the lateral sulcus of macaque monekeys. J. Neurosci. 15, 3821–3839.
LaMotte, R. H. and Srinivasan, M. A. 1996. Neural encoding of shape: responses of cutaneous mechanoreceptors to a wavy surface stroked across the monkey fingerpad. J. Neurophysiol. 76, 3787–3797.
Lederman, S. J. and Klatzky, R. L. 1993. Extracting object properties through haptic exploration. Acta. Psychol. (Amst.) 84, 29–40.
Loo, C. K., Hall, L. A., McCloskey, D. I., and Rowe, M. J. 1983. Proprioceptive contributions to tactile identification of figures: dependence on figure size. Behav. Brain Res. 7, 383–386.
Loomis, J. M., Klatzky, R. L., and Lederman, S. J. 1991. Similarity of tactual and visual picture recognition with limited field of view. Perception 20, 167–177.
Meftah, E. M., Shenasa, J., and Chapman, C. E. 2002. Effects of a cross-modal manipulation of attention on somatosensory cortical neuronal responses to tactile stimuli in the monkey. J. Neurophysiol. 88, 3133–3149.
Merabet, L., Thut, G., Murray, B., Andrews, J., Hsiao, S., and Pascual-Leone, A. 2004. Feeling by sight or seeing by touch? Neuron 42, 173–179.
Mountcastle, V. B., Lynch, J. C., Georgopoulos, A. P., Sakata, H., and Acuna, C. 1975. Posterior parietal association cortex of the monkey: command functions for operations within extrapersonal space. J. Neurophysiol. 38, 871–908.
Murray, E. A. and Mishkin, M. 1984. Relative contributions of SII and area 5 to tactile discrimination in monkeys. Behav. Brain. Res. 11, 67–85.
Newell, F. N., Ernst, M. O., Tjan, B. S., and Bulthoff, H. H. 2001. Viewpoint dependence in visual and haptic object recognition. Psychol. Sci. 12, 37–42.
Oldfield, S. R. and Phillips, J. R. 1983. The spatial characteristics of tactile form perception. Perception 12, 615–626.
Ostry, D. J. and Romo, R. 2001. Tactile shape processing. Neuron 31, 173–174.
Phillips, J. R. and Johnson, K. O. 1981a. Tactile spatial resolution. II. Neural representation of bars, edges, and gratings in monkey primary afferents. J. Neurophysiol. 46, 1192–1203.
Phillips, J. R. and Johnson, K. O. 1981b. Tactile spatial resolution. III. A continuum mechanics model of skin

predicting mechanoreceptor responses to bars, edges, and gratings. J. Neurophysiol. 46, 1204–1225.
Pons, T. P and Kaas, J. H. 1985. Connections of area 2 of somatosensory cortex with the anterior pulvinar and subdivisions of the ventroposterior complex in macaque monkeys. J. Comp. Neurol. 240, 16–36.
Pons, T. P., Garraghty, P. E., and Mishkin, M. 1992. Serial and parallel processing of tactual information in somatosensory cortex of rhesus monkeys. J. Neurophysiol. 68, 518–527.
Pont, S. C., Kappers, A. M. L., and Koenderink, J. J. 1999. Similar mechanisms underlie curvature comparison by static and dynamic touch. Percept. Psychophys. 61, 874–894.
Porter, L. L. and Izraeli, R. 1993. The effects of localized inactivation of somatosensory cortex, area 3a, on area 2 in cats. Somatosens. Mot. Res. 10, 399–413.
Randolph, M. and Semmes, J. 1974. Behavioral consequences of selective ablations in the postcentral gyrus of *Macaca mulatta*. Brain Res. 70, 55–70.
Ridley, R. M. and Ettlinger, G. 1978. Further evidence of impaired tactile learning after removal of the second somatosensory projection cortex (SII) in monkey. Exp. Brain Res. 31, 475–488.
Rinker, M. A. and Craig, J. C. 1994. The effect of spatial orientation on the perception of moving tactile stimuli. Percept. Psychophys. 56, 356–362.
Robinson, C. J. and Burton, H. 1980a. Somatic submodality distribution within the second somatosensory (SII), 7b, retroinsular, postauditory, and granular insular cortical areas of *M. fascicularis*. J. Comp. Neurol. 192, 93–108.
Robinson, C. J. and Burton, H. 1980b. Somatotopographic organization in the second somatosensory area of *M. fascicularis*. J. Comp. Neurol. 192, 43–67.
Roland, P. E., Eriksson, L., Widen, L., and Stone-Elander, S. 1988. Changes in regional cerebral oxidative metabolism induced by tactile learning and recognition in man. Eur. J. Neurosci. 1, 3–18.
Sadato, N., Pascual-Leone, A., Grafman, J., Ibanez, V., Delber, M. P., Dold, G. R., and Hallett, M. 1996. Activation of the primary visual cortex by Braille reading in blind subjects. Nature 380, 526–528.
Sakata, H. and Iwamura, Y. 1978. Cortical Processing of Tactile Information in the First Somatosensory and Parietal Association Areas in the Monkey. In: The Mechanism of Recognition of Objects by Manipulation: A Multi-Disciplinary Approach (*ed*. G. Gordon), pp. 55–72. Pergamon.
Seitz, R. J., Roland, P. E., Bohm, C., Greitz, T., and Stone-Elander, S. 1991. Somatosensory discrimination of shape: tactile exploration and cerebral activation. Eur. J. Neurosci. 3, 481–492.
Semmes, J. and Turner, B. H. 1977. Effects of cortical lesions on somatosensory tasks. J. Invest. Dermatol. 69, 181–189.
Smith, A. M. and Scott, S. H. 1996. Subjective scaling of smooth surface friction. J. Neurophysiol. 75, 1957–1962.
Srinivasan, M. A. and LaMotte, R. H. 1995. Tactual discrimination of softness. J. Neurophysiol. 73, 88–101.
Srinivasan, M. A. and LaMotte, R. H. 1996. Tactual Discrimination of Softness: Abilities and Mechanisms. In: Somesthesis and the Neurobiology of the Somatosensory Cortex (*eds*. O. Franzén, R. S. Johansson, and L. Terenius), pp. 123–135. Birkhäuser.
Srinivasan, M. A., Whitehouse, J. M., and LaMotte, R. H. 1990. Tactile detection of slip: surface microgeometry and peripheral neural codes. J. Neurophysiol. 63, 1323–1332.
Sripati, A. P., Bensmaia, S. J., and Johnson, K. O. 2006a. A continuum mechanical model of mechanoreceptive afferent responses to indented spatial patterns. J. Neurophysiol. 95, 3852–3864.
Sripati, A. P., Yoshioka, T., Denchev, P., Hsiao, S. S., and Johnson, K. O. 2006b. Spatiotemporal receptive fields of peripheral afferents and cortical area 3b and 1 neurons in the primate somatosensory system. J. Neurosci. 26, 2101–2114.
Steinmetz, P. N., Roy, A., Fitzgerald, P. J., Hsiao, S. S., Johnson, K. O., and Niebur, E. 2000. Attention modulates synchronized neuronal firing in primate somatosensory cortex. Nature 404, 187–190.
Sur, M. 1980. Receptive fields of neurons in areas 3b and 1 of somatosensory cortex in monkeys. Brain Res. 198, 465–471.
Thakur, P. H., Fitzgerald, P. J., Lane, J. W., and Hsiao, S. S. 2006. Receptive field properties of the macaque second somatosensory cortex: nonlinear mechanisms underlying the representation of orientation within a finger pad. J. Neurosci. 26, 13567–13575.
Vega-Bermudez, F. and Johnson, K. O. 1999. SA1 and RA receptive fields, response variability, and population responses mapped with a probe array. J. Neurophysiol. 81, 2701–2710.
Vega-Bermudez, F., Johnson, K. O., and Hsiao, S. S. 1991. Human tactile pattern recognition: active versus passive touch, velocity effects, and patterns of confusion. J. Neurophysiol. 65, 531–546.
Voisin, J., Benoit, G., and Chapman, C. E. 2002a. Haptic discrimination of object shape in humans: two-dimensional angle discrimination. Exp. Brain Res. 145, 239–250.
Voisin, J., LaMarre, Y., and Chapman, C. E. 2002b. Haptic discrimination of object shape in humans: contribution of cutaneous and proprioceptive inputs. Exp. Brain Res. 145, 251–260.
Westling, G. and Johansson, R. S. 1987. Responses in glabrous skin mechanoreceptors during precision grip in humans. Exp. Brain Res. 66, 128–140.
Wheat, H. E. and Goodwin, A. W. 2001. Tactile discrimination of edge shape: limits on spatial resolution imposed by parameters of the peripheral neural population. J. Neurosci. 21, 7751–7763.
Yoshioka, T., Gibb, B., Dorsch, A. K., Hsiao, S. S., and Johnson, K. O. 2001. Neural coding mechanisms underlying perceived roughness of finely textured surfaces. J. Neurosci. 21, 6905–6916.
Zangaladze, A., Epstein, C. M., Grafton, S. T., and Sathian, K. 1999. Involvement of visual cortex in tactile discrimination of orientation. Nature 401, 587–590.

6.05 Tactile Sensory Control of Object Manipulation in Humans

R S Johansson, Umeå University, Umeå, Sweden

J R Flanagan, Queen's University, Kingston, ON, Canada

Published by Elsevier Inc.

6.05.1	**Organization of Object Manipulation Tasks**	68
6.05.2	**Sensory Systems Supporting Object Manipulation**	68
6.05.2.1	Tactile Sensory Innervation of the Human Hand	70
6.05.2.2	Deformational Properties of the Fingertips and Coding of Tactile Information in Ensembles of Afferents	71
6.05.2.3	Relative Spike Timing Provides Fast Information about Mechanical Fingertip Events	76
6.05.3	**Predictions and Control Points in the Tactile Modality**	77
6.05.3.1	Control of Reach	77
6.05.3.2	Control of Grasp Stability	77
6.05.3.3	Control of Motion of Objects in Hand	81
6.05.4	**Predictions and Control Points in Other Modalities**	82
6.05.5	**Conclusions**	84
References		85

Glossary

action-phase controller Represents a sensorimotor control policy for reaching a subgoal of an overall action plan by using sensory information and predictions in a specific way, each. As such, it is conceptually related to the notion of internal models in motor control that involve neural circuits that mimic the behavior of the motor system and environment and capture the mapping between motor outputs and sensory inputs (Wolpert, D. M. *et al.*, 2001).

grasp stability control The control of grip forces such that they are adequate to prevent accidental slips but not so large as to cause unnecessary fatigue or damage to the object or hand.

haptic Refers to the ability to experience the environment through active exploration, typically with our hands, as when palpating an object to gauge its shape and material properties.

microneurography A method using metal microelectrodes to investigate directly neural signals in efferent and afferent peripheral nerves *in situ* in conscious human subjects, able to participate in sophisticated and cooperative experimental tests. Tungsten microelectrodes with an epoxy resin-insulated shaft having diameter of about 200 μm, a tip diameter of about 5 μm, and an impedance around 500 kΩ measured at 1 kHz are generally used for recording action potentials in single axons. For an early review detailing this technique see Vallbo, Å. B. *et al.* (1979).

precision grip The grip formed when grasping an object with the distal tips of digits. Usually refers to grasping with the tips of the thumb and index finger on either side of an object.

sensorimotor control points Contact events that denote completion of action goals and give rise to discrete and distinct sensory signals in one or more sensory modalities.

sensorimotor control The use of both predicted and unexpected sensory information in the control of action.

tactile Refers to signals conveyed to the brain by low-threshold mechanoreceptive afferent neurons that innervate the skin and subcutaneous tissues in glabrous skin areas and oral mucosa, i.e., body areas used primarily for object interactions.

6.05.1 Organization of Object Manipulation Tasks

Most natural object manipulation tasks involve a series of actions or phases where each phase accomplishes a specific goal or subgoal of the overall task. Distinct mechanical contact events typically signify goal attainments. For example, consider the task of lifting, holding, and replacing a box on a tabletop. This task involves a series of action phases separated by contact events that involve either the making or the breaking of contact (Figure 1(a)) (Johansson, R. S. and Westling, G., 1984a). Thus, the goal of the initial reach phase is marked by the digits contacting the box and the goal of the subsequent load phase, during which forces are applied under isometric conditions to overcome object weight, is marked by the breaking of contact between the object in hand and the support surface. These and subsequent contact events give rise to distinct and discrete sensory signals in the tactile modality and, in many cases, other modalities (Figure 1(a)). These sensory signals not only provide information about the timing of the events but also about the characteristics of the mechanical interaction. Thus, a given object manipulation task can be represented as a sensory plan specifying a sequence of sensory goals in one or more sensory modalities (Flanagan, J. R. *et al.*, 2006). The implementation of such a plan requires the selection and execution of a corresponding sequence of basic actions, or action-phase controllers, to achieve the sensory goals (Figure 1(a)).

The task of each action-phase controller is to generate motor commands that will lead to the successful attainment of the sensory goal. When possible, the controller uses knowledge of object properties, combined with information about the current state of the system (including the motor apparatus and objects in the environment), to predictively tailor motor commands to the task at hand. For example, during the load phase of lifting, people normally scale the rate of change of force output to the predicted weight of the object. At the same time, the controller generates predictions about the sensory consequences of the motor output, including sensory signals associated with contact events. By comparing predicted and actual sensory feedback, task progression can be monitored (Figure 1(a)). If a mismatch occurs, the brain can launch learned task- and phase-specific corrective actions (or smart reflexes) that are part and parcel of the controller (Figure 1(a)). If the mismatch is due to erroneous predictions about object properties, memory representations related to these properties can be updated so as to improve predictive control in subsequent phases of the task and in other tasks with the same object.

Predictions about the terminal sensory state of each action phase provide initial state information for the next action-phase controller. In the absence of such predictions, this state information would have to be obtained by a peripheral afferent signal at the start of each phase. This would prevent smooth transitions between action phases because of substantial time delays in sensorimotor control loops. Due to delays associated with receptor transduction and encoding, afferent and efferent neural conduction, central processing, and muscle activation, it takes approximately 100 ms before signals from tactile sensors in the digits can bring about meaningful adjustments of fingertip actions. Even longer delays, in excess of 200 ms, are usually required to transform visual events into purposeful fingertip actions. Anticipatory control policies support dexterous object manipulation by avoiding these long time delays.

6.05.2 Sensory Systems Supporting Object Manipulation

In addition to multiple motor systems (arm, hand, postural), most natural object manipulation tasks engage multiple sensory systems. Vision can provide important information for planning and controlling task kinematics. For example, vision is used to locate target objects and to identify contact sites that are both stable and advantageous for actions we want to perform with the grasped object. Furthermore, visual cues about the identity, size, and shape of an object can be used for predictively adapting fingertip forces. For example, visual cues related to object weight and mass distribution can be used to predict force magnitudes and visual cues about shape to predict stable force directions. However, vision is of limited utility when objects are out of sight or partially occluded and for assessing contact sites for digits contacting the backside of objects. Furthermore, vision only provides indirect information about mechanical interactions that is based on statistical correlations learned through experience. Similarly, proprioception can only provide indirect information about contact mechanics. For example, signals related to muscle length, joint angle, and muscle force do not directly code the contact state between the hands and objects, and the sensitivity of nondigital

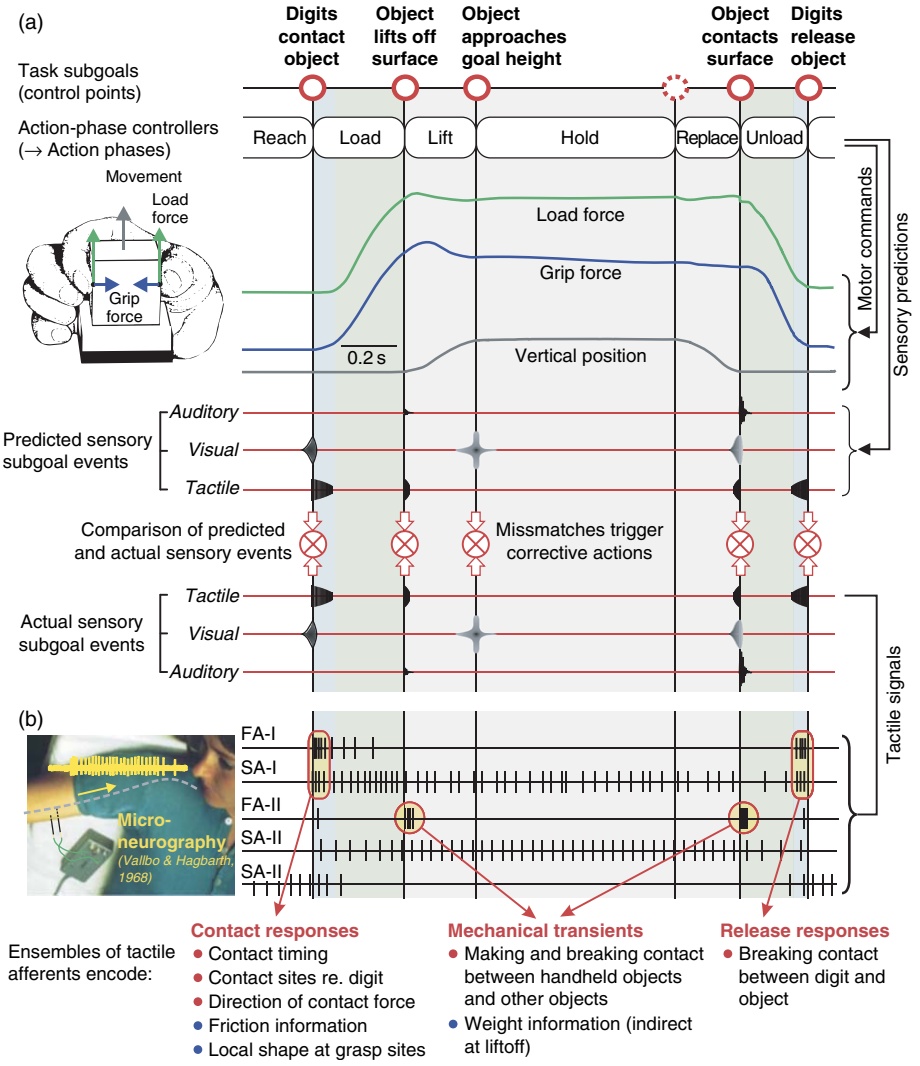

Figure 1 A person grasps and lifts an instrumented test object from a table, holds it in the air, and then replaces it, using the precision grip. (a) The contact events shown at the top define subgoals of the task (i.e., goals of each action phase). Sequentially implemented action-phase controllers generate motor commands that bring about the required action phases. After digits contact the object, the grip force increases in parallel with the tangential (load) force applied during isometric conditions to the object to overcome gravity. When the load force overcomes the force of gravity, the object lifts off. After the object is replaced such that it contacts the support surface, the load and grip forces decline in parallel until the object is released. In conjunction with generating motor command, the action-phase controllers predict internally the sensory consequences of these commands in one or more modalities (predicted sensory subgoal events) whereas the actual sensory consequences are signaled in one or more modalities (actual sensory subgoal events). For example, when the object is replaced on the surface, the contact between the object and the surface gives rise to tactile, visual, and auditory sensory events. By comparing predicted and actual sensory events, the sensorimotor system can monitor task progression and detect mismatches used to bring about corrective actions tailored to the action phase (see Figures 7 and 8). The predicted sensory events from each action phase can be used to provide initial state estimates for the next phase (not illustrated). (b) Schematic illustration of signals in four types of tactile afferents innervating the human fingertips as recorded from the median nerve at the level of the upper arm using the technique of microneurography. At four points corresponding to subgoal events of the task, tactile afferents show distinct burst discharges: (1) contact responses preferentially in fast-adapting type I (FA-I) and slowly adapting type I (SA-I) afferents when the object is first contacted, (2) responses in the fast-adapting type II (FA-II) afferents related to the mechanical transients at liftoff, and (3) when objects contact the support surface, and (4) responses primarily in FA-I afferents when the object is released (goal of the unloading phase). In addition to these event-related responses, slowly adapting type II (SA-II) afferents and many SA-I afferents show ongoing impulse activity when forces are applied to the object. Some spontaneously active SA-II units are unloaded during the lift and cease firing. (a) Compiled from data presented in Westling, G. and Johansson, R. S. 1987. Responses in glabrous skin mechanoreceptors during precision grip in humans. Exp. Brain Res. 66, 128–140. (b) From Vallbo, Å. B. and Hagbarth, K.-E. 1968. Activity from skin mechanoreceptors recorded percutaneously in awake human subjects. Exp. Neurol. 21, 270–289.

mechanoreceptive afferents (e.g., musculotendinous afferents) to fingertip events is very low in comparison to that of tactile sensors (*cf.* Macefield, V. G. and Johansson, R. S., 1996; Macefield, V. G. *et al.*, 1996; see also Häger-Ross, C. and Johansson, R. S., 1996).

Conversely, the tactile sensors directly provide information about mechanical interactions and thus play a pivotal role in the control of dexterous manipulation. The importance of tactile afferent signals in manipulation tasks is most apparent in people with impaired digital sensibility who have great difficulty with routine tasks even under visual guidance. For example, they often drop objects, may easily crush fragile objects, and have tremendous difficulties with everyday activities such as buttoning a shirt or picking up a match. About 2000 tactile afferents innervate each fingertip and some 10 000 afferent neurons innervate the remaining glabrous skin on the volar surface of the digits and the palm. As discussed below, these afferents provide various types of contact information critical for the control of the hands in dexterous object manipulation (see also Figure 1(b)). Because tactile information in object manipulation is used in control processes that generally operate automatically, transiently, and quickly, traditional studies of tactile sensory mechanisms, where perceptual (declarative) phenomena are examined in psychophysical experiments, provide limited information about the function of these mechanisms in manipulation.

6.05.2.1 Tactile Sensory Innervation of the Human Hand

Microneurography recordings of signals in single peripheral neurons in humans have shown that four different types of tactile afferents supply the inside of the hand (Johansson, R. S. and Vallbo, Å. B., 1983; Vallbo, A. B. and Johansson, R. S., 1984). Figure 2 summarizes characteristic features of these four types of afferents. Two types, termed fast-adapting type I (FA-I) and fast-adapting type II (FA-II) afferents, respond only during dynamic phases of tissue deformation. The other two types, called slowly adapting type I (SA-I) and slowly adapting type II (SA-II) afferents, respond to sustained skin deformation with a graded sustained discharge.

The type I afferents (FA-I and SA-I) terminate in end organs located at the dermal–epidermal margin. If delineated by weak point indentations of the skin, both types have small and well-defined cutaneous receptive fields ($\sim$10 mm^2), which in humans comprise multiple ($\sim$4–17) highly sensitive zones corresponding to individual terminal branches of the afferent axon (Johansson, R. S., 1978; Phillips, J. R. *et al.*, 1992). The receptive fields of both types exhibit enhanced representations of spatial discontinuities with comparable spatial resolution when tested with edge contours indenting the skin (Johansson, R. S. *et al.*, 1982b) and embossed dots scanned over the receptive field (Phillips, J. R. *et al.*, 1992). Their density in the skin increases stepwise in the distal direction of the hand (Figure 2(a)) and is especially high in the very tips of the digits where there are $\sim$140 FA-I afferents and $\sim$70 SA-I afferents per square centimeter of skin area (Figure 2). Hence, these afferents can transmit detailed spatial information about mechanical fingertip events, including the location and distribution of contact events. The FA-I and SA-I afferents provide complementary temporal information, with the SA-Is encoding static tissue deformations and deformation changes of lower frequencies (Johansson, R. S. *et al.*, 1982a). Accordingly, intraneural microstimulation of FA-I afferents typically evokes subjective sensations akin to wobbling, fluttering, or tapping feelings that are sharply delimited on the skin surface whereas stimulation of SA-I afferents typically evokes sensations of light pressure located more diffusely slightly below the skin surface (Vallbo, A. B. *et al.*, 1984; Torebjörk, H. E. *et al.*, 1987).

The predominance of FA-I afferents in the hand, and especially in the fingertips, indicates the premium placed on extracting with high-fidelity spatiotemporal features of dynamic mechanical events. Such events occur when objects are contacted and are often superimposed on low-frequency and large forces typically present when holding and maneuvering objects, including tools. Indeed, there is a predominance of FA-I afferents (or afferents similar to FA-Is) on other body areas used for accurate object interactions, such as the lips, the tip of the tongue (Trulsson, M. and Essick, G. K., 1997), and the sole of the foot (Kennedy, P. M. and Inglis, J. T., 2002). In contrast, hairy skin areas have no Meissner corpuscles (i.e., no FA-I sensors) and a predominance of slowly adapting sensors (Nordin, M. and Hagbarth, K. E., 1989; Edin, B. B. and Abbs, J. H., 1991; Edin, B. B. *et al.*, 1995; Vallbo, A. B. *et al.*, 1995).

The type II afferents (FA-II and SA-II) innervate the hand with a lower and more uniform density compared to the type I afferents. Their cutaneous receptive fields are an order of magnitude larger (Johansson, R. S., 1978), presumably partly because they terminate in the deeper dermal and subdermal

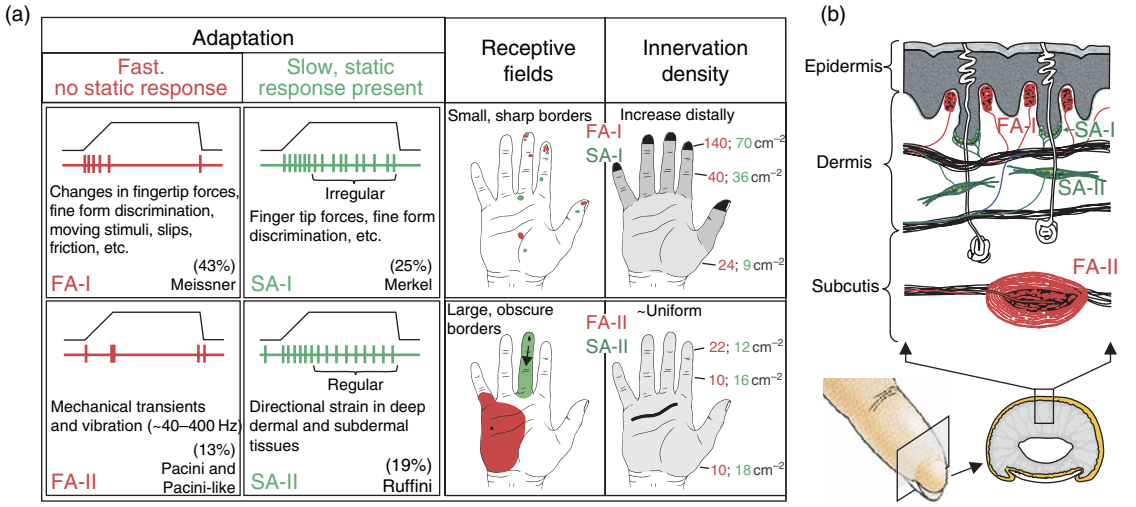

Figure 2 Types of tactile (mechanoreceptive) sensors in the glabrous skin of the inside of the human hand. (a) Graphs schematically show the impulse discharge (lower traces) to perpendicular ramp indentations of the skin (upper traces) for each sensor type. Two types (fast-adapting type I (FA-I) and fast-adapting type II (FA-II)) show fast adaptation to maintained tissue deformation, i.e., they only respond to deformation changes. These afferents were originally termed RA (rapidly adapting) and PC (Pacinian). Two types adapt slowly (slowly adapting type I (SA-I) and slowly adapting type II (SA-II)), that is, they show an ongoing response related to the strength of maintained tissue deformation. The type I sensors (FA-I and SA-I) have small and well-defined cutaneous receptive fields (typically 10 mm^2) when defined by light pointed stimuli (patches in the drawing of the hand represents the fields of 15 different sensors). The density of these sensors increases stepwise in the proximo-distal direction of the hand, with one step from the palm to the main parts of the digits and one at the border between the proximal to the distal half of the distal phalanx (see the rightmost drawing of the hand where the number of afferents per square centimeter of skin area is indicated for the fingertips, fingers, and palm, respectively). In contrast, the fast-adapting type II (FA-II) and SA-II sensors show lower and about uniform densities over the hand and their receptive fields are larger and less well defined. The FA-IIs are especially responsive to mechanical transients that propagate through the tissues whereas the SA-IIs sense strain in the dermal and subdermal fibrous tissues, often with a remote origin. The relative frequency of occurrence in the glabrous skin and the probable morphological correlate are indicated for each type of sensor. (b) Diagrammatic vertical section of a fingertip showing the organized nerve terminals corresponding to the four types of tactile sensors. Compiled from data reviewed in Johansson, R. S. and Vallbo, Å. B. 1983. Tactile sensory coding in the glabrous skin of the human hand. Trends Neurosci. 6, 27–31 and in Vallbo, A. B. and Johansson, R. S. 1984. Properties of cutaneous mechanoreceptors in the human hand related to touch sensation. Hum. Neurobiol. 3, 3–14.

tissues (Figure 2(b)). The FA-II afferents efficiently encode transient mechanical events containing high frequencies (~40–400 Hz) because of high-pass filtering properties of their end organs (Pacinian and Pacinian-like corpuscles) (Loewenstein, W. R. and Skalak, R., 1966). Such events arise in manipulation tasks when handheld objects form and break contacts with other objects and give rise to traveling waves in the tissues that can excite FA-II afferents located remotely from the contact areas. For example, it has been estimated that some 500–1000 FA-II afferents respond at liftoff and at support contact when objects are lifted and replaced, as illustrated in Figure 1 (Westling, G. and Johansson, R. S., 1987). The SA-II afferents sense directional strain in deep dermal and subdermal tissues (Johansson, R. S., 1978), including shear strain generated by forces tangential to the skin in object manipulation tasks (Westling, G. and Johansson, R. S., 1987). The fact that afferents with functional and structural properties akin to the type II afferents of the hand terminate in all fibrous tissues in the body, e.g., interosseous membranes, muscle fascias, and joint capsules and ligaments, suggests that they constitute a general mechanoreceptive system that supports proprioceptive in addition to tactile function.

6.05.2.2 Deformational Properties of the Fingertips and Coding of Tactile Information in Ensembles of Afferents

Signals in ensembles of afferents from the entire distal phalanx can contribute to the encoding of tactile information in natural object manipulation tasks because the interaction between the fingertips and objects typically causes widespread distributions of complex stresses

and strains throughout the engaged fingertips, including in the skin (Birznieks, I. *et al.*, 2001; Jenmalm, P. *et al.*, 2003). Hence, afferents that terminate outside regions of direct contact with objects can be vigorously excited, including FA-I and SA-I afferents, and constitute a part of the population code (Figure 3(b)). This applies, for example, to the encoding of fingertip force direction. Firing rates of individual tactile afferents distributed over the fingertips are tuned broadly to a preferred direction of fingertip force and this preferred direction varies amongst afferents such that ensembles of afferents can encode force direction (Figure 3(c) and 3(d)) (Birznieks, I. *et al.*, 2001). Directional preferences of individual afferents of specific types could, for example, be combined in population models such as the vector model of direction proposed for neurons in the motor cortex (Georgopoulos, A. P. *et al.*, 1986) and for encoding the direction of tooth loads by periodontal mechanoreceptors (Trulsson, M. *et al.*, 1992). In a similar vein, it has been proposed that the centroid of the population response can encode the position of a stimulus on the skin surface (Goodwin, A. W. and Wheat, H. E., 2004).

Firing rates in ensembles of tactile afferents also encode shape of contacted surfaces. Most studies of neural encoding of shape have concerned fine form

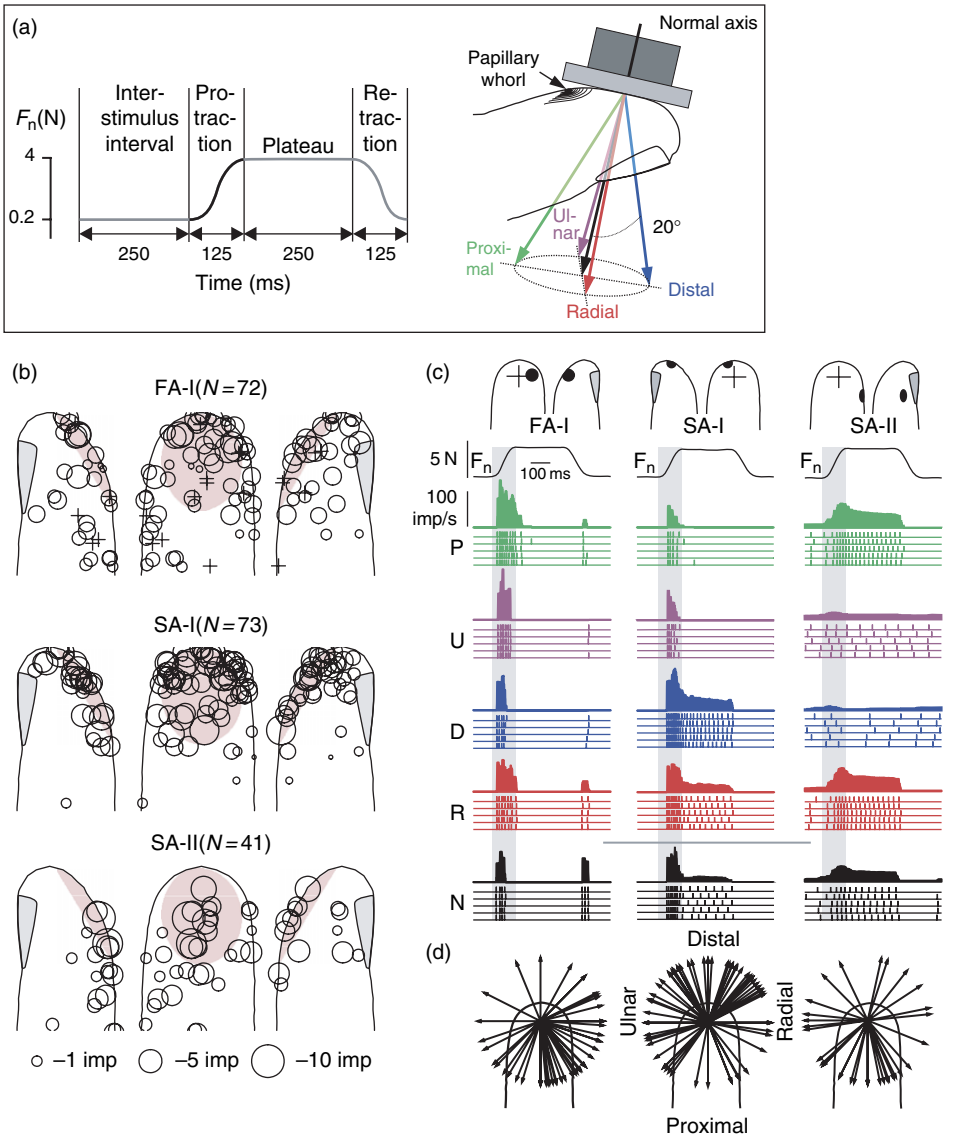

Figure 3 (*Continued*)

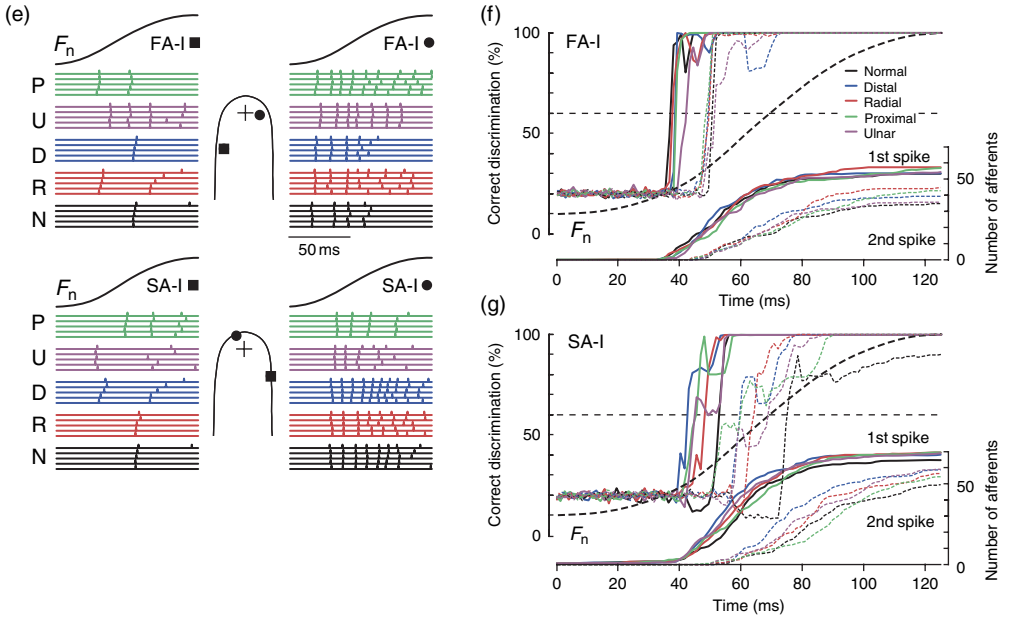

Figure 3 Signals in human tactile afferents under stimulation conditions representative for object manipulation tasks: Encoding of direction of fingertip forces. (a) Superimposed on a 0.2 N normal force (F_n), force was applied to the fingertip in the normal direction only (N), together with tangential components in the proximal (P), ulnar (U), distal (D), or radial (R) directions. Each stimulus consisted of a force protraction phase (125 ms), a plateau phase (4 N force), and a retraction phase (125 ms) and was applied with a flat contact surface at a standard site on the fingertip that serves as a primary target for object contact in grasping and manipulation of small objects. (b) The centers of the circles mark the location of the centers of the receptive fields of 186 tactile afferents, and the area of the circles represents the number of impulses evoked during the protraction phase with stimuli in the normal direction only. Nearly all afferent responded; crosses indicate locations of sampled afferents that did not respond. Pink zone represents the area of contact at 4 N normal force. (c) Impulse ensembles exemplifying responses in a single highly responsive fast-adapting type I (FA-I), slowly adapting type I (SA-I), and slowly adapting type II (SA-II) afferent to repeated force stimuli ($n = 5$) applied in each force direction (P, U, D, R, and N). Traces above show the instantaneous discharge frequency averaged over the five trials. Top traces show the normal force component (F_n) superimposed for all trials. Circles on the finger indicate the location of the afferents' termination and the cross the primary site of stimulation. (d) Distributions of preferred direction of tangential force components for 68 SA-I, 53 FA-I, and 32 SA-II afferents from the fingertip shown as unit vectors (arrows) with reference to the primary site of stimulation. These afferents terminate at various locations on a terminal phalanx (*cf*. (b)). Preferred directions were estimated by vector summation of the mean firing rates during the force protraction phase (gray zone in (c)) obtained with different directions of the tangential force component. (e–g) Discrimination of force direction by FA-I and SA-I afferents based on the relative timing of first spikes and on first-interspike intervals. Impulse ensembles in (e) exemplify responses during the force protraction phase in two FA-I and two SA-I afferents to repeated force stimuli ($n = 5$) applied in each of five force directions (see (a)). Force direction influenced consistently the first-spike latencies of all of these afferents. (f and g) Top graph: Solid curves show the probability of correct discrimination of stimuli in each of the five force directions (coded by different colors) by afferents' recruitment sequence as a function of time during the force protraction phase; dashed curve shows the development of the normal force component (F_n). Horizontal line indicates the probability for one-half of the stimuli being discriminated correctly, i.e., with force direction a probability of 60% given that chance performance is 20% (i.e., five force directions). Thin dashed curves show the time-varying probability of correct discrimination based on first-interspike intervals. Bottom graph: Solid curves give the number of sampled afferents recruited as a function of time for stimuli in each force direction, i.e., cumulative distributions of first-spike latencies. Thin dashed curves show the corresponding data for the second spike. (a–d) Adapted from Birznieks, I., Jenmalm, P., Goodwin, A., and Johansson, R. 2001. Encoding of direction of fingertip forces by human tactile afferents. J. Neurosci. 21, 8222–8237 and (e–g) from Johansson, R. S. and Birznieks, I. 2004. First spikes in ensembles of human tactile afferents code complex spatial fingertip events. Nat. Neurosci. 7, 170–177.

geometric features (e.g., Braille-like patterns and gratings), including markedly curved surfaces (radii $<\sim 5$ mm, i.e., curvatures $>\sim 200\ m^{-1}$), gently stimulating the fingertips in monkeys (Johnson, K. O., 2001; Goodwin, A. W. and Wheat, H. E., 2004). Such stimuli primarily engage afferents that terminate in the area of contact. However, objects that humans grasp in most everyday situations (e.g., cups, knobs, handles,

pens, fruit) involve larger curvatures (curvatures $\leq \sim 200\ m^{-1}$), and the control of fingertip actions in dexterous object manipulations depends critically on tactile information about these gross geometrical features (Jenmalm, P. and Johansson, R. S., 1997; Jenmalm, P. *et al.*, 2000). Recent findings in humans suggest that, in contrast to the encoding of fine form shapes, encoding of gross shapes engages ensembles of afferents terminating over the entire terminal phalanx (Jenmalm, P. *et al.*, 2003). Shape changes robustly influence firing rates in the majority of responsive SA-I, SA-II, and FA-I afferents, including afferents that terminate at the sides and end of the fingertip. For each afferent type, roughly half the afferents for which response intensity correlate with curvature showed a positive correlation and half a negative correlation (Figure 4(a) and 4(b)); afferents terminating at the sides and end of the fingertip tend to show negative correlations. Consequently, there is a curvature contrast signal within the populations of tactile afferents. This contrast signal may aid curvature recognition even though the overall discharge rates of afferent populations are influenced by various factors, e.g., the magnitude, direction, and rate of change of the contact force and changes in viscoelastic properties of the fingertip related to previous interactions with objects. Although the FA-I, SA-I, and SA-II afferents

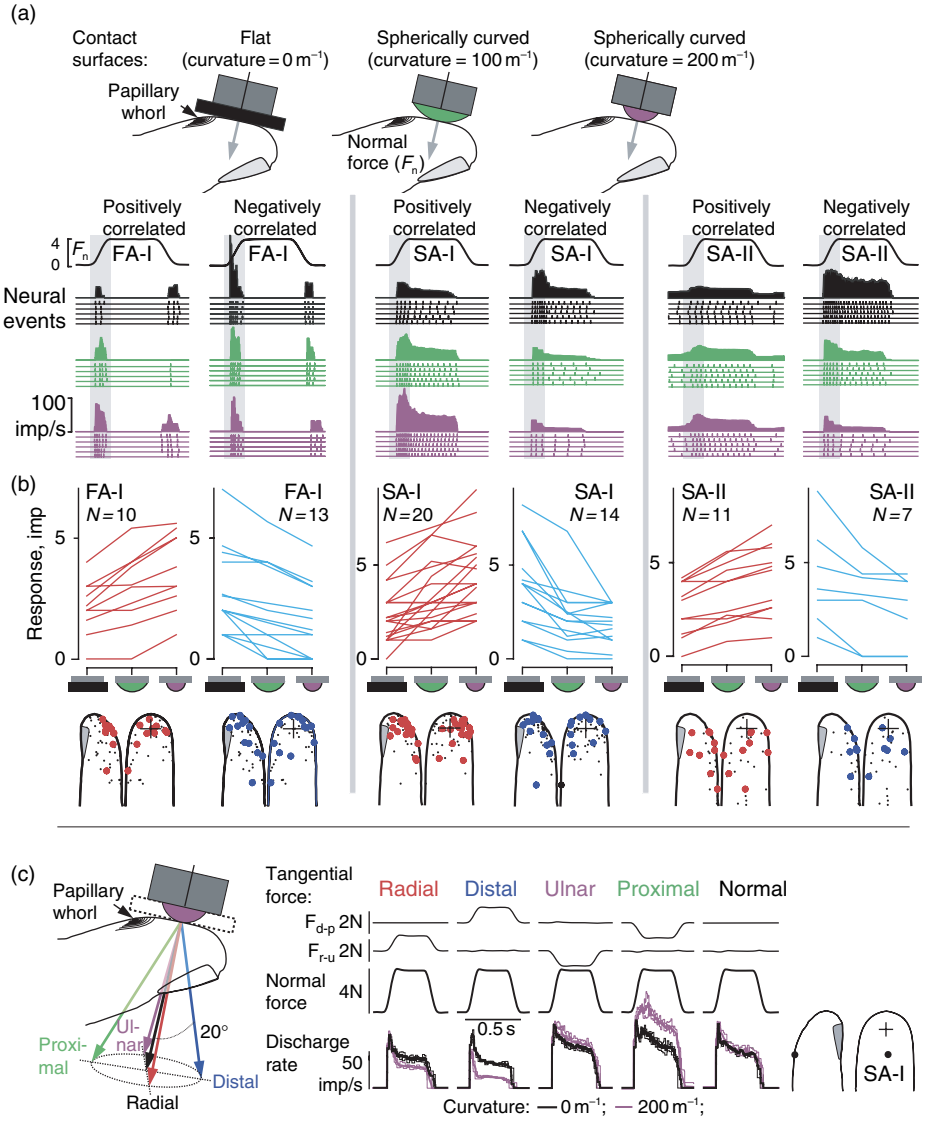

Figure 4 (*Continued*)

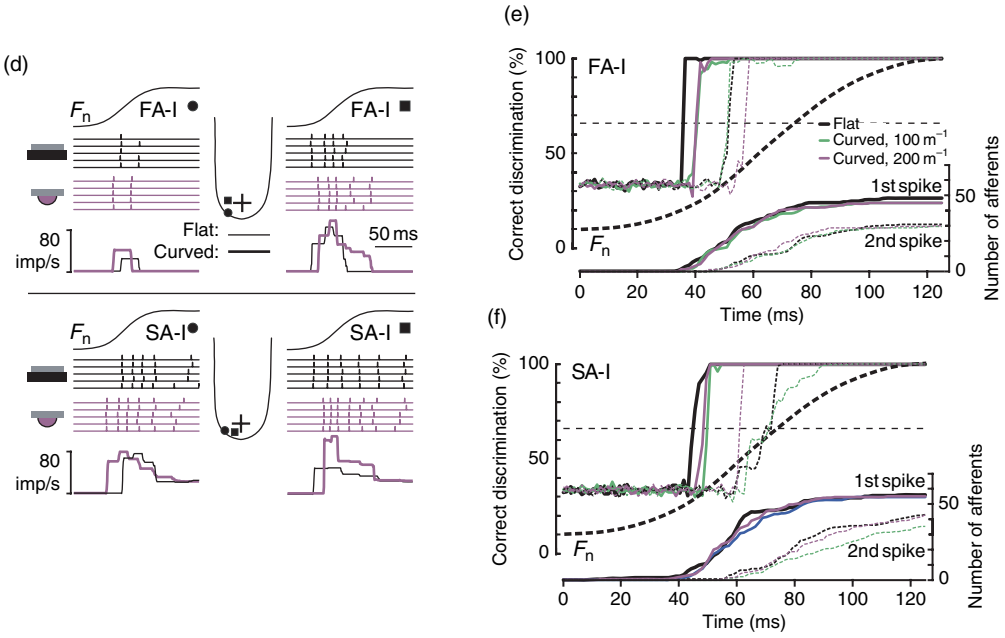

Figure 4 Signals in human tactile afferents under stimulation conditions representative for object manipulation tasks: Encoding of shape of spherically curved surfaces contacting the fingertips. (a) Impulse ensembles show responses to repeated stimuli ($n = 5$) of two single fast-adapting type I (FA-I), slowly adapting type I (SA-I), and slowly adapting type II (SA-II) afferents with forces applied in the normal direction with each of three surface curvatures 0, 100, and 200 m^{-1} (force stimulation as in Figure 3(a)). Traces above show the instantaneous discharge frequency averaged over the five trials. Top traces show the normal force. Left and right panels for each afferent type represent afferents for which response intensity increased (positively correlated) and decreased (negatively correlated) with an increase in curvature. (b) Left and right panels show, for each type of afferent, afferents with responses positively and negatively correlated with surface curvature, respectively; response is represented as the mean number of impulses evoked during the protraction phase (gray zone in (a)) with each curvature. Solid circles on the fingertip indicate the location of the receptive field centers of the afferents and the cross the stimulation site; the side view of the fingertip includes afferents located on either side of the finger. (c) Interaction effects between curvature and force direction on afferent responses illustrated by responses in one SA-I afferent during stimulation with forces in five directions (see Figure 3(a)) with the flat (0 m^{-1}) and most curved (200 m^{-1}) surface. Force profiles shown for the normal force component and for the tangential force components ($F_{d\text{-}p}$, $F_{r\text{-}u}$); radial, distal, ulnar, and proximal refer to the direction of the tangential force component. Profiles of instantaneous discharge frequency show responses to the 0 and 200 m^{-1} curvature; the center line indicates the mean instantaneous firing rates averaged over repeated stimuli ($n = 5$) and the thin lines represent the recorded maximum and minimum of the five rates. The dots on the fingertip indicate the afferents' receptive field center, the cross marks the stimulation site. (d–f) Discrimination of shape of stimulus surface by FA-I and SA-I afferents based on relative timing of the first spikes evoked in ensembles of tactile afferents and on the first-interspike intervals. (d) Impulse ensembles illustrate the effect of shape of stimulus surface on first-spike latencies of two single FA-I and SA-I afferents during five normal force stimuli with the flat (0 m^{-1}) and the most curved surface (200 m^{-1}). Traces above show normal force (F_n) and traces below instantaneous discharge frequency averaged over the five trials. Surface influenced consistently the first-spike latencies of all of these afferents. (e and f) Solid curves in the top graph show the probability of correct discrimination of each shape (coded by different colors) based on afferents' recruitment sequence as a function of time during the force protraction phase. Thin horizontal line indicates the probability for one-half of the stimuli being discriminated correctly, i.e., a probability of 66.5% given that chance performance is 33.3%. See caption of Figure 3(e–g). (a–c) Adapted from Jenmalm, P., Birznieks, I., Goodwin, A. W., and Johansson, R. S. 2003. Influences of object shape on responses in human tactile afferents under conditions characteristic for manipulation. Eur. J. Neurosci. 18, 164–176 and (d–f) from Johansson, R. S. and Birznieks, I. 2004. First spikes in ensembles of human tactile afferents code complex spatial fingertip events. Nat. Neurosci. 7, 170–177.

might all contribute information on object shape and contact forces, the SA-II population likely provides coarser information than the SA-I and especially the FA-I populations because of the lower innervation density of SA-II afferents.

Because tactile afferents respond to the complex patterns of strain/stress that occur in the fingertip when objects are contacted, various contact parameters can show complex interaction effects on the afferent responses. Interactions between force

direction and object shape on the responses of SA-I, SA-II, and FA-I afferents have been demonstrated (Jenmalm, P. *et al.*, 2003). That is, changing the direction of force generally affects an afferent's sensitivity to curvature and *vice versa*. Figure 4(c) illustrates such an interaction for a single SA-I afferent. How the brain deals with interactions among different parameters of fingertip stimulation in natural tasks poses important problems for future research. Presumably, many computational requirements for decoding tactile messages in manipulation tasks are satisfied by the somatosensory pathways functionally modeling the mechanics of the fingertips in the tactile sensory domain by, in effect, filtering information predictively in a manner that depends on context, task, and task phase. For example, corollary discharges associated with the execution of action plans (Sommer, M. A. and Wurtz, R. H., 2002) could, through descending corticothalamic, corticocuneate, and corticospinal projections, dynamically control the signal processing in ascending somatosensory pathways (Harris, F. *et al.*, 1965; Adkins, R. J. *et al.*, 1966; Ergenzinger, E. R. *et al.*, 1998). As such, there is ample evidence that the processing of sensory stimuli is controlled by top-down influences that constantly create predictions about forthcoming sensory events (Engel, A. K. *et al.*, 2001) including contract events (Bays, P. M. *et al.*, 2005).

6.05.2.3 Relative Spike Timing Provides Fast Information about Mechanical Fingertip Events

Traditionally, it is posited that tactile information is coded by the firing rates of afferents. To estimate firing rates, at least two impulses in a given neuron are required and given the stochastic properties of interspike intervals, reliable rate estimation may require that neural responses be averaged over a substantial time window and over several trials. However, in manipulation, typically, the brain quickly extracts information from dynamic tactile events and expresses this information in fingertip actions faster than can be readily explained by rate codes. Recent findings indicate that the relative timing of impulses from ensembles of individual different afferents conveys information about important contact parameters faster than the fastest possible rate code and fast enough to account for the use of tactile signals in natural manipulation (Johansson, R. S. and Birznieks, I., 2004). Specifically, the sequence in which different afferents initially discharge in response to discrete fingertip events provides information about the direction of fingertip force and the shape of the contacted surface. Presumably, the order of recruitment of members of the populations of tactile afferents can code other parameters of tactile stimuli used in the control of manual actions as well.

The relative timing of the first spikes contains information about force direction and object shape because changes in either of these parameters differentially influences the first-spike latency of individual afferents rather than having systematic effects on the latencies within an afferent population (Figures 3(e) and 3(g) and 4(d) and 4(f)). For example, with a single stimulus delivered to the fingertip in a given force direction, the responsive afferents will be recruited in a particular order. With another force direction, the order will be different because some afferents are recruited earlier and others later. The efficacy of this code for conveying early information to the brain depends on the variability and noise in first-spike latencies and the speed of recruitment of afferents. The FA-I population provide correct discrimination faster than the SA-I afferents of both force direction (*cf.* Figure 3(f) and 3(g)) and surface curvature (*cf.* Figure 4(e) and 4(f)). Effective discrimination takes place after as few as some five FA-I afferents are recruited, which occur a few milliseconds after the appearance of the first impulse in the population response (Figure 3(f) and 3(e)). For the SA-Is, about twice as many (but still very few) afferents had to be recruited for reliable discrimination primarily because of a larger variability in first-spike latencies. Even under the most favorable conditions, discrimination based on firing rates (first-interspike rate) takes on average 15–20 ms longer than discrimination based on first-spike latency (*cf.* dashed and solid curves in Figure 3(f) and 3(g) and 4(e) and 4(f)). Populations of SA-II are much poorer in discriminating force direction or object shape based on both first-spike latencies and firing rate, in part because of the background discharge in many of these afferents. Encoding and decoding of sensory information based on the timing of neural discharges, rather than (or in addition to) their rate, has received increasing attention in the past decade and it has become clear that the timing, with precision in the order of milliseconds or even less, of individual spikes can carry far more information than average rates alone (Heil, P., 2004; VanRullen, R. *et al.*, 2005).

6.05.3 Predictions and Control Points in the Tactile Modality

6.05.3.1 Control of Reach

Most manipulation tasks require that we first reach for the object to grasp it. One goal of this reach phase is to place the fingertips on the object in locations that will allow the development of a stable grasp in the context of the actions that will be performed with the object. Likewise, it is usually important that the fingertips contact the object at around the same time and that the fingertip force vectors sum to zero. These and other features of the contacts between the fingertips and object are robustly encoded by tactile signals. For each digit, contact responses in ensembles of afferents convey information about contact timing, the contact location on the digit, and the direction of contact force (Figure 1(b) and 3). Thus, the initial contact events represent control points where predicted and actual sensory feedback related to object geometry, location, and orientation can be compared. Mismatches between predicted and actual contact responses can be used to calibrate and uphold calibration of future reach commands (Gentilucci, M. *et al*., 1997; Lackner, J. R. and DiZio, P. A., 2000; Rao, A. K. and Gordon, A. M., 2001; Monzée, J. *et al*., 2003; Säfström, D. and Edin, B. B., 2004).

6.05.3.2 Control of Grasp Stability

After contact is obtained with an object, most manipulation tasks require application of forces tangential to the contacted surfaces (load forces). For example, to lift an object with the digits at the sides, vertical load forces must be applied to overcome the weight of the object (Figure 1(a)). If we lift a bar from one end, we must also apply tangential torque to prevent it from rotating when lifted. To deal with these potentially destabilizing tangential forces, the motor system generates grip forces normal to the grasped surface that are synchronous with, and proportional to, the tangential loads applied (Figures 1(a) and 5) (Johansson, R. S. and Westling, G., 1984a; Goodwin, A. W. *et al*., 1998; Johansson, R. S. *et al*., 1999). The grip forces are strong enough to prevent the object from slipping (either linearly or rotationally), while at the same time not excessive. This coordination of grip and load force supports grasp stability in virtually all maneuvers that we perform with objects. For example, it operates at the level of individual digits when people use two or more digits of the same or both hands to lift and further manipulate objects (Edin, B. B. *et al*., 1992; Flanagan, J. R. *et al*., 1999). Likewise, grip forces predict changes in load forces on a hand-held object that occur when we jump up and down (Flanagan, J. R. and Tresilian, J. R., 1994) and in bimanual tasks where the hands have different and complementary roles, such as when we use one hand to add things into, or remove things from, a receptacle held by the other hand (Johansson, R. S. and Westling, G., 1984a; 1988b). Coupling between grip and load forces also operates when we move objects with different complex dynamics (combinations of inertial, elastic and viscous loads) even though this involves altering the mapping between motor commands that generate load forces and those that generate grip forces (Flanagan, J. R. and Wing, A. M., 1997).

The control of grasp stability requires, however, that the balance between the grip and load forces be adapted to the properties of the contacted surfaces. Indeed, irrespective of surface friction and object shape, people typically use grip forces that exceed the minimum required to prevent slips by a safety margin of 10–40% of the applied grip force (gray areas in the force coordination plots of Figure 5). By varying the ratio between grip force change and load force change, people parametrically adapt to different frictional conditions and use greater grip forces with more slippery surfaces (Figure 5(b)). In the same vein, they adapt the grip-to-load force ratio to the shape of the contacted surface. For example, when lifting tapered objects, a greater grip-to-load force ratio is required when the grip surfaces are tapered upward as compared to downward (Figure 5(c)). Similarly, the greater the curvature of a spherically curved grasp surface, the larger the grip force required to generate a given tangential torque (Figure 5(d)).

Tactile signals are critical for forming, updating, and upholding predictions used by action-phase controllers when adapting forces to object surface properties. Indeed, people with digital sensory impairments fail to adapt grip-to-load force ratios to object surface properties and, instead, consistently use large grip forces (*cf.* Figure 6(b) and 6(c)) (Johansson, R. S. and Westling, G., 1984a; Westling, G. and Johansson, R. S., 1984; Jenmalm, P. and Johansson, R. S., 1997; Jenmalm, P. *et al*., 2000; Monzée, J. *et al*., 2003; Nowak, D. A. *et al*., 2004). Signals in ensembles of tactile afferents – primarily in FA-Is – rapidly convey information related to

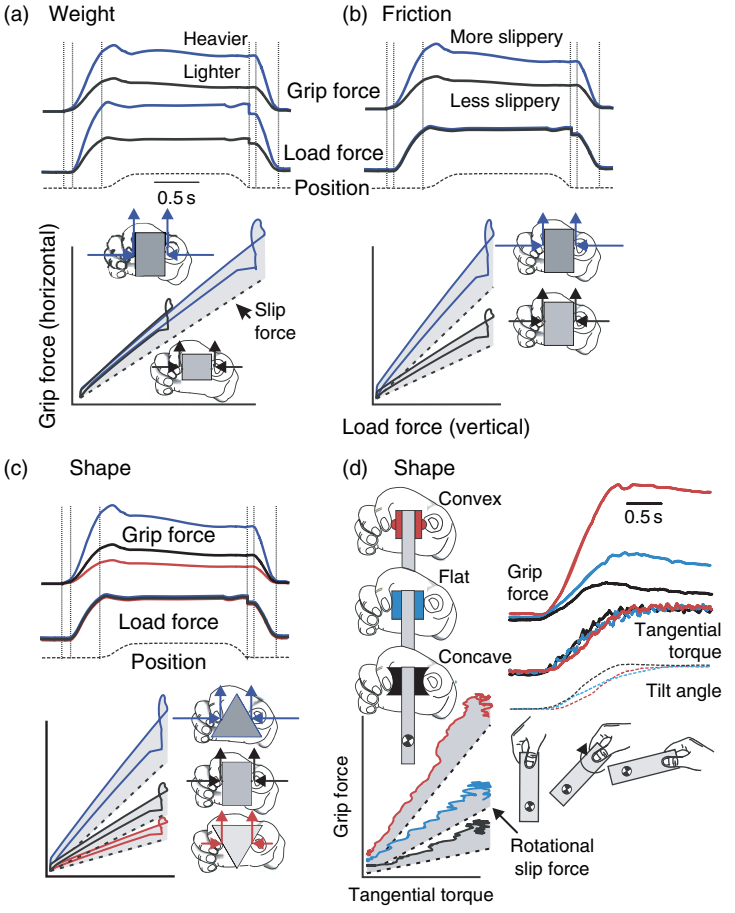

Figure 5 Parametric adjustments of fingertip forces to object weight, friction between the object and skin, and shape of the contact surface. (a–c) Subject lifts an instrumented test object from a table, holds it in the air, and then replaces it, using a precision grip (*cf*. Figure 1). Upper graphs show the horizontally oriented grip force, the vertically oriented load force (lift force), and the object's vertical position as a function of time for superimposed trials, indicated by differently colored curves. The lower graphs show the grip force as a function of the load for the corresponding data. Dashed lines indicate the minimum grip force to prevent slips; the safety margin against slips is indicated by hatching. (a) With weight variations the parallel change in grip and lift forces coordinated by the action-phase controllers ensures grasp stability when lifting objects of different weights. (b) The balance between grip force and load force is adjusted to deal with changes in friction. (c) A similar scaling of the grip-to-load force ratio is observed when object shape is varied. In either instance, the coordination of grip and load force ensures an adequate safety margin against slips. (d) An already lifted object is tilted by 65° around the grip axis, which caused tangential torques at the grasp surfaces. The three superimposed curves (color coded) refer to a trial with a spherically convex grip surface (radius 5 mm; curvature 200 m^{-1}), a flat (curvature 0 m^{-1}), and a spherically concave surface (radius 20 mm; curvature 50 m^{-1}). The top traces show the grip force, the tangential torque, and the tilt angle against time. Note the effect of surface curvature on the coordination between grip force and tangential torque, which is in the bottom graph that plots the grip force against tangential torque load for the corresponding data. The shading indicates a similar safety margin against rotational slips irrespective of curvature. (a, b) Adapted from Johansson, R. S. and Westling, G. 1984a. Roles of glabrous skin receptors and sensorimotor memory in automatic control of precision grip when lifting rougher or more slippery objects. Exp. Brain Res. 56, 550–564; Johansson, R. S. and Westling, G. 1988a. Coordinated isometric muscle commands adequately and erroneously programmed for the weight during lifting task with precision grip. Exp. Brain Res. 71, 59–71. (c) Jenmalm, P. and Johansson, R. S. 1997. Visual and somatosensory information about object shape control manipulative finger tip forces. J. Neurosci. 17, 4486–4499. (d) Goodwin, A. W., Jenmalm, P., and Johansson, R. S. 1998. Control of grip force when tilting objects: effect of curvature of grasped surfaces and of applied tangential torque. J. Neurosci. 18, 10724–10734, respectively.

surface friction (Figure 6(d)) and shape (Figures 4 and 7(a)) when a surface is contacted. Thus, the initial contact event represents a critical control point where predicted and actual sensory feedback related to surface properties can be compared. Mismatches between predicted and actual contact responses lead to an updating of the grip-load force coordination about 100 ms after contact. Figure 7(a)

illustrates such updating when repeatedly lifting objects with tapered grasp surfaces without visual cues about object shape. The tapering was changed between trials in a pseudo-random order. In all trials, the tapering (and hence force requirements) in the previous trial determined the initial increase in grip force. This indicates that predictions based on knowledge about the status of the object obtained in previous trials specify the force coordination. After a change in tapering, the grip force output is modified about 100 ms after contact with the object and tuned for the actual object properties (Figure 7(a)). By the second trial after the change, the force coordination is appropriately adapted right from the onset of force application. Thus, when a prediction error occurs, tactile information obtained at initial contact with the object rapidly initiates a corrective action accompanied with an updating of the representation of the object used to control forces in future interactions with the object. Knowledge about object surface properties remains critical for controlling grip forces for grasp stability when transporting held objects and using them as tools to impose forces on other environmental objects. A coupled decrease in the load and grip forces ensuring grasp stability also applies to the unloading phase where grip and load forces decrease in parallel in order to release an object placed on a support surface (Figures 1 and 5). Sensory events, especially in ensamples of FA-I afferents, related to the breaking of contact between the digits and the surface of the object represent the sensory goal of this phase (see release responses in Figure 1(b); see also responses in FA-I afferents to the retraction phase in Figures 3 and 4).

Under favorable conditions, visual geometric cues about object shape can provide state information for predictive parameterization of fingertip forces such that the grip-to-load force coordination is adapted to the prevailing shape right from the beginning of the force application (Figure 7(b)) (Jenmalm, P. and Johansson, R. S., 1997; Jenmalm, P. *et al.*, 2000). Once the object is contacted, tactile signals also provide state information about object shape that can override visual predictions if necessary. With regard to friction between the hand and an object, it appears that vision is unhelpful for feedforward adaptation of

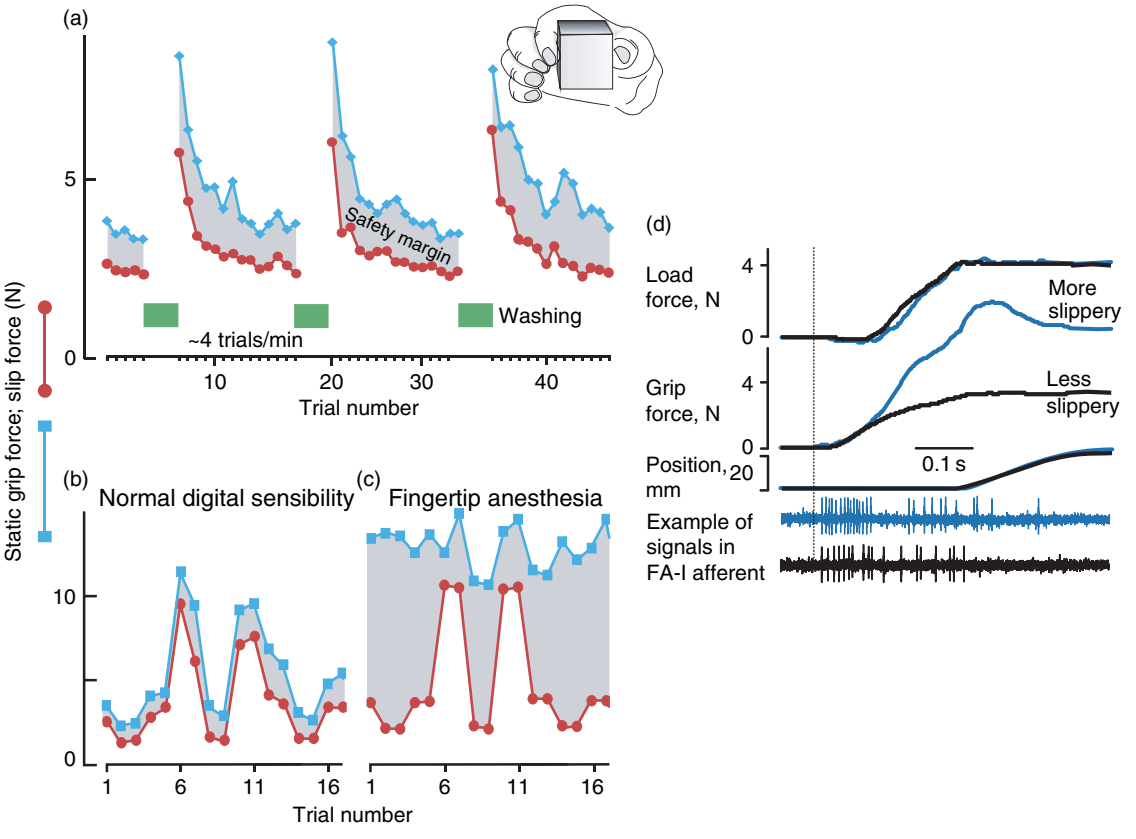

Figure 6 (*Continued*)

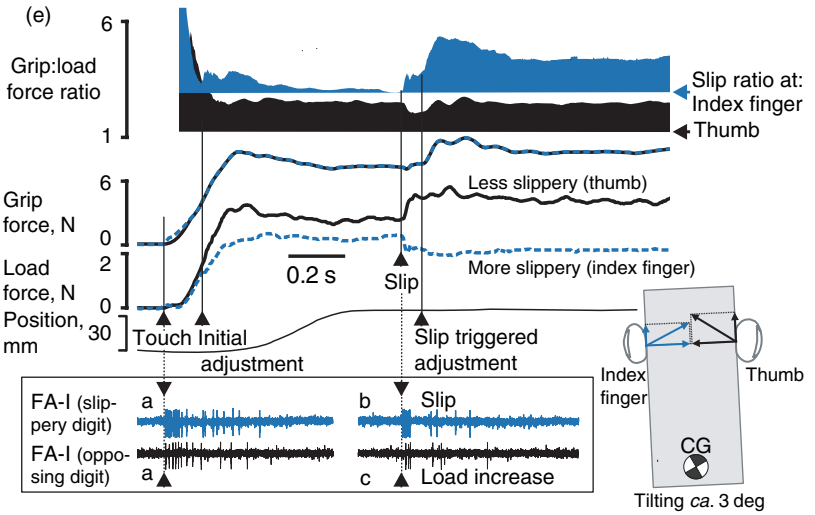

Figure 6 Adjustment of grip force to frictional changes in everyday situations. (a) Static grip force when holding an object in air using a precision grip (diamonds) and the corresponding minimum grip forces to prevent slips (slip force, dots) before and after the subject's hand was washed (soap and water) and dried (towel); 48 consecutive lifts with suede as surface structure (single subject, weight constant at 400 g). (b and c) Corresponding grip force data during frictional changes between lifts caused by changing the grasped surfaces among fine-grain sandpaper, and suede and smooth rayon, during normal digital sensibility (b) and with anesthetized finger tips (c). (d) The influence of friction on force output and initial contact responses in an fast-adapting type I (FA-I) afferent. Two lifting trials are superimposed, one with the grasped surfaces being less slippery (sandpaper; black lines) and a subsequent trial with more slippery surfaces (silk; blue lines). The sandpaper trial was preceded by a trial with sandpaper and therefore the force coordination is initially set for the higher friction. The vertical line indicates initial touch. (e) Digit-specific adjustments of force coordination to the frictional condition. The participant lifted a test object with low center of gravity (CG) from a support surface, and held it still in the air. The index finger contacted a more slippery surface (silk; blue curves) than that contacted by the thumb (sandpaper; black curves). The grip-to-load force ratio and corresponding slip ratios are shown for each digit; the blue and black areas indicate the safety margin to prevent slips at the index finger and at the thumb, respectively. In a previous lifting trial, both the index finger and the thumb had contacted fine-grain sandpaper. An initial adjustment to the new frictional condition occurs during the load phase, ~100 ms after the object is contacted. The index finger generates less load force than the thumb, which results in a higher grip-to-load force ratio at the index finger. A slip event occurring at the index finger later in the trial triggers a secondary adjustment to the frictional condition. The slip event is evident by a rapid decrease of the load force at that digit and a concomitant increase of the load force at the thumb. Less than 100 ms later, a grip force increase raises the grip-to-load force ratio at the index finger and restores the ratio at the thumb. Nevertheless, because of the uneven load force distribution between the digits, the test object tilts a bit when aloft. The inset shows signals in single FA-I afferents reconstructed based on microneurography recordings during similar lifting trials in a study by Johansson R. S. and Westling. G. (1987). Note the influence of the surface material on the impulse rate on the initial contact responses (a), the burst response to the slip in the afferent terminating in the tip of the slipping digit (b), and the response to the increase of the load force at the opposing digit. (a) Adapted from Johansson, R. S. and Westling, G. 1984b. Influences of Cutaneous Sensory Input on the Motor Coordination During Precision Manipulation. In: Somatosensory Mechanisms (*eds.* C. von Euler, O. Franzen, U. Lindblom, and D. Ottoson), pp. 249–260. Macmillan Press; (b and c) from Johansson, R. S. and Westling, G. 1991. Afferent Signals During Manipulative Tasks in Man. In: Somatosensory Mechanisms (*eds.* O. Franzen and J. Westman), pp. 25–48. Macmillan Press; (d) from Johansson, R. S. and Westling, G. 1987. Signals in tactile afferents from the fingers eliciting adaptive motor responses during precision grip. Exp. Brain Res. 66, 141–154; and (e) from Edin, B. B., Westling, G., and Johansson, R. S. 1992. Independent control of fingertip forces at individual digits during precision lifting in humans. J. Physiol. 450, 547–564.

force coordination. Presumably, this is because friction depends not only on the object surface but also on sweating rate and the greasiness and wetness of the skin (and objects) (Figure 6(a)). Thus, predictions of frictional conditions are based on the memory of recent haptic experiences with the same or similar objects. By varying the frictional condition independently at individual digits in two-digit and multidigit object lifting tasks it has been shown that the grip-to-load force ratios employed at each of the digits engaged can be independently controlled (Edin, B. B. *et al.*, 1992; Burstedt, M. K. O. *et al.*, 1999). When gripping and lifting an object using a precision grip, the digit that contacts a more slippery surface can exert less vertical lifting force than the digit in contact with a less slippery surface. Unpredicted

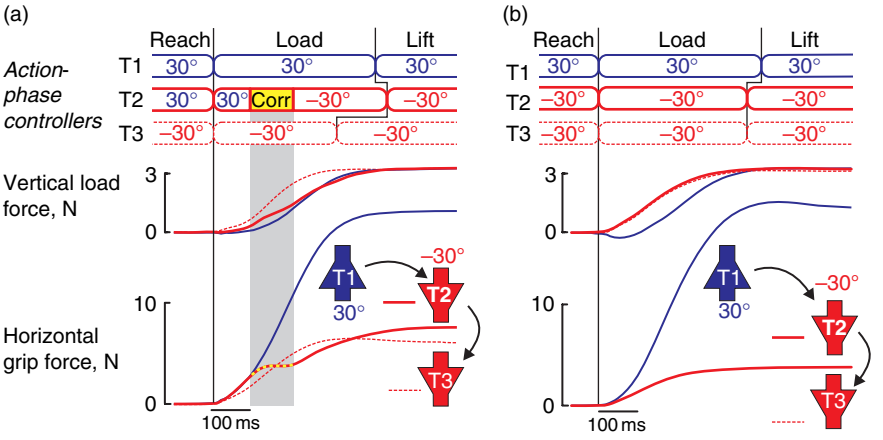

Figure 7 Adaptation of fingertip forces to changes in object shape. Vertical load force and horizontal grip force shown as a function of time for trials (a) without and (b) with vision of the contacted surfaces from a lift series in which surface angle was unpredictably varied between lifts. The blue curves refer to the last trial with the 30° object before the switch (T1; upward tapered grasp surfaces). (This trial was preceded by a trial with a 30° object.) The solid red curves show the next trial (T2) performed with the −30° object (downward tapered grasp surfaces). These curves thus illustrate adjustments to the smaller angle. The dashed yellow segment in the grip force curve in (a) indicates the epoch of the corrective action elicited by the new surface angle. The thin dashed red curves show the following trial, again with the −30° object. The top diagram represents the status of the sequentially implemented action-phase controllers. In T1 they are parameterized for the 30° object throughout. In T2, without vision of the contacted surfaces (a), a corrective action (Corr) is triggered about 100 ms after contact based on a mismatch between predicted and actual tactile information obtained at contact related to object shape. This action is interspersed during the loading phase and involves a change in the ratio between the grip force change and load force change, which, in turn, change the balance between grip and load forces to better suit the −30° object for the remainder of the trial (see also Figure 3(c)). In T3, the controllers remain updated to the −30° object. With vision of the contacted surfaces (b), visual cues about object geometry provide state information for anticipatory parametric adaptation of the motor output after the change in tapering (T2) and no corrective action is triggered. (a and b) Compiled from data presented in Jenmalm, P. and Johansson, R. S. 1997. Visual and somatosensory information about object shape control manipulative finger tip forces. J. Neurosci. 17, 4486–4499.

asymmetries in the frictional conditions at the digits can influence the development of the tangential forces during the load phase some 100 ms after contact (Figure 6(e)). Likewise, the average friction of the grasped surfaces influences the rate of increase of the grip force after this point.

Occasionally, the updating of frictional and shape representations that typically occurs at initial contact is inadequate and may result in an accidental slip later in the task. When an object is held in air after being lifted, such a slip usually results in a transitory and partial unloading at one digit (the slipping digit) and this increases the loads on the other digits engaged (Figure 6(e)). Such transient redistribution of the tangential force triggers a grip force increase. The net outcome is an increased safety margin at the slipping digit for the remainder of the task but a virtually unaffected safety margin at the other digits. This updated force coordination is used as default coordination for subsequent trials with the same object, again indicating that the force coordination is controlled by memory representations related to object properties. While slips during the hold phase lead to an increase in grip force, slips during the load phase in lifting lead to a slowing down of the subsequent increase in load force at the slipping digit (Johansson, R. S. and Westling, G., 1984a; 1987). Hence, different action-phase controllers are associated with different smart reflex mechanisms that support grasp stability and help achieve the current subgoal of the task.

6.05.3.3 Control of Motion of Objects in Hand

Tactile control points can also support planning and control of transport of grasped objects. The goal of many action phases in object manipulation (including tool use) is to move a held object so as to break or form contact between it and another object. The held object transmits various features of these contact events that tactile afferents can signal. Likewise, sensory plans in manipulation tasks integrate and thus predict the occurrence and nature of such signals, which allow

for comparison of predicted and actual sensory events at the level of the appropriate action-phase controllers. This applies, for example, when we lift an object, hold it in air, and then replace it on the support surface (Figure 1). The object breaking contact with the support surface at liftoff represents the sensory goal of the load phase and constitutes a control point for the load-phase controller. Likewise, the contact event that occurs when the object lands on the support surface represents the sensory goals of the controller that replaces the object. Because of their exquisite sensitivity to mechanical transients, ensembles of FA-II afferents most quickly and reliably signal the incidence and the dynamics of both the liftoff and the landing event (Westling, G. and Johansson, R. S., 1987).

Because no sensory information is available about weight until liftoff in object lifting, a natural, smooth, and critically damped lifting motion requires that the load force drive at liftoff, which accelerates the object, be scaled predictively to object weight. People form such predictions based on sensorimotor memory of the object derived from previous interactions with the object (Johansson, R. S. and Westling, G., 1988a). Familiar objects can be identified visually (or by haptic exploration) for retrieval of weight estimates (Gordon, A. M. *et al.*, 1991), and size–weight associations can be used to predict the weights of familiar objects that are organized into families of objects where the items can vary in size (e.g., cups, books, loafs of bread) (Gordon, A. M. *et al.*, 1993). Erroneous weight predictions often result in pronounced performance errors. For example, when we lift an object that is lighter than predicted and the load phase is programmed for a heavier weight, we typically make jerky movements and lift the object higher than intended (Figure 8(a), T2). The sensory events elicited by the liftoff occur before the predicted events that are part of the sensory plan (*cf.* predicted and actual neural events in Figure 8(a)). This mismatch automatically triggers a learned corrective action (smart reflex) that involves termination of the load-phase force followed by corrective motor commands that bring the object back to the intended position. However, due to the substantial delays in sensorimotor control loops, this corrective action pattern kicks in too late to avoid an overshoot in the lifting movement (see position signal in Figure 8(b)). When lifting an object that is heavier than expected, the load phase becomes slow and hesitant because the force drive is targeted for a lighter weight and additional increases in force are required to bring the object aloft (Figure 8(b), T2). In this case, the predicted sensory event related to liftoff does not occur at the predicted time (*cf.* predicted and actual neural events in Figure 8(b)). Hence, again there is a mismatch between actual and predicted sensory events. The corrective action triggered by the mismatch now involves slow, probing increases in fingertip forces until terminated reactively by sensory events signaling liftoff. Thus, the sensorimotor system reacts to both the presence of an unpredicted event and the absence of a predicted sensory event. Importantly, in addition to triggering corrective actions, these sensory mismatches lead to an updating of memory representations related to object weight, which in turn, improves predictive control in subsequent action phases and tasks that engage the same object. In natural situations, this updating generally occurs in a single trial (see Figure 8) while with objects with unusual dynamics (relating applied force to motion) (Flanagan, J. R. and Wing, A. M., 1997; Flanagan, J. R. *et al.*, 2003) or in the presence of misleading cues (Gordon, A. M. *et al.*, 1991; Flanagan, J. R. and Beltzner, M. A., 2000), updating may require repeated lifts or movements of the object.

6.05.4 Predictions and Control Points in Other Modalities

Studies of eye movements in object manipulation indicate that contact events that demarcate action phases can also be predicted and monitored in the visual modality (Land, M. *et al.*, 1999; Johansson, R. S. *et al.*, 2001; Land, M. F., 2006). Accordingly, people use saccades to direct their gaze to successive contact locations as they gain salience in the evolving manipulation task. For example, when people pick up a bar, move the bar in hand to contact a target switch, and then replace the bar, gaze is successively directed to the grasp site on the bar, the target, and the landing surface where the bar is replaced (Johansson, R. S. *et al.*, 2001). Both hand and eye movements are specified based on peripheral vision about the contact location (or on memorized landmark locations), but gaze reaches the contact location well before the hand (or object in hand) because the saccadic eye movements are quick. Gaze typically remains at the contact location until around the time of goal completion (e.g., until the grasp is established, the target switch is released, or the bar is replaced in the target contact task). This indicates that the visual system, like the tactile system, can monitor control points linked to the completion of task subgoals.

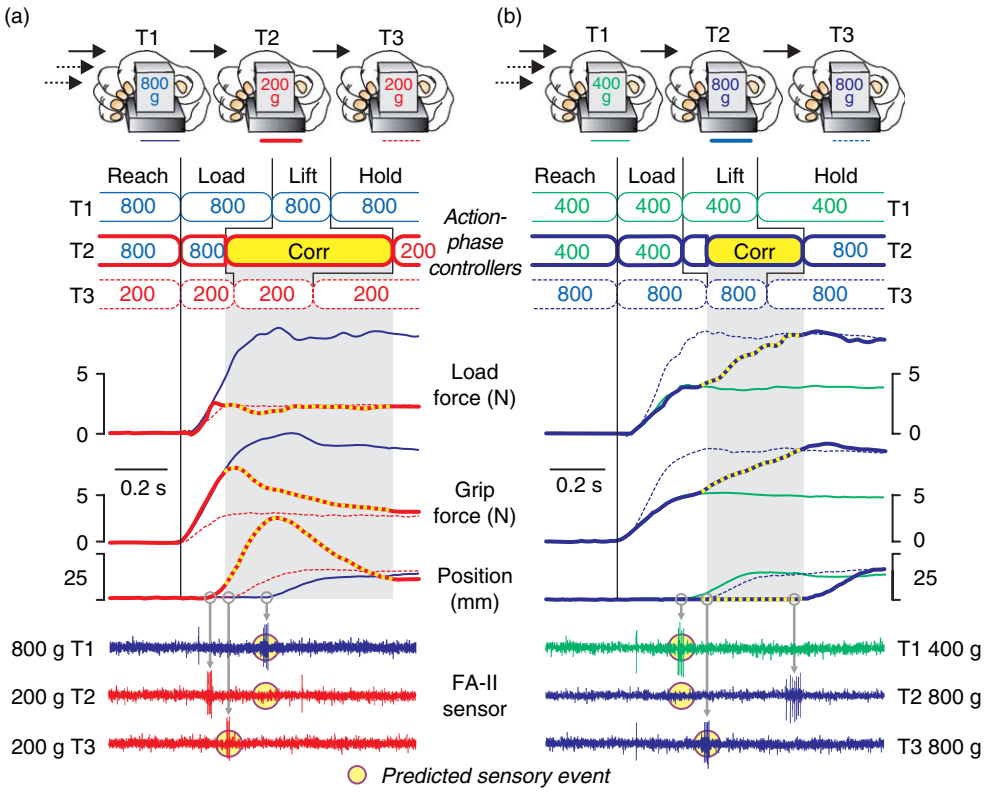

Figure 8 Adaptation of motor output to object weight. Single-unit tactile afferent responses and adjustments in force to unexpected changes in object weight. Data from single lift trials aligned on initial touch (vertical line). Gray circles and vertical lines indicate the moment of liftoff for each trial and the arrowheads point at the actual sensory events generated by the liftoff in a fast-adapting type II (FA-II) afferent. The circles behind the nerve traces indicate the corresponding predicted sensory events. (a) Three successive trials (T1–T3) in which the subject lifted an 800 g object (blue curves), a 200 g object (solid red curves), and then the 200 g object again (dashed red curves). The forces exerted in the first lift are adequately programmed – they had previously lifted the 800 g object. The forces are erroneously programmed in the first 200 g lift (T2), i.e., they are tailored for the heavier 800 g object lifted in the previous trial. The sensory information about the start of movement occurs earlier than expected (*cf.* actual and predicted sensory events), which initiates a corrective action (yellow–dashed red curves). The strong force drive of the ongoing load phase is terminated but still results in overshoots in position due to the reflex delay and a corrective motor command is launched that brings the object back to the intended position. (b) The participant performed an adequately programmed lift with a 400 g weight (T1, green curves), followed by a lift with 800 g, erroneously programmed for the lighter 400 g weight lifted in the previous trial (T2, solid blue curves), and then a lift with the 800 g object again (T3, dashed blue curves). The absence of burst responses in fast-adapting type II (FA-II) afferents at the predicted point for the erroneously programmed 800 g trial (*cf.* actual and predicted sensory event) elicits a corrective action (yellow–dashed blue curves). This involves abortion of the lift-phase command followed by triggering of a second load-phase command that involves a slow, discontinuous, and parallel increase in grip and load forces until terminated by sensory input signaling liftoff. The top diagram in (a) and (b) represents the status of the sequentially implemented action-phase controllers. In T1 they are parameterized for the 800 g (b) and 400 g (b) weight throughout. In T2, a corrective action (Corr) is triggered about 100 ms after the occurrence of the mismatch between predicted and actual sensory information related to object liftoff. This action involves abortion of the operation of the current action-phase controller and the implementation of corrective action patterns that allow the task to continue. The corrective action is linked to an updating of the subsequently implemented controllers for the new weight. In T3, the controllers remain updated to this weight. (a–b) Developed from Johansson, R. S. and Cole, K. J. 1992. Sensory-motor coordination during grasping and manipulative actions. Curr. Opin. Neurobiol. 2, 815–823.

Furthermore, the gaze behavior indicates that goal completion can be predicted in sensorimotor systems. That is, the time of gaze shift to the contact location associated with the next action phase occurs around the time of goal completion and is not delayed until sensory feedback verifying goal completion triggers the gaze shift. The latter strategy would lead to substantial lags in gaze behavior because of the time delays in sensorimotor control loops. That both gaze and hand movement commands are initiated in

anticipation of goal completion reinforces the idea that sensory predictions about the terminal state of each action phase provide initial state information for the controller responsible for executing the subsequent action phase.

Although there is no question that contact points predicted and monitored in the tactile modality are essential for skilled object manipulation, there are contact events that do not give rise to tactile events. For example, when we drop a ball onto a surface, we typically direct our gaze to the predicted contact point between the ball and surface. Here, sensory feedback related to contact is only available through vision (and possibly audition). Thus, vision and the tactile system can play complementary roles in predicting and monitoring contact events. Prediction of contact events in the visual modality without the tactile modality being engaged is evident from studies of eye movements when people observe an actor performing familiar manipulation tasks. In this situation, the gaze of both the actor and observer predicts forthcoming contact sites (e.g., where blocks are grasped and replaced in a predictable block stacking task) and gaze is maintained at each contact site until around the time of goal completion (grasp contact and block landing) (Flanagan, J. R. and Johansson, R. S., 2003). By comparing actual and predicted visual feedback related to contact events, both observers and actors may be able to obtain valuable information about outcomes of actions that can be exploited by the sensorimotor system when learning, planning, and controlling future actions. These findings also support the notion that understanding of observed actions performed by others involves a mechanism that maps observed actions onto sensorimotor representations in the observers' brain implemented in real time (Rizzolatti, G. *et al.*, 2001; Flanagan, J. R. and Johansson, R. S., 2003; Rotman, G. *et al.*, 2006).

6.05.5 Conclusions

Dexterity in object manipulation tasks depends on anticipatory control policies that rely on knowledge about movement–effect relationships when interacting with environmental objects. The tactile modality plays a pivotal role in gaining such knowledge because signals from tactile afferents provide direct information about mechanical interactions between the body and objects in the environment. The usefulness of visual and proprioceptive mechanisms in guiding the hands in object manipulation depends on learned associations between visual and proprioceptive cues and their mechanical meaning derived from tactile mechanisms. Signals in ensembles of tactile afferents of different types convey complementary information related to both the timing and the physical nature of the various kinds of contact events that represent the outcomes of motor commands to the hand. Populations of tactile afferents encode time courses, magnitudes, directions, and spatial distributions of contact forces relative to the hand. They likewise encode information related to surface properties of contacted objects such as shape and texture of contacted surfaces and frictional conditions between these surfaces and the skin. In addition to critically supporting the control of fingertip actions in manipulation, the brain uses tactile afferent information for establishing sensorimotor correlations that underlie haptic object identification as well as representations of object affordances used in planning of object manipulation activities.

Such action plans are composed of sequences of action phases implemented to attain task subgoals specified (and verified) in terms of sensory signals. Thus, manipulatory tasks involve a sensory plan that specifies the sequence of task subgoals and provides a scaffold for the selection and shaping of the action-phase controllers implemented for achieving sensory subgoals. Distinct contact events signaled in the tactile modality generally represent subgoals, but these subgoals can also be represented in the visual and auditory modalities. When the brain successfully predicts the actual sensory signals at a given contact event, no corrective action is required and the task runs in a feedforward fashion based on predictions derived from internal representations of object properties gained in previous interactions with objects. When a prediction error arises, a learned corrective action, the nature of which depends on the task and its action phase, is generated and representations of object properties are updated. Prediction of the terminal sensorimotor state of each action phase prevents stuttering phase transitions that would result if the brain relied on peripheral afferent information to confirm subgoal completion and update state information before launching the next action phase. The fact that contact events give rise to distinct sensory signals in multiple modalities permits the sensorimotor system to simultaneously monitor multiple aspects of task performance and, if prediction errors arise, respond to the pattern of errors observed in different modalities. Finally, contact events often give rise to multimodal sensory events that are linked in time

and space and this provides an opportunity for intermodal alignment helpful for learning and upholding multimodal sensorimotor correlations necessary for prediction of purposeful motor commands.

References

Adkins, R. J., Morse, R. W., and Towe, A. L. 1966. Control of somatosensory input by cerebral cortex. Science 153, 1020–1022.

Bays, P. M., Wolpert, D. M., and Flanagan, J. R. 2005. Perception of the consequences of self-action is temporally tuned and event driven. Curr. Biol. 15, 1125–1128.

Birznieks, I., Jenmalm, P., Goodwin, A., and Johansson, R. 2001. Encoding of direction of fingertip forces by human tactile afferents. J. Neurosci. 21, 8222–8237.

Burstedt, M. K. O., Flanagan, R., and Johansson, R. S. 1999. Control of grasp stability in humans under different frictional conditions during multi-digit manipulation. J. Neurophysiol. 82, 2393–2405.

Edin, B. B. and Abbs, J. H. 1991. Finger movement responses of cutaneous mechanoreceptors in the dorsal skin of the human hand. J. Neurophysiol. 65, 657–670.

Edin, B. B., Essick, G. K., Trulsson, M., and Olsson, K. A. 1995. Receptor encoding of moving tactile stimuli in humans. 1. Temporal pattern of discharge of individual low-threshold mechanoreceptors. J. Neurosci. 15, 830–847.

Edin, B. B., Westling, G., and Johansson, R. S. 1992. Independent control of fingertip forces at individual digits during precision lifting in humans. J. Physiol. 450, 547–564.

Engel, A. K., Fries, P., and Singer, W. 2001. Dynamic predictions: oscillations and synchrony in top-down processing. Nat. Rev. Neurosci. 2, 704–716.

Ergenzinger, E. R., Glasier, M. M., Hahm, J. O., and Pons, T. P. 1998. Cortically induced thalamic plasticity in the primate somatosensory system. Nat. Neurosci. 1, 226–229.

Flanagan, J. R. and Beltzner, M. A. 2000. Independence of perceptual and sensorimotor predictions in the size–weight illusion. Nat. Neurosci. 3, 737–741.

Flanagan, J. R. and Johansson, R. S. 2003. Action plans used in action observation. Nature 424, 769–771.

Flanagan, J. R. and Tresilian, J. R. 1994. Grip load force coupling: a general control strategy for transporting objects. J. Exp. Psychol. Hum. Percept. Perform. 20, 944–957.

Flanagan, J. R. and Wing, A. M. 1997. The role of internal models in motion planning and control: evidence from grip force adjustments during movements of hand-held loads. J. Neurosci. 17, 1519–1528.

Flanagan, J. R., Bowman, M. C., and Johansson, R. S. 2006. Control strategies in object manipulation tasks. Curr. Opin. Neurobiol. 16, 650–659.

Flanagan, J. R., Burstedt, M. K. O., and Johansson, R. S. 1999. Control of fingertip forces in multi-digit manipulation. J. Neurophysiol. 81, 1706–1717.

Flanagan, J. R., Vetter, P., Johansson, R. S., and Wolpert, D. M. 2003. Prediction precedes control in motor learning. Curr. Biol. 13, 146–150.

Gentilucci, M., Toni, I., Daprati, E., and Gangitano, M. 1997. Tactile input of the hand and the control of reaching to grasp movements. Exp. Brain Res. 114, 130–137.

Georgopoulos, A. P., Schwartz, A. B., and Kettner, R. E. 1986. Neuronal population coding of movement direction. Science 233, 1416–1419.

Goodwin, A. W. and Wheat, H. E. 2004. Sensory signals in neural populations underlying tactile perception and manipulation. Annu. Rev. Neurosci. 27, 53–77.

Goodwin, A. W., Jenmalm, P., and Johansson, R. S. 1998. Control of grip force when tilting objects: effect of curvature of grasped surfaces and of applied tangential torque. J. Neurosci. 18, 10724–10734.

Gordon, A. M., Forssberg, H., Johansson, R. S., and Westling, G. 1991. Integration of sensory information during the programming of precision grip: comments on the contributions of size cues. Exp. Brain Res. 85, 226–229.

Gordon, A. M., Westling, G., Cole, K. J., and Johansson, R. S. 1993. Memory representations underlying motor commands used during manipulation of common and novel objects. J. Neurophysiol. 69, 1789–1796.

Häger-Ross, C. and Johansson, R. S. 1996. Non-digital afferent input in reactive control of fingertip forces during precision grip. Exp. Brain Res. 110, 131–141.

Harris, F., Jabbur, S. J., Morse, R. W., and Tow, A. L. 1965. Influence of the cerebral cortex on the cuneate nucleus of the monkey. Nature 208, 1215–1216.

Heil, P. 2004. First-spike latency of auditory neurons revisited. Curr. Opin. Neurobiol. 14, 461–467.

Jenmalm, P. and Johansson, R. S. 1997. Visual and somatosensory information about object shape control manipulative finger tip forces. J. Neurosci. 17, 4486–4499.

Jenmalm, P., Birznieks, I., Goodwin, A. W., and Johansson, R. S. 2003. Influences of object shape on responses in human tactile afferents under conditions characteristic for manipulation. Eur. J. Neurosci. 18, 164–176.

Jenmalm, P., Dahlstedt, S., and Johansson, R. S. 2000. Visual and tactile information about object curvature control fingertip forces and grasp kinematics in human dexterous manipulation. J. Neurophysiol. 84, 2984–2997.

Johansson, R. S. 1978. Tactile sensibility in the human hand: receptive field characteristics of mechanoreceptive units in the glabrous skin area. J. Physiol. 281, 101–125.

Johansson, R. S. and Birznieks, I. 2004. First spikes in ensembles of human tactile afferents code complex spatial fingertip events. Nat. Neurosci. 7, 170–177.

Johansson, R. S. and Cole, K. J. 1992. Sensory-motor coordination during grasping and manipulative actions. Curr. Opin. Neurobiol. 2, 815–823.

Johansson, R. S. and Vallbo, Å.B. 1983. Tactile sensory coding in the glabrous skin of the human hand. Trends Neurosci. 6, 27–31.

Johansson, R. S. and Westling, G. 1984a. Roles of glabrous skin receptors and sensorimotor memory in automatic control of precision grip when lifting rougher or more slippery objects. Exp. Brain Res. 56, 550–564.

Johansson, R. S. and Westling, G. 1984b. Influences of Cutaneous Sensory Input on the Motor Coordination During Precision Manipulation. In: Somatosensory Mechanisms (*eds*. C. von Euler, O. Franzen, U. Lindblom, and D. Ottoson), pp. 249–260. Macmillan Press.

Johansson, R. S. and Westling, G. 1987. Signals in tactile afferents from the fingers eliciting adaptive motor responses during precision grip. Exp. Brain Res. 66, 141–154.

Johansson, R. S. and Westling, G. 1988a. Coordinated isometric muscle commands adequately and erroneously programmed for the weight during lifting task with precision grip. Exp. Brain Res. 71, 59–71.

Johansson, R. S. and Westling, G. 1988b. Programmed and triggered actions to rapid load changes during precision grip. Exp. Brain Res. 71, 72–86.

Johansson, R. S. and Westling, G. 1991. Afferent Signals During Manipulative Tasks in Man. In: Somatosensory Mechanisms

(*eds*. O. Franzen and J. Westman), pp. 25–48. Macmillan Press.

Johansson, R. S., Backlin, J. L., and Burstedt, M. K. O. 1999. Control of grasp stability during pronation and supination movements. Exp. Brain Res. 128, 20–30.

Johansson, R. S., Landström, U., and Lundström, R. 1982a. Responses of mechanoreceptive afferent units in the glabrous skin of the human hand to sinusoidal skin displacements. Brain Res. 244, 17–25.

Johansson, R. S., Landström, U., and Lundström, R. 1982b. Sensitivity to edges of mechanoreceptive afferent units innervating the glabrous skin of the human head. Brain Res. 244, 27–35.

Johansson, R. S., Westling, G., Bäckström, A., and Flanagan, J. R. 2001. Eye-hand coordination in object manipulation. J. Neurosci. 21, 6917–6932.

Johnson, K. O. 2001. The roles and functions of cutaneous mechanoreceptors. Curr. Opin. Neurobiol. 11, 455–461.

Kennedy, P. M. and Inglis, J. T. 2002. Distribution and behaviour of glabrous cutaneous receptors in the human foot sole. J. Physiol. 538, 995–1002.

Lackner, J. R. and DiZio, P. A. 2000. Aspects of body self-calibration. Trends Cogn. Sci. 4, 279–288.

Land, M. F. 2006. Eye movements and the control of actions in everyday life. Prog. Retin. Eye Res. 25, 296–324.

Land, M., Mennie, N., and Rusted, J. 1999. The roles of vision and eye movements in the control of activities of daily living. Perception 28, 1311–1328.

Loewenstein, W. R. and Skalak, R. 1966. Mechanical transmission in a Pacinian corpuscle. An analysis and a theory. J. Physiol. 182, 346–378.

Macefield, V. G. and Johansson, R. S. 1996. Control of grip force during restraint of an object held between finger and thumb: responses of muscle and joint afferents from the digits. Exp. Brain Res. 108, 172–184.

Macefield, V. G., Häger-Ross, C., and Johansson, R. S. 1996. Control of grip force during restraint of an object held between finger and thumb: responses of cutaneous afferents from the digits. Exp. Brain Res. 108, 155–171.

Monzée, J., Lamarre, Y., and Smith, A. M. 2003. The effects of digital anesthesia on force control using a precision grip. J. Neurophysiol. 89, 672–683.

Nordin, M. and Hagbarth, K. E. 1989. Mechanoreceptive units in the human infra-orbital nerve. Acta Physiol. Scand. 135, 149–161.

Nowak, D. A., Glasauer, S., and Hermsdorfer, J. 2004. How predictive is grip force control in the complete absence of somatosensory feedback? Brain 127, 182–192.

Phillips, J. R., Johansson, R. S., and Johnson, K. O. 1992. Responses of human mechanoreceptive afferents to embossed dot arrays scanned across fingerpad skin. J. Neurosci. 12, 827–839.

Rao, A. K. and Gordon, A. M. 2001. Contribution of tactile information to accuracy in pointing movements. Exp. Brain Res. 138, 438–445.

Rizzolatti, G., Fogassi, L., and Gallese, V. 2001. Neurophysiological mechanisms underlying the understanding and imitation of action. Nat. Rev. Neurosci. 2, 661–670.

Rotman, G., Troje, N. F., Johansson, R. S., and Flanagan, J. R. 2006. Eye movements when observing predictable and unpredictable actions. J. Neurophysiol. 96, 1358–1369.

Säfström, D. and Edin, B. B. 2004. Task requirements influence sensory integration during grasping in humans. Learn. Mem. 11, 356–363.

Sommer, M. A. and Wurtz, R. H. 2002. A pathway in primate brain for internal monitoring of movements. Science 296, 1480–1482.

Torebjörk, H. E., Vallbo, A. B., and Ochoa, J. L. 1987. Intraneural microstimulation in man. Its relation to specificity of tactile sensations. Brain 110, 1509–1529.

Trulsson, M. and Essick, G. K. 1997. Low-threshold mechanoreceptive afferents in the human lingual nerve. J. Neurophysiol. 77, 737–748.

Trulsson, M., Johansson, R. S., and Olsson, K. A. 1992. Directional sensitivity of human periodontal mechanoreceptive afferents to forces applied to the teeth. J. Physiol. 447, 373–389.

Vallbo, Å.B. and Hagbarth, K.-E. 1968. Activity from skin mechanoreceptors recorded percutaneously in awake human subjects. Exp. Neurol. 21, 270–289.

Vallbo, A. B. and Johansson, R. S. 1984. Properties of cutaneous mechanoreceptors in the human hand related to touch sensation. Hum. Neurobiol. 3, 3–14.

Vallbo, Å.B., Hagbarth, K.-E., Torebjörk, H. E., and Wallin, B. G. 1979. Somatosensory, proprioceptive and sympathetic activity in human peripheral nerves. Physiol. Rev. 59, 919–957.

Vallbo, A. B., Olausson, H., Wessberg, J., and Kakuda, N. 1995. Receptive field characteristics of tactile units with myelinated afferents in hairy skin of human subjects. J. Physiol. 483, 783–795.

Vallbo, A. B., Olsson, K. A., Westberg, K. G., and Clark, F. J. 1984. Microstimulation of single tactile afferents from the human hand. Sensory attributes related to unit type and properties of receptive fields. Brain 107, 727–749.

VanRullen, R., Guyonneau, R., and Thorpe, S. J. 2005. Spike times make sense. Trends Neurosci. 28, 1–4.

Westling, G. and Johansson, R. S. 1984. Factors influencing the force control during precision grip. Exp. Brain Res. 53, 277–284.

Westling, G. and Johansson, R. S. 1987. Responses in glabrous skin mechanoreceptors during precision grip in humans. Exp. Brain Res. 66, 128–140.

Wolpert, D. M., Ghahramani, Z., and Flanagan, J. R. 2001. Perspectives and problems in motor learning. Trends Cogn. Sci. 5, 487–494.

6.06 Physiological Characteristics of Second-Order Somatosensory Circuits in Spinal Cord and Brainstem

W D Willis Jr, University of Texas Medical Branch, Galveston, TX, USA

© 2008 Elsevier Inc. All rights reserved.

6.06.1	Introduction	87
6.06.2	Second-Order Somatosensory Circuits in the Spinal Cord	88
6.06.2.1	Mechanoreceptive Circuits	88
6.06.2.1.1	Touch–pressure	88
6.06.2.1.2	Flutter–vibration	90
6.06.2.1.3	Proprioception	91
6.06.2.1.4	Visceral sensation	92
6.06.2.2	Thermoreceptive Circuits	94
6.06.2.3	Nociceptive Circuits	95
6.06.2.4	Spinal Cord Projection Neurons	96
6.06.2.4.1	Spinothalamic tract neurons	96
6.06.2.4.2	Spinocervical neurons	98
6.06.2.4.3	Postsynaptic dorsal column neurons	98
6.06.2.4.4	Spinoreticular neurons	100
6.06.2.4.5	Spinoparabrachial neurons	101
6.06.2.4.6	Spinohypothalamic and other spinolimbic neurons	101
6.06.2.5	Descending Control Systems	102
6.06.2.5.1	Descending control pathways	102
6.06.3	Second-Order Somatosensory Circuits in the Brainstem	102
6.06.3.1	Cranial Nerve Somatosensory Afferents	102
6.06.3.2	Mechanoreceptor Circuits	106
6.06.3.2.1	Main sensory nucleus of V	106
6.06.3.2.2	Spinal nucleus of V	106
6.06.3.2.3	Mesencephalic nucleus of V	106
6.06.3.3	Thermoreceptive Circuits	106
6.06.3.4	Nociceptive Circuits	107
6.06.3.4.1	Cutaneous pain	107
6.06.3.4.2	Corneal pain	107
6.06.3.4.3	Joint pain	107
6.06.3.4.4	Dental pain	108
6.06.3.4.5	Meningeal pain	108
6.06.3.5	Brainstem Projection Neurons	108
6.06.3.5.1	Trigeminothalamic neurons	108
6.06.3.5.2	Trigeminoreticular neurons	109
6.06.3.5.3	Trigeminoparabrachial neurons	109
6.06.3.5.4	Other trigeminal projection neurons	109
6.06.3.6	Descending Control Systems	109
References		110

6.06.1 Introduction

As all medical students know, pain is the most common reason for a person to consult with a physician. Under ordinary circumstances, pain has a useful, protective function. It encourages the individual to avoid activities that aggravate the pain, allowing faster recovery from tissue damage. The physician can

often tell from the nature of the pain what its source may be. In most cases, treatment of the underlying condition resolves the pain. However, some kinds of pain are the result of difficult to treat or untreatable conditions and are persistent.

6.06.2 Second-Order Somatosensory Circuits in the Spinal Cord

In discussing second-order somatosensory neural circuits in the spinal cord gray matter, the projections of particular classes of primary afferent neurons to the spinal cord will first be described, as well as the responses of spinal cord interneurons to inputs from these afferents. Then, the responses of sensory projection neurons to somatosensory stimuli and the effects of descending control systems will be considered.

6.06.2.1 Mechanoreceptive Circuits

Mechanoreceptive afferents from the skin that project to the spinal cord innervate various types of cutaneous sensory receptors. Some of the sensory receptors adapt slowly to a maintained stimulus and are thought to mediate a spectrum of sensations described as touch–pressure; other cutaneous sensory receptors are rapidly adapting and are responsible for flutter–vibration sensations (Johansson, R. S. and Vallbo, A. B., 1979a; 1979b; 1993; see review by Willis, W. D. and Coggeshall, R. E., 2004). Slowly adapting receptors in muscles that supply muscle spindles are not only responsible for the stretch reflex but they also provide proprioceptive information about the position and movements of joints (Matthews, P. B. C., 1972). In addition to triggering the inverse stretch reflex, the activity of Golgi tendon organs reflects the tension developed in tendons, because of stretch of the muscles or muscular contractions (Matthews, P. B. C., 1972). Although the sensation evoked by afferents from some viscera, such as the ureter, may be restricted to pain (Cervero, F. and Sann, A., 1989; Giamberardino, M. A. *et al.*, 1995), afferents from other viscera can convey nonpainful mechanical sensations, such as distention, depending on the type of afferents activated and in some cases the firing rate (Jänig, W. and Kolzenburg, M., 1991) (for reviews of the properties of somatosensory and visceral receptors, see Cervero, F and Morrison, J. F. B., 1986; Gebhart, G. F., 1995; Willis, W. D. and Coggeshall, R. E., 2004).

6.06.2.1.1 Touch–pressure

Touch–pressure sensation refers to the perception of a maintained distortion of the skin, such as an indentation. The sensation increases in a linear fashion as skin indentation increases. The sensory receptors responsible for touch–pressure sensation are slowly adapting cutaneous mechanoreceptors. Both glabrous (nonhairy) and hairy skin contain slowly adapting mechanoreceptors, including SA I or Merkel cell endings and SA II or Ruffini endings (Figure 1; Darian-Smith, I., 1984; Guinard, D. *et al.*, 1998; Rice, F. L. and Rasmusson, D. D., 2000; Paré, M. *et al.*, 2002).

The threshold for activating human SA I receptors can be as low as 0.15 g, which is near the threshold for a sensation of touch in hairy skin (Hensel, H. and Boman, K. K. A., 1960; Järvilehto, T. *et al.*, 1981). Studies using intraneural microneurography have found that the conduction velocities of the axons of SA I receptors in humans average nearly $60\,m\,s^{-1}$, indicating that the axons are large myelinated or Aβ fibers (Knibestöl, M., 1975). SA I receptors have one or a few small, spot-like receptive fields that presumably

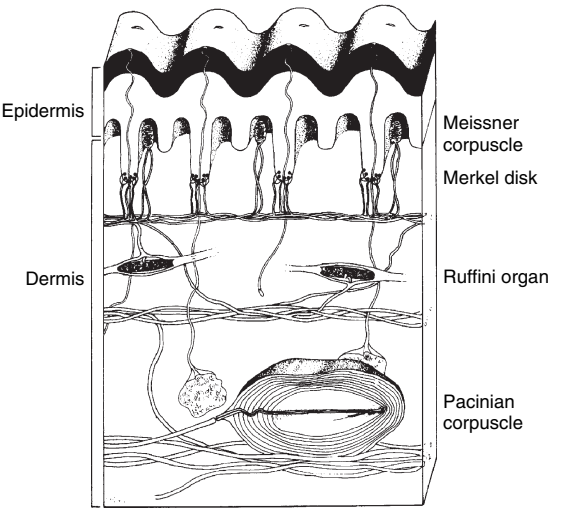

Figure 1 Tactile sensory receptors found in the glabrous skin of a monkey's hand. Meissner corpuscles are shown in several dermal papillae, and Merkel cell endings on ridges of the epidermis that extend into the dermis. Ruffini endings are in the dermis and Pacinian corpuscles in the deep dermis or in subcutaneous tissue. From Darian-Smith, I. 1984. The sense of touch: performance and peripheral neural processes. In: (*eds*. J. M. Brookhart and V .B. Mountcastle), Handbook of Physiology, Section 1: The Nervous System, Vol. III, Sensory Processes, Part 2, pp. 739–788. American Physiological Soc, Bethesda.

reflect the locations of one or more Merkel cell complexes (Johansson, R. S., 1978). These receptors characteristically lack spontaneous activity and do not respond to skin stretch, but they do respond dynamically to stimuli applied directly to the receptive field, and they have a variable firing rate during a maintained stimulus (see Willis, W. D and Coggeshall, R. E., 2004). They are especially responsive to edges. When the axons of human SA I receptors are stimulated repetitively through a microneurography electrode, their activity results in a sensation of continuous pressure (Torebjörk, H. E. *et al.*, 1987). Increasing the frequency of stimulation increases the intensity of the sensation (Ochoa, J. and Torebjörk, E., 1983). SA I receptors are highly likely to contribute to touch–pressure sensation and to the discrimination of form (reviewed in Willis, W. D and Coggeshall, R. E., 2004; see also Werner, G. and Mountcastle, V. B., 1965, and Mountcastle, V. B. *et al.*, 1966).

SA II receptors (or Ruffini organs; Figure 1) also have large myelinated axons. They may or may not display spontaneous activity, and they respond both to indentation and to stretch of the skin. The receptive fields may be near joints or fingernails. Their dynamic sensitivity is low and, when stimulated, they have a regular discharge (see Willis, W. D and Coggeshall, R. E., 2004). Activation of the axon of an SA II receptor through a microneurography electrode usually fails to evoke any sensation (Ochoa. J. and Torebjörk, E., 1983; Schady, W. J. L. and Torebjörk, H. E., 1983), perhaps because spatial summation is required before this type of receptor can elicit a sensory experience. However, stimulation of an occasional SA II unit can result in a sensation of sustained pressure or of joint movement (Macefield, G. *et al.*, 1990), suggesting that SA II receptors can contribute to touch–pressure and proprioception.

The large myelinated primary afferents from slowly adapting mechanoreceptors pass through the medial part of the appropriate dorsal roots to enter the spinal cord. Collaterals of some of these afferents join the dorsal funiculus. However, the axons of most slowly adapting receptors from the hind limb do not ascend all the way to the brainstem, but rather synapse in Clarke's column. By contrast, those from the forelimb often project directly to the main cuneate nucleus and/or the lateral cuneate nucleus (see Willis, W. D. and Coggeshall, R. E., 2004). Other collaterals of these slowly adapting mechanoreceptive afferents terminate in the gray matter of the spinal cord.

Afferents that supply SA I and SA II receptors end in Rexed's laminae III–V (Figure 2; Brown, A. G., 1977; Brown, A. G. *et al.*, 1978; Woolf, C. J., 1987; see Rexed, B., 1952; 1954, for a description of the laminar arrangement of the spinal cord gray matter).

Recordings have been made from a population of neurons in laminae III–VI that respond to input from slowly adapting cutaneous mechanoreceptors, but not to input from proprioceptors (Wall, P. D., 1967; Brown, P. B., 1969; Tapper, D. N. *et al.*, 1973). Rudomin's group has identified interneurons that generate primary afferent depolarization through

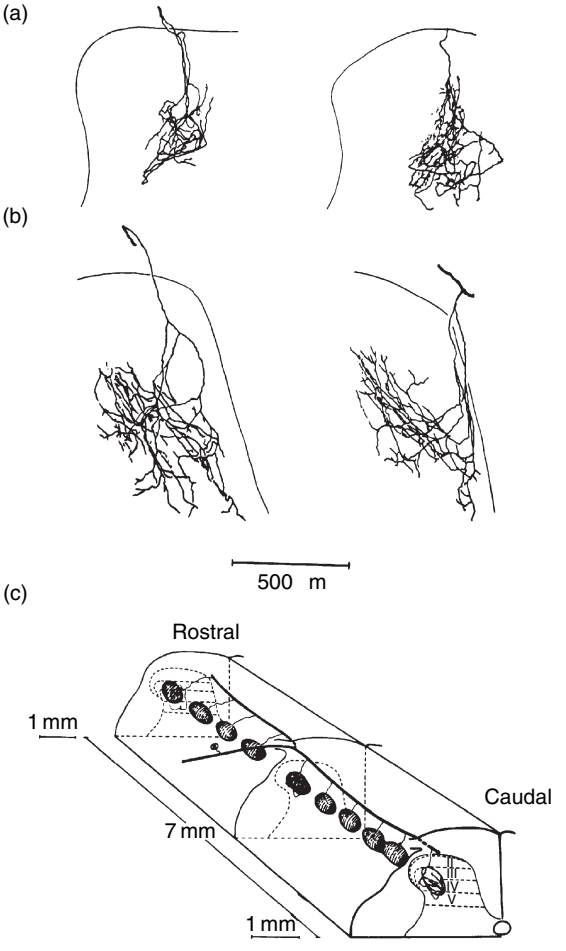

Figure 2 (a) The terminals of the axons of SA I receptors in the dorsal horn of a cat. (b) The terminals of SA II receptors. (c) The longitudinal distribution of the branches of an SA I afferent. (b) From Brown, A. G. 1977. Cutaneous axons and sensory neurons in the spinal cord. Br. Med. Bull. 33: 109–112. (c) From Brown, A. G., Rose, P. K. and Snow, P. J. 1978. Morphology and organization of axon collaterals from afferent fibres of slowly adapting type I units in cat spinal cord. J. Physiol. 277: 15–27.

synaptic actions on afferent terminals, or that excite motor neurons, or both (Rudomin, P. *et al.*, 1987). Spike-triggered averaging has shown that some of the interneurons in laminae V and VI with cutaneous input evoke excitatory or inhibitory postsynaptic potentials in motor neurons and are therefore premotor interneurons in reflex pathways (Hongo, T. *et al.*, 1989a; 1989b). More experiments like these are needed to define more completely the components of the various dorsal horn (and brainstem) circuits.

Information from slowly adapting cutaneous receptors is also transmitted by postsynaptic dorsal column neurons to the dorsal column nuclei through axons that ascend either in the dorsal columns or in the dorsal part of the lateral funiculus (see Willis, W. D. and Coggeshall, R. E., 2004). A sensory experience would then result from transmission of this sensory information from the dorsal column nuclei to the contralateral ventral posterior lateral (VPL) thalamic nucleus and from there to the somatosensory cortex. Recordings from neurons in the gracile nucleus of monkeys and cats that project to the VPL nucleus of the thalamus have demonstrated responses of some low-threshold (LT) gracile neurons to maintained indentation of the skin (Figures 3(a)–3(f)). Other gracile neurons were classified as wide dynamic range (WDR) neurons, as they could be excited by innocuous and noxious stimuli (Figures 3(g)–3(i); Ferrington, D. G. *et al.*, 1988; Cliffer, K. D. *et al.*, 1992; see also Figure 12). These gracile neurons are likely to reflect the activity generated in postsynaptic dorsal column neurons and then transmitted to the gracile neurons. However, more direct evidence is needed in support of this assumption.

6.06.2.1.2 Flutter–vibration

Rapidly adapting receptors in glabrous skin include FA I endings or Meissner's corpuscles and FA II endings or Pacinian corpuscles (see Figure 1; Johannsson, R. S and Vallbo, A. B. 1979a; 1979b;

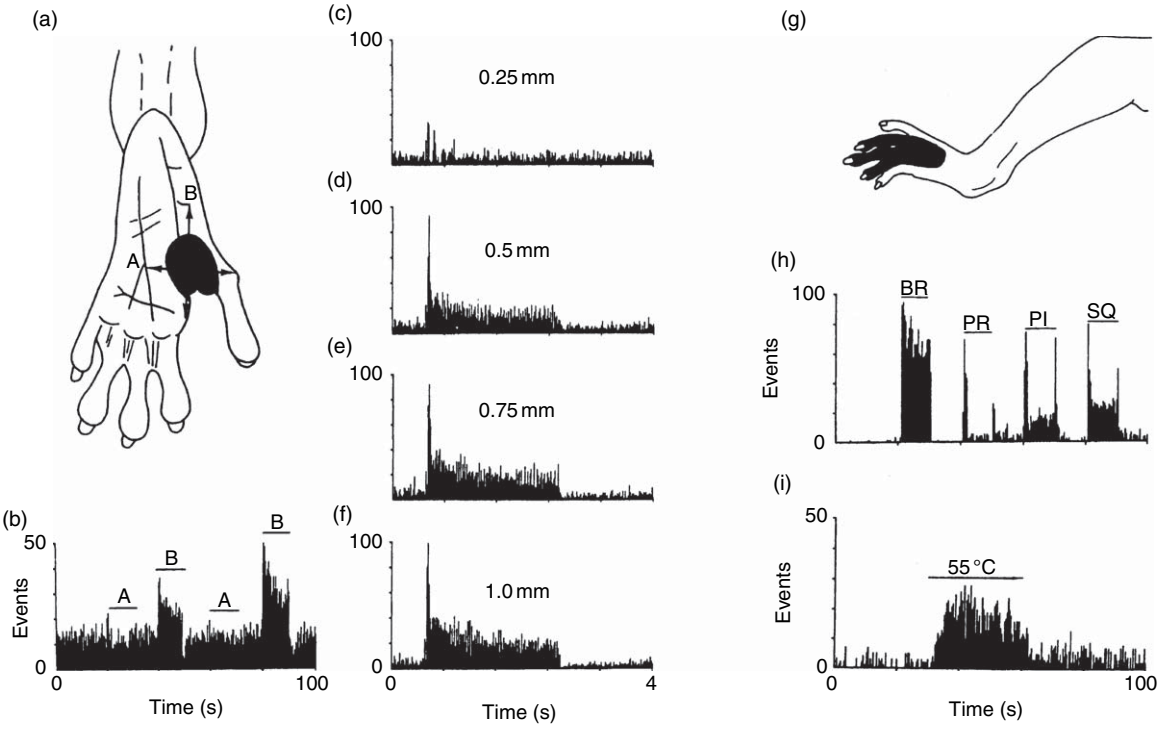

Figure 3 (a–f) Responses of a neuron in the gracile nucleus of a monkey to skin stretch and skin indentation. (a) The area and direction of hind paw skin that was stretched to produce the responses in (b). (c–f) Poststimulus time histograms of the responses of the same gracile neuron to graded indentations of the skin. The amounts of indentation are indicated; the duration is evident from the duration of the enhanced discharge rate. (g–i) The responses of a gracile neuron to graded mechanical stimulation and to noxious heat. (g) The receptive field. (h) The responses to brushing (BR), application of pressure using an arterial clip with a weak grip (PR), pinching the skin by an arterial clip with a strong grip (PI), and squeezing the skin with serrated forceps (SQ). (i) The response to a 55 °C heat stimulus that lasted 30 s. From Ferrington, D. G., Downie, J. W. and Willis, W. D. 1988. Primate nucleus gracilis neurons: responses to innocuous and noxious stimuli. J. Neurophysiol. 59: 886–907.

Schady, W. J. L. and Torebjörk, H. E., 1983; Johansson, O., *et al.*, 1999; Paré, M. *et al.*, 2001; 2002). Instead of FA I endings, the hairy skin contains hair follicle receptors (which are rapidly adapting and in effect substitute for FA I receptors) and field receptors, in addition to FA II, SA I, and SA II receptors (Vallbo, A. B. *et al.*, 1979; Halata, Z., 1993). There are several kinds of hair follicle receptors, including G_1, G_2, and T receptors, which are supplied by large myelinated ($A\beta$) afferents, and down hair receptors that are innervated by small myelinated ($A\delta$) afferents (Brown, A. G. and Iggo, A., 1967; Burgess, P. R. *et al.*, 1968; Perl, E. R., 1968). Field receptors respond to tactile stimulation of the skin, but not to movement of hair follicles; the morphology of field receptors is as yet undetermined. In addition, unmyelinated (or C fiber) afferents supply C mechanoreceptors, which are very responsive to mechanical stimuli that move slowly across the skin (sometimes referred to as caress detectors; Iggo, A., 1960; Bessou, P. *et al.*, 1971; Nordin, M., 1990; Vallbo, A. B. *et al.*, 1999).

FA I and hair follicle receptors are responsible for the sensation of flutter and FA II receptors for the sensation of vibration. Flutter sensation reflects the low-frequency components of moving stimuli (best frequency of about 30 Hz), whereas vibration sensation is triggered by the high-frequency components (best frequency of about 250 Hz). These different sensations can be distinguished experimentally by anesthetizing the skin (Talbot, W. H. *et al.*, 1968). When this is done, the threshold for flutter is elevated, whereas that for vibration is not. This shows that the receptors for flutter are located superficially within the skin and those for vibration are deep to the epidermis. The hypothesis that flutter depends on the activity of FA I receptors in glabrous skin and hair follicle and field receptors in hairy skin (Mountcastle, V. B. *et al.*, 1972) is supported by microneurography experiments in which stimulation of the axons of FA I and FA II receptors generally produce sensations related to flutter and vibration, respectively (Ochoa, J. and Torebjörk, E., 1983; Macefield, G. *et al.*, 1990).

The afferents from FA I and FA II receptors project to laminae III–VI of the dorsal horn (Figure 4; Brown, A. G. *et al.*, 1977; see also Wall, P. D., 1967; Brown, P.B., 1969; Tapper, D. N. *et al.*, 1973). The recurrent branches of hair follicle afferents within the dorsal horn have been referred to as flame-shaped arbors (Figures 4(a) and 4(b); Scheibel, M. E and Scheibel, A. B., 1968; Willis, W. D. and Coggeshall, R. E., 2004). Terminals of FA I and FA II afferents have also been traced into the inner part of lamina II (Woolf, C. J., 1987; Shortland, P. and Woolf, C. J., 1993).

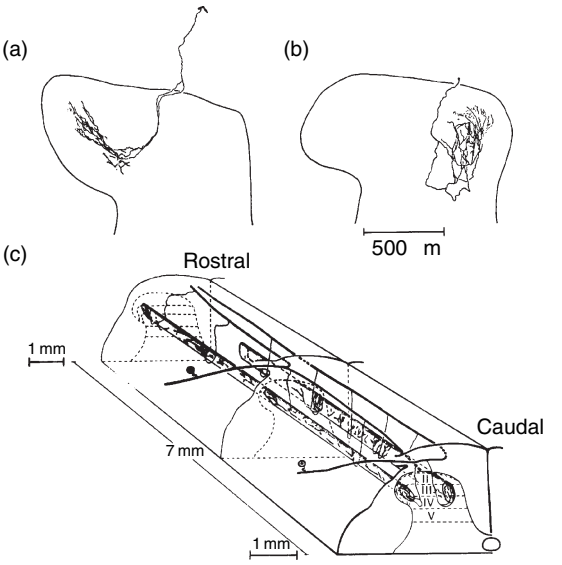

Figure 4 (a) and (b) The terminals of hair follicle afferents in the cat dorsal horn. Such endings have been called flame-shaped arbors. (c) The longitudinal arrangement of the branches of two hair follicle afferents in sagittal sheets within lamina III of the lateral and medial parts of the cat dorsal horn. From Brown, A. G., Rose, P. K., and Snow, P. J. 1977. The morphology of hair follicle afferent fibre collaterals in the spinal cord of the cat. J. Physiol. 272: 779–797.

Collaterals of some FA I, hair follicle afferents and field receptors project directly to the dorsal column nuclei through the dorsal columns. In addition, these afferents can activate postsynaptic dorsal column neurons, spinocervical tract (SCT), and spinothalamic tract (STT) neurons. Thus, there are multiple ascending pathways that share responsibility for signaling flutter sensation (see Willis, W. D. and Coggeshall, R. E., 2004). FA II receptors also have direct projections to the dorsal column nuclei through the dorsal columns and indirect projections by the way of postsynaptic dorsal column neurons; however, neither SCT nor STT neurons respond to FA II afferents.

6.06.2.1.3 Proprioception

Muscle is richly innervated. Proprioceptors in muscle include muscle spindles and Golgi tendon organs. These receptors subserve the position sense and the sensation of limb movement (kinesthesia) at proximal joints (Barker, D., 1962; Goodwin, G. M. *et al.*, 1972a;

1972b; Grigg, P. *et al.*, 1973; McCloskey, D. I., 1973; McCloskey, D. I., *et al.*, 1983; Horch, K. W. *et al.*, 1975; Clark, F. J. *et al.*, 1979). However, proprioception at distal joints, such as those of the digits, also involves SA II and joint receptors (Browne, K. *et al.*, 1954; Provins, K. A., 1958; Goodwin, G. M. *et al.*, 1972a, 1972b; Knibestöl, M., 1975; Gandevia, S. C. *et al.*, 1983; Ferrell, W. R. and Smith, A., 1987).

Recordings have been made from the Group Ia and II afferents that terminate in human muscle spindles as primary and secondary endings and from Group Ib afferents that end in human Golgi tendon organs (Hagbarth, K. E. and Vallbo, A. B., 1968; 1969; Hagbarth, K. E. *et al.*, 1975). The responses resemble those of similar receptors in animals. However, human muscle spindles do not appear to have any background fusimotor drive when the muscle is completely relaxed (Hagbarth, K. E. and Vallbo, A. B., 1968; Hagbarth, K. E. *et al.*, 1970; Burke, D. *et al.*, 1976). Human muscle spindle afferents usually discharge when the muscle contracts, presumably because of the activity of fusimotor neurons (Burke, D. *et al.*, 1978). Electrical stimulation of groups of large muscle afferents can result in illusions of movements (Gandevia, S. C. *et al.*, 1992), as can stimulation of cutaneous or joint afferents at distal joints (Gandavia, S. C., 1985; Macefield, G. *et al.*, 1990).

Group Ia and II muscle spindle afferents project to laminae VI, VII, and IX of the spinal cord gray matter (Figures 5(a)–5(d); Brown, A. G. and Fyffe, R. E. W., 1978; Fyffe, R. E. W., 1979; Brown, A. G., 1981). Group Ib afferents from Golgi tendon organs end in laminae VI and VII (Figures 5(e) and 5(f); Brown, A. G. and Fyffe, R. E. W., 1979; Brown, A. G., 1981). Afferents from these receptors synapse on proprioceptive interneurons (Eccles, J .C., 1965; Lucas, M. E. and Willis, W. D., 1974) and, in the case of muscle spindle afferents, also directly on motor neurons (Eccles, J. C., 1964; Burke, R. E. and Glenn, L. L., 1996). Many of these interneurons are likely to be involved in reflexes, although some may participate in sensory experience. Interneurons in the intermediate region (laminae VI and VII) that respond to volleys in group Ia afferents from muscle spindles or group Ib afferents from Golgi tendon organs include the inhibitory interneurons that produce reciprocal inhibition in the stretch reflex and inverse stretch reflex pathways (Eccles, J. C., 1964).

Like slowly adapting cutaneous receptors, proprioceptors of the lower extremity do not send axonal projections all the way to the dorsal column nuclei, although similar afferents from the upper extremity do project to the main cuneate and lateral cuneate nuclei (see Willis, W. D. and Coggeshall, R. E., 2004). Instead, collaterals of proprioceptive axons ascending in the dorsal column from stretch receptors of the hind limb terminate in Clarke's column, and the axons of some neurons in this nucleus accompany the dorsal spinocerebellar tract but terminate in nucleus z, a small nucleus just rostral to the nucleus gracilis whose neurons respond to proprioceptive inputs from the lower extremity (Figure 6; Pompeiano, O. and Brodal, A., 1957; Magherini, P. C. *et al.*, 1974; McIntyre, A. K. *et al.*, 1985). Nucleus z projects to the contralateral VPL and ventral lateral thalamic nuclei (Grant, G. *et al.*, 1973), and proprioceptive information is relayed from there to the sensorimotor cortex (Landgren, S. *et al.*, 1967; Landgren, S. and Silfvenius, H., 1971). In addition to its presence in several animal species, this spinomedullothalamic pathway is also likely to occur in humans, since a nucleus z has been described in the human brainstem (Sadjapour, K. and Brodal, A., 1968).

6.06.2.1.4 Visceral sensation

Mechanical events that occur in the viscera are often unaccompanied by sensation. Even very strong stimuli may not reach the level of consciousness (Lennander, K. G., 1907). This may be because many visceral nociceptors, like many cutaneous and articular nociceptors, are not normally responsive to mechanical stimuli (or alternatively because Lennander premedicated his patients with analgesics). However, insensitive nociceptors can be sensitized, after which they respond to weak mechanical and other stimuli and contribute to pain sensation (Häbler, H. J. *et al.*, 1993; Michaelis, M. *et al.*, 1996). Other visceral nociceptors can be activated by the distension of a hollow visceral organ, such as the colon, and produce pain (e.g., Ness, T. J. *et al.*, 1990; Sengupta, J. N. and Gebhart, G. F., 1994). Weak mechanical stimuli can be detected in certain viscera. For example, the urethra contains stretch receptors that detect urine flow (Shafik, A. *et al.*, 2003). These urethral stretch receptors are thought to provide feedback as part of a urethrovesical reflex. Many visceral receptors appear not to function in perception but rather provide sensory data for autonomic or other reflex activities.

Visceral afferents project to the dorsal horn of the spinal cord and are widely distributed, synapsing in laminae I, II, IV–V, and X (Figure 7; Sugiura, Y. *et al.*, 1989). Some cross the midline to end in the contralateral spinal cord gray matter. Furthermore, visceral

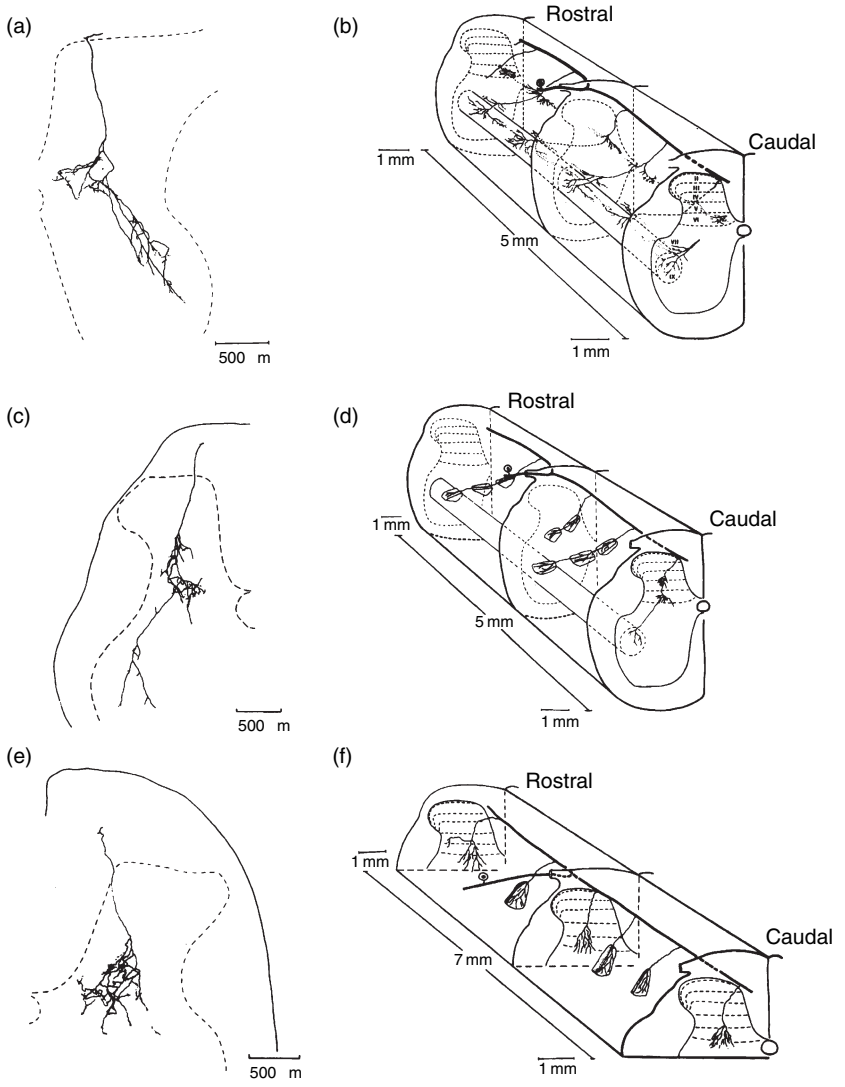

Figure 5 (a) An intrafiber injection of horseradish peroxidase (HRP) allows the visualization of the spinal cord projection of a group Ia afferent belonging to the cat lateral gastrocnemius–soleus (LGS) muscle group. (b) How the collaterals of an LGS group Ia fiber are distributed longitudinally in the lumbosacral spinal cord are shown. (c) and (d) Comparable depictions of the distribution of the terminals of a group II LGS afferent fiber and (e) and (f) of a group Ib fiber. (a, b) From Brown, A .G. and Fyffe, R. E. W. 1978. The morphology of group Ia afferent fibre collaterals in the spinal cord of the cat. J. Physiol. 274: 111–127. (c–f) From Brown, A. G. 1981. Organization in the Spinal Cord: The Anatomy and Physiology of Identified Neurones, Springer-Verlag.

afferents project rostrocaudally in the spinal cord for as many as six segments (Sugiura, Y. *et al.*, 1989), in contrast to cutaneous afferents, which terminate within one to two segments of their level of entry through a dorsal root (Sugiura, Y. *et al.*, 1989). Consistent with this, Fos expression has been demonstrated in spinal cord interneurons located in laminae I, V, and X following intraperitoneal injection of acetic acid in rats (Menétrey, D. *et al.*, 1989). The interneurons in lamina I that show Fos expression extend over many segments. The wide distribution of visceral afferents in the spinal cord may contribute to the common observation that visceral sensations are poorly localized.

Electrophysiological recordings have also demonstrated neurons near the central canal (lamina X) that respond to visceral as well as to somatic stimuli, and some that respond just to visceral stimuli (Honda, C. N., 1985). Ness T. J. and Gebhart G. F. (1987) found that many neurons in the area of lamina X that respond to

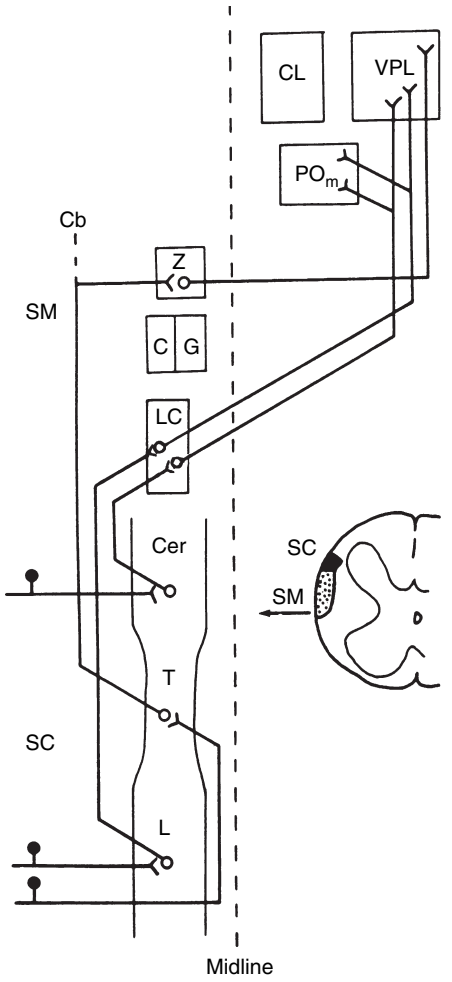

Figure 6 Diagram of the arrangement of the sensory pathways that ascend in the dorsal part of the lateral funiculus of the spinal cord. These pathways include the spinocervical (SC) tract and the spinomedullary (SM) tract. On the left is a schematic view of the connections of these pathways. At the right is a drawing of a cross section of the spinal cord showing the locations of the SC and SM tracts in the lateral funiculus. Primary afferent fibers end in the lumbar (L) and cervical (C) levels of the spinal cord. SC neurons project from these parts of the spinal cord to the lateral cervical nucleus (LC). The LC in turn projects to the contralateral thalamus, with terminations in the ventral posterior lateral (VPL) nucleus and the medial part of the posterior complex (PO$_m$). Branches of proprioceptive afferents are shown to ascend in the posterior funiculus to the thoracic level (T) and to end on neurons of Clarke's column. These neurons then project to the cerebellum (Cb) but also to nucleus z (z). Nucleus z in turn projects to the contralateral VPL thalamic nucleus. From Willis, W. D. and Coggeshall, R. E. 2004. 3rd edn., Sensory Mechanisms of the Spinal Cord, Kluwer Academic/Plenum.

noxious colorectal distention are projection neurons. These cells often have somatic receptive fields in the peroneal region or are activated when the tail is moved.

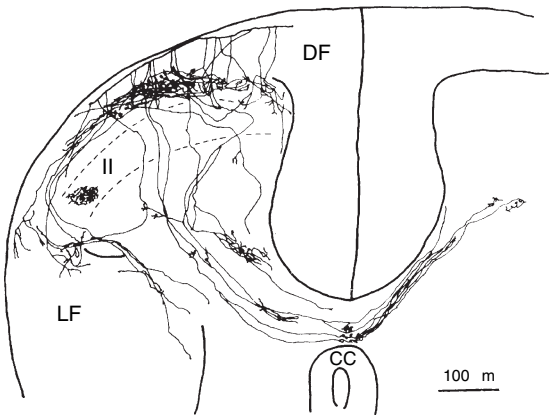

Figure 7 Spinal cord terminations of a visceral C fiber afferent whose cell body was injected with phaseolus vulgaris leucoagglutinin (PHA-L). The projections of the afferent are shown at one transverse level but they actually extended longitudinally over six segments. Note the dense terminations in lamina I and the decussation to the contralateral dorsal horn. From Sugiura, Y., Terui, N. and Hosoya, Y. 1989. Difference in distribution of central terminals between visceral and somatic unmyelinated (C) primary afferent fibers. J. Neurophysiol. 62: 834–840.

6.06.2.2 Thermoreceptive Circuits

Innocuous thermal sensations are signaled by two types of specific thermoreceptors: cold receptors and warm receptors (Hensel, H., 1974). When the skin temperature is in the neutral range, 32–34 °C, there is no experience of a thermal sensation. A slight deviation of the skin temperature from the neutral range results in a sensation of cooling or warmth because of the activation of cold or warm receptors and a reduction in the activity of the other type of thermoreceptor (reviewed in Willis, W. D. and Coggeshall, R. E., 2004). Thermal sensation adapts slowly (Kenshalo, D. R. and Scott, H. A., 1966). Extremes of temperature change lead to cold or heat pain by activating thermal nociceptors (see Section 6.06.2.3).

Cold and warm receptors have spot-like receptive fields (Dallenbach, K. M., 1927). Recordings have been made from afferents that supply each of these types of receptor, not only in animals but also in humans (see Willis, W. D. and Coggeshall, R. E., 2004). Cold receptors are thought generally to be supplied by Aδ fibers and warm receptors by C fibers in humans; however, some cold receptors in both humans and animals appear to be innervated by C fibers.

Thermoreceptors do not respond to mechanical stimuli. However, cold receptors (and cold sensation) can be activated by chemical substances, such as

menthol (Hensel, H. and Zotterman, Y., 1951). Recently, transducer proteins that permit cold and warm receptors to respond to certain ranges of temperature have been identified. These proteins form a family of TRP (transient receptor potential) receptors. For example, specific cold receptors contain TRPM8 that responds to cooling (<28 °C) and to menthol (McKemy, D. D. *et al.*, 2002; Peier, A. M. *et al.*, 2002). On the other hand, warm receptors that contain TRPV3 or TRPV4 respond to temperatures in the ranges of 34–38 °C and 27–34 °C, respectively (Patapoutian, A. *et al.*, 2003). These transducer proteins are found in both sensory neurons and keratinocytes (leading to the proposal that keratinocytes might contribute in some way to thermal sensation; Chung, M. K. *et al.*, 2004). The presence of these transducer molecules should lead to the identification of primary afferent terminals in the skin, dorsal root ganglion cells, and primary afferent terminals in the spinal cord that belong to cold or warm receptors through the use of immunocytochemical staining (just as nociceptors that contain TRPV1 receptors can be identified in this fashion).

Although the axons of individual thermoreceptors have not yet been traced into the spinal cord gray matter by labeling them with an anterograde marker or by identifying them immunocytochemically, as suggested above, electrophysiological recordings from dorsal horn neurons indicate that thermoreceptors project to laminae I–III of the superficial dorsal horn (SDH). Neurons in these laminae have been described that respond to the application of cold or warm stimuli to the skin (Christensen, B. N. and Perl, E. R., 1970; Courtney, K. *et al.*, 1972; Kumazawa, T. *et al.*, 1975; Iggo, A. and Ramsey, R. L., 1976; Kumazawa, T. and Perl, E. R., 1976; Kanui, T. I., 1988). Some of the responsive neurons in lamina I are STT cells (Craig, A. D. and Kniffki, K. D., 1985; Ferrington, D. G. *et al.* 1987; Kanui, T. I., 1988; Dostrovsky, J. O. and Craig, A. D., 1996; Han, Z. S. *et al.*, 1998; Andrew, D. and Craig, A. D., 2001; Craig, A. D. *et al.*, 2001). The axons from thermoreceptive STT neurons cross to the contralateral side and then ascend in the middle of the lateral funiculus, dorsal to the axons of STT neurons originating from deeper laminae (see Figure 12; Zhang, X. *et al.*, 2000a). This observation is consistent with the report by Foerster O. and Gagel O. (1932) that the thermal projections of the STT are posterior to the projections related to pain sensation.

There is a controversy about the destination in the thalamus of the terminations of lamina I STT neurons that signal cold or pain (see next section). Craig and his co-workers claim that essentially all lamina I STT neurons project to a nucleus located medial to VPL and named by them VMpo (Craig, A. D. *et al.*, 1994; Blomqvist, A. *et al.*, 2000; Craig, A. D., 2004). This has been disputed (Willis, W. D. *et al.*, 2002; Graziano, A. and Jones, E. G., 2004). Several lines of evidence indicate that the axons of many of these lamina I STT neurons terminate in the VPL nucleus (Applebaum, A. E. *et al.*, 1979; Zhang, X. *et al.*, 2000b; Willis, W. D. *et al.*, 2001) and lamina I trigeminothalamic neurons have been shown to project largely to the ventral posterior medial (VPM) nucleus (Graziano, A. and Jones, E. G., 2004).

6.06.2.3 Nociceptive Circuits

Pain is generally signaled by nociceptors, although pain can occur in the absence of activity in primary afferent fibers (e.g., pain can be evoked by stimulation of central neurons belonging to nociceptive circuits; see Mayer, D. J. *et al.*, 1975; Lenz, F. A. *et al.*, 1993; 1994). Primary afferent nociceptors are sensory receptors that signal stimuli that threaten damage or that produce overt damage to the body (Sherrington, C. S., 1906). In addition to pain sensation, nociceptors can evoke a variety of pain-related reactions, including nociceptive reflexes, emotional responses, autonomic activity, endocrine responses, and escape behavior.

There are various types of nociceptors. These are generally classified according to the sizes of the afferent axons that supply them and the kinds of noxious stimuli that activate them. For example, cutaneous Aδ mechanical and Aδ mechanoheat nociceptors are supplied by fine myelinated axons and are distinguished by their responses to noxious mechanical stimuli or to noxious mechanical and heat stimuli, respectively. Other nociceptors are supplied by unmyelinated or C fibers and include C mechanoheat, C heat, and C polymodal nociceptors. The latter are activated by noxious mechanical, thermal, and chemical stimuli. There is also a relatively small population of cutaneous nociceptors with axons that conduct in the Aβ range (see Willis, W. D. and Coggeshall, R. E., 2004).

Under normal conditions, nociceptors do not display spontaneous activity, and pain may not occur even if nociceptors are activated at a low level (Van Hees, J. 1976a; b). Their activity must exceed a threshold level before pain is perceived. Different kinds of pain are produced by different types of nociceptors. For example, activation of Aδ nociceptors in human

cutaneous nerves produces pricking pain, whereas excitation of C polymodal nociceptors results in dull or burning pain or sometimes itch (Konietzny, F. *et al.*, 1981; Ochoa, J. and Torebjörk, E., 1989; Torebjörk, H. E., and Ochoa, J. L., 1983; 1990; Schmelz, M. *et al.*, 1997). Stimulation of human muscle nociceptors evokes cramping pain (Marchettini, P. *et al.*, 1996).

As mentioned, many nociceptors are unresponsive to noxious mechanical stimuli under normal conditions (e.g., the sleeping nociceptors of Schaible, H. G. and Schmidt, R. F., 1985; 1988). However, such afferents can be sensitized following damage or inflammation (see Willis, W. D. and Coggeshall, R. E., 2004). The sensitized nociceptors often develop background activity and become responsive to even weak mechanical stimuli, leading to ongoing pain and to primary allodynia and hyperalgesia (Meyer, R. A. and Campbell, J. N., 1981). Secondary allodynia and hyperalgesia may also develop in neighboring undamaged areas because of changes in the responses of central nociceptive neurons, a process known as central sensitization (LaMotte, R. H. *et al.*, 1991; Simone, D. A. *et al.*, 1991; see Willis, W. D. and Coggeshall, R. E., 2004). Peripheral sensitization results from the activation of membrane proteins, such as TRPV1 receptors (Tominaga, M. *et al.*, 1998; Caterina, M. J. and Julius, D., 2001) or tetrodotoxin-resistant sodium channels (Gold, M. S. *et al.*, 1996; 1998). Central sensitization following intradermal injection of capsaicin appears to result (at least in part) from the phosphorylation of glutamate receptors (Zou, X. *et al.*, 2000; Fang. L. *et al.*, 2003).

Cutaneous Aδ nociceptors terminate in the spinal cord chiefly in laminae I and V and sometimes send collaterals to end in the lateral part of the contralateral lamina V (Figure 8(a); Light, A. R. and Perl, E. R., 1979), whereas C polymodal nociceptors end mostly in laminae I and II (Figure 8(b); Sugiura, Y. *et al.*, 1986).

Many interneurons in laminae I, II, and V, as well as in the adjacent laminae, respond to noxious inputs. Some respond to both innocuous and noxious mechanical stimuli, although best to noxious inputs (Figure 9(b)); these are termed WDR neurons (Mendell, L. M., 1966). Others respond solely or primarily to noxious stimuli and can be regarded as narrow dynamic range neurons. These are referred to as high-threshold (HT) or nociceptive-specific (NS) cells (Figure 9(c)). Other narrow dynamic range neurons, termed LT neurons, respond selectively to tactile stimuli (Figure 9(d)). This classification scheme is still in common use (see Willis, W. D. and Coggeshall, R. E., 2004). Although HT neurons are often said to be located principally in lamina I, they are in fact distributed widely in the dorsal horn, as are WDR range neurons. In monkeys, WDR STT neurons in lamina I appear to outnumber HT STT neurons in the same lamina (Owens, C. M. *et al.*, 1992). LT neurons are common in laminae III and IV.

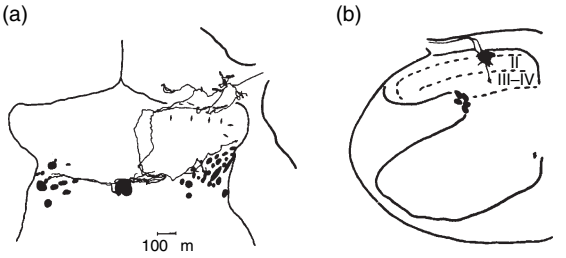

Figure 8 (a) The spinal cord distribution of the terminal branches of an Aδ mechanical nociceptive afferent fiber that had been injected with horseradish peroxidase (HRP) in a monkey. Note the endings in lamina I on one side and near the central canal, and in the deep dorsal horn bilaterally. From Light, A. R. and Perl, E. R. 1979. Spinal termination of functionally identified primary afferent neurons with slowly conducting myelinated fibers. J. Comp. Neurol. 186: 133–150. (b) The terminals of a C polymodal nociceptor in the dorsal horn of a guinea-pig. The cell body of the afferent was injected with phaseolus vulgaris leucoagglutinin (PHA-L). From Sugiura, Y., Lee, C. L. and Perl, E. R. 1986. Central projections of identified, unmyelinated (C) afferent fibers innervating mammalian skin. Science 234: 358–361.

Nociceptive information is transmitted to the brain by way of several different ascending tracts. In addition to the STT (Willis, W. D. *et al.*, 1974; Price, D. D. *et al.*, 1978; Chung, J. M. *et al.*, 1979; Kenshalo, D. R. *et al.*, 1979; Surmeier, D. J. *et al.*, 1988; Owens, C. M. *et al.*, 1992), ascending tracts with a nociceptive component include the SCT, spinoreticular, spinomesencephalic, spinohypothalamic, spinoparabrachial, and spinolimbic pathways (Willis, W. D. and Westlund, K. N., 1997; Willis, W. D. and Coggeshall, R. E., 2004; cf., Noordenbos, W. and Wall, P. D., 1976; Gybels, J. M. and Sweet, W. H., 1989). The postsynaptic dorsal column pathway appears to be particularly important for signaling visceral pain (Hirshberg, R. M. *et al.*, 1996; Al-Chaer, E. D. *et al.*, 1996a; b; Nauta, H. J. W. *et al.*, 2000).

6.06.2.4 Spinal Cord Projection Neurons

6.06.2.4.1 Spinothalamic tract neurons

The STT is generally considered the most important pathway to convey nociceptive information from the spinal cord to the brain. The somas of the cells of

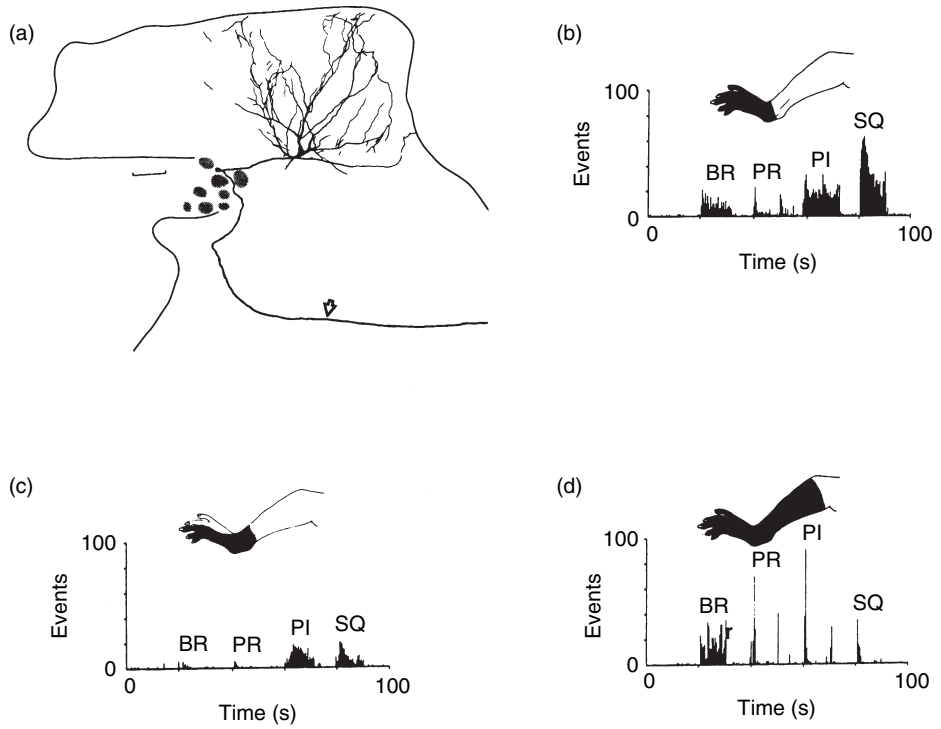

Figure 9 (a) A drawing of a wide dynamic range (WDR) primate spinothalamic tract cell that was injected intracellularly with horseradish peroxidase (HRP). Note that its dendritic tree extends dorsally into lamina I. The axon en route to its decussation in the anterior white commissure is indicated by the open arrow head. (b) The responses of this neuron to brush (BR), pressure (PR), pinch (PI), and squeeze (SQ) stimuli. (c, d) The responses of a high-threshold (HT) and a low-threshold (LT) spinothalamic tract neuron. From Surmeier, D. J., Honda, C. N. and Willis, W. D. 1988. Natural groupings of primate spinothalamic neurons based on cutaneous stimulation: Physiological and anatomical features. J. Neurophysiol. 59: 833–860.

origin of the STT are scattered widely in the spinal cord gray matter of monkeys. Many are concentrated in laminae I and V–VI, but some are located in lamina IV and in the ventral horn (Figure 10; Willis, W. D. *et al.*, 1979; 2001; Apkarian, A. V. and Hodge, C. J., 1989).

Primate STT cells project to several contralateral thalamic nuclei, including the VPL and central lateral nuclei, as well as the posterior complex, as shown by anterograde and retrograde labeling and by antidromic mapping of the terminations of the axons of STT cells (Figure 11; Applebaum, A. E. *et al.*, 1979; Giesler, G. J. *et al.*, 1981; Zhang, X. *et al.*, 2000a; 2000b). Apkarian A. V. and Hodge C. J. (1989) provide evidence that in macaque monkeys about 18 000 STT cells project to one side of the thalamus.

Primate STT cells in lamina I tend to be oriented longitudinally in the spinal cord; their configurations are described as fusiform, pyramidal, or multipolar (Zhang, E. T. and Craig, A. D., 1997). However, intracellularly labeled primate STT cells in laminae IV–VI are oriented transversely and often have long dendrites that can extend dorsally to reach laminae I and II (Figure 9(a); Surmeier, D. J. *et al.*, 1988; see Willis, W. D. and Coggeshall, R. E., 2004). The axons of STT cells in the deep layers of the dorsal horn decussate in the ventral white commissure at a level near the cell body. They then ascend to the thalamus at first in the ventral and then in the lateral funiculus (Willis, W. D. *et al.*, 1979; Apkarian, A. V. and Hodge, C. J., 1989). The axons of lamina I STT cells are concentrated in the middle of the contralateral lateral funiculus (Craig, A. D., 2000), whereas those from STT cells of the deep dorsal horn (DDH) are located more ventrally in the lateral funiculus (Figure 12; Zhang, X. *et al.*, 2000a; 2000b). The STT axons in the lateral funiculus are arranged somatotopically (Applebaum, A. E. *et al.*, 1975; Zhang, X. *et al.*, 2000a; b). The conduction velocities of the axons of primate STT neurons in lamina V average 45.5 m s^{-1} and those in lamina I average 20.3 m s^{-1} (Trevino, D. L. *et al.*, 1973).

The thalamic synaptic terminals of STT cells are enriched in glutamate, suggesting that they release

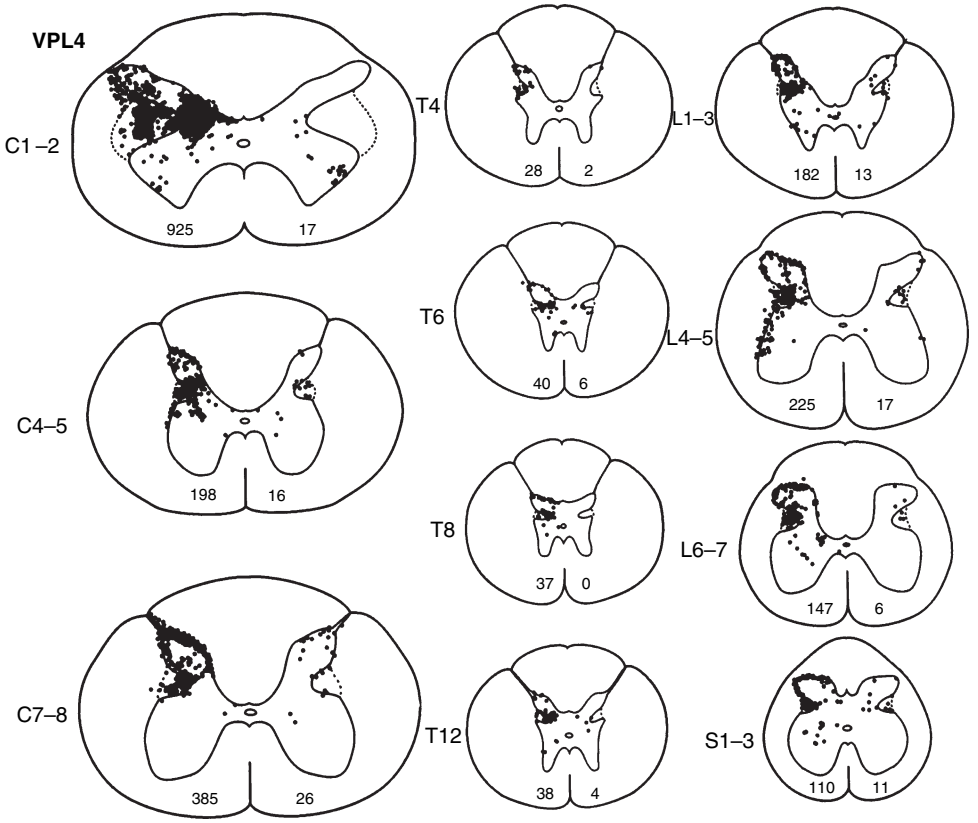

Figure 10 Distribution of the cell bodies of primate spinothalamic tract neurons as shown by retrograde labeling, using a circumscribed injection of the tracer, cholera toxin subunit B, into the ventral posterior lateral (VPL) nucleus of one side. The filled circles indicate the locations of individual neurons at different segmental levels plotted on drawings of transverse sections. The numbers in the ventral funiculi are cell counts. Most of the labeled neurons were contralateral to the injection. From Willis, W. D., Zhang, X., Honda, C. N. and Giesler, G. J. 2001. Projections from the marginal zone and deep dorsal horn to the ventrobasal nuclei of the primate thalamus. Pain 92: 267–276.

glutamate as an excitatory neurotransmitter (Ericson, A. C. *et al.*, 1995; Blomqvist, A. *et al.*, 1996). Some STT cells are thought to contain peptide neurotransmitters, such as substance P (SP) (see review by Willis, W. D. and Coggeshall, R. E., 2004). A variety of substances have been demonstrated immunocytochemically in synaptic endings on STT cells, including glutamate, gamma amino butyric acid (GABA), SP, calcitonin gene-related peptide (CGRP), enkephalin, and serotonin (Ruda, M. A. *et al.*, 1984; Westlund, K. N. *et al.*, 1992; Carlton, S. M. *et al.*, 1990; 1992). Release of these neurotransmitters can excite or inhibit STT cells (see Willis, W. D. and Coggeshall, W. D., 2004).

6.06.2.4.2 Spinocervical neurons

Most SCT neurons are located in lamina IV of the spinal cord dorsal horn, and they project ipsilaterally through the dorsal part of the lateral funiculus to the lateral cervical nucleus, which is in the uppermost cervical spinal cord (Figure 6; reviewed in Willis, W. D. and Coggeshall, R. E., 2004). Axons from neurons in the lateral cervical nucleus decussate immediately and then ascend through the brainstem to the contralateral VPL thalamic nucleus in company with the medial lemniscus. The number of SCT neurons in primates is not known, and it is uncertain if there is a lateral cervical nucleus in the human spinal cord.

Many SCT neurons are activated by hair follicle afferents (Brown, A. G. and Franz, D. N. 1969) and are therefore likely to mediate flutter sensation. However, some are nociceptive and can be classified as WDR or HT neurons Cervero, F. *et al.*, 1977).

6.06.2.4.3 Postsynaptic dorsal column neurons

The postsynaptic dorsal column pathway originates from projection neurons, most of which are located in

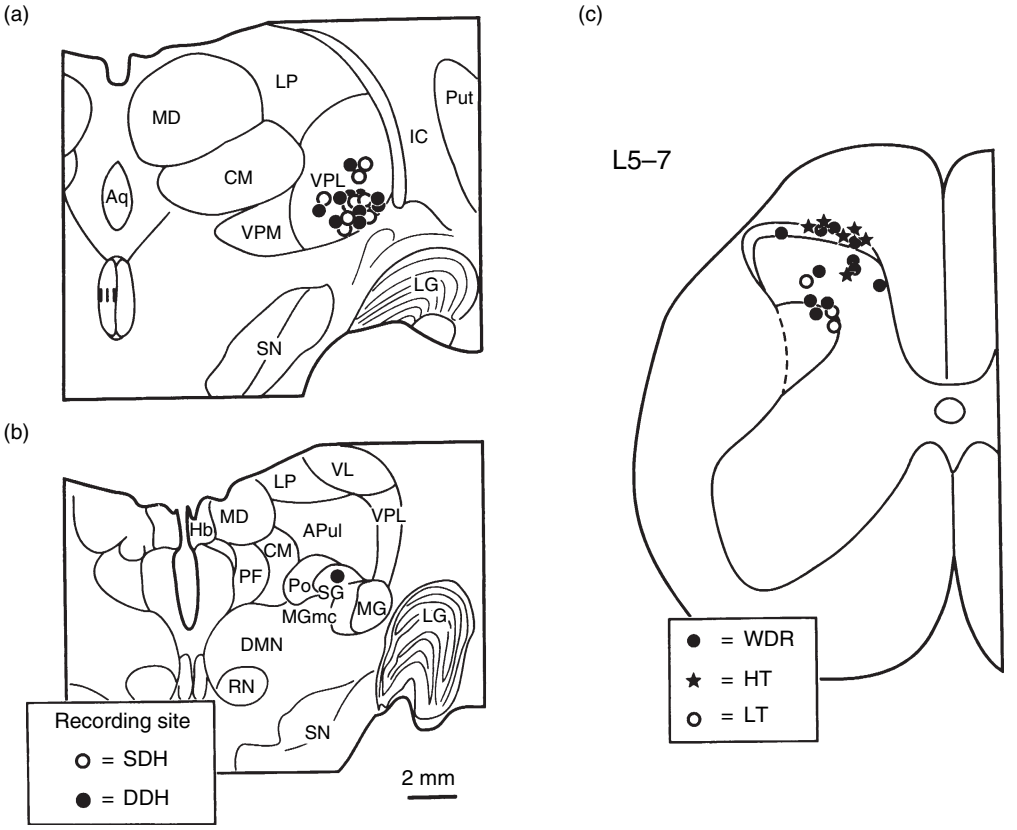

Figure 11 (a, b) The low-threshold (LT) sites determined by antidromic mapping to locate the terminations of primate spinothalamic tract (STT) neurons in the contralateral thalamus are shown. As indicated by the symbols, terminals of STT cells from both the superficial dorsal horn (SDH) and the deep dorsal horn (DDH) were in the VPL nucleus, with the exception of one cell of the DDH that projected to the suprageniculate (SG) nucleus of the posterior complex. (c) The locations of the cell bodies of the STT cells at the L5–7 levels that were antidromically activated in this experiment are shown. Wide dynamic range (WDR) cells are indicated by filled circles, high-threshold (HT) cells by asterisks, and LT cells by open circles. From Zang, X. *et al.*, 2000b.

the dorsal horn (reviewed in Willis, W. D. and Coggeshall, R. E., 2004). In monkeys, the cell bodies of these neurons are concentrated in laminae IV–VI (Rustioni, A. *et al.*, 1979), although some are also found in laminae III, VII, and X (Bennett, G. J. *et al.*, 1983). The dendrites of postsynaptic dorsal column neurons can project dorsally into lamina II and even I (Brown, A. G. and Fyffe, R. E. W. 1981). The axons of these neurons are medium-sized myelinated fibers that ascend to the caudal medulla in the dorsal column (although some of the axons are instead in the dorsal part of the lateral funiculus) to end in the ipsilateral dorsal column nuclei, along with the collaterals of dorsal root ganglion cells that project directly to the dorsal column nuclei (see Willis, W. D. and Coggeshall, R. E., 2004). Sensory information is then conducted from the dorsal column nuclei to the contralateral VPL thalamic nucleus through the medial lemniscus.

The postsynaptic dorsal column pathway was first recognized in recordings from second-order axons in the dorsal columns by Uddenberg N. (1968), who found that neurons in this pathway can respond to noxious mechanical stimuli, as well as to tactile stimuli. For example, in cats, these neurons are activated both by tactile stimuli and by noxious heat, and the responses to mechanical stimuli become sensitized after repeated heat stimuli (Kamogawa, H. and Bennett, G. J., 1986). Recently, it has been found that a population of postsynaptic dorsal column neurons is activated by noxious visceral stimuli, such as colorectal distention (Al-Chaer, E. D. *et al.*, 1996a; 1996b). Interruption of the dorsal columns or pharmacological blockade of the synaptic input from

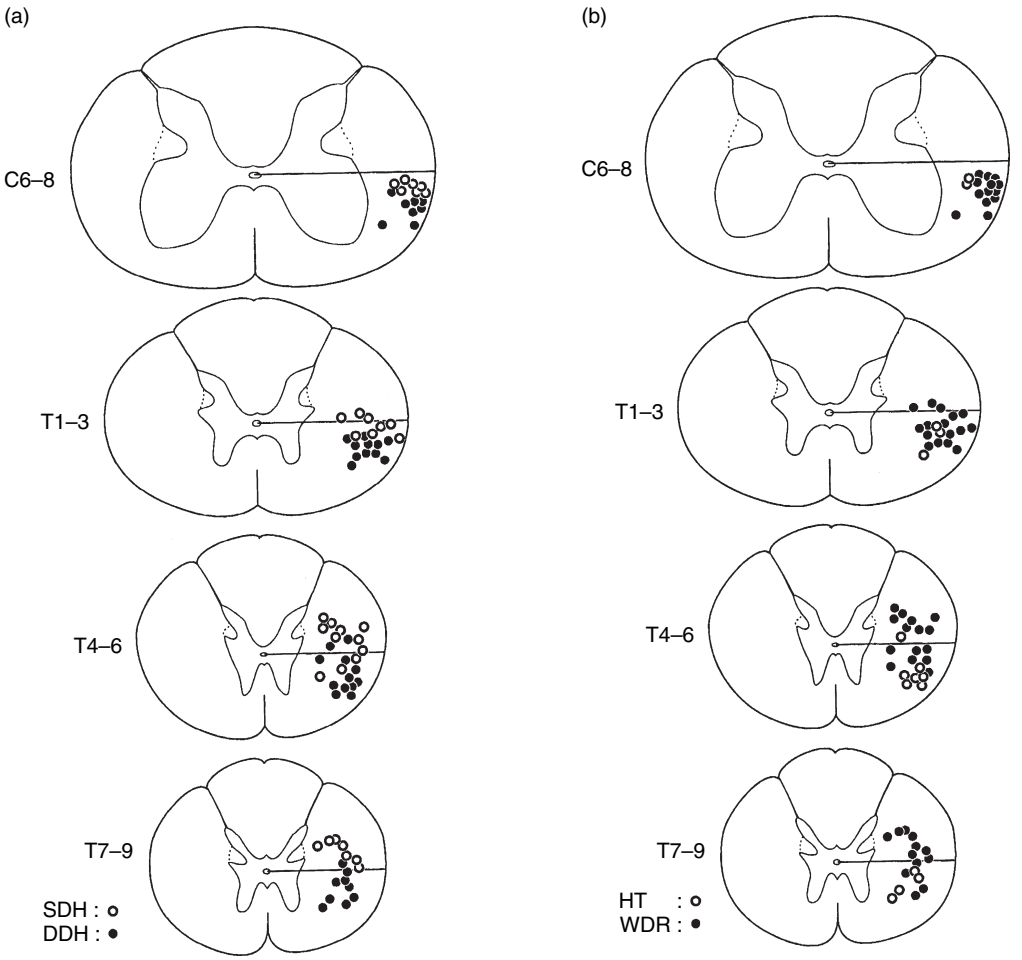

Figure 12 The positions of the axons of monkey spinothalamic tract (STT) cells within the spinal cord white matter and en route to the thalamus are shown at different segmental levels. The axons were activated antidromically by stimulation in the thalamus and the low-threshold points in the spinal cord were marked. (a) The symbols indicate axons from STT cells located in the superficial dorsal horn (SDH; open circles) or the deep dorsal horn (DDH; filled circles). (b) The symbols indicate whether the same axons belonged to high-threshold (HT) (open circles) or wide dynamic range (WDR) (filled circles) STT neurons. From Zhang, X. *et al.*, 2000.

primary afferents that excites these neurons prevents the responses of neurons in the nucleus gracilis (Figure 13) and in the VPL thalamic nucleus to noxious visceral stimuli (Al-Chaer, E. D. *et al.*, 1996b). This observation made in animal experiments helps explain the beneficial effects of midline myelotomy in human patients in relieving the pain of pelvic cancer (Hirshberg, R. M. *et al.*, 1996; Nauta, H. J. W. *et al.*, 2000).

6.06.2.4.4 Spinoreticular neurons

Spinoreticular neurons project to the brainstem reticular formation, including several reticular nuclei in the medulla and pons, such as the nucleus reticularis gigantocellularis (NGc) and the nucleus reticularis pontis caudalis (reviewed in Willis, W. D. and Coggeshall, R. E., 2004). Many of the cells of origin of the spinoreticular tract in monkeys are concentrated in the upper cervical spinal cord. Those found in the spinal cord enlargements are located mostly in lamina VII, although some are in laminae V and VIII (Kevetter, G. A. *et al.*, 1982). The axons of these neurons are myelinated and most cross the midline and ascend in the ventral white matter of the spinal cord. Spinoreticular neurons are often excited by noxious stimuli applied to large cutaneous or deep somatic receptive fields, but inhibitory responses and responses to visceral stimuli are also seen (reviewed by Willis, W. D. and Coggeshall, R. E., 2004).

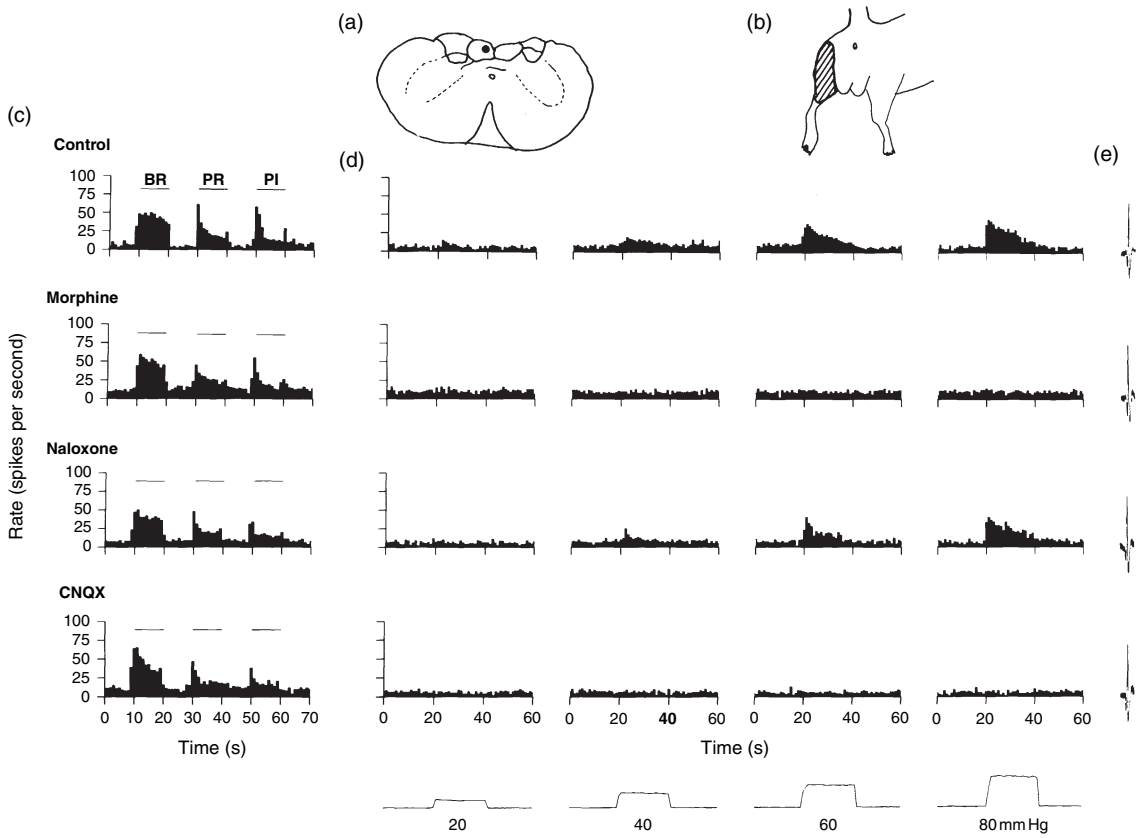

Figure 13 Activation of a neuron in the rat gracile nucleus by visceral input. The input from the colon was limited to that traversing the pelvic nerves by transecting the hypogastric nerves bilaterally. (a) The location of the gracile neuron. (b) Somatic receptive field of the gracile neuron. The peristimulus time histograms in (c) show the responses of the neuron to mechanical stimuli applied to the receptive field. The responses in (d) were to graded colorectal distention (20, 40, 60, and 80 mm Hg, as indicated by the monitor pulses below the histograms). (e) Spikes recorded from the neuron during different phases of the experiment to show that the recording was stable. A microdialysis fiber was placed across the sacral spinal cord to allow the intraspinal administration of drugs. Infusion of morphine blocked the responses to colorectal distention ((d), second row of records), as did the non-NMDA (*N*-methyl-D-aspartate) glutamate receptor antagonist, CNQX ((d), fourth row). Systemic administration of naloxone reversed the action of morphine ((d), third row). The drugs had little effect on the responses to mechanical stimulation (c). The actions of morphine and CNQX were presumably on the synaptic input to postsynaptic dorsal column neurons in the sacral cord; these drugs had a similar effect on the responses of identified postsynaptic dorsal column neurons within the sacral cord. From Al-Chaer, E. D., Lawand, N. B., Westlund, K. N. and Willis, W. D. 1996b. Pelvic visceral input into the nucleus gracilis is largely mediated by the postsynaptic dorsal column pathway. J. Neurophysiol. 76: 2675–2690.

6.06.2.4.5 Spinoparabrachial neurons

The spinoparabrachial tract is a component of the spinomesencephalic projections, which also include the spinotectal tract (to the superior colliculus and intercollicular region) and the spinoannular tract (to the periaqueductal gray (PAG)). Spinoparabrachial neurons are located in lamina I and also in deep layers of the dorsal horn, and their axons terminate in several nuclei in the parabrachial region, including not only the parabrachial nuclei proper but also the locus coeruleus and the Kölliker-Fuse nucleus (Bernard, J. F. *et al.*, 1995; reviewed in Willis, W. D. and Westlund, K. N., 1997). Nociceptive spinoparabrachial neurons activate neurons in the parabrachial region that project to the central nucleus of the amygdala (Bernard, J. F. and Besson, J. M., 1990; Bernard, J. F. *et al.*, 1989; 1992).

6.06.2.4.6 Spinohypothalamic and other spinolimbic neurons

Direct projections have been described from the spinal cord to the hypothalamus of rats, cats, and monkeys (Burstein, R. *et al.*, 1990; Katter, J. T. *et al.*, 1991; Zhang, X. *et al.*, 1999). Branches of the axons of

these neurons have been found to decussate in the hypothalamus and then to descend into the brainstem, where they terminate bilaterally in many nuclei in the diencephalon and brainstem (Zhang, X. *et al.*, 1995). The cells of origin of spinohypothalamic neurons are in the SDH and DDH and in the intermediate region. Most are WDR or HT neurons (Burstein, R. *et al.*, 1991).

Direct spinal cord projections to the amygdala, septal nuclei, nucleus accumbens, and other limbic system structures have also been reported (Burstein, R. *et al.*, 1987; Burstein, R. and Giesler, G. J., 1989; Cliffer, K. D. *et al.*, 1991).

6.06.2.5 Descending Control Systems

Pathways that descend from the brain to the spinal cord (and also to the brainstem) provide a means by which the brain can control its somatosensory input. These descending controls can either inhibit sensory input or facilitate it. The best-known descending controls are those that are capable of inhibiting nociceptive signals. These pathways are generally known collectively as the endogenous analgesia system. However, there are also pronociceptive descending controls, and not only pain but also tactile and other sensory inputs are regulated by such pathways.

6.06.2.5.1 Descending control pathways

6.06.2.5.1.(i) Cortical projections Corticospinal and corticobulbar projections that originate in the sensorimotor areas of the cerebral cortex (Weiberg, J. A. and Rustioni, A., 1977; see reviews by Willis, W. D., 1982; Willis, W. D. and Coggeshall, R. E., 2004) can exert inhibitory or excitatory influences on the activities of sensory neurons in the spinal cord dorsal horn, as well as in the brainstem, such as in the dorsal column nuclei (Jabbur, J. L. and Towe, A. L. 1961; Towe, A. L. and Jabbur, A. L. 1961).

STT neurons in monkeys are generally excited following stimulation in the primary motor cortex or in the medullary pyramid but inhibited by stimulation in the somatosensory cortex (Figure 14; Yezierski, R. P. *et al.*, 1983).

6.06.2.5.1.(ii) Periaqueductal gray and nucleus raphe magnus In addition to direct cortical projections to the spinal cord and brainstem, there are indirect projections to these from cortical and subcortical structures (such as the amygdala and the hypothalamus) by way of the gray matter that surrounds the cerebral aqueduct (PAG). Stimulation in the appropriate part of the PAG in awake, behaving rats results in analgesia so profound that it is possible to perform abdominal surgery without chemical anesthesia (Reynolds, D. V., 1969). In anesthetized monkeys, stimulation in the PAG results in the inhibition of STT cells (Hayes, R. L. *et al.*, 1979; Gerhart, K. D. *et al.*, 1984; see Willis, W. D. and Coggeshall, R. E., 2004). A review of the role of the PAG in defensive behavior and other responses can be found in Depaulis A. and Bandler R. (1991).

Very few neurons in the PAG project directly to the spinal cord. The effects of PAG stimulation at the spinal cord level are mediated by connections of neurons in the PAG with spinally projecting neurons in other parts of the brainstem, including the nucleus raphe magnus (NRM) and adjacent reticular formation (Figure 15), a region often referred to as the rostral ventral medulla (RVM) (Fields, H. L. and Besson, J. M. 1988).

Many of the bulbospinal neurons in the RVM contain serotonin; others may release peptides or other transmitters. Additional projections from the brainstem to the spinal cord arise from the locus coeruleus, subcoeruleus, and Kölliker-Fuse nuclei, which contain noradrenergic neurons. Other inhibitory neurotransmitters released by descending control systems, either from the terminals of descending projections or from spinal cord interneurons include GABA, glycine (Sorkin, L. S. *et al.*, 1993), enkephalin, and the recently discovered endomorphins I and II (Zadina, J. E. *et al.*, 1997; Wu, S. Y. *et al.*, 1999; see review by Willis, W. D. and Coggeshall, R. E., 2004). The actions of several of these neurotransmitters on dorsal horn neurons have been tested by their iontophoretic release in the vicinity of STT cells (Willcockson, W. S. *et al.*, 1984a; 1984b).

Some brainstem projections to the spinal cord have excitatory actions. For example, stimulation in certain parts of the reticular formation can excite primate STT neurons (Figure 16; Haber, L. H. *et al.*, 1980; Giesler, G. J. *et al.*, 1981). Candidate excitatory neurotransmitters released in the spinal cord following brainstem stimulation include the excitatory amino acids, glutamate, and aspartate (Sorkin, L. S. *et al.*, 1993).

6.06.3 Second-Order Somatosensory Circuits in the Brainstem

6.06.3.1 Cranial Nerve Somatosensory Afferents

Most of the somatosensory primary afferent fibers from the head enter the brainstem through the

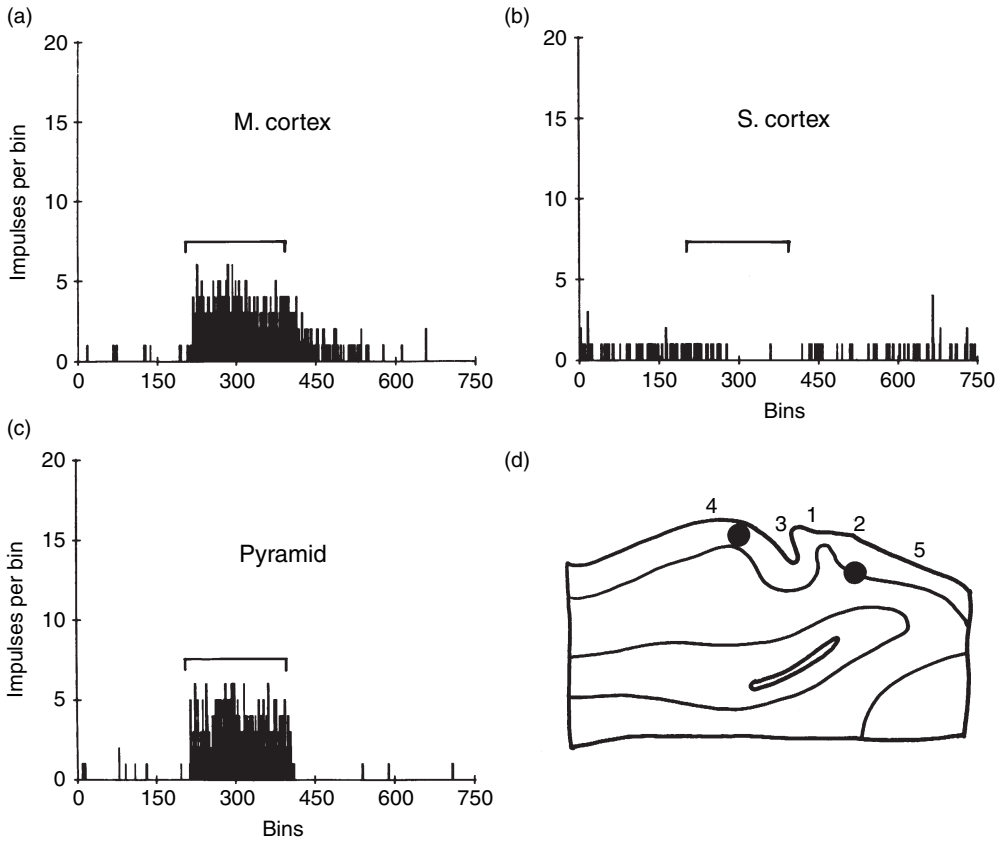

Figure 14 (a) The histogram shows the excitatory response of a primate spinothalamic tract (STT) cell to electrical stimulation in the motor cortex (area 4; 200-ms trains, 100 μA strength pulses). By contrast, (b) shows that stimulation in the somatosensory cortex (area 2; 200-ms trains, 200 μA pulses) inhibited the background activity of the cell. (c) The excitation of the neuron by stimulation in the medullary pyramid. (d) The Two sites in the sensorimotor cortex used for stimulation in (a) and (b). From Yezierski, R. P., Gerhart, K. D., Schrock, B. J. and Willis, W. D. 1983. A further examination of effects of cortical stimulation on primate spinothalamic tract cells. J. Neurophysiol. 49: 424–441.

trigeminal nerve, although some that supply the region of the external ear join other cranial nerves, including the facial, glossopharyngeal and vagus nerves, and somatosensory afferents that innervate the back of the head enter the central nervous system (CNS) through the upper cervical dorsal roots (Arvidsson, J. and Thomander, L., 1984; see a standard neuroanatomy textbook, such as Carpenter, M. B. and Sutin, J., 1983, or Nolte, J., 2002). Many of these somatosensory afferents have their cell bodies in the trigeminal ganglion; others have their cell bodies in the geniculate ganglion of the facial nerve, the superior ganglia of the glossopharyngeal and vagus nerves, or in dorsal root ganglia. Their axons terminate directly in the main sensory nucleus of the trigeminal nerve and/or in the spinal nucleus of the trigeminal nerve after passing caudally through the brainstem in the spinal tract of the trigeminal nerve. The trigeminal nerve, ganglion and nuclei have a somatotopic organization, as shown by tracing the central projections and the synaptic connections of receptors in the distributions of the three peripheral trigeminal branches (ophthalmic, maxillary, and mandibular divisions).

Large myelinated somatosensory afferents that signal touch–pressure and flutter–vibration end in the main sensory nucleus of the trigeminal nerve, whereas small myelinated and unmyelinated somatosensory afferents conveying tactile, pain and temperature information synapse in one or more of the subnuclei of the spinal nucleus of V (subnuclei oralis, interpolaris, and caudalis). The cell bodies of proprioceptive afferents of the trigeminal nerve are located in the CNS in the mesencephalic nucleus. The central processes of these proprioceptive afferent neurons synapse monosynaptically on motor neurons in the motor nucleus of the trigeminal nerve to form the afferent limb of the jaw jerk reflex,

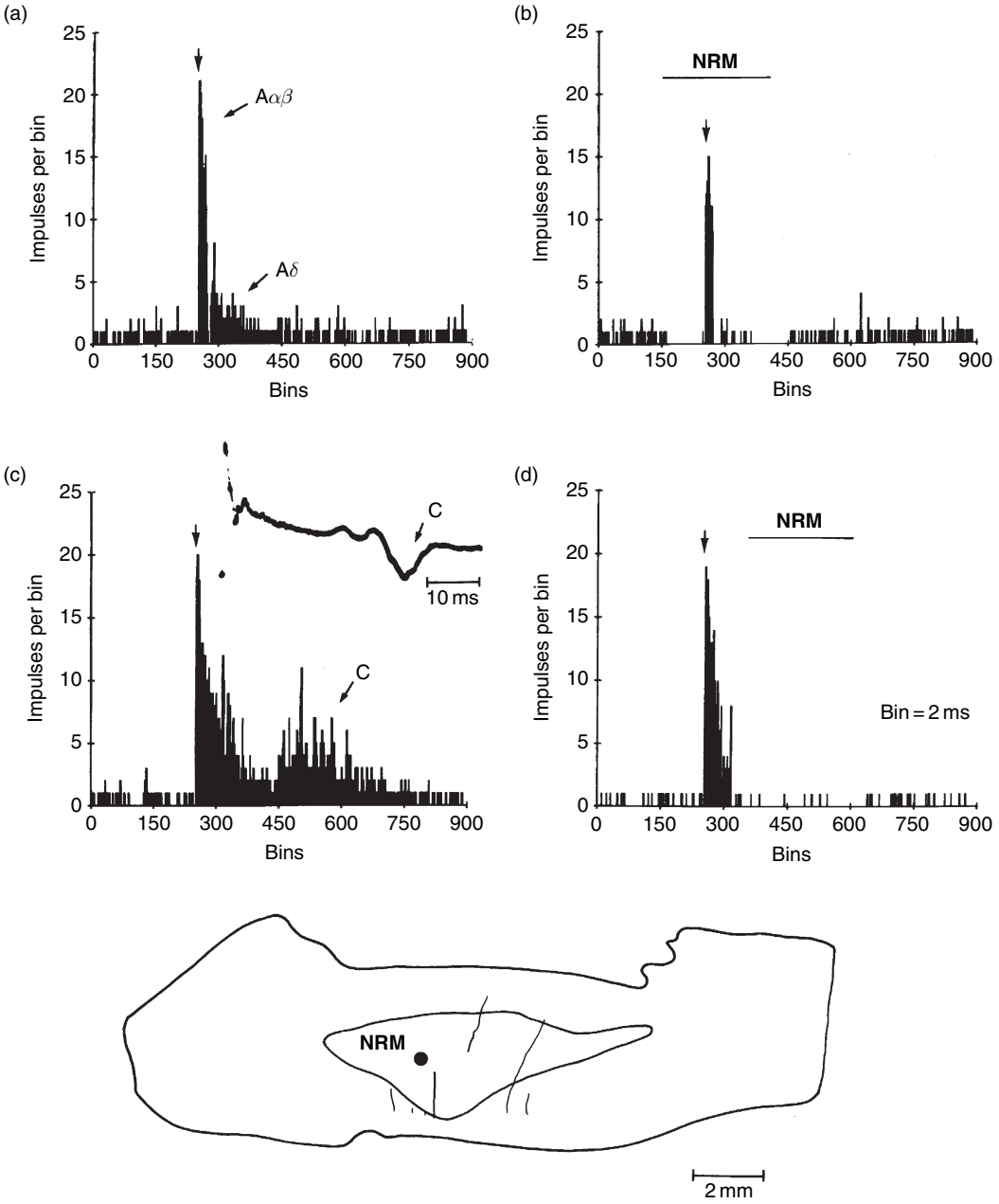

Figure 15 Inhibition of the responses of a wide dynamic range (WDR) primate spinothalamic tract (STT) cell to volleys in the sural nerve following stimulation in the nucleus raphe magnus (NRM). (a) and (b) The STT cell was activated by stimulation of the sural nerve at a strength that activated A$\alpha\beta$ and Aδ afferent fibers. (b) Conditioning stimuli were applied in the NRM during the time indicated by the bar (500 ms trains of 0.1 ms, 150 μA pulses at 333 Hz). Note the reduction in the response. The strength of the stimulus applied to the sural was increased to activate C fibers (1 ms pulses; inset shows compound action potential with the C fiber volley recorded from the sural nerve proximal to the site of stimulation). (d) The NRM was stimulated during the period of the C fiber response of the STT cell. The response was virtually eliminated. The drawing shows the marked position of the tip of the stimulating electrode in the NRM. From Gerhart, K. D. *et al.*, 1981.

a stretch reflex that involves the muscles of mastication. Proprioceptive information is also conveyed from the mesencephalic nucleus to the main sensory nucleus of V. The different nuclei of the trigeminal sensory complex are interconnected in a complicated fashion by ascending and descending projections within the brainstem (Nasution, I. D. and Shigenaga, Y., 1987).

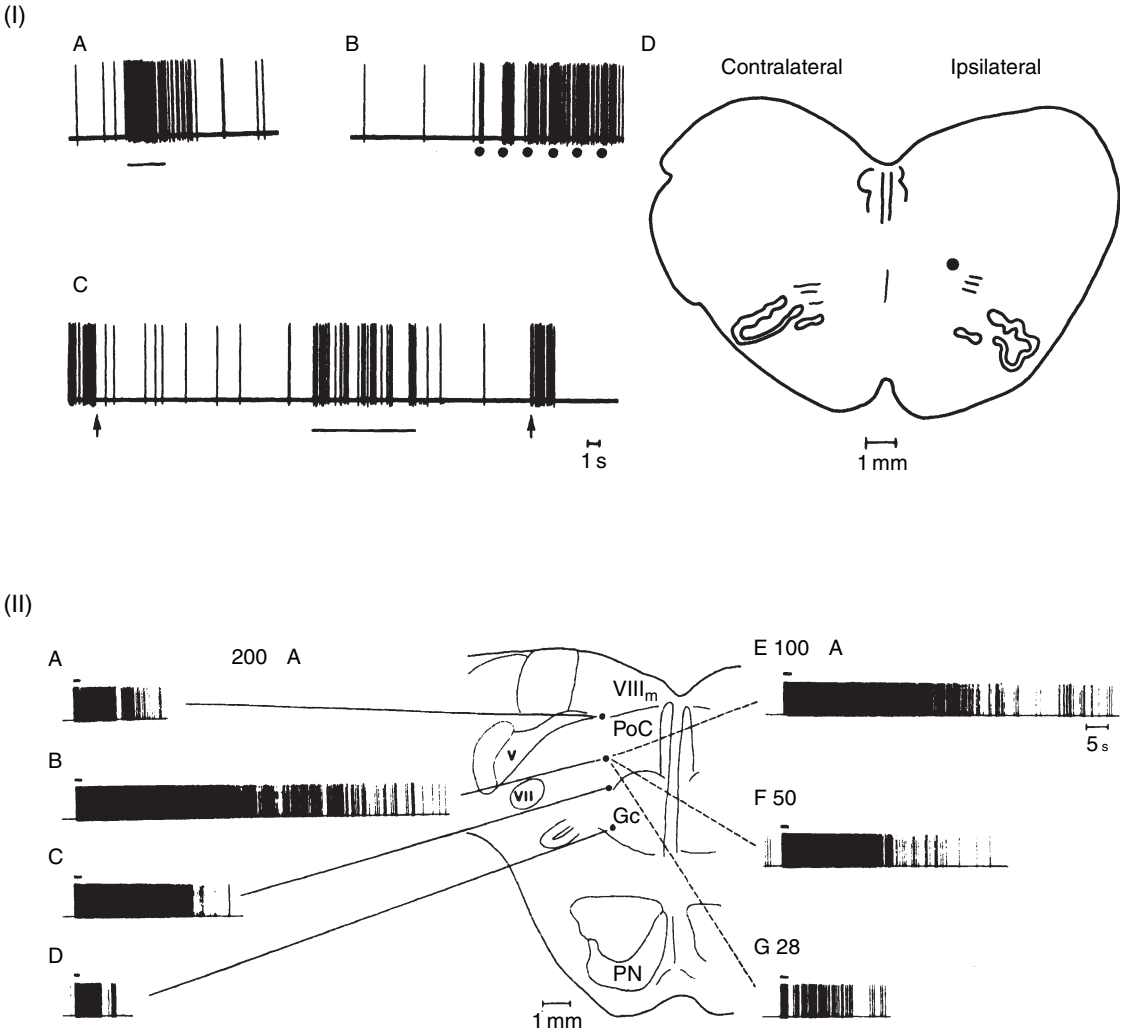

Figure 16 Excitation of primate spinothalamic tract (STT) cells by stimulation in the reticular formation. (I) Excitation and windup of excitation of a primate STT following stimulation in the nucleus reticularis gigantocellularis (NGc). A shows an excitatory burst followed by an after discharge in response to a train of stimuli in the NGc (50 μA, 333 Hz) during the period indicated by the horizontal bar. B shows windup produced by repetitive stimulation in the NGc (repeated 200-ms trains, 100 μA, 333 Hz). C shows that stimulation in the NGc (200 μA, 333 Hz) could interrupt the inhibition of the STT cell produced by squeezing the skin during the time between the two arrows. D is a drawing of a transverse section through the medulla showing the marked stimulus site (filled circle). (II) Long-lasting excitation of a medially projecting STT cell following stimulation in different parts of the pontine reticular formation of a monkey and at different strengths at one location. The drawing of a transverse section of the brainstem shows the locations of the nucleus pontis caudalis (PoC) and the nucleus gigantocellularis (Gc). The responses of STT cells at the left resulted from repetitive stimulation (200 μA, 0.1-ms pulses at 333 Hz) at the locations indicated (filled circles). The responses at the right were recorded from the point in the PoC in response to 100, 50, and 28 μA stimuli. (I) from Haber, L. H, *et al*., 1980. (II) From Giesler, G. J., Yezierski, R. P., Gerhart, K. D. and Willis, W.D. 1981. Spinothalamic tract neurons that project to medial and/or lateral thalamic nuclei: Evidence for a physiological novel population of spinal cord neurons. J. Neurophysiol. 46: 1285–1308.

Somatosensory information related to discriminative touch and proprioception is distributed contralaterally through a part of the trigeminothalamic tract that ascends adjacent to the medial lemniscus to the VPM thalamic nucleus, which then conveys somatosensory information to the face area of the somatosensory cortex. This arrangement for trigeminal sensations is comparable to the dorsal column–medial lemniscus pathway for the body. There is also a projection to the ipsilateral VPM nucleus. Pain and temperature (as well as crude touch) information is transmitted from the spinal

nucleus to the contralateral VPM nucleus through another component of the trigeminothalamic tract that ascends to the thalamus in a position adjacent to the STT. Nociceptive signals are also transmitted to the thalamus indirectly by the way of the reticular formation.

Visceral afferents, including those that supply taste buds, the carotid sinus and carotid body, and other visceral structures innervated by cranial nerves have their cell bodies in the geniculate ganglion of the facial nerve, the inferior ganglion of the glossopharyngeal nerve, or the inferior (nodosal) ganglion of the vagus nerve. They enter the brainstem through the facial (intermediate nerve), glossopharyngeal, and vagus nerves, and pass through the solitary tract to terminate in the nucleus of the solitary tract. Particular types of visceral afferents terminate in the corresponding subdivisions of the nucleus of the solitary tract (Blessing, W. W. *et al.*, 1999). Ascending projections from the solitary nucleus convey visceral information to nuclei that regulate the activity of the autonomic nervous system (Blessing, W. W., 1997; Ruggiero, D. A. *et al.*, 2000) and also to the parvocellular part of the VPM nucleus (VPMpo), which provides information about taste to the cerebral cortex.

6.06.3.2 Mechanoreceptor Circuits

6.06.3.2.1 Main sensory nucleus of V

LT mechanoreceptive afferents have been traced to their terminals in the main sensory nucleus and the subnucleus oralis of the spinal nucleus (Shigenaga, Y. *et al.*, 1990). Both rapidly and slowly adapting receptors that innervated either hairy or glabrous skin were included in the study. Many neurons in the main sensory nucleus have receptive fields on the lips (Arvidsson, J. *et al.*, 1991) or face. Some respond to activation of a single facial whisker or of groups of whiskers (Veinante, P. and Deschenes, M., 1999). Others discharge during mastication (as shown by experiments in which fictive mastication was elicited) and may contribute to the central pattern generator for mastication. Afferent input is from muscle spindles and periodontal receptors (Tsuboi, A. *et al.*, 2003; see also Tabata, T. and Karita, K., 1991).

6.06.3.2.2 Spinal nucleus of V

The axons of sensory neurons that innervate the lips in the rat terminate at several levels of the trigeminal nuclear complex, including not only the main sensory nucleus but also the subnuclei oralis, interpolaris, and caudalis of the spinal nucleus (Shigenaga, Y. *et al.*, 1990; Arvidsson, J. *et al.*, 1992). In addition, sensory axons descend in the spinal tract into the upper cervical spinal cord.

Some neurons in the subnucleus caudalis have been shown to respond in a rapidly adapting manner to hair movement or gentle tactile stimuli; others are activated by light touch and pressure, but the discharges are slowly adapting. These neurons are located in the magnocellular layer of the subnucleus caudalis, and their input is from Aβ afferent fibers (Price, D. D. *et al.*, 1976). Afferents that supply the mystacial vibrissae project to laminae III–V of the subnucleus caudalis and the dorsal horn at C1 (Arvidsson, J. and Rice, F. L., 1991).

6.06.3.2.3 Mesencephalic nucleus of V

Although neurons of the mesencephalic nucleus of V are the cell bodies of primary afferent neurons, they nevertheless receive synaptic input from neighboring nuclei (Verdier, D. *et al.*, 2004). Several different neurotransmitters have been identified in interneurons and in synaptic endings in the nucleus, including GABA and such peptides as galanin, neuropeptide Y, and CGRP (Lazarov, N. E., 2000). Synaptic input has been suggested to modulate the activity of the mesencephalic nucleus neurons, leading to synchronous firing. This may assist with rapid biting movements and with mastication of food. This arrangement of synapses on the cell bodies of primary afferent neurons is unusual, since such synapses do not occur on neuronal cell bodies in dorsal root ganglia or the trigeminal ganglion. Perhaps this unusual synapse formation is related to the fact that the cell bodies of the mesencephalic nucleus of V are in the CNS, rather than in the periphery.

6.06.3.3 Thermoreceptive Circuits

Burton H. *et al.* (1979) reported evidence about the processing of thermal information in the brainstem. They found neurons in the subnucleus caudalis of the trigeminal complex of cats that are thermoreceptive, as shown by their responses to cooling the tongue. These neurons were located in the marginal zone of the medullary dorsal horn, a position comparable to that of second-order thermoreceptive neurons in the spinal cord dorsal horn.

6.06.3.4 Nociceptive Circuits

6.06.3.4.1 Cutaneous pain

Responses of a monkey to noxious stimulation of the face were tested after destruction of the main sensory nucleus and the rostral part of the subnucleus oralis on one side (Lisney, S. J., 1985). Despite the lesion, there were no differences in the nociceptive responses on the two sides of the face, indicating that the rostral parts of the trigeminal sensory nuclear complex are unnecessary for nociception. It was concluded that the main synaptic connections made by facial nociceptive afferents are in the subnucleus caudalis. This is consistent with the presence of SP-containing synaptic terminals in laminae I and II of the subnucleus caudalis (Priestley, J. V. *et al.*, 1982). However, TRPV1 receptors are associated not only with small- and medium-sized neurons in the trigeminal ganglion but also with axons and their terminals in the main sensory nucleus and in the subnuclei oralis, interpolaris, and caudalis of the spinal nucleus. TRPV1 receptors are often colocalized with SP and CGRP (Bae, Y. C., *et al.*, 2004).

The relationship between the speed for detection by a monkey of a noxious heat stimulus applied to the face and the activity of medullary dorsal horn neurons was determined by Dubner R. *et al.* (1989; see also Kenshalo, D. R. *et al.*, 1989 and Maixner, W. *et al.*, 1989). The responses of WDR neurons correlated significantly with detection speed, whereas there was no correlation between the activity of NS neurons and the detection speed.

6.06.3.4.2 Corneal pain

The central terminals of afferent fibers that supply the cornea in monkeys have been traced using horseradish peroxidase (HRP) conjugated to wheatgerm agglutinin (WGA) (Marfurt, C. F. and Echtenkamp, S. F., 1988). Terminals were observed in all of the subdivisions of the trigeminal complex, but the density of the endings of corneal afferents varied. There was a heavy projection to the subnucleus interpolaris and the rostral part of subnucleus caudalis and a lighter projection to the main sensory nucleus, the subnucleus oralis, and the caudal part of the subnucleus caudalis.

The response properties of neurons that have corneal input and are located either in the transition zone between the subnucleus interpolaris and the caudalis or at the transition between the subnucleus caudalis and the cervical spinal cord were compared in experiments by Meng I. D. *et al.* (1997). Nociceptive neurons were classified as WDR, NS, or deep (D). All of the neurons recorded in the caudalis/spinal cord transition zone were WDR or NS, all responded to noxious thermal and mustard oil stimulation, most demonstrated diffuse noxious inhibitory controls (DNIC; see Le Bars, D. *et al.*, 1979a; 1979b), and most could be activated antidromically from the parabrachial area. However, over half of the neurons in the interpolaris/caudalis transition zone had no cutaneous receptive field; most of those that did were LT neurons, although some were WDR or D cells. Many failed to respond to thermal or mustard oil stimulation, few showed DNIC, and none could be activated antidromically from the parabrachial area. It was suggested that neurons in the two transition zones have distinct functions.

Many neurons in the subnuclei interpolaris and caudalis in rats show responses to stimulation of the surface of the cornea by CO_2 pulses. The responses were demonstrated either by increased expression of Fos protein (McEchron, M. D. *et al.*, 1996) or by changes in electrophysiological activity (Hirata, H. *et al.*, 1999). A large proportion of these neurons were also sensitive to mechanical stimulation. Interestingly, some of the neurons in the interpolaris and caudalis subnuclei responded to the CO_2 pulses only after the administration of morphine, whereas neurons in the transition zone between the caudalis nucleus and the C1 dorsal horn were inhibited by morphine (Hirata, H. *et al.*, 1999), and the inhibition could be reversed by naloxone. About one-third of the neurons in the caudalis/C1 transition could be activated antidromically from the contralateral thalamic posterior complex but not from VPM or the nucleus submedius; none of the units in the subnuclei interpolaris and caudalis region with corneal receptive fields could be activated antidromically from these thalamic nuclei. It was concluded that neurons in the caudalis/C1 transition zone that are responsive to corneal stimulation mediate ocular pain due to corneal irritation and that the corneal neurons in the subnuclei interpolaris and caudalis are likely to have some other function.

6.06.3.4.3 Joint pain

Afferents innervating the temporomandibular joint (TMJ) in cats were traced into the brainstem, using WGA–HRP (Capra, N, F., 1987). As in the case of corneal afferents, temporomandibular afferents project to all parts of the trigeminal complex. The greatest density of innervation was in the main sensory nucleus and the subnucleus oralis of the spinal

nucleus. Terminals were also found in laminae I–III of the subnucleus caudalis.

Inflammation induced by injection of complete Freund's adjuvant into TMJ resulted in significantly enhanced responses of WDR neurons in the medullary dorsal horn to mechanical stimuli (Iwata, K. *et al.*, 1999). Inflammation of the perioral skin also resulted in increased responses of these neurons, but was less effective than TMJ inflammation.

6.06.3.4.4 Dental pain

Injection of HRP into tooth pulp results in the labeling of afferent terminals in the main sensory nucleus and in the subnuclei oralis, interpolaris, and caudalis of the spinal trigeminal nucleus (Arvidsson, J. and Gobel, S., 1981; cf., Dong, W. K. *et al.*, 1990). Terminals in the medullary dorsal horn are in laminae I, II_{outer}, and V. HRP injected into the teeth of very young cats yields similar findings (Henry, M. A. and Westrum, L. E., 1990). In addition, cell bodies are also labeled in the mesencephalic nucleus of V. These presumably belong to mechanoreceptors. Electrical stimulation of the tooth pulp in human subjects can produce nonpainful sensations, as well as pain, depending on the stimulus parameters (McGrath, P. A. *et al.*, 1983). Therefore, some of the terminals of tooth pulp afferents in parts of the trigeminal complex may not relate to the processing of pain.

Park S. J. *et al.* (2001) found that application of mustard oil to the tooth pulp of a maxillary molar tooth in rats results in plastic changes in the activity of neurons of the subnucleus oralis similar to those seen in the subnucleus caudalis. There is an increase in spontaneous activity and receptive field size, and an increased sensitivity to mechanical stimuli in WDR, HT, and other nociceptive neurons, but not in LT neurons of the subnucleus oralis. These changes can be prevented by pretreatment with MK-801, an antagonist of *N*-methyl-D-aspartate (NMDA) receptors.

6.06.3.4.5 Meningeal pain

The dura is innervated by nociceptors belonging to the trigeminal nerve. As with nociceptors supplying other types of tissue, recordings from fine, mostly unmyelinated afferents that innervate the superior sagittal sinus and surrounding dura (Bove, G. M. and Moskowitz, M. A., 1997) show that these afferents respond to several modalities of stimulation, including mechanical, thermal, and chemical stimuli (capsaicin, inflammatory mediators, low pH). Application of inflammatory mediators, including lowered pH, to the dura enhances the sensitivity of nociceptive neurons in the subnucleus caudalis to mechanical stimulation of the dura and also to mechanical and thermal stimulation of the skin (Burstein, R. *et al.*, 1998). Ongoing activity develops in WDR and HT but not in LT neurons. Local anesthetic application to the dura blocks the responses to dural stimulation but not to cutaneous stimulation. Strassman A. M. and Levy D. (2006) confirmed that dural nociceptors exhibit chemosensitivity and showed that they can undergo peripheral sensitization.

6.06.3.5 Brainstem Projection Neurons

6.06.3.5.1 Trigeminothalamic neurons

Trigeminothalamic neurons can be identified by antidromic activation from the VPM and/or posterior thalamic nuclei (Price, D. D. *et al.*, 1976). Several classes of trigeminothalamic neurons can be recognized, based on their responses to mechanical stimulation. The classification scheme utilized applies both to trigeminothalamic cells and to presumed interneurons. Class 1 units have rapidly adapting responses to hair movement or light touch and are activated by Aβ afferents. Class 2 units have slowly adapting responses to light touch and pressure and are also activated by Aβ fibers. These two classes correspond to sets of LT neurons. Class 3 units are activated by light touch and pressure but maximally to pinch; these cells are excited by Aβ, Aδ, and C fibers and can also be classified as WDR neurons. Class 4 units respond to pressure and pinch and are excited by Aδ and sometimes C fibers. Class 5 units respond only to pinch and input is only from Aδ fibers. These two sets of neurons can also be classified as NS or HT cells. Receptive fields of the LT and HT neurons tend to be small, whereas the receptive fields of the WDR cells are large. HT neurons are prominent in the marginal zone of the subnucleus caudalis, although some WDR neurons are also found there, but no LT cells are. Instead, the LT cells are in the superficial part of the magnocellular layer. Deeper in this layer are WDR and HT cells.

Bushnell M. C. *et al.* (1984) confirmed that nociceptive trigeminothalamic tract neurons in the medullary dorsal horn include WDR and HT neurons. Both types of neuron respond to noxious heat stimuli. The responses are greater when associated with a thermal discrimination task, suggesting that

these neurons are involved in the discrimination of thermal stimuli.

Trigeminothalamic projections have been demonstrated by De Chazeron I. *et al.* (2004), using anterograde tracing with phaseolus vulgaris leucoagglutinin (PHA-L). The thalamic targets of these projections include the VPM nucleus and the posterior complex; in addition, terminals are found in the parvocellular part of VPM, suggesting that the subnucleus oralis is involved not only in the processing of somatosensory but also of gustatory information. Guy N. *et al.* (2005) confirmed by retrograde tracing in rats that trigeminothalamic neurons that project to the VPM nucleus and to the Po complex are located not only in the subnucleus caudalis but also in the subnucleus oralis.

Consistent with observations concerning the response properties of trigeminothalamic neurons, it has been reported that both WDR and HT neurons, as well as LT neurons, can be recorded in the VPM thalamic nucleus (Yokota, T. *et al.*, 1985; see also Bushnell, M. C. *et al.*, 1993; Tremblay, N. *et al.*, 1993). Furthermore, injections of lidocaine into the VPM nucleus in awake, behaving monkeys have shown that this nucleus is important for the perception of noxious and innocuous thermal stimuli, as well as for the detection of tactile stimuli (Duncan, D. H. *et al.*, 1993).

6.06.3.5.2 Trigeminoreticular neurons

Esser M. J. *et al.* (1998) did an anterograde tracing study in which biotinylated dextran was injected into the subnucleus caudalis. Dense labeling was found in several areas of the reticular formation and light labeling near the dendrites of catecholaminergic neurons in the C1, A1, and A5 regions. Injections into the dorsal medullary reticular formation resulted in dense labeling in the ventral medullary and pontine reticular formation, with numerous terminals near catecholaminergic neurons. It was suggested that reflex cardiovascular responses produced by painful stimulation in the trigeminal distribution involve indirect projections to the dorsal medullary and pontine reticular formation and connections from there to ventral medullary and pontine catecholaminergic neurons.

Krout K. E. *et al.* (2002) used retrograde tracing with cholera toxin subunit B to demonstrate projections from the brainstem reticular formation to intralaminar and midline nuclei of the thalamus in rats. The possible roles of the brainstem–thalamic pathways in arousal, somatosensory processing, and visceral control are discussed.

6.06.3.5.3 Trigeminoparabrachial neurons

Dallel R. *et al.* (2004) performed an anterograde tracing study that demonstrated projections from the subnucleus oralis of the spinal nucleus of the trigeminal nerve to the ipsilateral parabrachial nucleus and also to an area near the Kölliker-Fuse nucleus.

They suggest that these connections contribute to the processing of gustatory and nociceptive information. The dendrites of nociceptive parabrachial neurons have been shown to be located within the anterogradely labeled zones of termination of lamina I neurons of the medullary and spinal cord dorsal horns (Bourgeais, L. *et al.*, 2003).

6.06.3.5.4 Other trigeminal projection neurons

Iwata K. *et al.* (1998) performed an anterograde tracing study using injection of PHA-L into the medullary dorsal horn. Large injections resulted in labeling in the contralateral anterior pretectal area, superior colliculus, and the rostral linear raphe nucleus in the midbrain, as well as in the ipsilateral parabrachial nucleus. There were different labeling patterns when the label was injected into the SDH versus the DDH, indicating the presence of at least two different pathways.

6.06.3.6 Descending Control Systems

As for second-order somatosensory circuits in the spinal cord, brainstem somatosensory circuits are regulated by pathways that descend from higher levels of the brain. Corticobulbar projections influence these circuits, as well as do projections from the PAG and NRM (Sessle, B. J. *et al.*, 1981; Sunada, T. *et al.*, 1990). For example, electrical stimulation of the S II somatosensory cortex in rats was shown by Gojyo F. *et al.* (2002) to reduce the number of Fos-expressing neurons in the contralateral subnucleus caudalis following a bilateral injection of formalin into the lower lip. There are also descending projections from the parabrachial region to both the trigeminal sensory nuclei and the spinal cord dorsal horn. The parabrachial projections originate from the ventrolateral parabrachial area, including the Kölliker-Fuse nucleus and terminate in the main sensory nucleus and in the subnuclei oralis, interpolaris, and caudalis of the spinal nucleus, as well as in the spinal cord dorsal horn.

References

Al-Chaer, E. D., Lawand, N. B., Westlund, K. N., and Willis, W. D. 1996a. Visceral nociceptive input into the ventral posterolateral nucleus of the thalamus: A new function for the dorsal column pathway. J. Neurophysiol. 76: 2661–2674.

Al-Chaer, E. D., Lawand, N. B., Westlund, K. N., and Willis, W. D. 1996b. Pelvic visceral input into the nucleus gracilis is largely mediated by the postsynaptic dorsal column pathway. J. Neurophysiol. 76: 2675–2690.

Andrew, D. and Craig, A. D. 2001. Spinothalamic lamina I neurones selectively responsive to cutaneous warming in cats. J. Physiol. 537: 489–495.

Apkarian, A. V. and Hodge, C. J. 1989. The primate spinothalamic pathways: I. A quantitative study of the cells of origin of the spinothalamic pathway. J. Comp. Neurol. 288: 447–473.

Applebaum, A. E., Beall, J. E., Foreman, R. D., and Willis, W. D. 1975. Organization and receptive fields of primate spinothalamuc tract neurons. J. Neurophysiol. 38: 572–586.

Applebaum, A. E., Leonard, R. B., Kenshalo, D. R., Martin, R. F., and Willis, W. D. 1979. Nuclei in which functionally identified spinothalamic tract neurons terminate. J. Comp. Neurol. 188: 575–586.

Arvidsson, J. and Gobel, S. 1981. An HRP study of the central projections of primary trigeminal neurons which innervate tooth pulps in the cat. Brain Res. 210: 1–16.

Arvidsson, J. and Rice, F. L. 1991. Central projections of primary sensory neurons innervating different parts of the vibrissae follicles and intervibrissal skin on the mystacial pad of the rat. J. Comp. Neurol. 309: 1–16.

Arvidsson, J. and Thomander, L. 1984. An HRP study of the central course of sensory intermediate and vagal fibers in peripheral facial nerve branches in the cat. J. Comp. Neurol. 223: 35–45.

Arvidsson, J., Pfaller, K., and Gmeiner, S. 1992. The ganglionic origins and central projections of primary sensory neurons innervating the upper and lower lips in the rat. Somatosens. Mot. Res. 9: 199–209.

Bae, Y. C., Oh, J. M., Hwang, S. J., Shigenaga, Y., and Valtschanoff, J. G. 2004. Expression of vanilloid receptor TRPV1 in the rat trigeminal sensory nuclei. J. Comp. Neurol. 478: 62–71.

Barker, D. 1962. The structure and distribution of muscle receptors. In: (*ed*. D. Barker) Symposium on Muscle Receptors pp. 227–240. Hong Kong University Press.

Bennett, G. J., Seltzer, Z., Lu, G. W., Nishikawa, N., and Dubner, R. 1983. The cells of origin of the dorsal column postsynaptic projection in the lumbosacral enlargements of cats and monkeys. Somatosens. Res. 1: 131–149.

Bernard, J. F. and Besson, J. M. 1990. The spino (trigemino) pontoamygdaloid pathway: Electrophysiological evidence for an involvement in pain processes. J. Neurophysiol. 63: 473–489.

Bernard, J. F., Huang, G. F., and Besson, J. M. 1992. The nucleus centralis of the amygdala and the globus pallidus ventralis: electrophysiological evidence for an involvement in pain processes. J. Neurophysiol. 68: 551–569.

Bernard, J. F., Peschanski, M., and Besson, J. M. 1989. A possible spino (trigemino)-ponto-amygdaloid pathway for pain. Neurosci. Lett. 100: 83–88.

Bernard, J. F., Dallel, R., Raboisson, P., Villanueva, L., and Le Bars, D. 1995. Organization of the efferent projections from the spinal cervical enlargement to the parabrachial area and periaqueductal gray: a PHA-L study in the rat. J. Comp. Neurol. 353: 480–505.

Bessou, P., Burgess, P. R., Perl, E. R., and Taylor, C. B. 1971. Dynamic properties of mechanoreceptors with unmyelinated (C) fibers. J. Neurophysiol. 34: 116–131.

Blessing, W. W. 1997. The Lower Brainstem and Bodily Homeostasis, Oxford University Press.

Blessing, W. W., Yu, Y., and Nalivaiko, E. 1999. Medullary projections of rabbit carotid sinus nerve. Brain Res. 816: 405–410.

Blomqvist, A., Ericson, A. C., Craig, A. D., and Broman, J. 1996. Evidence for glutamate as a neurotransmitter in spinothalamic tract terminals in the posterior region of owl monkeys. Exp. Brain Res. 108: 33–44.

Blomqvist, A., Zhang, E. T., and Craig, A. D. 2000. Cytoarchitecture and immunohistochemical characterization of a specific pain and temperature relay, the posterior portion of the ventral medial nucleus, in the human thalamus. Brain 123: 601–619.

Bourgeais, L., Gauriau, C., Moncondut, L., Villanueva, L., and Bernard, J. F. 2003. Dendritic domains of nociceptive-responsive parabrachial neurons match terminal fields of lamina I neurons in the rat. J. Comp., Neurol. 464: 238–256.

Bove, G. M. and Moskowitz, M. A. 1997. Primary afferent neurons innervating guinea pig dura. J. Neurophysiol. 77: 299–308.

Brown, A. G. 1977. Cutaneous axons and sensory neurons in the spinal cord. Br. Med. Bull. 33: 109–112.

Brown, A. G. 1981. Organization in the Spinal Cord: The Anatomy and Physiology of Identified Neurones, Springer-Verlag.

Brown, A. G. and Franz, D. N. 1969. Responses of spinocervical tract neurons to natural stimulation of identified cutaneous receptors. Exp. Brain Res. 7: 231–249.

Brown, A. G. and Fyffe, R. E. W. 1978. The morphology of group Ia afferent fibre collaterals in the spinal cord of the cat. J. Physiol. 274: 111–127.

Brown, A. G. and Fyffe, R. E. W. 1979. The morphology of group Ib afferent fibre collaterals in the spinal cord of the cat. J. Physiol. 296: 215–228.

Brown, A. G. and Fyffe, R. E. W. 1981. Form and function of dorsal horn neurons with axons ascending the dorsal columns in cat. J. Physiol. 321: 31–47.

Brown, A. G. and Iggo, A. 1967. A quantitative study of the cutaneous receptors and afferent fibers in the cat and rabbit. J. Physiol. 193: 707–733.

Brown, A. G., Rose, P. K., and Snow, P. J. 1977. The morphology of hair follicle afferent fibre collaterals in the spinal cord of the cat. J. Physiol. 272: 779–797.

Brown, A. G., Rose, P. K., and Snow, P. J. 1978. Morphology and organization of axon collaterals from afferent fibres of slowly adapting type I units in cat spinal cord. J. Physiol. 277: 15–27.

Brown, P. B. 1969. Response of cat dorsal horn cells to variations of intensity, location, and area of cutaneous stimuli. Exp. Neurol. 23: 249–265.

Browne, K., Lee, J., and Ring, P. A. 1954. The sensation of passive movement at the metatarso-phalangeal joint of the great toe in man. J. Physiol. 126: 448–458.

Burgess, P. R., Petit, D., and Warren, R. M. 1968. Receptor types in cat hairy skin supplied by myelinated fibers. J. Neurophysiol. 31: 833–848.

Burke, D., Hagbarth, K. E., and Lofstedt, L. 1978. Muscle spindle activity in man during shortening and lengthening contractions. J. Physiol. 227: 131–142.

Burke, D., Hagbarth, K. E., Lofstedt, L., and Wallin, B. G. 1976. The responses of human muscle spindle endings to vibration during isometric contraction. J. Physiol. 261: 695–711.

Burke, R. E. and Glenn, L. L. 1996. Horseradish peroxidase study of the spatial and electrotonic distribution of group Ia synapses on type-identified ankle extensor motoneurons in the cat. J. Comp. Neurol. 372: 465–485.

Burstein, R. and Giesler, G. J. 1989. Retrograde labeling of neurons in spinal cord that project directly to nucleus accumbens or the septal nuclei in the rat. Brain Res. 497: 149–154.

Burstein, R., Cliffer, K. D., and Giesler, G. J. 1987. Direct somatosensory projections from the spinal cord to the hypothalamus and telencephalon. J. Neurisci. 7: 4159–4164.

Burstein, R., Cliffer, K. D., and Giesler, G. J. 1990. Cells of origin of the spinohypothalamic tract in the rat. J. Comp. Neurol. 291: 329–344.

Burstein, R., Dado, R. J., Cliffer, K. D., and Giesler, G. J. 1991. Physiological characterization of spinohypothalamic tract neurons in the lumbar enlargement of rats. J. Neurophysiol. 66: 261–284.

Burstein, R., Yamamura, H., Malick, A., and Strassmanm, A. M. 1998. Chemical stimulation of the intracranial dura induces enhanced responses to facial stimulation in brain stem trigeminal neurons. J. Neurophysiol. 79: 964–982.

Burton, H., Craig, A. D., Poulos, D. A., and Molt, J. T. 1979. Efferent projections from temperature sensitive recording loci within the marginal zone of the nucleus caudalis of the spinal trigeminal complex in the cat. J. Comp. Neurol. 183: 753–777.

Bushnell, M. C., Duncan, G. H., Dubner, R., and He, L. F. 1984. Activity of trigeminothalamic neurons in medullary dorsal horn of awake monkeys trained in a thermal discrimination task. J. Neurophysiol. 52: 170–187.

Bushnell, M. C., Duncan, G. H., and Tremblay, N. 1993. Thalamic VPM nucleus in the behaving monkey. I. Multimodal and discriminative properties of thermosensitive neurons. J. Neurophyiol. 69: 739–752.

Capra, N. F. 1987. Localization and central projections of primary afferent neurons that innervate the temporomandibular joint in cats. Somatosens. Res. 4: 201–213.

Carlton, S. M., Westlund, K. N., Zhang, D. X., Sorkin, L. K. S., and Willis, W. D. 1990. Calcitonin gene-related peptide containing primary afferent fibers synapse on primate spinothalamic tract cells. Neurosci. Lett. 109: 76–81.

Carlton, S. M., Westlund, K. N., Zhang, D., and Willis, W. D. 1992. GABA-immunoreactive terminals synapse on primate spinothalamic tract cells. J. Comp. Neurol. 322: 528–537.

Carpenter, M. B. and Sutin, J. 1983. Human Neuroanatomy, 8th edn., Williams and Wilkins.

Caterina, M. J. and Julius, D. 2001. The vanilloid receptor: A molecular gateway to the pain pathway. Annu. Rev. Neurosci. 24: 487–517.

Cervero, F. and Morrison, J.F.B. (eds.) (1986) Visceral Sensation. Progress in Brain Research Vol. 67. Elsevier.

Cervero, F. and Sann, H. 1989. Mechanically evoked responses of afferent fibres innervating the guinea-pig's ureter: An *in vitro* study. J. Physiol. 412: 245–266.

Cervero, F., Iggo, A., and Molony, V. 1977. Responses of spinocervical tract neurons to noxious stimulation of the skin. J. Physiol. 267: 537–558.

Christensen, B. N. and Perl, E. R. 1970. Spinal neurons specifically excited by noxious or thermal stimuli: Marginal zone of the dorsal horn. J. Neurophysiol. 33: 293–307.

Chung, J. M., Kenshalo, D. R., Gerhart, K. D., and Willis, W. D. 1979. Excitation of primate spinothalamic neurons by cutaneous C-fiber volleys. J. Neurophysiol. 42: 1354–1369.

Chung, M. K., Lee, H., Mizuno, A., Suzuki, M., and Caterina, M. J. 2004. TRPV3 and TRPV4 mediate warmth-evoked currents in primary mouse keratinocytes. J. Biol. Chem. 279: 21569–21575.

Clark, F. J., Horch, K. W., Bach, S. M., and Larsen, G. F. 1979. Contributions of cutaneous and joint receptors to static knee-position sense in man. J. Neurophysiol. 42: 877–888.

Cliffer, K. D., Burstein, R., and Giesler, G. J. 1991. Distribution of spinothalamic, spinohypothalamic, and spinotelencephalic fibers revealed by anterograde transport of PHA-L in rats. J. Neurosci. 11: 852–868.

Cliffer, K. D., Hasegawa, T., and Willis, W. D. 1992. Responses of neurons in the gracile nucleus of cats to innocuous and noxious stimuli: Basic Characterization and antidromic activation from the thalamus. J. Neurophysiol. 68: 818–832.

Courtney, K., Brengelman, K., and Sundsten, J. W. 1972. Evidence for spinal cord unit activity responsive to peripheral warming in the primate. Brain Res. 43: 657–661.

Craig, A. D. 2004. Distribution of trigeminothalamic and spinothalamic lamina I terminations in the macaque monkey. J. Comp. Neurol. 477: 119–148.

Craig, A. D. and Kniffki, K. D. 1985. Spinothalamic lumbosacral lamina I cells responsive to skin and muscle stimulation in the cat. J. Physiol. 365: 197–221.

Craig, A. D., Bushnell, M. C., Zhang, E. T., and Blomqvist, A. 1994. A thalamic nucleus specific for pain and temperature sensation. Nature 372: 770–773.

Craig, A. D., Krout, K., and Andrew, D. 2001. Quantitative response characteristics of thermoreceptive and nociceptive lamina I spinthalamic neurons in the cat. J. Neurophysiol. 86: 1459–1480.

Dallel, R., Ricard, O., and Raboisson, P. 2004. Organization of parabrachial projections from the spinal trigeminal nucleus oralis: an anterograde tracing study in the rat. J. Comp. Neurol. 470: 181–191.

Dallenbach, K. M. 1927. The temperature spots and end-organs. Am. J. Psychol. 39: 402–427.

Darian-Smith, I. 1984. The sense of touch: performance and peripheral neural processes. In: (*eds*. J. M. Brookhart and V. B. Mountcastle), Handbook of Physiology, Section 1: The Nervous System, Vol. III, Sensory Processes, Part 2, pp. 739–788. American Physiological Soc, Bethesda.

De Chazeron, I., Raboisson, P., and Dallel, R. 2004. Organization of diencephalic projections from the spinal trigeminal nucleus oralis: an anterograde tracing study in the rat. Neuroscience 127: 921–928.

Depaulis, A. and Bandler, R. (eds.) (1991). The Midbrain Periaqueductal Gray Matter: Functional, Anatomical, and Neurochemical Organization. Plenum.

Dong, W. K., Chudler, E. H., and Kawakami, Y. 1990. Tooth pulp-evoked potentials in the trigeminal brainstem nuclear complex. Brain Res. 529: 131–142.

Dostrovsky, J. O. and Craig, A. D. 1996. Cooling-specific spinothalamic tract neurons in the monkey. J. Neurophysiol. 76: 3656–3665.

Dubner, R., Kenshalo, D. R., Maixner, W., Bushnell, M. C., and Oliveras, J. L. 1989. The correlation of monkey medullary dorsal horn neuronal activity and the perceived intensity of noxious heat stimuli. J. Neurophysiol. 62: 450–457.

Duncan, G. H., Bushnell, M. C., Oliveras, J., Bastrash, N., and Tremblay, N. 1993. Thalamic VPM nucleus in the behaving monkey. III. Effects of reversible inactivation by lidocaine on thermal and mechanical discrimination. J. Neurophysiol. 70: 2086–2096.

Eccles, J. C. 1964. The Physiology of Synapses, Springer.

Eccles, R. M. 1965. Interneurons activated by higher threshold group I muscle afferents. In: (*eds*. D. R. Curtis and A. K. McIntyre) Studies in Physiology, pp. 59–64. Springer, New York.

Ericson, A. C., Blomqvist, A., Craig, A. D., Ottersen, O. P., and Broman, J. 1995. Evidence for glutamate as neurotransmitter in trigemino- and spinothalamic tract terminals in the nucleus submedius of cats. Eur. J. Neurosci. 7: 305–317.

Esser, M. J., Pronych, S. P., and Allen, G. V. 1998. Trigeminal-reticular connections: possible pathways for nociception-induced cardiovascular reflex responses in the rat. J. Comp. Neurol. 391: 526–544.

Fang, L., Wu, J., Lin, Q., and Willis, W. D. 2003. Protein kinases regulate the phosphorylation of the GluR1 subunit of AMPA receptors of spinal cord in rats following noxious stimulation. Mol. Brain Res. 118: 160–165.

Ferrell, W. R. and Smith, A. 1987. The effect of digital nerve block on position sense at the proximal interphalangeal joint of the human index finger. Brain Res. 425: 369–371.

Ferrington, D. G., Downie, J. W., and Willis, W. D. 1988. Primate nucleus gracilis neurons: responses to innocuous and noxious stimuli. J. Neurophysiol. 59: 886–907.

Ferrington, D. G., Sorkin, L. S., and Willis, W. D. 1987. Responses of spinothalamic tract cells in the superficial dorsal horn of the primate lumbar spinal cord. J. Physiol. 388: 681–703.

Fields, H.L. Besson, J.M. (eds.) 1988. Pain Modulation. In: Progress in Brain Research, Vol. 77, Elsevier.

Foerster, O. and Gagel, O. 1932. Die Vorderseitenstrangdurchschneidung beim Menschen: Eine klinisch-pathophysiologisch-anatomische Studie. Z. Ges. Neurol. Psychia 138: 1–92.

Fyffe, R. E. W. 1979. The morphology of group II muscle afferent fibre collaterals. J.Physiol. 296: 39–40.

Gandevia, S. C. 1985. Illusory movements produced by electrical stimulation of low-threshold muscle afferents from the hand. Brain 108: 965–981.

Gandevia, S. C., Hall, L. A., McCloskey, D. I., and Potter, E. K. 1983. Proprioceptive sensation at the terminal joint of the middle finger. J. Physiol. 335: 507–517.

Gandevia, S. C., McCloskey, D. I., and Burke, D. 1992. Kinaesthetic signals and muscle contraction. Trends Neurosci. 15: 62–65.

Gebhart, G.F. (ed.) 1995. Visceral Pain. Progress in Pain Research and Management, Vol. 5, IASP Press, Seattle.

Gerhart, K. D., Yezierski, R. P., Wilcox, T. K., and Willis, W. D. 1984. Inhibition of primate spinothalamic tract neurons by stimulation in periaqueductal gray of midbrain reticular formation. J. Neurophysiol. 51: 450–466.

Giamberardino, M. A., Valente, R., de Bigotina, P., and Vecchiet, L. 1995. Artificial ureteral calculosis in rats: behavioural characterization of visceral pain episodes and their relationship with referred lumbar muscle hyperalgesia. Pain 61: 459–469.

Giesler, G. J., Yezierski, R. P., Gerhart, K. D., and Willis, W. D. 1981. Spinothalamic tract neurons that project to medial and/or lateral thalamic nuclei: Evidence for a physiological novel population of spinal cord neurons. J. Neurophysiol. 46: 1285–1308.

Gojyo, F., Sugiyo, S., Kuroda, R., Kawabata, A., Varathan, V., Shigenaga, Y., and Takemura, M. 2002. Effects of somatosensory cortical stimulation on expression of c-Fos in rat medullary dorsal horn in response to formalin-induced noxious stimulation. J. Neurosci. Res. 68: 479–488.

Gold, M. S., Levine, J. D., and Correa, A. M. 1998. Modulation of TTX-R I_{Na} by PKC and PKA and their role in PGE_2-induced sensitization of rat sensory neurons *in vitro*. J. Neurosci. 18: 10345–10355.

Gold, M. S., Reichling, D. B., Schuster, M. J., and Levine, J. D. 1996. Hyperalgesic agents increase a tetrodotoxin-resistant Na^+ current in nociceptors. PNAS USA, 93: 1108–1112.

Goodwin, G. M., McCloskey, D. I., and Matthews, P. B. C. 1972a. The persistence of appreciable kinesthesia after paralyzing joint afferents but preserving muscle afferents. Brain Res. 37: 326–329.

Goodwin, G. M., McCloskey, D. I., and Matthews, P. B. C. 1972b. The contribution of muscle afferents to kinaesthesia shown by vibration induced illusions of movement and by the effects of paralyzing joint afferents. Brain 95: 705–748.

Grant, G., Boivie, J., and Silfvenius, H. 1973. Course and termination of fibres from the nucleus z of the medulla oblongata. An experimental light microscopical study in the cat. Brain Res. 55: 55–70.

Graziano, A. and Jones, E. G. 2004. Widespread thalamic terminations of fibers arising in the superficial medullary dorsal horn of monkeys and their relation to calbindin immunoreactivity. J. Neurosci. 24: 248–256.

Grigg, P., Finerman, G. A., and Riley, L. H. 1973. Joint-position sense after total hip replacement. J. Bone Joint Surg. 55A: 1016–1025.

Guinard, D., Usson, Y., Guillermet, C., and Saxod, R. 1998. Merkel complexes of human digital skin: Three-dimensional imaging with confocal laser microscopy and double immunofluoresecnce. J. Comp. Neurol. 398: 98–104.

Guy, N., Chalis, M., Dallel, R., and Voisin, D. L. 2005. Both oral and caudal parts of the spinal trigeminal nucleus project to the somatosensory thalamus in the rat. Eur. J. Neurosci. 21: 741–754.

Gybels, J. M. and Sweet, W. H. 1989. Neurosurgical Treatment of Persistent Pain. Karger, Basel.

Häbler, H. J., Jänig, W., and Koltzenburg, M. 1993. Receptive properties of myelinated primary afferents innervating the inflamed urinary bladder of the cat. J. Neurophysiol. 69: 395–405.

Haber, L. H., Martin, R. F., Chung, J. M., and Willis, W. D. 1980. Inhibition and excitation of primate spinothalamic tract neurons by stimulation in region of nucleus reticularis gigantocellularis. J. Neurophysiol. 43: 1578–1593.

Hagbarth, K. E. and Vallbo, A. B. 1968. Discharge characteristics of human muscle afferents during muscle stretch and contraction. Exp. Neurol. 22: 674–694.

Hagbarth, K. E. and Vallbo, A. B. 1969. Single unit recordings from muscle nerves in human subjects. Acta Physiol. Scand. 76: 321–334.

Hagbarth, K. E., Hongel, A., Hallin, R. G., and Torebjörk, H. E. 1970. Afferent impulses in median nerve fascicles evoked by tactile stimuli of the human hand. Brain Res. 24: 423–442.

Hagbarth, K. E., Wallin, G., and Lofstedt, L. 1975. Muscle spindle activity in man during voluntary fast alternating movements. J. Neurol. Neurosurg. Psychiat. 38: 625–635.

Halata, Z. 1993. Sensory innervation of the hairy skin (light- and electron-microscopic study). J. Invest. Dermatol. 101: 75S–81S.

Han, Z. S., Zhang, E. T., and Craig, A. D. 1998. Nociceptive and thermoreceptive lamina I neurons are anatomically distinct. Nature neurosci. 1: 218–225.

Hayes, R. L., Price, D. D., Ruda, M. A., and Dubner, R. 1979. Suppression of nociceptive responses in the primate by electrical stimulation of the brain or morphine administration: Behavioral and electrophysiological comparisons. Brain Res. 167: 417–421.

Henry, M. A. and Westrum, L. E. 1990. Central representation of dental structures in the kitten, including projections to the mesencephalic trigeminal nucleus. Somatosens Mot. Res. 7: 447–462.

Hensel, H. 1974. Thermoreceptors. Ann. Rev. Physiol. 36: 233–249.

Hensel, H. and Boman, K. K. A. 1960. Afferent impulses in cutaneous sensory nerves in human subjects. J. Neurophysiol. 23: 564–578.

Hensel, H. and Zotterman, Y. 1951. The effect of menthol on the thermoreceptors. Acta Physiol. Scand. 24: 27–34.

Hirata, H., Hu, J. W., and Bereiter, D. A. 1999. Responses of medullary dorsal horn neurons to corneal stimulation by CO_2 pulses in the rat. J. Neurophyiol. 82: 2092–2107.

Hirshberg, R. M., Al-Chaer, E. D., Lawand, N. B., Westlund, K. N., and Willis, W. D. 1996. Is there a pathway in the posterior funiculus that signals visceral pain? Pain 67: 291–305.

Honda, C. N. 1985. Visceral and somatic afferent convergence onto neurons near the central canal in the sacral spinal cord of the cat. J. Neurophysiol. 53: 1059–1078.

Hongo, T., Kitazawa, S., Ohki, Y., Sasaki, M., and Xi, M. C. 1989a. A physiological and morphological study of premotor interneurones in the cutaneous reflex pathways in cats. Brain Res. 505: 163–166.

Hongo, T., Kitazawa, S., Ohki, Y., and Xi, M. C. 1989b. Functional identification of last-order interneurones of skin reflex pathways in the cat forelimb segments. Brain Res. 505: 167–170.

Horch, K. W., Clark, F. J., and Burgess, P. R. 1975. Awareness of knee joint angle under static conditions. J. Neurophysiol. 38: 1436–1447.

Iggo, A. 1960. Cutaneous mechanoreceptors with afferent C fibres. J. Physiol. 152: 337–353.

Iggo, A. and Ramsey, R. L. 1976. Thermosensory mechanisms in the spinal cord of monkeys. In: (*ed*. Y. Zotterman) Sensory Functions of the Skin in Primates with Special Reference to Man, pp. 285–304. Pergamon.

Iwata, K., Tashiro, A., Tsuboi, Y., Imai, T., Sumino, R., Morimoto, T., Dubner, R., and Ren, K. 1999. Medullary dorsal horn neuronal activity in rats with persistent temporomandibular joint and perioral inflammation. J. Neurophysiol. 82: 1244–1253.

Iwata, K., Tsuboi, Y., Tashiro, A. S., Sakamoto, M., Hagiwara, S., Kohno, M., and Sumino, R. 1998. Mesencephalic projections from superficial and deep laminae of the medullary dorsal horn. J. Oral Sci. 40: 159–163.

Jabbur, S. J. and Towe, A. L. 1961. Cortical excitation of neurons in dorsal column nuclei of cat, including an analysis of pathways. J. Neurophysiol. 24: 499–509.

Jänig, W. and Koltzenburg, M. 1991. Receptive properties of sacral primary afferent neurons supplying the colon. J. Neurophysiol. 65: 1067–1077.

Järvilehto, T., Hämäläinen, H., and Soininen, K. 1981. Peripheral neural basis of tactile sensations in man: II. Characteristics of human mechanoreceptors in the hairy skin and correlations of their activity with tactile sensations. Brain Res. 219: 13–27.

Johannson, O., Fantini, F., and Hu, H. 1999. Neuronal structural proteins, transmitters, transmitter enzymes and neuropeptides in human Meissner's corpuscles: A reappraisal using immunohistochemistry. Arch. Dermatol. Res. 291: 419–424.

Johansson, R. S. 1978. Tactile sensibility in the human hand: Receptive field characteristics of mechanoreceptive units in the glabrous skin area. J. Physiol. 281: 101–123.

Johansson, R. S. and Vallbo, A. B. 1979a. Tactile sensibility in the human hand: Relative and absolute densities of four types of mechanoreceptive units in glabrous skin. J. Physiol. 286: 283–300.

Johansson, R. S. and Vallbo, A. B. 1979b. Detection of tactile stimuli: Threshold of afferent units related to psychophysical thresholds of the human hand. J. Physiol. 297: 405–422.

Kamogawa, H. and Bennett, G. J. 1986. Dorsal column postsynaptic neurons in the cat are excited by myelinated nociceptors. Brain Res. 364: 386–390.

Kanui, T. I. 1988. Receptive field organization and electrophysiological responses of spinal cord thermoreactive neurons in the rat. Exp. Brain Res. 71: 508–514.

Katter, J. T., Burstein, R., and Giesler, G. J. 1991. The cells of origin of the spinohypothalamic tract in cats. J. Comp. Neurol. 303: 101–112.

Kenshalo, D. R. and Scott, H. A. 1966. Temporal course of thermal adaptation. Science 151: 1095–1096.

Kenshalo, D. R., Anton, F., and Dubner, R. 1989. The detection and perceived intensity of noxious thermal stimuli in monkey and in human. J. Neurophysiol. 62: 429–436.

Kenshalo, D. R., Leonard, R. B., Chung, J. M., and Willis, W. D. 1979. Responses of primate spinothalamic neurons to graded and to repeated noxious heat stimuli. J. Neurophysiol. 42: 1370–1389.

Kevetter, G. A., Haber, L. H., Yezierski, R. P., Chung, J. M., Martin, R. F., and Willis, W. D. 1982. Cells of origin of the spinoreticular tract in the monkey. J. Comp. Neurol. 207: 61–74.

Knibestöl, M. 1975. Stimulus-response functions of slowly adapting mechanoreceptors in the human glabrous skin area. J. Physiol. 245: 63–80.

Konietzny, F., Perl, E. R., Trevino, D., Light, A., and Hensel, H. 1981. Sensory experiences in man evoked by intraneural electrical stimulation of intact cutaneous afferent fibers. Exp. Brain Res. 42: 219–222.

Krout, K. E., Belzer, R. E., and Loewy, A. D. 2002. Brainstem projections to midline and intralaminar thalamic nuclei of the rat. J. Comp. Neurol. 448: 53–101.

Kumazawa, T. and Perl, E. R. 1976. Differential excitation of dorsal horn marginal and substantia gelatinosa neurons by primary afferent units with fine (A-delta and C) fibers. In: (*ed*. Y. Zotterman) Sensory Functions of the Skin with Especial Reference to Man, pp. 67–89. Pergamon.

Kumazawa, T., Perl, E. R., Burgess, P. R., and Whitehorn, D. 1975. Ascending projections from marginal zone (lamina I) neurons of the spinal dorsal horn. J. Comp. Neurol. 162: 1–12.

LaMotte, R. H., Shain, C. N., Simone, D. A., and Tsai, E. F. P. 1991. Neurogenic hyperalgesia: Psychophysical studies of underlying mechanisms. J. Nuerophysiol. 66: 190–211.

Landgren, S. and Silfvenius, H. 1971. Nucleus z, the medullary relay in the projection path to the cerebral cortex of group I muscle afferents from the cat's hind limb. J. Physiol. 218: 551–571.

Landgren, S., Silfvenius, H., and Wolsk, D. 1967. Somato-sensory paths to the second cortical projection area of the group I muscle afferents. J. Physiol. 191: 543–559.

Lazarov, N. E. 2000. The mesencephalic trigeminal nucleus n the cat. Adv. Anat. Embryol. Cell Biol. 153: 1–103.

Le Bars, D., Dickenson, A. H., and Besson, J. M. 1979a. Diffuse noxious inhibitory controls (DNIC): I Effects on dorsal horn convergent neurons in the rat. Pain 6: 283–304.

Le Bars, D., Dickenson, A. H., and Besson, J. M. 1979b. Diffuse noxious inhibitory controls (DNIC): II. Lack of effect on non-convergent neurons, supraspinal involvement and theoretical implications. Pain 6: 305–327.

Lennander, K. G. 1907. Abdominal pain, especially pain in connection with ileus. JAMA, p. 1013.

Lenz, F. A., Gracely, R. H., Hope, E. J., Baker, F. H., Rowland, L. H., Dougherty, P. M., and Richardson, R. T. 1994. The sensation of angina can be evoked by stimulation of the human thalamus. Pain 59: 119–125.

Lenz, F. A., Seike, M., Richardson, R. T., Lin, Y. C., Baker, F. H., Khoja, I., Jaeger, C. J., and Gracely, R. H. 1993. Thermal and pain sensations evoked by microstimulation in the area of human ventrocaudal nucleus. J. Neurophysiol. 70: 200–212.

Light, A. R. and Perl, E. R. 1979. Spinal termination of functionally identified primary afferent neurons with slowly conducting myelinated fibers. J. Comp. Neurol. 186: 133–150.

Lisney, S. J. 1985. Observations on facial nociception in a monkey after destruction of the rostral part of the trigeminal sensory nuclear complex. Pain 21: 129–135.

Lucas, M. E. and Willis, W. D. 1974. Identification of muscle afferents which activate interneurons in the intermediate nucleus. J. Neurophysiol. 37: 282–293.

Macefield, G., Gandevia, S. C., and Burke, D. 1990. Perceptual responses to microstimulation of single afferents innervating joints, muscles and skin of the human hand. J. Physiol. 429: 113–129.

Magherini, P. C., Pompeiano, O., and Seguin, J. J. 1974. The responses of nucleus z neurons to sinusoidal stretch of hindlimb extensor muscles. Brain Res. 73: 343–349.

Maixner, W., Dubner, R., Kenshalo, D. R., Bushnell, M. C., and Oliveras, J. L. 1989. Responses of monkey medullary dorsal horn neurons during the detection of noxious heat stimuli. J. Neurophysiol. 62: 437–449.

Marchetinni, P., Simone, D. A., Caputi, G., and Ochoa, J. L. 1996. Pain from excitation of identified muscle nociceptors in humans. Brain Res. 740: 109–116.

Marfurt, C. F. and Echtenkamp, S. F. 1988. Central projections and trigeminal ganglion location of corneal afferent neurons in the monkey, *Macaca fascicularis*. J. Comp. Neurol. 272: 370–382.

Matthews, P. B. C. 1972. Mammalian Muscle Receptors and Their Central Actions, Williams and Wilkins.

Mayer, D. J., Price, D. D., and Becker, D. P. 1975. Neurophysiological characterization of the anterolateral spinal cord neurons contributing to pain perception in man. Pain 1: 51–58.

McCloskey, D. I. 1973. Differences between the senses of movement and position shown by the effects of loading and vibration of muscles in man. Brain Res. 63: 119–131.

McCloskey, D. I., Cross, M. J., Honner, R., and Potte, E. K. 1983. Sensory effects of pulling or vibrating exposed tendons in man. Brain 106: 21–37.

McEchron, M. D., McCabe, P. M., Green, E. J., Hitchcock, J. M., and Schneiderman, N. 1996. Immunohistochemical expression of the c-Fos protein in the spinal trigeminal nucleus following presentation of a corneal airpuff stimulus. Brain Res. 710: 112–120.

McGrath, P. A., Gracely, R. H., Dubner, R., and Heft, M. W. 1983. Non-pain and pain sensations evoked by tooth pulp stimulation. Pain 15: 377–388.

McIntyre, A. K., Proske, U., and Rawson, J. A. 1985. Pathway to the cerebral cortex for impulses from tendon organs in the cat's hindlimb. J. Physiol. 369: 115–126.

McKemy, D. D., Neuhausser, W. M., and Julius, D. 2002. Identification of a cold receptor reveals a general role for TRP channels in thermosensation. Nature 416: 52–58.

Mendell, L. M. 1966. Physiological properties of unmyelinated fiber projection to the spinal cord. Exp. Neurol. 16: 316–332.

Menétrey, D., Gannon, J. D., Levine, J. D., and Basbaum, A. I. 1989. Expression of c-fos protein in interneurons and projection neurons of the rat spinal cord in response to noxious somatic, articular, and visceral stimulation. J. Comp. Neurol. 285: 177–195.

Meng, I. D., Hu, J. W., Benetti, A. P., and Bereiter, D. A. 1997. Encoding of corneal input in two distinct regions of the spinal trigeminal nucleus in the rat: cutaneous receptive field properties, responses to thermal and chemical stimulation, modulation by diffuse noxious inhibitory controls, and projections to the parabrachial area. J. Neurophysiol. 77: 43–56.

Meyer, R. A. and Campbell, J. N. 1981. Myelinated nociceptive afferents account for the hyperalgesia that follows a burn to the hand. Science 213: 1527–1529.

Michaelis, M., Häbler, H. J., and Jänig, W. 1996. Silent afferents: A separate class of primary afferents? Clin. Exp. Pharmacol. Physiol. 23: 99–105.

Mountcastle, V. B., LaMotte, R. H., and Carli, G. 1972. Detection threshold for stimuli in humans and monkeys: Comparison with threshold events in mechanoreceptive afferent nerve fibers innervating the monkey hand. J. Neurophysiol. 35: 122–136.

Mountcastle, V. B., Talbot, W. H., and Kornhuber, H. H. 1966. The neural transformation of mechanical stimuli delivered to the monkey's hand. In: (*eds*. A. V. S. de Reuck and J. Knight) Touch, Heat and Pain, pp. 325–345. Churchill.

Nasution, I. D. and Shigenaga, Y. 1987. Ascending and descending internuclear projections within the trigeminal sensory nuclear complex. Brain Res. 425: 234–247.

Nauta, H. J. W., Soukup, V. M., Fabian, R. H, Lin, J. T., Grady, J. J., Williams, C. G. A., Campbell, G. A., Westlund, K. N., and Willis, W. D. 2000. Punctate mid-line myelotomy for the relief of visceral cancer pain. J. Neurosurg. (Spine I) 92: 125–130.

Ness, T. J and Gebhart, G. F. 1987. Characterization of neuronal responses to noxious visceral and somatic stimuli in the medial lumbosacral spinal cord of the rat. J. Neurophysiol. 57: 1867–1892.

Ness, T. J., Metcalf, A., and Gebhart, G. F. 1990. A psychophysical study in humans using phasic colonic distension as a noxious visceral stimulus. Pain 43: 377–386.

Nolte, J. 2002. The Human Brain: An Introduction to its Functional Anatomy, 5th edn., St. Louis, Mosby.

Noordenbos, W. and Wall, P. D. 1976. Diverse sensory functions with an almost totally divided spinal cord: A case of spinal cord transaction with preservation of part of one anterolateral quadrant. Pain 2: 185–195.

Nordin, M. 1990. Low-threshold mechanoreceptive and nociceptive units with unmyelinated (C) fibres in the human supraorbital nerve. J. Physiol. 426: 229–240.

Ochoa, J. and Torebjörk, E. 1983. Sensations evoked by intraneural microstimulation of single mechanoreceptor units innervating the human hand. J. Physiol. 342: 633–654.

Ochoa, J. and Torebjörk, E. 1989. Sensations evoked by intraneural microstimulation of C nociceptor fibres in human skin nerves. J. Physiol. 415: 583–599.

Owens, C. M., Zhang, D., and Willis, W. D. 1992. Changes in the response states of primate spinothalamic tract cells caused by mechanical damage of the skin or activation of descending controls. J. Neurophysiol. 67: 1509–1527.

Paré, M., Elde, R., Mazurkiewicz, J. E., Smith, A. M., and Rice, F. L. 2001. The Meissner corpuscle revised: A multiafferented mechanoreceptor with nociceptor immunochemical properties. J. Neurosci. 21: 7236–7246.

Paré, M., Smith, A. M., and Rice, F. L. 2002. Distribution and terminal arborizations of cutaneous mechanoreceptors in the glabrous finger pads of the monkey. J. Comp. Neurol. 445: 347–359.

Park, S. J., Chiang, C. Y., Hu, J. W., and Sessle, B. J. 2001. Neuroplasticity induced by tooth pulp stimulation in trigeminal subnucleus oralis involves NMDA receptor mechanisms. J. Neurophysiol. 85: 1836–1846.

Patapoutian, A., Peier, A. M., Story, G. M., and Viswaneth, V. 2003. ThermoTRP channels and beyond: mechanisms of temperature sensation. Nature Rev. Neurosci. 4: 529–539.

Peier, A. M., Moqrich, A., Hergarden, A. C., Reeve, A. J., Andersson, D. A., Story, G. M., Earley, T. J., Dragoni, I., McIntyre, P., Bevan, S., and Patapoutian, A. 2002. A TRP channel that senses cold stimuli and menthol. Cell 108: 705–715.

Perl, E. R. 1968. Myelinated afferent fibres innervating the primate skin and their response to noxious stimuli. J. Physiol. 197: 593–615.

Pompeiano, O. and Brodal, A. 1957. Spino-vestibular fibers in the cat. An experimental study. J. Comp. Neurol. 108: 353–382.

Price, D. D., Dubner, R., and Hu, J. W. 1976. Trigeminothalamic neurons in nucleus caudalis responsive to tactile, thermal, and nociceptive stimulation of monkey's face. J. Neurophysiol. 39: 936–953.

Price, D. D., Hayes, R. L., Ruda, M., and Dubner, R. 1978. Spatial and temporal transformations of input to spinothalamic tract neurons and their relation to somatic sensations. J. Neurophysiol. 41: 933–947.

Priestley, J. V., Somogyi, P., and Cuello, A. C. 1982. Immunocytochemical localization of substance P in the spinal trigeminal nucleus of the rat: a light and electron microscopic study. J. Comp. Neurol. 211: 31–49.

Provins, K. A. 1958. The effect of peripheral nerve block on the appreciation and execution of finger movements. J. Physiol. 143: 55–67.

Reynolds, D. V. 1969. Surgery in the rat during electrical analgesia induced by focal brain stimulation. Science 164: 444–445.

Rexed, B. 1952. The cytoarchitectonic organization of the spinal cord in the cat. J. Comp. Neurol. 96: 415–466.

Rexed, B. 1954. A cytoarchitectonic atlas of the spinal cord in the cat. J. Comp. Neurol. 100: 297380.

Rice, F. L. and Rasmusson, D. D. 2000. Innervation of the digit on the forepaw of the raccoon. J. Comp. Neurol. 417: 467–490.

Ruda, M. A., Coffield, J., and Dubner, R. 1984. Demonstration of postsynaptic opioid modulation of thalamic projection neurons by the combined techniques of retrograde horseradish peroxidase and enkephalin immunocytochemistry. J. Neurosci. 4: 2117–2132.

Rudomin, P., Solodkin, M., and Jiménez, I. 1987. Synaptic potentials of primary afferent fibers and motoneurons evoked by single intermediate nucleus interneurons in the cat spinal cord. J. Neurophysiol. 57: 1288–1313.

Ruggiero, D. A., Underwood, M. D., Mann, J. J., Anwar, M., and Arango, V. 2000. The human nucleus of the solitary tract: visceral pathways revealed with an ''in vitro'' postmortem tracing method. J. Auton. Nerve. Syst. 79: 181–190.

Rustioni, A., Hayes, N. L., and O'Neill, S. 1979. Dorsal column nuclei and ascending spinal afferents in macaques. Brain 102: 95–125.

Sadjapour, K. and Brodal, A. 1968. The vestibular nuclei in man: A morphological study in the light of experimental findings in the cat. J. Hirnforsch. 10: 299–319.

Schady, W. J. L. and Torebjörk, H. E. 1983. Projected and receptive fields. A comparison of projected areas of sensations evoked by intraneural stimulation of mechanoreceptive units and their innervation territories. Acta physiol. Scand. 119: 267–275.

Schaible, H. G. and Schmidt, R. F. 1985. Effects of an experimental arthritis on the sensory properties of fine articular afferent units. J. Neurophysiol. 54: 1109–1126.

Schaible, H. G. and Schmidt, R. F. 1988. Time course of mechanosensitivity changes in articular afferents during developing experimental arthritis. J. Neurophysiol. 60: 2180–2195.

Scheibel, M. E. and Scheibel, A. B. 1968. Terminal axon patterns in cat spinal cord: II. The dorsal horn. Brain Res. 9: 32–58.

Schmelz, M., Schmidt, R., Bickel, A., Handwerker, H. O., and Torebjörk, H. E. 1997. Specific C-receptors for itch in human skin. J. Neurosci. 17: 8003–8008.

Sengupta, J. N. and Gebhart, G. F. 1994. Characterization of mechanosensitive pelvic nerve afferent fibers innervating the colon of the rat. J. Neurophysiol. 71: 2046–2060.

Sessle, B. J., Hu, J. W., Dubner, R., and Lucier, G. E. 1981. Functional properties of neurons in cat trigeminal subnucleus caudalis (medullary dorsal horn). II. Modulation of responses to noxious and nonnoxious stimuli by periaqueductal gray, nucleus raphe magnus, cerebral cortex, and afferent influences, and effect of naloxone. J. Neurophysiol. 45: 193–207.

Shafik, A., Shafik, A. A., El-Sibai, O., and Ahmed, I. 2003. Role of positive urethrovesicle feedback in vesical evacuation. The concept of a second micturition reflex: the urethrovesical reflex. World J. Urol. 21: 167–170.

Sherrington, C. S. 1906. The Integrative Action of the Nervous System. (2nd ed.,1947) Yale University Press, New Haven.

Shigenaga, Y., Otani, K., and Suemune, S. 1990. Morphology of central terminations of low-threshold trigeminal primary afferents from facial skin in the cat– intra-axonal staining with HRP. Brain Res. 523: 23–50.

Shortland, P. and Woolf, C. J. 1993. Chronic peripheral nerve section results in a rearrangement of the central axonal arborizations of axotomized A beta primary afferent neurons in the rat spinal cord. J. Comp. Neurol. 330: 65–92.

Simone, D. A., Sorkin, L. S., Oh, U., Chung, J. M., Owens, C., LaMotte, R. H., and Willis, W. D. 1991. Neurogenic hyperalgesia: Central neural correlates in responses of spinothalamic tract neurons. J. Neurophysiol. 66: 228–246.

Sorkin, L. S., McAdoo, D. J., and Willis, W. D. 1993. Raphe magnus stimulatioin-induced antinociception in the cat is associated with release of amino acids as well as serotonin in the lumbar dorsal horn. Brain Res. 618: 95–108.

Strassman, A. M. and Levy, D. 2006. Response properties of dural nociceptors in relation to headache. J. Neurophysiol. 95: 1298–1306.

Sugiura, Y., Lee, C. L., and Perl, E. R. 1986. Central projections of identified, unmyelinated (C) afferent fibers innervating mammalian skin. Science 234: 358–361.

Sugiura, Y., Terui, N., and Hosoya, Y. 1989. Difference in distribution of central terminals between visceral and somatic unmyelinated (C) primary afferent fibers. J. Neurophysiol. 62: 834–840.

Sunada, T., Kurasawa, I., Hirose, Y., and Nakamura, Y. 1990. Intracellular response properties of neurons in the spinal trigeminal nucleus to peripheral and cortical stimulation in the cat. Brain Res. 514: 189–197.

Surmeier, D. J., Honda, C. N., and Willis, W. D. 1988. Natural groupings of primate spinothalamic neurons based on cutaneous stimulation: Physiological and anatomical features. J. Neurophysiol. 59: 833–860.

Tabata, T. and Karita, K. 1991. Response properties of the periodontal mechanosensitive neurons in the trigeminal main sensory nucleus of the cat. Exp. Brain Res. 84: 583–590.

Talbot, W. H., Darian-Smith, I., Kornhuber, H. H., and Mountcastle, V. B. 1968. The sense of flutter-vibration: Comparison of the human capacity with response patterns of mechanoreceptive afferents from the monkey hand. J. Neurophysiol. 31: 301–334.

Tapper, D. N., Brown, P. B., and Moraff, H. 1973. Functional organization of the cat's dorsal horn: Connectivity of myelinated fiber systems of hairy skin. J. Neurophysiol. 36: 817–826.

Tominaga, M., Caterina, M. J., Malmberg, A. B., Rosen, T. A., Gilbert, H., Skinner, K., Raumann, B. E., Basbaum, A. I., and Julius, D. 1998. The cloned capsaicin receptor integrates multiple pain-producing stimuli. Neuron 21: 531–543.

Torebjörk, H. E. and Ochoa, J. L. 1983. Selective stimulation of sensory units in man. Adv. Pain Res. Therap. 5: 99–104.

Torebjörk, H. E. and Ochoa, J. L. 1990. New method to identify nociceptor units innervating glabrous skin of the human hand. Exp. Brain Res. 81: 509–514.

Torebjörk, H. E., Vallbo, A. B., and Ochoa, J. L. 1987. Intraneural microstimulation in man. Its relation to specificity of tactile sensations. Brain 110: 1509–1529.

Towe, A. L. and Jabbur, S. J. 1961. Cortical inhibition of neurons in dorsal column nuclei of cat. J. Neurophysiol. 24: 488–498.
Tremblay, N., Bushnell, M. C., and Duncan, G. H. 1993. Thalamic VPM nucleus in the behaving monkey. II. Response to air-puff stimulation during discrimination and attention tasks. J Neurophysiol. 69: 753–763.
Trevino, D. L., Coulter, J. D., and Willis, W. D. 1973. Location of cells of origin of spinothalamic tract in lumbar enlargement of the monkey. J. Neurophysiol. 36: 750–761.
Tsuboi, A., Kolta, A., Chen, C. C., and Lund, J. P. 2003. Neurons of the trigeminal main sensory nucleus participate in the generation of rhythmic motor patterns. Eur. J. Neurosci. 17: 229–238.
Uddenberg, N. 1968. Functional organization of long, second-order afferents in the dorsal funiculus. Exp. Brain Res. 4: 377–382.
Vallbo, A. B., Hagbarth, K. E., Torebjörk, H. E., and Wallin, B. G. 1979. Somatosensory, proprioceptive and sympathetic activity in human peripheral nerves. Physiol. Rev. 59: 919–957.
Vallbo, A. B., Olausson, H., and Wessberg, J. 1999. Unmyelinated afferents constitute a second system coding tactile stimuli of the human hairy skin. J. Neurophysiol. 81: 2753–2763.
Van Hees, J. 1976a. Human C fibre input during painful and nonpainful skin stimulation with radiant heat. In: (eds. J. J. Bonica and D. Albe-Fessard), Advances in Pain Research and Therapy, pp. 35–40. Raven.
Van Hees, J. 1976b. Since afferent C fiber activity in the human nerve during painful and nonpainful skin stimulation with radiant heat. In: (*ed*. Y. Zotterman) Sensory Functions of the Skin in Primates, pp. 503–505. Pergamon.
Veinante, P. and Deschenes, M. 1999. Single- and multi-whisker channels in the ascending projections from the principal trigeminal nucleus in the rat. J. Neurosci. 19: 5085–5095.
Verdier, D., Lund, J. P., and Kolta, A. 2004. Synaptic inputs to trigeminal primary afferent neurons cause firing and modulate intrinsic oscillatory activity. J. Neurophysiol. 92: 2444–2455.
Wall, P. D. 1967. The laminar organization of dorsal horn and effects of descending impulses. J. Physiol. 188: 403–423.
Weiberg, J. A. and Rustioni, A. 1977. Cortical cells projecting to the dorsal column nuclei of Rhesus monkey. Exp. Brain Res. 28: 521–528.
Werner, G. and Mountcastle, V. B. 1965. Neural activity in mechanoreceptive cutaneous afferents: Stimulus-response relations, Weber functions, and information transmission. J. Neurophysiol. 28: 359–397.
Westlund, K. N., Carlton, S. M., Zhang, D., and Willis, W. D. 1992. Glutamate-immunoreactive terminals synapse on primate spinothalamic tract cells. J. Comp. Neurol. 322: 519–527.
Willcockson, W. S., Chung, J. M., Hori, Y., Lee, K. H., and Willis, W. D. 1984a. Effects of iontophoretically released amino acids and amines on primate spinothalamic tract cells. J. Neurosci. 4: 732–740.
Willcockson, W. S., Chung, J. M., Hori, Y., Lee, K. H., and Willis, W. D. 1984b. Effects of iontophoretically released peptides on primate spinothalamic tract cells. J. Neurosci. 4: 741–750.
Willis, W. D. 1982. Control of nociceptive transmission in the spinal cord. In: Progress in Sensory Physiology 3, D. Ottoson (Ed.-In-Chief) Springer Verlag, Heidelberg.
Willis, W. D. and Coggeshall, R. E. 2004. 3rd edn., Sensory Mechanisms of the Spinal Cord, Kluwer Academic/Plenum.
Willis, W. D. and Westlund, K. N. 1997. Neuroanatomy of the pain system and of the pathways that modulate pain. J. Clin. Neurophysiol. 14: 2–31.
Willis, W. D., Kenshalo, D. R., and Leonard, R. B. 1979. The cells of origin of the primate spinothalamic tract. J. Comp. Neuirol. 188: 543–574.
Willis, W. D., Trevino, D. L., Coulter, J. D., and Maunz, R. A. 1974. Responses of primate spinothalamic tract neurons to natural stimulation of hindlimb. J. Neurophysiol. 37: 358–372.
Willis, W. D., Zhang, X., Honda, C. N., and Giesler, G. J. 2001. Projections from the marginal zone and deep dorsal horn to the ventrobasal nuclei of the primate thalamus. Pain 92: 267–276.
Willis, W. D., Zhang, X., Honda, C. N., and Giesler, G. J. 2002. A critical review of the role of the proposed VMpo nucleus in pain. J. Pain 3: 79–94.
Woolf, C. J. 1987. Central terminations of cutaneous mechanoreceptive afferents in the rat lumbar spinal cord. J. Comp. Neurol. 261: 105–119.
Wu, S. Y., Dun, S. L., Wright, M. T., Chang, J. K., and Dun, N. J. 1999. Endomorphin-like immunoreactivity in the rat dorsal horn and inhibition of substantia gelatinosa neurons in vitro. Neuroscience 89: 317–321.
Yezierski, R. P., Gerhart, K. D., Schrock, B. J., and Willis, W. D. 1983. A further examination of effects of cortical stimulation on primate spinothalamic tract cells. J. Neurophysiol. 49: 424–441.
Yokota, T., Koyama, N., and Matsumoto, N. 1985. Somatotopic distribution of trigeminal nocicepetive neurons in ventrobasal complex of cat thalamus. J. Neurophysiol. 53: 1387–1400.
Zadina, J. E., Hackler, L., Ge, L. J., and Kastin, A. J. 1997. A potent and selective endogenous agonist for the mu-opiate receptor. Nature 386: 499–502.
Zhang, E. T. and Craig, A. D. 1997. Morphology and distribution of spinothalamic lamina I neurons in the monkey. J. Neurosci. 17: 3274–3284.
Zhang, X., Kostarczyk, E., and Giesler, G. J. 1995. Spinohypothalamic tract neurons in the cervical enlargement of rats: Descending axons in the ipsilateral brain. 1995. J. Neurosci. 15: 8393–8407.
Zhang, X., Wenk, H. N., Gokin, S. P., Honda, C. N., and Giesler, G. J. 1999. Physiological studies of spinohypothalamic tract neurons in the lumbar enlargement of monkeys. J. Neurophysiol. 82: 1054–1058.
Zhang, X., Wenk, H. N., Honda, C. N., and Giesler, G. J. 2000a. Locations of spinothalamic tract axons in cervical and thoracic spinal cord white matter in monkeys. J. Neurophysiol. 83: 2869–2880.
Zhang, X., Honda, C. N., and Giesler, G. J. 2000b. Position of spinothalamic tract axons in upper cervical spinal cord of monkeys. J. Neurophysiol. 84: 1180–1185.
Zou, X., Lin, Q., and Willis, W. D. 2000. Enhanced phosphorylation of NMDA receptor NR1 subunits in spinal cord dorsal horn and spinothaamic tract neurons following intradermal injection of capsaicin in rats. J. Neurosci. 20: 6989–6997.

Further Reading

Johansson, R. S. and Vallbo, A. B. 1983. Tactile sensory coding in the glabrous skin of the human hand. Trends Neurosci. 6: 27–32.
Yoshida, A., Chen, K., Moritani, M. M., Yabuta, N. H., Nagase, Y., Takemura, M., and Shigenaga, Y. 1997. Organization of the descending projections from the parabrachial nucleus to the trigeminal sensory nuclear complex and spinal dorsal horn in the rat. J. Comp. Neurol. 383: 94–111.

6.07 The Somatosensory Thalamus and Associated Pathways

J H Kaas, Vanderbilt University, Nashville, TN, USA

© 2008 Elsevier Inc. All rights reserved.

6.07.1	Introduction	118
6.07.2	Somatosensory Afferents and Afferent Pathways	119
6.07.3	Somatosensory Relay Nuclei of the Medulla and Upper Spinal Cord	120
6.07.3.1	The Dorsal Column–Trigeminal Complex	122
6.07.4	The Nuclei of the Somatosensory Thalamus, Their Spinal Cord and Brainstem Somatosensory Inputs, and Their Cortical Projections	125
6.07.5	The Ventroposterior Nucleus	126
6.07.6	The Ventroposterior Superior Nucleus	131
6.07.7	The Ventroposterior Inferior Nucleus	133
6.07.8	Other Nuclei: The Anterior Pulvinar, the Lateral Posterior Nucleus, the Posterior Group, the Ventroposterior Parvocellular Nucleus, and the Ventromedial Posterior Nucleus	135
6.07.9	Cortical Projections to the Somatosensory Thalamus and Dorsal Column Nuclei	136
References		136

Glossary

anterior pulvinar A subdivision of the pulvinar complex of the dorsal thalamus that is somatosensory rather than visual in function. The anterior pulvinar receives inputs from areas of the somatosensory cortex and projects back to areas of the somatosensory cortex.

dorsal column–trigeminal complex A group of three main subnuclei in the lower brainstem and upper spinal cord that receives cutaneous receptor afferents from the body, via the dorsal columns of the spinal cord, and from the head, via the trigeminal nerve. The complex projects to the ventroposterior nucleus (VP) of the contralateral thalamus. The subnuclei, often called nuclei, include the gracile nucleus for the lower body, the cuneate nucleus for the upper body and forelimb, and the trigeminal nucleus for the face and mouth.

dorsal root ganglia The structures that contain the cell bodies of afferents that course in peripheral nerves and enter the spinal cord via the dorsal roots of peripheral nerves.

dorsal thalamus A major component of the diencephalon, which also includes the epithalamus, ventral thalamus, hypothalamus, and pretectum. The dorsal thalamus, the division that is largest in mammals, receives ascending sensory pathways and projects to the neocortex.

low-threshold mechanoreceptor afferents Four types of low-threshold mechanoreceptors subserve the glabrous skin. The type I class is a slowly adapting afferent (SA-I) that is activated by receptors called Merkel disks, which respond to light pressure. The type II class (SA-II) is activated by Ruffini corpuscles that respond to skin stretch. The type I rapidly adapting afferent (RA-I) is activated by Meissner corpuscles and signals changes in skin indentation. The rapidly adapting type II (RA-II) or Pacinian afferent stems from Pacinian corpuscles that respond to vibration.

thalamic nucleus A collection of neurons and glia in the thalamus that is united by a common function. A nucleus is typically identified as a group of cells that is distinguished from adjoining groups of cells by differences in the sizes and packing of neurons. Many other histological characteristics are used to distinguish nuclei. Each nucleus should also have a distinct set of connections with the neocortex and other structures, and have neurons that have a distinct set of physiological response characteristics.

ventroposterior nucleus A nucleus in the thalamus that receives somatosensory afferents from the contralateral brainstem, systematically represents the cutaneous receptors of the contralateral body, and projects to the primary somatosensory cortex.

6.07.1 Introduction

This chapter describes structures in the early stages of processing in the somatosensory system. The focus is on the ascending sensory inputs to the somatosensory thalamus, the organization of the somatosensory thalamus, and the relay of somatosensory information from the thalamus to the cortex. Most of this description concentrates on what is known about the somatosensory system of anthropoid primates (monkeys, apes, and humans), as this information is most relevant to understanding how somatosensory information is processed in the human brain. Because the types of studies of somatosensory systems that can be conducted using apes and humans are limited, much of the data discussed here comes from investigations on monkeys. Thus, it is important to remember that many features of even the early stages of processing in somatosensory systems are variable across species. The somatosensory system of humans resembles those of monkeys, while being different in many ways. In addition, there are approximately 4500 species of mammals, now divided into six superorders. This impressive radiation of mammalian species has resulted in a number of distinctly different specializations of somatosensory systems (see Chapters The Evolution of Parietal Areas Involved in Hand Use in Primates and Specialized Somatosensory Systems), of which only a few have been studied in any detail. While an extensive comparative approach is not possible here, observations on the somatosensory systems of some of the more fully studied nonprimate mammals are included.

The parts of the somatosensory system of primates covered in this review are depicted schematically in Figure 1. In brief, peripheral nerve afferents related to receptors in the skin, muscles, and joints of each side of the body enter the spinal cord and lower brainstem where they branch to terminate locally in the dorsal horn of the spinal cord. Other branches of these afferents ascend in the ipsilateral dorsal columns or join the trigeminal pathways to terminate in the dorsal column–trigeminal nucleus complex or proprioceptive nuclei in the upper spinal cord and lower brainstem. Neurons in these nuclei send axons across the midline to form the medial lemniscus, a pathway that terminates in the ventroposterior complex of the contralateral thalamus. In addition, a small proportion of these neurons, largely neurons representing afferents devoted to the teeth and tongue, project into the ipsilateral medial lemniscus to the ipsilateral thalamus. Thus, parts of the oral cavity become represented in both the ipsilateral and the contralateral ventroposterior complex, as well as in the cortex. Another source of somatosensory information to the ventroposterior complex is from the spinothalamic pathway. Afferents that terminate in the dorsal horn of the spinal cord, and the equivalent part of the trigeminal nuclei of the lower brainstem, synapse on neurons that send axons across the midline to form the ventrolateral spinothalamic pathway that terminates in several subdivisions of the contralateral somatosensory thalamus. Thalamic neurons in the ventroposterior complex send axons to subdivisions of the anterior parietal cortex and other somatosensory areas such as the second somatosensory area (S2). In anthropoid primates, the anterior parietal cortex consists of the architectonic fields 3a, 3b, 1, and 2 of Brodmann K. (1909). Each of these fields receives a different pattern of projections from the somatosensory thalamus, and each contains a separate, complete representation of peripheral nerve afferents, mainly those from the contralateral half of the body. Thus, each area represents the contralateral body, from tail (if present) to tongue, in a mediolateral sequence across the cortex. The representations of ipsilateral afferents from the tongue and teeth activate the lateral extremes of these representations. Another thalamic nucleus, the anterior pulvinar of primates, receives inputs from areas of the somatosensory cortex, and contains neurons that project back to areas of the somatosensory cortex.

Descriptions of the somatosensory thalamus and cortex of cats and rats, and other well-studied nonprimate mammals, differ from those of anthropoid primates in that several subdivisions of the somatosensory thalamus and cortex are not recognized, or they have different names. In the thalamus, for example, the anterior pulvinar and the ventroposterior inferior nuclei (VPI) are not generally recognized, and the question that arises is whether these nuclei have emerged only in primates, have been named differently in other mammals, or have not been identified in other mammals. Likewise, in the cortex of anthropoid primates, four parallel representations exist in the anterior parietal cortex (areas 3a, 3b, 1, and 2), but only area 3b appears to correspond to the primary somatosensory area, S1, as commonly defined in other mammals. Are the other areas (3a, 1, and 2) unrecognized, differently named, or a derivation of anthropoid primates? Thus, descriptions and discussions of especially the organization of the

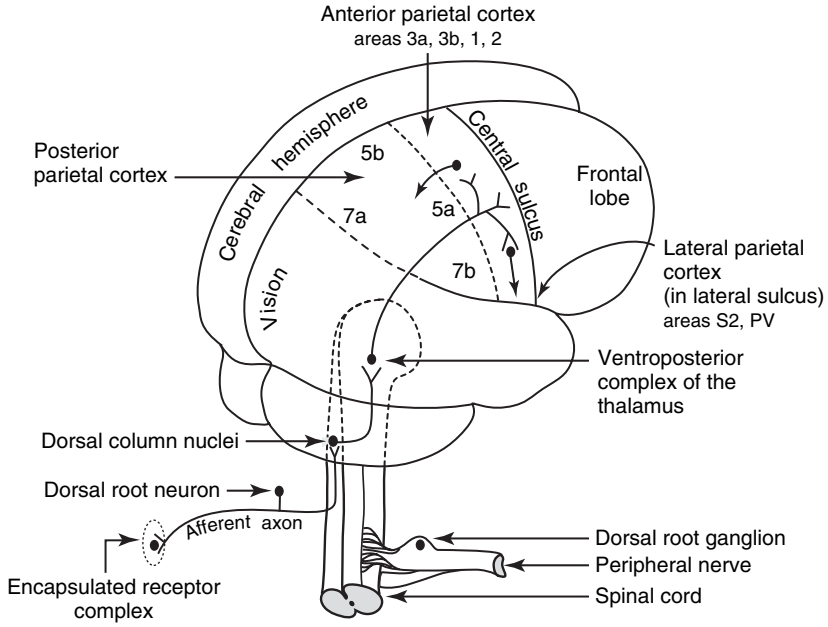

Figure 1 The basic components of the somatosensory system shown on a posterolateral view of a primate brain. Afferents subserving receptors in the skin, muscles, and joints travel in peripheral nerves to enter the spinal cord or brainstem to send axon branches into the dorsal column nuclei or divisions of the trigeminal complex. Neurons in these nuclei send axons to the ventroposterior nucleus (VP) and the ventroposterior superior nucleus (VPS) of the ventroposterior complex of the contralateral thalamus. Neurons in VP and VPS project to areas 3a, 3b, 1, and 2 of the anterior parietal cortex. Information from the anterior parietal cortex is distributed further to areas of the lateral parietal cortex, including the second somatosensory area (S2), the parietal ventral area (PV), the parietal rostral area (PR), and the ventral somatosensory area (VS). Other projections from the anterior and lateral parietal cortex spread somatosensory information to subdivisions of the posterior parietal cortex, shown here as divided into the classical areas of Brodmann K. (1909) numbered 5a, 5b, 7a, and 7b for general locations (this cortex is now known to be more complexly organized). Other afferents (see Figure 2) terminate in the dorsal horn of the spinal cord where neurons contribute to the contralateral spinothalamic tract, which terminates in the ventroposterior inferior nucleus (VPI) where neurons project to areas of the anterior and lateral parietal cortex. From Kaas, J. H. 2004. Somatosensory System. In: The Human Nervous System, 2nd edn. (*eds*. G. Paxinos and J. K. Mai), pp. 1059–1092. Elsevier Academic Press.

thalamus and cortex that go beyond our focus on primates and include other well-studied mammals are complicated by species differences in the appearances and names of brain structures.

6.07.2 Somatosensory Afferents and Afferent Pathways

Because several other chapters in this volume (see Chapters Cutaneous Mechanisms of Tactile Perception: Morphological and Chemical Organization of the Innervation to the Skin, Merkel Cells, Physiological Responses of Sensory Afferents in Glabrous and Hairy Skin of Humans and Monkeys, and Physiological Characteristics of Second-Order Somatosensory Circuits in Spinal Cord and Brainstem) review the functional organization of the peripheral somatosensory system, only a brief overview is necessary here (also see Kaas, J. H., 2004). Our main focus is on the low-threshold mechanoreceptors of the glabrous and hairy skin, as these provide the input that is critical for making fine tactile discriminations and tactile recognition. However, afferents from joint and muscle receptors for proprioception are equally important, as object recognition and localization by touch depend on knowing the articulation of the digits relative to each other, and the relationship between activity from cutaneous and proprioceptors. Low-threshold afferents from the glabrous skin include the slowly adapting type I (SA-I) subserved by Merkel cells, rapidly adapting type I (RA-1) from Meissner corpuscles, slowly adapting type II (SA-II) with Ruffini-like receptors, and rapidly adapting type II, emanating from Pacinian corpuscles. Hairy skin

afferents are similar, except that RA-I and SA-I receptors are also found in hair follicles around shafts of hairs where hair movement disturbs the base. Merkel cell receptors for SA-I afferents may be aggregated in touch domes or spots, and RA-II Pacinian receptors are found in deeper tissues rather than the skin. Other cutaneous afferents include the wide dynamic range (WDR) and other more slowly conducting afferents that respond to touch and more intense stimuli, and contribute to the spinothalamic pathway. In deeper tissues, the muscle spindle receptor afferents are very important for proprioception, perhaps aided by afferents from Ruffini and Golgi types of receptors in and around joints.

Afferents from peripheral receptors combine to form small nerve fascicles that join other fascicles and motor efferent axons to form peripheral nerves that then segregate afferents from efferents as they approach the spinal cord to form the dorsal sensory and ventral motor roots, as sensory afferents enter the spinal cord (and brainstem) and motor neuron axons leave.

Afferents entering the spinal cord terminate locally on neurons in the ipsilateral dorsal horn of the spinal cord to form an elongated representation of the ipsilateral half of the body (e.g., Florence, S. L. *et al.*, 1988; 1989). Terminations of the axon arbors of different classes of afferents distribute differently over the layers of the dorsal horn, maintaining a segregation of types of information. The low-threshold mechanoreceptors and muscle spindle receptor afferents also branch to send a collateral toward the brainstem to terminate either in the dorsal horn at higher levels or in the dorsal column–trigeminal complex of the lower brainstem (Figure 2). These collaterals contribute to the dorsal (posterior) column and dorsolateral column afferent pathways. WDR, nociceptive, and temperature-sensitive afferents terminate locally in the dorsal horn of the spinal cord on neurons that send axons across the midline of the spinal cord to ascend in the ventrolateral white matter to form the spinothalamic pathway, known as a relay of information about pain, temperature, and crude touch (Willis, W. D. and Coggeshall, R. E., 2004).

Primary afferents from oral and facial structures course in the trigeminal (fifth cranial) nerve to branch and terminate in the principal trigeminal nucleus (combining with the dorsal column nuclei to form a complete representation of the tactile receptors of the ipsilateral body surface), the mesencephalic trigeminal nucleus for muscle spindle afferents, and the spinal trigeminal nucleus for WDR and other afferents.

Second-order neurons in the spinal trigeminal nucleus send axons to the opposite ascending spinothalamic pathway. Thus, afferents entering the brainstem sort themselves to terminate with similar types in nuclei with second-order neurons that project contralaterally to form the medial lemniscus or spinothalamic pathways to the somatosensory thalamus.

In addition to neurons in the dorsal horn of the spinal cord that contribute to the spinothalamic tract, a long column of neurons outside the dorsal horn that extends from about the fourth cervical segment to the caudal medulla is known as the lateral cervical nucleus (Kaas, J. H., 2004). In humans, the lateral cervical nucleus is usually only a rudimentary structure, but it may contain up to 8000 neurons in cats where it is well developed. The lateral cervical nucleus receives a wide range of somatosensory inputs, and projects via the spinocervicothalamic pathway to the contralateral somatosensory thalamus to terminate in the septal regions of VP (Broman, J. and Zhang, M., 1996) in conjunction with spinothalamic tract terminations.

6.07.3 Somatosensory Relay Nuclei of the Medulla and Upper Spinal Cord

A collection of nuclei in the lower brainstem and upper spinal cord receive inputs from ipsilateral low-threshold mechanoreceptors and project to the contralateral ventroposterior complex of the thalamus (Figure 2). By tradition, several nuclei have been distinguished and named in this complex, but such subdivisions are best considered subnuclei, that is, parts of a functional system differing mainly in what parts of the body they represent, rather than nuclei that are devoted to distinct functions. Thus, the gracile, cuneate, and principal trigeminal nuclei all receive inputs from the low-threshold mechanoreceptors of the skin, and represent the hindlimb, the trunk and forelimb, and face plus oral cavity in a mediolateral sequence of subnuclei in the lower brainstem and upper spinal cord (e.g., Johnson, J. I. *et al.*, 1968; Xu, J. and Wall, J. T., 1996). Some investigators even distinguish a more medial cell group as Bischoff's nucleus (e.g., Johnson, J. I. *et al.*, 1968), a midline cell group that receives afferent inputs from the tail (Qi, H.-X. and Kaas, J. H., 2006). These subnuclei combine to form a functional unit, the dorsal column–trigeminal complex. However, there are other nuclei or subnuclei associated with the complex, as inputs from muscle spindle and joint

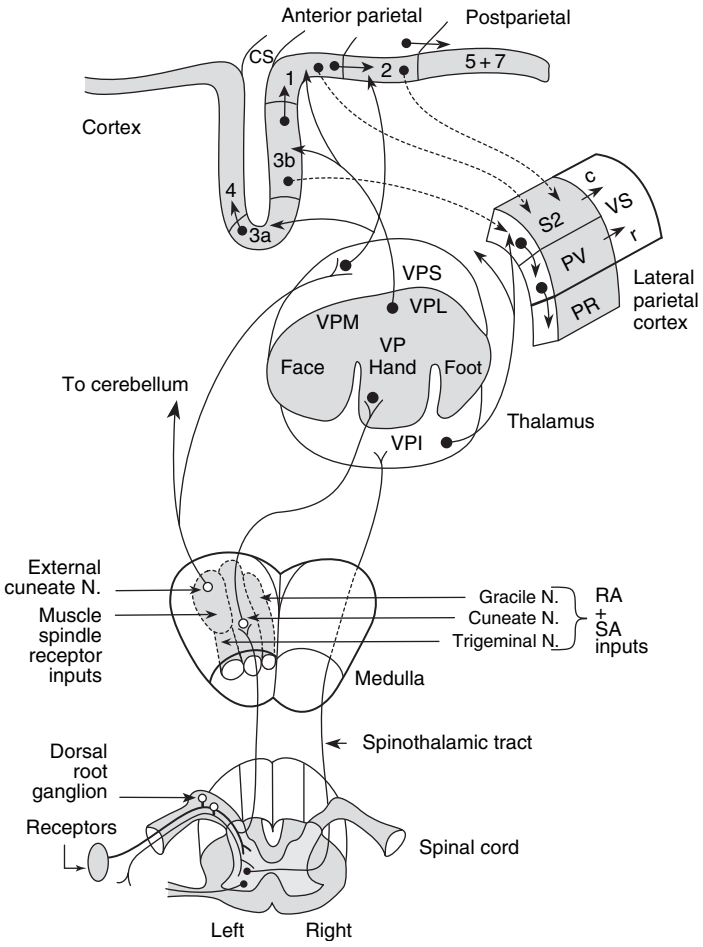

Figure 2 A more detailed schematic of components of the somatosensory system of anthropoid primates. Afferents from low-threshold, rapidly adapting (RA), and slowly adapting (SA) mechanoreceptors in the skin enter the spinal cord and brainstem to send branches that terminate in the gracile and cuneate nuclei (N) of the principal nucleus of the trigeminal nuclear complex, to synapse on neurons that project via the medial lemniscus nucleus (VP), where the ventroposterior lateral division (VPL) represents the foot, trunk, and hand, and the ventroposterior medial division (VPM) represents the face and oral structures. Afferents from muscle spindle receptors enter the spinal cord or brainstem to send branches to the external cuneate nucleus and other nuclei that project via the medial lemniscus to the contralateral ventroposterior superior nucleus (VPS). Other afferents terminate in the dorsal horn of the spinal cord or its equivalent in the trigeminal nuclear complex where neurons project via the contralateral spinothalamic tract to the ventroposterior inferior (VPI) nucleus. Arrows indicate projections of the three thalamic nuclei to the Brodmann K. (1909) areas of the anterior parietal cortex (3a, 3b, 1, and 2), and the lateral parietal cortex (ventral somatosensory area, VS, with caudal and rostral divisions, c and r, second somatosensory area (S2), parietal ventral area (PV), and parietal rostral area (PR)). Arrows also denote cortical connections that further distribute somatosensory information from the anterior parietal cortex, including a projection from area 3a to area 4 of the motor cortex. The bend in the cortical sheet corresponds to the central sulcus (CS). From Kaas, J. H. 2004. Somatosensory System. In: The Human Nervous System, 2nd edn. (*eds*. G. Paxinos and J.K. Mai), 1059–1092. Elsevier Academic Press.

receptor afferents terminate separately in several cell groups that relay to a separate nucleus of the contralateral ventroposterior thalamus, the ventroposterior superior nucleus (VPS) (Figure 2). Thus, two small medullary nuclei, termed X and Z by Pompeiano O. and Brodal A. (1957), receive inputs from muscle spindle afferents of the lower limb, the external cuneate nucleus is activated by muscle spindle afferents from the trunk and upper limb, while the mesencephalic trigeminal nucleus receives muscle spindle afferents from the face. These cell groups form a second functional unit in the lower brainstem that relays proprioceptive information to the contralateral thalamus.

6.07.3.1 The Dorsal Column–Trigeminal Complex

The sensory inputs to the subnuclei of the medullary complex that represent the forelimb, trunk, and hindlimb travel in the dorsal (posterior) columns of the spinal cord, while the inputs from the face and oral cavity course both dorsally and caudally after entering the midpontine brainstem to innervate the principal nucleus and other subnuclei of the trigeminal complex. The two major divisions of the dorsal column pathway are the gracile tract that carries information from the lower limb, lower trunk, and tail (if present) and the cuneate tract subserving the upper limb, upper trunk, and neck. The axons in the dorsal columns include the ascending branches of large, myelinated dorsal root fibers that enter the spinal cord at various levels while subserving adjoining skin regions. As the branches enter the dorsal columns from lower to higher spinal cord levels, the branches at higher levels add to the pathways laterally, resulting in a rough somatotopic pattern from medial to lateral across the dorsal columns (Whitsel, B. L. *et al*., 1972). A further refinement of this pattern occurs as the terminations of these axons sort themselves somatotopically in the dorsal column nuclei. Other axons in the dorsal columns originate from spinal cord neurons in the dorsal horn that either course in the dorsal column for several spinal cord segments to exit or continue to terminate in dorsal column nuclei or associated nuclei. Thus, the dorsal column pathway contains both branches of peripheral nerve axons, and axons that originate in second- or higher-order neurons of the dorsal horn of the spinal cord.

The gracile and cuneate tracts contain mixtures of functional classes of axons (Whitsel, B. L. *et al*., 1972). At lower spinal cord levels, the gracile tract contains a mixture of cutaneous afferents and muscle spindle afferents. The muscle spindle afferents leave at higher levels to innervate proprioceptive nuclei for the lower limb. The remaining afferents appear to be largely of the rapidly adapting RA-I type, but the smaller numbers of RA-II (Pacinian) and SA-I afferents likely course in this pathway as well to terminate in the gracile nucleus. The fate of the SA-II afferents, sensitive to skin stretch and thereby joint movement, is uncertain, but they may enter and then leave the tract to join with muscle spindle afferents to contribute to proprioception (McCloskey, P. I., 1978). The cuneate tract also contains a mixture of axonal branches of cutaneous and muscle spindle afferents, with the muscle spindle afferents separating to terminate in the external (proprioceptive) cuneate nucleus.

Complete lesions of the dorsal column in humans produce major defects in their ability to detect the speed and direction of moving contacts on the skin, but simple contacts can be felt and roughly localized (Nathan, P. W. *et al*., 1986; see Mountcastle, V. B., 2005, for review). The ability to judge the position and movement of the limbs is also greatly impaired, as there can be a major loss of the afferents carrying proprioceptive information. Thus, monkeys and humans with such lesions tend to not use the affected limb, and are impaired in the positioning and control of finger and hand movements (Glendenning, D. S. *et al*., 1992; Cooper, B. Y. *et al*., 1993).

The subnuclei of the dorsal column–trigeminal complex are organized somewhat differently from each other. However, all are elongated in the rostrocaudal dimension (Figure 2), and are largely composed of discrete clusters of cells separated from each other by a matrix of axons and glia. The cell clusters or nests have long been recognized (e.g., Cajal, S. R. Y., 1911). These clusters express higher levels of the inhibitory neurotransmitter, GABA, the calcium-binding proteins calbindin and parvalbumin, the activity-dependent enzyme nitric oxide synthase, and brain-derived neurotropic factor (Strata, F. *et al*., 2003) than the surrounding neuropil. In addition, the cell clusters express higher levels of the metabolic enzyme, cytochrome oxidase (CO), which is commonly used as a histological marker for these nuclei (Figure 3). Thus, the cell clusters are centers of metabolic activity in the nuclei where neurotransmitters are released and high levels of synaptic activity occur. While the majorities of neurons in the clusters are excitatory and project to the contralateral thalamus, roughly 30% of the neurons are inhibitory, and have local connections within the nuclei where they constrain the sizes of receptive fields (Schwark, H. D. *et al*., 1999; Wang, X. and Wall, J. T., 2006). Areas of the somatosensory cortex also project to the cell clusters, and these inputs appear to modulate the response properties of the relay neurons (Willis, W. D. and Coggeshall, R. E., 2004; Wang, X. and Wall, J. T., 2005).

The segregation of neurons into small clusters that are activated by a similar input may be a reflection of developmental mechanisms that isolate particular groups of neurons so that other axons are less likely to inadvertently grow into an inappropriate cluster (Massey, J. M. *et al*., 2006). The cell

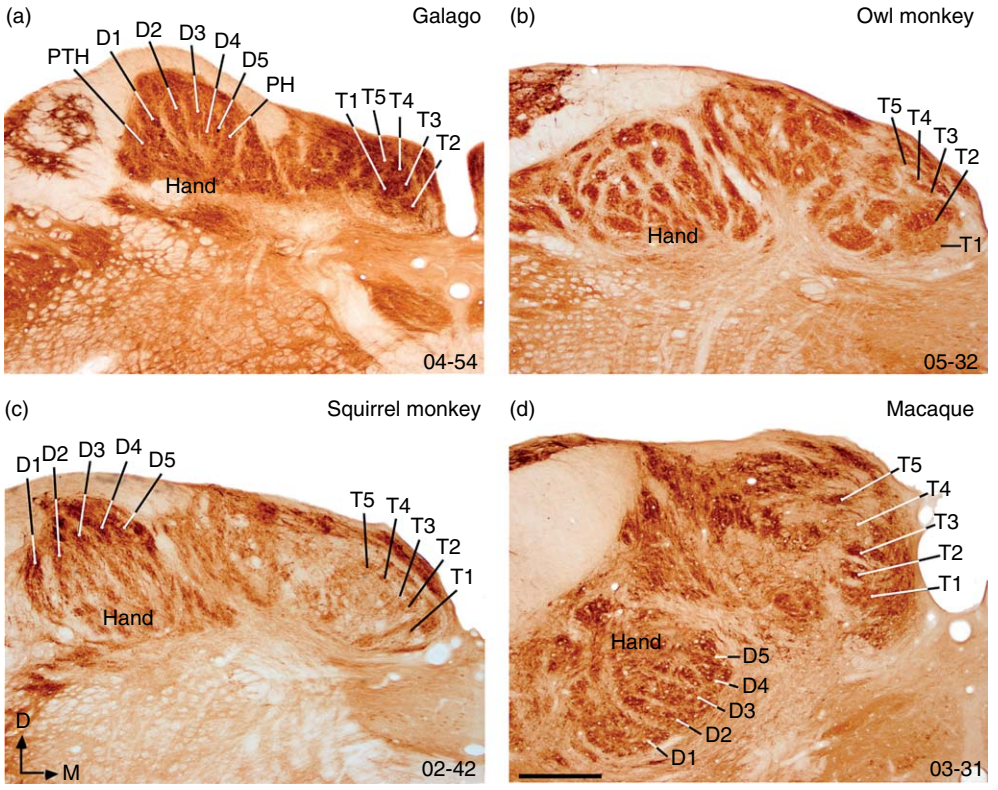

Figure 3 The gracile and cuneate nuclei of (a) a prosimian primate, galago; (b) a New World owl monkey; (c) a New World squirrel monkey; and (d) an Old World macaque monkey. The transverse brainstem sections through the rostral third of the nuclei have been processed for cytochrome oxidase (CO) to reveal CO-dense ovals or islands of tissue that are densely packed with neurons and surrounded by CO-light septa that have few neurons. The CO-dense modules for each primate receive slowly adapting (SA) or rapidly adapting (RA) afferents from different body parts so that collectively they represent the trunk, limbs, and tail, with afferents from the face and oral structures terminating in the principal nucleus of the trigeminal complex (not shown). In each section, dorsal (D) is up and medial (M) is to the right. Note that the toes of the foot (TI–T5) are represented in a mediolateral sequence in the more medial gracile nucleus, while the digits of the hand (D1–D5) are represented in a lateromedial sequence in the more lateral cuneate nucleus. CO-dense cell clusters activated from the thenar pad (Pth) and hyperthenarpad (PH) of the hand are also shown for the galago. The detailed organization of the cuneate nucleus in owl monkeys has not yet been determined. Dorsal (D) and medial (M) are indicated by arrows. Scale bar = 0.5 mm. From Qi, H.-X. and Kaas, J. H. 2006. The organization of primary afferent projections to the gracile nucleus of the dorsal column system of primates. J. Comp. Neurol. 499, 183–217.

clusters are most prominent in the central parts of the nuclei. While these isolated groups of neurons are activated by afferents from the same body part, they may also be receiving a different class of inputs from that body part. In the cuneate nucleus of cats, at least, microelectrode recordings have revealed a mosaic of restricted locations where cell neurons are activated by rapidly adapting type I inputs, Pacinian type II inputs, or slowly adapting inputs, probably type I (Dykes, R. W. *et al.*, 1982). This type of evidence is consistent with the premise that three or four of the major types of cutaneous mechanoreceptor afferents terminate in the nuclei of the dorsal column–trigeminal complex, and that separate groups of cells are activated by each class of input. Nevertheless, the inputs are organized overall into a somatotopic pattern.

The patches of dense expression of CO that correspond to cell clusters are shown for four species of primates in Figure 3. The figure also indicates the clusters that are innervated by afferents from different parts of the hand in the cuneate nucleus, and the foot in the gracile nucleus. These patterns of representation were determined by injecting tracers into restricted portions of the skin, which were then transported by afferents from the skin to terminations in cell clusters (Florence, S. L. *et al.*, 1988; 1989; 1991; Strata, F. *et al.*, 2003; Qi, H.-X. and Kaas, J. H., 2006).

Note that the digits are represented in order from lateral to medial by a series of CO-dense patches in the cuneate nucleus (not shown for the owl monkey, as the relevant experiments have not been done in this primate). Curiously, the glabrous hand is represented ventral to that of the digits in New World monkeys and dorsal to the hand in Old World monkeys (and probably in humans), while parts of the hand are represented both dorsal and ventral to that of the digits in prosimian galagos. In other mammals, the dorsal representation of the digits is often represented with a part of the dorsal and ventral hand (see Florence, S. L. *et al.*, 1991). Because the pattern of organization of the cuneate nucleus in prosimian galagos (Figure 3(a)) resembles patterns seen in other mammals, rather than the patterns seen in monkeys, it is likely that the organization of the cuneate in galagos reflects a primitive pattern of organization for this nucleus. Differences across primate taxa may relate to the increased use of the digits as a sensory surface in macaques, and to a lesser extent squirrel and owl monkeys, over prosimian galagos.

As the dorsal column nuclei are elongated rostrocaudally, a fuller appreciation of the somatotopic organization of these nuclei can be obtained by examining a series of transverse sections. In Figure 4, the gracile nucleus of a prosimian galago is color coded across a series of spinal cord and brainstem sections to show the overall somatotopic organization, and to show that the same body part is represented over most or all of the nucleus. Thus, the representations of the tail, foot, lower leg, and upper leg form a mediolateral sequence, while the representation of each of these skin surfaces is disjunctively focused within separated cell clusters along the rostrocaudal length of the nucleus. Results from other primates are similar, with a certain amount of species-specific variation. The reasons for separate clusters of neurons being activated by inputs from the same body part are not clear, but separate clusters could relate to different classes of afferent inputs, as noted above. The representation of skin receptors in the gracile nucleus seems to be more discontinuous and complex than in the cuneate nucleus.

The trigeminal component of the dorsal column–trigeminal nuclear group is more complex than the gracile and cuneate nuclei, as the trigeminal complex has been traditionally divided into five sensory nuclei: the principal sensory nucleus (Pr5), three spinal nuclei (oralis (Sp5o), interpolaris (SP5i), caudalis (Sp5c)), and

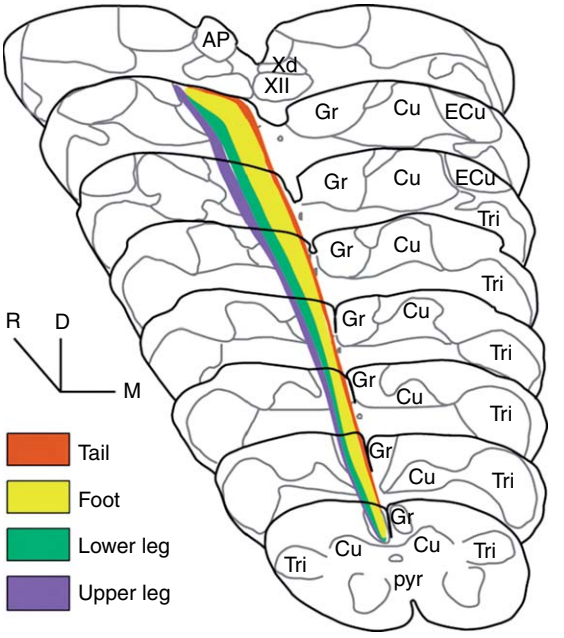

Figure 4 The somatotopic organization of the gracile nucleus in monkeys shown on a rostral (R) to caudal (C) series of brain sections through the dorsal column nuclei. Note that the tail, foot, lower leg, and upper leg are represented in a mediolateral sequence. A more lateral representation of the trunk joins the gracile with the cuneate nucleus for the forelimb. On the individual brain sections, the gracile nucleus (Gr), the cuneate nucleus (Cu), the trigeminal nuclear complex (Tri), and the external cuneate nucleus (ECu) are outlined. The locations of the pyramidal tracts (Pyr), motor nucleus of the twelfth cranial nerve (XII), and dorsal nucleus of the tenth nerve (Xd) and area postrema (AP) are shown for reference. From Qi, H.-X. and Kaas, J. H. 2006. The organization of primary afferent projections to the gracile nucleus of the dorsal column system of primates. J. Comp. Neurol. 499, 183–217.

the mesencephalic nucleus (Me5) for proprioception. Together they form a long column of cells that extends from the rostral pons to the upper segments of the cervical spinal cord (Waite, P. M. E. and Ashwell, K. W. S., 2004). The principal nucleus receives low-threshold mechanoreceptor afferents from the ipsilateral face and mouth, and it is the trigeminal component of the dorsal column–trigeminal complex. Neurons in the principal nucleus project across the midline to join the contralateral medial lemniscus and ascend to terminate in the ventroposterior medial subnucleus of VP. The principal nucleus is somatotopically organized (Kerr, F. W. L. *et al.*, 1968; Florence, S. L. and Lakshman, S., 1995; May, P. J. and Porter, J. D., 1998) and has the CO-dense patches of cells that also characterize the dorsal column nuclei (Noriega, A. L. and Wall, J. T., 1991).

The three spinal trigeminal nuclei all appear to contain separate representations of inputs from the face and oral cavity. CO patches found in the principal nucleus are not evident in the spinal nuclei in primates, but patches representing vibrissae of the face can be found in nucleus interpolaris and nucleus caudalis of rodents and cats (see Noriega, A. L. and Wall, J. T., 1991, for review). These nuclei are analogous to cells located in the dorsal horn of the spinal cord and cells in the proprioceptive nuclei for the lower body. As such, they contribute to the relay of muscle spindle afferent information to the contralateral thalamus, as well as a relay of mechanoreceptor, WDR, and nociceptive afferent information via the trigeminal contribution to the spinothalamic tract.

In addition to the contralateral projections from neurons in the trigeminal complex, both the principal and the spinal nuclei of the complex project ipsilaterally to the ventroposterior thalamus (Ganchrow, D., 1978; Jones, E. G. *et al.*, 1986). This ipsilateral component of a bilateral projection seems to be species variable, being large in sheep and small or absent in rats (Bombardieri, R. A. *et al.*, 1975). Across species, the ipsilateral relay is largely of inputs from the mouth, but ipsilateral inputs from the side of the head and lips are also observed in sheep (Cobral, R. J. and Johnson, J. I., 1971). In monkeys, the ipsilateral projections from the principal nucleus relay information from periodontal receptors that are responsive to light touch on the teeth and from cutaneous receptors on the tongue and inner cheek (Bombardieri, R. A. *et al.*, 1975; Jones, E. G. *et al.*, 1986). Other types of information are relayed from the spinal nuclei.

The mesencephalic trigeminal nucleus is another component of the trigeminal complex. The neurons of this nucleus are unique in that they are the cell bodies of peripheral nerve afferents. Instead of being located in the dorsal root ganglia for peripheral nerves, as for the cell bodies of other peripheral nerve afferents, these cell bodies are located within the central nervous system, mainly in the pons of the upper brainstem (Waite, P. M. E. and Ashwell, K. W. S., 2004). The cell bodies are of several types, mainly the pseudounipolar type that is characteristic of dorsal root ganglion cells, but also bipolar and multipolar neurons (Luo, P. *et al.*, 1991). The afferents of these cell bodies conduct proprioceptive impulses from muscle spindle receptors in the jaw muscles and from periodontal mechanoreceptors (see Luo, P. *et al.*, 1991, for review). The central projections of the cell bodies of the mesencephalic trigeminal nucleus terminate in the principal trigeminal nucleus (Luo, P. *et al.*, 1991; 1995), which in turn, relays proprioceptive information to the contralateral (and possibly ipsilateral) ventroposterior complex (e.g., Williams, M. N. *et al.*, 1994). Thus, most or all of the second-order neurons in the principal trigeminal nucleus that are responsive to proprioceptive inputs are activated by first-order afferent neurons with cell bodies in the mesencephalic trigeminal nucleus.

The trigeminal complex also includes a motor nucleus (Mo5) with cells projecting to muscles of the face and tongue. Some of the inputs to Mo5 are from Me5. The supratrigeminal nucleus and the intertrigeminal nucleus are additional motor nuclei associated with the trigeminal complex (Waite, P. M. E. and Ashwell, K. W. S., 2004).

6.07.4 The Nuclei of the Somatosensory Thalamus, Their Spinal Cord and Brainstem Somatosensory Inputs, and Their Cortical Projections

The somatosensory thalamus of primates includes three major nuclei (Figure 2): VP, VPS, and VPI. VP is the main relay of tactile information to the somatosensory cortex, and is a nucleus that has been identified in all studied mammals. VPS relays information from deep receptors in muscles and joints to the cortex. This nucleus has not been recognized as such in mammals other than primates, but a homologue likely exists in all or most mammals. VPI has spinothalamic inputs and projects broadly to somatosensory cortical areas. As for VPS, VPI is not generally recognized in nonprimate mammals, but has been recognized in squirrels, raccoons, and cats (Herron, P., 1983; Herron, P. and Dykes, R. W., 1986; Krubitzer, L. A. and Kaas, J. H., 1987). In addition to these three nuclei, the anterior pulvinar of primates is associated with somatosensory processing as it has reciprocal connections with the somatosensory cortex. Another subdivision of the pulvinar complex, the medial pulvinar, has connections with posterior parietal cortical fields involved in generating visually directed reaching and grasping and multisensory integration, which suggests that this nucleus is involved in higher-order functions. The lateral posterior nucleus, a less well-defined structure, also has connections with subdivisions of the posterior parietal cortex. However, in cats and a number of other mammals, components of the visual pulvinar have been included in the lateral posterior nucleus or

complex. In most mammals, one or more nuclei have been defined as belonging to the posterior complex (Po), which has somatosensory and multisensory functions. Finally, the ventromedial posterior nucleus, VMpo, has been proposed as a nucleus involved in the sensation of pain and temperature (Craig, A. D. *et al.*, 1994), and the parvocellular ventroposterior medial nucleus (VPMpc) is involved in relaying information about both touch and taste to the cortex (Kaas, J. H. *et al.*, 2006). The focus here is on the three main nuclei of the VP complex: VP, VPS, and VPI.

6.07.5 The Ventroposterior Nucleus

VP is a basic subdivision of the mammalian thalamus (Welker, W. I., 1973; Jones, E. G., 2007) that is easily identified by its densely packed, darkly stained neurons (Figure 5(b)) and its ventral location just posterior to the motor thalamus in coronal brain sections stained for cell bodies (Nissl stain). Neurons in VP express high levels of the metabolic enzyme CO (Figure 5(a)), and the calcium-binding protein parvalbumin (Rausell, E. *et al.*, 1992). In contrast, VP expresses very little of the calcium-binding protein calbindin (Figure 5(c)). These are some of the histochemical features that distinguish VP from the adjacent thalamic nuclei in primates: VPS and VPI. Neurons in VPS and VPI are less densely packed and less darkly stained for Nissl substance, and express less CO and more calbindin. The histological features that distinguish VP are also present in other primary sensory nuclei of the thalamus (the lateral geniculate nucleus and the ventral nucleus of the medial geniculate complex). The distinction between the VP and the VPS is less pronounced in macaque monkeys (see Figure 7) (e.g., Paxinos, G. *et al.*, 2000) and humans (e.g., Morel, A. *et al.*, 1997), where VPS more closely resembles VP in cytoarchitecture than in prosimian galagos (Figure 5) and New World monkeys (Figure 6; Krubitzer, L. A. and Kaas, J. H., 1992). Thus, most early studies of the connections and physiology of VP in macaques did not distinguish between VP and VPS and combined results from both nuclei. The clear architectonic distinctions between VP and VPS in prosimian primates and New World monkeys reflect major differences in the functional properties of neurons in the two structures, and in their patterns of cortical connections. These anatomical and functional differences are also found in macaque monkeys. Thus, there are reasons for distinguishing VP from VPS in all primates.

Another characteristic of VP is that the nucleus is divided into separate masses of cells by narrow cell-poor bands or septa (Figures 5–7). The most conspicuous of these across species is the band that separates the more medial part of VP representing the face from the more lateral part representing the body. These two divisions of VP, the ventroposterior medial division (VPM) and the ventroposterior lateral division (VPL), are typically distinguished as two nuclei separated by a prominent septum called the arcuate lamina, but they are more accurately considered major divisions of VP. Other septa are species variable, but common. In primates, a more lateral septum is present that separates the representations of the forelimb from the hindlimb, and often a narrow, less apparent septum separates a narrow band of cells on the lateral margin of VP, representing the tail from more medial cells representing the hindlimb. In favorable preparations, even septa separating representations of the digits of the hand are apparent in the subnucleus devoted to the hand. In the medial division of VP (VPM), other septa are apparent as they separate groups of cells devoted to different parts of the face and mouth. These septa are also apparent in brain sections processed for CO, myelin, or parvalbumin. Septa are especially numerous in VPM of macaque monkeys (Rausell, E. and Jones, E. G., 1991), although the assignment of specific cell clusters to parts of the face and mouth representations has not been fully determined. Septa separating cell groups that represent distinct body parts, or even individual facial whiskers of some rodents, commonly occur at different levels of the somatosensory system, including the dorsal column–trigeminal complex, the VP of the thalamus, and the primary somatosensory cortex (Welker, W. I., 1973; Killackey, H. and Rhoades, R. W., 1995). These segregating septa may emerge in development as a consequence of perturbations in the balance of target-selection factors by axons based on neural activity patterns and position-dependent attractions (Kaas, J. H. and Catania, K. C., 2002). The septa correspond to discontinuities or disruptions in the distribution of receptors in the skin, and these segregating septa are determined by the body form, including the separation of fingers and the isolation of receptors at the base of each protruding sensory hair from those for other hairs. The sizes of the segregated cell clusters in the thalamus and elsewhere vary according to the number and sizes of the afferents they subserve.

In addition, the cell clusters often have places where they merge with other clusters, as groups of peripheral receptors are usually not completely isolated from each other. Receptor populations for the fingers, for example, are isolated from each other except where the fingers join the palm at their base. These isolated cell clusters in the somatosensory brainstem, thalamus, and cortex are not equivalent to the classical cortical columns (Mountcastle, V. B., 1997), which correspond to alternating patches of cortical neurons that are activated by one class of peripheral afferent or another (e.g., Sur, M. *et al.*, 1984).

Although there are clear disruptions in the continuity of the somatotopy in VP, the overall pattern is consistent across mammals (Welker, W. I., 1973). From medial to lateral, the representation transitions from mouth to face, forelimb, hindlimb, and tail. When they have been demonstrated, the representations of the ipsilateral tongue and teeth are most medial (Bombardieri, R. A. *et al.*, 1975; Jones, E. G. *et al.*, 1986). The distal limbs are represented ventrally, or ventrorostrally, and the proximal limbs and trunk are represented dorsally. This somatotopy is portrayed in more detail for VP of the squirrel monkey in Figure 8. Note that the digits of the hand and the toes of the foot (1–5) are represented in order from medial to lateral in the subnuclei devoted to the hand and foot. Moreover, the digit and toe tips are represented ventrally, while the bases are represented dorsally. In detail, the representations are complicated by separating septa and by folds in the continuous parts of the representation (Kaas, J. H. *et al.*, 1984). In addition, there is likely to be a segregation of clusters of neurons activated by the SA-I class of peripheral afferents from those activated by the RA-I class (Dykes, R. W. *et al.*, 1981; Zhang, H. Q. *et al.*, 2001). Thus, VP likely contains at least two interdigitated maps of the cutaneous receptors of the contralateral body: one for RA receptors and one for SA receptors (see Sur, M. *et al.*, 1984 for cortex). As in other parts of the somatosensory system, the representations of body parts in VP are proportional to receptor density, so that, for example, the distal phalanges of the digits with high concentrations of afferents have proportionally larger representations than those of the proximal phalanges with fewer afferents. Lee C. C. and Woolsey C. N. (1975) have called this a peripheral scaling factor. In rare instances, the representation of important sensory surfaces can be greater than that predicted by the proportional representation of peripheral afferents. Such an overrepresentation has been called afferent magnification (Catania, K. C. and Kaas, J. H., 1997).

The major activating inputs to VP are from the SA-I and RA-I afferents relayed from the dorsal column–trigeminal complex via the medial lemniscus (Figure 2; Smith, R. L., 1975; Berkley, K., 1980; Kalil, K., 1981; Asanuma, H. *et al.*, 1983). Neurons responding to Pacinian (RA-II) inputs have been detected along the ventral margin of the nucleus (Dykes, R. W. *et al.*, 1981), but their distribution within VP is uncertain. Possibly SA-II afferents also activate VP neurons, but this is unknown. As SA-II afferents may contribute to a sense of digit position (McCloskey, P. I., 1974), they seem functionally more related to VPS, which is involved in proprioception. A few neurons in VP are activated by WDR afferents (e.g., Kenshalo, D. R. J. *et al.*, 1980). These neurons respond to light tactile stimuli, but respond with increasing magnitude as the stimulus intensity increases into the painful range. These neurons in the WDR category likely correspond to the small neurons in the septal regions of VP that have spinothalamic inputs (Rausell, E. *et al.*, 1992). Because some of these septal regions merge ventrally with VPI, which also has spinothalamic inputs and histologically resembles VP septal zones, one interpretation of the VP septa is that they are extensions of VPI (Krubitzer, L. A. and Kaas, J. H., 1992; Wilson, P. *et al.*, 1999). However, VP appears to receive most of its spinothalamic inputs from WDR neurons in layer 5 of the dorsal horn of the spinal cord, while VPI also receives inputs from the nociceptive neurons of layer 1 (Craig, A. D., 2006). A few neurons in VP are responsive to afferents that innervate the bladder, colon, and esophagus, and most of these were WDR or nociceptive, also often responding to afferents from skin (Brüggemann, J. *et al.*, 1994). In addition, spinothalamic axons terminate in a number of small patches along the rostral and caudal borders of VP (Stepniewska, I. *et al.*, 2003). These patches seem to be at least partly outside of VP (Figure 9).

In summary, SA-I and RA-I inputs dominate VP, but other inputs are expressed as well. In humans, electrical stimulation of neurons in VP generally results in a feeling of numbness or tingling in some skin location, rather than touch (e.g., Davis, K. D. *et al.*, 1996; Lenz, F. A. *et al.*, 1998), and localized lesions of VP are followed by persistent numbness in some skin region (e.g., Domino, E. F. *et al.*, 1965).

The inputs to VP of other mammals, judging from the well-studied cats and rats, appear to be similar to those of primates in that the dominating

somatosensory input is from the dorsal column–trigeminal complex. In rats, dorsal column nuclei project densely to VP (Lund, R. D. and Webster, K. E., 1967a), while spinothalamic afferents terminate along the caudal and rostral borders of VP, and more sparsely within VP (Lund, R. D. and Webster, K. E., 1967b; Ma, W. *et al.*, 1986). Spinothalamic afferents from lamina 1 of the dorsal horn of the spinal cord, which carry nociceptive and thermoreceptive information, terminate at the caudal margin of VP (Gauriau, C. and Bernard, J. F., 2004), possibly in a separate nucleus, as in VPMpo of primates (Craig, A. D., 2007). In cats, the dominant inputs to VP are from the dorsal column–trigeminal complex

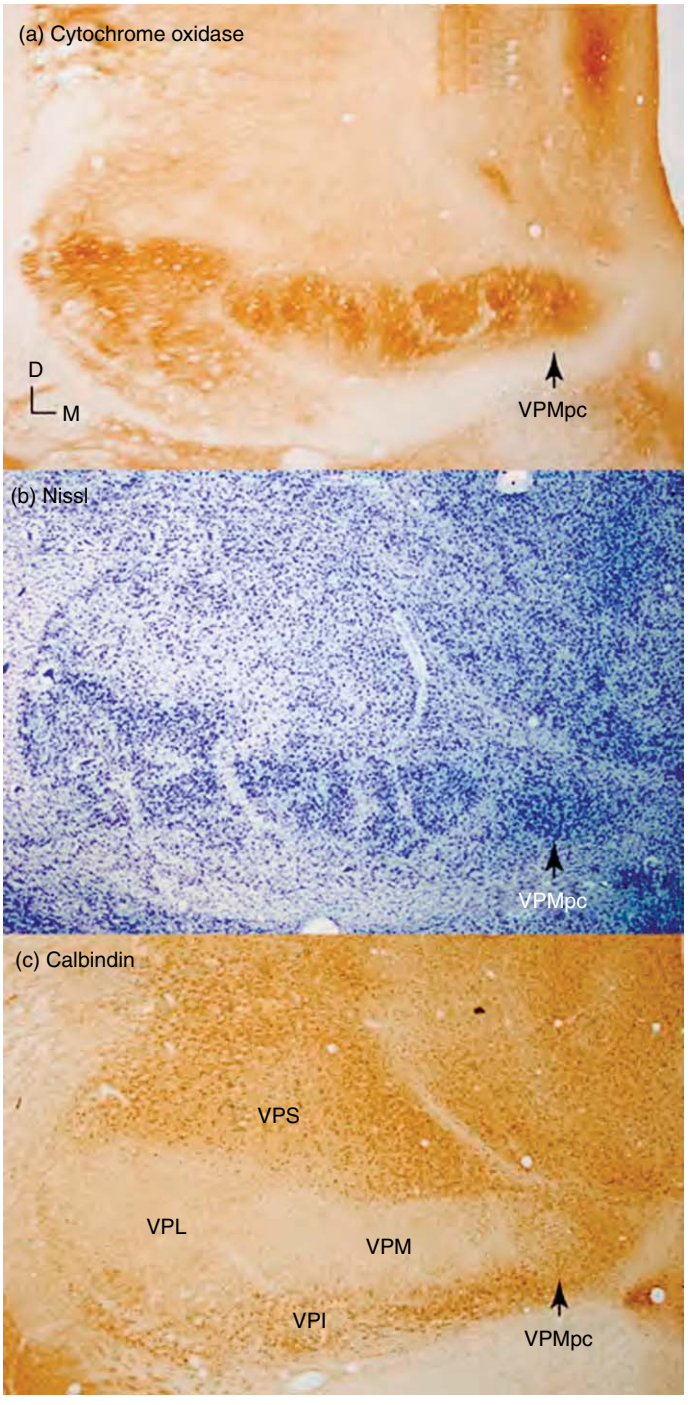

(Berkley, K., 1980), while the spinothalamic afferents project mainly to the ventral border of VP (Craig, A. D. and Burton, H., 1985) in VPI (Herron, P. and Dykes, R. W., 1986).

As for other thalamic nuclei, VP includes both relay neurons projecting to the cortex and about 30% interneurons with connections within the nucleus (e.g., Spreafico, R. *et al.*, 1983; Chmielowska, J. and Pons, T. P., 1995). The interneurons are inhibitory GABAergic neurons. Curiously, rats and possibly other rodents have very few (1%) GABAergic neurons in VP (Harris, R. M. and Hendrickson, A. E., 1987), and inhibitory functions in the nucleus largely depend on inputs from GABAergic neurons in the thalamic reticular nucleus. These reticular nucleus neurons are activated by collaterals of VP relay neurons projecting to S1, and by cortical neurons in S1, which also provide feedback to VP (Deschênes, M. *et al.*, 1998). Besides inputs to VP from the somatosensory sector of the reticular nucleus (Crabtree, J. W., 1996), VP and other thalamic nuclei receive modulatory inputs from the ascending dorsal tegmental cholinergic system and from other diffusely organized modulatory systems (Sherman, S. M. and Guillery, R. W., 2006; Jones, E. G., 2007).

In all mammals, the major cortical projections of VP are to S1 (see Krubitzer, L. A. and Kaas, J. H., 1987, for review), which corresponds to area 3b of primates (Kaas, J. H., 1982). In most mammals, VP also projects to two adjoining areas, S2 and the parietal ventral somatosensory area, PV (see Krubitzer, L. A. and Kaas, J. H., 1987). This allows S2 and PV to be activated in parallel with S1.

Therefore, S2 and PV can be activated via VP after lesions of S1 (Garraghty, P. E. *et al.*, 1991). However, anthropoid primates (monkeys, apes, and humans), as well as raccoons, appear to have lost most of their VP inputs to S2 (Friedman, D. P. and Murray, E. A., 1986; Krubitzer, L. A. and Kaas, J. H., 1992; Disbrow, E. *et al.*, 2002; see Herron, P., 1983 for raccoons). In macaque monkeys, lesions of the anterior parietal cortex (area 3a, 3b, 1, and 2) result in a loss of 94% of the non-GABA-containing projection neurons, leaving few neurons to project to other areas, including S2 (Chmielowska, J. and Pons, T. P., 1995). Thus, S1 (3b) lesions deactivate S2 and PV in these mammals (Burton, H. *et al.*, 1990; Garraghty, P. E. *et al.*, 1990b; Pons, T. P. *et al.*, 1992). Across species, the major VP inputs to S1 (3b) are to layer 4 (e.g., Jones, E. G., 1975), where they have a powerful activating influence. In addition, the small cells in the septa of VP that are related to spinothalamic input project to the more superficial layers of area 3b (Rausell, E. and Jones, E. G., 1991; Jones, E. G., 1998), and possibly play a modulatory role. Some of these cells also project to other areas including S2 and PV (Stevens, R. T. *et al.*, 1993).

In anthropoid primates, VP has additional projections to two other areas of the anterior parietal cortex: area 1 (the posterior cutaneous field) and area 2 (the deep receptor field of the anterior parietal cortex). While architectonic fields 3a, 3b, 1, and 2 were once all considered to be parts of S1 in primates, there has been long-standing evidence that each of these fields is functionally distinct and contains a separate representation of the contralateral body (see below). In keeping with the functional distinctions between

Figure 5 Architectonic features of the nuclei of the ventroposterior complex of a prosimian primate (galago). In the lower panel (c), showing a coronal brain section, processed for the calcium-binding protein calbindin (Cb), the two major divisions of the ventroposterior nucleus (VP), the ventroposterior lateral (VPL) and the ventroposterior medial (VPM) subnuclei, correspond to the Cb-light central region. Just ventral to VP, the ventroposterior inferior nucleus (VPI) is characterized by neurons and neural processes that express moderate levels of Cb, as does the ventromedially located ventroposterior medial parvocellular nucleus (VPMpc) for taste, touch, and other functions. In the middle panel (b), an adjacent brain section was processed for Nissl substance to reveal the cell bodies of neurons. VP is characterized by densely packed, large neurons that are darkly stained. Groups of neurons within VP are separated from each other by lightly stained, cell-poor septa. The most notable septum separates VPL from VPM, but other septa are visible as well, including a septum in the middle of VPL that separates more lateral neurons representing the foot from more lateral neurons representing the hand. VPMpc has slightly smaller neurons, while VPI and ventroposterior superior nucleus (VPS) both have smaller, more scattered neurons so that the nuclei are less darkly stained. In the upper panel (a), both VP and VPMpc express moderate to dense levels of the metabolic enzyme, cytochrome oxidase (CO). Within VP, a CO-light septum separates VPL from VPM, and several CO-light septa are apparent in VPM. A septum in the middle of VPL is faintly visible. VPI expresses very little CO, while CO is faintly expressed in VPS. These architectonic distinctions, especially evident in some primates such as galagos, provide part of the evidence that VP, VPI, and VPS are separate nuclei within the ventroposterior complex. From Kass, J. H., Qi, H.-X., and Iyengar, S. 2006. Cortical network for representing the teeth and tongue in primates. Anat. Rec. 288A, 182–190.

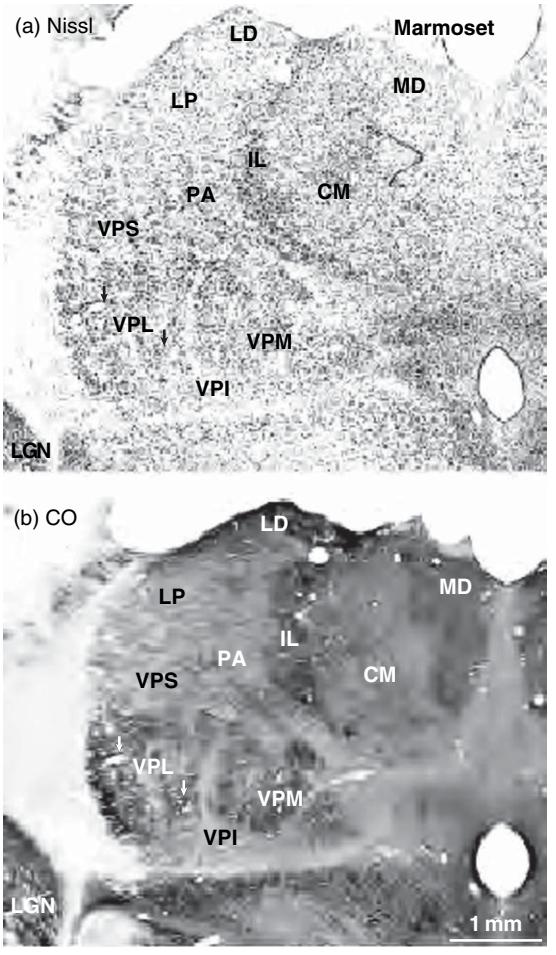

Figure 6 The architectonic subdivisions of the somatosensory thalamus of a marmoset, a small New World monkey. (a) A Nissl-stained section showing cell bodies. (b) An adjacent section processed for cytochrome oxidase (CO). Arrows mark the same two blood vessels for aligning the two sections. Note the darker cells and denser expression of CO in ventroposterior nucleus (VP) (ventroposterior lateral (VPL) and ventroposterior medial (VPM)). A cell-poor, CO-light septum separates VPL from VPM. The Nissl-stained cells in the ventroposterior superior nucleus (VPS) are notably lighter than those in VP, but darker than in the ventroposterior inferior nucleus (VPI) of galagos, making the boundary between VP and VPS less obvious. However, the expression of CO is notably less in VPS than in VP. VPI is less darkly stained than VP in both preparations. The locations of the anterior pulvinar (PA) and the lateral posterior nucleus (LP), both with somatosensory functions, are indicated. The lateral dorsal (LD) nucleus, the intralaminar nucleus (IL), the center median nucleus (CM), the medial dorsal nucleus (MD), and the lateral geniculate nucleus (LGN) are labeled for reference. From Qi, H.-X., Lyon, D. C., and Kaas, J. H. 2002. Cortical and thalamic connections of the parietal ventral somatosensory area in marmoset monkeys (*Callithrix jacchus*). J. Comp. Neurol. 443, 168–182.

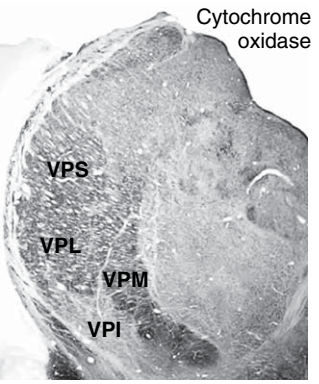

Figure 7 A coronal brain section through the somatosensory thalamus of a two-month-old macaque monkey that has been processed for cytochrome oxidase (CO). Note that the ventroposterior nucleus (VP) (ventroposterior lateral (VPL) and ventroposterior medial (VPM)) densely expresses CO, and a septum separating VPM from VPL is prominent. Ventroposterior superior nucleus (VPS) expresses only slightly less CO than VP. Because VPS is also only slightly less darkly stained in Nissl preparations than VP of macaque monkeys, the two nuclei were considered to be a single nucleus, VP, in early studies. Ventroposterior inferior nucleus (VPI) expresses little CO.

areas 3b, 1, and 2, which can be considered successively higher levels of cortical processing (e.g., Felleman, D. J. and Van Essen, D. C., 1991), VP projects less densely to area 1, and the axons of the neurons projecting to area 1 are thinner, and more slowly conducting than those projecting to area 3b. Further, the terminations of these axons in area 1 are in layer 3 rather than layer 4 (Jones, E. G., 1975). Locations in VP project to somatotopically matched locations in all parts of both the representations in area 3b and in area 1 (Lin, C.-S. *et al.*, 1979; Nelson, R. J. and Kaas, J. H., 1981; Mayner, L. and Kaas, J. H., 1986; Darian-Smith, C. *et al.*, 1990; Krubitzer, L. A. and Kaas, J. H., 1992). More neurons in VP project to area 3b than to area 1 (Nelson, R. J. and Kaas, J. H., 1981), and it is possible that only the RA-I class of VP relay cells projects to area 1. However, perhaps as many as 20% of VP neurons project via collaterals to both areas 3b and 1 (Cusick, C. G. *et al.*, 1985). In addition, parts of area 2 and even area 5 that are most responsive to cutaneous stimuli, those representing the glabrous hand and face, receive sparse inputs from VP, at least in macaque monkeys (Pons, T. P. and Kaas, J. H., 1985). Finally, a few neurons in VP of macaques project to the part of area 5 that is responsive to light tactile stimuli on the forelimb (Pons, T. P. and Kaas, J. H., 1985).

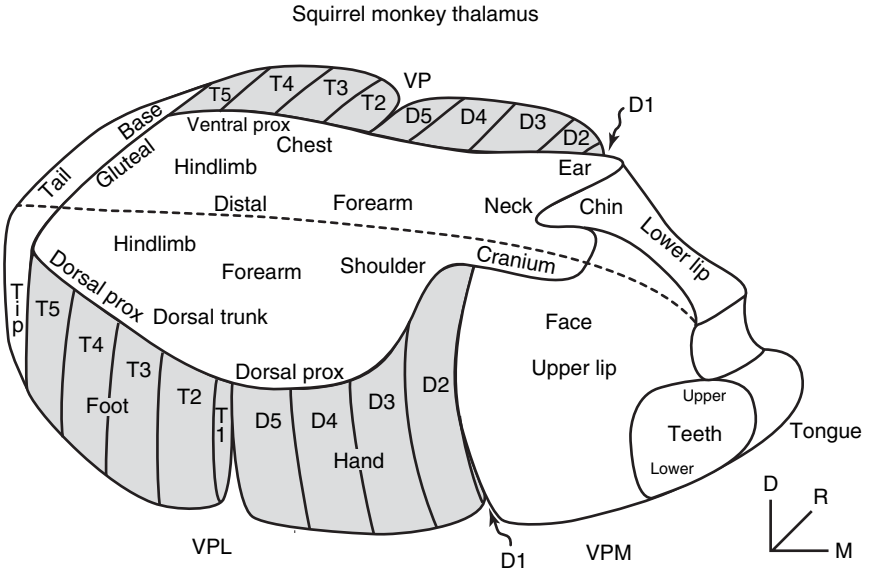

Figure 8 The somatotopic organization of the ventroposterior (VP) nucleus of squirrel monkeys. This 3D rendition is viewed from the back. The medial division of VP, the ventroposterior medial (VPM) subnucleus, devotes large territories to the lips, teeth, and tongue. A most medial portion also represents the ipsilateral teeth and tongue (not shown). A septum separates VPM from the lateral division, ventroposterior lateral nucleus (VPL). A septum within VPL separates the more medial representation of the hand from the more lateral representation of the foot. The tail is represented most laterally. A dorsal cap of VP represents the limbs, trunk, and cranium. Note that digits (D1–D5) and toes (T1–T5) are represented in order. Adapted from Kaas, J. H., Nelson, R. J., Sur, M., Dykes, R. W., and Merzenich, M. M. 1984. The somatotopic organization of the ventroposterior thalamus of the squirrel monkey, *Saimiri sciureus*. J. Comp. Neurol. 226, 111–140.

6.07.6 The Ventroposterior Superior Nucleus

The VPS forms a dorsal cap on the VP of primates. Although the region had long been recognized as having a concentration of inputs from receptors in deep tissues, muscles, and joints, in contrast to VP proper where inputs relayed from cutaneous receptors predominate, traditionally, the VPS region was usually included in VPL (e.g., Poggio, G. F. and Mountcastle, V. B., 1963). VPS was distinguished as a separate nucleus after the results of extensive microelectrode recording experiments were related to thalamic architecture in squirrel monkeys (Kaas, J. H. *et al.*, 1984). The results indicated that VPS is architectonically distinct from VP, and that each nucleus contains a separate representation of the contralateral body with VPS devoted to muscle spindle receptors, while VP is devoted to cutaneous receptors. In general, VPS has neurons that are less darkly stained in Nissl preparations, and less densely packed than neurons in VP. Further, VPS expresses less CO (Krubitzer, L. A. and Kaas, J. H., 1992) and less acetylcholinesterase (Pons, T. P. and Kaas, J. H., 1985) than does VP. VPS also expresses more calbindin and less parvalbumin (Figure 5). Inputs to VPS are from neurons in brainstem and upper spinal cord nuclei, such as the external cuneate nucleus. These inputs are activated by muscle spindle afferents and they send axons into the contralateral medial lemniscus (Berkley, K., 1980; Boivie, J. and Boman, K., 1981). Recordings in VPS, previously recognized as a rostral cap of VP (Maendly, R. *et al.*, 1981) or an anterodorsal shell of VP (Friedman, D. P. and Jones, E. G., 1981), indicate that the vast majority of neurons are activated by muscle spindle receptors (Wiesendanger, M. and Miles, T. S., 1982). VPS projects to areas 3a and 2 (Jones, E. G. *et al.*, 1979; Friedman, D. P. and Jones, E. G., 1980; 1981; Cusick, C. G. *et al.*, 1985; Pons, T. P. and Kaas, J. H., 1985; Darian-Smith, C. *et al.*, 1990; Akbarian, S. *et al.*, 1992; Darian-Smith, C. and Darian-Smith, I., 1993; Huffman, K. J. and Krubitzer, L. A., 2001). Possibly as many as 40% of the relay neurons in VPS project via collaterals to somatotopically matched locations in both area 3b and area 2 (Cusick, C. G. *et al.*, 1985), as both of these fields contain systematic tail-to-tongue representations of deep receptors in mediolateral

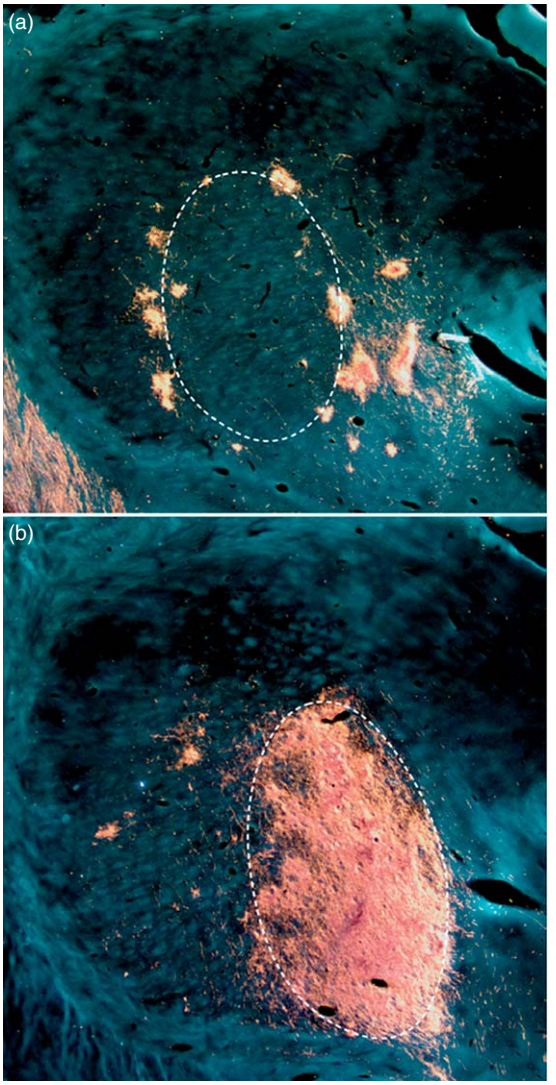

Figure 9 Parasagittal brain sections through the somatosensory thalamus after being processed for axon terminals labeled with wheatgerm agglutinin conjugated to horseradish peroxidase (WGA–HRP). In panel (a), an injection of WGA–HRP into the cervical spinal cord of a macaque monkey labeled patches of terminals along the rostral (left) and caudal borders of the ventroposterior nucleus, VP. Other patches of labeled terminals are in divisions of the posterior nuclei caudal to VP. In panel (b), an injection of WGA–HRP was placed in the contralateral dorsal column nuclei and VP was densely labeled. A few patches of labeled terminals were rostral to VP in the motor thalamus. In both panels, VP is outlined. (a) From Stepniewska, I., Sakai, S. T., Qi, H.-X., and Kaas, J. H. 2003. Distribution of somatosensory pathways in relation to thalamic neurons relaying information to the motor and premotor cortex in the macaque monkey. Soc. Neurosci. Abstr. 29, 60.16.

sequences that parallel those of areas 3b and 1 (e.g., Kaas, J. H. *et al.*, 1979; Pons, T. P. *et al.*, 1985; Huffman, K. J. and Krubitzer, L. A., 2001; Krubitzer, L. A. *et al.*, 2004).

As expected from the more extensive evidence from monkeys, an orderly representation of deep receptors has been described as just rostrodorsal to the representation of cutaneous receptors in VP of humans (Lenz, F. A. *et al.*, 1990; Ohye, C. *et al.*, 1993; Seike, M., 1993).

This human VPS represents receptors activated by movements of the jaw, digits, arm, and leg in a mediolateral sequence. Human VPS is located in a region of thalamus that has been variously identified, but most recently termed anterior VP or anterior VPL (Morel, A. *et al.*, 1997). Rather than an anterior or anterodorsal division of VP, the evidence for distinctly different inputs and outputs, as well as histological differences, justifies distinguishing the region as a separate nucleus in the ventroposterior complex, VPS.

There is also evidence for VPS in nonprimate mammals, although the nucleus may not be well differentiated. However, a problem in identifying VPS in nonprimates is that the cortical targets of VPS in primates, areas 3a and 2, often have not been identified. However, in all mammals, it appears that the primary somatosensory cortex, S1 or area 3b, is bordered rostrally by a narrow zone of the cortex that likely subserves proprioception and is also, based on position and function, a likely homologue of area 3a (Krubitzer, L. A. *et al.*, 2004; Kaas, J. H., 2007b). In rodents, the evidence for area 3a is most clear for squirrels, although there is supporting evidence from rats. In both rodents, S1 is histologically very distinct in preparations of sections cut parallel to the surface of the flattened cortex as a highly granular zone (packed with densely stained, small neurons) that also expresses high levels of CO and myelin (Krubitzer, L. A. and Kaas, J. H., 1987; Jain, N. *et al.*, 2003). The cortex along the rostral border of this S1 has been called dysgranular cortex (Chapin, J. K. and Lin, C. S., 1984), as layer 4 is less pronounced than in S1. In squirrels and rats, part of this dysgranular zone protrudes caudally between the representatives of the face and the forelimb in S1. The larger size of this protrusion of area 3a into S1 of squirrels made it a suitable target for injection of tracers that revealed the connections of the dysgranular cortex (Gould, H. J. *et al.*, 1989). The thalamic inputs to this dysgranular cortex were largely from a thalamic zone along the dorsal border of VP that has been referred to by

various names, but in rodents is called the posterior nucleus with medial (POm) and lateral (POl) divisions (e.g., Jones, E. G., 2007). More recently, Francis J. T. *et al.* (2003) used the results of microelectrode recordings to divide the somatosensory thalamus of rats into a middle zone of VP that responds to cutaneous somatosensory stimuli and a rostral subnucleus of VP that responded mainly to proprioceptive inputs. Furthermore, projections from the external cuneate nucleus in rats (Mantle-St. John, L. A. and Tracey, D. J., 1987), which carry muscle spindle information, terminate in the same rostrodorsal region of the somatosensory thalamus. Thus, rodents have a thalamic nucleus for proprioception that has been variously considered a subnucleus of VP or a rostrodorsal capping nucleus of VP, just as has VPS of primates. The nucleus projects to the dysgranular cortex that appears to be a homologue of area 3a of primates.

Other evidence comes from experiments in carnivores. Most notably, in raccoons, microelectrode recordings from the somatosensory thalamus identified a distinct zone of proprioceptive neurons responsive to receptors in muscles, tendons, and joints that were located rostrodorsal to the zone responsive to cutaneous stimulation (Wiener, S. I. *et al.*, 1987). As the functionally distinct zones were architectonically similar, they were termed cutaneous and kinesthetic divisions of VP (termed Vb for ventrobasal nucleus), although the kinesthetic division of VP was described as having less cell density (Wiener, S. I. *et al.*, 1987). The kinesthetic thalamic zone projects to a 3a-like strip of the dysgranular cortex rostral to S1 (Doetsch, G. S. *et al.*, 1988; Feldman, S. H. and Johnson, J. I., 1988). In cats, the situation is similar, as a rostrodorsal cap on VP has been identified as a proprioceptive nucleus with inputs from muscle spindle receptors (Andersson, S. A. *et al.*, 1966; Maendly, R. *et al.*, 1981; Wiesendanger, M. and Miles, T. S., 1982; Kniffki, K.-D. and Mizumura, K., 1983). This thalamic region, which Dykes R. W. *et al.* (1986) called the ventroposterior oralis nucleus (VPO), appears to correspond to VPS of monkeys. In cats, the cortex between S1 (area 3b) and the primary motor cortex (M1) has long been considered to be area 3a on architectonic grounds (Hassler, R. and Muhs-Clement, K., 1964). This 3a of cats is activated by receptors in muscles and joints (e.g., Dykes, R. W. *et al.*, 1980) and it receives projections from VPO (Dykes, R. W. *et al.*, 1986; Zheng, A.-H. *et al.*, 1986). Thus, at least in carnivores and rodents, there is evidence of a proprioceptive nucleus in the thalamus that is in the relative position of VPS of primates and projects to area 3a or a 3a-like area, as does VPS of primates. A difference is that VPS of moneys also projects to area 2, a subdivision of the somatosensory cortex that may not exist in nonprimate mammals (Kaas, J. H., 2004; 2007a), although the cortex caudal to S1 has been classified as area 1–2 (presumably, a composite of areas 1 and 2) in some instances.

An area 2 is sometimes distinguished in the somatosensory cortex of cats, although this appears to be a misidentification, as some investigators distinguish areas 3b, 1, and 2 within a single area 3b body representation (see for review, Felleman, J. D. *et al.*, 1983). In a detailed reinvestigation of the organization of the somatosensory cortex of cats, Myasinkov A. A. *et al.* (1994) found evidence for two representations of body receptors in the cortex caudal to S1 (they identified S1 as area 3b), with neither corresponding to previously proposed areas 1 and 2, and neither activated by deep receptors. Even in prosimian primates, there is no clear evidence for an area 2, and the cortex caudal to S1 (area 3b) in the position of area 1 is not very responsive to cutaneous stimuli in anesthetized animals, so there are uncertainties even about area 1 (e.g., Wu, C. W.-H. and Kaas, J. H., 2003). Furthermore, the presence of an area 2 has been questioned for some New World monkeys (Padberg, J. *et al.*, 2005), further complicating the use of projections to area 2, as well as those to area 3a, in identifying VPS.

Presently, the evidence suggests that a nucleus responsive to proprioceptive inputs, termed VPS here, is segregated from VP in a wide range of mammals, and this nucleus projects to a proprioceptive zone of the cortex at the rostral border of S1 that is recognized as area 3a in primates and cats, but is variously recognized and named in other mammals. The comparative evidence suggests that area 2, as a secondary target of VPS, emerged with the evolution of anthropoid primates (Kaas, J. H., 2007a), although an area 2 with a mixed representation of deep and cutaneous receptors is not clearly present in all investigated New World anthropoids.

6.07.7 The Ventroposterior Inferior Nucleus

VPI was first distinguished by Crouch R. L. (1934) in macaque monkeys, where it was described as a cell-sparse region ventral to VP. Jones E. G. (2007)

considered VPI to be distinct only in the brains of primates, although the nucleus is obvious in the brains of raccoons (Herron, P. *et al.*, 1997), carnivores with specialized hand use, as in primates. The neurons in VPI are smaller and less densely stained in Nissl preparations than neurons in VP, and VPI expresses less CO and parvalbumin, and more calbindin than VP (Figures 5–7; also see Rausell, E. and Jones, E. G., 1991; Krubitzer, L. A. and Kaas, J. H., 1992). The septal regions that separate the subnuclei of VP are almost identical in histological appearance with VPI proper, and spinothalamic inputs and projections to superficial cortical layers are shared, so it seemed parsimonious to include these septal regions with the main body of VPI as a single nucleus (Krubitzer, L. A. and Kaas, J. H., 1992; also see Wilson, P. *et al.*, 1999). However, there is evidence that the sources of spinothalamic inputs to VPI proper and the septal regions of VP are somewhat different, with the WDR neurons of lamina 5 of the dorsal horn of the spinal cord projecting to septa within VP, and both lamina 5 and nociceptive neurons in lamina 1 projecting to VPI proper (Craig, A. D. and Zhang, E. T., 2006). Thus, there are also arguments for not including septal regions of VP in VPI.

In monkeys, the major source of sensory information to VPI is from the spinothalamic tract, including inputs from the spinal trigeminal nuclei (Mehler, W. R. *et al.*, 1960; Boivie, J., 1980; Burton, H. and Craig, A. D., 1983; Mantyh, P. W., 1983; Apkarian, A. V. and Hodge, C. J., 1989; Ralston, H. J. and Ralston, D. D., 1992). There have been suggestions for a relay of Pacinian afferents, as well (Dykes, R. W. *et al.*, 1981; Herron, P. and Dykes, R. W., 1986), but this seems unlikely as the small cells of VPI and their superficial cortical projections seem incongruent with a low-threshold, rapidly conducting pathway for a Pacinian RA-II subsystem. In addition, Pacinian afferents would relay from dorsal column nuclei rather than from spinothalamic neurons. Some inputs may be from vestibular nuclei, but they are sparse (Deecke, L. *et al.*, 1974; Lang, W. *et al.*, 1979). Recordings indicate that VPI contains a somatotopic representation of afferents from the contralateral body that parallels the representation in VP, and that the major activating input is from WDR peripheral nerve afferents (Craig, A. D., 2007).

In monkeys, the major cortical projections of VPI are to higher-order somatosensory areas, S2 and PV (Friedman, D. P. and Murray, E. A., 1986; Krubitzer, L. A. and Kaas, J. H., 1992; Disbrow, E. *et al.*, 2002; Qi, H.-X. *et al.*, 2002; Coq, J. O. *et al.*, 2004). VPI projects much less densely to other somatosensory areas, such as 3b and 1. Projections to areas 3b and 1 also come from neurons in the embedded septal regions of VP (Penny, G. R. *et al.*, 1982; Rausell, E. and Jones, E. G., 1991). The VPI projections and septal neuron projections are to the superficial layers of the somatosensory cortex, rather than layer 4, and thus are likely to be modulatory instead of driving. This supposition is supported by the observations that S2 and PV, with dense VPI inputs, depend on areas 3a and 3b for activation (Garraghty, P. E. *et al.*, 1990a; Pons, T. P. *et al.*, 1992), and that neurons in S2 and PV respond vigorously to light tactile stimulation (see Coq, J. O. *et al.*, 2004, for review), while VPI neurons do not.

In addition to being recognized in primates, VPI has been described as a distinct nucleus in both cats and raccoons (see Herron, P., 1983; Craig, A. D. and Burton, H., 1985). As in primates, VPI of these carnivores consists of a narrow band of small cells that are lightly stained in Nissl preparations. VPI is just ventral to VP, and the septal regions in VP have lightly stained cells, as in VPI, and are continuous with VPI. Spinothalamic terminations terminate both in VPI proper and in and around VP septal zones (e.g., Berkley, K., 1980; Craig, A. D. and Burton, H., 1985). VPI is larger and more distinct in raccoons, and it appears to receive denser spinothalamic inputs. As in monkeys, there is evidence that Pacinian inputs activate neurons in VPI of cats and raccoons (Herron, P. and Dykes, R. W., 1986), but others place the Pacinian-responsive neurons in ventral VP (Fisher, G. R. *et al.*, 1983). In raccoons, Herron P. (1983) showed for the first time in a convincing manner that VPI projects strongly to S2, although there was some evidence for this from an earlier study in cats (Rinvik, E., 1968). Later studies more conclusively demonstrated VPI projections to S2 in cats (Herron, P. and Dykes, R. W., 1986).

In rats, there is not much of a region ventral to VP that can be identified as VPI (Jones, E. G., 2007), and spinothalamic axons terminate mainly on the rostral and caudal borders of VP (McAllister, J. P. and Wells, J., 1981). However, in squirrels, a small, thin VPI that contains small, lightly stained (Nissl) neurons has been identified (Krubitzer, L. A. and Kaas, J. H., 1987). While no connections were demonstrated between S2 and this VPI, connections with PV were found. A few connections with S1 were also revealed.

In conclusion, most of the evidence for the existence of VPI comes from studies on primates,

although a comparable region of the thalamus has been identified in raccoons, cats, and squirrels. It is not certain from the limited attempts to identify and characterize VPI if the nucleus is a basic component of the mammalian thalamus, although usually not a very distinctive part, or if a nucleus with similar histological characteristics and connections arose independently in primates, carnivores, and some rodents. The main function of VPI seems to be to relay modulating influences based on spinothalamic inputs activated by WDR afferents, to cortical areas S2 and PV, and to a lesser extent S1 and bordering somatosensory fields. The suggestions of Pacinian inputs to VPI deserve further study, but the limited evidence is open to the interpretation that the Pacinian-like thalamic cells are in ventral VP rather than VPI.

6.07.8 Other Nuclei: The Anterior Pulvinar, the Lateral Posterior Nucleus, the Posterior Group, the Ventroposterior Parvocellular Nucleus, and the Ventromedial Posterior Nucleus

A number of other thalamic nuclei contribute to somatosensory function in primates and other mammals. In monkeys, the anterior (oral) pulvinar, which has been identified only in primates, has widespread interconnections with somatosensory areas of anterior, posterior, and lateral subdivisions of the parietal cortex (e.g., Pons, T. P. and Kaas, J. H., 1985; Cusick, C. G. and Gould, H. J. I., 1990; Padberg, J. and Krubitzer, L. A., 2006). As the anterior pulvinar receives inputs from the somatosensory cortex and it projects back to the somatosensory cortex, the anterior pulvinar spreads activity (Sherman, S. M. and Guillery, R. W., 2006) across somatosensory areas, possibly coordinating activities in several areas, rather than providing an additional source of sensory information. Another subdivision of the pulvinar complex, the medial pulvinar, has connections with areas of the posterior parietal cortex that are multisensory or somatosensory, as well as areas of cingulate and the frontal cortex (see Stepniewska, I. *et al.*, 2004, for review). These nuclei of the primate thalamus have no obvious homologues in nonprimates.

The lateral posterior nucleus or region in primates also has interconnections with regions of the posterior and lateral parietal cortex (see Padberg, J. and Krubitzer, L. A., 2006). Comparisons with nonprimates are complicated by the common use of the term lateral posterior complex or nucleus to refer to part of or all of the visual pulvinar. Thus, different parts of the thalamus are called lateral posterior across taxa. Another region, the Po is also defined somewhat differently across species. In rats, the posterior nucleus is divided into medial and lateral nuclei. Both receive a mixture of somatosensory inputs from the brainstem and spinal cord and are interconnected with S1 and S2, and possibly other areas of the somatosensory cortex (see Groenewegen, H. J. and Witter, M. P., 2004). Similar nuclei, POm and POl, have been described in cats, where POl is mainly involved in processing auditory information, while POm has connections with the somatosensory areas of the cortex (Jones, E. G., 2007). A more caudal region of the thalamus is defined as the posterior complex in primates, where connections are with the somatosensory and multisensory cortex of the lateral fissure (Burton, H. and Jones, E. G., 1976).

A nucleus in the medioventral margin of VP, VPMpc (also known as the basal ventral medial nucleus, VMb) is sometimes referred to as the thalamic taste nucleus, although it receives inputs relayed from cutaneous and other somatosensory afferents in addition to those for gustation. In primates, VPMpc projects to the representation of the tongue in S1 (area 3b) and to a gustatory region, area G, in the cortex of the rostral part of the lateral sulcus (Kaas, J. H. *et al.*, 2006; Iyengar, S. *et al.*, 2007). Similar connections are likely in other mammals (Lundy, R. F. and Norgren, R., 2004).

Finally, Craig A. D. *et al.* (1994) have identified a region of the posterolateral thalamus of monkeys as the posterior ventral medial nucleus (VMpo). This nucleus, on the medial margin of VP just caudal to VPMpc, receives trigeminothalamic and spinothalamic inputs from nociceptive second-order neurons (Craig, A. D., 2004; 2007) and projects to the dorsal anterior insular cortex in the lateral sulcus. The nucleus is identified in part by its dense calbindin-positive fiber plexus. Craig A. D. (2004) regarded VMpo as novel to primates, and proposed that this relay in rats and cats involves VPI and VP (also see Zhang, X. *et al.*, 2006). This interpretation of the significance of VMpo has been criticized by Willis W. D. *et al.* (2002) for ignoring the nociceptive inputs to VP of primates that relay to S1 and S2. Jones E. G. (2007) has argued against the concept of VMpo. The proposal of Craig A. D. *et al.* (1994) has

provoked some thought and support, as well as disagreement, and further study is needed.

6.07.9 Cortical Projections to the Somatosensory Thalamus and Dorsal Column Nuclei

Cortical projections to the thalamus are obviously important in the functions of the somatosensory thalamus, as they are many times more numerous than the thalamocortical connections. These connections emerge from pyramidal neurons in layers 5 and 6, with the projections from layer 6 being denser while having smaller terminal endings. The less abundant projections from layer 5 terminate in the thalamus with large endings. The layer 6 projections are postulated to have weak, modulatory effects, while the layer 5 projections are considered to be feedforward, driving connections (Sherman, S. M. and Guillery, R. W., 2006). This laminar pattern of projections exists across cortical areas and mammalian species, with most thalamic nuclei receiving a mixture of layer 5 and layer 6 projections (Rouiller, E. M. and Welker, W. I., 2000). However, in rats, the S1 projection to VP originates entirely from layer 6 neurons (Killackey, H. P. and Sherman, S. M., 2003). The cortical projections to the somatosensory thalamus largely follow the general pattern that areas project back to the same thalamic regions that project to them. But thalamic nuclei also receive projections from somatotopically mismatched parts of a field, or fields without input from that nucleus. The layer 5 and 6 projections to the thalamus are excitatory, and they terminate on both relay neurons and inhibitory interneurons (see Li, L. and Ebner, F. F., 2007). Thalamic neurons may be influenced indirectly via cortical projections to the thalamic reticular nucleus, which has GABAergic inhibitory neurons projecting to the thalamus (Crabtree, J. W., 1996).

The corticothalamic projections to relay nuclei appear to alter the receptive field characteristics of projection neurons, sometimes by increasing the selectivity of these neurons according to behavioral state. For example, Li L. and Ebner F. F. (2007) found that microstimulation of neurons in the S1 cortex of rats rotates the angle of the directional selectivity for whisker movements of VPM neurons toward the direction that cortical neurons prefer. Cortical projections also help constrain the sizes of receptive field for VP neurons. When activity of neurons in S1 (area 3b) of macaque monkeys was suppressed, the receptive fields of neurons in VP increased in size (Ergenzinger, E. R. *et al.*, 1998). Similar results have been obtained in rats (Krupa, D. J. *et al.*, 1999; Chowdhury, S. A. *et al.*, 2004). Other cortical projections, especially those to the intrinsic nuclei such as the anterior pulvinar, may activate relay neurons so that information is transferred from one cortical area to another via the thalamus (Sherman, S. M. and Guillery, R. W., 2006).

The somatosensory cortex also projects to the contralateral dorsal column–trigeminal complex (Rustioni, A. and Sotelo, C., 1974; Wise, S. P. and Jones, E. G., 1977; Weinberg, R. J. *et al.*, 1990; Lue, J.-H. *et al.*, 1997; Martinez-Lorenzana, G., *et al.*, 2001;). One of the suggested functions of these cortical inputs is to activate intrinsic inhibitory neurons to selectively constrain the sizes of receptive fields for neurons in the nuclear complex (Wang, X. and Wall, J. T., 2005).

References

Akbarian, S., Grüsser, O. J., and Guldin, W. O. 1992. Thalamic connections of the vestibular cortical fields in the squirrel monkey (*Saimiri sciureus*). J. Comp. Neurol. 326, 423–441.

Andersson, S. A., Landgren, G., and Wolsk, D. 1966. The thalamic relay and cortical projection of group I muscle afferents from the forelimb of the cat. J. Physiol. 183, 576–591.

Apkarian, A. V. and Hodge, C. J. 1989. Primate spinothalamic pathways. III. Thalamic terminations of the dorsolateral and ventral spinothalamic pathways. J. Comp. Neurol. 288, 493–511.

Asanuma, H., Thach, W. T., and Jones, E. G. 1983. Distribution of cerebellar terminations and their relation to other afferent terminations in the ventral lateral thalamic region of the monkey. Brain Res. Rev. 5, 237–265.

Berkley, K. 1980. Spatial relationships between the terminations of somatic sensory and motor pathways in the rostral brainstem of cats and monkeys. I. Ascending somatic sensory inputs to lateral diencephalon. J. Comp. Neurol. 193, 283–317.

Boivie, J. 1980. Thalamic projections from lateral cervical nucleus in monkey. A degeneration study. Brain Res. 198, 13–26.

Boivie, J. and Boman, K. 1981. Termination of a separate (proprioceptive?) cuneothalamic tract from external cuneate nucleus in monkey. Brain Res. 224, 235–246.

Bombardieri, R. A., Johnson, J. I., and Campos, G. B. 1975. Species differences in mechanosensory projections from the mouth to the ventrobasal thalamus. J. Comp. Neurol. 163, 41–64.

Brodman, K. 1909. Vergleichende Lokalisationslehre der Grosshirnrhinde. Barth.

Broman, J. and Zhang, M. 1996. The cerviothalamic tract terminates in Cat-301-sparse regions of the cat VPL. Neuroreport 7, 1493–1496.

Brüggemann, J., Shi, T., and Apkarian, A. V. 1994. Squirrel monkey lateral thalamus. II. Viscerosomatic convergent

representation of urinary bladder, colon, and esophagus. J. Neurosci. 14, 6796–6914.
Burton, H. and Craig, A. D. 1983. Spinothalamic Projections in Cat, Raccoon and Monkey: A Study Based on Anterograde Transport of Horseradish Peroxidase. In: Somatosensory Integration in the Thalamus (*eds*. G. Macchi, A. Rustioni, and R. Spreafico), pp. 17–41. Elsevier.
Burton, H. and Jones, E. G. 1976. The posterior thalamic region and its cortical projection in New World and Old World monkeys. J. Comp. Neurol. 168, 249–302.
Burton, H., Sathian, K., and Shao, D. H. 1990. Altered responses to cutaneous stimuli in the second somatosensory cortex following lesions of the postcentral gyrus in infant and juvenile macaques. J. Comp. Neurol. 291, 395–414.
Cajal, S. R. Y. 1911. Histology of the Nervous System. (*trans*. N. Swanson and L. W. Swanson) Oxford University Press.
Catania, K. C. and Kaas, J. H. 1997. Somatosensory fovea in the star-nosed mole: behavioral use of the star in relation to innervation patterns and cortical representation. J. Comp. Neurol. 387, 215–233.
Chapin, J. K. and Lin, C. S. 1984. Mapping the body representation in the SI cortex of anesthetized and awake rats. J. Comp. Neurol. 229, 199–213.
Chmielowska, J. and Pons, T. P. 1995. Patterns of thalamocortical degeneration after ablation of somatosensory cortex in monkeys. J. Comp. Neurol. 360, 377–392.
Chowdhury, S. A., Grek, K. A., and Rasmusson, D. D. 2004. Changes in corticothalamic modulation of receptive fields during peripheral injury-induced reorganization. Proc. Natl. Acad. Sci. U. S. A. 101, 7135–7140.
Cobral, R. J. and Johnson, J. I. 1971. The organization of mechanoreceptive projections in the ventrobasal thalamus of the sheep. J. Comp. Neurol. 141, 17–36.
Cooper, B. Y., Glendenning, D. S., and Vierck, C. J. 1993. Finger movement deficits in the stumptail macaque following lesions of the fasciculus cuneatus. Somatosens. Mot. Res. 10, 17–29.
Coq, J. O., Qi, H.-X., Collins, C. E., and Kaas, J. H. 2004. Anatomical and functional organization of somatosensory areas of the lateral fissure of the New World titi monkey (*Callicebus moloch*). J. Comp. Neurol. 476, 363–387.
Crabtree, J. W. 1996. Organization in the somatosensory section of the cat's thalamic reticular nucleus. J. Comp. Neurol. 366, 207–222.
Craig, A. D. 2004. Distribution of trigeminothalamic and spinothalamic lamina. I. Terminations in the macaque monkey. J. Comp. Neurol. 477, 119–148.
Craig, A. D. 2006. Retrograde analyses of spinothalamic projections in the macaque monkey: input to ventral posterior nuclei. J. Comp. Neurol. 499, 965–978.
Craig, A. D. 2007. Evolution of Pain Pathways. In: Evolution of Nervous Systems in Mammals (*eds*. J. H. Kaas and L. A. Krubitzer), pp. 227–235. Elsevier.
Craig, A. D. and Burton, H. 1985. The distribution and topographical organization in the thalamus of anterogradely-transported horseradish peroxidase after spinal injection in cat and raccoon. Exp. Brain Res. 58, 227–254.
Craig, A. D. and Zhang, E. T. 2006. Retrograde analyses of spinothalamic projections in the macaque monkey: input to posterolateral thalamus. J. Comp. Neurol. 499, 953–964.
Craig, A. D., Bushnell, M. C., Zhang, E. T., and Blomqvist, A. 1994. A thalamic nucleus specific for pain and temperature sensation. Nature 372, 770–773.
Crouch, R. L. 1934. The nuclear configuration of the thalamus of *Macacus rhesus*. J. Comp. Neurol. 59, 451–485.
Cusick, C. G. and Gould, H. J. I. 1990. Connections between area 3b of the somatosensory cortex and subdivisions of the ventroposterior nuclear complex and the anterior pulvinar nucleus in squirrel monkeys. J. Comp. Neurol. 292, 83–102.
Cusick, C. G., Steindler, D. A., and Kaas, J. H. 1985. Corticocortical and collateral thalamocortical connections of postcentral somatosensory cortical areas in squirrel monkeys: a double-labeling study with radiolabeled wheatgerm agglutinin and wheat germ agglutinin conjugated to horseradish peroxidase. Somatosens. Res. 3, 1–31.
Darian-Smith, C. and Darian-Smith, I. 1993. Thalamic projections to areas 3a, 3b and 4 in the sensorimotor cortex of the mature and infant macaque monkey. J. Comp. Neurol. 335, 173–199.
Darian-Smith, C., Darian-Smith, I., and Cheema, S. S. 1990. Thalamic projections to sensorimotor cortex in the macaque monkey. Use of multiple retrograde fluorescent tracers. J. Comp. Neurol. 299, 17–46.
Davis, K. D., Kiss, Z. H. T., Tasker, R. R., and Destrovsky, J. O. 1996. Thalamic relay site for cold perception in humans. J. Neurophysiol. 81, 1970–1973.
Deecke, L., Schwarz, D. W. F., and Fredickson, V. M. 1974. Nucleus ventroposterior inferior (VPI) as the vestibular thalamic relay in the rhesus monkey. I. Field potential investigation. Exp. Brain Res. 20, 88–100.
Deschênes, M., Veinante, P., and Zhang, Z. W. 1998. The organization of corticothalamic projections: reciprocity versus parity. Brain Res. Rev. 28, 286–308.
Disbrow, E., Litinas, E., Recanzone, G. H., Slutsky, D. A., and Krubitzer, L. A. 2002. Thalamocortical connections of the parietal ventral area (PV) and the second somatosensory area (S2) in macaque monkeys. Thalamus Relat. Syst. 1, 289–302.
Doetsch, G. S., Standage, G. P., Johnston, K. W., and Lin, C.-S. 1988. Thalamic connections of two functional subdivisions of the somatosensory forepaw cerebral cortex of the raccoon. J. Neurosci. 8, 1873–1886.
Domino, E. F., Matsuoka, S., Waltz, J., and Cooper, I. S. 1965. Effects of cryogenic thalamic lesions on the somesthetic evoked response in man. Electroencephalogr. Clin. Neurophysiol. 53, 143–165.
Dykes, R. W., Herron, P., and Lin, C.-S. 1986. Ventroposterior thalamic regions projecting to cytoarchitectonic areas 3a and 3b in the cat. J. Neurophysiol. 56, 1521–1541.
Dykes, R. W., Rasmussen, D. D., and Hoeltzell, P. B. 1980. Organization of primary somatosensory cortex in the cat. J. Neurophysiol. 43, 1527–1546.
Dykes, R. W., Rasmussen, D. D., Survetavan, D., and Rehman, M. B. 1982. Submodality segregation and receptive field sequences in cuneate, gracile, and external cuneate nuclei of the cat. J. Neurophysiol. 47, 389–416.
Dykes, R. W., Sur, M., Merzenich, M. M., Kaas, J. H., and Nelson, R. J. 1981. Regional segregation of neurons responding to quickly adapting, slowly adapting, deep and Pacinian receptors within thalamic ventroposterior lateral and ventroposterior inferior nuclei in the squirrel monkey (*Saimiri sciureus*). Neuroscience 6, 1687–1692.
Ergenzinger, E. R., Glasier, M. M., Hahm, J. O., and Pons, T. P. 1998. Cortically induced thalamic plasticity in the primate somatosensory system. Nat. Neurosci. 1, 226–229.
Feldman, S. H. and Johnson, J. I. 1988. Kinesthetic cortical area anterior to primary somatic sensory cortex in the raccoon (*Procyon lotor*). J. Comp. Neurol. 277, 80–95.
Felleman, D. J. and Van Essen, D. C. 1991. Distributed hierarchical processing in the primate cerebral cortex. Cereb. Cortex 1, 1–47.
Felleman, J. D., Nelson, R. J., Sur, M., and Kaas, J. H. 1983. Representations of the body surface in areas 3b and 1 of postcentral parietal cortex of cebus monkeys. Brain Res. 268, 15–26.

Fisher, G. R., Freeman, B., and Rowe, M. J. 1983. Organization of parallel projections from Pacinian afferent fibers to somatosensory cortical areas I and II in the cat. J. Neurophysiol. 49, 75–97.

Florence, S. L. and Lakshman, S. 1995. Topography of primary afferent projections in the trigeminal sensory nuclei of rats. Acta Neurobiol. Exp. 55, 193–200.

Florence, S. L., Wall, J. T., and Kaas, J. H. 1988. The somatotopic pattern of afferent projections from the digits to the spinal cord and cuneate nucleus in macaque monkeys. Brain Res. 452, 388–392.

Florence, S. L., Wall, J. T., and Kaas, J. H. 1989. Somatotopic organization of inputs from the hand to the spinal gray and cuneate nucleus of monkeys with observations on the cuneate nucleus of humans. J. Comp. Neurol. 286, 48–70.

Florence, S. L., Wall, J. T., and Kaas, J. H. 1991. Central projections from the skin of the hand in squirrel monkeys. J. Comp. Neurol. 311, 563–578.

Francis, J. T., Xu, S., Rodriguez, D., and Chapin, J. K. 2003. Mapping the ventroposterior lateral thalamus: Cutaneous and proprioceptive representations. Soc. Neurosci. Abstrs. 60.5.

Friedman, D. P. and Jones, E. G. 1980. Focal projection of electrophysiologically defined groupings of thalamic cells on the monkey somatic sensory cortex. Brain Res. 191, 249–252.

Friedman, D. P. and Jones, E. G. 1981. Thalamic input to areas 3a and 2 in monkeys. J. Neurophysiol. 45, 59–85.

Friedman, D. P. and Murray, E. A. 1986. Thalamic connectivity of the second somatosensory area and neighboring somatosensory fields of the lateral sulcus of the macaque. J. Comp. Neurol. 252, 348–373.

Ganchrow, D. 1978. Intratrigeminal and thalamic projections of nucleus caudalis in the squirrel monkey (*Saimiri sciureus*): a degeneration and autoradiographic study. J. Comp. Neurol. 178, 281–312.

Garraghty, P. E., Florence, S. L., and Kaas, J. H. 1990a. Ablations of areas 3a and 3b of monkey somatosensory cortex abolish cutaneous responsivity in area 1. Brain Res. 528, 165–169.

Garraghty, P. E., Florence, S. L., Tenhula, W. N., and Kaas, J. H. 1991. Parallel thalamic activation of the first and second somatosensory areas in prosimian primates and tree shrews. J. Comp. Neurol. 311, 289–299.

Garraghty, P. E., Pons, T. P., and Kaas, J. H. 1990b. Ablations of areas 3b (S-I proper) and 3a of somatosensory cortex in marmosets deactivate the second and parietal ventral somatosensory areas. Somatosens. Mot. Res. 7, 125–135.

Gauriau, C. and Bernard, J. F. 2004. A comparative reappraisal of projections from the superficial laminae of the dorsal horn in the rat: the forebrain. J. Comp. Neurol. 468, 24–56.

Glendenning, D. S., Cooper, B. Y., Vierck, C. J., and Leonard, C. M. 1992. Altered precision grasping in stumptail macaques after fasciculus cuneatus lesions. Somatosens. Mot. Res. 9, 61–73.

Gould, H. J., Whitworth, R. H., and LeDoux, M. S. 1989. Thalamic and extrathalamic connections of the dysgranular unresponsive zone in the grey squirrel (*Sciurus carolinensis*). J. Comp. Neurol. 287, 38–63.

Groenewegen, H. J. and Witter, M. P. 2004. Thalamus. In: The Rat Nervous System (*ed*. G. Paxinos), pp. 407–453. Elsevier.

Harris, R. M. and Hendrickson, A. E. 1987. Local circuit neurons in the rat ventrobasal thalamus – a GABA immunocytochemical study. Neuroscience 21, 229–236.

Hassler, R. and Muhs-Clement, K. 1964. Architektonischer aufbau des sensomotorischen und parietalen cortex der katze. J. Hirnforsch. 6, 377–420.

Herron, P. 1983. The connections of cortical somatosensory areas I and II with separate nuclei in the ventroposterior thalamus in the raccoon. Neuroscience 8, 243–257.

Herron, P. and Dykes, R. W. 1986. The ventroposterior inferior nucleus in the thalamus of cats: a relay nucleus in the Pacinian pathway to somatosensory cortex. J. Neurophysiol. 56, 1475–1497.

Herron, P., Baskerville, K. A., Chang, H. T., and Doetsch, G. S. 1997. Distribution of neurons immunoreactive for parvalbumin and calbindin in the somatosensory thalamus of the raccoon. J. Comp. Neurol. 388, 120–129.

Huffman, K. J. and Krubitzer, L. A. 2001. Area 3a: topographic organization and cortical connections in marmoset monkeys. Cereb. Cortex 11, 849–867.

Iyengar, S., Qi, H.-X., Jain, N., and Kaas, J. H. 2007. Cortical and thalamic connections of the representations of the teeth and tongue in the somatosensory cortex of New World monkeys. J. Comp. Neurol. 501, 95–120.

Jain, N., Diener, P. S., Coq, J. O., and Kaas, J. H. 2003. Patterned activity via spinal dorsal quadrant inputs is necessary for the formation of organized somatosensory maps. J. Neurosci. 23, 10321–10330.

Johnson, J. I., Welker, W. I., and Pubols, B. H. 1968. Somatotopic organization of raccoon dorsal column nuclei. J. Comp. Neurol. 132, 1–44.

Jones, E. G. 1975. Lamination and differential distribution of thalamic afferents within the sensory-motor complex of the squirrel monkey. J. Comp. Neurol. 160, 167–203.

Jones, E. G. 1998. Viewpoint: the core and matrix of thalamic organization. Neuroscience 85, 331–345.

Jones, E. G. 2007. The Thalamus, 2nd edn. Cambridge University Press.

Jones, E. G., Schwark, H. D., and Callahan, P. A. 1986. Extent of the ipsilateral representation in the ventral posterior medial nucleus of the monkey thalamus. Exp. Brain Res. 63, 310–320.

Jones, E. G., Wise, S. P., and Coulter, J. C. 1979. Differential thalamic relationships of sensory-motor and parietal cortical fields in monkeys. J. Comp. Neurol. 183, 833–882.

Kaas, J. H. 1982. The Somatosensory Cortex and Thalamus in Galago. In: The Lesser Bush Baby (Galago) as an Animal Model: Selected Topics (*ed*. E. E. Haines), pp. 169–181. CRC Press.

Kaas, J. H. 2004. Somatosensory System. In: The Human Nervous System, 2nd edn. (*eds*. G. Paxinos and J. K. Mai), pp. 1059–1092. Elsevier Academic Press.

Kaas, J. H. 2007a. The Evolution of Sensory and Motor Systems in Primates. In: The Evolution of Primate Nervous Systems (*eds*. J. H. Kaas and T. M. Preuss), pp. 35–57. Elsevier.

Kaas, J. H. 2007b. The Evolution of the Dorsal Thalamus in Mammals. In: The Evolution of Nervous Systems in Mammals (*eds*. J. H. Kaas and L. A. Krubitzer), pp. 500–516. Elsevier.

Kaas, J. H. and Catania, K. C. 2002. How do features of sensory representations develop? Bioessays 24, 334–343.

Kaas, J. H., Nelson, R. J., Sur, M., Dykes, R. W., and Merzenich, M. M. 1984. The somatotopic organization of the ventroposterior thalamus of the squirrel monkey, *Saimiri sciureus*. J. Comp. Neurol. 226, 111–140.

Kaas, J. H., Nelson, R. J., Sur, M., Lin, C. S., and Merzenich, M. M. 1979. Multiple representations of the body within the primary somatosensory cortex of primates. Science 204, 521–523.

Kaas, J. H., Qi, H.-X., and Iyengar, S. 2006. Cortical network for representing the teeth and tongue in primates. Anat. Rec. 288A, 182–190.

Kalil, K. 1981. Projections of the cerebellar and dorsal column nuclei upon the thalamus of the rhesus monkey. J. Comp. Neurol. 195, 25–50.

Kenshalo, D. R. J., Giesler, G. J., Leonard, R. B., and Willis, W. P. 1980. Responses of neurons in primate ventral posterior lateral nucleus to noxious stimuli. J. Neurophysiol. 43, 1594–1614.

Kerr, F. W. L., Kruger, L., Schwassmann, H. O., and Stern, R. 1968. Somatotopic organization of mechanoreceptor units in the trigeminal nuclear complex of the macaque. J. Comp. Neurol. 134, 127–144.

Killackey, H. and Rhoades, R. W. 1995. The formation of a cortical somatotopic map. Trends Neurosci. 18, 202–407.

Killackey, H. P. and Sherman, S. M. 2003. Corticothalamic projections from the rat primary somatosensory cortex. J. Neurosci. 23, 7381–7384.

Kniffki, K.-D. and Mizumura, K. 1983. Responses of neurons in VPL and VPL-VL region of the cat to algesic stimulation of muscle and tendon. J. Neurophysiol. 49, 649–661.

Krubitzer, L. A. and Kaas, J. H. 1987. Thalamic connections of three representations of the body surface in somatosensory cortex of gray squirrels. J. Comp. Neurol. 265, 549–580.

Krubitzer, L. A. and Kaas, J. H. 1992. The somatosensory thalamus of monkeys: cortical connections and a redefinition of nuclei in marmosets. J. Comp. Neurol. 319, 1–18.

Krubitzer, L. A., Huffman, K. J., Disbrow, E., and Recanzone, G. 2004. Organization of area 3a in macaque monkeys: contributions to the cortical phenotype. J. Comp. Neurol. 471, 97–111.

Krupa, D. J., Ghazanfar, A. A., and Nicolelis, M. A. L. 1999. Immediate thalamic sensory plasticity depends on corticothalamic feedback. Proc. Natl. Acad. Sci. U. S. A. 96, 8200–8205.

Lang, W., Büttner-Ennever, J. A., and Bittner, U. 1979. Vestibular projections to monkey thalamus: an autoradiographic study. Brain Res. 177, 3–17.

Lee, C. C. and Woolsey, C. N. 1975. A proportional relationship between peripheral innervation and cortical neuron number in the somatosensory system of the mouse. Brain Res. 99, 349–353.

Lenz, F. A., Garonzik, I. M., Zirh, T. A., and Dougherty, P. M. 1998. Neuronal activity in the region of the thalamic principal sensory nucleus (ventralis caudalis) in patients with pain following amputations. Neuroscience 86, 1065–1081.

Lenz, F. A., Kwan, H. C., Dostrovsky, J. O., Tasker, R. R., Murphy, J. T., and Lenz, Y. E. 1990. Single unit analysis of the human ventral thalamic nuclear group: activity correlated with movement. Brain 113, 1795–1821.

Li, L. and Ebner, F. F. 2007. Cortical modulation of spatial and angular tuning maps in the rat thalamus. J. Neurosci. 27, 167–179.

Lin, C.-S., Merzenich, M. M., Sur, M., and Kaas, J. H. 1979. Connections of areas 3b and 1 of the parietal somatosensory strip with the ventroposterior nucleus in the owl monkey, *Aotus trivirgatus*. J. Comp. Neurol. 185, 355–372.

Lue, J.-H., Lai, S.-M., Wang, T.-J., Shieh, J.-Y., and Wen, C.-Y. 1997. Synaptic relationships between corticocuneate terminals and glycine-immunoreactive neurons in the rat cuneate nucleus. Brain Res. 771, 167–171.

Lund, R. D. and Webster, K. E. 1967a. Thalamic afferents from the dorsal column nuclei. an experimental anatomical study in the rat. J. Comp. Neurol. 130, 301–312.

Lund, R. D. and Webster, K. E. 1967b. Thalamic afferents from the spinal cord and trigeminal nuclei. An experimental anatomical study in the rat. J. Comp. Neurol. 130, 313–328.

Lundy, R. F. and Norgren, R. 2004. Gustatory System. In: The Rat Nervous System (*ed*. G. Paxinos), pp. 891–921. Elsevier.

Luo, P., Wang, B. R., Peng, Z. Z., and Li, J. S. 1991. Morphological characteristics and terminating patterns of masseteric neurons of the mesencephalic trigeminal nucleus in the rat: an intracellular horseradish peroxidase labeling study. J. Comp. Neurol. 303, 286–299.

Luo, P., Wong, R., and Dessem, D. 1995. Ultrastructural basis for synaptic transmission between jaw-muscle spindle afferents and trigeminothalamic neurons in the rostral trigeminal sensory nuclei of the rat. J. Comp. Neurol. 363, 109–128.

Ma, W., Peschanski, M., and Besson, J. M. 1986. The overlap of spinothalamic and dorsal column nuclei projections in the ventrobasal complex of the rat thalamus: a double anterograde labeling study using light microscopy analysis. J. Comp. Neurol. 245, 531–540.

Maendly, R., Rüegg, D. G., Wiesendanger, M., Wiesendanger, R., Lagowska, J., and Hess, B. 1981. Thalamic relay for group I muscle afferents of forelimb nerves in the monkey. J. Neurophysiol. 46, 901–917.

Mantle-St. John, L. A., and Tracey, D. J. 1987. Somatosensory nuclei in the brainstem of the rat: independent projections to the thalamus and cerebellum. J. Comp. Neurol. 255, 259–271.

Mantyh, P. W. 1983. The spinothalamic tract in the primate: a re-examination using wheatgerm agglutinin conjugated to horseradish peroxidase. Neuroscience 9, 847–862.

Martinez-Lorenzana, G., Machin, R., and Avendano, C. 2001. Definite segregation of cortical neurons projecting to the dorsal column nuclei in the rat. Neuroreport 12, 413–416.

Massey, J. M., Hubscher, C. H., Wagoner, M. R., Decker, J. A., Amps, J., Silver, J., and Onifer, S. M. 2006. Chondroitinase ABC digestion of the perineuronal net promotes functional collateral sprouting in the cuneate nucleus after cervical spinal cord injury. J. Neurosci. 26, 4406–4414.

May, P. J. and Porter, J. D. 1998. The distribution of primary afferent terminals from the eyelids of macaque monkeys. Exp. Brain Res. 123, 368–381.

Mayner, L. and Kaas, J. H. 1986. Thalamic projections from electrophysiologically defined sites of body surface representations in areas 3b and 1 of somatosensory cortex of Cebus monkeys. Somatosens. Res. 4, 13–29.

McAllister, J. P. and Wells, J. 1981. The structural organization of the ventral posterolateral nucleus in the rat. J. Comp. Neurol. 197, 271–301.

McCloskey, P. I. 1974. Muscular and cutaneous mechanisms in the estimation of the weights of grasped objects. Neuropsychologia 12, 513–529.

McCloskey, P. I. 1978. Kinesthetic sensibility. Physiol. Rev. 58, 763–820.

Mehler, W. R., Feferman, M. E., and Nauta, W. J. H. 1960. Ascending axon degeneration following anterolateral cordotomy. An experimental study in the monkey. Brain 83, 718–750.

Morel, A., Magnin, M., and Jeanmonod, D. 1997. Multiarchitectonic and stereotactic atlas of the human thalamus. J. Comp. Neurol. 387, 588–630.

Mountcastle, V. B. 1997. The columnar organization of the neocortex. Brain 120, 701–722.

Mountcastle, V. B. 2005. The Sensory Hand. Harvard University Press.

Myasinkov, A. A., Dykes, R. W., and Avendano, C. 1994. Cytoarchitecture and responsiveness of the medial ansate region of the cat primary somatosensory cortex. J. Comp. Neurol. 349, 401–427.

Nathan, P. W., Smith, M. C., and Cook, A. W. 1986. Sensory effects in man of lesions of the posterior columns and of some other afferent pathways. Brain 109, 1003–1041.

Nelson, R. J. and Kaas, J. H. 1981. Connections of the ventroposterior nucleus of the thalamus with the body surface representations in cortical areas 3b and 1 of the cynomolgus macaque (*Macaca fascicularis*). J. Comp. Neurol. 199, 29–64.

Noriega, A. L. and Wall, J. T. 1991. Parcellated organization in the trigeminal and dorsal column nuclei of primates. Brain Res. 565, 188–194.

Ohye, C., Shihazaki, T., Hirai, T., Kawashima, Y., Hirato, M., and Matsumura, K. 1993. Tremor-mediated thalamic zone studied in humans and in monkeys. Stereotact. Funct. Neurosurg. 6, 12–23.

Padberg, J. and Krubitzer, L. A. 2006. Thalamocortical connections of anterior and posterior parietal cortical areas in New World titi monkeys. J. Comp. Neurol. 497, 416–435.

Padberg, J., Disbrow, E., and Krubitzer, L. 2005. The organization and connections of anterior and posterior parietal cortex in titi monkeys: do New World monkeys have an area 2? Cereb. Cortex 12, 1938–1963.

Paxinos, G., Huang, X. F., and Toya, A. W. 2000. The Rhesus Monkey Brain. Academic Press.

Penny, G. R., Itoh, K., and Diamond, I. T. 1982. Cells of different sizes project to different layers of the somatic cortex in the cat. Brain Res. 242, 55–65.

Poggio, G. F. and Mountcastle, V. B. 1963. The functional properties of ventrobasal thalamic neurons studied in unanesthetized monkeys. J. Neurophysiol. 26, 775–806.

Pompeiano, O. and Brodal, A. 1957. Spino-vestibular fibers in the cat. An experimental study. J. Comp. Neurol. 108, 353–378.

Pons, T. P. and Kaas, J. H. 1985. Connections of area 2 of somatosensory cortex with the anterior pulvinar and subdivisions of the ventroposterior complex in macaque monkeys. J. Comp. Neurol. 240, 16–36.

Pons, T. P., Garraghty, P. E., Cusick, C. G., and Kaas, J. H. 1985. A sequential representation of the occiput, arm, forearm and hand across the rostrocaudal dimension of areas 1, 2 and 5 in macaque monkeys. Brain Res. 335, 350–353.

Pons, T. P., Garraghty, P. E., and Mishkin, M. 1992. Serial and parallel processing of tactual information in somatosensory cortex of rhesus monkeys. J. Neurophysiol. 68, 518–527.

Qi, H.-X. and Kaas, J. H. 2006. The organization of primary afferent projections to the gracile nucleus of the dorsal column system of primates. J. Comp. Neurol. 499, 183–217.

Qi, H.-X., Lyon, D. C., and Kaas, J. H. 2002. Cortical and thalamic connections of the parietal ventral somatosensory area in marmoset monkeys (*Callithrix jacchus*). J. Comp. Neurol. 443, 168–182.

Ralston, H. J. and Ralston, D. D. 1992. The primate dorsal spinothalamic tract: evidence for a specific termination in the posterior nuclei (Po/SG) of the thalamus. Pain 48, 107–118.

Rausell, E. and Jones, E. G. 1991. Chemically distinct compartments of the thalamic VPM nucleus in monkeys relay principal and spinal trigeminal pathways to different layers of the somatosensory cortex. J. Neurosci. 11, 226–237.

Rausell, E., Bae, C. S., Vinuela, A., Huntlery, G. W., and Jones, E. G. 1992. Calbindin and parvalbumin cells in monkey VPL thalamic nucleus: distribution, laminar cortical projections, and relations to spinothalamic terminations. J. Neurosci. 12, 4088–4111.

Rinvik, E. 1968. The re-evaluation of the cytoarchitecture of the ventral nuclear complex of the cat's thalamus on the basis of corticothalamic connections. Brain Res. 8, 237–254.

Rouiller, E. M. and Welker, W. I. 2000. A comparative analysis of the morphology of corticothalamic projections in mammals. Brain Res. 53, 727–741.

Rustioni, A. and Sotelo, C. 1974. Synaptic organization of the nucleus gracilis of the cat. Experimental identification of dorsal root fibers and cortical afferents. J. Comp. Neurol. 155, 441–468.

Schwark, H. D., Tennison, C. F., Ilyinsky, O. B., and Fuchs, J. L. 1999. Inhibitory influences on receptive field size in the dorsal column nuclei. Exp. Brain Res. 126, 439–442.

Seike, M. 1993. A study of the area of distribution of the deep sensory neurons of the human ventral thalamus. Stereotact. Funct. Neurosurg. 61, 12–23.

Sherman, S. M. and Guillery, R. W. 2006. Exploring the Thalamus and Its Role in Cortical Function. MIT Press.

Smith, R. L. 1975. Axonal projections and connections of the principal sensory trigeminal nucleus in the monkey. J. Comp. Neurol. 163, 347–376.

Spreafico, R., Schmechel, D. E., Ellis, L. C., and Rustioni, A. 1983. Cortical relay neurons and interneurons in the N. ventralis posterolateralis of cats: a horseradish peroxidase, electron-microscopic, Golgi and immuno-cytochemical study. Neuroscience 9, 491–509.

Stepniewska, I., Collins, C. E., and Kaas, J. H. 2004. Connection patterns of dorsolateral visual cortex in macaques suggest the dorsal and ventral boundaries of V4. Cereb. Cortex 15, 809–822.

Stepniewska, I., Sakai, S. T., Qi, H.-X., and Kaas, J. H. 2003. Distribution of somatosensory pathways in relation to thalamic neurons relaying information to the motor and premotor cortex in the macaque monkey. Soc. Neurosci. Abstr. 29, 60.16.

Stevens, R. T., London, S. M., and Apkarian, A. V. 1993. Spinothalamocortical projections to the secondary somatosensory cortex (S-II) in squirrel monkey. Brain Res. 63, 241–246.

Strata, F., Coq, J. O., and Kaas, J. H. 2003. The chemo- and somatotopic architecture of the Galago cuneate and gracile nuclei. Neuroscience 116, 831–850.

Sur, M., Wall, J. T., and Kaas, J. H. 1984. Modular distribution of neurons with slowly adapting and rapidly adapting responses in area 3b of somatosensory cortex in monkeys. J. Neurophysiol. 51, 724–744.

Waite, P. M. E. and Ashwell, K. W. S. 2004. The Trigeminal Sensory System. In: The Human Nervous System (*eds*. G. Paxinos and J. K. Mai), pp. 1093–1124. Elsevier.

Wang, X. and Wall, J. T. 2005. Cortical influences on sizes and rapid plasticity of tactile receptive fields in the dorsal column nuclei. J. Comp. Neurol. 489, 241–248.

Wang, X. and Wall, J. T. 2006. Cortical influences on rapid brainstem plasticity. Brain Res. 1095, 73–84.

Weinberg, R. J., Pierce, J. P., and Rustioni, A. 1990. Single fiber studies of ascending input to the cuneate nucleus of cats: I. Morphometry of primary afferent fibers. J. Comp. Neurol. 300, 113–133.

Welker, W. I. 1973. Principles of organization of the ventrobasal complex in mammals. Brain Behav. Evol. 7, 253–336.

Whitsel, B. L., Petrucelli, L. M., Ha, H., and Dryer, D. A. 1972. The resorting of spinal afferents as antecedent to the body representation in the postcentral gyrus. Brain Behav. Evol. 5, 303–342.

Wiener, S. I., Johnson, J. I., and Ostapoff, E.-M. 1987. Demarcations of the mechanosensory projection zones in the raccoon thalamus, shown by cytochrome oxidase, acetylcholinesterase, and Nissl stains. J. Comp. Neurol. 258, 509–526.

Wiesendanger, M. and Miles, T. S. 1982. Ascending pathway of low-threshold muscle afferents to the cerebral cortex and its possible role in motor control. Physiol. Rev. 62, 1234–1270.

Williams, M. N., Zahm, D. S., and Jacquin, M. F. 1994. Differential foci and synaptic organization of the principal and spinotrigeminal projections to the thalamus in the rat. Eur. J. Neurosci. 6, 429–453.

Willis, W. D. and Coggeshall, R. E. 2004. Sensory Mechanisms of the Spinal Cord. Kluwer Academic.

Willis, W. D., Zhang, X., Honda, C. N., and Giesler, J., Jr. 2002. A critical review of the role of the proposed VMpo nucleus in pain. J. Pain 3, 79–94.

Wilson, P., Kitchener, P. D., and Snow, P. J. 1999. Cutaneous receptive field organization in the ventral posterior nucleus of the thalamus in the common marmoset. J. Neurophysiol. 82, 1865–1875.

Wise, S. P. and Jones, E. G. 1977. Cells of origin and terminal distribution of descending projections of the rat somatic sensory cortex. J. Comp. Neurol. 175, 129–158.

Wu, C. W.-H. and Kaas, J. H. 2003. Somatosensory cortex of prosimian galagos: physiological recording, cytoarchitecture, and corticocortical connections of anterior parietal cortex and cortex of the lateral sulcus. J. Comp. Neurol. 457, 263–292.

Xu, J. and Wall, J. T. 1996. Cutaneous representations of the hand and other body parts in the cuneate nucleus of a primate, and some relationships to previously described cortical representations. Somatosens. Mot. Res. 13, 187–197.

Zhang, X., Davidson, S., and Giesler, G. J. J. 2006. Thermally identified subgroups of marginal zone neurons project to distinct regions of the ventral posterior lateral nucleus in rats. J. Neurosci. 26, 5215–5223.

Zhang, H. Q., Murray, G. M., Coleman, G. T., Turman, A. B., Zang, S. P., and Rowe, M. J. 2001. Functional characteristics of the parallel SI and SII projecting neurons of the thalamic ventroposterior nucleus in the marmoset. J. Neurophysiol. 85, 1805–1822.

Zheng, A.-H., Wu, C.-P., and Xi, M.-C. 1986. Thalamic projection to motor area and area 3a of the cat cerebral cortex. Brain Res. 380, 389–393.

6.08 Somatosensory Areas of the Cerebral Cortex: Architectonic Characteristics and Modular Organization

H-X Qi, Vanderbilt University, Nashville, TN, USA

T M Preuss, Emory University, Atlanta, GA, USA

J H Kaas, Vanderbilt University, Nashville, TN, USA

© 2008 Elsevier Inc. All rights reserved.

6.08.1	Introduction	144
6.08.2	The Somatosensory Cortex of Nonprimate Mammals	145
6.08.3	The Somatosensory Cortex of Prosimian Primates	149
6.08.4	The Anterior Parietal Cortex of New World Monkeys	151
6.08.5	Other Somatosensory Areas of New World Monkeys	153
6.08.6	Modules in Area 3b of Old World and New World Monkeys	154
6.08.7	The Anterior Parietal Cortex of Old World Monkeys, Apes, and Humans	157
6.08.8	Architectonic Areas of Lateral and Posterior Parietal Cortex	163
6.08.9	Conclusions	164
References		165

Glossary

area 1 A somatosensory area that is recognized in anthropoid primates that may exist in other mammals. Area 1 contains a systematic representation of cutaneous receptors of the opposite side of the body and has a less pronounced layer 4 of small neurons than S1 (area 3b), is located immediately caudal to S1, and depends on S1 inputs for activation.

area 2 A somatosensory area that is generally recognized in anthropoid primates but has not been identified with certainty in other mammals. Area 2 is located immediately caudal to area 1, and it contains complex representations or representations of a mixture of cutaneous receptor, information relayed from areas 3b and 1, and muscle spindle information relayed from the ventroposterior superior nucleus of the thalamus. Layer 4 of area 2 is somewhat more distinct than in area 1.

area 3a A subdivision of the somatosensory cortex that is recognized in primates and sometimes other mammals that may be present in most or all mammals. Area 3a is just rostral to S1 (area 3b), is activated by muscle spindle receptors, and has a less pronounced layer 4 of small neurons than S1 (area 3b).

cortical architecture The histological appearance of a cortical area in brain sections stained for cell bodies (cytoarchitecture), myelin (myeloarchitecture), or processed for proteins or other features of cortical tissue. Regional differences in cortical architecture are used to identify cortical areas.

cortical area The classical subdivision of neocortex that is often architectonically distinct, is characterized by a unique pattern of connections with other areas and subcortical structures, and performs a unique set of functions. Somatosensory areas usually contain a complete representation of the opposite side of the body.

cortical modules or columns Subdivisions of cortical areas that differ by being activated by one or another class of peripheral receptor, or by representing segregated inputs from the peripheral, such as receptors for specific whiskers on the face.

parietal ventral area (PV) A somatosensory area that adjoins S2 and represents receptors of the opposite half of the body in a pattern that mirrors the representation in S2. In early studies, PV was not distinguished from S2, but considerable evidence now suggests that PV exists in most and perhaps all mammals.

primary somatosensory cortex (S1) A subdivision of the somatosensory cortex that is present in all mammals. S1 contains a systematic representation of the cutaneous receptors of the opposite side of the body and is directly activated by afferents from the ventroposterior nucleus of the thalamus. Of all somatosensory areas, S1 has the most pronounced architectonic features of the sensory cortex, especially the well-developed layer 4 of small neurons. For historical reasons,

investigators often include other areas in S1 of anthropoid primates, but only area 3b is homologous to S1 of other mammals.

second somatosensory area (S2) A smaller representation of cutaneous and other receptors of the contralateral body that is located just lateral (ventral) to S1. S2 receives inputs from S1 and, in most mammals, from the ventroposterior inferior nucleus of the thalamus. S2 has less pronounced architectonic features than S1, but it is difficult to distinguish architectonically from other adjoining somatosensory areas, such as PV.

6.08.1 Introduction

The somatosensory cortex varies across mammals in how it is divided into areas or fields and how it is divided into modules within areas. Areas are the large functionally distinct subdivisions of cortex that Brodmann K. (1909) called the organs of the brain. For the somatosensory cortex, areas are expected to contain a complete representation of a class or classes of somatosensory afferents from the opposite side of the body (with perhaps some representation of ipsilateral inputs as well), patterns of connections with other parts of the brain that are distinctly different from those of other areas, similar but not necessarily identical types of connections for all parts of the area, and structural specializations within individual areas that reflect the functional specializations of each area. Additionally, the collective response properties of neurons in any area are expected to differ from those of other areas, and the functional consequences of activating or deactivating each area also should differ. Areas are well defined when all or most of these characteristics have been identified, while a correct identification is less certain when an area is incompletely characterized. Most mammals have four or five well-defined areas of the somatosensory cortex while monkeys and other anthropoid primates have more.

Modules are subdivisions of areas that have been defined in various ways, and often the term is used interchangeably with the term cortical column (Kaas, J. H., 1993; Krubitzer, L. A. and Hunt, D. L., 2007). However, cortical column sometimes refers to the vertical organization of cortex, the observations that the succession of neurons in a vertical array through the depth of cortex are highly interconnected and share such features as receptive field location and a number of other response properties. As all cortical areas have this vertical organization, we use the less confusing term module here to refer to two different types of subdivisions within the areas of the somatosensory cortex. One type of module corresponds to Mountcastle's V. B. (1957) original concept of cortical columns as consisting of alternating patches of cortex, from surface to white matter, that are distinguished from each other by being activated by one class of peripheral afferents or another, and have sharp boundaries. As these modules are expected to be small, 500 μm or less in diameter, a large cortical area could have quite a number of modules of at least two types (Towe, A. L., 1975). There is only limited evidence for such modules in the somatosensory cortex, but this evidence is covered briefly. The other type of module is one that is devoted to afferents from some body part, such as from one of the digits of the hand, and is segregated from afferents from adjoining body parts, such as adjacent digits of the hand, by narrow septa that are architectonically distinct. These segregating septa are apparent in the primary somatosensory cortex (S1) of many mammals, but they are rare in other somatosensory areas (for review, see Purves, D. *et al.*, 1992; Catania, K. C. and Kaas, J. H., 1995; Remple, M. S. *et al.*, 2006). The best-known example is the cortical barrel for each sinus hair of the face of rodents in the primary somatosensory cortex (Woolsey, T. A. and Van der Loos, H., 1970). Each barrel focuses inputs related to a single sinus hair, and each barrel is visible as a distinct structure, but they are anatomically and functionally similar. Some of these modules are described here. Their types and occurrences are quite variable across species.

The main focus of this review is the structural or architectonic features of the cortex. Other features are mentioned, but not in detail. The architectonic features of cortical areas that can be described are perhaps limitless. Traditionally, thin slices of cortex that have been stained for Nissl substance to reveal cell bodies (cytoarchitecture) or myelin to reveal myelinated fibers (myeloarchitecture) are examined. Probably the most popular additional procedure has

been to process brain sections for the expression of the metabolic enzyme, cytochrome oxidase (CO) (Wong-Riley, M., 1979). In general, the primary sensory areas are distinguished from adjoining areas by being densely packed in the middle cortical layers with darkly stained, small neurons in Nissl preparations, and by being densely myelinated and expressing high levels of CO. Other cortical areas are lighter in Nissl-stained sections, and harder to distinguish from each other. Fortunately, there are a number of other processing procedures for cortical sections that can be used to help divide cortex into presumptive areas. Antibodies that label proteins that are differentially distributed across the cortex are very useful for architectonic parcellation. For example, the monoclonal antibody SMI-32 labels a neurofilament protein that is expressed in a subset of cortical pyramidal cells (Campbell, M. J. and Morrison, J. H., 1989) in a laminar pattern that varies between cortical areas (e.g., Preuss, T. M. *et al.*, 1997). Another monoclonal antibody that has been useful for defining areas is Cat-301 (McKay, R. D. and Hockfield, S. J., 1982), which recognizes an antigen on the surface of neurons in a pattern that varies across cortical areas and layers (e.g., Jain, N. *et al.*, 1994). Also valuable are antibodies to the calcium-binding proteins, parvalbumin and calbindin, which are distributed differently in primary and secondary areas of the sensory cortex (e.g., Hackett, T. A. *et al.*, 1998). Another useful procedure has been to histochemically process brain sections for the enzyme acetylcholinesterase (AChE), which degrades the neurotransmitter acetylcholine, a neuromodulator associated with neuroplasticity in the developing and mature brain (e.g., Juliano, S. L. *et al.*, 1990). AChE is often expressed at high levels early in the development of primary sensory areas, but it remains at high levels in the primary auditory cortex of adult monkeys (e.g., Morel, A. *et al.*, 1993). Finally, the use of autoradiography for localizing the receptors for the neurotransmitters gamma-amino butyric acid (GABA), glutamate, acetylcholine, noradrenaline, and serotonin has been a powerful tool for demonstrating areal differences in the densities and laminar distributions of receptors (Zilles, K. *et al.*, 2002). These arrays of histological methods allow architectonic borders of cortical areas to be determined with much greater assurance than when Nissl and myelin preparations are examined alone. The results are especially convincing when borders based on the different histological procedures are congruent, and where such histological borders are also compatible with other anatomical and electrophysiological data.

6.08.2 The Somatosensory Cortex of Nonprimate Mammals

In a number of ways, the organization of the somatosensory cortex of mammals is extremely varied across species. Some of this variability is described in other chapters in this volume (see Specialized Somatosensory Systems and The Evolution of Parietal Areas Involved in Hand Use in Primates). Nevertheless, many mammals have a rather limited somatosensory system with perhaps five cortical areas devoted primarily to the processing of information from cutaneous receptors (Kaas, J. H., 2004). For example, marsupial opossums appear to have five somatosensory areas (Beck, P. D. *et al.*, 1996) that are widely shared by other mammals (Kaas, J. H., 2004; 2007). Opossums have a large primary area, S1, that has been identified in all mammals studied to date (Figure 1). S1 is characterized by a systematic representation of the cutaneous receptors of the contralateral body from tail to tongue in a medial-to-lateral cortical sequence, by activating inputs from the ventroposterior nucleus of the thalamus, and by histological features that include dense myelination, high levels of CO, and a layer 4 of densely packed, small

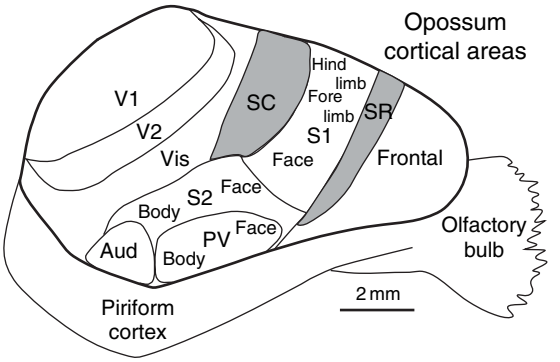

Figure 1 Proposed subdivisions of the somatosensory cortex in North American opossums (*Dedelphis marsupialis*). The areas are shown on a dorsolateral view of the brain. Somatosensory areas include the primary area, S1; the second somatosensory area, S2; the parietal ventral somatosensory area, PV; a caudal somatosensory area, SC; and a rostral somatosensory area, SR. Similar subdivisions of the somatosensory cortex have been identified in a wide range of mammalian species, with SC and SR given various names (see text). Some of the features of somatotopy in S1, PV, and S2 are noted. Cortex also includes the primary visual area (V1), the second visual area (V2), and the more lateral visual (Vis) cortex. Auditory cortex (Aud) may include more than one area. Adapted from Beck, P. D., Pospichal, M. W., and Kaas, J. H. 1996. Topography, architecture, and connections of somatosensory cortex in opossums: evidence for five somatosensory areas. J. Comp. Neurol. 366(1), 109–133.

neurons. Bands of somatosensory cortex rostral (area SR) and caudal (area SC) to S1 are known to have somatosensory functions in that they receive inputs from S1, and they may receive inputs from the ventroposterior complex as well, but they do not respond very well to tactile stimuli, at least in anesthetized animals (see Karlen, S. J. and Krubitzer, L., 2007, for an extensive review of somatosensory cortex organization in marsupials). There is evidence from some mammals, such as rats and cats, that the rostral somatosensory belt, SR, receives a relay of muscle spindle information from the thalamus, as does area 3a on the rostral border of S1 (area 3b) of primates. Thus, SR may be the homolog of area 3a of primates and other mammals where the term 3a is used. SC is in the position of area 1 or areas 1 and 2 of primates, but the relation of SR to areas 1 and 2 is less certain. Both SR and SC have a less prominent layer 4, less myelination, and less CO expression. In rats, the rostral zone has been called the dysgranular cortex (Chapin, J. K. and Lin, C. S., 1984) because the fourth layer of granular cells is poorly developed. Just lateral and ventral to S1, the second area, S2, and the parietal ventral, PV, somatosensory areas are found. The second area, S2, has long been recognized (e.g., Woolsey, C. N. and Fairman, O., 1946) as a distinct representation of the contralateral body surface just ventral to S1 in a wide range of mammals. S2 adjoins S1 where their face representations meet, but S2 represents the forelimb and hindlimb more ventrally, separate from S1. PV has been more recently described, first in squirrels (Krubitzer, L. A. *et al.*, 1986), and then in enough other species of mammals to indicate that PV is likely to be present in the common ancestor of extant mammals (see Disbrow, E. *et al.*, 2000, for humans; Remple, M. S. *et al.*, 2003; Benison, A. M. *et al.*, 2007, for rats). As PV forms a representation of the contralateral body surface in parallel to the one in S2, it may have been confused with S2 in early studies where observations were not made in enough detail to detect two parallel representations. However, in some mammals, a careful search for PV has not provided evidence for the area (e.g., Catania, K. C. *et al.*, 2000). S2 and PV both respond well to cutaneous stimulation and receive inputs from S1 as well as (in most mammals) from the ventroposterior nucleus of the thalamus (see Chapter The Somatosensory Thalamus and Associated Pathways). S2 and PV generally have less CO, myelin, and layer 4 development than S1, but more than SR and SC. In brain sections cut parallel to the surface of the cortex and processed for myelin or CO, S1 usually stands out as a darker region than surrounding areas of the cortex (Figures 2 and 3), as do primary auditory and visual areas. In some mammals, however, areas S2 and PV appear to be fairly similar in histological appearance to S1 (Figure 2; also see Huffman, K. J. *et al.*, 1999).

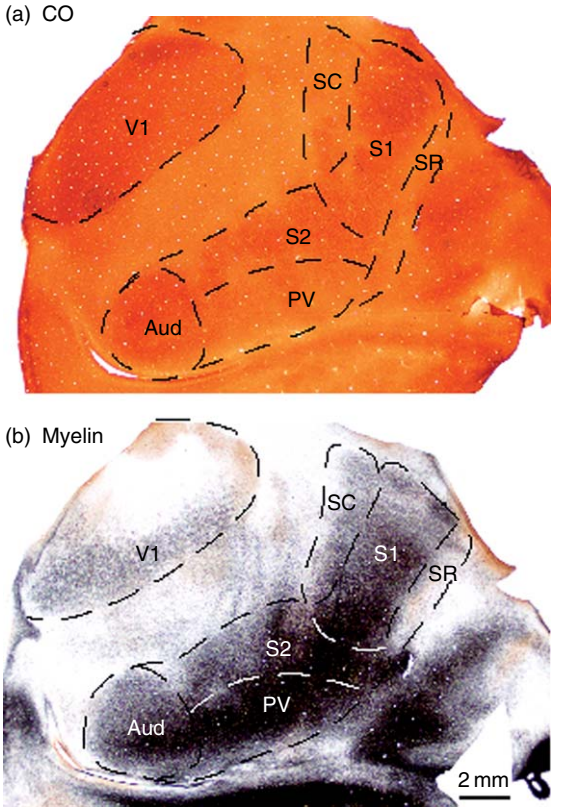

Figure 2 Architectonic characteristics of the somatosensory cortex in opossums. The cortex has been manually flattened and cut parallel to the surface so that it appears as a single sheet in each section. In (a), the section has been processed for cytochrome oxidase (CO). The primary sensory areas, S1, V1, and Aud, express high levels of CO, as does the frontal cortex. However, the CO level in S2 is also quite high. Unlike V1 and Aud, the CO expression in S1 and S2 is somewhat patchy, suggesting an uneven expression related to the somatotopy of the areas (see text). In (b), the brain section has been processed for myelin. Note that S1, S2, PV, and Aud are all densely myelinated. The lighter and uneven level of myelin in V1 is a result of laminar differences in expression, with the level of the section being superficial to the densely myelinated layer 4 of V1. Scale bar = 2 mm. Compare with Figure 1. Reproduced from Beck, P. D., Pospichal, M. W., and Kaas, J. H. 1996. Topography, architecture, and connections of somatosensory cortex in opossums: evidence for five somatosensory areas. J. Comp. Neurol. 366(1), 109–133.

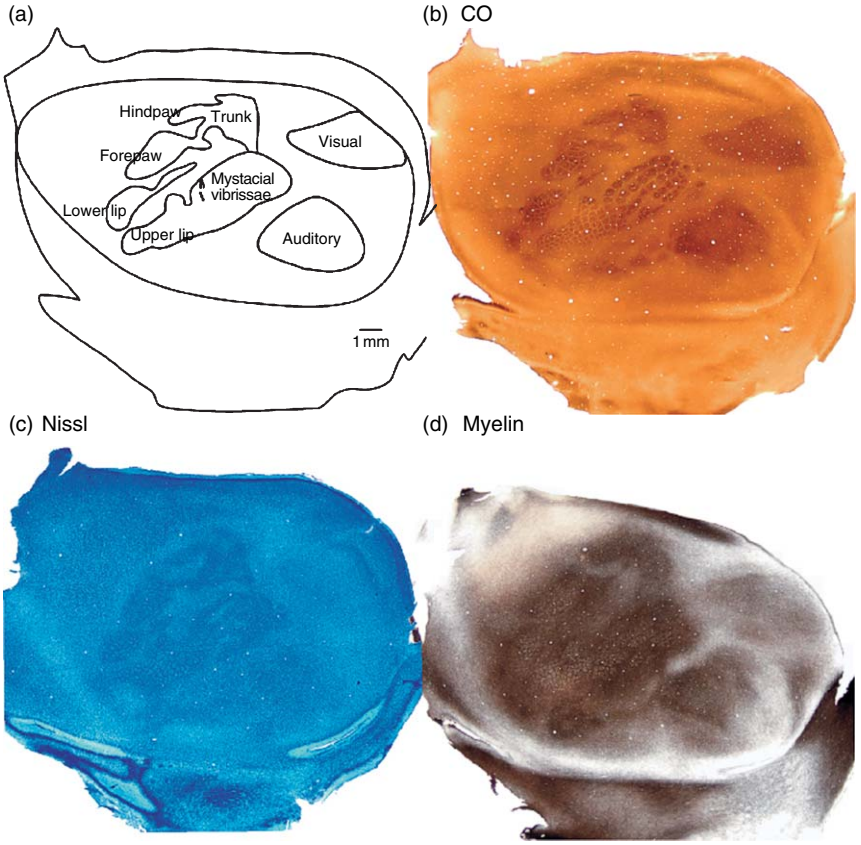

Figure 3 Architectonic characteristics of the somatosensory cortex in rats. As in Figure 2, the cortex has been flattened and cut parallel to the surface so that all of the neocortex can be seen in each brain section. In (a), the brain section is outlined and the portion of neocortex visible in a dorsolateral view is circumscribed. The primary somatosensory cortex is outlined and the portions representing major body parts are labeled. The locations of auditory and primary visual cortex are also indicated. In (c), a brain section has been stained for cell bodies (Nissl-stained). Note that even in this traditional stain, the major parts of S1 can be identified as darker due to the densely stained and packed cells in layer 4 cells of S1. In this section, even barrel-like structures with cell-poor hollows are apparent in parts of S1. In (b), the section has been processed for cytochrome oxidase (CO). Again, the locations of the representations of major body parts in S1 are apparent as CO-dark regions. The larger barrels of the mystacial barrel field stand out as CO-dark ovals, and the smaller barrels of the representation of hairs of the upper lip are also visible. Modular subdivisions of the representations of the forepaw and the lower lip are also apparent. The S2-PV region below S1 has a patchy pattern of CO expression, but the relationship of this pattern to somatotopy has not been established. Primary visual and auditory cortex are CO dense. In (d), the brain section has been stained for myelin. Due to the depth of the section, S1 is less clear, but overall S1 is densely myelinated. Note the less-dense myelination of the hallows of barrels in some locations. The primary visual and the auditory cortex are also more myelinated than the surrounding cortex. Reproduced from Jain, N., Diener, P. S., Coq, J. O., and Kaas, J. H. 2003. Patterned activity via spinal dorsal quadrant inputs is necessary for the formation of organized somatosensory maps. J. Neurosci. 23(32), 10321–10330. Copyright 2003 by the Society for Neuroscience, with permission.

In surface views, S1 typically has a rather mottled appearance, especially in surface views of CO preparations (Figures 2 and 3). This unevenness reflects the modular organization of S1, where small territories of the cortex are activated by inputs from one body part or another (somatotopic modules). The association of CO patches and ovals of cortex in S1 with representation of specific body parts has been demonstrated by correlating the results of mapping the somatotopy of S1 with microelectrodes with the CO pattern in detailed studies in numerous species of mammals (e.g., Krubitzer, L. A. *et al.*, 1986; 1995; Catania, K. C. and Kaas, J. H., 1995; Catania, K. C. and Remple, M. S., 2002; Remple, M. S. *et al.*, 2003). The details of the CO pattern differ with species, according to what types of sensory inputs are prominent, but a visible pattern of CO-dense modules that reflects the somatotopy of S1 in each species is common. Such associations between modular architecture and somatotopy are not usually seen in S2 and PV, as

CO staining is usually not that pronounced as in S1. However, some mammals, such as the star-nosed mole (Catania, K. C. and Kaas, J. H., 1995), do exhibit obvious modules in S2, and a patchy pattern of CO expression is apparent in S2 and PV of opossums (Beck, P. D. *et al*., 1996), rats (Remple, M. S. *et al*., 2003), and tree shrews (Remple, M. S. *et al*., 2007).

Perhaps the best-known example of somatic modularity in S1 is the so-called barrel field of rats and mice. The barrel field was named by Woolsey T. A. and Van der Loos H. (1970) when they discovered that the pattern of patches apparent in Nissl-stained sections through the lateral part of S1 correspond to the pattern of the mystacial vibrissae on the contralateral face, with each whisker activating neurons within a specific barrel. Sections stained for cell bodies (Nissl) cut through layer 4 revealed a pattern of ovals created by cell bodies with thalamic afferents arriving in the cortex of each oval, and cell-poor septa separating the ovals from each other (Figure 3). Subsequent studies revealed that the ovals, including the cell-poor hollows, are CO-dense (e.g., Land, P. W. and Simons, D. J., 1985), and can be revealed by histochemical stains for other mitochondrial enzymes, such as succinate dehydrogenase (Dawson, D. R. and Killackey, H. P., 1987). The barrels were best seen in brain sections cut parallel to the cortical surface. Certain lectins were also found to label the septal regions that separated the barrels (Cooper, N. G. and Steindler, D. A., 1986). In addition, it soon became apparent that the modular organization of S1 extends beyond the barrel field: another region of S1, termed the posteriomedial barrel subfield (PMBSF) that has barrel-like structures that correspond to the sinus hairs on the upper lip and hairy buccal pad, and the hairs of the lower lip, was described (Figure 3, see Jain, N. *et al*., 2003). A more medial group of succinic dehydrogenase and CO-dense ovals corresponded to representation of digits and pads of the forepaw (Dawson, D. R. and Killackey, H. P., 1987; Waters, R. S. *et al*., 1995), while a medial most group of ovals represented the toes and pads of the hindpaw (Dawson, D. R. and Killackey, H. P., 1987). These studies also revealed the protrusion of the SR dysgranular zone well into S1 to separate the representation of the face from the forepaw, the forepaw from the hindpaw, and the lower lip from the upper lip (Figure 3). Thus, histological features of S1 in rats and mice nicely illustrate both the architectonic distinctiveness of S1 and its modular organization, where the modules are devoted to parts of the sensory surface that are distinct by being activated by protruding sensory hairs or semi-segregated body parts such as digits.

Modules based on somatotopy are common in S1 of mammals, as discussed above and below for monkeys. In contrast, functionally distinct modules for different classes of receptors from the same body part have not been described in S1 of most mammals. In rats, however, the CO expression within the barrels of the barrel subfield is not uniformly dense, as CO-dark subbarrels, corresponding to functionally distinct inputs where neurons are differentially responsive to the angle of whisker deflection, are separated by narrow CO-sparse clefts (Bruno, R. M. *et al*., 2003; Andermann, M. L. and Moore, C. I., 2006; Louderback, K. M. *et al*., 2006). A more conspicuous example of such functionally segregating modules is the S1 representation of the receptors of the bill of the duck-billed platypus where separate, alternating islands of cells represent tactile and electrosensory inputs (Krubitzer, L. A. *et al*., 1995). Finally, modules of cells responding to either slowly adapting (SA) or rapidly adapting (RA) afferents have been described in S1 (area 3b) of monkeys (see below).

S1 of most mammals can be distinguished using a number of other histological preparations in additional Nissl and CO staining. In squirrels (Wong and Kaas in preparation), for example, parvalbumin is more densely expressed in layer 4 and inner layer 3 of S1 than in adjoining areas. Parvalbumin is expressed at a lower level in S2 and PV than in S1, but at a level that is higher than in the rostral and caudal somatosensory areas (SC and SR, also known as Pm and 3a). Primary sensory areas, including S1, are also marked by a wide layer 4 that is almost free of synaptic zinc (Figure 4), because the thalamocortical terminations that predominate in layer 4 are zinc poor, whereas the corticocortical terminations prominent in other layers are zinc rich. S1 and other primary areas also express more vesicular glutamate transporter 2, as visualized with immunohistochemical procedures. Other markers revealed by receptor autoradiography have been well studied in rats. Thus, S1 of rats expresses higher levels of the $GABA_A$ and cholinergic muscarinic M2 receptors than adjacent areas, and there are low levels of kainate receptor labeling in the middle layers (Palomero-Gallagher, N. and Zilles, K., 2004).

In summary, S1 is architectonically distinct in all mammals examined. Modules that segregate representations of body parts are often histologically apparent as they are isolated by cell-poor septa. In the rat barrel field, there is evidence of minimodules

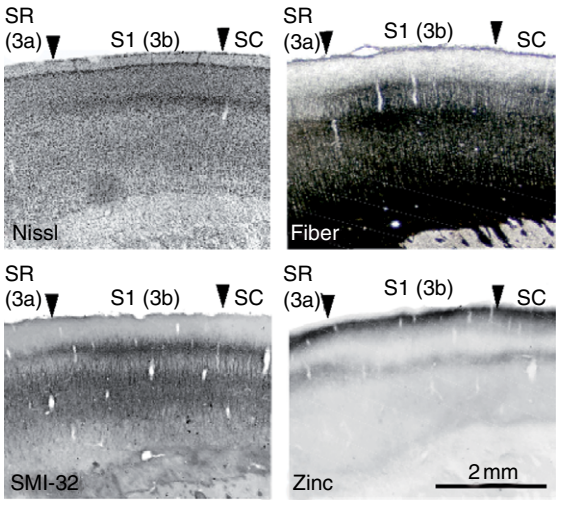

Figure 4 Some architectonic features of the somatosensory cortex of squirrels (*Sciurus carolenenisis*). Brain sections were cut at the parasagittal plane through SR, S1, and SC (rostral in the left). In a Nissl-stained section (upper left), S1 is characterized by a layer 4 that is densely packed with darkly stained neurons. This feature is less pronounced in SC, and much less so in SR such that SR is also called the dysgranular cortex. In sections stained for myelin (fibers; upper right), the middle layers of cortex are more densely myelinated in S1 than in SR or SC. Other layers are also more myelinated in S1, but the difference between S1 and SR or SC is most obvious in layer 4. In sections processed for the neurofilament protein revealed by the antibody SMI-32 (lower left), the staining of neurons and dendrites is more pronounced in layers 3 and 5 of S1 than in SC and PM. In sections processed for synaptic zinc (lower right), which is not expressed in thalamocortical terminations, S1 has a broader zinc-free (white) region in layer 4 and deeper layer 3 than SR or PM. Thus, S1 is distinguished from adjoining areas in all four preparations. Scale bar = 2 mm. Wong and Kaas (unpublished data).

within barrels that relate to groups of neurons with different response properties, and S1 of the duck-billed platypus has histologically visible modules for neurons related to electroreception or tactile sensations. These two examples suggest that the search for additional modules of the functional type would be rewarding. S2 and PV are difficult to distinguish histologically. They have histological characteristics that are similar to those of S1, but less pronounced. These characteristics are also variable, S2 being more or less like S1 in different species. The rostral (SR) and caudal (SC) somatosensory areas bordering S1 have a less well-developed layer 4, especially in SR (area 3a), which has been referred to as dysgranular cortex. A narrow zone of histologically indistinct posterior parietal cortex found in rats (Remple, M. S. *et al.*, 2003) and many other mammals also has somatosensory as well as multisensory functions. In rats, the region identified as the posterior parietal cortex (Reep, R. L. *et al.*, 1994) includes the caudal somatosensory area, SC (or Pm) of this review; so it is uncertain if a separate posterior parietal area exists. In some shrews, which have very small brains, there appears to be no cortex between S1 and the primary visual cortex, V1 (Catania, K. C., *et al.*, 1999). Thus, SC may not exist in all mammals. However, in tree shrews (mammalian order Scandentia), which are close relatives of primates, a posterior parietal region about the width of SC is present just caudal to SC. This posterior parietal region resembles SC histologically (Remple, M. S. *et al.*, 2006), but it has dense connections with the motor cortex, while SC of tree shrew and other mammals has dense connections with S1 (Remple, M. S. *et al.*, 2007).

6.08.3 The Somatosensory Cortex of Prosimian Primates

Prosimians represent one of the three major branches of primate evolution (prosimians, tarsiers, and anthropoids). The prosimians include present-day lemurs, lorises, and galagos. The somatosensory cortex is likely organized in a similar manner in most of the prosimians, but experimental data are largely from the slow lorises (Krishnamurti, A. *et al.*, 1976) and especially galagos (e.g., Wu, C. W. and Kaas, J. H., 2003). As in most mammals, the anterior parietal cortex of galagos consists of three areas (Figure 5): a systematic representation of the contralateral body surface (Sur, M. *et al.*, 1980), corresponding to area S1 or 3b, and rostral and caudal zones that are described as being unresponsive to cutaneous stimulation in anesthetized animals (.Carlson, M. and Welt, C., 1980; Sur, M. *et al.*, 1980; Wu, C. W. and Kaas, J. H., 2003) but have strong connections with S1 (Wu, C. W. and Kaas, J. H., 2003). The S1 representation has a somatotopic organization that is similar to S1 of anthropoid primates (Sur, M. *et al.*, 1980), dense inputs from the ventroposterior nucleus, and architectonic characteristics of the primary sensory cortex (Figure 6; Preuss, T. M. and Goldman-Rakic, P. S., 1991a). Based on its position in the cortical mantle and its architectonic features, the SR somatosensory cortex along the rostral border of S1 appears to be area 3a (e.g., Preuss, T. M. and Goldman-Rakic, P. S., 1991a). Thalamic inputs to SR arise from the ventroposterior superior nucleus, as do inputs to area 3a in anthropoid

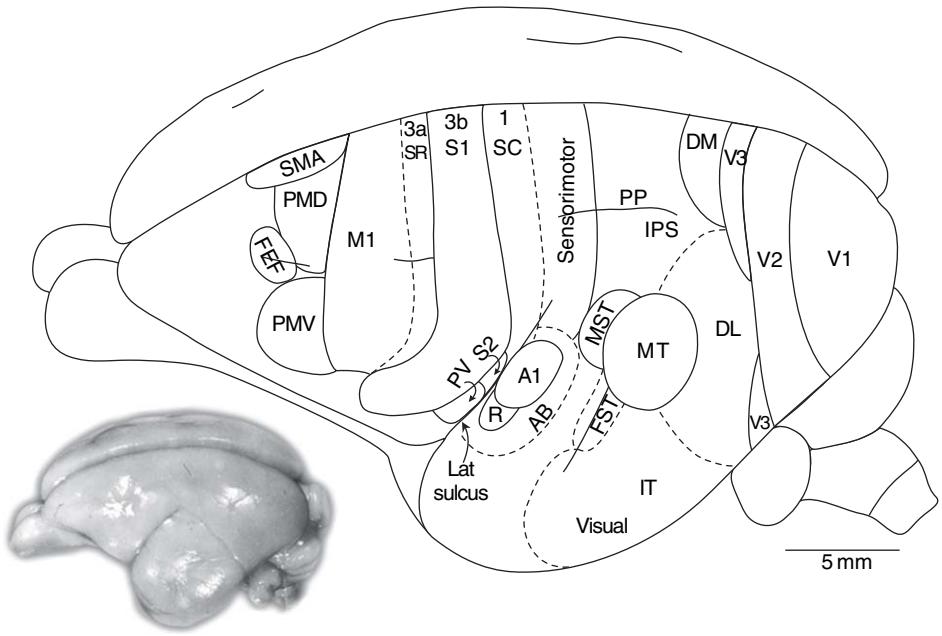

Figure 5 Somatosensory areas on a dorsolateral view of the left cerebral hemisphere of a galago (*Otolemur garnetti*), a prosimian primate. The anterior parietal cortex includes the three areas found in other mammals, S1 or area 3b, SR or area 3a, and area SC, which is in the position of area 1 in anthropoid primates. The second somatosensory area (S2), and the parietal ventral somatosensory area (PV), have been defined just lateral to S1 in the cortex on the upper bank of the lateral sulcus. A rostral strip of the posterior parietal cortex has dense cortical connections with other areas of the somatosensory cortex and with motor and premotor areas (M1, primary cortex; PMD, dorsal premotor cortex area; PMV, ventral premotor area; SMA, supplementary motor area). Other areas shown for reference include visual areas, V1, V2, and V3, dorsomedial (DM) and dorsolateral (DL) visual areas, inferior temporal (IT) cortex, the middle temporal (MT), medial superior temporal (MST), and fundal superior temporal (FST) visual areas. The auditory cortex includes the primary auditory area, A1, and the rostral auditory area, R, as well as an auditory belt (AB) of several areas. Note the lateral (Lat) sulcus and the intraparietal sulcus (IPS). Scale bar = 5 mm. FEF, frontal eye field.

primates (Franca, J. G. *et al.*, 2003). In an earlier architectonic study of another prosimian primate, the slow loris, Sanides F. and Krishnamurti A. (1967) concluded that the cytoarchitecture of S1 (their somatic koniocellular area) identified it as area 3b, while the strip of cortex on the rostral border of 3b was area 3a. The identity of the strip of cortex along the caudal border of 3b is less certain. By position, this cortex should be area 1, but the area has been variously identified as areas 2 + 5 (Preuss, T. M. and Goldman-Rakic, P. S., 1991a) or 1 + 2 (Sanides, F. and Krishnamurti, A., 1967; Wu, C. W. and Kaas, J. H., 2003). The lateral somatosensory cortex, located along the upper bank of the lateral sulcus, contains the second somatosensory area, S2, and the parietal ventral area, PV (Burton, H. and Carlson, M., 1986; Garraghty, P. E. *et al.*, 1991; Wu, C. W. and Kaas, J. H., 2003). S2 and PV of galagos receive dense inputs from the ventroposterior nucleus, as in other mammals with the exception of anthropoid primates, as well as inputs from the ventroposterior inferior nucleus, in common with anthropoid primates. The cortical connections of S2 and PV, together with limited results from microelectrode recordings, suggest the existence of additional areas in the lateral sulcus and insula, which have been designated as the ventral somatosensory area (VS), retroinsular area (Ri) and parietal rostral area (PR) (Wu, C. W. and Kaas, J. H., 2003). Histological distinctions between subdivisions of the lateral parietal cortex have been described in prosimian primates (Sanides, F. and Krishnamurti, A., 1967; Zilles, K. *et al.*, 1979b), but they are not pronounced. The posterior parietal cortex of galagos includes a rostral division having connections with motor and somatosensory areas of cortex, and a caudal division that receives inputs from the visual cortex and is connected with the rostral division (Fang, P. C. *et al.*, 2005; Stepniewska, I. *et al.*, 2005). Both regions have been included in an area 7 (with subdivisions) by Preuss T. M. and Goldman-Rakic P. S. (1991a; 1991b).

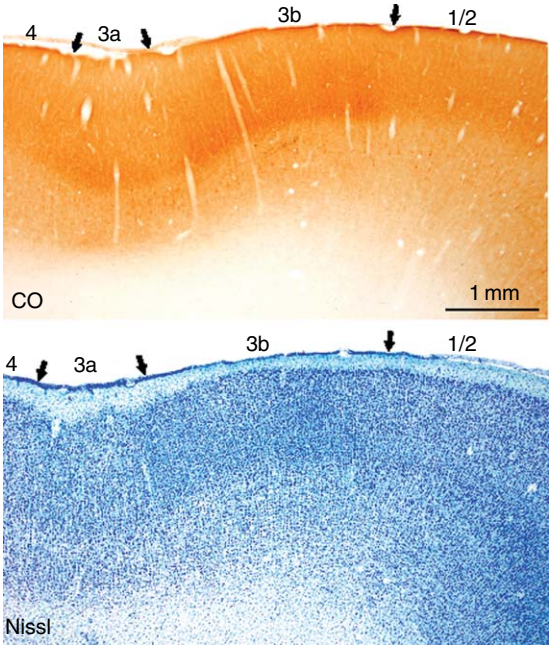

Figure 6 Architectonic characteristics of the somatosensory cortex of prosimian galagos. Brain sections cut in the parasagittal plane were processed for the expression of cytochrome oxidase (CO), above, or Nissl staining of cell bodies, below. CO levels were highest in the metabolically active layer 4 and the inner third of layer 3. This expression of CO was most dense in area 3b (S1), clearly marking the rostral and caudal boundaries of the area. Layer 4 expressed a moderate level of CO in area 3a, which was absent in agranular area 4 (primary motor cortex). The expression of CO in granular (4) and supragranular (3) layers of area 1/2 was much less than in area 3b. In tradition Nissl-stained sections, area 3b was characterized by densely packed, small cells in layers 4 and 3 such that these layers appear to fuse. This fused region of small cells corresponds to the CO-dense region. Layer 4 was less well developed in both area 3a and area 1/2. Scale bar = 1 mm.

Of the proposed architectonic subdivisions of the somatosensory cortex of galagos and other prosimians, such as slow loris (Sanides, F. and Krishnamurti, A., 1967) and microcebus murinus (Zilles, K. *et al.*, 1979a), areas 3b and 3a are most distinct, area 3b because it has the pronounced features of the primary sensory cortex and area 3a because this dysgranular cortex stands out between the highly granular cortex of area 3b and the agranular cortex of area 4 of the primary motor cortex. Nevertheless, the granular appearance of layer 4 in area 3b of prosimians is not as pronounced as in anthropoid primates, and this misled Brodmann K. (1909) into identifying area 3b of prosimian lemurs as area 1. However, layer 4 of area 3b of galagos is thick and densely packed with small neurons, as is area 3b of other primates, and layers 3 and 6 are densely packed with cells as well. The middle layers of area 3b of galagos are more myelinated and express more CO than in adjacent areas, making the field stand out. Area 3b of galagos (Figure 5) corresponds in location and extent to the area 1 of Brodmann K. (1909), area 3 of von Bonin G. (1945), area postcentralis 1 of Zilles K. *et al.* (1979b), and 3b of Preuss T. M. and Goldman-Rakic P. S. (1991a) in galagos and other prosimian primates.

In brain sections cut parallel to the surface of the cortex and processed for myelin, area 3b of galagos has modular subdivisions of the myelin-dense region that are separated by myelin-light septa, (Kaas, J. H. *et al.*, 2006), as in anthropoid primates. One prominent septum separates the forelimb representation from that of the face. Other septa separate representations of parts of the face, the teeth, and the tongue. These modular divisions of area 3b are similar to those found in monkeys, as described further below.

Descriptions of other architectonic areas in prosimians are more variable, reflecting the relative lack of sharp distinctions between areas. The most extensive description of the cytoarchitecture of the parietal cortex of prosimian is that of Preuss T. M. and Goldman-Rakic P. S. (1991a), where a number of subdivisions of their area 7 were identified and homologies with divisions of area 7 in macaque monkeys were proposed. These authors also recognized an S2 region that is extensive enough to include S2 and PV, as well as additional cortex in the lateral sulcus. The cytoarchitecture of a smaller galago (*Galago demidovii*) and of the prosimian mouse lemur (*Microcebus murinus*) has also been studied and S1 (area 3b) was obvious as an area with a pronounced layer 4, but areas SC and SR were not noted (Zilles, K., 1979a; 1979b). In a similar manner, the earlier study of the cytoarchitecture of cortex in galagos by von Bonin G. (1945) only identified S1 (3b).

6.08.4 The Anterior Parietal Cortex of New World Monkeys

The somatosensory cortex of anthropoid primates differs from that of prosimian primates and other mammals in that the anterior parietal cortex usually has four major divisions, areas 3a, 3b, 1, and 2, as an area 2 has been added to the three areas present in prosimians. The lateral parietal cortex is somewhat

expanded, and may have more areas. The posterior parietal cortex is variably expanded, being relatively small, as in galagos, in some New World monkeys, but considerably expanded in others, such as in Old World macaques. The somatosensory areas of New World owl monkeys are shown in Figure 7.

The anterior parietal cortex of New World monkeys is somewhat variable across species in histological appearance and the distinctiveness of subdivisions. At one extreme, these are the small New World marmosets and tamarins in which only area 3b (S1) responds well to cutaneous stimulation (Carlson, M. *et al*., 1986; Krubitzer, L. A. and Kaas, J. H., 1990). As area 1 and, to some extent, area 2 can be identified by having characteristic representations of cutaneous receptors that are separate and distinct from the representation in area 3b, the weakly responsive cortex caudal to area 3b (S1) of marmosets is more like the caudal somatosensory area of galagos and other mammals than area 1 of other anthropoid primates. Area 3b of marmosets (Figure 8) has densely packed granule cells in layer 4, as in other primates. The packing of cells in layers 4 and 3 is less pronounced in the cortex caudal to area 3b in the position of area 1, and a transition more caudally to cortex with somewhat less cell packing in layers 4 and 6 may signify the presence of an area 2. But there is no convincing physiological or connectional evidence for an area 2 in these primates. Cortex rostral to area 3b in marmosets has the typical appearance of area 3a, with a

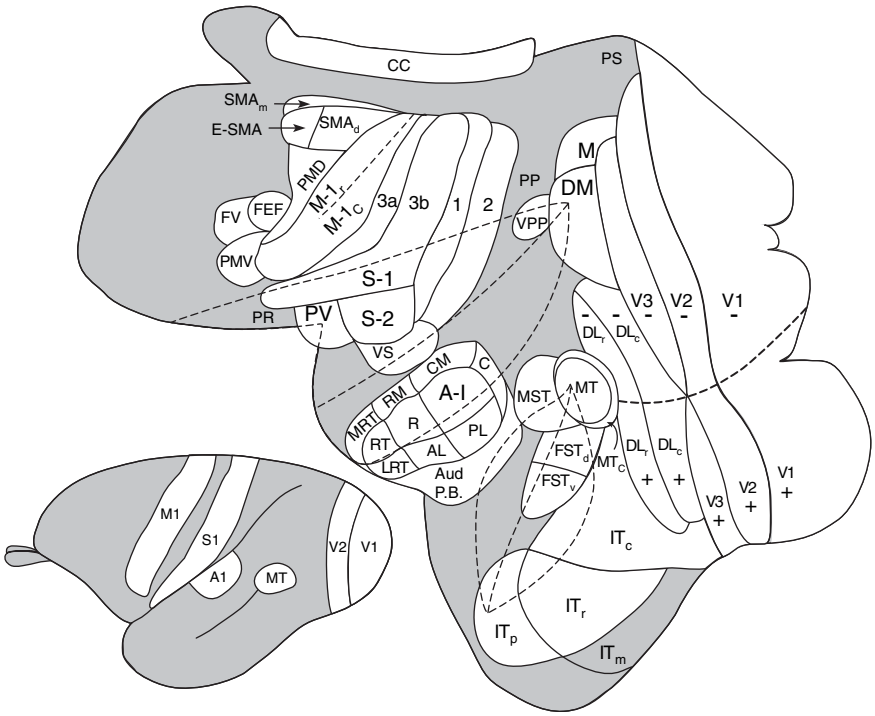

Figure 7 Somatosensory areas of a New World monkey (owl monkey, *Aotus*). On the lower left, a lateral view of the brain shows the locations of primary somatosensory (S1 or area 3b) and primary motor areas (M1), as well as the primary visual cortex (V1) for reference. The second visual area, V2, and the middle temporal area, MT, are also shown. On the upper right, cortical areas are indicated on a larger view of neocortex after it has been separated from the rest of the brain, fissures opened, and the cortex flattened. Somatosensory areas include areas 3a, 3b, 1, and 2 of Brodmann K. (1909), S2, PV, the parietal rostral area (PR), rostral and caudal divisions of the ventral somatosensory area (VSr and VSc), and the retroinsular area (Ri). The posterior parietal cortex (PP) includes a ventral posterior parietal (VPP) area with visual inputs. Other subdivisions are uncertain. Motor areas include rostral and caudal divisions of the primary motor cortex (M1r and M1c), dorsal and ventral premotor areas (PMD and PMV), dorsal and medial supplementary motor areas (SMAd and SMAm), caudal and rostral cingulate motor areas (CMv and CMc), a frontal eye field (FEF), frontal visual area (FV), and a supplementary eye field (E-SMA). Auditory areas include A1, a rostral area (R), and a rostrotemporal area (RT), as well as areas of the auditory belt (Aud B) and parabelt (Aud P.B.). Visual areas include V1, V2, V3, DM, DL with rostral and caudal divisions, MT, MST, FSTd, FSTv, and IT with caudal, rostral, medial and polar divisions (see Figure 5 for abbreviations). The medial visual area (M) and the MT crescent (MTc) are also indicated. CC, corpus callosum.

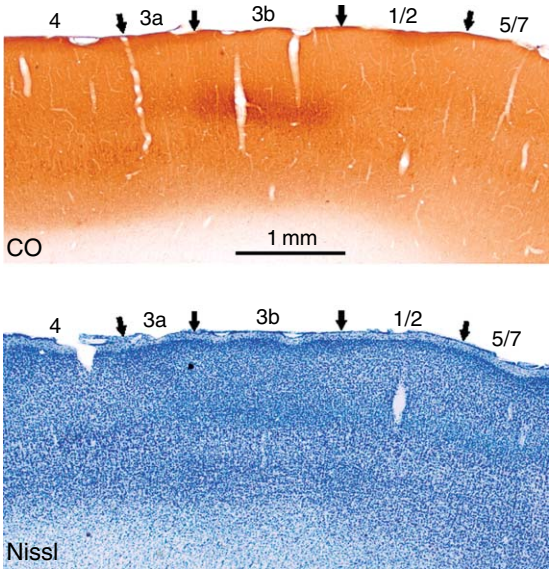

Figure 8 Architectonic characteristics of the anterior parietal somatosensory cortex in marmosets (*Callithrix jacchus*). Brain sections cut in the parasagittal plane have been processed for cytochrome oxidase (CO), above, or stained for cell bodies (Nissl), below. As in galagos (Figure 6), CO was densely expressed in layer 4 and inner layer 3 of area 3b (S1), with more focused and denser CO expression than in area 3b of galagos. The CO expression in layer 4 of area 3a was much less, with even less expression in layer 6 of area 4. Area 1/2 had little layer 4 CO expression, while layer 4 CO expression increased slightly in area 5/7. In area 3b, dense packing of small cells in layer 1 and the adjoining part of layer 3 was the most prominent defining feature, although layer 6 was also densely packed with cells. Layer 4 was less pronounced in area 3a, while the appearance of large pyramidal cells in layer 5 marked the translation to area 4. Layer 4 was moderately well developed in area 1/2, and even more pronounced in area 5/7. The use of the terms 1/2 and 5/7 for areas caudal to area 3b reflects uncertainties over the identities of these fields (see text). Scale bar = 1 mm.

poorly developed layer 4 and a scattering of larger layer 5 pyramidal cells. In addition, the connections of this cortex with the ventroposterior superior nucleus of the thalamus reinforce the identification of this rostral band of cortex as area 3a (Huffman, K. J. and Krubitzer, L., 2001).

In squirrel monkeys (Sanides, F., 1968; Jones, E. G. *et al.*, 1978; Sur, M. *et al.*, 1982; Cusick, C. G. *et al.*, 1985;) and owl monkeys (Merzenich, M. M. *et al.*, 1978), there is architectonic, connectional, and physiological evidence for areas 3a, 3b, 1, and 2. The microelectrode recording evidence for a separate representation of the body in area 2 is limited and has not been published in full. The large cebus monkeys also have architectonic fields corresponding to areas 3a, 3b, 1 and 2, and parallel representation of cutaneous receptor has been described in areas 3b and 1, while limited recordings suggest additional, mainly deep receptor representations in areas 3a and 2 (Felleman, D. J. *et al.*, 1983).

6.08.5 Other Somatosensory Areas of New World Monkeys

Areas of the posterior parietal cortex and the lateral parietal cortex have been difficult to delineate architectonically in primates, and these regions have been less well studied in New World monkeys than in Old World monkeys. In addition, the great range of brain sizes in New World monkeys suggests that subdivisions and architectonic feature vary across taxa, and descriptions developed for one or a few species may not apply to all. Brodmann K. (1909) used a marmoset brain as an example of a New World monkey, and divided all of the posterior parietal cortex into an anterior area 5 and a posterior area 7. Cortex in the positions of areas 1 and 2 of Old World monkeys was included in area 5. Neither area 5 nor area 7 was subdivided. Subdivisions of cortex in the lateral fissure were not identified. Later, Peden, J. K. and von Bonin G. (1947) also concluded that the parietal cortex of marmosets is not well differentiated into areas. These investigators also divided the posterior parietal cortex into an anterior region, PC, and a posterior region, PE, with PC including cortex up to the border of area 3b (their PB, which they stated "hardly deserves to be called koniocortex as in higher primates"). Much of the cortex on the upper bank of the lateral sulcus was included in an area PFD, which has a well-defined granular layer. PFD includes the regions of S2 and PV in marmosets, which have not been distinguished architectonically (Krubitzer, L. A. and Kaas, J. H., 1990).

Other early architectonic studies were those of von Bonin G. (1938) on cebus monkeys and of Lashley K. S. and Clark G. (1946) on spider monkeys, both being New World monkeys with large brains. In cebus monkeys, von Bonin described a narrow intermediate area, corresponding largely to area 2, between granular somatosensory cortex (area 3b) and a large, undivided posterior parietal region. The lengthy paper of Lashley K. S. and Clark G. (1946) on spider monkeys is known for its critical review of the cytoarchitectonic method for dividing cortex into areas, as the two authors independently produced different subdivisions of cortical organization.

Taking a position that now seems extreme, they concluded that only area 3a of the anterior parietal cortex could be reliably identified in spider and cebus monkeys, and that the proposed areas 5 and 7 of the posterior parietal cortex could not be "identified by any consistent characters and certainly do not represent functionally distinct units." Lashley and Clark described a large portion of the insular cortex in the lateral sulcus as the granular cortex.

More recent studies have not led to a clearer understanding of how the posterior parietal cortex is subdivided into areas in New World monkeys. Experimental and architectonic evidence for the array of fields proposed for the cortex of the intraparietal sulcus of macaques has not been obtained for New World monkeys. While an area 2 and an area 5, immediately caudal to area 2, have been described in squirrel monkeys (Rosabal, F., 1967; Jones, E. G. *et al.*, 1978), Padberg J. *et al.* (2005) propose that area 2 is missing in at least some New World monkeys so that area 5 extends to area 1 or even to the area 3b border. For now, a reasonable conclusion is that the origination of the posterior parietal cortex is not well understood in New World monkeys and that further studies combining histological techniques with studies of connections and function are needed.

In the lateral parietal cortex within the lateral fissure of New World monkeys, areas S2, PV, VS, and PR have been defined on the bases of somatotopic patterns and connections (Cusick, C. G. *et al.*, 1989; Krubitzer, L. A. and Kaas, J. H., 1990; Qi, H. X. *et al.*, 2002; Coq, J. O. *et al.*, 2004). All these areas have a moderately well-developed layer 4, and histological distinctions between the areas are not marked. The physiological and connectional data, together with the architectonic results, have not yet resolved the issue of whether areas S2 and PV immediately adjoin area 3b, which presents a clear architectonic border, or whether 3b is separated from S2 and PV by a narrow area 1 (or even an area 2) that cytoarchitectonically resembles S2 and PV. The architectonic border of S2 with VS is more apparent, as layer 4 is broader in S2 in both Nissl and CO preparations (Cusick,C. G. *et al.*, 1989). In squirrel monkeys, Jones E. G. and Burton H. (1976) include most of S2 and PV in the cortex designated as areas S2 and 1–2, while VS is located largely within their granular insular area, Ig. The region of area PR overlaps the cortex identified as gustatory by Sanides F. (1968). The insular cortex was divided from caudal to rostral by Jones E. G. and Burton H. (1976) into granular (Ig), dysgranular (Id), and agranular (Ia) fields. The VS region overlaps most of Ig. Just caudal to the granular insular cortex, a retroinsular region was distinguished as having more clearly separated layers. Thus, there are clear subdivisions of the lateral parietal cortex, but architectonic distinctions between the proposed somatosensory areas (S2, PV, VS, PR) of this region are not pronounced.

6.08.6 Modules in Area 3b of Old World and New World Monkeys

In brain sections cut parallel to the surface and stained for myelin, area 3b of marmosets stands out as a densely myelinated band of cortex that extends mediolaterally from the medial wall to near the lateral sulcus, at which point area 3b curves rostrally into the frontal lobe (.Krubitzer, L. A. and Kaas, J. H., 1990; Qi, H. X. *et al.*, 2002). This strip of densely myelinated cortex has a conspicuous septum crossing its width near the lateral end where it curves rostrally. This septum separates the mediolateral portion, which represents the foot, trunk, and forelimb in a mediolateral sequence, from the caudorostral segment representing the face, tongue, and teeth. Other septa divide the caudorostral segment into a series of ovals that represent different parts of the face, the contralateral teeth, the contralateral tongue, the ipsilateral teeth, and the ipsilateral tongue in a caudal-to-rostral sequence. These isolated ovals of cortex are visibly apparent modules in area 3b that relate to the functional isolation of body parts in the representation, rather than to differing functional classes of inputs. These modular features of area 3b are even more apparent in other New World monkeys (Figure 9; Jain, N. *et al.*, 2001; Iyengar, S. *et al.*, 2007), where septa can be seen dividing the representations of individual digits as well (Jain, N. *et al.*, 1998; 2001). Similar modular subdivisions of area 3b that represent digits, parts of the face, and the oral cavity have been described in area 3b of Old World macaque monkeys (Figure 10, Qi, H. X. and Kaas, J. H., 2004). Some of the modules can be seen, although less clearly, in area 3b of prosimian galagos (Kaas, J. H. *et al.*, 2006). They are likely to be visible in appropriately cut and stained brain sections of area 3b of apes and humans as well, but this has not yet been shown. The septa in area 3b of macaque are apparent soon after birth (Qi, H. X. and Kaas, J. H. 2004), so they are unlikely to depend on postnatal sensory experience. These septa, which separate parts of area 3b with few intrinsic

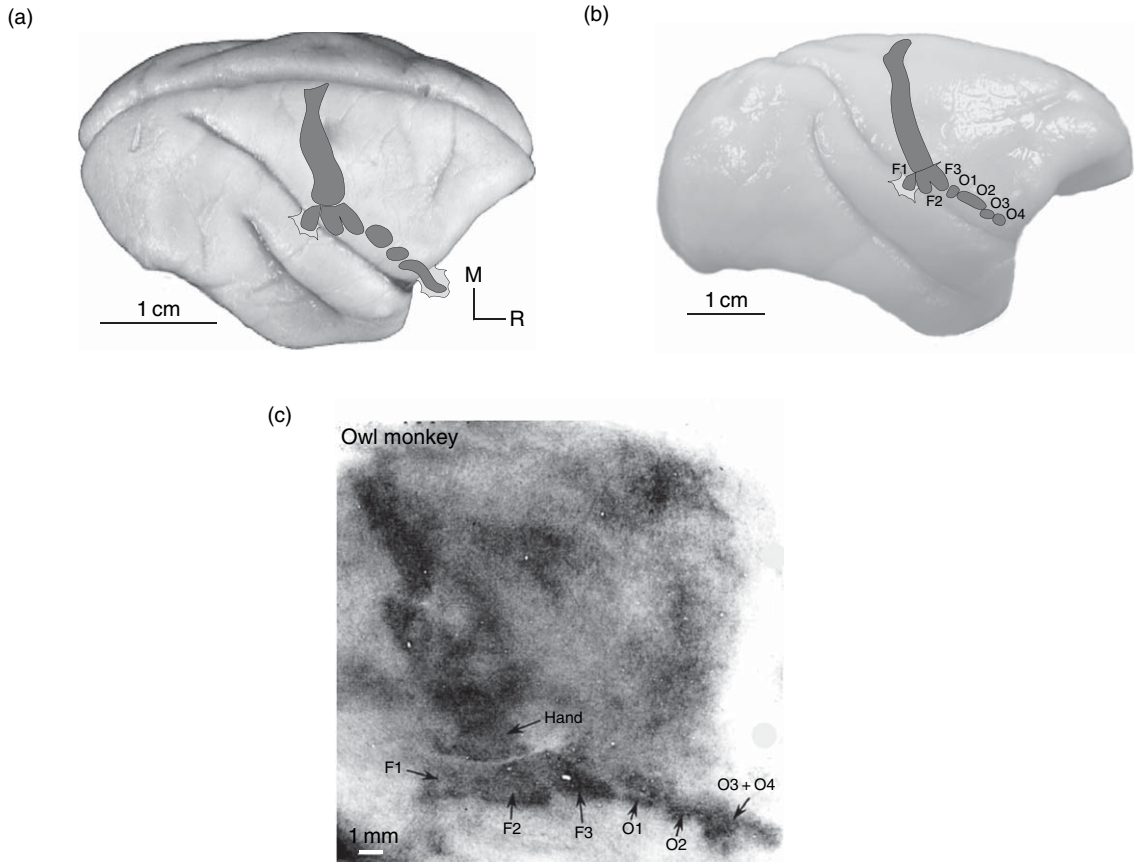

Figure 9 Modular subdivisions of the myeloarchitecture of area 3b (shaded) on lateral views of the right cerebral hemisphere of an owl monkey (a) and a squirrel monkey (b). The long mediolateral extent of area 3b represents the hand and other parts of the lower body, while the subdivided lower part represents the face and oral cavity. In the lower part, the modular subdivisions or ovals, F1–F3, represent the upper face, upper lip, and lower lip in a caudorostral sequence, while oral ovals, O1–O4, successively represent the contralateral teeth, the contralateral tongue, the ipsilateral teeth, and the ipsilateral tongue. The lateral sulcus (LS) and the superior temporal sulcus (STS) are indicated, and the marker bars = 1 cm. Ovals O3 + O4 fold onto the ventral surface of the frontal lobe in owl monkeys and F1 extends onto the upper bank of the lateral sulcus. In (c), a brain section cut parallel to the surface of unfolded and flattened cortex is stained for myelin. The myelin-dark region is area 3b. Lateral (ventral) to the hand representation, a myelin-light septum separates the hand representation from that of the face. Other septa that separate the F1–F3 and the O1–O4 ovals are variably apparent in this section. Other, less apparent, septa that separate the representations of the digits in the hand region need to be viewed at a higher magnification (see Jain, N. *et al.*, 1998). Scale bar = 1 mm. Adapted from Jain, N., Qi, H. X., Catania, K. C., and Kaas, J. H. 2001. Anatomic correlates of the face and oral cavity representations in the somatosensory cortical area 3b of monkeys. J. Comp. Neurol. 429(3), 455–468 and Kaas, J. H., Qi, H. X., and Iyengar, S. 2006. Cortical network for representing the teeth and tongue in primates. Anat. Rec. A Discov. Mol. Cell Evol. Biol. 288(2), 182–190.

interconnections, serve as useful anatomical guides to the somatotopy of area 3b.

The other type of module that appears to exist in area 3b of anthropoid primates is a functional one that divides the area into alternating patches of cortex that are activated by either SA or RA low-threshold cutaneous mechanoreceptors. These modules are not histologically distinct, and they have been demonstrated so far only in the territory of the hand representations of owl monkeys and macaque monkeys (Sur, M. *et al.*, 1981; 1984). The portions of area 3b that were devoted to each digit were divided into regions with inputs from RA receptors and regions devoted to SA receptors. The segregation of these two types of input was most apparent in arrays of microelectrode recordings from layer 4, where the thalamocortical projections from the ventroposterior nucleus terminate. The SA and RA domains revealed by these recordings were about 0.5 mm wide in macaques, and somewhat smaller in owl monkeys. Similar

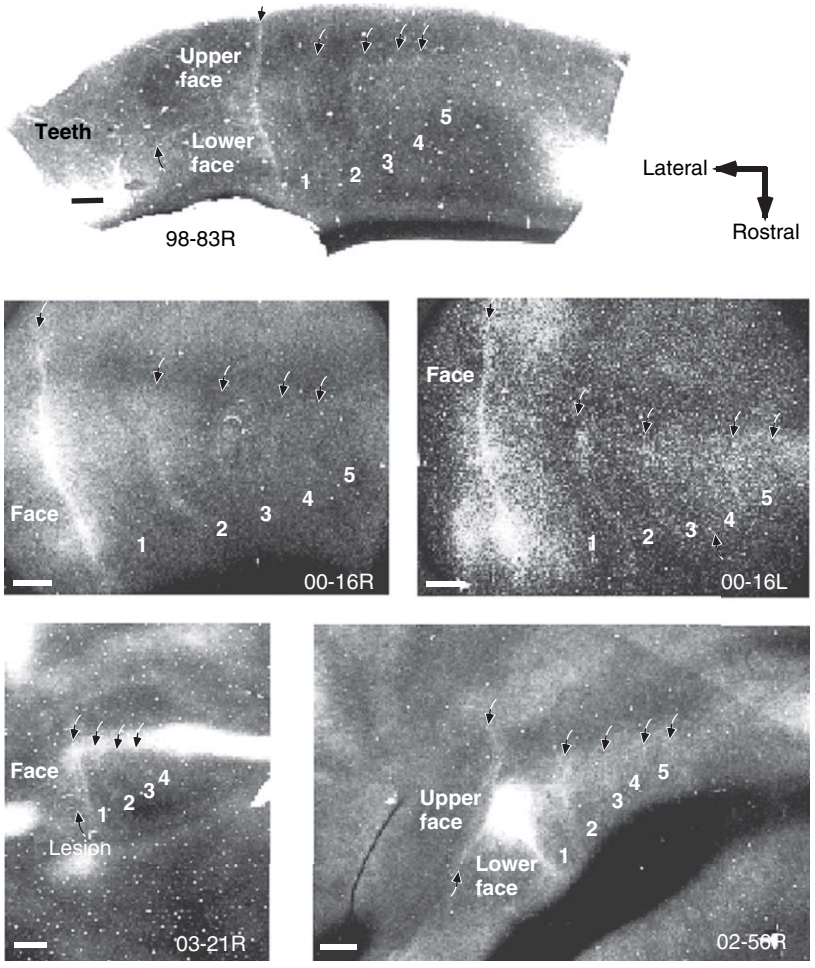

Figure 10 Modular subdivisions of area 3b representing individual digits in area 3b of macaque monkeys. Myelin-stained brain sections have been cut parallel to the surface of area 3b of macaque monkeys. The cortex corresponds to the caudal bank of the central sulcus with the fundus of the sulcus below (rostral). Narrow myelin-poor septa divide this cortex. The conspicuous lateralmost septa separates the representation of the face from that of the hand, while the progressively more medial and less apparent septa separate the representation of the digits, 1–5. A narrow septum separating the upper and lower face representation is apparent in the upper main section. Sections are numbered by case and cerebral hemisphere (R and L). Scale bars = 1 mm. Reproduced from Qi, H. X. and Kaas, J. H. 2004. Myelin stains reveal an anatomical framework for the representation of the digits in somatosensory area 3b of macaque monkeys. J. Comp. Neurol. 477(2), 172–187.

results have more recently been obtained in optical imaging studies of area 3b of squirrel monkeys (Chen, L. M. *et al.*, 2001). Presumably, all parts of area 3b have these modules, which correspond to the functionally distinct type of modules postulated by Mountcastle V. B. (1957). As further evidence for SA and RA modules in area 3b, microstimulation of regions of RA activation in area 3b of macaque monkeys appears to be interpreted by the monkeys as a sensation of flutter matching the frequency of the stimulation (Romo, R., *et al.*, 2000). This result suggests that the RA but not the SA modules participate in the somatosensory sensation of flutter.

Less is known about the existence of functional modules in other areas of the somatosensory cortex, but Friedman R. M. *et al.* (2004) have used optical imaging to determine what parts of the hand representation in area 1 are activated by frequencies of skin indentation that would preferentially activate SA (1–5 Hz, pressure), RA (30 Hz, flutter), or Pacinian RA-II (200 Hz, vibration) afferents. These results suggest that area 1 is divided into small domains-activated SA, RA, or PC afferents, with domains being roughly 200–300 μm in width. Other somatosensory areas may also be subdivided into interdigitating arrays of functionally distinct modules, but in higher-order areas

would be expected to have more complex functional types than the functional types that are closely tied to receptor type as in areas 3b and 1.

6.08.7 The Anterior Parietal Cortex of Old World Monkeys, Apes, and Humans

In Old World monkeys, apes, and humans, motor areas of the frontal lobe are separated from somatosensory areas of the parietal lobe by a deep central sulcus (Figure 11). The anterior parietal cortex includes the cortex in the depths of the central sulcus, and extends to the postcentral sulcus. In humans and Old World monkeys, the four major architecture fields of Brodmann K. (1909) divide the anterior parietal cortex into areas 3, 1, and 2 as a sequence of mediolateral strips of cortex extending from deep in the central fissure, anteriorly, to rostral bank of the postcentral gyrus. While Brodmann K. (1909) described the portion of area 3 lining the fundus of the central fissure as transitional, having architectonic features intermediate between the area 3 proper and the motor cortex (area 4), Vogt C. and Vogt O. (1919) distinguished the fundal cortex, with its narrow layer 4 and prominent layer 5 pyramidal cells, as area 3a, distinct from the hypergranular cortex located on the caudal bank of the central suclus, which they designated as area 3b. The four areas of the anterior parietal cortex distinguished by the Vogts (3a, 3b, 1, and 2) were combined in a single primary somatosensory field, S1, in early physiological studies on macaque monkeys (Marshall, W. H. *et al.*, 1937). As recording electrodes were placed only on the cortical surface in these experiments, recordings were made mainly from areas 1 and 2, and the separate representations of body parts in each of the architectonic fields were not apparent. Areas 3a, 3b, 1, and 2 are now widely recognized as

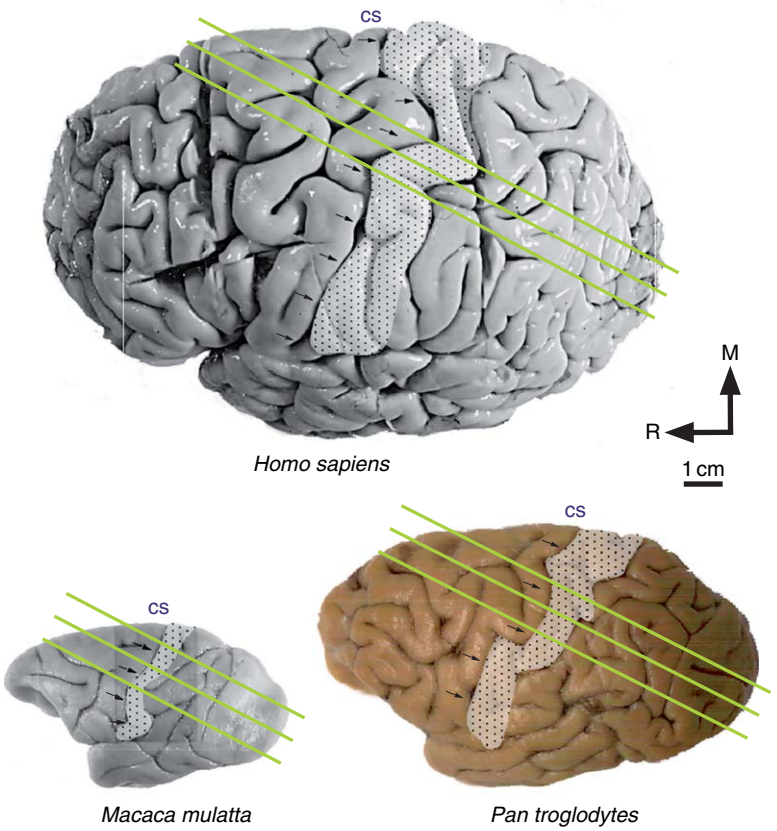

Figure 11 Dorsolateral views of the left cerebral hemisphere of macaque, chimpanzee, and human brains showing the locations of the central sulcus (CS) and the anterior parietal cortex. In these primates, most of area 3b is on the caudal bank of the central sulcus, and the postcentral gyrus is largely occupied by areas 1 and 2. Parallel lines indicate the planes of section for sections illustrated in Figure 13.

separate somatosensory areas, each containing a different representation of the body (Kaas, J. H. *et al.*, 1979). As in New World monkeys, the representations parallel each other while forming mirror reversals of somatotopy at their common borders. In contrast to New World marmosets, area 1 is highly responsive to cutaneous stimuli in Old World monkeys. Unlike New World monkeys such as owl and squirrel monkeys, much of area 2 in Old World monkeys is also responsive to cutaneous stimuli.

A summary of the somatotopic organizations of areas 3a, 3b, 1, and 2 of macaque monkeys, based on the reports of Nelson R. J. *et al.* (1980) and Pons T. P. *et al.* (1985), is shown in Figure 12. As area 3a is located in the depth of the central sulcus, it is the area that was least thoroughly examined in those

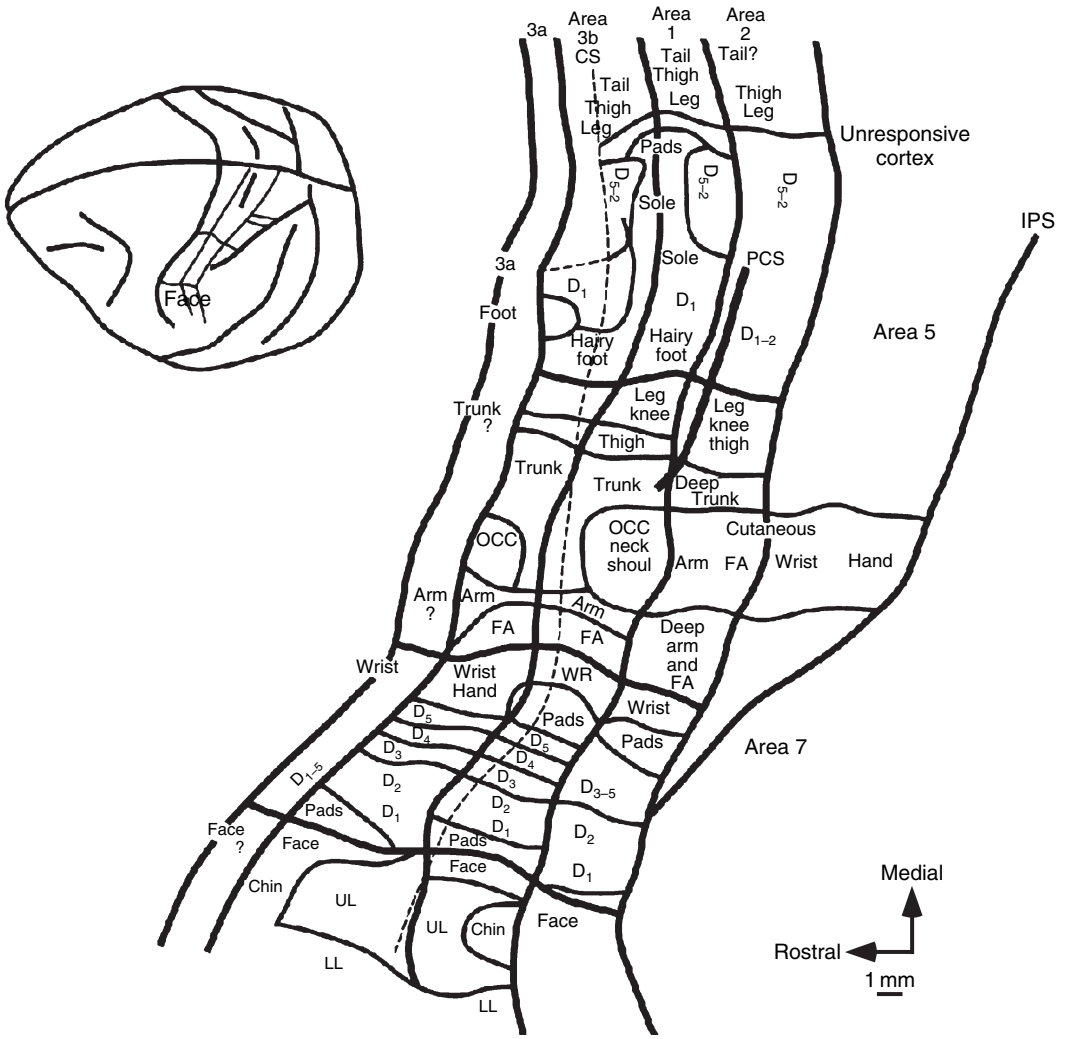

Figure 12 A summary of the somatotopic organization of the anterior parietal cortex of macaque monkeys based on the results of microelectrode recordings through this cortex by Nelson R. J. *et al.* (1980) and Pons T. P. *et al*. (1985). The explored region of the postcentral cortex is indicated on a dorsolateral view of the left cerebral hemisphere on the left. The diagram on the right is of the unfolded cortex of the central sulcus together with the postcentral gyrus, including some of area 5. The upper part of the diagram includes cortex unfolded from the medial wall of the cerebral hemisphere, while the most lateral extents of areas 3a, 3b, 1, and 2 were not explored (however, see Manger, P. R. *et al.*, 1996). Question marks indicate uncertainties about area 3a, which was not fully explored (however, see Krubitzer, L. *et al.*, 2004). A dashed line marks the crown of the central sulcus (CS). Note the location of the intraparietal sulcus (IPS). D1–D5, digits of the hand or foot, UL, upper lip; LL, lower lip; FA, forearm; Should, shoulder; OCC, occiput; Wr, wrist. Reproduced from Pons, T. P., Garraghty, P. E., Cusick, C. G., and Kaas, J. H. 1985. The somatotopic organization of area 2 in macaque monkeys. J. Comp. Neurol. 241(4), 445–466.

studies. A more complete portrayal of area 3a somatotopy in macaques has been presented by Krubitzer L. *et al.* (2004). The most lateral portion of these areas represents the face and receptors of the oral cavity. These parts of the representations have been more extensively described by Manger P. R. *et al.* (1996).

The somatosensory organization of the anterior parietal cortex in chimpanzee is largely unknown. However, some limited mapping of the anterior somatosensory cortex occurred in early studies in chimpanzees, with most of the recordings along the junction of area 1 with area 2 (Woolsey, C. N. *et al.*, 1943). The few recordings from surface sites in this study revealed a mediolateral somatotopic pattern that resembles that of macaque monkeys and humans (see Bailey, P. *et al.*, 1950, for maps of the motor cortex in chimpanzees).

In humans, the mediolateral somatotopy of the anterior parietal cortex, at least at a crude level, is well established (e.g., Penfield, W. and Boldrey, E., 1937; see Kaas, J. H., 2004, for review). However, the recording and stimulating sites in most studies were from the parts of the anterior parietal cortex exposed on the postcentral gyrus. Additional information has come from functional magnetic resonance imaging (MRI) studies. The overall somatotopic pattern is much like that reported for macaque monkeys and other primates. More recently, it has been possible to demonstrate separate representations of the glabrous hands in areas 3b and 1 of humans, with mirror image organizations as in monkeys. Thus, the digit tips are represented at the border of areas 3b and 3a, and again at the caudal border of area 1 with area 2 (Sato, K. *et al.*, 2002; Blankenburg, F. *et al.*, 2003). In addition, it is clear that area 2 contains another representation of the hand in humans (Krause, T. *et al.*, 2001). More laterally in the anterior parietal somatosensory cortex, the lower lip, teeth, and tongue are represented in a sequence that is similar to that of monkeys (Miyamoto, J. J. *et al.*, 2006). Thus, from the limited data available, the areas of the anterior parietal cortex of humans seem to be somatotopically organized in a manner that is similar to that described in monkeys.

Recently, we have started to compare the architectonic features of areas 3a, 3b, 1, and 2 of the anterior parietal cortex of macaque monkeys with those of areas in chimpanzees and humans. One reason to make these comparisons is to determine the extent to which the architectonic features of areas of the anterior parietal cortex vary across these primates, as structural differences may suggest functional differences. A second reason is to help resolve uncertainties about the boundaries of these areas in humans and chimpanzees. In macaques, the proposed boundaries of areas of the anterior parietal cortex are based on the results of studies of the anatomical connections, neuronal response properties, and somatotopic patterns of representation of the anterior parietal cortex. These results have been compatible with previously proposed boundaries of areas 3a and 3b, but, in our opinion, some depictions place the caudal boundary of area 1 too far caudally, and this is even more of a problem with area 2, which has often been shown extending caudally well onto the rostral bank of the intraparietal sulcus. These uncertainties reflect the fact that the architectonic borders of areas 1 and 2 are less obvious than those of area 3b and area 3a. However, the physiological data on somatotopy and neuron response properties and the data on area-specific connection patterns converge to clearly indicate where the caudal border of area 2, as a functional division of cortex, should be in macaques, and an architectonic change does take place at this location. The architectonic border between area 2 and area 5 (Pons, T. P. *et al.*, 1985; Pons, T. P. and Kaas, J. H., 1985) has recently been verified as conforming to a change in the response properties of neurons and somatotopy by Lewis J. W. *et al.* (1999).

As there are almost no data on connection patterns or somatotopy that would establish the significance of architectonic studies in chimpanzees, and very little in humans, consistent features of architectonic areas in macaques, chimpanzees, and humans allow architectonic criteria that have been validated in macaques to be applied to chimpanzees and humans (Figure 13).

Because of the supporting experimental data, the proposed architectonic subdivisions of the anterior parietal cortex of macaque monkeys serve as a standard for interpreting the architecture of the anterior parietal cortex in humans and chimpanzees. In all these primates, most of the anterior parietal cortex is buried in the central fissure, which is roughly 7 mm deep and 30 mm long in macaques, up to 10 mm deep and 65 mm long in chimps, and as much as 20 mm deep and 90 mm long in humans. Area 3b, which occupies much of the caudal bank of the central sulcus, is the most easily recognized subdivision of the anterior parietal cortex in all three primates. In Nissl-stained sections, area 3b of macaques is clearly distinguished from adjoining area 3a in the fundus of the central sulcus and area 1 near the top of the sulcus by a thick layer 4 that is densely packed with darkly

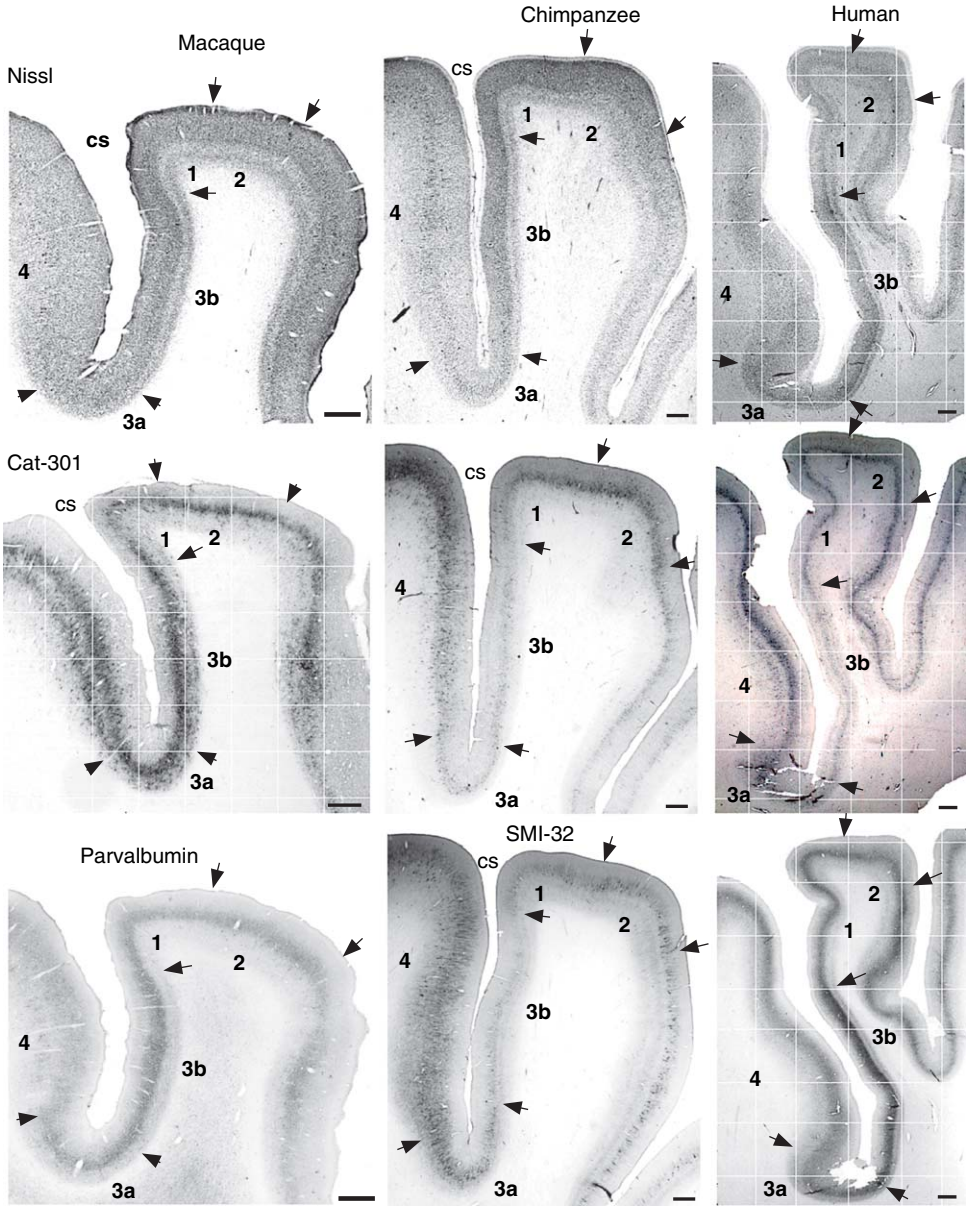

Figure 13 Some of the architectonic features of areas of the anterior parietal cortex of macaques, chimpanzees, and humans. In each column, a series of brain sections (see Figure 11) have been processed for cell bodies with a Nissl stain (top), the antigen for the Cat-301 antibody (middle), or the calcium-binding protein, parvalbumin (bottom, except for chimpanzee, where a section processed for SMI-32 has been substituted). The deep central sulcus (CS) is indicated, while the more caudal sulcus is the intraparietal sulcus. Arrows marking the boundaries of areas 4, 3a, 3b, 1, and 2 are indicated in a rostrocaudal sequence. Rostral is to the left. Scale bar = 1 mm. Unpublished illustration from Qi H-X. *et al.* (1997; 1998).

stained neurons. Layer 6 is also more darkly stained in area 3b than in adjoining areas. These same features mark area 3b of chimps and humans. These cytoarchitectonic features of area 3b are shown at higher magnifications in Figure 14, where the well-developed layer 4 is obvious. Lower-magnification photomicrographs are more useful in showing the pattern of change at the borders of areas. The monoclonal antibody, Cat-301, which is recognized by a proteoglycan antigen that is differentially expressed by different types of neurons (McKay, R. D. and Hockfield, S. J., 1982), has been useful in distinguishing some cortical areas, although not necessarily to the same extent or in the same way across species

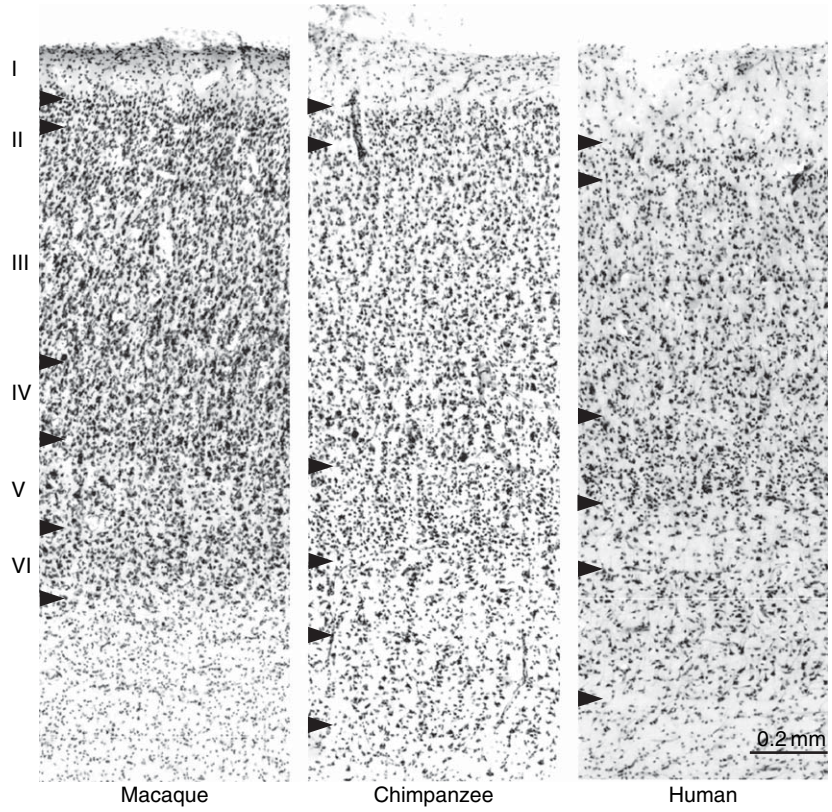

Figure 14 The cytoarchitecture of area 3b of a macaque, chimpanzee, and human at a higher magnification than that shown in Figure 13. Layers 1–6 (I–VI) are indicated. In each primate, a dense packing of small, darkly stained neurons in layer 4 is apparent.

(e.g., Jain, N. *et al.*, 1994). In our preparations, Cat-301 densely labeled layer 3 of area 3b of macaques, while layer 3 of area 1 was much less densely labeled (Figure 13). Layer 3 was also densely labeled in area 3a, thereby failing to clearly mark a 3a–3b border. In contrast, area 3b was not densely labeled by Cat-301 in chimps or humans, while area 1 expressed more of the antigen for Cat-301.

Immunostaining for the calcium-binding protein parvalbumin has also been used to reveal patterns of differential staining in the cortex of primates and has been very successful in demarcating primary sensory areas (e.g., Hackett, T. A. *et al.*, 1998). In area 3b of macaque monkeys, parvalbumin is densely expressed in layer 4 and inner layer 3 (Figure 13). Less parvalbumin is present in areas 1 and 3a. In chimps, the same pattern was present (Figure 15), but overall staining was not always as pronounced as in macaques. In humans the expression of parvalbumin in layer 4 and lower layer 3 was very dense in area 3b, and less dense in areas 1 and 3a. In sections processed for SMI-32 (only shown for chimpanzees; Figure 13; middle bottom; Figure 15, lower left), areas 3a and 3b can be clearly demarcated from area 4, and both the rostral and caudal borders of area 2 were apparent in all three primate species. Overall, area 3b is a very distinct area, and boundaries can be identified in several preparations, although the effectiveness of particular preparations can vary with the species, and with the state of the brain when processed.

Area 3a is also very distinct. In Nissl preparations, area 3a is characterized by a layer 4 that is less pronounced than in area 3b, but more developed than in the adjoining agranular motor cortex, area 4. Area 3a is not completely homogenous in appearance in Nissl preparations, but the significance of these variations is unknown (Jones, E. G. and Porter, R., 1980). Yet, the boundaries of area 3a are clear in macaques, chimps, and humans. In our Cat-301 preparations, the rostral border of area 3a with area 4 is very sharply marked in macaque monkeys, as neurons and neuropil are stained in a bilaminar pattern in area 4 that is not apparent in area 3a. In humans, the bilaminar pattern was weaker in area 4, but the border with area 3a was revealed by the

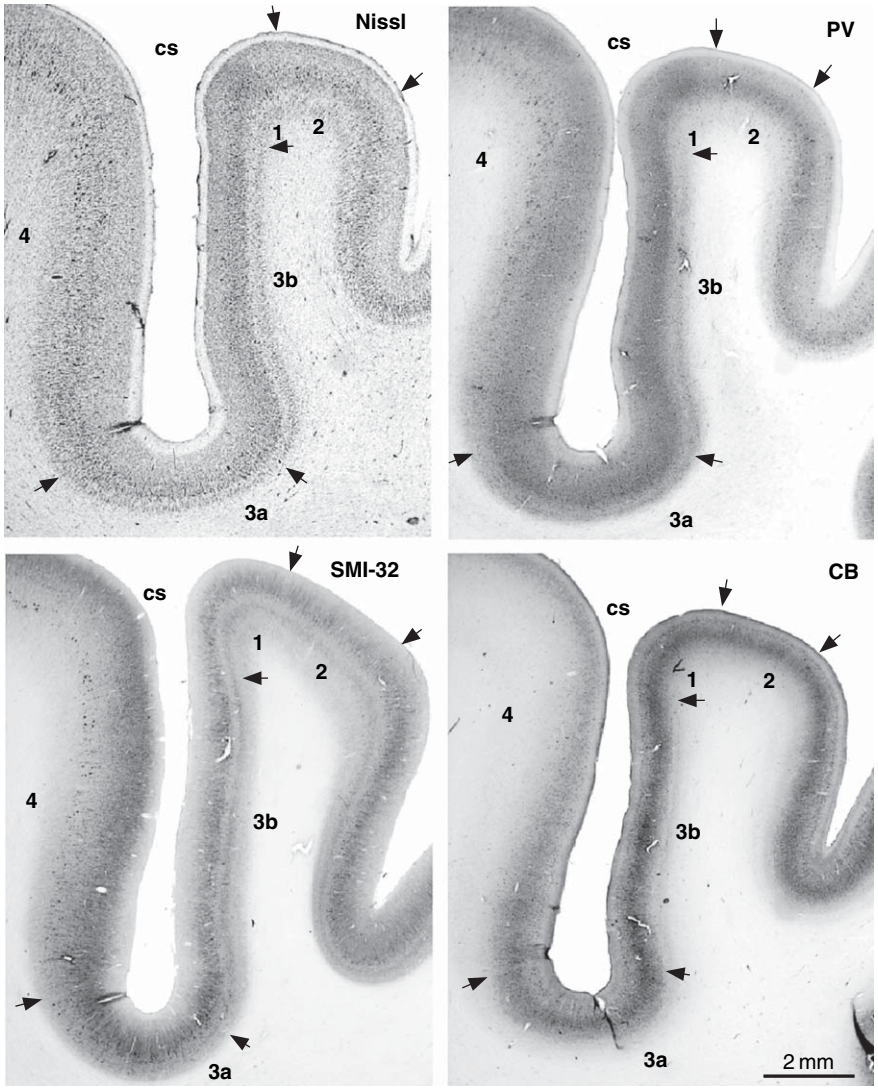

Figure 15 Photomicrographs of a series of adjacent parasagittal sections from the somatosensory cortex of a chimpanzee (case 95–93), illustrating the boundaries of areas 4, 3a, 3b, 1, and 2 in brain sections immunostained for calbindin, parvalbumin, or SMI-32 and a traditional Nissl stain for cell bodies. The deep central sulcus (CS) is indicated, while the more caudal sulcus is the intraparietal sulcus. Arrows mark the boundaries of areas 4, 3a, 3b, 1, and 2. Rostral is to the left. Scale bar = 2 mm. Unpublished illustration from Qi, H.-X., Jain, N., Preuss, T. M., and Kaas, J. H. 1997. Histochemical organization of somatosensory area 3b and surrounding cortex in chimpanzees. Soc. Neurosci. Abst. 23. Qi, H.-X., Jain, N., Preuss, T. M., and Kaas, J. H. 1998. Comparative architecture of areas 3a, 3b, and 1 of somatosensory cortex in chimpanzees, humans and macaques. Soc. Neurosci. Abst. 24, 1125.

denser expression of the Cat-301 antigen in layer 3 in area 4. In chimps, despite overall weak staining for the Cat-301 antigen (which has been noted in other cortical regions; Preuss, T. M. and Coleman, G. Q., 2002), it was still possible to detect the transition from the lighter staining of area 3a to the darker staining in area 4. As parvalbumin was more strongly expressed in layers 4 and 3 of area 3a than of area 4, this preparation also helped identify the rostral border of area 3a.

In Nissl preparations of area 1, layers 4 and 6 were less densely packed with neurons and less densely stained than in area 3b. In area 2, however, both of these layers were more pronounced, so that the border of area 1 with area 2 was reliably detected in macaques, chimps, and humans (Figures 13, 14, and 15). A similar change in appearance can be observed in brain sections processed for parvalbumin, which was more densely expressed in layer 4 and inner layer 3 of area 3b than

in area 1. Cat-301 preparations were also useful in delineating area 1, as area 2 expressed more of the antigen for Cat-301 than area 1 in all these primates, thereby marking the border of area 1 with area 2. The caudal border of area 2 with area 5 is not so obvious, and this has resulted in uncertainties and different opinions about where this border is located. However, patterns of somatotopic organization and connections with other areas and thalamic nuclei have helped to locate this border in macaques (Pons, T. P. *et al.*, 1985; Pons, T. P. and Kaas, J. H., 1985; 1986), and it corresponds in location in Old World monkeys to where the caudal boundary of area 2 was placed by Brodmann K. (1909), while others (e.g., Vogt, C. and Vogt, O., 1919 and Powell, T. P. and Mountcastle, V. B., 1959a; 1959b) placed the border further caudally in the rostral bank of the intraparietal sulcus. At the caudal border of area 2, cells in layers 4 and 6 became less darkly stained and less densely packed than in area 2 (Pons, T. P. *et al.*, 1985). The location of the physiological border in macaques also corresponds to a change in the laminar distribution of myelin and the neurofilament protein labeled by the SMI-32 antibody (Lewis, J. W. *et al.*, 1999). In chimps and humans, the border of area 2 with area 5 can be detected in similar fashion (Figures 13 and 15), although it is not always obvious. In sections processed for parvalbumin, the expression of parvalbumin in layer 4 and deeper layer 3 was somewhat less diffuse and more focused in area 2 than in area 5, providing some suggestion of a border. The Cat-301 preparations provided inconsistent results across these primates: chimpanzees exhibited stronger labeling of area 2 than of area 1, but the distinction between the areas was less clear in humans and macaques. The medial and lateral boundaries of area 2 have not been established (Lewis, J. W. *et al.*, 1999), but area 2 is generally depicted as extending along the full border of area 1.

Recent descriptions of the cytoarchitecture of the anterior parietal cortex of humans include those of Rademacher J. *et al.* (1993), White L. E. *et al.* (1997), and Geyer S. *et al.* (1999). The study of Geyer S. *et al.* (1999) is particularly noteworthy as it introduces an objective, observer-independent method of determining areal borders based on changes in Nissl-staining density profiles taken through the thickness of the cortex from pia to white matter. The results produced borders of areas 3a and 3b similar to those indicated in Figure 13(b), but area 1 was more extensive, including cortex onto the rostral bank of the postcentral sulcus, and area 2 was placed deep within the postcentral sulcus. Although the use of density profiles allows an objective determination of borders, the authors recognized that the classification (naming) of areas is an interpretation. In our view, area 1 was too extensive, and area 2 was misplaced in the study of Geyer S. *et al.* (1999). This supposition is supported by the results of a recent functional MRI study in humans that placed the systematic representation of the hand that characterizes area 3b on the caudal bank of the central sulcus, as expected, and the mirror image representation that denotes area 1 in the cortex extending from the upper part of the caudal bank of the central sulcus onto the crown of the postcentral gyrus (Blankenburg, F. *et al.*, 2003), similar to the extent of area 1 in Figure 13. This interpretation would also relocate the border of area 2 with area 1 to a more rostral position.

Differences in CO activity also have been used to characterize areas of the anterior parietal cortex in humans, as areas 3a and 3b have a darkly stained band in layer 4 and inner layer 3 that distinguishes these areas from areas 1 and 2 (Eskenasy, A. C. and Clark, S., 2000). In addition, Hilbig H. *et al.* (2001) have used a plant lectin, *Wisteria floribunda* agglutinin (WFA), which like Cat-301 is a marker of the proteoglycan-rich perineuronal nets, to distinguish area 3a from areas 3b and 4 in the human somatosensory cortex. Regional and laminar patterns in the distribution of neural receptors are also used to identify areas of the anterior parietal cortex in humans (.Geyer, S. *et al.*, 1997; Zilles, K. *et al.* 2002) and macaques (e.g., Huntsman, M. M. *et al.*, 1995). In humans, area 3b is associated with the expression of high levels of receptors for acetylcholine (muscarinic cholinergic M2 and nicotinic cholinergic receptors). These various architectonic approaches have the potential for revealing a number of other proposed divisions of the somatosensory cortex.

6.08.8 Architectonic Areas of Lateral and Posterior Parietal Cortex

Additional areas of the somatosensory cortex have been described and characterized architectonically in macaques and humans. These areas typically are difficult to distinguish from each other, so there are a number of uncertainties. Descriptions of the subdivisions and names of lateral and posterior parietal cortex vary across reports. In the lateral parietal cortex of macaques, where areas S2, PV, and VS are contained, Preuss T. M. and Goldman-Rakic P. S. (1989) described a large SII region that may include both S2 and PV. Jones E. G. and Burton H. (1976) and

Mesulam, M. M. and Mufson E. J. (1982) provide a similar description that includes a large SII, the retroinsular cortex, and granular, dysgranular, and agranular insular regions. Another region identified by Eickhoff S. B. *et al.* (2006a) may correspond to the parietal ventral area (Coq, J. O. *et al.*, 2004). A fourth architectonic region appears to correspond to the parieto-insular vestibular cortex of macaques (Eickhoff, S. B. *et al.*, 2006b). Other regions identified by Eickhoff S. B. *et al.* (2006b) and Eickhoff S. B. *et al.* (2007) may correspond to rostral and caudal divisions of the parietal ventral area (Coq, J. O. *et al.*, 2004).

The posterior parietal cortex of Old World monkeys, apes, and humans includes at least two major divisions, the caudal part being largely dominated by visual inputs and the rostral part by somatosensory and, to a lesser extent, auditory inputs (Lewis, J. W. and Van Essen, D. C., 2000; Kaas, J. H., 2004). The most significant outputs, in terms of sensorimotor function, are to motor and premotor areas of the frontal cortex. A number of alternative ways of subdividing the posterior parietal cortex have been proposed. Brodmann K. (1909) suggested a division into areas 5 and 7, and Vogt C. and Vogt O. (1919) subsequently divided these areas further, recognizing areas 5a, 5b, 7a, and 7b. More recent studies have proposed additional subdivisions, based either on Brodmann's nomenclature (e.g., the subdivisions of area 7 suggested by Cavada, C. and Goldman-Rakic, P. S., 1989, and by Preuss, T. M. and Goldman-Rakic, P. S., 1991a), or on extensions of von Economo's C. V.(1929) nomenclature (i.e., PE, PF, PFG, PG, Opt; see Pandya, D. N. and Seltzer, B., 1982). In addition, differences in connection patterns and physiological evidence, together with architectonic distinctions, have been used to divide the cortex of the intraparietal sulcus of macaque monkeys into medial (MIP), lateral (LIP), ventral (VIP), and anterior (AIP) areas, with MIP sometimes included in a larger parietal reach region (PRP) (see Lewis, J. W. and Van Essen, D. C., 2000; Kaas, J. H., 2004). Similar subdivisions have been proposed for the human posterior parietal cortex (e.g., Bremmer, F. *et al.*, 2001; Grefkes, C. *et al.*, 2002; .Simon, O. *et al.*, 2002), although there are uncertainties about how similar or different these regions are in humans and macaques (see Rushworth, M. F. *et al.*, 2001). While Brodmann K. (1909) argued that the inferior parietal lobule of humans contained areas (39 and 40) not found in monkey brains, several later investigations concluded that areas 39 and 40 are homologous to the inferior parietal lobe areas (areas 7b and 7a, respectively) of macaques (Bonin, G. and Bailey, P., 1947; Eidelberg, D. and Galaburda, A. M., 1984). In contrast, Zilles K. and Palomero-Gallagher N. (2001) concluded that area 7 of monkeys is not the same as area 7 of humans. Thus, considerable caution is needed in considering any view of how the posterior parietal cortex is subdivided into areas based on architecture or other types of data.

The difficulty in obtaining a reliable parcellation of the posterior parietal areas of macaque monkeys has been stressed by Lewis J. W. and Van Essen D. C. (2000), who illustrated six current partitioning schemes for this cortex, while they themselves charted 17 architectonic subdivisions in and near the intraparietal sulcus. These proposed subdivisions were characterized in terms of the density and laminar pattern of myelination and SMI-32 immunoreactivity. They denoted new areas as subdivisions of previously identified areas. Thus, LIP had ventral (LIPv) and dorsal (LIPd) subdivisions, while VIP had medial (VIPm) and lateral (VIPl) subdivisions. In the intraparietal cortex of humans, Zilles and coworkers (Choi, H. J. *et al.*, 2006) have recently identified two cytoarchitectonically different fields, human IP1 and IP2, that they propose correspond to VIP and AIP of monkeys.

6.08.9 Conclusions

1. Even small-brained mammals with little neocortex appear to have at least five areas of the somatosensory cortex, including a primary area S1, rostral (SR) and caudal (SC) somatosensory bands of cortex along the borders of S1, and the second (S2) and parietal ventral (PV) areas just lateral to S1. S1 is architectonically distinct in most histological preparations: S1 has a well-developed layer 4 that is densely packed with small neurons, although not to the same extent as in most anthropoid primates where this cortex (area 3b) is referred to as koniocortex because of the very small cells of layer 4. The bordering strips of the somatosensory cortex, SR and SC, have less distinct architectonic features, but they are easily distinguished from S1 and, if present, motor cortex. S1 is activated by cutaneous afferents via projections from the ventroposterior nucleus of the thalamus. Area SR is in the position of area 3a of primates, and may get proprioceptive information from the thalamus, in common with area 3a of primates. Area SC is in the position of area 1

or areas 1 plus 2 of primates. It is tempting to consider SC as a homologue of area 1 or of areas 1 and 2 combined, but the evidence for this is limited. S2 and PV resemble each other architectonically.

2. S1 of many mammals is not uniform in architectonic appearance, but instead is subdivided into patches or modules of granular cortex that receive dense inputs from the ventroposterior nucleus and express high levels of CO. These modules are separated by dysgranular cortex with low levels of CO. The narrow separation zones of dysgranular cortex separate the representations of distinct body parts in S1, such as the representations of individual mystacial vibrissae on the faces of rodents, where the CO-dense modules make up the so-called barrel field. Other types of isolating septa relating to somatotopic divisions are common. The isolated CO-dense, granular zones constitute one type of modular organization that is found in S1.
3. Many mammals have very little cortex that could be properly called posterior parietal cortex. This region of the cortex is greatly expanded in most anthropoid primates.
4. The somatosensory cortex of prosimian primates that have been examined has not been greatly modified from the pattern of organization commonly found in other mammals. SR clearly corresponds to area 3a of anthropoid primates, but the relationship of SC to areas 1 and 2 of anthropoid primates is still in question. The lateral parietal cortex includes one or more divisions of the ventral somatosensory area, VS, and there is evidence for a parietal rostral area, PR. A posterior parietal region is clearly present, and it is divided into a rostral region with connections with areas of the somatosensory and motor cortex, and a caudal region with visual inputs and projections to the rostral half of the posterior parietal cortex. Together, they presumably guide visuomotor behavior via connections with the primary motor cortex and premotor areas. The broad rostral and caudal regions of the posterior parietal cortex have functional subdivisions that have not been well defined.
5. New World monkeys differ from prosimians in that the posterior parietal cortex is usually more extensive, although functional subdivisions have not been well defined. In the anterior parietal cortex, an area 2 that represents both deep and cutaneous receptor is usually present (although not clearly so in marmosets and several other smaller New World monkeys). Areas 3a and 2 have been shown to receive proprioceptive information via projections from a distinct subdivision of the ventroposterior thalamus, the ventroposterior superior nucleus.
6. In both New World and Old World monkeys, dysgranular septa are often apparent that separate the face from the hand representations in area 3b (S1), digits from each other in the hand representation, and parts of the face, the tongue, and the teeth from each other in the face–mouth portion of area 3b. In addition, at least the hand representation of area 3b is divided into small territories or modules receiving either SA afferent activation or RA afferent activation from the ventroposterior nucleus. Thus, area 3b has modules that reflect somatotopic disjunctions and modules that reflect classes of activating neurons.
7. The anterior parietal cortex of Old World macaques, apes, and humans is divided into areas 3a, 3b, 1, and 2, with each of these areas being architectonically distinct. Other areas of the lateral and the posterior parietal cortex have been defined by architectonic and other criteria, but some of these areas, especially in the greatly expanded posterior parietal cortex, have not been well defined. However, a series of areas of the cortex of the intraparietal sulcus of macaques and humans are similar enough in relative position and functional roles to suggest that they are homologous.

References

Andermann, M. L. and Moore, C. I. 2006. A somatotopic map of vibrissa motion direction within a barrel column. Nat. Neurosci. 9(4), 543–551.

Bailey, P., Bonin, G. V., and McCulloch, W. S. 1950. The Isocortex of the Chimpanzee. The University of Illinois Press.

Beck, P. D., Pospichal, M. W., and Kaas, J. H. 1996. Topography, architecture, and connections of somatosensory cortex in opossums: evidence for five somatosensory areas. J. Comp. Neurol. 366(1), 109–133.

Benison, A. M., Rector, D. M., and Barth, D. S. 2007. Hemispheric mapping of secondary somatosensory cortex in the rat. J. Neurophysiol. 97(1), 200–207.

Blankenburg, F., Ruben, J., Meyer, R., Schwiemann, J., and Villringer, A. 2003. Evidence for a rostral-to-caudal somatotopic organization in human primary somatosensory cortex with mirror-reversal in areas 3b and 1. Cereb. Cortex 13(9), 987–993.

Von Bonin, G. 1938. The cerebral cortex of the cebus monkey. J. Comp. Neurol. 69, 181–227.

Von Bonin, G. 1945. The Cortex of Galago: Its Relation to the Pattern of the Primate Cortex. The University of Illinois Press.

Von Bonin, G. and Bailey, P. 1947. The Neocortex of *Macaca mulata*. The University of Illinois Press.

Bremmer, F., Schlack, A., Duhamel, J. R., Graf, W., and Fink, G. R. 2001. Space coding in primate posterior parietal cortex. Neuroimage 14(1 Pt 2), S46–S51.

Brodmann, K. 1909. Vergleichende Lokalisationsiehre der Grosshirnrinde in ihren Prinzipien Dargestellt auf Grund des Zellenbaues. Barth.

Bruno, R. M., Khatri, V., Land, P. W., and Simons, D. J. 2003. Thalamocortical angular tuning domains within individual barrels of rat somatosensory cortex. J. Neurosci. 23(29), 9565–9574.

Burton, H. and Carlson, M. 1986. Second somatic sensory cortical area (SII) in a prosimian primate, *Galago crassicaudatus*. J. Comp. Neurol. 247(2), 200–220.

Campbell, M. J. and Morrison, J. H. 1989. Monoclonal antibody to neurofilament protein (SMI-32) labels a subpopulation of pyramidal neurons in the human and monkey neocortex. J. Comp. Neurol. 282(2), 191–205.

Carlson, M. and Welt, C. 1980. Somatic sensory cortex (Sml) of the prosimian primate *Galago crassicaudatus*: organization of mechanoreceptive input from the hand in relation to cytoarchitecture. J. Comp. Neurol. 189(2), 249–271.

Carlson, M., Huerta, M. F., Cusick, C. G., and Kaas, J. H. 1986. Studies on the evolution of multiple somatosensory representations in primates: the organization of anterior parietal cortex in the New World callitrichid, *Saguinus*. J. Comp. Neurol. 246(3), 409–426.

Catania, K. C. and Kaas, J. H. 1995. Organization of the somatosensory cortex of the star-nosed mole. J. Comp. Neurol. 351(4), 549–567.

Catania, K. C. and Remple, M. S. 2002. Somatosensory cortex dominated by the representation of teeth in the naked mole-rat brain. Proc. Natl. Acad. Sci. U. S. A. 99(8), 5692–5697.

Catania, K. C., Jain, N., Franca, J. G., Volchan, E., and Kaas, J. H. 2000. The organization of somatosensory cortex in the short-tailed opossum (*Monodelphis domestica*). Somatosens. Mot. Res. 17(1), 39–51.

Catania, K. C, Lyon, D. C., Mock, O. B., and Kaas, J. H. 1999. Cortical organization in shrews: evidence from five species. J. Comp. Neurol. 410(1), 55–72.

Cavada, C. and Goldman-Rakic, P. S. 1989. Posterior parietal cortex in rhesus monkey: II. evidence for segregated corticocortical networks linking sensory and limbic areas with the frontal lobe. J. Comp. Neurol. 287(4), 422–445.

Chapin, J. K. and Lin, C. S. 1984. Mapping the body representation in the SI cortex of anesthetized and awake rats. J. Comp. Neurol. 229(2), 199–213.

Chen, L. M., Friedman, R. M., Ramsden, B. M., LaMotte, R. H., and Roe, A. W. 2001. Fine-scale organization of SI (area 3b) in the squirrel monkey revealed with intrinsic optical imaging. J. Neurophysiol. 86(6), 3011–3029.

Choi, H. J., Zilles, K., Mohlberg, H., Schleicher, A., Fink, G. R., Armstrong, E., and Amunts, K. 2006. Cytoarchitectonic identification and probabilistic mapping of two distinct areas within the anterior ventral bank of the human intraparietal sulcus. J. Comp. Neurol. 495(1), 53–69.

Cooper, N. G. and Steindler, D. A. 1986. Lectins demarcate the barrel subfield in the somatosensory cortex of the early postnatal mouse. J. Comp. Neurol. 249(2), 157–169.

Coq, J. O., Qi, H., Collins, C. E., and Kaas, J. H. 2004. Anatomical and functional organization of somatosensory areas of the lateral fissure of the New World titi monkey (*Callicebus moloch*). J. Comp. Neurol. 476(4), 363–387.

Cusick, C. G., Steindler, D. A., and Kaas, J. H. 1985. Corticocortical and collateral thalamocortical connections of postcentral somatosensory cortical areas in squirrel monkeys: a double-labeling study with radiolabeled wheatgerm agglutinin and wheatgerm agglutinin conjugated to horseradish peroxidase. Somatosens. Res. 3(1), 1–31.

Cusick, C. G., Wall, J. T., Felleman, D. J., and Kaas, J. H. 1989. Somatotopic organization of the lateral sulcus of owl monkeys: area 3b, S-II, and a ventral somatosensory area. J. Comp. Neurol. 282(2), 169–190.

Dawson, D. R. and Killackey, H. P. 1987. The organization and mutability of the forepaw and hindpaw representations in the somatosensory cortex of the neonatal rat. J. Comp. Neurol. 256(2), 246–256.

Disbrow, E., Roberts, T., and Krubitzer, L. 2000. Somatotopic organization of cortical fields in the lateral sulcus of *Homo sapiens*: evidence for SII and PV. J. Comp. Neurol. 418(1), 1–21.

Economo, C. V. 1929. The cytoarchitectonics of the human cerebral cortex. Oxford University Press.

Eickhoff, S. B., Schleicher, A., Zilles, K., and Amunts, K. 2006a. The human parietal operculum. I. Cytoarchitectonic mapping of subdivisions. Cereb. Cortex 16(2), 254–267.

Eickhoff, S. B., Grefkes, C., Zilles, K., and Fink, G. R. 2007. The somatotopic organization of cytoarchitectonic areas on the human parietal operculum. Cereb. Cortex 17, 1800–1811.

Eickhoff, S. B., Weiss, P. H., Amunts, K., Fink, G. R., and Zilles, K. 2006. Identifying human parieto-insular vestibular cortex using fMRI and cytoarchitectonic mapping. Hum. Brain Mapp. 27, 611–621.

Eidelberg, D. and Galaburda, A. M. 1984. Inferior parietal lobule. Divergent architectonic asymmetries in the human brain. Arch. Neurol. 41(8), 843–852.

Eskenasy, A. C. and Clarke, S. 2000. Hierarchy within human SI: supporting data from cytochrome oxidase, acetylcholinesterase and NADPH-diaphorase staining patterns. Somatosens. Mot. Res. 17(2), 123–132.

Fang, P. C., Stepniewska, I., and Kaas, J. H. 2005. Ipsilateral cortical connections of motor, premotor, frontal eye, and posterior parietal fields in a prosimian primate, *Otolemur garnetti*. J. Comp. Neurol. 490(3), 305–333.

Franca, J. G., Qi, H. S., and Kaas, J. H. 2003. Cortical connections and architecture of the somatosensory thalamus of prosimian galagos. Soc. Neurosci. Abst. 29, 173–180.

Felleman, D. J., Nelson, R. J., Sur, M., and Kaas, J. H. 1983. Representations of the body surface in areas 3b and 1 of postcentral parietal cortex of cebus monkeys. Brain Res. 268(1), 15–26.

Friedman, R. M., Chen, L. M., and Roe, A. W. 2004. Modality maps within primate somatosensory cortex. Proc. Natl. Acad. Sci. U. S. A. 101(34), 12724–12729.

Garraghty, P. E., Florence, S. L., Tenhula, W. N., and Kaas, J. H. 1991. Parallel thalamic activation of the first and second somatosensory areas in prosimian primates and tree shrews. J. Comp. Neurol. 311(2), 289–299.

Geyer, S., Schleicher, A., and Zilles, K. 1997. The somatosensory cortex of human: cytoarchitecture and regional distributions of receptor-binding sites. Neuroimage 6(1), 27–45.

Geyer, S., Schleicher, A., and Zilles, K. 1999. Areas 3a, 3b, and 1 of human primary somatosensory cortex. Neuroimage 10(1), 63–83.

Grefkes, C., Weiss, P. H., Zilles, K., and Fink, G. R. 2002. Crossmodal processing of object features in human anterior intraparietal cortex: an fMRI study implies equivalencies between humans and monkeys. Neuron 35(1), 173–184.

Hackett, T. A., Stepniewska, I., and Kaas, J. H. 1998. Subdivisions of auditory cortex and ipsilateral cortical connections of the parabelt auditory cortex in macaque monkeys. J. Comp. Neurol. 394(4), 475–495.

Hilbig, H., Bidmon, H. J., Blohm, U., and Zilles, K. 2001. *Wisteria floribunda* agglutinin labeling patterns in the human cortex: a

tool for revealing areal borders and subdivisions in parallel with immunocytochemistry. Anat. Embryol. (Berl.) 203(1), 45–52.
Huffman, K. J. and Krubitzer, L. 2001. Thalamo-cortical connections of areas 3a and M1 in marmoset monkeys. J. Comp. Neurol. 435(3), 291–310.
Huffman, K. J., Nelson, J., Clarey, J., and Krubitzer, L. 1999. Organization of somatosensory cortex in three species of marsupials, *Dasyurus hallucatus*, *Dactylopsila trivirgata*, and *Monodelphis domestica*: neural correlates of morphological specializations. J. Comp. Neurol. 403(1), 5–32.
Huntsman, M. M., Woods, T. M., and Jones, E. G. 1995. Laminar patterns of expression of GABA-A receptor subunit mRNAs in monkey sensory motor cortex. J. Comp. Neurol. 362(4), 565–582.
Iyengar, S., Qi, H. X., Jain, N., and Kaas, J. H. 2007. Cortical and thalamic connections of the representations of the teeth and tongue in somatosensory cortex of New World monkeys. J. Comp. Neurol. 501(1), 95–120.
Jain, N., Catania, K. C., and Kaas, J. H. 1998. A histologically visible representation of the fingers and palm in primate area 3b and its immutability following long-term deafferentations. Cereb. Cortex 8(3), 227–236.
Jain, N., Diener, P. S., Coq, J. O., and Kaas, J. H. 2003. Patterned activity via spinal dorsal quadrant inputs is necessary for the formation of organized somatosensory maps. J. Neurosci. 23(32), 10321–10330.
Jain, N., Preuss, T. M., and Kaas, J. H. 1994. Subdivisions of the visual system labeled with the Cat-301 antibody in tree shrews. Vis. Neurosci. 11(4), 731–741.
Jain, N., Qi, H. X., Catania, K. C., and Kaas, J. H. 2001. Anatomic correlates of the face and oral cavity representations in the somatosensory cortical area 3b of monkeys. J. Comp. Neurol. 429(3), 455–468.
Jones, E. G. and Burton, H. 1976. Areal differences in the laminar distribution of thalamic afferents in cortical fields of the insular, parietal and temporal regions of primates. J. Comp. Neurol. 168(2), 197–247.
Jones, E. G. and Porter, R. 1980. What is area 3a? Brain Res. 203(1), 1–43.
Jones, E. G., Coulter, J. D., and Hendry, S. H. 1978. Intracortical connectivity of architectonic fields in the somatic sensory, motor and parietal cortex of monkeys. J. Comp. Neurol. 181(2), 291–347.
Juliano, S. L., Ma, W., Bear, M. F., and Eslin, D. 1990. Cholinergic manipulation alters stimulus-evoked metabolic activity in cat somatosensory cortex. J. Comp. Neurol. 297(1), 106–120.
Kaas, J. H. 1993. Evolution of multiple areas and modules within neocortex. Perspect. Dev. Neurobiol. 1(2), 101–107.
Kaas, J. H. 2004. Evolution of somatosensory and motor cortex in primates. Anat. Rec. A Discov. Mol. Cell Evol. Biol. 281(1), 1148–1156.
Kaas, J. H. 2007. Reconstructing the Organization of Neocortex of the First Mammals and Subsequent Modifications. In: Evolution of Nervous Systems (*eds*. J. H. Kaas and L. A. Krubitzer), Vol. 3, pp. 27–48. Elsevier.
Kaas, J. H., Nelson, R. J., Sur, M., Lin, C. S., and Merzenich, M. M. 1979. Multiple representations of the body within the primary somatosensory cortex of primates. Science 204(4392), 521–523.
Kaas, J. H., Qi, H. X., and Iyengar, S. 2006. Cortical network for representing the teeth and tongue in primates. Anat. Rec. A Discov. Mol. Cell Evol. Biol. 288(2), 182–190.
Karlen, S. J. and Krubitzer, L. 2007. The functional and anatomical organization of marsupial neocortex: Evidence for parallel evolution across mammals. Prog. Neurobiol. (In Press).
Krause, T., Kurth, R., Ruben, J., Schwiemann, J., Villringer, K., Deuchert, M., Moosmann, M., Brandt, S., Wolf, K., Curio, G., and Villringer, A. 2001. Representational overlap of adjacent fingers in multiple areas of human primary somatosensory cortex depends on electrical stimulus intensity: an fMRI study. Brain Res. 899(1–2), 36–46.
Krishnamurti, A., Sanides, F., and Welker, W. I. 1976. Microelectrode mapping of modality-specific somatic sensory cerebral neocortex in slow loris. Brain Behav. Evol. 13(4), 267–283.
Krubitzer, L. A. and Hunt, D. L. 2007. Captured in the Net of Space and Time: Understanding Cortical Field Evolution. In: Evolution of Nervous System (*eds*. J. H. Kaas and L. A. Krubitzer), pp. 49–72. Elsevier.
Krubitzer, L. A. and Kaas, J. H. 1990. The organization and connections of somatosensory cortex in marmosets. J. Neurosci. 10(3), 952–974.
Krubitzer, L., Huffman, K. J., Disbrow, E., and Recanzone, G. 2004. Organization of area 3a in macaque monkeys: contributions to the cortical phenotype. J. Comp. Neurol. 471(1), 97–111.
Krubitzer, L. A., Manger, P., Pettigrew, J., and Calford, M. 1995. Organization of somatosensory cortex in monotremes: in search of the prototypical plan. J. Comp. Neurol. 351(2), 261–306.
Krubitzer, L. A., Sesma, M. A., and Kaas, J. H. 1986. Microelectrode maps, myeloarchitecture, and cortical connections of three somatotopically organized representations of the body surface in the parietal cortex of squirrels. J. Comp. Neurol. 250(4), 403–430.
Land, P. W. and Simons, D. J. 1985. Cytochrome oxidase staining in the rat SmI barrel cortex. J. Comp. Neurol. 238(2), 225–235.
Lashley, K. S. and Clark, G. 1946. The cytoarchitecture of the cerebral cortex of ateles: a critical examination of architectonic studies. J. Comp. Neurol. 85, 223–305.
Lewis, J. W. and Van Essen, D. C. 2000. Mapping of architectonic subdivisions in the macaque monkey, with emphasis on parieto-occipital cortex. J. Comp. Neurol. 428(1), 79–111.
Lewis, J. W., Burton, H., and Van Essen, D. C. 1999. Anatomical evidence for the posterior boundary of area 2 in the macaque monkey. Somatosens. Mot. Res. 16(4), 382–390.
Louderback, K. M., Glass, C. S., Shamalla -Hannah, L., Erickson, S. L., and Land, P. W. 2006. Subbarrel patterns of thalamocortical innervation in rat somatosensory cortical barrels: organization and postnatal development. J. Comp. Neurol. 497(1), 32–41.
Manger, P. R., Woods, T. M., and Jones, E. G. 1996. Representation of face and intra-oral structures in area 3b of macaque monkey somatosensory cortex. J. Comp. Neurol. 371(4), 513–521.
Marshall, W. H, Woolsey, C. N., and Bard, P. 1937. Cortical representation of tactile sensibility as indicated by cortical potentials. Science 85, 388–390.
McKay, R. D. and Hockfield, S. J. 1982. Monoclonal antibodies distinguish antigenically discrete neuronal types in the vertebrate central nervous system. Proc. Natl. Acad. Sci. U. S. A. 79(21), 6747–6751.
Merzenich, M. M., Kaas, J. H., Sur, M., and Lin, C. S. 1978. Double representation of the body surface within cytoarchitectonic areas 3b and 1 in ''SI'' in the owl monkey (*Aotus trivirgatus*). J. Comp. Neurol. 181(1), 41–73.
Mesulam, M. M. and Mufson, E. J. 1982. Insula of the Old World monkey. I. Architectonics in the insulo-orbito-temporal component of the paralimbic brain. J. Comp. Neurol. 212(1), 1–22.
Miyamoto, J. J., Honda, M., Saito, D. N., Okada, T., Ono, T., Ohyama, K., and Sadato, N. 2006. The representation of the human oral area in the somatosensory cortex: a functional MRI study. Cereb. Cortex 16(5), 669–675.

Morel, A., Garraghty, P. E., and Kaas, J. H. 1993. Tonotopic organization, architectonic fields, and connections of auditory cortex in macaque monkeys. J. Comp. Neurol. 335(3), 437–459.

Mountcastle, V. B. 1957. Modality and topographic properties of single neurons of cat's somatic sensory cortex. J. Neurophysiol. 20(4), 408–434.

Nelson, R. J., Sur, M., Felleman, D. J., and Kaas, J. H. 1980. Representations of the body surface in postcentral parietal cortex of *Macaca fascicularis*. J. Comp. Neurol. 192(4), 611–643.

Padberg, J., Disbrow, E., and Krubitzer, L. 2005. The organization and connections of anterior and posterior parietal cortex in titi monkeys: do New World monkeys have an area 2? Cereb. Cortex 15(12), 1938–1963.

Palomero-Gallagher, N. and Zilles, K. 2004. Isocortex. In: The Rat Nervous System (*ed*. G. Paxinos), Third Edn. Elsevier.

Pandya, D. N. and Seltzer, B. 1982. Intrinsic connections and architectonics of posterior parietal cortex in the rhesus monkey. J. Comp. Neurol. 204(2), 196–210.

Peden, J. K. and Bonin, G.v. 1947. The neocortex of Hapale. J. Comp. Neurol. 86, 37–63.

Penfield, W. and Boldrey, E. 1937. Somatic motor and sensory representation in the cerebral cortex of man as studied by electrical stimulation. Brain 60, 389–443.

Pons, T. P. and Kaas, J. H. 1985. Connections of area 2 of somatosensory cortex with the anterior pulvinar and subdivisions of the ventroposterior complex in macaque monkeys. J. Comp. Neurol. 240(1), 16–36.

Pons, T. P. and Kaas, J. H. 1986. Corticocortical connections of area 2 of somatosensory cortex in macaque monkeys: a correlative anatomical and electrophysiological study. J. Comp. Neurol. 248(3), 313–335.

Pons, T. P., Garraghty, P. E., Cusick, C. G., and Kaas, J. H. 1985. The somatotopic organization of area 2 in macaque monkeys. J. Comp. Neurol. 241(4), 445–466.

Powell, T. P. and Mountcastle, V. B. 1959a. The cytoarchitecture of the postcentral gyrus of the monkey *Macaca mulatta*. Bull. Johns Hopkins. Hosp. 105, 108–131.

Powell, T. P. and Mountcastle, V. B. 1959b. Some aspects of the functional organization of the cortex of the postcentral gyrus of the monkey: a correlation of findings obtained in a single unit analysis with cytoarchitecture. Bull. Johns Hopkins Hosp. 105, 133–162.

Preuss, T. M. and Coleman, G. Q. 2002. Human-specific organization of primary visual cortex: alternating compartments of dense Cat-301 and calbindin immunoreactivity in layer 4A. Cereb. Cortex 12(7), 671–691.

Preuss, T. M. and Goldman-Rakic, P. S. 1989. Connections of the ventral granular frontal cortex of macaques with perisylvian premotor and somatosensory areas: anatomical evidence for somatic representation in primate frontal association cortex. J. Comp. Neurol. 282(2), 293–316.

Preuss, T. M. and Goldman-Rakic, P. S. 1991a. Architectonics of the parietal and temporal association cortex in the strepsirhine primate galago compared to the anthropoid primate *Macaca*. J. Comp. Neurol. 310(4), 475–506.

Preuss, T. M. and Goldman-Rakic, P. S. 1991b. Ipsilateral cortical connections of granular frontal cortex in the strepsirhine primate galago, with comparative comments on anthropoid primates. J. Comp. Neurol. 310(4), 507–549.

Purves, D., Riddle, D. R., and LaMantia, A. S. 1992. Iterated patterns of brain circuitry (or how the cortex gets its spots). Trends Neurosci. 15(10), 362–368.

Preuss, T. M., Stepniewska, I., Jain, N., and Kaas, J. H. 1997. Multiple divisions of macaque precentral motor cortex identified with neurofilament antibody SMI-32. Brain Res. 767(1), 148–153.

Qi, H. X. and Kaas, J. H. 2004. Myelin stains reveal an anatomical framework for the representation of the digits in somatosensory area 3b of macaque monkeys. J. Comp. Neurol. 477(2), 172–187.

Qi, H. X., Lyon, D. C., and Kaas, J. H. 2002. Cortical and thalamic connections of the parietal ventral somatosensory area in marmoset monkeys (*Callithrix jacchus*). J. Comp. Neurol. 443(2), 168–182.

Qi, H.-X., Jain, N., Preuss, T. M., and Kaas, J. H. 1997. Histochemical organization of somatosensory area 3b and surrounding cortex in chimpanzees. Soc. Neurosci. Abst. 23.

Qi, H.-X., Jain, N., Preuss, T. M., and Kaas, J. H. 1998. Comparative architecture of areas 3a, 3b, and 1 of somatosensory cortex in chimpanzees, humans and macaques. Soc. Neurosci. Abst. 24, 1125.

Rademacher, J., Caviness, V. S., Jr, Steinmetz, H., and Galaburda, A. M. 1993. Topographical variation of the human primary cortices: implications for neuroimaging, brain mapping, and neurobiology. Cereb. Cortex 3(4), 313–329.

Reep, R. L, Chandler, H. C., King, V., and Corwin, J. V. 1994. Rat posterior parietal cortex: topography of corticocortical and thalamic connections. Exp. Brain Res. 100(1), 67–84.

Remple, M. S., Henry, E. C., and Catania, K. C. 2003. Organization of somatosensory cortex in the laboratory rat (*Rattus norvegicus*): evidence for two lateral areas joined at the representation of the teeth. J. Comp. Neurol. 467(1), 105–118.

Remple, M. S., Reed, J. L., Stepniewska, I., and Kaas, J. H. 2006. Organization of frontoparietal cortex in the tree shrew (*Tupaia belangeri*). I. Architecture, microelectrode maps, and corticospinal connections. J. Comp. Neurol. 497(1), 133–154.

Remple, M. S., Reed, J. L., Stepniewska, I., Lyon, D. C., and Kaas, J. H. 2007. The organization of frontoparietal cortex in the tree shrew (*Tupaia belangeri*): II connectional evidence for a frontal-posterior parietal network. J. Comp. Neurol. 501(1), 121–149.

Romo, R., Hernandez, A., Zainos, A., Brody, C. D., and Lemus, L. 2000. Sensing without touching: psychophysical performance based on cortical microstimulation. Neuron 26(1), 273–278.

Rosabal, F. 1967. Cytoarchitecture of the frontal lobe of the squirrel monkey. J. Comp. Neurol. 130(2), 87–108.

Rushworth, M. F., Paus, T., and Sipila, P. K. 2001. Attention systems and the organization of the human parietal cortex. J. Neurosci. 21(14), 5262–5271.

Sanides, F. 1968. The architecture of the cortical taste nerve areas in squirrel monkey (*Saimiri sciureus*) and their relationships to insular, sensorimotor and prefrontal regions. Brain Res. 8(1), 97–124.

Sanides, F. and Krishnamurti, A. 1967. Cytoarchitectonic subdivisions of sensorimotor and prefrontal regions and of bordering insular and limbic fields in slow loris (*Nycticebus coucang coucang*). J. Hirnforsch. 9(3), 225–252.

Sato, K., Nariai, T., Sasaki, S., Yazawa, I., Mochida, H., Miyakawa, N., Momose -Sato, Y., Kamino, K., Ohta, Y., Hirakawa, K., and Ohno, K. 2002. Intraoperative intrinsic optical imaging of neuronal activity from subdivisions of the human primary somatosensory cortex. Cereb. Cortex 12(3), 269–280.

Simon, O., Mangin, J. F., Cohen, L., Le Bihan, D., and Dehaene, S. 2002. Topographical layout of hand, eye, calculation, and language-related areas in the human parietal lobe. Neuron 33(3), 475–487.

Stepniewska, I., Fang, P. C., and Kaas, J. H. 2005. Microstimulation reveals specialized subregions for different complex movements in posterior

parietal cortex of prosimian galagos. Proc. Natl. Acad. Sci. U. S. A. 102(13), 4878–4883.
Sur, M., Nelson, R. J., and Kaas, J. H. 1980. Representation of the body surface in somatic koniocortex in the prosimian galago. J. Comp. Neurol. 189(2), 381–402.
Sur, M., Nelson, R. J., and Kaas, J. H. 1982. Representations of the body surface in cortical areas 3b and 1 of squirrel monkeys: comparisons with other primates. J. Comp. Neurol. 211(2), 177–192.
Sur, M., Wall, J. T., and Kaas, J. H. 1984. Modular distribution of neurons with slowly adapting and rapidly adapting responses in area 3b of somatosensory cortex in monkeys. J. Neurophysiol. 51(4), 724–744.
Towe, A. L. 1975. Notes on the hypothesis of columnar organization in somatosensory cerebral cortex. Brain Behav. Evol. 11(1), 16–47.
Vogt, C. and Vogt, O. 1919. Allgemeinere ergebnisse unserer hirnforschung. J. Psychol. Neurol. (Leipzig) 25, 277–462.
Waters, R. S., Li, C. X., and McCandlish, C. A. 1995. Relationship between the organization of the forepaw barrel subfield and the representation of the forepaw in layer IV of rat somatosensory cortex. Exp. Brain Res. 103(2), 183–197.
White, L. E., Andrews, T. J., Hulette, C., Richards, A., Groelle, M., Paydarfar, J., and Purves, D. 1997. Structure of the human sensorimotor system. I: Morphology and cytoarchitecture of the central sulcus. Cereb. Cortex 7(1), 18–30.
Wong-Riley, M. 1979. Changes in the visual system of monocularly sutured or enucleated cats demonstrable with cytochrome oxidase histochemistry. Brain Res. 171(1), 11–28.
Woolsey, C. N. and Fairman, O. 1946. Contralateral, ipsilateral and bilateral representation of cutaneous receptors in somatic areas I and II of cerebral cortex of pig, sheep and other mammals. Surgery 19, 684–702.
Woolsey, T. A. and Van der Loos, H. 1970. The structural organization of layer IV in the somatosensory region (SI) of mouse cerebral cortex. The description of a cortical field composed of discrete cytoarchitectonic units. Brain Res. 17(2), 205–242.
Woolsey, C. N., Marshall, W. H., and Bard, P. 1942. Representation of cutaneous tactile sensibility in the cerebral cortex of the monkey as indicated by evoked patentials. Bull. Johns Hopkins Hosp. 70, 399–441.
Woolsey, C. N., Marshall, W. H., and Bard, P. 1943. Note on the organization of the tactile sensory area of the cerebral cortex of the chimpanzee. J. Neurophysiol. 6, 287–291.
Wu, C. W. and Kaas, J. H. 2003. Somatosensory cortex of prosimian galagos: physiological recording, cytoarchitecture, and corticocortical connections of anterior parietal cortex and cortex of the lateral sulcus. J. Comp. Neurol. 457(3), 263–292.
Zilles, K. and Palomero-Gallagher, N. 2001. Cyto-, myelo-, and receptor architectonics of the human parietal cortex. Neuroimage 14(1 Pt 2), S8–S20.
Zilles, K., Rehkamper, G., and Schleicher, A. 1979a. A quantitative approach to cytoarchitectonics. V. The areal pattern of the cortex of microcebus murinus (E. Geoffroy 1828), (Lemuridae, primates). Anat. Embryol. (Berl.) 157(3), 269–289.
Zilles, K., Rehkamper, G., Stephan, H., and Schleicher, A. 1979b. A quantitative approach to cytoarchitectonics. IV. The areal pattern of the cortex of *Galago demidovii* (E. Geoffroy, 1796), (lorisidae, primates). Anat. Embryol. (Berl.) 157(1), 81–103.
Zilles, K., Schleicher, A., Palomero-Gallagher, N., and Amunts, K. 2002. Quantitative Analysis of Cyto- and Receptoarchitecture of the Human Brain. In: Brain Mapping: The Methods (*eds*. A. W. Toga and J. C. Mazziotta), 2nd edn., pp. 573–602.

Further Reading

Wallace, M. T., Ramachandran, R., and Stein, B. E. 2004. A revised view of sensory cortical parcellation. Proc. Natl. Acad. Sci. U. S. A. 101(7), 2167–2172.
Weller, W. L. 1993. SmI cortical barrels in an Australian marsupial, *Trichosurus vulpecula* (brush-tailed possum): structural organization, patterned distribution, and somatotopic relationships. J. Comp. Neurol. 337(3), 471–492.
Woolsey, T. A., Welker, C., and Schwartz, R. H. 1975. Comparative anatomical studies of the SmL face cortex with special reference to the occurrence of ''barrels'' in layer IV. J. Comp. Neurol. 164(1), 79–94.

6.09 Development of the Somatosensory Cortex and Patterning of Afferent Projections

R S Erzurumlu, University of Maryland School of Medicine, Baltimore, MD, USA

© 2008 Elsevier Inc. All rights reserved.

6.09.1	Introduction	172
6.09.2	Differentiation of the Somatosensory Cortex	172
6.09.2.1	Areal Specification	172
6.09.2.2	Laminar Specification	174
6.09.3	Development of Thalamocortical Projections	174
6.09.3.1	Thalamocortical Axon Guidance	174
6.09.3.2	Arrival of Thalamocortical and Other Afferents to the Somatosensory Cortex	176
6.09.3.3	Patterning of Afferent Projections	176
6.09.3.3.1	Positional cues underlying topography	176
6.09.3.3.2	Role of neuronal activity in patterning of the somatosensory cortex	177
6.09.3.3.3	Intracellular signaling pathways	179
References		179

Glossary

adenylate cyclase type I (AC1) Adenylate cyclases are enzymes that catalyze the conversion of ATP to cAMP and pyrophosphate. There are nine members of adenylate cyclases; AC1 is neuronal and is activated by glutamate. AC1 knockout mice, also known as barelless mice, fail to develop whisker-specific cellular aggregates, barrels, in their somatosensory cortex.

areal specification Division of the neocortical mantle into distinct functional and cytoarchitectural zones that represent various sensory and motor modalities and association areas. Both intrinsic and extrinsic molecular cues play a role in this specification during development. Neural activity plays a role in sharpening of the boundaries and specializations within them.

barrel cortex Region of the parietal cortex where layer IV cells form cylindrical, barrel-like modules that correspond to single whiskers, sinus hairs or receptor densities in the digits.

barreloids Whisker- and digit-specific neural modules that develop in the somatosensory thalamus.

cajal-retzius cells One of the earliest generated cells of the telencephalic vesicles that ultimately reside in layer I.

cortical maps Topographic representation of the sensory or motor periphery in specific neocortical areas.

dorsal column lemniscal and trigeminal pathways Axonal projections from the dorsal column nuclei *gracilis* and *cuneatus*, and from the brainstem trigeminal nuclei to the ventroposterolateral and ventroposteromedial nuclei of the thalamus, respectively. These inputs relay the somatic sensory information from the peripheral receptors and dorsal root ganglia and the trigeminal ganglion to the thalamus.

FGF 8 Fibroblast growth factor 8 FGFs are a family of growth factors involved in a variety of cellular and developmental processes. There are about 22 members of the FGF family.

GABA-ergic neurons Generally inhibitory interneurons that synthesize and release gamma-aminobutyric acid.

GAP-43 A 43kD growth-associated phosphoprotein involved in developmental and synaptic plasticity.

glutamate glutamic acid (Glu) A major excitatory neurotransmitter in the nervous system.

mGluR5 Metabotropic glutamate receptor subtype 5. Metaboptropic glutamate receptors are members of the C family of G-protein coupled receptors that bind glutamate.

MAOA Monoamine oxidase A. Monoamine oxidases catalyze the oxidation of monoamines. MAOA mainly breaks down serotonin and also other monoamines norepinephrine and epinephrine. *MAOA* knockout mice lack the gene that

encode MAOA, thus have increased brain serotonin levels.

NMDA receptor N-methyl d-aspartate receptor NMDAR is an ionotropic glutamate receptor. It is both voltage-dependent and ligand-gated. When the postsynaptic neuron is sufficiently depolarized, glutamate binding results in activation of NMDARs which then allow flow of Ca^{2+} ions. Calcium influx through NMDARs leads to intracellular signaling mechanisms that are thought to play a critical role in various forms of synaptic plasticity during development and at mature state.

serotonin 5-Hydroxytryptamine, or 5-HT a monoamine neurotransmitter synthesized by serotonergic neurons mostly located in the midbrain raphe nuclei. It has regulatory effects on excitatory neurotransmission in the mammalian brain.

somatosensory cortex Portions of the parietal cortex that receive primary and secondary ascending somatosensory inputs from the thalamus.

thalamocortical axons (TCAs) Axonal projections from various thalamic nuclei to predominantly layer IV of neocortex.

transcription factor Proteins that mediate RNA polymerase binding and initiation of transcription. These factors either stimulate or repress transcription of a specific gene.

ventricular zone Layer of proliferating cells along the ventricles of the telencephalic vesicles. These cells give rise to multiple layers of the neocortex, and different classes of neurons glia.

6.09.1 Introduction

In all mammals, the position of the somatosensory cortex (as are the cases with other primary sensory and motor cortices) is relatively constant, located within the parietal aspect of the cortical mantle. Areal specification of the somatosensory cortex (as well as other sensory-motor and association cortices), and the role of afferent innervation from the sensory thalamus in this process have been the focus of long-standing research. In late 1980s, results from a variety of experimental studies led to two contradicting hypotheses: The protomap and the protocortex (Rakic, P., 1988; O'Leary, D. D. M., 1989). Does the cortical ventricular zone impart its signature on areal specification of the neocortex (protomap), or do thalamocortical afferents (TCAs) claim specific territories and parcellate an otherwise a tabula rasa cortical sheet (protocortex)? Experiments involving lesioning of peripheral sensory receptor organs, before these inputs reach the sensory thalamus or genetic aberrations, that interfere with this connectivity lent support for the former, while observations on the whisker-specific patterning of the somatosensory cortex in mice with supernumerary whiskers, rerouting of sensory thalamic inputs to different cortical loci, or heterotopic neocortical transplants in newborn rodents lent support for the latter (reviewed in O'Leary, D. D. *et al.*, 1994). Since then, advanced technical tools in the fields of molecular genetics, *in vivo* imaging, and functional assays dissolved the dichotomous views. Areal specification of the neocortex and the positioning of the somatosensory cortex involve a cascade of molecular cues intrinsic to the developing cortical primordium. It is within this *tabula praeforma* engraved with multiple guidance cues, that TCAs find their proper targets and confer specificity and patterning through activity-dependent mechanisms.

6.09.2 Differentiation of the Somatosensory Cortex

6.09.2.1 Areal Specification

Regionalization or areal specification of the neocortex, and subsequent positioning of the primary somatosensory cortex, is a result of the coordinated action of secreted proteins from patterning centers and gradients of transcription factor expression in the ventricular zone, which eventually gives rise to the six-layered neocortex. The first clear indication of such intrinsic cues came from a transgenic mouse line, in which beta-galactosidase expression in the neocortex was largely restricted to the layer IV neurons of the somatosensory cortex, revealing a distinct body map with patterned whisker representations (Cohen-Tannoudji, M. *et al.*, 1994). Ectopic transplantation of embryonic parietal cortex from these mice further confirmed the intrinsic nature of the

transgene expression. In recent years, molecular identities of positioning cues have been emerging.

A striking example of this is the fibroblast growth factor (FGF) 8 secreted in the rostral pole of the cortical primordium, the commissural plate. Overexpression of FGF 8 by the commissural plate pushes the location of the somatosensory cortex caudally, soaking up endogenous FGF 8 by FGF receptors, or FGF 8 hypomorphism pulls it rostrally, and misexpression of FGF 8 caudally leads to duplication of the somatosensory cortical map in a mirror image (Fukuchi-Shimogori, T. and Grove, E. A., 2001; reviewed in Shimogori, T. and Grove, E. A., 2006). Curiously, the duplicated barrel cortex seems to attract branches of TCAs destined for the primary barrel cortex (Shimogori, T. and Grove, E. A., 2005). Other factors such as Wnt3a, Wnt8b, bone morphogenetic proteins (BMPs), and sonic hedgehog (Shh) are secreted along the telencephalic vesicles (Sur, M. and Rubenstein, J. L. R., 2005; Rash, B. G. and Grove, E. A., 2006), indicating a highly orchestrated signaling from multiple patterning centers that play a role in allocation of specific territories to the somatosensory and other primary sensory and motor cortical areas (Figure 1).

Several genes encoding transcription factors (e.g., Foxg1, COUPTF1, Emx2, Lef1, Lhx2, Pax6) are expressed in gradients along the rostracaudal and mediolateral axes of the developing cortical mantle, and they regulate neurogenesis, proliferation, migration and survival of neurons, and possibly axon guidance during wiring of the cortex (Sur, M. and Rubenstein, J. L. R., 2005; Pratt, T. and Price, D., 2006; Shimogori, T. and Grove, E. A., 2006). Potential consequence of secreted molecules from patterning centers described above could be in the patterning of the graded expression of transcription factors, and subsequent parcellation of the cortical sheet.

Targeted deletions of the homeodomain-containing transcription factors *Emx2* and *Pax6* in mice revealed some clues. In the embryonic mouse cortex, Emx2 is expressed along a caudal to rostral gradient (complementary to that of FGF 8 expression), and Pax6 expression follows a rostral to caudal gradient. *Emx2* knockout mice display a compression of caudal cortical areas and expansion of rostral areas such as the somatosensory and motor cortices (Bishop, K. M. *et al.*, 2000; Mallamaci, A. *et al.*, 2000), while *Pax6* knockout mice, or transgenic mice over-expressing Emx2

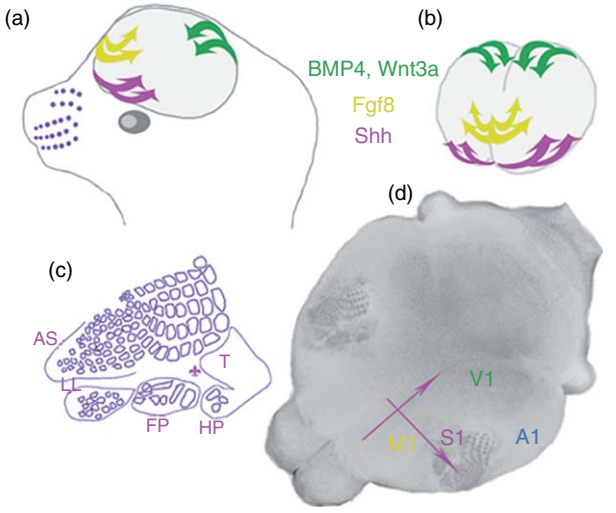

Figure 1 Regionalization and areal specification of the neocortex. Graded expression of transcription factors and secreted proteins from signaling centers help position sensory maps. (a) and (b) side and frontal views of the embryonic telencephalic vesicles with signaling centers expressing BMP4, Wnt3, Fgf8, and Shh. (c) and (d) illustrate parcellation of the somatosensory body map and its relative position with respect to other primary sensory coprtical areas such as visual (V1), auditory (A1), and primary motor cortex (M1). It is within this molecular regionalization that subcortical cues direct the space claimed by different thalamic nuclei resulting in areal specification of the neocortex. Experimental manipulations of the expression of a variety of proteins and transcription factors can alter the relative position and size of the sensory cortical parcels along the rostrocaudal and mediolateral axes. In the somatosensory map cartoon illustrated in **C**: AS: anterior snout, LL: lower lip, FP: fore paw, HP: hind paw, and T: trunk representation areas.

caudally display reduced somatosensory and motor cortical areas and expansion of caudal visual cortical and possibly auditory cortical areas (Bishop, K. M. *et al.*, 2000; Mallamaci, A. *et al.*, 2000; Hamasaki, T. *et al.*, 2004). Unaltered expression of FGF 8 but altered expression of Pax6 in Emx2 over-expressing cortex suggest that Emx2 action in cortical arealization is independent of FGF 8 action, but might take place by repressing *Pax6* expression (Hamasaki, T. *et al.*, 2004). An earlier study, employing electroporation-mediated gene transfer *in utero,* noted that over-expressing *Emx2* altered the cortical area map when ectopic Emx2 overlapped with the FGF 8 source (Fukuchi-Shimogori, T. and Grove, E. A., 2003). In addition, FGF 8 levels were decreased by excess Emx2, and increased in *Emx2* knockout mice. Thus, FGF 8 and Emx2 may act independently or in cooperation.

Clearly, overall positioning of different cortical areas, and the space allocated to each are determined by secreted proteins from patterning centers and graded expression of transcription factors (reviewed in Pratt, T. and Price, D., 2006; Rash, B. G. and Grove, E. A., 2006). On the other hand, patterning within sensory maps can be altered without affecting expression of positional markers or conversely, can occur in their absence. For example, while various manipulations of FGF 8 expression have been shown to shift the positioning of the somatosensory cortex (even duplication of it), whisker-specific patterning within the face representation area of the body map still develops. Another recent example is unaltered expression of primary sensory cortex layer-specific molecular markers Cux-1 and Cux2 (orthologues of the Drosophila homeobox *Cut* gene) in layer IV of barrel-defective mouse strains (Ferrere, A. *et al.*, 2006).

6.09.2.2 Laminar Specification

As in other primary sensory areas, the somatosensory cortex is characterized by six laminae with distinct cytoarchitecture and connectivity patterns (Figure 2). Glutamatergic neurons of the subplate and layers VI to II are produced sequentially in an inside-out fashion by the progenitors along the ventricular zone. Gamma-aminobutyric acid-(GABA)-ergic interneurons are mostly produced by the subcortical progenitors along the ganglionic eminence and migrate into the neocortex (Parnavelas, J. G. *et al.*, 2002). Cajal-Retzius cells of layer 1, which are generated about the same time as subplate neurons, are produced in the dorsal-most ventricular zone of the cortical anlage. Layer VI cells send projections to the thalamus; layer V cells project to subcortical targets such as the basal ganglia, midbrain, and brainstem. Layer IV cells receive projections from the thalamus and project to upper cortical layers. Layers II and III house neurons that project to other cortical areas (reviewed in Marin, O. and Rubenstein, J. L., 2003). Molecular specification of cortical laminar identity has been suspected for a long time, beginning with *in vitro* studies employing cocultures of thalamus and cortex or other targets of cortical cells (reviewed in Bolz, J., 1994). In cocultures of the developing neocortex with a variety of afferent–efferent sources, incoming fibers and cortical projection neurons establish layer-specific connectivity. Recent studies have begun to address molecular profiling of specific subsets of neurons that reside in different layers such as corticospinal projection neurons of Layer V and glutamatergic neurons of Layer IV (Arlotta, P., *et al.*, 2005; Ferrere, A. *et al.*, 2006) (Figure 2).

Thalamocortical axons have a specific affinity for Layer IV neurons (reviewed in Yamamoto, N. *et al.*, 2006). Whether in cocultures of thalamic neurons seeded on a cortical sheet (Emerling, D. E. and Lander, A. D., 1994), in explant cocultures of thalamus and cortex (Bolz, J., 1994), or in Reeler mouse with an inverted cortical lamination due to migration defects, TCAs seek layer IV neurons and terminate there (López-Bendito, G. and Molnár, Z., 2002). Membrane carpet assays have also indicated the presence of a stop signal in Layer IV (Castellani, V. and Bolz, J., 1997). A number of studies suggest that cell adhesion molecules such as N-cadherin (Poskanzer, K. *et al.*, 2003); neurotrophins BDNF and NT-3 (Yamamoto, N. and Hanamura, K., 2005), axon guidance molecules, such as Ephrins (Vanderhaeghen, P. and Polleux, F., 2004), as well as NMDA receptor-mediated signaling from postsynaptic cells (Lee, L. J. *et al.*, 2005) play a role in layer-specific terminations of TCAs (also reviewed in López-Bendito, G. and Molnár, Z., 2002; Polleux, F., 2005; Molnár, Z. *et al.*, 2006). Clearly multiple signals must act cooperatively in layer-specific targeting of TCAs.

6.09.3 Development of Thalamocortical Projections

6.09.3.1 Thalamocortical Axon Guidance

Motor and specific sensory (somatosensory, auditory and visual) thalamic nuclei are roughly aligned along the rostrocaudal axis of the developing dorsal

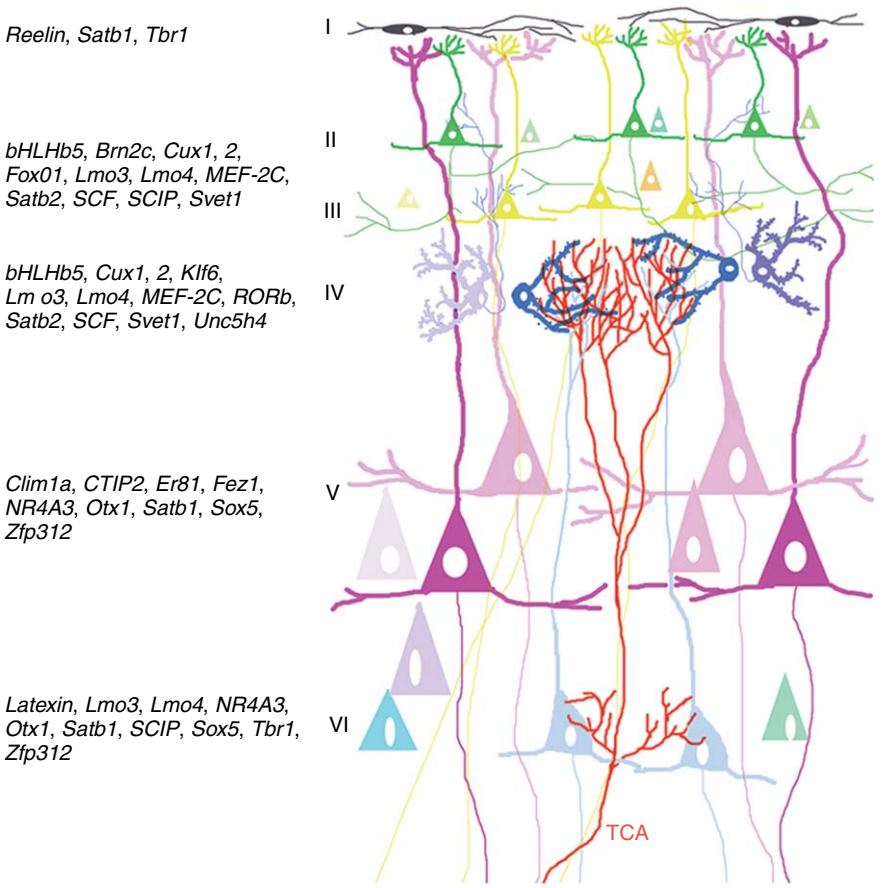

Figure 2 Layer- and cell type-specific genetic markers and lamination of the somatosensory cortex. During late embryonic development, the six-layered sensory cortex is generated in an inside out fashion. Overall, each cortical lamina is comprised of cells that receive specific inputs and project to distinct cortical or subcortical targets. In the rodent primary somatosensory cortex, whisker-specific thalamocortical afferents (TCAs) form discrete clusters that replicate the patterned array of whiskers on the contralateral snout. Their primary postsynaptic partners, layer IV spiny stellate cells, orient their dendrites towards these presynaptic terminal clusters, and their cell bodies form cylindrical aggregate, the barrels. In recent years, increasing numbers of molecular cues, genes, and transcription factors have been associated with specific cortical laminae, and subclasses of cells within each lamina; some are indicated on the left of the diagram (compiled from (Arimatsu *et al.*, 1999; Arlotta, P. *et al.*, 2005; Bulchand *et al.*, 2003; Chen *et al.*, 2005; Ferrere, A. *et al.*, 2006; Frantz *et al.*, 1994; Hevner *et al.*, 2003; Molyneaux *et al.*, 2005; Nieto *et al.*, 2004; Tarabykin *et al.*, 2001; Weimann *et al.*, 1999; Yoneshima *et al.*, 2006; Zhong *et al.*, 2004; Zimmer *et al.*, 2004.)

thalamus. Projections from each of these nuclei follow stereotypic routes to the neocortex where they colonize well-delineated territories along a similar axis. Several axon guidance cues, in particular ephrins and their receptors, are expressed in a graded fashion and in complementary patterns in the dorsal thalamus and neocortex, suggesting a role for these molecules in interareal topography formation between the thalamus and cortex (reviewed in Marin, O., 2003; Uziel, D. *et al.*, 2006). It has also been suggested that as the developing TCAs and corticothalamic axons (CTAs) meet in the internal capsule, axon–axon interactions guide the reciprocal topographic projections (the handshake hypothesis of Molnár, Z. and Blakemore, C., 1995; Molnár, Z. *et al.*, 1998).

Evidence from a variety of mutant mice is consistent with this hypothesis. For example, in the absence of transcription factors Tbr1, Gbx2, Pax6, or Emx2 (which pattern the cortex or thalamus), TCA and CTA axon pathfinding is disrupted (reviewed in Molnár, Z. *et al.*, 2006).

More recent studies, however, have underscored the role of positional cues such as graded expression of ephrins in the ventral telencephalon in guidance of TCAs (reviewed in Garel, S. and Rubenstein, J. L.,

2004; Polleux, F., 2005; Uziel, D. *et al.*, 2006). While EphA/ephrin-A signaling in the target tissue guides reciprocal TCA and CTA projections, it does not appear to be interdependent as predicted by the handshake hypothesis (Tori, M. and Levitt, P., 2006).

6.09.3.2 Arrival of Thalamocortical and Other Afferents to the Somatosensory Cortex

The primary somatosensory cortex receives inputs from a variety of sources, such as the somatosensory thalamus (glutamatergic inputs), serotonergic projections from the midbrain raphé nuclei, noradrenergic projections from locus coeruleus (D'Amato, R. J. *et al.*, 1987; Bennett-Clarke, C. A. *et al.*, 1991; Simpson, K. L., *et al.*, 2006). Afferents from the dorsal thalamus, as well as raphé cortical projections, show patterning in the barrel cortex. Noradrenergic inputs are not patterned according to cytoarchitectural landmarks.

Immunohistochemical localization of serotonin (5-HT) combined with autoradiographic imaging of serotonin-uptake sites in the neonatal rat somatosensory cortex showed a transient, dense, serotonergic innervation with dense patches over the cortical barrels (D'Amato, R.J. *et al.*, 1987).

Later studies confirmed the origin of these terminal patches from the raphé nuclei and raised the possibility that serotonergic inputs may aid TCAs in barrel-specific patterning. A dual labeling study with lipophilic tracers in fixed embryonic brains showed that thalamic afferents arrive in the somatosensory cortex well ahead of those projections from the raphé nuclei (Erzurumlu, R. S. and Jhaveri, S., 1992). Thus, it became apparent that TCAs are the first corticopetal projections to arrive in the somatosensory cortex and confer periphery-related patterns (Erzurumlu, R. S. and Jhaveri, S., 1990, 1992). Double labeling experiments further demonstrated that the patterning of TCAs in the rodent somatosensory cortex precedes other afferent terminals and extracellular matrix patterning seen in the developing barrel cortex (Blue, M. E. *et al.*, 1991; Jhaveri, S. *et al.*, 1991).

In mice, TCAs reach the somatosensory cortex after embryonic day 15, and begin probing the developing cortical plate by E18. Topographically organized TCAs invade the cortical plate by birth (gestation 19 days), as simple axons with very few branches (Senft, S. L. and Woolsey, T. A., 1991; Rebsam, A. *et al.*, 2002; Lee, L. J., *et al.*, 2005). Two days later, focalized terminal branches can be seen in layer IV and to a lesser extent in layer VI. Very few branches are seen in other layers. Developing TCAs can be visualized *en masse* by immunostaining for markers such as serotonin transporter. This approach allows for detection of emergence of the entire body map from a diffuse projection to partitioning of it into hindpaw and forepaw (lemniscal afferents) representation zones, lower lip and mystacial vibrissae representation zones (the posteromedial barrel subfield, and the representation area of the anterior snout with small sinus hairs. Once the body map is partitioned into these subterritories on postnatal day 2, further patterning into whisker-related rows (postnatal day 3), and between postnatal days 35 sensory periphery-related patterning, that is, patchy distribution of TCAs emerge (Rebsam, A. *et al*, 2002; Rebsam, A. and Gaspar, P., 2006) (Figure 3). As barreloids (whisker- and digit-specific neural modules) develop in the thalamus, TCA terminal fields and arbors in the cortex partition into Gaussian patches (Senft, S. L. and Woolsey, T. A., 1991), before the barrels appear as cellular modules (Figure 3). From postnatal day 5 onwards, selective pruning of overshooting collaterals, addition of more branches within focalized fields take place and TCAs consolidate their focal terminal arbors in layer IV with fewer terminal arbors in layer VI. Bifurcation points of axon arbors and terminal tips are mostly distributed in layer IV (about 75–80% of the total number), with some in layer VI (10–15%) (Lee, L. J. *et al.*, 2005).

6.09.3.3 Patterning of Afferent Projections

6.09.3.3.1 Positional cues underlying topography

The current understanding is that the general topography of TCA projections (as other axonal links along the subcortical somatosensory pathways) is established via gene expression gradients and chemoattractive and repulsive cues present along the route of the TCAs, as well as in their targets (reviewed in López-Bendito, G. and Molnár, Z., 2002; Molnár, Z. *et al.*, 2006). For example, ephrins and their Eph receptors have been implicated in topographic alignment of TCAs in the barrel cortex, as well as their topographic positioning along the ventral telencephalon (reviewed in Marin, O., 2003; Vanderhaeghen, P. and Polleux, F., 2004; Polleux, F., 2005). Developing TCAs also express high levels of the growth-associated phosphoprotein GAP43 (Erzurumlu, R. S. *et al.*, 1990). In *GAP43* knockout mice, TCA topography is disrupted, and TCA

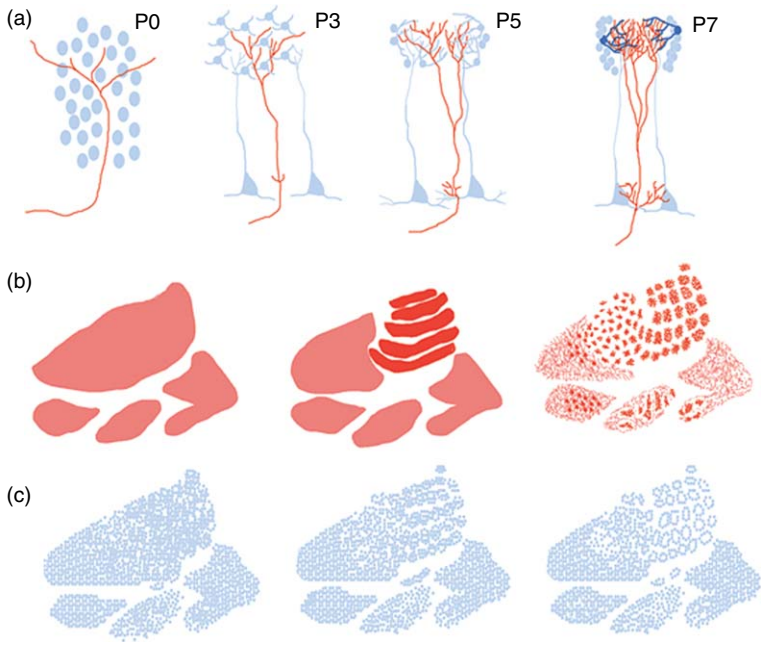

Figure 3 Development of thalamocortical axons (TCAs) projections to the barrel cortex and patterning of the somatosensory map. (a) Between postnatal days 0 and 7, TCAs develop focalized terminal arbors in layer IV and layer IV spiny stellate cells orient their dendrites toward these terminal clusters forming the barrels. (b) Cartoons illustrating emergence of first the body map, then the rows representing whiskers, and finally the patterning between P0 and P5. (c) Cellular organization in layer IV as routinely seen in tangential sections of the flattened cortex between P0 and P5.

terminals form aberrant patches (Maier, D. L. *et al.*, 1999). However, since these mice also have disrupted serotonergic projections to the neocortex (Donovan, S. L. *et al.*, 2002) it is not clear to what extent absence of GAP-43 in TCAs alone contribute to the barrel cortex phenotype. Once the molecular cues help guide and shape TCA topography, neural activity-mediated mechanisms play a major role in patterning of neural connections and consolidation of synapses in the somatosensory cortex.

6.09.3.3.2 Role of neuronal activity in patterning of the somatosensory cortex

Glutamatergic transmission and its regulation by serotonin in the early postnatal somatosensory cortex are key players in patterning of pre- and postsynaptic elements (reviewed in Erzurumlu, R. S. and Kind, P. C., 2001; Gaspar, P. *et al.*, 2003). Knockout mice with disrupted glutamatergic synaptic transmission (Iwasato, T. *et al.*, 1997, 2000; Hannan, A. J. *et al.*, 1998; 2001; Erzurumlu, R. S. and Iwasato, T., 2006), serotonergic modulation of presynaptic activity (Cases, O. *et al.*, 1996; Vitalis, T. *et al.*, 1998; Salichon, N. *et al.*, 2001; Rebsam, A. and Gaspar, P., 2006), downstream signaling molecules (Welker, E. *et al.*, 1996; Abdel-Majid, R. M. *et al.*, 1998; Hannan, A. J. *et al.*, 2001), all show abnormal patterning of the primary somatosensory cortex (Figure 4).

NMDA receptors have been shown to play a significant role in the patterning of body maps all along the murine somatosensory pathway leading to the somatosensory cortex (reviewed in Erzurumlu, R. S. and Iwasato, T., 2006). Recent evidence also indicates that NMDA receptor-mediated signaling is involved in parcellation of body map subdivisions (Lee, L. J. and Erzurumlu, R. S., 2005). In transgenic mice with low levels of *NR1* (the essential subunit of NMDAR), expression along the trigeminal pathway, subcortical and cortical face representation areas are reduced. Cortex-specific *NMDAR1* knockout (Cx*NR1*ko) mice show distinct somatosensory cortical defects. These mice fail to develop barrels as cellular modules and asymmetrical dendritic orientation of normal barrel cells is absent (Iwasato, T. *et al.*, 2000; Datwani, A. *et al.*, 2002). In these mutants, TCAs, corresponding to large whiskers develop small, faint patches as seen with histochemical and immunohistochemical markers. Single axon analyses between postnatal days 1–7 (Lee. L. J. *et al.*, 2005) revealed that in the somatosensory cortex without functional

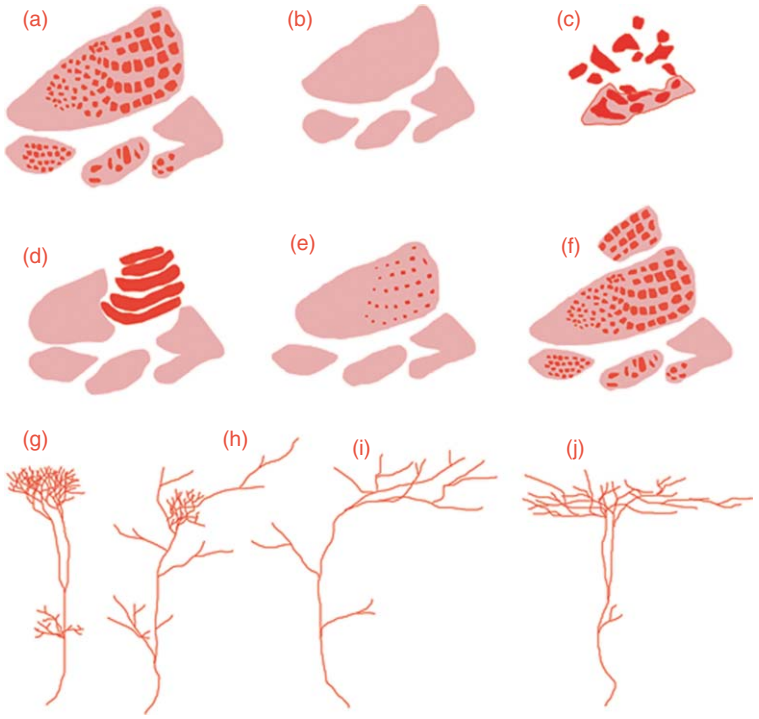

Figure 4 Examples of aberrant barrel cortex phenotypes in mutant or experimentally altered mice. (a). Normal body map and patterning of TCAs within it. In most mutants depicted in this cartoon there is no cellular patterning. In *PLCβ1* and *PKARIIβ* (protein kinase A IIβ subunit) knockout mice, TCAs form patterns similar to normal but there is no cellular (barrel) patterning (Hannan, A. J. *et al.*, 1998; Watson *et al.*, 2006) or there is partial patterning (Inan *et al.*, 2006). Body map can be discerned without the patterning of TCA projections (b) in *MAOA* knockout and barrelless (*Ac1* knockout) mice (Cases *et al.*, 1996; Abdel-Majid, R. M. *et al.*, 1998). In *GAP-43* knockout mice (Maier, D. L. *et al.*, 1999), there is no cellular patterning and TCAs form aberrant clusters, which can also be visualized with other histochemical markers (c). (d) In some mutants, without barrels, TCA projections into rows can be detected as in *MgluR5* and *Syngap* (Synaptic RAS GTPase activating protein) knockout mice (Hannan, A. J. *et al.*, 2001; Barnett, M. W. *et al.*, 2006b). (e) In Cx*NR1* knockout mice, there are small patches of clustered TCAs in the large whisker representation area (Iwasato, T. *et al.*, 2000; Lee, L. J. *et al.*, 2005). (f) Ectopic expression of Fgf8 in caudal cortex leads to partial duplication of the large whiskers (Fukuchi-Shimogori, T. and Grove, E. A. 2001). So far, single axon terminals have been examined only in a few of these mutants. (g-j). Stylized illustrations of single axons and their terminals. (g) An example of a normal TCA in P5 mouse cortex. (h) In Cx*NR1* knockout mice, TCA terminals are widespread with small focalizations in layer IV. TCAs are widespread without any patterning in *MAOA* (i) and spread out in layer IV in *AC1* (j) knockout mice.

NMDARs in excitatory cell, TCAs initially target proper cortical layers and begin arborization similar to that seen in controls. However, over time, these axons develop exuberant arbors in multiple cortical layers and fail to focalize within layer IV. In addition, their arbors are wider along the mediolateral extent. Despite these large arbors, zones of terminal condensations are seen in layer IV, which correspond to the rudimentary patterning seen with histochemical and immunohistochemical markers. Defects similar to those of Cx*NR1*ko mice are also observed in metabotropic glutamate receptor, *mGluR5* knockout mice (Hannan, A. J. *et al.*, 2001; Barnett, M. W. *et al.*, 2006a), which display segregation of TCAs representing large whiskers into rows but not individual whisker-specific patches within rows, and completely lack cellular, barrel organization. Loss of barrels indicates that mGluR5 signaling is critical for the normal development and transfer of patterns from TCAs to their postsynaptic partners. These results suggest that NMDARs and mGluR5 act synergistically during pattern formation.

Presynaptic, and subsequently postsynaptic, pattern defects in the barrel cortex can also be seen following disruption of the cortical serotonin levels which regulate glutamatergic transmission from TCAs (Rebsam, A. and Gaspar, P., 2006). *In vitro* recordings from thalamocortical slices indicate that 5-HT has a strong presynaptic inhibitory effect on glutamatergic transmission between TCAs and barrel

cortex cells via the activation of 5-HT1B receptors (Rhoades, R. W. *et al.*, 1994; Laurent, A. *et al.*, 2002). Developing TCAs express serotonin 1B (5HT-1B) receptors, serotonin transporters and autoregulate their glutamatergic transmission via presynaptic mechanisms using 5-HT present in their target field (Gaspar, P. *et al.*, 2003). In monoamine oxidase A (*MAOA*) knockout mice, excess brain serotonin levels prevent segregation of TCAs in the barrel cortex and subsequently formation of barrels as cellular entities (Cases, O. *et al.*, 1996; Vitalis, T. *et al.*, 1998; Gaspar, P. *et al.*, 2003). This defect can be corrected both at the pre- and postsynaptic levels by treatment with para-chlorophenylalanine (PCPA), which reduces excess serotonin levels in *MAOA* knockout mice (Rebsam *et al.*, 2005) or by genetic deletion of 5HT1B receptors (Salichon *et al.*, 2001). Rebsam *et al.* (2002) described the development of barrel patterns and TCA arbors in *MAOA* knockout and *MAOA/5-HT1B* receptor double knockout mice. In both of these phenotypes, TCAs target the barrel cortex and appropriate cortical laminae by P1 as in normal mice. At P7, however, a significant reduction of terminal branches in layer IV and an increase in the mediolateral span of TCA arbors become apparent in *MAOA* knockout mice. In contrast, these defects were not seen in double knockout animals. Presently, the specific roles of serotonin in the patterning and plasticity of the barrel cortex are not clear. While excess cortical serotonin prevents formation of barrel patterns, significant pharmacological reductions of cortical serotonin in neonatal rodents does not affect the TCA patterning and barrel formation, except for a delay of 1 day in the emergence of patterns (Blue, M. E. et al., 1991). Similarly, delaying the emergence of barrel patterns by a combination of genetic and pharmacological approach also does not change the time course of the critical period plasticity following neonatal whisker lesions in mice (Rebsam, A. et al., 2005).

6.09.3.3.3 Intracellular signaling pathways

Intracellular signaling pathways downstream from glutamatergic signaling and regulation by serotonin, which lead to communication between pre- and postsynaptic elements, leading to distinct neural patterns in the barrel cortex, are emerging (reviewed in Barnett *et al.*, 2006a; Rebsam and Gaspar, 2006). A spontaneous mutation with absent barrel phenotype was noted in 1996 (Welker *et al.*, 1996). These mice termed barrelless exhibited normal laminar and topographic distribution of TCAs, but the overall thalamocortical projection field was larger, much like that seen in *MAOA* knockout mice. The mutation was later identified as the adenylate cyclase type I (*AC1*) gene (Abdel-Majid, R. M. *et al.*, 1998). While there are several members of adenylate cyclases, AC1 is exclusively neuronal and is activated by glutamate, NMDA receptor stimulation, and voltage-gated calcium channels. This membrane-bound enzyme regulates production of cAMP and protein kinase A (PKA) in response to calcium entry. Presence of AC1, both at the pre- and postsynaptic sites, has made it difficult to pinpoint whether TCA and barrel defects seen in AC1 knockout mice arise from pre- or postsynaptic effects. Other mutant mice relevant to intracellular signaling molecules include phospholipase C-β1 (*PLC-β1*) knockout mice, which exhibit barrel cortex defects (Hannan *et al.*, 2001). Phospholipase C (PLC) subtypes beta, gamma, and delta are activated by cell surface receptors. These phosphodiasterases hydrolyze lipid phosphatidylinositol 4,5-bisphosphate [PI(4,5)P2], generating inositol 1,4,5-trisphosphate (InsP3), a calcium-mobilizer from internal stores, and diacylglycerol (DAG), an activator of protein kinase C (Rebecchi and Pentyala, 2000; Rhee S.G. 2001). PLC-β1 class of phospholipases are downstream from synaptic activity, hence a role in activity-dependent refinement and patterning in the barrel cortex. SynGAP, a synaptic Ras GTPase activating protein also appears to be essential in patterning of the somatosensory thalamocortical projections. Examination of the *SynGAP* knockout mouse phenotype revealed that somatosensory thalamic patterning as well as TCA patterning is impaired and barrels failed to form (Barnett *et al.*, 2006b). Collectively, all of these experimental findings reveal multifaceted role of neural activity in patterning connections within topographically organized sensory maps in the brain, in particular in the somatosensory cortex. Targeted gene mutations or experimental alterations will undoubtedly reveal many if not all the key players of developmental mechanisms underlying somatosensory cortical differentiation and patterning.

References

Abdel-Majid, R. M., Leong, W. L., Schalkwyk, L. C., Smallman, D. S., Wong, S. T., Storm, D. R., Fine, A., Dobson, M. J., Guernsey, D. L., and Neumann, P. E. 1998. Loss of adenylyl cyclase I activity disrupts patterning of mouse somatosensory cortex. Nat. Genet. 19, 289–291.

Arimatsu, Y., Ishida, M., Sato, M., and Kojima, M. 1999. Corticocortical associative neurons expressing latexin: specific cortical connectivity formed in vivo and in vitro. Cerebral Cortex. 9, 569–576.

Arlotta, P., Molyneaux, B. J., Chen, J., Inoue, J., Kominami, R., and Macklis, J. D. 2005. Neuronal subtype-specific genes that control corticospinal motor neuron development in vivo. Neuron. 45, 207–221.

Barnett, M. W., Watson, R. F., and Kind, P. C. 2006a. Pathways to Barrel Development. In: Development and Plasticity in Sensory Thalamus and Cortex (*eds*. R. Erzurumlu, W. Guido, and Z. Molnár), pp. 138–157. Springer.

Barnett, M. W., Watson, R. F., Vitalis, T., Porter, K., Komiyama, N. H., Stoney, P. N., Gillingwater, T. H., Grant, S. G., and Kind, P. C. 2006b. Synaptic Ras GTPase activating protein regulates pattern formation in the trigeminal system of mice. J. Neurosci. 26, 1355–1365.

Bennett-Clarke, C. A., Chiaia, N. L., Crissman, R. S., and Rhoades, R. W. 1991. The source of the transient serotoninergic input to the developing visual and somatosensory cortices in rat. Neuroscience. 43, 163–183.

Bishop, K. M., Goudreau, G., and O'Leary, D. D. 2000. Regulation of area identity in the mammalian neocortex by Emx2 and Pax6. Science. 288, 344–349.

Blue, M. E., Erzurumlu, R. S., and Jhaveri, S. 1991. A comparison of pattern formation by thalamocortical and serotonergic afferents in the rat barrel field cortex. Cereb. Cortex. 1, 380–389.

Bolz, J. 1994. Cortical circuitry in a dish. Curr. Opin. Neurobiol. 4, 545–549.

Bulchand, S., Subramanian, L., and Tole, S. 2003. Dynamic spatiotemporal expression of LIM genes and cofactors in the embryonic and postnatal cerebral cortex. Developmental Dynamics. 226, 460–469.

Cases, O., Vitalis, T., Seif, I., De Maeyer, E., Sotelo, C., and Gaspar, P. 1996. Lack of barrels in the somatosensory cortex of monoamine oxidase A-deficient mice: role of a serotonin excess during the critical period. Neuron. 16, 297–307.

Castellani, V. and Bolz, J. 1997. Membrane-associated molecules regulate the formation of layer-specific cortical circuits. Proc. Natl. Acad. Sci. USA 94, 7030–7035.

Chen, J. G., Rasin, M. R., Kwan, K. Y., and Sestan, N. 2005. Zfp312 is required for subcortical axonal projections and dendritic morphology of deep-layer pyramidal neurons of the cerebral cortex. Proc. Natl. Acad. Sci. USA 102, 17792–17797.

Cohen-Tannoudji, M., Babinet, C., and Wassef, M. 1994. Early determination of a mouse somatosensory cortex marker. Nature. 368, 460–463.

D'Amato, R. J., Blue, M. E., Largent, B. L., Lynch, D. R., Ledbetter, D. J., Molliver, M. E., and Snyder, S. H. 1987. Ontogeny of the serotonergic projection to rat neocortex: transient expression of a dense innervation to primary sensory areas. Proc. Natl. Acad. Sci. USA 84, 4322–4326.

Datwani, A., Iwasato, T., Itohara, S., and Erzurumlu, R. S. 2002. NMDA receptor-dependent pattern transfer from afferents to postsynaptic cells and dendritic differentiation in the barrel cortex. Mol. Cell. Neurosci. 21, 477–492.

Donovan, S. L., Mamounas, L. A., Andrews, A. M., Blue, M. E., and McCasland, J. S. 2002. GAP-43 is critical for normal development of the serotonergic innervation in forebrain. J. Neurosci. 22, 3543–3552.

Emerling, D. E. and Lander, A. D. 1994. Laminar specific attachment and neurite outgrowth of thalamic neurons on cultured slices of developing cerebral neocortex. Development. 120, 2811–2822.

Erzurumlu, R. S. and Iwasato, T. 2006. Patterning of the somatosensory maps with NMDA receptors. In: Development and Plasticity in Sensory Thalamus and Cortex (*eds*. R. Erzurumlu, W. Guido, and Z. Molnár), pp. 158–182. Springer.

Erzurumlu, R. S. and Jhaveri, S. 1990. Thalamic axons confer a blueprint of the sensory periphery onto the developing rat somatosensory cortex. Develop. Brain Res. 56, 229–34.

Erzurumlu, R. S. and Jhaveri, S. 1992. Emergence of connectivity in the embryonic rat parietal cortex. Cereb. Cortex. 2, 336–352.

Erzurumlu, R. S. and Kind, P. C. 2001. Neural activity: sculptor of 'barrels' in the neocortex. Trends Neurosci. 24, 589–595.

Erzurumlu, R. S., Jhaveri, S., and Benowitz, L. I. 1990. Transient patterns of GAP-43 expression during the formation of barrels in the rat somatosensory cortex. J. Comp. Neurol. 292, 443–456.

Ferrere, A., Vitalis, T., Gingras, H., Gaspar, P., and Cases, O. 2006. Expression of Cux-1 and Cux-2 in the developing somatosensory cortex of normal and barrel-defective mice. Anat. Rec. A Discov. Mol. Cell. Evol. Biol. 288, 158–165.

Frantz, G. D., Weimann, J. M., Levin, M. E., and McConnell, S. K. 1994. Otx1 and Otx2 define layers and regions in developing cerebral cortex and cerebellum. J. Neurosci. 14, 5725–5740.

Fukuchi-Shimogori, T. and Grove, E. A. 2001. Neocortex patterning by the secreted signaling molecule FGF8. Science 294, 1071–1074.

Fukuchi-Shimogori, T. and Grove, E. A. 2003. Emx2 patterns the neocortex by regulating FGF positional signaling. Nat. Neurosci. 6, 825–831.

Garel, S. and Rubenstein, J. L. 2004. Intermediate targets in formation of topographic projections: inputs from the thalamocortical system. Trends Neurosci. 27, 533–539.

Gaspar, P., Cases, O., and Maroteaux, L. 2003. The developmental role of serotonin: news from mouse molecular genetics. Nat. Rev. Neurosci. 4, 1002–1012.

Hannan, A. J., Kind, P. C., and Blakemore, C. 1998. Phospholipase C-beta1 expression correlates with neuronal differentiation and synaptic plasticity in rat somatosensory cortex. Neuropharmacology. 37, 593–605.

Hannan, A. J., Blakemore, C., Katsnelson, A., Vitalis, T., Huber, K. M., Bear, M., Roder, J., Kim, D., Shin, H. S., and Kind, P. C. 2001. PLC-beta1, activated via mGluRs, mediates activity-dependent differentiation in cerebral cortex. Nat. Neurosci. 4, 282–288.

Hamasaki, T., Leingartner, A., Ringstedt, T., and O'Leary, D. D. 2004. EMX2 regulates sizes and positioning of the primary sensory and motor areas in neocortex by direct specification of cortical progenitors. Neuron. 43, 359–372.

Hevner, R. F., Daza, R. A., Rubenstein, J. L., Stunnenberg, H., Olavarria, J. F., and Englund, C. 2003. Beyond laminar fate: toward a molecular classification of cortical projection/pyramidal neurons. Dev. Neurosci. 25, 139–151.

Iwasato, T., Erzurumlu, R. S., Huerta, P. T., Chen, D. F., Sasaoka, T., Ulupinar, E., and Tonegawa, S. 1997. NMDA receptor-dependent refinement of somatotopic maps. Neuron. 19, 1201–1210.

Iwasato, T., Datwani, A., Wolf, A. M., Nishiyama, H., Taguchi, Y., Tonegawa, S., Knopfel, T., Erzurumlu, R. S., and Itohara, S. 2000. Cortex-restricted disruption of NMDAR1 impairs neuronal patterns in the barrel cortex. Nature. 406, 726–731.

Jhaveri, S., Erzurumlu, R. S., and Crossin, K. 1991. Barrel construction in rodent neocortex: role of thalamic afferents versus extracellular matrix molecules. Proc. Natl. Acad. Sci. U. S. A. 88, 4489–4493.

Laurent, A., Goaillard, J. M., Cases, O., Lebrand, C., Gaspar, P., and Ropert, N. 2002. Activity-dependent presynaptic effect of serotonin 1B receptors on the somatosensory thalamocortical transmission in neonatal mice. J. Neurosci. 22, 886–900.

Lee, L. J. and Erzurumlu, R. S. 2005. Altered parcellation of neocortical somatosensory maps in *N*-methyl-D-aspartate receptor-deficient mice. J. Comp. Neurol. 485, 57–63.

Lee, L. J., Iwasato, T., Itohara, S., and Erzurumlu, R. S. 2005. Exuberant thalamocortical axon arborization in cortex-specific NMDAR1 knockout mice. J. Comp. Neurol. 485, 280–292.

López-Bendito, G. and Molnár, Z. 2002. Thalamocortical development: how are we going to get there? Nat. Rev. Neurosci. 4, 276–289.

Maier, D. L., Mani, S., Donovan, S. L., Soppet, D., Tessarollo, L., McCasland, J. S., and Meiri, K. F. 1999. Disrupted cortical map and absence of cortical barrels in growth-associated protein (GAP)-43 knockout mice. Proc. Natl. Acad. Sci. U S A. 96, 9397–9402.

Mallamaci, A., Muzio, L., Chan, C. H., Parnavelas, J., and Boncinelli, E. 2000. Area identity shifts in the early cerebral cortex of Emx2-/- mutant mice. Nat. Neurosci. 3, 679–686.

Marin, O. 2003. Thalamocortical topography reloaded: it's not where you go, but how you get there. Neuron. 39, 388–391.

Marin, O. and Rubenstein, J. L. 2003. Cell migration in the forebrain. Annu. Rev. Neurosci. 26, 441–483.

Molnár, Z. and Blakemore, C. 1995. How do thalamic axons find their way to the cortex? Trends Neurosci. 18, 389–397.

Molnár, Z., Adams, R., and Blakemore, C. 1998. Mechanisms underlying the early establishment of thalamocortical connections in the rat. J. Neurosci. 18, 5723–5745.

Molnár, Z., Lopez-Bendito, G., Blakey, D., Thompson, A., and Higashi, S. 2006. The Earliest Thalamocortical Interactions. In: Development and Plasticity in Sensory Thalamus and Cortex, (*eds*. R. Erzurumlu, W. Guido, and Z. Molnár), pp. 54–78. Springer.

Molyneaux, B. J., Arlotta, P., Hirata, T., Hibi, M., and Macklis, J. D. 2005. Fezl is required for the birth and specification of corticospinal motor neurons. Neuron. 47, 817–831.

Nieto, M., Monuki, E. S., Tang, H., Imitola, J., Haubst, N., Khoury, S. J., Cunningham, J., Gotz, M., and Walsh, C. A. 2004. Expression of Cux-1 and Cux-2 in the subventricular zone and upper layers II-IV of the cerebral cortex. J. Comp. Neurol. 479, 168–180.

O'Leary, D. D. M. 1989. Do cortical areas emerge from a protocortex? Trends Neurosci. 12, 400–406.

O'Leary, D. D., Schlaggar, B. L., and Tuttle, R. 1994. Specification of neocortical areas and thalamocortical connections. Annu. Rev. Neurosci. 17, 419–439.

Parnavelas, J. G., Alifragis, P., and Nadarajah, B. 2002. The origin and migration of cortical neurons. Prog. Brain Res. 136, 73–80.

Polleux, F. 2005. Genetic mechanisms specifying cortical connectivity: let's make some projections together. Neuron. 46, 395–400.

Poskanzer, K., Needleman, L. A., Bozdagi, O., and Huntley, G. W. 2003. N-cadherin regulates ingrowth and laminar targeting of thalamocortical axons. J Neurosci. 23, 2294–2305.

Pratt, T. and Price, D. 2006. Dual roles of transcription factors in forebrain morphogenesis and development of axonal pathways. In: Development and Plasticity in Sensory Thalamus and Cortex (*eds*. R. Erzurumlu, W. Guido, and Z. Molnár), pp. 19–41. Springer.

Rakic, P. 1988. Specification of cerebral cortical areas. Science. 241, 170–176.

Rash, B. G. and Grove, E. A. 2006. Area and layer patterning in the developing cerebral cortex. Curr. Opin. Neurobiol. 16, 25–34.

Rebecchi, M. J. and Pentyala, S. N. 2000. Structure, function, and control of phosphoinositide-specific phospholipase C. Physiol. Rev. 80, 1291–1335.

Rebsam, A. and Gaspar, P. 2006. Presynaptic signaling mechanisms controlling axon arbor remodeling in the thalamocortical and retinogeniculate systems. In: Development and Plasticity in Sensory Thalamus and Cortex, (*eds*. R. Erzurumlu, W. Guido, and Z. Molnár), pp. 183–207. Springer.

Rebsam, A., Seif, I., and Gaspar, P. 2002. Refinement of thalamocortical arbors and emergence of barrel domains in the primary somatosensory cortex: a study of normal and monoamine oxidase a knock-out mice. J. Neurosci. 22, 8541–8552.

Rebsam, A., Seif, I. and Gaspar, P. 2005. Dissociating barrel development and lesion-induced plasticity in the mouse somatosensory cortex. J. Neurosci. 25, 706–710.

Rhee, S. G. 2001. Regulation of phosphoinositide-specific phospholipase C. Annu. Rev. Biochem. 70, 281–312.

Rhoades, R. W., Bennett-Clarke, C. A., Shi, M. Y., and Mooney, R. D. 1994. Effects of 5-HT on thalamocortical synaptic transmission in the developing rat. J. Neurophysiol. 72, 2438–2450.

Salichon, N., Gaspar, P., Upton, A. L., Picaud, S., Hanoun, N., Hamon, M., De Maeyer, E., Murphy, D. L., Mossner, R., Lesch, K. P., Hen, R., and Seif, I. 2001. Excessive activation of serotonin (5-HT) 1B receptors disrupts the formation of sensory maps in monoamine oxidase a and 5-ht transporter knock-out mice. J. Neurosci. 21, 884–896.

Senft, S. L. and Woolsey, T. A. 1991. Growth of thalamic afferents into mouse barrel cortex. Cereb. Cortex. 1, 308–335.

Shimogori, T. and Grove, E. A. 2005. Fibroblast growth factor 8 regulates neocortical guidance of area-specific thalamic innervation. J. Neurosci. 25, 6550–6560.

Shimogori, T. and Grove, E. A. 2006. Subcortical and neocortical guidance of area-specific thalamic innervation. In: Development and Plasticity in Sensory Thalamus and Cortex, (*eds*. R. Erzurumlu, W. Guido, and Z. Molnár), pp. 42–53. Springer.

Simpson, K. L., Waterhouse, B. D., and Lin, R. C. 2006. Characterization of neurochemically specific projections from the locus coeruleus with respect to somatosensory-related barrels. Anat. Rec. A. Discov. Mol. Cell. Evol. Biol. 288, 166–173.

Sur, M. and Rubenstein, J. L. R. 2005. Patterning and plasticity of the cerebral cortex. Science. 310, 805–810.

Tarabykin, V., Stoykova, A., Usman, N., and Gruss, P. 2001. Cortical upper layer neurons derive from the subventricular zone as indicated by Svet1 gene expression. Development 128, 1983–1993.

Tori, M. and Levitt, P. 2006. Dissociation of corticothalamic and thalamocortical axon targeting by an EphA7-mediated mechanism. Neuron. 48, 563–575.

Uziel, D., Garcez, P., Lent, R., Peuckert, C., Niehage, R., Weth, F., and Bolz, J. 2006. Connecting thalamus and cortex: the role of ephrins. Anat. Rec. A Discov. Mol. Cell. Evol. Biol. 288, 135–142.

Vanderhaeghen, P. and Polleux, F. 2004. Developmental mechanisms patterning thalamocortical projections: intrinsic, extrinsic and in between. Trends Neurosci. 27, 384–391.

Vitalis, T., Cases, O., Callebert, J., Launay, J. M., Price, D. J., Seif, I., and Gaspar, P. 1998. Effects of monoamine oxidase A inhibition on barrel formation in the mouse somatosensory cortex: determination of a sensitive developmental period. J. Comp. Neurol. 393, 169–184.

Weimann, J. M., Zhang, Y. A., Levin, M. E., Devine, W. P., Brulet, P., and McConnell, S. K. 1999. Cortical neurons require Otx1 for the refinement of exuberant axonal projections to subcortical targets. Neuron. 24, 819–831.

Welker, E., Armstrong-James, M., Bronchti, G., Ourednik, W., Gheorghita-Baechler, F., Dubois, R., Guernsey, D. L., Van der Loos, H., and Neumann, P. E. 1996. Altered sensory processing in the somatosensory cortex of the mouse mutant barrelless. Science. 271, 1864–1867.

Yamamoto, N. and Hanamura, K. 2005. Formation of the thalamocortical projection regulated differentially by BDNF- and NT-3-mediated signaling. Rev. Neurosci. 16, 223–231.

Yamamoto, N., Takemoto, M., Hattori, Y., and Hanamura, K. 2006. Molecular basis for the formation of lamina-specific thalamocortical projections. In: Development and Plasticity in Sensory Thalamus and Cortex, (*eds*. R. Erzurumlu, W. Guido, and Z. Molnár), pp. 79–91. Springer.

Yoneshima, H., Yamasaki, S., Voelker, C. C., Molnar, Z., Christophe, E., Audinat, E., Takemoto, M., Nishiwaki, M., Tsuji, S., Fujita, I., and Yamamoto, N. 2006. Er81 is expressed in a subpopulation of layer 5 neurons in rodent and primate neocortices. Neuroscience. 137, 401–412.

Zhong, Y., Takemoto, M., Fukuda, T., Hattori, Y., Murakami, F., Nakajima, D., Nakayama, M., and Yamamoto, N. 2004. Identification of the genes that are expressed in the upper layers of the neocortex. Cerebral Cortex. 14, 1144–1152.

Zimmer, C., Tiveron, M. C., Bodmer, R., and Cremer, H. 2004. Dynamics of Cux2 expression suggests that an early pool of SVZ precursors is fated to become upper cortical layer neurons. Cerebral Cortex 14, 1408–1420.

6.10 The Evolution of Parietal Areas Involved in Hand Use in Primates

L Krubitzer, Department of Psychology, Center for Neuroscience, University of California, Davis, CA, USA

E Disbrow, Department of Neurology, Center for Neuroscience, University of California, Davis; Department of Radiology, San Francisco, CA, USA

Submitted, 2005; Published by Elsevier Inc.

6.10.1	**Introduction**	184
6.10.2	**Sensory Versus Association Cortex**	184
6.10.3	**Organization of Anterior Parietal Cortex in Primates (Areas 3b, 3a, 1, and 2)**	186
6.10.4	**Area 3b or S1**	187
6.10.4.1	Functional Organization	187
6.10.4.2	Connections	191
6.10.5	**Area 3a**	195
6.10.5.1	Functional Organization	195
6.10.5.2	Connections	198
6.10.6	**Area 1**	198
6.10.6.1	Functional Organization	198
6.10.6.2	Connections	200
6.10.7	**Area 2**	200
6.10.7.1	Functional Organization	200
6.10.7.2	Connections	203
6.10.8	**Posterior Parietal Area 5 in Primates**	203
6.10.8.1	Functional Organization	203
6.10.8.2	Connections	204
6.10.9	**Is Area 5 Homologous Across Mammals?**	206
6.10.10	**The Evolution of Anterior and Posterior Parietal Cortex**	206
References		208

Glossary

acallosal A neural pathway that does not project to the contralateral hemisphere and does not receive inputs via the corpus callosum. Such a region can be determined in studies of callosal connections by noting an absence of callosally projecting axon terminals in an otherwise terminal-rich area.

analogous A structure that has the same function. An analogous structure need not be homologous.

callosal A neural pathway that projects to the contralateral hemisphere via the corpus callosum. A callosal zone refers to a region of the cortex that receives inputs via the corpus callosum.

caudal Anatomical location – toward the tail.

contralateral A relative term referring to the opposite side of the brain or body.

deep receptors Peripheral receptor in the skin, muscles, or joints.

extrastriate Visual cortex that does not include V1 (striate cortex).

glabrous Regions of the skin lacking hairs, e.g., the pads of hands and feet.

homologous A structure that is inherited from a common ancestor. A homologous structure is not always analogous.

interdigitate To interweave two or more structures.

lateral Anatomical location – away from the midline of the brain or body.

medial Anatomical location – toward the midline of the brain or body.

myelin A material composed of lipids and lipoproteins that surrounds certain axons and functions as an electrical insulator. Myelin stains are often used to demarcate cortical areas and thalamic nuclei.

optokinetic Movement of the eyes when a moving visual stimulus is viewed.
rapidly adapting receptor A mechanoreceptor that responds to the initial presentation of a stimulus but stops responding or reduces its firing rate throughout the presentation of a sustained stimulus.
rostral Anatomical location – toward the rostrum or snout.
slowly adapting receptor A mechanoreceptor that responds throughout the presentation of a sustained stimulus.
topographic organization A feature of cortical organization in which adjacent points within a cortical field represent adjacent points on the sensory epithelium.
vibrissae Whiskers and/or stiff hair located on the face of an animal that often function as a tactile organ.

6.10.1 Introduction

Anthropocentric /, anθrəpəˈsɛntrik/*a.* M19. [f. prec. + CENTRIC] Centering in humans; regarding humanity as the central fact of the universe (*The New Shorter Oxford English Dictionary*).

As a beginning for a review on areas of the primate brain involved in generating frames of reference and ultimately a sense of self, the definition of anthropocentrism may seem misplaced. Yet anthropocentrism is, paradoxically, central to this scientific endeavor: our fascination with ourselves is simultaneously the driving force behind our desire to understand biological organisms and the activities they generate (including anthropocentrism itself) and probably the largest stumbling block to achieve an objective understanding. That we are anthropocentric is without question. Indeed, when not actually pursuing activities necessary for our literal survival, we spend the majority of our time pursuing an understanding of ourselves. We strive to understand our uniqueness, our past, our future, how we behave together, how we behave individually, how we think, how we expend our resources, and how to determine if there is any other sentient being out there like us. These pursuits encompass a variety of disciplines such as psychology, sociology, philosophy, anthropology, history, and economics, to name a few. All of these disciplines are based on the premise that humans are radically different from other animals – that we abide by a different set of rules, that we are unconstrained by evolution, and that we have miraculously developed emergent properties, such as a mind, intelligence, language, and even a soul. While we poke fun at this egocentric drive that all of us possess and the anthropocentric nature of our institutions, we must concede that this magnificent sense of self is biologically driven. Specifically, there are regions of the neocortex that are involved in generating a sense of our own body with respect to the world around us. These regions allow us to distinguish ourselves from external animate and inanimate objects and to interact with them via highly specialized morphological tools, such as our hands.

Despite this natural preoccupation with ourselves, and our need to understand how complexity has arisen in our species, many authors believe that it is more informative, when trying to appreciate our unique attributes with respect to other species, to examine similarities across groups, rather than trying to explain this uniqueness or variability in isolation. For example, are there similar principles of organization for all mammal brains? Once this question has been answered, then one can examine the departures from the common plan of organization to determine how these departures or modifications are achieved, and ultimately how they generate variable behavior like that described above for humans. A good illustration of this approach, and the focus of this review, is provided by an examination of the somatosensory areas of anterior and posterior parietal cortex in both primate and nonprimate mammals. These regions appear to have expanded in humans and are proposed to be associated with a number of sophisticated behaviors.

6.10.2 Sensory Versus Association Cortex

Traditionally, the mammalian neocortex has been divided into three broad categories: motor cortex, sensory cortex (including primary and second sensory fields such as S1, S2, V1, V2, A1, and R), and association cortex. This broad classification became popular in the middle part of the twentieth century, at which time electrophysiological mapping studies demonstrated that all mammals possessed

motor cortex and primary and second sensory cortices, and that primates in particular had a great deal of association cortex (Woolsey, C. N. and Fairman, D., 1946; Woolsey, C. N., 1958; see Kaas, J. H. and Collins, C. E., 2004, for review). Association cortex, as defined by modern textbooks, includes temporal, prefrontal, and posterior parietal cortex and is hypothesized to mediate complex behaviors such as perception, attention, cognition, and other high-level mental functions (Saper, C. B. *et al.*, 2000). The argument for defining cortex as association is somewhat circular and is based on the premise, which emerged from earlier mapping studies of Woolsey and colleagues, that the amount of cortex that could not be defined as unimodal sensory cortex in primates was relatively large compared to other mammals (Figure 1). Since primates were thought to be more cognitively complex than other mammals, this expanded cortex became associated with higher mental processes and was considered a primate phenomenon.

Unfortunately, the early mapping studies that provided support for these ideas were hampered by technical difficulties such as suboptimal anesthetics, recording methods, and stimulation parameters, all of which made it difficult to elicit responses from neurons in cortex other than primary and secondary sensory fields. Despite these limitations, these early studies fostered several ideas regarding the human brain that still persist today. Probably the most noteworthy are that primary fields are evolutionarily older, and that association cortex is a new evolutionary phenomenon found mainly in human and nonhuman primates. Thus, association cortex is proposed to be the hallmark of human brain evolution.

These ideas were firmly entrenched for most of the twentieth century. Indeed, a number of psychologists still hold this view, and it is currently circulated as the reigning model in most popular textbooks (e.g., Carlson, N. R., 1998; Saper, C. B. *et al.*, 2000). However, work in the early 1970s by Allman J. M. and Kaas J. H. (1971; 1974; 1975; 1976) upended these traditional views by demonstrating in nonhuman primates that much of extrastriate cortex that was considered association cortex actually contained a number of unimodal visual fields (also see

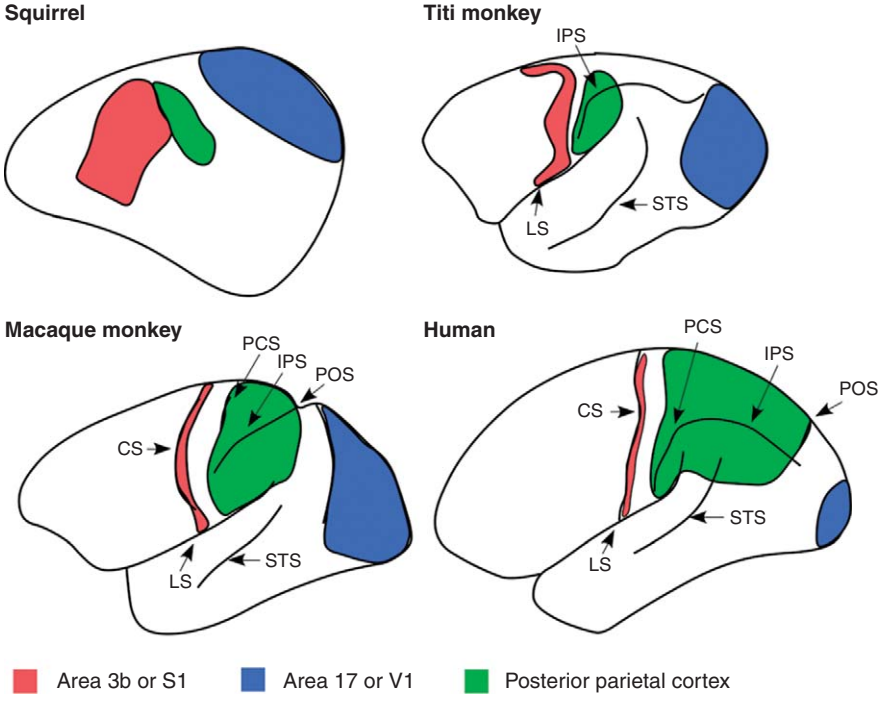

Figure 1 The location of association cortex (green) relative to the primary somatosensory area (red) and the primary visual area (blue) in four mammalian species. In mammals with a small neocortex, such as the gray squirrel, primary sensory areas occupy a relatively large portion of the cortical sheet. In mammals with a large neocortex such as monkeys, these primary sensory areas occupy relatively less cortex. In human primates, primary sensory areas occupy a very small portion of the neocortex, while association cortex, including posterior parietal cortex, occupies a large expanse of the cortical sheet.

Felleman, D. J. and Van Essen, D. C., 1991). Somewhat later, work in both somatosensory (Merzenich, M. M. *et al.*, 1978; Robinson, C. J. and Burton, H., 1980a; 1980b; Pons, T. P. *et al.*, 1985; Krubitzer, L. A. and Kaas, J. H., 1990; Krubitzer, L. *et al.*, 1995a) and auditory cortex (e.g., Imig, T. J. *et al.*, 1977; Hackett, T. A. *et al.*, 1998) demonstrated that parietal cortex and portions of temporal cortex that were thought to be association regions were occupied by somatosensory and auditory cortical fields, respectively (see Kaas, J. H. and Collins, C. E., 2004, for review).

Despite the ever-dwindling classical association cortex in primate brains (including human primates), there are still a few strongholds that seem indomitable, namely, prefrontal and posterior parietal cortex. Work on prefrontal cortex in humans demonstrates that it is involved in higher-order cognitive processes such as the ability to detect and respond to novel events, to discriminate internally motivated versus externally driven models of the world, and to "extract oneself from the present and fluidly move forward and backward in time" (p. 1319; Knight, R. T. and Graboweicky, M., 2000, for review). However, this region of cortex also has a number of visuomotor, olfactory, and limbic functions.

In humans, posterior parietal cortex is considered to be involved in coding the spatial location of objects within a particular frame of reference, both egocentric and extracentric (e.g., Mishkin, M. *et al.*, 1983; Behrmann, M., 2000; Robertson, L. C. and Rafal, R., 2000, for review). In nonhuman primates, posterior parietal cortex is divided into a number of cortical areas that are thought to be involved in visuospatial processing related to limb and hand use such as monitoring limb location during visually guided reaching and grasping, converting sensory locations into motor coordinates for intentional movement, and perceiving the movements of the body in extrapersonal space (Andersen, R. A. *et al.*, 1997; Snyder, L. H. *et al.*, 1997; Wise, S. P. *et al.*, 1997; Debowy, D. J. *et al.*, 2001; Andersen, R. A. and Buneo, C. A., 2002). Thus, much of the region traditionally defined as posterior parietal association cortex has actually evolved in primates as a consequence of and for the generation of specialized hand use rather than for general higher mental functions.

The following review will focus on several fields in anterior parietal cortex (areas 3a, 3b, 1, and 2) involved in processing somatic inputs from the skin, muscles, and joints, as well as one area of posterior parietal cortex (area 5) involved in manual dexterity, bilateral coordination of the hands, intentional reaching and grasping, and interhemispheric transfer of information. We contend that our sense of self, or an internal representation of our body with respect to the external world, is a concrete characteristic common to all mammals. This internal representation is generated by interactions between visual, proprioceptive, and vestibular systems, all of which are intricately intertwined with the motor system. Such an interaction allows an individual to interface an internal representation of self with the external world via a particular morphological structure, such as a hand, thereby generating a sensorimotor feedback loop that allows one to distinguish self from nonself.

6.10.3 Organization of Anterior Parietal Cortex in Primates (Areas 3b, 3a, 1, and 2)

Somatosensory cortex in primates is divided into three major divisions: anterior parietal cortex, posterior parietal cortex, and cortex of the lateral sulcus (see Kaas, J. H. and Pons, T. P., 1988, for review). Each of these major divisions contains several cortical areas. Anterior parietal cortex includes the primary somatosensory area, S1, which corresponds to area 3b in primates (see Kaas, J. H., 1983, for review), area 3a, area 1, and area 2. Posterior parietal cortex has been subdivided differently by different investigators, but most would agree that at least one of these regions, area 5, processes somatic inputs. Finally, like posterior parietal cortex, cortex in the lateral sulcus has been subdivided differently by different investigators. Recently, our laboratory and others have examined this region of cortex using multiunit electrophysiological recording techniques and neuroanatomical tracing methods combined with architectonic analysis, and we have divided this cortex into several fields including the second somatosensory area, S2, the parietal ventral area, PV, the ventral somatosensory area, VS, and the rostroventral parietal area, PR (e.g., Krubitzer, L. A. and Kaas, J. H., 1990; Krubitzer, L. *et al.*, 1995a; Disbrow, E. *et al.*, 2002; 2003; Wu, C.-H. and Kaas, J., 2003).

In this chapter we focus only on somatosensory areas of the anterior and posterior parietal cortex. While several anterior parietal fields such as areas 3a, 3b, 1 and 2 are architectonically distinct in some primates, architectonic comparisons across species

are difficult to make for fields other than areas 3b and 3a. Ideally, the consideration of homology should be based on a number of criteria such as architecture, electrophysiological recording data, cortical and subcortical connections, and lesions to cortical fields and resultant behavioral deficits (Kaas, J. H., 1982). Indeed, determining homology based on architecture alone, in the absence of corroborative electrophysiological data, leads to too many inaccuracies in subdividing the neocortex and erroneous conclusions regarding the evolution of cortical fields. For this reason, the following review focuses primarily on electrophysiological recording studies, studies of connections and studies of lesions, rather than studies which only use architecture to subdivide the cortex.

Cortical fields

A1	primary auditory area
AIP	anterior intraparietal area
C1	caudal region 1
C2	caudal region 2
DSG	dysgranular zone
LIP	lateral intraparietal area
M1	primary motor area
MIP	medial intraparietal area
PM	parietal medial area
PP	posterior parietal cortex
PR	rostroventral parietal area
PV	parietal ventral area
R	rostral area
R1	rostral region 1
R2	rostral region 2
S1	primary somatosensory area
S2	secondary somatosensory area
S3	third somatosensory area
SMA	supplementary motor area
UZ	unresponsive zone
V1	primary visual area
VIP	ventral intraparietal area
VPZ	ventral posterior nucleus, recipient zone

Sulci

CS	central sulcus
IPS	intraparietal sulcus
LS	lateral sulcus
PCS	post central sulcus
POS	parietal occipital sulcus
STS	superior temporal sulcus

Thalamic nuclei

CL	central lateral nucleus
MG	medial geniculate nucleus
Pa	anterior pulvinar
PO	posterior nucleus
VL	ventral lateral nucleus
VP	ventral posterior nucleus
Vpi	ventral posterior nucleus, inferior division
VPl	ventral posterior nucleus, lateral division
VPm	ventral posterior nucleus, medial division
VPs	ventral posterior nucleus, superior division

Body parts

ch	chin
ck	cheek
dig	digits
D1	digit one
D2	digit two
D3	digit three
D4	digit four
D5	digit five
F or ft	foot
fa	forearm
fl	forelimb
fp	forepaw
gen	genitals
hl	hindlimb
hp	hindpaw
j	jaw
l	lip
nb	nail bed
ne	neck
sh	shoulder
sn	snout
t	toes
te	teeth
to	tongue
tr	trunk
ut	upper trunk
vib	vibrissae
w	wing
web	finger web
wr	wrist

Neuroanatomical directions

dor	dorsal
prox	proximal

(*Continued*)

6.10.4 Area 3b or S1

6.10.4.1 Functional Organization

The topographic organization of the primary somatosensory area, S1 or area 3b, has been described in a variety of primates including Old World macaque monkeys (Nelson, R. J. *et al.*, 1980); New World monkeys such as owl (Merzenich, M. M. *et al.*, 1978), squirrel (Sur, M. *et al.*, 1982), cebus (Felleman, D. J. *et al.*, 1983), spider (Pubols, B. and Pubols, L., 1971), titi (Padberg, J. P. *et al.*, 2005), tamarin (Carlson, M. *et al.*, 1986), and marmoset monkeys (Krubitzer, L. A. and Kaas, J. H., 1990); prosimian galagos (Sur, M. *et al.*, 1980); and humans (e.g., Penfield, W. and Rasmussen, T., 1968; Woolsey,

C. *et al.*, 1979; Fox, P. T. *et al.*, 1987; Moore, C. *et al.*, 2000; Blankenburg, F. *et al.*, 2003, for review; Hlushchuk, Y. *et al.*, 2003). In all primates investigated, area 3b forms a systematic representation of the contralateral body surface with the tail, genitals and feet represented most medially, followed by the representations of the hindlimb, trunk, forelimb, hand, face, and oral structures in a mediolateral progression (Figure 2).

Single unit studies demonstrate that neurons in area 3b have small receptive fields compared to other anterior parietal fields (e.g., Gardner, E., 1988) and along with optical imaging studies show that neurons are rapidly or slowly adapting to cutaneous stimulation (e.g., Sur, M. *et al.*, 1984; Chen, L. *et al.*, 2001) and respond to high-frequency stimulation (e.g., Lebedev, M. and Nelson, R., 1996), pressure, and flutter (Chen, L. *et al.*, 2001). In awake behaving monkeys, firing rates are modulated by contact with an object (DeBowy, D. J. *et al.*, 2001), and neurons respond prior to wrist movements (Nelson, R. *et al.*, 1991). It is proposed that area 3b is involved in texture and form discrimination (Johnson, K. O. and Lamb, G. D., 1981; Chapman, C. E. and Ageranioti-Bélanger, S., 1991; Sinclair, R. J. and Burton, H., 1991; Ageranioti-Belanger, S. A. and Chapman, C. E., 1992; Tremblay, F. *et al.*, 1996; Jiang, W. *et al.*, 1997; DiCarlo, J. *et al.*, 1998; see Johnson, K. and Yoshioka, T., 2002, for review) as well as topographic tactile learning (e.g., Romo, R. *et al.*, 1998; 2000; Diamond, M. *et al.*, 2002, for review). While most researchers have examined the neural response to stimulation of the hand or have designed behavioral tasks associated with the hand, one group of studies examined the properties of neurons in area 3b in response to tongue and face movements (Lin, L.-D. *et al.*, 1994a; 1994b). These investigators found that neurons in area 3b (and area 1) increase their firing rate for preferred tongue directions and suggest that neurons in 3b and 1 provide sensory inputs to M1 necessary for generating coordinated tongue and facial movements. Such a homologous processing network in primates could form the basis, in a modified form, for the highly derived articulation behaviors that have evolved in humans.

Studies in which area 3b has been lesioned in monkeys are consistent with single unit studies. For example, lesions in area 3b result in an inability to make discriminations of roughness, hardness, and angle of an object (Randolph, M. and Semmes, J., 1974). Other studies demonstrate that lesions in area 3b result in an inability to make static tactile discriminations (detection of edges), as well as tactile discriminations that require movement, such as discriminating a many-sided object (Schwartz, A., 1983). While the studies of Lamotte R. H. and Mountcastle V. B. (1979) support these findings, the lesions in their study encompassed the entire postcentral gyrus, making it difficult to relate a particular deficit with a specific cortical area.

A primary somatosensory area has also been identified in a wide range of nonprimate mammals including monotremes (e.g., Krubitzer, L. *et al.*, 1995b), marsupials (e.g., Pubols, B. H. *et al.*, 1976; Beck, P. D. *et al.*, 1996; Huffman, K. *et al.*, 1999; Frost, S. B. *et al.*, 2000), and eutherians (e.g., Felleman, D. J. *et al.*, 1983; see Kaas, J. H., 1983; Chapin, J. K. and Lin, C.-S., 1984; Ledoux, M. S. *et al.*, 1987; Johnson, J. I., 1990; Catania, K. C. *et al.*, 1993; Krubitzer, L., 1995, for review). Like area 3b in primates, S1 or area 3b in other mammals is topographically organized with the foot represented most medially, followed by the representation of the trunk, forelimb, forepaw, and face in a mediolateral progression (Figure 3). While single units have been recorded in the barrel field of some rodents, a full description of work in barrel cortex is beyond the scope of this chapter. However, Diamond M. *et al.* (2002) propose that S1 in whisking rodents may be involved in topographic learning via the whiskers, as is the hand representation in area 3b in monkeys. For our purpose, it is important to note that not only is the gross topographic organization of S1 similar in all species examined, but also the types of systems-level modifications to S1, or the rules of change, are consistent across species.

Probably the most salient modification in S1 across species is the amount of neocortex that represents body parts associated with specialized use, which we term behaviorally relevant body surfaces. For example, animals such as the duck-billed platypus have evolved electrosensory receptors that run in parallel strips along the bill (Figure 4). Together with mechanosensory receptors, platypus use electrosensory receptors almost exclusively for prey capture, navigation, and most other activities (Scheich, H. *et al.*, 1986; Manger, P. R. and Pettigrew, J. D., 1995; see Krubitzer, L., 1998, for review). The importance of this morphological structure is reflected in the neocortical organization in that a large percentage of S1, and indeed most of the neocortex, is devoted to the representation of the bill (Krubitzer, L. *et al.*, 1995b). Other examples of cortical magnification of specialized morphology (Figure 3) include the nose representation of the star-nosed mole (Catania, K. C. *et al.*, 1993), the

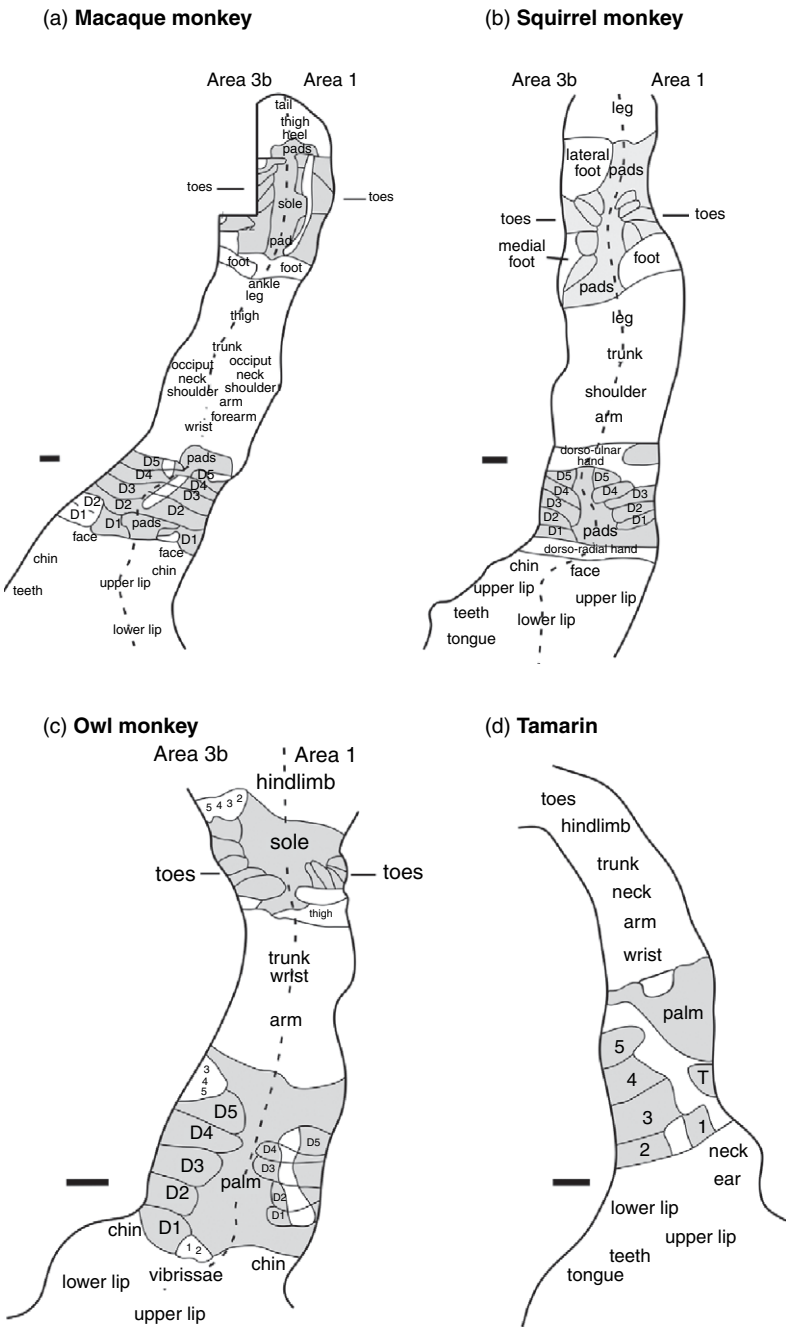

Figure 2 The topographic organization of the primary somatosensory area (S1 or 3b) and area 1 in New and Old World monkeys. Both areas 3b and 1 contain a systematic representation of the contralateral body surface and form mirror representations of each other. In some primates (a–c) area 1 is very well developed, while in other primates (d) area 1 has not been identified. We propose that area 1 coevolved with a well-developed, glabrous hand in some lineages. This is supported by the fact that tamarins have a more primitive hand with claws, compared to the other primates shown. (a) From Nelson, R. J., Sur, M., Felleman, D. J., and Kaas, J. H. 1980. Representations of the body surface in postcentral parietal cortex of *Macaca fascicularis.* J. Comp. Neurol. 192, 611–643; (b) From Sur, M., Nelson, R. J., and Kaas, J. H. 1982. Representations of the body surface in cortical areas 3b and 1 of squirrel monkeys: comparisons with other primates. J. Comp. Neurol. 211, 177–192; (c) From Merzenich, M. M., Kaas, J. H., Sur, M., and Lin, C.-S. 1978. Double representation of the body surface within cytoarchitectonic areas 3b and 1 in ''SI'' in the owl monkey (*Aotus trivirgatus*). J. Comp. Neurol. 181, 41–74; (d) From Carlson, M., Huerta, M. F., Cusick, C. G., and Kaas, J. H. 1986. Studies on the evolution of multiple somatosensory representations in primates: the organization of anterior parietal cortex in the New World Callitrichid, *Saguinus.* J. Comp. Neurol. 246, 409–426.

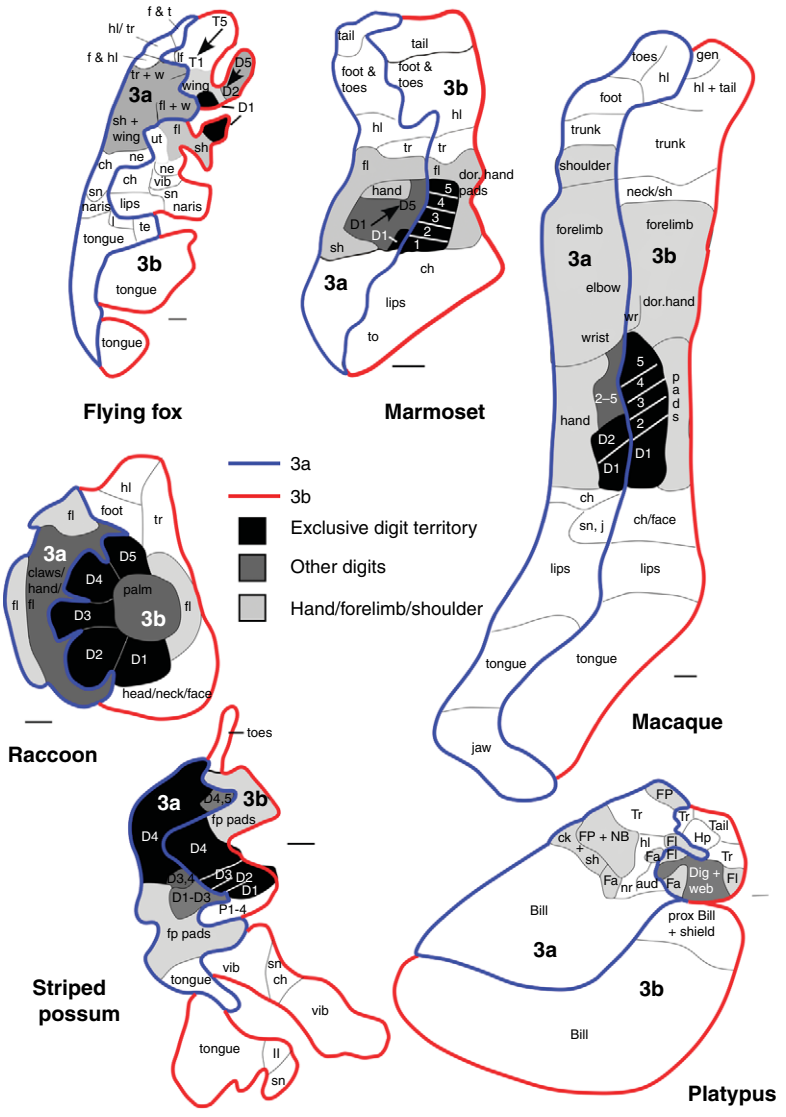

Figure 3 The topographic organization of areas 3b (red) and 3a (blue) in a variety of mammals including primates (macaques and marmosets), megachiropteran bats (flying fox), carnivores (raccoon), marsupials (striped possum), and monotremes (duck-billed platypus). Although the region of cortex immediately rostral to area 3b is termed differently in different mammals, there are a number of features of organization that are similar across groups of mammals including neural responsiveness to stimulation of deep receptors, dense connections with motor and posterior parietal cortical areas, and a large magnification of behaviorally relevant body parts. For these reasons, we believe that area 3a is a homologous cortical field in mammals. The exaggerated representation of specialized peripheral sensory receptor arrays in area 3a argues that the evolution of this field is highly dependent on the use of a particular body part and suggests that the motor system plays a crucial role in the development of area 3a. This figure was adapted from Krubitzer, L., Huffman, K. J., Disbrow, E., and Recanzone, G. 2004. Organization of area 3a in macaque monkeys: contributions to the cortical phenotype. J. Comp. Neurol. 471, 97–111.

digit 4 (D4) representation of the striped possum (Huffman, K. *et al.*, 1999), the D1 and tongue representation of the flying fox (e.g., Calford, M. B. *et al.*, 1985; Krubitzer, L. *et al.*, 1998), and the hand representation of the raccoon (Welker, W. I. and Seidenstein, S., 1959; Johnson, J. I. *et al.*, 1982).

Most primates, including humans, have a large representation of the glabrous hand in area 3b that reflects the special use of the hand in discrimination of texture and form, and a larger representation of oral structures (Figure 4; e.g., Cusick, C. G. *et al.*, 1986), possibly involved in discriminations necessary

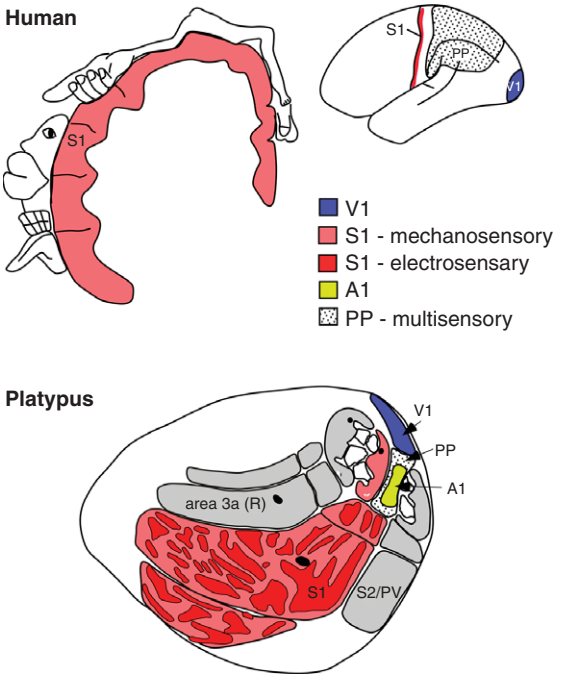

Figure 4 A schematic rendition that demonstrates the cortical magnification of behaviorally relevant body part representations in area 3b across different mammals. In humans, the hand, lips, and oral structure representations are magnified, while in platypus, the bill representation is magnified. Although such magnification occurs for different body part representations, the rules of modification of S1 are similar in both groups of mammals despite approximately 200 million years of independent evolution. This observation indicates that S1 is highly constrained in evolution. The schematic of the human is adapted from Penfield, W. and Rasmussen, T. 1968. Secondary Sensory and Motor Representation. In: Cerebral Cortex of Man. A Clinical Study of Localization of Function (Chapter VI), pp. 109–134. Hafner Publishing Company and the schematic of the platypus is adapted from Krubitzer L. *et al*. (1995).

for omnivorous feeding and for the articulation of species-specific sounds. Similarly, some primates have a relative enlargement of other body parts that are related to specialized use. For example, cebus and spider monkeys have an enlarged representation of their prehensile tail (Felleman, D. J. *et al*., 1983; Pubols, B. and Pubols, L., 1971). While this magnification of S1 in different species is related to innervation density at the periphery (e.g., Lee, K. and Woolsey, T., 1975; Catania, K. C. and Kaas, J. H., 1997), recent evidence also indicates that the use, or the unique pattern of activity from peripheral sensory receptor arrays, also contributes to this cortical magnification (Recanzone, G. H., 1992b; Catania, K. C. and Kaas, J. H., 1997; Xerri, C. *et al*., 1996). It has been proposed that this magnification generates the high spatial resolution necessary for texture and form discriminations made with specialized structures (see Johnson, K. and Yoshiako, T., 2002, for review).

A second type of consistent modification that has evolved in a number of different lineages is the segregation of inputs from similar body parts into distinct isomorphs, or modules, defined electrophysiologically or histochemically (Figure 5). For example, in primates, rapidly adapting and slowly adapting inputs are segregated into separate clusters or bands within S1 (e.g., Sur, M. *et al*., 1984; Chen, L. *et al*., 2001), and the face representation is divided into myelin light and dense zones that segregate different portions of the face and oral structures (Krubitzer, L. A. and Kaas, J. H., 1990; Jain, N. *et al*., 2001). In a number of rodents, inputs from the vibrissae are segregated into cortical barrels (Woolsey, T. A. and Van der Loos, H., 1970), in the star-nosed mole, nose follicles form isomorphs (Catania, K. C. *et al*., 1993), and in the duck-billed platypus, electrosensory and mechanosensory inputs are segregated into interdigitating bands (Krubitzer, L. *et al*., 1995b). The evolutionary and developmental significance of modules has been discussed previously (Krubitzer, L., 1995; Krubitzer, L., and Kahn, D., 2003). In brief, we hypothesize that modules represent a stage in the evolution of a cortical field and that selection for shorter connection length and/or increased speed of transmission has led to the aggregation of modules in different cortical fields and different species over time. If this is the case, then it suggests that a cortical field is actually a pattern of activation (connectivity) from a variety of sources including the thalamus and ipsilateral and contralateral hemispheres that shifts and redistributes across the cortical sheet within an individual lifetime (development) and across species over time (evolution).

6.10.4.2 Connections

The ipsilateral cortical connections of area 3b have been described in macaque monkeys (e.g., Jones, E. G. *et al*., 1978; Pearson, R. C. A. and Powel, T. P. S., 1985; Shanks, M. F. *et al*., 1985b; Juliano, S. *et al*., 1990; Darian-Smith, C. *et al*., 1993; Burton, H. and Fabri, M., 1995; Burton, H. *et al*., 1995), New World titi monkeys (Coq, J. O. *et al*., 2004; Padberg, J. P. *et al*., 2005), marmosets (Krubitzer, L. A. and Kaas, J. H., 1990),

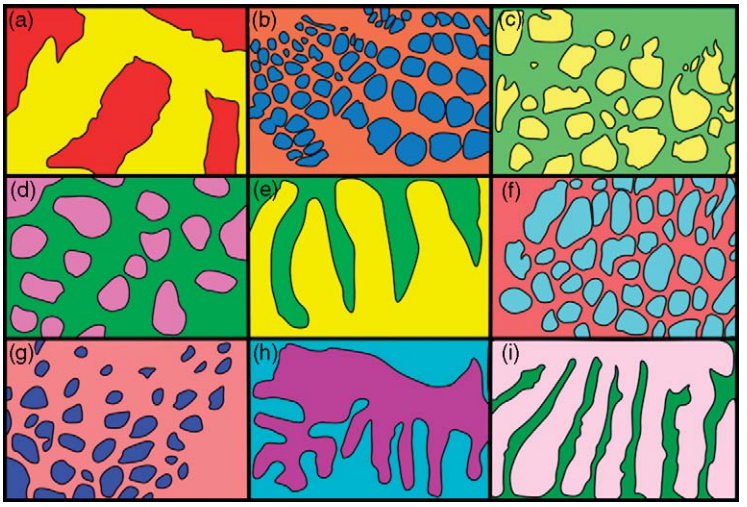

Figure 5 A schematic illustrating a second type of modification, modular organization, that has been observed in slices of flattened sensory cortex in a variety of different mammals. (a) Myelin bands in area 18 of squirrel monkeys; (b) the barrel field in S1 of rats; (c) modules in the insula of dolphin neocortex; (d) entorhinal clusters in macaque monkeys; (e) ocular dominance columns in monkeys; (f) entorhinal clusters in humans; (g) the barrel field in S1 of brush-tailed possums; (h) mechanosensory and electrosensory bands in S1 of duck-billed platypuses; and (i) nose follicle representation of S1 in star-nosed moles. This figure was adapted from Manger, P., Sum, M., Szymanski, M., Ridyway, S., and Krubitzer, L. 1998. Modular subdivisions of dolphin anterior ensular cortex: does evolutionary history repeat itself? J. Cogn. Neurosci. 10(2), 153–166.

and prosimian galagos (Wu, C.-H. and Kaas, J., 2003). In these primates, restricted injections in area 3b result in a relatively tight distribution of connections predominantly with adjacent somatosensory cortical fields including areas 3a, cortex immediately caudal to area 3b (areas 1 and 2 in macaque monkeys, area 1/2 in New World monkeys and galagos), S2 (and PV where described), and primary motor cortex (Figure 6). In primates, thalamic connections of area 3b are predominantly from the ventral posterior nucleus, both VPm and VPl (e.g., Jones, E. G. *et al.*, 1979; Nelson, R. J. and Kaas, J. H., 1981; Mayner, L. and Kaas, J., 1986; Darian-Smith, C. *et al.*, 1990; Krubitzer , L. A. and Kaas, J. H., 1992; Rausell, E. and Jones, E. G., 1995; Coq, J. O. *et al.*, 2004; Padberg, J. and Krubitzer, L., 2006). However, sparse projections from VPi, VPs, and Pa have also been observed (e.g., Cusick, C. G. and Gould, H. J. I., 1990).

Both the cortical and subcortical connections of area 3b (S1) have been described in a number of mammals such as rodents (e.g., Wise, S. P. and Jones, E. G., 1976; Akers, R. M. and Killackey, H. P., 1978; Krubitzer, L. A. *et al.*, 1986; Chapin, J. K. *et al.*, 1987; Krubitzer, L. and Kaas, J., 1987; Koralek, K. A. *et al.*, 1990; Fabri, M. and Burton, H., 1991; Paperna, T. and Malach, R., 1991), carnivores (Alloway, K. D. and Burton, H., 1985; Barbaresi, P. *et al.*, 1987; Herron, P. and Johnson, J. I, 1987), and marsupials (Beck, P. D. *et al.*, 1996; Elston, G. N. and Manger, P. R., 1999; see Johnson, J. I., 1990, for review). As in primates, S1 is densely connected with area 3a (R, UZ, and dysgranular cortex), M1, and S2/PV. The major thalamic projection to S1 is from VPl and VPm, and connections are also observed with the posterior nucleus, PO.

The total pattern of callosal connections of areas 3b, 1, 2, and 5 indicates that the hand representation of area 3b is almost completely acallosal in primates (e.g., Pandya, D. N. and Vignolo, L. A., 1968; Killackey, H. P. *et al.*, 1983; Shanks, M. F. *et al.*, 1985a; 1985b). Surprisingly, specific callosal connections of individual anterior parietal fields have only been described for a few species of primates (e.g., Manzoni, T. *et al.*, 1986; Krubitzer, L. A. and Kaas, J. H., 1990; Padberg *et al.*, 2005). In macaque monkeys it was found that while the hand representation of area 3b does not project to the hand representation of area 3b of the opposite hemisphere, it does project to S2 (e.g., Manzoni, T. *et al.*, 1986). In marmosets, electrophysiologically defined body part representations in area 3b are differentially interconnected across hemispheres. Myelin light portions of area 3b appear to be strongly interconnected, while myelin dense portions of area 3b are acallosal. Furthermore, as described in early studies, the hand representation of area 3b appears to be mostly acallosal. Area 3b is also

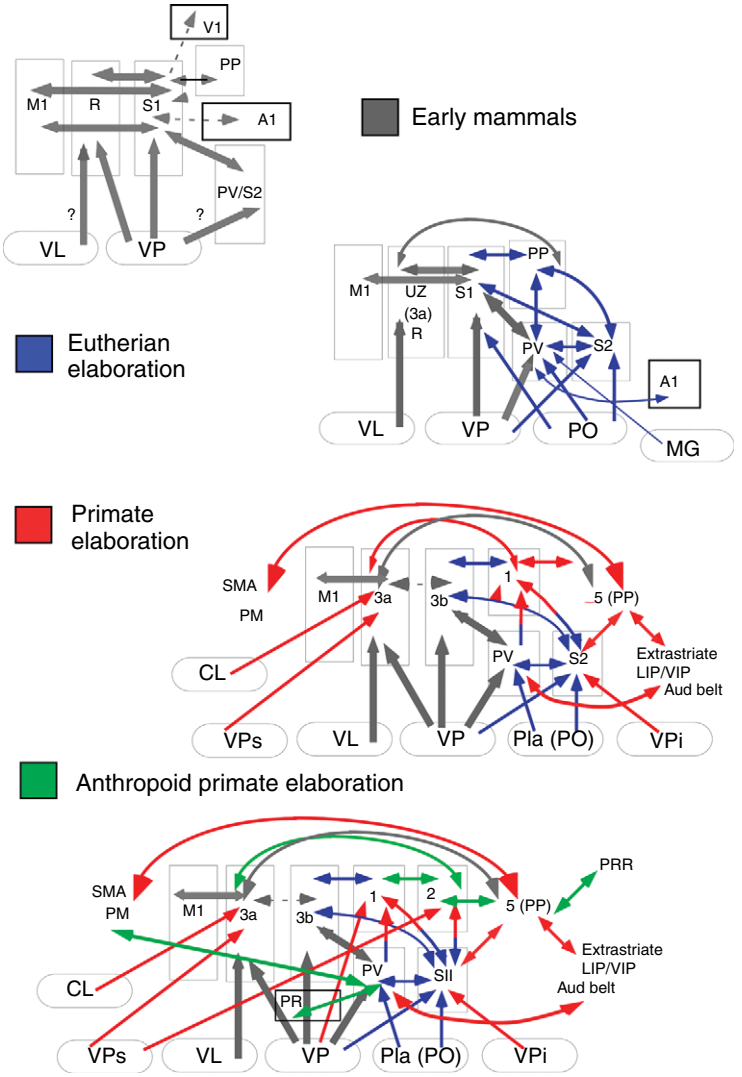

Figure 6 An overview of the cortical and thalamocortical connections of anterior parietal cortical fields, lateral sulcus fields, and posterior parietal area 5 in mammals. This figure is not an exhaustive overview of the connections of particular fields in different mammals. Rather, this figure depicts that particular patterns of connections can be identified in all groups of mammals due to retention from a common ancestor (gray arrows). Such connections are homologous. Additional connections arose later in mammalian evolution and have been added to this retained network in eutherian mammals (blue arrows). In different lineages, such as primates, these networks were further elaborated with the addition of new cortical areas, modules to existing cortical areas, and new thalamic nuclei. Such modifications to the neocortex make determining homologous areas and connection patterns difficult. Furthermore, these types of anatomical modifications suggest that homologous cortical fields may not be analogous (Figure 8).

interconnected with S2 and PV of the opposite hemisphere. Similar findings were reported in titi monkeys in which the hand representation was acallosal, and myelin light regions formed callosal zones in area 3b (Padberg *et al.*, 2004).

Callosal connections have been described for area 3b or S1 in rats (e.g., Wise, S. P. and Jones, E. G., 1976; Akers, R. K. and Killackey, H. P., 1978), mice (White, E. L. and DeAmicis, R. A., 1977), cats (e.g., Ebner, F. F. and Myers, R. E., 1965; Caminiti, R. *et al.*, 1979; McKenna, T. M. *et al.*, 1981), raccoons (Ebner, F. F. and Myers, R. E., 1965; Herron, P. and Johnson, J. I., 1987), flying foxes (Krubitzer, L. *et al.*, 1998), rabbits (Ledoux, M. S. *et al.*, 1987), and tree shrews (Cusick, C. G. *et al.*, 1985; Weller, R. E. *et al.*, 1987; see Krubitzer, L. *et al.*, 1998, for review). As in primates,

there is a heterogeneity of callosal connectivity of different body parts that appear to be associated with use. For example, the representations of specialized body parts in area 3b are acallosal, and zones such as the unresponsive zone in squirrels, the dysgranular zone (septa) in rats, the heterogeneous zones of raccoons, and the myelin light area 1/2 interdigitations in flying foxes are rich in callosal connections, as is the unmyelinated region in monkeys. Thus, studies of callosal connectivity for all mammals investigated report that S1 contains callosal zones related to different body part representations often associated with distinct myelin light zones (Figure 7; see Krubitzer, L. *et al.*, 1998, for review). Body part representations associated with specialized use such as the barrels in rodents, lateral face representations in rabbits, and the hand representations in primates are devoid of callosal connections. Previous studies suggest that callosal free zones are the regions of cortex where thalamocortical afferents terminate (e.g., Wise, S. P. and Jones, E. G., 1976; Gould, H. J. I. and Kaas, J. H., 1981; Krubitzer, L. A. and Kaas, J. H., 1990; Krubitzer, L. *et al.*, 1998). It appears that selection for specialized peripheral morphology in the form of receptor-dense regions like finger tips also operates on cortical representations to both conserve discrete receptive

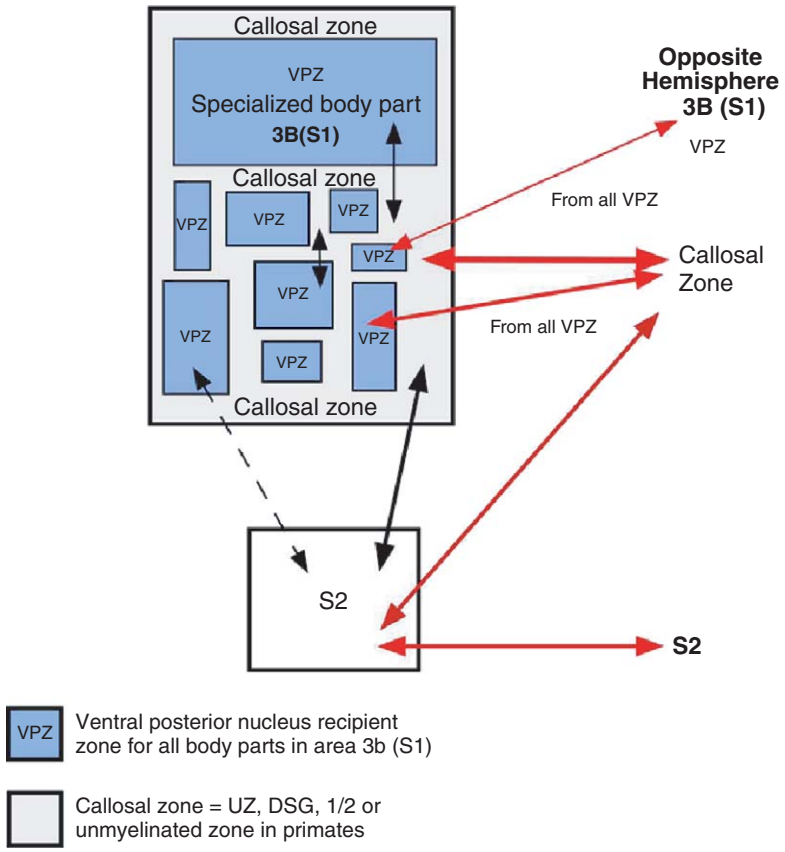

Figure 7 An illustration of the callosal connections of the primary somatosensory area (3b or S1) that depicts some common features of connectivity across all mammals. This figure demonstrates that area 3b appears to be modularly organized based on several important principles. First, S1 is broken into thalamocortical recipient zones (VPZ) and callosal recipient zones. Thalamocortical recipient zones of behaviorally relevant body parts (e.g., hand, bill, nose, and wing) are acallosal. Some of the VPZs have sparse callosal connections with VPZs in the opposite hemisphere and more dense connections to callosal zones in the opposite hemisphere. Finally, information from 3b can also reach the opposite hemisphere indirectly via S2. We and others propose that this type of organization evolved to maintain close intracortical connections between neurons in the same VPZ, uninterrupted by connections from the opposite hemisphere. This type of organization would allow for the maintenance of small receptive fields in neurons over a large region of cortex and would allow the integrity of sensory discriminations derived from inputs from behaviorally significant body parts to be maintained.

fields of neurons created by thalamocortical inputs and preserve neuroanatomical interactions between neighboring specialized skin regions. This conservation of thalamocortical inputs carrying information from specialized skin regions, and of short intrinsic cortical connections within the representation of these specialized skin regions, results in cortical zones or islands that are uninterrupted by callosal afferents (Herron, P. and Johnson, J. I., 1987; Ledoux, M. S. *et al.*, 1987; Krubitzer, L. *et al.*, 1998). We further suggest that in area 3b this type of connection labyrinth may be necessary to maintain the integrity of sensory discriminations derived from inputs from behaviorally significant body parts and as such constrains the evolution of S1.

Taken together, the data illustrate that there is a common organization of S1 across species and that modifications to this field take a similar form reflected as a magnification of the representation of specialized peripheral sensory morphology. How this magnification is related to specialized behavior is not clear, and why this mode of cortical specialization has emerged (compared to any number of potential types of modification) is not known. However, Kaas J. H. (1997) suggests that it is a byproduct of development that has been functionally optimized. Regardless of the functional significance of this magnification, comparative surveys demonstrate that the neocortex must be highly constrained since only a few modifications to S1, other than cortical magnification, have emerged. In addition to cortical magnification, the cortex has been modified to segregate subclasses of input, such as the segregation of rapidly adapting and slowly adapting inputs as well as the callosal and acallosal zones described above. Again, it is not understood why this feature has emerged independently in a number of different lineages, but it has been proposed that it reflects developmental contingencies and is therefore highly constrained (e.g., Krubitzer, L., 1995; Kaas, J. H., 1997; Krubitzer, L. and Kahn, D., 2003).

As with cortical organization, connections of S1 also have similar patterns across mammals. This homologous network may in part subserve similar functions, but it is likely that with the addition of new fields and connections (as in primates), and a reweighting of existing synaptic interactions, new functions or at least a species-specific refinement of particular behaviors is likely to have emerged (Figures 6 and 8). This observation, of course, implies that even for primary fields, direct extrapolation between nonhuman and human primates regarding function is problematic.

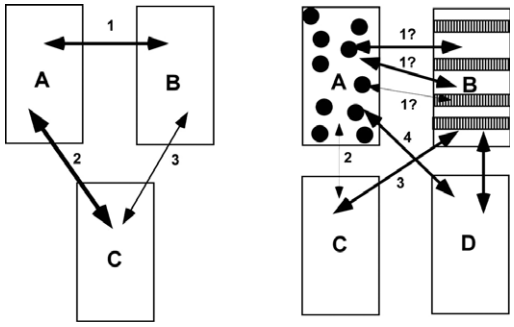

Figure 8 A theoretical rendition of the evolution of cortical fields and their connections. This figure illustrates the difficulties inherent in assigning homology across groups of mammals. It also illustrates the problems with making direct extrapolations regarding analogy of cortical fields, and their circuitry, between any groups of mammals (such as macaque monkeys and humans). Hypothetical cortical fields include field A, B, and C with connection patterns 1, 2, and 3 (*left*). When comparing cortical organization and connections across groups to determine homology, several problems arise. First, new cortical fields have been added in some groups (D). Second, modules may have been added to existing cortical fields (A and B). Third, the density of connections between fields may have changed (connection 2). Fourth, existing connections have been modified by the generation of modules (connection 1). Finally, new connections (4) have developed between retained fields (A) and new fields (D). All of these events are complicated by the fact that connection patterns are often used to determine homology between fields. Thus, even when one can convincingly determine the homology of cortical fields in different groups of animals, it is unlikely that homologous fields are strictly analogous.

6.10.5 Area 3a

6.10.5.1 Functional Organization

A representation of deep receptors of the contralateral body, termed area 3a, is located immediately rostral to area 3b. Area 3a was originally described as an architectonically distinct cortical field in humans by Vogt C. and Vogt O. (1919) but has since been described in a variety of mammals. The functional organization of area 3a in primates has been described for marmosets (Huffman, K. J. and Krubitzer, L., 2001a) and macaque monkeys (Krubitzer, L. *et al.*, 2004) in multiunit recording studies, and recently in humans using modern imaging techniques (Moore, C. *et al.*, 2000). These studies demonstrate that area 3a contains a topographically organized representation of deep receptors and musculature of the contralateral body that parallels that of area 3b (Figure 3) and ultimately receives input

from proprioceptors of the muscles and joints (Phillips, C. B. *et al.*, 1971; Schwarz, D. W. *et al.*, 1973; Heath, C. J. *et al.*, 1975; Hore, J. *et al.*, 1976; see Tanji, J. and Wise, S., 1981, for review). Single unit studies in awake monkeys report that neurons in area 3a modulate activity prior to wrist flexion and extension (Nelson, R., 1987) and are active under a variety of joint movements (Gardner, E., 1988). Neural activity in area 3a increases with maintained limb position and is modulated with the velocity of movement toward a limb position, as well as the ultimate position of the limb (Tanji, J., 1975; Wise, S. and Tanji, J., 1981). Furthermore, lateral portions of area 3a (termed 3aV) contain neurons that respond to vestibular stimulation (Guldin, W. O. *et al.*, 1992). Thus, area 3a in primates is a proprioceptive field that is closely involved in the kinetics of movement. This contention is supported by microstimulation studies in monkeys which demonstrate that body movements can be elicited by stimulating area 3a with very small currents (e.g., Stepniewska, I. *et al.*, 1993).

Studies in other mammals have identified a region of cortex just rostral to area 3b in which neurons respond to stimulation of deep receptors. In carnivores such as cats (e.g., Oscarsson, O. and Rosén, I., 1963; 1966; Oscarsson, O. *et al.*, 1966; Landgren, S. and Silfvenius, H., 1969; Zarzecki, P. *et al.*, 1978; Felleman, D. J. *et al.*, 1983), raccoons (Johnson, J. I. *et al.*, 1982; Feldman, S. H. and Johnson, J. I., 1988), and ferrets (Hunt, D. L. *et al.*, 2000), a region just rostral to area 3b exhibits a number of characteristics of area 3a in monkeys, such as neural response to stimulation of deep receptors, architectonic appearance, and gross topographic organization (Figure 3). This field has been termed area 3a in cats and ferrets and kinesthetic cortex in raccoons. In other mammals such as marsupials (see Huffman,K. *et al.*, 1999), rodents (see Slutsky, D. A. *et al.*, 2000, for review), insectivores (Krubitzer, L. *et al.*, 1997), and monotremes (Krubitzer, L. *et al.*, 1995b), these features are observed in a field just rostral to S1, termed the rostral field, R (Figure 9). In all of these mammals, this cortical area immediately rostral to S1 and caudal to area 4 contains a gross mediolateral organization that mirrors that of area 3b, although there is a great deal of variability across groups. Thus, all mammals have a cortical field located just rostral to area 3b that receives inputs from deep receptors of the contralateral body and is distinguished from motor cortex (area 4) based on a number of criteria including functional organization, neural stimulus preference, architectonic distinctiveness, and when known cortical and subcortical connectivity. We propose that area 3a is homologous in all mammals.

As demonstrated for area 3b, there are several features of area 3a organization that have been consistently modified in different lineages, and these modifications appear to be more related to the use of behaviorally relevant body parts than in area 3b. For instance, when the topographic organization of area 3b is compared with that of area 3a in macaque monkeys, area 3b is observed to be more topographically precise, particularly for representations of the digits where every digit is represented in an exclusive cortical zone. This aspect of representation in area 3b has been observed in every primate examined regardless of the use of the hand or whether the primate in question has an opposable thumb. In contrast, in area 3a in macaque monkeys, exclusive cortical territory is devoted to the representation of D1 and D2, while digits 3 through 5 are represented together. In area 3a in marmosets, little if any cortical territory is devoted to the exclusive representation of a single digit. Digit representation in area 3a in the two species appears to parallel differences in use (Figure 3). Macaque monkeys have opposable thumbs and are highly skilled graspers who employ two general techniques. The first technique is to oppose D1 to D2 (precision grip), and the second technique is to oppose all four remaining digits to the palm (power grip; Welles, J. F., 1976; Roy, A. *et al.*, 2000). Marmoset monkeys, on the other hand, generally employ only a power grip, and their cortical representation in area 3a reflects this behavior. These observations suggest that in primates, area 3a emerges in development and evolution as a result of the actual use of the body part, and therefore, the motor system must play an important role in its construction.

Studies of the organization of area 3a in a variety of other species who use the hand quite differently than primates support this contention (Figure 3). For instance, the flying fox has a highly derived hand in which the digits have evolved membranes that span between them. This digit/membrane configuration functions as a whole unit, the wing, which is adapted for flight. Consequently, all digits form a single representation in area 3a, the wing, and there is no cortical territory that exclusively represents any one digit (Krubitzer, L. *et al.*, 1998), although such exclusive digit representation is present in area 3b in these mammals (Calford, M. B. *et al.*, 1985; Krubitzer, L. A. and Calford, M. B., 1992). Another interesting

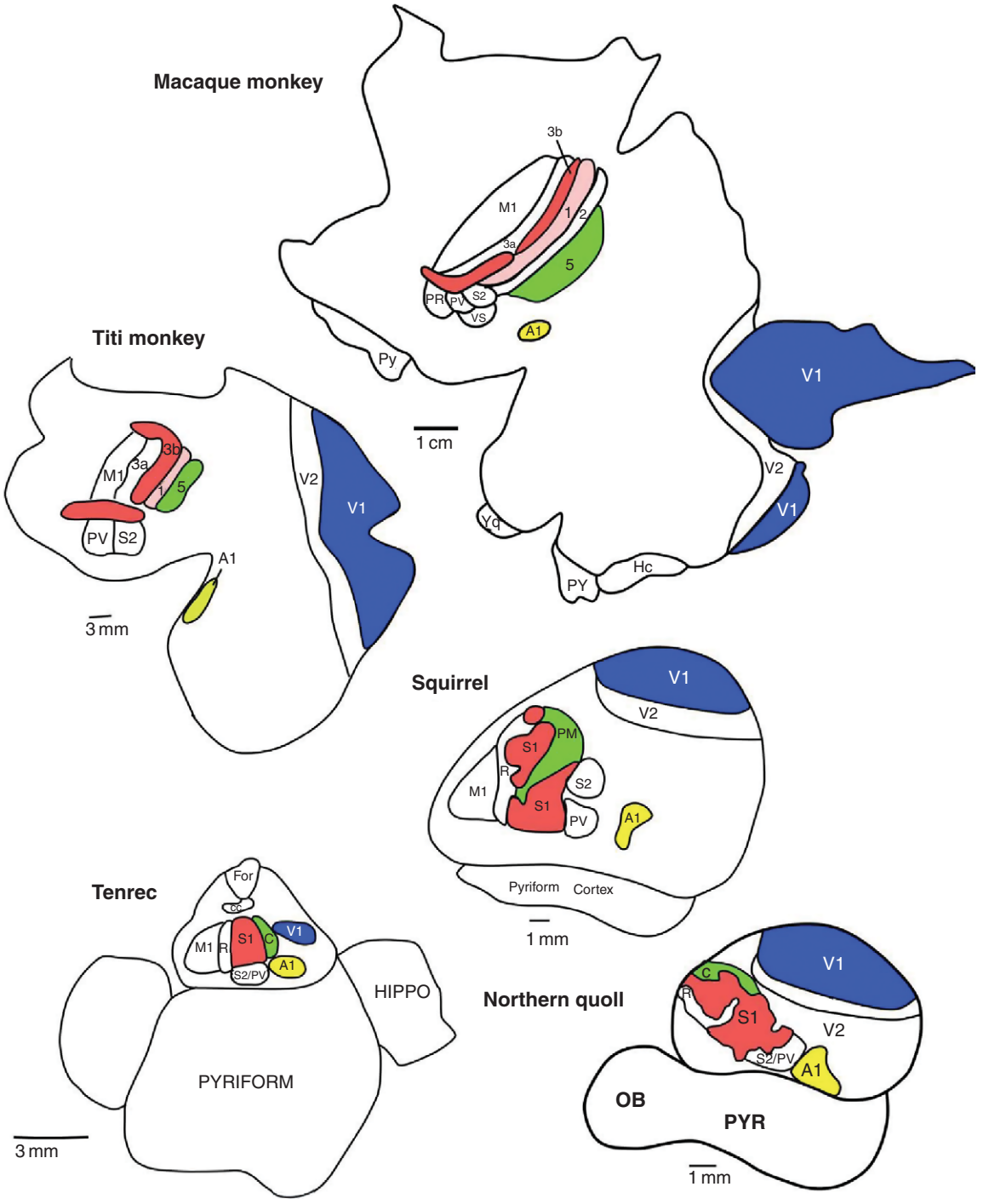

Figure 9 The organization of neocortex in several different mammals. This figure demonstrates that assigning homology of a cortical field based on the location of a particular field relative to another field is problematic. For instance, in mammals with large brains, such as macaque monkeys, area 1 is immediately caudal to area 3b, area 5 is close to the caudal boundary of area 1, and both are very far removed from V1 and V2. In mammals such as squirrels, cortex immediately caudal to area 3b, PM, is relatively close to V2 compared to macaque monkeys. In tenrecs, cortex immediately caudal to area 3b (S1) is also immediately adjacent to V1. If one were to assign homology based solely on location, this cortex in tenrecs could as easily be termed area 1 as it could be termed V2.

example of use-dependent organization of area 3a is the marsupial striped possum. This animal has a specialized D4 that it uses almost entirely to capture insects (Van Dyck, S., 1983). While exclusive cortical territory for all of the digits is observed in area 3b (with a magnification of D4), only D4 is represented in area 3a. Differences in use between members of the same species can produce a good deal of variability in the topographic organization of area 3a (e.g., Recanzone, G. H. *et al.*, 1992b), and this variability is even more pronounced across species due to specialized motor sequences or exaggerated behaviors that coevolved with specialized peripheral morphology and associated sensory receptor arrays (Krubitzer, L. *et al.*, 2004).

6.10.5.2 Connections

There are several studies of the connections of area 3a in primates including macaque monkeys (e.g., Jones, E. G. *et al.*, 1978; Darian-Smith, C. *et al.*, 1993), squirrel monkeys (Guldin, W. O. *et al.*, 1992), and marmosets (Huffman, K. J. and Krubitzer, L., 2001a). These studies demonstrate that area 3a is densely connected with M1, SMA, area 2 (or cortex caudal to area 3b), S2/PV, cingulate cortex, insular cortex, and posterior parietal cortex (area 5; Figure 6). The surprising result from these previous studies is that area 3a has more numerous connections with motor and posterior parietal areas of the neocortex than with traditionally defined somatosensory areas. Studies of thalamic connections of area 3a in Old World (Jones, E. G. *et al.*, 1979; Darian-Smith, C. *et al.*, 1990) and New World monkeys (Akbarian, S. *et al.*, 1992; Huffman, K. J. and Krubitzer, L. A., 2001b) indicate that area 3a receives input from somatic nuclei such as the ventral posterior superior nucleus (VPs, VPLc of Jones, E. G. *et al.*, 1979; Friedman, D. and Jones, E., 1981 and Darian-Smith, C. *et al.*, 1993) and the anterior pulvinar (Pla), some of which (e.g., VPi, VPs, and VLc) are also associated with vestibular processing (e.g., Lang, W. *et al.*, 1979). Area 3a also receives input from nuclei associated with the motor system such as the ventral lateral (VL), ventral anterior (VA), and central lateral (CL) nucleus of the thalamus.

The cortical and subcortical connections of area 3a, or cortex in the location of area 3a, has only been described in a few mammals such as squirrels (Gould, H. J. *et al.*, 1989; dysgranular UZ), flying foxes (Krubitzer, L. *et al.*, 1998), cats (e.g., Avendano, C. *et al.*, 1992), and briefly for ferrets (e.g., Hunt, D. L. *et al.*, 2000). While there is variability in the patterns of cortical connections of area 3a across animals, there are consistent patterns of connections with motor cortex, areas of the lateral sulcus such as S2/PV, and with cortex immediately caudal to S1 (Figure 6; termed area 5, PP, 1/2, and C in different animals). Thalamic connections of the UZ/R region of squirrels (area 3a) were from nuclei situated rostral, dorsal, and caudal to VP and from the central medial nucleus (Gould, H. J. *et al.*, 1989).

As with 3b, in most studies, the total pattern of callosal connections of anterior parietal fields 3a, 3b, 1, and 2 has been examined rather than the specific connections of area 3a (e.g., Jones, E. G. and Powell, T. P. S., 1969a; Killackey, H. P. *et al.*, 1983; Shanks, M. F. *et al.*, 1985a). These studies suggest that like area 3b, the hand representation of area 3a is acallosal. There are only a few studies of callosal connections of area 3a in primates and other mammals. In marmosets, specific connections of the hindlimb and forelimb representation in area 3a have been described (e.g., Huffman, K. J. and Krubitzer, L., 2001a). Interestingly, at least for the marmoset, the hand representation of area 3a does have callosal connections with the hand representation of area 3a in the opposite hemisphere. Furthermore, area 3a is callosally connected to areas M1 and SMA as well. Similar findings were demonstrated for the wing representation of the flying fox (Krubitzer, L. *et al.*, 1998).

Taken together, the data indicate that area 3a is a proprioceptive area that integrates somatic and vestibular inputs with the motor system. This cortical field is involved in the kinetics of movement (determining the load and force), in maintaining posture and limb position, and in regulating the velocity of limb movement.

6.10.6 Area 1

6.10.6.1 Functional Organization

A third somatosensory cortical field just caudal to area 3b, termed area 1, has been described in macaque monkeys and three species of New World monkeys including owl, squirrel, and cebus monkeys (Merzenich, M. M. *et al.*, 1978; Nelson, R, J. *et al.*, 1980; Sur, M. *et al.*, 1982; Felleman, D. J. *et al.*, 1983 respectively). Recent evidence indicates that area 1 is present in humans as well (e.g., Krause, R. *et al.*, 2001; Blankenburg, F. *et al.*, 2003). In some primates, such as macaques, squirrel monkeys, and owl monkeys, area

1 forms a mirror reversal representation of area 3b and contains a precise, topographically organized representation of the contralateral body surface, much like that of area 3b (Figure 2). As in area 3b, there is a magnification of the glabrous hand and oral structures, and receptive fields for neurons are small and limited to single digits. In other primates, only a rudimentary area 1 has been observed (e.g., titi monkeys, Coq, J. O. *et al.*, 2004; Padberg, J. P. *et al.*, 2005) or is absent under similar recording conditions (e.g., tamarins, Carlson, M. *et al.*, 1986; marmosets, Krubitzer, L. A. and Kaas, J. H., 1990; prosimian galagos, Sur, M. *et al.*, 1980). Although we and others have termed cortex caudal to area 3b 'area 1/2' in previous studies in marmoset monkeys (e.g., Krubitzer, L. A. and Kaas, J. H., 1990) and galagos (Wu, C.-H. and Kaas, J., 2003), this terminology was based solely on position with respect to area 3b, rather than any solid electrophysiological data. Indeed, in these species, cortex caudal to area 3b contains neurons that are either unresponsive to any type of sensory stimulation under the anesthetic conditions utilized or are inconsistently driven by stimulation of deep receptors or high-threshold cutaneous receptors of the contralateral body (Figure 11). Thus, area 1 is well developed in only a few primates including Old World macaque monkeys and a few New World monkeys. Given that these species have a well-developed glabrous hand compared to the clawed New World marmoset and tamarin monkeys, we hypothesize that this field coevolved with the highly specialized glabrous hand and is associated with sophisticated hand use.

Single unit studies demonstrate that like neurons in area 3b, neurons in area 1 are modulated by contact with an object (e.g., Debowy, D. J. *et al.*, 2001), are selective for motion across the skin, and are involved in edge orientation (e.g., Gardner, E., 1988). Furthermore, neurons in area 1 respond to noxious stimulation (Kenshalo, D. *et al.*, 2000). Lesions that are restricted to area 1 in primates demonstrate that animals are unable to discriminate between hard versus soft and rough versus smooth objects (Randolph, M. and Semmes, J., 1974; Carlson, M., 1981).

There is very limited evidence for an area 1 in other mammals. While investigators have subdivided cat cortex into architectonic areas 3a, 3b, 1, and 2 (e.g., Hassler, R. and Muhs-Clement, K., 1964), electrophysiological recording experiments in which this cortex was densely surveyed demonstrate that only a single representation of the contralateral body surface (area 3b or S1) resides in anterior parietal cortex of the cat (e.g., Felleman, D. J. *et al.*, 1983). Although cortex caudolateral to area 3b has been electrophysiologically explored and termed S3 by Garraghty P. E. *et al.* (1987), these investigators propose that S3 may be homologous to S2 or PV in other mammals, rather than area 1. The data in ferrets are equivocal. Some laboratories report multiple cutaneous representations in anterior parietal cortex (termed C1, C2, R1, and R2; e.g., LeClerc, S. S. *et al.*, 1993), while others report that neurons in cortex caudal to area 3b respond to stimulation of deep receptors (Hunt, D. L. *et al.*, 2000). In the former study, only the snout representation was explored. It is not clear if indeed four separate cutaneous representations exist in ferrets since the mapping data were limited; or if they do exist, which of the four corresponds to area 3b and area 1. Finally, a field termed area 1/2 has been described for the flying fox (e.g., Krubitzer, L. A. and Calford, M. B., 1992). This region of cortex interdigitates with area 3b and contains neurons that respond to cutaneous stimulation of the contralateral body surface as well as islands of neurons that respond to stimulation of deep receptors. Like area 1 in primates, area 1/2 in the flying fox contains a complete representation of the contralateral body surface.

In all other mammals investigated, cortex caudal to area 3b contains neurons that respond to stimulation of deep receptors (Figure 11). For example, in rodents (Slutsky *et al.*, 2000), insectivores (Krubitzer, L. *et al.*, 1997), monotremes (Krubitzer, L. *et al.*, 1995b), and marsupials (Beck, P. D. *et al.*, 1996; Huffman, K. *et al.*, 1999), cortex immediately caudal to 3b contains neurons that respond to stimulation of deep receptors of the contralateral body, which are often multimodal (e.g., short-tailed possums and platypus). This field has been called the caudal field (C), the caudal somatosensory area (SC), the parietal medial field (PM), PPC, or area 1/2 in different mammals and has been proposed to correspond to posterior parietal cortex including area 5 or a combination of areas 1 and 2 (Reep, R. L. *et al.*, 1994; Krubitzer, L. *et al.*, 1997; 1998; Huffman, K. *et al.*, 1999; Slutsky, D. A. *et al.*, 2000, for review). Interestingly, studies in which the behavioral effects of lesions in PPC were examined in rats report that these animals have deficits in spatial attention and navigation (Kolb, B. *et al.*, 1994). Similar types of deficits are observed when posterior parietal cortex (rather than area 1) is lesioned in primates (see below).

It seems unlikely that cortex immediately caudal to area 3b in nonprimate mammals is homologous to area 1 in primates for three reasons. The first is that there are only two nonprimate mammals in which neurons in

cortex that adjoins area 3b at its caudal boundary respond to cutaneous stimulation, and this cortex has only been thoroughly explored in one of these species (e.g., flying fox). In all other mammals, cortex immediately caudal to 3b contains neurons that respond to stimulation of deep receptors that are often multimodal. Second, the location of an area 1 described in these animals as just caudal to S1 is not a conclusive indicator of homology because in small-brained mammals such as tenrecs and marsupial northern quolls, cortex immediately caudal to area 3b is also immediately rostral to V1 or V2 (Figure 9). Therefore, assigning homology based on position alone is problematic. Finally, prosimians, marmosets, and tamarins do not appear to have an area 1, which suggests that this field arose later in primate evolution and is therefore a purely primate phenomenon, with the cutaneous field immediately caudal to area 3b arising independently in flying foxes (and possibly ferrets, if area 1 does indeed exist in these animals), and serving different, although overlapping functions in these species (see below).

6.10.6.2 Connections

Highly restricted injections into electrophysiologically identified portions of area 1 have only been made in macaque monkeys (Pons, T. P. and Kaas, J. H., 1986; Burton, H. and Fabri, M., 1995; Burton, H. *et al.*, 1995) and titi monkeys (Coq, J. O. *et al.*, 2004; Padberg, J. P. *et al.*, 2005). Connections of area 1 in macaque monkeys are more broadly distributed than those in area 3b and are observed with areas 3b, 2, S2/PV, 5, AIP/7b, and sparsely with areas 3a, M1, and frontal cortex. Previous reports on connections of the architectonically defined area 1 with local parietal cortical areas support these electrophysiological studies (e.g., Jones, E. G. *et al.*, 1978; Vogt, B. A. and Pandya, D. N., 1978; Pearson, R. C. A. and Powell, T. P. S., 1985; Shanks, M. F. *et al.*, 1985b). In macaque monkeys, thalamocortical connections from electrophysiologically identified locations in area 1 indicate that like area 3b, area 1 receives the majority of its inputs from VP proper (e.g., Nelson, R. J. and Kaas, J. H., 1981; Pons, T. P. and Kaas, J. H., 1985). However, in New World titi monkeys, thalamocortical connections of area 1 are also from VL, Pa, and VPs (e.g., Padberg, J. and Krubitzer, L., 2006).

Examination of callosal connections of areas 3a, 3b, 1, and 2 indicates that the hand representation of area 1 is acallosal (e.g., Pandya, D. N. and Vignolo, L. A., 1968; Killackey, H. P. *et al.*, 1983; Shanks, M. F. *et al.*, 1985a; Conti, F. *et al.*, 1986). Recent work in titi monkeys in our laboratory in which the injections in area 1 were made under electrophysiological guidance demonstrates sparse callosal connections for the hand representation in area 1 (Padberg, J. and Krubitzer, L., 2006). In this primate, area 1 was most densely interconnected with areas 5 and AIP/7 of the opposite hemisphere.

Connections, lesions, and single unit studies in macaque monkeys indicate that areas 3b and 1 in primates are involved in integrating local inputs from restricted portions of the glabrous hand necessary for fine tactile discriminations such as ascertaining object texture and form (Randolph, M. and Semmes, J., 1974; LaMotte, R. H. and Mountcastle, V. B., 1979; Carlson, M., 1981; Sinclair, R. J. and Burton, H., 1991; Ageraniotis-Belanger, S. A. and Chapman, C. E., 1992; Jiang, W. *et al.*, 1997). We propose that area 1 is a recently evolved field restricted to primates, although some species (e.g., flying foxes) have independently evolved a cutaneous representation caudal to area 3b. The location of this field in flying foxes is similar to that of area 1 in primates, but comparative data and examination of behavior in this species indicate that it is unlikely that this area is homologous, or strictly analogous to area 1 in primates since flying foxes do not use their wings for making form and texture discriminations of objects. It is possible that this area arose with the modification of the distal forelimb for flight and is involved in making fine tactile discriminations regarding small changes in air pressure and velocity across the wing during flight.

6.10.7 Area 2

6.10.7.1 Functional Organization

The functional organization of area 2 has only been investigated in one species of nonhuman primate, the macaque monkey (e.g., Pons, T. P. *et al.*, 1985; Toda, T. and Taoka, M., 2001; 2002). In macaque monkeys, area 2 contains a complete representation of deep receptors of the contralateral body, and the gross mediolateral topography is much like that described for areas 3b and 1, although the somatotopic organization is not as precise. The representation of the hand and forelimb in area 2 is highly magnified, more so than in areas 3a, 3b, and 1 (Figure 10).

Studies of response properties of neurons in area 2 (e.g., Hyvärinen, J. and Poranen, A., 1978; Taoka, M. *et al.*, 1998; 2000; Iwamura, Y. *et al.*, 2002) report that neurons here respond well to stimulation of deep

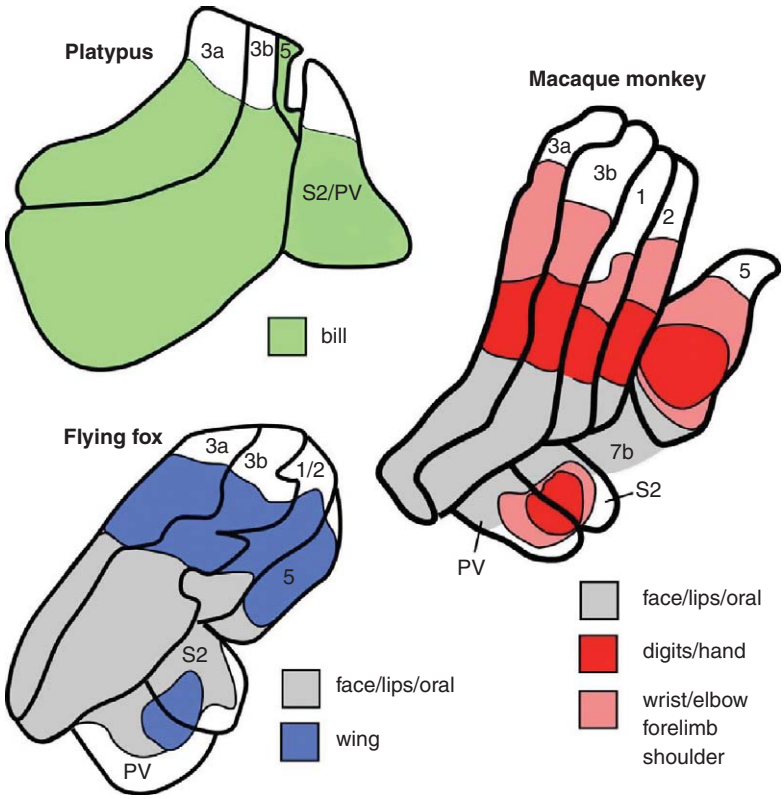

Figure 10 This figure demonstrates that parietal cortex obeys similar rules of construction regardless of which body part has been specialized. For example, the platypus has only three somatosensory areas and, we propose, a posterior parietal area (area 5). The three somatosensory areas are dominated by the representation of the bill, and area 5 exclusively represents the bill. In other groups, more cortical fields have been added between areas 3b and 5, such as areas 1 and 2 in macaque monkeys. These fields contain an enlarged representation of the hand and oral structures, as do 3b and 3a. Like the bill representation of area 5 in the platypus, area 5 in primates almost exclusively represents the hand. Even in species with a derived hand, such as the wing of the bat, similar principles of expansion and magnification are upheld.

receptors, although in some portions of area 2 neurons also responded to cutaneous stimulation (e.g., Pons, T. P. *et al.*, 1985; Ageranioti-Belanger, S. A. and Chapman, C. E., 1992), and may participate with areas 3b and 1 in texture discriminations (e.g., Salimi, I. *et al.*, 1999). Receptive fields for neurons in area 2 are relatively large (sometimes bilateral) when compared to areas 3b and 1 (e.g., Taoka, M. *et al.*, 2000; Iwamura, Y. *et al.*, 2002). In awake behaving monkeys, neurons in area 2 respond to both passive and active flexion of joints (Wolpaw, J., 1980; Gardner, E., 1988) and are facilitated or inhibited during grasping (Debowy, D. J. *et al.*, 2001). Furthermore, neuronal burst duration is correlated with arm movement duration (Burbaud, P. *et al.*, 1991), suggesting that area 2 directly participates in the online maintenance of movement. There is limited evidence for an area 2 in humans, and the organization and the subclass of receptors represented appears to be similar to that of macaque monkeys (e.g., Moore, C. *et al.*, 2000). Lesions in macaque monkeys that include area 2 affect the animal's ability to discriminate object shape, size, and curvature (Randolph, M. and Semmes, J., 1974; Carlson, M., 1981). Furthermore, the animal is unable to make discriminations that require active exploration with the hands (Schwartz, A., 1983).

Cortex immediately caudal to area 1 has been explored in a limited fashion in New World monkeys. Neurons in this region have been reported to be unresponsive to somatic stimulation, responsive only at the caudal border of area 1, or sometimes responsive to stimulation of deep receptors (Figure 11; e.g., Merzenich, M. M. *et al.*, 1978; Carlson, M. *et al.*, 1986; Huffman, K. J. and Krubitzer, L., 2001a). Thus, unlike macaque monkeys, it appears that New World monkeys do not possess an area 2. As noted above, cortex caudal to area 3b in nonprimate mammals contains

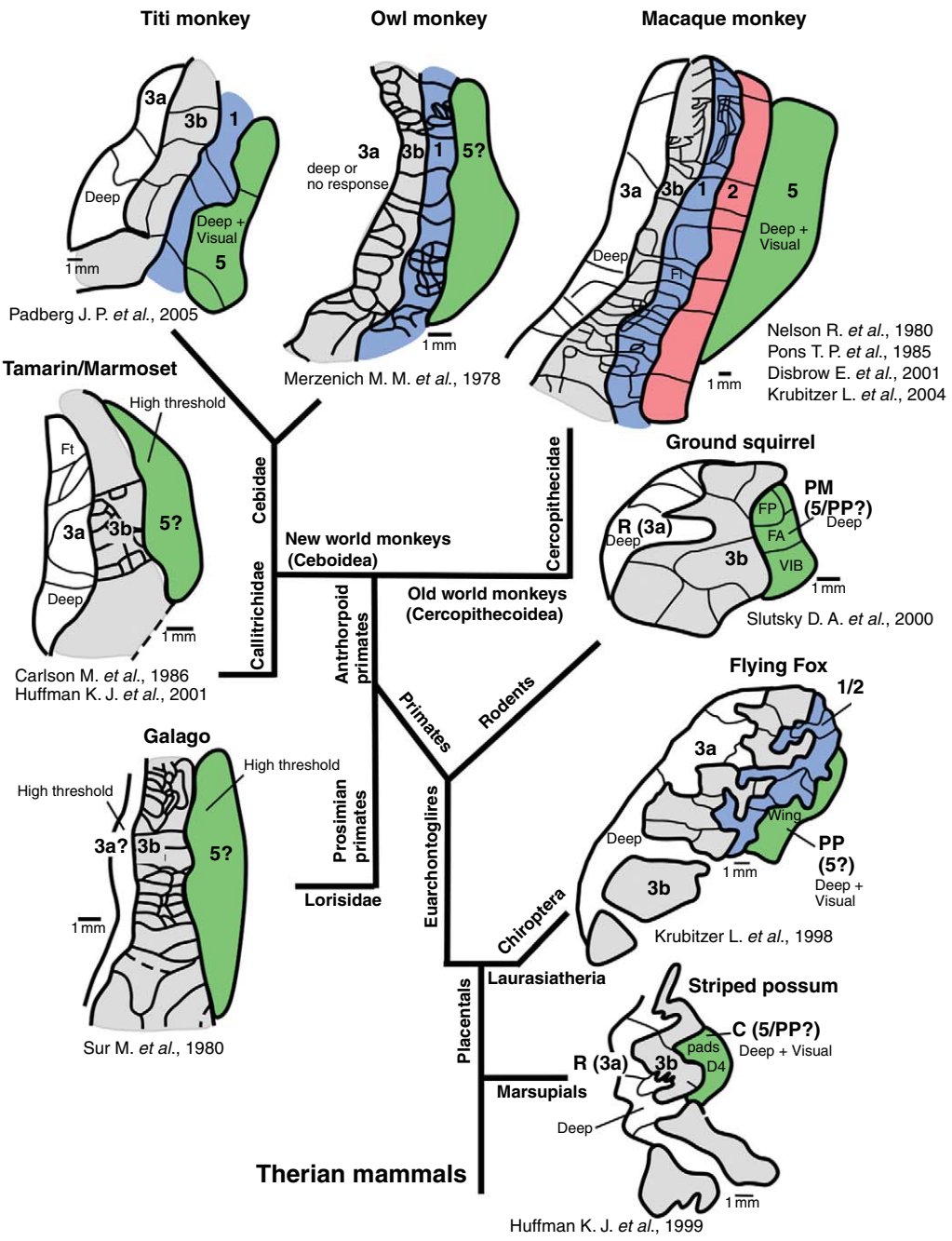

Figure 11 A simplified cladogram depicting the phylogenetic relationship of primates and other mammals and the organization of anterior and posterior parietal cortex in several species. Comparative data from these and other mammals indicate that early therian mammals possessed a primary somatosensory area (3b or S1, light gray), a rostral field (3a or R, white), and a caudal area (5 or PP, green). Some species, such as simian primates, have evolved a low-threshold cutaneous representation just caudal to 3b, termed area 1 (blue). Since area 1 has not been identified in other mammals, or even in prosimian primates, it is likely that area 1 evolved after the simian and prosimian divergence. Area 2 (orange) has only been identified in macaque monkeys. Comparisons across mammals indicate that areas 3a, 3b, and 5 are evolutionarily old fields and that new, unimodal somatosensory fields such as areas 1 and 2 evolved later in some lineages and are interspersed between existing fields (i.e., are not added hierarchically). We propose that areas 1 and 2 evolved with the modified morphology of the hand in anthropoid primates and that older, retained field, such as area 5, were modified both functionally and connectionally for sophisticated hand use. Phylogenetic relationships come from Murphy, W. J., Eizirik, E., O'Brein, S. J., Madsen, O., Scally, M., Douady, C. J., Teeling, E., Ryder, O. A., Stanhope, M. J., de Jong, W. W., and Springer, M. S. 2001. Resolution of the early placental mammal radiation using Bayesian phylogenetics. Science 294, 2348–2351 and Eisenberg, J. H. 1981. The mammalian radiations: an analysis of trends in evolution, adaptation and behavior. Continuum. Cortical organization of different species depicted here is taken from studies listed below each species.

neurons that respond to stimulation of deep receptors. While these regions could correspond to area 2 in these mammals and New World monkeys, it is also possible that they correspond to area 5. We suggest that this is the case based on several lines of evidence including the organization and magnification of representations in these fields, location relative to visual and somatosensory cortex, and the presence of neurons that also respond to stimulation of other sensory modalities (see below) but are often hard to drive under any given anesthetic condition (unlike neurons in area 2).

6.10.7.2 Connections

Studies of connections of area 2 in which injections were placed under electrophysiological guidance indicate that this field is connected with other somatosensory cortical areas such as 3b, 1, 3a, and S2, as well as with M1 and area 5 (Pons, T. P. and Kaas, J. H., 1985). Earlier studies of the connections of architectonically defined area 2 with local parietal cortical areas support these later studies (e.g., Jones, E. G. *et al.*, 1978). Area 2 receives thalamic input predominantly from VPs (VPLc of Friedman, D. and Jones, E., 1981) and the anterior pulvinar (Pa; Pons, T.P. and Kaas, J. H., 1985). The callosal connections of area 2 have only been described collectively with other anterior parietal fields. Unlike areas 3b and 1, the hand representation of area 2 does have callosal connections (see Manzoni, T., 1997). Taken together, all data indicate that area 2 is a proprioceptive area that is involved in the discrimination of shape and in the online maintenance of hand and forelimb movements necessary for reaching and grasping and is only present in Old World monkeys and humans (and likely great apes).

6.10.8 Posterior Parietal Area 5 in Primates

6.10.8.1 Functional Organization

Area 5 was first described as a very large cortical field that occupied the entire rostral bank of the IPS and much of the caudal postcentral gyrus (e.g., Brodmann, K., 1909). However, modern electrophysiological and anatomical studies indicate that area 5 is much smaller and resides in the middle of the rostral bank of the IPS and folds around the sulcal crown to spread onto the adjacent postcentral gyrus (e.g., Pons, T. P. *et al.*, 1985; Iwamura, Y., 2000, for review). Most data pertaining to posterior parietal cortex, and to area 5 in particular, have been collected in macaque monkeys and recently in titi monkeys (Figure 11), with limited information available in humans (Culham, J. C. and Kanwisher, N. G., 2001). In all of these primates, area 5 is dominated by the representation of the hand and forelimb (Figure 10); neurons in area 5 have contralateral, ipsilateral, and bilateral receptive fields (particularly on the hand and forelimb), and most neurons respond to the stimulation of deep receptors of the skin and joints (e.g., Sakata, H. *et al.*, 1973; Mountcastle, V. B. *et al.*, 1975; Taoka, M. *et al.*, 2000; Iwamura, Y. *et al.*, 1994; 2002; Padberg, J. P. *et al.*, 2005; see Iwamura, Y., 2000, for review). Single unit studies in awake behaving macaque monkeys indicate that area 5 is involved in coordinating or programming intention of movement (Snyder, L. H. *et al.*, 1997; Debowy, D. J. *et al.*, 2001), in preshaping the hand before grasping an object (e.g., Debowy, D. J. *et al.*, 2001), and in generating body- or shoulder-centered, rather than eye-centered coordinates for reaching (Ferraina, S. and Bianchi, L., 1994; Lacquaniti, F. *et al.*, 1995; see Wise, S. P. *et al.*, 1997, for review). Furthermore, area 5 appears to be involved in the kinematics (e.g., spatiotemporal coordinates) rather than the kinetics (e.g., load and force of muscle) of reaching (see Kalaska, J. F., 1996; Wise, S. P. *et al.*, 1997, for review). The proposition that area 5 is involved in the kinematics of movement is in part supported by studies which demonstrate that a large proportion of neurons are active prior to an arm movement, that these neurons are direction-selective for arm movement, and that activity is dependent on the behavioral context in which the movement will occur (Burbaud, P. *et al.*, 1991).

Recent studies indicate that neurons in area 5 are involved in generating an internal representation of the body that can be modified by experience (Graziano, M. S. A. *et al.*, 2000). For example, neurons in area 5 can change their receptive field size and location when a limb used to perform a task is artificially extended with a tool (Iriki, A. *et al.*, 1996). Furthermore, Iriki A. and colleagues (2001) demonstrated that monkeys can be trained to recognize an image in a video monitor as part of their own body and that neurons in the IPS, in the location of what we consider to be area 5, change their visual receptive fields to incorporate changes in hand location and size, as viewed on the video monitor, into an internal frame of reference. In these studies, the position and the size of the visual receptive field was

modified with respect to modifications of the image in the monitor (e.g., expansions, contractions, and displacement of the hand). These investigators speculate that a symbolic representation of the self in humans has a precursor in monkeys that is latent and can be activated with training. We would argue that these monkeys always possess an internal frame of reference, much like that in humans, and that the experimenters devised a clever and objective way in which to evaluate this internal representation in a nonhuman mammal. We would further argue that such a representation is a critical characteristic of most living things and constitutes a sense of self. Thus, this sense of self is present in all mammals and the region of cortex we propose to be involved in generating this behavioral characteristic (area 5 or PP) is homologous across groups of mammals.

Our recent studies in New World titi monkeys, as well as preliminary findings in macaque monkeys, indicate that many neurons in area 5 can be driven by visual stimulation (Disbrow, E. A. *et al.*, 2001; Padberg, J. P. *et al.*, 2005; Figure 11). While responsiveness to visual stimulation has not been described in previous studies for area 5, the studies often did not test whether or not neurons would be responsive to visual stimulation. This issue of whether neurons in area 5 respond to visual stimulation is important for our discussion of the evolution of posterior parietal cortex in mammals, since as noted above, cortex immediately caudal to 3b in many primitive mammals contains neurons that respond to both somatic and visual stimulation.

There are several studies in which lesions, that include area 5, were made in posterior parietal cortex in monkeys. For example, studies in which unilateral lesions included areas 5, MIP, and 7b demonstrated that animals had deficits in coordinating arm velocity with hand velocity, that the postural relationship between the arm and wrist was disrupted, and that there were disruptions in coordinating the hand in shoulder-centered space (Rushworth, M. F. S. *et al.*, 1997). However, these lesions did not affect the range or velocity of movements or the hand's trajectory. In a related investigation in which areas 5, 7b, and MIP (which may have also included V6) were bilaterally ablated, the monkey had deficits in reaching to the same target under different starting positions (Rushworth, M. F. S. *et al.*, 1998). Finally, a study in green monkeys in which bilateral ablations were made to area V6A (but may have incorporated portions of area 5) demonstrated that monkeys showed a reluctance to move and had deficits in reaching, grasping, and wrist orientation (Battaglini, P. P. *et al.*, 2002). While previous work on the effects of posterior parietal lesions on behavior are difficult to interpret because the size of the lesion was so large (e.g., Ettlinger, G. and Kalsbeck, J. E., 1962; Hartje, W and Ettlinger, G., 1973; Brown, J. V. *et al.*, 1983), they do indicate that lesions to posterior parietal cortex result in nonvisually guided reaching deficits but spare roughness discrimination abilities (Brown, J. V. *et al.*, 1983; Murray, E. A. and Mishkin, M., 1984).

There are a number of studies in humans on the deficits that occur with insults to posterior parietal cortex. These studies indicate that the most severe deficit, termed spatial hemineglect, is in coding spatial location of objects within a particular frame of reference (see Robertson, L. C. and Rafal, R., 2000; Behrmann, M., 1999, for review). While the data suggest that there are several egocentric frames of reference, including that of the forelimb or shoulder, there are little data on areas of posterior parietal cortex that contribute to these frames of reference. Furthermore, in these studies, the lesions are extremely large and encompass a number of cortical areas, and it is difficult to interpret which area is associated with which aspect of the deficit.

6.10.8.2 Connections

There are only a few studies of connections of area 5 in the macaque monkey, and those that exist are limited in scope. For example, only one study used electrophysiological guidance to place injections in area 5, and in this study, only one injection in one animal was performed, and the injection spread into area 2 (Pons, T. P. and Kaas, J. H., 1986). Furthermore, only local connections, or connections in neighboring fields, were examined. This previous investigation demonstrated connections with areas 1, 7b, S2, M1, and premotor cortex, which is a subset of the connections we describe for area 5 in titi monkeys (Padberg, J. P. *et al.*, 2005). Early studies of connections of architectonically defined area 5 to local parietal cortical areas support these recent findings in macaques (e.g., Jones, E. G. and Powell, T. P. S., 1969b; Jones, E. G. *et al.*, 1978; Pandya, D. N. and Seltzer, B., 1982). In titi monkeys, area 5 connections are widespread compared to anterior parietal fields, and some of the strongest connections of area 5 are with motor and premotor cortex, the supplementary motor area, S2, PV, extrastriate visual areas, 7b, and cingulate cortex (Figure 6; Padberg, J. P. *et al.*, 2005). Studies of vestibular processing in human and

nonhuman primates indicate that cortex at the juncture of areas 5 and 7b projects to vestibular brainstem nuclei, contains neurons that respond to optokinetic and vestibular stimulation, and is interconnected with other areas of the neocortex that process vestibular information (Akbarian, S. *et al.*, 1988; Guldin, W. O. *et al.*, 1992; Akbarian, S. *et al.*, 1993; 1994; Brandt, T. and Dieterich, M., 1999; Lobel, E. *et al.*, 1999; see Guldin, W. and Grüsser, O.-J., 1998, for review).

Most studies that examine callosal connectivity have studied total patterns of connections of large regions of cortex (e.g., Karol, E. A. and Pandya, D. N., 1971; Killackey, H. P. *et al.*, 1983), or connections of several fields grouped together such as 3a, 3b, 1, 2, and 5 collectively (e.g., Jones, E. G. and Powell, T. P. S., 1969a; Boyd, E. H. *et al.*, 1971; Jones, E. G. *et al.*, 1975; Jones, E. G. *et al.*, 1979; Shanks, M. F. *et al.*, 1985a). A consistent observation is that area 5 receives callosal inputs throughout the field (i.e., including the hand representation). There is one study in which the connections of cortex in the location of area 5 were examined, although the location of the injection site was not verified electrophysiologically (Caminiti, R. and Sbriccoli, A., 1985). In this study in macaque monkeys, label in the hemisphere contralateral to that injected was observed throughout area 5, the supplementary motor area, 7b, and on the dorsal bank of the lateral sulcus (in the S2/PV region). Our recent studies in titi monkeys indicate that the hand representation of area 5 has dense callosal connections with the contralateral area 5 in the expected location of the hand representation (Padberg, J. P. *et al.*, 2005). Area 5 in titi monkeys is also connected with areas 7b/AIP, S2/PV, motor, premotor, and cingulate cortex, a finding similar to that of Caminiti R. and Sbriccoli A. (1985). Thus, area 5 is one of the few somatosensory cortical areas involved in integrating inputs between the hands and in the interhemispheric transfer of information necessary for limb and hand coordination.

This latter notion is supported by studies of the behavioral consequences of lesions to the posterior portions of the corpus callosum through which axons from posterior parietal cortex travel (Seltzer, B. and Pandya, D. N., 1983). For example, after lesions to the posterior portion of the corpus callosum, monkeys have deficits in intermanual transfer of information about shape, roughness, or size of an object (Manzoni, T. *et al.*, 1984; Hunter, M. *et al.*, 1976; Myers, R. E. and Ebner, F. F., 1976). However, if animals were allowed to view the manual task to be transferred, thus supplying visual input regarding the task to both hemispheres, there was no noticeable deficit in information transfer across hemispheres (Kohn, B. and Meyers, R. E., 1969). Studies of tactile and tactuomotor transfer in humans who have undergone complete section of the corpus callosum or partial sections of the posterior portion of the corpus callosum indicate a number of abnormalities associated with transferring manual information regarding one hand to the opposite hemisphere. For example, complete section of the corpus callosum (Geffen, G. *et al.*, 1985) or a section in the portion of the callosum through which axons connecting the posterior parietal cortex of each hemisphere travel (Geffen, G. *et al.*, 1985; Risse, G. L. *et al.*, 1989), result in an inability to perform cross-localization, intermanual tasks (Geffen, G. *et al.*, 1985; Lassonde, M. *et al.*, 1986; Risse, G. L. *et al.*, 1989). Other studies demonstrate that with sections of the posterior corpus callosum, individuals cannot perform posture matching tasks (kinesthesis) in which they are required to match the position of one forelimb and hand with the opposite forelimb and hand in the absence of visual guidance (Risse, G. L. *et al.*, 1989). Finally, humans with sections of the corpus callosum performed poorly on the transfer of information regarding object shape, and the magnitude of the effect was dependent on the difficulty of the task (Lassonde, M. *et al.*, 1986). The studies described above in both human and nonhuman primates indicate that the connections between the posterior parietal cortex of each hemisphere, including area 5, transfer crucial information necessary for intermanual tactile learning and coordination of the hands.

Taken together, electrophysiological, connection, and lesion studies in nonhuman primates indicate that area 5 is involved in generating an egocentric, shoulder-centered frame of reference necessary for object exploration with the hands. Related abilities such as kinesthetic-visual matching, which may require an understanding of both object permanence and body part objectification, are proposed to be generated by regions in posterior parietal cortex (possibly area 5) in humans as well (see Mitchell, R. W., 2005, for review). This field also is involved in coordinating both hands to accomplish visually guided and perhaps nonvisually guided tasks and for interhemispheric transfer of information between the hands. While area 5 alone may not be responsible for generating an internal representation of the self, the activity of neurons in area 5 is coincident with tasks that require the animal to have such an internal representation, and receptive fields for neurons in

area 5 are modified in a manner consistent with alterations in the internal frame of reference.

6.10.9 Is Area 5 Homologous Across Mammals?

Throughout the text we intimated that cortex caudal to area 3b or S1 in nonprimate mammals is homologous to area 5. Although traditionally cortex immediately caudal to 3b is considered to be area 1 in nonprimate mammals such as cats, the predominant evidence for this traditional view is that this presumptive area is immediately caudal to area 3b. Furthermore, there is a tendency to make the cat somatosensory system both homologous and analogous to the primate somatosensory system, despite the fact that cats have a derived forepaw that is not used in a fashion analogous to that of the hand of primates. Indeed, Johnson J. I. (1990) states in his comparative analysis of mammal somatosensory cortex:

> Doubtless due to the great number of investigations rather than the specializations of the species, no less than five distinct somatic sensory areas have been identified and formally numbered in cat neocortex. (p. 399)

It should be noted that in a number of species in which cortex caudal to area 3b has been mapped, this cortex is rostrally adjacent to V2 (which would make it V3 if one were to assume homology based solely on relative location; Figure 9). As noted above, cortex immediately caudal to 3b, and immediately rostral to V1 or V2, has been explored using electrophysiological recording techniques in a variety of mammals and has been termed C, PP, PM, or SC. Like area 5 in primates, there is an extreme magnification of particular body parts, such that a complete representation of the body surface is often not present (Figures 10 and 11). For example, in murine rodents, this cortex is dominated by the representation of the vibrissae and in squirrels by the representation of the forepaw. In marsupials such as the striped possum, with its specialized fourth digit, this cortex represents only D4. Also like area 5 and unlike areas 1 and 2, neurons in this cortex often respond to visual stimulation as well as to stimulation of deep receptors. Species such as the flying fox have a cortical field immediately caudal to 3b in which neurons respond to cutaneous and deep stimulation, termed area 1/2 (see above). Just caudal to this region, a cortical field in which neurons respond to the stimulation of deep receptors as well as to visual stimulation has been described and termed the posterior parietal cortex or PP (Krubitzer, L. A. and Calford, M. B., 1992). While studies of connections of this caudal region of cortex in a variety of mammals would allow us to more accurately infer homology, we believe that most evidence supports the hypothesis that this field (termed C, SC, PM, and PP) is more like area 5 in primates than like area 1 or 2.

6.10.10 The Evolution of Anterior and Posterior Parietal Cortex

All mammals examined have a primary somatosensory area, S1 or 3b, in which the organization clearly reflects specializations of peripheral morphology, innervation density of peripheral receptors, and use. Furthermore, there appears to be a basic pattern of interconnections with several cortical and subcortical areas, suggesting that there is a network that has been inherited from a common ancestor but modified in different lineages with the evolution of peripheral morphology, as well as with the addition of new cortical fields and thalamic nuclei to the network. (Figures 6 and 8). While one would like to speculate as to the function of S1, most single unit recording studies in awake behaving animals and/or lesions of S1 have been done in primates, namely, macaque monkeys. Thus, these data must be interpreted with caution when discussing other species since homologous fields need not be analogous. In primates, area 3b appears to be involved in texture and form discrimination, and such discriminations are made with the glabrous hands. Although the representation of the oral structures in area 3b of primates is greatly magnified, suggesting some behavioral specialization related to the mouth, most studies only examine response to stimulation of the hand, or the activity of neurons in area 3b during discriminations made with the hand. If S1 serves as a general-purpose processor of cutaneous inputs necessary for fine discriminations using a morphologically distinct and specialized structure for a particular animal, then one would expect different magnifications of different body parts for different animals. One would also expect that the greatest variability within a species would be for the specialized body part that is used extensively, such as the hand (e.g., Merzenich, M. M. *et al.*, 1987) and lips (Cusick, C. G. *et al.*, 1986) of

primates, versus a less actively used body part such as the trunk, which appears to be the case.

Like area 3b, area 3a appears to be part of a common plan of cortical organization in all mammals (Figure 11). Area 3a is a proprioceptive area involved in integrating somatic and vestibular inputs (at least in primates) with the motor system to generate specialized behavior that allows the animal to maximally interface receptor-dense morphological structures (e.g., hand, nose, and bill) with an external object or animal to be explored. Such a sensorimotor interface likely contributes to an enlarged representation of a specialized peripheral structure not only in area 3a, but also in all anterior parietal fields. While the body part in question may be different for different animals, the same rules of modification are implemented in all mammals.

The presence of an area 1 or a rudimentary area 1 in several New World primates and macaque monkeys, and what appears to be the absence of area 1 in marmosets, tamarins, prosimian galagos, as well as other mammals, indicates that this cortical field arose later in primate evolution (Figure 11). We believe that the most parsimonious explanation for the observations made about anterior parietal cortex in a variety of primates is that in early primates, areas 3b and 3a were present. A rudimentary area 1 arose after the simian and prosimian divergence, and this was lost or greatly reduced in some lineages (e.g., Callitricidae), retained in a primitive form in some lineages (e.g., titi monkeys), or became well developed in some lineages (e.g., squirrel monkeys and macaque monkeys), possibly with the evolution of the hand and consequent tactile abilities associated with hand use. It should be noted that the two species of New World monkey (tamarins and marmosets) that do not possess an area 1 have a modified hand with claws used to a large extent for climbing, and to a lesser extent for tactile discrimination.

The functional organization of area 2 has only been investigated in one species of nonhuman primates, the macaque monkey (Pons, T. P. *et al.*, 1985). While cortex immediately caudal to area 1 has been explored in New World monkeys and prosimian galagos, neurons in this region have been reported to be unresponsive to somatic stimulation, responsive only at the caudal border of area 1, or sometimes responsive to the stimulation of deep receptors, features generally associated with area 5 in macaque monkeys. Thus, if one relies on electrophysiological mapping data, it appears that New World monkeys do not possess an area 2 (e.g., Padberg, J. P. *et al.*, 2005; Figure 11). It is tempting to postulate that area 2 arose or coevolved with the emergence of an opposable thumb and is related to the behaviors associated with using a variety of grips for tactile exploration and identification.

The presence of an area 5 in both New World and Old World monkeys, and a rudimentary form of area 5 (posterior parietal cortex) in most mammals studied, suggests that this posterior parietal field arose early in evolution and has been retained in most or all mammals (Figure 11). While area 5 may be a homologous cortical area in all mammals, the addition of new areas, such as 1 and 2, and new connections likely promotes new functions of this cortical field in primates (Figures 6 and 8). For example, PM in squirrels and PP in flying foxes may be homologous to area 5 in primates, but not strictly analogous. Much like the magnification of behaviorally relevant body parts in area 3b, in area 5 these representations and associated functions are magnified to the extreme in particular lineages. An important point of these observations in primate and nonprimate mammals is that cortical fields are not added in a functional hierarchy in evolution but rather are interspersed between existing fields. Indeed, we believe that the data indicate that areas 3a and 3b and 5 are evolutionarily old fields and that areas 1 and 2 are recent primate phenomenon, likely associated with sophisticated hand use.

With respect to the ideas put forward in the beginning of this chapter regarding the evolution of association cortex, we propose a modified scenario based on data in a variety of other mammals. In primates, unimodal somatosensory cortex has expanded with the addition of areas 1 and 2. Posterior parietal area 5 in primates, although homologous to area 5 in other mammals, has undergone a number of changes including a magnification of the hand and forelimb representation, the preponderance of neurons active under different reaching and grasping paradigms, and the broad distribution of ipsilateral and contralateral connections of the hand and limb representation with proprioceptive, limbic, and motor cortex (Figure 6). All of these features are coincident with the evolution of the hand and opposable thumb in a number of primates, as well as with a larger repertoire of grips and manual and bimanual hand configurations (Napier, J., 1960; 1962; Welles, J. F., 1976). A reasonable hypothesis is that anterior parietal cortex in primates has expanded as a result of sophisticated hand use, which distinguishes primates, and humans in particular, from other

mammals. An evolutionary old cortical area, area 5, has been modified due to the addition of these new anterior parietal fields and the evolution of highly derived manual behavior. Thus, modification of homologous cortical fields (area 5), and the addition of new unimodal cortical fields (e.g., areas 1 and 2) devoted to hand use, is one of the hallmarks of human brain evolution.

The evolution of sophisticated, visually guided, hand use and the addition of anterior parietal fields and the elaboration of posterior parietal cortical areas associated with this behavior may ultimately have led to the emergence of a more refined and species-specific internal representation of self, and an increased number of permutations of how this internal representation can interact with objects in extrapersonal space via the hands. It should be noted that this species-specific internal representation is not a static, enigmatic property that emerged in anthropoid primates alone but is a dynamic sensorimotor loop that all mammals possess in a derived form based on their morphological distinctions and distribution of sensory receptors. Studies of connections as well as electrophysiological recording data indicate that the motor system is a critical component for distinguishing self from nonself, an attribute traditionally delegated solely to association cortex. It follows then that any discussion of an internal representation of self and how an individual distinguishes itself from nonself should incorporate the motor system in this more than human phenomenon.

Acknowledgements

This work was supported by an NINDS grant (R01-NS035103-11) and McDonnell Foundation grant to Leah Krubitzer.

References

Ageranioti-Belanger, S. A. and Chapman, C. E. 1992. Discharge properties of neurones in the hand area of primary somatosensory cortex in monkeys in relation to the performance of an active tactile discrimination task. II. Area 2 as compared to areas 3b and 1. Exp. Brain Res. 91, 207–228.

Akbarian, S., Berndl, K., Grusser, O.-J., Guldin, W., Pause, M., and Schreiter, U. 1988. Responses of single neurons in the parietoinsular vestibular cortex of primates. Ann. N. Y. Acad. Sci. 545, 187–202.

Akbarian, S., Grusser, O. J., and Guldin, W. O. 1992. Thalamic connections of the vestibular cortical fields in the squirrel monkeys (*Saimiri sciureus*). J. Comp. Neurol. 326, 423–441.

Akbarian, S., Grusser, O. J., and Guldin, W. O. 1993. Corticofugal projections to the vestibular nuclei in squirrel monkeys: further evidence of multiple cortical vestibular fields. J. Comp. Neurol. 332, 89–104.

Akbarian, S., Grusser, O.-J., and Guldin, W. 1994. Corticofugal connections between the cerebral cortex and brainstem vestibular nuclei in the macaque monkey. J. Comp. Neurol. 339, 421–437.

Akers, R. M. and Killackey, H. P. 1978. Organization of corticocortical connections in the parietal cortex of the rat. J. Comp. Neurol. 181, 513–538.

Allman, J. M. and Kaas, J. H. 1971. A representation of the visual field in the caudal third of the middle temporal gyrus of the owl monkey (*Aotus trivirgatus*). Brain Res. 31, 85–105.

Allman, J. M. and Kaas, J. H. 1974. A crescent-shaped cortical visual area surrounding the middle temporal area (MT) in the owl monkey (*Aotus trivirgatus*). Brain Res. 81, 199–213.

Allman, J. M. and Kaas, J. H. 1975. The dorsomedial cortical visual area: a third tier area in the occipital lobe of the owl monkey (*Aotus trivirgatus*). Brain Res. 100, 473–487.

Allman, J. H. and Kaas, J. H. 1976. Representation of the visual field on the medial wall of the occipital-parietal cortex in the owl monkey. Science 191, 572–576.

Alloway, K. D. and Burton, H. 1985. Homotypical ipsilateral cortical projections between somatosensory areas I and II in the cat. Neuroscience 14, 15–35.

Andersen, R. A. and Buneo, C. A. 2002. Intentional maps in posterior parietal cortex. Annu. Rev. Neurosci. 25, 189–220.

Andersen, R. A., Snyder, L. H., Bradley, D. C., and Xing, J. 1997. Multimodal representation of space in the posterior parietal cortex and its use in planning movements. Annu. Rev. Neurosci. 20, 303–330.

Avendano, C., Isla, A. J., and Rausell, E. 1992. Area 3a in the cat. II. Projections to the motor cortex and their relations to other corticocortical connections. J. Comp. Neurol. 321, 373–386.

Barbaresi, P., Fabri, M., Conti, F., and Manzoni, T. 1987. D-[^{3}H]Aspartate retrograde labelling of callosal and association neurones of somatosensory areas I and II of cats. J. Comp. Neurol. 263, 159–178.

Battaglini, P. P., Muzur, A., Galletti, C., Skrap, M., Brovelli, A., and Fattori, P. 2002. Effects of lesions in area V65 in monkeys. Exp. Brain Res. 144, 419–422.

Beck, P. D., Pospichal, M. W., and Kaas, J. H. 1996. Topography, architecture, and connections of somatosensory cortex in opossums: evidence for five somatosensory areas. J. Comp. Neurol. 366, 109–133.

Behrmann, M. 2000. Spatial Reference Frames and Hemispatial Neglect. In: The New Cognitive Neurosciences (*ed*. M. Gazzaniga), pp. 651–666. MIT Press.

Blankenburg, F., Ruben, J., Meyer, R., Schwiemann, J., and Villringer, A. 2003. Evidence for a rostral-to-caudal somatotopic organization in human primary somatosensory cortex with mirror-reversal in areas 3b and 1. Cereb. Cortex 13, 987–993.

Boyd, E. H., Pandya, D. N., and Bignall, K. E. 1971. Homotopic and nonhomotopic interhemispheric cortical projections in the squirrel monkey. Exp. Neurol. 32, 256–274.

Brandt, T. and Dieterich, M. 1999. The vestibular cortex, its locations, functions, and disorders. Ann. N. Y. Acad. Sci. 871, 293–312.

Brodmann, K. 1909. Vergleichende Lokalisationsiehre der Grosshirnrinde in ihren Prinzipien Dargestellt auf Grund des Zellenbaues. Barth.

Brown, J. V., Ettlinger, G., and Garcha, H. S. 1983. Visually guided reaching and tactile discrimination in the monkey: the effects of removals of parietal cortex soon after birth. Brain Res. 267, 67–79.

Burbaud, P., Doegle, C., Gross, C., and Bioulac, B. 1991. A quantitative study of neuronal discharge in areas 5, 2 and 4 of the monkey during fast arm movements. J. Neurophysiol. 66, 429–443.

Burton, H. and Fabri, M. 1995. Ipsilateral intracortical connections of physiologically defined cutaneous representations in areas 3b and 1 of macaque monkeys: projections in the vicinity of the central sulcus. J. Comp. Neurol. 355, 508–538.

Burton, H., Fabri, M., and Alloway, K. 1995. Cortical areas within the lateral sulcus connected to cutaneous representations in areas 3b and 1: a revised interpretation of the second somatosensory area in macaque monkeys. J. Comp. Neurol. 355, 539–562.

Calford, M. B., Graydon, M. L., Huerta, M. F., Kaas, J. H., and Pettigrew, J. D. 1985. A variant of the mammalian somatotopic map in the bat. Nature 313, 477–479.

Caminiti, R. and Sbriccoli, A. 1985. The callosal system of the superior parietal lobule in the monkey. J. Comp. Neurol. 2237, 85–99.

Caminiti, R., Innocenti, G. M., and Manzoni, T. 1979. The anatomical substrate of callosal messages from SI and SII in the cat. Brain Res. 35, 295–314.

Carlson, M. 1981. Characteristics of sensory deficits following lesions of Brodmann's areas 1 and 2 in the postcentral gyrus of *Macaca mulatta*. Brain Res. 204, 424–430.

Carlson, N. R. 1998. Physiology of Behavior, 6th edn. Allyn and Bacon.

Carlson, M., Huerta, M. F., Cusick, C. G., and Kaas, J. H. 1986. Studies on the evolution of multiple somatosensory representations in primates: the organization of anterior parietal cortex in the New World Callitrichid, *Saguinus*. J. Comp. Neurol. 246, 409–426.

Catania, K. C. and Kaas, J. H. 1997. Somatosensory fovea in the star-nosed mole: behavioral use of the star in relation to innervation patterns and cortical representation. J. Comp. Neurol. 387, 215–233.

Catania, K. C., Northcutt, R. G., Kaas, J. H., and Beck, P. D. 1993. Nose stars and brain stripes. Nature 364, 493.

Chapin, J. K. and Lin, C.-S. 1984. Mapping the body representation in the SI cortex of anesthetized and awake rats. J. Comp. Neurol. 229, 199–213.

Chapin, J. K., Sadeq, M., and Guise, J. L. U. 1987. Corticocortical connections within the primary somatosensory cortex of the rat. J. Comp. Neurol. 263, 326–346.

Chapman, C. E. and Ageranioti-Bélanger, S. 1991. Discharge properties of neurones in the hand area of primary somatosensory cortex in monkeys in relation to the performance of an active tactile discrimination task. I. Areas 3b and 1. Exp. Brain Res. 87, 319–339.

Chen, L., Friedman, R., Ramsden, B., LaMotte, R., and Roe, A. 2001. Fine-scale organization of S1 (area 3b) in the squirrel monkey revealed with intrinsic optical imaging. J. Neurophysiol. 86, 3011–3029.

Conti, F., Fabri, M., and Manzoni, T. 1986. Bilateral receptive fields and callosal connectivity of the body midline representation in the first somatosensory area of primates. Somatosens. Res. 3, 273–289.

Coq, J. O., Qi, H., Collins, C. E., and Kaas, J. H. 2004. Anatomical and functional organization of somatosensory areas of the lateral fissure of the new world titi monkey (*Callicebus moloch*). J. Comp. Neurol. 476, 363–387.

Culham, J. C. and Kanwisher, N. G. 2001. Neuroimaging of cognitive functions in human parietal cortex. Curr. Opin. Neurobiol. 11, 157–163.

Cusick, C. G. and Gould, H. J. I. 1990. Connections between area 3b of the somatosensory cortex and subdivisions of the ventroposterior nuclear complex and the anterior pulvinar nucleus in squirrel monkeys. J. Comp. Neurol. 292, 83–102.

Cusick, C. G., MacAvoy, M. G., and Kaas, J. H. 1985. Interhemispheric connections of cortical sensory areas in tree shrews. J. Comp. Neurol. 235, 111–128.

Cusick, C. G., Wall, J., and Kaas, J. 1986. Representations of the face, teeth and oral cavity in areas 3b and 1 of somatosensory cortex in squirrel monkeys. Brain Res. 370, 359–364.

Darian-Smith, C., Darian-Smith, I., Burman, K., and Ratcliffe, N. 1993. Ipsilateral cortical projections to areas 3a, 3b, and 4 in the macaque monkey. J. Comp. Neurol. 335, 200–213.

Darian-Smith, C., Darian-Smith, I., and Cheema, S. S. 1990. Thalamic projections to sensorimotor cortex in the macaque monkey: use of multiple retrograde fluorescent tracers. J. Comp. Neurol. 299, 17–46.

Debowy, D. J., Ghosh, S., Ro, J. Y., and Gardner, E. P. 2001. Comparison on neuronal firing rates in somatosensory and posterior parietal cortex during prehension. Exp. Brain Res. 137, 269–291.

Diamond, M., Harris, J., and Petersen, R. 2002. Sensory Learning and the Brain's Body Map. In: The Somatosensory System, Deciphering the Brain's Own Body Image (*ed*. R. Nelson), pp. 183–195. CRC Press.

Dicarlo, J., Johnson, J. K., and Hsiao, S. 1998. Structure of receptive fields in area 3b of primary somatosensory cortex in the alert monkey. J. Neurosci. 18, 2626–2645.

Disbrow, E., Litinas, E., Recanzone, G., Padberg, J. P., and Krubitzer, L. A. 2003. Cortical connections of the parietal central area and the second somatosensory area in macaque monkeys. J. Comp. Neurol. 462, 382–399.

Disbrow, E., Litinas, E., Recanzone, G., Slutsky, D., and Krubitzer, L. A. 2002. Thalamocortical connections of the parietal ventral area (PV) and the second somatosensory area (S2) in macaque monkeys. Thalamus Relat. Syst. 1, 289–302.

Disbrow, E. A., Murray, S. O., Roberts, T. P., Litinas, E. D., and Krubitzer, L. A. 2001. Sensory integration in human posterior parietal area 5. Soc. Neurosci. Abst. 27, 511–526.

Ebner, F. F. and Myers, R. E. 1965. Distribution of corpus callosum and anterior commissure in cat and raccoon. J Comp. Neurol. 124, 353–356.

Eisenberg, J. H. 1981. The mammalian radiations: an analysis of trends in evolution, adaptation and behavior. Continuum.

Elston, G. N. and Manger, P. R. 1999. The organization and connections of somatosensory cortex in the brush-tailed possum (*Trichosurus vulpecula*): evidence for multiple, topographically organized and interconnected representations in an Australian marsupial. Somatosens. Mot. Res. 16, 312–337.

Ettlinger, G. and Kalsbeck, J. E. 1962. Changes in tactile discrimination in visual reaching after successive and simultaneous bilateral posterior parietal ablations in the monkey. J. Neurol. Neurosurg. Psychiatry 25, 256–268.

Fabri, M. and Burton, H. 1991. Topography of connections between primary somatosensory cortex and posterior complex in rat: a multiple fluorescent tracer study. Brain Res. 538, 351–357.

Feldman, S. H. and Johnson, J. I. 1988. Kinesthetic cortical area anterior to primary somatic sensory cortex in the raccoon (*Procyon lotor*). J. Comp. Neurol. 277, 80–95.

Felleman, D. J. and Van Essen, D. C. 1991. Distributed hierarchical processing in primate cerebral cortex. Cereb. Cortex 1, 1–47.

Felleman, D. J., Wall, J. T., Cusick, C. G., and Kaas, J. H. 1983. The representation of the body surface in S-I of cats. J. Neurosci. 3, 1648–1669.

Ferraina, S. and Bianchi, L. 1994. Posterior parietal cortex: functional properties of neurons in area 5 during an instructed-delay reaching task within different parts of space. Exp. Brain Res. 99, 175–178.

Fox, P. T., Burton, H., and Raichle, M. E. 1987. Mapping human somatosensory cortex with positron emission tomography. J. Neurosurg. 67, 34–43.

Friedman, D. and Jones, E. 1981. Thalamic input to areas 3a and 2 in monkeys. J. Neurophysiol. 45, 59–85.

Frost, S. B., Milliken, G. W., Plautz, E. J., Masterton, R. B., and Nudo, R. J. 2000. Somatosensory and motor representations in cerebral cortex of a primitive mammal (*Monodelphis domestica*): a window into the early evolution of sensorimotor cortex. J. Comp. Neurol. 421, 29–51.

Gardner, E. 1988. Somatosensory cortical mechanisms of feature detection in tactile and kinesthetic discrimination. Can. J. Physiol. Pharmacol. 66, 439–454.

Garraghty, P. E., Pons, T. P., Huerta, M. F., and Kaas, J. H. 1987. Somatotopic organization of the third somatosensory area (SIII) in cats. Somatosens. Res. 4, 333–357.

Geffen, G., Nilsson, J., and Quinn, K. 1985. The effects of lesions of the corpus callosum on finger localization. Neuropsychologia 23, 497–514.

Gould, H. J. I. and Kaas, J. H. 1981. The distribution of commissural terminations in somatosensory areas I and II of the grey squirrel. J. Comp. Neurol. 196, 489–504.

Gould, H. J., 3rd, Whitworth, R. H., Jr., and LeDoux, M. S. 1989. Thalamic and extrathalamic connections of the dysgranular unresponsive zone in the grey squirrel (*Sciurus carolinensis*). J. Comp. Neurol. 287, 38–63.

Graziano, M. S. A., Cooke, D. F., and Taylor, C. S. R. 2000. Coding the location of the arm by sight. Science 290, 1782–1786.

Guldin, W. and Grusser, O.-J. 1998. Is there a vestibular cortex? Trends Neurosci. 21, 254–259.

Guldin, W. O., Akbarian, S., and Grusser, O. J. 1992. Cortico-cortical connections and cytoarchitectonics of the primate vestibular cortex: a study in squirrel monkeys (*Saimiri sciureus*). J. Comp. Neurol. 326, 375–401.

Hackett, T. A., Stepniewska, I., and Kaas, J. H. 1998. Subdivisions of auditory cortex and ipsilateral cortical connections of the parabelt auditory cortex in macaque monkeys. J. Comp. Neurol. 394, 475–495.

Hartje, W. and Ettliner, G. 1973. Reaching in light and dark after unilateral posterior parietal ablations in the monkey. Cortex 9, 346–354.

Hassler, R. and Muhs-Clement, K. 1964. Architectonic construction of the sensomotor and parietal cortex in the cat. J. Hirnforsch. 20, 377–420.

Heath, C. J., Hore, J., and Philips, C. G. 1975. Inputs from low threshold muscle and cutaneous afferents of hand and forearm to areas 3a and 3b of baboon's cerebral cortex. J. Physiol. (Lond.) 257, 199–227.

Herron, P. and Johnson, J. I. 1987. Organization of intracortical and commissural connections in somatosensory cortical areas I and II in the raccoon. J. Comp. Neurol. 257, 359–371.

Hlushchuk, Y., Forss, N., and Hari, R. 2003. Distal-to-proximal representation of volar index finger in human area 3b. NeuroImage 21, 696–700.

Hore, J., Preston, J. B., and Cheney, P. D. 1976. Responses of cortical neurons (areas 3a and 4) to ramp stretch of hindlimb muscles in the baboon. J. Neurophysiol. 39, 484–500.

Huffman, K. J. and Krubitzer, L. 2001a. Area 3a: topographic organization and cortical connections in marmoset monkeys. Cereb. Cortex 11, 849–867.

Huffman, K. J. and Krubitzer, L. A. 2001b. Thalamo-cortical connections of areas 3a and M1 in marmoset monkeys. J. Comp. Neurol. 435, 291–310.

Huffman, K., Nelson, J., Clarey, J., and Krubitzer, L. 1999. The organization of somatosensory cortex in three species of *marsupials*, *Dasyurus hallucatus*, *Dactylopsila trivirgata*, and *Monodelphis domestica*: neural correlates of morphological specializations. J. Comp. Neurol. 403, 5–32.

Hunt, D. L., Slutsky, D. A., and Krubitzer, L. A. 2000. The organization of somatosensory cortex in the ferret. Soc. Neurosci. Abst. 26, 243.13.

Hunter, M., Maccabe, J. J., and Ettlinger, G. 1976. Intermanual transfer of tactile training in the monkey: the effects of bilateral parieto-prestriate ablations. Neuropsychologia 14, 385–389.

Hyvärinen, J. and Poranen, A. 1978. Receptive field integration and submodality convergence in the hand area of the post-central gyrus of the alert monkey. J. Physiol. 283, 539–556.

Imig, T. J., Ruggero, M. A., Kitzes, L. M., Javel, E., and Brugge, J. F. 1977. Organization of auditory cortex in the owl monkey (*Aotus trivirgatus*). J. Comp. Neurol. 171, 111–128.

Iriki, A., Tanaka, M., and Iwamura, Y. 1996. Coding of modified body schema during tool use by macaque postcentral neurons. NeuroReport 7, 2325–2330.

Iriki, A., Tanaka, M., Obayashi, S., and Iwamura, Y. 2001. Self-images in the video monitor coded by monkey intraparietal neurons. J. Neurosci. Res. 40, 163–173.

Iwamura, Y. 2000. Bilateral receptive field neurons and callosal connections in the somatosensory cortex. Philos. Trans. R. Soc. Lond. B Biol. Sci. 355, 267–273.

Iwamura, Y., Iriki, A., and Tanaka, M. 1994. Bilateral hand representation in the postcentral somatosensory cortex. Nature 369, 554–556.

Iwamura, Y., Tanaka, M., Iriki, A., Taoka, M., and Toda, T. 2002. Processing of tactile and kinesthetic signals from bilateral sides of the body in the postcentral gyrus of awake monkeys. Behav. Brain Res. 135, 185–190.

Jain, N., Qi, H.-X., Catania, K., and Kaas, J. 2001. Anatomic correlates of the face and oral cavity representations in the somatosensory cortical area 3b of monkeys. J. Comp. Neurol. 429, 455–468.

Jiang, W., Tremblay, F., and Chapman, C. E. 1997. Neuronal encoding of texture changes in the primary and the secondary somatosensory cortical areas of monkeys during passive texture discrimination. J. Neurophysiol. 77, 1656–1662.

Johnson, J. I. 1990. Comparative Development of Somatic Sensory Cortex. In: Cerebral Cortex (*eds*. E. G. Jones and A. Peters), pp. 335–449. Plenum.

Johnson, K. O. and Lamb, G. D. 1981. Neural mechanisms of spatial tactile discrimination: neural patterns evoked by Braille-like dot patterns in the monkey. J. Physiol. 310, 117–144.

Johnson, K. and Yoshioka, T. 2002. Neural Mechanisms of Tactile Form and Texture Perception. In: The Somatosensory System, Deciphering the Brain's Own Body Image (*ed*. R. Nelson), pp. 73–101. CRC Press.

Johnson, J. I., Ostapoff, E.-M., and Warach, S. 1982. The anterior border zones of primary somatic sensory (SI) neocortex and their relation to cerebral convolutions, shown by micromapping of peripheral projections to the region of the fourth forepaw digit representation in raccoons. Neuroscience 7, 915–936.

Jones, E. G. and Powell, T. P. S. 1969a. Connexions of the somatic sensory cortex of the rhesus monkey II contralateral cortical connexions. Brain 92, 717–730.

Jones, E. G. and Powell, T. P. S. 1969b. Connexions of the somatic sensory cortex of the rhesus monkey: I. Ipsilateral cortical connections. Brain 92, 477–502.

Jones, E. G., Burton, H., and Porter, R. 1975. Commissural and cortico-cortical ''columns'' in the somatic sensory cortex of primates. Science 190, 572–574.

Jones, E. G., Coulter, J. D., and Hendry, S. H. C. 1978. Intracortical connectivity of architectonic fields in the somatic sensory, motor and parietal cortex of monkeys. J Comp. Neurol. 181, 291–348.

Jones, E. G., Wise, S. P., and Coulter, J. C. 1979. Differential thalamic relationships of sensory-motor and parietal cortical fields in monkeys. J Comp. Neurol. 183, 833–882.

Juliano, S., Friedman, D., and Eslin, D. 1990. Corticocortical connections predict patches of stimulus-evoked metabolic activity in monkey somatosensory cortex. J. Comp. Neurol. 298, 23–39.

Kaas, J. H. 1982. The segregation of function in the nervous system: why do the sensory systems have so many subdivisions? Contrib. Sens. Physiol. 7, 201–240.

Kaas, J. H. 1983. What, if anything, is SI? Organization of first somatosensory area of cortex. Physiol. Rev. 63, 206–230.

Kaas, J. H. 1997. Topographic maps are fundamental to sensory processing. Brain Res. Bull. 44(2), 107–112.

Kaas, J. H. and Collins, C. E. 2004. The Resurrection of Multimodal Cortex in Primates: Connection Patterns that Integrate Modalities. In: Handbook of Mulitsensory Processing (*eds*. G. Calvert, C. Spence, and B. E. Stein), MIT Press. pp. 285–293.

Kaas, J. H. and Pons, T. P. 1988. The somatosensory system of primates. Comp. Primate Biol. 4, 421–468.

Kalaska, J. F. 1996. Parietal cortex area 5 and visuomotor behavior. Can. J. Physiol. Pharmacol. 74, 483–498.

Karol, E. A. and Pandya, D. N. 1971. The distribution of the corpus callosum in the rhesus monkey. Brain 94, 471–786.

Kenshalo, D., Iwata, K., Sholas, M., and Thomas, D. 2000. Response properties and organization of nociceptive neurons in area 1 of monkey primary somatosensory cortex. J. Neurophysiol. 84, 719–729.

Killackey, H. P., Gould, H. J. I., Cusick, C. G., Pons, T. P., and Kaas, J. H. 1983. The relation of corpus callosum connections to architectonic fields and body surface maps in sensory motor cortex of new and old world monkeys. J. Comp. Neurol. 219, 384–419.

Knight, R. T. and Grabowecky, M. 2000. Prefrontal Cortex, Time and Consciousness. In: The New Cognitive Neurosciences (*ed*. M. Gazzaniga), pp. 1319–1330. MIT Press.

Kohn, B. and Myers, R. E. 1969. Visual information and intermanual transfer of latch box problem solving in monkeys with commissures sectioned. Exp. Neurol. 23, 303–309.

Kolb, B., Buhrmann, K., McDonald, R., and Sutherland, R. J. 1994. Dissociation of the medial prefrontal, posterior parietal, and posterior temporal cortex for spatial navigation and recognition memory in the rat. Cereb. Cortex 4, 664–680.

Koralek, K. A., Olavarria, J., and Killackey, H. P. 1990. Areal and laminar organization of corticocortical projections in rat somatosensory cortex. J. Comp. Neurol. 299, 133–150.

Krause, R., Kurth, R., Ruben, J., Schwiemann, J., Villringer, K., Deuchert, M., Moosmann, M., Brandt, S., Wolf, K., Curio, G., and Villringer, A. 2001. Representational overlap of adjacent fingers in multiple areas of human primary somatosensory cortex depends on electrical stimulus intensity: an fMRI study. Brain Res. 899, 36–46.

Krubitzer, L. 1995. The organization of neocortex in mammals: are species differences really so different? Trends Neurosci. 18, 408–417.

Krubitzer, L. 1998. What can monotremes tell us about brain evolution? Philos. Trans. R. Soc. Lond. B Biol. Sci. 353, 1127–1146.

Krubitzer, L. A. and Calford, M. B. 1992. Five topographically organized fields in the somatosensory cortex of the flying fox: microelectrode maps, myeloarchitecture, and cortical modules. J. Comp. Neurol. 317, 1–30.

Krubitzer, L. and Kaas, J. 1987. Thalamic connections of three representations of the body surface in somatosensory cortex of grey squirrels. J. Comp. Neurol. 265, 549–580.

Krubitzer, L. A. and Kaas, J. H. 1990. The organization and connections of somatosensory cortex in marmosets. J. Neurosci. 10, 952–974.

Krubitzer, L. A. and Kaas, J. H. 1992. The somatosensory thalamus of monkeys: cortical connections and a redefinition of nuclei in marmosets. J. Comp. Neurol. 319(1), 123–140.

Krubitzer, L. and Kahn, D. 2003. Nature vs. nurture: an old idea with a new twist. Prog. Neurobiol. 70, 33–52.

Krubitzer, L., Clarey, J., Tweedale, R., and Calford, M. 1998. Interhemispheric connections of somatosensory cortex in the flying fox. J. Comp. Neurol. 402(4), 538–539.

Krubitzer, L., Clarey, J., Tweedale, R., Elston, G., and Calford, M. 1995a. A redefinition of somatosensory areas in the lateral sulcus of macaque monkeys. J. Neurosci. 15, 3821–3839.

Krubitzer, L., Huffman, K. J., Disbrow, E., and Recanzone, G. 2004. Organization of area 3a in macaque monkeys: contributions to the cortical phenotype. J. Comp. Neurol. 471, 97–111.

Krubitzer, L., Künzle, H., and Kaas, J. 1997. Organization of sensory cortex in a madagascan insectivore, the tenrec (*Echinops telfairi*). J. Comp. Neurol. 379, 399–414.

Krubitzer, L., Manger, P., Pettigrew, J., and Calford, M. 1995b. The organization of somatosensory cortex in monotremes: in search of the prototypical plan. J. Comp. Neurol. 351, 261–306.

Krubitzer, L. A., Sesma, M. A., and Kaas, J. H. 1986. Microelectrode maps, myeloarchitecture, and cortical connections of three somatotopically organized representations of the body surface in the parietal cortex of squirrels. J. Comp. Neurol. 250, 403–430.

Lacquaniti, F., Guigon, E., Bianchi, L., Ferraina, S., and Caminiti, R. 1995. Representing spatial information for limb movement: the role of area 5 in monkey. Cereb. Cortex 5, 391–409.

LaMotte, R. H. and Mountcastle, V. B. 1979. Disorders in somesthesis following lesions in parietal lobe. J. Neurophysiol. 42, 400–419.

Landgren, S. and Silfvenius, H. 1969. Projection to cerebral cortex of group I muscle afferents from the cat's hind limb. J. Physiol. 200, 353–372.

Lang, W., Büttner-Ennever, J. A., and Büttner, U. 1979. Vestibular projections to the monkey thalamus: an autoradiographic study. Brain Res. 177, 3–17.

Lassonde, M., Sauerwein, H., Geoffroy, G., and DèCarie, M. 1986. Effects of early and late transection of the corpus callosum in children. Brain 109, 953–967.

Lebedev, M. and Nelson, R. 1996. High-frequency vibratory sensitive neurons in monkey primary somatosensory cortex: entrained and non-entrained responses to vibration during the performance of vibratory-cued hand movements. Exp. Brain Res. 111, 313–325.

Leclerc, S. S., Rice, F. L., Dykes, R. W., Pourmoghadam, K., and Gomez, C. M. 1993. Electrophysiological examination of the representation of the face in the suprasylvan gyrus of the ferret: a correlative study with cytoarchitecture. Somatosens. Motor Res. 10, 133–159.

Ledoux, M. S., Whitworth, R. H., and Gould, H. J. I. 1987. Interhemispheric connections of the somatosensory cortex in the rabbit. J. Comp. Neurol. 258, 145–157.

Lee, K. and Woolsey, T. 1975. A proportional relationship between peripheral innervation density and cortical neuron number in the somatosensory system of the mouse. Brain Res. 99, 349–353.

Lin, L.-D., Murray, G., and Sessle, B. 1994a. Functional properties of single neurons in the primate face primary

somatosensory cortex. I. relations with trained orofacial motor behaviors. J. Neurophysiol. 71, 2377–2390.
Lin, L.-D., Murray, G., and Sessle, B. 1994b. Functional properties of single neurons in the primate face primary somatosensory cortex. II relations with different directions of trained tongue protrusion. J. Neurophysiol. 71, 2391–2400.
Lobel, E., Kleine, J., Leroy-Willig, A., Van de Moortele, P.-F., Le Bihan, D., Grusser, O.-J., and Berthoz, A. 1999. Cortical areas activated by bilateral galvanic vestibular stimulation. Ann. N. Y. Acad. Sci. 871, 313–323.
Manger, P. R. and Pettigrew, J. D. 1995. Electroreception and feeding behaviour of the platypus. Philos. Trans. R. Soc. Lond. B Biol. Sci. 347, 359–381.
Manger, P., Sum, M., Szymanski, M., Ridyway, S., and Krubitzer, L. 1998. Modular subdivisions of dolphin anterior ensular cortex: does evolutionary history repeat itself? J. Cogn. Neurosci. 10(2), 153–166.
Manzoni, T. 1997. The callosal connections of the hierarchically organized somatosensory areas of primates. J. Neurosurg. Sci. 41, 1–13.
Manzoni, T., Barbaresi, P., and Conti, F. 1984. Callosal mechanism for the enter hemispheric transfer of hand somatosensory information in the monkey. Behav. Brain Res. 11, 155–170.
Manzoni, T., Conti, F., and Fabri, M. 1986. Callosal projections from area SII to SI in monkeys: anatomical organization and comparison with association projections. J. Comp. Neurol. 252, 245–263.
Mayner, L. and Kaas, J. 1986. Thalamic projections from electrophysiologically defined sites of body surface representations in areas 3b and 1 of somatosensory cortex of cebus monkeys. Somatosens. Res. 4, 13–29.
McKenna, T. M., Whitsel, B. L., Dreyer, D. A., and Metz, C. B. 1981. Organization of cat anterior parietal cortex: relations among cytoarchitecture, single neuron functional properties, and interhemispheric connectivity. J. Neurophysiol. 45, 667–697.
Merzenich, M. M., Kaas, J. H., Sur, M., and Lin, C.-S. 1978. Double representation of the body surface within cytoarchitectonic areas 3b and 1 in ''SI'' in the owl monkey (*Aotus trivirgatus*). J. Comp. Neurol. 181, 41–74.
Merzenich, M. M., Nelson, R. J., Kaas, J. H., Stryker, M. P., Jenkins, W. M., Zook, J. M., Cynader, M. S., and Schoppmann, A. 1987. Variability in hand surface representations in area 3b and 1 in adult owl and squirrel monkeys. J. Comp. Neurol. 258, 281–296.
Mishkin, M., Ungerleider, L. G., and Macko, K. A. 1983. Object vision and spatial vision: two cortical pathways. Trends Neurosci. 6, 414–417.
Mitchell, R. W. 2005. Mirrors and Matchings: Limitation from the Perspective of Mirror-Self Recognition, and Why the Parietal Region Is Involved in Both. In: Spatial Perception, Spatial Cognition (*eds*. F. Dolins and R. W. Mitchell). Cambridge University Press (in press).
Moore, C., Stern, C., Corkin, S., Fischl, B., Gray, A., Rosen, B., and Dale, A. 2000. Segregation of somatosensory activation in the human rolandic cortex using fMRI. J. Neurophysiol. 84, 558–569.
Mountcastle, V. B., Lynch, J. C., Georgopoulos, A., Sakata, H., and Acuña, C. 1975. Posterior parietal association cortex of the monkey: command functions for operations within extrapersonal space. J. Neurophysiol. 38, 871–908.
Murphy, W. J., Eizirik, E., O'Brein, S. J., Madsen, O., Scally, M., Douady, C. J., Teeling, E., Ryder, O. A., Stanhope, M. J., de Jong, W. W., and Springer, M. S. 2001. Resolution of the early placental mammal radiation using Bayesian phylogenetics. Science 294, 2348–2351.
Murray, E. A. and Mishkin, M. 1984. Relative contributions of SII and area 5 to tactile discrimination in monkeys. Behav. Brain Res. 11, 67–83.
Myers, R. E. and Ebner, F. F. 1976. Localization of function in corpus callosum: tactual information transmission in *Macaca mulatta*. Brain Res. 103, 455–462.
Napier, J. 1962. The evolution of the hand. Sci. Am. 207, 56–61.
Napier, J. R. 1960. Studies of the hands of living primates. Proc. Zool. Soc. Lond. 134, 647–657.
Nelson, R. 1987. Activity of monkey primary somatosensory cortical neurons changes prior to active movement. Brain Res. 406, 402–407.
Nelson, R. J. and Kaas, J. H. 1981. Connections of the ventroposterior nucleus of the thalamus with the body surface representations in cortical areas 3b and 1 of the cynomologus macaque, *Macaca fascicularis*. J. Comp. Neurol. 199, 29–64.
Nelson, R., Smith, B., and Douglas, V. 1991. Relationship between sensory responsiveness and premovement activity of quickly adapting neurons in areas 3b and 1 of monkey primary somatosensory cortex. Exp. Brain Res. 84, 75–90.
Nelson, R. J., Sur, M., Felleman, D. J., and Kaas, J. H. 1980. Representations of the body surface in postcentral parietal cortex of *Macaca fascicularis*. J. Comp. Neurol. 192, 611–643.
Oscarsson, O. and Rosen, I. 1963. Projection to cerebral cortex of large muscle-spindle afferents in forelimb nerves of the cat. J. Physiol. 169, 924–945.
Oscarsson, O. and Rosen, I. 1966. Short-latency projections to the cat's cerebral cortex from skin and muscle afferents in the contralateral forelimb. J. Physiol. 182, 164–184.
Oscarsson, O., Rosen, I., and Sulg, I. 1966. Organization of neurones in the cat cerebral cortex that are influenced from group I muscle afferents. J. Physiol. 183, 189–210.
Padberg, J. and Krubitzer, L. 2006. Thalamocortical connections of anterior and posterior parietal cortical areas in New World titi monkeys. J. Comp. Neurol. 497, 416–435.
Padberg, J. P., Disbrow, E., and Krubitzer, L. 2005. The organization and connections of anterior and posterior parietal cortex in titi monkeys: do New World monkeys have an area 2? Cereb. Cortex 15, 1938–1063.
Pandya, D. N. and Seltzer, B. 1982. Intrinsic connections and architectonics of posterior parietal cortex in the rhesus monkey. J. Comp. Neurol. 204, 196–210.
Pandya, D. N. and Vignolo, L. A. 1968. Interhemispheric neocortical projections of somatosensory areas I and II in the rhesus monkey. Brain Res. 7, 300–303.
Paperna, T. and Malach, R. 1991. Patterns of sensory intermodality relationships in the cerebral cortex of the rat. J. Comp. Neurol. 308, 432–456.
Pearson, R. C. A. and Powell, T. P. S. 1985. The projection of the primary somatic sensory cortex upon area 5 in the monkey. Brain Res. Rev. 9, 89–107.
Penfield, W. and Rasmussen, T. 1968. Secondary Sensory and Motor Representation. In: Cerebral Cortex of Man. A Clinical Study of Localization of Function (Chapter VI), pp. 109–134. Hafner Publishing Company.
Phillips, C. B., Powell, T. P. S., and Wiesandanger, M. 1971. Projections from low threshold muscle afferents of hand and forearm to area 3a of baboon's cortex. J. Physiol. 217, 419–446.
Pons, T. P. and Kaas, J. H. 1985. Connections of area 2 of somatosensory cortex with the anterior pulvinar and subdivisions of the ventroposterior complex in macaque monkeys. J. Comp. Neurol. 240, 16–36.
Pons, T. P. and Kaas, J. H. 1986. Corticocortical connections of area 2 of somatosensory cortex in macaque monkeys: a

correlative anatomical and electrophysiological study. J. Comp. Neurol. 248, 313–335.
Pons, T. P., Garraghty, P. E., Cusick, C. G., and Kaas, J. H. 1985. The somatotopic organization of area 2 in macaque monkeys. J. Comp. Neurol. 241, 445–466.
Pubols, B. and Pubols, L. 1971. Somatotopic organization of spider monkey somatic sensory cerebral cortex. J. Comp. Neurol. 141, 63–76.
Pubols, B. H., Pubols, L. M., DePette, D. J., and Sheely, J. C. 1976. Opossum somatic sensory cortex: a microelectrode mapping study. J. Comp. Neurol. 165, 229–246.
Randolph, M. and Semmes, J. 1974. Behavioral consequences of selective subtotal Ablations in the postcentral gyrus of *Macaca mulatta*. Brain Res. 70, 55–70.
Rausell, E. and Jones, E. G. 1995. Extent of intracortical arborization of thalamocortical axons as a determinant of representational plasticity in monkey somatic sensory cortex. J. Neurosci. 15, 4270–4288.
Recanzone, G. H., Merzenich, M. M., Jenkins, W. M., Grajski, K. A., and Dinse, H. R. 1992b. Topographic reorganization of the hand representation in cortical area 3b of owl monkeys trained in a frequency discrimination task. J. Neurophysiol. 67, 1031–1056.
Reep, R. L., Chandler, H. C., King, V., and Corwin, J. V. 1994. Rat posterior parietal cortex: topography of corticocortical and thalamic connections. Exp. Brain Res. 100, 67–84.
Risse, G. L., Gates, J., Lund, G., Maxwell, R., and Rubens, A. 1989. Interhemispheric transfer in patients with incomplete section of the corpus callosum. Arch. Neurol. 46, 437–443.
Robertson, L. C. and Rafal, R. 2000. Disorders of visual attention. In: The New Cognitive Neurosciences (*ed*. M. Gazzaniga), pp. 633–649. MIT Press.
Robinson, C. J. and Burton, H. 1980a. Organization of somatosensory receptive fields in cortical areas 7b, retroinsula, postauditory, and granular insula of *M. fascicularis*. J. Comp. Neurol. 192, 69–92.
Robinson, C. J. and Burton, H. 1980b. Somatotopographic organization in the second somatosensory area of *M. fascicularis*. J. Comp. Neurol. 192, 43–67.
Romo, R., Hernandez, A., Zainos, A., Brody, C., and Lemus, L. 2000. Sensing without touching: psychophysical performance based on cortical microstimulation. Neuron 26, 273.
Romo, R., Hernandez, A., Zainos, A., and Salinas, E. 1998. Somatosensory discrimination based on cortical microstimulation. Nature 392, 387.
Roy, A., Paulignan, Y., Farne, A., Jouffrais, C., and Boussaoud, D. 2000. Hand kinematics during reaching and grasping in macaque monkey. Behav. Brain Res. 117, 75–82.
Rushworth, M. F. S., Johansen-Berg, H., and Young, S. A. 1998. Parietal cortex and spatial-postural transformation during arm movements. J. Neurophysiol. 79, 478–482.
Rushworth, M. F. S., Nixon, P. D., and Passingham, R. E. 1997. Parietal cortex and movement. Exp. Brain Res. 117, 311–323.
Sakata, H., Takaoka, Y., Kawarasaki, A., and Shibutani, H. 1973. Somatosensory properties of neurons in the superior parietal cortex (area 5) of the rhesus monkey. Brain Res. 64, 85–102.
Salimi, I., Brochier, T., and Smith, A. 1999. Neuronal activity in somatosensory cortex of monkeys using a precision grip. II. Responses to object texture and weights. J. Neurophysiol. 81, 835–844.
Saper, C. B., Iversen, S., and Frackowiak, R. 2000. Integration of Sensory and Motor Function: The Association Areas of the Cerebral Cortex and the Cognitive Capabilities of the Brain. In: Principles of Neural Science (*eds*. E. R. Kandel, J. H. Schwartz, and R. M. Jessel), pp. 349–380. McGraw-Hill Companies Inc.
Scheich, H., Langner, G., Tidemann, C., Coles, R. B., and Guppy, A. 1986. Electroreception and electrolocation in platypus. Nature 319, 401–402.
Schwartz, A. 1983. Functional relationship between somatosensory cortex and specialized afferent pathways in the monkey. Exp. Neurol. 79, 316–328.
Schwarz, D. W., Deeck, L., and Fredrickson, J. M. 1973. Cortical projections of group I muscle afferents to areas 2, 3a, and the vestibular field in the rhesus monkey. Exp. Brain Res. 17, 516–526.
Seltzer, B. and Pandya, D. N. 1983. The Distribution of posterior parietal fibers in the corpus callosum of the rhesus monkey. Exp. Brain Res. 49, 147–150.
Shanks, M. F., Pearson, R. C. A., and Powell, T. P. S. 1985a. The callosal connexions of the primary somatic sensory cortex in the monkey. Brain Res. Rev. 9, 43–65.
Shanks, M. F., Pearson, R. C. A., and Powell, T. P. S. 1985b. The ipsilateral cortico-cortical connexions between the cytoarchitectonic subdivisions of the primary somatic sensory cortex in the monkey. Brain Res. Rev. 9, 67–88.
Sinclair, R. J. and Burton, H. 1991. Neuronal activity in the primary somatosensory cortex in monkeys (*Macaca mulatta*) during active touch of textured surface gratings: responses to groove width, applied force, and velocity of motion. J. Neurophysiol. 66, 153–169.
Slutsky, D. A., Manger, P. R., and Krubitzer, L. 2000. Multiple somatosensory areas in the anterior parietal cortex of the California ground squirrel (*Spermophilus beecheyii*). J. Comp. Neurol. 416, 521–539.
Snyder, L. H., Batista, A. P., and Andersen, R. A. 1997. Coding of intention in the posterior parietal cortex. Nature 386, 167–170.
Stepniewska, I., Preuss, T. M., and Kaas, J. H. 1993. Architectonics, somatotopic organization, and ipsilateral cortical connections of the primary motor area (MI) of owl monkeys. J. Comp. Neurol. 330, 238–271.
Sur, M., Nelson, R. J., and Kaas, J. H. 1980. Representation of the body surface in somatic koniocortex in the prosimian *Galago*. J. Comp. Neurol. 189, 381–402.
Sur, M., Nelson, R. J., and Kaas, J. H. 1982. Representations of the body surface in cortical areas 3b and 1 of squirrel monkeys: comparisons with other primates. J. Comp. Neurol. 211, 177–192.
Sur, M., Wall, J. T., and Kaas, J. H. 1984. Modular distribution of neurons with slowly adapting and rapidly adapting responses in area 3b of somatosensory cortex in monkeys. J. Neurophysiol. 51, 724–744.
Tanji, J. 1975. Activity of neurons in cortical area 3a during maintenance of steady postures by the monkey. Brain Res. 88, 549–553.
Tanji, J. and Wise, S. 1981. Submodality distribution in sensorimotor cortex of the unanesthetized monkey. J. Neurophysiol. 45, 467–481.
Taoka, M., Toda, T., Iriki, A., Tanaka, M., and Iwamura, Y. 2000. Bilateral receptive field neurons in the hindlimb region of the postcentral somatosensory cortex in awake macaque monkeys. Exp. Brain Res. 134, 139–146.
Taoka, M., Toda, T., and Iwamura, Y. 1998. Representation of the midline trunk, bilateral arms, and shoulders in the monkey postcentral somatosensory cortex. Exp. Brain Res. 123, 315–322.
Toda, T. and Toaka, M. 2001. The complexity of receptive fields of periodontal mechanoreceptive neurons in the postcentral area 2 of conscious macaque monkey brains. Arch. Oral Biol. 46, 1079–1084.
Toda, T. and Taoka, M. 2002. Integration of the upper and lower lips in the postcentral area 2 of conscious macaque monkeys (*Macaca fuscata*). Arch. Oral Biol. 47, 449–456.

Tremblay, F., Ageranioti-Belanger, S. A., and Chapman, C. E. 1996. Cortical mechanisms underlying tactile discrimination in the monkey. I. Role of primary somatosensory cortex in passive texture discrimination. J. Neurophysiol. 76, 3382–3403.
Van Dyck, S. 1983. The Complete Book of Australian Mammals. Angus and Robertson.
Vogt, B. A. and Pandya, D. N. 1978. Cortico-cortical connections of somatic sensory cortex (areas 3, 1 and 2) in the Rhesus monkey. J. Comp. Neurol. 177, 179–192.
Vogt, C. and Vogt, O. 1919. Allgemeinere ergelnisse unserer hirnforschung. J. Psychol. (Leipzig) 25, 279–462.
Welker, W. I. and Seidenstein, S. 1959. Somatic sensory representation in the cerebral cortex of the raccoon (*Procyon lotor*). J. Comp. Neurol. 111, 469–501.
Weller, R. E., Sur, M., and Kaas, J. H. 1987. Callosal and ipsilateral cortical connections of the body surface representations in SI and SII of tree shrews. Somatosens. Res. 5, 107–133.
Welles, J. F. 1976. A comparative study of manual prehension in anthropoids. Saugetierkundliche Mittielungen 24, 26–38.
White, E. L. and DeAmicis, R. A. 1977. Afferent and efferent projections of the region in mouse SmI cortex which contains the posteromedial barrel subfield. J. Comp. Neurol. 175, 455–481.
Wise, S. P. and Jones, E. G. 1976. The organization and postnatal development of the commissural projection of the rat somatic sensory cortex. J. Comp. Neurol. 168, 313–344.
Wise, S. and Tanji, J. 1981. Neuronal responses in sensorimotor cortex to ramp displacements and maintained positions imposed on hindlimb of the unanesthetized monkey. J. Neurophysiol. 45, 482–500.
Wise, S. P., Boussaoud, D., Johnson, P. B., and Caminiti, R. 1997. Premotor and parietal cortex: corticocortical connectivity and combinatorial computations. Annu. Rev. Neurosci. 20, 25–42.
Wolpaw, J. 1980. Correlations between task-related activity and responses to perturbation in primate sensorimotor cortex. J. Neurophysiol. 44, 1122–1138.
Woolsey, C. N. 1958. Organization of Somatic Sensory and Motor Areas of the Cerebral Cortex. University of Wisconsin Press.
Woolsey, C. N. and Fairman, D. 1946. Contralateral, ipsilateral, and bilateral representation of cutaneous receptors in somatic areas I and II of the cerebral cortex of pig, sheep, and other mammals. Surgery 19, 684–702.
Woolsey, T. A. and Van der Loos, H. 1970. The structural organization of layer IV in the somatosensory region (SI) of the mouse cerebral cortex: the description of a cortical field composed of discrete cytoarchitectonic units. Brain Res. 17, 205–242.
Woolsey, C., Erickson, T., and Gilson, W. 1979. Localization in somatic sensory and motor areas of human cerebral cortex as determined by direct recording of evoked potentials and electrical stimulation. J. Neurosurg. 51, 476–506.
Wu, C.-H. and Kaas, J. 2003. Somatosensory cortex of prosimian galagos: physiological recording, cytoarchitecture, and corticocortical connections of anterior parietal cortex and cortex of the lateral sulcus. J. Comp. Neurol. 457, 263–292.
Xerri, C., Coq, J. O., Merzenich, M. M., and Jenkins, W. M. 1996. Experience-induced plasticity of cutaneous maps in the primary somatosensory cortex of adult monkeys and rats. J. Physiol. (Paris) 90, 277–287.
Zarzecki, P., Shinoda, Y., and Asanuma, H. 1978. Projection from area 3a to the motor cortex by neurons activated from group I muscle afferents. Exp. Brain Res. 33, 269–282.

Further Reading

LaMotte, R. H. and Acuña, C. 1978. Defects in accuracy of reaching after removal of posterior parietal cortex in monkeys. Brain Res. 139, 309–326.
Recanzone, G. H., Merzenich, M. M., and Jenkins, W. M. 1992a. Frequency discrimination training engaging a restricted skin surface results in an emergence of a cutaneous response zone in cortical area 3a. J. Neurophysiol. 67, 1057–1070.
Rosa, M., Gattass, R., and Soares, J. 1991. A quantitative analysis of cytochrome oxidase-rich patches in the primary visual cortex of cebus monkeys: topographic distribution and effects of late monocular enucleation. Exp. Brain Res. 84, 195–209.
Savaki, H. E., Kennedy, C., Sokoloff, L., and Mishkin, M. 1993. Visually guided reaching with the forelimb contralateral to a ''blind'' hemisphere: a metabolic mapping study in monkeys. J. Neurosci. 13, 2772–2789.
Xerri, C., Merzenich, M., Jenkins, W. M., and Santucci, S. 1999. Representational plasticity in cortical area 3b paralleling tactual-motor skill acquisition in adult monkeys. Cereb. Cortex 9, 1047–3211.

This work was originally submitted in 2005 and since then several relevant studies have been published which could not be incorporated into the text of the current chapter. These include:

Berryman, L. J., Yau, J. M., and Hsiao S. S. 2006. Representation of object size in the somatosensory system. J. Neurophysiol. 96, 27–39.
Fitzgerald, P. J., Lane, J. W., Thakur, P. H., and Hsiao, S. S. 2006. Receptive field (RF) properties of the macaque second somatosensory cortex: RF size, shape, and somatotopic organization. J. Neurosci. 26, 6485–95.
Fitzgerald, P. J., Lane, J. W., Thakur, P. H., and Hsiao, S. S. 2006. Receptive field properties of the macaque second somatosensory cortex: representation of orientation on different finger pads. J. Neurosci. 26, 6473–84.
Padberg, J., Franca, J. G., Cooke, D. F., Soares, J. G., Rosa, M. G., Fiorani, M. Jr, Gattass, R., and Krubitzer, L. 2007. Parallel evolution of cortical areas involved in skilled hand. J. Neurosci. 27, 10106–15.
Wang, X., Zhang, M., Cohen, I. S., and Goldberg, M. E. 2007. The proprioceptive representation of eye position in monkey somatosensory cortex.

6.11 Role of Primary Somatosensory Cortex in Perceptual Touch Detection and Discrimination

R Romo, A Hernández, V de Lafuente, A Zainos, L Lemus, R Luna, V Nácher, and M Alvarez, Universidad Nacional Autónoma de México, México

© 2008 Elsevier Inc. All rights reserved.

6.11.1	Introduction	216
6.11.2	Sensory Detection	217
6.11.3	Psychophysics of Sensory Detection	217
6.11.4	S1 Responses during Vibrotactile Detection	217
6.11.5	S1 Responses and Perceptual Reports	218
6.11.6	Further Comments on the Functional Role of S1 in Sensory Detection	218
6.11.7	Sensory Discrimination	220
6.11.8	Neural Coding of Vibrotactile Stimuli in S1	222
6.11.9	Neuronal Correlates of Flutter Discrimination in S1	222
6.11.10	Artificial Induction of Activity in S1 Underlying Flutter Discrimination	226
6.11.11	Further Comments on the Functional Role of S1 to Flutter Discrimination	228
6.11.12	Conclusion	230
References		231

Glossary

choice A choice is required when an organism is confronted with alternatives for which an action is necessary to acquire or avoid one or more of the alternatives because of a desire, goal, or preference.

choice probability A trial-to-trial correlation between neuronal signals and the monkey's choice behavior.

detection The simplest perceptual experiences that is a prerequisite for any further sensory processing. In detection tasks repeated presentations of a near-threshold stimulus might unpredictably fail or succeed in producing sensory percept.

discrimination The capacity to determine the difference between two stimuli.

difference limen In flutter discrimination, the difference limen is a measure of how a small increase in the frequency of a vibrotactile stimulus can be detected when compared to a standard stimulus frequency. A smaller difference limen implies a higher discrimination capacity.

flutter A type of somatosensory stimulation that is felt when touching an object that vibrates at frequencies between ~10 and ~50 Hz.

functional magnetic resonance imaging (fMRI) The use of MRI to measure the hemodynamic response related to neural activity in the brain or spinal cord of humans or other animals. It is one of the most recently developed forms of neuroimaging.

intracortical microstimulation A neurophysiological technique that is used to activate a population of neurons within a restricted cortical locus. Pulses of electric current delivered through a microelectrode drive the activation.

memory An organism's ability to store, retain, and subsequently recall information.

neurometric curve A plot of the percentage of correct behavioral responses that an ideal observer would make on the basis of observing the neuronal responses that are elicited by a given test stimulus.

perception The process of acquiring, interpreting, selecting, and organizing sensory information. The word perception comes from the Latin *capere*, meaning to take, the prefix per meaning completely.

primary somatosensory cortex (S1) It is located in the poscentral gyrus and in the depths of the central sulcus. It consists of four functional areas: Brodmann's areas 1, 2, 3a, and 3b, each of which has a somewhat different role in somatic sensation.

Projections from the thalamus to S1 arise chiefly from the ventral posterior nucleus, are somatotopically organized, and transmit information from the contralateral body.

psychometric curve A plot of the percentage of correct behavioral responses as function of changes in the properties of the test stimulus.

psychophysics A subdiscipline of psychology dealing with the relationship between physical stimuli and their subjective correlates, or percepts.

receptive field The area of the sensory space in which stimulus presentation leads to the response of a particular sensory neuron.

receiver operating characteristic (ROC) ROC analysis is often used to evaluate the results of a detection task with weak signals. A ROC curve is generated by plotting the probability of true positives (hits) against the probability of false positives (false alarms) for a binary classifier system and its criterion is varied. In neurophysiology, it is used to test whether an ideal observer could reliably identify a given stimulus or a behavior based on a neural response.

sensory threshold A theoretical concept used in psychophysics. A stimulus that is less intense than the sensory threshold will not elicit any sensation. The concept can be applied to detection and perception in all senses. Several different sensory thresholds have been defined:

- *Absolute threshold.* The lowest level at which a stimulus can be detected.
- *Recognition threshold.* The level at which a stimulus can not only be detected but also recognized.
- *Differential threshold.* The level at which an increase in a detected stimulus can be perceived.
- *Terminal threshold.* The level beyond which a stimulus is no longer detected.

stimulus A detectable change in the internal or external environment.

top-down* and *bottom-up Strategies of information processing. The first is applied to cerebral signals that transmit information derived from past experience and the second is applied to cerebral signals that transmit sensory information.

vibrotactile stimulus A mechanical oscillation in time delivered on the skin.

Weber fraction Weber made the observation that, within a fairly large range, the increase in a stimulus that is just noticeable (ΔI) is a constant proportion of the initial stimulus (I) from any one sense. The proportion $\Delta I/I$ is the Weber fraction.

6.11.1 Introduction

A fundamental goal of neuroscience is to understand how sensory experiences arise from activity in the brain (Adrian, E. D., 1928). A major component of this problem involves understanding how the brain represents sensory features. Pioneering investigations in several sensory systems have shown how neural activity represents the physical parameters of the sensory stimuli both in the periphery and in the central areas of the brain (Mountcastle, V. B. *et al.*, 1967; Talbot, W. H. *et al.*, 1968; Hubel, D. H. and Wisel, T. N., 1998). These investigations have paved the way for new questions that are more closely related to cognitive processing. For example, where and how in the brain do the neuronal responses that encode the sensory stimuli translate into responses that encode a perceptual decision (Romo, R. and Salinas, E., 2001; Schall, J. D., 2001)? What components of the neuronal activity evoked by a sensory stimulus are directly related to perception (Newsome, W. T. *et al.*, 1989; Romo, R. *et al.*, 1998)? Where and how in the brain sensory information is stored in memory (Romo, R. *et al.*, 1999)? These questions have been investigated in behavioral tasks where the sensory stimuli are under precise quantitative control and the subject's psychophysical performances are quantitatively measured (Hernández, A. *et al.*, 1997; de Lafuente, V. and Romo, R., 2005). One of the main challenges of this approach is that even the simplest cognitive tasks engage a large number of cortical areas, and each one might render the sensory information in a different way (Romo, R. and Salinas, E., 2003; Romo, R. *et al.*, 2004). Also, the sensory information might be combined in these cortical areas with other types of stored signals representing, for example, past experience and future actions (Hernández, A. *et al.*, 2002; Romo, R. *et al.*, 2002; 2004). Thus, an important issue in neuroscience is to decode from the neuronal activity all these processes that might be related to perception.

In this chapter, we review results obtained using the somatic modalities and that are relevant for understanding the link between neural representations of sensory events in areas 3b and 1 of the

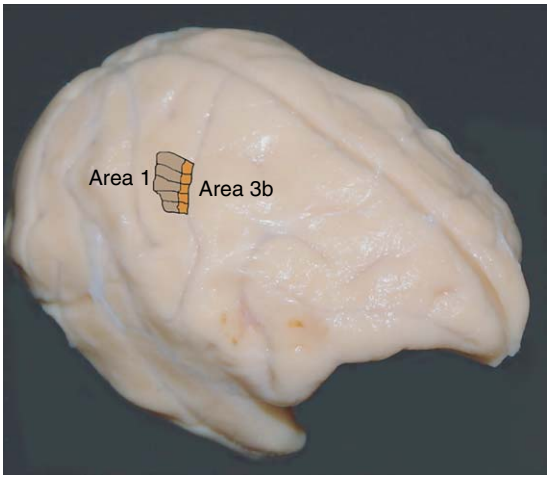

Figure 1 Picture of brain surface of one of the monkeys used to investigate the response properties of primary somatosensory cortex (S1) neurons during touch perception. Recordings were made in areas 3b and 1 of S1.

primary somatosensory cortex (S1; Figure 1) and psychophysically quantified behaviors during detection and discrimination tasks.

6.11.2 Sensory Detection

The detection of sensory stimuli is among the simplest perceptual experiences and is a prerequisite for any further sensory processing. A fundamental problem posed by the sensory detection tasks is that repeated presentation of a near-threshold stimulus might unpredictably fail or succeed in producing a sensory percept. Where in the brain are the neuronal correlates of these varying perceptual judgments? Pioneering studies on the neuronal correlates of sensory detection showed that in the case of vibrotactile stimuli the responses of S1 neurons account for the measured psychophysical accuracy (Mountcastle, V. B. *et al.*, 1969). However, direct comparisons between S1 responses and detection performance was not directly addressed and, therefore, it is not clear whether the activity of S1 accounts for the variability of the behavioral responses. Psychophysical performance was measured in human observers and S1 recordings were made in anesthetized monkeys.

6.11.3 Psychophysics of Sensory Detection

This problem has been recently addressed (de Lafuente, V. and Romo, R., 2005; 2006). These authors trained monkeys to perform a detection task. In each trial, the animal had to report whether the tip of a mechanical stimulator vibrated or not (Figure 2(a)). Stimuli were sinusoidal, had a fixed frequency of 20 Hz, and were delivered to the glabrous skin of one fingertip. Crucially, they varied in amplitude across trials. Stimulus-present trials were interleaved with an equal number of stimulus-absent trials in which no mechanical vibrations were delivered (Figure 2(a)). Depending of the monkeys' responses, trials could be classified into four types of responses: hits and misses in the stimulus-present condition, and correct rejections and false alarms in the stimulus-absent condition (Figure 2(b)). Stimulus detection thresholds were calculated from the behavioral responses (Figure 2(c)). Thus an important issue in this and similar tasks is to determine the neuronal correlates that account for these behavioral reports.

6.11.4 S1 Responses during Vibrotactile Detection

de Lafuente V. and Romo R. (2005) simultaneously characterized the activity of S1 neurons (areas 3b and 1) and the monkey's psychophysical performance by recording the extracellular spike potentials of single S1 neurons while the monkeys performed the detection task. Figures 2(c) and 3(a) show, respectively, the monkey's psychometric curve and the spike trains of an S1 neuron in the same trials. The firing rate of this example neuron varied smoothly as a function of stimulus amplitude, and no clear modulations in its firing rate could be appreciated during the stimulus-absent trials.

To test whether the responses of S1 neurons accounted for the monkey's psychophysical performance, de Lafuente V. and Romo R. (2005) calculated neurometric detection curves and compared them with the psychometric curves (Figures 3(b) and 3(c)). The proportion of yes responses for neurometric curves was defined, for a given amplitude, as the proportion of trials in which the neuron's firing rate reached or exceeded a criterion value (Green, D. M. and Swets, J. A., 1966;

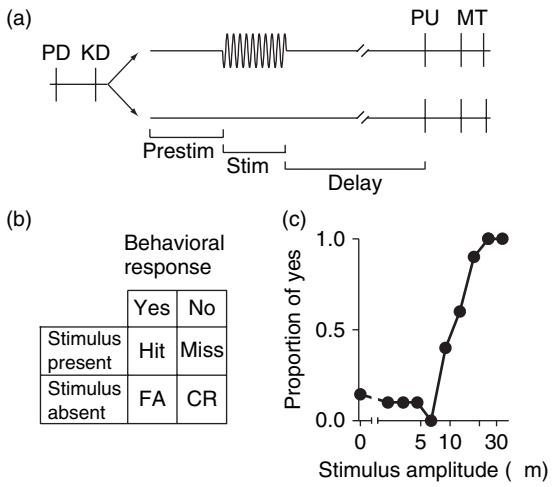

Figure 2 Detection task. (a) Trials began when the stimulator probe indented the skin of one fingertip of the right, restrained hand (probe down, PD). The monkey then placed its free left hand in an immovable key (key down, KD). On half of the randomly selected trials, after a variable prestimulus period (2.5–3.5 s), a vibratory stimulus (20 Hz, 0.5 s) was presented or not. Then, after a fixed delay period (3 s), the stimulator probe moved up (probe up, PU), indicating to the monkey that the response movement (MT) to one of the two push buttons could be made. The button pressed indicated whether the stimulus was felt or not (henceforth referred to as yes and no responses, respectively). (b) Depending on whether the stimulus was present or absent, and on the behavioral response, the trial outcome was classified as a hit, miss, false alarm, or correct rejection. Trials were pseudorandomly chosen; 90 trails were stimulus-absent (amplitude = 0) and 90 trials were stimulus-present with varying amplitudes (9 amplitudes with ten repetitions each). (c) Classical psychometric detection curve obtained by plotting the proportion of yes responses as a function of stimulus amplitude. Adapted from de Lafuente, V. and Romo, R. 2005. Neuronal correlates of subjective sensory experience. Nat. Neurosci. 12, 1698–1703.

de Lafuente, V. and Romo, R., 2005). For each neuron, this criterion was chosen to maximize the number of correct responses (Figure 3(b)). Pairwise comparisons of detection thresholds obtained from logistic fits to the simultaneously obtained neurometric and psychometric data showed that the detection thresholds of individual S1 neurons were not significantly different from the animals' psychophysical thresholds, and the two thresholds measures highly covaried. In addition, the shape of the mean neurometric curve resulting from the activity of the S1 neurons showed close correspondence with the shape of the mean psychometric curve (Figure 3(c)).

6.11.5 S1 Responses and Perceptual Reports

An important question addressed in this study is whether the activity of S1 neurons covaries with the perceptual yes–no judgments that the monkeys made on a trial-by-trial basis (de Lafuente, V. and Romo, R., 2005). To test this, these authors compared the activity during hit and miss trials for the near-threshold stimulus as well as for the corresponding activity in correct reject and false alarm trials in the stimulus-absent condition (Figure 4). They found no significant differences in the activity of S1 neurons between hits and misses (Figure 4, upper left panel) or between correct rejections and false alarms (Figure 4, upper right panel). This indicated that the activity of individual S1 neurons did not predict the monkey's behavior. To further quantify this, de Lafuente V. and Romo R. (2005) calculated a choice probability index, which estimates the probability with which the behavioral outcome can be predicted from the neuronal responses (Britten, K. H. *et al.*, 1996; Hernández, A. *et al.*, 2002). As shown in the lower panels of Figure 4, again they found no significant differences between hits and misses, or between correct rejections and false alarms trials.

6.11.6 Further Comments on the Functional Role of S1 in Sensory Detection

The low choice probability values are consistent with a detection model in which the activity of S1 serves as input to an additional processing stage(s) that determines whether a stimulus has occurred or not. Under this hypothesis, correlation between S1 activity and the final decision about the stimulus presence or absence is highly dependent on the amount of correlated noise among sensory neurons (Zohary, E. *et al.*, 1994). Indeed, de Lafuente V. and Romo R. (2005) found that the mean noise correlation coefficient across pairs of S1 neurons was 0.16 ± 0.02. This amount of correlated noise is similar to those reported in previous studies (Zohary, E. *et al.*, 1994; Bair, W. *et al.*, 2001; Romo, R. *et al.*, 2003), and is also consistent with the near chance choice probability values reported in the study of de Lafuente V. and Romo R. (2005). These results further support a detection model in which a central area(s) must be observing the activity of S1 neurons to judge about the stimulus

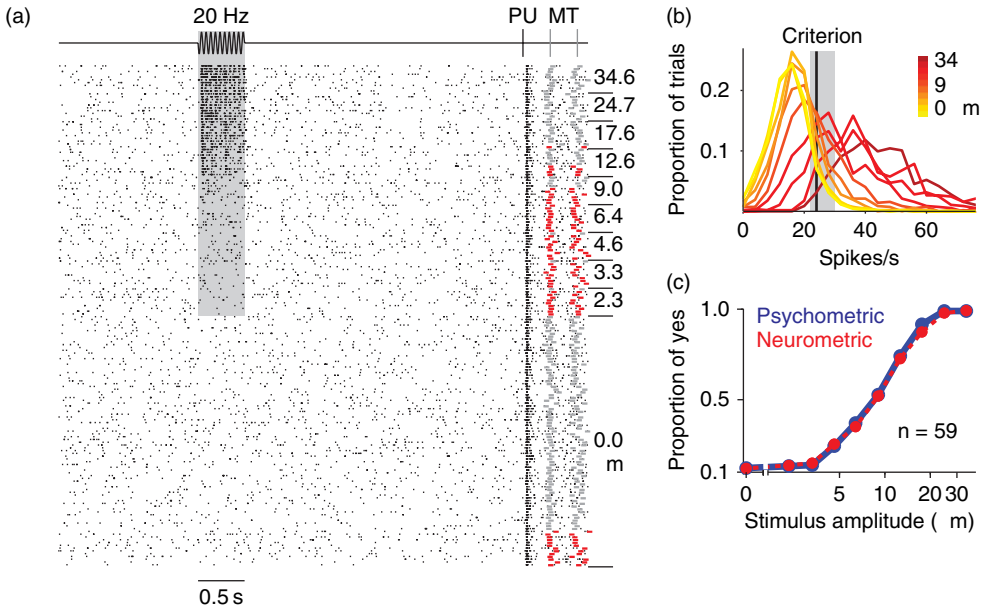

Figure 3 Activity of primary somatosensory cortex (S1) neurons during the detection task. (a) Raster plot of the spiking activity of an S1 neuron during the 180 trials of a typical detection experiment run. Each tick represents the time of spike occurrence and each row is a trial. Trials are arranged by stimulus amplitude, shown at right. Red markers at the end of the trial denote misses in stimulus-present trials, and false alarms in stimulus-absent trials. Gray box marks the time of stimulus presentation. (b) Activity distributions of the 59 neurons recorded in S1, grouped by stimulus amplitude (see calibration bar). Black vertical line marks the median criterion value (22 spikes per second) used to produce the neurometric proportion of yes for each neuron. Gray box indicates interquartile range. (c) Mean psychometric and neurometric detection curves (590 trials for each stimulus amplitude data point; 5310 trials for zero-amplitude data point). Adapted from de Lafuente, V. and Romo, R. 2005. Neuronal correlates of subjective sensory experience. Nat. Neurosci. 12, 1698–1703.

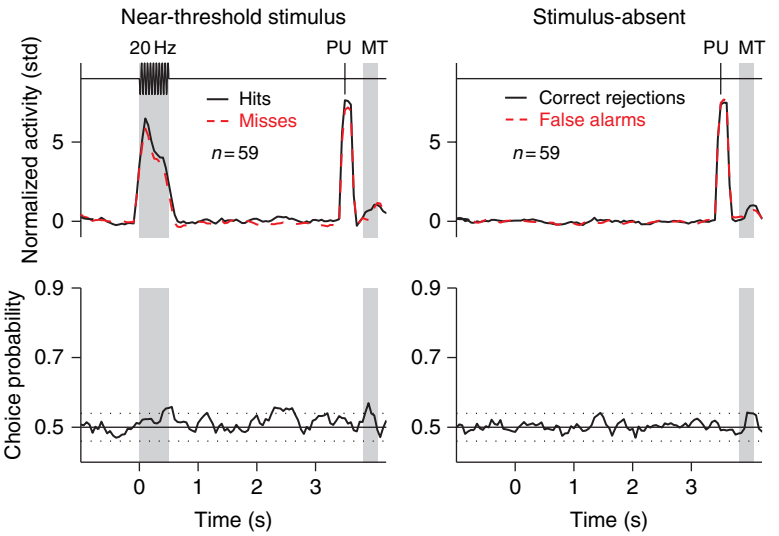

Figure 4 Correlation between psychophysical performance and neuronal responses during the detection task. Upper panels show the comparison of normalized neuronal population activity during hits and misses for near-threshold stimuli, and during correct rejections and false alarms in stimulus-absent trials. Lower panels show the choice probability index as a function of time. This index estimates the probability with which a trial's outcome can be predicted from the activity of neurons. Dotted lines mark significance levels (0.5 means chance levels) and *n* is the number of neurons. Adapted from de Lafuente, V. and Romo, R. 2005. Neuronal correlates of subjective sensory experience. Nat. Neurosci. 12, 1698–1703.

presence or absence. Therefore, the functional role of S1 in this and other perceptual tasks may be mainly to generate a neural representation of the sensory stimulus for further processing in areas central to it (Romo, R. *et al.*, 1999; Hernández, A. *et al.*, 2000; Salinas, E. *et al.*, 2000; Romo, R. *et al.*, 2002; 2003). However, a previous study found that functional magnetic resonance imaging (fMRI) signals in primary visual cortex (V1) reflected the percepts of human subjects rather than the encoded stimulus features (Ress, D. and Heeger, D. J., 2003). This result suggests that in V1 top-down signals (nonsensory inputs delivered to V1 via feedback projections) can be combined with bottom-up (sensory) information and this can contribute to sensory percepts (Ress, D. and Heeger, D. J., 2003). S1 data did not show evidence of this type of neural interaction; rather, they indicated that S1 represents the physical properties of stimuli and contributes little to near-threshold percepts (de Lafuente, V. and Romo, R., 2005). The discrepancy could be due to fundamentally different organizations across sensory cortices, or to differences between species. Another possibility to consider is that the modulation revealed through fMRI may have an effect that is invisible from the point of view of single neurons. This would happen if, for instance, such modulation acted only to synchronize the spikes of multiple target neurons (Fries, P. *et al.*, 2001a; 2001b).

6.11.7 Sensory Discrimination

The sensory detection task discussed above addressed the fundamental problem of whether the activity of S1 accounts for sensory detection. The results indicate that the S1 responses do not account for perceptual judgments in the detection task. However, there are reports suggesting a role for early sensory cortices in cognitive functions previously asigned to more central cortices. A more interesting cognitive task – sensory discrimination – was introduced by Mountcastle and colleagues several years ago (LaMotte, R. H. and Mountcastle, V. B., 1975; Mountcastle, V. B. *et al.*, 1990), and served to further explore the role of sensory cortices in perception. In the discrimination task they designed (LaMotte, R. H. and Mountcastle, V. B., 1975; Mountcastle, V. B. *et al.*, 1990), animals had to indicate whether the frequency of a comparison stimulus was lower or higher than the frequency of a base stimulus presented earlier (Figure 5). In principle, the task can be conceptualized as a chain of neural operations or cognitive steps: encoding the first stimulus frequency, maintaining it in working memory, encoding the second frequency and comparing it to the memory trace left by the first stimulus, and communicating the result of the comparison to the motor apparatus. Thus the flutter task offers a number of advantages as a model for sensory processing in the brain (Romo, R. and Salinas, E., 2001; 2003): not only do humans and monkeys perform similarly, but the items to be compared are spread out across time and always activate the same well-defined population of primary receptors (Mountcastle, V. B. *et al.*, 1967; Talbot, W. H. *et al.*, 1968; Ochoa, J. and Torebjörk, E., 1983; Macefield, G. *et al.*, 1990; Vallbo, A. B., 1995). So spatial variations are basically taken out of the picture. However, for the flutter task to be a useful model it is essential that it generate a reliable sequence of cognitive events like the one just mentioned. How do we know that this is so?

A crucial step is to scrutinize the psychophysics. Importantly, in the original paradigm the base frequency did not vary from trial to trial during a run (LaMotte, R. H. and Mountcastle, V. B., 1975; Mountcastle, V. B. *et al.*, 1990). When Romo and colleagues reexamined the flutter discrimination task, they found the paradigm to be ambiguous: when the base stimulus frequency is kept constant, the task can be solved either by comparing the two stimuli or by categorizing the second stimulus as high or low, ignoring the base stimulus (Hernández, A. *et al.*, 1997). What were the monkeys actually doing? When the base frequency was held constant during long blocks of trials, as done originally, the measured discrimination limens (DLs) and Weber fractions were similar to those reported before. If the monkeys had been discriminating the differences in frequency between the two stimuli, they would also have been able to do so when the frequency of the base stimulus changed from trial to trial. However, this was not the case: their performance dropped to chance levels. It seemed that the monkeys were paying attention only to the second stimulus, categorizing it as low or high with respect to an internal reference, perhaps the base frequency used during training. To test this possibility, in separate runs the base stimulus was removed and single stimuli were delivered in each trial. In this new condition the monkeys were rewarded for correctly categorizing stimulus frequency as lower or higher than an arbitrary reference (20, 30, or 40 Hz) kept constant during a block of trials; monkeys had to determine this reference by trial and error. The monkeys learned this task very quickly, and the

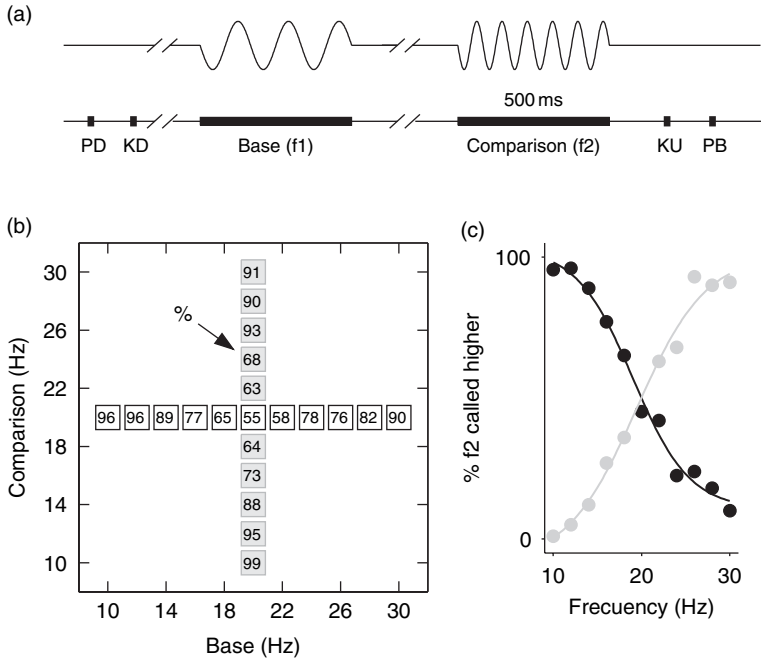

Figure 5 Discrimination task. (a) Sequence of events during discrimination trials. The mechanical probe is lowered, indenting the glabrous skin of one digit of the hand (PD); the monkey places his free hand on an immovable key (KD); the probe oscillates vertically, at the base frequency; after a delay, a second mechanical vibration is delivered at the comparison frequency; the monkey releases the key (KU) and presses one of two push buttons (PB) to indicate whether the comparison frequency was higher or lower than the base. (b) Stimulus set used to estimate psychometric thresholds. Each box indicates a base frequency/comparison frequency stimulus pair used; the number inside the box indicates overall percent correct trials for that base/comparison pair. (c) Psychometric curves computed from (b). Adapted from Romo, R., Hernández, A., Zainos, A., Brody, C. D., and Lemus, L. 2000. Sensing without touching: psychophysical performance based on cortical microstimulation. Neuron 26, 273–278 and Romo, R., Hernández, A., Zainos, A., and Salinas, E. 1998. Somatosensory discrimination based on cortical microstimulation. Nature 392, 387–390.

psychometric curves (Hernández, A. *et al.*, 1997) measured in this condition were practically identical to those measured during the classical discrimination task (Mountcastle, V. B. *et al.*, 1990).

For true discrimination, monkeys were retrained using multiple pairs of base and comparison frequencies. The key was to vary the base frequency in each trial but such that each frequency could be followed either by a higher or by a lower comparison; this forced the subjects to compare (Hernández, A. *et al.*, 1997). After retraining, which took a few months, performance in this situation was similar to that in the classical discrimination task. From these results it seems almost certain that the animals truly learned to discriminate between frequencies on a trial-by-trial basis.

The lesson is that although monkeys may indeed learn to discriminate they can also develop alternate strategies to solve a task, as suggested earlier based on theoretical arguments (Johnson, K. O., 1980). In particular, in the classical flutter discrimination paradigm, monkeys tend not to compare the two stimuli at every trial; instead they classify the second stimulus, possibly setting the limits of each category during the first few trials in a run. Whenever animals are assumed to discriminate, this problem should not be underestimated, regardless of sensory modality (Johnson, K. O., 1980; Vogel, R. and Orban, G., 1990; Vázquez, P. *et al.*, 2000).

This appears as a simple observation, but it may reflect fundamentally different mechanisms at work. Consider a task that involves variations in a single feature across trials. To identify or classify a current sensory stimulus, it must be compared to a reference stored in long-term memory, but it is not clear how the comparison process can be studied in this situation. How is information stored in long-term memory read out and made comparable to current sensory events? Where is this information stored and how does it differ from the original sensory-evoked activity? In contrast, in discrimination tasks in which two stimuli are presented sequentially in each trial, the

comparison is made against the short-term memory trace left by the first stimulus. This means that if we can identify the neural correlate of the working-memory component, it might be possible to study the comparison or decision-making mechanisms that underlie task performance. Indeed, such neural correlate has been reported recently (Hernández, A. *et al.*, 2002; Romo, R. *et al.*, 2002; 2004).

6.11.8 Neural Coding of Vibrotactile Stimuli in S1

Mountcastle and colleagues recorded S1 responses in behaving monkeys trained to detect and discriminate the frequencies of flutter stimuli (Mountcastle, V. B. *et al.*, 1990). The results support previous findings (Mountcastle, V. B. *et al.*, 1969). First, it was found that quickly adapting (QA) neurons of S1 (areas 3b and 1), like their afferent fibers, fire periodically, in phase with mechanical oscillations. Second, their firing rates seem to change little in the flutter range (this conclusion was based, however, on data from 17 neurons). Third, psychophysical performance matched the inferred performance based on the discriminability of the periodic interspike intervals (Mountcastle, V. B. *et al.*, 1990). It followed that, as proposed before, stimulus frequency could not be encoded by S1 firing rates; stimulus frequency had to be encoded temporally, in the serial order of evoked spikes (Talbot, W. H. *et al.*, 1968; Mountcastle, V. B. *et al.*, 1969; 1990).

In support of this proposal, using flutter stimuli, Merzenich and colleagues compared psychophysical data from monkeys to S1 recordings in separate experiments from the same animals (Recanzone, G. H. *et al.*, 1992). The comparison was consistent with a temporal coding mechanism, and firing rates were not seen to vary with stimulus frequency (however, the range of frequencies tested was quite narrow, and animals were anaesthetized). Merzenich and colleagues made another important observation: that spike timing associated with the sine wave was much more precise in trained animals than in untrained monkeys (Recanzone, G. H. *et al.*, 1992). Thus, based on these results, a psychophysical observer should exploit the periodic, spike timing evoked in the QA neurons of the S1 cortex for sensory discrimination.

Arguments in favor of the proposal reviewed above can be strengthened if a large number of neurons are studied and if neurons are studied in behaving animals during the flutter discrimination task. To this end, Romo and colleagues trained monkeys to discriminate between flutter stimulus frequencies and recorded many neurons with QA properties in areas 3b and 1 of S1 (Hernández, A. *et al.*, 2000; Salinas, E. *et al.*, 2000; Luna, R. *et al.*, 2005). Each recorded neuron with QA properties was studied during the discrimination task. There were three major results. First, the majority of neurons from S1 were phase-locked to the input stimulus frequency (Figures 6(a) and 6(b)); however, almost a third of QA neurons modulated their firing rates as a function of the stimulus frequency (Figures 7(a) and 7(b); Hernández, A. *et al.*, 2000; Salinas, E. *et al.*, 2000; Luna, R. *et al.*, 2005). Second, the QA neurons that modulate their firing rates were affected by the task condition; that is, they increased their transmitted information about the stimulus frequency during task performance (Salinas, E. *et al.*, 2000). Third, only those neurons that varied their firing rates as a function of the stimulus frequency were affected in error trials (Salinas, E. *et al.*, 2000).

These findings question a unique role of periodic, spike timing in discrimination of flutter stimuli, and suggest that a firing rate code cannot be discarded (Salinas, E. *et al.*, 2000). But, apart from this, what do these findings suggest? They suggest the presence of two subpopulations of QA neurons in S1 that behave differently in response to a periodic mechanical stimulus (Hernández, A. *et al.*, 2000; Salinas, E. *et al.*, 2000; Luna, R. *et al.*, 2005). These two subpopulations might be arranged in a hierarchical fashion: QA neurons that respond periodically might be closer to the input stimulus, and those that modulate their firing rates might integrate the responses of the periodic neurons and transform them into a rate code (Hernández, A. *et al.*, 2000). Such last-order neurons of the QA circuit could distribute the neural representation to those structures anatomically linked to S1, in order to solve the sensory discrimination task. However, further studies are needed to see whether this is so.

6.11.9 Neuronal Correlates of Flutter Discrimination in S1

A more direct test for the role of periodicity in flutter discrimination is measuring the discrimination capabilities of these subtypes of QA neurons associated with the psychophysical performance (Figures 6(c) and 6(d) and Figures 7(c) and 7(d)). A second test is to prove whether the evoked neural activity during discrimination in S1 cortex is sufficient for sensory performance. Finally, whether the temporal order of the spikes is important for sensory discrimination. These are

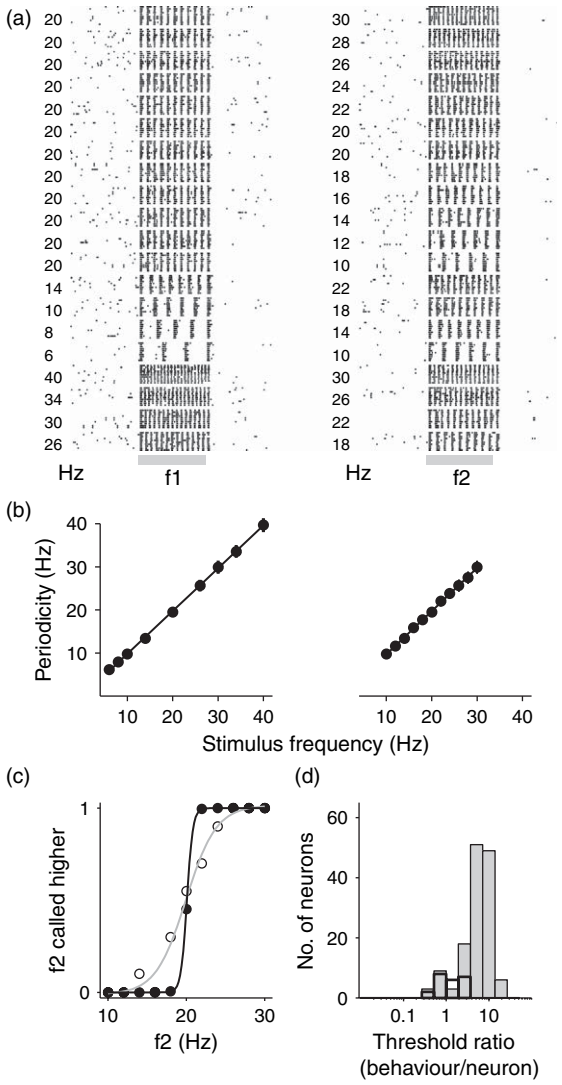

Figure 6 Periodic responses of a quickly adapting (QA) neuron of area 1 during the discrimination task. (a) Raster plots. Each row of ticks represents a trial, and each tick represents an action potential. Trials were randomly delivered. Gray horizontal lines indicate the first (f1) and the second (f2) stimulus. (b) Periodicity (±SD) as a function of the first (f1) and second stimulus (f2) frequencies. (c) Relationship between psychometric and neurometric discrimination functions. This is plotted as the probability that the second stimulus is judged higher than the first; data and sigmoidal fits (χ^2 test, $P < 0.001$) for 11 pairs of stimulus frequencies in which the base frequency was 20 Hz. Gray and black lines represent psychometric and neurometric functions, respectively. (d) Thresholds ratios (psychometric/neurometric thresholds) calculated from neurons with periodicity (gray bars). Open bars represent the threshold ratios between psychometric and neurometric thresholds calculated from a small number of neurons with modulations in their firing rate. Adapted from Hernández, A., Zainos, A., and Romo, R. 2000. Neuronal correlates of sensory discrimination in the somatosensory cortex. Proc. Natl. Acad. Sci. U. S. A. 97, 6091–6096.

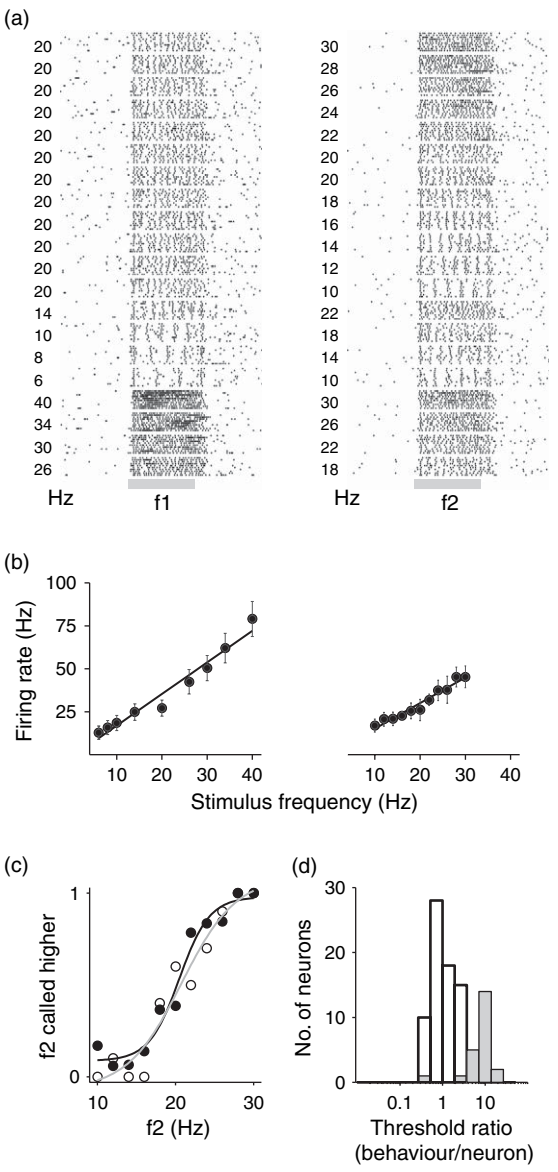

Figure 7 Firing rate modulation of a quickly adapting (QA) neuron of area 3b during the discrimination task. Same format as in Figure 6. (a) Raster plots. (b) Mean firing rate (±SD) as a function of the stimulus frequency. (c) Relationship between psychometric and neurometric discrimination functions. (d) Threshold ratios calculated between psychometric and neurometric thresholds for each neuron, which varied the firing rate as a function of the stimulus frequency (open bars). Gray bars represent the threshold ratios between psychometric and neurometric thresholds calculated from a small number of neurons that show periodicity. Adapted from Hernández, A., Zainos, A., and Romo, R. 2000. Neuronal correlates of sensory discrimination in the somatosensory cortex. Proc. Natl. Acad. Sci. U. S. A. 97, 6091–6096.

incisive tests to validate the meaning of the neural encoding of the flutter stimuli in the S1 cortex.

The vibrotactile discrimination task requires the comparison of the second stimulus frequency against the first (Hernández, A. *et al.*, 1997). As indicated above, Romo and colleagues found two types of responses in QA neurons of the S1 cortex: one that is periodically entrained by the stimulus frequency, and a second that, although not periodically entrained, has average firing rates during the stimulus period that are modulated as a function of the stimulus frequency (Hernández, A. *et al.*, 2000; Salinas, E. *et al.*, 2000; Luna, R. *et al.*, 2005). To investigate which of these two representations is associated with the psychophysical performance, these authors determined the probability that an observer (a cortical region central to S1 cortex) could distinguish the difference between the two stimuli (Hernández, A. *et al.*, 2000; Salinas, E. *et al.*, 2000; Luna, R. *et al.*, 2005). This could be based on a comparison of the neuronal response distributions of the second stimulus frequency made against the neuronal response distributions of the first stimulus frequency. According to this, the observer could use a simple rule: if the number of spikes during the second stimulus is higher than during the first stimulus, then the second stimulus is higher than the first. The same rule can be used when considering the periodicity values: if the periodicity (estimated as the frequency with greatest power in a Fourier transform of the spiking responses) during the second stimulus period is higher than during the first stimulus period, then the second stimulus is higher than the first. The effect of this type of rule is equivalent to determining the area under the curve ROC (receiver operating characteristic; Green, D. M. and Swets, J. A., 1966) generated by the neuronal response distributions for each pair of stimulus frequencies, using both periodicity and firing rate values (Hernández, A. *et al.*, 2000; Luna, R. *et al.*, 2005). The areas under each of these two ROC curves are an estimate of the proportion of correct trials that an optimal observer would obtain by comparing the number of spikes or periodicity. In pairs of stimulus frequencies where the neuronal response distributions during the second stimulus are much higher than the neuronal distributions of the first stimulus, ROC values are close to 1; if the neuronal response distributions during the stimulus are much lower than the neuronal response distributions of the first stimulus, ROC values are close to 0; for overlapping distributions, intermediate ROC values are found. The ROC values were then used to compute neurometric functions. Psychophysical and neuronal discrimination thresholds are calculated as half the difference between the stimulus frequency identified as higher than the standard in 75% of trials and that frequency identified as higher in 25% of the trials. These are read directly from the logistic functions expressed in terms of hertz. Using this analysis, Romo and colleagues are in the position to address the question of which of the two representations is meaningful for frequency discrimination.

Neurometric functions based on periodicity (Figures 6(c) and 6(d)) or firing rate (Figures 7(c) and (d)) of single S1 neurons were directly compared to the psychometric thresholds (Hernández, A. *et al.*, 2000). The results of this analysis show that neurometric threshold values based on periodicity are far lower than the psychometric thresholds (Figure 6(d)). This is not the case when neurometric thresholds based on firing rate are compared to the psychometric thresholds (Figure 7(d)). They are very close to the psychometric thresholds. The goal of computing neurometric functions was not only to reveal the relationship between the neuronal responses of S1 to the mechanical stimulus, but also to discern whether these neural signals account for the psychometric behavior. However, what is then the functional meaning of the periodic neural signal in S1? One possible role is that they simply represent the temporal structure of the stimulus and that monkeys do not use this exquisite representation for frequency discrimination. This would be the case if, for example, discrimination were based on the mean number of spikes (or bursts) fired by the population of QA neurons as a function of the stimulus frequency. Consistent with this idea, Hernández A. *et al.* (2000) found that QA neurons in S1 whose firing rates are modulated by the stimulus frequencies and their neurometric thresholds based on firing rates are closely similar to the monkey's psychophysical thresholds. However, these correlations do not prove they are sufficient for discrimination (Romo, R. *et al.*, 1998; 2000).

One experiment that could give an insight about the functional meaning of the periodic spike structure of the evoked activity in S1 is testing whether monkeys could discriminate the difference between the two stimuli when periodicity is broken. If monkeys fail to discriminate the difference in mean frequency between the two stimuli, this would strengthen the proposal that discrimination of flutter stimuli depends on the periodic structure of the spike trains evoked in S1 (Figure 8). However, monkeys were able to extract the mean frequency from the nonperiodic signals and the psychophysical measures were almost identical with the periodic stimuli (Romo, R. *et al.*, 1998).

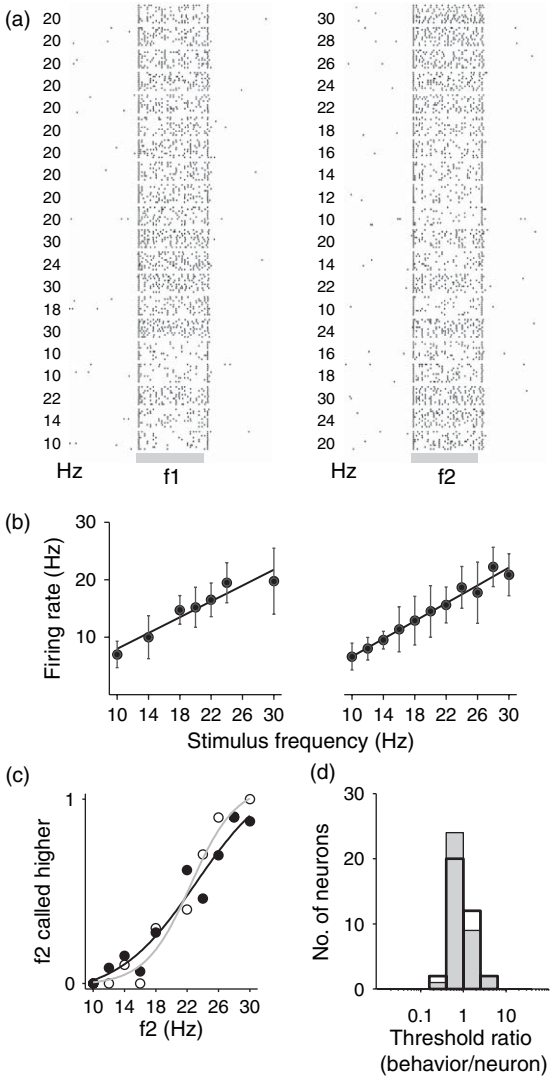

Figure 8 Firing rate modulation of a quickly adapting (QA) neuron of area 1 during the discrimination of aperiodic stimuli. Same format as in Figure 6, but both base (f1) and comparison (f2) frequencies (mean frequencies) lack periodicity. (a) Raster plots. (b) Mean firing rate (±SD) as a function of the stimulus frequency. (c) Relationship between psychometric and neurometric discrimination functions. (d) Threshold ratios calculated between psychometric and neurometric thresholds for each neuron during the discrimination of a periodic stimulus frequencies (open bars). Gray bars represent threshold ratios between psychometric and neurometric thresholds during the discrimination of aperiodic frequencies. Adapted from Hernández, A., Zainos, A., and Romo, R. 2000. Neuronal correlates of sensory discrimination in the somatosensory cortex. Proc. Natl. Acad. Sci. U. S. A. 97, 6091–6096.

Romo and colleagues then studied QA neurons in each of the two conditions: while monkeys discriminated between periodic stimuli and while monkeys discriminated between aperiodic stimuli (Hernández, A. *et al.*, 2000). Due to the aperiodic stimulus design, even highly stimulus-entrained neurons do not carry information about stimulus frequency in their periodicity. Clearly, neurometric thresholds based on the firing rate were again closely associated with the psychometric thresholds (Figures 8(c) and 8(d)). As in the periodic condition, a psychophysical observer could exploit firing rate for frequency discrimination of aperiodic stimuli. These results suggest that an observer could solve this task with a precision similar to that of the monkey, based only on the firing rate produced during the stimulus periods.

There are, however, some further unexplored possibilities. For example, QA neurons of S1 typically respond to each stimulus pulse with a discrete burst of spikes. Encoding of vibrotactile stimuli could therefore be based on the number or rate of events, where each event is defined as a burst instead of being defined as a single spike. An observer counting bursts would obtain a good estimate of the count of stimulus pulses, and this estimate would be independent of variability in the number of spikes fired in response to each pulse. Indeed, there is experimental evidence suggesting that bursting activity could efficiently encode the stimulus features (Reinagel, P. *et al.*, 1999; Martínez-Conde, S. *et al.*, 2000; Kepecs, A. *et al.*, 2002; Krahe, R. and Gabbiani, F., 2004). But whether bursting actually contributes directly to the psychophysical behavior is not known. Finally, the temporal window on which vibrotactile discrimination is based has not been determined. In previous experiments carried out by Romo and colleagues, stimulus periods were always 500 ms long. Under these conditions, the use of a code based on counting events and the use of a code based on the rate of events could not be distinguished.

To distinguish between all these alternatives, Romo and colleagues conducted new combined psychophysical and neurophysiological experiments in the vibrotactile discrimination task (Luna, R. *et al.*, 2005). They reasoned that if an observer uses a firing rate, a bursting rate, or a measure of periodicity, then increases or decreases in the duration of either of the two stimuli used in each trial of the task should not lead to a systematic bias in discrimination, in either of the two possible directions. (On the other hand, under this hypothesis, stimulus duration could affect the sensory signal-to-noise ratio and therefore affect the psychometric threshold.) Alternatively, if the observer uses a strategy based on the total number of spikes or bursts fired in response to each stimulus, then manipulation of

the stimulus duration should systematically bias performance, with longer stimuli being perceived as having been of higher frequencies than they actually were. Romo and colleagues found that when the duration of one of the two stimuli was changed by 50% relative to the other stimulus, monkeys indeed biased their discrimination performance (Luna, R. *et al.*, 2005). Monkeys treated shortened stimuli as if the applied stimulus frequency had been slightly but significantly lower than it actually was; conversely, monkeys treated lengthened stimuli as if the applied frequency had been slightly but significantly higher than it actually was. These effects were observed with both periodic and aperiodic stimuli. These investigators then sought an explanation for these psychophysical biases by recording QA neurons of S1 while the monkeys performed in variable-stimulus-length conditions (Luna, R. *et al.*, 2005). They found that the effects can be qualitatively explained if one assumes that the neural signal used by the observer to solve the task is an integral of either spikes or bursts over a time window that concentrates most of its mass within the first 250 ms of the stimulus, but also has a small tail into later parts of the stimulus. Finally, examining trial-by-trial covariations of weighted counts of spikes and weighted counts of bursts, they found that only the weighted count of spikes covaried with performance on a trial-by-trial basis.

In summary, firing rates that vary as functions of stimulus frequency are seen in multiple areas activated during the task, in particular in S1, and there is evidence that these rate variations have a significant impact on behavior. Clearly, the brain must be able to extract at least some information from the precise timing of S1 spikes evoked during the task; for instance, humans can easily distinguish periodic stimuli from aperiodic. However, Romo and colleagues found no indication that the high periodicity found in S1 contributes to frequency discrimination, although this possibility is hard to rule out entirely.

6.11.10 Artificial Induction of Activity in S1 Underlying Flutter Discrimination

How can we be sure that the activity recorded in S1 is actually related to perception and behavior? Intracortical microstimulation is a powerful technique capable of establishing a causal link – not just a correlation – between the activity of localized neuronal populations and specific cognitive functions (Salzman, D. *et al.*, 1990; Britten, K. H. and van Wezel, R. J., 1998; Romo, R. *et al.*, 1998; 2000). For flutter discrimination, this approach has provided the most compelling evidence that all the cognitive processes of the task may be triggered directly by the QA circuit in S1, and has also allowed us to explore questions about the neural code for flutter stimuli (Romo, R. *et al.*, 1998; 2000). Importantly, S1 is organized in modules of neurons sharing the same receptive field and mechanoreceptor submodality (Mountcastle, V. B., 1957; Powell, T. P. S. and Mountcastle, V. B., 1959; Sur, M. *et al.*, 1984). The experiments described below were aimed to drive a column(s) of S1 – mostly of the QA type – in a way that matched the dynamic responses recorded when mechanical stimuli were applied to a patch of skin of the fingertips.

Initially, the idea was to manipulate the comparison stimulus only (Romo, R. *et al.*, 1998). The monkeys first learned to discriminate the frequencies of two sinusoidal vibrations delivered successively to the fingertips. Once they mastered the task, neurophysiological recordings were made in area 3b of S1, which allowed the identification of clusters of QA neurons. An applied microstimulation current spreads around a certain cortical area, activating many neighboring units. Thus, a key for the success of microstimulation experiments is that the microelectrode must be located in the midst of a functionally homogeneous cluster of neurons. Fortunately, area 3b is indeed organized into modules of units with similar properties, or into columns (Sur, M. *et al.*, 1984). So, after the identificaton of a set of QA neurons, the comparison stimulus was substituted with microstimulation in one half of the trials. Artificial stimuli consisted of periodic current bursts delivered at the same comparison frequencies as mechanical stimuli. Microstimulation sites in S1 were selected to have QA neurons with receptive fields on the fingertip at the location of the mechanical stimulating probe. Remarkably, the monkeys discriminated the mechanical (base) and electrical (comparison) signals with performance profiles indistinguishable from those obtained with mechanical stimuli only (Figure 9(a)), so the artificially induced sensations probably resembled natural flutter quite closely (Romo, R. *et al.*, 1998).

Going back to the question of whether periodicity is crucial for frequency discrimination, Romo and colleagues applied aperiodic microstimulation patterns that mimicked the random trains of mechanical pulses discussed earlier (Figure 9(b)). The same mean frequencies were used in this condition – 20 Hz still corresponded to 10 current bursts delivered

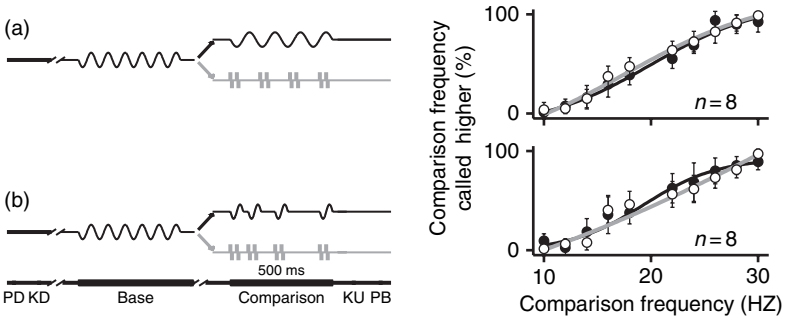

Figure 9 Psychophysical performance in frequency discrimination with natural mechanical stimuli and with artificial electrical stimuli injected into clusters of quickly adapting (QA) neurons of area 3b. The diagrams on the left show two types of trials that were interleaved during the experiments. In half of the trials, the monkeys compared two mechanical vibrations delivered on the skin. In the other half, one or both stimuli could be replaced by electrical frequencies microinjected into clusters of QA neurons of area 3b. The curves on the right show the animals' performance in the different situations, illustrated on the left. Filled and open circles indicate mechanical and electrical stimuli, respectively. In (a) and (b), the *y*-axis corresponds to the percentage of times the monkeys called the second stimulus frequency (*x*-axis) higher than the first (20 Hz). (a) Psychophysical performance using periodic stimuli; the comparison stimulus could be either mechanical or electrical frequencies. (b) Psychophysical performance when the comparison stimulus could be either aperiodic, mechanical or electrical stimulus frequencies. PD, indentation of the glabrous skin by the mechanical probe; KD, detection of indentation; KU, detection of the end of the comparison stimulus; PB, the monkeys presses one of two push buttons to indicate whether the second stimulus frequency was higher or lower than the first. Adapted from Romo, R., Hernández, A., Zainos, A., and Salinas, E. 1998. Somatosensory discrimination based on cortical microstimulation. Nature 392, 387–390.

in 500 ms – but the bursts were separated by random time intervals. Everything else proceeded as before, with mechanical and stimulation trials interleaved, as indicated in Figure 9(b). From the very first trials, the animals were able to discriminate both mechanical and electrical aperiodic signals (Figure 9(b)), with practically the same performance level reached with mechanical, periodic vibrations (Romo, R. *et al.*, 1998).

An interesting effect was observed as the intensity of the microstimulation current was varied. At very low intensities, artificial stimuli were not detected; the monkeys simply kept waiting. At intermediate intensities the monkeys detected the stimuli – they reacted and pushed a button – but their psychophysical behavior was at chance levels, as if they could determine the presence but not the frequency of the artificial stimuli. At higher intensities they discriminated normally (Romo, R. *et al.*, 1998). These transitions parallel those observed when the amplitude of mechanical vibrations is gradually increased; in particular, there is an atonal interval in which stimuli can be detected but their frequencies cannot be ascertained (LaMotte, R. H. and Mountcastle, V. B., 1975; Mountcastle, V. B. *et al.*, 1990). In an extra control experiment these authors investigated the effect of stimulus amplitude, which could potentially act as an alternate discrimination signal (Romo, R. *et al.*, 1998). Four frequency pairs and all stimuli were mechanical, and the other half of the comparison stimulus was electrical. In both cases, the amplitude of the comparison could take one of three values, a standard amplitude A, 0.6A, or 1.4A. The changes in amplitude were, in terms of percentage, of the same magnitude (40%) as the differences between base and comparison frequencies. The results showed that performance was not affected by the large variations in amplitude; had the monkeys been guided by the amplitudes changes, one of the three combinations for each frequency pair would have fallen to <25% correct, because performance was normally >75% correct. Amplitude corrections, like those mechanical stimuli, were also applied to electrical currents in ~60% of all runs; they had no marked impact on performance (Romo, R. *et al.*, 1998).

Because of the design of the paradigm, comparison of the second stimulus is made against a memory trace of the first one (Hernández, A. *et al.*, 1997). Having shown that the monkeys could use an artificial stimulus during the comparison, Romo and colleagues wondered whether they would be able to memorize and use an electrical stimulus delivered during the base period (Romo, R. *et al.*, 2000). In this case, in one half of the trials the base stimulus consisted of electrical microstimulation at a frequency equal to f1 (Figure 10), with the electric

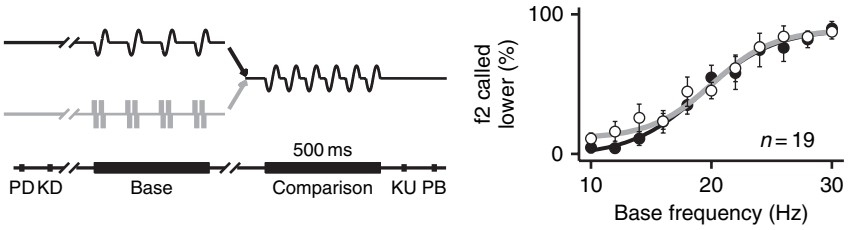

Figure 10 Psychophysical performance when the base stimulus could be either periodic, mechanical or electrical stimulus frequencies injected into clusters of quickly adapting (QA) neurons in area 3b. The same protocols and labels as in Figure 9, but here the base mechanical stimulus frequency was substituted by electrical stimulus frequencies. The *y*-axis corresponds to the percentage of times the monkeys called the comparison stimulus (20 Hz) lower than base stimuli at the frequency specified in the *x*-axis. Adapted from Romo, R., Hernández, A., Zainos, A., Brody, C.D., and Lemus, L. 2000. Sensing without touching: psychophysical performance based on cortical microstimulation. Neuron 26, 273–278.

current again being injected into QA neurons. The frequency pairs and event sequence during the task were the same as in previous experiments with natural stimuli; we stress this because careful design of the stimulus sets was particularly crucial here, in order to ensure that the monkeys paid attention to the base stimulus and stored it in working memory (Romo, R. *et al.*, 1999). The monkeys' psychophysical behavior was again indistinguishable from that observed with natural stimuli only (Figure 10), showing that the signals evoked by mechanical and artificial stimuli could be stored and recalled with approximately the same fidelity (Romo, R. *et al.*, 2000). Finally, they also investigated whether monkeys could perform the entire task on the basis of purely artificial stimuli. In most sessions in which the two mechanical stimuli were replaced by microstimulation patterns, monkeys were able to reach discrimination levels close to those measured with mechanical stimuli delivered to the fingertips. This demonstrates that activation of QA neurons is sufficient to drive all the cognitive processes involved in the task with little degradation in performance (Romo, R. *et al.*, 2000).

A couple of additional observations derived from these experiments are also noteworthy. First, early experiments with primary afferents had demonstrated that the flutter sensation is specifically mediated by QA fibers (Ochoa, J. and Torebjörk, E., 1983; Vallbo, A. B., 1995), but this was more difficult to test at the level of S1 (Romo, R. *et al.*, 1998). When microstimulation was applied to clusters of neurons identified as having slowly adapting (SA) properties (Figure 11(a)), the monkeys could barely discriminate, if at all (Romo, R. *et al.*, 2000). As the electrode was advanced to the border between SA and QA clusters, performance became somewhat better (Figure 11(b)), and it reached its usual degree of accuracy when QA properties became most evident in the recordings (Figure 11(c); Romo, R. *et al.*, 2000). Hence, QA and SA units are still functionally segregated in S1, consistent with previous observations (Sur, M. *et al.*, 1984).

In some sessions, Romo and colleagues were able to introduce three microelectrodes into a cluster of QA neurons of area 3b that shared the same receptive field (Romo, R. *et al.*, 2000). They knew that the most anterior microelectrode was placed in the superficial layers, because another microelectrode was placed in front of it and recorded units in primary motor cortex that were driven by spontaneous or passive movements of the fingers and lacked cutaneous receptive fields. The most posterior microelectrode was placed, they believe, in the lower layers, and the microelectrode between these two in the middle layers. In separate runs, the frequency pairs and event sequence were the same in both mechanical and microestimulation trials, except that in the microstimulation trials the first mechanical stimuli were substituted with train of current pulses delivered at the frequency of the mechanical stimulus they were substituting. Figure 12 shows that discrimination is triggered by microstimulating each of the three different clusters. Thus, activation of any part of the cluster of neurons (probably a QA column) with similar functional properties is sufficient to initiate discrimination in this task (Romo, R. *et al.*, 2000).

6.11.11 Further Comments on the Functional Role of S1 to Flutter Discrimination

The results obtained in these sets of experiments suggest that QA neurons from S1 represent the stimulus frequencies both in the periodic spike intervals and

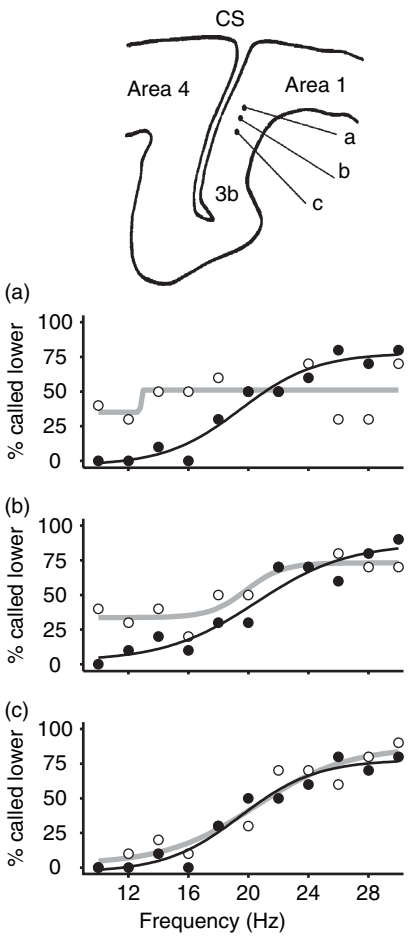

Figure 11 Psychophysical performance elicited by microstimulating at the base stimulus frequency in three different sites of area 3b. Same protocol and labels as in Figure 9. (a–c). Data collected in three separate runs during the same electrode penetration. (a) Psychophysical performance when microstimulation was applied in the center of cluster of slowly adapting (SA) neurons. (b) Psychophysical performance when microstimulation was applied in the border between quickly adapting (QA) and SA neurons. (c) Psychophysical performance when microstimulation was applied in a cluster of QA neurons. CS, central sulcus. Adapted from Romo, R., Hernández, A., Zainos, A., Brody, C.D., and Lemus, L. 2000. Sensing without touching: psychophysical performance based on cortical microstimulation. Neuron 26, 273–278.

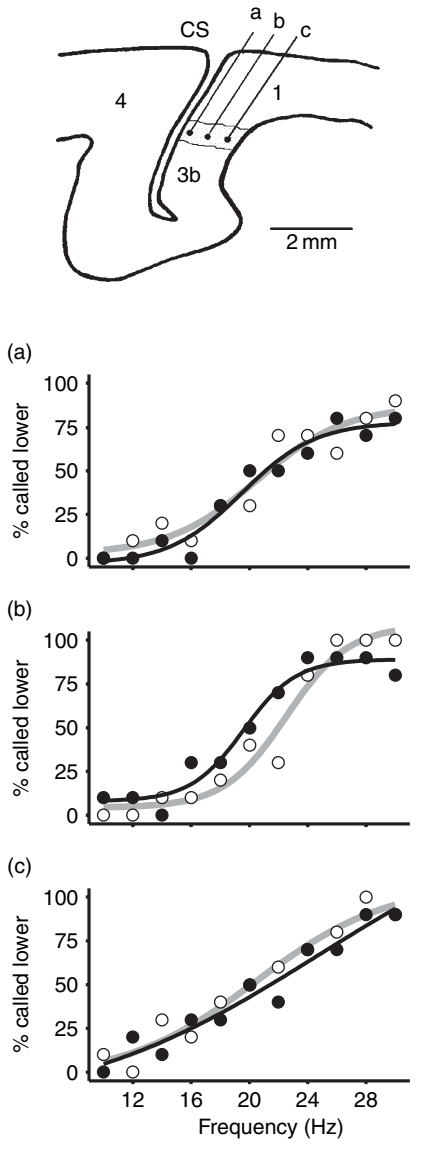

Figure 12 Psychophysical performance elicited by microstimulating at the base stimulus frequency in three independent microelectrodes in three different sites of a cluster of quickly adapting (QA) neurons of area 3b. Protocols and labels as in Figure 9. CS, central sulcus. Adapted from Romo, R., Hernández, A., Zainos, A., Brody, C.D., and Lemus, L. 2000. Sensing without touching: psychophysical performance based on cortical microstimulation. Neuron 26, 273–278.

in the firing rate (Hernández, A. *et al*., 2000; Salinas, E. *et al*., 2000), and that activation of the QA circuit is sufficient to activate the entire chain of discrimination processes of this task (Romo, R. *et al*., 1998; 2000).

The conclusion previously found in the literature – that frequency discrimination is based on periodicity – came from the observation that a small number of studied QA neurons from S1 reproduce in their activity the periodicity of the mechanical stimulus frequency, and also from the fact that these neurons did not have average firing rates that were modulated by the stimulus frequency (Mountcastle, V. B. *et al*., 1990). However, the study that reached this conclusion only determined the relationship between the

neuronal responses to the mechanical stimulus frequencies; no attempt was made to quantify the neurometric thresholds based on periodicity and to compare these to the psychophysical thresholds. Romo and colleagues observed that neurometric thresholds using the periodicity values are far lower than the psychometric thresholds (Hernández, A. *et al.*, 2000). What is then the functional meaning of this neural signal? One possible role is that this simply represents the temporal structure of the stimulus and that monkeys do not use this exquisite representation for frequency discrimination. Consistent with this interpretation, these authors found QA neurons in S1 whose firing rates are modulated by the stimulus frequencies (Salinas, E. *et al.*, 2000), and their neurometric thresholds based on this measure are similar to the monkey's psychophysical thresholds (Hernández, A. *et al.*, 2000).

These results also suggest that QA neurons of S1, which are classified according to their capacity to react to a slight mechanical indentation applied to the center of their receptive fields, may in fact be composed of two subpopulations, each of which behaves differently in response to a periodic mechanical stimulus. These two subpopulations might be organized in a hierarchical fashion: QA neurons that respond periodically might be closer to the input stimulus, and those that modulate their firing rate might integrate the responses of the periodic neurons and transform them into a rate code. Such last-order neurons of the QA circuit could distribute the neural representation of the stimulus to those structures anatomically linked to S1 (Burton, H. and Fabri, M., 1995; Burton, H. *et al.*, 1995), to solve the sensory discrimination task. Relevant to this interpretation is the fact that neurons in secondary somatosensory cortex (S2) respond by encoding the stimulus frequencies in their firing rates and this encoding correlates closely with the subject's discrimination performance (Salinas, E. *et al.*, 2000; Romo, R. *et al.*, 2002; 2003). Ascending the cortical hierarchy, neurons in the prefrontal cortex and in the premotor cortices respond, encoding the entire sequence of the discrimination task, and correlate closely with the decision motor report (Romo, R. *et al.*, 1999; Hernández, A. *et al.*, 2002; Brody. C. D. *et al.*, 2003; Romo, R. *et al.*, 2004).

The results obtained in the microstimulation experiments show that the relationship between the neuronal responses and the animal's behavior in the flutter discrimination task are not simple coincidences (Romo, R. *et al.*, 1998; 2000). Monkeys were able to discriminate the stimulus frequencies either delivered to the fingertips or artificially injected into a cluster of QA neurons. The specificity of QA stimulation for frequency discrimination is suggested by the fact that SA stimulation cannot produce discrimination (Romo, R. *et al.*, 2000). Interestingly, it has been shown that activity in a single cutaneous afferent fiber could produce localized somatic sensations (Ochoa, J. and Torebjörk, E., 1983; Macefield, G. *et al.*, 1990; Vallbo, A. B., 1995), and frequency microstimulation of QA afferents linked to Meissner's corpuscles produced the sensation of flutter (Vallbo, A. B., 1995). These observations strongly support the notion that the activity initiated in specific mechanoreceptors is read out by S1; this reading is then widely distributed to those anatomical structures that are linked to S1 (Romo, R. and Salinas, E., 2001). The whole sequence of events associated with this sensory discrimination task must depend on this distributed neural signal (Romo, R. *et al.*, 1999; Hernández, A. *et al.*, 2002; Romo, R. *et al.*, 2002; Brody, C. D. *et al.*, 2003; Romo, R. and Salinas, E., 2003; Romo, R. *et al.*, 2004).

6.11.12 Conclusion

The highly simplified sensory tasks used here require perception of the stimuli and producing a decision that is communicated to the motor apparatus. The most salient result obtained in the detection task is that the S1 activity does not account for the variability in the detection responses at near-threshold stimuli. However, the S1 neural representation of the stimulus is necessary for further central processing. Indeed, the activity of areas central to S1 did covary with trial-by-trial judgments in the detection task (not reviewed here). This suggests that perceptual judgments in this task arise in the activity of those areas linked to S1. Experiments not reviewed here show that covariations between neuronal activities and perceptual judgments increase gradually, from lower covariations in the somatosensory cortices of the parietal lobe to higher covariations in some areas of the frontal lobe. Experiments in the vibrotactile discrimination task suggest that S1 transforms the phase-locked responses into a firing rate code that accounts for the variability of the discrimination performance. Activation of the QA circuit of S1 appears sufficient for vibrotactile discrimination; however, similar to the detection task, perceptual judgments arise in the activity of more central areas linked to S1.

Acknowledgments

The research of R. Romo was supported in part by an International Research Scholars Award from the Howard Hughes Medical Institute and from grants from CONACYT and DGAPA-UNAM.

References

Adrian, E. D. 1928. The Basis of Sensation. The Action of the Sense Organs. Christophers.

Bair, W., Zohary, E., and Newsome, W. T. 2001. Correlated firing in macaque visual MT: time scales and relationship to behavior. J. Neurosci. 21, 1676–1697.

Britten, K. H. and van Wezel, R. J. 1998. Electrical microstimulation of cortical MST biases heading perception in monkeys. Nat. Neurosci. 1, 59–63.

Britten, K. H., Newsome, W. T., Shadlen, M. N., Celebrini, S., and Movshon, J. A. 1996. A relationship between behavioral choice and the visual responses of neurons in macaque MT. Vis. Neurosci. 13, 87–100.

Brody, C. D., Hernández, A., Zainos, A., and Romo, R. 2003. Timing and neural encoding of somatosensory parametric working memory in macaque monkey. Cereb. Cortex 13, 1196–1207.

Burton, H. and Fabri, M. 1995. Ipsilateral intracortical connections of physiologically defined cutaneous representations in areas 3b and 1 of macaque monkeys. J. Comp. Neurol. 355, 508–538.

Burton, H., Fabri, M., and Alloway, K. 1995. Cortical areas within the lateral sulcus connected to cutaneous representations in areas 3b and 1: a revisited interpretation of the second somatosensory area in macaque monkeys. J. Comp. Neurol. 355, 539–562.

Fries, P., Neueschwander, S., Engel, A. K., Goebel, R., and Singer, W. 2001a. Rapid feature selective neuronal synchronization through correlated latency shifting. Nat. Neurosci. 4, 194–200.

Fries, P., Reynolds, J. H., Rorie, A. E., and Desimone, R. 2001b. Modulation of oscillatory neuronal synchronization by selective visual attention. Science 291, 1560–1563.

Green, D. M. and Swets, J. A. 1966. Signal Detection Theory and Psychophysics. Wiley.

Hernández, A., Salinas, E., Garcia, R., and Romo, R. 1997. Discrimination in the sense of flutter: new psychophysical measurements in monkeys. J. Neurosci. 17, 6391–6400.

Hernández, A., Zainos, A., and Romo, R. 2000. Neuronal correlates of sensory discrimination in the somatosensory cortex. Proc. Natl. Acad. Sci. U. S. A. 97, 6091–6096.

Hernández, A., Zainos, A., and Romo, R. 2002. Temporal evolution of a decision-making process in medial premotor cortex. Neuron 33, 959–972.

Hubel, D. H. and Wiesel, T. N. 1998. Early exploration of the visual cortex. Neuron 20, 401–412.

Johnson, K. O. 1980. Sensory discrimination: neural processes preceding discrimination decision. J. Neurophysiol. 43, 1793–1815.

Kepecs, A., Wang, X. J., and Lisman, J. 2002. Bursting neurons signal input slope. J. Neurosci. 22, 9053–9062.

Krahe, R. and Gabbiani, F. 2004. Burst firing in sensory systems. Nat. Rev. Neurosci. 5, 13–24.

de Lafuente, V. and Romo, R. 2005. Neuronal correlates of subjective sensory experience. Nat. Neurosci. 12, 1698–1703.

de Lafuente, V. and Romo, R. 2006. Neural correlate of subjective sensory experience gradually builds up across cortical areas. Proc. Natl. Acad. Sci. U. S. A. 10, 1266–1271.

LaMotte, R. H. and Mountcastle, V. B. 1975. Capacities of humans and monkeys to discriminate between vibratory stimuli of different frequency and amplitude: correlation between neural events and psychophysical measurements. J. Neurophysiol. 38, 539–559.

Luna, R., Hernández, A., Brody, C. D., and Romo, R. 2005. Neural codes for perceptual discrimination in primary somatosensory cortex. Nat. Neurosci. 8, 1210–1219.

Macefield, G., Gandevia, S. C., and Burke, D. 1990. Perceptual responses to microstimulation of single afferents innervating joints, muscles and skin of the human hand. J. Physiol. 429, 113–129.

Martínez-Conde, S., Mckinik, S. L., and Hubel, D. H. 2000. The function of bursts of spikes during visual fixation in the awake primate lateral geniculate nucleus and primary visual cortex. Proc. Natl. Acad. Sci. U. S. A. 99, 13920–13925.

Mountcastle, V. B. 1957. Modality and topographic properties of single neurons of cat's somatic sensory cortex. J. Neurophysiol. 20, 408–434.

Mountcastle, V. B., Talbot, W. H., Darian-Smith, I., and Kornhuber, H. H. 1967. Neural basis of the sense of flutter-vibration. Science 155, 597–600.

Mountcastle, V. B., Talbot, W. H., Sakata, H., and Hyvärinen, J. 1969. Cortical neuronal mechanisms in flutter-vibration studied in unanesthetized monkeys. Neuronal periodicity and frequency discrimination. J. Neurophysiol. 32, 452–484.

Mountcastle, V. B., Steinmetz, M. A., and Romo, R. 1990. Frequency discrimination in the sense of flutter: psychophysical measurements correlated with postcentral events in behaving monkeys. J. Neurosci. 10, 3032–3044.

Newsome, W. T., Britten, K. H., and Movshon, J. A. 1989. Neural correlates of a perceptual decision. Nature 341, 52–54.

Ochoa, J. and Torebjörk, E. 1983. Sensations evoked by intraneural microstimulation of single mechanoreceptor units innervating the human hand. J. Physiol. 342, 633–654.

Powell, T. P. S. and Mountcastle, V. B. 1959. Some aspects of the functional organization of the cortex of the postcentral gyrus of the monkey: a correlation of findings obtained in a single unit analysis with cytoarchitecture. Bull. Johns Hopkins Hosp. 105, 133–162.

Recanzone, G. H., Merzenich, M. M., and Schreiner, C. E. 1992. Changes in the distributed temporal response properties of SI cortical neurons reflect improvements in performance on a temporally based tactile discrimination task. J. Neurophysiol. 67, 1071–1091.

Reinagel, P., Godwin, D., Sherman, M., and Koch, C. 1999 Encoding of visual information by LGN bursts. J. Neurophysiol. 81, 2558–2569.

Ress, D. and Heeger, D. J. 2003. Neuronal correlates of perception in early visual cortex. Nat. Neurosci. 6, 414–420.

Romo, R. and Salinas, E. 2001. Touch and go: decision-making mechanisms in somatosensation. Annu. Rev. Neurosci. 24, 107–137.

Romo, R. and Salinas, E. 2003. Flutter discrimination: neural codes, perception, memory and decision making. Nat. Rev. Neurosci. 4, 203–218.

Romo, R., Brody, C. D., Hernández, A., and Lemus, L. 1999. Neuronal correlates of parametric working memory in the prefrontal cortex. Nature 399, 470–473.

Romo, R., Hernández, A., and Zainos, A. 2004. Neuronal correlates of a perceptual decision in ventral premotor cortex. Neuron 41, 165–173.

Romo, R., Hernández, A., Zainos, A., Brody, C. D., and Lemus, L. 2000. Sensing without touching: psychophysical performance based on cortical microstimulation. Neuron 26, 273–278.

Romo, R., Hernández, A., Zainos, A., Lemus, L., and Brody, C. D. 2002. Neuronal correlates of decision-making in secondary somatosensory cortex. Nat. Neurosci. 5, 1217–1225.

Romo, R., Hernández, A., Zainos, A., and Salinas, E. 1998. Somatosensory discrimination based on cortical microstimulation. Nature 392, 387–390.

Romo, R., Hernández, A., Zainos, A., and Salinas, E. 2003. Correlated neuronal discharges that increase coding efficiency during perceptual discrimination. Neuron 38, 649–657.

Salinas, E., Hernández, A., Zainos, A., and Romo, R. 2000. Periodicity and firing rate as candidate neural codes for the frequency of vibrotactile stimuli. J. Neurosci. 20, 5503–5515.

Salzman, D., Britten, K. H., and Newsome, W. T. 1990. Cortical microstimulation influences perceptual judgements of motion direction. Nature 346, 174–177.

Schall, J. D. 2001. Neural basis of deciding, choosing and acting. Nat. Rev. Neurosci. 2, 583–591.

Sur, M., Wall, J. T., and Kaas, J. H. 1984. Modular distribution of neurons with slowly adapting and rapidly adapting responses in area 3b of somatosensory cortex in monkeys. J. Neurophysiol. 51, 724–744.

Talbot, W. H., Darian-Smith, I., Kornhuber, H. H., and Mountcastle, V. B. 1968. The sense of flutter-vibration: comparison of the human capacity response patterns of mechanoreceptive afferents from the monkey hand. J. Neurophysiol. 31, 301–334.

Vallbo, A. B. 1995. Single-Afferent Neurons and Somatic Sensation in Humans. In: The Cognitive Neurosciences (*ed*. M. S. Gazzaniga), pp. 237–252. MIT Press.

Vázquez, P., Cano, M., and Acuña, C. 2000. Discrimination of line orientation in humans and monkeys. J. Neurophysiol. 83, 2639–2648.

Vogel, R. and Orban, G. 1990. How well do response changes of striate neurons signal differences in orientation: a study in the discriminating monkey. J. Neurosci. 10, 3543–3558.

Zohary, E., Shadlen, M. N., and Newsome, W. T. 1994. Correlated neuronal discharge rate and its implications for psychophysical performance. Nature 370, 140–143.

Further Reading

Mountcastle, V. B., LaMotte, R. H., and Carli, G. 1972. Detection thresholds for stimuli in humans and monkeys: comparison with thresholds events in mechanoreceptive afferent nerve fibers innervating the monkey hand. J. Neurophysiol. 25, 122–136.

Vallbo, A. B. and Johansson, R. S. 1984. Properties of cutaneous mechanoreceptors in the human hand related to touch sensations. Hum. Neurobiol. 3, 3–14.

6.12 Dorsal and Ventral Streams in the Sense of Touch

Esther P Gardner, Department of Physiology and Neuroscience, New York University School of Medicine, New York, NY, USA

© 2008 Elsevier Ltd. All rights reserved.

6.12.1	Introduction	233
6.12.2	Anatomical Localization of the Posterior Parietal Cortex	234
6.12.3	Physiological Studies of Posterior Parietal Cortex	237
6.12.3.1	Reaching as a Model System for Analyzing Sensorimotor Integration	238
6.12.3.2	Role of Posterior Parietal Cortex in Motor Planning and the Neural Representation of Space	239
6.12.3.3	Grasping and Hand Manipulation Neurons in Posterior Parietal Cortex	242
6.12.4	Bilateral Coordination of the Hands	249
6.12.5	Posterior Parietal Cortex and Active Touch	251
6.12.6	Conclusions	252
References		253

Glossary

haptics The study of touch and tactile sensations, especially as a means of communication. Haptic sensations are derived primarily from active touch, in which proprioceptive and cutaneous inputs are combined to define object properties.

intention Direction of the mind or attention to a particular action, goal, or effort. Intention also implies understanding the meaning, significance, import, purpose, design, or aim of an action. In its strongest usage, intention describes the volition or determination to carry out a particular action.

kinematics The science concerned with movements of the parts of the body.

kinaesthesia (kinesthesis) The sense of muscular effort and perception of movement that accompanies a voluntary motion of the body. This sense is mediated by end organs located in muscles, tendons, and joints stimulated by bodily movements and tensions.

prehension The action of taking possession of and grasping or holding something. The term is also applied to mental comprehension, the action of grasping with the mind.

proprioception The sense or perception, usually at a subconscious level, of the movements and posture of the body and especially its limbs, independent of vision. This sense is mediated by sensory nerve terminals in muscles and tendons (muscle spindles) and the fibrous capsule of joints combined with input from the vestibular apparatus.

stereognosis The appreciation and recognition of the form of solid objects by means of touch.

tactile agnosia The inability to recognize objects by touch, in the presence of intact cutaneous and proprioceptive hand sensation. This deficit is caused by a lesion in the contralateral parietal lobe, and is also termed astereognosis.

6.12.1 Introduction

One of the key concepts to illuminate our understanding of sensory processing in the cerebral cortex was set forth in a seminal paper by Ungerleider L. G. and Mishkin M. (1982). They proposed that visual information from the retina enters the cortex in the primary visual area, V1, is transmitted to V2 cortex, and then split into two parallel pathways directed to the temporal and parietal lobes. These pathways analyze the same sensory information in different ways that came to be known as the what and where streams.

The ventral stream – transmitted through the inferotemporal cortex – is the putative 'what' pathway. These cortical areas analyze the visual signals to derive cognitive information about the size, shape, and color of the stimulus. These intrinsic properties allow us to recognize such stimuli as distinct objects, persons, or places. The dorsal stream – transmitted through the parietal lobe – forms the where pathway. It analyzes the extrinsic properties of the image, defining the spatial and temporal properties of the stimulus with respect to the observer and the environment.

Later studies of these pathways by Milner A. D. and Goodale M. A. (1995) suggested a more sophisticated view, based on their clinical studies of patients with lesions localized to the parietal or temporal cortex. They proposed that the ventral stream forms a vision-for-cognition pathway that allows us to name objects, contributing to semantic memory. The dorsal stream forms a vision-for-action network that provides spatial information for guiding behavior. The parietal pathway creates a pragmatic representation of the world needed for immediate action, and for the formation of procedural memories underlying skilled behavior. The Milner–Goodale hypothesis can be summarized as what and how networks.

Mishkin M. (1979) also proposed a similar dual organization of the somatosensory pathways for touch and proprioception. In his formulation, the somatosensory ventral stream originates in the projections from the primary somatic sensory cortex (S-I) to the second somatic sensory area (S-II cortex), including the neighboring zones along the upper bank of the Sylvian (lateral) fissure and the parietal operculum. The ventral network has strong anatomical links through the insular cortex to the medial temporal lobe and hippocampus (Friedman, D. P. *et al.*, 1986; Felleman, D. J. and Van Essen, D. C., 1991), providing a cortico-limbic circuit for object memory acquired through touch.

The somatosensory dorsal stream is conveyed through the posterior parietal cortex (PPC), particularly the region bordering the intraparietal sulcus (IPS) in humans and monkeys. The dorsal stream represents the actions of the subject when interacting with the environment, as gleaned by touch and proprioception. The PPC projects primarily to the premotor areas of the frontal lobe, providing a pathway for initiating and controlling motor behavior. These frontal–parietal networks play a key role in voluntary movement, particularly the skilled behaviors of the hand and arm: reaching, grasping, and tool use.

In this chapter, I review the anatomical, physiological, and clinical evidence for a dorsal stream pathway in the sense of touch. The discussion is focused on actions of the hand and arm, as physiological studies have concentrated on the role of PPC in reach and grasp behaviors. The properties of the ventral stream network in the sense of touch are described in the chapters by Leah Krubitzer, Steven Hsiao, and Ranulfo Romo in this volume.

6.12.2 Anatomical Localization of the Posterior Parietal Cortex

The cortical areas surrounding the IPS in monkeys are referred to collectively as the posterior parietal cortex. PPC is normally subdivided anatomically into a rostral division – the superior parietal lobule (SPL) – and a caudal zone – the inferior parietal lobule (IPL). The SPL and IPL in monkeys were named areas 5 and 7 by Brodmann K. (1909). Vogt C. and Vogt O. (1919) subdivided the SPL into caudal and rostral regions (areas 5a and 5b), and the IPL into areas 7a and 7b. Later anatomists further subdivided the SPL into areas PE, PEc, and PEa, and the IPL convexity into areas PF, PFG, PG, and Opt (von Economo, C. and Koskinas, G. N., 1925; von Bonin, G. and Bailey, P., 1947; Pandya, D. N. and Selzer, B., 1982; Gregoriou, G. G. *et al.*, 2006) (Figure 1). Anatomical distinctions were also made for the regions buried within the wall of the IPS (areas MIP, LIP, AIP, and VIP) and those bordering the parietal operculum (PFop and PGop).

More recent physiological, cytoarchitectural, myeloarchitectural, and connectionist studies have resulted in further fractionation of this region into 17 distinct areas concerned primarily with vision and/or somatic sensation (Lewis, J. W. and Van Essen, D. C., 2000a; 2000b; Van Essen, D. C. *et al.*, 2001). Visual areas are situated primarily in the IPL, and along the midline at the parietal–occipital (PO) junction; these include areas 7a, LIPv, LIPd, VIPm, VIPl, PO (V6A), PIP, V3, V3A, MDP, and LOP. Somatosensory areas are situated primarily in the SPL, and in the rostral and lateral regions of the IPL (areas 5d, 5v, MIP, AIP, 7b, and 7t) (Figure 2). To add to the confusion of terminology, the regions of the SPL in the human brain called BA5 and BA7 do not coincide with their namesakes in the macaque cortex; their properties as revealed in functional imaging studies suggest instead that they correspond to areas PE, PEa, and PEc in the macaque (Galletti, C.

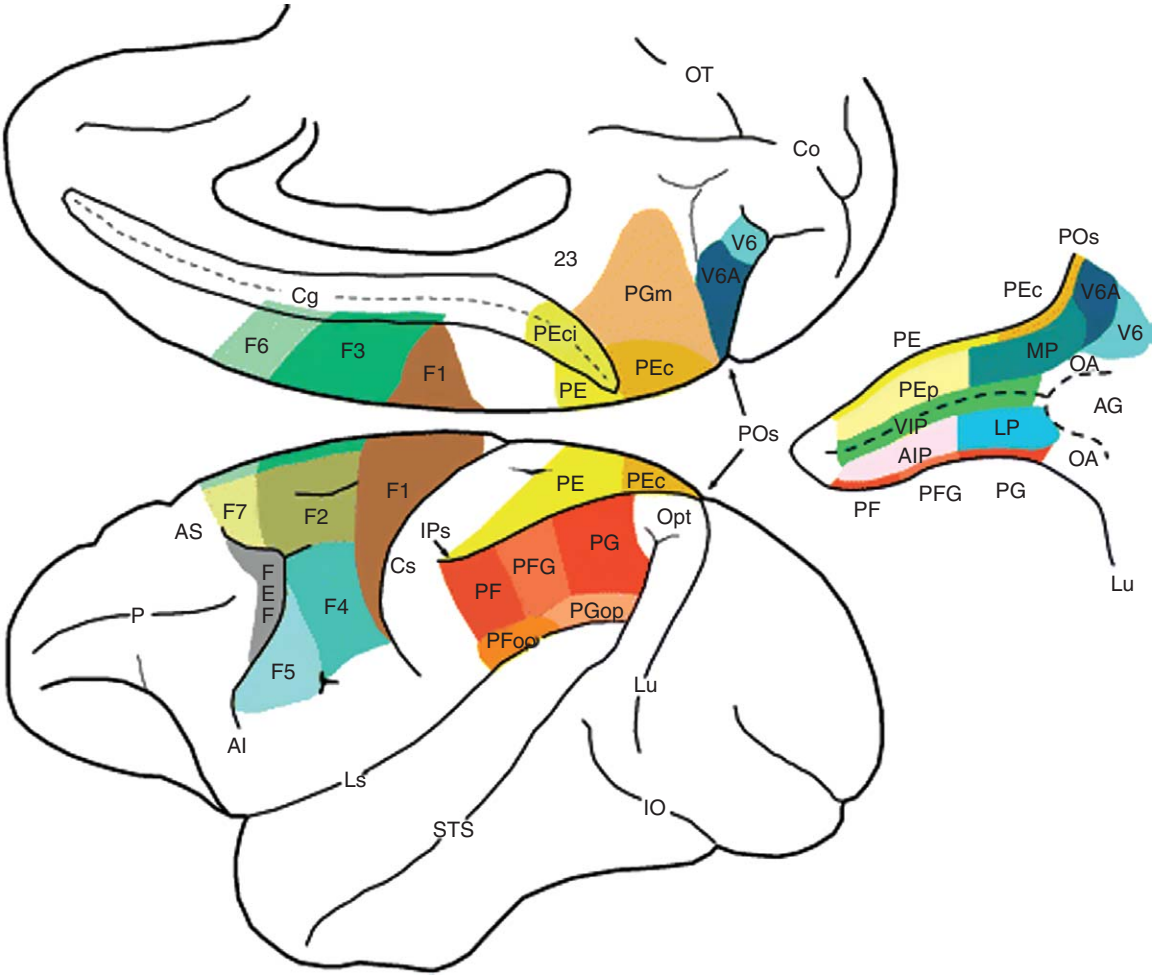

Figure 1 Lateral and medial views of the macaque cerebral cortex showing the anatomical locations of the posterior parietal cortex (areas PE, PEc, PO, PF, PFG, PG, Opt, PFop, and PGop) and frontal motor areas (areas F1, F2/F3, F7/F6, F4, F5, and FEF). The inset shows the areas lying within the intraparietal sulcus (IPS). Reproduced from Rizzolatti, G. and Matelli, M. 2003. Two different streams form the dorsal visual system: anatomy and functions. Exp. Brain Res. 153, 146–157; figure 1).

et al., 1997; Binkofski, F. *et al.*, 1999a). Similarly, the human BA39 and 40 are functionally related to the macaque areas 7a and 7b.

The anatomical connections of somatosensory areas of the PPC are schematized in Figure 3. The principal somatosensory input to area 5 originates from S-I cortex, particularly from area 2 (Jones, E. G. and Powell, T. P. S., 1969; 1970; Pearson, R. C. A. and Powell, T. P. S., 1985). These feed-forward projections are somatotopic. The hand representation in S-I projects to the lateral end of the IPS in areas 5d and 5v that is involved in grasping behaviors (Mountcastle, V. B. *et al.*, 1975; Gardner, E. P. *et al.*, 1999; 2002; 2007a). The arm and shoulder regions project to more medial and caudal regions in the SPL – designated the parietal reach region (PRR) – that are involved in reaching (reviewed in Caminiti, R. *et al.*, 1996; Andersen, R. A. *et al.*, 1997; Kalaska, J. F. *et al.*, 1997; Caminiti, R. *et al.*, 1998; Burnod, Y. *et al.*, 1999; Andersen, R. A. and Buneo, C. A., 2002). The face representation projects to area VIP, located at the fundus of the IPS at its rostral end; this region may be involved in hand–mouth coordination during feeding (Colby, C. L. *et al.*, 1993; Duhamel, J. R. *et al.*, 1998; Colby, C. L. and Goldberg, M. E., 1999).

Tracer injection studies reveal extensive interconnections between different subregions of the SPL and IPL. For example, the primary output targets of neurons in the hand region of area 5 are the more caudal regions of the SPL involved in reaching (Seltzer, B. and Pandya, D. N., 1980; Pandya, D. N. and Selzer, B., 1982; Lewis, J. W. and Van Essen, D.

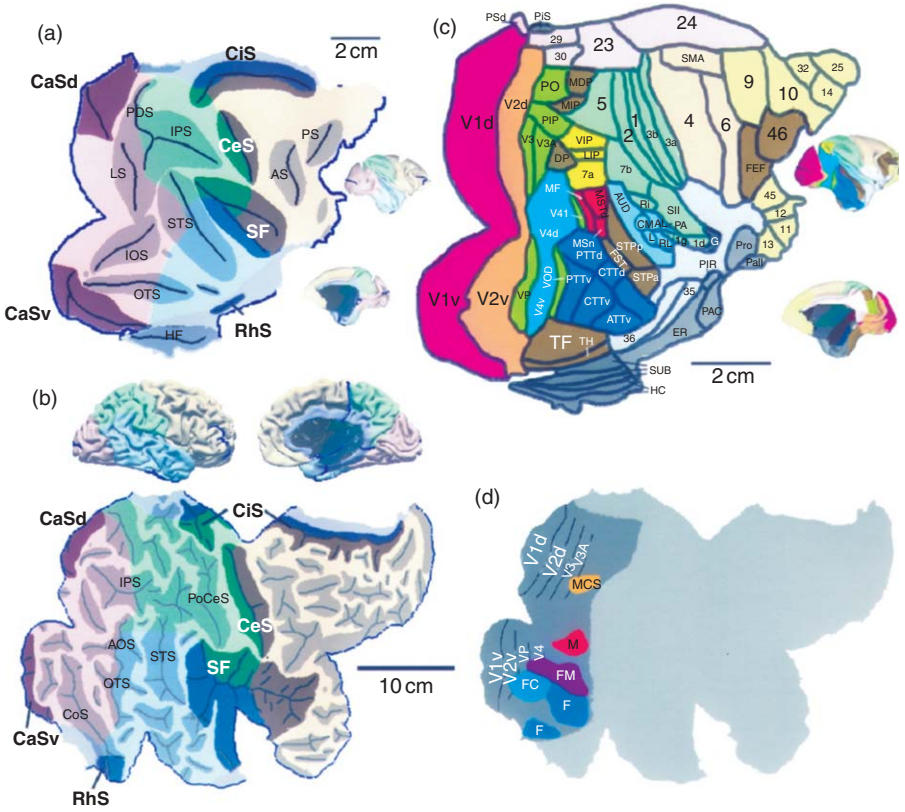

Figure 2 Flat maps showing the spatial relationship between somatosensory, visual, auditory, and motor areas of the cerebral cortex in macaques (a and c) and humans (b and d). The surface is colored to delineate the different cortical lobes. *Shaded regions* on the flat map indicate cortex buried within various sulci (AS, arcuate sulcus; CaS, calcarine sulcus (dorsal and ventral); CeS, central sulcus; CiS, cingulate sulcus; HF, hippocampal fissure; IOS, inferior occipital sulcus; IPS, intraparietal sulcus; LS, lunate sulcus; OTS, occipito-temporal sulcus; POS, parieto-occipital sulcus; PS, principal sulcus; RhS, rhinal sulcus; SF, Sylvian fissure; STS, superior temporal sulcus). Cortical areas in the macaque are labeled according to the partitioning scheme of Felleman D. J. and Van Essen D. C. (1991). Posterior parietal visual areas along the midline are colored chartreuse green (PO, PIP, V3, and V3A), and those buried in the IPS (AIP and VIP) and adjacent bank of the IPL (7a) are colored yellow. Somatosensory areas (3a, 3b, 1, 2, 5, 7b, SII, Ri, and Ig) are shown in pale green. Brown areas between the parietal visual and somatosensory regions (MDP, MIP, and DP) form portions of the parietal reach region (PRR). Dark blue regions in the temporal lobe indicate the ventral visual areas; no distinction is made in this figure between dorsal and ventral somatosensory areas. Reproduced from Van Essen, D. C. and Drury, H. A. 1997. Structural and functional analyses of human cerebral cortex using a surface-based atlas. J. Neurosci. 17, 7079–7107; figure 13).

C., 2000b), providing anatomical pathways to coordinate reach and grasp during goal-directed hand behaviors. Neurons in the hand representation of area 5 project to mirror-image sites in the contralateral hemisphere, providing circuitry for bilateral coordination of the left and right hands (Jones, E. G. *et al.*, 1978; Padberg, J. *et al.*, 2005). This is the first site of bilateral hand interactions in the dorsal pathway, as the hand representation in S-I is apparently acallosal (Jones, E. G. *et al.*, 1978; 1979; Caminiti, R. and Sbriccoli, A., 1985; Shanks, M. F. *et al.*, 1985; Padberg, J. *et al.*, 2005).

Neurons in the hand representation of area 5 also provide prominent somatosensory inputs to areas AIP and 7b in the IPL (Neal, J. W. *et al.*, 1986; 1987; Cavada, C. and Goldman-Rakic, P., 1989a), thereby linking tactile and visual information needed for grasping. The connections between SPL and IPL neurons are reciprocal, allowing exchange of tactile and visual information between cortical areas. Area 7b also receives somatosensory inputs from S-II cortex (Disbrow, E. *et al.*, 2003).

Area 5 also has strong projections to motor areas of the frontal lobe, particularly to the premotor cortex. Medial regions of area 5 that represent the arm project primarily to the dorsal premotor cortex (PMd or F2), while the lateral regions representing the hand and face project to ventral premotor cortex

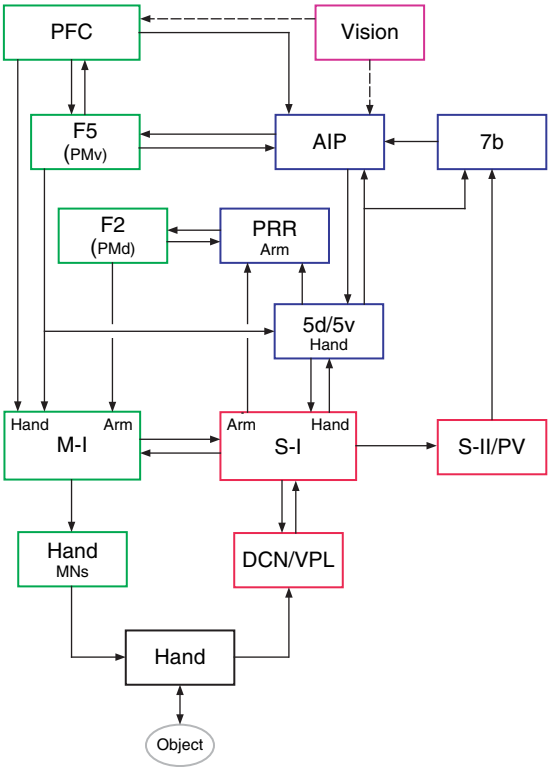

Figure 3 Simplified block diagram of the input–output circuits for grasping. Somatosensory areas (red): DCN/VPL (dorsal column nuclei and ventral posterolateral nucleus of the thalamus), S-I (primary somatosensory cortex, areas 3a, 3b, 1, and 2), S-II/PV (secondary somatosensory and parietal ventral cortex). Posterior parietal areas (blue): 5d/5v (rostral end of superior parietal lobule), PRR (parietal reach region, caudal end of superior parietal lobule), AIP (anterior intraparietal area of inferior parietal lobule), and 7b (lateral convexity of the inferior parietal lobule). Frontal motor areas (green): PFC (prefrontal cortex), F5 (ventral premotor cortex), F2 (dorsal premotor cortex), and M-I (primary motor cortex). Other important frontal motor areas that project to M-I, such as the supplementary motor area (SMA) and cingulate motor area (CMA), are not shown, nor are the corticomotor pathways to spinal interneurons from M-I and F5. Visual areas (violet): For simplicity, the visual pathways from the retina to areas AIP, PRR, and PFC have been compressed into a single box that includes important visuomotor centers of PPC such as areas LIP, CIP, 7a, and V6A; the dashed arrows denote polysynaptic pathways. Reproduced from Gardner, E. P., Ro, J. Y., Babu, K. S., and Ghosh, S. 2007b. Neurophysiology of prehension: II. Response diversity in primary somatosensory (S-I) and motor (M-I) cortices. J. Neurophysiol. 97, 1656–1670; figure 10).

(PMv or F5/F4) (Petrides, M. and Pandya, D. N., 1984; Matelli, M. *et al.*, 1986; Cavada, C. and Goldman-Rakic, P., 1989b; Kurata, K., 1991; Ghosh, S. and Gattera, R., 1995; Johnson, P. B. *et al.*, 1996; Wise, S. P. *et al.*, 1997; Matelli, M. *et al.*, 1998; Luppino, G. *et al.*, 1999; Matelli, M. and Luppino, G., 2001; Tanne-Gariepy, J. T. *et al.*, 2002; Rizzolatti, G. and Matelli, M., 2003).

Neurons in the IPL also receive somatosensory information, but it arrives not from the primary somatic sensory cortex, but from area 5 and S-II cortex. Actions of the arm are represented primarily in area 7a, and those of the hand in more lateral zones, particularly areas AIP and 7b. However, visual inputs exert a stronger influence on these neurons than the somatosensory modality (reviewed in Felleman, D. J. and Van Essen, D. C., 1991; Fogassi, L. and Luppino, G., 2005; Jeannerod, M. *et al.*, 1995; Andersen, R. A. *et al.*, 1997; Rizzolatti, G. *et al.*, 1997; Sakata, H. *et al.*, 1997; Colby, C. L. and Goldberg, M. E., 1999; Van Essen, D. C. *et al.*, 2001; Andersen, R. A. and Buneo, C. A., 2002; Buneo, C. A. and Andersen, R. A., 2006). Hand manipulation neurons in areas AIP and 7b receive visual inputs from area LIP (Lewis, J. W. and Van Essen, D. C., 2000b; Nakamura, H. *et al.*, 2001), project to ventral premotor cortex (PMv or F5), and receive reciprocal connections from these frontal motor areas (Matelli, M. *et al.*, 1986; Rizzolatti, G. *et al.*, 1987; Matelli, M. *et al.*, 1988; Cavada, C. and Goldman-Rakic, P., 1989b; Preuss, T. M. and Goldman-Rakic, P. S., 1991; Fogassi, L. and Luppino,G., 1995; Rizzolatti, G. *et al.*, 1997; Ghosh, S. and Gattera, R., 1995; Luppino, G. *et al.*, 1999; Matelli, M. and Luppino, G., 2001; Rizzolatti, G. and Luppino, G., 2001).

6.12.3 Physiological Studies of Posterior Parietal Cortex

The anatomical connections of PPC suggest that this region is a higher-order somatosensory and visual area important for feature detection for one or both modalities (Gardner, E. P., 1988; Felleman, D. J. and Van Essen, D. C., 1991; Van Essen, D. C. *et al.*, 2001). Its connections to the frontal motor areas also provide sensory feedback networks for guiding movements. Early physiological studies seemed to support the notion of serial hierarchical processing of tactile input in PPC for the purpose of exteroception and object recognition (Iwamura, Y. and Tanaka, M., 1978; Darian-Smith, I. *et al.*, 1984; Koch, K. W. and Fuster, J. M., 1989; Felleman, D. J. and Van Essen, D. C., 1991; Ageranioti-Bélanger, S. A. and Chapman, C. E., 1992; Iwamura, Y. *et al.*, 1993, 1995). Neurons recorded along the rostral bank of the IPS were shown to have complex tactile receptive fields that distinguish the roughness of textures (Ageranioti-Bélanger, S. A. and Chapman, C.

E., 1992), the spatial frequency and/or orientation of gratings scanned by the fingers (Darian-Smith, I. *et al.*, 1984), and the shape of objects touched by the hand (Iwamura, Y. and Tanaka, M., 1978; Iwamura, Y. *et al.*, 1995), or aid recognition of the surface features of objects previously grasped in the hand (Koch, K. W. and Fuster, J. M., 1989). Other neurons recorded in this region receive proprioceptive signals from multiple joints that aid perception of integrated body postures (Duffy, F. H. and Burchfiel, J. L., 1971; Sakata, H. *et al.*, 1973). Although many of these physiological studies attributed recording sites in the superior bank of the IPS to area 2, anatomists such as Pandya D. N. and Selzer B. (1982), Pons T. P. *et al.* (1985), and Lewis, J. W. *et al.* (1999) have included this region in Brodmann's area 5, calling it area PEa or 5v. Interestingly, most of the complex tactile responses reported in the physiological studies cited above were evoked by active hand movements that were rewarded, such as grasping objects or palpating surfaces.

Our view of PPC was changed dramatically by the pioneering studies of Vernon Mountcastle and Juhani Hyvärinen and their collaborators (Hyvärinen, J. and Poranen, A., 1974; Mountcastle, V. B. *et al.*, 1975; Leinonen, L. *et al.*, 1979; Hyvärinen, J., 1981; 1982a; 1982b). They found that neurons in areas 5 and 7 in the macaque cortex did not respond to the traditional types of tactile stimuli used to study S-I, such as pressure pulses or vibration. In a later historical review, Mountcastle V. B. (1995) described these cells as "neurons that were active if and only if the animal 'had a mind' to deal with the stimulus in a behaviorally meaningful way!" They responded to goal-directed actions of the hand and arm "aimed at securing for the animal an object he desires, such as food when he is hungry; or, as in our experimental paradigm, contacting a switch or pulling a lever that provides fluid when he is thirsty" (Mountcastle, V. B. *et al.*, 1975). Mountcastle and coworkers distinguished two classes of neurons in PPC: arm projection neurons involved in reaching to targets in immediate extrapersonal space and hand manipulation neurons engaged in hand movements such as grasping or foraging for objects with the fingers. Both types were influenced by visual information, particularly neurons recorded in area 7. Reaching and grasping behaviors activated neurons in different portions of PPC, as arm projection neurons were recorded at more medial sites in areas 5 and 7 than hand manipulation neurons. These actions are also segregated anatomically into medial and lateral zones in human parietal cortex, as revealed in functional imaging studies (Chieffi, S. and Gentilucci, M., 1993; Grafton, S. T. *et al.*, 1996; Binkofski, F. *et al.*, 1998; 1999a; Ehrsson, H. H. *et al.*, 2000; 2001; Culham, J. C. *et al.*, 2003; Connolly, J. D. *et al.*, 2003; Ehrsson, H. H. *et al.*, 2003; Shikata, E. *et al.*, 2003; Culham, J. C., 2004; Frey, S. H. *et al.*, 2005; Culham, J. C. and Valyear, K. F., 2006).

The studies by Mountcastle, Hyvärinen, and their collaborators played a seminal role in subsequent investigations of PPC that have focused on reaching movements of the arm, grasping actions of the hand, and goal-directed eye movements to salient targets. They led to the development of new behavioral tasks that tested not only sensory discrimination and motor behaviors, but also the role of memory, intention, and planning of such actions. The correlation of neuronal firing patterns with hand actions also provided an impetus for detailed analyses of the kinematics of reach and grasp behaviors. Collectively, these studies implicate PPC in sensorimotor transformations that couple perceptions to actions needed to direct the hand to objects of behavioral interest such as food and acquire them for consumption.

6.12.3.1 Reaching as a Model System for Analyzing Sensorimotor Integration

Neurons in the SPL appear to play an important role in perception of the body, and its relation to external space during reaching, pointing, and grasping. Reaching is primarily a visuomotor action in which the subject projects the arm toward a target object to touch or grasp it (reviewed in Jeannerod, M., 1994; Jeannerod, M. *et al.*, 1995; Paulignan, Y. and Jeannerod, M., 1996). Reaching occurs in a smooth trajectory in which the peak velocity of the wrist occurs at 40% of the movement time in humans (Jeannerod, M., 1984) and 50% in monkeys (Georgopoulos, A. P. *et al.*, 1982; Roy, A. C. *et al.*, 2000). Ipsilateral reaches take proportionately less time than those to contralateral sites at the same distance. Reaches toward small objects take longer than those toward large ones (Wing, A. M. *et al.*, 1986; Marteniuk, R. G. *et al.*, 1990; Paulignan, Y. and Jeannerod, M., 1996; Roy, A. C. *et al.*, 2000; Roy, A. *et al.*, 2002), presumably because a small object requires more precise aim and finger placement for accurate grip.

Reach and grasp are temporally synchronized but controlled by distinct networks of neurons in parietal cortex (Chieffi, S. and Gentilucci, M., 1993; Grafton, S. T. *et al.*, 1996; Binkofski, F. *et al.*, 1998; 1999; Ehrsson, H. H. *et al.*, 2000; 2001; 2003; Astafiev, S. V. *et al.*, 2003; Culham, J. C. *et al.*, 2003; Rizzolatti, G. and Matelli, M., 2003; Shikata, E. *et al.*, 2003; Frey, S. H. *et al.*, 2005; Hu,

Y. *et al.*, 2005; Tunik, E. *et al.*, 2005). Reach targets are encoded by neurons in the shoulder representation of area 5, the PRR including areas MIP, 7a, PEc, and the PO zone (areas V6, V6A, and 7m) on the medial surface of the hemisphere. These regions have been studied using a variety of reaching tasks (Kalaska, J. F. *et al.*, 1983; Crammond, D. J. and Kalaska, J. F., 1989; Snyder, L. H. *et al.*, 1998a; 1998b; Kalaska, J. F. *et al.*, 1990; Galletti, C. *et al.*, 1993; Kalaska, J. F. and Crammond, D. J., 1995; Lacquaniti, F. *et al.*, 1995; Caminiti, R. *et al.*, 1996; Ferraina, S. *et al.*, 1997; Kalaska, J. F. *et al.*, 1997; Rizzolatti, G. *et al.*, 1997; Caminiti, R. *et al.*, 1998; Batista, A. P. *et al.*, 1999; Battaglia-Mayer, A. *et al.*, 2000; Batista, A. P. and Andersen, R. H., 2001; Ferraina, S. *et al.*, 2001; Andersen, R. A. and Buneo, C. A., 2002; Galletti, C. *et al.*, 2003; Fattori, P. *et al.*, 2004; Fogassi, L. and Luppino, G., 2005; Buneo, C. A. and Andersen, R. A., 2006).

The notion that goal-directed reaches are mediated through area 5 was first analyzed by Kalaska J. F. *et al.* (1983) and Georgopoulos, *et al.* (1884). They developed a behavioral paradigm – called the center-out task – that has been widely used to study reaching and other goal-directed behaviors such as eye movements (Georgopoulos, A. P. *et al.*, 1982). In this task, monkeys are trained to grasp a handle, place it at a central start point, and then displace it to one of eight targets surrounding the origin (Figure 4, *upper panels*). Each trial requires the animal to reach in a specific direction to a visually defined endpoint. They found that most neurons in area 5 respond to a broad range of reach directions, with maximum firing in one preferred direction, and minimum rates along the opposite path. The directional tuning curves of firing rates for the eight different directions can be approximated by a sine wave (Figure 4, *lower panel*), allowing them to derive preferred reach directions for each cell studied. Although the individual neurons do not by themselves provide a strong directional signal, collectively the population of neurons precisely specifies the reach direction on each trial. This notion was further extended to three dimensions in later studies (Georgopoulos, A. P. *et al.*, 1988; Schwartz, A. B. *et al.*, 1988; Lacquiniti *et al.*, 1995). Kalaska and colleagues (1990) later discovered that the tuning of area 5 neurons to particular reach directions reflects the movement kinematics, that is, the particular muscle groups needed to direct the arm in specific directions. Area 5 firing rates are independent of the amount of muscle force needed to pull or push the handle toward the specified target.

The time course of neural responses during reaches also has important implications concerning the sensorimotor role of PPC. The onset of neuronal responses in area 5 coincides with the start of reach and overlaps motor activity in primary motor cortex (M-I) and in the dorsal premotor cortex (PMd) (Kalaska, J. F. *et al.*, 1983; Crammond, D. J. and Kalaska, J. F., 1989; Kalaska, J. F. *et al.*, 1990; Burbaud, P. *et al.*, 1991; Kalaska, J. F. and Crammond, D. J., 1995). In addition, Seal J. *et al.* (1982) and Seal J. and Commenges D. (1985) found that area 5 neurons in deafferented monkeys respond to reaching movements in the absence of somatosensory feedback, suggesting that an efference copy of motor commands from the frontal lobe is also transmitted to PPC (Mountcastle, V. B. *et al.*, 1975). These findings led to the proposal that area 5 receives convergent central and peripheral signals that allow it to compare central motor commands with peripheral sensory feedback during task performance. These circuits provide a network for planning intended movements and updating ongoing actions as they proceed. Kalaska and colleagues (1997) described this role as a "sequence of sensorimotor coordinate transformations between a signal of spatial location and a pattern of muscle activity."

6.12.3.2 Role of Posterior Parietal Cortex in Motor Planning and the Neural Representation of Space

Further clues about the sensorimotor function of PPC have been derived from instructed delay tasks when the animal was able to plan reaches or saccades to cued spatial targets. In these studies, the motor plans or intentions of the animal are distinguished from subsequent actions during motor performance of the task. During delayed reaching tasks, neurons in areas 5 and PRR show strongly enhanced firing rates prior to the onset of movement that are tuned to the location of the visual target and that specify potential actions that can be performed there (Crammond, D. J. and Kalaska, J. F., 1989; Andersen, R. A., 1995; Kalaska, J. F. and Crammond, D. J., 1995; Kalaska, J. F., 1996; Batista, A. P. and Andersen, R. H., 2001). The initial hand position modifies the strength of responses of neurons in area 5 (Crammond, D. J. and Kalaska, J. F., 1989; Kalaska, J. F. and Crammond, D. J., 1995), but not those in PRR (Andersen, R. A. *et al.*, 1997; Batista, A. P. and Andersen, R. H., 2001; Buneo, C. A. and Andersen, R. A., 2006), suggesting that these regions respond to different aspects of the sensory cue. These studies support the notion that PPC activity reflects the intention to execute a specific motor program.

Premovement activity during the instructed delay period has been variously described as motor intentions (Andersen, R. A. *et al.*, 1997; Andersen, R. A. and

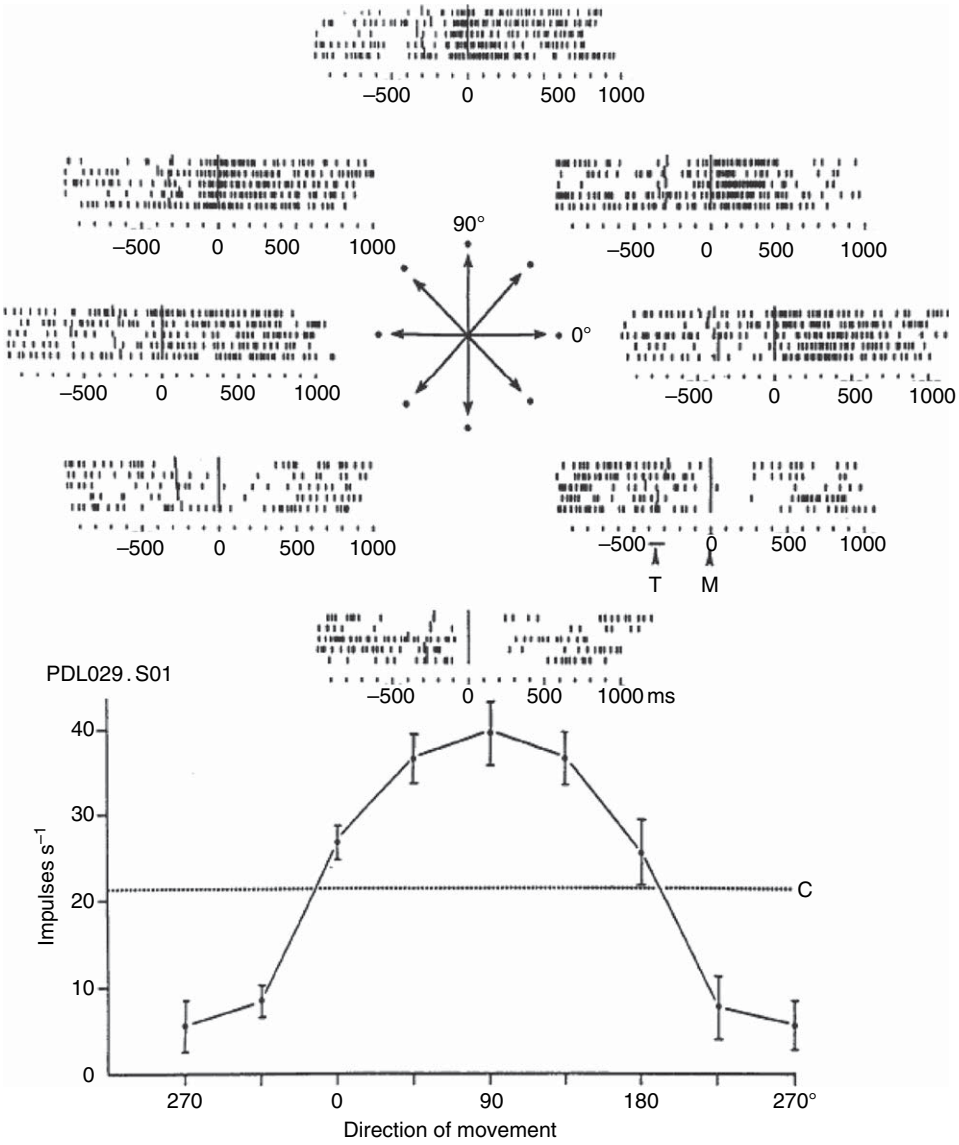

Figure 4 Tuning of responses of an area 5 neuron to the direction of reach in the center-out task. Upper panels: Rasters illustrating five trials in the stated directions aligned to the start of reach (M); the neuron responded most vigorously to upward movements (90°) and was inhibited by movement in the opposite direction (270°). Note that neural responses precede the start of movement, and continue until the hand reaches the specified target. Lower panel: Mean firing rate during the movement time; the neuron responded to movement over most of the range tested. *C*, mean firing rate during the control period before the target cue light was illuminated. Reproduced from Kalaska, J. F., Caminiti, R., and Georgopoulos, A. P. 1983. Cortical mechanisms related to the direction of two-dimensional arm movements: relations in parietal area 5 and comparison with motor cortex. Exp. Brain Res. 51, 247–260; figure 3).

Buneo, C. A., 2002; Buneo, C. A. and Andersen, R. A., 2006), spatial attention (Colby, C. L., 1998; Duhamel, J. R. *et al.*, 1998; Colby, C. L. and Goldberg, M. E., 1999; Bisley, J. W. and Goldberg, M. E., 2003), or perceptual decision-making (Platt, M. L. and Glimcher, P. W., 1999; Shadlen, M. N. and Newsome, W. T., 2001; Glimcher, P. W., 2003; Dorris, M. C. and Glimcher, P. W., 2004; Sugrue, L. P. *et al.*, 2004; 2005). We refer to this early activity as motor planning, because it reflects high-level cognitive plans for movement without the implication of emotional commitment to such behaviors.

Motor plans for reaching require transformation of a visual signal concerning the target position in the

workspace into a motor signal that selects the appropriate muscle groups needed to transport the hand to the specified place. The intended goal of the reach is often described as a motor error signal, that is, the difference between the starting hand and arm position, and the desired goal (reviewed in Buneo, C. A. and Andersen, R. A., 2006). Actions of the arm are represented in a variety of coordinate systems along the SPL including eye-centered (Figure 5), head-centered, arm-centered, and hand-centered reference frames, or combinations of these expressed as gain fields (Crammond, D. J. and Kalaska, J. F., 1989; Pause, M. and Freund, H.-J., 1989; Galletti, C. *et al.*, 1993; Kalaska, J. F. and Crammond, D. J., 1995; Lacquaniti, F. *et al.*, 1995; Caminiti, R. *et al.*, 1996; Andersen, R. A. *et al.*, 1997; Ferraina, S. *et al.*, 1997; Kalaska, J. F. *et al.*, 1997; Caminiti, R. *et al.*, 1998; Colby, C. L., 1998; Snyder, L. H. *et al.*, 1998a; 1998b; Batista, A. P. *et al.*, 1999; Burnod, Y. *et al.*, 1999; Ferraina, S. *et al.*, 2001; Battaglia-Mayer, A. *et al.*, 2003; 2006; Buneo, C. A. and Andersen, R. A., 2006). This is a hotly debated and somewhat controversial subject. In a recent review, Buneo C. A. and Andersen R. A. (2006) proposed that PPC contains both a "representation of target and hand position in eye coordinates, and a representation of motor error in hand-centered coordinates." They seem to recognize that different coordinate systems are arrayed along the IPS but that their relative importance may depend on the specific task requirements. Multiple coordinate frames are useful for achieving flexibility when reaching is the prelude to subsequent hand actions such as grasping, pointing, pulling, pushing, or turning that require a variety of motor synergies.

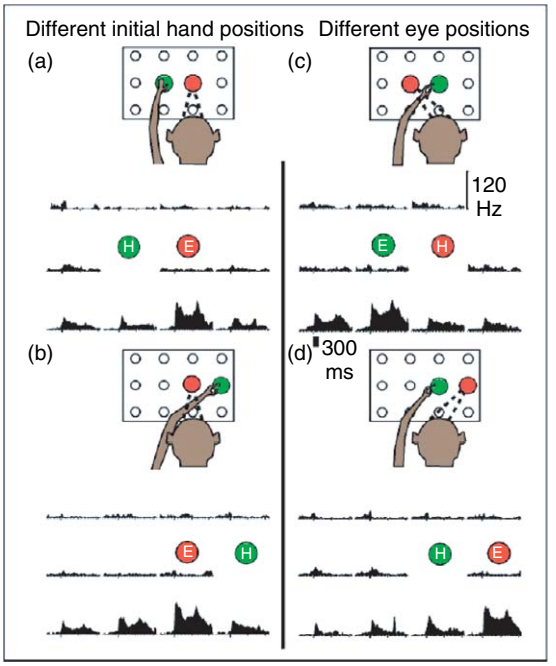

Figure 5 Sensitivity of a neuron in the parietal reach region (PRR) to eye and hand position during the instructed delay period of a reach task. The initial hand position and the point of visual fixation are represented by green and red circles, respectively, in the behavioral cartoons. The animal is instructed to reach to one of the other 11 positions when the GO signal occurs while maintaining fixation of gaze on the red circle. The spike density histograms below the cartoons illustrate the averaged response to the cue; in each case the strongest response occurred when the animal was instructed to reach to the location below the center of gaze, regardless of the starting point of the hand or the direction of reach. The authors conclude that the neuron encodes the required movement in terms of the target location on the retina. Modified from Andersen, R. A. and Buneo, C. A. 2002. Intentional maps in posterior parietal cortex. Annu. Rev. Neurosci. 25, 189–220; figure 5).

Spatial maps may play a critical role in the dysmetrias and neglect syndromes characteristic of damage to PPC (reviewed in Hyvärinen, J., 1982b; Pause, M. *et al.*, 1989; Milner, A. D. and Goodale, M. A., 1995; Ghika, J. *et al.*, 1998; Pouget, A. and Driver, J., 2000; Freund, H.-J., 2001; Goodale, M. A. and Westwood, D. A., 2004; Battaglia-Mayer, A. *et al.*, 2006). Ben-Hamed and Duhamel reported that the population of neurons in area VIP of each hemisphere responded to stimulation of the entire visual field, both ipsilateral and contralateral, but the relative distribution of neurons responding at each eccentricity was skewed, with peak numbers ~15° contralateral to the recording side (Figure 1 in Pouget, A. and Driver, J., 2000). This coincides with the location of the fingertips when the arm is extended forward of the body. From a bilateral perspective, the greatest number of neurons represents the workspace between the shoulders, with equal representation at the midline for left and right sides, and a gradual bias toward the contralateral side that accelerates lateral to the shoulder. The large population monitoring the intramanual space endows it as the preferred site of skilled bimanual actions. If one hemisphere is disabled, the skewed representation of visual space biases reaches and attention toward the contralateral side. This model predicts hypometric reaches toward ipsilateral targets, because fewer than 10% of cells in the intact hemisphere represent eccentricities >20° in that space. Similarly, modulation of visual gain fields by eye and head position could further skew neuronal responses to contralaterally displaced reach targets (Andersen, R. A. *et al.*, 1985; Snyder, L. H. *et al.*, 1998a; 1998b).

6.12.3.3 Grasping and Hand Manipulation Neurons in Posterior Parietal Cortex

Prehension is an object-oriented behavior that is fundamental to skilled actions of the hand. As Lederman S. J. (1994) notes, "the grasp would appear to be a privileged movement pattern of the human hand, inasmuch as it provides varied somatosensory inputs that may be used to guide both motoric and perceptual functions." Skilled grasping behaviors are strongly influenced by both visual and somatosensory information. Visual information about the object's size, shape, and orientation is required during reaching for proper orientation of the hand and for preshaping of the fingers prior to acquisition (Jeannerod, M., 1984; 1994; Milner, A. D. and Goodale, M. A., 1995; Paulignan, Y. and Jeannerod, M., 1996; Connolly, J. D. and Goodale, M. A., 1999; Castiello, U., 2005). The grip aperture of the fingers is proportional to object size and is maximum at 75% of the movement time as the hand decelerates near the target (Jeannerod, M., 1986; Chieffi, S. and Gentillucci, M., 1993; Jeannerod, M., 1994; Jeannerod, M. *et al.*, 1995; Lemon, R. N. *et al.*, 1995; Roy, A. *et al.*, 2002; Hu, Y. *et al.*, 2005). Hand preshaping to object size and shape is characteristic of normal primate hand function and is disrupted by lesions of PPC (LaMotte, R. H. and Acuña, C., 1978; Gallese, V. *et al.*, 1994; Jeannerod, M. *et al.*, 1994; Milner, A. D. and Goodale, M. A., 1995; Fogassi, L. *et al.*, 2001; Tunik, E. *et al.*, 2005). Johansson and coworkers (Jenmalm, P. and Johansson, R. S., 1997; Jenmalm, P. *et al.*, 2000; Johansson, R. S. *et al.*, 2001) demonstrated that visual information helps guide the choice of grasp points on an object to promote stability and efficient manipulation. The development of grasp forces is determined initially by visual identification of the object and retrieval of implicit memory information concerning its physical properties (Johansson, R. S. and Westling, G., 1984; Gordon, A. M. *et al.*, 1993).

Grasping is also influenced by somatosensory information from previous encounters with objects. Through experience we learn how and where to grasp objects, and the rate and amount of force required to lift and manipulate them. Roland Johansson and Göran Westling have shown that when we grasp objects, we do so delicately applying just enough force to secure it in the hand without slippage (reviewed in Johansson, R. S., 1996). The tactile information transmitted by receptors in the hand as objects are handled allows us to develop skills and learn new behaviors that can be used as templates for future action.

Johansson R. S. (1996) proposed that prehension is governed by two control mechanisms operating in parallel: anticipatory parameter control and sensory-driven event control (see chapter by Johansson and Flanagan, this volume). Anticipatory parameter control is used for motor planning of prehension. Subjects anticipate what an object should feel like in the hand when it is viewed and formulate a grasp program. Visual and somatosensory inputs are combined with sensorimotor memories to construct an internal model of the hand shape and grip forces needed for prehension and manipulation of the object. These modalities set a context in which ascending tactile information is interpreted after the object is touched. Anticipatory parameter control also involves the conjoint application of grip and load forces to the object in order to execute a smooth lift without the application of excessive grip force. Discrete event, sensory-driven control describes the sensory information that signals completion of one action such as grasping to allow rapid transition to another behavior such as manipulation. It also includes error signals when a mismatch occurs between expectation and execution of the task, requiring corrective responses. For example, tactile afferents in the hand can detect slippage due to unexpected contours, textures, or weight that require adjustment in hand position or force. Anticipatory parameter control provides an efficient mechanism of sensorimotor control, because long-loop feedback to the cortex is not needed for the initiation of sequential actions. It allows rapid movement execution by relying on experience to control the timing of muscle activation in the hand. Sensory feedback monitors how the task proceeds; this information strengthens grasp motor programs when implemented properly and initiates corrective actions if errors such as slippage occur.

Studies of the neurophysiology of prehension using single unit recordings in monkeys indicate that PPC responses are predictive rather than reactive to touch receptor stimulation during prehension (Mountcastle, V. B. *et al.*, 1975; Leinonen, L. *et al.*, 1979; Taira, M. *et al.*, 1990; Sakata, H. *et al.*, 1995; Murata, A. *et al.*, 1996; Sakata, H. *et al.*, 1997; Gardner, E. P. *et al.*, 1999; Murata, A. *et al.*, 2000; Ro, J. Y. *et al.*, 2000; Debowy, D. J. *et al.*, 2001; Gardner, E. P. *et al.*, 2002; Fogassi, L. and Luppino, G., 2005; Gardner, E. P. *et al.*, 2007a). Other studies demonstrate that sensory-driven control is mediated primarily by neurons in S-I (Iwamura, Y. and Tanaka, M., 1978; Hikosaka, O. *et al.*, 1985; Wannier, T. M. *et al.*, 1986; Wannier, T. M. *et al.*, 1991; Iwamura, Y. *et al.*, 1995; Iwamura, Y. and Tanaka, M., 1996; Brochier, T. *et al.*, 1999; Gardner, E.

P. *et al.*, 1999; Salimi, I. *et al.*, 1999; Ro, J. Y. *et al.*, 2000; Debowy, D. J. *et al.*, 2001; Gardner, E. P. *et al.*, 2002; 2007b; Jenmalm, P. *et al.*, 2006).

Mountcastle V. B. *et al.* (1975) described neurons in areas 5 and 7 activated during exploratory hand movements such as foraging for raisins in small containers. They named these cells 'hand manipulation' neurons but did not document their firing patterns beyond a textual description. They noted that hand manipulation neurons in area 7 responded to both visual and tactile modalities when the stimuli occupied the same spatial location. These cells fired during visual fixation or tracking of desired objects such as food but responded at highest rates during projection of the arm toward the object or manipulation of it in the hand. The eye–hand coordination neurons were situated in the posterior bank of the IPS in the most anterior portion of area 7, a region that is now called the anterior intraparietal (AIP) area. Leinonen L. *et al.* (1979) described similar hand manipulation neurons in the adjacent convexity of the IPL (area 7b) that were active as monkeys tried to acquire raisins or other food morsels from the experimenter and ceased firing as the food was grasped and brought to the mouth.

The first systematic studies of hand manipulation neurons in monkeys were performed by Hideo Sakata and coworkers, who developed a prehension task to study neural responses in area AIP (Taira, M. *et al.*, 1990; Sakata, H. *et al.*, 1995; Murata, A. *et al.*, 1996; Sakata, H. *et al.*, 1997; 1999; Murata, A. *et al.*, 2000). They trained the animals to grasp and pull handles of different shapes located on a turntable in the middle of the workspace. In order to test the visual sensitivity of these neurons, and to measure its effect on hand movements, the task included an instructed delay period in which the animal viewed an object (FIX, Figure 6) before a GO cue signaled the start of the movement period. Some of the task trials were also conducted in the dark where only tactile and proprioceptive signals were available to aid task performance. Sakata and colleagues subdivided the population of hand manipulation neurons into five classes according to their relative sensitivity to vision and somatosensory modalities. The most common class was visuomotor 'object-type' neurons (28%) that were similar to the eye–hand coordination neurons originally reported by Mountcastle V. B. *et al.* (1975). These neurons combined visual and tactile inputs, displaying higher overall firing rates during manipulation in light – in which the animal viewed the object and the hand grasping it – than in the dark when neither hand nor object was visible (Figure 6a). It is unclear whether the enhanced responses resulted from somatosensory input from the hand, efference copy of the motor commands for hand preshaping and grasping, or visual stimulation as the hand entered foveal receptive fields. Responses during the visuomotor and motor tasks were higher than during object fixation, when the object was displayed and viewed but not grasped. Fourteen percent of the neurons tested responded only to the conjunction of vision and hand actions during manipulation in the light (visual nonobject, Figure 6d), showing no response to object presentation during fixation, nor during manipulation in the dark. Another 16% had purely visual inputs, responding only when the object was visible, without increasing their firing rates during reach or grasping actions (visual object, Figure 6c). The remaining 42% of cells did not have overt visual responses; they responded only during the reach and grasp stages of the task (visuomotor nonobject or motor, Figure 6b and e).

The firing rates of hand manipulation neurons were also tuned to broad categories of object shapes tested in this task (Murata, A. *et al.*, 2000). Visuomotor neurons displayed the same preferences during viewing and grasping objects, suggesting that they might provide relevant information about the size, shape, and composition of objects needed to grasp them. However, Murata and coworkers concluded that AIP neurons signaled the type of manipulatory action performed by the hand, rather than object properties, because the neurons did not distinguish between objects of different shape that were grasped using the same or similar hand postures.

Likewise, neurons in areas F5 and F2vr (the primary projection targets of area AIP) responded primarily to the grasp posture of the hand rather than the object form (Murata, A. *et al.*, 1997; Raos, V. *et al.*, 2004; 2006). Raos V. and coworkers (2006) noted that "although the object-related visual responses of AIP neurons reflect the objects' common geometrical features, the object-related visual responses of F5 neurons reflect the chosen grip." These circuits create 'pragmatic representations' of objects in which their intrinsic properties are encoded in terms of the hand postures normally used to grasp them. Since neurons in area AIP respond both to direct view of an object to be grasped and to the actual performance of grasp, they are postulated to be involved in the sensorimotor transformation of the visual representation of object features into the hand posture needed for grasping (Jeannerod, M. *et al.*, 1995; Sakata, H. *et al.*, 1997; Fagg, A. H. and Arbib, M. A., 1998; Rizzolatti, G. and Luppino, G., 2001; Fogassi, L. and Luppino, G., 2005).

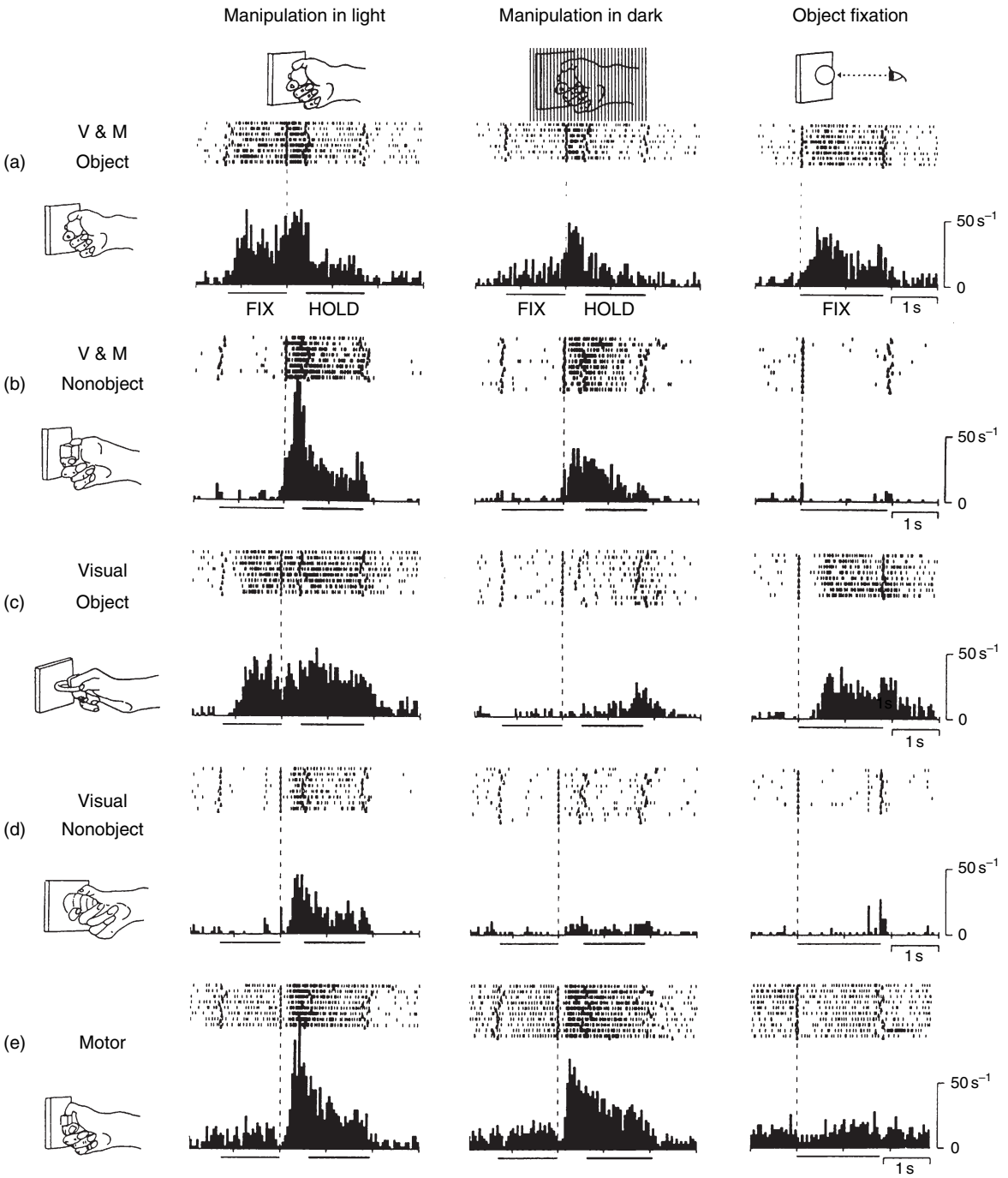

Figure 6 Classes of hand manipulation neurons recorded in area AIP during a prehension task. Responses illustrated in the rasters and peristimulus–time histograms (PSTHs) are aligned to the onset of reach; different neurons are illustrated in each row. At the start of each trial, the animal had to maintain gaze on the test object for ~2 s while pressing a button with the test hand (FIX). The animal was trained to reach toward the test object after a GO signal, grasp and pull it, and maintain the pull posture during the HOLD period. All of these neurons fired at highest rates during reach and grasp actions, and most continued to respond during holding, although at lower rates. Object-type neurons responded to viewing the object during the FIX period; nonobject-type responded only to hand actions but not to visual stimulation. Motor type neurons responded equally well to manipulation in light and in darkness. Reproduced from Murata, A., Gallese, V., Luppino, G., Kaseda, M., and Sakata, H. 2000. Selectivity for the shape, size and orientation of objects for grasping in neurons of monkey parietal area AIP. J. Neurophysiol. 83, 2580–2601; figure 2).

Hand manipulation neurons in area 5 also signal how an object is grasped. Using digital video methods to quantify hand kinematics, Esther Gardner and colleagues found that area 5 neurons responded to the actions of the hand during object acquisition and manipulation (Ro, J. Y. *et al.*, 1998; Gardner, E. P. *et al.*, 1999; Ro, J. Y. *et al.*, 2000; Debowy, D. J. *et al.*, 2001; 2002; Gardner, E. P. *et al.*, 2002; 2007a). Activity in area 5 spanned the period from the start of reach through object manipulation (Figures 7b and 8). Responses began before the hand was stimulated directly by the object when approach was initiated. Firing rates peaked during hand preshaping or at contact and declined after the object was securely grasped in the hand. Neural activity during lifting and holding was weaker than during acquisition and concluded when the object was released from the hand.

Selectivity of neuronal firing rates for particular objects occurred most often after contact and during grasping and lifting actions. For example, the neuron in Figure 9e responded most vigorously to grasp and lift of a large round object (stages 3 and 4) but showed little distinction in firing rates between the test objects during approach or at contact. Most neurons

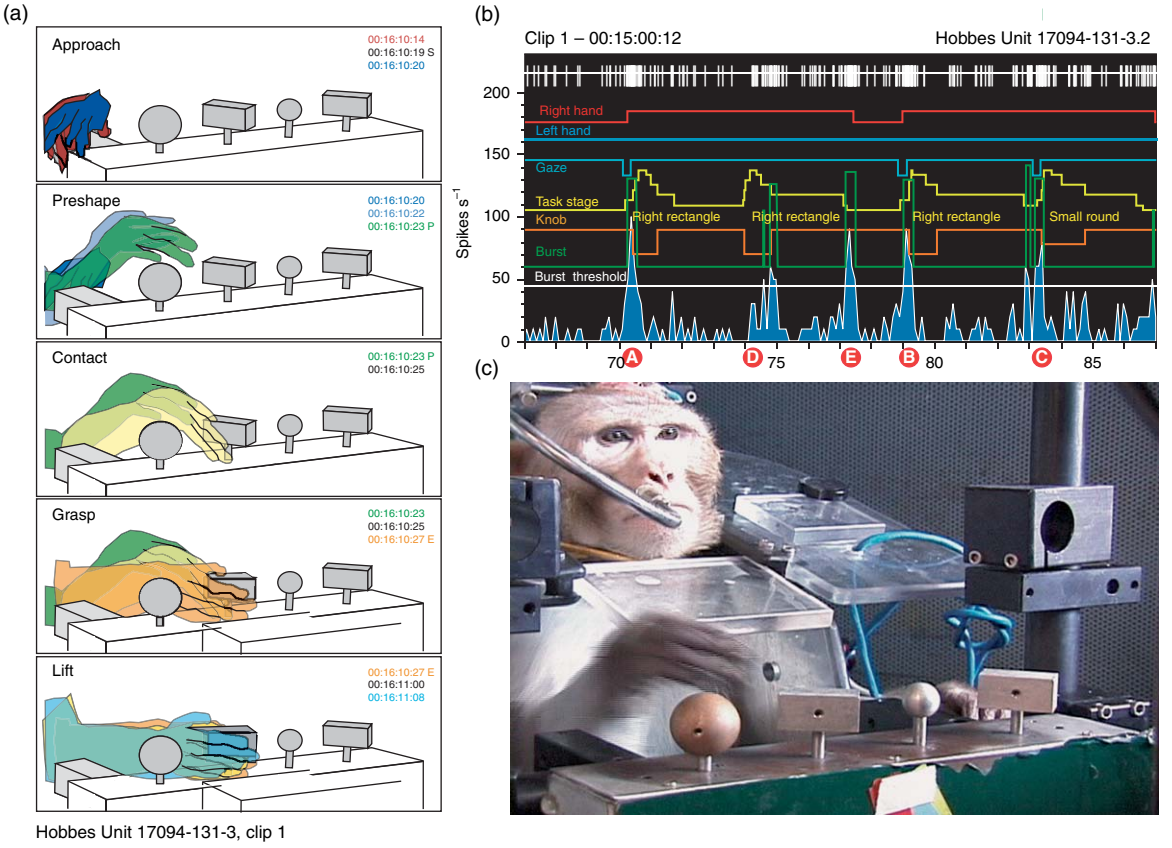

Figure 7 Hand kinematics and neural responses in area 5 during a prehension task. The animal was trained to grasp and lift one of four knobs designated by icons on a video monitor. (a) Kinematic actions of the hand during sequential stages of the task traced from digital video images of a single trial. Labels describe the action performed in the top image of each set. (b) Burst analysis graphs of continuous neural and behavioral activity recorded during the task. Neural responses evoked during the trial in Panel (a) are marked by the red A below the graph. Each burst in this 20 s record coincides with the initiation of a task trial (A–D), or grasp of the chair frame (E). Green burst trace: Periods of firing 1 SD above the mean rate for the entire analysis period. *Yellow task stage trace*: Each stepped pyramid marks a single trial. Upward deflections denote the start of stages 1–4 (approach, contact, grasp, and lift); downward deflections mark the onset of stages 5–8 (hold, lower, relax, and release). *Orange knob trace:* Downward pulses indicate knob location in the workspace and duration of hand contact. Other traces illustrate spontaneous actions of the two hands (red and blue) and gaze fixation on the target object (cyan, downward deflection). (c) Video image captured at the peak of burst A; maximum activity occurred during hand preshaping prior to contact. Modified from Gardner, E. P., Babu, K. S., Reitzen, S. D., Ghosh, S., Brown, A. M., Chen, J., Hall, A. L., Herzlinger, M. D., Kohlenstein, J. B., and Ro, J. Y. 2007a. Neurophysiology of prehension: I. Posterior parietal cortex and object-oriented hand behaviors. J. Neurophysiol. 97, 387–406; figures 4 and 5).

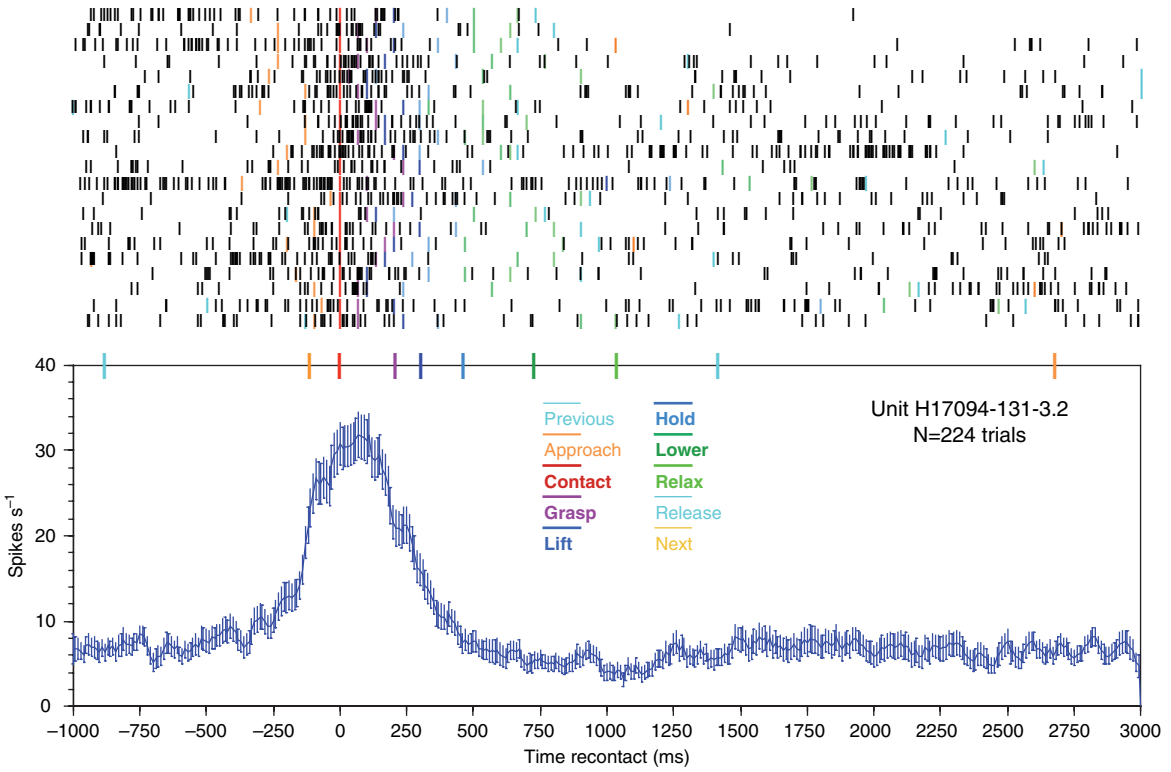

Figure 8 Raster and spike density plot of neural responses during the prehension task aligned to hand contact with the objects; error bars show SEM during each time epoch. Same neuron as in Figure 7. Colored lines on rasters and markers above the spike density graph indicate the onset times of the task stages relative to contact. Responses began ~250 ms before contact at the start of approach and peaked at contact. Modified from Gardner, E. P., Babu, K. S., Reitzen, S. D., Ghosh, S., Brown, A. M., Chen, J., Hall, A. L., Herzlinger, M. D., Kohlenstein, J. B., and Ro, J. Y. 2007a. Neurophysiology of prehension: I. Posterior parietal cortex and object-oriented hand behaviors. J. Neurophysiol. 97, 387–406; figure 7).

in area 5 displayed weak and subtle distinctions between objects as in Figure 9f. The slight preference of this neuron for the smallest object during grasping appears to reflect the tightly flexed posture of the fingers (Figure 9a–d).

The similarity of the hand postures used to grasp these objects and the overlap in evoked firing patterns throughout most of the task suggest that neurons in area 5, like those in area AIP, represent grasp actions of the hand rather than the particular shape of the grasped object. The persistence of neural activity after contact indicates that neurons in area 5 also monitor the success or failure of object acquisition. Dynamic error correction occurred when an incorrect object was touched, and it was reflected in immediate alteration of responses of area 5 neurons (Gardner, E. P. *et al.*, 2007a).

The strong responses observed during approach suggest that the motor commands for hand preshaping and grasping may originate in area 5 and as well as in AIP. Alternatively, area 5 neurons may receive an efference copy of motor commands from the ventral premotor cortex (area F5) that is itself activated from visuomotor signals originating in area AIP. Like reach neurons in the more medial regions of area 5, hand manipulation neurons in the SPL may provide a body schema of hand actions that allow them to compare the predictions of feed-forward grasping plans with feedback sensory information from the hand.

We were somewhat surprised by the weak selectivity for object shape in the area 5 population, as Iwamura and coworkers had reported shape-specific responses in the anterior bank of the IPS during spontaneous grasp of objects such as fruits, rulers, or blocks (Iwamura, Y. and Tanaka, M., 1978; Iwamura, Y. *et al.*, 1985; 1995; Iwamura, Y. and Tanaka, M., 1996). However, it is possible that the selectivity for shape described in their studies may actually reflect the animal's intentions or interest in the test objects. It is clear from Mountcastle's original observations that the intentions motivating grasp of food are different from those directed toward inedible wooden objects. Alternatively, the

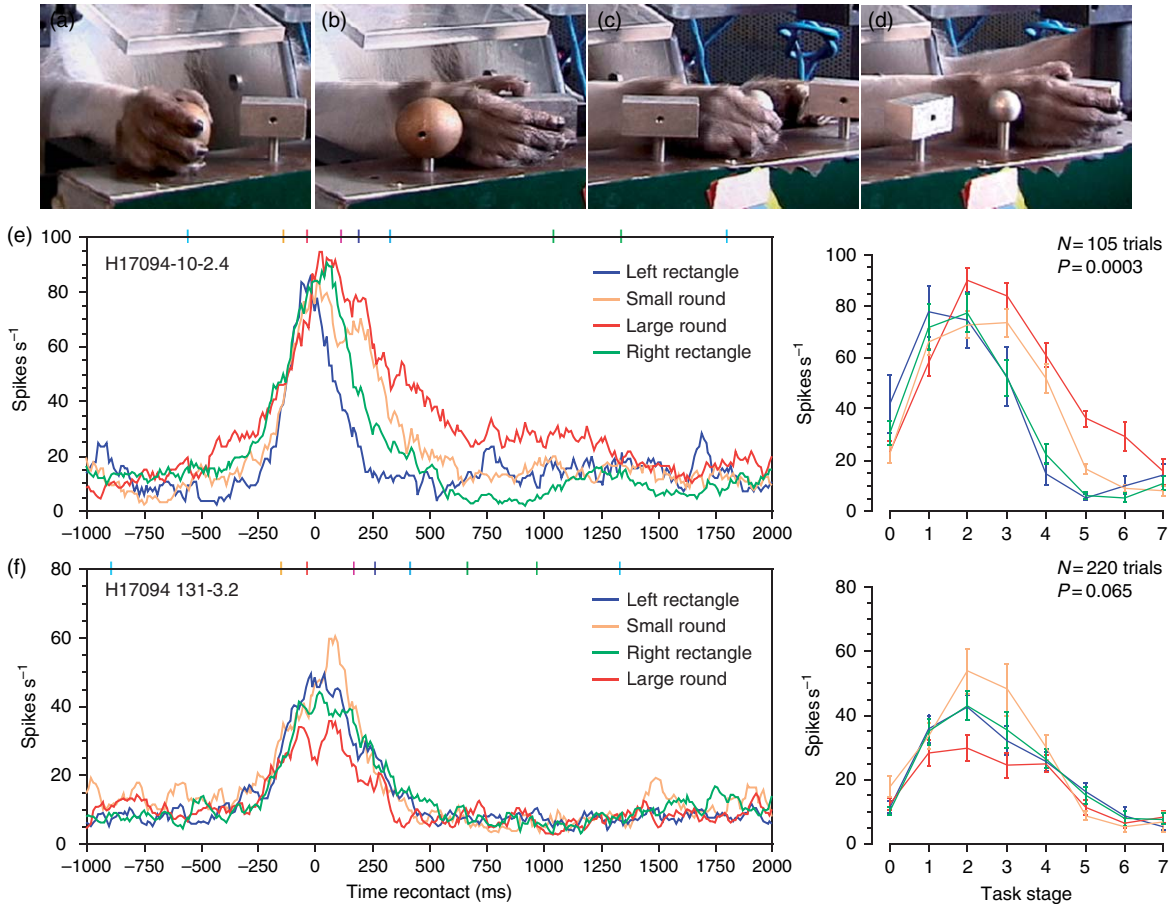

Figure 9 Shape selectivity of two different area 5 neurons during performance of the prehension task. (a–d) Video images of the grasp posture used for each knob captured during recordings from Unit H17094-131-3. (e–f) *Left panels*: Superimposed spike density plots evoked by the four test objects. Right panels: Average firing rates per task stage evoked by each object. The neuron in (e) responded most vigorously to grasp of the large round knob, particularly during lift and hold. The neuron in (f) preferred the small round knob and had the weakest response to the large one; responses to the two rectangles were similar, as these objects were grasped with the same posture.

apparent shape selectivity reported in the Iwamura and Tanaka studies may reflect the diverse hand postures and distinctive muscle activation patterns used to grasp their test objects (Brochier, T. *et al.*, 2004).

Hand manipulation neurons in areas 5 and 7 differ in their sensitivity to visual inputs. As noted above, 58% of the neurons recorded in area AIP responded to viewing as well as grasping objects, and most responded more vigorously during the task when both the hand and objects were visible. Mirror neurons recorded more caudally in area 7b responded to observation as well as performance of grasping, suggesting that they signal action recognition as well as motor planning (Rizzolatti, G. *et al.*, 2001; Rizzolatti, G. and Craighero, L., 2004; Fogassi, L. *et al.*, 2005).

Visual receptive fields in area 5 are rare and, when present, seem linked to view of the animal's own hand rather than to view of the object. Iriki A. and coworkers (1996; 2001) reported that such neurons respond to salient objects (such as food morsels) approaching the hand and fire at peak rates when the object is in range for grasp regardless of where the gaze is directed. These fields may extend beyond the hand when the animal uses a tool to rake in distant food morsels. Maravita A. and Iriki A. (2004) proposed that area 5 neurons may contribute to the animal's own body schema, the conscious perception of one's own actions.

Functional magnetic resonance imaging (fMRI) studies in humans have revealed similar areas for grasping in the human cerebral cortex (Figure 10). The first of these studies by Binkofski, F. *et al.* (1998) demonstrated that patients with lesions that included the anterior intraparietal sulcus had impairments of grasping behaviors whereas patients with PPC lesions sparing this

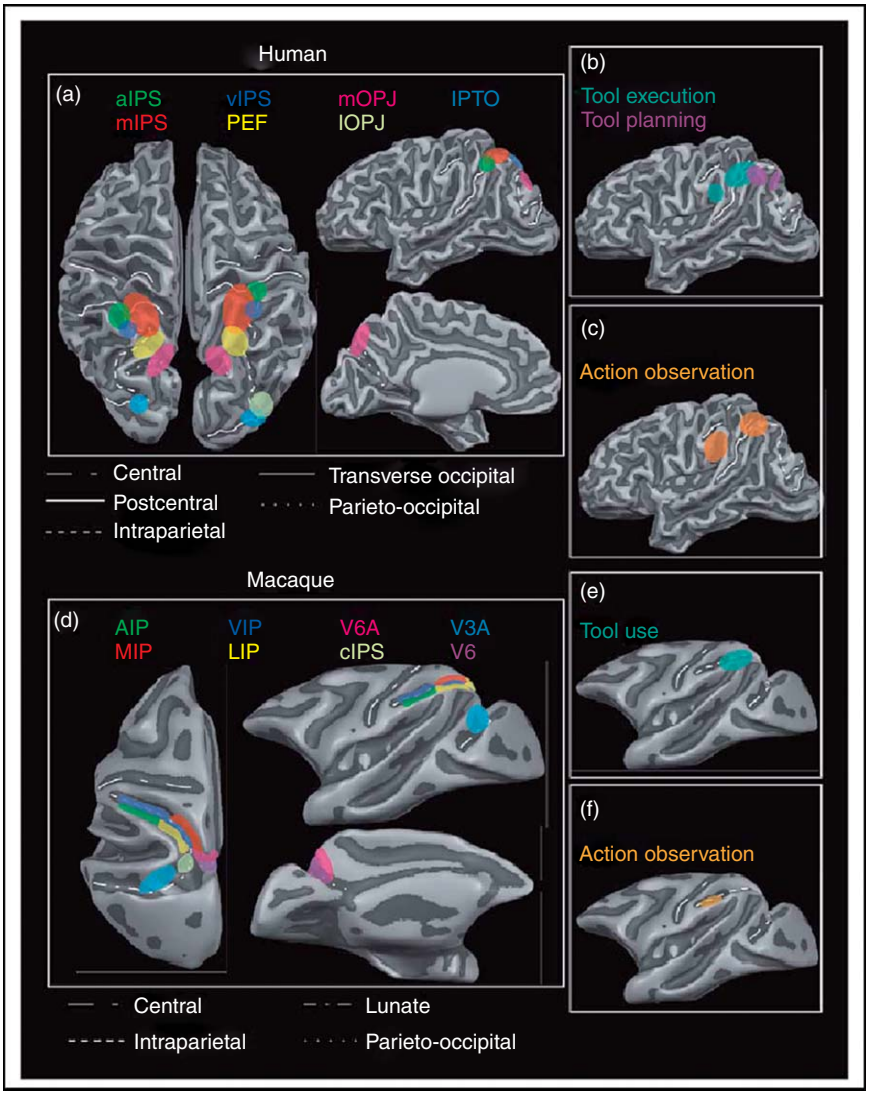

Figure 10 Inflated brain maps of the macaque and human brain showing regions of posterior parietal cortex (PPC) involved in various skilled tasks. Reproduced from Culham, J. C. and Valyear, K. F. 2006. Human parietal cortex in action. Curr. Opin. Neurobiol. 16, 205–212; figure 1).

region did not. The deficits in hand preshaping included slower hand opening during reach, and unusually large apertures betweeen the thumb and index finger of the contralesional hand before contact, compared to age-matched control subjects, and to their own ipsilesional hand. fMRI scans of neurologically normal adults in this same study revealed a focus of activation in the lateral bank of the anterior intraparietal sulcus (aIPS) when they grasped and manipulated rectangular blocks. The activation sites in the aIPS during grasping have been confirmed in subsequent studies comparing grasping and reaching behaviors (Culham, J. C., *et al.*, 2003; Frey, S. H., *et al.*, 2005). These same brain areas are also activated by viewing grasping actions performed by other individuals (Buccino, G., *et al.*, 2001; Fogassi, L., *et al.*, 2005; Shmuelof, L. and Zohary, E., 2005, 2006). More detailed descriptions of areas in the human brain involved in grasping are provided in several excellent reviews recently published (Culham, J. C., and Valyear, K. F., 2006; Culham, J. C., *et al.*, 2006; Grefkes, C., and Fink, G. R., 2005; Tunik, E., *et al.*, 2007).

In summary, hand manipulation neurons in areas 5 and 7 participate in sensorimotor networks involved in grasp planning, prediction of sensory stimulation, and monitoring of appropriate execution of the desired actions. Firing patterns of these neurons appear to

reflect the internal motor commands needed to accomplish task goals, as well as the sensory events resulting from self-generated movement. The onset of firing seems best correlated with the preparation of specific actions. The external tactile stimulation of the hand by the grasped object appears to reinforce the motor plans by signaling the accomplishment of the desired action when successful or provides an error signal for corrective maneuvers when it fails.

6.12.4 Bilateral Coordination of the Hands

Neurons in both the dorsal and ventral stream pathways for touch respond to tactile stimulation of both the contralateral and ipsilateral hands. Anatomical studies indicate that callosal connections within the hand representation do not occur in S-I but first appear in S-II (reviewed in Disbrow, E. *et al.*, 2003) and in PPC (Jones, E. G. *et al.*, 1978; Padberg, J. *et al.*, 2005). Bilateral receptive fields on the hands of monkeys have been found in S-II cortex (Whitsel, B. L. *et al.*, 1969; Robinson, C. J. and Burton, H., 1980a; 1980b; Burton, H., 1986; Disbrow, E. *et al.*, 2003; Fitzgerald, P. J. *et al.*, 2004; 2006) and in PPC (Mountcastle, V. B. *et al.*, 1975; Leinonen, L. *et al.*, 1979; Koch, K. W. and Fuster, J. M., 1989; Iwamura, Y. *et al.*, 1994; Iwamura, Y., 2000; Iwamura, Y. *et al.*, 2002; Padberg, J. *et al.*, 2005), and on midline structures in S-I (Taoka, M. *et al.*, 1998; Iwamura, Y., 2000).

The functional role of distal bilateral receptive fields is unclear and has not been tested rigorously in monkeys. Using digital video, we analyzed how hand kinematics are related to neuronal spike trains recorded in area 5 as monkeys performed trained prehension tasks and spontaneous behaviors engaging both hands (Gardner, E. P. *et al.*, 2001). Many of the cells analyzed responded equally to grasp by either hand. These bimanual neurons represented equivalent actions of the right and the left hand in a common cell population. For example, the neurons shown in Figure 11 responded equally to grasp of a raisin with the ipsilateral left hand (burst D) and the contralateral right hand (burst E). The responses to precision grip were similar to those evoked in the same neurons during the trained task (Figure 7). Like the hand manipulation neurons described by

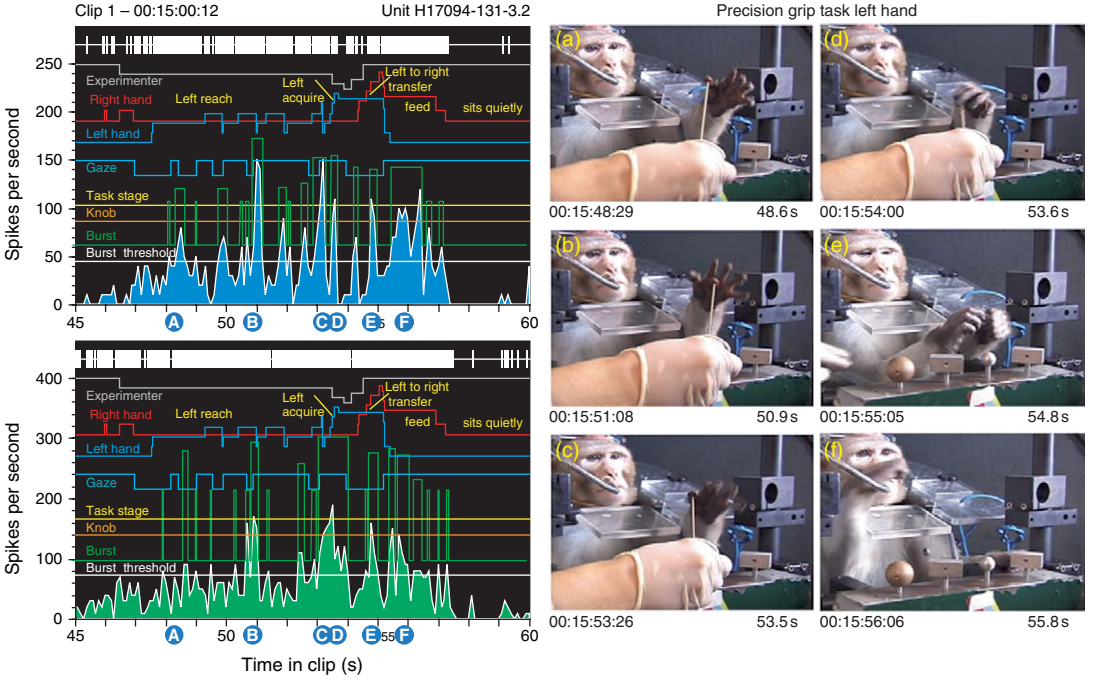

Figure 11 Responses of two simultaneously recorded area 5 neurons to acquisition of a raisin with the ipsilateral (left) hand. Natural grasping actions of the right and left hands (red and blue traces) are represented in the burst analysis records using the same format as the task stages in Figure 7. Each attempt to grasp the raisin was accompanied by a burst of impulses (A–D). Video images captured at the times marked by letters below the burst analysis graphs; note that when reaching toward a moving target, the animal opened the fingers using a baseball glove-like posture to maximize contact area on the hand. Once the stick was immobilized, the animal plucked the raisin using a precision grip between the thumb and digits 2 and 3.

Leinonen L. *et al.* (1979) in area 7b, these area 5 neurons fired at high rates as the hand tracked movements of the raisin by the experimenter (bursts A, B, and C). Activity declined once the raisin was acquired in the hand (burst D), or when the animal withdrew the hand as the target moved beyond reach. These neurons also responded strongly as the hand brought the raisin to the mouth to eat it (burst F).

Other neurons in area 5 fired most intensely when bilateral actions were coordinated between the left and the right hand, as when food morsels were transferred between them (Figure 12). These

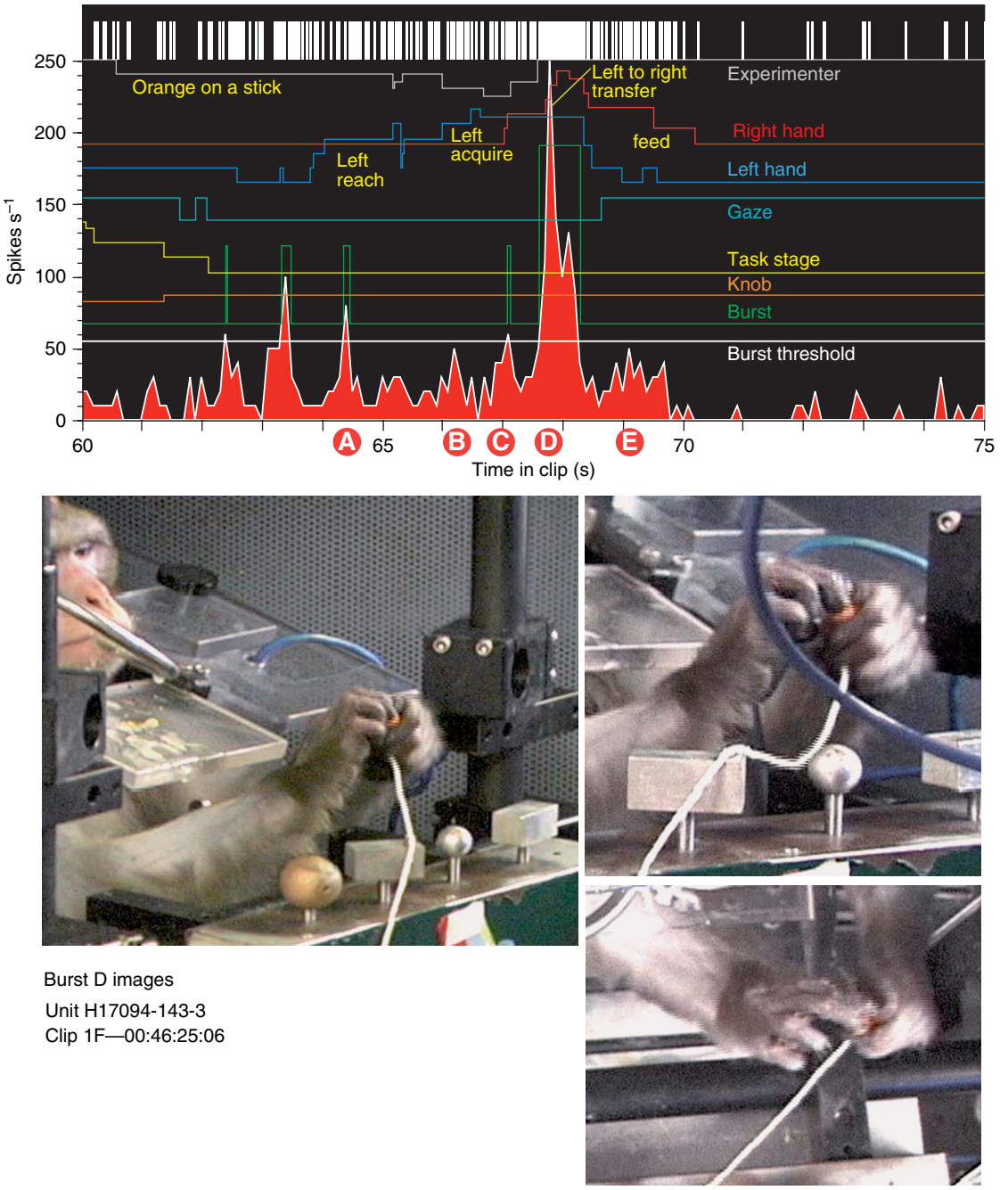

Figure 12 Responses of an intrapersonal-coordinated neuron in area 5 to precision grasp of an orange segment; the strongest responses were obtained when the orange was transferred from the left to the right hand (burst D). Images captured at the time of peak firing on three different cameras.

intrapersonal-coordinated neurons did not just encode equivalent tactile information from either side but preferentially signaled coincident somatosensory data shared between hemispheres during synergistic hand actions. They responded more vigorously to manipulatory actions of the two hands during bimanual transfer than to acquisition or release of food by either hand alone. Kinematic analyses of the hand actions indicated that hand-to-hand transfer integrated two prehensile actions: one hand slowly released grip as the other acquired the object. Bimanual and intrapersonal coordination neurons thus provide somesthetic feedback from both limbs, encoding whether the hands act independently or in concert. Consequently, frontal motor areas receive information, allowing them to coordinate the actions of both hands.

Two complementary mechanisms have been envisaged for bilateral coordination of the left and right hands. Temporal coordination involves a bilateral schema in which each hand is controlled separately in the contralateral hemisphere. Coordinated actions between the hands would need to be synchronized temporally by simultaneous activity in homologous regions on both sides of the brain (Gerloff, C. and Andres, F. G., 2002; Serrien, D. J. and Brown, P., 2002; Swinner, S. P., 2002; Serrien, D. J. *et al.*, 2006). Spatial specialization is a unilateral mechanism in which each hemisphere has neurons activated by bimanual actions (Kermadi, I. *et al.*, 2000; Donchin, *et al.*, 1998, 2002). Specific classes of these bilateral neurons would be engaged when coordinated bimanual activity is required. Although the temporal coordination hypothesis is the traditional view, the spatial specialization hypothesis provides an attractive mechanism for bilateral control for various reasons. In addition to the obvious advantage of providing redundant circuits for recovery from cortical damage, autonomous bilateral control is a prerequisite for hemispheric specialization and unilateral dominance. It also could explain some bilateral interactions observed between the hands during skilled tasks. Grasp forces exerted by each hand are interdependent regardless of whether the hands manipulate the same or different objects (Marteniuk, R. G. *et al.*, 1984; Paulignan, Y. *et al.*, 1989; Geffen, G. M. *et al.*, 1994; Wiesendanger, M. *et al.*, 1996; Ohki, Y. and Johansson, R. S., 1999; Birznieks, I. *et al.*, 2001; Serrien, D. J. and Wiesendanger, M., 2001; Serrien, D. J. *et al.*, 2006); a common output pathway would provide a simple circuit for coordinating grip force during bimanual grasp. PPC is a likely source of such bilateral control, as lesions to the posterior corpus callosum have been associated with losses of coordinated actions between the hands (Eliassen, J. C. *et al.*, 1999; Serrien, D. J. *et al.*, 2001).

6.12.5 Posterior Parietal Cortex and Active Touch

In their original study, Mountcastle V. B. *et al.* (1975) emphasized the difficulty of evoking responses in areas 5 and 7 to light tactile stimuli applied to the hand. However, these neurons were successfully activated when the animal's attention was directed toward the stimuli as a mechanism for reward or during active palpation of surfaces during tactile discrimination tasks. Like the studies of reach and grasp described above, the active touch studies involved goal-directed hand movements. However, the hand actions were directed not toward acquiring objects, but rather to acquiring sensory information needed for reward. Although many of these studies attributed recording sites in the rostral bank of the IPS to area 2, this region is now properly included in area 5 (Pandya D. N. and Selzer B., 1982; Pons, T. P. *et al.*, 1985; Lewis, J. W. *et al.* 1999).

Darian-Smith I. and colleagues (1984) trained monkeys to scan their fingers over gratings using a back-and-forth sinusoidal pattern. About one-third of the cells recorded in their area 5 population responded to the direction of hand movement but failed to signal the spatial properties of the grating surface. Indeed these authors expressed disappointment at the failure to find a greater population of neurons sensitive to the properties of the textured surface. Similarly, Ageranioti-Bélanger S. A. and Chapman C. E. (1992) classified area 5 responses to scans of gratings and smooth surfaces as either texture-related (25%) or movement-related (26%). These neurons were presumed to underlie the analysis of surface texture and the representation of the physical parameters of movement, respectively. Their movement-related cells showed monotonic increases in firing rates precisely timed to the onset and end of hand movement and were independent of whether the surface texture was rough or smooth. In addition, 35% of the texture-related units responded more vigorously during active performance of the scanning movement than to passive stimulation of the fingers with the same surfaces (texture- and movement-related cells); no such units were found in area 3b, and only one was encountered in area 1.

Lastly, they described neurons that were silent during the scanning movement but subsequently fired a burst that was stronger for rough surfaces, suggesting that they signaled the perceptual decision made by the animal.

Studies using procedural memory tasks – in which the animal had to retain visual information about a target's shape or location during a delay period – are consistent with the notion that PPC activity may express the intention to execute a specific motor program. Fifty percent of neurons tested in areas 2, 5, and 7 by Joaquin Fuster and colleagues showed sustained activity during a delayed visual–haptic match-to-sample task related to the surface texture of a viewed object (Koch, K. W. and Fuster, J. M., 1989; Zhou, Y. D. and Fuster, J. M., 1996; 1997; 2000); tactile responses to palpation of the object were of matching sign. These authors proposed that alterations of firing prior to hand contact with an object may represent long-term tactile memory associations with objects previously perceived by touch or by vision. Zhou Y. D. and Fuster J. M. (2000) suggested that, by association, the visual cue might activate the internal representation of the object's tactile features to enable the correct choice. Alternatively, the firing patterns could represent the upcoming exploratory procedures used during palpation by the hand to distinguish the object properties (Klatzky, R. A. *et al.*, 1985; Bodegård, A. *et al.*, 2001).

Object manipulation activates similar regions in the human brain (Binkofski, F., *et al.*, 1999; Bodegård, A. *et al.*, 2001; Grefkes, C., *et al.*, 2002; Stoeckel, M. C., *et al.*, 2004), including area aIPS and the anterior portion of the superior parietal cortex (aSPL) that corresponds to the macaque area 5 hand representation. Activation of aSPL was particularly strong when subjects had to palpate the surfaces to discriminate object dimensions or form, while area aIPS was preferentially activated in cross-modal visual–tactile matching tasks. Neurological tests of stereognosis in humans and psychophysical tests of complex tactile discrimination in humans and animals can be considered goal-directed actions in which the aim is to acquire information about objects, rather than to gain possession of objects as in prehension tasks. The common neurological substrate of both types of behaviors supports hypotheses that the principal function of the dorsal stream involves both the planning of such behaviors and on-line control and adjustment of hand actions to achieve the intended goal.

6.12.6 Conclusions

We have shown in this chapter that goal-directed hand and arm movements seem to play a key role in the responses of neurons in PPC. Although most of the current research has analyzed reaching, pointing, and grasping behaviors, studies of active touch should also be included in analyses of PPC function. The common feature of all of these studies has been the importance of directing actions of the hand to internally generated task goals such as acquiring objects or information about them that are beneficial or desirable to the subject. Repeated experience and practice allows the subject, whether human or monkey, to plan the action efficiently and to monitor successful execution. The feedback circuits between parietal and frontal cortex allow dynamic error correction and updating of existing motor programs. They help guide hand movements to salient targets on an object, whether for efficient grasp or for exploratory palpation. The sensory feedback provided to S-I cortex from the hand may in turn call forth more information by redirecting the hand elsewhere on the object. As such, these circuits enable acquisition of new skills and the maintenance of a repertoire of learned adaptive behaviors of the hand.

Lesions of the hand representation of PPC result in paucity of exploratory and skilled movements of the hand in humans and deficits in stereognosis and other complex tactile recognition tasks (reviewed in Pause, M. *et al.*, 1989; Ghika, J. *et al.*, 1998; Binkofski, F. *et al.*, 2001; Freund, H.-J., 2001; Jäncke, L. *et al.*, 2001). The importance of PPC in monitoring and guiding sensorimotor functions of the hand may explain the neurophysiological basis of such disorders.

Acknowledgments

Major funding for studies from my laboratory described in this chapter has been provided by Research Grant R01 NS11862 from the National Institute of Neurological Diseases and Stroke (NINDS) and from Human Brain Project Research Grant R01 NS44820 funded jointly by the National Institute of Neurological Diseases and Stroke (NINDS), National Institute of Mental Health (NIMH), and the National Institute of Aging (NIA). I thank my colleagues Drs. Daniel J. Debowy,

Soumya Ghosh, Jin Y. Ro, K. Srinivasa Babu, Jessie Chen, and Shari D. Reitzen for their many contributions to these studies, and Dr. Daniel Gardner for insightful comments and criticisms of this chapter.

References

Ageranioti-Bélanger, S. A. and Chapman, C. E. 1992. Discharge properties of neurones in the hand area of primary somatosensory cortex in monkeys in relation to the performance of an active tactile discrimination task. II. Area 2 as compared to areas 3b and 1. Exp. Brain Res. 91, 207–228.

Andersen, R. A. 1995. Coding of intention and spatial location in the posterior parietal cortex. Cereb. Cortex 5, 457–469.

Andersen, R. A. and Buneo, C. A. 2002. Intentional maps in posterior parietal cortex. Annu. Rev. Neurosci. 25, 189–220.

Andersen, R. A., Essick, G. K., and Siegel, R. M. 1985. Encoding of spatial location by posterior parietal neurons. Science 230, 456–458.

Andersen, R. A., Snyder, L. H., Bradley, D. C., and Xing, J. 1997. Multimodal representation of space in the posterior parietal cortex and its use in planning movements. Annu. Rev. Neurosci. 20, 303–330.

Astafiev, S. V., Shulman, G. L., Stanley, C. M., Snyder, A. Z., Van Essen, D. C., and Corbetta, M. 2003. Functional organization of human intraparietal and frontal cortex for attending, looking and pointing. J. Neurosci. 23, 4689–4699.

Batista, A. P. and Andersen, R. H. 2001. The parietal reach region codes the next planned movement in a sequential reach task. J. Neurophysiol. 85, 539–544.

Batista, A. P., Buneo, C. A., Snyder, L. H., and Andersen, R. A. 1999. Reach plans in eye-centered coordinates. Science 285, 257–260.

Battaglia-Mayer, A., Archambault, P. S., and Caminiti, R. 2006. The cortical network for eye-hand coordination and its relevance to understanding motor disorders of parietal patients. Neuropsychologia 44, 2594–2606.

Battaglia-Mayer, A., Caminiti, R., Lacquaniti, F., and Zago, M. 2003. Multiple levels of representation of reaching in the parieto-frontal network. Cereb. Cortex, 13, 1009–1022.

Battaglia-Mayer, A., Ferraina, S., Mitsuda, T., Marconi, B., Genovesio, A., Onorati, P., Lacquaniti, F., and Caminiti, R. 2000. Early coding of reaching in the parieto-occipital cortex. J. Neurophysiol. 83, 2374–2391.

Binkofski, F., Buccino, G., Stephan, K. M., Rizzolatti, G., Seitz, R. J., and Freund, H. J. 1999a. A parieto-premotor network for object manipulation: evidence from neuroimaging. Exp. Brain Res. 128, 210–213.

Binkofski, F., Buccino, G., Posse, S., Seitz, R. J., Rizzolatti, G., and Freund, H. J. 1999b. A fronto-parietal circuit for object manipulation in man: evidence from an fMRI-study. Eur. J. Neurosci. 11, 3276–3286.

Binkofski, F., Dohle, C., Posse, S., Stephan, K., Hefter, H., Seitz, R., and Freund, H. 1998. Human anterior intraparietal area subserves prehension: a combined lesion and functional MRI activation study. Neurology 50, 1253–1259.

Binkofski, F., Kunesch, E., Classen, J., Seitz, R. J., and Freund, H. J. 2001. Tactile apraxia: unimodal apractic disorder of tactile object exploration associated with parietal lobe lesions. Brain 124, 132–144.

Bisley, J. W. and Goldberg, M. E. 2003. Neuronal activity in the lateral intraparietal area and spatial attention. Science 299, 81–86.

Birznieks, I., Jenmalm, P., Goodwin, A. W., and Johansson, R. S. 2001. Encoding of the direction of fingertip forces by human tactile afferents. J. Neurosci. 21, 8222–8237.

Bodegård, A., Geyer, S., Grefkes, C., Zilles, K., and Roland, P. E. 2001. Hierarchical processing of shape in the human brain. Neuron 31, 317–328.

von Bonin, G. and Bailey, P. 1947. The Neocortex of *Macaca mulatta*, University of Illinois.

Brochier, T., Boudreau, M.-J., Paré, M., and Smith, A. M. 1999. The effects of muscimol inactivation of small regions of motor and somatosensory cortex on independent finger movements and force control in the precision grip. Exp. Brain Res. 128, 31–40.

Brochier, T., Spinks, R. L., Umilta, M. A., and Lemon, R. N. 2004. Patterns of muscle activity underlying object-specific grasp by the Macaque monkey. J. Neurophysiol. 92, 1770–1782.

Brodmann, K. 1909. Vergleichende Lokalisationsiehre der Grosshirnrinde in ihren Prinzipien Dargestellt auf Grund des Zellenbaues. Leipzig.

Buccino, G., Binkofski, F., Fink, G. R., Fadiga, L., Fogassi, L., Gallese, V., Seitz, R. J., Zilles, K., Rizzolatti, G., and Freund, H. J. 2001. Action observation activates premotor and parietal areas in a somatotopic manner: an fMRI study. Eur. J. Neurosci. 13, 400–404.

Buneo, C. A. and Andersen, R. A. 2006. The posterior parietal cortex: sensorimotor interface for the planning and online control of visually guided movements. Neuropsychologia 44, 2594–2606.

Burbaud, P., Doegle, C., Gross, C., and Bioulac, B. 1991. A quantitative study of neuronal discharge in areas 5, 5 and 4 of the monkey during fast arm movements. J. Neurophysiol. 66, 429–443.

Burnod, Y., Baraduc, P., Battaglia-Mayer, A., Guigon, E., Koechlin, E., Ferraina, S., Lacquaniti, F., and Caminiti, R. 1999. Parieto-frontal coding of reaching: an integrated framework. Exp. Brain Res. 129, 325–346.

Burton, H. 1986. Second Somatosensory Cortex and Related Areas. In: Cerebral Cortex, Vol. 5, (*eds*. E. G. Jones and A. Peters), pp. 31–98. Plenum Press.

Caminiti, R. and Sbriccoli, A. 1985. The callosal system of the superior parietal lobule in the monkey. J. Comp. Neurol. 2237, 85–2299.

Caminiti, R., Ferraina, S., and Johnson, P. B. 1996. The sources of visual information to the primate frontal lobe: a novel role for the superior parietal lobule. Cereb. Cortex 6, 319–328.

Caminiti, R., Ferraina, S., and Mayer, A. B. 1998. Visuomotor transformations: early cortical mechanisms of reaching. Curr. Opin. Neurobiol. 8, 753–761.

Castiello, U. 2005. The neuroscience of grasping. Nat. Neurosci. Rev. 6, 726–736.

Cavada, C. and Goldman-Rakic, P. 1989a. Posterior parietal cortex in rhesus monkey. I. Parcellation of areas based on distinctive limbic and sensory corticocortical connections. J. Comp. Neurol. 287, 393–421.

Cavada, C. and Goldman-Rakic, P. 1989b. Posterior parietal cortex in rhesus monkey. II. Evidence for segregated corticocortical networks linking sensory and limbic areas with the frontal lobe. J. Comp. Neurol. 287, 422–445.

Chieffi, S. and Gentilucci, M. 1993. Coordination between the transport and the grasp component during prehension movements. Exp. Brain Res. 94, 471–477.

Colby, C. L. 1998. Action-oriented spatial reference frames in cortex. Neuron 20, 15–24.

Colby, C. L. and Goldberg, M. E. 1999. Space and attention in parietal cortex. Annu. Rev. Neurosci. 22, 319–349.

Colby, C. L., Duhamel, J. R., and Goldberg, M. E. 1993. Ventral intraparietal area of the macaque: anatomic

location and visual response properties. J. Neurophysiol. 69, 902–914.
Connolly, J. D. and Goodale, M. A. 1999. The role of visual feedback of hand position in the control of manual prehension. Exp. Brain Res. 125, 281–286.
Connolly, J. D., Andersen, R. A., and Goodale, M. A. 2003. FMRI evidence for a 'parietal reach region' in the human brain. Exp. Brain Res. 153, 140–1145.
Crammond, D. J. and Kalaska, J. F. 1989. Neuronal activity in primate parietal cortex area 5 varies with intended movement direction during an instructed-delay period. Exp. Brain Res. 76, 458–462.
Culham, J. C. 2004. Human Brain Imaging Reveals a Parietal Area Specialized for Grasping. In: Attention and Performance XX: Functional Brain Imaging of Visual Cognition (*eds*. N. Kanwisher and J. Duncan), pp. 417–438. Oxford University Press.
Culham, J. C. and Valyear, K. F. 2006. Human parietal cortex in action. Curr. Opin. Neurobiol. 16, 205–212.
Culham, J. C., Cavina-Pratesi, C., and Singhal, A. 2006. The role of parietal cortex in visuomotor control: what have we learned from neuroimaging? Neuropsychologia 44, 2668–2684.
Culham, J. C., Danckert, S. L., DeSouza, J. F., Gati, J. S., Menon, R. S., and Goodale, M. A. 2003. Visually guided grasping produces fMRI activation in dorsal but not ventral stream brain areas. Exp. Brain Res. 153, 180–189.
Darian-Smith, I., Goodwin, A., Sugitani, M., and Heywood, J. 1984. The Tangible Features of Textured Surfaces: Their Representation in the Monkey's Somatosensory Cortex. In: Dynamic Aspects of Neocortical Function (*eds*. G. W. Edelman, E. Gall, and W. M. Cowan), pp. 475–500. John Wiley.
Debowy, D. J., Babu, K. S., Hu, E. H., Natiello, M., Reitzen, S., Chu, M., Sakai, J., and Gardner, E. P. 2002. New Applications of Digital Video Technology for Neurophysiological Studies of Hand Function. In: The Somatosensory System: Deciphering the Brain's Own Body Image (*eds*. R. Nelson and F. L. BocaRaton), pp. 219–241. CRC Press.
Debowy, D. J., Ghosh, S., Ro, J. Y., and Gardner, E. P. 2001. Comparison of neuronal firing rates in somatosensory and posterior parietal cortex during prehension. Exp. Brain Res. 137, 269–291.
Disbrow, E., Litinas, E., Recanzone, G., Padberg, J., and Krubitzer, L. 2003. Cortical connections of the parietal ventral area and the second somatosensory area in macaque monkeys. J. Comp. Neurol. 462, 382–1399.
Dorris, M. C. and Glimcher, P. W. 2004. Activity in posterior parietal cortex is correlated with the relative subjective desirability of action. Neuron 44, 365–378.
Duhamel, J. R., Colby, C. L., and Goldberg, M. E. 1998. Ventral intraparietal area of the macaque: congruent visual and somatic response properties. J. Neurophysiol. 80, 126–136.
Duffy, F. H. and Burchfiel, J. L. 1971. Somatosensory system: organizational hierarchy from single units in monkey area 5. Science 172, 273–275.
von Economo, C. and Hoskinas, G. N. 1925. Die Cytoarchitektonik der Hirnrindedes erwachsenen Menschen, Springer.
Ehrsson, H. H., Fagergren, E., and Forssberg, H. 2001. Differential fronto-parietal activation depending on force used in a precision grip task: an fMRI study. J. Neurophysiol. 85, 2613–2623.
Ehrsson, H. H., Fagergren, A., Johansson, R. S., and Forssberg, H. 2003. Evidence for the involvement of the posterior parietal cortex in coordination of fingertip forces for grasp stability in manipulation. J. Neurophysiol. 90, 2978–2986.
Ehrsson, H. H., Fagergren, A., Jonsson, T., Westling, G., Johansson, R. S., and Forssberg, H. 2000. Cortical activity in precision- versus power-grip tasks: an fMRI study. J. Neurophysiol. 83, 528–536.
Eliassen, J. C., Baynes, K., and Gazzaniga, M. S. 1999. Direction information coordinated via the posterior third of the corpus callosum during bimanual movements. Exp. Brain Res. 128, 573–577.
Fagg, A. H. and Arbib, M. A. 1998. Modeling parietal-premotor interactions in primate control of grasping. Neural Netw. 11, 1277–1303.
Fattori, P., Breveglieri, R., Amoroso, K., and Galletti, C. 2004. Evidence for both reaching and grasping activity in the medial parieto-occipital cortex of the macaque. Eur. J. Neurosci. 20, 2457–2466.
Felleman, D. J. and Van Essen, D. C. 1991. Distributed hierarchical processing in the primate cerebral cortex. Cereb. Cortex 1, 1–47.
Ferraina, S., Battaglia-Mayer, A., Genovesio, A., Marconi, B., Onorati, P., and Caminiti, R. 2001. Early coding of visuomanual coordination during reaching in parietal area PEc. J. Neurophysiol. 85, 462–467.
Ferraina, S., Johnson, P. B., Garasto, M. R., Battaglia-Mayer, A., Ercolani, L., Bianchi, L., Lacquaniti, F., and Caminiti, R. 1997. Combination of hand and gaze signals during reaching: activity in parietal area 7m of the monkey. J. Neurophysiol. 77, 1034–1038.
Fitzgerald, P. J., Lane, J. W., Thakur, P. H., and Hsiao, S. S. 2004. Receptive field properties of the macaque second somatosensory cortex: evidence for multiple functional representations. J. Neurosci. 24, 11193–11204.
Fitzgerald, P. J., Lane, J. W., Thakur, P. H., and Hsiao, S. S. 2006. Receptive field (RF) properties of the macaque second somatosensory cortex: RF size, shape, and somatotopic organization. J. Neurosci. 26, 6485–6495.
Fogassi, L. and Luppino, G. 2005. Motor functions of the parietal lobe. Curr. Opin. Neurobiol. 15, 626–631.
Fogassi, L., Ferrari, P. F., Gesierich, B., Rozzi, S., Chersi, F., and Rizzolatti, G. 2005. Parietal lobe: from action organization to intention understanding. Science 308, 662–667.
Fogassi, L., Gallese, V., Buccino, G., Craighero, L., Fadiga, L., and Rizzolatti, G. 2001. Cortical mechanism for the visual guidance of hand grasping movements in the monkey: a reversible inactivation study. Brain 124, 571–586.
Freund, H.-J. 2001. The parietal lobe as sensorimotor interface: a perspective from clinical and neuroimaging data. Neuroimage 14, S142–S146.
Frey, S. H., Vinton, D., Norlund, R., and Grafton, S. T. 2005. Cortical topography of human anterior intraparietal cortex active during visually guided grasping. Cogn. Brain Res. 23, 397–405.
Friedman, D. P., Murray, E. A., O'Neill, J. B., and Mishkin, M. 1986. Cortical connections of the lateral sulcus of macaques: evidence for a corticolimbic pathway for touch. J. Comp. Neurol. 252, 323–347.
Gallese, V., Murata, A., Kaseda, M., Niki, N., and Sakata, H. 1994. Deficit of hand preshaping after muscimol injection in monkey parietal cortex. Neuroreport 5, 1525–1529.
Galletti, C., Battaglini, P. P., and Fattori, P. 1993. Parietal neurons encoding spatial locations in craniotopic coordinates. Exp. Brain Res. 96, 221–229.
Galletti, C., Battaglini, P. P., and Fattori, P. 1997. The posterior parietal cortex in humans and monkeys. NIPS 12, 166–171.
Galletti, C., Gamberini, M., Breveglieri, R., and Fattori, P. 2003. Role of the medial parieto-occipital cortex in the control of reaching and grasping movements. Exp. Brain Res. 153, 158–170.
Gardner, E. P. 1988. Somatosensory cortical mechanisms of feature detection in tactile and kinesthetic discrimination. Can. J. Physiol. Pharmacol. 66, 439–454.
Gardner, E. P., Babu, K. S., Natiello, M., and Debowy, D. J. 2001. How the right hand coordinates with the left during

synergistic hand interactions. Soc. Neurosci. Abstr. 27: Program No. 21.9.
Gardner, E. P., Babu, K. S., Reitzen, S. D., Ghosh, S., Brown, A. M., Chen, J., Hall, A. L., Herzlinger, M. D., Kohlenstein, J. B., and Ro, J. Y. 2007a. Neurophysiology of prehension: I. Posterior parietal cortex and object-oriented hand behaviors. J. Neurophysiol. 97, 387–406.
Gardner, E. P., Debowy, D., Ro, J. Y., Ghosh, S., and Babu, K. S. 2002. Sensory monitoring of prehension in the parietal lobe: a study using digital video. Behav. Brain Res. 135, 213–224.
Gardner, E. P., Ro, J. Y., Babu, K. S., and Ghosh, S. 2007b. Neurophysiology of prehension: II. Response diversity in primary somatosensory (S-I) and motor (M-I) cortices. J. Neurophysiol. 97, 1656–1670.
Gardner, E. P., Ro, J. Y., Debowy, D., and Ghosh, S. 1999. Facilitation of neuronal firing patterns in somatosensory and posterior parietal cortex during prehension. Exp. Brain Res. 127, 329–354.
Geffen, G. M., Jones, D. L., and Geffen, L. B. 1994. Interhemispheric control of manual motor activity. Behav. Brain Res. 64, 131–140.
Georgopoulos, A. P., Caminiti, R., and Kalaska, J. F. 1984. Static spatial effects in motor cortex and area 5: quantitative relations in a two dimensional space. Exp. Brain Res. 54, 446–454.
Georgopoulos, A. P., Kalaska, J. F., Caminiti, R., and Massey, J. T. 1982. On the relations between the direction of two-dimensional arm movements and cell discharge in primate motor cortex. J. Neurosci. 2, 1527–1537.
Georgopoulos, A. P., Kettner, R. E., and Schwartz, A. B. 1988. Primate motor cortex and free arm movements to visual targets in three-dimensional space. II. Coding of the direction of movement by a neuronal population. J. Neurosci. 8, 2928–2937.
Ghika, J., Ghika-Schmid, F., and Bogousslasvky, J. 1998. Parietal motor syndrome: a clinical description in 32 patients in the acute phase of pure parietal strokes studied prospectively. Clin. Neurol. Neurosurg. 100, 271–282.
Ghosh, S. and Gattera, R. 1995. A comparison of the ipsilateral cortical projections to the dorsal and ventral subdivisions of the macaque premotor cortex. Somatosens. Mot. Res. 12, 359–378.
Glimcher, P. W. 2003. The neurobiology of visual-saccadic decision making. Annu. Rev. Neurosci. 26, 133–179.
Goodale, M. A. and Westwood, D. A. 2004. An evolving view of duplex vision: separate but interacting cortical pathways for perception and action. Curr. Opin. Neurobiol. 14, 203–211.
Gordon, A. M., Westling, G., Cole, K. J., and Johansson, R. S. 1993. Memory representations underlying motor commands used during manipulation of common and novel objects. J. Neurophysiol. 69, 1789–1796.
Grafton, S. T., Fagg, A. H., Woods, R. P., and Arbib, M. A. 1996. Functional anatomy of pointing and grasping in humans. Cereb. Cortex 6, 226–237.
Grefkes, C. and Fink, G. R. 2005. The functional organization of the intraparietal sulcus in humans and monkeys. J. Anat. 207, 3–17.
Grefkes, C., Weiss, P. H., Zilles, K., and Fink, G. R. 2002. Crossmodal processing of object features in human anterior intraparietal cortex: an fMRI study implies equivalencies between humans and monkeys. Neuron 35, 173–184.
Gregoriou, G. G., Borra, E., Matelli, M., and Luppino, G. 2006. Architectonic organization of the inferior parietal convexity of the macaque monkey. J. Comp. Neurol. 496, 422–1451.
Hikosaka, O., Tanaka, M., Sakamoto, M., and Iwamura, Y. 1985. Deficits in manipulative behaviors induced by local injections of muscimol in the first somatosensory cortex of the conscious monkey. Brain Res. 325, 375–380.
Hu, Y., Osu, R., Okada, M., Goodale, M. A., and Kawato, M. A. 2005. model of the coupling between grip aperture and hand transport during human prehension. Exp. Brain Res. 167, 301–304.
Hyvärinen, J. 1981. Regional distribution of functions in parietal association area 7 of the monkey. Brain Res. 206, 287–303.
Hyvärinen, J. 1982. Posterior parietal lobe of the primate brain. Physiol. Rev. 62, 1060–1129.
Hyvärinen, J. 1982b. The Parietal Cortex of Monkey and Man, Springer-Verlag.
Hyvärinen, J. and Poranen, A. 1974. Function of the parietal associative area 7 as revealed from cellular discharges in alert monkeys. Brain 97, 673–692.
Iriki, A., Tanaka, M., and Iwamura, Y. 1996. Coding of modified body schema during tool use by macaque postcentral neurones. Neuroreport 7, 2325–2330.
Iriki, A., Tanaka, M., Obayashi, S., and Iwamura, Y. 2001. Self-images in the video monitor coded by monkey intraparietal neurons. Neurosci. Res. 40, 163–173.
Iwamura, Y. 2000. Bilateral receptive field neurons and callosal connections in the somatosensory cortex. Phil. Trans. R. Soc. Lond. B. 355, 267–273.
Iwamura, Y. and Tanaka, M. 1978. Postcentral neurons in hand region of area 2: their possible role in the form discrimination of tactile objects. Brain Res. 150, 662–666.
Iwamura, Y. and Tanaka, M. 1996. Representation of reaching and grasping in the monkey postcentral gyrus. Neurosci. Lett. 214, 147–150.
Iwamura, Y., Iriki, A., and Tanaka, M. 1994. Bilateral hand representation in the postcentral somatosensory cortex. Nature 369, 554–556.
Iwamura, Y., Tanaka, M., Hikosaka, O., and Sakamoto, M. 1995. Postcentral neurons of alert monkeys activated by the contact of the hand with objects other than the monkey's own body. Neurosci. Lett. 186, 127–130.
Iwamura, Y., Tanaka, M., Iriki, A., Taoka, M., and Toda, T. 2002. Processing of tactile and kinesthetic signals from bilateralsides of the body in the postcentral gyrus of awake monkeys. Behav. Brain Res. 135, 185–190.
Iwamura, Y., Tanaka, M., Sakamoto, M., and Hikosaka, O. 1985. Vertical neuronal arrays in the postcentral gyrus signaling active touch: a receptive field study in the conscious monkey. Exp. Brain Res. 58, 412–420.
Iwamura, Y., Tanaka, M., Sakamoto, M., and Hikosaka, O. 1993. Rostrocaudal gradients in neuronal receptive field complexity in the finger region of the alert monkey's postcentral gyrus. Exp. Brain Res. 92, 360–368.
Jäncke, L., Kleinschmidt, A., Mirzazade, S., Shah, N. J., and Freund, H.-J. 2001. The role of the inferior parietal cortex in linking the tactile perception and manual construction of object shapes. Cereb. Cortex 11, 114–121.
Jeannerod, M. 1984. The timing of natural prehension movements. J. Mot. Behav. 16, 235–254.
Jeannerod, M. 1986. The formation of finger grip during prehension: a cortically mediated visuomotor pattern. Behav. Brain Res. 19, 99–116.
Jeannerod, M. 1994. The hand and the object: the role of posterior parietal cortex in forming motor representations. Can. J. Physiol. Pharmacol. 72, 535–541.
Jeannerod, M., Arbib, M. A., Rizzolatti, G., and Sakata, H. 1995. Grasping objects: the cortical mechanisms of visuomotor transformation. Trends Neurosci. 18, 314–320.
Jeannerod, M., Decety, J., and Michel, F. 1994. Impairment of grasping movements following a bilateral posterior parietal lesion. Neuropsychologia 32, 369–380.
Jenmalm, P. and Johansson, R. S. 1997. Visual and somatosensory information about object shape control manipulative fingertip forces. J. Neurosci. 17, 4486–4499.
Jenmalm, P., Dahlstedt, S., and Johansson, R. S. 2000. Visual and tactile information about object-curvature control

fingertip forces and grasp kinematics in human dextrous manipulation. J. Neurophysiol. 84, 2984–2997.
Jenmalm, P., Schmitz, C., Forssberg, H., and Ehrsson, H. H. 2006. Lighter or heavier than predicted: neural correlates of corrective mechanisms during erroneously programmed lifts. J. Neurosci. 26, 9015–9021.
Johansson, R. S. 1996. Sensory Control of Dexterous Manipulation in Humans. In: Hand and Brain (*eds*. A. M. Wing, P. Haggard, and J. R. Flanagan), pp. 381–414. Academic Press.
Johansson, R. S. and Westling, G. 1984. Roles of glabrous skin receptors and sensorimotor memory in automatic control of precision grip when lifting rougher or more slippery objects. Exp. Brain Res. 56, 550–564.
Johansson, R. S., Westling, G., Backstrom, A., and Flanagan, J. R. 2001. Eye-hand coordination in object manipulation. J. Neurosci. 21, 6917–6932.
Johnson, P. B., Ferraina, S., Bianchi, L., and Caminiti, R. 1996. Cortical networks for visual reaching: physiological and anatomical organization of frontal and parietal lobe arm regions. Cereb. Cortex 6, 102–119.
Jones, E. G. and Powell, T. P. S. 1969. Connexions of the somatic sensory cortex of the rhesus monkey. I. Ipsilateral cortical connexions. Brain 92, 477–502.
Jones, E. G. and Powell, T. P. S. 1970. An anatomical study of converging sensory pathways within the cerebral cortex of the monkey. Brain 93, 793–820.
Jones, E. G., Coulter, J. D., and Hendry, S. H. C. 1978. Intracortical connectivity of architectonic fields in the somatic sensory, motor and parietal cortex of monkeys. J. Comp. Neurol. 181, 291–348.
Jones, E. G., Coulter, J. D., and Wise, S. 1979. Commissural columns in the sensory-motor cortex of monkeys. J. Comp. Neurol. 188, 113–1136.
Kalaska, J. F. 1996. Parietal cortex area 5 and visuomotor behavior. Can. J. Physiol. Pharmacol. 74, 483–498.
Kalaska, J. F. and Crammond, D. J. 1995. Deciding not to GO: neural correlates of response selection in a GO/NOGO task in primate premotor and parietal cortex. Cereb. Cortex 5, 410–428.
Kalaska, J. F., Caminiti, R., and Georgopoulos, A. P. 1983. Cortical mechanisms related to the direction of two-dimensional arm movements: relations in parietal area 5 and comparison with motor cortex. Exp. Brain Res. 51, 247–260.
Kalaska, J. F., Cohen, D. A. D., Prud'Homme, M. J. L., and Hyde, M. L. 1990. Parietal area 5 neuronal activity encodes movement kinematics, not movement dynamics. Exp. Brain Res. 80, 351–364.
Kalaska, J. F., Scott, S. H., Cisek, P., and Sergios, L. E. 1997. Cortical control of reaching movements. Curr. Opin. Neurobiol. 7, 849–859.
Kermadi, I., Liu, Y., and Rouiller, E. M. 2000. Do bimanual motor actions involve the dorsal premotor (PMd), cingulate (CMA) and posterior parietal (PPC) cortices? Comparison with primary and supplementary motor cortical areas. Somatosens. Mot. Res. 17, 255–271.
Klatzky, R. A., Lederman, S. J., and Metzger, V. A. 1985. Identifying objects by touch: an ''expert system''. Percept. Psychophys. 37, 299–302.
Koch, K. W. and Fuster, J. M. 1989. Unit activity in monkey parietal cortex related to haptic perception and temporary memory. Exp. Brain Res. 76, 292–306.
Kurata, K. 1991. Corticocortical inputs to the dorsal and ventral aspects of the premotor cortex of macaque monkeys. Neurosci. Res. 12, 263–280.
Lacquaniti, F., Guigon, E., Bianchi, L., Ferraina, S., and Caminiti, R. 1995. Representing spatial information for limb movement: role of area 5 in the monkey. Cereb. Cortex 5, 391–409.
LaMotte, R. H. and Acuña, C. 1978. Defects in accuracy of reaching after removal of posterior parietal cortex in monkeys. Brain Res. 139, 309–326.
Lederman, S. J. 1994. The adaptive control of prehension. Can. J. Physiol. Pharmacol. 72, 506–510.
Leinonen, L., Hyvärinen, J., Nyman, G., and Linnankowski, I. 1979. Functional properties of neurons in lateral part of associative area 7 in awake monkey. Exp. Brain Res. 34, 299–320.
Lemon, R. N., Johansson, R. S., and Westling, G. 1995. Corticospinal control during reach, grasp and precision lift in man. J. Neurosci. 15, 6145–6156.
Lewis, J. W., Burton, H., and Van Essen, D. C. 1999. Anatomical evidence for the posterior boundary of area 2 in the macaque monkey. Somatosens. Mot. Res. 16, 382–390.
Lewis, J. W. and Van Essen, D. C. 2000a. Mapping of architectonic subdivisions in the macaque monkey, with emphasis on parieto-occipital cortex. J. Comp. Neurol. 428, 79–1111.
Lewis, J. W. and Van Essen, D. C. 2000b. Corticocortical connections of visual, sensorimotor, and multimodal processing areas in the parietal lobe of the macaque monkey. J. Comp. Neurol. 428, 112–1137.
Luppino, G., Murata, A., Govoni, P., and Matelli, M. 1999. Largely segregated parietofrontal connections linking rostral intraparietal cortex (areas AIP VIP) and the ventral premotor cortex (areas F5 and F4). Exp. Brain Res. 128, 181–187.
Maravita, A. and Iriki, A. 2004. Tools for the body (schema). Trends Cogn. Sci. 8, 79–86.
Marteniuk, R. G., Leavitt, J. L., MacKenzie, C. L., and Athenes, S. 1990. Functional relationships between grasp and transport components in a prehension task. Hum. Mov. Sci. 9, 149–176.
Marteniuk, R. G., MacKenzie, C. L., and Baba, D. M. 1984. Bimanual movement control: information processing and interaction effects. Q. J. Exp. Psychol. 36A, 335–365.
Matelli, M. and Luppino, G. 2001. Parietofrontal circuits for action and space perception in the macaque monkey. NeuroImage 14, S27–S32.
Matelli, M., Camarda, R., Glickstein, M., and Rizzolatti, G. 1986. Afferent and efferent projections of the inferior area 6 in the macaque monkey. J. Comp. Neurol. 251, 281–298.
Matelli, M., Govoni, P., Galletti, C., Kutz, D. F., and Luppino, G. 1998. Superior area 6 afferents from the superior parietal lobule in the macaque monkey. J. Comp. Neurol. 402, 327–1352.
Milner, A. D. and Goodale, M. A. 1995. The Visual Brain in Action, Oxford University Press.
Mishkin, M. 1979. Analogous neural models for tactual and visual learning. Neuropsychologia 17, 139–151.
Mountcastle, V. B. 1995. The parietal system and some higher brain functions. Cereb. Cortex 5, 377–390.
Mountcastle, V. B., Lynch, J. C., Georgopoulos, A., Sakata, H., and Acuna, C. 1975. Posterior parietal association cortex of the monkey: command functions for operations within extrapersonal space. J. Neurophysiol. 38, 871–908.
Murata, A., Fadiga, L., Fogassi, L., Gallese, V., Raos, V., and Rizzolatti, G. 1997. Object representation in the ventral premotor cortex (area F5) of the monkey. J. Neurophysiol. 78, 2226–2230.
Murata, A., Gallese, V., Kaseda, M., and Sakata, H. 1996. Parietal neurons related to memory-guided hand manipulation. J. Neurophysiol. 75, 2180–2186.
Murata, A., Gallese, V., Luppino, G., Kaseda, M., and Sakata, H. 2000. Selectivity for the shape, size and orientation of objects for grasping in neurons of monkey parietal area AIP. J. Neurophysiol. 83, 2580–2601.
Nakamura, H., Kuroda, T., Wakita, M., Kusunoki, M., Kato, A., Mikami, A., Sakata, H., and Itoh, K. 2001. From three-dimensional space vision to prehensile hand movements:

the lateral intraparietal area links the area V3A and the anterior intraparietal area in macaque monkeys. J. Neurosci. 21, 8174–8187.

Neal, J. W., Pearson, R. C. A., and Powell, T. P. S. 1986. The organization of the corticocortical projection of area 5 upon area 7 in the parietal lobe of the monkey. Brain Res. 381, 164–1167.

Neal, J. W., Pearson, R. C. A., and Powell, T. P. S. 1987. The cortico-cortical connections of area 7b, PF, in the parietal lobe of the monkey. Brain Res. 419, 341–1346.

Ohki, Y. and Johansson, R. S. 1999. Sensorimotor interactions between pairs of fingers in bimanual and unimanual manipulative tasks. Exp. Brain Res. 127, 43–153.

Padberg, J., Disbrow, E., and Krubitzer, L. 2005. The organization and connections of anterior and posterior parietal cortex in Titi monkeys: Do new world monkeys have an area 2? Cereb. Cortex 15, 1938–1963.

Pandya, D. N. and Seltzer, B. 1982. Intrinsic connections and architectonics of posterior parietal cortex in the rhesus monkey. J. Comp. Neurol. 204, 196–210.

Paulignan, Y. and Jeannerod, M. 1996. Prehension Movements: The Visuomotor Channels Hypothesis Revisited. In: Hand and Brain (*eds*. A. M. Wing, P. Haggard, and J. R. Flanagan), pp. 265–282. Academic Press.

Paulignan, Y., Dufosse, M., Hugon, M., and Massion, J. 1989. Acquisition of co-ordination between posture and movement in a bimanual task. Exp. Brain Res. 77, 337–348.

Pause, M. and Freund, H.-J. 1989. Role of the parietal cortex for sensorimotor transformation. Evidence from clinical observations. Brain Behav. Evol. 33, 136–140.

Pause, M., Kunesch, E., Binkofski, F., and Freund, H.-J. 1989. Sensorimotor disturbances in patients with lesions of the parietal cortex. Brain 112, 1599–1625.

Pearson, R. C. A. and Powell, T. P. S. 1985. The projection of the primary somatic sensory cortex upon area 5 in the monkey. Brain Res. Rev. 9, 89–107.

Petrides, M. and Pandya, D. N. 1984. Projections to the frontal cortex from the posterior parietal region in the rhesus monkey. J. Comp. Neurol. 228, 105–1116.

Platt, M. L. and Glimcher, P. W. 1999. Neural correlates of decision variables in parietal cortex. Nature 400, 233–1238.

Pons, T. P., Garraghty, P. E., Cusick, C. G., and Kaas, J. H. 1985. The somatotopic organization of area 2 in macaque monkeys. J. Comp. Neurol. 241, 445–466.

Pouget, A. and Driver, J. 2000. Relating unilateral neglect to the neural coding of space. Curr. Opin. Neurosci. 10, 242–249.

Preuss, T. M. and Goldman-Rakic, P. S. 1991. Architectonics of the parietal and temporal association cortex in the strepsirhine primate *Galago* compared to the anthropoid primate Macaca. J. Comp. Neurol. 310, 475–506.

Raos, V., Umiltá, M. A., Gallese, V., and Fogassi, L. 2004. Functional properties of grasping-related neurons in the dorsal premotor area F2 of the macaque monkey. J. Neurophysiol. 92, 1990–2002.

Raos, V., Umiltá, M. A., Murata, A., Fogassi, L., and Gallese, V. 2006. Functional properties of grasping-related neurons in the ventral premotor area F5 of the macaque monkey. J. Neurophysiol. 95, 709–729.

Rizzolatti, G. and Craighero, L. 2004. The mirror-neuron system. Annu. Rev. Neurosci. 27, 169–192.

Rizzolatti, G. and Luppino, G. 2001. The cortical motor system. Neuron 31, 889–901.

Rizzolatti, G. and Matelli, M. 2003. Two different streams form the dorsal visual system: anatomy and functions. Exp. Brain Res. 153, 146–157.

Rizzolatti, G., Fogassi, L., and Gallese, V. 1997. Parietal cortex: from sight to action. Curr. Opin. Neurobiol. 7, 562–567.

Rizzolatti, G., Fogassi, L., and Gallese, V. 2001. Neurophysiological mechanisms underlying the understanding and imitation of action. Nat. Rev. Neurosci. 2, 661–670.

Rizzolatti, G., Gentilucci, M., Fogassi, L., Luppino, G., and Ponzoni-Maggi, S. 1987. Neurons related to goal-directed motor acts in inferior area 6 of the macaque monkey. Exp. Brain Res. 67, 220–224.

Ro, J. Y., Debowy, D., Lu, S., Ghosh, S., and Gardner, E. P. 1998. Digital video: A tool for correlating neuronal firing patterns with hand motor behavior. J. Neurosci. Methods 82, 215–231.

Ro, J. Y., Debowy, D., Ghosh, S., and Gardner, E. P. 2000. Depression of neuronal activity in somatosensory and posterior parietal cortex during prehension. Exp. Brain Res. 135, 1–211.

Robinson, C. J. and Burton, H. 1980a. Somatotopographic organization in the second somatosensory area of *M. fascicularis.*. J. Comp. Neurol. 192, 43–268.

Robinson, C. J. and Burton, H. 1980b. The organization of somatosensory receptive fields in cortical areas 7b, retroinsular, postauditory and granular insular cortical areas of *M. fascicularis.* J. Comp. Neurol. 192, 69–292.

Roy, A. C., Paulignan, Y., Farne, A., Jouffrais, C., and Boussaoud, D. 2000. Hand kinematics during reaching and grasping in the macaque monkey. Behav. Brain. Res. 117, 75–182.

Roy, A., Paulignan, Y., Meunier, M., and Boussaoud, D. 2002. Prehension movements in the macaque monkey: effects of object size and location. J. Neurophysiol. 88, 1491–1499.

Sakata, H., Taira, M., Kusunoki, M., Murata, A., and Tanaka, Y. 1997. The parietal association cortex in depth perception and visual control of hand action. Trends Neurosci. 20, 350–357.

Sakata, H., Taira, M., Kusunoki, A., Murata, A., Tsutsui, K.-I, Tanaka, Y., Shein, W. N., and Miyashita, Y. 1999. Neural representation of three-dimensional features of manipulation objects with stereopsis. Exp. Brain Res. 128, 160–169.

Sakata, H., Taira, M., Murata, A., and Mine, S. 1995. Neural mechanisms of visual guidance of hand action in the parietal cortex of the monkey. Cereb. Cortex 5, 429–438.

Sakata, H., Takaoka, A., Hawarasaki, A., and Shibutani, H. 1973. Somatosensory properties of neurons in superior parietal cortex (area 5) of the rhesus monkey. Brain Res. 64, 85–102.

Salimi, I., Brochier, T., and Smith, A. M. 1999. Neuronal activity in somatosensory cortex of monkeys using a precision grip. I. Receptive fields and discharge patterns. J. Neurophysiol. 81, 825–834.

Schwartz, A. B., Kettner, R. E., and Georgopoulos, A. P. 1988. Primate motor cortex and free arm movements to visual targets in three-dimensional space. I. Relations between single cell discharge and direction of movement. J. Neurosci. 8, 2913–2927.

Seal, J. and Commenges, D. 1985. A quantitative analysis of stimulus- and movement-related responses in the posterior parietal cortex of the monkey. Exp. Brain Res. 58, 144–153.

Seal, J., Gross, C., and Bioulac, B. 1982. Activity of neurons in area 5 during a simple arm movement in monkey before and after deafferentation of the trained limb. Brain Res. 250, 229–1243.

Seltzer, B. and Pandya, D. N. 1980. Converging visual and somatic sensory cortical input to the intraparietal sulcus of the rhesus monkey. Brain Res. 192, 339–351.

Serrien, D. J. and Brown, P. 2002. The functional role of interhemispheric synchronization in the control of bimanual timing tasks. Exp. Brain Res. 147, 268–272.

Serrien, D. J. and Wiesendanger, M. 2001. Dissociation of grip/load-force coupling during a bimanual manipulative assignment. Exp. Brain Res. 136, 417–420.

Serrien, D. J., Ivry, R. B., and Swinnen, S. P. 2006. Dynamics of hemispheric specialization and integration in the context of motor control. Nat. Rev. Neurosci. 7, 160–166.
Serrien, D. J., Nirkko, A. C., Lovblad, K. O., and Wiesendanger, M. 2001. Damage to the parietal lobe impairs bimanual coordination. Neuroreport 12, 2721–2724.
Shadlen, M. N. and Newsome, W. T. 2001. Neural basis of a perceptual decision in the parietal cortex (area LIP) of the rhesus monkey. J. Neurophysiol. 86, 1916–1936.
Shanks, M. F., Pearson, R. C. A., and Powell, T. P. S. 1985. The callosal connexions of the primary somatic sensory cortex in the monkey. Brain Res. Rev. 9, 43–65.
Shikata, E., Hamzei, F., Glauche, V., Koch, M., Weiller, C., Binkofski, F., and Buchel, C. 2003. Functional properties and interaction of the anterior and posterior intraparietal areas in humans. Eur. J. Neurosci. 17, 1105–1110.
Shmuelof, L. and Zohary, E. 2005. Dissociation between ventral and dorsal fMRI activation during object and action recognition. Neuron 47, 457–470.
Shmuelof, L. and Zohary, E. 2006. A mirror representation of others' actions in the human anterior parietal cortex. J. Neurosci. 26, 9736–9742.
Snyder, L. H., Batista, A. P., and Andersen, R. A. 1998a. Change in motor plan, without a change in the spatial locus of attention, modulates activity in posterior parietal cortex. J. Neurophysiol. 79, 2814–2819.
Snyder, L. H., Grieve, K., Brotchie, P., and Andersen, R. A. 1998b. Separate body- and world-referenced representations of visual space in parietal cortex. Nature 394, 887–891.
Stoeckel, M. C., Weder, B., Binkofski, F., Choi, H. J., Amunts, K., Pieperhoff, P., Shah, N. J., and Seitz, R. J. 2004. Left and right superior parietal lobule in tactile object discrimination. Eur. J. Neurosci. 19, 1067–1072.
Sugrue, L. P., Corrado, G. S., and Newsome, W. T. 2004. Matching behavior and the representation of value in the parietal cortex. Science 304, 1782–1787.
Sugrue, L. P., Corrado, G. S., and Newsome, W. T. 2005. Choosing the greater of two goods: neural currencies for valuation and decision making. Nat. Rev. Neurosci. 6, 363–375.
Taira, M., Mine, S., Georgopoulos, A. P., Murata, A., and Sakata, H. 1990. Parietal cortex neurons of the monkey related to the visual guidance of hand movement. Exp. Brain Res. 83, 29–136.
Tanne-Gariepy, J. T., Rouiller, E. M., and Boussaoud, D. 2002. Parietal inputs to dorsal versus ventral premotor areas in the macaque monkey: evidence for largely segregated visuomotor pathways. Exp. Brain Res. 145, 91–1103.
Taoka, M., Toda, T., and Iwamura, Y. 1998. Representation of the midline trunk, bilateral arms, and shoulders in the monkey postcentral somatosensory cortex. Exp. Brain. Res. 123, 315–322.
Tunik, E., Frey, S., and Grafton, S. 2005. Virtual lesions of the anterior intraparietal area disrupt goal-dependent on-line adjustments of grasp. Nat. Neurosci. 8, 505–511.
Tunik, E., Rice, N. J., Hamilton, A., and Grafton, S. T. 2007. Beyond grasping: representation of action in human anterior intraparietal sulcus. Neuroimage 36, T77–T86.
Ungerleider, L. G. and Mishkin, M. 1982. Two Cortical Visual Systems. In: Analysis of Visual Behavior (*eds*. D. G. Ingle, M. A. Goodale, and R. J. W. Mansfield), pp. 549–586. MIT Press.
Van Essen, D. C. and Drury, H. A. 1997. Structural and functional analyses of human Cerebral Cortex using a surface-based atlas. J. Neurosci. 17, 7079–7107.
Van Essen, D. C., Lewis, J. W., Drury, H. A., Hadjikhani, N., Tootell, R. B. H., Bakircioglu, M., and Miller, M. I. 2001. Mapping visual cortex in monkeys and humans using surface-based atlases. Vision Res. 41, 1359–1378.
Vogt, C. and Vogt, O. 1919. Allgemeinere ergebnisse unserer hirnforschung. J. Psychol. Neurol. (Leipzig) 25, 277–462.
Wannier, T. M., Maier, M. A., and Hepp-Reymond, M. C. 1991. Contrasting properties of monkey somatosensory and motor cortex neurons activated during the control of force in precision grip. J. Neurophysiol. 65, 572–589.
Wannier, T. M., Toltl, M., and Hepp-Reymond, M. C. 1986. Neuronal activity in the postcentral cortex related to force regulation during a precision grip task. Brain Res. 382, 427–432.
Whitsel, B. L., Petrucelli, L. M., and Werner, G. 1969. Symmetry and connectivity in the map of the body surface in somatosensory area II of primates. J. Neurophysiol. 32, 170–183.
Wiesendanger, M., Kazennikov, O., Perrig, S., and Kaluzny, P. 1996. Two hands – One action. The Problem of Bimanual Coordination. In: Hand and Brain (*eds*. A. M. Wing, P. Haggard, and J. R. Flanagan), pp. 283–300. Academic Press.
Wing, A. M., Turton, A., and Fraser, C. 1986. Grasp size and accuracy of approach in reaching. J. Mot. Behav. 18, 245–260.
Wise, S. P., Boussaoud, D., Johnson, P. B., and Caminiti, R. 1997. Premotor and parietal cortex: corticocortical connectivity and combinatorial computations. Annu. Rev. Neurosci. 20, 25–42.
Zhou, Y. D. and Fuster, J. M. 1996. Mnemonic neuronal activity in somatosensory cortex. Proc. Nat. Acad. Sci. U. S. A. 93, 10533–10537.
Zhou, Y. D. and Fuster, J. M. 1997. Neuronal activity of somatosensory cortex in a cross-modal (visuo-haptic) memory task. Exp. Brain Res. 116, 551–555.
Zhou, Y. D. and Fuster, J. M. 2000. Visuo-tactile cross-modal associations in cortical somatosensory cells. Proc. Nat. Acad. Sci. U. S. A. 97, 9777–9782.

Further Reading

Donchin, O., Gribova, A., Steinberg, O., Bergman, H., and Vaadia, E. 1998. Primary motor cortex is involved in bimanual coordination. Nature 395, 274–278.
Donchin, O., Gribova, A., Steinberg, O., Mitz, A. R., Bergman, H., and Vaadia, E. 2002. Single-unit activity related to bimanual arm movements in primary and supplementary motor cortices. J. Neurophysiol. 88, 3498–3517.
Gerloff, C. and Andres, F. G. 2002. Bimanual coordination and interhemispheric interaction. Acta Psychologica 110, 161–186.
Swinner, S. P. 2002. Intermanual coordination: from behavioral principles to neural-network interactions. Nat. Rev. Neurosci. 3, 350–361.

6.13 Plasticity of Somatosensory Function during Learning, Disease and Injury

C Darian-Smith, Stanford University School of Medicine, Stanford, CA, USA

© 2008 Elsevier Inc. All rights reserved.

6.13.1	**Introduction**	260
6.13.2	**The Functional Anatomy of the Somatosensory System**	261
6.13.2.1	Functional Circuitry of the Spinal Cord – Comparing Primates and Rodents	263
6.13.2.2	Representational Maps	266
6.13.3	**Somatosensory Plasticity Following Injury**	267
6.13.3.1	Reorganization Following Injury to the Primary Afferent	267
6.13.3.1.1	Peripheral nerve injuries and amputation	267
6.13.3.1.2	Dorsal rhizotomy – root cut	268
6.13.3.1.3	Deafferentation of the dorsal column nuclei	269
6.13.3.2	Behavioral Changes Following Primary Afferent Injury	273
6.13.3.2.1	Nonhuman primate studies	273
6.13.3.2.2	Behavioral studies in the rodent	275
6.13.4	**Somatosensory Plasticity in Learning and Experience**	276
6.13.4.1	Cortical Reorganization in Response to Learning	276
6.13.4.1.1	Activity-dependent changes in synaptic transmission – hebbian learning and long-term potentiation	276
6.13.4.2	Cortical Plasticity in Braille Readers	277
6.13.4.3	Musicians: Training, Focal Hand Dystonia, and Rehabilitative Training	278
6.13.4.3.1	Rehabilitative strategies	279
6.13.4.4	The Dynamics of the Somatosensory Cortex during Learned Sensorimotor Tasks	279
6.13.5	**Somatosensory Plasticity in Response to Disease**	280
6.13.5.1	Changes in Response to Somatosensory Cortical Ablation, Ischemia, or Stroke	280
6.13.5.2	Cortical Plasticity in Multiple Sclerosis	283
6.13.5.3	Cortical Plasticity in Response to Other Diseases	285
6.13.5.4	Cortical Reorganization and Chronic Pain	286
6.13.6	**Neural Basis/Mechanisms of Somatosensory Plasticity**	288
6.13.6.1	Pathway Divergence and Disinhibition	288
6.13.6.2	Structural Plasticity	289
6.13.6.2.1	Injury-induced structural changes: axonal sprouting	289
6.13.6.2.2	Injury- and experience-induced structural changes in dendrites	290
6.13.6.2.3	Atrophy, transneuronal atrophy, and degeneration	291
References		292

Glossary

ablation For example, cortical ablation. Removal or excision of a region of cortex.

afferent For example, afferent nerve, of primary afferent neuron. Nerve or neuron that carries impulses toward the central nervous system. The opposite of an afferent nerve is an efferent nerve that carries impulses away from the CNS. To deafferent, is to cut or block afferent input.

brachial plexus A network or plexus of spinal nerves that originate in the back of the neck, extend through the axilla (armpit), and innervate the hand and upper limb. Nerve fibers of the brachial plexus enter or leave the spinal cord from cervical segment 5 (C5) to thoracic segment 1 (T1).

CNS Central nervous system.

D1, D2,. . .,D5 Digits 1–5 where D1 is the thumb and D5 is the little finger.
dermatome A region of skin that is innervated by the sensory fibers of a single dorsal root
contralateral Opposite side of body, ipsilateral refers to the same side of the body
dystonia For example, focal hand dystonia. Disabling movement disorder characterized by sustained contraction of muscles, or muscle spasms that cause abnormal postures or uncontrolled twisting.
fractionated digit movements Independent voluntary control of individual fingers.
Fasciculu Nerve fiber tract
glial scarring Following an injury that causes neuronal cell death in the CNS, glial cells infiltrate the region to phagocytose degenerating neurons. This gradually results in the formation of a glial scar. Astrocytes and oligodendrocytes in the glial scar have been shown to release inhibitory factors that prevent the growth or invasion of axons into or through the glial scar.
hemiparesis Weakness or paralysis affecting one side of the body.
hemorrhagic cyst A cyst containing blood or resulting from the encapsulation of a hematoma.
infarct An area of tissue that undergoes necrosis (cell death) due to the obstruction of the local blood supply.
ischemia A decrease of the blood flow to a part of the brain (or other body part) which is caused by the constriction or obstruction of the blood vessels.
neuraxis The axial unpaired part of the central nervous system, comprising the spinal cord, brainstem, thalamus, and cerebral cortex.
nociceptors Sensory receptors that respond to pain produced by noxious, chemical, or mechanical stimuli.
parvocellular: parvo = small Refers to the small cell component of a neuronal structure. For example, the parvocellular red nucleus refers to that component that comprises small neurons. Large celled = magnocellular
phantom limb A term used to describe abnormal sensations (painful or nonpainful) perceived on a previously amputated limb.
spinal contusion injury An injury caused by the application of a weight of set force to the dorsal surface of the spinal cord. Frequently used to create a rodent model of clinical spinal cord injury.
somatotopy Orderly topographic relationship of receptors in the body from periphery to subsequent levels of the pathway (e.g., brainstem nuclei, thalamic projection nuclei) to functional areas of the cerebral cortex (e.g., primary somatosensory cortical areas 3a, 3b, 1, and 2) in the CNS.
rhizotomy Surgical cutting or severance of spinal nerve roots. A dorsal rhizotomy refers to the transection of just the dorsal nerve roots or rootlets that make up the root.
thalamotomy A stereotaxic surgical technique that destroys a part of the thalamus (typically for therapeutic purposes)
thenar eminence Fleshy region of the palm at the base of the thumb.
transneuronal degeneration Degeneration across synapses from one neuron to the next affecting multiple steps of a pathway.

6.13.1 Introduction

The field of somatosensory plasticity has come a long way in the last two decades. It is now generally accepted that after an especially malleable period during development and early life, the mammalian brain retains a surprising plasticity into adulthood. We still have much to learn about the details of this plasticity; details of where and under what circumstances it occurs, its cellular and molecular bases, functional relevance, and so forth. What is clear, however, is that the brain, from the cortical or subcortical representational map to the underlying synaptic connectivity, continues to respond to ever-changing peripheral and central inputs, or extrinsic and intrinsic environmental circumstances. Inputs can be manipulated in a great variety of ways. Injury, disease, and alterations in behavior brought about by learning, have all been shown to alter the activation and wiring of the somatosensory, as well as the visual, auditory, and motor pathways. System level plasticity has been studied intensively in these

systems for over two decades and the purpose of this chapter is to bring the reader up-to-date with much of the current knowledge and concepts relating to plasticity in the somatosensory system. A good deal of the research being done is broadly directed toward a clinical application, in which reorganizing principles might be used to manipulate and alter neural circuitry to benefit or improve behavioral outcome in the patient. For this and reasons of personal bias, much of the work reviewed in this chapter focuses on primate research, both human and nonhuman. Much excellent work has also been accomplished in the somatosensory system in other mammalian species, most notably the rodent. It has not been possible to address this work in depth in this chapter, and the reader is referred to reviews where possible. However, a section (further in the chapter) has been included that describes some of the most important differences between the rodent and the primate in the organization of the sensorimotor pathways, particularly in the spinal cord. My hope is that some readers will find this summary useful for the interpretation of data in the literature and when comparing specifics of rodent and primate lesion models.

The term plasticity is used in this chapter to refer to the capacity of the brain to reorganize itself in response to changes in input, be it the removal of input following injury, or a change in the activity (amplitude, synchrony, tuning) of inputs to a specific cortical or subcortical region. Neural plasticity can be demonstrated in many ways, and is generally defined according to the technique being used to measure it – an altered behavior, representational map, cellular response, neuronal activity, protein expression, and so forth.

The definition of somatosensory also deserves comment from the outset. In the context of even a simple voluntary task, such as the exploration of an object with the hand, there is a complex interplay between somatosensory feedback and motor control (Jeannerod, M., 1999). Somatosensory plasticity is therefore inherently sensorimotor in nature. For this reason, motor pathways directly associated with changes in the somatosensory system are mentioned throughout this chapter.

Another goal in this chapter has been to address changes that occur at multiple levels of the pathway. Though the early emphasis of study was to look at cortical responses and cortical reorganization, it is now broadly accepted, particularly in work in the somatosensory system, where there is a spinal cord and spatially distributed connectivity from periphery to cortex, that modifications at one level of the neuraxis seldom, if ever, occur independently of other levels. Data is therefore presented for multiple levels of the CNS (see Wall, J. T. *et al.*, 2002 for review of subcortical involvement).

6.13.2 The Functional Anatomy of the Somatosensory System

The primary somatosensory pathway comprises the afferent projections of the sensorimotor system, from peripheral receptors (mechanoceptors, thermoreceptors, nociceptors, etc.) to the spinal cord, brainstem, thalamus, and cortex (Darian-Smith, I. *et al.*, 1996; Darian-Smith, I. and Darian-Smith, C., 2005; Mountcastle, V. B., 2005). If we take hand function as an example, information received by mechanoreceptors of the skin, muscles, tendons, and joints of the hand surface is transmitted via the dorsal roots to the dorsal horn of the spinal cord (see Figure 1). Fibers in the dorsal column project to the ipsilateral cuneate nucleus of the brainstem, and cross the midline in the medial lemniscus before terminating in the contralateral ventral posterolateral nucleus (VPLc) of the thalamus. The cell bodies of the spinothalamic neurons originate in the cervical dorsal horn and cross the midline within 1–2 spinal segments before terminating primarily in the same thalamic VPLc nucleus. In the monkey and human, spinothalamic fibers also terminate more caudally in the anterior pulvinar (Pul.o) of the thalamus, and more rostrally in the posterior nucleus of the ventral lateral complex (VLp). Rodents (and even the cat) do not have an anterior somatosensory component to their thalamic pulvinar, which evolved exclusively in primates with a greater sophistication of hand function. In primates, thalamocortical projections from the thalamic VPLc nucleus terminate within the primary somatosensory cortex (Brodmann's areas 3a, 3b, 1, and 2). Projections from the Pul.o also terminate within these regions, the posterior parietal cortex, and even the caudal primary motor cortex. Figure 1 shows these pathways at their simplest level of organization in the macaque monkey. In rodents, that have only one body map representation in the primary somatosensory cortex (primates have up to 4), and an additional representation in somatosensory area II (SII), thalamocortical projections are far simpler, with projections from the thalamic ventrobasal complex terminating within just the primary somatosensory cortex.

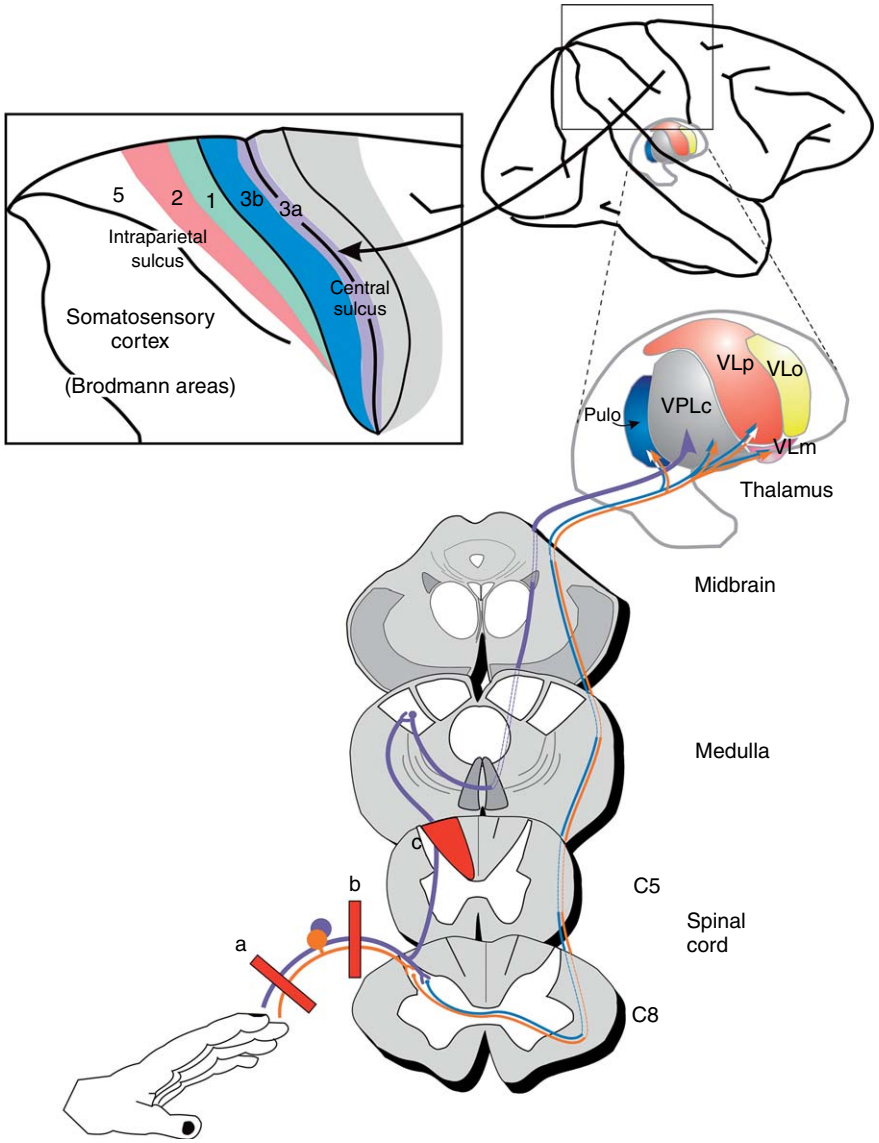

Figure 1 The primary somatosensory pathway showing the two major afferent projections, and the different levels at which reorganization can occur in the primary afferent following injury. a–c mark the three levels at which primary afferent neuronal populations can be blocked following a peripheral nerve (a), dorsal root (b), or central dorsal column (c) injury. In the macaque monkey and human, the primary somatosensory cortex (S1) comprises four functional subdivisions, areas 3a, 3b, 1, and 2, each named according to Brodmann K. (1908). Each area receives input from the full body surface, though there is greater representation of the digits and mouth, or those parts of the body having greater somatosensory receptor density and somesthetic importance. Reproduced from Darian-Smith, I. and Darian-Smith, C. 2005. Touch, Tangible Surfaces and Their Neuronal Representation. In: Encyclopedia of Neuroscience, 3rd edn. (*eds*. G. Adelman and B. Smith). Elsevier, with permission from Elsevier.

In both primates and rodents, additional afferent projections also transmit sensory information to higher levels (e.g., spinoreticular, spinocerebellar, spinocervical), and feedback loops from higher levels of the pathway can be found at every step (Figure 1). For example, the somatosensory cortex (e.g., the hand region in monkeys) projects directly to the cuneate nucleus and to the dorsal horn of the cervical spinal cord, as part of the corticospinal tract. In the execution of fine manipulative tasks that involve ongoing

tactile and proprioceptive feedback from the monkey or human hand, many of these pathways and feedback loops are continuously involved.

6.13.2.1 Functional Circuitry of the Spinal Cord – Comparing Primates and Rodents

The somatosensory and motor circuitry of the spinal cord has been described elsewhere in great detail (Snow, P. J. and Wilson, P., 1991; Willis, W. D. and Coggeshall, R. E., 2004 for reviews), and is only briefly addressed here to help guide the reader through various spinal injury models in different species. Some of the important differences between the primate (including humans) and rodent spinal cord organization are not easily found in a brief overview of the literature and are important to keep in mind when assessing studies that correlate the rodent with the human condition. Figure 2 shows the general layout of the major afferent and efferent pathways of the spinal cord in the primate and rodent, as they relate to the left hand or forepaw and the cervical spinal cord. Primary afferent pathways are shown in color. In addition to the major somatosensory pathways, smaller pathways including the spinoreticular, spinomesencephalic, and spinocerebellar tracts are indicated. The spinoreticular and spinomesencephalic tracts are mainly ipsilateral, terminate in the reticular complex and periaqueductal gray in the midbrain, respectively, and respond to noxious stimuli. Neither pathway transmits cutaneous information. The spinocerebellar pathways transmit signals from muscle spindles and Golgi tendon organs as well as cutaneous information (mainly of the lower body) to the cerebellar nuclei. Cutaneous information also reaches the cerebellum via the cuneocerebellar pathway that receives input directly from dorsal column fibers.

More than 65 million years of evolution divide the early rodent-like mammals and the modern primates. It is therefore unsurprising that there are some notable differences between rodent and primate neuroanatomy. In rats, somatosensory input arising from the forelimb and coursing through the nerves of the brachial plexus, terminates bilaterally in the dorsal horn, from cervical segments C1–C5 (Webster, K. E. and Kemplay, S. K., 1987) (Figure 3). This bilateral projection does not occur in the monkey or human. Rats have an ipsilateral projection (~5%) from the dorsal column nuclei to the thalamus (Wree, A. *et al.*, 2005) which is also not observed in primates. This suggests a greater bilaterality of afferent projections at multiple levels of the somatosensory pathway in the rodent, and such differences may play a role in the adaptive plastic changes observed following peripheral or central injuries. In addition, while the spinocervical tract has been described in the rodent and some primate species, and is particularly prominent in the cat (Willis, W. D. and Coggeshall, R. E., 2004), it is generally associated with the hindlimb and does not appear to play a significant role in primate forelimb circuitry.

Peripheral nerves are also organized somewhat differently in the rat compared with the monkey, and this is important to keep in mind when comparing peripheral nerve and dorsal root injuries in rats and monkeys. As an example, the mechanosensory median nerve innervates a large part of the medial glabrous hand in the monkey and human and projects via dorsal roots to terminate in the dorsal horn through segments C5–C8. In rodents, the median nerve also innervates part of the forepaw, but terminates in the dorsal horn over a greater rostrocaudal distance, from C3 to T2 (LaMotte, C. *et al.*, 1991).

There are also important differences in the organization of descending pathways (Figures 2(c) and 2(d)). The corticospinal tract (CST) has been the subject of numerous investigations over the decades, since it plays a critical role in fine directed movements of the hand and digits in monkeys and humans (Galea M. P. and Darian-Smith, I., 1997a; 1997b). In primates, the corticospinal tract originates from multiple regions of the somatosensory and motor cortex, and is the most functionally important control pathway in voluntary manual dexterity. In the primate, 90% of fibers that project to the cervical cord are contralateral and descend in the dorsolateral CST. An additional 8% of fibers course in the ipsilateral dorsolateral tract and there is a further bilateral component in the ventral tract (~2%). The rubrospinal tract is relatively insignificant in monkeys, and almost nonexistent in the human, and projections from the magnocellular red nucleus of the midbrain have diminished as the parvocellular component has evolved into a more prominent feedback loop to the cortex via the inferior olive and lateral cerebellar hemispheres (Burman, K. *et al.*, 2000a; 2000b). In contrast in the rat, the CST relays mainly in the medial columns (see Figure 2(d)) ventral to the dorsal columns (Brosamle, C. and Schwab, M. E., 1997). A small number of fibers (between 5% and 15%) descend within the contralateral dorsolateral CST and within the ipsilateral ventral CST (<5%). The medial positioning of the CST in the rat is important when

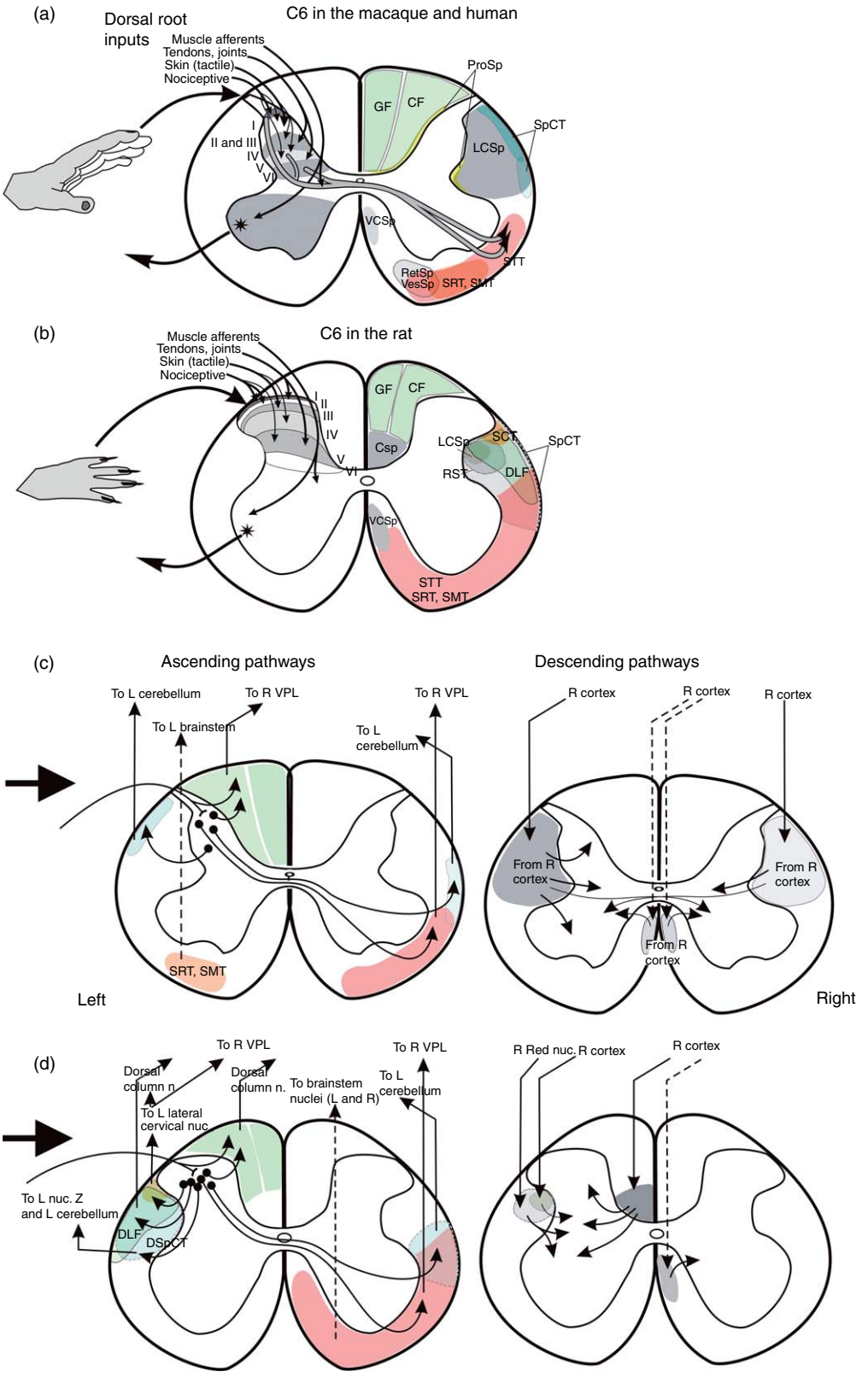
(a)
Dorsal root inputs
C6 in the macaque and human
Muscle afferents
Tendons, joints
Skin (tactile)
Nociceptive
I
II and III
IV
V
VI
GF
CF
ProSp
SpCT
LCSp
VCSp
STT
RetSp
VesSp
SRT, SMT
(b)
C6 in the rat
Muscle afferents
Tendons, joints
Skin (tactile)
Nociceptive
I
II
III
IV
V
VI
GF
CF
Csp
LCSp
SCT
SpCT
RST
DLF
VCSp
STT
SRT, SMT
(c)
Ascending pathways
Descending pathways
To L cerebellum
To L brainstem
To R VPL
To R VPL
To L cerebellum
SRT, SMT
R cortex
R cortex
R cortex
From R cortex
From R cortex
From R cortex
Left
Right
(d)
To R VPL
To R VPL
Dorsal column n.
Dorsal column n.
To brainstem nuclei (L and R)
To L cerebellum
To L lateral cervical nuc.
To L nuc. Z and L cerebellum
DLF
DSpCT
R Red nuc.
R cortex
R cortex

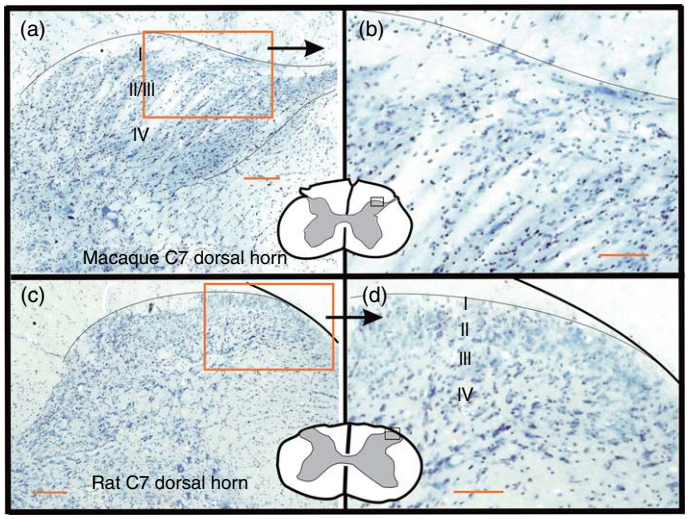

Figure 3 The cytoarchitecture of the cervical (C7) dorsal horn in the macaque monkey and rat, stained with the Nissl stain cresyl violet, showing some of the species differences. (a) In the monkey, large diameter myelinated primary afferents course through the superficial layers, evident as streaks of white matter. Laminae II–III are also difficult to differentiate, and have mostly small diameter (8–10 μm diameter) neurons, with large nuclei and little cytoplasm. (b) Shows the characteristic layering and uniform soma packing density in laminae, which is typical of rodent dorsal horn. Scale bars = 50 μm (a, c), 25 μm (b, d).

considering the effects of a dorsal transection or spinal contusion. In the monkey, sectioning the dorsomedial cord blocks the major cutaneous mechanoreceptor pathway. In the rodent, both the dorsal column and CST pathways are cut. In contusion injuries in the rat, the corticospinal pathway is likely to be involved by the lesion, but this is not the case in a similar injury in the monkey or human. The rubrospinal tract plays a more prominent role in voluntary movements of the limbs than it does in primates, and courses in the contralateral dorsolateral tract.

At a behavioral level, the quadrupedal rodent mainly uses its limbs to locomote efficiently through its external environment. Though their forelimbs and forepaws are used to reach and grasp, in locomotion they are moved in a bilaterally synchronous gate with the hindlimbs. Even with a total transection of the thoracic cord, the hindlimbs can be trained to step when the appropriate sensory feedback is applied to the hindpaws and the body weight-supported. This demonstrates a local spinal circuitry that is capable of orchestrating coordinated limb movement, independent of cortical or brainstem control. Studies that demonstrate the recovery of walking in rodents following cord transection should therefore be interpreted in the context of the rodent.

In humans, a very rudimentary stepping behavior can be learned in patients with a technically complete spinal cord transection. However, while the therapies that simulate synchronous walking in such

Figure 2 (a, b) Shows terminal distributions for the different primary afferent subpopulations into the cervical dorsal horn (left side), and the major ascending (color), and descending (grayscale) tracts involved in the transmission of somatosensory and motor information relevant to sensorimotor control (right). (a, b) The general pattern of input to the different laminae of the dorsal horn is similar in the rodent and macaque monkey, though details and fine circuitry differ. Though the local circuitry and neurochemical composition are complex, and primary afferent inputs less segregated than originally thought, dominant primary afferent inputs have been broadly characterized. In both species, the predominant primary afferent input into lamina I is from Aδ and C fibers. Lamina II is the main recipient layer for collaterals from fine, mainly unmyelinated, sensory fibers, including Aδ and C fibers, but at least in monkeys, this layer also receives some coarse primary afferent input. Large diameter mechanosensory afferents terminate in laminae II (medially) III and IV, but input from large myelinated fibers is dominant in III–IV. Lamina V in both monkeys and rats receives input from heterogeneous sources including collaterals from deeper tissues. (c, d) Shows the major ascending and descending tracts at the level of C6 in both the monkey and rat as they relate to the left forelimb. See text. CF, cuneate fasciculus; GF, gracile fasciculus; SpCT, spinocerebellar tract (dorsal and ventral combined; STT, spinothalamic tract; SRT, spinoreticular tract; SMT, spinomesencephalic tract; DLF, dorsal lateral funiculus; SCT, spinocervical tract; ProSp, propriospinal tract; Csp, corticospinal tract; LCSp, dorsolateral corticospinal tract; VCSp, ventral corticospinal tract; RST, rubrospinal tract; RetSp, reticulospinal; VesSp, vestibulospinal.

patients can lead to important collateral health benefits, these patients are not able to step without complete assistance. This is because the circuitry required for walking is particularly complex, and complicated further by the weight-bearing needs of the large human biped.

Forelimbs in the human are no longer used for weight-bearing synchronous locomotion, and have not been for 3–4 million years, when our ancestral bipedal *Australopithecines* lived. Along with an expanding forebrain, primates have evolved pathways that uniquely serve precision manual dexterity and hand–eye coordination. With such an emphasis on hand function, it is perhaps not surprising that primates are the only mammals with corticospinal pathways that directly synapse with motor neurons innervating the hand and forelimb (corticomotoneuronal projections). In the cat and rodent, all corticospinal input to the cord synapses first on interneurons or networks of interneurons within the intermediate zone (Porter, R and Lemon, R. N., 1993). Rodents do not perform fractionated digit movements, have no opposing digits, and can perform only rudimentary sensorimotor tasks of grasping and holding with the forepaws. Paw behavior is not easily compared with primate hand use.

Another neuronal pathway worth mentioning is that of the short and long propriospinal neurons (PSNs). Long PSNs link forelimb and hindlimb activity during locomotion (e.g., walking or running). They originate in C3–C5, travel in the ventral and lateral columns and terminate in the ventral horn of the lumbosacral enlargement. They are spared in midthoracic dorsal hemisection and are able to bridge spinal segments above and below such a lesion. Long ascending PSNs have also recently been reported to project from lumbosacral segments to the contra- and ipsilateral (to a lesser extent) upper cervical cord in the rat (Dutton, R. M. *et al.*, 2006), though the presence of this contralateral projection in the primate is unclear. Primates, including humans, also have long propriospinal neurons that connect fore- and hindlimbs and play a role in coordinating arm with leg swing during locomotion. However, there is no evidence in humans with midthoracic spinal cord injury (SCI) that long PSNs can contribute significantly to the recovery of locomotion postinjury (Dietz, V., 2002). Short PSNs only connect the rostral and caudal cervical cord (C3–C4 and C6–T1) (Bareyre, F. M. *et al.*, 2004).

In the rodent and the cat, which have no direct corticomotoneuronal connections (CM), a substantial amount of corticospinal (CST) excitation reaches the forelimb motor neurons via cervical propriospinal projections. In contrast, in the macaque monkey and particularly in the human, where CST neurons innervate motor neurons directly, the propriospinal pathway plays little part in the transmission of cortical commands to motor neurons innervating the forelimb (Nakajima, K., *et al.*, 2000).

6.13.2.2 Representational Maps

The skin and fascia of the body surface are represented at each level of the somatosensory pathway, in much the same way as the retina of the visual pathway and cochlea of the auditory system. These representations are topographic in their organization or, in the case of the somatosensory system, somatotopic (Merzenich, M. M., *et al.*, 1978; Kaas, J. H. *et al*, 1979). This means that the inputs from adjacent body parts are always located adjacent to each other at subsequent levels of the neuraxis (e.g., within the cuneate nucleus, the VPL nucleus, and the primary somatosensory cortex). The primate hand is also like the retinal fovea in providing the sharpest somatosensory image of the world within reach. As such, the digits of the primate hand have a greater mechanoreceptor density than elsewhere (Darian-Smith, I., 1984), and the skin of the digit pads occupies a disproportionately large region of S1, and subcortical nuclei. Somatotopic body representations can be mapped at any level of the pathway by recording the unitary activity of the component neurons, and receptive fields can be plotted while stimulating the skin surface or deeper fascia. Such maps have been used extensively over the last two decades to explore the mutability of the adult brain following injury, disease, and other manipulations (e.g., learning paradigms).

In adult mammals, map somatotopy remains stable over time, and maps obtained months and even years apart will be largely indistinguishable at the population level. However, when the activity of the constituent neuron populations is modified significantly with, for example, the instigation of a training regiment (Fox, K. and Wong, R., 2005) or following an injury of the peripheral or central pathways, then these central maps alter and adapt to the new circumstances. Cortical reorganization has been demonstrated extensively across species and systems since the early seminal studies of Merzenich and colleagues (Merzenich, M. M. *et al.*, 1983a; 1983b; 1984) who reported significant alterations in the cortical map following a median nerve cut and digit amputation.

Reorganization also occurs at subcortical levels, and has been fully appreciated only in the last decade (see Wall, J. T. *et al.*, 2002 for review). Earlier studies generally focused on the cortical map, because it represents the processing center for all primary pathway inputs, and is easily accessed for electrophysiological recordings. A corticocentricity may also reflect real differences in the organization of visual and somatosensory pathways. In the visual pathway, which has long led sensory system neuroscience research, the receptor sheet in the form of the retina is physically small, and afferent projections to the lateral geniculate nucleus (of the thalamus) and cortex are spatially tightly organized. As such, the most dramatic plastic changes occur in the cortex (Darian-Smith, C. and Gilbert, C. D., 1995). In contrast, the receptor sheet for the somatosensory pathway is comparatively vast and multilayered (skin, muscles, joints) and there is a spinal cord, with its complex spatially distributed parallel circuitry, which is unique to the somatosensory system. This provides more opportunity for subcortical circuit reorganization.

The primate somatosensory cortex is unique amongst mammals in having multiple representations of the body map. The prosimian galago brain has at least three representations of the body surface, divided into the functional subdivisions denoted as Brodmann areas 3a, 3b, and 1.

6.13.3 Somatosensory Plasticity Following Injury

6.13.3.1 Reorganization Following Injury to the Primary Afferent

The somatosensory pathways respond differently to injury, depending on whether the primary afferent neuron is cut or damaged peripherally, centrally to the dorsal root ganglion, or centrally within the CNS (e.g., in the dorsal column; see Figure 1). The extent to which fibers are spared by the lesion, the size of the injury, and the postlesion time period at which changes are examined, will also affect outcome.

The postlesion time period can be divided into several stages of postinjury reorganization. These generally include an acute phase (minutes to hours), a chronic phase (days, weeks, early months), and an extended chronic phase (years). For example, immediately following a digit amputation or median nerve cut, a silent region is produced within the corresponding contralateral cortical hand map, and there is a rapid expansion of the representation of parts of the hand lying adjacent to the silenced or deafferented region. This expansion can occur within minutes to hours, and may persist for weeks to months. During the chronic second stage (weeks to months), there is opportunity for the establishment of new connections from spared inputs and there is a consolidation of the cortical and subcortical body maps. A final stage (years) involves the eventual atrophy of chronically deafferented neuronal populations. This was shown more than a decade after monkeys received a dorsal rhizotomy that deafferented the forelimb (see Jones, E. G., 2000). The cuneate nucleus of the brainstem and the VPLc nucleus of the thalamus reduced substantially in volume over this period (Woods, T. M. *et al.*, 2000), and the face representation expanded proportionately within the somatosensory cortex. This suggests that when the deafferentation is complete and extensive, consolidation involving cell shrinkage and death can continue slowly over many years and even decades.

The patterns of deafferentation that result from injuries to primary afferent neuron populations relaying sensory information from the hand to the cortex, have been studied extensively (Buonomano, D. V. and Merzenich, M. M., 1998; Belyantseva, I. A. and Lewin, G. R., 1999; Bradbury, E. J. *et al.*, 2000; Jones, E. G., 2000; Wall, J. T. *et al.*, 2002; Kaas, J. H., 2002; Ding, Y. *et al.*, 2005, for reviews). They include investigations into peripheral nerve injury (Xu, J. and Wall, J. T., 1999), amputations (Florence, S. L. and Kaas, J. H., 1995), dorsal rhizotomies (Darian-Smith, C. and Brown, S., 2000), and more central injuries to the spinal cord and dorsal column (Jain, N. *et al.*, 1997; 2000; Weng, H. R. *et al.*, 2003).

The following sections briefly summarize what happens when injuries involve different components of the primary afferent pathway, as shown in Figures 1(a)–1(c).

6.13.3.1.1 Peripheral nerve injuries and amputation

Peripheral nerves retain the capacity to regenerate following injury, and will do so unless blocked by a physical or chemical barrier (Sunderland, S., 1991), so the central map changes that result following nerve cut are often relatively minor. Even so, studies in the macaque monkey have shown that if a nerve is cut and then rejoined to enable regeneration, the cortical somatotopic map does not completely recover. Many neurons in the reorganized cortex

develop abnormal multiple receptive fields on non-adjacent skin regions, and the map becomes disorganized (Florence, S. L. *et al.*, 1994). This mislocalization is avoided following nerve crush, presumably because individual fibers are able to regenerate to innervate their original peripheral target.

When nerves are prevented from reaching their original target (e.g., following nerve ligation), cortical reorganization is far more substantial. Following peripheral nerve transection, for example, a silent zone is initially observed within the corresponding somatosensory map, where the digits and/or skin surface have been deafferented. Within minutes to hours the silent zone is surrounded by an expanded representation of the adjacent body parts, and over a period of weeks to months, there is a gradual filling in or expansion of the representation of the adjacent skin surface until the new organization stabilizes. In an early example of this, median and ulnar nerves were sectioned in squirrel monkeys (Garraghty, P. E. and Kaas, J. H., 1991). This resulted in a corresponding deprived region of cortex, which responded over many months to inputs originating from the back of the hand.

Following the amputation of the hand or digits, where afferent and efferent nerves are both cut, the pattern of cortical reorganization mimics that seen following the permanent section of both sensory and motor nerves supplying the hand. Thus, following digit amputation, the representation of the stump region (or adjacent hand) expands into the deprived region of the cortical map. This again takes weeks to months to occur, and parts of the cortex may remain chronically silent if the injury is sufficiently large.

When the whole of the forelimb is amputated in monkeys, there is some expansion of the face representation (which lies adjacent to hand representation) into the hand cortex. Imaging studies in humans with hand or forearm amputations, similarly report face responses within the deprived hand cortex months or even years following the amputation. Though the neural substrate for these observations remains unclear, the longer timeframe suggests that local neuronal growth, synapse formation and modification, and perhaps even some transneuronal atrophy (where years have elapsed since the injury) may contribute (see Section 6.13.6.2.3).

In studies of nerve section or amputation, changes observed within the cortex reflect subcortical reorganization. Cutting nerves supplying the hand in the squirrel monkey, for example, results in the reorganization of the hand map in both the brainstem cuneate nucleus, and the thalamic ventroposterior lateral nucleus (Churchill, J. *et al.*, 2001). Reorganization within the brainstem and thalamus was found to be similar in extent to that observed in the cortex of these monkeys.

6.13.3.1.2 Dorsal rhizotomy – root cut

Mott and Sherrington (Mott, F. W. and Sherrington, C. S., 1895) demonstrated over a century ago that cutting dorsal roots C4–T2 causes an extensive deafferentation of the macaque's hand and forearm, and a profound and lasting impairment of voluntary manipulative movements. In humans, the loss of sensory feedback from the hand (e.g., following brachial plexus injury) also results in a severe impairment in dexterity (Nagano, A., 1998).

When dorsal roots that innervate the digits of the hand are sectioned, the central axons of the primary afferents that are cut degenerate, while their cell bodies within the dorsal root ganglion and peripheral axons remain alive. Thirty years ago, Basbaum A. I. and Wall P. D. (1976) showed that when dorsal roots supplying the hindlimb were cut in the cat, initially deafferented dorsal horn neurons developed novel cutaneous receptive field. Though this work indicated central neuronal plasticity in response to dorsal rhizotomy, the mechanisms were not determined.

Early studies that looked at dorsal root injury in nonhuman primates, focused on a unique group of macaque monkeys, the so-called Silver Spring Monkeys, that received massive dorsal root sections (C2–T4), for an unrelated series of studies, some 12–20 years earlier (Pons, T. P. *et al.*, 1991). These lesions completely deafferented the forelimb, and in some cases part of the trunk, and the arm was rendered completely nonfunctional. The data from these studies demonstrated several things. First, it was shown that chronic deafferentation of such a large magnitude results in significant transneuronal degeneration over many years (Jones, E. G. and Pons, T. P., 1998). Not surprisingly, there was an extensive reorganization of the body map within the thalamic somatosensory nucleus VPLc, and within the primary somatosensory cortex (S1) cortex. In the cortex, no unresponsive zones were detected, but the face was represented over a larger region and abutted the trunk representation in the absence of any input from the deafferented limb. There was also significant atrophy within the cuneate fasciculus of the spinal cord, the cuneate nucleus of the brainstem (37–48%

shrinkage by volume; Woods, T. M. *et al.*, 2000), the thalamic VPLc nucleus and possibly even the somatosensory cortex, though the latter was not determined. Perhaps surprisingly, only 5–15% of neurons were lost within the cuneate nucleus even up to 20 years postinjury. This indicated that shrinkage by volume was associated with a loss of neuropil, axons, and possibly dendrites, rather than a loss of neurons.

In recent investigations in the macaque monkey, we investigated acute, chronic, and long-term changes (>8 months) that accompany substantially smaller dorsal rhizotomies. In these experiments, only dorsal rootlets innervating the first 2–3 digits of one hand were cut (Figure 4). Immediately following one of these lesions, there is no detectable input from the experimentally deafferented digits, and a silent region is present in the corresponding spinal dermatomal map, and in somatotopic maps at the level of the brainstem (Figure 5; Darian-Smith, C. and Ciferri, M., 2006), and somatosensory cortex (Darian-Smith, C. and Brown, S., 2000). These silent zones persist for many weeks at all levels of the pathway and correspond to what can be a severe behavioral deficit initially (see further, Figures 4 and 6). Gradually, over the course of many weeks, and with constant hand use, there is some recovery of digit use (see Figures 4(c), 6(b), and 6(c)), and as this occurs, there is a corresponding reorganization within the cuneate nucleus of the brainstem (Figure 5) and cortex (Figures 4 and 6). Within dorsal root fascicles immediately adjacent to the lesion, cutaneous responses can also be elicited where this was not previously possible.

To examine the neural basis of these changes, a series of anatomical experiments were conducted in monkeys with a similar lesion (Darian-Smith, C., 2004). These indicated that a small population of spared afferent fibers continued to innervate the deafferented digits. These entered the cord adjacent to the lesion site, and for many weeks following the lesion, were presumably too weak in response to drive the somatotopic map at any level of the pathway. The axon terminals of these spared fibers were shown to sprout locally within the spinal dorsal horn and cuneate nucleus over several postlesion months. It was proposed that these sprouts form additional connections with input-deprived postsynaptic target neurons to play a role in driving reorganization at the spinal and higher levels of the neuraxis.

Importantly, these studies also demonstrated a limit to the amount of reorganization and recovery that can occur. Quite extensive postlesion reorganization can occur in the spinal dorsal horn (and at higher levels) as long as a small population (<5%) of uninjured primary afferents remain intact, and continue to transmit information from the impaired digits. For example, in monkeys with lesions that removed most input from the thumb and index finger, there was a complete re-emergence of the cortical map over the first 3–4 postlesion months (Figure 4(b)). However, in macaques with a slightly larger lesion (2–3 segments; Figure 6(a)), the hand map never completely re-emerged. This was true for the cuneate nucleus (Figure 5) and cortex (Figures 4(b) and 6(a)) (Darian-Smith, C. and Ciferri, M., 2005, for additional examples).

6.13.3.1.3 Deafferentation of the dorsal column nuclei

Studies that have investigated the effects of partial or complete deafferentation of the cuneate or gracile nuclei, have shown that deafferented neurons can immediately enlarge or express new peripheral receptive fields from the same or surrounding regions of the body surface, depending on the extent of deafferentation (Millar, J. *et al.*, 1976; Pettit, M. J. and Schwark, H. D., 1993; Kalaska, J. and Pomeranz, B., 1982; Wang, X. and Wall, J. T., 2005). Longer-term changes, such as those described in the previous section and following dorsal rhizotomy (Darian-Smith, C. and Ciferri, M., 2006), also demonstrate substantial reorganization within these nuclei following partial deafferentation. These changes reflect much of the reorganization seen in the somatosensory cortex, and clearly demonstrate that the dorsal column/medial lemniscal pathway plays a role in cortical reorganization.

But what happens when the afferent input to the dorsal column nuclei is completely blocked following a dorsal column section? Some insight into how the somatosensory system can respond is provided in a study of owl monkeys (Jain, N. *et al.*, 1997) in which a high cervical dorsal column lesion (at C3–C4) removed input from the entire extent of the dorsal column nuclei (Figure 7). Though the spinothalamic pathway remained intact, these neurons could not independently transmit sufficient afferent information from the forelimb to reactivate the cortical map. When even a small afferent population was spared, this input was able to reactivate the corresponding cortex and expand its representation into the cortical map. When no afferents were spared within the dorsal columns, face inputs expanded to utilize the adjacent silent forelimb cortex. A subsequent anatomical study showed that preserved inputs from the face had

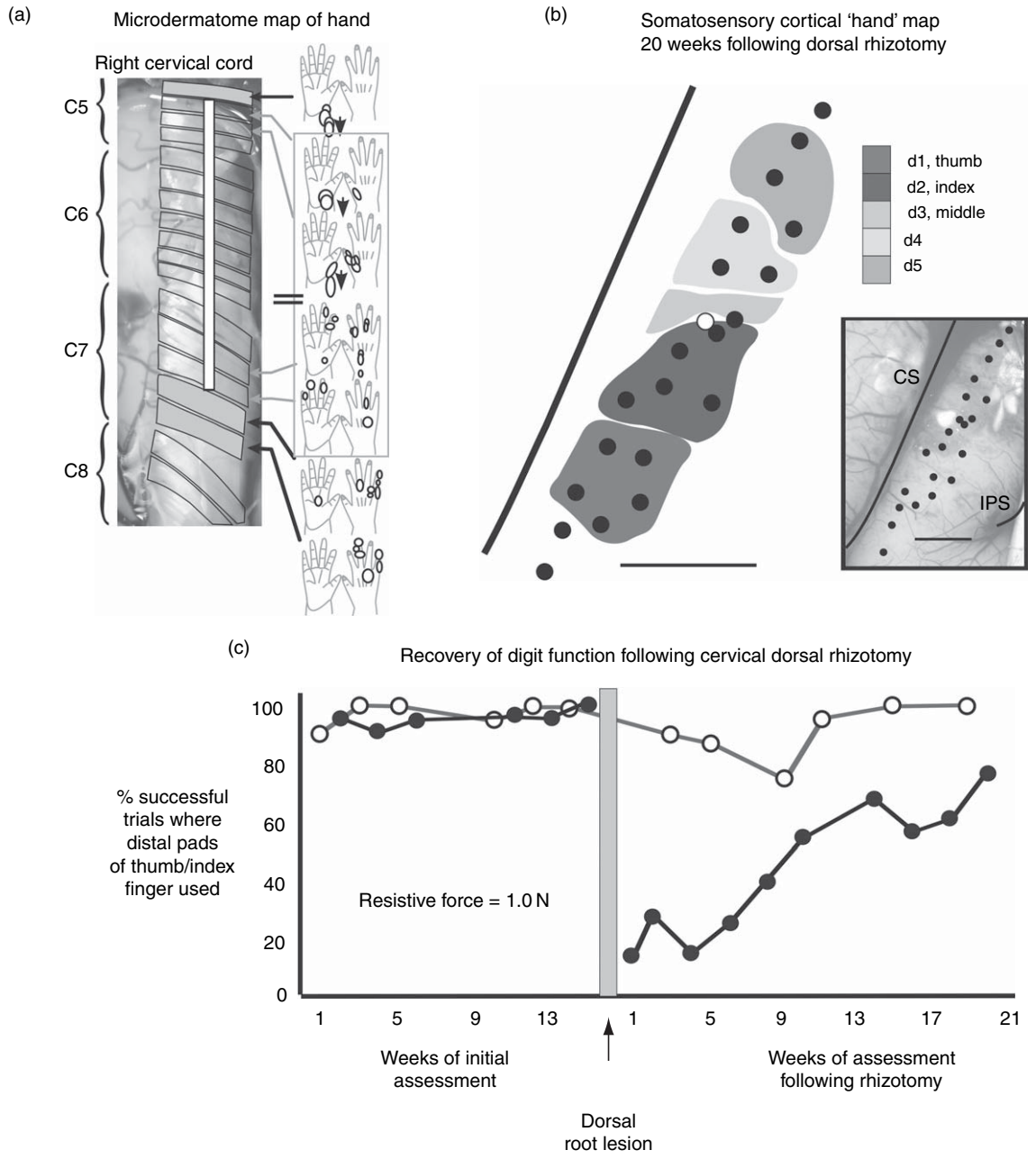

Figure 4 Changes following a dorsal rhizotomy. (a) Shows a laminectomy in a monkey (M-2) in which tactile input was selectively removed from the thumb and index finger. Cartoons of the hand show the distribution of cutaneous receptive fields on the palmar and dorsal surface of the hand in rootlets along the borders of the lesion zone, before rootlets were cut. The white bar marks extent of the lesion. Gray-shaded rootlets identify fascicles that were left intact following the lesion. Afferent fibers within these rootlets altered in their responses over several postinjury months such that cutaneous receptive fields could be mapped on the deafferented digits where this was not previously possible. (b) Shows the corresponding cortical hand map for the same monkey, 20 weeks following the lesion. By this time a complete hand map had reemerged and a silent region was not observed. Black dots indicate recording sites. Color coding shows digit representation as indicated. d1, thumb; d2, index finger; etc. (c) Shows the accompanying recovery of performance of a reach retrieval task in the same monkey over 20 postinjury weeks. The opposition of the pads of the index finger and thumb was the preferred stratagem used by the monkey before the lesion, and in the control hand (open circles). The use of this stratagem was lost immediately following the rhizotomy (black circles) but was gradually recovered over 20 postlesion weeks. The time of the dorsal rootlet section is indicated by the gray bar. Adapted from Darian-Smith, C. and Ciferri, M. 2005. Loss and recovery of voluntary hand movements in the macaque following a cervical dorsal rhizotomy. J. Comp. Neurol. 491, 27–45.

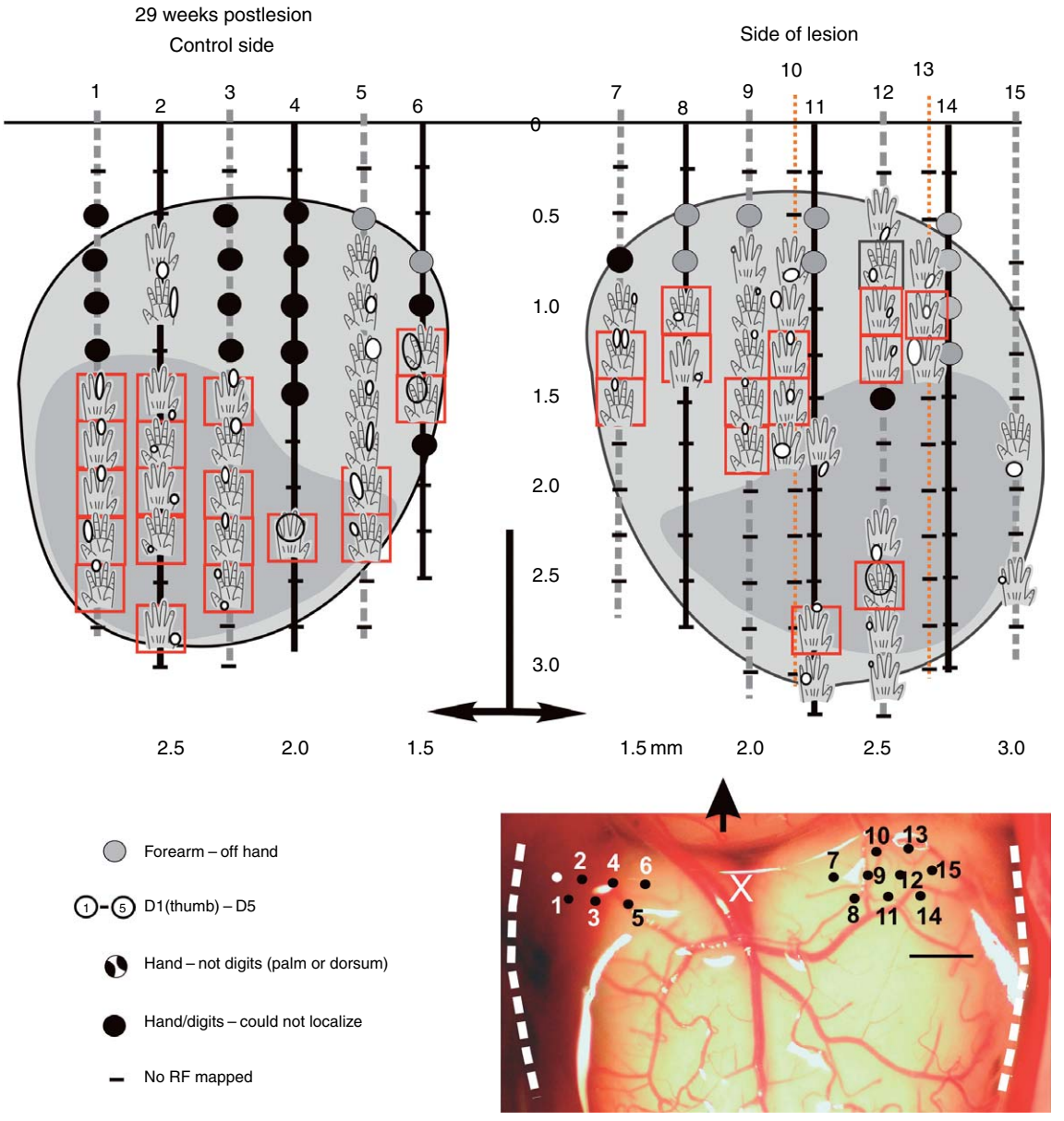

Figure 5 Changes in the pars rotunda of the cuneate nucleus in a monkey that received a DRL that removed input from the thumb, index, and middle fingers. At 2 weeks following the lesion, there were no inputs mapped in the cuneate nucleus on the first three digits of the hand. Twenty-nine weeks following the lesion, shown here, a silent region remained, but surrounding parts of the cuneate nucleus responded to stimulation of the initially deprived digits. Monkeys with slightly smaller lesions also showed a substantial reorganization of the hand map in the cuneate >16 weeks following the lesion, but did not have a silent zone. Electrode penetration sites are on photograph of the dorsal surface of the brainstem. Different rostrocaudal rows of penetrations are identified with different line formatting. Cutaneous receptive fields (RFs) on the digits are shown on cartoons of the hand surface. Shaded regions in the cuneate map on the normal side (right) outline the distribution of D1–D3 RFs. This input zone is transposed to the side of the lesion to help define the original region of input of the experimentally deafferented digits. Scale in photo = 1 mm; numbers refer to electrode penetrations. Adapted from Darian-Smith, C. and Ciferri, M. 2006. Cuneate nucleus reorganization following cervical dorsal rhizotomy in the macaque monkey: its role in the recovery of manual dexterity. J. Comp. Neurol. 498, 552–565.

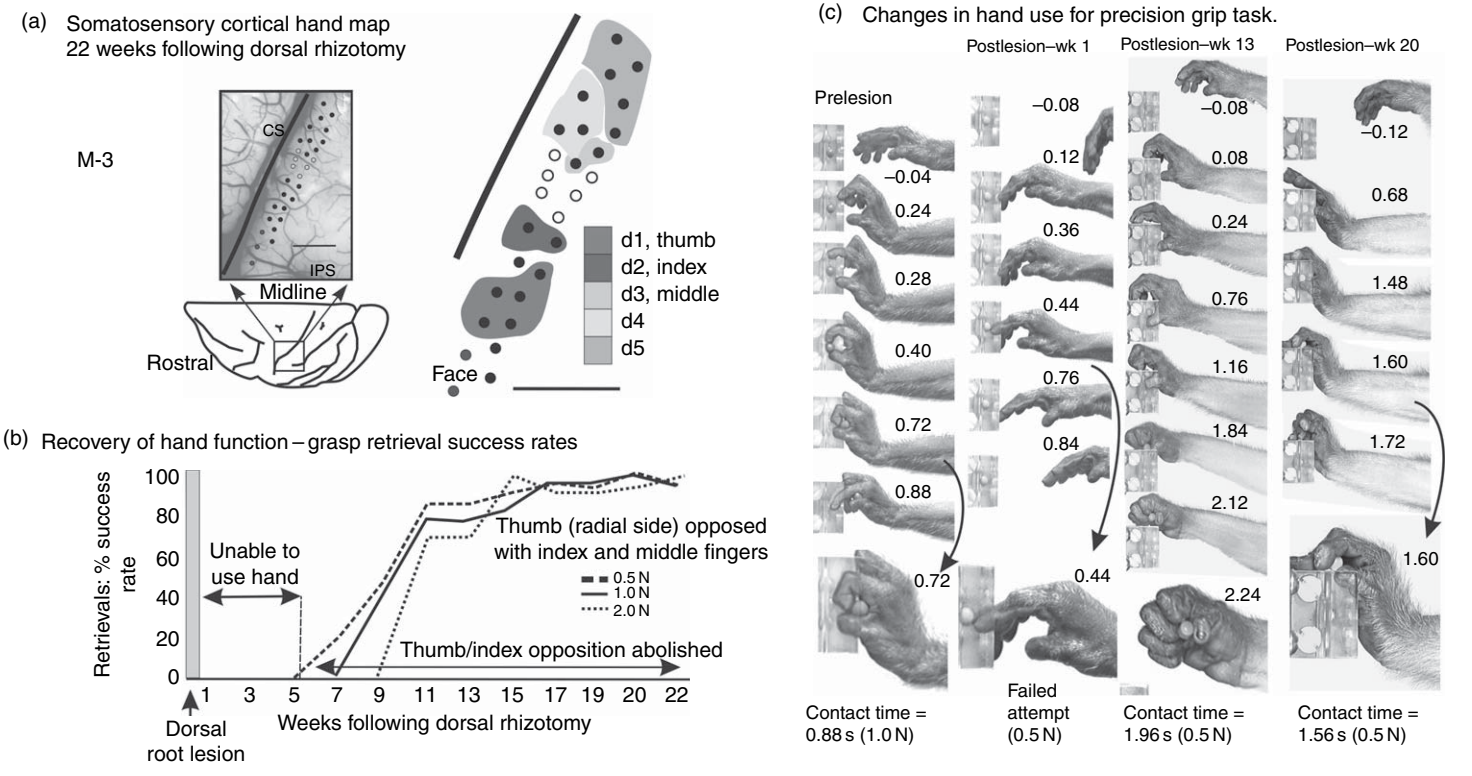

Figure 6 Data from a monkey that received a larger lesion than that shown in Figure 4. Here the dorsal rhizotomy removed all detectable sensory input from the thumb, index, middle finger, and thenar palm of the right hand. This monkey was initially unable to use its left hand at all and could not successfully perform a reach–retrieval task requiring cutaneous feedback for more than 2 months. (a) Shows the partial re-emergence of the somatosensory cortical hand map in this monkey 22 weeks following the lesion. Note that while there was a significant re-emergence of the digit map, a silent region remained. (b) Shows the rate of success of retrieving a target reward following the lesion. Data is given for three clamp forces holding the target, that the monkey had to overcome to retrieve the object. These correspond to increasing levels of difficulty with 2.0 N force being the most difficult and last to be successfully achieved. (c) Shows changes in the strategy used to perform the grasp–retrieval task. The prelesion stratagem shown in column 1, shows the target being grasped and removed by the opposing index finger and thumb. At one week postlesion, the monkey failed to perform the task, or preshape the digits. By the thirteenth postlesion week, the object could be grasped using an abnormal use of the first three digits, and by the twentieth postlesion week, cutaneous sensation had recovered sufficiently so that the monkey was able to retrieve the object 100% of the time, using opposition of the thumb and index fingers. Adapted from Darian-Smith, C. and Ciferri, M. 2005. Loss and recovery of voluntary hand movements in the macaque following a cervical dorsal rhizotomy. J. Comp. Neurol. 491, 27–45.

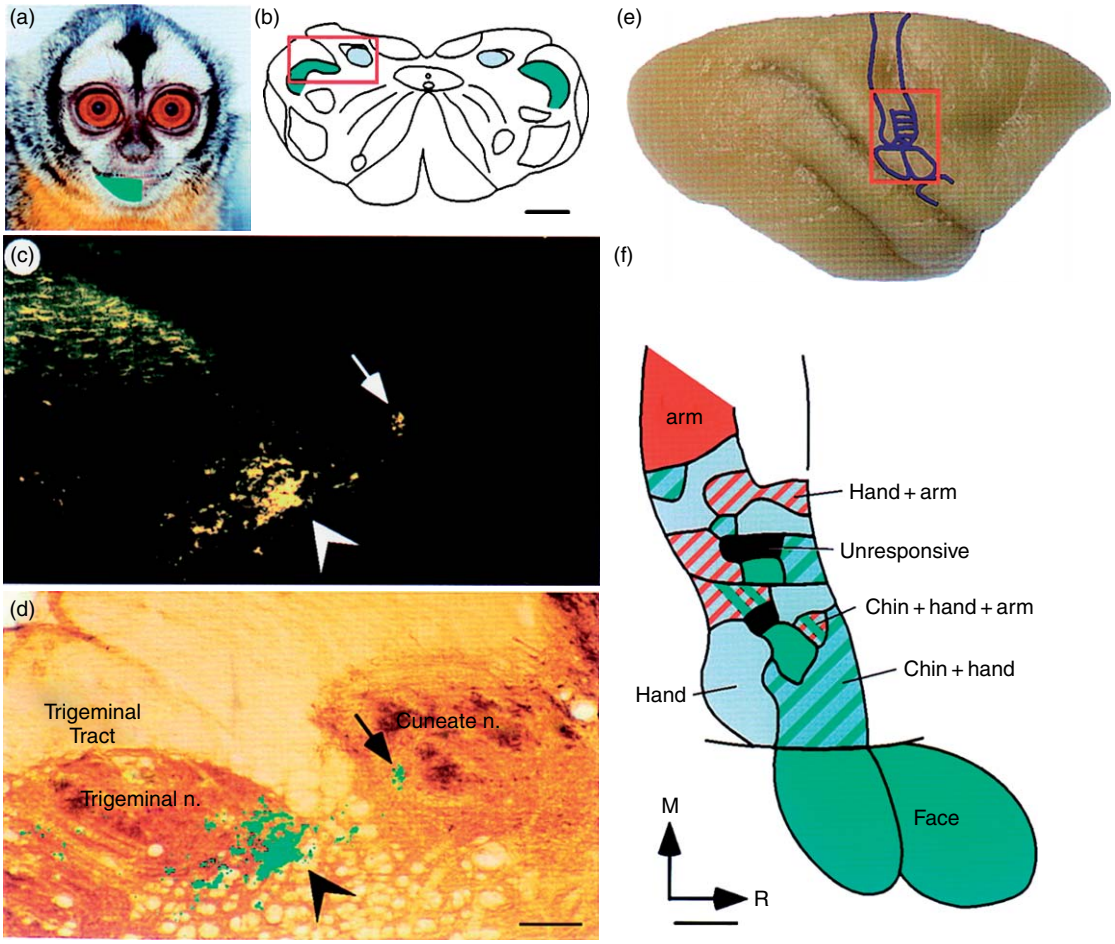

Figure 7 Jain N. *et al*. (2000) showed axon terminal growth from the trigeminal nucleus into the cuneate nucleus in an adult owl monkey 18 months following a complete cuneate fasciculus transection. (a) Shows the location of injections of the tracer B-HRP made into the chin. (b) Shows the cuneate (blue) and trigeminal nuclei (green) in a coronal section through the medulla. (c–d) Show brainstem section and corresponding cytochrome oxidase stained section. B-HRP labeling can be seen in the cuneate nucleus (arrow) following the injections made into the chin. Far stronger normal terminations of inputs from the face are indicated in the trigeminal nucleus (arrowhead). (e) A view of an owl monkey brain showing the somatosensory area 3b and the location of the map shown in (f). (f) Shows a reorganized somatotopy in area 3b following an incomplete dorsal column lesion at C4/C5 (right side). Inputs from the chin, and remaining parts of the hand and arm were observed in the deafferented hand region. Regions that only responded to chin stimulation = green, chin and hand = green and blue hatch, and chin, hand, and arm = green, blue, and red hatch. Regions responsive to hand stimulation = blue, and both hand and arm = blue and red hatch. R, rostral; M, medial; n., nucleus. Scale bar = 1 mm (b, f), 200 μm (d). Reproduced from Jain, N., Florence, S. L., Qi, H. X. and Kass, J. H. 2000. Growth of new brainstem connections in adult monkeys with massive sensory loss. Proc. Natl. Acad. Sci. U. S. A. 97(10), 5546–5550.

grown, over many months, from the adjacent trigeminal nucleus into denervated regions of the cuneate nucleus (Jain, N. *et al*., 2000). These results imply that the spinothalamic pathway does not play a defining role in the cortical reorganization observed, though some controversy regarding the compensatory role of mechanoreceptor afferents within the spinothalamic tract remains (Wall, J. T. *et al*., 2002).

In humans, spinal injuries are rarely restricted to the dorsal column, so it is more difficult to assess the neural bases of acute or chronic changes following such an injury.

6.13.3.2 Behavioral Changes Following Primary Afferent Injury

6.13.3.2.1 Nonhuman primate studies

Though behavioral testing has been used widely to provide a coarse assessment of dexterity (e.g., with the use of Kluver boards) over the years, surprisingly few

nonhuman primate studies have systematically examined behavioral changes following somatosensory pathway injuries, and linked these back to neuronal reorganization.

Investigations that have looked into the effects of dorsal column lesions on hand and digit use over the last several decades, have also been inconsistent in their findings. Deficits described for ostensibly similar lesions have ranged from subtle and insignificant (Leonard, C. M. *et al.*, 1992) to chronic and debilitating. A likely reason for the confusion stems from the lack of lesion reconstruction at the completion of many of these studies, and thus a lack of correlation between the anatomical and behavioral deficits. In studies by Vierck and colleagues, who made this link, transection of the dorsal spinal column was found to initially impair the monkey's ability to discriminate textures, or specifically – the frequency or duration of tactile stimulation (Vierck, C. J. and Cooper, B. Y., 1998). Some monkeys recovered this ability over several months of testing, and others did not. In the monkeys that did recover, it was proposed that they learned to use alternate cues and pathways to assess and discriminate textures (see Figure 8).

The behavioral effects of a spinal hemisection, which also involves the dorsal column, in addition to the corticospinal tract and other ascending and descending pathways on the lesion side of the cord, have also been studied in the macaque (Figure 7; Darian-Smith, I. *et al.*, 1996; Galea, M. P. and Darian-Smith, I., 1997b). Monkeys with a near-complete hemisection at spinal segments C3–C4 initially presented with a severe hemiparesis, but regained the ability to pick up objects with the impaired hand within one month of the lesion. By the end of the third postlesion month, monkeys were able to use their hand and digits quite efficiently in a reach-grasp-retrieval task, though recovery was never fully complete (up to 3 years postinjury). Persistent impairments included a less direct trajectory and preshaping of the hand during the reach component of the task, and some weakness of the opposing digits. The somatosensory component of the task was also clearly impaired, but not as completely as might have been expected. Somatotopic maps of the body representation showed a considerable reorganization of the deprived cortex and a greatly reduced hand map

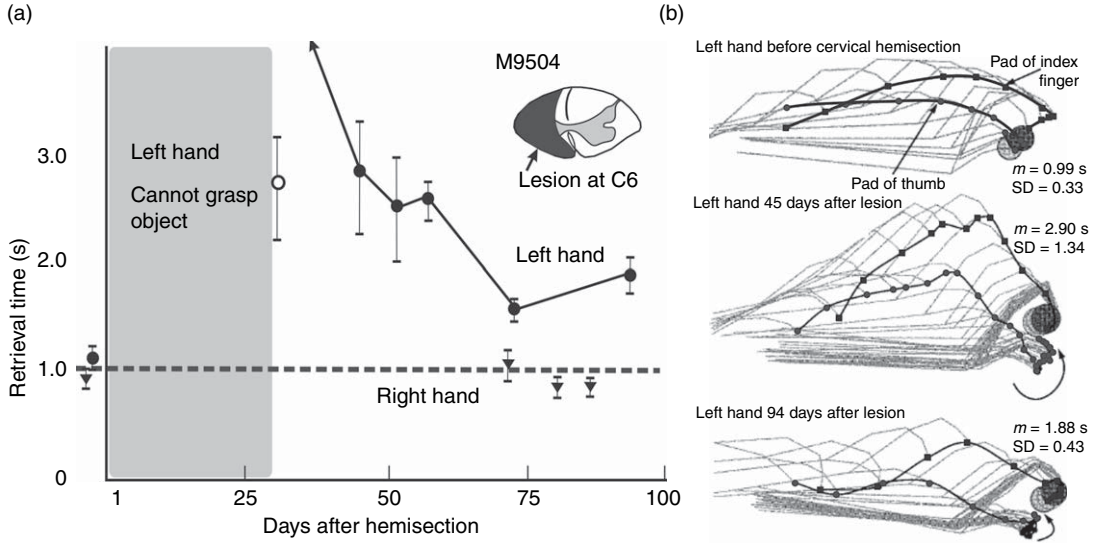

Figure 8 Behavioral changes following a cervical hemisection. (a) Shows changes in the time taken for the monkey to execute a reach–retrieval task following a near-complete left hemisection at C6. Solid circles = mean retrieval time for left hand, triangles = right hand. This monkey could not perform the task with the left hand for the first month following hemisection. (b) Shows stick figure sequences of trajectories of the pads of the index finger (squares) and thumb (circles) of the left hand of the same monkey. Sequences show retrieval prelesion, and at 45 and 94 days after hemisection. Interval period was 80 ms. Postlesion sequences show a slower, clumsier reaching trajectory and thumb opposition. Performance at day 94 was considerably improved from day 45. Adapted from Galea, M. P. and Darian-Smith I. 1997b. Manual dexterity and corticospinal connectivity following unilateral section of the cervical spinal cord in the macaque monkey. J. Comp. Neurol. 381, 307–319.

with abnormally large cutaneous receptive fields. In these studies, previously existing crossover corticospinal projections were thought, at least in part, to mediate behavioral recovery. It was also proposed that the localized sprouting of these or other preexisting pathways may also play a role. Recent examination of the behavioral effects of cervical hemisections supports these findings (Tuszynski and colleagues, personal communication).

Mott F. W. and Sherrington C. S. (1895) showed that sectioning the dorsal roots of spinal segments C4–T4 in the macaque completely blocked somatic sensation in the hand and voluntary digit movements, while sparing some controlled movements of the elbow and shoulder. They also observed that if a single dorsal root was cut in the same range of cervical segments, there was no identifiable impairment of voluntary hand function. In more recent studies of reaching movements following cervical dorsal root transection, some return of gross limb movement was reported in the monkey forelimb. Vierck C. (1982) studied the effects of a dorsal rhizotomy (C3–T3) on forelimb reaching to points in space and found an initially severe deficit, followed by a gradual recovery of some directed limb movements, after many months of training. However, voluntary hand function was not systematically examined.

What happens following a more circumscribed dorsal rhizotomy? Returning to work in our lab, we recently examined the effects of a restricted cervical dorsal rhizotomy on the macaque's ability to perform a voluntary task requiring cutaneous feedback (Darian-Smith, C. and Ciferri, M., 2005). Monkeys were divided into two groups and trained to retrieve a target object from a clamp (Figure 6(c)), using the thumb and index finger in opposition. In group 1, dorsal rootlets containing fibers supplying the thumb and index finger were cut, and in group 2, additional rootlets innervating the middle finger and thenar eminence, were also cut. Performance parameters were assessed before and following the lesion, and included (1) % successful retrievals; (2) digital stratagem (the pattern of digit opposition); and (3) the contact time (or duration of digit contact with the object prior to retrieval). During the first postoperative week, hand function was severely impaired in all monkeys, but over the following weeks, group 1 monkeys recovered the ability to retrieve the object by opposing the index finger and thumb in >80% of trials. Figure 4 shows the gradual recovery of the prelesion digit use over 21 postlesion weeks in one such monkey. Group 2 monkeys with the larger lesion also regained function in the impaired hand. Though this recovery was sometimes dramatic, as in the case of M-3 in Figure 6, it was never complete. Each of these monkeys quickly adopted a stratagem for grasping the target, using digits that were incompletely deafferented. At the end of these experiments, hand representations were mapped within the contralateral somatosensory cortex, and in the cuneate nucleus (Darian-Smith, C. and Ciferri, M., 2006) to define hand deafferentation and cortical reactivation, and in all cases, a tight correspondence was observed between these somatotopic maps and digit use. For example, if the monkey regained function in the thumb and middle finger but never again used the index finger, digit maps consistently showed a re-emergence of input from the thumb and middle finger, and a silent zone for the index finger.

These behavioral studies, which focus on hand sensorimotor function, consistently demonstrate that the sparing of even very small numbers of somatosensory fibers (<5%) can lead to quite dramatic behavioral recovery during the early postinjury months.

6.13.3.2.2 Behavioral studies in the rodent

A number of behavioral testing paradigms have been developed in recent years to assess sensorimotor deficits and recovery in rats following various injuries. Due to the relatively undifferentiated use of the forepaw in rodents compared with primate hand and digit function, the measurements that can be made in rodent limb behavior studies are inherently crude. However, they do provide a consistent measure of a particular sensorimotor capacity that can be followed over time. A full description of these sensorimotor tasks and rodent study outcomes falls outside the scope of this chapter (see Basso, D. M. *et al.*, 2002; Cenci, M. *et al.*, 2002; Nudo, R. J. *et al.*, 2006 for reviews and original articles). However, some examples for testing fore- and hindlimb function include the following. What is commonly referred to as the sticky tape test, involves placing stickers on the forepaws following a unilateral cortical (or subcortical) injury. Determining which sticker is removed first and the speed of removal measures sensorimotor deficit asymmetry. Rod, beam, and grid walking tests are commonly used to measure forepaw placement and thus sensorimotor coordination. Reach training has also been used to test and encourage the use of an impaired forelimb and paw following, for example, cortical ischemia (Biernaskie,

J. and Corbett, D., 2001), and finally, the Basso–Beattie–Bresnehan (BBB) scale is becoming widely used to test open field locomotion (Basso, D. M. *et al.*, 1995). Variations of a reach-grasp task are also used to measure grip force following spinal injuries that implicate descending as well as ascending sensorimotor pathways (Courtine, G. *et al.*, 2005). In studies looking at questions relating to plasticity in the barrel fields, a large number of whisker deflection, and object discrimination tasks involving the stimulation of one or more whiskers are used to alter or measure behavioral outcome.

6.13.4 Somatosensory Plasticity in Learning and Experience

A pervading theme through this chapter is that neuronal connections and cortical maps are continuously shaped and reshaped throughout life in accord with changes in our experience. This holds for injury, as we have seen; it equally holds for extensive training or use of a particular somatosensory or sensorimotor task. A persistent change in behavior is therefore sufficient to drive cortical and subcortical reorganization, which highlights the relevance of neuronal plasticity in our daily lives (Pascual-Leone, A. and Torres, F., 1993; Elbert, T. *et al.*, 1995; Buonomano, D. V. and Merzenich, M. M., 1998; Braun, C. *et al.*, 2001; Elbert, T. and Rockstroh, B., 2004).

6.13.4.1 Cortical Reorganization in Response to Learning

The somatosensory cortex lends itself well to the investigation of the role of sensory experience and learning in shaping neuronal circuitry, both because the S1 cortex is accessible, and because sensorimotor performance can be readily manipulated and assessed behaviorally. Merzenich and colleagues conducted seminal work on this during the early 1990s (Jenkins, W. M. *et al.*, 1990; Recanzone, G. H. *et al.*, 1992a; 1992b; 1992c; 1992d), in which monkeys were trained in various behavioral tasks that increased cutaneous stimulation to one part of the hand. A number of findings emerged, which have gathered much experimental support since. It was found that intensive repetitive stimulation of a skin surface, or the use of a part of the hand in a tactile discrimination task involving training over weeks and months, results in (1) the expansion of the representation of the stimulated skin surface in the corresponding somatosensory cortical map, (2) a decrease in RF size in the same region, signifying a greater sensitivity or focus of processing of input from this area, and (3) some shifting and reorganization of the surrounding cortical map representing adjacent parts of the hand. In tactile frequency discrimination tasks, where monkeys were rewarded for correct performance, an increased incidence of overlapping receptive fields (RFs) was also observed in areas 3b and 3a in regions representing the trained skin surfaces (Recanzone G. H. *et al.*, 1992a; 1992b; 1992c). Importantly, these and more recent investigations, have shown that spatial, as well as temporal response properties of cortical neurons can be altered with coherent, behaviorally relevant, and temporally coincident peripheral input. Behavioral relevance infers motivation, which can be correlated directly with more significant alterations to the cortex and improved motor performance (Jenkins, W. M. *et al.*, 1990; Lotze, M. *et al.*, 2003). Behaviorally induced cortical reorganization generally requires an intense training schedule, from several hours per day for many days, to a daily regimen over many weeks to months, and examples of this in humans (e.g., Braille-reading, instrumental playing) are discussed ahead. Training raises the activity level of the corresponding cortical and subcortical pathways, and leads to changes in the morphology and neurophysiology of the constituent neuron populations.

6.13.4.1.1 Activity-dependent changes in synaptic transmission – hebbian learning and long-term potentiation

An abundance of studies, primarily in the cortex, have shown that synaptic transmission and strength is greatly influenced by experience and learning. This activity-dependence, which follows Hebbian, or Hebbian-like rules (Hebb, D. O., 1949; Cooper, S. J., 2005), is important for altering synaptic efficacy, in response to changes in the input from the periphery (i.e., through injury, disease, or skill learning). The basic premise of Hebbian-based learning is that synaptic strength increases between neurons that are activated together. That is, synapses are modified when there is simultaneous activation of the presynaptic and postsynaptic neuron. More specifically, when the presynaptic action potential precedes the firing of the postsynaptic neuron, the synaptic response increases (long-term potentiation (LTP)).

Conversely, when the postsynaptic action potential precedes that of the presynaptic cell, the synaptic response decreases (long-term depression (LTD)). The temporal correlation of inputs (typically around a time window of ~100 ms) is therefore critical to synaptic state. Also critical to Hebbian learning is a cellular mechanism for detection of rapid successive pre- and postsynaptic activation. The *N*-methyl-D-aspartic acid (NMDA) receptor (a subtype of glutamate receptor) performs this role by enabling Ca^{2+} influx in the presence of Glu and postsynaptic depolarization, a step that is critical to LTP induction. NMDA-receptor activation requires sufficient depolarization to enable LTP induction, so the balance of inhibition and excitation is critical to synaptic plasticity. As such, a large number of studies have looked at the regulation of GABAergic pathways in the brain following injury, learning, and disease.

LTP has primarily been associated with learning in the hippocampus, but has also been demonstrated *in vivo* in sensory and motor cortex (Baranyi, A. and Feher, O., 1981; Iriki, A. *et al*., 1989; 1991; Baranyi, A. *et al*., 1991; Aou, S. *et al*., 1992; for reviews see Weinberger, N. M., 1995; Buonomano, D. V. and Merzenich, M. M., 1998; Garraghty, P. E. and Muja, N., 1996; Myers, W. A. *et al*., 2000; Elbert, T. and Rockstroh, B., 2004; Fox, K. and Wong, R., 2005). Either LTP or LTP-like mechanisms are inferred in all neuronal reorganization, and are thought to play a fundamental role in mediating the maintenance and modification of somatosensory plasticity, including plasticity that occurs with skill learning.

6.13.4.2 Cortical Plasticity in Braille Readers

A particularly striking example of tactile skill learning or use-dependent cortical reorganization can be seen in blind Braille readers (see Figure 9). Braille-reading involves intense stimulation of the digit pads of the reading fingers, sometimes for many hours per day, and over many years. With considerable experience, proficient Braille readers, and particularly those who use multiple fingers and both hands, are capable of reading speeds of 200 or more words per minute (Foulke, E., 1991). The sensorimotor cortex activated by the reading digits of Braille readers, has been shown to be enlarged relative to their

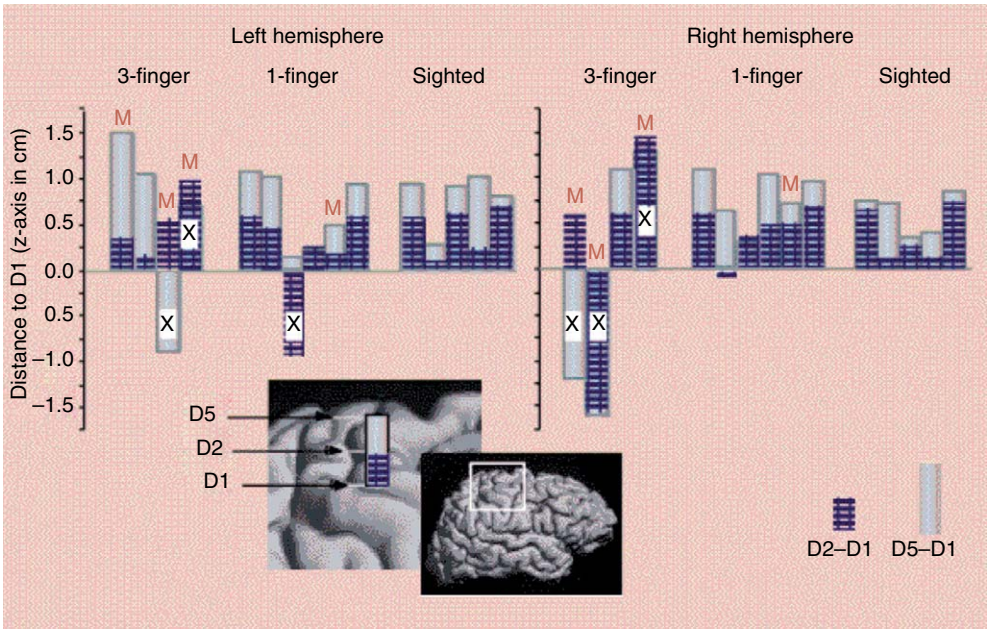

Figure 9 Using magnetic source imaging, Sterr A. *et al*. (1998a) showed that finger representations were topographically disordered in blind Braille readers who used 3 digits from both hands. These individuals also misidentified touched digits. Figure shows the distances between the centers of cortical activation. Distances are illustrated with reference to D1, which is shown as the zero line. The inset shows the relationship of responses of D1 (thumb), D2 (index), and D5 (little finger), as seen in a sighted subject. X – shows hemispheres where digit representation was disordered. M – indicates hemispheres where location of the tactile stimulation of the digits was mislocalized. Reproduced from Sterr, A., Muller, M., Elbert, T., Rockstroh, B., Pantev, C. and Taub, E. 1998a. Changed perceptions in Braille readers. Nature 391, 134–135.

nonreading digits (Pascual-Leone, A. and Torres, F., 1993; Sterr, A. *et al*., 1998b; 2003). This fits with other examples of use-dependent cortical reorganization following, for example, tactile discrimination or motor tasks in monkeys (Hlustik, P., *et al*., 2004; Recanzone, G. H. *et al*., 1992b), and string playing in musicians (see below).

In addition, blind Braille readers who use multiple fingers of the hands when reading, are able to very precisely attribute the Braille, but frequently mislocalize, or misidentify the digits of their hands when touched with a tactile stimulus (Sterr, A. *et al*., 1998a; 2003). When Sterr and colleagues used magnetic source imaging to examine the representation of the digits in S1 cortex in multidigit readers, they found that digit representations were also frequently disordered. The same was not true for single-digit users. It is plausible that the smearing of cortical digit representations has, in the example of multifinger Braille reading, an advantageous effect, and Sterr and colleagues suggest that a greater efficiency in information processing, when the incoming information can be processed as a whole. These data do, however, imply a dissociation between the perception of the position of the digits and the accurate localization of the tactile stimuli (i.e., the Braille). The neural basis of this distinction, however, is not yet understood.

Though several theories have been proposed to account for the phenomenon of mislocalization (Sterr, A. *et al*., 2003), perhaps the most plausible one suggests that the increased somatosensory input that occurs with Braille-reading, changes neural networks underlying cortical digit representations (in a Hebbian manner). Finger representations are disordered, overlapping, and enlarged in multidigit Braille readers who mislocalize, and by inference there will be a greater overlap of the neural networks processing information for each digit. When stimulus conditions provide a low signal-to-noise ratio in the underlying neuronal populations (which occurs with light tactile stimulation of the fingertips using von Frey hairs), the probability of stimulus mislocalization increases. In the same individuals, when the signal-to-noise ratio increases, as when the individual attends to the stimulus more carefully, or when the stimulus itself is more intense, the output from the network is more accurate and few, if any, errors occur. Since the reading digit representation dominates the cortical hand map in blind Braille readers, mislocalization occurs least often with the reading finger/s. However, when stimulation of surrounding digits results in mislocalization, the subject most commonly attributes the stimulus to the reading digit/s.

Digit mislocalization can also be demonstrated in sighted trained and untrained subjects. When Schweizer R. *et al.* (2001) applied near-threshold stimuli to the center of the subject's fingertips to evoke mislocalizations from fingers other than the one stimulated, they found a different response in trained and untrained individuals. In untrained subjects the digits adjacent to the stimulated digits were mislocalized more often than the digits further away. However, when the thumb and little fingers were simultaneously stimulated over many hours, these digits were more frequently mislocalized with each other and the incidence of mislocalizing adjacent fingers decreased. The first of these results harks back to findings in Braille readers and is not surprising, given that adjacent mislocalized digits have overlapping receptive fields and somatotopic positions within the pathway and cortex. The second finding is perhaps more surprising but does suggest some fusing of representations of the two simultaneously stimulated digits.

In another study, Braun C. *et al.* (2000) passively stimulated digits D1 and D5, and measured responses using high resolution EEG. They observed similar mislocalizations to the fourth rather than the first adjacent finger over time and were able to correlate the perceptual changes with an enlargement of the representations of the stimulated digits within S1 cortex, whereby D1 and D5 representations were closer together. Such findings suggest that tactile stimulus training strengthens the functional bond between the simultaneously trained areas. Where this perceptual fusion takes place is not yet known, but it may occur in higher somatosensory areas (i.e., areas 2 and 5) where RFs are larger and overlap to a greater extent than in area 3b.

6.13.4.3 Musicians: Training, Focal Hand Dystonia, and Rehabilitative Training

As with Braille readers, musicians provide excellent examples of the trained brain, and the adjustments made to brain organization throughout life that reflect the experiences of the individual. Magnetic source imaging studies have shown an increased representation of the digits of the left hand of string players (Elbert, T. *et al*., 1995), with digit representation correlated with the age of playing onset, with those training from a younger age having a larger

digit representation. Recent fMRI analysis of professional versus amateur musicians (Lotze, M. *et al.*, 2003) has also shown that sensorimotor and auditory cortical activation are more focused in the professional musician's brain than in the amateur. This supports the idea that task-specific neural networks are established and strengthened over a long period of training, and that these networks provide a greater efficiency of neuronal activation during performance. Task-specific networks also enable additional connections to be formed with higher order regions of the brain. In support of this, professional musicians show activation of regions of the auditory and somatosensory cortex not observed in the amateur, and it is thought that this may account for higher performance (e.g., the application of emotion and nuance to the playing) in such individuals (Lotze, M. *et al.*, 2003).

Overtraining in musicians can lead to a painless motor disorder known as focal hand dystonia, characterized by the loss of independent finger control (usually 2–3 adjacent digits) during the performance of the trained task. This condition is greatly feared by professional musicians and generally effects string, piano, keyboard, and wind players, who move their digits in rapid, repetitive, synchronous, and stereotyped ways and who hold their hands in abnormal or awkward postures over long periods. Seminal work in the owl monkey (Byl, N. N. *et al.*, 1996; 1997) provided a nonhuman primate model for the study of this syndrome, though there remains some question as to the model's equivalence with focal hand dystonia in humans (Chen, R. and Hallett, M., 1998). In the first of the studies by Byl and colleagues, monkeys were trained to repetitively grasp a handpiece that opened and closed over short distances, and the task was repeated at least 300 times per day. After many months of training, monkeys deteriorated in their motor performance and were unable to make complete contact with the handpiece. In a second study, two monkeys were trained to actively squeeze a hand grip that then vibrated. In one monkey that squeezed the handpiece using the digits, performance degraded from 80–90% to <50% over 5 months, before the digit representation was mapped electrophysiologically within the S1 cortex. In both studies, cortical area 3b was found to be remarkably degraded compared with the untrained hand. RFs were greatly enlarged in size (~10 times), overlapped extensively, and there was a breakdown of the normal segregation of RFs on the hand. These, and follow-up studies from the same lab (Blake, D. *et al.*, 2002a; 2002b; 2002c), showed that digit representations in S1 cortex degrades when inputs from multiple digits of the hand to the cortex are synchronous, repetitive, spatially stereotyped, and cognitively important to the monkey.

To investigate similarities in the human, Elbert T. *et al.* (1998) used magnetic source imaging to investigate changes in dystonic musicians. As with the owl monkey studies, they found significant disruptions of the cortical map, with fusion of the digit representations in the S1 cortex of dystonic musicians compared with nondystonic musicians and nonmusician controls.

Recordings made in the somatosensory thalamus in humans undergoing thalamotomies showed similar degradation in the thalamus of dystonic patients, such that there were greater numbers of RFs with multiple overlapping body parts (Lenz, F. and Byl, N., 1999). Similar findings have also been reported in the thalamus of dystonic monkeys (Blake, D. *et al.*, 2002a).

6.13.4.3.1 Rehabilitative strategies

From these studies and a growing understanding of cortical and subcortical use-dependent reorganization, new techniques have recently been developed to treat focal hand dystonia (Pantev, C. *et al.*, 2001; Candia, V. *et al.*, 2003; 2005). Termed sensorimotor retuning (SMR), this form of rehabilitation is context-specific and involves the splinting of one or two digits while subjects perform sequential extensions of the fingers and train in a manner that breaks the synchrony and repetition of dystonic digit use. Figure 10 shows functional improvements in dystonic fingers following SMR treatment in one of many such subjects (Candia, V *et al.*, 2003; 2005). magnetoencephalography (MEG) studies indicate that S1 cortical digit representations alter over the course of treatment to resemble the contralateral normal side. Beneficial changes also persist in string players for more than 2 years.

6.13.4.4 The Dynamics of the Somatosensory Cortex during Learned Sensorimotor Tasks

Once training of a precision sensorimotor task (e.g., learning a musical instrument, handwriting, or typing) has occurred and the underlying connectivity has been altered and set to accommodate the learned task, recent studies (Moore, C. I. *et al.*, 1999; Braun, C. *et al.*, 2000; 2001) suggest that the somatosensory cortex can then switch dynamically between

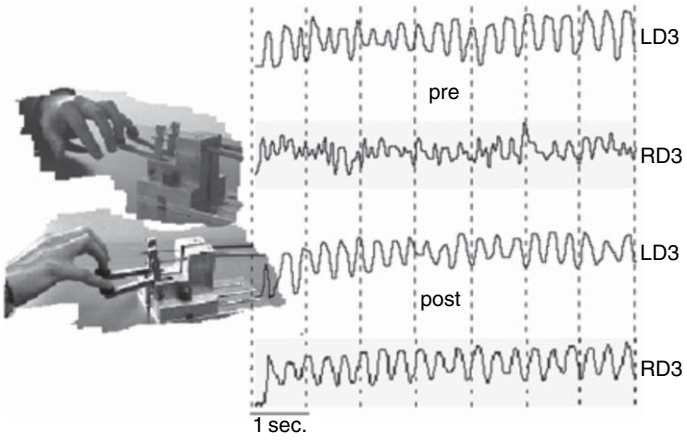

Figure 10 A dexterity displacement device is illustrated which was used for SMR in a subject with focal hand dystonia. Segments of pre- and posttreatment movement slopes are shown for the right D3 (RD3) and left D3 (LD3) during the execution of a trill-like task. Prior to treatment, movements of the dystonic digit (RD3) were uneven and uncontrolled (upper RD3 profile) compared with the control LD3 (upper LD3 profile) finger. Following treatment, the RD3 movements resemble performance in LD3 (lower LD3 and RD3 profiles, respectively). Only D4 and D5 are shown. Reproduced from Candia, V., Wienbruch, C., Elbert, T., Rockstroh, B. and Ray, W. 2003. Effective behavioral treatment of focal hand dystonia in musicians alters somatosensory cortical organization. PNAS 100, 7942–7946.

concurrently preexisting representational maps (or neural networks), according to the requirements of the task. Braun C. *et al.* (2001), for example, obtained MEG data from the somatosensory cortex while subjects wrote with their left or right hands, and compared the distance between the center of D1 and D5 activation during the writing and rest states. As shown in Figure 11, the distance between D1 and D5 activation increased significantly while subjects were writing, compared with rest. This was interpreted as demonstrating the activation of a preexisitng task-specific map. This and other studies in the motor cortex (Karni, A. *et al.*, 1995; 1998; Korman, M. *et al.*, 2003; Lotze, M. *et al.*, 2003) suggest that optimal performance of highly trained sensorimotor tasks may be achieved by the rapid activation of task-specific cortical networks, which develop over time.

Karni and colleagues (Karni, A. *et al.*, 1998) have proposed several distinct phases for learned motor skill acquisition, including (1) an initial rapid learning phase, (2) a longer phase of consolidation of the learned task, and (3) a slow learning phase where small incremental gains in performance occur with continued practice. In sensorimotor learning, as in injury-induced plasticity, initial rapid changes are followed by a longer period of correlated activity, possibly accompanied by structural changes to sensorimotor neuronal populations specific to the sensorimotor task. At least superficially, it seems likely that many of the same mechanisms may be involved.

6.13.5 Somatosensory Plasticity in Response to Disease

Models of disease such as stroke and ischemia, multiple sclerosis, spinal neuropathies, and pain-related disorders, are also associated with the loss of somatosensory and motor information, and frequently result in quite severe behavioral disturbances. As with peripheral and central injuries, and task learning, the adult CNS shows a remarkable capacity for reorganization in response to such disease states.

6.13.5.1 Changes in Response to Somatosensory Cortical Ablation, Ischemia, or Stroke

Somatosensory cortex damage can result in an impaired capacity for directed voluntary movement and tactile discrimination. In monkeys, the removal of the distal forelimb region in S1 cortex, for example, results in a severe loss of tactile discriminatory ability (see LaMotte, R. H. and Mountcastle, V. B., 1979), while the ablation of different functional subdivisions of the somatosensory cortex produces region modality-specific deficits (Randolph, M. and Semmes, J., 1974; Murray, E. A. and Mishkin, M.,

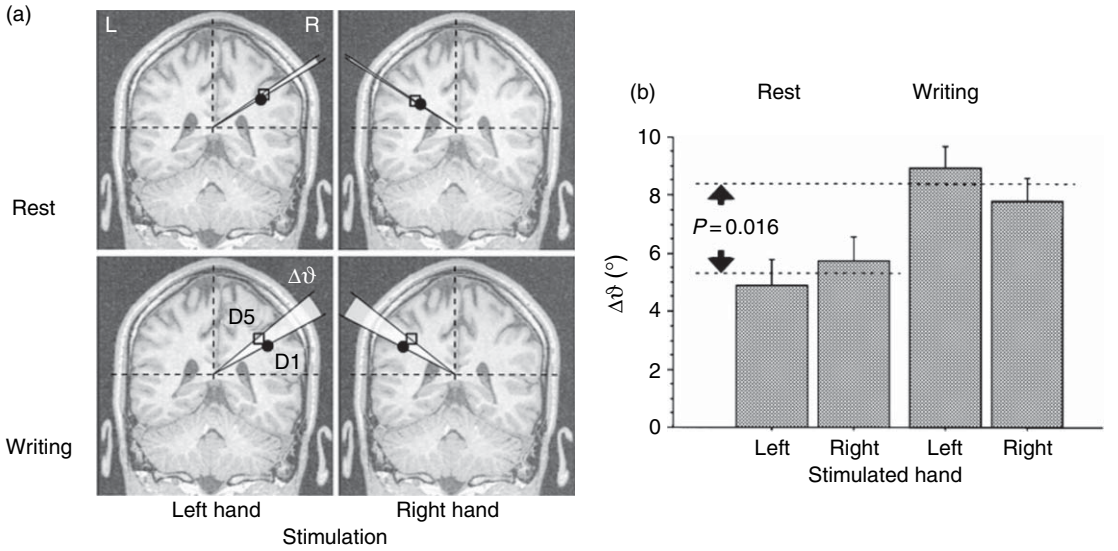

Figure 11 Braun C. *et al*. (2001) used source localization to look at the distance between D1 and D2 activation during an overlearned handwriting task. (a) Data are shown for the contralateral S1 cortex in this subject, at rest (top), and while writing (bottom). The distance between D1 (filled circle) and D5 (open square) was shown to be significantly greater during the writing task compared to rest. (b). Group data (means and standard error) are given for the cortical distance between D1 and D5 representation for the left and right hand during rest and writing. Reproduced from Braun, C., Heinz, U. *et al*. 2001. Dynamic organization of the somatosensory cortex induced by motor activity. Brain 124, 2259–2267.

1984). For example, the removal of area 3b leaves only a gross ability to detect size, while the ablation of area 2 leaves tactile discriminatory abilities intact and results in the loss of shape recognition only (Randolph, M and Semmes, J., 1974; Carlson, M., 1981). Such studies, combined with our understanding of the anatomy of the system, support the view that the connections between somatosensory functional subdivisions, including SII, are parallel, distributed, and hierarchical, and are structurally and functionally interdependent. Complex sensorimotor tasks require the coactivation of area 3b and numerous other specialized somatosensory and motor cortical and subcortical regions. How these different neuronal networks are activated and interact during normal and impaired sensorimotor performance, however, remains unclear.

That the S1 cortex is capable of functional recovery following cortical injury has long been recognized (Cole, J. and Glees, P., 1954; Glassman, R., 1971) but has been examined in more detail in recent decades. Monkey studies have been fundamental to this. Jenkins W. M. and Merzenich M. M. (1987) used intracortical microelectrode mapping techniques in owl monkeys to look at changes in the somatosensory hand map following focal ischemic lesions in somatosensory area 3b (see Figure 12). Several months following the lesion, they observed the emergence of a new map within a part of area 3b left intact following the lesion. The new map was smaller than in the normal cortex and somatotopy was greatly reorganized, with RFs observed on that part of the hand previously ablated by the lesion site. Soon after, Doetsch G. S. *et al.* (1990) reported a similar finding in the raccoon. In their study, digit 3 representation was ablated within S1, and the region mapped electrophysiologically 4 months later. They observed the emergence of a new representation of digit 3 within intact cortex adjacent to the lesion site, and substantial changes in the response properties of neurons within the reorganized cortex, including enlarged, and overlapping RFs.

The neural basis of skill recovery has also been examined following cortical lesions, such as might occur following stroke. Xerri C. *et al.* (1998) trained owl and squirrel monkeys to perform a sensorimotor retrieval task, and then removed functionally relevant parts of area 3b using a series of microlesions. Monkeys were behaviorally impaired in task performance following the lesion, but were retrained to perform the same task over several weeks with the initially impaired digits. Maps obtained across the S1 hand representation following functional recovery showed a newly emerged representation of

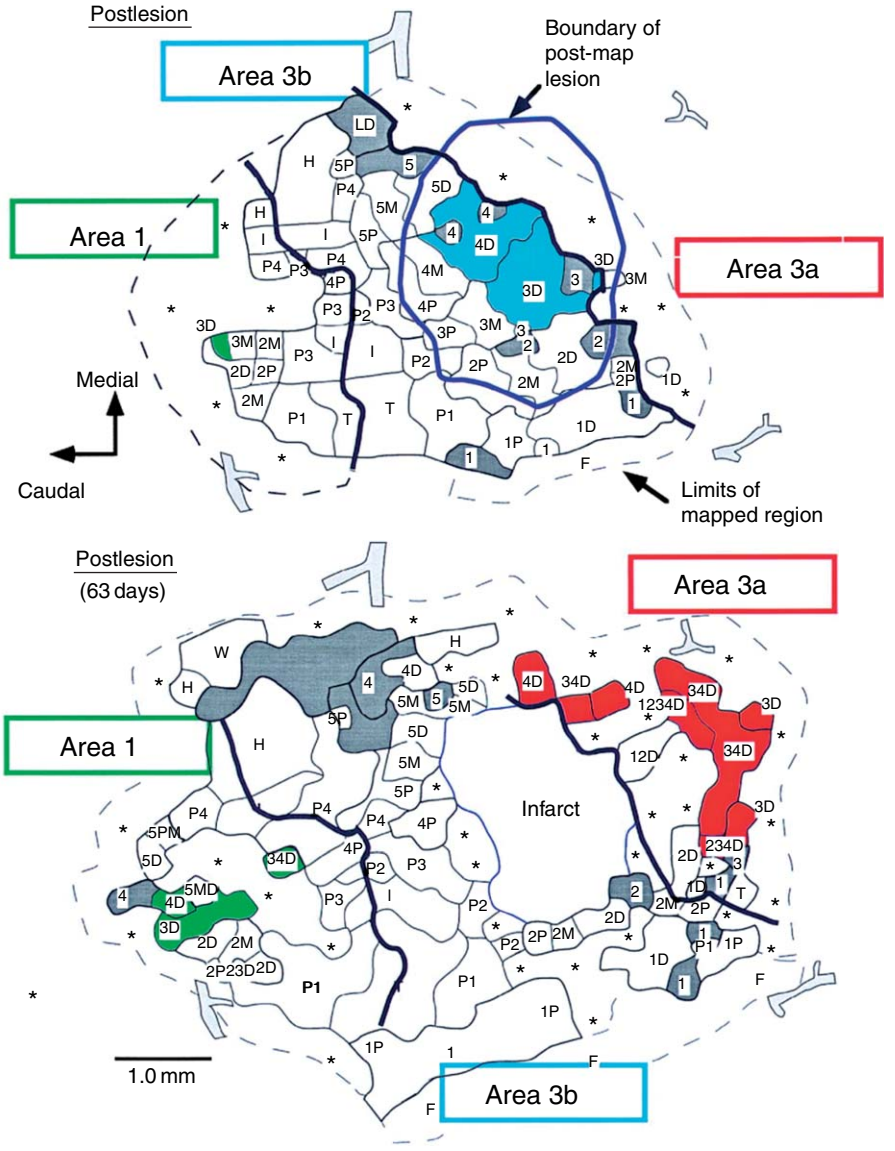

Figure 12 Reorganization of the hand map in primary somatosensory cortex in an owl monkey, following a cortical lesion. Top panel shows the somatotopically organized hand map before a cortical lesion was made in the region of digit representation in area 3b. Lower panel shows the same region of cortex as it was mapped 98 days after the cortical lesion. There was an emergence of cutaneous representational zones in both area 3a and area 1. Cortical representation of the tips of digits 3 and 4, that were heavily used in recovered behavior, are colored: blue indicates area 3b representations, green = area 1, red for area 3a. Numbers 1–5 denote the digits (i.e., 1 = thumb); D, M, and P, distal, middle, and proximal phalanges, respectively W, wrist; F, face; LD, large dorsum surfaces; * indicate where no receptive fields could be mapped. Estimated area 3a–3b border is delineated with dark gray lines. From Xerri, C., Merzenich, M. M. *et al*. 1998. Plasticity of primary somatosensory cortex paralleling sensorimotor skill recovery from stroke in adult monkeys. J. Neurophysiol. 79(4), 2119–2148.

the same fingertips in a novel region of area 3b. New and enlarged cutaneous inputs were also observed in area 3a from the same region of the hand. Though results were variable between monkeys, all showed newly emerged fields, and a disproportionate representation of the fingertips relevant to the task (whose cortical fields had originally been destroyed). In effect, regions of S1 cortex that normally played a nondominant role in cutaneous activation, gradually adopted the role of the missing cortex. Similar changes have also been reported in the primary motor cortex hand area of

squirrel monkeys following focal vascular infarct (Nudo, R. J. and Milliken, G. W., 1996; Nudo, R. J. *et al.*, 1996), which suggests a generalized response to cortical injury.

Topographic reorganization also occurs in cortical regions remote to the site of the lesion. This was shown in monkeys in the second somatosensory area (SII) following damage to the primary somatosensory cortex (Pons, T. P. *et al.*, 1988), where ablation of the hand area in cortical areas 3b, 1, and 2 enabled the target zone in SII to respond to input from the foot. Similar changes have now been seen in motor cortex, where post-ischemia reorganization has been observed in premotor cortex; a region which is functionally and anatomically aligned but spatially distant to the injury site (Frost, S. *et al.*, 2003).

These data suggest that connected regions of the cortex, regardless of whether they are adjacent to, or spatially remote from the injury site, reorganize in response to brain injury. Rodent studies, particularly in the barrel cortex, have provided additional insights into the plastic changes that accompany somatosensory cortical ablation (see Sachdev, R. N. S. *et al.*, 2001 for review).

In humans, changes that occur following ischemic brain disease have been investigated extensively using a range of imaging techniques, including transcranial magnetic stimulation (TMS), fMRI, PET, and MEG, or combinations of these. These techniques show changes in regional activity (e.g., regional cerebral blood flow, regional cerebral metabolism of glucose, oxygen, or neuroreceptor or transmitter systems) in the brain during specific sensorimotor tasks. Such studies can be difficult to interpret, both technically, and because brain injury following a cerebral artery infarct, for example, can be difficult to define in the individual, since it changes from the acute to chronic phases. It is also often difficult to find patients with sufficiently similar injuries that they can reasonably be compared. Even so, several patterns of reorganization have been identified that accompany the recovery of sensorimotor function following injury to the hand/forearm region of the somatosensory and motor cortex. Since middle cerebral artery (MCA) infarcts are common and cause the most circumscribed damage to the sensorimotor cortex in a region supplying the hand and forelimb, data pertinent to MCA infarcts will mainly be reviewed here.

A number of groups have shown significant contrainfarct sensorimotor cortex activation but little additional perilesion cortical reorganization following an MCA infarct (Seitz, R. J. *et al.*, 1998; 2004). For example, when Cramer S. *et al.* (1997) asked MCA stroke patients with good recovery to perform a finger-tapping sequence, they found increased activation in the contralesion sensorimotor cortex (hand representation), but little, if any, increased activation in the ipsilateral hemisphere adjacent to the injury site. In addition, when infarction involved just the motor cortex, activity was localized to the primary somatosensory cortex, and when it involved the somatosensory cortex, sensorimotor activity centered around the motor cortex. In contrast, Butefisch C. *et al.* (2005) reported bilateral sensorimotor and SMA activation during finger tapping in patients with cortical MCA infarcts, compared with control subjects where only the sensorimotor cortex contralateral to the performing hand was activated during hand performance (see Figure 13). In yet another study, Carey J. *et al.* (2002) used fMRI to show that when MCA stroke patients received training in a finger-tracking dexterity task, sensorimotor cortical areas were activated in both the contralateral and ipsilateral hemispheres (Figure 14). In untrained stroke patients, activation was observed mainly on the side contralateral to the infarct or ipsilateral to the performing hand. In healthy control subjects, activity is localized to the hemisphere contralateral to the moving hand.

From these and other clinical studies (see Seitz, R. J. *et al.*, 2004 for review; Nelles, G. *et al.*, 1999), it is clear that the hemisphere contralateral to the lesion plays an important compensatory role in postischemic reorganization (Johansson, B., 2000).

6.13.5.2 Cortical Plasticity in Multiple Sclerosis

Multiple sclerosis (MS) is a disease that causes the breakdown and destruction of the myelin sheath surrounding neurons and thus the disturbance of signal transmission. The disease is progressive with episodes of near-complete functional recovery and relapse, though eventually symptoms become chronic as the myelin and axonal injury become irreversible (DeStefano, N. *et al.*, 1998; Scolding, N., 1999 for review). Through the different phases of the disease the brain undergoes reorganization, presumably as a compensatory or adaptive response to initially temporary, and later chronic functional loss. Though MS does not specifically target somatosensory and motor regions of the cortex and related subcortical structures, it does eventually involve

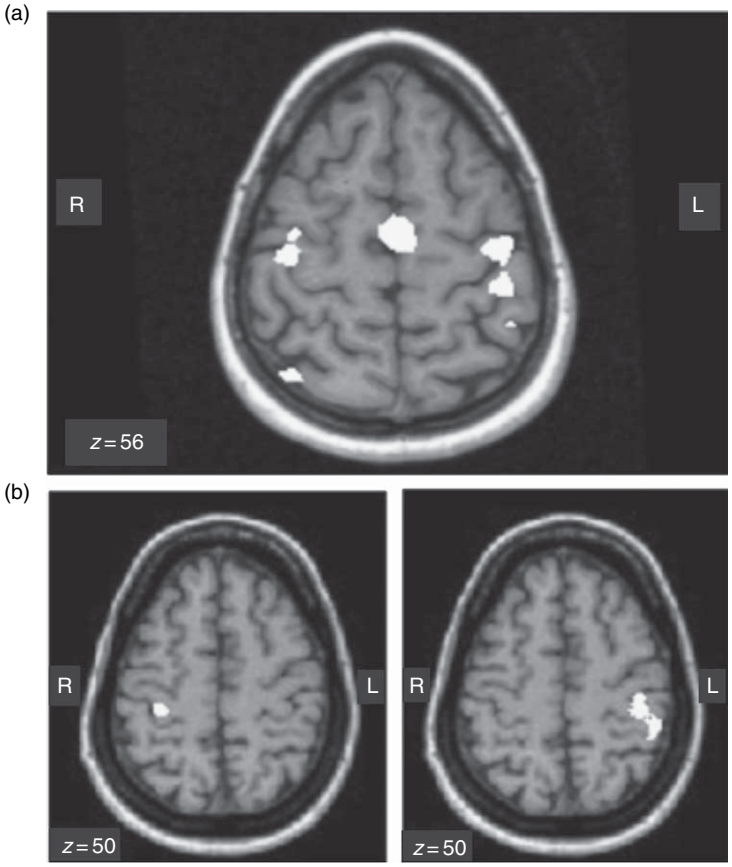

Figure 13 fMRIs showing mean activation during a fingertapping sequence with the affected hand in five patients with cortical MCA infarcts (a) and in controls (b). In (a) the right hemisphere r corresponds to the affected hemisphere and l refers to the unaffected hemisphere. The activation of the contralesion side is evident during the hand task in (b) control subjects performed the finger-tapping sequence with the left and right hands, respectively, and activation is evident in the pericentral gyrus only on the side contralateral to the performing hand. This patient had excellent recovery of function at 6 weeks postinfarction. Adapted from Butefisch, C., Kleiser, R., Korber, B., Muller, K., Wittsack, H. -J., Homberg, V. and Seitz, R. J. 2005. Recruitment of contralesional motor cortex in stroke patients with recovery of hand function. Neurology 64, 1067–1069.

these regions of the brain and cause sensorimotor dysfunction. A number of studies have used fMRI to look at changes in cortical activation during simple passive or active sensorimotor tasks during different phases of MS to determine patterns of reorganization that might characterize disease progression (Buckle, G., 2005 for review). In spite of individual differences in disease phenotype and response, cortical activation patterns do alter with disease progression. At early stages of MS, as the patient performs a simple voluntary manual task with their dominant hand, more contralateral sensorimotor cortical regions normally associated with movement are recruited compared with healthy controls. In patients experiencing relapse and remission, these same regions are activated bilaterally and there is some recruitment of the premotor and supplementary motor areas either ipsilaterally or bilaterally. Figure 15 shows an example of a patient at this stage (Lee, M. *et al.*, 2000). Late in the disease, additional regions are recruited (e.g., middle and the inferior frontal gyrus bilaterally, the ipsilateral cingulate motor area and the inferior parietal lobule), that are normally only activated in normal subjects during more complex tasks (Reddy, H. *et al.*, 2002; Rocca, M. *et al.*, 2005). Though studies differ in their detail, they do provide consistent evidence of a progressive adaptive ongoing reorganization in the brain that involves the gradual recruitment of bilateral and then higher order neural networks. Such changes are presumed to reflect and enable true functional compensation.

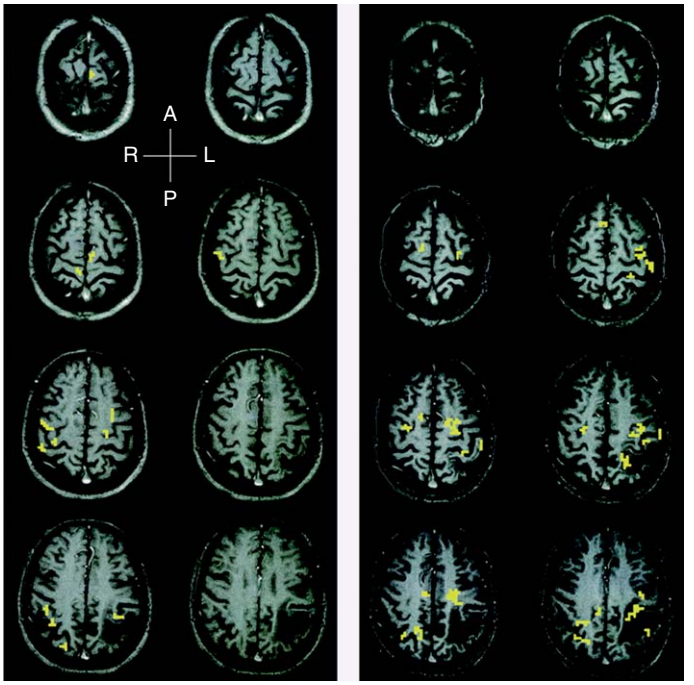

Figure 14 fMRIs from a subject in a stroke treatment group who underwent finger-tracking training. (Subject had stroke 9.4 years previously.) Images were taken while the partially paralysed right hand performed a finger-movement tracking test before (pretest) and after (posttest) 20 sessions of training. The infarct is visible in left parietal cortex in the lower three images in each panel. Cortical activation was evident mainly on the side ipsilateral to the paretic hand (or contralateral to the infarct) prior to training. After training, activation was predominantly contralateral to the paretic hand (or ipsilateral to the infarct). Reproduced from Carey, J., T. Kimberley, T. Lewis, S., Auerbach, E., Dorsey, L., Rundquist, P. and Ugurbil, K. 2002. Analysis of fMRI and finger tracking training in subjects with chronic stroke. Brain 125, 773–788.

6.13.5.3 Cortical Plasticity in Response to Other Diseases

Cortical plasticity also contributes to functional recovery from diseases that affect the spinal cord. One example of this is myelitis, a transient inflammatory disease of the spinal cord that seldom involves the brain. Patients exhibit a wide range of sensorimotor deficits, and while there is residual damage to the cord, there is frequently some return of function following the disease. Cramer S. *et al.* (2001) used fMRI to examine potential cortical contributions to the restoration of hand function in patients with cervical myelitis. They found that the return of upper limb function (in the form of a finger-tapping task) correlated with an increased activation volume in the contralateral primary sensorimotor and premotor cortex. The extent to which additional cortex was activated, directly correlated with the daily use of the affected hand, meaning that use of the recruited circuitry was critical to its formation and stability. Though some cortical activation was probably the result of spinal recovery following the disease, the increase in regional activation demonstrated compensatory plasticity and reorganization.

However, not all diseases induce adaptive plastic responses. In Huntington's disease (HD), for example, it seems that one of the earliest signs of the disease is the lack of normal plastic neuronal responses. A defining feature of Huntington's disease (caused by a CAG repeat in chromosome 4) is that it is progressive and results in extensive neurodegeneration in the striatum and cerebral cortex. Symptoms include motor disturbances such as chorea, athetosis, and cognitive impairment. Mazarakis N. *et al.* (2005), recently used a presymptom mouse model of Huntington's disease to assess possible abnormalities in neocortical plasticity and synaptic function. To do this they used a known model of plasticity in the rodent barrel cortex which involved the cutting of all but one row of whiskers. In normal control mice this resulted in an enlarged representation of the remaining whiskers,

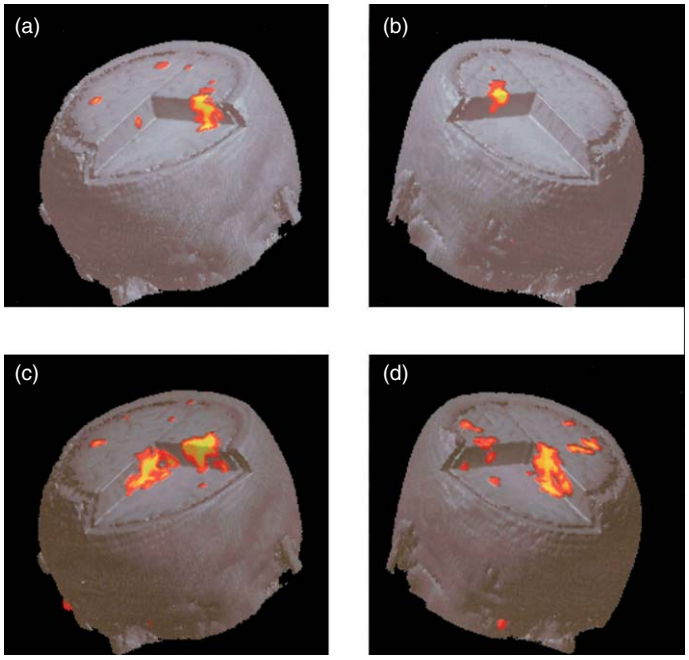

Figure 15 fMRI 3D rendered reconstructions showing patterns of cortical activation associated with finger-tapping in a normal control subject ((a) right hand and (b) left hand), and a patient with MS ((c) right hand and (d) left hand). Note activation of the sensorimotor cortex contralateral to the moving limb and supplementary motor cortex (SMA). In the MS patient, there was an increased activation in the ipsilateral sensorimotor cortex and the SMA. The right hemisphere is to the viewer's left. Reproduced from Lee, M., Reddy, H., Johansen-Berg, H., Pendlebury, S., Jenkinson, M., Smith, S., Palace, J. and Matthews, P. 2000. The motor cortex shows adaptive functional changes to brain injury from multiple sclerosis. Ann. Neurol. 47, 606–613.

but such changes were not observed in the HD mice. In addition, HD mice showed a severe impairment of somatosensory discrimination learning in a whisker discrimination learning task that required an intact cortex. Thus the HD mice exhibited somatosensory cortical dysfunction and an abnormal plastic response before exhibiting any motor disturbances symptomatic of the disease state.

6.13.5.4 Cortical Reorganization and Chronic Pain

While the neural basis of pain is covered in Volume 3, pain is mentioned briefly here in the context of somatosensory plasticity. Pain is complex, involves multiple levels of the somatosensory pathway and cortex to varying degrees, and is caused by multiple mechanisms. It can be divided into physiological, inflammatory, and neuropathic categories. Physiological pain is initiated by nociceptors responding to noxious stimuli, either from chemical irritants, or noxious heat/cold differentials. These pathways are subject to activity-dependent plasticity, so that increased activation can eventually result in an increased response, or a lowering of the high-threshold nociceptor terminal response to the stimulus. Inflammatory pain is induced following inflammation or damage to tissue, and neuropathic pain by injury. Both produce hypersensitivity at and surrounding the injury site. During the normal course of healing, the hypersensitivity produced by inflammation usually dissipates and goes away. Neuropathic pain, however, remains and manifests long after the injury site has healed, and is an expression of aberrant neuronal function rather than a response to the initial pathology.

Phantom limb pain is a form of neuropathic pain. It occurs with the loss of input following amputation, and is usually associated with cortical reorganization. In upper limb amputees who experience phantom limb sensation, stimulation of the face can elicit a point-to-point referred sensation on the phantom limb or hand, and perceived sensations on the phantom match the stimulus modality (e.g., vibration, heat, and painful stimuli are all perceived as such on the phantom limb). Ramachandran V. S. *et al.*

(1992; Ramachandran, V. S., 2005 for review) described this clinically known phenomenon in some detail, and proposed that phantom sensations, including pain, were likely to be the perceptual correlate of cortical reorganization. Since the hand and forelimb are represented adjacent to each other in the cortex, it seemed reasonable that inputs from the adjacent mouth and face region, that invaded what was previously the hand region, could form the neural substrate for phantom sensation and pain. This was tested in imaging studies in humans (Elbert, T. *et al.*, 1994; Yang, T. T. *et al.*, 1994), with somewhat surprising results. As with the earlier animal studies, cortical reorganization was demonstrated in upper extremity amputees, with the mouth representation shifted into the former hand/limb representation. However, cortical reorganization occurred irrespective of whether the patient perceived phantom limb sensation or not. Studies on chronic back pain subsequently showed a positive correlation between the amount of pain and the extent of cortical reorganization, and this relationship was then tested in patients with phantom limb pain. It was shown that as with chronic back pain (Flor, H. *et al.*,1995), the magnitude of phantom pain, rather than the referred sensation, correlated significantly with the extent of cortical reorganization. The same correlation was not seen in amputees without chronic pain.

More studies in the early 2000s (Grusser, S. *et al.*, 2004; Karl, A. B. N. *et al.*, 2001) have shown that stimulation of body parts far from the region of amputation (e.g., the foot) can also elicit referred sensation on the amputated limb. Current evidence suggests that nonpainful phantom limb sensations are associated with changes in area 5 and SII, in addition to S1 reorganization that does not involve large shifts of face representation into the hand/arm cortex. It has also been proposed that phantom limb sensation involves the coactivation of nonadjacent representations rather than somatotopic cortical reorganization (Moore, C. I. *et al.*, 2000). Phantom limb pain, on the other hand, is strongly correlated with the magnitude of S1 reorganization (Figure 16; Flor, H. *et al.*, 2000; Flor, H., 2002; 2003; Grusser, S. *et al.*, 2004).

In addition to cortical changes, it is likely that a number of subcortical mechanisms also contribute to phantom limb pain. Nerve endings that have been directly damaged by the amputation may, for example, grow erroneously within the stump region and develop abnormal discharge that is perceived as painful. Evidence for peripheral involvement comes from Birbaumer N. *et al.* (1997), who used brachial plexus nerve blocks to anesthetize the forearm in upper extremity amputees suffering from phantom limb pain. They found that the symptoms were eliminated in about 50% of patients. Neuroelectric source imaging showed that in individuals relieved of their phantom limb pain, cortical reorganization was reversed, and in individuals not relieved, cortical reorganization was increased. These data suggest that peripheral input plays a large role in phantom limb pain in some patients and in others, symptoms are caused or maintained by factors independent of the periphery. In addition to cortical reorganization, and maladaptive input from the periphery, changes may also take place within the dorsal root ganglia, the spinal dorsal horn, and/or the thalamus that cause or maintain phantom pain. In the spinal circuitry, for example, localized axon terminal growth of the injured neurons within the spinal dorsal horn may contribute.

Additional studies suggest that chronic back pain may also lead to an expansion of the cortical

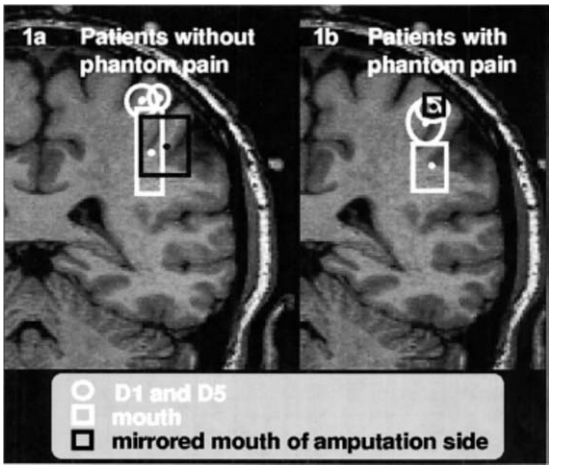

Figure 16 Flor and colleagues used neuromagnetic imaging techniques to demonstrate differences between phantom limb sensation and phantom limb pain in human subjects. Panel (1a) shows the mean and standard deviations of digit (circles) and mouth (rectangles) localization in patients without phantom limb pain. Mouth representations were symmetrical bilaterally and clearly separated from the digits. In panel (1b) the same representations are illustrated for a group of upper extremity amputees, all with phantom limb pain. Where phantom pain is present, the mouth representation on the affected side was found to have moved into the cortical hand region. From Flor, H. 2002. The modification of cortical reorganization and chronic pain by sensory feedback. Appl. Psychophysiol. Biofeedback 27, 215–227.

Figure 17 Using mirror visual feedback (MVF) in treating complex regional pain syndrome. Left panel shows a subject viewing a nonreflective surface with the painful limb hidden on the other side. Right panel shows the same subject viewing the nonpainful limb in the mirror with the painful limb hidden. McCabe and colleagues found that in early complex regional pain syndrome patients (CRPS) of $\leq$ 8 weeks, the MVF immediately stopped the pain. In patients with CRPS $\leq$ 1 year, stiffness in the limb was reduced, and in chronic patients there was no effect. From McCabe, C., Haigh, R., Ring, E., Halligan, P., Wall, P. and Blake, D. 2003. A controlled pilot study of the utility of mirror visual feedback in the treatment of complex regional pain syndrome (type 1). Rheumatology (Oxford) 42, 97–101.

representation of the pain region, and that this is often accompanied by a lower pain response threshold. The magnitude of the cortical expansion of the back region is positively correlated with the chronicity of the back pain, so that the longer the patient has experienced the pain, the greater the cortical representation of the nociceptor input. Nociceptor response thresholds also decrease with chronicity (Flor, H., 2002 for review).

Rehabilitation methods and models of phantom limb and chronic pain are now beginning to take these data into consideration. The idea that chronic pain states lead to somatosensory pain memories, which may lead to pain perception in the absence of noxious stimuli, has gained considerable attention in recent years. This means that patients who experience pain for an extended period prior to forelimb amputation are more likely to suffer the effects of phantom limb pain postoperatively, than those experiencing only acute pain prior to amputation. The implication is that there is a pain memory trace. Innovative techniques that use mirrors and visual input to trick the brain into counterlearning these memory traces, are meeting with some success (McCabe, C. *et al.*, 2003; Ramachandran, V. S., 2005). As illustrated in Figure 17, McCabe and colleagues found that when patients with early complex regional pain syndrome (CRPS) of less than 8 weeks onset visually experience movements of the phantom hand (or leg), with mirror images of the normal side, the analgesic effect is immediate. By one year of CRPS onset, the benefit is reduced to a reduction in the stiffness of the limb, and in chronic sufferers, the visual feedback had no impact on the condition. These findings indicate that visual input from the normal limb can be enough during the early months to re-establish the pain-free connections between the sensory feedback and the movement. However, the chronic state becomes less plastic in its ability to re-establish a pain-free relationship between feedback and movement execution. Consequently, in chronic patients the phantom limb pain is commonly intractable.

6.13.6 Neural Basis/Mechanisms of Somatosensory Plasticity

6.13.6.1 Pathway Divergence and Disinhibition

The somatosensory pathways are divergent and hierarchical in their organization, from their point of entry to the spinal cord, to the brainstem nuclei, the thalamus, and cortex. This divergence is undoubtedly responsible for some plasticity within the system, particularly during the acute phase of the injury. This is well demonstrated in the cortical map, immediately following a peripheral nerve cut, where receptive fields from adjacent body parts enlarge and fill in the edges of the deafferented (silent) cortex (up to 1 mm). This can occur within minutes to hours and is enabled by the normal

divergence of thalamocortical afferents (up to 2 mm in the monkey) within the cortex, and the unmasking or disinhibition of connections that normally keep receptive fields in check. Unmasking during the acute phase occurs when excitatory inputs to inhibitory neurons within the cortex are removed by the lesion. This removes local GABAergic inhibition to latent excitatory synapses within adjacent cortex, and unmasks or disinhibits the underlying preexisting circuitry. Available data indicates that disinhibition can also operate at subcortical levels. The demonstration that GABAergic pathways are modulated following peripheral lesions (or by pharmacological blockade) demonstrates the importance of this neurotransmitter in cortical and subcortical plasticity, particularly during the initial acute phase of injury (for reviews see Chen, R. *et al.*, 2002; Ding, *et al.*, 2005; Ojakangas, C. L. and Donoghue, J. P., 2006).

Longer-term changes following injury, skill learning, or disease involve additional synaptic mechanisms, including LTP or LTP-like events (Malenka, R. C. and Nicoll, R. A., 1999), in addition to some of the structural changes described ahead.

6.13.6.2 Structural Plasticity

A substantial body of evidence shows that the adult somatosensory system retains some capacity for neuronal structural plasticity in response to changes in input. Both axons and dendrites can undergo structural modification in response to injury, and determining the conditions that best support this plasticity in a way that benefits functional recovery, remains a major direction of study in the field.

6.13.6.2.1 Injury-induced structural changes: axonal sprouting

Neurons in the adult mammalian CNS generally show only a limited capacity for repair, particularly when compared with peripheral or embryonic neuronal populations. Despite this, axonal sprouting can occur in response to injury in the adult mammal, and has now been demonstrated in different species and across different levels of the neuraxis. Axon terminal growth that leads to functional recovery generally takes weeks to many months to occur. This has to do with the growth process – axon extension, the assemblage of new synapses, and an activity-driven dynamic process of pruning, strengthening, and stabilization of new connectivity along Hebbian-like principles.

It has been known for several decades that primary afferent sprouting can occur centrally when the peripheral axon of proliferating neurons is itself damaged (Liu, C. N. and Chambers, W. W., 1958; Goldberger, M. E. and Murray, M., 1974; Molander, C. *et al.*, 1988; LaMotte, C. and Kapadia, S. E., 1993; Woolf, C. J. *et al.*, 1995; Florence, S. L. and Kaas, J. H., 1995; Jain, N. *et al.*, 2000). More recently, it has become evident that central as well as uninjured neurons also retain some capacity for axonal growth in adult mammals. Most reports in the rodent are from spinal cord or barrel cortex (for reviews see Feldman, D. E. and Brecht, M., 2005; Maier, I. and Schwab, M., 2006). In the mouse barrel cortex, for example, neurons that have their principle whisker input spared following vibrissectomy, project their axons further than cells in deprived barrel columns (Kossut, M. and Juliano, S., 1999). In another recent example, Bareyre and colleagues (Bareyre, F. M. *et al.*, 2004), showed that following a partial thoracic spinal injury, transected hindlimb corticospinal tract axons sprouted into the cervical gray matter to form new connections with propriospinal neurons (PSNs). Over 3 months, sprouts that contacted long PSNs that bridged the injury, were maintained, and those contacting short PSNs, that did not bridge the injury, were lost. Such studies are important mechanistically, though the relevance of long PSNs, in the latter example, to the human in SCI compensation, remains questionable, given inherent species differences (Nakajima, K. *et al.*, 2000; Lemon, R. *et al.*, 2004).

In nonhuman primates, axonal sprouting has been shown in response to various forms of deafferentation in the spinal cord (Florence, S. L. *et al.*, 1993; 1998; Florence, S. L. and Kaas, J. H., 1995; Wu, C. W. and Kaas, J. H., 2002; Darian-Smith, I., 2004), in visual (Darian-Smith, C. and Gilbert, C. D., 1994) and somatosensory cortex (Florence, S. L. *et al.*, 1998), and in the cuneate nucleus of the brainstem (Jain, N. *et al.*, 2000; Wu, C. W. and Kaas, J. H., 2002; Darian-Smith, I., 2004).

Importantly, recent primate studies have demonstrated that central neurons left intact following an injury (but adjacent to the injury site), are capable of localized terminal sprouting in the adult primate sensorimotor pathways (Darian-Smith, C. and Gilbert, C. D., 1994; 1995; Florence, S. L. *et al.*, 1998). Jain and colleagues (Jain, N. *et al.*, 2000) showed this in monkeys with dorsal column lesions or arm amputation. Over many months, face afferents from the trigeminal nucleus were found to grow into

the adjacent cuneate nucleus. This likely accounted for the expansion of the face representation into the S1 cortical hand region, that occurred following the deafferentation. The sprouting of spared primary afferents also occurs in macaque monkeys following a cervical dorsal rhizotomy (Darian-Smith, C., 2004). Primary afferents that are spared by the injury, sprout locally within the spinal dorsal horn and cuneate nucleus (Darian-Smith, C., 2004). This process takes several months and likely leads to cuneate nucleus map reorganization (Darian-Smith, C. and Ciferri, M., 2006) and the circuitry changes that mediate recovery of dexterity in the deprived digits (Darian-Smith, C. and Ciferri, M., 2005). Evidence supports the idea that axon terminal sprouting enables local synapse formation on deprived postsynaptic neurons, which then amplifies an initially weak signal from the periphery to suprathreshold levels (using an LTP-like process). The benefit gained by such sprouting is behaviorally important (Darian-Smith, C. and Ciferri, M., 2005), but nonetheless limited. If the initial deafferentation of one or more digits is complete, the proliferation of primary afferent terminals does not compensate for the loss.

There are few other examples of injury-induced axonal growth in the somatosensory and motor pathways of the adult monkey. Corticospinal axonal sprouting following hemisection or other spinal injuries may mediate circuit reorganization and functional compensation, but the normal collateral branching of descending fibers has so far made this difficult to assess (Galea, M. P. and Darian-Smith, I., 1997a).

The reduced capacity for axon growth in the adult CNS, as opposed to the embryonic or peripheral nervous system, appears to be determined not by specific differences in the CNS neurons themselves, but according to the permissiveness of the cellular environment. This has long been recognized in primary afferent neurons, with their peripheral and central axonal branches having different capacities for regeneration, and was demonstrated more than 25 years ago in experiments (Richardson, P. *et al.*, 1980; David, S. and Aguayo, A., 1981) in which CNS axons were able to grow into peripheral nerve grafts.

Both physical (e.g., glial scarring hemorrhagic cysts) and chemical barriers, can act to inhibit growth in the CNS, and a number of proteins and neurotrophic factors have been identified that inhibit or augment axon growth (e.g., myelin-associated proteins, chondroitin sulphate proteoglycans, semaphorin-3A, Nogo-A). Amongst the better studied of the myelin-associated inhibitors is Nogo-A, which is synthesized mainly in oligodendrocytes and localized in myelin (Schwab, M. E., 2004; Maier, I. and Schwab, M., 2006 for reviews). By using one of two neutralizing antibodies now available against Nogo-A (mAb IN-1), Schwab and others have begun investigating the role of this growth inhibitor in the adult CNS. In adult control rats, transection of the corticospinal tract leads to minimal terminal growth. In contrast, in adult rodents treated with mAB IN-1 after a complete transection of the corticospinal tract, new collaterals were shown to sprout from the rubrospinal tract into the cervical spinal ventral horn, where they synapsed with forelimb motor neurons not normally receiving rubrospinal input (Raineteau, O. *et al.*, 2001; 2002). In another series of studies, adult rats treated with mAb IN-1 following a focal cortical ischemic lesion, recovered the ability to perform a forelimb reaching task (Papadopoulos, C. *et al.*, 2002; Weissner, C. *et al.*, 2003). In similarly treated rats, motor cortical neurons also showed an increased dendritic arbor complexity and spine density (Papadopoulos, C. *et al.*, 2006), suggesting significant remodeling of the cortical circuitry. Corticospinal axon terminal sprouting has recently been reported in marmoset (Fouad, K. *et al.*, 2004) and macaque monkeys (Freund, P. *et al.*, 2006) that received mAB IN-1 following a unilateral corticospinal lesion. Though potentially exciting, these results should be interpreted with a modicum of caution. For example, in the recent work of Freund and colleagues (Freund, P. *et al.*, 2006), unilateral corticospinal lesions were made in macaque monkeys at cervical level C7–C8, and manual dexterity and corticospinal axon density assessed over the first 7–8 postinjury weeks. Since there is interanimal variability in the exact location of motor neuron pools that innervate the hand, the behavioral recovery reported may be due in part to small variations in the placement of the lesion, and not to the effects of the Nogo-A specific antibody treatment. In addition, nothing is known about how or if sprouts find functionally relevant targets, and whether or not these results are clinically meaningful. Despite such hurdles, such studies hold enormous potential.

6.13.6.2.2 Injury- and experience-induced structural changes in dendrites

Dendritic spines are the postsynaptic target for most excitatory cortical synapses, and because they are easily visualized, they can be quantified as an indirect

measure of synapse density along dendrites. With the recent introduction of 2-photon imaging (in rodent models), it is also now possible to study the dynamics of dendrites in living neurons *in vivo* that express fluorescent proteins (i.e., GFP; Lendvai, B. *et al.*, 2000; Hickmott, P. and Ethell, I., 2006 for review). Most studies of dendritic structure modification have been done in rodents.

A number of studies have looked at synaptic changes in the form of dendritic spine density and dynamics with respect to experience, in the adult S1. In the barrel cortex, spine loss has been shown to be regulated by experience during adolescence (Zuo, Y. *et al.*, 2005), and in adult mice, whisker stimulation over just 24 h increases the co-innervation of layer IV spines by excitatory and inhibitory inputs by 36% (Knott, G. *et al.*, 2002). These and other studies (Kleim J. A. *et al.*, 2002; Trachtenberg, J. *et al.*, 2002; for reviews see Feldman, D. E. and Brecht, M., 2005; Fox, K. and Wong, R., 2005) indicate that activity-driven changes in synaptic circuitry occur throughout life in the cortex, and that sensory information flow is modified according to changes in experience.

An increase in dendritic arborizaton has also been reported in cortical layer V pyramidal neurons following sensorimotor cortical lesions (forelimb region) in the adult rat (Jones, T. A. and Schallert, T., 1994), and this was directly related to forelimb use. With use of both forelimbs, or just the limb ipsilateral to the lesion, neuronal arbor size was found to peak by 3 postlesion weeks, and then prune back over time. Restricted forelimb use on the side ipsilateral to the lesion, however, blocked dendritic growth.

Dendritic arbor bias can also alter following denervation. For example, layer III barrel neurons tend to project their dendrites toward the center of their home barrel, but 2–3 months after their home follicle is ablated, dendrites lose this orientation and extend in all directions (Tailby, C. *et al.*, 2005). In a similar way to barrel architecture, the dendrites of pyramidal neurons in the S1 of the rat have a direction bias away from the border of the forepaw/jaw representation (Hickmott, P. and Merzenich, M., 1999). When Hickmott and Steen (Hickmott, P. and Steen, P., 2005) cut the radial and median nerves to the forelimb, they showed a shift in dendritic bias over 2–4 weeks, that matched the resulting new functional border between the forepaw and jaw. These studies suggest that dendritic structural changes are induced by altered activity patterns in the cortex resulting from denervation, and not by degenerative changes within the cortex. Two-photon imaging studies have shown that following whisker trimming, which is known to induce functional reorganization, spine turnover is substantial (Trachtenberg, J. *et al.*, 2002). This suggests synaptic plasticity, but changes in dendritic branch complexity have yet to be demonstrated following whisker deprivation.

Little equivalent work has been completed in the primate. However, similar changes in dendritic structure have been demonstrated in S1 in the monkey following peripheral nerve cut that partially denervated the hand (Churchill, J. *et al.*, 2004). In this study, it was shown that there was increased complexity in the distal branches of dendrites in deprived cortex, compared with those in cortex unaffected by the lesion. Further investigations are needed to determine the underlying relevance of changes in dendritic structure to functional reorganization.

Increased dendritic complexity implies that the neuron is primed to receive new input. That is, it has a greater surface area available for receipt of new inputs and synapse formation. Changing connectivity patterns across a network of neurons likely facilitates changes in the role of the neuronal population in signal processing, which may then lead to the functional map changes described throughout this chapter. See Hickmott P. and Ethell I. (2006) for a review of the various cues that have been linked with the modification of neuronal structural elements (e.g., hormones, neurotrophins, neurotransmitters).

6.13.6.2.3 Atrophy, transneuronal atrophy, and degeneration

Atrophy and degeneration (e.g., Wallerian) occur in any chronic peripheral nerve or central injury that involves the death of axons entering, or coursing through the spinal cord.

In monkeys that received large-scale dorsal root injuries (C4–T2), 12–20 years earlier, transneuronal atrophy was considerable, and occurred at the level of the cuneate nucleus and the thalamus. In these monkeys, the brainstem cuneate and thalamic VPLc nuclei were reduced in overall volume by as much as 50%, though volume loss involved neuropil more than the total neuron numbers. As expected, somatotopic maps were greatly altered in these monkeys but after this length of time, no inactive or silent regions remained. These studies indicate that following a large peripheral injury, long-term transneuronal atrophy continues over many years and is a slow but dynamic process (see Jones, E. G., 2000 for review).

In the shorter term and to some extent, chronically, a number of nonneuronal cells types (e.g., macrophages, oligodendrocytes, microglia, and astrocytes) are recruited and activated. These cells perform many roles in addition to cleaning up and managing the structural integrity of the injury site. In chronic injuries, and most obviously in traumatic injuries of the spinal cord and CNS, astrocytes are known to play a major role in gliosis and scar formation. Activated astrocytes within the scar tissue secrete molecules (e.g., chondroitin sulphate proteoglycans, ephrins,), that can either permit or inhibit axon terminal growth and synapse formation (Fawcett, J. W. and Asher, R. A., 1999; Ullian, E. M. *et al.*, 2004; Miller, J. H. and Silver, J., 2006). Their secretion of inhibitory factors can present a major barrier to axon growth and recovery following traumatic spinal injury, and the effects of these cells on neuronal reorganization forms an important focus of investigation. Their role in somatosensory plasticity, however, is complex, and requires further investigation.

References

Aou, S., Woody, C., and Birt, D. 1992. Changes in the activity of units of the cat motor cortex with rapid conditioning and extinction of a compound eye blink movement. J. Neurosci. 12, 549–559.

Baranyi, A. and Feher, O. 1981. Synaptic facilitation requires paired activationof convergent pathways in the neocortex. Nature 290, 413–415.

Baranyi, A., Feher, O., and Woody, C. 1991. Properties of associative long-lasting potentiation induced by cellular conditioning in the motor cortex of conscious cats. Neuroscience 42, 321–334.

Bareyre, F. M., Kerschensteiner, M., Raineteau, O., Mettenleiter, T. C., Weinmann, O., and Schwab, M. E. 2004. The injured spinal cord spontaneously forms a new intraspinal circuit in adult rats. Nat. Neurosci. 7, 206–208.

Basbaum, A. I. and Wall, P. D. 1976. Chronic changes in the response of cells in adult cat dorsal horn following partial deafferentation: the appearance of responding cells in a previously non-responsive region. Brain Res. 116(2), 181–204.

Basso, D. M., Beattie, M. S., and Bresnahan, J. C. 1995. A sensitive and reliable locomotor rating scale for open field testing in rats. J. Neurotrauma 12, 1–21.

Basso, D. M., Beattie, M. S., and Bresnahan, J. O. 2002. Descending systems contributing to locomotor recovery after mild or moderate spinal cord injury in rats: experimental evidence and a review of literature. Restor. Neurol. and Neurosci. 20, 189–218.

Belyantseva, I. A. and Lewin, G. R. 1999. Stability and plasticity of primary afferent projections following nerve regeneration and central degeneration. Eur. J. Neurosci. 11, 457–468.

Biernaskie, J. and Corbett, D. 2001. Enriched rehabilitative training promotes improved forelimb motor function and enhanced dendritic growth after focal ischemic injury. J. Neurosci. 21, 5272–5280.

Birbaumer, N., Lutzenberger, W., Montoya, P., Larbig, W., Unert, K., Topfner, S., Grodd, W., Taub, E., and Flor, H. 1997. Effects of regional anesthesia on phantom limb pain are mirrored in changes in cortical reorganization. J. Neurosci. 17, 5503–5508.

Blake, D., Byl, N., Cheung, S., Bedenbaugh, P., Nagarajan, S., Lamb, M., and Merzenich, M. M. 2002a. Sensory representation abnormalities that parallel focal hand dystonia in a primate model. Somatosens. Mot. Res. 19, 347–357.

Blake, D., Byl, N., and Merzenich, M. M. 2002b. Representation of the hand in the cerebral cortex. Behav. Brain Res. 135, 179–184.

Blake, D., Strata, F., Chrurchland, A., and Merzenich, M. M. 2002c. Neural correlates of instrumental learning in primary auditory cortex. PNAS 99, 10114–10119.

Bradbury, E. J., McMahon, S. B., and Ramer, M. S. 2000. Keeping in touch: sensory neurone regeneration in the CNS. Trends Pharmacol. Sci. 21(10), 389–394.

Braun, C., Heinz, U., Schweizer, R., Wiech, K., Birbaumer, N., and Topka, H. 2001. Dynamic organization of the somatosensory cortex induced by motor activity. Brain 124, 2259–2267.

Braun, C., Schweizer, R., Elbert, T., Birbaumer, N., and Taub, E. 2000. Differential activation in somatosensory cortex for different discrimination tasks. J. Neurosci. 20, 446–450.

Brodmann, K. 1908. Die vergleichende Lokalisationslehre der Großhirnrinde. Barth, Leipzig, English translation: Garey, L., 1992. Localisation in the cerebral cortex. Smith-Gordon.

Brosamle, C. and Schwab, M. E. 1997. Cells of origin, course, and termination patterns of the ventral, uncrossed component of the mature rat corticospinal tract. J. Comp. Neurol. 386, 293–303.

Buckle, G. 2005. Functional magnetic resonance imaging in multiple sclerosis: the evidence for neuronal plasticity. J. Neuroimaging 15, 82S–93S.

Buonomano, D. V. and Merzenich, M. M. 1998. Cortical plasticity: From synapses to maps. 21, 149–186.

Burman, K., Darian-Smith, C., and Darian-Smith, I. 2000a. Macaque red nucleus: origins of spinal and olivary projections and terminations of cortical inputs. J. Comp. Neurol. 423, 179–196.

Burman, K., Darian-Smith, C., and Darian-Smith, I. 2000b. Geometry of rubrospinal, rubroolivary, and local circuit neurons in the macaque red nucleus. J. Comp. Neurol. 423, 197–219.

Butefisch, C., Kieizer, R., Korber, B., Muller, K., Wittsack, H- J., Homberg, V, and Seitz, R. J. 2005. Recruitment of contralesional motor cortex in stroke patients with recovery of hand function. Neurology 64, 1067–1069.

Byl, N., Merzenich, M. M., Cheung, S. , Bedenbaugh, P., Nagarajan, S., and Jenkins, W. 1997. A primate model for studying focal dystonia and repetitive strain injury: effects on the primary somatosensory cortex. Phys. Ther. 77, 269–284.

Byl, N. N., Merzenich, M. M., and Jenkins, W. M. 1996. A primate genesis model of focal dystonia and repetitive strain injury: I. Learning-induced dedifferentiation of the representation of the hand in the primary somatosensory cortex in adult monkeys. Neurology 47(2), 508–520.

Candia, V., Rosset-liobet, J., Elbert, T., and Pascual-Leone, A. 2005. Changing the brain through therapy for musicians' hand dystonia. Ann. N. Y. Acad. Sci. 1060, 335–342.

Candia, V., Wienbruch, C., Elbert, T., Rockstroh, B., and Ray, W. 2003. Effective behavioral treatment of focal hand dystonia in musicians alters somatosensory cortical organization. PNAS 100, 7942–7946.

Carey, J., Kimberley, T., Lewis, S., Auerbach, E., Dorsey, L., Rundquist, P., and Ugurbil, K. 2002. Analysis of fMRI and

finger tracking training in subjects with chronic stroke. Brain 125, 773–788.
Carison, M. 1981. Characteristics of sensory deficits following lesions of Brodmann's areas 1 and 2 in the postcentral gyrus of Macaca mulatta. Brain Res. 1981(204), 424–430.
Cenci, M., Whishaw, I., and Schallert, T. 2002. Animal models of neurological deficits: how relevant is the rat? Nat. Rev. Neurosci. 3, 574–579.
Chen, R., Cohen, L., and Hallett, M. 2002. Nervous system reorganization following injury. Neuroscience 111, 761–773.
Chen, R. and Hallett, M. 1998. Focal dystonia and repetitive motion disorders. Clinical Orthop. 351, 102–106.
Churchill, J., Arnold, L., and Garraghty, P. 2001. Somatotopic reorganization in the brainstem and thalamus following peripheral nerve injury in adult primates. Brain Res. 910, 142–152.
Churchill, J., Tharp, J., Wellman, C., Sengelaub, D., and Garraghty, P. 2004. Morphological correlates of injury-induced reorganization in primate somatosensory cortex. BMC Neurosci. 5, 43.
Cole, J. and Glees, P. 1954. Effects of small lesions in sensory cortex in trained monkeys. J. Neurophysiol. 17, 1–13.
Cooper, S. J. 2005. Donald O. Hebb's synapse and learning rule: a history and commentary. Neurosci. and Biobehav. Rev. 28, 851–874.
Courtine, G., Roy, R. R., Raven, J., Hodgson, J., McKay, H., Yang, H., Zhong, H., and Tuszynski, M. H. 2005. Performance of locomotion and foot grasping following a unilateral thoracic corticospinal tract lesion in monkeys (Macaca mulatta). Brain 128, 2338–2358.
Cramer, S., Fray, E., Tievsky, A., Parker, R., Riskind, P., Stein, M., and Wedeen, V. 2001. Changes in motor cortex activation after recovery from spinal cord inflammation. Mult. Scler. 7, 364–370.
Cramer, S., Nelles, G., Benson, R., Kaplan, J., Parker, R., Kwong, k., Kennedy, D., Finklestein, S., and Rosen, B. 1997. A functional MRI study of subjects recovered from hemiparetic stroke. Stroke 28, 2518–2527.
Darian-Smith, C. 2004. Primary afferent terminal sprouting after a cervical dorsal rootlet section in the macaque monkey. J. Comp. Neurol. 470, 134–150.
Darian-Smith, C. and Brown, S. 2000. Functional changes at periphery and cortex following dorsal root lesions in adult monkeys. Nat. Neurosci. 3, 476–481.
Darian-Smith, C. and Cifern, M. 2005. Loss and recovery of voluntary hand movements in the macaque following a cervical dorsal rhizotomy. J. Comp. Neurol. 491, 27–45.
Darian-Smith, C. and Ciferri, M. 2006. Cuneate nucleus reorganization following cervical dorsal rhizotomy in the macaque monkey: its role in the recovery of manual dexterity. J. Comp. Neurol. 498, 552–565.
Darian-Smith, C. and Gilbert, C. D. 1994. Axonal sprouting accompanies functional reorganization in adult cat striate cortex. Nature 368, 737–740.
Darian-Smith, C. and Gilbert, C. D. 1995. Topographic reorganization in the striate cortex of the adult cat and monkey is cortically mediated. J. Neurosci. 15, 1631–1647.
Darian-Smith, I. 1984. The Sense of Touch: Performance and Peripheral Neural Processes. In: *Handbook of Physiology.* Section 1. The Nervous System (*eds*. I. Darian-Smith, J. M. Brookhart, and V. B. Mountcastle), pp. 739–788. Bethesda.
Darian-Smith, I. and Darian-Smith, C. 2005. Touch, Tangible Surfaces and Their Neuronal Representation. In: Encyclopedia of Neuroscience, 3rd edn. (*eds*. G. Adelman and B. Smith). Elsevier.
Darian-Smith, I., Galea, M. P., Darian-Smith, C., Sugitani, M., Tan, A., and Burman, K. 1996. The Anatomy of Manual Dexterity. Springer.
David, S. and Aguayo, A. 1981. Axonal elongation into peripheral nervous system ''bridges'' after central nervous system injury in adult rats. Science 214, 931–933.
DeStefano, N., Matthews, P., Fu, L., Narayamanan, S., Stanley, J., and Francis, G. 1998. Axonal damage correlates with disability in patients with relapsing-remitting multple sclerosis. Results of a longitudinal magnetic resonance spectroscopy study. Brain 121, 1469–1477.
Dietz, V. 2002. Do human bipeds use quadrupedal coordination? Trends Neurosci. 25, 462–467.
Ding, Y., Kastin, A., and Pan, W. 2005. Neural plasticity after spinal cord injury. Curr. Pharm. Des. 11, 1441–1450.
Doetsch, G. S., Johnston, K., and Hannan, G. 1990. Physiological changes in the somatosensory forepaw cerebral cortex of adult raccoons following lesions of a single cortical digit representation. Exp. Neurol. 108, 162–175.
Dutton, R., Carstens, M., Antognini, J., and Carstens, E. 2006. Long ascending propriospinal projections from lumbosacral to upper cervical spinal cord in the rat. Brain Res. 1119, 76–85.
Elbert, T., Candia, V., Altenmuller, E., Rau, H., Sterr, A., Rockstroh, B., Pantev, C., and Taub, E. 1998. Alteration of digital representations in somatosensory cortex in focal hand dystonia. Neuroreport 9: 3571–3575.
Elbert, T., Flor, H., Birbaumer, N., Knecht, S., Hampson, S., Larbig, W., and Taub, E. 1994. Extensive reorganisation of the somatosensory cortex in adult humans after nervous system injury. Neuroreport 5: 2593–2597.
Elbert, T., Pantev, C., Wienbruch, C., Rockstroh, B., and Taub, E. 1995. Increased cortical representation of the fingers of the left hand in string players. Science 270(5234). 305–307.
Elbert, T. and Rockstroh, B. 2004. Reorganization of human cerebral cortex: the range of changes following use and injury. Neuroscientist 10, 129–141.
Fawcett, J. W. and Asher, R. A. 1999. The glial scar and central nervous system repair. Brain. Res. Bull. 49, 377–391.
Feldman, D. E. and Brecht, M. 2005. Map plasticity in somatosensory cortex. Science 310, 810–815.
Flor, H. 2002. The modification of cortical reorganization and chronic pain by sensory feedback. Appl. Psychophysiol. Biofeedback 27, 215–227.
Flor, H. 2003. Cortical reorganization and chronic pain: implications for rehabilitation. J. Rehabil. Med. Suppl. 41, 66–72.
Flor, H., Elbert, T., Knecht, S., Wienbruch, C., Pantev, C., Birbaumer, N., Larbig, W., and Taub, E. 1995. Phantom-Limb pain as a perceptual correlate of cortical reorganization following arm amputation. Nature 375, 482–484.
Flor, H., Muhinickel, W., Karl, A., Denke, C., Grusser, S., Kurth, R., and Taub, E. 2000. A neural substratefor nonpainful phantom limb phenomena. Neuroreport 11, 1407–1411.
Florence, S. L., Garraghty, P. E., Carlson, M., and Kass, J. H. 1993. Sprouting of peripheral nerve axons in the spinal cord of monkeys. Brain Res. 601, 343–348.
Florence, S. L., Garraghty, P. E., Wall, J. T., and Kass, J. H. 1994. Sensory afferent projections and area 3b somatotopy following median nerve cut and repair in macaque monkeys. Cereb. Cortex 4(4), 391–407.
Florence, S. L. and Kass, J. H. 1995. Large-scale reorganization at multiple levels of the somatosensory pathway follows therapeutic amputation of the hand in monkeys. J. Neurosci. 15(12), 8083–8095.
Florence, S. L., Taub, E., and Kass, J. H. 1998. Large-scale sprouting of cortical connections after peripheral injury in adult macaque monkeys. Science 282, 1117–1121.
Fouad, K., Klusman, I., and Schwab, M. E. 2004. Regenerating corticospinal fibers in the Marmoset (Callitrix jacchus) after spinal cord lesion and treatment with the anti-Nogo-A antibody IN-1. Eur. J. Neurosci. 20, 2479–2482.

Foulke, E. 1991. Braille. In: *The Psychology of Touch (eds*. M. Heller and W. Schiff), pp. 219–233. Lawrence Erlbaum Associated Publishers.

Fox, K. and Wong, R. 2005. A comparison of experience-dependent plasticity in the visual and somatosensory systems. Neuron 48, 465–477.

Freund, P., Schmidlin, E., Wannier, T., Bloch, J., Mir, A., Schwab, M. E., and Rouiller, E. M. 2006. Nogo-A-specific antibody treatment enhances sprouting and functional recovery after cervical lesion in adult primates. Nat. Med. 12, 790–792.

Frost, S., Barbay, S., Friel, K. M., Plautz, E. J., and Nudo, R. J. 2003. Reorganization of remote cortical regions after ischemic brain injury: a potential substrate for stroke recovery. J. Neurophysiol. 89, 3205–3214.

Galea, M. P. and Darian-Smith, I. 1997a. Corticospinal projection patterns following unilateral section of the cervical spinal cord in the newborn and juvenile macaque monkey. 381, 282–306.

Galea, M. P. and Darian-Smith, I. 1997b. Manual dexterity and corticospinal connectivity following unilateral section of the cervical spinal cord in the macaque monkey. J. Comp. Neurol. 381, 307–319.

Garraghty, P. E. and Kaas, J. H. 1991. Functional reorganization in adult monkey thalamus after peripheral nerve injury. Neuroreport 2, 747–750.

Garraghty, P. E. and Muja, N. 1996. NMDA receptors and plasticity in adult primate somatosensory cortex. J. Comp. Neurol. 367(2), 319–326.

Glassman, R. 1971. Recovery following sensorimotor cortical damage: evoked potentials, brain stimulation and motor control. Exp. Neurol. 33, 16–29.

Goldberger, M. E. and Murray, M. 1974. Restitution of function and collateral sprouting in the cat spinal cord: the deafferented animal. J. Comp. Neurol. 158, 37–53.

Grusser, S., Muhinickel, W., Schaefer, M., Villringer, K., Christmann, C., Koeppe, C., and Flor, H. 2004. Remote activation of referred phantom sensation and cortical reorganization in human upper extremity amputees. Exp. Brain Res. 154, 97–102.

Hebb, D. O. 1949. The Organization of Behavior: A Neuropsychological Theory. Wiley.

Hickmott, P. and Ethell, I. 2006. Dendritic plasticity in the adult neocortex. Neuroscientist 12, 16–28.

Hickmott, P. and Merzenich, M. 1999. Dendritic bias of neurons in rat somatosensory cortex associated with a functional boundary. J. Comp. Neurol. 409, 385–399.

Hickmott, P. and Steen, P. 2005. Large-scale changes in dendritic structure during reorganization of adult somatosensory cortex. Nat. Neurosci. 8, 140–142.

Hlushk, P., Solodkin, A., Noll, D. C., and Small, S. L. 2004. Corhcal plasticity during three-week motor skill learning. J. Clin. Neurophysiol. 21, 180–191.

Iriki, A., Pavlides, C., Keller, A., and Asanuma, H. 1989. Long-term potentiation in the motor cortex. Science 245, 1385–1387.

Iriki, A., Pavlides, C., Keller, A., and Asanuma, H. 1991. Long-term potentiation of thalamic input to the motor cortex induced by coactivation of thalamocortical and corticocortical afferents. J. Neurophysiol. 65, 1435–1441.

Jain, N., Catania, K. C., and Kaas, J. H. 1997. Deactivation and reactivation of somatosensory cortex after dorsal spinal cord injury. Nature 386(6624), 495–498.

Jain, N., Florence, S. L., Qi, H. X., and Kaas, J. H. 2000. Growth of new brainstem connections in adult monkeys with massive sensory loss. Proc. Natl. Acad. Sci. USA. 97(10), 5546–5550.

Jeannerod, M. 1999. The 25th Bartlett Lecture. To act or not to act: perspectives on the representation of actions. Quart. J. Exp. Psychol. A. 52, 1–29.

Jenkins, W. M. and Merzenich, M. M. 1987. Reorganization of neocortical representations after brain injury: a neurophysiological model of the bases of recovery from stroke. Prog. Brain Res. 71, 249–266.

Jenkins, W. M., Merzenich, M. M., Ochs, M. T., Allard, T., and Guic-Robles, E. 1990. Functional reorganization of primary somatosensory cortex in adult owl monkeys after behaviorally controlled tactile stimulation. J. Neurophysiol. 63, 82–104.

Johansson, B. 2000. Brain plasticity and stroke rehabilitation. Stroke 31, 223–230.

Jones, E. G. 2000. Cortical and subcortical contributions to activity-dependent plasticity in primate somatosensory cortex. Ann. Rev. Neurol. 23, 1–37.

Jones, E. G. and Pons, T. P. 1998. Thalamic and brainstem contributions to large-scale plasticity of primate somatosensory cortex. Science 282, 1121–1125.

Jones, T. A. and Schallert, T. 1994. Use dependent growth of pramidal neurons after neocortical damage. J. Neurosci. 14, 2140–2152.

Kass, J. H. 2002. Sensory loss and cortical reorganization in mature primates. Progress in Brain Res. 138, 167–176.

Kass, J. H., Nelson, R. J., Sur, M., Lin, C. S., and Merzenich, M. M. 1979. Multiple representations ofhte body within 'S-1' of primates. Science 204, 521–523.

Kalaska, J. and Pomeranz, B. 1982. Chronic peripheral nerve injuries alter the somatotopic organization of the cuneate nucleus in kittens. Brain Res. 236, 35–47.

Karl A, B. N., Lutzenberger, W., Cohen, LG, and Flor, H. 2001. Reorganization of motor and somatosensory cortex in upper extremity amputees with phantom limb pain. J. Neurosci. 21, 3609–3618.

Karni, A., Meyer, G., Jezzard, P., Adams, M., Turner, R., and Ungerleider, L. 1995. Functional MRI evidence for the adult motor cortical plasticity during motor skill learning. Nature 377, 155–158.

Karni, A., Meyer, G., Rey-Hipoloto, C., Jezzard, P., Adams, M., Turner, R., and Ungerleider, L. 1998. The acquisition of skilled motor performance: Fast and slow experience-driven changes in primary motor cortex. PNAS 95, 861–868.

Kleim JA, B. S., Cooper, NR, Hogg, TM, Reidel, CN, Remple, MS, and Nudo, RJ 2002. Motor learning-dependent synaptogenesis is localized to functionally reorganized motor cortex. Neurobiol. Learn. Mem. 77, 63–77.

Knott, G., Quairiaux, C., Genoud, C., and Welker, E. 2002. Formation of dendritic spines with GABAergic synapses induced by whisker stimulation in adult mice. Neuron 34, 265–273.

Korman, M., Raz, N., Flash, T., and Kami, A. 2003. Multiple shifts in the representation of a motor sequence during the acquisition of skilled performance. PNAS 100, 12492–12497.

Kossut, M. and Juliano, S. 1999. Anatomical correlates of representational map reorganization induced by partial vibrissectomy in the barrel cortex of adult mice. Neuroscience 92, 807–817.

LaMotte, C., Kapadia, S., and Shapiro, C. 1991. Central projections of the sciatic, saphenous, median, and ulnar nerves of the rat demonstrated by transganglionic transport of choleragenoid-HRP (B-HRP) and wheat germ agglutinin-HRP (WGA-HRP). J. Comp. Neurol. 311, 546–562.

LaMotte, C. and Kapadia, S. E. 1993. Deafferentation-induced terminal field expansion of myelinated saphenous affarents in the adult rat dorsal horn and the nucleus gracilis following pronase injection of the sciatic nerve. J Comp. Neurol. 330, 83–94.

LaMotte, R. H. and Mountcastle, V. B. 1979. Disorders in somesthesis following lesions of parietal lobe. J. Neurophysiol. 42, 400–419.

Lee, M., Reddy, H., Johansen-Berg, H., Pendlebury, S., Jenkinson, M., Smith, S., Palace, J., and Matthews, P. 2000. The motor cortex shows adaptive functional changes to

brain injury from multiple sclerosis. Ann. Neurol. 47, 606–613.
Lemon, R., Kirkwood, P., Maier, M., Nakajima, K., and Nathan, P. 2004. Direct and indirect pathways for corticospinal control of upper limb motoneurons in the primate. Prog. Brain Res. 143, 63–79.
Lendvai, B., Stern, E., Chen, B., and Svoboda, K. 2000. Experience-dependent plasticity of dendritic spines in the developing rat barrel cortex in vivo. Nature 404, 876–881.
Lenz, F. and Byl, N. 1999. Reorganization in the cutaneous core of the human thalamic principal somatic sensory nucleus (ventral caudal) in patients with dystonia. J. Neurophysiol. 82, 3204–3212.
Leonard, C. M., Glendinning, D. S., Wilfong, T., Cooper, B. Y., and Vierck, C. J., Jr 1992. Alterations of natural hand movements after interruption of fasciculus cuneatus in the macaque. Somatosens. Mot. Res. 9(1), 75–89.
Liu, C. N. and Chambers, W. W. 1958. Intraspinal sprouting of dorsal root axons; development of new collaterals and preterminals following partial denervation of the spinal cord in the cat. AMA Arch. Neurol. Psychiatry 79, 46–61.
Lotze, M., Scheler, G., Tan, H.-R., Braun, C., and Birbaumer, N. 2003. The musician's brain: functional imaging of amateurs and professionals during performance and imagery. Neuroimage 20, 1817–1829.
Maier, I. and Schwab, M. 2006. Sprouting, regeneration and circuit formation in the injured spinal cord: factors and activity. Philos. Trans. R. Soc. Lond. B Biol, Sci. 361, 1611–1634.
Malenka, R. C. and Nicoll, R. A. 1999. Long-term potentiation- A decade of progress? Science 285, 1870–1874.
Mazarakis, N., Cybulska-Klosowicz, A., Grote, H., Pang, T., Van Dellen, A., Kossut, M., Blakemore, C., and Hannan, A. 2005. Deficits in experience-dependent cortical platicity and sensory-discrimination learning in presymptomatic Huntington's disease mice. J. Neurosci. 25, 3059–3066.
McCabe, C., Haigh, R., Ring, E., Halligan, P., Wall, P., and Blake, D. 2003. A controlled pilot study of the utility of mirror visual feedback in the treatment of complex regional pain syndrome (type 1). Rheumatology (Oxford) 42, 97–101.
Merzenich, M. M., Kass, J. H., Sur, M., and Lin, C. S. 1978. Double representation of the body surface within cytoarchitectonic areas 3b and 1 in 'S-1' in teh owl monkey (Aotus trivirgatus). J. Comp. Neurol. 181, 41–74.
Merzenich, M. M., Kass, J. H., Wall, J. T., Nelson, R. J., Sur, M., and Felleman, D. 1983a. Topographic reorganization of somatosensory cortical areas 3b and 1 in adult monkeys following restricted deafferentation. Neuroscience 8, 33–55.
Merzenich, M. M., Kass, J. H., Wall, J. T., Sur, M., Nelson, R. J., and Felleman, D. 1983b. Progression of change following median nerve section in the cortical representations of the hand in areas 3b and 1 in adult owl and squirrel monkeys. Neuroscience 10, 639–665.
Merzenich, M. M., Nelson, R. J., Stryker, M. P., Cynader, M. S., Schoppmann, A., and Zook, J. M. 1984. Somatosensory cortical map changes following digital amputation in adult monkeys. J Comp. Neurol. 224, 591–605.
Millar, J., Basbaum, A. I., and Wall, P. D. 1976. Restructuring of the somatotopic map and appearance of abnormal neuronal activity in the gracile nucleus after partial deafferentation. Exp. Neurol. 50(3), 658–672.
Miller, J. H. and Silver, J. 2006. Effects of the Glial Scar and Extracellular Matrix Molecules on Axon Regeneration. In: Textbook of Neural Repair and Rehabilitation. Neural Repair and Plasticity (*eds*. M. Selzer, S. Clarke, L. Cohen, P. Duncan, and F. Gage), Vol. 1, pp. 390–404. Cambrige University Press.
Molander, C., Kinnman, E., and Aldskogius, H. 1988. Expansion of spinal cord primary sensory afferent projection following combined sciatic nerve resection and saphenous nerve crush: a horseradish peroxidase study in the adult rat. J Comp. Neurol. 276, 436–441.
Moore, C. I., Nelson, S. B., and Sur, M. 1999. Dynamics of neuronal processing in rat somatosensory cortex. Trends Neurosci. 22, 513–520.
Moore, C. I., Stern, C., Dunbar, C., Kostyk, S., Gehi, A., and Corkin, S. 2000. Referred phantom sensations and cortical reorganization after spina cord injury in humans. PNAS 97, 14703–14708.
Mott, F. W. and Sherrington, C. S. 1895. Experiments upon the influence of sensory nerves upon. movement and nutrition of the limbs. Proc. R. Soc. B 57, 481–488.
Mountcastle, V. B. 2005. The Sensory Hand. Neural Mechanisms of Somatic Sensation Harvard Unversity Press.
Murray, E. A. and Mishkin, M. 1984. Relative contributions of SII and area 5 to tactile discrimination in monkeys. Behav. Brain Res. 11, 67–83.
Myers, W. A., Churchill, J. D., Muja, N., and Garraghty, P. E. 2000. Role of NMDA receptors in adult primate cortical somatosensory plasticity. J. Comp. Neurol. 418(4), 373–382.
Nagano, A. 1998. Treatment of brachial plexus injury. J. Orthop. Sci. 3, 71–80.
Nakajima, K., Majer, M., Kirkwood, P., and Lemon, R. 2000. Striking differences in transmission of corticospinal excitation to upper limb motoneurons in two primate species. J. Neurophysiol. 84, 698–709.
Nelles, G., Spiekermann, G., Jueptner, M., Leonhardt, G., Muller, S., Gerhard, H., and Diener, H. C. 1999. Reorganization of sensory and motor systems in hemiplegic stroke patients. A positron emission tomography study. Stroke 30, 1510–1516.
Nudo, R. J., Eisner-janowicz, I., and Stowe, A. M. 2006. Plasticity After Brain Lesions. In: *Textbook of Neural Repair and Rehabilitiation. Neural repair and Plasticity (eds*. M. Selzer, S. Clarke, L. Cohen, P. Duncan, and F. Gage). Cambridge University Press 1.
Nudo, R. J. and Milliken, G. W. 1996. Reorganization of movement representations in primary motor cortex following focal ischemic infarcts in adult squirrel monkeys. J. Neurophysiol. 75(5), 2144–2149.
Nudo, R. J., Wise, B. M., SiFuentes, F., and Milliken, G. W. 1996. Neural substrates for the effects of rehabilitative training on motor recovery after ischemic infarct. Science 272, 1791–1794.
Obata, S., Obata, J., Das, A., and Gilbert, C. D. 1999. Molecular correlates of topographic reorganisation in primary visual cortex following retinal lesions. Cereb. Cortex 9, 238–248.
Ojakangas, C. L. and Donoghue, J. P. 2006. Plasticity of Cerebral Motor Functions: Implications for Repair And Rehabilitation. In: Textbook of Neural Repair and Rehabilitation. Neural Repair and Plasticity (*eds*. M. Selzer, S. Clarke, L. Cohen, P. Duncan, and F. Gage), Vol. 1, pp. 126–146. Cambridge University Press.
Pantev, C., Engelien, A., Candia, V., and Elbert, T. 2001. Representational cortex in musicians. Plastic alterations in response to musical practice. Ann. N. Y. Acad. Sci. 930, 300–314.
Papadopoulos, C., Tsai, S., Alsbiei, T., O'Brien, T., Schwab, M., and Kartje, G. 2002. Functional recovery and neuroanatomical plasticity following middle cerebral artery occlusion and IN-1 antibody treatment in the adult rat. Ann. Neurol. 51, 433–441.
Papadopoulos, C., Tsai, S., Cheatwood, J., Bollnow, M., Kolb, B., Schwab, M., and Kartje, G. 2006. Dendritic plasticity in the adult rat following middle cerebral artery occlusion and Nogo-a neutralization. Cereb. Cortex 16, 529–536.
Pascual-Leone, A. and Torres, F. 1993. Plasticity of the sensorimotor cortex representation of the reading finger in Braille readers. Brain 116, 39–52.

Pettit, M. J. and Schwark, H. D. 1993. Receptive field reorganization in dorsal column nuclei during temporary denervation. Science 262, 2054–2056.

Pons, T. P., Garraghty, P. E., and Mishkin, M. 1988. Lesion-induced plasticity in the second somatosensory cortex of adult macaques. Neurobiology 85, 5279–5281.

Pons, T. P., Garraghty, P. E., Ommaya, A. K., Kaas, J. H., Taub, E., and Mishkin, M. 1991. Massive cortical reorganization after sensory deafferentation in adult macaques. Science 252, 1857–1860.

Porter, R. and Lemon, R. N. 1993. Corticospinal Function and Voluntary Movement. Clarendon.

Raineteau, O., Fouad, K., Bareyre, F., and Schwab, M. 2001. Functional switch between motor tracts in the presence of the mAb IN-1 in the adult rat. PNAS 98, 6929–6934.

Raineteau, O., Fouad, K., Noth, P., Thallmair, M., and Schwab, M. 2002. Reorganization of descending motor tracts in the rat spinal cord. Eur. J. Neurosci. 16, 1761–1771.

Ramachandran, V. S. 2005. Plasticity and functional recovery in neurology. Clin. Med. 5, 368–373.

Ramachandran, V. S., Rogers-Ramachandran, D., and Stewart, M. 1992. Perceptual correlates of massive cortical reorganization. Science 258(5085), 1159–1160.

Randolph, M. and Semmes, J. 1974. Behavioral consequences of selective subtotal ablations in the postcentral gyrus of Macaca mulatta. Brain Res. 70, 55–70.

Recanzone, G. H., Merzenich, M. M., and Dinse, H. R. 1992a. Expansion of the cortical representation of a specific skin field in primary somatosensory cortex by intracortical microstimulation. Cereb. Cortex 2, 181–196.

Recanzone, G. H., Merzenich, M. M., and Jenkins, W. M. 1992b. Frequency discrimination training engaging a restricted skin surface results in an emergence of a cutaneous response zone in cortical area 3a. J. Neurophysiol. 67(5), 1057–1070.

Recanzone, G. H., Merzenich, M. M., Jenkins, W. M., Gregory, T. L., and Dinse, H. R. 1992c. Topographical reorganisation of the hand representation in cortical area 3b of owl monkeys trained in a frequency-discrimination task. J. Neurophysiol. 67(5), 1031–1056.

Recanzone, G. H., Merzenich, M. M., and Schreiner, C. E. 1992d. Changes in the distributed temporal response properties of S1 cortical neurons reflect imporovements in performance on a temporally based tactile discrimination task. J. Neurophysiol. 67(5), 1071–1091.

Reddy, H., Narayamanan, S., Woolrich, M., Mitsumori, T., Lapierre, Y., Arnold, D., and Matthews, P. 2002. Functional brain reorganization for hand movement in patients with multiple sclerosis: defining distinct effects of injury and disability. Brain 125, 2646–2657.

Richardson, P., McGuinness, U., and Aguayo, A. 1980. Axons from CNS neurons regenerate into PNS grafts. Nature 284, 264–265.

Rocca, M., Colombo, B., Falini, A., Ghezzi, V., Martinelli, V., Scotti, G., Comi, G., and Filippi, M. 2005. Cortical adaptation in patients with MS: a cross-sectional functional MRI study of disease phenotypes. Lancet Neurol. 4, 618–626.

Sachdev, R. N. S., Jenkinson, E., Zeigier, H. P., and Eoner, F. F. 2001. Sensorimotor Plasticity in the Rodent Vibrissa System. In: The Mutable Brain. Dynamic and Plastic Features of the Developing and Mature Brain (*ed*. J. H. Kaas). Harwood Academic Publishers.

Schwab, M. E. 2004. Nogo and axon regeneration. Curr. Opin. Neurobiol. 14, 118–124.

Schweizer, R., Braun, C., Fromm, C., Wilms, A., and Birbaumer, N. 2001. The distribution of mislocalizations across fingers demonstrates training-induced neuroplastic changes in somatosensory cortex. Exp. Brain. Res. 139, 435–442.

Scolding, N. 1999. Therapeutic strategies in multiple sclerosis . II. Long-term repair. Philos.Trans. R. Soc. Lond. B Biol. Sci. 354, 1711–1720.

Seitz, R. J., Butefisch, C., Kleizer, R., and Hornberg, V. 2004. Reorganization of cerebral circuits in human ischemic brain disease. Restor. Neurol. and Neurosci. 22, 207–229.

Seitz, R. J., Hoflich, P., Binkofski, F., Tellmann, L., Herzog, H., and Freund, H. J. 1998. Role of the premotor cortex in recovery from middle cerebral artery infarction. Arch. Neurol. 55, 1081–1088.

Snow, P. J. and Wilson, P. 1991. Plasticity in the Somatosensory System of Developing and Mature Mammals – The Effects of Injury to the Central and Peripheral Nervous System. In: Progress in Sensory Physiology (*ed*. D. Ottoson), vol. 11, pp. 1–482. Springer.

Sterr, A., Green, L., and Elbert, T. 2003. Blind Braille readers mislocate tactile stimuli. Biol. Psychol. 63, 117–127.

Sterr, A., Muller, M., Elbert, T., Rockstroh, B., Pantev, C., and Taub, E. 1998a. Changed perceptions in Braille readers. Nature 391, 134–135.

Sterr, A., Muller, M., Elbert, T., Rockstroh, B., Pantev, C., and Taub, E. 1998b. Perceptual correlates of changes in cortical representation of fingers in blind multifinger braille readers. J. Neurosci. 18, 4417–4423.

Sunderland, S. 1991. Nerve Injuries and Their Repair: A Critical Appraisal. Churchill Livingstone.

Tailby, C., Wright, L., Metha, A., and Calford, M. 2005. Activity-dependent maintenance and growth of dendrites in adult cortex. PNAS 102, 4631–4636.

Trachtenberg, J., Chen, B., Knott, G., Feng, G., Sanes, J., Welker, E., and Svoboda, K. 2002. Long-term in vivo imaging of experience-dependent synaptic plasticity in adult cortex. Nature 420, 788–794.

Ullian, E. M., Christopherson, K. S., and Barres, B. A. 2004. Role for glia in synaptogenesis. Glia 47, 209–216.

Vierck, C. 1982. Comparison of the effects of dorsal rhizotomy or dorsal column transection on motor performance of monkeys. Exp. Neurol. 75, 566–575.

Vierck, C. J. and Cooper, B. Y. 1998. Cutaneous texture discrimination following transection of the dorsal spinal column in monkeys. Somatosens. Mot. Res. 15, 309–315.

Wall, J. T., Xu, J., and Wang, X. 2002. Human brain plasticity: an emerging view of the multiple substrates and mechanisms that cause cortical changes and related sensory dysfunctions after injuries of sensory inputs from the body. Brain Res. Rev. 39, 181–215.

Wang, X. and Wall, J. T. 2005. Cortical influences on sizes and rapid plasticity of tactile receptive fields in the dorsal column nuclei. J. Comp. Neurol. 489, 241–248.

Webster, K. E. and Kemplay, S. K. 1987. Distribution of primary afferent fibres from the forelimb of the rat to the upper cervical spinal cord in relation to the location of spinothalamic neuron populations. Neurosci. Lett. 76, 18–24.

Weinberger, N. M. 1995. Dynamic regulation of receptive fields and maps in the adult sensory cortex. Ann. Rev. Neurosci. 19, 129–158.

Weng, H. R., Lenz, F. A., Vierck, C., and Dougnerty, P. 2003. Physiological changes in primate somatosensory thalamus induced by deafferentation are dependent on the spinal funiculi that are sectioned and time following injury. Neuroscience 116, 1149–1160.

Wiessner, C., Bareyre, F., Allegrini, P., Mir, A., Frentzel, S., Zurini, M., Schnell, L., Oertle, T., and Schwab, M. 2003. Anti-Nogo-A antibody infusion 24 hours after experimental stroke improved behavioral outcome and corticospinal plasticity in normotensive and spontaneously hypertensive rats. J. Cereb. Blood Flow Metab. 23, 154–165.

Willis, W. D. and Coggeshall, R. E. 2004. Sensory Mechanisms of the Spinal Cord. Primary Afferent Neurons and the Spinal Dorsal Horn. Volume 1. Kluwer Academic/ Plenum.

Woods, T. M., Cusick, C. G., Pons, T. P., Taub, E., and Jones, E. G. 2000. Progressive transneuronal changes in the brainstem and thalamus after long-term dorsal rhizotomies in adult macaque monkeys. J. Neurosci. 20, 3884–3899.

Woolf, C. J., Shortland, P., *et al.* 1995. Reorganization of central terminals of myelinated primary afferents in the rat dorsal horn following peripheral axotomy. J. Comp. Neurol. 360, 121–134.

Wree, A. D., Itzev, E., *et al.* 2005. Neurons in the dorsal column nuclei of the rat emit a moderate projection to the ipsilateral ventrobasal thalamus. Anat. Embryol. 210, 155–162.

Wu, C. W. and Kaas, J. H. 2002. The effects of long-standing limb loss on anatomical reorganization of the somatosensory afferents in the brainstem and spinal cord. Somatosens. Mot. Res. 19, 153–163.

Xerri, C., Merzenich, M. M., *et al.* 1998. Plasticity of primary somatosensory cortex paralleling sensorimotor skill recovery from stroke in adult monkeys. J. Neurophysiol. 79(4), 2119–2148.

Xu, J. and Wall, J. T. 1999. Evidence for brain stem and supra-brain stem contributions to rapid corhcal plasticity in adult monkeys. J. Neurosci. 19, 7578–7590.

Yang, T. T., Gallen, C. C., *et al.* 1994. Noninvasive detection of cerebral plasticity in adult human somatosensory cortex. Neuroreport 5(6), 701–704.

Zuo, Y., Yang, G., *et al.* 2005. Long-term sensory deprivation prevents dendritic spine loss in primary somatosensory cortex. Nature 436, 261–265.

Further Reading

Banati, R. B., Cagnin, A., Brooks, D. J., Gunn, R. N., Myers, R., Jones, T., Birch, R., and Anand, P. 2001. Long-term trans-synaptic glial responses in the human thalamus after peripheral nerve injury. Neuroreport 12(16), 3439–3442.

Bjarkam, C. R., Pedersen, M., and Sorensen, J. O. 2001. New strategies for embedding, orientation and sectioning of small brain specimens enable direct correlation to MR-images, brain atlases, or use of unbiased stereology. J. Neurosci. Methods 108(2), 153–159.

Das, A. and Gilbert, C. D. 1995. Long-range horizontal connections and their role in cortical reorganization revealed by optical recording of cat primary visual cortex. Nature 375(6534), 780–784.

Luo, L., Ryan, A. F., and Saint Marie, R. L. 1999. Cochlear ablation alters acoustically induced c-fos mRNA expression in the adult rat auditory brainstem. J. Comp. Neurol. 404, 271–283.

Williamson, A. M., Ohara, P. T., Ralston, D. D., Milroy, A. M., and Ralston, H. J.r. 1994. Analysis of gamma-aminobutyric acidergic synaptic contacts in the thalamic reticular nucleus of the monkey. J. Comp. Neurol. 349(2), 182–192.

6.14 Intrinsic Signal Imaging of Somatosensory Function in Nonhuman Primates

A W Roe, L M Chen, and R Friedman, Vanderbilt University, Nashville, TN, USA

© 2008 Elsevier Inc. All rights reserved.

6.14.1	**Intrinsic Signal Imaging of Somatosensory Cortex Organization**	299
6.14.2	**Topographic Representation in Primary Somatosensory Cortex**	301
6.14.2.1	Topography in Somatosensory Cortex	301
6.14.2.2	Optical Imaging of Cortical Topography in Anesthetized Monkeys	301
6.14.2.3	Optical Imaging of Cortical Topography in Alert Monkeys	301
6.14.3	**Topographic Representation of Tactile Perception in the Somatosensory Cortex**	303
6.14.3.1	The Funneling Illusion	303
6.14.3.2	Two-Point Stimulation Produces Cortical Merging in Area 3b	304
6.14.3.3	Intensity of Funneling Percept	304
6.14.4	**Modality Representation in the Somatosensory Cortex**	306
6.14.4.1	Presence of Interdigitated Multiple Maps	306
6.14.4.2	Relationship of Vibrotactile Domains to Topography	309
6.14.5	**A New Model of Somatosensory Cortex Organization**	309
References		310

6.14.1 Intrinsic Signal Imaging of Somatosensory Cortex Organization

This chapter reviews some exciting new studies on primate somatosensory cortex (SI) using intrinsic signal optical imaging methods. Previous electrophysiological approaches have provided a great deal of information regarding neural processes in the SI. However, there is a limited understanding of the functional organization of such representation in SI. Optical imaging is a method well suited for revealing such functional organizations. In the visual cortex, understanding functional organization has offered significant insight into the segregation and integration of different visual perceptual channels and has inspired a large number of studies. The hope is that greater understanding of functional organizations in SI will similarly illuminate the role of SI in tactile perceptual behaviors.

This chapter will be restricted to the imaging of intrinsic optical signals *in vivo* (i.e., without the use of dyes; *cf.* Bonhoeffer, T. and Grinvald, A. 1996, for review). The intrinsic signal arises from various sources including changes in blood volume due to local capillary recruitment, activity-dependent changes in the oxygen saturation level of hemoglobin (increase or decrease in deoxyhemoglobin), and light-scattering changes that accompany cortical activation. In this method, stimulus-induced changes in neural activity produce local decreases in blood oxygenation detected as local decreases in tissue reflectance. These minute changes in optical absorption (typically in the 0.1% range), which are recorded by a charge-coupled device (CCD) camera, can be highly spatially localized because local capillary-related blood flow is highly localized. Thus, functional organizations in sensory cortices can be mapped at high resolution, permitting the visualization of 100-μm-sized structures. The magnitude and timecourse of reflectance change is dependent on the illumination wavelength used (Vanzetta, I. *et al.*, 2005). In the visual cortex, the typical intrinsic signal timecourse (under 600–630 nm illuminant, wavelengths at which the oxymetry component is relatively large) peaks within 2–4 s followed by a several-second undershoot (Bonhoeffer, T. and Grinvald, A., 1996; Vnek, N. *et al.*, 1999). The optical signal in primate SI is similar in timecourse and magnitude (Chen, L. M. *et al.*, 2001; 2003; 2005; for different wavelengths, see Tommerdahl, M. *et al.*, 1998; 1999). Although intrinsic imaging lacks the temporal resolution offered by dyes, it is a high-spatial-resolution imaging method that does not require application of any external agents to the brain. The intrinsic signal has been associated with so-called initial dip in blood-oxygen-level-dependent functional magnetic resonance imaging (BOLD fMRI)

studies (e.g., Kim, D. S. *et al.*, 2000; Cannestra, A. F. *et al.*, 2001; Devor, A. *et al.*, 2003; Sheth, S. *et al.*, 2003; Thompson, J. K. *et al.*, 2003; Fukuda, M. *et al.*, 2006; Roe, A. W. *et al.*, 2006) and has been shown to be correlated with both spiking and subthreshold components of neural response. For a recent review and Zepeda A. *et al.* (2004).

New World monkeys are an attractive species for optical imaging studies because their lissencephalic cortex allows unobstructed viewing of multiple visual cortical areas in both dorsal and ventral streams (see Figure 1(a), *cf.* for visual cortex Malach, R. *et al.*, 1994; Lyon, D. C. *et al.*, 2002; Xu, X. *et al.*, 2004; Roe, A. W. *et al.*, 2005). Thus, it is possible, for example, to image areas 3a, 3b, 1, and 2 simultaneously by optical methods. The functional organization of SI in New World monkeys largely parallels those in Old World monkeys (*cf.* Sur, M. *et al.*, 1982) and has been studied extensively in physiological, anatomical, and behavioral studies, making them prime candidates for studies of functional organization of sensation and sensory behavior. For this reason, the studies summarized in this chapter are mostly derived from studies on New World monkeys.

To underscore the importance of this developing approach, one of the challenges of optical imaging is to understand the modular basis of cognition. How do networks of modules within and across cortical areas achieve vision or memory or emotion? Visualization of such modular activations during behavior is tantamount to watching the brain at work. Over the past decade, researchers have developed methods to visualize activations through implanted windows on the brain (e.g., Chen, L. M. *et al.*, 2002). By applying these methods to the awake, behaving animal, it is hoped that this method can open new vistas in our understanding of the neural basis of cognitive function. Furthermore, the ability of these studies to forge a critical link between a large body of work on animal models and functional imaging in humans will be invaluable. There are now a handful of optical

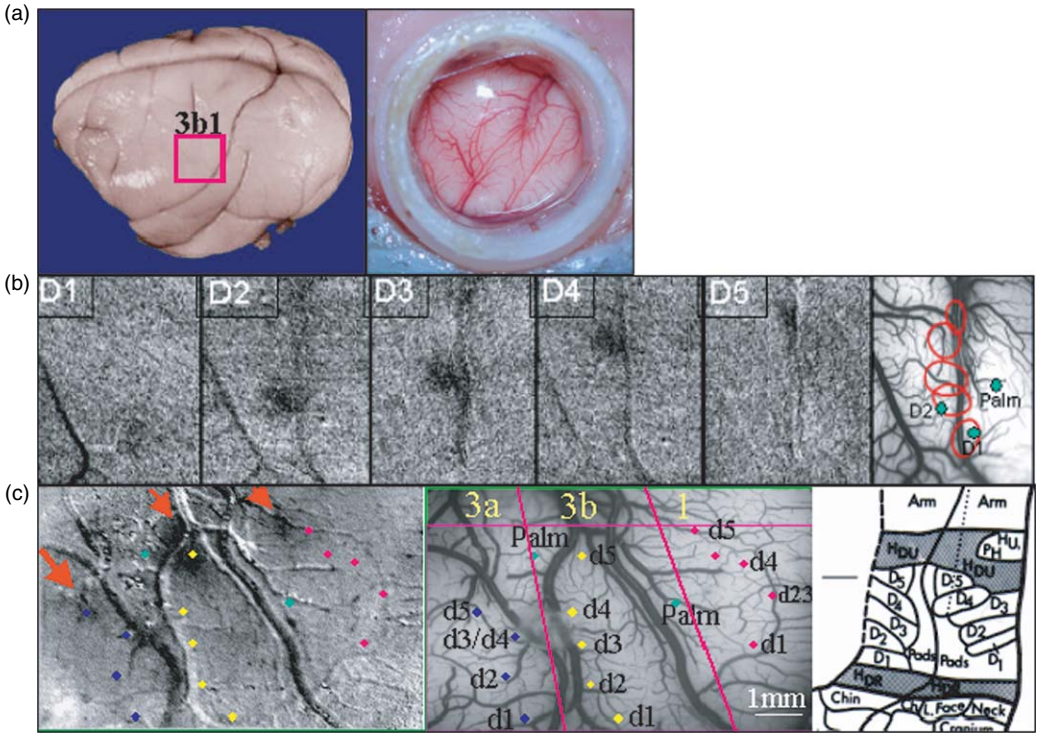

Figure 1 Optical imaging of digit topography in somatosensory cortex (SI) of anesthetized squirrel monkey. (a) Locations of areas 3b and 1 in squirrel monkey brain. Optical window over this area (Sur, M. *et al.*, 1982). (b) Five images obtained in response to indentation of digits D1–D5, respectively. Dark pixels indicate cortical activation. D1–D5 activation locations overlaid on blood vessel map (from Chen, L. M. *et al.*, 2001). (c) Imaging of areas 3a, 3b, and 1 in squirrel monkey in response to indentation of digit D5. D5 activation zones (orange arrows) correlate well with electrophysiological map (dots). Topography and size of focal activations (0.5–1 mm) area consistent with published maps (Sur, M. *et al.*, 1982).

imaging studies on visual behaviors in the awake monkey (Grinvald, A. *et al.*, 1991; Vnek, N. *et al.*, 1999; Shtoyerman, E. *et al.*, 2000; Seidemann, E. *et al.*, 2002; Slovin, H. *et al.*, 2002; Siegel, R. M. *et al.*, 2003; Roe, A. W. *et al.*, 2004). However, such studies in alert tactile behaviors are still few (Chen, L. M. *et al.*, 2005).

6.14.2 Topographic Representation in Primary Somatosensory Cortex

6.14.2.1 Topography in Somatosensory Cortex

Orderly topographic sensory maps in primary SI serve as an anchor for our understanding of somatosensory cortical organization (Woolsey, C. N. *et al.*, 1942; Nelson, R. J. *et al.*, 1980; Sur, M. *et al.* 1982; Pons, T. P. *et al.*, 1985; 1987). Primate primary SI in the postcentral gyrus contains four complete topographic maps of the body surface that fall within the architectonically defined Brodmann's areas 3a, 3b, 1, and 2 (e.g., Woolsey, C. N. *et al.*, 1942; Powell, T. P. and Mountcastle, V. B., 1959; Kaas, J. H. *et al.*, 1979; Nelson, R. J. *et al.*, 1980; Sur, M. *et al.* 1982; Pons, T. P. *et al.*, 1985; 1987). Areas 3b and 1 receive input primarily from cutaneous afferents where areas 3a and 2 receive input from deep afferents (muscle spindles and joints) (e.g., Tanji, J. and Wise, S. P., 1981). Other parietal areas, such as areas 5 and 7, also process somatosensory information (Murray, E. A. and Mishkin, M., 1984; Dong, W. K. *et al.*, 1994; Burton, H. *et al.*, 1997; Duhamel, J. R. *et al.*, 1998; Debowy, D. J. *et al.*, 2001). Somatotopic maps are also found laterally in SII and adjacent area PV (Burton, H. *et al.*, 1995; Krubitzer, L. *et al.*, 1995), and there are other somatosensory areas in insular cortex that receive cutaneous and visceral information (Robinson, C. J. and Burton, H., 1980; Schneider, R. J. *et al.* 1993; Craig, A. D., 2003).

6.14.2.2 Optical Imaging of Cortical Topography in Anesthetized Monkeys

A number of studies have employed the optical imaging approach to examine topographic representation in SI. Such studies have revealed organizations quite consistent with previous electrophysiological studies of SI topography (e.g., in rats: Masino, S. A. and Frostig, R. D., 1996; Sheth, B. R., *et al.*, 1998; Goldreich, D. *et al.*, 1998; in non-human primates and humans: Narayan, S. M. *et al.* 1994; Cannestra, A. F. *et al.*, 1998; Schwartz, T. H. *et al.*, 2004). In the nonhuman primate, studies of somatotopy have produced images of the body map in the squirrel monkey (radial interdigital pad, D2 fingertip, and similar sites on the leg and foot) (Tommerdahl, M. *et al.*, 1999), distal fingerpads of the squirrel monkey (Chen, L. M. *et al.*, 2001), and area 1 of the macaque monkey (Shoham, D. and Grinvald, A., 2001).

As shown in Figure 1(b), focal activations roughly 0.5–1 mm in size are obtained following stimulation of individual digit tips with indenting probes. Comparison of D1 (thumb) to D5 digit tip activations reveals an orderly map within area 3b of the squirrel monkey. These maps are quite consistent with published maps obtained with electrophysiological methods (e.g., Sur, M. *et al.* 1982; Merzenich, M. M. *et al.*, 1987). Imaging a larger field of view reveals multiple representations, which include areas 3a, 3b, and 1 (Figure 1(c)). For example, stimulation of a single digit tip (D5) elicits three activations in areas 3a, 3b, and 1, respectively (Figure 1(c), orange arrows); the locations of these activations are consistent with electrophysiological recordings in this case (colored dots). Thus, intrinsic signal imaging is a useful tool for quickly and clearly revealing tactile topography in primates.

6.14.2.3 Optical Imaging of Cortical Topography in Alert Monkeys

Our view of somatosensory topography is largely based on data collected in the anesthetized animal. However, little is known about these topographies in the awake primate (McKenna, T. M. *et al.*, 1982; Iwamura, Y. *et al.*, 1993; Blankenburg, F. *et al.*, 2003). The question remains as to whether the fundamental structure of topographic maps is the same in the anesthetized and the awake, behaving animal. For example, does topography remain stable over time in the awake animal or is it dependent on behavioral context? Neither is much known regarding the relative activations of different cortical areas (within primary SI of the primate are cortical areas 3a, 3b, 1, and 2). Since different cortical areas are characterized by distinct stimulus preferences (Mountcastle, V. B. and Powell, T. P. S., 1959; Hyvarinen, J. and Poranen, A., 1978; Costanzo, R. M. and Gardner, E. P., 1980; Carlson, M., 1981; Sur, M. *et al.*, 1985; Iwamura, Y. *et al.*, 1993), it is possible that different cortical areas become dominant under changing stimulus and behavioral contexts. A number of studies have investigated behavioral modulation of neuronal response within single cortical areas (Iwamura, Y.

et al., 1983; Nelson, R. J., 1987; Nelson, R. J. *et al.*, 1991; Burton, H. and Sinclair, R. J., 2000; Meftah, el-M. *et al.*, 2002; Fitzgerald, P. J. *et al.*, 2006); however, little is known about the modulation of interareal dominance or of patterned area-specific functional organizations during behavior (Hsiao, S. S. *et al.*, 1993; Buchel, C. and Friston, K. J. 1997; Friston, K. J., 1998; Kastner, S. *et al.*, 1998; Mesulam, M. M., 1998; Ungerleider, L. G. *et al.*, 1998). Indeed, what is the behavioral relevance of known functional organizations and topographies? Such studies would provide important constraints for studies on feedforward versus feedback influences in cortical processing (*cf.* Roe, A. W., 2003).

One recent optical imaging study in SI revealed that activation patterns can differ significantly between anesthetized and awake preparations. Using intrinsic signal optical imaging of areas 3b and 1, awake squirrel monkeys were imaged repeatedly for over a period of 2 years in awake and anesthetized states in response to vibrotactile and electrocutaneous stimuli presented to individual fingerpads (Figure 2). Imaged somatotopic maps were in general stable over this period in both the anesthetized and the awake states, consistent with electrophysiologically recorded maps in areas 3b and 1 in the anesthetized state.

However, in the awake animal, signal sizes were larger and more variable, leading to larger activations (both in area and in amplitude), suggesting a less precise topography. Topographically, the map in the awake state appears less precise and also different from that in the anesthetized state. As shown in Figure 3, in the awake state the activations to D3 and D4 stimulation are highly overlapped. The significance of this finding remains to be explored. Larger activations and larger receptive field sizes are traditionally associated with less refined topography and perhaps decreased discriminability. However, the possibility remains that larger imaged activations reflect a substrate for greater cortical dynamics. Indeed, these findings are consistent with some previous studies in the awake animal that have shown large receptive fields and dynamic changes in receptive fields (such as increases in receptive field size, shifting hot spots, or changes in spatial sensitivity profiles within receptive fields) or other modulation of cortical activity within the behavioral context (Chapin, J. K. and Lin, C. S., 1984; Nelson, R. J., 1987; Lee, C. J. and Whitsel, B. L., 1992; Nicolelis, M. A. *et al.*, 1993; Schroeder, C. E. *et al.*, 1995). Thus, topographic organizations present in the anesthetized animal may be used in different ways in the awake animal.

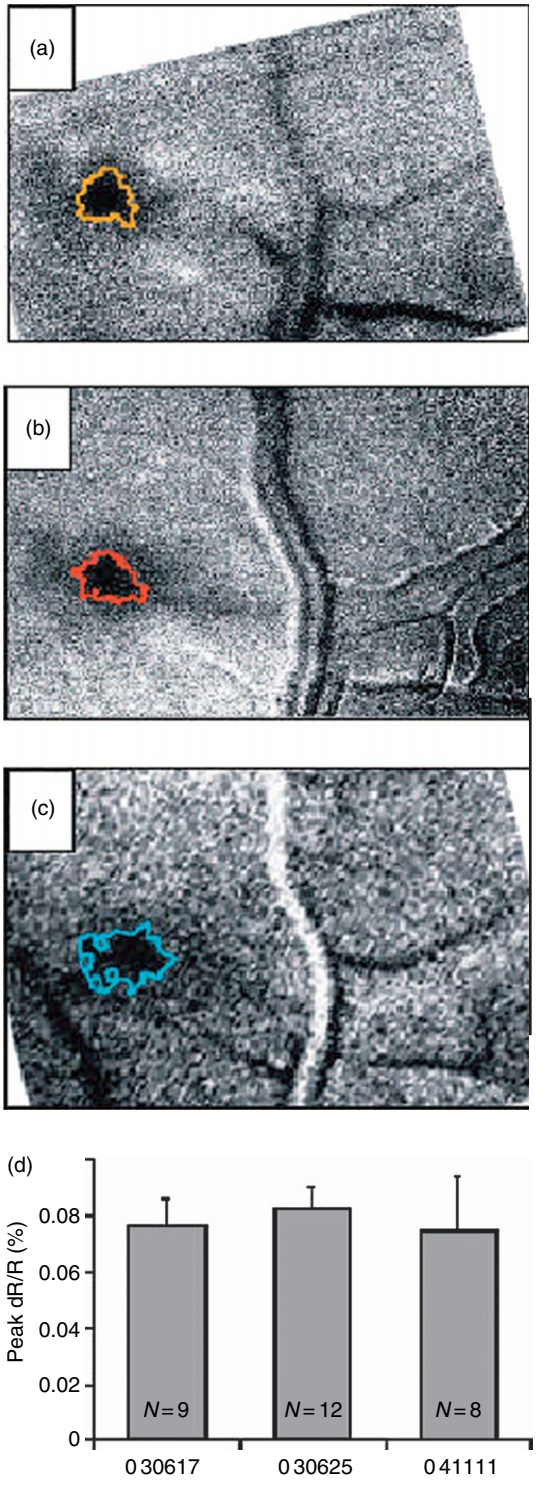

Figure 2 Cortical topography is stable over time in awake squirrel monkey somatosensory cortex (SI) (from Chen, L. M., Friedman, R. M., and Roe, A. W. 2005. Optical imaging of SI topography in anesthetized and awake squirrel monkey. J. Neurosci. 25, 7648–7659). Images taken over three different imaging sessions.

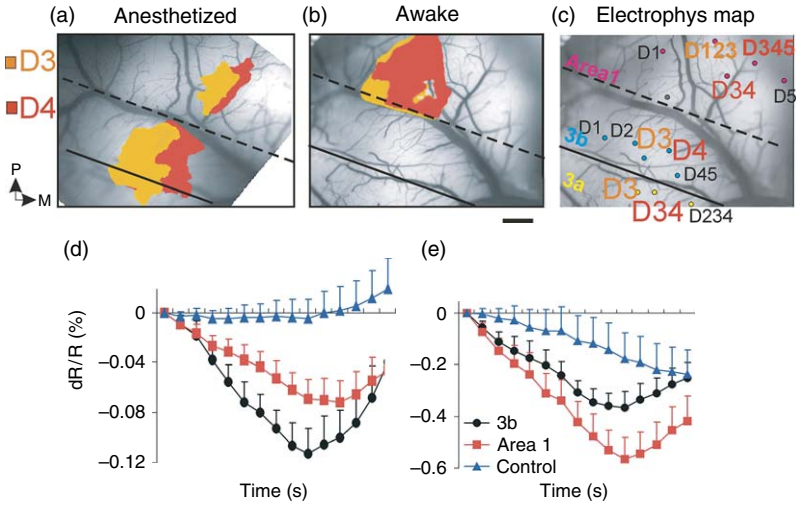

Figure 3 Comparison of topographic activations in the anesthetized and awake states. Cortical response to vibrotactile stimulation of D3 (orange) and D4 (red) in the squirrel monkey. (a) Anesthetized activation is more prominent in area 3b (see (d)). (b) Awake activation is more prominent in area 1 (see (e)). (c) Electrophysiological mapping of areas 3a, 3b, and 1. (d) and (e) Optical signal time course for D4 locations in anesthetized (d) and D3 locations in awake (e) in areas 3b and 1.

Another difference between anesthetized and awake activation patterns lies in the strength of activations across cortical areas. Whereas in the anesthetized animal strongest imaging signals are obtained from area 3b, in the awake animal area 1 activation dominates over that in area 3b, suggesting that interareal interactions in the alert animal differ substantially from that in the anesthetized animal. In the anesthetized state, we generally observe stronger activations in area 3b than in area 1 (Figure 3(d)). The opposite is observed in the awake state, where area 1 activations are more prominent (Figure 3(e)). These results suggest significant awake versus anesthetized differences in somatosensory activations, due to differences in neural response and/or vacular response.

6.14.3 Topographic Representation of Tactile Perception in the Somatosensory Cortex

The long-standing view that sensory topography in SI reflects a body map is well supported. However, a recent study has called into question traditional views of somatosensory cortical maps (Chen, L. M. *et al.*, 2003). This study used the so-called funneling illusion to demonstrate that topographic maps in SI can reflect the perceived location of tactile stimulation rather than the location of physical stimulation on the skin. This finding suggested that, in contrast to previous views, the topographic map in area 3b is a perceptual map rather than a physical one.

6.14.3.1 The Funneling Illusion

The funneling illusion is the illusory perception of skin stimulation at a single site central to a line of multiple stimulation sites (Sherrick, C. E., 1964; von Bekesy, G., 1967; Gardner, E. P. and Spencer, W. A., 1972; Gardner, E. P. and Tast, J. M., 1981; Hashimoto, I. *et al.*, 1999). Inputs at lateral sites are funneled centrally so that perceived intensity at the central site is greater than that to stimulation at the middle site alone. With two-point stimulation, a funneled sensation is produced at a central location that is without direct stimulation. This illusion has been reported on the forearm, palm, and fingers. When two digit tips are simultaneously stimulated, subjects report sensations such as a mound or trapezoid centered over a finger, a mound or trapezoid bridging fingers, or a mound bridging fingers with two lateral humps (Chen, L. M. *et al.*, 2003 supplemental material). Thus, the funneling illusion is characterized by a perception of spatial mislocalization and increased tactile intensity. The neural basis for this illusion is thought to involve a complex integration of inhibitory interactions. Previous studies have shown that the funneling illusion is encoded in primary SI, and not peripherally at the skin (Gardner, E. P. and

Spencer, W. A., 1972). Responses of SI neurons to three-point skin stimulation have demonstrated that a broad distribution of cortical neurons are recruited (Gardner, E. P. and Spencer, W. A., 1972; Gardner, E. P. and Costanzo, R. M., 1980).

6.14.3.2 Two-Point Stimulation Produces Cortical Merging in Area 3b

The central representation of this phenomenon was not expected to be in primary SI. Since the illusion involves integration across multiple digits, it was unlikely to occur in area 3b where receptive fields are confined to single-digit tips. However, a recent study has demonstrated that this integration does indeed occur in early somatosensory areas. Figure 4 illustrates that stimulation of D2 alone (a,b), D3 alone (c,d) or D4 alone (e,f) elicits single focal millimeter-sized activations. However, stimulation of adjacent digits D4 + D3 (g,h) produces a single activation site whose center lies between the D3 and D4 sites (l). This merged activation is not observed for nonadjacent digits D4 + D2 together (i,j) (n). Thus, stimulation of each location alone activates spatially distinct locations in the cortex, but together produces a single centrally located peak of activation.

6.14.3.3 Intensity of Funneling Percept

The second notable characteristic of multipoint stimulation (two or more points) is the increased intensity of the funneled sensation in comparison to stimulation of a single point. Gardner E. P. and Costanzo R. M. (1980) demonstrated that responses of cortical neurons to multipoint stimulation were often similar in magnitude to single-point stimulation and were always less than the sum of component single-point responses. From this, they suggested that the increased intensity is not due to greater neuronal firing rates, but rather due to recruitment of a broader distribution of neurons. Such broader distribution can be reflected in either greater area of activation or greater amplitude of imaged signal.

Chen L. M. *et al.* (2003) found that both the area and the amplitude of activation produced by paired digit stimulation (both adjacent and nonadjacent) is smaller than the sum of the single-digit activation areas. This reduction was observed in all digit pairs examined (both adjacent and nonadjacent). Thus, two-finger stimulation leads to a reduction in activation area (for both adjacent and nonadjacent digit pairs).

Electrophysiological recording of single units also show similar reductions in activation. As shown in Figure 5, two units (one rapidly adapting (RA) and one slowly adapting (SA)) were recorded with receptive fields on the D4 fingerpad. Stimulation of D4 alone (left column) revealed an early transient component and a weak late component (indicated by arrows) in both of the RA and SA cells' responses. Stimulation of either adjacent D3 or nonadjacent D2 alone produced no initial transient and relatively weak late response. Simultaneous stimulation of two adjacent fingerpads (right column, D4 + D3) reduced the amplitude of the initial transient. This reduction of the initial transient was not observed with simultaneous stimulation of nonadjacent fingerpads (right, D4 + D2). Thus, adjacent digit stimulation leads to weakening of digit activation as evidenced by decreased area and amplitude of optical signal, late component suppression in optical signal (not shown, Chen, L. M. *et al.*, 2003), and decline in size of single-unit response.

We suggest that the decreased cortical activation observed during two-digit stimulation may be due to inhibitory interdigit interactions. Lateral inhibition is a well-described phenomenon in the somatosensory pathways. Somatosensory afferents produce both inhibition and excitation in central neurons, including the dorsal horn, dorsal column nuclei, the ventrobasal complex, and SI. These inhibitory processes are thought to be mediated by local feedforward or feedback circuits within the target nuclei. The spatial profiles of inhibition are often larger than that of excitation, producing a center-surround receptive field organization (e.g., Janig, W. *et al.*, 1979); this sharpening has also been referred to as coning. Stimulus-induced inhibition has longer latencies than excitation and may last for 100 ms or more (e.g., Laskin, S. E. and Spencer, W. A., 1979). These lateral inhibitory processes may serve to limit the spatial extent of discharge zones and enhance stimulus contrast, thereby improving spatial and form discrimination.

In sum, simultaneous digit stimulation produces a reduced activation at the sites of digit representation. This reduction is coupled with an increased response amplitude in the merged zone (where no actual stimulation occurs); this increased response at the merged zone is comparable in magnitude to that of single-digit activations. In other words, even though no physical stimulus occurs at the merged site, the response is similar in size to that of an actual single-digit stimulus. We speculate that a change in the balance of interaction between neurons at the merged

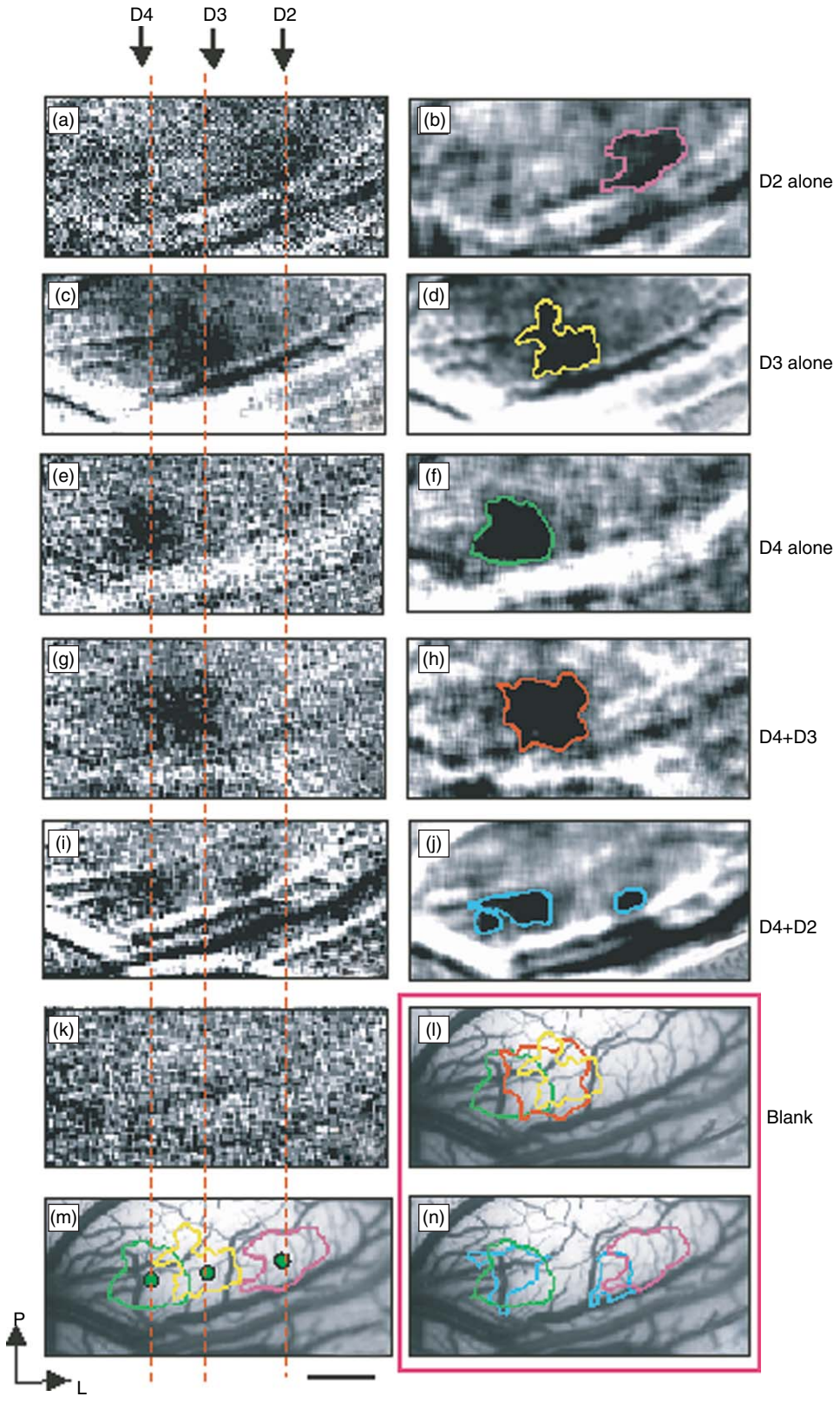

Figure 4 Cortical activations by one- and two-digit stimulation in area 3b. Raw images of D2, D3, D4, D3 + D4, D2 + D4 stimulation (a,c,e,g,i); low-passed images with threshold outlines (b,d,f,h,j). Digit activation centers are indicated by red dashed lines. (k), blank condition. (l–n) overlay of outlines of adjacent digit (l), single digit (m), and nonadjacent digit (n) activations. (m) penetrations show lateral to medial topographic locations of D2, D3, and D4 (green dots). Scale bar: 1 mm.

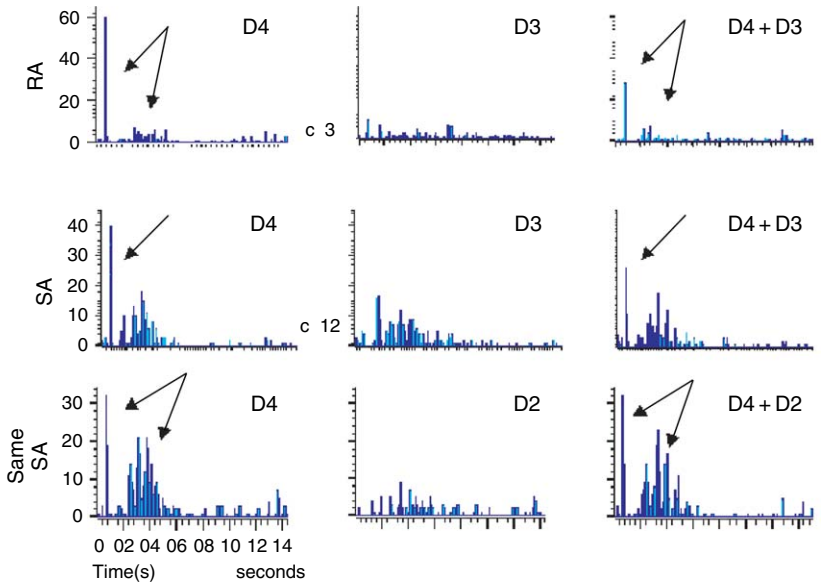

Figure 5 Two units recorded on D4 fingerpad. Top row: Rapidly adapting (RA) cell response to D4, D3, and D4 + D3 stimulation. Middle row: Slowly adapting (SA) cell response to D4, D3, and D4 + D3 stimulation. Bottom row: Same SA cell response to D4, D2, and D4 + D2 stimulation. Twenty trials, bin width 100 ms. Arrows specify early and late components of response.

site (increased amplitude) and those at nearby sites (decreased amplitudes) serves to heighten the perceived intensity and sharpen the focus (decreased area) during the funneling illusion (Figure 6). The fact that activation of nearby cortical sites leads to single merged activations suggests that spatial percepts are strongly dictated by central representations. Indeed, physical perception can occur where no physical stimulus occurred. This study further suggests that, under certain contextual situations, receptive fields of neurons in area 3b can span more than a single digit. The extent of these contextual influences are likely to be determined by mechanisms dependent on intracortical distance, center and surround interactions, and cortical feedback.

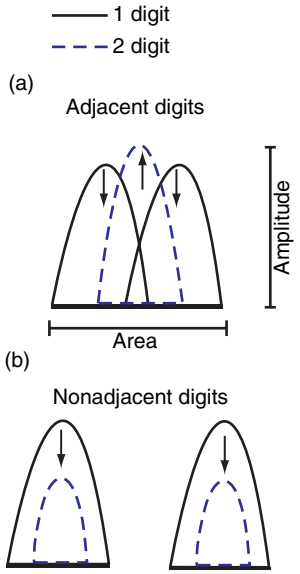

Figure 6 Summary of cortical merging. (a) Adjacent digit stimulation results in merging to a single central site, and increased signal amplitude at the merged location concomitant with decreased amplitudes nearby. (b) Nonadjacent digit stimulation results in decreased signal area and amplitude at each of the stimulation sites.

6.14.4 Modality Representation in the Somatosensory Cortex

6.14.4.1 Presence of Interdigitated Multiple Maps

Both anatomical and physiological evidence suggests labeled lines of modality-specific cutaneous information (Verrillo, R. T., 1966; Talbot, W. H. *et al.*, 1968; Verrillo, R. T. and Bolanowski, S. J., 1986). Psychophysically, vibrotactile stimuli produce three distinct sensations on the skin (Johansson, R. S. *et al.*, 1982):

1. A pressure sensation is induced by stimuli below 2 Hz.
2. A flutter sensation is evoked by stimulation in the 2- to 40-Hz range.
3. A vibration sensation is evoked by higher frequencies (40–200 Hz).

These pressure, flutter, and vibratory sensations are mediated by SA, RA, and pacinian (PC) receptors, respectively (Mountcastle, V. B. *et al*., 1972; LaMotte, R. H. and Mountcastle, V. B., 1975; Cohen, R. H. and Vierck, C. J., 1993). These modalities remain largely separate in their central projections. For example, direct electrical stimulation of single identified low-threshold mechanoreceptive afferents (SA, RA, or PC) evokes only one type of perception (pressure, flutter, or vibration, respectively) (Torebjork, H. E. and Ochoa, J. L., 1980; Vallbo, A. B., 1981). Psychophy-sical studies fail to find vibrotactile masking and adaptation between stimulus frequencies that produce pressure (0.5 Hz), flutter (20 Hz), and vibratory sensations (200 Hz) (Gescheider, G. A. *et al*., 1979; 1985; Bolanowski, S. J. *et al*., 1988). In addition, frequency-specific electrical stimulation of a cortical RA-dominated site in area 3b mimics the effect of stimulating RA receptors of the skin (Romo, R. *et al*., 1998). Remarkably, even the transfer of tactile learning from one digit to another is modality-specific (Harris, J. A. *et al*., 2001). These studies suggest a marked degree of separation in the experiences of pressure, flutter, and vibration, mediated by separate populations of receptors that remain separate in their central projections, and perhaps even to higher cortical areas involved in tactile learning and memory (also Romo, R. *et al*., 2000). Thus, both psychophysical and neurophysiological studies suggest some degree of modality-specific functional segregation in SI.

Anatomical and physiological evidence also suggest parallel modality-specific pathways, from periphery through the dorsal column nuclei, to the thalamus, and into early somatosensory cortical areas. Dykes R. W. *et al*. (1981) have described the segregation of RA, SA, and PC responses in the VPL and VPI. Jones E. G. and coworkers (1982) have suggested that rods of topography and modality-specific cells project to similar modality-specific bands in area 3b, and perhaps also area 1. Connections between areas 3b and 1 are topographically homotopic, with feedforward projections being more robust than feedback (e.g., Jones, E. G. and Powell, T. P. S., 1969; Jones, E. G. *et al*., 1978; Cusick, C. G. *et al*., 1985; Burton, H. and Fabri, M., 1995). Using 2-deoxyglucose labeling methods combined with anatomical tracer injections, Juliano S. L. *et al*. (1990) suggest that excitatory information is transmitted from area 3b to area 1 in a way that connects clusters of cells with similar response properties.

However, there is limited evidence as to whether different tactile features form multiple functional domains within each of areas 3a, 3b, 1, and 2. Electrophysiological mapping studies describe zones of neurons with SA, RA, and PC mechanoreceptor responses within area 3b (Paul, R. L. *et al*. 1972; Sur, M. *et al*., 1981; Sretavan, D. and Dykes, R. W., 1983; Sur, M. *et al*., 1984). Based on densely spaced electrode penetrations, Sur M. *et al*. (1981; 1984) found a segregation of SA and RA cells in the middle layers of area 3b and suggested that these are organized in irregular anteroposterior bands. This ground-breaking work was the first to suggest the presence of multiple maps in single cortical areas in SI.

Recently, studies using optical imaging methods have revealed networks of vibrotactile domains in SI. Vibrotactile stimulation of the digit fingerpads at frequencies that produce the sensations of pressure (1 Hz), flutter (30 Hz), and vibration (200 Hz) was used in the anesthetized squirrel monkey. These stimuli produced characteristic SA-dominated, RA-dominated, or PC-dominated responses, respectively. Intrinsic signal optical maps were obtained in response to each of these stimuli. A vector summation method was used to determine a pixel-by-pixel weighted response to the pressure, flutter, and vibration stimuli (similar to that used for visual cortical orientation maps, methodology details are described in Friedman R. M. *et al*. (2004)). Clusters of pixels with saturated color indicate that one vector magnitude dominates the other two. Three examples of such pixel-wise SA/RA/PC vector summation are illustrated in Figure 7(a–c). Pixel locations with a dominant SA response appear bright red, those with a dominant RA response appear bright green, and those with a dominant PC response appear bright blue. Patches of cortex that are coded white indicate areas with strong response to each of the pressure, flutter, and vibratory stimuli. These vibrotactile domains are typically 200–300 μm in size in both area 3b and area 1 (Figure 8).

Imaging using near-infrared signals has also shown a fine topography consistent with previous electrophysiological methods. Further research using 25-Hz flutter and 200-Hz vibratory stimuli on the palm found that flutter stimulation led to focal topographic activation in area 3b, whereas vibration only led to delayed reduced activation or an inhibition in areas 3a and 3b that was supported by a reduced activation to paired stimulation (Tommerdahl, M. *et al*., 1999). The apparent contradiction between a

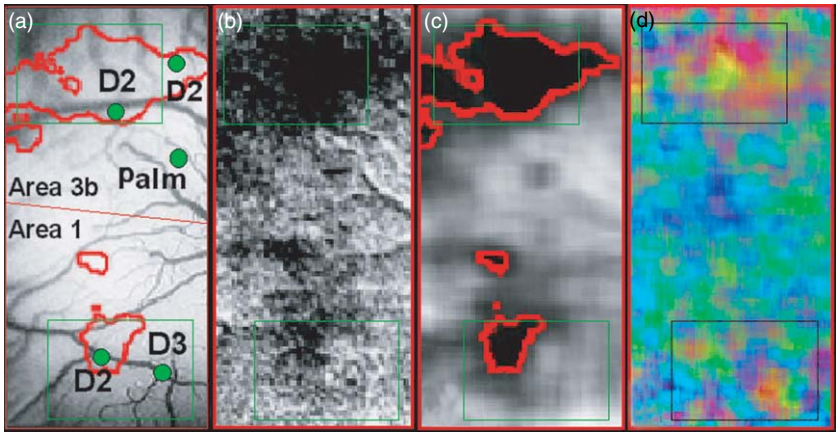

Figure 7 Relationship of topography and vibrotactile response. D2 activation in areas 3b and 1. (a) Vessel map. D2 activations in area 3b (above) and area 1 (below). (b–c) Raw and filtered image of D2 indentation. Red outline delineates strongest activation zones. (d) Modality vector map (red, green, blue: response for somatosensory cortex (SA), rapidly adapting (RA), and pacinian (PC), respectively) shows strongest activation in centers.

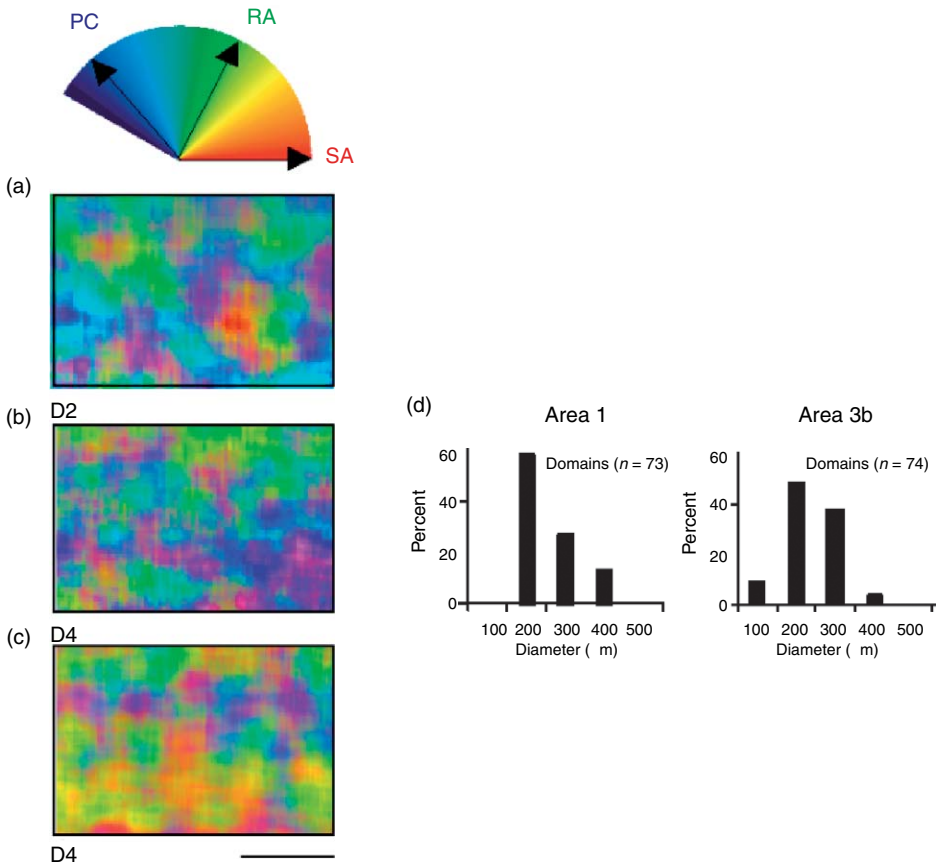

Figure 8 Modality maps in somatosensory cortex (SI). Top: Vibrotactile frequency-specific responses are plotted in different directions of color space (red: slowly adapting (SA), 1 Hz; green: rapidly adapting (RA), 30 Hz; blue: pacinian (PC), 200 Hz). (a–c) Three cases: vector maps obtained through pixel-by-pixel vector summation. Domains dominated by single colors indicate regions preferentially responsive to a single vibrotactile frequency. Scale bar: 1 mm. (d) Size distribution of vibrotactile domains in area 1 (left) and area 3b (right).

lack of activation to 200-Hz vibration in studies by Tommerdahl M. *et al.* (2005) and the focal activation observed by Chen L. M. *et al.* (2001) and Friedman R. M. *et al.* (2004) in areas 3b and 1 has been reconciled by the finding that the responses to vibration are site-dependent (i.e., digits vs. palm). Further research has shown that the extent and magnitude of cortical response to flutter stimuli is duration-dependent (Simons, S. B. *et al.*, 2007; see also Simons, S. B. *et al.*, 2005; Chiu, J. S. *et al.*, 2005), with longer (2–5 s) stimulation leading to suppression in surrounding regions. This finding parallels the improved ability to spatially localize following presentation of longer-adapting stimulation (Tannan, V. *et al.*, 2006). Surprising evidence demonstrates that ipsilateral input can modify responses in SI, suggesting significant interhemispheric interactions (Tommerdahl, M. *et al.*, 2006). In sum, the research of Tommerdahl and associates in anterior parietal cortex has revealed complex spatial and temporal responses to relatively simple tactile stimuli that might reflect the sensations in humans to the same kinds of stimuli (Tommerdahl, M. *et al.*, 2005; Tannan, V. *et al.*, 2005; 2006).

6.14.4.2 Relationship of Vibrotactile Domains to Topography

It is evident that the modality-specific response extends beyond the classically defined topographic map as revealed by simple indentation stimuli. As shown in Figure 7(b), an indentation stimulus (which activates all three receptors types) to digit D2 produces a fairly focal activation in both area 3b and area 1 (outline in red in Figure 7(c)). In response to pressure, flutter, and vibration stimulation, the vector summation map reveals that the strongest responses (most saturated red, green, and blue regions) correspond with the topographic digit locations. However, clustered responses, though weaker, are also evident away from the location of D2 representation (outside the boxes). This additional nontopographic activation is reminiscent of the finding in visual cortex in which complete orientation maps are obtained even though only a single eye is stimulated (Blasdel, G. G., 1992). Thus, modality maps and topographic maps exhibit some degree of independence. Whether this extended nontopographic region of activation is due to spiking and/or subthreshold activity remains to be determined.

6.14.5 A New Model of Somatosensory Cortex Organization

The finding that somatosensory cortical domains are roughly 200–300 μm in size strengthens the view that modularity is a common organizational feature of cortical representation. Cortical domains of similar size have been described in multiple cortical areas (in V1 and V2 (see Roe, A. W., 2003 for review), and V4 (Felleman, D. J. *et al.*, 1997), IT (Tsunoda, K. *et al.*, 2001), area 7 (Siegel, R. M. *et al.*, 2003), and in prefrontal areas (Kritzer, L. and Goldman-Rakic, P. S., 1995)). These findings suggest a revision of previous views of SI organization that were based primarily on electrophysiological recordings. Previously, each cortical hypercolumn was thought to contain segregated SA and RA columns innervated predominantly by thalamocortical fibers of a single vibrotactile modality (Sur, M. *et al.*, 1980). Optical imaging evidence now suggests a modification of this view (Figure 9). As shown by reconstruction of single thalamocortical arbors (Garraghty, P. E. *et al.*, 1989), inputs to SI have multiple arbors (200–300 μm in size) that span several millimeters of the cortex (see also Jones, E. G. *et al.*, 1982). These and other cortico-cortical arbors are likely to give rise to clustered activations that have been observed in 2-deoxyglucose studies (Juliano, S. L. *et al.*, 1981; Juliano, S. L. and Whitsel, B. L., 1987; Juliano, S. L. *et al.*, 1990; *cf.* Burton, H. and Fabri, M.,

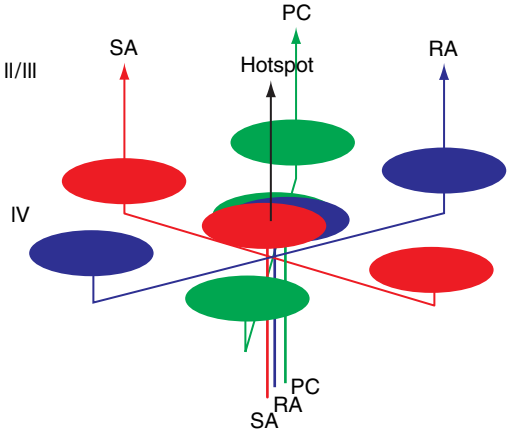

Figure 9 Proposed model of vibrotactile representation in somatosensory cortex (SI). Single slowly adapting (SA) (red), rapidly adapting (RA) (blue), or pacinian (PC) (green) fibers terminate in layer IV, each with several arbors (colored disks). These arbors project in turn to superficial layers II/III (vertical arrows). Thus, some cortical columns are dominated by a single SA, RA, or PC input, while others have mixed input (central overlapping disks).

1995). Such arbors could give rise to either an array of discrete clusters or, by varying arbor overlap, continuous modality maps. Thus, regions dominated by single SA, RA, or PC inputs would give rise to SA (red), RA (blue), or PC (green) domains. Regions of some overlap would appear as magenta or yellow-green colors (not depicted). And regions of high SA, RA, and PC overlap could underlie the so-called hotspots commonly described in SI receptive fields (in optical images these locations would appear as black, gray, or white domains); these would be well activated by broadband stimuli such as skin indentation. Other arbors extend to nontopographic locations away from the hotspot and establish locally some degree of modality-specific dominance (*cf.* Figure 9). Thus, not unlike the way horizontal iso-orientation, networks in V1 give rise to resulting orientation map structure; the observed maps result from overlapping horizontal networks of patchy, modality-specific dominance. In sum, in the revised view, each digit representation is served by collections of interdigitating SA, RA, and PC columns. The effect of topographic stimulation is therefore no longer so discrete and can, under certain stimulation conditions, have nontopographic consequences.

Acknowledgment

This work was supported by the NINDS, Packard Foundation.

References

von Bekesy, G. 1967. *Sensory Inhibition*. Princeton University Press.

Blankenburg, F., Ruben, J., Meyer, R., Schwiemann, J., and Villringer, A. 2003. Evidence for a rostral-to-caudal somatotopic organization in human primary somatosensory cortex with mirror-reversal in areas 3b and 1. Cereb. Cortex 13(9), 987–993.

Blasdel, G. G. 1992. Differential imaging of ocular dominance and orientation selectivity in monkey striate cortex. J. Neurosci. 12, 3115–3138.

Bolanowski, S. J. Jr., Gescheider, G. A., Verrillo, R. T., and Checkosky, C. M. 1988. Four channels mediate the mechanical aspects of touch. J. Acoust. Soc. Am. 84, 1680–1694.

Bonhoeffer, T. and Grinvald, A. 1996. Optical imaging based on intrinsic signals. The methodology. In: Brain Mapping. The Methods (*eds*. A. W. Toga and J. C. Mazziota), pp. 55–97. Academic Press.

Burton, H. and Fabri, M. 1995. Ipsilateral intracortical connections of physiologically defined cutaneous representations in areas 3b and 1 of macaque monkeys: projections in the vicinity of the central sulcus. J. Comp. Neurol. 355, 508–538.

Burton, H. and Sinclair, R. J. 2000. Tactile-spatial and cross-modal attention effects in the primary somatosensory cortical areas 3b and 1-2 of rhesus monkeys. Somatosens. Mot. Res. 17, 213–228.

Burton, H., Fabri, M., and Alloway, K. 1995. Cortical areas within the lateral sulcus connected to cutaneous representations in areas 3b and 1: a revised interpretation of the second somatosensory area in macaque monkeys. J. Comp. Neurol. 355(4), 539–562.

Burton, H., Sinclair, R. J., Hong, S. Y., Pruett, J. R. Jr., and Whang, K. C. 1997. Tactile-spatial and cross-modal attention effects in the second somatosensory and 7b cortical areas of rhesus monkeys. Somatosens. Mot. Res. 14(4), 237–267.

Cannestra, A. F., Pouratian, N., Bookheimer, S. Y., Martin, N. A., Beckerand, D. P., and Toga, A. W. 2001. Temporal spatial differences observed by functional MRI and human intraoperative optical imaging. Cereb. Cortex 11(8), 773–782.

Cannestra, A. F., Pouratian, N., Shomer, M. H., and Toga, A. W. 1998. Refractory periods observed by intrinsic signal and fluorescent dye imaging. J. Neurophysiol. 80(3), 1522–1532.

Carlson, M. 1981. Characteristics of sensory deficits following lesions of Brodmann's areas 1 and 2 in the postcentral gyrus of *Macaca mulatta*. Brain Res. 204(2), 424–430.

Chapin, J. K. and Lin, C. S. 1984. Mapping the body representation in the SI cortex of anesthetized and awake rats. J. Comp. Neurol. 229(2), 199–213.

Chen, L. M., Friedman, R. M., and Roe, A. W. 2003. Optical imaging of a tactile illusion in Area 3b of primary somatosensory cortex. Science 302, 881–885.

Chen, L. M., Friedman, R. M., and Roe, A. W. 2005. Optical imaging of SI topography in anesthetized and awake squirrel monkey. J. Neurosci. 25, 7648–7659.

Chen, L. M., Friedman, R. M., Ramsden, B. M., LaMotte, R. H., and Roe, A. W. 2001. Fine-scale organization of primary somatosensory cortex (Area 3b) in the squirrel monkey revealed with intrinsic optical imaging. J. Neurophysiol. 86, 3011–3029.

Chen, L. M., Heider, B., Healy, F. L., Ramsden, B. R., Williams, G. V., and Roe, A. W. 2002. A chamber and artificial dura method for long-term optical imaging in primates. J. Neurosci. Meth. 113, 41–49.

Chiu, J. S., Tommerdahl, M., Whitsel, B. L., and Favorov, O. V. 2005. Stimulus-dependent spatial patterns of response in SI cortex. BMC. Neurosci. 6, 47p.

Cohen, R. H. and Vierck, C. J. 1993. Population estimates for responses of cutaneous mechanoreceptors to a vertically indenting probe on the glabrous skin of monkeys. Exp. Brain Res. 94, 105–119.

Costanzo, R. M. and Gardner, E. P. 1980. A quantitative analysis of responses of direction sensitive neurons in somatosensory cortex of awake monkeys. J. Neurophysiol. 43, 139–1341.

Craig, A. D. 2003. Pain mechanisms: labeled lines versus convergence in central processing. Annu. Rev. Neurosci. 26, 1–30.

Cusick, C. G., Steindler, D. A., and Kaas, J. H. 1985. Corticocortical and collateral thalmocortical connections of postcentral somatosensory cortical areas in squirrel monkeys: a double-labeling study with radiolabeled wheatgerm agglutinin and wheatgerm agglutinin conjugated to horseradish peroxidase. Somatosens. Res. 3, 1–31.

Debowy, D. J., Ghosh, S., Ro, J. Y., and Gardner, E. P. 2001. Comparison of neuronal firing rates in somatosensory and posterior parietal cortex during prehension. Exp. Brain Res. 137(3–4), 269–291.

Devor, A., Dunn, A. K., Andermann, M. L., Ulbert, I., Boas, D. A., and Dale, A. M. 2003. Coupling of total hemoglobin concentration, oxygenation, and neural activity in rat somatosensory cortex. Neuron 39(2), 353–359.

Dong, W. K., Chudler, E. H., Sugiyama, K., Roberts, V. J., and Hayashi, T. 1994. Somatosensory, multisensory, and task-related neurons in cortical area 7b (PF) of unanesthetized monkeys. J. Neurophysiol. 72(2), 542–564.

Duhamel, J. R., Colby, C. L., and Goldberg, M. E. 1998. Ventral intraparietal area of the macaque: congruent visual and somatic response properties. J. Neurophysiol. 79(1), 126–136.

Dykes, R. W., Sur, M., Merzenich, M. M, Kaas, J. H., and Nelson, R. J. 1981. Regional segregation of neurons responding to quickly adapting, slowly adapting, deep and pacinian receptors within thalamic ventroposterior lateral and ventroposterior inferior nuclei in the squirrel monkey (*Saimiri sciureus*). Neuroscience 6, 1687–1692.

Friston, K. J. 1998. Imaging neuroscience: principles or maps? Proc. Natl. Acad. Sci. U. S. A. 95(3), 796–802.

Felleman, D. J., Xiao, Y., and McClendon, E. 1997. Modular organization of occipito-temporal pathways: cortical connections between visual area 4 and visual area 2 and posterior inferotemporal ventral area in macaque monkeys. J. Neurosci. 17(9), 3185–3200.

Fitzgerald, P. J., Lane, J. W., Thakur, P. H., and Hsiao, S. S. 2006. Receptive field properties of the macaque second somatosensory cortex: representation of orientation on different finger pads. J. Neurosci. 26(24), 6473–6484.

Friedman, R. M., Chen, L. M., and Roe, A. W. 2004. Modality maps within primate somatosensory cortex. Proc. Natl. Acad. Sci. U. S. A. 101, 12724–12729.

Fukuda, M., Wang, P., Moon, C. H., Tanifuji, M., and Kim, S. G. 2006. Spatial specificity of the enhanced dip inherently induced by prolonged oxygen consumption in cat visual cortex: implication for columnar resolution functional MRI. Neuroimage 30(1), 70–87. Epub. 27 Oct 2005.

Gardner, E. P. and Costanzo, R. M. 1980. Spatial integration of multiple-point stimuli in primary somatosensory cortical receptive fields of alert monkeys. J. Neurophysiol. 43, 420–443.

Gardner, E. P. and Spencer, W. A. 1972. Sensory funneling. I. Psychophysical observations of human subjects and responses of cutaneous mechanoreceptive afferents in the cat to patterned skin stimuli. J. Neurophysiol. 35, 925–953.

Gardner, E. P. and Tast, J. M. 1981. Psychophysical measurements of perceived intensity of single-point and multiple-point cutaneous stimuli in humans and subhuman primates. J. Neurophysiol. 46(3), 479–495.

Garraghty, P. E., Pons, T. P., Sur, M., and Kaas, J. H. 1989. The arbors of axons terminating in middle cortical layers of somatosensory area 3b in owl monkeys. Somatosens Mot. Res. 6(4), 401–411.

Gescheider, G. A., Frisina, R. D., and Verrillo, R. T. 1979. Selective adaptation of vibrotactile thresholds. Sens. Process. 3, 37–48.

Gescheider, G. A., Sklar, B. F., Van Doren, C. L., and Verrillo, R. T. 1985. Vibrotactile forward masking: psychophysical evidence for a triplex theory of cutaneous mechanoreception. J. Acoust. Soc. Am. 78(2), 534–543.

Goldreich, D., Peterson, B. E., and Merzenich, M. M. 1998. Optical imaging and electrophysiology of rat barrel cortex. II. Responses to paired-vibrissa deflections. Cereb. Cortex 8, 184–192.

Grinvald, A., Frostig, R. D., Siegel, R. M., and Bartfeld, E. 1991. High-resolution optical imaging of functional brain architecture in the awake monkey. Proc. Natl. Acad. Sci. U. S. A. 88, 11559–11563.

Harris, J. A., Harris, I. M., and Diamond, M. E. 2001. The topography of tactile learning in humans. J. Neurosci. 21, 1056–1061.

Hashimoto, I., Yoshikawa, K., and Kimura, T. 1999. Sensory funneling of liminal multiple-point air-puff stimulation produces dramatic reduction in reaction time but relatively invariant P300 somatosensory evoked potential. Neuroreport 10(15), 3201–3205.

Hsiao, S. S., O'Shaughnessy, D. M., and Johnson, K. O. 1993. Effects of selective attention on spatial form processing in monkey primary and secondary somatosensory cortex. J. Neurophysiol. 70(1), 444–447.

Hyvarinen, J. and Poranen, A. 1978. Movement-sensitive and direction and orientation-selective cutaneous receptive fields in the hand area of the post-central gyrus in monkeys. J. Physiol. (Lond.) 283, 523–537.

Iwamura, Y., Tanaka, M., Sakamoto, M., and Hikosaka, O. 1983. Converging patterns of finger representation and complex response properties of neurons in Area 1 of the first somatosensory cortex of the conscious monkey. Exp. Brain Res. 51, 327–337.

Iwamura, Y., Tanaka, M., Sakamoto, M., and Hikosaka, O. 1993. Rostrocaudal gradients in the neuronal receptive field complexity in the finger region of the alert monkey's postcentral gyrus. Exp. Brain. Res. 92(3), 360–368.

Janig, W., Spencer, W. A., and Younkin, S. G. 1979. Spatial and temporal features of afferent inhibition of thalamocortical relay cells. J. Neurophysiol. 42, 1450–1460.

Johansson, R. S., Landstrom, U., and Lundstrom, R. 1982. Responses of mechanoreceptive afferent units in the glabrous skin of the human hand to sinusoidal skin displacements. Brain Res. 244, 17–25.

Jones, E. G. and Powell, T. P. S. 1969. Connexions of the somatic sensory cortex of the rhesus monkey. I. Ipsilateral connections. Brain 92, 477–502.

Jones, E. G., Coulter, J. D., and Hendry, S. H. C. 1978. Intracortical connectivity of architectonic fields in the somatic sensory, motor and parietal cortex of monkeys. J. Comp. Neurol. 181, 291–347.

Jones, E. G., Friedman, D. P., and Hendry, S. H. C. 1982. Thalamic basis of place- and modality-specific columns in monkey somatosensory cortex: a correlative anatomical and physiological study. J. Neurophysiol. 48, 545–568.

Juliano, S. L., Hand, P. F., and Whitsel, B. L. 1981. Patterns of increased metabolic activity in somatosensory cortex of monkeys *Macaca fascicularis*, subjected to controlled cutaneous stimulation: a 2-deoxyglucose study. J. Neurophysiol. 46, 1260–1284.

Juliano, S. L. and Whitsel, B. L. 1987. A combined 2-deoxyglucose and neurophysiological study of primate somatosensory cortex. J. Comp. Neurol. 263, 514–525.

Juliano, S. L., Friedman, D. P., and Eslin, D. E. 1990. Corticocortical connections predict patches of stimulus-evoked metabolic activity in monkey somatosensory cortex. J. Comp. Neurol. 298, 23–39.

Kaas, J. H., Nelson, R. J., Sur, M., Lin, C. S., and Merzenich, M. M. 1979. Multiple representations of the body within the primary somatosensory cortex of primates. Science 204, 521–523.

Kastner, S., De Weerd, P., Desimone, R., and Ungerleider, L. G. 1998. Mechanisms of directed attention in the human extrastriate cortex as revealed by functional MRI. Science 282(5386), 108–111.

Kim, D. S., Duong, T. Q., and Kim, S. G. 2000. High-resolution mapping of iso-orientation columns by fMRI. Nat. Neurosci. 3(2), 164–169.

Kritzer, M. F. and Goldman-Rakic, P. S. 1995. Intrinsic circuit organization of the major layers and sublayers of the

dorsolateral prefrontal cortex in the rhesus monkey. J. Comp. Neurol. 359(1), 131–143.
Krubitzer, L., Clarey, J., Tweedale, R., Elston, G., and Calford, M. 1995. A redefinition of somatosensory areas in the lateral sulcus of macaque monkeys. J. Neurosci. 15, 3821–3839.
LaMotte, R. H. and Mountcastle, V. B. 1975. Capacities of humans and monkeys to discriminate vibratory stimuli of different frequency and amplitude: a correlation between neural events and psychological measurements. J. Neurophysiol. 38, 539–559.
Laskin, S. E. and Spencer, W. A. 1979. Cutaneous masking. I. Psychophysical observations on interactions of multipoint stimuli in man. J. Neurophysiol. 42, 1048–1060.
Lee, C. J. and Whitsel, B. L. 1992. Mechanisms underlying somatosensory cortical dynamics: I. In vivo studies. Cereb. Cortex 2(2), 81–106.
Lyon, D. C., Xu, X., Casagrande, V. A., Stefansic, J. D., Shima, D., and Kaas, J. H. 2002. Optical imaging reveals retinotopic organization of dorsal V3 in New World owl monkeys. Proc. Natl. Acad. Sci. U. S. A. 99, 15735–15742.
Malach, R., Tootell, R. B. H., and Malonek, D. 1994. Relationship between orientation domains, cytochrome oxidase stripes, and intrinsic horizontal connections in squirrel monkey area V2. Cereb. Cortex 4, 151–165.
Masino, S. A. and Frostig, R. D. 1996. Quantitative long-term imaging of the functional representation of a whicker in rat barrel cortex. Proc. Natl. Acad. Sci. U. S. A. 93, 4942–4947.
McKenna, T. M., Whitsel, B. L., and Dreyer, D. A. 1982. Anterior parietal cortical topographic organization in macaque monkey: a reevaluation. J. Neurophysiol. 48(2), 289–317.
Meftah, el-M., Shenasa, J., and Chapman, C. E. 2002. Effects of a cross-modal manipulation of attention on somatosensory cortical neuronal responses to tactile stimuli in the monkey. J. Neurophysiol. 88(6), 3133–3149.
Merzenich, M. M., Nelson, R. J., Kaas, J. H., Stryker, M. P., Jenkins, W. M., Zook, J. M., Cynader, M. S., and Schoppmann, A. 1987. Variability in hand surface representations in areas 3b and 1 in adult owl and squirrel monkeys. J. Comp. Neurol. 258, 281–296.
Mesulam, M. M. 1998. From sensation to cognition. Brain 121(Pt 6), 1013–1052.
Mountcastle, V. B. and Powell, T. P. S. 1959. Neural mechanisms subserving cutaneous sensibility, with special reference to the role of afferent inhibition in sensory perception and discrimination. Bull. Johns Hopkins Hosp. 105, 201–232.
Mountcastle, V. B., LaMotte, R. H., and Carli, G. 1972. Detection thresholds for stimuli in humans and monkeys: comparison with threshold events in mechanoreceptive afferent nerve fibers innervating the monkey hand. J. Neurophysiol. 35, 122–136.
Murray, E. A. and Mishkin, M. 1984. Relative contributions of SII and area 5 to tactile discrimination in monkeys. Behav. Brain Res. 11(1), 67–83.
Narayan, S. M., Santori, E. M., and Toga, A. W. 1994. Mapping functional activity in rodent cortex using optical intrinsic signals. Cereb. Cortex 4(2), 195–204.
Nelson, R. J. 1987. Activity of monkey primary somatosensory cortical neurons changes prior to active movement. Brain Res. 406(1–2), 402–407.
Nelson, R. J., Sur, M., Felleman, D. J., and Kaas, J. H. 1980. Representations of the body surface in postcentral parietal cortex of Macaca fascicularis. J. Comp. Neurol. 192(4), 611–643.
Nelson, R. J., Smith, B. N., and Douglas, V. D. 1991. Relationships between sensory responsiveness and premovement activity of quickly adapting neurons in areas 3b and 1 of monkey primary somatosensory cortex. Exp. Brain Res. 84, 75–90.
Nicolelis, M. A., Lin, R. C., Woodward, D. J., and Chapin, J. K. 1993. Dynamic and distributed properties of many-neuron ensembles in the ventral posterior medial thalamus of awake rats. Proc. Natl. Acad. Sci. U. S. A. 90(6), 2212–2216.
Paul, R. L., Merzenich, M., and Goodman, H. 1972. Representation of slowly and rapidly adapting cutaneous mechanoreceptors of the hand in Brodmann's areas 3 and 1 of Macaca mulatta. Brain Res. 36(2), 229–249.
Pons, T. P., Garraghty, P. E., Cusick, C. G., and Kaas, J. H. 1985. A sequential representation of the occiput, arm, forearm and hand across the rostrocaudal dimension of areas 1, 2 and 5 in macaque monkeys. Brain Res. 335(2), 350–353.
Pons, T. P., Wall, J. T., Garraghty, P. E., Cusick, C. G., and Kaas, J. H. 1987. Consistent features of the representation of the hand in area 3b of macaque monkeys. Somatosens. Res. 4, 309–331.
Powell, T. P. and Mountacstle, V. B. 1959. The cytoarchitecture of the postcentral gyrus of the monkey Macaca mulatta. Bull. Johns Hopkins Hosp. 105, 108–131.
Robinson, C. J. and Burton, H. 1980. Organization of somatosensory receptive fields in cortical areas 7b, retroinsula, postauditory and granular insula of *M. fascicularis*. J. Comp. Neurol. 192(1), 69–92.
Roe, A. W. 2003. Modular complexity of Area V2 in the Macaque monkey. In: The Primate Visual System (*eds*. C. Collins and J. Kaas), pp. 109–138. CRC Press.
Roe, A. W., Fristches, K., and Pettigrew, J. D. 2005. Optical imaging of functional organization in V1 and V2 of marmoset visual cortex. Anat. Rec. 287, 1213–1225.
Roe, A. W., Walled, D., Sybirska, E., and Goldman-Rakic, P. S 2004. Optical imaging of prefrontal cortex during oculomotor delay response task in Macaque monkey. Soc. Neurosci. Abstract .
Roe, A. W., Lu, H., Kamitani, Y., and Tong, F. 2006. Orientation-selective information in the late positive optical intrinsic signal: implications for fMRI. Human Brain Mapping.
Romo, R., Hernandez, A., Zainos, A., and Salinas, E. 1998. Somatosensory discrimination based on cortical microstimulation. Nature 392, 387–390.
Romo, R., Hernandez, A., Zainos, A., Brody, C. D., and Lemus, L. 2000. Sensing without touching: psychophysical performance based on cortical microstimulation. Neuron 26, 273–278.
Schneider, R. J., Friedman, D. P., and Mishkin, M. 1993. A modality-specific somatosensory area within the insula of the rhesus monkey. Brain Res. 621(1), 116–120.
Schroeder, C. E., Seto, S., Arezzo, J. C., and Garraghty, P. E. 1995. Electrophysiological evidence for overlapping dominant and latent inputs to somatosensory cortex in squirrel monkeys. J. Neurophysiol. 74(2), 722–732.
Schwartz, T. H., Chen, L. M., Friedman, R. M., Spencer, D. D., and Roe, A. W. 2004. Intraoperative Optical Imaging of Face Topography in Human Somatosensory Cortex. Neuroreport 15, 1527–1532.
Seidemann, E., Arieli, A., Grinvald, A., and Slovin, H. 2002. Dynamics of depolarization and hyperpolarization in the frontal cortex and saccade goal. Science 295(5556), 862–865.
Sherrick, C. E. 1964. Effects of double simultaneous stimulation of the skin. Am. J. Psychol. 77, 42–53.
Sheth, B. R., Moore, C. I., and Sur, M. 1998. Temporal modulation of spatial borders in rat barrel cortex. J. Neurophysiol. 79(1), 464–470.
Sheth, S., Nemoto, M., Guiou, M., Walker, M., Pouratian, N., and Toga, A. W. 2003. Evaluation of coupling between optical intrinsic signals and neuronal activity in rat somatosensory cortex. Neuroimage 19(3), 884–894.

Shoham, D. and Grinvald, A. 2001. The cortical representation of the hand in macaque and human Area S-I: high resolution optical imaging. J. Neurosci. 21(17), 6820–6835.

Shtoyerman, E., Arieli, A., Slovin, H., Vanzetta, I., and Grinvald, 2000. A. Long-term optical imaging and spectroscopy reveal mechanisms underlying the intrinsic signal and stability of cortical maps in V1 of behaving monkeys. J. Neurosci. 20, 8111–8121.

Siegel, R. M., Raffi, M., Phinney, R. E., Turner, J. A., and Jando, G. 2003. Functional architecture of eye position gain fields in visual association cortex of behaving monkey. J. Neurophysiol. 90(2), 1279–1294.

Simons, S. B., Chiu, J., Favorov, O. V., Whitsel, B. L., and Tommerdahl, M. 2007. Duration-dependent response of SI to vibrotactile stimulation in squirrel monkey. J. Neurophysiol. 97(3), 2121–2129.

Simons, S. B., Tannan, V., Chiu, J., Favorov, O. V., Whitsel, B. L., and Tommerdahl, M. 2005. Amplitude-dependency of response of SI cortex to flutter stimulation. BMC Neurosci. 6(1), 43p.

Slovin, H., Arieli, A., Hildesheim, R., and Grinvald, A. 2002. Long-term voltage-sensitive dye imaging reveals cortical dynamics in behaving monkeys. J. Neurophysiol. 88(6), 3421–3438.

Sretavan, D. and Dykes, R. W. 1983. The organization of two cutaneous submodalities in the forearm region of area 3b of cat somatosensory cortex. J. Comp. Neurol. 213, 381–398.

Sur, M., Garraghty, P. E., and Bruce, C. J. 1985. Somatosensory cortex in macaque monkeys: laminar differences in receptive field size in areas 3b and 1. Brain Res. 342, 391–395.

Sur, M., Merzenich, M. M., and Kaas, J. H. 1980. Magnification, receptive-field area, and ''hypercolumn'' size in areas 3b and 1 of somatosensory cortex in owl monkeys. J. Neurophysiol. 44, 295–311.

Sur, M., Nelson, R. J., and Kaas, J. H. 1982. Representations of the body surface in cortical areas 3b and 1 of squirrel monkeys: comparisons with other primates. J. Comp. Neurol. 211, 177–192.

Sur, M., Wall, J. T., and Kaas, J. H. 1981. Modular segregation of functional cell classes within the postcentral somatosensory cortex of monkeys. Science 212, 1059–1061.

Sur, M., Wall, J. T., and Kaas, J. H. 1984. Modular distribution of neurons with slowly adapting and rapidly adapting responses in area 3b of somatosensory cortex in monkeys. J. Neurophysiol. 51, 724–744.

Talbot, W. H., Darian-Smith, I., Kornhuber, H. H., and Mountcastle, V. B. 1968. The sense of flutter-vibration: comparison of the human capacity with response patterns of mechanoreceptive afferents from the monkey hand. J. Neurophysiol. 31, 301–334.

Tanji, J. and Wise, S. P. 1981. Submodality distribution in sensorimotor cortex of the unanesthetized monkey. J. Neurophysiol. 45, 467–481.

Tannan, V., Dennis, R. G., and Tommerdahl, M. 2005. Stimulus-dependent effects on tactile spatial acuity. Behav. Brain. Funct. 1(1), 18p.

Tannan, V., Whitsel, B. L., and Tommerdahl, M. A. 2006. Vibrotactile adaptation enhances spatial localization. Brain Res. 1102(1), 109–116.

Thompson, J. K., Peterson, M. R., and Freeman, R. D. 2003. Single-neuron activity and tissue oxygenation in the cerebral cortex. Science 299(5609), 1070–1072.

Tommerdahl, M., Delemos, K. A., Favorov, O. V., Metz, C. B., Vierck, C. J. Jr., and Whitsel, B. L. 1998. Response of anterior parietal cortex to different modes of same-site skin stimulation. J. Neurophysiol. 80, 3272–3283.

Tommerdahl, M., Delemos, K. A., Whitsel, B. L., Favorov, O. V., and Metz, C. B. 1999. Response of anterior parietal cortex to cutaneous flutter versus vibration. J. Neurophysiol. 82(1), 16–33.

Tommerdahl, M., Favorov, O. V., and Whitsel, B. L. 2005. Effects of high-frequency skin stimulation on SI cortex: mechanisms and functional implications. Somatosens. Mot. Res. 22(3), 151–169.

Tommerdahl, M., Hester, K. D., Felix, E. R., Hollins, M., Favorov, O. V., Quibrera, P. M., and Whitsel, B. L. 2005. Human vibrotactile frequency discriminative capacity after adaptation to 25 Hz or 200 Hz stimulation. Brain Res. 1057(1–2), 1–9.

Tommerdahl, M., Simons, S. B., Chiu, J. S., Favorov, O., and Whitsel, B. L. 2006. Ipsilateral input modifies the primary somatosensory cortex response to contralateral skin flutter. J. Neurosci. 26(22), 5970–5977.

Torebjork, H. E. and Ochoa, J. L. 1980. Specific sensations evoked by activity in single identified sensory units in man. Acta. Physiol. Scand. 110, 445–447.

Tsunoda, K., Yamane, Y., Nishizaki, M., and Tanifuji, M. 2001. Complex objects are represented in macaque inferotemporal cortex by the combination of feature columns. Nat. Neurosci. 4(8), 832–838.

Ungerleider, L. G., Courtney, S. M., and Haxby, J. V. 1998. A neural system for human visual working memory. Proc. Natl. Acad. Sci. U. S. A. 95(3), 883–890.

Vallbo, A. B. 1981. Sensations evoked from the glabrous skin of the human hand by electrical stimulation of unitary mechanosensitive afferents. Brain Res. 215(1–2), 359–363.

Vanzetta, I., Hildesheim, R., and Grinvald, A. 2005. Compartment-resolved imaging of activity-dependent dynamics of cortical blood volume and oximetry. J. Neurosci. 25, 2233–2244.

Verrillo, R. T. 1966. Vibrotactile thresholds for hairy skin. J. Exp. Psychol. 72(1), 47–50.

Verrillo, R. T. and Bolanowski, S. J. Jr. 1986. The effects of skin temperature on the psychophysical responses to vibration on glabrous and hairy skin. J. Acoust. Soc. Am. 80, 528–532.

Vnek, N., Ramsden, B. M., Hung, C. P., Goldman-Rakic, P. S., and Roe, A. W. 1999. Optical imaging of functional domains in the cortex of the awake and behaving monkey. Proc. Natl. Acad. Sci. U. S. A. 96, 4057–4060.

Xu, X., Bosking, W., Sary, G., Stefansic, J., Shima, D., and Casagrande, V. 2004. Functional organization of visual cortex in the owl monkey. J. Neurosci. 24(28), 6237–6247.

Woolsey, C. N., Marshall, W. H., and Bard, P. 1942. Representation of cutaneous tactile sensibility in the cerebral cortex of the monkey as indicated by evoked potentials. Bull. Johns. Hopkins Hosp. 70, 399–441.

Zepeda, A., Ariasa, C., and Sengpiel, F. 2004. Optical imaging of intrinsic signals: recent developments in the methodology and its applications. J. Neurosci. Meth. 136, 1–21.

Further Reading

Alloway, K. D. and Burton, H., 1991. Differential effects of GABA and bicuculline on rapidly- and slowly-adapting neurons in primary somatosensory cortex of primates. Exp. Brain Res. 85(3), 598–610.

Buchel, C. and Friston, K. J. 1997. Modulation of connectivity in visual pathways by attention: cortical interactions evaluated with structural equation modelling and fMRI. Cereb. Cortex 7(8), 768–778.

6.15 Twenty-Five Years of Multielectrode Recordings in the Somatosensory System: It is All about Dynamics

M C Wiest, E Thomson, and M A L Nicolelis, Duke University, Durham, NC, USA

© 2008 Elsevier Inc. All rights reserved.

6.15.1	**Introduction**	316
6.15.2	**Single-Whisker Stimulation**	317
6.15.2.1	Location Coding	317
6.15.2.2	Spatiotemporal Receptive Fields Point to Multiwhisker Integration over Time	318
6.15.3	**Multiwhisker Stimulation**	320
6.15.3.1	Bilateral Interactions	321
6.15.4	**Coordinated Firing of Simultaneously Recorded Neurons**	323
6.15.5	**Plasticity**	324
6.15.5.1	Modified Inputs	324
6.15.5.2	Operant Conditioning	325
6.15.6	**Behavioral Modulation of Tactile Responses**	325
6.15.7	**Conclusion and Outlook**	327
References		328

Glossary

barrel Region in layer IV of S1 with a patchwork of regions that stain dark with cytochrome oxidase. Neurons in each barrel respond most vigorously to a particular body part. Barrels are arranged somatotopically across S1, and in the rat the whisker barrels make up almost half of barrel cortex. The regions of S1 that do not contain barrels are known as dysgranular cortex.

barrelet A cluster of brainstem neurons corresponding to a single facial whisker.

barreloid A cluster of thalamic neurons corresponding to a single facial whisker.

bilateral On both sides of the body.

contralateral On the opposite side of the body.

deafferentation The elimination or interruption of sensory nerve inputs.

$GABA_A$ Fast-responding receptors for the brain's main inhibitory neurotransmitter.

granular layer Cortical layer IV.

infragranular layers Cortical layers deeper than layer IV.

ipsilateral On the same side of the body.

mystacial pad The thick muscular pad on the side of the face of the rat that contains the whisker follicles.

plasticity Long-term changes in anatomy, topographic maps, or neuronal responses.

principal whisker (PW) The whisker that evokes the greatest response in a particular neuron.

receptive field (RF) The region of stimulus space that evokes a response in a neuron. In the somatosensory system, an RF is defined as the part of the body whose stimulation evokes a response.

somatotopic A topographic neural representation of the body's surface, such that neighboring neurons respond to neighboring body regions.

supragranular layers Cortical layers superficial to layer IV.

trigeminal nerve The fifth cranial nerve, through which sensory inputs from the face enter the brainstem. The nerve is split into three divisions, the mandibular, maxillary, and ophthalmic. The whisker information comes in through the infraorbital branch of the maxillary division.

vibrissa The large stiff facial whiskers of mammals such as rats and cats.

whisking The rhythmic large-amplitude 9 Hz back-to-front movement of the facial whiskers. The behavior is exhibited by rats during active exploration, used to sample certain tactile objects, and possibly also to enhance olfaction.

6.15.1 Introduction

The modern era of somatosensory neurophysiology was inaugurated in 1983 by the discovery of widespread plastic functional reorganization in the primary somatosensory cortex (S1) of adult monkeys (Merzenich, M. M. *et al.*, 1983a; 1983b). In essence, this discovery marked the first evidence that the somatotopic representations found in the S1 cortex are rather dynamical entities, whose functional organization can be shaped over time as a function of the state of the body's periphery (Merzenich, M. M. *et al.*, 1983a; 1983b) or the animal's sensory experience (Jenkins, W. M. *et al.*, 1990). Yet, in these first few studies the dynamics of such a process of functional reorganization was measured on a timescale of days or even months.

Soon after the original findings of Mike Merzenich and Jon Kaas, the process of plastic reorganization in the somatosensory system was found to occur in a matter of seconds and minutes (Calford, M. B. and Tweedale, R., 1991a; 1991b; 1991c; Nicolelis, M. A. *et al.*, 1993).

As these discoveries unfolded, a new neurophysiological method began to be employed to investigate the functional properties of the somatosensory system in behaving animals (Chapin, J. K. and Woodward, D. J., 1981; 1982; Nicolelis, M. A. *et al.*, 1993). Known as chronic, multielectrode recordings, this approached allowed for the first time the simultaneous quantification of the physiological properties of small populations of single neurons, distributed across distinct cortical and subcortical structures that form the mammalian somatosensory system (Nicolelis, M. A. *et al.*, 1995). These studies indicated the existence of a dynamic functional organization throughout the somatosensory system on a timescale of tens of milliseconds (Nicolelis, M. A. and Chapin, J. K., 1994). Moreover, such a dynamic structure was suggested to serve as the basis through which the process of plastic reorganization could be triggered (Faggin, B. M. *et al.*, 1997).

The goal of this review, therefore, is to provide a brief description of the findings that followed the introduction, 25 years ago, of the multielectrode recording method as an experimental tool to characterize the functional organization of the somatosensory system, with particular emphasis on the rat trigeminal system.

Since the 1970s, the facial vibrissal system of the rat (Figure 1) has been a popular model for studying somatosensory processing (Woolsey, T. A. and Van der Loos, H., 1970; Jones, E. and Diamond, M., 1995; Nicolelis, M. A. and Fanselow, E. E., 2002a; 2002b). This interest is due to a confluence of several attractive features. First, rats are known to employ their whiskers flexibly for a variety of sensitive discrimination, recognition, and navigation tasks (Whishaw, I. and Kolb, B., 2005). A variety of behavioral tasks now exist that probe the limits of this behavioral repertoire. Second, the central brain representation of the whiskers is large, facilitating electrophysiological study. That is, almost half of the S1 cortex is responsive to whisker stimulation (Woolsey, T. A. and Van der Loos, H., 1970). Moreover, early anatomical and single-unit electrophysiological studies of the rat vibrissae system revealed a relatively simple organization such that neurons that respond preferentially to individual whiskers are anatomically segregated into topographically arranged modules (barrellets in the brainstem, barreloids in the thalamus, and barrel columns in the S1 cortex) (Jones, E. and Diamond, M., 1995). This later feature suggests a conceptually simple model of coding in which the activity in these modules represents stimulation of specific whiskers on the contralateral face.

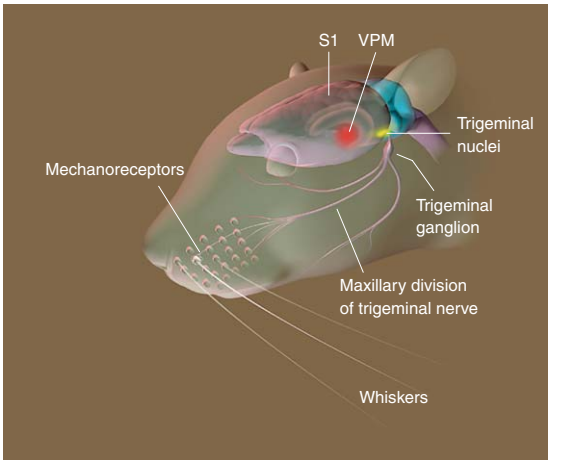

Figure 1 Schematic of the rat whisker system. Whisker stimulation activates mechanoreceptors whose somata lie in the trigeminal ganglion (at the root of the fifth cranial nerve). These primary afferents synapse onto neurons in multiple trigeminal brain stem nuclei. The primary pathway proceeds from the trigeminal nuclei of the brainstem, across the midline via the medial lemniscus, onto neurons in the ventral posterior medial (VPM) nucleus of the thalamus. VPM neurons synapse onto neurons in primary somatosensory (S1) cortex.

6.15.2 Single-Whisker Stimulation

6.15.2.1 Location Coding

The anatomical organization of the whisker system suggests that it consists of arrays of dedicated detectors that function to indicate the deflection of individual contralateral whiskers (Welker, C., 1971). However, it was soon observed that whiskers other than the principal whisker (PW) modulate responses in a barrel or a barreloid. For instance, ventral posterior medial nucleus of the thalamus (VPM, see Figure 1) neurons in both awake and anesthetized animals have large multiwhisker receptive fields (RFs) (Armstrong-James, M. and Fox, K., 1987; Nicolelis, M. A. and Chapin, J. K., 1994), and the same is true for S1 barrel neurons (primary somatosensory cortex layer IV; Figure 1) (Zhu, J. J. and Connors, B. W., 1999; Ghazanfar, A. A. and Nicolelis, M. A., 2001). In the supra- and infragranular layers of S1, intercolumnar connections are more common, and RFs in these layers are correspondingly larger, including up to 20 whiskers (Armstrong-James, M. *et al.*, 1992; Ghazanfar, A. A. *et al.*, 2000; Schubert, D. *et al.*, 2001).

These results suggest that stimulus location on the mystacial pad is coded in a distributed manner across the rat S1 cortex. With the advent of multielectrode array (MEA) technology, it has been possible to test specific hypotheses about how activity in S1 encodes information about which whisker was deflected. Candidate codes include the number of spikes following stimulation, time-varying firing rate, and correlated activity between neurons.

In one study, researchers implanted 16-electrode arrays into S1 and VPM and delivered mechanical stimuli to each whisker of the anesthetized rat (300 trials per whisker) (Ghazanfar, A. A. *et al.*, 2000). They used classification algorithms to estimate which whisker was deflected on each trial, quantifying discrimination performance as the percentage of stimuli correctly predicted by the classifier (Ghazanfar, A. A. *et al.*, 2000; Thomson, E. E. and Kristan, W. B., 2005). The study revealed many details of how ensembles of cortical neurons encode stimulus location. First, the ensemble of S1 neurons discriminated much better than any individual neuron, suggesting that S1 encodes stimulus location using a population of neurons rather than individual neurons. They also showed, by repeating the analysis with different numbers of neurons from their data, that the discrimination performance decreased gradually with the number of neurons, suggesting that no individual neuron is privileged in this distributed representation of stimulus location (Figure 2). In a related study, it was found that the knowledge of the activity of additional neurons within a column, in contrast to activity of neurons in different columns, provided little new information about stimulus location (Petersen, R. S. *et al.*, 2001).

In addition to examining the effects of neuronal population size, studies described in Ghazanfar A. A. *et al.* (2000) examined a set of possible ensemble codes for stimulus location. Overall, the analysis showed that while the firing rate of neurons in an ensemble contributes most to stimulus discrimination, the temporal structure of the neural response provides a significant boost in performance. For instance, by shifting the spike trains in time, such that the single-neuron temporal patterns of spikes would remain the same but the onset times (i.e., latencies) would be randomized, they found a small but significant reduction in discrimination. This suggests that the onset time of evoked activity in a population of somatosensory neurons codes for stimulus location, a conclusion confirmed in a later study (Petersen, R. S. *et al.*, 2001).

In the same study, Ghazanfar A. A. *et al.* (2000) parametrically varied the bin widths of neural response histograms between 40 and 1 ms and found that classifier performance was reduced by a small but significant amount when larger bin widths were used. This analysis suggested the importance of temporal patterning of spike trains. On the other hand, when trials were shuffled to eliminate correlated firing among neurons while preserving time-varying firing rates, the discrimination performance was not significantly affected. This suggests that synchronous activity, and cross-correlations more generally, over and above that expected due to stimulus-locked firing rate modulations, do not encode the location of single whisker stimuli. A similar study performed during recording of multiple units in S1 and S2 of monkey found similar results in S1, but found that in S2 stimulus location discrimination was impaired when correlations between neurons were disrupted by shuffling (Nicolelis, M. A. *et al.*, 1998). This suggests that S2 uses a strategy different than S1 for coding the location of point stimuli.

The findings of multiwhisker RFs and distributed stimulus coding are in some tension with the single-whisker modular model of S1 stimulus coding, but do not rule it out. Petersen R. S. *et al.* (2001) have recently noted that the earliest evoked spike after a

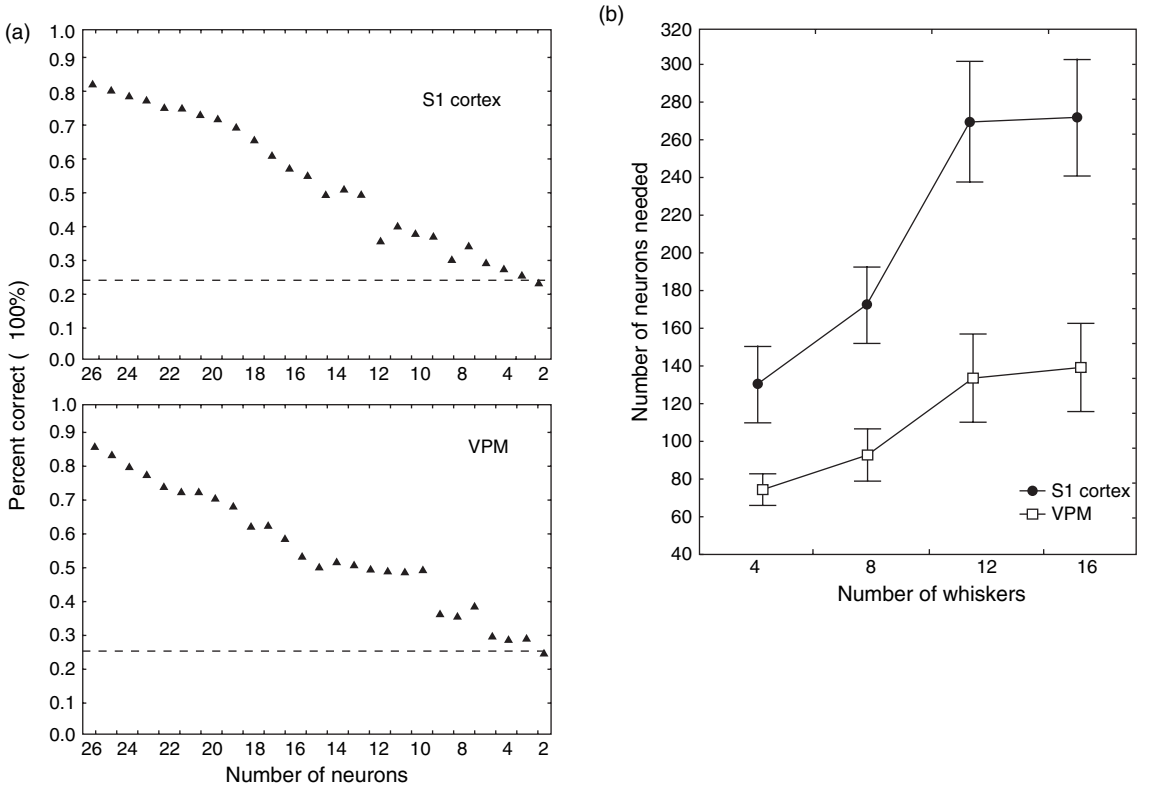

Figure 2 Neuron-dropping analysis suggests a distributed code. (a) Graceful degradation of ensemble performance discriminating four different whiskers after the sequential one-by-one removal of the best predictor neuron from an S1 ensemble (top panel) and a ventral posterior medial nucleus of the thalamus (VPM) ensemble (bottom panel). The dashed line at 25% indicates chance performance. (b) The number of neurons needed within a cortical or a thalamic population to achieve 99.9% correct performance was extrapolated from their average performance discriminating 4, 8, 12, and 16 whiskers. The number of cortical neurons needed to achieve near-perfect performance was approximately twice as many for discriminating 16 versus 4 whiskers (black line). The plateau between 12 and 16 whiskers suggests that the number of neurons needed is not linearly related to the number of classes to be discriminated. From Ghazanfar, A. A., Stambaugh, C. R., *et al.* 2000. Encoding of tactile stimulus location by somatosensory thalamocortical ensembles. J. Neurosci. 20(10), 3761–3775.

single-whisker stimulus contains most of the information about which whisker was stimulated. From this they concluded that later activity, reflecting interactions between different barrels, was largely redundant for neural coding of stimulus identity. In line with a model of barrel columns as single-whisker processing units, Brumberg J. C. *et al.* (1996) proposed that inhibitory circuitry within barrels functions to "increase the 'principal whiskerness' of the cortical column" by suppressing weaker responses so that "only . . . the initial perturbation of the principal whiskers will overcome the . . . cortical inhibition." Mirabella proposed that inhibitory intercolumnar interactions may also function to maintain a dynamic range and to prevent response saturation (Mirabella, G. *et al.*, 2001).

6.15.2.2 Spatiotemporal Receptive Fields Point to Multiwhisker Integration over Time

The finding that multiwhisker RFs are dynamic over poststimulus time (Nicolelis, M. A. and Chapin, J. K., 1994; Ghazanfar, A. A. and Nicolelis, M. A., 1999; Ghazanfar, A. A. *et al.*, 2000) makes it more difficult to interpret neural tactile responses solely in terms of the stimulation of individual whiskers. Ghazanfar A. A. and Nicolelis M. A. (2001) characterized both spatial and temporal aspects of single-neuron responses in VPM and S1 cortex to single-whisker stimulation. A single neuron's responses to deflections of each whisker in a 5×5 spatial array on the face were divided into time bins. The PW, or RF center, at each poststimulus time bin was defined as the whisker that led to the strongest

response at that poststimulus time, leading the generalized notion of a spatiotemporal RF whose center or PW drifts across the whisker pad over poststimulus time.

Similarly, recordings in VPM through multisite chronic microwire arrays revealed VPM neurons whose poststimulus RF center moved over poststimulus time, and others whose RF center was fixed at one whisker (Nicolelis, M. A. and Chapin, J. K., 1994). The dynamic RF centers tended to shift in a caudal-to-rostral direction. In other words, caudal whiskers dominated short-latency responses of these neurons, whereas the response to more rostral whiskers grew large at longer poststimulus times. The neurons with fixed RF centers, on the other hand, invariably had their PW in the rostral part of the whisker pad among the small and immobile vibrissae.

An analogous multielectrode study of layer V S1 neurons in anesthetized rats (Ghazanfar, A. A. and Nicolelis, M. A., 1999) found more heterogeneous spatiotemporal RFs than in VPM. They observed time-dependent RF-center shifts in 88% of these cortical output neurons. In contrast to VPM neurons, the pattern of RF-center shifts varied widely, including rostral-to-caudal, caudal-to-rostral, dorsal-to-ventral, and ventral-to-dorsal trajectories. Moore saw similar poststimulus variation in the center of subthreshold RFs of neurons in all cortical layers using *in vivo* whole-cell recordings in anesthetized rats (Moore, C. I. and Nelson, S. B., 1998).

Ghazanfar reviewed evidence for analogous spatiotemporal RFs in the auditory and visual systems and suggested the hypothesis that tactile spatiotemporal RFs function to integrate time-varying multiwhisker inputs (Ghazanfar, A. A. and Nicolelis, M. A., 2001). The discovery of single-neuron spatiotemporal RFs in which the PW varies over poststimulus time suggests that each neuron will respond maximally to a specific spatiotemporal sequence of whisker deflections. The Ghazanfar study therefore predicted that multiwhisker stimuli constructed to match the spatiotemporal RF of a neuron should evoke supralinear responses (Ghazanfar, A. A. and Nicolelis, M. A., 2001). Such combination selectivity would encode particular temporal sequences of stimulation, as has been shown in the rat auditory system (Irvine, D. R. *et al.*, 1995). In support of this possibility, DiCarlo found that a delayed inhibitory component of the responses of neurons in primate S1 (area 3b) to tactile stimuli scanned across the fingertips was at a different latency for different scanning directions (DiCarlo, J. J. and Johnson, K. O., 2000). This sensitivity to the direction of scanning movements is an example of sensitivity to distributed spatiotemporal patterns of tactile stimulation.

Nicolelis hypothesized that spatiotemporal RFs of tactile neurons at each level arise from the asynchronous convergence of multiple feedforward and feedback pathways (Nicolelis, M. A. and Chapin, J. K., 1994). For example, the short-latency component of VPM RFs would result from the fast ascending lemniscal pathways from the principal and spinal trigeminal brainstem nuclei (which reach VPM at different latencies). The long-latency component could be due to feedback connections from cortical somatosensory areas (Veinante, P. *et al.*, 2000).

These ideas were tested in the Nicolelis lab by combining multielectrode recordings with methods to reversibly inactivate specific afferent inputs and specific sources of descending feedback onto VPM neurons. The contribution of feedforward inputs to VPM spatiotemporal RFs was assessed by temporary deafferentation using subcutaneous infusions of lidocaine, a local anesthetic, into a small region of the whisker pad (Nicolelis, M. A. *et al.*, 1993). The effect of deafferentation was a temporal shift due to the reduction of early components from the anesthetized area, and enhancement of later components, together with a spatial shift of RFs to outside the anesthetized region. The contribution of corticothalamic feedback to spatiotemporal RFs in VPM was assessed by temporarily inactivating the S1 cortex with the gamma-amino butyric acid $(GABA)_A$ agonist muscimol (Krupa, D. J. *et al.*, 1999; Ghazanfar, A. A. *et al.*, 2001). Spatiotemporal RF mapping of VPM neurons in the presence and the absence of cortical feedback revealed that corticofugal projections contributed to both the short and long latency components of VPM responses. These effects likely reflect both direct cortical inputs to VPM and indirect cortical influences via the thalamic reticular nucleus (Lee, S. M. *et al.*, 1994) and the trigeminal brainstem (Jacquin, M. F. *et al.*, 1990).

Subsequent studies addressed whether the development of spatiotemporal RF properties is related to whisking, a fundamental behavior that rats use to explore their environment. This idea was hinted by the above-mentioned finding that fixed PWs of VPM neurons were the small rostral whiskers that are not involved in whisking. To test whether spatiotemporal RFs of VPM neurons reflect the pattern of spatiotemporal inputs that occurs during active whisking over object surfaces, Nicolelis denervated the facial muscles used for whisking by cutting the facial nerve early in postnatal life (Nicolelis, M. A. *et al.*, 1996).

Preventing voluntary whisker movements in this way, which does not affect the sensory innervation of the vibrissae, led to (1) a dramatic reduction in VPM neurons' RF size from 13 to 6 whiskers and (2) a dramatic reduction in the percentage of VPM neurons with caudal short-latency PWs exhibiting time-varying PWs, from 100% in normal animals to 19% in animals whose facial motor nerve had been cut. These results suggest that active whisking plays an important role in sculpting VPM spatiotemporal RFs.

In summary, detailed investigation of single-neuron responses to single-whisker deflections led to the idea that single somatosensory neurons may code for specific spatiotemporal patterns of stimulation of multiple whiskers.

6.15.3 Multiwhisker Stimulation

In general, the large size of somatosensory RFs, and their spatiotemporal structure, suggests significant degrees of functional intercolumnar connectivity, convergence from multiple whiskers, or modulation from other cortical areas. Some authors propose that such interactions lead to redundant activity (Armstrong-James, M., 1995; Petersen, R. S. *et al.*, 2001). In contrast, Simons D. J. (1985) concluded "that an important function of the S1 cortex is to integrate information from different, individual vibrissae on the contralateral face". He suggested that intercolumnar integration functioned to make S1 neurons sensitive to spatiotemporal patterns of whisker activity characterizing the movement of particular objects across the contralateral whisker pad (Simons, D. J., 1985). Experimental findings of spatiotemporal RFs, as reviewed above, and supralinear interactions of multiple whiskers (Ghazanfar, A. A. and Nicolelis, M. A., 1997; Shimegi, S. *et al.*, 2000), as reviewed below, led to a more detailed prediction that single neurons should respond preferentially to the specific time-varying multiwhisker stimulation patterns that match their spatiotemporal RFs (Ghazanfar, A. A. and Nicolelis, M. A., 2001).

Direct measurements of spatiotemporal integration of multiwhisker inputs in the rat whisker system have found evidence of both inhibitory and excitatory interactions. Extra- and intracellular studies of S1 responses to combinations of unilateral stimuli found inhibitory interactions dominating between pairs of neighboring whiskers (Simons, D. J., 1985; Brumberg, J. C. *et al.*, 1996; Higley, M. J. and Contreras, D., 2003) at interstimulus intervals (ISIs) of around 10–20 ms. Responses to pairs of synchronous stimuli were found to sum linearly (Simons, D. J. and Carvell, G. E., 1989; Mirabella, G. *et al.*, 2001), whereas Mirabella reported that synchronous stimulation of four whiskers usually resulted in sublinear response summation (Mirabella, G. *et al.*, 2001). These studies focused on responses of neurons in middle and supragranular layers of S1 in immobilized or anesthetized rats.

Using chronic multisite recordings in freely moving rats, Fanselow found comparable temporal interactions of multiple unilateral inputs by neurons in S1 layer V (Fanselow, E. E. and Nicolelis, M. A., 1999). Responses to the second of a pair of unilateral electrical stimulations of the infraorbital (IO) nerve in awake rats were suppressed, with the strongest effect at ISIs of around 25–50 ms. This suppression was most pronounced when rats were in a quiet behavioral state as compared to the whisking and active exploring states. Recent recordings using moveable MEAs in freely moving rats engaged in an active whisker-dependent discrimination task have suggested that inhibitory response modes in all layers are significantly more common in the discriminating animals as compared to passively stimulated animals and moreover that inhibitory response modulations contribute significantly to encoding the behaviorally discriminated tactile feature (Krupa, D. J. *et al.*, 2004). (We will return to discuss these experiments further below.)

However, not all unilateral multiwhisker interactions are inhibitory: synchronous multiple-whisker deflections have also been reported to sum supralinearly. Shimegi S. *et al.* (2000) reported supralinear summation of neighboring single-whisker stimuli in 37% of S1 neurons, primarily by cells in supragranular layers. They noted that enhanced responses were often selective for specific combinations of stimulus features such as whisker position, angle of deflection, and relative timing of multiwhisker stimuli, supporting the idea that S1 cells code for spatiotemporal patterns of whisker stimulation. Ghazanfar found that 81% of units in S1 layer V showed supralinear responses to simultaneous stimulation of triplets of whiskers as compared to single-whisker stimulations (Ghazanfar, A. A. and Nicolelis, M. A., 1997). They reported a bias toward supralinear summation of within-column triplets as compared to within-row triplets. They pointed out that their findings were consistent with the reports of sublinear summation of unilateral stimuli, since sublinear spatial summation was reported in studies of responses to pairs of neighboring whiskers in granular and

supragranular layers, as opposed to the layer V responses to stimulation of triplets of relatively distant whiskers in their study. Together these findings suggest excitatory as well as inhibitory nonlinear interactions among multiple-whisker stimuli, which could encode spatiotemporal patterns of unilateral whisker stimulations.

Combining the methods for inactivating specific neural inputs with ensemble recordings led to a further important conclusion that the integration of multiwhisker stimuli by somatosensory neurons is shaped not only by intrinsic local properties of neurons and their neighbor connections, but also by interactions among multiple levels of the somatosensory system. As mentioned above, Ghazanfar A. A. *et al.* used muscimol to reversibly inactivate the S1 cortex and to evaluate the contribution of corticothalamic feedback projections to the definition of tactile responses in populations of VPM neurons (Ghazanfar, A. A. *et al.*, 2001). S1 inactivation effectively linearized VPM responses, abolishing the supralinear summation of VPM neural responses to multiwhisker stimuli. These results show that the response properties of VPM neurons to multiwhisker stimuli are shaped by corticothalamic feedback from S1. In Section 6.15.6, we review evidence that tactile responses in S1 are similarly shaped by descending inputs when rats are performing a whisker-guided discrimination task.

6.15.3.1 Bilateral Interactions

All the studies mentioned above have in common that neural activity in the whisker cortex (or VPM barreloid field) is interpreted as a topographic map of whisker deflections exclusively on the contralateral whisker pad. This picture is overly restrictive. It has long been known that callosal cross-projections connect the two S1 hemispheres (White, E. L. and DeAmicis, R. A., 1977; Olavarria, J. *et al.*, 1984; Koralek, K. A. *et al.*, 1990; Cauller, L. J. *et al.*, 1998). Interhemispheric projections are concentrated in the homologous portions of the barrel field, innervating primarily but not exclusively the supra- and infragranular layers (Hayama, T. and Ogawa, H., 1997). Those callosal connections that do innervate layer IV are concentrated in the regions outside the barrel centers, called septa (Olavarria, J. *et al.*, 1984; Hayama, T. and Ogawa, H., 1997), as are unilateral interbarrel connections in layer IV (Kim, U. and Ebner, F. F., 1999).

One potential function of the commissural interhemispheric connections is to transfer learned associations from one hemisphere to the other (Ebner, F. F. and Myers, R. E., 1962; Calford, M. B. and Tweedale, R., 1990). Such transfer of plasticity on relatively long timescales might be assumed to preserve the unambiguous representation of the contralateral whisker pad in each S1 hemisphere implied by the traditional models mentioned above.

However, growing evidence points to robust synaptic interactions between the S1 hemispheres on millisecond timescales. Pidoux B. and Verley R. (1979) recorded S1 local field potential (LFP) responses to ipsilateral whisker stimulation in anesthetized rats, the first electrophysiological evidence of cross talk between the S1 hemispheres. Shuler, M. G. *et al.*, (2001) used bilateral MEA recordings to demonstrate that whisker stimulation on either side of the face of an anesthetized rat could evoke responses in the same layer V S1 neuron. This result has been recently confirmed by intracellular recordings (Manns, I. D. *et al.*, 2004). By reversibly inactivating individual hemispheres of S1 using micro infusion of the $GABA_A$ agonist muscimol, Shuler also showed that S1 single-neuron responses to ipsilateral whisker deflection likely propagate across the corpus callosum from the contralateral S1 hemisphere where neurons receive the primary afferent sensory signal from the whisker pad (Shuler, M. G. *et al.*, 2001). Other studies have shown that the responses of individual neurons in S1 are suppressed in the absence of activity in the contralateral hemisphere (Shin, H. C. *et al.*, 1997). Rema V. and Ebner F. F. (2003) found similar response suppression as well as changes in whisker-pairing plasticity in all layers, due to contralateral lesions.

Following Shuler M. G. *et al.* (2001), Wiest used bilateral multielectrode recordings of layer V S1 neurons to characterize responses to bilateral whisker stimulation in head-immobilized awake rats (Wiest, M. C. *et al.*, 2005). This study revealed that S1 neurons continue to respond to bilateral whisker stimuli in the awake state (Figure 3(a)). S1 neurons integrated bilateral inputs over more than 100 ms, with suppressive interactions dominating at ISIs of about 30 ms, in agreement with recordings in anesthetized rats. As in the anesthetized state, responses to ipsilateral whisker stimulation tended to appear at longer latencies than contralateral responses (24 vs. 15 ms), consistent with the afferent ipsilateral input's propagation across the corpus callosum from the contralateral to the ipsilateral S1 hemisphere.

In anesthetized rats the contralateral stimulus universally suppressed the responses to simultaneously presented ipsilateral stimuli. This is understandable

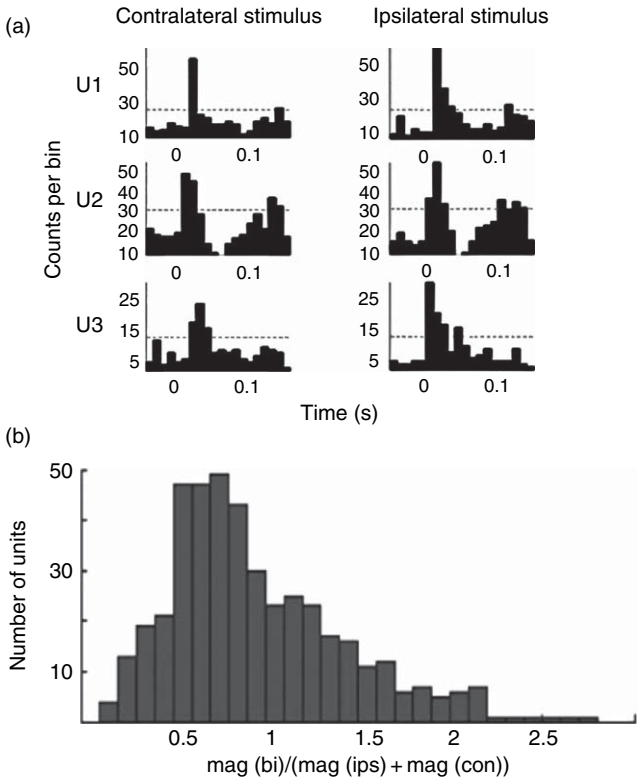

Figure 3 S1 neurons in awake rats integrate bilateral whisker inputs. (a) Example of a single-unit responses to whisker stimulation on either side of the face. Each row shows poststimulus time histograms (PSTHs, 10 ms bins) of one layer V single unit to contralateral (left column) and ipsilateral (right column) whisker stimulation at $t = 0$. Dashed lines show the 99% confidence limit for the spike counts based on the prestimulus baseline firing rate. (b) Histogram of the ratio of multiunit response magnitudes to simultaneous bilateral whisker stimulation over the sum of contralateral and ipsilateral response magnitudes. A ratio >1 indicates supralinear summation of the two whisker arc stimuli; a ratio <1 indicates sublinear summation of bilateral inputs. In contrast to bilateral interactions in anesthetized rats (Shuler, M. G. *et al.*, 2001), which are exclusively sublinear, many units summed bilateral inputs supralinearly in awake S1 rats. Adapted from Wiest, M. C., Bentley, N., *et al.* 2005. Heterogeneous integration of bilateral whisker signals by neurons in primary somatosensory cortex of awake rats. J. Neurophysiol. 93(5), 2966–2973.

since the latency for the contralateral response is shorter, so the ipsilateral excitatory response can be suppressed before it occurs by the inhibitory phase of the contralateral response. In contrast, in the awake rats many individual units showed significant supralinear spatial summation as well as sublinear summation of synchronous bilateral inputs (Figure 3(b)). This difference suggests that the profile of excitatory and inhibitory contributions to ongoing S1 responses to bilateral stimuli is substantially altered in the anesthetized animal. The heterogeneity of responses we observed in the awake animals could function to enhance discrimination of multiwhisker patterns of whisker stimulation (Maass, W. *et al.*, 2002).

The cross talk between S1 hemispheres observed in both anesthetized and waking animals, as reviewed above, challenges the conception of the S1 barrel cortex as an encoder for exclusively contralateral whisker activity and suggests the potential importance of bilateral interactions in S1 for whisker-guided behavior.

We do not know yet whether neural activity in one hemisphere of S1 could interfere with stimulus representations in the contralateral S1, or if in some behavioral contexts, rats can make positive use of bilateral interactions in S1 to solve tactile discrimination tasks. Previous behavioral experiments have demonstrated that rats use whisker signals from both sides of the face in tactile discrimination tasks (Krupa, D. J. *et al.*, 2001; Maass, W. *et al.*, 2002; Shuler, M. G. *et al.*, 2002). In fact, rats used bilateral whisker signals even in an aperture-width discrimination task that in principle could be solved without integrating information from both sides of the face

(Oliveira, L. M. *et al.*, 2003; Krupa, D. J. *et al.*, 2004), suggesting that bilateral interactions are functionally important. S1 is the first locus of bilateral interactions (Waite, P. M., 1969; Smith, R. L., 1973; Erzurumlu, R. S. and Killackey, H. P., 1980). Accordingly, Shuler M. G. *et al.* (2002) found that intact S1 cortex in both hemispheres was required for successful performance of a bilateral tactile discrimination task. These connections between the S1 hemispheres are fully functional in awake rats (Wiest, M. C. *et al.*, 2005), suggesting that S1 is a potential site of bilateral integration used by the animals for discrimination performance, rather than merely a conduit for sensory information that is integrated at higher processing stages.

Just as the variety of cortical spatiotemporal RFs suggested a basis for discriminating different spatiotemporal patterns of unilateral multiwhisker stimulation, the heterogeneity of bilateral interactions in S1 neurons might provide the basis for discriminating different spatiotemporal patterns of bilateral whisker stimulation.

Over longer timescales, if a rat's different behavioral goals require attention to different aspects of the bilateral pattern of whisker deflections, integration may be optimized (see also Sections 6.15.5. and 6.15.6. below) by changes in the functional connectivity between the hemispheres. Studying bilateral integration of whisker sensory signals in S1 may offer an advantageous window on the larger issue of the dynamic integration of distributed sensory representations, because the peripheral signals to be integrated are clearly segregated in space and may be independently manipulated up to the level of the S1 cortex, and so it may be possible to gain experimental access to the brain's mechanisms for adjusting the functional connectivity between neural populations in the two hemispheres.

6.15.4 Coordinated Firing of Simultaneously Recorded Neurons

In the past 30 years, correlated activity among neurons has received a great deal of attention for its potential role in the binding of sensory features into complex objects and scenes (Singer, W., 1999), motor coordination (Sanes, J. N. and Truccolo, W., 2003), and attention (Tiesinga, P. H. *et al.*, 2004). The only way to empirically determine the extent of such correlations is by recording the responses of multiple neurons simultaneously. We have already touched on the role of temporal patterning across multiple neurons in the context of coding the location of single-whisker stimuli. In that context it was found that S1 ensembles code stimulus location in the relative response latencies of their neurons, but not in single-trial covariations among the neurons (Nicolelis, M. A. *et al.*, 1998; Ghazanfar, A. A. *et al.*, 2000). In S2 of the primate, on the other hand, single-trial covariations among multiple neurons did contribute significantly to coding the location of a punctate stimulus (Nicolelis, M. A. *et al.*, 1998; Ghazanfar, A. A. *et al.*, 2000).

It seems theoretically plausible that the importance of such correlated activity among populations of neurons should increase when more complex spatiotemporal patterns of multiwhisker deflections are to be discriminated. While the investigation of the functional role of correlated firing in somatosensory behavior is still at an early stage, there is some empirical support for this idea. For example, it was recently shown that, in response to the simultaneous deflection of multiple whiskers, there is a higher prevalence of synchronous responses between neurons in the infragranular layers of S1 than in other layers (Boyden, E. S. *et al.*, 2005; Zhang, M. and Alloway, K. D., 2006). Even if such synchrony does not mathematically improve stimulus discrimination using local ensemble activity, it might be more likely to generate responses in downstream neurons (Tiesinga, P. H. *et al.*, 2004). Ahrens K. F. and Kleinfeld D. (2004) showed that activity in S1 is correlated with large-amplitude whisking even after the sectioning of the infraorbital nerve (IO), suggesting close coordination with activity in the motor cortex (the IO nerve is a branch of the trigeminal nerve that carries sensory information from the vibrissae to the CNS).

Another set of studies has recorded synchronous activity among ensembles of neurons at multiple levels of the lemniscal pathway, recording from the spinal trigeminal nucleus in the brainstem (Vg), VPM, and S1. It was found that, before bouts of high-frequency low-amplitude whisker twitching, correlated activity in the range of 7–12 Hz began in S1 and then emerged in VPM and the spinal nucleus (Nicolelis, M. A. *et al.*, 1995). Such correlated activity remains even after the transection of the facial nerve, which suggests that such synchronous activity is generated centrally. Although the high coherence among large populations of neurons associated with this oscillatory 7–12 Hz brain state suggested the absence of seizures to a number of authors (Marescaux, C. *et al.*, 1992; Shaw, F. Z. *et al.*, 2006; Shaw, F. Z., 2007), a direct test showed that rats respond robustly to mild tactile stimulation during bouts of 7–12 Hz oscillations in S1, contradicting the absence

of interpretation (Wiest, M. C. and Nicolelis, M. A., 2003). Subsequent work showed that under analogous oscillatory activity in the gustatory cortex, the neural representation of the tastant palatability was actually enhanced (Fontanini, A. and Katz, D. B., 2006).

Recent multielectrode recordings in the primary auditory cortex during somatosensory stimulation (Lakatos, P. *et al.*, 2007) support the general idea that oscillatory activity could modulate neural coding in functionally important ways. These authors reported that somatosensory stimulation resets the phase of ongoing oscillatory activity in the auditory cortex, such that responses to synchronous auditory stimulation were enhanced whereas responses to asynchronous auditory stimuli were suppressed. They suggested that this oscillatory phase-resetting effect could account for aspects of auditory–somatosensory integration psychophysics.

Finally, results in Section 6.15.5., suggest that long-term plasticity between cortical barrels in S1 can be induced more easily during bouts of synchronous firing (Erchova, I. A. and Diamond, M. E., 2004).

6.15.5 Plasticity

The primary somatosensory cortex is not a static entity whose functional role is fixed after a critical developmental period. Rather, a range of experiments suggests that the cortex is organized to adaptively adjust its responses to the statistical structure of inputs received as well as to the specific demands that an organism faces (as was hypothesized in Gilbert, C. D., 1996; Buonomano, D. V. and Merzenich, M. M., 1998; Plumbley, M. D., 1999; Calford, M. B., 2002; Elbert, T. and Rockstroh, B., 2004). The somatosensory system has been a font of insight into the phenomenology and mechanisms of such neuronal plasticity (we define plasticity as the induction of long-term changes in anatomy, topographic maps, or response properties of neurons). For a review, see Ebner F. (2005).

We will focus mainly on studies that have employed multielectrode recordings to monitor plasticity in the adult primary somatosensory cortex (for a review of plasticity during development, see Feldman, D. E. and Brecht, M., 2005). Studies of adult plasticity typically fall into two categories: first, plasticity induced by directly modifying the inputs from the periphery and second, plasticity induced by operant conditioning on discrimination tasks. We will discuss these two lines of evidence in turn.

6.15.5.1 Modified Inputs

The organization of the somatosensory cortex can be drastically altered when the inputs from the periphery are modified (Gilbert, C. D. *et al.*, 2001). In a classic study, the inputs to the palm of one hand in monkeys were removed by transection of the median nerve (Merzenich, M. M. *et al.*, 1983a). This removal of inputs induced drastic changes in the topographic map of the corresponding region of S1: single-unit mapping of cortical RFs showed that the representation of adjoining regions of the hand expanded and filled in the space in the deafferented region (Merzenich, M. M. *et al.*, 1983a). Such topographic plasticity has been extensively investigated in the barrel cortex of rats following whisker removal (Fox, K. *et al.*, 2000; Feldman, D. E. and Brecht, M., 2005). For example, when all but two adjacent whiskers were clipped, many neurons in the two corresponding barrels exhibited long-lasting enhanced responses to both whiskers (Diamond, M. E. *et al.*, 1993). Interestingly, a follow-up study showed that when pairs of adjacent whiskers were mechanically costimulated (Erchova, I. A. and Diamond, M. E., 2004), the induction of the two-whisker RF plasticity was seen only when the stimulation was delivered during peaks in synchronous bursts across S1 (Erchova, I. A. and Diamond, M. E., 2004).

While it takes months for cortical maps to stabilize following deafferentation (Merzenich, M. M. *et al.*, 1983a; 1983b), such reorganization is probably initiated by a series of events that takes place immediately after deafferentation (Calford, M. B., 2002). Merzenich M. M. *et al.* (1983a; 1983b) examined RFs of individual neurons in the somatotopic map corresponding to deafferented regions of the hand. Many RFs from other regions of the hand were unmasked, often at a similar location on the digit but on the other side of the hand. Similarly, reversibly interrupting localized inputs from the mystacial pad of the rat with local anesthesia result in immediate unmasking of RFs in the brainstem spinal trigeminal nucleus (SpV), VPM, and S1 (Faggin, B. M. *et al.*, 1997). Such immediate changes, too rapid to be brought about by anatomical reorganization of cortical circuitry, are likely induced via a release from inhibitory effects of interneurons that were previously tonically activated by the anesthetized mystacial region (Moore, C. I. *et al.*, 1999).

The series of steps between deafferentation and stabilization of the new somatotopic map are presently being elucidated with the help of

multielectrode recordings. For instance, in one study, researchers recorded from layers II/III and layer IV neurons in single S1 columns in anesthetized rats before and after the removal of PW of that column (Celikel, T. *et al.*, 2004). They found that after such removal, the number of evoked spikes when all uncut whiskers were stimulated remained unchanged, but the order of firing in layers IV and II/III was reversed, such that layer IV neurons tended to fire after supragranular neurons (Celikel, T. *et al.*, 2004). This suggests that deprivation-induced changes in the topographic map are partly caused by spike-timing-dependent plasticity, a hypothesis that has been supported by subsequent studies (Bender, K. J. *et al.*, 2006; Jacob, V. *et al.*, 2007).

6.15.5.2 Operant Conditioning

Task-dependent plasticity has been observed in multiple modalities and species (Calford, M. B., 2002). In a classic study in monkeys, the area of the somatosensory cortical representation was increased specifically for those fingers the monkey used to perform a flutter-vibration discrimination task, and these neurons had smaller RFs when compared with the neurons in untrained digits (Recanzone, G. H. *et al.*, 1992). This plasticity was not observed in VPM, suggesting a cortical origin (Wang, X. *et al.*, 1995). In a particularly noteworthy study, a 7×7 MEA was chronically implanted in the hand representation in S1 of monkeys (area 3b) such that the electrodes sampled from regions corresponded to the two digits used in the discrimination task (Blake, D. T. *et al.*, 2005). Initially, none of the units' RFs included both digits, but during the initial month of training, 40% of the neurons acquired RFs that included responses to the two digits used to perform the task.

Another study revealed interesting functional consequences of the topographic organization of the representation of the whiskers in S1 (Harris, J. A. *et al.*, 1999; Blake, D. T. *et al.*, 2005). Researchers first trained rats to perform a gap-crossing task with a single intact whisker (in the gap-crossing tasks, rats are trained to leap across a gap between two platforms when they contact the target platform with their whiskers). After that single whisker was cut, the rats were able to relearn the task when researchers attached a prosthetic whisker attached to a single whisker stub. Interestingly, the time the rats took to relearn the task increased with the distance between the prosthetic whisker and the original whisker used to learn the task. In a second group of rats, they recorded from S1 in rats with 100 electrode arrays and found that the relearning speed was highly correlated with the degree of overlap between the cortical representation of the original whisker and the prosthetic whisker (Blake, D. T. *et al.*, 2005).

6.15.6 Behavioral Modulation of Tactile Responses

It is important to note that the localist or the labeled line approach and the distributed approach to somatosensory coding sketched above need not be mutually exclusive, but could reflect different processing strategies appropriate in different behavioral contexts. Previous studies have shown that S1 is not a simple recorder of events that occur on the periphery, but is modulated by the behavioral state of the animal (Nelson, R. J., 1996). This has also been observed in the rat whisker system where different S1 responses are observed in the quiet waking state as compared to the whisking state (Fanselow, E. E. and Nicolelis, M. A., 1999; Moore, C. I. *et al.*, 1999; Nicolelis, M. A. and Fanselow, E. E., 2002a; 2002b; Castro-Alamancos, M. A., 2004; Moore, C. I., 2004).

By measuring neuronal tactile responses during clearly distinguishable behavioral states, Fanselow E. E. *et al.* (2001) showed that the response properties of S1 and VPM neurons depend strongly on a rat's behavioral state (Fanselow, E. E. and Nicolelis, M. A., 1999; Nicolelis, M. A. and Fanselow, E. E., 2002a; 2002b). In one set of experiments, a nerve cuff electrode was used to stimulate the IO nerve. Individual stimuli were delivered to freely behaving rats, and the cortical and thalamic sensory responses produced when the rats were not moving their whiskers were compared to those observed during periods when the animals were engaged in four different types of behaviors (during quiet immobility, large-amplitude low-frequency whisking, and small-amplitude high-frequency whisker twitching). Overall, the magnitudes of the neural responses in S1 and VPM neurons were significantly reduced during whisker movements. This was not the case when there was motor activity that did not include the whiskers (e.g., movement of the head or the body) or during the period of quiet immobility. This corroborates work in cats (Coulter, J. D., 1974) and in humans (Schmidt, R. F. *et al.*, 1990a; 1990b).

Nicolelis M. A. and Fanselow E. E. (2002) proposed that greater response magnitudes during the quiet state could perform a gross detection function, and the decreased adaptation during the whisking state

would allow for better discrimination of stimuli with a dynamic spatiotemporal structure. Based on the finding that the area of the cortex activated by the stimulation of a vibrissa is relatively smaller during whisking than during an isolated passive contact, some authors have further speculated that a more spatially focused sensory representation during whisking could improve tactile discrimination (Moore, C. I. *et al.*, 1999; Castro-Alamancos, M. A., 2004; Moore, C. I., 2004).

Another study recorded the activity of ensembles of S1 neurons when performing a tactile discrimination task (Krupa, D. J. *et al.*, 2004). In this task, rats learned to behaviorally discriminate between a wide and a narrow aperture width using only their whiskers as sensors (Figures 4(a) and 4(b); see also Krupa, D. J. *et al.*, 2001). By recording from populations of S1 neurons at different cortical depths in the whisker representation, they found that populations

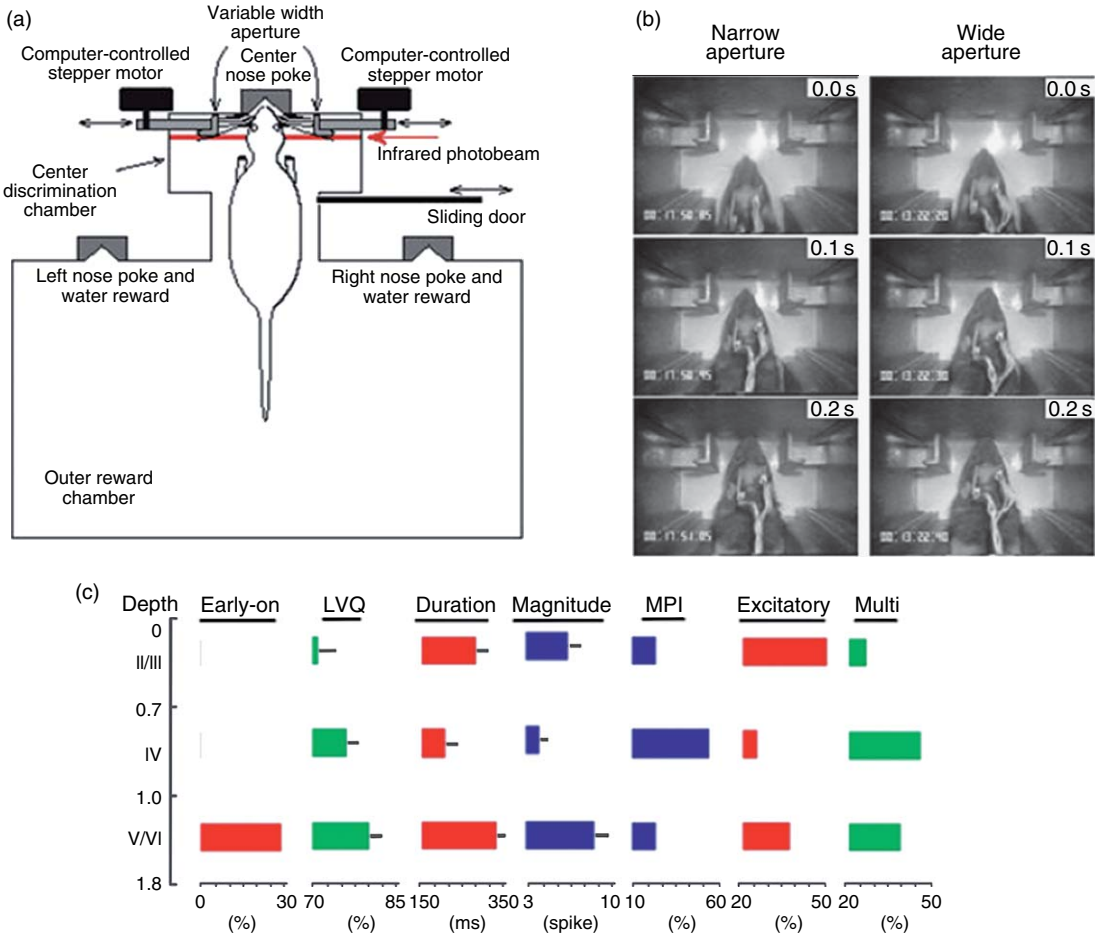

Figure 4 S1 single-unit responses during a freely moving tactile aperture-width discrimination task. (a) Schematic of the behavioral task. Trials begin when a sliding door into the discrimination chamber opens. Rats then sample the variable width aperture with their whiskers and retreat to the left for reward if the aperture was narrow (60 mm) and to the right if the aperture was wide (68 mm). (b) Video frame captures over a 0.2 s period showing a rat approaching and sampling the narrow and wide apertures (left and right panels). (c) Summary diagram showing salient response properties of neurons in different layers of S1. The vertical axis measures recording depth in millimeters. Early-on: percentage of units showing early-onset responses that begin before whisker stimulation; *LVQ:* mean (SEM) wide versus narrow categorization performance of an artificial neural network using population neural activities recorded at different depths. Duration: mean (SEM) excitatory response duration. Magnitude: mean (SEM) magnitude of excitatory responses. MPI: distribution of units with multiphasic responses that began with an inhibitory phase. Excitatory: percentage of units with excitatory responses. Multi: percentage of multiphasic responses. The difference between responses during the active discrimination and responses to passive whisker stimulation (not shown) could not be attributed to differences in the stimuli, suggesting that top-down inputs to S1 sculpt the active discrimination responses. LVQ, learning vector quantization; MPI, multiphasic inhibitory. Adapted from Krupa, D. J., Wiest, M. C., *et al.* 2004. Layer-specific somatosensory cortical activation during active tactile discrimination. Science 304(5679), 1989–1992.

of infragranular neurons encoded aperture width better than the granular and supragranular layers (Figure 4(c), learning vector quantization (LVQ) column), where encoding was quantified using percent correct of a classification algorithm as discussed above in the section on location coding.

In the same study, Krupa D. J. *et al.* (2004) examined the effects of performing the active task on S1 neurons by delivering physically similar stimuli to both anesthetized and awake head-fixed rats. The study demonstrated several differences between S1 responses in the active versus the passive context. First, during active discrimination, S1 neurons produced longer-duration responses (lasting hundreds of milliseconds) of much higher magnitude. Second, a much higher percentage of inhibitory S1 tactile responses was seen when performing the aperture-width discrimination task (49% inhibitory responses vs. 7% during passive stimulation). Third, a novel functional class of S1 neurons was observed during the execution of this task: 30% of infragranular neurons exhibited profound modulation of their firing rate several hundred milliseconds before the animal's whiskers contacted the discriminandum. These anticipatory firing modulations could involve either an increase or a decrease in firing rate, or both. Figure 4(c) summarizes S1 response properties during active tactile discrimination at different cortical depths.

Multiple lines of evidence support the conclusion that these differences between active and passive neural responses are due to top-down modulation of S1 rather than the result of differences in the stimulus itself (see online supplement for Krupa, D. J. *et al.*, 2004). For example, anticipatory firing modulations obviously cannot be accounted for in terms of bottom-up stimulus-driven responses. Similarly, recordings in the peripheral trigeminal ganglion during the active discrimination task show short-duration neural responses (unpublished data), suggesting that long-duration responses at the cortical level are not stimulus-driven. As activity in S1 is modulated by the phase within the whisking cycle and by M1 activity, M1 is a candidate source of top-down inputs (Ahrens, K. F. and Kleinfeld, D., 2004). S2 represents another potential source of contextual modulation of S1 responses (Jackson, M. E. and Cauller, L. J., 1998). The contribution of these and other candidate top-down inputs to S1 may be quantified by combining reversible inactivation of specific candidate areas with multielectrode recordings when performing the tactile discrimination task.

6.15.7 Conclusion and Outlook

We have reviewed recent progress in somatosensory neurophysiology with an emphasis on chronic multielectrode recordings in the rat whisker system. The results suggest that as the typical experimental paradigm shifts from studies of single-whisker stimulus coding in a neutral behavioral context towards more complex stimuli and more active behavioral states, the neural representation of tactile stimuli shifts towards more dynamic and distributed codes. In fact, neural responses within the primary thalamocortical loop, even to simple whisker stimuli, are widely distributed across the two hemispheres. Moreover, the results of reversibly inactivating S1 while recording in VPM showed that thalamic tactile response properties are partly determined by descending feedback from S1, supporting the idea that tactile responses in general reflect the asynchronous convergence of inputs from multiple levels of the somatosensory system. Finally, we found that the importance of the relative timing of responses among neurons tends to increase with the number of whiskers stimulated. Achieving these results was greatly facilitated by multielectrode recording methods – and the last result is currently not attainable in any other way.

The other major shift in our understanding of the somatosensory system came as neurophysiologists found that the functional organization of the somatosensory system was plastic on increasingly fast timescales, down to milliseconds. The evidence that principles of somatosensory coding depend strongly on the behavioral state of the rat, together with observations of task-related plasticity, suggests that the rat's brain adjusts its functional architecture to optimize the performance in different behavioral contexts. This hypothesis provides a framework for interpreting changes in tactile responses in varying contexts and will be most naturally explored and tested using simultaneous recordings of neurons distributed across multiple brain areas involved in somatosensory behavior.

Multielectrode, behavioral, pharmacological, and quantitative methods have evolved to the point where we can now effectively test these ideas about somatosensory coding by neuronal ensembles in the awake-behaving rat. Technical improvements in three directions will facilitate the discovery of the neuronal underpinnings of somatosensory behavior. First, more fine-grained circuit analysis techniques

will reveal specific cell-types, their precise locations, geometry, and channel distributions, leading to refinements of biologically realistic models of the specific transformations being carried out by the somatosensory system. Markram H. (2006) discusses a research program along these lines.

Second, techniques to evoke neuronal activity in precise spatiotemporal patterns will shed light on the effects of such perturbations on downstream networks and behavior. Recent advances in such techniques are discussed in Boyden E. S. *et al.* (2005). Third, as the focus of somatosensory electrophysiology shifts to questions of somatosensory function in awake-behaving animals, behavioral methods will assume increasing importance. For example, advances in whisker sensory physiology will likely follow improvements in our ability to monitor whisker movements using optoelectronic whisker monitoring (Bermejo, R. *et al.*, 1998), video analysis (Knutsen, P. M. *et al.*, 2005), and physical modeling of whisker dynamics (Hartmann, M. J. *et al.*, 2003).

These and related advances will allow experimenters to determine the limits and mechanisms of the fast representational flexibility observed in the mammalian somatosensory system as a result of the past 25 years of multielectrode recordings.

References

Ahrens, K. F. and Kleinfeld, D. 2004. Current flow in vibrissa motor cortex can phase-lock with exploratory rhythmic whisking in rat. J. Neurophysiol. 92(3), 1700–1707.

Armstrong-James, M. 1995. The Nature and Plasticity of Sensory Processing within Adult Rat Barrel Cortex. In: The Barrel Cortex of Rodents (*eds*. E. Jones and M. Diamond), pp. 333–373. Plenum.

Armstrong-James, M. and Fox, K. 1987. Spatiotemporal convergence and divergence in the rat S1 barrel cortex. J. Comp. Neurol. 263(2), 265–281.

Armstrong-James, M., Fox, K., *et al.* 1992. Flow of excitation within rat barrel cortex on striking a single vibrissa. J. Neurophysiol. 68(4), 1345–1358.

Bender, K. J., Allen, C. B., *et al.* 2006. Synaptic basis for whisker deprivation-induced synaptic depression in rat somatosensory cortex. J. Neurosci. 26(16), 4155–4165.

Bermejo, R., Houben, D., *et al.* 1998. Optoelectronic monitoring of individual whisker movements in rats. J. Neurosci. Methods 83(2), 89–96.

Blake, D. T., Strata, F., *et al.* 2005. Experience-dependent plasticity in S1 caused by noncoincident inputs. J. Neurophysiol. 94(3), 2239–2250.

Boyden, E. S., Zhang, F., *et al.* 2005. Millisecond-timescale, genetically targeted optical control of neural activity. Nat. Neurosci. 8(9), 1263–1268.

Brumberg, J. C., Pinto, D. J., *et al.* 1996. Spatial gradients and inhibitory summation in the rat whisker barrel system. J. Neurophysiol. 76(1), 130–140.

Buonomano, D. V. and Merzenich, M. M. 1998. Cortical plasticity: from synapses to maps. Annu. Rev. Neurosci. 21, 149–186.

Calford, M. B. 2002. Dynamic representational plasticity in sensory cortex. Neuroscience 111(4), 709–738.

Calford, M. B. and Tweedale, R. 1990. Interhemispheric transfer of plasticity in the cerebral cortex. Science 249(4970), 805–807.

Calford, M. B. and Tweedale, R. 1991a. Acute changes in cutaneous receptive fields in primary somatosensory cortex after digit denervation in adult flying fox. J. Neurophysiol. 65(2), 178–187.

Calford, M. B. and Tweedale, R. 1991b. C-fibres provide a source of masking inhibition to primary somatosensory cortex. Proc. Biol. Sci. 243(1308), 269–275.

Calford, M. B. and Tweedale, R. 1991c. Immediate expansion of receptive fields of neurons in area 3b of macaque monkeys after digit denervation. Somatosens. Mot. Res. 8(3), 249–260.

Castro-Alamancos, M. A. 2004. Absence of rapid sensory adaptation in neocortex during information processing states. Neuron 41(3), 455–464.

Cauller, L. J., Clancy, B., *et al.* 1998. Backward cortical projections to primary somatosensory cortex in rats extend long horizontal axons in layer I. J. Comp. Neurol. 390(2), 297–310.

Celikel, T., Szostak, V. A., *et al.* 2004. Modulation of spike timing by sensory deprivation during induction of cortical map plasticity. Nat. Neurosci. 7(5), 534–541.

Chapin, J. K. and Woodward, D. J. 1981. Modulation of sensory responsiveness of single somatosensory cortical cells during movement and arousal behaviors. Exp. Neurol. 72(1), 164–178.

Chapin, J. K. and Woodward, D. J. 1982. Somatic sensory transmission to the cortex during movement: gating of single cell responses to touch. Exp. Neurol. 78(3), 654–669.

Coulter, J. D. 1974. Sensory transmission through lemniscal pathway during voluntary movement in the cat. J. Neurophysiol. 37(5), 831–845.

Diamond, M. E., Armstrong-James, M., *et al.* 1993. Experience-dependent plasticity in adult rat barrel cortex. Proc. Natl. Acad. Sci. U. S. A. 90(5), 2082–2086.

DiCarlo, J. J. and Johnson, K. O. 2000. Spatial and temporal structure of receptive fields in primate somatosensory area 3b: effects of stimulus scanning direction and orientation. J. Neurosci. 20(1), 495–510.

Ebner, F. 2005. Neural Plasticity in Adult Somatic Sensory-Motor Systems. CRC Press.

Ebner, F. F. and Myers, R. E. 1962. Corpus callosum and the interhemispheric transmission of tactual learning. J. Neurophysiol. 25, 380–391.

Elbert, T. and Rockstroh, B. 2004. Reorganization of human cerebral cortex: the range of changes following use and injury. Neuroscientist 10(2), 129–141.

Erchova, I. A. and Diamond, M. E. 2004. Rapid fluctuations in rat barrel cortex plasticity. J. Neurosci. 24(26), 5931–5941.

Erzurumlu, R. S. and Killackey, H. P. 1980. Diencephalic projections of the subnucleus interpolaris of the brainstem trigeminal complex in the rat. Neuroscience 5(11), 1891–1901.

Faggin, B. M., Nguyen, K. T., *et al.* 1997. Immediate and simultaneous sensory reorganization at cortical and subcortical levels of the somatosensory system. Proc. Natl. Acad. Sci. U. S. A. 94(17), 9428–9433.

Fanselow, E. E. and Nicolelis, M. A. 1999. Behavioral modulation of tactile responses in the rat somatosensory system. J. Neurosci. 19(17), 7603–7616.

Fanselow, E. E., Sameshima, K., *et al.* 2001. Thalamic bursting in rats during different awake behavioral states. Proc. Natl. Acad. Sci. U. S. A. 98(26), 15330–15335.

Feldman, D. E. and Brecht, M. 2005. Map plasticity in somatosensory cortex. Science 310(5749), 810–815.
Fontanini, A. and Katz, D. B. 2006. State-dependent modulation of time-varying gustatory responses. J. Neurophysiol. 96(6), 3183–3193.
Fox, K., Glazewski, S., *et al.* 2000. Plasticity and stability of somatosensory maps in thalamus and cortex. Curr. Opin. Neurobiol. 10(4), 494–497.
Ghazanfar, A. A. and Nicolelis, M. A. 1997. Nonlinear processing of tactile information in the thalamocortical loop. J. Neurophysiol. 78(1), 506–510.
Ghazanfar, A. A. and Nicolelis, M. A. 1999. Spatiotemporal properties of layer V neurons of the rat primary somatosensory cortex. Cereb. Cortex 9(4), 348–361.
Ghazanfar, A. A. and Nicolelis, M. A. 2001. Feature article: the structure and function of dynamic cortical and thalamic receptive fields. Cereb. Cortex 11(3), 183–193.
Ghazanfar, A. A., Krupa, D. J., *et al.* 2001. Role of cortical feedback in the receptive field structure and nonlinear response properties of somatosensory thalamic neurons. Exp. Brain Res. 141(1), 88–100.
Ghazanfar, A. A., Stambaugh, C. R., *et al.* 2000. Encoding of tactile stimulus location by somatosensory thalamocortical ensembles. J. Neurosci. 20(10), 3761–3775.
Gilbert, C. D. 1996. Learning and receptive field plasticity. Proc. Natl. Acad. Sci. U. S. A. 93(20), 10546–10547.
Gilbert, C. D., Sigman, M., *et al.* 2001. The neural basis of perceptual learning. Neuron 31(5), 681–697.
Harris, J. A., Petersen, R. S., *et al.* 1999. Distribution of tactile learning and its neural basis. Proc. Natl. Acad. Sci. U. S. A. 96(13), 7587–7591.
Hartmann, M. J., Johnson, N. J., *et al.* 2003. Mechanical characteristics of rat vibrissae: resonant frequencies and damping in isolated whiskers and in the awake behaving animal. J. Neurosci. 23(16), 6510–6519.
Hayama, T. and Ogawa, H. 1997. Regional differences of callosal connections in the granular zones of the primary somatosensory cortex in rats. Brain Res. Bull. 43(3), 341–347.
Higley, M. J. and Contreras, D. 2003. Nonlinear integration of sensory responses in the rat barrel cortex: an intracellular study in vivo. J. Neurosci. 23(32), 10190–10200.
Irvine, D. R., Park, V. N., *et al.* 1995. Responses of neurons in the inferior colliculus of the rat to interaural time and intensity differences in transient stimuli: implications for the latency hypotheses. Hear. Res. 85(1–2), 127–141.
Jackson, M. E. and Cauller, L. J. 1998. Neural activity in SII modifies sensory evoked potentials in SI in awake rats. Neuroreport 9(15), 3379–3382.
Jacob, V., Brasier, D. J., *et al.* 2007. Spike timing-dependent synaptic depression in the *in vivo* barrel cortex of the rat. J. Neurosci. 27(6), 1271–12784.
Jacquin, M. F., Wiegand, M. R., *et al.* 1990. Structure-function relationships in rat brain stem subnucleus interpolaris. VIII. Cortical inputs. J. Neurophysiol. 64(1), 3–27.
Jenkins, W. M., Merzenich, M. M., *et al.* 1990. Functional reorganization of primary somatosensory cortex in adult owl monkeys after behaviorally controlled tactile stimulation. J. Neurophysiol. 63(1), 82–104.
Jones, E. and Diamond, M. (*eds*.) 1995. Barrel Cortex of Rodents. Plenum.
Kim, U. and Ebner, F. F. 1999. Barrels and septa: separate circuits in rat barrels field cortex. J. Comp. Neurol. 408(4), 489–505.
Knutsen, P. M., Derdikman, D., *et al.* 2005. Tracking whisker and head movements in unrestrained behaving rodents. J. Neurophysiol. 93(4), 2294–2301.
Koralek, K. A., Olavarria, J., *et al.* 1990. Areal and laminar organization of corticocortical projections in the rat somatosensory cortex. J. Comp. Neurol. 299(2), 133–150.
Krupa, D. J., Ghazanfar, A. A., *et al.* 1999. Immediate thalamic sensory plasticity depends on corticothalamic feedback. Proc. Natl. Acad. Sci. U. S. A. 96(14), 8200–8205.
Krupa, D. J., Matell, M. S., *et al.* 2001. Behavioral properties of the trigeminal somatosensory system in rats performing whisker-dependent tactile discriminations. J. Neurosci. 21(15), 5752–5763.
Krupa, D. J., Wiest, M. C., *et al.* 2004. Layer-specific somatosensory cortical activation during active tactile discrimination. Science 304(5679), 1989–1992.
Lakatos, P., Chen, C. M., *et al.* 2007. Neuronal oscillations and multisensory interaction in primary auditory cortex. Neuron 53(2), 279–292.
Lee, S. M., Friedberg, M. H., *et al.* 1994. The role of GABA-mediated inhibition in the rat ventral posterior medial thalamus. II. Differential effects of GABAA and GABAB receptor antagonists on responses of VPM neurons. J. Neurophysiol. 71(5), 1716–1726.
Maass, W., Natschlager, T., *et al.* 2002. Real-time computing without stable states: a new framework for neural computation based on perturbations. Neural. Comput. 14(11), 2531–2560.
Manns, I. D., Sakmann, B., *et al.* 2004. Sub- and suprathreshold receptive field properties of pyramidal neurones in layers 5A and 5B of rat somatosensory barrel cortex. J. Physiol. 556(Pt 2), 601–622.
Marescaux, C., Vergnes, M., *et al.* 1992. Genetic absence epilepsy in rats from Strasbourg – a review. J. Neural Transm. Suppl. 35, 37–69.
Markram, H. 2006. The blue brain project. Nat. Rev. Neurosci. 7(2), 153–160.
Merzenich, M. M., Kaas, J. H., *et al.* 1983a. Topographic reorganization of somatosensory cortical areas 3b and 1 in adult monkeys following restricted deafferentation. Neuroscience 8(1), 33–55.
Merzenich, M. M., Kaas, J. H., *et al.* 1983b. Progression of change following median nerve section in the cortical representation of the hand in areas 3b and 1 in adult owl and squirrel monkeys. Neuroscience 10(3), 639–665.
Mirabella, G., Battiston, S., *et al.* 2001. Integration of multiple-whisker inputs in rat somatosensory cortex. Cereb. Cortex 11(2), 164–170.
Moore, C. I. 2004. Frequency-dependent processing in the vibrissa sensory system. J. Neurophysiol. 91(6), 2390–2399.
Moore, C. I. and Nelson, S. B. 1998. Spatio-temporal subthreshold receptive fields in the vibrissa representation of rat primary somatosensory cortex. J. Neurophysiol. 80(6), 2882–2892.
Moore, C. I., Nelson, S. B., *et al.* 1999. Dynamics of neuronal processing in rat somatosensory cortex. Trends Neurosci. 22(11), 513–520.
Nelson, R. J. 1996. Interactions between motor commands and somatic perception in sensorimotor cortex. Curr. Opin. Neurobiol. 6(6), 801–810.
Nicolelis, M. A. and Chapin, J. K. 1994. Spatiotemporal structure of somatosensory responses of many-neuron ensembles in the rat ventral posterior medial nucleus of the thalamus. J. Neurosci. 14(6), 3511–3532.
Nicolelis, M. A. and Fanselow, E. E. 2002a. Dynamic shifting in thalamocortical processing during different behavioural states. Philos. Trans. R. Soc. Lond. B Biol. Sci. 357(1428), 1753–1758.
Nicolelis, M. A. and Fanselow, E. E. 2002b. Thalamocortical [correction of Thalamcortical] optimization of tactile processing according to behavioral state. Nat. Neurosci. 5(6), 517–523.
Nicolelis, M. A., Baccala, L. A., *et al.* 1995. Sensorimotor encoding by synchronous neural ensemble activity at multiple levels of the somatosensory system. Science 268(5215), 1353–1358.

Nicolelis, M. A., De Oliveira, L. M., *et al.* 1996. Active tactile exploration influences the functional maturation of the somatosensory system. J. Neurophysiol. 75(5), 2192–2216.

Nicolelis, M. A., Ghazanfar, A. A., *et al.* 1998. Simultaneous encoding of tactile information by three primate cortical areas. Nat. Neurosci. 1(7), 621–630.

Nicolelis, M. A., Lin, R. C., *et al.* 1993. Induction of immediate spatiotemporal changes in thalamic networks by peripheral block of ascending cutaneous information. Nature 361(6412), 533–536.

Olavarria, J., Van Sluyters, R. C., *et al.* 1984. Evidence for the complementary organization of callosal and thalamic connections within rat somatosensory cortex. Brain Res. 291(2), 364–348.

Oliveira, L. M., Wiest, M. C., *et al.* 2003. Integration of bilateral whisker stimuli in primary somatosensory cortex in awake rats. In: *Society for Neuroscience Annual Meeting,* New Orleans, LA, USA.

Petersen, R. S., Panzeri, S., *et al.* 2001. Population coding of stimulus location in rat somatosensory cortex. Neuron 32(3), 503–514.

Pidoux, B. and Verley, R. 1979. Projections on the cortical somatic I barrel subfield from ipsilateral vibrissae in adult rodents. Electroencephalogr. Clin. Neurophysiol. 46(6), 715–726.

Plumbley, M. D. 1999. Do cortical maps adapt to optimize information density? Network 10(1), 41–58.

Recanzone, G. H., Merzenich, M. M., *et al.* 1992. Topographic reorganization of the hand representation in cortical area 3b owl monkeys trained in a frequency-discrimination task. J. Neurophysiol. 67(5), 1031–1056.

Rema, V. and Ebner, F. F. 2003. Lesions of mature barrel field cortex interfere with sensory processing and plasticity in connected areas of the contralateral hemisphere. J. Neurosci. 23(32), 10378–10387.

Sanes, J. N. and Truccolo, W. 2003. Motor binding: do functional assemblies in primary motor cortex have a role? Neuron 38(1), 3–5.

Schmidt, R. F., Schady, W. J., *et al.* 1990a. Gating of tactile input from the hand. I. Effects of finger movement. Exp. Brain Res. 79(1), 97–102.

Schmidt, R. F., Torebjork, H. E., *et al.* 1990b. Gating of tactile input from the hand. II. Effects of remote movements and anaesthesia. Exp. Brain Res. 79(1), 103–108.

Schubert, D., Staiger, J. F., *et al.* 2001. Layer-specific intracolumnar and transcolumnar functional connectivity of layer V pyramidal cells in rat barrel cortex. J. Neurosci. 21(10), 3580–3592.

Shaw, F. Z. 2007. 7–12 Hz high-voltage rhythmic spike discharges in rats evaluated by antiepileptic drugs and flicker stimulation. J. Neurophysiol. 97(1), 238–247.

Shaw, F. Z., Lee, S. Y., *et al.* 2006. Modulation of somatosensory evoked potentials during wake-sleep states and spike-wave discharges in the rat. Sleep 29(3), 285–293.

Shimegi, S., Akasaki, T., *et al.* 2000. Physiological and anatomical organization of multiwhisker response interactions in the barrel cortex of rats. J. Neurosci. 20(16), 6241–6248.

Shin, H. C., Won, C. K., *et al.* 1997. Interhemispheric modulation of sensory transmission in the primary somatosensory cortex of rats. Neurosci. Lett. 230(2), 137–139.

Shuler, M. G., Krupa, D. J., *et al.* 2001. Bilateral integration of whisker information in the primary somatosensory cortex of rats. J. Neurosci. 21(14), 5251–5261.

Shuler, M. G., Krupa, D. J., *et al.* 2002. Integration of bilateral whisker stimuli in rats: role of the whisker barrel cortices. Cereb. Cortex 12(1), 86–97.

Simons, D. J. 1985. Temporal and spatial integration in the rat SI vibrissa cortex. J. Neurophysiol. 54(3), 615–635.

Simons, D. J. and Carvell, G. E. 1989. Thalamocortical response transformation in the rat vibrissa/barrel system. J. Neurophysiol. 61(2), 311–330.

Singer, W. 1999. Neuronal synchrony: a versatile code for the definition of relations? Neuron 24(1), 49–65, 111–125.

Smith, R. L. 1973. The ascending fiber projections from the principal sensory trigeminal nucleus in the rat. J. Comp. Neurol. 148(4), 423–445.

Thomson, E. E. and Kristan, W. B. 2005. Quantifying stimulus discriminability: a comparison of information theory and ideal observer analysis. Neural Comput. 17(4), 741–778.

Tiesinga, P. H., Fellous, J. M., *et al.* 2004. Inhibitory synchrony as a mechanism for attentional gain modulation. J. Physiol. (Paris) 98(4–6), 296–314.

Veinante, P., Lavallee, P., *et al.* 2000. Corticothalamic projections from layer 5 of the vibrissal barrel cortex in the rat. J. Comp. Neurol. 424(2), 197–204.

Waite, P. M. 1969. Organization of whisker responses in the rat thalamus. J. Physiol. 202(2), 51P–53P.

Wang, X., Merzenich, M. M., *et al.* 1995. Remodelling of hand representation in adult cortex determined by timing of tactile stimulation. Nature 378(6552), 71–75.

Welker, C. 1971. Microelectrode delineation of fine grain somatotopic organization of (SmI) cerebral neocortex in albino rat. Brain Res. 26(2), 259–275.

Whishaw, I. and Kolb, B. 2005. The Behavior of the Laboratory Rat. Oxford.

White, E. L. and DeAmicis, R. A. 1977. Afferent and efferent projections of the region in mouse SmL cortex which contains the posteromedial barrel subfield. J. Comp. Neurol. 175(4), 455–482.

Wiest, M. C. and Nicolelis, M. A. 2003. Behavioral detection of tactile stimuli during 7–12 Hz cortical oscillations in awake rats. Nat. Neurosci. 6(9), 913–914.

Wiest, M. C., Bentley, N., *et al.* 2005. Heterogeneous integration of bilateral whisker signals by neurons in primary somatosensory cortex of awake rats. J. Neurophysiol. 93(5), 2966–2973.

Woolsey, T. A. and Van der Loos, H. 1970. The structural organization of layer IV in the somatosensory region (SI) of mouse cerebral cortex. The description of a cortical field composed of discrete cytoarchitectonic units. Brain Res. 17(2), 205–242.

Zhang, M. and Alloway, K. D. 2006. Intercolumnar synchronization of neuronal activity in rat barrel cortex during patterned airjet stimulation: a laminar analysis. Exp. Brain Res. 169(3), 311–325.

Zhu, J. J. and Connors, B. W. 1999. Intrinsic firing patterns and whisker-evoked synaptic responses of neurons in the rat barrel cortex. J. Neurophysiol. 81(3), 1171–1183.

6.16 Specialized Somatosensory Systems

J I Johnson, Michigan State University, East Lansing, MI, USA

R L Reed, University of Florida, Gainesville, FL, USA

© 2008 Elsevier Inc. All rights reserved.

6.16.1	**Introduction**	332
6.16.2	**Thermal Sensory Systems**	332
6.16.2.1	Receptor Structure and Function	332
6.16.2.2	Location	333
6.16.2.3	Pathways to and through the Central Nervous System	334
6.16.2.4	Heat-Sensory Pit Organs of Snakes	334
6.16.2.4.1	Location, structure, and function of receptors	335
6.16.2.4.2	Pathways to and through the central nervous system	335
6.16.2.4.3	Role in behavior	335
6.16.3	**Electrosensory System of Monotremes**	335
6.16.3.1	Receptor Structure and Function	335
6.16.3.2	Location	336
6.16.3.3	Pathways to and through the Central Nervous System	336
6.16.3.4	Role of Electrosensation in Specialized Behaviors of Platypus and Echidnas	337
6.16.3.5	Comparison of the Trigeminal Electrosensory System of Monotremes with the Octavolateral Electrosensory Systems of Fishes	337
6.16.4	**Specialized Mechanosensory Systems**	337
6.16.4.1	Telemechanosensory Specializations	337
6.16.4.1.1	Structural extensions of the skin in fishes	337
6.16.4.1.2	Feathers and bristles in birds	337
6.16.4.1.3	Vibrissae in mammals	337
6.16.4.2	Endomechanosensory Specializations	343
6.16.4.2.1	The dome pressure receptor systems of crocodilian reptiles	343
6.16.4.2.2	Specialized relatively hairless regions of skin in mammals	343
6.16.4.3	Combined Endo- and Telomechanosensory Specializations	345
6.16.4.3.1	Elephant trunks	345
6.16.4.3.2	Stars of star-nosed moles	345
6.16.5	**Overview**	346
References		350

Glossary

endomechanosensory Tactile specializations in certain areas within the skin.

follicle-sinus complex (F-SC) The mechanosensory apparatus found in the follicles at the base of vibrissae and other hairs.

oripulation Working with objects in the environment using lips and other perioral tissues.

ringwulst A dense collar of connective tissue that in many mammals is seen inside the ring sinus portion of the blood sinus around the follicles of vibrissae.

telemechanosensory Apparatus for achieving tactile sensation at some distance from the main body mass.

vibrissa A stiff hair that serves as a tactile organ.

6.16.1 Introduction

By way of introducing the contents of this chapter, a bit of deconstruction of the chapter title will help. Specialized means something is other than the usual, and has a unique character or identity. Somatosensory refers to a group of sensory modalities that are found over wide extensive regions of the body, and is nearly coterminous with general, meaning not special, sensation. So specialized somatosensory is something of a two-word oxymoron. We will take advantage of this inherent self-contradiction to make use of several different meanings of specialized.

The general run of somatosensory modalities respond to mechanical displacement of body tissue, so one kind of specialized somatosensations can be those that respond to stimuli other than mechanical displacement. One of these, the sensation of pain, is sufficiently widespread and important that it is allotted a volume of its own in this series.

Another modality, taste, has long been classified as a special sense since in humans the sensory surface is concentrated in a particular location, as are the organs of the other special senses. Studies of fishes have shown, however, that it could as well be regarded as a general rather than a special sense spread over widespread bodily regions with its receptors intermingled with those of painful and mechanosensory modalities. This topic shares a separate volume in the series with the olfactory sense.

A third traditional somatosensory modality is that of temperature, yielding sensations of heat and cold to stimulation by changing the thermodynamic flow of thermal energy in bodily tissues.

A fourth and newly recognized modality is that of electroreception, which in one of its manifestations in the mammalian monotremes shares receptor locations and neural pathways with the mechanosensory, nociceptive, gustatory, and temperature-sensing systems.

We will begin our treatment of specialized somatosensory systems by reviewing the last two of these widespread receptor modalities, thermoreception and electroreception, which share the somatosensory neural pathways with those of mechanoreceptors, but which are not represented elsewhere in this series of volumes.

Following this we will consider the varieties of unusually organized groups of mechanosensory receptors and pathways that have arisen in the course of chordate evolution. The topic of somatosensation in invertebrates is covered in another volume in this series.

6.16.2 Thermal Sensory Systems

Among the vertebrates, there are two sensory systems that respond to different states of temperature, and particularly, to changes in the temperature of objects in the vicinity of the thermal receptors. One of these systems – that of the cold sensors – responds to loss of heat energy to other objects in the near environment, and to changes in the rate of that loss. The second, less extensive – the warmth-sensing system – responds to the gain of heat from objects that are warmer than the receptive tissues.

The cold and warm systems have different receptors, and activate different pathways within the overall somatosensory pathways to and through the central nervous system. More is known about the cold-sensing system, because it is more widespread in the body and includes several times more cells and fibers than does the warmth-sensing system.

6.16.2.1 Receptor Structure and Function

This account is based mostly on Hensel H. (Hensel, H. *et al.*, 1974; Hensel, H., 1981), with a few later additions cited individually. Both cold and warm receptors are located in unencapsulated free nerve endings, as are the pain and many mechanosensory receptors (Figure 1). The nerve endings are the terminals of small myelinated (A-delta) and unmyelinated (C) fibers. As judged by conduction velocities, all of the warmth-sensitive fibers are believed to be unmyelinated, while there is evidence that cold-sensitive fibers include both myelinated and unmyelinated types.

Some of the cold-sensitive fibers, and possibly some of the warmth-sensitive fibers as well, also respond to painful stimulation with no concurrent change in temperature. Others respond only to changes in temperature. This has led to classifications of receptive endings and fibers as innocuous cold and innocuous warm in contrast to nociceptive cold and nociceptive warm. No innocuous cold and warm endings and fibers have been identified.

In the cellular slime mold amoebas *Dictyostelium discoideum* (Darcy, P. K. *et al.*, 1994), changes in cyclic guanosine monophosphate (cGMP) levels occur in response to thermal stimulation. This finding suggested speculation that transduction processes in thermal receptors may in some ways be analogous to the transduction processes in visual receptors, where a chain of molecular and enzymatic effects brought about by

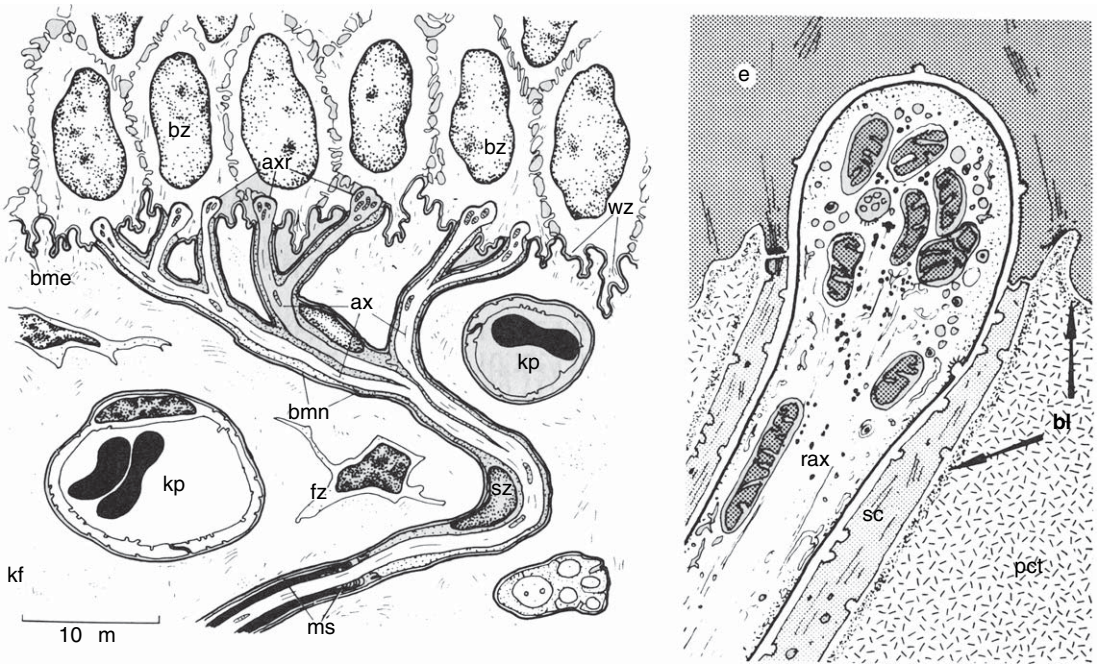

Figure 1 Left: Semischematic diagram of nerve endings at the site of an electrophysiologically identified cold receptor in the hairy skin of the cat nose. ms, myelin sheath of afferent nerve fiber; sz, nonmyelinated Schwann cell accompanying terminal axons (ax) to the basement membrane (bme) of epidermis; bmn, basement membrane of nerve terminals; axr, receptive endings with mitochondria; bz, basal epidermal cells; wz, root feet of basal cells; kp, capillaries; fz, fibrocyte; kf, collagen fibrils of stratum papillare. Right: Schematic representation of a cold receptor axon. The terminal protrudes into a basal epidermal cell. The typical structures of the receptor matrix are present below the receptor membrane. rax, receptor axon;sc, Schwann cell; e, epidermis; pct, papillary connective tissue; bl, basal lamina. Reproduced from Pflügers Arch., Vol. 352, 1974, 1–10, Structure and function of cold receptors, Hensel, H., Andres, K. H. and Düring, M. von., figure 6, with kind permission of Springer Science and Buisness Media. and figure 4.2 in Hensel, H. 1981. Thermoreception and temperature regulation. Monogr. Physiol. Soc. 38, 1–321.

photic stimulation results in changes in cGMP levels that are involved in the initiation of neuronal activity.

More closely related to the actual transduction process, genetic analysis of molecular structure has identified a set of receptor membrane channels known as transient receptor potential (TRP) channels. These channels play a role in the neural activation of receptor cells in a great variety of sensory modalities, and understanding of their function is advanced in the cases of temperature and pain sensation. The subdivision of somatic sensation through free nerve endings may soon be revealed as a graded distribution of the sensitivities of various TRP channels, in the membranes of receptive endings, to restricted ranges of ambient temperatures. These observed ranges fill in the range of perceptible temperature changes, and nociceptive results are obtained by activations beyond these restricted ranges at both the hot and cold ends of the range. Before long we may see a reunification of the separate modalities of heat, cold, pain, and mechanical sensation into a common somatic sensory modality with gradations based on TRP channels of graded sensitivities.

The TRP channels, when activated by their appropriate range of temperature change or other environmental alteration, open to permit the flow of calcium and magnesium through the membrane of the receptive ending. Many contemporary reviews describe the history and details of this developing science of temperature, pain, and mechanical sensation (McKemy, D. D. *et al.*, 2002; Jordt, S.-E. *et al.*, 2003; Patapoutian, A. *et al.*, 2003; Voets, T. *et al.*, 2004; Caterina, M. J. and Montell, C., 2005; Voets, T. *et al.*, 2005; Montell, C., 2006).

6.16.2.2 Location

Based on reaction times to application of cold and warm stimuli, it appears that cold receptive endings in the skin are located immediately below the

epidermis, while warm receptive endings are found deeper, in the upper layers of the corium. In any given region, cold, warm, and nociceptive endings are found, but within a region there are distinct cold and warm spots.

6.16.2.3 Pathways to and through the Central Nervous System

Both cold and warm fibers, along with many nociceptive and mechanosensitive fibers, terminate in the outermost layer of spinal and medullary dorsal horns, in the marginal lamina (Lamina 1 of Rexed). For all of these modalities there are fibers of marginal lamina cells, which project to the ventroposterolateral (VPL) thalamic nucleus in a somatotopic order. In rats there is a distinctive region within VPL that responds only to cold stimulation through a special group of cold-sensory second-order axons of marginal lamina cells (Zhang, X. *et al.*, 2006). Cells of VPL in many and possibly all mammalian species project to parietal regions of the cerebral cortex.

Functional magnetic resonance imaging (fMRI) study has shown the cortex of the superior parietal lobule and other brain regions responding to stimulation by thermal stimuli, which is perceived by human subjects as being warm or cold. These regions include the insular and orbitofrontal regions of the cerebral cortex (Hua, L. H. *et al.*, 2005; Craig, A. D. *et al.*, 2006) (Figure 2).

6.16.2.4 Heat-Sensory Pit Organs of Snakes

Snakes of the subfamily Crotalinae (Viperidae), and others of the family Boidae, possess concentrations of warm receptors in special organs known as pits, depressions between the scales on the face between the eyes,

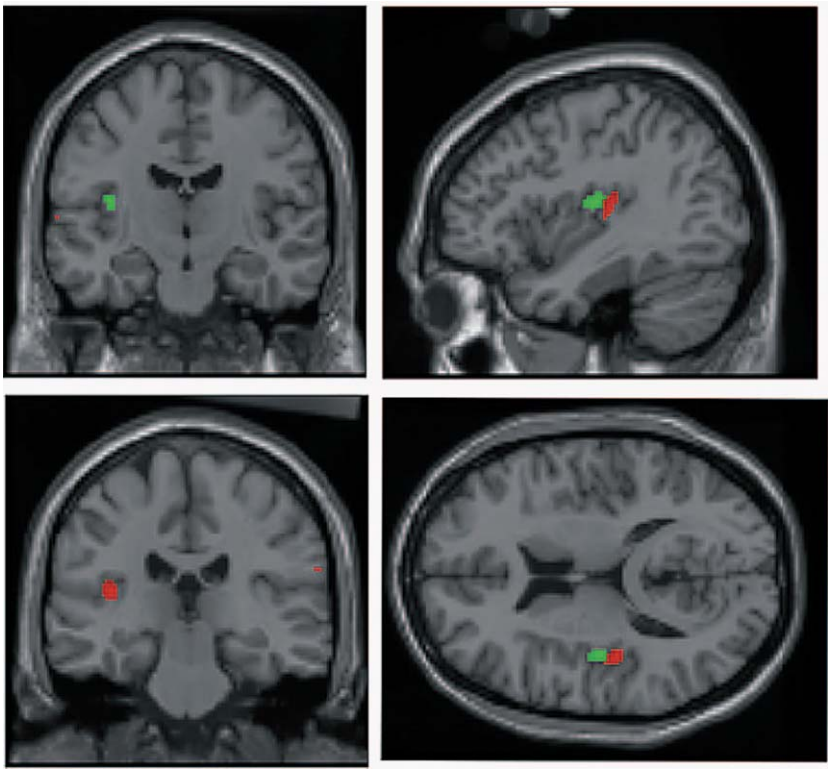

Figure 2 Somatotopographical organization of hand (red) and neck (green) activation foci in the human dorsal posterior insula superimposed on a standard brain anatomic volume. This activation, viewed with functional magnetic resonance imaging (fMRI), was produced by stimulation of the hand or neck with an innocuous cooling stimulus. Reproduced from Figure 5 in Hua, L. H., Strigo, I. A., Baxter, L. C., Johnson, S. C., and Craig, A. D. 2005. Anteroposterior somatotopy of innocuous cooling activation focus in human dorsal posterior insular cortex. Am. J. Physiol. Regul. Integr. Comp. Physiol. 289, R319–R325, used with permission.

nares, and mouth. The boids have several small sensory pits, while the crotalines have a single large pit on each side of the head. This account is based largely on contemporary reviews by Krochmal A. R. and Bakken G. S. (2003) and by Pappas T. C. *et al.* (2004).

6.16.2.4.1 Location, structure, and function of receptors

Within the crotaline pits the receptors are concentrated in a thin membrane that stretches between the edges of the pit, and this membrane is accompanied by a concentration of capillaries that can serve as a drain for removing heat accumulated in the pit, analogous to the role of the pigment epithelium in the visual retina that absorbs light after light has excited the layer of photoreceptors. Evidence now shows that the pit receptors are sensitive to ambient temperatures rather than to photons reporting the location of infrared radiation. The pit organs contain the greatest number and density of heat-sensitive cells known in the animal kingdom. They have the capability of giving the snakes a finely detailed picture of the temperature map of their environment.

The heat receptors are in the endings of neurons in the trigeminal ganglia. The mode of transduction of the dynamic patterns of heat energy into patterns of nerve impulses in the trigeminal nerve is not known, but electrophysiological evidence suggests that it may be similar to that which utilizes TRP channels and cGMP activation in mammalian temperature and nociceptive receptors.

6.16.2.4.2 Pathways to and through the central nervous system

The trigeminal temperature-sensitive cells project to the optic tectum, where the information they supply appears to complement that received from the visual system. Many individual tectal cells receive both visual and thermosensory input.

6.16.2.4.3 Role in behavior

The temperature information appears to supply deficiencies in the visual information due to decrease in ambient light during the dark part of the diurnal cycle, giving the snake a continuous 24 h visual–thermal picture of the environment and events therein. The thermal aspect of the informational input has been put to use by snakes as an aid in locating warm-blooded prey, and also to help find warm places to rest and to nest.

6.16.3 Electrosensory System of Monotremes

The egg-laying monotreme mammals have developed a unique system, within the trigeminal somatic sensory system, that is sensitive to electrical states and currents in the environment (reviewed by Proske, U. *et al.*, 1998; Pettigrew, J. D., 1999).

6.16.3.1 Receptor Structure and Function

The electroreceptors are nerve endings associated with the ducts of large mucus-secreting glands (Gregory, J. E. *et al.*, 1988; Manger, P. R. and Pettigrew, J. D., 1996). They respond to steady DC electrical fields and to rapid potential transients. The neurons with the receptive endings are excited by cathodal (negative) pulses and inhibited by anodal (positive) pulses (Proske, U. *et al.*, 1998). Figure 3 shows the organization of nerve endings around and in the duct of the gland. There are many other mucous glands without the receptor innervation.

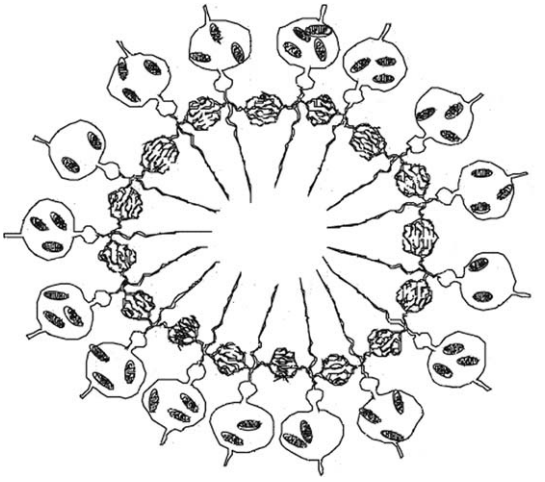

Figure 3 Diagrammatic representation of a monotreme mucous gland electroreceptor showing the tangential arrangement of afferent nerve endings around the pore. The bulbous expansions of each nerve fiber are packed with mitochondria. The terminal naked filaments pierce a high-resistance layer in the epidermis and extend toward the mucous-filled duct. The lateral branches of each fiber extend toward each other. It is not known whether they are electrically coupled. Reproduced from figure 3 in Pettigrew, J. D. 1999. Electroreception in monotremes. J. Exp. Biol. 202, 1447–1454, with permission.

6.16.3.2 Location

In platypus the mucous gland electroreceptors are arranged in a series of rostrocaudal bands with electroreceptor-free bands between them, over almost the whole extent of the inner and outer surfaces of the upper and lower bill (Figure 4; Manger, P. R. and Pettigrew, J. D., 1996; Pettigrew, J. D., 1999). This is in contrast to the distribution of another set of mechanoreceptors peculiar to monotremes, called the push-rod receptors, which are arrangements of stiff rods in the skin of the bill that enhance the mechanical stimulation of sets of Merkel cells and lamellated corpuscles when the bill is touched. (Their structure and function have many features in common with Eimer's organs; see Figure 10.) The push-rod receptors are distributed more evenly across the whole surface of the bill.

Another type of receptor, called serous gland receptors located in the ducts of glands smaller than the mucous receptors, is found along the lateral margins of the bill. It was speculated that the serous gland receptors might be another type of electroreceptor sensitive only to electrical events in close proximity to small regions of the skin of the bill.

These receptor types are also found in the two extant monotreme species of echidnas (spiny anteaters), but are restricted to a small region near the tip of the bill, where the skin is kept moist by nasal secretions (Gregory, J. E. *et al.*, 1989; Manger, P. R. *et al.*, 1997).

6.16.3.3 Pathways to and through the Central Nervous System

In echidnas the electrosensory receptors were found to project through the infraorbital branch of the maxillary division of the trigeminal nerve (Gregory, J. E. *et al.*, 1989).

In platypus electroreceptors were reported to project to the somatosensory region of the cerebral cortex, with some cortical cells activated by either electrosensory or mechanosensory stimulation of bill receptors (Iggo, A. *et al.*, 1992; Proske, U. and Gregory, E., 2003). Pettigrew J. D. (1999) reported alternating electrosensory and mechanosensory modality columns in this cerebral cortical region.

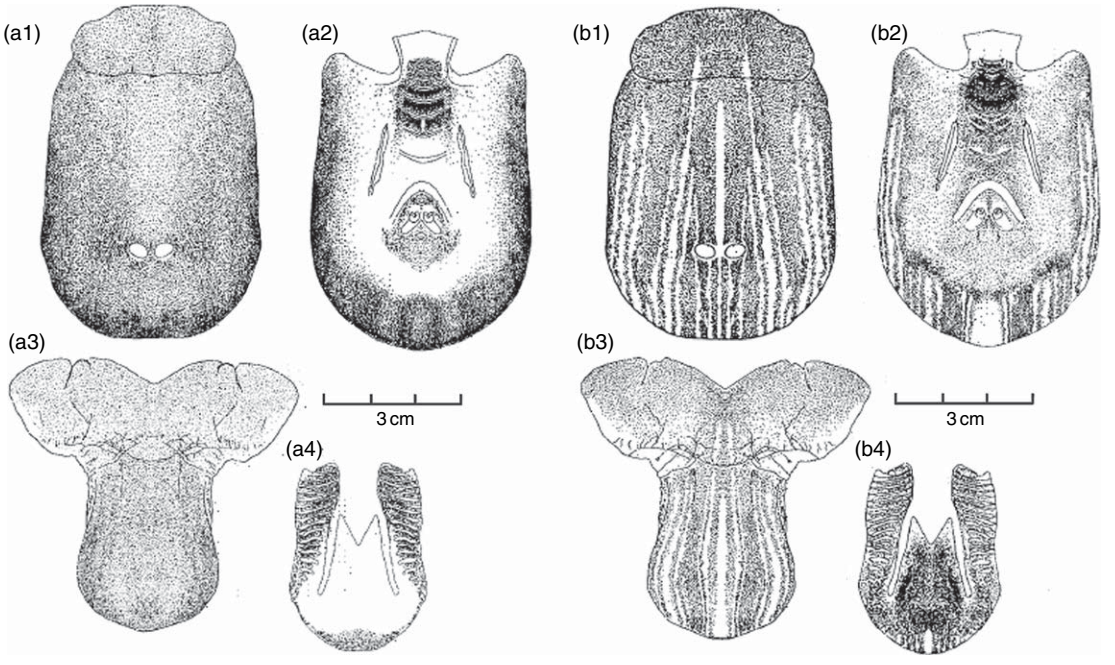

Figure 4 Distribution of push-rod mechanoreceptors (a) (visible as a touch dome in the dissecting microscope) and (b) mucous electroreceptors (visible as a large pit) in platypus. Note the parasagittal arrays of electroreceptors. The total number of electroreceptors, counting both the outside (1,3) and the inside (2,4) surfaces of both the upper (1,2) and lower (3,4) bills, is approximately 40 000. There are approximately 60 000 mechanoreceptors. Reproduced with permission from Manger, P. R. and Pettigrew, J. D. 1996. Ultrastructure, number, distribution and innervation of electroreceptors and mechanoreceptors in the bill skin of the platypus, *Ornithorhynchus anatinus*. Brain Behav. Evol. 48, 27–54 as it appears in figure 2 of Pettigrew, J. D. 1999. Electroreception in monotremes. J. Exp. Biol. 202, 1447–1454.

6.16.3.4 Role of Electrosensation in Specialized Behaviors of Platypus and Echidnas

Pettigrew J. D. (1999) provides an extensive discussion of the possible roles of the striated arrangement of electroreceptors on the platypus bill, and the alternating stripes of electrosensory and mechanosensory projections in the sensory cerebral cortex, in prey localization. These features appear to work optimally in combination with a saccadic side-to-side movement of the bill over the aquatic substrate where voltage-generating prey are found. One interesting feature revealed in behavioral studies is that the whole moving platypus can detect smaller voltage changes than can the individual receptors. It is speculated that echidnas employ their more modest electrosensory endowment in a similar fashion in searching for ants in a sandy environment.

6.16.3.5 Comparison of the Trigeminal Electrosensory System of Monotremes with the Octavolateral Electrosensory Systems of Fishes

Electrosensory systems have arisen convergently and independently at least three times in the evolution of the vertebrate chordates. In two of these cases, both in fishes, electrical sensation takes place through derivatives of the eighth cranial nerve placode; the third case is that in monotremes, where the system derives from the fifth cranial nerve placode (Pettigrew, J. D., 1999). In the octavolateral systems, transduction takes place in specialized epithelial receptive hair cells. In the trigeminal system, transduction takes place in naked nerve endings in ducts of secreting glands, although these naked endings have an elaborate formal arrangement in the daisy chains seen in Figure 3. In the trigeminal monotreme system, most central processing takes place in the cerebral cortex of the forebrain; in the octavolateral fish systems most central processing takes place in the brain stem and cerebellum of the hindbrain. In all three systems receptors are located at the depth of pores in the surface skin.

6.16.4 Specialized Mechanosensory Systems

We have sorted specialized mechanosensory systems into two categories. The first category is that of telemechanosensory specializations, whereby mechanical stimulation is amplified or spatially extended by the use of projections reaching out from the body surface. These are represented by extension of the skin, by sensory endings related to feathers in birds, and most extensively by specialized hairs extending from the skin of mammals. In birds and mammals, these structures embedded in, and projecting out from the skin, function in locomotion, or body heat conservation, or as tools with which to accomplish specific behavioral ends, but in the cases to be described they also add to the animals' sensation of objects and events in the more distant environment.

The second category is that of endomechanosensory specializations, such as touch spots or regions – adaptive groupings of receptors within particular regions of skin, in locations of importance to adaptive behaviors peculiar to particular species or groups of species.

6.16.4.1 Telemechanosensory Specializations

6.16.4.1.1 Structural extensions of the skin in fishes

Among the best-known projections of skin for the purpose of extending sensory surfaces into the environment are the barbels seen around the oral regions of several species of bony fishes. In many species these are outgrowths of the taste system (see references in Zhang, G. *et al.*, 2006). The barbels extend the sensory surface into the surrounding environment. In one species, the Antarctic plunderfish, there is a single midline barbel that has no taste buds and is entirely mechanosensory, which is not used for probing the substrate but rather for gathering information about the presence and activity of prey in the water (Roule, L. *et al.*, 1913; Eastman, J. T. and Lannoo, M. J., 2003) (Figure 5).

6.16.4.1.2 Feathers and bristles in birds

In birds there is a rich network of sensory nerve fibers around the base of feathers (Saxod, R. *et al.*, 1996). This suggests a role of feathers in amplifying tactile sensation of mechanical contact.

Bristles, which are actually modified feathers around the mouth and eyes, appear to have a tactile sensory protective function inducing reflex closure of these openings (Lederer, R. J., 1972; Conover, M. L. and Miller, D. E., 1980).

6.16.4.1.3 Vibrissae in mammals

All mammals possess hair of some kind during at least some phase of their ontogeny. Vibrissae are hairs that are specialized for sensory functions. Terrestrial

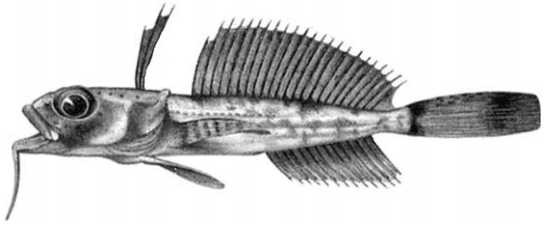

Figure 5 A tactile barbel with no taste function. Antarctic plunderfish *Dolloidraco longedorsalis* (TL = 123 mm) showing overall morphology, barbel, eyes, and location of nasal pore. In life the barbel is usually oriented about 45° above the substrate. Reproduced with permission from Roule, L., Angel, F., and Despax, R. 1913. Poissons. In: Deuxième Expédition Antarctique Française (1908–1910), (*eds.* J. Charcot and L. Joubin), p. 24. Masson as it appears in figure 1 in Eastman, J. T. Lannoo, M. J. 2003. Anatomy and histology of the brain and sense organs of the Antarctic plunderfish *Dolloidraco longedorsalis* (perciformes: notothenioidei: artedidraconidae), with comments on the brain morphology of other artedidraconids and closely related harpagiferids. J. Morphol. 255, 358–377.

mammals possess vibrissae on restricted regions of the body, most notably the face (Pocock, R. I., 1914; Eisenberg, J. F., 1981). However, monotremes, some marsupials, and humans lack vibrissae (Ling, J. K., 1966). Some rodents possess a few carpal, antebrachial, or tarsal vibrissae, and six to eight vibrissae are found on the trunk in two squirrel species (Hyvärinen, H. *et al.*, 1977; Sokolov, V. E. and Kulikov, V. F., 1987). Rock hyraxes (*Procavia capensis*) have vibrissae on the trunk (Sale, J. B., 1970; Sokolov, V. E., 1982). Among aquatic mammals, pinnipeds and cetaceans have vibrissae on the face only (Ling, J. K., 1977). Baleen whales have ~100 thin vibrissae on the upper and lower jaws. In most odontocete cetaceans, hair is present only as prenatal vibrissae, which atrophy, leading to a completely hairless condition postnatally. An important exception is the freshwater river dolphins, with well-developed vibrissae along the upper and lower jaws. Sirenians possess vibrissae over the entire body (Reep, R. L. *et al.*, 2001; 2002).

Vibrissae are known to convey detailed information about shapes and textures of objects in the immediate environment through direct tactile contact (Dykes, R. W., 1975; Brecht, M. *et al.*, 1997), and they enable detection of hydrodynamic stimuli in some aquatic mammals (Dehnhardt, G. *et al.*, 1998a; 2001). The use of mystacial vibrissae by terrestrial mammals is well documented, and includes the findings that rodents use rhythmic whisking motions (Welker, W. I., 1964) and that each row of mystacial vibrissae operates as a functional unit by sampling highly overlapping spatial information perpendicular to the rostrocaudal axis (Brecht, M. *et al.*, 1997). Sokolov V. E. and Kulikov V. F. (1987) performed vibrissae ablation experiments indicating that nocturnal and crepuscular rodents, which possess relatively long mystacial vibrissae, rely primarily on touch for orientation whereas diurnal species, which have short vibrissae, rely principally on vision. Vibrissal follicles are referred to as follicle-sinus complexes (F-SCs) because of their specialized structural features, including a well-defined circumferential blood sinus, dense connective tissue capsule, and substantial innervation (Andres, K. H., 1966; Stephens, R. J. *et al.*, 1973; Rice, F. L. *et al.*, 1986; 1997; Ebara, S. *et al.*, 2002). Furthermore, in many taxa, specializations exist in the brain stem, thalamic, and cortical regions that process information from F-SC afferents (Van der Loos, H., 1976; Jones, E. G., 1983; Ladygina, T. F. *et al.*, 1985; Land, P. W. and Simons, D. J., 1985; Nomura, S. and Mizuno, N., 1986; Florence, S. L. and Lakshman, S., 1995; Rice, F. L., 1995).

All the major hair types possess innervated mechanoreceptors. Vibrissae are the most extensively innervated and have numerous mechanoreceptors, including Merkel cells, lanceolate endings, and free nerve endings (Zelena, J., 1994). Receptor types and innervation patterns have been studied in a variety of mammals including rodents (Munger, B. L. and Rice, F. L., 1986; Rice, F. L. *et al.*, 1986; Mosconi, T. M. *et al.*, 1993; Rice, F. L., 1993; Rice, F. L. *et al.*, 1993; 1997; Ebara, S. *et al.*, 2002), rabbits and cats (Rice, F. L. *et al.*, 1986; Rice, F. L., 1993; Ebara, S. *et al.*, 2002), primates (Halata, Z. and Munger, B. L., 1980), tammar wallabies (Marotte, L. R. *et al.*, 1992), hippopotamuses (Bachteler, D. *et al.*, 1998), manatees (Reep, R. L. *et al.*, 2001; 2002; Sarko, D. K. *et al.*, 2007), sea lions (Stephens, R. J. *et al.*, 1973), ringed seals (Hyvärinen, H., 1995), and bearded seals (Marshall, C. D. *et al.*, 2006). A deep vibrissal nerve contains 100–200 axons that terminate in receptors located in the outer root sheath and mesenchymal sheath. Some aquatic mammals possess far greater numbers of axons per follicle (Hyvärinen, H., 1995; Dehnhardt, G. *et al.*, 1999; Marshall, C. D. *et al.*, 2006).

It is not known exactly how vibrissae work. However, integrity of the sinus capsule is necessary for normal function (Gottschaldt, K.-M. *et al.*, 1973). Rapidly adapting vibrissal afferent axons code stimulus onset and appear to be associated with encapsulated endings (Ebara, S. *et al.*, 2002). Slowly adapting units code aspects of stimulus intensity, and are associated with Merkel cells and possibly lanceolate and club-like endings (Gottschaldt, K.-M. *et al.*, 1973; Dykes, R. W., 1975; Ebara, S. *et al.*, 2002). Reticular and spiny endings

are candidates for transducing directionally selective responses seen in some slowly adapting units (Dykes, R. W., 1975; Ebara, S. *et al.*, 2002). Blood pressure may set the mechanical tension (and thus response sensitivity) of the tissue in which lanceolate endings and Merkel cells are located (Woolsey T. A. *et al.*, 1981; Rice, F. L. *et al.*, 1986). Therefore, the neural response properties of individual vibrissa follicles would depend on at least the following attributes at the microanatomical level: (1) hair length, diameter, and stiffness, both external to the skin surface and within the follicle; (2) follicle geometry, especially follicle length and diameter, capsule wall thickness, and ring sinus size and shape; (3) innervation density and types and distributions of nerve endings; (4) Merkel cell density and distribution.

6.16.4.1.3.(i) Nonmystacial vibrissae in terrestrial mammals The intense focus on mystacial vibrissae as a neurobiological model system has tended to obscure the fact that many mammals also possess vibrissae in other body locations. Among rodents, collectively, vibrissae are found in nine other regions of the face and eight other regions of the postfacial body (Sokolov, V. E. and Kulikov, V. F., 1987), with individual species exhibiting various subsets of these. In a morphological study of squirrel carpal and abdominal vibrissae, Hyvärinen H. *et al.* (1977) found that these have structural features similar to mystacial vibrissae, including the same types of receptors. Fox squirrels exhibit a wide expanse of somatosensory projections to the dorsolateral medulla oblongata from the outer hairs of the forelimb (Ostapoff, E.-M. *et al.*, 1983). Jerboas hang their longest mystacial vibrissae on the ground in front of where their feet will land, apparently sampling the substrate prior to landing (Sokolov, V. E. and Kulikov, V. F., 1987). This is especially apparent during jumping. The ventral abdominal vibrissae in squirrels may perform a similar function (Hyvärinen, H. *et al.*, 1977; Sokolov, V. E. and Kulikov, V. F., 1987).

In microchiropteran bats, touch domes along the wings are heavily invested with Merkel cells and free nerve endings that appear to detect air flow and aid in navigation and maneuvering (Zook, J. M., 2007).

Hyraxes are unusual in having vibrissae scattered over the entire body, intermingled with dense pelage fur. Sale J. B. (1970) based this conclusion upon external morphological features including the greater length and thickness of these hairs, and their relatively sparse distribution, and suggested that this array of vibrissae may be used for tactile exploration and orientation within rock crevices and tunnels under low-light conditions. Sokolov V. E. (1982) also reported that three species of hyraxes have vibrissae on the trunk as well as the face. Diana Sarko (unpublished observations) has used histological criteria to confirm the identification of these hairs as vibrissae (Figure 6). Thus, hyraxes are apparently unique among extant terrestrial mammals in having vibrissae distributed over the entire body surface. Naked mole rats may represent a case of convergent evolution in this regard. They possess sparsely distributed, evenly spaced vibrissae-like body hairs on their otherwise unfurred bodies, and these hairs are densely innervated though they lack blood sinuses (Park, T. J. *et al.*, 2003). This system of tactile hairs is used in behavioral orientation (Crish, S. D. *et al.*, 2003).

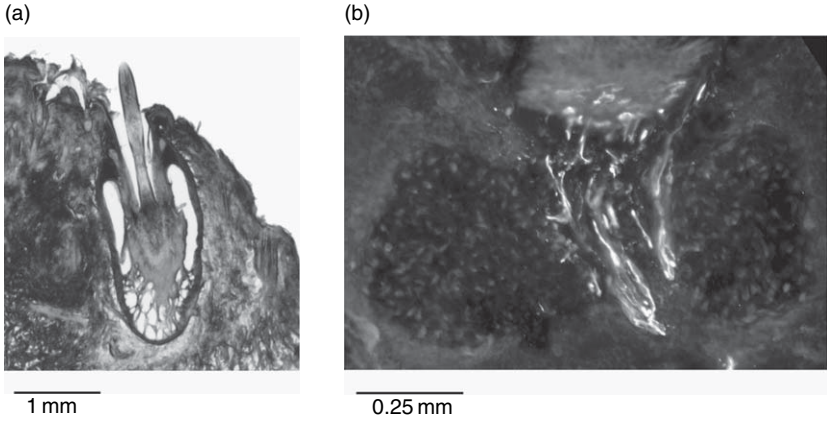

Figure 6 Follicle-sinus complexes (F-SCs) from the dorsal body region of the rock hyrax (*Procavia capensis*). As shown in (a), the blood sinus is surrounded by a dense capsule, and its lower portion is trabeculated. (b) Illustrates nerve endings positive for protein gene product 9.5 in the mesenchymal sheath, flanked by the sinus to the left and right. Photo courtesy of Dr. Diana Sarko.

6.16.4.1.3.(ii) Functions of vibrissae in aquatic mammals The aquatic medium presents two features that have a significant impact on somatosensory processes. First, the greater density of water compared to air changes the dynamics of interaction between a moving vibrissa and the follicle wall containing mechanoreceptors. Some pinniped vibrissae are oval and stiff (Marshall, C. D. *et al.*, 2006); others are flattened and exhibit a wavy, beaded edge (Hyvärinen, H. and Katajisto, H., 1984; Watkins, W. A. and Wartzok, D., 1985; Hyvärinen, H., 1989; Dehnhardt, G. and Kaminski, A., 1995), features that may reduce vibratory movements generated by swimming (Hanke, W., personal communication). Second, many aquatic environments are turbid, which reduces the usefulness of visual cues. Although odontocete cetaceans have developed high-frequency echolocation in order to locate prey and navigate underwater, other aquatic mammals have not.

Hydrodynamic stimuli occur when there is motion in a fluid medium. Hydrodynamic reception is intermediate between touch and hearing and it has been suggested that mammalian vibrissae may serve a function complementary to audition at low frequencies (Griffin, D. R., 1959; Marler, P. and Hamilton, W. J., 1966; Yohro, T., 1977; Gerstein, E. R. *et al.*, 1999; Reep, R. L. *et al.*, 2002). In nonmammals hydrodynamic receptors act as low-pass filters that respond proportional to velocity or acceleration of stimuli, in the frequency range of 1–150 Hz (Bleckmann, H., 1994). Fishes and some amphibians possess a lateral line system that detects hydrodynamic stimuli with frequencies in the range of <100 Hz. Evidence suggests that pinnipeds, sirenians, and some aquatic rodents possess vibrissal specializations that represent adaptations for direct tactile contact and for the detection of low-frequency hydrodynamic stimuli in the aquatic environment. In the latter context they may be considered mammalian analogs of the lateral line system.

Psychophysical studies and behavioral observations suggest that vibrissae are very important in the lives of aquatic mammals. Harbor seals can discriminate objects using their facial vibrissae as effectively as monkeys do when using their hands (Weber fraction of ~9%; Dehnhardt, G. and Kaminski, A., 1995). Manatees perform tactile discriminations using their facial vibrissae as well, as do elephants when using their trunks (Weber fraction of ~14%; Bachteler, D. and Dehnhardt, G., 1999), and much better than sea lions do when using their facial vibrissae (Weber fraction of ~20%; Dehnhardt, G. and Ducker, G., 1996). Walruses can distinguish shapes with surface areas as low as 0.4 cm^2 (Kastelein, R. A. and van Gaalen, M. A., 1988). Pinnipeds wave their long vibrissae in the air during display behaviors and tactile exploration (Peterson, R. S. and Bartholomew, G. A., 1967; Miller, E. H., 1975; Kastelein, R. A. and van Gaalen, M. A., 1988; Dehnhardt, G., 1994; Dehnhardt, G. and Kaminski, A., 1995; Dehnhardt, G. and Ducker, G., 1996). Freshwater river dolphins (Platanistidae) have reduced visual systems but relatively well-developed bristle-like vibrissae on the upper and lower jaws. These nonmobile vibrissae are likely used to detect fishes and crustacean prey along river bottoms (Norman, J. R. and Fraser, F. C., 1948; Layne, J. N. and Caldwell, D. K., 1964, cited in Ling, J. K., 1977). The Australian water rat is an aquatically adapted murid rodent that uses its long mystacial vibrissae to locate prey underwater. It also dips its vibrissae in the water while the remainder of its body is on land, presumably to sample the hydrodynamic environment prior to diving after prey with its eyes closed (Woollard, P. *et al.*, 1978; Dehnhardt, G. *et al.*, 1999). Marshall C. D. *et al.* (2006) have drawn attention to the relationship between feeding strategy and vibrissae elaboration. Bearded seals and walruses are benthic foragers and they possess more numerous vibrissae arranged on a broad, flat muzzle compared to the lateral placement of fewer vibrissae in pinnipeds that are nonbenthic foragers. Walruses and sirenians use their perioral vibrissae not only for tactile investigation, but also to move food and inanimate objects (Fay, F. H., 1982; Marshall, C. D. *et al.*, 1998a; 1998b; 2003).

In manatees the perioral bristles are located in six regions. A subset of these perioral vibrissae engages in true grasping to gather and ingest plants during feeding (Marshall, C. D. *et al.*, 1998a; 1998b; Reep, R. L. *et al.*, 1998). We have named this unique behavior oripulation. (Oripulation is a term we use to denote grasping or handling behavior using the vibrissae and associated perioral musculature (Reep, R. L. *et al.*, 2001). This distinguishes it from the term manipulation, which connotes the use of the manus or hand.) The oral disk, the expanded mystacial region of the sirenian face, contains a dense array of thin vibrissae intermediate in stiffness and innervation between perioral bristles and postcranial body hairs. These thinner vibrissae are used during tactile investigation of novel objects or food items (Hartman, D. S., 1979; Marshall, C. D. *et al.*, 1998b; Bachteler, D. and Dehnhardt, G., 1999). About 3000 vibrissae are distributed on the postfacial body, each with a relatively independent field of movement (Reep, R. L. *et al.*, 2002). Each postcranial follicle is supplied by 20–50

axons, compared to 50–250 axons innervating follicles of the perioral bristles and oral disk (Reep, R. L. *et al.*, 2001; 2002). This widespread postfacial distribution of vibrissae is unique among mammals. In nonmammals, hydrodynamic sensors spread over the body surface record the spatial distribution of a stimulus, and thus extract important 3D information (Teyke, T., 1989; Bleckmann, H., 1994). For example, many fishes use the lateral line for discrimination and avoidance of objects in the aquatic environment (Hassan, E. S., 1986). Stationary underwater objects create distortions in the flow fields generated by animals moving through water, and unequivocal information about object size and distance can be obtained by analyzing the velocity distribution of the flow field over the body (Hassan, E. S., 1989). These capacities may be enhanced in manatees due to the widespread distribution of vibrissae and large body size.

Vibrissae of nonsirenian aquatic mammals appear to be used not only in direct tactile contact, but also to detect water movements, often caused by other animals. Harbor seals can use their facial vibrissae to detect controlled low-frequency underwater vibratory stimuli (Mills, F. H. J. and Renouf, D., 1986) and hydrodynamic trails like those produced by swimming fishes (Dehnhardt, G. *et al.*, 1998a; 2001). The Australian water rat preys on fishes and is able to detect constant velocity but not oscillatory hydrodynamic stimuli (Hanke, W., personal communication).

6.16.4.1.3.(iii) Follicle structure and follicle-sinus complexes in aquatic mammals Vibrissae follicles in aquatic mammals exhibit several structural differences from those in terrestrial mammals, likely reflecting the different functional requirements of operating in the aquatic medium. Mystacial vibrissae of terrestrial rodents exhibit a circumferential ring sinus with a ringwulst (ring body), as well as a ventrally adjacent trabeculated cavernous sinus (Vincent, S., 1913; Melaragno, H. P. and Montagna, W., 1953; Wineski, L. E., 1985; Rice, F. L. *et al.*, 1986; 1997; Dehnhardt, G. *et al.*, 1999). Facial vibrissae in pinnipeds and manatees exhibit elongated F-SCs with a ring sinus flanked by upper and lower cavernous sinuses (Ling, J. K., 1966; 1972; Stephens, R. J. *et al.*, 1973; Hyvärinen, H. and Katajisto, H., 1984; Reep, R. L. *et al.*, 2001; 2002; Marshall, C. D. *et al.*, 2006), and trabeculae found in the cavernous sinuses of manatees are innervated by a novel type of nerve ending (Sarko, D. K. *et al.*, 2007). Ling J. K. (1977) noted a variety of sinus configurations among cetaceans. One effect of increased F-SC size and the addition of an upper cavernous sinus is to increase thermal compensation. Low temperature reduces the sensitivity of mechanoreceptors, but at least some taxa (harbor seals) exhibit selective heating in F-SCs (Mauck, B. *et al.*, 2000), which preserves tactile sensitivity under conditions of low ambient water temperature (Dehnhardt, G. *et al.*, 1998b).

Pinniped F-SCs possess a ringwulst, but sirenian follicles do not. The ringwulst in southern elephant seals is relatively small compared to the ringwulst in rats (Ling, J. K., 1966). The largest F-SCs of manatees exhibit rigidly attached appendages rather than a suspended ringwulst, whereas smaller manatee F-SCs have no appendages and reduced ring sinuses (Reep, R. L. *et al.*, 2001; 2002). Stephens R. J. *et al.* (1973) suggested that the ringwulst may transmit vibratory energy from the hair shaft to the ring sinus, and this conjecture may also apply with some modification to the appendages in manatee F-SCs. Postfacial F-SCs in manatees are smaller than the facial F-SCs, lack a ring sinus and ringwulst, and have only cavernous tissue with a widened region where one would expect to find the ring sinus (Reep, R. L. *et al.*, 2002). This condition is also seen in F-SCs of rhesus monkeys (Van Horn, R. N., 1970), tammar wallabies (Marotte, L. R. *et al.*, 1992), and brush-tailed possums (Hollis, D. E. and Lyne, A. G., 1974). Hippopotamus facial F-SCs have a similar configuration, in which the sinus contains umbrella-like appendages invested with Merkel cells (Bachteler, D. *et al.*, 1998).

In the Australian water rat, mystacial F-SCs exhibit an asymmetrical ring sinus that is larger rostrally than caudally (Dehnhardt, G. *et al.*, 1999), and this may bias each follicle toward directionally selective responding. Water rat follicles also exhibit specialized sandwich nerve endings that may be adaptations for low-frequency detection of hydrodynamic stimuli.

6.16.4.1.3.(iv) Innervation density Several variables undoubtedly influence the functional responses of F-SCs. These include follicle size; hair shaft size, shape, and composition; sinus geometry and blood pressure; receptor types and their distribution; and innervation density. The last factor is somewhat difficult to quantify because one first needs to know the effective region of contact when the hair shaft is deflected. Although this parameter is not usually known, it can be approximated by the perimeter or area of the ring sinus around which most receptors are located.

Some aquatic mammals possess more axons and mechanoreceptors per follicle than terrestrial taxa, perhaps suggesting that vibrissae in aquatic mammals have

greater discriminative power than those of terrestrial taxa. Facial vibrissae in rodents, rabbits, cats, and monkeys are innervated by 80–200 axons originating from the deep vibrissal nerves (Halata, Z. and Munger, B. L., 1980; Rice, F. L. *et al.*, 1986; 1997). However, in the Australian water rat, each caudal mystacial F-SC receives over 500 myelinated axons (Dehnhardt, G. *et al.*, 1999). As many as 1300 axons innervate single F-SCs in ringed seals (Hyvärinen, H., 1995) and bearded seals (Marshall, C. D. *et al.*, 2006). Nerve estimates in cetacean F-SCs range from 40 to 290 axons per F-SC (Ling, J. K., 1977). Manatee caudal mystacial vibrissae (U2 field) are innervated by ~200 axons (Reep, R. L. *et al.*, 2001). Hyvärinen H. (1995) estimated that individual follicles in ringed seals possess 10 000–20 000 Merkel cell–neurite complexes compared to 500–2000 for terrestrial taxa, and 1000–4000 lanceolate endings versus 20–100 for terrestrials.

Implicit in the conjecture that these data suggest higher acuity for aquatic follicles is the assumption that higher numbers of axons and receptors equate with higher innervation density, a major determinant of acuity. However, this assumption is complicated by the fact that follicles tend to be larger in aquatic species. Larger follicles have ring sinuses that are longer and of greater circumference than those in smaller follicles. Consequently, the area to be innervated is greater, requiring a greater number of mechanoreceptors in order to preserve the same innervation density found in smaller follicles. Therefore, it may be that more axons are required in aquatic follicles to match the same innervation density seen in terrestrial follicles. To what extent do axon numbers in aquatic taxa exceed this expected increase? The Australian water rat exhibits ~500 axons per follicle of ~6.3 mm length, whereas terrestrial rats exhibit ~200 axons per follicle of ~4.0 mm, suggesting a surplus in water rats of ~185 axons per follicle beyond the number required to meet expected linear scaling to preserve innervation density. Ringed seals and bearded seals possess a surplus of ~950 axons when scaled to terrestrial rats, and somewhat fewer axons than predicted by scaling to water rats. Therefore, these admittedly crude estimates support the claim that at least some aquatic taxa possess relatively high innervation density. One confounding factor is that the most relevant size variable is likely to be area innervated rather than the total follicle length. Thus, this issue cannot be resolved fully until sufficient quantitative data exist.

In manatees there are significant linear correlations between number of axons and ring sinus perimeter and area for facial follicles, suggesting that larger follicles have more axons simply because the ring sinus is larger (Reep, R. L. *et al.*, 2001). Thus, innervation density may be relatively similar in small and large manatee follicles. This would suggest that differently sized follicles are specialized to respond to different types of stimuli. We know that manatees utilize vibrissae of the oral disk for tactile investigation whereas perioral vibrissae are used in oripulation (Marshall, C. D. *et al.*, 1998a; 1998b), and we have hypothesized that the postfacial vibrissae are used in hydrodynamic reception (Reep, R. L. *et al.*, 2002). Each of these groups of vibrissae exhibits characteristic attributes, not only of follicle size, but also of sinus geometry, hair shaft geometry, and receptor types and distribution (Reep, R. L. *et al.*, 2001; 2002; Sarko, D. K. *et al.*, 2007). Interestingly, Marshall C. D. *et al.* (2006) found no such relationship between the number of axons and the perimeter of the mesenchymal sheath in bearded seals.

Another factor that is significant in considerations of innervation density is axon branching. Because the extent and geometry of branching among the axons supplying mechanoreceptors has not generally been quantified, it is not known whether these parameters influence innervation density and the types of information processed by single axons. Different types of mechanoreceptive endings are likely to be associated with differing degrees of branching. The simplest assumption is that the overall degree of branching is conserved across taxa. If so, it follows that an increase in axon number would be required in aquatic taxa to match the innervation density seen in terrestrial taxa.

6.16.4.1.3.(v) Evolution and vibrissae Species-level variation in the distribution of vibrissae on the body raises interesting questions concerning the evolution and development of these patterns of variation. Sirenians and at least some hyraxes possess vibrissae over the entire body. Interestingly, these groups are both members of the Afrotheria (Waddell, P. J. and Shelley, S., 2003; Reyes, A. *et al.*, 2004) and their extant taxa represent closest living relatives. This relatively close relationship suggests that a body-wide distribution of vibrissae may have been present in the common ancestor of sirenians and hyraxes. Evidence that postfacial vibrissae in manatees and hyraxes have similar molecular pathways of development would provide support for this conjecture. The body-wide distribution of tactile hairs in naked mole rats suggests at least two possible scenarios: first, a body-wide distribution of vibrissae may be a plesiomorphic trait in

mammals generally, and naked mole rats have evolved a modified type of vibrissa; second, naked mole rats may have evolved their peculiar type of tactile hairs independently. In the absence of relevant fossil evidence, molecular developmental studies would be of particular importance in generating strong inferences to resolve these possibilities. (It is also significant that we have no data on the status of these traits in many living taxa, including tenrecs, hippopotamuses, and elephants.) As reviewed above, many terrestrial mammals have retained some nonfacial vibrissae, raising the issue of whether these arose via sculpting of an ancestral body-wide distribution pattern or by addition to an ancestral facial-only distribution. It is possible that pelage hair could transform rather easily into vibrissae through alterations in developmental pathways, but not enough is known about the relevant molecular events to address this possibility.

6.16.4.2 Endomechanosensory Specializations

Another form of mechanosensory specialization is in the relatively high density of receptors in particular locations in the skin, accompanied by expanded connections in the central nervous system, which are related to distinctive behavioral needs. Several examples have been documented.

6.16.4.2.1 The dome pressure receptor systems of crocodilian reptiles

This account of a reptilian specialized mechanosensory system derives from that of Soares D. (2007). Tactile papillas are found in all reptiles. Those in lizards have bristles that indicate sensitive areas of skin, which contain a variety of sensory terminals such as Merkel cells, discoid terminals, and free nerve endings in dermal layers. All reptilian touch papillas have a modified keratin layer, where a more flexible region is located over the sensory organ.

Dome pressure receptor organs are a specialized form of tactile papilla found in the crocodilian reptiles: families Alligatoridae, Crocodylidae, and Gavialidae. The alligatorids have dome pressure receptors around the face and mouth; in the other two families they are found on the caudal portions of most scales over the whole body surface, including the belly, legs, tail, and cloaca. They possess a pigmented epidermal evagination, with thinner epidermis and a more compact keratin layer, which contains highly branched nerve bundles. The secondary and tertiary branches lie directly under the epidermis. In alligatorids there are some, more distal, unmyelinated branches issuing from more proximal myelinated branches; they project, via foramina in the maxillary and mandibular bones, which can be recognized in fossils, to the trigeminal sensory nuclei of the brain stem. These nuclei are greatly enlarged, forming lateral lobes visible on the surface of the brain stem.

The dome receptors in alligators have been shown experimentally to be used to detect the precise locations of the sources of perturbations in the air–water interface where alligators habitually lurk. Their natural stimulation by such disturbances provokes instantaneous coordinated predatory attack on the locus of the source of the disturbance. These receptor organs may also participate in courtship rituals of alligators, which include bellowing by both sexes, which produces informative patterns of disturbances in the air–water interface.

6.16.4.2.2 Specialized relatively hairless regions of skin in mammals

Like the alligators, most mammals (and probably most vertebrates, and even most members of the animal kingdom) have an extraordinary density of receptors, including mechanoreceptors, around the face and mouth. One extreme of this is seen in sheep, where thalamic and cerebral cortical projections from lips and oral structures occupy the major portion of these cerebral parts of the somatic sensory system (Figure 7), particularly the glabrous region between hairy skin of the face and the mucous lining of the mouth, along with the glabrous rhinarium between hairy skin and the mucous lining of the nasal cavity. Sheep, like most of the grazing artiodactyls, show facility in oripulation using perioral tissues, but without the involvement of long vibrissae as seen in manatee oripulation.

In raccoons, a striking expansion of medullary, thalamic, and cortical projections from sensory surfaces on the digits and palm of the forelimb result in separate lobules and gyruses in the brain regions to which they project (Welker, W. I. and Seidenstein, S., 1959; Welker W. I. and Johnson, J. I., 1965; Johnson, J. I. *et al.*, 1968) (Figure 8). Parallel subdivisions resembling these are seen in medullary and thalamic forelimb, and some hindlimb, projections in primates (Florence, S. L. *et al.*, 1989; 1991).

In raccoons this density of projections results in more than simple discriminative sensation: there is a positive motivational component for the animal in stimulation of this system.

The scientific name of raccoons is *Procyon lotor*, owing to their presumed habit of washing, often

thought of as a food-cleaning behavior. In fact, all objects, particularly smooth or metallic ones, are washed in any available water as a rewarding leisure time activity, which may have evolutionary significance for training animals to discriminate submerged food items that cannot be readily seen.

Similar expansions of central nervous projections, from the snout, are seen in marsupial wombats (Johnson, J. I., 1980), carnivore coatimundis (Welker, W. I. and Campos, G. B., 1963), and artiodactyl pigs (Woolsey, C. N. and Fairman, D., 1946; Craner, S. L. and Ray, R. H., 1991), where the location of the nostril in the cerebral cortical body representation is marked by a constant sulcus (Figure 9).

The receptive surface contributing to these specialized arrangements in brain structures is different

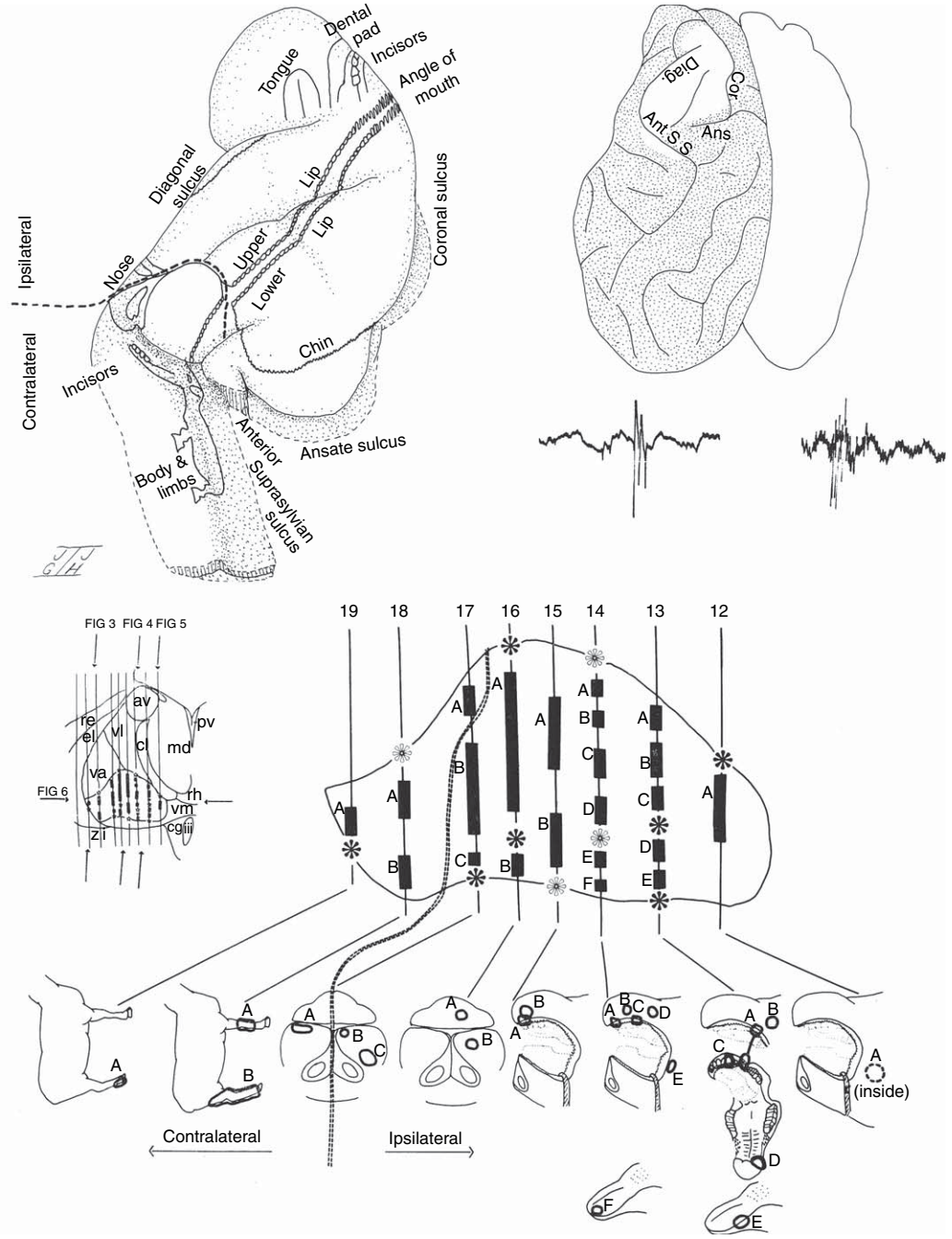

in different groups of species where the tactile skin surface has been well investigated. Those common to the extremities in primates, tree shrews, and arboreal marsupials have been summarized by Preuss T. M. (2006) as follows. Mechanosensorily (tactile, haptic) specialized surfaces on the extremities consist of dermatoglyphic glabrous (hairless) skin with complex patterns of epidermal ridges. In some platyrrhine New World monkeys such as in the genera Cebus and Ateles (e.g., spider monkeys) and Cebus (e.g., capuchin monkeys) there is an additional patch of such dermatoglyphic skin near the distal end of a fifth extremity – a prehensile tail. A special internal neural feature of this skin is a population of distinctive Meissner corpuscles, a nerve ending ensheathed in a capsule of nonneural cells, making them hypersensitive to deformation of the skin. In raccoon hands, in contrast, there are no Meissner corpuscles or epidermal ridges (Rice, F. L. and Rasmusson, D. D., 2000).

All of these skin regions specialized for touch, on the extremities of the forelimbs, hindlimbs, and in some cases the tail, have greatly enlarged representations in the various regions of the brain somatic sensory system to which they project.

6.16.4.3 Combined Endo- and Telomechanosensory Specializations

There are two other examples, from mammals, of elaborate specializations in the immediate vicinity of the olfactory portal and the opening of the mouth, like the perioral–nasal skin of pigs, sheep, and wombats. But unlike the ones that we have described, in these two examples the skin itself is carried out for a distance to extend the reach: the trunks of elephants and the stars of the star-nosed moles. These can be considered both telemechanosensory and endomechanosensory in that they extend the spatial reach of tactile surfaces, but possess the entire sensory apparatus within the skin.

6.16.4.3.1 Elephant trunks

A mechanosensorily specialized patch of skin in elephants is situated at the end of greatly elongated and motile nostrils, the well-known trunk, with which the animal can reach into, over, and under objects in the environment in a range of the same order as that of vibrissae in other mammals. Furthermore, the trunk contains sufficient musculature to act as a grasping organ and is the chief means through which elephants can manipulate objects in their local environment, in ways similar to the ways primates and raccoons both sense and manipulate using their hands, and many herbivores use prehensile lips. At the distal end of the trunk, above the narial openings, there is a distinctive finger, a flexible, pointed, but more rigid structure that is used for detailed exploration, grasping, fine manipulation, and enhanced tactile sensation. The skin of the finger contains epidermal ridges, multiple clusters of peripheral nerve endings, and what are described as Meissner-like endings, but no true Meissner corpuscles. The finger also has an olfactory role in that it can be used to insert samples of items of interest into the openings of the vomeronasal organ to obtain an increased level of discriminatory stimulation (Rasmussen, L. E. L. and Munger, B. L., 1996; Hoffman, J. N. *et al*., 2004). Stone J. and Halasz P. (1989) speculated that a peculiar distribution of retinal ganglion cells might have developed in elephants to provide fine visual monitoring of movements of the finger of the trunk.

6.16.4.3.2 Stars of star-nosed moles

The skin around the nares in talpid moles contains specialized assemblies of mechanoreceptors, known as Eimer's organs (Figure 10). In star-nosed moles the

Figure 7 Approximate locations of projections from peripheral receptors to somatosensory cerebral cortex and thalamus in sheep. The diagram at upper right shows the location of the somatosensory cortex (the unstippled region) on the left cerebral hemisphere between or along the ansate (Ans.), anterior suprasylvian (Ant. s. s.), coronal (Cor.), and diagonal (Diag.) sulci. Rostral is toward the top. The diagram at the upper left shows the somatosensory region as dissected free from the rest of the hemisphere, and with the anterior suprasylvian sulcus spread open. The locations of projections forming sensory representations of major body parts are indicated. Particularly prominent are projections from the glabrous, papillated lips, and the neighboring hairy skin. At the center right are examples of activity of neuronal units in response to mechanical stimulation. The diagram at lower right represents a section through the somatosensory thalamus and shows the paths of recording electrodes through the thalamus. Black bars illustrate the location of neural responses to stimulation of receptive fields whose locations are depicted on drawings of the body surface. Most of the sensory thalamus and cortex of sheep is devoted to processing information from very small receptive fields in and around the ipsilateral mouth and rhinarium. Reproduced from: upper diagrams Johnson, J. I., Rubel, E. W., Hatton, G. I. 1975. Mechanosensory projections to cerebral cortex of sheep. J. Comp. Neurol. 158, 81–108, with permission and lower diagrams Cabral, R. J. and Johnson, J. I. 1971. The organization of mechanoreceptive projections in the ventrobasal thalamus of sheep. J. Comp. Neurol. 141, 17–36, with permission.

skin is shaped into a star-shaped assemblage of skin extensions or rays around the nares (Catania, K. C., 1999; 2000; 2005).

Skin of all the rays contains Eimer's organs and those of two central foveal rays have a much greater density of these organs and smaller receptive fields (Catania, K. C. and Remple, F. E., 2004). The rays are motile and objects of interest are moved from other rays on to the foveal rays for closer mechanosensory examination. There is a central nervous elaboration related to projections from the rays, particularly the foveal rays: using appropriate histological markers the pattern of the rays and the much larger region containing projections from the foveal rays form a distorted somatotopic image of the star in the cerebral isocortex (Figure 10).

There is an olfactory role for the star as well, animals underwater will exhale air past objects of potential olfactory interest, then the rays act as a scoop to gather up the olfactant-filled air and direct it into the nares (Catania, K. C., 2006).

6.16.5 Overview

This account has been a survey of multiple ways in which a particular somatosensory system can be special. Most somatic sensory systems have been considered to be mechanosensory; so other bodily ubiquitous forms of energy transduction into neural signals can be considered special. The familiar triad of energy transductions that occur in free nerve endings would, in this view, constitute the basis of one general sensory modality, mechanosensory, and two special modalities, nociceptive and thermosensory (thermosensory is often divided into two submodalities, sensation of warmth and of cold).

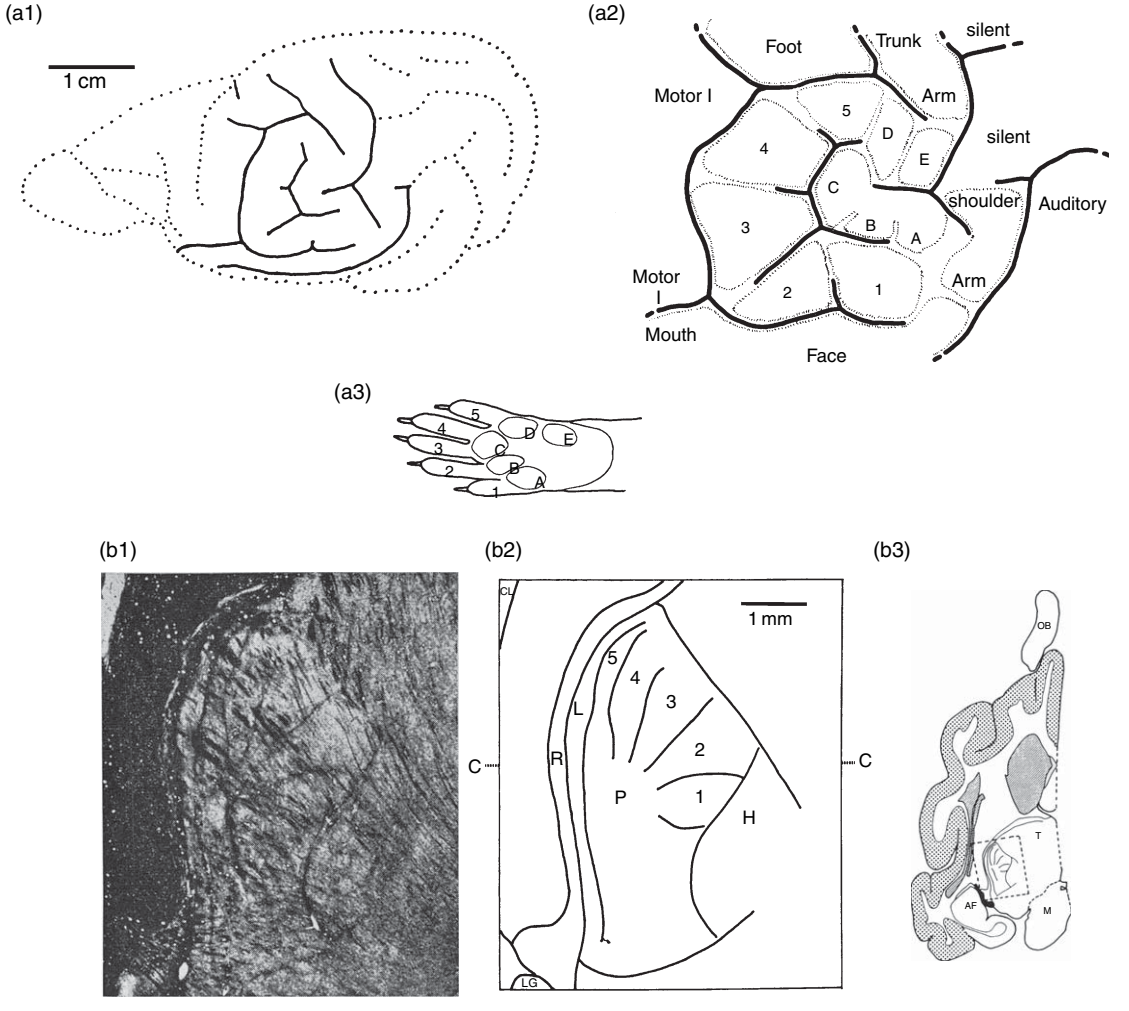

Figure 8 (*Continued*)

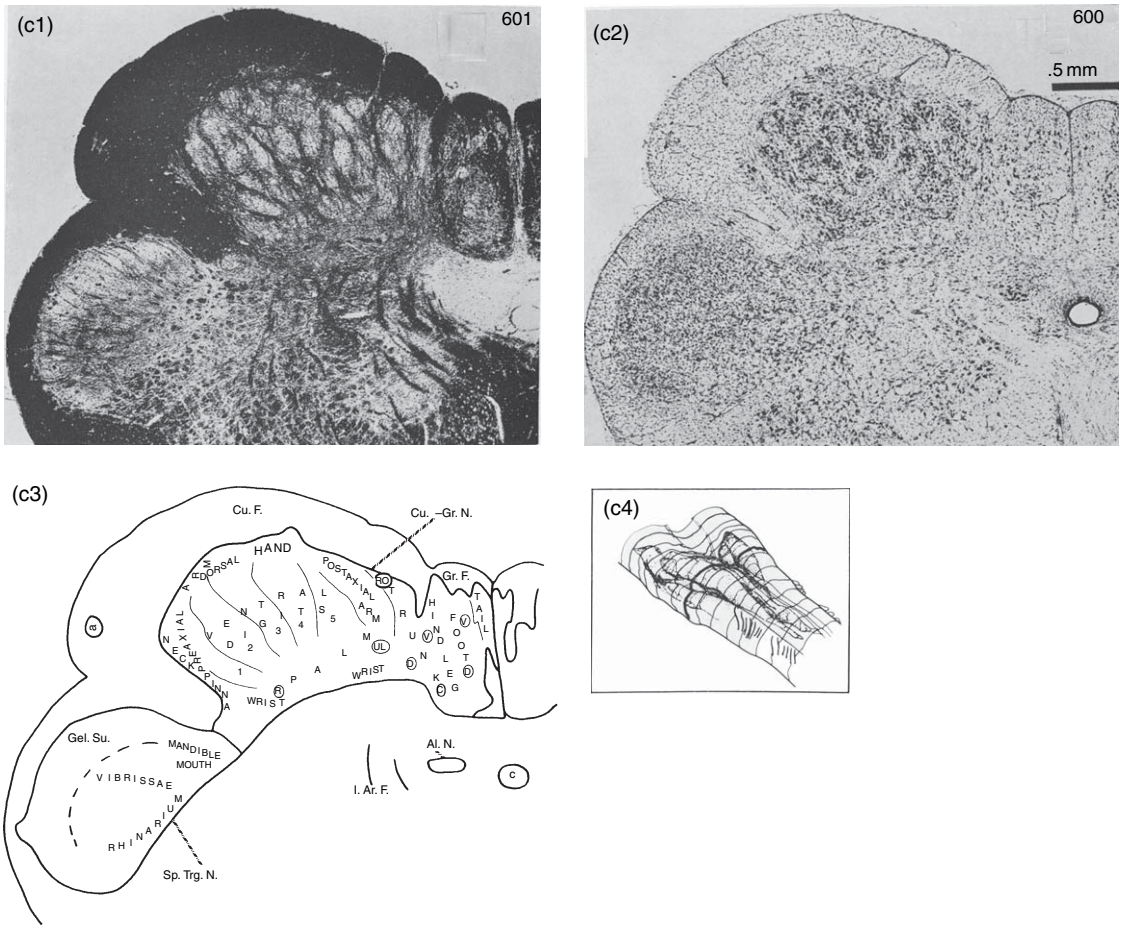

Figure 8 Mechanosensory projections from the volar hand in cerebral cortex, thalamus, and cuneate nucleus of raccoon. (a1) Outline drawing of left cerebral hemisphere with solid lines showing gyral formations in the somatic sensory region. Anterior is to the left. (a2) Projections from hand digits and palm pads, and other body parts and their relation to gyri and sulci. (a3) Positions of volar digital and palm pads on the skin of the hand. (b1) Section through the somatosensory thalamus stained for myelin, showing fiber bundles segregating the nucleus into lobules. (b2) Outline drawing of lobules showing the projection regions of head h, volar surfaces of digits 1, 2, 3, 4, 5, hind limb l, palm p, head, thalamic reticular nucleus r. (b3) Location of b2 in a horizontal section through the brain. Anterior is toward the top. (c1) Section 601 through a dorsal caudal medulla oblongata stained for myelin, showing fiber bundles segregating the cuneate nucleus into lobules containing projections from volar surfaces of individual digits of the hand. (c2) Neighboring section 600 stained with thionin for ribonucleic acid (Nissl method) showing the location of neuronal cell bodies organized into clumps forming the digit lobules. (c3) Outline diagram of the sections identifying the receptive fields projecting to the different parts of the cuneate, gracile, and spinal trigeminal nuclei. (c4) A 3D reconstruction showing the location of the sections and the dorsal column and spinal trigeminal nuclei in the medulla oblongata. C, caudal; D, dorsal; R, radial; RO, rostral; UL ulnar; V, ventral; an external cuneate nucleus; Al. N., alar nucleus; c, central canal; Cu. F., cuneate fasciculus; Cu.–Gr. N., cuneate–gracile nuclear complex; Gel. Su., substantia gelatinosa; Gr. F., gracile fasciculus; I. Ar. F., internal arcuate fibers; Sp. Trg. N., spinal trigeminal nucleus. (a1–a3) Reproduced from Welker, W. I. and Seidenstein, S. 1959. Somatic sensory representation in the cerebral cortex of the racoon (*Procyon lotor*). J. Comp. Neurol. 111, 469–501. (b1–3) Reproduced from Welker, W. I. and Johnson, J. I. 1965. Correlation between nuclear morphology and somatotopic organization in ventrobasal complex of the raccoon's thalamus. J. Anat. 99, 761–790, with permission from Blackwell publishing Ltd. (c1–4) Reproduced from Johnson, J. I., Welker, W. I., Pubols, B. H. 1968. Somatotopic organization of raccoon dorsal column nuclei. J. Comp. Neurol. 132, 1–44.

We have seen in Section 6.16.2.1 that current work on the role of TRP channels in thermal and nociceptive transduction in free nerve endings suggests a common cellular mechanism for touch, heat, cold, and painful sensation and that the distinction between these modalities is based on distinctive ranges of sensitivities that overlap and together comprise a continuous spectrum of sensed energy

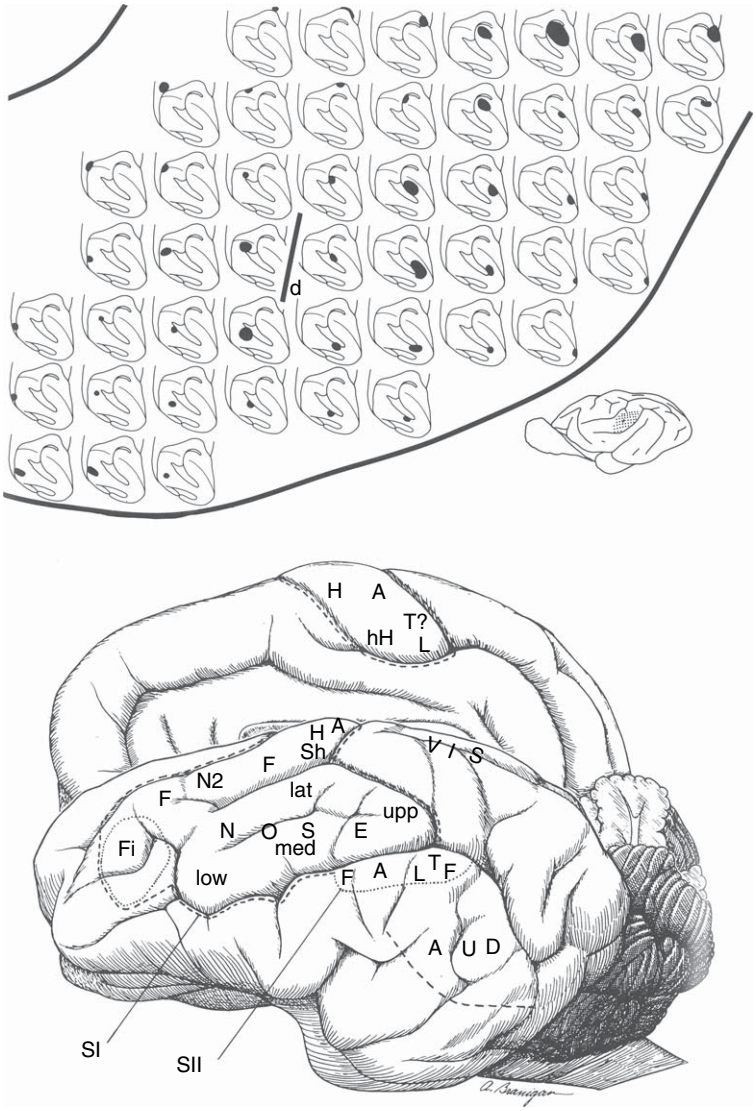

Figure 9 Top: Map of the relatively large somatosensory representation of the contralateral rhinarium on the crown of the coronal gyrus in the coatimundi (*Nasua narica*). A small dimple (solid line: d) commonly appears within the coati's rhinarial representation at a location (indicated in brain diagram at lower right) that is surrounded by a slightly elevated gyral formation that contains peripheral projections from the ring of highly innervated rhinarium that surrounds the nostril. Bottom: Locations of somatic sensory projections to primary (SI) and secondary (SII) cortical regions of pigs (*Sus scrofa*) as described in Adrian E. D. (1943), Woolsey C. N. and Fairman D. (1946), and Craner S. L. and Ray R. H. (1991). The left cerebral hemisphere is depicted, showing both the lateral surface and the mesial surface as it would be reflected in a mirror. Anterior is to the left. A, arm or foreleg; F, face; Fi, ipsilateral face; H, forehoof; hH, hindhoof; L, hind leg; lat, lateral; low, lower; med, median; upp, upper, aspects of the large representation of the flat rostrum of the rhinarium (NOSE), which occupies a large elliptical gyrus around a sulcus that occurs where the nostril is located in the cortical representation (a giant narial sulcus, Johnson, J. I., 1980); N2, a second complete representation of the nose in SI; Sh, shoulder; T?, site of occasional few and inconsistent responses to stimulation of the trunk. The face (F) is represented twice in SII, at its anterior and posterior poles. (Top) Adapted from Welker, W. I. 1990. Why Does Cerebral Cortex Fissure and Fold? A Review of Determinants of Gyri and Sulci. In Cerebral Cortex: Vol. 8B: Comparative Structure and Evolution of Cerebral Cortex, Part II (*eds*. E. G. Jones and A. Peters), pp. 3–136. Plenum; and Welker, W. I. and Campos, G. B. 1963. Physiological significance of sulci in somatic sensory cerebral cortex in mammals of the family procyonidae. J. Comp. Neurol. 120, 19–36, with permission. (Bottom) Adapted from Craner, S. L. and Ray, R. H. 1991. Somatosensory cortex of the neonatal pig: I. Topographic organization of the primary somatosensory cortex (SI). J. Comp. Neurol. 306, 24–38, with permission; and Johnson, J. I. 1990. Comparative Development of Somatic Sensory Cortex. In: Cerebral Cortex: Vol. 8B: Comparative Structure and Evolution of Cerebral Cortex, Part II (*eds*. E.G. Jones and A. Peters), pp. 331–445. Plenum.

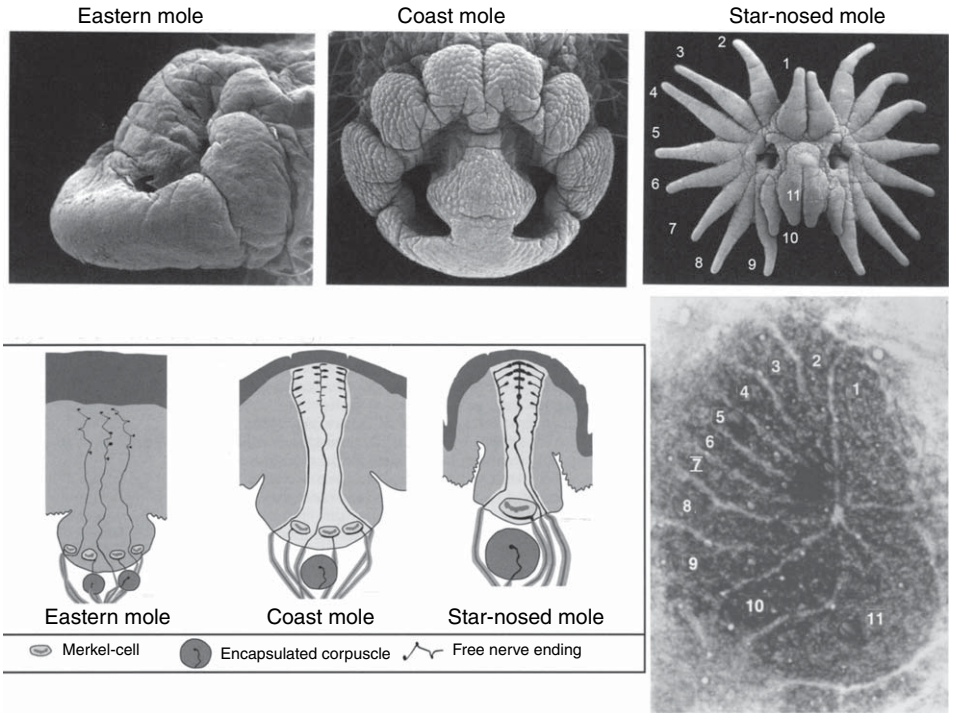

Figure 10 Top: The glabrous rhinarium of three species of talpid moles covered with thousands of mechanosensory organs called Eimer's organs. The elaborate rhinarium of the star-nosed mole, consisting of 22 nasal appendages is covered with 25,000 Eimer's organs. Below, left: Drawings of sections through individual Eimer's organs from each of the three species. Each organ consists of a small swelling in the epidermis, and contains a circular configuration of free nerve endings, one or more Merkel cell-neurite complexes, and an encapsulated corpuscle in the underlying dermis. Below, right: A section through the flattened neocortex processed for the metabolic enzyme cytochrome oxidase, showing the area to where touch information from the star projects. The 11 modules in the cortex each represent one of the 11 appendages of the contralateral side of the star. Note the greatly expanded representation of the tactile fovea (appendage 11). Adapted with permission from Catania K. C. (2005a, b).

alterations. This in turn points the way toward considering these various modalities as a single modality that is present in most body tissues of animals and perhaps plants and other life forms as well. The nociceptive modality is at least as ubiquitous as the mechanosensory, such that pain is allotted a volume of its own in this series of handbook volumes.

We have included the generally distributed thermosensitive systems here as specialized somatosensory systems largely because they are not treated elsewhere in the series. Within the thermal modality there is at least one truly specialized apparatus – that of the heat-sensitive pit organs found in crotaline and some boid snakes, described in Section 6.16.2.4.3

Another form of specialization is represented by the electrosensory apparatus of the monotreme mammals, discussed in Section 6.16.3.5. In this case, in a restricted taxonomic grouping, a truly specialized system has evolved, but it works in concert with the general mechanoreceptive system with which it shares the same trigeminal-to-cerebral-cortical pathway and associated brain processing regions.

The remainder of the specialized systems we described were elaborations and variations in mechanosensory capabilities. One set of these specialties are those that take advantage of peripheral structures, in many cases developed to serve other vital functions such as alimentation and locomotion, to increase the range of mechanical recognition of environmental features and events. This was done by attaching mechanoreceptive nerve endings to such structures as lips, limbs, barbels of fishes, feathers of birds, and hairs of mammals. A great deal of scientific attention has been paid to vibrissae, mammalian hairs that have become specialized for mechanoreceptive functions. We classify these spatial range-extending specialties as telemechanosensory – touching at a distance.

An alternative type of specializations we call endoreceptive. They consist of unusual concentrations of receptors within certain regions of skin, such as lips of the oral cavity.

Both telemechanoreceptive and endomechanoreceptive specialties include brain elaborations and expansions to process the increased amount of information delivered by the specialized receptive interfaces with the environment.

Many systems incorporate both telemechanoreceptive and endomechanoreceptive properties. Among these we have considered the hands of raccoons, the tails of some New World monkeys, the trunks of elephants, and the stars of star-nosed moles. Significantly, all of these enhanced sensory surfaces are also mechanically prehensile, revealing the collaborative nature of motor and sensory specialization of particular body parts.

Our selection, and that of science in general, of specialized somatosensory systems is in no way exhaustive. Those presented here are certain instances of sensory system evolution that have caught the attention of astute observers. They constitute an instructive exhibit of the evolutionary possibilities that have been realized in variations and additions to basic sensory equipment.

Acknowledgment

Preparation of this work was supported by Grant IBN 0131267 from the US National Science Foundation.

References

Adrian, E. D. 1943. Afferent areas in the brain of ungulates. Brain 66, 89–103.

Andres, K. H. 1966. Über die Feinstruktur der Rezeptoren an Sinushaaren. Z. Zellforsch. 75, 339–365.

Bachteler, D. and Dehnhardt, G. 1999. Active touch performance in the Antillean manatee: evidence for a functional differentiation of facial tactile hairs. Zoology 102, 61–69.

Bachteler, D., Klauer, G. J., and Dehnhardt, G. 1998. The morphology of the vibrissae of *Hippopotamus amphibius*. Euro-Am. Mammal Cong. Abst. 669.

Bleckmann, H. 1994. Reception of hydrodynamic stimuli in aquatic and semiaquatic animals. Prog. Zool. 41, 1–115.

Brecht, M., Preilowski, B., and Merzenich, M. M. 1997. Functional architecture of the mystacial vibrissae. Behav. Brain Res. 84, 81–97.

Cabral, R. J. and Johnson, J. I. 1971. The organization of mechanoreceptive projections in the ventrobasal thalamus of sheep. J. Comp. Neurol. 141, 17–36.

Catania, K. C. 1999. A nose that looks like a hand and acts like an eye: the unusual mechanosensory system of the star-nosed mole. J. Comp. Physiol. A 185, 367–372.

Catania, K. C. 2000. Cortical organization in insectivora: the parallel evolution of the sensory periphery and the brain. Brain Behav. Evol. 55, 311–321.

Catania, K. C. 2005a. Evolution of sensory specializations in insectivores. Anat. Rec. 287A, 1038–1050.

Catania, K. C. 2005b. Star-nosed moles. Curr. Biol. 15, R863–R864.

Catania, K. C. 2006. Olfaction: underwater 'sniffing' by semiaquatic mammals. Nature 444, 1024–1025.

Catania, K. C. and Remple, F. E. 2004. Tactile foveation in the star-nosed mole. Brain Behav. Evol. 63, 1–12.

Caterina, M. J. and Montell, C. 2005. Take a TRP to beat the heat. Genes Dev. 19, 415–418.

Conover, M. L. and Miller, D. E. 1980. Rictal bristle function in willow flycatcher. Condor 82, 469–471.

Craig, A. D., Chen, K., Bandy, D., and Reiman, E. M. 2000. Thermosensory activation of insular cortex. Nat. Neurosci. 3, 184–190.

Craner, S. L. and Ray, R. H. 1991. Somatosensory cortex of the neonatal pig: I. Topographic organization of the primary somatosensory cortex (SI). J. Comp. Neurol. 306, 24–38.

Crish, S. D., Rice, F. L., Park, T. J., and Comer, C. M. 2003. Somatosensory organization and behavior in naked mole-rats I: vibrissa-like body hairs comprise a sensory array that mediates orientation to tactile stimuli. Brain Behav. Evol. 62, 141–151.

Darcy, P. K, Wilczynska, Z., and Fisher, P. R. 1994. The role of cGMP in photosensory and thermosensory transduction in *Dictyostelium discoideum*. Microbiology 140, 1619–1632.

Dehnhardt, G. 1994. Tactile size discrimination by a California sea lion (*Zalophus californianus*) using its mystacial vibrissae. J. Comp. Physiol. A 175, 791–800.

Dehnhardt, G. and Ducker, G. 1996. Tactual discrimination of size and shape by a California sea lion (*Zalophus californianus*). Anim. Learn. Behav. 24, 366–374.

Dehnhardt, G. and Kaminski, A. 1995. Sensitivity of the mystacial vibrissae of harbour seals (*Phoca vitulina*) for size differences of actively touched objects. J. Exp. Biol. 198, 2317–2323.

Dehnhardt, G., Hyvärinen, H., Palviainen, A., and Klauer, G. 1999. Structure and innervation of the vibrissal follicle-sinus complex in the Australian water rat, *Hydromys chrysogaster*. J. Comp. Neurol. 411, 550–562.

Dehnhardt, G., Mauck, B., and Bleckmann, H. 1998a. Seal whiskers detect water movements. Nature 394, 235–236.

Dehnhardt, G., Mauck, B., Hanke, W., and Bleckmann, H. 2001. Hydrodynamic trail-following in harbor seals (*Phoca vitulina*). Science 293, 102–104.

Dehnhardt, G., Mauck, B., and Hyvärinen, H. 1998b. Ambient temperature does not effect the tactile sensitivity of mystacial vibrissae in harbor seals. J. Exp. Biol. 201, 3023–3029.

Dykes, R. W. 1975. Afferent fibers from mystacial vibrissae of cats and seals. J. Neurophysiol. 38, 650–662.

Eastman, J. T. and Lannoo, M. J. 2003. Anatomy and histology of the brain and sense organs of the Antarctic plunderfish *Dolloidraco longedorsalis* (perciformes: notothenioidei: artedidraconidae), with comments on the brain morphology of other artedidraconids and closely related harpagiferids. J. Morphol. 255, 358–377.

Ebara, S., Kumamoto, K., Matsuura, T., Mazurkiewicz, J. E., and Rice, F. L. 2002. Similarities and differences in the innervation of mystacial vibrissal follicle-sinus complexes in the rat and cat: a confocal microscopic study. J. Comp. Neurol. 449, 103–119.

Eisenberg, J. F. 1981. The Mammalian Radiations. The University of Chicago Press.

Fay, F. H. 1982. Ecology and biology of the Pacific walrus, *Odobenus rosmarus divergens* Illiger. United States

Department of Interior, Fish and Wildlife Service, North American Fauna, Washington, DC, 74, 1–279.
Florence, S. L. and Lakshman, S. 1995. Topography of primary afferent-projections in the trigeminal sensory nuclei of rats. Acta Neurobiol. Exp. 55, 193–200.
Florence, S. L., Wall, J. T., and Kaas, J. H. 1989. Somatotopic organization of inputs from the hand to the spinal gray and cuneate nucleus of monkeys with observations on the cuneate nucleus of humans. J. Comp. Neurol. 286, 48–70.
Florence, S. L., Wall, J. T., and Kaas, J. H. 1991. Central projections from the skin of the hand in squirrel monkeys. J. Comp. Neurol. 311, 563–578.
Gerstein, E. R., Gerstein, L., Forsythe, S., and Blue, J. 1999. Underwater audiogram of a West Indian Manatee (*Trichechus manatus*). J. Acoust. Soc. Am. 105, 3575–3583.
Gottschaldt, K.-M., Iggo, A., and Young, D. W. 1973. Functional characteristics of mechanoreceptors in sinus hair follicles of the cat. J. Physiol. 235, 287–315.
Gregory, J. E., Iggo, A., McIntyre, A. K., and Proske, U. 1988. Receptors in the bill of the platypus. J. Physiol. 400, 349–366.
Gregory, J. E., Iggo, A., McIntyre, A. K., and Proske, U. 1989. Responses of electroreceptors in the snout of the echidna. J. Physiol. 414, 521–538.
Griffin, D. R. 1959. Listening in the Dark. Yale University Press.
Halata, Z. and Munger, B. L. 1980. Sensory nerve endings in rhesus monkey sinus hairs. J. Comp. Neurol. 192, 645–663.
Hartman, D. S. 1979. Ecology and behavior of the manatee (*Trichechus manatus*) in Florida. Am. Soc. Mamm. Spec. Pub. 5, 1–153.
Hassan, E. S. 1986. On the discrimination of spatial intervals by the blind cave fish (*Anoptichthys jordani*). J. Comp. Physiol. A 159, 701–710.
Hassan, E. S. 1989. Hydrodynamic Imaging of the Surroundings by the Lateral Line of the Blind Cave Fish *Anoptichthys jordani*. In: The Mechanosensory Lateral Line, Neurobiology and Evolution (*eds*. S. Coombs, P. Gorner, and H. Munz), pp. 217–227. Springer.
Hensel, H. 1981. Thermoreception and temperature regulation. Monogr. Physiol. Soc. 38, 1–321.
Hensel, H., Andres, K. H., and Düring, M.von 1974. Structure and function of cold receptors. Pflügers Arch. 352, 1–10.
Hoffman, J. N., Montag, A. G., and Dominy, N. J. 2004. Meissner corpuscles and somatosensory acuity: the prehensile appendages of primates and elephants. Anat. Rec. A 281A, 1138–1147.
Hollis, D. E. and Lyne, A. G. 1974. Innervation of vibrissa follicles in the marsupial *Trichosurus vulpecula*. Aust. J. Zool. 22, 263–276.
Hua, L. H., Strigo, I. A., Baxter, L. C., Johnson, S. C., and Craig, A. D. 2005. Anteroposterior somatotopy of innocuous cooling activation focus in human dorsal posterior insular cortex. Am. J. Physiol. Regul. Integr. Comp. Physiol. 289, R319–R325.
Hyvärinen, H. 1989. Diving in darkness: whiskers as sense organs of the ringed seal. J. Zool. (Lond.) 218, 663–678.
Hyvärinen, H. 1995. Structure and Function of the Vibrissae of the Ringed Seal (*Phoca hispada* L). In: Sensory Systems of Aquatic Mammals (*eds*. R. A. Kastelein, J. A. Thomas, and P. A. Nachtigall), pp. 429–445. De Spil Publishers.
Hyvärinen, H. and Katajisto, H. 1984. Functional structure of the vibrissae of the ringed seal (*Phoca hispida* Schr.). Acta Zool. Fenn. 171, 17–30.
Hyvärinen, H., Kangasperko, H., and Puera, R. 1977. Functional structure of the carpal and ventral vibrissae of the squirrel (*Sciurus vulgaris*). J. Zool. (Lond.) 182, 457–466.
Iggo, A., Gregory, J. E., and Proske, U. 1992. The central projection of electrosensory information in the platypus. J. Physiol. 447, 449–465.
Johnson, J. I. 1980. Morphological Correlates of Specialized Elaborations in Somatic Sensory Neocortex. In: Comparative Neurology of the Telencephalon (*ed*. S. O. E. Ebbesson), pp. 423–447. Plenum.
Johnson, J. I. 1990. Comparative Development of Somatic Sensory Cortex. In: Cerebral Cortex: Vol. 8B: Comparative Structure and Evolution of Cerebral Cortex, Part II (*eds*. E. G. Jones and A. Peters), pp. 331–445. Plenum.
Johnson, J. I., Rubel, E. W., and Hatton, G. I. 1975. Mechanosensory projections to cerebral cortex of sheep. J. Comp. Neurol. 158, 81–108.
Johnson, J. I., Welker, W. I., and Pubols, B. H. 1968. Somatotopic organization of raccoon dorsal column nuclei. J. Comp. Neurol. 132, 1–44.
Jones, E. G. 1983. Organization of the Thalamocortical Complex and Its Relation to Sensory Process. In: Handbook of Physiology – The Nervous System, Vol. III, Chap. 5 (*ed*. I. Darian-Smith), pp. 49–212. American Physiological Society.
Jordt, S.-E., McKemy, D. D., and Julius, D. 2003. Lessons from peppers and peppermint: the molecular logic of thermosensation. Curr. Opin. Neurobiol. 13, 487–492.
Kastelein, R. A. and van Gaalen, M. A. 1988. The tactile sensitivity of the mystacial vibrissae of a Pacific Walrus (*Odobenus rosmarus divergens*). Part 1. Aquat. Mamm. 14, 123–133.
Krochmal, A. R. and Bakken, G. S. 2003. Thermoregulation is the pits: use of thermal radiation for retreat site selection by rattlesnakes. J. Exp. Biol. 206, 2539–2545.
Ladygina, T. F., Popov, V. V., and Supin, A. Y. 1985. Somatotopic projections in the cerebral cortex of the fur seal (*Callorhinus ursinus*). Acad. Sci. Moskow 17, 344–351.
Land, P. W. and Simons, D. J. 1985. Metabolic and structural correlates of the vibrissae representation in the thalamus of the adult rat. Neurosci. Lett. 60, 319–324.
Layne, J. N. and Caldwell, D. K. 1964. Behavior of the Amazon dolphin, *Inia geoffrensis* (Blainville), in captivity. Zoologica 49, 81–108.
Lederer, R. J. 1972. The role of avian rictal bristles. Wilson Bull. 84, 193–197.
Ling, J. K. 1966. The skin and hair of the southern elephant seal, *Mirounga leonina* (Linn.). I. The facial vibrissae. Aust. J. Zool. 14, 855–866.
Ling, J. K. 1972. Vibrissa follicles of the Ross seal. Br. Antarct. Surv. Bull. 27, 19–24.
Ling, J. K. 1977. Vibrissae of Marine Mammals. In: Functional Anatomy of Marine Mammals (*ed*. J. B. Harrison), Vol. 3, pp. 387–415. Academic Press.
Manger, P. R. and Pettigrew, J. D. 1996. Ultrastructure, number, distribution and innervation of electroreceptors and mechanoreceptors in the bill skin of the platypus, *Ornithorhynchus anatinus*. Brain Behav. Evol. 48, 27–54.
Manger, P. R., Collins, R., and Pettigrew, J. D. 1997. Histological observations on presumed electroreceptors and mechanoreceptors in the beak skin of the long-beaked echidna, *Zaglossus bruinjii*. Proc. R. Soc. Lond. B 264, 165–172.
Marler, P. and Hamilton, W. J. 1966. Mechanisms of Animal Behavior, pp. 397–425. Wiley.
Marotte, L. R., Rice, F. L., and Waite, P. M. E. 1992. The morphology and innervation of facial vibrissae in the tammar wallaby, *Macropus eugenii*. J. Anat. 180, 401–417.
Marshall, C. D., Amin, H., Kovacs, K. M., and Lydersen, C. 2006. Microstructure and innervation of the mystacial vibrissal follicle-sinus complex in bearded seals, *Erignathus barbatus* (Pinnipedia: Phocidae). Anat. Rec. A 228A, 13–25.
Marshall, C. D., Clark, L. A., and Reep, R. L. 1998a. The muscular hydrostat of the Florida manatee (*Trichechus manatus latirostris*) and its role in the use of perioral bristles. Mar. Mamm. Sci. 14, 290–303.

Marshall, C. D., Huth, G. D., Edmonds, V. M., Halin, D. L., and Reep, R. L. 1998b. Prehensile use of perioral bristles during feeding and associated behaviors of the Florida manatee (*Trichechus manatus latirostris*). Mar. Mamm. Sci. 14, 274–289.

Marshall, C. D., Maeda, H., Iwata, M., Furuta, M., Asano, A., Rosas, F., and Reep, R. L. 2003. Orofacial morphology and feeding behaviour of the dugong, Amazonian, West African and Antillean manatees (Mammalia: Sirenia): Functional morphology of the muscular–vibrissal complex. J. Zool. (Lond.) 259, 1–16.

Mauck, B., Eysel, U., and Dehnhardt, G. 2000. Selective heating of vibrissal follicles in seals (*Phoca vitulina*) and dolphins (*Somalia fluviatilis guianensis*). J. Exp. Biol. 203, 2125–2131.

McKemy, D. D., Neuhausser, W. M., and Julius, D. 2002. Identification of a cold receptor reveals a general role for TRP channels in thermosensation. Nature 416, 52–58.

Miller, E. H. 1975. A comparative study of facial expressions of two species of pinnipeds. Behaviour 53, 268–284.

Mills, F. H. J. and Renouf, D. 1986. Determination of the vibration sensitivity of harbour seal *Phoca vitulina* (L.) vibrissae. J. Exp. Mar. Biol. Ecol. 100, 3–9.

Montell, C. 2006. A mint of mutations in TRPM8 leads to cool results. Nat. Neurosci. 9, 466–468.

Mosconi, T. M., Rice, F. L., and Song, M. J. 1993. Sensory innervation in the inner conical body of the vibrissal follicle-sinus complex of the rat. J. Comp. Neurol. 328, 232–251.

Munger, B. L. and Rice, F. L. 1986. Sequential maturation of cutaneous receptors in the rat mystacial pad. J. Comp. Neurol. 252, 404–411.

Nomura, S. and Mizuno, N. 1986. Histochemical demonstration of vibrissae-representing patchy patterns of cytochrome-oxidase activity within the trigeminal sensory nuclei in the cat. Brain Res. 380, 167–171.

Norman, J. R. and Fraser, F. C. 1948. Giant Fishes, Whales and Dolphins. Putnam.

Ostapoff, E. M., Johnson, J. I., and Albright, B. C. 1983. Mechanosensory projections to cuneate, gracile, and external cuneate nuclei in a tree squirrel (fox squirrel, *Sciurus niger*). Neuroscience 9, 107–127.

Pappas, T. C., Mohamed, M., and Christensen, B. N. 2004. Unique temperature-activated neurons from pit viper thermosensors. Am. J. Physiol. Cell Physiol. 287, C1219–C1228.

Park, T. J., Comer, C., Carol, A., Lu, Y., Hong, H.-S., and Rice, F. L. 2003. Somatosensory organization and behavior in naked mole-rats. II. Peripheral structures, innervation, and selective lack of neuropeptides associated with thermoregulation and pain. J. Comp. Neurol. 465, 104–120.

Patapoutian, A., Peier, A. M., Story, G. M., and Viswanath, V. 2003. Thermo TRP channels and beyond: mechanisms of temperature sensation. Nat. Rev. Neurosci. 4(7), 529–539.

Peterson, R. S. and Bartholomew, G. A. 1967. The natural history and behavior of the California sea lion. Am. Soc. Mamm. Spec. Pub. 1, 1–79.

Pettigrew, J. D. 1999. Electroreception in monotremes. J. Exp. Biol. 202, 1447–1454.

Pocock, R. I. 1914. On the facial vibrissae of mammalia. Proc. Zool. R. Soc. Lond. 40, 889–912.

Preuss, T. M. 2006. Primate Brain Evolution in Phylogenetic Context. In: Evolution of Nervous Systems. A Comprehensive Reference, Vol. 5: Primates (*eds*. J. H. Kaas and T. M. Preuss), pp. 1–34. Elsevier.

Proske, U. and Gregory, E. 2003. Electrolocation in the platypus – some speculations. Comp. Biochem. Physiol. A Mol. Integr. Physiol. 136, 821–825.

Proske, U., Gregory, J. E., and Iggo, A. 1998. Sensory receptors in monotremes. Philos. Trans. R. Soc. Lond. B Biol. Sci. 353, 1187–1198.

Rasmussen, L. E. L. and Munger, B. L. 1996. The sensorineural specializations of the trunk tip (finger) of the Asian elephant, *Elephas maximus*. Anat. Rec. 246, 127–134.

Reep, R. L., Marshall, C. D., and Stoll, M. L. 2002. Tactile hairs on the postcranial body in Florida manatees: a mammalian lateral line? Brain Behav. Evol. 59, 141–154.

Reep, R. L., Marshall, C. D., Stoll, M. L., and Whitaker, D. M. 1998. Distribution and innervation of facial bristles and hairs in the Florida manatee (*Trichechus manatus latirostris*). Mar. Mamm. Sci. 14, 257–273.

Reep, R. L., Stoll, M. L., Marshall, C. D., Homer, B. L., and Samuelson, D. A. 2001. Microanatomy of facial vibrissae in the Florida manatee: the basis for specialized sensory function and oripulation. Brain Behav. Evol. 58, 1–14.

Reyes, A., Gissi, C., Catzeflis, F., Nevo, E., Pesole, G., and Saccone, C. 2004. Congruent mammalian trees from mitochondrial and nuclear genes using Bayesian methods. Mol. Biol. Evol. 21, 397–403.

Rice, F. L. 1993. Structure, vascularization and innervation of the mystacial pad of the rat as revealed by the lectin *Griffonia simplicifolia*. J. Comp. Neurol. 337, 386–399.

Rice, F. L. 1995. Comparative Aspects of Barrel Structure and Development. In: Cerebral Cortex, Vol. 11, The Barrel Cortex of Rodents (*eds*. E. G. Jones and I. T. Diamond), pp. 1–75. Plenum.

Rice, F. L. and Rasmusson, D. D. 2000. Innervation of the digit on the forepaw of the raccoon. J. Comp. Neurol. 417, 467–490.

Rice, F. L., Fundin, B. T., Arvidsson, J., Aldskogius, H., and Johansson, O. 1997. Comprehensive immunofluorescence and lectin binding analysis of vibrissal follicle sinus complex innervation in the mystacial pad of the rat. J. Comp. Neurol. 385, 149–184.

Rice, F. L., Kinnman, E., Aldskogius, H., Johansson, O., and Arviddson, J. 1993. The innervation of the mystacial pad of the rat as revealed by PGP 9.5 immunofluorescence. J. Comp. Neurol. 337, 366–385.

Rice, F. L., Mance, A., and Munger, B. L. 1986. A comparative light microscopic analysis of the innervation of the mystacial pad. I. Vibrissal follicles. J. Comp. Neurol. 252, 154–174.

Roule, L., Angel, F., and Despax, R. 1913. Poissons. In: Deuxième Expédition Antarctique Française (1908–1910) (*eds*. J. Charcot and L. Joubin), p. 24. Masson.

Sale, J. B. 1970. Unusual external adaptations in the rock hyrax. Zool. Afr. 5, 101–113.

Sarko, D. K., Reep, R. L., Mazurkiewicz, J. E., and Rice, F. L. 2007. Innervation of follicle-sinus complexes in the Florida manatee. J. Comp. Neurol, in press.

Saxod, R., Pays, L., and Hemming, F. J. 1996. Development of the cutaneous nervous system. Pathol. Biol. (Paris) 44, 838–848.

Soares, D. 2007. The Evolution of Dome Pressure Receptors in Crocodiles. In: Non-Mammalian Vertebrates, Vol 2 (*eds*. J. H. Kaas and T. H. Bullock), pp. 157–162. In: Evolution of Nervous Systems. A Comprehensive Reference (*ed.* J. H. Kaas). Elsevier.

Sokolov, V. E. 1982. Mammal Skin, pp. 453–458. University of California Press.

Sokolov, V. E. and Kulikov, V. F. 1987. The structure and function of the vibrissal apparatus in some rodents. Mammalia 51, 125–138.

Stephens, R. J., Beebe, I. J., and Poulter, T. C. 1973. Innervation of the vibrissae of the California sea lion, *Zalophus californianus*. Anat. Rec. 176, 421–442.

Stone, J. and Halasz, P. 1989. Topography of the retina in the elephant *Loxodonta africana*. Brain Behav. Evol. 34, 84–95.

Teyke, T. 1989. Learning and remembering the environment in the blind cave fish *Anoptichthys jordani*. J. Comp. Physiol. A 164, 655–662.

Van der Loos, H. 1976. Barreloids in the mouse somatosensory thalamus. Neurosci. Lett. 2, 1–6.

Van Horn, R. N. 1970. Vibrissae structure in the rhesus monkey. Folia Primatol. 13, 241–285.
Vincent, S. 1913. The tactile hair of the white rat. J. Comp. Neurol. 23, 1–36.
Voets, T., Droogmans, G., Wissenbach, U., Janssens, A., Flockerzi, V., and Nilius, B. 2004. The principle of temperature-dependent gating in cold- and heat-sensitive TRP channels. Nature 430, 748–754.
Voets, T., Talavera, K., Owsianik, G., and Nilius, B. 2005. Sensing with TRP channels. Nat. Chem. Biol. 1, 85–92.
Waddell, P. J. and Shelley, S. 2003. Evaluating placental interordinal phylogenies with novel sequences including RAG1, gamma-fibrinogen, ND6, and mt-tRNA, plus MCMC-driven nucleotide, amino acid, and codon models. Mol. Phylogenet. Evol. 28, 197–224.
Watkins, W. A. and Wartzok, D. 1985. Sensory biophysics of marine mammals. Mar. Mamm. Sci. 1, 219–260.
Welker, W. I. 1964. Analysis of sniffing of the albino rat. Behaviour 22, 223–244.
Welker, W. I. 1990. Why Does Cerebral Cortex Fissure and Fold? A Review of Determinants of Gyri and Sulci. In: Cerebral Cortex: Vol. 8B: Comparative Structure and Evolution of Cerebral Cortex, Part II (*eds*. E. G. Jones and A. Peters), pp. 3–136. Plenum.
Welker, W. I. and Campos, G. B. 1963. Physiological significance of sulci in somatic sensory cerebral cortex in mammals of the family procyonidae. J. Comp. Neurol. 120, 19–36.
Welker, W. I. and Johnson, J. I. 1965. Correlation between nuclear morphology and somatotopic organization in ventro-basal complex of the raccoon's thalamus. J. Anat. 99, 761–790.
Welker, W. I. and Seidenstein, S. 1959. Somatic sensory representation in the cerebral cortex of the racoon (*Procyon lotor*). J. Comp. Neurol. 111, 469–501.
Wineski, L. E. 1985. Facial morphology and vibrissal movement in the golden hamster. J. Morphol. 183, 199–217.
Woollard, P., Vestjens, W. J. M., and MacLean, L. 1978. Ecology of eastern water rat *Hydromys chrysogaster* at Griffith, NSW food and feeding habits. Austr. Wild. Res. 5, 59–73.
Woolsey, C. N. and Fairman, D. 1946. Contralateral, ipsilateral, and bilateral representation of cutaneous receptors in somatic areas I and II of the cerebral cortex of pig, sheep, and other mammals. Surgery 19, 684–702.
Woolsey, T. A., Durham, D., Harris, R. M., Simons, D. J., and Valentino, K. L. 1981. Somatosensory development. Dev. Percept. 1, 259–292.
Yohro, T. 1977. Structure of the sinus hair follicle in the big-clawed shrew, *Sorex unguiculatus*. J. Morph. 153, 333–354.
Zelena, J. 1994. Nerves and Mechanoreceptors. Chapman and Hall.
Zhang, G., Deng, S., Zhang, H., Li, H., and Li, L. 2006. Distribution of different taste buds and expression of a-gustducin in the barbels of yellow catfish (*Pelteobagrus fulvidraco*). Fish Physiol. Biochem. 32, 55–62.
Zhang, X., Davidson, S., and Giesler, G. J. 2006. Thermally identified subgroups of marginal zone neurons project to distinct regions of the ventral posterior lateral nucleus in rats. J. Neurosci. 26, 5215–5223.
Zook, J. M. 2007. Somatosensory Adaptations of Flying Mammals. In: Evolution of Nervous Systems. A Comprehensive Reference Vol. 3 mammal (*eds*. J. H. Kaas and L. A. Krubitzer), pp. 215–226. Elsevier.

Further Reading

Melaragno, H. P. and Montagna, W. 1953. The tactile hair follicle in the mouse. Anat. Rec. 115, 29–50.

6.17 Somatosensation in Invertebrates

A Büschges, University of Cologne, Cologne, Germany

R A DiCaprio, Ohio University, Athens, OH, USA

© 2008 Elsevier Inc. All rights reserved.

6.17.1	**Introduction**	355
6.17.2	**Sensors Reporting Discriminative Touch, Temperature, and Proprioception**	356
6.17.2.1	Trichoid Sensillae	356
6.17.2.2	Basiconic Sensillae	357
6.17.2.3	Campaniform Sensillae	357
6.17.3	**Mapping in Invertebrates**	357
6.17.4	**Case Studies Illustrating Principles of Somatosensory Organization and Processing in Invertebrates**	357
6.17.4.1	The Insect Cercal System	357
6.17.4.1.1	Central processing of cercal afferent information	359
6.17.4.1.2	Mapping of the surface of the insect leg by mechanosensory signals in the locust nervous system	360
References		361

Glossary

cercal system In insects, the cercal system consists of a bilateral pair of tapered spike-shaped structures (cerci) extending posteriorly from the last abdominal segment. Each cercus has several hundred mechanoreceptive hairs, organized into regular rows and columns, and each hair is mechanically coupled to a single afferent neuron. This system is responsible for the detection and monitoring of wind currents on the body surface.

campaniform sensillae Campaniform sensillae are sensory receptors located in the cuticle and respond to stress on the cuticle. Associated with the flexible ovoid cuticular dome is a single sensory neuron which inserts into the surrounding tissue. Compression of the cuticle perpendicular to the length axis of the sensillum excites the sensory neuron.

hair sensillae Hair sensillae are sensory receptors located in the cuticle on various parts of the body. Based on their detailed morphology and function two kinds of hair sensillae are distinguished: trichoid senillae and basiconic sensillae. The dendrite of a sensory neuron extends into the shaft of the hair and transduces movements of the hair into spike discharges. While trichoid sensillae serve exclusively as mechanoreceptors with one single mechanoreceptive sensory neuron innervating at the base of the hair, basiconic sensillae act in addition as chemoreceptors with chemoreceptive sensory neurons located at their work base and connected by the shaft to the pore at the tip.

6.17.1 Introduction

The somatosensory system is often considered to be an exclusive organizational feature of vertebrate central nervous systems (CNSs), although the sensory modalities and (equivalent) receptors involved are found in invertebrates as well. The somatosensory system encompasses receptors, modalities, and pathways that underlie the representation of sensory stimuli from the surface of the organism as well as the relative positioning of body appendages relative to each other and in space. The primary sensory modality associated with somatosensation is tactile input from the surface of an organism. As such, discriminative touch is the sensory modality that many textbooks refer to first when introducing somatosensation. Additional secondary modalities included in the somatosensory system are the senses for pain and temperature and proprioceptive

sensation. In addition to the types of receptors involved, the most prominent architectural feature of the somatosensory system in vertebrate nervous systems is the mapping of the body surface to a spatially coherent internal map in a designated cortical (neuronal) space.

It is this latter aspect that has probably limited the use of somatosensation in invertebrate neuroscience more widely, which can easily be tested by running a search for this term together with the term invertebrate. This is true despite the fact that (1) representation of all three aspects of body sensations, that is, touch, temperature, and proprioception, exist in invertebrate phylae; (2) mapping of sensory signals according to their origin or function is widely found in the invertebrate CNS; and (3) a variety of invertebrate directional motor behaviors have contributed substantially to our current understanding of how animal nervous systems operate.

The distributed and decentralized nature of invertebrate nervous systems precludes the strict application of the term somatosensation, as the vertebrate definition does not readily apply to this neural architecture. As the CNS of invertebrates is largely distributed along the body axis, there is no single central cortical structure with a global representation of the body surface as found in the sensory cortex of mammals. Instead, invertebrate nervous systems are subdivided into segments and ganglia that have a substantial degree of independence with respect to the organization of local sensory and motor processing. Secondly, although a highly centralized representation of the body surface does not exist in invertebrates, sensory information processing on a local level possesses numerous features that appear similar to, or functionally parallel with, the characteristics of vertebrate somatosensory systems. We will introduce several examples in order to illustrate similarities, functional parallels, and also differences.

We first list the sensors that report somatosensory information from the surface of the body, and then describe the principles of sensory mapping found in invertebrates, as well as the neural substrates and present two different examples of somatosensation in invertebrates.

6.17.2 Sensors Reporting Discriminative Touch, Temperature, and Proprioception

Invertebrates with a soft cuticle, like annelids, have sensory cells in each of their homologous segmental ganglia that respond to touch and pressure, and to noxious stimuli. One annelid model system that has contributed to our present understanding of decision making in CNSs in general is the medical leech, *Hirudo medicinalis* (Muller, K. J. *et al*, 1981; Kristan, W. B. and Shaw, B. K., 1997; Kristan, W. B., Jr., 2000). Three major groups of sensory neurons, named for their specific modality, are the T (touch), P (pressure), and N (nocioceptive) neurons. The T and P cells each have specific receptive fields that cover part of the body surface in each segment. For example, the four P cells per segment divide up the circumference of the body wall into dorsal left and right and ventral left and right quadrants with overlapping receptive fields (Nicholls, J. G. and Baylor, D. A., 1968). These sensory neurons provide the sensory inputs to the CNS underlying a variety of motor functions such as directionally specific avoidance reflexes (Lewis, J. E. and Kristan, W. B., 1998).

Invertebrates with a tough cuticle made from chitin, that is, arthropods, have a variety of sensory cells that can report discriminative touch and proprioception from the body surface. Among those are three major receptor types: two types of hair sensillae and cuticular stress receptors, the campaniform sensillae.

6.17.2.1 Trichoid Sensillae

Trichoid sensillae are typical mechanosensory hair sensillae that possess a single sensory neuron at their base, just below the socket in which the hair shaft is articulated, that is sensitive to displacement of the tactile hair (e.g., Klee, S. and Thurm, U., 1986). Trichoid hairs can vary in length from as short as 60 μm to more than 750 μm (Newland, P. L., 1991a; 1991b). The thickness of the hair shaft can vary in different regions of the body. Filiform hairs are long and thin while bristle hairs are short and thick. Correlated with these changes in thickness are changes in stiffness of the socket of the hairs, which determines whether a trichoid hair can be very sensitive to small forces exerted by sound pressure or small air currents (e.g., Pflüger, H. J. and Tautz, J., 1982; Shimozawa, T. and Kanou, M., 1984) or sensitive only to stronger mechanosensory stimuli, like touch, as in case of the bristle hairs. In many cases trichoid sensillae also exhibit directional sensitivity (e.g., Newland, P. L., 1991a; 1991b). A case study illustrating the role of these receptors in sensing air currents and predator avoidance is the insect cercal system (see below).

6.17.2.2 Basiconic Sensillae

Basiconic sensillae are peg-like structures with a shaft that is generally much shorter than trichoid hair sensillae, often in the range of 30–50 µm (Newland, P. L. and Burrows, M., 1994). Most often basiconic sensillae exhibit directional sensitivity (ibid). The sensitivity of the basiconic sensillae to displacement is very high, and is on the order of a few degrees. These sensillae are much more sensitive than the trichoid sensillae. In addition, the shaft of the basiconic sensilae has a pore at its tip that allows access for chemicals to the dendrites of chemosensory neurons inside the hair. Each basiconic sensillum is innervated by five to ten sensory neurons, with one of them being a chemoreceptive sensory neuron (e.g., Newland, P. L. *et al.*, 2000). Together with the trichoid receptors, these sensillae are the relevant input elements for several simple targeted movement patterns in insects (Berkowitz, A. and Laurent, G., 1996; Matheson, T., 1997; Page, K. L. and Matheson, T., 2005).

6.17.2.3 Campaniform Sensillae

Campaniform sensillae reside in the cuticle and respond to stress and torsion of the cuticle. Their outer appearance is best described as an ovoid depression of the cuticle. Underneath the flexible central cuticular dome, a single sensory neuron inserts into the surrounding tissue. Compression of the cuticle perpendicular to the length axis of the ovoid sensillum excites the sensory neuron (Spinola, S. M. and Chapman, K. M., 1975). Individual campaniform sensillae are found on the insect leg (Burrows, M. and Pflüger, H. J., 1995; Hustert, R. *et al.*, 1981; Zill, S. N. and Moran, D. T., 1981; Zill, S. N. *et al.*, 2004) or they may be arranged in groups, most often close to the joints (Hustert, R. *et al.*, 1981; Bässler, U. and Hofmann, T., 1986; Mücke, A., 1991; Akay, T. *et al.*, 2001). The mechanics of the campaniform sensillae also make this receptor directionally sensitive. Torsion of the cuticle, and excitation of the receptor, may arise either from active muscle contractions or from passive externally imposed stress (Delcomyn, F., 1991). Considering the first kind of activation of the campaniform sensillae, that is, torsion of the cuticle upon muscle activity, the campaniform sensillae serve a function in motor control that parallels closely the role of group Ib afferents, that is, the Golgi tendon organs in vertebrates (cf. Pearson, K. G., 2000; Zill, S. N. *et al.*, 2004; Büschges, A., 2005).

6.17.3 Mapping in Invertebrates

A characteristic feature of CNSs is that sensory information is represented as neural maps at one or more levels of their processing. These maps may be organized with respect to the location of the sensory neuron or organized with respect to the parameter space encoded by the sensory signals. As such, the projections of mechanosensory neurons on the limbs of invertebrates form somatotopic maps in which the spatial location of each signal is maintained (e.g., Zill, S. N. *et al.*, 1980; Murphey, R. K., 1981; Pflüger, H. J. *et al.*, 1981; Levine, R. B. *et al.*, 1985; Newland, P. L., 1991a; 1991b). Maps of the other sensory modalities can be organized differently, for example, for the eyes by forming retinotopic maps in the visual pathway (Strausfeld, N. S., 1976) or for auditory signals by forming tonotopic maps (Oldfield, B. P., 1982; Römer, H., 1983; Römer, H. *et al.*, 1988). In invertebrates, these maps are formed at a given morphological level where information processing takes place and they are not dependent on, or attributed to, any hierarchical level of the nervous system. Somatotopic mechanosensory maps are found in the segmental ganglia, retinotopical maps in the invertebrate brain and tonotopic maps in thoracic ganglia.

6.17.4 Case Studies Illustrating Principles of Somatosensory Organization and Processing in Invertebrates

The sensory processing in somatosensation is related to the representation of the body surface on a higher order level in sensory processing. Therefore, somatosensation can only be present in invertebrates that have a CNS, that is, in organisms from articulates, like annelids, onwards. Several arthropod systems have been investigated in detail that exhibit features related to vertebrate somatosensation. In the following section we will introduce two different examples for somatosensation in invertebrates (insects) where they have most thoroughly been studied.

6.17.4.1 The Insect Cercal System

The cercal system of insects is responsible for the detection and monitoring of wind currents on the body surface. This system consists of a bilateral pair of cerci which are tapered spike-shaped structures

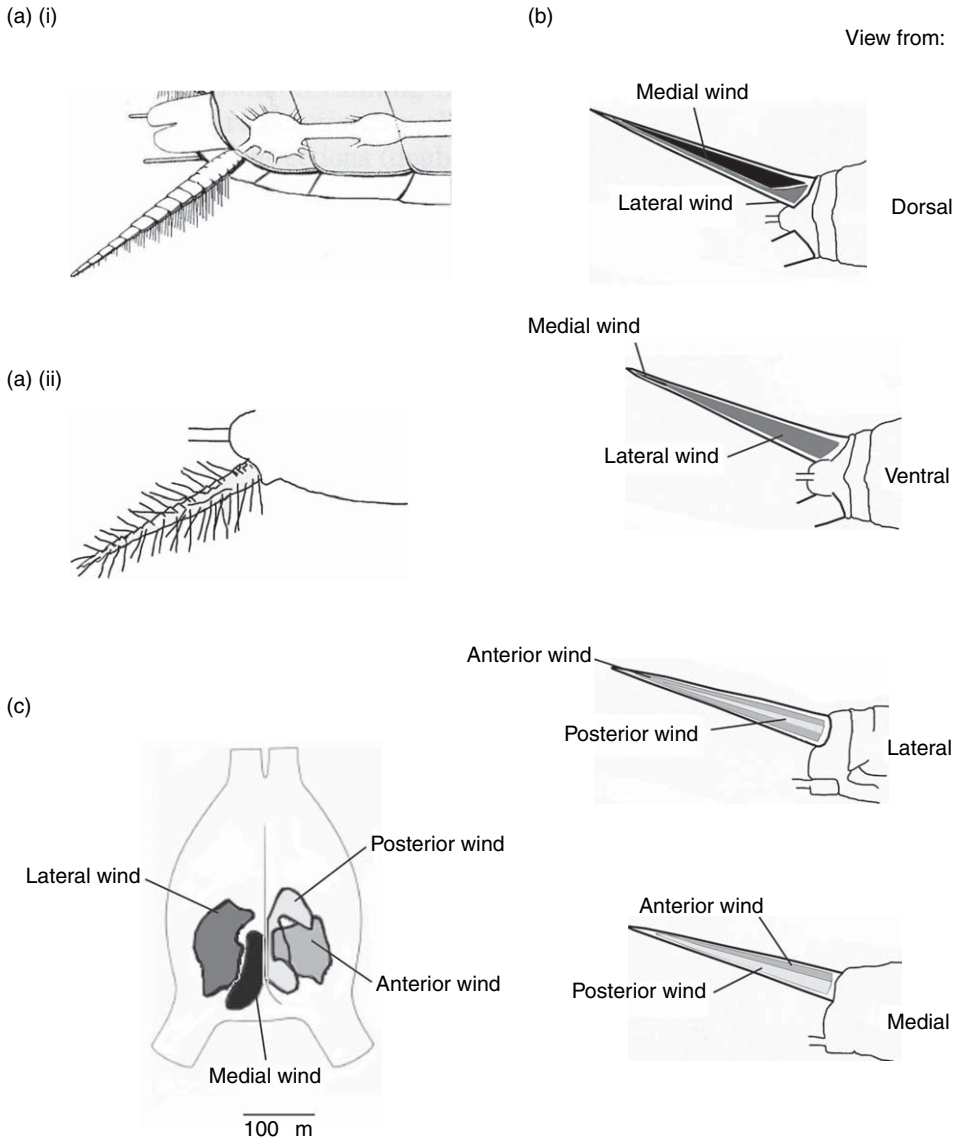

Figure 1 Mapping of cercal hair receptors in the cockroach and cricket. (a) (i) Schematic drawing of a single cercus and the last abdominal ganglion in the cockroach, (ii) schematic drawing of a circus and filiform hairs in the cricket. (b) Mapping of the directional sensitivity of the hairs on the surface (dorsal, ventral, lateral, and medial) of the cricket cercus. (c) The functional organization of the cereal glomerulus in the ganglionic neuropil. There are four almost entirely nonoverlapping neuropil regions corresponding to different wind from four quadrants.

extending posteriorly from the last abdominal segment of the animal. Each cercus has several hundred filiform mechanoreceptive hairs that are organized into regular rows and columns and each hair is mechanically coupled to a single afferent neuron. In the cockroach (Figure 1(a)(i)) these hairs are arranged in rows of nine long (0.5–1.0 mm) hairs on each of the 19 cercal segments except for the basal and tip segments. The homologous hairs at a given position along the segment are organized in columns of similarly oriented hairs that are aligned along the length of the cercus. The hairs in a given column are functionally equivalent in that they are all oriented with respect their axis of (easiest) mechanical deflection (Nicklaus, R., 1965). This precise arrangement of sensory hairs is also seen in the cricket cercal system (Figure 1(a)(ii)), where the circumferential location of the hair is precisely correlated with the directional tuning of the hairs (Palka, J. *et al.*, 1977; Bacon, J. P. and Murphey, R. K., 1984).

The afferent neurons are tonicly active and deflection in the preferred direction depolarizes and hence increases the firing rate of the afferent, while deflection in the opposite direction (−180°) inhibits the neuron and decreases the firing rate. The orientation of the optimal deflection axis is different for each of the columns and the angular orientation of the deflection is shifted sequentially from column to column in a given row. The response tuning curves to wind stimulation are rather broad, but are generally restricted to wind input from a single spatial quadrant (Westin, J., 1979). The different mechanical properties of the hairs results in different coding properties. In the cricket, long hairs are more flexible, respond to low-frequency air currents and code for wind velocity, while short hairs are stiffer, respond only to high frequencies, and code for wind acceleration (Shimozawa, T. and Kanou, M., 1984). The cercal hairs therefore constitute a receptor system that encode wind direction information and dynamics and the ensemble of receptors can completely map air currents on the body surface and hence in space around the animal.

Multiple inputs from cercal afferents are processed by interneurons in the terminal abdominal ganglion of the CNS in order to construct higher order maps of the sensory space. These convergent inputs have been extensively described in the cricket and cockroach CNS. There are seven giant interneurons (GI 1–7) in the cockroach that integrate cercial afferent inputs (Westin, J. *et al.*, 1977). The interneuronal tuning curves are generally broader than the individual afferent tuning curves and the distribution of afferent inputs and their synaptic strengths determine the directional tuning of the individual GIs. The interneurons also appear to receive inputs of differing sign from specific receptors that serves to sculpt their response properties.

6.17.4.1.1 Central processing of cercal afferent information

A feature of the central organization of somatosensory systems is the relatively strict topographic organization of sensory space in the CNS. For example in the mammalian somatosensory system, touch or pressure receptors that innervate an area on the body surface are mapped to similar adjacent higher-order neurons in somatosensory cortex, resulting from a projection of adjacent sensory neurons to adjacent cortical cells. This somatotopic mapping produces the classical homunculus representation of the body surface in the cortex. However, in many systems such as the visual and auditory systems, maps of sensory features in the cortex are often computational maps (Konishi, M., 1986; Knudsen, E. I., 1987) that are not organized on a topological basis, but rather serve to map the variation of some derived parameter of sensory input to higher-order neurons. A simple variant of a computational map appears to be present in the interneurons that receive inputs from cercial primary afferents in the cricket.

As in the cockroach, the cercal hairs of the cricket are arranged circumferentially along the cercus and each hair has a preferred stimulus direction of stimulation (Figure 1(b); Palka, J. *et al.*, 1977; Bacon, J. P. and Murphey, R. K., 1984). However, unlike the arrangement in the cockroach, the hairs are more randomly arranged on the cercus with respect to their preferred direction (Figure 1(b); Walthall, W. W. and Murphey, R. K., 1986) although they are clustered with respect to their preferred direction. The hairs therefore are not continuously mapped topographically on the surface of the cercus. However, the presynaptic arborization of individual afferent terminals in the abdominal ganglion project to specific regions in the ganglionic neuropil that are correlated with the directional specificity of the individual hair, thus establishing a map of the sensory array in the CNS (Murphey, R. K., 1981; Bacon, J. P. and Murphey, R. K., 1984; Jacobs, G. A. and Nevin, R., 1991).

Cercal afferents can be grouped into four major classes based on their directional sensitivity (Figure 1; Bacon, J. P. and Murphey, R. K., 1984.) The afferent terminals of these four classes have been shown to terminate in specific regions of the neuropil of the terminal abdominal ganglion that define four corresponding regions of directional sensitivity in the second-order sensory interneurons in the ganglion (Figure 1(c)). Centrally, the circumferential position of each hair on the cercus, and its longitudinal position, is associated with a specific terminal arborization (Thompson, K. S. *et al.*, 1992).

A simple model of the directional sensitivity of the interneurons based on their monosynaptic inputs from the cercal afferents can account for the major features of the directional sensitivity of the interneurons (Bacon, J. P. and Murphey, R. K., 1984; Shephard, D. and Murphey, R. K., 1986). In a more detailed study of the central processing of cercal input, Jacobs G. A. *et al.* (1986) demonstrated that for one interneuron (10-3) there are distinct dendritic branches of this interneuron that receive afferent

input and these regions have different receptive fields. Summation of the individual receptive fields could account for the interneuron's total receptive field, but the precise directional sensitivity could not be predicted by simple linear summation. Specific afferents were identified that inhibited interneuron 10-3 via polysynaptic connections and the electrotonic structure of the interneuron was also found to play an important role in this overall computation.

A detailed analysis of the neuroanatomical organization of the projections of wind-sensitive afferents in the CNS revealed that the central map of wind direction was formed by projections of afferents with similar direction aborizing adjacent to each other, thus composing a global map of wind direction in the CNS (Jacobs, G. A. and Theunissen, F. E., 1996). The projections of the afferents form a spiral shape with stimulus direction mapped continuously along the spiral. The conclusion was that there was not a topographic projection of the sensory epithelium to the CNS, but rather that the continuous central representation of wind direction was synthesized by the anatomic organization of the afferent terminals, that were independent of the location of the specific afferent on the cercus.

6.17.4.1.2 Mapping of the surface of the insect leg by mechanosensory signals in the locust nervous system

The surface of an insect leg (Figure 2(a)) is covered by exteroceptors, the most prominent ones being hair sensillae and campaniform sensillae. These sensors provide information from the surface of the leg and can monitor contact of an object with the cuticle. In addition to these receptors, proprioceptors are located on and in the leg that provide information about movement and position of the joints. In his detailed account of the neurobiology of the locust, Burrows M. (1996) estimated that there are a few hundred proprioceptive afferent axons in locust leg nerves, while the majority of the approximately 10 000 sensory axons from the leg arise from exteroceptors, including the hair sensillae. The mechanosensory trichoid and basiconic hair sensillae send their afferent axons into the segmental ganglion, with the latter being accompanied by chemoreceptive afferents (Newland, P. L. and Burrows, M., 1994; 1997). The afferents from the trichoid sensillae all project to a common region in the most ventral portion of the neuropil of the thoracic ganglia, that is, the ventral, anterior, and lateral ventral association center (VAC; Figure 2(b)). In this region of the ganglion almost exclusively arborizations of interneurons are present, while almost no arborizations of leg motorneurons are present. The arborizations of the hair sensillae in the segmental ganglion are arranged in a way that represents their origin on the surface of the segmental appendage (Newland, P. L. and Burrows, M., 1997; Newland, P. L. *et al*., 2000). Clear topographical maps reflecting the legs surface can be found for the arborizations of afferents of hair sensors in the locust (Figure 2(b)). Afferents from the leg arborize so that the surface of the leg is closely represented in the internal neural map of the leg (Figure 2(c)). Afferents from the tarsus project to more lateral regions as compared to afferents from the trochanter and coxa, and the opposite is the case for afferents from more centrally located afferents (Newland, P. L. *et al*., 2000). Similarly, arborizations of hair sensillae are different for hairs on the ventral, dorsal, anterior, and posterior surface of the leg. The subsequent neural levels of processing mirror this mapping so that interneurons exhibit receptive fields that result from their specific dendritic branching pattern in the area of the VAC (Newland, P. L., 1991a; 1991b; Burrows, M. and Newland, P. L., 1993). These interneurons are the neural elements in a variety of local reflex circuits that are generated in response to touch stimuli of the leg. These reflexes act to ensure posture and maintain the mobility of the leg by moving the leg away from the assumed origin of stimulation. For example, when the dorsal femur is touched the trochater is depressed, the tibia flexed, and the tarsus levated and when the ventral tibiae is touched the trochanter is levated the tibia extended and the tarsus depressed (summary in Burrows, M., 1996).

It appears that the somatosensory mapping of the locust leg within the CNS not only reflects a topological organization, but also bears some relation to the sensorimotor transformations involving individual afferents. In that respect the somatotopic mapping of the locust leg in the CNS may share similarities to findings on cutaneous somatotopy in the spinal cord of vertebrates (Willis, W. D. and Coggeshall, R. E., 1991; Woodbury, C. J. and Scott, S. A., 1991; Levinsson, A. *et al*., 2002). However, although current data suggest that somatotopic disruption is common in the vertebrate spinal cord (Molander, C. and Grant, G., 1985; Florence, S. L. *et al*., 1991), it does not appear to exist for somatosensory projections of leg afferents in the insect CNS.

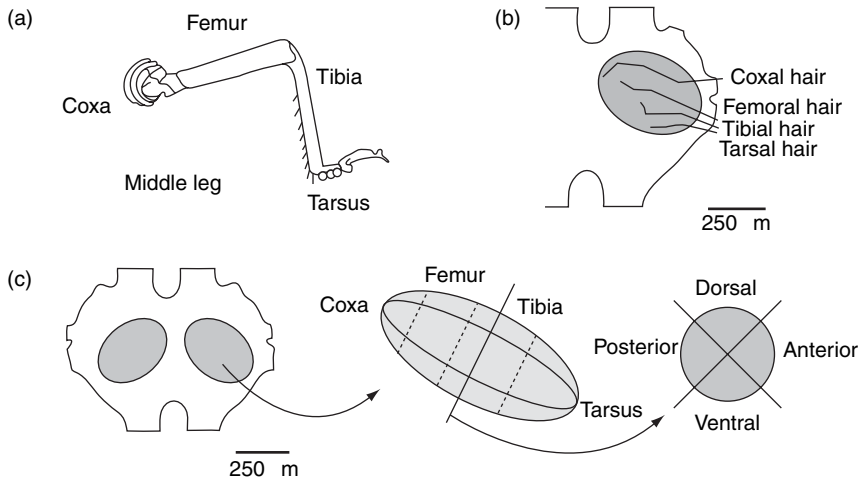

Figure 2 Mapping of exteroreceptive afferents in the mesothoracic ganglion of the locust. (a) Schematic drawing of the locust middle leg and its four main partitions (see also Burrows, M., 1996). (b) Schematic representation of the branching of the primary neurites of trichoid hairs from coxa, femur, tibia, and tarsus of the locust middle leg. (c) Schematic drawing of the main arborization area of leg exteroceptors in the mesothoracic ganglion in the ventral association center (VAC). The first inset in the middle shows a top view of the spatial mapping of afferents from the leg segments in that area. The second inset to the right gives a transection of the VAC showing the order of topographical mapping of leg afferents with respect to their location in three-dimensional space on a given segment.

Acknowledgments

We are grateful to Dr. Tim Mentel for his suggestions on the manuscript and Sharon Meyen-Southard for technical support in editing the text and preparing the figures.

References

Akay, T., Bässler, U., Gerharz, P., and Büschges, A. 2001. The role of sensory signals from the insect coxa-trochanteral joint in controlling motor activity of the femur-tibia joint. J. Neurophysiol. 85, 594–604.

Bacon, J. P. and Murphey, R. K. 1984. Receptive fields of cricket giant interneurones are related to their dendritic structure. J. Physiol. 352, 601–623.

Bässler, U. and Hofmann, T. 1986. Response characteristics of single trochanteral campaniform sensilla in the stick insect, *Cuniculina impigra*. Physiol. Entomol. 11, 17–21.

Berkowitz, A. and Laurent, G. 1996. Local control of leg movements and motor patterns during grooming in locusts. J. Neurosci. 16, 8067–8078.

Büschges, A. 2005. Sensory control and organization of neural networks mediating coordination of multisegmental organs for locomotion. J. Neurophysiol. 93, 1127–1135.

Burrows, M. 1996. The Neurobiology of an Insect Brain. Oxford University Press.

Burrows, M. and Newland, P. L. 1993. Correlation between the receptive fields of locust interneurons, their dendritic morphology, and the central projections of mechanosensory neurons. J. Comp. Neurol. 329, 412–426.

Burrows, M. and Pflüger, H. J. 1995. Action of locust neuromodulatory neurons is coupled to specific motor patterns. J. Neurophysiol. 74, 347–357.

Delcomyn, F. 1991. Perturbation of the motor system in freely walking cockroaches. J. Exp. Biol. 156, 503–517.

Florence, S. L., Wall, J. T., and Kaas, J. H. 1991. Central projections from the skin of the hand in squirrel monkeys. J. Comp. Neurol. 311, 563–578.

Hustert, R., Pflüger, H. J., and Braunig, P. 1981. Distribution and specific central projections of mechanorecptors in the thorax and proximal leg joints of locusts III. The external mechanoreceptors: the Campaniform sensilla. Cell Tiss. Res. 216, 97–111.

Jacobs, G. A. and Nevin, R. 1991. Anatomical relationships between sensory afferent arborizations in the cricket cercal system. Anat. Rec. 231, 563–572.

Jacobs, G. A. and Theunissen, F. E. 1996. Functional organization of a neural map in the cricket cercal sensory system. J. Neurosci. 16, 769–784.

Jacobs, G. A., Miller, J. P., and Murphey, R. K. 1986. Integrative mechanisms controlling directional sensivity of an identified sensory interneuron. J. Neurosci. 6, 2298–2311.

Klee, S. and Thurm, U. 1986. Mechanorezeptive fadenhaar-sensillen mit zwei sinneszellen von *Locusta migratoria* L. Verh. Dtsch. Zool. Ges. 79, 220.

Knudsen, E. I. 1987. Neural derivation of sound source localization in the barn owl – an example of a computational map. Ann. New York Acad. Sci. 510, 33–38.

Konishi, M. 1986. Centrally synthesized maps of sensory space. Trends Neurosci. 9, 163–167.

Kristan, W. B., Jr. 2000. Dezentrale Verarbeitung gegen engagierte Neuronen in der Produktion der einfachen Verhaltenstaten. In: Vor-rationale Intelligenz: Anpassungsfähiges Verhalten und intelligente Systeme ohne die Symbole und Logik-Volumen 1 (*eds*. H. Cruse, J. Dekan and U. H. Ritter), pp. 243–266. Kluwer.

Kristan, W. B. and Shaw, B. K. 1997. Population coding and behavioral choice. Curr. Opin. Neurobiol. 7, 826–831.

Levine, R. B., Pak, C., and Linn, D. 1985. The structure, function and metamorphic reorganization of somatatopically projecting sensory neurons in *Manduca sexta* larvae. J. Comp. Physiol. A 157, 1–13.

Levinsson, A., Holmberg, H., Broman, J., Zhang, M., and Schouenborg, J. 2002. Spinal sensorimotor transformation: relation between cutaneous somatotopy and a reflex network. J. Neurosci. 22, 8170–8182.
Lewis, J. E. and Kristan, W. B. 1998. Quantitative analysis of a directed behavior in the medicinal leech: implications for organizing motor output. J. Neurosci. 18, 1571–1582.
Matheson, T. 1997. Hindleg targeting during scratching in the locust. J. Exp. Biol. 200, 93–100.
Mücke, A. 1991. Innervation pattern and sensory supply of the midleg of *Schistocerca gregaria* (Insecta, Orthopteroidea). Zoomorphology 110, 175–187.
Molander, C. and Grant, G. 1985. Cutaneous projections from the rat hind limb foot ot the substantia gelatinosa of the spinal cord studied by transganglionic transport of WGA-HRP conjugate. J. Comp. Neurol. 273, 476–484.
Muller, K. J., Nicholls, J. G., and Stent, G. S. *(eds)* 1981. Neurobiology of the Leech. Cold Spring Harbor publications.
Murphey, R. K. 1981. The structure and development of a somatotopic map in crickets: the cercal afferent projection. Dev. Biol. 88, 236–246.
Newland, P. L. 1991a. Morphology and somatotopic organisation of the central projections of afferents from tactile hairs on the hind leg of the locust. J. Comp. Neurol. 312, 493–508.
Newland, P. L. 1991b. Physiological properties of afferents from tactile hairs on the hindlegs of the locust. J. Exp. Biol. 155, 487–503.
Newland, P. L. and Burrows, M. 1994. Processing of mechanosensory information from gustatory receptors on a hind leg of the locust. J. Comp. Physiol. A 174, 399–410.
Newland, P. L. and Burrows, M. 1997. Processing of tactile information in neuronal networks controlling leg movements of the locust. J. Insect Physiol. 43, 107–128.
Newland, P. L., Rogers, S. M., Gaaboub, I., and Matheson, T. 2000. Parallel somatotopic maps of gustatory and mechanosensory neurons in the central nervous system of an insect. J. Comp. Neurol. 425, 82–96.
Nicholls, J. G. and Baylor, D. A. 1968. Specific modalities and receptive fields of sensory neurons in CNS of the leech. J. Neurophysiol. 31, 740–756.
Nicklaus, R. 1965. Die Erregung einzelner fadenhaare von periplaneta americana in abhängigkeit von der größe und richtung der auslenkung. Z. vergl. Physiol. 50, 331–362.
Oldfield, B. P. 1982. Tonotopic organisation of auditory receptors in Tettigonniidae (Orthoptera: Ensifera). J. Comp. Physiol. 147, 461–469.
Page, K. L. and Matheson, T. 2005. Wing hair sensilla underlying aimed hindleg scratching of the locust. J. Exp. Biol. 207, 2691–2703.
Palka, J., Levine, R., and Schubiger, M. 1977. The cercus-to-giant interneuron system of crickets. 1: Some attributes of the sensory cells. J. Comp. Physiol. A 119, 267–283.
Pearson, K. G. 2000. Neural adaptation in the generation of rhythmic behavior. Ann. Rev. Physiol. 62, 723–753.
Pflüger, H. J., Braunig, P., and Hustert, R. 1981. Distribution and specific central projections of mechanoreceptors in the thorax and proximal leg joints of locusts II. the external mechanoreceptors: hair plates and tactile hairs. Cell Tiss. Res. 216, 79–96.
Pflüger, H. J. and Tautz, J. 1982. Air movement sensitive hairs and interneurons in *Locusta migratoria*. J. Comp. Physiol. 145, 369–380.
Römer, H. 1983. Tonotopic organization of the auditory neuropile in the bushcricket *Tettigonia viridissima*. Nature 306, 60–62.
Römer, H, Marquart, V., and Hardt, M. 1988. The organization of a sensory neuropile in the auditory pathways of two groups of Orthoptera. J. Comp. Neurol. 275, 201–215.
Shepherd, D. and Murphey, R. K. 1986. Competition regulates the efficacy of an identified synapse in crickets. J. Neurosci. 6, 3152–3160.
Shimozawa, T. and Kanou, M. 1984. Varieties of filiform hairs: range fractionation by sensory afferents and cercal interneurons of a cricket. J. Comp. Physiol. A 155, 485–493.
Spinola, S. M. and Chapman, K. M. 1975. Proprioceptive indentation of the campaniform sensilla of cockroach legs. Comp. Physiol. 96, 257–272.
Strausfeld, N. S. 1976. Atlas of an Insect Brain. Springer Verlag.
Thompson, K. S., Blagburn, J. M., Gibbon, C. R., and Bacon J. P. 1992. Correlation of filiform hair position with sensory afferent morphology and synaptic connections in the second instar cockroach. J. Comp. Neurol. 320, 213–227.
Walthall, W. W. and Murphey, R. K. 1986. Positional information, compartments, and the cercal sensory system of crickets. Dev. Biol. 113, 182–200.
Westin, J. 1979. Responses to wind recorded from the cercal nerve of the cockroach *Periplaneta americana*. I. Response properties of single sensory neurons. J. Comp. Physiol. A 133, 97–102.
Westin, J., Langberg, J. J., and Camhi, J. 1977. Responses of giant interneurons of the cockroach *Periplaneta americana* to wind puffs of different directions and velocities. J. Comp. Physiol. 121, 307–324.
Willis, W. D. and Coggeshall, R. E. 1991. *Sensory Mechanisms of the Spinal Cord*. Plenum.
Woodbury, C. J. and Scott, S. A. 1991. Somatotopic organization of hindlimb skin sensory inputs to the dorsal horn of hatchling chicks (*Gallus g. domesticus*). J. Comp. Neurol. 314, 237–256.
Zill, S. N. and Moran, D. T. 1981. The exosceleton and insect proprioception. I. Responses of tibial campanofiorm sensillae to external and muscle regnerated forces in the American cockroach, *Periplaneta Americana*. J. Exp. Biol. 91, 1–24.
Zill, S. N., Schmitz, J., and Büschges, A. 2004. Load sensing and the control of posture and locomotion. Arth. Struct. Dev. 33, 273–286.
Zill, S. N., Underwood, M. A., Rowley, J. C., and Moran, D. T. 1980. A somatotopic organization of groups of afferents in insect peripheral nerves. Brain Res. 198, 253–269.

Further Reading

Field, L. H. and Matheson, T. 1998. Chordotonal organs of insects. Adv. Insect Physiol. 27, 1–228.
Jacobs, G. A. 1995. Detection and analysis of air currents by crickets – a special insect sense. BioScience 45, 776–785.
Mill, P. J. 1976. Structure and Function of Proprioceptors in the Invertebrates. Chapman and Hall.
Molander, C. and Grant, G. 1987. Spinal cord projections from hindlimb muscle nerves in the rat studied by transganglionic transport of horseradish peroxidase, wheat germ agglutinin conjugated horseradish peroxidase, or horseradish peroxidase with dimethylsulfoxide. J. Comp. Neurol. 260, 246–255.

6.18 Visual Deprivation Effects on Somatosensory and Visual Systems: Behavioral and Cortical Changes

H Burton, Washington University School of Medicine, St. Louis, MO, USA

D G McLaren, University of Wisconsin, Madison, WI, USA

© 2008 Elsevier Inc. All rights reserved.

6.18.1	**Reading by Touch**	365
6.18.1.1	Somatosensory Aspects of Braille Reading	365
6.18.1.2	Shape or Texture Processing	366
6.18.1.3	One- or Two-Handed Braille Reading	366
6.18.2	**Tactile Acuity Following Visual Deprivation**	367
6.18.2.1	Heightened Tactile Acuity	367
6.18.2.2	The Effects of Practice and Enhanced Attentive Skills	368
6.18.2.3	Visual Deprivation and Enhanced Attentive Skills	369
6.18.2.4	The Blind Artist	369
6.18.2.5	Spatial Cognition and Blindness	371
6.18.3	**Somatosensory Cortex Changes in Response to Visual Deprivation**	372
6.18.3.1	Evidence for Reorganized Somatosensory Cortex	372
6.18.3.2	Does Reorganization Follow a Hebbian Model?	373
6.18.3.3	Response Dynamics in S1 and S2	374
6.18.4	**Visual Cortex Adjustments in Response to Visual Deprivation**	375
6.18.4.1	Metabolic Changes	375
6.18.4.2	Studies in Animals	376
6.18.4.3	Studies in Humans	377
6.18.4.3.1	Cross-modal visual cortex activation: event-related potential/magnetoencephalography recordings	377
6.18.4.3.2	Disrupted tactile processing: effects of repetitive transcranial magnetic stimulation and stroke	377
6.18.4.3.3	Regional distribution of visual cortex activity – perceptual processing	378
6.18.4.3.4	Regional distribution of visual cortex activity – cognitive processing	381
6.18.5	**Possible Sources of Cross-Modal Visual Cortex Activity**	383
6.18.5.1	An Innate Network	383
6.18.5.2	Connections with Multisensory Areas	383
6.18.5.3	Tactile Activation of Visual Areas in Sighted People	384
6.18.5.4	Altered Physiology	384
6.18.6	**Conclusions**	385
References		386

Glossary

BOLD Blood oxygen level-dependent (BOLD) responses are the measured signals in functional magnetic imaging studies. BOLD indicates brain regions, especially in the cortex, where blood flows have increased due to heightened neural activity in the underlying tissue. The blood flows are greater than the metabolism needed to support the activity, which leads to greater oxygenation in the affected site. As oxygenated blood is less paramagnetic, there is lower suppression of the magnetic fields and hence, larger measured local magnetic signals in the region of increased neural activity.

compensatory processing An eighteenth-century concept that described substitution of heightened acuity in retained sensory capacities in response to severe sensory deprivation such as blindness or deafness.

dot-gap densities An aspect of braille cell patterns involves the location of raised dots within a standard two column by three row array. Adjacent braille cells that spell words vary as to whether comparably positioned dots are raised in adjoining series of letters. These differences create variations in the size and frequency of spaces between dots in any given row within a word and between adjacent words.

dot numerosity An aspect of braille cell patterns involves the number of raised dots. More raised dots for a particular braille letter indicate greater dot numerosity.

event-related potentials (ERPs) A technique that measures synchronized electrical responses in the brain through electrodes attached to the scalp. Usually some external stimulus is used to elicit these stereotypical responses. ERPs are seen only after averaging recordings from dozens or hundreds of synchronized events. The timing of recorded negative and positive potentials reflects ongoing brain activity, including possible cognitive processes such as attention.

GABA Gamma-aminobutyric acid is an inhibitory neurotransmitter found throughout the vertebrate central nervous system.

global–holistic An entire object is perceived as a single entity.

haptics An object's properties are perceived through touch by actively moving a portion of skin, usually a fingertip, over the object.

isomorphic response patterns See spatial response profiles.

odd-ball targets A paradigm in which a repeated series of similar stimuli is interrupted by presentation of a stimulus with different parameters. Detecting these unusual and infrequent events often requires attention.

oxygen extraction fraction (OEF) A measure of brain activity related to the ratio of fractional changes in cerebral blood flow (CBF) and cerebral metabolic rate of oxygen consumption ($CMRO_2$): $CBF/CMRO_2$.

PET Positron emission tomography is a nuclear medicine imaging technique that is based on scanning the brain (or other organ) after intravenously injecting (or inhaling) a short-lived radioactive tracer isotope, which decays by emitting a positron. Detection occurs when a burst of light is produced where positrons encounter and annihilate with an electron to produce a pair of photons. Coincident detection of photon pairs by arrays of photodetectors and back-projection algorithms localize the source of the positrons.

phosphene A sensation of seeing light is caused by nonvisual stimulation of the retina or visual cortex.

retinopathy of prematurity A potentially blinding disease of the retina that mainly affects prematurely born babies. The condition develops as a consequence of abnormal retinal vessel growth in areas where normal retinal vascularization has not yet occurred. Normally retinal blood vessel growth is mostly complete in full-term babies. In premature infants, before normal blood vessels reach the edges of the retina, normal vessel growth is replaced. The abnormal blood vessels are fragile, can leak, and consequently can scar the retina and even lead to retinal detachment.

S1 First or primary somatosensory cortex is located along the postcentral gyrus of parietal cortex in primates. Historically, it was the first cortical region identified that responded to stimulation of peripheral mechanoreceptors which are responsible for the sense of touch.

S2 Second somatosensory cortex is located lateral to S1 and along the parietal operculum in primates. Historically, it was the second cortical region identified that responded to stimulation of peripheral mechanoreceptors.

SA-I afferent activity A type of peripheral mechanoreceptor that shows persistent, slowly adapting responses to constant pressure.

spatial response profiles A topographically distributed representation of neural responses evoked by sequential, spatially iterated stimulation, usually across a tactile object. The spatially represented responses are directly triggered by the structure of the touched object. The response pattern is said to be isomorphic where it faithfully maps an object's shape.

transcranial magnetic stimulation (TMS) A noninvasive technique through which neurons in the brain can be excited. Short duration, rapidly changing magnetic pulses are passed through to the underlying brain from a coil placed on a section of skull. Cortical activity in the affected region is excited by induced electric currents momentarily induced by the magnetic fields. Pulse application is most effective when applied repetitively.

two-point threshold A measurement of the minimum detectable distance between two points simultaneously applied to the skin.

vibrissae Elongated hairs used as tactile sensing organs and mostly concentrated on the faces of furry animals.

von Frey filament von Frey, a nineteenth-century psychophysicist, first described using fine wires or hairs of varying diameter to study the sense of contact force against the skin. His studies utilized Hook's principle that a constant force is delivered and proportional to the extent of recoverable inwards bends. Filaments of different diameters have different spring constants and therefore produce a constant force proportional to the filament diameter. von Frey calibrated the forces produced by different diameter filaments (cat's vibrissal hairs) at the first bend and used these to determine the minimum detectable tactile contact force on different regions of skin.

6.18.1 Reading by Touch

6.18.1.1 Somatosensory Aspects of Braille Reading

Braille reading involves pattern recognition of mechanical stimulation arising from small scale, 2D coded, embossed dot arrays (Millar, S., 1997; Mountcastle, V. B., 2005). Each braille cell is based on a six-dot pattern arranged into two columns of three each (Figure 1), which provides 64 different dot patterns. In the standard braille matrix, dots are ~1 mm in diameter and ~0.45 mm high. Interdot spacing within a cell is 2.28 mm and between cells is 6.35 mm. Dot spacing is above human thresholds of 0.7–0.9 mm on the fingertip (Mountcastle, V. B., 2005). Braille letter patterns are more distinguishable, and therefore easier to read than embossed letters or even letters made with braille-like dots (Loomis, J. M., 1981). It is the patterns rather than the dots *per se* that makes braille more legible. Braille patterns lack multiple distinctive features since the presence or absence of any dot changes the character. Each dot arrangement defines a unique letter or a word in contracted braille (Figure 1).

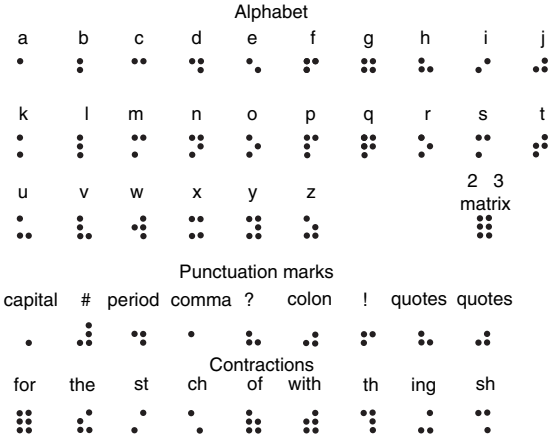

Figure 1 American braille cell patterns for alphabet, punctuation marks, and some braille II contractions.

The lateral scanning movements of skilled braillists evoke distinct tactile stimulation from each braille cell and a rapid, complex stream of intermittent stimulation from every word and line of text. These scanning movements across the dots effectively activate afferent nerve endings found in the glabrous skin finger tip (Mountcastle, V. B., 2005). The slowly adapting Merkel cell-associated afferents (SA-I) especially resolve individual dots in typical braille cells (Johnson, K. O. and Lamb, G. D., 1981). Reconstructed population spatial response profiles from various peripheral afferents showed that only SA-I afferents coded the spatial structure of braille cell dot patterns (Phillips, J. *et al.*, 1990). SA-I spatial response profiles persist with scanning at 20–120 mm s^{-1}, speeds that span the typical range of braille reading rates of 60–175 words per minute. Other low-threshold peripheral afferents are also activated by braille dot arrays (Johnson, K. O. and Lamb, G. D., 1981), but their contribution to braille reading is less certain because the spatial response profiles are less distinctive for different braille patterns.

A nearly isomorphic transformation of the peripheral SA-I activity reaches area 3b and some area 1 cells in the primary somatosensory cortex (Phillips, J. R. *et al.*, 1988). These faithful replications of peripheral responses transmit information to the cortex where subsequent decoding and linkage to linguistics support tactile reading. Mountcastle V. B. (2005) lists several hypotheses plausibly underlying observed isomorphic cortical responses:

1. Each synaptic stage between periphery and cortex must respond nearly simultaneously.
2. Temporal dispersion between peripheral receptor to cortical responses must be minimal despite conduction times and synaptic delays.

3. Transient responses are most critical at each synapse because only 75–100 ms is available for perceptual processing of a braille cell in skilled braillists.
4. Activation from successive braille cells is independent of each other.
5. Isomorphic transmission of braille cell patterns relies on spatially distributed activity from peripheral receptors and the population of activated cortical neurons.

6.18.1.2 Shape or Texture Processing

The possible braille cell physical attributes perceived during reading are dot numerosity, texture, and spatial shape (Millar, S., 1985). Additionally, a tactile feature produced by fluent braille reading is sensing lateral shearing produced by the density of dot gaps within individual braille cells (Millar, S., 1987; Pring, L., 1994). Thus, flowing lateral movements of the reading finger across the text transform braille cell static spatial shapes into a dynamically changing spatial–temporal pattern. These patterns vary with braille letters and characters due to differences in dot-gap densities, a texture feature, which the SA-I afferent nerve endings also excel at coding (Connor, C. E. *et al.*, 1990; Connor, C. E. and Johnson, K. O., 1992). Thus, fluid hand movements in fluent reading highlight the possibility of temporally extended dynamic patterns (Millar, S., 1997).

Good readers presumably do not use global–holistic letter or word shape coding (Nolan, C. and Kederis, C., 1969; Millar, S., 1984a; Pring, L., 1985; Millar, S., 1987; Pring, L., 1994). In contrast, a global shape hypothesis receives strong buttressing from neurophysiological findings that braille spatial patterns are coded isomorphically. However, many S1 (primary somatosensory cortex) cells and all other activated cortical areas do not show isomorphic response patterns that are tied to the global shapes of braille cells. Whether nonisomorphic response patterns solely derive from input projected by SA-I afferent activity or indicate input from other activated peripheral afferents is unknown. Decoding nonisomorphic response patterns remains an important unresolved issue. Current physiology also does not adequately encompass the actual events in fluent text reading in which top-down linguistic content drives perceptual processing (Millar, S., 1997). Thus, detection of the spatial structure of individual braille cells probably becomes subservient to content-driven discrimination of the text.

6.18.1.3 One- or Two-Handed Braille Reading

A critical aspect of reading braille is simultaneously processing both spatial and verbal components of the text (Millar, S., 1997). The resulting integration of the spatial and verbal domains is often shared across two hands, especially in more proficient readers (Davidson, P. W. *et al.*, 1992). Nevertheless, there is discrepant evidence on the cerebral lateralization of braille reading (Semenza, C. *et al.*, 1996), which, as a linguistic task dominated by left hemisphere processing (Burton, H. *et al.*, 2002a), might predict a right-hand preference. Consistent with left linguistic lateralization, one study demonstrated a right-hand advantage when a matching task required processing name identities (e.g., a verbal code) as opposed to the physical identities of letters (Semenza, C. *et al.*, 1996). However, according to Millar, there is no best hand for braille reading (Millar, S., 1984b) because proficient reading depends on simultaneous verbal and spatial information processing that commonly involves two-handed reading. In addition, reading proficiency appears related to task demands and an individual's proclivities as opposed to any left hemisphere specialization for linguistic factors in braille reading (Millar, S., 1997).

Most readers prefer to use two hands, and bimanual reading is faster (Davidson, P. W. *et al.*, 1992). Reading strategies also vary widely wherein the first segment of a line might be explored by the left hand, a second segment conjointly and a third by the right hand (Bertelson, P. *et al.*, 1985). Analyses of braille reading based on photographing the hands from below transparent braille text showed no evidence for simultaneous, parallel text reading even with conjoint hand movements across the text (Millar, S., 1997). One finger reads while the other marks spatial features of the text (e.g., spaces, line position). Two fingers never show simultaneous skin compression over textual dots that characterize reading even when both fingers are simultaneously over different text (Millar, S., 1997). One fingertip pressed against the dots while the other sequentially was pushed into spaces between braille cells or adjacent words in instances of apparently tandem and juxtaposed reading (Millar, S., 1997). Thus, one finger reads while the other simultaneously tracks the layout of the text.

6.18.2 Tactile Acuity Following Visual Deprivation

6.18.2.1 Heightened Tactile Acuity

Blind people are traditionally believed to be better at perceiving tactile stimuli that go unnoticed by sighted individuals possibly because of obligatory expanded experience with haptics. In 1749, Diderot proposed the concept of compensatory processing in remaining senses after the loss of one sensory system. In 1890, William James suggested that compensation led to acquiring superior acuity in the intact senses (cited in Röder, B. and Rösler, F., 2004). However, in blind and sighted people, equivalent tactile receptor sensitivity thresholds are found over approximately a six-decade age range (Stevens, J. *et al.*, 1996), and tactile acuity thresholds on the fingers rise at nearly identical rates with age (Stevens, J. *et al.*, 1996; Goldreich, D. and Kanics, I. M., 2003). Threshold increases with age presumably reflect decreases in peripheral receptor densities and/or central neuron populations that are not affected by blindness. Thus, it is doubtful that peripheral receptor sensitivity changes in blind people. The one exception to these findings is peripheral neuropathy in individuals whose blindness arises from diabetic retinopathy (Hollins, M., 1989). In contrast are reports of enlarged and elongated facial vibrissae (e.g., peripheral tactile organs) in cats and mice visually deprived at birth (Rauschecker, J. P. *et al.*, 1992). Altered vibrissae anatomy possibly was a consequence of increased haptic usage (Rauschecker, J. P. *et al.*, 1992). As noted below, learned skills are a more probable explanation for superior tactile acuity in blind humans because age of blindness onset, extent of visual experience, and level of retained light sensitivity did not affect the uniformity of tactile acuity findings across blind subgroups (Stevens, J. *et al.*, 1996).

No differences in tactile thresholds between blind and sighted people have been reported for tactile tasks that are based on detecting probable differences in the magnitude of peripheral receptor activity. For example, blind people show no superiority in von Frey filament force detection thresholds (Axelrod, S., 1959; Pascual-Leone, A. and Torres, F., 1993; Sterr, A. *et al.*, 2003). No group threshold differences were reported even with servo-controlled application of contact force that was distributed over a fingertip (Goldreich, D. and Kanics, I. M., 2003). Blind and sighted individuals are also equally adept at distinguishing the lengths of thin bars pressed against the finger (Stevens, J. *et al.*, 1996). Both groups comparably discern tactile roughness differences between horizontal gratings with variable ridge widths (Grant, A. C. *et al.*, 2000) or textures such as sandpaper or abrasive stones, whether actively or passively touched (Heller, M. A., 1989a). Each of these tasks involves detecting stimulus magnitude differences, which reflect response vigor in activated peripheral receptors and/or the number and types of activated receptors.

Distinctions in tactile acuity between blind and sighted people have been mixed when using the classic test of the minimum detectable distance between two, passively applied points. The ambiguity arises because traditional two-point assessments are prone to intensity differences from stimulating more or less skin with, respectively, two or one point (Johnson, K. O. and Phillips, J. R., 1981). Study protocols that ignored this confound reported no two-point threshold differences between blind and sighted persons (Axelrod, S., 1959; Pascual-Leone, A. and Torres, F., 1993). In contrast, Stevens J. *et al.* (1996) reported that people with early- and late-onset blindness, and some with residual light perception, similarly detected ~15% shorter gap distances than sighted. Stevens and co-workers' study utilized a two-alternative forced choice task in which the intensity confound based on perceived stimulation length was balanced. The task involved discriminating between a two-point gap versus an uninterrupted narrow bar whose length equaled the distance between the two points. Blind people also differentiated transverse compared to longitudinal orientation of two-point stimulation with ~40% shorter distances between points compared to sighted people (Stevens, J. *et al.*, 1996). All blind participants were braille literate, and the test results were obtained from the preferred braille reading index finger.

Greater acuity on these tests possibly reflected practice in attending to features of braille dot displays. For example, learning to distinguish braille dot patterns that differ by dot numerosity (Figure 1, e.g., f vs. p) possibly provides practice with detecting two points as in the test used by Stevens and co-workers. Similarly, learning to read braille letters based on the angle of dots across the first and second column (Figure 1, e.g., e vs. i) might provide practice in noting the orientation of two-point stimulation. Another consequence of these developed skills is that blind braillists recognize braille-like tactile patterns better than sighted, but only for dot pattern

arrays whose size (3×3 and 4×4) resembled standard braille (e.g., 2×3) (Foulke, E. and Warm, J. S., 1967). Cognitive guidance subsequent to extensive practice is also relatively specific to the task and learned tactile patterns, because blind and sighted performance differences did not occur when participants discriminated patterns created from unfamiliar, larger embossed dot matrices (e.g., 5×5 or 6×6), even when using the practiced braille reading finger (Foulke, E. and Warm, J. S., 1967).

Heightened sensitivity in blind people is also observed with tactile stimuli unrelated to braille. A grating orientation task involves discriminating between transverse and longitudinal orientations of passively applied square-wave gratings (e.g., equal groove and ridge widths), where the variable parameter is groove width (Van Boven, R. W. and Johnson, K. O., 1994). The minimal groove width is an index of tactile spatial acuity. However, the orientation task involves a fine tactile spatial discrimination for which groove width contributes to the perceptions. Two studies found that blind people detected orientation differences for gratings with smaller groove widths (Van Boven, R. W. *et al.*, 2000; Goldreich, D. and Kanics, I. M., 2003). All blind subgroups had lower groove width thresholds than the sighted group when gratings were applied with calibrated force levels, using a servo-controlled device (Goldreich, D. and Kanics, I. M., 2003), or were applied manually (Van Boven, R. W. *et al.*, 2000). Superior tactile spatial acuity did not correlate with braille reading factors (e.g., years reading, daily usage, age when learned) (Goldreich, D. and Kanics, I. M., 2003). However, tactile acuity on the reading finger was superior to the other fingers; although all fingers were superior compared to sighted individuals (Van Boven, R. W. *et al.*, 2000). Group differences were not found in another study that used the same grating orientation task and manual stimulation (Grant, A. C. *et al.*, 2000). The divergent findings might involve procedural differences.

6.18.2.2 The Effects of Practice and Enhanced Attentive Skills

Superior tactile acuity plausibly ensues from learned sensorimotor skills (Hollins, M., 1989; Davidson, P. W. *et al.*, 1992; Millar, S., 1997; Morgan, M., 1999; Grant, A. C. *et al.*, 2000; D'Angiulli, A. and Waraich, P., 2002) and attention strategies (Millar, S., 1974; Röder, B. and Rösler, F., 2003; Collignon, O. *et al.*, 2006). A real-life example is that reading comprehension persists relatively unchanged in older braillists despite significant declines in braille reading speeds. Age-related structural changes possibly do not affect fluent braillists because they attend to contextual, linguistic content to guide perceptual processing (Millar, S., 1997). In the absence of age-associated cognitive impairments, such lexical skills are probably less affected by age. However, training that leads to superior acuity tends to be confined to the practiced skin surface. For example, late-onset blind individuals have >20% lower thresholds in the grating orientation task on the dominant compared with the nondominant hand (Sathian, K., 2000). In contrast, skin surfaces that normally are not exposed to extensive experience in haptic exploration or tactile literacy, such as the lips, show no tactile discrimination differences between blind and sighted persons (Stevens, J. *et al.*, 1996).

Another study explicitly evaluated the effects of practice and learning to attend tactile differences in a more refined embossed dot detection paradigm (Grant, A. C. *et al.*, 2000). Multiple blind subgroups and sighted individuals detected whether a central dot in a three-dot linear array was offset (Grant, A. C. *et al.*, 2000). On the first assessment, early blind were 50% and late-onset blind were 33% more sensitive than sighted participants. They detected offsets of less than 1 mm, which is considered an example of hyperacuity because the differences are below the limits of tactile spatial acuity. However, there were no group differences after practice. Thresholds declined nearly 50% in sighted, >20% decrease in early blind, and 0% in late-onset blind participants. Irrespective of the tested hand, early- and late-onset subgroups were also not significantly different. Amongst the early blind participants, there were no threshold differences between preferred and nonpreferred braille reading hands. These results indicate that practice rapidly improves performance on a tactile task involving braille-like embossed dots, but only in individuals who have little or no prior experience with attending to tactile distinctions. Smaller or no threshold improvements in the blind participants and an absence of threshold differences between the hands suggest that prior braille literacy had already optimized and generalized cognitive skills affecting tactile perceptual acuity.

Practice effects on tactile acuity are not limited to blind people. Adult professional pianists, who have practiced daily from early childhood, have lower

two-point spatial discrimination thresholds than age-matched nonmusicians and, for the musicians, more hours of daily practice inversely correlated with the magnitudes of lower discrimination thresholds (Ragert, P. *et al.*, 2004).

6.18.2.3 Visual Deprivation and Enhanced Attentive Skills

Superior tactile acuity in blindness might not solely rely on expanded haptic experience because visual deprivation alone possibly induces cognitive changes that contribute to heightened acuity (Goldreich, D. and Kanics, I. M., 2003). Permanent visual deprivation during some critical developmental period is not necessary to demonstrate behaviorally enhanced tactile acuity because sighted individuals improved performance on tactile tasks after blindfolding. In one study (Kauffman, T. *et al.*, 2002), two groups of sighted individuals wore blindfolds for 5 days. One subgroup additionally received 4 h of daily practice learning braille and 2 h of intense tactile stimulation. Two control groups were not blindfolded, and one of these was also exposed to enhanced tactile stimulation. Performance was assessed at days 1, 3, and 5 using two-alternative forced choice identification of whether stimulation was with the same or different braille cell patterns. Blindfolded participants made significantly fewer errors than both groups without visual deprivation. Surprisingly, the blindfolded subgroup that did not receive tactile training performed significantly better than the stimulated group (Théoret, H. *et al.*, 2004), which contradicts reports of heightened acuity following practice on the dot-offset task (Grant, A. C. *et al.*, 2000) and evidence of greater skill in braillists in recognizing braille-like patterns (Foulke, E. and Warm, J. S., 1967). Additionally, shorter-term visual deprivations of 90 min lowered thresholds on a grating orientation task (Facchini, S. and Aglioti, S. M., 2003) and 120 min of blindfolding enhanced accuracy in identifying tactile shapes (Weisser, V. *et al.*, 2005). Awareness of somatosensory and auditory sensations probably increased during blindfolding, which possibly enhanced resource allocations to tactile stimulation during threshold testing.

Tactile encoding might be enhanced by practice-induced improvement in memory recognition of haptically explored objects. For example, blind were faster, but less accurate in recalling tactile nonsense shapes than sighted participants (Millar, S., 1974). The speed–accuracy trade-off might reflect a behavioral strategy rather than recognition recall differences in blind people. Early- and late-onset blind are also better than sighted participants at recalling tangible letters. However, letters presented in a practiced modality (braille for blind and visually for sighted) were remembered with equivalent accuracy by blind and sighted participants (Bliss, I. *et al.*, 2004). However, it is more probable that blind people are superior at directing attention toward selected targeted stimulation (Hötting, K. *et al.*, 2004; Collignon, O. *et al.*, 2006) and at dividing or switching attention between targets (Kujala, T. *et al.*, 1997a). Thus, congenitally blind process the spatial location of attended tactile or auditory stimuli faster in both selective and divided attention conditions (Collignon, O. *et al.*, 2006) and ignore irrelevant stimulation better (Hötting, K. *et al.*, 2004). These differences indicate that in the absence of vision, congenitally/early blind people are qualitatively less distracted by nontarget stimuli and are better at processing target stimuli within intact modalities. Without visual deprivation, sighted people have difficulty dissociating visual and tactile information even when performing tactile tasks (Hollins, M., 1989).

A possible consequence of extensive practice with tactile skills is "a higher-order plasticity" that "alters somatosensory information processing and sensory perception beyond training-specific constraints" (Ragert, P. *et al.*, 2004, p. 477). However, several findings indicate that such metaplastic phenomena might not be universal. For example, equivalent tactile reading speeds occur in blind and sighted people following practice with the Optacon device (Craig, J., 1988), a vibrator-based tactile reading device. Blind people do not show any advantage in learning to read with the Optacon device despite prior developed tactile skills for braille literacy. In addition, those who had the least prior tactile learning showed greater improvement in tactile acuity with practice, as noted above by performance of sighted individuals on the dot-offset task following practice (Grant, A. C. *et al.*, 2000) and on the braille pattern detection task in blindfolded participants who received no extra tactile practice (Théoret, H. *et al.*, 2004).

6.18.2.4 The Blind Artist

A traditional view is that congenitally/early blind people have limited competence to create pictures because they fail to incorporate perceptions of outlines and perspective that are not readily perceived through touch (Hollins, M., 1989). Haptic

perceptions are necessarily atomistic, which possibly makes it difficult to relate parts to an overview of a complex display (Heller, M. A. *et al.*, 2003). Generally, haptic exploration places greater emphasis on substance properties, successive integration of inputs, and the manipulative complexity of hand movements (Klatzky, R. L. *et al.*, 1989). Because of the successive nature of touch, even extensive practice with haptics might not compensate for the structural compartmentalization of form experienced by blind individuals. A possible consequence is that congenitally/early blind people are unable to understand such structural linkages as interposition or covering and perspective. In contrast, Révész G. (1950) hypothesized that late-onset blind people probably retain visual imagery, which directs manual dexterity and helps fuse haptic inputs. Prior visual experience and greater haptic skills possibly allow late-onset blind to perform better on a haptic-embedded figures test (Heller, M. A. *et al.*, 2003) and on identifying tangible drawings (Heller, M. A., 1989b). A contrary view is that congenitally/early blind people can appreciate perspective, overlapping objects, and structural relationships across 3D objects and can interpret external scenes. Examples of these skills are the ability to identify objects in tangible drawings (Kennedy, J., 1993), to perceive separate objects within complex backgrounds (Heller, M. A. *et al.*, 2003), and to draw pictures (Kennedy, J., 1993; 2003; Kennedy, J. M. and Igor, J., 2003; Kennedy, J. and Juricevic, I., 2006).

Spatial perception might not be inherently visual but depends on familiarity and practice to learn rules like linear perspective, convergence, vantage point and depth in pictorial representation (Heller, M. A., 1989b; Heller, M. A. and Kennedy, J. M., 1990; Heller, M. A. *et al.*, 2002; Kennedy, J. M., 2003; Kennedy, J. M. and Igor, J., 2003; Kennedy, J. and Juricevic, I., 2006). Greater superiority in picture naming observed in late-onset blind participants might indicate that the translational rules in pictorial representation were learned from prior visual experience (Heller, M. A., 1989b; Kennedy, J. M. and Igor, J., 2003). A consequence of no familiarity or practice with these rules is that raised outline drawings produced by congenitally/early blind individuals often appear distorted and unrealistic (Figures 2(a)–2(e)). However, even blindfolded sighted participants, who relied only on tactile feedback, produced unrepresentative perspectives in their raised outline drawings of angled stimulus objects (Heller, M. A. *et al.*, 2002), which indicate the need to practice drawing correct perspectives irrespective of visual status.

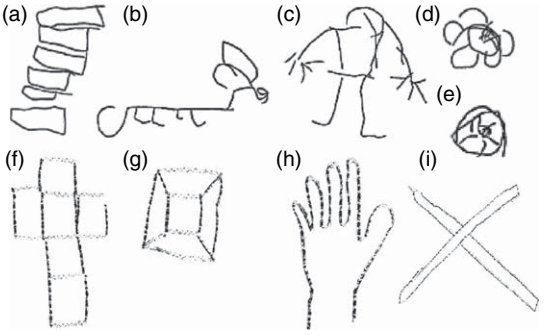

Figure 2 Tangible, raised line drawings produced by early blind individuals. (a)–(e) Drawings made by a 10-year-old blinded at age 21/2. (a) Hexagonal box drawn as six rectangular sides. (b) Stick figure of a dog. (c) Stick figure of a man. (d) Spinning wheel shown with extra loops around the edge for movement. (e) Static wheel drawn with spokes arranged around the center. (f)–(i) Drawings made by a 12–13-year-old blind since birth. (f) A foldout drawing of a cube with all six sides. (g) A cube drawn with vertical sides. (h) A hand. (i) Overlapping pencils showing one on top of the other, note the bottom pencil has its sides occluded. Reproduced from Kennedy, J. 1993. Drawing and the Blind: Pictures to Touch. Yale University Press; Kennedy, J. M. 2003. Drawings from Gaia, a blind girl. Perception 32, 321–340, with permission from Yale University Press.

Because raised outline, tactile drawings predominantly portray visual perceptions as opposed to those obtained through touch, they present a somewhat arbitrary depiction to blind people. As a consequence, tangible drawings produced by congenitally/early blind individuals can appear distorted, especially when the attempt is to show features with a possible haptic provenance (Kennedy, J., 1993). The drawing might incorporate some metaphorical device like a spinning wheel (Figure 2(d)) or an individual running that is not visually representative in 2D drawings (Kennedy, J., 1993). However, blind people can identify objects represented with 3D perspective in tactile pictures (Kennedy, J., 1993; Heller, M. A. *et al.*, 2002) and can recognize raised outline shapes with accuracy comparable to sighted (Heller, M. A. and Kennedy, J. M., 1990). Blind individuals can also create drawings that employ perspective (Figures 2(f)–2(i)) including object overlap (Figure 2(i)) and other visual conventions (Kennedy, J., 1993; Kennedy, J. M., 2003; Kennedy, J. M. and Igor, J., 2003; Kennedy, J. and Juricevic, I., 2006). With practice and feedback that teaches the representational rules, tangible drawings produced by congenitally/early blind individuals can be reasonable

Figure 3 Photograph and self-portrait of Ernesto Masuelli. Reproduced by permission from Révész, G. 1950. Psychology and Art of the Blind. Longmans, Green and Co.

depictions (Kennedy, J., 1993; Kennedy, J. M., 2003; Kennedy, J. M. and Igor, J., 2003) that even indicate foreshortening and convergence (Kennedy, J. and Juricevic, I., 2006). However, the ability to understand perspective is more variable in congenitally/early compared to late-onset blind people (Heller, M. A. *et al.*, 2002).

Révész G. (1950) evaluated whether sculpture produced by congenitally/early blind and late blind individuals had aesthetic qualities. Truly aesthetic accomplishments were noted only in creative and technically trained people with late-onset blindness (Révész, G., 1950). Révész G. concluded that congenitally blind individuals are incapable of creating truly aesthetic sculptures because they lack a unifying sense of form and space. He hypothesized that in a late-blind individual, previous visual world experiences presumably provide a guiding spatial, symmetrical conception that suffuses true aesthetics.

An example of art produced by a late-onset blind person is shown in Figure 3. Masuelli was an artist who first began sculpting 14 years after losing sight through a shell splinter in World War I (Révész, G., 1950). His remarkable artistic ability is highlighted by a comparison between a photograph of the artist and a particularly captivating self-portrait (Figure 3). The aesthetics revealed in Masuelli's sculpture relies on 3D spatial skills.

6.18.2.5 Spatial Cognition and Blindness

Individuals with congenital/early compared to late-onset blindness have diminished processing abilities for spatial information mainly because of difficulties in encoding external cues, frames of reference or configurations (Millar, S., 1994; Gaunet, F. *et al.*, 1997). Absence of early visual experience is especially deleterious to appreciating metrical information obtained through haptic exploration of space even when topological positions are accurately retained (Gaunet, F. *et al.*, 1997). Most congenitally and early-onset blind individuals, even subsequent to improved performance learned through feedback guidance, were unable to learn with comparable accuracy the spatial representations of complex 3D haptic arrays. Late-onset blind and trained blindfolded sighted individuals were similar in performing with greater accuracy (Gaunet, F. *et al.*, 1997). However, contrary findings indicated that a true spatial metric probably is available to even congenitally blind people if they are given more time to establish a representation of space (Heller, M. A. and Kennedy, J. M., 1990). For example, congenitally blind participants had smaller absolute displacement errors in the raised outline drawings they created to represent a top-down perspective of a haptically explored, multiobject scene. Additionally, blind participants had lower absolute distance errors compared to blindfolded sighted participants in a pointing task to memorized proprioceptive targets (Gaunet, F. and Rossetti, Y., 2006).

The role early visual experience plays in integrating and mapping somatosensory stimuli into external spatial coordinates is especially demonstrated by the effects that crossing the hands over the body midline has on tactile perceptions. When sighted, blindfolded sighted, and late-onset blind people detected the temporal order between two tactile stimuli, they required longer interstimulus intervals with the hands held crossed compared to resting in a normal uncrossed position. In contrast, congenitally blind individuals have better temporal resolution of two successive tactile stimuli compared to sighted and late-onset blind for the crossed and uncrossed posture (Röder, B. *et al.*, 2004). In sighted people, for whom vision dominates other sensory modalities, the localization of external tactile events is subjugated to a visual spatial reference frame (Eimer, M., 2004). Crossing the hands creates a conflict between left and right visual space and anatomical left and right hands. Computations are slowed when body-centered proprioceptive and externally referenced tactile coordinates are in conflict (Röder, B. *et al.*, 2004). Visual instruction to the somatosensory system never occurs in congenitally blind. Consequently, these people do not perceive a conflict between

body-centered and externally referenced tactile coordinates because the latter never develops. Therefore, they do not experience computation differences when the hands are crossed. Finding that late-onset blind individuals have delayed perceptions similar to those observed in sighted people with crossed hands posture suggests that early visual experience permanently instructs the somatosensory system with a visually established external coordinate reference frame. These effects persist for life and are probable contributors to the work of blind artists such as Masuelli.

6.18.3 Somatosensory Cortex Changes in Response to Visual Deprivation

6.18.3.1 Evidence for Reorganized Somatosensory Cortex

Extensive sensorimotor experiences involving isolated body regions (e.g., fingers) causes the S1 representation for the affected peripheral anatomy to expand in animals and humans (Jenkins, W. M. *et al.*, 1990; Recanzone, G. H. *et al.*, 1992b; Merzenich, M. M. and Jenkins, W. M., 1993; Elbert, T. *et al.*, 1995; Buonomano, D. V. and Merzenich, M. M., 1998, Ramachandran, V. S. and Hirstein, W., 1998; Pleger, B. *et al.*, 2003). S1 reorganization revealed in animal studies is mostly subsequent to repetitive and stereotypical tactile stimulation protocols. An important feature is neuroplasticity in adult animals, long after any critical developmental period. S1 reorganization in adult animals predict similar S1 changes in both congenitally/early-onset and late-onset blind people. Additionally, in animal studies, a reorganized cortical representation correlated with enhanced tactile discrimination performance (Jenkins, W. M. *et al.*, 1990; Recanzone, G. H. *et al.*, 1992a; 1992c; Xerri, C. *et al.*, 2005), which suggests heightened tactile acuity in blind people might similarly involve S1 reorganization. Neuroplasticity in S1 of congenital/early blind proficient braillists was suggested by a larger distribution of contralateral parietal cortex surface potentials to braille-like stimulation compared to sighted individuals (Pascual-Leone, A. and Torres, F., 1993). Responses were evoked by stimulating the index finger on the reading hand while participants judged whether braille patterns in a pair matched or differed. Two correlative findings involved the application of repetitive transcranial magnetic stimulation (rTMS) to the contralateral sensorimotor cortex. Normally, rTMS to parietal cortex disrupts perception of tactile stimulation (Cohen, L. G. *et al.*, 1991). In blind participants, tactile perceptions were disturbed by rTMS applied over a larger number of contralateral parietal cortex sites (Pascual-Leone, A. and Torres, F., 1993). Supporting evidence for an expanded S1 representation for the right index fingertip also was obtained using vibrotactile stimulation to elicit functional magnetic imaging (fMRI) responses (Burton, H. *et al.*, 2004). Only early-onset blind participants showed an expanded activity distribution across the contralateral S1.

S1 reorganization in blind people was not found in an event-related potential (ERP) study (Röder, B. *et al.*, 1996) that reported similar topographic distributions of the somatosensory evoked N1 component in blind and sighted individuals. (The very short latency early negative component of the ERP (N1 component) reaches maximum amplitude over primary sensory areas and is hypothesized to be a reflection of primary, low-level sensory processing (Röder, B. *et al.*, 1996).) Participants tracked the frequency of odd-ball tactile dot-pattern stimulation. Attention was additionally manipulated by presenting stimulation patterns that were easy or difficult to discriminate. One potential basis for the contrasting results concerns the reading styles of the blind participants. In the study by Pascual-Leone A. and Torres F. (1993), the cortical distribution of ERPs in the blind participants was greater for the preferred reading hand compared to the ERP extent for the opposite homologous finger, which suggests that these participants might have been predominantly one-handed braillists. Reading preference was not specified in the study by Röder B. and co-workers. However, because most fluent braillists read with two hands (see Section 6.18.1.3), S1 reorganization might plausibly be bilateral. Consequently, no hemispheric differences in ERP distributions might occur in two-handed braillists.

S1 reorganization can also involve changes other than selective expanded representations. For example, in a magnetoencephalography study involving multifinger and single-finger braillists (Sterr, A. *et al.*, 1998a), the S1 neuromagnetic dipole distribution in the multifinger braillists was disorganized and enlarged. In contrast, dipole distance was unchanged in single-finger blind braillists compared to sighted individuals. A behavioral correlate of these distinguishable S1 organizations was that multifinger

braillists made more errors when asked to identify the finger on the reading hand that was focally touched (Sterr, A. *et al.*, 1998a; 1998b; 2003). Tactile thresholds were either lower or equal to those in sighted participants (Sterr, A. *et al.*, 1998a; 2003). Currently, these are the only results that link S1 reorganization to tactile acuity in blindness.

Adult animals and humans showed S1 reorganization when they were forced to rely on tactile experience from a restricted limb. However, no S1 reorganization was found in late-onset blind people in one ERP study (Röder, B. *et al.*, 1996) and in several fMRI studies that involved tactile stimulation (Burton, H. *et al.*, 2002a; 2004; 2006). The evidence for S1 expansions has only been obtained in early-onset blind people who are haptically experienced from infancy (Pascual-Leone, A. and Torres, F., 1993; Burton, H. *et al.*, 2004). The absence of S1 expansion in late-onset blind people was neither attributable to differences in extent of tactile stimulation nor to the duration of blindness. The demographic data indicated that early- and late-onset blind participants had similar sensorimotor experiences such as reading braille daily and depending on tactile information in everyday life (Burton, H. *et al.*, 2002a; 2004; 2006).

Transient reorganization of S1 in normally sighted individuals potentially explains the negative findings in late-onset blind people. S1 representation for stimulated fingers reversibly changes when sighted people attend to tasks that involve processing somatosensory stimulation on the hands and fingers (Buchner, H. *et al.*, 1995; Noppeney, U. *et al.*, 1999; Braun, C. *et al.*, 2002; Iguchi, Y. *et al.*, 2005; Schaefer, M. *et al.*, 2005; 2006). In these studies, the distance between neuromagnetic dipoles or ERPs associated with selected fingers expands when attention is directed toward a particular finger. These short-term neuroplasticity effects arise without protracted practice or visual deprivation but depend on the attended focus. Dynamic switching in S1 organization has been hypothesized as cognitive influences on an existing and earlier established stable representation (Braun, C. *et al.*, 2002). Importantly, these rapid transient changes in somatosensory cortex have been observed in cognitive tasks that last less than 10 min (Schaefer, M. *et al.*, 2005) and when tactile stimulation is synchronized with seen touch attributed to the stimulated finger (Schaefer, M. *et al.*, 2006). A key question is whether S1 reorganization observed in congenitally/early-onset blind individuals involves similar attention-based mechanisms and, as such, is plausibly the result of prolonged transient effects. As noted in Section 6.18.2, heightened tactile acuity in blind people is best explained by practice in attending to touch. It is therefore possible that reorganized S1 maps in blind people indicate improved attention skills that are invoked whenever a blind person addresses a tactile task. Consequently, inconsistent evidence regarding S1 expansions might plausibly depend on the attentive demands associated with the stimulation protocols used in different studies and on the tactile attention skills of early- compared to late-onset blind people.

Tactile stimulation also activates lateral parietal cortex bilaterally in blind and sighted people. The affected cortex includes the parietal operculum, adjoining inferior supramarginal gyrus (SMGi), parietal cortex medial to the intraparietal sulcus, and the superior aspect of the supramarginal gyrus (SMGs), which involves previously identified second somatosensory cortex (S2) (Burton, H. *et al.*, 1993; Ledberg, A. *et al.*, 1995; Burton, H., 2001; Eickhoff, S. B. *et al.*, 2006a; 2006b) and an SMGi region possibly analogous to monkey area 7b (Eidelberg, D. and Galaburda, A. M., 1984; Burton, H., 2001). Blind and sighted people show similar distributions of bilateral parietal opercular activity during vibrotactile (Burton, H. *et al.*, 2004), embossed letter (Burton, H. *et al.*, 2006), and braille stimulation (Sadato, N. *et al.*, 2002). Early- and late-onset blind people also showed similar activity distributions in S2 during braille reading (Burton, H. *et al.*, 2002a). These results suggest that blindness or the age of blindness onset does not differentially induce reorganization in lateral parietal somatosensory regions.

6.18.3.2 Does Reorganization Follow a Hebbian Model?

A Hebbian learning model for increased synaptic efficacy has been proposed as a mechanism responsible for cortical reorganization following extensive use or training (Buonomano, D. V. and Merzenich, M. M., 1998; Ramachandran, V. S. and Hirstein, W., 1998). Key features are that repetitive and synchronized neural activity enhances plasticity. In an attempt to implement such synchronization, passive, long duration (3 h) punctate tactile stimulation was applied through small solenoids worn on the right index fingerpad. Participants did not explicitly attend or discriminate the stimulation but engaged in unrelated activity. Tactile stimulation was presented with pulse durations of 10 ms, at an average frequency of 1 Hz, and with pseudorandomized intervals of 100–3000 ms. Stimulation was applied in one group using a probe tip of 50 mm^2 and to a

second group using a smaller 0.8 mm^2 tip (Pleger, B. *et al.*, 2003). The larger probe tip coactivated a greater number of receptors. S1 and S2 finger representation expanded only in the group that was stimulated over the larger skin surface. In the affected group and in the stimulated skin region, two-point spatial discrimination thresholds were lower and single-point localization was disturbed immediately following the stimulation interval. Several issues challenge whether the results based on coactivated stimulation apply to somatosensory cortex reorganization in blindness. In contrast to the stereotypical protocols used by Pleger B. *et al.* (2003), haptic exploration and tactile reading in blind people is tactilely diverse and less sustained. Braille reading also does not produce spatially and temporally correlated tactile stimulation. Neural activation during braille reading is probably not synchronous, although a temporally dynamic signal distributes tactile stimulation across most of the reading fingerpad (Millar, S., 1997). Stimulation timing changes with dot density differences; any possible stimulation synchrony is interrupted as the finger moves across lines and as reading shifts between hands with two-handed reading. Few braillists read continuously for several uninterrupted hours. Thus, tactile reading implausibly replicates the intensity, synchrony and duration of stimulation used to demonstrate S1 and S2 changes immediately following coactive tactile stimulation (Pleger, B. *et al.*, 2003). Despite these differences in stimulation, careful assessments find that blind people also have lower two-point spatial discrimination thresholds (see Section 6.18.2.1). One possibility is that the multiyear training to learn braille and to develop tactile attention skills provides sufficient repetition to satisfy a Hebbian model for somatosensory cortex neuroplasticity. However, supporting evidence for differences in the organization in S1 is contradictory in congenitally/early-onset blind, negative in late-onset blind people, and absent for S2. Potentially, expanded maps in late-blind and sighted individuals are the same as those maps in early-blind. Thus, top-down cognitive effects from attention provide a more probable mechanism for mobilizing resources in tactile tasks. As noted, blind people are more skilled in attending, and attention focused on selected fingers can transiently reorganize S1. It is unknown whether these transient changes can be long lasting and permanent. Consequently, current results do not support a Hebbian mechanism in somatosensory cortex of blind people.

6.18.3.3 Response Dynamics in S1 and S2

Extended exposure to vibrotactile stimulation changes the temporal patterns of S1 single neuron responses in animals (Recanzone, G. H. *et al.*, 1992c). The question is whether similar dynamic changes in brain activity occur in blind people. In imaging studies, some global indices of brain physiology are response magnitude and time course. Response magnitude is expressed as greater regional cerebral blood flow (rCBF) with positron emission tomography (PET), as amplitudes of regional blood oxygen level-dependent (BOLD) signals in fMRI, and as greater voltage of component waveforms in ERPs. For fMRI or ERPs, response time courses are expressed as component latencies and durations. Selective changes in these measures possibly suggest enhanced processing of information.

Evidence of response magnitude distinctions between blind and sighted persons is contradictory. Tactile stimulation did not evoke larger evoked potentials over parietal cortex in blind compared to sighted people in an ERP study where both groups were equally accurate in detecting rare target stimuli (Röder, B. *et al.*, 1996). Blind and sighted individuals showed no BOLD magnitude differences in S1 or S2 when discriminating vibrotactile stimuli (Burton, H. *et al.*, 2004) or embossed capital letters (Burton, H. *et al.*, 2006). In both fMRI studies, performance accuracy was >75% in all groups. In a PET study, only early blind showed greater rCBF in sensorimotor cortex contralateral to the preferred braille reading finger when discriminating braille cell patterns (Sadato, N. *et al.*, 2002). In the latter study, however, late-onset blind and sighted individuals performed at chance, while early-onset blind participants correctly discriminated the braille patterns. These discrepant findings on response magnitudes in S1 are best explained by behavioral performance differences between groups (Burton, H. *et al.*, 2004) and suggest that response magnitudes in S1 do not correlate with blindness.

Congenitally blind have shorter reaction times than sighted individuals when detecting odd-ball tactile or auditory targets (Röder, B. *et al.*, 1996; Kujala, T. *et al.*, 1997b), identifying embossed block capital letters (Burton, H. *et al.*, 2006), recalling tactile nonsense shapes (Millar, S., 1974), and encoding and transforming the spatial orientation of haptic images (Röder, B. *et al.*, 1997). Blind people, and especially those with late-onset blindness, identify tangible drawings faster (Heller, M. A., 2002; Heller, M. A. *et al.*, 2002; 2003). Shorter latency cortical responses possibly underly

speeded responses. Blind exhibit shortened N1 component latencies over parietal cortex to tactile stimulation (Feinsod, M. *et al.*, 1973; Röder, B. *et al.*, 1996). In addition, earlier time-to-peak were noted in S1 and S2 BOLD responses during an embossed letter identification task from early-onset blind compared to late-onset and sighted individuals (Figure 4). An inference from these results is that speeded performance in early-onset blind is causally linked to more efficient processing, and hence, earlier response latencies to tactile stimulation in somatosensory cortex. Greater skill in attending to tactile stimulation possibly accounts for such speeded neural responses.

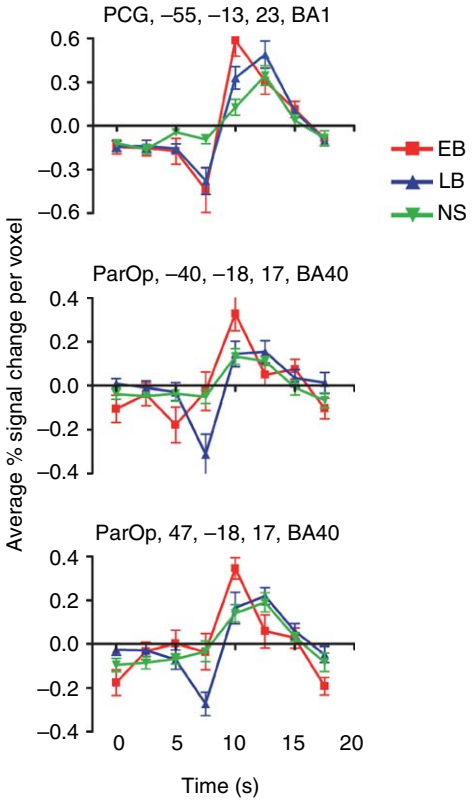

Figure 4 Regional S1 (PCG) and S2 (ParOp) BOLD response time courses during identification of an embossed capital letter with the right index finger in early- (EB), late-onset blind (LB), and sighted (NS) participants. S1 and S2 parietal cortex regions included significant voxels from the time-by-event-type factor in a random effect ANOVA analysis. Repeated measures MANOVA-assessed group differences in the time course profiles from these regions (as described in Burton, H. *et al.*, 2006). Responses in EB differed significantly from those noted in both other groups in left S1 ($p < 0.001$ vs. NS; $p = 0.024$ vs. LB; $p = 0.034$ LB vs. NS), from LB in left S2 ($p = 0.05$; $p = 0.01$ LB vs. NS), and from NS in the right S2 ($p = 0.006$; $p = 0.041$ LB vs. NS). In a *post hoc* analysis, a gamma function was fitted to the estimated hemodynamic response per event type for each participant and region (Liu, H. L. *et al.*, 2004; de Zwart, J. A. *et al.*, 2005). Time-to-peak of the gamma function, taken as the latency to the BOLD response peak, showed significantly earlier time-to-peak in BOLD responses from EB compared to NS. BA, Brodmann area; BOLD, blood oxygen level dependent; PCG, postcentral gyrus; ParOp, parietal operculum.

6.18.4 Visual Cortex Adjustments in Response to Visual Deprivation

6.18.4.1 Metabolic Changes

Metabolism and cerebral blood flow measurements address the important question of whether visual cortex remains active in blindness. Congenitally/early blind individuals show elevated glucose metabolism (Wanet-Defalque, M. C. *et al.*, 1988; Veraart, C. *et al.*, 1990), oxygen utilization and lower oxygen extraction fractions (OEFs) (De Volder, A. G. *et al.*, 1997) and heightened cerebral blood flow (CBF) (Uhl, F. *et al.*, 1993; De Volder, A. G. *et al.*, 1997; Mishina, M. *et al.*, 2003; Wittenberg, G. F. *et al.*, 2004). Studies that found similar glucose (Veraart, C. *et al.*, 1990) and CBF measurements (De Volder, A. G. *et al.*, 1997; Mishina, M. *et al.*, 2003; Wittenberg, G. F. *et al.*, 2004) in sighted people at rest, but with open eyes (e.g., an activated state) support the notion of an active visual cortex in blindness. The metabolic differences noted in these studies were generally identified in visual areas that included Brodmann areas 17–19.

By contrast, late-onset, totally blind have slightly lower glucose utilization compared to sighted individuals with eyes closed (Veraart, C. *et al.*, 1990) and lower resting CBF in visual areas (Wittenberg, G. F. *et al.*, 2004). The depressed glucose and CBF levels might indicate reduced visual cortex activity in late-onset blindness. Visual cortex glucose metabolism differences between early- and late-onset blindness and the relation to results in sighted people indicate that the potential for functional adaptations to visual deprivation possibly decreases with age of blindness onset.

From studies in adult animals, glucose metabolism in late-onset blind people might be expected to be normal or minimally elevated, but not depressed after several years of blindness. Visual cortex metabolic markers were transiently depressed in adult animals following visual deprivation. For example, glucose metabolism in visual cortex decreased and then recovered to normal levels within 16–17 days in monocular enucleated adult rats (Cooper, R. M. and Thurlow, G. A., 1985). Similarly, CBF decreased and then recovered within 45 days in monocular

enucleated adult mice (Madar, I. *et al.*, 1994). Consistent with an expected normal activity level is evidence that late-onset blind and sighted individuals have comparable occipital cortex TMS excitability thresholds for evoked phosphenes (Gothe, J. *et al.*, 2002). Clearly, additional studies of visual cortex in late-onset blind people are needed to confirm or refute findings of lower glucose metabolism (Veraart, C. *et al.*, 1990) or CBF (Wittenberg, G. F. *et al.*, 2004).

Changes in gamma-aminobutyric acid (GABA)ergic, inhibitory circuits are possibly responsible for enhanced excitability in visual cortex despite blindness. In support of this notion are findings of decreased GABA and glutamate decarboxylase (GAD) immunoreactivity in adult monkey's visual cortex following monocular visual deprivation (Hendry, S. H. C. and Jones, E. G., 1988). Presumably regional deafferentation yields decreased synaptic inhibition, which associates with increased regional cortical excitability. Visual cortex excitability also increased in sighted participants within a few hours of complete visual deprivation (Boroojerdi, B. *et al.*, 2000). The excitability changes from short-term blindfolding were blocked when participants received a benzodiazepine agonist, *N*-methyl-D-aspartic acid (NMDA) antagonist, or a muscarinic acetylcholine antagonist (Boroojerdi, B. *et al.*, 2001). These results are comparable to evidence of heightened cortical neuron excitability from reversibly blocking GABA inhibitory synapses in animals (Sillito, A. M., 1975; Alloway, K. D. *et al.*, 1989). However, visual deprivation probably has only a transient effect on cortical activity via inhibitory circuits because even early blind individuals show a normal distribution of $GABA_A$ receptors in visual cortex (Mishina, M. *et al.*, 2003). Consequently, because inhibitory circuits might not be permanently altered by visual deafferentation, alternative mechanisms possibly foster visual cortex activity in blindness (see Section 6.18.6).

6.18.4.2 Studies in Animals

Several animal models have demonstrated that peripherally induced blindness fostered cross-modal responses in normally visually activated cortex (Hyvärinen, J. *et al.*, 1981; Rauschecker, J. P. and Korte, M., 1993; Toldi, J. *et al.*, 1996; Kahn, D. M. and Krubitzer, L., 2002; Newton, J. R. *et al.*, 2002). The possible source for cross-modal reorganization must be evaluated relative to the neurodevelopment stage when blindness occurred. The critical factor is whether blindness was instantiated before or after completion of cell migrations to visual cortex because novel connections might only be possible while cortical and subcortical development is in progress. In monkeys, there was little alteration in the cellular and synaptic structure of visual cortex area 17 following binocular enucleations *in utero* after the gestational stage for cortical cell proliferation and migration (Rakic, P., 1988). Thus, any observed cross-modal adjustments noted after postmigrational development are presumably based on adjustments within extant circuitry. The demographic data on most blind human participants in metabolic, recording, or brain imaging studies cite loss of sight subsequent to peripheral eye structure pathology that primarily occurred late in gestation (e.g., retinopathy of prematurity in congenitally/early-onset blind) and well past postnatal sensitive periods in late-onset blind people. Therefore, human visual cortex connections and structure are probably minimally altered by peripheral eye pathology in most early- and all late-onset blind people.

In a study with monkeys, eyelids were sutured throughout the first year of life and then opened just prior to recording neuronal activity from occipital cortex (Hyvärinen, J. *et al.*, 1981). The model of induced blindness in the monkeys resembles some instances of human early-onset blindness. Somatosensory activity was recorded in extrastriate, Brodmann area 19, a visual association region normally selective for visual inputs (Hyvärinen, J. *et al.*, 1981). After year-long visual deprivation, 20% of multineuron responses were exclusively activated by tactile and 40% were driven by visual stimulation (Hyvärinen, J. *et al.*, 1981). Another study examined the effects of monocular enucleation in adult rabbits. The rabbit's striate visual cortex primarily receives crossed monocular inputs. Consequently, functional adjustments in the deprived contralateral visual cortex in rabbits plausibly correlate with total blindness effects in human late-onset blind people. The proportion of tactile responsive neurons in the rabbit primary visual cortex (V1) increased from 0% to 31%, although generally there were fewer responsive neurons (Newton, J. R. *et al.*, 2002).

Animal studies where visual deprivation was imposed prior to maturation of subcortical connections (Toldi, J. *et al.*, 1996; Kahn, D. M. and Krubitzer, L., 2002) also reported cross-modal activity in normally visual cortical regions. However, it is theoretically possible that in the aforementioned

animal studies, subcortical somatosensory and auditory relay nuclei project to the lateral geniculate nucleus to convey nonvisual information to visual cortex. An equivalent result has been demonstrated in the auditory system of ferrets following peripheral auditory deafferentation prior to maturation of subthalamic and thalamocortical connections. New projections developed from retained subcortical visual nuclei (e.g., superior colliculus), and these connected through the deafferented medial geniculate nucleus to convey visual information to auditory cortex (e.g., Sur, M. *et al.*, 1990; Sur, M. and Leamey, C. A., 2001). New subcortical projections probably do not explain most instances of cross-modal visual cortex activity in human early-onset and no cases of late-onset blindness, but such connections might arise in some cases of congenital anophthalmia.

6.18.4.3 Studies in Humans

6.18.4.3.1 Cross-modal visual cortex activation: event-related potential/ magnetoencephalography recordings

ERP recordings were the first to reveal occipital cortex activation to nonvisual stimulation in blind humans. A prominent sustained negativity was topographically recorded from occipital leads in early-onset blind participants during braille reading compared to passive stimulation with embossed dots. Tactile reading of embossed text did not evoke similar slow negativity from occipital sites in sighted participants (Uhl, F. *et al.*, 1991). The same experimenters also found occipital negativities in early-onset blind and sighted participants while they imagined feeling textured surfaces with the fingertips (Uhl, F. *et al.*, 1994). The authors suggested that the mechanisms in visual cortex responsible for visual imagery were similarly responsible for tactile imagery even in the blind participants who had no prior visual perceptions. This was the first suggestion that visual cortex activity in blind humans serves cognitive processes that were similar to those in sighted people.

Cross-modal auditory responses in occipital cortex were also demonstrated using a detection task involving rare deviant target tones. Evoked short latency, fast ERP components were recorded from posterior-occipital leads in early- and late-onset blind people (Kujala, T. *et al.*, 1995a; 1997a). Observing similar activity irrespective of age at blindness onset suggests that even mature brains can reorganize (Kujala, T. *et al.*, 1997a). Magnetoencephlography (MEG) more explicitly localized these auditory-evoked responses to visual cortex (Kujala, T. *et al.*, 1995b).

The specificity of cross-modal activation of visual cortex was examined by comparing the distribution of slow negative potentials during low-level perceptual or high-level cognitive processing and by determining whether task difficulty affected response distributions. In perceptual tasks, participants detected rare tactile display patterns or tone frequencies (Röder, B. *et al.*, 1996) or perceived and stored in working memory a standard tactile display (Röder, B. *et al.*, 1997). In the cognitive processing task, participants were required to mentally rotate a test tactile display and compare it to a recalled standard (Röder, B. *et al.*, 1997). Extended perceptual detection of both tactile and auditory target stimuli evoked sustained negative ERP potentials from occipital-posterior leads in early-onset blind but not sighted participants. ERP topographies were coincident for tactile and auditory stimulation (Röder, B. *et al.*, 1996). Similar occipital-posterior ERP response distributions were obtained during cognitive perceptual encoding and subsequent mental rotation of tactile stimulus orientations (Röder, B. *et al.*, 1997). Thus, ERP topographies were similar for low- and high-level processes. Task difficulty directly affected ERP magnitudes, but not distributions. In contrast, the topography and magnitudes of negative slow potentials recorded from nonoccipital sites were similar between the groups during the same tasks and difficulty levels. Activated nonoccipital sites especially respected modality specific topographies associated with the tasks – parietal for somatosensory and temporal for auditory.

6.18.4.3.2 Disrupted tactile processing: effects of repetitive transcranial magnetic stimulation and stroke

An important question is whether visual deprivation induces functionally diverse and yet behaviorally relevant cross-modal plasticity in visual cortex that contributes to adaptive adjustments. Behavioral relevance was shown by findings that rTMS applied to occipital cortex in blind people can transiently disrupt performance on various tasks. rTMS is known to disrupt task performance if the stimulated region contributes to task pertinent processing (Cohen, L. G. *et al.*, 1997; 1999). rTMS over a mid-occipital site causes congenitally/early-onset blind participants to make more errors when identifying braille or embossed Roman letters (Cohen, L. G. *et al.*, 1997; 1999). The rTMS caused distorted tactile

sensations that involved noting absent, extra, or confusing dots. However, neither blind nor sighted participants detected any tactile stimulation when single pulse TMS was applied to parietal cortex 20–40 ms after presentation of real or nonsense braille patterns (Hamilton, R. H. and Pascual-Leone, A., 1998; Pascual-Leone, A. *et al.*, 2005). When single pulse TMS was applied to occipital cortex 50–80 ms after peripheral stimulation, blind, but not sighted participants, were unable to identify braille patterns or distinguish them from nonsense dot patterns (Hamilton, R. H. and Pascual-Leone, A., 1998; Pascual-Leone, A. *et al.*, 2005). Both groups detected when they were touched by the embossed dots. These timing differences indicate that initial tactile detection still occurs in dedicated somatosensory–parietal cortex. After a delay, presumably needed for output from parietal cortex to reach occipital cortex, cognitive processing critical to letter identification utilizes posterior occipital cortex in blind people.

Occipital rTMS had no effect on tactile reading in late-onset blind and sighted participants. According to Cohen L. G. *et al.* (1999), the negative findings in late-onset blind participants indicated that cross-modal reorganization of visual cortex is possibly limited by the age of blindness onset. However, the mid-occipital rTMS site studied previously possibly spared a critical occipital region in late-onset blind people. When these individuals read braille, activity primarily was found in lower tier visual areas ipsilateral to the reading hand and mostly in inferior occipital cortex (Burton, H. *et al.*, 2002a). More importantly, occipital rTMS disrupts braille letter discrimination in sighted individuals after 5 days of visual deprivation (Pascual-Leone, A. and Hamilton, R., 2001). Additionally, occipital rTMS in sighted participants not subjected to blindfolding transiently disrupted judgments of the relative distance between raised dot patterns (Merabet, L. *et al.*, 2004). These findings strongly suggest that there is no critical period for the reorganization of visual cortex following blindness and that visual cortex normally contributes to macrogeometric tactile discriminations of spatial distance (Merabet, L. *et al.*, 2004).

Clinical evidence further indicates that visual cortex contributes to tactile perceptions when a blind person reads braille. Specifically, a congenitally blind individual developed alexia for braille without tactile agnosia or aphasia for heard language following a bilateral posterior occipital ischemic stroke (Hamilton, R. *et al.*, 2000). The patient had been a highly fluent braille reader. Her touch sensations were unimpaired and she recognized touched braille, but was nevertheless unable to read. Her microgeometric judgments of roughness were intact, while detection of tactile spatial distances was severely depressed (Merabet, L. *et al.*, 2004). Magnetic resonance (MR) structural images revealed no parietal sensorimotor or frontal language area lesions. Overall the rTMS results and clinical case show that reading by touch, a cognitive language function, depends on reorganized visual cortex in blindness. Whether a visual cortex contribution to tactile spatial discriminations relates to braille reading remains to be investigated.

6.18.4.3.3 Regional distribution of visual cortex activity – perceptual processing

Brain imaging studies in blind people provide numerous examples of visual cortex activation during tactile stimulation (Figure 5(c) and Sadato, N. *et al.*, 1996; 1998; 2002; Gizewski, E. R. *et al.*, 2003; Burton, H. *et al.*, 2004; 2006). However, several studies did not distinguish between regional activity for perceptual processing of tactile stimulation from cognitive language processing when participants read braille words, an explicit language task (Uhl, F. *et al.*, 1991; 1993; Sadato, N. *et al.*, 1996; 1998; Melzer, P. *et al.*, 2001; Burton, H. *et al.*, 2002a; Amedi, A. *et al.*, 2003; Gizewski, E. R. *et al.*, 2003). A similar language confound is present in tasks that required discriminating between successive braille letter displays (Büchel, C. *et al.*, 1998; Sadato, N. *et al.*, 2002) because fluent braillists indirectly incorporate linguistic processes when they recognize letter patterns. Consequently, in these studies activity due to cognition cannot be dissociated from that due to processing tactile stimulation. Generally, less visual cortex activity was elicited by tactile stimulation when discriminating angles, groove widths, or Roman letters compared to tactile inputs when distinguishing between braille words and nonwords (Sadato, N. *et al.*, 1996; 1998). These pioneering PET studies reported widespread, bilateral activation of medial occipital cortex, including striate and extrastriate cortex (Sadato, N. *et al.*, 1996; 1998), but did not differentiate regional activation differences between tasks. However, significant visual cortex responses consistently occurred only when blind people attended to sensory inputs (Sadato, N. *et al.*, 1996; Gizewski, E. R. *et al.*, 2003; Kujala, T. *et al.*, 2005), which suggests a task-relevant contribution

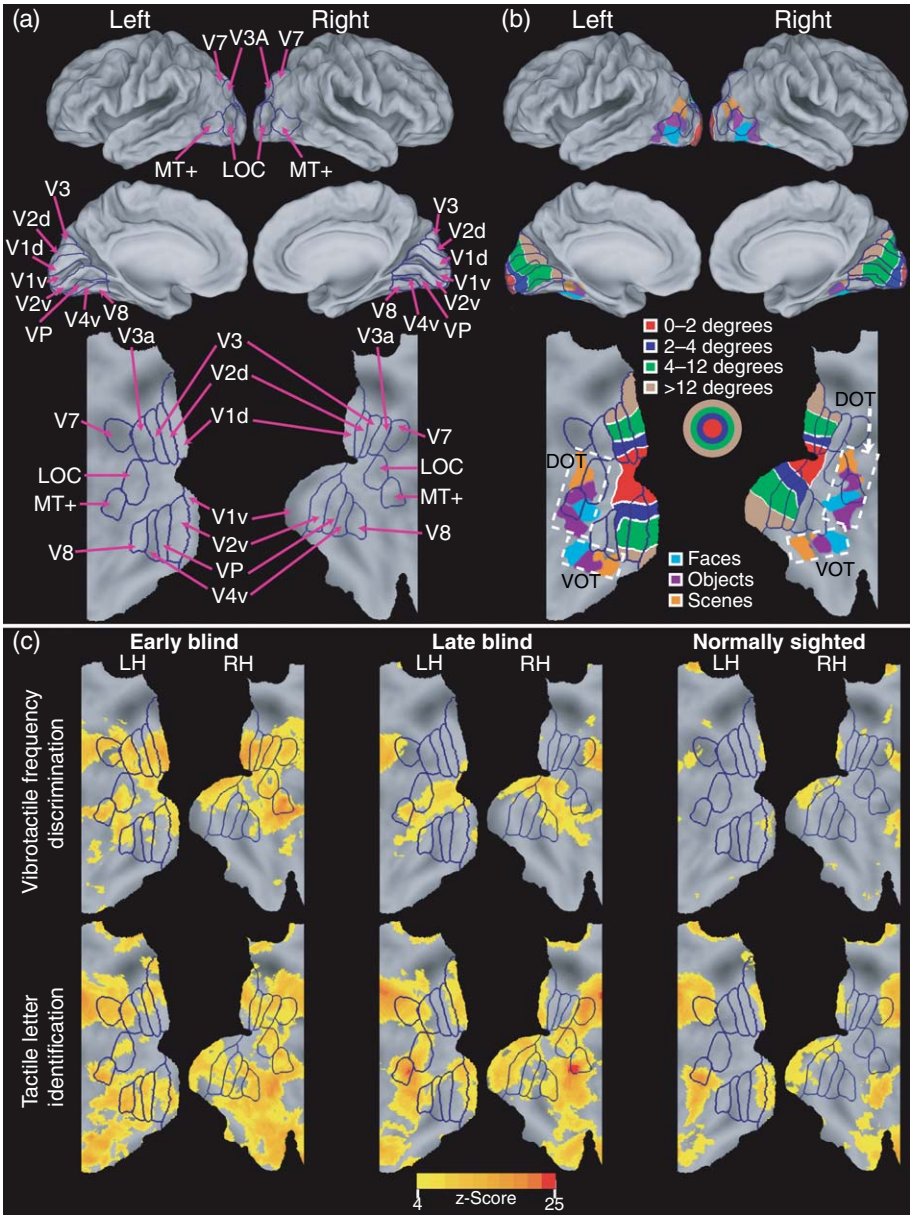

Figure 5 (a) Projection of visual areas onto a standard surface-based cerebral cortex reconstruction (VAN ESSEN, D. C., 2005). Top and middle: Fiducial reconstructions show lateral and medial hemisphere views, respectively. Bottom: Flattened reconstructions of the occipital lobe show visual area borders that are from prior identifications in sighted people (Hadjikhani, N. *et al.*, 1998; Van Essen, D. C., 2004). LOC, lateral occipital complex; MT+, medial temporal area; V1d and V1v, dorsal and ventral primary visual areas; V2d and V2v, dorsal and ventral second visual areas; V3 and V3a, third visual areas; V4v, ventral fourth visual area; VP, ventral posterior visual area; V7, seventh visual area; V8, eighth visual area. (b) Projection of receptive field eccentricity bands for lower tier visual areas onto a standard surface-based reconstruction. Concentric colored circles indicate different degrees of eccentricity. In the fiducial views, foveal to peripheral ordering of eccentricity bands occupies, respectively, posterior to anterior Talairach atlas coordinates (Talairach, J. and Tournoux, P., 1988). In the flattened view, foveal to peripheral eccentricity bands align from bottom to top in dorsal visual areas and from top to bottom in ventral visual areas. In addition, item selective regions in ventral and dorsal occipito-temporal partitions (VOT and DOT) were projected onto the standard surface reconstruction using spheres centered on previously reported centers-of-mass coordinates (Hasson, U. *et al.*, 2003). Colored boxes indicate regions activated when viewing faces, objects, or scenes (Hasson, U. *et al.*, 2003). (c) Distribution of increased activity in the occipital lobe for two tactile tasks. Maps show results by group during a vibrotactile frequency discrimination task (Burton, H. *et al.*, 2004) and a tactile letter identification task (Burton, H. *et al.*, 2006). Scale is for group average cross correlation magnitude *z*-scores greater than 4. LH, left hemisphere; RH, right hemisphere.

to performance as opposed to reactive stimulus–response effects.

Perceptual processing occurred during tactile stimulation in a task that involved vibrotactile stimulation passively applied to the right index finger. Early- and late-onset blind and blindfolded sighted participants attended paired vibrations (25 and 100 Hz) to detect when they differed in frequency. No activity was found in traditional language areas during this frequency discrimination task (Burton, H. *et al.*, 2004). Thus, verbal tagging was absent and long-term recognition/recall was not required because the interval between stimuli was 300 ms. The vibrotactile discrimination task evoked some bilateral visual cortex activity in all groups. Early blind participants showed the greatest activation of visual cortex including portions of all lower tier retinotopic areas, that is, V1–VP (Figures 5(a) and 5(c)). These areas additionally show an orthogonal regional representation of different eccentricity axes (e.g., center–periphery maps) (Figure 5(b) and Hasson, U. *et al.*, 2002; 2003; Grill-Spector, K. and Malach, R., 2004). Within the eccentricity representation, the vibrotactile task activated the most significant responses in foveal and parafoveal eccentricity bands (Figures 5(b) and 5(c)). No lower tier visual areas selectively responded except for activation along the upper bank of the calcarine sulcal cortex, which in sighted people normally represents lower visual space. Similar lower tier visual subdivisions were activated in late-onset blind participants in whom, however, responses principally affected foveal eccentricity band cortex (Figure 5(c)).

Higher tier visual areas in the inferior and middle occipital gyri and posterior inferior temporal sulcus and gyrus were also bilaterally activated in early blind participants during a vibrotactile task. The same regions had smaller responses that were less extensively distributed in late-onset blind participants (Burton, H. *et al.*, 2004). The affected higher tier regions included V7, V8, LOC, and MT+ (Figures 5(a) and 5(c) and Tootell, R. B. *et al.*, 1996; Amedi, A. *et al.*, 2002; Grill-Spector, K. and Malach, R., 2004; Van Essen, D. C., 2004). Included within, but extending beyond these higher visual areas is a second tier organization that involves dorsal occipito-temporal (DOT) and ventral occipito-temporal (VOT) partitions (Figure 5(b)). In sighted people, activity associated with these partitions selectively deal with visual images of faces, objects, and scenes compared to textures (Figure 5(b) and Malach, R. *et al.*, 1995; Kanwisher, N. *et al.*, 1997; Levy, I. *et al.*, 2001; Hasson, U. *et al.*, 2002; Malach, R. *et al.*, 2002; Hasson, U. *et al.*, 2003; Levy, I. *et al.*, 2004; Yovel, G. and Kanwisher, N., 2004). Within these partitions, visual information from faces or letters activates cortex just anterior to foveal eccentricities; cortex associated with parafoveal eccentricities selectively process pictures of objects; and cortex associated with peripheral eccentricities are preferentially activated by views of buildings or scenes (Figure 5(b)). Activity evoked by the vibrotactile stimulation in blind people encompassed the face and object but not the scene locations in DOT and VOT partitions in both groups of blind participants (Figures 5 (b) and 5(c)). The most significant activity especially overlapped the face or central gaze eccentricity, especially in late-onset blind participants (Figure 5(c)). Only three sighted participants showed small patches of V1 activity that principally involved the parafoveal eccentricity band (Burton, H. *et al.*, 2004).

These results show that a tactile task requiring some discrimination, but no language area involvement, cross-modally activated lower and higher tier visual cortex subdivisions in blindness. Although domain specificity was not observed, activation of foveal and central gaze regions might have reflected focal attention to the stimulated fingertip, which normally is seen in lower visual space.

Vibrotactile activation of visual areas has few parallels with visual stimulus attributes and, therefore, constitutes an unusual cross-modal adjustment to blindness even in higher tier areas that respond to complex tactile features in sighted people (see Section 6.18.5). In contrast, the vibrotactile task evoked a delayed and sustained negative BOLD response in most visual areas in sighted people (Burton, H. *et al.*, 2004), which normally indicates suppressed activity (Haxby, J. V. *et al.*, 1994; Drevets, W. C. *et al.*, 1995; Gusnard, D. A. and Raichle, M. E., 2001). Positive BOLD responses were found in somatosensory cortex of all groups. Hence, the positive BOLD responses in visual areas of blind people represent an adjustment and addition to tactile perceptual processing even of a relatively uncomplicated vibration frequency attribute.

Identifying embossed block letters is a tactile task that incorporates perceptual processing of tactile shapes and a sublexical linguistic task. Tactile reading of letters can readily be accomplished with little training by sighted and blind people (Loomis, J. M., 1981; Vega-Bermudez, F. *et al.*, 1991), even when letters are passively translated across a fingertip (Vega-Bermudez, F. *et al.*, 1991). Compared to findings with vibrotactile stimulation, tactile letter identification

activated a greater bilateral extent of visual cortex in blind and sighted people, but the activity in blind participants was most prominent (Figure 5(c)) (Burton, H. *et al.*, 2006). In V1 and V2, late-onset blind and sighted participants exhibited similar bilateral activity distributions across near foveal and parafoveal eccentricities; early-onset blind participants showed sparing of the foveal eccentricity (Figure 5(c)). Compared to the vibrotactile task data, activity in the remaining lower tier areas was more evident in both blind groups and was greater along the lower bank of calcarine sulcal cortex. Positive BOLD responses occurred in V2d, V3 and V3a, and VP and V4v in early and late blind participants. Activity was suppressed in the same areas in sighted participants. Activity was also relatively enhanced in higher tier visual areas. Highly significant responses were noted in MT+ and adjacent occipital–temporal cortex in all groups. All domains were activated in DOT and VOT partitions in early, but not late blind participants. Known letter identification areas in anterior fusiform gyral cortex (BA 37) (Puce, A. *et al.*, 1996; Garrett, A. S. *et al.*, 2000; Polk, T. A. *et al.*, 2002; Flowers, D. L. *et al.*, 2004) were similarly activated in blind and sighted groups (Burton, H. *et al.*, 2006).

By adding a simple sublexical language task to perceptual processing of tactile shapes, activity was enhanced generally and expanded to several lower and higher tier visual areas. The similar findings in both early and late blind participants indicate cross-modal adaptations persist despite different ages of blindness onset. The contrast between activity distributions with vibrotactile stimulation and letter identification indicate potentially different strategies when processing the letter shapes. For example, MT+ activity plausibly reflected moving tactile letters across the fingertip, an effective feature for MT+ (Hagen, M. C. *et al.*, 2002) in all groups. However, both cognitive recognition of the felt letter and greater skill in attending to tactile motion in blind participants possibly contributed to bilateral and generally more significant activity in MT+. Additionally, activity in V8 and neighboring nonvisuotopic portions of parieto-occipital cortex (BA 19) might indicate attention to tactile shape orientations (Zangaladze, A. *et al.*, 1999). Striking activity differences in the foveal eccentricity between vibrotactile stimulation and letter identification (Figure 5(c)) in late blind might indicate perceptually processing vibration features of focal stimulation compared to extracting multiple tactile object features for letters. Another example of possible special processing was larger responses in VOT in blindness. Prior reports in sighted people observed preferential VOT activation for item viewing (Malach, R. *et al.*, 1995; 2002). Thus, VOT response enhancements in blind people might have contributed to the processing of tactile letters as objects (Garrett, A. S. *et al.*, 2000; Flowers, D. L. *et al.*, 2004), especially when attending to letter identification.

6.18.4.3.4 Regional distribution of visual cortex activity – cognitive processing

Language tasks activated a greater extent of visual cortex than perceptual processing of tactile stimulation, especially in early blind people (Figure 6). For example, a phonological task that involved identifying a common rhyme for heard words (Burton, H. *et al.*, 2003) activated nearly all visual areas bilaterally in early blind, some of posterior V1 in late blind, and nothing in sighted participants. A more difficult language task that required identifying a common meaning for a list of heard words evoked yet more significant and extensive activation of visual cortex in early blind participants than the rhyming task (Figure 6 and Burton, H. *et al.*, 2003). The same semantic task led to a lesser distribution of activity across several lower and higher tier visual areas in late blind and barely any responses in sighted participants. Figure 6 shows that comparable findings were obtained with the semantic task of generating a verb to an offered noun irrespective of whether the noun was heard (Burton, H. *et al.*, 2002b) or read through braille (Burton, H. *et al.*, 2002a). Verb generation to heard words also activated V1 and V2 areas bilaterally in a few sighted people (Figure 6). In early blind participants, especially, any of the semantic language tasks activated the most significant activity in cortex associated with lower tier parafoveal eccentricity bands (Figure 6). Semantic tasks also evoked highly significant responses throughout several higher tier visual areas (e.g., V7, LOC, MT+, and V8). In reference to the selective domains in DOT and VOT partitions, the most significant activity spared the peripheral eccentricity zones normally associated with viewing scenes (Figure 6). Generally, however, activated visual cortex shows no distinctive topography in early blind people in whom semantic language tasks activate nearly all visual areas. In late blind, the affected regions are less extensive and more heterogeneous.

The only substantive topographic distinction was the more significant activity in the left hemispheres of early blind participants for semantic tasks with heard

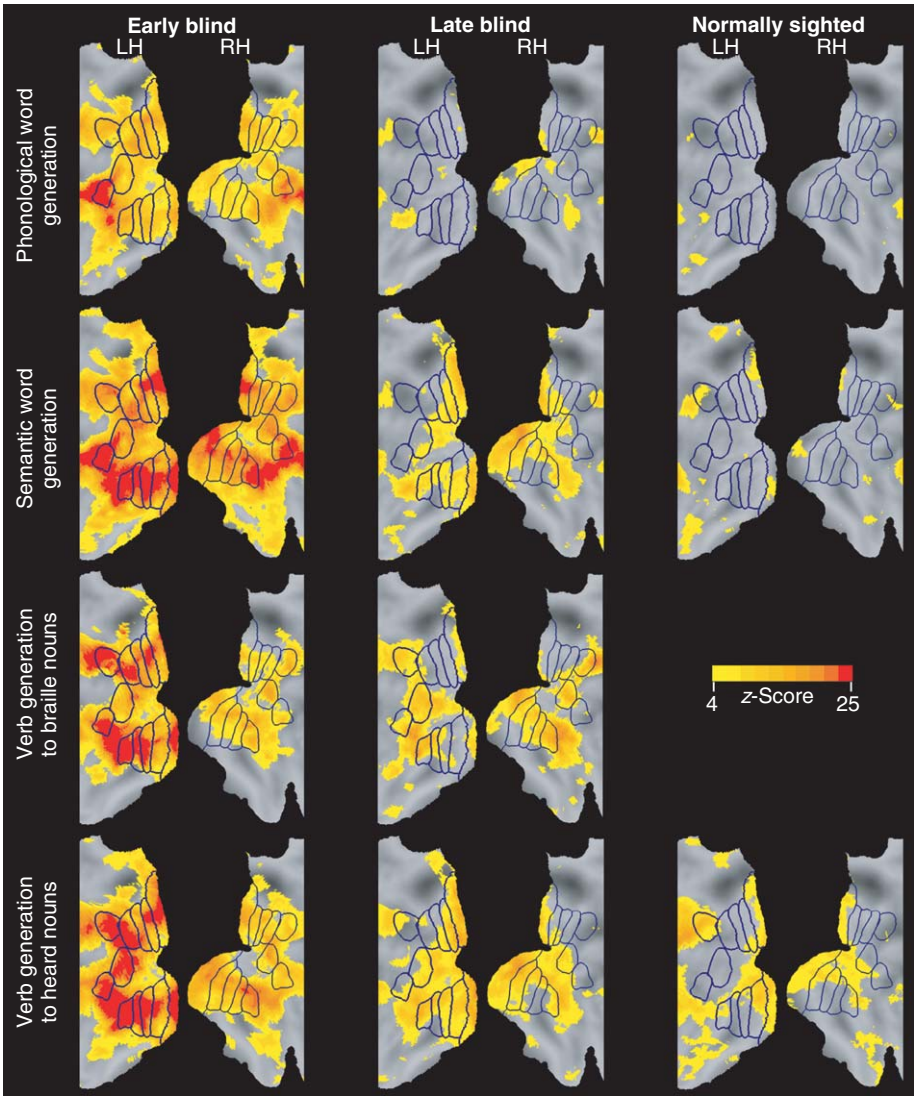

Figure 6 Distribution of increased activity observed in the occipital lobe during four language tasks. Row 1: During a phonological task, participants generated a word that matched the common rhyme in a group of 16 heard words (Burton, H. *et al.*, 2003). Row 2: During a semantic task, participants generated a word that matched a common meaning in a group of 16 words (Burton, H. *et al.*, 2003). During the semantic task of verb generation, participants read through braille (Burton, H. *et al.*, 2002a) (Row 3) or heard (Burton, H. *et al.*, 2002b) (Row 4) the nouns. Word generation was covert in all tasks. Scale is for group average cross correlation magnitude *z*-scores greater than 4. Borders and enclosed visual areas are shown in Figure 5.

words (Burton, H. *et al.*, 2002b; Röder, B. *et al.*, 2002; Amedi, A. *et al.*, 2003; Noppeney, U. *et al.*, 2003), imagery of sounds (De Volder, A. G. *et al.*, 2001), and braille reading (Sadato, N. *et al.*, 1998; Burton, H. *et al.*, 2002a). In contrast, activity predominated in the right hemisphere in late blind participants when they read braille, but was more symmetrically bilateral when generating verbs to heard nouns (Figure 6).

These results plausibly suggest a contribution to semantic language processing from striate and extrastriate visual cortex in blindness. A similar conclusion was proposed to explain greater BOLD response magnitudes with increased semantic and syntactic complexity of heard sentences (Röder, B. *et al.*, 2002) and during a semantic retrieval task (Noppeney, U. *et al.*, 2003). The functional relevance of occipital cortex to semantic processing was demonstrated when rTMS over left striate and extrastriate regions transiently increased errors in verb generation to heard nouns in blind but not sighted

participants; there was little interference with articulation of responses (Amedi, A. *et al.*, 2004). Activation of visual cortex during a variety of high-level language tasks is coupled with activity in traditional left-lateralized frontal, temporal, and parietal language areas (Röder, B. *et al.*, 2002; Burton, H. *et al.*, 2002a; 2002b; 2003; Noppeney, U. *et al.*, 2003); areas that have increased effective connectivity with occipital cortex in blindness (Noppeney, U. *et al.*, 2003).

The role of occipital cortex in language processing possibly needs qualification because any semantic task depends on retrieving word associations (Amedi, A. *et al.*, 2003). Thus, findings from two fMRI studies showed a stronger relationship between retention performance and visual cortex activity, especially in V1, than with verb generation. For example, V1 response magnitudes were more positively correlated with verbal retention performance (Amedi, A. *et al.*, 2003) and the accuracy of long-term episodic memory (Raz, N. *et al.*, 2005) in congenitally/early blind participants. These authors concluded that verbal memory processes underlay findings of visual cortex responses during verb generation.

These studies collectively indicate that reorganized visual cortex contributes to a range of perceptual, cognitive/language, and memory processes. The intensity of activation, however, is possibly greater for higher-order cognitive functions. But much remains unresolved about the spatial pattern of functional specializations in reorganized cortex. For example, there is little evidence of language-specific domains aside from the observation that linguistic tasks preferentially activate left visual areas in congenitally/early blind individuals. Tactile perceptual, sublexical language, and phonological processing all activate fewer visual areas than more demanding higher-level verbal processing. The distinction that more of visual cortex is needed for more complex cognitive processes might reflect effort and level of attention utilized in different tasks. Implied by this suggestion are concerns regarding visual cortex excitability and activity specificity and relevance. In future studies, controls for task difficulty and performance equalization between groups are sorely needed to assess the notion of nonselective visual cortex activity. Additionally, despite evidence of cross-modal auditory activation (Weeks, R. *et al.*, 2000; Arno, P. *et al.*, 2001; Röder, B. and Rösler, F., 2003; Gougoux, F. *et al.*, 2004; Gougoux, F. *et al.*, 2005), the topography of auditory perceptual processing has not been evaluated in the context of defined visual areas. At issue is whether reorganized visual cortex is amodal and the same regions are activated by tactile and auditory inputs. Furthermore, more topography comparisons are needed amongst various groups of visually deprived participants: congenitally/early blind, late-onset blind, low vision, and transiently blindfolded sighted people.

6.18.5 Possible Sources of Cross-Modal Visual Cortex Activity

6.18.5.1 An Innate Network

Findings following short-term visual deprivation of 90 min to 5 days in sighted people show that existing networks are capable of cross-modal processing. These intervals of transient visual deprivation are too brief for growing new connections. Blindfolding made visual cortex more excitable (Boroojerdi, B. *et al.*, 2000) and responsive to tactile stimulation during discrimination of braille letters as well as during a tone-matching task (Pascual-Leone, A. and Hamilton, R., 2001; Pascual-Leone, A. *et al.*, 2005). Blindfolding also induced performance improvements in distinguishing tactile grating orientation (Facchini, S. and Aglioti, S. M., 2003) and braille characters (Kauffman, T. *et al.*, 2002). These alterations reversed within 2 h after restoration of sight. Undoubtedly, visual cortex activity in late blind relies on extant networks. Even in early blind, similar connections probably support cross-modal visual cortex activity, especially when blindness occurred after neuronal migration ended during development. A recent tract tracing study found no new thalamocortical connections to primary visual cortex in early blind individuals (Shimony, J. *et al.*, 2006), which supports the notion that intracortical network changes are probably responsible for cross-modal visual cortex reorganization after permanent blindness. (Subcortical multisensory inputs from the superior colliculus or basal ganglia are also possible sources for cross-modal inputs (Macaluso, E. and Driver, J., 2005). These have yet to be investigated in blind people.)

6.18.5.2 Connections with Multisensory Areas

Projections to occipital cortex from temporal and parietal multisensory areas (Distler, C. *et al.*, 1993; Falchier, A. *et al.*, 2002; Rockland, K. S. and Ojima, H., 2003) possibly provide the anatomical substrate for activity not normally observed without visual

deprivation. These temporal and parietal multisensory areas densely project to peripheral and parafoveal axes of lower tier visual areas (Lewis, J. W. and Van Essen, D. C., 2000; Falchier, A. *et al.*, 2002; Rockland, K. S. and Ojima, H., 2003). Greater activation of the parafoveal eccentricity band illustrated in Figure 6 plausibly reflects these connections. Linkages are also available to prefrontal language areas indirectly through a temporal cortex link from visual to frontal cortex (Distler, C. *et al.*, 1993; Rempel-Clower, N. L. and Barbas, H., 2000), which possibly is a conduit for more complex cognitive operations in reorganized visual cortex, for example, verbal memory or semantics. Even primary sensory areas receive heteromodal inputs, a finding that questions traditional models of unimodal information processing (Cappe, C. and Barone, P., 2005). Additionally, all visual areas are intricately interconnected with feedforward and feedback connections (Felleman, D. J. and Van Essen, D. C., 1991). The higher tier visual areas also have more direct connections with multisensory areas and, as a consequence, are positioned to convey nonvisual information directly to lower tier regions. Visual cortex connections are consequently of sufficient diversity and breadth that a challenge will be to discern the pathways responsible for deprivation induced cross-modal plasticity (Cappe, C. and Barone, P., 2005).

6.18.5.3 Tactile Activation of Visual Areas in Sighted People

A possible functional basis for visual cortex responses to touch is enhanced processing of tactile stimulation in visual areas that already respond to somatosensory inputs in sighted people. For example, the visual motion area, V5/MT+, responds while attending to tactile motion (Hagen, M. C. *et al.*, 2002; Burton, H. *et al.*, 2006); LOC responds to 2D (Prather, S. C. *et al.*, 2004) and 3D macrospatial tactile object features (Amedi, A. *et al.*, 2002; James, T. W. *et al.*, 2002; Stoesz, M. R. *et al.*, 2003); V8/parieto-occipital regions activate when imagining spatial locations of tactile objects (Arno, P. *et al.*, 2001; Vanlierde, A. *et al.*, 2003); and a parieto-occipital area responds to tactile grating orientation (Sathian, K. *et al.*, 1997; Zhang, M. M. *et al.*, 2005). Selected visual area activation in nonvisual tasks are possibly instances where vision and touch involve the same perception, that is, stimulus motion, spatial orientation, and object identification. Normal tactile responsiveness might expand to other tactile stimulation features because visual deprivation removes afferent drive to inhibitory circuits that normally suppress tactile input to these regions.

6.18.5.4 Altered Physiology

Another possible source for reorganized visual cortex activity is altered intracortical flow of information from cortical locations that exhibit multisensory interactions. Example cortical multisensory regions are the ventral intraparietal area, caudal superior temporal region, and ventral premotor cortex, regions shown to contain heteromodal neurons in monkeys and overlapping activation from different modalities in human imaging data (Macaluso, E. and Driver, J., 2005). In sighted people, convergent feedforward information from unimodal sensory regions provides a plausible mechanism for multimodal responses, especially for stimulation occurring in overlapping space (Macaluso, E. and Driver, J., 2005). Additionally, cognitive factors, such as attention to targets in a specified space, might enable cross-modal activity in multisensory regions to affect processing in unimodal visual areas (Macaluso, E. *et al.*, 2000; 2002; Macaluso, E. and Driver, J., 2005). Any enhanced reversal of information flow from multisensory to visually deprived areas might easily funnel auditory or tactile inputs to visual cortex, including presumptive unimodal lower tier visual areas. A demonstration of a change in effective connectivity was increments in lower tier visual cortex rCBF in early but not late blind or sighted blind participants following application of rTMS to S1 cortex (Wittenberg, G. F. *et al.*, 2004). These effects occurred without evidence of rCBF alterations in thalamus. Thus, reorganized visual cortex becomes activated through heightened transfer of intracortical connections to visual cortex (Sadato, N. *et al.*, 2002). Prior evidence for these kinds of transfers was shown in physiological studies where the flow of cross-modal activity in the auditory system and superior colliculus was altered through convergent feedforward connections from specific sensory areas, feedback connections from higher level cortical areas or possible convergent projections to specific sensory areas (Foxe, J. J. *et al.*, 2002; Meredith, M. A., 2002; Schroeder, C. E. and Foxe, J. J., 2002). Rapid and reversible changes in effective connectivity following blindfolding in sighted people indicate that the potential for plasticity is already present and does not necessarily involve structural changes (Pascual-Leone, A. *et al.*, 2005). However, sustained visual

deprivation might cause more permanent shifts in connectivity.

Convergence effects might also entail temporally synchronized multimodal stimulation whose coincidence leads to multisensory interactions that again can affect activity in visual cortex (Macaluso, E. *et al.*, 2004; Macaluso, E. and Driver, J., 2005). An example observed in sighted participants was greater rCBF changes for target detection of a category word while viewing a speaking face and during temporal coincidence of heard words and visual inputs associated with speech (Macaluso, E. *et al.*, 2004). The increases occurred in ventral occipital and multisensory superior temporal sulcal cortex with audiovisual synchrony but not spatial congruency and in dorsolateral occipital cortex with synchrony and congruency (Macaluso, E. *et al.*, 2004). The enhanced visual cortex responses are potentially a model for acquired tactile activation of visual cortex when blind people learn braille. During learning, additive cross-modal effects are associated with prolonged practice that connects the feel of braille fields and heard phonemic information (Nolan, C. and Kederis, C., 1969; Pring, L., 1985; 1994; Millar, S., 1997). The temporal synchrony between sound and touch possibly activates multisensory areas more vigorously, which additionally influences and enhances activity in ventral visual cortex similarly to the events during speech perception. An expected subsequent effect from such training might generalize to tactile activation of visual cortex without braille reading. A secondary consequence with progressive tactile literacy is guidance to braille reading from contextual semantic meaning (Millar, S., 1997). Thus, tactile stimulation is coupled to semantic content, which possibly leads to coincident activation from tactile and frontal language area inputs – thereby developing and enhancing language activation of visual cortex.

6.18.6 Conclusions

New skills for enhanced processing of nonvisual stimuli develop in blind people. Adjustments include tactile reading and attentive skills for all nonvisual inputs. Positively reinforced practice heightens acuity on tasks requiring subtle perceptual and cognitive distinctions. Practice in attending to sensory subtleties also heightens tactile acuity in sighted people. Additionally, short-term visual deprivation alone improves tactile acuity in sighted individuals. Thus, better performance in blind people does not depend on more sensitive peripheral receptors. Nevertheless, especially early blind people have impoverished spatial awareness, presumably because without vision they do not project body-centered coordinates to external topography. A consequence for most early blind individuals is an inability to create representative drawings or sculptures. However, some blind people make tangible drawings that show perspective and external spatial features. Late-onset blind artists with past visual experience are more likely to produce aesthetic works.

Evidence of reorganization is inconsistent in primary somatosensory cortex and absent from any other somatosensory cortical areas in blind people. Reported alterations are potentially an instantiation of transient changes arising from attention effects and not Hebbian in nature. Specifically, in tasks requiring tactile attention and equal performance across groups, S1 shows similar response distributions. However, response dynamics are possibly speeded in early blind people.

Neuroplasticity has been observed in visual cortex of blind individuals at any age of blindness onset. For example, visual cortex metabolic activity in congenital/early blind people is comparable to levels obtained in sighted people with their eyes open. The metabolism is suggestive of normal neuronal activity. Cross-modal activation of visual cortex in blind people has been extensively documented. The activity appears relevant to behavior because disruption of visual cortex by posterior occipital strokes or TMS deteriorates tactile reading and semantic language performance in blind people. These changes garner surprise only when sensory areas are viewed as unimodal processors that funnel computations into a cascade of cortical areas, including multisensory regions. A bias regarding dedicated sensory cortical areas predicts a silent visual cortex following blindness. Heteromodal activity in reorganized visual cortex most parsimoniously reflects innate intracortical connections between cortical areas that normally exhibit nonvisual responsiveness in sighted people. These connections possibly lead to resurgent GABA receptor levels, plausibly normal inhibitory synaptic activity in deafferented visual cortex, and frank metamodal functions (Pascual-Leone, A. and Hamilton, R., 2001; Pascual-Leone, A. *et al.*, 2005).

Two plausible critical factors for heightened tactile acuity in blindness are reorganized visual cortex and altered response dynamics in visual and nonvisual areas. An important question is whether separate

visual cortex areas service different perceptual and cognitive processes and whether any distribution selectivity conforms to that noted in sighted people (Grill-Spector, K. and Malach, R., 2004). Hypothetically, some combination of visuotopic areas and eccentricity axes might apply to reorganized visual cortex. Low-level perceptual processing might only evoke lower tier visual areas wherein nonvisual stimulus features are analyzed; more complex cognitive tasks might evoke occipito-temporal and occipito-parietal areas possibly within selective eccentricity axes. Additionally, activation of dorsal and ventral occipito-temporal cortical partitions in sighted people is invariant with respect to many visual features (Hasson, U. *et al*., 2002; 2003; Grill-Spector, K. and Malach, R., 2004), which thereby suggest a capacity for processes independent of visual input. Thus, the global nature of selective domain specialization is possibly applicable to cognitive processing in blindness.

Acknowledgment

This work was supported by grant NS37237 from the National Institutes of Health.

References

Alloway, K. D., Rosenthal, P., and Burton, H. 1989. Quantitative measurements of receptive field changes during antagonism of GABAergic transmission in primary somatosensory cortex of cats. Exp. Brain Res. 78, 514–532.

Amedi, A., Floel, A., Knecht, S., Zohary, E., and Cohen, L. G. 2004. Transcranial magnetic stimulation of the occipital pole interferes with verbal processing in blind subjects. Nat. Neurosci. 7, 1266–1270.

Amedi, A., Jacobson, G., Hendler, T., Malach, R., and Zohary, E. 2002. Convergence of visual and tactile shape processing in the human lateral occipital complex. Cereb. Cortex 12, 1202–1212.

Amedi, A., Raz, N., Pianka, P., Malach, R., and Zohary, E. 2003. Early 'visual' cortex activation correlates with superior verbal memory performance in the blind. Nat. Neurosci. 6, 758–766.

Arno, P., De Volder, A. G., Vanlierde, A., Wanet-Defalque, M. C., Streel, E., Robert, A., Sanabria-Bohorquez, S., and Veraart, C. 2001. Occipital activation by pattern recognition in the early blind using auditory substitution for vision. Neuroimage 13, 632–645.

Axelrod, S. 1959. Effects of Early Blindness: Performance of Blind and Sighted Children on Tactile and Auditory Tasks. American Foundation for the Blind.

Bertelson, P., Mousty, P., and D'Alimonte, G. 1985. A study of braille reading. 2. Patterns of hand activity in one-handed and two-handed reading. Q. J. Exp. Psychol. A 37, 235–256.

Bliss, I., Kujala, T., and Hamalainen, H. 2004. Comparison of blind and sighted participants' performance in a letter recognition working memory task. Cogn. Brain Res. 18, 273–277.

Boroojerdi, B., Battaglia, F., Muellbacher, W., and Cohen, L. G. 2001. Mechanisms underlying rapid experience-dependent plasticity in the human visual cortex. Proc. Natl. Acad. Sci. U. S. A. 98, 14698–14701.

Boroojerdi, B., Bushara, K. O., Corwell, B., Immisch, I., Battaglia, F., Muellbacher, W., and Cohen, L. G. 2000. Enhanced excitability of the human visual cortex induced by short-term light deprivation. Cereb. Cortex 10, 529–534.

Braun, C., Haug, M., Wiech, K., Birbaumer, N., Elbert, T., and Roberts, L. E. 2002. Functional organization of primary somatosensory cortex depends on the focus of attention. Neuroimage 17, 1451–1458.

Büchel, C., Price, C., Frackowiak, R. S., and Friston, K. 1998. Different activation patterns in the visual cortex of late and congenitally blind subjects. Brain 121, 409–419.

Buchner, H., Kauert, C., and Radermacher, I. 1995. Short-term changes of finger representation at the somatosensory cortex in humans. Neurosci. Lett. 198, 57–59.

Buonomano, D. V. and Merzenich, M. M. 1998. Cortical plasticity: from synapses to maps. Annu. Rev. Neurosci. 21, 149–186.

Burton, H. 2001. Brain Imaging Studies of Human Somatosensory Cortical Regions: Results from Brain Imaging Studies in Humans. In: The Somatosensory System: Deciphering the Brain's Own Body Image (*ed*. R. J. Nelson), pp. 27–72. CRC Press.

Burton, H., Diamond, J. B., and McDermott, K. B. 2003. Dissociating cortical regions activated by semantic and phonological tasks to heard words: a fMRI study in blind and sighted individuals. J. Neurophysiol. 90, 1965–1982.

Burton, H., McLaren, D., and Sinclair, R. 2006. Reading embossed capital letters: a fMRI study in blind and sighted individuals. Hum. Brain Mapp. 27, 325–339.

Burton, H., Sinclair, R., and McLaren, D. 2004. Cortical activity to vibrotactile stimulation: a fMRI study in blind and sighted individuals. Hum. Brain Mapp. 23, 210–228.

Burton, H., Snyder, A. Z., Conturo, T. E., Akbudak, E., Ollinger, J. M., and Raichle, M. E. 2002a. Adaptive changes in early and late blind: a fMRI study of Braille reading. J. Neurophysiol. 87, 589–611.

Burton, H., Snyder, A. Z., Diamond, J., and Raichle, M. E. 2002b. Adaptive changes in early and late blind: a fMRI study of verb generation to heard nouns. J. Neurophysiol. 88, 3359–3371.

Burton, H., Videen, T. O., and Raichle, M. E. 1993. Tactile-vibration-activated foci in insular and parietal-opercular cortex studied with positron emission tomography: mapping the second somatosensory area in humans. Somatosens. Mot. Res. 10, 297–308.

Cappe, C. and Barone, P. 2005. Heteromodal connections supporting multisensory integration at low levels of cortical processing in the monkey. Eur. J. Neurosci. 22, 2886–2902.

Cohen, L. G., Bandinelli, S., Sato, S., Kufta, C., and Hallett, M. 1991. Attenuation in detection of somatosensory stimuli by transcranial magnetic stimulation. Electroencephalogr. Clin. Neurophysiol. 81, 366–376.

Cohen, L. G., Celnik, P., Pascual-Leone, A., Corwell, B., Faiz, L., Dambrosia, J., Honda, M., Sadato, N., Gerloff, C., Catala, M. D., and Hallett, M. 1997. Functional relevance of cross-modal plasticity in blind humans. Nature 389, 180–183.

Cohen, L. G., Weeks, R. A., Sadato, N., Celnik, P., Ishii, K., and Hallett, M. 1999. Period of susceptibility for cross-modal plasticity in the blind. Ann. Neurol. 45, 451–460.

Collignon, O., Renier, L., Bruyer, R., Tranduy, D., and Veraart, C. 2006. Improved selective and divided spatial attention in early blind subjects. Brain Res. 1075, 175–182.

Connor, C. E. and Johnson, K. O. 1992. Neural coding of tactile texture: comparison of spatial and temporal mechanisms for roughness perception. J. Neurosci. 12, 3414–3426.

Connor, C. E., Hsiao, S. S., Phillips, J. R., and Johnson, K. O. 1990. Tactile roughness: neural codes that account for psychophysical magnitude estimates. J. Neurosci. 10, 3823–3836.

Cooper, R. M. and Thurlow, G. A. 1985. Depression and recovery of metabolic activity in rat visual system after eye removal. Exp. Neurol. 89, 322–336.

Craig, J. 1988. The role of experience in tactual pattern perception: a preliminary report. Int. J. Rehabil. Res. 11, 167–183.

D'Angiulli, A. and Waraich, P. 2002. Enhanced tactile encoding and memory recognition in congenital blindness. Int. J. Rehabil. Res. 25, 143–145.

Davidson, P. W., Appelle, S., and Haber, R. N. 1992. Haptic scanning of braille cells by low- and high-proficiency blind readers. Res. Dev. Disabil. 13, 99–111.

De Volder, A. G., Bol, A., Blin, J., Robert, A., Arno, P., Grandin, C., Michel, C., and Veraart, C. 1997. Brain energy metabolism in early blind subjects: neural activity in the visual cortex. Brain Res. 750, 235–244.

De Volder, A. G., Toyama, H., Kimura, Y., Kiyosawa, M., Nakano, H., Vanlierde, A., Wanet-Defalque, M. C., Mishina, M., Oda, K., Ishiwata, K., and Senda, M. 2001. Auditory triggered mental imagery of shape involves visual association areas in early blind humans. Neuroimage 14, 129–139.

Distler, C., Boussaoud, D., Desimone, R., and Ungerleider, L. G. 1993. Cortical connections of inferior temporal area TEO in macaque monkeys. J. Comp. Neurol. 334, 125–150.

Drevets, W. C., Burton, H., Videen, T. O., Snyder, A. Z., Simpson, J. R., Jr., and Raichle, M. E. 1995. Blood flow changes in human somatosensory cortex during anticipated stimulation. Nature 373, 249–252.

Eickhoff, S. B., Amunts, K., Mohlberg, H., and Zilles, K. 2006a. The human parietal operculum. II. Stereotaxic maps and correlation with functional imaging results. Cereb. Cortex 16, 268–279.

Eickhoff, S. B., Schleicher, A., Zilles, K., and Amunts, K. 2006b. The human parietal operculum. I. Cytoarchitectonic mapping of subdivisions. Cereb. Cortex 16, 254–267.

Eidelberg, D. and Galaburda, A. M. 1984. Inferior parietal lobule: divergent architectonic asymmetries in the human brain. Arch. Neurol. 41, 843–852.

Eimer, M. 2004. Multisensory integration: how visual experience shapes spatial perception. Curr. Biol. 14, R115–R117.

Elbert, T., Pantev, C., Wienbruch, C., Rockstroh, B., and Taub, E. 1995. Increased cortical representation of the fingers of the left hand in string players. Science 270, 305–307.

Facchini, S. and Aglioti, S. M. 2003. Short term light deprivation increases tactile spatial acuity in humans. Neurology 60, 1998–1999.

Falchier, A., Clavagnier, S., Barone, P., and Kennedy, H. 2002. Anatomical evidence of multimodal integration in primate striate cortex. J. Neurosci. 22, 5749–5759.

Feinsod, M., Bach-y-Rita, P., and Madey, J. M. 1973. Somatosensory evoked responses: latency differences in blind and sighted persons. Brain Res. 60, 219–223.

Felleman, D. J. and Van Essen, D. C. 1991. Distributed hierarchical processing in the primate cerebral cortex. Cereb. Cortex 1, 1–47.

Flowers, D. L., Jones, K., Noble, K., VanMeter, J., Zeffiro, T. A., Wood, F. B., and Eden, G. F. 2004. Attention to single letters activates left extrastriate cortex. Neuroimage 21, 829–839.

Foulke, E. and Warm, J. S. 1967. Effects of complexity and redundancy on the tactual recognition on metric figures. Percept. Mot. Skills 25, 177–187.

Foxe, J. J., Wylie, G. R., Martinez, A., Schroeder, C. E., Javitt, D. C., Guilfoyle, D., Ritter, W., and Murray, M. M. 2002. Auditory–somatosensory multisensory processing in auditory association cortex: an fMRI study. J. Neurophysiol. 88, 540–543.

Garrett, A. S., Flowers, D. L., Absher, J. R., Fahey, F. H., Gage, H. D., Keyes, J. W., Porrino, L. J., and Wood, F. B. 2000. Cortical activity related to accuracy of letter recognition. Neuroimage 11, 111–123.

Gaunet, F. and Rossetti, Y. 2006. Effects of visual deprivation on space representation: immediate and delayed pointing toward memorised proprioceptive targets. Perception 35, 107–124.

Gaunet, F., Martinez, J.-L., and Thinus-Blanc, C. 1997. Early-blind subjects' spatial representation of manipulatory space: exploratory strategies and reaction to change. Perception 26, 345–366.

Gizewski, E. R., Gasser, T., de Greiff, A., Boehm, A., and Forsting, M. 2003. Cross-modal plasticity for sensory and motor activation patterns in blind subjects. Neuroimage 19, 968–975.

Goldreich, D. and Kanics, I. M. 2003. Tactile acuity is enhanced in blindness. J. Neurosci. 23, 3439–3445.

Gothe, J., Brandt, S. A., Irlbacher, K., Roricht, S., Sabel, B. A., and Meyer, B. U. 2002. Changes in visual cortex excitability in blind subjects as demonstrated by transcranial magnetic stimulation. Brain 125, 479–490.

Gougoux, F., Lepore, F., Lassonde, M., Voss, P., Zatorre, R. J., and Belin, P. 2004. Pitch discrimination in the early blind. Nature 430, 309.

Gougoux, F., Zatorre, R. J., Lassonde, M., Voss, P., and Lepore, F. 2005. A functional neuroimaging study of sound localization: visual cortex activity predicts performance in early-blind individuals. PLoS Biol. 3, 324–333.

Grant, A. C., Thiagarajah, M. C., and Sathian, K. 2000. Tactile perception in blind Braille readers: a psychophysical study of acuity and hyperacuity using gratings and dot patterns. Percept. Psychophys. 62, 301–312.

Grill-Spector, K. and Malach, R. 2004. The human visual cortex. Annu. Rev. Neurosci. 27, 649–677.

Gusnard, D. A. and Raichle, M. E. 2001. Searching for a baseline: functional imaging and the resting human brain. Nat. Rev. Neurosci. 2, 685–694.

Hadjikhani, N., Liu, A. K., Dale, A. M., Cavanagh, P., and Tootell, R. B. 1998. Retinotopy and color sensitivity in human visual cortical area V8. Nat. Neurosci. 1, 235–241.

Hagen, M. C., Franzen, O., McGlone, F., Essick, G., Dancer, C., and Pardo, J. V. 2002. Tactile motion activates the human middle temporal/V5 (MT/V5) complex. Eur. J. Neurosci. 16, 957–964.

Hamilton, R. H. and Pascual-Leone, A. 1998. Cortical plasticity associated with Braille learning. Trends Cogn. Sci. 2, 168–174.

Hamilton, R., Keenan, J. P., Catala, M., and Pascual-Leone, A. 2000. Alexia for Braille following bilateral occipital stroke in an early blind woman. Neuroreport 11, 237–240.

Hasson, U., Harel, M., Levy, I., and Malach, R. 2003. Large-scale mirror-symmetry organization of human occipito-temporal object areas. Neuron 37, 1027–1041.

Hasson, U., Levy, I., Behrmann, M., Hendler, T., and Malach, R. 2002. Eccentricity bias as an organizing principle for human high-order object areas. Neuron 34, 479–490.

Haxby, J. V., Horwitz, B., Ungerleider, L. G., Maisog, J. M., Pietrini, P., and Grady, C. L. 1994. The functional organization of human extrastriate cortex: a PET–rCBF study

of selective attention to faces and locations. J. Neurosci. 14, 6336–6353.
Heller, M. A. 1989a. Texture perception in sighted and blind observers. Percept. Psychophys. 45, 49–54.
Heller, M. A. 1989b. Picture and pattern perception in the sighted and the blind: the advantage of the late blind. Perception 18, 379–389.
Heller, M. A. 2002. Tactile picture perception in sighted and blind people. Behav. Brain Res. 135, 65–68.
Heller, M. A. and Kennedy, J. M. 1990. Perspective taking, pictures, and the blind. Percept. Psychophys. 48, 459–466.
Heller, M. A., Brackett, D. D., Scroggs, E., Steffen, H., Heatherly, K., and Salik, S. 2002. Tangible pictures: viewpoint effects and linear perspective in visually impaired people. Perception 31, 747–769.
Heller, M. A., Wilson, K., Steffen, H., Yoneyama, K., and Brackett, D. D. 2003. Superior haptic perceptual selectivity in late-blind and very-low-vision subjects. Perception 32, 499–511.
Hendry, S. H. C. and Jones, E. G. 1988. Activity-dependent regulation of GABA expression in the visual cortex of adult monkeys. Neuron 1, 701–712.
Hollins, M. 1989. Understanding Blindness: An Integrative Approach. Lawrence Erlbaum.
Hötting, K., Rösler, F., and Röder, B. 2004. Altered auditory–tactile interactions in congenitally blind humans: an event-related potential study. Exp. Brain Res. 159, 370–381.
Hyvärinen, J., Carlson, S., and Hyvarinen, L. 1981. Early visual deprivation alters modality of neuronal responses in area 19 of monkey cortex. Neurosci. Lett. 26, 239–243.
Iguchi, Y., Hoshi, Y., Tanosaki, M., Taira, M., and Hashimoto, I. 2005. Attention induces reciprocal activity in the human somatosensory cortex enhancing relevant- and suppressing irrelevant inputs from fingers. Clin. Neurophysiol. 116, 1077–1087.
James, T. W., Humphrey, G. K., Gati, J. S., Servos, P., Menon, R. S., and Goodale, M. A. 2002. Haptic study of three-dimensional objects activates extrastriate visual areas. Neuropsychologia 40, 1706–1714.
Jenkins, W. M., Merzenich, M. M., Ochs, M. T., Allard, T., and Guic-Robles, E. 1990. Functional reorganization of primary somatosensory cortex in adult owl monkeys after behaviorally controlled tactile stimulation. J. Neurophysiol. 63, 82–104.
Johnson, K. O. and Lamb, G. D. 1981. Neural mechanisms of spatial tactile discrimination: neural patterns evoked by braille-like dot patterns in the monkey. J. Physiol. (Lond.) 310, 117–144.
Johnson, K. O. and Phillips, J. R. 1981. Tactile spatial resolution. I. Two-point discrimination, gap detection, grating resolution, and letter recognition. J. Neurophysiol. 46, 1177–1191.
Kahn, D. M. and Krubitzer, L. 2002. Massive cross-modal cortical plasticity and the emergence of a new cortical area in developmentally blind mammals. Proc. Natl. Acad. Sci. U. S. A. 99, 11429–11434.
Kanwisher, N., McDermott, J., and Chun, M. M. 1997. The fusiform face area: a module in human extrastriate cortex specialized for face perception. J. Neurosci. 17, 4302–4311.
Kauffman, T., Theoret, H., and Pascual-Leone, A. 2002. Braille character discrimination in blindfolded human subjects. Neuroreport 13, 571–574.
Kennedy, J. 1993. Drawing and the Blind: Pictures to Touch. Yale University Press.
Kennedy, J. M. 2003. Drawings from Gaia, a blind girl. Perception 32, 321–340.
Kennedy, J. M. and Igor, J. 2003. Haptics and projection: drawings by Tracy, a blind adult. Perception 32, 1059–1071.
Kennedy, J. and Juricevic, I. 2006. Foreshortening, convergence and drawings from a blind adult. Perception 31, 893–894.
Klatzky, R. L., Lederman, S. J., and Reed, C. 1989. Haptic integration of object properties: texture, hardness, and planar contour. J. Exp. Psychol. Hum. Percept. Perform. 15, 45–57.
Kujala, T., Alho, K., Huotilainen, M., Ilmoniemi, R. J., Lehtokoski, A., Leinonen, A., Rinne, T., Salonen, O., Sinkkonen, J., Standertskjold-Nordenstam, C. G., and Naatanen, R. 1997a. Electrophysiological evidence for cross-modal plasticity in humans with early- and late-onset blindness. Psychophysiology 34, 213–216.
Kujala, T., Alho, K., Kekoni, J., Hamalainen, H., Reinikainen, K., Salonen, O., Standertskjold-Nordenstam, C. G., and Naatanen, R. 1995a. Auditory and somatosensory event-related brain potentials in early blind humans. Exp. Brain Res. 104, 519–526.
Kujala, T., Huotilainen, M., Sinkkonen, J., Ahonen, A., Alho, K., Hamalainen, M., Ilmoniemi, R., Kajola, M., Knuutila, J., Lavikainen, J., Salonen, O., Simola, J., Standerskjold-Nordenstam, C.-G., Tiitinen, H., Tissari, S., and Naatanen, R. 1995b. Visual cortex activation in blind humans during sound discrimination. Neurosci. Lett. 183, 143–146.
Kujala, T., Lehtokoski, A., Alho, K., Kekoni, J., and Naatanen, R. 1997b. Faster reaction times in the blind than sighted during bimodal divided attention. Acta Psychol. 96, 75–82.
Kujala, T., Palva, M. J., Salonen, O., Alku, P., Huotilainen, M., Jarvinen, A., and Naatanen, R. 2005. The role of blind humans' visual cortex in auditory change detection. Neurosci. Lett. 379, 127–131.
Ledberg, A., O'Sullivan, B. T., Kinomura, S., and Roland, P. E. 1995. Somatosensory activations of the parietal operculum of man. A PET study. Eur. J. Neurosci. 7, 1934–1941.
Levy, I., Hasson, U., Avidan, G., Hendler, T., and Malach, R. 2001. Center–periphery organization of human object areas. Nat. Neurosci. 4, 533–539.
Levy, I., Hasson, U., Harel, M., and Malach, R. 2004. Functional analysis of the periphery effect in human building related areas. Hum. Brain Mapp. 22, 15–26.
Lewis, J. W. and Van Essen, D. C. 2000. Corticocortical connections of visual, sensorimotor, and multimodal processing areas in the parietal lobe of the macaque monkey. J. Comp. Neurol. 428, 112–137.
Liu, H. L., Liao, W. T., Fang, S. Y., Chu, T. C., and Tan, L. H. 2004. Correlation between temporal response of fMRI and fast reaction time in a language task. Magn. Reson. Imaging 22, 451–455.
Loomis, J. M. 1981. On the tangibility of letters and braille. Percept. Psychophys. 29, 37–46.
Macaluso, E. and Driver, J. 2005. Multisensory spatial interactions: a window onto functional integration in the human brain. Trends Neurosci. 28, 264–271.
Macaluso, E., Frith, C. D., and Driver, J. 2000. Modulation of human visual cortex by crossmodal spatial attention. Science 289, 1206–1208.
Macaluso, E., Frith, C. D., and Driver, J. 2002. Crossmodal spatial influences of touch on extrastriate visual areas take current gaze direction into account. Neuron 34, 647–658.
Macaluso, E., George, N., Dolan, R., Spence, C., and Driver, J. 2004. Spatial and temporal factors during processing of audiovisual speech: a PET study. Neuroimage 21, 725–732.
Madar, I., Scheffel, U., and Frost, J. J. 1994. Transient increase in the *in vivo* binding of the benzodiazepine antagonist [^{3}H]flumazenil in deafferented visual areas of the adult mouse brain. Synapse 18, 79–85.

Malach, R., Levy, I., and Hasson, U. 2002. The topography of high-order human object areas. Trends Cogn. Sci. 6, 176–184.

Malach, R., Reppas, J. B., Benson, R. R., Kwong, K. K., Jiang, H., Kennedy, W. A., Ledden, P. J., Brady, T. J., Rosen, B. R., and Tootell, R. B. 1995. Object-related activity revealed by functional magnetic resonance imaging in human occipital cortex. Proc. Natl. Acad. Sci. U. S. A. 92, 8135–8139.

Melzer, P., Morgan, V. L., Pickens, D. R., Price, R. R., Wall, R. S., and Ebner, F. F. 2001. Cortical activation during Braille reading is influenced by early visual experience in subjects with severe visual disability: a correlational fMRI study. Hum. Brain Mapp. 14, 186–195.

Merabet, L., Thut, G., Murray, B., Andrews, J., Hsiao, S., and Pascual-Leone, A. 2004. Feeling by sight or seeing by touch? Neuron 42, 173–179.

Meredith, M. A. 2002. On the neuronal basis for multisensory convergence: a brief overview. Cogn. Brain Res. 14, 31–40.

Merzenich, M. M. and Jenkins, W. M. 1993. Reorganization of cortical representations of the hand following alterations of skin inputs induced by nerve injury, skin island transfers, and experience. J. Hand Ther. 6, 89–104.

Millar, S. 1974. Tactile short-term memory by blind and sighted children. Br. J. Psychol. 65, 253–263.

Millar, S. 1984a. Strategy choices by young Braille readers. Perception 13, 567–579.

Millar, S. 1984b. Is there a ''best hand'' for braille? Cortex 20, 75–87.

Millar, S. 1985. The perception of complex patterns by touch. Perception 14, 293–303.

Millar, S. 1987. Perceptual and task factors in fluent braille. Perception 16, 521–536.

Millar, S. 1994. Understanding and Representing Space. Theory and Evidence from Studies with Blind and Sighted Children. Clarendon.

Millar, S. 1997. Reading By Touch. Routledge.

Mishina, M., Senda, M., Kiyosawa, M., Ishiwata, K., De Volder, A. G., Nakano, H., Toyama, H., Oda, K., Kimura, Y., Ishii, K., Sasaki, T., Ohyama, M., Komaba, Y., Kobayashi, S., Kitamura, S., and Katayama, Y. 2003. Increased regional cerebral blood flow but normal distribution of GABAA receptor in the visual cortex of subjects with early-onset blindness. Neuroimage 19, 125–131.

Morgan, M. 1999. Sensory perception: supernormal hearing in the blind? Curr. Biol. 9, R53–R54.

Mountcastle, V. B. 2005. The Sensory Hand: Neural Mechanisms of Somatic Sensation. Harvard University Press.

Newton, J. R., Sikes, R. W., and Skavenski, A. A. 2002. Cross-modal plasticity after monocular enucleation of the adult rabbit. Exp. Brain Res. 144, 423–429.

Nolan, C. and Kederis, C. 1969. Perceptual factors in Braille word recognition. American Foundation for the Blind.

Noppeney, U., Friston, K. J., and Price, C. J. 2003. Effects of visual deprivation on the organization of the semantic system. Brain 126, 1620–1627.

Noppeney, U., Waberski, T. D., Gobbele, R., and Buchner, H. 1999. Spatial attention modulates the cortical somatosensory representation of the digits in humans. Neuroreport 10, 3137–3141.

Pascual-Leone, A. and Hamilton, R. 2001. The metamodal organization of the brain. Prog. Brain Res. 134, 427–445.

Pascual-Leone, A. and Torres, F. 1993. Plasticity of the sensorimotor cortex representation of the reading finger in Braille readers. Brain 116 (Pt 1), 39–52.

Pascual-Leone, A., Amedi, A., Fregni, F., and Merabet, L. B. 2005. The plastic human brain cortex. Annu. Rev. Neurosci. 28, 377–401.

Phillips, J., Johansson, R., and Johnson, K. 1990. Representation of braille characters in human nerve fibers. Exp. Brain Res. 81, 589–592.

Phillips, J. R., Johnson, K. O., and Hsiao, S. S. 1988. Spatial pattern representation and transformation in monkey somatosensory cortex. Proc. Natl. Acad. Sci. U. S. A. 85, 1317–1321.

Pleger, B., Foerster, A.-F., Ragert, P., Dinse, H. R., Schwenkreis, P., Malin, J.-P., Nicolas, V., and Tegenthoff, M. 2003. Functional imaging of perceptual learning in human primary and secondary somatosensory cortex. Neuron 40, 643–653.

Polk, T. A., Stallcup, M., Aguirre, G. K., Alsop, D. C., D'Esposito, M., Detre, J. A., and Farah, M. J. 2002. Neural specialization for letter recognition. J. Cogn. Neurosci. 14, 145–159.

Prather, S. C., Votaw, J. R., and Sathian, K. 2004. Task-specific recruitment of dorsal and ventral visual areas during tactile perception. Neuropsychologia 42, 1079–1087.

Pring, L. 1985. Processes involved in braille reading. J. Vis. Impair. Blind. 79, 252–255.

Pring, L. 1994. Touch and go: learning to read braille. Read Res. Quart. 29, 67–74.

Puce, A., Allison, T., Asgari, M., Gore, J. C., and McCarthy, G. 1996. Differential sensitivity of human visual cortex to faces, letterstrings, and textures: a functional magnetic resonance imaging study. J. Neurosci. 16, 5205–5215.

Ragert, P., Schmidt, A., Altenmuller, E., and Dinse, H. R. 2004. Superior tactile performance and learning in professional pianists: evidence for meta-plasticity in musicians. Eur. J. Neurosci. 19, 473–478.

Rakic, P. 1988. Specification of cerebral cortical areas. Science 241, 170–176.

Ramachandran, V. S. and Hirstein, W. 1998. The perception of phantom limbs. The D. O. Hebb lecture. Brain 121, 1603–1630.

Rauschecker, J. P. and Korte, M. 1993. Auditory compensation for early blindness in cat cerebral cortex. J. Neurosci. 13, 4538–4548.

Rauschecker, J. P., Tian, B., Korte, M., and Egert, U. 1992. Crossmodal changes in the somatosensory vibrissa/barrel system of visually deprived animals. Proc. Natl. Acad. Sci. U. S. A. 89, 5063–5067.

Raz, N., Amedi, A., and Zohary, E. 2005. V1 Activation in congenitally blind humans is associated with episodic retrieval. Cereb. Cortex 15, 1459–1468.

Recanzone, G. H., Merzenich, M. M., and Jenkins, W. M. 1992a. Frequency discrimination training engaging a restricted skin surface results in an emergence of a cutaneous response zone in cortical area 3a. J. Neurophysiol. 67, 1057–1070.

Recanzone, G. H., Merzenich, M. M., Jenkins, W. M., Grajski, K. A., and Dinse, H. R. 1992b. Topographic reorganization of the hand representation in cortical area 3b of owl monkeys trained in a frequency-discrimination task. J. Neurophysiol. 67, 1031–1056.

Recanzone, G. H., Merzenich, M. M., and Schreiner, C. E. 1992c. Changes in the distributed temporal response properties of SI cortical neurons reflect improvements in performance on a temporally based tactile discrimination task. J. Neurophysiol. 67, 1071–1091.

Rempel-Clower, N. L. and Barbas, H. 2000. The laminar pattern of connections between prefrontal and anterior temporal cortices in the Rhesus monkey is related to cortical structure and function. Cereb. Cortex 10, 851–865.

Révész, G. 1950. Psychology and Art of the Blind. Longmans, Green and Co.

Rockland, K. S. and Ojima, H. 2003. Multisensory convergence in calcarine visual areas in macaque monkey. Int. J. Psychophysiol. 50, 19–26.

Röder, B. and Rösler, F. 2003. Memory for environmental sounds in sighted, congenitally blind and late blind adults: Evidence for cross-modal compensation. Int. J. Psychophysiol. 50, 27–39.

Röder, B. and Rösler, F. 2004. Compensatory Plasticity as a Consequence of Sensory Loss. In: Handbook of Multisensory Processing (*eds*. G. Calbert, C. Spence, and B. E. Stein), pp. 719–747. The MIT Press.

Röder, B., Rösler, F., and Hennighausen, E. 1997. Different cortical activation patterns in blind and sighted humans during encoding and transformation of haptic images. Psychophysiology 34, 292–307.

Röder, B., Rösler, F., Hennighausen, E., and Näcker, F. 1996. Event-related potentials during auditory and somatosensory discrimination in sighted and blind human subjects. Cogn. Brain Res. 4, 77–93.

Röder, B., Rösler, F., and Spence, C. 2004. Early vision impairs tactile perception in the blind. Curr. Biol. 14, 121–124.

Röder, B., Stock, O., Bien, S., Neville, H., and Rosler, F. 2002. Speech processing activates visual cortex in congenitally blind humans. Eur. J. Neurosci. 16, 930–936.

Sadato, N., Okada, T., Honda, M., and Yonekura, Y. 2002. Critical period for cross-modal plasticity in blind humans: a functional MRI study. Neuroimage 16, 389–400.

Sadato, N., Pascual-Leone, A., Grafman, J., Deiber, M. P., Ibanez, V., and Hallett, M. 1998. Neural networks for Braille reading by the blind. Brain 121, 1213–1229.

Sadato, N., Pascual-Leone, A., Grafman, J., Ibanez, V., Deiber, M. P., Dold, G., and Hallett, M. 1996. Activation of the primary visual cortex by Braille reading in blind subjects. Nature 380, 526–528.

Sathian, K. 2000. Practice makes perfect – sharper tactile perception in the blind. Neurology 54, 2203–2204.

Sathian, K., Zangaladze, A., Hoffman, J., and Grafton, S. 1997. Feeling with the mind's eye. Neuroreport 8, 3877–3881.

Schaefer, M., Flor, H., Heinze, H.-J., and Rotte, M. 2006. Dynamic modulation of the primary somatosensory cortex during seeing and feeling a touched hand. Neuroimage 29, 587–592.

Schaefer, M., Heinze, H. J., and Rotte, M. 2005. Task-relevant modulation of primary somatosensory cortex suggests a prefrontal–cortical sensory gating system. Neuroimage 27, 130–135.

Schroeder, C. E. and Foxe, J. J. 2002. The timing and laminar profile of converging inputs to multisensory areas of the macaque neocortex. Cogn. Brain Res. 14, 187–198.

Semenza, C., Zoppello, M., Gidiuli, O., and Borgo, F. 1996. Dichaptic scanning of Braille letters by skilled blind readers: lateralization effects. Percept. Mot. Skills 82, 1071–1074.

Shimony, J., Burton, H., Epstein, A., McLaren, D., Sun, S., and Snyder, A. 2006. Diffusion tensor imaging reveals white matter reorganization in early blind humans. Cereb. Cortex 16(11), 1653–1661.

Sillito, A. M. 1975. The contribution of inhibitory mechanisms to the receptive field properties of neurons in the striate cortex of the cat. J. Physiol. (Lond.) 250, 305–329.

Sterr, A., Green, L., and Elbert, T. 2003. Blind Braille readers mislocate tactile stimuli. Biol. Psychol. 63, 117–127.

Sterr, A., Muller, M. M., Elbert, T., Rockstroh, B., Pantev, C., and Taub, E. 1998a. Perceptual correlates of changes in cortical representation of fingers in blind multifinger Braille readers. J. Neurosci. 18, 4417–4423.

Sterr, A., Muller, M. M., Elbert, T., Rockstroh, B., Pantev, C., and Taub, E. 1998b. Changed perceptions in Braille readers. Nature 391, 134–135.

Stevens, J., Foulke, E., and Patterson, M. 1996. Tactile acuity, aging, and braille reading in long-term blindness. J. Exp. Psychol. Appl. 2, 91–106.

Stoesz, M. R., Zhang, M., Weisser, V. D., Prather, S. C., Mao, H., and Sathian, K. 2003. Neural networks active during tactile form perception: common and differential activity during macrospatial and microspatial tasks. Int. J. Psychophysiol. 50, 41–49.

Sur, M. and Leamey, C. A. 2001. Development and plasticity of cortical areas and networks. Nat. Rev. Neurosci. 2, 251–262.

Sur, M., Pallas, S. L., and Roe, A. W. 1990. Cross-modal plasticity in cortical development: differentiation and specification of sensory neocortex. Trends Neurosci. 13, 227–233.

Talairach, J. and Tournoux, P. 1988. Coplanar Stereotaxic Atlas of the Human Brain. Thieme Medical.

Théoret, H., Merabet, L., and Pascual-Leone, A. 2004. Behavioral and neuroplastic changes in the blind: evidence for functionally relevant cross-modal interactions. J. Physiol. (Paris) 98, 221–233.

Toldi, J., Feher, O., and Wolff, J.-R. 1996. Neuronal plasticity induced by neonatal monocular (and binocular) enucleation. Prog. Neurobiol. 48, 191–218.

Tootell, R. B., Dale, A. M., Sereno, M. I., and Malach, R. 1996. New images from human visual cortex. Trends Neurosci. 19, 481–489.

Uhl, F., Franzen, P., Lindinger, G., Lang, W., and Deecke, L. 1991. On the functionality of the visually deprived occipital cortex in early blind persons. Neurosci. Lett. 124, 256–259.

Uhl, F., Franzen, P., Podreka, I., Steiner, M., and Deecke, L. 1993. Increased regional cerebral blood flow in inferior occipital cortex and cerebellum of early blind humans. Neurosci. Lett. 150, 162–164.

Uhl, F., Kretschmer, T., Lindinger, G., Goldenberg, G., Lang, W., Oder, W., and Deecke, L. 1994. Tactile mental imagery in sighted persons and in patients suffering from peripheral blindness early in life. Electroencephalogr. Clin. Neurophysiol. 91, 249–255.

Van Boven, R. W. and Johnson, K. O. 1994. A psychophysical study of the mechanisms of sensory recovery following nerve injury in humans. Brain 117(Pt 1), 149–167.

Van Boven, R. W., Hamilton, R. H., Kauffman, T., Keenan, J. P., and Pascual-Leone, A. 2000. Tactile spatial resolution in blind braille readers. Neurology 54, 2230–2236.

Van Essen, D. C. 2004. Organization of Visual Areas in Macaque and Human Cerebral Cortex. In: The Visual Neurosciences (*eds*. L. Chalupa and J. S. Werner), pp. 507–521. MIT Press.

Van Essen, D. C. 2005. A population-average, landmark- and surface-based (PALS) atlas of human cerebral cortex. Neuroimage 23(3), 635–662.

Vanlierde, A., De Volder, A. G., Wanet-Defalque, M. C., and Veraart, C. 2003. Occipito-parietal cortex activation during visuo-spatial imagery in early blind humans. Neuroimage 19, 698–709.

Vega-Bermudez, F., Johnson, K. O., and Hsiao, S. S. 1991. Human tactile pattern recognition: active versus passive touch, velocity effects, and patterns of confusion. J. Neurophysiol. 65, 531–546.

Veraart, C., De Volder, A. G., Wanet-Defalque, M. C., Bol, A., Michel, C., and Goffinet, A. M. 1990. Glucose utilization in human visual cortex is abnormally elevated in blindness of early onset but decreased in blindness of late onset. Brain Res. 510, 115–121.

Wanet-Defalque, M. C., Veraart, C., De Volder, A., Metz, R., Michel, C., Dooms, G., and Goffinet, A. 1988. High metabolic activity in the visual cortex of early blind human subjects. Brain Res. 446, 369–373.

Weeks, R., Horwitz, B., Aziz-Sultan, A., Tian, B., Wessinger, C. M., Cohen, L. G., Hallett, M., and Rauschecker, J. P. 2000. A positron emission tomographic study of auditory localization in the congenitally blind. J. Neurosci. 20, 2664–2672.

Weisser, V., Stilla, R., Peltier, S., Hu, X., and Sathian, K. 2005. Short-term visual deprivation alters neural processing of tactile form. Exp. Brain Res. 166, 572–582.

Wittenberg, G. F., Werhahn, K. J., Wassermann, E. M., Herscovitch, P., and Cohen, L. G. 2004. Functional connectivity between somatosensory and visual cortex in early blind humans. Eur. J. Neurosci. 20, 1923–1927.

Xerri, C., Bourgeon, S., and Coq, J.-O. 2005. Perceptual context-dependent remodeling of the forepaw map in the SI cortex of rats trained on tactile discrimination. Behav. Brain Res. 162, 207–221.

Yovel, G. and Kanwisher, N. 2004. Face perception: domain specific, not process specific. Neuron 44, 889–898.

Zangaladze, A., Epstein, C. M., Grafton, S. T., and Sathian, K. 1999. Involvement of visual cortex in tactile discrimination of orientation. Nature 401, 587–590.

Zhang, M. M., Mariola, E., Stilla, R., Stoesz, M., Mao, H., Hu, X. P., and Sathian, K. 2005. Tactile discrimination of grating orientation: fMRI activation patterns. Hum. Brain Mapp. 25, 370–377.

de Zwart, J. A., Silva, A. C., van Gelderen, P., Kellman, P., Fukunaga, M., Chu, R., Koretsky, A. P., Frank, J. A., and Duyn, J. H. 2005. Temporal dynamics of the BOLD fMRI impulse response. Neuroimage 24, 667–677.

6.19 Cross-Modal and Multisensory Interactions between Vision and Touch

S Lacey and K Sathian, Emory University School of Medicine, Atlanta, GA, USA

© 2008 Elsevier Inc. All rights reserved.

6.19.1	Functional Involvement of Visual Cortical Areas in Tactile Perception	393
6.19.1.1	Macrospatial versus Microspatial Tasks	393
6.19.1.2	Motion, Texture, and Form	395
6.19.2	Visual Imagery and Multisensory Representations	396
6.19.3	Top-Down and Bottom-Up Processing	399
6.19.4	Cross-Modal Conflict, Enhancement, and Perceptual Illusions	399
6.19.5	Conclusions	401
References		402

Glossary

amodal Devoid of sensory modality reference.
cross-modal Reflecting the effect of a stimulus in one sensory modality on processing in another.
encoding With respect to memory, the process of storing information at initial exposure.
extrastriate visual cortex Nonprimary visual cortex.
functional magnetic resonance imaging (fMRI) A method for measuring brain activity using MRI.
haptic Sensing by touch through active manual exploration.
multisensory Reflecting processing of inputs from more than one modality.
positron emission tomography (PET) A method for measuring functional brain activity as indexed by regional cerebral blood flow, using a positron-emitting isotope.
priming Unconscious effect of one stimulus on processing of another.
retrieval The process of recalling previously encoded and stored information from memory.
tactile Sensing by touch through passive stimulation of the skin surface.
transcranial magnetic stimulation (TMS) A method for testing the function of discrete brain regions by applying magnetic pulses to the head.
visual imagery Mental reconstruction of a pictorial representation (seeing with the mind's eye).

6.19.1 Functional Involvement of Visual Cortical Areas in Tactile Perception

6.19.1.1 Macrospatial versus Microspatial Tasks

Activation of extrastriate visual cortical areas during tactile perception was first demonstrated in a positron emission tomographic (PET) study from our laboratory (Sathian, K. *et al.*, 1997), in which participants were asked to discriminate the orientation of gratings presented to the immobilized right index fingerpad. When this task was contrasted with a control task requiring discrimination of grating groove width, activation was found at a focus in the left extrastriate visual cortex, close to the parieto-occipital fissure. Since this focus was known to be active during visual discrimination of grating orientation (Sergent, J. *et al.*, 1992) and spatial imagery (Mellet, E. *et al.*, 1996), it was considered to mediate spatial processes common to vision and touch (Sathian, K. *et al.*, 1997). The location of this activity near the parieto-occipital fissure indicates possible homology with an area in the macaque parieto-occipital fissure known as V6 or PO where a large proportion of neurons appear to be orientation selective (Galletti, C. *et al.*, 1991). Indeed, the focus of activation in our PET study (Sathian, K. *et al.*, 1997) is in the vicinity of the human V6 complex of areas (Pitzalis, S. *et al.*, 2006).

These results suggested that tactile analogs of visual tasks potentially activate the same cortical areas as the visual tasks and that the visual cortex responds to certain tasks independently of the sensory modality in which the task is presented. A fairly extensive series of studies have since established that cerebral cortical areas previously regarded as exclusively visual are activated by haptic/tactile input in a task- and stimulus-specific manner, as reviewed below.

A subsequent functional magnetic resonance imaging (fMRI) study from our laboratory (Zhang, M. *et al.*, 2005) confirmed left parieto-occipital cortical activation during discrimination of grating orientation (relative to discrimination of grating groove width) with the right index fingerpad, and also found selective activation in other cortical areas. Among these areas were the right postcentral sulcus (PCS) and the left anterior intraparietal sulcus (aIPS). The PCS corresponds to Brodmann's area 2 (Grefkes, C. *et al.*, 2001) and is considered to be part of S1 (primary somatosensory cortex), while the aIPS has been consistently identified as a multisensory region, as will become increasingly evident as this chapter progresses. Other groups have corroborated the role of the aIPS in tactile discrimination of grating orientation, using fMRI: one group reported bilateral activity in this region during performance of this task with either hand, relative to discrimination of small changes in grating location on the fingerpad (van Boven, R. W. *et al.*, 2005). Activity was greater on the left than the right in this study, regardless of which hand was used. Another group scanned gratings over the fingerpad and found right-lateralized activity in the PCS–aIPS region during discrimination of grating orientation with either hand, relative to discrimination of grating roughness (Kitada, R. *et al.*, 2006). The right aIPS part of this region was directly established as multisensory by the demonstration that it was also activated by visual discrimination of grating orientation, relative to discrimination of grating color.

At the time we reported cross-modal parieto-occipital cortical activation during tactile discrimination of grating orientation (Sathian, K. *et al.*, 1997) this was an unusual finding and hence we wished to confirm that the finding was not merely epiphenomenal. This possibility was ruled out using transcranial magnetic stimulation (TMS) to test whether disrupting the function of this cortical region was detrimental to performance. Applying single-pulse TMS directly over the parieto-occipital focus and at sites close to it, at the appropriate interval (180 ms after the onset of tactile stimulation), significantly impaired discrimination of grating orientation but not of grating groove width, whilst TMS at more distant sites did not affect performance on either task (Zangaladze, A. *et al.*, 1999). This allowed us to infer that the activation found in the earlier PET study was not accidental but, in fact, functionally meaningful. A more recent study (Merabet, L. *et al.*, 2004) used repetitive TMS (rTMS) at 1 Hz (hertz, unit of frequency (cycles per second)) to decrease local cortical excitability. This study exploited a known dissociation between subjective magnitude estimates of perceived tactile interdot distance, which increase with physical interdot distance (up to 8 mm), and those of perceived tactile roughness, which peak at intermediate values (around 3 mm). The main finding was that rTMS over S1 disrupted judgments of roughness, but not interdot distance, whereas rTMS over medial occipital cortex impaired distance but not roughness judgments. In addition, a congenitally blind patient with bilateral occipital lesions following a stroke was impaired on tactile judgments of interdot spacing but not roughness (Merabet, L. *et al.*, 2004).

Two conclusions can be drawn from these observations, together with the studies of the grating orientation task reviewed above (Sathian, K. *et al.*, 1997; Zangaladze, A. *et al.*, 1999; Zhang, M. *et al.*, 2005). First, visual cortical activation may be necessary for some tactile tasks because performance on these is disrupted when these cortical areas are deactivated by TMS or damaged by lesions. Second, visual cortical involvement occurs in macrospatial (large-scale) tactile tasks, but not in microspatial (small-scale) tasks where the parameters of interest vary in the range of $\leq$3 mm. This conclusion is consistent with psychophysical studies suggesting that macrospatial tactile tasks are preferentially associated with visual processing (Klatzky, R. L. *et al.*, 1987), and that vision seems to be better than touch for perceiving macrospatial features, the reverse being true for microspatial features (Heller, M. A., 1989).

An fMRI study from our laboratory focused on the macrospatial–microspatial dichotomy (Stoesz, M. *et al.*, 2003). As a macrospatial task, we used a global form condition in which participants were asked to distinguish between the upside-down letters T and V, contrasting this with detection of a 3 to 4 mm gap in a bar as the microspatial task. Activity in the lateral occipital complex (LOC) was greater bilaterally in the form task than in the gap task, in agreement with the studies reviewed so far indicating

that macrospatial tactile tasks are more likely to evoke visual cortical activity during tactile tasks. The LOC is located within the ventral visual pathway, which is specialized for form processing and is a visual object-selective area (Malach, R. *et al.*, 1995) thought to be homologous to macaque inferotemporal cortex (Grill-Spector, K. *et al.*, 1998). A recent fMRI study from our laboratory confirmed the conclusion that visual cortical activation during microspatial tasks is minimal (Stilla and Sathian, unpublished observations). In this study, a three-dot array was presented to the immobilized fingerpad with the array oriented along the long axis of the finger, the central dot in the array being offset to the left or right by <2 mm. Subjects were asked to indicate the direction of offset. Activation in this spatial task was contrasted against that due to discrimination of the duration of stimulation with an array that lacked a spatial offset, thus isolating activity associated with tactile microspatial processing. The key point here is that there was only minimal activation of the LOC bilaterally, although there was strong and extensive activation in multiple parietal cortical areas, including the left PCS, bilateral aIPS, bilateral posterior IPS (pIPS), and bilateral posterior insula (Stilla and Sathian, unpublished observations).

6.19.1.2 Motion, Texture, and Form

Several studies have shown that an area involved in perception of visual motion, the human MT complex (which is considered to be the human homolog of macaque MT, a visual motion-processing area), is also active during presentation of tactile motion stimuli, even in the absence of any task (Hagen, M. C. *et al.*, 2002; Blake, R. *et al.*, 2004). Psychophysical studies point to a common representation of motion across vision and touch: tactile motion perception can be used to disambiguate the direction of motion in an ambiguous visual motion display (Blake, R. *et al.*, 2004), and facilitates such disambiguation when presentation of the visual motion display is delayed (James, T. W. and Blake, R., 2004). However, when the direction of motion is unambiguous but incongruent between vision and touch, visual motion disrupts tactile motion perception (Craig, J. C., 2006).

In a recent fMRI study, we contrasted activations during shape and texture perception in both haptic and visual modalities (Stilla and Sathian, submitted). We found somatosensory areas that were selectively activated during haptic texture perception, in the parietal operculum and posterior insula bilaterally. We also found that there was haptic texture selectivity in the right medial occipital cortex, probably in visual area V2. This focus overlapped with a visually texture-selective area that was primarily in area V1 (primary visual cortex), the multisensory overlap being on the border between V1 and V2. This result is interesting not merely because it extends the range of visual areas that respond to tactile tasks into areas quite early in the visual cortical hierarchy, but also because, for the first time, visual areas were shown to be active in a microspatial tactile task. It remains to be seen whether this is an exception to the general rule that microspatial tactile tasks do not recruit visual cortical activity, or whether such tasks might tend to evoke activity in particular early visual cortical areas under the appropriate conditions.

Conversely, the LOC was bilaterally active during shape perception in both haptic and visual modalities (Stilla and Sathian, submitted), consistent with numerous earlier fMRI studies (Deibert, E. *et al.*, 1999; Amedi, A. *et al.*, 2001; 2002; James, T. W. *et al.*, 2002; Stoeckel, M. C. *et al.*, 2003; Reed, C. L. *et al.*, 2004; Zhang, M. *et al.*, 2004). As mentioned above, we found bilateral activation of the LOC during tactile 2D form discrimination, distinguishing between upside-down Ts and Vs, when this task was contrasted with gap detection (Stoesz, M. *et al.*, 2003). We also found activation of the right LOC in the same form task, relative to bar orientation discrimination, in a PET study (Prather, S. C. *et al.*, 2004). Thus, the LOC appears to be consistently active during tactile perception of either 2D or 3D form. Studies of patients with lesions involving the LOC suggest, moreover, that it is actually necessary for haptic as well as visual shape perception. One patient with visual agnosia (inability to recognize objects), following a lesion of the left occipitotemporal cortex that probably included the LOC, also turned out to have tactile agnosia, although somatosensory cortex and basic somatic sensation were intact (Feinberg, T. E. *et al.*, 1986). Another patient who developed bilateral lesions of the LOC was impaired at learning unfamiliar objects using either touch or vision (James, T. W. *et al.*, 2006a). Multisensory object selectivity in the LOC appears to be confined to a subregion, which responds more strongly to graspable visual objects (such as tools) than to other stimuli (such as buildings or faces) but does not appear to be object selective in the auditory modality (Amedi, A. *et al.*, 2002).

Our study (Stilla and Sathian, submitted) also found multisensory shape selectivity bilaterally in

the PCS, and at multiple foci within the IPS, including the aIPS, pIPS, and ventral IPS (vIPS). Multisensory shape selectivity had been reported previously in the left aIPS (Grefkes, C. *et al.*, 2002) and in a caudal region of the IPS located between our pIPS and vIPS foci (Saito, D. N. *et al.*, 2003). Multisensory shape processing in the IPS fits with the description of multisensory responses in various parts of the IPS in monkeys (Iriki, A. *et al.*, 1996; Duhamel, J. R. *et al.*, 1998), although the homologies with humans remain uncertain. The demonstration of extensive multisensory overlap in the cortical processing of shape raises the possibility that both visual and haptic shape perception may engage a unitary neural representation, as in the case of motion perception. This is supported by cross-modal priming effects between visual and haptic object presentations in two fMRI studies, although the effects were in opposite directions in the two studies (Amedi, A. *et al.*, 2001; James, T. W. *et al.*, 2002). Additional psychophysical evidence bearing on the issue of a common visuo-haptic representation of shape is considered in the next section. Of some interest is the finding of multisensory shape processing in the PCS, which, as pointed out earlier in this chapter, corresponds to Brodmann's area 2 (Grefkes, C. *et al.*, 2001), part of S1. Along with the finding of multisensory texture selectivity in V2 described above, this underscores the ubiquity of multisensory processing, with its presence even in regions early in the sensory hierarchies.

Face perception is a special case of form perception. Obviously, sighted humans perform face recognition almost exclusively using vision, but they can also identify faces haptically. Like the patients described in the studies of object perception (see above), a prosopagnosic patient (i.e., one who could not recognize faces visually) was found to be unable to recognize faces haptically (Kilgour, A. R. *et al.*, 2004). Face recognition also occurs cross-modally between vision and touch (Kilgour, A. R. and Lederman, S., 2002), albeit not without a cost relative to within-modal recognition (Casey, S. J. and Newell, F. N., 2007). This cost in cross-modal performance is unrelated to the encoding modality or to differences in encoding procedures and suggests that, unlike object and motion perception, face recognition may not rely on a representation that is common to both vision and touch (Casey, S. J. and Newell, F. N., 2007). Recent fMRI studies fit with this idea: face-selective voxels in ventral and inferior temporal cortex are mostly nonoverlapping between the two modalities (Pietrini, P. *et al.*, 2004); the left fusiform gyrus is activated during haptic face recognition, whereas the right fusiform gyrus is more active during visual face recognition (Kilgour, A. R. *et al.*, 2005); and left fusiform activity increases when the faces are familiar compared to unfamiliar while the right fusiform remains relatively inactive (James, T. W. *et al.*, 2006b). Differential activation of the left versus right fusiform gyrus for haptic versus visual face perception may reflect processing of modality-specific featural face information, whilst modality-independent configural face information is dealt with elsewhere in the brain (Casey, S. J. and Newell, F. N., 2007). Since imagery of visually presented faces produces greater activation in the left than in the right fusiform gyrus (Ishai, A. *et al.*, 2002), another possibility is that haptic face perception may involve imagery mechanisms, although one study found no correlation between performance on haptic face recognition and imagery ratings (Kilgour, A. R. and Lederman, S., 2002). Further studies are needed to resolve the neural basis of multisensory face perception, and its differences from multisensory object perception.

6.19.2 Visual Imagery and Multisensory Representations

The studies reviewed so far establish that visual cortical processing is routinely involved in normal tactile perception in the sighted, especially during macrospatial tasks but potentially during microspatial tasks as well. Such processing is quite task specific, so that extrastriate visual cortical areas known to be specialized for particular visual tasks are involved during performance of the same tasks in touch. So far we have considered whether vision and touch share a common representation (e.g., for objects and motion) or separate representations (e.g., for faces). In this section we consider the nature of these representations in more detail. It was formerly thought that cross-modal performance was mediated by language, but cross-modal abilities have been demonstrated in preverbal infants and in several nonhuman primate and nonprimate species (see Rose, S. A., 1994 for a brief review). However, whilst linguistic competence may not be necessary, it may play a facilitatory role: it is possible to produce a verbal description of unfamiliar objects (Easton, R. D. *et al.*, 1997a) and a verbal secondary task disrupts both visual and haptic encoding of unfamiliar objects such that subsequent

cross-modal recognition is impaired (Lacey, S. and Campbell, C., 2006a).

A more fundamental explanation for cross-modal recruitment of the visual cortex into nonvisual tasks is that these tasks might involve visual imagery. This is an intuitively appealing explanation, especially since subjects consistently report mental visualization of tactile stimuli during macrospatial tasks such as discrimination of grating orientation or tactile form, which are associated with visual cortical recruitment. This is not true of microspatial tasks such as discrimination of grating groove width or gap detection, which tend to not involve visual cortical activity (Sathian, K. *et al.*, 1997; Zangaladze, A. *et al.*, 1999; Stoesz, M. *et al.*, 2003; Zhang, M. *et al.*, 2005). Visual imagery might be triggered by lack of familiarity with the tactile stimuli or tasks used; indeed, such cross-modal translation may be a general phenomenon, especially during complex information processing (Freides, D., 1974). Consistent with the idea that visual imagery mediates visual cortical activity in touch, an fMRI study from our laboratory (Zhang, M. *et al.*, 2004) found that interindividual variations in the magnitude of haptic shape-selective activity in the right LOC (ipsilateral to the hand used for haptic perception) were strongly predicted by ratings of the vividness of visual imagery. In contrast, activation strengths in the left LOC were uncorrelated with these visual imagery scores, pointing to an additional role for factors other than visual imagery in cross-modal visual cortical recruitment (Zhang, M. *et al.*, 2004). Left-lateralized activity has, however, been found in the LOC when either geometric or material object properties are retrieved from memory in the absence of visual or haptic input (Newman, S. D. *et al.*, 2005) and in both the blind and the sighted while generating mental images of shape derived from haptic and visual experience, respectively (De Volder, A. G. *et al.*, 2001). (Although this last report did not specifically identify the LOC, the illustrations and coordinates of activation clearly indicate it.)

If the representation of haptically perceived objects is indeed primarily visual, there should be a relationship between cross-modal memory performance and visual imagery ability. Several studies show that children's visuo-spatial abilities are indeed correlated with cross-modal memory performance for both familiar (Johnson, C. L. *et al.*, 1989) and unfamiliar objects (Stoltz-Loike, M. and Bornstein, M. H., 1987). Furthermore, good imagers (as measured by scores on the Vividness of Visual Imagery Questionnaire, VVIQ; Marks, D. F., 1973) are better at cross-modal memory than are poor imagers (Cairns, E. and Coll, P., 1977). However, this approach has its limitations. One is that visual imagery is a multicomponent process: images have to be generated and maintained, and once retrieved can be inspected, scanned, rotated, or otherwise manipulated (Kosslyn, S. M., 1980; 1994). Furthermore, individuals may vary in ability on one or more of these components (Kosslyn, S. M. *et al.*, 1990; 1984). Thus, a single test of visual imagery ability may not be appropriate since it may not capture the relevant component and thus may not be sensitive to the relevant individual differences. Secondly, it has been argued that the VVIQ only measures a subjective aspect of the experience of imagery rather than imagery processes and abilities *per se* (Pearson, D. *et al.*, 2001; Dean, G. and Morris, P. E., 2003). Moreover, the superiority of good imagers might stem not from greater proficiency at imagery but from better use of strategically important information (Baddeley, A. D. and Andrade, J., 2000). In addition, different aspects of visual imagery may contribute differentially to cross-modal memory and perceptual representations. For example, spatial recall predicts cross-modal performance whereas mental rotation does not (Stoltz-Loike, M. and Bornstein, M. H., 1987).

Some have argued that the LOC activity observed during haptic shape perception is not due to visual imagery since visual imagery evoked less activity in the LOC than did haptic object recognition (Amedi, A. *et al.*, 2001). However, this reduced activation might have been due to object familiarity and/or the lack of a requirement to maintain images online during the entire scan. Nonetheless, other possible explanations should be considered for visual cortical recruitment during tactile perception. Vision and touch can both encode object shape, and visual cortical activation during tactile perception might reflect a multisensory representation rather than a specifically visual image. Psychophysical observations indicate, for example, that cross-modal visuo-haptic priming is essentially as effective as within-modal priming (Easton, R. D. *et al.*, 1997a; 1997b; Reales, J. M. and Ballesteros, S., 1999), and that cross-modal shape matching can be quite effective even when the objects are highly similar (Norman, J. F. *et al.*, 2004). An alternative approach to the relationship between visual and haptic representations argues that vision and touch encode object properties common to both modalities into a single representation that is multisensory (Sathian, K., 2004) or amodal (e.g., Lewkowicz, D. J.,

1994). It is our view that the amodal label is best suited to processing of information that cannot be derived directly from sensory systems and that must be represented linguistically or perhaps propositionally. We prefer instead the term multisensory, referring to a representation that is accessible from multiple sensory systems, but in which the modality tags of the associated inputs are preserved (Sathian, K., 2004). In the case of vision and touch, modality-independent representations can be specified as spatial in format since both these sensory systems can encode spatial information such as size, shape, and the relative positions of different object features. An important question is the precise nature of the modality-independent representation.

The format of visuo-haptic object representation has been investigated behaviorally using interference tasks in a cross-modal memory paradigm. In one study (Lacey, S. and Campbell, C., 2006a), both visual and verbal interference disrupted encoding of unfamiliar objects, significantly reducing subsequent cross-modal recognition, while haptic interference was ineffective and familiar objects were immune to any form of interference. These results suggested that encoding in both modalities resulted in a common representation linked to a strategy of covert verbal description. Since the visual interference task (dynamic visual noise) is known to disrupt visual imagery mnemonics for recall of word lists (Quinn, J. G. and McConnell, J., 1996) and the use of visual imagery in symbolic comparison tasks (Dean, G. M. *et al.*, 2005), these results suggested that the common representation could be a visual image. Interference might have been more important for the unfamiliar objects because cross-modal memory for familiar objects is probably supported by closely interconnected representations in several formats – for example, visual, verbal, and haptic (Lacey, S. and Campbell, C., 2006a).

Lacey S. and Campbell C. (2006b) showed that spatial interference disrupted both encoding and retrieval, independent of the modality in which the interference task was presented, whereas nonspatial interference in either modality had no effect. Thus the common representation could be a modality-independent spatial one, rather than visual. It remains uncertain whether this reflects a single, multisensory spatial representation or separately derived visual and haptic spatial representations that are compared cross-modally. A recent neuroimaging study is instructive in this regard, showing that category selectivity within human inferotemporal cortex is relatively independent of whether the input modality is visual or haptic (Pietrini, P. *et al.*, 2004). Subjects with early-onset blindness had similar patterns of category-selective responses during haptic object perception in this study, although there were some differences in the locations of the category-selective responses between blind and sighted subjects. These findings suggest a single multisensory representation for objects that may be spatially rather than visually based. This interpretation is suggested by the recent work by Kozhevnikov and co-workers (Kozhevnikov, M. *et al.*, 2002; 2005; Blajenkova, O. *et al.*, 2006) showing that visual imagery is of two distinct types. Object imagery refers to images that are more pictorial and detailed in terms of shape, color, brightness, etc., whilst spatial imagery refers to images that are more concerned with the spatial relations of objects and object parts and hence may facilitate spatial transformations. Thus, an interesting question is how these different types of imagery are related to cross-modal performance: for example, are spatial imagers better at haptically deriving representations than object imagers?

If haptic and visual perception engage a modality-independent imagery system, we might expect to see similarities between visually and haptically accessed component processes of this system. For example, scanning times in visual imagery increase with the spatial distance to be inspected in the image, implying preservation of metric spatial information in visual images (Kosslyn, S. M., 1973; Kosslyn, S. M. *et al.*, 1978). The same effect is observed in scanning haptically derived representations, implying that these are also spatial and that similar, if not identical, imagery processes operate in both modalities (Röder, B. and Rösler, F., 1998). Similarly, studies of mental rotation of visual stimuli show that the time taken to judge whether two objects are the same or mirror images increases linearly with increasing angular disparity between the stimuli (Shepard, R. N. and Metzler, J., 1971). This also holds true for haptic and tactile stimuli (Marmor, G. S. and Zaback, L. A., 1976; Carpenter, P. A. and Eisenberg, P., 1978; Hollins, M., 1986; Dellantonio, A. and Spagnolo, F., 1990; Prather, S. C. and Sathian, K., 2002; Prather, S. C. *et al.*, 2004). A PET study from our laboratory (Prather, S. C. *et al.*, 2004) investigated the mental rotation of tactile stimuli – upside-down Js presented in one of two mirror-image configurations. Contrasting a mental rotation condition (stimuli at 135–180° angle with respect to the long axis of the finger) with a pure mirror-image discrimination condition (stimuli at 0°)

revealed activity in the left aIPS, at a focus that is also active during mental rotation of visual stimuli (Alivisatos, S. and Petrides, M., 1997), lending further support to the idea that similar spatial imagery processes operate on both visually and haptically derived representations.

Interestingly, these similarities between visually and haptically derived representations are observed in both the early-blind and the late-blind as well as the sighted (Carpenter, P. A. and Eisenberg, P., 1978; Röder, B. and Rösler, F., 1998). The blind are reported to be slower than the sighted at haptic mental rotation (Marmor, G. S. and Zaback, L. A., 1976) but Hollins M. (1986) suggests that, after controlling for greater variability in the use of frames of reference by the sighted, this difference is more apparent than real. Taken together, these studies indicate that common processes are engaged when generating, retrieving, and manipulating representations derived from both vision and touch.

6.19.3 Top-Down and Bottom-Up Processing

If mental imagery underlies tactile activation of the visual cortex, we would expect to find direct, bottom-up somatosensory projections into the visual cortical areas that are implicated in tactile perception, as opposed to the top-down projections from prefrontal into visual cortical areas that would be required to support a process such as visual imagery (Mechelli, A. *et al.*, 2004). These are possibilities that can be tested empirically, either by studying connectivity in experimental animals or by analyzing fMRI data to reveal effective connectivity. A study from our laboratory (Peltier, S. *et al.*, 2007) probed effective connectivity using structural equation modeling, based on the correlation matrix between the time courses of fMRI activity in various regions. This study revealed both bottom-up and top-down paths in a network of haptically shape-selective areas, including foci in the PCS, the IPS, and the LOC. This suggests that potential neural substrates exist for both visual imagery and multisensory representations, in relation to visual cortical involvement during haptic shape perception.

Neurophysiological and neuroanatomic studies in monkeys have also illuminated understanding of cross-modal visual cortical recruitment. Some neurons in area V4 (a nonprimary area in the ventral visual pathway) were selective for the orientation of a tactile grating when it served as a cue for matching to a subsequently presented visual stimulus, but not when it was task irrelevant (Haenny, P. E. *et al.*, 1988). The requirement for task relevance implicates top-down, rather than bottom-up, inputs. Multisensory inputs have been reported in early sensory cortical areas that are traditionally considered unisensory, including V1 (Falchier, A. *et al.*, 2002; Rockland, K. S. and Ojima, H., 2003) and auditory association cortex (Schroeder, C. E. *et al.*, 2001; Schroeder, C. E. and Foxe, J. J., 2002; Schroeder, C. E. *et al.*, 2003). Analysis of the laminar profile of these projections suggests that both top-down (Falchier, A. *et al.*, 2002; Schroeder, C. E. and Foxe, J. J., 2002; Rockland, K. S. and Ojima, H., 2003; Schroeder, C. E. *et al.*, 2003) and bottom-up (Schroeder, C. E. and Foxe, J. J., 2002; Schroeder, C. E. *et al.*, 2003) inputs exist. Thus, the sum total of the evidence to date indicates the probable existence of multisensory representations that are flexibly accessible via both vision and touch, with the potential to involve interactions between bottom-up sensory inputs and top-down processes such as visual imagery.

6.19.4 Cross-Modal Conflict, Enhancement, and Perceptual Illusions

If vision and touch produce separate representations, how do these affect each other? Classic research suggested that vision dominates touch (Rock, I. and Victor, J., 1964). When the visual width of an object was distorted by a lens, individuals who both saw and felt the object were unaware of the cross-modal conflict and reported the distorted width perceived visually, rather than the true width perceived tactually. Thus this sensory conflict was resolved in favor of the visual percept. More recent research has shown the situation to be more complex and to depend on the specific object property (Klatzky, R. L. *et al.*, 1987). For example, under neutral instructions the haptic salience of object properties is hardness > texture > shape and under haptically biased instructions this changes to texture > shape > hardness. However, in combined visual and haptic perception, and in haptic perception with concurrent visual imagery, this saliency is reversed and changes to shape > texture > hardness/size (Klatzky, R. L. *et al.*, 1987). Visual imagery can therefore influence tactile perception in the absence of visual perception and, moreover, different modalities may be optimal for

different object properties (Klatzky, R. L. *et al.*, 1993). Thus, there is not a simple dominance of visual over tactile perception.

Another interesting phenomenon is the asymmetry normally observed in cross-modal memory performance: in general, performance is better when visual encoding is followed by haptic retrieval than the reverse (e.g., Jones, B., 1981; Streri, A. and Molina, M., 1994; Lacey, S. and Campbell, C., 2006a; 2006b). Asymmetric performance appears to be a consistent aspect of cross-modal memory but, while many studies address the difference between within- and cross-modal performance, the difference between the two cross-modal conditions receives less attention (e.g., Easton, R. D. *et al.*, 1997a; 1997b; Reales, J. M. and Ballesteros, S., 1999; Nabeta, T. and Kawahara, J., 2006). It has been suggested that if cross-modal memory relied on a common representation, based on properties that can be represented equally well by different modalities (Lewkowicz, D. J., 1994), then performance should be similar in the two cross-modal conditions (Freides, D., 1974; Streri, A. and Molina, M., 1994). The fact that asymmetric performance occurs suggests otherwise, but given that the basis for the asymmetry still requires explanation, it would be premature to rule out a common representation solely on this basis. One explanation for asymmetry may be that, although vision and touch are both encoding the same information about an object into the same modality-independent format, this information may not be encoded equally well because of competition from other, more salient, modality-specific information. As noted above, visual imagery instructions alter the haptic salience of object properties (Klatzky, R. L. *et al.*, 1987) – without the imagery-biased instructions it might have been more difficult to encode shape because of the more salient hardness and texture information.

In a study using an *n*-back letter recognition task, Bliss I. and Hämäläinen H. (2005) showed that haptic working memory capacity appears to be limited and variable. A simple explanation for asymmetry may therefore be that haptic working memory is more error prone than visual working memory. An alternative is that haptic representations may simply decay faster than visual representations. Indeed, the decay function in haptic memory, rather than being progressive, appears to occur entirely in a band of 15–30 s poststimulus (Kiphart, M. J. *et al.*, 1992). This suggests that performance might be lower in the haptic–visual condition of the cross-modal memory task because haptically encoded representations have substantially decayed by the time that visual retrieval is required. However, several cross-modal memory studies show that increasing the delay between encoding and retrieval up to 30 s did not affect haptic–visual performance more than visual–haptic performance (Garvill, J. and Molander, B., 1973; Woods, A. T. *et al.*, 2004) and so it seems that the explanation will be more complicated than a simple function of haptic memory properties alone. Interestingly, asymmetry is also observed in cross-modal studies involving very young infants (e.g., Streri, A. and Molina, M., 1994). These studies attribute asymmetric performance to constraints imposed by different stages of motor development (Streri, A. and Molina, M., 1994), but since asymmetry persists beyond early development into more mature motor systems (Easton, R. D. *et al.*, 1997a; 1997b; Bushnell, E. W. and Baxt, C., 1999; Lacey, S. and Campbell, C., 2006a; 2006b), it is likely that other representationally important factors are involved.

Haptic versions of visual illusions have been used to investigate the relationship between vision and touch. In the Müller–Lyer illusion, two lines of identical length and endcapped with fins that point either outward or inward are seen as shorter or longer, respectively, than the true length. This visual illusion has also been demonstrated in a haptic format (Heller, M. A. *et al.*, 2002; Millar, S. and Al-Attar, Z., 2002) and appears to be independent of visual experience since blindfolded, normally sighted individuals as well as those with low vision, late-blind subjects, and congenitally blind individuals were all equally susceptible to the illusion (Heller, M. A. *et al.*, 2002). Length distortion is an illusion that was first described haptically and subsequently found to also occur in vision. Length distortion refers to overestimation of the distance between two points as a function of the increasing length of an indirect pathway between them. The same effect can be observed, albeit of a smaller magnitude, in the visual version of the task (Balakrishnan, J. D. *et al.*, 1989). These studies suggest a common visuo-haptic representation of space that may be based on body-centered reference points (e.g., the body midline or the positions of the hands relative to each other), since instructions to use these in judging Müller–Lyer line length virtually eliminated the illusion in both modalities whilst external reference points (a frame surrounding the illusion figure) had no effect (Millar, S. and Al-Attar, Z., 2002). The use of these body-centered reference points may be a common mechanism for integrating spatial information from vision and touch.

Other approaches have identified interactions between vision and somatosensory representations of the body. One line of research has demonstrated that noninformative vision of the body can improve tactile spatial acuity, as measured using grating orientation discrimination (Taylor-Clarke, M. *et al.*, 2004), and that this cross-modal enhancement is abolished by TMS over S1 (Fiorio, M. and Haggard, P., 2005). In related work, visual stimuli (light flashes from light-emitting diodes (LEDs) on the finger) have been shown to increase the proportion of concomitant electrotactile stimuli that are detected; however, signal detection analyses showed only a small change in perceptual sensitivity – most of the effect apparently arose from criterion shift (Johnson, R. M. *et al.*, 2006). Similarly, a patient with a right hemispheric lesion was reported to perceive touch on the contralesional hand only when viewing the tactile stimulation (Halligan, P. *et al.*, 1996). Another line of research pertains to the rubber hand illusion. When a rubber hand is positioned in alignment with one's own, invisible hand, if one sees the rubber hand being touched, one experiences illusory touch, indicating a feeling of ownership of the synthetic hand (Botvinick, M. and Cohen, J., 1998). Such a feeling of ownership is associated with activity in the ventral premotor cortex (Ehrsson, H. H. *et al.*, 2004), a region where, in monkeys, neurons exhibit visual receptive fields that are anchored to the arm and move with it (Graziano, M. S. *et al.*, 1994).

Yet another line of work stems from observations that tactile stimuli can be referred ipsilaterally from intact body parts to phantoms of resected body parts (Ramachandran, V. S. and Hirstein, W., 1998; Aglioti, S., 1999). Tactile stimuli applied to the intact hand of arm amputees have been shown to evoke contralateral percepts referred topographically to the phantom hand (Ramachandran, V. S., 1995), and similar contralateral mirror-symmetric referral of sensations also occurs in patients with sensory loss due to neurological lesions (Sathian, K., 2000). The referral is evoked for touch but typically not other kinds of somatosensory stimuli, such as pain or temperature (Ramachandran, V. S., 1995; Sathian, K., 2000). The referred sensations tend to be relatively high threshold, crudely localized, and lacking spatial organization, leading to the conclusion (Sathian, K., 2000) that they are unlikely to depend on neurons in area 3b, which exhibit fine-grained spatial resolution and topographic organization (DiCarlo, J. J. *et al.*, 1998). Also, since the hand representation in area 3b has sparse callosal connectivity (Killackey, H. P. *et al.*, 1983) and normally lacks neurons with bilateral receptive fields (Pons, T. P. *et al.*, 1987), transcallosal referral probably occurs more posteriorly in S1, in areas 1 and 2, or in the parietal opercular cortex, where bilateral somatosensory responsiveness (Robinson, C. J. and Burton, H., 1980a; 1980b; Iwamura, Y. *et al.*, 1994) and callosal connectivity (Killackey, H. P. *et al.*, 1983; Manzoni, T. *et al.*, 1984) are found in the hand representation. Interestingly, in both amputees (Ramachandran, V. S., 1995) and patients with sensory loss (Sathian, K., 2000), visual input via a mirror tended to strengthen referred percepts, suggesting a role for multisensory convergence. Use of a mirror to create conflict between the vision of touch (present) and the feeling of touch (absent) enhanced subsequent sensitivity to touch; the effect was eliminated by TMS over posterior parietal cortex (Ro, T. *et al.*, 2004). Provision of illusory visual input using a mirror has been exploited as a rehabilitative method to improve arm function affected by strokes (Altschuler, E. L. *et al.*, 1999; Sathian, K. *et al.*, 2000). These studies point to the existence of intricate and multifaceted interactions between visual and tactile processing that may be beneficial during normal perception as well as in neurological rehabilitation – such interactions offer fertile ground for future basic and clinical investigation.

6.19.5 Conclusions

In this chapter, we have outlined a plethora of cross-modal and multisensory interactions that occur in a variety of circumstances. Such interactions underscore the generality of multisensory processing, and are increasingly being recognized by researchers. The effects of visual deprivation that are reviewed by Burton (see Chapter Visual Deprivation Effects on Somatosensory and Visual Systems: Behavioral and Cortical Changes) should be interpreted in the context of these normal interactions, although a unifying framework is inchoate. The development of this framework remains a major challenge for future work.

Acknowledgments

Current research support from the National Eye Institute, National Science Foundation, and the Veterans Administration is gratefully acknowledged.

References

Aglioti, S. 1999. ''Anomalous'' Representations and Perceptions: Implications for Human Neuroplasticity. In: Neuronal Plasticity: Building a Bridge from the Laboratory to the Clinic (*eds*. J. Grafman and Y. Christen), pp. 79–91. Springer.

Alivisatos, B. and Petrides, M. 1997. Functional activation of the human brain during mental rotation. Neuropsychologia 36, 111–118.

Altschuler, E. L., Wisdom, S. B., Stone, L., Foster, C., Galasko, D., Llewellyn, D. M. E., and Ramachandran, V. S. 1999. Rehabilitation of hemiparesis after stroke with a mirror. Lancet 353, 2035–2036.

Amedi, A., Jacobson, G., Hendler, T., Malach, R., and Zohary, E. 2002. Convergence of visual and tactile shape processing in the human lateral occipital complex. Cereb. Cortex 12, 1202–1212.

Amedi, A., Malach, R., Hendler, T., Peled, S., and Zohary, E. 2001. Visuo-haptic object-related activation in the ventral visual pathway. Nat. Neurosci. 4, 324–330.

Baddeley, A. D. and Andrade, J. 2000. Working memory and the vividness of imagery. J. Exp. Psychol. Gen. 129, 126–145.

Balakrishnan, J. D., Klatzky, R. L., Loomis, J. M., and Lederman, S. J. 1989. Length distortion of temporally extended visual displays: similarity to haptic spatial perception. Percept. Psychophys. 46, 387–394.

Blajenkova, O., Kozhevnikov, M., and Motes, M. A. 2006. Object-spatial imagery: a new self-report imagery questionnaire. Appl. Cognit. Psychol. 20, 239–263.

Blake, R., Sobel, K. V., and James, T. W. 2004. Neural synergy between kinetic vision and touch. Psychol. Sci. 15, 397–402.

Bliss, I. and Hämäläinen, H. 2005. Different working memory capacity in normal young adults for visual and tactile letter recognition task. Scand. J. Psychol. 46, 247–251.

Botvinick, M. and Cohen, J. 1998. Rubber hands 'feel' touch that eyes see. Nature 391, 756.

van Boven, R. W., Ingeholm, J. E., Beauchamp, M. S., Bikle, P. C., and Ungerleider, L. G. 2005. Tactile form and location processing in the human brain. Proc. Natl. Acad. Sci. U. S. A. 102, 12601–12605.

Bushnell, E. W. and Baxt, C. 1999. Children's haptic and cross-modal recognition with familiar and unfamiliar objects. J. Exp. Psychol. Human. Percep. Perf. 25, 1867–1881.

Cairns, E. and Coll, P. 1977. The role of visual imagery in visual, tactual and cross-modal matching. Brit. J. Psychol. 68, 213–214.

Carpenter, P. A. and Eisenberg, P. 1978. Mental rotation and the frame of reference in blind and sighted individuals. Percept. Psychophys. 23, 117–124.

Casey, S. J. and Newell, F. N. 2007. Are representations of unfamiliar faces independent of encoding modality? Neuropsychologia 45, 506–513.

Craig, J. C. 2006. Visual motion interferes with tactile motion perception. Perception 35, 351–367.

Dean, G. and Morris, P. E. 2003. The relationship between self-reports of imagery and spatial ability. Brit. J. Psychol. 94, 245–273.

Dean, G. M., Dewhurst, S. A., Morris, P. E., and Whittaker, A. 2005. Selective interference with the use of visual images in the symbolic distance paradigm. J. Exp. Psychol. Learn. 31, 1043–1068.

Deibert, E., Kraut, M., Kremen, S., and Hart, J., Jr. 1999. Neural pathways in tactile object recognition. Neurology 52, 1413–1417.

Dellantonio, A. and Spagnolo, F. 1990. Mental rotation of tactual stimuli. Acta Psychol. 73, 245–257.

De Volder, A. G., Toyama, H., Kimura, Y., Kiyosawa, M., Nakano, H., Vanlierde, A., Wanet-Defalque, M.-C., Mishima, M., Oda, K., Ishiwata, K., and Senda, M. 2001. Auditory triggered mental imagery of shape involves visual association areas in early blind humans. NeuroImage 14, 129–139.

DiCarlo, J. J., Johnson, K. O., and Hsiao, S. S. 1998. Structure of receptive fields in area 3b of primary somatosensory cortex in the alert monkey. J. Neurosci. 18, 2626–2645.

Duhamel, J. R., Colby, C. L., and Goldberg, M. E. 1998. Ventral intraparietal area of the macaque: congruent visual and somatic response properties. J. Neurophysiol. 79, 126–136.

Easton, R. D., Greene, A. J., and Srinivas, K. 1997a. Transfer between vision and haptics: memory for 2-D patterns and 3-D objects. Psychon. Bull. Rev. 4, 403–410.

Easton, R. D., Srinivas, K., and Greene, A. J. 1997b. Do vision and haptics share common representations? Implicit and explicit memory within and between modalities. J. Exp. Psychol. Learn Mem. Cogn. 23, 153–163.

Ehrsson, H. H., Spence, C., and Passingham, R. E. 2004. That's my hand! Activity in premotor cortex reflects feeling of ownership of a limb. Science 305, 875–877.

Falchier, A., Clavagnier, S., Barone, P., and Kennedy, H. 2002. Anatomical evidence of multimodal integration in primate striate cortex. J. Neurosci. 22, 5749–5759.

Feinberg, T. E., Rothi, L. J., and Heilman, K. M. 1986. Multimodal agnosia after unilateral left hemisphere lesion. Neurology 36, 864–867.

Fiorio, M. and Haggard, P. 2005. Viewing the body prepares the brain for touch: effects of TMS over somatosensory cortex. Eur. J. Neurosci. 22, 773–777.

Freides, D. 1974. Human information processing and sensory modality: cross-modal functions, information complexity, memory and deficit. Psychol. Bull. 81, 284–310.

Galletti, C., Battaglini, P. P., and Fattori, P. 1991. Functional properties of neurons in the anterior bank of the parieto-occipital sulcus of the macaque monkey. Eur. J. Neurosci. 3, 452–461.

Garvill, J. and Molander, B. 1973. Effects of standard modality, comparison modality and retention interval on matching of form. Scand. J. Psychol. 14, 203–206.

Graziano, M. S., Yap, G. S., and Gross, C. G. 1994. Coding of visual space by premotor neurons. Science 266, 1054–1057.

Grefkes, C., Geyer, S., Schormann, T., Roland, P., and Zilles, K. 2001. Human somatosensory area 2: observer-independent cytoarchitectonic mapping, interindividual variability, and population map. NeuroImage 14, 617–631.

Grefkes, C., Weiss, P. H., Zilles, K., and Fink, G. R. 2002. Crossmodal processing of object features in human anterior intraparietal cortex: an fMRI study implies equivalencies between humans and monkeys. Neuron 35, 173–184.

Grill-Spector, K., Kushnir, T., Hendler, T., Edelman, S., Itzchak, Y., and Malach, R. 1998. A sequence of object-processing stages revealed by fMRI in the human occipital lobe. Hum. Brain Mapp. 6, 316–328.

Haenny, P. E., Maunsell, J. H. R., and Schiller, P. H. 1988. State dependent activity in monkey visual cortex. II. Retinal and extraretinal factors in V4. Exp. Brain Res. 69, 245–259.

Hagen, M. C., Franzen, O., McGlone, F., Essick, G., Dancer, C., and Pardo, J. V. 2002. Tactile motion activates the human middle temporal/V5 (MT/V5) complex. Eur. J. Neurosci. 16, 957–964.

Halligan, P., Hunt, M., Marshall, J., and Wade, D. 1996. When seeing is feeling: acquired synaesthesia or phantom touch? Neurocase 2, 21–29.

Heller, M. A. 1989. Texture perception in sighted and blind observers. Percept. Psychophys. 45, 49–54.

Heller, M. A., Brackett, D. D., Wilson, K., Yoneyama, K., and Boyer, A. 2002. The haptic Müller–Lyer illusion in sighted and blind people. Perception 31, 1263–1274.

Hollins, M. 1986. Haptic mental rotation: more consistent in blind subjects? J. Visual. Impair. Blin. 80, 950–952.
Iriki, A., Tanaka, M., and Iwamura, Y. 1996. Coding of modified body schema during tool use by macaque postcentral neurones. NeuroReport 7, 2325–2330.
Ishai, A., Haxby, J. V., and Ungerleider, L. G. 2002. Visual imagery of famous faces: effects of memory and attention revealed by fMRI. NeuroImage 17, 1729–1741.
Iwamura, Y., Iriki, A., and Tanaka, M. 1994. Bilateral hand representation in the postcentral somatosensory cortex. Nature 369, 554–556.
James, T. W. and Blake, R. 2004. Perceiving object motion using vision and touch. Cognit. Affect. Behav. Neurosci. 4, 201–207.
James, T. W., Humphrey, G. K., Gati, J. S., Servos, P., Menon, R. S., and Goodale, M. A. 2002. Haptic study of three-dimensional objects activates extrastriate visual areas. Neuropsychologia 40, 1706–1714.
James, T. W., James, K. H., Humphrey, G. K., and Goodale, M. A. 2006a. Do Visual and Tactile Object Representations Share the Same Neural Substrate? In: Touch and Blindness: Psychology and Neuroscience (*eds*. M. A. Heller and S. Ballesteros), pp. 139–155. Lawrence Erlbaum Associates.
James, T. W., Servos, P., Kilgour, A. R., Huh, E., and Lederman, S. 2006b. The influence of familiarity on brain activation during haptic exploration of 3-D facemasks. Neurosci. Lett. 397, 269–273.
Johnson, R. M., Burton, P. C., and Ro, T. 2006. Visually induced feelings of touch. Brain Res. 1073–1074, 398–406.
Johnson, C. L., Paivio, A. U., and Clark, J. M. 1989. Spatial and verbal abilities in children's cross-modal recognition: a dual-coding approach. Can. J. Psychol. 43, 397–412.
Jones, B. 1981. The Developmental Significance of Cross-Modal Matching. In: Intersensory Perception and Sensory Integration (*eds*. R. D. Walk and H. L. Pick Jr.), pp. 109–136. Plenum.
Kilgour, A. R. and Lederman, S. 2002. Face recognition by hand. Percept. Psychophys. 64, 339–352.
Kilgour, A. R., de Gelder, B., and Lederman, S. 2004. Haptic face recognition and prosopagnosia. Neuropsychologia 42, 707–712.
Kilgour, A. R., Kitada, R., Servos, P., James, T. W., and Lederman, S. J. 2005. Haptic face identification activates ventral occipital and temporal areas: an fMRI study. Brain Cogn. 59, 246–257.
Killackey, H. P., Gould, H. J., Cusick, C. G., Pons, T. P, and Kaas, J. H. 1983. The relation of corpus callosum connections to architectonic fields and body surface maps in sensorimotor cortex of New and Old World monkeys. J. Comp. Neurol. 219, 384–419.
Kiphart, M. J., Hughes, J. L., Simmons, J. P., and Cross, H. A. 1992. Short-term haptic memory for complex objects. Bull. Psychon. Soc. 30, 212–214.
Kitada, R., Kito, T., Saito, D. N., Kochiyama, T., Matsumura, M., Sadato, N., and Lederman, S. J. 2006. Multisensory activation of the intraparietal area when classifying grating orientation: a functional magnetic resonance imaging study. J. Neurosci. 26, 7491–7501.
Klatzky, R. L., Lederman, S. J., and Matula, D. E. 1993. Haptic exploration in the presence of vision. J. Exp. Psychol. Human Percep. Perf. 19, 726–743.
Klatzky, R. L., Lederman, S. J., and Reed, C. 1987. There's more to touch than meets the eye: the salience of object attributes for haptics with and without vision. J. Exp. Psychol. Gen. 116, 356–369.
Kosslyn, S. M. 1973. Scanning visual images: some structural implications. Percept. Psychophys. 14, 90–94.
Kosslyn, S. M. 1980. Image and Mind. Harvard University Press.
Kosslyn, S. M. 1994. Image and Brain: The Resolution of the Imagery Debate. MIT Press.
Kosslyn, S. M., Ball, T. M., and Reiser, B. J. 1978. Visual images preserve metric spatial information: evidence from studies of image scanning. J. Exp. Psychol. Human Percep. Perf. 4, 47–60.
Kosslyn, S. M., Brunn, J., Cave, K. R., and Wallach, R. W. 1984. Individual differences in mental imagery ability. Cognition 18, 195–243.
Kosslyn, S. M., Van Kleeck, M. H., and Kirby, K. N. 1990. A Neurologically Plausible Model of Individual Differences in Visual Mental Imagery. In: Imagery: Current Developments (*eds*. P. J. Hampson, D. F. Marks, and J. T. E. Richardson), pp. 39–77. Routledge.
Kozhevnikov, M., Hegarty, M., and Mayer, R. E. 2002. Revising the visualiser–verbaliser dimension: evidence for two types of visualisers. Cognit. Instruct. 20, 47–77.
Kozhevnikov, M., Kosslyn, S. M., and Shepard, J. 2005. Spatial versus object visualisers: a new characterisation of cognitive style. Mem. Cognit. 33, 710–726.
Lacey, S. and Campbell, C. 2006a. Mental representation in visual/haptic crossmodal memory: evidence from interference effects. Q. J. Exp. Psychol. 59, 361–376.
Lacey, S. and Campbell, C. 2006b. Object representation in visual/haptic cross-modal memory. Abstract, 7th International Multisensory Research Forum.
Lewkowicz, D. J. 1994. Development of Intersensory Perception in Human Infants. In: The Development of Intersensory Perception: Comparative Perspectives (*eds*. D. J. Lewkowicz and R. Lickliter), pp. 165–203. Lawrence Erlbaum Associates.
Malach, R., Reppas, J. B., Benson, R. R., Kwong, K. K., Jiang, H., Kennedy, W. A., Ledden, P. J., Brady, T. J., Rosen, B. R., and Tootell, R. B. 1995. Object-related activity revealed by functional magnetic resonance imaging in human occipital cortex. Proc. Natl. Acad. Sci. U. S. A. 92, 8135–8139.
Manzoni, T., Barbaresi, P., and Conti, F. 1984. Callosal mechanism for the interhemispheric transfer of hand somatosensory information in the monkey. Behav. Brain Res. 11, 155–170.
Marks, D. F. 1973. Visual imagery differences in the recall of pictures. Brit. J. Psychol. 64, 17–24.
Marmor, G. S. and Zaback, L. A. 1976. Mental rotation by the blind: does mental rotation depend on visual imagery? J. Exp. Psychol. Hum. Percept. Perform 2, 515–521.
Mechelli, A., Price, C. J., Friston, K. J., and Ishai, A. 2004. Where bottom-up meets top-down: neuronal interactions during perception and imagery. Cereb. Cortex 14, 1256–1265.
Mellet, E., Tzourio, N., Crivello, F., Joliot, M., Denis, M., and Mazoyer, B. 1996. Functional anatomy of spatial imagery generated from verbal instructions. J. Neurosci. 16, 6504–6512.
Merabet, L., Thut, G., Murray, B., Andrews, J., Hsiao, S., and Pascual-Leone, A. 2004. Feeling by sight or seeing by touch? Neuron 42, 173–179.
Millar, S. and Al-Attar, Z. 2002. The Müller–Lyer illusion in touch and vision: implications for multisensory processes. Percept. Psychophys. 64, 353–365.
Nabeta, T. and Kawahara, J. 2006. Congruency effect of presentation modality on false recognition of haptic and visual objects. Memory 14, 307–315.
Newman, S. D., Klatzky, R. L., Lederman, S. J., and Just, M. A. 2005. Imagining material versus geometric properties of objects: an fMRI study. Cognit. Brain Res. 23, 235–246.
Norman, J. F., Norman, H. F., Clayton, A. M., Lianekhammy, J., and Zielke, G. 2004. The visual and haptic perception of natural object shape. Percept. Psychophys. 66, 342–351.
Pearson, D., De Beni, R., and Cornoldi, C. 2001. The Generation, Maintenance and Transformation of Visuo-Spatial Mental Images. In: Imagery, Language and Visuo-Spatial Thinking (*eds*. M. Denis, R. H. Logie,

C. Cornoldi, M. de Vega, and J. Engelkamp), pp. 1–27. Psychology Press.
Peltier, S., Stilla, R., Mariola, E., LaConte, S., Hu, X., and Sathian, K. 2007. Activity and effective connectivity of parietal and occipital cortical regions during haptic shape perception Neuropsychologia 45, 476–483.
Pietrini, P., Furey, M. L., Ricciardi, E., Gobbini, M. I., Wu, W.-H. C., Cohen, L., Guazzelli, M., and Haxby, J. V. 2004. Beyond sensory images: object-based representation in the human ventral pathway. Proc. Natl. Acad. Sci. U. S. A. 101, 5658–5663.
Pitzalis, S., Galletti, C., Huang, R. S., Patria, F., Committeri, G., Galati, G., Fattori, P., and Sereno, M. I. 2006. Wide-field retinotopy defines human cortical visual area V6. J. Neurosci. 26, 7962–7973.
Pons, T. P., Wall, J. T., Garraghty, P. E., Cusick, C. G., and Kaas, J. H. 1987. Consistent features of the representation of the hand in area 3b of macaque monkeys. Somatosens. Res. 4, 309–331.
Prather, S. C. and Sathian, K. 2002. Mental rotation of tactile stimuli. Cognit. Brain Res. 14, 91–98.
Prather, S. C., Votaw, J. R., and Sathian, K. 2004. Task-specific recruitment of dorsal and ventral visual areas during tactile perception. Neuropsychologia 42, 1079–1087.
Quinn, J. G. and McConnell, J. 1996. Indications of the functional distinction between the components of visual working memory. Psychol. Beitr. 53, 355–367.
Ramachandran, V. S. 1995. Touching the phantom limb. Nature 377, 489–490.
Ramachandran, V. S. and Hirstein, W. 1998. The perception of phantom limbs: the DO Hebb Lecture. Brain 121, 1603–1630.
Reales, J. M. and Ballesteros, S. 1999. Implicit and explicit memory for visual and haptic objects: cross-modal priming depends on structural descriptions. J. Exp. Psychol. Learn Mem. Cogn. 25, 644–663.
Reed, C. L., Shoham, S., and Halgren, E. 2004. Neural substrates of tactile object recognition: an fMRI study. Hum. Brain Mapp. 21, 236–246.
Ro, T., Wallace, R., Hagedorn, J., Farne, A., and Pienkos, E. 2004. Visual enhancing of tactile perception in the posterior parietal cortex. J. Cogn. Neurosci. 16, 24–30.
Robinson, C. J. and Burton, H. 1980a. Organization of somatosensory receptive fields in cortical areas 7b, retroinsula, postauditory and granular insula of *M. fascicularis*. J. Comp. Neurol. 192, 69–92.
Robinson, C. J. and Burton, H. 1980b. Somatotopographic organization in the second somatosensory area of *M. fascicularis*. J. Comp. Neurol. 192, 43–67.
Rock, I. and Victor, J. 1964. Vision and touch: an experimentally created conflict between the two senses. Science 143, 594–596.
Rockland, K. S. and Ojima, H. 2003. Multisensory convergence in calcarine visual areas in macaque monkey. Int. J. Psychophysiol. 50, 19–26.
Röder, B. and Rösler, F. 1998. Visual input does not facilitate the scanning of spatial images. J. Mental Imagery 22, 165–181.
Rose, S. A. 1994. From Hand To Eye: Findings and Issues in Infant Cross-Modal Transfer. In: The Development of Intersensory Perception: Comparative Perspectives (*eds*. D. J. Lewkowicz and R. Lickliter), pp. 265–284. Lawrence Erlbaum Associates.
Saito, D. N., Okada, T., Morita, Y., Yonekura, Y., and Sadato, N. 2003. Tactile-visual cross-modal shape matching: a functional MRI study. Cognit. Brain Res. 17, 14–25.
Sathian, K. 2000. Intermanual referral of sensation to anesthetic hands. Neurology 54, 1866–1868.
Sathian, K. 2004. Modality, quo vadis? Behav. Brain Sci. 27, 413–414.
Sathian, K., Greenspan, A. I., and Wolf, S. L. 2000. Doing it with mirrors: a case study of a novel approach to neurorehabilitation. Neurorehabilit. Neural Repair 14, 73–76.
Sathian, K., Zangaladze, A., Hoffman, J. M., and Grafton, S. T. 1997. Feeling with the mind's eye. NeuroReport 8, 3877–3881.
Schroeder, C. E. and Foxe, J. J. 2002. The timing and laminar profile of converging inputs to multisensory areas of the macaque neocortex. Cognit. Brain Res. 14, 187–198.
Schroeder, C. E., Lindsley, R. W., Specht, C., Marcovici, A., Smiley, J. F., and Javitt, D. C. 2001. Somatosensory input to auditory association cortex in the macaque monkey. J. Neurophysiol. 85, 1322–1327.
Schroeder, C. E., Smiley, J., Fu, K. G., McGinnis, T., O'Connell, M. N., and Hackett, T. A. 2003. Anatomical mechanisms and functional implications of multisensory convergence in early cortical processing. Int. J. Psychophysiol. 50, 5–17.
Sergent, J., Ohta, S., and MacDonald, B. 1992. Functional neuroanatomy of face and object processing. A positron emission tomography study. Brain 115, 15–36.
Shepard, R. N. and Metzler, J. 1971. Mental rotation of three-dimensional objects. Science 171, 701–703.
Stoeckel, M. C., Weder, B., Binkofski, F., Buccino, G., Shah, N. J., and Seitz, R. J. 2003. A fronto-parietal circuit for tactile object discrimination: an event-related fMRI study. NeuroImage 19, 1103–1114.
Stoesz, M., Zhang, M., Weisser, V. D., Prather, S. C., Mao, H., and Sathian, K. 2003. Neural networks active during tactile form perception: common and differential activity during macrospatial and microspatial tasks. Int. J. Psychophysiol. 50, 41–49.
Stoltz-Loike, M. and Bornstein, M. H. 1987. The roles of imagery, language and metamemory in cross-modal transfer in children. Psychol. Res. 49, 63–68.
Streri, A. and Molina, M. 1994. Constraints on Intermodal Transfer between Touch and Vision in Infancy. In: The Development of Intersensory Perception: Comparative Perspectives (*eds*. D. J. Lewkowicz and R. Lickliter), pp. 285–307. Lawrence Erlbaum Associates.
Taylor-Clarke, M., Kennett, S., and Haggard, P. 2004. Persistence of visual–tactile enhancement in humans. Neurosci. Lett. 354, 22–25.
Woods, A. T., O'Modhrain, S., and Newell, F. N. 2004. The effect of temporal delay and spatial differences on crossmodal object recognition. Cogn. Affect. Behav. Neurosci. 4, 260–269.
Zangaladze, A., Epstein, C. M., Grafton, S. T., and Sathian, K. 1999. Involvement of visual cortex in tactile discrimination of orientation. Nature 401, 587–590.
Zhang, M., Mariola, E., Stilla, R., Stoesz, M., Mao, H., Hu, X., and Sathian, K. 2005. Tactile discrimination of grating orientation: fMRI activation patterns. Hum. Brain Mapp. 25, 370–377.
Zhang, M., Weisser, V. D, Stilla, R., Prather, S. C., and Sathian, K. 2004. Multisensory cortical processing of object shape and its relation to mental imagery. Cognit. Affect. Behav. Neurosci. 4, 251–259.

Further Reading

Sathian, K. 2000. Intermanual referral of sensation to anesthetic hands. Neurology 54, 1866–1868.